FORTIETH EDITION

Anatomy

The Anatomical Basis of Clinical Practice

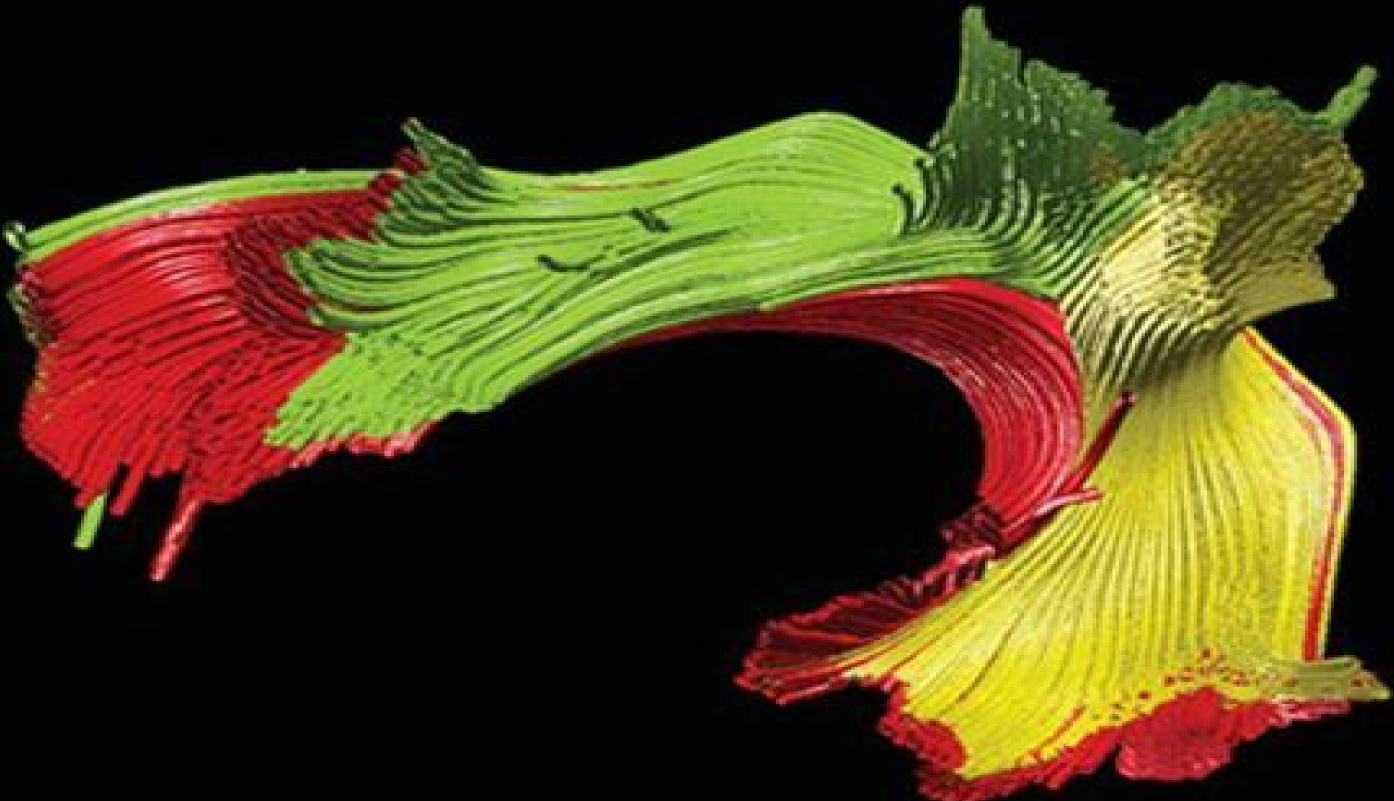

ANNIVERSARY EDITION
150 YEARS
One Hundred and Fiftieth Year

Editor-in-Chief
Susan Standring

Gray's Anatomy

The Anatomical Basis of Clinical Practice

Fortieth Edition

EDITOR-IN-CHIEF

Susan Standring, PhD, DSc, FKC
Emeritus Professor of Anatomy, King's College London, London, UK

SECTION EDITORS

Neil R Borley, FRCS, FRCS(Ed), MS
Consultant Colorectal Surgeon, Department of Gastrointestinal Surgery, Cheltenham General Hospital, Gloucestershire Hospitals NHS Trust, Cheltenham, UK

Patricia Collins, PhD
Associate Professor of Anatomy, Anglo-European College of Chiropractic, Bournemouth, UK

Alan R Crossman, PhD, DSc
Professor of Anatomy, Faculty of Life Sciences, The University of Manchester, Manchester, UK

Michael A Gatzoulis, MD, PhD, FESC, FACC
Professor of Cardiology, Congenital Heart Disease

Consultant Cardiologist, Adult Congenital Heart Centre and Centre for Pulmonary Hypertension, Royal Brompton Hospital, and the National Heart and Lung Institute, Imperial College, London, UK

Jeremiah C Healy, MA, MB BChir, MRCP, FRCR
Consultant Radiologist, Chelsea and Westminster Hospital; Honorary Senior Lecturer Imperial College, London, UK

David Johnson, MA, BM BCh, DM, FRCS(Eng)
Consultant in Plastic, Reconstructive and Craniofacial Surgery, Department of Plastic and Reconstructive Surgery, Radcliffe Infirmary, Oxford, UK

Vishy Mahadevan, PhD, FRCS(Ed), FRCS(Eng)
Professor of Surgical Anatomy and Barbers' Company Reader in Anatomy, Raven Department of Education, The Royal College of Surgeons of England, London, UK

Richard LM Newell, BSc, MB BS, FRCS

Honorary Consultant Orthopaedic Surgeon, Royal Devon and Exeter Healthcare NHS Trust, Exeter, UK

Caroline B Wigley, BSc, PhD
Senior Honorary, University Teaching Fellow, College of Medicine and Dentistry Peninsula, Exeter, UK

CHURCHILL LIVINGSTONE

Table of Contents

Instructions for online access

Title page

Copyright

PREFACE

ACKNOWLEDGEMENTS

CONTRIBUTORS

REVIEWERS

INTERNATIONAL REVIEWERS

HISTORICAL INTRODUCTION

ANATOMICAL NOMENCLATURE

BIBLIOGRAPHY OF SELECTED TITLES

Section 1: CELLS, TISSUES AND SYSTEMS

- Chapter 1: Basic structure and function of cells
- Chapter 2: Integrating cells into tissues
- Chapter 3: Nervous system
- Chapter 4: Blood, lymphoid tissues and haemopoiesis
- Chapter 5: Functional anatomy of the musculoskeletal system
- Chapter 6: Smooth muscle and the cardiovascular and lymphatic systems

  - Chapter 7: Skin and its appendages
- Section 2: EMBRYOGENESIS
  - Chapter 8: Preimplantation development
  - Chapter 9: Implantation and placentation
  - Chapter 10: Cell populations at gastrulation
  - Chapter 11: Embryonic induction and cell division
  - Chapter 12: Cell populations at the start of organogenesis
  - Chapter 13: Early embryonic circulation
  - Chapter 14: Pre- and postnatal development
- Section 3: NEUROANATOMY
  - Chapter 15: Overview of the nervous system
  - Chapter 16: Ventricular system and subarachnoid space
  - Chapter 17: Vascular supply and drainage of the brain
  - Chapter 18: Spinal cord: internal organization
  - Chapter 19: Brain stem
  - Chapter 20: Cerebellum
  - Chapter 21: Diencephalon
  - Chapter 22: Basal ganglia
  - Chapter 23: Cerebral hemisphere
  - Chapter 24: Development of the nervous system
- Section 4: HEAD AND NECK
  - Chapter 25: Head and neck: overview and surface anatomy

Chapter 26: External skull

Chapter 27: Intracranial region

Chapter 28: Neck

Chapter 29: Face and scalp

Chapter 30: Oral cavity

Chapter 31: Infratemporal and pterygopalatine fossae and temporomandibular joint

Chapter 32: Nose, nasal cavity and paranasal sinuses

Chapter 33: Pharynx

Chapter 34: Larynx

Chapter 35: Development of the head and neck

Chapter 36: External and middle ear

Chapter 37: Inner ear

Chapter 38: Development of the ear

Chapter 39: The orbit and accessory visual apparatus

Chapter 40: The eye

Chapter 41: Development of the eye

Section 5: THE BACK

Chapter 42: The back

Chapter 43: Spinal cord and spinal nerves: gross anatomy

Chapter 44: Development of the back

Section 6: PECTORAL GIRDLE AND UPPER LIMB

Chapter 45: Pectoral girdle and upper limb: overview and surface anatomy

Chapter 46: Pectoral girdle, shoulder region and axilla

Chapter 47: Upper arm

Chapter 48: Elbow

Chapter 49: Forearm

Chapter 50: Wrist and hand

Chapter 51: Development of the limbs

Chapter 52: Development of the pectoral girdle and upper limb

Section 7: THORAX

Chapter 53: Thorax: overview and surface anatomy

Chapter 54: Chest wall and breast

Chapter 55: Mediastinum

Chapter 56: Heart and great vessels

Chapter 57: Pleura, lungs, trachea and bronchi

Chapter 58: Diaphragm

Chapter 59: Development of the thorax

Section 8: ABDOMEN AND PELVIS

Chapter 60: Abdomen and pelvis: overview and surface anatomy

Chapter 61: Anterior abdominal wall

Chapter 62: Posterior abdominal wall and retroperitoneum

Chapter 63: True pelvis, pelvic floor and perineum

Chapter 64: Peritoneum and peritoneal cavity

Chapter 65: Abdominal oesophagus and stomach

Chapter 66: Small intestine

Chapter 67: Large intestine

Chapter 68: Liver

Chapter 69: Gallbladder and biliary tree

Chapter 70: Pancreas

Chapter 71: Spleen

Chapter 72: Suprarenal (adrenal) gland

Chapter 73: Development of the peritoneal cavity, gastrointestinal tract and its adnexae

Chapter 74: Kidney and ureter

Chapter 75: Bladder, prostate and urethra

Chapter 76: Male reproductive system

Chapter 77: Female reproductive system

Chapter 78: Development of the urogenital system

Section 9: PELVIC GIRDLE AND LOWER LIMB

Chapter 79: Pelvic girdle and lower limb: overview and surface anatomy

Chapter 80: Pelvic girdle, gluteal region and thigh

Chapter 81: Hip

Chapter 82: Knee

Chapter 83: Leg

Chapter 84: Ankle and foot

Chapter 85: Development of the pelvic girdle and lower limb

INDEX

Copyright

CHURCHILL LIVINGSTONE ELSEVIER

is an imprint of Elsevier.

© 2008, Elsevier Limited. All rights reserved.

Fortieth edition published 2008

First edition JW Parker & Son 1858

The right of Susan Standring, Neil R Borley, Patricia Collins, Alan R Crossman, Michael A Gatzoulis, Jeremiah C Healy, David Johnson, Vishy Mahadevan, Richard LM Newell and Caroline Wigley to be identified as authors of this work has been asserted by them in accordance with the Copyright, Designs and Patents Act 1988.

No part of this publication may be reproduced or transmitted in any form or by any means, electronic or mechanical, including photocopying, recording, or any information storage and retrieval system, without permission in writing from the publisher. Permissions may be sought directly from Elsevier's Rights Department: phone: (+1) 215 239 3804 (US) or (+44) 1865 843830 (UK); fax: (+44) 1865 853333; e-mail: healthpermissions@elsevier.com. You may also complete your request on-line via the Elsevier website at http://www.elsevier.com/permissions.

Expert Consult ISBN: 978-0-443-06684-9

International Edition ISBN: 978-0-8089-2371-8

British Library Cataloguing in Publication Data

A catalogue record for this book is available from the British Library

Library of Congress Cataloging in Publication Data

A catalog record for this book is available from the Library of Congress

Notice

No responsibility is assumed by the Publishers, Editors or Contributors for any loss or injury and/or damage to persons or property arising out of or related to any use of the material contained in this book. It is the responsibility of the treating practitioner, relying upon independent expertise and knowledge of the patient, to determine the best treatment and method of application for the patient.

Every effort has been made to contact holders of copyright to obtain permission to reproduce copyright material. However, if any have been inadvertently overlooked, the Publisher will be pleased to make the necessary arrangements at the first opportunity.

The Publisher

Printed in Spain

Last digit is the print number: 9 8 7 6 5 4 3 2 1

Commissioning Editors: Madelene Hyde and Inta Ozols

Development Editors: Martin Mellor, Gavin Smith and Alison Whitehouse

Head of Development (Global Medicine): Louise Cook

Editorial Assistants: Julie Goolsby and Liam Jackson

Project Managers: Glenys Norquay and Bryan Potter

Illustration Managers: Merlyn Harvey, Bruce Hogarth and Gillian Richards

Illustrators (39th and 40th editions): Antbits (Paul Banville, Michael Courtney, Jonathan Dimes, Paul Richardson, Richard Tibbitts), Robert Britton, Joe Chovan, Peter Cox, Ethan Danielson, Brian Evans, Sandie Hill, Bruce Hogarth, Gillian Lee, Debbie Maizels, Annabel Milne, Philip Wilson, Martin Woodward

Page Design: Jayne Jones

Cover Design: Stewart Larking

Copyeditors: Carolyn Holleyman, with Alyson Colley
Proofreader: Ian Ross
Indexer: Susan Boobis
Marketing Managers: Jeremy Bowes (UK) and Lisa Damico (US)

COVER IMAGE

‘Tractography reconstruction of the perisylvian language pathways’ from Catani M, Jones DK & ffytche DH, *Ann Neurol* 2005; 57(1):8–16 with permission of John Wiley & Sons. After almost 120 years this tractography reconstruction of the language pathways has updated the anatomy of the language networks. Image courtesy of Marco Catani, Natbrainlab, Centre for Neuroimaging Sciences and Section of Brain Maturation, Department of Psychological Medicine, Institute of Psychiatry, King’s College London.

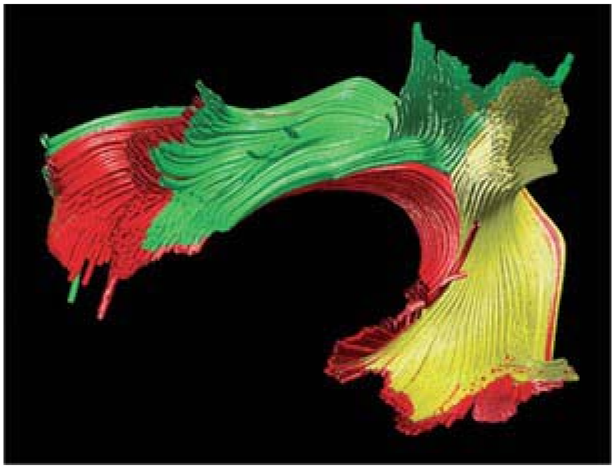

PREFACE

The 40th edition of *Gray's Anatomy* celebrates 150 years of continuous publication of an extraordinary book. Although this edition looks very different from the first edition (see Ruth Richardson's historical introduction on page xvii), the essential aim of Henry Gray and the illustrator Henry Vandyke Carter, to describe the clinically relevant anatomy of the human body, particularly (but not exclusively) for the practicing surgeon, has not changed over the years. Anatomy may be struggling to retain its foothold in many undergraduate medical curricula, but it is enjoying a renaissance at the postgraduate level. A detailed knowledge of clinical anatomy which would have been undreamed of in the first edition, is now essential for clinicians working in technologically driven fields such as imaging, endoscopic and robotic surgery.

Nine Section Editors (Neil Borley, Pat Collins, Alan Crossman, Michael Gatzoulis, Jeremiah Healy, David Johnson, Vishy Mahadevan, Richard Newell and Caroline Wigley) have worked with me in preparing the 40th edition. They have brought their extensive experience as anatomists, cell biologists and clinicians to the task, and I thank them for their dedication and enthusiastic support. Pat Collins, Jeremiah Healy and Caroline Wigley also worked closely with all members of the editorial team in updating the text and artworks for embryology, imaging and microstructure respectively throughout the book. Harold Ellis has meticulously edited the section on eponyms which is available on the website, and has commented on many of the chapters.

Each Section Editor was assisted by a group of Contributors – experienced anatomists and clinicians (sometimes both) who contributed text and/or artworks and original micrographs. The page proofs were scrutinized by a core team of Reviewers and finally a panel of

International Reviewers: their comments have been incorporated into the text and I acknowledge their critical input. Working at this level of detail I have often been impressed by how much anatomy remains controversial or is simply unknown: surgeons, radiologists and embryologists often disagree passionately about structural relationships or developmental processes. Gray's continues to flag up these uncertainties and to present different perspectives.

As a general rule, the orientation of diagrams and photographs throughout the book has been standardized to show the left side of the body, irrespective of whether a lateral or medial view is presented, and transverse sections are viewed from below to facilitate comparison with clinical images. Clinicopathological examples have been selected where the pathology is either a direct result of, or a consequence of, the anatomy, or where the anatomical features are instrumental in the diagnosis/treatment/management of the condition. All of the pre 39th edition artworks, and the great majority of the images and micrographs of histological and embryological specimens have been replaced: wherever possible, the photomicrographs illustrate human histology and embryology, and non human sources have been acknowledged in the captions. New artworks have either been generated *de novo* or have been taken from other texts (principally *Sobotta's Atlas of Anatomy, Books 1 and 2* or *Gray's Atlas of Anatomy*), making this the first full-colour edition of *Gray's Anatomy*.

I am often asked why *Gray's Anatomy* does not contain *even more* detailed surgical and radiological anatomy, with further examples of anatomical variants and of laparoscopic and endoscopic anatomy, and why we exclude all but a very few references. The answer is that we would love to do this, and to include some systematic anatomy, but we have reached a point where there is no room for more material in a single volume. Short reference lists are provided at the ends of each chapter to guide further reading, and a list of general texts and references covering material presented in more than one chapter, e.g. the distribution of angiosomes, appears on page xxiv. The Bibliography, which collated all of the references cited in a number of earlier editions 35–38, is retained on the website.

I offer my sincere thanks to the editorial team at Elsevier, initially under the leadership of Inta Ozols and latterly of Madelene Hyde, for their guidance, professionalism, good humour and unfailing support. In particular, I thank Alison Whitehouse, Gavin Smith, Martin Mellor and Louise Cook, for being at the end of a phone or e-mail whenever I needed advice. I am especially grateful to my dear husband, Guy Standring, for his tolerance while he has shared his life with *Gray's Anatomy*, and I dedicate my work in this book to him.

Susan Standring

May 2008

ACKNOWLEDGEMENTS

Within individual figure captions, we have acknowledged all figures kindly loaned from other sources. However, we would particularly like to thank the following authors who have generously loaned so many figures from other books published by Elsevier:

Drake R, Vogl W, Mitchell AWM 2004 Gray's Anatomy for Students. Edinburgh: Churchill Livingstone.

Drake R, Vogl W, Mitchell AWM, Tibbitts R, Richardson P 2008 Gray's Atlas of Anatomy. Edinburgh: Churchill Livingstone.

Putz R, Pabst R 2006 Sobotta: Atlas der Anatomie des Menschen. Band 1. Kopf, Hals, obere Extremitat. 22 Auflage. Munchen: Elsevier.

Much of the illustration in *Gray's Anatomy* has as its basis the work of illustrators and photographers who contributed towards earlier editions, their figures sometimes being retained almost unchanged though more often being used as the foundation for figures that are new to this edition. The Publishers would like to thank them. For illustration reused from the 39th edition, we particularly thank its photographer Sarah-Jane Smith and the artists listed on page iv.

The Publishers would also like to thank: Anne-Marie Childs BSc, MB ChB, MRCP, FRCPCH, Consultant Paediatric Neurologist, The General infirmary at Leeds; James M McCall BSc, MBBS, MRCP, FRCR, Consultant Radiologist, Chelsea and Westminster Hospital, London, and Romney JE Pope MA, MRCP, FRCR, Consultant Radiologist, Royal Marsden and Chelsea and Westminster Hospitals, London, for their help in preparing material for the new edition.

CONTRIBUTORS

Michael A. Adams, BSc, PhD
Reader in Spine Biomechanics, Department of Anatomy, University of Bristol, Bristol, UK

Andrew Amis, PhD, DSc(Eng), FIMechE
Professor of Orthopaedic Biomechanics, Imperial College London, London, UK

Robert H. Anderson, BSc, MD, FRCPath
Formerly Professor of Paediatric Cardiac Morphology, Institute of Child Health, University College, London, UK

Professor of Paediatrics, Medical University of South Carolina, Charleston, South Carolina, USA

Tipu Aziz, BSc, MBBS, MD, FRCS, FRCS(SN), DMedSci
Professor of Neurosurgery, University of Oxford, Oxford, UK

Timothy J. Beale, MBBS FRCS FRCR
Consultant Radiologist, Royal National Throat Nose and Ear Hospital, London, UK

Sue M. Black, OBE, BSc, PhD, DSc, FRSE, Hon FRCPS (Glasg)
Professor, Head of Anatomy and Human Identification, College of Life Sciences, University of Dundee, Dundee, UK

Nikolai Bogduk, BSc (Med), MB BS, PhD, MD, DSc, DipAnat, Dip Pain Med, FAFRM, FAFMM, FFPM(ANZCA)
Professor of Pain Medicine, University of Newcastle, Newcastle, New South Wales, Australia

Peter R. Braude, PhD, FRCOG, FMedSci
Professor and Head of Department of Women's Health, King's College London

Honorary Consultant in Reproductive Medicine, Guy's and St Thomas' Foundation Trust, London, UK

Jonathan L. Brown, MA, MSc, MD, FRCP, DTMH
Professor and Consultant Physician and Gastroenterologist, Gloucestershire Hospitals NHS Trust, Gloucester, UK

Anthony Bull, BEng, DIC CEng, PhD, FIMechE
Reader in Musculoskeletal Mechanics, Department of Bioengineering, Imperial College London, London, UK

Andrew Bush, MB BS (Hons), MA MD FRCP, FRCPCH

Professor of Paediatric Respirology, Department of Paediatric Respiratory Medicine, Imperial College and Royal Brompton Hospital, London, UK

Declan JP. Cahill, BSc, MSc, FRCS (Urol)
Consultant Urologist, Department of Urology, Guy's and St Thomas' NHS Trust, London, UK

Cécile Chalouni, PhD
Technical Director and Associate Research Scientist in Cell Biology, Department of Cell Biology, Ludwig Institute for Cancer Research, Yale University School of Medicine, New Haven, CT, USA

Ashish Chandra, FRCPath, DipRCPath (Cyto)
Consultant Histopathologist, Guy's and St. Thomas' Hospital NHS Foundation Trust, London, UK

Roger Chinn, MB BS, MRCP, FRCR
Consultant Radiologist, Department of Radiology, Chelsea and Westminster NHS Foundation Trust, London, UK

Bodo EA. Christ, MD, PhD, h.c.
Professor, Director of the Institute of Anatomy and Cell Biology, University of Freiburg, Freiburg, Germany

Alfred Cutner, MD, FRCOG
Consultant Gynaecologist, Department of Obstetrics and Gynaecology, University College London Hospitals, London, UK

Catriona L. Davies, MB BS, MRCP, FRCR
Consultant Radiologist, Chelsea and Westminster Hospital, London, UK

Patricia Dolan, BSc, PhD
Reader in Biomechanics, Department of Anatomy, University of Bristol, Bristol, UK

Ronald H. Douglas, BSc, PhD
Professor of Visual Science, Department of Optometry and Visual Science, City University, London, UK

Justin A. Durham, BDS, MFDS, RCS (Ed), FHEA
Clinical Fellow and Honorary Specialist Registrar in Oral Surgery, School of Dental Sciences, Newcastle University, Newcastle, UK

William C. Earnshaw, PhD, FRSE
Professor and Wellcome Trust Principal Research Fellow, Wellcome Trust Centre for Cell Biology, University of Edinburgh, Edinburgh, UK

David M. Evans, FRCS
Consultant Hand Surgeon, Clinical Director, The Hand Clinic, Windsor, UK

Paul A. Felts, PhD
Senior Lecturer, Centre for Anatomy and Human Identification, University of Dundee, Dundee, UK

Alex Freeman, MSc, MBBS, MD, MRCPath
Consultant Urological Pathologist, University College London Hospitals NHS Foundation Trust, London, UK

David Furness, PhD
Reader in Auditory Neuroscience, MacKay Institute of Communication and Neuroscience, The School of Life Sciences Keele University, Keele, UK

Andrew JT. George, MA, PhD, FRCPath, FRSA
Professor of Molecular Immunology, Department of Immunology, Division of Medicine, Faculty of Medicine, Imperial College London, London, UK

Jonathan M. Glass, BSc, MB BS, FRCS (Urol)
Urologist, Department of Urology, Guy’s and St Thomas’ Hospitals, London, UK

Michael Gleeson, MD, FRCS
Consultant Otolaryngologist and Skull Base Surgeon to Guy’s, Kings and St. Thomas’ Hospitals, London

Professor of Skull Base Surgery, National Hospital for Neurology and Neurosurgery, London

Honorary Skull Base Surgeon to the Great Ormond Street Hospital for Sick Children, London, UK

David JA. Goldsmith, MA, FRCP
Consultant Nephrologist, Kidney Unit, Guy’s Hospital, London, UK

Anthony Graham, BSc (Hons), PhD
Professor of Developmental Biology, MRC Centre for Developmental Neurobiology and Division of Anatomy and Human Sciences, School of Biomedical and Health Sciences, Guy’s Campus, King’s College London, London, UK

Paul D. Griffiths, MB ChB, PhD, FRCR
Professor of Radiology, Academic Unit of Radiology, Division of Clinical Science, University of Sheffield, Sheffield, UK

Gerald PH. Gui, MS, FRCS, FRCS(Ed)
Consultant Surgeon, Academic Surgery (Breast Unit), Royal Marsden NHS Foundation Trust, London, UK

Chinmay M. Gupte, FRCS(Tr & Orth), PhD, MA (Oxon), MRCS
Specialist Registrar, St Mary’s Hospital and North West Thames, London, UK

Carole M. Hackney, BSc (Hons), PhD
Professor of Auditory Neuroscience, MacKay Institute of Communication and Neuroscience, School of Life Sciences, Keele University, Keele, UK

Peter A. Helliwell, FIBMS, CSci, CBA, Cert Ed
Chief Scientist and Manager, Molecular and Cell Biology Unit, Department of Cellular Pathology, Royal Cornwall Hospital, Truro, UK

John M. Hutson, AO

Professor of Paediatric Surgery, University of Melbourne, Department of Urology, Royal Children's Hospital, Parkville, Australia

Alan Jackson, BSc (Hons), PhD, MRCP, FRCR, FRCP

Professor of Radiology Imaging, Science and Biomedical Engineering, Wolfson Molecular Imaging Centre, The University of Manchester, Manchester, UK

Bruce W. Jafek, MD, FACS, FRSM

Professor and Former Chairman (1976–1998), Department of Otolaryngology, Head and Neck Surgery, University of Colorado School of Medicine, Denver, Colorado, USA

Eric R. Jauniaux, MD, PhD, MRCOG

Professor and Consultant in Materno-Fetal Medicine, Department of Obstetrics and Gynaecology, University College London Medical School, London, UK

Jonathan C. Kentish, MA, PhD

Professor of Cellular Cardiology, Cardiovascular Division, King's College London, London, UK

Aadil A. Khan, BM BCh, MPH, MRCS(Eng)

Speciality Trainee in Plastic Surgery, Oxford Region, UK

Khan Nasir, MBBS, MRCP, FRCR

Consultant Radiologist, Chelsea and Westminster Hospital

Royal Marsden Hospital, London, UK

W Niall A. Kirkpatrick, BDS, MB BS, MD, FRCS, FRCS(Plast)

Consultant Craniofacial Plastic Surgeon, Craniofacial Unit, Chelsea and Westminster Hospital, London, UK

John G. Lawrenson, BSc, PhD, MCOptom

Professor of Clinical Visual Science, Department of Optometry and Visual Science, City University, London, UK

Justin Lee, BSc, MBBS, MRCS(Eng), FRCR

Consultant Radiologist, Department of Radiology, Chelsea and Westminster Hospital, London, UK

David Lowe, MD, FRCS, FRCPath, FIBiol

Consultant Histopathologist, The London Clinic, London, UK

Andres Lozano, MD, PhD, FRCSC

Professor, Division of Neurosurgery, University of Toronto, Toronto, Ontario, Canada

Joseph Mathew, MBBS, FMCPath, FRCPath, CertTLHE, PGCE, CertBusStud, FHEA

Consultant in Histopathology, Department of Histopathology, Royal Cornwall Hospitals Trust, Truro, UK

Stephen McHanwell, BSc, PhD

Professor of Anatomical Sciences, School of Dental Sciences, The Dental School, Framlington Place, Newcastle-Upon-Tyne, UK

Mary-Clare C. Miller, MA (Cantab), MB BS, MRCS (Eng)
Specialty Registrar in Plastic Surgery, London Deanery, London, UK

Sukhbinder Minhas, MD, FRCS (Urol)
Consultant Uro-andrologist and Senior Lecturer, The Institute of Urology, University College Hospital, London, UK

Zoltán Molnár, MD, DPhil
Professor of Developmental Neuroscience, Department of Physiology, Anatomy and Genetics, University of Oxford, Oxford, UK

Michael Monteiro, BDS, FDSRCS, MB BCH, MRCS
Specialist Registrar, Department of Oral and Maxillofacial Surgery, Brighton and Sussex University Hospitals NHS Trusts, Brighton, UK

Louise A. Moore, MB ChB, Dip Paeds, FRANZCR
Consultant Radiologist, Department of Radiology, Tauranga Hospital, Tauranga, New Zealand

Antoon FM. Moorman, PhD
Professor of Embryology and Molecular, Biology of Cardiovascular Diseases, Head, Department of Anatomy and Embryology, Academic Medical Center, Amsterdam, The Netherlands

Gillian M. Morriss-Kay, BSc (Hons), PhD, DSc
Professor Emeritus, Department of Physiology, Anatomy and Genetics, University of Oxford, Oxford, UK

Timothy AJ Mould, MA (Oxon), DM (Oxon), FRCOG
Consultant Gynaecological Oncologist, University College London Hospitals Gynaecological Cancer Centre, University College London Hospitals, London, UK

Jagdeep Nanchahal, BSc, PhD, MBBS, FRCS(plast), FRACS
Professor of Hand, Plastic and Reconstructive Surgery, Kennedy Institute of Rheumatology and Charing Cross Hospital, Imperial College, London, UK

David Neary, MD, FRCP
Professor of Neurology, The Greater Manchester Neuroscience Centre, Salford Royal Hospital, University of Manchester, Manchester, UK

Niri S. Niranjan, MBBS, LRCP, MS, FRCS, FRCS(Plast), FRCS Ed, FRCS Eng
Consultant Plastic, Reconstructive and Cosmetic Surgeon, St. Andrew’s Centre for Burns and Plastic Surgery, Broomfield Hospital, Chelmsford, UK

Simon Padley, BSc, MBBS, FRCP, FRCR
Consultant Radiologist, Royal Brompton and Harefield NHS Trust, Honorary Senior Lecturer, Imperial College Medical School, London, UK

Pranav P. Pandya, BSc, MRCOG, MD

Consultant and Honorary Senior Lecturer in Fetal Medicine and Obstetrics, Institute for Women's Health, Department of Obstetrics and Gynaecology, University College London Hospitals, London, UK

Terence A. Partridge, BSc, PhD, FMed. Sci

Research Faculty, Research Center for Genetic Medicine, Children's National Medical Center, Washington, DC, USA

Hannes Petersen, MD, PhD

Head of Department and Associate Professor, Department of Anatomy and Otorhinolaryngology, Head and Neck Surgery, University of Iceland and Landspitali University Hospital, Reykjavik, Iceland

Raj Prasad, MS, MCh, FRCS

Consultant Surgeon, Hepatobiliary and Transplant Unit, St James's University Hospital, Leeds, UK

Donald J. Reid, PhD

Lecturer in Oral Anatomy, The Dental School, School of Dental Sciences, Newcastle-Upon-Tyne, UK

Patricia A. Reynolds, BDS, MBBS, MAODE(Open), PhD, FDSRCS(Eng)(Edin)

Professor of Dental Education, King's College London Dental Institute, London, UK

Paul D. Robinson, PhD, MBBS, BDS, FDSRCS

Oral and Maxillofacial Surgeon (Retired from), Department of Maxillofacial Surgery, King's College London Dental Institute, London, UK

Pallav L. Shah, MD, MBBS, FRCP

Consultant Physician, Royal Brompton Hospital, London, UK

Jane Sowden, PhD

Senior Lecturer, Developmental Biology Unit, University College London Institute of Child Health, University College London, London, UK

Jonathan Spratt, BA, MB BChir, MA (Cantab), FRCS(Eng), FRCS(Glasg), FRCR

Consultant Clinical Radiologist, University Hospital of North Durham

Visiting Professor of Radiology, University of Wisconsin, Madison, USA

Visiting Fellow in Anatomy, University of Northumbria, Newcastle, UK

Cheryll Tickle, MA, PhD

Foulerton Research Professor of the Royal Society, Department of Biology and Biochemistry, University of Bath, Bath, UK

Graham Tytherleigh-Strong, MB BS, FRCS (Orth), FFESM (UK), DSportMed

Consultant Orthopaedic Surgeon, Division of Orthopaedics, Addenbrooke's Hospital, Cambridge University Teaching Hospital Trust, Cambridge, UK

Bart Wagner, BSc, CSci, FIBMS
Chief Biomedical Scientist, Regional Electron Microscopy Unit, Histopathology Department, Northern General Hospital, Sheffield, UK

Jeremy PT. Ward, BSc, PhD
Head of Department of Physiology and Professor of Respiratory Cell Physiology, Division of Asthma Allergy and Lung Biology, King's College London, London, UK

Ming Zhang, MB(Anhui), MMed (Anhui), PhD(Otago)
Senior Lecturer of Clinical Anatomy, Department of Anatomy and Structural Biology, University of Otago, Dunedin, New Zealand

REVIEWERS

Andrew Amis, PhD, DSc (Eng), FiMechE

Professor of Orthopaedic Biomechanics, Imperial College London, London, UK

Anthony Bull, BEng, DIC CEng, PhD, FiMechE

Reader in Musculoskeletal Mechanics, Department & Bioengineering, Imperial College London, London, UK

Robert F. Brooks, BSc, PhD

Senior Lecturer, Department of Anatomy and Human Sciences, School of Biomedical and Health Sciences, King's College London, London, UK

Michael Gleeson, MD, FRCS

Consultant Otolaryngologist and Skull Base Surgeon to Guy's, Kings and St Thomas' Hospitals, London

Professor of Skull Base Surgery, National Hospital for Neurology and Neurosurgery London, UK

Honorary Skull Base Surgeon to the Great Ormond Street Hospital for Sick Children, London, UK

Chinmay M. Gupte, FRCS (Tr&Orth), PhD, MA(Oxon), MRCS

Specialist Registrar, St Mary's Hospital and North West Thames, London, UK

Peter Goldstraw, FRCS

Consultant Thoracic Surgeon, Department of Thoracic Surgery, Royal Brompton Hospital, London, UK

John Granton, MD, FRCPC

Associate Professor of Medicine, Director, Pulmonary Hypertension Program, University Health Network Director, Toronto General Hospital, Toronto, Ontario, Canada

Siew Yen Ho, PhD, FRCPath

Reader and Honorary Consultant, Head of Cardiac Morphology, National Heart and Lung Institute, Imperial College London, Royal Brompton and Harefield NHS Trust, London, UK

Nick Jones, MB, BDS, FRCS, FRCS (Oto)

Consultant Otorhinolaryngologist, Division of Otorhinolaryngology, School of Medical and Surgical Science, The University of Nottingham, Nottingham, UK

Mark R. Johnson, MBBS, PhD, MRCP, MRCOG

Reader in Obstetrics, Imperial College

Consultant Obstetrician and Obstetric Physician, Department of Obstetrics and Gynaecology, Chelsea and Westminster Hospital, London, UK

E Birgitte Lane, PhD, FRSE, FMedSci

*Professor and Executive Director, A*STAR Institute of Medical Biology, Singapore*

Roger J. Morris

Head of the School of Health and Life Sciences, King's College London, Guy's Campus, London, UK

Andrew G. Nicholson, MD, MRCPath

Professor and Consultant Histopathologist, Royal Brompton Hospital, London, UK

Koichiro Niwa, MD, PhD, FACC

Director Departments of Adult Congenital Heart Disease and Paediatric Cardiology, Chiba Cardiovascular Center, Chiba, Japan

Jaideep J. Pandit, MA, BM, DPhil, FRCA

Consultant Anaesthetist and Fellow of St John's College, Nuffield Department of Anaesthetics, John Radcliffe Hospital, Oxford, UK

John Pepper, MChir, FRCS

Professor of Cardiac Surgery, Imperial College School of Medicine, London, UK

Michael I. Polkey, MB ChB, FRCP

Professor of Respiratory Medicine, Royal Brompton Hospital and National Heart and Lung Institute, London, UK

Darryl Shore, FRCS

Consultant Cardiac Surgeon, Director of Paediatric and Adult Congenital Surgery, Royal Brompton and Harefield NHS Trust, London, UK

Christos Tolias, MBBS, PhD, FRCS(Engl), FRCS(SN)

Consultant Neurosurgeon and Honorary Senior Lecturer, Department of Neurosurgery, Kings College Hospital, London, UK

Giles Toogood, MA DM FRCS

Consultant Hepatobiliary Surgeon, Hepatobiliary and Transplant Unit, St James's University Hospital, Leeds, UK

Eleftherios Tsiridis, MD, MSc, PhD, FRCS

Consultant Orthopaedic and Trauma Surgeon, Academic Orthopaedic Unit, Leeds General Infirmary and Chapel Allerton, Leeds Teaching Hospitals, Leeds, UK

Graham Tytherleigh-Strong, MB BS, FRCS(Orth), FFESM (UK), DSportMed

Consultant Orthopaedic Surgeon, Division of Orthopaedics, Addenbrooke's Hospital, Cambridge University, Teaching Hospital Trust, Cambridge, UK

Anselm Uebing, MD

Fellow in Adult Congenital Heart Disease, Adult Congenital Heart Centre, Royal Brompton Hospital, London, UK

Hideki Uemura, MD, FRCS

Consultant Cardiac Surgeon, Department of Cardio-thoracic Surgery, Royal Brompton Hospital, London, UK

Christopher R. Weatherley, MD, FRCS, FRCSEd, FRCSEd (Orth)

Consultant Spinal Surgeon, Princess Elizabeth Orthopaedic Centre, Royal Devon and Exeter Hospital, Exeter, UK

Gary D. Webb, MD, FRCP(C)

Director, Philadelphia Adult Congenital Heart Center, Philadelphia, Pennsylvania, USA

Roy O. Weller, BSc, MD, PhD, FRCPath

Emeritus Professor of Neuropathology, Clinical Neurosciences, University of Southampton School of Medicine, Southampton, UK

INTERNATIONAL REVIEWERS

Masood Ahmed, MBBS, MS

Professor, Department of Anatomy, Baqai Medical University, Karachi, Pakistan

Sadakazu Aiso, MD, PhD

Professor, Department of Anatomy, Keio University, School of Medicine, Keio, Japan

Saad Al-Ali, MB ChB, PhD

Senior Lecturer, Department of Anatomy with Radiology, University of Auckland, Auckland, New Zealand

PD. Athavia, MB BS, MS, DHA, DHRD

Professor and Head, Department of Anatomy, Lokmanaya Tilak Municipal Medical College, Sion Hospital, Mumbai, India

Brion Benninger, MD, MS

Clinical Anatomy Directer, Departments of Surgery, Oral Maxillofacial Surgery and Integrated Biosciences, Oregon Health and Science University, Oregon, USA

Rolfe Birch, MChir, FRCS

Consultant Orthopaedic Surgeon, Peripheral Nerve Injury Unit, Royal National Orthopaedic Hospital, Stanmore, UK

Phil Blyth, PhD

Lecturer in Anatomy, Department of Anatomy with Radiology, University of Auckland, Auckland, New Zealand

Chris Briggs, Dip Ed, BSc, MSc, PhD

Associate Professor, Department of Anatomy and Cell Biology, University of Melbourne, Melbourne, Australia

Stuart Bunt, MA, DPhil (Oxon)

Professorial Fellow, School of Anatomy and Human Biology, University of Western Australia, Perth, Australia

Robert Callister, PhD

Professor of Anatomy, School of Biomedical Sciences, University of Newcastle, Newcastle, Australia

John Corson, MD

Professor of Surgery, University of New Mexico

Chief of Surgery, New Mexico Veterans Administration Center, Albuquerque, New Mexico, USA

Richard Drake, PhD

Director of Anatomy and Professor of Surgery, Cleveland Clinic, Lerner College of Medicine, Case Western Reserve University, Cleveland, Ohio, USA

Norman Eizenberg, MBBS

Senior Lecturer, Department of Anatomy and Cell Biology, The University of Melbourne, Melbourne, Australia

Harold Ellis, CBE, Mch, FRCS

Emeritus Professor of Surgery, Department of Anatomy and Human Sciences, Biomedical and Health Sciences, King's College London, London, UK

Darrell JR. Evans, PhD

Professor of Developmental Tissue Biology, Department of Anatomy, Brighton and Sussex Medical School, Brighton, UK

Richard Faull, BMed Sc, MB ChB, PhD, DSc, FRSNZ

Professor of Anatomy, Department of Anatomy with Radiology, University of Auckland, Auckland, New Zealand

Mark K. Ferguson, MD

Professor of Surgery, University of Chicago, Chicago, USA

David Green, BSc (Hons), PhD (Cantab)

Professor, Head of Department, Department of Anatomy and Structural Biology, University of Otago, Dunedin, New Zealand

Rod Green, BSc (Hons), DipEd, MSc, PhD

Senior Lecturer and Anatomy Discipline Coordinator, School of Human Biosciences, La Trobe University, Bundoora, Australia

JP. Gunasegaran, MSc PhD(Anat)

Professor, Department of Anatomy, Rajah Muthiah Medical College, Annamalai University, Chidambaram, India

Nobutaka Hirokawa, MD, PhD

Professor, Department of Cell Biology and Anatomy, Graduate School of Medicine, University of Tokyo, Tokyo, Japan

Cynthia Jensen, PhD

Head of Department of Anatomy with Radiology and Associate Professor, University of Auckland, Auckland, New Zealand

D Gareth Jones, CNZM, BSc(Hons), MBBS(Lond), MD(Otago), DSc(W Aust), CBiol, FIBiol

Professor, Department of Anatomy and Structural Biology, University of Otago, Dunedin, New Zealand

John Paul Judson, MBBS, MS, DHA

Associate Professor of Anatomy and Head of Human Biology Department, International Medical University, Kuala Lampur, Malaysia

Yogendra Kumar Kadian, MD

Associate Professor and Head, Department of Anatomy, Sikkim Manipal Institute of Medical Sciences, Sikkim, India

Mitsuhiro Kawata, MD

Professor, Department of Anatomy and Neurobiology, Kyoto Prefectural University of Medicine, Kyoto, Japan

Jeffrey Kerr, PhD

Associate Professor, Anatomy and Developmental Biology, Monash University, Victoria, Australia

Rachel Koshi, MBBS, MS, PhD

Professor of Anatomy in Surgery, Weill Cornell Medical College in Qatar, Doha, Qatar

Ashwin Kumaria, BSc (Hons)

Research Associate, Department of Neurosurgery, Kings College Hospital, London, UK

Nancy M. Major, MD

Associate Professor Radiology and Surgery, Biological Anthropology and Anatomy, Musculoskeletal Division, Director Medical Student Radiology, Duke University Medical Center, Durham, USA

Robert Mansel, MS, FRCS

Professor of Surgery, University Department of Surgery, Cardiff University, University Hospital of Wales, Cardiff, UK

Keith Moore, PhD, FIAC, FRSM, FAAA

Professor Emeritus, Department of Surgery, Faculty of Medicine, Division of Anatomy, University of Toronto, Toronto, Ontario, Canada

Tim O’Brien, MA, DM, FRCS (Urol)

Consultant Urological Surgeon, Department of Urology, Guy’s and St Thomas’s NHS Trust, London, UK

Ronan O’Rahilly, MD, DSc, Dr hc

Professor Emeritus, Faculty of Medicine, University of California, Davis, California, USA

TH. Quinn, PhD

Professor of Anatomy and Surgery, Creighton University School of Medicine, Omaha, Nebraska, USA

John Reynard, DM, MA, FRCS (Urol)

Consultant Urological Surgeon, Nuffield Department of Surgery, University of Oxford, Oxford, UK

Sue Runciman, BSc, PhD, DipEd

Senior Lecturer, Department of Anatomy and Histology, Flinders University, Adelaide, SA, Australia

Ashok Sahai, BSc, MBBS, MS (Anat)

Professor and Head, Department of Anatomy, CSM Medical University (Upgraded King George’s Medical College), Lucknow, India

Tatsuo Sakai, DMedSci

Professor, Department of Anatomy, School of Medicine, Juntendo University, Tokyo, Japan

Sujatha Salgado, MBBS, MPhil

Senior Lecturer, Department of Anatomy, Faculty of Medicine, University of Kelaniya, Ragama, Sri Lanka

John H. Shepherd, FRCS, FRCOG, FRACOG

Professor of Surgical Gynaecology, St Bartholomew's Hospital

Consultant Surgeon, Royal Marsden Hospital, London, UK

Yosaburo Shibata, DMedSci, PhD

Professor, Department of Developmental Molecular Anatomy, Graduate School of Medical Sciences, Kyushu University, Fukuoka, Japan

Kohei Shiota, MD, PhD

Professor and Chairman, Department of Anatomy and Developmental Biology, Director, Congenital Anomaly Research Center, Kyoto University Graduate School of Medicine, Kyoto, Japan

Fiona Stewart, MBBS, BSc

Associate Professor, School of Rural Medicine, University of New England, Armidate, NSW, Australia

Mark David Stringer, BSc, MBBS, MRCP, FRCP, FRCS, MS, FRCS (Edin)

Clinical Anatomist, Department of Anatomy and Structural Biology, University of Otago, Dunedin, New Zealand

(Formerly Professor of Paediatric Surgery, Leeds, UK)

Mark Sullivan, MBBS, BSc, MD, FRCS (Urol)

Consultant Urological Surgeon & Honorary Senior Lecturer, Churchill Hospital, Oxford, UK

Tim Terry, BSc, MBBS, LRCP, FRCS, MS

Consultant Urological Surgeon and Honorary Senior Lecturer, Department of Urology, Leicester General Hospital, Leicester, UK

Grant Townsend, BDS, BScDent (Hons), PhD, DDSc, FADI

Professor of Dental Science, School of Dentistry, The University of Adelaide, Adelaide, South Australia

Wayne Vogl, PhD

Professor, Department of Cellular and Physiological Sciences, Faculty of Medicine, The University of British Columbia, Vancouver, Canada

Dzung Vu, MBBS, MD, DipAnat, GradCertHEd

Senior Lecturer, Department of Anatomy, University New South Wales, New South Wales, Australia

Anil H. Walji, MD, PhD

Professor and Director, Division of Anatomy, Professor of Radiology and Diagnostic Imaging, Professor of Surgery, Faculty of Medicine and Dentistry, University of Alberta, Alberta, Canada

Colin Wendell-Smith, AO, MBBS, PhD, LLD Hon, FRANZCOG

Professor Emeritus, Department of Anatomy and Physiology, University of Tasmania, Tasmania, Australia

John A. Windsor, BSc MBChB DipObst MD FRACS FACS

Professor of Surgery, Head, Department of Surgery, Faculty of Medical and Health Sciences, The University of Auckland, Auckland, New Zealand

Ming Zhang, MB (Anhui), MMed (Anhui), PhD (Otago)

Senior Lecturer of Clinical Anatomy, Department of Anatomy and Structural Biology, University of Otago, Dunedin, New Zealand

HISTORICAL INTRODUCTION

The year 2008 sees the 150th anniversary of the publication of *Gray's Anatomy*. The book is a rarity in textbook publishing in having been in continuous publication on both sides of the Atlantic Ocean, for so long. One and a half centuries is an exceptionally long era for a textbook, and of course the volume published now is very different from the one Mr. Henry Gray first created with his colleague Dr Henry Vandyke Carter, in mid-Victorian London. In this introductory essay, I shall explain the long history of Gray's, from those Victorian days right up to today.

The shortcomings of existing anatomical textbooks probably impressed themselves upon Henry Gray when he was still a student at St George's Hospital Medical School, near London's Hyde Park Corner, in the early 1840s. He began thinking about creating a new anatomy textbook a decade later, while war was being fought in the Crimea. New legislation was being planned which would establish the General Medical Council (1858) to regulate professional education and standards.

Gray was twenty-eight years old, and a teacher himself at St George's. He was very able, hard-working, and highly ambitious, already a Fellow of the Royal Society, and of the Royal College of Surgeons. Although little is known about his personal life, his was a glittering career thus far, achieved while he served and taught on the hospital wards and in the dissecting room (Fig. 1). (1)

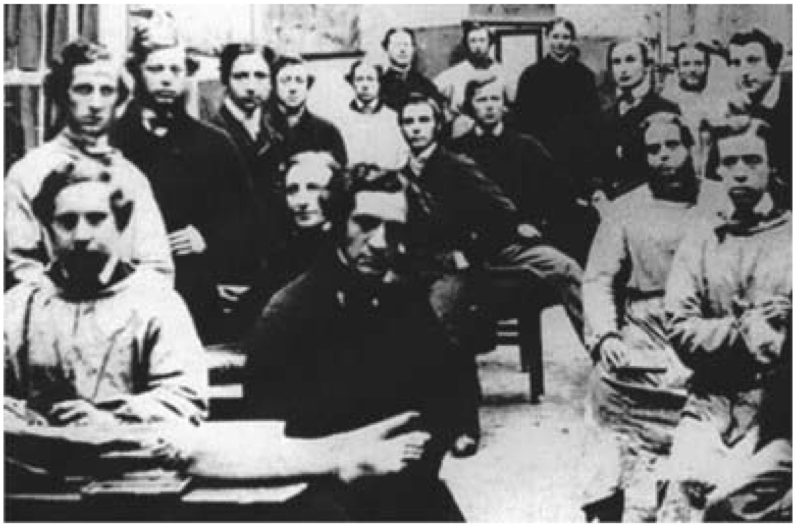

Fig. 1 Henry Gray (1827–1861) is shown here in the foreground, seated by the feet of the cadaver. The photograph was taken by a medical student, Joseph Langhorn. The room is the dissecting room of St George’s Hospital medical school in Kinnerton Street, London. Gray is shown surrounded by staff and students. When the photo was taken, on 27th March 1860, Carter had left St George’s, to become Professor of Anatomy and Physiology at Grant Medical College, in Bombay (nowadays Mumbai). The second edition of *Gray’s Anatomy* was in its proof stages, to appear in December 1860. Gray died just over a year later, in June 1861, at the height of his powers.

Gray shared the idea for the new book with a talented colleague on the teaching staff at St George’s, Henry Vandyke Carter, in November 1855. Carter was from a family of Scarborough artists, and was himself a clever artist and microscopist. He had produced fine illustrations for Gray’s scientific publications before, but could see that this idea was a much more complex kind of a project. Carter recorded in his diary:

> Little to record. Gray made proposal to assist by drawings in bringing out a Manual for students: a good idea but did not come to any plan … too exacting, for would not be a simple artist. (2)

Neither of these young men was interested in producing a pretty book, or an expensive one. Their purpose was to supply an affordable, accurate teaching aid for people like their own students, who might soon be required to operate on real patients, or on soldiers injured at Sebastopol or some other battlefield. The book they planned together was a practical one, designed to encourage youngsters to study anatomy, help them pass exams, and assist them as budding surgeons. It was not simply an anatomy textbook, but a guide to dissecting procedure, and to the major operations.

Gray and Carter belonged to a generation of anatomists ready to infuse the study of human anatomy with a new, and respectable, scientificity. Disreputable aspects of the profession's history, acquired during the days of bodysnatching, were assiduously being forgotten. The Anatomy Act of 1832 had legalized the requisition of unclaimed bodies from workhouse and hospital mortuaries, and the study of anatomy (now with its own Inspectorate) was rising in respectability in Britain. The private anatomy schools which had flourished in the Regency period were closing their doors, and the major teaching hospitals were erecting new purpose-built dissection rooms. (3)

The best-known student works when Gray and Carter had qualified were probably Erasmus Wilson's *Anatomist's Vade Mecum*, and *Elements of Anatomy* by Jones Quain. Both works were small – pocket-sized – but Quain came in two thick volumes. Both Quain's and Wilson's works were good books in their way, but their small pages of dense type, and even smaller illustrations, were somewhat daunting, seeming to demand much nose-to-the-grindstone effort from the reader.

The planned new textbook's dimensions and character were serious matters. Pocket manuals were commercially successful because they appealed to students by offering much knowledge in a small compass. But pocket-sized books had button-sized illustrations. Knox's *Manual of Human Anatomy*, for example, was a good book, but was only six inches by four (17 × 10 cm) and few of its illustrations occupied more than a third of a page. Gray and Carter must have discussed this matter between themselves, and with Gray's publisher JW Parker & Son, before decisions were taken about the size and girth of the new book, and especially the size of its illustrations.

The two men were earnestly engaged for the following eighteen months in the work which formed the basis of the book. All the dissections were undertaken jointly, Gray wrote the text, and Carter the illustrations. While Gray and Carter were working, a new edition of Quain's was published: this time it was a 'triple-decker' – in three volumes – of 1740 pages in all. Gray and Carter's working days were long, all the hours of daylight, eight or nine hours at a stretch – right through 1856, and well into 1857. We can infer from the warmth of Gray’s appreciation of Carter in his published acknowledgements that their collaboration was a happy one.

The Author gratefully acknowledges the great services he has derived in the execution of this work, from the assistance of his friend, Dr. H. V. Carter, late Demonstrator of Anatomy at St George’s Hospital. All the drawings from which the engravings were made, were executed by him. (4)

With all the dissections done, and Carter’s inscribed wood-blocks at the engravers, Gray took six months’ leave from his teaching at St George’s to work as a personal doctor for a wealthy family. It was probably as good a way as any to get a well-earned break from the dissecting room and the dead-house. (5)

Carter sat the examination for medical officers in the East India Company, and sailed for India in the spring of 1858, when the book was still in its proof stages. Gray had left a trusted colleague, Timothy Holmes, to see the book through the press.

Gray looked over the final galley proofs, just before the book finally went to press. Timothy Holmes’s association with the book’s first edition would later prove vital to its survival.

THE FIRST EDITION

The book Gray and Carter had created together, *Anatomy, Descriptive and Surgical* appeared at the very end of August 1858, to immediate acclaim. Reviews in the *Lancet* and *British Medical Journal* were highly complimentary, and students flocked to buy.

It is not difficult to understand why it was a runaway success. Gray's *Anatomy* knocked its competitors into a cocked hat. The book holds well in the hand, it feels substantial, and it contains everything required. It was considerably smaller and more slender than the doorstopper with which modern readers are familiar. To contemporaries it was small enough to be portable, but large enough for decent illustrations: 'royal octavo' – nine-and-a-half inches by six (24 × 15 cm) – about two-thirds of modern A4 size. Its medium size, single volume format was far removed from *Quain*, yet double the size of Knox's *Manual*.

Simply organized and well designed, the book explains itself confidently and well: the clarity and authority of the prose is manifest. But what made it unique for its day was the outstanding size and quality of the illustrations. Gray thanked the wood engravers Butterworth and Heath for the 'great care and fidelity' they had displayed in the engravings, but it was really to Carter that the book owed its extraordinary success.

The beauty of Carter's illustrations resides in their diagrammatic clarity, quite atypical for their time. The images in contemporary anatomy books were usually *proxy labelled*: dotted with tiny numbers or letters (often hard to find, or read) or bristling with a sheaf of numbered arrows, referring to a key situated elsewhere, usually in a footnote which was sometimes so lengthy it wrapped round onto the following page. Proxy labels require the reader's eye to move to and fro: from the structure to the proxy label to the legend and back again. There was plenty of scope for slippage, annoyance and distraction. Carter's illustrations, by contrast, unify name and structure, enabling the eye to assimilate both at a glance. We are so familiar with Carter's images that it is hard to appreciate how incredibly modern they must have seemed in 1858. The volume made human anatomy look new, exciting, accessible, and do-able.

The first edition was covered in a light brown bookbinder's cloth embossed all over in a dotted pattern, and a double picture-frame border. Its spine was lettered in gold blocking:

with ‘**DESCRIPTIVE AND SURGICAL**’ in small capitals underneath. *Gray’s Anatomy* is how it has been referred to ever since. Carter was given credit with Gray on the book’s titlepage for undertaking all the dissections on which the book was based, and sole credit for all the illustrations, though his name appeared in a significantly smaller type, and for some obscure reason he was described as the ‘Late Demonstrator in Anatomy at St George’s Hospital’ rather than being given his full current title, which was Professor of Anatomy and Physiology at Grant Medical College, Bombay. Perhaps Gray was concerned not be upstaged, as he was still only a Lecturer at St George’s. Gray may have been aware that his words had been upstaged by the quality of Carter’s anatomical images. He need not have worried: Gray is the famous name on the spine of the book.

Gray was paid £150 for every thousand copies sold. Carter never received a royalty payment, just a one-off fee at publication, which may have allowed him to purchase the long-wished for microscope he took with him to India (Fig. 2).

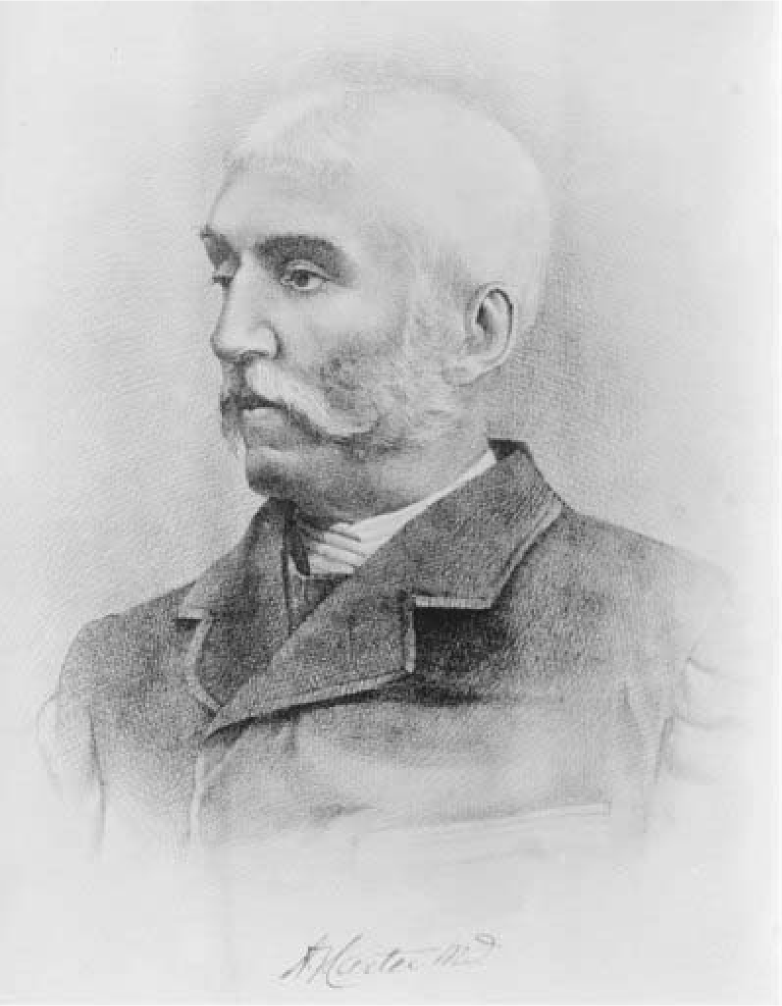

Fig. 2 Henry Vandyke Carter (1831–1897). Carter was appointed Honorary Surgeon to the Queen in 1890.

The first edition print-run of 2000 copies sold out swiftly. A parallel edition was published in the United States in 1859, and Gray must have been deeply gratified to have to revise an enlarged new English edition in 1859–60, though he was surely saddened and worried by the death of John Parker junior, at the young age of 40, while the book was going through the press. The second edition came out in the December of 1860 and it too sold like hot cakes, as indeed has every subsequent edition.

The following summer, in June 1861, at the height of his powers and full of promise, Henry Gray died unexpectedly at the age of only 34. Gray had contracted smallpox while nursing his little nephew Charles. A new strain of the disease was more virulent than the one with which Gray had been vaccinated as a child: the disease became confluent, and Gray died in a matter of days.

Within months the whole country would be pitched into the mourning for the death of Prince Albert and the creative era over which he had presided – especially the decade which had flowered since the Great Exhibition of 1851 – would be history.

THE BOOK SURVIVES

Anatomy Descriptive and Surgical could have died too. With Carter in India, the death of Gray, so swiftly after the younger Parker, might have spelled catastrophe. Certainly, at St George’s there was a sense of calamity. The grand old medical man Sir Benjamin Brodie, Sergeant-Surgeon to the Queen, and the great supporter of Gray to whom *Anatomy* had been dedicated, cried forlornly: ‘Who is there to take his place?’ (1)

But old J.W. Parker ensured the survival of *Gray’s* by inviting Timothy Holmes, the doctor who had helped proof-read the first edition, and who had filled Gray’s shoes at the medical school, to serve as Editor for the next edition. Other long-running anatomy works such as Quain, remained in print in a similar way, co-edited by other hands. (6)

Holmes (1825–1907) was another gifted George’s man, a scholarship boy who had won an exhibition to Cambridge, where his brilliance was recognized. Holmes was a Fellow of the Royal College of Surgeons at 28. John Parker junior had commissioned him to edit *A System of Surgery* (1860–64), an important essay series by distinguished surgeons on subjects of their own choosing. Many of Holmes’s authors remain important figures, even today: John Simon, James Paget, Henry Gray, Ernest Hart, Jonathan Hutchinson, Brown Séquard, and Joseph Lister. Holmes had lost an eye in an operative accident, and he had a gruff manner which terrified students, yet he published a lament for young Parker which reveals him capable of deep feeling. (7)

John Parker senior’s heart, however, was no longer in publishing. His son’s death had closed down the future for him. The business, with all its stocks and copyrights, was sold to Messrs Longman. Parker retired to the village of Farnham, where he later died.

With Holmes as editor, and Longmans as publisher, the immediate future of Gray’s *Anatomy* was assured. The third edition appeared in 1864 with relatively few changes, Gray’s estate receiving the balance of his royalty after Holmes was paid £100 for his work.

THE MISSING OBITUARY

Why no obituary appeared for Henry Gray in *Gray's Anatomy* is curious. Gray had referred to Holmes as his 'friend' in the preface to the first edition, yet it would also be true to say that they were rivals. Both had just applied for a vacant post at St George's, as Assistant Surgeon. Had Gray lived, it is thought that Holmes may not have been appointed, despite his seniority in age. (1)

Later commentators have suggested, as though from inside knowledge, that Holmes's 'proof-reading' included improving Gray's writing style. This could be a reflection of Holmes's own self-regard, but there may be some truth in it. There can be no doubt that as Editor of seven subsequent editions of *Gray's Anatomy* (3rd to 9th editions, 1863 – 1880) Holmes added new material, and had to correct and compress passages, but it is also possible that back in 1857, Gray's original manuscript had been left in a poor state for Holmes to sort out. In other works, Gray's writing style was lucid, but he always seems to have paid a copyist to transcribe his work prior to submission. The original manuscript of *Gray's Anatomy*, sadly, has not survived, so it is impossible to be sure how much of the finished version had actually been written by Holmes.

It may be that Gray's glittering career, or perhaps the patronage which unquestionably advanced it, created jealousies among his colleagues, or that there was something in Gray's manner which precluded affection, or which created resentments among clever social inferiors like Carter and Holmes, especially if they felt their contributions to his brilliant career were not given adequate credit. Whatever the explanation, no reference to Gray's life or death appeared in *Gray's Anatomy* itself until the twentieth century. (8)

A SUCCESSION OF EDITORS

Holmes expanded areas of the book that Gray himself had developed in the 2nd edition (1860), notably in ‘general’ anatomy (histology) and ‘development’ (embryology). In Holmes’s time as editor the volume grew from 788 pages in 1864 to 960 in 1880 (9th edition), with the histological section paginated separately in roman numerals at the front of the book. Extra illustrations were added, mainly from other published sources.

The connections with Gray and Carter, and with St George’s were maintained with the appointment of the next editor, T. Pickering Pick, who had been a student at St George’s in Gray’s time. From 1883 (10th edition) onwards, Pick kept up with current research, rewrote and integrated the histology and embryology into the volume, dropped Holmes from the titlepage, removed Gray’s preface to the first edition, and added emboldened subheadings which certainly improved the appearance and accessibility of the text. Pick said he had ‘tried to keep before himself the fact that the work is intended for students of anatomy rather than for the Scientific Anatomist’ (13th edition 1893).

Pick also introduced colour printing (in 1887, 11th edition) and experimented with the addition of illustrations using the new printing method of half-tone dots: for colour (which worked) and for new black-and-white illustrations (which didn’t). Half-tone shades of grey compared poorly with Carter’s wood engravings, still sharp and clear by comparison.

What Henry Vandyke Carter made of these changes is a rich topic for speculation. He returned to England in 1888, having retired from the Indian Medical Service, full of honours – Deputy Surgeon General, and in 1890, was made Honorary Surgeon to Queen Victoria. Carter had continued researching throughout his clinical medical career in India, and became one of India’s foremost bacteriologists/tropical disease specialists before there was really a name for either discipline. Carter made some important discoveries, including the fungal cause of mycetoma, which he described and named. He was also a key figure in confirming scientifically in India some major international discoveries, such as Hansen’s discovery of the cause of leprosy, Koch’s discovery of the organism causing tuberculosis, and Laveran’s discovery of the organism which causes malaria. Carter married late in life, and had two young children when he died in Scarborough in 1897, aged 65. Like Gray, he received no obituary in the book.

When Pick was joined on the titlepage by Robert Howden (a professional anatomist from the University of Durham) in 1901 (15th edition), the volume was still easily recognizable as the book Gray and Carter had created. Although many of Carter's illustrations had been revised or replaced, many others still remained. Sadly, though, an entire section (embryology) was again separately paginated, as its revision had taken longer than anticipated. *Gray's* had grown, seemingly inexorably, and was now quite thick and heavy, 1244 pages weighing 5lb8oz/2.5 kg. Both co-editors, and perhaps also its publisher, were dissatisfied with it.

KEY EDITION: 1905

Serious decisions were taken well in advance of the next edition, which turned out to be Pick's last with Howden. Published 50 years after Gray had first suggested the idea to Carter, the 1905 (16th) edition was a landmark edition.

The period 1880–1930 was a difficult time for anatomical illustration, because the new techniques of photo-lithography and half-tone were not as yet perfected, and in any case could not provide the bold simplicity of line required for a book like *Gray's* which depended so heavily on clear illustration, and clear lettering. Recognizing the inferiority of half-tone illustrations by comparison with Carter's wood engraved originals, Pick and Howden courageously decided to jettison the second-rate half-tones altogether. Most of the next edition's illustrations were either Carter's, or old supplementary illustrations inspired by his work, or newly commissioned wood engravings or line drawings, intended 'to harmonize with Carter's original figures'. They successfully emulated Carter's verve. Having fewer pages and lighter paper, the 1905 (16th edition) weighed less than its predecessor, at 4lb11oz/2.1 kg. Typographically, the new edition was superb.

Howden took over as sole editor in 1909 (17th edition) and immediately stamped his personality on *Gray's*. He excised 'Surgical' from the title, changing it to *Anatomy Descriptive and Applied*, and removed Carter's name altogether. He also instigated the beginnings of an editorial board of experts for *Gray's*, by adding to the titlepage: 'Notes on Applied Anatomy' by AJ Jex-Blake and W Fedde Fedden, both St George's men. For the first time, the number of illustrations exceeded one thousand. Howden was responsible for the significant innovation of a short historical note on Henry Gray himself, nearly 60 years after his death, which included a portrait photograph (1918, 20th edition).

THE NOMENCLATURE CONTROVERSY

Howden’s era, and that of his successor TB Johnston (of Guy’s) was overshadowed by a cloud of international controversy concerning anatomical terminology. European anatomists were endeavouring to standardize anatomical terms, often using Latinate constructions, a move resisted in Britain and the United States. *Gray’s* became mired in these debates for over twenty years. The endeavour to be fair to all sides by using multiple terms doubtless generated much confusion amongst students, until a working compromise was at last arrived at in 1955 (32nd edition, 1958).

Johnston oversaw the second re-titling of the book (in 1938, 27th edition): it was now, officially, *Gray’s Anatomy*, finally ending the fiction that it had ever been known as anything else. *Gray’s* suffered from paper shortages and printing difficulties in World War II, but successive editions nevertheless continued to grow in size and weight, while illustrations were replaced and added as the text was revised. Between Howden’s first sole effort (1909, 17th edition) to Johnston’s last edition (1958, 32nd edition) *Gray’s* expanded by over 300 pages – from 1296 to 1604 pages, and almost 300 additional illustrations brought the total to over 1300. Johnston also introduced X-ray plates (1938) and in 1958 (32nd edition) electron micrographs by AS Fitton-Jackson, one of the first occasions on which a woman was credited with a contribution to *Gray’s*. Johnston felt compelled to mention that she was ‘a blood relative of Henry Gray himself’, perhaps by way of mitigation.

AFTER WORLD WAR II

The editions of *Gray's* issued in the decades immediately following the Second World War give the impression of intellectual stagnation. Steady expansion continued in an almost formulaic fashion, with the insertion of additional detail.

The central historical importance of innovation in the success of *Gray's* seems to have been lost sight of by its publishers and editors – Johnston (1930–58, 24th to 32nd editions); J Whillis (co-editor with Johnston 1938–54) DV Davies (1958–1967, 32nd to 34th editions) and F Davies (co-editor with DV Davies 1958–64, 32nd to 33rd editions). *Gray's* had become so pre-eminent that perhaps complacency crept in, or editors were too daunted or too busy to confront the 'massive undertaking' of a root and branch revision. (9) The unexpected deaths of three major figures associated with *Gray's* in this era, James Whillis, Francis Davies, and David Vaughan Davies – all of whom had been groomed to take the editorial reins – may have contributed to retard the process. The work became somewhat dull.

KEY EDITION: 1973

DV Davies had recognized the need for modernization, but his unexpected death left the work to other hands. Two Professors of Anatomy at Guy's, Roger Warwick and Peter Williams, the latter of whom had been involved as an indexer for *Gray's* for several years, regarded it as an honour to fulfill Davies' intentions.

Their 35th edition of 1973 was a significant departure from tradition. Over 780 pages (of 1471) were newly written, almost a third of the illustrations were newly commissioned, and the illustration captions were freshly written throughout. With a complete retypesetting of the text in larger double-column pages, a new index, and the innovation of a bibliography, this edition of *Gray's* looked and felt quite unlike its 1967 (34th edition) predecessor, and much more like its modern incarnation.

This 1973 edition departed from earlier volumes in other significant ways. The editors made explicit their intention to try to counter the impetus towards specialization and compartmentalization in twentieth century medicine, by embracing and attempting to reintegrate the complexity of the available knowledge. Warwick and Williams openly renounced the pose of omniscience adopted by many textbooks, believing it important to accept and mention areas of ignorance or uncertainty. They shared with the reader the difficulty of keeping abreast in the sea of research, and accepted with a refreshing humility the impossibility of fulfilling their own ambitious programme.

Warwick and Williams' 1973 edition had much in common with Gray and Carter's first edition. It was bold and innovative: respectful of its heritage, while also striking out into new territory. It was visually attractive and visually informative. It embodied a sense of a treasury of information laid out for the reader. (10) It was published simultaneously in the United States (the American *Gray's* had developed a distinct character of its own in the interval), and sold extremely well there. (10)

The influence of the Warwick and Williams's edition was forceful and long-lasting, and set a new pattern for the following quarter century. As has transpired several times before, wittingly or unwittingly a new editor was being prepared for the future: Dr Susan Standring (of Guy's) who created the new bibliography for the 1973 edition of *Gray's*, went on to serve on the editorial board, and has served as Editor-in-Chief for the last two editions (2004–2008, 39th and 40th editions). Both editions are important for different reasons.

For the 39th edition, the entire content of *Gray's* was reorganized, from systematic to regional anatomy. This great sea-change was not just organizational, but historic, because since its outset *Gray's* had prioritized bodily systems, with subsidiary emphasis on how the systems interweave in the regions. Professor Standring explained that the change of emphasis to the regions of the body had long been asked for by readers and users of *Gray's*, and that new imaging techniques in our era have raised the clinical importance of local anatomy. (11) The change was facilitated by an enormous collective effort on the part of the editorial team and the illustrators.

The current edition consolidates that momentous change, and is of historic importance because it is the *fortieth* edition, published on the 150th anniversary of Gray's original publication in autumn 1858 (see Table 1).

Table 1 Gray's Anatomy Editions

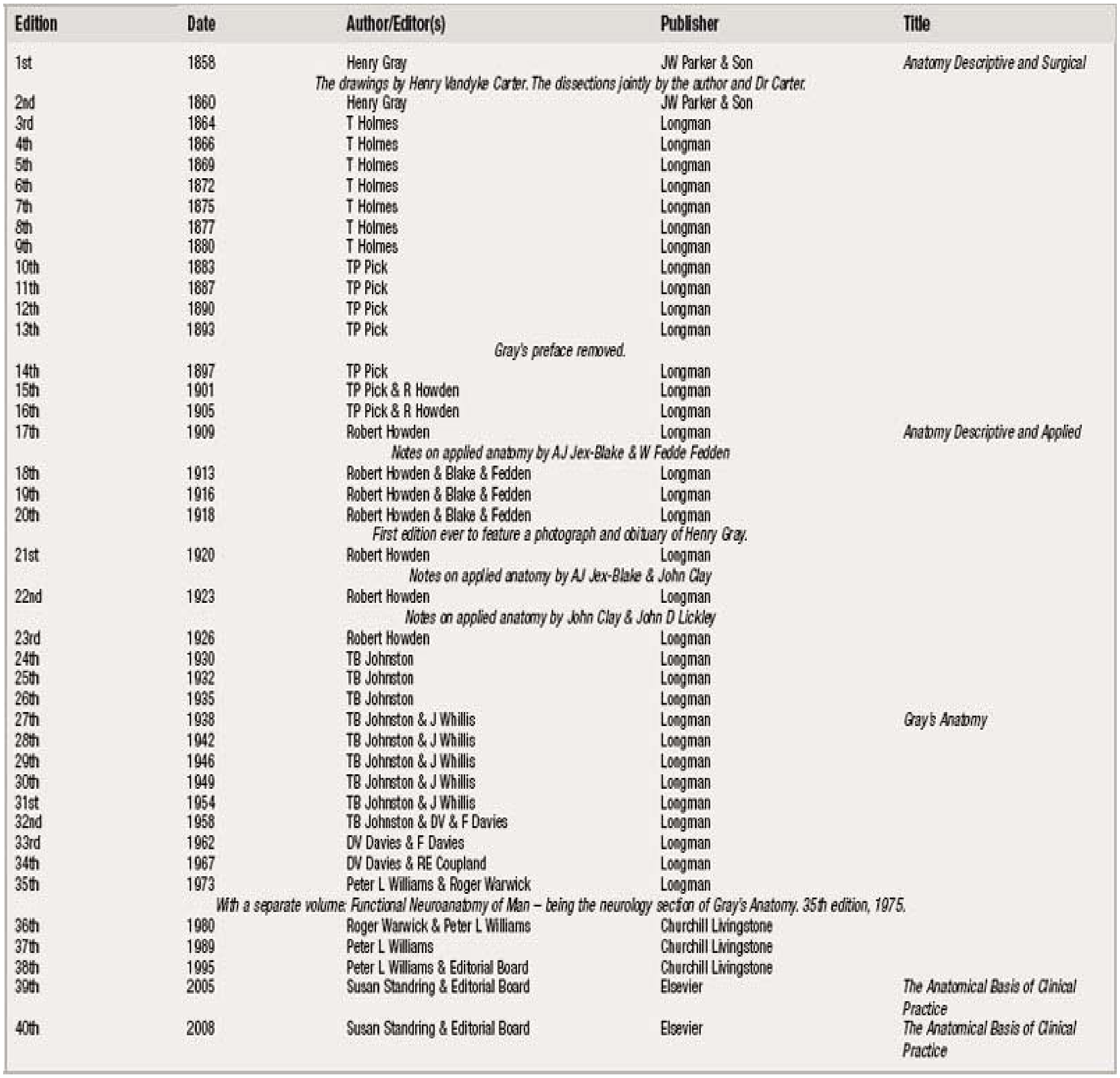

Edition	Date	Author/Editor(s)	Publisher	Title
1st	1858	Henry Gray	JW Parker & Son	*Anatomy Descriptive and Surgical*
		The drawings by Henry Vandyke Carter. The dissections jointly by the author and Dr Carter.		
2nd	1860	Henry Gray	JW Parker & Son	
3rd	1864	T Holmes	Longman	
4th	1866	T Holmes	Longman	
5th	1869	T Holmes	Longman	
6th	1872	T Holmes	Longman	
7th	1875	T Holmes	Longman	
8th	1877	T Holmes	Longman	
9th	1880	T Holmes	Longman	
10th	1883	TP Pick	Longman	
11th	1887	TP Pick	Longman	
12th	1890	TP Pick	Longman	
13th	1893	TP Pick	Longman	
		Gray's preface removed.		
14th	1897	TP Pick	Longman	
15th	1901	TP Pick & R Howden	Longman	
16th	1905	TP Pick & R Howden	Longman	
17th	1909	Robert Howden	Longman	*Anatomy Descriptive and Applied*
		Notes on applied anatomy by AJ Jex-Blake & W Fedde Fedden		
18th	1913	Robert Howden & Blake & Fedden	Longman	
19th	1916	Robert Howden & Blake & Fedden	Longman	
20th	1918	Robert Howden & Blake & Fedden	Longman	
		First edition ever to feature a photograph and obituary of Henry Gray.		
21st	1920	Robert Howden	Longman	
		Notes on applied anatomy by AJ Jex-Blake & John Clay		
22nd	1923	Robert Howden	Longman	
		Notes on applied anatomy by John Clay & John D Lickley		
23rd	1926	Robert Howden	Longman	
24th	1930	TB Johnston	Longman	
25th	1932	TB Johnston	Longman	
26th	1935	TB Johnston	Longman	
27th	1938	TB Johnston & J Whillis	Longman	*Gray's Anatomy*
28th	1942	TB Johnston & J Whillis	Longman	
29th	1946	TB Johnston & J Whillis	Longman	
30th	1949	TB Johnston & J Whillis	Longman	
31st	1954	TB Johnston & J Whillis	Longman	
32nd	1958	TB Johnston & DV & F Davies	Longman	
33rd	1962	DV Davies & F Davies	Longman	
34th	1967	DV Davies & RE Coupland	Longman	
35th	1973	Peter L Williams & Roger Warwick	Longman	
		With a separate volume: Functional Neuroanatomy of Man – being the neurology section of Gray's Anatomy. 35th edition, 1975.		
36th	1980	Roger Warwick & Peter L Williams	Churchill Livingstone	
37th	1989	Peter L Williams	Churchill Livingstone	
38th	1995	Peter L Williams & Editorial Board	Churchill Livingstone	
39th	2005	Susan Standring & Editorial Board	Elsevier	*The Anatomical Basis of Clinical Practice*
40th	2008	Susan Standring & Editorial Board	Elsevier	*The Anatomical Basis of Clinical Practice*

THE DOCTORS' BIBLE

Neither Gray nor Carter, young men who – by their committed hard work between 1856 and 1858 – created the original *Gray's Anatomy*, would have conceived that years after their deaths their book would not only be a household name, but regarded as a work of such pre-eminent importance that a novelist half a world away would rank it as cardinal – alongside the Bible and Shakespeare – to a doctor's education. (11)

Now, in this 40th edition of *Gray's Anatomy*, we can look back over 150 years of continuous publication to appraise the long term value of their efforts. We can discern how the book they created triumphed over its competitors, and has survived pre-eminent. *Gray's* is a remarkable publishing phenomenon. Although the volume now looks quite different to the original, and contains so much more, its kinship with the *Gray's Anatomy* of 1858 is easily demonstrable by direct descent, every edition updated by Henry Gray's successor. Works are rare indeed that have had such a long history of continuous publication on both sides of the Atlantic, and such a useful one.

With this fine new 150th anniversary edition, the book goes marching on.

Ruth Richardson, MA, DPhil, FRHistSoc

Affiliated Scholar in the History & Philosophy of Science, University of Cambridge; Senior Visiting Research Fellow in History, University of Hertfordshire at Hatfield.

ACKNOWLEDGEMENTS

For their assistance while I was undertaking the research for this essay, I should like to thank the Librarians and Archivists and Staff at the British Library, Society of Apothecaries, London School of Hygiene & Tropical Medicine, Royal College of Surgeons, Royal Society of Medicine, St Bride Printing Library, St George's Hospital Tooting, Scarborough City Museum & Art Gallery, University of Reading, Wellcome Institute Library, Westminster City Archives and Windsor Castle; and the following individuals: Anne Bayliss, Gordon Bell, David Buchanan, Dee Cook, Arthur Credland, Chris Hamlin, Victoria Killick, Louise King, Keith Nicol, Sarah Potts, Mark Smalley, Nallini Thevakarrunai. Above all, my thanks to Brian Hurwitz, who has read and advised on the evolving text.

REFERENCES

Anon. *Henry Gray. St George's Hospital Gazette*. 1908;16(4):49-54.

Carter HV: Diary. Wellcome Western Manuscript 5818: Nov 25th 1855.

Richardson R. Death, Dissection & the Destitute. Chicago: Chicago University Press, 2000;193-249. 287, 357.

Gray H. Anatomy: Descriptive and Surgical. London: JW Parker & Son, 1858. Preface.

Nicol KE. Henry Gray of St George's Hospital: a Chronology. London: Published by the Author, 2002.

Quain J. Sharpey W, Ellis GV. Elements of Anatomy. London: Walton & Maberly, 1856.

Holmes T, editor. A System of Surgery. London: JW Parker & Son, 1860. I: Preface.

Gray's Anatomy. London: Longmans, 1918.

Tansey EM. A Brief History of Gray's Anatomy. Gray's Anatomy. London: Churchill Livingstone, 1995;xvii-xvxx.

Gray's Anatomy. London: Churchill, 1973. preface.

Gray's Anatomy. 39th edition. London: Elsevier; 2005. Preface.

Sinclair Lewis 1925: Arrowsmith. Place, Harcourt Brace: 4.

ANATOMICAL NOMENCLATURE

Anatomy is the study of the structure of the body. It is conventionally divided into topographical or gross anatomy (which includes surface, or ‘living’, anatomy, neuroanatomy, endoscopic and imaging anatomy), microscopic anatomy or histology and embryology (the study of the embryo and fetus).

Anatomical language is one of the fundamental languages of medicine. The unambiguous description of thousands of structures is impossible without an extensive and often highly specialized vocabulary. Ideally, these terms, which are often derived from Latin or Greek, should be used to the exclusion of any other, throughout the world. In reality, many terms are vernacularized. The *Terminologia Anatomica*, drawn up by the Federative Committee on Anatomical Terminology (FCAT) in 1998, has served as our guide in preparing the 39th and 40th Editions of *Gray’s Anatomy*. Where we have anglicized some of the Latin terms, we have given the official form, at least once, in parentheses. We have also included eponyms, since these are often used, possibly more so by clinicians than anatomists. Indeed, certain eponyms are so firmly entrenched in the language of the clinician that to avoid them could lead to confusion: the eponymous term is often the only way to describe a particular structure, because there is no simple alternative anatomical term. (Short biographical details of the clinicians and anatomists whose names are used in this way are included in the electronic version of the book.)

PLANES, DIRECTIONS AND RELATIONSHIPS

To avoid ambiguity, all anatomical descriptions assume that the body is in the conventional ‘anatomical position’, i.e. standing erect and facing forwards, upper limbs by the side with the palms facing forwards, and lower limbs together with the toes facing forwards (Fig. 1). Descriptions are based on four imaginary planes, median, sagittal, coronal and horizontal, applied to a body in the anatomical position. The median plane passes longitudinally through the body and divides it into right and left halves. The sagittal plane is any vertical plane parallel with the median plane: although often used, ‘parasagittal’ is therefore redundant. The coronal (frontal) plane is orthogonal to the median plane and divides the body into anterior (front) and posterior (back). The horizontal (transverse) plane is orthogonal to both median and sagittal planes. Radiologists refer to transverse planes as (trans)axial: convention dictates that axial anatomy is viewed as though looking from the feet towards the head.

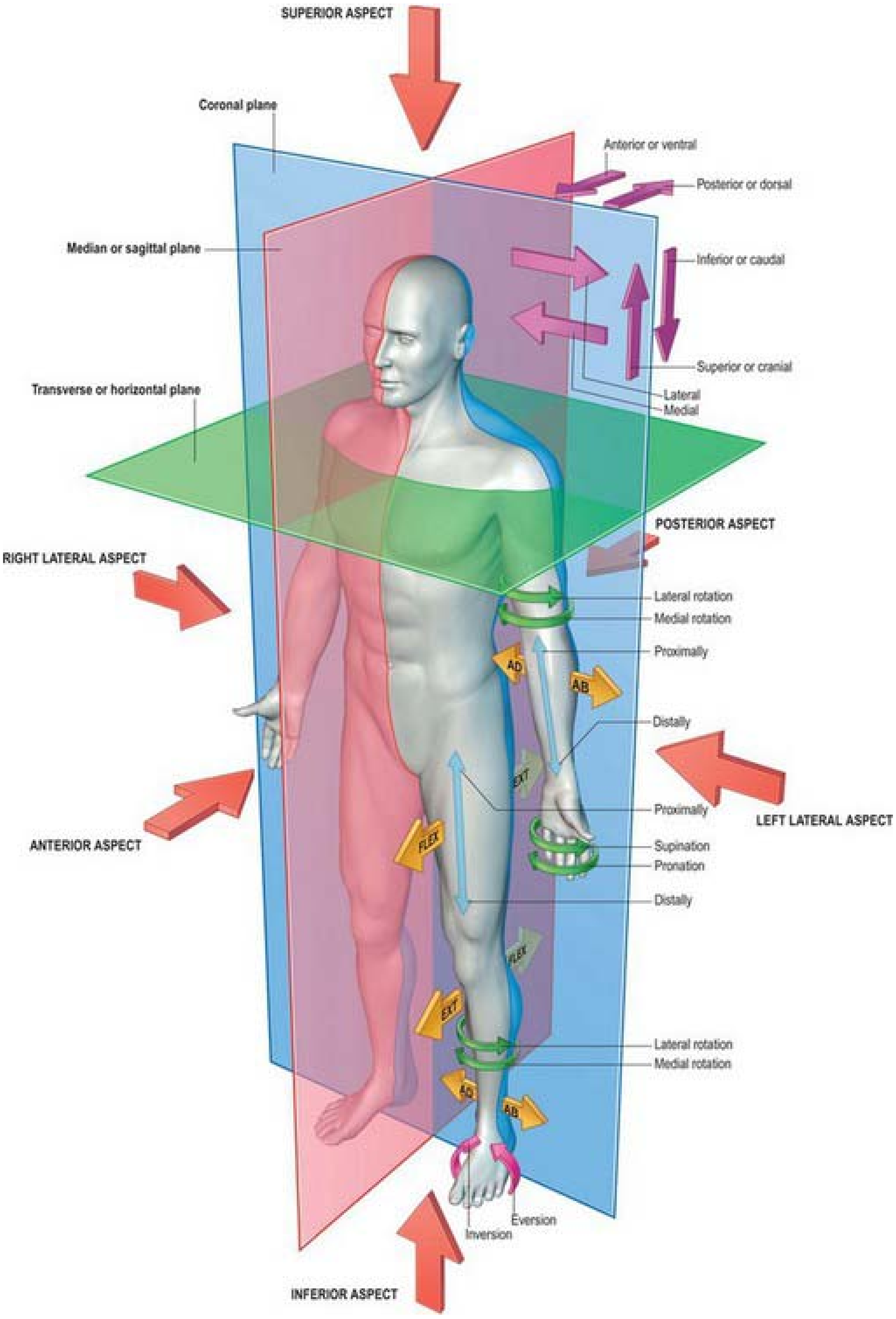
SUPERIOR ASPECT
Coronal plane
Anterior or ventral
Posterior or dorsal
Median or sagittal plane
Inferior or caudal
Superior or cranial
Transverse or horizontal plane
Lateral
Medial
POSTERIOR ASPECT
RIGHT LATERAL ASPECT
Lateral rotation
Medial rotation
Proximally
AD
AB
Distally
EXT
Proximally
LEFT LATERAL ASPECT
Supination
ANTERIOR ASPECT
FLEX
Pronation
Distally
FLEX
EXT
Lateral rotation
Medial rotation
AD
AB
Eversion
Inversion
INFERIOR ASPECT

Fig. 1 The terminology widely used in descriptive anatomy. Abbreviations shown on arrows: AD, adduction; AB, abduction; FLEX, flexion (of the thigh at the hip joint); EXT, extension (of the leg at the knee joint).

Structures nearer the head are superior, cranial or (sometimes) cephalic, whereas structures closer to the feet are inferior; caudal is most often used in embryology to refer to the tail end of the embryo. Medial and lateral indicate closeness to the median plane, medial being closer than lateral: in the anatomical position, the little finger is medial to the thumb, the great toe is medial to the little toe. Specialized terms may also be used to indicate medial and lateral. Thus, in the upper limb, ulnar and radial are used to mean medial and lateral respectively, and in the lower limb, tibial and fibular (peroneal) are used to mean medial and lateral respectively. Terms may be based on embryological relationships: the border of the upper limb that includes the thumb, and the border of the lower limb that includes the great toe are the pre-axial borders, whilst the opposite borders are the post-axial borders. Various degrees of obliquity are acknowledged using compound terms, e.g. posterolateral.

When referring to structures in the trunk and upper limb we have used freely the synonyms anterior, ventral, flexor, palmar, volar, and posterior, dorsal and extensor. We recognize that these synonyms are not always satisfactory, e.g. the extensor aspect of the leg is anterior with respect to the knee and ankle joints, and superior in the foot and digits; the plantar (flexor) aspect of the foot is inferior. Dorsal (dorsum) and ventral are terms used particularly by embryologists and neuroanatomists: they therefore feature most often in Sections 2 and 3.

Distal and proximal are used particularly to describe structures in the limbs, taking the datum point as the attachment of the limb to the trunk (sometimes referred to as the root), such that a proximal structure is closer to the attachment of the limb than a distal structure. However, proximal and distal are also used in describing branching structures, e.g. bronchi, vessels and nerves.

External (outer) and internal (inner) refer to the distance from the centre of an organ or cavity, e.g. the layers of the body wall, or the cortex and medulla of the kidney. Superficial and deep are used to describe the relationships between adjacent structures. Ipsilateral refers to the same side (of the body, organ or structure), bilateral to both sides, and contralateral to the opposite side.

Teeth are described using specific terms which indicate their relationship to their neighbours and to their position within the dental arch: these terms are described in Chapter 30.

MOVEMENTS

Movements at joints, e.g. flexion, extension, adduction and abduction, and the many possible combinations of these ‘pure’ movements, are described in Chapter 5. Specialized movements, such as those that occur at the elbow, wrist, ankle and temporomandibular joints, are described in the appropriate chapters.

BIBLIOGRAPHY OF SELECTED TITLES

The following references contain information relevant to numerous chapters in this edition. They are therefore cited here rather than at the end of individual chapters. For an extended historical bibliography, all references from the 38th edition are available on the website which accompanies *Gray's Anatomy*.

TERMINOLOGY

Federative Committee on Anatomical Terminology 1998 Terminologia Anatomica. International Anatomical Nomenclature. Stuttgart: Thieme.

Dorland, 2007, Dorland’s Illustrated Medical Dictionary, 31st edn. Philadelphia: W B Saunders.

BASIC SCIENCES

Abrahams P, Boon H, Spratt J, and Hutchings R 2008 McMinn's Clinical Atlas of Human Anatomy, 6th edn. London: Churchill Livingstone.

Alberts B, Johnson A, Lewis J, Raff M, Roberts K, Walter P 2002 Molecular Biology of the Cell, 4th edn. New York: Garland Science Publishing.

Berkovitz BKB, Kirsh C, Moxham BJ, Alusi G, Cheeseman T 2002 Interactive Head and Neck. London: Primal Pictures.

Boron W, Boulpaep E 2004 Medical Physiology, updated edn. Philadelphia: W B Saunders.

Crossman AR, Neary D 2005 Neuroanatomy, An Illustrated Colour Text, 3rd edn. Edinburgh: Churchill Livingstone.

Fitzgerald MJT, Folan-Curran J 2006 Clinical Neuroanatomy and Related Science, 5th edn. Edinburgh: Churchill Livingstone.

Guyton AC, Hall JE 2005 Textbook of Medical Physiology, 11th edn. Philadelphia: W B Saunders.

Kerr JB 1999 Atlas of Functional Histology. London: Mosby.

Kierszenbaum AL 2007 Histology and Cell Biology: An Introduction to Pathology, 2nd edn. St Louis: Mosby.

Moore KL, Persaud TVN 2008 Before We Are Born: Essentials of Embryology and Birth Defects, 7th edn. Philadelphia: W B Saunders.

Pollard TD, Earnshaw WC 2007 Cell Biology, 2nd edn. Philadelphia: W B Saunders.

Male D, Brostoff J, Roth D, Roitt I, 2006 Immunology, 7th edn. London: Mosby.

Salmon M 1994 Anatomic Studies: Book 1 Arteries of the Muscles of the Extremities and the Trunk, Book 2 Arterial Anastomotic Pathways of the Extremities. Ed. by Taylor GI, Razaboni RM. St Louis: Quality Medical Publishing Inc.

Stevens A, Lowe JS 2004 Human Histology, 3rd edn. London: Mosby.

Young B, Lowe JS, Stevens A, Heath JW 2006 Wheater's Functional Histology: A Text and Colour Atlas, 5th edn. Edinburgh: Churchill Livingstone.

IMAGING AND RADIOLOGY/RADIOLOGICAL ANATOMY

Butler P, Mitchell AWM, Ellis H 1999 Applied Radiological Anatomy. New York: Cambridge University Press.

Ellis H, Dixon A, Logan BM 1999 Human Sectional Anatomy: Atlas of Body Sections, CT and MRI Images, 2nd edn. Oxford: Oxford University Press.

Haaga JR, Lanzieri CF, Gilkeson RC 2002 CT and MR Imaging of the Whole Body, 4th edn. St Louis: Mosby.

Lasjaunias P, Berenstein A, ter Brugge K 2001 Surgical Neuroangiography, vol 1. Clinical Vascular Anatomy and Variations, 2nd edn. Berlin, New York: Springer.

Meyers MA 2000 Dynamic Radiology of the Abdomen: Normal and Pathologic Anatomy, 5th edn. New York: Springer.

Pomeranz SJ 1992 MRI Total Body Atlas. Cincinnati: MRI-EFI Publications.

Sutton D, Reznek R, Murfitt J 2002 Textbook of Radiology and Imaging, 7th edn. Edinburgh: Churchill Livingstone.

Weir J, Abrahams PH 2003 Imaging Atlas of Human Anatomy, 3rd edn. London: Mosby.

Wicke L 1998 Atlas of Radiologic Anatomy, 7th edn. Philadelphia: Saunders.

Whaites E 2006 Essential of Dental Radiography and Radiology, 4th edn. Edinburgh: Churchill Livingstone.

CLINICAL

Birch R, Bonney G, Wynn Parry CB 1998 Surgical Disorders of the Peripheral Nerves. Edinburgh: Churchill Livingstone.

Bogduk N 2005 Clinical Anatomy of the Lumbar Spine and Sacrum, 4th edn. Edinburgh: Churchill Livingstone.

Borges AF 1984 Relaxed skin tension lines (RSTL) versus other skin lines. Plast Reconstr Surg 73: 144–50.

Burnand KG, Young AE, Lucas JD, Rowlands B, Scholefield J 2005 The New Aird's Companion in Surgical Studies, 3rd edn. Edinburgh: Churchill Livingstone.

Canale ST, Beaty JH 2008 Campbell's Operative Orthopaedics, 11th edn. Philadelphia: Mosby.

Cormack GC, Lamberty BGH 1994 The Arterial Anatomy of Skin Flaps. Edinburgh: Churchill Livingstone.

Dyck PJ, Thomas PK 2005 Peripheral Neuropathy, 4th edn. Philadelphia: W B Saunders.

Ellis H 2002 Clinical Anatomy: A Revision and Applied Anatomy for Clinical Students, 10th edn. Maldem MA: Blackwell Scientific Publications.

Ellis H, Feldman S, Harrop-Griffiths W 2003 Anatomy for Anaesthetists, 8th edn. Oxford: Blackwell Science.

Rosai J 2004 Rosai and Ackerman's Surgical Pathology, 9th edn. London: Mosby.

Shah J 2003 Head and Neck Surgery and Oncology, 3rd edn. London: Mosby.

Taylor GI, Palmer JH, McManamy D 1987 The vascular territories of the body (angiosomes): experimental study and their clinical applications. In McCarthy JG, 1990, Plastic Surgery, vol I General Principles. Philadelphia: W B Saunders.

Zancolli E A, Cozzi E P 1992 Atlas of Surgical Anatomy of the Hand, Edinburgh: Churchill Livingstone.

CLINICAL EXAMINATION

Aids to the Examination of the Peripheral Nervous System, 4th Edition. London: W B Saunders, 2000.

Lumley JSP 2002 Surface Anatomy: The Anatomical Basis of Clinical Examination, 3rd edn. Edinburgh: Churchill Livingstone.

Section 1

CELLS, TISSUES AND SYSTEMS

CHAPTER 1

Basic structure and function of cells

CELL STRUCTURE

GENERAL CHARACTERISTICS OF CELLS

The shapes of mammalian cells vary widely depending on their interactions with each other, their extracellular environment and internal structures. Their surfaces are often highly folded when absorptive or transport functions take place across their boundaries. Cell size is limited by rates of diffusion, either that of material entering or leaving cells, or of diffusion within them. Movement of macromolecules can be much accelerated and also directed by processes of active transport across membranes and by transport mechanisms within the cell. According to the location of absorptive or transport functions, apical microvilli (Fig. 1.1) or basolateral infoldings create a large surface area for transport or diffusion.

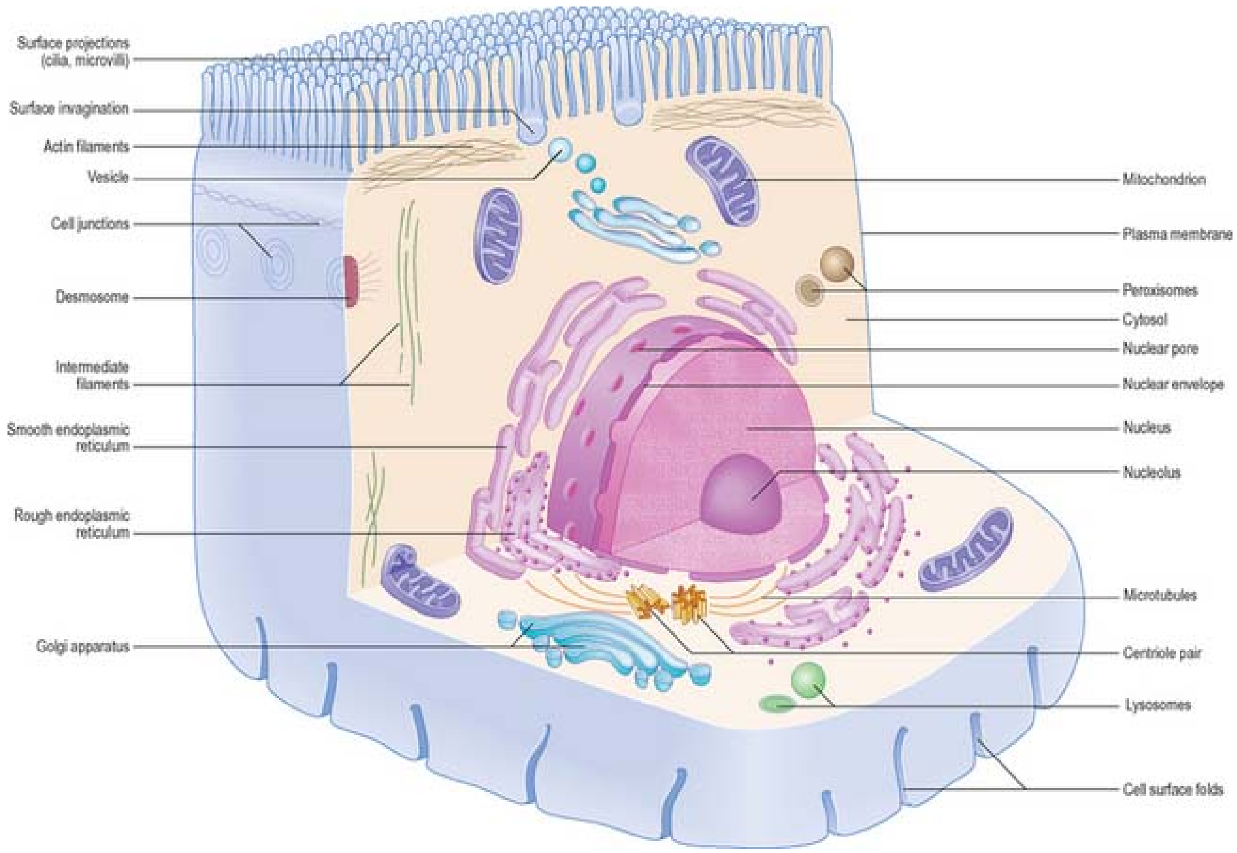
Surface projections (cilia, microvilli)
Surface invagination
Actin filaments
Vesicle
Cell junctions
Desmosome
Intermediate filaments
Smooth endoplasmic reticulum
Rough endoplasmic reticulum
Golgi apparatus
Mitochondrion
Plasma membrane
Peroxisomes
Cytosol
Nuclear pore
Nuclear envelope
Nucleus
Nucleolus
Microtubules
Centriole pair
Lysosomes
Cell surface folds

Fig. 1.1 The main structural components and internal organization of a generalized cell.

Motility is a characteristic of most cells, in the form of movements of cytoplasm or specific organelles from one part of the cell to another. It also includes: the extension of parts of the cell surface such as pseudopodia, lamellipodia, filopodia and microvilli; locomotion of entire cells as in the amoeboid migration of tissue macrophages; the beating of flagella or cilia to move the cell (e.g. in spermatozoa) or fluids overlying it (e.g. in respiratory epithelium); cell division and muscle contraction. Cell movements are also involved in the uptake of materials from their environment (endocytosis, phagocytosis) and the passage of large molecular complexes out of cells (exocytosis, secretion).

Cells rarely operate independently of each other and commonly form aggregates by adhesion, often assisted by specialized intercellular junctions. They may also communicate with each other either by generating and detecting molecular signals that diffuse across intercellular spaces, or more rapidly by membrane contact, which may involve small, transient, transmembrane channels or interactions between membrane-bound signalling molecules. Cohesive groups of cells constitute tissues and more complex assemblies of tissues form functional systems or organs.

Most cells are between 5–50 μm in diameter: e.g. resting lymphocytes are 6 μm across, red blood cells 7.5 μm and columnar epithelial cells are 20 μm tall and 10 μm wide (all measurements are approximate). Some cells are much larger than this: e.g. megakaryocytes of the bone marrow are more than 200 μm in diameter. Large neurones and skeletal muscle cells have relatively enormous volumes because of their extended shapes, some of the former being over 1 metre in length.

CELLULAR ORGANIZATION

Each cell is contained within its limiting plasma, or surface, membrane which encloses the cytoplasm. All cells except mature red blood cells also contain a nucleus that is surrounded by a nuclear membrane or envelope (Fig. 1.1, Fig. 1.2). The nucleus includes the genome of the cell contained within the chromosomes, the nucleolus, and other sub-nuclear organelles. The cytoplasm contains several systems of organelles. These include a series of membrane-bound structures that form separate compartments within the cytoplasm, such as rough and smooth endoplasmic reticulum, Golgi apparatus, lysosomes, peroxisomes, mitochondria and vesicles for transport, secretion and storage of cellular components. There are also structures that lie free in the non-membranous, cytosolic compartment. They include ribosomes and several filamentous protein networks known collectively as the cytoskeleton. The cytoskeleton determines general cell shape and supports specialized extensions of the cell surface (microvilli, cilia, flagella). It is involved in the assembly of new filamentous organelles (e.g. centrioles) and controls internal movements of the cytoplasm and cytoplasmic vesicles. The cytosol contains many soluble proteins, ions and metabolites.

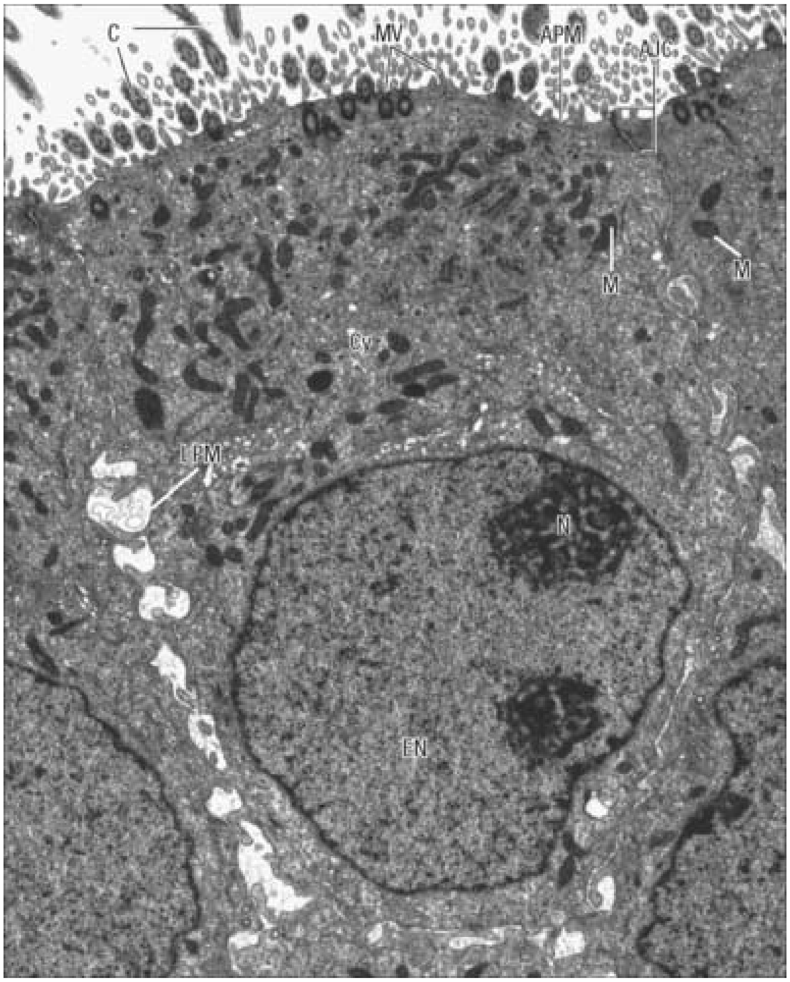

Fig. 1.2 The structural organization and some principal organelles of a typical cell. This example is a ciliated columnar epithelial cell from human nasal mucosa. The central cell, which occupies most of the field of view, is closely apposed to its neighbours along their lateral plasma membranes. Within the apical junctional complex, these membranes form a tightly sealed zone (tight junction) that isolates underlying tissues from, in this instance, the nasal cavity. AJC, apical junctional complex; APM, apical plasma membrane; C, cilia; Cy, cytoplasm; EN, euchromatic nucleus; LPM, lateral plasma membrane; M, mitochondria; MV, microvilli; N, nucleolus.

Cell polarity and domains

Epithelia (including endothelia and mesothelia) are organized into sheets or more complex structures (see Ch. 2) with very different environments on either side. These cells actively transfer macromolecules and ions between the two surfaces and are thus polarized in structure and function (Fig. 1.3). In polarized cells, particularly in epithelia, the cell is generally subdivided into domains that reflect the polarization of activities within it. The free surface, e.g. that facing the intestinal lumen or airway, is the apical surface, and its adjacent cytoplasm is the apical cell domain. This is where the cell interfaces with a specific body compartment (or, in the case of the epidermis, with the outside world). The apical surface is specialized to act as a barrier, restricting access of substances from this compartment to the rest of the body. Specific components are selectively absorbed from, or added to, the external compartment by the active processes, respectively, of active transport and endocytosis inwardly or exocytosis and secretion outwardly. The apical surface is often covered with small protrusions of the cell surface, microvilli, which increase the surface area, particularly for absorption.

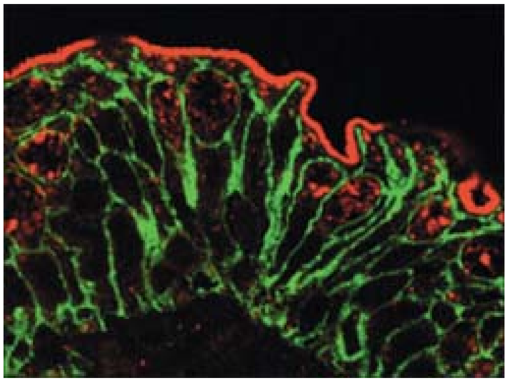

Fig. 1.3 Absorptive epithelium from human colon, immunolabelled to show the functional division of cell surface domains. CD66 antigen expression (red) is concentrated in the apical domain facing the gut lumen (top), on striated border microvilli; diffuse labelling is present throughout the cytoplasm but is excluded from the basal zone occupied by nuclei. The intestinal cell antigen A33 (green) is a member of the immunoglobulin superfamily of transmembrane proteins, expressed here on basolateral cell surfaces.

(By courtesy of Cécile Chalouni, Ludwig Institute for Cancer Research, Yale University School of Medicine.)

The surface of the cell opposite to the apical surface is the basal surface, with its associated basal cell domain. In a single-layered epithelium, this surface is apposed to the basal lamina. The remaining surfaces are known as the lateral cell surfaces. In many instances the lateral and basal surfaces perform similar functions and the cellular domain is termed the basolateral domain. Cells actively transport substances, such as digested nutrients from the intestinal lumen or endocrine secretions, across their basal (or basolateral) surfaces into the subjacent connective tissue matrix and the blood capillaries within it. Dissolved non-polar gases (oxygen and carbon dioxide) diffuse freely between the cell and the bloodstream across the basolateral surface. Apical and basolateral surfaces are separated by a tight intercellular seal, the tight junction, which prevents the passage of even small ions through the space between adjacent cells and thus maintains the difference between environments either side of the epithelium.

PLASMA MEMBRANE

Cells are bounded by a distinct plasma membrane, which shares features with the system of internal membranes that compartmentalize the cytoplasm and surround the nucleus. They are all composed of lipids (mainly phospholipids, cholesterol and glycolipids) and proteins, in approximately equal ratios. Plasma membrane lipids form a layer two molecules thick, the lipid bilayer. The hydrophobic ends of each lipid molecule face the interior of the membrane and the hydrophilic ends face outwards. Most proteins are embedded within, or float in, the lipid bilayer as a fluid mosaic. Some proteins, because of extensive hydrophobic regions of their polypeptide chains, span the entire width of the membrane (transmembrane proteins), whereas others are only superficially attached to the bilayer by lipid groups. Both are integral (intrinsic) membrane proteins, as distinct from peripheral (extrinsic) membrane proteins, which are membrane-bound only through their association with other proteins. Carbohydrates in the form of oligosaccharides and polysaccharides are bound either to proteins (glycoproteins) or to lipids (glycolipids), and project mainly into the extracellular domain.

Combinations of biochemical, biophysical and biological techniques have revealed that lipids are not homogenously distributed in membranes, but that some are organized into microdomains in the bilayer, called ‘detergent-resistant membranes’ or lipid ‘rafts’, rich in sphingomyelin and cholesterol (Morris et al 2004). The ability of select subsets of proteins to partition into different lipid microdomains has profound effects on their function, e.g. in T-cell receptor and neurotrophin signalling. The highly organized environment of the domains provides a signalling, trafficking and membrane fusion environment very different from that found in the disorganized fluid mosaic membrane.

In the electron microscope, membranes fixed and contrasted by heavy metals such as osmium appear in section as two densely stained layers separated by an electron-translucent zone – the classic unit membrane (Fig. 1.4). The total thickness is about 5 nm. Freeze-fracture cleavage planes usually pass along the midline of each membrane, where the hydrophobic tails of phospholipids meet. This technique has also demonstrated intramembranous particles embedded in the lipid bilayer; these are in the 5–15 nm range and in most cases represent large transmembrane protein molecules or complexes of molecules. Intramembranous particles are distributed asymmetrically between the two half-membranes, usually adhering more to one face than to the other. In plasma membranes, the inner or protoplasmic (cytoplasmic) half-membrane carries most particles, seen on its surface facing the exterior (the P face). Where they have been identified, particles usually represent channels for the transmembrane passage of ions or molecules.

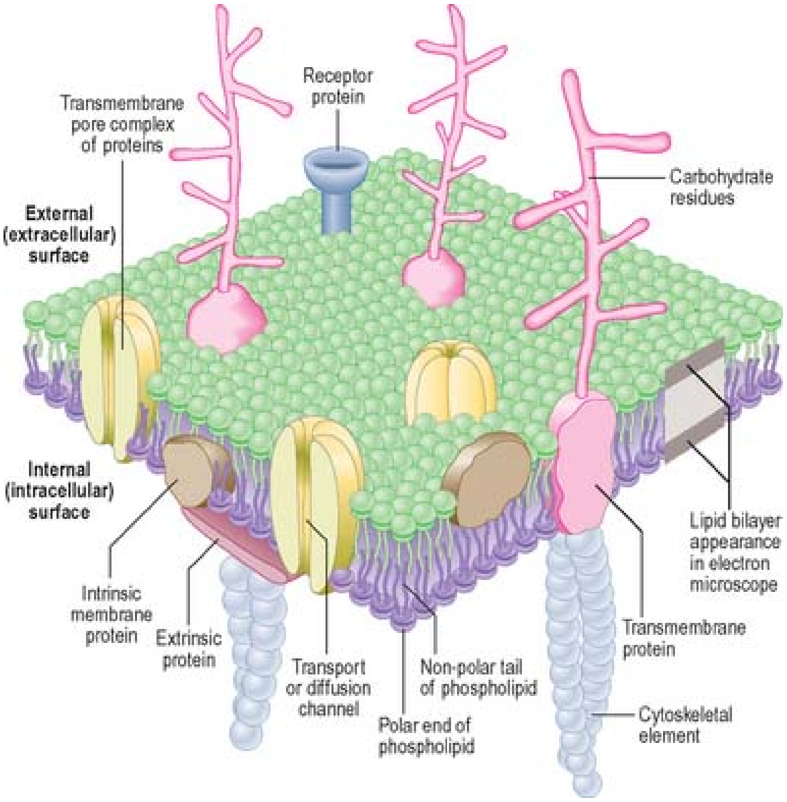
Receptor protein
Transmembrane pore complex of proteins
External (extracellular) surface
Carbohydrate residues
Internal (intracellular) surface
Lipid bilayer appearance in electron microscope
Intrinsic membrane protein
Extrinsic protein
Transport or diffusion channel
Non-polar tail of phospholipid
Polar end of phospholipid
Transmembrane protein
Cytoskeletal element

Fig. 1.4 The molecular organization of the plasma membrane, according to the fluid mosaic model of membrane structure. Intrinsic or integral membrane proteins include diffusion or transport channel complexes, receptor proteins and adhesion molecules. These may span the thickness of the membrane (transmembrane proteins) and can have both extracellular

and cytoplasmic domains. Transmembrane proteins have hydrophobic zones, which cross the phospholipid bilayer and allow the protein to ‘float’ in the plane of the membrane. Some proteins are restricted in their freedom of movement where their cytoplasmic domains are tethered to the cytoskeleton.

Biophysical measurements show the lipid bilayer to be highly fluid, allowing diffusion in the plane of the membrane. Thus proteins are able to move freely in such planes unless anchored from within the cell. Membranes in general, and the plasma membrane in particular, form boundaries selectively limiting diffusion and creating physiologically distinct compartments. Lipid bilayers are impermeable to hydrophilic solutes and ions and so membranes actively control the passage of ions and small organic molecules such as nutrients, through the activity of membrane transport proteins. However, lipid-soluble substances can pass directly through the membrane so that, for example, steroid hormones enter the cytoplasm freely. Their receptor proteins are either cytosolic or nuclear, rather than being located on the cell surface.

Plasma membranes are able to generate electrochemical gradients and potential differences by selective ion transport, and actively take up or export small molecules by energy dependent processes. They also provide surfaces for the attachment of enzymes, sites for the receptors of external signals, including hormones and other ligands, and sites for the recognition and attachment of other cells. Internally, plasma membranes can act as points of attachment for intracellular structures, in particular those concerned with motility and other cytoskeletal functions. Cell membranes are synthesized by the rough endoplasmic reticulum in conjunction with the Golgi apparatus.

The cell coat (glycocalyx)

The plasma membrane differs structurally from internal membranes in that it possesses an external, diffuse, carbohydrate-rich coat, the cell coat or glycocalyx. The cell coat forms an integral part of the plasma membrane, projecting as a diffusely filamentous layer 2–20 nm or more from the lipoprotein surface (see Fig. 1.5). The overall thickness of the plasma membrane is therefore variable, but is typically 8–10 nm. The cell coat is composed of the carbohydrate portions of glycoproteins and glycolipids embedded in the plasma membrane (Fig. 1.4).

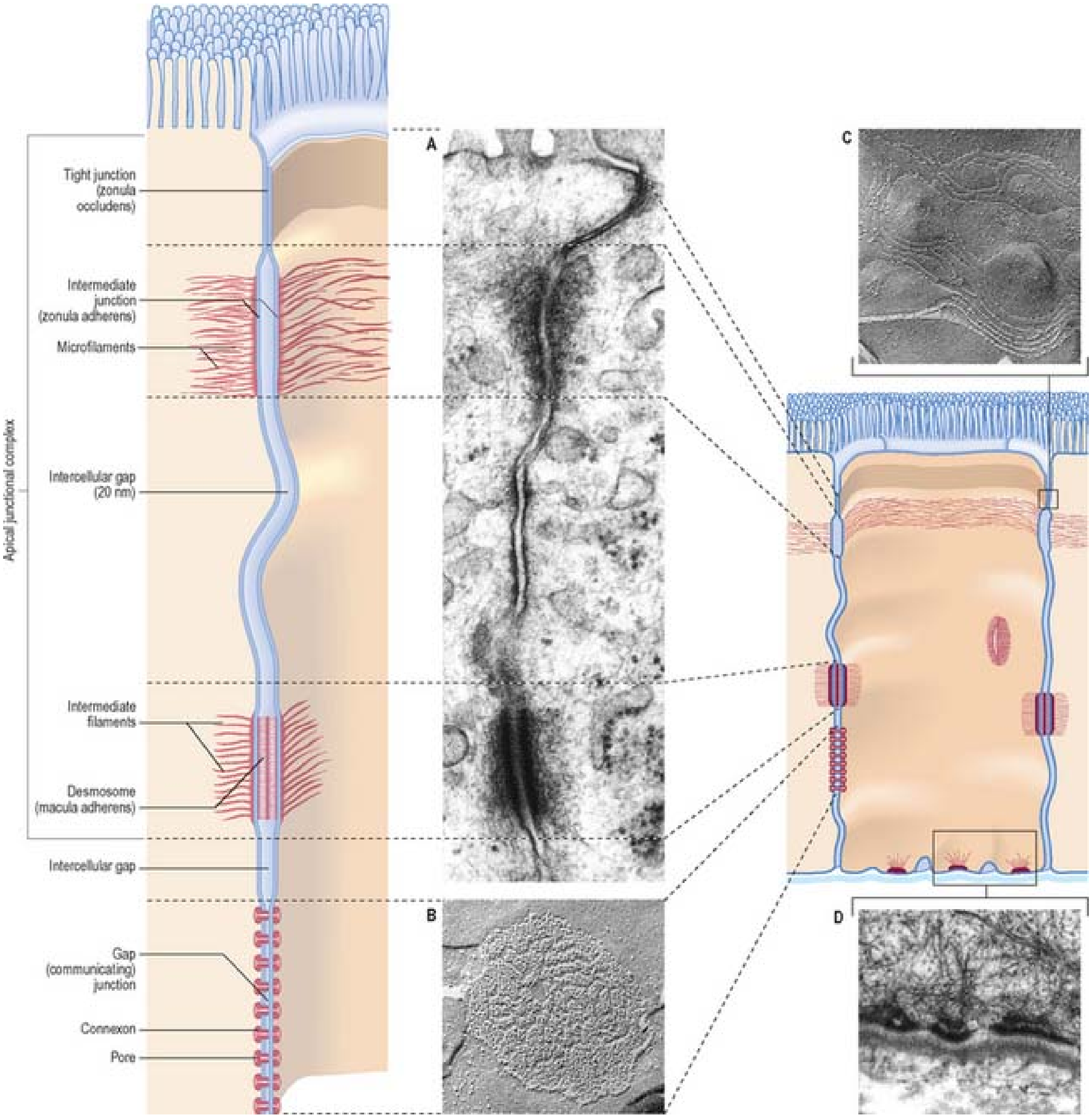
Apical junctional complex
Tight junction (zonula occludens)
Intermediate junction (zonula adherens)
Microfilaments
Intercellular gap (20 nm)
Intermediate filaments
Desmosome (macula adherens)
Intercellular gap
Gap (communicating) junction
Connexon
Pore
A
B
C
D

Fig. 1.5 Intercellular junctions. The positions of the apical junctional complex and other junctional specializations of epithelial cells are shown, along with their electron microscopic appearances (see **A–D**; B and C are

freeze fractured preparations). **B** shows how, in a gap junction, numerous channels (pores within connexons) are clustered to form a plaque-like junctional region between adjacent plasma membranes. **C** shows the anastomotic network of contacts between adjacent cell membranes forming a tight junction. **D** shows the attachments of basal plasma membrane to basal lamina at hemidesmosomes.

(Part B by courtesy of Professor Dieter Hülser, University of Stuttgart. Part C by courtesy of Dr Andrew Kent, King's College London.) A,D from human tissue.

The precise composition of the glycocalyx varies with cell type: many tissue and cell type-specific antigens are located in the coat, including the major histocompatibility antigen systems and, in the case of erythrocytes, blood group antigens. It also contains adhesion molecules, which enable cells to adhere selectively to other cells or to the extracellular matrix. They have important roles in maintaining the integrity of tissues and in a wide range of dynamic cellular processes, e.g. the formation of intercommunicating neural networks in the developing nervous system and the extravasation of leukocytes. Cells tend to repel each other because of the predominance of negatively charged carbohydrates at cell surfaces. There is consequently a distance of at least 20 nm between the plasma membranes of adjacent cells, other than at specialized junctions.

Cell surface contacts

The plasma membrane is the surface which establishes contact with other cells and with structural components of extracellular matrices. These contacts may have a predominantly adhesive role, or initiate instructive signals within and between cells, or both; they frequently affect the behaviour of cells. Structurally, there are two main classes of contact, both associated with cell adhesion molecules. One class is associated with specializations at discrete regions of the cell surface that are ultrastructurally distinct. These are described on page 6. The second, general, class of adhesive contact has no obvious associated ultrastructural features.

General adhesive contacts

One class of transmembrane or membrane-anchored glycoproteins that project externally from the plasma membrane, and which form adhesive contacts, are the cell adhesion molecules. There are a number of molecular subgroups, which are broadly divisible on the basis of their calcium dependence. Their numerous functions include tissue formation and morphogenesis and there is evidence for coordinated interaction between the subgroups.

Calcium-dependent adhesion molecules

Cadherins, selectins and integrins are calcium-dependent adhesion molecules. Cadherins are transmembrane proteins, with five heavily glycosylated external domains. They are responsible for strong general intercellular adhesion, as well as being components of some specialized adhesive contacts, and are attached by linker proteins (catenins) at their cytoplasmic ends to underlying cytoskeletal fibres (either actin or intermediate filaments). Different cell types possess different members of the cadherin family, e.g. N-cadherins in nervous tissue, E-cadherins in epithelia, and P-cadherins in the placenta. These molecules bind to those of the same type in other cells (homophilic binding), so that cells of the same class adhere to each other preferentially, forming tissue aggregates or layers, as in epithelia. For a review of cadherin-mediated adhesion in morphogenesis, see Gumbiner (2005).

Selectins are found on leukocytes, platelets and vascular endothelial cells. They are transmembrane lectin glycoproteins that can bind with low affinity to the carbohydrate groups on other cell surfaces to permit movement between the two, e.g. the rolling adhesion of leukocytes on the walls of blood vessels (p. 136). They function cooperatively in sequence with integrins, which strengthen the selectin adhesion.

Integrins are glycoproteins that typically mediate adhesion between cells and extracellular matrix components such as fibronectin, collagen, laminin. They integrate interactions between the matrix and the cell cytoskeleton to which they are linked, and so facilitate cell migration within the matrix. An integrin molecule is formed of two subunits (α and β), each of which has several subtypes. Combinations of alternative subunits provide some 24 known integrin heterodimers, each one directed to a particular extracellular molecule, although there is considerable overlap in specificity. Some integrins depend for their binding on magnesium, rather than calcium.

Calcium-independent adhesion molecules

The best known calcium-independent adhesion molecules are glycoproteins that have external domains related to immunoglobulin molecules. Most are transmembrane proteins. Some are entirely external, either attached to the plasma membrane by a glycosylphosphatidylinositol anchor, or secreted as soluble components of the extracellular matrix. Different types are expressed in different tissues. Neural cell adhesion molecules (N-CAMs) are found on a number of cell types, but are expressed widely by neural cells. Intercellular adhesion molecules (I-CAMs) are expressed on vascular endothelial cells. Cell adhesion molecule binding is predominantly homophilic, although some use a heterophilic mechanism, e.g. vascular intercellular adhesion molecule (VCAM), which can bind to integrins.

For further information on all aspects of cell adhesion molecules and intercellular contacts, see Pollard & Earnshaw (2007).

Specialized adhesive contacts

Specialized adhesive contacts, some of which mediate activities other than simple mechanical cohesion, are localized regions of the cell surface with particular ultrastructural characteristics. Three major classes exist: occluding, adhesive and communicating junctions (Fig. 1.5).

Occluding junctions (tight junctions, zonula occludens)

Occluding junctions create diffusion barriers in continuous layers of cells, including epithelia, mesothelia and endothelia, and prevent the passage of materials across the cellular layer through intercellular spaces. They form a continuous belt (zonula) around the cell perimeter, near the apical surface in cuboidal or columnar epithelial cells. At a tight junction, the membranes of the adjacent cells come into contact, so that the gap between them is obliterated. Freeze-fracture electron microscopy shows that the contacts between the membranes lie along branching and anastomosing ridges formed by the incorporation of chains of intramembranous protein particles on the P face of the lipid bilayer (Fig. 1.5C).

This arrangement ensures that substances can only pass through the layer of cells by diffusion or transport through their apical membranes and cytoplasm. The cells thus selectively modify the environment on either side of the layer. Occluding junctions also create regional differences in the plasma membranes of the cells in which they are found. For example, in epithelia, the composition of the apical plasma membrane differs from that of the basolateral regions (see Fig. 1.3), and this allows these regions to engage in functions such as directional transport of ions and uptake of macromolecules. Because tight junctions have high concentrations of fixed transmembrane proteins, they act as barriers to lateral diffusion of lipid and protein within membranes. The integrity of tight junctions is calcium-dependent. Cells can transiently alter the permeability of their tight junctions to increase passive paracellular transport in some circumstances.

Adhesive junctions

Adhesive junctions include intercellular and cell–extracellular matrix contacts, where cells adhere strongly to each other or to adjacent matrix components. Intercellular contacts can be subdivided according to the extent and location of the contact. They all display a high concentration of cell adhesion molecules, which externally bind adjacent cells, and internally link to the cytoskeleton via intermediary proteins.

Zonula adherens (intermediate junction)

A zonula adherens is a continuous, belt-like zone of adhesion around the apical perimeters of epithelial, mesothelial and endothelial cells, parallel and just basal to the tight junction in epithelia. High concentrations of cadherins occur in this zone; their cytoplasmic ends are anchored via the proteins vinculin and α-actinin to a layer of actin microfilaments. These junctions help to reinforce the intercellular attachment of the tight junction and prevent its mechanical disruption. The gap between cell surfaces is about 20 nm. Usually, no electron-dense material is observed within this intercellular space.

Fascia adherens

A fascia adherens is similar to a zonula adherens, but is more limited in extent and forms a strip or patch of adhesion, e.g. between smooth muscle cells, in the intercalated discs of cardiac muscle cells and between glial cells and neurones. The junctions involve cadherins attached indirectly to actin filaments on the inner side of the membrane.

Desmosomes (maculae adherentes)

Desmosomes are limited, plaque-like areas of particularly strong intercellular contact. They can be located anywhere on the cell surface. In epithelial cells, there may be a circumferential row of desmosomes parallel to the tight and intermediate junctional zones, an arrangement that forms the third, most basally situated, component of the epithelial apical junctional complex (Fig. 1.5). The intercellular gap is approximately 25 nm, is filled with electron-dense filamentous material running transversely across it and is also marked by a series of densely staining bands running parallel to the cell surfaces. Adhesion is mediated by calcium-dependent cadherins, desmoglein and desmocollin. Within the cells on either side, a cytoplasmic density underlies the plasma membrane and includes the anchor proteins desmoplakin and plakoglobin, into which the ends of intermediate filaments are inserted. The type of intermediate filament depends on cell type, e.g. keratins are found in epithelia and desmin filaments in cardiac muscle cells. Desmosomes form strong anchorage points, likened to spot-welds, between cells subject to mechanical stress, e.g. in the prickle cell layer of the epidermis, where they are extremely numerous and large.

Hemidesmosomes

Hemidesmosomes are best known as anchoring junctions between the bases of epithelial cells and the basal lamina. Ultrastructurally, they resemble a single-sided desmosome, anchored on one side to the plasma membrane, and on the other to the basal lamina and adjacent collagen fibrils (Fig. 1.5D and see Fig. 7.5). On the cytoplasmic side of the membrane there is a dense plaque into which keratin filaments are inserted. Hemidesmosomes use integrins as their adhesion molecules, whereas desmosomes use cadherins.

Less highly structured attachments with a similar arrangement exist between many other cell types and their surrounding matrix, e.g. between smooth muscle cells and their matrix fibrils, and between the ends of skeletal muscle cells and tendon fibres. The smaller, punctate adhesions resemble focal adhesion plaques.

Focal adhesion plaques

Focal adhesion plaques are regions of local attachment between cells and the extracellular matrix. They are typically situated at or near the ends of actin filament bundles (stress fibres), which are anchored through intermediary proteins to the cytoplasmic domains of integrins. In turn, these are attached at their external ends to collagen or other filamentous structures in the extracellular matrix. They are usually short-lived: their formation and subsequent disruption are part of the motile behaviour of migratory cells.

Gap junctions (communicating junctions)

Gap junctions resemble tight junctions in transverse section, but the two apposed lipid bilayers are separated by an apparent gap of 3 nm which is bridged by numerous transmembrane channels (connexons). Connexons are formed by a ring of six connexin proteins in each membrane. Their external surfaces meet those of the adjacent cell in the middle. A minute central pore links one cell to the next (Fig. 1.5). These channels may exist in small numbers, and this makes them difficult to detect structurally. However, they lower the transcellular electrical resistance and so can be detected by microelectrodes. Larger assemblies of many thousands of channels are often packed in hexagonal arrays (Fig. 1.5B). Such junctions form limited attachment plaques rather than continuous zones, and so allow free passage of substances within the adjacent intercellular space, unlike tight junctions. They occur in numerous tissues including the liver, epidermis, pancreatic islet cells, connective tissues, cardiac muscle and smooth muscle, and are also common in embryonic tissues. In the central nervous system, they are found in the ependyma and between neuroglial cells, and they form electrical synapses between some types of neurone, although this is rare in humans. Very recently, a second family of gap junctional proteins has been discovered, the pannexins. In humans, expression of pannexins has been most extensively studied in the nervous system (reviewed in Litvin et al 2006).

Although gap junctions form diffusion channels between cells, the size of their apertures limits diffusion to small molecules and ions (up to a molecular weight of about 1000 kDa). Thus they admit sodium, potassium and calcium ions, various second messenger components, and a number of metabolites, but they exclude messenger RNA and other macromolecules. In some excitable tissues (e.g. cardiac and smooth muscle), one cell can activate another electrically by current flow through gap junctions. Communicating junctions probably permit metabolic cooperation between groups of adjacent cells; the significance of this activity in embryogenesis, normal tissue function, homeostasis and repair is only beginning to be understood.

Other types of junction

Chemical synapses and neuromuscular junctions are specialized areas of intercellular adhesion where neurotransmitters secreted from a neuronal terminal gain access to specialized receptor molecules on a recipient cell surface. They are described on pages 44 and 62, respectively.

Cell signalling

Cellular systems in the body communicate with each other to coordinate and integrate their functions. This occurs through a variety of processes known collectively as cell signalling, in which a signalling molecule produced by one cell is detected by another, almost always by means of a specific receptor protein molecule. The recipient cell transduces the signal, which it most usually detects at the plasma membrane, into intracellular chemical messages that change cell behaviour.

The signal may act over a long distance, e.g. endocrine signalling through the release of hormones into the bloodstream, or neuronal synaptic signalling via electrical impulse transmission along axons and subsequent release of chemical transmitters of the signal at synapses (p. 44) or neuromuscular junctions (p. 62). A specialized variation of endocrine signalling (neurocrine or neuroendocrine signalling) occurs when neurones or paraneurones (e.g. chromaffin cells of the suprarenal medulla) secrete a hormone into interstitial fluid and the bloodstream.

Alternatively, signalling may occur at short range through a paracrine mechanism, in which cells of one type release molecules into the interstitial fluid of the local environment, to be detected by nearby cells of a different type that express the specific receptor protein. Neurocrine cell signalling uses chemical messengers found also in the central nervous system which may act in a paracrine manner via interstitial fluid or reach more distant target tissues in the bloodstream. Cells may generate and respond to the same signal. This is autocrine signalling, a phenomenon that reinforces the coordinated activities of a group of like cells, which respond together to a high concentration of a local signalling molecule. The most extreme form of short-distance signalling is contact-dependent (juxtacrine) signalling, where one cell responds to transmembrane proteins of an adjacent cell that bind to surface receptors in the responding cell membrane. Contact-dependent signalling also includes cellular responses to integrins on its surface binding to elements of the extracellular matrix. Juxtacrine signalling is important during development and in immune responses.

These different types of intercellular signalling mechanism are illustrated in Figure 1.6. For further reading, see Alberts et al (2002) and Pollard & Earnshaw (2007).

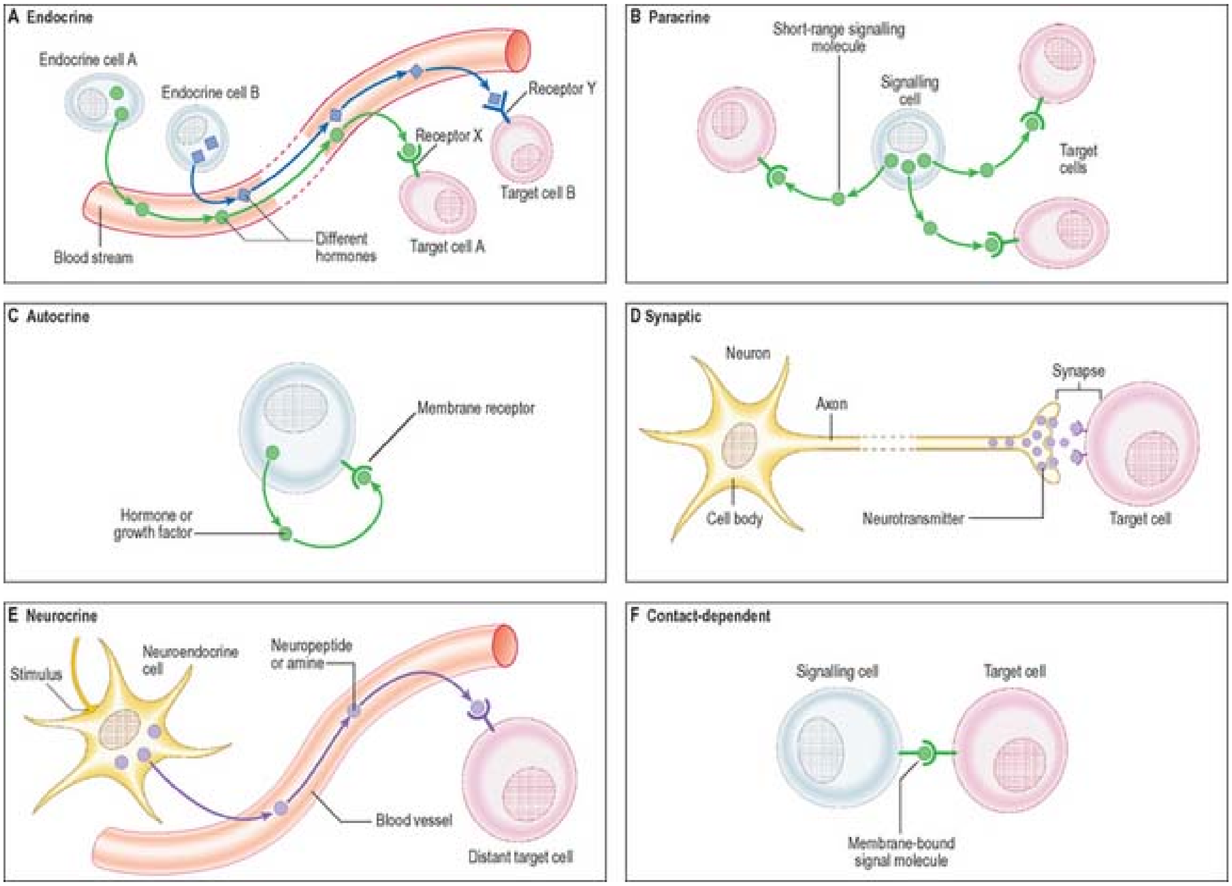
A Endocrine
Endocrine cell A
Endocrine cell B
Receptor Y
Receptor X
Target cell B
Blood stream
Different hormones
Target cell A
B Paracrine
Short-range signalling molecule
Signalling cell
Target cells
C Autocrine
Membrane receptor
Hormone or growth factor
D Synaptic
Neuron
Axon
Synapse
Cell body
Neurotransmitter
Target cell
E Neurocrine
Stimulus
Neuroendocrine cell
Neuropeptide or amine
Blood vessel
Distant target cell
F Contact-dependent
Signalling cell
Target cell
Membrane-bound signal molecule

Fig. 1.6 The different modes of cell–cell signalling.

Signalling molecules and their receptors

The majority of signalling molecules (ligands) are hydrophilic. They cannot cross the plasma membrane of a recipient cell to effect changes intracellularly unless they first bind to a plasma membrane receptor protein. Ligands are mainly proteins (usually glycoproteins), polypeptides or highly charged biogenic amines. They include: classic peptide hormones of the endocrine system; cytokines, which are mainly of haemopoietic cell origin and involved in inflammatory responses and tissue remodelling (e.g. the interferons, interleukins, tumour necrosis factor, leukaemia inhibitory factor); polypeptide growth factors (e.g. the epidermal growth factor superfamily, nerve growth factor, platelet-derived growth factor, the fibroblast growth factor family, transforming growth factor beta and the insulin-like growth factors). Polypeptide growth factors are multifunctional molecules with more widespread actions and cellular sources than their names suggest. They and their receptors are commonly mutated or aberrantly expressed in certain cancers. The cancer-causing gene variant is termed a transforming oncogene and the normal (wild-type) version of the gene is a cellular oncogene or proto-oncogene. The activated receptor acts as a transducer to generate intracellular signals, which are either small diffusible second messengers (e.g. calcium, cyclic adenosine monophosphate or the plasma membrane lipid-soluble diacylglycerol), or larger protein complexes that amplify and relay the signal to target control systems. For further reading on growth factors and other signalling molecules, see Epstein (2003).

Some signals are hydrophobic and able to cross the plasma membrane freely. Classic examples are the steroid hormones, thyroid hormones, retinoids and vitamin D. Steroids, for instance, enter cells non-selectively, but elicit a specific response only in those target cells which express specific cytoplasmic or nuclear receptors. Light stimuli also cross the plasma membranes of photoreceptor cells and interact intracellularly, at least in rod cells, with membrane-bound photosensitive receptor proteins. Hydrophobic ligands are transported in the bloodstream or interstitial fluids, generally bound to carrier proteins, and they often have a longer half-life and longer-lasting effects on their targets than do water-soluble ligands.

A separate group of signalling molecules that are able to cross the plasma membrane freely is typified by the gas, nitric oxide. The principal target of short-range nitric oxide signalling is smooth muscle, which relaxes in response. Nitric oxide is released from vascular endothelium as a result of the action of autonomic nerves that supply the vessel wall. It causes local relaxation of smooth muscle and dilation of vessels. In the penis, this mechanism is responsible for penile erection. Nitric oxide is unusual among signalling molecules in having no specific receptor protein; instead, it acts directly on intracellular enzymes of the response pathway.

Receptor proteins

There are some 20 different families of receptor proteins, each with several isoforms responding to different ligands. The great majority of these receptors are transmembrane proteins. Members of each family share structural features that indicate either shared ligand-binding characteristics in the extracellular domain or shared signal transduction properties in the cytoplasmic domain, or both. There is little relationship either between the nature of a ligand and the family of receptor proteins to which it binds and activates, or the signal transduction strategies by which an intracellular response is achieved. The same ligand may activate fundamentally different types of receptor in different cell types.

Cell surface receptor proteins are generally grouped according to their linkage to one of three intracellular systems: ion channel-linked receptors; G-protein-coupled receptors; receptors that link to enzyme systems. Other receptors do not fit neatly into any of these categories. All the known G-protein-coupled receptors belong to a structural group of proteins that pass through the membrane seven times in a series of serpentine loops. These receptors are thus known as seven-pass transmembrane receptors or, because the transmembrane regions are formed from α-helical domains, as seven-helix receptors. The most well-known of this large group of phylogenetically ancient receptors are the odorant-binding proteins of the olfactory system, the light-sensitive receptor protein, rhodopsin, and many of the receptors for clinically useful drugs. A comprehensive list of receptor proteins, their activating ligands and examples of the resultant biological function, is given in Pollard & Earnshaw (2007).

Intracellular signalling

A wide variety of small molecules carry signals within cells, conveying the signal from its source (e.g. activated plasma membrane receptor) to its target (e.g. the nucleus). These second messengers convey signals as fluctuations in local concentration, according to rates of synthesis and degradation by specific enzymes (e.g. cyclases involved in cyclic nucleotide (cAMP, cGMP) synthesis), or, in the case of calcium, according to the activities of calcium channels and pumps. Other, lipidic, second messengers such as phosphatidylinositol, derive from membranes and may act within the membrane to generate downstream effects. For further consideration of the complexity of intracellular signalling pathways, see Pollard & Earnshaw (2007).

Transport across cell membranes

Lipid bilayers are increasingly impermeable to molecules as they increase in size or hydrophilicity. Transport mechanisms are therefore required to carry essential polar molecules, including ions, nutrients, nucleotides and metabolites of various kinds, across the plasma membrane and into or out of membrane-bound intracellular compartments. Transport is facilitated by a variety of membrane transport proteins, each with specificity for a particular class of molecule, e.g. sugars. Transport proteins fall mainly into two major classes, channel proteins and carrier proteins.

Channel proteins form aqueous pores in the membrane, which open and close under the regulation of intracellular signals, e.g. G-proteins, to allow the flux of solutes (usually inorganic ions) of specific size and charge. Transport through ion channels is always passive and ion flow through an open channel depends only on the ion concentration gradient and its electronic charge, and the potential difference across the membrane. These factors combine to produce an electrochemical gradient, which governs ion flux. Channel proteins are utilized most effectively by the excitable plasma membranes of nerve cells, where the resting membrane potential can change transiently from about −80 mV (negative inside the cell) to +40 mV (positive inside the cell) when stimulated by a neurotransmitter (as a result of the opening and subsequent closure of channels selectively permeable to sodium and potassium).

Carrier proteins bind their specific solutes, such as amino-acids, and transport them across the membrane through a series of conformational changes. This latter process is slower than ion transport through membrane channels. Transport by carrier proteins can occur either passively by simple diffusion, or actively against the electrochemical gradient of the solute. Active transport must therefore be coupled to a source of energy, such as ATP generation, or energy released by the coordinate movement of an ion down its electrochemical gradient. Linked transport can be in the same direction as the solute, in which case the carrier protein is described as a symporter, or in the opposite direction, when the carrier acts as an antiporter.

Translocation of proteins across intracellular membranes

Proteins are generally synthesized on ribosomes in the cytosol or on the rough endoplasmic reticulum. A few are made on mitochondrial ribosomes. Once synthesized, many proteins remain in the cytosol, where they carry out their functions. Others, such as integral membrane proteins or proteins for secretion, are translocated across intracellular membranes for post-translational modification and targeting to their destinations. This is achieved by the signal sequence, an addressing system contained within the protein sequence of amino-acids, which is recognized by receptors or translocators in the appropriate membrane. Proteins are thus sorted by their signal sequence (or set of sequences that become spatially grouped as a signal patch when the protein folds into its tertiary configuration), so that they are recognized by and enter the correct intracellular membrane compartment.

Exocytosis and endocytosis

Secreted proteins, lipids, mucins, small molecules such as amines and other cellular products destined for export from the cell are transported to the plasma membrane in small vesicles released from the *trans* face of the Golgi apparatus. This pathway is either constitutive, in which transport and secretion occur more or less continuously, or it is regulated by external signals, as in the control of salivary secretion by autonomic neural stimulation. In regulated secretion, the secretory product is stored temporarily in membrane-bound secretory granules or vesicles. Exocytosis is achieved by fusion of the secretory vesicular membrane with the plasma membrane and release of the vesicle contents into the extracellular domain.

In polarized cells, e.g. most epithelia, exocytosis occurs at the apical plasma membrane and the cells secrete into a duct lumen or onto a free surface such as the lining of the stomach. In hepatocytes, bile is secreted across a very small area of plasma membrane forming the wall of the bile canaliculus. This region is defined as the apical plasma membrane, and is the site of exocrine secretion, whereas secretion of hepatocyte plasma proteins into the bloodstream is targeted to the basolateral surfaces facing the sinusoids. Packaging of different secretory products into appropriate vesicles takes place in the *trans*-Golgi network. Delivery of secretory vesicles to their correct plasma membrane domains is achieved by sorting sequences in the cytoplasmic tails of vesicular membrane proteins.

There are other mechanisms in which initial delivery of secretory products is less selective, but is followed by selective retention (or degradation) or reprocessing and redistribution by endosomes. Ultimately, secretory vesicles undergo docking, priming (to prepare the vesicle for a regulatory signal, where secretion is regulation-dependent) and fusion with the plasma membrane to release their contents. The process of exocytosis also delivers integral membrane components to the cell surface in the normal turnover and recycling of the plasma membrane. However, excess plasma membrane generated by vesicle fusion during exocytosis is rapidly removed by concurrent endocytosis.

The process of endocytosis involves the internalization of vesicles derived from the plasma membrane. The vesicles may contain: engulfed fluids and solutes from the extracellular interstitial fluid (pinocytosis); larger macromolecules, often bound to surface receptors (receptor-mediated endocytosis); particulate matter, including microorganisms or cellular debris (phagocytosis). Pinocytosis generally involves small fluid-filled vesicles and is a marked property of capillary endothelium, e.g. where vesicles containing nutrients and oxygen dissolved in blood plasma are transported from the vascular lumen to the endothelial basal plasma membrane (see Fig. 6.11). Interstitial fluid containing dissolved carbon dioxide is also taken up by pinocytosis for simultaneous transportation across the endothelial cell wall in the opposite direction, for release into the bloodstream by exocytosis. This shuttling of pinocytotic vesicles is also termed transcytosis. Larger volumes of fluid are engulfed by dendritic cells, e.g. in the process of sampling interstitial fluids by macropinocytosis in immune surveillance for antigens (p.

79). Interstitial fluid is inevitably taken up during receptor-mediated endocytosis when ligands are internalized.

Receptor-mediated endocytosis, also known as clathrin-dependent endocytosis, is initiated at specialized regions of the plasma membrane known as clathrin-coated pits. Clathrin is a protein that cross-links adjacent adaptor protein (adaptin) complexes to form a basket-like structure, bending the membrane inwards into a hemisphere. Much, but not all, fluid-phase pinocytosis also utilizes clathrin-coated pits. Ligands such as the iron-transporting protein, transferrin, and the cholesterol-transporting low-density lipoprotein bind to their receptors, which cluster in clathrin-coated pits through an interaction with adaptins. The pits then invaginate and pinch off from the plasma membrane, internalizing both receptor and ligand. The processing of endocytic vesicles and their contents is described on p. 12. For further details of the molecular mechanisms of endocytosis, see Alberts et al (2002) or Pollard & Earnshaw (2007).

Phagocytosis

Phagocytosis is a property of many cell types, but is most efficient in cells specialized for this activity. The professional phagocytes of the body belong to the monocyte lineage of haemopoietic cells, in particular the tissue macrophages (p. 78). Other effective phagocytes are neutrophil granulocytes and most dendritic cells (p. 79), which are also of haemopoietic origin. Phagocytosis plays an important part in the immune defence system of the body, in which the amoeboid process of ingestion of organisms for nutrition has evolved into a mechanism for the clearance of microorganisms invading the body. Macrophages also ingest particulate material including inorganic matter, such as inhaled dust particles, in addition to debris from dead cells and protein aggregates such as immune complexes in the blood, airways, interstitial spaces and connective tissue matrices.

Phagocytosis is a triggered process, initiated when a phagocytic cell binds to a particle or organism, often through a process of molecular recognition. Typically, a pathogenic microorganism may first be coated by antibodies, which are bound in turn by receptors for the Fc portion of the antibody molecule expressed by macrophages and neutrophils; in this way the microorganism is attached to the cell. This triggers the production of large pseudopodia, which engulf the organism and internalize it, as their pseudopod tips fuse together. The process appears to depend on actin–myosin-based cellular motility and, unlike receptor-mediated endocytosis, it is energy dependent. Phagosomes thus formed are as large as the body they engulf and can be a considerable proportion of the volume of the phagocytic cell. Inside the cell, the phagosome fuses with lysosomes, which degrade its contents.

CYTOPLASM

Compartments and functional organization

The cytoplasm is highly concentrated, with about 200 mg/ml of proteins (about twice the concentration in blood) that must be precisely organized for correct molecular interactions to occur. It normally has extremely low levels of Ca^{2+}, high K^+ and low Na^+ ions in comparison to extracellular fluid, differences which are important in cell signalling. Cytoplasm is also reductive, a state maintained by a high concentration of thiol-containing glutathione. The cell is able to undertake completely opposite reactions simultaneously (e.g. the synthesis and degradation of proteins; growth at one end of a cell with retraction at another) by partitioning them into different regions of the cytoplasm. The most fundamental divide is the use of oxidative reactions within the reductive cytoplasm, achieved by the compartmentalization of different environments within membranes. For example, the endoplasmic reticulum is comprised of stacks of tubules, whose lumen resembles the extracellular environment in being oxidative and Ca^{2+}-rich, predominantly encrusted on the external (cytoplasmic) face with attached ribosomes (rough endoplasmic reticulum). Ribosomes are macromolecular machines for protein synthesis and those attached to RER are engaged in synthesizing proteins that will undergo post-translational modification to adapt them (in the RER lumen and within the Golgi apparatus and associated vesicles) for exposure to the oxidative extracellular environment. A key development in the evolution of the modern cell was the ability to use oxygen as an energy source. This is possible due to one organelle, the mitochondrion, whose separate genes and dual membranes suggest its origins as a symbiotic bacterium.

The key organizer of the cytoplasm, and thence of the entire cell, is the cytoskeleton (see below). This is composed of three distinct elements. Intermediate filaments are relatively stable cables of approximately 10 nm diameter that provide strength. Actin microfilaments (6–8 nm diameter) form highly branched scaffolds under the cell surface, organizing the shape of the cell surface and its specialized functions, including extracellular interactions such as signalling and adhesion, by binding to the intracellular domains of receptors and adhesive proteins, respectively. The actin scaffold under the cell surface is highly labile, forming, branching and dissolving in response to extracellular signals. Specialized myosin-family motor proteins attach to actin filaments, generating force to move membranes and to relay vesicles between the surface and the tubulin network. The tubulin network, however, is the core organizer of the cell; it is polarized, which allows motor proteins to move directionally along the tubules and convey vesicular traffic around the cell.

Endoplasmic reticulum

Endoplasmic reticulum is a system of interconnecting membrane-lined channels within the cytoplasm (Fig. 1.7). These channels take various forms, including cisternae (flattened sacs), tubules and vesicles. The membranes divide the cytoplasm into two major compartments. The intramembranous compartment includes the space where secretory products are stored or transported to the Golgi complex and cell exterior. The extramembranous cytosol is made up of the colloidal proteins such as enzymes, carbohydrates and small protein molecules, together with ribosomes and ribonucleic acids, and elements of the cytoskeleton.

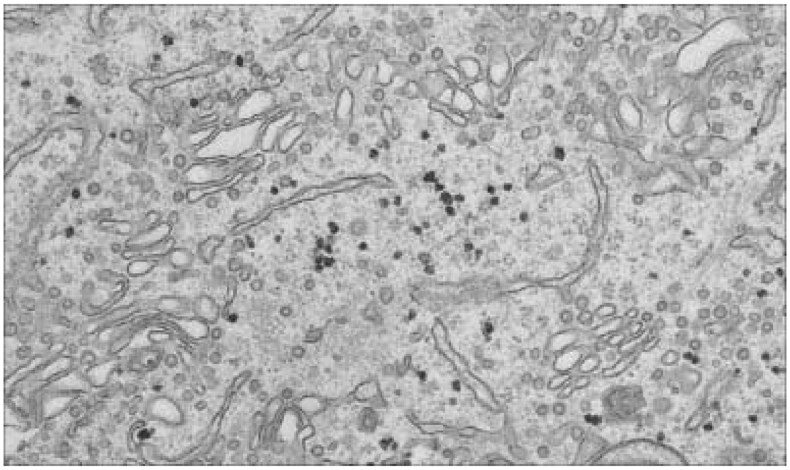

Fig. 1.7 Smooth endoplasmic reticulum with associated vesicles. The dense particles are glycogen granules.

(By courtesy of Rose Watson, Cancer Research UK.)

Structurally, the channel system can be divided into rough or granular endoplasmic reticulum, which has ribosomes attached to its outer cytosolic surface, and smooth or agranular endoplasmic reticulum, which lacks ribosomes. Functionally, the endoplasmic reticulum is compartmentalized into specialized regions with unique functions. For further reading see Levine & Rabouille (2005).

Rough endoplasmic reticulum

The rough endoplasmic reticulum, studded with ribosomes, is a site of protein synthesis (Fig. 1.8). Most proteins pass through its membranes and accumulate within its cisternae, although some integral membrane proteins, e.g. plasma membrane receptors, are inserted into the rough endoplasmic reticulum membrane, where they remain. After passage from the rough endoplasmic reticulum, proteins remain in membrane-bound cytoplasmic organelles such as lysosomes, become incorporated into new plasma membrane, or are secreted by the cell. Some carbohydrates are also synthesized by enzymes within the cavities of the rough endoplasmic reticulum and may be attached to newly formed protein (glycosylation). Vesicles are budded off from the rough endoplasmic reticulum for transport to the Golgi as part of the protein-targeting mechanism of the cell.

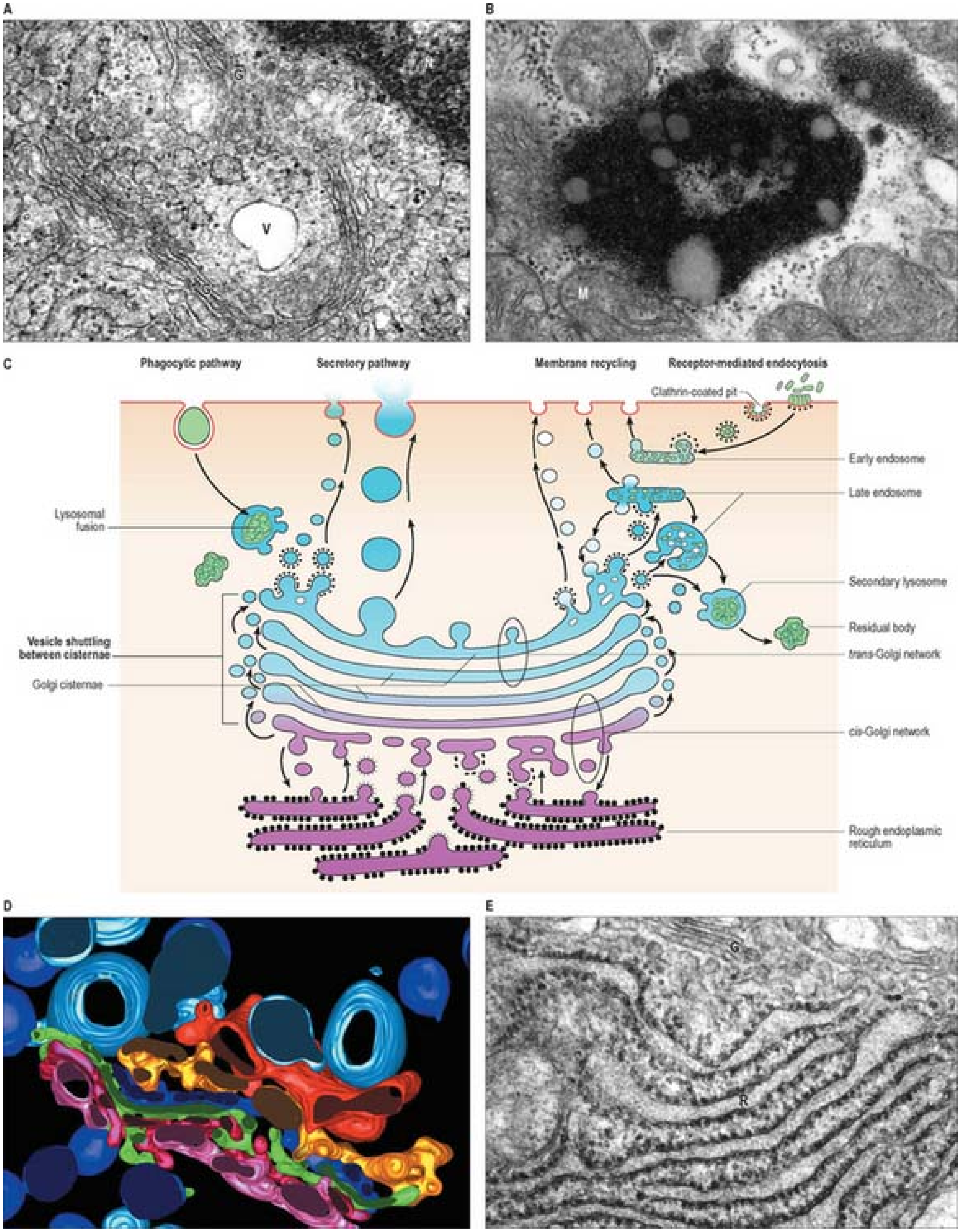
A
G
V
B
M
C
Phagocytic pathway
Secretory pathway
Membrane recycling
Receptor-mediated endocytosis
Clathrin-coated pit
Early endosome
Late endosome
Lysosomal fusion
Secondary lysosome
Residual body
Vesicle shuttling between cisternae
trans-Golgi network
Golgi cisternae
cis-Golgi network
Rough endoplasmic reticulum
D
E
G
R

Fig. 1.8 The Golgi apparatus and functionally related organelles. **A**, Golgi apparatus (G) adjacent to the nucleus (N) (V = vesicle). **B**, Large residual body (tertiary lysosome) in a cardiac muscle cell (M = mitochondrion). **C**, Functional relationships between the Golgi apparatus and associated cellular

structures. **D**, 3-dimensional reconstruction of the Golgi apparatus in a pancreatic beta cell showing stacks of Golgi cisternae from the *cis*-face (pink), *cis*-medial cisternae (red, green), to the *trans*-Golgi network (blue, yellow, orange-red); immature proinsulin granules (condensing vesicles) shown in pale blue and mature (crystalline) insulin granules in dark blue. The flat colour areas represent cut faces of cisternae and vesicles; **E**, Rough endoplasmic reticulum (R), associated with the Golgi apparatus (G).

(Part D by courtesy of Dr Brad Marsh, Institute for Molecular Bioscience, University of Queensland, Brisbane.) ***A,B,E*** *from human tissue.*

Smooth endoplasmic reticulum

The smooth endoplasmic reticulum (Fig. 1.7) is associated with carbohydrate metabolism and many other metabolic processes, including detoxification and synthesis of lipids, cholesterol and other steroids. The membranes of the smooth endoplasmic reticulum serve as surfaces for the attachment of many enzyme systems, e.g. the enzyme cytochrome P450, which is involved in important detoxification mechanisms and is thus accessible to its substrates, which are generally lipophilic. They also cooperate with the rough endoplasmic reticulum and the Golgi apparatus to synthesize new membranes; the protein, carbohydrate and lipid components are added in different structural compartments. Highly specialized types of endoplasmic reticulum are present in some cells. For example, in skeletal muscle cells, the smooth endoplasmic reticulum (sarcoplasmic reticulum) stores calcium ions, which are released into the cytosol to initiate contraction after stimulation initiated by a motor neurone at the neuromuscular junction (p. 62).

Ribosomes

Ribosomes are macromolecular machines that catalyse the synthesis of proteins from amino-acids. They are granules approximately 15 nm in diameter, composed of ribosomal RNA (rRNA) molecules assembled into two unequal subunits. A large number of proteins, mostly small and basic, are applied mainly to the surfaces of the subunit cores of RNA. The subunits can be separated by their sedimentation coefficients (S) in an ultracentrifuge, into larger 60S and smaller 40S components. These are associated with 73 different proteins (40 in the large subunit and 33 in the small), which have structural and enzymatic functions. Three small, highly convoluted rRNA strands (28S, 5.8S and 5S) make up the large subunit, and one strand (18S) is in the small subunit. Their synthesis and assembly into subunits takes place in the nucleolus, and includes association with ribosomal proteins translocated from their site of synthesis in the cytoplasm. The individual subunits are then transported into the cytoplasm, where they remain separate from each other when not actively synthesizing proteins.

A typical cell contains millions of ribosomes. They may be solitary, relatively inactive structures, or may form groups (polyribosomes or polysomes) attached to messenger RNA (mRNA), which they translate during protein synthesis. Polysomes may be attached to the membranes of the rough endoplasmic reticulum (see Fig. 1.8) or may lie free in the cytosol, where they synthesize proteins for use outside the system of membrane compartments, including enzymes of the cytosol and cytoskeletal proteins. Some of the cytosolic products include proteins that can be inserted directly into (or through) membranes of selected organelles, such as mitochondria and peroxisomes.

In a mature polysome, all the attachment sites of the mRNA are occupied as ribosomes move along it, synthesizing protein according to its nucleic acid sequence. Consequently, the number of ribosomes in a polysome indicates the length of the mRNA molecule and hence the size of the protein being made. The two subunits have separate roles in protein synthesis. The 40S subunit is the site of attachment and translation of mRNA. The 60S subunit is responsible for the release of the new protein and, where appropriate, attachment to the endoplasmic reticulum via an intermediate docking protein that directs the newly synthesized protein through the membrane into the cisternal space.

Protein synthesis on ribosomes may be suppressed by a class of RNA molecule known as small interfering RNA (siRNA) or silencing RNA. These molecules are typically 20–25 nucleotides in length and bind (as a complex with proteins) to specific mRNA molecules via their complementary sequence. This triggers the enzymatic destruction of the mRNA or prevents the movement of ribosomes along it. Synthesis of the encoded protein is thus prevented. Their normal function may have anti-viral or other protective effects; there is also potential for developing artificial siRNAs as a therapeutic tool for silencing disease-related genes.

Golgi apparatus (Golgi complex)

The Golgi apparatus is a distinct cytoplasmic region near the nucleus, and is particularly prominent in secretory cells when stained with silver or other metallic salts. The Golgi apparatus forms part of the pathway by which proteins synthesized in the rough endoplasmic reticulum undergo post-translational modification and are targeted to the cell surface for secretion or for storage in membranous vesicles. As with the endoplasmic reticulum, the Golgi apparatus is compartmentalized spatially, in a labile manner, to carry out specific functions.

Ultrastructurally, the Golgi apparatus is a membranous organelle (Fig. 1.8) consisting of a stack of several flattened membranous cisternae, together with clusters of vesicles surrounding its surfaces. Seen in vertical section, it is often cup-shaped. Small transport vesicles from the rough endoplasmic reticulum, generated by a process of budding and pinching off, are received at one face of the Golgi stack, the convex *cis*-face (entry or forming surface). Here, they deliver their contents to the first cisterna in the series by membrane fusion. From the edges of this cisterna, the protein is transported to the next cisterna by vesicular budding and then fusion, and this process is repeated until the final cisterna at the concave *trans* face (exit or condensing surface) is reached. Here, larger vesicles are formed for delivery to other parts of the cell.

In addition to these cisternae, there are other membranous structures that form an integral part of the Golgi apparatus, termed the *cis*-Golgi and *trans*-Golgi networks. The *cis*-Golgi network is a region of complex membranous channels interposed between the rough endoplasmic reticulum and the Golgi *cis* face (Golgi–rough endoplasmic reticulum complex), which receives and transmits vesicles in both directions. Its function is to select appropriate proteins synthesized on the rough endoplasmic reticulum for delivery by vesicles to the Golgi stack, while inappropriate proteins are shuttled back to the rough endoplasmic reticulum.

The *trans*-Golgi network, at the other side of the Golgi stack, is also a region of interconnected membrane channels engaged in protein sorting. Here, modified proteins processed in the Golgi cisternae are packaged selectively into vesicles and dispatched to different parts of the cell. The packaging depends on the detection, by the *trans*-Golgi network, of particular amino-acid signal sequences, leading to their enclosure in membranes of appropriate composition that will further modify their contents, e.g. by extracting water to concentrate them or by pumping in protons to acidify their contents. The membranes contain specific signal proteins, which may allocate them to microtubule-based transport pathways and allow them to dock with appropriate targets elsewhere in the cell, e.g. the plasma membrane in the case of secretory vesicles. Vesicle formation and budding at the *trans*-Golgi network involves the addition of clathrin on their external surface, to form coated pits.

Within the Golgi stack proper, proteins undergo a series of sequential chemical modifications that started in the rough endoplasmic reticulum. These include: changes in glycosyl groups, e.g. removal of mannose, addition of *N*-acetyl glucosamine and sialic acid; sulphation of attached glycosaminoglycans; protein phosphorylation. Lipids formed in the endoplasmic reticulum are also routed for incorporation into vesicles.

The role of the Golgi apparatus in the synthesis of primary lysosomes is a major activity in cells with abundant lysosomes, such as those with phagocytic roles. In glandular cells with an apical secretory zone, the Golgi apparatus lies between the secretory surface and the nucleus. In fibroblasts, there are two or more groups of Golgi stacks; up to 50 groups are found in liver cells. The Golgi apparatus is often closely associated with the centrosome (a region of the cell containing a centriole pair and related microtubules), reflecting a link with the microtubule-mediated vesicle transport system.

Endosomes, lysosomes, proteasomes and peroxisomes

The endosome system of vesicles originates in small endocytic vesicles (clathrin-coated vesicles and caveolae) or larger phagosomes and macropinocytic vesicles taken up by the cell from the exterior. Clathrin-dependent endocytosis occurs at specialized patches of plasma membrane called coated pits; this mechanism is also used to internalize ligands bound to surface receptor molecules and is also termed receptor-mediated endocytosis. Caveolae (little caves) are structurally distinct vesicles most widely used by endothelial and smooth muscle cells, where they are involved in transcytosis, signal transduction and possibly other functions. For further reading, see Pollard & Earnshaw (2007).

The endocytic system is linked functionally to a second series of membranous structures, the lysosomes. Lysosomes contain acid hydrolases, which process or degrade exogenous materials (heterophagy), and intracellular organelles that are exhausted, damaged or no longer required (autophagy). There is a continual exchange of vesicles between this system and the Golgi–rough endoplasmic reticulum complex, so that the endosomal/lysosomal system is provided with hydrolytic enzymes and the Golgi receives depleted vesicles for recharging. Once internalized, endocytic vesicles shed their coat of adaptin and clathrin, and fuse with a tubular cisterna termed an early endosome, where the receptor molecules release their bound ligands. Membrane and receptors from the early endosomes can be recycled to the cell surface as exocytic vesicles.

Late endosomes

After a brief period in the early endosomes, materials can be passed on to late endosomes, which are a more deeply placed set of tubules, vesicles or cisternae. Late endosomes receive lysosomal enzymes via vesicles (small lysosomes) transported from the Golgi apparatus. The pH of late endosomes is low (about 5.0) and this activates lysosomal acid hydrolases to degrade the endosomal contents. The products of hydrolysis are either passed through the membrane into the cytosol, or may be retained in the endosome. Late endosomes (Fig. 1.8) may grow considerably in size by vesicle fusion to form multivesicular bodies and the enzyme concentration may increase greatly to form the large, dense classic lysosomes described by de Duve (1963). However, such large organelles do not appear in all cells, perhaps because late endosomes often deal very rapidly with endocytosed material.

Lysosomes

Lysosomes are dense, spheroidal, membrane-bound bodies 80–800 nm in diameter (Fig. 1.8, Fig. 1.9), often with complex inclusions of material undergoing hydrolysis (secondary lysosomes). They contain acid hydrolases able to degrade a wide variety of substances. To date, more than 40 lysosomal enzymes have been described, including proteases, lipases, carbohydrases, esterases and nucleases. The enzymes are heavily glycosylated, and are maintained at a low pH by proton pumps in the lysosomal membranes.

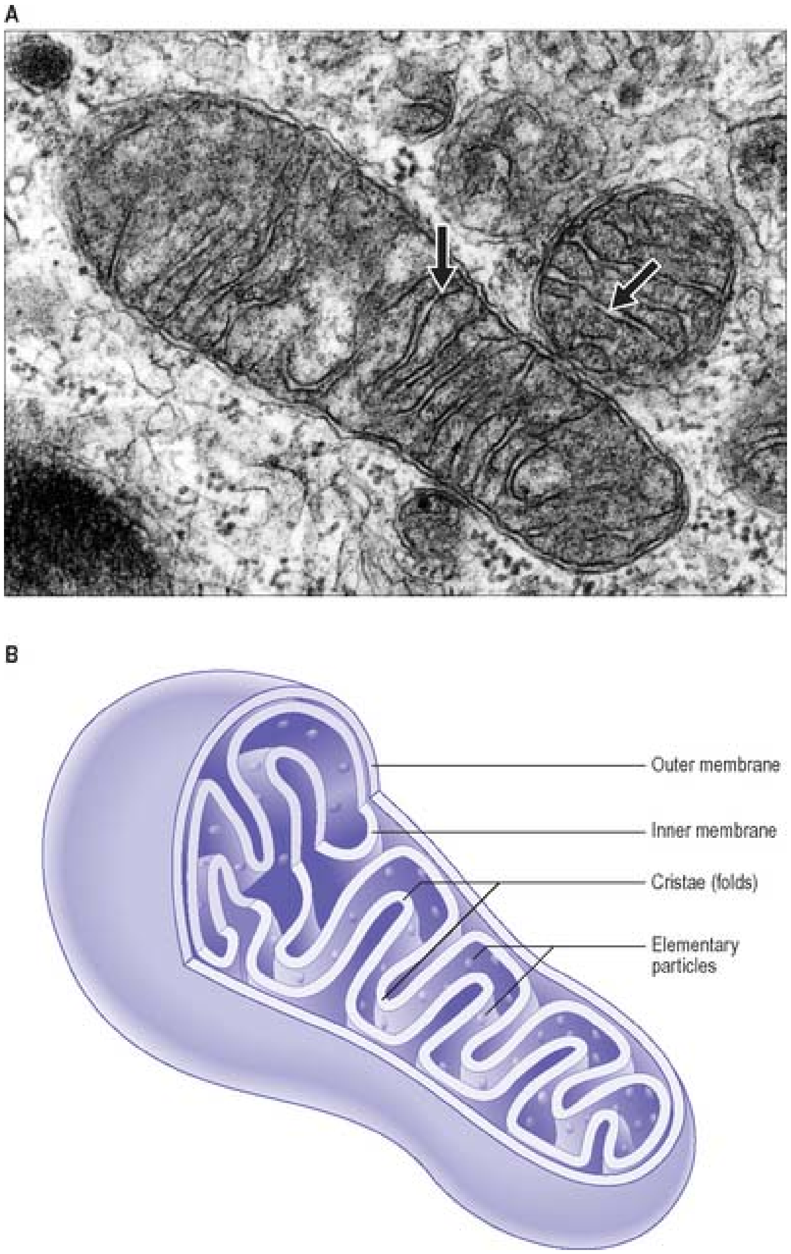
A
B
Outer membrane
Inner membrane
Cristae (folds)
Elementary particles

Fig. 1.9 **A**, Mitochondria in human cardiac muscle. The folded cristae (arrows) project into the matrix from the inner mitochondrial membrane. **B**, The location of the elementary particles which couple oxidation and phosphorylation reactions.

Lysosomes are numerous in actively phagocytic cells, e.g. macrophages and neutrophil granulocytes, in which lysosomes are responsible for destroying phagocytosed bacteria. In these cells, the phagosome containing the bacterium may fuse with several lysosomes. Lysosomes are also frequent in cells with a high turnover of organelles, e.g. exocrine gland cells and neurones. Effete organelles are targeted for demolition by a process that is not fully understood, but which results in engulfment of areas of cytoplasm, including entire organelles, in a membranous cisterna. The structure then fuses with lysosomes and the contents are rapidly degraded.

Material that has been hydrolysed within late endosomes and lysosomes may be completely degraded to soluble products, e.g. amino-acids, which are recycled through metabolic pathways. However degradation is usually incomplete, and some debris remains. A debris-laden vesicle is called a residual body or tertiary lysosome (Fig. 1.8B), and may be passed to the cell surface, where it is ejected by exocytosis; alternatively, it may persist inside the cell as an inert residual body. Considerable numbers of residual bodies can accumulate in long-lived cells, often fusing to form larger dense vacuoles with complex lamellar inclusions. As their contents are often darkly pigmented, this may change the colour of the tissue, e.g. in neurones the end-product of lysosomal digestion, lipofuscin (neuromelanin or senility pigment), gives ageing brains a brownish-yellow colouration.

Lysosomal enzymes may also be secreted – often as part of a process to alter the extracellular matrix, as in osteoclast erosion of bone (p. 88). Abnormal release of enzymes can cause tissue damage, as in certain types of arthritis. Some drugs, e.g. cortisone, can stabilize lysosomal membranes and may therefore inhibit many lysosomal activities, including the secretion of enzymes, and their fusion with phagocytic vesicles.

Lysosomal storage diseases

If any of the lysosomal enzymes are defective because of gene mutations, the materials that they normally degrade will accumulate within late endosomes and lysosomes. Many such lysosomal storage diseases are known, e.g. Tay–Sachs disease, in which a faulty hexosaminidase leads to the accumulation of ganglioside in neurones, causing death during childhood. In Hurler’s syndrome, failure to metabolize certain mucopolysaccharides causes the accumulation of large amounts of matrix within connective tissue, which distorts growth of many parts of the body.

Proteasomes

Intracellular proteolysis occurs via two pathways, one mediated via lysosomes and the other via proteasomes. Eukaryote proteasomes are non-membranous, large barrel-shaped complexes composed of about 28 distinct protein subunits which form a highly ordered ring-shaped structure (20S ring) in both the cytoplasm and the nucleoplasm. The active sites are on the inner surfaces of the barrel; terminal apertures restrict access of substrates to these sites. Proteasomes degrade proteins, including those that are misfolded and tagged for degradation by ubiquitin, and play an important role in the cleavage of intracellular antigens (e.g. those derived from viral infection) for presentation to immune system effector cells.

Peroxisomes

Peroxisomes are membrane-bound vacuoles 0.5–0.15 μm across, present in all nucleated cell types. They often contain dense cores or crystalline interiors composed mainly of high concentrations of the enzyme urate oxidase. Large (0.5 μm) peroxisomes are particularly numerous in hepatocytes and kidney tubule cells. Peroxisomes are important in the oxidative detoxification of various substances taken into or produced within cells, including ethanol and formaldehyde. Oxidation is carried out by a number of enzymes, including D-amino-acid oxidase and urate oxidase, which generate hydrogen peroxide as a source of molecular oxygen. Excess amounts of hydrogen peroxide are broken down by the enzyme, catalase. Peroxisomes also oxidize fatty acid chains by β-oxidation.

The formation of peroxisomes is unusual in that they appear to be derived by the growth and fission of previously existing peroxisomes. Their internal proteins, including oxidative enzymes, are passed from the cytosol directly through channels in their membranes, rather than by packaging from the rough endoplasmic reticulum and Golgi apparatus. These features are also found in mitochondria, although peroxisomal proteins are coded for entirely in the nucleus. Genetic abnormalities in peroxisome biogenesis are seen in Zellweger syndrome, and include gene mutations in a peroxisome enzyme transporter protein. In homozygotes, this is usually fatal shortly after birth.

Mitochondria

Mitochondria are membrane-bound organelles (Fig. 1.9). They are the principal source of chemical energy in most cells. Mitochondria are the site of the citric acid (Krebs', tricarboxylic acid) cycle and the electron transport (cytochrome) pathway by which complex organic molecules are finally oxidized to carbon dioxide and water. This process provides the energy to drive the production of ATP from ADP and inorganic phosphate (oxidative phosphorylation). The various enzymes of the citric acid cycle are located in the mitochondrial matrix, whereas those of the cytochrome system and oxidative phosphorylation are localized chiefly in the inner mitochondrial membrane. It is now known that in many tissues, especially smooth muscle, mitochondria also play an important role in cell signalling, especially intracellular calcium homeostasis. They are also major producers of reactive oxygen species and oxidant stress, and are involved in activation of apoptosis.

The numbers of mitochondria in a particular cell reflect its general energy requirements; e.g. in hepatocytes there may be as many as 2000, whereas in resting lymphocytes there are usually very few. Mature erythrocytes lack mitochondria altogether. Cells with few mitochondria generally rely largely on glycolysis for their energy supplies. These include some very active cells, e.g. fast twitch skeletal muscle fibres, which are able to work rapidly, but for only a limited duration. Mitochondria appear in the light microscope as long thin threads in the cytoplasm of most cells, particularly those with a high metabolic rate, e.g. secretory cells in exocrine glands. In living cells, mitochondria constantly change shape and intracellular position; they multiply by growth and fission and may undergo fusion.

In the electron microscope, mitochondria usually appear as round or elliptical bodies 0.5–2.0 µm long. Each mitochondrion is lined by an outer and an inner unit membrane, separated by a variable gap termed the intermembrane space. The lumen is surrounded by the inner membrane and contains the mitochondrial matrix. The outer membrane is smooth and sometimes attached to other organelles, particularly microtubules. The inner membrane is deeply folded to form incomplete transverse or longitudinal tubular invaginations, cristae, which create a relatively large surface area of membrane. Mitochondrial shape, and the shape and organization of the cristae, vary with the cell type. Cristae are most numerous and complex in cells with a high metabolic rate, e.g. cardiac muscle cells. The permeabilities of the two mitochondrial membranes differ considerably: the outer membrane is freely permeable to many substances because of the presence of large non-specific channels formed by proteins (porins), whereas the inner membrane is permeable to only a narrow range of molecules. The presence of cardiolipin, a phospholipid, in the inner membrane may contribute to this relative impermeability.

The mitochondrial matrix is an aqueous environment. It contains a variety of enzymes, and strands of mitochondrial DNA with the capacity for transcription and translation of a unique set of mitochondrial genes (mitochondrial mRNAs and transfer RNAs, mitochondrial ribosomes with rRNAs). The DNA forms a closed loop, about 5 µm across; several identical copies are present in each mitochondrion. The ratio between its bases differs from that of nuclear DNA, and the RNA sequences also differ in the precise genetic code used in protein synthesis. At least 13 respiratory chain enzymes of the matrix and inner membrane are encoded by the small number of genes along the mitochondrial DNA. The great majority of mitochondrial proteins are encoded by nuclear genes and made in the cytosol, then inserted through special channels in the mitochondrial membranes to reach their destinations. Their membrane lipids are synthesized in the endoplasmic reticulum.

Mitochondrial ribosomes are smaller and quite distinct from those of the rest of the cell; they (and mitochondrial nucleic acids) resemble those of bacteria. This similarity underpins the theory that mitochondrial ancestors were oxygen-utilizing bacteria that existed in a symbiotic relationship with eukaryotic cells unable to metabolize the oxygen produced by early plants. As mitochondria are formed only from previously existing ones, it follows that all mitochondria in the body are descended from those in the cytoplasm of the fertilized ovum. It has also been shown that mitochondria are of maternal origin because the mitochondria of the sperm are not generally incorporated into the ovum at fertilization. Thus mitochondria (and mitochondrial genetic variations and mutations) are passed only through the female line.

Mitochondria are distributed within a cell according to regional energy requirements, e.g. near the bases of cilia in ciliated epithelia, in the basal domain of the cells of proximal convoluted tubules in the renal cortex (where considerable active transport occurs) and around the proximal end of the flagellum in spermatozoa. They may be involved with tissue-specific metabolic reactions, e.g. various urea-forming enzymes in liver cell mitochondria. Moreover, a number of genetic diseases of mitochondria affect particular tissues exclusively, e.g. mitochondrial myopathies (skeletal muscle) and mitochondrial neuropathies (nervous tissue). For further information see Graff et al (2002).

Cytosolic organelles

The aqueous cytosol surrounds the membranous organelles described above. It also contains various non-membranous organelles, including free ribosomes, a system of filamentous proteins known as the cytoskeleton, and other inclusions, such as storage granules (e.g. glycogen) and lipid vacuoles.

Lipid vacuoles

Lipid vacuoles are spherical bodies of various sizes found within many cells, but are especially prominent in the adipocytes (lipocytes) of adipose connective tissue. They do not belong to the Golgi-related vacuolar system of the cell. They are not membrane bound, but are droplets of lipid suspended in the cytosol. In cells specialized for lipid storage the vacuoles reach 80 µm or more in diameter.

Lipid vacuoles are often surrounded by cytoskeletal filaments that help to stabilize them within cells and to prevent their fusion with the membranes of other organelles, including the plasma membrane. They function as stores of chemical energy, thermal insulators and mechanical shock absorbers in adipocytes. In many cells, they may represent end-products of other metabolic pathways, e.g. in steroid-synthesizing cells, where they are a prominent feature of the cytoplasm. They may also be secreted, as in the alveolar epithelium of the lactating breast.

Cytoskeleton

The cytoskeleton is a system of filamentous intracellular proteins of different shapes and sizes that form a complex, often interconnected, network throughout the cytoplasm. It provides mechanical support, maintains cell shape and rigidity, and enables cells to adopt highly asymmetric or irregular profiles, e.g. in neurones. The cytoskeleton plays an important part in establishing structural polarity and different functional domains within a cell. It also provides mechanical support for projections from the cell surface such as microvilli and cilia, and anchors them into the cytoplasm.

The cytoskeleton restricts specific organelles to particular cellular locations, e.g. the Golgi apparatus is near the nucleus and endoplasmic reticulum, and mitochondria are near sites of energy requirement. Most specifically, the cytoskeleton is concerned with motility, either within the cell (e.g. shuttling vesicles and macromolecules between cytoplasmic sites, or the movement of chromosomes during mitosis), or of the entire cell (e.g. in embryonic morphogenesis or the chemotactic migration of leukocytes). One of the most highly developed and specialized functions of the cytoskeleton is seen in the contractility of muscle cells.

The catalogue of cytoskeletal structural proteins is extensive and still increasing. The major filamentous structures found in non-muscle cells are microfilaments (actin), microtubules (tubulin), and intermediate filaments (assemblies of cell type-specific intermediate filament proteins). Other important components are proteins that bind to the principal filamentous types to link them together or to generate movement. These include actin-binding proteins such as myosin, which in some cells can assemble into thick filaments, and microtubule-associated proteins. Pathologies involving cytoskeletal abnormalities are reviewed in Ramaekers & Bosman (2004).

Actin filaments (microfilaments)

Actin filaments are flexible filaments with a width of 6–8 nm (Fig. 1.10), and a solid cross-section. Within most cell types, actin constitutes the most abundant protein and in some motile cells its concentration may exceed 200 μM (10 mg protein per ml cytoplasm). The filaments are formed by the ATP-dependent polymerization of actin monomer (with a molecular mass of 43 kDa) into a characteristic linear form in which the subunits are arranged in a single tight helix with a distance of 13 subunits between turns. The polymerized form is termed F-actin (fibrillar actin) and the unpolymerized form is G-actin (globular actin). Each monomer has an asymmetric structure. When monomers polymerize, they confer a defined polarity on the filament: the plus end favours monomer addition, and the minus end favours monomer dissociation. Myosins bind to filamentous actin at an angle to give the appearance of a series of arrowheads pointing towards the minus end of the filament, and the barbs point towards the plus end. There is a dynamic equilibrium between G-actin and F-actin: in most cells about 50% of the actin is estimated to be in the polymerized state.

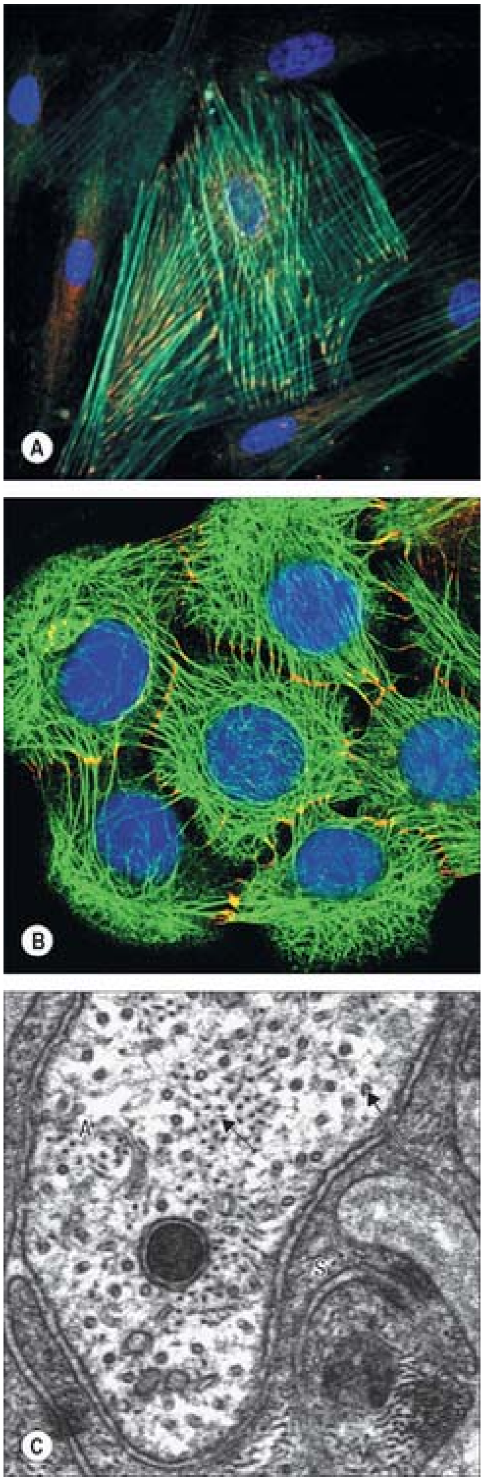

Fig. 1.10 The cytoskeleton. **A**, Immunofluorescence micrograph of α actin microfilaments (green) in human airway smooth muscle cells in culture. The actin-binding protein, vinculin (red), is localized at the ends of actin filament bundles; nuclei are blue. **B**, Immunofluorescence micrograph

of keratin intermediate filaments (green) in human keratinocytes in culture. Desmosome junctions are labelled with antibody against desmoplakin (red). Nuclei are stained blue (Hoechst). By courtesy of Prof. Dr. W.W. Franke, German Cancer Research Centre, Heidelberg. **C**, Electron micrograph of human nerve showing microtubules (small, hollow structures in cross-section, long arrow) in a transverse section of an axon (A), engulfed by a non-myelinating Schwann cell (S). Neuronal intermediate filaments (neurofilaments) are the solid, electron-dense profiles, also in transverse section (short arrow).

(By courtesy of Dr T Nguyen, Professor J Ward, Dr SJ Hirst, Kings College London.)

Actin-binding proteins

A wide variety of actin-binding proteins are capable of modulating the form of actin within the cell. These interactions are fundamental to the organization of cytoplasm and to cell shape. Actin-binding proteins can be grouped into bundling proteins, gel-forming proteins and filament severing proteins.

Bundling proteins tie actin filaments together in longitudinal arrays to form cables or core structures. The bundles may be closely spaced, e.g. in microvilli, microspikes and filopodia, where parallel filaments are tied tightly together to form stiff bundles orientated in the same direction. Proteins with this function include fimbrin and villin (also classified as a severing protein). Other actin-bundling proteins form rather looser bundles of filaments that run anti-parallel to each other with respect to their plus and minus ends. They include myosin II, which can form cross-links with ATP-dependent motor activity, and cause adjacent actin filaments to slide on each other, and either change the shape of cells or (if the actin bundles are anchored into the cell membrane at both ends), maintain a degree of active rigidity.

Gel-forming proteins, such as filamin, interconnect adjacent actin filaments to produce loose filamentous meshworks (gels) composed of randomly orientated F-actin. These networks are frequently found in the outer cortical regions of cells, e.g. fibroblasts. They form a semi-rigid zone from which most other organelles are excluded. Severing proteins, such as gelsolin and severin, bind to F-actin filaments and sever them, which produces profound changes within the actin cytoskeleton and in its coupling to the cell surface.

Other classes of actin-binding protein link the actin cytoskeleton to the plasma membrane either directly or indirectly through a variety of membrane-associated proteins. The latter may also create links via transmembrane proteins to the extracellular matrix. Best known of these is the family of spectrin-like molecules, which can bind to actin and also to each other and various membrane-associated proteins to create supportive networks beneath the plasma membrane. Defects in such molecules are linked to a number of inherited diseases (reviewed in Bennett & Healy 2008). Spectrin is found in erythrocytes, and closely related molecules are present in many other cells; for instance, fodrin is found in nerve cells, and dystrophin occurs in muscle cells, linking the contractile apparatus with the extracellular matrix via integral membrane proteins. Proteins such as ankyrin (which also binds actin directly), vinculin, talin, zyxin and paxillin connect actin-binding proteins to integral plasma membrane proteins such as integrins (directly or indirectly), and thence to focal adhesions. Myosin I and other unconventional myosins connect actin filaments to membranous structures, including the plasma membrane and transport vesicle membranes. Tropomyosin, an important regulatory protein of muscle fibres, is also present in non-muscle cells, where its function may be primarily to stabilize actin filaments against depolymerization. For further reading see Pollard & Earnshaw (2007).

Myosins – the motor proteins

The myosin family of microfilaments is often classified within a distinct category of motor proteins. Myosin proteins have a globular head region consisting of a heavy and a light chain. The heavy chain bears an α-helical tail of varying length. The head has an ATPase activity and can bind to and move along actin filaments – the basis for myosin function as a motor protein. The best-known class is myosin II, which occurs in muscle and in many non-muscle cells. Its molecules have two heads and two tails, intertwined to form a long rod. The rods can bind to each other to form long, thick filaments, as seen in striated and smooth muscle fibres, myoepithelial cells and myofibroblasts. Myosin II molecules can also assemble into smaller groups, especially dimers, which can cross-link individual actin microfilaments in stress fibres and other F-actin arrays. The ATP-dependent sliding of myosin on actin forms the basis for muscle contraction and the extension of microfilament bundles, as seen in cellular motility or in the contraction of the ring of actin and myosin around the cleavage furrow of dividing cells. There are a number of known subtypes of myosin II: they assemble in different ways and have different dynamic properties. In skeletal muscle the myosin molecules form bipolar filaments 15 nm thick. Because these filaments have a symmetric anti-parallel arrangement of subunits, the midpoint is bare of head regions. In smooth muscle the molecules form thicker, flattened ribbons and are orientated in different directions on either face of the ribbon. These arrangements have important consequences for the contractile force characteristics of the different types of muscle cell.

Related molecules include the myosin I subfamily of single-headed molecules with tails of varying length. Functions of myosin I include the movements of membranes in endocytosis, microspike formation in neuronal growth cones, actin–actin sliding and attachment of actin to membranes, e.g. of microvilli. Myosin V is implicated in the movements of membranous organelles on actin filaments. So, for example, vesicles track along F-actin in a similar manner to kinesin and dynein-related movements along microtubules. Other myosins have been isolated; the significance of their diversity is not fully understood.

Other thin filaments

A heterogeneous group of filamentous structures with diameters of 2–4 nm occur in various cells. The two most widely studied forms, titin and nebulin, constitute around 13% of the total protein of skeletal muscle. They are amongst the largest known molecules, and have subunit weights of around 10^6; native molecules are about 1 μm in length. Their repetitive bead-like structure gives them elastic properties that are important for the effective functioning of muscle, and possibly for other cells.

Intermediate filaments

Intermediate filaments are about 10 nm thick and formed by a heterogeneous group of filamentous proteins. They are found in different cell types and are often present in large numbers, either where structural strength is needed (Fig. 1.10B,C), or to provide scaffolding for the attachment of other structures. It is likely that more complex, non-mechanical functions of intermediate filaments, with implications for human disease, remain to be discovered (see Toivola et al 2005). Intermediate filaments of different molecular classes are characteristic of particular tissues or states of maturity. They are therefore important indicators of the origins of cells or levels of differentiation, and are of considerable value in histopathology.

Of the different classes of intermediate filaments, keratin (cytokeratin) proteins are found in epithelia, where keratin filaments are always composed of equal ratios of types I (acidic) and II (basic to neutral) keratins. About 20 types of each of the acidic and basic/neutral keratin proteins are known. Within the epidermis, expression of keratin heterodimer combinations changes as keratinocytes mature during their transition from basal to superficial layers. Genetic abnormalities of keratins are known to affect the mechanical stability of epithelia. For example, the disease epidermolysis bullosa simplex causes lysis of epidermal basal cells and blistering of the skin after mechanical trauma. It is caused by defects in genes encoding keratins 5 and 14, which produce cytoskeletal instability and thus cellular fragility in the basal cells. When keratins 1 and 10 are affected, cells in the prickle cell layer of the epidermis lyse, and this produces the intraepidermal blistering of epidermolytic hyperkeratosis. For a review, see Porter & Lane (2003).

Vimentins occur in mesenchyme-derived cells of connective tissue, desmins in muscle cells, glial fibrillary acidic protein in glial cells, and peripherin in peripheral axons. Neurofilaments are a major cytoskeletal element in neurones, particularly in axons (Fig. 1.10C), where they are the dominant protein. They are heteropolymers of low, medium and high molecular weight neurofilament proteins; the low molecular weight form is always present in combination with either the medium- or the high-molecular weight neurofilament. Abnormal accumulations of neurofilaments (neurofibrillary tangles) are characteristic features of a number of neuropathological conditions.

Other intermediate filament proteins include nestin, a molecule resembling neurofilament protein which forms intermediate filaments in neurectodermal stem cells in particular. Nuclear lamins are intermediate filaments that line the inner surface of the nuclear envelope of all nucleated cells. They provide a mechanical framework for the nucleus and act as attachment sites for a number of proteins that organize the chromatin at the periphery of the nucleus. They are unusual in that they form an irregular anastomosing network of filaments rather than linear bundles.

The exact manner in which intermediate filament proteins polymerize to form linear filaments is much more complex than that of tubulin or actin, and has not been fully determined. The individual intermediate filament proteins are chains with a middle α-helical region flanked on either side by non-helical domains. The proteins associate as coiled coil dimers that form short rods about 48 nm long. These assemble in pairs in a staggered antiparallel formation to form soluble tetramers, eight of which pack together laterally and twist into the rope-like 10 nm intermediate filament. The 32 α-helices in parallel give the filaments their tensile strength. However, unlike actin and myosin, the antiparallel arrangement of the dimers produces a filamentous protein with no intrinsic polarity. The non-coiled regions of the subunits project outwards as side arms that can link intermediate filaments into bundles or attach them to other structures. The existence of different combinations of subunit proteins within one filament is the basis of their functional diversity. In the living cell they have been shown to be quite dynamic structures, possibly as a result of reversible phosphorylation.

Microtubules

Microtubules are polymers of tubulin with the form of hollow, relatively rigid cylinders, approximately 25 nm in diameter and of varying length (up to 70 μm in spermatozoan flagella). They are present in most cell types, and are particularly abundant in neurones (Fig. 1.10C), leukocytes and blood platelets. They are the predominant constituent of the mitotic spindles of dividing cells. They also form part of the structure of cilia, flagella and centrioles.

There are two major classes of tubulin: α- and β-tubulins. Before microtubule assembly, tubulins are associated as dimers with a combined molecular mass of 100 kDa (50 kDa each). Each protein subunit is approximately 5 nm across and arranged along the long axis in straight rows of alternating α- and β-tubulins, forming protofilaments. Typically, 13 protofilaments (the number can vary between 11 and 16), associate in a ring to form the wall of a hollow cylindrical microtubule. Each longitudinal row is slightly out of alignment with its neighbour, so that a spiral pattern of alternating α and β subunits appears when the microtubule is viewed from the side. There is a dynamic equilibrium between the dimers and assembled microtubules: dimeric asymmetry creates polarity (α-tubulins are all orientated towards the minus end, β-tubulins towards the plus end). Tubulin is added preferentially to the plus end; the minus end is relatively slow growing. Microtubules exhibit a dramatic behaviour, known as dynamic instability, in which growing tubules can undergo a ‘catastrophe’, abruptly shifting from net growth to rapid shrinkage. This can result in disappearance of the microtubule, or the catastrophe can be rescued and growth resumed. Tubulins are guanosine triphosphate (GTP)-binding proteins, and growth is accompanied by hydrolysis of GTP. This may regulate the dynamic behaviour of the tubules. Microtubule growth is initiated at specific sites known as microtubule-organizing centres, the best known of which are centrosomes, from which most cellular microtubules polymerize and basal bodies, from which cilia grow.

Various drugs (e.g. colcemid, vinblastine, griseofulvin, nocodazole) cause microtubule depolymerization by binding the soluble tubulin dimers and so shifting the equilibrium towards the unpolymerized state. Microtubule disassembly causes a wide variety of effects, including the inhibition of cell division by disruption of the mitotic spindle. Conversely, the drug taxol stabilizes microtubules and promotes abnormal microtubule assembly. This can cause a peripheral neuropathy, but taxol is widely used as an effective chemotherapeutic agent in the treatment of cancer.

Different microtubules possess varying degrees of stability, e.g. microtubules in cilia are generally unaffected by many drugs that cause microtubular demolition. There are also differences between tissues, e.g. neurones have a special tubulin subclass. Microtubule organizing centres include a specialized tubulin isoform known as γ-tubulin, that is essential for the nucleation of microtubule growth.

Microtubule-associated proteins

Various proteins that can bind to assembled tubulins may be concerned with structural properties or associated with motility. One important class of microtubule-associated proteins (MAPs) consists of proteins that associate with the plus ends of microtubules. They regulate the dynamic instability of microtubules as well as interactions with other cellular substructures. Structural MAPs form cross-bridges between adjacent microtubules or between microtubules and other structures such as intermediate filaments, mitochondria and the plasma membrane. Microtubule-associated proteins found in neurones include: MAPs 1A and 1B, which are present in neuronal dendrites and axons; MAPs 2A and 2B, found chiefly in dendrites; and tau, found only in axons. MAP 4 is the major microtubule-associated protein in many other cell types. Structural microtubule-associated proteins are implicated in microtubule formation, maintenance and demolition, and are therefore of considerable significance in cell morphogenesis, mitotic division, and the maintenance and modulation of cell shape. Motility-associated microtubule-associated proteins are found in situations in which movement occurs over the surfaces of microtubules, e.g. the transport of cytoplasmic vesicles, bending of cilia and flagella, and some movements of mitotic spindles. They include a large family of motor proteins, the best known of which are the dyneins and kinesins. Another protein, dynamin, is involved in endocytosis. The kinetochore proteins assemble at the chromosomal centromere during mitosis and meiosis. They attach (and thus attach chromosomes) to spindle microtubules; some of the kinetochore proteins are responsible for chromosomal movements in mitotic and meiotic anaphase.

All of these microtubule-associated proteins bind to microtubules and either actively slide along their surfaces or promote microtubule assembly or disassembly. Kinesins and dyneins can simultaneously attach to membranes such as transport vesicles and convey them along microtubules for considerable distances, thus enabling selective targeting of materials within the cell. Such movements occur in both directions along microtubules. Kinesin-dependent motion is usually towards the plus ends of microtubules, e.g. from the cell body towards the axon terminals in neurones, and away from the centrosome in other cells. Conversely, dynein-related movements are in the opposite direction, i.e. to the minus ends of microtubules. Dyneins also form the arms of peripheral microtubules in cilia and flagella, where they make dynamic cross-bridges to adjacent microtubule pairs. When these tethered dyneins try to move, the resulting shearing forces cause the axonemal array of microtubules to bend, generating ciliary and flagellar beating movements. Kinesins form a large and diverse family of related microtubule-stimulated ATPases. Some kinesins are motors that move cargo, others cause microtubule disassembly, whilst still others cross-link mitotic spindle microtubules to push the two centriolar poles apart during mitotic prophase.

Centrioles, centrosomes and basal bodies

Centrioles are microtubular cylinders 0.2 μm in diameter and 0.4 μm long (Fig. 1.11). They are formed by a ring of nine microtubule triplets linked by a number of other proteins. At least two centrioles occur in all animal cells that are capable of mitotic division (eggs, which undergo meiosis instead of mitosis, lack centrioles). They usually lie close together, at right angles or, most usually, at an oblique angle to each other (an arrangement often termed a diplosome), within the centrosome, a densely filamentous region of cytoplasm at the centre of the cell. The centrosome is the major microtubule-organizing centre of most cells; it is the site at which new microtubules are formed and the mitotic spindle is generated during cell division. Centriole biogenesis is a complex process that takes more than a single cell cycle to complete. At the beginning of the S phase (DNA replication phase) of the cell cycle, a new daughter centriole forms at right angles to each separated maternal centriole. Each mother–daughter pair forms one pole of the next mitotic spindle, and the daughter centriole becomes fully mature only as the progeny cells are about to enter the next mitosis. Because centrosomes are microtubule organizing centres, they lie at the centre of a network of microtubules all of which have their minus ends proximal to the centrosome. The association of membrane vesicles with dynein motors means that certain membranes (including the Golgi apparatus) concentrate near the centrosome. This is convenient, as the microtubules provide a means of targeting Golgi vesicular products to different parts of the cell.

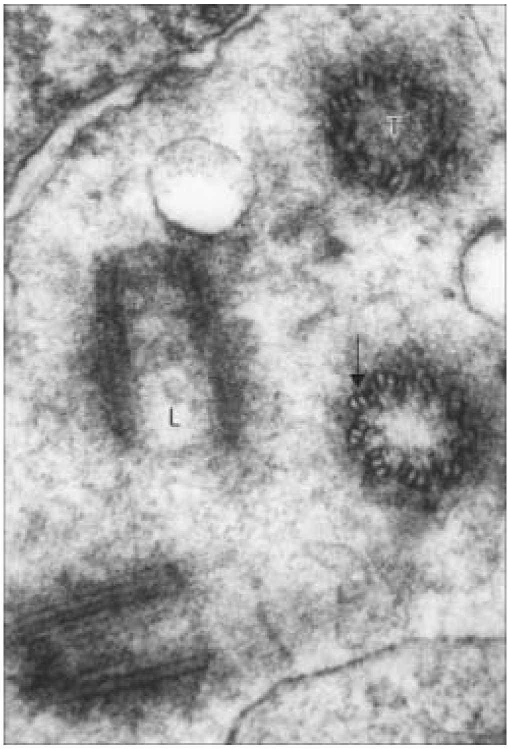

Fig. 1.11 A duplicated pair of centrioles in a human carcinoma specimen. Each centriole pair consists of a mother and daughter, oriented

approximately at right angles to each other so that one is sectioned transversely (T) and the other longitudinally (L). The transversely sectioned centrioles are seen as rings of microtubule triplets (arrowed).

The microtubule-organizing centre contains complexes of γ-tubulin that nucleate microtubule polymerization at the minus ends of microtubules. Basal bodies are microtubule-organizing centres that are closely related to centrioles, and are believed to be derived from them. They are located at the bases of cilia and flagella, which they anchor to the cell surface. The outer microtubule doublets of cilia and flagella originate from two of the microtubules in each triplet of the basal body.

Cell surface projections

The surfaces of many different types of cell are specialized to form structures that project from the surface. These projections may permit movement of the cell itself (flagella), or of fluids across the apical cell surface (cilia), or increase the surface area available for absorption (microvilli). Infoldings of the basolateral plasma membrane also increase the area for transport across this surface of the cell. In most non-dividing epithelial cells, the centriole gives rise to a non-motile primary cilium, which has an important sensory role.

Cilia and flagella

Cilia and flagella are motile, hair-like projections of the cell surface which create currents in the surrounding fluid, movements of the cell to which they are attached, or both. Cilia occur on many internal surfaces of the body, in particular: the epithelia of most of the respiratory tract; parts of the male and female reproductive tracts; the ependyma that line the central canal of the spinal cord and ventricles of the brain. They also occur at the endings of olfactory receptors and vestibular hair cells, and, in modified form, as portions of the rods and cones of the retina. A single cell may bear many cilia, e.g. in bronchial epithelium, or only one or two. Each male gamete possesses a single flagellum 70 μm long.

A cilium or flagellum consists of a shaft (0.25 μm diameter) constituting most of its length, a tapering tip and a basal body at its base, which lies within the surface cytoplasm of the cell (Fig. 1.12). Other than at its base, the entire structure is covered by plasma membrane. The core of the cilium is the axoneme, a cylinder of nine microtubule doublets that surrounds a central pair of single microtubules (Fig. 1.12). However, there is a class of cilia (primary cilia and nodal cilia) that are composed of nine microtubule doublets and no central microtubules.

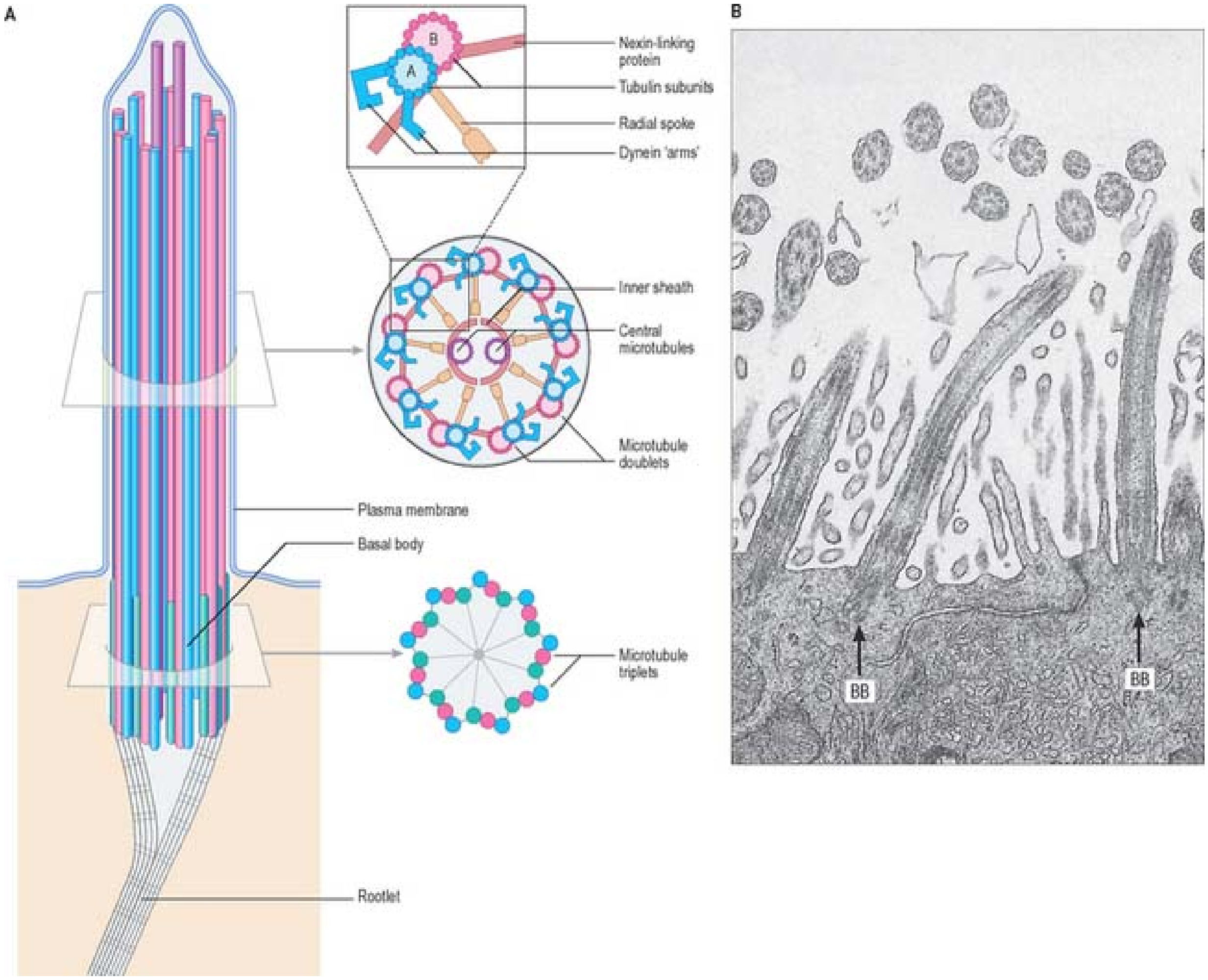
A
B
Nexin-linking protein
Tubulin subunits
Radial spoke
Dynein 'arms'
Inner sheath
Central microtubules
Microtubule doublets
Plasma membrane
Basal body
Microtubule triplets
Rootlet
B
BB
BB

Fig. 1.12 **A**, Structure of a cilium shown in longitudinal (left) and transverse (right) section. A and B are subfibres of the peripheral

microtubule doublets (see text); the basal body is structurally similar to a centriole, but with microtubule triplets. **B**, Apical region of respiratory epithelial cells, showing the proximal parts of three cilia sectioned longitudinally, anchored into the cytoplasm by basal bodies (BB). Other cilia project out of the plane of section and are cut transversely, showing the ‘9 + 2′ arrangement of microtubules.

(Part B by permission from Young B, Heath JW 2000 Wheater’s Functional Histology. Edinburgh: Churchill Livingstone.)

Several filamentous structures are associated with the microtubules in the shaft, e.g. radial spokes extend inwards from the outer microtubules towards the central pair. The outer doublet microtubules bear two rows of tangential dynein arms attached to the A subfibre of the doublet, which point towards the B subfibre of the adjacent doublet. Adjacent doublets are also linked by thin filaments. Other filaments partially encircle the central pair of microtubules, which are also united by ladder-like spokes.

Movements of cilia and flagella are broadly similar. Flagella move by rapid undulation, which passes from the attached to the free end. In human spermatozoa there is an additional helical component to this motion. In cilia, the beating is planar, but asymmetric. In the effective stroke, the cilium remains stiff except at the base, where it bends to produce an oar-like stroke. The recovery stroke follows, during which the bend passes from base to tip, returning the cilium to its initial position for the next cycle. The activity of groups of cilia is usually coordinated so that the bending of one is rapidly followed by the bending of the next and so on, resulting in long travelling waves of metachronal synchrony. These pass over the tissue surface in the same direction as the effective stroke.

When a cilium bends, the microtubules do not change in length, but slide on one another. The dynein arms of peripheral doublets slant towards the base of the cilium from their attached ends. Dynein has an ATPase activity, which causes mutual sliding of adjacent doublets by initially attaching sideways to the next pair, then swinging upwards towards the tip of the cilium. There is a group of genetic diseases (reviewed in Afzelius 2004) in which cilia beat either ineffectively or not at all, e.g. Kartagener's immotile cilia syndrome. Affected cilia exhibit various ultrastructural defects, such as a lack of dynein arms or missing spokes. Patients with this syndrome suffer various respiratory problems caused by the accumulation of particles in the lungs; males are typically sterile because of the loss of sperm motility, and 50% have an alimentary tract that is a mirror image of the usual pattern (situs inversus) – i.e. it rotates in the opposite direction during early development.

Microvilli

Microvilli are finger-like cell surface extensions usually 0.1 µm in diameter and up to 2 µm long (Fig. 1.13). When arranged in a regular parallel series, they constitute a striated border, as typified by the absorptive surfaces of the epithelial enterocytes of the small intestine. When they are less regular, as in the gallbladder epithelium and proximal kidney tubules, the term brush border is used.

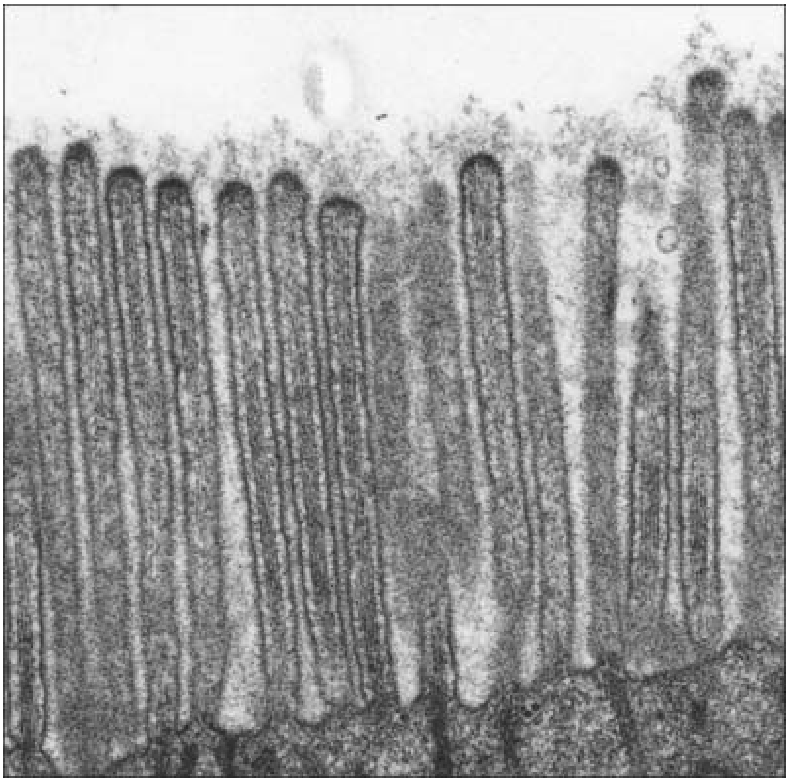

Fig. 1.13 Microvilli sectioned longitudinally in the striated border of an intestinal absorptive cell in a human duodenal biopsy specimen. Actin filaments fill the cores of the microvilli and insert into the apical cytoplasm. There is a prominent glycocalyx (formed by the extracellular domains of plasma membrane glycoproteins), seen as a fuzzy coat at the tips of and between microvilli; it includes enzymes concerned with the final stages of digestion.

Microvilli are covered by plasma membrane and supported internally by closely packed bundles of actin filaments linked by cross-bridges of the actin-bundling proteins, fascin and fimbrin. Other bridges composed of myosin I and calmodulin connect the filament bundles to the plasma membrane. At the tip of each microvillus, the free ends of microfilaments are inserted into a dense mass that includes the protein, villin. The actin filament bundles of microvilli are embedded in the apical cytoplasm amongst a meshwork of transversely running actin filaments stabilized by spectrin to form the terminal web, which is underlain by keratin intermediate filaments.

The web is anchored laterally to the zonula adherens of the apical epithelial junctional complex. Myosin II and tropomyosin are also found in the terminal web, which may explain its contractile activity.

Microvilli greatly increase the area of cell surface (up to 40 times), particularly at sites of active absorption. In the small intestine, they have a very thick cell coat or glycocalyx, which reflects the presence of integral membrane glycoproteins, including enzymes concerned with digestion and absorption. Irregular microvilli, filopodia, are also found on the surfaces of many types of cell, particularly free macrophages and fibroblasts, where they may be associated with phagocytosis and cell motility.

Long, regular microvilli are called stereocilia, an early misnomer, as they are not motile and lack microtubules. They are found on cochlear and vestibular receptor cells, where they act as sensory transducers, and also in the absorptive epithelium of the epididymis.

NUCLEUS

The nucleus (Figs 1.1, 1.2) is generally the largest intracellular structure and is usually spherical or ellipsoid in shape, with a diameter of 3–10 µm. Histological stains used to identify nuclei in tissue sections mainly detect the acidic molecules of deoxyribonucleic acid (DNA), which are largely confined to the nucleus.

Nuclear membrane

The nucleus is surrounded by two concentric lipid bilayers which together form the nuclear membrane or envelope. The outer membrane bilayer and the lumen between the two bilayers are continuous with the rough endoplasmic reticulum. Like the rough endoplasmic reticulum, the outer membrane of the nuclear envelope is studded with ribosomes that are active in protein synthesis; the newly synthesized proteins pass into the perinuclear space between the two membrane layers.

A special class of intermediate filaments known as lamins is associated with the inner surface of the nuclear membrane. The lamins form a dense meshwork beneath the membrane, the nuclear lamina. The lamin filaments cross each other at right angles to create an irregular anastomosing network that covers the interior surface of the nuclear membrane. In so doing, they reinforce the nuclear membrane mechanically, determine the shape of the nucleus and provide a binding site for a range of proteins that anchor chromatin. Nuclear lamin A, with over 350 mutations, is the most mutated protein linked to human disease. Lamin A mutations cause a surprisingly wide range of diseases, from progeria to various dystrophies (reviewed in Mattout et al 2006 and Pollard and Earnshaw 2007).

Condensed chromatin (heterochromatin) also tends to aggregate near the nuclear membrane during interphase. At the end of mitotic and meiotic prophase (see below), the lamin filaments disassemble, causing the nuclear membranes to vesiculate and disperse into the endoplasmic reticulum. During the final stages of mitosis (telophase), proteins of the nuclear periphery, including lamins, associate with the surface of the chromosomes, providing docking sites for membrane vesicles. Fusion of these vesicles reconstitutes the nuclear compartment.

The transport of molecules between the nucleus and the cytoplasm occurs via specialized nuclear pore structures that perforate the nuclear membrane (Fig. 1.14A). They act as highly selective directional molecular filters, permitting proteins such as histones and gene regulatory proteins (which are synthesized in the cytoplasm but function in the nucleus) to enter the nucleus, and molecules that are synthesized in the nucleus but destined for the cytoplasm (e.g. ribosomal subunits, transfer RNAs and messenger RNAs), to leave the nucleus.

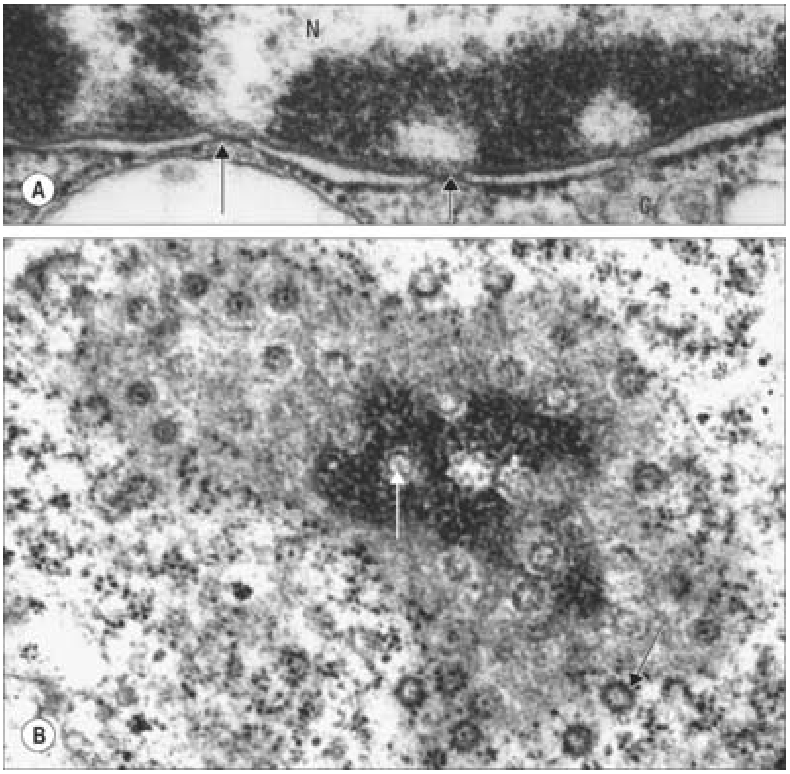

Fig. 1.14 **A**, Nuclear envelope with nuclear pores (arrowed) in transverse section, showing the continuity between the inner and outer phospholipid layers of the envelope on either side of the pore. The fine ‘membrane’ appearing to span the pore is formed by proteins of the pore complex. Note that the chromatin is less condensed in the region of nuclear pores. Nucleus (N); cytoplasm (C). **B**, Nuclear pores seen ‘en face’ as spherical structures (arrows) in a tangential section through the nuclear envelope. The

appearance of the envelope varies in electron density as the plane of section passes through different regions of the curved double membrane, which is interrupted at intervals by pores through the envelope (see also **Fig. 1.1**). The surrounding cytoplasm with ribosomes is less electron-dense. Human tissues.

Ultrastructurally, nuclear pores appear as disc-like structures with an outer diameter of 130 nm and an inner pore with an effective diameter for free diffusion of 9 nm (Fig. 1.14B). The nuclear membrane of an active cell is bridged by up to 4000 such pores. The nuclear pore complex has an octagonal symmetry and is formed by an assembly of more than 50 proteins, the nucleoporins. The inner and outer nuclear membranes fuse around the pore complex (Fig. 1.14A). Nuclear pores are freely permeable to small molecules, ions and proteins up to about 17 kDa. Most proteins that enter the nucleus do so as complexes with specific transport receptor proteins known as importins. Importins shuttle back and forth between the nucleus and cytoplasm. Binding of the cargo to the importin requires a short sequence of amino acids known as a nuclear localization sequence (NLS), and can be either direct or via an adapter protein. Interactions of the importin with components of the nuclear pore move it together with its cargo through the pore by an energy-independent process still not understood. A complementary cycle functions in export of proteins and RNA molecules from the nucleus to the cytoplasm using transport receptors known as exportins. For further explanation, see Pollard & Earnshaw (2007).

Chromatin

DNA is organized within the nucleus in a DNA–protein complex known as chromatin. The protein constituents of chromatin are the histones and the non-histone proteins. Non-histone proteins are an extremely heterogeneous group that includes structural proteins, DNA and RNA polymerases and gene regulatory proteins. Histones are the most abundant group of proteins in chromatin, primarily responsible for the packaging of chromosomal DNA into its primary level of organization, the nucleosome. There are four core histone proteins: H2A, H2B, H3 and H4 that combine in equal ratios to form a compact octameric nucleosome core. A fifth histone, H1, is involved in further compaction of the chromatin. The DNA molecule (one per chromosome) winds twice around each nucleosome core, taking up 165 nucleotide pairs. This packaging organizes the DNA into a chromatin fibre 11 nm in diameter, and imparts to this form of chromatin the electron microscopic appearance of beads on a string, in which each bead is separated by a variable length of DNA, typically about 35 nucleotide pairs long. The nucleosome core region and one of the linker regions constitute the nucleosome proper, which is typically about 200 nucleotide pairs in length. However, chromatin rarely exists in this simple form and is usually packaged further into a 30 nm thick fibre, involving a single H1 histone per nucleosome, which interacts with both DNA and protein to impose a higher order of nucleosome packing. Usually, 30 nm fibres are further coiled or folded into larger domains. Individual domains are believed to decondense and extend during active transcription. In a typical interphase nucleus, euchromatin (nuclear regions that appear pale in appropriately stained tissue sections, or relatively electron-lucent in electron micrographs; Fig. 1.2) is likely to consist mainly of 30 nm fibres and loops, and contains the transcriptionally active genes. Transcriptionally active cells, such as most neurones, have nuclei that are predominantly euchromatic and often described as ‘open face’ nuclei.

Heterochromatin (nuclear regions that appear dark in appropriately stained tissue sections or electron-dense in electron micrographs) is characteristically located mainly around the periphery of the nucleus, except over the nuclear pores (Fig. 1.14A), and around the nucleolus (Fig. 1.2). It is a relatively compacted form of chromatin in which the histone proteins carry a specific set of post-translational modifications, including methylation at characteristic residues. This facilitates the binding of specific heterochromatin-associated proteins. Heterochromatin includes non-coding regions of DNA, such as centromeric regions, which are known as constitutive heterochromatin. DNA that is inactivated (becoming resistant to transcription) in some cells as they differentiate during development or cell maturation contributes to heterochromatin, and is known as facultative heterochromatin. The inactive X chromosome in females is an example of facultative heterochromatin and can be identified in the light microscope as the deeply staining Barr body (drumstick chromosome), often located near the nuclear periphery.

In transcriptionally inactive cells, chromatin is predominantly in the condensed, heterochromatic state, and may comprise as much as 90% of the total. Examples of such cells are mature neutrophil leukocytes (in which the condensed chromatin is present in a multilobed, densely staining nucleus), and the highly condensed nuclei of orthochromatic erythroblasts (late-stage erythrocyte precursors). In most mature cells, a mixture of the two occurs, indicating that only a proportion of the DNA is being transcribed. A particular instance of this is seen in the mature B lymphocyte (plasma cell), in which much of the chromatin is in the condensed condition and is arranged in regular masses around the perimeter of the nucleus, producing the so-called ‘clock-face’ nucleus (Figs 4.6, 4.12). Although this cell is actively transcribing, much of its protein synthesis is of a single immunoglobulin type, and consequently much of its genome is in an inactive state.

During mitosis, the chromatin is further reorganized and condensed to form the much shortened chromosomes characteristic of metaphase. This shortening is achieved through further levels of close packing of the chromatin. The mechanism of condensation is unknown, but the condensed chromosomes are stabilized by protein complexes known as condensins. Progressive folding of the chromosomal DNA by interactions with specific proteins can reduce 5 cm of chromosomal DNA by 10,000 fold, to a length of 5 μm in the mitotic chromosome.

Chromosomes and karyotypes

The nuclear DNA of eukaryotic cells is organized into linear units called chromosomes. The DNA in a normal human diploid cell contains 6×10^9 nucleotide pairs organized in the form of 46 chromosomes (44 autosomes and two sex chromosomes). The largest human chromosome (number 1) contains

2.5×10^8 nucleotide pairs, and the smallest (the Y chromosome) 5×10^7 nucleotide pairs.

Each chromosomal DNA molecule contains a number of specialized nucleotide sequences that are associated with its maintenance. One is the centromere. During mitosis, a disc-shaped structure composed of a complex array of proteins, the kinetochore, forms as a substructure of the centromeric region of DNA in order to attach it to the microtubular spindle. Another sequence, the telomere, defines the end of each chromosomal DNA molecule. Telomeres consist of hundreds of repeats of the nucleotide sequence $(TTAGGG)_n$. The very ends of the chromosomes cannot be replicated by the same DNA polymerase as the rest of the chromosome, and are maintained by a specific enzyme called telomerase which contains an RNA subunit which acts as the template for lengthening the TTAGGG repeats. Thus telomerase is a specialized type of polymerase known as a reverse transcriptase that turns sequences in RNA back into DNA. The number of tandem repeats of the telomeric DNA sequence varies. It appears to shorten with successive cell divisions, because telomerase activity reduces or is absent in differentiated cells with a finite lifespan. It is believed that this mechanism contributes to regulation of cell senescence and may protect against proliferative disorders, including cancer (reviewed in Flores et al 2006).

Classification of human chromosomes

A number of genetic abnormalities can be directly related to the chromosomal pattern. The characterization or karyotyping of chromosome number and structure is therefore of considerable diagnostic importance. The identifying features of individual chromosomes are most easily seen during metaphase, although prophase chromosomes can be used for more detailed analyses.

Lymphocytes separated from blood samples, or cells taken from other tissues, are used as a source of chromosomes. Diagnosis of fetal chromosome patterns is generally carried out on samples of amniotic fluid containing fetal cells aspirated from the uterus by amniocentesis, or on a small piece of chorionic villus tissue removed from the placenta. Whatever their origin, the cells are cultured *in vitro* and stimulated to divide by treatment with agents that stimulate cell division. Mitosis is interrupted at metaphase with spindle inhibitors. The chromosomes are dispersed by first causing the cells to swell in a hypotonic solution, then the cells are gently fixed and mechanically ruptured on a slide to spread the chromosomes. They are subsequently stained in various ways to allow the identification of individual chromosomes by size, shape and distribution of stain (Fig. 1.15). General techniques show the obvious landmarks, e.g. lengths of arms and positions of constrictions. Banding techniques demonstrate differential staining patterns, characteristic for each chromosome type. Fluorescence staining with quinacrine mustard and related compounds produces Q bands, and Giemsa staining (after treatment that partially denatures the chromatin) gives G bands (Fig. 1.15A). Other less widely used methods include: reverse-Giemsa staining, in which the light and dark areas are reversed (R bands); the staining of constitutive heterochromatin with silver salts (C-banding); T-banding to stain the ends (telomeres) of chromosomes. Collectively, these methods permit the classification of chromosomes into numbered autosomal pairs in order of decreasing size, from 1 to 22, plus the sex chromosomes.

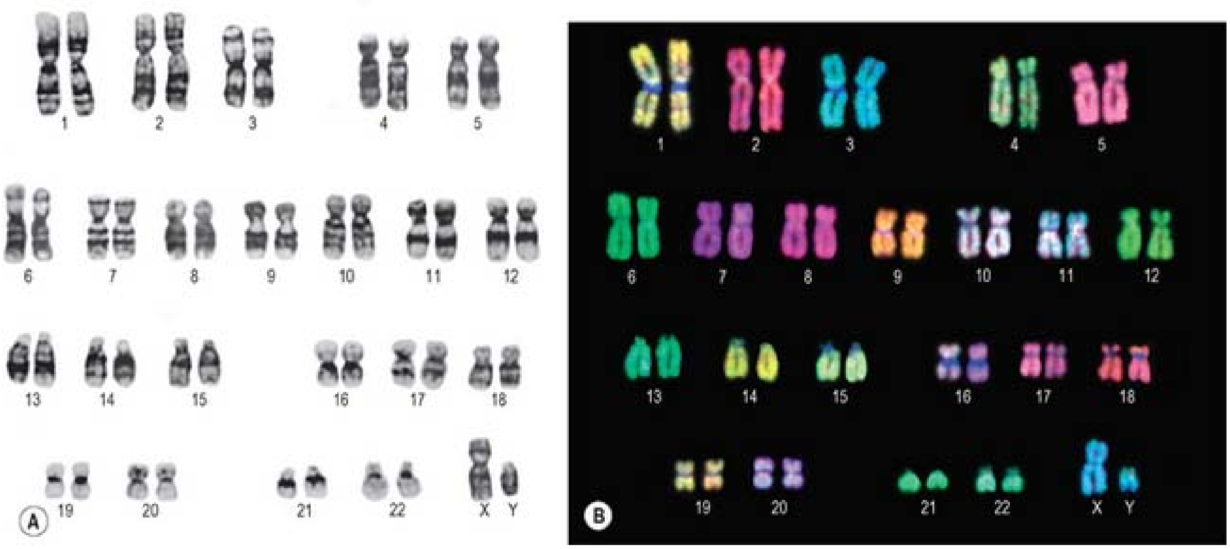

Fig. 1.15 Chromosomes from normal males, arranged as karyotypes. **A**, G-banded preparation; **B**, preparation stained by multiplex fluorescence *in situ* hybridization to identify each chromosome.

(By courtesy of Dr Denise Sheer, Cancer Research UK.)

A summary of the major classes of chromosomes is given below:

Group	**Features**
1–3 (A)	Large metacentric chromosomes
4–5 (B)	Large submetacentric chromosomes
6–12 + X (C)	Metacentrics of medium size
13–15 (D)	Medium-sized acrocentrics with satellites
16–18 (E)	Shorter metacentrics (16) or submetacentrics (17,18)
19–20 (F)	Shortest metacentrics
21–22 + Y (G)	Short acrocentrics; 21, 22 with satellites, Y without

Methodological advances in banding techniques improved the recognition of abnormal chromosome patterns. The use of *in situ* hybridization with fluorescent DNA probes specific for each chromosome (Fig. 1.15B) permits the identification of even very small abnormalities.

Nucleolus

Nucleoli are a prominent feature of an interphase nucleus (Fig. 1.2). They are the site of most of the synthesis of rRNA and assembly of ribosome subunits. Ultrastructurally, the nucleolus appears as a pale fibrillar region (non-transcribed DNA), containing dense fibrillar cores (sites of rRNA gene transcription) and granular regions (sites of ribosome subunit assembly) within a diffuse nucleolar matrix. Five pairs of chromosomes carry rRNA genes organized in clusters of tandemly repeated units on each chromosome. Each rRNA unit is transcribed individually and encodes a large precursor RNA that is processed to yield the 28S, 18S and 5.8S rRNA molecules. This processing takes place in the nucleolus, as does the processing of a number of other stable RNAs, including the RNA component of the signal recognition particle (SRP), which is essential for protein secretion. During mitosis the nucleolus breaks down. It reforms after nuclear envelope reformation in telophase, in a process associated with the onset of transcription in nucleolar organizing centres on each chromosome. The 28S, 18S and 5.8S rRNA molecules are assembled into their ribosomal subunits in the granular region of the nucleolus together with the 5S rRNA, which is not synthesized in the nucleolus. The newly formed ribosomal subunits are then translocated to the cytoplasm through the nuclear pores.

CELL DIVISION AND THE CELL CYCLE

During prenatal development, most cells undergo repeated division as the body grows in size and complexity. As cells mature, they differentiate structurally and functionally. Some cells, such as neurones, lose the ability to divide. Others may persist throughout the lifetime of the individual as replication-competent stem cells, e.g. cells in the haemopoietic tissue of bone marrow. Many stem cells divide infrequently, but give rise to daughter cells that undergo repeated cycles of mitotic division as transit (or transient) amplifying cells. Their divisions may occur in rapid succession, as in cell lineages with a short lifespan and similarly fast turnover and replacement time. Transit amplifying cells are all destined to differentiate and ultimately to die and be replaced, unlike the population of parental stem cells, which self-renews.

Patterns and rates of cell division within tissues vary considerably. In many epithelia, such as the crypts between intestinal villi, the replacement of damaged or effete cells by division of stem cells can be rapid. Rates of cell division may also vary according to demand, as occurs in the healing of wounded skin, in which cell proliferation increases to a peak and then returns to the normal replacement level (see Ch. 7). The rate of cell division is tightly coupled to the demand for growth and replacement. Where this coupling is faulty, tissues either fail to grow or replace their cells, or they can overgrow, producing neoplasms.

The cell cycle is the period of time between the birth of a cell and its own division to produce two daughter cells. It generally lasts a minimum of 12 hours, but in most adult tissues can be considerably longer, and is divided into four distinct phases, which are known as G_1, S, G_2 and M. The combination of G_1, S and G_2 phases is known as interphase. M is the mitotic phase. G_1 is the period when cells respond to growth factors directing the cell to initiate another cycle; once made, this decision is irreversible. It is also the phase in which most of the molecular machinery required to complete another cell cycle is generated. Cells that retain the capacity for proliferation, but which are no longer dividing, have entered a phase called G_0 and are described as quiescent even though they may be quite active physiologically. Growth factors can stimulate quiescent cells to leave G_0 and re-enter the cell cycle, whereas the proteins encoded by certain tumour suppressor genes (e.g. the gene mutated in retinoblastoma, *Rb*) block the cycle in G_1. DNA synthesis (replication of the genome) occurs during S phase, at the end of which the DNA content of the cell has doubled. During G_2, the cell prepares for division; this period ends with the onset of chromosome condensation and breakdown of the nuclear membrane. The times taken for S, G_2 and M are similar for most cell types, and occupy 6–8, 2–4 and 1–2 hours respectively. In contrast, the duration of G_1 shows considerable variation, sometimes ranging from less than 2 hours in rapidly dividing cells, to more than 100 hours within the same tissue.

Cell cycle progression is driven in part by changes in the activity of cyclin-dependent protein kinases, CDKs (protein kinases which are activated by binding of a cyclin subunit). Each cell cycle stage is characterized by the activity of one or more CDK-cyclin pairs. Transitions between cell cycle stages are triggered by highly specific proteolysis of the cyclins and other key components. The targets for proteolysis are marked for destruction by E3 ubiquitin ligases, which decorate them with polymers of the small protein ubiquitin, a sign for recognition by the proteasome. To give one example, the transition from G2 to mitosis is driven by activation of CDK1 by its partners the A- and B-type cyclins: the characteristic changes in cellular structure that occur as cells enter mitosis are largely driven by phosphorylation of proteins by active CDK1-cyclin A and CDK1-cyclin B (further details are beyond the scope of this book). Cells exit from mitosis when the anaphase promoting complex/cyclosome (APC/C), an E3 ubiquitin ligase, marks the cyclins for destruction. The APC/C also triggers for destruction another protein whose function is to protect the cohesion between sister chromatids. An analogous process of protein phosphorylation coupled with targeted destruction drives the transition between G1 and S phase as cells commit to another cycle of proliferation.

There are important checkpoints in the cell cycle at which progress will be arrested if, for instance, DNA replication or mitotic spindle assembly and chromosome attachment are incomplete. Negative regulation systems also operate to delay cell cycle progression when DNA has been damaged by radiation or chemical mutagens. Cells with checkpoint defects, such as loss of the protein p53, which is a major negative control element in the division cycle of all cells, are commonly associated with the development of malignancy. Cells lacking one of the critical checkpoint functions are able to progress through the cycle carrying defects, thus increasing the probability that further abnormalities will accumulate in their progeny. The p53 gene is an example of a tumour suppressor gene. For further reading, see Blow & Tanaka (2005); Pollard & Earnshaw (2007).

MITOSIS AND MEIOSIS

Mitosis is the process that results in the distribution of identical copies of the parent cell genome to the two daughter somatic cells. In meiosis, the divisions immediately before the final production of gametes halve the number of chromosomes to the haploid number, so that at fertilization the diploid number is restored. Moreover, meiosis includes a phase in which exchange of genetic material occurs between homologous chromosomes. This allows a reassortment of genes to take place, which means that the daughter cells differ from the parental cell in both their precise genetic sequence and their haploid state. Mitosis and meiosis are alike in many respects, and differ principally in chromosomal behaviour during the early stages of cell division. In meiosis, two divisions occur in succession, without an intervening S phase. Meiosis I is distinct from mitosis, whereas meiosis II is more like mitosis.

Mitosis

New DNA is synthesized during the S phase of the cell cycle interphase. This means that the amount of DNA in diploid cells has doubled to the tetraploid value by the onset of mitosis, although the chromosome number is still diploid. During mitosis, this amount is halved between the two daughter cells, so that DNA quantity and chromosome number are diploid in both cells. The cellular changes that achieve this distribution are conventionally divided into four phases called prophase, metaphase, anaphase and telophase (Fig. 1.16, Fig. 1.17).

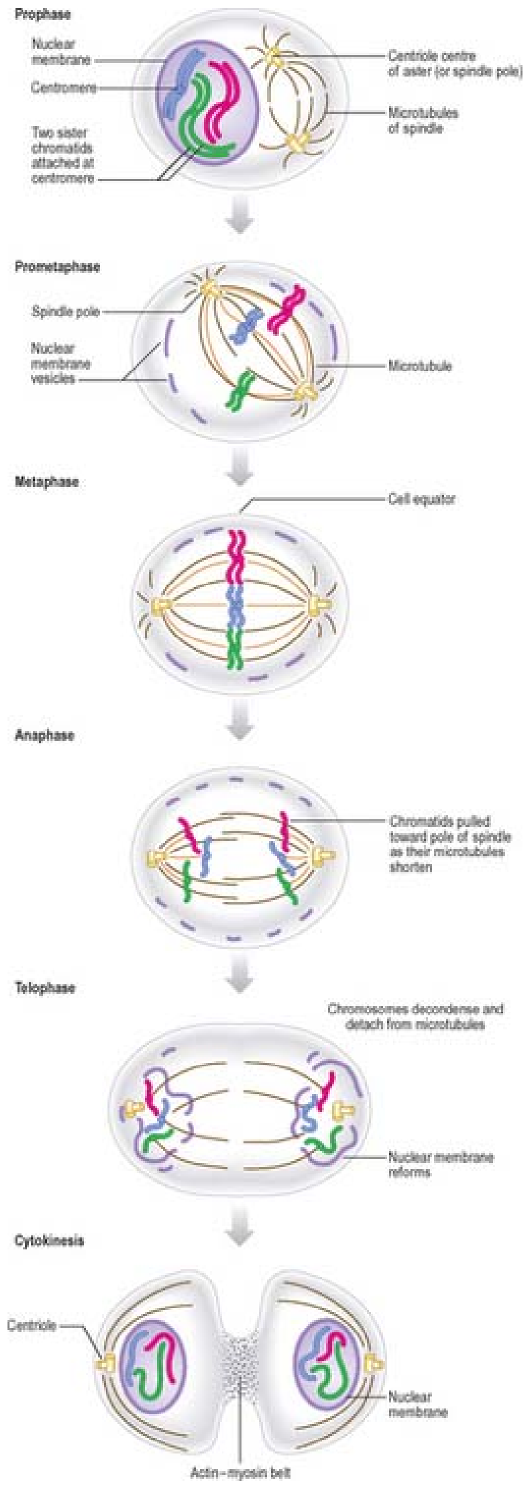
Prophase
Nuclear membrane
Centromere
Two sister chromatids attached at centromere
Centriole centre of aster (or spindle pole)
Microtubules of spindle
Prometaphase
Spindle pole
Nuclear membrane vesicles
Microtubule
Metaphase
Cell equator
Anaphase
Chromatids pulled toward pole of spindle as their microtubules shorten
Telophase
Chromosomes decondense and detach from microtubules
Nuclear membrane reforms
Cytokinesis
Centriole
Nuclear membrane
Actin–myosin belt

Fig. 1.16 The stages in mitosis, including the appearance and distribution of the chromosomes.

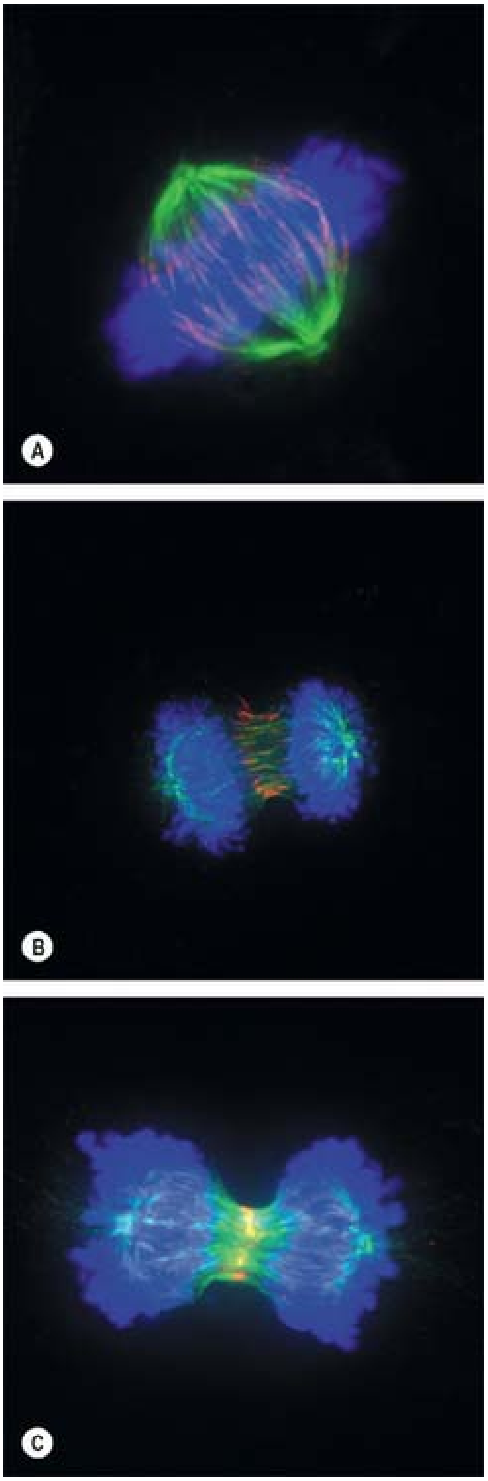

Fig. 1.17 Immunofluorescence images of stages in mitosis in human carcinoma cells in culture. **A**, Metaphase, with spindle microtubules (green), the microtubule-stabilizing protein (HURP; red) and chromosomal DNA (blue). **B**, Anaphase, with spindle microtubules (green), the central spindle

(Aurora-B kinase, red) and segregated chromosomes (blue). **C**, Late anaphase, with spindle microtubules (green), the central spindle (Plk1 kinase, red, appearing yellow where co-localized with microtubule protein) and segregated chromosomes (blue).

(By courtesy of Dr Herman Silljé, Max-Planck-Institute fur Biochemie, Martinsried, Germany.)

Prophase

During prophase, the strands of chromatin, which are highly extended during interphase, shorten, thicken and resolve themselves into recognizable chromosomes. Each chromosome is made up of duplicate chromatids (the products of DNA replication) joined at their centromeres. Outside the nucleus, the two centriole pairs begin to separate, and move towards opposite poles of the cell. Parallel microtubules are assembled between them to create the mitotic spindle, and others radiate to form the asters, which come to form the spindle poles. As prophase proceeds, the nucleoli disappear, and the nuclear membrane suddenly disintegrates to release the chromosomes, an event that marks the end of prophase.

Prometaphase–metaphase

As the nuclear membrane disappears, the spindle microtubules extend into the central region of the cell, attaching to the chromosomes which subsequently move towards the equator of the spindle (prometaphase). The grouping of chromosomes at the spindle equator is called the metaphase or equatorial plate. The chromosomes, attached at their centromeres, appear to be arranged in a ring when viewed from either pole of the cell, or to lie linearly across this plane when viewed from above. Cytoplasmic movements during late metaphase effect the approximately equal distribution of mitochondria and other organelles around the cell periphery.

Anaphase

By the end of metaphase every chromosome consists of a pair of sister chromatids attached to opposing spindle poles by bundles of microtubules associated with the centromeres. The onset of anaphase begins with the proteolytic cleavage of a key subunit of a complex known as cohesin, which holds the replicated sister chromatids together. This cleavage releases the cohesion between sister chromatids, which each then move towards opposite spindle poles as the microtubule bundles attached to the centromeres shorten and move polewards. At the end of anaphase the sister chromatids are grouped at either end of the cell, and both clusters are diploid in number. An infolding of the cell equator begins, and deepens during telophase as the cleavage furrow.

Telophase

During telophase the nuclear membranes reform, beginning with the association of membranous vesicles with the surface of the chromosomes. Later, after the vesicles have fused and the nuclear envelope is complete, the chromosomes decondense and the nucleoli reform. At the same time, cytoplasmic division, which usually begins in early anaphase, continues until the new cells separate, each with its derived nucleus. The spindle remnant now disintegrates. While the cleavage furrow is active, a peripheral band or belt of actin and myosin appears in the constricting zone: contraction of this band is responsible for furrow formation.

Failure of disjunction of chromatids, so that sister chromatids pass to the same pole, may sometimes occur. Of the two new cells, one will have more, and the other fewer, chromosomes than the diploid number. Exposure to ionizing radiation promotes non-disjunction and may, by chromosomal damage, inhibit mitosis altogether. A typical symptom of radiation exposure is the failure of rapidly dividing epithelia to replace lost cells, with consequent ulceration of the skin and mucous membranes. Mitosis can also be disrupted by chemical agents, particularly colchicine, taxol and their derivatives. These compounds either disassemble spindle microtubules or interfere with their dynamics. As a result, mitosis is arrested in metaphase. Taxol and its derivatives are widely used in the treatment of breast cancer. Colchicine is widely used for the treatment of gout, but the mechanism is not known and may have nothing to do with mitotic regulation.

Meiosis

There are two cell divisions during meiosis (Fig. 1.18). Details of this process differ at a cellular level for male and female lineages.

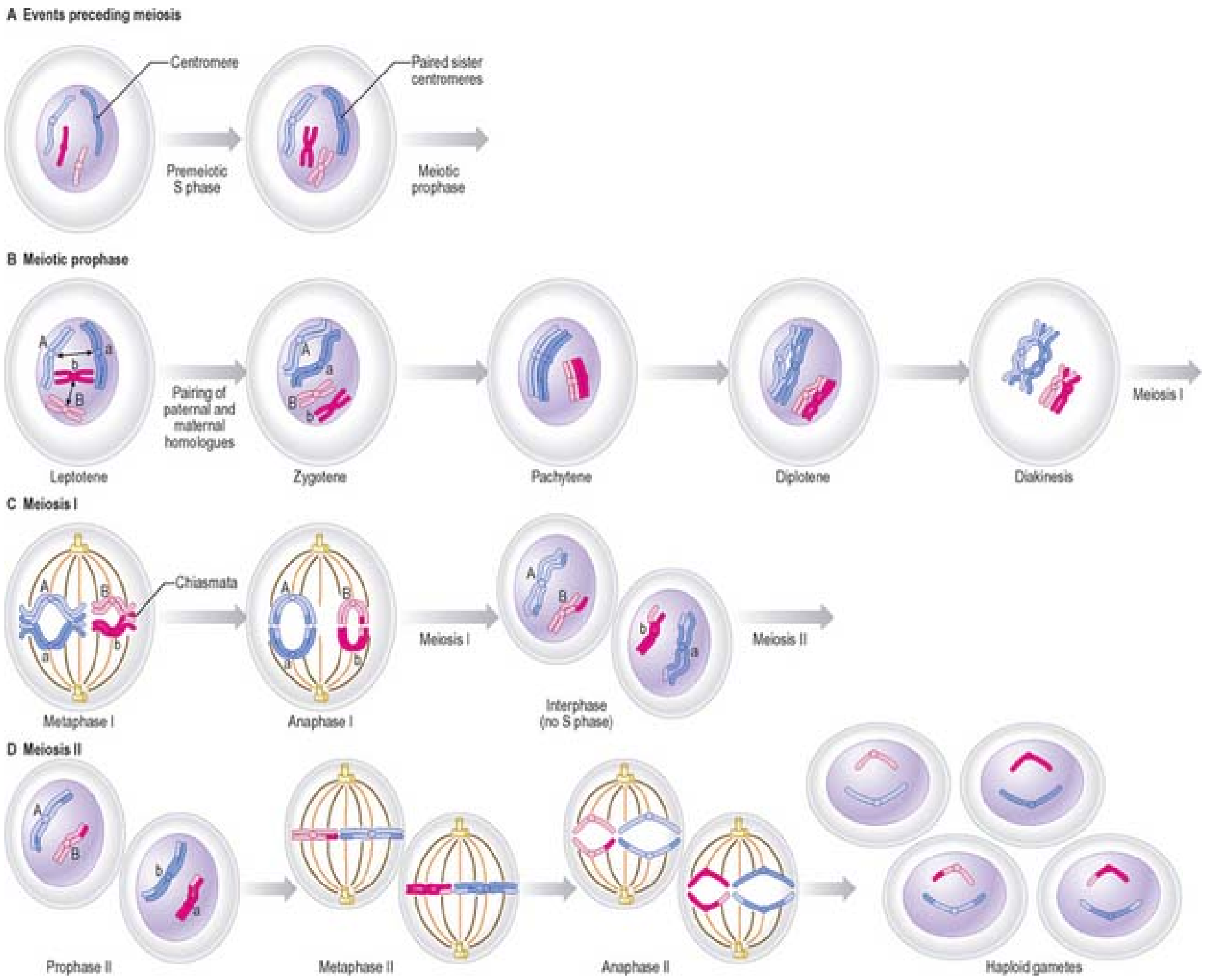
A Events preceding meiosis
Centromere
Premeiotic S phase
Paired sister centromeres
Meiotic prophase
B Meiotic prophase
A
a
b
B
Pairing of paternal and maternal homologues
Leptotene
Zygotene
Pachytene
Diplotene
Diakinesis
Meiosis I
C Meiosis I
Chiasmata
Metaphase I
Anaphase I
Meiosis I
Interphase (no S phase)
Meiosis II
D Meiosis II
Prophase II
Metaphase II
Anaphase II
Haploid gametes

Fig. 1.18 The stages in meiosis, depicted by two pairs of maternal and paternal homologues (dark and pale colours). DNA and chromosome complement changes and exchange of genetic information between homologues are indicated.

Meiosis I

Prophase I

Meiotic prophase I is a long and complex phase that differs considerably from mitotic prophase and is customarily divided into five substages, called leptotene, zygotene, pachytene, diplotene and diakinesis (see Pollard & Earnshaw 2007).

Leptotene stage

During leptotene, homologous chromosomes (maternal and paternal copies of the same chromosome), which were replicated in a preceding S phase and each consist of sister chromatids joined at the centromere (see above), locate one another within the nucleus, and the process of genetic recombination is initiated. Cytologically, chromosomes begin to condense, appearing as individual threads that are attached via their telomeres to the nuclear membrane. They often show characteristic beading throughout their length.

Zygotene stage

During zygotene, the homologous chromosomes initiate a process known as synapsis, during which they become intimately associated with one another. Synapsis may begin near the telomeres at the inner surface of the nuclear membrane, and during this stage the telomeres often cluster to one side of the nucleus (a stage known as the bouquet because the chromosomes resemble a bouquet of flowers). The pairs of synapsed homologues, also known as bivalents, are linked together by a highly structured fibrillar band, the synaptonemal complex.

The sex chromosomes also synapse during zygotene. In males, with distinct X and Y chromosomes, synapsis involves a short region of shared DNA sequence known as the pseudoautosomal region. The unpaired sex-specific regions adopt a special hypercondensed structure known as the sex vesicle.

Chromosome behaviour in meiosis is intimately linked with the process of genetic recombination. This begins during leptotene, as homologous chromosomes first locate one another at a distance. Synapsis is thought to represent the completion of recombination, as sites of genetic exchange are turned into specialized structures known as chiasmata. Chiasmata are topological ‘knots’ that hold homologous chromosomes together.

Pachytene stage

When synapsis is complete for all chromosomes, the cell is said to be in pachytene. Each bivalent looks like a single structure, but is actually two pairs of sister chromatids held together by the synaptonemal complex. Genetic recombination is completed at this point, with sites where it has occurred (usually one per chromosome arm) appearing as nodules in the center of the synaptonemal complex.

Diplotene stage

During diplotene, the synaptonemal complex disassembles, and pairs of homologous chromosomes, now much shortened, separate except where crossing over has occurred (chiasmata). At least one chiasma forms between each homologous pair, exchanging maternal and paternal sequences, and up to five have been observed. In the ovaries, primary oocytes become diplotene by the fifth month *in utero* and each remains at this stage until the period before ovulation (up to 50 years).

Diakinesis

Diakinesis is the prometaphase of the first meiotic division. The chromosomes, still as bivalents, become even shorter and thicker. They gradually attach to the spindle and become aligned at a metaphase plate. In eggs, the spindle forms without centrosomes. Microtubules first nucleate and are stabilized near the chromosomes, and the action of various motor molecules eventually sorts them into a bipolar spindle. Perhaps surprisingly, this spindle is as efficient a machine for chromosome segregation as the spindle of mitotic cells with centrosomes at the poles.

Metaphase I

Metaphase I resembles mitotic metaphase, except that the bodies attaching to the spindle microtubules are bivalents, not single chromosomes. These become arranged so that the homologous pairs occupy the equatorial plane of the spindle. The centromeres of each pair of sister chromatids function as a single unit, facing a single spindle pole. Homologous chromosomes are pulled towards opposite spindle poles, but are held paired at the spindle midzone by chiasmata. Thus, recombination is essential for the mechanics of the meiosis I division – without it the chromosomes cannot align properly, and errors in chromosome segregation (known as non-disjunction) lead to the production of aneuploid progeny. Most human aneuploid embryos are non-viable, and this is the major cause of fetal loss (spontaneous abortion), particularly during the first trimester of pregnancy in humans. The most common form of viable aneuploid progeny in humans is Down syndrome (trisomy for chromosome 21), which is relatively rare in young mothers, but exhibits a dramatic increase with maternal age.

Anaphase and telophase I

Anaphase I of meiosis begins with the release of cohesion between the arms of sister chromatids, much as it does during mitosis. In meiosis, this ‘unties’ the topological knots of the chiasmata, and allows homologous chromosomes to separate and migrate to opposite spindle poles. As positioning of bivalent pairs is random, assortment of maternal and paternal chromosomes in each telophase nucleus is also random. Critically, sister centromeres, and thus chromatids, do not separate during anaphase I.

During meiosis I, cytoplasmic division occurs by specialized mechanisms. In females, the division is highly asymmetric, producing one egg and one tiny cell known as a polar body. In males, the process does not go to full completion, resulting in production of spermatocytes that remain joined by small cytoplasmic bridges.

Meiosis II

Meiosis II commences after only a short interval during which no DNA synthesis occurs. The centromeres of sister chromatids remain paired, but rotate so that each one can face an opposite spindle pole. Onset of anaphase II is triggered by loss of cohesion between the centromeres, as it is in mitosis. This second division is more like mitosis, in that chromatids separate during anaphase, but, unlike mitosis, the separating chromatids are genetically different (the result of genetic recombination). Cytoplasmic division also occurs and thus, in the male, four haploid cells result from meiosis I and II.

CELL DIFFERENTIATION

As the embryo develops, its cells pass through a series of changes in gene expression, reflected in alterations of cell structure and behaviour. They begin to diversify, separating first into two main tissue arrangements, epithelium and embryonic mesenchyme, then into more restricted subtypes of tissue, until finally they mature into cells of their particular adult lineage. In this process, and in the maturation of functioning cells of the different lineages from their stem cells, there is a sequential pattern of gene expression that changes and limits the cell to a particular specialized range of activities. Such changes involve alterations in cell structure and biochemical characteristics, particularly in the types of proteins that are synthesized. At the genetic level, differentiation is based on a change in the pattern of repression and activation of the DNA sequences encoding proteins specific to that stage of development.

A cell may be committed to a particular differentiated fate without manifesting its commitment until later. Once switched in this way, cells are not usually able to revert to an earlier stage of commitment to a differentiation pathway, so that an irreversible repression of some gene sequences must have occurred. Differentiation signals include interactions between cells that are mediated by diffusible signalling molecules elaborated by one cell and detected by another, and by contactmediated signalling (such as Delta–Notch signalling). The latter is particularly important in establishing boundaries between different cell populations in development.

Differentiation may also depend in some instances on a temporal sequence, but probably not the number of previous cell divisions. In mature tissues in which cell turnover occurs, similar mechanisms appear to ensure the final differentiation to a functional end cell. This may be linked to the presence of a physiological stimulus, e.g. B lymphocytes respond to exposure to an antigen by differentiating into plasma cells that secrete a neutralizing antibody. In other cases, particularly where a cell is part of a highly organized tissue system, more subtle mechanisms exist to ensure a balance between cell proliferation, differentiation and programmed cell death (apoptosis). This balance is disturbed when tissue is damaged and different cell types respond differently to repair the damage. Liver hepatocytes are able to revert to a functionally less well-differentiated phenotype and re-enter the cell cycle, in order to restore cell numbers and tissue mass. Other cell types (such as skeletal muscle fibres) are unable to do so and depend on the proliferation of precursor cells (stem cells) for repair. In many tissues such as skin, where normal cell turnover is continuous, wound repair includes up-regulation of proliferation in the stem cell and transit amplifying cell compartments.

There are few instances of the transdifferentiation of one differentiated cell type into another (metaplasia, see Ch. 2), but there is evidence that stem cells in the developing embryo and in certain mature tissues (e.g. bone marrow) may have the potential to differentiate into more diverse phenotypes than was once believed. This plasticity depends on environmental cues and offers the prospect of engineering tissues for clinical therapy. For further reading, see Alberts et al (2002).

CELL FUSION

A small number of cell types undergo a process of fusion, the regulation of which is not well understood, as part of their normal programme of differentiation. A variable number of precursor cells fuse their plasma membranes and form syncytia, with their nuclei occupying a common cytoplasm. The best known examples are: skeletal muscle, where many hundreds of mononucleated myoblasts fuse to form a myotube which differentiates further to form the mature skeletal muscle fibre; osteoclasts (bone resorbing cells) form from the fusion of up to 30 precursor haemopoietic cells of the monocytic lineage. Such multinucleated cells do not divide. Oocyte and spermatocyte fusion initiates embryonic development, and because the gametes are haploid, mitotic division of the diploid zygote follows.

Some normal polyploid cells, which may also have more than one nucleus, arise however by a different mechanism. Cells replicate their DNA (endoreduplication) to produce a tetraploid or octaploid nucleus, or may proceed to nuclear division and become binucleate, but fail to complete cytokinesis. Liver hepatocytes, some cardiac myocytes and the superficial cells of the urinary bladder are examples.

Other examples of cell fusion are pathological and usually result from viral infection. Measles, mumps and human immunodeficiency virus (HIV) are all fusogenic. Most cells fused as a result of viral infection do not divide and die without causing adverse effects.

APOPTOSIS

Cells die as a result of either tissue injury (necrosis) or the internal activation of a ‘suicide’ programme (apoptosis) in response to extrinsic or intrinsic cues. Apoptosis (programmed cell death, regulated cell suicide) is a central mechanism controlling multicellular development. During morphogenesis, apoptosis mediates activities such as the separation of the developing digits, and has an important role in regulating the number of neurones in the nervous system (the majority of neurones die during development). Apoptosis also ensures that inappropriate or inefficient cells of the acquired immune system are eliminated.

The morphological changes exhibited by necrotic cells are very different from those seen in apoptotic cells (Fig. 1.19). Necrotic cells swell and subsequently rupture; the resulting debris may induce an inflammatory response (see Ch. 4, Ch. 7). Apoptotic cells shrink, their nuclei and chromosomes fragment, forming apoptotic bodies, and their plasma membranes undergo conformational changes that act as a signal to local phagocytes. The dead cells are removed rapidly, and as their intracellular contents are not released into the extracellular environment, inflammatory reactions are avoided; the apoptotic fragments also stimulate macrophages to release anti-inflammatory cytokines.

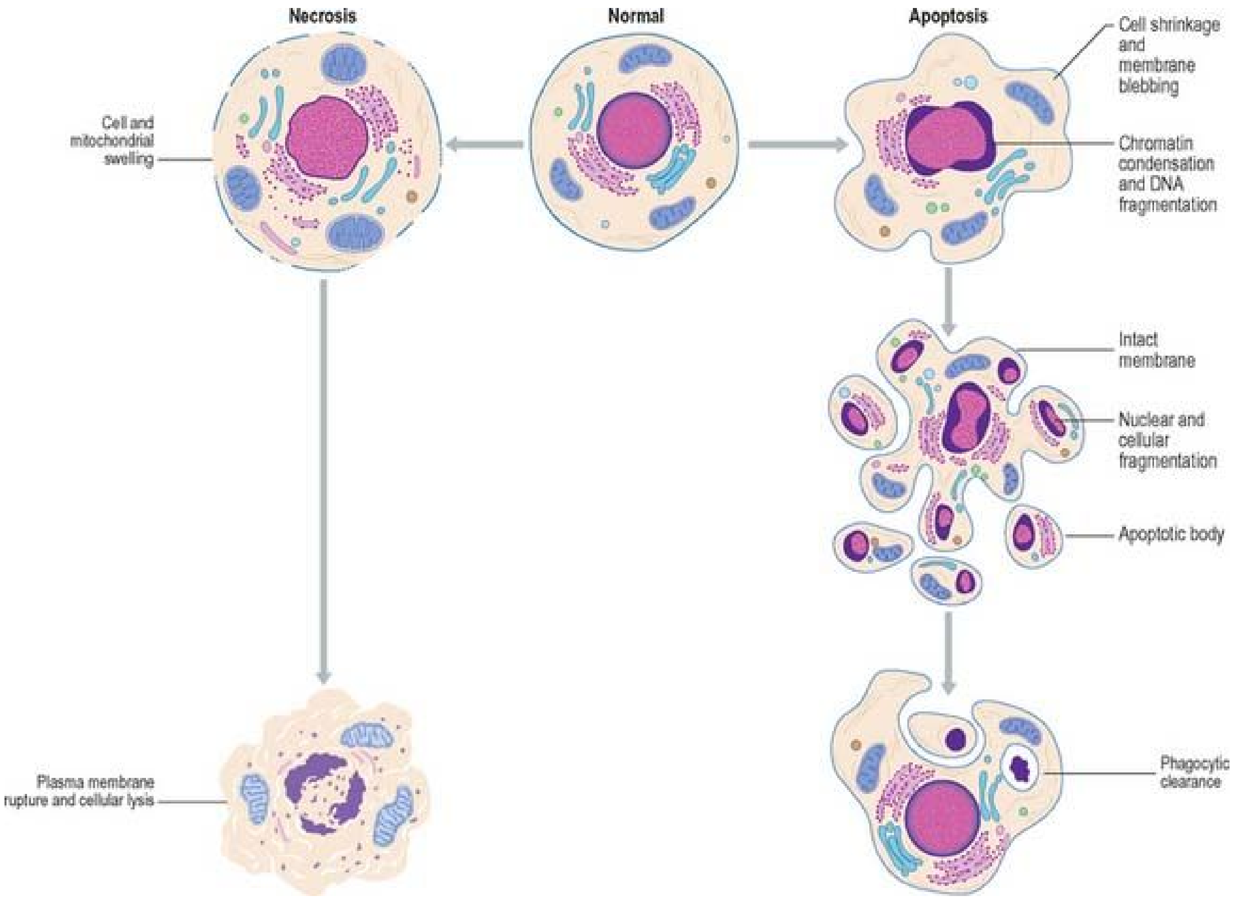
Necrosis
Normal
Apoptosis
Cell shrinkage and membrane blebbing
Cell and mitochondrial swelling
Chromatin condensation and DNA fragmentation
Intact membrane
Nuclear and cellular fragmentation
Apoptotic body
Plasma membrane rupture and cellular lysis
Phagocytic clearance

Fig. 1.19 Comparison between the changes in cellular structure during cell death by apoptosis and necrosis.

Apoptosis and cell proliferation are intimately coupled: several cell cycle regulators can influence both cell division and apoptosis. The signals that trigger apoptosis include withdrawal of survival factors or exposure to inappropriate proliferative stimuli. The current model of the intracellular pathway(s) that leads to apoptosis implicates permeabilization of the mitochondrial membrane, the release of cytochrome *c* (from the space between the inner and outer mitochondrial membranes) into the cytosol, and subsequent activation of a family of cysteine proteases known as caspases. Caspases are the intracellular mediators of apoptosis: when activated, they initiate a cascade of degradative processes targeting proteins throughout the cell. Caspase cleavage inactivates many systems that normally promote damage repair and support cell viability in general. They also activate a number of proteins which promote the death and disassembly of the cell.

Subversion of the apoptotic response is a key characteristic of many cancer cells. Thus the tumour suppressor gene *p53* (which functions in cell-cycle control, regulation of apoptosis and the maintenance of genetic stability), is mutated in about 50% of all human cancers. For further details, see Pollard & Earnshaw (2007).

REFERENCES

zelius BA. Cilia-related diseases. *J Pathol*. 2004;204:470-477.

berts B, Johnson A, Lewis J, Raff M, Roberts K, Walter P. Molecular Biology of the Cell, 4th edn. New York: Garland Press, 2002.

nnett V, Healy J. Organising the fluid membrane bilayer: diseases linked to spectrin and ankyrin. *Trends Mol Med*. 2008;14:28-36.

ow JJ, Tanaka TU. The chromosome cycle: coordinating replication and segregation. *EMBO Reports*. 2005;6:1028-1034.

Duve C. The lysosome. *Sci Am*. 1963;208:64-72.

stein RJ. Human Molecular Biology. In *An Introduction to the Molecular Basis of Health and Disease*. Cambridge: Cambridge University Press; 2003.

Reviews signalling molecules and their receptors in the context of human disease..

ores I, Benetti R, Blasco MA. Telomerase regulation and stem cell behaviour. *Curr Op Cell Biol*. 2006;18:1-7.

aff C, Bui T-H, Larsson N-G. Mitochondrial diseases. *Best Pract Res Clin Obstet Gynaecol*. 2002;16:715-728.

Reviews clinical conditions related to the inheritance of maternal mitochondrial gene mutations..

mbiner BM. Regulation of cadherin-mediated adhesion in morphogenesis. *Nature Rev Mol Cell Biol*. 2005;6:622-634.

vine T, Rabouilee C. Endoplasmic reticulum: one continuous network compartmentalized by extrinsic cues. *Curr Op Cell Biol*. 2005;17:362-368.

tvin O, Tiunova A, Connell-Alberts Y, Panchin Y, Baranova A. What is hidden in the pannexin treasure trove: the sneak peek and the guesswork. *J Cell Mol Med*. 2006;10:613-634.

attout A, Dechat T, Adam SA, Goldman RD, Gruenbaum Y. Nuclear lamins, diseases and aging. *Curr Op Cell Biol*. 2006;18:335-341.

orris R, Cox H, Mombelli E, Quinn P. Rafts, little caves and large potholes: how lipid structure interacts with membrane proteins to create functionally diverse membrane environments. Quinn PJ, editor. Subcellular Biochemistry. vol 37. New York: Kluwer Academic/Plenum Publishers; 2004:35-118.

Reviews how lipids partition proteins into different environments within membranes, and the benefits that accrue to the proteins as a result..

llard TD, Earnshaw WC. Cell Biology. Philadelphia: Saunders, 2007.

Reviews current principles and theories on the structure and functions of the cell. Extends the scope of this chapter, particularly where indicated in the text..

rter RM, Lane EB. Phenotypes, genotypes and their contribution to understanding keratin function. *Trends Genet*. 2003;19:278-285.

Reviews the largest family of intermediate filament proteins, providing evidence for the functional roles of this diverse group, and addresses inherited tissue fragility disorders resulting from keratin gene mutations..

maekers FCS, Bosman FT. The cytoskeleton and disease. *J Pathol*. 2004;204:351-505.

ivola DM, Tao G-Z, Habtezion A, Liao J, Omary MB. Cellular integrity plus: organelle-related and protein-targeting functions of intermediate filaments. *Trends Cell Biol*. 2005;15:608-617.

CHAPTER 2

Integrating cells into tissues

Cells evolved as single, free-living organisms, but natural selection favoured more complex communities of cells, multicellular organisms, where groups of cells specialize during development to carry out specific functions for the body as a whole. This allowed the emergence of larger organisms with greater control over their internal environment and to the evolution of highly specialized organic structures such as the brain. The human body contains more than 200 different cell types, sharing the same genome but with different patterns of gene expression.

Some cells in the body are essentially migratory, but most exist as cellular aggregates in which individual cells carry out similar or closely related functions in a coordinated manner. These aggregates are termed tissues, and can be classified into a fairly small number of broad categories on the basis of their structure, function and molecular properties. On the basis of their structure, most tissues are divided into four major types: epithelia, connective or supporting tissue, muscle and nervous tissue. Epithelia are continuous layers of cells with little intercellular space, which cover or line surfaces, or have been so derived. In connective tissues, the cells are embedded in an extracellular matrix which, typically, forms a substantial and important component of the tissue. Muscle consists largely of specialized contractile cells. Nervous tissue consists of cells specialized for conducting and transmitting electrical and chemical signals and the cells that support this activity.

There is molecular evidence that this structure-based scheme of classification has validity. Thus the intermediate filament proteins (p. 15) characteristic of all epithelia are keratins; those of connective tissue are vimentins; those of muscle are desmins; and those of nervous tissue are neurofilament and glial fibrillary acidic proteins. However, cells such as myofibroblasts, neuroepithelial sensory receptors and ependymal cells of the central nervous system have features of more than one tissue type. Despite its anomalies, the scheme is useful for descriptive purposes and widely used, and will be adopted here.

In this section, two of the major tissue categories, epithelia and general connective and supporting tissues, will be described. Specialized skeletal connective tissues, i.e. cartilage and bone, together with skeletal muscle, are described in detail in Chapter 5 as part of the musculoskeletal system overview. Smooth muscle and cardiac muscle are described in Chapter 6. Nervous system tissues are described in Chapter 3. Specialized defensive cells, which also form a migrant population within the general connective tissues, are considered in more detail in Chapter 4, with blood, lymphoid tissues and haemopoiesis.

EPITHELIA

The term epithelium is applied to the layer or layers of cells that cover the body surfaces or line the body cavities that open on to it. Developmentally, epithelia are derived from all three layers of the early embryo (p. 198). The ectoderm gives rise to the epidermis, glandular tissue of the breast, cornea and the junctional zones of the buccal cavity and anal canal. The endoderm forms the epithelial lining of the alimentary canal and its glands, most of the respiratory tract and the distal parts of the urogenital tract. Mesodermal derivatives include the epithelia of the kidney, the suprarenal (adrenal) cortex and endocrine cells of the ovary and testis. These endocrine cells are atypical epithelia in that they differentiate from embryonic mesenchyme and, in common with endocrine cells in general, they lack a free surface that communicates with the exterior. This atypical category also includes endothelia that line blood vessels and lymphatics (p. 135), and the epithelium-like cell layers of mesodermal (and mesenchymal) origin that line internal cavities of the body and are usually classified separately as mesothelia: they line the pericardial, pleural and peritoneal cavities.

Epithelia function generally as selective barriers that facilitate, or inhibit, the passage of substances across the surfaces they cover. In addition, they may: protect underlying tissues against dehydration, chemical or mechanical damage; synthesize and secrete products into the spaces that they line; function as sensory surfaces. In this respect, many features of nervous tissue can be regarded as those of a modified epithelium and the two tissue types share an origin (p. 186) in embryonic ectoderm.

Epithelia (Fig. 2.1) are predominantly cellular and the little extracellular material they possess is limited to the basal lamina. Intercellular junctions, which are usually numerous, maintain the mechanical cohesiveness of the epithelial sheet and contribute to its barrier functions. A series of three intercellular junctions forms a typical epithelial junctional complex: in sequence from the apical surface, this consists of a tight junctional zone, an adherent (intermediate) junctional zone and a region of discrete desmosome junctions (p. 6). Epithelial cell shape is most usually polygonal and partly determined by cytoplasmic features such as secretory granules. The basal surface of an epithelium lies in contact with a thin layer of filamentous protein and proteoglycan termed the basal lamina, which is synthesized predominantly by the epithelial cells. The basal lamina is described on p. 33.

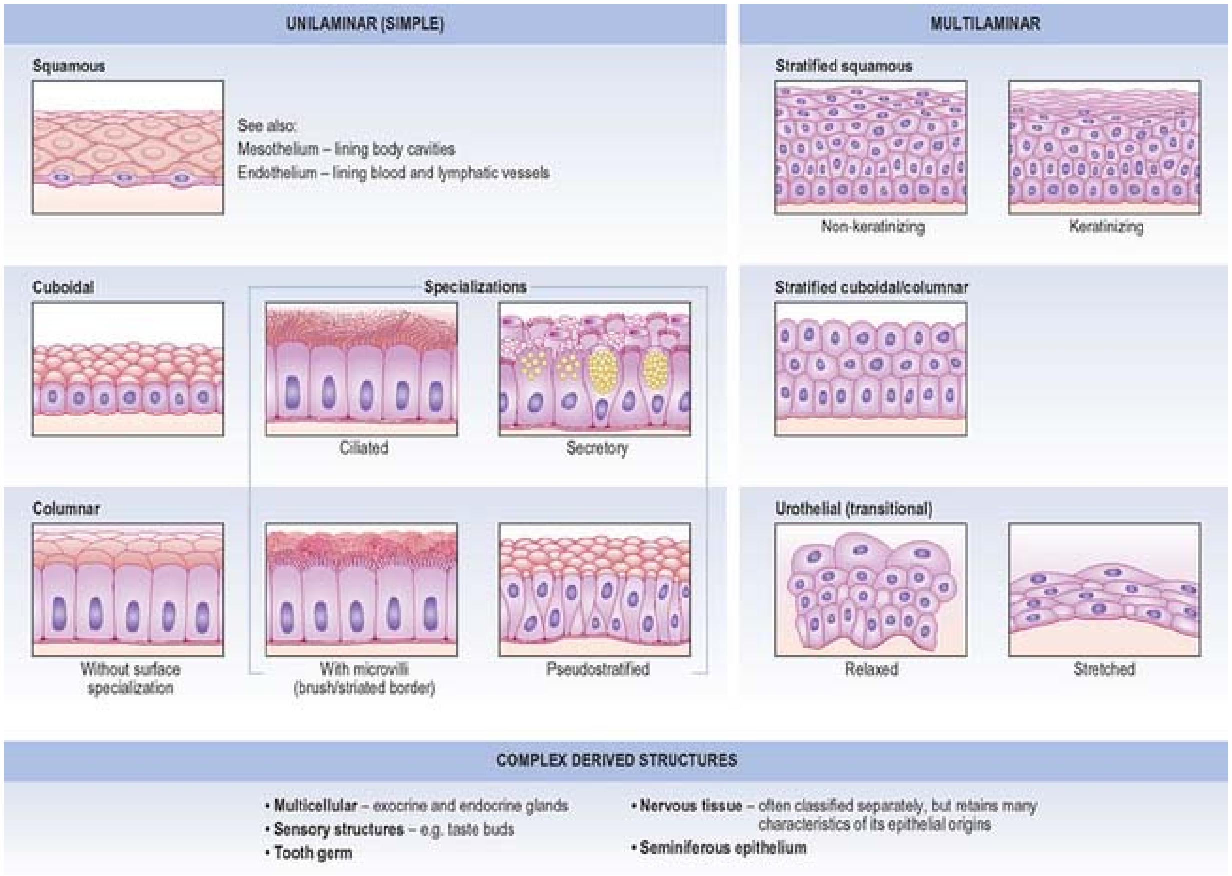
UNILAMINAR (SIMPLE)
MULTILAMINAR
Squamous
See also:
Mesothelium – lining body cavities
Endothelium – lining blood and lymphatic vessels
Stratified squamous
Non-keratinizing
Keratinizing
Cuboidal
Specializations
Ciliated
Secretory
Stratified cuboidal/columnar
Columnar
Without surface specialization
With microvilli (brush/striated border)
Pseudostratified
Urothelial (transitional)
Relaxed
Stretched
COMPLEX DERIVED STRUCTURES
• Multicellular – exocrine and endocrine glands
• Sensory structures – e.g. taste buds
• Tooth germ
• Nervous tissue – often classified separately, but retains many characteristics of its epithelial origins
• Seminiferous epithelium

Fig. 2.1 Classification of epithelial tissues and cells.

Epithelia can usually regenerate when injured. Indeed, many epithelia continuously replace their cells to offset cell loss caused by mechanical abrasion (reviewed in Blanpain et al 2007). Blood vessels do not penetrate typical epithelia and so cells receive their nutrition by diffusion from capillaries of neighbouring connective tissues. This arrangement limits the maximum thickness of living epithelial cell layers. Epithelia, together with their supporting connective tissue, can often be removed surgically as one layer, which is collectively known as a membrane. Where the surface of a membrane is moistened by mucous glands it is called a mucous membrane or mucosa (p. 39), whereas a similar layer of connective tissue covered by mesothelium is called a serous membrane or serosa (p. 39).

CLASSIFICATION

Epithelia can be classified as unilaminar (single-layered, simple), in which a single layer of cells rests on a basal lamina, or multilaminar, in which the layer is more than one cell thick. The latter includes: stratified squamous epithelia, in which superficial cells are constantly replaced from the basal layers; urothelium (transitional epithelium), which serves special functions in the urinary tract; and other multilaminar epithelia such as those lining the largest ducts of some exocrine glands, which, like urothelium, are replaced only very slowly under normal conditions. Seminiferous epithelium is a specialized multilaminar tissue found only in the testis.

Unilaminar (simple) epithelia

Unilaminar epithelia are further classified according to the shape of their cells, into squamous, cuboidal, columnar and pseudostratified types. Cell shape may, in some cases, be related to cell volume. Where little cytoplasm is present, there are generally few organelles and therefore low metabolic activity and cells are squamous or low cuboidal. Highly active cells, e.g. secretory epithelia, contain abundant mitochondria and endoplasmic reticulum and are typically tall cuboidal or columnar. Unilaminar epithelia can also be subdivided into those which have special functions, such as those with cilia, numerous microvilli, secretory vacuoles (in mucous and serous glandular cells), or sensory features. Myoepithelial cells, which are contractile, are found as isolated cells associated with glandular structures, e.g. salivary and mammary glands.

Squamous epithelium

Simple squamous epithelium is composed of flattened, tightly apposed, polygonal cells (squames). This type of epithelium is described as tessellated when the cells have complex, interlocking borders rather than straight boundaries. The cytoplasm may in places be only 0.1 µm thick and the nucleus usually bulges into the overlying space (Fig. 2.2A). These cells line the alveoli of the lungs, where their surface area is huge and cytoplasmic volume correspondingly large, and they form the outer capsular wall of renal corpuscles, the thin segments of the renal tubules and various parts of the inner ear. Because it is so thin, simple squamous epithelium allows rapid diffusion of gases and water across its surface; it may also engage in active transport, as indicated by the presence of numerous endocytic vesicles in these cells. Tight junctions between adjacent cells ensure that materials pass primarily through cells, rather than between them.

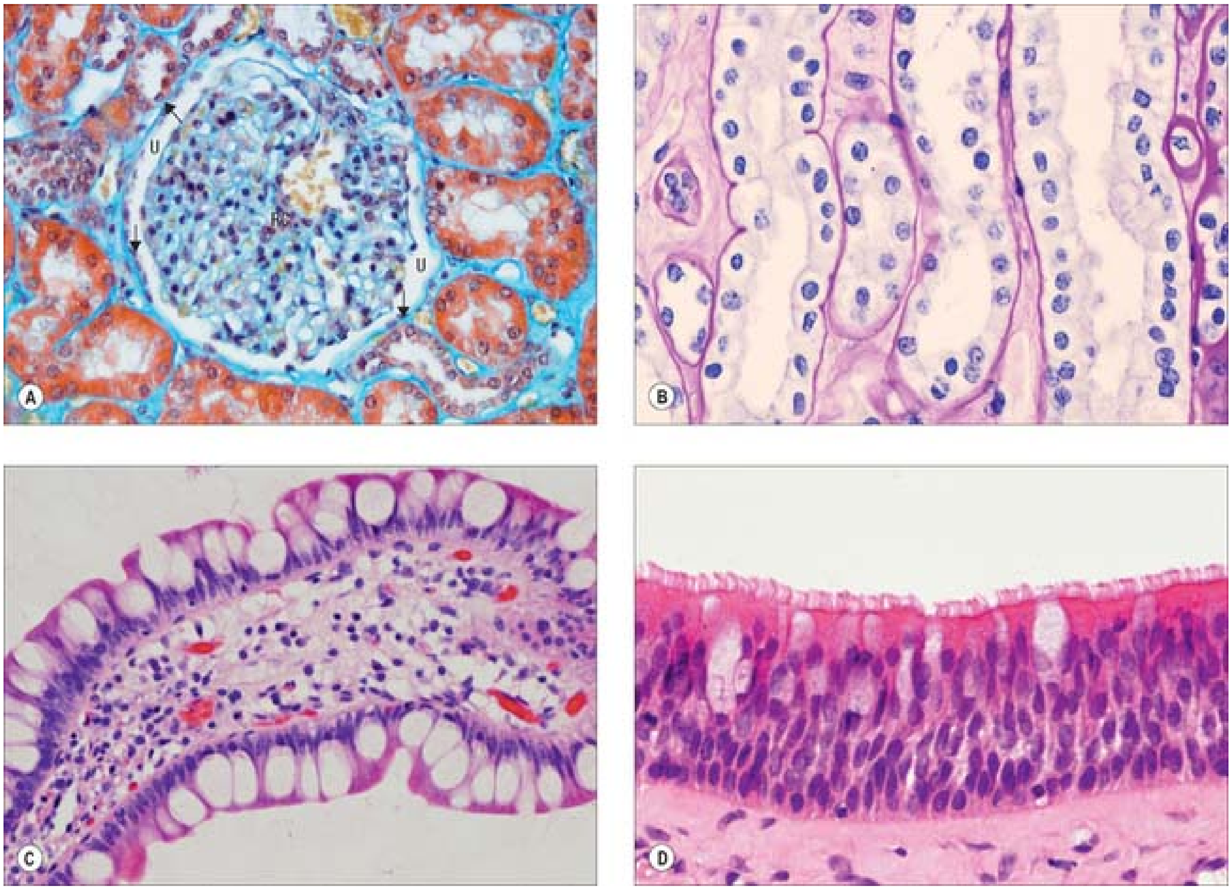

Fig. 2.2 **A**, Simple squamous epithelium lining the outer parietal layer (arrows) of Bowman’s capsule in the renal corpuscle (RC), stained with the trichrome, MSB. Oval epithelial nuclei project into the urinary space (U), within a highly attenuated cytoplasm. **B**, Simple cuboidal epithelium lining a group of collecting ducts sectioned longitudinally in the renal medulla. The basement membranes are stained magenta with periodic–acid Schiff (PAS) reagent. **C**, Simple columnar epithelium covering the tip (off field,

right) of a villus in the ileum. Tall, columnar absorptive cells with oval, vertically-orientated nuclei, bear a striated border of microvilli, just visible as a deeper-stained apical fringe. Numerous, interspersed goblet cells are present, with pale apical cytoplasm filled with mucinogen secretory granules and dark, flattened, basally-situated nuclei. **D**, Ciliated columnar pseudostratified epithelium in the respiratory tract, and interspersed goblet cells, with pale, mucinogen granule-filled apical cytoplasm. All human tissues.

Cuboidal and columnar epithelia

Cuboidal and columnar epithelia consist of regular rows of cylindrical cells (Fig. 2.2B, Fig. 2.2C). Cuboidal cells are approximately square in vertical section, whereas columnar cells are taller than their diameter, and both are polygonal when sectioned horizontally. Commonly, microvilli (Ch. 1) are found on their free surfaces, which considerably increases the absorptive area, e.g. in the epithelia of the small intestine (columnar cells with a striated border of very regular microvilli), the gallbladder (columnar cells with a brush border) and proximal convoluted tubules of the kidney (large cuboidal to low columnar cells with brush borders).

Ciliated columnar epithelium lines most of the respiratory tract, except for the lower pharynx and vocal folds, and it is pseudostratified (Fig. 2.2D) as far as the larger bronchioles; some of the tympanic cavity and auditory tube; the uterine tube; the efferent ductules of the testis. Submucosal mucous glands and mucosal goblet cells secrete mucus on to the luminal surface of much of the respiratory tract and cilia sweep a layer of mucus and trapped dust particles etc., from the lung towards the pharynx in the mucociliary rejection current, which clears the respiratory passages of inhaled particles. Cilia in the uterine tube assist the passage of oocytes and fertilized ova to the uterus (Ch. 77).

Some columnar cells are specialized for secretion and aggregates of such cells may be described as glandular tissue. Their apical domains (p. 4) typically contain mucus- or protein-filled (zymogen) vesicles, e.g. mucin-secreting and chief cells of the gastric epithelium. Where mucous cells lie among non-secretory cells, e.g. in the intestinal epithelium, their apical cytoplasm and its secretory contents often expand to produce a characteristic cell shape, and they are known as goblet cells (Fig. 2.2D). For further details of glandular tissue, see page 31 and for the characteristics of mucus, see page 39.

Pseudostratified epithelium

Pseudostratified epithelium is a single-layered (simple) columnar epithelium in which nuclei lie at different levels in a vertical section (Fig. 2.2D). All cells are in contact with the basal lamina throughout their lifespan, but not all cells extend through the entire thickness of the epithelium. Some constitute an immature basal cell layer of smaller cells, which are often mitotic and able to replace damaged mature cells. Migrating lymphocytes and mast cells within columnar epithelia may also give a similar, pseudostratified appearance because their nuclei are found at different depths. Much of the ciliated lining of the respiratory tract is of the pseudostratified type, and so is the sensory epithelium of the olfactory area.

Sensory epithelia

Sensory epithelia are found in special sense organs of the olfactory, gustatory and vestibulocochlear receptor systems. All of these contain sensory cells surrounded by supportive, non-receptor cells. Olfactory receptors are modified neurones, and their axons pass directly to the brain, but the other types are specialized epithelial cells that synapse with terminals of afferent (and sometimes efferent) nerve fibres.

Myoepithelial cells

Myoepithelial cells, which are also sometimes termed basket cells, are fusiform or stellate in shape (Fig. 2.3), contain actin and myosin filaments, and contract when stimulated by nervous or endocrine signals. They surround the secretory portions and ducts of some glands, e.g. mammary, lacrimal, salivary and sweat glands, and lie between the basal lamina and the glandular or ductal epithelium. Their contraction assists the initial flow of secretion into larger conduits. Myoepithelial cells are ultrastructurally similar to smooth muscle cells in the arrangement of their actin and myosin, but differ from them because they originate, like the glandular cells, from embryonic ectoderm or endoderm. They can be identified immunohistochemically on the basis of the co-localization of myofilament proteins (which signify their contractile function), and keratin intermediate filaments (which accords with their epithelial lineage).

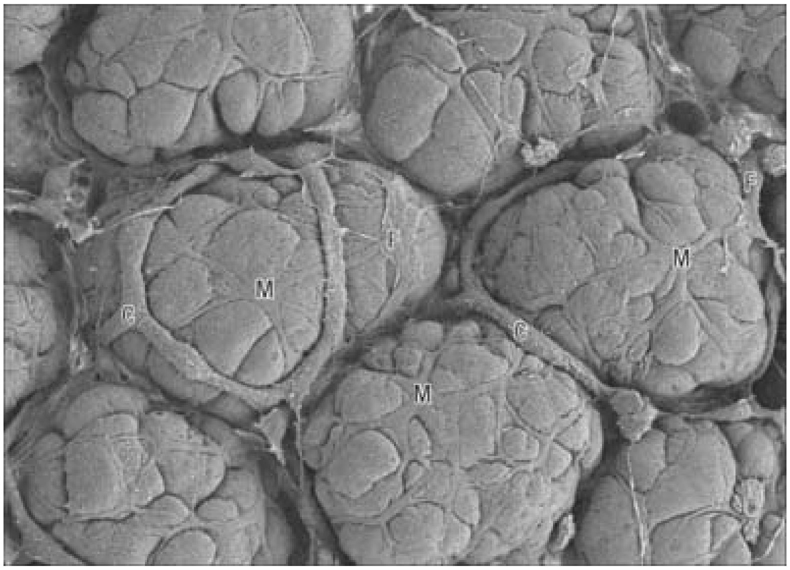

Fig. 2.3 Stellate myoepithelial cells (M) wrapped around secretory acini in the lactating mouse mammary gland, seen in the scanning electron microscope after enzymatic depletion of extracellular matrix. Blood capillaries (C) and fibroblasts (F) are also indicated.

(By courtesy of Prof. Toshikazu Nagato, Fukuoka Dental College, Japan.)

Multilaminar (stratified) epithelia

Multilaminar epithelia are found at surfaces subjected to mechanical damage or other potentially harmful conditions. They can be divided into those which continue to replace their surface cells from deeper layers, designated stratified squamous epithelia, and others in which replacement is extremely slow except after injury.

Stratified squamous epithelia

Stratified squamous epithelia are multilayered tissues in which the formation, maturation and loss of cells is continuous, although the rates of these processes can change, e.g. after injury. New cells are formed in the most basal layers by the mitotic division (p. 21) of stem cells and transit (or transient) amplifying cells. The daughter cells move more superficially, changing gradually from a cuboidal shape to a more flattened form and are eventually shed from the surface as a highly flattened squame. Typically, the cells are held together by numerous desmosomes to form strong, contiguous cellular sheets that provide protection to the underlying tissues against mechanical, microbial and chemical damage. Stratified squamous epithelia may be broadly subdivided into keratinized and non-keratinized types.

Keratinized epithelium

Keratinized epithelium (Fig. 2.4A) is found at surfaces that are subject to drying or mechanical stresses, or are exposed to high levels of abrasion. These include the entire epidermis and the mucocutaneous junctions of the lips, nostrils, distal anal canal, outer surface of the tympanic membrane and parts of the oral lining (gingivae, hard palate and filiform papillae on the anterior part of the dorsal surface of the tongue). Their cells, keratinocytes, are described in more detail on page 146. A distinguishing feature of keratinized epithelia is that cells of the superficial layer, the stratum corneum, are anucleate, dead, flattened squames that eventually flake off from the surface. In addition, the tough keratin intermediate filaments become firmly embedded in a matrix protein. This unusual combination of strongly coherent layers of living cells and more superficial strata made of plates of inert, mechanically robust protein complexes, interleaved with water-resistant lipid, makes this type of epithelium an efficient barrier against different types of injury, microbial invasion and water loss.

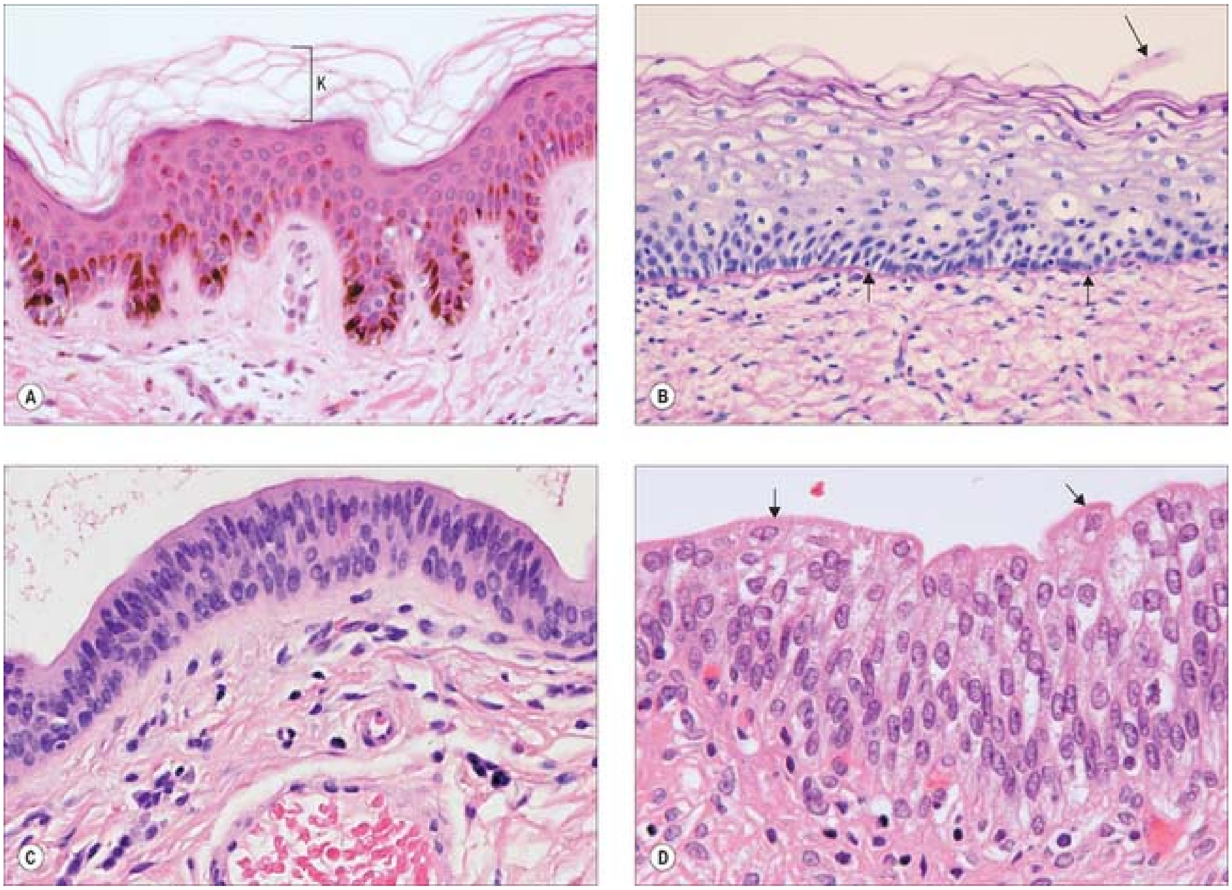

Fig. 2.4 **A**, Keratinized stratified squamous epithelium in thin skin. Pigmented melanocytes are seen in the basal layer and a few keratinocytes of the prickle cell layer also contain melanin granules. The dead, keratinized layer (K) lacks nuclei. **B**, Non-keratinized stratified squamous epithelium of the uterine ectocervix, stained with periodic–acid Schiff (PAS) reagent. The basement membrane (short arrows) and superficial squames, which retain their nuclei, are PAS-positive; squames sloughing off the surface are indicated (long arrow). **C**, Stratified low columnar epithelium of an interlobular excretory duct of the sublingual salivary gland. **D**, Urothelium (transitional epithelium) lining the relaxed urinary bladder. The most superficial cells have a thickened plasma membrane as a result of the presence of intramembranous plaques, which give an eosinophilic appearance to the luminal surface (arrows). All human tissues.

Non-keratinized epithelium

Non-keratinized epithelium is present at surfaces that are subject to abrasion but protected from drying (Fig. 2.4B). These include: the buccal cavity (except for the areas noted above); oropharynx and laryngopharynx; oesophagus; part of the anal canal; vagina; distal uterine cervix; distal urethra; cornea; inner surfaces of the eyelids; the vestibule of the nasal cavities. Cells go through the same transitions in general shape as are seen in the keratinized type, but they do not fill completely with keratin or secrete glycolipid, and they retain their nuclei until they desquamate at the surface. In sites where considerable abrasion occurs, e.g. parts of the buccal cavity, the epithelium is thicker and its most superficial cells may partly keratinize, so that it is referred to as parakeratinized, in contrast to the orthokeratinized state of fully keratinized epithelium. Diets deficient in vitamin A may induce keratinization of such epithelia, and excessive doses may lead to its transformation into mucus-secreting epithelium.

Stratified cuboidal and columnar epithelia

Two or more layers of cuboidal or low columnar cells (Fig. 2.4C) are typical of the walls of the larger ducts of some exocrine glands, e.g. the pancreas, salivary glands and the ducts of sweat glands and they presumably provide more strength than a single layer. Parts of the male urethra are also lined by stratified columnar epithelium. The layers are not continually replaced by basal mitoses and there is no progression of form from base to surface, but they can repair themselves if damaged.

Urothelium (urinary or transitional epithelium)

Urothelium (Fig. 2.4D) is a specialized epithelium that lines much of the urinary tract and prevents its rather toxic contents from damaging surrounding structures. It extends from the ends of the collecting ducts of the kidneys, through the ureters (p. 1242) and bladder (p. 1250), to the proximal portion of the urethra. In males it covers the urethra as far as the ejaculatory ducts, then becomes intermittent and is finally replaced by stratified columnar epithelium in the membranous urethra. In females it extends as far as the urogenital membrane. During development, part of it is derived from mesoderm and part from ectoderm and endoderm.

The epithelium appears to be four to six cells thick, and lines organs that undergo considerable distension and contraction. It can therefore stretch greatly without losing its integrity. In stretching, the cells become flattened, without altering their positions relative to each other, as they are firmly connected by numerous desmosomes. However, the urothelium appears to be reduced to two or three cells thick. The epithelium is called transitional because of the apparent transition between a stratified cuboidal epithelium and a stratified squamous epithelium, which occurs as it is stretched to accommodate urine, particularly in the bladder. The basal cells are basophilic, with many ribosomes, uninucleate (diploid), and are cuboidal when relaxed. More apically, they form large binucleate, or, more often, polyploid uninucleate cells. The surface cells are largest and may even be octaploid: in the relaxed state, they typically bulge into the lumen as dome-shaped cells with a thickened, eosinophilic glycocalyx or cell coat (p. 4). Their luminal surfaces are covered by a specialized plasma membrane in which plaques of intramembranous glycoprotein particles are embedded. These plaques stiffen the membrane. When the epithelium is in the relaxed state, and the surface area of the cells is reduced, the plaques are partially internalized by the hinge-like action of the more flexible interplaque membrane regions. They re-emerge onto the surface when it is stretched.

Normally, cell turnover is very slow; cell division is infrequent and is restricted to the basal layer. However, when damaged, the epithelium regenerates quite rapidly.

Seminiferous epithelium

Seminiferous epithelium is a highly specialized, complex stratified epithelium. It consists of a heterogeneous population of cells that form the lineage of the spermatozoa (spermatogonia, spermatocytes, spermatids), together with supporting cells (Sertoli cells). It is described in detail in Chapter 76 (p. 1266).

GLANDS

One of the features of many epithelia is their ability to alter the environment facing their free surfaces by the directed transport of ions, water or macromolecules. This is particularly well demonstrated in glandular tissue, in which the metabolism and structural organization of the cells is specialized for the synthesis and secretion of macromolecules, usually from the apical surface. Such cells may exist in isolation amongst other non-secretory cells of an epithelium, e.g. goblet cells in the absorptive lining of the small intestine, or may form highly coherent sheets of epithelium with a common secretory function, e.g. the mucous lining of the stomach and, in a highly invaginated structure, the complex salivary glands.

Glands may be subdivided into exocrine glands and endocrine glands. Exocrine glands secrete, usually via a duct, onto surfaces that are continuous with the exterior of the body, including the alimentary tract, respiratory system, urinary and genital ducts and their derivatives, and the skin. Endocrine glands are ductless and secrete hormones directly into interstitial fluid and thence the circulatory system, which conveys them throughout the body to affect the activities of other cells. In addition to strictly epithelial glands, some tissues derived from the nervous system, including the suprarenal medulla (p. 1200) and neuro-hypophysis (p. 321), are neurosecretory.

Paracrine glandular cells are similar to endocrine cells, but their secretions diffuse locally to cellular targets in the immediate vicinity; many of these are classed as neuroendocrine cells since they secrete molecules used elsewhere in the nervous system as neurotransmitters or neuromodulators (Ch. 3). Modes of signalling by secretory cells are illustrated in Fig. 1.6.

EXOCRINE GLANDS

Types of secretory process

The mechanism of secretion varies considerably. If the secretions are initially packaged into membrane-bound vesicles, these are conveyed to the cell surface (p. 9), where they are discharged. In merocrine secretion, which is by far the most common secretory mechanism, vesicle membranes fuse with the plasma membrane to release their contents to the exterior (Fig. 2.5). Specialized transmembrane molecules in the secretory vesicle wall recognize marker proteins on the cytoplasmic side of the plasma membrane and bind to them. This initiates interactions with other proteins that cause the fusion of the two membranes and the consequent release of the vesicle contents. The stimulus for secretion varies with the type of cell, but often appears to involve a rise in intracellular calcium. Glands such as the simple sweat glands of the skin, where ions and water are actively transported from plasma as an exudate, were once classified as eccrine glands. They are now known to synthesize and secrete small amounts of protein by a merocrine mechanism, and are thus reclassified as merocrine glands.

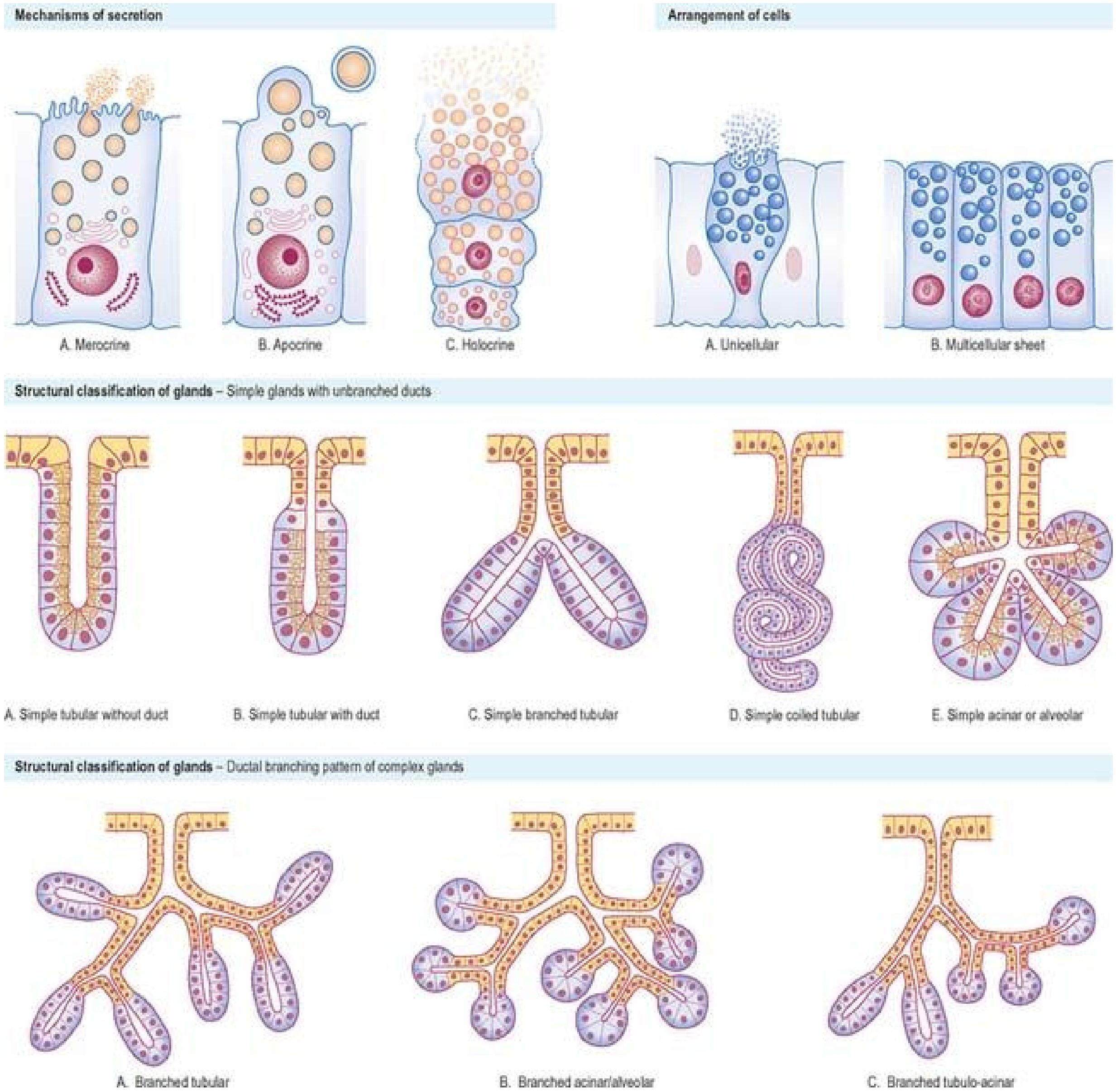
Mechanisms of secretion
A. Merocrine
B. Apocrine
C. Holocrine
Arrangement of cells
A. Unicellular
B. Multicellular sheet
Structural classification of glands – Simple glands with unbranched ducts
A. Simple tubular without duct
B. Simple tubular with duct
C. Simple branched tubular
D. Simple coiled tubular
E. Simple acinar or alveolar
Structural classification of glands – Ductal branching pattern of complex glands
A. Branched tubular
B. Branched acinar/alveolar
C. Branched tubulo-acinar

Fig. 2.5 Classification of the different types of epithelial gland.

In apocrine glands, some of the apical cytoplasm is pinched off with the contained secretions, which are stored in the cell as membrane-free droplets (Fig. 2.5). The best understood example of this is the secretion of milk fat by mammary gland cells (p. 936), in which a small amount of cytoplasm is incorporated into the plasma membrane-bound lipid globule as it is released from the cell. Larger amounts of cytoplasm are included in secretions by specialized apocrine sweat glands in the axilla and anogenital regions of the body. In some tissues there is a combination of different types of secretion, e.g. mammary gland cells secrete milk fat by apocrine secretion and milk protein, casein, by merocrine secretion.

In holocrine glands (Fig. 2.5), e.g. sebaceous glands in the skin, the cells first fill with secretory products (lipid droplets or sebum, in this instance) and then the entire cell disintegrates to liberate the accumulated mass of secretion into the duct or, more usually, hair follicle.

Structural and functional classification

Exocrine glands are either unicellular or multicellular. The latter may be in the form of simple sheets of secretory cells, e.g. the lining of the stomach, or may be structurally more complex and invaginated to a variable degree. Such glands (Fig. 2.5) may be simple units or their connection to the surface may be branched. Simple unbranched tubular glands exist in the walls of many of the hollow viscera, e.g. the small intestine and uterus, whereas some simple glands have expanded, flask-like ends (acini or alveoli). Such glands may consist entirely of secretory cells, or may have a blind-ending secretory portion that leads through a non-secretory duct to the surface, in which case the ducts may modify the secretions as they pass along them.

Glands with ducts may be branched (compound), and sometimes form elaborate ductal trees. Such glands generally have acinar or alveolar secretory lobules, as in the exocrine pancreas, but the secretory units may alternatively be tubular or mixed tubulo-acinar. More than one type of secretory cell may occur within a particular secretory unit, or individual units may be specialized to just one type of secretion (e.g. serous acini of salivary glands).

Exocrine glands are also classified by their secretory products. Secretory cells in mucus-secreting or mucous glands have frothy cytoplasm and basal, flattened nuclei. They stain deeply with metachromatic stains and periodic acid–Schiff (PAS) methods that detect carbohydrate residues. However, in general (i.e. non-specific) histological preparations they are weakly stained because much of their content of water-rich mucin is extracted by the processing procedures. Secretory cells in serous glands have centrally placed nuclei and eosinophilic secretory storage granules in their cytoplasm. They secrete mainly glycoproteins (including lysozyme) and digestive enzymes.

Some glands are almost entirely mucous (e.g. the sublingual salivary gland), whereas others are mainly serous (e.g. the parotid salivary gland). The submandibular gland is mixed, in that some lobules are predominantly mucous and others serous. In some regions, mucous acini share a lumen with clusters of serous cells (seen in routine preparations as serous demilunes). Although this simple approach to classification is useful for general descriptive purposes, the diversity of molecules synthesized and secreted by glands is such that complex mixtures often exist within the same cell.

ENDOCRINE GLANDS

Endocrine glands secrete directly into connective tissue interstitial fluid and the circulation. Their cells are grouped around beds of capillaries or sinusoids (p. 133) which typically are lined by fenestrated endothelia (Ch. 6) to allow the rapid passage of macromolecules through their walls. Endocrine cells may be arranged in clusters within vascular networks, in cords between parallel vascular channels or as hollow structures (follicles) surrounding their stored secretions. In addition to the cells of specialized ductless endocrine glands (e.g. pituitary, pineal, thyroid and parathyroid), hormone-producing cells also form components of other organ systems. These include: the cells of the pancreatic islets; thymic epithelial cells; renin-secreting cells of the kidney juxtaglomerular apparatus; erythropoietin-secreting cells of the kidney; circumventricular organs; interstitial testicular (Leydig) cells; interstitial follicular and luteal ovarian cells; in pregnancy, placental cells. Some cardiac myocytes, particularly in the walls of the atria, also have endocrine functions. These are all described within the appropriate regional sections.

Isolated endocrine cells also exist scattered amongst other tissues as part of the dispersed (diffuse) neuroendocrine system (p. 56), e.g. throughout the alimentary and respiratory tracts. Neuroendocrine cells are generally situated within a mucosal epithelium and their bases often rest on the basal lamina (see below). In response to an external stimulus, they secrete their product basally into interstitial fluid. A typical neuroendocrine cell is shown in Fig. 2.6. The secretory granules vary in shape, size and ultrastructure in the different cell types, many of which take the name of their secretion, e.g. gastrin-secreting G cells of the small intestine. Neuroendocrine cells share many of their secretory products with chemical mediators (p. 47) in the nervous system.

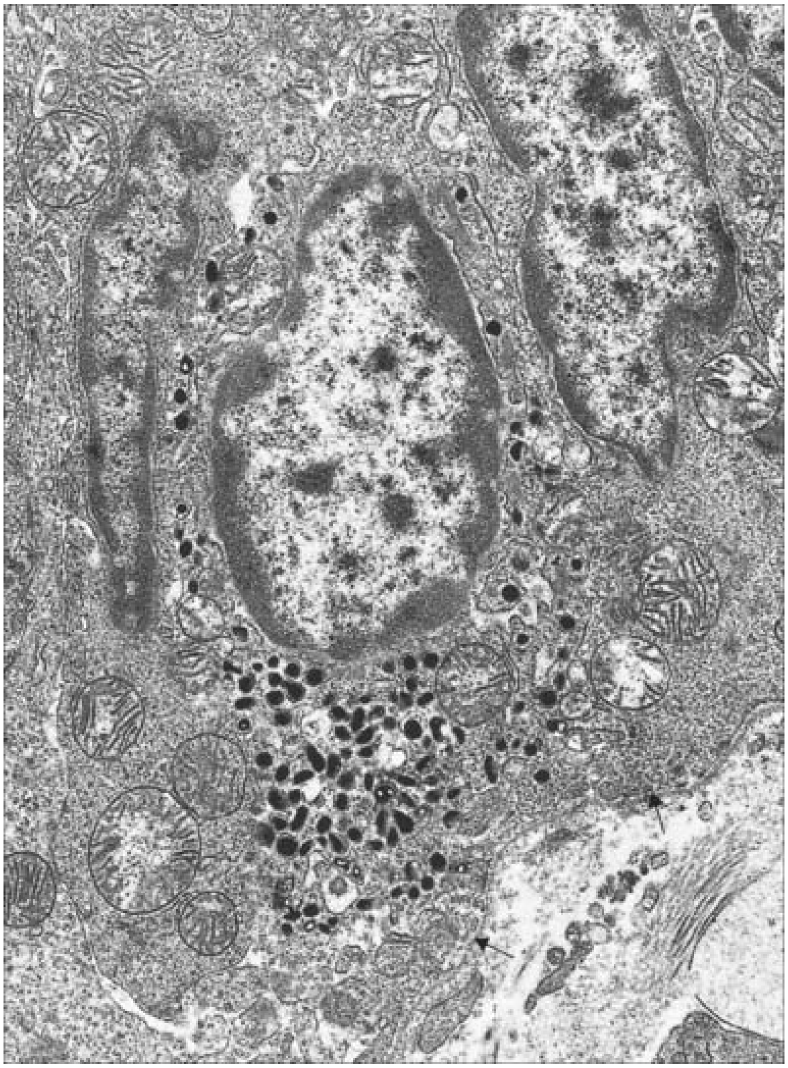

Fig. 2.6 Electron micrograph of a neuroendocrine cell between two absorptive cells in the colon (rat tissue). Dense neurosecretory granules are seen in the basal cytoplasm, apposed to the basal lamina (arrows).

(By courtesy of Michael Crowder.)

CONTROL OF GLANDULAR SECRETION

The activities of cells in the various tissue and organ systems of the body are tightly regulated by the coordinated activity of the endocrine and autonomic nervous systems (Ch. 15). Endocrine (and paracrine) signals (Ch. 1) reach target cells in interstitial fluid, often via blood plasma, and together with autonomic nervous signals they ensure that the body responds to normal physiological stimuli and adjusts to changes in the external environment. Hormone secretion is itself controlled in a number of ways, e.g. by neural control, regulatory feedback loops or according to various cyclical, rhythmical or pulsatile patterns of release. Endocrine glands have a rich vascular supply and their blood flow is controlled by autonomic vasomotor nerves, which can thus modify glandular activity.

Glandular activity may also be controlled directly by autonomic secretomotor fibres, which may either form synapses on the bases of gland cells (e.g. in the suprarenal medulla) or release neuromediators in the vicinity of the glands, to reach them by diffusion. Alternatively, the autonomic nervous system may act indirectly on gland cells, e.g. on neuroendocrine G cells via histamine, released neurogenically from another neuroendocrine cell in the gastric lining (Ch. 65). Such paracrine activities of neuroendocrine cells (Ch. 1) are important in the respiratory, as well as the gastrointestinal system. Circulating hormones from the adenohypophysis stimulate synthesis and secretion by target cells in many endocrine glands. Such signals, mostly detected by receptors at the cell surface and mediated by second messenger systems, may increase the synthetic activity of gland cells, and may cause them to discharge their secretions by exocytosis. Secretions from certain exocrine glandular cells are expressed rapidly from those glands by the contraction of associated myoepithelial cells (Fig. 2.3) that enclose the secretory units and smaller ducts. Myoepithelial cells may be under direct neural control, as in the salivary glands, or they may respond to circulating hormones, e.g. such cells in the mammary gland respond to the concentration of circulating oxytocin.

Feedback loops and endocrine axes

The pituitary gland, in particular the adenohypophysis, is often termed the master gland, because of its central role in endocrine physiological processes. It provides the means by which the central nervous system regulates and integrates, by non-neural mechanisms, the widespread functions of the body, including the activities of other endocrine glands and, often indirectly, exocrine glands such as the breast. Regulatory hormones from the adenohypophysis stimulate synthesis and secretion in target cells of many endocrine glands; these glands therefore respond to, in addition to generating, hormonal signals.

The hypothalamus of the brain and the adenohypophysis are central to most regulatory feedback loops within the endocrine system. Loops can be either positive or negative, e.g. the hypothalamus stimulates release of follicle stimulating hormone (FSH) by the adenohypophysis, which in turn stimulates ovarian follicular maturation and secretion of oestradiol, which acts on breast and endometrial target tissues. Oestradiol, in this case, also acts back on the adenohypophysis and hypothalamus to reinforce their function positively in a feedback loop. In contrast, hypothalamic and adenohypophysial stimulation of testicular production of testosterone, which acts on targets such as skeletal muscle, are negatively regulated in a feedback loop generated by circulating testosterone. Such negative feedback regulation is a widely utilized physiological mechanism.

BASEMENT MEMBRANE AND BASAL LAMINA

There is a narrow layer of extracellular matrix (p. 36), which stains strongly for carbohydrates, at the interface between connective and other tissues, e.g. between epithelia and their supporting connective tissues. In early histological texts this layer was termed the basement membrane. As almost all of its components are synthesized by the epithelium or other tissue (e.g. muscle), rather than the adjacent connective tissue, it will be discussed here.

Electron microscopy revealed that the basement membrane is composed of two distinct components. A thin, finely fibrillar layer, the basal lamina, is associated closely with the basal cell surface (Fig. 2.7). A variable reticular lamina of larger fibrils and glycosaminoglycans of the extracellular matrix underlies this layer and is continuous with the connective tissue proper, although it is much reduced or largely absent in some tissues, e.g. surrounding muscle fibres, Schwann cells and capillary endothelia. In other tissues, the basal lamina separates two layers of cells and there are no intervening typical connective tissue elements. This occurs in the thick basal lamina of the renal glomerular filter (p. 1238) and the basal lamina of the thin portions of the lung interalveolar septa across which gases exchange between blood and air (p. 998).

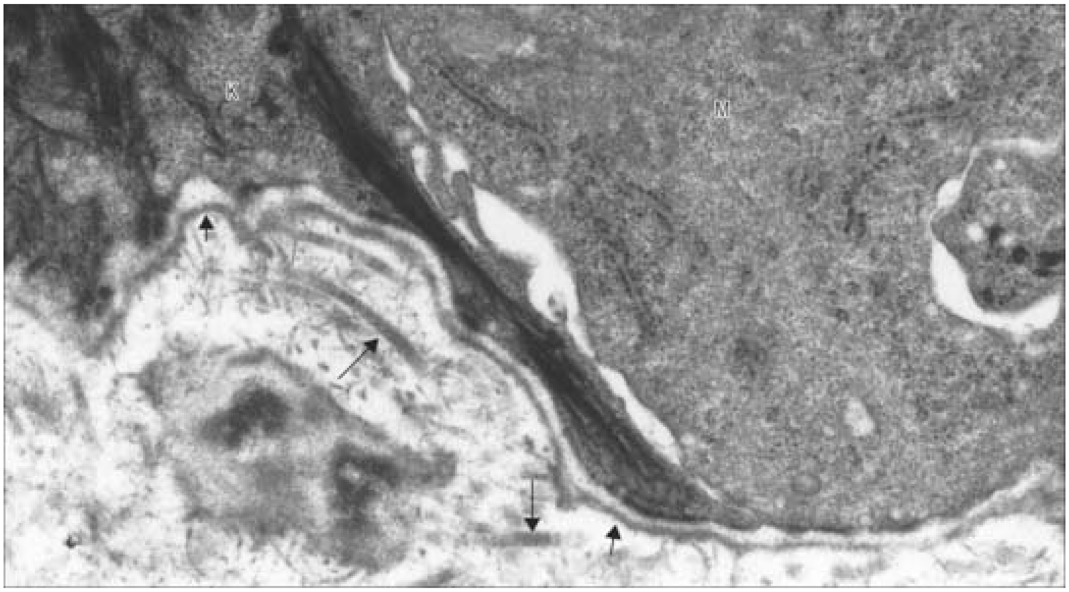

Fig. 2.7 The basal lamina as seen in an electron micrograph, underlying the basal epithelial layer of human skin. The finely fibrillar dense layer (short arrows) corresponds to the lamina densa and fine collagen fibrils (long arrows) lie in the subjacent connective tissue. These contribute to the appearance of the basement membrane in light microscope preparations stained for carbohydrate-rich structures. The cell on the left is a keratinocyte (K) with dense keratin filaments in its cytoplasm, anchoring into contacts with the basal lamina, and the cell on the right is a melanocyte (M).

The basal lamina is usually about 80 nm thick, varying between 40 and 120 nm, and consists of a sheet-like fibrillar layer, the lamina densa (20–50 nm wide), separated from the plasma membrane of the cell it supports by a narrow electron-lucent zone, the lamina lucida. The lamina lucida is absent from tissues prepared by rapid freezing and so may be an artefact. In many tissues this zone is crossed by integral plasma membrane proteins, e.g. keratinocyte hemidesmosomes (Chs 1 and 7) are anchored into the lamina densa in the basal lamina of the epidermis. The basal lamina is a delicate felt-like network composed largely of two glycoprotein polymers, laminin and type IV collagen, which self-assemble into two-dimensional sheets interwoven with each other. Early embryonic basal lamina is formed only of the laminin polymer. Two other molecules cross-link and stabilize the network: entactin (nidogen) and perlecan (a large heparan sulphate proteoglycan).

Although all basal laminae have a similar form, their thickness and precise molecular composition vary between tissues and even within a tissue, e.g. between the crypts and villi of the small intestine. The isoforms of laminin and collagen type IV differ in various tissues, thus Schwann cells and muscle cells express laminin-2 (merosin) rather than the prototypical laminin-1. Laminin-5, although not itself a basal lamina component, is found in the hemidesmosomes of the basal epidermis and links the basal lamina with epidermal transmembrane proteins, α_6 β_4 integrin and collagen type XVII (formerly known as bullous pemphigoid antigen, one of the targets of the autoimmune blistering skin disease, bullous pemphigoid). The particular isoform of collagen type IV in the basal lamina of different tissues is reflected in tissue-specific disease patterns. Mutations in a collagen expressed by muscle and kidney glomeruli cause Alport’s syndrome, a form of renal failure. Renal failure also occurs in Goodpasture’s syndrome, in which renal basal lamina collagen is targeted by autoantibodies.

In Descemet’s membrane in the cornea, collagen type VIII replaces collagen type IV in the much thickened (increasing with age, up to 10 µm,) endothelial basal lamina. The basal lamina of the neuromuscular junction (p. 62) contains agrin, a heparan sulphate proteoglycan, which plays a part in the clustering of muscle acetylcholine receptors in the plasma membrane at these junctions.

RETICULAR LAMINA

The reticular lamina consists of a dense extracellular matrix that contains collagen. In skin, it contains fibrils of type VII collagen (anchoring fibrils), which bind the lamina densa to the adjacent connective tissue. The high concentration of proteoglycans in the reticular lamina is responsible for the positive reaction of the entire basement membrane to stains for carbohydrates, seen in sections prepared for light microscopy.

FUNCTIONS OF BASAL LAMINA

Basal laminae perform a number of important roles (Iozzo 2005). They form selectively permeable barriers (anionic filters) between adjacent tissues, e.g. in the glomerular filter of the kidney; they anchor epithelial and connective tissues and so stabilize and orientate the tissue layers; they may exert instructive effects on adjacent tissues, and so determine their polarity, rate of cell division, cell survival etc.; they regulate angiogenesis. In addition, they may act as pathways for the migration and pathfinding of growing cell processes, both in development and in tissue repair, e.g. in guiding the outgrowth of axons and the reestablishment of neuromuscular junctions during regeneration after injury in the peripheral nervous system. Changes in basal lamina thickness are often associated with pathological conditions, e.g. the thickening of the glomerular basal lamina in glomerulonephritis and diabetes.

CONNECTIVE AND SUPPORTING TISSUES

The connective tissues are defined as those composed predominantly of intercellular material, the extracellular matrix, which is secreted mainly by the connective tissue cells. The cells are therefore usually widely separated by their matrix, which is composed of fibrous proteins and a relatively amorphous ground substance (Fig. 2.8). Many of the special properties of connective tissues are determined by the composition of the matrix, and their classification is also largely based on its characteristics. In some types of connective tissue, the cellular component eventually dominates the tissue, even though the tissue originally has a high matrix:cell ratio, e.g. adipose tissue. Connective tissues are derived from embryonic mesoderm or, in the head region, largely from neural crest.

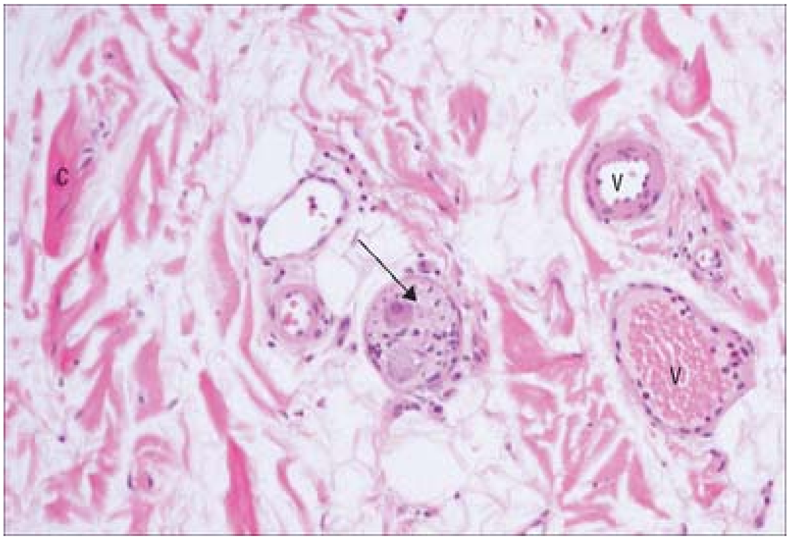

Fig. 2.8 General loose connective tissue (human), with bundles of collagen fibres (C) within an amorphous ground substance, penetrated by blood vessels (V), lymphatics and nerves. A small autonomic ganglion is arrowed.

Connective tissues have several essential roles in the body. These may be subdivided into structural roles, which largely reflect the special mechanical properties of the extracellular matrix components, and defensive roles, in which the cellular component has the dominant role. Connective tissues often also play important trophic and morphogenetic parts in organizing and influencing the growth and differentiation of surrounding tissues, e.g. in the development of glands from an epithelial surface.

Structural connective tissues are divided into ordinary (or general) types, which are widely distributed, and special skeletal types, i.e. cartilage and bone, which are described in Chapter 5. A third type, haemolymphoid tissues, consists of peripheral blood cells, lymphoid tissues and their precursors; these tissues are described in Chapter 4. They are often grouped with other types of connective tissue, because of their similar mesenchymal origins and because the various defensive cells of the blood also form part of a typical connective tissue cell population. They reach connective tissues via the blood circulation and migrate into them through the endothelial walls of vessels.

CELLS OF GENERAL CONNECTIVE TISSUES

Cells of general connective tissues can be separated into the resident cell population (fibroblasts, adipocytes, mesenchymal stem cells, etc.) and a population of migrant cells with various defensive functions (macrophages, lymphocytes, mast cells, neutrophils and eosinophils), which may change in number and moderate their activities according to demand. Embryologically, fibroblasts and adipocytes arise from mesenchymal stem cells, some of which may remain in the tissues to provide a source of replacement cells postnatally. As noted above, the cells of haemopoietic origin migrate into the tissue from bone marrow and lymphoid tissue.

Resident cells

Fibroblasts

Fibroblasts are usually the most numerous resident cells. They are flattened and irregular in outline, with extended processes, and in profile they appear fusiform or spindle-shaped (Fig. 2.9; see also Fig. 2.11). Fibroblasts synthesize most of the extracellular matrix of connective tissue (Fig. 2.9); accordingly they have all the features typical of cells active in the synthesis and secretion of proteins. Their nuclei are relatively large and euchromatic and possess prominent nucleoli. In young, highly active cells, the cytoplasm is abundant and basophilic (reflecting the high concentration of rough endoplasmic reticulum), mitochondria are abundant and several sets of Golgi apparatus are present. In old and relatively inactive fibroblasts (often termed fibrocytes) the cytoplasmic volume is reduced, the endoplasmic reticulum is sparse and the nucleus is flattened and heterochromatic.

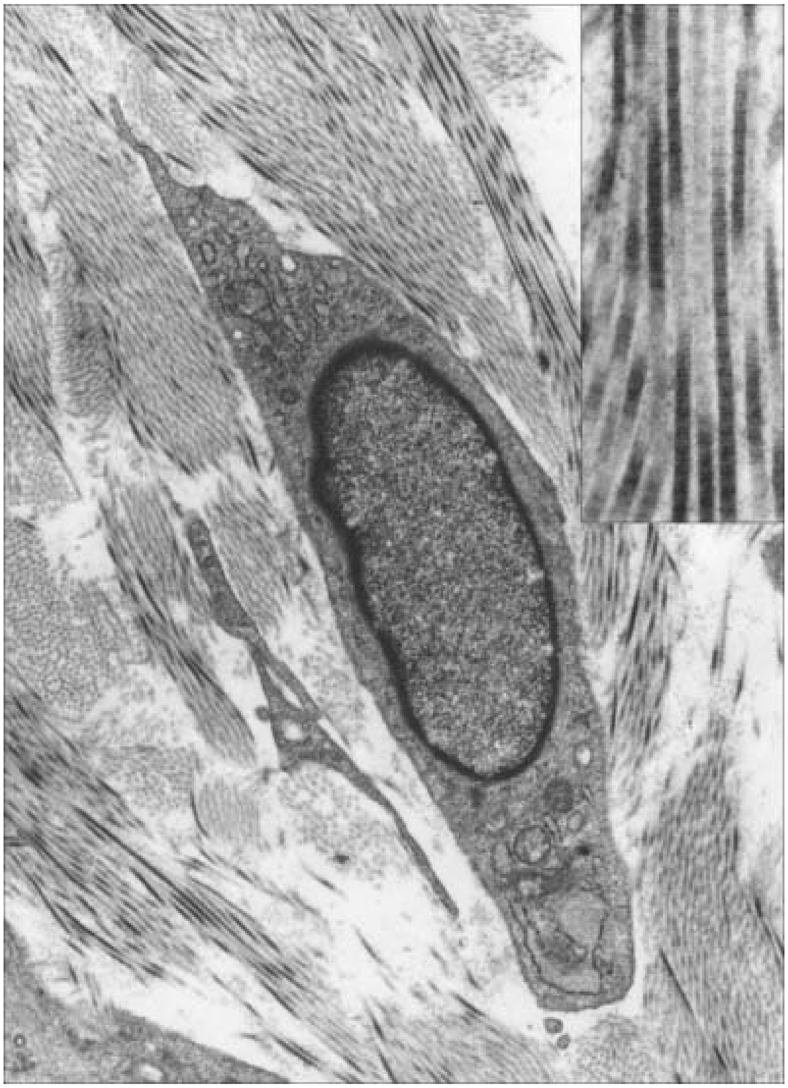

Fig. 2.9 Electron micrograph of a fibroblast in human connective tissue, surrounded by bundles of finely banded collagen fibrils (shown at high magnification in the insert) which they secrete.

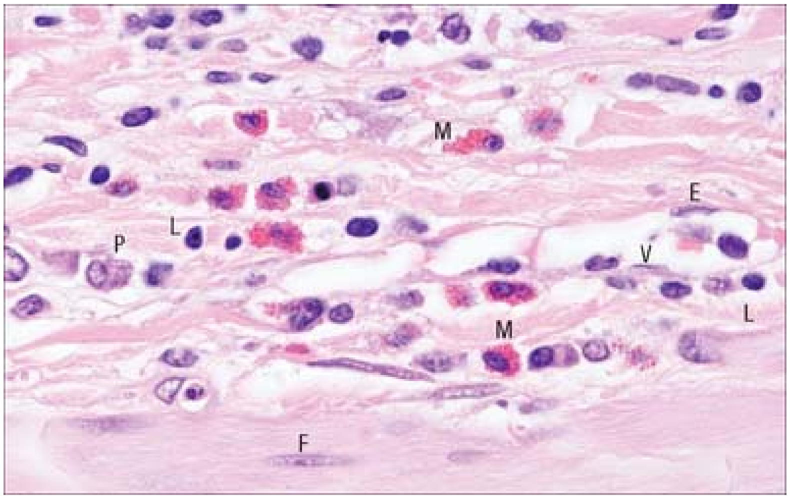

Fig. 2.11 Macrophages (M) in chronically inflamed human connective tissue, showing prominent eosinophic cytoplasmic granules. Also seen are plasma cells (P), small lymphocytes (L) and fibroblasts (F), and the endothelial lining (E) of small vessels (V).

Fibroblasts are usually adherent to the fibres of the matrix (collagen and elastin), which they lay down. In some highly cellular structures, e.g. liver, kidney and spleen, and in most lymphoid tissue, fibroblasts and delicate collagenous fibres (type III collagen; reticular fibres) form fibrocellular networks which are often called reticular tissue. The fibroblasts may then be termed reticular cells or reticulocytes.

Fibroblasts are particularly active during wound repair (Ch. 7) following traumatic injury or inflammation, when tissue mass is lost through cell death. They proliferate and lay down a fibrous matrix that becomes invaded by numerous blood vessels (granulation tissue). Contraction of wounds is at least in part caused by the shortening of specialized contractile fibroblasts (myofibroblasts) with smooth muscle-like properties, which differentiate from fibroblasts in granulation tissue (reviewed in McAnulty 2007). In cases where the specialized cells of the damaged region cannot divide and regenerate functional tissue, e.g. cardiac muscle cells after infarction, connective tissue fibroblasts and their extracellular matrix fill the void to form a scar. An exception is the central nervous system, where glial scars are formed. Fibroblast activity is influenced by various factors such as steroid hormone concentrations, dietary content and prevalent mechanical stresses. In vitamin C deficiency, there is an impairment of collagen formation.

Adipocytes (lipocytes, fat cells)

Adipocytes occur singly or in groups in many, but not all, connective tissues. They are numerous in adipose tissue (Fig. 2.10). Individually, the cells are oval or spherical in shape, but when packed together they are polygonal. They vary in diameter, averaging 50 µm. Each cell consists of a peripheral rim of cytoplasm, in which the nucleus is embedded, surrounding a single large central globule of fat, which consists of glycerol esters of oleic, palmitic and stearic acids. There is a small accumulation of cytoplasm around the nucleus, which is oval in shape and compressed against the cell membrane by the lipid droplet, as is the Golgi complex. Many cytoskeletal filaments, some endoplasmic reticulum and a few mitochondria lie around the lipid droplet, which is in direct contact with the surrounding cytoplasm and not enclosed within a membrane. In sections of tissue not specially treated to preserve lipids, the lipid droplet is usually dissolved out by the solvents used in routine preparations, so that only the nucleus and the peripheral rim of cytoplasm surrounding a central empty space remain.

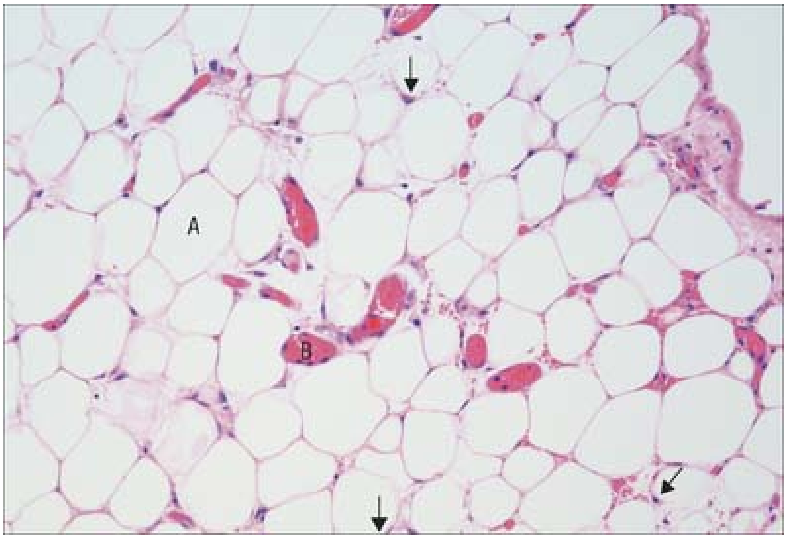

Fig. 2.10 Adipose tissue (human). Adipocytes (A) are distended polygonal cells filled with lipid, which has been extracted by the tissue

processing. This leaves only the plasma membranes with scant cytoplasm and nuclei (arrows), occasionally visible compressed against the cell periphery. Small blood vessels (B) penetrate the adipose tissue.

In neonates, a special form of adipose tissue known as brown fat is present in the interscapular region and may be more widespread. Brown fat is characterized by the presence of a large cell type in which the fat is present as several separate droplets (multilocular adipose tissue) and not as a single globule (typical of unilocular adipose tissue), and the mitochondria have unusually large and numerous cristae. These deposits of fat are concerned with heat production, mediated by mitochondria.

The mobilization of fat is under nervous or hormonal control: noradrenaline (norepinephrine) released at sympathetic nerve endings in adipose tissue is particularly important in this respect. No new adipose tissue is formed after the immediate postnatal period and accumulation of body fat, as in obesity, is due to excessive accumulation of lipid in existing adipocytes, which become very large. Conversely, weight loss results from the mobilization and metabolism of lipid from adipocyte stores, with the consequent shrinkage of the cells.

Mesenchymal stem cells

Mesenchymal stem cells are normally inconspicuous cells in connective tissues. They are derived from embryonic mesenchyme and are able to differentiate into the mature cells of connective tissue during normal growth and development, in the turnover of cells throughout life and, most conspicuously, in the repair of damaged tissues in wound healing (p. 162). There is evidence that, even in mature tissues, mesenchymal stem cells remain pluripotent and able to give rise to all the resident cells of connective tissues in response to local signals and cues.

Migrant cells

Macrophages

Macrophages are typically numerous in connective tissues (Fig. 2.11), where they are either attached to matrix fibres or are motile and migratory. They are relatively large cells, 15–20 μm in diameter, with indented and relatively heterochromatic nuclei and a prominent nucleolus. Their cytoplasm is slightly basophilic, contains many lysosomes (p. 12) and typically has a foamy appearance under the light microscope. Macrophages are important phagocytes, and form part of the mononuclear phagocyte system (p. 78). They can engulf and digest particulate organic materials, such as bacteria, and are also able to clear dead or damaged cells from a tissue. They are also the source of a number of secreted cytokines that have profound effects on many other cell types. Macrophages are able to proliferate in connective tissues to a limited extent, but are derived and replaced primarily from haemopoietic stem cells (p. 75) in the bone marrow, which circulate in the blood as monocytes before migrating through vessel walls into connective tissues.

Many properties of macrophages in general connective tissue are similar to those of related cells in other sites. These include: circulating monocytes, from which they are derived; alveolar macrophages in the lungs; phagocytic cells in the lymph nodes, spleen and bone marrow; Kupffer cells of the liver sinusoids; microglial cells of the central nervous system.

Lymphocytes

Lymphocytes are typically present in small numbers and are numerous in general connective tissue only in pathological states, when they migrate in from adjacent lymphoid tissue or from the circulation. The majority are small cells (6–8 μm) with highly heterochromatic nuclei, but they enlarge when stimulated. Two major functional classes exist, termed B and T lymphocytes (p. 70). B lymphocytes originate in the bone marrow, then migrate to various lymphoid tissues, where they proliferate. When antigenically stimulated, they undergo further mitotic divisions, then enlarge as they mature, commonly in general connective tissues, to form plasma cells that synthesize and secrete antibodies (immunoglobulins). Mature plasma cells are rounded or ovoid, up to 15 μm across, and have an extensive rough endoplasmic reticulum. Their nuclei are spherical, often eccentrically situated and have a characteristic ‘clock-face’ configuration of heterochromatin (see p. 70 and Fig. 4.12) that is regularly distributed in peripheral clumps. The prominent Golgi complex is visible with a light microscope as a pale region to one side of the nucleus and the remaining cytoplasm is deeply basophilic because of the abundant endoplasmic reticulum. Mature plasma cells do not divide.

T lymphocytes originate from precursors in bone marrow haemopoietic tissue, but later migrate to the thymus, where they develop T-cell identity, before passing into the peripheral lymphoid system where they continue to multiply. When antigenically stimulated, T cells enlarge and their cytoplasm becomes filled with free polysome clusters. The functions of T lymphocytes are numerous: different subsets recognize and destroy virus-infected cells, tissue and organ grafts, or interact with B lymphocytes and several other defensive cell types (p. 71).

Mast cells

Mast cells are important defensive cells which occur particularly in loose connective tissues and often in the fibrous capsules of certain organs such as the liver. They are characteristically numerous around blood vessels and nerves. Mast cells are round or oval, approximately 20 μm in diameter, with many filopodia extending from the cell surface. The nucleus is centrally placed and relatively small, and is surrounded by large numbers of prominent vesicles and a well developed Golgi apparatus, but scant endoplasmic reticulum. The vesicles have a high content of glycosaminoglycans and show a strongly positive reaction with the periodic acid–Schiff (PAS) stain for carbohydrates. The vesicles, which are membrane-bound, vary in size and shape (mean diameter 0.5 μm) and also have a rather heterogeneous content of dense, lipid-containing material, which may be finely granular, lamellar or in the form of membranous whorls.

The major granule components, many of them associated with inflammation, are the proteoglycan heparin, histamine, tryptase, superoxide dismutase, aryl sulphatase, β-hexosaminidase and various other enzymes, together with chemotactic factors for neutrophil and eosinophil granulocytes.

Mast cells may be disrupted to release some or all of their contents, either by direct mechanical or chemical trauma, or after contact with particular antigens to which the body has previously been exposed. The consequences of granule release include alteration of capillary permeability, smooth muscle contraction, and activation and attraction to the locality of various other defensive cells. Responses to mast cell degranulation may be localized, e.g. urticaria, or there may occasionally be a generalized response to the release of large amounts of histamine into the circulation (anaphylactic shock). Mast cells closely resemble basophil granulocytes of the general circulation but are thought to develop as distinct descendants of an earlier myeloid lineage precursor (Ch. 4). It is believed that they are generated in the bone marrow and circulate to the tissues as immature basophil-like cells, migrating through the capillary and venule walls to their final destination. For further reading, see Bischoff (2007).

Granulocytes (polymorphonuclear leukocytes)

Neutrophil and eosinophil granulocytes are immigrant cells from the circulation. Relatively infrequent in normal connective tissues, their numbers may increase dramatically in infected tissues, where they are important components of cellular defence. Neutrophils are highly phagocytic, especially towards bacteria. The functions of eosinophils are less well understood. These cells are described further in Chapter 4.

CELLS OF SPECIALIZED CONNECTIVE TISSUES

Skeletal tissues, namely cartilage and bone, are generally classified with the connective tissues, but their structure and functions are highly specialized; they are described in Chapter 5. As with the general connective tissues, these specialized types are characterized by their extracellular matrix, which forms the major component of the tissues and is responsible for their properties. The resident cells are different from those in general connective tissues. Cartilage is populated by chondroblasts, which synthesize the matrix, and by mature chondrocytes. Bone matrix is elaborated by osteoblasts. Their mature progeny, osteocytes, are embedded within the matrix, which they help to mineralize, turn over and maintain. A third cell type, the osteoclast, has a different lineage origin and is derived from haemopoietic tissue; osteoclasts are responsible for bone degradation and remodelling in collaboration with osteoblasts.

EXTRACELLULAR MATRIX

The term extracellular matrix is applied collectively to the extracellular components of connective and supporting tissues. Essentially it consists of a system of insoluble protein fibres, adhesive glycoproteins and soluble complexes composed of carbohydrate polymers linked to protein molecules (proteoglycans and glycosaminoglycans), which bind water. The extracellular matrix distributes the mechanical stresses on tissues and also provides the structural environment of the cells embedded in it, forming a framework to which they adhere and on which they can move (reviewed in Even-Ram & Yamada 2005). With the exception of bone matrix, it provides a highly hydrated medium, through which metabolites, gases and nutrients can diffuse freely between cells and the blood vessels traversing it or, in the case of cartilage, passing nearby. There are many complex interactions between connective tissue cells and the extracellular matrix. The cells continually synthesize, secrete, modify and degrade extracellular matrix components, and themselves respond to contact with the matrix in the regulation of cell metabolism, proliferation and motility. Tissue remodelling depends on the controlled degradation of extracellular matrix by secreted metalloproteinases (reviewed in Mott & Werb 2004), regulated by their specific inhibitors, as occurs for instance during wound healing and involution, e.g. of the postpartum uterus. Pathological, uncontrolled degradation of matrix can lead to disease states such as emphysema and arthritis. In the process of matrix degradation, bioactive peptides are liberated that act as growth factors, cytokines and other signalling molecules to change the behaviour of cells in the vicinity.

The insoluble fibres are mainly of two types of structural protein: members of the collagen family, and elastin (Fig. 2.12). The interfibrillar matrix (ground substance) includes a number of adhesive glycoproteins that perform a variety of functions in connective tissues, including cell–matrix adhesion and matrix–cell signalling. These glycoproteins include fibronectin, laminin, tenascin and vitronectin, in addition to a number of other less well characterized proteins. The glycosaminoglycans of the interfibrillar matrix are, with one notable exception, post-translationally modified proteoglycan molecules in which long polysaccharide side chains are added to short core proteins during transit through the secretory pathway between the rough endoplasmic reticulum and the *trans*-Golgi network. The exception, the polymeric disaccharide, hyaluronan, has no protein core and is synthesized entirely by cell surface enzymes. For further reading on extracellular matrix molecules, see Pollard and Earnshaw (2007). Functional attributes of connective tissues vary and depend on the abundance of its different components. Collagen fibres resist tension, whereas elastin provides a measure of resilience to deformation by stretching. The highly hydrated, soluble polymers of the interfibrillar material (proteoglycans and glycosaminoglycans, mainly hyaluronan) generally form a stiff gel resisting compressive forces. Thus tissues that are specialized to resist tensile forces (e.g. tendons) are rich in collagen fibrils, tissues that accommodate changes in shape and volume (e.g. mesenteries) are rich in elastic fibres and those that absorb compressive forces (e.g. cartilages) are rich in glycosaminoglycans and proteoglycans. In bone, mineral crystals take the place of most of the soluble polymers, and endow the tissue with incompressible rigidity.

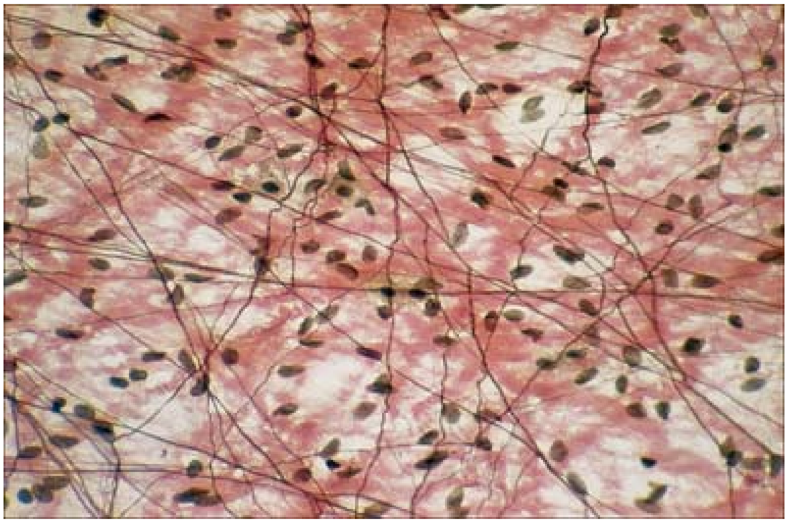

Fig. 2.12 Elastic fibres, seen as fine, dark, relatively straight fibres in a whole-mount preparation of mesentery, stained for elastin. The wavy pink bands are collagen bundles and oval grey nuclei are mainly of fibroblasts.

Fibrillar matrix

Collagens

Collagens make up a very large proportion (approximately 30%) of all the proteins of the body. They consist of a wide range of related molecules that have various roles in the organization and properties of connective (and some other) tissues. The first collagen to be characterized was type I, the most abundant of all the collagens and a constituent of the dermis, fasciae, bone, tendon, ligaments, blood vessels and the sclera of the eyeball. The characteristic collagen of cartilage and the vitreous body of the eye, with a slightly different chemical composition, is type II, whereas type III is present in several tissues, including the dermis and blood vessels, and type IV is in basal lamina. The other types are widely distributed in various tissues. Five of the collagens, types I, II, III, V and XI, form fibrils; types IV, VIII and X form sheets or meshworks; types VI, VII, IX, XII, XIV and XVIII have an anchoring or linking role; types XIII and XVII are transmembrane proteins.

Biochemically, all collagens have a number of features in common. Unlike most other proteins, they contain high levels of hydroxyproline and all are composed of three polypeptides that form triple helices and are substantially modified post-translationally. After secretion, individual molecules are further cross-linked to form stable polymers. Functionally, collagens are structural proteins with considerable mechanical strength. Just a few of their distinguishing structural features are described below. For further reading on the molecular structure and functions of the collagens, see Pollard and Earnshaw (2007).

Type I collagen

Type I collagen is very widely distributed. It forms inextensible fibrils in which collagen molecules (triple helices) are aligned side by side in a staggered fashion, with three-quarters of the length of each molecule in contact with neighbouring molecules. The fibril has well-marked bands of charged and uncharged amino-acids arranged across it; these stain with heavy metals in a banding pattern that repeats every 65 nm in longitudinal sections viewed in the electron microscope (Fig. 2.9 insert).

Fibril diameters vary between tissues and with age. Developing tissues often have thinner fibrils than mature tissues. Corneal stroma fibrils are of uniform and thin diameter, whereas tendon fibrils may be up to 20 times thicker and quite variable. Tissues in which the fibrils are subject to high tensile loading tend to have thicker fibrils. Thick fibrils are composites of uniform thin fibrils with a diameter of 8–12 nm. The fibrils themselves are relatively flexible, but when mineralized (as in bone) or surrounded by high concentrations of proteoglycan (as in cartilage), the resulting fibre-reinforced composite materials are rigid.

Fresh type I collagen fibres are tightly packed assemblies of parallel fibrils and are white and glistening. They form variably wavy (crimped) bundles of various sizes that are generally visible at the light microscope level. The component fibres may leave one bundle and interweave with others. In some situations, collagen fibrils are laid down in precise geometrical patterns, in which successive layers alternate in direction, e.g. corneal stroma, where the high degree of order is essential for transparency. Tendons, aponeuroses and ligaments are also highly ordered tissues (Ch. 5).

Types II, III, V and XI collagens

Types II, III, V and XI collagens can also aggregate to form linear fibrils. Type II collagen occurs in extremely thin (10 nm) short fibrils in the vitreous humour and in very thick fibrils in ageing human cartilage. The amino-acid sequence and banding pattern are very similar to those of type I collagen, as are the post-translational modifications of the triple helical protein molecule. The fine fibrils in the vitreous may fuse into thicker aggregates in older tissue.

Type III collagen is very widely distributed, particularly in young and repairing tissues. It usually co-localizes with type I collagen, and covalent links between Type I and Type III collagen have been demonstrated. In skin, many fibrils are probably composites of Types I and III collagens.

Reticular fibres

Fine branching and anastomosing reticular fibres form the supporting mesh framework of many glands, including the liver (Fig. 2.13), the kidney and lymphoreticular tissue (lymph nodes, spleen, etc.). Classically, these fibres stained intensely with silver salts, although they are poorly stained using conventional histological techniques. They associate with basal laminae and are often found in the neighbourhood of collagen fibre bundles. Reticular fibres are formed principally of type III collagen.

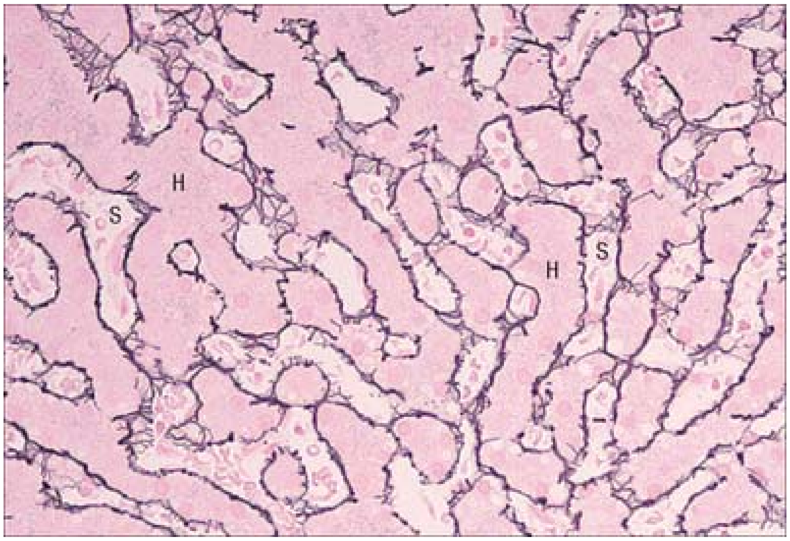

Fig. 2.13 Reticular fibres (type III collagen; reticulin) in the human liver, forming a delicate meshwork within the space of Disse, between hepatocytes (H) plasma membranes and the sinusoidal (S) endothelia.

Elastin

Elastin is a 70 kDa protein, rich in the hydrophobic amino-acids valine and alanine. Elastic fibrils, which also contain fibrillin, are highly cross-linked via two elastin-specific amino-acids, desmosine and iso-desmosine, which are formed extracellularly from lysine residues. They are less widely distributed than collagen, yellowish in colour, typically cross-linked and are usually thinner (10–20 nm) than collagen fibrils. They can be thick, e.g. in the ligamenta flava and ligamentum nuchae. Unlike collagen type I, they show no banding pattern in the electron microscope. They stain poorly with routine histological stains, but are stained with orcein-containing preparations (see Fig. 2.12). They sometimes appear as sheets, as in the fenestrated elastic lamellae of the aortic wall. Elastin-rich structures stretch easily with almost perfect recoil, although they tend to calcify with age and lose elasticity. Elastin is highly resistant to attack by acid and alkali, even at high temperatures.

Interfibrillar matrix

Glycosaminoglycans

The structural soluble polymers characteristic of the extracellular matrix are the acidic glycosaminoglycans, which are unbranched chains of repeating disaccharide units, each unit carrying one or more negatively charged groups (carboxylate or sulphate esters, or both). The anionic charge is balanced by cations (Na^+, K^+, etc.) in the interstitial fluid. Their polyanionic character endows the glycosaminoglycans with high osmotic activity, which helps keep the fibrils apart, confers stiffness on the porous gel that they collectively create and gives the tissue a varying degree of basophilia. Glycosaminoglycans are named according to the tissues in which they were first found, e.g. hyaluronan (vitreous body), chondroitins (cartilage), dermatan (skin), keratan (cornea), heparan (liver). This terminology is no longer relevant, as most glycosaminoglycans are very widely distributed, whereas, conversely, some corneas contain little or no keratan sulphate. Of the glycosaminoglycans, all except hyaluronan have short protein cores and are highly variable in their carbohydrate side chain structure.

Hyaluronan

Hyaluronan was formerly called hyaluronic acid (or hyaluronate, as only the salt exists at physiological pH). It is a very large, highly hydrated molecule (25,000 kDa). Hyaluronan is found in all extracellular matrices and in most tissues and is a prominent component of embryonic and developing tissues.

Hyaluronan is important in the aggregation of proteoglycans and link proteins that possess specific hyaluronan binding sites (e.g. laminin). Indeed, the very large aggregates that are formed may be the essential compression-resisting units in cartilage. Hyaluronan also forms very viscous solutions, which are probably the major lubricants in synovial joints. Because of its ability to bind water, it is often present in semi-rigid structures (e.g. vitreous humour in the eye), where it co-operates with sparse but regular meshworks of thin collagen fibrils.

Proteoglycans

Proteoglycans have been classified according to the size of their protein core: their nomenclature is under review. The same core protein can bear different glycosaminoglycan side chains in different tissues. The functions of many proteoglycans are poorly understood. Some of the better known proteoglycans are: aggrecan in cartilage, perlecan in basal laminae, decorin associated with fibroblasts in collagen fibril assembly, and syndecan in embryonic tissues.

Adhesive glycoproteins

These proteins include molecules that mediate adhesion between cells and the extracellular matrix, often in association with collagens, proteoglycans or other matrix components. All of them are glycosylated and they are, therefore, glycoproteins. General connective tissue contains the well known families of fibronectins (and osteonectin in bone), laminins and tenascins; there is a rapidly growing list of other glycoproteins associated with extracellular adhesion (Pollard & Earnshaw 2007). They possess binding sites for other extracellular matrix molecules and for cell adhesion molecules (p. 5), especially the integrins; in this way they enable cells selectively to adhere to appropriate matrix structures (e.g. the basal lamina). They also function as signalling molecules, which are detected by cell surface receptors and initiate changes within the cytoplasm (e.g. to promote the formation of hemidesmosomes or other areas of strong adhesion; reorganize the cytoskeleton; promote or inhibit locomotion and cell division).

Fibronectin

Fibronectin is a large glycoprotein consisting of a dimer joined by disulphide links. Each subunit is composed of a string of large repetitive domains linked by flexible regions. Fibronectin subunits have binding sites for collagen, heparin and cell surface receptors, especially integrins, and so can promote adhesion between all these elements. In connective tissues, the molecules are able to bind to cell surfaces in an orderly fashion, to form short fibronectin filaments. The liver secretes a related protein, plasma fibronectin, into the circulation. The selective adhesion of different cell types to the matrix during development and in postnatal life is mediated by numerous isoforms of fibronectin generated by alternative splicing. Isoforms found in embryonic tissues are also expressed during wound repair, when they facilitate tissue proliferation and cell movements; the adult form is re-expressed once repair is complete.

Laminin

Laminin is a large (850 kDa) flexible molecule composed of three polypeptide chains (designated α, β, and γ). There are many isoforms of the different chains, and at least 18 types of laminin. The prototypical molecule has a cruciform shape, in which the terminal two-thirds are wound round each other to form the stem of a cross, and the shorter free ends form the upright and transverse members. Laminin bears binding sites for other extracellular matrix molecules such as heparan sulphate, type IV collagen and entactin and also for laminin receptor molecules (integrins) situated in cell plasma membranes. Laminin molecules can assemble themselves into flat regular meshworks, e.g. in the basal lamina.

Tenascin

Tenascin is large glycoprotein composed of six subunits that are joined at one end to form a structure that resembles the spokes of a wheel. There is a family of tenascin molecules, generated by alternative splicing of the tenascin gene transcript. Tenascin is abundant in embryonic tissues, but its distribution is restricted in the adult. It appears to be important in guiding cell migration and axonal growth in early development: it may either promote or inhibit these activities depending on the cell type and tenascin isoform.

CLASSIFICATION OF CONNECTIVE TISSUES

Connective and supporting tissues differ considerably in appearance, consistency and composition in different regions. These differences reflect local functional requirements and are related to the predominance of the cell types, the concentration, arrangement and types of fibre and the characteristics of the interfibrillar matrix. On these bases, general connective tissues can be classified into irregular and regular types, according to the degree of orientation of their fibrous components.

Irregular connective tissues

Irregular connective tissues can be further subdivided into loose, dense and adipose connective tissue.

Loose (areolar) connective tissue

Loose connective tissue is the most generalized form and is extensively distributed. Its chief function is to bind structures together, while still allowing a considerable amount of movement to take place. It constitutes the submucosa in the digestive tract and other viscera lined by mucosae, and the subcutaneous tissue in regions where this is devoid of fat (e.g. eyelids, penis, scrotum and labia), and it connects muscles, vessels and nerves with surrounding structures. It is present in the interior of organs, where it binds together the lobes and lobules of glands, forms the supporting layer (lamina propria) of mucosal epithelia and vascular endothelia, and lies within and between fascicles of muscle and nerve fibres.

Loose connective tissue consists of a meshwork of thin collagen and elastin fibres interlacing in all directions (see Fig. 2.12) to give a measure of both elasticity and tensile strength. The large meshes contain the soft, semi-fluid interfibrillar matrix or ground substance, and different connective tissue cells, which are scattered along the fibres or in the meshes. It also contains adipocytes, usually in small groups, and particularly around blood vessels.

A variant of loose connective tissue occurs in the choroid and the sclera of the eye, where large numbers of pigment cells (melanocytes) are also present.

Dense irregular connective tissue

Dense irregular connective tissue is found in regions that are under considerable mechanical stress and where protection is given to ensheathed organs. The matrix is relatively acellular and contains a high proportion of collagen fibres organized into thick bundles interweaving in three dimensions and imparting considerable strength. There are few active fibroblasts, which are usually flattened with heterochromatic nuclei. Dense irregular connective tissue occurs in: the reticular layer of the dermis; the superficial connective tissue sheaths of muscle and nerves and the adventitia of large blood vessels; the capsules of various glands and organs (e.g. testis, sclera of the eye, periostea and perichondria).

Adipose tissue

A few adipocytes occur in loose connective tissue in most parts of the body. However, they constitute the principal component of adipose tissue (see Fig. 2.10), where they are embedded in a vascular loose connective tissue, usually divided into lobules by stronger fibrous septa carrying the larger blood vessels. Adipose tissue only occurs in certain regions. In particular it is found in: subcutaneous tissue; the mesenteries and omenta; the female breast; bone marrow; as retro-orbital fat behind the eyeball; around the kidneys; deep to the plantar skin of the foot; as localized pads in the synovial membrane of many joints. Its distribution in subcutaneous tissue shows characteristic age and sex differences. Fat deposits serve as energy stores, sources of metabolic lipids, thermal insulation (subcutaneous fat) and mechanical shock-absorbers (e.g. soles of the feet, palms of the hands, gluteal region and synovial membranes).

Regular connective tissues

Regular connective tissues include highly fibrous tissues in which fibres are regularly orientated, either to form sheets such as fasciae and aponeuroses, or as thicker bundles such as ligaments or tendons (Fig. 2.14). The direction of the fibres within these structures is related to the stresses which they undergo, moreover, fibrous bundles display considerable interweaving, even within tendons, which increases their structural stability and resilience.

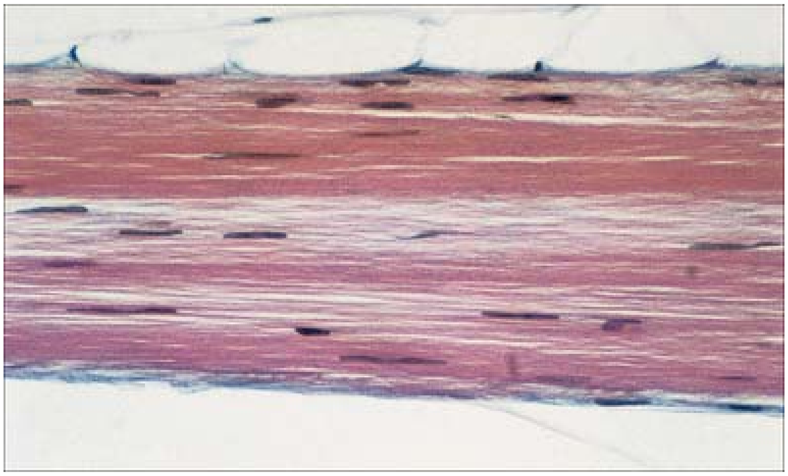

Fig. 2.14 Dense regular connective tissue in a tendon. Thick parallel bundles of type 1 collagen (stained pink) give tendon its white colour in life. The elongated nuclei of inactive fibroblasts (tendon cells) are visible between collagen bundles.

The fibroblasts that secrete the fibres may eventually become trapped within the fibrous structure, where they become compressed, relatively inactive cells with stellate profiles and small heterochromatic nuclei. These cells are called tendon cells. Fibroblasts on the external surface may be active in continued fibre formation and they constitute a pool of cells available for repair of injured tissue.

Although regular connective tissue is predominantly collagenous, some ligaments contain significant amounts of elastin, e.g. the ligamenta flava of the vertebral laminae and the vocal folds. The collagen fibres may form precise geometrical patterns, as in the cornea (p. 678).

Mucoid tissue

Mucoid tissue is a fetal or embryonic type of connective tissue, found chiefly as a stage in the development of connective tissue from mesenchyme. It exists in Wharton’s jelly, which forms the bulk of the umbilical cord, and consists substantially of extracellular matrix, largely made up of hydrated mucoid material and a fine meshwork of collagen fibres, in which nucleated, fibroblast-like cells with branching process are found. Fibres are usually rare in typical mucoid tissue, although the full-term umbilical cord contains perivascular collagen fibres. Postnatally, mucoid tissue is seen in the pulp of a developing tooth, the vitreous body of the eye (a persistent form of mucoid tissue that contains few fibres or cells) and the nucleus pulposus of the intervertebral disc.

TRANSDIFFERENTIATION AND METAPLASIA

Transitions occur between populations of cells forming an epithelium (sheets of polarized cells) and mesenchymal types (where the cells lack polarity) during normal development (Section 3), but all well-described transitions between morphologically different cell types in postnatal life do not cross the epithelial–mesenchymal boundary. They are transitions between types of epithelial cell or, less frequently, between mesenchymal (connective tissue) cell types. Most instances of such transdifferentiation (metaplasia) are adaptive, to changing environmental conditions or trauma, and almost all are pathological; the altered cells are termed metaplastic. A very common and physiologically normal example is the squamous metaplasia of columnar secretory epithelium of the distal endocervical canal (Section 8), when exposed to the hormonally-stimulated vaginal environment. Gastric metaplasia of the lower oesophagus may occur when chronic reflux of gastric juices exposes its stratified squamous epithelial lining to acid, and the original epithelium is replaced by a mucus-secreting columnar epithelium typical of the stomach (Barrett's oesophagus): this is pathological and susceptible to malignant change. Similarly, the respiratory epithelium (see Fig. 2.2D) of the upper airway often develops foci of stratified squamous metaplasia in response to irritants in cigarette smoke. Mesenchymal (osseous) metaplasia can occur, for example, in the fibrous connective tissue of muscles subjected to repeated damage, where trabeculi of bone develop. It is thought that stem cells (rather than the differentiated cells) in the affected tissue respond to changes in their environment by altering their differentiation pathway, a process which may be reversible if the stimulus is removed.

MUCOSA (MUCOUS MEMBRANE)

A mucosa or mucous membrane lines many internal hollow organs in which the inner surfaces are moistened by mucus, such as the intestines, conducting portions of the airway, and the genital and urinary tracts. The mucosa proper consists of an epithelial lining, which may have mucosal glands opening on to its surface, the underlying loose connective tissue, the lamina propria, and a thin layer of smooth muscle, the muscularis mucosae. This last layer is either absent from some mucosae, or is replaced by a layer of elastic fibres. The term mucous membrane reflects the fact that these tissues can all be peeled away as a sheet or membrane from underlying structures; the plane of separation occurs along the muscularis mucosae.

Submucosa is a layer of supporting connective tissue, which usually lies below the muscularis mucosae. It may contain mucous or seromucous submucosal glands, which convey their secretions through ducts to the mucosal surface. Most mucosae are also supported by one or more layers of smooth muscle, the muscularis externa. Contraction of this muscle may constrict the mucosal lumen (e.g. in the airway) or, where there are two or more muscle layers orientated in opposing directions (e.g. in the intestines), cause peristaltic movement of the viscus and the contents of its lumen. The outer surface of the muscle may be covered by a serosa or, where the structure is retroperitoneal or passes through the pelvic floor, by a connective tissue adventitia.

MUCUS

Mucus is a viscous suspension of complex glycoproteins (mucins) of various kinds, and is secreted by scattered individual epithelial (goblet) cells, a secretory surface epithelium (e.g. the stomach lining) or mucous and sero-mucous glands. The precise composition of the mucus varies with the tissue and secretory cells that produce it. All mucins consist of filamentous core proteins to which are attached carbohydrate chains, usually branched; salivary mucus contains nearly 600 chains. Carbohydrate residues include glucose, fucose, galactose and *N*-acetylglucosamine (sialic acid). The terminals of some carbohydrate chains are identical with the blood group antigens of the ABO group in the majority of the population (secretors, bearing the secretor gene S^e), and can be detected in salivary mucus by means of appropriate clinical tests. The long polymeric carbohydrate chains bind water and protect surfaces against drying; they also provide good lubricating properties. In concentrated form, mucins form viscous layers that protect the underlying tissues against damage.

Synthesis of mucus starts in the rough endoplasmic reticulum. It is then passed to the Golgi complex, where it is conjugated with sulphated carbohydrates to form the glycoprotein, mucinogen, and this is exported in small, dense, membrane-bound vesicles, which swell as they approach the cell surface, with which they fuse before releasing their contents.

SEROSA (SEROUS MEMBRANE)

Serosa consists of a single layer of squamous mesothelial cells supported by an underlying layer of loose connective tissue that contains numerous blood and lymphatic vessels. Serosal cells are derived from embryonic mesenchyme and so share a common lineage with connective tissue cells. However, structurally they resemble squamous epithelia and they express keratin intermediate filaments. Serosa lines the pleural, pericardial and peritoneal cavities, covers the external surfaces of organs lying within those cavities and, in the abdomen, the mesenteries that envelop them. A potential space, filled with a small amount of protein-containing serous fluid – largely an exudate of interstitial fluid – exists between the outer parietal and the inner visceral layer of the serosa.

FASCIA

Fascia is a term applied to masses of connective tissue large enough to be visible to the unaided eye. Its structure is highly variable but, in general, collagen fibres in fascia tend to be interwoven and seldom show the compact, parallel orientation seen in tendons and aponeuroses.

Fascia that is organized into condensations on the surfaces of muscles – and their epimysial sheaths – and other tissues is termed investing fascia. Between muscles that move extensively, it takes the form of loose areolar connective tissue and provides a degree of mechanical isolation. It constitutes the loose packing of connective tissue around peripheral nerves, blood and lymph vessels as they pass between other structures and often links them together as neurovascular bundles. It forms a dense connective tissue layer investing some large vessels, e.g. the common carotid and femoral arteries, and its presence here may be functionally significant, aiding venous return by approximating large veins to pulsating arteries.

SUPERFICIAL FASCIA

Superficial fascia is a layer of loose connective tissue of variable thickness that merges with the deep aspect of the dermis; it is thus also known as the hypodermis. It is often adipose, particularly between muscle and skin. It allows increased mobility of skin, and the adipose component contributes to thermal insulation and constitutes a store of energy for metabolic use. Subcutaneous nerves, vessels and lymphatics travel in the superficial fascia; their main trunks lie in its deepest layer, where adipose tissue is sparse. In the head and neck, superficial fascia also contains a group of striated muscles – collectively termed the muscles of facial expression (Ch. 29) – which are a remnant of more extensive sheets of skin-associated musculature found in other mammals (panniculus carnosus).

The quantity and distribution of subcutaneous fat differs in the sexes. It is generally more abundant and widely distributed in females. In males, it diminishes from the trunk to the extremities; this distribution becomes more obvious in middle age, when the total amount increases in both sexes. There is an association with climate (rather than race), and superficial fat is more abundant in colder geographical regions. Superficial fascia is most distinct on the lower anterior abdominal wall, where it contains much elastic tissue and appears many-layered as it passes through the inguinal regions into the thighs. It is well differentiated in the limbs and the perineum, but is thin where it passes over the dorsal aspects of the hands and feet, the sides of the neck and face, around the anus and over the penis and scrotum, and is almost absent from the external ears. Typical superficial fascia is lacking in the palms and soles, where numerous strong connective tissue collagenous bands tether the dermis of the skin to underlying structures. Also atypical is the skin of the scalp, where dense dermal connective tissue and the epicranial aponeurosis are bound together as a layer that ‘rides’ on loose connective tissue overlying the periosteum of the skull.

DEEP FASCIA

Deep fascia is also composed mainly of collagenous fibres, but these are compacted and in many cases arranged so regularly that the deep fascia may be indistinguishable from aponeurotic tissue. In limbs, where deep fascia is well developed, the collagen fibres are longitudinal or transverse, and condense into tough, inelastic sheaths around the musculature.

REFERENCES

schoff SC. Role of mast cells in allergic and non-allergic immune responses: comparison of human and murine data. *Nat Rev Immunol*. 2007;7:93-104.

anpain C, Horsley V, Fuchs E. Epithelial stem cells: turning over new leaves. *Cell*. 2007;128:445-458.

en-Ram S, Yamada KM. Cell migration in 3D matrix. *Curr Opin Cell Biol*. 2005;17:524-532.

nz B, Gabbiani G. Cell-matrix and cell-cell contacts of myofibroblasts: role in connective tissue remodeling. *Thromb Haemost*. 2003;90:993-1002.

zzo RV. Basement membrane proteoglycans: from cellar to ceiling. *Nat Rev Mol Cell Biol*. 2005;6:646-656.

cAnulty RJ. Fibroblasts and myofibroblasts: their source, function and role in disease. *Int J Biochem & Cell Biol*. 2007;39:666-671.

ott JD, Werb Z. *Curr Opin Cell Biol*. 2004;16:558-564.

llard TD, Earnshaw WC. Cell Biology. Philadelphia: Saunders, 2007. Section VIII, Cell adhesion and the extracellular matrix

CHAPTER 3

Nervous system

The nervous system has two major divisions, the central nervous system (CNS) and the peripheral nervous system (PNS). The CNS consists of the brain and spinal cord and contains the majority of neuronal cell bodies. The PNS includes all nervous tissue outside the central nervous system and is subdivided into the cranial and spinal nerves, peripheral autonomic nervous system (ANS) (including the enteric nervous system of the gut wall, ENS) and special senses (taste, olfaction, vision, hearing and balance). It is composed mainly of the axons of sensory and motor neurones that pass between the CNS and the body. However, the ENS contains as many intrinsic neurones in its ganglia as the entire spinal cord, is not connected directly to the CNS, and may be considered separately as a third division of the nervous system (Gershon 1998).

The CNS is derived from the neural tube (Ch. 24). The cell bodies of neurones are often grouped together in discrete areas termed nuclei, or they may form more extensive layers or masses of cells; collectively they constitute grey matter. Neuronal dendrites and synaptic contacts are mostly confined to areas of grey matter, and they form part of its meshwork of neuronal and glial processes termed the neuropil. Their axons join bundles of nerve fibres that tend to be grouped separately to form tracts. In the spinal cord, cerebellum, cerebral cortices (Chs 20, 22) and some other areas, concentrations of tracts constitute the white matter, so called because the axons are often ensheathed in lipid-rich sheaths of myelin which is white when fresh (Fig. 3.1).

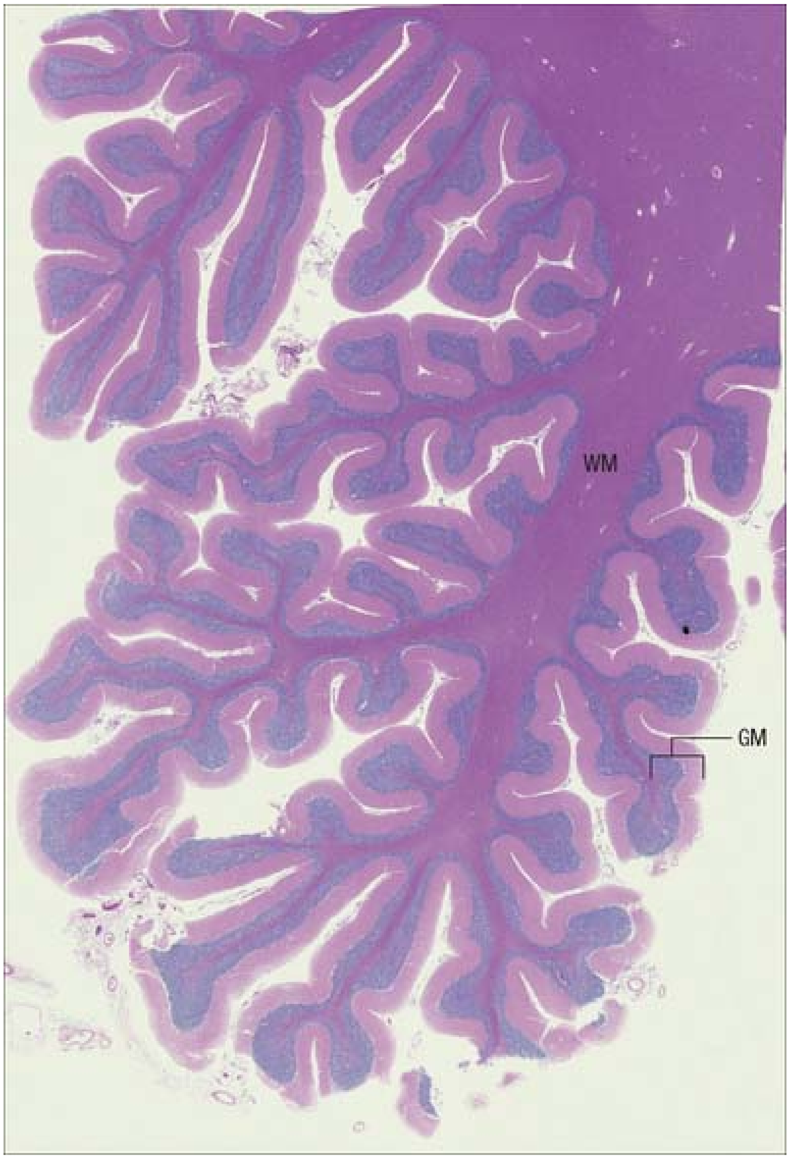

Fig. 3.1 Section through the human cerebellum stained to show the arrangement in the brain of the central white matter (WM, deep pink), and the highly folded outer grey matter (GM). In the cerebellum, GM consists of an inner granular layer of tightly packed small neurones (blue) and an outermost molecular layer (pale pink) where neuronal processes make synaptic contacts.

The PNS is composed of the efferent axons (fibres) of motor neurones situated inside the CNS, and the cell bodies of sensory neurones (grouped together as ganglia) and their afferent processes. Sensory cells in dorsal root ganglia give off both centrally and peripherally directed processes: there are no synapses on their cell bodies. Also included are ganglionic neurones of the ANS, which receive synaptic contacts from the peripheral fibres of preganglionic autonomic neurones whose cell bodies lie within the CNS. Neuronal cell bodies in peripheral ganglia are all derived embryologically from cells which migrate from the neural crest (p. 201).

When the neural tube is formed during prenatal development its walls thicken greatly but do not completely obliterate the cavity within. The latter remains in the spinal cord as the narrow central canal, and in the brain it becomes greatly expanded to form a series of interconnected cavities called the ventricular system. In the fore- and hindbrains, parts of the neural tube roof do not generate nerve cells but become thin folded sheets of secretory tissue which are invaded by blood vessels and are called the choroid plexuses. The plexuses secrete cerebrospinal fluid (CSF) which fills the ventricles and subarachnoid spaces and penetrates the intercellular spaces of the brain and spinal cord to create their interstitial fluid. The CNS has a rich blood supply, which is essential to sustain its high metabolic rate. The blood–brain barrier places considerable restrictions on the substances which can diffuse from the bloodstream into the nervous tissue.

Neurones encode information, conduct it over considerable distances, and then transmit it to other neurones or to various non-neural cells. The movement of this information within the nervous system depends on the rapid conduction of transient electrical impulses along neuronal plasma membranes. Transmission to other cells is mediated by secretion of neurotransmitters at special junctions either with other neurones (synapses), or with cells outside the nervous system, e.g. muscle cells (neuromuscular junctions), gland cells, adipose tissue, etc. and this causes changes in their behaviour.

The nervous system contains large populations of non-neuronal cells, neuroglia or glia, which, whilst not electrically active in the same way, are responsible for creating and maintaining an appropriate environment in which neurones can operate efficiently. Indeed, it is now known that two-way communication between neurones and glial cells is essential for normal neural activity (reviewed in Fields & Stevens-Graham 2002). In the CNS, glia outnumber neurones by 10–50 times and consist of microglia and macroglia. Macroglia are further subdivided into three main types, oligodendrocytes, astrocytes and ependymal cells. The principal glial cell of the PNS is the Schwann cell. Satellite cells surround each neuronal soma in ganglia.

NEURONES

Most of the neurones in the CNS are either clustered into nuclei, columns or layers, or dispersed within grey matter. Neurones of the PNS are confined to ganglia. Irrespective of location, neurones share many general features, which are discussed here in the context of central neurones. Special characteristics of ganglionic neurones and their adjacent tissues are discussed on page 55–6.

Neurones exhibit great variability in their size (cell bodies range from 5 to 100 µm diameter) and shapes. Their surface areas are extensive because most neurones display numerous narrow branched cell processes. They usually have a rounded or polygonal cell body (perikaryon or soma). This is a central mass of cytoplasm which encloses a nucleus and gives off long, branched extensions, with which most intercellular contacts are made. Typically, one of these processes, the axon, is much longer than the others, the dendrites (Fig. 3.2). Dendrites conduct electrical signals towards a soma whereas axons conduct impulses away from it.

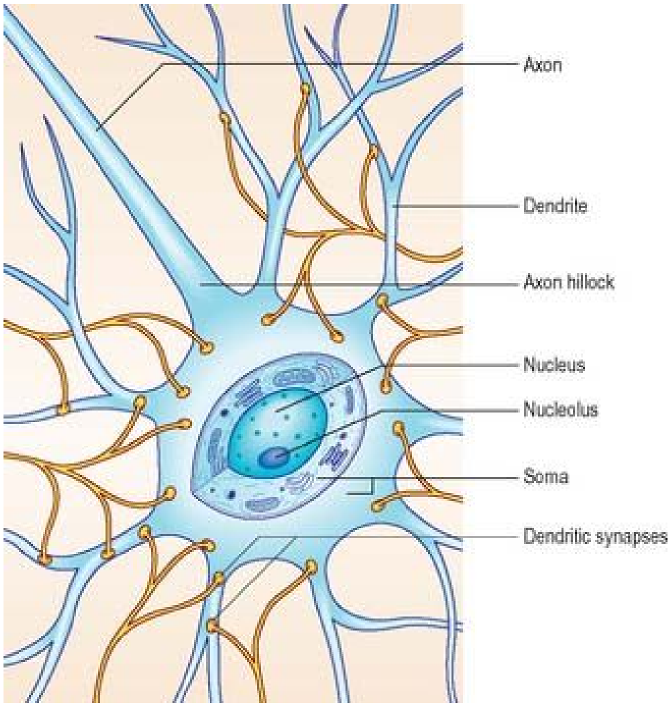

Fig. 3.2 Schematic view of a typical neurone showing the soma (cut away to show the nucleus and cytoplasmic organelles), the dendritic tree with synaptic contacts (also shown contacting the soma), the axon hillock and the proximal part of the axon.

Neurones can be classified according to the number and arrangement of their processes. Multipolar neurones (Fig. 3.3) are common: they have an extensive dendritic tree which arises from either a single primary dendrite or directly from the soma, and a single axon. Bipolar neurones, which typify neurones of the special sensory systems, e.g. the retina (p. 697), have only a single dendrite which emerges from the soma opposite the axonal pole. Unipolar neurones which transmit general sensation, e.g. dorsal root ganglion neurones, have a single short process which bifurcates into peripheral and central processes (p. 55). This arrangement arises by the fusion of the proximal axonal and dendritic processes of a bipolar neurone during development: they may also, therefore, be termed pseudounipolar. Neurones are also classified according to whether their axons terminate locally on other neurones (interneurones), or transmit impulses over long distances, often to distinct territories via defined tracts (projection neurones).

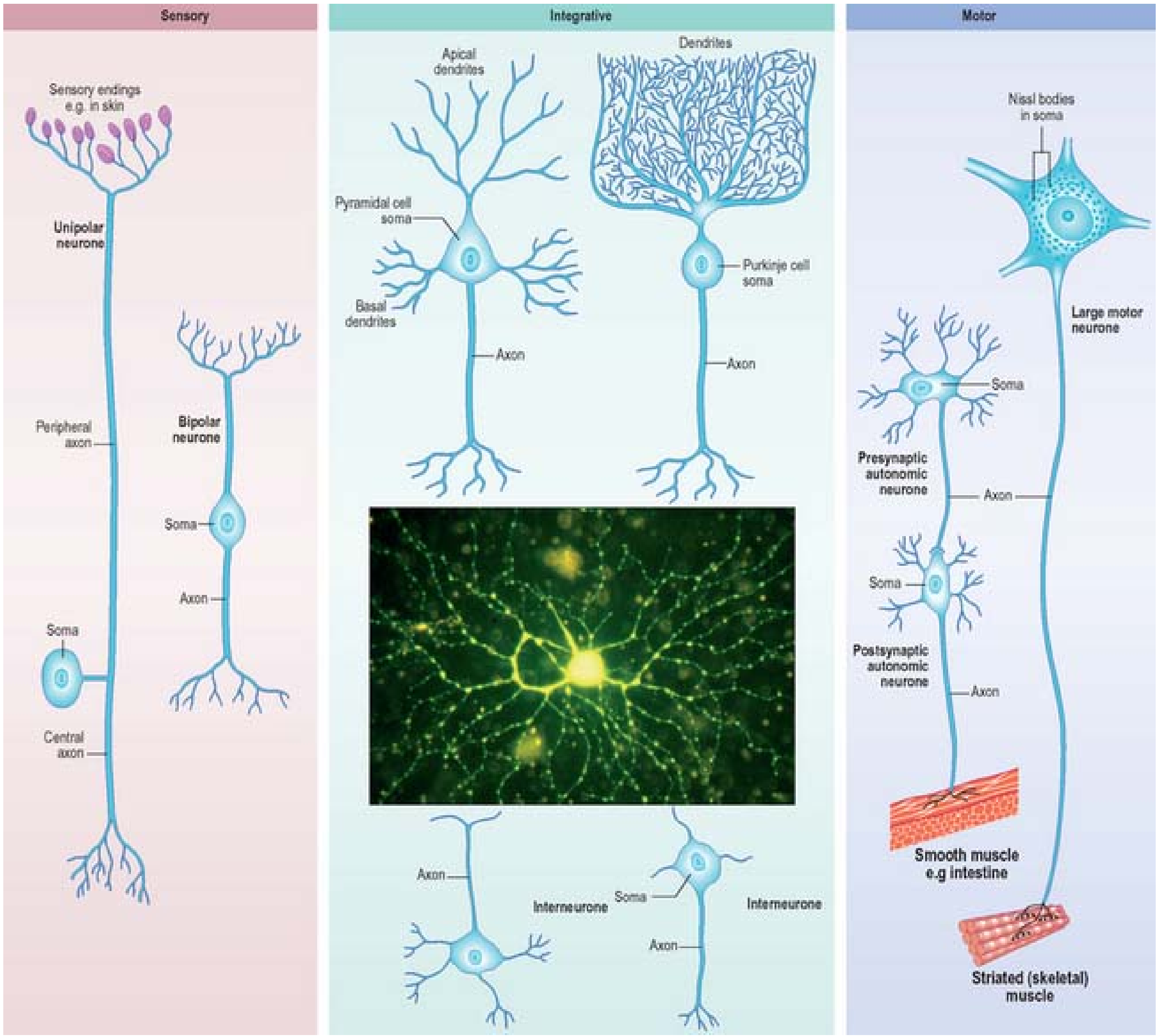
Sensory
Integrative
Motor
Sensory endings e.g. in skin
Unipolar neurone
Peripheral axon
Soma
Central axon
Bipolar neurone
Soma
Axon
Apical dendrites
Pyramidal cell soma
Basal dendrites
Axon
Dendrites
Purkinje cell soma
Axon
Axon
Interneurone
Soma
Interneurone
Axon
Nissl bodies in soma
Large motor neurone
Soma
Presynaptic autonomic neurone
Axon
Axon
Soma
Postsynaptic autonomic neurone
Axon
Smooth muscle e.g intestine
Striated (skeletal) muscle

Fig. 3.3 The variety of shapes of neurones and their processes. The inset shows a human multipolar retinal ganglion cell, filled with fluorescent dye by microinjection.

(Inset by courtesy of Drs Richard Wingate, James Morgan and Ian Thompson, King's College, London.)

Neurones are postmitotic cells and, with few exceptions, they are not replaced when lost.

SOMA

The plasma membrane of the soma is unmyelinated and contacted by inhibitory and excitatory axosomatic synapses: very occasionally, somasomatic and dendrosomatic contacts may be made. The non-synaptic surface is covered by either astrocytic or satellite oligodendrocyte processes.

The cytoplasm of a typical soma (Fig. 3.2) is rich in rough and smooth endoplasmic reticulum and free polyribosomes, indicating a high level of protein synthetic activity. Free polyribosomes often congregate in large groups associated with the rough endoplasmic reticulum. These aggregates of RNA-rich structures are visible by light microscopy as basophilic Nissl bodies or granules. They are more obvious in large, highly active cells, such as spinal motor neurones (Fig. 3.4), which contain large stacks of rough endoplasmic reticulum and polyribosome aggregates. Maintenance and turnover of cytoplasmic and membranous components are necessary in all cells: the huge total volume of cytoplasm within the soma and processes of many neurones requires a considerable commitment of protein synthetic machinery. Neurones also synthesize other proteins (enzyme systems, etc.) involved in the production of neurotransmitters and in the reception and transduction of incoming stimuli. Various transmembrane channel proteins and enzymes are located at the surfaces of neurones where they are associated with movements of ions. The apparatus for protein synthesis (including RNA and ribosomes) occupies the soma and dendrites, but is usually absent from axons.

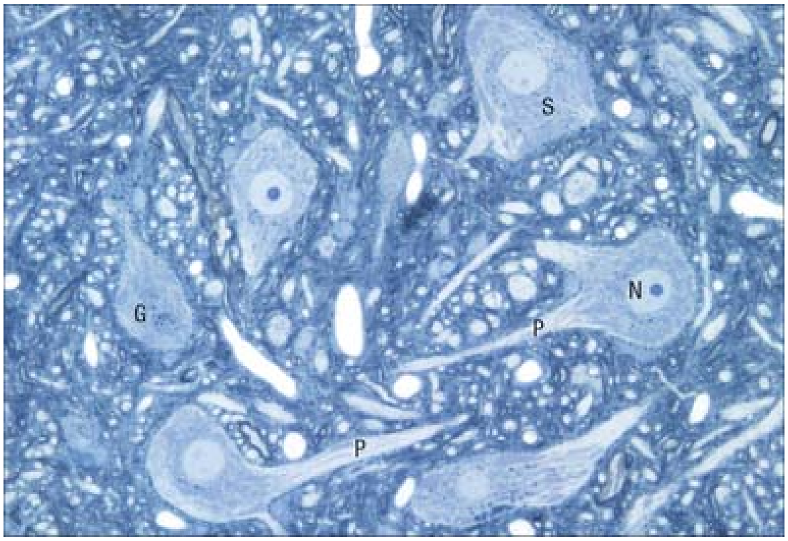

Fig. 3.4 Spinal motor neurones (toluidine blue stained resin section, rat tissue) showing a group of cell bodies (somata, S), some with the proximal parts of axonal and dendritic processes (P) visible. Their nuclei (N) typically have prominent, deeply staining nucleoli, indicative of metabolically highly active cells; two are visible in the plane of section. Nissl granules (G) are seen in the cytoplasm. Surrounding the neuronal somata is the neuropil, consisting of the interwoven processes of these and other neurones and of glial cells.

The nucleus is characteristically large, round and euchromatic and contains at least one prominent nucleolus; these are features typical of all cells engaged in substantial levels of protein synthesis. The cytoplasm contains many mitochondria and moderate numbers of lysosomes. Golgi complexes are usually close to the nucleus, near the bases of the main dendrites and opposite the axon hillock.

The neuronal cytoskeleton is a prominent feature of its cytoplasm and gives shape, strength and support to the dendrites and axons. A number of neurodegenerative diseases are characterized by abnormal aggregates of cytoskeletal proteins (reviewed in Cairns et al 2004). Neurofilaments (the intermediate filaments of neurones) and microtubules are abundant in the soma and along dendrites and axons: the proportions vary with the type of neurone and cell process. Bundles of neurofilaments constitute neurofibrils which can be seen by light microscopy in silver stained or immunolabelled sections. Neurofilaments are heteropolymers of proteins assembled from three polypeptide subunits, NF-L (68 kilodaltons [kDa]), NF-M (160 kDa) and NF-H (200 kDa). NF-M and NF-H have long C-terminal domains which project as side arms from the assembled neurofilament and bind to neighbouring filaments. They can be heavily phosphorylated, particularly in the highly stable neurofilaments of mature axons, and are thought to give axons their tensile strength. Some axons are almost filled by neurofilaments.

Microtubules are important in axonal transport, although dendrites usually have more microtubules than axons. Centrioles persist in mature postmitotic neurones, where they are concerned with the generation of microtubules rather than cell division. Centrioles are associated with cilia on the surfaces of developing neuroblasts. Their significance, other than at some sensory endings (e.g. the olfactory mucosa, p. 553), is not known.

Pigment granules (Fig. 3.5) appear in certain regions, e.g. neurones of the substantia nigra contain neuromelanin, probably a waste product of catecholamine synthesis. In the locus coeruleus a similar pigment, rich in copper, gives a bluish colour to the neurones. Some neurones are unusually rich in certain metals which may form a component of enzyme systems, e.g. zinc in the hippocampus and iron in the oculomotor nucleus. Ageing neurones, especially in spinal ganglia, accumulate granules of lipofuscin (senility pigment) in residual bodies, which are lysosomes packed with partially degraded lipoprotein material (corpora amylaceae).

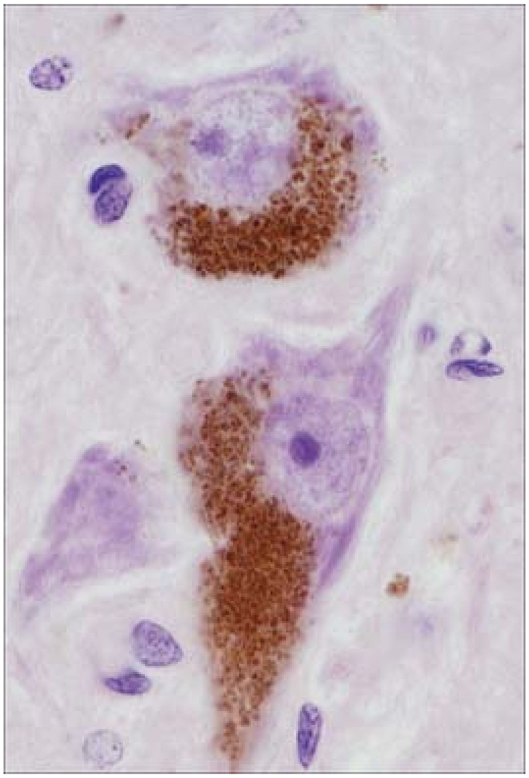

Fig. 3.5 Neurones in the substantia nigra of the human midbrain, showing cytoplasmic granules of neuromelanin pigment.

DENDRITES

Dendrites are highly branched, usually short processes which project from the soma (Fig. 3.2). The branching patterns of many dendritic arrays are probably established by random adhesive interactions between dendritic growth cones and afferent axons that occur during development. There is an overproduction of dendrites in early development, and this is pruned in response to functional demand as the nervous system matures and information is processed through the dendritic tree. There is evidence that dendritic trees may be plastic structures throughout adult life, expanding and contracting as the traffic of synaptic activity varies through afferent axodendritic contacts (for review see Wong & Ghosh 2002). Groups of neurones with similar functions have a similar stereotypic tree structure (Fig. 3.6), suggesting that the branching patterns of dendrites are important determinants of the integration of the afferent inputs that converge on the tree.

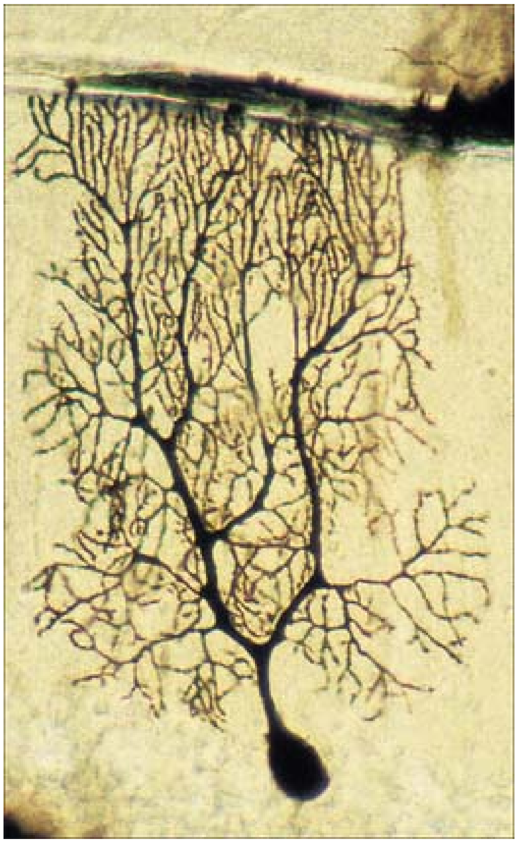

Fig. 3.6 Purkinje neurone from the cerebellum of a rat stained by the Golgi–Cox method, showing the extensive two-dimensional array of dendrites.

(By courtesy of Martin Sadler and M Berry, Division of Anatomy and Cell Biology, GKT School of Medicine, London.)

Dendrites differ from axons in many respects. They represent the afferent rather than the efferent system of the neurone, and receive both excitatory and inhibitory axodendritic contacts. They may also make dendrodendritic and dendrosomatic connections (see Fig. 3.9), some of which are reciprocal. Synapses occur either on small projections called dendritic spines or on the smooth dendritic surface. Dendrites contain ribosomes, smooth endoplasmic reticulum, microtubules, neurofilaments, actin filaments and Golgi complexes. Their neurofilament proteins are poorly phosphorylated and their microtubules express the microtubule-associated protein (MAP)-2 almost exclusively in comparison with axons.

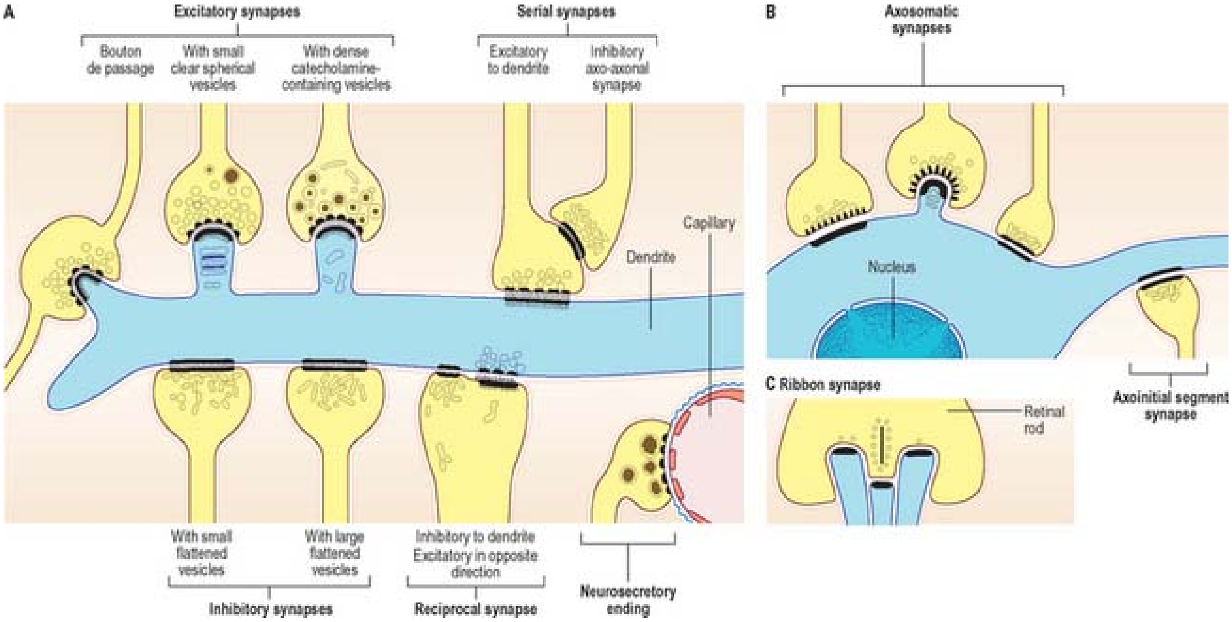
A
Excitatory synapses
Bouton de passage
With small clear spherical vesicles
With dense catecholamine-containing vesicles
Serial synapses
Excitatory to dendrite
Inhibitory axo-axonal synapse
Capillary
Dendrite
With small flattened vesicles
With large flattened vesicles
Inhibitory synapses
Inhibitory to dendrite Excitatory in opposite direction
Reciprocal synapse
Neurosecretory ending
B
Axosomatic synapses
Nucleus
Axoinitial segment synapse
C Ribbon synapse
Retinal rod

Fig. 3.9 The structural arrangements of different types of synaptic contact.

The shapes of dendritic spines range from simple protrusions to structures with a slender stalk and expanded distal end. Most spines are not more than 2 μm long, and have one or more terminal expansions; they can also be short and stubby, branched or bulbous. Free ribosomes and polyribosomes are concentrated at the base of the spine. Ribosomal accumulations near synaptic sites provide a mechanism for activity-dependent synaptic plasticity through the local regulation of protein synthesis.

AXONS

The axon originates either from the soma or from the proximal segment of a dendrite, at a specialized region free of Nissl granules, the axon hillock (Fig. 3.2). Action potentials are initiated here. The axonal plasma membrane (axolemma) is undercoated at the hillock by a concentration of cytoskeletal molecules, including spectrin and actin fibrils, which are important in anchoring numerous voltage-sensitive channels to the membrane. The axon hillock is unmyelinated and often participates in inhibitory axo-axonal synapses. It is unique because it contains ribosomal aggregates immediately below the postsynaptic membrane.

In the CNS, small, unmyelinated axons lie free in the neuropil, whereas in the PNS they are embedded in Schwann cell cytoplasm. Myelin, which is formed around almost all axons >2 μm diameter by oligodendrocytes in the CNS and Schwann cells in the PNS, begins at the distal end of the axon hillock. Nodes of Ranvier are specialized constricted regions of myelin-free axolemma where action potentials are generated and where an axon may branch. In both CNS and PNS, the territory of a myelinated axon between adjacent nodes is called an internode: the region close to a node, where the myelin sheath terminates, is called the paranode. Myelin thickness and internodal lengths are, in general, positively correlated with axon diameter. The density of sodium channels in the axolemma is highest at nodes of Ranvier, and very low along internodal membranes: sodium channels are spread more evenly within the axolemma of unmyelinated axons. Fast potassium channels are present in the paranodal regions of myelinated axons. Fine processes of glial cytoplasm (astrocytic in the CNS, Schwann cell in the PNS) surround the nodal axolemma.

The terminals of an axon are unmyelinated and most expand into presynaptic boutons which may form connections with axons, dendrites, neuronal somata or, in the periphery, muscle fibres, glands and lymphoid tissue. Exceptions include the free afferent sensory endings in e.g. the epidermis, which are unspecialized structurally, and the peripheral terminals of afferent sensory fibres with encapsulated endings (see Fig. 3.30). Axon terminals may themselves be contacted by other axons, forming axoaxonal presynaptic inhibitory circuits. Further details of neuronal microcircuitry are given in Kandel et al (2000).

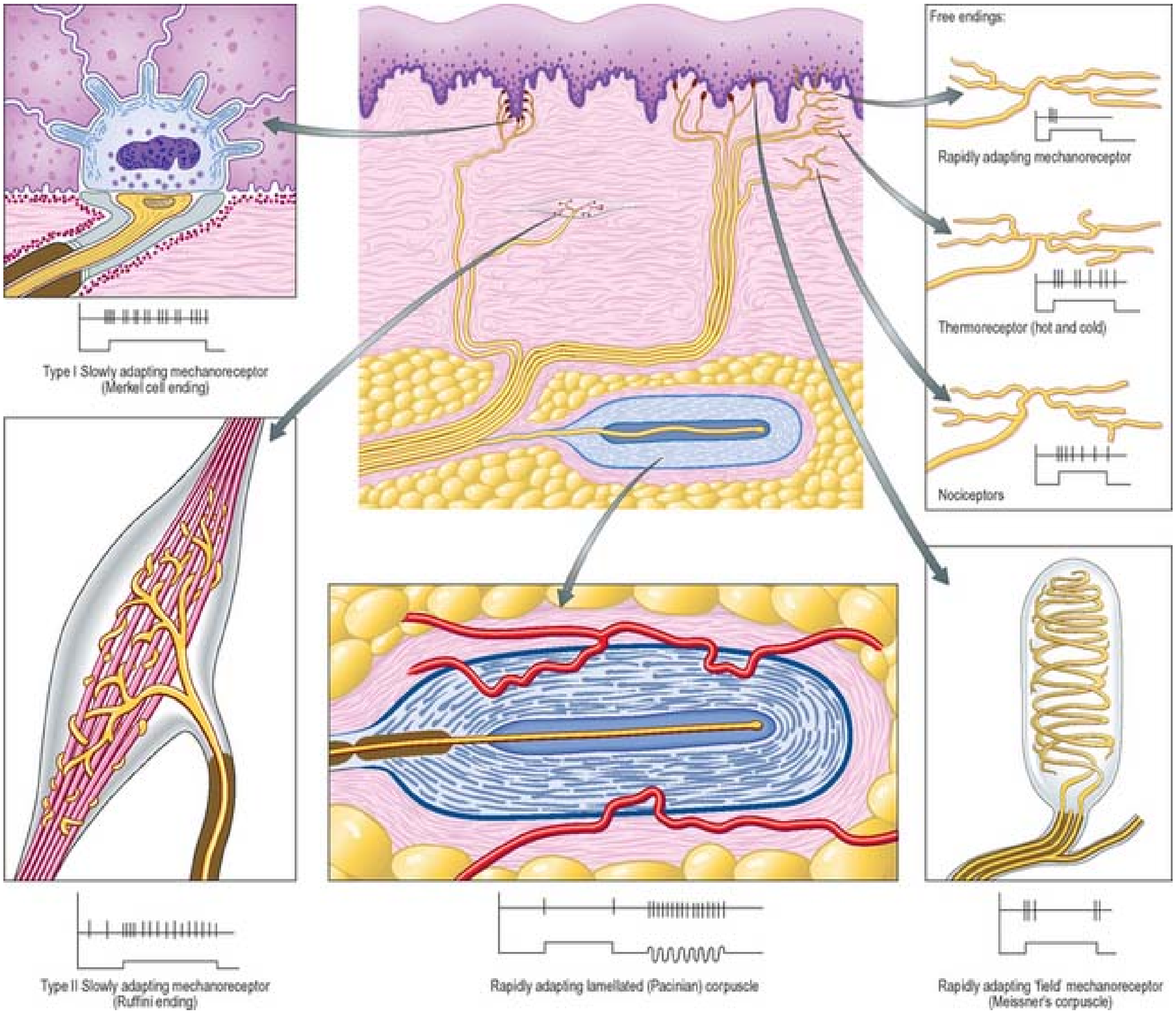
Free endings:
Rapidly adapting mechanoreceptor
Thermoreceptor (hot and cold)
Nociceptors
Type I Slowly adapting mechanoreceptor (Merkel cell ending)
Type II Slowly adapting mechanoreceptor (Ruffini ending)
Rapidly adapting lamellated (Pacinian) corpuscle
Rapidly adapting 'field' mechanoreceptor (Meissner's corpuscle)

Fig. 3.30 Some major types of sensory ending of general afferent fibres (omitting neuromuscular, neurotendinous and hair-related types). The traces below each type of ending indicate (top) their response (firing rate [vertical lines] and adaption with time) to an appropriate stimulus (below) of the duration indicated. The Pacinian corpuscle response to vibration (rapid sequence of on-off stimuli) is also shown.

Axons contain microtubules, neurofilaments, mitochondria, membrane vesicles, cisternae, and lysosomes. Axons do not usually contain ribosomes or Golgi complexes, except at the axon hillock: exceptionally, the neurosecretory fibres of hypothalamo-hypophysial neurones contain the mRNA of neuropeptides. Organelles are differentially distributed along axons, e.g. there is a greater density of mitochondria and membrane vesicles in the axon hillock, at nodes, and in presynaptic endings. Axonal microtubules are interconnected by cross-linking MAPs, of which tau is the most abundant. Microtubules have an intrinsic polarity, and in axons all microtubules are uniformly orientated with their rapidly growing ends directed away from the soma towards the axon terminal. Neurofilament proteins ranging from high to low molecular weights are highly phosphorylated in mature axons, whereas growing and regenerating axons express a calmodulin-binding membrane-associated phosphoprotein, growth-associated protein-43 (GAP-43), as well as poorly phosphorylated neurofilaments.

Neurones respond differently to injury depending on whether the damage occurs in the CNS or the PNS. The glial microenvironment of a damaged central axon does not facilitate axonal regrowth, consequently reconnection with original synaptic targets does not normally occur. In marked contrast, the glial microenvironment in the PNS is capable of facilitating axonal regrowth. However, functional outcome of clinical repair of a large mixed peripheral nerve, especially if the injury occurs some distance from the target organ, or produces a long defect in the damaged nerve, is frequently unsatisfactory.

Axoplasmic flow

Neuronal organelles and cytoplasm are in continual motion. Bidirectional streaming of vesicles along axons results in a net transport of materials from the soma to the terminals, with more limited movement in the opposite direction. Two major types of transport occur, one slow, and one relatively fast. Slow axonal transport is a bulk flow of axoplasm only in the anterograde direction, carrying cytoskeletal proteins and soluble, non-membrane bound proteins from the soma to the terminals at a rate of approximately 0.1–3 mm a day. In contrast, fast axonal transport carries membrane-bound vesicular material (endosomes and lysosomal autophagic vacuoles) and mitochondria at approximately 200 mm a day in the retrograde direction (towards the soma) and approximately 40 mm per day anterogradely (in particular, synaptic vesicles containing neurotransmitters).

Rapid flow depends on microtubules. Vesicles with side projections line up along microtubules and are transported along them by their side-arms. Two microtubule-based motor proteins with ATPase activity are involved in fast transport: kinesin family proteins are responsible for the fast component of anterograde transport, and cytoplasmic dynein is responsible for retrograde transport. Microtubule-dependent axonal transport is reviewed in Guzik and Goldstein (2004). Retrograde transport mediates the movement of neurotrophic viruses, e.g. herpes zoster, rabies and polio, from peripheral terminals, and their subsequent concentration in the neuronal soma.

SYNAPSES

Transmission of impulses across specialized junctions (synapses) between two neurones is largely chemical and depends on the release of neurotransmitters from the presynaptic side. This causes a change in the electrical state of the postsynaptic neuronal membrane, resulting in either its depolarization or hyperpolarization.

The patterns of axonal termination vary considerably. A single axon may synapse with one neurone (e.g. climbing fibres ending on cerebellar Purkinje neurones), or more often with many neurones (e.g. cerebellar parallel fibres, which provide an extreme example of this phenomenon (p. 302). In synaptic glomeruli, e.g. in the olfactory bulb and cerebellum, and synaptic cartridges, groups of synapses between two or many neurones form interactive units encapsulated by neuroglia (Fig. 3.7).

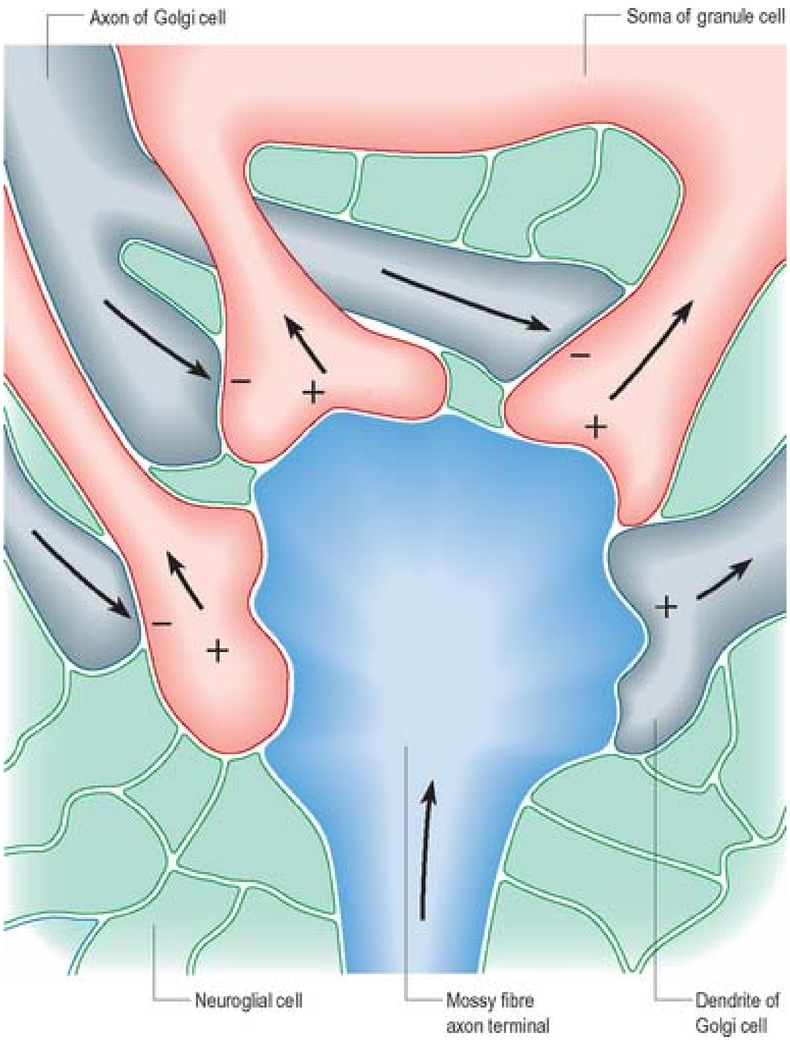
Axon of Golgi cell
Soma of granule cell
−
+
−
+
−
+
+
Neuroglial cell
Mossy fibre axon terminal
Dendrite of Golgi cell

Fig. 3.7 The arrangement of a complex synaptic unit. A cerebellar synaptic glomerulus with excitatory ('+') and inhibitory ('−') synapses grouped around a central axonal bouton. The directions of transmission are shown by the arrows.

Electrical synapses (direct communication via gap junctions) are rare in the human CNS and are confined largely to groups of neurones with tightly coupled activity, e.g. the inspiratory centre in the medulla. They will not be discussed further here.

Classification of chemical synapses

Chemical synapses have an asymmetric structural organization (Fig. 3.8 and Fig. 3.9) in keeping with the unidirectional nature of their transmission. Typical chemical synapses share a number of important features. They all display an area of presynaptic membrane apposed to a corresponding postsynaptic membrane: the two are separated by a narrow (20–30 nm) gap, the synaptic cleft. Synaptic vesicles containing neurotransmitter lie on the presynaptic side, clustered near a dense plaque on the cytoplasmic aspect of the presynaptic membrane. A corresponding region of submembrane density is present on the postsynaptic side. Together these define the active zone, the area of the synapse where neurotransmission takes place.

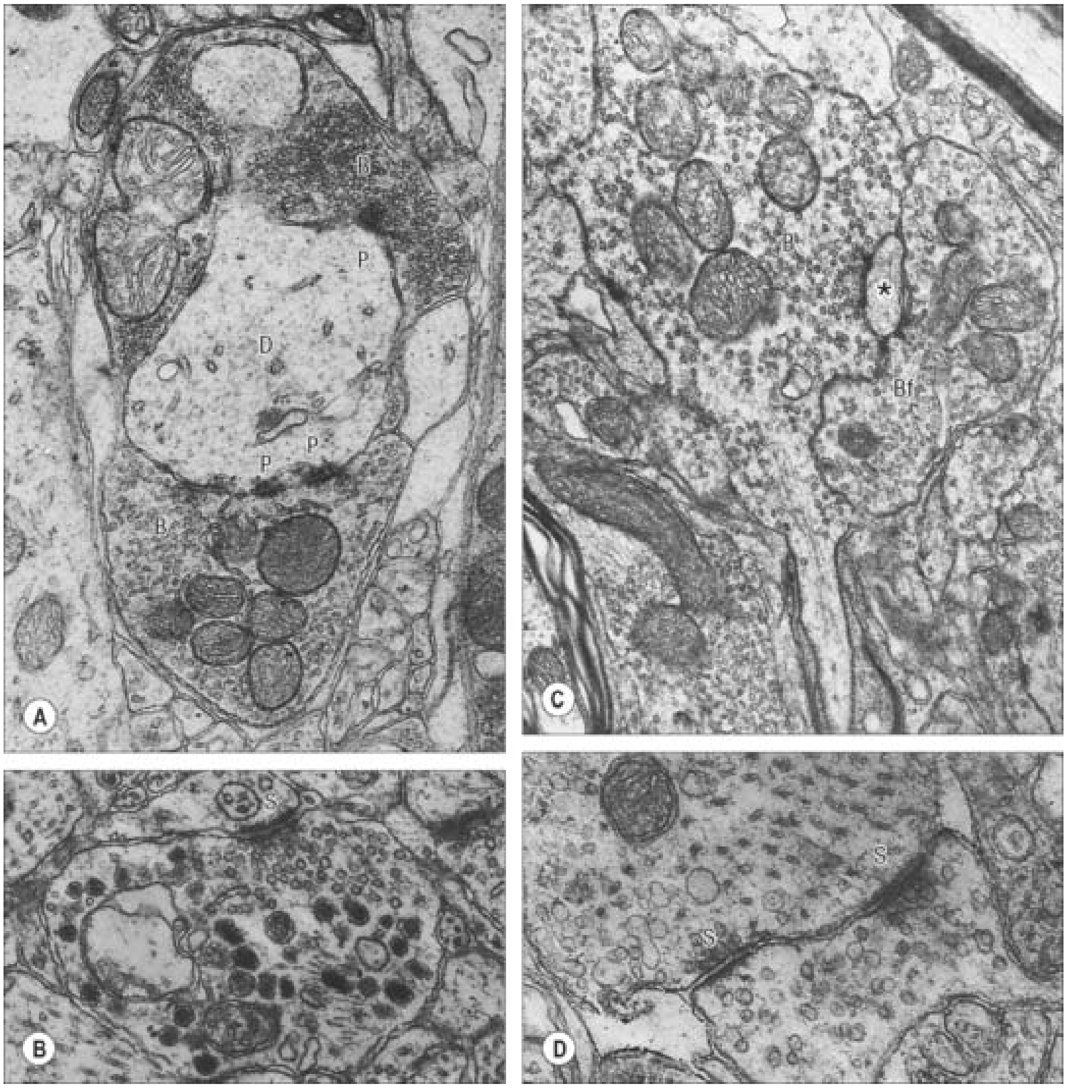

Fig. 3.8 Electron micrographs demonstrating various types of synapse. **A**, Cross-section of a dendrite (D) upon which two synaptic boutons (B) end. The upper bouton contains round vesicles, and the lower bouton contains flattened vesicles of the small type. A number of pre- and postsynaptic (P) thickenings mark the specialized zones of contact. **B**, A type I synapse (S, postsynaptic site) containing both small, round, clear vesicles and also large dense-cored vesicles of the neurosecretory type. **C**, A large terminal bouton (B) of an optic nerve afferent fibre, which is making contact with a number of postsynaptic processes, in the dorsal lateral geniculate nucleus of the rat. One of the postsynaptic processes (*) also receives a synaptic contact from a bouton (Bf) containing flattened vesicles. **D**, Reciprocal synapses (S) between two neuronal processes in the olfactory bulb.

(By courtesy of Professor AR Lieberman, Department of Anatomy, University College, London.)

Chemical synapses can be classified according to a number of different parameters including the neuronal regions forming the synapse, their ultrastructural characteristics, the chemical nature of their neurotransmitter(s) and their effects on the electrical state of the postsynaptic neurone. The following classification is limited to associations between neurones. Neuromuscular junctions share many (though not all) of these parameters, and are often referred to as peripheral synapses. They are described separately on page 63.

Synapses can occur between almost any surface regions of the participating neurones. The most common type occurs between an axon and either a dendrite or a soma, when the axon is expanded as a small bulb or bouton (Fig. 3.8, Fig. 3.9). This may be a terminal of an axonal branch (terminal bouton) or one of a row of bead-like endings, when the axon makes contact at several points, often with more than one neurone (bouton de passage). Boutons may synapse with dendrites, including dendritic spines or the flat surface of a dendritic shaft, a soma (usually on its flat surface, but occasionally on spines), the axon hillock and the terminal boutons of other axons.

The connection is classified according to the direction of transmission, and the incoming terminal region is named first. Most common are axodendritic synapses, although axosomatic connections are frequent. All other possible combinations are found but are less common, i.e. axoaxonic, dendroaxonic, dendrodendritic, somatodendritic or somatosomatic. Axodendritic and axosomatic synapses occur in all regions of the CNS and in autonomic ganglia, including those of the ENS. The other types appear restricted to regions of complex interaction between larger sensory neurones and microneurones, e.g. in the thalamus.

Ultrastructurally, synaptic vesicles may be internally clear or dense, and of different size (loosely categorized as small or large) and shape (round, flat or pleomorphic, i.e. irregularly shaped). The submembranous densities may be thicker on the postsynaptic than on the presynaptic side (asymmetric synapses), or equivalent in thickness (symmetrical synapses). Synaptic ribbons are found at sites of neurotransmission in the retina and inner ear. They have a distinctive morphology, in that the synaptic vesicles are grouped around a ribbon- or rod-like density orientated perpendicular to the cell membrane (Fig. 3.9).

Synaptic boutons make obvious close contacts with postsynaptic structures, but many other terminals lack specialized contact zones. Areas of transmitter release occur in the varicosities of unmyelinated axons, where effects are sometimes diffuse, e.g. the aminergic pathways of the basal ganglia and in autonomic fibres in the periphery. In some instances, such axons may ramify widely throughout extensive areas of the brain and affect the behaviour of very large populations of neurones, e.g. the diffuse cholinergic innervation of the cerebral cortices. Pathological degeneration of these pathways can therefore cause widespread disturbances in neural function.

Neurones express a variety of neurotransmitters, either as one class of neurotransmitter per cell or more often as several. Good correlations exist between some types of transmitter and specialized structural features of synapses. In general, asymmetric synapses with relatively small spherical vesicles are associated with acetylcholine (ACh), glutamate, serotonin (5-

hydroxytryptamine, 5-HT), and some amines; those with dense-core vesicles include many peptidergic synapses and other amines (e.g. noradrenaline (norepinephrine), adrenaline (epinephrine), dopamine). Symmetrical synapses with flattened or pleomorphic vesicles have been shown to contain either γ-aminobutyric acid (GABA) or glycine.

Neurosecretory endings found in various parts of the brain and in neuroendocrine glands and cells of the dispersed neuroendocrine system (see below; p. 31) share many features with presynaptic boutons. They all contain peptides or glycoproteins within dense-core vesicles. The latter are of characteristic size and appearance: they are often ellipsoidal or irregular in shape, and relatively large, e.g. oxytocin and vasopressin vesicles in the neurohypophysis may be up to 200 nm across.

Synapses may cause depolarization or hyperpolarization of the postsynaptic membrane, depending on the neurotransmitter released and the classes of receptor molecule in the postsynaptic membrane. Depolarization of the postsynaptic membrane results in excitation of the postsynaptic neurone, whereas hyperpolarization has the effect of transiently inhibiting electrical activity. Subtle variations in these responses may also occur at synapses where mixtures of neuromediators are present and their effects are integrated.

Type I and II synapses

There are two broad categories of synapse: type I synapses, in which the cytoplasmic density is thicker on the postsynaptic side, and type II synapses, in which the pre- and post-synaptic densities are more symmetrical but thinner. Type I boutons contain a predominance of small spherical vesicles approximately 50 nm in diameter, and type II boutons contain a variety of flat forms. Throughout the CNS, type I synapses are generally excitatory and type II, inhibitory. In a few instances types I and II synapses are found in close proximity, orientated in opposite directions across the synaptic cleft (a reciprocal synapse).

Mechanisms of synaptic activity

Synaptic activation begins with arrival of one or more action potentials at the presynaptic bouton, which causes the opening of voltage-sensitive calcium channels in the presynaptic membrane. The response time in typical fast-acting synapses is then very rapid; classic neurotransmitter (e.g. ACh) is released in less than a millisecond, which is faster than the activation time of a classic second messenger system on the presynaptic side. The influx of calcium activates Ca^{2+}-dependent protein kinases. This uncouples synaptic vesicles from a spectrin-actin meshwork within the presynaptic ending, to which they are bound via synapsins I and II. The vesicles dock with the presynaptic membrane, through processes not yet fully understood, and their membranes fuse to open a pore through which neurotransmitter diffuses into the synaptic cleft.

Once the vesicle has discharged its contents, its membrane is incorporated into the presynaptic plasma membrane and is then more slowly recycled back into the bouton by endocytosis around the edges of the active site. The time between endocytosis and re-release may be approximately 30 seconds; newly recycled vesicles compete randomly with previously stored vesicles for the next cycle of neurotransmitter release. The fusion of vesicles with the presynaptic membrane is responsible for the observed quantal behaviour of neurotransmitter release, both during neural activation and spontaneously, in the slightly leaky resting condition.

Postsynaptic events vary greatly, depending on the receptor molecules and their related molecular complexes. Receptors are generally classed as either ionotropic or metabotropic. Ionotropic receptors function as ion channels, so that conformational changes induced in the receptor protein when it binds the neurotransmitter cause the opening of an ion channel within the same protein assembly, thus causing a voltage change within the postsynaptic cell. Examples are the nicotinic ACh receptor and the N-methyl-D-aspartate (NMDA) glutamate receptor. Alternatively, the receptor and ion channel may be separate molecules, coupled by G-proteins, some via a complex cascade of chemical interactions (a second messenger system), e.g. the adenylate cyclase pathway. Postsynaptic effects are generally rapid and short-lived, because the transmitter is quickly inactivated either by an extracellular enzyme (e.g. acetylcholinesterase, AChE), or by uptake by neuroglial cells. Examples of such metabotropic receptors are the muscarinic Ach receptor and 5-HT receptor.

Neurohormones

Neurohormones are included in the class of molecules with neurotransmitter-like activity. They are synthesized in neurones and released into the blood circulation by exocytosis at synaptic terminal-like structures. As with classic endocrine gland hormones, they may act at great distances from their site of secretion. Neurones secrete into the CSF or local interstitial fluid to affect other cells, either diffusely or at a distance. To encompass this wide range of phenomena the general term neuromediation has been used, and the chemicals involved are called neuromediators.

Neuromodulators

Some neuromediators do not appear to affect the postsynaptic membrane directly, but they can affect its responses to other neuromediators, either enhancing their activity (by increasing or prolonging the immediate response), or perhaps limiting or inhibiting their action. These substances are called neuromodulators. A single synaptic terminal may contain one or more neuromodulators in addition to a neurotransmitter, usually (though not always) in separate vesicles. Neuropeptides (see below) are nearly all neuromodulators, at least in some of their actions. They are stored within dense granular synaptic vesicles of various sizes and appearances.

Development and plasticity of synapses

Embryonic synapses first appear as inconspicuous dense zones flanking synaptic clefts. Immature synapses often appear after birth, suggesting that they may be labile, and are reinforced if transmission is functionally effective, or withdrawn if redundant. This is implicit in some theories of memory, which postulate that synapses are modifiable by frequency of use, to establish preferential conduction pathways. Evidence from hippocampal neurones suggests that even brief synaptic activity can increase the strength and sensitivity of the synapse for some hours or longer (long-term potentiation, LTP). During early postnatal life, the normal developmental increase in numbers and sizes of synapses and dendritic spines depends on the degree of neural activity and is impaired in areas of damage or functional deprivation.

Neurotransmitter molecules

Until recently the molecules known to be involved in chemical synapses were limited to a fairly small group of classic neurotransmitters, e.g. ACh, noradrenaline, adrenaline, dopamine and histamine, all of which had well-defined rapid effects on other neurones, muscle cells or glands. However, many synaptic interactions cannot be explained on the basis of classic neurotransmitters, and it is now known that other substances, particularly some amino acids such as glutamate, glycine, aspartate, GABA and the monoamine, serotonin, also function as transmitters. Substances first identified as hypophysial hormones or as part of the dispersed neuroendocrine system (see below) of the alimentary tract, can be detected widely throughout the CNS and PNS, often associated with functionally integrated systems. Many of these are peptides: more than 50 (together with other candidates), function mainly as neuromodulators and influence the activities of classic transmitters.

Acetylcholine

Acetylcholine (ACh) is perhaps the most extensively studied neurotransmitter of the classic type. Its precursor, choline, is synthesized in the neuronal soma and transported to the axon terminals where it is acetylated by the enzyme choline acetyl transferase (ChAT), and stored in clear spherical vesicles approximately 50 nm in diameter. ACh is synthesized by motor neurones and released at all their motor terminals on skeletal muscle. It is released by preganglionic fibres at synapses in parasympathetic and sympathetic ganglia, and many parasympathetic, and some sympathetic, ganglionic neurones are cholinergic. In some sites e.g. at neuromuscular junctions, ACh is also associated with the degradative extracellular enzyme AChE.

The effects of ACh on nicotinic receptors (i.e. those in which nicotine is an agonist) are rapid and excitatory. In the peripheral autonomic nervous system, the slower, more sustained excitatory effects of cholinergic autonomic endings are mediated by muscarinic receptors via a second messenger system.

Monoamines

Monoamines include the catecholamines (noradrenaline, adrenaline and dopamine), and the indoleamine serotonin (5-hydroxytryptamine, 5-HT) and histamine. They are synthesized by neurones in sympathetic ganglia and by their homologues, the chromaffin cells of the suprarenal medulla and paraganglia. Within the CNS, the somata of monoaminergic neurones lie mainly in the brainstem, although their axons ramify widely into all parts of the nervous system. Monoaminergic cells are also present in the retina.

Noradrenaline is the chief transmitter present in sympathetic ganglionic neurones with endings in various tissues, notably smooth muscle and glands, and in other sites including adipose and haemopoietic tissues, and the corneal epithelium. It is also found at widely distributed synaptic endings within the CNS, many of them terminals of neuronal somata situated in the locus coeruleus in the medullary floor. The actions of noradrenaline depend on its site of action, and vary with the type of postsynaptic receptor. In some cases, e.g. the neurones of the submucosal plexus of the intestine and of the locus coeruleus, it is strongly inhibitory via actions on the α_2-adrenergic receptor, whereas the β-receptors, e.g. of vascular smooth muscle, mediate depolarization and therefore vasoconstriction. Adrenaline is present in central and peripheral nervous pathways and occurs with noradrenaline in the suprarenal medulla. Both adrenaline and noradrenaline are found in dense-cored synaptic vesicles approximately 50 nm diameter.

Dopamine is a neuromediator of considerable clinical importance, found mainly in neurones with cell bodies in the telencephalon, diencephalon and mesencephalon. A major dopaminergic neuronal population in the midbrain constitutes the substantia nigra, so called because its cells contain neuromelanin, a black granular byproduct of dopamine synthesis. Dopaminergic endings are particularly numerous in the corpus striatum, limbic system and cerebral cortex. Structurally, dopaminergic synapses contain numerous dense-cored vesicles that resemble those containing noradrenaline. Pathological reduction in dopaminergic activity has widespread effects on motor control, affective behaviour and other neural activities, as seen in Parkinson’s syndrome (Ch. 22).

Serotonin and histamine are found in neurones mainly within the CNS. Serotonin is typically synthesized in small midline neuronal clusters in the brainstem, mainly in the raphe nuclei: the axons from these neurones ramify extensively throughout the entire brain and spinal cord. Synaptic terminals contain rounded, clear vesicles approximately 50 nm diameter and are of the asymmetrical type. Histaminergic neurones appear to be relatively sparse, and are restricted largely to the hypothalamus.

Amino acids

GABA is a major inhibitory transmitter released at the terminals of local circuit neurones within the brainstem and spinal cord (e.g. the recurrent inhibitory Renshaw loop), cerebellum (where it is the main transmitter of Purkinje cells), basal ganglia, cerebral cortex, thalamus and subthalamus. It is stored in flattened or pleomorphic vesicles within symmetrical synapses. GABA may be inhibitory to the postsynaptic neurone, or may mediate either presynaptic inhibition or facilitation, depending on the synaptic arrangement.

Glutamate and aspartate are major excitatory transmitters present widely within the CNS, including the major projection pathways from the cortex to the thalamus, tectum, substantia nigra and pontine nuclei. They are found in the central terminals of the auditory and trigeminal nerves, and glutamate is present in the terminals of parallel fibres ending on Purkinje cells in the cerebellum. Structurally, glutamate and aspartate are associated with asymmetrical synapses containing small (approximately 30 nm) round, clear synaptic vesicles.

Glycine is a well-established inhibitory transmitter of the CNS, particularly the lower brainstem and spinal cord, where it is mainly found in local circuit neurones.

Nitric oxide

Nitric oxide (NO) is of considerable importance at autonomic and enteric synapses, where it mediates smooth muscle relaxation. NO has been implicated in the mechanism of long-term potentiation. It is able to diffuse freely through cell membranes, and so is not under such tight quantal control as vesicle-mediated neurotransmission.

Neuropeptides

Many neuropeptides coexist with other neuromediators in the same synaptic terminals. As many as three peptides often share a particular ending with a well-established neurotransmitter, in some cases within the same synaptic vesicles. Some peptides occur both in the CNS and PNS, particularly in the ganglion cells and peripheral terminals of the ANS, whilst others are entirely restricted to the CNS. Only a few examples are given here.

Most of the neuropeptides are classified according to the site where they were first discovered. For example, the gastrointestinal peptides were initially found in the gut wall, and a group that includes releasing hormones, adenohypophysial and neurohypophysial hormones was first associated with the pituitary gland. Some of these peptides are closely related to each other in their chemistry, because they are derived from the same gene products (e.g. the pro-opiomelanocortin group), which are cleaved to produce smaller peptides.

Substance P (SP) was the first of the peptides to be characterized as a gastrointestinal neuromediator and is considered to be the prototypic neuropeptide. It is an 11-amino acid polypeptide that belongs to the tachykinin neuropeptide family, and is a major neuromediator in the brain and spinal cord. Contained within large granular synaptic vesicles, SP is found in approximately 20% of dorsal root and trigeminal ganglion cells, in particular in small nociceptive neurones, and in some fibres of the facial, glossopharyngeal and vagal nerves. Within the CNS, SP is present in several apparently unrelated major pathways, and has been described in the limbic system, basal ganglia, amygdala and hypothalamus. Its known action is prolonged postsynaptic excitation, particularly from nociceptive afferent terminals, which sustains the effects of noxious stimuli. SP is one of the main neuropeptides that trigger an inflammatory response in the skin and has also been implicated in the vomiting reflex, changes in cardiovascular tone, stimulation of salivary secretion, smooth muscle contraction, and vasodilation.

Vasoactive intestinal polypeptide (VIP), another gastrointestinal peptide, is widely present in the CNS, where it is probably an excitatory neurotransmitter or neuromodulator. It is found in distinctive bipolar neurones of the cerebral cortex; small dorsal root ganglion cells, particularly of the sacral region; the median eminence of the hypothalamus, where it may be involved in endocrine regulation; intramural ganglion cells of the gut wall; sympathetic ganglia.

Somatostatin (ST, somatotropin release inhibiting factor) has a broad distribution within the central nervous system, and may be a central neurotransmitter or neuromodulator. It also occurs in small dorsal root ganglion cells. β-Endorphin, leu- and metenkephalins and the dynorphins belong to a group of peptides called the naturally occurring opiates that possess analgesic properties. They bind to opiate receptors in the brain where, in general, their action seems to be inhibitory. Enkephalins have been localized in many areas of the brain. Their particular localization in the septal nuclei, amygdaloid complex, basal ganglia and hypothalamus, suggests that they are important mediators in the limbic system and in the control of endocrine function. They have also been implicated strongly in the central control of pain pathways, because they are found in the periaqueductal grey matter of the midbrain, a number of reticular raphe nuclei, the spinal nucleus of the trigeminal nerve and the substantia gelatinosa of the spinal cord. The enkephalinergic pathways exert an important presynaptic inhibitory action on nociceptive afferents in the spinal cord and brainstem. Like many other neuromediators, enkephalins also occur widely in other parts of the brain in lower concentrations.

CENTRAL GLIA

Glial (neuroglial) cells vary considerably in type and number in different regions of the CNS. There are two major groups, macroglia (astrocytes and oligodendrocytes) and microglia, classified according to origin. Macroglia arise within the neural plate, in parallel with neurones, and constitute the great majority of glial cells. Their functions are diverse and are now known to extend beyond a passive supporting role (reviewed in He & Sun, 2007). Microglia are smaller cells, generally considered to be monocytic in origin, and are derived from haemopoietic tissue (see Fig. 3.21).

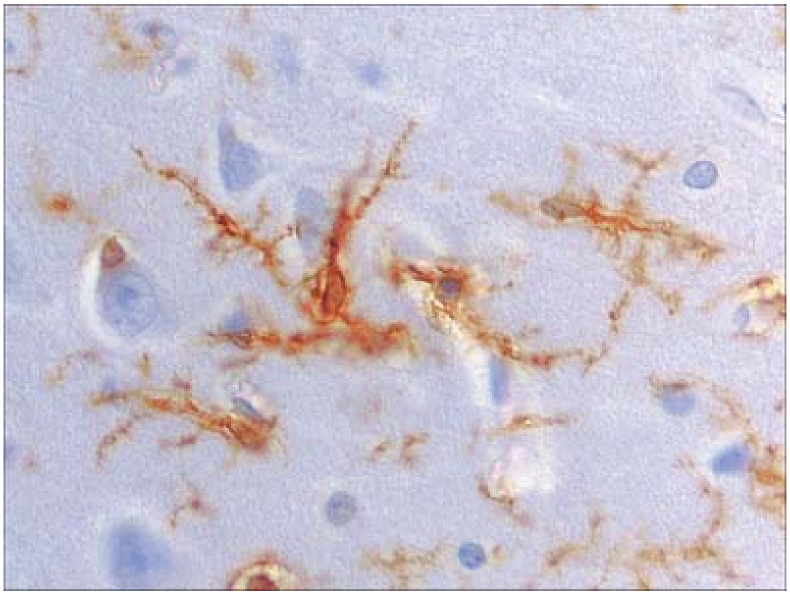

Fig. 3.21 Activated microglial cells in the human central nervous system, in a biopsy from a patient with Rasmussen’s encephalitis, visualized using MHC class II antigen immunohistochemistry.

(By courtesy of Dr Norman Gregson, Division of Neurology, GKT School of Medicine, London.)

ASTROCYTES

Astrocytes are star-shaped glia (Fig. 3.10). Their processes, which ramify through the entire central neuropil (Fig. 3.11), are coupled functionally at gap junctions, forming an interconnected network which ensheathes all neurones, other than at synapses and along the myelinated segments of axons. Some astrocyte processes terminate as end-feet on the basal lamina of blood vessels, and at the pial surface, where they form the glia limitans (glial limiting membrane).

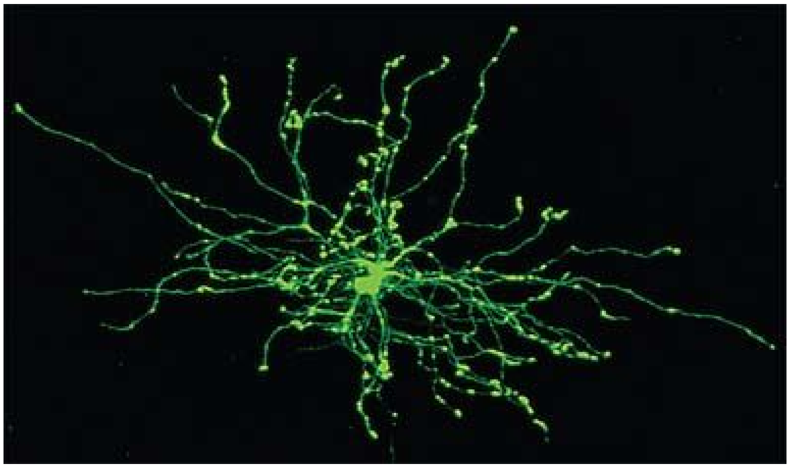

Fig. 3.10 Confocal micrograph of an astrocyte in an adult rat optic nerve, iontophoretically filled with an immunofluorescent dye by intracellular microinjection. (Prepared by Professor A Butt, Portsmouth, and Kate Colquhoun, formerly of Division of Physiology, GKT School of Medicine, London.)

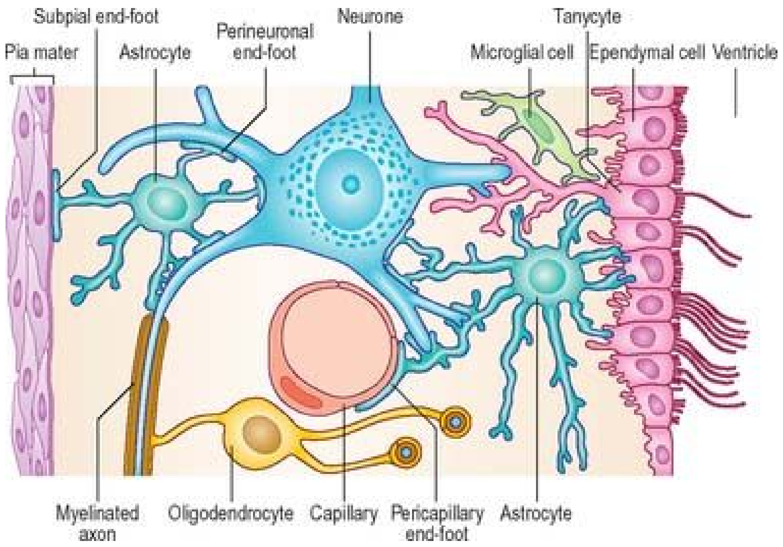
Subpial end-foot
Pia mater
Astrocyte
Perineuronal end-foot
Neurone
Tanycyte
Microglial cell
Ependymal cell
Ventricle
Myelinated axon
Oligodendrocyte
Capillary
Pericapillary end-foot
Astrocyte

Fig. 3.11 The different types of non-neuronal cell in the CNS and their structural organization and interrelationships with each other and with neurones.

Astrocytes have been divided into two subtypes, fibrous and protoplasmic, on morphological grounds. Fibrous astrocytes occur predominantly in white matter and protoplasmic astrocytes are found mainly in grey matter. The significance of these subtypes is unclear since there are few known functional differences between fibrous and protoplasmic astrocytes. Astrocytes typically have a pale nucleus with a narrow rim of heterochromatin, although this is variable. Their cytoplasm is pale and contains glycogen, lysosomes, Golgi complexes and bundles of glial intermediate filaments that extend into their processes (these last are found particularly in fibrous astrocytes). Glial intermediate filaments are formed from glial fibrillary acidic protein (GFAP): its presence can be used clinically to identify tumour cells of glial origin.

Astrocytes are now thought to provide a network of communication, providing integration and regulation of function in the brain (reviewed in Fields 2004, Volterra & Meldolesi 2005). One form of communication, with other astrocytes, is via interconnecting low resistance gap junctional complexes. There is recent evidence that astrocytic (and other neural) gap junctions may be formed by a novel family of proteins, the pannexins (see p.

7). They signal to each other using intracellular calcium wave propagation, triggered by synaptically-released glutamate. Signalling presumably co-ordinates astrocyte functions that are essential for efficient neuronal activity, such as ion (particularly potassium) buffering; neurotransmitter uptake and metabolism (e.g. of excess glutamate, which is excitotoxic); membrane transport; the secretion of peptides, amino acids, trophic factors etc. The complexity of astrocytic function and dysfunction in neurological disorders is reviewed in Seifert et al (2006).

Injury to the CNS induces astrogliosis, seen as a local increase in the number and size of cells expressing GFAP, and in the production of an extensive meshwork of processes to form a glial scar. It is thought that the microenvironment of a glial scar, which may also include cells of oligodendrocyte lineage and myelin debris, plays an important role in inhibiting regrowth of damaged CNS axons.

Pituicytes are glial cells found in the neural parts of the pituitary gland, the infundibulum and neurohypophysis. They resemble astrocytes, but their processes end mostly on endothelial cells in the neurohypophysis and tuber cinereum.

Blood–brain barrier

Proteins circulating in the blood enter most tissues of the body except those of the brain, spinal cord or peripheral nerves. This concept of a blood–brain or a blood–nerve barrier applies to many substances – some are actively transported across the blood–brain barrier, others are actively excluded. The blood–brain barrier is located at the capillary endothelium within the brain and is dependent upon the presence of tight junctions between endothelial cells coupled with a relative lack of transcytotic vesicular transport. The tightness of the barrier depends upon the close apposition of astrocytes, which direct the formation of endothelial tight junctions, to blood capillaries (reviewed in Abbott et al 2006) (Fig. 3.12, Fig. 3.13).

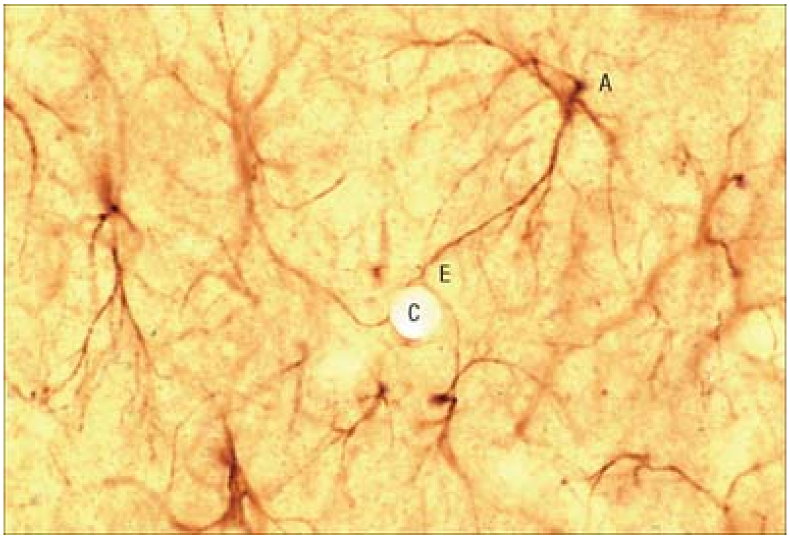

Fig. 3.12 Astrocytes (A) in rat brain, immunolabelled to show glial fibrillary acidic protein (brown). Fine processes form end-feet (E) on brain capillaries (C). Note that astrocytes have extremely dense, numerous processes: immunostaining only reveals a proportion of the processes. (Prepared by Mr Marios Hadjipavlou, King's College, London.)

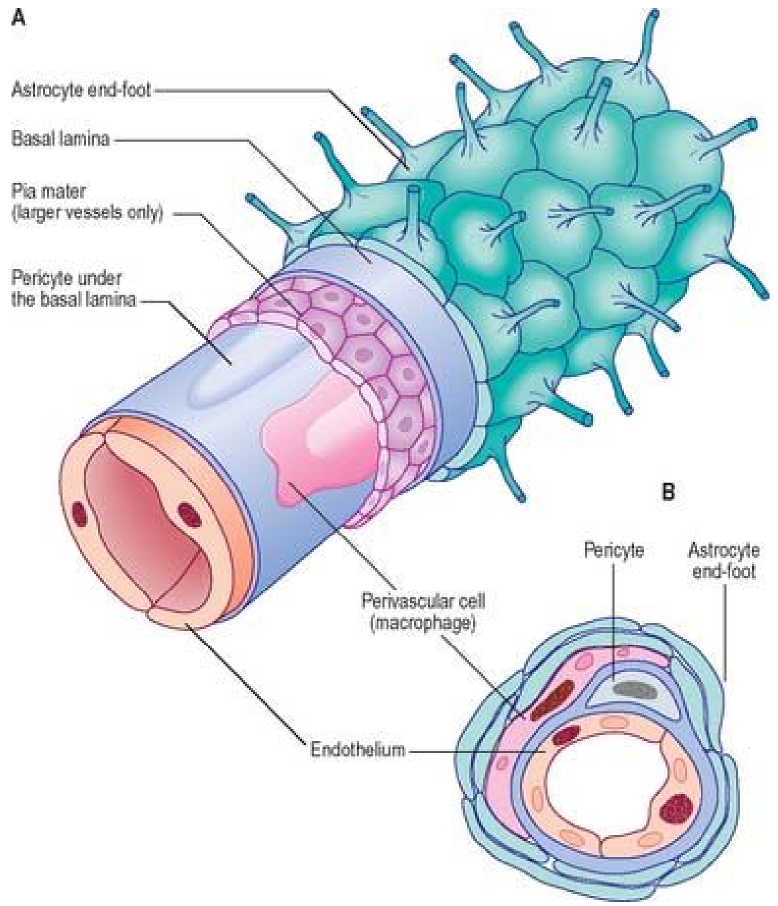
A
Astrocyte end-foot
Basal lamina
Pia mater
(larger vessels only)
Pericyte under
the basal lamina
Perivascular cell
(macrophage)
Endothelium
B
Pericyte
Astrocyte
end-foot

Fig. 3.13 The relationship between the glia limitans, perivascular cells and blood vessels within the brain, in longitudinal and transverse section. A sheath of astrocytic end-feet wraps around the vessel and, in vessels larger than capillaries, its investment of pial meninges. Vascular endothelial cells are joined by tight junctions and supported by pericytes; perivascular macrophages lie outside the endothelial basal lamina.

The blood–brain barrier develops during embryonic life but may not be fully completed by birth. There are certain areas of the adult brain where the endothelial cells are not linked by tight junctions, which means that a free exchange of molecules occurs between blood and adjacent brain. Most of these areas are situated close to the ventricles and are known as circumventricular organs (p. 240). Elsewhere, unrestricted diffusion through the blood–brain barrier is only possible for substances that can cross biological membranes because of their lipophilic character. Lipophilic molecules may be actively re-exported by the brain endothelium.

Breakdown of the blood–brain barrier occurs when the brain is damaged by ischaemia or infection, and is also associated with primary and metastatic cerebral tumours. Reduced blood flow to a region of the brain alters the permeability and regulatory transport functions of the barrier locally: the increased stress on compromised endothelial cells results in leakage of fluid, ions, serum proteins and intracellular substances into the extracellular space of the brain. The integrity of the barrier can be evaluated clinically using CT and fMRI. Breakdown of the blood–brain barrier may be seen at postmortem in jaundiced patients who have had an infarction. Normally, the brain, spinal cord and peripheral nerves remain unstained by the bile post mortem, although the choroid plexus is often stained a deep yellow. However, areas of recent infarction (1–3 days) will also be stained by bile pigment because of the localized breakdown of the blood–brain barrier.

OLIGODENDROCYTES

Oligodendrocytes myelinate CNS axons and are most commonly seen as intrafascicular cells in myelinated tracts (Fig. 3.14, Fig. 3.15). They usually have round nuclei and their cytoplasm contains numerous mitochondria, microtubules and glycogen. They display a spectrum of morphological variation, from cells with large euchromatic nuclei and pale cytoplasm, to cells with heterochromatic nuclei and dense cytoplasm. Oligodendrocytes may enclose up to 50 axons in separate myelin sheaths, and the largest calibre axons are usually ensheathed on a 1 : 1 basis. Some oligodendrocytes are not associated with axons, and are either precursor cells or perineuronal (satellite) oligodendrocytes whose processes ramify around neuronal somata.

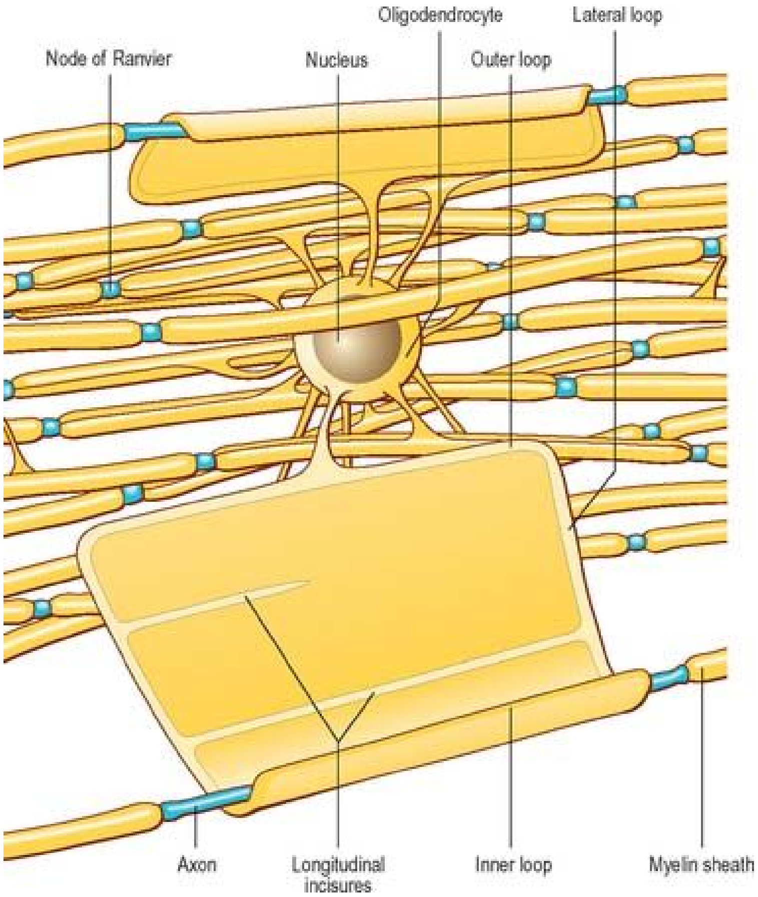
Oligodendrocyte
Lateral loop
Node of Ranvier
Nucleus
Outer loop
Axon
Longitudinal incisures
Inner loop
Myelin sheath

Fig. 3.14 The ensheathment of a number of axons by the processes of an oligodendrocyte. The oligodendrocyte soma is shown in the centre and its

myelin sheaths are unfolded to varying degrees to show their extensive surface area.

(Modified from Morell & Norton 1980 by Raine 1984, by permission.)

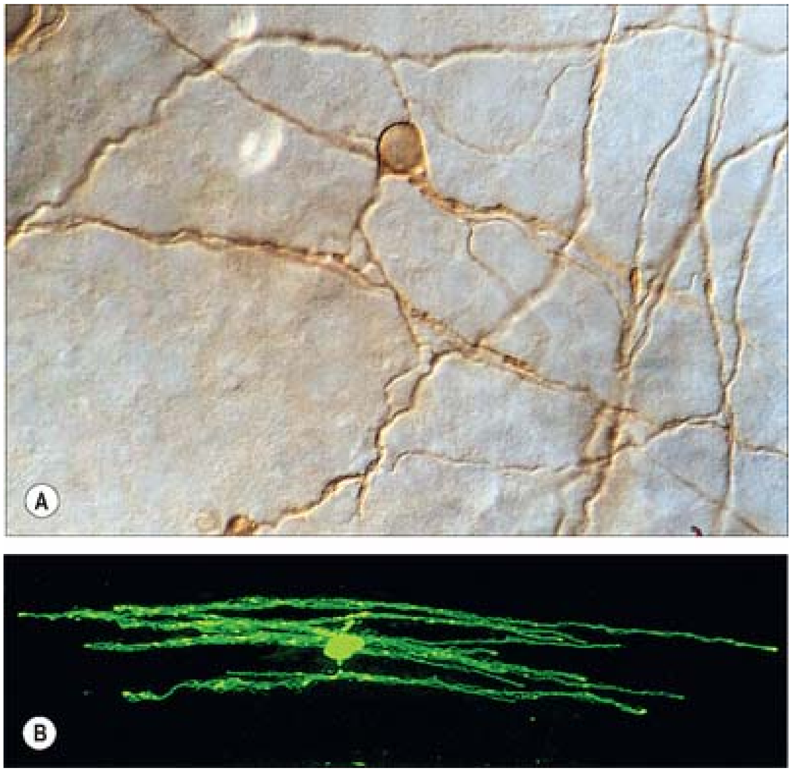

Fig. 3.15 **A**, An oligodendrocyte enwrapping several axons with myelin, demonstrated in a whole-mounted rat anterior medullary velum, immunolabelled with antibody to an oligodendrocyte membrane antigen. **B**, Confocal micrograph of a mature myelin forming oligodendrocyte in an adult rat optic nerve, iontophoretically filled with an immunofluorescent dye by intracellular microinjection.

*(**A**, By courtesy of Fiona Ruge; **B**, prepared by Professor A Butt, Portsmouth, and Kate Colquhoun, formerly Division of Physiology, GKT School of Medicine, London.)*

Within tracts, interfascicular oligodendrocytes are arranged in long rows interspersed with single astrocytes at regular intervals. Since oligodendrocyte processes are radially aligned to the axis of each row, myelinated tracts typically consist of cables of axons myelinated by a row of oligodendrocytes running down the axis of each cable.

Oligodendrocytes originate from the ventricular neurectoderm and the subependymal layer in the fetus (p. 368), and continue to be generated from the subependymal plate postnatally. Stem cells migrate and seed into white and grey matter to form a pool of adult progenitor cells which may later differentiate to replenish lost oligodendrocytes, and possibly remyelinate pathologically demyelinated regions.

Nodes of Ranvier and incisures of Schmidt–Lanterman

The territory ensheathed by an oligodendrocyte (or Schwann cell) process defines an internode, the interval between internodes is called a node of Ranvier (Fig. 3.16) and the territory immediately adjacent to the nodal gap is a paranode, where loops of oligodendrocyte cytoplasm abut the axolemma. Nodal axolemma is contacted by fine filopodia of perinodal cells which have been shown in animal studies to have a presumptive adult oligodendrocyte progenitor phenotype: their function is unknown (reviewed in Butt et al 2005). Schmidt–Lanterman incisures are helical decompactions of internodal myelin where the major dense line of the myelin sheath splits to enclose a spiral of oligodendrocyte cytoplasm. Their structure suggests that they may play a role in the transport of molecules across the myelin sheath, but their function is not known.

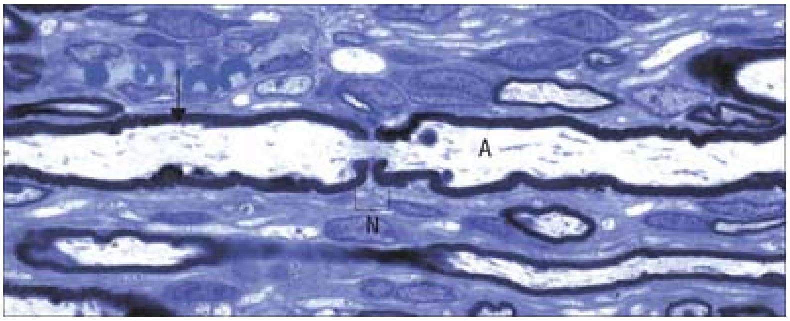

Fig. 3.16 A node of Ranvier (N) in the central nervous system. The pale-staining axon (A) is ensheathed by oligodendrocyte myelin (arrow), apart

from a short, exposed region at the node. Toluidine blue stained resin section (rat tissue).

(By courtesy of Dr Clare Farmer, King’s College, London.)

MYELIN AND MYELINATION

Myelin is formed by oligodendrocytes (CNS) and Schwann cells (PNS). A single oligodendrocyte may ensheathe up to 50 separate axons, depending upon calibre, whereas myelinating Schwann cells ensheathe axons on a 1 : 1 basis.

In general, myelin is laid down around axons above 2 μm diameter. However, the critical minimal axon diameter for myelination is smaller and more variable in the CNS than in the PNS (approximately 0.2 μm in the CNS compared with 1–2 μm in the PNS). There is considerable overlap between the size of the smallest myelinated and the largest unmyelinated axons, and so axonal calibre is unlikely to be the only factor in determining myelination. Moreover, the first axons to become ensheathed ultimately attain larger diameters than those that are ensheathed at a later date. There is a reasonable linear relationship between axon diameter and internodal length and myelin sheath thickness: as the sheath thickens from a few lamellae to up to 200, the axon may also grow from 1 to 15 μm in diameter. Internodal lengths increase about tenfold during the same time.

It is not known precisely how myelin is formed in either PNS or CNS, but in the CNS it has been shown recently to depend in part on expression of a protein (Wiskott–Aldrich syndrome protein family verprolin homologous; WAVE), which influences the actin cytoskeleton, oligodendrocyte lamellipodia formation and myelination (Kim et al 2006). The ultrastructural appearance of myelin is usually explained in terms of the spiral wrapping of an extensive, flat glial process (lamellipodium) around an axon, and the subsequent extrusion of cytoplasm from the sheath at all points other than incisures and paranodes. In this way, the compacted external surfaces of the plasma membrane of the ensheathing glial cell are thought to produce the minor dense lines, and the compacted inner cytoplasmic surfaces, the major dense lines, of the mature myelin sheath (Fig. 3.17). These lines, first described in early electron microscope studies of the myelin sheath, correspond to the intraperiod and period lines respectively defined in X-ray studies of myelin. The inner and outer zones of occlusion of the spiral process are continuous with the minor dense line and are called the inner and outer mesaxons.

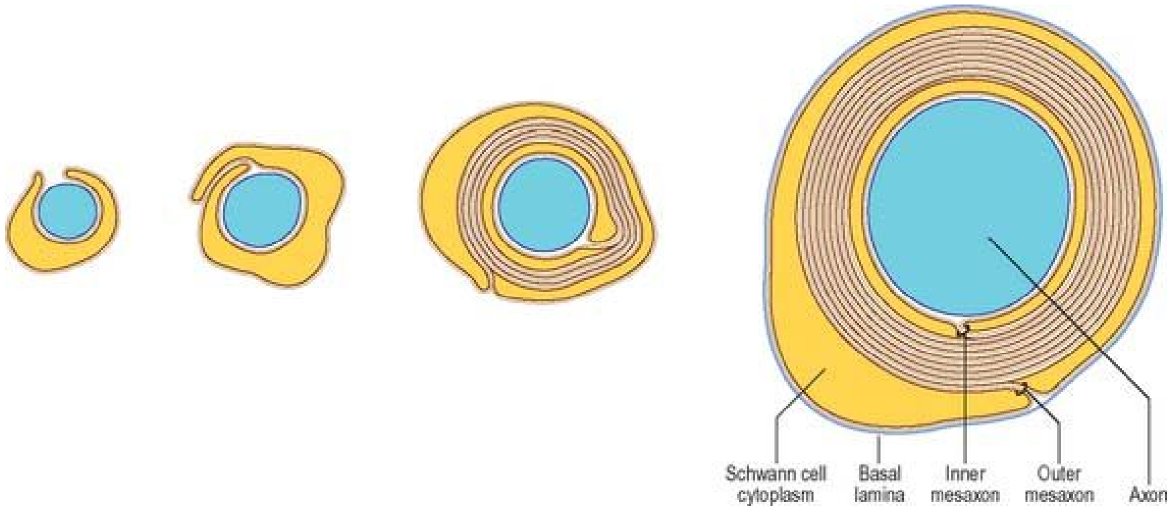

Fig. 3.17 Stages in myelination of a peripheral axon.

There are significant differences between central and peripheral myelin, reflecting the fact that oligodendrocytes and Schwann cells express different proteins during myelinogenesis. The basic dimensions of the myelin membrane are different. CNS myelin has a period repeat thickness of 15.7 nm whereas PNS myelin has a period to period line thickness of 18.5 nm, and the major dense line space is approximately 1.7 nm in CNS myelin, compared with 2.5 nm in PNS myelin. Myelin membrane contains protein, lipid and water, which forms at least 20% of the wet weight. It is a relatively lipid-rich membrane and contains 70–80% lipid. All classes of lipid have been found; perhaps not surprisingly, the precise lipid composition of PNS and CNS myelin is different. The major lipid species are cholesterol (the commonest single molecule), phospholipids and glycosphingolipids. Minor lipid species include galactosylglycerides, phosphoinositides and gangliosides. The major glycolipids are galactocerebroside and its sulphate ester, sulphatide: these lipids are not unique to myelin, but they are present in characteristically high concentrations. CNS and PNS myelin also contain low concentrations of acidic glycolipids, which constitute important antigens in some inflammatory demyelinating states. Gangliosides, which are glycosphingolipids characterized by the presence of sialic acid (N-acetylneuraminic acid), account for less than 1% of the lipid in myelin.

A relatively small number of protein species account for the majority of myelin protein. Some of these proteins are common to both PNS and CNS myelin, but others are different. Proteolipid protein (PLP) and its splice variant DM20 are found only in CNS myelin, whereas myelin basic protein (MBP) and myelin associated glycoprotein (MAG) occur in both. MAG is a member of the immunoglobulin supergene family, and is localized specifically at those regions of the myelin segment where compaction starts, namely, the mesaxons and inner periaxonal membranes, paranodal loops and incisures, in both CNS and PNS sheaths. It is thought to have a functional role in membrane adhesion.

In the developing CNS, axonal outgrowth precedes the migration of oligodendrocyte precursors, and oligodendrocytes associate with and myelinate axons after their phase of elongation: oligodendrocyte myelin gene expression is not dependent on axon-association. In marked contrast, Schwann cells in the developing PNS are associated with axons during the entire phase of axonal growth. Myelination does not occur simultaneously in all parts of the body in late fetal and early postnatal development. White matter tracts and nerves in the periphery have their own specific temporal patterns which relate to their degree of functional maturity.

Mutations of the major myelin structural proteins have now been recognized in a number of inherited human neurological diseases. As would be expected, these mutations produce defects in myelination, and in the stability of nodal and paranodal architecture, which are consistent with the suggested functional roles of the relevant proteins in maintaining the integrity of the myelin sheath. The molecular organization of myelinated axons is described in Scherer & Arroyo (2002).

EPENDYMA

Ependymal cells line the ventricles (Fig. 3.18; see Fig. 3.11) and central canal of the spinal cord. They form a single-layered epithelium which varies from squamous to columnar in form. At the ventricular surface, cells are joined by gap junctions and occasional desmosomes. Their apical surfaces have numerous microvilli and cilia which contribute to the flow of CSF. There is considerable regional variation in the ependymal lining of the ventricles, but four major types have been described. These are: general ependyma which overlies grey matter; general ependyma which overlies white matter; specialized areas of ependyma in the third and fourth ventricles; choroidal epithelium.

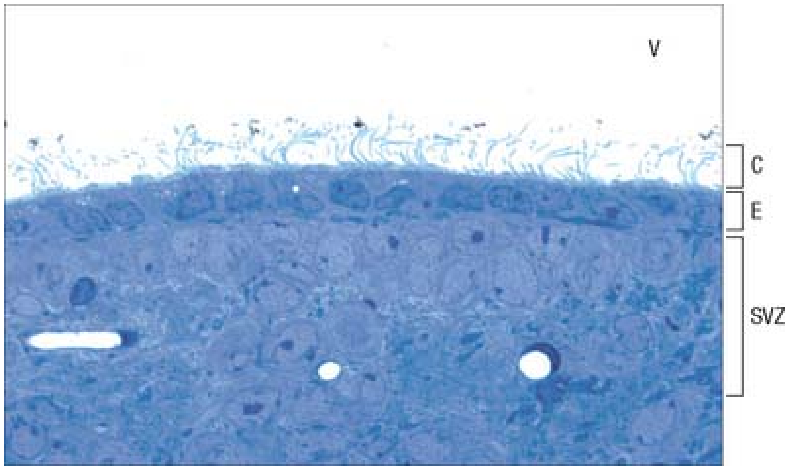

Fig. 3.18 Ciliated columnar epithelial lining of the lateral ventricle (V), overlying the subventricular zone (SVZ). C, cilia; E, ependymal cells. Mouse tissue, toluidine blue stained resin section.

The ependymal cells overlying areas of grey matter are cuboidal; each cell bears approximately 20 central apical cilia, surrounded by short microvilli. The cells are joined by gap junctions and desmosomes and do not have a basal lamina. Beneath them there may be a subependymal (or subventricular) zone, from two to three cells deep, consisting of cells which generally resemble ependymal cells. The capillaries beneath them have no fenestrations and few transcytotic vesicles, which is typical of the CNS. Where the ependyma overlies myelinated tracts of white matter, the cells are much flatter and few are ciliated. There are gap junctions and desmosomes between these cells, but their lateral margins interdigitate, unlike their counterparts overlying grey matter. No subependymal zone is present.

Specialized areas of ependymal cells called the circumventricular organs are found in four areas around the margins of the third ventricle, namely the lining of the median eminence of the hypothalamus; the subcommissural organ; the subfornical organ and the vascular organ of the lamina terminalis. The area postrema, at the inferoposterior limit of the fourth ventricle, has a similar structure. In all of these sites the ependymal cells are only rarely ciliated and their ventricular surfaces bear many microvilli and apical blebs. They have numerous mitochondria, well-formed Golgi complexes and a rather flattened basal nucleus. They are joined laterally by tight junctions which form a barrier to the passage of materials across the ependyma, and by desmosomes. Many of the cells are tanycytes (ependymal astrocytes) and have basal processes which project into the perivascular space surrounding the underlying capillaries. Significantly these capillaries are fenestrated and therefore do not form a blood–brain barrier. It is believed that neuropeptides can pass from nervous tissue into the CSF by active transport through the ependymal cells in these specialized areas, and in this way access a wide population of neurones via the permeable ependymal lining of the rest of the ventricle.

The ependyma is highly modified where it lies adjacent to the vascular layer of the choroid plexuses.

Choroid plexus

The choroid plexus forms the CSF and actively regulates the concentration of molecules in the CSF. It consists of highly vascularized masses of pia mater enclosed by pockets of ependymal cells. The ependymal cells resemble those of the circumventricular organs, except that they do not have basal processes, but form a cuboidal epithelium which rests on a basal lamina adjacent to the enclosed fold of meningeal pia mater and its capillaries (Fig. 3.19, Fig. 3.20).

The cells have numerous long microvilli with only a few cilia interspersed between them. They also have many mitochondria, large Golgi complexes and basal nuclei, features that are consistent with their secretory activity: they produce most components of the CSF. They are linked by tight junctions that form a transepithelial barrier (a component of the blood–CSF barrier), and by desmosomes. Their lateral margins are highly folded.

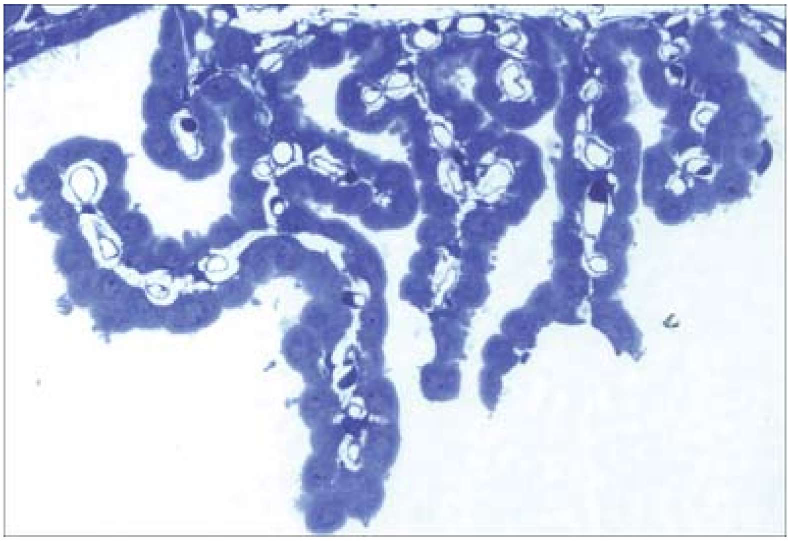

Fig. 3.19 Choroid plexus within the lateral ventricle. Frond-like projections of vascular stroma derived from the pial meninges are covered with a low columnar epithelium which secretes cerebrospinal fluid. Mouse tissue, toluidine blue stained resin section.

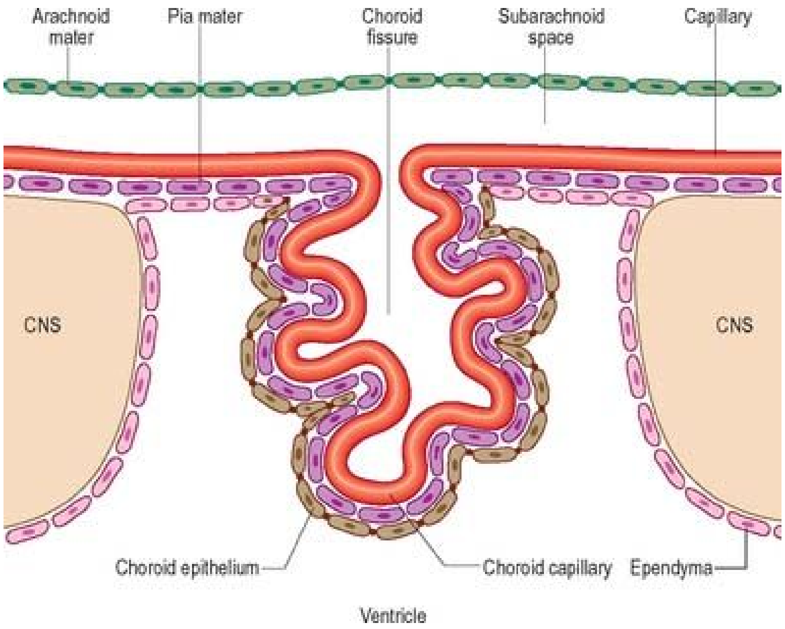
Arachnoid mater
Pia mater
Choroid fissure
Subarachnoid space
Capillary
CNS
CNS
Choroid epithelium
Choroid capillary
Ependyma
Ventricle

Fig. 3.20 The arrangement of tissues forming the choroid plexus.

The choroid plexus has a villous structure where the stroma is composed of pial meningeal cells, and contains fine bundles of collagen and blood vessels. Choroidal capillaries are lined by a fenestrated endothelium. During fetal life, erythropoiesis occurs in the stroma, which is occupied by bone marrow-like cells. In adult life, the stroma contains phagocytic cells, which, together with the cells of the choroid plexus epithelium, phagocytose particles and proteins from the ventricular lumen.

Age-related changes occur in the choroid plexus which can be detected by neuroimaging. Calcification of the choroid plexus can be detected by X-ray or CT scan in 0.5% of individuals in the first decade of life and in 86% in the eighth decade. The incidence of calcification rises sharply, from 35% of CT scans in the fifth decade to 75% in the sixth decade. Visible calcification is usually restricted to the glomus region of the choroid plexus, i.e. the vascular bulge in the choroid plexus as it curves to follow the anterior wall of the lateral ventricle into the temporal horn.

MICROGLIA

Microglia are small dendritic cells found throughout the CNS (Fig. 3.21) including the retina (p. 692). They are thought to be derived from fetal monocytes or their precursors; the haematogenous cells cross the walls of neural blood vessels and invade CNS tissue prenatally as amoeboid cells. Later they lose their motility and transform into typical microglia which bear branched processes that ramify in non-overlapping territories within the brain. All microglial domains, defined by their dendritic fields, are equivalent in size, and form a regular mosaic throughout the brain. The expression of microglia-specific antigens changes with age and many are downregulated when microglia attain the mature dendritic form.

Microglia have elongated nuclei with peripheral heterochromatin. Their scant cytoplasm is pale staining and contains granules, scattered cisternae of rough endoplasmic reticulum and Golgi complexes at both poles. Two or three primary processes stem from the opposite poles of each cell body and then branch repeatedly to form short terminal processes. The function of microglia in the normal brain is obscure. Like astrocytes, microglia are activated by both traumatic and ischaemic injury. In many diseases including Parkinson’s disease, Alzheimer’s disease, multiple sclerosis, acquired immunodeficiency syndrome (AIDS), amyotrophic lateral sclerosis (motor neurone disease) and paraneoplastic encephalitis, microglia become phagocytic and are actively involved in synaptic stripping and clearance of neuronal debris. Some transform into amoeboid, motile cells.

ENTRY OF INFLAMMATORY CELLS INTO THE BRAIN

Although the CNS has long been considered to be an immunologically privileged site, lymphocyte surveillance of the brain may be a normal, low-grade activity that is enhanced in disease. Lymphocytes can enter the brain in response to virus infections and as part of the autoimmune response in multiple sclerosis. Activated, but not resting, lymphocytes pass through the endothelium of small venules, a process that requires the expression of recognition and adhesion molecules (induced following cytokine activation) and subsequently migrate into the brain parenchyma. Within the CNS, microglia and astrocytes can be induced by T-cell cytokines to act as efficient antigen-presenting cells. After leaving the CNS, lymphocytes probably drain along lymphatic pathways to regional cervical lymph nodes.

Polymorphonuclear leukocyte entry into the CNS is less common than lymphocyte entry, but occurs in the early stages of infarction and autoimmune disease and, in particular, in pyogenic infections. They probably enter the nervous system by passing through the endothelial layer. Monocytes may follow similar pathways in the later stages of inflammation. Within the subarachnoid space, polymorphonuclear leukocytes and lymphocytes pass through the endothelium of large veins into the CSF during the inflammatory phase of meningitis.

PERIPHERAL NERVES

Afferent nerve fibres connect peripheral receptors to the CNS: they are derived from neuronal cell bodies located either in special sense organs (e.g. the olfactory epithelium) or in the sensory ganglia of the craniospinal nerves. Efferent nerve fibres connect the CNS to the effector cells and tissues: they are the peripheral axons of neurones with somata in the central grey matter.

Peripheral nerve fibres are grouped in widely variable numbers into bundles (fasciculi). The size, number and pattern of fasciculi vary in different nerves and at different levels along their paths (Fig. 3.22). Their number increases and their size decreases some distance proximal to a point of branching. Where nerves are subjected to pressure, e.g. deep to a retinaculum, fasciculi are increased in number but reduced in size, and the amount of associated connective tissue and degree of vascularity also increase. At these points, nerves may occasionally show a pink, fusiform dilatation, sometimes termed a pseudoganglion or gangliform enlargement.

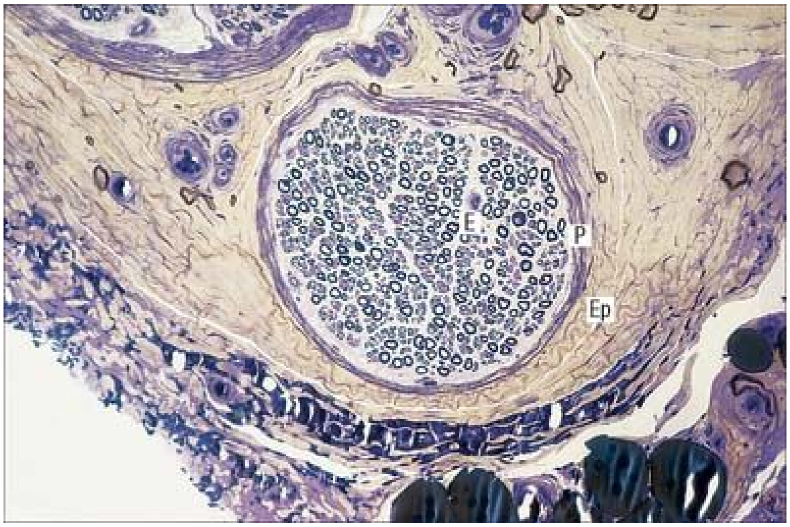

Fig. 3.22 Transverse section through a human peripheral nerve, showing the arrangement of its connective tissue sheaths. Individual axons, myelinated and unmyelinated, are arranged in a small fascicle bounded by a perineurium. P, perineurium; Ep, epineurium; E, endoneurium.

(By courtesy of Professor Susan Standring, GKT School of Medicine, London.)

PERIPHERAL NERVE FIBRES

Classification of peripheral nerve fibres is based on various parameters such as conduction velocity, function and fibre diameter. Of two classifications in common use, the first divides fibres into three major classes, designated A, B and C, corresponding to peaks in the distribution of their conduction velocities. In man, group A fibres are subdivided into α, β, δ and γ subgroups: fibre diameter and conduction velocity are proportional in most fibres. Group Aα fibres are the largest and conduct most rapidly, and C fibres are the smallest and slowest.

The largest afferent axons (Aα fibres) innervate encapsulated cutaneous mechanoreceptors, Golgi tendon organs and muscle spindles, and some large alimentary enteroceptors. Aβ fibres form secondary endings on some muscle spindle (intrafusal) fibres and also innervate cutaneous and joint capsule mechanoreceptors. Aδ fibres innervate thermoreceptors, stretch-sensitive free endings, hair receptors and nociceptors, including those in dental pulp, skin and connective tissue. Aγ fibres are exclusively fusimotor to plate and trail endings on intrafusal muscle fibres. B fibres are myelinated autonomic preganglionic efferent fibres. C fibres are unmyelinated and have thermoreceptive, nociceptive and interoceptive functions, including the perception of slow, burning pain and visceral pain. This scheme can be applied to fibres of both spinal and cranial nerves except perhaps those of the olfactory nerve, where the fibres form a uniquely small and slow group. The largest somatic efferent fibres (Aα) are up to 20 μm in diameter. They innervate extrafusal muscle fibres (at motor end plates) exclusively and conduct at a maximum of 120 m/s. Fibres to fast twitch muscles are larger than those to slow twitch muscle. Smaller (Aγ) fibres of gamma motor neurones, and autonomic preganglionic (B) and postganglionic (C) efferent fibres conduct, in order, progressively more slowly (40 m/s – less than 10 m/s).

A different classification divides fibres into groups I–IV on the basis of their calibre; groups I–III are myelinated and group IV is unmyelinated. Group I fibres are large (12–22 μm), and include primary sensory fibres of muscle spindles (Group Ia) and smaller fibres of Golgi tendon organs (Group Ib). Group II fibres are the secondary sensory terminals of muscle spindles, with diameters of 6–12 µm. Group III fibres, 1–6 µm in diameter, have free sensory endings in the connective tissue sheaths around and within muscles and are nociceptive and, in skin, also thermosensitive. Group IV fibres are unmyelinated, with diameters below 1.5 µm: they include free endings in skin and muscle, and are primarily nociceptive.

CONNECTIVE TISSUE SHEATHS

Nerve trunks, whether uni- or multifascicular, are surrounded by an epineurium. Individual fasciculi are enclosed by a multilayered perineurium, which in turn surrounds the endoneurium or intrafascicular connective tissue (Fig. 3.22).

Epineurium

Epineurium is a condensation of loose (areolar) connective tissue derived from mesoderm. As a general rule, the more fasciculi present in a peripheral nerve, the thicker the epineurium. Epineurium contains fibroblasts, collagen (types I and III), and variable amounts of fat, and it cushions the nerve it surrounds. Loss of this protective layer may be associated with pressure palsies seen in wasted, bedridden patients. The epineurium also contains lymphatics (which probably pass to regional lymph nodes) and blood vessels, vasa nervorum, that pass across the perineurium to communicate with a network of fine vessels within the endoneurium.

Perineurium

Perineurium extends from the CNS–PNS transition zone to the periphery, where it is continuous with the capsules of muscle spindles and encapsulated sensory endings, but ends openly at unencapsulated endings and neuromuscular junctions. It consists of alternating layers of flattened polygonal cells (thought to be derived from fibroblasts) and collagen. It can often contain 15–20 layers of such cells, each layer enclosed by a basal lamina up to 0.5 μm thick. Within each layer the cells interdigitate along extensive tight junctions; their cytoplasm typically contains vesicles and bundles of microfilaments and their plasma membrane often shows evidence of pinocytosis. These features are consistent with the function of the perineurium as a metabolically active diffusion barrier; together with the blood–nerve barrier the perineurium is thought to play an essential role in maintaining the osmotic milieu and fluid pressure within the endoneurium.

Endoneurium

Strictly speaking, the term endoneurium is restricted to intrafascicular connective tissue and excludes the perineurial partitions within fascicles. Endoneurium consists of a fibrous matrix composed predominantly of type III collagen (reticulin) fibres, characteristically organized in fine bundles lying parallel to the long axis of the nerve, and condensed around individual Schwann cell–axon units and endoneurial vessels. The fibrous and cellular components of the endoneurium are bathed in endoneurial fluid at a slightly higher pressure than that outside in the surrounding epineurium. The major cellular constituents of the endoneurium are Schwann cells and endothelial cells; minor components are fibroblasts (constituting approximately 4% of the total endoneurial cell population), resident macrophages and mast cells. Schwann cell–axon units and blood vessels are enclosed within individual basal laminae and therefore isolated from the other cellular and acellular components of the endoneurium.

Endoneurial arterioles have a poorly developed smooth muscle layer, and do not autoregulate well. In sharp contrast, epineurial and perineurial vessels have a dense perivascular plexus of peptidergic, serotoninergic and adrenergic nerves.

SCHWANN CELLS

Schwann cells are the major glial type in the PNS. *In vitro* they are fusiform in appearance. Both *in vitro* and *in vivo*, Schwann cells ensheathe peripheral axons, and myelinate those greater than 2 μm diameter. In a mature peripheral nerve, they are distributed along the axons in longitudinal chains: the precise geometry of their association depends on whether the axon is myelinated or unmyelinated. In myelinated axons the territory of a Schwann cell defines an internode.

The molecular phenotype of mature myelin-forming Schwann cells is different from that of mature non-myelinating Schwann cells. Adult myelin-forming Schwann cells are characterized by the presence of several myelin proteins, some, but not all, of which are shared with oligodendrocytes and central myelin. In contrast, expression of the low affinity neurotrophin receptor ($p75^{NTR}$) and GFAP intermediate filament protein (which differs from the CNS form in its post-translational modification), characterize adult non-myelin forming Schwann cells.

Schwann cells arise from multipotent cells of the very early migrating neural crest that can also give rise to peripheral neurones. Neuronal signals regulate many aspects of Schwann cell behaviour in developing and postnatal nerves. Axon-associated signals appear to control the proliferation of developing Schwann cells and their precursors; the developmentally programmed death of those precursors in order to match numbers of axons and glia within each peripheral nerve bundle; the production of basal laminae by Schwann cells; the induction and maintenance of myelination. Relatively little is known about either Schwann cell–axon or Schwann cell–Schwann cell signalling in normal nerves. An extensive literature supports the view that Schwann cells are key players in the acute injury response in the PNS, helping to provide a microenvironment that facilitates axonal regrowth. Few Schwann cells persist in chronically denervated nerves.

Unmyelinated axons

Unmyelinated axons (Fig. 3.23) are commonly 1.0 μm in diameter, although some may be 1.5 μm or even 2 μm in diameter. Groups of up to 10 small axons (0.15–2.0 μm in diameter) are enclosed within a chain of overlapping Schwann cells that is surrounded by a basal lamina. Within each Schwann cell, individual axons are usually sequestered from their neighbours by delicate processes of cytoplasm. Axons move between Schwann cell chains as they pass proximodistally along a nerve fasciculus. It seems likely, on the basis of quantitative studies in subhuman primates, that axons from adjacent cord segments may share Schwann cell columns: this phenomenon may play a role in the evolution of neuropathic pain after nerve injury. In the absence of a myelin sheath and nodes of Ranvier, conduction along unmyelinated axons is not saltatory but electrotonic, and the passage of impulses is therefore relatively slow (approximately 0.5–4.0 m/s).

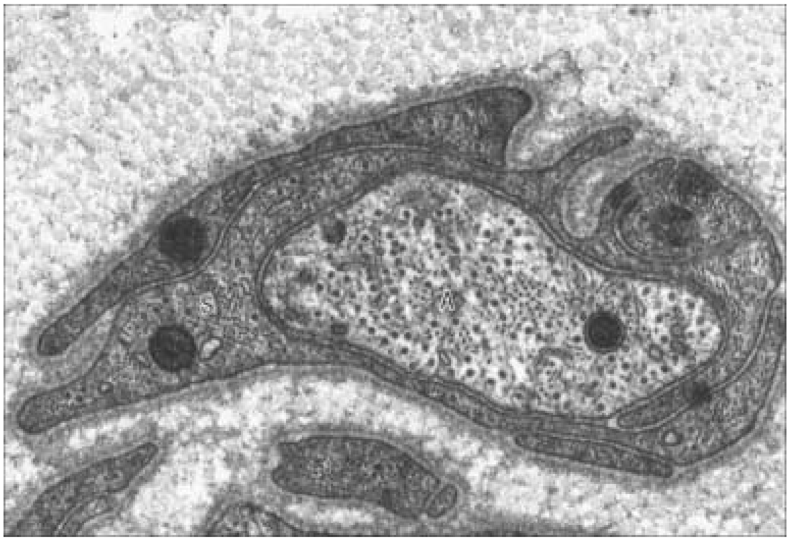

Fig. 3.23 An unmyelinated axon (A), enclosed by cytoplasmic processses of a Schwann cell (S) and its basal lamina (arrow), from a biopsy of human sural nerve.

Myelinated axons

Myelinated axons (Fig. 3.24) have a 1 : 1 relationship with their ensheathing Schwann cells. The territory of an individual Schwann cell defines an internode (Fig. 3.25): internodal length varies directly with the diameter of the fibre, from 150 to 1500 μm. The interval between two internodes is a node of Ranvier. In the PNS, the myelin sheaths on either side of a node terminate in asymmetrically swollen paranodal bulbs. Schwann cell cytoplasm only forms a continuous layer in the perinuclear (mid-internodal) and paranodal regions. Between these sites, internodal Schwann cytoplasm forms a delicate network over the inner (abaxonal) surface of the myelin sheath. The outer (adaxonal) layer of Schwann cell cytoplasm is frequently discontinuous, and axons are surrounded by a narrow periaxonal space (15–20 nm) which, although nominally part of the extracellular space, is functionally isolated from it at the paranodes. For further details, see Scherer & Arroyo (2002).

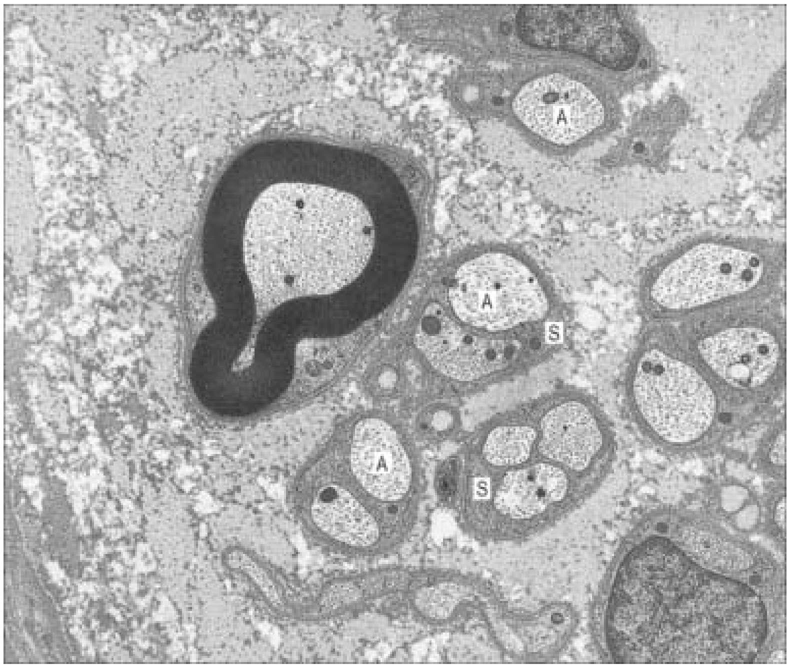

Fig. 3.24 Transverse section of sciatic nerve showing a myelinated axon and several non-myelinated axons (A), ensheathed by Schwann cells (S), from a biopsy of human sural nerve.

(By courtesy of Professor Susan Standring, GKT School of Medicine, London.)

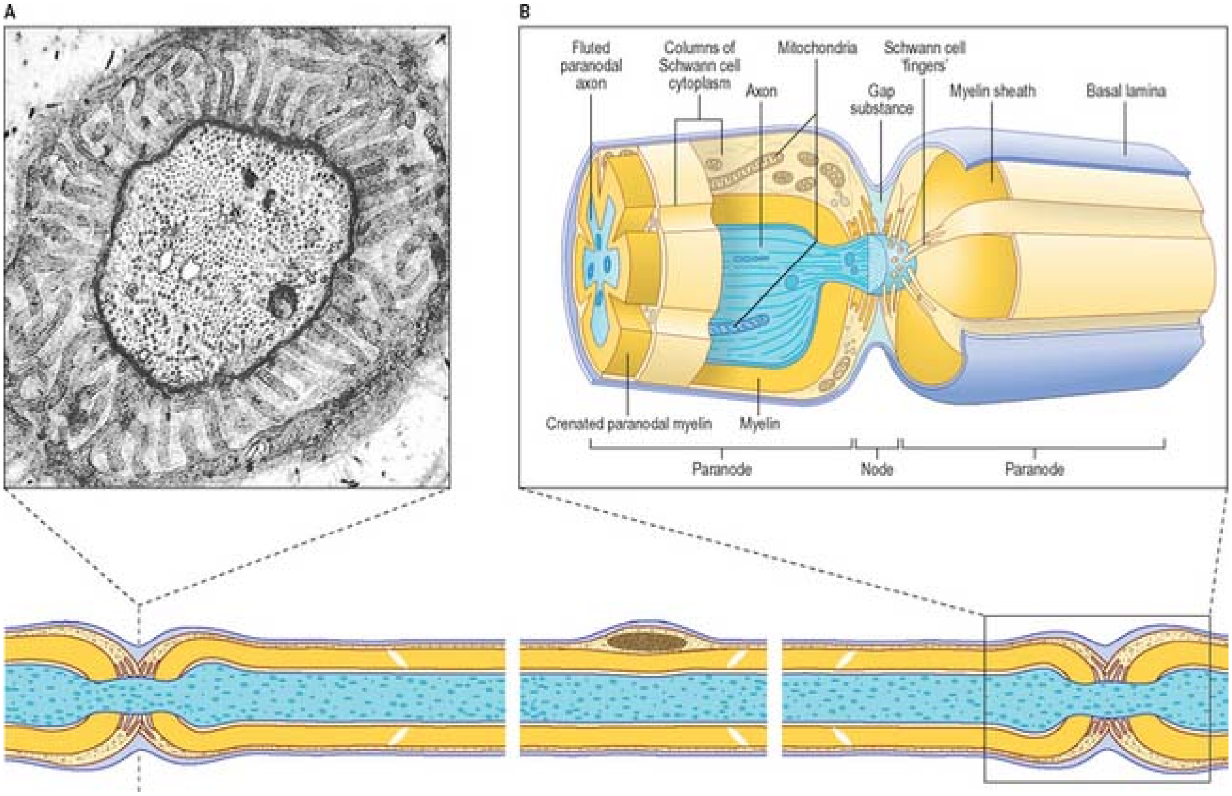
A
B
Fluted paranodal axon
Columns of Schwann cell cytoplasm
Mitochondria
Schwann cell 'fingers'
Axon
Gap substance
Myelin sheath
Basal lamina
Crenated paranodal myelin
Myelin
Paranode
Node
Paranode

Fig. 3.25 General plan of a myelinated nerve fibre in longitudinal section including one complete internodal segment and two adjacent paranodal bulbs, used as a key for the more detailed microarchitecture of specific subregions. **A**, Transverse electron microscope section through the centre of a node of Ranvier, with numerous finger-like processes of adjacent Schwann cells converging towards the nodal axolemma. Many microtubules and neurofilaments are visible within the axoplasm. **B**, The arrangement of the axon, myelin sheath and Schwann cell cytoplasm at the node of Ranvier and in the paranodal bulbs.

*(**A**, By courtesy of Professor Susan Standring, GKT School of Medicine, London. **B**, Redrawn from a figure provided by PL Williams and DN Landon.)*

Nodes of Ranvier

PNS nodes of Ranvier (Fig. 3.25) are typically approximately 0.8–1.1 µm in length. The calibre of the nodal axon is characteristically reduced relative to that of the internodal axon: this is most marked in the largest calibre axons.

Node gaps are filled with an amorphous gap substance and processes of Schwann cell cytoplasm, and are surrounded by a continuous basal lamina elaborated by the ensheathing Schwann cells. In large calibre axons the surfaces of the paranodal bulbs and of the underlying axon are fluted as they approach the nodes. Fluting produces grooves in the external surface of the myelin sheath that are filled by Schwann cell cytoplasm characterized by large numbers of mitochondria. In smaller fibres this arrangement is less obvious, although the paranodal cytoplasm usually contains mitochondria.

Schmidt–Lanterman incisures

Schmidt–Lanterman incisures are helical decompactions of internodal myelin that occur in every sheath, irrespective of thickness. At an incisure the major dense line of the myelin sheath splits to enclose a continuous spiral band of granular cytoplasm that passes between the abaxonal and adaxonal layers of Schwann cell cytoplasm. The minor dense line of the incisural myelin sheath separates to create a long channel that potentially connects the periaxonal space with the extracellular fluid in the endoneurium. The function of incisures is not known: their structure suggests that they may participate in transport of molecules across the myelin sheath.

SATELLITE CELLS

Many non-neuronal cells of the nervous system have been called satellite cells, including small round extracapsular cells in peripheral ganglia, ganglionic capsular cells, Schwann cells, any cell that is closely associated with neuronal somata, and precursor cells associated with striated muscle fibres (p. 117). Within the nervous system, the term is most commonly reserved for flat, epithelioid cells (ganglionic glial cells, capsular cells) that surround the neuronal somata of peripheral ganglia (Fig. 3.26). Their cytoplasm resembles that of Schwann cells, and their deep surfaces interdigitate with reciprocal infoldings in the membranes of the enclosed neurones. Capsular cells are succeeded by similar cells that enclose the initial part of the dendroaxonal process of unipolar sensory neurones in dorsal spinal ganglia, and these in turn are continuous with the Schwann cells that surround the peripheral and central processes of the neurones.

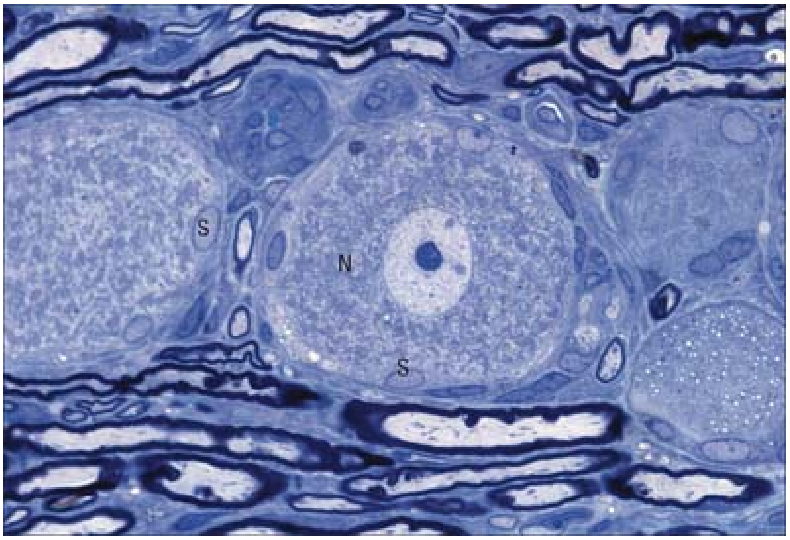

Fig. 3.26 Sensory neurones in a dorsal root ganglion (rat). Neurones (N) are typically variable in size but all are encapsulated by satellite cells (S). Myelinated fibres are seen above and below the neuronal somata. Toluidine blue stained resin section.

(By courtesy of Dr Clare Farmer, King’s College, London.)

Enteric glia

Enteric nerves lack an endoneurium and so do not have the collagenous coats of other peripheral nerves. The enteric ganglionic neurones are supported by glia that closely resemble astrocytes: they contain more glial fibrillary acidic protein (GFAP) than non-myelinating Schwann cells, and do not produce a basal lamina.

Olfactory ensheathing glia

Olfactory ensheathing glia share a common origin with olfactory receptor neurones in the olfactory placode. They ensheathe olfactory sensory axons in a manner that is reminiscent of the relationship between Schwann cells and axons in very immature peripheral nerves, i.e. they surround, but do not segregate, bundles of up to 50 fine unmyelinated fibres to form approximately 20 fila olfactoria. Olfactory ensheathing glia accompany olfactory axons from the lamina propria of the olfactory epithelium to their synaptic contacts in the glomeruli of the olfactory bulbs. This unusual arrangement is unique: elsewhere in the nervous system the territories of peripheral and central glia are clearly demarcated at CNS–PNS transition zones.

Ensheathing glia, and the end-feet of astrocytes that lie between olfactory axon bundles, both contribute to the glia limitans at the pial surface of the olfactory bulbs. Ensheathing glia have a malleable phenotype, indeed there may be more than one subtype. Some express GFAP as fine cytoplasmic filaments, and some express $p75^{NTR}$.

BLOOD SUPPLY OF PERIPHERAL NERVES

The blood vessels supplying a nerve end in a capillary plexus that pierces the perineurium. The branches of the plexus run parallel with the fibres, connected by short transverse vessels, forming narrow, rectangular meshes similar to those found in muscle. The blood supply of peripheral nerves is unusual. Endoneurial capillaries have atypically large diameters and intercapillary distances are greater than in many other tissues. Peripheral nerves have two separate, functionally independent vascular systems: an extrinsic system (regional nutritive vessels and epineurial vessels) and an intrinsic system (longitudinally running microvessels in the endoneurium). Anastomoses between the two systems produce considerable overlap between the territories of the segmental arteries. This unique pattern of vessels, together with a high basal nerve blood flow relative to metabolic requirements, means that peripheral nerves possess a high degree of resistance to ischaemia.

Blood–nerve barrier

Just as the neuropil within the CNS is protected by a blood–brain barrier, the endoneurial contents of peripheral nerve fibres are protected by a blood–nerve barrier and by the cells of the perineurium. The blood–nerve barrier operates at the level of the endoneurial capillary walls, where the endothelial cells are joined by tight junctions, are non-fenestrated and surrounded by continuous basal laminae. The barrier is much less efficient in dorsal root ganglia and autonomic ganglia and in the distal parts of peripheral nerves.

GANGLIA

Ganglia are aggregations of neuronal somata and are of varying form and size. They occur in the dorsal roots of spinal nerves; in the sensory roots of the trigeminal, facial, glossopharyngeal, vagal and vestibulocochlear cranial nerves; in autonomic nerves and in the enteric nervous system. Each ganglion is enclosed within a capsule of fibrous connective tissue and contains neuronal somata and neuronal processes. Some ganglia, particularly in the ANS, contain fibres from cell bodies that lie elsewhere in the nervous system and that either pass through, or terminate within, the ganglia.

Sensory ganglia

The sensory ganglia of dorsal spinal roots (Fig. 3.26) and the ganglia of the trigeminal, facial, glossopharyngeal and vagal cranial nerves are enclosed in periganglionic connective tissue that resembles the perineurium surrounding peripeheral nerves. Ganglionic neurones are unipolar. They have spherical or oval somata of varying size, aggregated in groups between fasciculi of myelinated and unmyelinated nerve fibres. For each neurone, the single axodendritic process bifurcates into central and peripheral processes: in myelinated fibres the junction occurs at a node of Ranvier. The peripheral process reaches a sensory ending and, since it conducts impulses towards the soma, strictly speaking it functions as an elongated dendrite. However, since it has the typical structural and functional properties of a peripheral axon, it is conventionally described as an axon.

Each neuronal soma is surrounded by a capsule of glial satellite cells (see above). Each axodendritic process and its peripheral and central divisions, ensheathed by Schwann cells, lies outside the capsule. All of the cells in the ganglion lie within a delicate vascular connective tissue that is continuous with the endoneurium of the nerve root. Sensory ganglionic neurones are not confined to discrete craniospinal ganglia, and often occupy heterotopic positions, either singly or in small groups, distal or proximal to their ganglia.

Herpes zoster

Primary infection with the varicella zoster virus causes chickenpox. Following recovery, the virus remains dormant within dorsal root ganglia: its reactivation leads to shingles, which involves the dermatome(s) supplied by the affected sensory nerve(s). Severe pain and a rash similar to chickenpox, often confined to one of the divisions of the trigeminal nerve, or to a spinal nerve dermatome, are diagnostic. Herpes zoster involving the geniculate ganglion compresses the facial nerve and results in a lower motor neurone facial paralysis, known as Ramsay Hunt syndrome. Occasionally, if the vestibulocochlear nerve becomes involved, there is vertigo, tinnitus and some deafness.

Autonomic ganglia

Autonomic ganglia are largely relay stations. Their neurones are multipolar and have dendritic trees on which preganglionic autonomic motor axons synapse (Fig. 3.27). The neurones are surrounded by a mixed neuropil of afferent and efferent fibres, dendrites, synapses and non-neural cells. There is considerable variation in the ratio of pre- and postganglionic fibres in different types of ganglion. Thus preganglionic sympathetic axons may synapse with many postganglionic neurones for the wide dissemination and perhaps amplification of sympathetic activity, a feature not found to the same degree in parasympathetic ganglia. Dissemination may also be achieved by connections with ganglionic interneurones or by the diffusion within the ganglion of transmitter substances produced either locally (paracrine effect) or elsewhere (endocrine effect). A small fraction of the fibres within a ganglion are either efferent fibres en route to another ganglion, or are afferent fibres from the viscera and glands: none of these fibres will synapse in the ganglion.

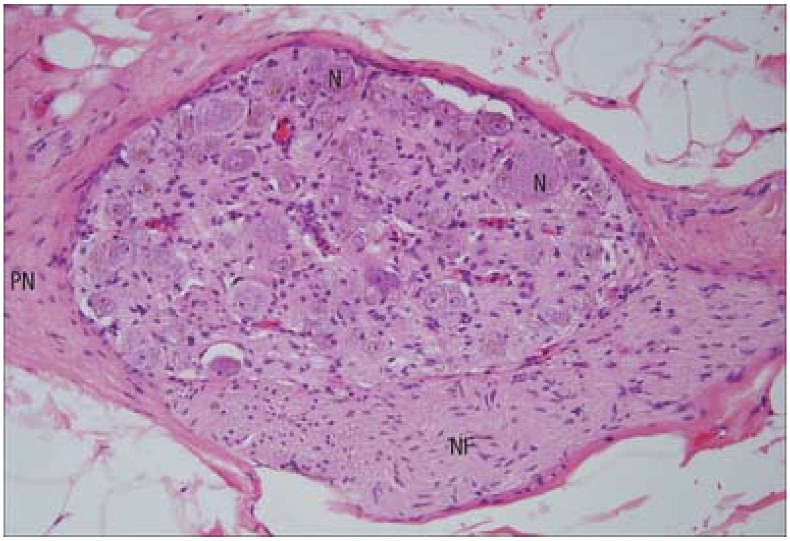

Fig. 3.27 Autonomic ganglion (human) on a peripheral nerve (PN) in adipose connective tissue. Neuronal somata (N) and a nerve fibre layer (NF) are visible within the ganglion.

Most neurones of autonomic ganglia have somata ranging from 25–50 μm; a less frequent type is smaller, 15–20 μm, and often clustered in groups. Dendritic fields of these multipolar neurones are complex and dendritic glomeruli have been observed in many ganglia. Clusters of small granular adrenergic vesicles occupy the soma and dendrites, probably representing the storage of catecholamines. Ganglionic neurones receive many axodendritic synapses from preganglionic nerve fibres; axosomatic synapses are less numerous. Postganglionic fibres commonly arise from the initial stem of a large dendrite and produce few or no collateral processes.

Enteric ganglia

The enteric nervous system is composed of ganglionic neurones (Fig. 3.28) and associated nerves serving different functions, including regulation of gut motility and mucosal transport (see Chs 15 and 60). Extrinsic autonomic fibres supply the gut wall and, together with intrinsic enteric ganglionic neurones, and the endocrine and cardiovascular systems, they integrate the activities of the digestive system either as a result of interaction with enteric neurones (e.g. via vagal fibres), or the direct regulation of the local blood flow (via postganglionic sympathetic fibres).

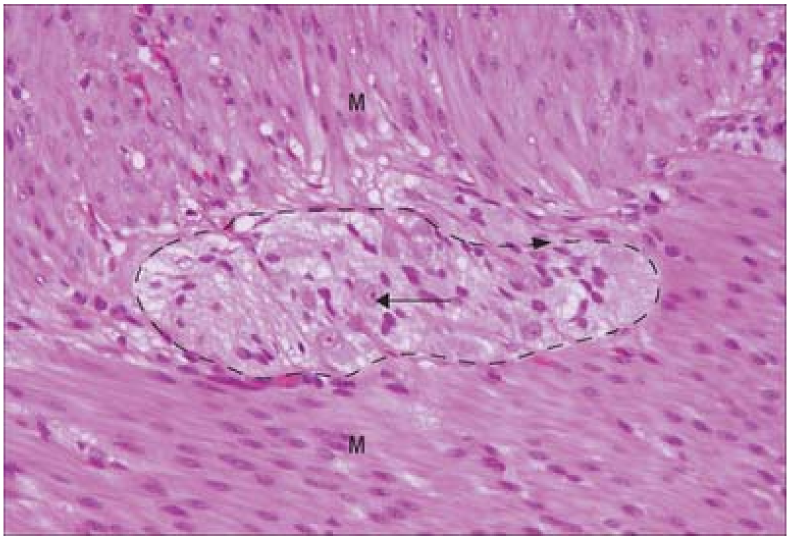

Fig. 3.28 Enteric ganglion (outlined) of the myenteric (Auerbach's) plexus between the inner circular and outer longitudinal layers of smooth muscle (M) in the wall of the human intestine. An enteric ganglionic neurone is arrowed.

Enteric ganglionic neurones are predominantly peptidergic or monoaminergic and can be classified accordingly. Other neurones express nitric oxide synthase and release NO. There are regional differences in the numbers of ganglia and the classes of neurone they contain. For example, myenteric plexus ganglia are less frequent in oesophageal smooth muscle (1.5 per cm) than in the small and large intestines (approximately 10 per cm length of bowel). Oesophageal enteric neurones all coexpress vasoactive polypeptide (VIP) and neuropeptide Y (NPY), whereas gastrin- and somatostatin-containing fibres are rare. In contrast, gastrin and somatostatin-containing neurones are abundant in the small and large intestines, and although both types are present, very few VIP neurones coexpress NPY.

Correlations can be made between some phenotypic classes of enteric neurone and their functional properties, although much remains undetermined. Cholinergic neurones are excitatory, cause muscular contraction and mainly project orally. NO-releasing neurones are generally larger and project for longer distances, mainly anally. They are inhibitory neurones, some of which also express VIP, and they promote muscular relaxation.

DISPERSED NEUROENDOCRINE SYSTEM

Although the nervous, neuroendocrine and endocrine systems all operate by intercellular communication, they differ in the mode, speed and degree or localization of the effects produced. The autonomic nervous system uses impulse conduction and neurotransmitter release to transmit information, and the responses induced are rapid and localized. The dispersed neuroendocrine system uses only secretion. It is slower and the induced responses are less localized, because the secretions, e.g. neuromediators, can act either on contiguous cells, or on groups of nearby cells reached by diffusion, or on distant cells via the bloodstream. Many of its effector molecules operate in both the nervous system and the neuroendocrine system. The endocrine system proper, which consists of clusters of cells and discrete, ductless, hormone-producing glands, is even slower and less localized, although its effects are specific and often prolonged. These regulatory systems overlap in function, and can be considered as a single neuroendocrine regulator of the metabolic activities and internal environment of the organism, acting to provide conditions in which it can function successfully. Neural and neuroendocrine axes appear to cooperate to modulate some forms of immunological reaction: the extensive system of vessels, circulating hormones and nerve fibres that link the brain with all viscera are thought to constitute a neuroimmune network (Fig. 3.29). For further reading see Furness (2006); Shepherd et al (2005).

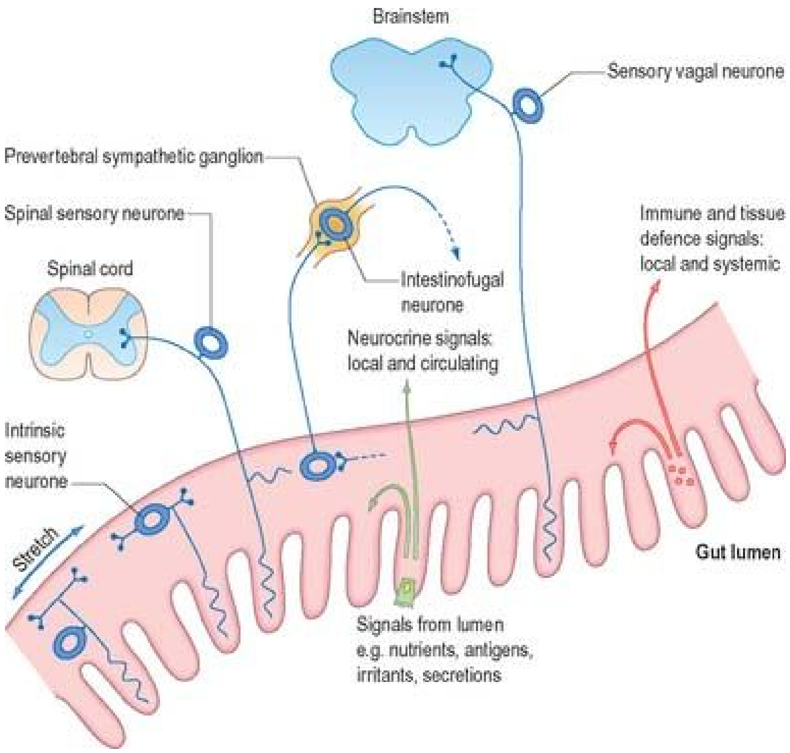
Brainstem
Sensory vagal neurone
Prevertebral sympathetic ganglion
Spinal sensory neurone
Spinal cord
Intestinofugal neurone
Immune and tissue defence signals: local and systemic
Neurocrine signals: local and circulating
Intrinsic sensory neurone
Stretch
Gut lumen
Signals from lumen e.g. nutrients, antigens, irritants, secretions

Fig. 3.29 The ways in which the nervous system, neuroendocrine system and immune system are integrated, demonstrated in the intestine. Neurocrine signals from enteric neuroendocrine cells and signals from immune defence cells (e.g. lymphocytes, macrophages and mast cells) act on other cells of those systems and on neurones with sensory endings in the intestinal wall, either locally or at a distance. Some neuronal soma lie within enteric ganglia in the gut wall, others have their bodies in peripheral ganglia. Neuronal signals may act locally, be transmitted to the CNS or enter a reflex pathway via sympathetic ganglia.

Some cells can take up and decarboxylate amine precursor compounds (amine precursor uptake and decarboxylation or APUD cells. They are characterized by dense-core cytoplasmic granules (see Fig. 2.6), similar to the neurotransmitter vesicles seen in some types of neuronal terminal. The group includes cells described as chromaffin cells (phaeochromocytes), derived from neuroectoderm and innervated by preganglionic sympathetic nerve fibres. Chromaffin cells synthesize and secrete catecholamines (dopamine, noradrenaline or adrenaline). Their name refers to the finding that their cytoplasmic store of catecholamines is sufficiently concentrated to give an intense yellow-brown colouration, the positive chromaffin reaction, when they are treated with aqueous solutions of chromium salts, particularly potassium dichromate. Classic chromaffin cells include clusters of cells in the suprarenal medulla; the para-aortic bodies, which secrete noradrenaline; paraganglia (see Ch. 15); certain cells in the carotid bodies; small groups of cells irregularly dispersed among the paravertebral sympathetic ganglia, splanchnic nerves and prevertebral autonomic plexuses.

The alimentary tract contains a large population of cells of a similar type (previously called neuroendocrine or enterochromaffin cells) in its wall. These cells act as sensory transducers, activating intrinsic and extrinsic primary afferent neurones via their release of 5-hydroxytryptamine (5-HT). The neonatal respiratory tract contains a prominent system of neuroendocrine cells, both dispersed and aggregated (neuroepithelial bodies): the numbers of both types decline during childhood. Merkel cells in the basal epidermis of the skin store neuropeptides which they release to associated nerve endings in response to pressure. Experimental animal studies have revealed 5-HT-containing intraepithelial paraneurones in the urothelial lining of the urethra: these cells are thought to relay information from the luminal surface of the urethra to underlying sensory nerves.

A number of descriptions and terms have been applied to cells of this system in the older literature. They include: clear cells (so named because of their poor staining properties in routine preparations); argentaffin cells (reduce silver salts); argyrophil cells (absorb silver); small intensely fluorescent cells; peptide-producing cells (particularly of the hypothalamus, hypophysis, pineal and parathyroid glands and placenta); Kulchitsky cells in the lungs; paraneurones. Many cells of the dispersed (or diffuse) neuroendocrine system, DNES, are derived embryologically from the neural crest. Some, in particular cells from the alimentary system, are now known to be endodermal in origin. For further reading, see Day and Salzet (2002).

SENSORY ENDINGS

GENERAL FEATURES OF SENSORY RECEPTORS

There are three major forms of sensory receptor, neuroepithelial, epithelial and neuronal (Fig. 3.30).

A neuroepithelial receptor is a neurone with a soma lying near a sensory surface and an axon that conveys sensory signals into the CNS to synapse on second order neurones. This is an evolutionarily primitive arrangement, and the only example in man is the sensory neurone of the olfactory epithelium.

An epithelial receptor is a cell that is modified from a non-nervous sensory epithelium and innervated by a primary sensory neurone with a soma lying near the CNS. Examples are epidermal Merkel cells, auditory receptors and taste buds. When activated, this type of receptor excites its neurone by neurotransmission across a synaptic gap.

A neuronal receptor is a primary sensory neurone that has a soma in a craniospinal ganglion and a peripheral axon ending in a sensory terminal. All cutaneous sensors (with the exception of Merkel cells) and proprioceptors are of this type: their sensory terminals may be encapsulated or linked to special mesodermal or ectodermal structures to form a part of the sensory apparatus. The extraneural cells are not necessarily excitable, but create an appropriate environment for the excitation of the neuronal process.

The receptor stimulus is transduced into a graded change of electrical potential at the receptor surface (receptor potential), and this initiates an all-or-none action potential that is transmitted to the CNS. This may occur either in the receptor, when this is a neurone, or partly in the receptor and partly in the neurone that innervates it, in the case of epithelial receptors. Transduction varies with the modality of the stimulus, and usually causes depolarization of the receptor membrane (or hyperpolarization, in the retina). In mechanoreceptors, transduction may involve the deformation of membrane structure, which causes strain- or voltage-sensitive transducing protein molecules to open ion channels. In chemoreceptors, receptor action may resemble that for ACh at neuromuscular junctions. Visual receptors share similarities with chemoreceptors: light causes changes in receptor proteins, which activate G proteins, resulting in the release of second messengers and altered membrane permeability.

The quantitative responses of sensory endings to stimuli vary greatly and increase the flexibility of the functional design of sensory systems. Although increased excitation with increasing stimulus level is a common pattern (‘on’ response), some receptors respond to decreased stimulation (‘off’ response). Even unstimulated receptors show varying degrees of spontaneous background activity against which an increase or decrease in activity occurs with changing levels of stimulus. In all receptors studied, when stimulation is maintained at a steady level, there is an initial burst (the dynamic phase) followed by a gradual adaptation to steady level (the static phase). Though all receptors show these two phases, one or other may predominate, providing a distinction between rapidly adapting endings which accurately record the rate of stimulus onset, and slowly adapting endings which signal the constant amplitude of a stimulus, e.g. position sense. Dynamic and static phases are reflected in the amplitude and duration of the receptor potential and also in the frequency of action potentials in the sensory fibres. The stimulus strength necessary to elicit a response in a receptor, i.e. its threshold level, varies greatly between receptors, and provides an extra level of information about stimulus strength.

For further information on sensory receptors, see Nolte (2002).

FUNCTIONAL CLASSIFICATION OF RECEPTORS

Receptors have been classified in several ways. They may be classified by the modalities to which they are sensitive, such as mechanoreceptors (which are responsive to deformation, e.g. touch, pressure, sound waves, etc.), chemoreceptors, photoreceptors and thermoreceptors. Some receptors are polymodal, ie. they respond selectively to more than one modality: they usually have high thresholds and respond to damaging stimuli associated with irritation or pain (nociceptors).

Another widely used classification divides receptors on the basis of their distribution in the body into exteroceptors, proprioceptors and interoceptors. Exteroceptors and proprioceptors are receptors of the somatic afferent components of the nervous system, while interoceptors are receptors of the visceral afferent pathways.

Exteroceptors respond to external stimuli and are found at, or close to, body surfaces. They can be subdivided into the general or cutaneous sense organs and special sensory organs. General sensory receptors include free and encapsulated terminals in skin and near hairs. Special sensory organs are the olfactory, visual, acoustic, vestibular and taste receptors.

Proprioceptors respond to stimuli to deeper tissues, especially of the locomotor system, and are concerned with detecting movement, mechanical stresses and position. They include Golgi tendon organs, neuromuscular spindles, Pacinian corpuscles, other endings in joints, and vestibular receptors. Proprioceptors are stimulated by the contraction of muscles, movements of joints and changes in the position of the body. They are essential for the coordination of muscles, the grading of muscular contraction, and the maintenance of equilibrium.

Interoceptors are found in the walls of the viscera, glands and vessels, where their terminations include free nerve endings, encapsulated terminals and endings associated with specialized epithelial cells. Nerve terminals are found in the layers of visceral walls and the adventitia of blood vessels, but the detailed structure and function of many of these endings are not well-established. Encapsulated (lamellated) endings occur in the heart, adventitia, and mesenteries. Free terminal arborizations occur in the endocardium, the endomysium of all muscles, and connective tissue generally. Visceral nerve terminals are not usually responsive to stimuli which act on exteroceptors, and do not respond to localized mechanical and thermal stimuli. Tension produced by excessive muscular contraction or by visceral distension often causes pain, particularly in pathological states, which is frequently poorly localized and of a deep-seated nature. Visceral pain is often referred to the corresponding dermatome (see Fig. 15.12). Polymodal nociceptors (irritant receptors) respond to a variety of stimuli such as noxious chemicals or damaging mechanical stimuli. They are mainly the free endings of fine, unmyelinated fibres that are widely distributed in the epithelia of the alimentary and respiratory tracts: they may initiate protective reflexes.

Interoceptors include vascular chemoreceptors, e.g. the carotid body, and baroceptors, which are concerned with the regulation of blood flow and pressure and the control of respiration.

FREE NERVE ENDINGS

Sensory endings that branch to form plexuses occur in many sites (Fig. 3.30). They occur in all connective tissues, including those of the dermis, fasciae, capsules of organs, ligaments, tendons, adventitia of blood vessels, meninges, articular capsules, periosteum, perichondrium, Haversian systems in bone, parietal peritoneum, walls of viscera and the endomysium of all types of muscle. They also innervate the epithelium of the skin, cornea, buccal cavity, and the alimentary and respiratory tracts and their associated glands. Within epithelia, free sensory endings lack Schwann cell ensheathment and are enveloped instead by epithelial cells. Afferent fibres from free terminals may be myelinated or unmyelinated but are always of small diameter and low conduction velocity. When afferent axons are myelinated, their terminal arborizations are not. These terminals serve several sensory modalities. In the dermis, they may be responsive to moderate cold or heat (thermoreceptors); light mechanical touch (mechanoreceptors); damaging heat, cold or deformation (unimodal nociceptors); damaging stimuli of several kinds (polymodal nociceptors). Similar fibres in deeper tissues may also signal extreme conditions, which are experienced, as with all nociceptors, as pain. Free endings in the cornea, dentine and periosteum may be exclusively nociceptive.

Special types of free ending are associated with epidermal structures in the skin. They include terminals associated with hair follicles (peritrichial receptors) which branch from myelinated fibres in the deep dermal cutaneous plexus: the number, size and form of the endings are related to the size and type of hair follicle innervated. These endings respond mainly to movement when hair is deformed and belong to the rapidly adapting mechanoreceptor group.

Merkel tactile endings lie either at the base of the epidermis or around the apical ends of some hair follicles, and are innervated by large myelinated axons. Each axon expands into a disc that is applied closely to the base of a Merkel cell in the basal layer of the epidermis. The cells, which are believed to be derived from the neural crest, contain many large (50–100 nm) dense-cored vesicles, presumably containing transmitters, which are concentrated near the junction with the axon. Merkel endings are slow-adapting mechanoreceptors and are responsive to sustained pressure and sensitive to the edges of applied objects.

ENCAPSULATED ENDINGS

Encapsulated endings are a major group of special endings that includes lamellated corpuscles of various kinds (e.g. Meissner’s, Pacinian), Golgi tendon organs, neuromuscular spindles and Ruffini endings (Fig. 3.30). They exhibit considerable variety in their size, shape and distribution, but share a common feature, in that each axon terminal is encapsulated by non-excitable cells.

Meissner’s corpuscles

Meissner’s corpuscles are found in the dermal papillae of all parts of the hand and foot, the anterior aspect of the forearm, the lips, palpebral conjunctiva and mucous membrane of the apical part of the tongue. They are most concentrated in thick hairless skin, especially of the finger pads, where there may be up to 24 corpuscles per cm^2 in young adults. Mature corpuscles are cylindrical in shape, approximately 80 µm long and 30 µm across, with their long axes perpendicular to the skin surface. Each corpuscle has a connective tissue capsule and central core composed of a stack of flat modified Schwann cells (Fig. 3.31). Meissner’s corpuscles are rapidly adapting mechanoreceptors, sensitive to shape and textural changes in exploratory and discriminatory touch: their acute sensitivity provides the neural basis for reading Braille text.

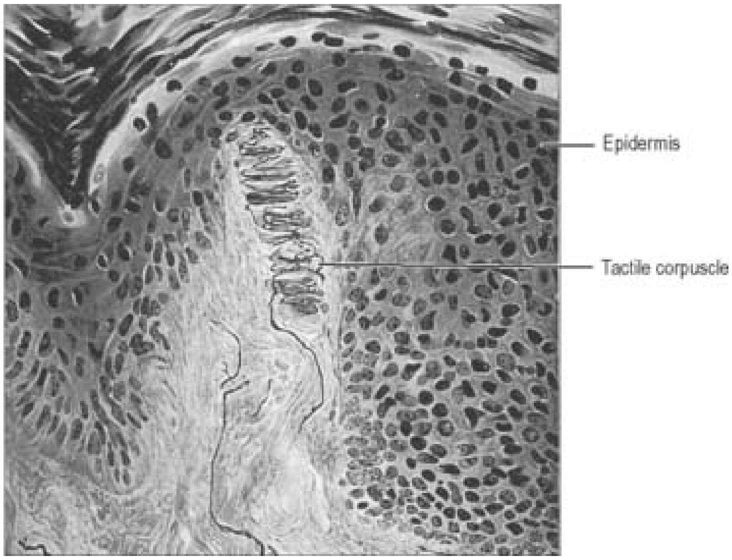

Fig. 3.31 A tactile Meissner's corpuscle in a dermal papilla in the skin, demonstrated using the modified Bielschowsky silver stain technique.

(By courtesy of N Cauna, University of Pittsburgh.)

Pacinian corpuscles

Pacinian corpuscles are situated subcutaneously in the palmar and plantar aspects of the hand and foot and their digits; the external genitalia; arm; neck; nipple; periostea; interosseous membranes; near joints, and within the mesenteries. They are oval, spherical or irregularly coiled and measure up to 2 mm in length and 100–500 µm or more across: the larger ones are visible to the naked eye. Each corpuscle has a capsule, an intermediate growth zone and a central core that contains an axon terminal. The capsule is formed by approximately 30 concentrically arranged lamellae of flat cells approximately 0.2 µm thick (Fig. 3.32). Adjacent cells overlap and successive lamellae are separated by an amorphous proteoglycan matrix that contains circularly orientated collagen fibres, closely applied to the surfaces of the lamellar cells. The amount of collagen increases with age. The intermediate zone is cellular and its cells become incorporated into the capsule or core, so that it is not clearly defined in mature corpuscles. The core consists of approximately 60 bilateral, compacted lamellae lying on both sides of a central nerve terminal.

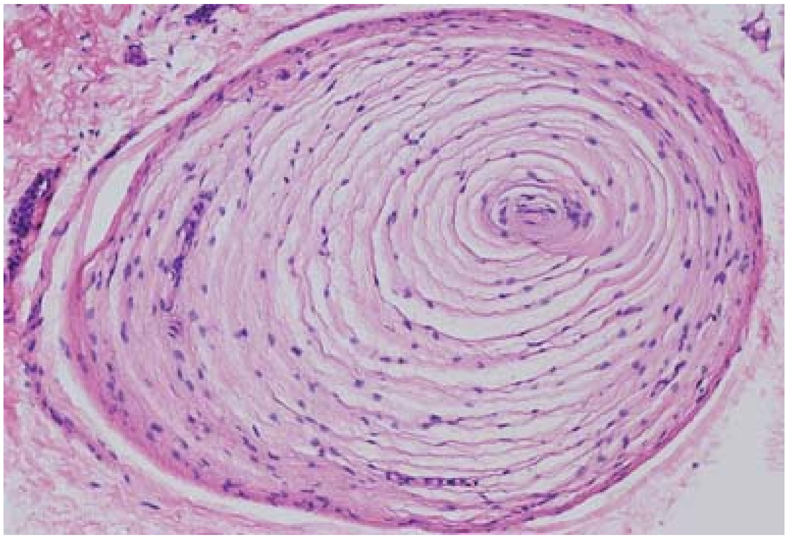

Fig. 3.32 A Pacinian corpuscle in human dermis.

Each corpuscle is supplied by a myelinated axon, which initially loses its myelin sheath and subsequently loses its ensheathing Schwann cell at its junction with the core. The naked axon runs through the central axis of the core and ends in a slightly expanded bulb. It is in contact with the innermost core lamellae, is transversely oval and sends short projections of unknown function into clefts in the lamellae. The axon contains numerous large mitochondria, and minute vesicles, approximately 5 nm in diameter, which aggregate opposite the clefts. The cells of the capsule and core lamellae are thought to be specialized fibroblasts but some may be Schwann cells. Elastic fibrous tissue forms an overall external capsule to the corpuscle. Pacinian corpuscles are supplied by capillaries that accompany the axon as it enters the capsule.

Pacinian corpuscles act as very rapidly adapting mechanoreceptors. They respond only to sudden disturbances and are especially sensitive to vibration. The rapidity may be partly due to the lamellated capsule acting as a high pass frequency filter, damping slow distortions by fluid movement between lamellar cells. Groups of corpuscles respond to pressure changes, e.g. on grasping or releasing an object.

Ruffini endings

Ruffini endings are slowly adapting mechanoreceptors. They are found in the dermis of thin, hairy skin, where they function as dermal stretch receptors and are responsive to maintained stresses in dermal collagen. They consist of the highly branched, unmyelinated endings of myelinated afferents. They ramify between bundles of collagen fibres within a spindle-shaped structure which is enclosed partly by a fibrocellular sheath derived from the perineurium of the nerve. Ruffini endings appear electrophysiologically similar to Golgi tendon organs, which they resemble, although they are less organized structurally. Similar structures appear in joint capsules (see below).

Golgi tendon organs

Golgi tendon organs are found mainly near musculotendinous junctions (Fig. 3.33), where more than 50 may occur at any one site. Each terminal is related closely to a group of muscle fibres (up to 20) as they insert into the tendon. Golgi tendon organs are approximately 500 µm long and 100 µm in diameter, and consist of small bundles of tendon fibres enclosed in a delicate capsule. The collagen bundles (intrafusal fasciculi) are less compact than elsewhere in the tendon, the collagen fibres are smaller and the fibroblasts larger and more numerous. A single, thickly myelinated 1b afferent nerve fibre enters the capsule and divides. Its branches, which may lose their ensheathing Schwann cells, terminate in leaf-like enlargements containing vesicles and mitochondria, which wrap around the tendon. A basal lamina or process of Schwann cell cytoplasm separates the nerve terminals from the collagen bundles that constitute the tendon. Golgi tendon organs are activated by passive stretch of the tendon, but are much more sensitive to active contraction of the muscle. They are important in providing proprioceptive information that complements the information coming from neuromuscular spindles. Their responses are slowly adapting and they signal maintained tension.

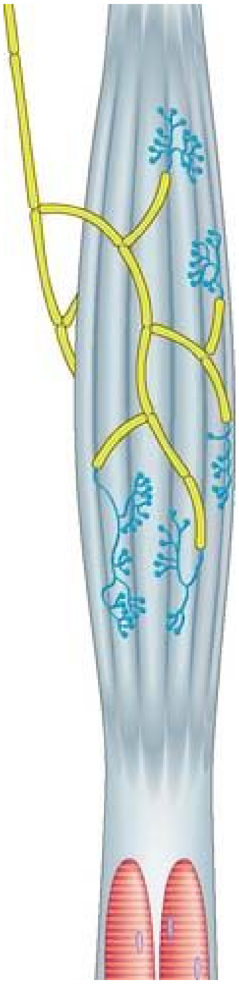

Fig. 3.33 The structure and innervation of a Golgi tendon organ. For clarity the perineurium and endoneurium have been omitted to show the distribution of nerve fibres ramifying between the collagen fibre bundles of the tendon.

NEUROMUSCULAR SPINDLES

Neuromuscular spindles are essential for the control of muscle contraction. Each spindle contains a few small, specialized intrafusal muscle fibres, innervated by both sensory and motor nerve fibres (Fig. 3.34, Fig. 3.35). The whole is surrounded equatorially by a fusiform spindle capsule of connective tissue, consisting of an outer perineurial-like sheath of flattened fibroblasts and collagen and an inner sheath that forms delicate tubes around individual intrafusal fibres (Fig. 3.36). A gelatinous fluid rich in glycosaminoglycans fills the space between the two sheaths.

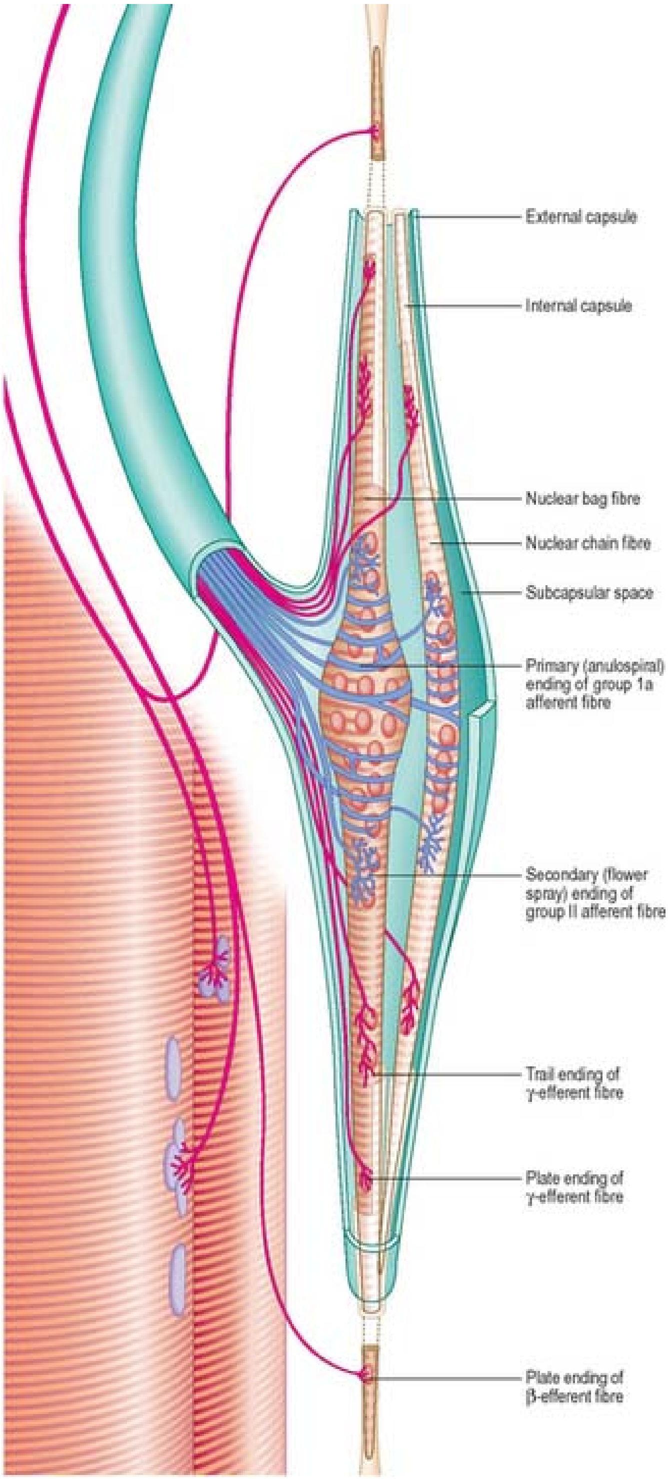
External capsule
Internal capsule
Nuclear bag fibre
Nuclear chain fibre
Subcapsular space
Primary (anulospiral) ending of group 1a afferent fibre
Secondary (flower spray) ending of group II afferent fibre
Trail ending of γ-efferent fibre
Plate ending of γ-efferent fibre
Plate ending of β-efferent fibre

Fig. 3.34 A neuromuscular spindle, showing nuclear bag and nuclear chain fibres within the spindle capsule (green); these are innervated by the sensory anulospiral and ‘flower spray’ afferent fibre endings (blue) and by the γ and β fusimotor (efferent fibre) endings (red). The β efferent fibres are

collaterals of fibres innervating extrafusal slow twitch muscle cells (pink, bottom left).

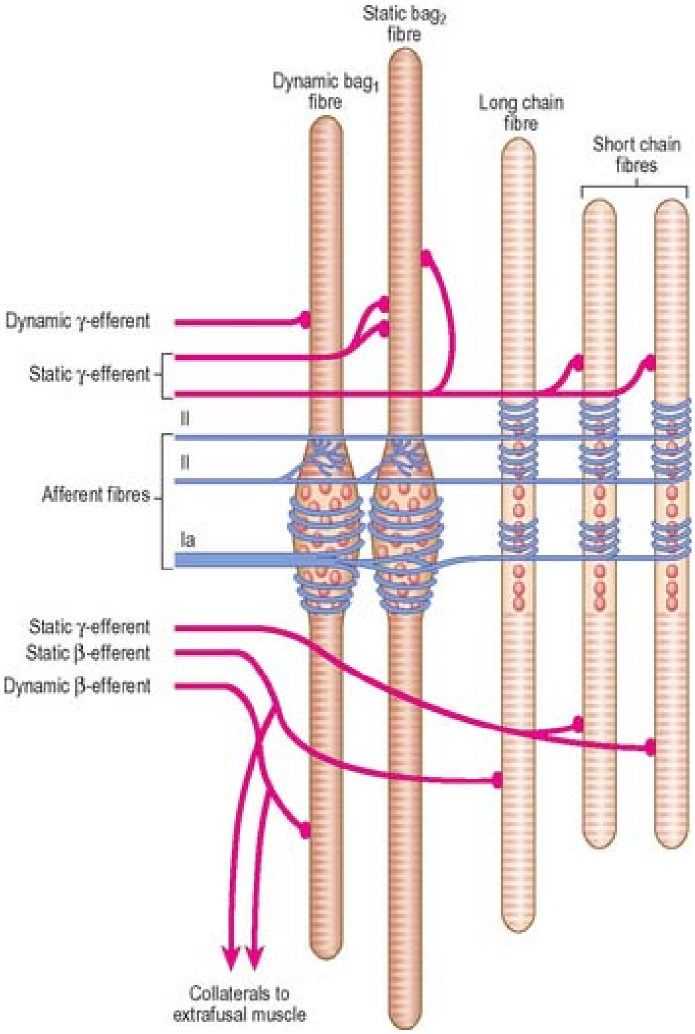
Static bag$_2$ fibre
Dynamic bag$_1$ fibre
Long chain fibre
Short chain fibres
Dynamic γ-efferent
Static γ-efferent
II
II
Afferent fibres
Ia
Static γ-efferent
Static β-efferent
Dynamic β-efferent
Collaterals to extrafusal muscle

Fig. 3.35 Nuclear bag and nuclear chain fibres in a neuromuscular spindle. Dynamic β- and γ-efferents innervate dynamic bag 1 intrafusal fibres, whereas static β- and γ-efferents innervate static bag 2 and nuclear chain intrafusal fibres.

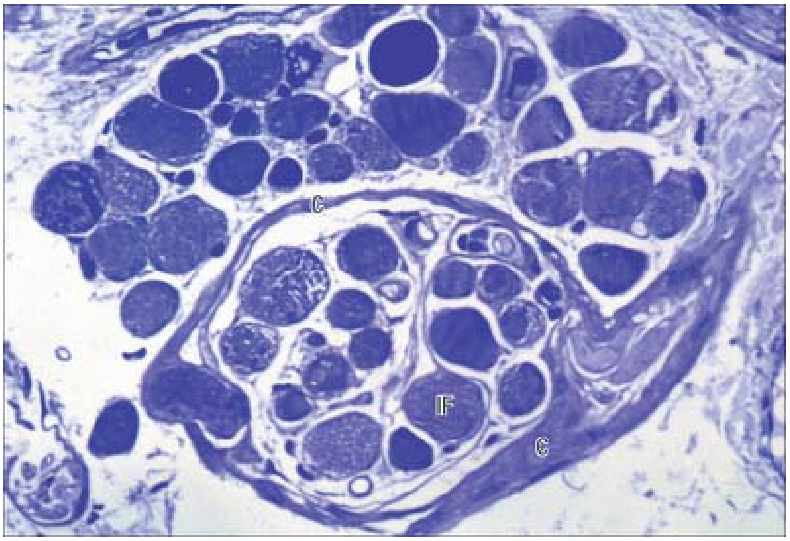

Fig. 3.36 Neuromuscular spindle in transverse section in human extraocular muscle. The spindle capsule (C) encloses intrafusal fibres (IF) of varying diameters. Typical muscle fibres (M) in transverse section are shown above the spindle. Toluidine blue stained resin section.

There are usually 5–14 intrafusal fibres (the number varies between muscles) and two major types of fibre, nuclear bag and nuclear chain fibres, which are distinguished by the arrangement of nuclei in their sarcoplasm. In nuclear bag fibres, an equatorial cluster of nuclei makes the fibre bulge slightly, whereas the nuclei in nuclear chain fibres form a single axial row. Nuclear bag fibres are greater in diameter than chain fibres and extend beyond the surrounding capsule to the endomysium of nearby extrafusal muscle fibres. Nuclear chain fibres are attached at their poles to the capsule or to the sheaths of nuclear bag fibres.

The intrafusal fibres resemble typical skeletal muscle fibres, except that the zone of myofibrils is thin around the nuclei. One subtype of nuclear bag fibre (dynamic bag 1) generally lacks M lines, possesses little sarcoplasmic reticulum and has an abundance of mitochondria and oxidative enzymes, but little glycogen. A second subtype of bag fibre (static bag 2) has distinct M lines and abundant glycogen. Nuclear chain fibres have marked M lines, sarcoplasmic reticulum and T-tubules, and abundant glycogen, but few mitochondria. These variations reflect the contractile properties of different intrafusal fibres (Boyd 1985).

Muscle spindles receive two types of sensory innervation via the unmyelinated terminations of large myelinated axons. Primary (anulospiral) endings are equatorially placed and form spirals around the nucleated parts of intrafusal fibres. They are the endings of large sensory fibres (Group Ia afferents), each of which sends branches to a number of intrafusal muscle fibres. Each terminal lies in a deep sarcolemmal groove in the spindle plasma membrane beneath its basal lamina. Secondary (flowerspray) endings, which may be spray-shaped or anular, are largely confined to nuclear chain fibres, and are the branched terminals of somewhat thinner myelinated (Group II) afferents. They are varicose and spread in a narrow band on both sides of the primary endings. They lie close to the sarcolemma, though not in grooves. In essence primary endings are rapidly adapting, while secondary endings have a regular, slowly adapting, response to static stretch.

There are three types of motor endings in muscle spindles. Two are from fine, myelinated, fusimotor (γ) efferents and one is from myelinated (β) efferent collaterals of axons that supply extrafusal slow twitch muscle fibres. The fusimotor efferents terminate nearer the equatorial region where their terminals either resemble the motor end-plates of extrafusal fibres (plate endings) or are more diffuse (trail endings). Stimulation of the fusimotor and β efferents causes contraction of the intrafusal fibres and consequently, activation of their sensory endings.

Muscle spindles signal the length of extrafusal muscle both at rest and throughout contraction and relaxation, the velocity of their contraction and changes in velocity. These modalities may be related to the different behaviours of the three major types of intrafusal fibre and their sensory terminals. The sensory endings of one type of nuclear bag fibre (dynamic bag 1) are particularly concerned with signalling rapid changes in length that occur during movement, whilst those of the second bag fibre type (static bag 2), are less responsive to movement. The afferents from chain fibres have relatively slowly adapting responses at all times. These elements can therefore detect complex changes in the state of the extrafusal muscle surrounding spindles and can signal fluctuations in length, tension, velocity of length change and acceleration. Moreover, they are under complex central control: efferent (fusimotor) nerve fibres, by regulating the strength of contraction, can adjust the length of the intrafusal fibres and thereby the responsiveness of spindle sensory endings. In summary, the organization of spindles allows them to monitor muscle conditions actively in order to compare intended and actual movements, and to provide a detailed input to spinal, cerebellar, extrapyramidal and cortical centres about the state of the locomotor apparatus.

JOINT RECEPTORS

The arrays of receptors situated in and near articular capsules provide information on the position, movements and stresses acting on joints. Structural and functional studies have demonstrated at least four types of joint receptor: their proportions and distribution vary with site. Three are encapsulated endings, the fourth a free terminal arborization.

Type I endings are encapsulated corpuscles of the slowly adapting mechanoreceptor type and resemble Ruffini endings. They lie in the superficial layers of the fibrous capsules of joints in small clusters and are innervated by myelinated afferent axons. Being slowly adapting, they provide awareness of joint position and movement, and respond to patterns of stress in articular capsules. They are particularly common in joints where static positional sense is necessary for the control of posture (e.g. hip, knee).

Type II endings are lamellated receptors, and resemble small versions of the large Pacinian corpuscles found in general connective tissue. They occur in small groups throughout joint capsules, particularly in the deeper layers and other articular structures (e.g. the fat pad of the temporomandibular joint). They are rapidly adapting, low-threshold mechanoreceptors, sensitive to movement and pressure changes, and they respond to joint movement and transient stresses in the joint capsule. They are supplied by myelinated afferent axons, but are probably not involved in the conscious awareness of joint sensation.

Type III endings are identical to Golgi tendon organs in structure and function: they occur in articular ligaments, but not in joint capsules. They are high-threshold, slowly adapting receptors and may serve, at least in part, to prevent excessive stresses at joints by reflex inhibition of the adjacent muscles. They are innervated by large myelinated afferent axons.

Type IV endings are free terminals of myelinated and unmyelinated axons that ramify in articular capsules, the adjacent fat pads and around the blood vessels of the synovial layer. They are high-threshold, slowly adapting receptors and are thought to respond to excessive movements, providing a basis for articular pain.

NEUROMUSCULAR JUNCTIONS

SKELETAL MUSCLE

The most intensively studied effector endings are those that innervate muscle, particularly skeletal muscle. All neuromuscular (myoneural) junctions are axon terminals of somatic motor neurones. They are specialized for the release of neurotransmitter on to the sarcolemma of skeletal muscle fibres, causing a change in their electrical state which leads to contraction. Each axon branches near its terminal to innervate from several to hundreds of muscle fibres, the number depending on the precision of motor control required.

The detailed structure of a motor terminal varies with the type of muscle innervated. Two major types of ending are recognized, innervating either extrafusal muscle fibres, or the intrafusal fibres of neuromuscular spindles. In the former type, each axonal terminal usually ends midway along a muscle fibre in a discoidal motor end-plate (Fig. 3.37), and usually initiates action potentials that are rapidly conducted to all parts of the muscle fibre. In the latter type, the axon gives off numerous branches that form a cluster of small expansions extending along the muscle fibre; in the absence of propagated muscle excitation, these excite the fibre at several points. Both types of ending are associated with a specialized receptive region of the muscle fibre, the sole plate, where a number of muscle cell nuclei are grouped within the granular sarcoplasm.

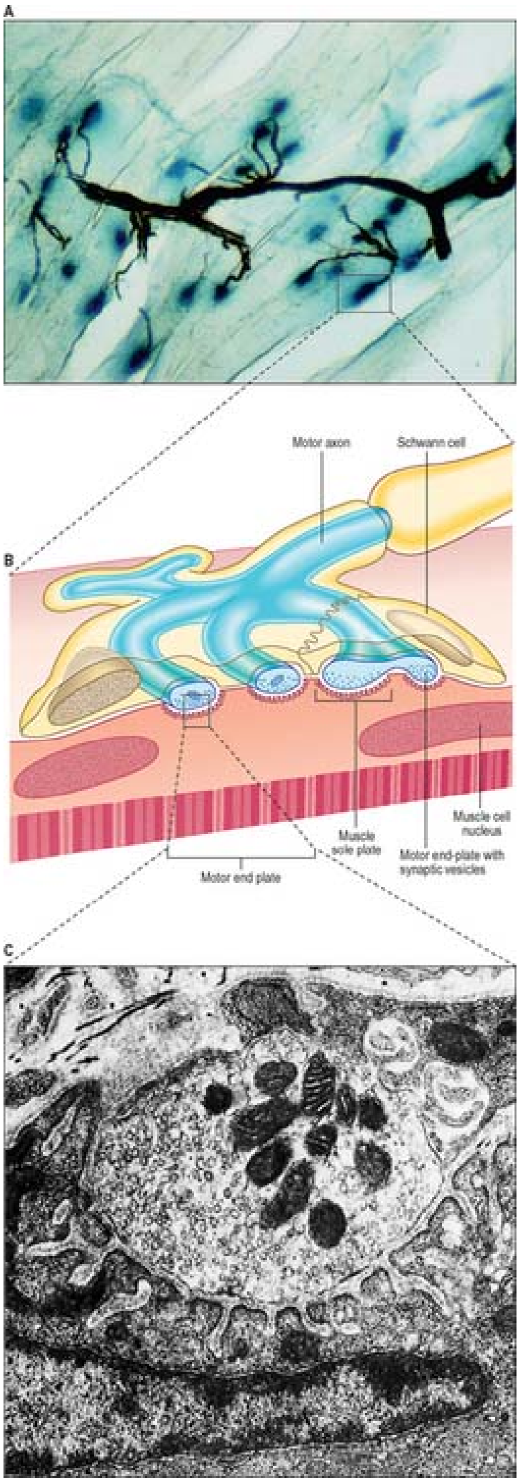
A
Motor axon
Schwann cell
B
Muscle cell nucleus
Muscle sole plate
Motor end-plate with synaptic vesicles
Motor end plate
C

Fig. 3.37 The neuromuscular junction. **A**, Whole-mount preparation of teased skeletal muscle fibres (pale, faintly striated, diagonally orientated structures). The terminal part of the axon (silver-stained, brown) branches to form motor end-plates on adjacent muscle fibres. The sole plate recesses in

the sarcolemma, into which the motor end-plates fit, are demonstrated by the presence of acetylcholinesterase (shown by enzyme histochemistry, blue). **B**, Diagrammatic representation of the axonal motor end-plate and the deeply infolded sarcolemma. **C**, Electron micrograph showing the expanded motor end-plate of the axon filled with vesicles containing synaptic transmitter (ACh) (above); the deep infoldings of the sarcolemmal sole plate (below) form subsynaptic gutters.

*(**A** By courtesy of Dr Norman Gregson, Division of Neurology, GKT School of Medicine, London; **C** By courtesy of Professor DN Landon, Institute of Neurology, University College London.)*

The sole plate contains numerous mitochondria, endoplasmic reticulum and Golgi complexes. The terminal branches of the axon are plugged into shallow grooves in the surface of the sole plate (primary clefts), from where numerous pleats extend for a short distance into the underlying sarcoplasm (secondary clefts) (Fig. 3.37B,C). The axon terminal contains mitochondria and many clear, 60 nm spherical vesicles similar to those in presynaptic boutons, which are clustered over the zone of membrane apposition. It is ensheathed by Schwann cells whose cytoplasmic projections extend into the synaptic cleft. The plasma membranes of the axon terminal and the muscle cell are separated by a 30–50 nm gap and an interposed basal lamina which follows the surface folding of the sole plate membrane into the secondary clefts. The basal lamina contains specialized components including specific isoforms of type IV collagen and laminin and the heparan sulphate proteoglycan, agrin. Endings of fast and slow twitch muscle fibres (p. 111) differ in detail: the sarcolemmal grooves are deeper, and the presynaptic vesicles more numerous, in the fast fibres.

Junctions with skeletal muscle are cholinergic; the release of ACh changes the ionic permeability of the muscle fibre. Clustering of ACh receptors at the neuromuscular junction depends in part on the presence in the muscle basal lamina of agrin, which is secreted by the motor neurone, and is important in establishing the post-junctional molecular machinery. When the depolarization of the sarcolemma reaches a particular threshold, it initiates an all-or-none action potential in the sarcolemma, which is then propagated rapidly over the whole cell surface and also deep within the fibre via the invaginations (T-tubules) of the sarcolemma (p. 108), causing contraction. The amount of ACh released by the arrival of a single nerve impulse is sufficient to trigger an action potential. However, because ACh is very rapidly hydrolysed by the enzyme AchE, present at the sarcolemmal surface of the sole plate, a single nerve impulse only gives rise to one muscle action potential, i.e. there is a one-to-one relationship between neural and muscle action potentials. Thus the contraction of a muscle fibre is controlled by the firing frequency of its motor neurone.

Neuromuscular junctions are partially blocked by high concentrations of lactic acid, as in some types of muscle fatigue.

AUTONOMIC MOTOR TERMINATIONS

Autonomic neuromuscular junctions differ in several important ways from the skeletal neuromuscular junction and from synapses in the CNS and PNS. There is no fixed junction with well defined pre- and post-junctional specializations. Unmyelinated, highly branched, postganglionic autonomic axons become beaded or varicose as they reach the effector smooth muscle. These varicosities are not static but move along axons. They are packed with mitochondria and vesicles containing neurotransmitters which are released from the varicosities during conduction of an impulse along the axon. The distance (cleft) between the varicosity and smooth muscle membrane varies considerably depending on the tissue, from 20 nm in densely innervated structures such as the vas deferens to 1–2 μm in large elastic arteries. Unlike skeletal muscle, the effector tissue is a muscle bundle rather than a single cell. Gap junctions between individual smooth muscle cells are low resistance pathways which allow electronic coupling and the spread of activity within the effector bundle: they vary in size from punctate junctions to junctional areas of more than 1 μm in diameter.

Adrenergic sympathetic postganglionic terminals contain dense-cored vesicles. Cholinergic terminals, which are typical of all parasympathetic and some sympathetic endings, contain clear spherical vesicles like those in the motor end-plates of skeletal muscle. A third category of autonomic neurones has non-adrenergic, non-cholinergic endings which contain a wide variety of chemicals with transmitter properties. Conjugated purine (ATP, a nucleoside), is probably the neurotransmitter at these terminals, which are thus classed as purinergic. For further reading on purinergic signalling, see Burnstock (2006). Typically, their axons contain large, 80–200 nm, dense opaque vesicles, congregated in varicosities at intervals along axons. Such terminals are formed in many sites, including the external muscle layers and sphincters of the alimentary tract, lungs, walls of blood vessels, urogenital tract and in the CNS (see Chapter 15). In the intestinal wall, neuronal somata lie in the myenteric plexus, and their axons spread caudally for a few millimetres, mainly to innervate circular muscle. Purinergic neurones are under cholinergic control from preganglionic sympathetic neurones, via postganglionic sympathetic fibres. Their endings mainly hyperpolarize smooth muscle cells, causing relaxation, e.g. preceding peristaltic waves, opening sphincters and, probably, causing reflex distension in gastric filling.

Autonomic efferents also innervate glands, myoepithelial cells, adipose and lymphoid tissues.

CNS–PNS TRANSITION ZONE

The transition between CNS and PNS usually occurs some distance from the point at which nerve roots emerge from the brain or the spinal cord. The segment of root that contains components of both CNS and PNS tissue is called the CNS–PNS transition zone (TZ). All axons in the PNS, other than postganglionic autonomic neurones, cross such a TZ. Macroscopically, as a nerve root is traced towards the spinal cord or the brain, it splits into several thinner rootlets which may, in turn, subdivide into minirootlets. The TZ is located within either rootlet or minirootlet (Fig. 3.38). The arrangement of roots and rootlets varies according to whether the root trunk is ventral, dorsal or cranial. Thus, in dorsal roots, the main root trunk separates into a fan of rootlets and minirootlets which enter the spinal cord in sequence along the dorsolateral sulcus. In certain cranial nerves the minirootlets come together central to the TZ and enter the brain as a stump of white matter.

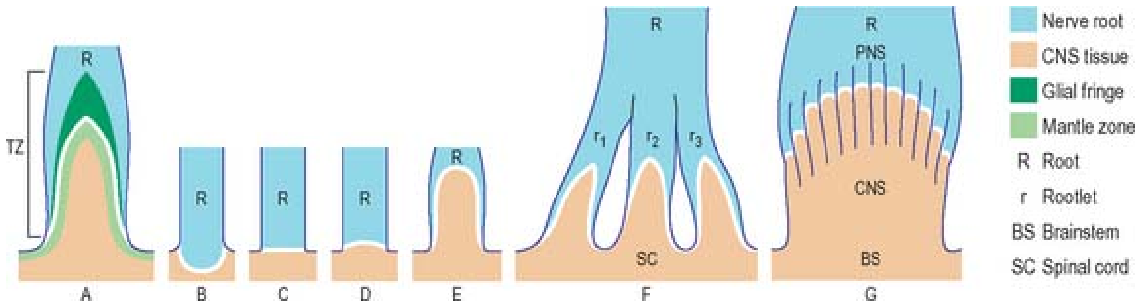

Fig. 3.38 Schematic representation of the nerve root–spinal cord junction. **A–G**, Different CNS–PNS borderline arrangements. **A**, Pointed borderline. The extent of the transitional zone (TZ) is indicated. **B–G**, glial fringe omitted; **B**, Concave borderline (white line) and inverted TZ. **C**, Flat borderline situated at the level of the root (R)–spinal cord junction. **D** and **E**, Convex, dome-shaped borderline; the CNS expansion into the rootlet is moderate in **D** and extensive in **E**. **F**, The root (R) splits into rootlets (r), each with its own TZ and attaching separately to the spinal cord (SC). **G**, Arrangement found in several cranial nerve roots (e.g. vestibulocochlear nerve). The PNS component of the root separates into a bundle of closely

packed minirootlets, each equipped with a TZ. The minirootlets reunite centrally.

Microscopically, the TZ is characterized by an axial CNS compartment surrounded by a PNS compartment. The zone lies more peripherally in sensory than in motor nerves, but in both, the apex of the TZ is described as a glial dome, whose convex surface is usually directed distally. The centre of the dome consists of fibres with a typical CNS organization, surrounded by an outer mantle of astrocytes (corresponding to the glia limitans). From this mantle, numerous glial processes project into the endoneurial compartment of the peripheral nerve where they interdigitate with its Schwann cells. The astrocytes form a loose reticulum through which axons pass. Peripheral myelinated axons usually cross the zone at a node of Ranvier, which is here termed a PNS–CNS compound node.

A novel cell type, the boundary cap (BC) cell, has been described recently in avian and mammalian species. BCs are derived from the neural crest and form transient clusters in the presumptive dorsal root TZ of the embryonic spinal cord: they are thought to prevent cell mixing at this interface and to help dorsal root ganglion afferents navigate their path to targets in the spinal cord. It has been proposed that within dorsal root ganglia, BC-derived cells are the progenitors of neurones, mainly nociceptive afferents, satellite cells and all Schwann cell precursors that migrate into the dorsal roots (see Maro et al 2004).

CONDUCTION OF THE NERVOUS IMPULSE

All cells generate a steady electrical potential across their plasma membranes (a membrane potential) by maintaining ionic concentrations inside the cell that differ from the extracellular fluid (Fig. 3.39). In neurones this membrane potential is known as the resting potential, and at approximately −80 mV (potential inside the cell measured relative to the outside of the cell), it is similar to that of non-excitable cells. However unlike non-excitable cells, neurones receive, conduct, and transmit information across their surfaces using minute fluctuations in membrane potential that result from changes in transmembrane ion fluxes. Sodium or, in some sites, calcium, entry causes depolarization of the cell, while chloride influx or potassium efflux results in hyperpolarization. Plasma membrane permeability to these ions is altered by the opening or closing of ion-specific transmembrane channels, triggered by chemical or electrical stimuli.

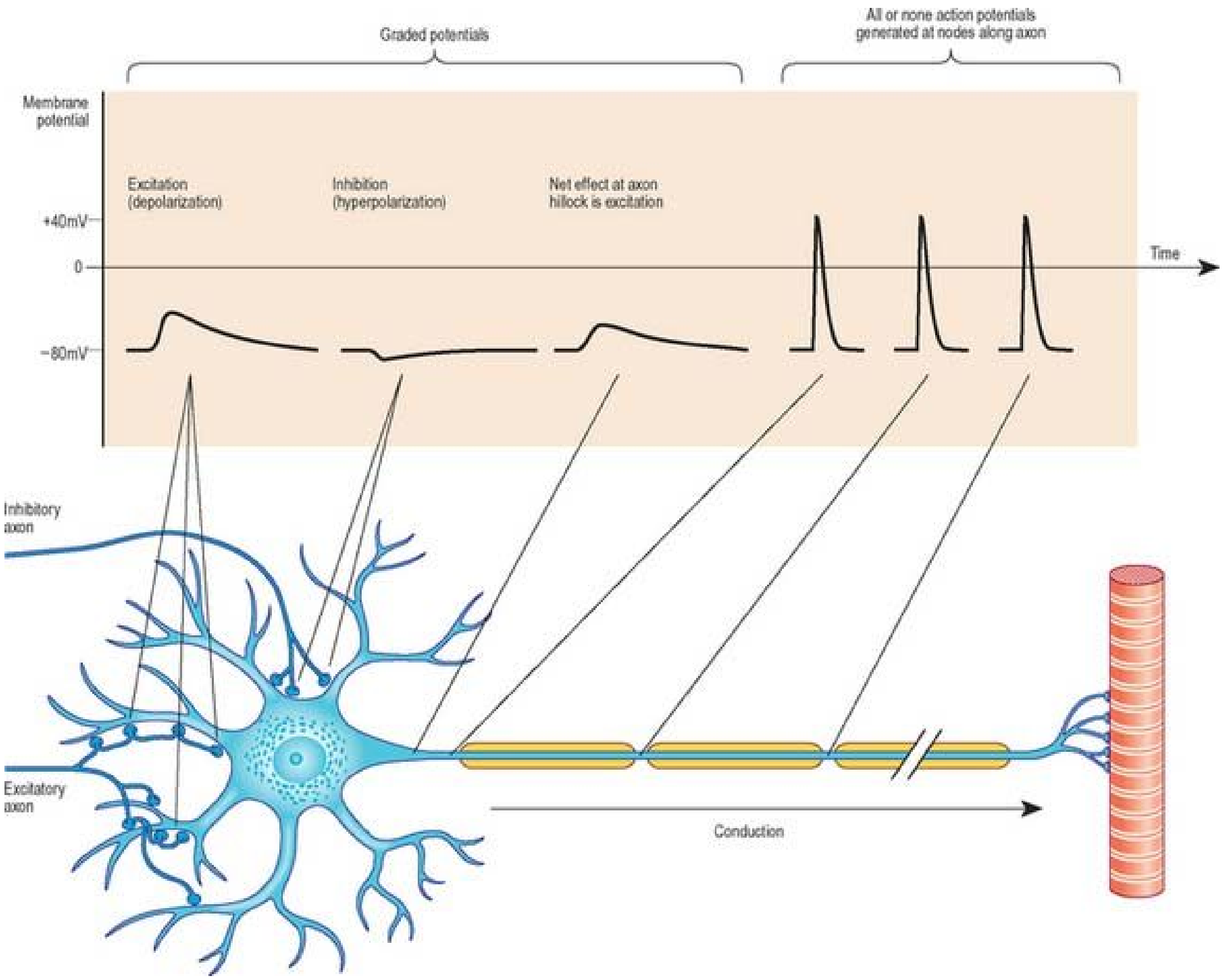
Graded potentials
All or none action potentials
generated at nodes along axon
Membrane potential
Excitation (depolarization)
Inhibition (hyperpolarization)
Net effect at axon hillock is excitation
+40mV
0
−80mV
Time
Inhibitory axon
Excitatory axon
Conduction

Fig. 3.39 The types of change in electrical potential that can be recorded across the cell membrane of a motor neurone at the points indicated. Excitatory and inhibitory synapses on the surfaces of the dendrites and soma cause local graded changes of potential which summate at the axon hillock and may initiate a series of all-or-none action potentials, which in turn are conducted along the axon to the effector terminals.

Chemically triggered ionic fluxes may be either direct, where the chemical agent (neurotransmitter) binds to the channel itself to cause it to open, or indirect, where the neurotransmitter is bound by a transmembrane receptor molecule that activates a complex second messenger system within the cell to open separate transmembrane channels. Electrically induced changes in membrane potential depend on the presence of voltage-sensitive ion channels which, when the transmembrane potential reaches a critical level, open to allow the influx or efflux of specific ions. In all cases, the channels remain open only transiently, and the numbers which open and close determine the total flux of ions across the membrane.

The types and concentrations of transmembrane channels and related proteins, and therefore the electrical activity of the membranes, vary in different parts of the cell. Dendrites and neuronal somata depend mainly on neurotransmitter action and show graded potentials, whereas axons have voltage-gated channels that give rise to action potentials.

In graded potentials, a flow of current occurs when a synapse is activated: the influence of an individual synapse on the membrane potential of neighbouring regions decreases with distance. Thus synapses on the distal tips of dendrites may, on their own, have relatively little effect on the membrane potential of the cell body. The electrical state of a neurone therefore depends on many factors, including the numbers and positions of thousands of excitatory and inhibitory synapses, their degree of activation, and the branching pattern of the dendritic tree and geometry of the cell body. The integrated activity directed toward the neuronal cell body is converted to an output directed away from the soma at the site where the axon leaves the cell body, the axon hillock. Voltage sensitive channels are concentrated at the axon hillock (unlike the dendrites or soma), and when this region is sufficiently depolarized, an action potential is generated and is subsequently conducted along the axon.

ACTION POTENTIAL

The action potential is a brief, self-propagating reversal of membrane polarity. It depends on an initial influx of sodium ions which causes a reversal of polarity to about +40 mV, followed by a rapid return towards the resting potential as potassium ions flow out (the detailed mechanism differs somewhat between CNS and PNS). The rapid reversal process is completed in approximately 0.5 msec, followed by a slower recovery phase of up to 5 msec, when the resting potential is fully restored. Once the axon hillock reaches threshold, propagation of the action potential is independent of the initiating stimulus, thus the size and duration of action potentials are always the same (described as all-or-none) for a particular neurone, no matter how much a stimulus may exceed the threshold value.

Once initiated, an action potential spreads spontaneously and at a relatively constant velocity, within the range of 4–120 m/s. Conduction velocity depends on a number of factors related to the way in which the current spreads, e.g. axonal cross-sectional area, the numbers and positioning of ion channels, and membrane capacitance (influenced particularly by the presence of myelin). In axons lacking myelin, action potential conduction is analogous to a flame moving along a fuse. Just as each segment of fuse is ignited by its upstream neighbour, each segment of axon membrane is driven to threshold by the depolarization of neighbouring membrane. Sodium channels within the newly depolarized segment open and positively charged sodium ions enter, driving the local potential inside the axon toward positive values. This inward current in turn depolarizes the neighbouring, downstream, nondepolarized membrane, and the cyclic propagation of the action potential is completed.

Myelinated fibres are electrically insulated by their myelin sheaths along most of their lengths, except at nodes of Ranvier. The distance between nodes, referred to as the internodal distance, is directly related to axon diameter and varies between 0.2 and 2.0 mm. Voltage-gated sodium channels are clustered at nodes, and the nodal membrane is the only place where high densities of inward sodium current can be generated across the axon membrane. Like conduction in unmyelinated axons, conduction in myelinated axons is self-propagating, but instead of physically adjacent regions of membrane acting to excite one another, it is the depolarization occurring in the neighbouring upstream node that excites a node to threshold. Reaching threshold causes the sodium channels at the node to open and generate inward sodium current, but instead of this acting on the adjacent membrane, the high resistance and low capacitance of the myelin sheath directs the current toward the next downstream node, exciting it to threshold and completing the cycle. The action potential thus jumps from node to node, a process known as saltatory conduction, which greatly increases the conduction velocity.

A number of disorders of the CNS and PNS include demyelination as a characteristic feature. Perhaps most common amongst these is multiple sclerosis, which is characterized by primary demyelination at scattered sites within the white matter of the CNS (it is now recognized that axonal loss also contributes to the progression of multiple sclerosis). Primary demyelination is the loss of the myelin sheath with axonal preservation, and is usually segmental, ie. it rarely extends along the entire length of an affected axon. The phenomenon is associated with conduction block because the newly exposed, previously internodal, axolemma contains relatively few voltage-sensitive Na^+ channels. There is experimental evidence that conduction can be restored in some demyelinated axons, and experimental and clinical evidence that remyelinated axons can conduct at near normal speeds, because even though their sheaths are thinner than the original myelin sheaths, the safety factor (i.e. the factor by which the outward current at a quiescent node next to an excited node exceeds the minimum current required to evoke a response) is greater than 1. The myelin loss that occurs in the early stages of Wallerian degeneration in both CNS and PNS, usually distal to a site of trauma but also in response to a prolonged period of ischaemia or exposure to a neuronotoxic substance, is accompanied by axonal degeneration (the term secondary demyelination is sometimes used to describe this form of myelin loss).

In both myelinated and unmyelinated fibres there is an irreducible interval at the end of an action potential, termed the refractory period, during which another action potential cannot be triggered. This determines the maximum frequency at which action potentials can be conducted along a nerve fibre: its value differs in different neurones and affects the amount of information which can be carried by an individual fibre.

Axonal conduction is naturally unidirectional, from dendrites and soma to axon terminals. When an action potential reaches the axonal terminals, it causes depolarization of the presynaptic membrane and as a result, quanta of neurotransmitter (which correspond to the content of individual vesicles) are released to change the degree of excitation of the next neurone, muscle fibre or glandular cell. For further information, see Kandel et al (2000).

REFERENCES

bott NJ, Rönnbäck L, Hansson E. Astrocyte-endothelial interactions at the blood-brain barrier. *Nature Rev Neurosci*. 2006;7:41-53.

yd IA. Muscle spindles and stretch reflexes. In: Swash M, Kennard C. *Scientific Basis of Clinical Neurology*. Edinburgh: Churchill Livingstone; 1985:74-97.

A detailed account of the functional aspects of neuromuscular spindles..

rnstock G. Pathophysiology and therapeutic potential of purinergic signaling. *Pharmacol Rev*. 2006;58:58-86.

tt AM, Hamilton N, Hubbard P, Pugh M, Ibrahim M. Synantocytes: the fifth element. *J Anat*. 2005;207:695-706.

Describes the characteristics of a novel glial cell which contacts nodes of Ranvier in the central nervous system..

irns NJ, Lee VM-Y, Trojanowski JQ. The cytoskeleton in neurodegenerative disease. *J Pathol*. 2004;204:438-449.

y R, Salzet M. The neuroendocrine phenotype, cellular plasticity, and the search for genetic switches: redefining the diffuse neuroendocrine system.

Neuroendocrinol Lett. 2002;23:379-384.

elds RD. The other half of the brain. *Sci Am (April)*. 2004:54-61.

elds RD, Stevens-Graham B. New insights into neuron-glia communication. *Science*. 2002;298:552-556.

Reviews the evidence for two-way signalling between neurones and glia, essential in axonal conduction, synaptic transmission, and information processing..

ırness JB. Novel gut afferents: Intrinsic afferent neurons and intestinofugal neurons. *Auton Neurosci*. 2006;125:81-85.

ershon MD. The Second Brain. New York: HarperCollins, 1998.

ızik BW, Goldstein LSB. Microtubule-dependent transport in neurons: steps towards an understanding of regulation, function and dysfunction. *Curr Opin Cell Biol*. 2004;16:443-450.

Reviews axonal transport mechanisms and their involvement in acquired and inherited neural disorders..

F, Sun YE. Glial cells more than support cells? *Int J Biochem Cell Biol*. 2007;39:661-665.

ındel ER, Schwartz JH, Jessel T. Principles of Neural Science, 4th edn. New York: McGraw-Hill, 2000.

m H-J, DiBernardo AB, Sloane JA, et al. TK WAVE1 is required for oligodendrocyte morphogenesis and normal CNS myelination. *J Neurosci*. 2006;26:5849-5859.

aro GS, Vermeren M, Voiculescu O, et al. Neural cap boundary cells constitute a source of neuronal and glial cells of the PNS. *Nature Neurosci*. 2004;7:930-938. P

Describes the characteristics and developmental fate of a novel type of cell, boundary cap (BC) cell, concerned with establishing the boundary between central and peripheral nervous systems during embryogenesis. Proposes that BCs constitute a source of PNS components that migrate into the PNS after the major neural crest ventrolateral migratory stream..

olte J. The Human Brain. In *An Introduction to Functional Anatomy*, 5th edn., Edinburgh: Mosby; 2002:197-222. Ch. 9

herer SS, Arroyo EJ. Recent progress on the molecular organization of myelinated axons. *J Peripheral Nerv Syst*. 2002;7:1-12.

Review of the molecular architecture of myelinated peripheral axons and their myelin sheaths..

ifert G, Schilling K, Steinhäuser C. Astrocyte dysfunction in neurological disorders: a molecular perspective. *Nature Rev Neurosci*. 2006;7:194-206.

epherd AJ, Downing JEG, Miyan JA. Without nerves, immunology remains incomplete – *in vivo veritas*. *Immunology*. 2005;116:145-163.

Reviews evidence for neural mechanisms that contribute to specific categories of host defence. Complements the established view of neuroendocrine-immune modulation..

olterra A, Meldolesi J. Astrocytes, from brain glue to communication elements: the revolution continues. *Nat Rev Neurosci*. 2005;6:626-640.

ong RO, Ghosh A. Activity-dependent regulation of dendritic growth and patterning. *Nature Rev Neurosci*. 2002;25:803-812.

CHAPTER 4

Blood, lymphoid tissues and haemopoiesis

In postnatal life blood cells are formed in the bone marrow. Haemopoiesis produces red cells (erythrocytes), and a wide variety of defensive cells (white blood cells, or leukocytes). The latter include neutrophil, eosinophil and basophil granulocytes, B lymphocytes and monocytes. T lymphocytes develop in the thymus from bone marrow-derived progenitors. Platelets are produced in the bone marrow as cellular fragments of megakaryocytes. Only erythrocytes and platelets are generally confined to the blood vascular system, whereas all leukocytes can leave the circulation and enter extravascular tissues. The numbers of cells doing so increases greatly during inflammation caused by local infections and diseases.

The lymphoid tissues are the thymus, lymph nodes, spleen and the lymphoid follicles associated mainly with the alimentary and respiratory tracts. Lymphocytes populate lymphoid tissues and are concerned with various types of immune defence. Lymphoid tissue also contains supportive stromal cells which are non-haemopoietic in origin (e.g. thymic epithelium), non-haemopoietic follicular dendritic cells of lymph nodes and splenic follicles, haemopoietically-derived interdigitating dendritic cells, and macrophages of the mononuclear phagocyte system. Dendritic cells and blood monocyte-derived macrophages are found additionally in most tissues and organs where they function as immunostimulatory antigen-presenting cells (APCs).

CELLS OF PERIPHERAL BLOOD

BLOOD

Blood is an opaque fluid with a viscosity greater than that of water (mean relative viscosity 4.75 at 18°C), and a specific gravity of 1.06 at 15°C. It is bright red when oxygenated, in the systemic arteries, and dark red to purple when deoxygenated, in systemic veins. Blood is a mixture of a clear liquid, plasma, and cellular elements, and consequently the hydrodynamic flow of blood in vessels behaves in a complex manner that is not entirely predictable by simple Newtonian equations.

Plasma

Plasma is a clear, yellowish fluid which contains many substances in solution or suspension: low molecular weight solutes give a mean freezing-point depression of 0.54°C. Plasma contains high concentrations of sodium and chloride ions, potassium, calcium, magnesium, phosphate, bicarbonate, traces of many other ions, glucose, amino acids and vitamins. The colloids include high molecular weight plasma proteins, e.g. clotting factors, particularly prothrombin; immunoglobulins and complement proteins involved in immunological defence; glycoproteins, lipoproteins, polypeptide and steroid hormones and globulins for the transport of hormones and iron. Since most of the metabolic activities of the body are reflected in the plasma composition, its routine chemical analysis is of great diagnostic importance.

The precipitation of the protein fibrin from plasma to form a clot (Fig. 4.1) is initiated by the release of specific materials from damaged cells and blood platelets in the presence of calcium ions. If blood or plasma samples are allowed to stand, they will separate into a clot and a clear yellowish fluid, the serum. Clot formation is prevented by removal of calcium ions, e.g. by addition of citrate, oxalate or various organic calcium chelators (EDTA, EGTA) to the sample. Heparin is also widely used as an anticlotting agent, because it interferes with another part of the complex series of chemical interactions which lead to fibrin clot formation.

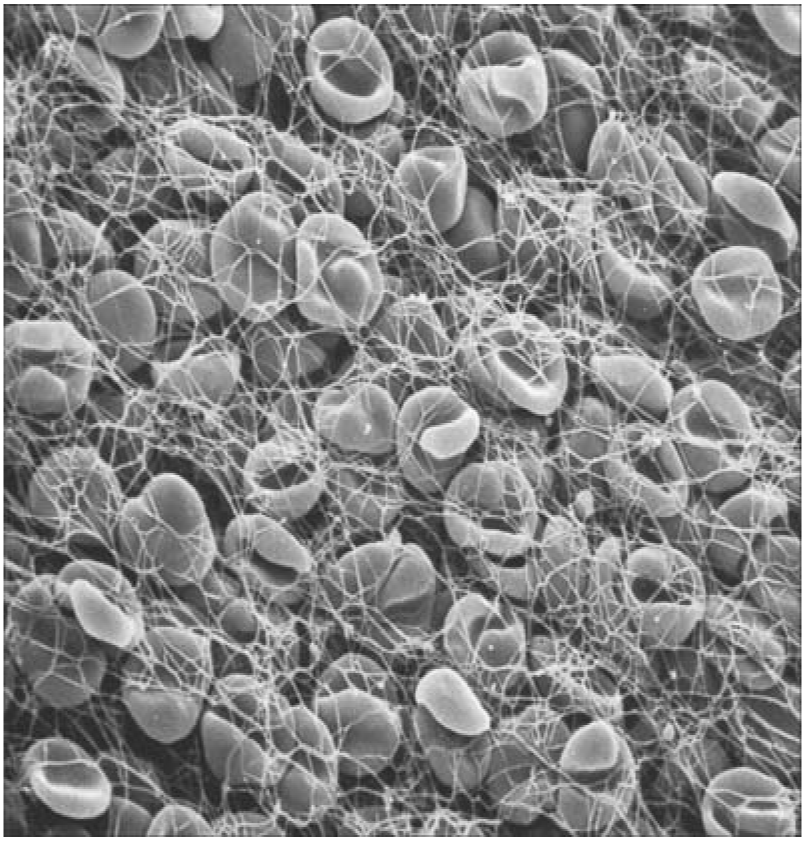

Fig. 4.1 Erythrocytes enmeshed in filaments of fibrin in a clot.

(By courtesy of Michael Crowder.)

ERYTHROCYTES

Erythrocytes (red blood cells, red blood corpuscles [RBC]) account for the largest proportion of blood cells (99% of the total number), with normal values of 4.1–6.0 × 10^6/µl in adult males and 3.9–5.5 × 10^6/µl in adult females. Polycythaemia (increased red cell mass) can occur in individuals living at high altitude, or pathologically in conditions resulting in arterial hypoxia. Reduction in red cell mass (anaemia) has many underlying causes but in rare instances can be due to structural defects in erythrocytes (see below).

Each erythrocyte is a biconcave disc (Fig. 4.1, Fig. 4.2) with a mean diameter in dried smear preparations of 7.1 µm; in fresh preparations the mean diameter is 7.8 µm, decreasing slightly with age. Mature erythrocytes lack nuclei. They are pale red by transmitted light, with paler centres because of their biconcave shape. The properties of their cell coat cause them to adhere to one another by their rims to form loose piles of cells (rouleaux). In normal blood, a few cells assume a shrunken star-like, crenated form: this shape can be reproduced by placing normal biconcave erythrocytes in a hypertonic solution, which causes osmotic shrinkage. In hypotonic solutions erythrocytes take up water and become spherical; they may eventually lyse to release their haemoglobin (haemolysis), leaving red cell ghosts.

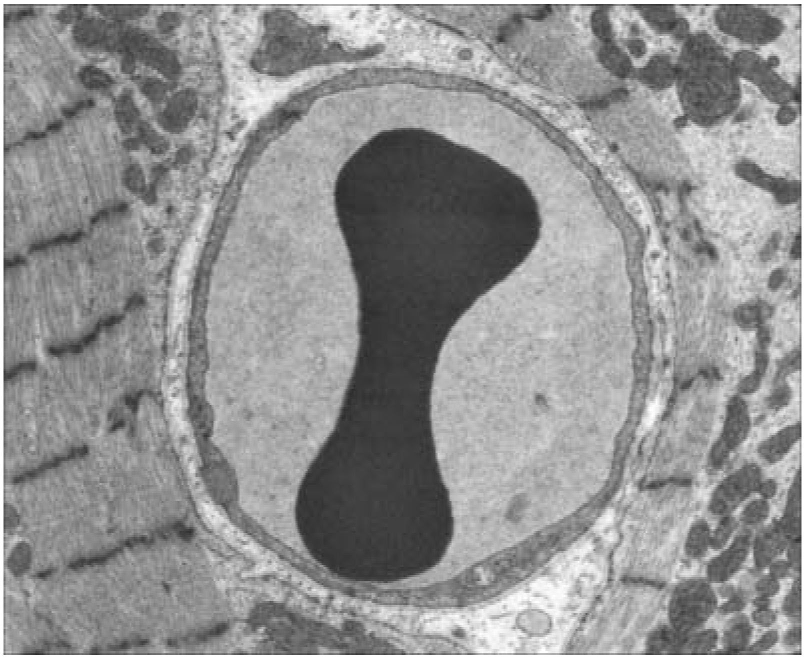

Fig. 4.2 A human heart muscle biopsy specimen, showing an erythrocyte within a capillary. The erythrocyte biconcave disc is typically electron dense and almost fills the capillary lumen.

Erythrocytes have a limiting plasma membrane which encloses mainly a single protein, haemoglobin, as a 33% solution. The plasma membrane of erythrocytes is 60% lipid and glycolipid, and 40% protein and glycoprotein. More than 15 classes of protein are present, including two major types. Glycophorins A and B (each with a molecular mass of approximately 50 kDa) span the membrane, and their negatively charged carbohydrate chains project from the outer surface of the cell. Their sialic acid groups confer most of the fixed charge on the cell surface. A second transmembrane macromolecule, band 3 protein, forms an important anion channel, exchanging bicarbonate for chloride ions across the membrane and allowing the release of CO_2 in the lungs. The ABO blood group antigens are all membrane glycolipids.

The shape of the erythrocyte is largely determined by the filamentous protein dimer, spectrin, a name which reflects its original isolation from red cell ghosts. Spectrin dimers associate as tetramers through their head regions, and are attached to the cytoplasmic domain of the anion carrier, band 3 protein, via ankyrin. Other proteins, including tropomyosin, tropomodulin and short actin filaments form junctional complexes which link spectrin to glycophorin transmembrane proteins, forming a stabilizing cytoskeletal network. This gives the membrane great flexibility: red cells are deformable but regain their biconcave shape and dimensions after passing through the smallest capillaries, which are 4 μm in diameter. Erythrocyte membrane flexibility also contributes to the normally low viscosity of blood. Defects in the cytoskeleton occur in autosomal dominant disorders (some cases of elliptocytosis result from mutations in spectrin and of spherocytosis from ankyrin dysfunction) which result in abnormalities of red cell shape, membrane fragility, premature destruction of erythrocytes in the spleen and haemolytic anaemia.

Fetal erythrocytes up to the fourth month of gestation differ markedly from those of adults, in that they are larger, are nucleated and contain a different type of haemoglobin (HbF). After this time they are progressively replaced by the adult type of cell.

Haemoglobin

Haemoglobin (Hb) is a globular protein with a molecular mass of 67 kDa. It consists of globulin molecules bound to haem, an iron-containing porphyrin group. The oxygen-binding power of haemoglobin is provided by the iron atoms of the haem groups, and these are maintained in the ferrous (Fe^{++}) state by the presence of glutathione within the erythrocyte. The haemoglobin molecule is a tetramer, made up of four subunits, each a coiled polypeptide chain holding a single haem group. In normal blood, five types of polypeptide chain can occur, namely; α, β and two β-like polypeptides, γ and δ. A third, β-like η chain is restricted to early fetal development. Each haemoglobin molecule contains two α-chains and two others, so that several combinations, and hence a number of different types of haemoglobin molecule, are possible. For example, haemoglobin A (HbA), which is the major adult class, contains 2α- and 2β-chains; a variant, HbA_2 with 2α and

2δ chains, accounts for only 2% of adult haemoglobin. Haemoglobin F (HbF), found in fetal and early postnatal life, consists of 2α- and 2γ-chains. Adult red cells normally contain less than 1% of HbF.

In the pathological genetic condition thalassaemia, only one type of chain is expressed normally, the mutant chain being absent or present at much reduced levels. Thus, a molecule may contain 4 α-chains (β-thalassaemia) or, more commonly, 4 β-chains (α-thalassaemia) where individuals affected carry haemoglobin H (HbH). In haemoglobin S (HbS) of sickle-cell disease, a point mutation in the β-chain gene (valine substituted for glutamine) causes a major alteration in the behaviour of the red cell and its oxygen-carrying capacity.

Lifespan

Erythrocytes last between 100 and 120 days before being destroyed. As erythrocytes age they become increasingly fragile, and their surface charges decrease as their content of negatively charged membrane glycoproteins diminishes. The lipid content of their membranes also reduces. Aged erythrocytes are eventually ingested by the macrophages of the spleen and liver sinusoids, usually without prior lysis, and are hydrolysed in phagocytic vacuoles where the haemoglobin is split into its globulin and porphyrin moieties. Globulin is further degraded to amino acids which pass into the general amino acid pool. Iron is removed from the porphyrin ring and either transported in the circulation bound to transferrin and used in the synthesis of new haemoglobin in the bone marrow, or stored in the liver as ferritin or haemosiderin. The remainder of the haem group is converted in the liver to bilirubin and excreted in the bile.

The recognition of effete erythrocytes by macrophages appears to depend in part on the exposure of normally inaccessible parts of membrane proteins, enabling autoantibodies to these erythrocyte senescence antigens to bind to them and flag them for macrophage removal. Red cells are destroyed at the rate of 5×10^{11} cells a day and are normally replaced from the bone marrow (see Fig. 4.12) at the same rate.

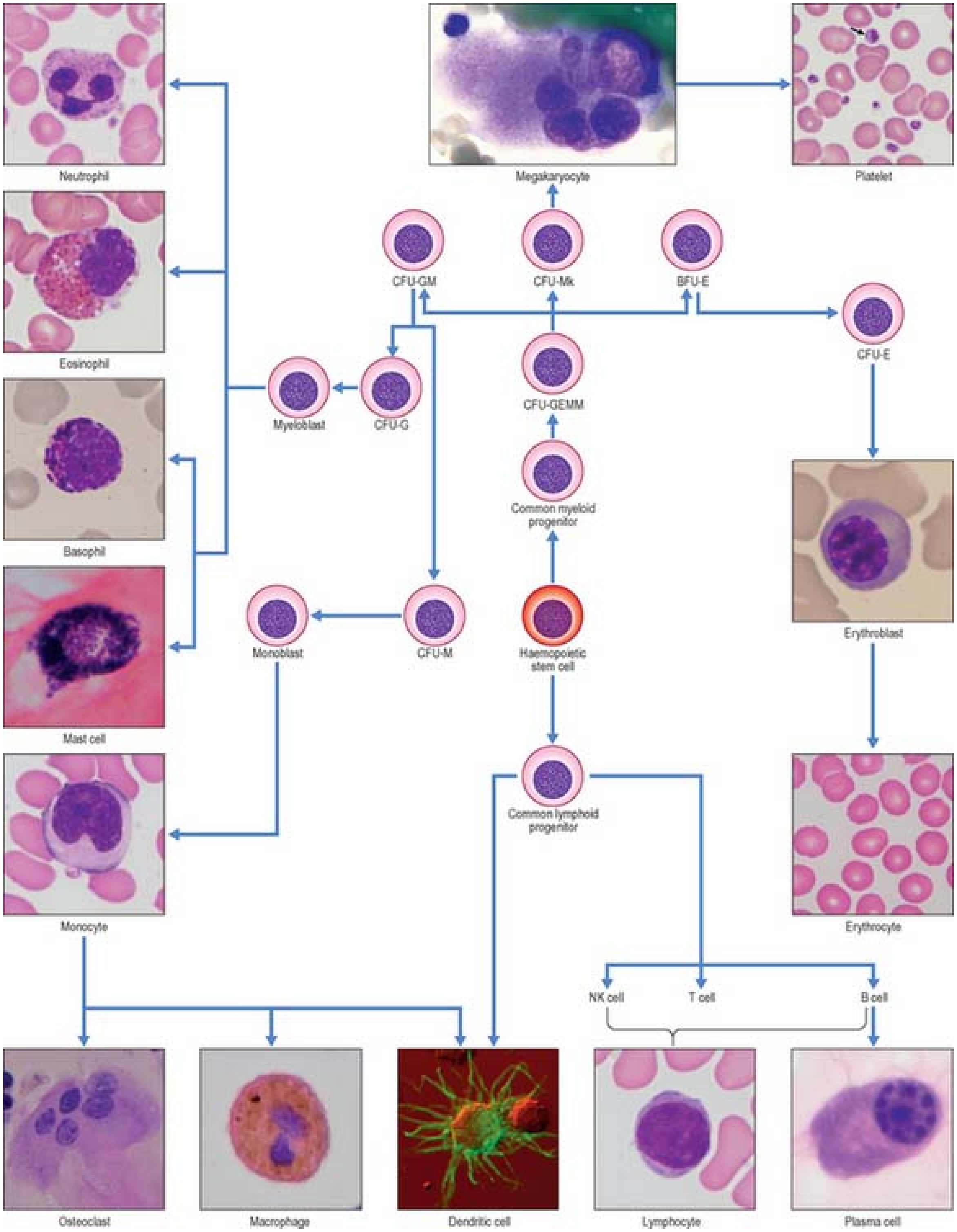
Neutrophil
Megakaryocyte
Platelet
Eosinophil
CFU-GM
CFU-Mk
BFU-E
CFU-E
Myeloblast
CFU-G
CFU-GEMM
Basophil
Common myeloid progenitor
Erythroblast
Mast cell
Monoblast
CFU-M
Haemopoietic stem cell
Monocyte
Common lymphoid progenitor
Erythrocyte
NK cell
T cell
B cell
Osteoclast
Macrophage
Dendritic cell
Lymphocyte
Plasma cell

Fig. 4.12 The origins and lineage relationships of haemopoietically-derived cells of the immune system. Mature cells and selected progenitors (all human) are illustrated (magnifications vary). The dendritic cell was

cultured from peripheral blood, immunolabelled to show HLA-DR and photographed using Nomarski optics. The megakaryocyte and erythroblast are from a bone marrow smear, stained with MGG; the remaining cells illustrated are from peripheral blood smears (Wright's stain), sections of connective tissue (plasma cell, mast cell), bone (osteoclast) and lung alveolus (macrophage). Platelets (one is arrowed) are subcellular fragments of bone marrow megakaryocytes. Note that circulating small lymphocytes cannot be classified further with routine staining methods. For further explanation of cellular structure and staining properties, see the text.

(by courtesy of Dr Cécile Chalouni, Ludwig Institute for Cancer Research, Yale University School of Medicine, USA)

Blood groups

Over 300 red cell antigens are recognizable with specific antisera. They can interact with naturally occurring or induced antibodies in the plasma of recipients of an unmatched transfusion, causing agglutination and lysis of the erythrocytes. Erythrocytes of a single individual can carry several different types of antigen, each type belonging to an antigenic system in which a number of alternative antigens are possible in different persons. So far, 19 major groups have been identified. They vary in their distribution frequencies between different populations, and include the ABO, Rhesus, MNS, Lutheran, Kell, Lewis, Duffy, Kidd, Diego, Cartwright, Colton, Sid, Scianna, Yt, Auberger, Ii, Xg, Indian and Dombrock systems. Clinically, the ABO and Rhesus groups are of most importance.

In the ABO system, two allelic genes are inherited in simple Mendelian fashion. Thus the genome may be homozygous and carry the AA complement, the blood group being A, or the BB complement which gives blood group B, or it may carry neither (OO), producing blood group O. In the heterozygous condition the following combinations can occur: AB (blood group AB), AO (blood group A) and BO (blood group B).

Individuals with group AB blood lack antibodies to both A and B antigens, and so can be transfused with blood of any group: they are termed universal recipients. Conversely, those with group O, universal donors, can give blood to any recipient, since anti-A and anti-B antibodies in the donated blood are diluted to insignificant levels. Normally, however, blood is only transfused between persons with precisely corresponding groups, because anomalous antibodies of the ABO system are occasionally found in blood and may cause agglutination or lysis. The anti-ABO agglutinins, unlike those of the Rhesus system, belong to the immunoglobulin M (IgM) class and do not cross the placenta during pregnancy.

The Rhesus antigen system is determined by three sets of alleles, namely Cc, Dd and Ee: the most important clinically is Dd. Inheritance of the Rh factor also obeys simple Mendelian laws and it is therefore possible for a Rhesus-negative mother to bear a Rhesus-positive child. Fetal Rh antigens can, under these circumstances, stimulate the production of anti-Rh antibodies by the mother: since these belong to the immunoglobulin G (IgG) class of antibodies they are able to cross the placental barrier (generally late in the last trimester) and cause agglutination of fetal erythrocytes. In the first such pregnancy little damage usually occurs because anti-Rh antibodies are present only at low levels, but in subsequent Rh-positive pregnancies massive destruction of fetal red cells (haemolytic disease of the newborn) may result, causing fetal or neonatal death. Sensitization of the maternal immune system can also result from abortion or miscarriage, or even occasionally amniocentesis, which may introduce fetal antigens into the maternal circulation. Treatment is by exchange transfusion of the neonate or, prophylactically, by giving Rh-immune (anti-D) serum to the mother after the first Rh-positive pregnancy, which destroys the fetal Rh antigen in her circulation before sensitization can occur.

Leukocytes also bear highly polymorphic antigens encoded by allelic gene variants. These belong to the group of major histocompatibility complex (MHC) antigens, also termed human leukocyte antigens (HLA) in man. HLA Class I antigens are expressed by all nucleated cells. Class II antigen expression is more restricted outside the immune system, but is inducible on many parenchymal cell types e.g. after exposure to interferon. HLA Class I and II antigens play important roles in cell–cell interactions in the immune system, particularly in the presentation of antigens to T lymphocytes by APCs.

LEUKOCYTES

Leukocytes (white blood cells) belong to at least five different categories (see Fig. 4.12), and are distinguishable by their size, nuclear shape and cytoplasmic inclusions. In practice, leukocytes are often divided into two main groups, namely those with prominent stainable cytoplasmic granules, the granulocytes, and those without.

Granulocytes

This group consists of eosinophil granulocytes, with granules which bind acidic dyes such as eosin; basophil granulocytes, with granules which bind basic dyes strongly; and neutrophil granulocytes, with granules which stain only weakly with either type of dye. Granulocytes (Fig. 4.3) all possess irregular or multilobed nuclei and belong to the myeloid series of blood cells (p. 77 see Fig. 4.12).

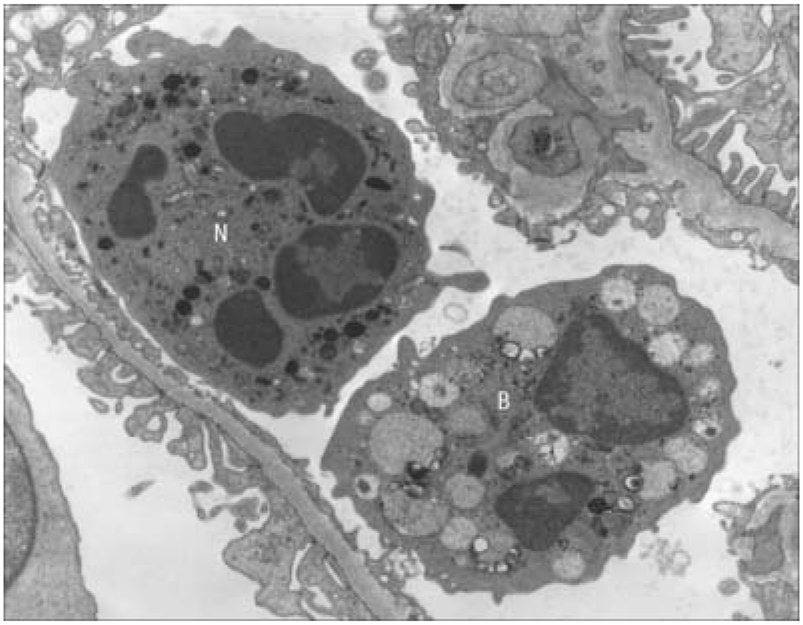

Fig. 4.3 Neutrophil (N) and basophil (B) granulocytes within a renal glomerular capillary in a human kidney biopsy. The neutrophil nucleus is more segmented (four lobes are visible) and the granules are smaller and more electron-dense than in the basophil.

Neutrophil granulocytes

Neutrophil granulocytes (neutrophils), are also referred to as polymorphonuclear leukocytes (polymorphs) because of their irregularly segmented (multilobed) nuclei. They form the largest proportion of the white blood cells (40–75% in adults, with a normal count of 2500–7500/μl) and have a diameter of 12–14 μm. The cells may be spherical in the circulation, but they can flatten and become actively motile within the extracellular matrix of connective tissues.

The numerous cytoplasmic granules are heterogeneous in size, shape and content, but all are membrane-bound and contain hydrolytic and other enzymes. Two major types can be distinguished according to their developmental origin and contents. Non-specific or primary (azurophilic) granules are formed early in neutrophil maturation. They are relatively large (0.5 μm) spheroidal lysosomes containing myeloperoxidase, acid phosphatase, elastase and several other enzymes. Specific or secondary granules are formed later, and occur in a wide range of shapes including spheres, ellipsoids and rods. These contain strong bacteriocidal components including alkaline phosphatase, lactoferrin and collagenase, none of which are found in primary granules. Conversely, secondary granules lack peroxidase and acid phosphatase. Some enzymes, e.g. lysozyme, are present in both types of granule.

In mature neutrophils the nucleus is characteristically multilobed with up to six (usually three or four) segments joined by narrow nuclear strands: this is known as the segmented stage. Less mature cells have fewer lobes. The earliest to be released under normal conditions are juveniles (band or stab cells) in which the nucleus is an unsegmented crescent or band. In certain clinical conditions, even earlier stages in neutrophil formation, when cells display indented or rounded nuclei (metamyelocytes or myelocytes) may be released from the bone marrow. In mature cells the edges of the nuclear lobes are often irregular. In females 3% of the nuclei of neutrophils show a conspicuous ‘drumstick’ formation which represents the sex chromatin of the inactive X chromosome (Barr body). Neutrophil cytoplasm contains few mitochondria but abundant cytoskeletal elements, including actin filaments, microtubules and their associated proteins, all characteristic of highly motile cells.

Neutrophils are important in the defence of the body against microorganisms. They can phagocytose microbes and small particles in the circulation and, after extravasation, they carry out similar activities in other tissues. They function effectively in relatively anaerobic conditions, relying largely on glycolytic metabolism, and they fulfil an important role in the acute inflammatory phase of tissue injury, responding to chemotaxins released by damaged tissue. Phagocytosis of cellular debris or invading microorganisms is followed by fusion of the phagocytic vacuole, first with specific granules, whose pH is reduced to 5.0 by active transport of protons, then with non-specific (primary) granules, which complete the process of bacterial killing and digestion. Actively phagocytic neutrophils are able to reduce oxygen enzymatically to form reactive oxygen species including superoxide radicals and hydrogen peroxide, which enhance bacterial destruction.

Phagocytosis is greatly facilitated by circulating antibodies to molecules such as bacterial antigens which the body has previously encountered. Antibodies coat the antigenic target and bind the plasma complement protein, C1, to their non-variable Fc regions. This activates the complement cascade, which involves some 20 plasma proteins synthesized mainly in the liver, and completes the process of opsonization. The complement cascade involves the sequential cleavage of the complement proteins into a large fragment, which generally binds to the antigenic surface, and a small bioactive fragment which is released. The final step is the recognition of complement by receptors on the surfaces of neutrophils (and macrophages), which promotes phagocytosis of the organism.

Neutrophils are short-lived; they spend some 6–7 hours circulating in the blood and a few days in connective tissues. The number of circulating neutrophils varies, and often rises during episodes of acute bacterial infection. They die after carrying out their phagocytic role: dead neutrophils, bacteria, tissue debris (including tissue damaged by neutrophil enzymes and toxins) and interstitial fluid form the characteristic, greenish-yellow pus of infected tissue. The colour is derived from the natural colour of neutrophil myeloperoxidase.

Granules may also be inappropriately released from neutrophils. Their enzymes are implicated in various pathological conditions, e.g. rheumatoid arthritis, where tissue destruction and chronic inflammation occur.

Eosinophil granulocytes

Eosinophil granulocytes (eosinophils) are similar in size (12–15 μm), shape and motile capacity to neutrophils, but are present only in small numbers in normal blood (100–400/μl). The nucleus has two prominent lobes connected by a thin strand of chromatin. Their cytoplasmic specific granules are uniformly large (0.5 μm) and give the living cell a slightly yellowish colour. The cytoplasm is packed with granules which are spherical or ellipsoid and membrane-bound. The core of each granule is composed of a lattice of major basic protein, which is responsible for its strong eosinophilic staining properties. The surrounding matrix contains several lysosomal enzymes including acid phosphatase, ribonuclease, phospholipase and a myeloperoxidase unique to eosinophils.

Like other leukocytes, eosinophils are motile. When suitably stimulated, they are able to pass into the extravascular tissues from the circulation. They are typical minor constituents of the dermis, and of the connective tissue components of the bronchial tree, alimentary tract, uterus and vagina. The total lifespan of these cells is a few days, of which some 10 hours is spent in the circulation, and the remainder in the extravascular tissues.

Eosinophil numbers rise (eosinophilia) in worm infestations and also in certain allergic disorders, and it is thought that they evolved as a primary defence against parasitic attack. They have surface receptors for IgE which bind to IgE-antigen complexes, triggering phagocytosis and release of granule contents. However, they are only weakly phagocytic and their most important function is the destruction of parasites too large to phagocytose. This anti-parasitic effect is mediated via toxic molecules released from their granules (e.g. eosinophil cationic protein and major basic protein). They also release histaminase, which limits the inflammatory consequences of mast cell degranulation. High local concentrations of eosinophils, e.g. in bronchial asthma and in cutaneous contact sensitivity and allergic eczema, can cause tissue destruction as a consequence of the release of molecules such as collagenase from their granules.

Basophil granulocytes

Slightly smaller than other granulocytes, basophil granulocytes are 10–14 μm in diameter, and form only 0.5–1% of the total leukocyte population of normal blood, with a count of 25–200/μl. Their distinguishing feature is the presence of large, conspicuous basophilic granules. The nucleus is somewhat irregular or bilobed, and is usually obscured in stained blood smears by the similar colour of the basophilic granules. The granules are membrane-bound vesicles which display a variety of crystalline, lamellar and granular inclusions: they contain heparin, histamine and several other inflammatory agents, and closely resemble those of tissue mast cells (see p. 36). Both basophils and mast cells have high affinity membrane receptors for IgE and are therefore coated with IgE antibody. If this binds to its antigen it triggers degranulation of the cells, producing vasodilation, increased vascular permeability, chemotactic stimuli for other granulocytes, and the symptoms of immediate hypersensitivity, e.g. in allergic rhinitis (hay fever). Despite these similarities, basophils and mast cells develop as separate lineages in the myeloid series, from haemopoietic stem cells in the bone marrow. Evidence from experimental animal models suggests that they are closely related (see Fig. 4.12) but studies on mast cell disorders in humans indicate that their lineages diverge from a more distant ancestral progenitor (Kocabas et al 2005).

Mononuclear leukocytes

Monocytes

Monocytes are the largest of the leukocytes (15–20 μm in diameter), but they form only a small proportion of the total population (2–8% with a count of 100–700/μl of blood). The nucleus, which is euchromatic, is relatively large and irregular, often with a characteristic indentation on one side. The cytoplasm is pale-staining, particulate and typically vacuolated. Near the nuclear indentation it contains a prominent Golgi complex and vesicles. Monocytes are actively phagocytic cells, and contain numerous lysosomes. Phagocytosis is triggered by recognition of opsonized material, as described for neutrophils. Monocytes are highly motile, and possess a well-developed cytoskeleton.

Monocytes express Class II MHC antigens and share other similarities to tissue macrophages and dendritic cells. Most monocytes are thought to be in transit via the bloodstream from the bone marrow to the peripheral tissues where they give rise to macrophages and dendritic cells; different monocyte subsets may target inflamed tissues. Like other leukocytes, they pass into extravascular sites through the walls of capillaries and venules.

Lymphocytes

Lymphocytes (Fig. 4.4, see Fig. 4.6, see Fig. 4.12) are the second most numerous type of leukocyte in adulthood, forming 20–30% of the total population (1500–2700/μl of blood). In young children they are the most numerous blood leukocyte. Most circulating lymphocytes are small, 6–8 μm in diameter; a few are medium-sized and have an increased cytoplasmic volume, often in response to antigenic stimulation. Occasionally, cells up to 16 μm are seen in peripheral blood. Lymphocytes, like other leukocytes, are found in extravascular tissues (including lymphoid tissue); however, they are the only white blood cells which return to the circulation. The lifespan of lymphocytes ranges from a few days (short-lived) to many years (long-lived). Long-lived lymphocytes play a significant role in the maintenance of immunological memory.

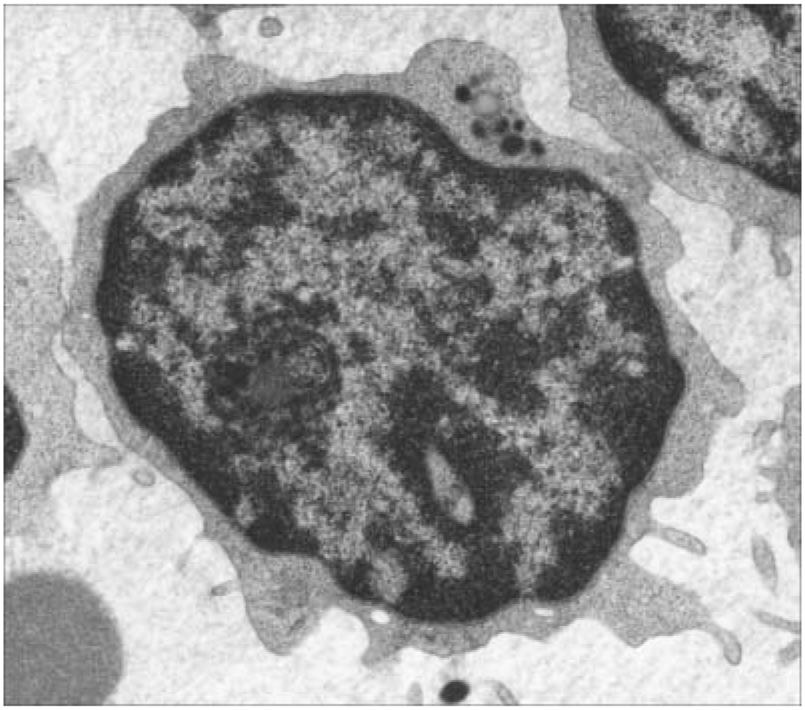

Fig. 4.4 A small, resting lymphocyte in human peripheral blood. The nuclear/cytoplasmic ratio is high and the cytoplasm contains few organelles, indicative of its quiescent state.

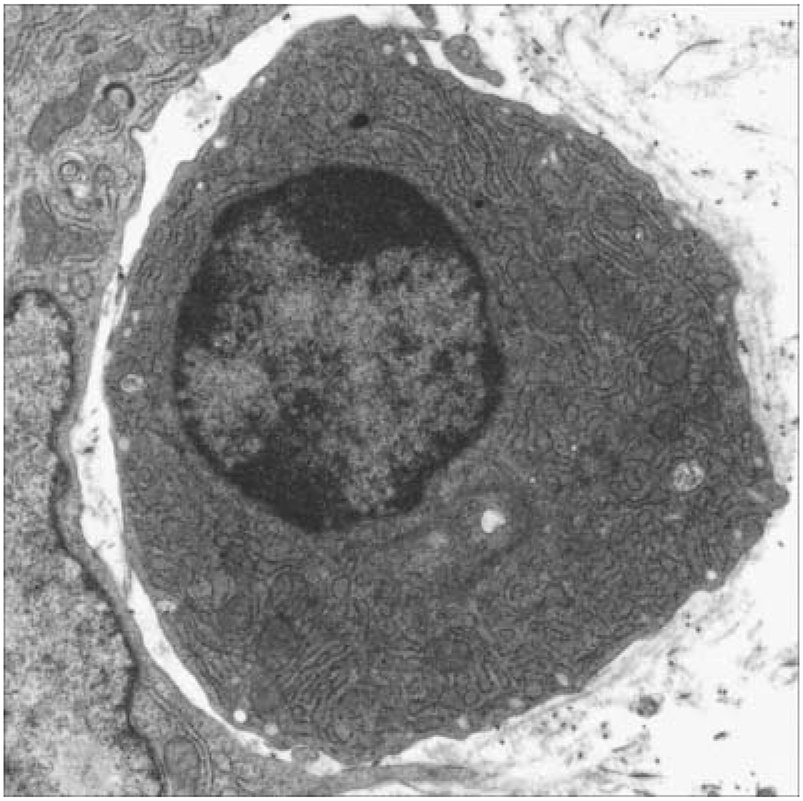

Fig. 4.6 A mature B cell (plasma cell) in human connective tissue. The abundant rough endoplasmic reticulum is typical of a cell actively synthesizing secretory protein, in this case immunoglobulin. The cell to the left is a fibroblast.

Blood lymphocytes are a heterogeneous collection mainly of B and T cells and consist of different subsets and different stages of activity and maturity. About 85% of all circulating lymphocytes in normal blood are T cells. Primary immunodeficiency diseases can result from molecular defects in T and B lymphocytes (reviewed in Cunningham-Rundles & Ponda 2005). Included with the lymphocytes, but probably a separate lineage subset, are the natural killer (NK) cells. NK cells most closely resemble large T cells morphologically.

Small lymphocytes (both B and T cells) contain a rounded, densely staining nucleus which is surrounded by a very narrow rim of cytoplasm, barely visible in the light microscope. In the electron microscope (Fig. 4.4), few cytoplasmic organelles can be seen apart from a small number of mitochondria, single ribosomes, sparse profiles of endoplasmic reticulum and occasional lysosomes: these features indicate a low metabolic rate and a quiescent phenotype. However, these cells become motile when they contact solid surfaces, and can pass between endothelial cells to exit from, or re-enter, the vascular system. They migrate extensively within various tissues, including epithelia (Fig. 4.5).

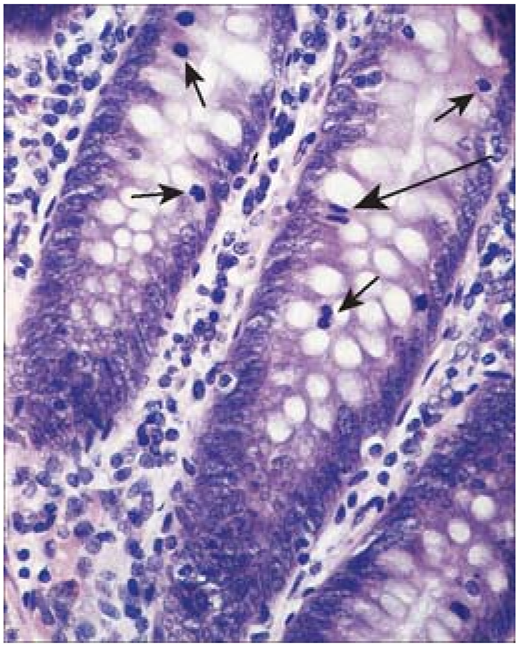

Fig. 4.5 Tubular glands in the appendix, showing intraepithelial lymphocytes (arrowed). A lymphocyte in anaphase is indicated (longer arrow).

Larger lymphocytes include T and B cells which are functionally activated or proliferating after stimulation by antigen, and NK cells. They contain a nucleus, which is at least in part euchromatic, a basophilic cytoplasm, which may appear granular, and numerous polyribosome clusters, consistent with active protein synthesis. The ultrastructural appearance of these cells varies according to their class and is described below.

B cells

B cells and the plasma cells that develop from them synthesize and secrete antibodies which can specifically recognize and neutralize foreign (non-self) macromolecules (antigens), and can prime various non-lymphocytic cells (e.g. neutrophils, macrophages and dendritic cells) to phagocytose pathogens. B cells differentiate from haemopoietic stem cells in the bone marrow. After deletion of autoreactive cells, the selected B lymphocytes then leave the bone marrow and migrate to peripheral lymphoid sites (e.g. lymph nodes). Here, following stimulation by antigen, they undergo further proliferation and selection, forming germinal centres in the lymphoid tissues. Following this, some B cells differentiate into large basophilic (RNA-rich) plasma cells, either within or outside the lymphoid tissues. Plasma cells produce antibodies in their extensive rough endoplasmic reticulum (Fig. 4.6) and secrete them into the adjacent tissues. They have a prominent pale-staining Golgi complex adjacent to an eccentrically-placed nucleus, typically with peripheral blocks of condensed heterochromatin resembling the numerals of a clock (clock-faced nucleus) (see Fig. 4.12). Other germinal centre B cells develop into long-lived memory cells capable of responding to their specific antigens not only with a more rapid and higher antibody output, but also with an increased antibody affinity compared with the primary response.

Antibodies are immunoglobulins, grouped into five classes according to their heavy polypeptide chain. Immunoglobulin G (IgG) forms the bulk of circulating antibodies. Immunoglobulin M (IgM) is normally synthesized early in immune responses. Immunoglobulin A (IgA) is present in breast milk, tears, saliva and other secretions of the alimentary tract, coupled to a secretory piece (a 70 kDa protein) which is synthesized by the epithelial cells and protects the immunoglobulin from proteolytic degradation: IgA thus contributes to mucosal immunity. IgA deficiency is relatively common, particularly in some ethnic groups (reviewed in Woof & Kerr 2006). Immunoglobulin E (IgE) is an antibody which binds to receptors on the surfaces of mast cells, eosinophils and blood basophils; it is found only at low concentrations in the circulation. Immunoglobulin D (IgD) is found together with IgM as a major membrane-bound immunoglobulin on mature, immunocompetent but naïve (prior to antigen exposure) B cells, acting as the cellular receptor for antigen.

When circulating antibodies bind to antigens they form immune complexes. If present in abnormal quantities, these may cause pathological damage to the vascular system and other tissues, either by interfering mechanically with the permeability of the basal lamina (e.g. some types of glomerulonephritis), or by causing local activation of the complement system which generates inflammatory mediators (e.g. C5a), attacks cell membranes and causes vascular disease. In pregnancy, maternal IgG crosses the placenta and confers passive immunity on the fetus. Maternal milk contains secretory immunoglobulins (IgA) which help to combat bacterial and viral organisms in the alimentary tract of the baby during the first few weeks of postnatal life.

T cells

There are a number of sub-sets of T (thymus-derived) lymphocytes, all progeny of haemopoietic stem cells in the bone marrow. They develop and mature in the thymus, and subsequently populate peripheral secondary lymphoid organs, which they constantly leave and re-enter via the circulation. As recirculating cells, their major function is immune surveillance. Their activation and subsequent proliferation and functional maturation is under the control of antigen-presenting cells. T cells undertake a wide variety of cell-mediated defensive functions which are not directly dependent on antibody activity, and which constitute the basis of cellular immunity. T cell responses focus on the destruction of cellular targets such as virus-infected cells, certain bacterial infections, fungi, some protozoal infections, neoplastic cells and the cells of grafts from other individuals (allografts) when the tissue antigens of the donor and recipient are not sufficiently similar. Targets may be killed directly by cytotoxic T cells, or indirectly by accessory cells (e.g. macrophages) which have been recruited and activated by cytokine-secreting helper T cells. A third group, regulatory T cells, acts to regulate or limit immune responses.

Functional groups of T cells are classified according to the molecules they express on their surfaces. The majority of cytokine-secreting helper T cells express CD4, while cytotoxic T cells are characterized by CD8. Regulatory T cells coexpress CD4 and CD25. The CD (cluster of differentiation) prefix provides a standard nomenclature for all cell surface molecules. At present, more than 330 different CD antigens have been designated: each one represents a cell surface molecule that can be identified by specific antibodies. Further details of the classification are beyond the scope of this publication and are given in Male et al (2006).

Structurally, T lymphocytes present different appearances depending on their type and state of activity. When resting, they are typical small lymphocytes and are morphologically indistinguishable from B lymphocytes. When stimulated, they become large (up to 15 μm), moderately basophilic cells, with a partially euchromatic nucleus and numerous free ribosomes, rough and smooth endoplasmic reticulum, a Golgi complex and a few mitochondria, in their cytoplasm. Cytotoxic T cells contain dense lysosome-like vacuoles which function in cytotoxic killing.

Cytotoxic T cells

Cytotoxic T lymphocytes (which express CD8 on their surface) are responsible for the direct cytotoxic killing of target cells (e.g. virus-infected cells): the requirement for direct cell–cell contact ensures the specificity of the response. Recognition of antigen, presented as a peptide fragment on MHC class I molecules, triggers the calcium-dependent release of lytic granules by the T cell. These lysosome-like granules contain perforin which forms a pore in the target cell membrane. They also contain several different serine protease enzymes (granzymes) which enter the target cell via the perforin pore and induce the programmed cell death (apoptosis; p. 24) of the target.

Helper T cells

Helper T cells (which express CD4) are characterized by the secretion of cytokines. Two major populations have been identified according to the range of cytokines produced. Th1 helper T cells typically secrete interleukin (IL)-2, tumour necrosis factor (TNF)-alpha and interferon gamma, while Th2 cells produce cytokines such as IL-4, IL-5 and IL-13. These two CD4-expressing populations are termed ‘helper’ T cells because one aspect of their function is to stimulate the proliferation and maturation of B lymphocytes and cytotoxic T lymphocytes (mediated via cytokines such as IL-4, IL-2 and interferon gamma), thus enabling and enhancing the immune responses mediated by those cells. In addition to Th1 and Th2 cells, other subsets of helper T cells have been described. Notably, Th17 cells (which secrete the cytokine IL-17) have recently been implicated in autoimmune diseases.

However, helper T cells are also important in directing the destruction of pathogens by recruiting accessory cells (e.g. macrophages, neutrophils, eosinophils) to the site of infection and by activating their effector functions. This process is tightly coordinated. For example, Th1 helper T cells secrete cytokines that not only attract and activate macrophages but also provide help for B cells and guide their immunoglobulin production to the subclasses that fix complement. Thus these antibodies opsonize the pathogen target which can then be recognized, ingested and destroyed by the macrophage accessory cells that bear receptors for complement and the Fc region of IgG. These Th1 cells are sometimes referred to as delayed type hypersensitivity T cells. In contrast, Th2 cells secrete cytokines that induce the development and activation of eosinophils, and also induce B cells to switch their immunoglobulins to non-complement fixing classes (e.g. IgE). Pathogens such as parasitic worms can then be coated with IgE antibody and hence recognized and destroyed by the effector functions of the eosinophil accessory cells which bear receptors for the Fc region of IgE.

If helper T-cell activities are non-functional, a state of immunodeficiency results. This means that potentially pathogenic organisms, which are normally kept in check by the immune system, may proliferate and cause overt pathology, e.g. in acquired immune deficiency syndrome (AIDS), where a virus (HIV) specifically infects and kills (predominantly) helper T cells, though some antigen-presenting cells are also killed.

Regulatory T cells

A third population of T cells, ‘regulatory’ T or ‘Treg’ cells has been identified within the last decade (reviewed in O’Garra & Vieira 2004). These $CD4^+$, $CD25^+$ cells have an immunomodulatory function and can dampen the effector functions of both cytotoxic and helper T cells. Regulatory T cells are produced in the thymus and are an important additional mechanism for maintaining self-tolerance. Treg function is antigen-specific and depends upon direct cell–cell contact. Molecules secreted or induced by Treg cells, such as interleukin (IL)-10 or transforming growth factor (TGF) β, may also play an important role in mediating Treg suppressive effects on the immune system. Similar regulatory T cells can be induced in the periphery and may be important in the induction of oral tolerance to ingested antigens as well as tolerance to tissue specific molecules that are not expressed in the thymus.

Natural killer (NK) cells

Natural killer (NK) cells have functional similarities to cytotoxic T cells. However they lack other typical lymphocyte features, and do not express antigen-specific receptors. They normally form only a small percentage of all lymphocyte-like cells and are usually included in the large granular lymphocyte category. When mature, NK cells have a mildly basophilic cytoplasm. Ultrastructurally, their cytoplasm contains ribosomes, rough endoplasmic reticulum and dense, membrane-bound vesicles 200–500 nm in diameter with crystalline cores. These contain the protein perforin (cytolysin), which is capable of inserting holes in the plasma membranes of target cells, and granzymes (serine proteases), which trigger subsequent target cell death by apoptosis. NK cells are activated to kill target cells by a number of factors. They can recognize and kill antibody coated target cells via a mechanism termed antibody-dependent cell-mediated cytotoxicity (ADCC). They also have receptors that inhibit NK destructive activity when they recognize MHC class I on normal cells. When NK cells detect the loss or downregulation of MHC class I antigens on certain virus-infected cells and some tumour cells, they activate apoptosis-inducing mechanisms which enable them to attack these abnormal cells, albeit relatively non-specifically. For further reading, see Vivier et al 2008.

Platelets

Blood platelets, also known as thrombocytes, are relatively small (2–4 μm across) irregular or oval discs present in large numbers (200,000–400,000/μl) in blood. In freshly harvested blood samples they readily adhere to each other and to all available surfaces, unless the blood is treated with citrate or other substances which reduce the availability of calcium ions. Platelets are anucleate cell fragments, derived from megakaryocytes in the bone marrow. They are surrounded by a plasma membrane with a thick glycoprotein coat, which is responsible for their adhesive properties. A band of 10 microtubules lies around the perimeter of the platelet beneath the plasma membrane: the microtubules are associated with actin filaments, myosin and other proteins related to cell contraction. The cytoplasm also contains mitochondria, glycogen, scant smooth endoplasmic reticulum, tubular invaginations of the plasma membrane, and three major types of membrane-bound vesicle, designated alpha, delta and lambda granules.

Alpha granules are the largest, and have diameters of up to 500 nm. They contain platelet-derived growth factor (PDGF), fibrinogen and other substances. Delta granules are smaller (up to 300 nm), and contain 5-hydroxytryptamine (serotonin) which has been endocytosed from the blood plasma. Lambda granules are the smallest (up to 250 nm) and contain lysosomal enzymes.

Platelets play an important role in haemostasis. When a blood vessel is damaged, platelets become activated, evert their membrane invaginations to form lamellipodia and filopodia, and aggregate at the site of injury, plugging the wound. They adhere to each other (agglutination), and to other tissues. Adhesion is a function of the thick platelet coat and is promoted by the release of ADP and calcium ions from the platelets in response to vessel injury. The contents of released alpha granules, together with factors released from the damaged tissues, initiate a complex sequence of chemical reactions in the blood plasma, which leads to the precipitation of insoluble fibrin filaments in a three-dimensional meshwork, the fibrin clot (Fig. 4.1). More platelets attach to the clot, inserting extensions of their surfaces, filopodia, deep into the spaces between the fibrin filaments, to which they adhere strongly. The platelets then contract (clot retraction) by actin–myosin interactions within their cytoplasm, and this concentrates the fibrin clot and pulls the walls of the blood vessel together, which limits any further leakage of blood. After repair of the vessel wall, which may be promoted by the mitogenic activity of PDGF, the clot is dissolved by enzymes such as plasmin. Plasmin is formed by plasminogen activators in the plasma, probably assisted by lysosomal enzymes derived from the lambda granules of platelets. Platelets typically circulate for 10 days before they are removed, mainly by splenic macrophages.

LYMPHOID TISSUES

Lymphocytes are located in many sites in the body, most obviously at strategic sites which are liable to infection, e.g. the oropharynx. The main areas of lymphocyte concentration are classified as primary or secondary lymphoid organs, according to whether they are involved in *de novo* lymphocyte generation (primary lymphoid organs, e.g. bone marrow, thymus) or the site of mature lymphocyte activation and initiation of an immune response (secondary lymphoid organs, e.g. lymph nodes, spleen).

All lymphocytes arise from pluripotent haemopoietic stem cells in the bone marrow. The B lymphocyte lineage develops through a series of differentiation stages within the bone marrow. The newly formed B cells then leave through the circulation and migrate to peripheral sites. In contrast, T lymphocyte development requires the thymus; the bone marrow-derived stem cells must therefore migrate via the blood circulation to the thymus. After their differentiation and maturation into immunocompetent T cells which have survived thymic selection processes (1–3%), they re-enter the circulation and are transported to peripheral sites where they join the pool of naïve lymphocytes which recirculate through the secondary lymphoid organs via blood and lymphatic circulation systems.

The secondary or peripheral lymphoid organs are the specialized sites where B and T lymphocytes and antigen presenting cells come together to initiate immune responses to foreign antigens. These secondary tissues include lymph nodes, spleen, and lymphoid tissue associated with epithelial surfaces (mucosa-associated lymphoid tissue, MALT), e.g. the palatine and nasopharyngeal tonsils, Peyer’s patches in the small intestine, lymphoid nodules in the respiratory and urogenital systems, the skin and conjunctiva of the eye. The microstructure of lymph nodes and of general MALT are described below. Details of all other lymphoid tissues and organs are included in the descriptions of the appropriate regional anatomy.

Lymphocytes enter secondary lymphoid tissues from the blood, usually by migration through the walls of capillaries or venules (high endothelial venules, HEV) and leave by the lymphatic system. In the spleen, lymphocyte entry and exit is via the marginal zone and venous drainage respectively. Antigen presenting cells (dendritic cells) enter via the lymphatics, bringing with them antigen from peripheral infected sites. In all the secondary tissues there are specific areas where either B or T cells are concentrated. After activation, functionally competent lymphocytes migrate to other sites in the body, where they combat the original infection.

LYMPH NODES

Lymph nodes (Fig. 4.7) are encapsulated centres of antigen presentation and lymphocyte activation, differentiation and proliferation. They generate mature, antigen-primed, B and T cells, and filter particles, including microbes, from the lymph by the action of numerous phagocytic macrophages. A normal young adult body contains up to 450 lymph nodes, of which 60–70 are found in the head and neck, 100 in the thorax and as many as 250 in the abdomen and pelvis. Lymph nodes are particularly numerous in the neck, mediastinum, posterior abdominal wall, abdominal mesenteries, pelvis and proximal regions of the limbs (axillary and inguinal lymph nodes). By far the greatest number lie close to the viscera, especially in the mesenteries.

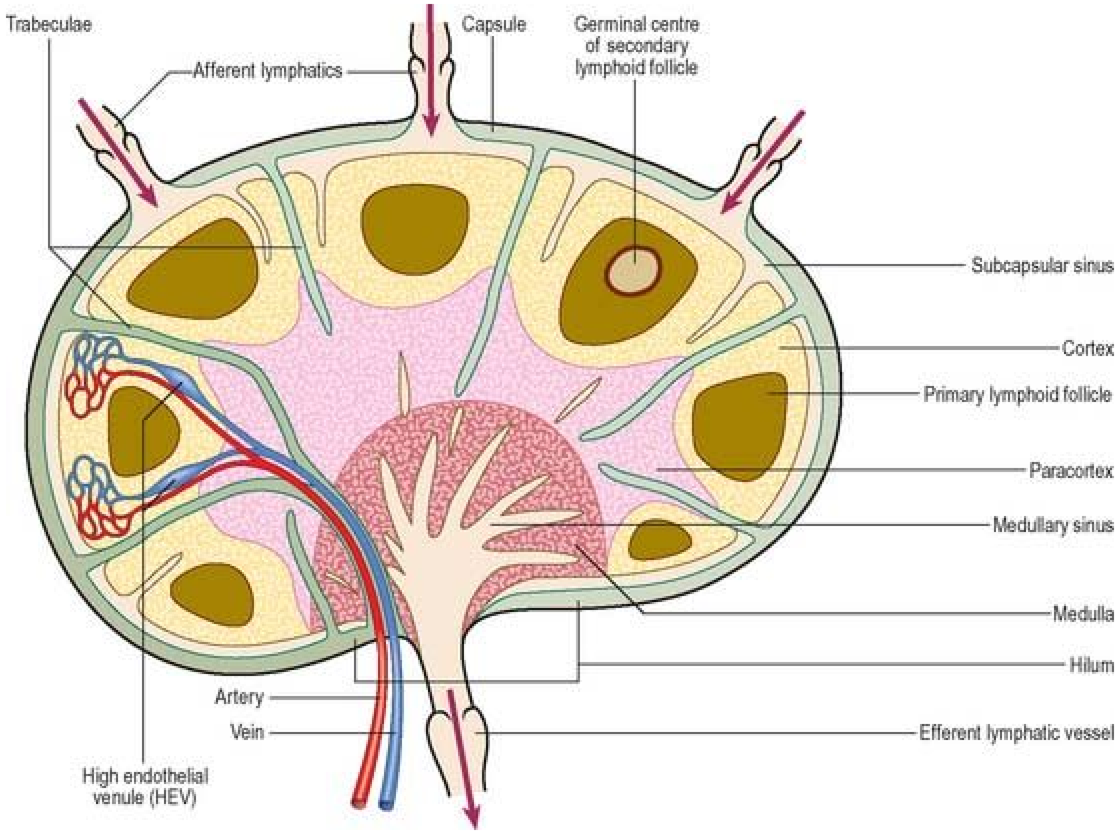
Trabeculae
Afferent lymphatics
Capsule
Germinal centre of secondary lymphoid follicle
Subcapsular sinus
Cortex
Primary lymphoid follicle
Paracortex
Medullary sinus
Medulla
Hilum
Efferent lymphatic vessel
Artery
Vein
High endothelial venule (HEV)

Fig. 4.7 The structure of a lymph node.

Microstructure

Lymph nodes (Fig. 4.8) are small, oval or kidney-shaped bodies, 0.1–2.5 cm long, lying along the course of the lymphatic vessels. Each usually has a slight indentation on one side, the hilum, through which blood vessels enter and leave and the efferent lymphatic vessel leaves. Several afferent lymphatic vessels enter the capsule around the periphery. Lymph nodes have a highly cellular cortex and a medulla which contains a network of minute lymphatic channels (sinuses) through which lymph from the afferent lymphatics is filtered, to be collected at the hilum by the efferent lymphatic. The cortex is absent at the hilum, where the medulla reaches the surface.

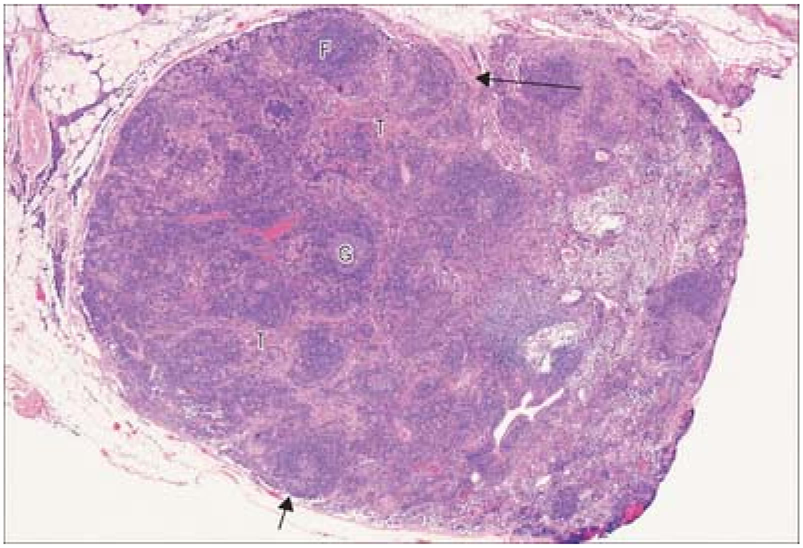

Fig. 4.8 Lymph node (human) sectioned mainly through cortical tissue, showing lymphoid follicles (F), some with germinal centres (G), and connective tissue trabeculae (T). Also shown is the subcapsular sinus (short arrow) and hilum (long arrow) with blood vessels.

The capsule is composed mainly of collagen fibres, elastin fibres (especially in the deeper layers), and a few fibroblasts. From the capsule, trabeculae of dense connective tissue extend radially into the interior of the node. They are continuous with a network of fine type III collagen (reticulin) fibrils which supports the lymphoid tissue. At the hilum, dense fibrous tissue may extend into the medulla, surrounding the efferent lymphatic vessel.

The fine reticulin bundles branch and interconnect to form a very dense network in the cortex: there are fewer fibres in the germinal centres of follicles (see below). They provide attachment for various cells, mostly dendritic cells, macrophages and lymphocytes. Reticulin and the associated proteoglycan matrix are produced by fibroblasts, a few of which are associated with the fibre network.

Lymphatic and vascular supply

Lymph nodes are permeated by channels through which lymph percolates after its entry from the afferent vessels. Macrophages line the channels or migrate along the reticulin which crosses them, and so lymph is exposed to their phagocytic activities, as well as to B and T lymphocytes which lie within the various regions of a node. Afferent lymphatic vessels enter at many points on the periphery, branch to form a dense intracapsular plexus, and then open into the subcapsular sinus, a cavity which is peripheral to the whole cortex except at the hilum (Fig. 4.7). Numerous radial cortical sinuses lead from the subcapsular sinus to the medulla, where they coalesce as larger medullary sinuses. The latter become confluent at the hilum with the efferent vessel which drains the node. All of these spaces are lined by a continuous endothelium and traversed by fine reticular fibres, which support sinus macrophages.

Arteries and veins serving lymph nodes pass through the hilum, giving off straight branches which traverse the medulla, and sending out minor branches as they do so. In the cortex, arteries form dense arcades of arterioles and capillaries in numerous anastomosing loops, eventually returning to highly branched venules and veins. Capillaries are especially profuse around the follicles, which contain fewer vessels. Postcapillary HEV are abundant in the paracortical zones. They form an important site of blood-borne lymphocyte extravasation into lymphoid tissue, apparently by migration through labile endothelial tight junctions. The density of the capillary beds increases greatly when lymphocytes multiply in response to antigenic stimulation. Veins leave a node through its principal trabeculae and capsule, and drain them and the surrounding connective tissue.

Cells and cellular zones of lymph nodes

Although most of the cells in a lymph node are B and T lymphocytes, their distribution is not homogeneous. In the cortex, cells are densely packed and in the outer cortical area they form lymphoid follicles or nodules (Fig. 4.8), which are populated mainly by B cells and specialized follicular dendritic cells (FDC) (see Fig. 4.15). The number, degree of isolation and staining characteristics of follicles vary according to their state of antigenic stimulation. A primary follicle is uniformly populated by small, quiescent lymphocytes, whereas a secondary follicle has a germinal centre (Fig. 4.9) which is composed mainly of antigen-stimulated B cells which are larger, less deeply staining and more rapidly dividing than those at its periphery.

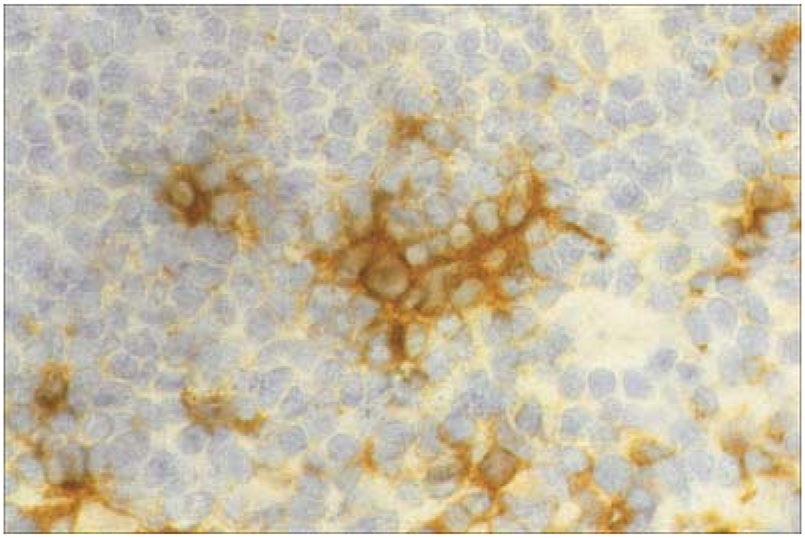

Fig. 4.15 Follicular dendritic cells (brown) in a germinal centre of the human palatine tonsil (immunoperoxidase labelled).

(By courtesy of Dr Marta Perry, UMDS, London.)

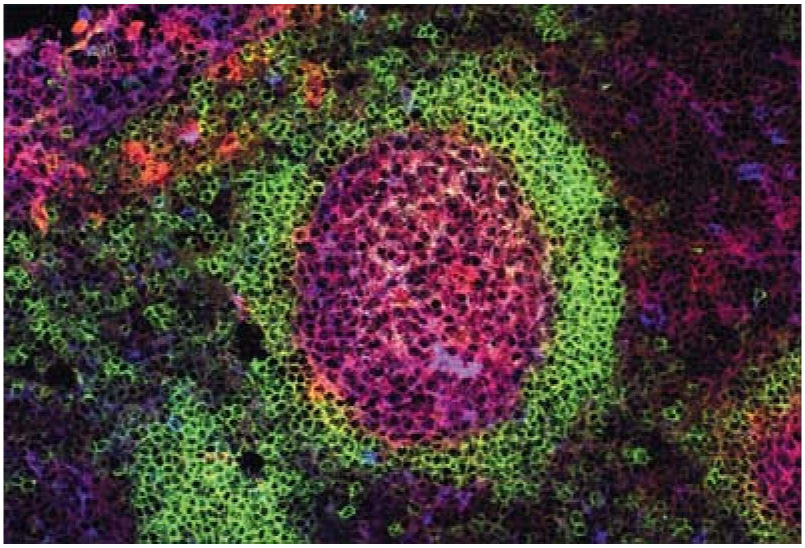

Fig. 4.9 A germinal centre in a human tonsil lymphoid follicle, immunolabelled to show CD 38-positive B cells in the germinal centre (red), IgD-positive naïve B cells (green) in the mantle zone and activated, transferrin receptor (CD 71)-positive cells of various lineages (blue).

(By courtesy of Dr Cécile Chalouni, Ludwig Institute for Cancer Research, Yale University School of Medicine, USA.)

The role of the germinal centre is to provide a microenvironment which allows the affinity maturation of the B cell response, so that as the immune response progresses the affinity or strength with which antibodies bind their antigen also increases. There are several zones in the germinal centre where this is allowed to happen. In the ‘dark zone’ the B cells (centroblasts) undergo rapid proliferation which is associated with hypermutation of their antibody molecules. They then move into the light zone (as centrocytes), where they can interact with the FDCs which carry intact unprocessed antigen on their surface. The centrocytes compete for binding to the antigen; those whose antibody has the highest affinity survive and the rest die. T cells are also present, helping the survival of the B cells and inducing class switching. Macrophages in the germinal centre phagocytose apoptotic lymphocytes (e.g. those B cells which die as part of the process of affinity maturation), and consequently macrophage cytoplasm becomes filled with engulfed lipid and nuclear debris.

The mantle zone (Fig. 4.9) is produced as surrounding cells are marginalized by the rapidly growing germinal centre. It is populated by cells similar to those found in primary follicles, mainly quiescent B cells with condensed heterochromatic nuclei and little cytoplasm (hence the deeply basophilic staining of this region in routine preparations; Fig. 4.10), a few helper T cells, FDCs and macrophages. After numerous mitotic divisions the selected B cells give rise to small lymphocytes, some of which become memory B cells and leave the lymph node to join the recirculating pool, while others leave to mature as antibody-secreting plasma cells either in the lymph node medulla or in peripheral tissues.

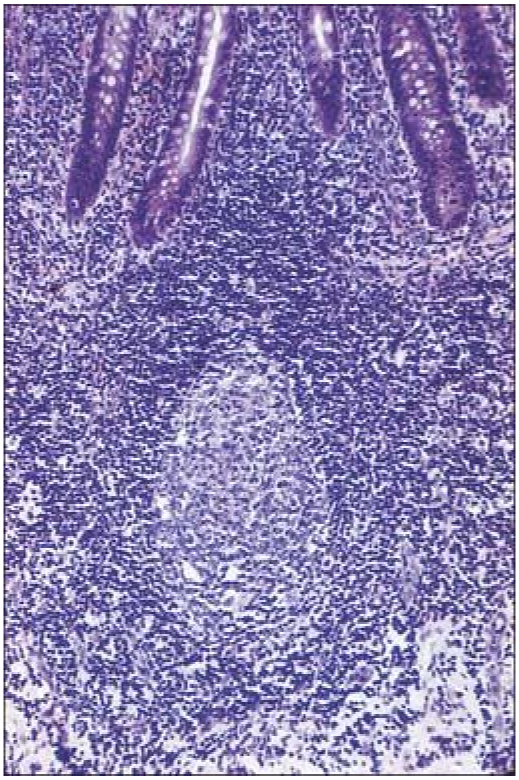

Fig. 4.10 Germinal centre in a follicle of mucosa-associated lymphoid tissue (MALT) in the mucosa and submucosa of the appendix. The bases of tubular glands of the mucosal epithelium are seen in the upper field.

The deep cortex or paracortex lies between the cortical follicles and the medulla, and is populated mainly by T cells, which are not organized into follicles. Both CD4 and CD8 T cell subsets are present. The paracortex also contains interdigitating dendritic cells. These dendritic cells include Langerhans cells from the skin and other squamous epithelia which have migrated as veiled cells via the afferent lymphatics into the draining lymph nodes (see Fig. 4.14). Their role is to present processed antigen to T cells. The region expands greatly in T cell-dominated immune responses, when its cells are stimulated to proliferate and disperse to peripheral sites.

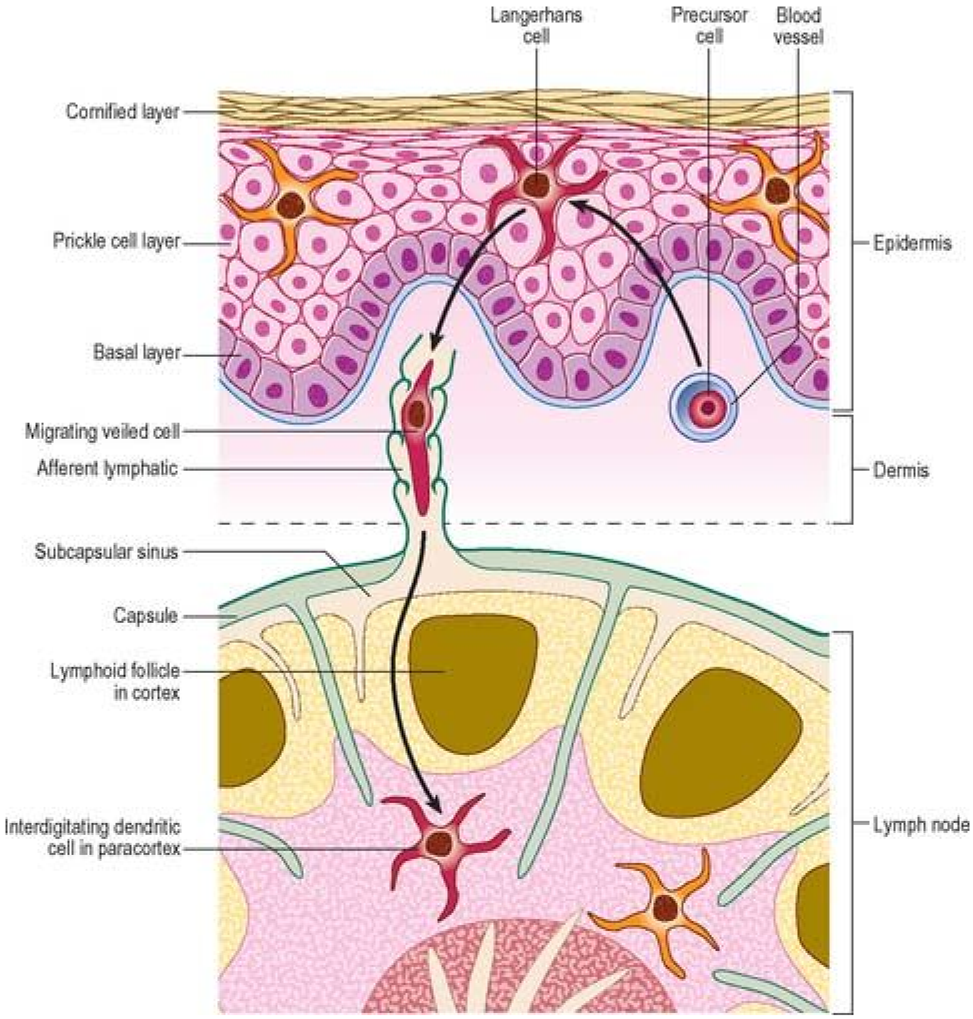
Langerhans cell
Precursor cell
Blood vessel
Cornified layer
Prickle cell layer
Basal layer
Migrating veiled cell
Afferent lymphatic
Subcapsular sinus
Capsule
Lymphoid follicle in cortex
Interdigitating dendritic cell in paracortex
Epidermis
Dermis
Lymph node

Fig. 4.14 Dendritic cells in the skin and lymphoid tissues. Their migratory routes are shown: from blood-borne, marrow-derived precursors, to immature dendritic cells (Langerhans cells) in skin, and then

to migrating veiled cells in afferent lymphatic vessels and interdigitating dendritic cells in lymph nodes. An example of each cell in the sequence (arrowed) is shown in red.

In the medulla, lymphocytes are much less densely packed, forming irregular, branching medullary cords between which the reticulin network is easily seen. Other cells include macrophages, which are more numerous in the medulla than in the cortex, plasma cells and a few granulocytes.

MUCOSA-ASSOCIATED LYMPHOID TISSUE (MALT)

Large amounts of unencapsulated lymphoid tissue exist in the walls of the alimentary, respiratory, reproductive and urinary tracts, and in the skin: they are collectively termed mucosa-associated lymphoid tissue (MALT). Some authorities distinguish between lymphoid tissues associated with different organ systems of the body. Although there may be functional differences between them related to the different antigenic challenges encountered, this is not evident in their microstructure. Anatomically, the main subclasses are gut-associated lymphoid tissue (GALT) and bronchus-associated lymphoid tissue (BALT).

Throughout the body, MALT includes an extremely large population of lymphocytes, principally because of the size of the alimentary tract. The lymphoid cells are located in the lamina propria and in the submucosa as discrete follicles or nodules. More scattered cells, derived from these follicles, are found throughout the lamina propria and in the base of the epithelium (Fig. 4.5, Fig. 4.10). MALT includes macroscopically visible lymphoid masses, notably the peripharyngeal lymphoid (Waldeyer's) ring of tonsillar tissue (palatine, nasopharyngeal, tubal and lingual), and the Peyer's patches of the small intestine (see Ch. 66) which are described elsewhere. Most MALT consists of microscopic aggregates of lymphoid tissue, and lacks a fibrous capsule. Lymphocyte populations are supported mechanically by a fine network of fine type III collagen (reticulin) fibres and associated fibroblasts, as they are in lymph nodes.

In common with lymph nodes, MALT provides centres for the activation and proliferation of B and T lymphocytes in its follicles and parafollicular zones, respectively. The function of cells in these zones, including antigen presenting cells (follicular dendritic cells and interdigitating dendritic cells) and macrophages as well as T and B cells, is similar to that found in lymph nodes. The close proximity of lymphocytes within the MALT to an epithelial surface facilitates their access to pathogens. The lymphocyte population in MALT is not fixed: lymphocytes migrate into MALT through its HEV and leave mainly via its efferent lymphatics, which drain interstitial fluid as lymph. MALT lacks afferent lymphatic vessels. Migration from MALT follows a different route from the major peripheral route of recirculation. After antigen activation, lymphocytes travel via the regional lymph nodes to disperse widely along mucosal surfaces to provide protective T- and B-cell immunity.

Follicle-associated epithelium

The epithelium covering mucosa-associated lymphoid tissue, which varies in type according to its location, is unusual in possessing cells which are involved in sampling antigens and passing them to the underlying tissues. The main function of B lymphocytes in MALT is to produce IgA for secretion into the lumen of the tracts which they line. They are exposed to antigens present in the lumen because the epithelium samples and transfers these antigens to antigen-presenting cells in the underlying tissues. Appropriate clones of T and B cells in local lymphoid tissues are then activated and amplified prior to their exit via the lymphatics. In the small and large intestine these specialized epithelial cells have characteristic short microvilli on their luminal surface and are known as microfold (M) cells. In the palatine tonsils they include modified stratified squamous reticulated epithelial cells.

Thus, many of the lymphocytes migrating between cells in the basal regions of epithelia (Fig. 4.5) are effector cytotoxic and helper T cells that have already been selected in lymphoid nodules and are engaged in immune responses. Similar cells, and activated IgA-producing B cells and plasma cells, are also scattered throughout the entire mucosal lamina propria.

HAEMOPOIESIS

Postnatally, blood cells are formed primarily in the bone marrow. Other tissues, particularly the spleen and liver, may develop haemopoietic activity once more, if production from the marrow is inadequate.

BONE MARROW

Bone marrow is a soft pulpy tissue which is found in the marrow cavities of all bones (Fig. 4.11) and even in the larger Haversian canals of lamellar bone. It differs in composition in different bones and at different ages and occurs in two forms, yellow and red marrow. In old age the marrow of the cranial bones undergoes degeneration and is then termed gelatinous marrow.

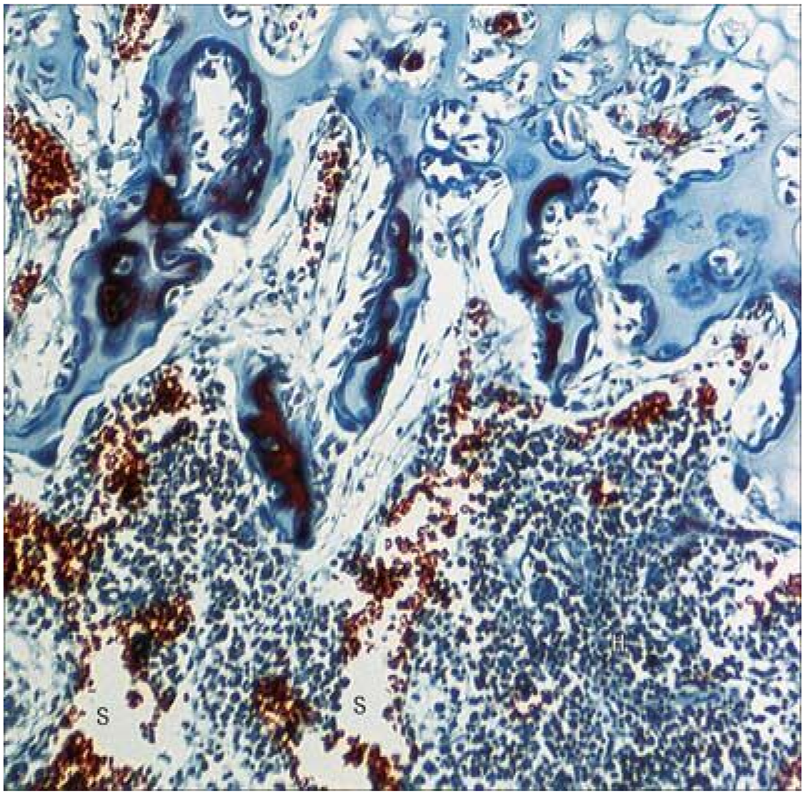

Fig. 4.11 Haemopoietic tissue (H) in the marrow cavity of a fetal long bone undergoing endochondral ossification (top). Islands of densely-packed nucleated haemopoietic cells of different lineages are separated by large vascular sinusoids (S) which are filled with mature red blood cells in the general circulation.

Yellow marrow

Yellow marrow consists of a framework of connective tissue which supports numerous blood vessels and cells, most of which are adipocytes. A small population of typical red marrow cells persists and may be reactivated when the demand for blood cells becomes sufficiently great.

Red marrow

Red marrow is found throughout the skeleton in the fetus and during the first years of life. After about the fifth year the red marrow, which represents actively haemopoietic tissue, is gradually replaced in the long bones by yellow marrow. The replacement starts earlier, and is generally more advanced, in the more distal bones. By 20–25 years of age, red marrow persists only in the vertebrae, sternum, ribs, clavicles, scapulae, pelvis, cranial bones and in the proximal ends of the femur and humerus.

Red bone marrow consists of a network of loose connective tissue, the stroma, which supports clusters of haemopoietic cells (haemopoietic cords or islands) and a rich vascular supply in which large, thin-walled sinusoids are the main feature (Fig. 4.11). The vascular supply is derived from the nutrient artery to the bone, which ramifies in the bone marrow, and terminates in thin-walled arterioles from which the sinusoids arise. These, in turn, drain into disproportionately large veins. Lymphatic vessels are absent from bone marrow. The stroma contains a variable amount of fat, depending on age, site and the haematological status of the body, and small patches of lymphoid tissue are also present. Marrow thus consists of vascular and extravascular compartments, both enclosed within a bony framework from which they are separated by a thin layer of endosteal cells (p. 91).

Stroma

Stroma is composed of a delicate network of fine type III collagen (reticulin) fibres secreted by highly branched, specialized fibroblast-like cells (reticular cells) derived from embryonic mesenchyme. When haemopoiesis stops, as occurs in most limb bones in adult life, these cells (or closely related cells) become distended with lipid droplets, and fill the marrow with yellow fatty tissue (yellow marrow). If there is a later demand for haemopoiesis, the stellate stromal cells reappear. The stroma also contains numerous macrophages attached to extracellular matrix fibres. These cells actively phagocytose cellular debris created by haemopoietic development, especially the extruded nuclei of erythroblasts, remnants of megakaryocytes and cells which have failed the B lymphocyte selection process. Stromal cells play a major role in the control of haemopoietic cell differentiation, proliferation and maturation.

Marrow sinusoids are lined by a single layer of endothelial cells, supported by reticulin on their basal surfaces. Although the endothelial cells are interconnected by tight junctions, their cytoplasm is extremely thin in places, and the underlying basal lamina is discontinuous. The passage of newly formed blood cells from the haemopoietic compartment into the bloodstream appears to occur through an interactive process with the endothelium, producing temporary apertures (large fenestrae) in their attenuated cytoplasm.

Haemopoietic tissue

Cords and islands of haematogenous cells consist of clusters of immature blood cells in various stages of development; several different cell lineages are typically represented in each focal group. One or more macrophages lie at the core of each such group of cells. These macrophages engage in phagocytic functions, are important in transferring iron to developing erythroblasts for haemoglobin synthesis, and may play a role, with other stromal cells, in regulating the rate of cell proliferation and maturation of the neighbouring haemopoietic cells.

CELL LINEAGES

Haemopoietic stem cells

Within the adult marrow there is a very small number (0.05% of haemopoietic cells) of self-renewing, pluripotent stem cells which are capable of giving rise to all blood cell types, including lymphocytes (Fig. 4.12). Although they cannot be identified morphologically in the marrow, they can be recognized in aspirates by the expression of specific cell surface marker proteins (e.g. CD34). It is thought that haemopoietic stem cells occupy specific environmental niches in the marrow associated with the endosteum of trabecular bone or with sinusoidal endothelium and that their microenvironment is important in homeostasis, the balance between self-renewal and differentiation. Stem cells can also be found (at lower concentrations) in the peripheral blood, particularly after treatment with appropriate cytokines.

Progressively more lineage-restricted committed progenitor cells develop from these ancestors (see Laiosa et al 2006 for a recent review) to produce the various cell types found in peripheral blood. The committed progenitor cells are often termed colony-forming units (CFU) of the lineage(s), e.g. CFU-GM cells give rise, after proliferation, to neutrophil granulocytes, monocytes and certain dendritic cells, whereas CFU-E produce only erythrocytes. Each cell type undergoes a period of maturation in the marrow, often accompanied by several structural changes, before release into the general circulation. In some lineages, e.g. the erythroid series, the final stages of maturation take place in the circulation, whereas in the monocytic lineage, they occur after the cells have left the circulation and entered peripheral tissues where they differentiate into macrophages and some dendritic cells.

To generate a complete set of blood cells from a single pluripotent cell may take some months. The later progenitor cells form mature cells of their particular lineages more quickly. However, because they are not self-renewing, grafts of these later cells eventually fail because the cells they produce all ultimately die. This is of considerable importance in bone marrow replacement therapy. The presence of pluripotent stem cells in the donor marrow is essential for success: only 5% of the normal number are needed to repopulate the marrow. Following replacement therapy, T lymphocytes reconstitute more slowly than the other haemopoietic lineages, reflecting the progressive reduction in size of the thymus with age (chronic involution).

Lymphocytes

Lymphocytes are a heterogeneous group of cells which may share a common ancestral lymphoid progenitor cell, distinct from the myeloid progenitor cell which gives rise to all of the cell types described above. The first identifiable progenitor cell is the lymphoblast, which divides several times to form prolymphocytes: both cells are characterized by a high nuclear to cytoplasmic ratio. B cells undergo differentiation to their specific lineage subset entirely within the bone marrow and migrate to peripheral or secondary lymphoid tissues as naïve B cells, ready to respond to antigen. However, T cells require the specialized thymic microenvironment for their development. During fetal and early postnatal life, and subsequently at lower levels throughout life, progenitor cells migrate to the thymus where they undergo a process of differentiation and selection as T cells, before leaving to populate secondary lymphoid tissues.

B cell development

B cells start their development in the subosteal region of the bone marrow, and move centripetally as differentiation progresses. Their development entails the rearrangement of immunoglobulin genes to create a unique receptor for antigen on each B cell, and the progressive expression of cell surface and intracellular molecules required for mature B lymphocyte function. Autoreactive cells which meet their self-antigen within the bone marrow are eliminated. Overall some 25% of B cells successfully complete these developmental and selection processes: those that fail die by apoptosis and are removed by macrophages. Bone marrow stromal cells (fibroblasts, fat cells and macrophages) express cell surface molecules and secreted cytokines which control B lymphocyte development. The mature naïve B lymphocytes leave via the central sinuses. They express antigen receptors (immunoglobulin) of IgM and IgD classes. Class switching to IgG, A and E occurs in the periphery following antigen activation in response to signals from T helper cells.

T-cell (thymocyte) development

T cells develop within the thymus from blood-borne bone marrow-derived progenitors which enter the thymus via HEVs at the corticomedullary junction. They first migrate to the outer (subcapsular) region of the thymic cortex and then, as in the bone marrow, move progressively inwards towards the medulla as development continues. T-cell development involves gene rearrangements in the T-cell receptor (TcR) loci to create unique receptors for antigen on each cell, together with the progressive expression of molecules required for mature T-cell function. Selection of the receptor repertoire is more stringent for T cells than for B cells because of the way in which mature T cells recognize cell-bound antigens presented in conjunction with specific proteins of the major histocompatibility complex (MHC) expressed on the surfaces of cells. Thus mature CD8 (cytotoxic) T cells recognize antigen in the form of short peptides complexed with the polymorphic MHC class I molecules, while CD4 (helper/regulatory) T cells recognize the peptides in the context of MHC class II molecules. Because the TcR recognizes both the peptide and the MHC molecule, the T cell will only recognize peptides bound to their own (self) type of MHC: they will not ‘see’ peptides in combination with allelically different MHC molecules (i.e. those from other individuals). This is termed MHC restriction of T-cell recognition. Selection of T cells in the thymus must ensure the survival of those T cells which can respond only to foreign antigens, bound to their own (self) class of MHC molecule. Cells which are incapable of binding to self MHC molecules, or which bind to self-antigens, are eliminated by apoptotic cell death: it is estimated that up to 95% of T cell progenitors undergo apoptosis in this way. Cells which express an appropriate TcR and have effective MHC-restricted binding properties survive to become mature, naïve T cells which leave the thymus and populate the periphery.

Thymic stromal cells play a crucial role in T-cell development and selection. Thymic epithelial cells in the cortex express both MHC class I and II molecules and are unique in their ability to select T cells which recognize self MHC (positive selection). Deletion of self-antigen reactive cells (negative selection) is mainly controlled by thymic dendritic cells located at the corticomedullary junction and in the medulla, although the epithelium can also perform this function. Apoptotic thymocytes are removed by thymic macrophages. The role of the thymic epithelium in thymocyte differentiation is complex and involves cell–cell contact as well as the secretion of soluble mediators such as cytokines, chemokines, neuroactive peptides (e.g. somatostatin) and thymic hormones (e.g. thymulin). Thymic fibroblasts and the extracellular matrix also play a role.

Erythrocytes

Erythrocytes and granulocytes belong to the myeloid lineage. The earliest identifiable erythroid progenitor cells are capable of rapid bursts of cell division to form numerous daughter cells; they have thus been named burst-forming units of the erythroid line (BFU-E). They give rise to the CFU-E, which, with their immediate progeny, are sensitive to the hormone erythropoietin. This hormone, produced in the kidney, induces further differentiation along the erythroid line.

The first readily identifiable cell of the erythroid series is the proerythroblast, which is a large (about 20 μm) cell with a large euchromatic nucleus and a moderately basophilic cytoplasm. It also responds to erythropoietin. The proerythroblast contains small amounts of ferritin and bears some of the protein spectrin on its plasma membrane. Proerythroblasts proliferate to produce smaller (12–16 μm) basophilic erythroblasts, rich in ribosomes, in which haemoglobin-RNA synthesis begins. The cytoplasm becomes partially, and then uniformly, eosinophilic (the polychromatic erythroblast and orthochromatic erythroblast respectively). These cells are only 8–10 μm in diameter and contain very little cytoplasmic RNA. The nucleus becomes pyknotic (dense, deep-staining, shrunken) and is finally extruded from the cell, leaving an anucleate reticulocyte, which enters a sinusoid. Its reticular staining pattern, visible using special stains, results from residual cytoplasmic RNA which is usually lost within 24 hours of entering the peripheral blood circulation. Reticulocyte numbers in peripheral blood are therefore a good indicator of the rate of red cell production. The whole process of erythropoiesis takes 5–9 days.

Granulocytes

Granulocyte formation involves major changes in nuclear morphology and cytoplasmic contents which are best known for the neutrophil. Initially, myeloid progenitor cells transform into large (10–20 μm) myeloblasts which are similar in general size and appearance to proerythroblasts. These proliferative cells have large euchromatic nuclei and lack cytoplasmic granules. They differentiate into slightly larger promyelocytes, in which the first group of specific proteins is synthesized in the rough endoplasmic reticulum and Golgi apparatus. The proteins are stored in large (0.3 μm) primary (non-specific) granules, which are large lysosomes containing acid phosphatase. Smaller secondary (specific) granules are formed in the smaller myelocyte, which is the last proliferative stage. The nucleus is typically flattened or slightly indented on one side in myelocytes.

In the next, metamyelocyte, stage, the cell size (10–15 μm) decreases, the nucleus becomes heterochromatic and horse-shoe shaped, and protein synthesis almost stops. As the neutrophil is released, the nucleus becomes first heavily indented (the juvenile stab or band form), and subsequently segmented into up to six lobes, characteristic of the mature neutrophil. The whole process usually takes 7 days to complete, of which 3 days are spent proliferating, and 4 days maturing. Neutrophils may then be stored in the marrow for a further 4 days, depending on demand, before their final release into the circulation.

Eosinophils and basophils pass through a similar sequence but their nuclei do not become as irregular as that of the neutrophil. It is thought that these cells each arise from distinct colony-forming units, which are separate from the CFU-GM.

Monocytes

Monocytes are formed in the bone marrow. Monocytes and neutrophils appear to be closely related cells: together with some of the antigen-presenting dendritic cells, they arise from a shared progenitor, the colony-forming unit for granulocytes and macrophages (CFU-GM). Different colony-stimulating factors (CSF) act on the common progenitor to direct its subsequent differentiation pathway. Monocyte progenitors pass through a proliferative monoblast stage (14 μm) and then form differentiating promonocytes, which are slightly smaller cells in which production of small lysosomes begins. After further divisions, monocytes (up to 20 μm) are released into the general circulation. Most migrate into perivascular and extravascular sites, which they then populate as macrophages, while others may give rise to certain dendritic cells, including Langerhans cells.

Platelets

Platelets arise in a unique manner by the shedding of thousands of cytoplasmic fragments from the tips of processes of megakaryocytes in the bone marrow. The first detectable cell of this line is the highly basophilic megakaryoblast (15–50 μm), followed by a promegakaryocyte stage (20–80 μm), in which synthesis of granules begins. Finally, the fully differentiated megakaryocyte, a giant cell (35–160 μm) with a large, dense, polyploid, multilobed nucleus, appears. Once differentiation is initiated from the CFU-Meg, DNA replicates without cytoplasmic division (endoreduplication), and the chromosomes are retained within a single polyploid nucleus which may contain up to 256n chromosomes (where n is the haploid complement present in gametes). Megakaryocyte lineage characteristics and disorders are reviewed in Sun et al (2006).

The cytoplasm contains fine basophilic granules and becomes partitioned into proplatelets by invaginations of the plasma membrane. These are seen ultrastructurally as a network of tubular profiles which coalesce to form cytoplasmic islands 3–4 μm in diameter. Individual platelets are shed into the circulation from a long, narrow process of megakaryocyte cytoplasm which is protruded through an aperture in the sinusoidal endothelium.

PHAGOCYTES AND ANTIGEN-PRESENTING CELLS

Macrophages and neutrophils (see above) are specialized phagocytes. Certain dendritic cells (see Fig. 4.12), e.g. Langerhans cells of the skin and other stratified squamous epithelia, are ‘professional’ antigen-presenting cells (APCs): they take up foreign material by endocytosis and macropinocytosis, and are uniquely capable of efficiently activating naïve as well as mature T lymphocytes. Macrophages are also able to process and present antigen to lymphocytes, but are less effective than dendritic cells. In addition they play an important role in the effector arm of the immune response, clearing the infectious agent by phagocytosis. The third major cell type involved in antigen presentation and T cell activation is the B lymphocyte, which is particularly efficient at taking up antigen that binds to its surface immunoglobulin (see above). Follicular dendritic cells of lymph nodes, MALT and the spleen are capable of presenting non-processed antigen to B lymphocytes, but are not classic APCs because they cannot present antigen to helper T cells.

APCs endocytose antigen, digest it intracellularly, mostly to peptide fragments, and present the fragments on their surfaces, generally in conjunction with MHC class II molecules. (Class II molecules are normally found only on APCs, although many other cells can express class II molecules in inflammatory situations.) Recognition of foreign antigen is controlled by a variety of APC cell surface receptors: Fc and complement receptors mediate uptake of opsonized material, while pattern recognition receptors of the innate immune system, e.g. Toll-like receptors and scavenger receptors, directly recognize pathogen-derived molecules.

MACROPHAGES

The mononuclear phagocyte system consists of the blood monocytes, from which the other types are derived, and various tissue macrophages, some of which have tissue-specific names. Certain dendritic cells are sometimes included in the mononuclear phagocyte system: although they share a common lineage ancestor, they appear to form a discrete branch of the family tree. Most monocytes and macrophages express class II MHC molecules.

Macrophages are very variable in size (generally 15–25 μm) and are found in many tissues of the body, where they constitute a heterogeneous family of cells (reviewed in Gordon & Taylor 2005). They are migrant cells in all general connective tissues, the alveolar macrophages in the lung, Kupffer cells in liver sinusoids, in bone marrow and in all lymphoid tissues. Macrophages often aggregate in subserous connective tissue of the pleura and peritoneum, where they are visible as milky spots near small lymphatic trunks. They cluster around the terminations of small (penicillar) arterioles in the spleen and are distributed, more diffusely, throughout the splenic cords.

Osteoclasts (up to 100 μm) in bone are closely related to macrophages. However they are syncytial cells derived from the fusion of up to 30 progenitor monocytes in bone tissue, where they differentiate further. Microglia of the central nervous system (CNS) are thought to be monocytic in origin: they migrate into the CNS during its development. They differ from macrophages in that normally they are quiescent cells in which MHC class II expression is downregulated, and they display little phagocytic activity.

Macrophages vary in structure depending on their location in the body. All have a moderately basophilic cytoplasm containing some rough and smooth endoplasmic reticulum, an active Golgi complex and a large, euchromatic and somewhat irregular nucleus. These features are consistent with an active metabolism: synthesis of lysosomal enzymes continues in mature cells. All macrophages have irregular surfaces with protruding filopodia and they contain varying numbers of endocytic vesicles, larger vacuoles and lysosomes. Some macrophages are highly motile, whereas others tend to remain attached and sedentary, e.g. in hepatic and lymphoid sinuses. Within connective tissues, macrophages may fuse to form large syncytia (giant cells) around particles which are too large to be phagocytosed, or when stimulated by the presence of infectious organisms, e.g. *Mycobacterium tuberculosis*.

When blood-borne monocytes enter the tissues through the endothelial walls of capillaries and venules, they can undergo a limited number of rounds of mitosis as tissue macrophages before they die and are replaced from the bone marrow, typically after several weeks. There is some evidence that alveolar macrophages of the lung are able to undergo many more mitoses than other macrophages.

Phagocytosis

The uptake of particulate material and microorganisms is carried out by macrophages in many tissues and organs. When present in general connective tissue, they ingest and kill invading microorganisms and remove debris that has been produced as a consequence of tissue damage. They recognize, engulf and rapidly ingest apoptotic cells in all situations: the mechanism of apoptotic cell uptake does not activate the phagocyte for antigen presentation, and so the process is immunologically silent. In the lung, alveolar macrophages constantly patrol the respiratory surfaces, to which they migrate from pulmonary connective tissue (Fig. 4.13). They engulf inhaled particles including bacteria, surfactant and debris and many enter the sputum (hence their alternative names, dust cells or, in cardiac disease, heart failure cells, which are full of extravasated erythrocytes). They perform similar scavenger functions in the pleural and peritoneal cavities. In lymph nodes, macrophages line the walls of sinuses and remove particulate matter from lymph as it percolates through them. In the spleen and liver, macrophages are involved in particle removal and in the detection and destruction of aged or damaged erythrocytes. They begin the degradation of haemoglobin for recycling iron and amino acids.

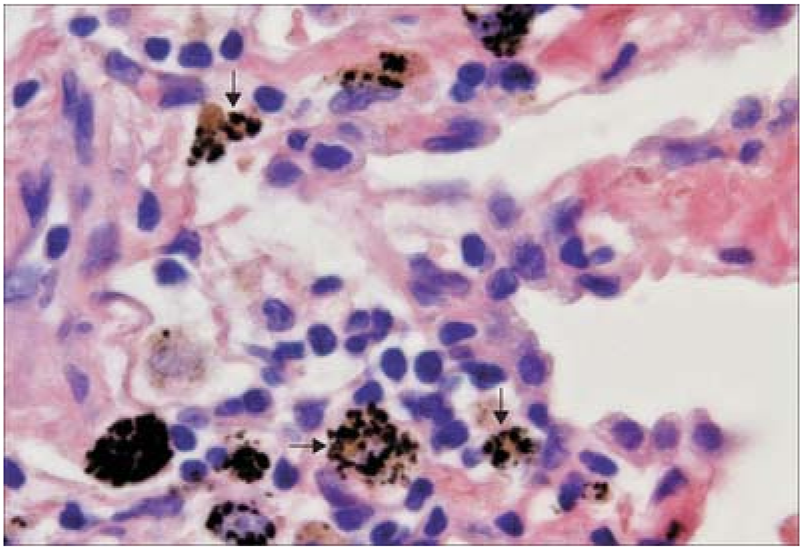

Fig. 4.13 Alveolar macrophages (dust cells, arrows) containing ingested carbon particles, in alveoli and interalveolar septa of the human lung.

Macrophages bear surface receptors for the Fc portions of antibodies and for the C3 component of complement. Phagocytic activity is greatly increased when the target has been coated in antibody (opsonized) or complement, or both. Once phagocytosis has occurred, the vacuole bearing the ingested particle fuses with endosomal vesicles which contain a wide range of lysosomal enzymes, including many hydrolases, and oxidative systems capable of rapid bacteriocidal action. These activities are much enhanced when macrophages are stimulated (activated macrophages) by cytokines, e.g. interferon (IFN)-γ, which are secreted by other cells of the immune system, especially T lymphocytes.

Close antibody-mediated binding may initiate the release of lysosomal enzymes onto the surfaces of the cellular targets to which the macrophages bind. This process of cytotoxicity is also used by other cells, including neutrophils and eosinophils, particularly if the targets are too large to be phagocytosed (e.g. nematode worm parasites).

Secretory activities

Activated macrophages can synthesize and secrete various bioactive substances, e.g. IL-1, which stimulate the proliferation and maturation of other lymphocytes, greatly amplifying the reaction of the immune system to foreign antigens. They also synthesize tumour necrosis factor (TNF)-α, which is able to kill small numbers of neoplastic cells. TNF-α depresses the anabolic activities of many cells in the body, and may be a major factor mediating cachexia (wasting) which typically accompanies more advanced cancers. Other macrophage products include plasminogen activator, which promotes clot removal; various lysosomal enzymes; several complement and clotting factors; and lysozyme (an antibacterial protein). In pathogenesis, these substances may be released inappropriately and damage healthy tissues, e.g. in rheumatoid arthritis and various other inflammatory conditions.

DENDRITIC CELLS

There are two distinct groups of dendritic cell, myeloid dendritic cells (also known as conventional dendritic cells) and plasmacytoid dendritic cells. Both groups of cells are derived from haematopoietic stem cells. Until recently it was thought that plasmacytoid dendritic cells were derived from the lymphoid precursor cells, while the myeloid dendritic cells were derived from the myeloid progenitor cell. However, it is now apparent that these cells can be derived from either lineage, possibly from a common stem cell indicating considerable plasticity in their developmental pathways. Both cells are involved in antigen presentation, though have somewhat different functional roles in controlling both the adaptive and innate immune system. The myeloid dendritic cells are professional antigen-presenting cells (APC), which are able to process and present antigen to T lymphocytes, including naïve T cells. They are present as immature dendritic cells in the epidermis of the skin (Fig. 4.14) and other stratified squamous epithelia, e.g. the oral mucosa (Langerhans cells), and in the dermis and most other tissues (interstitial dendritic cells), where they are concerned with immune surveillance. Immature dendritic cells have an antigen-capturing function. They respond to chemotactic signals, for example defensins released by epithelial cells in the small intestine and they express pattern recognition receptors (e.g. Toll-like receptors) on their surface. Binding of bacterial molecules (e.g. carbohydrate or DNA) to these receptors stimulates the dendritic cells to migrate via the lymphatics to nearby secondary lymphoid tissues where they mature and acquire an antigen-presenting function. Mature dendritic cells are known as veiled cells when in the afferent lymphatics and the subcapsular sinuses of lymph nodes, and as interdigitating dendritic cells once they are within the lymphoid tissue proper. Their function within the secondary lymphoid tissue is to present their processed antigen to T lymphocytes, and thus to initiate and stimulate the immune response. For a review of recent research on dendritic cell function, see Colonna et al (2006).

Langerhans cells

Langerhans cells (Fig. 4.14) are one of the most well-studied types of immature dendritic cell (reviewed in Berger et al 2006). They are present throughout the epidermis of skin, where they were first described, but are most clearly identifiable in the stratum spinosum (see Ch. 7). They have an irregular nucleus and a clear cytoplasm, and contain characteristic elongated membranous vesicles (Birbeck granules). Langerhans cells endocytose and process antigens, undergoing a process of maturation from antigen-capturing to antigen-presenting cells which express high levels of MHC class I and II molecules, co-stimulatory molecules and adhesion molecules. They migrate to lymph nodes to activate T lymphocytes.

Interdigitating dendritic cells

Immature dendritic cells are found all over the body, including peripheral blood, and function in antigen-processing and immune surveillance. Mature dendritic cells are present in T cell-rich areas of secondary lymphoid tissue (paracortical areas of lymph nodes, interfollicular areas of MALT, periarteriolar sheaths of splenic white pulp), where they are frequently referred to as interdigitating dendritic cells. Within the secondary lymphoid tissues, they are involved in the presentation to T lymphocytes of antigens associated with either MHC class I (CD8 T cells) or MHC class II (CD4 T cells) molecules. Naïve T cells can only respond to antigen presented by dendritic cells. The T cells are stimulated not only by recognition of the antigen-MHC complex by the TcR, but also by interaction with co-stimulatory molecules expressed by the dendritic cells, and by cytokines secreted by the cells. These cytokines not only help activate the T cell but can also direct the nature of the T-cell response (e.g. Th1 or Th2). Appropriate T cells are thus activated to proliferate and are primed for carrying out their immunological functions. Once primed, T cells can then be stimulated by any APC, including macrophages and B cells.

Follicular dendritic cells

Follicular dendritic cells, FDCs (Fig. 4.15), are a non-migratory population of cells found in the follicles of secondary lymphoid tissues, where they attract and interact with B cells. Unlike other dendritic cells, FDCs are not haemopoietic in origin, but are probably derived from the stromal cells of lymphoid tissues. They are unable to endocytose and process antigen, and they lack MHC class II molecules. However, Fc receptors and complement receptors CD21 and CD35 on FDCs allow the cells to bind immune complexes to their surface for subsequent presentation, as unprocessed antigen, to germinal centre B cells. Interactions between B cells, CD4 helper T cells and FDCs in the germinal centres are important in the selection of high affinity B cells and their maturation to either plasma cells or memory B lymphocytes.

REFERENCES

rger CL, Vasquez JG, Shofner J, Mariwalla K, Edelson RL. Langerhans cells: mediators of immunity and tolerance. *Int J Biochem Cell Biol*. 2006;38:1632-1636.

lonna M, Pulendran B, Iwasaki A. Dendritic cells at the host–pathogen interface. *Nature Immunol*. 2006;7:117-120.

nningham-Rundles C, Ponda PP. Molecular defects in T- and B-cell primary immunodeficiency diseases. *Nature Rev Immunol*. 2005;5:880-892.

rdon S, Taylor PR. Monocyte and macrophage heterogeneity. *Nat Rev Immunol*. 2005;5:953-964.

neway C, Walport M, Travers P. Immunobiology: The Immune System in Health and Disease, 5th edn. New York: Garland Publishing, 2004.

Emphasizes the unifying principles of structure and function of the immune system in health and disease..

cabas CN, Yavuz AS, Lipsky PE, Metcalfe DD, Akin C. Analysis of the lineage relationship between mast cells and basophile using the c-kit

D816V mutation as a biologic signature. *J Allergy Clin Immunol*. 2005;115:1155-1161.

iosa CV, Stadtfelt M, Graf T. Determinants of lymphoid-myeloid lineage diversification. *Ann Rev Immunol*. 2006;24:705-738.

u Y-J. Dendritic cell subsets and lineages, and their functions in innate and adaptive immunity. *Cell*. 2001;106:259-262.

Review of current research and a re-evaluation of the lineage of and functional relationships between different dendritic cell types..

ale D, Brostoff J, Roth DB, Roitt I. Immunology, 7th edn. London: Mosby, 2006.

Sets out the scientific principles of clinical immunology, integrated with histology, pathology and clinical examples..

Garra A, Vieira P. Regulatory T cells and mechanisms of immune system control. *Nat Med*. 2004;10:801-805.

n L, Hwang WYK, Aw SE. Biological characteristics of megakaryocytes: specific lineage commitment and associated disorders. *Int J Biochem Cell Biol*. 2006;38:1821-1826.

vier E, Tomasello E, Baratin M, Walzer T, Ugolini S. Functions of natural killer cells. *Nature Immunol*. 2008;9:503-510.

oof JM, Kerr MA. The function of immunoglobulin A in immunity. *J Path*. 2006;208:270-282.

CHAPTER 5

Functional anatomy of the musculoskeletal system

The skeletal system consists of the specialized supporting connective tissues of the bony skeleton and the associated tissues of joints, including cartilage. Cartilage is the fetal precursor tissue in the development of many bones; it also supports non-skeletal structures, as in the ear, larynx and tracheobronchial tree. Bone provides a rigid framework which protects and supports most of the soft tissues of the body and acts as a system of struts and levers which, through the action of attached skeletal muscles, permits movement of the body. Bones of the skeleton are connected with each other at joints which, according to their structure, allow varying degrees of movement. Some joints are stabilized by fibrous tissue connections between the articulating surfaces, while others are stabilized by tough but flexible ligaments. Skeletal muscles are attached to bone by strong flexible, but inextensible, tendons which insert into bone tissue. The entire assembly forms the musculoskeletal system; all its cells are related members of the connective tissue family and are derived from mesenchymal stem cells.

CARTILAGE

During early fetal life the human skeleton is mostly cartilaginous, but is subsequently largely replaced by bone. In adults, cartilage persists at the surfaces of synovial joints, in the walls of the larynx and epiglottis, trachea, bronchi, nose and external ears. Developmental replacement by bone is a complex process: cells in cartilaginous growth plates – which lie between ossifying epiphyses and the diaphyses of long bones (and elsewhere) – continue to proliferate, increasing the length of the bones concerned until they eventually ossify, when growth ceases.

MICROSTRUCTURE OF CARTILAGE

Cartilage is a type of load-bearing connective tissue. It has a low metabolic rate and its vascular supply is confined to its surface or to large cartilage canals. It has a capacity for continued and often rapid interstitial and appositional growth, and a high resistance to tension, compression and shearing, with some resilience and elasticity. Cartilage is covered by a fibrous perichondrium except at its junctions with bone and at synovial surfaces, which are lubricated by a secreted nutrient synovial fluid.

The cells of cartilage are chondroblasts and chondrocytes. Like connective tissues generally, the extracellular matrix is a dominant component and gives the tissue its distinguishing characteristics. The extracellular matrix of cartilage varies in appearance, composition and in the nature of its fibres in the different types of cartilage, namely, hyaline cartilage, white fibrocartilage and yellow elastic cartilage. A densely cellular cartilage, with thin septa of matrix between its cells, is typical of early embryonic cartilage. Hyaline cartilage is the prototypical form but it varies more in composition and properties according to age and location, than either elastic or fibrocartilage. Hyaline cartilage may become calcified as part of the normal process of bone development, or as an age-related, degenerative change.

Cartilage cells occupy small lacunae in the matrix which they secrete. Young cells (chondroblasts) are smaller, often flat and irregular in contour, and bear many surface processes, which fit into complementary recesses in the matrix. Newly generated chondroblasts often retain intercellular contacts, including gap junctions. These are lost when daughter cells are separated by the synthesis of new matrix. As cartilage cells mature, they lose the ability to divide and become metabolically less active. Some authors reserve the name chondrocytes for such cells, but this term is commonly employed, as it is here, to denote all cartilage cells embedded in matrix. Mature chondrocytes enlarge with age and become more rounded. The ultrastructure of chondrocytes is typical of cells which are active in making and secreting proteins. The nucleus is round or oval, euchromatic and possesses one or more nucleoli. The cytoplasm is filled with rough endoplasmic reticulum, transport vesicles and Golgi complexes, and contains many mitochondria and frequent lysosomes, together with numerous glycogen granules, intermediate filaments (vimentin) and pigment granules. When these cells mature to the relatively inactive chondrocyte stage, the nucleus becomes heterochromatic, the nucleolus smaller, and the protein synthetic machinery much reduced: the cells may also accumulate large lipid droplets.

Cartilage is often described as totally avascular. Most cartilage cells are usually distant from exchange vessels, which are mostly perichondrial, and so nutrient substances and metabolites diffuse along concentration gradients across the matrix between the perichondrial capillary network and chondrocytes. This limitation is reflected in the fact that most living cartilage tissue is restricted to a few millimetres in thickness. Cartilage cells situated further than this from a nutrient vessel do not survive, and their surrounding matrix typically becomes calcified. In the larger cartilages and during the rapid growth of some fetal cartilages, vascular cartilage canals penetrate the tissue at intervals, providing an additional source of nutrients. In some cases these canals are temporary structures, but others persist throughout life.

Extracellular matrix

The extracellular matrix is composed of collagen and, in some cases, elastic fibres, embedded in a highly hydrated but stiff ground substance (Fig. 5.1). The components are unique to cartilage, and endow it with unusual mechanical properties. The ground substance is a firm gel, rich in carbohydrates and predominantly acidic. The chemistry of the ground substance is complex. It consists mainly of water and dissolved salts, held in a meshwork of long interwoven proteoglycan molecules together with various other minor constituents, mainly proteins or glycoproteins.

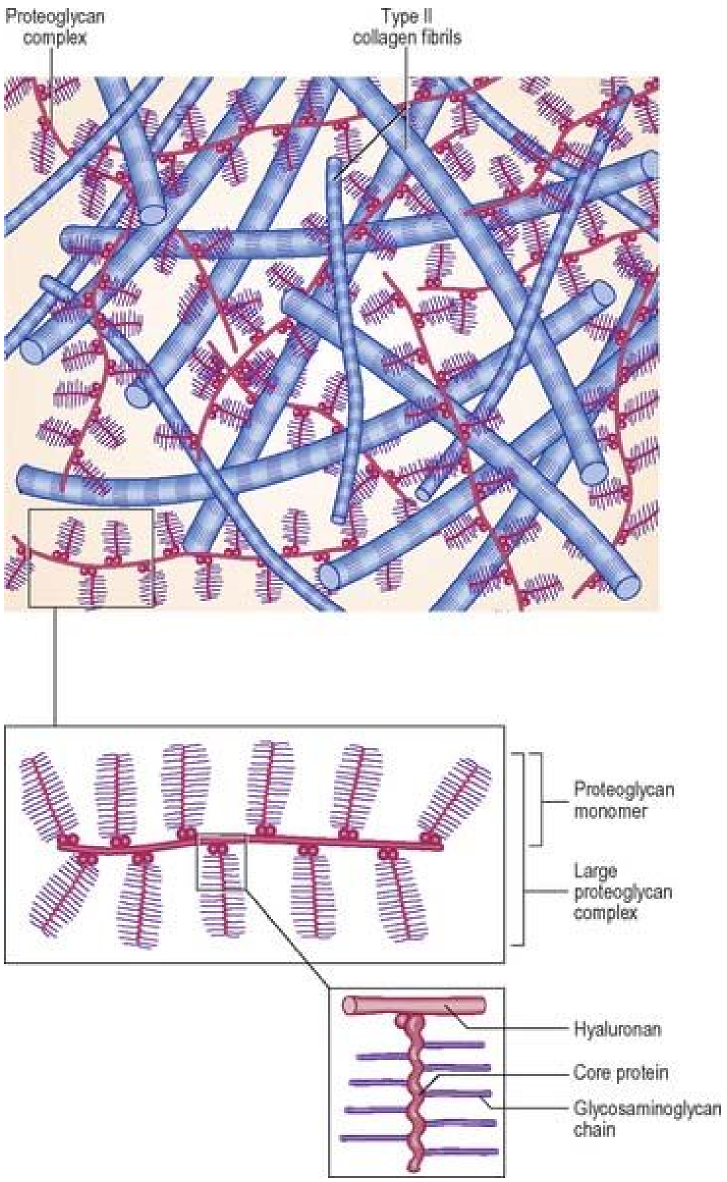
Proteoglycan complex
Type II collagen fibrils
Proteoglycan monomer
Large proteoglycan complex
Hyaluronan
Core protein
Glycosaminoglycan chain

Fig. 5.1 Fine structural organization of hyaline cartilage matrix. Depicted are large proteoglycan complexes and type II collagen fibres (cross-banded and of different diameters). Proteoglycan complexes bind to the surface of these fibres via their monomeric sidechains and link them together. The arrangement of glycosaminoglycans and core protein of the proteoglycan monomer is illustrated in the expansion.

Collagen

Collagen forms up to 50% of the dry weight of cartilage. It is chemically distinct from the collagen in most other tissues, and is classed as type II collagen. This variety is only found elsewhere in the notochord, the nucleus pulposus of the intervertebral disc, the vitreous body of the eye, and the primary corneal stroma. Its tropocollagen subunits are composed of triple helices of identical polypeptides (three α-1 chains). Collagen in the outer layers of the perichondrium and much of the collagen in white fibrocartilage is the general connective tissue type I.

The majority of the collagen fibres of cartilage are relatively short and thin (mainly 10–20 nm diameter), with a characteristic cross-banding (65 nm periodicity). They are interwoven to create a three-dimensional meshwork linked by lateral projections of the proteoglycans associated with their surfaces. Proteoglycans and other organic molecules link collagen fibres with the interfibrillar ground substance and with chondrocytes. The amount, size and orientation of collagen fibres vary in different types of cartilage, and with maturity and position within the cartilage mass. In articular cartilage, collagen fibres close to the surfaces of cells are particularly narrow (4–6 nm diameter) and resemble fibres of type II collagen in non-cartilaginous tissue, i.e. the vitreous body of the eye. Cartilage contains minor quantities of other classes unique to cartilage, including types IX, X and XI.

Proteoglycans and glycosaminoglycans (GAGs)

Proteoglycans are similar in general outline to those of general connective tissue, although with features peculiar to cartilage. Chondroitin sulphate and keratan sulphate play important roles in the water retention properties of cartilage.

Synthesis of matrix

Chondrocytes synthesize and secrete all of the major components of the matrix. Collagen is synthesized within the rough endoplasmic reticulum in the same way as in fibroblasts, except that type II rather than type I procollagen chains are made. These assemble into triple helices and some carbohydrate is added at this stage. After transport to the Golgi apparatus, where further glycosylation occurs, they are secreted as procollagen molecules into the extracellular space. Here, terminal registration peptides are cleaved from their ends, so forming tropocollagen molecules, and final assembly into collagen fibres takes place. Core proteins of the proteoglycan complexes are also synthesized in the rough endoplasmic reticulum and addition of GAG chains begins. The process is completed in the Golgi complex. Hyaluronan, which lacks a protein core, is synthesized by enzymes on the surface of the chondrocyte; it is not modified post-synthetically, and is extruded directly into the matrix without passing through the endoplasmic reticulum.

Hyaline cartilage

Hyaline cartilage has a homogeneous glassy, bluish opalescent appearance. It has a firm consistency and some elasticity. Costal, nasal, some laryngeal, tracheobronchial, all temporary (developmental) and most articular, cartilages are hyaline. The arytenoid cartilage changes from hyaline at its base, to elastic cartilage at its apex. Size, shape and arrangement of cells, fibres and proteoglycan composition vary at different sites and with age. The chondrocytes are flat near the perichondrium and rounded or angular, deeper in the tissue. They are often grouped in pairs, sometimes more, forming cell nests (isogenous cell groups) which are daughter cells of a common parent chondroblast: apposing cells have a straight outline. The matrix is typically basophilic (Fig. 5.2) and metachromatic, particularly in the lacunar capsule, where recently formed, territorial matrix borders the lacuna of a chondrocyte. The paler-staining interterritorial matrix between cell nests is older synthetically. Fine collagen fibres are arranged in a basket-like network (Fig. 5.3), but are often absent from a narrow zone immediately surrounding the lacuna. An isogenous cell group, together with the enclosing pericellular matrix, is sometimes referred to as a chondron.

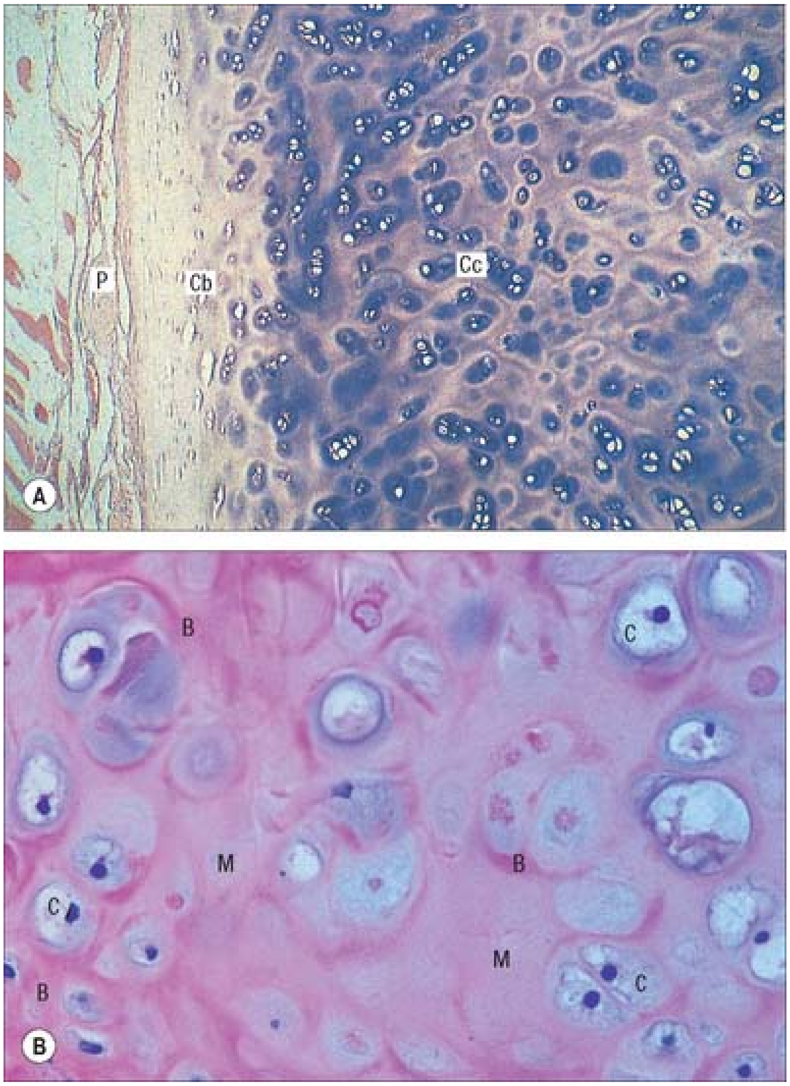

Fig. 5.2 Sections through hyaline cartilage. **A**, Low-power view of human rib, showing perichondrium (P, left), young chondroblasts (Cb) embedded in pale-staining interterritorial matrix and mature chondrocytes (Cc) embedded in the basophilic interterritorial matrix (centre and right). **B**, Higher magnification of hyaline cartilage in human bronchial wall, showing isogenous groups of chondrocytes (C). Note the more deeply-stained basophilic zones (B) (rich in acidic proteoglycans) around the cell clusters, with older, paler-staining matrix (M) between clusters.

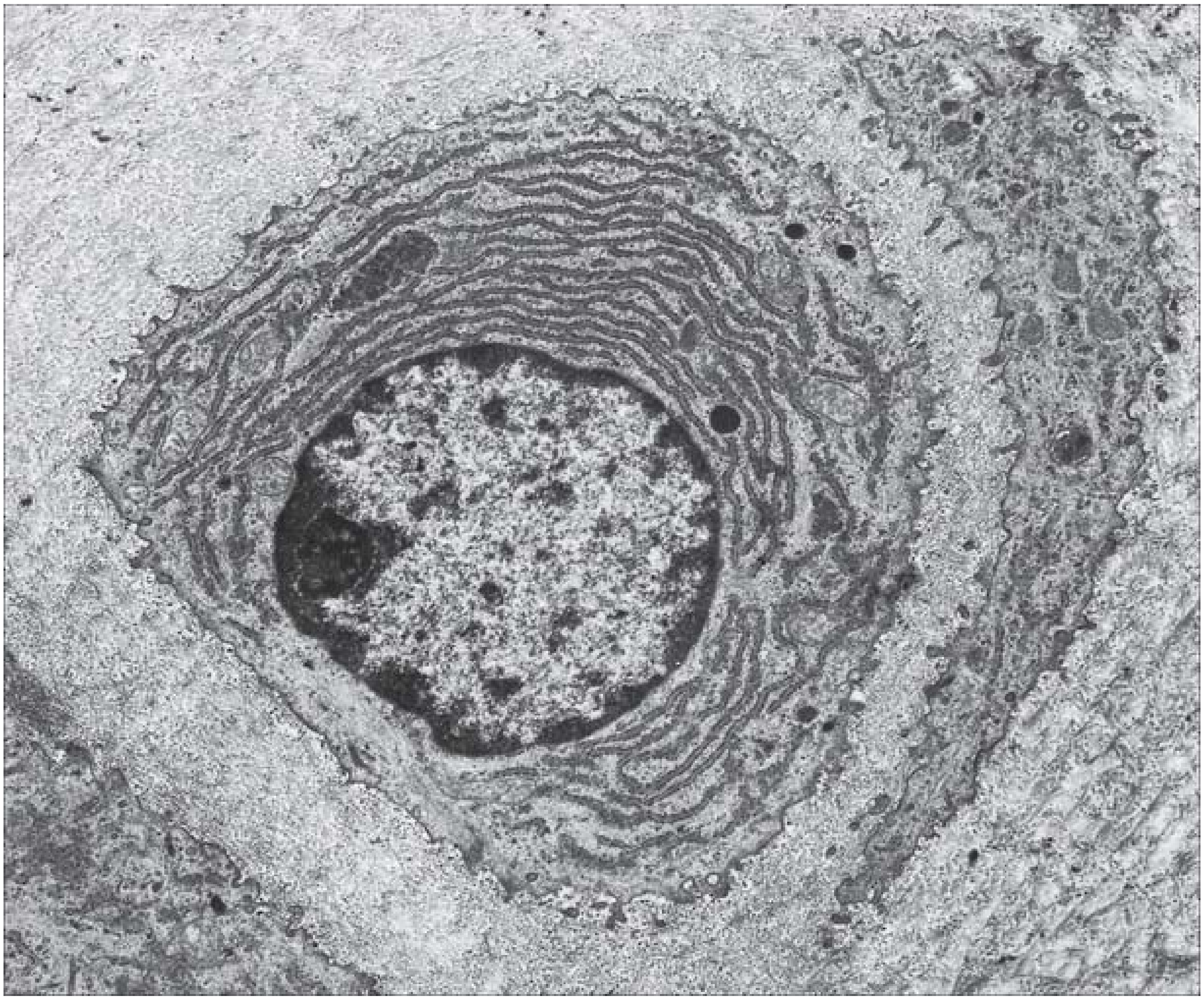

Fig. 5.3 Electron micrograph of chondroblasts in rabbit femoral condylar cartilage. The central cell has an active euchromatic nucleus with a prominent nucleolus, and its cytoplasm contains concentric cisternae of rough endoplasmic reticulum, scattered mitochondria, lysosomes and glycogen aggregates. The plasma membrane bears numerous short filopodia which project into the surrounding matrix. The latter shows a delicate feltwork of collagen fibrils within finely granular interfibrillary material. No pericellular lacuna is present; the matrix separates the central chondroblast from the cytoplasm of two adjacent chondroblasts (left, and crescentic profile).

(Preparation by courtesy of Susan Smith, Department of Anatomy, GKT School of Medicine, London.)

After adolescence, hyaline cartilages are prone to calcification, especially in costal and laryngeal sites. In costal cartilage, the matrix tends to fibrous striation, especially in old age when cellularity diminishes. The xiphoid process and the cartilages of the nose, larynx and trachea (except the elastic cartilaginous epiglottis and corniculate cartilages) resemble costal cartilage in microstructure. The regenerative capacity of hyaline cartilage is poor.

Articular hyaline cartilage

Articular hyaline cartilage covers articular surfaces in synovial joints (Fig. 5.4). It provides an extremely smooth, resistant surface bathed by synovial fluid, which allows almost frictionless movement. Its elasticity, together with that of other articular structures, dissipates stresses, and gives the whole articulation some flexibility, particularly near extremes of movement. Articular cartilage is particularly effective as a shock-absorber, and resists the large compressive forces generated by weight transmission, especially during movement.

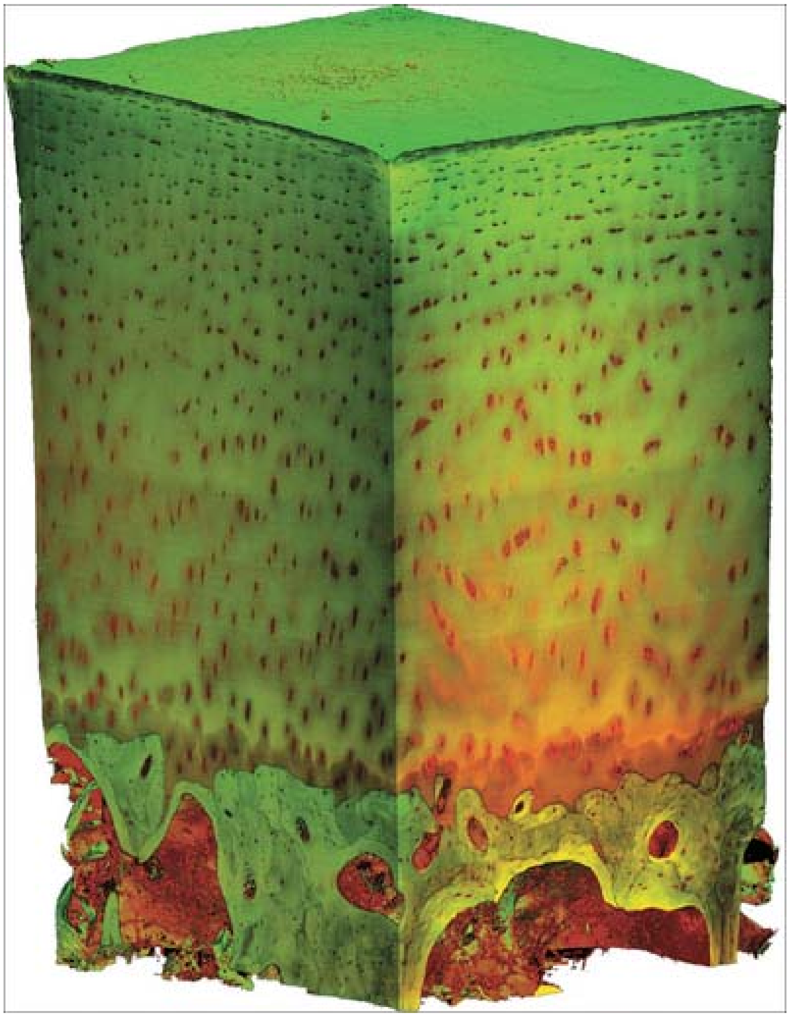

Fig. 5.4 Articular cartilage from the anterior region of the lateral femoral condyle of a young adult human female. Shown are the articular surface (top), articular cartilage and subchondral bone (below). Note the changes in size and spatial distribution of articular chondrocytes through the thickness of the cartilage. 3-D digital volumetric fluorescence imaging of serially sectioned, eosin-Y and acridine orange-stained tissue.

(Provided by courtesy of Professor Robert L Sah, Drs Won C Bae, Kyle D Jadin, Benjamin L Wong, Kelvin W. Li and Mrs Barbara L. Schumacher, Department of Bioengineering and Whitaker Institute of Biomedical Engineering, University of California, San Diego.)

Articular cartilage does not ossify. It varies from 1 to 7 mm in thickness and is moulded to the shape of the underlying bone, indeed it often accentuates and modifies the surface geometry of the bone. It is thickest centrally on convex osseous surfaces, and the reverse is true of concave surfaces. Its thickness decreases from maturity to old age. The surface of articular cartilage lacks a perichondrium; synovial membrane overlaps and then merges into its structure circumferentially (see Fig. 5.32).

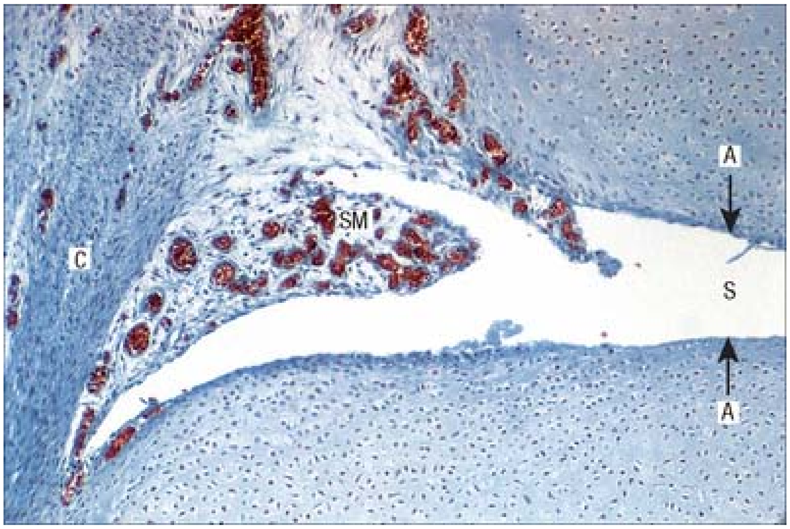

Fig. 5.32 A section of a synovial joint and its associated highly vascular (red) synovial membrane in a human fetal hand. The two articular cartilage surfaces (A, arrowed) are separated on the right by a layer of synovial fluid (S) secreted by the synovial membrane (SM) which extends a short distance into the joint space from the capsule (C).

Adult articular cartilage shows a structural zonation with increasing depth from the surface. The arrangement of collagen fibres has been variously described as plexiform, helical, or in the form of serial arcades which radiate from the deepest zone to the surface, where they follow a short tangential course before returning radially. If the surface of an articular cartilage is pierced by a needle, a longitudinal split-line remains after withdrawal. For any given joint, the patterns of split-lines are constant and distinctive and follow the predominant directions of collagen bundles in tangential zones of cartilage. These patterns may reveal tension trajectories set up in surrounding cartilage during joint movement.

Zone 1 is the superficial or tangential layer. The free articular surface is a thin, cell-free layer, 3 μm thick, which contains fine collagen type II fibrils covered superficially by a protein coating. The cells are small, oval or elongated and parallel to the surface, relatively inactive, and surrounded by fine tangential fibres. The collagen fibres deeper within this zone are regularly tangential, their diameters and density increase with depth. Zone 2 is the transitional or intermediate layer. The cells are larger, rounder, and are either single or in isogenous groups. Most are typical active chondrocytes, surrounded by oblique collagen fibres. Deeper still, in the radiate layer (zone 3), cells are large, round and often disposed in vertical columns, with intervening radial collagen fibres. As elsewhere, the cells, either singly or in groups, are encapsulated in pericellular matrix which has fine fibrils and contains fibronectin and types II, IX and XI collagen. The deepest layer or calcified layer (zone 4) lies adjacent to the subchondral bone (hypochondral osseous lamina) of the epiphysis. The adjacent surfaces show reciprocal fine ridges, grooves and interdigitations, which, with the confluence of their fibrous arrays, resist shearing stresses produced by postural changes and muscle action. The junction between zones 3 and 4 is called the tidemark. With age, articular cartilage thins and degenerates by advancement of the tidemark zone, and the replacement of calcified cartilage by bone.

Concentrations of GAGs vary according to site and, in particular, with age. The proportion of keratan sulphate increases linearly with depth, mainly in the older matrix between cell nests, whereas chondroitin sulphates are concentrated around lacunae. The turnover rates of GAGs in cartilage are faster than those of collagen, and the smaller, more soluble GAGs turn over fastest. Turnover decreases with age and distance from the cells. The proteoglycan turnover time is estimated at nearly 5 years for adult human articular cartilage.

The sequence of structural features outlined above is also typical of cartilaginous growth plates (see p. 95). During radial epiphysial growth, the extension of endochondral ossification into overlying calcified cartilage starts with the development of isogenous groups followed by the appearance of hypertrophic cells arranged in vertical columns. This ceases in maturity, but the zones persist throughout life. The same terminal mechanism also occurs in bones which lack epiphyses.

Cells of articular cartilage are capable of cell division, but mitoses are rare except in young bones and damage is not repaired in the adult. Superficial cells are lost progressively from normal young joint surfaces, and they are replaced by cells from deeper layers. Degenerating cells may occur in any of the four zones. This probably accounts for the progressive reduction in cellularity of cartilage with advancing age, particularly in superficial layers.

Articular cartilages derive nutrients by diffusion from vessels of the synovial membrane, synovial fluid and hypochondral vessels of an adjacent medullary cavity, some capillaries from which penetrate and occasionally traverse the calcified cartilage. The contributions from these sources are uncertain and may change with age. Small molecules freely traverse articular cartilage, with diffusion coefficients about half those in aqueous solution. Larger molecules have diffusion coefficients inversely related to their molecular size. The permeability of cartilage to large molecules is greatly affected by variations in its GAG, and hence water, content, e.g. a three-fold increase multiplies the diffusion coefficient a hundred-fold.

Fibrocartilage

Fibrocartilage is dense, fasciculated, opaque white fibrous tissue. It contains fibroblasts and small interfascicular groups of chondrocytes. The cells are ovoid and surrounded by concentrically striated matrix (Fig. 5.5). When present in quantity, as in intervertebral discs, fibrocartilage has great tensile strength and appreciable elasticity. In lesser amounts, as in articular discs, the glenoid and acetabular labra, and the cartilaginous lining of bony grooves for tendons and some articular cartilages, it provides strength, elasticity and resistance to repeated pressure and friction. It is resistant to degenerative change.

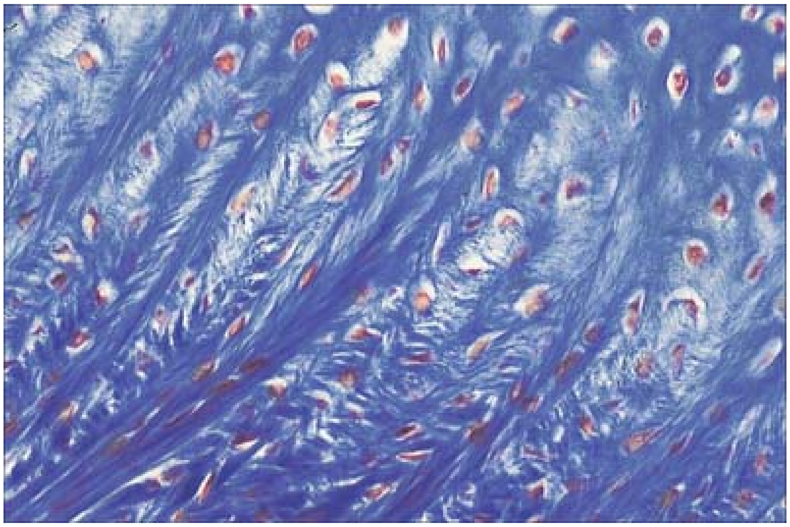

Fig. 5.5 White fibrocartilage in a late fetal intervertebral disc (human). Chondroblasts lie between coarse collagen type I fibres (blue) derived from the anulus fibrosus. Mallory's triple stain.

Fibrocartilage is unlike other types of cartilage in that it contains a considerable amount of type I (general connective tissue) collagen which is synthesized by the fibroblasts in its matrix. It is perhaps best regarded as a mingling of the two types of tissue, e.g. where a ligament or tendinous tissue inserts into hyaline cartilage, rather than as a separate type of cartilage. However, fibrocartilage in joints often lacks type II collagen altogether, and so possibly represents a distinct class of connective tissue.

The articular surfaces of bones which ossify in mesenchymal membranes (e.g. squamous temporal, mandible and clavicle) are covered by white fibrocartilage. The deep layers, adjacent to hypochondral bone, resemble calcified regions of the radial zone of hyaline articular cartilage. The superficial zone contains dense parallel bundles of thick collagen fibres, interspersed with typical dense connective tissue fibroblasts and little ground substance. Fibre bundles in adjacent layers alternate in direction, as they do in the cornea. A transitional zone of irregular bundles of coarse collagen and active fibroblasts separates the superficial and deep layers. The fibroblasts are probably involved in elaboration of proteoglycans and collagen, and may also constitute a germinal zone for deeper cartilage. Fibre diameters and types may differ at different sites according to the functional load.

Elastic cartilage

Elastic cartilage occurs in the external ear, corniculate cartilages, epiglottis and apices of the arytenoids. It contains typical chondrocytes, but its matrix is pervaded by yellow elastic fibres, except around lacunae (where it resembles typical hyaline matrix with fine type II collagen fibrils) (Fig. 5.6). Its elastic fibres are irregularly contoured and show no periodic banding. Most sites in which elastic cartilage occurs have vibrational functions, such as laryngeal sound wave production, or the collection and transmission of sound waves in the ear. Elastic cartilage is resistant to degeneration; it can regenerate to a limited degree following traumatic injury, e.g. the distorted repair of a ‘cauliflower ear’.

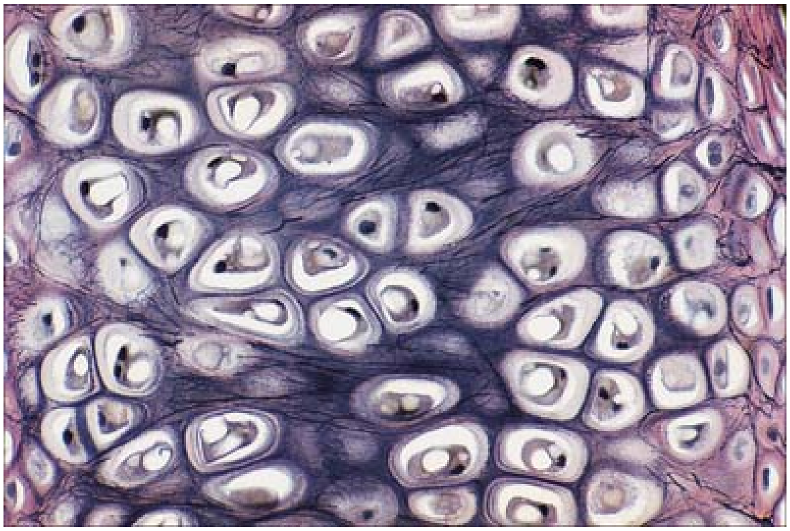

Fig. 5.6 Elastic cartilage, stained to demonstrate elastin fibres (blue-black). Chondroblasts and larger chondrocytes are embedded in the matrix, which also contains collagen type II fibres.

DEVELOPMENT AND GROWTH OF CARTILAGE

Cartilage is usually formed in embryonic mesenchyme. Mesenchymal cells proliferate and become tightly packed: the shape of their condensation foreshadows that of the future cartilage. They also become rounded, with prominent round or oval nuclei and a low cytoplasm: nucleus ratio. Adjacent cells are linked by gap junctions. Each cell next secretes a basophilic halo of matrix, composed of a delicate network of fine type II collagen filaments, type IX collagen and cartilage proteoglycan core protein, i.e. it differentiates into a chondroblast (Fig. 5.7). In some sites, continued secretion of matrix separates the cells, producing typical hyaline cartilage. Elsewhere, many cells become fibroblasts: collagen synthesis predominates and chondroblastic activity appears only in isolated groups or rows of cells which become surrounded by dense bundles of collagen fibres to form white fibrocartilage. In yet other sites, the matrix of early cellular cartilage is permeated first by anastomosing oxytalan fibres, and later by elastin fibres. In all cases, developing cartilage is surrounded by condensed mesenchyme which differentiates into a bilaminar perichondrium. The cells of the outer layer become fibroblasts and secrete a dense collagenous matrix lined externally by vascular mesenchyme. The cells of the inner layer contain differentiated, but mainly resting, chondroblasts or prechondroblasts.

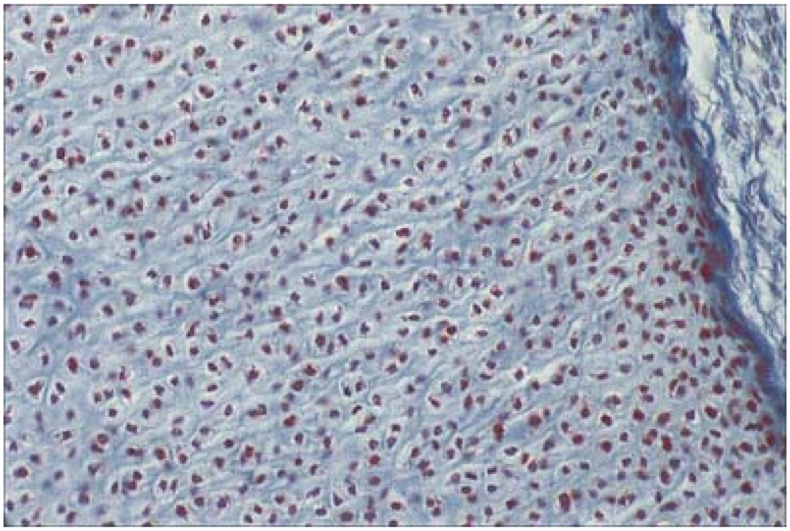

Fig. 5.7 Highly cellular fetal cartilage, human phalanx. The cells are small and almost uniform in distribution. Mallory's triple stain.

Cartilage grows by interstitial and appositional mechanisms. Interstitial growth is the result of continued mitosis of early chondroblasts throughout the tissue mass and is obvious only in young cartilage, where plasticity of the matrix permits continued expansion. When a chondroblast divides, its descendants temporarily occupy the same lacuna. They are soon separated by a thin septum of secreted matrix, which thickens and further separates the daughter cells. Continuing division produces isogenous groups. Appositional growth is the result of continued proliferation of the cells that form the internal, chondrogenic layer of the perichondrium. Newly formed chondroblasts secrete matrix around themselves, creating superficial lacunae beneath the perichondrium. This continuing process adds additional surface, while the entrapped cells participate in interstitial growth. Apposition is thought to be most prevalent in mature cartilages, but interstitial growth must persist for long periods in epiphysial cartilages. Relatively little is known about the factors which determine the overall shape of a cartilage.

BONE

Bone, and the struts and levers which it forms, is exquisitely adapted to resist stress with suitable resilience, support the body and provide leverage for movement. It is a highly vascular mineralized connective tissue: the great majority of its cells are embedded in an extracellular matrix composed of organic materials (about 40% dry weight in mature bone) and inorganic salts rich in calcium and phosphate.

MACROSCOPIC ANATOMY OF BONE

Macroscopically, living bone is white. Its texture is either dense like ivory (compact bone), or honeycombed by large cavities (trabecular, cancellous or spongy bone), where the bony element is reduced to a latticework of bars and plates (trabeculae) (Fig. 5.8, Fig. 5.9). Compact bone is usually limited to the cortices of mature bones (cortical bone) and is of great importance in providing their strength. Its thickness and architecture vary for different bones, according to their overall shape, position and functional roles. The cortex plus the hollow medullary canal of long bones allows combination of strength with low weight. Cancellous bone is usually internal, giving additional strength to cortices and supporting the bone marrow. Bone forms a reservoir of metabolic calcium (99% of body calcium is in the bony skeleton) and phosphate which is under hormonal and cytokine control.

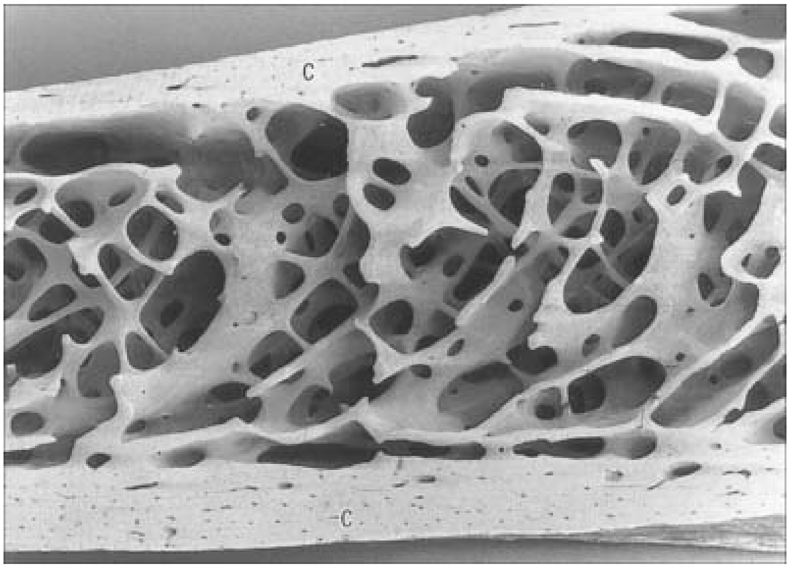

Fig. 5.8 Vertical section 2 cm below the anterosuperior border of the iliac crest (female, 42 years). The cancellous bone consists of intersecting curved plates and struts. Osteonal (Haversian) canals can just be seen in the two cortices (C) at this magnification.

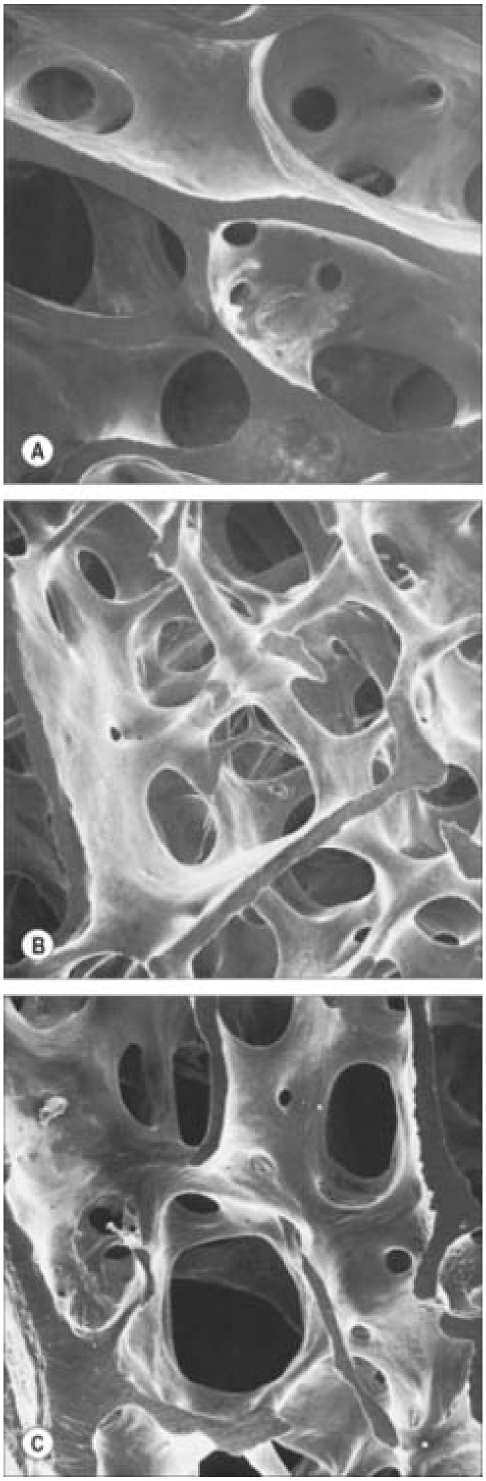

Fig. 5.9 Trabecular bone at different sites in the proximal part of the same human femur. All fields are at the same scale. **A**, Subcapital part of the neck; **B**, Greater trochanter; **C**, Rim of the articular surface of the head.

Note the wide variation in thickness, orientation and spacing of the trabeculae.

(Original photographs from Whitehouse WJ, Dyson ED 1974 Scanning electron microscope studies of trabecular bone in the proximal end of the human femur. J Anat 118: 417–414, by permission from Blackwell Publishing.)

The proportions of compact to cancellous bone vary greatly. In long bones, the diaphysis consists of a thick cylinder of compact bone with a few trabeculae and spicules on its inner surface. It encloses a large central medullary or marrow cavity that communicates freely with the intratrabecular spaces of the expanded bone ends. In other bones, especially flat bones such as the ribs, the interior is uniformly cancellous, and compact bone forms the surface. The cavities are usually filled with marrow, either red haemopoietic or yellow adipose, according to age and site. However, in some bones of the skull, notably the mastoid process of the temporal bone, and the paranasal sinuses of the maxilla, sphenoid and ethmoid, many of the internal cavities are filled with air, i.e. they are pneumatized.

Bones vary not only in their primary shape but also in lesser surface details, or secondary markings, which appear mainly in postnatal life. Most bones display features such as elevations and depressions (fossae), smooth areas and rough ridges. Numerous names are used to describe these secondary features. Some articular surfaces are called fossae (e.g. the glenoid fossa); lengthy depressions are grooves or sulci (e.g. the humeral bicipital sulcus); a notch is an incisura, and an actual gap is a hiatus. A large projection is termed a process or, if elongated and slender or pointed, a spine. A curved process is a hamulus or cornu (e.g. the pterygoid hamuli of the sphenoid bone and the cornua of the hyoid). A rounded projection is a tuberosity or tubercle, and occasionally a trochanter. Long elevations are crests, or lines, if they are less developed; crests are wider and present boundary edges or lips. An epicondyle is a projection close to a condyle and is usually a site where the common tendon of a superficial muscle group or the collateral ligament of the adjacent joint are attached. The terms protuberance, prominence, eminence and torus are less often applied to certain bony projections. The expanded proximal ends of many long bones are often termed the ‘head’ or caput (e.g. humerus, femur, radius). A hole in bone is a foramen, and becomes a canal when lengthy. Large holes may be called apertures or, if covered largely by connective tissue, fenestrae. Clefts in or between bones are fissures. A lamina is a thin plate; larger laminae may be called squamae (e.g. the temporal squama). Large areas on many bones are featureless and often smoother than articular surfaces, from which they differ because they are pierced by many visible vascular foramina. This texture occurs where muscle is directly attached to bone, and small blood vessels pass through the foramina from bone to muscle, and perhaps vice versa. Areas covered only by periosteum are similar, but vessels are less numerous.

Tendons are usually attached at roughened bone surfaces. Wherever any aggregation of collagen in a muscle reaches bone, surface irregularities correspond in form and extent to the pattern of such ‘tendinous fibres’. Such markings are almost always elevated above the general surface, as if ossification advanced into the collagen bundles from periosteal bone. How such secondary markings are induced is uncertain but they may result from the continued incorporation of new collagen fibres into the bone, perhaps necessary for minor functional adjustment. Evidence suggests that their prominence may be related to the power of the muscles involved and they increase with advancing years, as if the pull of muscles and ligaments exercised a cumulative effect over a limited area. Surface markings delineate the shape of attached connective tissue structures, whether these are an obvious tendon, intramuscular tendon or septum, aponeurosis, or tendinous fibres mediating what is otherwise a direct muscular attachment. These markings may be facets, ridges, nodules, rough areas or complex mixtures: they afford accurate indications of the junctions of bone with muscles, tendons, ligaments or articular capsules.

When a muscle is apparently attached directly to bone, its fibres do not themselves adhere directly to periosteum or bone. The route of transmission of tension from contracting muscle to bone is through the connective tissue that encapsulates (epimysium) and pervades (perimysium and endomysium) all muscles. These two forms of attachment of muscles, which are at the extremes of a range of admixtures, differ in the density of collagen fibres between muscle and bone. Where collagen is visibly concentrated, markings appear on the bone surface. In contrast, the multitude of microscopic connective tissue ties of direct attachment that occur over a larger area do not visibly mark the bone, and so it appears smooth to unaided vision and touch.

Bones display articular surfaces at synovial joints with their neighbours: if small, these are termed facets or foveae, larger, knuckle-shaped surfaces are condyles, and a trochlea is grooved like a pulley. Articular surfaces are smooth and adapted in shape to the movement of particular joints. In life they are covered by articular cartilage; they are smooth partly because they lack the vascular foramina typical of most other bone surfaces. Large tendons, e.g. those of adductor magnus and subscapularis, are attached to facets which lack the regular contours of articular surfaces, but which resemble them in texture, because they are poorly vascularized. These facets are sometimes depressed, but they may surmount large elevations, e.g. the humeral tubercles.

MICROSTRUCTURE OF BONE

Bone contains a mineralized extracellular matrix; specialized cells including osteoblasts, osteocytes and osteoclasts; and components of the periosteum, endosteum and marrow. These components will be described in detail below, first individually, and then in terms of their overall organization.

Bone matrix

Bone matrix is the mineralized extracellular material of bone; like general connective tissues, it consists of a ground substance in which numerous collagen fibres are embedded, usually ordered in parallel branching arrays (Fig. 5.10). In mature bone, the matrix is moderately hydrated, and 10–20% of its mass is water. Of its dry weight, 60–70% is made up of inorganic, mineral salts (mainly microcrystalline calcium and phosphate hydroxides, hydroxyapatite (see below), approximately 30% is collagen and the remainder is non-collagenous protein and carbohydrate, mainly conjugated as glycoproteins. The proportions of these components vary with age, location and metabolic status.

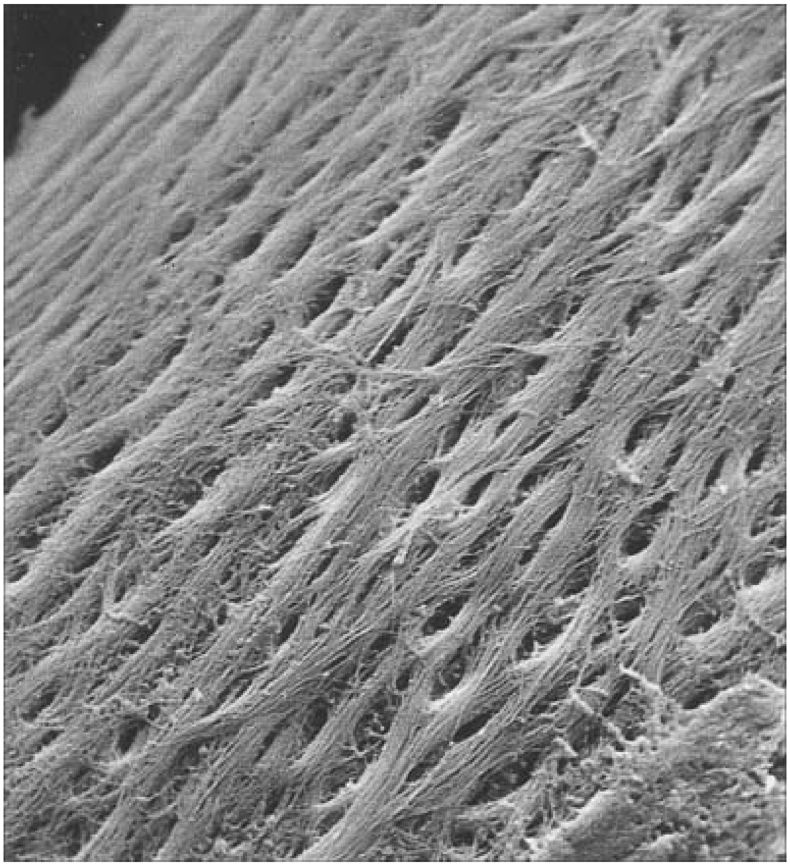

Fig. 5.10 Scanning electron micrograph of collagen fibres on the surface of human trabecular bone. Note branching fibres (female, 2 months, sixth rib).

Collagen

The collagen that is found in bone closely resembles that of many other connective tissues, and is mainly type I: there are trace amounts of type V which is thought to regulate fibrillogenesis. However, its molecular structure is unlike that of collagen in general connective tissue: it displays internal covalent cross-linkages, and the transverse spacings within its fibrils are somewhat larger. The cross-links make it stronger and chemically more inert, and the internal gaps provide the space for deposition of minerals. Up to two-thirds of the mineral content of bone is thought to be located within collagen fibrils. Crystal formation is probably initiated in the hole zones, which are gaps between the ends of tropocollagen subunits.

Collagen contributes greatly to the mechanical strength of bone, although its precise role in bone mechanics has yet to be clarified. As well as contributing to the tensile, compressive and shearing strengths of bone, the small degree of elasticity shown by collagen imparts a measure of resilience to the tissue, and helps to resist fracture when bone is mechanically loaded.

Collagen fibres are synthesized by osteoblasts, polymerize from tropocollagen extracellularly, and become progressively more cross-linked as they mature. In primary bone, they form a complex interwoven meshwork of non-lamellar woven or bundle bone, which in most sites is almost entirely replaced by regular laminar arrays of nearly parallel collagen fibres (lamellar bone). Partially mineralized collagen networks can be seen within osteoid on the outer and internal surfaces of bone, and in the endosteal linings of vascular canals. Collagen fibres from the periosteum are incorporated in cortical bone (extrinsic fibres), and anchor this fibrocellular layer at its surface. Terminal collagen fibres of tendons and ligaments are incorporated deep into the matrix of cortical bone. They may be interrupted by new osteons during cortical drift (modelling) and turnover (remodelling), and remain as islands of interstitial lamellae or even trabeculae.

Non-collagenous organic components

Small amounts of various complex macromolecules are attached to collagen fibres and surrounding bone crystals. These are secreted by osteoblasts and young osteocytes and include osteonectin, osteocalcin, the bone proteoglycans biglycan and decorin, the bone sialoproteins osteopontin and thrombospondin, many growth factors including transforming growth factor β (TGF-β), proteases and protease inhibitors, often in a latent form. The functions of some of these molecules are described with osteoblasts (see below).

Bone minerals

Bone minerals are the inorganic constituents of the bone matrix. They confer the hardness and much of the rigidity of bone, and are the main reason that bone is easily seen on radiographs (bone has to be 50% mineralized to be visible on radiographs produced with a standard X-ray unit). The mineral substances of bone are mostly acid-soluble. If they are removed, using calcium chelators such as citrates or ethylene diamine tetra-acetic acid (EDTA), the bone retains its shape but becomes highly flexible.

The mineral portion of mature bones is composed largely of crystals made of a substance generally referred to as hydroxyapatite (but with an important carbonate content, and a lower Ca/P ratio than pure hydroxyapatite (Ca_{10} $(PO_4)_6$ $(OH)_2$), together with a small amount of calcium phosphate. Bone crystals are small but have a large surface area. They take the form of thin plates or leaf-like structures and range in size up to 150 nm long × 80 nm wide × 5 nm thick, although most are half that size. They are often packed quite closely together, with their long axes nearly parallel to the axes of the collagen fibrils. The narrow gaps between the crystals contain associated water and organic macromolecules.

The major ions which make up the mineral part of bone include calcium, phosphate, hydroxyl and carbonate. Less numerous ions are citrate, magnesium, sodium, potassium, fluoride, chloride, iron, zinc, copper, aluminium, lead, strontium, silicon and boron, many of which are present only in trace quantities. Fluoride ions can substitute for hydroxyl ions, and carbonate can substitute for either hydroxyl or phosphate groups. Group IIA cations, e.g. radium, strontium and lead, all readily substitute for calcium and are therefore known as bone-seeking cations. Since they can be either radioactive or chemically toxic, their presence in bone, where they may be close to haemopoietic bone marrow, may cause illness and characteristic appearances on X-rays.

The concentration of mineral in young osteons is low but increases with age: it is highest in the older, more peripheral, lamellae. Mineral distribution is uniform in established, highly mineralized, osteons. Mineralization normally reaches 70–80% in 3 weeks. Immature woven bone mineralizes faster and can be identified from adjacent lamellar bone by its higher degree of mineralization. Osteons may show one or more highly mineralized arrest lines within their walls.

Osteoblasts

Osteoblasts are derived from osteoprogenitor (stem) cells of mesenchymal origin, which are present in the bone marrow and other connective tissues. They proliferate and differentiate, stimulated by bone morphogenetic proteins (BMPs), into osteoblasts prior to bone formation. Osteoblasts are basophilic, roughly cuboidal mononuclear cells 15–30 µm across. Ultrastructurally, they have features typical of protein-secreting cells. They are found on the forming surfaces of growing or remodelling bone, where they constitute a covering layer (Fig. 5.11). In relatively quiescent adult bones they appear to be present mostly on endosteal rather than periosteal surfaces, but they also occur deep within compact bone where osteons are being remodelled. They are responsible for the synthesis, deposition and mineralization of the bone matrix, which they secrete. Once embedded in the matrix, they become osteocytes.

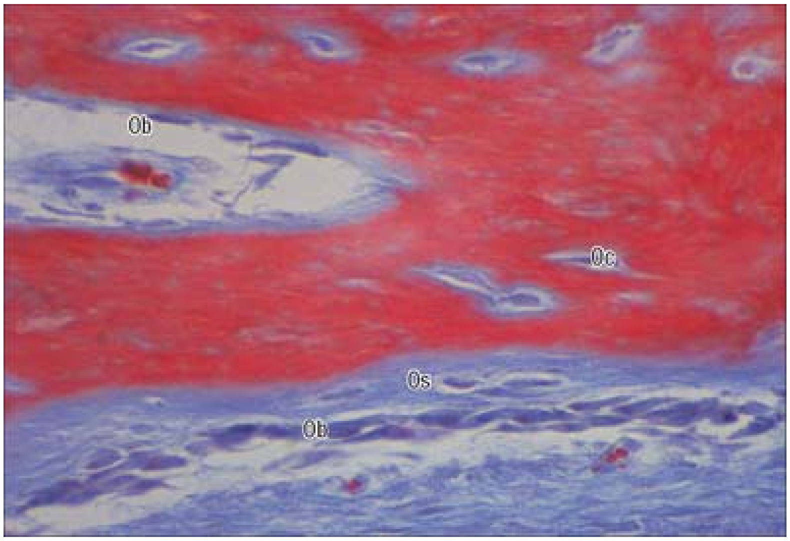

Fig. 5.11 Osteoblasts (Ob) covering the free surfaces of developing bone in a human fetal hand. Deep to the layer of osteoblasts in the lower field is a layer of osteoid matrix (Os, pale blue) which has yet to be mineralized. Osteocytes (Oc) are shown within lacunae in mineralized matrix (red).

Osteoblasts contain prominent bundles of actin, myosin and other cytoskeletal proteins which are associated with the maintenance of cell shape, attachment and motility. Their plasma membranes display many extensions, some of which contact neighbouring osteoblasts and embedded osteocytes at intercellular gap junctions. This arrangement facilitates coordination of the activities of groups of cells, e.g. in the formation of large domains of parallel collagen fibres.

Osteoblasts synthesize and secrete organic matrix, i.e. type I collagen, small amounts of type V collagen, and numerous other macromolecules involved in bone formation and resorption. Collagen synthesis occurs in the rough endoplasmic reticulum and Golgi apparatus, and type I collagen is secreted as monomers which assemble into the triple helical procollagen extracellularly. Other glycoprotein products include osteocalcin, which is required for bone mineralization, binds hydroxyapatite and calcium, and is used as a marker of new bone formation; osteonectin, a phosphorylated glycoprotein which binds strongly to hydroxyapatite and collagen – it may play a role in initiating hydroxyapatite crystallization, and may also be a cell adhesion factor; RANKL, the cell surface ligand for RANK (receptor for activation of nuclear factor kappa B), which is an osteoclast progenitor receptor (see below); osteoprotegerin (a soluble, high affinity decoy ligand for RANKL) which restricts osteoclast differentiation; the bone proteoglycans biglycan and decorin which bind TGF-β; bone sialoproteins, osteopontin and thrombospondin, which mediate osteoclast adhesion to bone surfaces via binding to osteoclast integrins; latent proteases and growth factors, including BMPs. TGF-β is secreted by osteoblasts as well as osteoclasts: it is activated in the acid conditions of the ruffled border zone of the osteoclast, and may be a coupling factor for stimulating new bone formation at resorption sites.

Extracellular fluid is supersaturated with respect to the basic calcium phosphates, yet mineralization is not a widespread phenomenon. Osteoblasts play a significant role in the mineralization of osteoid, the unmineralized organic matrix. They secrete osteocalcin which binds calcium weakly, but at levels sufficient to concentrate the ion locally. They also contain membrane-bound vesicles, 0.1–0.2 μm in diameter, which contain alkaline phosphatase (which can cleave phosphate ions from various molecules to elevate concentrations locally), and pyrophosphatase (which degrades inhibitory pyrophosphate in the extracellular fluid). The vesicles bud off from the cell surfaces of the osteoblasts into newly formed osteoid and are the sites of initiation of hydroxyapatite crystal formation in newly forming bone (see below). Crystals are then released into the osteoid matrix by an unknown mechanism. Some alkaline phosphatase reaches the blood circulation where it can be detected in conditions of rapid bone formation or turnover.

Osteoblasts play a key role in the hormonal regulation of bone resorption, since they express receptors for parathyroid hormone (PTH), 1,25-dihydroxy vitamin D3 and other promoters of bone resorption. During bone resorption, osteoblasts promote osteoclast differentiation via PTH-activated expression of cell surface RANKL, which binds to RANK on immature osteoclasts, establishes cell–cell contact and triggers contact-dependent osteoclast differentiation. In the presence of PTH, osteoblasts also downregulate secretion of osteoprotegerin, a soluble decoy ligand with higher affinity for RANKL. In conditions favouring bone deposition, secreted osteoprotegerin blocks RANKL binding to RANK and restricts numbers of mature osteoclasts. (For a recent review, see Blair et al 2007.)

Bone-lining cells are flattened epithelioid cells found on the surfaces of adult bone that is not undergoing active deposition or resorption, and are generally considered to be quiescent osteoblasts or osteoprogenitor cells. They form the outer boundary of the marrow tissue on the endosteal surface of marrow cavities, are present on the periosteal surface, and line the system of vascular canals within osteons.

Osteocytes

Osteocytes constitute the major cell type of mature bone, and are scattered within its matrix, interconnected by numerous dendritic processes to form a complex cellular network (Fig. 5.12). They are derived from osteoblasts and are enclosed within their matrix but, unlike chondrocytes, they do not divide. Bone growth is appositional: new layers are added only to pre-existing surfaces and so, again unlike chondrocytes, osteocytes enclosed in lacunae do not secrete new matrix. The rigidity of mineralized bone matrix prevents internal expansion, which means that interstitial growth, which is characteristic of most tissues, does not occur in bone. Osteocytes retain contacts with each other and with cells at the surfaces of bone (osteoblasts and bone-lining cells) throughout their lifespan.

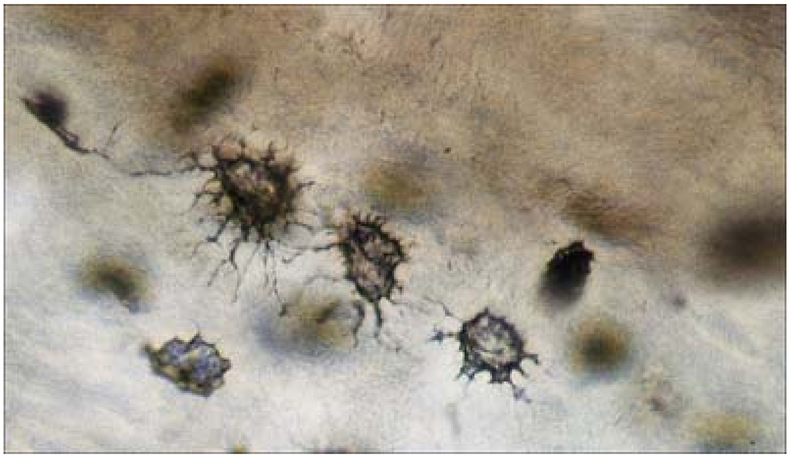

Fig. 5.12 Osteocyte lacunae shown at high magnification in a dry ground section of lamellar bone. The territories of three osteocytes are shown. Their branching dendrites contact those of neighbouring cells via the canaliculi seen here within the bone matrix. Several other osteocyte lacunae are present, out of the focal plane in this section, and tangential to the osteon axis.

Mature, relatively inactive, osteocytes possess an ellipsoid cell body with the longest axis (25 µm) parallel to the surrounding bony lamella. The rather narrow rim of cytoplasm is faintly basophilic, contains relatively few organelles and surrounds an oval nucleus. Osteocytes in woven bone are larger and more irregular in shape (Fig. 5.13).

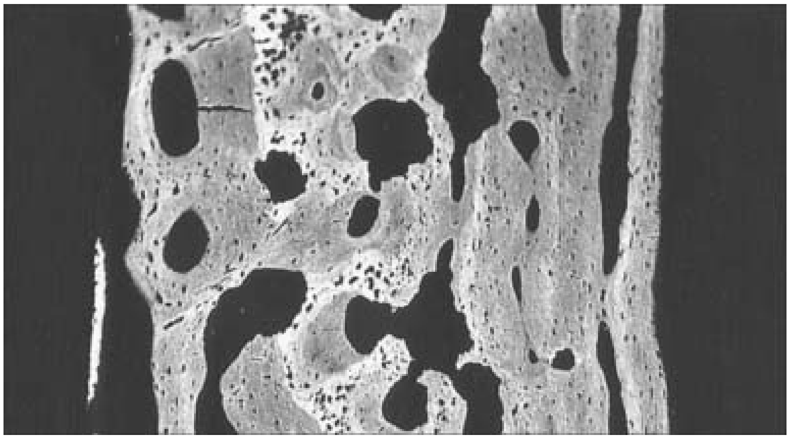

Fig. 5.13 Human parietal bone (male neonate) showing primary osteonal bone (grey) and woven bone (white) containing many connecting osteocyte lacunae (black). Internal resorption of the bone has produced large irregular dark spaces (trabecularization).

Numerous fine dendritic processes emerge from the cell body of each osteocyte and branch a number of times. They contain bundles of microfilaments and some smooth endoplasmic reticulum. At their distal tips they contact the processes of adjacent cells, i.e. other osteocytes and, at surfaces, osteoblasts and bone-lining cells. They form communicating gap junctions with these cells which means that they are in electrical and metabolic continuity.

Bone matrix surrounds the cell bodies and processes. There appears to be a variable space filled with extracellular fluid between each osteocyte and its enclosing wall. Each cell body lies in a lacuna from which many narrow, branched channels extend. These channels or canaliculi are 0.5–0.25 μm wide, and contain the dendritic processes of the osteocytes: they provide a route for the diffusion of nutrients, gases and waste products between the osteocytes and the blood vessels. Canaliculi do not usually extend through and beyond the reversal line surrounding an osteon and so do not communicate with neighbouring systems. The walls of lacunae may be lined with a variable (0.2–2 μm) layer of unmineralized organic matrix.

In well-vascularized bone, osteocytes are long-lived cells which actively maintain the bone matrix. The average lifespan of an osteocyte varies with the metabolic activity of the bone and the likelihood that it will be remodelled, but is measured in years. Old osteocytes may retract their processes from the canaliculi; when they die, their lacunae and canaliculi may become plugged with cell debris and minerals, which hinders diffusion through the bone. Dead osteocytes occur commonly in interstitial bone and the inner regions of trabecular bone which escape surface remodelling, and are particularly noticeable by the second and third decades. Bones which experience little turnover, e.g. the auditory ossicles, are most likely to contain aged osteocytes and low osteocyte viability.

Osteocytes play an essential role in the maintenance of bone: their death leads to the resorption of the matrix by osteoclast activity. They remain responsive to parathyroid hormone and 1,25$(OH)_2$ vitamin D_3, and it is possible that they are involved in mineral exchange at adjacent bone surfaces. Osteocytes themselves are often mineralized.

Osteoclasts

Osteoclasts are large (40 μm or more) polymorphic cells containing up to 20 oval, closely packed nuclei. They lie in close contact with the bone surface in resorption bays (Howship's lacunae). Their cytoplasm contains numerous mitochondria and vacuoles, many of which are acid phosphatase-containing lysosomes. The rough endoplasmic reticulum is relatively sparse given the size of cell, but the Golgi complex is extensive. The cytoplasm also contains numerous coated transport vesicles and microtubule arrays involved in the transport of the vesicles between the Golgi stacks and the ruffled membrane, which is the highly infolded cell surface of active osteoclasts at sites of local bone resorption. A well-defined zone of actin filaments and associated proteins occurs beneath the ruffled membrane around the circumference of the resorption bay, in a region termed the sealing zone.

Functionally, osteoclasts are responsible for the local removal of bone during bone growth and subsequent remodelling of osteons and surface bone (see Fig. 5.25). They cause demineralization by proton release, which creates an acidic local environment, and organic matrix destruction by releasing lysosomal (cathepsin K) and non-lysosomal (e.g. collagenase) enzymes.

Factors stimulating osteoclasts to resorb bone include osteoblast-derived signals; cytokines from other cells, e.g. macrophages and lymphocytes; blood-borne factors, e.g. parathyroid hormone and 1,25(OH)$_2$ vitamin D$_3$ (calcitriol). Calcitonin, produced by C cells of the thyroid follicle, reduces osteoclast activity.

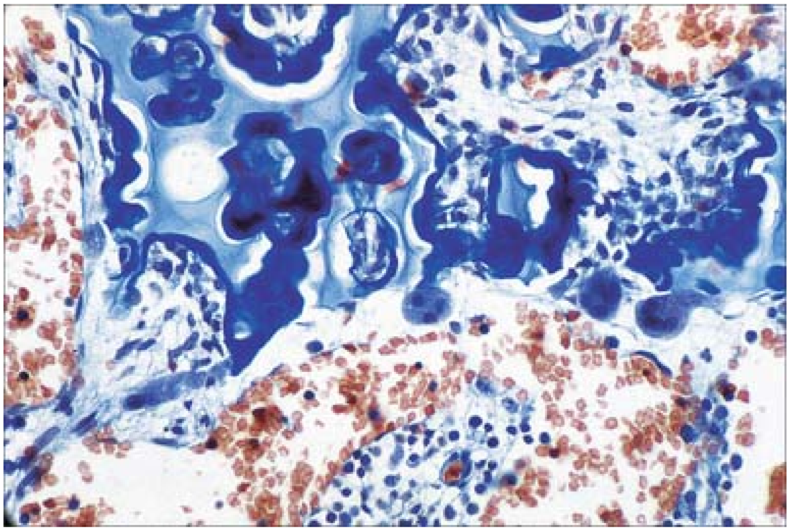

Fig. 5.25 Endochondral ossification in human fetal bone. Spicules of cartilage remnant (pale blue) serve as surfaces for the deposition of osteoid (dark blue), shown in the upper half of the field. Mineralized, woven bone is stained red. Three large multinucleate osteoclasts are seen centre right, further eroding cartilage and remodelling the developing bone. Blood sinusoids and haemopoietic tissue (below) fill the spaces between areas of ossification. Heidenhain's azan trichrome preparation.

Osteoclasts arise by fusion of monocytes derived from the bone marrow or other haemopoietic tissue. They probably share a common ancestor with macrophages within the granulocyte–macrophage lineage (see Fig. 4.12) but it is thought that they subsequently follow a distinct differentiation pathway.

Osteons

The mechanical properties of bone, particularly its strength and resilience, are dependent on the general composition of its matrix. Woven and lamellar bone display two quite distinct types of organization.

In woven, or bundle, bone, the collagen fibres and bone crystals are irregularly arranged. The diameters of the fibres vary, so that fine and coarse fibres intermingle, producing the appearance of the warp and weft of a woven fabric. Woven bone is typical of young fetal bones, but is also seen in adults during excessively rapid bone remodelling and repair of fractures (Fig. 5.14). It is formed by highly active osteoblasts during development, and is stimulated in the adult by fracture, growth factors, or prostaglandin E_2.

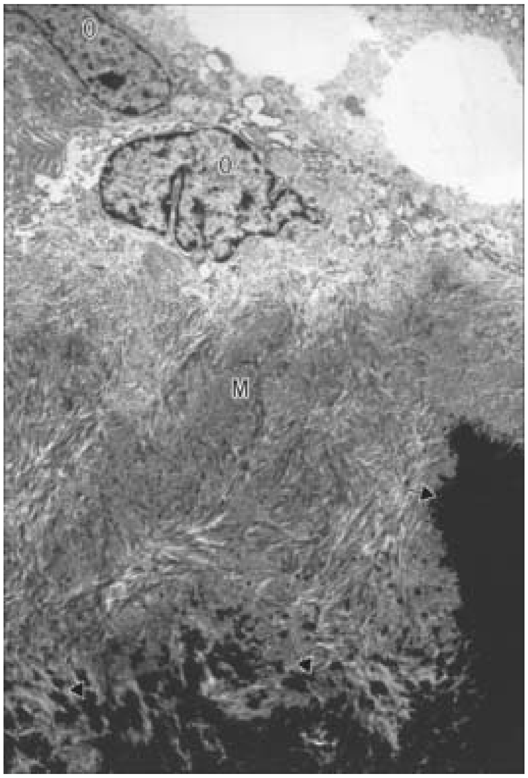

Fig. 5.14 Electron micrograph of woven bone from a failed fracture of human distal tibia. Two osteoblasts (O) lie on the free surface (top). Newly synthesized collagenous osteoid matrix (M) is seen in the centre field, with a mineralization front (electron-dense area) below (arrows).

Lamellar bone makes up almost all of an adult osseous skeleton (Fig. 5.15, Fig. 5.16). The precise arrangement of lamellae varies from site to site, particularly between compact cortical bone and the trabecular bone within. In many bones a few lamellae form continuous circumferential layers at the outer (periosteal) and inner (endosteal) surfaces. However, by far the greatest proportion of lamellae are arranged in concentric cylinders around neurovascular channels called Haversian canals, to form the basic units of bone tissue which are the Haversian systems or osteons. Osteons usually lie parallel with each other (Fig. 5.17) and, in elongated bones such as those of the appendicular skeleton, with the long axis of the bone. They may also spiral, branch or intercommunicate, and some end blindly.

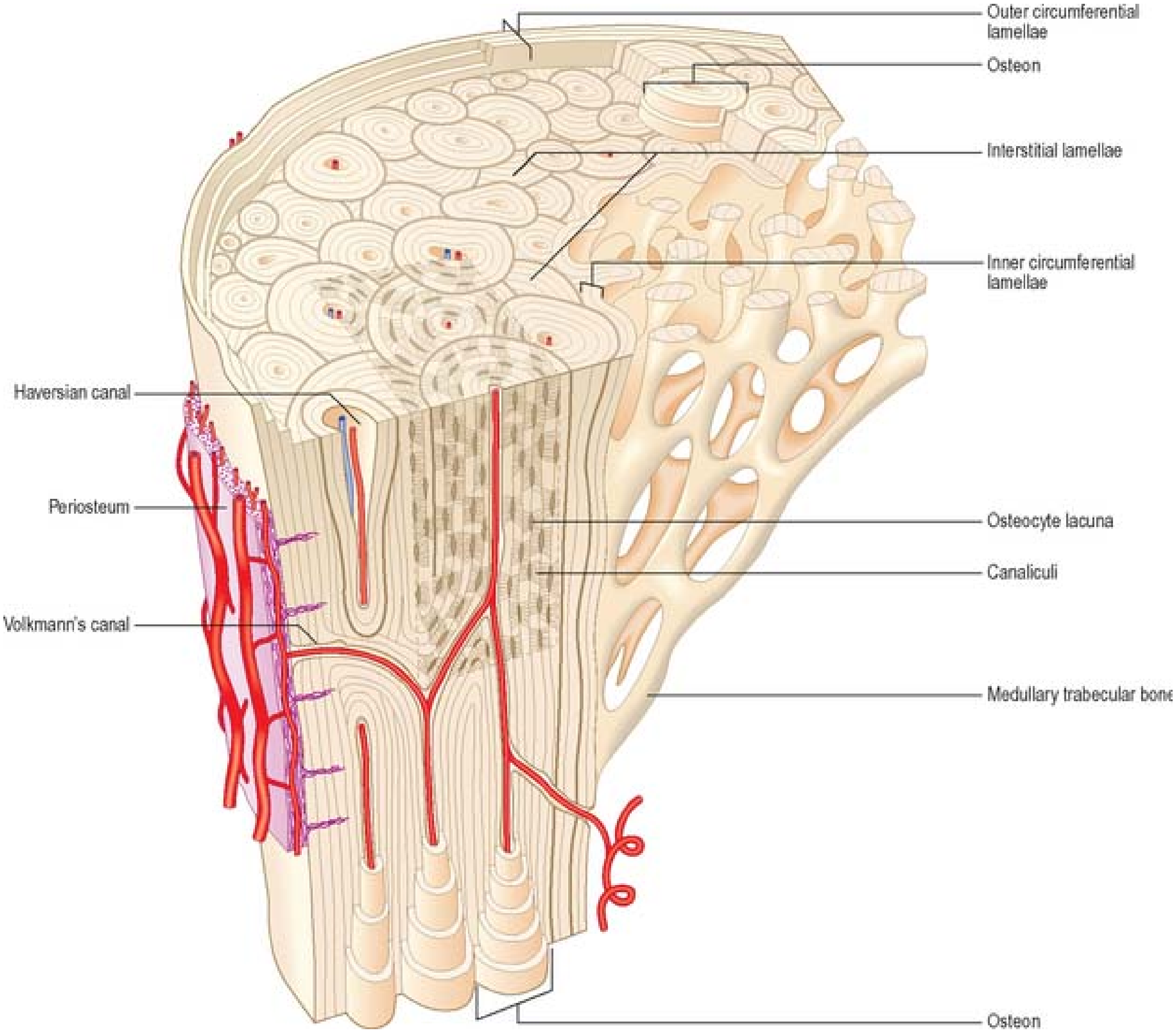
Outer circumferential lamellae
Osteon
Interstitial lamellae
Inner circumferential lamellae
Haversian canal
Periosteum
Volkmann's canal
Osteocyte lacuna
Canaliculi
Medullary trabecular bone
Osteon

Fig. 5.15 Main features of the microstructure of mature lamellar bone. Areas of compact and trabecular (cancellous) bone are included. Note the general construction of the osteons; distribution of the osteocyte lacunae;

Haversian canals and their contents; resorption spaces. Different views of the structural basis of bone lamellation.

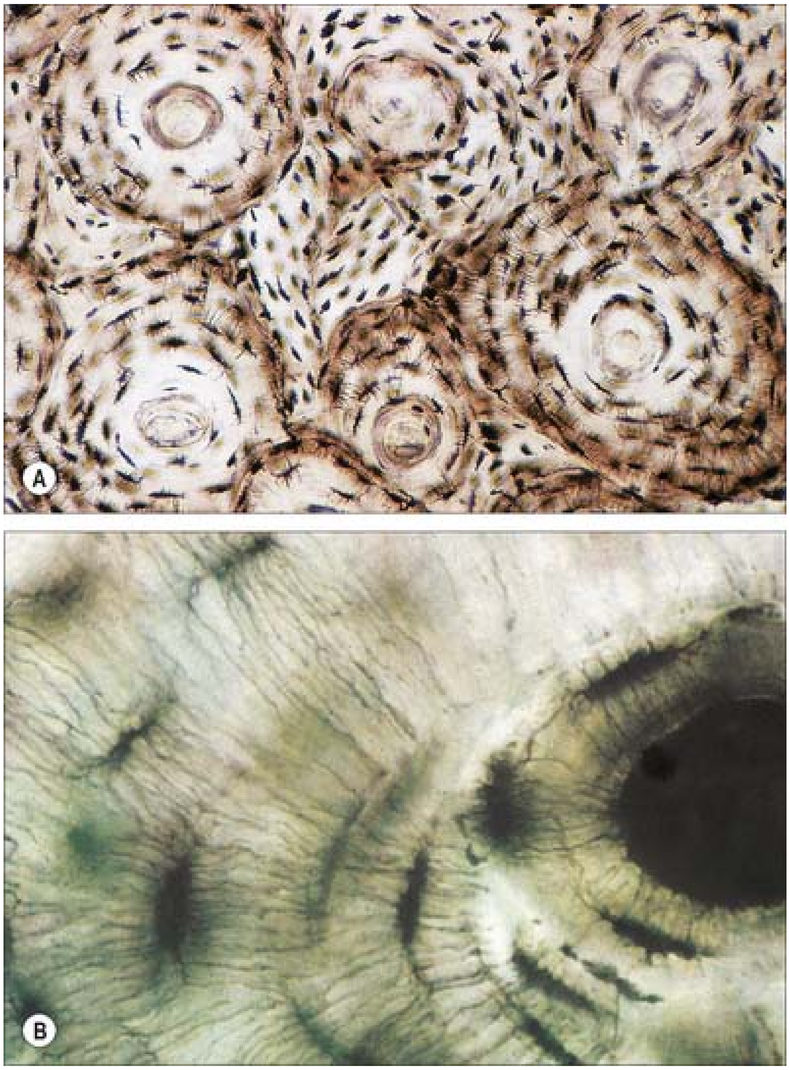

Fig. 5.16 **A**, Osteons in a dry ground transverse section of bone. Concentric lamellae surround the central Haversian canal of each complete osteon; they contain the dark lacunae of osteocytes and the canaliculi which are occupied in life by their dendrites. These canaliculi interconnect with canaliculi of osteocytes in adjacent lamellae. Incomplete (interstitial) lamellae (e.g. centre field) are the remnants of osteons remodelled by osteoclast erosion. **B**, High-power view of osteocytes within lamellae; a Haversian canal is seen on the right.

*(**B**, Photograph by Sarah-Jane Smith.)*

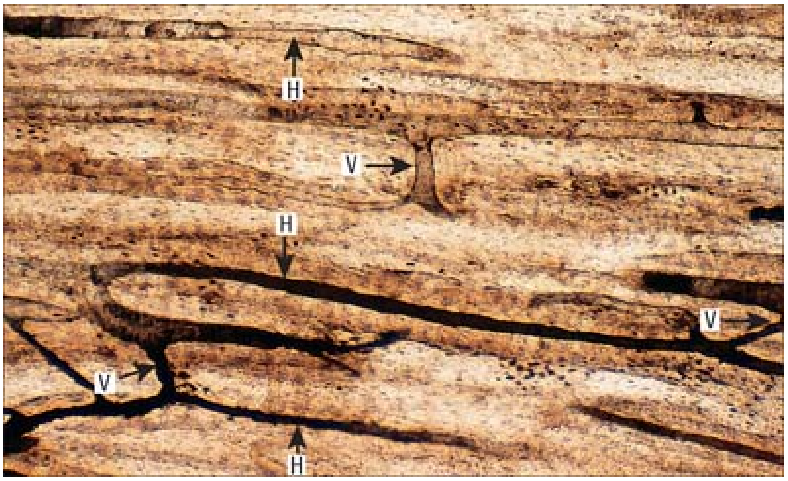

Fig. 5.17 Osteons in a dry ground longitudinal section of bone. The central Haversian canals (H: tubular structures, mainly dark) show transverse nutrient (Volkmann's) canals (V) which form bridges between adjacent osteons and their blood vessels.

It has been estimated that there are 21 million osteons in the adult skeleton. In transverse section they are round or ellipsoidal, varying from 100 to 400 µm in diameter. A medium-sized osteon contains about 30 lamellae, each approximately 3 µm thick. Each osteon is permeated with the canaliculi of its resident osteocytes, and these form pathways for diffusion of nutrients, gases, etc. between the vascular system and the osteocytes. The maximum diameter of an osteon ensures that no osteocyte is more than 200 µm from a blood vessel, a distance that may be a limiting factor in cellular survival. The spaces between osteons contain interstitial lamellae which are the fragmentary remains of osteons and the partially eroded circumferential lamellae of older bone (see below).

The central Haversian canals of osteons vary in size, with a mean diameter of 50 µm; those near the marrow cavity are somewhat larger. Each canal contains one or two capillaries lined by fenestrated endothelium and surrounded by a basal lamina which also encloses typical pericytes. They usually contain a few unmyelinated and occasional myelinated axons. The bony surfaces of osteonic canals are perforated by the openings of osteocyte canaliculi and are lined by collagen fibres.

Haversian canals communicate with each other and directly or indirectly with the marrow cavity via vascular (nutrient) channels called Volkmann's canals, which run obliquely or at right angles to the long axes of the osteons (Fig. 5.17). The majority of these channels appear to branch and anastomose, but some join large vascular connections with vessels in the periosteum and the medullary cavity.

Osteons are distinguished from their neighbours by a cement line which contains little or no collagen, and is strongly basophilic because it has a high content of glycoproteins and proteoglycans. Cement lines mark the limit of bone erosion prior to the formation of a new osteon, and are therefore also known as reversal lines. Canaliculi occasionally pass through cement lines, and so provide a route for exchange between interstitial bone lamellae and vascular channels within osteons. Basophilic lines can occur in the absence of erosion: they indicate where bony growth has been interrupted and then resumed and are called resting lines.

Each lamella consists of a sheet of mineralized matrix that contains collagen fibres of similar orientation locally, running in branching bundles 2–3 µm thick, and often extending the full width of a lamella. This interconnecting, three-dimensional construction increases the strength of the bone. The orientation of the collagen fibres and associated mineral crystals differs in adjacent lamellae: the difference varies between 0° and 90°, and is clearly shown by polarized light microscopy. A less perfect packing of collagen fibrils into bundles occurs at the borders of lamellae, where intermediate and random orientations predominate. The main direction of the collagen fibres within osteons of long bone shafts varies: the fibres are more longitudinal at sites which are subjected predominantly to tension, and more oblique at sites subjected mostly to compression. The peripheral lamellae of osteons contain more transverse fibres at any site in a diaphysis.

Trabecular bone

The organization of trabecular (cancellous, spongy) bone is basically lamellar, as shown most clearly under polarized light (Fig. 5.18). It takes the form of branching and anastomosing curved plates, tubes and bars of various widths and lengths which surround marrow cavities and are lined by endosteal tissue (Fig. 5.8, Fig. 5.9). Their thickness ranges from 50 to 400 μm. In general, bone lamellae are oriented parallel with the adjacent bone surface, and the arrangement of cells and matrix is similar to that found in circumferential and osteonic bone. Thick trabeculae and regions close to compact bone may contain small osteons, but blood vessels do not otherwise lie within the bony tissue, and osteocytes therefore rely on canalicular diffusion from adjacent medullary vessels. In young bone, calcified cartilage may occur in the cores of trabeculae, but this is generally replaced by bone during subsequent remodelling.

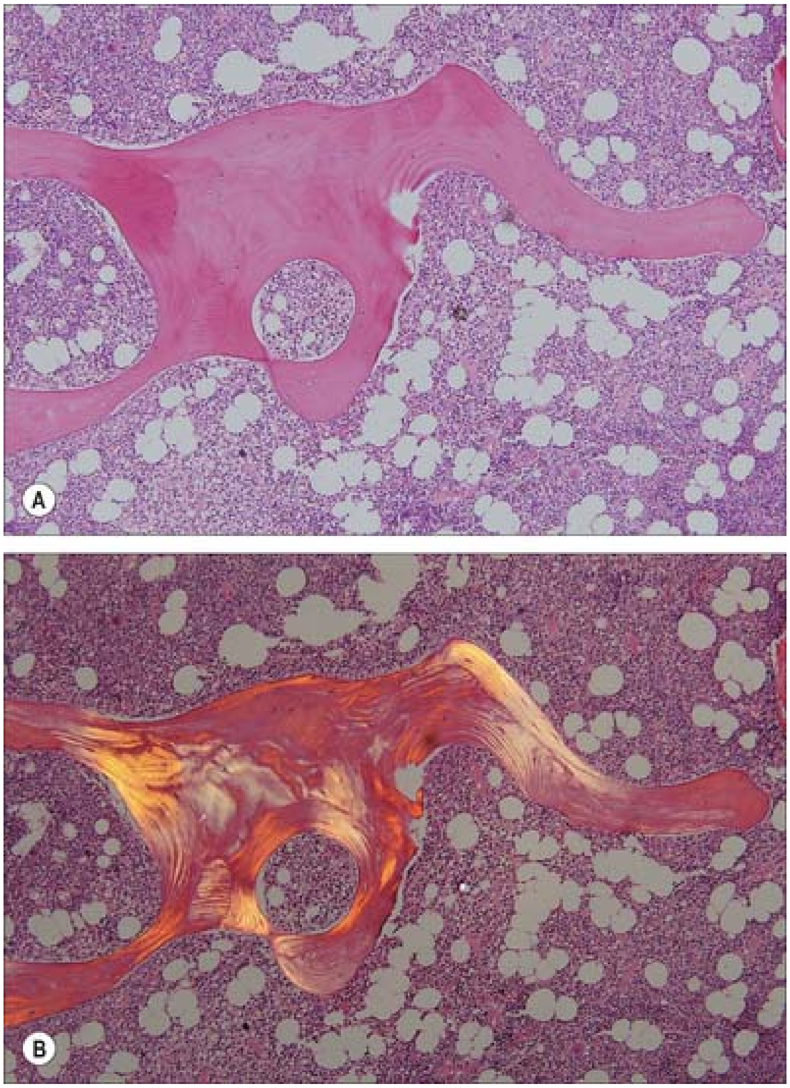

Fig. 5.18 Trabecular bone in a bone marrow sample taken from the human posterior iliac crest. **A**, Irregular trabeculae of bone, surrounded by bone marrow haemopoietic and adipose tissue (haematoxylin and eosin stain); **B**, the same field viewed under polarized light, demonstrating lamellar, non-osteonic bone with lamellae oriented in different directions in different regions. Osteocytes are just visible, embedded in the solid matrix.

Remodelling

Remodelling of the interior of a bone depends upon the balance of resorption and deposition of bone, i.e. on the balanced activities of osteoclasts and osteoblasts. Osteoclasts first excavate a cylindrical tunnel by concerted action. A ‘cutting cone’ is formed by groups of osteoclasts moving at 50 µm/day, followed by osteoblasts which fill in the space so created. The osteoblasts deposit new osteoid matrix concentrically around a centrally ingrowing blood vessel, starting at the peripheral surface of the tunnel. This forms a ‘closing cone’ with 4000 osteoblasts/mm^2. Deposition of successive, concentric lamellae follows, as cohorts of osteoblasts become embedded in the matrix they secrete, and are succeeded by new osteoblasts which line the free surface thus created, and secrete the next layer. In this way the walls of resorption cavities are lined with new lamellar matrix, and the vascular channels are progressively narrowed (Fig. 5.19). The pattern and extent of remodelling is dictated by the mechanical loads applied to the bone.

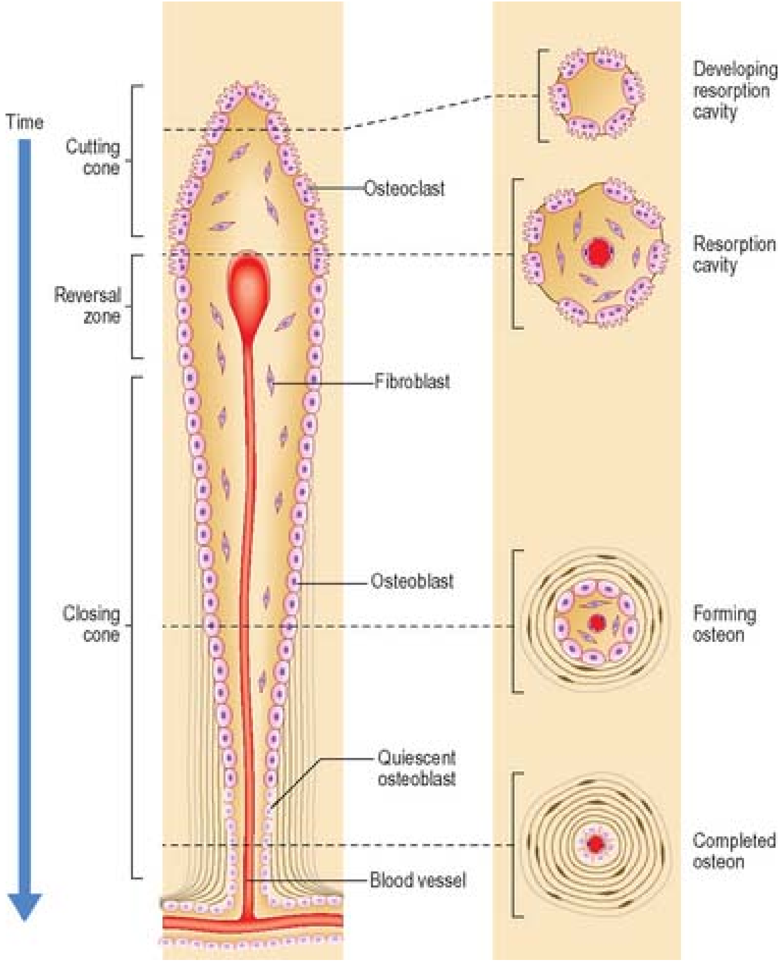
Time
Cutting cone
Reversal zone
Closing cone
Osteoclast
Fibroblast
Osteoblast
Quiescent osteoblast
Blood vessel
Developing resorption cavity
Resorption cavity
Forming osteon
Completed osteon

Fig. 5.19 Bone remodelling. Longitudinal and cross-sections of a time line illustrating the formation of an osteon. Osteoclasts cut a cylindrical

channel through bone. Osteoblasts follow, laying down bone on the surface of the channel until matrix surrounds the central blood vessel of the newly formed osteon (closing cone of a new osteon).

A hypermineralized basophilic cement line marks a site of reversal from resorption to deposition. Formation of osteons does not end with growth but continues variably throughout life. Remnants of circumferential lamellae of old osteons form interstitial lamellae between newer osteons (Fig. 5.15, Fig. 5.16A).

It has been estimated that approximately 10% of the adult bony skeleton turns over each year by the process of remodelling. The degree of remodelling varies with age and the number of osteons and osteon fragments have therefore been used in attempts to estimate the age of skeletal material at death.

Periosteum, endosteum and bone marrow

The outer surface of bone is covered by a condensed, fibrocollagenous layer, the periosteum. The inner surface is lined by a thinner, more cellular, endosteum. Osteoprogenitor cells, osteoblasts, osteoclasts and other cells important in the turnover and homeostasis of bone tissue lie in these layers.

The periosteal layer is tethered to the underlying bone by extrinsic collagen fibres, Sharpey's fibres, which penetrate deep into the outer cortical bone tissue. It is absent from articular surfaces, and from the points of insertion of tendons and ligaments (entheses) (see Fig. 5.46). The periosteum is highly active during fetal development, when it generates osteoblasts for the appositional growth of bone. These cells form a layer, two to three cells deep, between the fibrous periosteum and new woven bone matrix. Osteoprogenitor cells within the mature periosteum are indistinguishable morphologically from fibroblasts. Periosteum is important in the repair of fractures: where it is absent, e.g. within the joint capsule of the femoral neck, fractures are slow to heal.

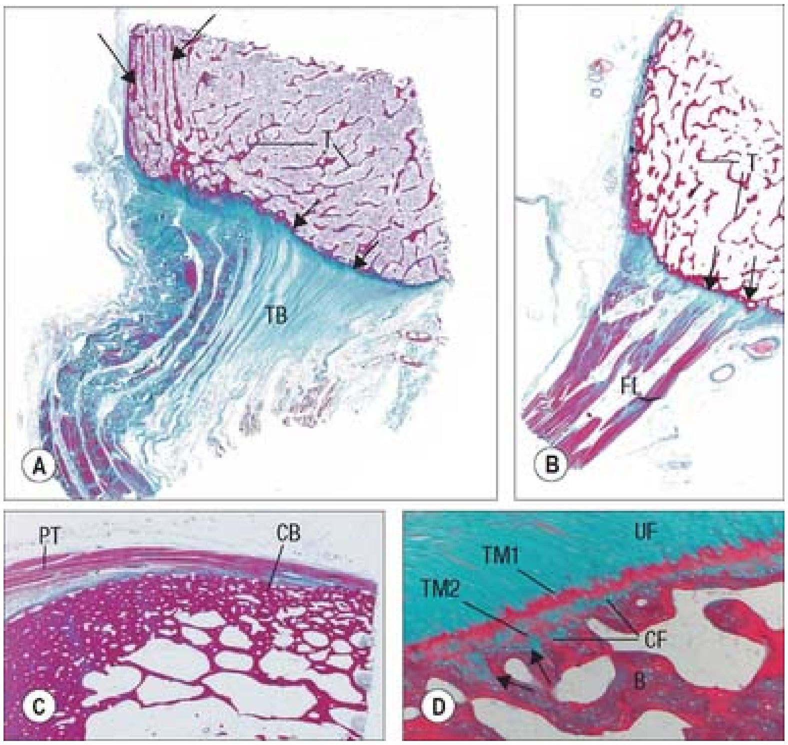

Fig. 5.46 The microstructure of bone at entheses. **A**, **B**, The cortical shell of bone (short arrows) is very thin at fibrocartilaginous attachment sites. In these examples showing the attachment of the tendons of triceps brachii (TB) and of fibularis longus (FL), it is approximately the same thickness as the underlying trabeculae (T). Note that in **A**, the superficial trabeculae (long arrows) are aligned along the direction of pull of the tendon of triceps. **C**, In marked contrast, the layer of cortical bone (CB) at the fibrous attachment site of pronator teres (PT) to the mid-shaft of the radius, is much thicker. **D**, Higher power view of the cortical calcified shell of tissue at a fibrocartilaginous attachment site (the Achilles tendon), which consists of bone (B) and calcified fibrocartilage (CF). In this specimen, there are two tidemarks, TM1 and TM2, associated with the cortical shell of calcified tissue. TM1 is adjacent to the zone of uncalcified fibrocartilage (UF), and marks the mechanical boundary between hard and soft tissues. TM2 lies nearer the bone and indicates an earlier phase of calcification. Note the relative straightness of the tidemarks but the highly irregular interface between calcified fibrocartilage and bone (arrows), which is important in

anchoring the tendon to the bone. Sections of human cadaveric bone stained with Masson’s trichrome.

(Photographs provided by courtesy of Professor Michael Benjamin from sections cut and stained by S. Redman.)

In resting adult bone, quiescent osteoblasts and osteoprogenitor cells are present chiefly on the endosteal surfaces, which act as the principal reservoir of new bone-forming cells for remodelling or repair. The endosteum provides a surface of approximately 7.5 m^2, thought to be important in calcium homeostasis. It is formed by flattened osteoblast precursor cells and reticular (type III collagen) fibres, and lines all the internal cavities of bone, including the Haversian canals. It overlies the endosteal circumferential lamellae, and encloses the medullary cavity.

NEUROVASCULAR SUPPLY OF BONE

Vascular supply and lymphatic drainage

The osseous circulation supplies bone tissue, marrow, perichondrium, epiphysial cartilages in young bones, and, in part, articular cartilages. The vascular supply of a long bone depends on several points of inflow which feed complex and regionally variable sinusoidal networks within the bone. The sinusoids drain to venous channels which leave through all surfaces that are not covered by articular cartilage. The flow of blood through cortical bone in the shafts of long bones is mainly centrifugal (Fig. 5.20).

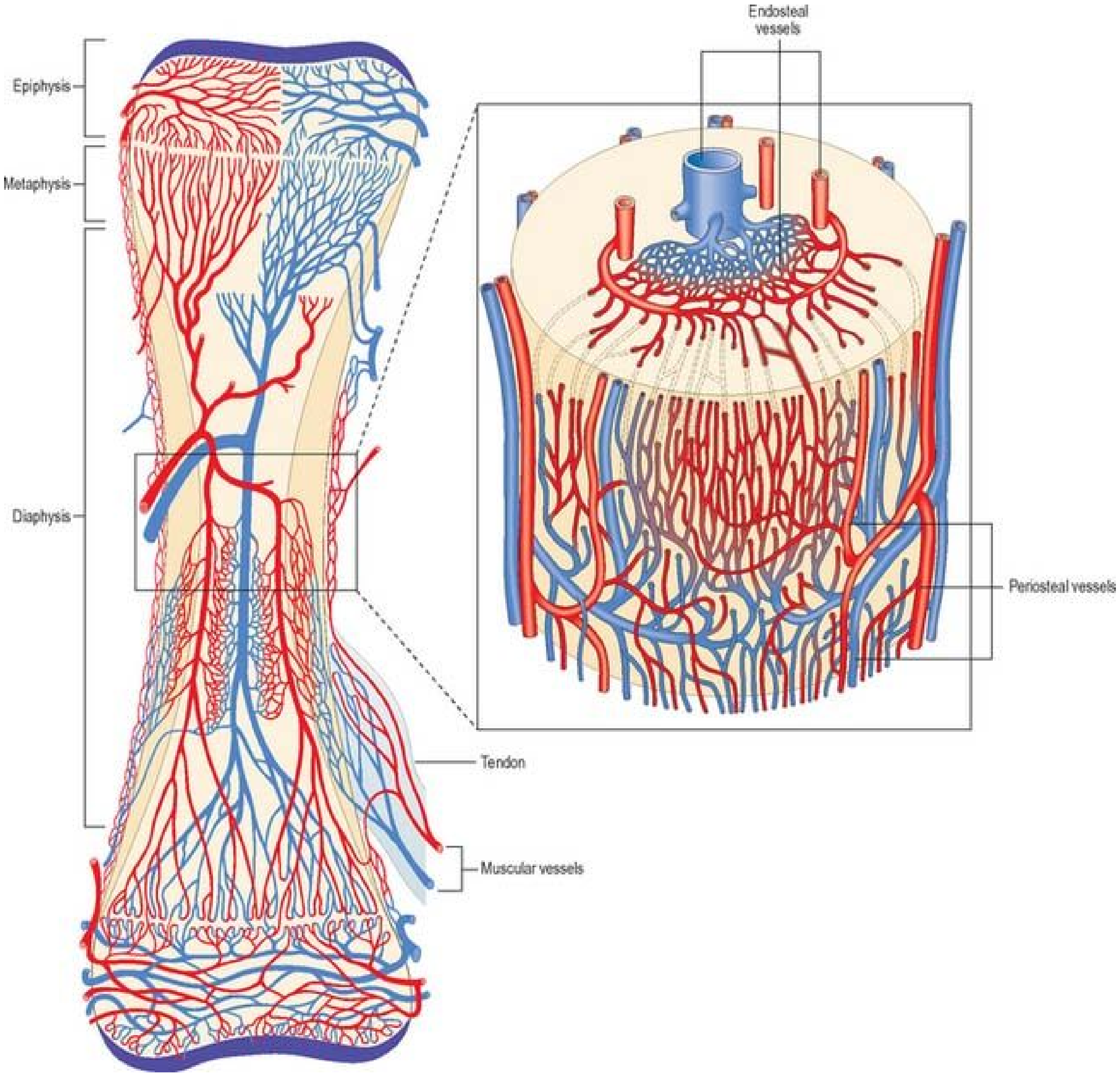
Endosteal vessels
Epiphysis
Metaphysis
Diaphysis
Periosteal vessels
Tendon
Muscular vessels

Fig. 5.20 The main features of the blood supply of a long bone. Note the contrasting supplies of the diaphysis, metaphysis and epiphysis, and their connections with periosteal, endosteal, muscular and periarticular vessels. The expansion shows part of the diaphysis in more detail. The marrow cavity contains a large central venous sinus, a dense network of medullary sinusoids, and longitudinal medullary arteries and their circumferential rami. Longitudinally oblique transcortical capillaries emerge through minute ‘cornet-shaped’ foramina to become confluent with the periosteal capillaries and venules. The obliquity of the cortical capillaries is emphasized for clarity. Not to scale.

One or two main diaphysial nutrient arteries enter the shaft obliquely through nutrient foramina which lead into nutrient canals. Their sites of entry and angulation are almost constant and characteristically directed away from the dominant growing epiphysis. Nutrient arteries do not branch in their canals, but divide into ascending and descending branches in the medullary cavity which approach the epiphyses, dividing repeatedly into smaller helical branches close to the endosteal surface. The endosteal vessels are vulnerable during operations which involve passing metal implants into the medullary canal, e.g. intramedullary nailing for fractures. Near the epiphyses they are joined by terminal branches of numerous metaphysial and epiphysial arteries. The former are direct branches of neighbouring systemic vessels, the latter come from periarticular vascular arcades formed on non-articular bone surfaces. Numerous vascular foramina penetrate bones near their ends, often at fairly specific sites; some are occupied by arteries, but most contain thin-walled veins. Within bone, the arteries are unusual in consisting of endothelium with only a thin layer of supportive connective tissue. The epiphysial and metaphysial arterial supply is richer than the diaphysial supply.

Medullary arteries in the shaft give off centripetal branches which feed a hexagonal mesh of medullary sinusoids that drain into a wide, thin-walled central venous sinus. They also possess cortical branches which pass through endosteal canals to feed fenestrated capillaries in osteons (Haversian systems). The central sinus drains into veins which retrace the paths of nutrient arteries, sometimes piercing the shaft elsewhere as independent emissary veins. Cortical capillaries follow the pattern of Haversian canals, and are mainly longitudinal with oblique connections via Volkmann’s canals (Fig. 5.17). At bone surfaces, cortical capillaries make capillary and venous connections with periosteal plexuses (Fig. 5.20). The latter are formed by arteries from neighbouring muscles which contribute vascular arcades with longitudinal links to the fibrous periosteum. From this external plexus a capillary network permeates the deeper, osteogenic periosteum. At muscular attachments, periosteal and muscular plexuses are confluent and the cortical capillaries then drain into interfascicular venules.

In addition to the centrifugal supply of cortical bone, there is an appreciable centripetal arterial flow to outer cortical zones from periosteal vessels. The large nutrient arteries of epiphyses form many intraosseous anastomoses, their branches passing towards the articular surfaces within the trabecular spaces of the bone. Near the articular cartilages these form serial anastomotic arcades (e.g. three or four in the femoral head), which give off end-arterial loops. These often pierce the thin hypochondral compact bone to enter, and sometimes traverse, the calcified zone of articular cartilage, before returning to the epiphysial venous sinusoids.

In immature long bones the supply is similar, but the epiphysis is a discrete vascular zone. Epiphysial and metaphysial arteries enter on both sides of the growth cartilage; there are few, if any, anastomoses between them. Growth cartilages probably receive a supply from both sources, and from an anastomotic collar in the adjoining periosteum. Occasionally, cartilage canals are incorporated into a growth plate. Metaphysial bone is nourished by terminal branches of metaphysial arteries and by primary nutrient arteries of the shaft which form terminal blind-ended sprouts or sinusoidal loops in the zone of advancing ossification. Young periosteum is more vascular, its vessels communicate more freely with those of the shaft than their adult counterparts, and they give off more metaphysial branches.

Large irregular bones, e.g. the scapula and innominate, receive a periosteal supply. In addition, they often have large nutrient arteries which penetrate directly into their cancellous bone: the two systems anastomose freely. Short bones receive numerous fine vessels which supply their compact and cancellous bone and medullary cavities from the periosteum. Arteries enter vertebrae close to the bases of their transverse processes. Each vertebral medullary cavity drains to two large basivertebral veins which converge to a foramen on the posterior surface of the vertebral body. Flatter cranial bones are supplied by numerous periosteal or mucoperiosteal vessels. Large thin-walled veins run tortuously in cancellous bone. Lymphatic vessels accompany periosteal plexuses but have not been convincingly demonstrated in bone.

Innervation

Nerves are most numerous in the articular extremities of long bones, vertebrae and larger flat bones, and in periosteum. Fine myelinated and unmyelinated axons accompany nutrient vessels into bone and marrow and lie in the perivascular spaces of Haversian canals. Bone has a complex autonomic and sensory innervation; osteoblasts possess receptors for several neuropeptides that are found in the nerves which supply bone, e.g. neuropeptide Y, calcitonin gene-related peptide, vasoactive intestinal peptide and substance P.

DEVELOPMENT AND GROWTH OF BONE

Most bones are formed by a process of endochondral ossification, in which preformed cartilage templates (models) define their initial shapes and positions, and the cartilage is replaced by bone in an ordered sequence. Bones such as those in the cranial vault are laid down within a fibrocellular mesenchymal membrane, by a process known as intramembranous ossification.

Intramembranous ossification

Intramembranous ossification is the direct formation of bone (membrane bone) within highly vascular sheets or ‘membranes’ of condensed primitive mesenchyme (Fig. 5.21). At centres of ossification, mesenchymal stem cells differentiate into osteoprogenitor cells which proliferate around the branches of a capillary network, forming incomplete layers of osteoblasts in contact with the primitive bone matrix. The cells are polarized because they secrete a fine mesh of collagen fibres and ground substance, osteoid, from the surface which faces away from the blood vessels. The earliest crystals appear in association with extracellular matrix vesicles produced by the osteoblasts; crystal formation subsequently extends into collagen fibrils in the surrounding matrix, producing an early labyrinth of woven bone, the primary spongiosa. As layers of calcifying matrix are added to these early trabeculae, the osteoblasts enclosed by matrix come to lie within primitive lacunae. New osteocytes retain intercellular contact by means of their fine cytoplasmic processes (dendrites) and, as these elongate, matrix condenses around them to form canaliculi.

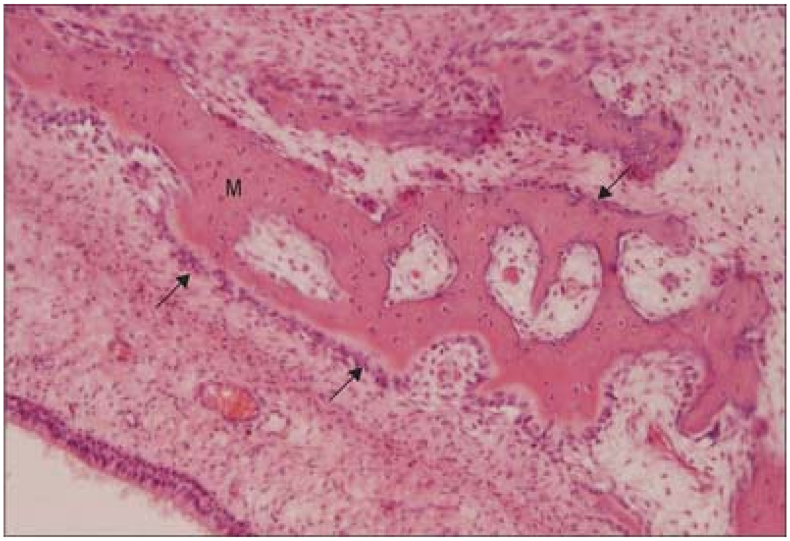

Fig. 5.21 Intramembranous ossification forming the nasal bones of a 7-month human fetus. Islands of bone (solid pink matrix [M], enclosing osteocytes) enlarge through the deposition of new matrix by osteoblasts (arrows). They subsequently fuse and are remodelled by osteoclasts to form mature lamellar bone.

As matrix secretion, calcification and enclosure of osteoblasts proceed, the trabeculae thicken and the intervening vascular spaces become narrower. Where bone remains trabecular, the process slows and the spaces between trabeculae become occupied by haemopoietic tissue. Where compact bone is forming, trabeculae continue to thicken and vascular spaces continue to narrow. Meanwhile the collagen fibres of the matrix, secreted on the walls of the narrowing spaces between trabeculae, become organized as parallel, longitudinal or spiral bundles, and the cells they enclose occupy concentric sequential rows. These irregular, interconnected masses of compact bone each have a central canal, and are called primary osteons (primary Haversian systems). They are later eroded, together with the intervening woven bone, and replaced by generations of mature (secondary) osteons.

While these changes are occurring, mesenchyme condenses on the outer surface to form a fibrovascular periosteum. Bone is laid down increasingly by new osteoblasts which differentiate from osteoprogenitor cells in the deeper layers of the periosteum. Modelling of the growing bone is achieved by varying rates of resorption and deposition at different sites.

Endochondral ossification

The hyaline cartilage model which forms during embryogenesis is a miniature template of the bone (cartilage bone) that will subsequently develop. It becomes surrounded by a condensed, vascular mesenchyme or perichondrium, which resembles the mesenchymal ‘membrane’ in which intramembranous ossification occurs. Its deeper layers contain osteoprogenitor cells.

The first appearance of a centre of primary ossification (Fig. 5.22) occurs when chondroblasts deep in the centre of the primitive shaft enlarge greatly, and their cytoplasm becomes vacuolated and accumulates glycogen. Their intervening matrix is compressed into thin, often perforated, septa. The cells degenerate and may die, leaving enlarged and sometimes confluent lacunae (primary areolae) whose thin walls become calcified during the final stages (Fig. 5.23). Type X collagen is produced in the hypertrophic zone of cartilage. Matrix vesicles originating from chondrocytes in the proliferation zone are most evident in the intercolumnar regions, where they appear to initiate crystal formation. At the same time, cells in the deep layer of perichondrium around the centre of the cartilage model differentiate into osteoblasts and form a peripheral layer of bone. Initially, this periosteal collar, formed by intramembranous ossification within the perichondrium, is a thin-walled tube which encloses and supports the central shaft (Fig. 5.22, Fig. 5.23). As it increases in diameter it also extends towards both ends of the shaft.

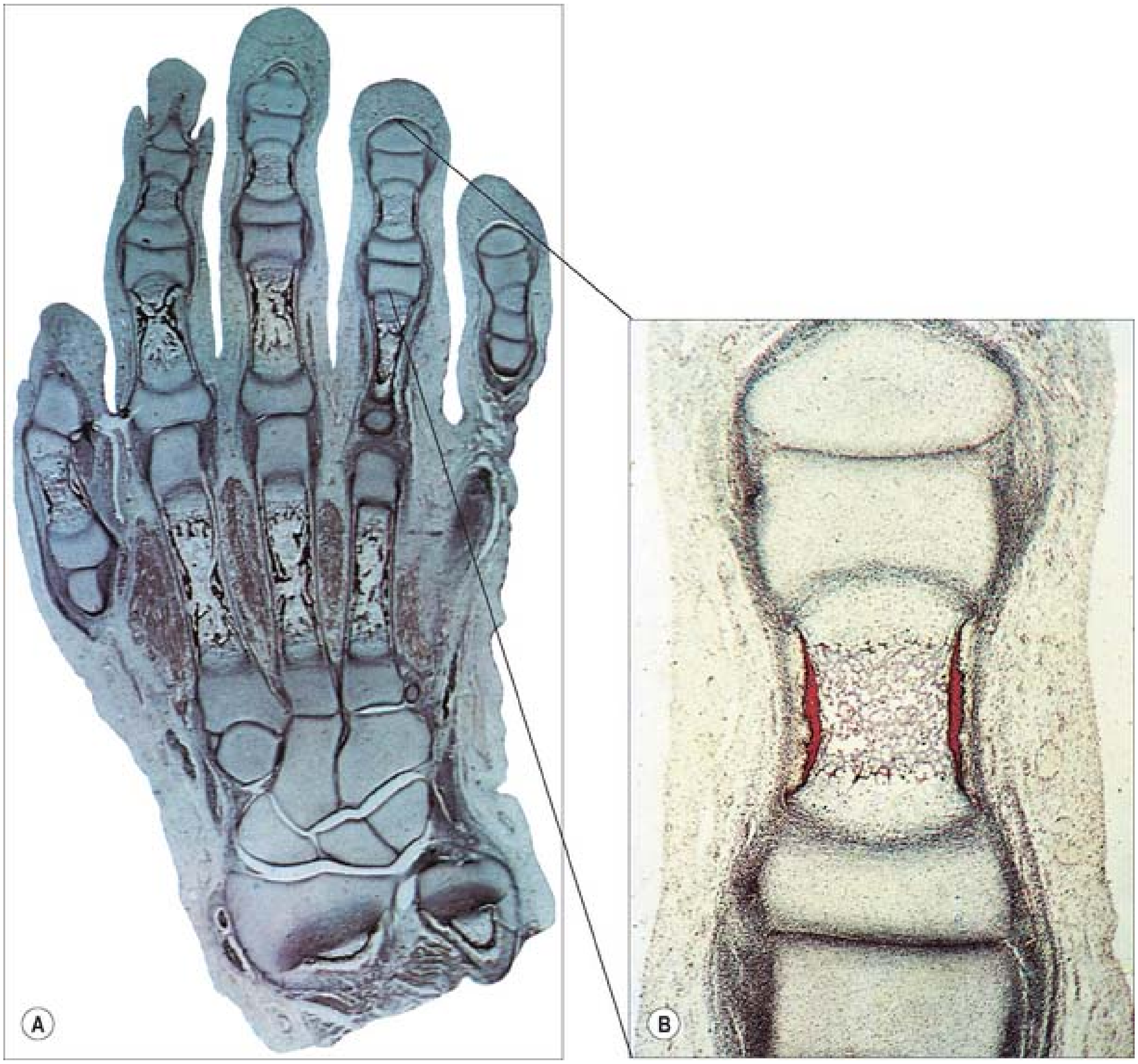

Fig. 5.22 **A,** Section of a human fetal hand showing cartilaginous models of the carpal bones, and the primary ossification centres, which display varying stages of maturity, in the metacarpals and phalanges. Note that none of the carpal elements shows any evidence of ossification. **B,** Higher power view of an early primary ossification centre. The cartilage cells in the shaft have hypertrophied and this region is surrounded by a delicate tube or collar of subperiosteal bone (red).

(Photograph by Kevin Fitzpatrick on behalf of GKT School of Medicine, London.)

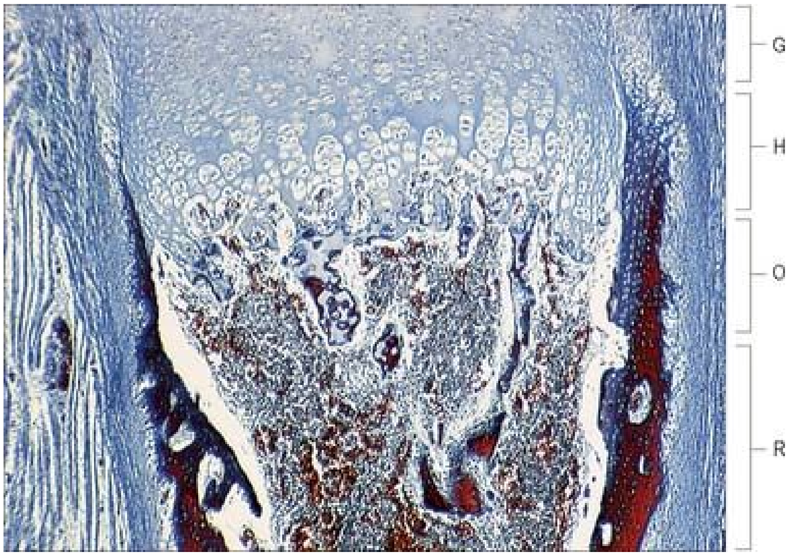

Fig. 5.23 The sequence of cellular events in endochondral ossification. This low magnification micrograph shows the primary ossification centre in a human fetal bone. See **Fig. 5.26** for further details. G, growth zone; H, hypertrophic zone; O, ossification zone; R, remodelling zone.

The periosteal collar which overlies the calcified cartilaginous walls of degenerate chondrocyte lacunae is invaded from the deep layers of the periosteum (formerly perichondrium) by osteogenic buds. These are blind-ended capillary sprouts and are accompanied by osteoprogenitor cells and osteoclasts. The latter excavate newly formed bone to reach adjacent calcified cartilage where they continue to erode the walls of primary chondrocyte lacunae (Fig. 5.24, Fig. 5.25). This process leads to their fusion into larger and irregular communicating spaces, secondary areolae, which fill with embryonic medullary tissue (vascular mesenchyme, osteoblasts and osteoclasts, haemopoietic and marrow stromal cells, etc.). Osteoblasts attach themselves to the delicate residual walls of calcified cartilage and lay down osteoid which rapidly becomes confluent, forming a continuous lining of bone. Further layers of bone are added, enclosing young osteocytes in lacunae, and narrowing the perivascular spaces. Bone deposition on the more central calcified cartilage ceases as the formation of subperiosteal bone continues.

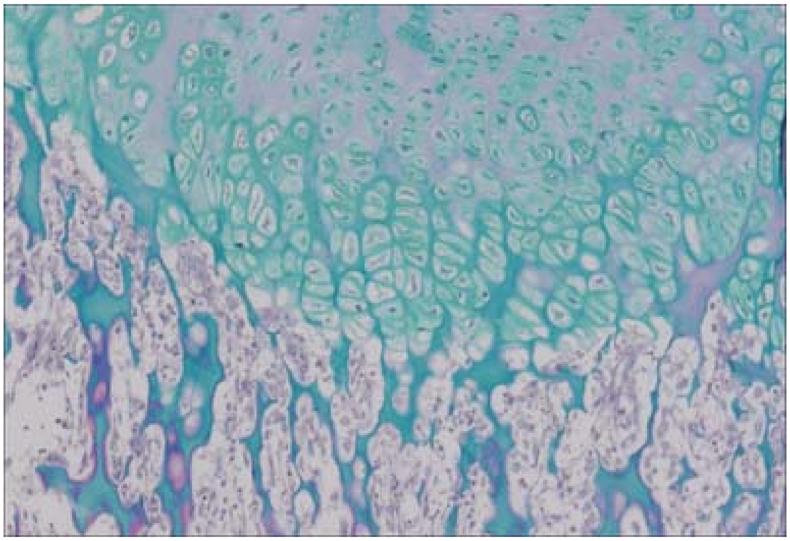

Fig. 5.24 Section showing the hypertrophy and palisading of cartilage cells as the ossifying (mineralising) front of an early primary centre of ossification is approached (below). Lacunae are enlarged, and matrix partitions are reduced in width and exhibit increased staining density following cartilage calcification. Alcian-blue PAS stained section of human fetal femur.

Osteoclastic erosion of the early bone spicules then creates a primitive medullary cavity in which only a few trabeculae, composed of bone with central cores of calcified cartilage (Fig. 5.24), remain to support the developing marrow tissues. These trabeculae soon become remodelled and replaced by more mature bone or by marrow. Meanwhile new, adjacent, cartilaginous regions undergo similar changes. Since these are most advanced centrally, and the epiphyses remain cartilaginous, the intermediate zones exhibit a temporospatial sequence of changes when viewed in longitudinal section (Fig. 5.26F). This region of dynamic change from cartilage to bone persists until longitudinal growth of the bone ceases.

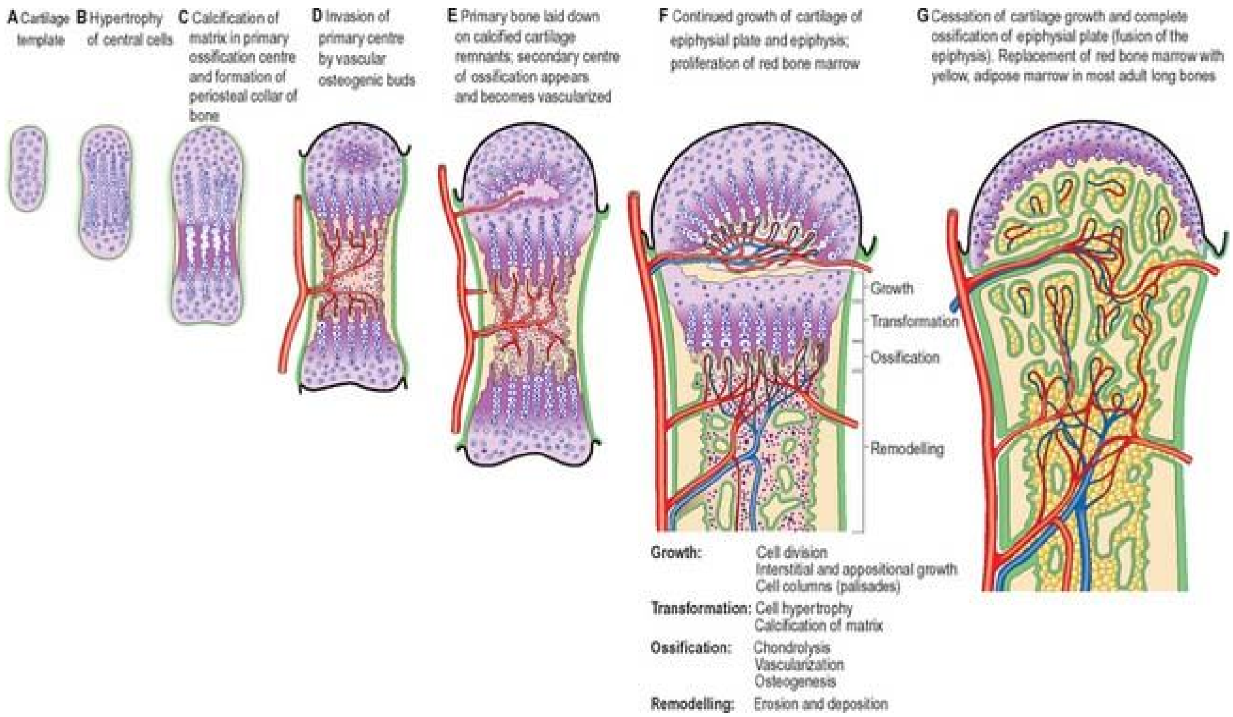
A Cartilage template
B Hypertrophy of central cells
C Calcification of matrix in primary ossification centre and formation of periosteal collar of bone
D Invasion of primary centre by vascular osteogenic buds
E Primary bone laid down on calcified cartilage remnants; secondary centre of ossification appears and becomes vascularized
F Continued growth of cartilage of epiphysial plate and epiphysis; proliferation of red bone marrow
G Cessation of cartilage growth and complete ossification of epiphysial plate (fusion of the epiphysis). Replacement of red bone marrow with yellow, adipose marrow in most adult long bones
Growth
Transformation
Ossification
Remodelling
Growth: Cell division
Interstitial and appositional growth
Cell columns (palisades)
Transformation: Cell hypertrophy
Calcification of matrix
Ossification: Chondrolysis
Vascularization
Osteogenesis
Remodelling: Erosion and deposition

Fig. 5.26 The stages of endochondral ossification in a long bone.

Expansion of the cartilaginous extremity (usually an epiphysis) keeps pace with the growth of the rest of the bone both by appositional and interstitial growth. The growth zone expands in all dimensions. Growth in thickness of a developing long bone is caused by occasional transverse mitoses in its chondrocytes, and by appositional growth as a result of matrix deposition by cells from the perichondrial collar or ring at this level. The future growth plate therefore expands in concert with the shaft and adjacent future epiphysis. A zone of relatively quiescent chondrocytes (the resting zone) lies on the side of the plate closest to the epiphysis. An actively mitotic zone of cells faces towards the shaft of the bone: the more frequent divisions in the long axis of the bone soon create numerous longitudinal columns (palisades) of disc-shaped chondrocytes, each in a flattened lacuna (Fig. 5.26). Proliferation and column formation occurs in this zone of cartilage growth (the proliferative zone), and its continued longitudinal interstitial expansion provides the basic mode of elongation of a bone.

The columns of cells show increasing maturity towards the centre of the shaft, as their chondrocytes increase in size and accumulate glycogen. In the hypertrophic zone, energy metabolism is depressed at the level of the mineralizing front (Fig. 5.24). The lacunae are now separated by transverse and longitudinal walls, and the latter are impregnated with apatite crystals (the zone of calcified cartilage). The calcified partitions enter the zone of bone formation and are invaded by vascular mesenchyme containing osteoblasts, osteoclasts, etc. The partitions, especially the transverse ones, are then partly eroded while osteoid deposition, bone formation and osteocyte enclosure occur on the surfaces of the longitudinal walls. Lysis of calcified partitions is mediated by osteoclast (chondroclast) action, aided by cells associated with the terminal buds of vascular sinusoids which occupy, and come into close contact with, each incomplete columnar trabecular framework.

Continuing cell division in the growth zone adds to the epiphysial ends of cell columns, and the bone grows in length as this sequence of changes proceeds away from the diaphysial centre. The bone also grows in diameter as further subperiosteal bone deposition occurs near the epiphyses, and its medullary cavity enlarges transversely and longitudinally. Internal erosion and remodelling of the newly formed bone tissue continues.

Growth continues in this way for many months or years in different bones but eventually one or more secondary centres of ossification usually appear in the cartilaginous extremities. These epiphysial centres (or the ends of bones which lack epiphyses) do not at first display cell columns. Instead, isogenous cell groups hypertrophy, with matrix calcification, and are then invaded by osteogenic vascular mesenchyme, sometimes from cartilage canals. Bone is formed on calcified cartilage, as described above. As an epiphysis enlarges, its cartilaginous periphery also forms a zone of proliferation in which cell columns are organized radially; hypertrophy, calcification, erosion and ossification occur at increasing depths from the surface. The early osseous epiphysis is thus surrounded by a superficial growth cartilage, and the growth plate adjacent to the metaphysis soon becomes the most active region.

As a bone reaches maturity, epiphysial and metaphysial ossification processes gradually encroach upon the growth plate from either side, eventually meeting when bony fusion of the epiphysis occurs and longitudinal growth of the bone ceases. The events which take place during fusion are broadly as follows. As growth ceases, the cartilaginous plate becomes quiescent and gradually thins, proliferation, palisading and hypertrophy of chondrocytes stop, and the cells form short, irregular conical masses. Patchy calcification is accompanied by resorption of calcified cartilage and some of the adjacent metaphysial bone, to form resorption channels which are invaded by vascular mesenchyme. Some endothelial sprouts pierce the thin plate of cartilage, and the metaphysial and epiphysial vessels unite. Ossification around these vessels spreads into the intervening zones and results in fusion of epiphysis and metaphysis.

This bone is visible in radiographs as a radiodense epiphysial line (a term which is also used to describe the level of the perichondrial collar or ring around the growth cartilage of immature bones, or the surface junction between epiphysis and metaphysis in a mature bone). In smaller epiphyses, which unite earlier, there is usually one initial eccentric area of fusion, and thinning of the residual cartilaginous plate. The original sites of fusion are subsequently resorbed and replaced by new bone. Medullary tissue extends into the whole cartilaginous plate until union is complete and no epiphysial ‘scar’ persists. In larger epiphyses, which unite later, similar processes also involve multiple perforations in growth plates, and islands of epiphysial bone often persist as epiphysial scars. Calcified cartilage coated by bone forms the epiphysial scar, and is also found below articular cartilage. It has been called metaplastic bone, a term also applied to sites of attachments of tendons, ligaments and other dense connective tissues to bone.

The cartilaginous surfaces of epiphyses that form synovial joints remain unossified, but the typical sequence of cartilaginous zones persists in them throughout life. A similar developmental sequence occurs at synchondroses, except that the proliferative rates of chondrocytes and the replacement of cartilage by bone are similar, although not identical, on either side of the synchondrosis.

Postnatal growth and maintenance

Modelling, by which is meant changes in general shape, occurs in all growing bones. The process has been studied mainly in cranial and long bones with expanded extremities. A bone such as the parietal thickens and expands during growth, but decreases in curvature. Accretion continues at its edges by proliferation of osteoprogenitor cells at sutures, and periosteal bone is mainly added externally and eroded internally, but not at uniform rates or at all times. The rate of formation increases with radial distance from the centre of ossification (in this case, the future parietal eminence), and formation may also occur endocranially as well as ectocranially, changing the curvature of the bone. As the skull bones thicken and grow at the sutures, the relative positions of the original centres of ossification change in three dimensions as the vault of the skull expands with growth of the brain. The development of diploë (trabeculae of spongy bone) and marrow space internally produces outer and inner cortical plates.

Long bones elongate mainly by extension of endochondral ossification into calcified zones of adjacent growth cartilages, which are continually replaced by the longitudinal interstitial growth of their proliferative zones, with minor additions by radial epiphysial growth. Simultaneously, diametric increases of growth cartilages and shafts occur by continuing subperiosteal deposition and endosteal erosion. However, in many bones growth occurs at different rates, and is even reversed, at different places. A bone which is initially tubular may thus become triangular in section, e.g. the tibia. Similarly, the waisted contours of metaphyses are preserved by differential rates of periosteal erosion and endosteal deposition, as metaphysial bone becomes diaphysial in position. The junction between a field of resorption and one of deposition on the surface of a bone during its growth is called a surface reversal line. The relative position of such a line may remain stable over long periods of cortical drift.

Lamellar bone forms at variable rates which reflect the slow turnover of osteons throughout adult life. A resorption canal (cutting cone) is typically 2 mm long and takes 1–3 months to form; a new osteon (closing cone) forms in a similar period (Fig. 5.19). Internal remodelling continuously supplies young osteons with labile calcium reserves, and provides a malleable bony architecture that is responsive to changing patterns of stress. The remodelling unit in cancellous bone, equivalent to the secondary osteon of compact bone, is the bone structural unit: it has an average thickness of 40–70 µm and an average length of 100 µm, but may be more extensive and irregular in shape.

The normal development and maintenance of bone requires adequate intake and absorption of calcium, phosphorus, vitamins A, C and D, and a balance between growth hormone (GH, somatotropin), thyroid hormones, oestrogens and androgens. Various other factors, including different prostaglandins and glucocorticoids, may also play important roles in the maintenance and turnover of bone. Prolonged deficiency of calcium causes loss of bone mineral via a loss of bone tissue (osteoporosis) and consequent bone fragility. Vitamin D influences intestinal transport of calcium and phosphate, and therefore affects circulatory calcium levels. In adults, prolonged deficiency (with or without low intake) produces bones which contain regions of deformable, uncalcified osteoid (osteomalacia). During growth, similar deficiencies lead to severe disturbance of growth cartilages and ossification, e.g. reductions of regular columnar organization in growth plates, and failure of cartilage calcification even though chondrocytes proliferate. Growth plates also become thicker and less regular than normal, as exemplified in classic rickets or juvenile osteomalacia. In rickets, the uncalcified or poorly calcified cartilage trabeculae are only partially eroded: osteoblasts secrete layers of osteoid, but these fail to ossify in the metaphysial region, and ultimately gravity deforms these softened bones.

Vitamin C is essential for the adequate synthesis of collagen and matrix proteoglycans in connective tissues. When vitamin C is deficient, growth plates become thin, ossification almost stops, and metaphysial trabeculae and cortical bone are reduced in thickness. This causes fragility and delayed healing of fractures. Vitamin A is necessary for normal growth, and for a correct balance of deposition and removal of bone. Deficiency retards growth as a result of the failure of internal erosion and remodelling, particularly in the cranial base. Foramina are narrowed, sometimes causing pressure atrophy of contained nerves, and the cranial cavity and spinal canal may fail to expand with the central nervous system, which impairs nervous function.

Conversely, excess vitamin A stimulates vascular erosion of growth cartilages, which become thin or totally lost, and longitudinal growth ceases. Retinoic acid, a vitamin A derivative, is involved in pattern formation in limb buds (see Ch. 51), and in the differentiation of osteoblasts.

Balanced endocrine functions are also essential to normal bone maturation, and disturbances in this balance may have profound effects. In addition to its role in calcium metabolism, excess parathyroid hormone (primary hyperparathyroidism) stimulates unchecked osteoclastic erosion of bone, particularly subperiosteally and later endosteally (osteitis fibrosa cystica). Growth hormone is required for normal interstitial proliferation in growth cartilages, and hence increase in stature. Termination of normal growth is imperfectly understood, but may involve a fall in hormone production or in the sensitivity of chondroblasts to insulin-like growth factors regulated by GH. Reduction of GH production in the young leads to quiescence and thinning of growth plates and hence pituitary dwarfism. Conversely, continued hypersecretion in the immature leads to gigantism, and in the adult results in thickening of bones by subperiosteal deposition; the mandible, hands and feet are the most affected, a condition known as acromegaly.

While continued longitudinal growth of bones depends on adequate levels of GH, effective remodelling to achieve a mature shape also requires the action of the thyroid hormones. Moreover, growth and skeletal maturity are closely related to endocrine activities of the ovaries, testes and suprarenal cortices. High oestrogen levels increase deposition of endosteal and trabecular bone, conversely, osteoporosis in postmenopausal women reflects reduced ovarian function. Fluctuations in the rate of growth and the timing of skeletal maturation are a function of circulating levels of suprarenal and testicular androgens. In hypogonadism, growth plate fusion is delayed and the limbs therefore elongate excessively, conversely, in hypergonadism, premature fusion of the epiphyses results in diminished stature.

Although the morphogenetic factors that determine the shape of a bone have yet to be fully defined, responses to strain are believed to play a major role. Bone resorption typically occurs when gravitational or other mechanical stresses are reduced, as occurs in bed rest, or in zero gravity conditions in space. Bone subjected to constant pressure also tends to resorb, a response that underpins much orthodontic treatment, since teeth can be made to migrate slowly through alveolar bone by the application of steady lateral or medial pressure. Conversely, with constant tension, bone is deposited, e.g. the bones in the racket arm of tennis players are more robust than in the contralateral limb.

Growth of individual bones

Ossification centres appear over a long period during bone growth, many in embryonic life, some in prenatal life, and others well into the postnatal growing period. Ossification centres are initially microscopic but soon become macroscopic, which means that their growth can then be followed by radiological and other scanning techniques.

Some bones, including carpal, tarsal, lacrimal, nasal, and zygomatic bones, inferior nasal conchae and auditory ossicles, ossify from a single centre which may appear between the eighth intrauterine week and the tenth year, a wide sequence for studying growth or estimating age. Most bones ossify from several centres, one of which appears in the centre of the future bone in late embryonic or early fetal life (seventh week to fourth month). Ossification progresses from the centres towards the ends, which are still cartilaginous at birth (Fig. 5.27). These terminal regions ossify from separate centres, which are sometimes multiple, and which appear between birth and the late teens: they are therefore secondary to the earlier primary centre from which much of the bone ossifies. This is the pattern in long bones, as well as in some shorter bones such as the metacarpals and metatarsals, and in the ribs and clavicles.

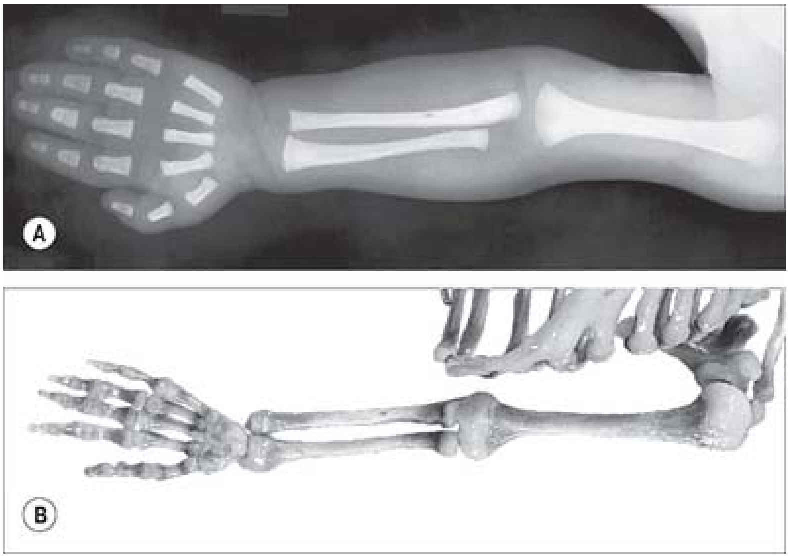

Fig. 5.27 **A**, Radiograph of a neonatal arm. Ossification from primary centres is well advanced in all of the limb bones except the carpals, which are still wholly cartilaginous. The gaps by which individual elements appear to be separated are filled by radiolucent hyaline cartilage, in which epiphysial or carpal ossification will subsequently occur. Note the flaring contours, narrow midshaft and relatively expanded metaphyses of the long bones, and the proportions of the limb segments, in particular the relatively large hand, which are characteristic of this age. **B**, The bones and cartilages of a neonatal left arm. Compare the radiolucent areas in the radiograph (**A**) with the preserved cartilaginous epiphyses and carpal elements in this specimen.

(Part B prepared by Michael C.E. Hutchinson; photographed by Kevin Fitzpatrick on behalf of GKT School of Medicine, London.)

At birth a bone such as the tibia is typically ossified throughout its diaphysis from a primary centre which appears in the seventh intrauterine week, whereas its cartilaginous epiphyses ossify from secondary centres. As the epiphyses enlarge almost all the cartilage is replaced by bone, except for a specialized layer of articular hyaline cartilage which persists at the joint surface, and a thicker zone between the diaphysis and epiphysis. Persistence of this epiphysial plate or disc (growth plate or growth cartilage) allows increase in bone length until the usual dimensions are reached, by which time the epiphysial plate has ossified. The bone has then reached maturity. Coalescence of the epiphysis and diaphysis is fusion, the amalgamation of separate osseous units into one.

Many long bones have epiphyses at both their proximal and distal extremities. Metacarpals, metatarsals and phalanges have only one epiphysis. Typical ribs have epiphyses for the head and articular tubercle and one for the non-articular area. The costal cartilages represent the unossified hyaline cartilage of the developing rib and therefore do not display epiphyses. Epiphysial ossification is sometimes complex, e.g. the proximal end of the humerus is wholly cartilaginous at birth, and subsequently develops three centres during childhood which coalesce into a single mass before they fuse with the diaphysis; only one of these centres forms an articular surface, the others form the greater and lesser tubercles which give muscular attachments. Similar composite epiphyses occur at the distal end of the humerus and in the femur, ribs and vertebrae.

Many cranial bones ossify from multiple centres. The sphenoid, temporal and occipital bones are almost certainly composites of multiple elements in their evolutionary history. Some show evidence of fusion between membrane and cartilage bones which unite during growth.

If the growth rate was uniform, ossification centres would appear in a strict descending order of bone size. However, disparate rates of ossification occur at different sites and do not appear to be related to bone size. The appearance of primary centres for bones of such different sizes as the phalanges and femora are separated by, at most, a week of embryonic life. Those for carpal and tarsal bones show some correlation between size and order of ossification, from largest (calcaneus in the fifth fetal month) to smallest (pisiform in the ninth to twelfth postnatal year). In individual bones, succession of centres is related to the volume of bone which each centre produces. The largest epiphyses, e.g. the adjacent ends of the femur and tibia, are the earliest to begin to ossify (immediately before or after birth, and of forensic interest). At epiphysial plates, the rate of growth is initially equal at both ends of those bones which possess two epiphyses. However, experimental observations in other species have revealed that one generally grows faster than the other after birth. Since the faster-growing end also usually fuses later with the diaphysis, its contribution to length is greater. Though faster rate has not been measured directly in human bones, later fusion has been documented radiologically.

The more active end of a long limb bone is often termed the growing end, but this is a misnomer. The rate of increase in stature, which is rapid in infancy and again at puberty, demonstrates that rates of growth at epiphyses vary. The spurt at puberty, or slightly before, decreases as epiphyses fuse in post-adolescent years, and has been the subject of much study.

Growth cartilages do not grow uniformly at all points, which presumably accounts for changes such as the alteration in angle between the humeral shaft and its neck. The junctions between epiphysis and diaphysis at growth plates are not uniformly flat on either surface. Osseous surfaces usually become reciprocally curved by differential growth, and the epiphysis forms a shallow cup over the convex end of the shaft, with cartilage intervening, an arrangement that may resist shearing forces at this relatively weak region. Reciprocity of bone surfaces is augmented by small nodules and ridges, as can be seen when the surfaces are stripped of cartilage. These adaptations emphasize the formation of many immature bones from several elements held together by epiphysial cartilages. Most human bones exhibit these complex junctions, at which bone is bonded to bone through cartilage throughout the active years of childhood and adolescence.

Forces at growth cartilages are largely compressive, but with an element of shear. Interference with epiphysial growth may occur as a result of trauma, but more frequently follows disease: the resulting changes in trabecular patterns of bone are visible radiographically as dense transverse lines of arrested growth (Harris’s growth lines). Several such lines may appear in the limb bones of children afflicted by successive illnesses.

Variation in skeletal development occurs between individuals, sexes and possibly also races. The timing rather than the sequence of events varies, and females antedate males in all groups studied: differences which are perhaps insignificant before birth may be as great as two years in adolescence.

JOINTS

Joints are the regions of the skeleton where two or more bones meet and articulate. These junctions are supported by a variety of soft tissue structures and their prime functions are either to facilitate growth or to transmit forces between bones, thereby enabling movement to occur or weight to be transferred. The simplest classifications of joints relate to either the range of movement possible or the nature of the intervening soft tissues: there is no satisfactory single classification. Free movement occurs at synovial joints, whereas restricted movement occurs at joints that are sometimes referred to as synarthroses. The latter are commonly subdivided into fibrous and cartilaginous joints, according to the principal type of intervening connective tissue. What follows are descriptions of the general characteristics of each type of joint. Features that are specific to individual joints are discussed in the relevant topographical chapters.

FIBROUS JOINTS

Fibrous joints lack intervening cartilage between the two bones, the articulation is therefore fixed and movement is very restricted. The three most definable types of fibrous articulation are sutures, gomphoses and syndesmoses (Fig. 5.28).

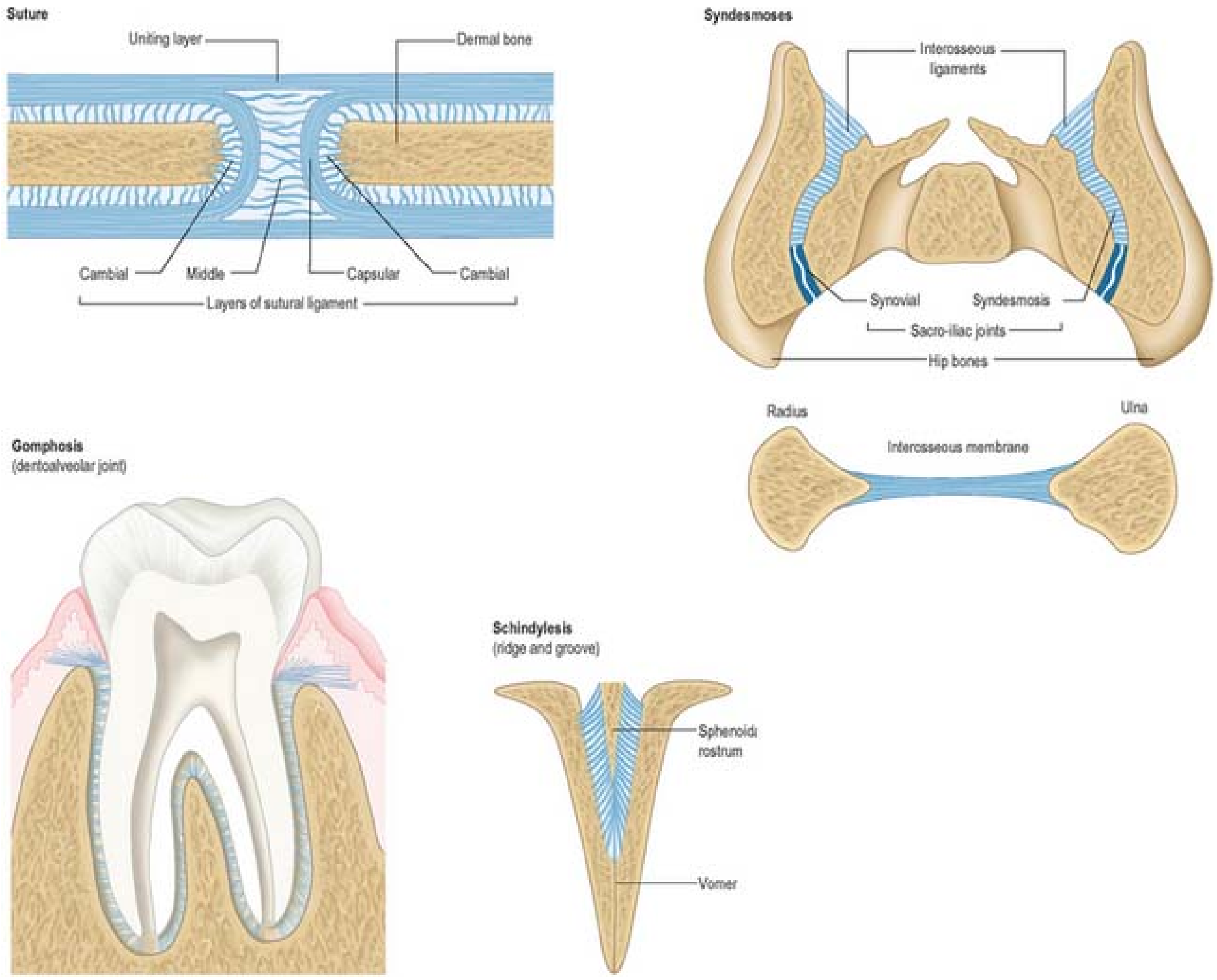
Suture
Uniting layer
Dermal bone
Cambial
Middle
Capsular
Cambial
Layers of sutural ligament
Syndesmoses
Interosseous ligaments
Synovial
Syndesmosis
Sacro-iliac joints
Hip bones
Radius
Ulna
Interosseous membrane
Gomphosis
(dentoalveolar joint)
Schindylesis
(ridge and groove)
Sphenoid
rostrum
Vomer

Fig. 5.28 Examples of the principal varieties of fibrous joints, each shown in section.

Suture

Sutures are restricted to the skull (see Ch. 26 for descriptions of individual sutures). In a suture, the two bones are separated by a layer of membrane-derived connective tissue. The sutural aspect of each bone is covered by a layer of osteogenic cells (cambial layer) overlaid by a capsular lamella of fibrous tissue which is continuous with the periosteum on both the endo- and ectocranial surfaces. The area between the capsular coverings contains loose fibrous connective tissue and decreases with age so that the osteogenic surfaces become apposed. On completion of growth, many sutures synostose and are obliterated. Synostosis occurs normally as the skull ages: it can begin in the early twenties and continues into advanced age. A schindylesis is a specialized suture in which a ridged bone fits into a groove on a neighboring element, e.g. where the cleft between the alae of the vomer receives the rostrum of the sphenoid.

Gomphosis

A gomphosis is a peg-and-socket junction between a tooth and its socket, where the two components are maintained in intimate contact by the collagen of the periodontium connecting the dental cement to the alveolar bone. Strictly speaking, a gomphosis is not an articulation between two skeletal structures.

Syndesmosis

A syndesmosis is a truly fibrous connection between bones. It may be represented by an interosseous ligament (inferior tibiofibular joint), a slender fibrous cord, or a more dense aponeurotic membrane (posterior part of sacroiliac joint).

CARTILAGINOUS JOINTS

Cartilaginous joints may be classified as primary (synchondrosis) or secondary (symphysis), depending upon the nature of the intervening cartilage. While the distinction between fibrous and cartilaginous joints is usually clear, some degree of admixture can occur in which either a predominantly fibrous articulation contains occasional islands of cartilage or a predominantly cartilaginous articulation contains aligned dense bundles of collagen. These joints tend to be less rigid than the fibrous articulations and some permit movement, albeit restricted in range (Fig. 5.29, Fig. 5.30).

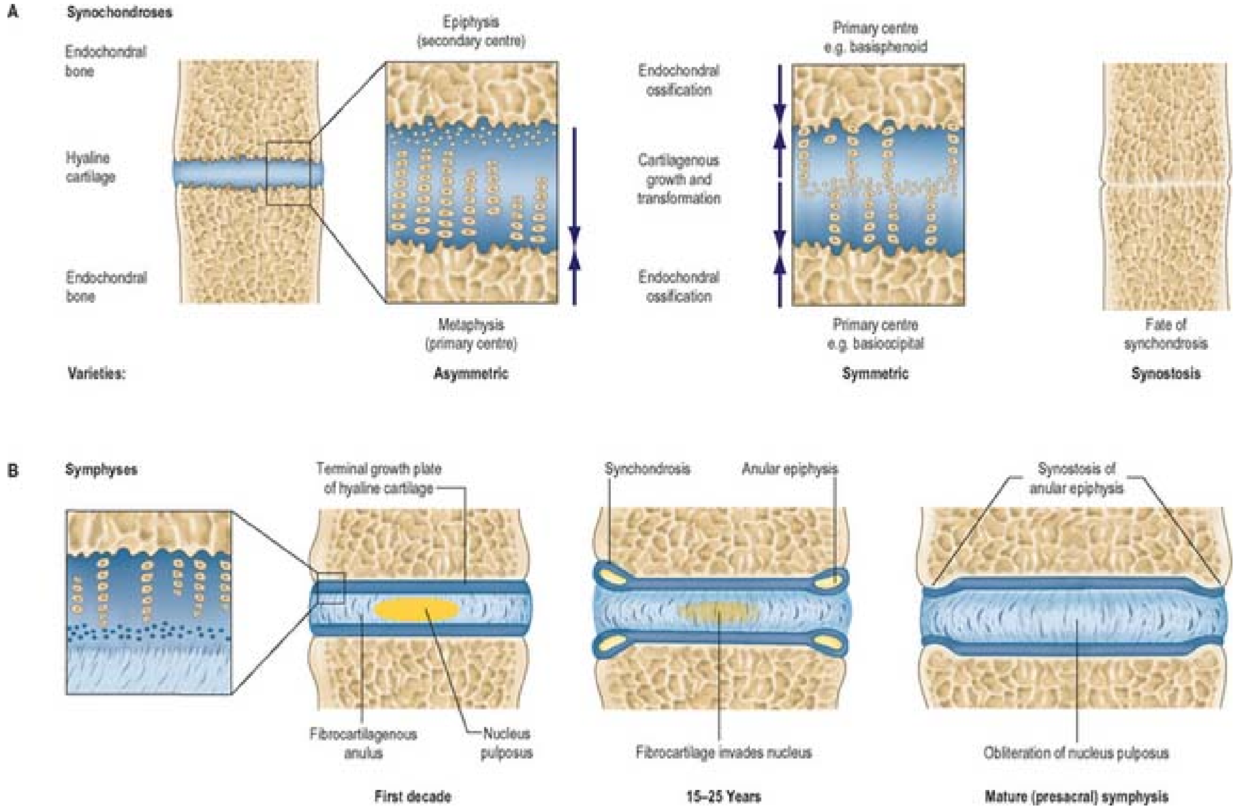
A
Synochondroses
Endochondral bone
Hyaline cartilage
Endochondral bone
Varieties:
Epiphysis (secondary centre)
Metaphysis (primary centre)
Asymmetric
Endochondral ossification
Cartilagenous growth and transformation
Endochondral ossification
Primary centre e.g. basisphenoid
Primary centre e.g. basioccipital
Symmetric
Fate of synchondrosis
Synostosis
B
Symphyses
Terminal growth plate of hyaline cartilage
Fibrocartilagenous anulus
Nucleus pulposus
First decade
Synchondrosis
Anular epiphysis
Fibrocartilage invades nucleus
15–25 Years
Synostosis of anular epiphysis
Obliteration of nucleus pulposus
Mature (presacral) symphysis

Fig. 5.29 Examples of varieties of cartilaginous joints (see also Fig. 5.30). **A**, Sectional view of the principal tissues involved, more detailed architecture and main growth patterns of symmetrical and asymmetrical synchondroses. Lesser degrees of asymmetry occur in some locations. Synostosis is the normal fate of almost all synchondroses when endochondral growth has ceased. **B**, Intervertebral symphyses (presacral),

shown in section, displaying age-related changes. Partial or complete synostosis is the normal fate of sacral and coccygeal symphyses.

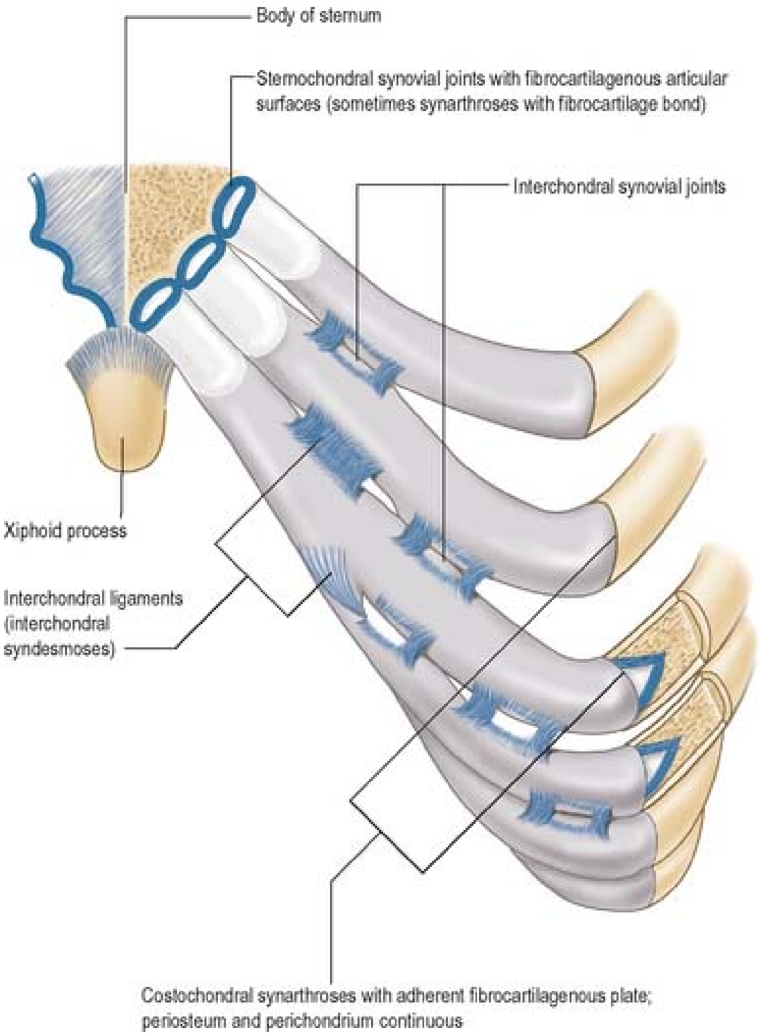
Body of sternum
Sternochondral synovial joints with fibrocartilagenous articular surfaces (sometimes synarthroses with fibrocartilage bond)
Interchondral synovial joints
Xiphoid process
Interchondral ligaments (interchondral syndesmoses)
Costochondral synarthroses with adherent fibrocartilagenous plate; periosteum and perichondrium continuous

Fig. 5.30 Less common interchondral and osseochondral junctions: see text for other locations. General periosteum and perichondrium omitted.

Primary cartilaginous joints

Primary cartilaginous joints or synchondroses occur where advancing centres of ossification are separated by an area of hyaline (non-articular) cartilage. They are present in all postcranial bones that form from more than one centre of ossification. Since hyaline cartilage retains the capability to ossify with age, synchondroses tend to synostose when growth is complete. Primary cartilaginous joints are almost exclusively associated with growth plates (see above): the detailed anatomy of specific joints is described in the appropriate topographical chapter. The location and growth of the spheno-occipital synchondrosis is discussed in Chapter 26.

Secondary cartilaginous joints

Secondary cartilaginous joints or symphyses are largely defined by the presence of an intervening pad or disc of fibrocartilage interposed between the articular hyaline cartilage that covers the ends of two bones. The pad or disc varies from a few millimetres to over a centimetre in width, and the whole region is generally bound by strong, tightly adherent, dense connective tissues. Collagenous ligaments extend from the periostea of the articulating bones across the symphysis and blend with the hyaline and fibrocartilaginous perichondria: they do not form a complete capsule and contain plexuses of afferent nerve terminals which also penetrate the periphery of the fibrocartilage. The combined strength of the ligaments and of the hyaline and fibrocartilage exceeds that of the associated bones, and is designed to withstand a range of stresses (compression, tension, shear and torsion). The range of movement in a symphysis is limited by the physical nature of the articulation and also by the restrictions imposed by other bones associated with the complex. Tears are usually the result of sudden, massive stresses that occur when the body is in an inappropriate posture.

All symphyses occur in the midline (mandibular, manubriosternal, pubic and intervertebral). All except the mandibular symphysis occur in the postcranial skeleton and resist synostosis. The mandibular symphysis (symphysis menti) is histologically different from the other symphyses, however, the widespread use of this descriptive term ensures that it remains, albeit probably inappropriately, within this category.

The concept that synchondroses are temporary and concerned with growth, whereas symphyses are permanent and concerned with movement, is an oversimplification and only partly correct. Both types of joint are concerned with strength and the ability to withstand and transmit considerable stresses, both are sites at which growth occurs, and both contribute either directly or indirectly to the total movement patterns of the parts involved. The strength and mechanical properties of cartilaginous joints are acknowledged, perhaps less attention is paid to the fact that the rigidity of synchrondroses also increases the efficiency of positive movements at related syndesmoses, symphyses and particularly at synovial joints. The movements that occur at a symphysis are not simple extrapolations based on the mechanical properties of a fibrocartilaginous pad or disc. For example, movement of a vertebra relative to its neighbours is a three-dimensional summation of the events that occur in all of the relevant intervertebral joints (syndesmoses, synovial joints, symphyses), each of which is subject to a particular array of stresses.

The prominent role of synchondroses in skeletal growth is widely recognized, whereas growth of symphyses has received less attention. Symphysial growth may, for convenience, be considered from two interrelated aspects, namely intrinsic growth of the fibrocartilaginous disc, and growth of the hyaline cartilaginous plates into which endochondral ossification progresses.

SYNOVIAL JOINTS

Synovial articulations are quite readily differentiated from both fibrous and cartilaginous joints (Fig. 5.31). Although the bones involved are linked by a fibrous capsule (which usually has intrinsic ligamentous thickenings), and often by internal or external accessory ligaments, the articulating bony surfaces are generally not in direct continuity. They are covered by hyaline articular cartilage of varying thickness and precise topology; contact is strictly limited between these cartilaginous surfaces, which have a very low coefficient of friction, facilitating free movement. Smooth movement of the opposing articular surfaces is aided by a viscous synovial fluid, which acts as a lubricant, but is also concerned with cellular maintenance in the articular cartilages. The production of synovial fluid requires the presence of a synovial membrane which is one of the defining characteristics of the joint type.

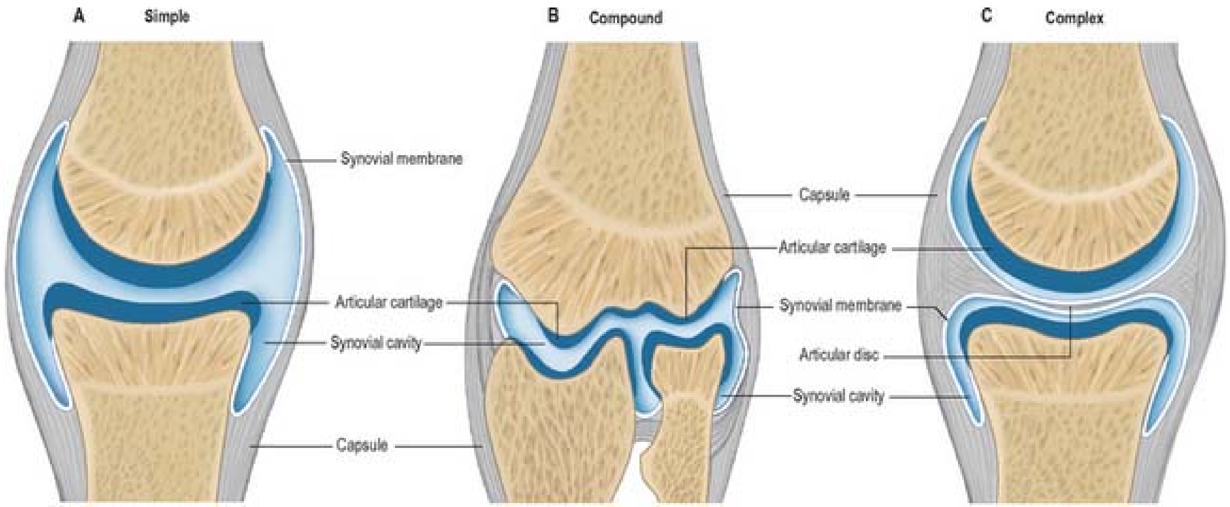
A
Simple
B
Compound
C
Complex
Synovial membrane
Articular cartilage
Synovial cavity
Capsule
Capsule
Articular cartilage
Synovial membrane
Articular disc
Synovial cavity

Fig. 5.31 Synovial joints, some main structural features and one elementary type of classification: **A**, simple; **B**, compound; **C**, complex joints. For clarity, the articular surfaces are artificially separated. A and C are purely diagrammatic and not related to particular joints. B, however, is a simplified representation of some features of an elbow joint; the complicated contours due to the olecranon, coronoid and radial fossae and profiles of articular fat pads have been omitted for clarity.

Articular surfaces

Articular surfaces are mostly formed by a specialization of hyaline cartilage, reflecting their preformation as parts of cartilaginous models in embryonic life. Exceptionally, surfaces of the sternoclavicular and acromioclavicular joints and both temporomandibular surfaces are covered by dense fibrous tissue which contains isolated groups of chondrocytes and little surrounding matrix – perhaps a legacy of their formation by intramembranous ossification. Articular cartilage has a wear-resistant, low-frictional, lubricated surface, which is slightly compressible and elastic and is thus ideally constructed for easy movement. It is also able to resist and distribute large forces of compression and shear generated by movement, body weight transfer and muscle contractions.

The thickness of articular cartilage may reach 5–7 mm in larger joints of young individuals but may be reduced to 1–2 mm in the elderly. Young cartilages are typically white, smooth, glistening and compressible, whereas ageing cartilages are thinner, less cellular, firmer and more brittle, with a less regular surface and a yellowish opacity.

Articular cartilages are moulded to bone (see Fig. 5.4), and variations in thickness often accentuate subjacent osseous surface shape. Typically, convex surfaces are thickest centrally, thinning peripherally, and concave surfaces are the reverse. The precise configuration, degree of congruence in various positions, and the dispositions of the surrounding capsule and ligaments, are all related to the types and ranges of movement permitted at a joint. Articular cartilage has no penetrating nerves or blood vessels (except occasional vascular loops). Its nutrition and maintenance therefore largely depend on diffusion from a peripheral vascular plexus in the synovial membrane (circulus vasculosus articuli), blood vessels in adjacent marrow spaces and synovial fluid: the relative importance of these contributions is uncertain.

The zone of articular cartilage next to the joint cavity is mainly a layer of collagen fibres arranged in various planes with small, oval chondrocytes lying deep to it in the matrix. Transmission electron microscopy of heavy metal stained preparations shows an interrupted electron-dense surface coat of a particulate or filamentous material, generally 0.03–0.1 μm thick, covering the cartilage. Synovial fluid and membranous debris, the product of chondrocytic necrosis, may contribute to this surface coat, which is transient in nature; the stable, permanent, articular surface is bounded by the most superficial collagen fibres. The ‘lamina splendens’, a structure that appears as a bright line at the free surface of articular cartilage when oblique sections are examined by negative phase contrast microscopy, is an artefact arising at the border between regions of different refractive index: it is not an anatomically distinct surface layer. The deeper zones of articular cartilage contain a highly complex, three-dimensional reticulum of interconnected fibrils, which have obvious functional implications.

With advancing age, undulations of articular surfaces deepen and develop minute, ragged projections, perhaps as a consequence of wear and tear. These changes are extremely slow in healthy joints: erosion occurs in pathologically ‘dry’ joints and where synovial fluid viscosity is altered. Mitosis is not observed in adult articular chondrocytes.

Fibrous capsule

A fibrous capsule completely encloses a joint except where it is interrupted by synovial protrusions (see descriptions of individual joints for specific details). It is composed of interlacing bundles of parallel fibres of white collagen and is attached continuously round the ends of the articulating bones. In small bones this attachment is usually near the periphery of the articular surfaces, but in long bones it varies considerably, and part or all of the attachment may be a significant distance from the articular surface. The capsule is perforated by vessels and nerves and may contain apertures through which synovial membrane protrudes as bursae. It is lined by a synovial membrane that also covers all non-articular surfaces (non-articular osseous surfaces, tendons and ligaments) that lie partly or wholly within the fibrous capsule, e.g. at the shoulder and knee. Where a tendon is attached inside a joint, an extension of synovial membrane usually accompanies it beyond the capsule. Some extracapsular tendons are separated from the capsule by a synovial bursa continuous with the interior of the joint. These protrusions are potential routes for the spread of infection into joints.

A fibrous capsule usually exhibits local thickenings of parallel bundles of collagen fibres, called capsular (intrinsic) ligaments, that are named by their attachments. Some capsules are reinforced or replaced by tendons of nearby muscles or expansions from them. Accessory ligaments are separate from capsules and may be extracapsular or intracapsular in position.

All ligaments, although yielding little to tension, are pliant. They are slightly elastic and protected from excessive tension by reflex contraction of appropriate muscles. They are taut at the normal limit of a particular movement but do not resist normal actions, since they are designed to check excessive or abnormal movements.

Synovial membrane

Synovial membrane lines fibrous capsules and covers exposed osseous surfaces, intracapsular ligaments, bursae and tendon sheaths (Fig. 5.32). It does not cover intra-articular discs or menisci and stops at the margins of articular cartilages in a transitional zone that occupies the peripheral few millimetres of the cartilage. Synovial membrane secretes and absorbs a fluid that lubricates the movement between the articulating surfaces.

Pink, smooth and shining, the internal synovial surface displays a few small synovial villi that increase in size and number with age. Folds and fringes of membrane may also project into a joint cavity; some are sufficiently constant to be named, e.g. the alar folds and ligamentum mucosum of the knee. Synovial villi are more numerous near articular margins and on the surfaces of folds and fringes, and become prominent in some pathological states.

Accumulations of adipose tissue (articular fat pads) occur in the synovial membrane in many joints. These pads, folds and fringes are flexible, elastic and deformable cushions that occupy the potential spaces and irregularities in joints that are not wholly filled by synovial fluid. During movement they accommodate to the changing shape and volume of the irregularities, they also increase synovial area and may promote the distribution of lubricant over articular surfaces (cf. intra-articular discs and menisci).

Synovial membrane is composed of a cellular intima resting on a fibrovascular subintimal layer (subsynovial tissue). The intima consists of pleomorphic synovial cells embedded in a granular, amorphous, fibre-free extracellular matrix. There is considerable regional variation in cell morphology and numbers. Human synovial cells are generally elliptical, and have numerous cytoplasmic processes. At least two morphologically distinct populations, type A and type B synovial cells, are responsible for synthesizing some of the components of the synovial fluid.

Type A cells are macrophage-like cells characterized by surface ruffles or lamellipodia, plasma membrane invaginations and associated pinocytotic vesicles, a prominent Golgi apparatus but little rough endoplasmic reticulum. Type B synovial cells, which predominate, resemble fibroblasts and have abundant rough endoplasmic reticulum but fewer vacuoles and vesicles, and have a less ruffled plasma membrane. It is thought that some of the hyaluronan and glycoproteins of synovial fluid are synthesized by synovial type B cells, whereas the fluid component is a transudate from synovial capillaries. Type A synovial cells synthesize and release lytic enzymes and phagocytose joint debris: potential damage to joint tissues is limited by the secretion of enzyme inhibitors by type B synovial cells. Synovial cells do not divide actively in normal synovial membranes, but their division rate increases dramatically in response to acute trauma and haemarthrosis. In such conditions the type B synovial cells divide in situ, while the type A cell population is increased by immigration of bone marrow-derived precursors.

The synovial cells of normal human joints form an interlacing, discontinuous layer, one to three cells and 20–40 μm deep, between the subintima and the joint cavity. They are not separated from the subintima by a basal lamina, and are distinguished from the subintimal cells only because they associate to form a superficial layer. In many locations, but particularly over loose subintimal tissue, areas are commonly found that are free from synovial cells. Over fibrous subintimal tissue the synovial cells may be flattened and closely packed, forming endothelioid sheets. Neighbouring cells are often separated by distinct gaps but their processes may interdigitate where they lie closer together.

The subintima is often composed of loose, irregular connective tissue, but also contains organized lamellae of collagen and elastin fibres lying parallel to the membrane surface, interspersed with occasional fibroblasts, macrophages, mast cells and fat cells. The elastic component may prevent formation of redundant folds during joint movement. Subintimal adipose cells form compact lobules surrounded by highly vascular fibroelastic interlobular septa that provide firmness, deformability and elastic recoil. The subintima merges with the synovial membrane where it covers the adjacent capsule, intracapsular ligament or tendon.

Synovial fluid

Synovial fluid occupies synovial joints, bursae and tendon sheaths. In synovial joints it is clear or pale yellow, viscous, slightly alkaline at rest (the pH lowers during activity), and contains a small mixed population of cells and metachromatic amorphous particles. Fluid volume is low: usually less than 0.5 ml can be aspirated from a large joint such as the knee.

The composition of synovial fluid is consistent with it being mainly a dialysate of blood plasma. It contains protein (approximately 0.9 mg/100 ml) derived from the blood. It also contains hyaluronan, which is thought to be a significant determinant of the viscoelastic and thixotropic (flow rate dependent) properties of synovial fluid. A small proportion (approximately 2%) of synovial protein differs from plasma protein and is probably produced by synovial type B cells, and a very small proportion (approximately 0.5%) of synovial protein appears to be a specialized lubricating glycoprotein. Synovial fluid contains a few cells (approximately 60 per ml in resting human joints), including monocytes, lymphocytes, macrophages, synovial intimal cells and polymorphonuclear leukocytes: higher counts are found in young individuals. The amorphous metachromatic particles and fragments of cells and fibrous tissue found in synovial fluid are presumed to be produced by wear and tear.

Intra-articular menisci, discs and fat pads

An articular disc or meniscus occurs between articular surfaces where congruity is low. It consists of fibrocartilage where the fibrous element usually predominates, and is not covered by synovial membrane. The term meniscus should be reserved for incomplete discs, like those in the knee joint and, occasionally, in the acromioclavicular joint. Complete discs, such as those in the sternoclavicular and inferior radio-ulnar joints, extend across a synovial joint, dividing it structurally into two synovial cavities; they often have small perforations. The disc in the temporomandibular joint may be complete or incomplete.

The main part of a disc is relatively acellular, but the surface may be covered by an incomplete stratum of flat cells, continuous at the periphery with adjacent synovial membrane. Discs are usually connected to their fibrous capsule by vascularized connective tissue, so that they become invaded by vessels and afferent and vasomotor sympathetic nerves. Sometimes the union between disc and capsule is closer and stronger, as occurs in the knee and temporomandibular joints.

The function of intra-articular fibrocartilages is uncertain. Deductions have been made from structural or phylogenetic data, aided by mechanical analogies; suggestions include shock absorption, improvement of fit between surfaces, facilitation of combined movements, checking of translation at joints such as the knee, deployment of weight over larger surface areas, protection of articular margins, facilitation of rolling movements, and spread of lubricant. The temporomandibular disc has attracted particular attention because of its exceptional, perhaps unique, design and biomechanical properties (see Ch. 31).

The functions of labra and fat pads, two other quite common types of intra-articular structure, are also uncertain. A labrum is a fibrocartilaginous annular lip, usually triangular in cross-section, attached to an articular margin (e.g. glenoid fossa and acetabulum). It deepens the socket and increases the area of contact between articulating surfaces, and may act as a lubricant spreader. Like menisci, labra may reduce the synovial space to capillary dimensions, thus limiting drag, but unlike menisci, labra are not compressed between articular surfaces. Small fibrous labra (connective tissue rims) have been described along the ventral or dorsal margins of the zygapophysial joints at lumbar levels, as have meniscus-shaped fibroadipose meniscoids at the superior or inferior poles of the same joints. Fat pads are soft and change shape to fill joint recesses that vary in dimension according to joint position.

Neurovascular supply

Vascular supply and lymphatic drainage

Joints receive blood from periarticular arterial plexuses whose numerous branches pierce the fibrous capsules to form subsynovial vascular plexuses. Some synovial vessels end near articular margins in an anastomotic fringe, the circulus articularis vasculosus. A lymphatic plexus in the synovial subintima drains along blood vessels to the regional deep lymph nodes.

Innervation

A movable joint is innervated by articular branches of the nerves that supply the muscles acting on the joint and that also supply the skin covering the joint (Hilton's law). Although there is overlap between the territories of different nerves, each nerve innervates a specific part of the capsule. The region made taut by muscular contraction is usually innervated by nerves that supply the antagonists. For example, stretching the portion of the capsule of the hip joint supplied by the obturator nerve during abduction elicits reflex contraction of the adductors that is usually sufficient to prevent damage.

Myelinated axons in articular nerves innervate Ruffini endings, lamellated articular corpuscles and structures resembling Golgi tendon organs. Ruffini endings respond to stretch and adapt slowly, whereas lamellated corpuscles respond to rapid movement and vibration and adapt rapidly; both types of receptor register the speed and direction of movement. Golgi tendon organs, innervated by the largest myelinated axons (10–15 μm diameter), are slow to adapt; they mediate position sense and are concerned in stereognosis, i.e. recognition of shape of held objects. Simple endings are numerous at the attachments of capsules and ligaments, and are thought to be the terminals of unmyelinated and thinly myelinated nociceptive axons.

Many unmyelinated postganglionic sympathetic axons terminate near vascular smooth muscle, and are presumably either vasomotor or vasosensory. The nerve endings in synovial membrane are believed to supply blood vessels exclusively, from which it is inferred that synovial membrane is relatively insensitive to pain.

Classification

Synovial joints may be classified (Fig. 5.33) according to their shape. While this has some practical value, it should be remembered that they are merely variations, sometimes extreme, of two basic forms. Articular surfaces are never truly flat, or complete spheres, cylinders, cones or ellipsoids. They are better described as parts of a single ovoid surface or a complex construction of more than one such surface.

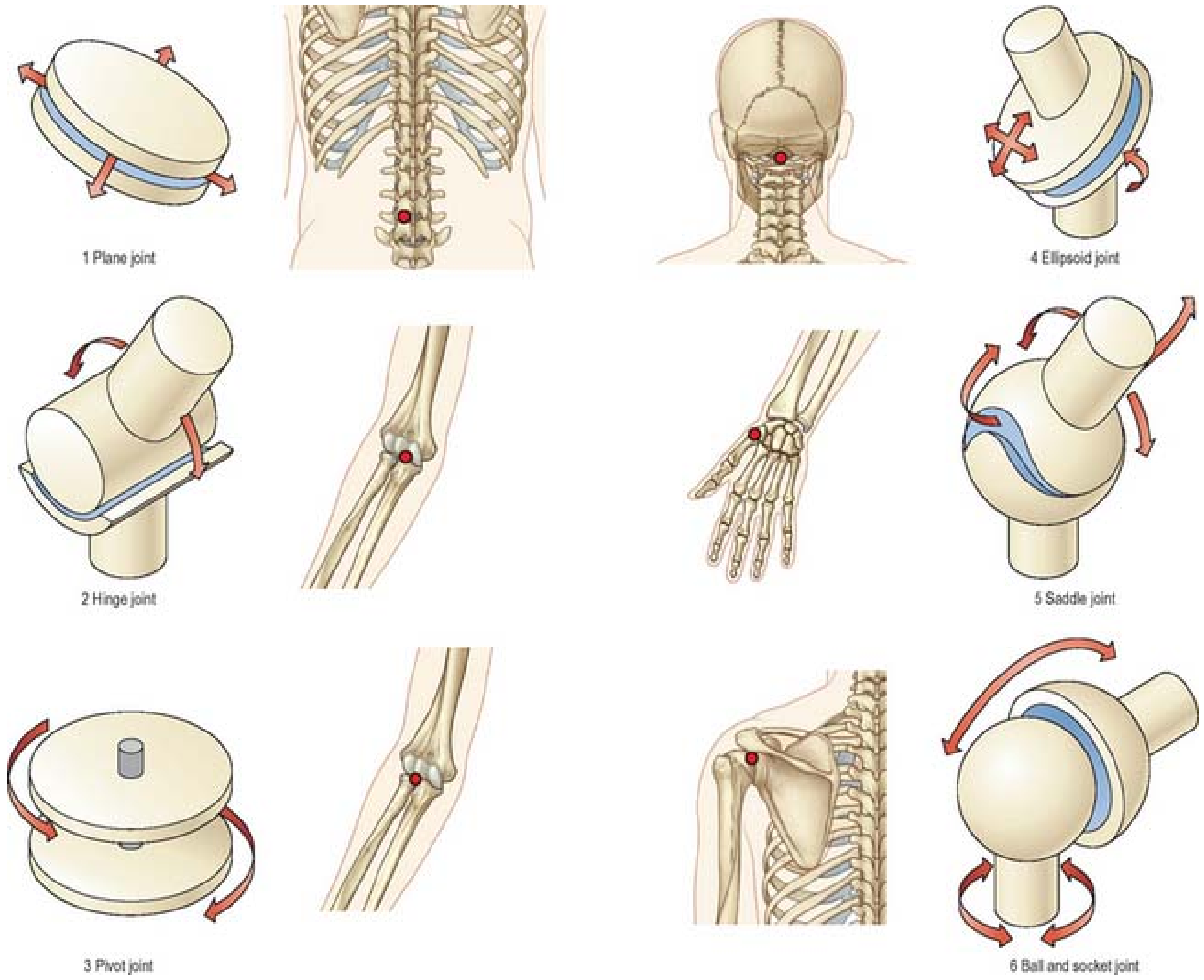
1 Plane joint
4 Ellipsoid joint
2 Hinge joint
5 Saddle joint
3 Pivot joint
6 Ball and socket joint

Fig. 5.33 Types of synovial joint, with selected examples.

Plane joints

Plane joints are appositions of almost flat surfaces, e.g. intermetatarsal and some intercarpal joints. Slight curvature although usual, is often disregarded, and movements are considered to be pure translations or sliding between bones, whereas, in precise dynamics, even slight curvatures cannot be ignored.

Hinge joints

These joints resemble hinges because movement is largely restricted to one plane, which means that they are uniaxial, e.g. interphalangeal and humero-ulnar joints. However, the surfaces of these biological hinges differ from regular mechanical cylinders because their profiles are not arcs but varyingly spiral, which means that motion does not truly occur about a single axis. Hinge joints possess strong collateral ligaments.

Pivot joints

These are uniaxial joints in which an osseous pivot in an osteoligamentous ring allows rotation only around the axis of the pivot. Pivots may rotate in rings, e.g. the head of the radius rotates within the anular ligament and ulnar radial notch, or rings may rotate around pivots, e.g. the atlas rotates around the dens of the axis.

Bicondylar joints

Bicondylar joints are predominantly uniaxial, with a main movement in one plane, but with limited rotation about a second axis orthogonal to the first. Bicondylar joints are so named because they are formed of two convex condyles (knuckles) which articulate with concave or flat surfaces (sometimes inappropriately also called condyles). The condyles may lie within a common fibrous capsule, e.g. the knee, or in separate capsules that necessarily cooperate in all movements as a condylar pair, e.g. temporomandibular joints.

Ellipsoid joints

Ellipsoid joints are biaxial, and consist of an oval, convex surface apposed to an elliptical concavity, e.g. radiocarpal and metacarpophalangeal joints. Primary movements occur around two orthogonal axes, e.g. flexion–extension, abduction–adduction, that may be combined as circumduction. Rotation around the third axis is largely prevented by general articular shape.

Saddle joints

Saddle joints are biaxial and have concavoconvex surfaces. Each is maximally convex in a particular direction, and is maximally concave at right angles to this direction. The convexity of the larger surface is apposed to the concavity of the smaller surface and vice versa. Primary movements occur in two orthogonal planes, but articular shape causes axial rotation of the moving bone. Such coupled rotation is never independent, and is functionally significant in habitual positioning and limitation of movement. The most familiar saddle joint is the carpometacarpal joint of the thumb, other examples include the ankle and calcaneocuboid joints.

Ball-and-socket joints

These joints are multiaxial and are formed by the reception of a globoid ‘head’ into an opposing cup, e.g. the hip and shoulder joints. Their surfaces, although resembling parts of spheres, are not strictly spherical but slightly ovoid, and consequently congruence is not perfect in most positions. Indeed, it occurs in only one position, at the end of the commonest movement.

Factors influencing movement

Movements at synovial joints depend upon a number of factors including the complexity and number of articulating surfaces and the number and position of the principal axes of movement.

Complexity of form

Most synovial joints have two surfaces and are simple articulations, e.g. the glenohumeral and interphalangeal joints. In some, one surface is wholly convex and greater in area than its opposing concave surface, and occasionally, both surfaces are concavoconvex. A joint with more than two articular surfaces is called a compound joint, e.g. the knee and the elbow. In all compound joints, articulating territories remain distinct. A synovial joint that contains an intra-articular disc or meniscus is called a complex joint, e.g. the tibiofemoral joint of the knee, the sternoclavicular and temporomandibular joints (see Fig. 5.31).

Degrees of freedom

Joint motion can be described by rotation and translation about three orthogonal axes. There are three possible rotations (axial, abduction–adduction, flexion–extension) and three possible translations (proximo-distal, mediolateral, anteroposterior). Each is a degree of freedom. For most joints, translations are negligible and do not need consideration (Fig. 5.34). A few joints have minor pure translatory movements, but most joint motion is by rotation.

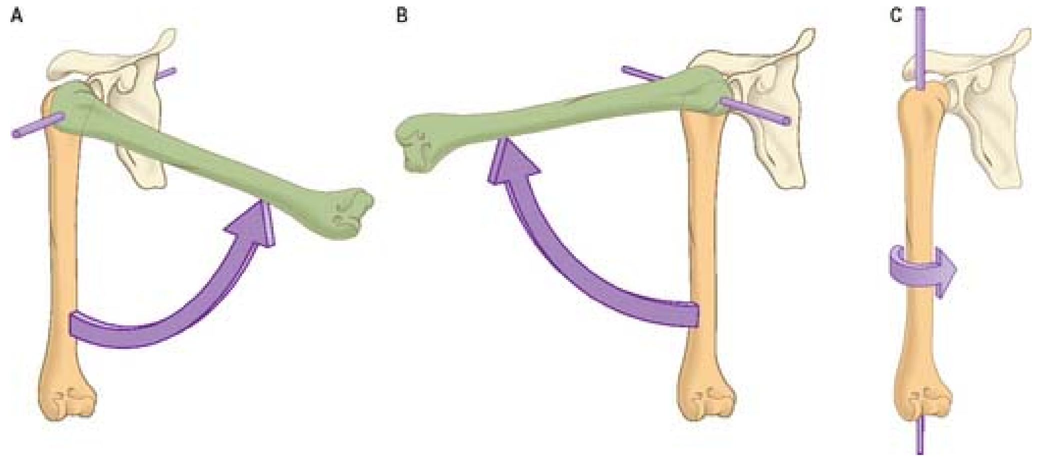

Fig. 5.34 The shoulder joint is multiaxial, and possesses three degrees of freedom. **A–C** show the three mutually perpendicular axes around which the principal movements of flexion–extension (**A**), abduction–adduction (**B**) and medial and lateral rotation (**C**) occur. Note that these axes are referred to the plane of the scapula and not to the coronal and sagittal planes of the erect body. Although an infinite variety of additional movements may occur at such a joint, e.g. movements involving intermediate planes or combinations, they can always be resolved mathematically into components related to the three axes illustrated.

When movement is practically limited to rotation about one axis, e.g. the elbow, a joint is termed uniaxial and has one degree of freedom. If independent movements can occur around two axes, e.g. the knee (flexion–extension and axial rotation), the joint is biaxial, and has two degrees of freedom. Since there are three axes for independent rotation, joints may have up to three degrees of freedom. This apparently simple classification is complicated by the complexity of joint structure, and has consequent effects on motion. Even though a true ‘ball and socket’ joint can rotate about many chosen axes, i.e. it is multiaxial, for each position there is a maximum of three orthogonal planes, which means that it can have, as a maximum, three degrees of freedom.

For a uniaxial hinge joint with a single degree of freedom, a single unchanging axis of rotation would be predicted. However, because the shapes of joint surfaces are complex, there is a variable radius of curvature (Fig. 5.35) and consequently the axis of rotation will vary as joint movement progresses. When the variation is minor, e.g. the elbow, it is often appropriate to describe a mean position for the axis. In others, e.g. the knee, the situation is more complex.

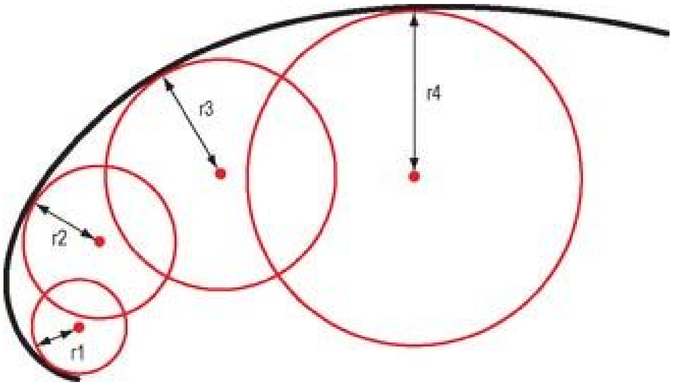

Fig. 5.35 Profile of a section through an ovoid surface showing that it may be considered as a series of segments of circles of changing radius. The radius of curvature of joint surfaces often changes from one location to another.

Simple movements are rarely such. Often motion in one direction is linked to motion in another in an obligatory fashion. There are two varieties of rotation: conjunct (coupled), which is an integral and inevitable accompaniment of the main movement, and adjunct, which can occur independently and may or may not accompany the principal movement.

Articular movements and mechanisms

Joint surfaces move by translation (gliding) and angulation (rotation), usually in combination, to produce gross movements at the joint. Where movement is slight, the reciprocal surfaces are of similar size; where it is wide, the habitually more mobile bone has the larger articular surface.

Translation

Translation is the simplest motion and involves gliding or sliding without appreciable angulation. Although frequently combined with other movements, it is often considered the only motion permitted in some carpal and tarsal articulations. However, cineradiography reveals that considerable angulation occurs during movements of the small carpal and tarsal bones.

Angulation

Angulation implies a change in angle between the topographical axes of articulating bones, e.g. flexion and extension; abduction and adduction. Angulation can be subdivided as follows.

Flexion

Flexion is a widely used term, but difficult to define. It often means approximation of two ventral surfaces around a transverse axis. However, the thumb is almost at right angles to the fingers: its ‘dorsal’ surface faces laterally so that flexion and extension at its joints occur around anteroposterior axes. At the shoulder, flexion is referred to an oblique axis through the centre of the humeral head in the plane of the scapular body, the arm moving anteromedially forwards and hence nearer to the ventral aspect of the trunk. At the hip, which has a transverse axis, flexion brings the morphologically dorsal (but topographically ventral) surface of the thigh to the ventral aspect of the trunk. Description of flexion at the ankle joint is complicated by the fact that the foot is set at a right angle to the leg. Elevation diminishes this angle and is usually termed flexion: since it is the approximation of two dorsal surfaces it might equally be called extension. Flexion has also been defined as the fetal posture, implying that elevation of the foot is flexion, a view supported by withdrawal reflexes in which elevation is always associated with flexion at the knee and hip. Definitions based on morphological and physiological considerations are thus contradictory: to avoid confusion, dorsiflexion and plantarflexion are used to describe ankle movements.

Abduction and adduction

Abduction and adduction occur around anteroposterior axes except at the first carpometacarpal and shoulder joints. The terms generally imply lateral or medial angulation, except in digits, where arbitrary planes are chosen (midlines of the middle digit of the hand and second digit of the foot), because these are least mobile in this respect. Abduction of the thumb occurs around a transverse axis and away from the palm. Similarly, abduction of the humerus on the scapula occurs in the scapular plane around an oblique axis at right angles to it.

Axial rotation

Axial rotation is a widely, but often imprecisely, used term. Its restricted sense denotes movement around some notional ‘longitudinal’ axis which may even be in a separate bone, e.g. the dens of the second cervical vertebra, on which the atlas rotates. An axis may be approximately the centre of the shaft of a long bone, e.g. in medial and lateral humeral rotation (Fig. 5.34). It may be at an angle to the topographical axis of a bone, e.g. in movement of the radius on the ulna in pronation and supination, where the axis joins the centre of the radial head to the base of the ulnar styloid process, or in medial and lateral femoral rotation, where the axis joins the centre of the femoral head to a (disputed) point in the distal femur. In these examples, rotations can be independent adjunct motions, constituting a degree of freedom, or conjunct (coupled) rotations, which always accompany some other main movement as a consequence of articular geometry. Obligatory conjunct (coupled) motion is frequently combined with a degree of voluntary adjunct motion, the latter dictating what proportion of the motion occurs above the minimum obligatory component.

Circumduction

Circumduction combines successive flexion, abduction, extension and adduction, and occurs when the distal end of a long bone circumscribes the base of a cone that has its apex at the joint in question, e.g. shoulder and hip joints.

DEVELOPMENT OF JOINTS

The development of joints is described in the context of limb development in Chapter 51.

MUSCLE

Most cells possess cytoskeletal elements that are capable of lengthening or shortening and so enable the cell to change its shape. This capacity is important in a variety of cellular functions, e.g. locomotion, phagocytosis, mitosis and extension of processes. Proteins referred to as molecular motors (see Ch. 1) can effect changes of length much more rapidly than systems that are dependent on polymerization–depolymerization mechanisms (actin, tubulin), by using energy from the hydrolysis of adenosine 5′-triphosphate (ATP). Of these ATP-dependent systems, one of the most widespread is based on the interaction of actin and myosin.

In muscle cells the filaments of actin and myosin and their associated proteins are so abundant that they almost fill the interior of the cell. Moreover they align predominantly in one direction, so that interactions at the molecular level are translated into linear contraction of the whole cell. The ability of these specialized cells to change shape has thus become their most important property. Assemblies of contractile muscle cells, the muscles, are machines for converting chemical energy into mechanical work. The forces generated move limbs, inflate the lungs, pump blood, close and open tubes, etc. In man, muscle tissue constitutes 40–50% of the body mass.

CLASSIFICATION OF MUSCLE

Muscle cells (fibres) are also known as myocytes (the prefixes myo- and sarco- are frequently used in naming structures associated with muscle). They differentiate along one of three main pathways to form skeletal, cardiac or smooth muscle. Both skeletal and cardiac muscle may be called striated muscle, because their myosin and actin filaments are organized into regular, repeating elements which give the cells a finely cross-striated appearance when they are viewed microscopically. Smooth muscle, in contrast, lacks such repeating elements and thus has no striations.

Other contractile cells, including myofibroblasts and myoepithelial cells, are different in character and developmental origin. They contain smooth muscle-like contractile proteins and are found singly or in small groups.

Striated muscle

Skeletal muscle

Skeletal muscle forms the bulk of the muscular tissue of the body and consists of parallel bundles of long, multinucleate fibres. This type of muscle is capable of powerful contractions (about 100 watts per kilogram) because of the regular organization of its contractile proteins. However, the price paid for this organization is a limited contractile range: wherever a larger range of movement is required, it is achieved through the amplification provided by the lever systems of the skeleton to which the muscle is attached (hence the name skeletal muscle) (see below).

Skeletal muscle is innervated by somatic motor nerves. It is sometimes referred to as voluntary muscle, because the movements in which it participates are often initiated under conscious control. However, this is a misleading term: skeletal muscle is involved in many movements, such as breathing, blinking, swallowing, and the actions of the muscles of the perineum and in the middle ear, which are usually or exclusively driven at an unconscious level.

Cardiac muscle

Cardiac muscle is found only in the heart, and in the walls of large veins where they enter the heart. It consists of a branching network of individual cells that are linked electrically and mechanically to function as a unit. Compared with skeletal muscle, cardiac muscle is much less powerful (3–5 watts per kilogram) but far more resistant to fatigue. It is provided with a continuous supply of energy by numerous blood vessels around the fibres, and abundant mitochondria within them. Cardiac muscle differs structurally and functionally from skeletal muscle in some important respects. It is, for example, intrinsically capable of rhythmic contraction, with a rate and strength which is nevertheless responsive to hormonal and autonomic nervous control.

Cardiac muscle is considered in detail in Chapter 6.

Smooth muscle

Smooth muscle is found in all systems of the body, in the walls of the viscera, including most of the gastrointestinal, respiratory, urinary and reproductive tracts, in the tunica media of blood vessels, in the dermis (as the arrector pili muscles), in the intrinsic muscles of the eye, and the dartos muscular layer of the scrotum. In some places, smooth muscle fasciculi are associated with those of skeletal muscle, e.g. the sphincters of the anus and the urinary bladder, the tarsal muscles of the upper and lower eyelids, the suspensory muscle of the duodenum, a transitional zone in the oesophagus, and fasciae and ligaments on the pelvic aspect of the pelvic diaphragm.

Smooth muscle contains actin and myosin, but they are not organized into repeating units, and its microscopic appearance is therefore unstriated (smooth). The elongated cells are smaller than those of striated muscle, and taper at the ends. They are capable of slow but sustained contractions, and although this type of muscle is less powerful than striated muscle, the amount of shortening can be much greater. These functional attributes are well illustrated by its role in the walls of tubes and sacs, where its action regulates the size of the enclosed lumen and, in some cases, the consequent movement of luminal contents.

A smooth muscle cell may be excited in several ways, most commonly by an autonomic nerve fibre, a blood-borne neurohormone, or conduction from a neighbouring smooth muscle cell. Since none of these routes is under conscious control, smooth muscle is sometimes referred to as involuntary muscle.

Smooth muscle is considered in detail in Chapter 6.

SKELETAL MUSCLE

Shape and fibre architecture

It is possible to classify muscles based on their general shape and the predominant orientation of their fibres relative to the direction of pull (Fig. 5.36). Muscles with fibres that are largely parallel to the line of pull vary in form from flat, short and quadrilateral (e.g. thyrohyoid) to long and strap-like (e.g. sternohyoid, sartorius). In such muscles, individual fibres may run for the entire length of the muscle, or over shorter segments when there are transverse, tendinous intersections at intervals (e.g. rectus abdominis). In a fusiform muscle, the fibres may be close to parallel in the 'belly', but converge to a tendon at one or both ends. Where fibres are oblique to the line of pull, muscles may be triangular (e.g. temporalis, adductor longus) or pennate (feather-like) in construction. The latter vary in complexity from unipennate (e.g. flexor pollicis longus) and bipennate (e.g. rectus femoris, dorsal interossei) to multipennate (e.g. deltoid). Fibres may pass obliquely between deep and superficial aponeuroses, in a type of 'unipennate' form (e.g. soleus), or muscle fibres may start from the walls of osteofascial compartments and converge obliquely on a central tendon in circumpennate fashion (e.g. tibialis anterior). Muscles may exhibit a spiral or twisted arrangement (e.g. sternocostal fibres of pectoralis major and latissimus dorsi, which undergo a 180° twist between their medial and lateral attachments), or may spiral around a bone (e.g. supinator, which winds obliquely around the proximal radial shaft), or may contain two or more planes of fibres arranged in differing directions, a type of spiral sometimes referred to as cruciate (sternocleidomastoid, masseter and adductor magnus are all partially spiral and cruciate). Many muscles display more than one of these major types of arrangement, and show regional variations which correspond to contrasting, and in some cases independent, actions.

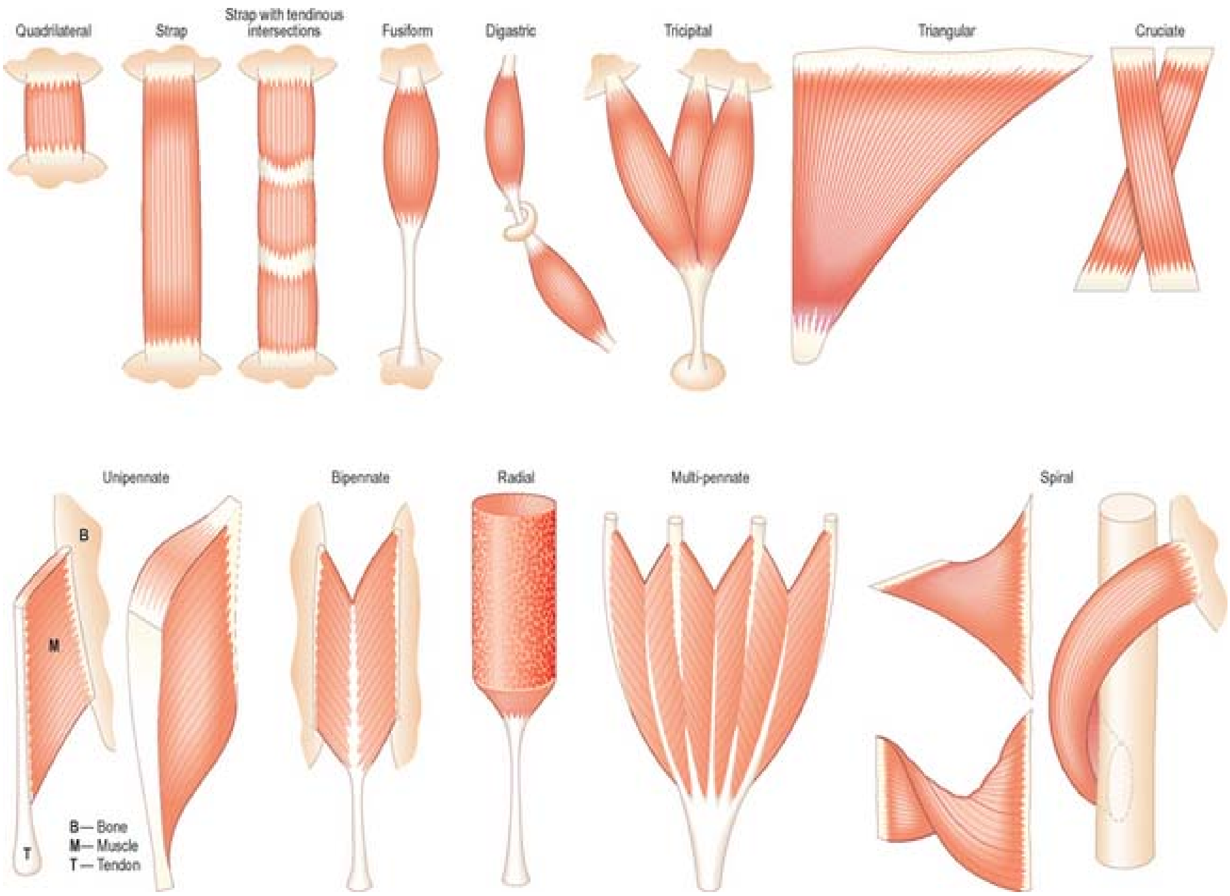
Quadrilateral
Strap
Strap with tendinous intersections
Fusiform
Digastric
Tricipital
Triangular
Cruciate
Unipennate
B
M
T
B—Bone
M—Muscle
T—Tendon
Bipennate
Radial
Multi-pennate
Spiral

Fig. 5.36 Morphological ‘types’ of muscle based on their general form and fascicular architecture.

Muscle nomenclature

The names given to individual muscles are usually descriptive, based on their shape, size, number of heads or bellies, position, depth, attachments, or actions. The meanings of some of the terms used are given in Table 5.1.

Table 5.1 Terms used in naming muscles.

Shape	**Number of heads or bellies**	**Position**
Deltoid (triangular)	Biceps (two heads)	Anterior, posterior, medial, lateral, superior, inferior, supra-, infra-

Quadratus (square) Rhomboid (diamond-shaped) Teres (round) Gracilis (slender) Rectus (straight) Lumbrical (worm-like)	Triceps (three heads) Quadriceps (four heads) Digastric (two bellies)	Interosseus (between bones) Dorsi (of the back) Abdominis (of the abdomen) Pectoralis (of the chest) Brachii (of the arm) Femoris (of the thigh) Oris (of the mouth) Oculi (of the eye)

Size	**Depth**	**Action**
Major, minor, longus (long) Brevis (short) Latissimus (broadest) Longissimus (longest)	Superficialis (superficial) Profundus (deep) Externus/externi (external) Internus/interni (internal)	Extensor, flexor Abductor, adductor Levator, depressor Supinator, pronator Constrictor, dilator

	Attachment	
	Sternocleidomastoid (from sternum and clavicle to mastoid process) Coracobrachialis (from the coracoid process to the arm)	

These terms are often used in combination, e.g. flexor digitorum longus (long flexor of the digits), latissimus dorsi (broadest muscle of the back). The functional roles implied by names should be interpreted with caution: the names given to individual muscles or muscle groups are often oversimplified, and terms denoting action may emphasize only one of a number of usual actions. Moreover, a given muscle may play different roles in different movements, and these roles may change if the movements are assisted or opposed by gravity.

Microstructure of skeletal muscle

The cellular units of skeletal muscle are enormous multinucleate muscle fibres (Fig. 5.37, Fig. 5.38) which develop by fusion of individual myoblasts (see below). Individual muscle fibres are long, cylindrical structures that tend to be consistent in size within a given muscle, but in different muscles may range from 10 to 100 µm in diameter and from millimetres to many centimeters in length. The cytoplasm of each fibre, sarcoplasm, is surrounded by a plasma membrane that is often called the sarcolemma. The contractile machinery is concentrated into myofibrils, long narrow structures (1–2 µm in diameter) that extend the length of the fibre and form the bulk of the sarcoplasm. Numerous moderately euchromatic, oval nuclei usually occupy a thin transparent rim of sarcoplasm between the myofibrils and the sarcolemma, and are especially numerous in the region of the neuromuscular junction (see Fig. 3.37). A transverse section of a muscle fibre may only reveal one or two nuclei, but there may be several hundred along the length of an entire fibre. Myogenic satellite cells lie between the sarcolemma and the surrounding basal lamina (see below).

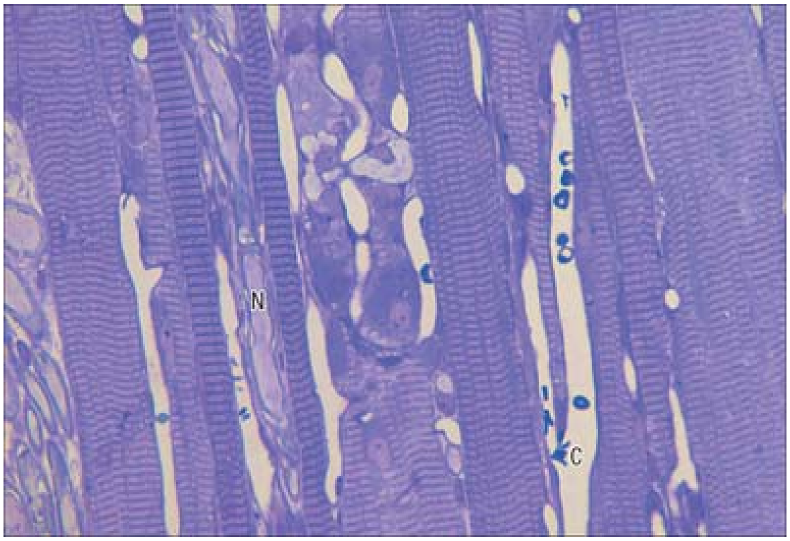

Fig. 5.37 Skeletal muscle fibres from human lateral rectus in longitudinal section, showing transverse striations representing the sarcomeric organization of actin and myosin filaments. The variation in fibre diameter is typical of extraocular muscles. Capillaries (C) and nerves (N) lie between the fibres, oriented mainly in parallel and so are also sectioned longitudinally. Toluidine blue stained resin section.

(Provided by courtesy of the Department of Optometry and Visual Science, City University, London.)

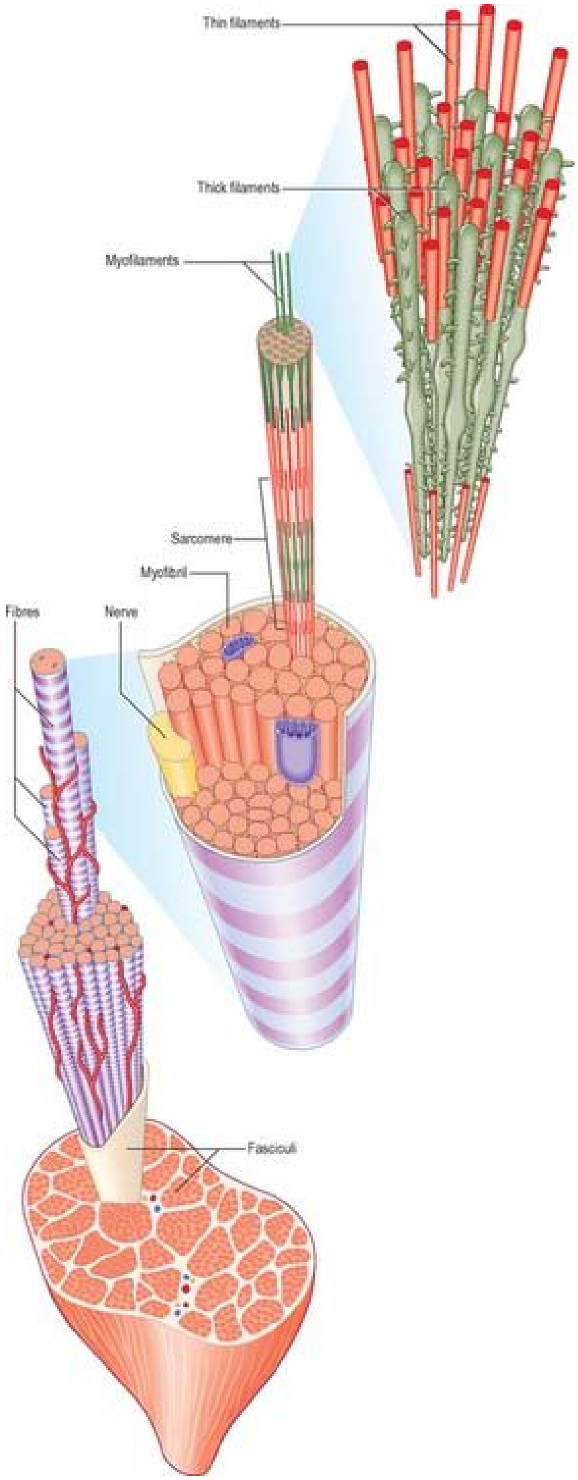
Thin filaments
Thick filaments
Myofilaments
Sarcomere
Myofibril
Fibres
Nerve
Fasciculi

Fig. 5.38 Levels of organization within a skeletal muscle, from whole muscle to fasciculi, single fibres, myofibrils and myofilaments.

The myofibrils are too tightly packed to be visible by routine light microscopy (see below). Of greater significance are transverse striations, produced by the alignment across the fibre of repeating elements, the sarcomeres, within neighbouring myofibrils. These cross-striations are usually evident in conventionally stained histological sections, but may be demonstrated more effectively using special stains. They are even more striking under polarized light when they appear as a pattern of alternating dark and light bands. The darker, anisotropic or A-bands, are birefringent and rotate the plane of polarized light strongly. The lighter, isotropic or I-bands, rotate the plane of polarized light to a negligible degree. In transverse section, the profiles of the fibres are usually polygonal (Fig. 5.38; see Fig. 5.40). The sarcoplasm often has a stippled appearance, because the transversely sectioned myofibrils are resolved as dots. Their packing density varies. In some muscles, e.g. the extrinsic muscles of the larynx, the muscle fibres tend not to be tightly packed, whereas in others, e.g. the group of jaw closing muscles, the fibres are closely packed and have rounded profiles.

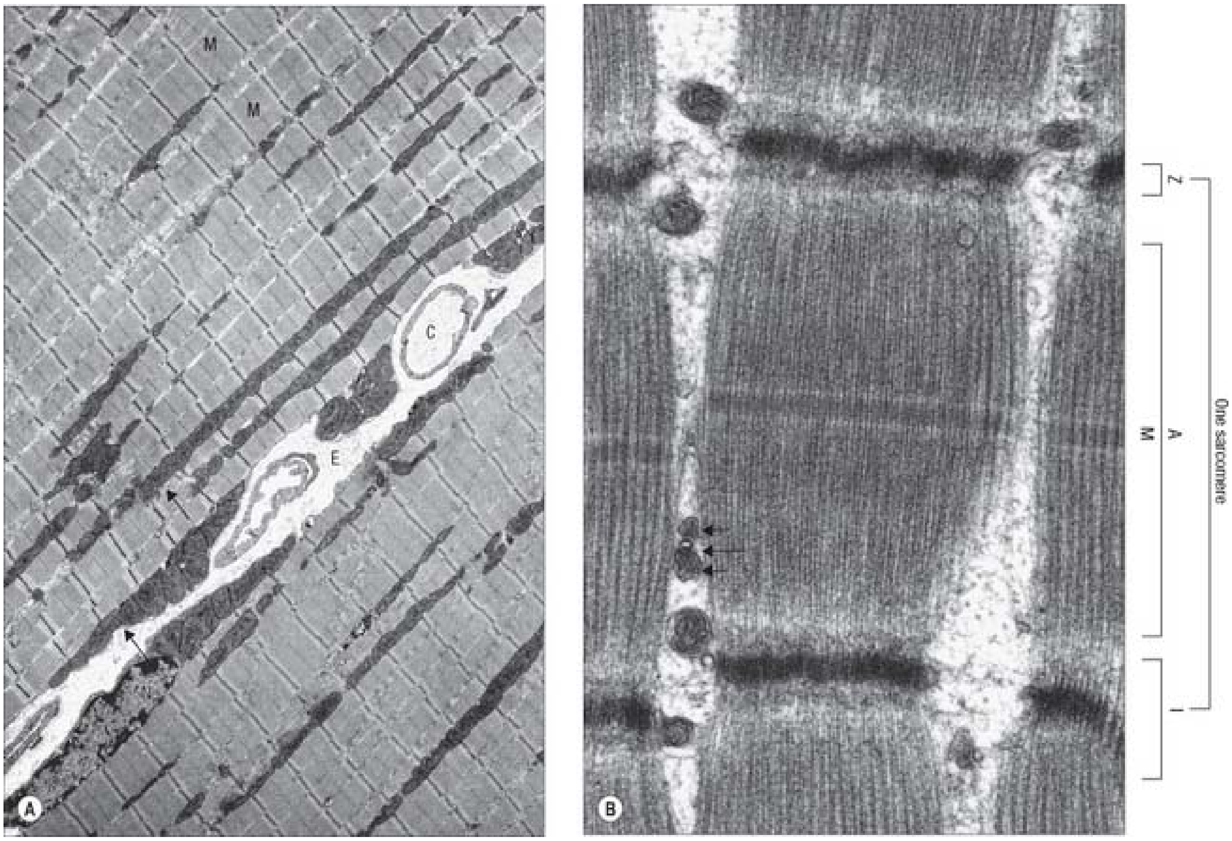

Fig. 5.40 The electron microscopic appearance of skeletal muscle in longitudinal section. **A**, Low-power view of parts of two adjacent muscle fibres, separated by endomysium (E) containing capillaries (C) and a peripherally-placed nucleus (N) in the fibre on the right. Mitochondria (arrows) are situated peripherally and between myofibrils (M). Myofibrils pack the cytoplasm, with their sarcomeres (contractile units) in register, as seen by the alignment of Z discs (dark transverse lines) across each muscle fibre. **B**, A sarcomere within a myofibril, and parts of two others. (A sarcomere is the distance between adjacent Z discs). Also seen are the A band, bisected by the M line, and I band, which here is almost obliterated in the contracted state (see **Fig. 5.41**). A triad is visible between myofibrils, comprised of a T-tubule (long arrow) and two terminal cisternae of sarcoplasmic reticulum (short arrows).

(Part A provided by courtesy of Professor Hans Hoppeler, Institute of Anatomy, University of Bern, Switzerland.)

In general, skeletal muscle fibres are large (there are a few exceptions, e.g. the intrinsic muscles of the larynx). This means that electron micrographs, unless of very low magnification, seldom show more than part of the interior of a fibre. Myofibrils, cylindrical structures about 1 μm diameter (Fig. 5.37), are the dominant ultrastructural feature of such micrographs. In longitudinal sections they appear as ribbons and are interrupted at regular intervals by thin, very densely stained transverse lines, which correspond to discsin the parent cylindrical structure. These are the Z-lines or, more properly, Z-discs (Zwischenscheiben = interval discs) that divide the myofibril into a linear series of repeating contractile units, sarcomeres, each of which is typically 2.2 μm long in resting muscle. At higher power, sarcomeres are seen to consist of two types of filament, thick and thin, organized into regular arrays (Fig. 5.38; Fig. 5.40). The thick filaments, which are approximately 15 nm in diameter, are composed mainly of myosin. The thin filaments, which are 8 nm in diameter, are composed mainly of actin. The arrays of thick and thin filaments form a partially overlapping structure in which electron density (as seen in the electron microscope) varies according to the amount of protein present. The A-band consists of the thick filaments, together with lengths of thin filaments that interdigitate with, and thus overlap, the thick filaments at either end (Fig. 5.40, Fig. 5.41). The central, paler region of the A-band, which is not penetrated by the thin filaments, is called the H-zone (Helle = light). At their centres, the thick filaments are linked together transversely by material that constitutes the M-line (Mittelscheibe = middle [of] disc), that is visible in most muscles. The I-band consists of the adjacent portions of two neighbouring sarcomeres in which the thin filaments are not overlapped by thick filaments. The thin filaments of adjacent sarcomeres are anchored in the Z-disc, which bisects the I-band. A third type of filament is composed of the elastic protein, titin.

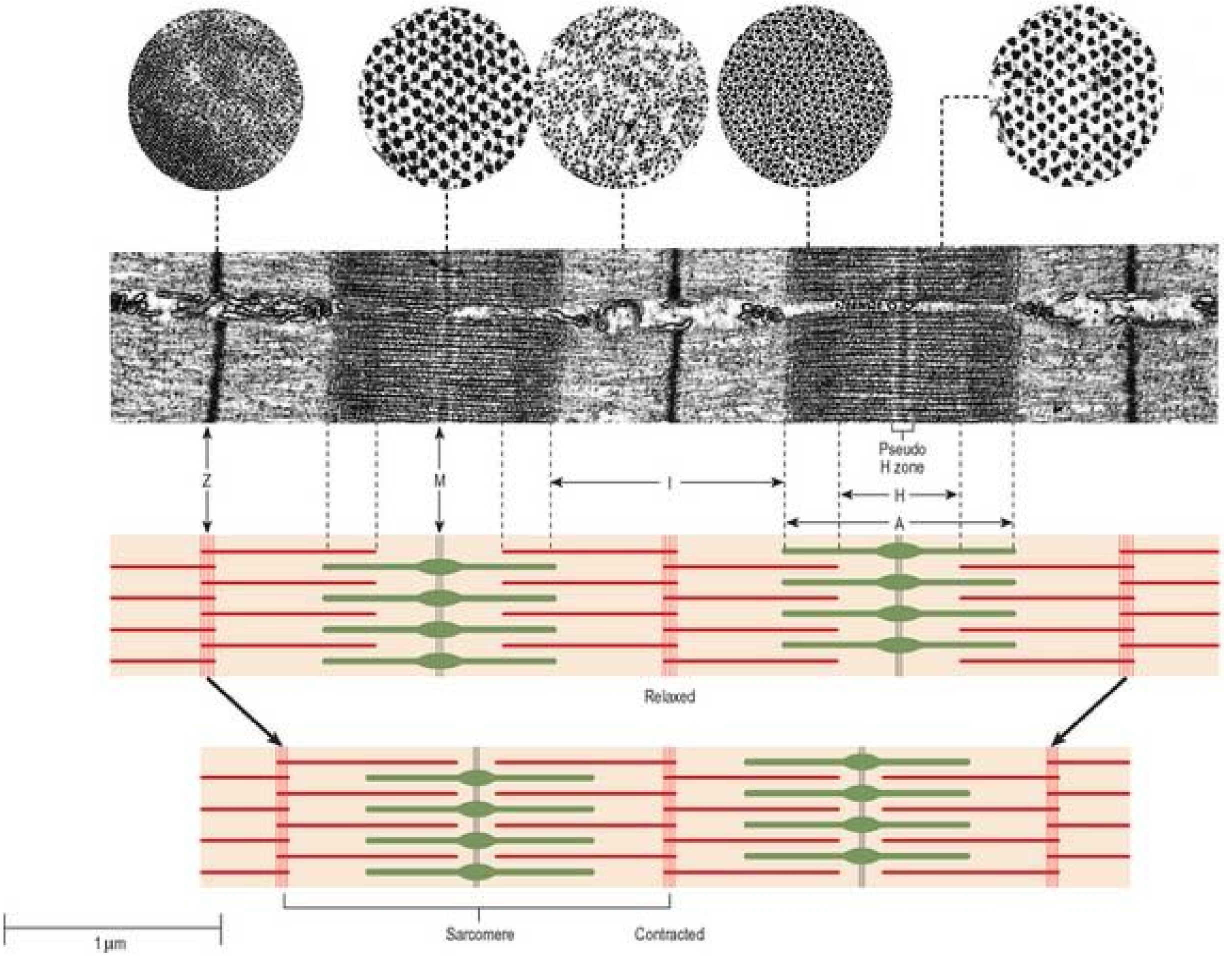

Fig. 5.41 Sarcomeric structures. The drawings below the electron micrograph (of two myofibrils sectioned longitudinally and with their long axes, orientated transversely) indicate the corresponding arrangements of thick and thin filaments. Relaxed and contracted states are shown to illustrate the changes which occur during shortening. Insets at the top show the electron micrographic appearance of transverse sections through the myofibril at the levels shown. Note that the packing geometry of the thin filaments changes from a square array at the Z-disc to a hexagonal array where they interdigitate with thick filaments in the A-band.

(Photographs by Professor Brenda Russell, Department of Physiology and Biophysics, University of Illinois at Chicago.)

The high degree of organization of the arrays of filaments is equally evident in electron micrographs of transverse sections (Fig. 5.41, Fig. 5.42).

The thick myosin filaments form a hexagonal lattice. In the regions where they overlap the thin filaments, each myosin filament is surrounded by six actin filaments at the trigonal points of the lattice. In the I-band, the thin filament pattern changes from hexagonal to square as the filaments approach the Z-disc, where they are incorporated into a square lattice structure.

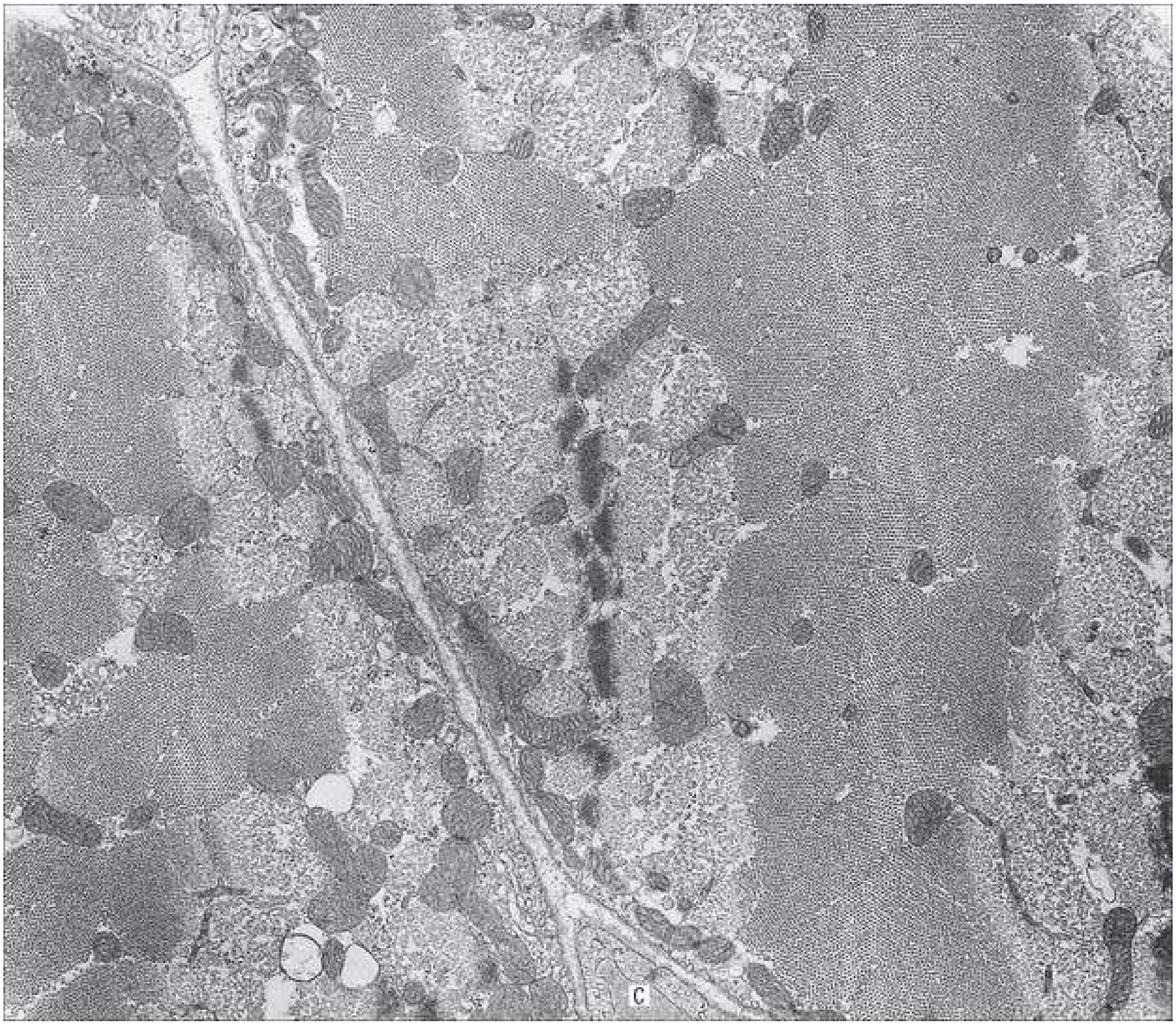

Fig. 5.42 Electron micrograph of skeletal muscle in transverse section, showing parts of two muscle fibres. Part of a capillary (C) is seen in transverse section in the endomysial space. The variation in the appearance of myofibrils in cross-section is explained in **Fig. 5.41**.

(Photograph by Professor Brenda Russell, Department of Physiology and Biophysics, University of Illinois at Chicago.)

The banded appearance of individual myofibrils is a function of the regular alternation of the thick and thin filament arrays. The size of myofibrils places them at the limit of resolution of light microscopy: cross-striations are only visible at that level because of the alignment in register of the bands in adjacent myofibrils across the width of the whole muscle fibre. In suitably stained relaxed material, the A-, I- and H-bands are quite distinct, whereas the Z-discs, which are such a prominent feature of electron micrographs, are thin and much less conspicuous in the light microscope, and M-lines cannot be resolved.

Muscle proteins

Myosin, the protein of the thick filament, constitutes 60% of the total myofibrillar protein and is the most abundant contractile protein. The thick filaments of skeletal and cardiac muscle are 1.5 μm long. Their composition from myosin heavy and light chain assemblies is described in Chapter 1. The other components of myosin, the regulatory proteins tropomyosin and troponin, play a major part in the control of contraction. Actin is the next most abundant contractile protein and constitutes 20% of the total myofibrillar protein. In its filamentous form, F-actin, it is the principal protein of the thin filaments. A number of congenital myopathies result from gene mutations in components of the thin filament assembly (reviewed in Clarkson et al 2004). The third type of long sarcomeric filament connects the thick filaments to the Z-disc, and is formed by the giant protein, titin, which has a molecular mass in the millions. Single titin molecules span the half-sarcomere between the M-lines and the Z-discs, into which they are inserted. They have a tethered portion in the A-band, where they are attached to thick filaments as far as the M-line, and an elastic portion in the I-band. The elastic properties of titin endow the relaxed muscle fibre with passive resistance to stretching and with elastic recoil.

A number of proteins which are neither contractile nor regulatory are responsible for the structural integrity of the myofibrils, particularly their regular internal arrangement. A component of the Z-disc, α-actinin, is a rod-shaped molecule which anchors the plus-ends of actin filaments from adjacent sarcomeres to the Z-disc. Nebulin inserts into the Z-disc, associated with the thin filaments, and regulates the lengths of actin filaments. An intermediate filament protein characteristic of muscle, desmin, encircles the myofibrils at the Z-disc and, with the linking molecule plectrin, forms a meshwork that connects myofibrils together within the muscle fibre and to the sarcolemma. Myomesin holds myosin filaments in their regular lattice arrangement in the region of the M line. Dystrophin is confined to the periphery of the muscle fibre, close to the cytoplasmic face of the sarcolemma. It binds to actin intracellularly and is also associated with a large oligomeric complex of glycoproteins, the dystroglycan/sarcoglycan complex, that spans the membrane and links specifically with merosin, the α2 laminin isoform of the muscle basal lamina. This stabilizes the muscle fibre and transmits forces generated internally on contraction to the extracellular matrix.

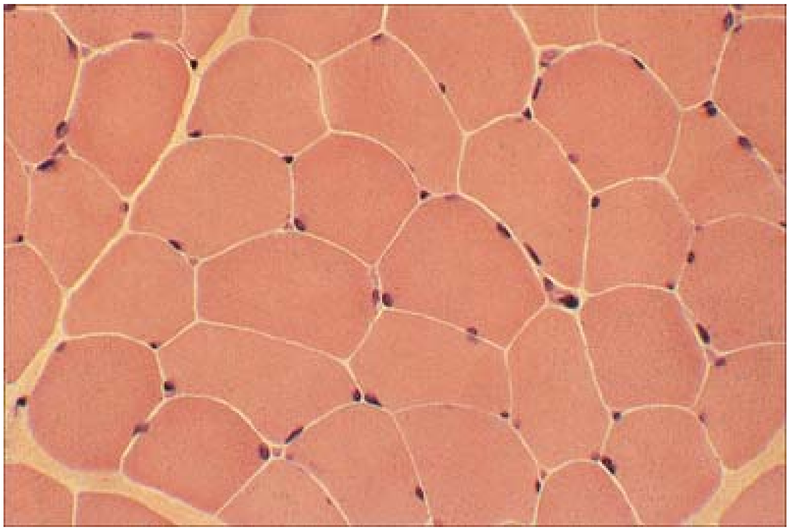

Fig. 5.39 Transverse cryostat section of adult human skeletal muscle. Note the tight packing of the fibres and the peripheral location of the dark stained nuclei.

(Photograph by Professor Stanley Salmons, from a specimen provided by courtesy of Tim Helliwell, Department of Pathology, University of Liverpool.)

Dystrophin is the product of the gene affected in Duchenne muscular dystrophy, a fatal disorder that develops when mutation of the gene leads to the absence of the protein. A milder form of the disease, Becker muscular dystrophy, is associated with a reduced size and/or abundance of dystrophin. Female carriers (heterozygous for the mutant gene) of Duchenne muscular dystrophy may also have mild symptoms of muscle weakness. At about 2500 kb, the gene is one of the largest yet discovered, which may account for the high mutation rate of Duchenne muscular dystrophy (approximately 35% of cases are new mutations). Other muscular dystrophies may involve deficiencies in proteins functionally associated with dystrophin, such as the dystroglycan/sarcoglycan complex or α2 laminin. The involvement in muscular dystrophy of defects in the dystrophin adhesion complex is reviewed in Batchelor & Winder (2006).

Other sarcoplasmic structures

Although myofibrils are the dominant ultrastructural feature of skeletal muscle, the fibres contain other organelles essential for cellular function, such as ribosomes, Golgi apparatus and mitochondria. Most of them are located around the nuclei, between myofibrils and the sarcolemma and, to a lesser extent, between the myofibrils. Mitochondria, lipid droplets and glycogen provide the metabolic support needed by active muscle. The mitochondria are elongated and their cristae are closely packed. The number of mitochondria in an adult muscle fibre is not fixed, but can increase or decrease quite readily in response to sustained changes in activity. Spherical lipid droplets, approximately 0.25 μm in diameter, are distributed uniformly throughout the sarcoplasm between myofibrils. They represent a rich source of energy that can be tapped only by oxidative metabolic pathways: they are therefore more common in fibres which have a high mitochondrial content and good capillary blood supply. Small clusters of glycogen granules are dispersed between myofibrils and among the thin filaments. In brief bursts of activity they provide an important source of anaerobic energy that is not dependent on blood flow to the muscle fibre.

Tubular invaginations of the sarcolemma penetrate between the myofibrils in a transverse plane at the limit of each A-band (Fig. 5.40). The lumina of these transverse (T-) tubules are thus in continuity with the extracellular space. At the ends of the muscle fibre, where force is transmitted to adjacent connective tissue structures, the sarcolemma is folded into numerous finger-like projections that strengthen the junctional region by increasing the area of attachment.

The sarcoplasmic reticulum (SR) is a specialized form of smooth endoplasmic reticulum and forms a plexus of anastomosing membrane cisternae that fills much of the space between myofibrils (Fig. 5.43). The cisternae expand into larger sacs, junctional sarcoplasmic reticulum or terminal cisternae, where they come into close contact with T-tubules, forming structures called triads (Fig. 5.40; Fig. 5.43). The membranes of the SR contain calcium–ATPase pumps that transport calcium ions into the terminal cisternae, where the ions are bound to calsequestrin, a protein with a high affinity for calcium, in dense storage granules. In this way, calcium can be accumulated and retained in the terminal cisternae at a much higher concentration than elsewhere in the sarcoplasm. Ca^{2+}-release channels (ryanodine receptors) are concentrated mainly in the terminal cisternae and form one half of the junctional ‘feet’ or ‘pillars’ that bridge the SR and T-tubules at the triads. The other half of the junctional feet is the T-tubule receptor that constitutes the voltage sensor.

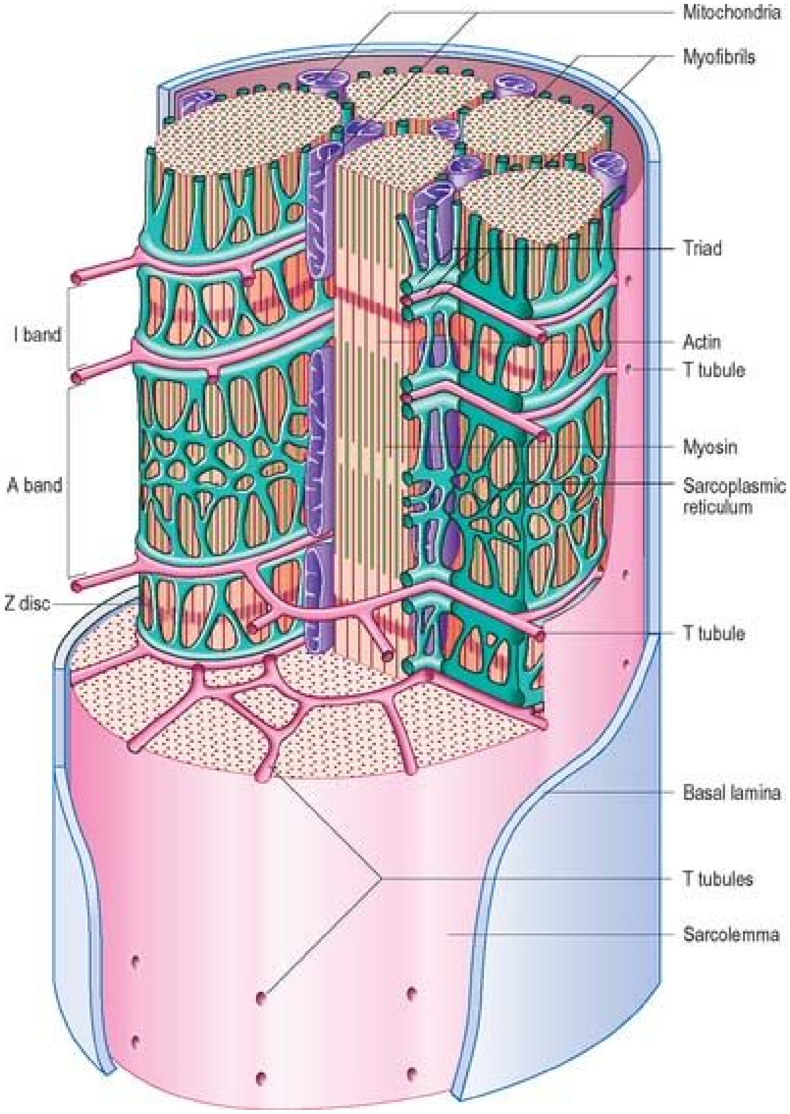
Mitochondria
Myofibrils
Triad
I band
Actin
T tubule
Myosin
A band
Sarcoplasmic reticulum
Z disc
T tubule
Basal lamina
T tubules
Sarcolemma

Fig. 5.43 Three-dimensional reconstruction of a mammalian skeletal muscle fibre, showing in particular the organization of the transverse tubules and sarcoplasmic reticulum. Mitochondria lie between the myofibrils. Note that transverse tubules are found at the level of the A/I junctions, where they form triads with the terminal cisternae of the sarcoplasmic reticulum.

Connective tissues of muscle

The endomysium is a delicate network of connective tissue that surrounds muscle fibres, and forms their immediate external environment. It is the site of metabolic exchange between muscle and blood, and contains capillaries and bundles of small nerve fibres. Ion fluxes associated with the electrical excitation of muscle fibres take place through its proteoglycan matrix. The endomysium is continuous with more substantial septa of connective tissue that constitute the perimysium. The latter ensheathes groups of muscle fibres to form parallel bundles or fasciculi, carries larger blood vessels and nerves and accommodates neuromuscular spindles. Perimysial septa are themselves the inward extensions of a collagenous sheath, the epimysium, which forms part of the fascia that invests whole muscle groups.

Epimysium consists mainly of type I collagen, perimysium contains type I and type III collagen, and endomysium contains collagen types III and IV. Collagen IV is associated particularly with the basal lamina that invests each muscle fibre.

The epimysial, perimysial and endomysial sheaths coalesce where the muscles connect to adjacent structures at tendons, aponeuroses, and fasciae (see below): this gives the attachments great strength, since the tensile forces are distributed in the form of shear stresses, which are more easily resisted. This principle is also seen at the ends of the muscle fibres, which divide into finger-like processes separated by insertions of tendinous collagen fibres. Although there are no desmosomal attachments at these myotendinous junctions, there are other specializations that assist in the transmission of force from the interior of the fibre to the extracellular matrix. Actin filaments from the adjacent sarcomeres, which would normally insert into a Z-disc at this point, instead penetrate a dense, subsarcolemmal filamentous matrix that provides attachment to the plasma membrane. This matrix is similar in character to the cytoplasmic face of an adherens junction. The structure as a whole is homologous to the intercalated discs of cardiac muscle. At the extracellular surface of the junctional sarcolemma, integrins provide contact with the basal lamina which in turn adheres closely to collagen and reticular fibres (type III collagen) of the adjacent tendon or other connective tissue structure.

Vascular supply and lymphatic drainage

In most muscles the major source artery enters on the deep surface, frequently in close association with the principal vein and nerve, which together form a neurovascular hilum. The vessels subsequently course and branch within the connective tissue framework of the muscle. The smaller arteries and arterioles ramify in the perimysial septa and give off capillaries which run in the endomysium: although the smaller vessels lie mainly parallel to the muscle fibres, they also branch and anastomose around the fibres, forming an elongated mesh.

Mathes & Nahai (1981) have classified the gross vascular anatomy of muscles into five types according to the number and relative dominance of vascular pedicles which enter the muscle (Fig. 5.44). This classification has important surgical relevance in determining which muscles will survive and therefore be useful for pedicled or free tissue transfer procedures using techniques of plastic and reconstructive surgery. Type I muscles possess a single vascular pedicle supplying the muscle belly, e.g. tensor faciae latae (supplied by the ascending branch of the lateral circumflex femoral artery) and gastrocnemius (supplied by the sural artery). Type II muscles are served by a single dominant vascular pedicle and several minor pedicles, and can be supported on a minor pedicle as well as the dominant pedicle, e.g. gracilis (supplied by the medial circumflex femoral artery in the dominant pedicle). Type III muscles are supplied by two separate dominant pedicles each from different source arteries, e.g. rectus abdominus (supplied by the superior and inferior epigastric arteries) and gluteus maximus (supplied by the superior and inferior gluteal arteries). Type IV muscles have multiple small pedicles which, in isolation, are not capable of supporting the whole muscle, e.g. sartorius and tibialis anterior: about 30% survive reduction onto a single vascular pedicle. Type V muscles have one dominant vascular pedicle and multiple secondary segmental pedicles, e.g. latissimus dorsi (supplied by the thoracodorsal artery as the primary pedicle, and thoracolumbar perforators from the lower six intercostal arteries and the lumbar arteries as the segmental supply), and pectoralis major (supplied by the pectoral branch of the thoracoacromial axis as the dominant pedicle, and anterior perforators from the internal thoracic vessels as the segmental supply).

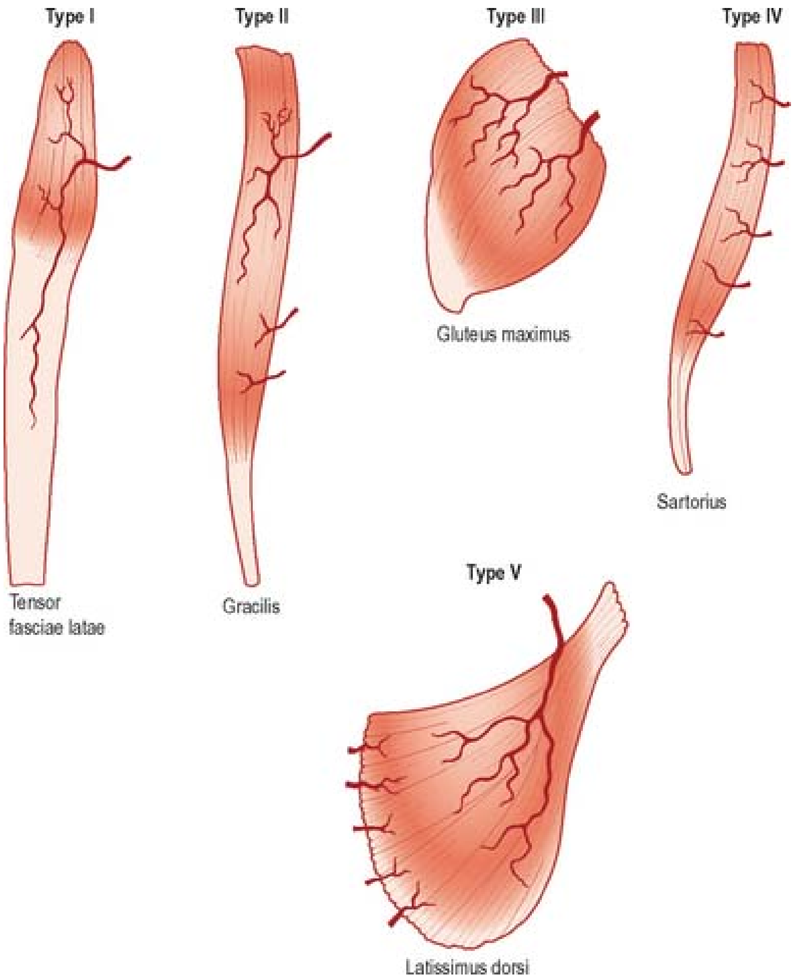
Type I
Type II
Type III
Type IV
Gluteus maximus
Sartorius
Tensor fasciae latae
Gracilis
Type V
Latissimus dorsi

Fig. 5.44 Classification of muscles according to their blood supply.

(By permission from Cormack GC, Lamberty BGH 1994 The Arterial Anatomy of Skin Flaps, 2nd edn. Edinburgh: Churchill Livingstone.)

In muscle cross-sections, the number of capillary profiles found adjacent to fibres usually varies from 0 to 3. Fibres that are involved in sustained activities, such as posture, are served by a denser capillary network than fibres that are recruited only infrequently. It is common for muscles to receive their arterial supply via more than one route. The accessory arteries penetrate the muscle at places other than the hilum, and ramify in the same way as the principal artery, forming vascular territories. The boundaries of adjacent territories are spanned by anastomotic vessels, sometimes at constant calibre, but more commonly through reduced-calibre arteries or arterioles which are referred to as ‘choke vessels’ (see Ch. 6). These arterial arcades link the territories into a continuous network.

Veins branch in a similar way, forming venous territories that correspond closely to the arterial territories. In the zones where the arterial territories are linked by choke vessels, the venous territories are linked by anastomosing veins, in this case without change of calibre. On either side of these venous bridges, the valves in the adjacent territories direct flow in opposite directions towards their respective pedicles, but the connecting veins themselves lack valves, and therefore permit flow in either direction.

Because of the potential for relative movement within muscle groups, vessels tend not to cross between muscles, but radiate to them from more stable sites or cross at points of fusion. Where a muscle underlies the skin, vessels bridge between the two. These may be primarily cutaneous vessels, i.e. they supply the skin directly, but contribute small branches to the muscle as they pass through it, or they may be the terminal branches of intramuscular vessels which leave the muscle to supplement the cutaneous blood supply. The latter are less frequent where the muscle is mobile under the deep fascia. The correspondence between the vascular territories in the skin and underlying tissues gave rise to the concept of angiosomes, whichare composite blocks of tissue supplied by named distributing arteries and drained by their companion veins (see Ch. 6).

The pressure exerted on valved intramuscular veins during muscular contraction functions as a ‘muscle pump’ that promotes venous return to the heart. In some cases this role appears to be amplified by veins which pass through the muscle after originating elsewhere in superficial or deep tissues (see Ch. 79). The extent to which the muscle capillary bed is perfused can be varied in accordance with functional demand. Arteriovenous anastomoses, through which blood can be returned directly to the venous system without traversing the capillaries, provide an alternative, regulated pathway.

The lymphatic drainage of muscles begins as lymphatic capillaries in epimysial and perimysial, but not endomysial, sheaths. These converge to form larger lymphatic vessels that accompany the veins and drain to the regional lymph nodes.

Innervation

Every skeletal muscle is supplied by one or more nerves. In the limbs, face and neck there is usually a single nerve, although its axons may be derived from neurons located in several spinal cord segments and their associated ganglia. Muscles such as those of the abdominal wall, which originate from several embryonic segments, are supplied by more than one nerve. In most cases, the nerve travels with the principal blood vessels within a neurovascular bundle, approaches the muscle near to its least mobile attachment, and enters the deep surface at a position which is more or less constant for each muscle.

Nerves supplying muscle are frequently referred to as ‘motor nerves’, but they contain both motor and sensory components. The motor component is mainly composed of large, myelinated α-efferent axons, which supply the muscle fibres, supplemented by small, thinly myelinated γ-efferents, or fusimotor fibres, which innervate the intrafusal muscle fibres of neuromuscular spindles, and fine, non-myelinated autonomic efferents (C fibres), which innervate vascular smooth muscle. The sensory component consists of large, myelinated IA and smaller group II afferents from the neuromuscular spindles, large myelinated IB afferents from the Golgi tendon organs, and fine myelinated and non-myelinated axons which convey pain and other sensations from free terminals in the connective tissue sheaths of the muscle.

Within muscles, nerves travel through the epimysial and perimysial septa before entering the fine endomysial tissue around the muscle fibres. α-Motor axons branch repeatedly before they lose their myelinated sheaths and terminate in a narrow zone towards the centre of the muscle belly known as the motor point. Clinically, this is the place on a muscle from which it is easiest to elicit a contraction with stimulating electrodes. Long muscles generally have two or more terminal, or end-plate bands, because many muscle fibres do not run the full length of an anatomical muscle. The terminal branch of an α-motor axon contacts a muscle fibre at a specialized synapse, the neuromuscular junction (see Fig. 3.37). It gives off several short, tortuous branches each ending in an elliptical area, the motor end plate. The underlying discoidal patch of sarcolemma, the sole plate or subneural apparatus, is thrown into deep synaptic folds. This discrete type of neuromuscular junction is an example of an en plaque ending and is found on muscle fibres which are capable of propagating action potentials. A different type of ending is found on slow tonic muscle fibres, which do not have this capability, e.g. in the extrinsic ocular muscles, where slow tonic fibres form a minor component of the anatomical muscle. In this case the propagation of excitation is taken over by the nerve terminals, which branch over an extended distance to form a number of small neuromuscular junctions (en grappe endings). Some muscle fibres of this type receive the terminal branches of more than one motor neurone. The terminals of the γ-efferents that innervate the intrafusal muscle fibres of the neuromuscular spindle also take a variety of different forms.

The terminal branches of α-motor axons are normally in a ‘one-to-one’ relationship with their muscle fibres: a muscle fibre receives only one branch, and any one branch innervates only one muscle fibre. When a motor neurone is excited, an action potential is propagated along the axon and all of its branches to all of the muscle fibres that it supplies. The motor neurone and the muscle fibres that it innervates can therefore be regarded as a functional unit, the motor unit: the arrangement accounts for the more or less simultaneous contraction of a number of fibres within the muscle. The size of a motor unit varies considerably. In muscles used for precision tasks, e.g. extraocular muscles, interossei and intrinsic laryngeal muscles, each motor neurone innervates perhaps 10 muscle fibres, whereas in a large limb muscle, a motor neurone may innervate several hundred muscle fibres. Within a muscle, the fibres belonging to one motor unit are distributed over a wide territory, without regard to fascicular boundaries, and intermingle with the fibres of other motor units. The motor units become larger in cases of nerve damage, because denervated fibres induce collateral or terminal sprouting of the remaining axons. Each new branch can reinnervate a fibre, thus increasing the territory of its parent motor neurone.

Muscle contraction: basic physiology

The arrival of an action potential at the motor end plate of a neuromuscular junction causes acetylcholine (ACh) to be released from storage vesicles into the highly infolded 30–50 nm synaptic cleft that separates the nerve ending from the sarcolemma (see Fig. 3.37). ACh is rapidly bound by receptor molecules located in the junctional folds, triggering an almost instantaneous increase in the permeability, and hence conductance, of the postsynaptic membrane. This generates a local depolarization (the end-plate potential), which initiates an action potential in the surrounding sarcolemma. The activity of the neurotransmitter is rapidly terminated by the enzyme acetylcholinesterase (AChE), which is bound to the basal lamina in the sarcolemmal junctional folds. The sarcolemma is an excitable membrane, and action potentials generated at the neuromuscular junction propagate rapidly over the entire surface of the muscle fibre.

The action potentials are conducted radially into the interior of the fibre via the T-tubules, extensions of the sarcolemma (see above), ensuring that all parts of the muscle fibre are activated rapidly and almost synchronously. Excitation–contraction coupling is the process whereby an action potential triggers the release of calcium from the terminal cisternae of the sarcoplasmic reticulum into the cytosol. This activates a calcium-sensitive switch in the thin filaments (see below) and so initiates contraction. At the end of excitation, the T-tubular membrane repolarizes, calcium release ceases, calcium ions are actively transported back to the calsequestrin stores in the sarcoplasmic reticulum by the calcium–ATPase pumps, and the muscle relaxes.

The lengths of the thick and thin filaments do not change during muscle contraction. The sarcomere shortens by the sliding of thick and thin filaments past one another, which draws the Z-discs towards the middle of each sarcomere (Fig. 5.41). As the overlap increases, the I- and H-bands narrow to near extinction, while the width of the A-bands remains constant. Filament sliding depends on the making and breaking of bonds (cross-bridge cycling) between myosin head regions and actin filaments. Myosin heads ‘walk’ or ‘row’ along actin filaments using a series of short power strokes, each resulting in a relative movement of 5–10 nm. Actin filament binding sites for myosin are revealed only in the presence of calcium, which is released into the sarcoplasm from the sarcoplasmic reticulum, causing a repositioning of the troponin–tropomyosin complex on actin (the calcium-sensitive switch). Myosin head binding and release are both energy dependent (ATP binding is required for detachment of bound myosin heads as part of the normal cycle). In the absence of ATP (as occurs postmortem) the bound state is maintained, and is responsible for the muscle stiffness known as rigor mortis.

The summation of myosin power strokes leads to an average sarcomere shortening of up to 1 μm: an anatomical muscle shortens by a centimetre or more, depending on the muscle, because each muscle has thousands of sarcomeres in series along its length. For further details of actin–myosin interactions in muscle contraction, see Alberts et al (2002) and Pollard & Earnshaw (2007) (see Bibliography of selected titles for publication details).

Slow twitch vs fast twitch

The passage of a single action potential through a motor unit elicits a twitch contraction where peak force is reached within 25–100 ms, depending on the motor unit type involved. However, the motor neurone can deliver a second nervous impulse in less time than it takes for the muscle fibres to relax. When this happens, the muscle fibres contract again, building the tension to a higher level. Because of this mechanical summation, a sequence of impulses can evoke a larger force than a single impulse and, within certain limits, the higher the impulse frequency, the more force is produced (‘rate recruitment’). An alternative strategy is to recruit more motor units. In practice, the two mechanisms appear to operate in parallel, but their relative importance may depend on the size and/or function of the muscle: in large muscles with many motor units, motor unit recruitment is probably the more important mechanism.

With the exception of rare tonic fibres, skeletal muscles are composed entirely of fibres of the twitch type. These fibres can all conduct action potentials, but they differ in other respects. Some fibres obtain their energy very efficiently by aerobic oxidation of substrates, particularly of fats and fatty acids. They have large numbers of mitochondria; contain myoglobin, an oxygen-transport pigment related to haemoglobin; and are supported by a well-developed network of capillaries that maintains a steady nutrient supply of oxygen and substrates. Such fibres are well suited to functions such as postural maintenance, in which moderate forces need to be sustained for prolonged periods. At the other end of the spectrum, some fibres have few mitochondria, little myoglobin, and a sparse capillary network, and store energy as cytoplasmic glycogen granules. Their immediate energy requirements are met largely through anaerobic glycolysis, a route that provides prompt access to energy but that is less sustainable than oxidative metabolism. They are capable of brief bursts of intense activity that must be separated by extended quiescent periods during which intracellular pH and phosphate concentrations, perturbed in fatigue, are restored to normal values and glycogen and other reserves are replenished.

Different types of fibre tend to be segregated into different muscles in some animals: some muscles have a conspicuously red appearance, reflecting their rich blood supply and high myoglobin content associated with a predominantly aerobic metabolism, whereas others have a much paler appearance, reflecting a more anaerobic character. These variations in colour led to the early classification of muscle into red and white types. This classification has now been largely superseded by myosin-based typing and the presence of specific disease-related enzymes.

In man, all muscles are mixed; fibres that are specialized for aerobic working conditions intermingle with fibres of a more anaerobic or intermediate metabolic character. The different types of fibre are not readily distinguished in routine histological preparations but are clear when specialized enzyme histochemical techniques are used. On the basis of metabolic differences, individual fibres can be classified as predominantly oxidative, slow twitch (red) fibres, or glycolytic, fast twitch (white) fibres. Muscles composed mainly of oxidative, slow twitch fibres correspond to the red muscles of classical descriptions. Muscles that are predominantly oxidative in their metabolism contract and relax more slowly than muscles relying on glycolytic metabolism. This difference in contractile speed is due in part to the activation mechanism (volume density of sarcotubular system and proteins of the calcium ‘switch’ mechanism), and in part to molecular differences between the myosin heavy chains of these types of muscle. These differences affect the ATPase activity of the myosin head, which in turn alters the kinetics of its interaction with actin, and hence the rate of cross-bridge cycling. Differences between myosin isoforms may be detected histochemically: ATPase histochemistry continues to play a significant role in diagnostic typing (Table 5.2). Two main categories have been described: type I fibres, which are slow-contracting, and type II, which are fast-contracting. Molecular analyses have revealed that type II fibres may be further subdivided according to their content of myosin heavy-chain isoforms into types IIA, IIB and IIX (Schiaffino & Reggiani 1996). There is a correlation between categories and metabolism, and therefore with fatigue resistance, such that type I fibres are generally oxidative (slow oxidative) and resistant to fatigue, type IIA are moderately oxidative, glycolytic (fast oxidative glycolytic) and fatigue resistant, and IIB largely rely on glycolytic metabolism (fast glycolytic) and so are easily fatigued.

Table 5.2 Physiological, structural and biochemical characteristics of the major histochemical fibre types.

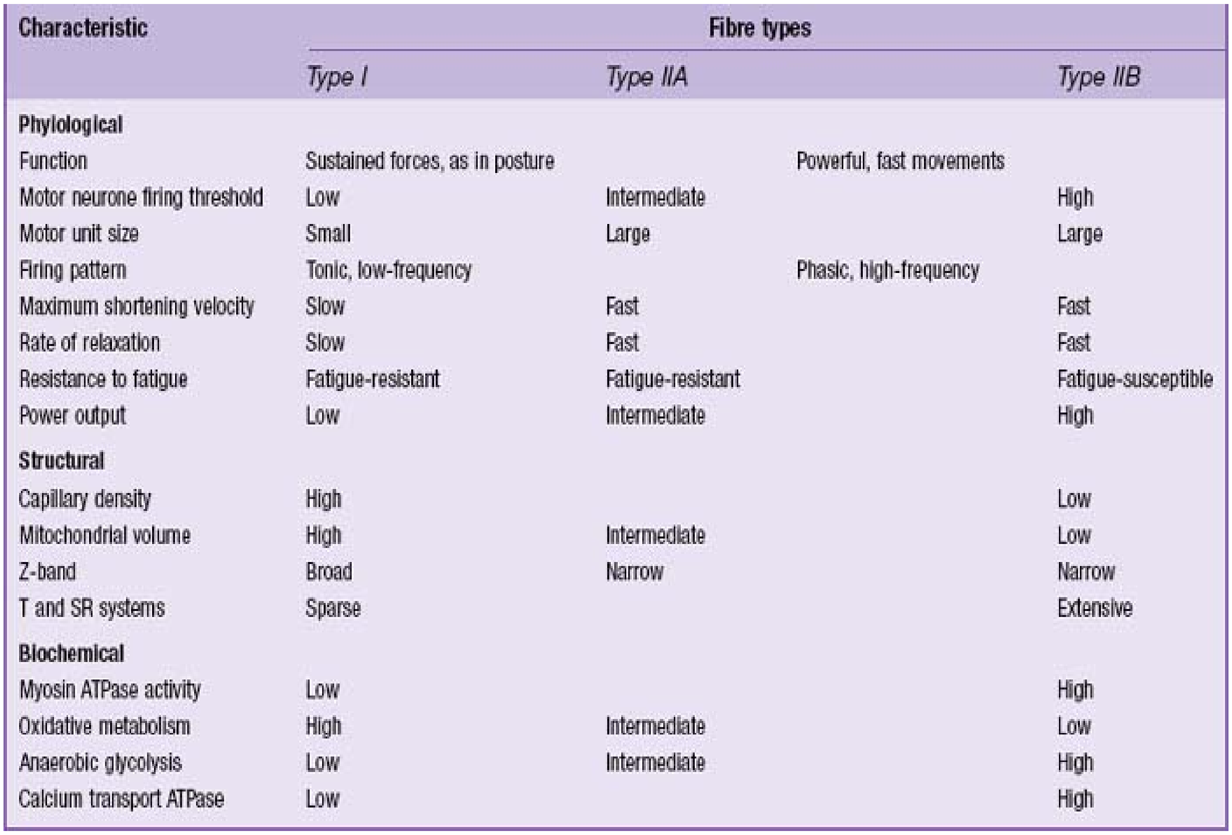

Characteristic	Fibre types		
	Type I	*Type IIA*	*Type IIB*
Phylological			
Function	Sustained forces, as in posture	Powerful, fast movements	
Motor neurone firing threshold	Low	Intermediate	High
Motor unit size	Small	Large	Large
Firing pattern	Tonic, low-frequency	Phasic, high-frequency	
Maximum shortening velocity	Slow	Fast	Fast
Rate of relaxation	Slow	Fast	Fast
Resistance to fatigue	Fatigue-resistant	Fatigue-resistant	Fatigue-susceptible
Power output	Low	Intermediate	High
Structural			
Capillary density	High		Low
Mitochondrial volume	High	Intermediate	Low
Z-band	Broad	Narrow	Narrow
T and SR systems	Sparse		Extensive
Biochemical			
Myosin ATPase activity	Low		High
Oxidative metabolism	High	Intermediate	Low
Anaerobic glycolysis	Low	Intermediate	High
Calcium transport ATPase	Low		High

Fibre type transformation

The fibre type proportions in a named muscle may vary between individuals of different age or athletic ability. Fibre type grouping, where fibres with similar metabolic and contractile properties aggregate, increases after nerve damage and with age. It occurs as a result of reinnervation episodes, where denervated fibres are ‘taken over’ by a sprouting motor neurone and their type properties transformed under direction of the new motor neurone. If the nerves to fast white and slow red muscles are cut and cross-anastomosed in experimental animals, so that each muscle is reinnervated by the other’s nerve, the fast muscle becomes slower-contracting, and the slow muscle faster-contracting (Buller et al 1960). There is evidence that fibre type transformation may be a response to the patterns of impulse traffic in the nerves innervating the muscles. If fast muscles are stimulated continuously for several weeks at 10 Hz, a pattern similar to that normally experienced by slow muscles, they develop slow contractile characteristics and acquire a red appearance and a resistance to fatigue even greater than that of slow muscles.

The initial phase of slowing can be explained by less rapid cycling of calcium, the result of a reduction in the extent of the sarcoplasmic reticulum and changes in the amount and molecular type of proteins involved in calcium transport and binding. Chronic stimulation also triggers the synthesis of myosin heavy and light chain isoforms of the slow muscle type: the associated changes in cross-bridge kinetics result in a lower intrinsic speed of shortening. The muscle becomes more resistant to fatigue through changes in the metabolic pathways responsible for the generation of ATP and a reduced dependence on anaerobic glycolysis. There is a switch to oxidative pathways, particularly those involved in the breakdown of fat and fatty acids, and an associated increase in capillary density and in the fraction of the intracellular volume occupied by mitochondria. If stimulation is discontinued, the sequence of events is reversed and the muscle regains, over a period of weeks, all of its original characteristics. The reversibility of transformation is one of several lines of evidence that the changes take place within existing fibres, and not by a process of degeneration and regeneration.

Many of the changes in the protein profile of a muscle that are induced by stimulation are now known to be the result of transcriptional regulation. For example, analysis of the messenger RNA species encoding myosin heavy chain isoforms shows that expression of the fast myosin heavy chain mRNA is downregulated within a few days of the onset of chronic stimulation, while the slow myosin heavy chain mRNA is upregulated. Although myosin isoform expression is responsive to the increase in use induced by chronic stimulation, it tends to be stable under physiological conditions unless these involve a sustained departure from normal postural or locomotor behaviour.

Attachments of skeletal muscles

The forces developed by skeletal muscles are transferred to bones by connective tissue structures: tendons, aponeuroses and fasciae.

Tendons

Tendons (Fig. 5.45) take the form of cords or straps of round or oval cross-section, and consist of dense, regular connective tissue. They contain fascicles of type I collagen, orientated mainly parallel to the long axis, but are to some extent interwoven. The fasciculi may be conspicuous enough to give tendons a longitudinally striated appearance to the unaided eye. Tendons generally have smooth surfaces, although large tendons may be ridged longitudinally by coarse fasciculi (e.g. the osseous aspect of the angulated tendon of obturator internus). Loose connective tissue between fascicles provides a conduit for small vessels and nerves, and condenses on the surface as a sheath or epitendineum, which may contain elastin and irregularly arranged collagen fibres. The loose attachments between this sheath and the surrounding tissue present little resistance to movements of the tendon, but in situations where greater freedom of movement is required, a tendon is separated from adjacent structures by a synovial sheath.

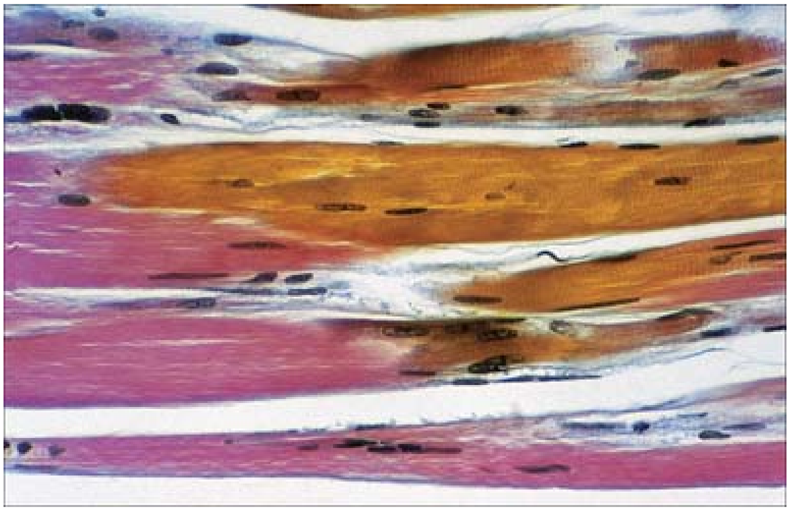

Fig. 5.45 Attachment of a tendon (orange) to skeletal muscle (pink). The regular dense connective tissue of the tendon consists of parallel bundles of type I collagen fibres which are orientated in the long axis of the tendon and the muscle to which it is attached. A few elongated fibroblast nuclei are visible in the tendon.

Tendons are strongly attached to bones, both at the periosteum and through fasciculi (extrinsic collagen fibres). Tendinous attachments (entheses or osteotendinous junctions) have been broadly categorized as either fibrocartilagenous or fibrous. In fibrocartilagenous entheses, four zones of tissue have been identified: pure dense fibrous connective tissue (continuous with and indistinguishable from the tendon), uncalcified fibrocartilage, calcified fibrocartilage and bone (continuous with and indistinguishable from the rest of the bone). There are no sharp boundaries between the zones, and the proportions of each component vary between entheses (Fig. 5.46A,B,D). At fibrous entheses, which are characteristic of the shafts of long bones, the tendon is attached to bone by dense fibrous connective tissue either directly or indirectly via the periosteum (Fig. 5.46C). It has been suggested that the greater area of the skeleton to which many fibrous entheses (e.g. pronator teres, deltoid) are attached compared with fibrocartilagenous entheses (e.g. rotator cuff tendons) is important in dissipating stress. (For a review of entheses and the concept of the ‘enthesis organ’, see Benjamin et al 2006.)

Tendons are slightly elastic and may be stretched by 6–10% of their length without damage. Recovery of the elastic ‘strain’ energy stored in tendons can make movement more economical. Although they resist extension, tendons are flexible and can therefore be diverted around osseous surfaces or deflected under retinacula to redirect the angle of pull. Since tendons are composed of collagen and their vascular supply is sparse, they appear white. However, their blood supply is not unimportant: small arterioles from adjacent muscle tissue pass longitudinally between the fascicles, branching and anastomosing freely, and accompanied by venae comitantes and lymphatic vessels. This longitudinal plexus is augmented by small vessels from adjacent loose connective tissue or synovial sheaths. Vessels rarely pass between bone and tendon at osseous attachments, and the junctional surfaces are usually devoid of foramina. A notable exception is the calcaneal tendon (Achilles tendon), which receives a blood supply across the osseotendinous junction. During postnatal development, tendons enlarge by interstitial growth, particularly at myotendinous junctions, where there are high concentrations of fibroblasts. Growth decreases along the tendon from the muscle to the osseous attachments. The thickness finally attained by a tendon depends on the size and strength of the associated muscle, but appears to be influenced by additional factors such as the degree of pennation of the muscle. The metabolic rate of tendons is very low but increases during infection or injury. Repair involves an initial proliferation of fibroblasts followed by interstitial deposition of new collagen fibres.

The nerve supply to tendons is largely sensory, and there is no evidence of any capacity for vasomotor control. Golgi tendon organs, specialized endings that are sensitive to force, are found near myotendinous junctions; their large myelinated afferent axons run within branches of muscular nerves or in small rami of adjacent peripheral nerves.

Form and function in skeletal muscles

Direction of action

Although muscles differ in their internal architecture, the resultant force is directed along the line of the tendon: any forces transverse to this direction must therefore be in balance (Fig. 5.36, Fig. 5.47). In strap-like muscles, the transverse component is negligible. In fusiform, bipennate and multipennate muscles, symmetry in the arrangement of the fibres produces a balanced opposition between transverse components, whereas in asymmetrical muscles, e.g. unipennate muscles, the fibres generate an unopposed lateral component of force which is balanced by intramuscular pressure.

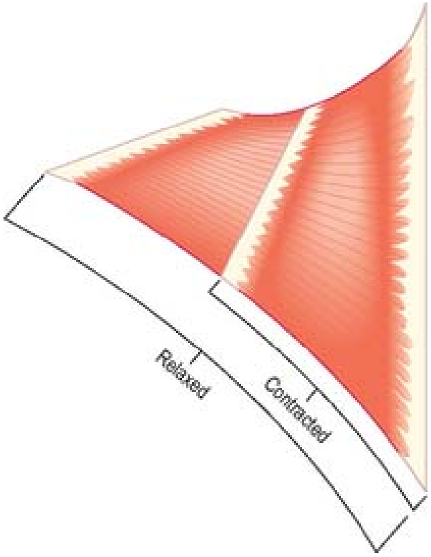

Fig. 5.47 The ‘detorsion’ or untwisting which results from the contraction of a spirally arranged muscle.

Muscles that incorporate a twist in their geometry unwind it as they contract, so that they tend not only to approximate their attachments but also to bring them into the same plane. Muscles that spiral around a bone tend to reduce the spiral on contraction, imparting rotational force.

Force and range of contraction

The force developed by an active muscle is the summation of the tractive forces exerted by millions of cross-bridges as they work asynchronously in repeated cycles of attachment and detachment. This force depends on the amount of contractile machinery that is assembled in parallel, and therefore on the cross-sectional area of the muscle. The phrase ‘contractile machinery’ has been chosen deliberately here. Mechanically, it matters little that the myofilaments are assembled into myofibrils, the myofibrils into fibres, and the fibres into fascicles (see Fig. 5.38): the total area occupied by myofilamentous arrays determines the force. If the fibres are small, the force will be influenced only to the extent that more of the cross-sectional area will be occupied by non-contractile elements, such as endomysial connective tissue. If there are many small fascicles, the amount of perimysial connective tissue in the cross-section will increase.

The range of contraction generated by an active muscle depends on the relative motion that can take place between the overlapping arrays of thick and thin filaments in each sarcomere. In vertebrate muscle, the construction of the sarcomere sets a natural limit to the amount of shortening that can take place: the difference between the minimum overlap and the maximum overlap of the thick and thin filaments represents a shortening of about 30%. Since the sarcomeres are arranged in series, the muscle fibres shorten by the same percentage. The actual movement that takes place at the ends of the fibres will depend on the number of sarcomeres in series, i.e. it will be proportional to fibre length. By way of illustration, compare the behaviour of two muscles, fixed at one end, both having fibres parallel to the line of pull and the same cross-sectional area. If one muscle is twice as long as the other, then the force developed by each muscle will be the same, but the maximum movement produced at the free ends will be twice as much for the longer muscle. Muscles in which the fibres are predominantly parallel to the line of pull are often long and thin (strap-like): they develop rather low forces, but are capable of a large range of contraction. Where greater force is required the cross-sectional area must be increased, as occurs in a pennate construction (Fig. 5.48). Here, the fibres are set at an angle to the axis of the tendon (the angle of pennation). The range of contraction produced by such a muscle will be less than that of a strap-like muscle of the same mass, because the fibres are short and a smaller fraction of the shortening takes place in the direction of the tendon. The obliquely directed force can be resolved vectorially into two components, one acting along the axis of the tendon, and one at 90° to this. In symmetrical forms (Fig. 5.48), the transverse force is balanced by fibres on the opposite side of the tendon. The functionally significant component is the one acting along the axis of the tendon. As the lengths of the vectors show, less force is available in this direction than is developed by the fibres themselves. In practice, this loss is not very great: angles of pennation are usually less than 30°, and so the force in the direction of the tendon may be 90% or more of that in the fascicles (cos 30° = 0.87). Angulation of a set of fibres reduces both the force and range of contraction along the axis of the tendon. However, these negative consequences are outweighed by the design advantage conferred by pennation, i.e. the opportunity to extend the tendinous aponeurosis, and so increase the area available for the attachment of muscle fibres. A given mass of muscle can then be deployed as a large number of short fibres, increasing the total cross-sectional area, and hence the force, available. In a multipennate muscle, the effective cross-sectional area is larger still, and the fibres tend to be even shorter. The ‘gearing’ effect of pennation on a muscle therefore results from an internal exchange of fibre length for total fibre area: this allows much greater forces to be developed, but at the expense of a reduced range of contraction.

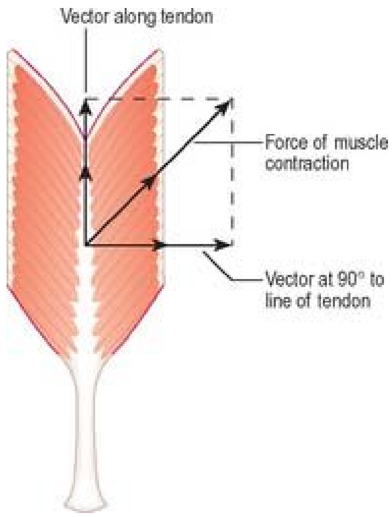

Fig. 5.48 Force vectors in an idealized pennate muscle. The increase in effective cross-sectional area made possible by this architecture outweighs the small reduction in the component of force acting in the direction of the tendon.

Although the terms power and strength are often used interchangeably with force, they are not synonymous. Power is the rate at which a muscle can perform external work and is equal to force × velocity. Since force depends on the total cross-sectional area of fibres, and velocity (the rate of shortening) depends on their length, power is related to the total mass of a muscle. Strength is usually measured on intact subjects in tasks which require the participation of several muscles, when it is as much an expression of the skillful activation and coordination of these muscles as it is a measure of the forces which they contribute individually. Thus it is possible for strength to increase without a concomitant increase in the true force-generating capacities of the muscles involved, especially during the early stages of training.

Muscles and movement

Historically, attempts were made to elucidate the actions of muscles by gross observation. The attachments were identified by dissection, and the probable action deduced from the line of pull. With the use of localized electrical stimulation it became possible to study systematically the actions of selected muscles in the living subject. This approach was pioneered above all by Duchenne de Boulogne in the mid 19th century. Such knowledge is necessarily incomplete: a study of isolated muscles, whether by dissection, postmortem or stimulation *in vivo*, cannot reveal the way in which those muscles behave in voluntary movements, in which several muscles may participate in a variety of synergistic and stabilizing roles. Duchenne appreciated this, and supplemented electrical stimulation with clinical observations on patients with partial paralysis to make more accurate deductions about the way in which muscles acted together in normal movement. Manual palpation can be used to detect contraction of muscles during the performance of a movement, but tends to be restricted to superficially placed muscles, with examination taking place under quasi-static conditions. Modern knowledge of muscle action has been acquired almost entirely by recording the electrical activity which accompanies mechanical contraction, a technique known as electromyography (EMG). This technique can be used to study voluntary activation of deep as well as superficial muscles, under static or dynamic conditions. Multiple channels of EMG can be used to examine coordination between the different muscles that participate in a movement. These data can be further supplemented by monitoring joint angle and ground reaction force, and by recording the movement on camera or with a three-dimensional motion analysis system.

Actions of muscles

Conventionally, the action of a muscle is defined as the movement that takes place when it contracts. However, this is an operational definition: equating ‘contraction’ with shortening, and ‘relaxation’ with lengthening is too simple in the context of whole muscles and real movements. Whether a muscle approximates its attachments on contraction depends on the degree to which it is activated, and the forces against which it has to act. The latter are generated by numerous factors: gravity and inertia, any external contact or impact, actively by opposing muscles, and passively by the elastic and viscous resistance of all the structures which undergo extension and deformation, some within the muscle itself, others in joints, inactive muscles and soft tissues. Depending on the conditions, an active muscle may therefore maintain its original length or shorten or lengthen, and during this time its tension may increase, decrease or not change. Movements that involve shortening of an active muscle are termed concentric, e.g. contraction of biceps/brachialis while raising a weight and flexing the elbow. Movements in which the active muscle undergoes lengthening are termed eccentric, e.g. in lowering the weight previously mentioned, biceps/brachialis ‘pays out’ length as the elbow extends. Eccentric contractions are associated with increased risk of muscle tears, especially in the hamstrings. Muscle contraction that does not involve change in muscle length is isometric.

Natural movements are accomplished by groups of muscles. Each muscle may be classified, according to its role in the movement, as a prime mover, antagonist, fixator or synergist. It is usually possible to identify one or more muscles which are consistently active in initiating and maintaining a movement: they are its prime movers. Muscles that wholly oppose the movement, or initiate and maintain the opposite movement, are antagonists, e.g. brachialis has the role of prime mover in elbow flexion, and triceps is the antagonist. To initiate a movement, a prime mover must overcome passive and active resistance and impart an angular acceleration to a limb segment until the required angular velocity is reached; it must then maintain a level of activity sufficient to complete the movement. Antagonists may be transiently active at the beginning of a movement, and thereafter they remain electrically quiescent until the deceleration phase, when units are activated to arrest motion. During the movement, the active prime movers are not completely unrestrained, and are balanced against the passive, inertial and gravitational forces mentioned above.

When prime movers and antagonists contract together they behave as fixators, stabilizing the corresponding joint by increased transarticular compression, and creating an immobile base on which other prime movers may act, e.g. flexors and extensors of the wrist co-contract to stabilize the wrist when an object is grasped tightly in the fingers. In some cases, sufficient joint stability can be afforded by gravity, acting either on its own, e.g. knee and hip joints when they are in or near the close-packed position in the erect posture, or in conjunction with a single prime mover, e.g. the shoulder joint when it is stabilized by supraspinatus with the arm pendent. In other cases, and whenever strong external forces are encountered, prime movers and antagonists contract together, holding the joint in any required position.

Acting across a uniaxial joint, a prime mover produces a simple movement. Acting at multiaxial joints, or across more than one joint, prime movers may produce more complex movements which contain elements that have to be eliminated by contraction of other muscles. The latter assist in accomplishing the movement, and are considered to be synergists, although they may act as fixators, or even as partial antagonists of the prime mover. For example, flexion of the fingers at the interphalangeal and metacarpophalangeal joints is brought about primarily by the long flexors, superficial and deep. However, these also cross intercarpal and radiocarpal joints, and if movement at these joints was unrestrained, finger flexion would be less efficient. Synergistic contraction of the carpal extensors eliminates this movement, and even produces some carpal extension, which increases the efficiency of the desired movement at the fingers.

In the context of different movements, a given muscle may act differently, as a prime mover, antagonist, fixator or synergist. Even the same movement may involve a muscle in different ways if it is assisted or opposed by gravity. For example, in thrusting out the hand, triceps is the prime mover responsible for extending the forearm at the elbow, and the flexor antagonists are largely inactive. However, when the hand lowers a heavy object, the extensor action of the triceps is replaced by gravity, and the movement is controlled by active lengthening, i.e. eccentric contraction, of the flexors. It is important to remember that all movements take place against the background of gravity, and its influence must not be overlooked.

Development of skeletal muscle

Most information about the early development of the skeletal musculature in man has been derived from other vertebrate species. However, where direct comparisons with the developing human embryo have been made, the patterns and mechanisms of muscle formation have been found to be the same.

A myogenic lineage, denoted by the expression of myogenic determination factors, can be demonstrated transiently in some cells shortly after their ingression through the primitive streak. Skeletal muscle found throughout the body is derived from this paraxial mesenchyme, which is formed from ingression at the streak and subsequently segmented into somites (see also the origin of extraocular muscles, Ch. 41).

Skeletal muscle originates from a pool of premyoblastic cells which arise in the dermatomyotome of the maturing somite and begin to differentiate into myoblasts at 4–5 weeks of gestation. By 6 weeks, cells have migrated from the dermatomyotomal compartment to form the myotome in the centre of the somite (see Fig. 44.3). These myotomal precursor cells are identified by the expression of myogenic determination factors; they will eventually differentiate within the somite to form the axial (or epaxial) musculature (erector spinae). A distinct cohort of precursor cells migrates away from the somite to invade the lateral regions of the embryo; there they form the muscles of the limbs (see Ch. 51), limb girdles and body wall (hypaxial musculature; see Fig. 44.3). Virtually all cells in the lateral half of the newly formed somite are destined to migrate in this way. Myogenic determination factors are not expressed in these cells until the muscle masses coalesce. The appearance of myotomal myoblasts, and the migration of myoblasts to the prospective limb region, occurs first in the occipital somites. Thereafter these processes follow the general craniocaudal progression of growth, differentiation and development of the embryo. The myoblastic cells from which the limb muscles develop do not arise *in situ* from local limb bud mesenchyme, as was once thought, but migrate from the ventrolateral border of those somites adjacent to the early limb buds.

Myogenic determination factors

The myogenic determination factors Myf-5, myogenin, MyoD and Myf-6 (herculin) are a family of nuclear phosphoproteins. They have in common a

70-amino-acid, basic helix-loop-helix (bHLH) domain that is essential for protein–protein interactions and DNA binding. Outside the bHLH domain there are sequence differences between the factors that probably confer some functional specificity. The myogenic bHLH factors play a crucial role in myogenesis. Forced expression of any of them diverts non-muscle cells to the myogenic lineage. They activate transcription of a wide variety of muscle-specific genes by binding directly to conserved DNA sequence motifs (–CANNTG–known as E-boxes) that occur in the regulatory regions (promoters and enhancers) of these genes. Their effect may be achieved cooperatively, and can be repressed, e.g. by some proto-oncogene products. Some of the bHLH proteins can activate their own expression. Accessory regulatory factors, whose expression is induced by the bHLH factors, provide an additional tier of control.

The myogenic factors do not all appear at the same stage of myogenesis (Buckingham et al 2003). In the somites, *Myf-5* is expressed early, before myotome formation, and is followed by expression of *myogenin*. *MyoD* is expressed relatively late together with the contractile protein genes. *Myf-6* is expressed transiently in the myotome and becomes the major transcript postnatally. Whether this specific timing is important for muscle development is not yet clear. The creation of mutant mice deficient in the bHLH proteins (gene ‘knock-out’) has shown that *myogenin* is crucial for the development of functional skeletal muscle, and that while neither *Myf-5* nor *MyoD* is essential to myogenic differentiation on their own, lack of both results in a failure to form skeletal muscle. In the limb bud (see Ch. 51) the pattern of expression of the bHLH genes is generally later than in the somite: *Myf-5* is expressed first but transiently, followed by *myogenin* and *MyoD*, and eventually *Myf-6*. These differences provide evidence at the molecular level for the existence of distinct muscle cell populations in the limb and somites. It may be that the myogenic cells that migrate to the limb differ at the outset from those that form the myotome, or their properties may diverge subsequently under the influence of local epigenetic factors.

Formation of muscle fibres

In both myotomes and limb buds, myogenesis proceeds in the following way. Myoblasts become spindle-shaped and begin to express muscle-specific proteins. The mononucleate myoblasts aggregate and fuse to form multinucleate cylindrical syncytia, or myotubes, in which the nuclei are aligned in a central chain (Fig. 5.49). These primary myotubes attach at each end to the tendons and developing skeleton. The initiation of fusion does not depend on the presence of nerve fibres, since these do not penetrate muscle primordia until after the formation of primary myotubes.

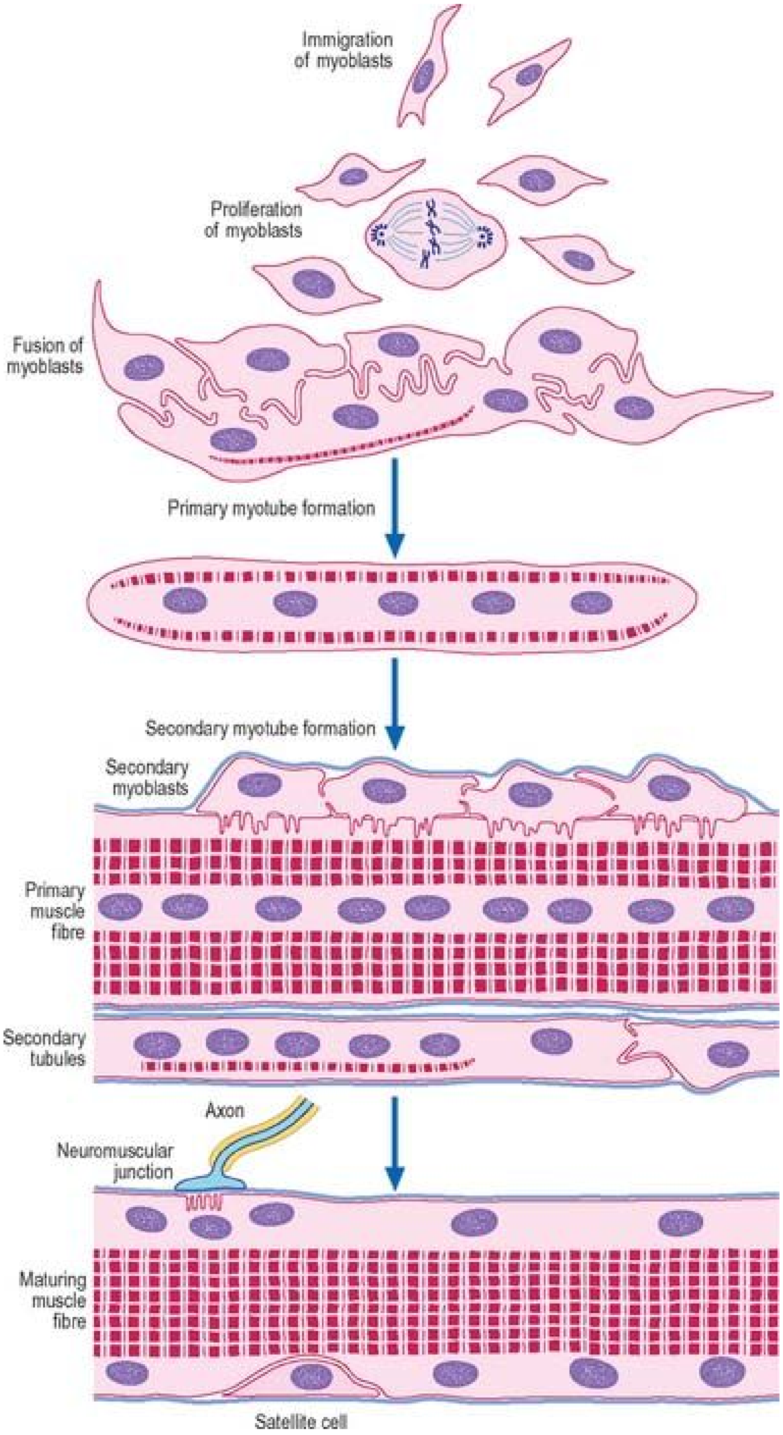
Immigration of myoblasts
Proliferation of myoblasts
Fusion of myoblasts
Primary myotube formation
Secondary myotube formation
Secondary myoblasts
Primary muscle fibre
Secondary tubules
Axon
Neuromuscular junction
Maturing muscle fibre
Satellite cell

Fig. 5.49 Stages in formation of skeletal muscle. Mononucleate myoblasts fuse to form multinucleate primary myotubes, characterized initially by central nuclei. Subsequently, other myoblasts align along the primary myotubes and begin to fuse with one another, forming secondary myotubes. In large animals, such as man, further generations of new muscle

fibres are similarly formed. As the contractile apparatus is assembled, the nuclei move to the periphery, cross-striations become visible and primitive features of the neuromuscular junction emerge. Later, small adult-type myoblasts – satellite cells – can be seen lying between the basal lamina and the sarcolemma of the mature muscle fibre. These too appear to be derived from cells that originated in the somites during early development.

(Redrawn from a figure provided by Terry Partridge, Department of Genetic Medicine, Children's National Medical Center, Washington DC.)

Although synthesis of the contractile machinery is not dependent upon fusion of myoblasts, it proceeds much more rapidly after fusion. Sarcomere formation begins at the Z-disc, which binds actin filaments constituting the I-band to form I–Z–I complexes. The myosin filaments assemble on the I–Z–I complexes to form A-bands. Nebulin and titin are among the first myofibrillar proteins to be incorporated into the sarcomere, and may well determine the length and position of the contractile filaments. Desmin intermediate filaments connect the Z-discs to the sarcolemma at an early stage, and these connections are retained.

Myogenic cells continue to migrate and to divide, and during weeks 7–9 there is extensive *de novo* myotube formation. Myoblasts aggregate near the midpoint of the primary myotubes and fuse with each other to form secondary myotubes, a process that may be related to early neural contact. Several of these smaller diameter myotubes may be aligned in parallel with each of the primary myotubes. Each develops a separate basal lamina and makes independent contact with the tendon. Initially, the primary myotube provides a scaffold for the longitudinal growth of the secondary myotubes, but eventually they separate. At the time of their formation, the secondary myotubes express an 'embryonic' isoform of the myosin heavy chains, whereas the primary myotubes express a 'slow' muscle isoform apparently identical to that found in adult slow muscle fibres. In both primary and secondary myotubes, sarcomere assembly begins at the periphery of the myotube and progresses inwards towards its centre. Myofibrils are added constantly and lengthen by adding sarcomeres to their ends. T-tubules are formed and grow initially in a longitudinal direction: since they contain specific proteins not found in plasma membranes, they are probably assembled via a different pathway from that which supports the growth of the sarcolemma. The sarcoplasmic reticulum wraps around the myofibrils at the level of the I-bands.

By 9 weeks, the primordia of most muscle groups are well defined, contractile proteins have been synthesized and the primitive beginnings of neuromuscular junctions can be observed, confined initially to the primary myotubes. Although some secondary fibre formation can take place in the absence of a nerve, most is initiated at sites of innervation of the primary myotubes. The pioneering axons branch and establish contact with the secondary myotubes. By 10 weeks these nerve–muscle contacts have become functional neuromuscular junctions and the muscle fibres contract in response to impulse activity in the motor nerves. Under this new influence the secondary fibres express fetal (sometimes referred to as neonatal) isoforms of the myosin heavy chains. At this stage several crucial events take place which may be dependent on, or facilitated by, contractile activity. As the myofibrils encroach on the centre of the myotube, the nuclei move to the periphery, and the characteristic morphology of the adult skeletal muscle myofibre is established. The myofibrils become aligned laterally, and A- and I-bands in register across the myotube produce cross-striations that are visible at the light microscopic level. T-tubules change from a longitudinal to a transverse orientation and adopt their adult positions: they may be guided in this process by the sarcoplasmic reticulum, which is more strongly bound to the myofibrils.

The myotubes and myofibres are grouped into fascicles by growing connective tissue sheaths, and the fascicles are assembled to build up entire muscles. As development proceeds, the increase in intramuscular volume is accommodated by remodelling of the connective tissue matrix.

At 14–15 weeks, primary myotubes are still in the majority, but by 20 weeks the secondary myotubes predominate. During weeks 16–17, tertiary myotubes appear: they are small and adhere to the secondary myotubes, with which they share a basal lamina. They become independent by 18–23 weeks, their central nuclei move to the periphery, and they contribute a further generation of myofibres. The secondary and tertiary myofibres are always smaller and more numerous than the primary myofibres. In some large muscles, higher order generations of myotubes may be formed.

Late in fetal life, a final population of myoblasts appears which will become the satellite cells of adult muscle. These normally quiescent cells lie outside the sarcolemma beneath the basal lamina (Fig. 5.49, Fig. 5.50). M-cadherin, a cell adhesion protein of possible regulatory significance, occurs at the site of contact between a satellite cell and its muscle fibre. In a young individual, there is one satellite cell for every 5–10 muscle fibre nuclei. The latter are incapable of DNA synthesis and mitosis, and satellite cells are therefore important as the sole source of additional muscle fibre nuclei during postnatal growth of muscle (to maintain the ratio of cytoplasmic volume per nucleus as fibres increase in mass). After satellite cells divide, one of the daughter cells fuses with the growing fibre, the other remains as a satellite cell capable of further rounds of division. Similar events may take place to support exercise-induced hypertrophy of adult skeletal muscle. Satellite cells provide a reservoir of myoblasts capable of initiating regeneration of an adult muscle after damage. Other stem cell populations may also be induced to begin a myogenic differentiation pathway, e.g. bone marrow stem cells and processed lipoaspirate cells (Mizuno et al 2002).

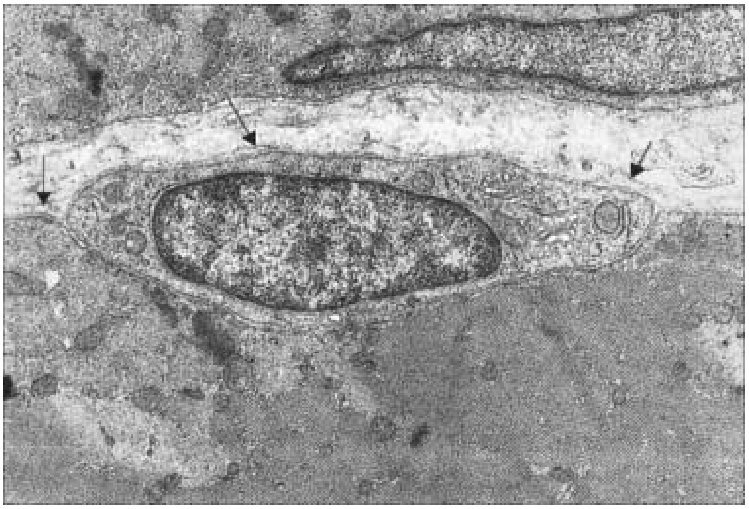

Fig. 5.50 Electron micrograph of a satellite cell. Note the two plasma membranes that separate the cytoplasm of the satellite cell from that of the muscle fibre, and the basal lamina (arrows) of the transversely-sectioned muscle fibre, which continues over the satellite cell (see also **Fig. 5.38**). Compare this appearance with the normal muscle nucleus which is seen in the adjacent fibre (above).

(Photograph by Dr Michael Cullen, School of Neurosciences, University of Newcastle upon Tyne.)

The development of fibre types

Developing myotubes express an embryonic isoform of myosin which is subsequently replaced by fetal and adult myosin isoforms. The major isoform of sarcomeric actin in fetal skeletal muscle is cardiac α-actin; only later is this replaced by skeletal α-actin. The significance of these developmental sequences is not known.

The pattern of expression is fibre-specific as well as stage-specific. In primary myotubes, embryonic myosin is replaced by adult slow myosin from about 9 weeks onwards. In secondary and higher order myotubes the embryonic myosin isoform is superseded first by fetal and then by adult fast myosin, and a proportion go on to express adult slow myosin. Other fibre-specific, tissue-specific and species-specific patterns of myosin expression have been described in mammalian limb muscles and jaw muscles.

The origin of this diversity in the temporal patterns of expression of different fibres, even within the same muscle, is far from clear. It has been suggested that intrinsically different lineages of myoblast emerge at different stages of myogenesis or in response to different extracellular cues. If this is the case, their internal programmes may be retained or overridden when they fuse with other myoblasts or with fibres that have already formed. The fibres that emerge from this process go on to acquire a phenotype that will depend on the further influence of hormones and neural activity.

In man, unlike many smaller mammals, muscles are histologically mature at birth, but fibre type differentiation is far from complete. In postural muscles, the expression of type I myosin increases significantly over the first few years of life; during this period the fibre type proportions in other muscles become more divergent. The presence in adult muscles of a small proportion of fibres with an apparently transitional combination of protein isoforms reinforces the view that changes in fibre type continue to some extent in all muscles and throughout adult life. Fibre type transitions also occur in relation to damage or neuromuscular disease; under these conditions, the developmental sequence of myosins may be recapitulated in regenerating fibres.

Growth and regulation of fibre length

Muscle fibres grow in length by addition of sarcomeres to the ends of the myofibrils. It is important that the number of sarcomeres is regulated throughout life, so that the mean sarcomere length, and hence filament overlap, is optimized for maximum force. This is achieved by addition or removal of sarcomeres in response to any prolonged change of length. For example, if a limb is immobilized in a plaster cast, the fibres of muscles that have been fixed in a shortened position lose sarcomeres, while those that have been fixed in a lengthened position add sarcomeres; the reverse process occurs after the cast has been removed.

Satellite cells and muscle repair

Until the mid 20th century, the mechanisms responsible for the maintenance and repair of skeletal muscle were unclear. These issues were largely resolved by the almost simultaneous discovery that multinucleated muscle fibres were formed by the fusion of mononucleated precursors, myoblasts, and that a population of satellite cells, so-called because of their position on the edge of the fibre, existed between the basal lamina of the mature muscle fibre and its sarcolemma. Although satellite cells constitute 2–5% of the nuclei enclosed by the basal lamina, their role in repair and regeneration of muscle was not resolved until quite recently, because they could be identified only by their anatomical position and quiescent appearance. In contrast, active myoblasts at sites of muscle injury lose both of these features. In recent years, the discovery of a number of myogenic differentiation genes whose expression is retained in the quiescent satellite cell has elucidated their role.

Studies in mouse models, where genetic analysis is possible, have shown that the functional properties of postnatal satellite cells are dependent on the expression of the *Pax7* gene, whereas the prenatal development of muscle is not similarly dependent. This implies that the satellite cells are not simply the relics of the prenatal myogenic population although they appear to be derived from the same embryonic source in the somites. Moreover, satellite cells are not a homogeneous population: no two differentiation markers concur completely. This is also the situation in human tissue (Fig. 5.51). It has yet to be determined whether this variation reflects a difference in position in the lineage, in functional status, or in the adjacent environment.

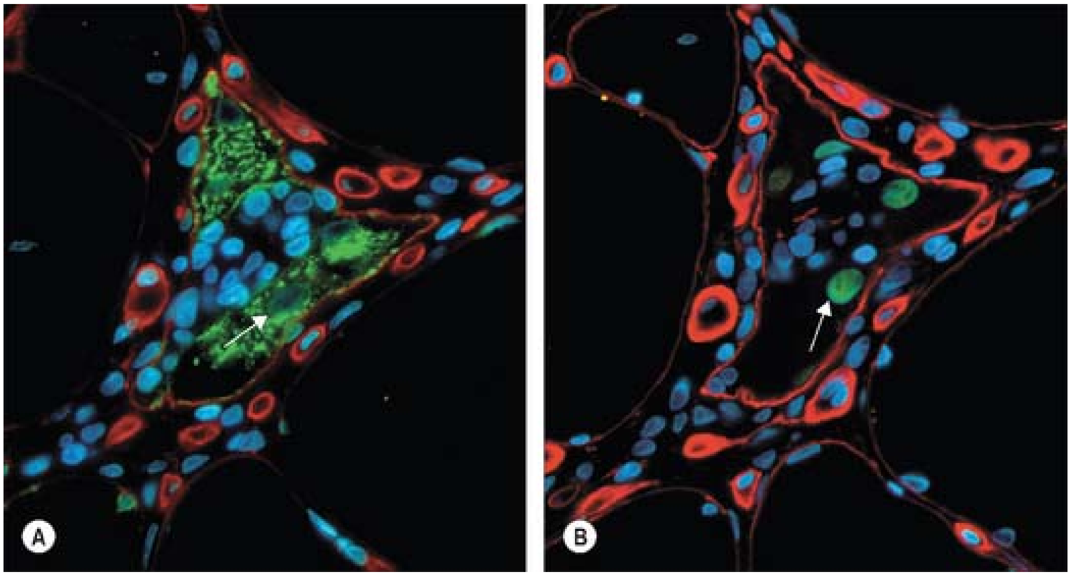

Fig. 5.51 Two adjacent sections, fluorescence-immunolabelled, of a regenerating muscle fibre in the trapezius muscle of a power-lifter. **A**, Anti-laminin antibody (red) shows basal lamina. Anti-CD56 (green) is a marker of myogenic cells and of newly-formed myotubes. **B**, Adjacent section, basal lamina (red) and myogenin-positive nuclei (green). Basal laminae outline the transversely-sectioned muscle fibres, including the original outline of the fibre being regenerated (centre field). Numerous small blood vessels also outlined by basement membranes, are present probably

reflecting local inflammation. Within the CD56 +ve zone, several nuclei (one arrowed) are positive for myogenin, indicating their terminally-differentiated status. Numerous other nuclei (Hoechst dye, blue) within the basement membrane surrounding the area of regeneration probably include proliferating myogenic cells and inflammatory cells.

(Provided by courtesy of Ms Mona Lindström and Professor Lars-Eric Thornell, Department of Anatomy, Umea University, Sweden.)

The satellite cell been rigorously established in mice as being both necessary and sufficient for effective regeneration of damaged skeletal muscle. The cells proliferate to replace their resident region of muscle in 3–4 days and to replenish the quiescent satellite cell population (Collins & Partridge 2005). In man, there is histological evidence of the rapid accumulation of myoblasts, presumably derived from local satellite cells, at sites of muscle damage.

A point of wide pathological interest is the demonstration that the failing regenerative potency of satellite cells in aging muscle seems in large part to be attributable to age-related changes in the systemic environment rather than a decline in the intrinsic capabilities of the satellite cells themselves (Conboy et al 2005).

BIOMECHANICS

The musculoskeletal system is essentially a mechanical system, designed to support, protect and move the body, and capable of adapting to changing mechanical demands (see Benjamin & Maganaris 2006, for a review of the ways in which different elements of the musculoskeletal system respond to exercise). Structures such as long bones and synovial joints have specific mechanical functions; the material properties of the skeletal tissues from which they are derived permit optimal adaptations to diverse mechanical demands.

The purpose of this section is to explain, in a non-mathematical way, how mechanical principles shape the human musculoskeletal system. Mechanical considerations explain why bones are stiff and tendons are tough, why the surfaces of some synovial joints are imperfectly matched, and why some tendons insert closer to joints than others. The emerging subject of ‘mechanobiology’ considers how cells adapt their matrix to prevailing mechanical demands and explains why some tissues are better at doing this than others.

MECHANICAL CONCEPTS

Forces, moments and torques

A force is an action which deforms an object, or which causes it to move, and can be termed compressive, tensile or shear, according to the manner in which it deforms objects (Fig. 5.52). A force F acting at the end of a lever of length L will generate a bending moment (F × L) acting about the pivot point of the lever. A torque or torsional moment (Fig. 5.52F) may be quantified in similar terms. The combined influence of several forces can be calculated as shown in Fig. 5.53. If the forces all act in the same direction, they may be added; if they act in different directions each force must be resolved into two imaginary components which act in two anatomically convenient directions at 90° to each other, using simple trigonometry. All components acting in the same direction are added to form two forces (S and C in Fig. 5.53) which can be used to calculate the magnitude and direction of the single resultant force (which has a similar effect to all of the individual forces combined). Forces acting on a stationary object are analysed according to the principle that all forces acting in any given direction must balance each other (i.e. add to zero) and all moments or torques acting about a given pivot point must also balance each other.

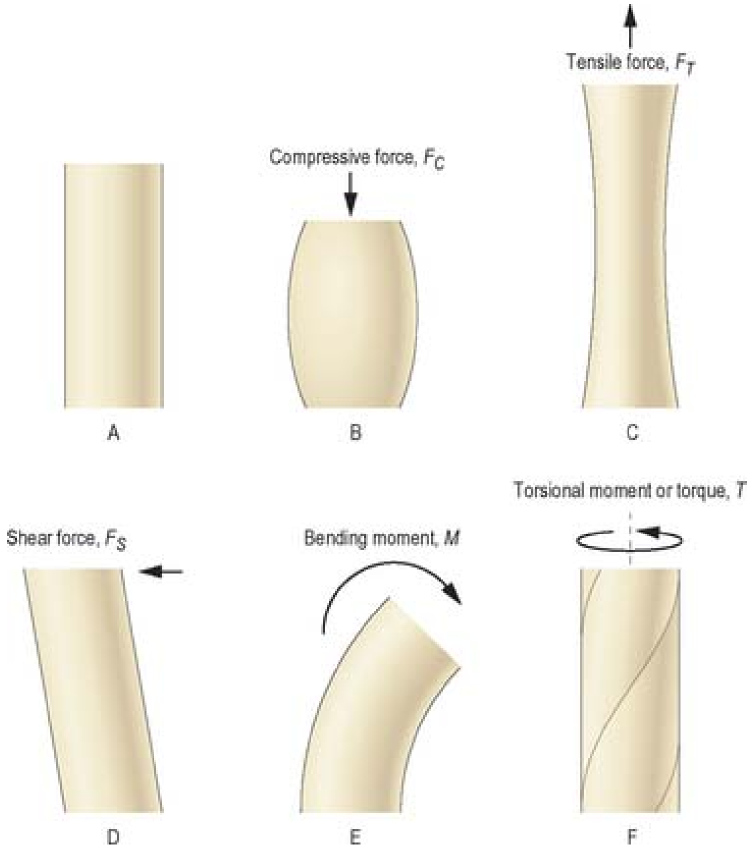
Tensile force, F_T
Compressive force, F_C
A
B
C
Torsional moment or torque, T
Shear force, F_S
Bending moment, M
D
E
F

Fig. 5.52 The effects of different types of loading on a solid object (shown in **A**) are illustrated in **B–F**.

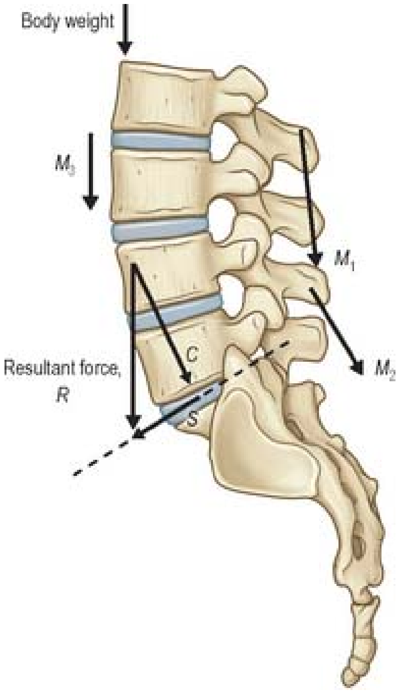

Fig. 5.53 The combined effect of several muscle forces (M_1–M_3) and body weight (W) can be calculated by resolving each force into two components acting in two anatomically-meaningful directions (in this case parallel and perpendicular to the mid-plane of the lumbosacral intervertebral disc). The components acting in these two directions are then summed to give the total compressive (C) and shear (S) forces acting on the disc. The magnitude and direction of the resultant force (R) which represent the combined effect of all four forces can be calculated using trigonometry.

Mechanical properties of structures

Most biological structures deform readily when a sufficient force is applied to them, but their resistance to deformation increases steadily as the magnitude of the force increases: the resulting graph of force against deformation resembles the one shown in Fig. 5.54. Stiffness is the ratio of force to deformation (typical units N/mm) and so is represented by the gradient of the graph. The initial region of low stiffness, or 'toe region', is followed by a stiffer region in which the graph is almost linear. In many biological structures, the 'toe region' can be explained by the straightening out of the zig-zag 'crimp' structure of collagen type I fibres, whereas the linear region represents direct stretching of the straightened collagen fibres. If the deformed structure springs back immediately to its original dimensions when the deforming force is removed, the deformation is termed elastic; a deformation that shows no sign of recovering is plastic, and one that recovers eventually, but gradually, is viscoelastic (see below). Strength is the force at which an object becomes damaged, and is usually interpreted either as the force at which the gradient of the graph first reduces (the elastic limit) or the force when the gradient falls to zero (the ultimate strength).

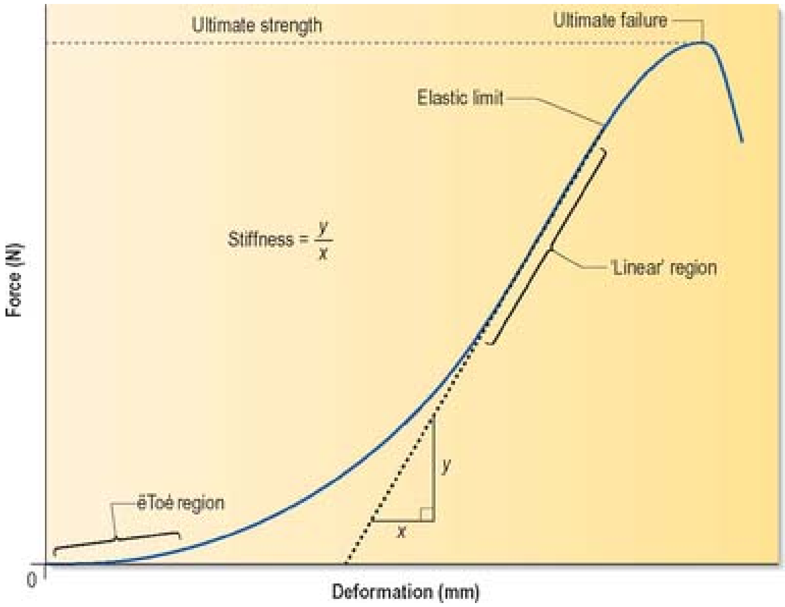

Fig. 5.54 A typical force-deformation graph for a skeletal structure subjected to mechanical loading. In the initial 'toe region', deformation increases rapidly with force, but this is followed by a linear region in which the deformation increases more slowly, and in proportion to the applied force. The gradient of the graph indicates the stiffness of the structure at any given load. Strength is the force at which an object becomes damaged, and this is usually interpreted either as the force at which the gradient first reduces (the elastic limit) or the force when the gradient falls to zero (the ultimate strength).

Properties of materials

The properties of materials must be expressed in such a way that they are independent of the size and shape of the structure they constitute. A force divided by the area over which that force is applied gives a stress value (force per unit area); the resulting deformation divided by the original length of the object gives a strain value (fractional or percentage deformation). Stress divided by strain is the size-independent material equivalent of the stiffness of an object, and is an important physical property termed the modulus. There are different types of modulus, but essentially they correspond to stiffness, or resistance to deformation.

Energy and shock absorption

Deforming an object may require a considerable expenditure of energy. Technically, the work done (or energy expended) is proportional to the average force exerted, multiplied by the distance moved. This is mathematically equivalent to the area under the graph in Fig. 5.55. For this reason, the area is referred to as the strain energy, i.e. the energy that has been expended in deforming the object. If the object has elastic properties, it will spring back to its original shape when the deforming force is removed, and all the strain energy is then released. (This release of energy explains why a stretched rope can recoil violently if it snaps.) Structures such as coiled springs, which can resist high forces and also deform extensively, are capable of storing large amounts of energy, and so can act as shock absorbers when they are continually compressed and stretched. Tendons act in a similar manner during locomotion: they store strain energy when their muscles contract, and release most of it as the muscles relax later in the gait cycle. A small fraction of the stored strain energy, the hysteresis energy, is dissipated as heat (Fig. 5.55), and can cause generation of heat in large tendons involved in vigorous repetitive activity. Any material or structure that is capable of absorbing large amounts of strain energy before failure is termed tough; otherwise it is brittle. From Fig. 5.55 it is apparent that tough materials must be both strong and extensible: examples of strong but brittle materials are glass and tooth enamel, which both undergo minimal deformation and so display very steep force-deformation graphs.

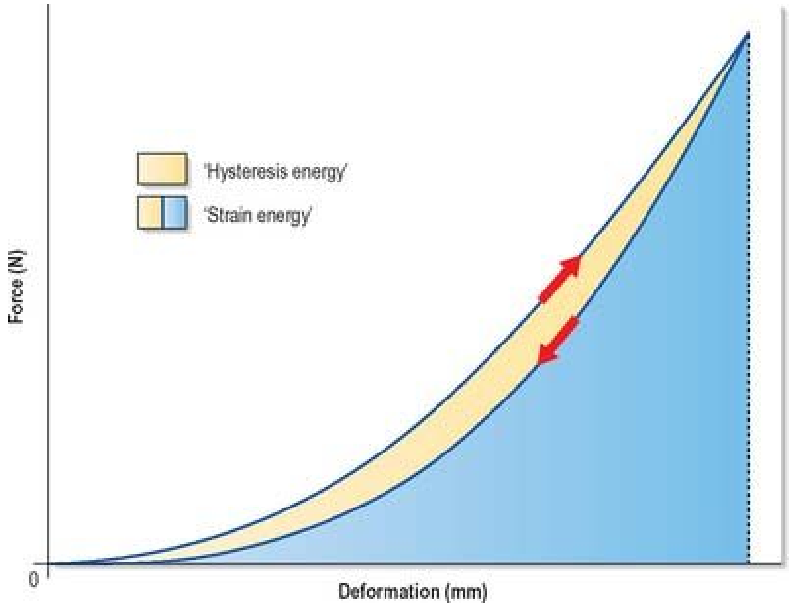

Fig. 5.55 This force–deformation graph shows how an object deforms when a force is applied to it (upwards arrow) and how it recovers its shape when the force is gradually released (downwards arrow). The area under the loading curve represents the strain energy that has been expended in deforming the object. The area under the unloading curve represents the energy that is given up when the object is allowed to spring back to its original shape. The small area in between represents energy which cannot be recovered but is dissipated as heat. This is the hysteresis energy.

Liquids

A liquid has negligible rigidity and so deforms readily to take the shape of its container. When compressed, it maintains practically the same volume, but it flows to equalize the intensity of loading within it. As a result, a static liquid under load exhibits a single internal pressure (force per unit area) that does not vary with location or direction. Even delicate objects are not deformed when immersed in a high pressure liquid if they themselves are filled with liquid, because the internal and external pressures on them are exactly equal, which explains why cells can survive high pressures in liquids without damage to their plasma membrane. Of the musculoskeletal tissues, only the nucleus pulposus of intervertebral discs exhibits true liquid behaviour, although other tissues such as bone and cartilage contain liquid which is able to move relative to the solid matrix that surrounds it.

Viscoelasticity

Materials are said to be viscoelastic if they behave partly like a thick (viscous) fluid and partly like an elastic solid. Viscoelastic deformations change with time, even when the deforming stress is constant, and complete recovery from such deformations also takes some time after the stress is removed (Fig. 5.56). In most biological materials, viscous behaviour occurs because applied loading causes fluid to flow from the most heavily loaded regions to the least loaded, by percolating through very small (nanometre-scale) pores in the matrix, a process which can take hours: for this reason, the term poroelastic is often preferred to viscoelastic when referring to tissues such as cartilage. Creep and stress relaxation are two important manifestations of viscoelasticity. Creep may be described as continuing deformation under constant load (Fig. 5.56), whereas stress relaxation is a gradual decrease in force resisted by a viscoelastic material when it is initially deformed by a certain amount, and then held with the same constant deformation.

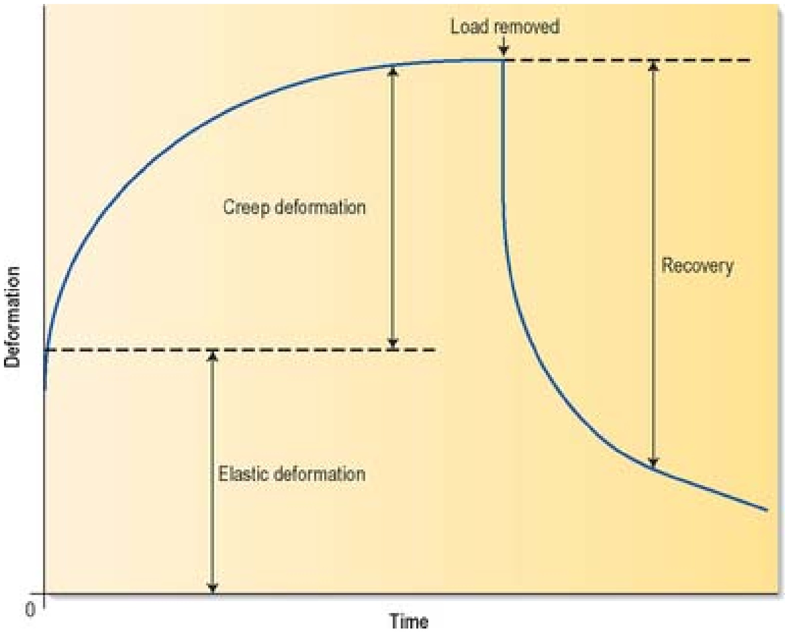

Fig. 5.56 The deformation of viscoelastic materials varies with time. In this example, a load is applied at zero time which causes an immediate elastic deformation, followed by a slowly increasing time-dependent deformation (creep). When the load is removed, some deformation is recovered immediately, but full recovery is achieved only slowly.

MATERIAL PROPERTIES OF SKELETAL TISSUES

The material properties of several skeletal tissues are compared in Table 5.3.

Table 5.3 Tensile materials properties of skeletal tissues. For comparison, alloy steel has a strength of 600 MPa and a modulus of 20,000 MPa.

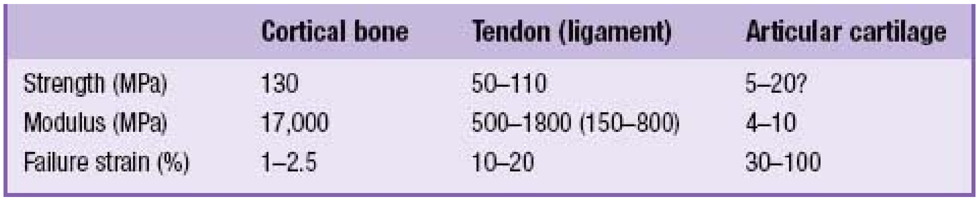

	Cortical bone	Tendon (ligament)	Articular cartilage
Strength (MPa)	130	50–110	5–20?
Modulus (MPa)	17,000	500–1800 (150–800)	4–10
Failure strain (%)	1–2.5	10–20	30–100

Bone

Bone consists mainly of collagen type I, and microcrystals of the mineral hydroxyapatite. Collagen gives bone considerable tensile strength, and renders it very tough when fractured, whereas the mineral component gives bone a very high compressive modulus and high compressive strength. Rigidity (stiffness) is the defining characteristic of bone: it enables the tissue to provide precisely shaped surfaces in synovial joints which will deform very little under load, and it also enables fast locomotion when muscles pull on bones. If bones were strong and tough but not rigid, rapid muscle contractions would cause them to bend alarmingly and would slow the angular movement of limbs.

Tendon, ligament and fascia

Tendons, ligaments and fascia consist primarily of densely packed collagen type I fibres, an arrangement that gives these structures very high tensile strength: the crimped structure of the collagen fibre bundles permits stretching by 10–15% before failure. This combination of strength and extensibility enables tendons, ligaments and fascia to absorb more strain energy per unit weight than any other biological material, and makes them very effective shock absorbers (Alexander, 1988). An important mechanical difference between tendons and ligaments is that ligaments often contain bundles of collagen fibres orientated in a range of directions, presumably because bones can be moved apart in a range of directions, whereas the fibres in a tendon are aligned only in the direction in which the muscle pulls on the tendon. Fascia usually contains collagen fibres aligned to resist forces in at least two different directions.

Hyaline cartilage

Hyaline cartilage consists mainly of very fine collagen type II fibrils and large proteoglycan molecules which have the property of attracting water and swelling. Collagen gives cartilage its tensile strength and stiffness, and the proteoglycans give the tissue a high water content that confers compressive ‘turgor’. During growth and healing, proteoglycans enable the growing cartilage to swell and occupy space that later will be strengthened by other components of the matrix. Articular cartilage is a particular type of hyaline cartilage that covers the ends of articulating bones: the high water content of the tissue enables it to distribute loading evenly on the underlying bone. Because cartilage is softer than bone, it exhibits a relatively greater degree of deformation when loaded. This increases the area of contact between articular surfaces and reduces the contact stress (Fig. 5.57). Sustained loading of a synovial joint for just a few minutes causes substantial cartilage creep, because water is expelled from the tissue. Creep causes the area of contact to increase, and further reduces the contact stress. Creep in articular cartilage also causes water to be exuded into the joint cavity, assisting in fluid film lubrication (see below). Articular cartilage ‘wear’ (measured in grammes) is the gradual loss of material from the surface in response to high and repetitive loading; it is minimized because the collagen type II fibrils in the superficial zone are aligned parallel to the surface, an arrangement that provides maximal resistance to surface splitting and the subsequent loss of tissue.

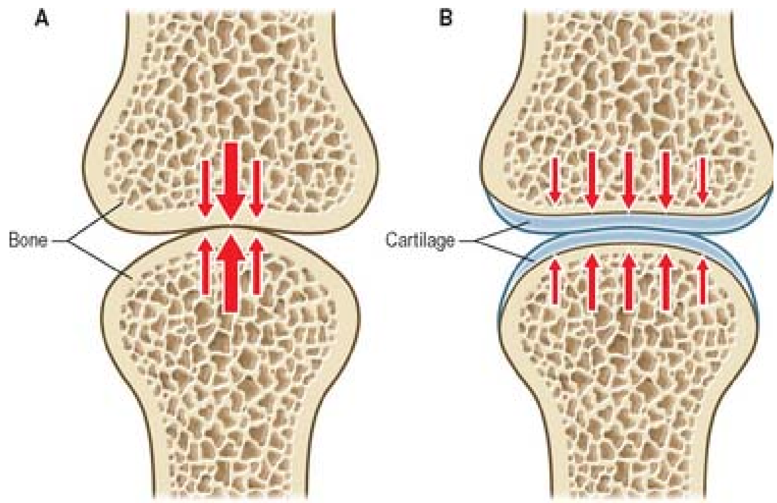

Fig. 5.57 Articular cartilage in a synovial joint is not as stiff as the underlying bone, so the presence of cartilage in a loaded joint increases the area of contact (**B**) compared to a joint without cartilage (**A**).

Fibrocartilage and elastic cartilage

Fibrocartilage and elastic cartilage combine the high proteoglycan and water content that characterizes cartilage with a high proportion of either thick collagen type I fibres (fibrocartilage) or elastin fibres (elastic cartilage). Collagen type I confers extra tensile strength and toughness, whereas elastin fibres provides elastic recoil, i.e. the ability to spring back to shape after large deformations.

MECHANICAL PROPERTIES OF SKELETAL STRUCTURES

Long bones

Long bones are characterized by enlarged ends covered in cartilage, a long hollow shaft, and various bony protuberances. The enlarged ends serve to reduce contact stress where long bones meet in synovial joints, and to increase the stability of such joints (Fig. 5.58). A different relationship between stability and mobility can exist in different anatomic planes, even for the same joint, e.g. the knee joint favours stability in the frontal plane, and mobility in the sagittal plane. The hollow shaft of a long bone confers high strength in bending, but also minimizes bone mass and so increases the speed of movement. Bending strength is increased by having as much bone mass as possible far from the axis of bending (Fig. 5.59). The precise cross-sectional shape of a long bone therefore gives a clear indication of the planes in which the shaft is most likely to be subjected to severe bending. Bony prominences or processes on long bones serve to increase the lever arm of muscles that are attached to them: if a large prominence is close to the centre of rotation of a joint, then the lever arm might increase by over 100%, and the maximum torque developed by the muscle about that centre of rotation would increase by the same amount.

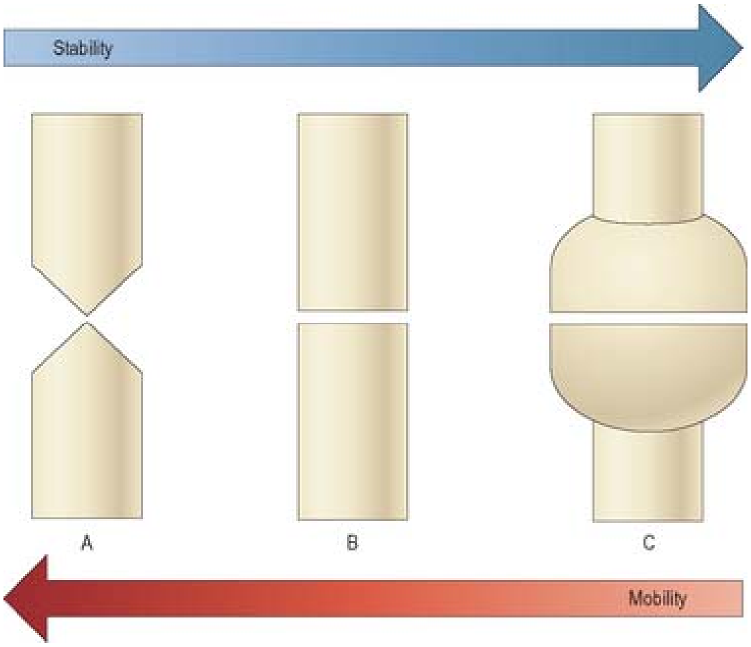

Fig. 5.58 In synovial joints, the shapes of the opposing bone ends largely determine how much movement is possible, and the stability of the joint. Tapered bone ends (**A**) lead to high mobility, but low stability (in the plane of the page). Conversely, very wide bone ends (**C**) lead to low mobility and high stability. Some joints resemble (**A**) in one plane, but (**B**) or (**C**) in others.

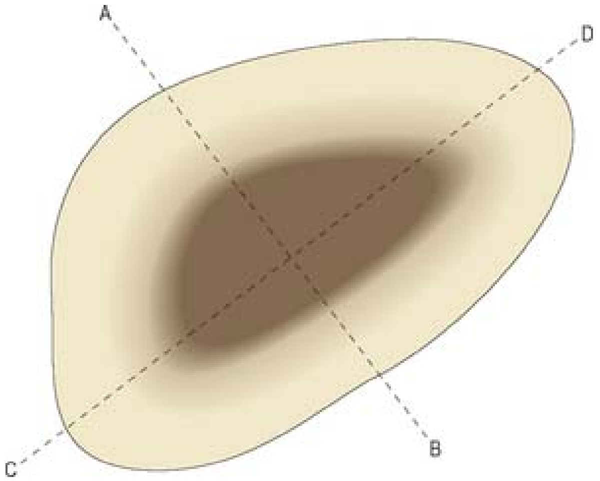

Fig. 5.59 Cross-section through the shaft of a long bone, showing how the irregular shape gives information about the bone's strength in bending about different axes. Strength will be greatest about the axis A–B because a high proportion of bone mass is located a long distance from this axis, and

so will resist bending very strongly. Strength will be minimal about the axis C–D for a similar reason.

Synovial joints

Typically, synovial joints are designed for full and free movements, but they must also provide some stability in specific planes (Fig. 5.58). In a joint with a small range of movement, intrinsic stability provided by the articular surfaces and ligaments of that joint may be more important than the extrinsic stability provided by surrounding muscles. Low friction movement is facilitated by the smooth surfaces of articular cartilage, made slippery by the presence of hydrophobic lubricants (surface-active phospholipids) which are bound to the cartilage surface. This boundary lubrication reduces friction during slow movements, especially when forces are high. During rapid movements, microscopic undulations in the cartilage surface trap small quantities of synovial fluid between the articular surfaces, so that fluid film lubrication (akin to aqua-planing) can also occur (Fig. 5.60), and friction and wear are greatly reduced. The sticky, viscous nature of synovial fluid enables it to persist between the cartilage surfaces for longer than water, which would be squeezed out much too quickly. Fluid film lubrication is assisted by joint incongruity, in which the opposing articular surfaces have slightly different curvatures (Fig. 5.61), producing a potential fluid filled gap which moves as the joint moves, washing synovial fluid across the cartilage surfaces. Incongruity can also help to reduce peak loading on the apex of the joint.

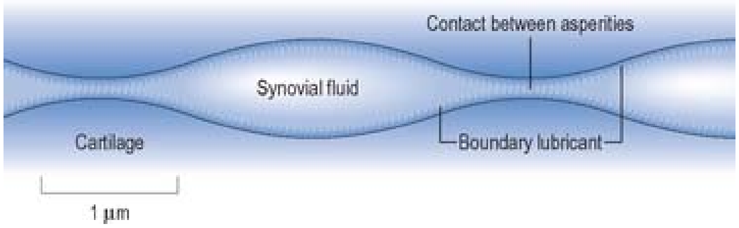

Fig. 5.60 The articular cartilage surfaces of synovial joints contain microscopic undulations which trap small quantities of synovial fluid between the surfaces. This enables fluid film lubrication to occur. Boundary lubrication at the points of contact between cartilage asperities is facilitated by lubricants adhering to the cartilage surface.

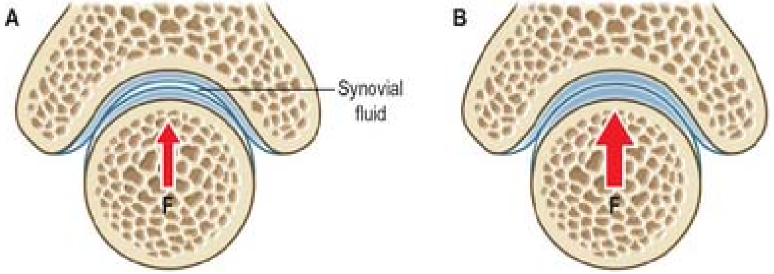

Fig. 5.61 Some synovial joints are incongruent in the sense that the opposing articular surfaces have slightly different curvatures. This ensures that there is a fluid-filled gap between them when the joint is subjected to low loading (**A**). Under high loading (**B**) this gap disappears, but peak loading at the apex of the joint remains lower than it would be if the surfaces had the same curvature, and this is a major advantage for an incongruent joint. The shape of the concave articular surface is sometimes referred to as a Gothic arch. F = Loading force.

Intervertebral discs

Intervertebral discs are composed of three tissues: the anulus fibrosus (fibrocartilage), the nucleus pulposus (a hydrated collagenproteoglycan gel), and the endplates (hyaline cartilage) (see Ch. 42). The water content of the nucleus pulposus can reach 90% in children and young adults, enabling the whole tissue to behave like a fluid. When compressive loading is applied to the vertebral column, the fluid pressure in the nucleus presses evenly on the adjacent vertebral bodies, even when they are orientated at small angles to each other. The anulus resists radial expansion of the nucleus, and can deform vertically to facilitate spinal bending in various planes. The relatively dense hyaline cartilage endplate helps to maintain a fluid pressure in the nucleus by slowing down water loss into the vertebral body through perforations in the vertebral endplate. Nevertheless, discs lose approximately 20% of their water gradually, in the course of the day. This nett loss of water is regained at night when, in recumbency, the load on the spine is relieved. Diurnal variations in disc water content cause adults to be approximately 2 cm taller in the early morning, and more flexible in the evening (see Ch. 42).

MUSCLES AND LEVER SYSTEMS

Collagenous architecture of muscle

Muscles are supported by a hierarchy of collagenous sheaths (endomysium, perimysium and epimysium) which surround individual muscle fibres, fascicles and whole muscles respectively. Muscles are bound together into functional groups by collagenous fascia. Together these sheaths create a strong honeycomb structure which contributes to the resistance of a muscle to tension. When muscle is stretched, high tensile forces in these collagenous structures contribute to the high forces which can be generated during eccentric (lengthening) muscle contractions.

Internal muscle forces

Generally speaking, muscle forces exert greater mechanical loading to the skeleton than does body weight. During relaxed standing, 50% of the compressive force acting on the lumbar spine arises from the antagonistic activity of the muscles of the back and abdomen, and 50% comes from superincumbent body weight. However, when bending the trunk to lift weights from the ground, more than 90% of the compressive force acting on the spine can be attributed to muscle tension (Fig. 5.62). Similarly, muscle forces acting on the knee can exceed body weight by a factor of 200–400% during stair climbing, and during deep squatting movements. Muscle forces can exceed the strength of adjacent bones if they contract in alarm, so that normal inhibitory reflexes are suppressed: it is not uncommon for vertebrae to be crushed by muscle tension during major epileptic fits. Muscle forces also rise to high levels when attempting to accelerate body parts. According to Newton’s 2nd Law of motion (force = mass × acceleration), it follows that any attempt to achieve maximum acceleration, e.g. during some sporting activity, will naturally require maximal muscle tension. The size and potential dangers of internal muscle forces are often overlooked, leading some authors to draw spurious distinctions between weight-bearing and non-weight-bearing joints, and suggesting erroneously that only the former are subjected to high loading: it is likely that a watch-maker’s finger joints are subjected to stresses as high, and as often, as those applied to his ankles.

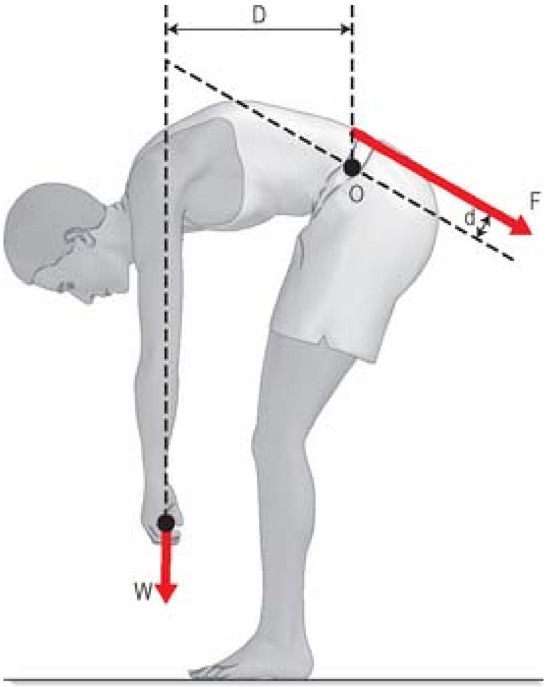

Fig. 5.62 During manual labour, muscle tension often rises to high levels in order to generate sufficient bending moment to move external objects. In this example, the back muscles act only a short distance (d) from the pivot point in the intervertebral discs, whereas the weight being lifted acts on a much bigger lever arm (D). In order for the moments to balance, the back muscle tension (F) must exceed the weight being lifted (W) by the ratio of D/d. In practice, this can lead to the lumbar spine being compressed by approximately 500 kg during moderate manual handling.

Muscle lever systems

Muscle tension generates bending moments and torques about joints. Moments and torques depend on lever arms as well as muscle forces. It is conventional (although not particularly instructive) to distinguish between three types of muscle lever system (Fig. 5.63). The length of the lever arm (the perpendicular distance between the muscle line of action and the centre of rotation of the joint) is more important than lever type (Fig. 5.64). If the lever arm is short, then a given muscle contraction will move the joint through a large angle, so the lever system is suited to large and/or rapid movements of that joint. Conversely, a long lever arm leads to small and/or slow movements, but greater moment generation. These considerations can reveal, for example, whether an animal's jaws are designed to catch insects, or to crush nuts. Elite weight-lifters may have muscle insertions with particularly large lever arms about particular joints.

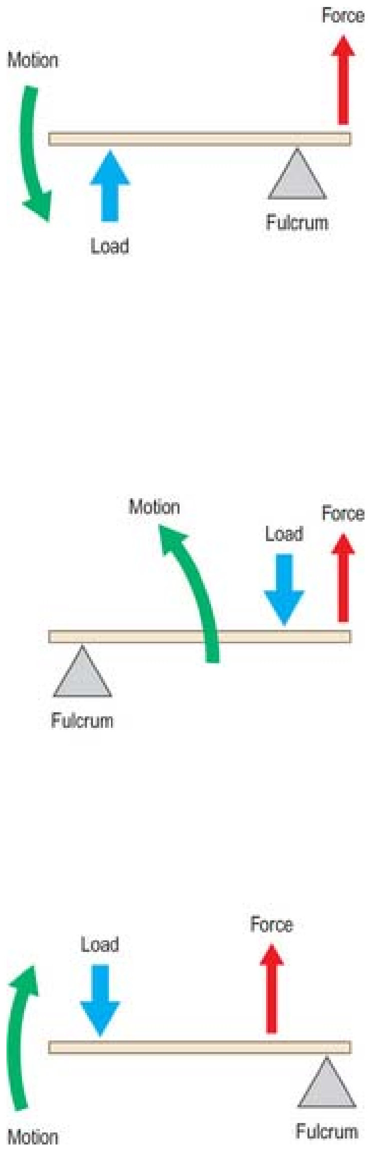
Force
Motion
Load
Fulcrum
Motion
Force
Load
Fulcrum
Force
Load
Motion
Fulcrum

Fig. 5.63 Muscle lever systems can be classified as First class (**A**), Second class (**B**) or Third class (**C**) according to the relative positions of the pivot, the muscle insertion, and the externally-applied force.

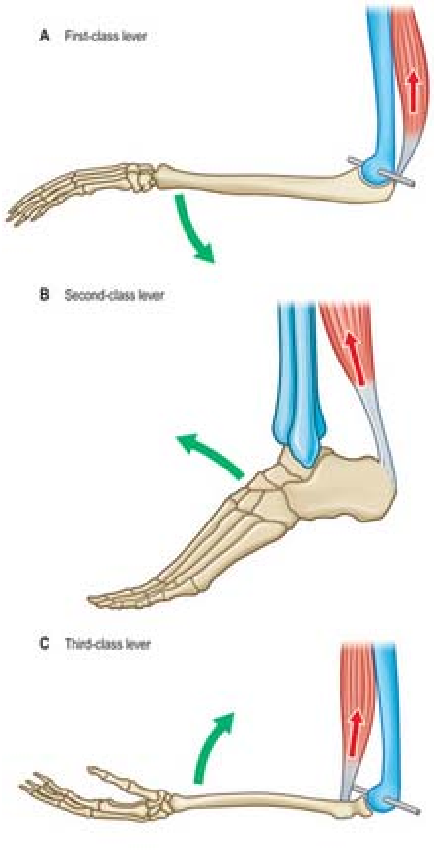
A First-class lever
B Second-class lever
C Third-class lever

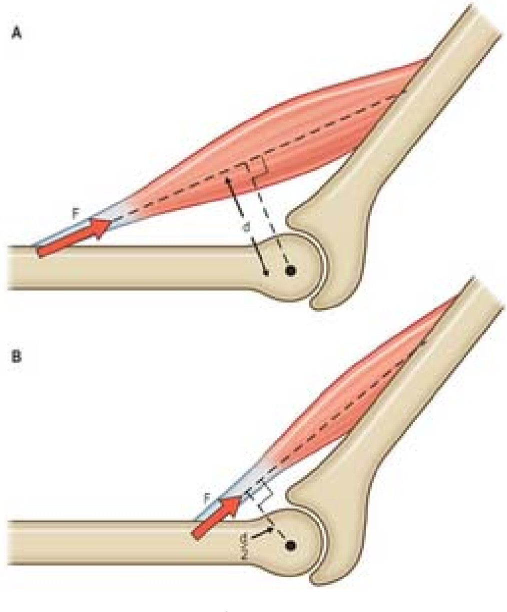

Fig. 5.64 The precise location of a muscle insertion relative to a joint greatly influences the function of that joint. **A**, If the perpendicular distance (d) between the muscle line of action and the centre of rotation of the joint (•) is large, then the joint is suited to slow but forceful movements. **B**, If d is small, then the joint is suited to rapid but less forceful movements.

MOVEMENTS

Movements of bones

Movement of a bone is referred to as translation if it does not involve any change in orientation relative to a fixed frame of reference (or to another bone). A pure rotation involves no translation, merely a pivoting of the bone about some fixed point or centre of rotation. Spin is the rotation of a bone about its mechanical axis, which for a long bone would coincide with its long axis. Spin can occur in conjunction with other joint rotations (Fig. 5.65). Most body movements involve some combination of rotation, translation, and spin, although the translational component is often small.

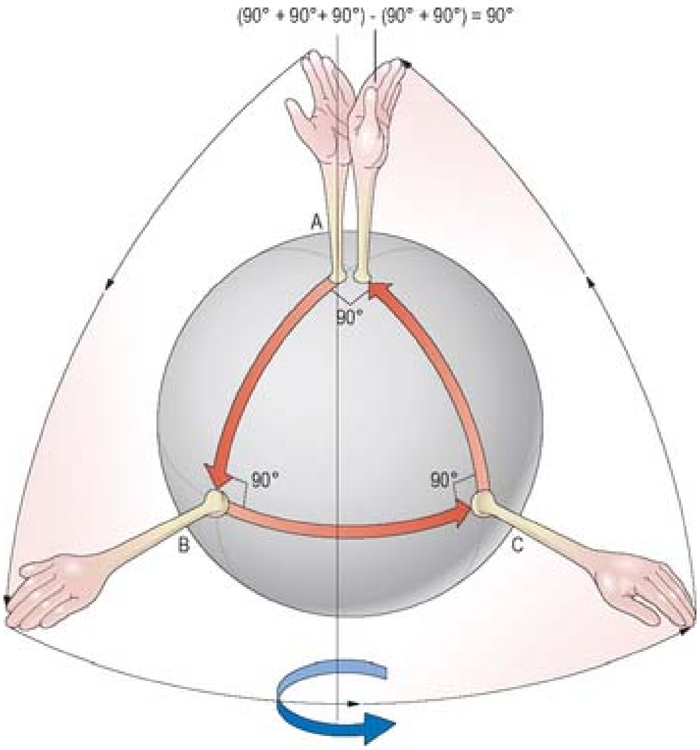

Fig. 5.65 Complex movements of the body’s joints are sometimes required to produce apparently simple movements of the limbs. In this example, moving the hand as shown from A to B to C requires a hidden ‘spin’ movement of the arm of 90° about its mechanical (long) axis.

Movements at articular surfaces

Opposing joint surfaces are never perfectly congruent. Nevertheless, substantial regions of opposing surfaces may fit together exactly in a certain position known as the close-packed position in which the joint is most stable, e.g. the close-packed position of the knee joint corresponds to full extension. In other (loose-packed) positions, the surfaces of incongruent joints are not perfectly matched, and are able to move relative to each other by a combination of spin, roll and slide (Fig. 5.66). In final close-packing, surfaces are fully congruent, in maximal contact and tightly compressed or ‘screwed-home’. The fibrous capsule and ligaments are maximally spiralized and tensed, and no further movement is possible. Close-packed surfaces cannot be separated by normal external force (as they may be in other positions), and bones can be regarded as temporarily locked, as if no joint existed. Close-packing is a final, limiting position, and any force which tends to further change can only be resisted by contraction of appropriate muscles. Failure to stop further movement results in injury to joint structures. Therefore movement just short of close-packing is physiologically most important.

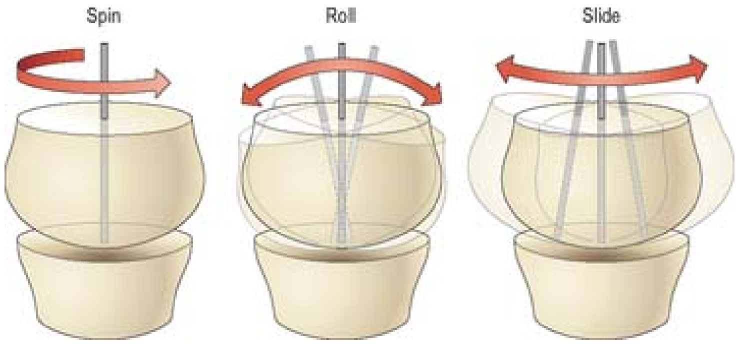

Fig. 5.66 The surfaces of incongruent joints move relative to each other by various combinations of spin, roll, and slide.

Ligaments and articular cartilage are to a small degree elastically deformable: in the final stages of close-packing the articular position is an equilibrium between the external moments and torques applied (often by gravity) and resistance to tissue deformation by the tense, twisted capsule and compressed cartilage surfaces. In symmetrical standing, the knee and hip joints approach close-packed positions sufficiently to maintain an erect posture with minimal energy. In all other positions the articular surfaces are not congruent and parts of the capsule are lax; the joint is said to be loose-packed. According to MacConaill & Basmajian (1977) the close- and loose-packed positions of joints are as shown in Table 5.4. Capsules are sufficiently lax near the mid-range of many movements to allow separation of the articulating surfaces by external forces. Opinions may vary in connection with some of the positions in Table 5.4, e.g. a close-packed position may possibly occur in occasional joints at both extremes of the range of movement. It is difficult to assess the situation in small tarsal and carpal joints and the first carpometacarpal joints. Intervertebral movements are the result of integrated simultaneous changes at all elements which make up the intervertebral articular complex, and perhaps should not be included in Table 5.4. However, most of the positions given do correspond with postures adopted when maximal stress is encountered.

Table 5.4 The close- and loose-packed positions of joints.

Joint	**Close-packed position**	**Loose-packed position**
Shoulder	Abduction + lateral rotation	Semiabduction
Ulnohumeral	Extension	Semiflexion
Radiohumeral	Semiflexion + semipronation	Extension + supination
Wrist	Dorsiflexion	Semiflexion
2nd–5th metacarpo-phalangeal	Full flexion	Semiflexion + ulnar deviation
Interphalangeal (fingers)	Extension	Semiflexion
1st carpometacarpal	Full opposition	Neutral position of thumb
Hip	Extension + medial rotation	Semiflexion
Knee	Full extension	Semiflexion
Ankle	Dorsiflexion	Neutral position
Tarsal joints	Full supination	Semipronation
Metatarsophalangeal	Dorsiflexion	Neutral position
Interphalangeal (toes)	Dorsiflexion	Semiflexion
Intervertebral	Extension	Neutral position

Data from MacConaill MA, Basmajian JV 1977 Muscles and Movements, 2nd edn. New York: Kriger.

Centre of rotation

The centre of rotation is a theoretical concept and may not correspond closely to any anatomical landmark. For a finite movement of one bone relative to a fixed reference (perhaps an anatomical plane), the centre of rotation can be located by (i) drawing theoretical lines between the initial and final positions of anatomical landmarks on the bone, and (ii) determining where the perpendicular bisectors of these lines meet (Fig. 5.67). Real movements of real joints often involve varying combinations of rotation and translation as the movement progresses. It can be instructive to break the whole movement down into a series of small movements, calculate the centre of rotation for each one, and then join up the centres to create the locus of the instantaneous centre of rotation for the whole movement. Joint disease sometimes leads to an abnormally long and tortuous locus of the centre of rotation, because degenerative changes can reduce the restraint to motion offered by one or more tissues.

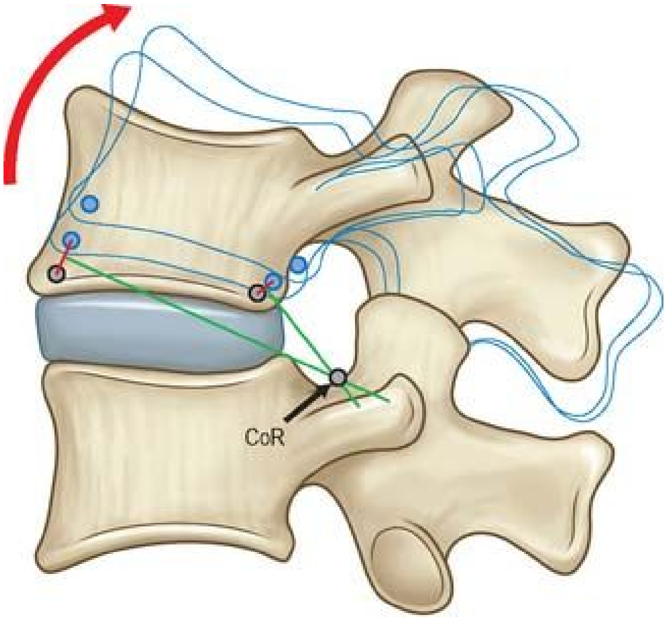

Fig. 5.67 When a bone is rotated, the centre of rotation (CoR) can be located by (i) drawing lines between the initial and final positions of anatomical landmarks on the bone, and (ii) determining where the perpendicular bisectors of these lines meet. The CoR may not correspond to a precise anatomical landmark.

Coupled movements

An attempt to move a joint in one plane sometimes causes articular surfaces to meet at an oblique angle, which can cause small rotations in other planes. These secondary rotations, which are usually smaller than the primary rotations, are referred to as coupled movements. As an example, lateral bending of the lumbar spine, which occurs in the coronal plane, also normally produces coupled axial rotations. Joint pathology can lead to abnormal coupled movements.

MECHANOBIOLOGY

Adaptive remodelling

Skeletal tissues are generally able to adapt their mechanical properties to match the forces applied to them. This process is best understood for bone, and bone biologists refer to this general principle as Wolff's Law. As illustrated in Fig. 5.68, the degree of deformation of a tissue is proportional to the amount of mechanical loading to which it is subjected. Cells detect this increased strain and respond by producing more extracellular matrix, which increases the modulus (stiffness) of the tissue and returns strain levels to normal. Similarly, reduced loading leads to reduced tissue strain, reduced matrix synthesis, and reduced modulus, so that tissue strain increases to normal values. This negative feedback system ensures that bone adapts (remodels) to suit its mechanical environment. Animal experiments suggest that as few as 36 relatively severe loading cycles per day are sufficient to produce a maximal hypertrophic response in bone, whereas fewer than four loading cycles per day leads to tissue resorption. Evidently, bone cells respond to maximal loading rather than time-averaged loading. There is some experimental evidence that cartilage and tendon likewise adapt to their mechanical environment. It would be unlikely that they did not, because the mechanical properties of adjacent tissues would rapidly become mismatched, increasing the risk of damage to one of them. However, it is equally evident that different tissues cannot adapt at the same rates. Highly vascularized tissues such as muscle and bone have the potential to adapt rapidly, whereas poorly vascularized tissues such as large tendons do not. Avascular tissues such as articular cartilage and intervertebral discs can adapt only very slowly, so that turnover times for some matrix macromolecules can be as long as 100 years. Large differences in adaptive potential between adjacent musculoskeletal tissues could lead to problems in the less well-vascularized tissue when levels of mechanical loading increase abruptly.

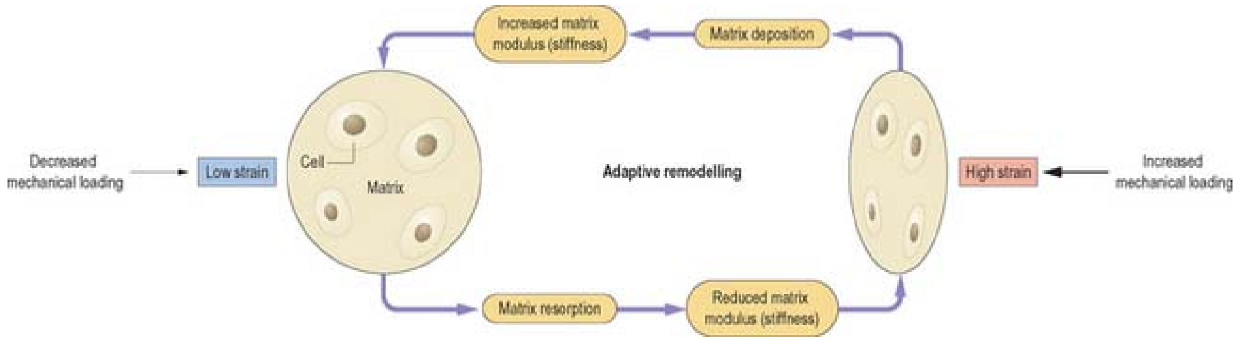
Increased matrix modulus (stiffness)
Matrix deposition
Decreased mechanical loading
Low strain
Cell
Matrix
Adaptive remodelling
High strain
Increased mechanical loading
Matrix resorption
Reduced matrix modulus (stiffness)

Fig. 5.68 Adaptive remodelling is the process by which musculoskeletal tissues adapt to prevailing mechanical demands. If a tissue is subjected to increased mechanical loading (right) it deforms more. Cells respond to this increased strain by depositing more matrix and increasing its modulus (stiffness) until strain levels return to normal. Similarly, reduced loading leads to reduced tissue strain (left), reduced modulus, and reduced matrix deposition until strain levels rise to normal.

Mechanotransduction

Various mechanisms have been proposed to explain how cells in musculoskeletal tissues detect mechanical loading. Cells in bone appear to respond to tissue strain, possibly by detecting fluid flow within the microscopic canaliculi of the matrix (reviewed in Klein-Nulend et al 2003). Cells in cartilage and ligaments also appear able to detect tissue strain, possibly because fluid flow in the surrounding matrix deforms the cells in shear (Fig. 5.52). Cells in articular cartilage and in the nucleus pulposus of intervertebral discs can detect hydrostatic pressure in the surrounding medium, although only the cells in the nucleus would normally experience such a pressure in life. Muscle cells respond to strain and microinjury. Mechanotransduction appears to be mediated by matrix molecules such as fibronectin, by transmembrane proteins such as integrins, and by a range of intracellular proteins such as titin in muscle.

Degeneration, injury and frustrated repair

Numerous theories have been propounded to explain degenerative changes in skeletal tissues. Most presume that the cells behave abnormally, possibly because of an unfavourable genetic inheritance, so that the matrix becomes weakened and physically disrupted. Alternatively, degenerative changes may represent an attempt by the cells to repair a matrix where the primary cause of damage has been excessive mechanical loading. In poorly vascularized tissues, such as cartilage and tendon, low cell density and inadequate transportation of metabolites could lead to a vicious circle of minor injury, frustrated repair, tissue weakening, and further injury.

REFERENCES

lams MA, Bogduk N, Burton K, Dolan P. The Biomechanics of Back Pain. Edinburgh: Churchill Livingstone, 2002.

exander RM. Elastic mechanisms in animal movement. Cambridge: Cambridge University Press, 1988.

tchelor CL, Winder SJ. Sparks, signals and shock absorbers: how dystrophin loss causes muscular dystrophy. *Trends Cell Biol*. 2006;16:198-205.

njamin M, Maganaris C (eds) 2006 Symposium on ‘The Anatomy of Exercise’. J Anat 208.

njamin M, Toumi H, Ralphs JR, Bydder G, Best TM, Milz S. Where tendons and ligaments meet bone: attachment sites (‘entheses’) in relation to exercise and/or mechanical load. *J Anat*. 2006;208:471-490.

air JM, Zheng Y, Dunstan CR. RANK ligand. *Int J Biochem Cell Biol*. 2007;39:1077-1081.

and-Saberi B, Christ B. Evolution and development of distinct cell lineages derived from somites. Current Topics in Developmental Biology. vol 48. New York: Academic Press; 2000.

ckingham M, Bajard L, Chang T, et al. The formation of skeletal muscle: from somite to limb. *J Anat*. 2003;202:59-68.

ller AJ, Eccles JC, Eccles RM. Interactions between motoneurones and muscles in respect of the characteristic speeds of their responses. *J Physiol*. 1960;150:417-439.

arkson E, Costa CF, Machesky L. Congenital myopathies: diseases of the actin cytoskeleton. *J Path*. 2004;204:407-417.

llins CA, Partridge TA. Self-renewal of the adult skeletal muscle satellite cell. *Cell Cycle*. 2005;4:1338-1341.

onboy IM, Conboy MJ, Wagers AJ, Girma ER, Weissman IL, Rando TA. Rejuvenation of aged progenitor cells by exposure to a young systemic environment. *Nature*. 2005;433:760-764.

urrey JD. Bones: structure and mechanics. Woodstock: Princeton University Press, 2002.

lgerton VR, Roy RR, Allen DL, Monti RJ. Adaptations in skeletal muscle disuse or decreased-use atrophy. *Am J Phys Med Rehabil*. 2002;81(11 Suppl):S127-S147.

oldring K, Partridge T, Watt D. Muscle stem cells. *J Pathol*. 2002;197:457-467.

Reviews the role of the satellite cell in growth and repair of muscle fibres..

ein-Nulend J, Nijweide PJ, Burger EH. Osteocyte and bone structure. *Curr Osteoporos Rep*. 2003;1:5-10.

eber RL, Friden J. Functional and clinical significance of skeletal muscle architecture. *Muscle Nerve*. 2000;23:1647-1666.

acConaill MA, Basmajian JV. Muscles and Movements. A Basis for Human Kinesiology. 2nd edn.. New York: Krieger; 1977.

altin CA, Delday MI, Sinclair KD, Steven J, Sneddon AA. Impact of manipulations of myogenesis in utero on the performance of adult skeletal muscle. *Reproduction*. 2001;122:359-374.

ankin HJ, Mow VC, Buckwalter JA, Iannotti JP, Ratcliffe A. Articular cartilage structure, composition and function. In: Buckwalter J, Einhorn TA, Simon SR. *Orthopaedic Basic Science: Biology and Biomechanics of the Musculoskeletal System*. 2nd edn. Illinois: American Academy of Orthopaedic Surgeons; 2000:427-463.

athes SJ, Nahai F. Classification of the vascular anatomy of muscles: experimental and clinical correlation. *Plast Reconstr Surg*. 1981;67:177-187.

izuno H, Zuk PA, Zhu M, Lorenz HP, Benhaim P, Hedrick MH. Myogenic differentiation by human processed lipoaspirate cells. *Plast Reconstr Surg*. 2002;109:199-209.

untoni F, Brown S, Sewry C, Patel K. Muscle development genes: their relevance in neuromuscular disorders. *Neuromusc Disord*. 2002;12:438-446.

njabi MM, White AAIII. Biomechanics in the Musculoskeletal System. Edinburgh: Churchill Livingstone, 2001.

hiaffino S, Reggiani C. Molecular diversity of myofibrillar proteins: gene regulation and functional significance. *Physiol Rev*. 1996;76:371-423.

CHAPTER 6

Smooth muscle and the cardiovascular and lymphatic systems

The cardiovascular system carries blood from the heart to all parts of the body through a series of tubes, all but the smallest of which are muscular. The muscle in these tubes is of two types: smooth muscle is characteristic of the walls of blood vessels and cardiac muscle provides the walls of the heart chambers with their powerful contractile pumping action. The general characteristics and classification of muscle tissues are given on page 103. Smooth muscle also forms an important contractile element in the walls of many other organ systems of the body, e.g. the gastrointestinal tract.

SMOOTH MUSCLE

In smooth muscle tissue the contractile proteins actin and myosin are not organized into regular sarcomeres, visible as transverse striations, so the cytoplasm has a smooth (unstriated) appearance. Smooth muscle is also referred to as involuntary muscle, because its activity is neither initiated nor monitored consciously. It is more variable, in both form and function, than either striated or cardiac muscle, a reflection of its varied roles in different systems of the body.

Smooth muscle cells (fibres) are smaller than those of striated muscle. Their length can range from 15 µm in small blood vessels to 200 µm, and even to 500 µm or more in the uterus during pregnancy. The cells are spindle-shaped, tapering towards the ends from a central diameter of 3–8 µm (Fig. 6.1). The nucleus is single, located at the midpoint, and often twisted into a corkscrew shape by the contraction of the cell. Smooth muscle cells aggregate with their long axes parallel and staggered longitudinally, so that the wide central portion of one cell lies next to the tapered end of another. Such an arrangement achieves both close packing and a more efficient transfer of force from cell to cell. In transverse section, smooth muscle is seen as an array of circular or slightly polygonal profiles of very varied size, and nuclei are present only in the centres of the largest profiles (Fig. 6.2). This appearance contrasts markedly with that of skeletal muscle cells, which show a consistent diameter in cross-section and peripherally placed nuclei throughout their length.

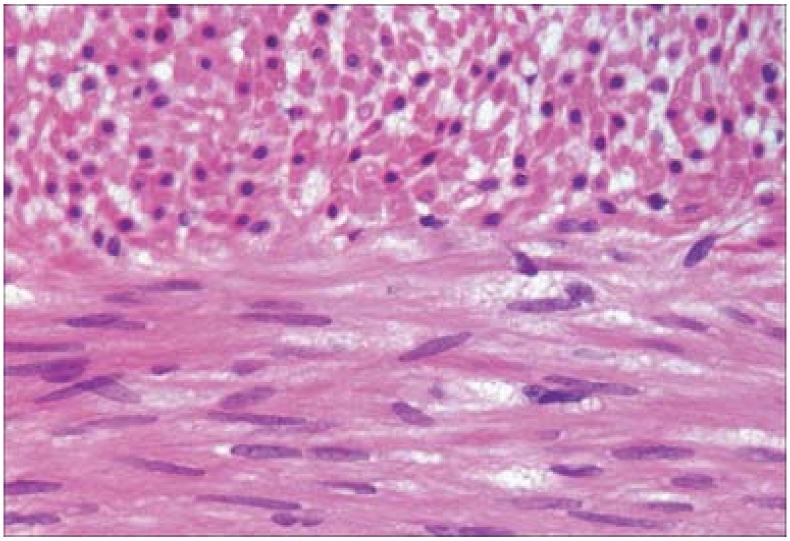

Fig. 6.1 Smooth muscle cells (fibres) in transverse (above) and longitudinal (below) section in the human intestinal wall. Individual cells are spindle-shaped with a single central nucleus, aligned in parallel with neighbouring cells in a fasciculus.

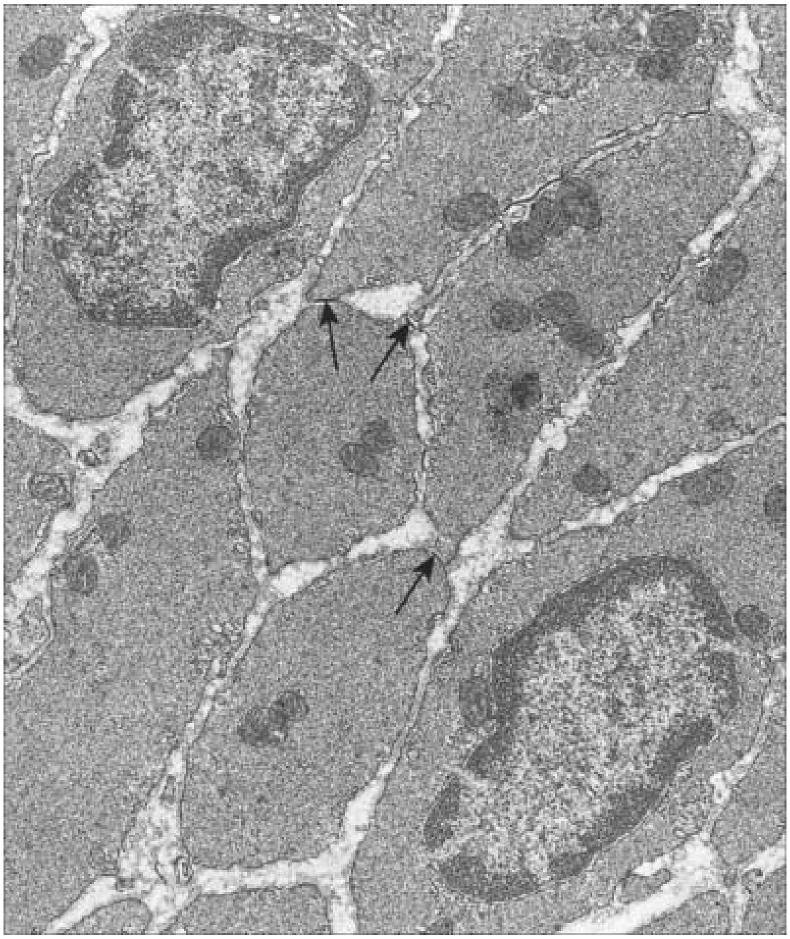

Fig. 6.2 Electron micrograph showing smooth muscle fibres in transverse section, two at the level of their single central nucleus. In several places, the plasma membranes of adjacent cells are closely approximated at gap junctions (arrows).

Smooth muscle is typically found in the walls of tubular structures and hollow viscera. It regulates diameter (e.g. in blood vessels, and branches of the bronchial tree); propels liquids or solids (e.g. in the ureter, hepatic duct, and intestines); or expels the contents (e.g. in the urinary bladder and uterus). The actual arrangement of the cells varies with the tissue. The account that follows will therefore be concerned with the generic properties of smooth muscle. The more specialized morphologies of smooth muscle are described in the appropriate regional chapters.

Smooth muscle has no attachment structures equivalent to the fasciae, tendons and aponeuroses associated with skeletal muscle. There is a special arrangement for transmitting force from cell to cell and, where necessary, to other soft tissue structures. Cells are separated by a gap of 40–80 nm. Each cell is covered almost entirely by a prominent basal lamina which merges with a reticular layer consisting of a network of fine elastin, reticular fibres (collagen type III) and type I collagen fibres (Fig. 6.3). These elements bridge the gaps between adjacent cells and provide mechanical continuity throughout the fascicle. The cell attaches to components of this extracellular matrix at dense plaques (see Fig. 6.4A) where the basal lamina is thickened; cell–cell attachment occurs at intermediate junctions or desmosomes, formed of two adjacent dense plaques. At the boundaries of fascicles, the connective tissue fibres become interwoven with those of interfascicular septa, so that the contraction of different fascicles is communicated throughout the tissue and to neighbouring structures. The components of the reticular network, the ground substance and collagen and elastic fibres, are synthesized by the smooth muscle cells themselves, not by fibroblasts or other connective tissue cells, which are rarely found within fasciculi.

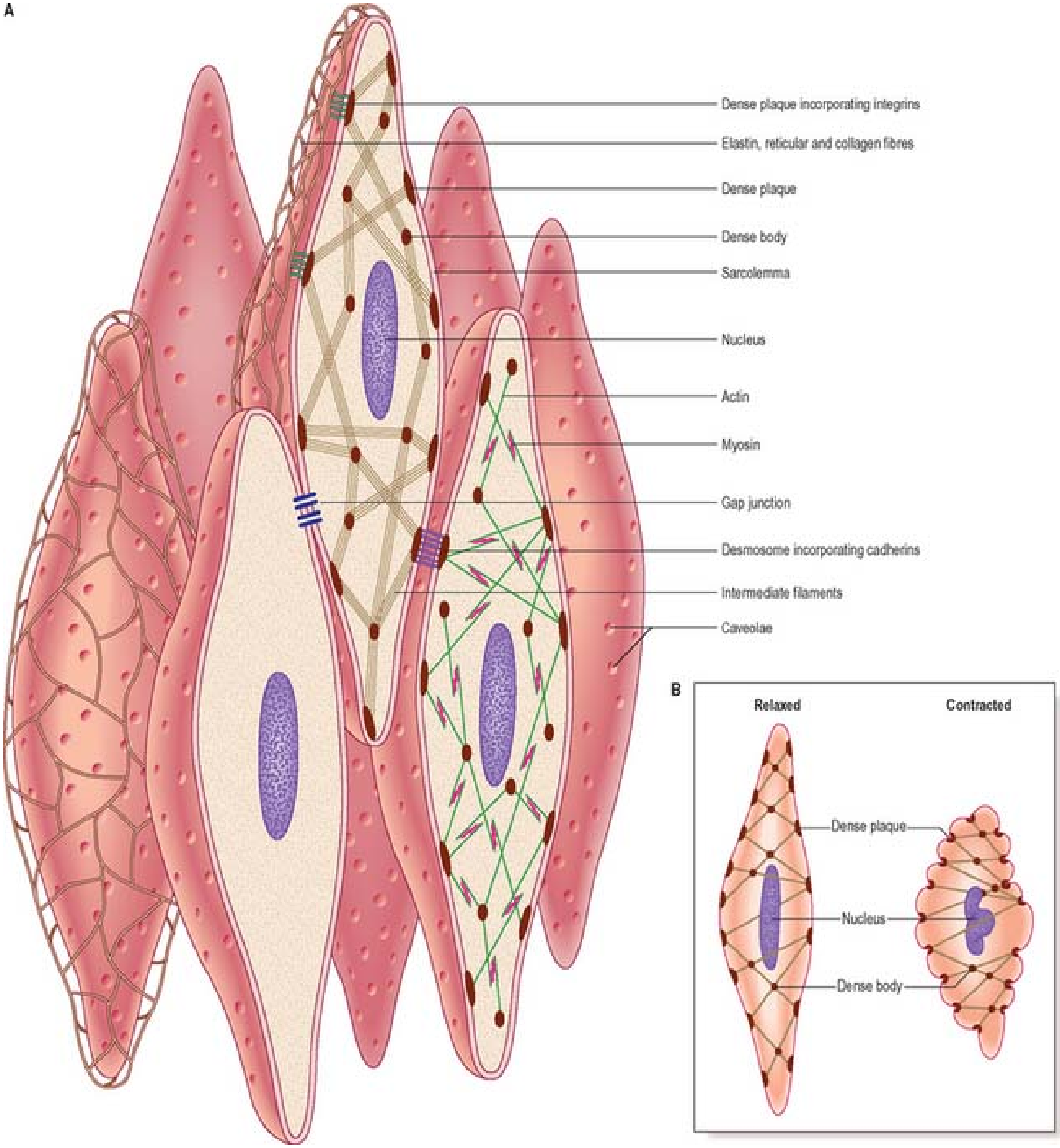
A
Dense plaque incorporating integrins
Elastin, reticular and collagen fibres
Dense plaque
Dense body
Sarcolemma
Nucleus
Actin
Myosin
Gap junction
Desmosome incorporating cadherins
Intermediate filaments
Caveolae
B
Relaxed
Contracted
Dense plaque
Nucleus
Dense body

Fig. 6.3 **A**, Three-dimensional representation of smooth muscle cells. For clarity, some structural features have been separated for illustration in different cells. The spindle-shaped cells interdigitate with their long axes parallel; mechanical continuity between the cells is provided by a reticular layer of elastin and collagen fibres. The cytoskeletal framework consists of intermediate filament arrays (mainly longitudinal) and bundles of actin and myosin filaments (shown in separate cells) inserted into cytoplasmic dense

bodies and submembraneous dense plaques to form a three-dimensional network. The sarcolemma contains anchoring desmosomes (adherens junctions), gap junctions and caveolae. **B**, The concertina-like change in shape of smooth muscle cells as they contract.

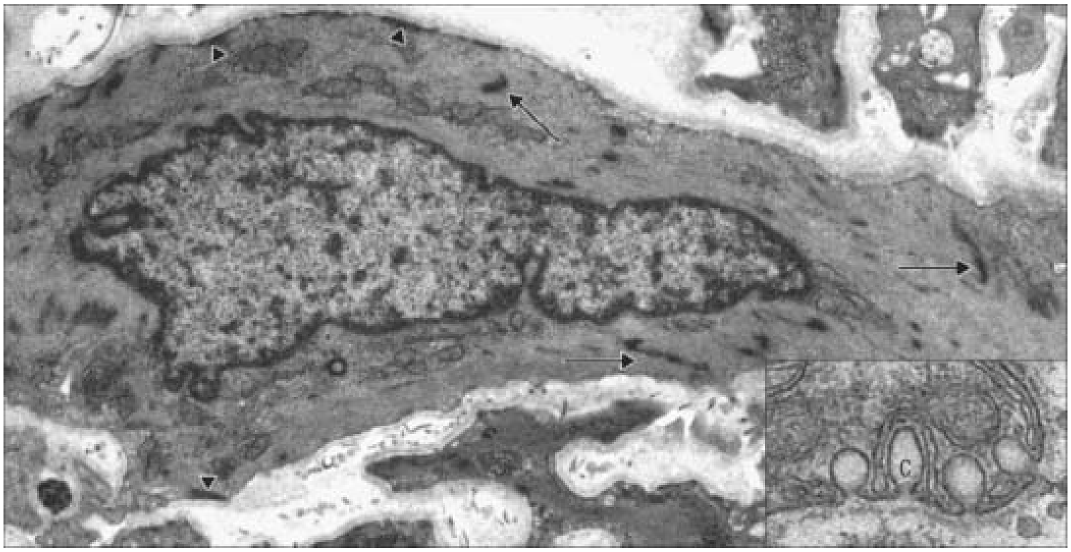

Fig. 6.4 Electron micrographs showing the characteristic features of smooth muscle cells. Vascular smooth muscle in human kidney tissue, showing a cytoplasm packed densely with microfilaments (actin and myosin), cytoplasmic dense bodies (arrows) and submembraneous dense plaques (arrowheads). A basal lamina encloses the cell. Inset shows four caveolae (C) (vesicular invaginations of the cell surface at high magnification. These are associated with receptors, enzymes and ion channels important in smooth muscle function.

(Inset courtesy of Professor Chun Y. Seow, University of British Columbia.)

In some blood vessels, notably those of the pulmonary circulation, and in the airways, and probably in other smooth muscle types, there is evidence for heterogeneity of cell phenotype. Some myofibroblast-like cells have a function that is more secretory than contractile. The secretory phenotype is often increased in disease (e.g. chronic severe asthma, pulmonary hypertension) and is associated with increased proliferation and remodeling, also the secretion of cytokines and other mediators. Many smooth muscles seem to exhibit considerable plasticity between these contractile and secretory phenotypes.

Discontinuities occur in the basal lamina between adjacent cells, and here the cell membranes approach to 2–4 nm of one another to form a gap junction (Fig. 6.2). These junctions are believed to be structurally similar to their counterparts in cardiac muscle. They provide a low-resistance pathway through which electrical excitation can pass between cells, producing a coordinated wave of contraction. The incidence of gap junctions varies with the anatomical site of the tissue: they appear to be more abundant in the type of smooth muscle which generates rhythmic (phasic) activity.

Although some smooth muscles can generate as much force per unit cross-sectional area as skeletal muscle, the force always develops much more slowly than in striated muscle. Smooth muscle can contract by more than 80%, a much greater range of shortening than the 30% or so to which striated muscle is limited. The significance of this property is illustrated by the urinary bladder, which is capable of emptying completely from an internal volume of 300 ml or more. Smooth muscles can maintain tension for long periods with very little expenditure of energy. Many smooth muscle structures are able to generate spontaneous contractions: examples are found in the walls of the intestines, ureter and uterine tube.

MICROSTRUCTURE OF SMOOTH MUSCLE AND THE CONTRACTILE MECHANISM

Although electron microscopy revealed the presence of filaments in smooth muscle some years ago, this observation alone provided little insight into their mode of function because of the lack of any obvious organization of the filaments. More recent work, using high-resolution immunocytochemistry, has revealed further details of the internal architecture of the cell and suggests a structural basis for contractile function. The model, which is illustrated in Fig. 6.3, depends on the mutual interaction of two systems of filaments, one forming the cytoskeleton and the other the contractile apparatus.

Excluding the perinuclear region, the cytoplasm of a smooth muscle cell effectively consists of two structural domains. The cytoskeleton forms a structural framework that maintains the spindle-like form of the cell and provides an internal scaffold with which other elements can interact. Its major structural component is the intermediate filament desmin, with the addition of vimentin (which may also be present alone) in vascular smooth muscle. The intermediate filaments are arranged mainly in longitudinal bundles, but some filaments interconnect the bundles with each other and with the sarcolemma to form a three-dimensional network. The bundles of intermediate filaments insert into focal, electron-dense bodies, approximately 0.1 μm in diameter, which are distributed uniformly throughout the cytoplasm and also attach to dense plaques underlying the plasma membrane (Fig. 6.3A). The cytoplasmic dense bodies and submembraneous dense plaques are equivalent to the Z-discs of striated muscle cells. They contain the actin-binding protein α-actinin and thus also anchor the actin filaments of the contractile apparatus. These form a lattice of obliquely arranged bundles throughout the cytoplasm, which transmit force to the plasma membrane and thus the basal lamina and extracellular matrix via dense plaques. These are associated with a highly structured arrangement of ancillary proteins, including vinculin and talin, which in turn attach to integrins that cross the membrane and provide attachment to components of the extracellular matrix.

An analogous arrangement underlies cell–cell attachment at desmosomes, but here the attachment between dense plaques is provided by transmembrane cadherin glycoproteins and intracellular catenins instead of integrins and talin. Mechanical deformation of the cell may be linked to cell signalling mechanisms via focal adhesion kinase (FAK) and its substrate paxillin; phosphorylation of talin and paxillin may modulate the deformability of the smooth muscle cell. Other regulatory proteins also associate specifically with actin, such as caldesmon and calponin. The cytoskeleton is therefore not a passive structure, and can adapt dynamically to load, presumably therefore contributing to the low energy requirements of smooth muscle contraction. The ratio of actin to myosin is about eight times greater in smooth compared to striated muscle, reflecting the greater length of actin filaments in smooth muscle.

Smooth muscle myosin filaments are 1.5–2 μm long, somewhat longer than those of striated muscle. Although smooth muscle cells contain less myosin, the longer filaments are capable of generating considerable force. The myosin filaments of smooth muscle are also assembled differently, such that their head regions lie symmetrically on either side of a ribbon-like filament, rather than imposing a bipolar organization on the filament. Actin filaments, to which they bind, can thus slide along the whole length of the myosin filament during contraction. This difference underpins the ability of smooth muscle to undergo much greater changes in length than striated muscle. Actin–myosin filament sliding generates tension which transmits to focal regions of the plasma membrane, changing the cell to a shorter, more rounded shape (Fig. 6.3B) and often deforming the nucleus to a corkscrew-like profile.

Caveolae, cup-like invaginations of the plasma membrane with a resemblance to endocytotic vesicles, are a characteristic feature of smooth muscle cells, and may form up to 30% of the membrane (Fig. 6.4). They are associated with many receptors, ion channels and kinases, and the peripheral sarcoplasmic reticulum and may thus act as sites for highly localized signalling pathways. They may also act as specialized pinocytotic structures involved in fluid and electrolyte transport into the cell. Other organelles (mitochondria, ribosomes etc) are largely confined to the filament-free perinuclear cytoplasm, although in some smooth muscle types, including vascular smooth muscle, peripheral mitochondria, sarcoplasmic reticulum and sarcolemma seem to form signalling microdomains. Recent studies using mitochondria-specific staining of such smooth muscle cells often show mitochondria forming a reticular network within the cytosol, which would be consistent with a cell signalling function, especially that concerned with intracellular calcium homeostasis.

VASCULAR SUPPLY

The blood supply of smooth muscle is less extensive than that of striated muscle. Where the tissue is not too densely packed, afferent and efferent vessels gain access via connective tissue septa, and capillaries run in the connective tissue between small fascicles. However, unlike striated muscle, capillaries are not found in relation to individual cells.

INNERVATION

Smooth muscle may contract in response to nervous or hormonal stimulation, or electrical depolarization transferred from neighbouring cells. Some muscles receive a dense innervation to all cells; these are often referred to as multi-unit smooth muscles, and most blood vessels are of this type. Such innervation can precisely define contractile activity, e.g. in the iris, specific nervous control can produce either pupillary constriction or dilation. Other muscles are more sparsely innervated. They tend to display myogenic activity, initiated spontaneously or in response to stretch, which may be markedly influenced by hormones. In these muscles, which include those in the walls of the gastrointestinal tract, urinary bladder, ureter, uterus and uterine tube, innervation tends to exert a more global influence on the rate and force of intrinsically generated contractions. These muscles have been referred to as unitary smooth muscles. The terms multi-unit and unitary smooth muscles are widely used, but in practice such distinctions are better regarded as the extremes of a continuous spectrum.

Smooth muscles are innervated by unmyelinated axons whose cell bodies are located in autonomic ganglia, either in the sympathetic chain or, in the case of parasympathetic fibres, closer to the point of innervation (Fig. 6.5). They ramify extensively, spreading over a large area of the muscle and sending branches into the muscle fasciculi. The terminal portion of each axonal branch is beaded, and consists of expanded portions, varicosities, packed with vesicles and mitochondria, separated by thin, intervaricose portions. Each varicosity is regarded as a transmitter release site, and, in the functional sense, is therefore a nerve ending. In this way the axonal arborization of a single autonomic neurone bears a very large number of nerve endings (up to tens of thousands), as opposed to a maximum of a few hundred in somatic motor neurones. The neuromuscular terminals of autonomic efferents are considered in more detail on page 62.

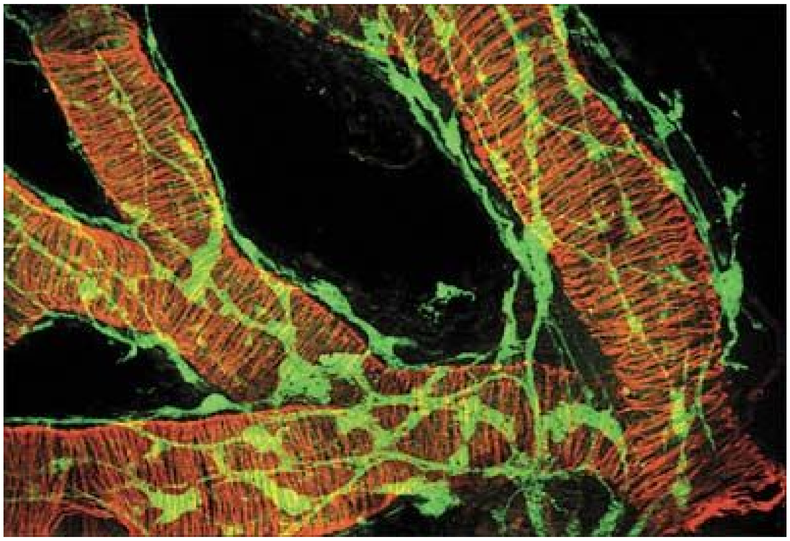

Fig. 6.5 Confocal fluorescence micrograph illustrating the innervation of airway smooth muscle in the developing human lung. Smooth muscle cells are arranged circumferentially and are labelled for actin (red); nerves and ganglia form a loose network around the smooth muscle, separated from it by up to 40 μm. Nervous tissue is labelled for PGP 9.5 (green).

Reproduced with permission from Sparrow MP, Weichselbaum M, McCray PB Jr 1999 Development of the innervation and airway smooth muscle in human fetal lung. Am J Respir Cell Mol Biol 20: 550–60.

The neuromuscular junctions in smooth muscles do not show the consistent appearance seen in skeletal muscles. The neurotransmitter diffuses across a gap that can vary from 10 to 100 nm: even separations up to 1 μm may still allow neuromuscular transmission to take place, although more slowly. The nerve ending is packed with vesicles, but the adjacent area of the muscle cell is not structurally differentiated from that of non-junctional regions – there is no distinct synapse.

Intramuscular afferent nerves are the peripheral processes of small sensory neurones in the dorsal root ganglia. Since they are unmyelinated, contain axonal vesicles and have a beaded appearance, they are difficult to distinguish from efferent fibres, except by differential staining for neurotransmitters.

EXCITATION–CONTRACTION COUPLING IN SMOOTH MUSCLE

Excitation–contraction coupling in smooth muscle may be electromechanical or pharmacomechanical. Electromechanical coupling involves depolarization of the cell membrane by an action potential, and may be generated when a membrane receptor, usually linked with an ion channel, is occupied by a neurotransmitter, hormone or other blood-borne substance. It is most commonly seen in unitary smooth muscles such as those of the viscera, with transmission of electrical excitation from cell to cell via gap junctions. In some types of smooth muscle, depolarization may be the consequence of other stimuli, such as cooling, stretching, and even light.

Pharmacomechanical coupling is a receptor-mediated and G-protein coupled process, which can activate constriction via several pathways. These include triggering the formation of inositol trisphosphate, which acts as a signal for intracellular calcium release from the sarcoplasmic reticulum, activation of voltage-independent calcium channels in the sarcolemma, and depolarization causing activation of voltage-dependent calcium channels. In addition, some receptors couple to kinases that modulate contraction in a calcium independent fashion, either via myosin phosphatase (see below), or via the actin cytoskeleton. Different types of smooth muscle use these pathways to differing extents.

The regulation of contraction of smooth muscle is however largely calcium-dependent. In the cytoplasm, calcium binds to calmodulin. The complex so formed regulates the activity of myosin light chain kinase, which phosphorylates myosin regulatory light chains and initiates the myosin-actin ATPase cycle (p. 111). The enzymatic activation process is therefore inherently slow. Unphosphorylated myosin II of smooth muscle cannot initiate actin binding, although it can maintain contraction, with little energy expenditure. Myosin phosphatase dephosphorylates myosin light chains, and thus promotes relaxation. Inhibition of the phosphatase, for example by Rho kinase, increases phosphorylation for any level of calcium (i.e. increases calcium sensitivity). This is now believed to be a very important component of the response to many constrictor agonists.

DEVELOPMENT

It was thought that all smooth muscle cells developed *in situ* exclusively from the splanchnopleuric mesenchyme in the walls of the anlagen of the viscera and around the endothelium of blood vessels. However, recent experimental studies have traced the progeny of cells proliferating from the epithelial plate of the somite and have identified endothelial and tunica media smooth muscle cells arising from individual somites (Scaal & Christ 2004). The origin of the smooth muscle of the iris is still unclear. This region of the eye develops from the optic cup, and so the smooth muscle which arises there is derived either from the neurectoderm of the original optic cup or from the neural crest mesenchyme which later invades the iris.

Following a period of proliferation, clusters of myoblasts become elongated in the same orientation. Dense bodies, associated with actin and cytoskeletal filaments, appear in the cytoplasm, and the surface membrane starts to acquire its specialized features, i.e. caveolae, adherens junctions and gap junctions. Cytoskeletal filaments extend to insert into the submembranous dense plaques and cytoplasmic dense bodies. Thick filaments are seen a few days after the first appearance of thin filaments and intermediate filaments, and from this time the cells are able to contract. During development, dense bodies increase in number and further elements of the cytoskeleton are added. In addition to synthesizing the cytoskeleton and contractile apparatus, the differentiating cells express and secrete components of the extracellular matrix.

In a developing smooth muscle all the cells express characteristics of the same stage of differentiation, and there are no successive waves of differentiation. From its earliest appearance to maturity, a smooth muscle increases several hundredfold in mass, partly by a 2- to 4-fold increase in the size of individual cells, but mainly by a very large increase in cell number. Growth occurs by division of cells in every part of the muscle, not just at its surface or ends. Mitosis occurs in cells in which differentiation is already well advanced, as evidenced by the presence of myofilaments and membrane specializations. Mitotic smooth muscle cells may be found at any stage of life, but their numbers peak before birth, at a time that differs for different muscles; they are rare in the adult unless the tissue is stimulated to hypertrophy (as in the pregnant uterus) or to repair. The ability of mature cells to undergo mitosis therefore differs between the three major types of muscle: skeletal muscle cells cannot divide at all after differentiation; cardiac muscle cells can divide, but only before birth; and smooth muscle cells appear to remain capable of division throughout life.

During the early stages of development, smooth muscle expresses embryonic and non-muscle isoforms of myosin. The proportions of these isoforms decrease progressively. Initially, SM-1 is the dominant or exclusive smooth muscle heavy chain isoform: the SM-2 isoform becomes more established later. For a review of the development of vascular smooth muscle see Owens, Kumar and Wamhoff (2004).

THE CARDIOVASCULAR AND LYMPHATIC SYSTEMS

GENERAL ORGANIZATION

Cells of peripheral blood, suspended in plasma, circulate through the body in the blood vascular system. Interstitial fluid from peripheral tissues returns to the blood vascular system via the lymphatic system, which also provides a channel for the migration of leukocytes and the absorption of certain nutrients from the gut.

The cardiovascular system carries nutrients, oxygen, hormones, etc. throughout the body and the blood redistributes and disperses heat. As a consequence of the hydrostatic pressure, the system also has mechanical effects, such as maintaining tissue turgidity and counteracting the effects of gravity. Blood circulates within a fast, high capacity system made up of the heart, which is the central pump and main motor of the system; arteries, which lead away from the heart and carry the blood to the peripheral parts of the body; and veins, which return the blood to the heart. The heart can be thought of as a pair of muscular pumps, one feeding a minor loop (pulmonary circulation), which serves the lungs and oxygenates the blood, the other feeding a major loop (systemic circulation), which serves the rest of the body. With limited exceptions, each loop is a closed system of tubes, so that blood *per se* does not usually leave the circulation.

From the centre to the periphery, the vascular tree shows three main modifications. The arteries increase in number by repeated bifurcation and by sending out side branches, in both the systemic and the pulmonary circulation. For example, the aorta, which carries blood from the heart to the systemic circulation, gives rise to about 4×10^6 arterioles and four times as many capillaries. The arteries also decrease in diameter, although not to the same extent as their increase in number, so that a hypothetical cross-section of all the vessels at a given distance will increase in total area with increasing distance from the heart. At its emergence from the heart, the aorta of an adult man has an outer diameter of approximately 30 mm (cross-sectional area of nearly 7 cm^2). The diameter decreases along the arterial tree until it is as little as 10 μm in arterioles (each with a cross-sectional area of about 80 μm^2). However, given the enormous number of arterioles, the total crosssectional area at this level is approximately 150 cm^2, more than 200 times that of the aorta. As a result, blood flow is faster near the heart than at the periphery.

The walls of arteries decrease in thickness towards the periphery, although this is not as substantial as the reduction in vessel diameter. Consequently, in the smallest arteries (arterioles), the thickness of the wall represents about half the outer radius of the vessel, whereas in a large vessel it represents between one-fifteenth and one-fifth, e.g. in the thoracic aorta the radius is approximately 17 mm and the wall thickness 1.1 mm.

Venules, which return blood from the periphery, converge on each other forming a progressively smaller number of veins of increasingly large size. As with arteries, the hypothetical total cross-sectional area of all veins at a given level reduces nearer to the heart. Eventually, only the two largest veins, the superior and inferior venae cavae, open into the heart from the systemic circulation. A similar pattern is found in the pulmonary circulation, but here the vascular loop is shorter and has fewer branch points, and consequently, the number of vessels is smaller than in the systemic circulation. The total end-to-end length of the vascular network in a typical adult is twice the circumference of the earth.

Large arteries, such as the thoracic aorta, subclavian, axillary, femoral and popliteal arteries, lie close to a single vein which drains the same territory as that supplied by the artery. Other arteries are usually flanked by two veins, satellite veins (venae comitantes), which lie on either side of the artery, and have numerous cross-connections: the whole is enclosed in a single connective tissue sheath. The artery and the two satellite veins are often associated with a nerve, and when they are surrounded by a common connective tissue sheath they form a neurovascular bundle.

The close association between the larger arteries and veins in the limbs allows the counterflow exchange of heat to take place. This mechanism promotes heat transfer from arterial to venous blood, and thus helps to preserve body heat. Counterflow heat exchange systems are found in certain organs, e.g. in the testis, where the pampiniform plexus of veins surrounds the testicular artery (this arrangement not only conserves body heat, but also maintains the temperature of the testis below average body temperature).

Counterflow ion exchange mechanisms are found in the microcirculation, as in the arterial and venous sinusoids of the vasa recta in the renal medulla. Here, countercurrent exchange retains sodium ions at a high concentration in the medullary interstitium, and efferent venous blood transfers sodium ions to the afferent arterial supply.

Arteries and veins are named primarily according to their anatomical position. In functional terms, three main classes of vessel are described: resistance vessels (arteries, but mainly arterioles), exchange vessels (capillaries, sinusoids and small venules) and capacitance vessels (veins). Structurally, arteries can also be divided into elastic and muscular types. Although muscle cells and elastic tissue are present in all arteries, the relative amount of elastic material is greatest in the largest vessels, whereas the relative amount of smooth muscle increases progressively towards the smallest arteries.

Arteries may also be subdivided into conducting and distributing, as well as resistance, vessels. The large conducting arteries which arise from the heart, together with their main branches, are characterized by the predominantly elastic properties of their walls. Distributing vessels are smaller arteries supplying the individual organs, and their wall is characterized by a well-developed muscular component. Resistance vessels are mainly arterioles. Small and muscular, they provide the main source of the peripheral resistance to blood flow, and they cause a marked drop in the pressure of blood which flows into the capillary beds within tissues.

Capillaries, sinusoids and small (postcapillary) venules are collectively termed exchange vessels. Their walls allow exchange between blood and the interstitial tissue fluid which surrounds all cells: this is the essential function of a circulatory system. Arterioles, capillaries and venules constitute the microvascular bed, the structural basis of the microcirculation.

Larger venules and veins form an extensive, but variable, large-volume, low-pressure system of vessels conveying blood back to the heart. The high capacitance of these vessels is due to the distensibility (compliance) of their walls, so that the content of blood is high even at low pressures. This part of the vascular bed contains the greatest proportion of blood, reflecting the large relative volume of veins.

Blood from the abdominal part of the digestive tube (with the exception of the lower part of the anal canal), and from the spleen, pancreas and gallbladder, drains to the liver via the portal vein. The portal vein ramifies within the substance of the liver like an artery and ends in the hepatic sinusoids. These drain into the hepatic veins which in turn drain into the inferior vena cava. Blood supplying the abdominal organs thus passes through two sets of capillaries before it returns to the heart. The first provides the organs with oxygenated blood, and the second carries deoxygenated blood, rich in absorption products from the intestine, through the liver parenchyma. A venous portal circulation also connects the median eminence and infundibulum of the hypothalamus with the adenohypophysis. In essence, a venous portal system is a capillary network that lies between two veins, instead of between an artery and a vein, which is the more usual arrangement in the circulation. A capillary network may also be interposed between two arteries, e.g. in the renal glomeruli, where the glomerular capillary bed lies between afferent and efferent arterioles. This maintains a relatively high pressure system, which is important for renal filtration.

A parallel circulatory system in the body is provided by the lymphatic vessels and lymph nodes. Lymphatic vessels originate in peripheral tissues as blind-ended endothelial tubes which collect excess fluid from the interstitial spaces between cells and conduct it as lymph. Lymph is returned to the blood vascular system via lymphatic vessels which converge on the large veins in the root of the neck.

The development of blood vessels is described on pages, 206–208.

General features of vessel walls

Blood vessels, irrespective of size, and with the exception of capillaries and venules, have walls consisting of three concentric layers (tunicae) (see Fig. 6.7). The intima (tunica intima), is the innermost layer. Its main component, the endothelium, lines the entire vascular tree, including the heart, and the lymphatic vessels. The media (tunica media) is made of muscle tissue, elastic fibres and collagen. While it is by far the thickest layer in arteries, the media is absent in capillaries and is comparatively thin in veins. The adventitia (tunica adventitia) is the outer coat of the vessel, and consists of connective tissue, nerves and vessel capillaries (vasa vasorum). It links the vessels to the surrounding tissues. Vessels differ in the relative thicknesses and detailed compositions of their layers and, in the smallest vessels, the number of layers represented.

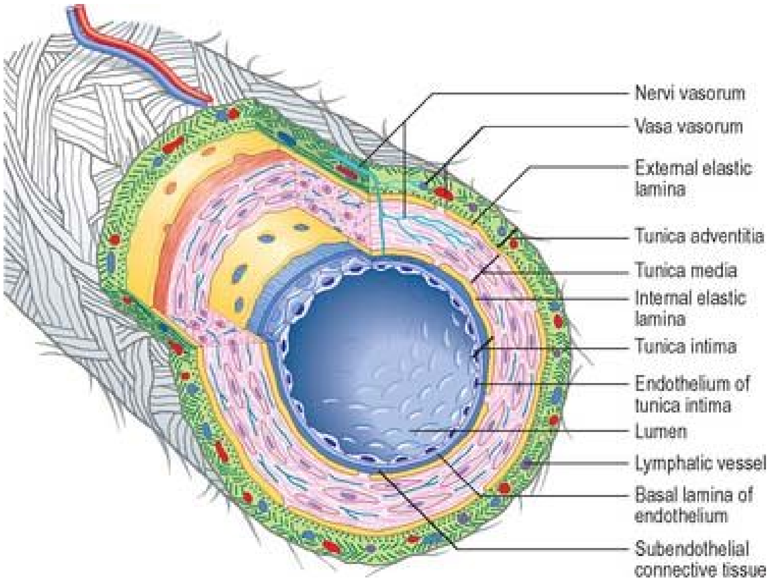
Nervi vasorum
Vasa vasorum
External elastic lamina
Tunica adventitia
Tunica media
Internal elastic lamina
Tunica intima
Endothelium of tunica intima
Lumen
Lymphatic vessel
Basal lamina of endothelium
Subendothelial connective tissue

Fig. 6.7 The principal structural features of the larger blood vessels as seen in a muscular artery.

Large elastic arteries

The aorta and its largest branches (brachiocephalic, common carotid, subclavian and common iliac arteries) are large elastic arteries which conduct blood to the medium-sized distributing arteries.

The intima is made of an endothelium, resting on a basal lamina, and a subendothelial connective tissue layer. The endothelial cells are flat, elongated and polygonal in outline, with their long axes parallel to the direction of blood flow (see Fig. 6.17). The subendothelial layer is well developed, contains elastic fibres and type I collagen fibrils, fibroblasts and small, smooth muscle-like myointimal cells. The latter accumulate lipid with age and in an extreme form, this feature contributes to atherosclerotic changes in the intima. Thickening of the intima progresses with age and is more marked in the distal than in the proximal segment of the aorta.

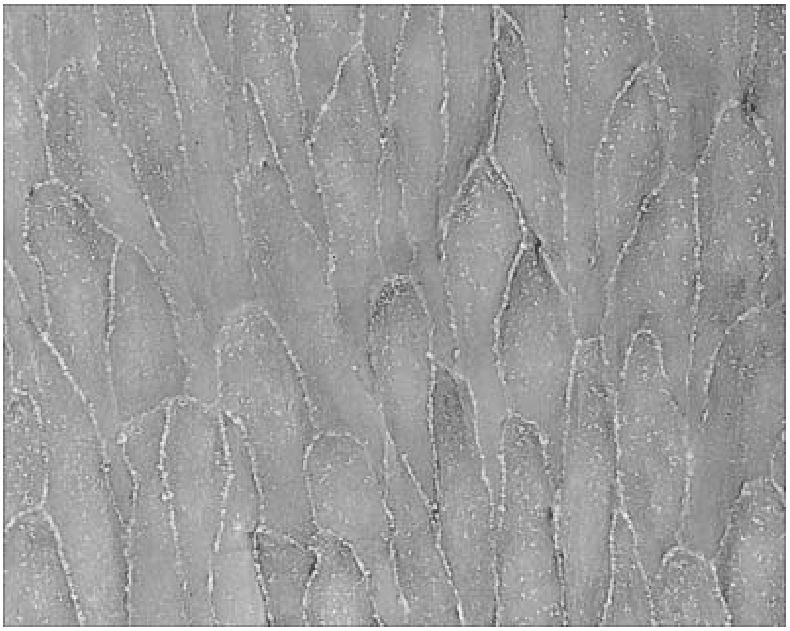

Fig. 6.17 Scanning electron micrograph of the luminal surface of the basilar artery. The tightly packed endothelial cells are elongated in the direction of blood flow.

(By courtesy of Masoud Alian, University College, London.)

A prominent internal elastic lamina, sometimes split, lies between intima and media. This lamina is smooth, measures about 1 μm in thickness, and, with the elastic lamellae of the media, is stretched under the effect of systolic pressure, recoiling elastically in diastole. Elastic arteries thus have the effect of sustaining blood flow despite the pulsatile cardiac output. They also smooth out the cyclical pressure wave. The media has a markedly layered structure, in which fenestrated layers of elastin (elastic lamellae) alternate with interlamellar smooth muscle cells (Fig. 6.6), collagen and fine elastic fibres. The arrangement is very regular, such that each elastic lamella and adjacent interlamellar zone is regarded as a ‘lamellar unit’ of the media.

In the human aorta there are approximately 52 lamellar units, measuring about 11 µm in thickness. Number and thickness of lamellar units increases during postnatal development, from 40 at birth.

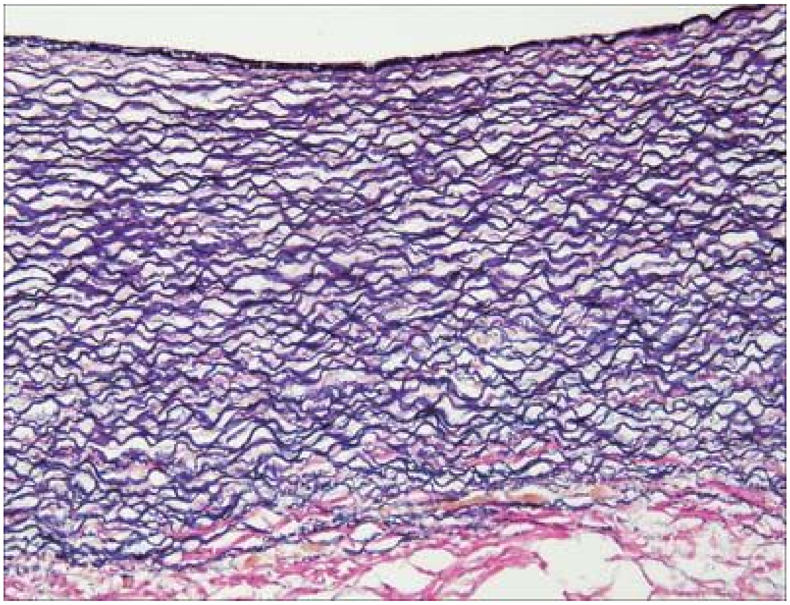

Fig. 6.6 Elastic artery (human aorta), stained for elastic fibres. The dense staining of the internal elastic lamina is seen close to the luminal surface (top); elastic lamellae fill the tunica media and merge with the external elastic lamina at its junction with the collagenous adventitia (red fibres, below). Compare with **Fig. 6.20**. Elastic van Gieson technique.

The adventitia is well developed. In addition to collagen and elastic fibres, it contains flattened fibroblasts with extremely long, thin processes, macrophages and mast cells, nerve bundles and lymphatic vessels. The vasa vasorum are usually confined to the adventitia.

Muscular arteries

Muscular arteries are characterized by the predominance of smooth muscle in the media (Fig. 6.8). The intima consists of an endothelium, similar to that of elastic arteries, which rests on a basal lamina and subendothelial connective tissue. The internal elastic lamina (Fig. 6.7, Fig. 6.8) is a distinct, thin layer, sometimes duplicated and occasionally absent. It is thrown into wavy folds as a result of contraction of smooth muscle in the media. Some 75% of the mass of the media consists of smooth muscle cells which run spirally or circumferentially around the vessel wall. The relative amount of extracellular matrix is therefore less than in large arteries, however, fine elastic fibres which run mainly parallel to the muscle cells are present. An external elastic lamina, composed of sheets of elastic fibres, forms a less compact layer than the internal lamina, and separates the media from the adventitia in the larger muscular arteries. The adventitia is made of fibroelastic connective tissue, and can be as thick as the media in the smaller arteries. The inner part of the adventitia contains more elastic than collagen fibres.

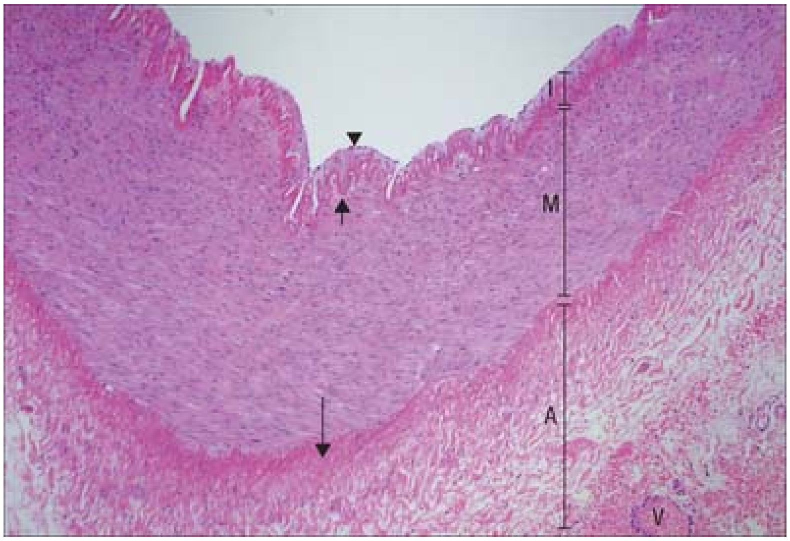

Fig. 6.8 The wall of a human muscular artery. The intima (I) forms the innermost layer, lined by an endothelium (arrowhead) and separated from the middle muscular layer, the media (M), by an internal elastic lamina (short arrow). A more diffuse external elastic lamina (long arrow) divides the media from the outermost collagenous adventitia (A), within which lie the vasa vasorum (V).

Arterioles

In arterioles (Fig. 6.9, Fig. 6.10) the endothelial cells are smaller than in large arteries, but their nuclear region is thicker and often projects markedly into the lumen. The nuclei are elongated and orientated parallel to the vessel length, as is the long axis of the cell. The basal surface of the endothelium contacts a basal lamina, but an internal elastic lamina is either absent or is highly fenestrated and traversed by the cytoplasmic processes of muscle cells or endothelial cells.

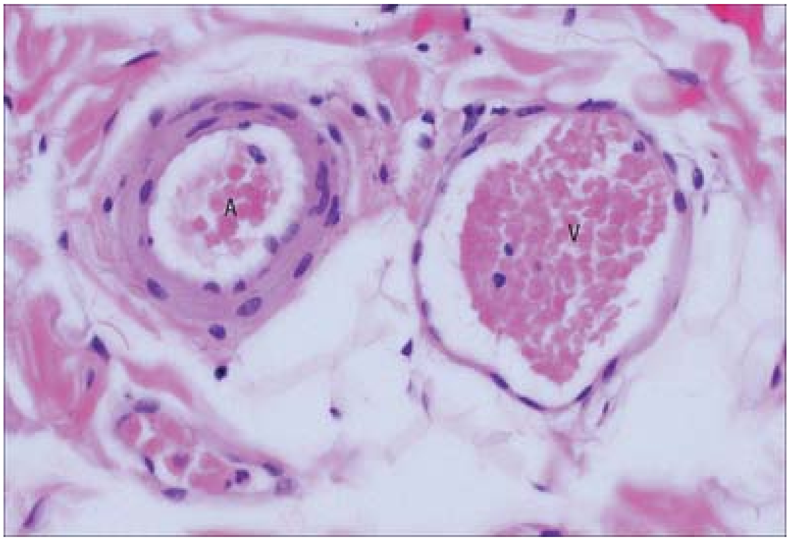

Fig. 6.9 A small arteriole (A) and accompanying venule (V) in loose connective tissue (human). Note the relative thicknesses of the vessel walls, in comparison with the diameters of their lumens.

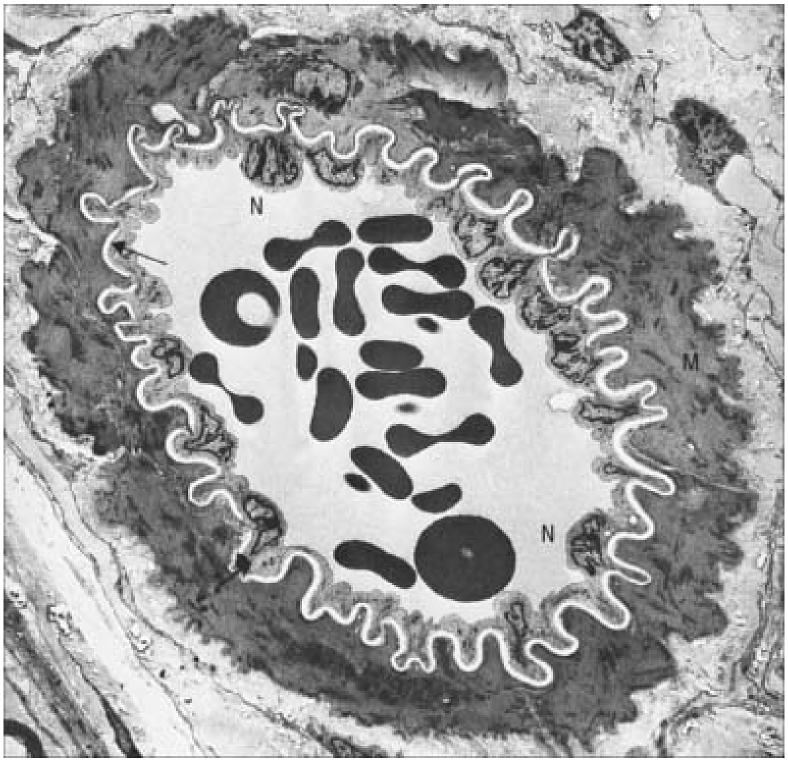

Fig. 6.10 Electron micrograph of a small arteriole in the epineurium of a peripheral nerve. The vessel lumen contains erythrocytes and is lined by endothelial cells (with nuclei, N, projecting into the lumen); note the electron-lucent internal elastic lamina (pale, wavy line, arrowed), the media containing densely filamentous smooth muscle cells (M) and the connective tissue of the adventitia (A) merging with that of the epineurium (E).

The muscle cells are larger in cytoplasmic volume than those of large arteries and they form a layer one or two cells thick. They are arranged circumferentially and are tightly wound around the endothelium. In the smallest arterioles each cell makes several turns, producing extensive apposition between parts of the same cell. Their contractility controls the flow of blood into the capillary bed, and they act functionally as precapillary sphincters. Constriction of the vessel lumen is thought to be under myogenic, rather than neurogenic, control and is responsive to local vasoactive and metabolic factors. Arteriolar adventitia is very thin.

Arterioles are usually densely innervated by sympathetic fibres, via small bundles of varicose axons packed with transmitter vesicles, mostly of the adrenergic type. The distance between axolemma and muscle cell membrane can be as little as 50–100 nm and the gap is occupied only by a basal lamina. Autonomic neuromuscular junctions are very common in arterioles.

Capillaries

The capillary wall (Fig. 6.11) is formed by an endothelium and its basal lamina, plus a few isolated pericytes. Capillaries are the vessels closest to the tissue they supply and their wall is a minimal barrier between blood and the surrounding tissues. Capillary structure varies in different locations. Capillaries measure 4–8 μm in diameter (much more in the case of sinusoids) and are hundreds of microns long. Their lumen is just large enough to admit the passage of single blood cells, usually with considerable deformation. However, the true bottleneck of the circulatory system occurs at the level of the arterioles, where muscle contraction can obliterate the lumen.

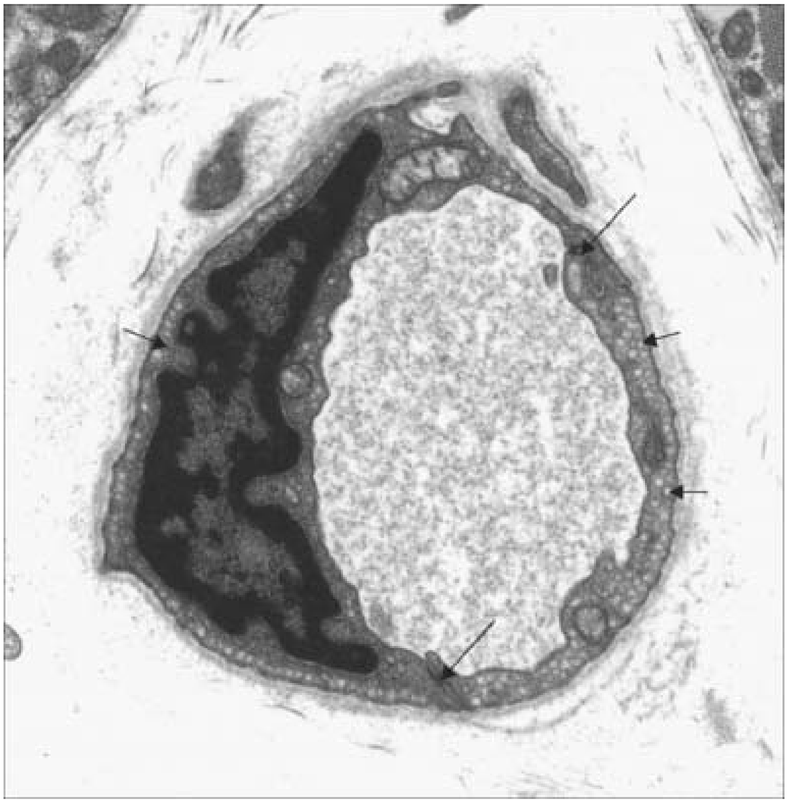

Fig. 6.11 Electron micrograph of a capillary in a human muscle biopsy specimen. An endothelial cell with its nucleus in the plane of section forms adherens junctions (long arrows) with a second cell, or an extension of itself. The cytoplasm contains numerous transcytotic vesicles (short arrows). A basal lamina surrounds the capillary.

Typically a single endothelial cell forms the wall of a capillary, so that the junctional complex occurs between extensions of the same cell. The endothelial cells of some capillaries have fenestrations, or pores, through their cytoplasm. Fenestrations are approximately circular, 50–100 nm in diameter, and at their edge the luminal and abluminal membranes of the endothelial cell come into contact with each other. The fenestration itself is usually occupied by a thin electron-dense diaphragm of unknown molecular composition. Fenestrated capillaries occur in renal glomeruli, where they lack a diaphragm, in intestinal mucosae, and in endocrine and exocrine glands. Fenestrations are almost invariably present in capillaries which lie close to an epithelium, including the skin.

Capillaries without fenestrations, such as those in the brain, striated and smooth muscles, lung and connective tissues, are known as continuous capillaries. Capillary permeability varies greatly among tissues, and this can be correlated partly with the type of endothelium. Where efficient barriers to diffusion of large molecules occur, e.g. brain, thymic cortex and testis, continuous capillary endothelial cells are joined by tight junctions.

Sinusoids

Sinusoids are expanded capillaries (Fig. 6.12), and are large and irregular in shape. They have true discontinuities in their walls, allowing intimate contact between blood and the parenchyma. The discontinuities are formed by gaps between endothelial cells, which are also fenestrated, such that the sinusoidal lining, and sometimes also the basal lamina, is incomplete. Sinusoids occur in large numbers in the liver (where a basal lamina is completely absent), spleen, bone marrow, adenohypophysis (Fig. 6.12) and suprarenal medulla.

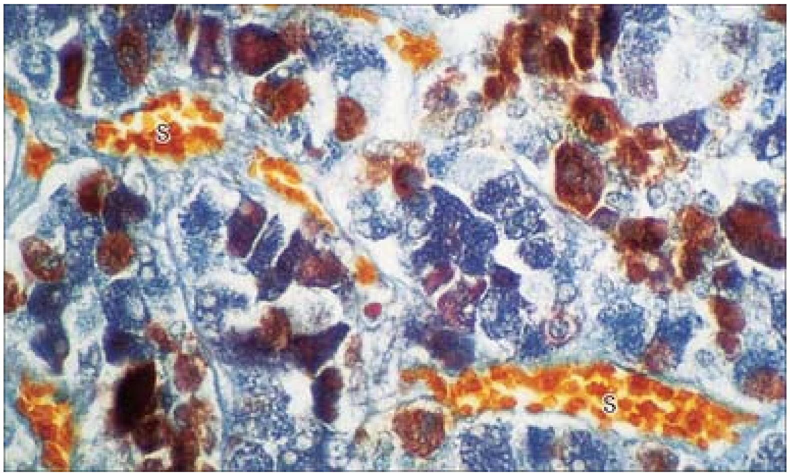

Fig. 6.12 Expanded sinusoids (S) typical of endocrine glands and certain other tissues, are seen here containing erythrocytes (orange) in the adenohypophysis. Endocrine cells stain blue, reddish-brown or are poorly stained in this trichrome preparation.

Venules

When two or more capillaries converge, the resulting vessel is larger (10–30 μm) and is known as a venule (postcapillary venule). Venules (Fig. 6.9) are essentially tubes of flat, oval or polygonal endothelial cells surrounded by basal lamina and, in the larger vessels, by a delicate adventitia of a few fibroblasts and collagen fibres mainly running longitudinally. Pericytes (see Fig. 6.21) support the walls of these venules.

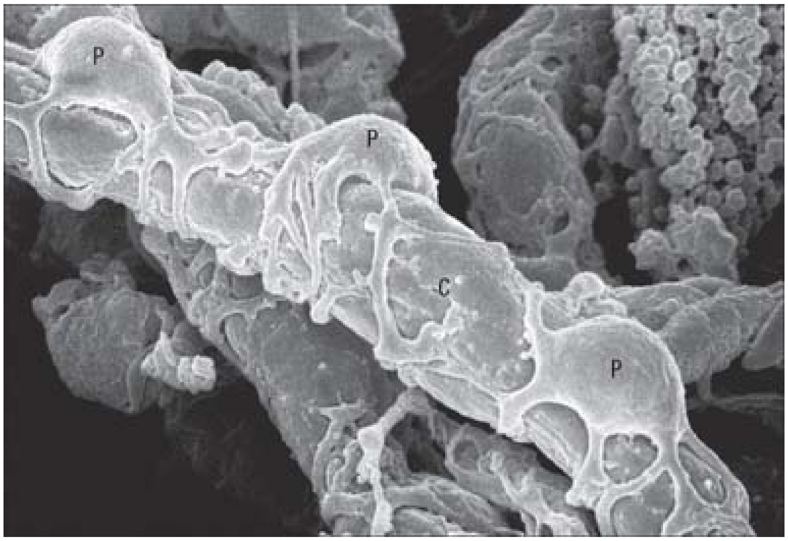

Fig. 6.21 Scanning electron micrograph of capillary (C) and pericytes (P) supporting the vessel wall.

(By courtesy of T. Fujiwara and Y. Uehara, Department of Anatomy, Ehime University School of Medicine, Japan.)

Postcapillary venules are sites of leukocyte migration. In venules of mucosa-associated lymphoid tissue (MALT), particularly of the gut and bronchi, and in the lymph nodes and thymus, endothelial cells are taller and have intercellular junctions through which lymphocytes and other blood components can readily pass. These are known as high endothelial venules (HEV) (see Figs 6.18, 6.19). Elsewhere, venules are believed to be a major site where migration of neutrophils, macrophages and other leukocytes into extravascular spaces occurs, and where neutrophils may temporarily attach, forming marginated pools.

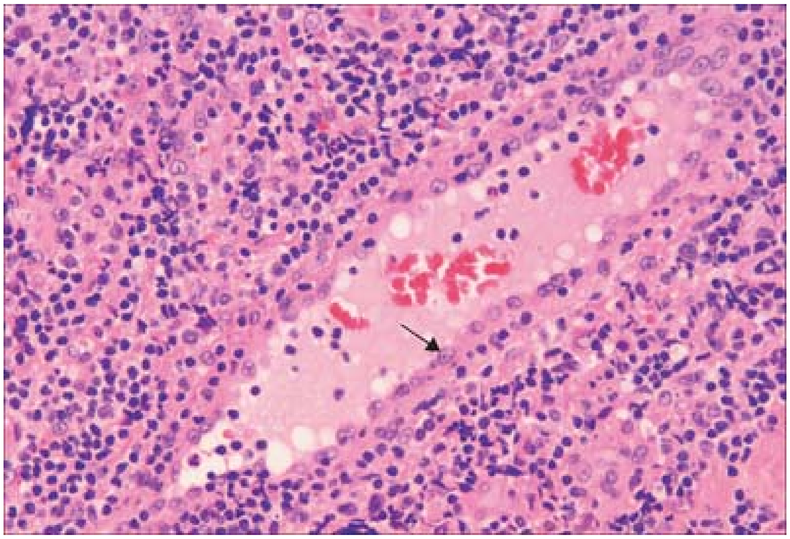

Fig. 6.18 A high endothelial venule in a human lymph node, sectioned longitudinally, lined by cuboidal endothelium (arrow). Erythrocytes and leukocytes (mainly lymphocytes and neutrophils) are seen in the lumen.

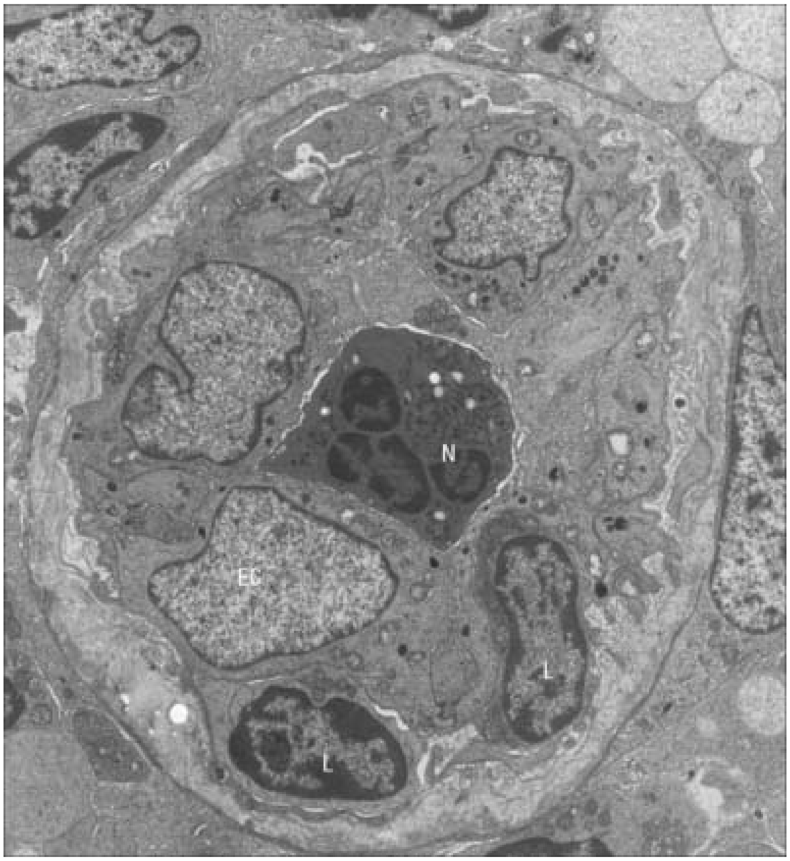

Fig. 6.19 A high endothelial venule in transverse section in the human palatine tonsil. The lumen is completely filled by a neutrophil (N). Cuboidal endothelial cells (EC) line the vessel. Two lymphocytes (L) with heterochromatic nuclei are seen below, in transit within the wall of the vessel.

(By courtesy of Dr Marta Perry, Department of Anatomy, St Thomas's Hospital Medical School, London.)

In general, the endothelium of venules has few tight junctions, and is relatively permeable. The intercellular junctions of venules are sensitive to inflammatory agents which increase their permeability to fluids and defensive cells, and facilitate leukocyte extravasation by diapedesis.

Venules do not acquire musculature until they are about 50 μm in outer diameter, when they are known as muscular venules. This distinction is important, because postcapillary venules, which lack muscle in their walls, are as permeable to solutes as capillaries and are thus part of the microcirculatory bed. At the level of the postcapillary venule the cross-sectional area of the vascular tree is at its maximum, and there is a dramatic fall in pressure (from 25 mmHg in the capillary to approximately 5 mmHg). Muscular venules converge to produce a series of veins of progressively larger diameter. Venules and veins are capacitance vessels, i.e. they have thin distensible walls which can hold a large volume of blood and accommodate luminal pressure changes.

Veins

Veins are characterized by a relatively thin wall in comparison to arteries of similar size and by a large capacitance. Wall thickness is not correlated exactly to the size of the vein, and varies in different regions, e.g. the wall is thicker in veins of the leg than it is in veins of a similar size in the arm.

The structural plan of the wall is similar to that of other vessels, except that the amount of muscle is considerably less than in arteries, while collagen and, in some veins, elastic fibres, predominate. In most veins, e.g. those of the limbs, the muscle is arranged approximately circularly. Longitudinal muscle is present in the iliac, brachiocephalic, portal and renal veins and in the superior and inferior venae cavae. Muscular tissue is absent in the maternal placental veins, dural venous sinuses and pial and retinal veins, veins of trabecular bone and the venous spaces of erectile tissue. These veins consist of endothelium supported by variable amounts of connective tissue. Distinction between the media and adventitial layers is often difficult, and a discrete internal elastic lamina is absent.

Tethering of some veins to connective tissue fasciae and other surrounding tissues may prevent collapse of the vessel even under negative pressure. Pressure within the venous system does not normally exceed 5 mmHg, and it decreases as the veins grow larger and fewer in number, approaching zero close to the heart. Because they contain only a small amount of muscle, veins have limited influence on blood flow. However, during a sudden fall in blood pressure, e.g. following a haemorrhage, elastic recoil and reflex constriction in veins compensate for the blood loss and tend to maintain venous return to the heart. Vasoconstriction in cutaneous veins in response to cooling is important in thermoregulation.

Most veins have valves to prevent reflux of blood (Fig. 6.13, Fig. 6.14). A valve is formed by an inward projection of the intima, strengthened by collagen and elastic fibres, and covered by endothelium which differs in orientation on its two surfaces. Surfaces facing the vessel wall have transversely arranged endothelial cells, whereas on the luminal surface of the valve, over which the main stream of blood flows, cells are arranged longitudinally in the direction of flow. Most commonly two, or occasionally three, valves lie opposite one another, sometimes only one is present. They are found in small veins or where tributaries join larger veins. The valves are semilunar (cusps) and attached by their convex edges to the venous wall. Their concave margins are directed with the flow and lie against the wall as long as flow is towards the heart. When blood flow reverses, the valves close and blood fills an expanded region of the wall, a sinus, on the cardiac side of the closed valve. This may give a ‘knotted’ (varicose) appearance to the distended veins, if these have many valves. In the limbs, especially the legs where venous return is against gravity, valves are of great importance to venous flow. Blood is moved towards the heart by the intermittent pressure produced by contractions of the surrounding muscles. Valves are absent in veins of the thorax and abdomen.

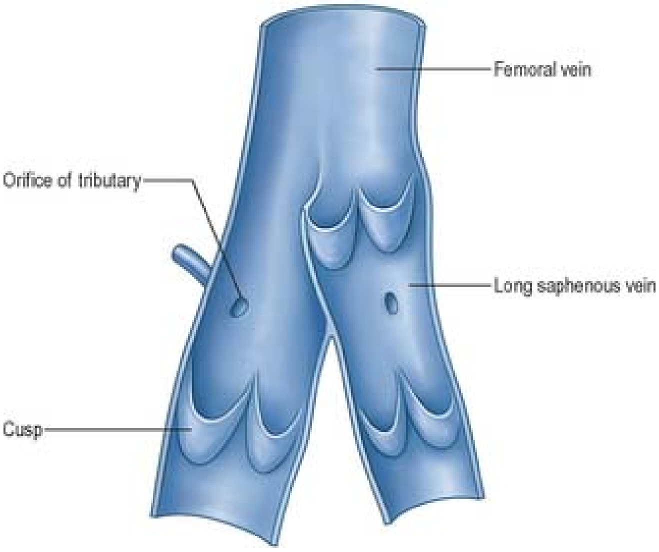

Fig. 6.13 The upper portions of the femoral and long saphenous veins laid open to show the valves. About two-thirds of the natural size.

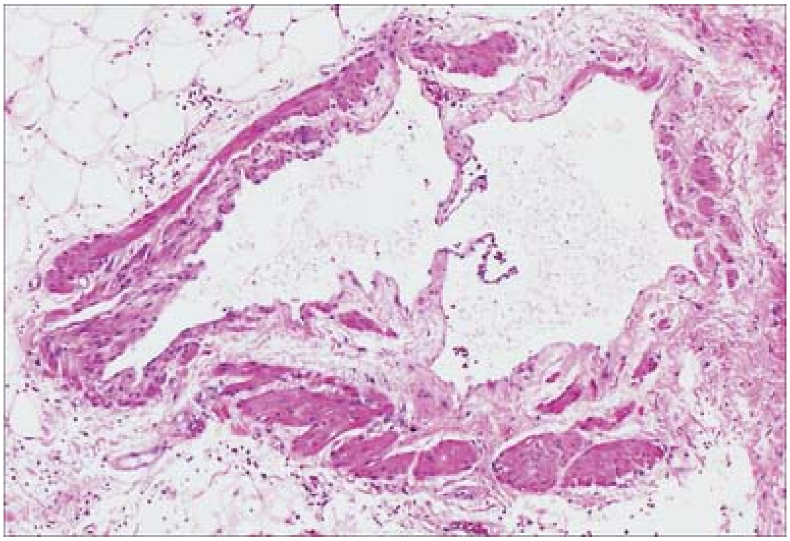

Fig. 6.14 A valve in a human small vein, formed from flap-like extensions of the intima which close when pressure increases on the proximal side, preventing backflow.

VASCULAR SHUNTS AND ANASTOMOSES

Arteriovenous shunts and anastomoses

Communications between the arterial and venous systems are found in many regions of the body. In some parts of the microcirculation (e.g. mesentery), the capillary circulation can be bypassed by wider thoroughfare channels formed by metarterioles (Fig. 6.15A). These have similarities to both capillaries and the smallest arterioles, and have a discontinuous layer of smooth muscle in their walls. Metarterioles can deliver blood directly to venules or to a capillary bed, according to local demand and conditions. When functional demand is low, blood flow is largely limited to the bypass channel. Periodic opening and closing of different arterioles irrigates different parts of the capillary network. The number of capillaries in individual microvascular units and the size of their mesh determine the degree of vascularity of a tissue: the smallest meshes occur in the lungs and the choroid of the eye.

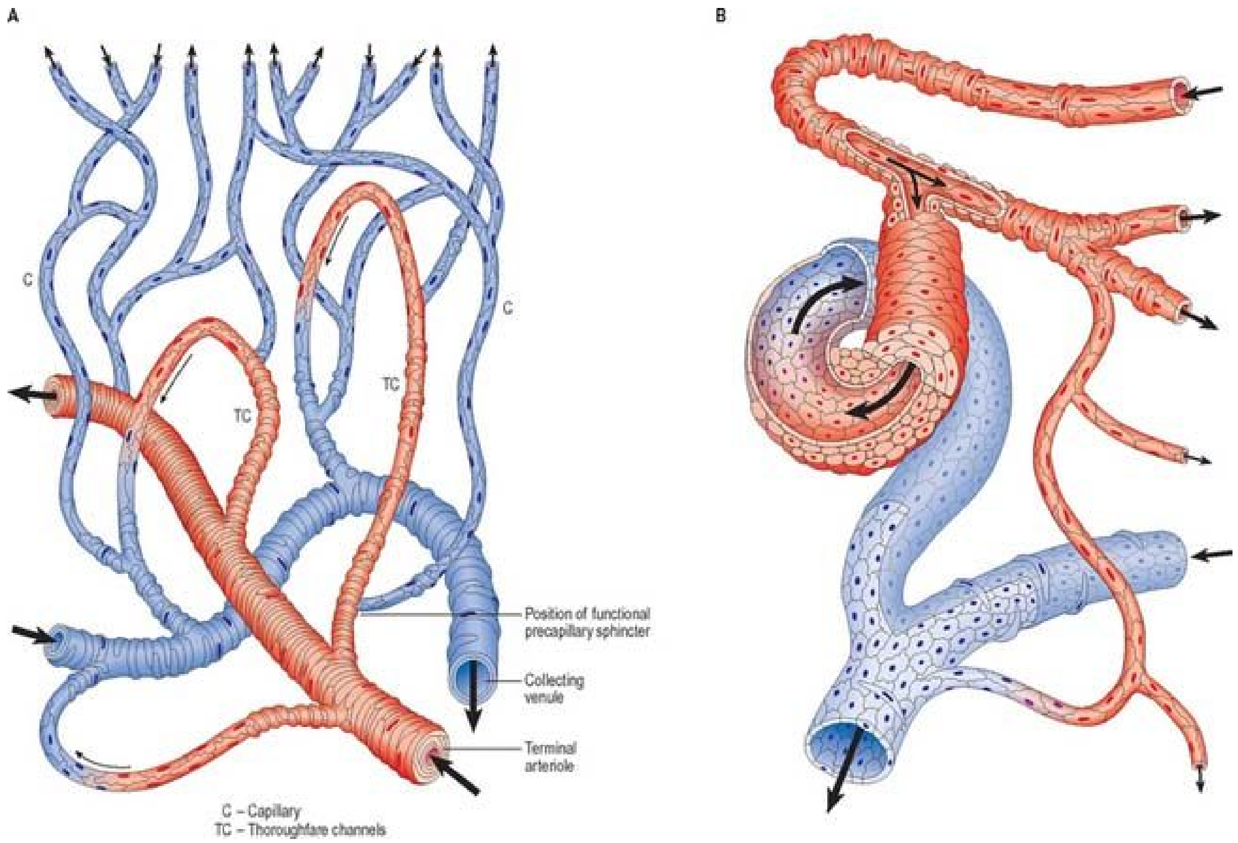
A
C
C
TC
TC
Position of functional precapillary sphincter
Collecting venule
Terminal arteriole
C – Capillary
TC – Thoroughfare channels
B

Fig. 6.15 **A**, A microcirculatory unit, showing a terminal arteriole, thoroughfare channels, capillaries and collecting venule. The distribution of smooth muscle cells and one of the precapillary sites where perfusion of the capillary bed is regulated are also shown. **B**, An arteriovenous anastomosis. Note the thick wall of the anastomotic channel composed of layers of modified smooth muscle cells.

Arteriovenous anastomoses (Fig. 6.15B) are direct connections between smaller arteries and veins. Connecting vessels may be straight or coiled, and often possess a thick muscular tunic. Under sympathetic control, the vessel is able to close completely, diverting blood into the capillary bed. When patent, the vessel carries blood from artery to vein, partially or completely excluding the capillary bed from the circulation. Simple arteriovenous anastomoses are widespread and occur notably in the skin of the nose, lips and ears, nasal and alimentary mucosae, erectile tissue, tongue, thyroid gland and sympathetic ganglia. In the newborn child, there are few arteriovenous anastomoses, but they develop rapidly during the early years. In old age they atrophy, sclerose and diminish in number. These factors may contribute to the less efficient temperature regulation which occurs at the two extremes of age.

In the skin of the hands and feet, especially in digital pads and nail beds (see Fig. 7.18), anastomoses form a large number of small units termed glomera. Each glomus organ has one or more afferent arteries, stemming from branches of cutaneous arteries which approach the surface. The afferent artery gives off a number of fine periglomeral branches and then immediately enlarges, makes a sinuous curve, and narrows again into a short funnel-shaped vein which opens at right angles into a collecting vein (Fig. 6.16).

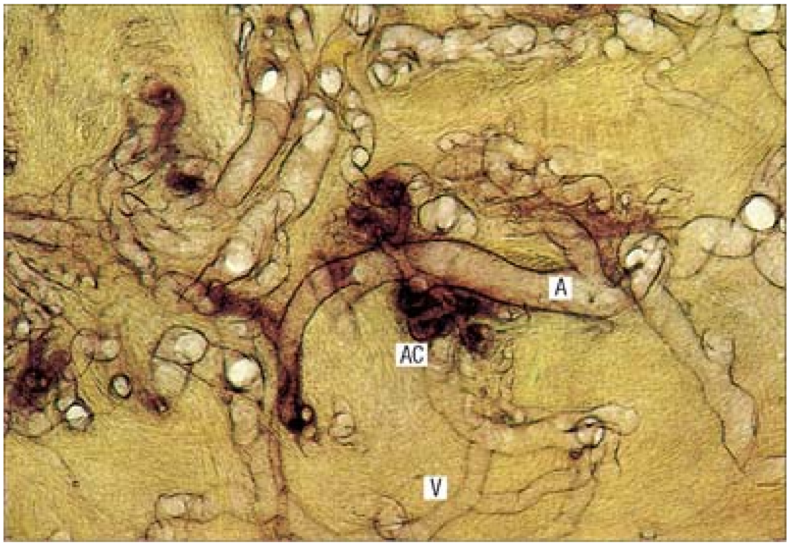

Fig. 6.16 Digital arteriovenous anastomosis prepared by intravascular perfusion of stain in a full thickness specimen of skin, followed by clearance. The heavily stained, thick-walled, tortuous anastomotic channels (AC) contrast with the central arterial stem (A) and the thin-walled venous (V) outflow channels.

(By courtesy of the late RT Grant, GKT School of Medicine, London.)

Arterial anastomoses

Arteries can be joined to each other by an anastomosis, so that one can supply the territory of the other. An end-to-end anastomosis occurs when two arteries communicate directly, e.g. the uterine and ovarian arteries, the right and the left gastroepiploic arteries, the ulnar artery and the superficial palmar branch of the radial artery. Anastomosis by convergence occurs when two arteries converge and merge, as happens when the vertebral arteries form the basilar artery at the base of the brain. A transverse anastomosis occurs when a short arterial vessel links two large arteries transversely, e.g. the anastomoses between the two anterior cerebral arteries; the posterior tibial artery and the fibular artery; and the radial and ulnar arteries at the wrist.

The angiosome concept and vascular territories

An angiosome is a three-dimensional block of tissue (known as an anatomical territory) supplied by a source artery and its accompanying veins. It can be a composite of skin, underlying fascia, muscle and bone. These blocks of tissue form a complex three-dimensional jigsaw puzzle: some pieces have a predominantly cutaneous component while others are predominantly muscular. Each angiosome is made up of arteriosomes and venosomes and they are linked to neighbouring angiosomes by either simple anastomoses composed of similar calibre vessels or reduced calibre vessels termed choke vessels. The anastomoses between adjacent angiosomes can occur within the skin or within muscle. Some muscles are supplied by a single artery and its accompanying veins and therefore lie within one angiosome, while other muscles are supplied by more than one vessel and therefore cross more than one angiosome.

The clinical relevance of the angiosome concept is reflected in the potential connections of adjacent vascular territories. Should the source vessels for one angiosome become blocked or damaged, then that anatomical territory can be ‘rescued’ by receiving a blood supply from the immediately neighbouring angiosome via the connecting simple and choke vessel anastomoses. A detailed knowledge of angiosomes and vascular territories is essential for plastic and reconstructive surgeons when designing and surgically raising flaps of tissue which can reliably be moved from one part of the body to another without disrupting their blood supply.

FUNCTIONAL MICROSTRUCTURE OF VESSELS

Intima

The intimal lining of blood vessels consists of an endothelium, and a variable amount of subendothelial connective tissue, depending on the vessel.

Endothelium

The endothelium is a monolayer of flattened polygonal cells which extends continuously over the luminal surface of the entire vascular tree (Fig. 6.17, see Fig. 6.10). Its structure varies in different regions of the vascular bed.

The endothelium is a key component of the vessel wall, and subserves several major physiological roles. Endothelial cells are in contact with the bloodstream and thus influence blood flow. They regulate the diffusion of substances and migration of cells out of and into the circulating blood. In the brain, endothelial cells of small vessels actively transport substances, e.g. glucose, into the brain parenchyma. Endothelial cells participate in the formation of blood clots (by secreting clot-promoting factors – von Willebrand factor); in minimizing clot formation (by secreting prostacyclin and thrombomodulin); and in the process of clot dissolution or fibrinolysis (by secreting tissue plasminogen activator). They have selective phagocytic activity and are able to extract substances from the blood. For example, the endothelium of pulmonary vessels removes and inactivates several polypeptides, biogenic amines, bradykinin, prostaglandins and lipids from the circulation. Endothelial cells secrete both vasoconstrictive (thromboxane) and vasodilator (prostacyclin) prostaglandins, nitric oxide (NO, relaxing factor) and endothelin (a vasoconstrictor), which affect the tone of smooth muscle in vessel walls. They are sensitive to stretch (e.g. increased pressure) and the shear effect of blood flow, via stretch-sensitive ion channels in the cell membrane. Endothelial cells synthesize components of the basal lamina. They proliferate to provide new cells during the growth in size of a blood vessel, to replace damaged endothelial cells, and to provide solid cords of cells which develop into new blood vessels (angiogenesis). Angiogenesis, which may be stimulated by endothelial production of autocrine growth factors (see Ch. 1) in response to locally low oxygen tension, is important in wound healing, and in the growth of tumours. Endothelial cells are also active participants in, and regulators of, inflammatory processes (reviewed in Pober & Sessa, 2007).

Endothelial cells are thin but extend over a relatively large surface area. They are generally elongated in the direction of blood flow, especially in arteries (see Fig. 6.17). They usually adhere firmly to each other at their edges, so that the lining of the lumen presents no discontinuity, other than in sinusoids. The thickness of endothelial cells is maximal at the level of their nucleus, where it can reach 2–3 µm, and this part of the cell often bulges slightly into the lumen (see Fig. 6.10). Elsewhere, the endothelial cell is thinner and laminar: in capillaries, these portions of the cell often measure as little as 0.2 µm in thickness.

Transcytotic (pinocytotic) vesicles (see Fig. 6.11) are present in all endothelial cells, but are particularly numerous in exchange vessels; they include caveolae (see Fig. 6.4) typical of smooth muscle cells. They shuttle small amounts of extracellular fluid or blood plasma across the endothelial cytoplasm and thus facilitate the bulk exchange of dissolved gases, nutrients and metabolites between these compartments. In spite of the factors known to be released by endothelial cells, they do not have the morphological characteristics of secretory cells.

An organelle which characterizes endothelial cells is the Wiebel–Palade body, an elongated cytoplasmic vesicle, 0.2 × 2–3 µm in length, which contains regularly spaced tubular structures parallel to its long axis. Wiebel–Palade bodies store the adhesion molecule, P-selectin, and a large glycoprotein known as von Willebrand factor, which is released into the subendothelial connective tissue; it mediates the binding of platelets to the extracellular matrix and platelet aggregation, after vascular injury. Von Willebrand factor is also produced by megakaryocytes and is stored in platelets. Plasma von Willebrand factor binds factor VIII clotting protein, which is secreted into the bloodstream by hepatocytes. Hereditary deficiency or defective function of von Willebrand factor causes a clotting disorder of the same name.

Endothelial cells adhere to adjacent cells through the junctional complex, an area of apposition where adherent and tight junctions are found. They also communicate via gap junctions. Tight junctions are most marked in continuous capillaries. Cell contacts between endothelial cells and smooth muscle cells are common in arterioles, where the separation between endothelium and media is reduced and the inner elastic lamina is either very thin or absent.

Endothelial–leukocyte interactions

The luminal surface of endothelial cells does not normally support the adherence of leukocytes or platelets. However, many functions of human vascular endothelial cells are dynamic rather than fixed. Activated endothelial cells and the characteristic endothelium of high endothelial venules (HEV) of lymphoid tissues, are sites of leukocyte attachment and diapedesis (see below).

HEV (Fig. 6.18) are located within the T cell domains, between and around lymphoid follicles in all secondary lymphoid organs and tissues except the spleen. They are specialized venules of 7–30 μm diameter, which possess a conspicuous cuboidal endothelial lining. The luminal aspect of HEVs shows a cobblestone appearance. The endothelial cells rest on a basal lamina and are supported by pericytes and a small amount of connective tissue (Fig. 6.19). They are linked by discontinuous adhesive junctions at their apical and basal aspects: the junctions are circumnavigated by migrating lymphocytes. Ultrastructurally, the endothelial cells have the characteristics of metabolically active secretory cells. They contain large, rounded euchromatic nuclei with one or two nucleoli, prominent Golgi complexes, many mitochondria, ribosomes and pinocytotic vesicles. Typically, they also possess Wiebel–Palade bodies (see above).

Many of the adhesion molecules which mediate interactions between blood leukocytes and HEVs or cytokine-activated endothelium have been identified. They can be divided into three general families: selectins, integrins and the immunoglobulin supergene family. Selectins and integrins are expressed on leukocytes and mediate adhesion of circulating cells to the endothelium, which expresses selectins and members of the immunoglobulin supergene family. Regulated expression of these molecules by both cell types provides the means by which leukocytes recognize the vessel wall (leukocyte homing antigens and vascular addressins), adhere to it and subsequently leave the circulation.

The first step in this cascade is the loose binding or tethering of leukocytes, and is initiated via L-, P- or E-selectin (see below). This weak, reversible adhesion allows leukocytes to roll along the endothelial surface of a vessel lumen at low velocity, making and breaking contact, and sampling the endothelial cell surfaces. Recognition of chemokines (chemotactic signalling molecules) presented by the endothelium leads to ‘inside-out’ signalling and conversion of integrins at the leukocyte surface into actively adhesive configurations which bind strongly to their endothelial ligands, resulting in stable arrest. Finally, the leukocyte migrates through the vessel wall (diapedesis), passing between (paracellular migration) or across (transcellular migration) endothelial cells. It is now thought that transcellular migration is the preferred pathway and endothelial transcytotic vesicles (caveolae), intermediate filaments (vimentin) and F-actin are important in the creation of transient transcellular channels through which leukocytes pass. They then cross the basal lamina and migrate into the surrounding tissue by mechanisms which involve CD31 antigen and matrix metalloproteinases (see Ch. 2).

Cell adhesion molecules

Three members of the selectin family of adhesive proteins are currently recognized. They are L-selectin (also known as lymphocyte homing receptor), E-selectin and P-selectin. L-selectin is expressed on most leukocytes. Endothelial cells of HEVs in lymphoid organs express its oligosaccharide ligand, although other molecules such as mucins may be alternative ligands. Thus, L-selectin mediates homing of lymphocytes, especially to peripheral lymph nodes, but also promotes the accumulation of neutrophils and monocytes at sites of inflammation. E-selectin is an inducible adhesion molecule which mediates adhesion of leukocytes to inflammatory cytokine-activated endothelium, and is only transiently expressed on endothelium. P-selectin is rapidly mobilized from Wiebel–Palade bodies, where it is stored, to the endothelial surface after endothelial activation. It binds to ligands expressed on neutrophils, platelets, and monocytes and, like E-selectin, tethers leukocytes to endothelium at sites of inflammation. However, since P-selectin is quickly endocytosed by the endothelial cells, its expression is short-lived.

The integrins are a large family of molecules which mediate cell-to-cell adhesion as well as interactions of cells with extracellular matrix. Certain β-1 integrin heterodimers are expressed on lymphocytes 2–4 weeks after antigenic stimulation (very late antigens, VLA), and bind to the extracellular matrix. Additionally, VLA-4 present on resting lymphocytes (the expression of which increases after activation), monocytes and eosinophils, binds to the vascular cell adhesion molecule-1 (VCAM-1), the ligand on activated endothelium. In contrast to β-1 integrins, which many cells express, the expression of β-2 integrins is limited to white blood cells. Although the leukocyte integrins are not constitutively adhesive, they become highly adhesive after cell activation and therefore play a key role in the events required for cell migration. The endothelial ligands for one such β-2 integrin are the intercellular adhesion molecules-1 and -2 (ICAM-1 and ICAM-2), which belong to the immunoglobulin superfamily.

Three members of the large immunoglobulin superfamily of proteins are involved in leukocyte-endothelial adhesion, providing integrin counter-receptors on the endothelial cell membrane. ICAM-1 and ICAM-2 are constitutively expressed but upregulated by inflammatory cytokines. VCAM-1 is absent from resting endothelium but is induced by cytokines on activated endothelium and promotes extravasation of lymphocytes at sites of inflammation.

Subendothelial connective tissue

The subendothelial connective tissue, also termed the lamina propria, is a thin but variable layer. It is largely absent in the smallest vessels, where the endothelium is supported instead by pericytes (see Fig. 6.21). It contains a typical fibrocollagenous extracellular matrix, a few fibroblasts and occasional smooth muscle cells. Endothelial von Willebrand factor concentrates in this layer and participates in the clotting process when the overlying endothelium is damaged.

Media

The media consists chiefly of concentric layers of circumferentially or helically arranged smooth muscle cells with variable amounts of elastin and collagen.

Smooth muscle

Smooth muscle forms most of the media of arteries (see Fig. 6.8) and arterioles. A thinner layer of smooth muscle is also found in venules and veins, with the exception of small segments of the pulmonary veins, where striated cardiac muscle is present in the portions nearest to the heart. Contraction of the smooth muscle in arteries and arterioles reduces the calibre of the vessel lumen, which reduces blood flow through the vessel and raises the pressure on the proximal side. This role is particularly effective in small resistance vessels where the wall is thick, relative to the diameter of the vessel. Smooth muscle can also alter the rigidity of the wall, without causing constriction (isometric contraction), and this affects the distensibility of the wall and propagation of the pulse.

The smooth muscle cells synthesize and secrete elastin, collagen and other extracellular components of the media which bear directly on the mechanical properties of the vessels. The mechanics of the musculature of the media are complex. Distensibility, strength, self-support, elasticity, rigidity, concentric constriction etc., are interrelated functions and are finely balanced in the different regions of the vascular bed.

In large arteries, where the blood pressure is high, the muscle cells are shorter (60–200 μm) and smaller in volume than in visceral muscle. In arterioles and veins, smooth muscle cells more closely resemble visceral muscle cells. The cells are packed with myofilaments and other elements of the cytoskeleton, including intermediate filaments. Vascular muscle cells have intermediate filaments of either vimentin alone or both vimentin and desmin; the intermediate filaments of visceral smooth muscle are exclusively of desmin. Intercellular junctions are mainly of the adhesive (adherens) type and provide mechanical coupling between the cells. In addition, there are gap (communicating) junctions which couple cells electrically. Junctions between muscle cells and the connective tissue matrix are particularly numerous, especially in arteries.

The muscle cells of the arterial media can be regarded as multifunctional mesenchymal cells. After damage to the endothelium, muscle cells migrate into the intima and proliferate, forming bundles of longitudinally oriented cells which reform the layer. In certain pathological conditions, muscle cells (and macrophages) undergo fatty degeneration and participate in the formation of atheromatous plaques.

Collagen and elastin

Components of the extracellular matrix are major constituents of vessel walls, and in large arteries and veins they make up more than half of the mass of the wall, mainly in the form of collagen and elastin. Other fibrous components such as fibronectin, and amorphous proteoglycans and glycosaminoglycans, are present in the interstitial space.

Elastin is found in all arteries and veins and is especially abundant in elastic arteries (see Fig. 6.6). Individual elastic fibres (0.1–1.0 μm in diameter) anastomose with each other to form net-like structures, which extend predominantly in a circumferential direction. More extensive fusion produces lamellae of elastic material, which though usually perforated and thus incomplete, separate the layers of muscle cells. A conspicuous elastic lamella, the internal elastic lamina, is seen in arteries, between intima and media. This is a tube of elastic material which allows the vessel to recoil after distension. When the intraluminal pressure falls below physiological limits (postmortem), the inner elastic lamina is compressed and it coils up into a regular corrugated shape (Fig. 6.20, see Figs 6.8, 6.10): in these conditions the lumen is much reduced but is not obliterated, and the profile of the artery remains circular. Fenestrations in the elastic lamina, which may also be split in thickness, allow materials to diffuse between intima and media. An outer elastic lamina, similar in appearance to, but markedly less well developed and less compact than the internal elastic lamina, lies at the outer aspect of the media at its boundary with the adventitia (see Fig. 6.8). These laminae are less evident in elastic arteries, where elastic fibres occupy much of the media (see Fig. 6.6).

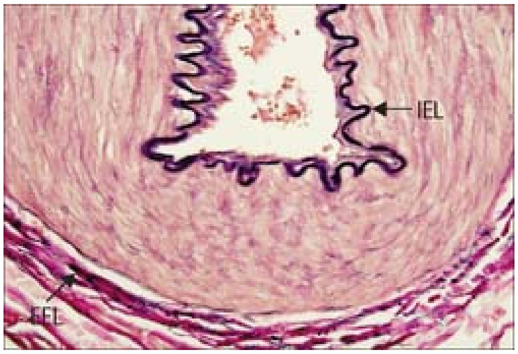

Fig. 6.20 The wall of a muscular artery (a biopsied human temporal artery), stained for elastin, showing the internal elastic lamina (black wavy line nearest to the lumen, IEL) and more diffuse external elastic lamina (EEL). Fine, incomplete elastic lamellae are interspersed between smooth muscle cells of the tunica media between the IEL and EEL. Elastic van Gieson technique.

Collagen fibrils are found in all three vessel layers. Type III collagen (reticulin) occupies much of the interstitial space between the muscle cells of the media, and is also found in the intima. Collagen is abundant in the adventitia, where type I collagen fibres form large bundles which increase in size from the junction with the media to the outer limit of the vessel wall. In veins, collagen is the main component of the vessel wall, and accounts for more than half its mass.

In general terms, collagen and elastic fibres in the media run parallel to, or at a small angle to, the axes of the muscle cells, and they are therefore mainly circumferentially arranged. In contrast, the predominant arrangement of collagen fibres in the adventitia is longitudinal. This arrangement imposes constraints on length change in large vessels under pressure, e.g. in large arteries, in which the radial distension under the effect of the pulse far exceeds the longitudinal distension. The outer sheath of type I collagen in the adventitia therefore has a structurally supportive role. The more delicate type III collagen network of the media provides attachment to the muscle cells and its role is to transmit force around the circumference of the vessel. In a distended vessel, the elastic fibres store energy and, by recoiling, help to restore the resting length and calibre.

The extracellular material of the media, including collagen and elastin, is produced by the muscle cells. Its turnover is slow compared to that in other tissues. In the adventitia, collagen is synthesized and secreted by fibroblasts, as in other connective tissues. During postnatal development, while vessels increase in diameter and wall thickness, there is an increase in elastin and collagen content. Subsequent changes in vessel structure, seen during ageing, include an increase in the collagen-to-elastin ratio, with a reduction in vessel elasticity.

Adventitia

The adventitia is formed of general connective tissue, varying in the thickness and density of its collagen fibre bundles.

Vasa vasorum

In smaller vessels, the nourishment of the tissues of the vessel wall is provided by diffusion from the blood circulating in the vessel itself. Large vessels have their own vascular supply within the adventitia (see Figs 6.7, 6.8), in the form of a network of small vessels, mainly of the microcirculation, which are called the vasa vasorum. The wall thickness at which simple diffusion from the lumen becomes insufficient is 1 mm.

The vasa vasorum originate from, and drain into, adjacent vessels which are peripheral branches of the vessel they supply. They ramify within the adventitia and, in the largest of arteries, penetrate the outermost part of the media. The larger veins are also supplied by vasa vasorum, but these may penetrate the wall more deeply, perhaps because of the lower oxygen tension.

Nervi vasorum

Blood vessels are innervated by efferent autonomic fibres which regulate the state of contraction of the musculature (muscular tone), and thus the diameter of the vessels, particularly the arteries and arterioles. These perivascular nerves branch and anastomose within the adventitia of an artery, forming a meshwork around it. In some of the large muscular arteries, nerves are occasionally found within the outermost layers of the media.

Nervi vasorum are small bundles of axons, which are almost invariably unmyelinated and typically varicose. Most are postganglionic fibres which issue from sympathetic ganglion neurones. Some vessels in the brain may be innervated by intrinsic cerebral neurones although neural control of brain vessels is of minor importance compared with metabolic and autoregulation (local response to stretch stimuli). The density of innervation varies in different vessels and in different areas of the body: it is usually sparser in veins and larger lymphatic vessels. Large veins with a pronounced muscle layer, such as the hepatic portal vein, are well-innervated.

The control of vascular smooth muscle is complex. Vasoconstrictor adrenergic fibres release noradrenaline (norepinephrine) which acts on adrenoceptors in the muscle cell membrane. In addition, circulating hormones and factors such as nitric oxide and endothelins, which are released from endothelial cells, exert a powerful effect on the muscle cells. The neurotransmitters reach the muscle from the adventitial surface of the media, and hormonal and endothelial factors diffuse from the intimal surface. In some tissues, sympathetic cholinergic fibres inhibit smooth muscle contraction and induce vasodilation.

Most arteries are accompanied by nerves which travel in parallel with them to the peripheral organs which they supply. However, these paravascular nerves are quite independent, and do not innervate the vessels they accompany.

Pericytes

Pericytes are present at the outer surface of capillaries and the smallest venules (postcapillary venules), where an adventitia is absent and there are no muscle cells. They are elongated cells, whose long cytoplasmic processes are wrapped around the endothelium. Pericytes are scattered in a discontinuous layer around the outer circumference of capillaries. They are generally absent from fenestrated capillaries, but form a more continuous layer around postcapillary venules (Fig. 6.21). They are gradually replaced by smooth muscle cells as vessels converge and increase in diameter.

Pericytes are enclosed by their own basal lamina, which merges in places with that of the endothelium. Most pericytes display areas of close apposition with endothelial cells, and occasionally form adherens junctions where their basal laminae are absent. Pericyte cytoplasm contains actin, myosin, tropomyosin and desmin, which suggests that these cells are capable of contractile activity. They also have the potential to act as mesenchymal stem cells, and they participate in repair processes by proliferating and giving rise to new blood vessel and connective tissue cells.

Cerebral vessels

Major branches of cerebral arteries that lie in the subarachnoid space over the surface of the brain have a thin outer coating of meningeal cells, usually one layer thick, where adjacent meningeal cells are joined by desmosomes and gap junctions. These arteries have a smooth muscle media and a distinct elastic lamina. Veins on the surface of the brain have very thin walls, and the smooth muscle layers in the wall are often discontinuous. They are coated externally by a monolayer of meningeal cells.

As arteries enter the subpial space and penetrate the brain, they lose their elastic laminae, and consequently the cerebral cortex and white matter typically contain only arterioles, venules and capillaries. The exceptions are the large penetrating vessels in the basal ganglia, where many arteries retain their elastic laminae and thick smooth muscle media. Enlarged perivascular spaces form around these large arteries in ageing individuals. Arterioles and venules in the cortex and white matter can be distinguished from each other because arterioles are surrounded by a smooth muscle coat, and the veins and venules have larger lumina and thinner walls.

Cerebral capillaries are the site of the blood–brain barrier (p. 49). They are lined by endothelial cells which are joined by tight junctions. The endothelial cytoplasm contains a few pinocytotic vesicles. The cells are surrounded by a basal lamina (see Fig. 3.13): at points of contact with perivascular astrocytes the intervening basal lamina is formed by fusion of the endothelial and glial basal laminae. Pericytes, completely surrounded by basal lamina, are present around capillaries. Perivascular macrophages are attached to the outer walls of capillaries and to other vessels: they are phenotypically distinct from parenchymal microglia, which are also of monocytic origin. A thin layer of meningeal cells derived from the pia mater surrounds arterioles but disappears at the level of capillaries. For further descriptions of cerebral vessels, see Ch. 17.

LYMPHATIC VESSELS

Lymphatic capillaries form wide-meshed plexuses in the extracellular matrices of most tissues. They begin as dilated, blind-ended tubes with larger diameters and less regular cross-sectional appearances than those of blood capillaries. A basal lamina is incomplete or absent and they lack associated pericytes. The smaller lymphatic vessels are lined by endothelial cells, which have numerous transcytotic vesicles within their cytoplasm, and so resemble blood capillaries. However, unlike capillaries, their endothelium is generally quite permeable to much larger molecules: they are readily permeable to large colloidal proteins and particulate material such as cell debris and microorganisms, and also to cells. Permeability is facilitated by gaps between the endothelial cells, which lack tight junctions, and by pinocytosis.

Lymph is formed from interstitial fluid, which is derived from blood plasma via the microcirculation. Much of this fluid is returned to the venous system. Lymphatic vessels take up residual fluid (about one tenth) by passive diffusion and the transient negative pressures in their lumina which are generated intrinsically by contractile activity of smooth muscle in the largest lymphatic vessel walls, and extrinsically, by movements of other tissues (muscles, arteries) locally. The unidirectional flow of lymph is maintained by the presence of valves in the larger vessels (see Fig. 6.22). Lymphatic capillaries are prevented from collapsing by anchoring filaments which tether their walls to surrounding connective tissue structures and exert radial traction.

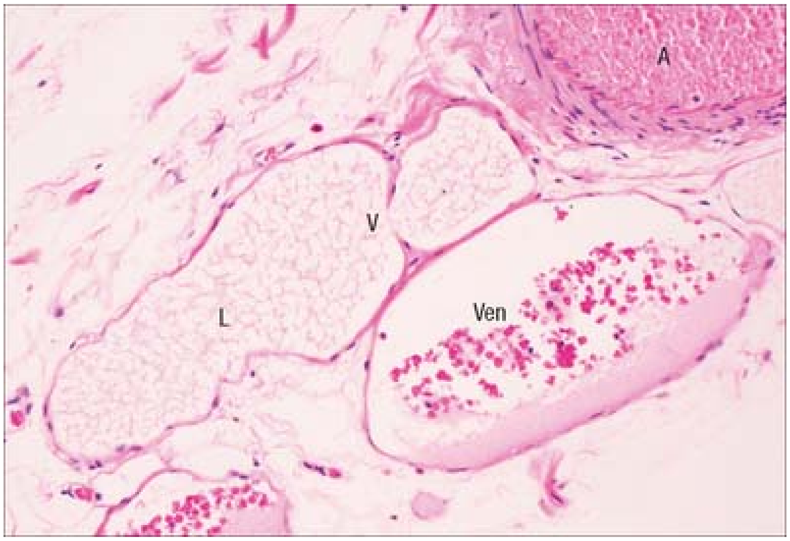

Fig. 6.22 A valve (V) in a lymphatic vessel (L), accompanying a small venule (Ven) and arteriole (A) in human connective tissue.

In most tissues, lymph is clear and colourless. In contrast, the lymph from the small intestine is dense and milky, reflecting the presence of lipid droplets (chylomicrons) derived from fat absorbed by the mucosal epithelium. The terminal lymphatic vessels in the mucosa of the small intestine are known as lacteals and the lymph as chyle. Lymphatic capillaries are not ubiquitous: they are not present in cornea, cartilage, thymus, the central or peripheral nervous system or bone marrow, and there are very few in the endomysium of skeletal muscles.

Lymphatic capillaries join into larger vessels which pass to local lymph nodes. Typically, lymph percolates through a series of nodes before reaching a major collecting duct. There are exceptions to this arrangement: the lymph vessels of the thyroid gland and oesophagus, and of the coronary and triangular ligaments of the liver, all drain directly to the thoracic duct without passing through lymph nodes. In the larger vessels, a thin external connective tissue coat supports the endothelium. The largest lymphatic vessels (200 µm) have three layers, like small veins, although their lumen is considerably larger than is the case in veins with a similar wall thickness. The tunica media contains smooth muscle cells, mostly arranged circumferentially.

Elastic fibres are sparse in the tunica intima, but form an external elastic lamina in the tunica adventitia.

The larger lymphatic vessels differ from small veins in having many more valves (Fig. 6.22). The valves are semilunar, generally paired and composed of an extension of the intima. Their edges point in the direction of the current, and the vessel wall downstream is expanded into a sinus, which gives the vessels a beaded appearance when they are distended. Valves are important in preventing the backflow of lymph.

Deep lymphatic vessels usually accompany arteries or veins, and almost all reach either the thoracic duct or the right lymphatic duct, which usually join the left or right brachiocephalic veins respectively at the root of the neck.

The thoracic duct is structurally similar to a medium-sized vein, but the smooth muscle in its tunica media is more prominent. Most lymphatic vessels anastomose freely, and larger ones have their own plexiform vasa vasorum and accompanying nerve fibres. If their walls are acutely infected (lymphangitis) this vascular plexus becomes congested, marking the paths of superficial vessels by red lines, which are visible through the skin, and tender to the touch.

Lymphatic vessels repair easily and new vessels readily form after damage. They begin as solid cellular sprouts from the endothelial cells of persisting vessels and later become canalized.

CARDIAC MUSCLE

In cardiac muscle, as in skeletal muscle, the contractile proteins are organized structurally into sarcomeres which are aligned in register across the fibres, producing fine cross-striations that are visible in the light microscope. They both contain the same contractile proteins (although many are cardiac isoforms), which are assembled in a similar way, and the molecular basis for contraction, but not its regulation, is the same. Release of calcium into the sarcoplasm triggers contraction, which corresponds to cardiac systole, the pumping phase of the heart cycle. Reuptake of calcium produces relaxation, which corresponds to cardiac diastole, the filling phase of the cycle.

Despite the similarities, there are major functional, morphological and developmental differences between cardiac and skeletal muscle. Some of the ways in which cardiac muscle differs morphologically from skeletal muscle are described below, before consideration of other features that are unique to cardiac muscle.

MICROSTRUCTURE

The myocardium, the muscular component of the heart, constitutes the bulk of its tissues. It consists predominantly of cardiac muscle cells, which are usually 120 μm long and 20–30 μm in diameter in a normal adult. Each cell has one or two large nuclei, occupying the central part of the cell, whereas skeletal muscle has multiple, peripherally placed nuclei. The cells are branched at their ends, and the branches of adjacent cells are so tightly associated that the light microscopic appearance is of a network of branching and anastomosing fibres (Fig. 6.23). Cells are bound together by elaborate junctional complexes, the intercalated discs (Fig. 6.23, Fig. 6.24, see Fig. 6.26).

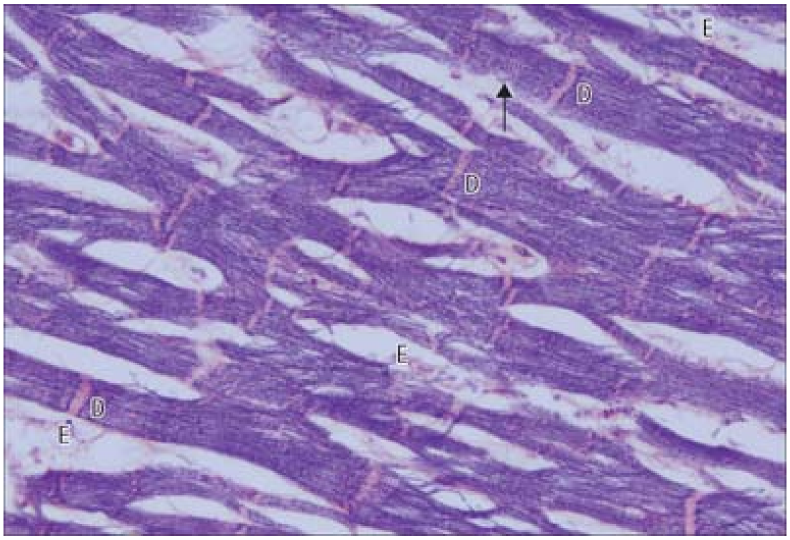

Fig. 6.23 Cardiac muscle fibres (human heart), sectioned longitudinally. Faint fine cross-striations are just visible (arrow) and indicate the intracellular organization of sarcomeres. The pale transverse lines (some appear stepped) are intercalated discs (D). Endomysium (E) contains nuclei of endothelial cells and fibroblasts.

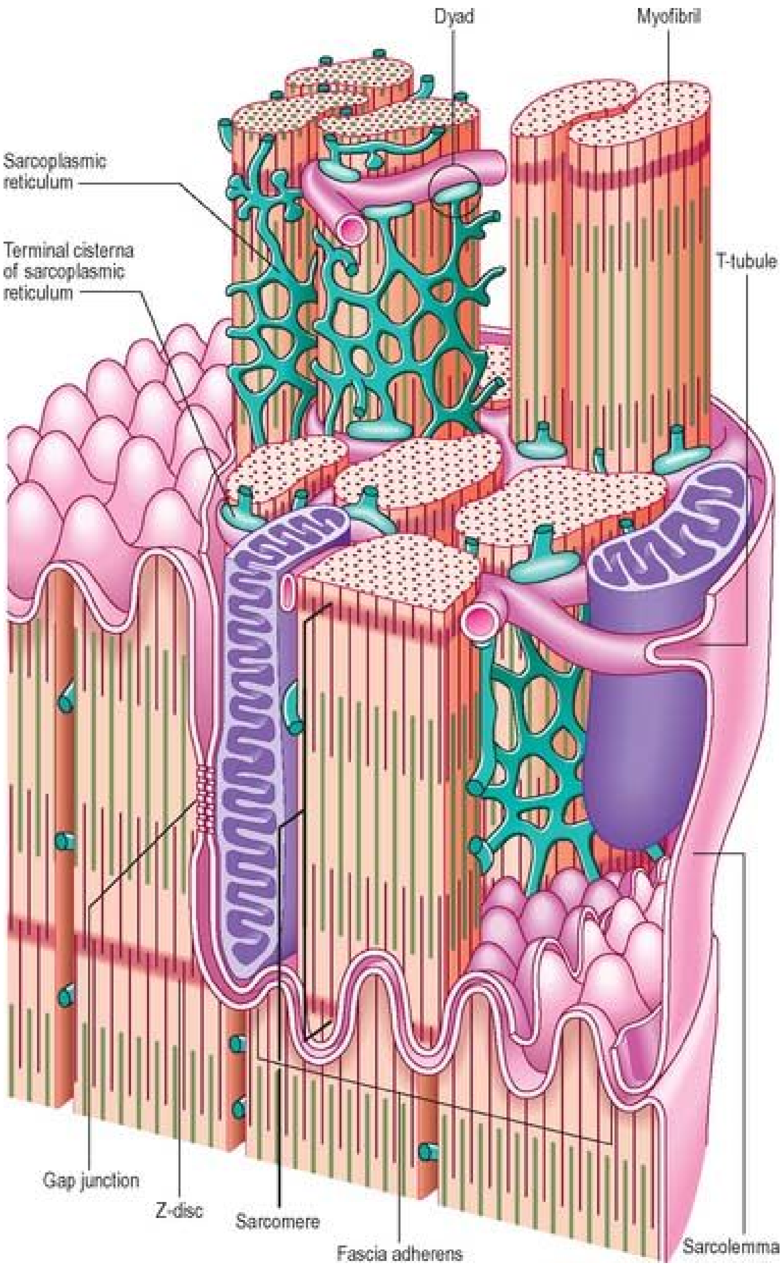
Dyad
Myofibril
Sarcoplasmic reticulum
Terminal cisterna of sarcoplasmic reticulum
T-tubule
Gap junction
Z-disc
Sarcomere
Fascia adherens
Sarcolemma

Fig. 6.24 Three-dimensional reconstruction of cardiac muscle cells in the region of an intercalated disc, a junctional complex between neighbouring cells. The interdigitating transverse parts of the intercalated disc form a fascia adherens, with numerous desmosomes; gap junctions are found in the longitudinal parts of the disc. The organization of the transverse tubules and sarcoplasmic reticulum is also shown.

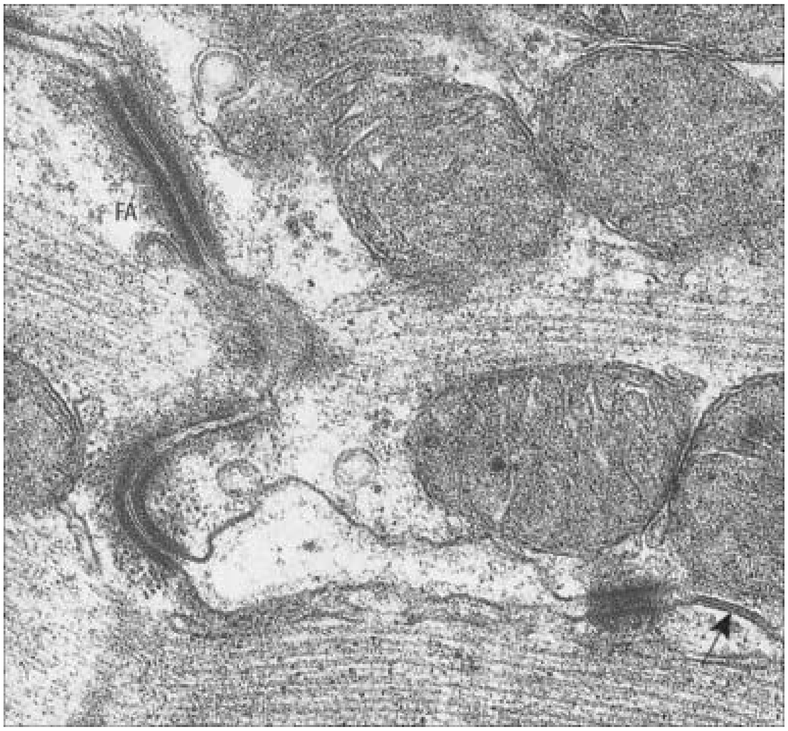

Fig. 6.26 An intercalated disc in cardiac muscle, with several zones of electron dense fascia adherens (FA) and a gap junction (arrow).

(By courtesy of Professor Brenda Russell, Department of Physiology and Biophysics, University of Illinois at Chicago.)

Fine fibrocollagenous connective tissue is found between cardiac muscle fibres. Although this is equivalent to the endomysium of skeletal muscle, it is less regularly organized because of the complex three-dimensional geometry imposed by the branching cardiac cells. Numerous capillaries and some nerve fibres are found within this layer. Coarser connective tissue, equivalent to the perimysium of skeletal muscle, separates the larger bundles of muscle fibres, and is particularly well developed near the condensations of dense fibrous connective tissue that form the ‘skeleton’ of the heart (see Ch. 56). The ventricles of the heart are composed of spiralling layers of fibres which run in different directions. Consequently, microscope sections of ventricular muscle inevitably contain the profiles of cells cut in a variety of orientations. A linear arrangement of cardiac muscle fibres is found only in the papillary muscles and trabeculae carneae.

Electron micrographs of cardiac muscle cells in longitudinal section (Fig. 6.25) show that the myofibrils separate before they pass around the nucleus, leaving a zone that is occupied by organelles, including sarcoplasmic reticulum, Golgi complex, mitochondria, lipid droplets, and glycogen. At the light microscopic level, these zones appear in longitudinal sections as unstained areas at the poles of each nucleus. They often contain lipofuscin granules, which accumulate there in individuals over the age of 10; the reddish-brown pigment may be visible even in unstained longitudinal sections.

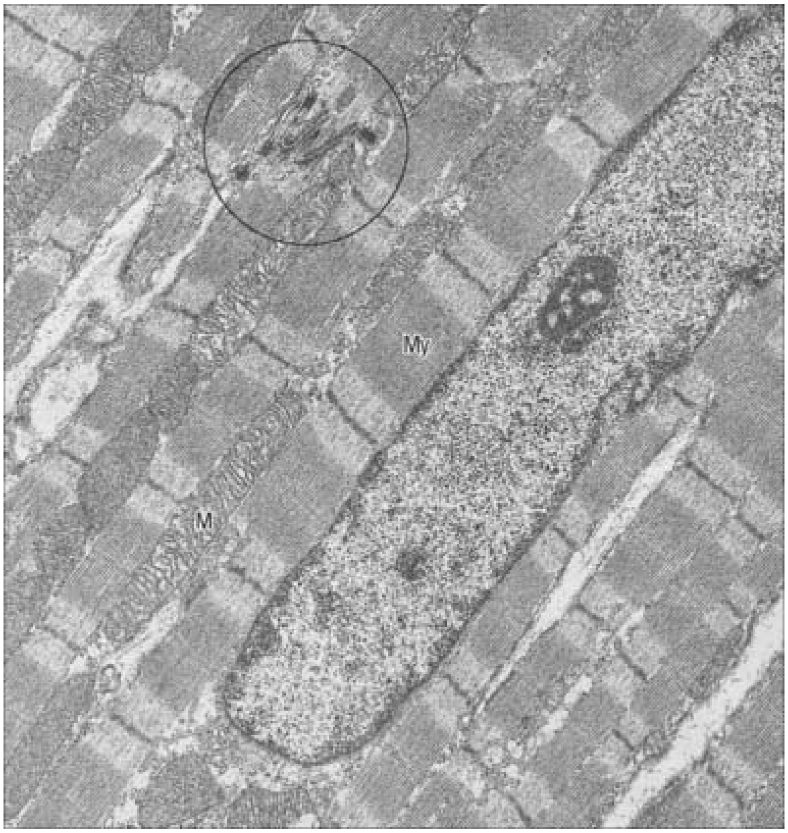

Fig. 6.25 Low power electron micrograph of cardiac muscle in longitudinal section, including the perinuclear zone of one of the fibres. Note the abundant large mitochondria (M) between myofibrils (My), and an intercalated disc (circled).

By courtesy of Professor Brenda Russell, Department of Physiology and Biophysics, University of Illinois at Chicago.)

The cross-striations of cardiac muscle are less conspicuous than those of skeletal muscle. This is because the contractile apparatus of cardiac muscle lies within a mitochondria-rich sarcoplasm. The myofibrils are less well delineated than they are in skeletal muscle: in transverse sections they often fuse into a continuous array of myofilaments, irregularly bounded by mitochondria and longitudinal elements of sarcoplasmic reticulum. The large mitochondria, with their closely spaced cristae, reflect the highly developed oxidative metabolism of cardiac tissue. The proportion of the cell volume occupied by mitochondria (approximately 35%) is even greater in cardiac muscle than it is in slow twitch skeletal muscle fibres. The high demand for oxygen is also reflected in high levels of myoglobin and an exceptionally rich network of capillaries around the fibres.

The force of contraction is transferred through the ends of the cardiac muscle cells via the junctional strength provided by the intercalated discs. As in skeletal muscle, force is also transmitted laterally to the sarcolemma and extracellular matrix via vinculin-containing elements which bridge between the Z-discs of peripheral myofibrils and the plasma membrane.

Atrial muscle cells are smaller than ventricular cells. The cytoplasm near the Golgi complexes at the poles of the nuclei exhibits dense membrane-bound granules, which contain the precursor of atrial natriuretic factor. This is a hormone whose action is to promote loss of sodium chloride and water in the kidneys, reducing body fluid volume and thereby lowering blood pressure. It is released in response to stretch of the atrial wall. The actions of atrial natriuretic factor are normally balanced by the opposing effects of aldosterone and antidiuretic hormone.

The sarcolemma of ventricular cardiac muscle cells invaginates to form T-tubules with a wider lumen than those of skeletal muscle; atrial muscle cells have few or no T-tubules. Unlike skeletal muscle, most T-tubules penetrate the sarcoplasm at the level of the Z-discs (Fig. 6.24). The T-tubules are interconnected at intervals by longitudinal branches to form a complex network. They probably serve a similar function in skeletal and cardiac muscle, i.e. to carry the wave of depolarization into the core of the cells. The actin-binding proteins, spectrin and dystrophin, are important components of the cardiac muscle cell cytoskeleton, which associate independently with the sarcolemma to provide mechanical support.

The sarcoplasmic reticulum is a membrane-bound tubular plexus which surrounds, and defines, sometimes incompletely, the outlines of individual myofibrils. Its main role, as in skeletal muscle, is the storage, release and reaccumulation of calcium ions. It comes into close contact with the T-tubules, leaving a 15 nm gap that is spanned by structures termed junctional processes. These processes are thought to be the cytoplasmic part of the calcium release channels (ryanodine receptors); similar processes are found in skeletal muscle at the junctional surface of the terminal cisternae. Sarcoplasmic reticulum which bears junctional processes has been termed junctional sarcoplasmic reticulum, to distinguish it from the free sarcoplasmic reticulum, which forms a longitudinal network. Junctional sarcoplasmic reticulum makes contact with both the T-tubules and the sarcolemma (of which the T-tubules are an extension). Sarcoplasmic reticulum forms small globular extensions (corbular sarcoplasmic reticulum) in the vicinity of the Z-discs, but not in immediate relation to T-tubules or the sarcolemma. Since the junctions between T-tubules and sarcoplasmic reticulum usually involve only one structure of each type, the corresponding profiles in electron micrographs are referred to as dyads, rather than triads as in skeletal muscle.

Intercalated discs

Intercalated discs are unique to cardiac muscle. In the light microscope they are seen as transverse lines crossing the tracts of cardiac cells (see Fig. 6.23). They may step irregularly within or between adjacent tracts, and may appear to jump to a new position as the plane of focus is altered. At the ultrastructural level these structures, which are complex junctions between the cardiac muscle cells, are seen to have transverse and lateral portions (see Fig. 6.24, Fig. 6.26). The transverse portions occur wherever myofibrils abut the end of the cell, and each takes the place of the last Z-disc. At this point, the actin filaments of the terminal sarcomere insert into a dense subsarcolemmal matrix which anchors them, together with other cytoplasmic elements such as intermediate filaments, to the plasma membrane. Prominent desmosomes, often with a dense line in the intercellular space, occur at intervals along each transverse portion. This junctional region is homologous with, and probably similar in composition to, the structure found on the cytoplasmic face of the myotendinous junction, and is a type of fascia adherens junction. It provides firm adhesion between cells, and a route for the transmission of contractile force from one cell to the next.

The lateral portions of the intercalated disc run parallel to the myofilaments, and the long axis of the cell, for a distance which corresponds to one or two sarcomeres before it turns again to form another transverse portion. It is therefore responsible for the stepwise progression of the intercalated disc which can be seen microscopically. The lateral portions contain gap junctions, which are responsible for the electrical coupling between adjacent cells (see Fig. 6.26). Conductance channels within these junctions enable the electrical impulse to propagate from one cell to the next, spreading excitation and contraction rapidly along the branching tracts of interconnected cells. In this way the activity of the individual cells of the heart is coordinated so that they function as if they were a syncytium.

VASCULAR SUPPLY AND LYMPHATIC DRAINAGE

The activity of the heart is equivalent to a constant power expenditure of 1.3 watts under basal conditions, and escalates to 3 watts or more during physical exertion. Cardiac muscle cells contain glycogen, which is a reserve during peaks of activity, but the majority of their energy requirement is continuous and supplied only through a highly developed oxidative metabolism, as is evident from the high proportion of the cell volume which is occupied by mitochondria. This metabolism has to be supported by a rich blood supply. Myocardium has a very high perfusion rate of 0.5 ml/min/g of tissue (five times that of liver and 15 times that of resting skeletal muscle). No cardiac muscle cell is more than 8 μm from a capillary, and vascular channels occupy a high proportion of the total interstitial space. Heart muscle is supplied by the coronary vessels. Although there is some variation in the detailed distribution of the arterial branches, the left ventricle, which has the highest workload, consistently receives the highest arterial blood flow. Branches run in the myocardium along the coarser aggregations of connective tissue and ramify extensively in the endomysial layer, creating a rich plexus of anastomosing vessels. This plexus includes lymphatic as well as blood capillaries, which is not the case in skeletal muscle.

The high oxygen requirement of the myocardium makes it vulnerable to ischaemic damage arising from atheroma or embolism in the coronary arteries. Arterial anastomoses, often more than 100 μm in diameter, are found throughout the heart and are an important factor in determining whether an adequate collateral circulation can develop after a coronary occlusion.

INNERVATION

Although the impulse-generating and conducting system of the heart establishes an endogenous rhythm, the rate and force of contraction are under neural influence. Both divisions of the autonomic nervous system supply non-myelinated postganglionic fibres to the heart. The innervation is derived bilaterally, but it is functionally asymmetrical. Activation of the left stellate ganglion (sympathetic) has little effect on heart rate but increases ventricular contractility, whereas activation of the right stellate ganglion influences both rate and contractility. Activation of the right vagus nerve (parasympathetic) slows heart rate mainly through its influence on the pacemaker region, the sinoatrial (SA) node, whereas activation of the left vagus slows propagation of the impulse mainly through its effect on the atrioventricular (AV) node. Vagal activity has little direct effect on ventricular contractility.

Sympathetic nerve fibres from the cervical sympathetic ganglia reach the heart via the cardiac nerves. Parasympathetic fibres in the heart originate in ganglion cells that are innervated by efferent fibres of the vagus nerve. Adrenergic, cholinergic and peptidergic endings have been demonstrated in the myocardium. Fibres often end close to muscle cells and blood vessels, but junctional specializations are not seen, and a gap of at least 100 nm remains between cell and nerve fibre. It is probable that neurotransmitters diffuse across this gap to the adjacent cells. Some of the endings represent efferent nerve terminals, others function as pain, mechano- or chemoreceptors.

EXCITATION–CONTRACTION COUPLING IN CARDIAC MUSCLE

The molecular interaction between actin and myosin that underlies the generation of force is initiated in the same way in cardiac and skeletal muscle. However, differences in the physical arrangement and molecular composition of these contractile elements have a profound influence on contractile function in cardiac muscle.

The calcium release channels of the sarcoplasmic reticulum are sensitive to the concentration of free calcium in the gap between the T-tubule and sarcoplasmic reticulum membranes. This underlies ‘calcium-induced calcium release’, which is believed to be the principal, and probably the only, mechanism involved in the liberation of calcium from the sarcoplasmic reticulum during physiological activation. The passage of an action potential depolarizes the sarcolemma and thereby opens sarcolemmal L-type calcium channels, which allows some calcium to enter from the extracellular space. This produces a localized rise in the intracellular free calcium concentration near the calcium release channels, which consequently open, allowing calcium ions to flow down their concentration gradient from the sarcoplasmic reticulum into the cytosol. The rise in cytosolic calcium concentration then activates the contractile machinery.

Systolic activation is terminated by reuptake of calcium from the cytosol. Although both the sarcolemma and the mitochondrial membrane have some capacity for calcium transport, the main route of uptake is into the sarcoplasmic reticulum, via a high-affinity, calcium-transporting ATPase. The activity of this ATPase controls the rate of decay of the calcium transient and is therefore a determinant of the rate of relaxation of the heart. The sarcoplasmic reticulum contains a cardiac form of calsequestrin, a distant homologue of the protein found in skeletal muscle. This calcium-binding protein buffers the free calcium concentration inside the sarcoplasmic reticulum, allowing it to store considerable amounts of total calcium without increasing the gradient against which the calcium-ATPase must pump.

One of the major functional differences between cardiac and skeletal muscle is the way in which contractile force is regulated. Smoothness and gradation of contraction in a skeletal muscle depend on the recruitment and asynchronous firing of different numbers of motor units. Individual motor units can also build up a contraction through a brief series of re-excitations. In the heart, the entire mass of muscle must be activated almost simultaneously, and mechanical summation by re-excitation is not possible, because the cells are electrically refractory until mechanical relaxation has taken place.

In cardiac muscle cells, as in skeletal muscle cells, contraction is initiated when calcium binds to troponin-C, a component of the regulatory protein complex on the thin filaments. During basal activity of the heart, the amount of calcium bound to troponin-C during each systole induces less than half-maximal activation of the contractile apparatus. There is therefore the potential for producing more force by increasing the amount of calcium bound to troponin-C. This can be achieved by controlling the amount of free calcium that is released into the cytosol during systole.

A special feature of the cardiac cell is the long duration of its action potential. The long-lasting plateau of depolarization allows a prolonged inward flux of calcium to take place via the L-type calcium channels in the sarcolemma. During the relaxation phase, the calcium is actively pumped into the sarcoplasmic reticulum: the extent to which the sarcoplasmic reticulum is loaded is crucially dependent on this entry of extracellular calcium. The greater the amount of calcium that is stored in the sarcoplasmic reticulum, the more is available for release during subsequent contractions. These calcium movements provide an automatic mechanism for matching any increase in heart rate with a progressive increase in contractile force. At higher heart rates, more calcium enters per unit time and is pumped into the sarcoplasmic reticulum. Each systole is then more forceful, because the amount of calcium that can be delivered into the cytosol is greater.

The most potent physiological means of enhancing cardiac contractility is through the action of β-adrenergic agents, such as adrenaline (epinephrine) and noradrenaline (norepinephrine). These increase calcium taken up by the sarcoplasmic reticulum in two ways. Firstly, β-adrenergic stimulation increases the amount of calcium that enters during depolarization by opening more L-type calcium channels. Secondly, β-adrenergic stimulation can enhance the activity of the calcium-pumping ATPase by phosphorylating an associated protein, phospholamban. This enables the calcium pump to lower the cytosolic free calcium more rapidly, which contributes to the accelerated relaxation produced by β-adrenergic agonists. In a coordinated manner, phosphorylation of troponin-I on the thin filament increases the rate of cross-bridge cycling to aid the acceleration of relaxation.

Because of the clinical significance of positive inotropic agents (substances which increase the strength of cardiac contraction), generally now used only in severe end-stage heart failure, there is great interest in the multiple control sites which might provide targets for pharmacological intervention. Some of these are related to another important set of ionic fluxes through the sarcolemma via the sodium–potassium pump and the bidirectional sodium–calcium exchange and sodium-hydrogen exchange transporter proteins.

DEVELOPMENT

Cardiac myocytes differentiate from the splanchnic coelomic cells of the pericardium initially subjacent to the endoderm. Myogenic activity begins at the beginning of stage 10, 22 days gestation, when the embryo has four somites. At this time the presumptive cardiac myocytes express myosin, actin, troponin and other contractile proteins. The cardiac myocytes do not fuse with their neighbours to form a syncytium as occurs in skeletal muscle, but remain mononucleated, branched cells connected via intercellular junctions.

Presumptive myocardial cells form a continuous sheet of cuboidal cells which line the ventral splanchnic wall of the pericardial cavity in stage 9 (unfolded) embryos. From this time, an endocardial plexus forms between the splanchnopleuric coelomic epithelium and the endoderm. The plexus cells coalesce to establish bilateral, hollow tubular structures which fuse in the midline to form a single endocardial tube. After head folding, the endocardium is separated from the myocytes of the primitive heart tube by a fine extracellular reticulum, formerly referred to as cardiac jelly, which is secreted by the myocardial cells. The extracellular matrix of the heart contains inductive signals, also secreted by the myocardial cells, which transform competent cells of the endocardial epithelium into free mesenchymal cells. Thus during cardiac development, presumptive myocardial cells engage in several processes at once: they divide and differentiate to form a functional myocardium; they secrete matrix and inductive factors that will modify the differentiation of other cells; and they participate in the bending and rotation of the primitive heart tube, and differential growth within its walls, which will ultimately produce the four-chambered adult heart.

Overt differentiation of the primitive myocardial cells begins at about the time of fusion of the endocardial tube. As the primitive heart tube is formed, the presumptive myocardial cells start to express genes that encode characteristic myocardial proteins, including myosin, actin, troponin and other components of the contractile apparatus. Myofibrils begin to appear in the developing muscle cells, and the first functional heart beats start soon afterwards.

The regulatory mechanisms underlying differentiation of cardiac muscle appear to be distinct from those of skeletal muscle. Although it is anticipated that counterparts will be found for the transcriptional factors Myf-5, myogenin, MyoD and Myf-6, which are responsible for inducing differentiation of skeletal muscle, the corresponding factors for cardiac myogenesis have yet to be identified. During fetal maturation, successive changes in gene expression give rise to the characteristics of fetal, neonatal and adult myocardium and are responsible for the divergence of the properties of atrial and ventricular muscle cells.

Committed cardiac myoblasts do not fuse to form multinucleated myotubes as occurs in skeletal muscle, but remain as single cells coupled physically and electrically through intercellular junctions. Moreover, differentiated cardiac muscle cells continue to divide during fetal development, and withdraw from the cell cycle only after birth. This is markedly different from skeletal muscle development, in which differentiation, including the activation of muscle-specific genes, coincides with withdrawal from the cell cycle.

Concurrent with development of the contractile proteins of cardiac muscle, cardiac muscle cells develop numerous specific heart granules which contain substances shown to induce natriuresis and diuresis, and a family of polypeptides generally known as atrial natriuretic peptides. Specific heart granules develop from the Golgi complex in both atria and ventricles during fetal life, but become restricted to atrial muscle in the adult. Atrial natriuretic peptide is measurable when the heart is recognizably four-chambered. Within the atria almost all cells are capable of its synthesis.

Contractile protein isoforms of cardiac muscle

As in skeletal muscle, the contractile proteins of cardiac muscle exist in a number of tissue- and stage-specific forms. The cardiac isoform of α-actin is not identical to the skeletal muscle form, and is encoded by a different gene, although the two are so similar as to be functionally interchangeable. Both skeletal and cardiac isoforms of sarcomeric actin are expressed in fetal ventricular muscle. The mRNA for skeletal α-actin increases postnatally and exceeds that of cardiac actin in the adult.

The myosin heavy chain of human cardiac muscle exists in two isoforms, α and β, both of which are present in the fetal heart. The α-form persists as the adult isoform in atrial muscle, whereas the β-form (which is associated with a slower rate of contraction) predominates in ventricular muscle. Interestingly, the β-form of myosin heavy chain in cardiac muscle is identical to the isoform in slow twitch skeletal muscle. This identity between cardiac and slow twitch skeletal protein isoforms is true of several proteins, including ventricular myosin light chains and cardiac troponin-C. Other proteins, such as troponin-I and -T, exist in cardiac-specific forms in the adult, although skeletal isoforms are expressed in the fetus and neonate. The appearance of cardiac-specific isoforms of troponin-I and -T in the blood, following their release from damaged cardiac cells, is now a standard diagnostic test for myocardial infarction.

Under some experimental conditions the contractile protein isoforms expressed by mature cardiac muscle may change in the adult mammal. Two established influences in this respect are thyroid hormone, and mechanical stretch induced by pressure overload. Transitions in both the heavy chains and light chains of myosin have been shown to take place in the human heart under conditions of pathological overload, but the functional significance of these changes is not clear.

Development of the impulse-conducting tissues

The impulse-generating and conducting system of the heart is formed from muscle cells that differ in their morphology from the working cardiac cells which make up the bulk of the myocardium. Cells of the mature conduction system retain some similarities to the myocardium of the early heart tube, and share with that embryonic tissue a distinctive pattern of expression of many genes, including those encoding contractile proteins and acetylcholinesterase. This suggests that divergence of conducting tissues and working myocardium takes place at an early embryonic stage. A cytological marker specific for the conduction system, the sulphate-3-glucuronyl carbohydrate moiety of glycoproteins, is expressed by 32 days of development and is downregulated during the later stages of cardiac septation. Its distribution strongly suggests that the conduction tissue in humans originates in a ring of specialized myocardial cells located at the interventricular foramen of the early heart.

Lack of regeneration of cardiac muscle

In skeletal muscle, a population of precursor cells, satellite cells, is retained in adult life, and constitutes a pool of myoblasts which is capable of dividing, fusing with existing muscle fibres, and initiating regeneration after damage. Cardiac muscle contains no equivalent of these cells, and is therefore incapable of regeneration. There is experimental evidence that temporary ischaemia injures cardiac cells in a reversible manner (Schwanger et al 1987), whereas longer periods of ischaemia produce irreversible damage.

REFERENCES

hof BA, Aurrand-Lions M. Angiogenesis and inflammation face-off. *Nat Med*. 2006;12:171-172.

wens GK, Kumar MS, Wamhoff BR. Molecular regulation of vascular smooth muscle cell differentiation in development and disease. *Physiol Rev*. 2004;84:767-801.

ber JS, Sessa WC. Evolving functions of endothelial cells in inflammation. *Nat Revs Immunol*. 2007;7:803-815.

aal M, Christ B. Formation and differentiation of the avian dermomyotome. *Anat Embryol*. 2004;208:411-424.

hwanger M, Fishbein MC, Block M, Wijns W, Selin C, Phelps ME, Schelbert HR. Metabolic and ultrastructural abnormalities during ischemia in canine myocardium: noninvasive assessment by positron emission tomography. *Mol Cell Cardiol*. 1987;19:25-89.

arrow MP, Weichselbaum M, McCray PBJr. Development of the innervation and airway smooth muscle in human fetal lung. *Am J Respir Cell Mol Biol*. 1999;20:550-560.

ichel Salmon: Anatomic Studies. In: Taylor GI, Razaboni RM. *Book 1, Arteries of the Muscles of the Extremities and the Trunk. Book 2, Arterial Anastomotic Pathways of the Extremities*. St Louis: Quality Medical Publishing, 1994.

Contains the translated work of Dr Michel Salmon describing the blood supply to muscle and the anastomotic pathways in the limbs..

CHAPTER 7

Skin and its appendages

In this chapter, the types and functions of skin in different parts of the body are described first, followed by the microstructure of the epidermis and dermis, and the appendages of skin including the pilosebaceous units and the sweat glands and nails. The development of skin, natural skin lines and age-related changes, and clinical aspects of skin, e.g. grafts, surgical skin flaps and wound healing, are also described. The integumental system includes the skin and its derivatives, hairs, nails, sweat and sebaceous glands; subcutaneous fat and deep fascia; the mucocutaneous junctions around the openings of the body orifices; and the breasts. Mucocutaneous junctions and breast tissues are covered in the appropriate regional sections.

TYPES AND FUNCTIONS OF SKIN

The skin covers the entire external surface of the body, including the external auditory meatus, the lateral aspect of the tympanic membrane and the vestibule of the nose. It is continuous with the mucosae of the alimentary, respiratory and urogenital tracts at their respective orifices, where the specialized skin of mucocutaneous junctions is present. It also fuses with the conjunctiva at the margins of the eyelids, and with the lining of the lachrymal canaliculi at the lachrymal puncta. Skin forms 8% of the total body mass. Its surface area varies with height and weight, e.g. in an individual of 1.8 m and weighing 90 kg, the surface area of the skin is approximately 2.2 m^2. Its thickness ranges from 1.5–4.0 mm, according to its state of maturation, ageing and regional specializations.

The skin forms a self-renewing interface between the body and its environment, and is a major site of intercommunication between the two. Within limits, it forms an effective barrier against microbial invasion, and has properties which can protect against mechanical, chemical, osmotic, thermal and UV radiation damage. It is an important site of immune surveillance against the entry of pathogens and the initiation of primary immune responses. Skin carries out many biochemical synthetic processes, including the formation of vitamin D under the influence of ultraviolet B (UVB) radiation and synthesis of cytokines and growth factors. Skin is the target of a variety of hormones. These activities can affect the appearance and function of individual skin components, such as the sebaceous glands, the hairs and the pigment-producing cells.

Control of body temperature is an important function of skin, and is effected mainly by regulation of heat loss from the cutaneous circulation through the rapid increase or reduction in the flow of blood to an extensive external surface area: the process is assisted by sweating. Skin is involved in sociosexual communication and, in the case of facial skin, can signal emotional states by means of muscular and vascular responses. It is a major sense organ, richly supplied by nerve terminals and specialized receptors for touch, temperature, pain and other stimuli.

Skin has good frictional properties, assisting locomotion and manipulation by its texture. It is elastic, and can be stretched and compressed within limits. The outer surface is covered by various markings, some of them are large and conspicuous and others are microscopic, or are only revealed after manipulation or incision of the skin. These markings are often referred to collectively as skin lines.

The colour of human skin is derived from, and varies with, the amount of blood (and its degree of oxygenation) in the cutaneous circulation, the thickness of the cornified layer, and the activity of specialized cells which produce the pigment melanin. Melanin has a protective role against ultraviolet radiation, and acts as a scavenger of harmful free radicals. Racial variations in colour are mainly due to differences in the amount, type and distribution of melanin, and are genetically determined.

The appearance of skin is affected by many other factors, e.g. size, shape and distribution of hairs and of skin glands (sweat, sebaceous and apocrine), changes associated with maturation, ageing, metabolism, pregnancy. The general state of health is reflected in the appearance and condition of the skin, and the earliest signs of many systemic disorders may be apparent in the skin. Examination of the skin, therefore, is of importance in the diagnosis of more than just skin disease.

CLASSIFICATION OF SKIN

Although skin in different parts of the body is fundamentally of similar structure, there are many local variations in parameters such as thickness, mechanical strength, softness, flexibility, degree of keratinization (cornification), sizes and numbers of hairs, frequency and types of glands, pigmentation, vascularity, innervation. Two major classes of skin are distinguished: they cover large areas of the body and show important differences of detailed structure and functional properties. These are thin, hairy (hirsute) skin, which covers the greater part of the body, and thick, hairless (glabrous) skin, which forms the surfaces of the palms of the hands, soles of the feet, and flexor surfaces of the digits (Fig. 7.1, Fig. 7.2, see Fig. 7.4).

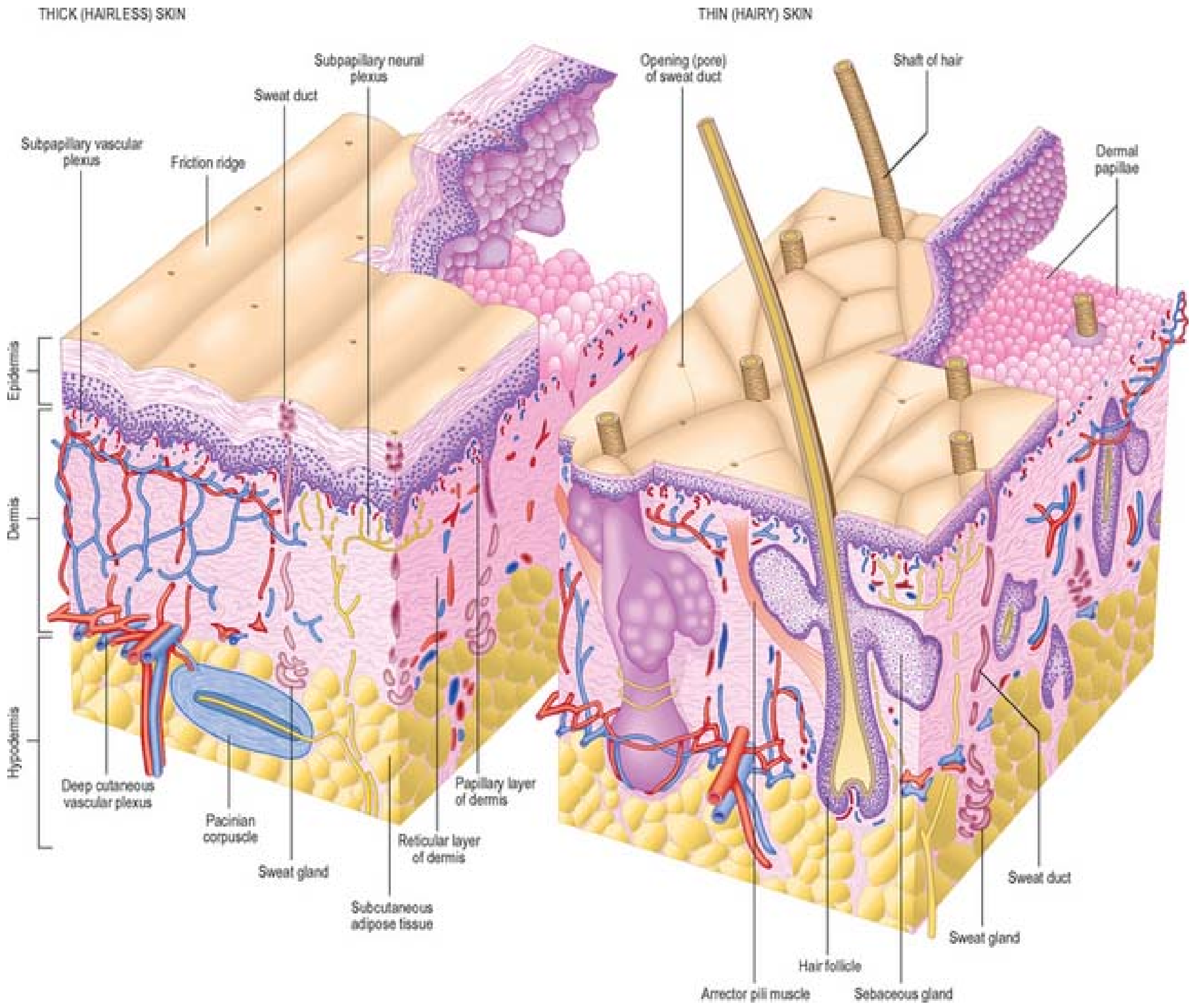
THICK (HAIRLESS) SKIN
THIN (HAIRY) SKIN
Subpapillary neural plexus
Sweat duct
Subpapillary vascular plexus
Friction ridge
Opening (pore) of sweat duct
Shaft of hair
Dermal papillae
Epidermis
Dermis
Hypodermis
Deep cutaneous vascular plexus
Pacinian corpuscle
Sweat gland
Subcutaneous adipose tissue
Papillary layer of dermis
Reticular layer of dermis
Sweat duct
Sweat gland
Hair follicle
Arrector pili muscle
Sebaceous gland

Fig. 7.1 The organization of skin, comparing the structures found in thick, hairless (plantar and palmar) skin with thin, hairy (hirsute) skin. The epidermis has been partially peeled back to show the interdigitating dermal and epidermal papillae.

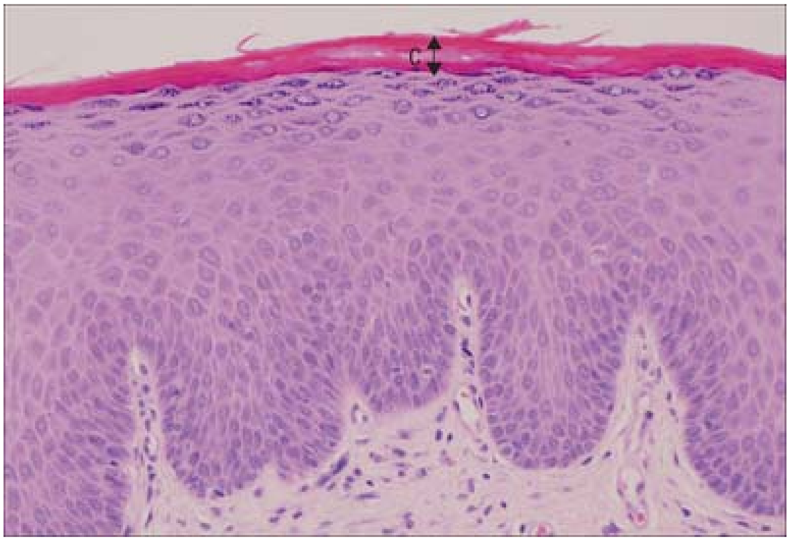

Fig. 7.2 The interfollicular epidermis of human thin skin. Note the thin cornified layer (C) in comparison with **Fig. 7.4** (which is also at a lower magnification).

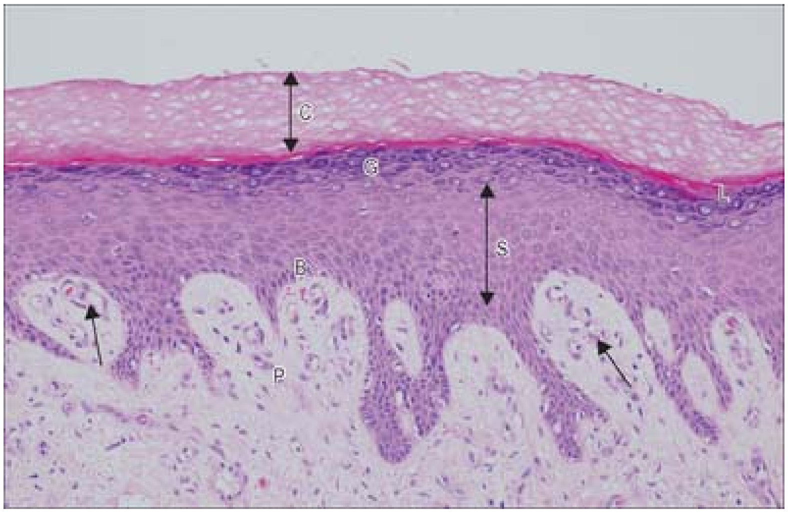

Fig. 7.4 The epidermis and papillary dermis (P) of human thick skin, showing the thick cornified layer (C, stratum corneum), the eosinophilic clear layer (L, stratum lucidum), the granular layer (G, stratum granulosum), the prickle cell layer (S, stratum spinosum) and the basal layer (B, stratum basale). Capillary loops (arrows) are seen entering the deep papillae (rete ridges) of the dermis, between downward-projecting epidermal rete pegs.

MICROSTRUCTURE OF SKIN AND SKIN APPENDAGES

EPIDERMIS

The epidermis (Fig. 7.2, Fig. 7.3) is a compound tissue consisting mainly of a continuously self-renewing, keratinized, stratified squamous epithelium: the principal cells are called keratinocytes. Nonkeratinocytes within the mature epidermis include melanocytes (pigment-forming cells from the embryonic neural crest), Langerhans cells (immature antigen-presenting dendritic cells derived from bone marrow), and lymphocytes. Merkel cells, which may function as sensory mechanoreceptors or possibly as part of the dispersed neuroendocrine system, are associated with nerve endings. Free sensory nerve endings are sparsely present within the epidermis. In routine histological preparations, the non-keratinocytes and Merkel cells are almost indistinguishable, and appear as clear cells surrounded by a clear space produced by shrinkage during processing. Their cytoplasm lacks prominent filament bundles.

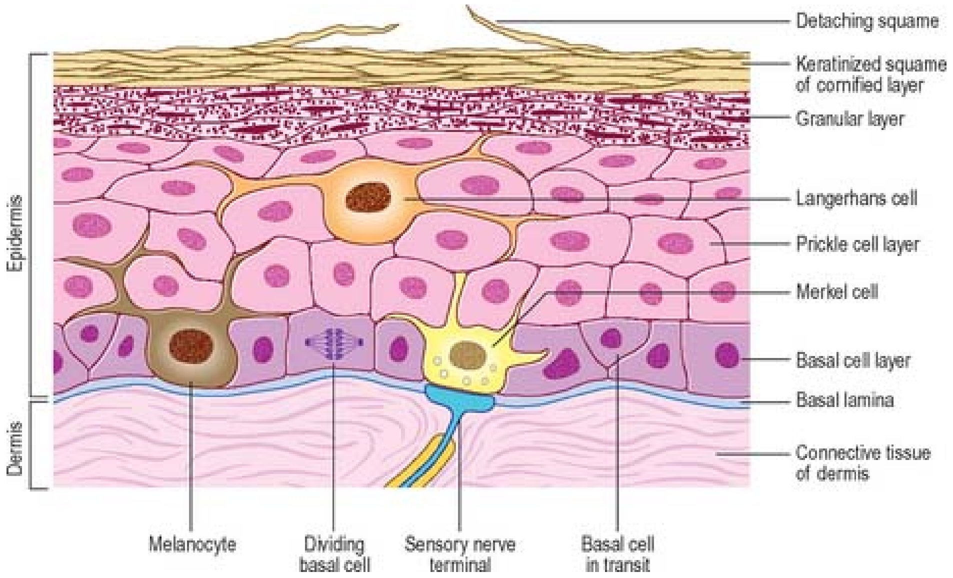
Detaching squame
Keratinized squame of cornified layer
Granular layer
Langerhans cell
Prickle cell layer
Merkel cell
Basal cell layer
Basal lamina
Connective tissue of dermis
Epidermis
Dermis
Melanocyte
Dividing basal cell
Sensory nerve terminal
Basal cell in transit

Fig. 7.3 The main features of the epidermis, including its cell layers and different cell types. Melanocytes and Merkel cells are derived from the neural crest and Langerhans cells are derived from bone marrow precursor cells.

The population of keratinocytes undergoes continuous renewal throughout life: a mitotic layer of cells at the base replaces those shed at the surface. As they move away from the base of the epidermis, keratinocytes undergo progressive changes in shape and content. They transform from polygonal living cells to non-viable flattened squames full of intermediate filament proteins (keratins) embedded in a dense matrix of cytoplasmic proteins to form mature keratin. The process is known as keratinization or, more properly, cornification.

The epidermis can be divided into a number of layers from deep to superficial as follows: basal layer (stratum basale), spinous or prickle cell layer (stratum spinosum), granular layer (stratum granulosum), clear layer (stratum lucidum) and cornified layer (stratum corneum) (Fig. 7.4). The first three of these layers are metabolically active compartments through which cells pass and change their form as they progressively differentiate. The more superficial layers of cells undergo terminal keratinization, or cornification, which involves not only structural changes in keratinocytes, but also alterations in their relationships with each other and with non-keratinocytes, and molecular changes within the intercellular space.

The epidermal appendages (pilosebaceous units, sweat glands and nails) are formed developmentally by ingrowth of the general epidermis, and the latter is thus referred to as the interfollicular epidermis.

Keratinocytes

Basal layer

The basal or deepest layer of cells, adjacent to the dermis, is the layer where cell proliferation in the epidermis takes place. This layer contacts a basal lamina (Fig. 7.5, see Fig. 2.7), which is a thin layer of specialized extracellular matrix, not usually visible by light microscopy. By routine electron microscopy the basal lamina appears as a clear lamina lucida (adjacent to the basal cell plasma membrane) and a darker lamina densa. The basal plasma membrane of the basal keratinocytes, together with the extracellular basal lamina (lamina lucida and lamina densa) and anchoring fibrils within the subjacent dermal matrix (the lamina fibroreticularis), which insert into the lamina densa and loop around bundles of collagen, collectively form the basement membrane zone (BMZ) which constitutes the dermo-epidermal junction. This is a highly convoluted interface, particularly in thick, hairless skin, where dermal papillae (rete ridges) project superficially into the epidermal region, interlocking with adjacent downward projections of the epidermis (rete pegs) (Fig. 7.4).

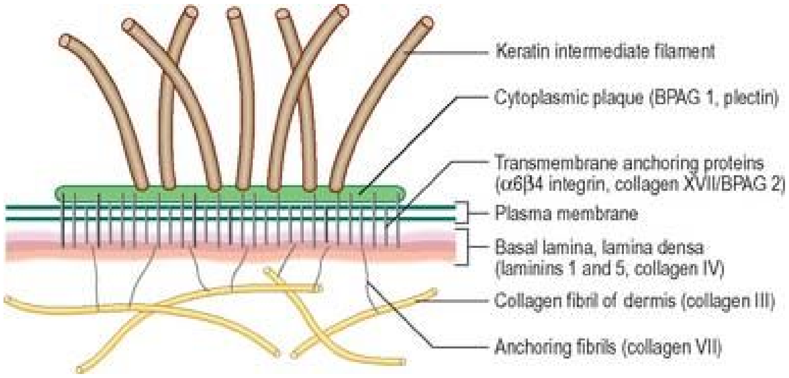
Keratin intermediate filament
Cytoplasmic plaque (BPAG 1, plectin)
Transmembrane anchoring proteins ($\alpha6\beta4$ integrin, collagen XVII/BPAG 2)
Plasma membrane
Basal lamina, lamina densa (laminins 1 and 5, collagen IV)
Collagen fibril of dermis (collagen III)
Anchoring fibrils (collagen VII)

Fig. 7.5 The major features of a hemidesmosome in the basement membrane zone (BMZ) of skin, including some of the important molecular components.

The majority of basal layer cells (Fig. 7.3) are columnar to cuboidal in shape, with large (relative to their cytoplasmic volume) mainly euchromatic nuclei and prominent nucleoli. The cytoplasm contains variable numbers of melanosomes and, characteristically, keratin filament bundles corresponding to the tonofilaments of classic electron microscopy. In the basal keratinocytes these keratins are mostly K5 and K14 proteins. The plasma membranes of apposed cells are connected by desmosomes, and the basal plasma membrane is linked to the basal lamina at intervals by hemidesmosomes (Fig. 7.5, see Fig. 1.5). Melanocytes (see Fig. 7.9), occasional Langerhans cells (see Fig. 7.3) and Merkel cells (see Fig. 3.30) are interspersed among the basal keratinocytes. Merkel cells are connected to keratinocytes by desmosomes, but melanocytes and Langerhans cells lack these specialized contacts. Intraepithelial lymphocytes are present in small numbers.

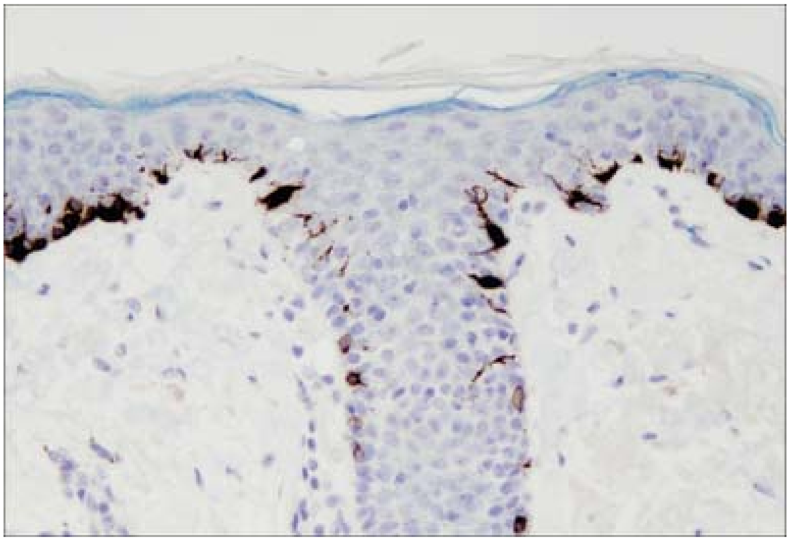

Fig. 7.9 Melanocytes in the basal layer of thin skin, including that of the follicular epidermis, in a biopsy of periauricular skin in a Caucasian male. The pigmented melanocytes, visualized immunocytochemically using antibody against a differentiation marker (Melan A/MART-1), extend dendritic processes between keratinocytes of the basal and lower prickle cell layers. Melanocytes are relatively inactive in this specimen, with no melanosomes visible in the surrounding keratinocytes.

At any one time the basal layer of the epidermis contains keratinocytes with different fates. These include multipotent stem cells. On division these may self-renew or produce a daughter cell which is committed to differentiate after undergoing further transit amplifying cell divisions. The activity of stem cells and transit amplifying cells in the basal layer provides a continuous supply of differentiating cells which enter the prickle cell layer. The great majority of these cells are postmitotic, although some cell division may occur in the more basal regions of the prickle cell layer. Stem cells are thought to reside mainly in the troughs of rete pegs, and in the outer root sheath bulge of the hair follicle, but they cannot easily be distinguished morphologically. The distribution of stem cells and the size of their proliferative units (see below) may be quite variable in human skin (Ghazizadeh & Taichman 2005).

The organization of the basal layer and overlying progeny cells is thought to form a series of columns. Several layers of prickle and granular cells overlie a cluster of six to eight basal cells, forming a columnar proliferative unit. Each group of basal cells consists of a central stem cell with an encircling ring of transit amplifying proliferative cells and postmitotic maturing cells. From the periphery of this unit, postmitotic cells transfer into the prickle cell layer. The normal total epidermal turnover time is between 52 and 75 days. In some pathologies of skin, turnover rates and transit times can be exceedingly rapid, e.g. in psoriasis, total epidermal turnover time may be as little as 8 days. The control of keratinocyte proliferation and differentiation is beyond the scope of this publication but is reviewed in Niemann & Watt (2002) and Byrne et al (2003).

Prickle cell layer

The prickle cell layer (Fig. 7.3, Fig. 7.6) consists of several layers of closely packed keratinocytes that interdigitate with each other by means of numerous cell surface projections. The cells are anchored to each other by desmosomes that provide tensile strength and cohesion to the layer. These suprabasal cells are committed to terminal differentiation and gradually move upwards towards the cornified layer as more cells are produced in the basal layer. When skin is processed for routine light microscopy, the cells tend to shrink away from each other except where they are joined by desmosomes, which gives them their characteristic spiny appearance. Prickle cell cytoplasm contains prominent bundles of keratin filaments, (mostly K1 and K10 keratin proteins) arranged concentrically around a euchromatic nucleus, and attached to the dense plaques of desmosomes. The cytoplasm also contains melanosomes, either singly or aggregated within membrane-bound organelles (compound melanosomes). Langerhans cells (see Fig. 7.11) and the occasional associated lymphocyte are the only non-keratinocytes present in the prickle cell layer.

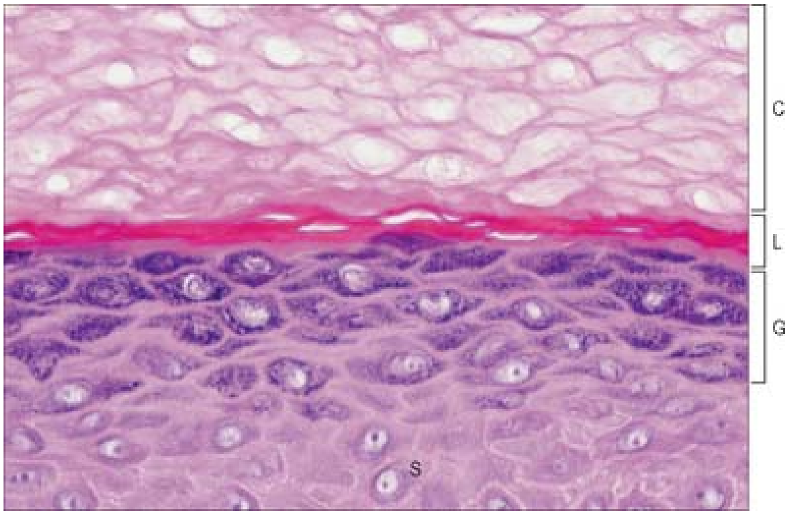

Fig. 7.6 The superficial layers of human thick skin at high magnification, showing the deeply stained keratohyalin granule-containing cells of the granular layer (G) between the prickle cell or spinous layer (S) and the clear (or lucid, L) and cornified (C) layers above. Note that the clear layer is only translucent in unstained preparations and appears eosinophilic, as here, after staining.

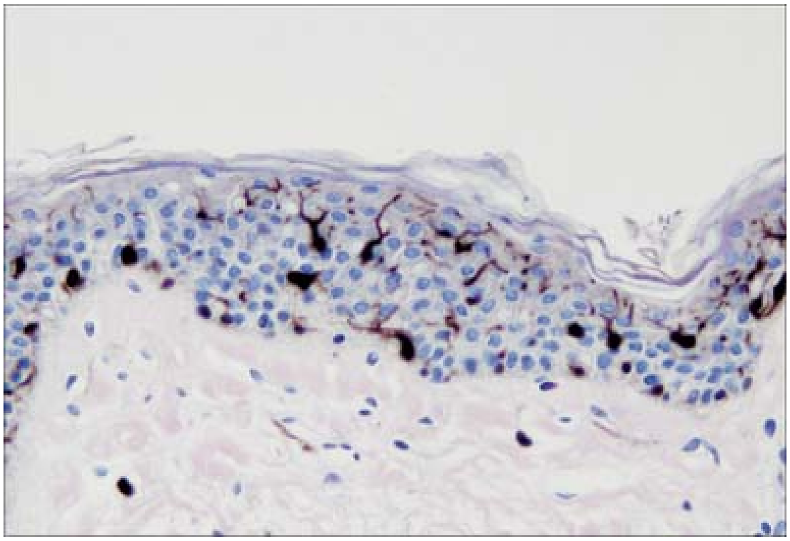

Fig. 7.11 Langerhans cells immunolabelled for the marker protein S100, extending dendrites between keratinocytes, mainly in the prickle cell layer of human thin skin. Basal layer melanocytes and scattered dermal cells (possibly of neural origin) are also positive for S100, visualized using a peroxidase method.

Granular layer

Extensive changes in keratinocyte structure occur in the three to four layers of flattened cells in the granular layer. The nuclei become pyknotic and begin to disintegrate; organelles such as ribosomes and membrane-bound mitochondria and Golgi bodies degenerate; and keratin filament bundles become more compact and associated with irregular, densely staining keratohyalin granules (Fig. 7.6). Small round granules (100 × 300 nm) with a lamellar internal structure (lamellar granules, Odland bodies, keratinosomes) also appear in the cytoplasm. Keratohyalin granules contain a histidine-rich, sulphur-poor protein (profilaggrin) which, when the cell reaches the cornified layer, becomes modified to filaggrin. The lamellar granules are concentrated deep to the plasma membrane, with which they fuse, releasing their hydrophobic glycophospholipid contents into the intercellular space within the layer and also between it and the cornified layer. They form an important component of the permeability barrier of the epidermis, rendering it relatively waterproof.

Clear layer

The clear layer is only found in thick palmar or plantar skin. It represents a poorly understood stage in keratinocyte differentiation. It stains more strongly than the cornified layer with acidic dyes (Fig. 7.6), is more refractile optically, and often contains nuclear debris. Ultrastructurally, its cells contain compacted keratin filaments and resemble the incompletely keratinized cells which are occasionally seen in the innermost part of the cornified layer of thin skin.

Cornified layer

The cornified layer (Fig. 7.3, Fig. 7.6) is the final product of epidermal differentiation, or cornification. It consists of closely packed layers of flattened polyhedral squames (Fig. 7.7), ranging in surface area from 800 to 1100 μm^2. These cells overlap at their lateral margins and interlock with cells of apposed layers by ridges, grooves and microvilli. In thin skin this layer may be only a few cells deep, but in thick skin it may be more than 50 cells deep. The plasma membrane of the squame appears thicker than that of other keratinocytes, partly due to the cross-linking of a soluble precursor, involucrin, at the cytoplasmic face of the plasma membrane, in the complex insoluble cornified envelope. The outer surface is also covered by a monolayer of bound lipid. The intercellular region contains extensive lamellar sheets of glycolipid derived from the lamellar granules of the granular layer. The cells lack a nucleus and membranous organelles, and consist solely of a dense array of keratin filaments embedded in a cytoplasmic matrix which is partly composed of filaggrin derived from keratohyalin granules.

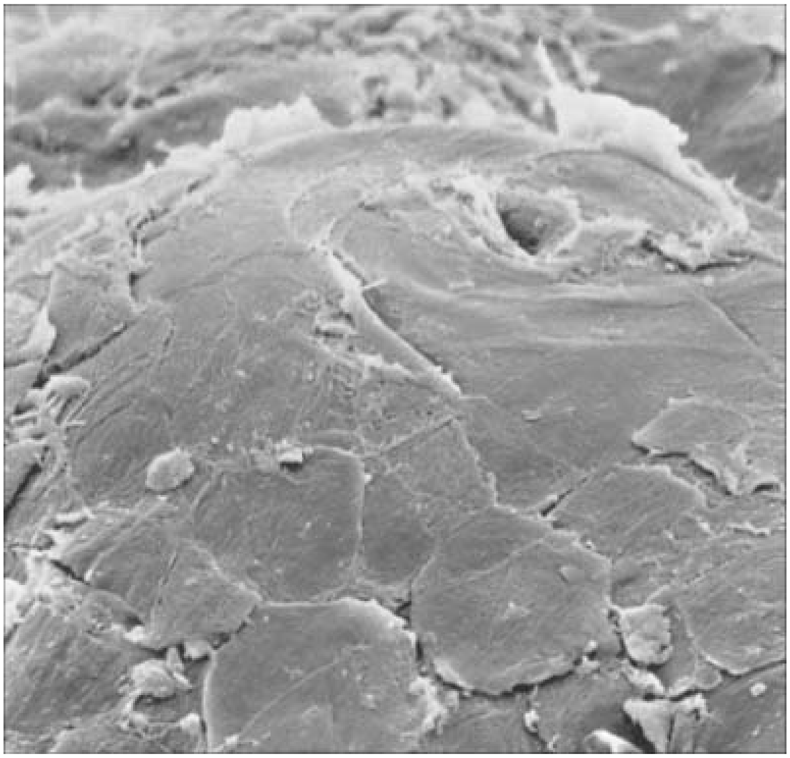

Fig. 7.7 The epidermal surface surrounding the aperture of a sweat duct. Several polygonal, scale-like keratinocytes (squames) of the superficial cornified layer are visible in this scanning electron micrograph.

Under normal conditions the production of epidermal keratinocytes in the basal layer is matched by loss of cells from the cornified layer.

Desquamation of these outer cells is normally imperceptible. When excessive, it appears in hairy regions as dandruff, and more extensively in certain diseases and, to a lesser extent, after sunburn, as peeling, scaling and exfoliation. The thickness of the cornified layer can be influenced by local environmental factors, particularly abrasion, which can lead to a considerable thickening of the whole epidermis including the cornified layer. The soles of the feet become much thickened if an individual habitually walks barefoot, and cornified pads develop in areas of frequent pressure, e.g. corns from tight shoes, palmar calluses in manual workers, and digital calluses in guitar players.

Keratins

Epidermal keratinization has historically been the term applied to the final stages of keratinocyte differentiation and maturation, during which cells are converted into tough cornified squames. However, this is now regarded as ambiguous because the term keratin is assumed to refer to the protein of epithelial intermediate filaments, rather than (as previously) to the whole complement of proteins in the terminally differentiated cell of the stratum corneum.

Keratins are the intermediate filament proteins found in all epithelial cells. There are two types, type I (acidic) and type II (neutral/basic); they form heteropolymers, are coexpressed in specific pairs and are assembled into 10 nm intermediate filaments. Fifty-four different keratin genes have been recognized and their protein products are numbered. The nomenclature for human keratins and keratin genes has recently been revised and is given in Schweizer et al (2006). Different keratin pairs are expressed according to epithelial cell differentiation; antibodies to individual keratins are useful analytical tools (Fig. 7.8). Keratins K5 and K14 are expressed by basal keratinocytes. New keratins, K1 and K10, are synthesized suprabasally. In the granular layer the filaments become associated with keratohyalin granules containing profilaggrin, a histidine-rich phosphorylated protein. As the cells pass into the cornified layer, profilaggrin is cleaved by phosphatases into filaggrin which causes aggregation of the filaments and forms the matrix in which they are embedded. Other types of keratin expression occur elsewhere, particularly in hair and nails, where highly specialized hard, or trichocyte, keratin is expressed. This becomes chemically modified and is much tougher than in the general epidermis. For a recent review of keratin function see Gu & Coulombe 2007.

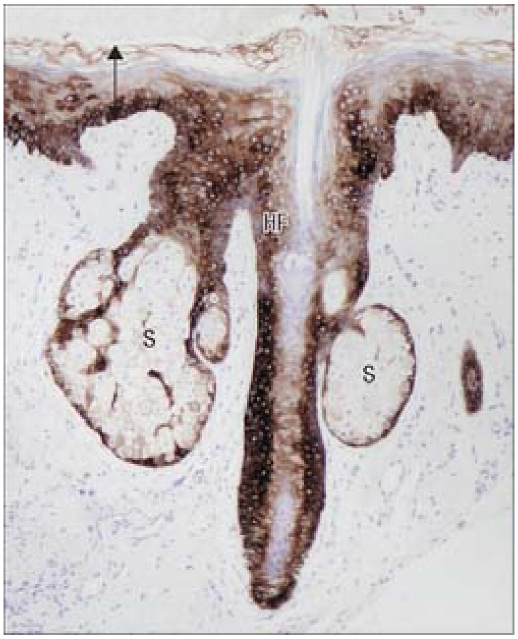

Fig. 7.8 Thin skin in the region of a human hair follicle, immunolabelled to detect keratins (including K5) in the basal and suprabasal interfollicular epidermis (between arrowheads), the hair follicle (HF) and associated sebaceous glands (S). The presence of keratins was visualized using a peroxidase technique.

Epidermal lipids

The epidermis serves as an important barrier to the loss of water and other substances through the body surface (apart from in sweating and sebaceous secretion). A variety of lipids are present and synthesized in the epidermis, including triglycerides and fatty acids, phospholipids, cholesterol, cholesterol esters, glycosphingolipids and ceramides. An intermediate in the synthesis of cholesterol, 7-dehydrocholesterol, is the precursor of vitamin D, which is also synthesized in the skin. The content and composition of epidermal lipids change with differentiation. Phospholipids and glycolipids at first accumulate within keratinocytes above the basal layer, but higher up they are broken down and are practically absent from the cornified layer. Cholesterol and its esters, fatty acids and ceramides accumulate towards the surface, and are abundant in the cornified layer. The lamellar arrangement of the extracellular lipids is a major factor in their barrier function.

Melanocytes

Melanocytes are melanin pigment-forming cells derived from the neural crest (Fig. 7.9, Fig. 7.10). They are present in the epidermis and its appendages, in oral epithelium, some mucous membranes, the uveal tract (choroid coat) of the eyeball, parts of the middle and internal ear and in the pial and arachnoid meninges at the base of the brain. The cells of the retinal pigment epithelium, developed from the outer wall of the optic cup, also produce melanin, and neurones in different locations within the brainstem (e.g. the locus coeruleus and substantia nigra) synthesize a variety of melanin called neuromelanin. True melanins are high molecular weight heteropolymers attached to structural protein. In humans there are two classes, the brown-black eumelanin, and the red-yellow phaeomelanin, both derived from the substrate tyrosine. Most natural melanins are mixtures of eumelanin and phaeomelanin, and phaeomelanic pigments, trichochromes, occur in red hair.

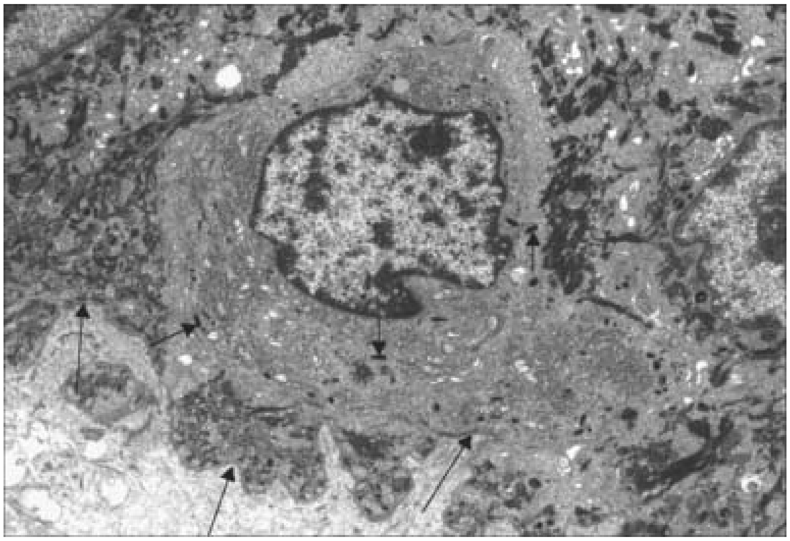

Fig. 7.10 Electron micrograph of a basal epidermal melanocyte, showing its nucleus and cytoplasm containing melanosomes (short arrows). There are no desmosomes connecting it with apposed keratinocytes. The cytoplasm of the keratinocytes is full of dense keratin filaments (absent from the melanocyte), as well as transferred melanosomes. The dermo-epidermal junction is indicated (long arrows). Human tissue.

Melanocytes are dendritic cells, and lack desmosomal contacts with apposed keratinocytes, though hemidesmosomal contacts with the basal lamina are present. In routine tissue preparations, melanocytes appear as clear cells in the basal layer of the epidermis; numbers per unit area of epidermis range from 2300 per mm^2 in cheek skin to 800 per mm^2 in abdominal skin. It is estimated that a single melanocyte may be in functional contact via its dendritic processes with up to 30 keratinocytes. The nucleus is large, round, and euchromatic, and the cytoplasm contains intermediate filaments, a prominent Golgi complex and vesicles and associated rough endoplasmic reticulum, mitochondria, and coated vesicles, together with a characteristic organelle, the melanosome.

The melanosome is a membrane-bound structure which undergoes a sequence of developmental stages during which melanin is synthesized and deposited within it by a tyrosine–tyrosinase reaction. Mature melanosomes move into the dendrites along the surfaces of microtubules and are transferred to keratinocytes through their phagocytic activity. Keratinocytes engulf and internalize the tip of the dendrite with the subsequent pinching off of melanosomes into the keratinocyte cytoplasm. Here, they may exist as individual granules in heavily pigmented skin, or be packaged within secondary lysosomes as melanosome complexes in lightly pigmented skin. In basal keratinocytes they can be seen to accumulate in a crescent-shaped cap over the distal part of the nucleus. As the keratinocytes progress towards the surface of the epidermis, melanosomes undergo degradation, and melanin remnants in the cornified layer form dust-like particles. Melanosomes are degraded more rapidly in Caucasian skin than in dark-skinned races, where melanosomes persist in cells of the more superficial layers.

Melanin has biophysical and biochemical properties related to its functions in skin. It protects against the damaging effects of UV radiation on DNA and is also an efficient scavenger of damaging free radicals. However a high concentration of melanin may adversely affect synthesis of vitamin D in darker-skinned individuals living in northern latitudes. Melanin pigmentation is both constitutive and facultative. Constitutive pigmentation is the intrinsic level of pigmentation and is genetically determined, whereas facultative pigmentation represents reversible changes induced by environmental agents, e.g. UV and X-radiation, chemicals, and hormones. Racial variations in pigmentation are due to differences in melanocyte morphology and activity rather than to differences in frequency or distribution. In naturally heavily pigmented skins the cells tend to be larger, more dendritic, and to contain more large, late-stage melanosomes than melanocytes of paler skins. The keratinocytes in turn contain more melanosomes, individually dispersed, whereas in light skins, the majority are contained within secondary lysosomes to form melanosome complexes.

Response to UV light includes immediate tanning, pigment darkening, which can occur within a matter of minutes, probably due to photo-oxidation of pre-existing melanin. Delayed tanning occurs after about 48 hours, and involves stimulation of melanogenesis within the melanocytes, and transfer of additional melanosomes to keratinocytes. There may also be some increase in size of active melanocytes, and in their apparent numbers, mainly through activation of dormant cells. Freckles in the skin of red-haired individuals are usually thought to be induced by UV, though they do not appear until several years after birth, despite exposure. Paradoxically, melanocytes are significantly fewer in freckles than in adjacent paler epidermis, but they are larger and more active. What determines the onset of freckles, or their individual location, is not known.

Adrenocorticotrophin (ACTH) is thought to affect melanocyte activity, and is probably responsible for the hyperpigmentation associated with pituitary and adrenal disorders. In pregnancy, higher levels of circulating oestrogens and progesterone are responsible for the increased melanization of the face, abdominal and genital skin, and the nipple and areola, much of which may remain permanently.

In albinism, the tyrosinase required for melanin synthesis is either absent or inactive, and melanocytes, though present, are relatively quiescent cells in an otherwise normal epidermis. Melanocytes decrease significantly in numbers in old age, and are absent from grey-white hair. For further reading on melanocyte function in health and disease, see Goding (2007).

Langerhans cells

Langerhans cells (Fig. 7.11) are immature dendritic antigen-presenting cells (see p. 79) regularly distributed throughout the basal and prickle cell layers of the epidermis and its appendages, apart from the sweat gland. They are also present in other stratified squamous epithelia, including the buccal, tonsillar and oesophageal epithelia, as well as the cervical and vaginal mucosae and the transitional epithelium of the bladder. They are found in the conjunctiva, but not in the cornea. In routine preparations they appear as clear cells, relatively high in the stratified layer. They enter the epidermis from the bone marrow during development to establish the postnatal population (460–1000/mm^2, 2–3% of all epidermal cells, with regional variations), and this is maintained by continual replacement from the marrow.

The nucleus is euchromatic and markedly indented and the cytoplasm contains a well-developed Golgi complex, lysosomes (which often contain ingested melanosomes), and a characteristic organelle, the Birbeck granule. The latter are discoid, cup-shaped, or have a distended vesicle resembling the head of a tennis racket; in section they often appear as a cross-striated rod 0.5 μm long and 30 nm wide. When stimulated by antigen, Langerhans cells migrate out of the epidermis to lymphoid tissues (see Fig. 4.14). Their numbers are increased in chronic skin inflammatory disorders, particularly of an immune aetiology, such as some forms of dermatitis.

Merkel cells

Merkel cells are present as clear oval cells, singly or in groups, in the basal layer of the epidermis, especially of thick skin. They are also present in the outer root sheath of some large hair follicles. Merkel cells are derived embryologically from the neural crest and are not related developmentally to keratinocytes, as was once thought. They can be distinguished histologically from other clear cells (melanocytes and Langerhans cells) only by immunohistochemical and ultrastructural criteria.

Short, stiff processes of their plasma membrane interdigitate with adjacent basal keratinocytes, to which the Merkel cell is attached by small desmosomes. The cytoplasm contains numerous closely-packed intermediate filaments (simple epithelial keratins, mostly K8 and K18 but also K19 and K20), and characteristic 80–110 µm dense-core granules. The basal plasma membrane is closely apposed to the membrane of an axonal terminal. Merkel cells are thought to function as neuroendocrine sensory receptors, and are slowly adapting mechanoreceptors which respond to directional deformations of the epidermis and direction of hair movement by releasing a transmitter from their dense-core cytoplasmic granules.

DERMIS

The dermis (Fig. 7.1, Fig. 7.4, see Fig. 7.17) is an irregular, moderately dense connective tissue. It has a matrix composed of an interwoven collagenous and elastic network in an amorphous ground substance of glycosaminoglycans, glycoproteins and bound water, which accommodates nerves, blood vessels, lymphatics, epidermal appendages and a changing population of cells. Mechanically, the dermis provides considerable strength to the skin by virtue of the number and arrangement of its collagen fibres (which give it tensile strength), and its elastic fibres (which give it elastic recoil). The density of its fibre meshwork, and therefore its physical properties, varies within an area, in different parts of the body, and with age and sex. The dermis is vital for the survival of the epidermis, and important morphogenetic signals are exchanged at the interface between the two both during development and postnatally. The dermis can be divided into two zones, a narrow superficial papillary layer and a deeper reticular layer: the boundary between them is indistinct.

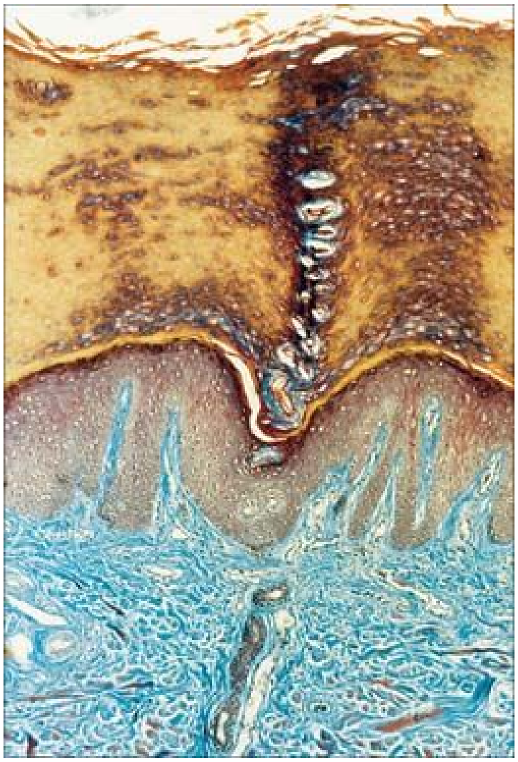

Fig. 7.17 A sweat duct in thick skin (trichrome-stained), spiralling through the dermis and epidermis, visible most clearly in the cornified superficial layer.

Adult dermal collagen is mainly of types I and III, in proportions of 80–85% and 15–20% respectively. The coarser-fibred type I is predominant in the deeper, reticular dermis, and the finer type III is found in the papillary dermis and around blood vessels. Type IV collagen is found in the basal lamina between epidermis and dermis, around Schwann cells of peripheral nerves and endothelial cells of vessels. Types V, VI and VII are minor collagenous components of the dermis. Elastic fibres form a fibrous network interwoven between the collagen bundles throughout the dermis, and are more prominent in some regions, e.g. the axilla.

Two major categories of cell are present in postnatal dermis, permanent and migrant, as is typical of all general connective tissues (see Ch. 2). The permanent resident cells include cells of organized structures such as nerves, vessels and cells of the arrector pili muscles, and the fibroblasts, which synthesize all components of the dermal extracellular matrix. The migrant cells originate in the bone marrow (Fig. 4.12) and include macrophages, mast cells, eosinophils, neutrophils, T and B cells (including antibody-secreting plasma cells), and dermal interstitial dendritic cells which are capable of immune surveillance and antigen presentation.

Layers of the dermis

Papillary layer

The papillary layer is immediately deep to the epidermis (Fig. 7.4), and is specialized to provide mechanical anchorage, metabolic support, and trophic maintenance to the overlying epidermis, as well as supplying sensory nerve endings and blood vessels. The cytoskeleton of basal epidermal keratinocytes is linked to the fibrous matrix of the papillary dermis through the attachment of keratin filament bundles to hemidesmosomes, then via anchoring filaments of the basal lamina, to the anchoring fibrils of type VII collagen which extend deep into the papillary dermis (Fig. 7.5). This arrangement provides a mechanically stable substratum for the epidermis.

The superficial surface of the dermis is shaped into numerous papillae or rete ridges, which interdigitate with rete pegs in the base of the epidermis and form the dermo-epidermal junction at their interface. The papillae have round or blunt apices which may be divided into several cusps. In thin skin, especially in regions with little mechanical stress and minimal sensitivity, papillae are few and very small, while in the thick skin of the palm and sole of the foot they are much larger, closely aggregated, and arranged in curved parallel lines following the pattern of ridges and grooves on these surfaces (Fig. 7.1). Lying under each epidermal surface ridge are two longitudinal rows of papillae, one on either side of the epidermal rete pegs through which the sweat ducts pass on the way to the surface. Each papilla contains densely interwoven, fine bundles of types I and III collagen fibres and some elastic fibrils. Also present is a capillary loop (Fig. 7.4), and in some sites, especially in thick hairless skin, Meissner's corpuscle nerve endings.

Reticular layer

The reticular layer merges with the deep aspect of the papillary layer. Its bundles of collagen fibres are thicker than those in the papillary layer and interlace with them and with each other to form a strong but deformable three-dimensional lattice, in which many fibres are parallel to each other, and which contain a variable number of elastic fibres. The predominant orientation of the collagen fibres may be related to the local mechanical forces on the dermis and thus may be involved in the development of skin lines.

Hypodermis

Also known as the superficial fascia, the hypodermis is a layer of loose connective tissue of variable thickness which merges with the deep aspect of the dermis. It is often adipose, particularly between the dermis and musculature of the body wall. It mediates the increased mobility of the skin, and the adipose component contributes to thermal insulation, acts as a shock absorber and constitutes a store of metabolic energy. Subcutaneous nerves, vessels and lymphatics travel in the hypodermis, their main trunks lying in its deepest part, where adipose tissue is scant. In the head and neck, the hypodermis also contains muscles, such as platysma, which are remnants of more extensive sheets of skin-associated musculature found in other mammals.

The quantity and distribution of subcutaneous fat differs in the sexes. It is generally more abundant and widely distributed in females. In males it diminishes from the trunk to the extremities, and this distribution is more obvious in middle age, when the total amount increases in both sexes. The amount of adipose tissue in the hypodermis, as elsewhere, reflects the quantity of lipid stored in its adipocytes rather than a change in the number of cells. There is an association with climate (rather than race), and superficial fat is more abundant in colder geographical regions. The hypodermis is most distinct on the lower anterior abdominal wall, where it contains much elastic tissue and appears many-layered as it passes through the inguinal regions into the thighs. It is similar in the limbs and the perineum, but is thin where it passes over the dorsal aspects of the hands and feet, the sides of the neck and face, around the anus, and over the penis and scrotum. It is almost absent from the external ears but is particularly dense in the scalp, palms and soles, where it is crossed by numerous strong connective tissue bands binding the hypodermis and skin to underlying structures: these are part of the deep fascia, but are known regionally as aponeuroses of the scalp, palm and sole.

PILOSEBACEOUS UNIT

The pilosebaceous unit consists of the hair and its follicle with an associated arrector pili muscle, sebaceous gland, and sometimes an apocrine gland (Fig. 7.1, Fig. 7.12). Not all elements of the unit occur together in all body regions.

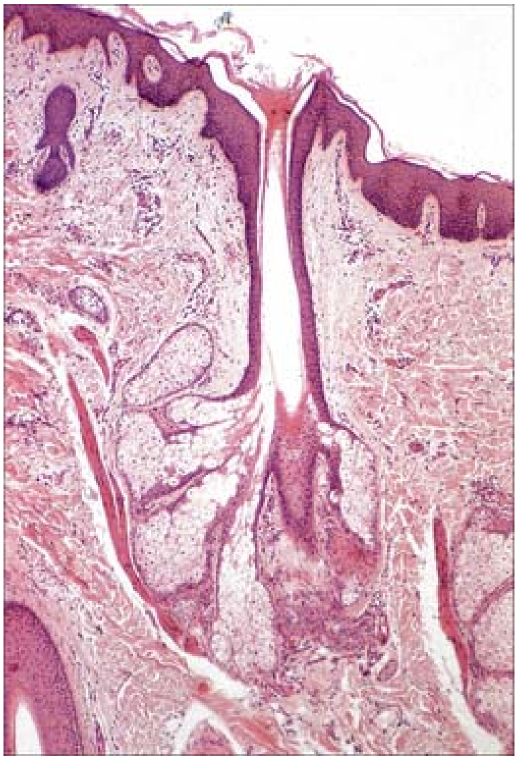

Fig. 7.12 A pilosebaceous unit in thin, hairy skin seen at low magnification. The hair follicle, hair shaft and hair root extend almost vertically through the field, the follicle joining the interfollicular epidermis (top). To the left of the follicle are the acini of a sebaceous gland, which is also sectioned tangentially through its capsule (centre bottom, below the portion of the hair follicle in section); the gland opens into the follicle in centre field. The associated arrector pili smooth muscle (thin red fibre bundle) is seen to the left of the sebaceous gland, following its contours.

Hairs

Hairs are filamentous cornified structures present over almost the entire body surface. They grow out of the skin at a slant (Fig. 42.1) as is evident in the sloping of the hairs on the dorsum of forearm, hand and fingers towards the ulnar side. Hairs are absent from several areas of the body, including the thick skin of the palms, soles, the flexor surfaces of the digits, the thin skin of the umbilicus, nipples, glans penis and clitoris, the labia minora and the inner aspects of the labia majora and prepuce. The presence, distribution and relative abundance of hair in certain regions such as the face (in males), pubis and axillae, are secondary sexual characteristics which play subtle roles in sociosexual communication. There are racial variations in density, form, distribution and pigmentation, as well as individual variations. Hairs assist minimally in thermoregulation: on the scalp they provide some protection against injury and the harmful effects of solar radiation. They have a sensory function.

Hairs vary from approximately 600 per cm^2 on the face to 60 per cm^2 on the rest of the body. In length they range from less than a millimetre to more than a metre, and in width from 0.005 to 0.6 mm. They vary in form, being straight, coiled, helical or wavy, and differ in colour depending on the type and degree of pigmentation. Curly hairs tend to have a flattened cross-section, and are weaker than straight hairs. In general, body hairs are longest and coarsest in Caucasians and least noticeable in Mongolian races. Over most of the body surface hairs are short and narrow (vellus hairs) and in some areas these hairs do not project beyond their follicles, e.g. in eyelid skin. In other regions they are longer, thicker and often heavily pigmented (terminal hairs); these include the hairs of the scalp, the eyelashes and eyebrows and the postpubertal skin of the axillae and pubis, and the moustache, beard and chest hairs of males. The presence in females of coarse terminal hairs in a male-like pattern is termed hirsutism and is usually a sign of an endocrine disorder and excess androgen production (Azziz 2003).

Hair follicle

The hair follicle (Fig. 7.1, Fig. 7.12, Fig. 7.13A) is a downgrowth of the epidermis containing a hair, which may extend deeply (3 mm) into the hypodermis, or may be more superficial (1 mm) within the dermis. Typically, the long axis of the follicle is oblique to the skin surface; with curly hairs it is also curved. There are cycles of hair growth and loss, during which the follicle presents different appearances. In the anagen phase the hair is actively growing and the follicle is at its maximum extent of development. In the involuting or catagen phase, hair growth ceases and the follicle shrinks. During the resting or telogen phase the inferior segment of the follicle is absent. This is succeeded by the next anagen phase. Further details of the hair growth cycle are given below, after the description of the anagen follicle and hair.

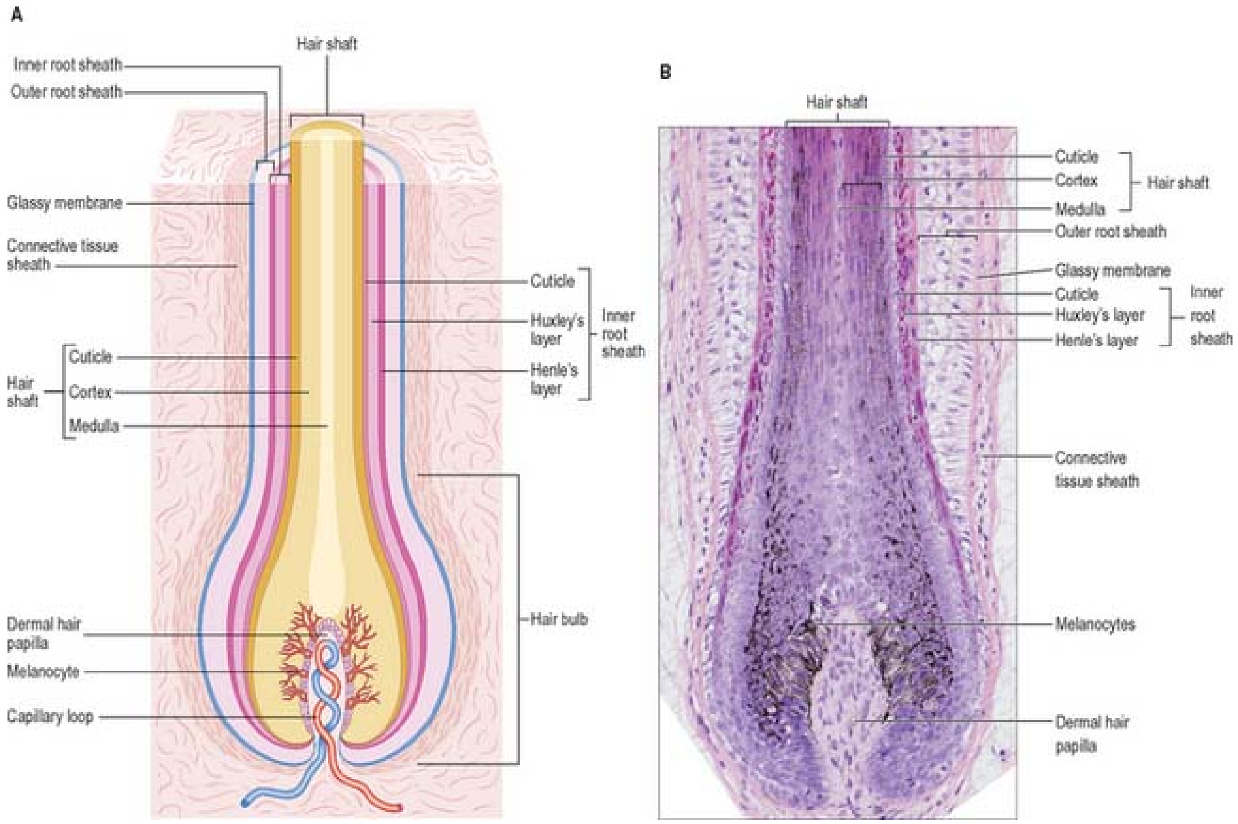
A
Hair shaft
Inner root sheath
Outer root sheath
Glassy membrane
Connective tissue sheath
Cuticle
Huxley's layer
Henle's layer
Inner root sheath
Hair shaft
Cuticle
Cortex
Medulla
Hair bulb
Dermal hair papilla
Melanocyte
Capillary loop
B
Hair shaft
Cuticle
Cortex
Medulla
Hair shaft
Outer root sheath
Glassy membrane
Cuticle
Huxley's layer
Henle's layer
Inner root sheath
Connective tissue sheath
Melanocytes
Dermal hair papilla

Fig. 7.13 **A**, The major structural features of the base of a hair follicle, showing the organization of the major layers of the hair and surrounding sheath, arising from the hair bulb. A dermal hair papilla invaginates the bulb, and along the basal layer of the epidermis, at its interface with the dermis, melanocytes insert their dendrites among the keratinocytes forming the hair. **B**, The hair bulb at the base of the human hair follicle. The dermal

hair papilla invaginates the bulb from its fibrous outer sheath, carrying a loop of capillaries. Melanocytes in the germinal matrix (equivalent to the basal layer of interfollicular epidermis) extend dendrites into the adjacent layers of keratinocytes, to which they pass melanosomes. The layers of the hair shaft and root sheaths are also indicated.

Anagen follicle

The anagen follicle has several regions. The deepest is the inferior segment which includes the hair bulb region extending up to the level of attachment of the arrector pili muscle at the follicular bulge. Between this point and the site of entry of the sebaceous duct is the isthmus, above which is the infundibulum, or dermal pilary canal, which is continuous with the intraepidermal pilary canal. Below the sebaceous duct, the hair shaft and follicular wall are intimately connected, and it is only towards the upper end of the isthmus that the hair becomes free in the pilary canal. Below the infundibulum the follicle is surrounded by a thick perifollicular dermal coat containing type III collagen, elastin, sensory nerve fibres and blood vessels, and into which the arrector pili muscle fibres blend. A thick, specialized basal lamina, the glassy membrane, marks the interface between dermis and the epithelium of large hair follicles.

Hair bulb

The hair bulb forms the lowermost portion of the follicular epithelium and encloses the dermal hair papilla of connective tissue cells (Fig. 7.13B). The dermal hair papilla is an important cluster of inductive mesenchymal cells which is required for hair follicle growth in each cycle throughout adult life: it is a continuation of the layer of adventitious mesenchyme that follows the contours of the hair follicle. The hair bulb generates the hair and its inner root sheath. A hypothetical line drawn across the widest part of the hair bulb divides it into a lower germinal matrix and an upper bulb. The germinal matrix is formed of closely packed, mitotically active pluripotential keratinocytes, among which are interspersed melanocytes, and some

Langerhans cells. The upper bulb consists of cells arising from the matrix. These migrate apically and differentiate along several lines. Those arising centrally form the hair medulla. Radially, successive concentric rings of cells give rise to the cortex and cuticle of the hair and outside this, to the three layers of the inner root sheath. The latter are, from within out, the cuticle of the inner root sheath, Huxley's layer and Henle's layer. Henle's layer is surrounded by the outer root sheath, which forms the cellular wall of the follicle (Fig. 7.13). Differentiation of cells in the various layers of the hair and its inner root sheath begins at the level of the upper bulb and is asynchronous, beginning earliest in Henle's layer and Huxley's layer.

Structure of hair and its sheaths

A fully developed hair shaft consists of three concentric zones which are, from outwards in, the cuticle, cortex and medulla. Each has different types of keratin filament proteins and different patterns of cornification. In finer hairs the medulla is usually absent. The cuticle forms the hair surface and consists of several layers of overlapping cornified squames directed apically and slightly outwards (Fig. 7.14). Immature cuticle cells have dense amorphous granules aligned predominantly along the outer plasma membrane with a few filaments. The cortex forms the greater part of the hair shaft and consists of numerous closely packed, elongated squames which may contain nuclear remnants and melanosomes. Immature cortical cells contain bundles of closely packed filaments but no dense granules, and when fully cornified, they have a characteristic thumb-print appearance with filaments arranged in whorls. The medulla, when present, is composed of loosely aggregated and often discontinuous columns of partially disintegrated cells containing vacuoles, scattered filaments, granular material and melanosomes. Air cavities lie between the cells or even within them.

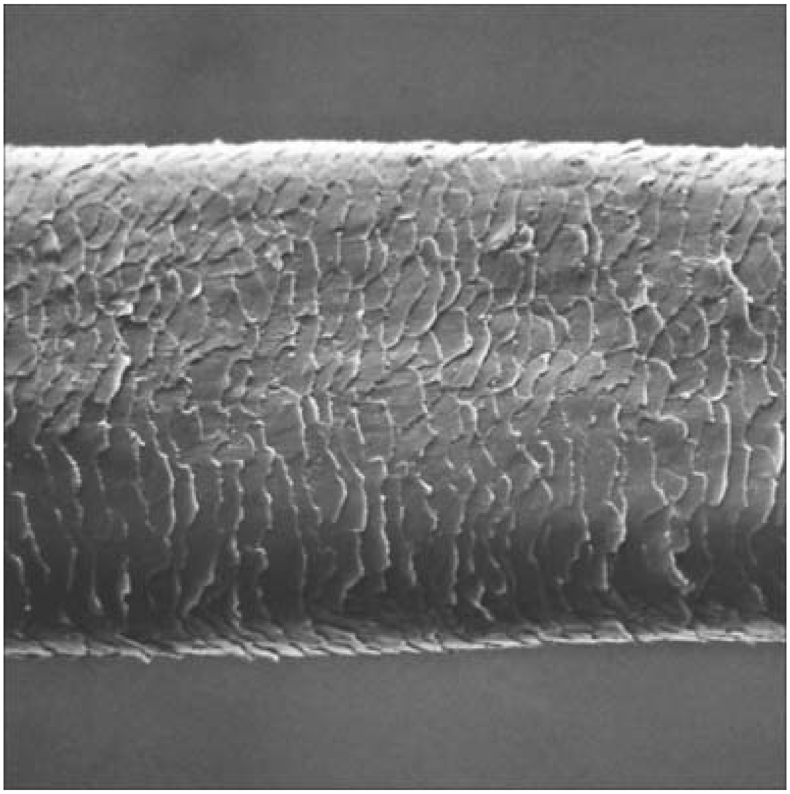

Fig. 7.14 A scalp hair showing details of surface structure as seen in the scanning electron microscope. Note that the cuticular cells overlap each other; their free ends point towards the apex of the hair.

(By courtesy of Michael Crowder.)

Henle’s layer and Huxley’s layer of the inner root sheath contain irregular dense keratohyalin granules and associated filaments in the precornified state. At the level of the upper bulb, Henle’s layer begins to cornify, as does Huxley’s layer at the middle of the inferior follicle. When fully differentiated, cells of both layers have a thickened cornified envelope enclosing keratin filaments embedded in a matrix. The cells of the inner root sheath cuticle undergo terminal differentiation at a level closer to the hair bulb than that of Huxley’s layer, but lack a clear-cut filament pattern such as is seen in the cortical cells of the hair shaft. As they cornify, the cuticle cells of the inner root sheath and hair become interlocked. At about the level of entry of the sebaceous duct, above the isthmus, the inner root sheath undergoes fragmentation, and the hair then lies free in the pilary canal.

The outer root sheath, beginning at the level of the upper bulb, is a single or double layer of undifferentiated cells containing glycogen. Higher up the follicle it becomes multilayered. At the isthmus all remaining cell layers of the follicle sheath become flattened, compressed and attenuated. On emerging from the isthmus, the outer root sheath assumes the stratified, differentiating characteristics of interfollicular epidermis, with which it becomes continuous. At the level of entry of the sebaceous duct, it forms the wall of the pilary canal.

Hair cycle and growth of hair

Recurrent cyclic activity of hair follicles involves growth, rest, and shedding of hair in phases. In humans, these occur in irregular cycles of variable duration: there are regional and other variations in the length of the individual phases. In the growing or anagen phase, follicle and hair are as described above. Melanocytes are active only in mid-anagen, and are capable of producing both phaeo- and eumelanosomes, which they pass to precortical and medullary keratinocytes. Changes in hair colour of an individual, usually in adolescence, are due to alterations in the dominant type of melanosome produced.

Anagen is followed by the involuting or catagen phase during which mitotic activity of the germinal matrix ceases, the base of the hair condenses into a club which moves upwards to the level of the arrector pili muscle, and the whole inferior segment of the follicle degenerates. The dermal papilla also ascends and remains close to the base of the shortened follicle and its enclosed club hair, a situation which persists during the resting or telogen phase. During telogen, melanocytes become amelanotic and can be identified only ultrastructurally. At the beginning of the next anagen, the epithelial cells at the base of the follicle divide to form a secondary hair rudiment which envelops the dermal papilla to form a new hair bulb. This grows downwards, reforming the inferior segment of the follicle, from which a new hair grows up alongside the club hair, which is eventually shed.

Postnatally, hairs exhibit regional asynchrony of cycle duration and phase leading to an irregular pattern of growth and replacement. In some regions, such as the scalp, the cycle is measured in years; in others, such as general body hair, the cycle is much shorter and hairs are therefore limited in length. At puberty, hair growth and generation of much thicker hairs occurs on the pubes and axillae in both sexes, and on the face and trunk in males. The actions of hormones on hair growth are complex, and involve not only sex hormones, but also those of the thyroid, suprarenal cortex and pituitary glands. Androgens stimulate facial and general body hair formation. After about the first 30 years, they tend to cause the thick terminal hairs of the scalp to change to small vellus hairs, which produces recession from the forehead and sometimes almost complete male pattern baldness. In females, oestrogens tend to maintain vellus hairs: postmenopausal reduction of oestrogens may permit stronger facial and bodily hair growth. In mid-pregnancy, hair growth may be particularly active but later, often post-partum, an unusually large number of hairs enter the telogen phase and are shed before the growth cycle recommences. In older men, growth of hairs on the eyebrows and within the nostrils and external ear canals increases, whereas elsewhere on the body, growth slows and the hairs become much finer.

Measurements of the rate of growth of individual hairs vary considerably, probably because of the influence of the factors mentioned above. A rate of 0.2–0.44 mm per 24 hours in males is usually given: the higher rate occurs on the scalp. Contrary to popular myth, shaving does not appear to affect the growth rate and hair ceases growth after death.

Sebaceous glands

Sebaceous glands are small saccular structures (Fig. 7.1, Fig. 7.12, Fig. 7.15) lying in the dermis; together with the hair follicle and arrector pili muscle, they constitute the pilosebaceous unit. They are present over the whole body except the thick hairless skin of the palm, soles and flexor surfaces of digits. Typically, they consist of a cluster of secretory acini which open by a short common duct into the dermal pilary canal of the hair follicle. They release their lipid secretory product, sebum, into the canal by a holocrine mechanism (see Ch. 2). In some areas of thin skin which lack hair follicles, their ducts open instead directly on to the skin surface, e.g. on the lips and corners of the mouth, the buccal mucosa, nipples, female breast areolae, penis, inner surface of the prepuce, clitoris and labia minora. At the margins of the eyelids, the large complex palpebral tarsal glands (Meibomian glands) are of this type. They are also present in the external auditory meatus.

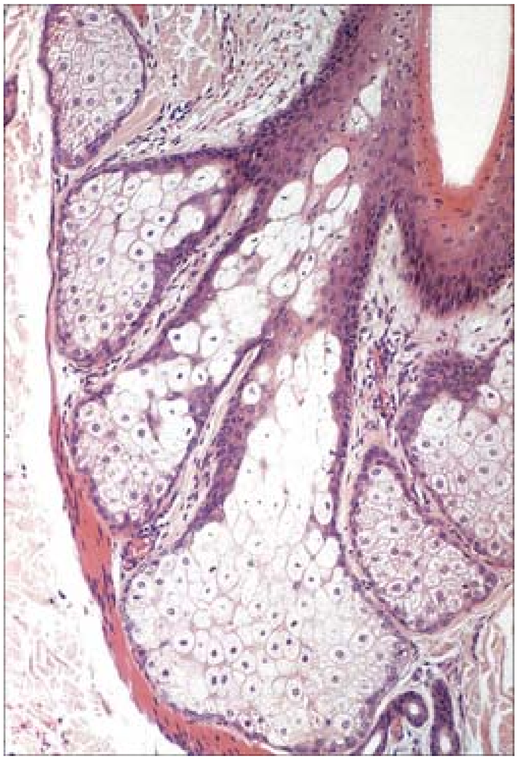

Fig. 7.15 A sebaceous gland, showing a group of secretory acini opening into a hair follicle (top right). The distended sebocytes are filled with their oily secretion (sebum), which is discharged into the hair follicle by the holocrine disintegration of secretory cells.

In general, numbers of sebaceous glands in any given area reflect the distribution of hair follicles, ranging from an average of 100/cm^2 over most of the body to as many as 400–900/cm^2 on the face and scalp. They are also numerous in the midline of the back. Individual sebaceous glands are particularly large on the face, around the external auditory meatus, chest and shoulders, and on the anogenital surfaces. Those on the face are often related to very small vellus hairs whose follicles have particularly wide apertures.

Microscopically, the glandular acini are enclosed in a basal lamina supported by a thin dermal capsule and a rich capillary network. Each acinus is lined by a single layer of small, flat, polygonal epithelial cells (sebocytes) which ultrastructurally resemble undifferentiated basal keratinocytes of interfollicular epidermis. They possess euchromatic nuclei and large nucleoli, scattered keratin filaments, free ribosomes, smooth endoplasmic reticulum and rounded mitochondria, and are attached to each other by desmosomes. Functionally, they are mitotically active stem cells whose progeny move gradually towards the centre of the acinus, increasing in volume and accumulating increasingly large lipid vacuoles. The nuclei become pyknotic as the cells mature. The huge distended cells ultimately disintegrate, filling the central cavity and its duct with a mass of fatty cellular debris (Fig. 7.15). The process takes 2–3 weeks. The secretory products pass through a wide duct lined with keratinized stratified squamous epithelium into the infundibulum of the hair follicle and then to the surface of the hair and the general epidermis.

The normal functions of sebum are the provision of a protective coating on hairs, possibly helping to waterproof the epidermis, discouragement of ectoparasites and contribution to a characteristic body odour. When first formed, sebum is a complex mixture of over 50% di- and triglycerides, with smaller proportions of wax esters, squalene, cholesterol esters, cholesterol and free fatty acids. At birth, sebaceous glands are quite large, regressing later until stimulated again at puberty. At that time, sebaceous gland growth and secretory activity increase greatly in both males and females, under the influence of androgens (testicular and suprarenal), which act directly on the gland. Excessive amounts of sebum may become impacted within the duct, and this, associated with hyperkeratinization, may lead to blockage and formation of a comedone. This may become infected and inflamed, and is the primary lesion of acne. Oestrogens have an effect opposite to that of androgens, and sebum secretion is considerably lower in women, becoming greatly decreased after the age of 50 years.

Apocrine glands

Apocrine glands are particularly large glands of the dermis or hypodermis, classed as a type of sweat gland. Since they develop as outgrowths of the hair follicle and discharge secretion into the hair canal, they are considered here. In the adult, they are present in the axillae, perianal region, areolae, periumbilical skin, prepuce, scrotum, mons pubis and labia minora. Ceruminous glands of the external auditory meatus and the ciliary glands of the palpebral margins (Moll's glands) are also usually included in this category, but their secretions are quite different and they should be considered as distinct, specialized subtypes.

An apocrine gland consists of a basal secretory coil and a straight duct which opens into either the pilary canal above the duct of the sebaceous gland, or directly onto the skin surface if there is no associated hair. The secretory region may be as much as 2 mm wide and its coils often anastomose to form a labyrinthine network. Each coil is lined by cuboidal secretory cells whose apical cytoplasm projects into the lumen and basally is in contact with a layer of myoepithelial cells within a thick basal lamina. The secretory cells contain vacuoles, vesicles and dense granules of varying size and internal structure: the numbers and character vary with the cycle of synthesis and discharge. The mechanism of secretion is still not clear, but may involve merocrine secretion of granules, apocrine secretion or complete holocrine disintegration of the cells (see Fig. 2.5).

Apocrine activity is minimal before puberty, after which it is androgen dependent and responsive to emotional stimuli. It is controlled by adrenergic nerves, and is sensitive to adrenaline (epinephrine) and noradenaline (norepinephrine). The secretion is initially sterile and odourless, but it undergoes bacterial decomposition to generate potent odorous, musky compounds, including short-chain fatty acids, and steroids such as 5α-androstenone. In many animals these are potent pheromonal signals but their role in humans is less certain. Obstruction of apocrine sweat ducts and associated upper hair follicles in the axillae, breast areolae and pubic region, mainly in women, is thought to underlie Fox–Fordyce disease.

Arrector pili muscles

The arrector pili muscles are small bundles of closely packed smooth muscle cells which form oblique links between the dermal sheaths of hair follicles and the papillary layer of the dermis (Fig. 7.1, Fig. 7.12). They show the typical features of smooth muscle cells and are separated by narrow spaces containing collagen fibres and unmyelinated noradrenergic sympathetic axons.

The muscles are attached to the bulge region of the follicles by elastin fibrils, and are directed obliquely and towards the side to which the hair slopes superficially. The sebaceous gland occupies the angle between the muscle and the hair follicle, and muscle contraction helps to expel the gland contents. Contraction tends to pull the hair into a more vertical position and to elevate the epidermis surrounding it into a small hillock (goose bump), dimpling the skin surface where the muscle is inserted superficially. Arrector pili muscles are absent from facial, axillary, and pubic hairs, from eyelashes and eyebrows, and from the hairs around the nostrils and the external auditory meatuses.

SWEAT GLANDS

The vast majority of sweat glands (Fig. 7.16) are often classified as eccrine, although their mode of secretion includes typical merocrine mechanisms (see Ch. 2). They are long unbranched tubular structures, each with a highly coiled, secretory portion up to 0.4 mm in diameter, situated deep in the dermis or hypodermis. From there, a narrower, straight or slightly helical ductal portion emerges (Fig. 7.1). The walls of the duct fuse with the base of epidermal rete pegs and the lumen passes between the keratinocytes, often in a tight spiral, particularly in thick hairless skin (Fig. 7.17), and opens via a rounded aperture (pore) onto the skin surface (Fig. 7.7). In thick hairless skin, sweat glands discharge along the centres of friction ridges, incidentally providing fingerprint patterns for forensic analysis. Sweat glands have an important thermoregulatory function, they contribute significantly to excretion and their secretion enhances grip and sensitivity of the palms and soles.

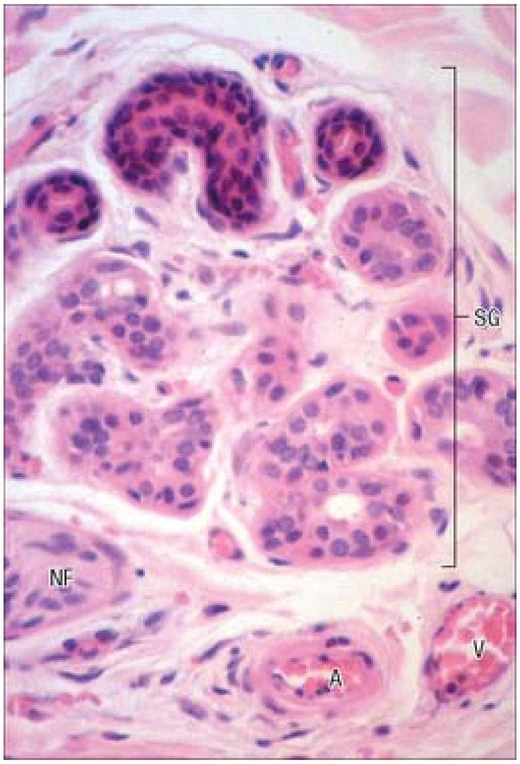

Fig. 7.16 The coiled secretory portion of a sweat gland (SG) in the reticular dermis. The deeper-stained profiles (above) are the origins of the duct. An autonomic nerve fibre (NF) and accompanying arteriole (A) and venule (V) are seen below.

Sweat glands are absent from the tympanic membrane, margins of the lips, nail bed, nipple, inner preputial surface, labia minora, penis and clitoris, where apocrine glands are located. Elsewhere they are numerous, their frequency ranging from 80 to over 600/cm^2, depending on position and genetic variation. The total number lies between 1.6 and 4.5 million, and is greatest on the plantar skin of the feet. There are many sweat glands on the face and flexor aspects of the hands, and fewest on the surfaces of the limbs. Racial groups indigenous to warmer climates tend to have more sweat glands than those indigenous to cooler regions.

Microscopically the secretory coil consists of a pseudostratified epithelium enclosing a lumen. Three types of cell have been described: clear cells from which most of the secretion derives, dark cells which share the same lumen, and myoepithelial cells. Clear cells are approximately pyramidal in shape, and their bases rest on the basal lamina or contact myoepithelial cells. Their apical plasma membranes line lateral intercellular canaliculi which connect with the main lumen. The basolateral plasma membranes are highly folded, interdigitating with apposed clear cells, and they have the basal membrane infoldings typical of cells involved in fluid and ion transport. Their cytoplasm contains glycogen granules, mitochondria, rough endoplasmic reticulum and a small Golgi complex, but few other organelles. The nucleus is round and moderately euchromatic. Dark cells are pyramidal, and lie closer to the lumen such that their broad ends form its lining. Their cytoplasm contains a well-developed Golgi complex, numerous vacuoles and vesicles and dense glycoprotein granules which they secrete by a typical merocrine mechanism. Myoepithelial cells resemble those associated with secretory acini of the salivary glands and breast, and contain abundant myofilaments.

The intradermal sweat duct is formed of an outer basal layer and an inner layer of luminal cells connected by numerous desmosomes. The intraepidermal sweat duct (acrosyringium) is coiled, and consists of two layers of cells which, developmentally, are different from the surrounding keratinocytes and can be distinguished from them by the presence of keratin K19. The outer cells near the surface contain keratohyalin granules and lamellar granules, and undergo typical cornification. The inner cells, from a midepidermal level, contain numerous vesicles, undergo an incomplete form of cornification, and are largely shed into the lumen at the level of the cornified epidermal layer.

Sweat is a clear, odourless fluid, hypotonic to tissue fluid, and contains mainly sodium and chloride ions, but also potassium, bicarbonate, calcium, urea, lactate, amino acids, immunoglobulins and other proteins. Excessive sweating can lead to salt depletion. Heavy metals and various organic compounds are eliminated in sweat, the greater part of which is thought to be produced by the clear cells. When first secreted, the fluid is similar in composition to interstitial fluid. It is modified as it passes along the duct by the action mainly of the basal cells, which resorb sodium and chloride and some water. The hormone aldosterone enhances this activity. The sweat glands are capable of producing up to 10 litres of sweat per day, in response to thermal, emotional and taste stimuli, mediated by unmyelinated sympathetic cholinergic fibres; the glands also respond to adrenaline. Thermoregulation involves a heat centre in the hypothalamus which reacts to changes in blood temperature and afferent stimuli from the skin, by controlling cutaneous blood supply and the rate and volume of sweat secretion for evaporation at the surface.

NAIL APPARATUS

Nails (Fig. 7.18) are homologous with the cornified layer of the general epidermis. They consist of compacted, anucleate, keratin-filled squames in two or three horizontal layers. Ultrastructurally, the squames contain closely packed filaments which lie transversely to the direction of proximodistal growth, and are embedded in a dense protein matrix. Unlike the general epidermis, squames are not shed from the nail plate surface. A variety of mineral elements are present in nail, including calcium. Calcium is not responsible for the hardness of nail: this is determined by the arrangement and cohesion of the layers of squames, and their internal fibres. The water content of nail is low, but nail is 10 times more permeable to water than the general epidermis. The softness and elasticity of the nail plate is related to its degree of hydration.

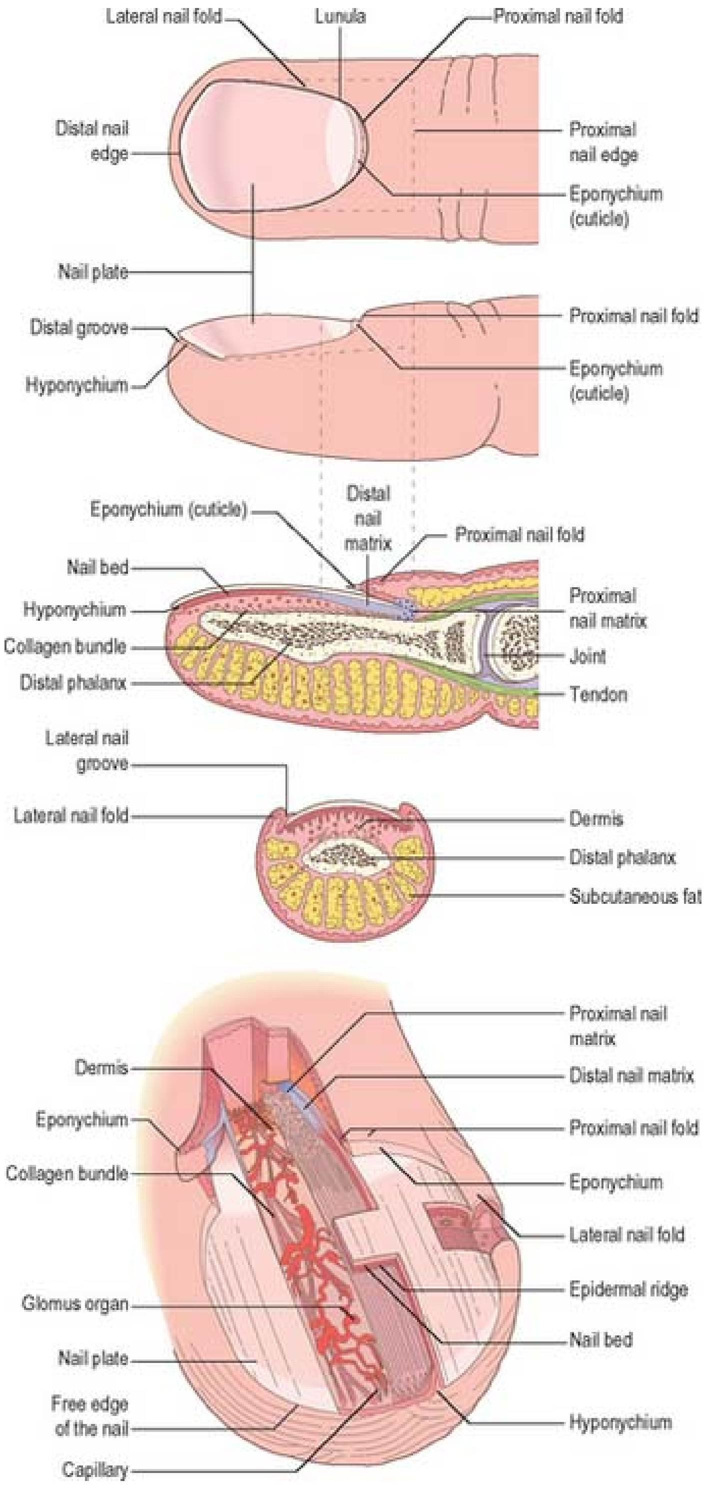
Lateral nail fold
Lunula
Proximal nail fold
Distal nail edge
Proximal nail edge
Eponychium (cuticle)
Nail plate
Distal groove
Hyponychium
Proximal nail fold
Eponychium (cuticle)
Eponychium (cuticle)
Distal nail matrix
Proximal nail fold
Nail bed
Hyponychium
Collagen bundle
Distal phalanx
Proximal nail matrix
Joint
Tendon
Lateral nail groove
Lateral nail fold
Dermis
Distal phalanx
Subcutaneous fat
Proximal nail matrix
Distal nail matrix
Dermis
Eponychium
Proximal nail fold
Collagen bundle
Eponychium
Lateral nail fold
Epidermal ridge
Glomus organ
Nail bed
Nail plate
Free edge of the nail
Hyponychium
Capillary

Fig. 7.18 The organization and terminology of the structures associated with a fingernail.

(By permission from Paus R, Peker S 2003 Biology of hair and nails. In: Bolognia JL, Jorizzo JL, Rapini RP (eds) Dermatology. London: Mosby.)

The nail apparatus consists of the nail plate, proximal and lateral nail folds, nail matrix, nail bed and hyponychium.

Nail plate

The nail plate is embedded within the proximal and lateral nail folds. It is approximately rectangular in shape and is mostly convex in both longitudinal and transverse axes: there is considerable inter- and intra-individual variation (Fig. 7.18). The thickness of the plate increases proximodistally from about 0.7 mm to 1.6 mm: the terminal thickness varies between individuals. The surface of the nail plate may show fine longitudinal ridges, and its undersurface is grooved by corresponding ridges in the nail bed. Disturbances of growth pattern or disease may lead to transverse ridging or grooves, and minute trapped air bubbles may produce white flecks. These defects move distally with growth of the plate.

The nail plate arises from compacted cornified epithelial cells derived from the dorsal, intermediate and ventral nail matrices. It is densely adherent to the matrices on its undersurface, but becomes a free structure distal to the onychodermal band, where it separates from the nail bed. The dorsal aspect of the nail plate originates from the more proximal regions of the germinal matrix, i.e. dorsal and intermediate matrices, whereas the deeper, volar aspect of the plate originates from the ventral matrix.

Nail folds

The sides of the nail plate are bordered by lateral nail folds which are continuous with the proximal fold (Fig. 7.18). The lateral nail folds enclose the lateral free edges of the nail plate and are bounded by the attachment of the skin to the lateral aspect of the distal phalanx margin and the lateral nail. The proximal nail fold provides the visible proximal border to the nail apparatus. It consists of two epidermal layers, superficial and deep, separated by a core of dermis. The epidermis of the superficial layer lacks hair follicles and epidermal ridges: its cornified distal margin extends over the nail plate for a little distance as the cuticle or eponychium. The deep layer merges with the nail matrix.

The eponychium is bounded by the fascial attachment of the skin to the base of the distal phalanx, distal to the insertion of the extensor tendon, and its distal free edge. It adheres to the dorsal aspect of the nail plate and overlies the root of the nail.

Nail matrix

The nail matrix is the main source of the nail plate, and it can be divided into three parts. Proximally, the dorsal matrix is defined as the volar surface (undersurface) of the proximal nail fold. The intermediate matrix (germinal matrix) starts where the dorsal matrix folds back on itself and extends as far as the distal portion of the lunule. The ventral matrix (sterile matrix) is the remainder of the nail bed: it starts at the distal border of the lunule and ends at the hyponychium.

The matrix epithelium consists of typical basal and prickle cell layer keratinocytes, among which are scattered melanocytes and Langerhans cells. Cornified cells of the dorsal and ventral aspects of the matrix are steadily extruded distally to form the nail plate: the proximal 50% of the nail matrix contributes 80% of the nail plate. This process continues into the nail bed at the distal edge of the lunule, which is formed where the distal portion of the ventral matrix underlies the nail plate.

The lunule is pale, opaque and convex and is more prominent in the thumb than the other digits. It is not known why the lunule is so pale compared with the more distal translucent pink nail bed. The lack of colour may reflect the thickness of the epidermis in the lunule and/or a paucity of capillaries in the dermis of the lunule.

Nail bed

The nail bed epidermis extends from the distal margin of the lunule to the hyponychium. The distal margin of the nail bed, at which point the nail plate becomes free of the nail bed, is called the onychodermal band. The surface of the nail bed is ridged and grooved longitudinally, corresponding to a similar pattern on the undersurface of the nail plate. This results in a tight interlocking of the two which prevents the invasion of microbes and the impaction of debris underneath the nail. The epidermis of the nail bed is thin and lacks a stratum granulosum. It consists of two to three layers of nucleated cells which lack keratohyalin granules, and a thin cornified layer which moves distally with the growing nail plate. It contains an occasional sweat gland distally.

The dermis of the nail bed is anchored to the periosteum of the distal phalanx without any intervening subcutaneous layer. It forms a distinct compartment, which means that infections of the nail bed, or other local causes of a rise in pressure (e.g. haematoma) may cause severe pain which is only relieved by excision of part or all of the nail plate. The dermis is richly vascularized. The blood vessels are arranged longitudinally and display numerous glomus bodies, which are encapsulated arteriovenous anastomoses involved in the physiological control of peripheral blood flow in relation to temperature (see Ch. 6 and Ch. 50). The dermis is well-innervated, and contains numerous sensory nerve endings, including Merkel endings and Meissner’s corpuscles.

Nail bed cells differentiate towards the nail plate, and contribute to its thickness ventrally.

Hyponychium

The hyponychium is the area under the free nail between the onychodermal band proximally and the distal groove. It is an epidermal ridge which demarcates the junction between the finger pulp and the subungual structures.

Growth of nail

Nail growth is determined by the turnover rate of the matrix cells, which varies with digit, age, environmental temperature and season, time of day, nutritional status, trauma and various diseases. Generally, its speed is related to the length of the digit, being fastest (approximately 0.1 mm per day) in the middle finger of the hand, and slowest in the little finger. Fingernails grow three to four times faster than toenails, quicker in summer than in winter, and faster in the young than in the old. A fingernail grows out in about 6 months, whereas a toenail is replaced, on average, in 18 months.

Genetic keratin disorders (Irvine & McLean 1999) may lead to nail dystrophies such as pachyonychia, where the nails become grossly thickened.

VASCULAR SUPPLY, LYMPHATIC DRAINAGE AND INNERVATION

VASCULAR SUPPLY AND LYMPHATIC DRAINAGE

The metabolic demands of the skin are not great, and yet, under normal conditions, its blood flow exceeds nutritional requirements by 10 times, and may amount to 5% of the cardiac output. This is because the cutaneous circulation has an important thermoregulatory function, and is arranged so that its capacity can be increased or decreased rapidly by as much as 20 times, in response to the required loss or conservation of heat.

The blood supply to the skin originates from three main sources, the direct cutaneous system, the musculocutaneous system and the fasciocutaneous system. The direct cutaneous system of vessels is derived from the main arterial trunks and accompanying veins. Vessels course in the subcutaneous fat parallel to the skin surface, and are confined to certain areas of the body, e.g. the supraorbital artery, the superficial circumflex iliac artery and the dorsalis pedis artery. The musculocutaneous perforators arise from the intramuscular vasculature, pass through the surface of the muscle, and pierce the deep fascia to reach the skin by spreading out in the subcutaneous tissues. The fasciocutaneous system consists of perforating branches from deeply located vessels (deep to the deep fascia) which pass along intermuscular septa and then fan out at the level of the deep fascia to reach the skin. Examples include the fasciocutaneous perforating vessels from the radial and ulnar arteries.

The direct cutaneous vessels, the musculocutaneous perforators and the fasciocutaneous perforators each contribute to six anastomosing horizontal reticular plexi of arterioles (Fig. 7.19) which have vascular connections between them and which ultimately provide the blood supply to the skin. Three plexi are located in the skin itself and supply all elements including the sweat glands and pilosebaceous units. The subpapillary plexus is located at the junction of the papillary and reticular layers of the dermis. It gives off small branches which form capillary loops in the dermal papillae (usually one loop per papilla) which are perpendicular to the skin surface (Fig. 7.1, Fig. 7.4, Fig. 7.20). The reticular dermal plexus is located in the middle portion of the dermis and is primarily venous. The deep dermal plexus is located in the deepest part of the reticular dermis and on the undersurface of the dermis. The close association between arteriolar and venous plexi permits exchange of heat between blood in vessels at different temperatures flowing in opposite directions (counter-current heat exchange).

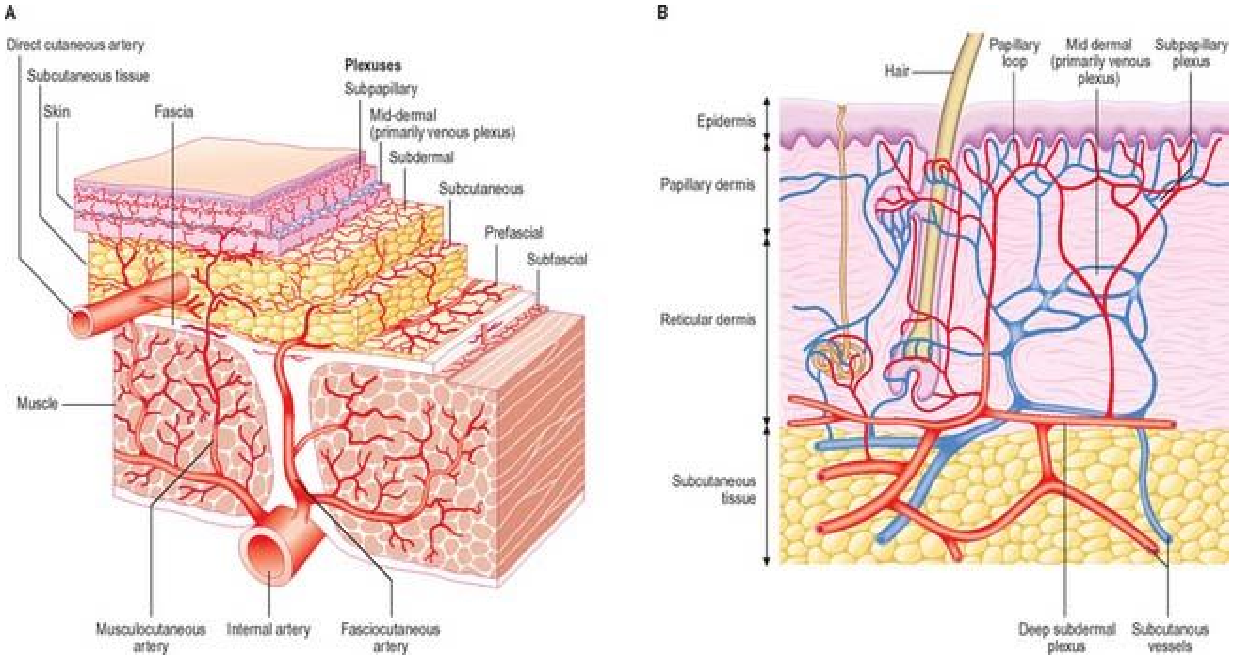
A
Direct cutaneous artery
Subcutaneous tissue
Skin
Fascia
Plexuses
Subpapillary
Mid-dermal (primarily venous plexus)
Subdermal
Subcutaneous
Prefascial
Subfascial
Muscle
Musculocutaneous artery
Internal artery
Fasciocutaneous artery
B
Hair
Papillary loop
Mid dermal (primarily venous plexus)
Subpapillary plexus
Epidermis
Papillary dermis
Reticular dermis
Subcutaneous tissue
Deep subdermal plexus
Subcutanous vessels

Fig. 7.19 Vascular supply to the skin. **A**, Note the various horizontal plexuses fed by direct cutaneous, fasciocutaneous and musculocutaneous arteries. **B**, Higher magnification of vascular supply.

*(**A**, redrawn from McCarthy JG (ed) Chapter 9 in Plastic Surgery, Vol 1. Philadelphia: Saunders. **B**, redrawn from Cormack GC, Lamberty BGH 1994 The Arterial Anatomy of Skin Flaps, 2nd edition. Edinburgh: Churchill Livingstone.)*

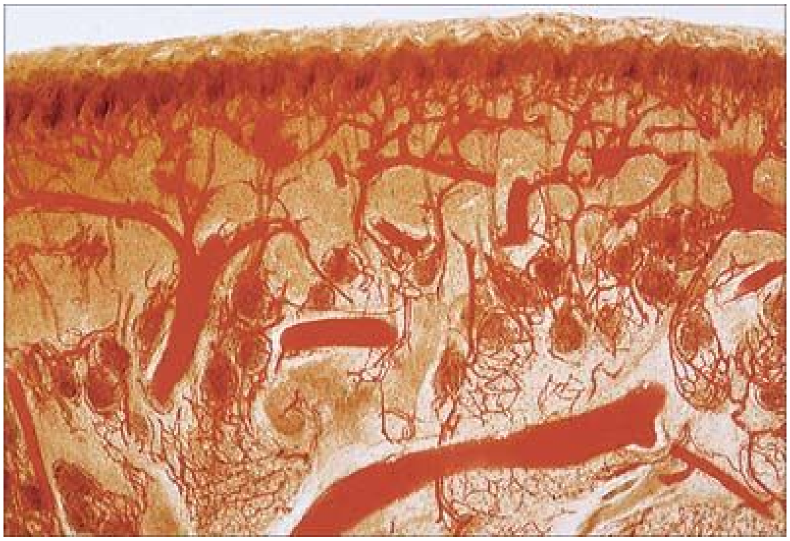

Fig. 7.20 A thick vertical section through palmar skin, the arteries, arterioles and capillaries of which have been injected with red gelatin to demonstrate the pattern of dermal vascularization. At the base of the dermis a broad, flat arterial plexus supplies a more superficial papillary plexus, which in turn gives off capillary loops which enter the dermal papillae.

The remaining three plexi are the subcutaneous plexus, and two plexi associated with the deep fascia. The deep fascia has a plexus on its deep surface and a more extensive plexus on its superficial surface. This arrangement is much more pronounced in the limbs than it is in the trunk.

The general structure and arrangement of the microvasculature is described in detail in Ch. 6, and so only features particular to skin will be considered here. In the deeper layers of the dermis, arteriovenous anastomoses are common, particularly in the extremities (hands, feet, ears, lips, nose), where, as glomera, they are surrounded by thick muscular coats. Under autonomic vasomotor control, these vascular shunts, when relaxed, divert blood away from the superficial plexus and so reduce heat loss, while at the same time ensuring some deep cutaneous circulation and preventing anoxia of structures such as nerves. Extensive capillary anastomoses are present. Generally, cutaneous blood flow is regulated according to thermoregulatory need, and also, in some areas of the body, according to emotional state. In very cold conditions, the peripheral circulation is greatly reduced by vasoconstriction, but intermittent spontaneous vasodilatation results in periodic increases in temperature which prevent cooling to the level at which frostbite might occur. This is thought to be due to a direct effect of oxygen lack on the arteriolar constrictor muscle, rather than to a neural influence.

The lymphatics of the skin, as elsewhere, are small terminal vessels which collect interstitial fluid and macromolecules for return to the circulation via larger vessels. They also convey lymphocytes, Langerhans cells and macrophages to regional lymph nodes. They begin as blind-ended, endothelial-lined tubes or loops just below the papillary dermis. These drain into a superficial plexus below the subpapillary venous plexus, which drains via collecting vessels into a deeper plexus at the junction of the reticular dermis and subcutis, and this, in turn, drains into the larger subcutaneous channels.

INNERVATION

Skin is a major sensory surface, with regional variations in sensitivity to different stimuli. It has a rich nerve supply, which is also concerned with autonomic functions, particularly related to thermoregulation. Cutaneous sense provides information about the external environment through receptors responsive to stimuli which may be mechanical (rapid or sustained touch, pressure, vibration, stretching, bending of hairs, etc.), thermal (hot and cold), or noxious (perceived as itching, discomfort or pain). Pacinian corpuscles subserve deep pressure and vibrational sensation, and are located deep in the dermis or in the hypodermis, particularly of the digits. Meissner's corpuscles are located in dermal papillae, close to the dermo-epidermal junction, and are sensitive to touch sensation. These receptors are particularly suited to detecting shape and texture during active exploratory touch as employed most skillfully by readers of Braille text.

The primary input is transmitted by neurones whose cell bodies lie in the spinal and cranial ganglia (see p. 55), and whose myelinated or unmyelinated axons are terminally distributed, mainly within the dermis. Efferent autonomic fibres are unmyelinated and noradrenergic or cholinergic. They innervate the arterioles, arrector pili muscles, and the myoepithelial cells of sweat and apocrine glands. In the scrotum, labia minora, perineal skin and nipples they also supply smooth muscle fasciculi of the dermis and adjacent connective tissue. Except in the nipples and genital area, activity of the autonomic efferent nerves is mainly concerned with regulation of heat loss by vasodilation and vasoconstriction, sweat production, and pilo-erection (although this is a minor function in humans).

On reaching the dermis, nerve fasciculi branch extensively to form a deep reticular plexus which serves much of the dermis, including most sweat glands, hair follicles and the larger arterioles. Many small fasciculi pass from this plexus to ramify in another superficial papillary plexus at the junction between the reticular and papillary layers of the dermis. Branches from this pass superficially into the papillary layer, ramifying horizontally and vertically, and terminate either in relation to encapsulated receptors, or as terminals reaching the level of the basal lamina. In some instances, they enter the epidermis as free endings, responsive to light pressure and touch sensation or to nociceptive stimuli. As these latter fasciculi terminate, they lose their epineurial and perineurial sheaths, leaving Schwann cell axonal complexes or naked axons enveloped by basal lamina, in direct contact with the matrix. These naked distal axonal terminals may be vulnerable to pathogens entering via a skin abrasion. The structure and classification of sensory endings are described in detail Chapter 3.

The segmental arrangement of the spinal nerves is reflected in the sensory supply of the skin: a dermatome is the area supplied by all the cutaneous branches of an individual spinal nerve through its dorsal and ventral rami (see Ch. 15 and Fig. 15.12). Typically, dermatomes extend round the body from the posterior to the anterior median line. The upper half of each zone is supplemented by the nerve above, the lower half by the nerve below. Dermatomes of adjacent spinal nerves overlap markedly, particularly in the segments least affected by development of the limbs.

DEVELOPMENT OF SKIN AND SKIN APPENDAGES

Skin is developed from the surface ectoderm and its underlying mesenchyme. Surface ectoderm gives rise to the cornifying general surface epidermis and its appendages, the pilosebaceous units, sweat glands and nail units, depending on interactions with the mesenchyme. Interactions between ectoderm and mesenchyme also give rise to the internal epithelium of the buccal cavity and the teeth and the nasal epithelia. The differentiated descendants of ectodermal cells are keratinocytes. Immigrant cells of different developmental origin constitute an important component of the epithelial sheet formed by the keratinocytes. The non-keratinocytes are melanocytes and Merkel cells derived from the neural crest, Langerhans cells of bone-marrow origin, and lymphocytes.

The dermis, composed of irregular connective tissue and some of the connective tissue sheaths of peripheral nerves, is derived from somatopleuric mesenchyme (in the limbs and trunk), and possibly somitic mesenchyme (covering the epaxial musculature), and from neural crest (in the head). Angiogenic mesenchyme gives rise to the blood vessels of the dermis. Nerves and associated Schwann cells, of neural crest origin, enter and traverse the dermis to reach their peripheral terminations during development.

EPIDERMIS AND APPENDAGES

General (interfollicular) epidermis

In the first 4–5 weeks, embryonic skin consists of a single layer of ectodermal cells overlying a mesenchyme containing cells of stellate dendritic appearance interconnected by slender processes and sparsely distributed in a loosely arranged microfibrillar matrix (Fig. 7.21). The interface between ectoderm and mesenchyme, known as the basement membrane zone (BMZ), is an important site of mutual interactions upon which the maintenance of the two tissues depends, both in prenatal and postnatal life. Ectodermal cells, which characteristically contain glycogen deposits, contact each other at gap and tight junctions. The layer so formed soon develops into a bilaminar epithelium, and desmosomes also appear. The basal germinative layer gives rise to the definitive postnatal epidermis, and the superficial layer to the periderm, a transient layer confined to fetal life. The periderm maintains itself, expresses different keratin polypeptides, and grows by the mitotic activity of its own cells, independent of those of the germinative layer. Originally flattened, the periderm cells increase in depth: the central area containing the nucleus becomes elevated and projects as a globular elevation towards the amniotic cavity. The plasma membrane develops numerous surface microvilli with an extraneous coat of glycosaminoglycans, and cytoplasmic vesicles become prominent deep to it. These developments reach a peak over the period 12–18 weeks, at which time the periderm is a major source of the amniotic fluid to which it may contribute glucose; it also has an absorptive function. From about 20 weeks onwards, the globular protrusions become undermined and pinched off to float free in the amniotic fluid. The now flattened periderm cells undergo a type of terminal differentiation to form what is regarded as a temporary protective layer for the underlying developing epidermis proper, against an amniotic fluid of changing composition as a result of the accumulation of products of fetal renal excretion. Up to parturition, periderm squames continue to be cast off into the amniotic fluid, and they contribute to the vernix caseosa, a layer of cellular debris which covers the fetal skin at birth.

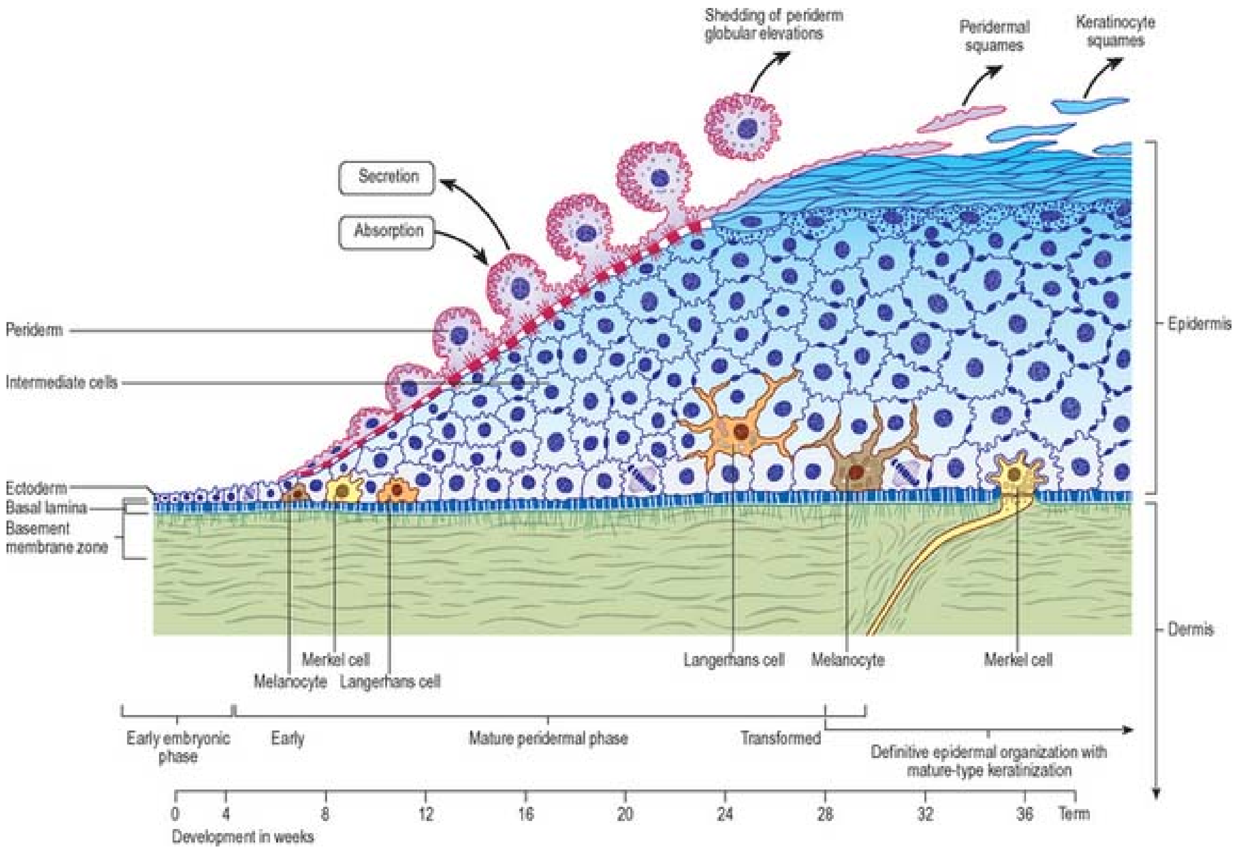
Shedding of periderm globular elevations
Peridermal squames
Keratinocyte squames
Secretion
Absorption
Periderm
Intermediate cells
Epidermis
Ectoderm
Basal lamina
Basement membrane zone
Dermis
Merkel cell
Melanocyte
Langerhans cell
Langerhans cell
Melanocyte
Merkel cell
Early embryonic phase
Early
Mature peridermal phase
Transformed
Definitive epidermal organization with mature-type keratinization
0
4
8
12
16
20
24
28
32
36
Term
Development in weeks

Fig. 7.21 Development of the skin.

Proliferation in the germinative layer leads to a stratified appearance with successive layers of intermediate cells between it and the periderm. From an early stage, cells of all layers are packed with glycogen granules, presumably a source of energy during this early replicative stage of differentiation. Differentiation of these layers is not synchronous throughout all regions of the developing skin, being more advanced cranially than caudally, and progressing on the body from the midaxillary line ventrally. Reduction in glycogen content of the cells is associated with a shift towards biosynthetic activity connected with terminal (cornifying) differentiation, manifested by the presence of different enzymes and expression of keratins. Simple epithelial keratins present from before implantation (K8 and K18) are replaced by typical keratinocyte basal cell keratins (K5 and K14), followed in the first suprabasal cell layer by those of higher molecular weight associated with differentiation (K1 and K10) at 10–12 weeks. This is soon followed by expression of profilaggrin and filaggrin, and the appearance of keratohyalin granules among filamentous bundles of the uppermost intermediate layer cells at approximately 20 weeks. The first fully differentiated keratinocytes appear shortly afterwards. By 24–26 weeks a definite cornified layer exists in some areas, and by 30 weeks or so, apart from some lingering glycogen in intermediate cells, the interfollicular epidermis is essentially similar to its postnatal counterpart (see Holbrook & Odland 1980, for further details).

Non-keratinocytes are present in developing epidermis from about 8 weeks' gestation. Langerhans cells can be seen in the epidermis by 5–6 weeks and are fully differentiated by 12–14 weeks. Their numbers increase at least partially by mitotic division *in situ*, but at 6 months are only 10–20% of those in the adult. It is not known if the Langerhans cell functions in immune surveillance in fetal skin. Melanocytes, of neural crest origin, are present in the bilaminar epidermis of cephalic regions as early as 8 weeks. By 12–14 weeks they can reach a density of 2300 per mm^2 reducing to 800 per mm^2 just before birth. Keratinocytes regulate the final ratio between themselves and melanocytes via growth factors, cell surface molecules and other signals. Fetal melanocytes produce melanized melanosomes and transfer them to keratinocytes: these are intrinsic activities clearly independent of ultraviolet (UV) irradiation, and suggest functions of melanin other than photoprotection.

Merkel cells originate from migratory neural crest cells (Szeder et al 2003) and begin to appear in the epidermis of the palm and sole of the foot between 8 and 12 weeks, and later in association with some hairs and with dermal axonal–Schwann cell complexes.

Pilosebaceous unit

Pilosebaceous units develop at about 9 weeks, first in the regions of the eyebrows, lips, and chin, and at progressively later stages elsewhere, proceeding caudally. The first rudiment is a crowding of cells in the basal layer of the epidermis, the hair placode, adjacent to a local concentration of mesenchymal cells which will become the dermal papilla. Further proliferation and elongation of the cells leads to a hair germ, which protrudes downwards into the mesenchyme in association with the primitive dermal papilla during weeks 13–15. With continued downward growth in a slanted direction, the hair germ becomes a hair peg, and when its bulbous lower end envelops the dermal papilla it is known as a bulbous peg. Melanocytes are individually present at the hair peg stage, and abundantly so and quite active in the bulbous peg. At this stage (approximately week 15) two or three swellings appear on the posterior wall. The uppermost is the rudiment of the apocrine gland (present only in some follicles), the middle forms the sebaceous gland and the lower one is the bulb, to which the arrector pili muscle (arising from underlying mesenchyme) later becomes attached, and where it is believed the main reservoir of hair follicle stem cells resides. The cells of the lowermost region of the bulb, the matrix, divide actively and produce a pointed hair cone. This grows upwards to canalize a developing hair tract, along which the fully formed hair, derived by further differentiation of cells advancing from the matrix, reaches the surface at approximately week 18 of gestation.

Sebaceous glands develop independently of hair follicles in the nostrils, eyelids (as tarsal glands) and in the anal region. Apocrine sweat glands are formed at the same time as eccrine (merocrine) sweat glands and are at first distributed widely over the body. Their number diminishes from 5 months' gestation, producing the distribution seen in the adult.

Hairs produced prenatally are called lanugo hairs; they are short and downy, lack a medulla, and in certain parts of the body are arranged in a vortex-like manner into tracts. Late in pregnancy, lanugo hairs are replaced by vellus hairs, and these in turn by intermediate hairs, which are the predominant type until puberty. New follicles do not develop in postnatal skin.

Eccrine sweat glands

Eccrine (merocrine) sweat glands are one type of sudoriferous gland. Sweat gland rudiments appear in the second and third months as cell buds associated with the primary epidermal ridges of the finger and toe pads of terminal digits. They elongate into the dermis and by 16 weeks the lower end begins to form the secretory coil, within which, by 22 weeks, secretory and myoepithelial cells are evident. The solid cord of cells connecting the coil to the epidermis becomes the intradermal duct, and the lumina of both are formed by dissolution of desmosomal contacts between the cells. The intraepidermal duct is foreshadowed by a coiled column of concentrically arranged inner and outer cells, within which, by fusion of lysosomal vacuoles, a lumen is formed which opens on the surface at 22 weeks. As with hair follicles, no new eccrine sweat glands develop postnatally. Emotional sweating, detected by skin conductance changes, occurs in preterm infants from 29 weeks' gestational age.

Epidermal ridges

The epidermal ridges are foreshadowed as regularly spaced small downgrowths of epidermal cells which appear in finger and toe pads during the second and third months. They are known as primary epidermal ridges, separated by corresponding dermal ridges. In the fifth month secondary ridges develop, the pattern becomes evident on the surface, and is finalized through further remodelling postnatally.

Nails

Fields of proliferative ectoderm appear on the tips of the terminal segments of the digits. They progressively reach a dorsal position, where at approximately 9 weeks, a flattened nail field limited by proximal, distal, and lateral nail grooves is apparent. The nail field ultimately forms the nail bed, and the primordium of the nail is formed of a wedge of cells which grows diagonally, proximally and deeply into the mesenchyme from the proximal groove towards the underlying terminal phalanx. The deeper cells of this wedge form the primordium of the matrix which gives rise to the nail plate. The latter emerges from under a, now proximal, nail fold at about 14 weeks and grows distally over an already keratinized nail bed. The nail matrix is usually considered to have dorsal and ventral (intermediate) components, but there are conflicting opinions as to the extent to which each contributes to the nail, both in ontogeny and postnatally: it is generally agreed that the ventral matrix contributes the major part. It has been claimed that the nail bed additionally contributes up to 20% of the postnatal nail plate, but embryological studies to date are not clear on this matter. Most texts state that keratohyalin is not involved in the cornification of nail. However, up to at least 16 weeks, the dorsal matrix granular layer cells which contribute cornified cells to the nail plate and eponychium (cuticle) contain typical keratohyalin granules, and the cells of the ventral matrix next to the nail plate contain single and compound granules similar to those present in granular layer cells of oral epithelia. Similar granules have been reported in matrix cells of postnatal human toenail.

At 20 weeks, the nail plate entirely covers the nail field (nail bed), now limited distally by a distal ridge, which, when the plate projects beyond the tip, becomes the hyponychium beneath it. At birth, the microstructure of the main nail unit components is similar to that postnatally; the nail is long and overhanging, and easily falls off during cleansing.

Abnormalities of the epidermis

Anomalous development of the epidermis and its derivatives is relatively common. Excessive or diminished growth, or even complete absence, may affect sebaceous or sudoriferous glands and hair, either locally or generally. Similarly, the epidermis may be excessively pigmented (melanism). Excessive production of the cornified layer leads to ichthyosis. A naevus or mole is a benign proliferation of melanocytes in the basal layer of the epidermis. Ectodermal dysplasia is a rare condition characterized by fine blond and scanty hair, reduced or absent eyelashes and eyebrows. The skin has deficient sweat and sebaceous glands. Teeth are usually peg- or cone-shaped, and absence of major salivary glands may occur. For information on keratin disorders, see Irvine & McLean 1999.

DERMIS

The embryonic dermis is far richer in cells than the adult dermis, and many of these mesenchymal cells are involved in an essential signalling dialogue which regulates ectodermal differentiation. The mesenchymal cells underlying the surface ectoderm and early bi- and trilaminar epidermis contact each other by slender processes to form an intercommunicating network. They secrete a matrix which is rich in ions, water, and macromolecules, proteoglycan/glycosaminoglycans, fibronectin, collagenous proteins of various types and elastin. Further development of these intrinsic components involves the differentiation of individual cell types, fibroblasts, endothelial cells, mast cells, etc. and the assembly of matrix components into organized fibrillar collagen fibres and elastic fibres. During embryogenesis, the matrix is heterogeneous with regard to its biochemical and macromolecular components. The main glycosaminoglycans of embryonic and fetal skin are glycuronic acid and dermatan sulfate. Collagens type I, III, V, and VI are distributed more or less uniformly regardless of fetal age, and there are some local concentrations of III and V, the levels of which are higher than in postnatal skin. Collagens type IV and VII are found predominantly in the BMZ.

The progressive morphological differentiation of the dermis involves its separation from the subcutis at about the third month; changes in composition and size of collagen fibrils and their organization into bundles amongst which cells become relatively fewer; downgrowth of epidermal appendages; the organization of nervous and vascular plexuses, and the relatively late appearance of elastic networks. The papillary and reticular regions are said to be evident as early as 14 weeks, but the overall organization of the dermis continues postnatally.

Vascular supply and lymphatic drainage

The dermal vasculature is generally thought to be developed *in situ* by transformation of angiogenic mesenchymal cells. Closed endothelial-lined channels containing nucleated red cells are present by 6 weeks underneath the ectoderm, and by the eighth week are arranged in a single plane parallel to the epidermis: they will ultimately form the subpapillary plexus. A second deeper horizontal plexus is evident by 50–70 days. Both plexuses extend by budding as development proceeds, and they give rise to the final patterns of arterioles, venules and capillaries which are established shortly after birth. Pericytes also develop from mesenchymal cells. Lymphatic vessels are formed by mesenchymal cells which become organized to enclose pools of proteinaceous fluid leaking from the developing capillaries.

Innervation

Sensory cutaneous nerves (axons and Schwann cells) are derived by outgrowth from the neural crest (via dorsal root ganglia). Motor fibres to vessels and glands arise from cells of sympathetic ganglia. As individual parts of the embryo grow, the nerves grow and lengthen with them. Small axons are present superficially at a stage when the epidermis is bilaminar, and by 8 weeks gestation there is already a functioning cutaneous plexus. By the fourth gestational month, the dermal plexuses are very richly developed, and Meissner and Pacinian corpuscles have appeared. The outer lamellar cells of Pacinian corpuscles in the dermis are homologous with the perineurium, but the source of the laminar cells of the Meissner corpuscle is unclear.

EPITHELIAL–MESENCHYMAL INTERACTIONS IN DEVELOPING SKIN

Epidermal–mesenchymal (dermal) interactions at the BMZ occur during development and throughout life. At the ectodermal stage, the BMZ consists of the basal plasma membrane of an ectodermal cell, paralleled on its cytoplasmic side by various cytoskeletal filaments, and beneath it, by a layer (0.1–0.2 μm) of microfibrillar-amorphous material deposited by the cell. At the bilaminar stage, a definite continuous lamina densa is present, separated from the basal plasma membrane by a lamina lucida traversed by loosely fibrillar material: similar filaments extend from the lamina densa into the mesenchymal matrix.

Hemidesmosomes begin to appear at 8 weeks as stratification starts, and anchoring fibrils at 9–10 weeks. By the end of the third month the basic morphology of the interfollicular BMZ is essentially similar to that of the postnatal BMZ.

Laminin and collagen type IV are present in the developing basal lamina at 6 weeks, and bullous pemphigoid antigen (BPAG, in hemidesmosomes) and anchoring fibril proteins are expressed later. These immunocytochemical and morphological observations are of importance for prenatal diagnosis of genetically determined diseases, e.g. epidermolysis bullosa. The basal lamina provides a physical supporting substrate and attachment for the developing epidermis, and is thought to be selectively permeable to macromolecules and soluble factors regulating epidermal–dermal morphogenetic interactions.

NEONATAL GROWTH

The surface area of the skin increases with growth. It has been estimated that the surface area of a premature neonate weighing 1505 g is approximately 1266 cm^2, whereas a neonate of 2980 g has a surface area of 2129 cm^2. The skin of the neonate is thinner than that of older infants and children. It cornifies over a period of 2–3 weeks which provides protection; however, in the premature infant the thin epidermal layer allows absorption of a variety of substances, e.g. chlorhexidine and boric acid and also permits a significantly higher transepidermal water loss than occurs in full term neonates. At birth the skin is richly vascularized by a dense subepidermal plexus. The mature pattern of capillary loops and of the subpapillary venous plexus is not present at birth but develops as a result of capillary budding with migration of endothelia at some sites and the absorption of vessels from other sites. Some regions mature faster than others. With the exceptions of the palms, soles and nail beds, the skin of the neonate has almost no papillary loops. It has a disordered capillary network which becomes more orderly from the second week when papillary loops appear; defined loops are not present until the fourth or fifth week, and all areas possess loops by 14–17 weeks postnatally.

Neonates exhibit a regional sequence of eccrine gland maturation. The earliest sweating occurs on the forehead, followed by the chest, upper arm and, later, more caudal areas. Acceleration of maturation of the sweating response occurs in premature babies after delivery.

NATURAL SKIN CREASES AND WRINKLES

SKIN LINES

The surface of the skin and its deeper structures show various linear markings, seen as grooves, raised areas and preferred directions of stretching. Some of these are clearly evident in intact skin, others only appear after some sort of intervention.

Surface pattern lines, tension lines and skin creases

Externally visible skin lines are related to various patterns of epidermal creasing, ridge formation, scarring and pigmentation. A simple lattice pattern of lines occurs on all major areas of the body other than the thick skin of volar and plantar surfaces. The lattice pattern typically consists of polygons formed by relatively deep primary creases visible to the naked eye, which are irregularly divided by finer secondary creases into triangular areas (Fig. 7.22, Fig. 7.23). These, in turn, are further subdivided by tertiary creases limited to the cornified layer of the epidermis, and, finally, at the microscopic level, by quaternary lines which are simply the outlines of individual squames (Fig. 7.7). Apart from the quaternary lines, all the others increase the surface area of the skin, permit considerable stretching and recoil and distribute stresses more evenly. Details of the pattern vary according to the region of the body; e.g. on the cheek the primary creases radiate from the hair follicles, on the scalp they form hexagons, while on the calf and thigh they form parallelograms. There is a relationship between type of pattern and local skin extensibility.

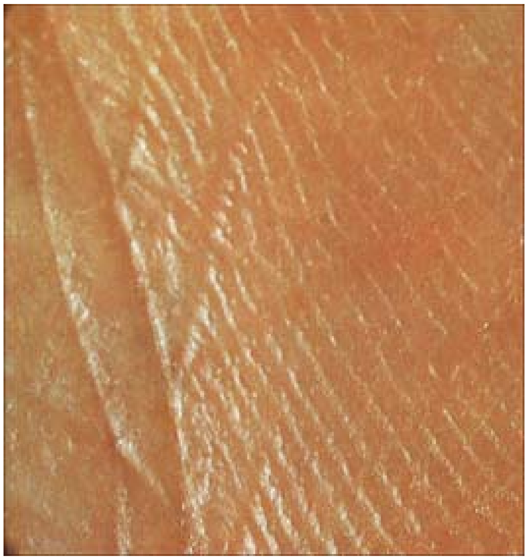

Fig. 7.22 The surface of hairless skin from the palm of the hand, showing epidermal friction (papillary) ridges and larger flexure lines (left).

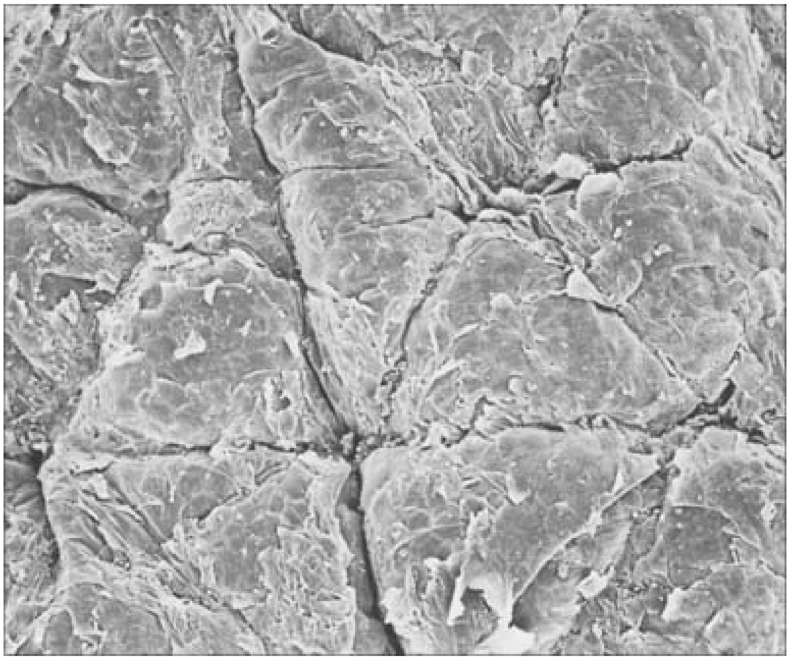

Fig. 7.23 Scanning electron micrograph of the surface of thin skin of the back, showing an interlacing network of fine creases and predominantly triangular areas between them.

Wrinkle lines

Wrinkle lines are caused by contraction of underlying muscles and are usually perpendicular to their axis of shortening. On the face they are known as lines of expression, and with progressive loss of skin elasticity due to ageing, they become permanent. Occupational lines are creases produced by repeated muscular contractions associated with particular trades or skills. Contour lines are lines of division at junctions of body planes, e.g. the cheek with the nose, and lines of dependency are produced by the effect of gravity on loose skin or fatty tissue, e.g. the creases associated with the pendulous fold beneath the chin in older age.

Flexure (joint) lines

Flexure (joint) lines are major markings found in the vicinity of synovial joints, where the skin is attached strongly to the underlying deep fascia (Fig. 7.22). They are conspicuous on the flexor surfaces of the palms, soles, and digits, and in combination with associated skin folds, they facilitate movement. The skin lines do not necessarily coincide with the associated underlying joint line. For example, the flexure lines demarcating the extended fingers from the palm lie approximately half an inch distal to the metacarpophalangeal joints, the positions of which are more closely related to the distal palmar crease (heart-line of palmistry). The patterns of flexure lines on the palms and soles may vary and are to some extent genetically determined. In Down syndrome, the distal and middle palmar creases tend to be united into a prominent single transverse crease, a sign which is of diagnostic importance.

Papillary ridges

Papillary ridges are confined to the palms and soles and the flexor surfaces of the digits, where they form narrow parallel or curved arrays separated by narrow furrows (Fig. 7.24, Fig. 7.25). The apertures of sweat ducts open at regular intervals along the summit of each ridge. The epidermal ridges correspond to an underlying interlocking pattern of dermal papillae, an arrangement which helps to anchor the two layers firmly together. The pattern of dermal papillae determines the early development of the epidermal ridges. This arrangement is stable throughout life, unique to the individual, and therefore significant as a means of identification. The ridge pattern can be affected by certain abnormalities of early development, including genetic disorders such as Down syndrome, and skeletal malformations such as polydactyly. Absence of epidermal ridges is extremely rare. Functionally, epidermal ridges increase the gripping ability of hands and feet, preventing slipping. The great density of tactile nerve endings beneath them means that they are also important sensory structures.

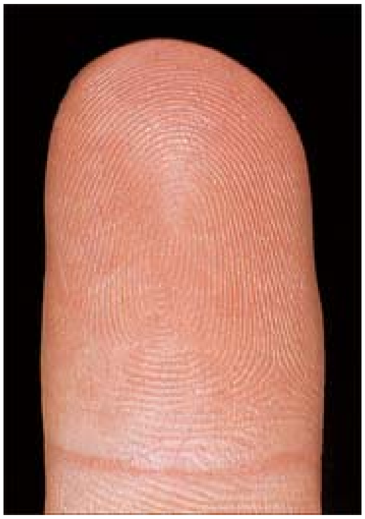

Fig. 7.24 The palmar aspect of a terminal phalanx to show fingerprint ridges. Note interphalangeal flexure line (below).

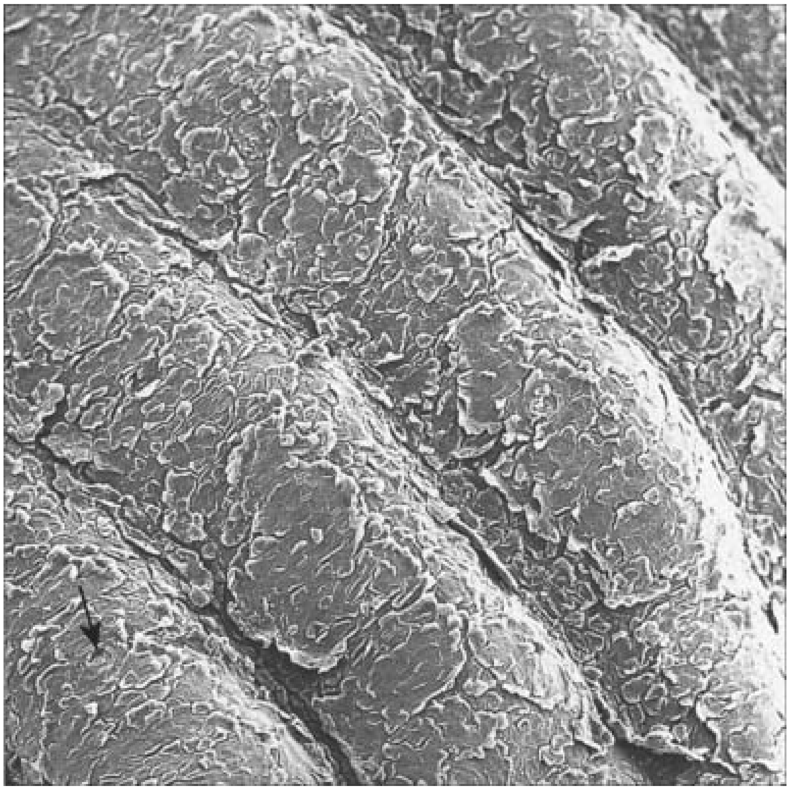

Fig. 7.25 Scanning electron micrograph of the surface of thick hairless skin from the volar surface of a human digit, showing friction ridges along which lines of sweat ducts open as pores (one pore is arrowed).

(By courtesy of Professor Lawrence Bannister and Dr Caroline Wigley.)

The analysis of ridge patterns by studying prints of them (fingerprints) is known as dermatoglyphics and is of considerable forensic importance. Measurable parameters include the frequency of ridges in particular patterns and the disposition of tri-radii, which are junctional areas where three sets of parallel ridges meet. Fingerprint ridge patterns can be separated into three major types (Fig. 7.24), arches (5%), loops (70%), and whorls (25%). Arches have no tri-radii, loops have one tri-radius, and whorls have two or more. Whorl finger patterns are more common on the right hand, and males generally have more whorls and fewer arches than females, in whom the ridges are relatively narrower. The frequency of individual patterns varies with particular fingers. Similar patterns are seen on the toes.

The precise positions, numbers and ridge-counts associated with the triradii have an inherited basis: in general the genetics are multifactorial and highly complex. However, the total ridge-count of all 10 digits of the hand appears to have a simpler inheritance.

If the mechanical demands placed on the skin are greater than the skin creases and the dermis can accommodate, the lateral cohesion of dermal collagen fibres is disrupted, and there is associated haemorrhage and cellular reaction, and eventually, formation of poorly vascularized scar tissue. These changes can be termed intrinsic, to distinguish them from scars formed by external wounding. Sites of dermal rupture are visible externally as lines or striae. They are initially pink in colour, later widen and become a vivid purple or red (striae rubrae), and eventually fade, becoming paler than the surrounding intact skin (striae albae). They develop on the anterior abdominal wall of some women in pregnancy when they are termed striae gravidarum (stretch marks).

Variation in pigmentation can also produce externally visible lines on the surface of the skin. Futcher's or Voigt's lines mark differences in pigmentation between the darker extensor and paler flexor surfaces of the arms, and occur along the anterior axial lines, extending from the sternum to the wrist. They are more common in darker-skinned races.

Lines detectable after manipulation or incision

In certain regions of the body, surgical wounds heal with a better and less conspicuous scar if they are lying in a particular direction. This finding is related to a number of factors including skin tension and naturally formed wrinkle lines. Skin is normally under tension and the direction in which this is greatest varies regionally. Tension is dependent on the protrusion of underlying structures, the direction of underlying muscles, and on joint movements. Many anatomists and surgeons have therefore attempted to produce a body map to indicate the best direction in which to make an elective incision to obtain the most aesthetic scar. These maps frequently differ, especially in the region of the face. Out of the multitude of described cleavage lines, the most commonly referred to are relaxed skin tension lines

(RSTLs), Langer’s lines, and Kraissl’s lines (Borges 1984). Of these, the RSTLs and Kraissl’s lines are probably more appropriate lines for surgical incision.

Relaxed skin tension lines

Relaxed skin tension lines (RSTLs) are those which correspond to the directional pull (which forms furrows) when the skin is relaxed: they do not always correspond to wrinkle lines. The tension across the RSTL is constant even during sleep but can be altered (increased, decreased or abolished) by underlying muscle contraction. The direction of the RSTLs can be determined by pinching the skin in different directions. Pinching at right angles to the RSTLs will result in fewer and higher furrows than pinching parallel to these lines.

Lines of Langer and Kraissl

Langer punctured the skin of cadavers with a circular awl and noted the subsequent elliptical-shaped openings. By connecting the long axis of these holes, he produced the cleavage lines named after him. These lines represent skin tension in rigor mortis but frequently do not relate to the lines of choice in making elective incisions. Indeed, Langer’s lines often run at right angles to the RSTLs on the face.

Kraissl’s lines are essentially exaggerated wrinkle lines obtained by studying the loose skin of elderly faces whilst contracting the muscles of facial expression. These lines for the most part correspond to RSTLs, but slight variation exists on the face, especially on the lateral side of the nose, the lateral aspect of the orbit, and the chin. For further information on lines of Langer and Kraissl, see Chapter 29.

Blaschko lines

Blaschko’s lines refer to the way in which patterns of naevi and related dermatological pathologies are distributed or develop along certain preferred cutaneous pathways. They do not appear to correspond to vascular or neural elements of the skin, and may be related to earlier developmental boundaries of a ‘mosaic’ nature.

AGE-RELATED SKIN CHANGES

Two main factors, chronological and environmental, are involved in skin ageing. Chronological changes are physiological or intrinsic in origin. A major environmental factor is chronic exposure to the sun, referred to as photoageing: emphasis is laid upon differences between the two because photoageing is to some extent preventable.

Intrinsic ageing

From about the third decade onwards there are gradual changes in the appearance and mechanical properties of the skin which reflect natural ageing processes. These become very marked in old age. Normal ageing is accompanied by epidermal and dermal atrophy, which result in some changes in the appearance, microstructure and function of the skin. Alterations include wrinkling, dryness, loss of elasticity, thinning and a tendency towards purpura on minor injury. Epidermal atrophy is expressed by general thinning and loss of the basal rete pegs with flattening of the dermo-epidermal junction, and this results in a reduction in contact area between the two which may affect epidermal nutrition. Flattening of the junction decreases resistance to shear, leading to poor adhesion of epidermis and its separation following minor injury. The thickness of the cornified layer is not reduced in old age, and its permeability characteristics seem little affected. Epidermal proliferative activity and rate of cell replacement decline with age, being reduced by up to 50% in elderly skin. Synthesis of vitamin D is also reduced. After middle age there is a 10–20% decline in the number of melanocytes, and Langerhans cells become sparser, which is associated with a reduction in immune responsiveness. Depigmentation and loss of hair, and some local increases (eyebrows, nose and ears in males, and face and upper lip in females) are commonly observed. Alterations in non-keratinocytes may be aggravated by chronic exposure to UV irradiation.

Dermal changes are mainly responsible for the appearance of aged skin, its stiffness, flaccidity and wrinkling, and loss of extensibility and elasticity. Its general thickness diminishes as a result of the decline in collagen synthesis by a reduced population of fibroblasts, though the relative proportion of type III collagen increases. Senile elastosis is a degenerative condition of collagen which may be partly due to excessive exposure to sun. Vascularization of the skin is reduced, the capillary loops of the dermal papillae are particularly affected, and the tendency towards small spontaneous purpuric haemorrhages indicates a general fragility of the cutaneous microvasculature. A decrease in sensitivity of sensory perception associated with some loss of specialized receptors occurs.

Photoageing

Photoageing is a major concern because of an association with epidermal cancer. The effects of chronic sun exposure on melanocytes (stimulatory) and Langerhans cells (destructive) are thought to be connected with the increasing incidence of malignant melanoma in some groups of individuals, where reduction in tumour monitoring activity by Langerhans cells may be a factor.

CUTANEOUS WOUND HEALING AND SCARRING

The end-point of healing of mammalian skin wounds is usually scar formation. Cutaneous scars result from injury to both the epidermis and underlying dermis; while the epidermis largely regenerates, dermal architecture is abnormal after repair and the undulating pattern of rete ridges at the dermo-epidermal junction is not reproduced. It is not known why scarring occurs. Scar tissue is biomechanically inferior to unwounded skin. Appendages such as hair follicles, sebaceous and sweat glands that are derived from the epidermis do not regenerate after wounding. It is possible that humans evolved to close wounds rapidly, at the expense of perfect regeneration.

The molecular biology of cutaneous repair involves the coordination of numerous cell types, signalling molecules and matrix proteins. Many such factors are pleiotropic in their effects and it is the complex balance of such mediators, rather than their individual action, that determines events in wound repair. Wound healing is often considered in four overlapping temporal phases, namely haemostasis, inflammation, proliferation and remodelling (Fig. 7.26). These events will be discussed separately for clarity, although this is an artificial division of the complex, inter-related processes that constitute the wound healing response. For further reading, see Miller & Nanchahal (2005).

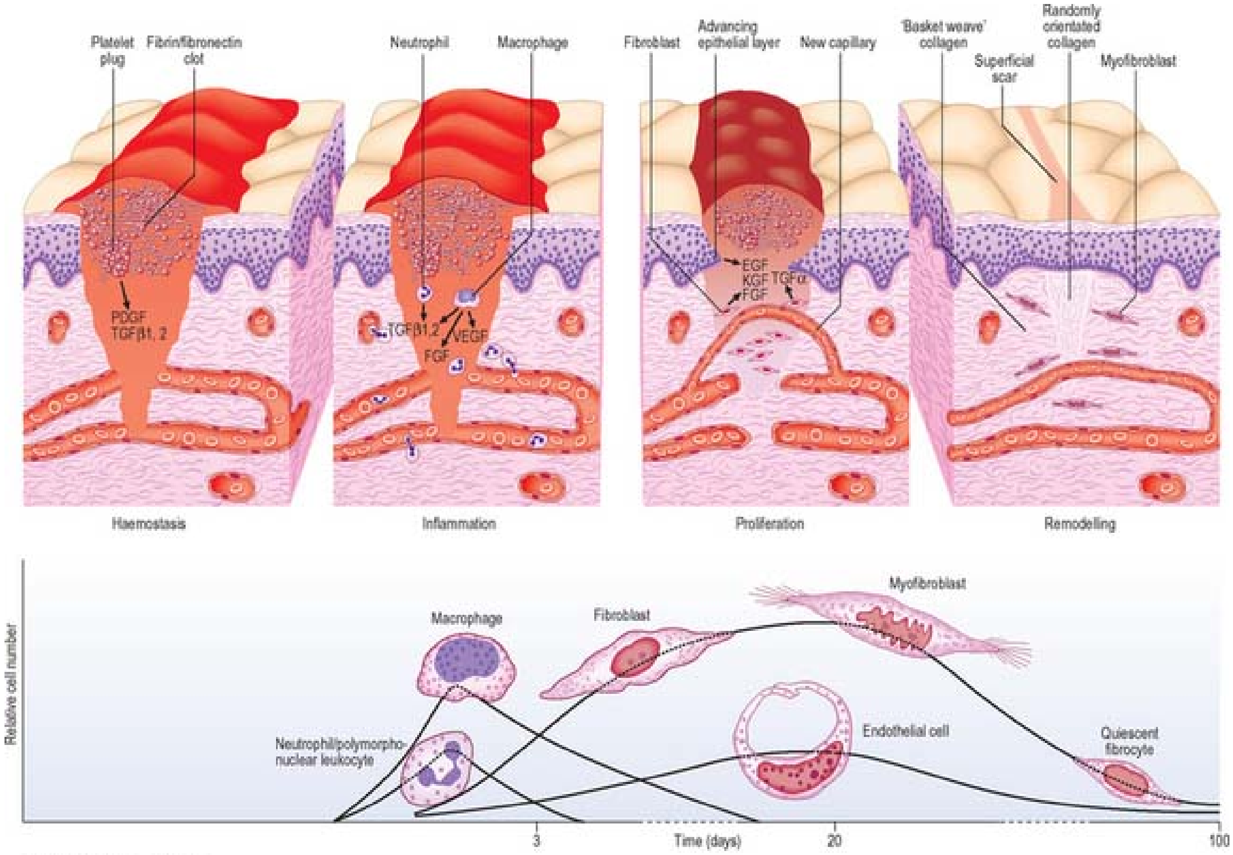
Platelet plug
Fibrin/fibronectin clot
PDGF
TGFβ1, 2
Haemostasis
Neutrophil
Macrophage
TGFβ1,2
VEGF
FGF
Inflammation
Fibroblast
Advancing epithelial layer
New capillary
EGF
KGF
FGF
TGFα
Proliferation
'Basket weave' collagen
Randomly orientated collagen
Superficial scar
Myofibroblast
Remodelling
Relative cell number
Macrophage
Fibroblast
Myofibroblast
Neutrophil/polymorpho-nuclear leukocyte
Endothelial cell
Quiescent fibrocyte
3
Time (days)
20
100

EGF: Epidermal growth factor
KGF: Keratinocyte growth factor
TGF: Transforming growth factor
FGF: Fibroblast growth factor
VEGF: Vascular endothelial growth factor
PDGF: Platelet derived growth factor

Fig. 7.26 Schematic illustration of the processes involved in the healing of a normal cutaneous wound.

HAEMOSTASIS

Wounding causing vascular injury initiates fibrin-fibronectin clot formation. The clot consists of platelets (promoted to aggregate by fibrillar collagens type I and III) embedded in a mesh of cross-linked fibrin and fibronectin fibres. It serves as a haemostatic plug, protects the denuded wound with a temporary physical shield, and forms a provisional matrix through and over which cells migrate during the repair process. The clot also acts as a reservoir of growth factors and cytokines, which are released as platelets de-granulate, and contribute to inflammatory cell recruitment.

INFLAMMATION

Neutrophils and monocytes are recruited to wound sites within minutes of injury by a variety of chemotactic signals, including complement factors, bacterial polysaccharides, cytokines and growth factors such as tumour necrosis factor (TNF)-α, interleukin (IL)-1, platelet-derived growth factor (PDGF), transforming growth factor (TGF)-α and TGF-β1,2, basic fibroblast growth factors (bFGF/FGF-2), serotonin, and monocyte chemotactic protein-1 (MCP-1).

Neutrophils act against contaminating bacteria. Monocytes differentiate into macrophages that phagocytose not only pathogenic organisms, but also expended neutrophils, cell and matrix debris. Both neutrophils and macrophages act as a further source of cytokines and growth factors to amplify stimuli already present in the wound site. Macrophages are also a source of additional factors such as TGFβ, FGF and vascular endothelial growth factor (VEGF) that activate resident fibroblasts, endothelial cells and keratinocytes, which in turn are central to the processes of re-epithelialization and formation of granulation tissue, as discussed below.

PROLIFERATION

The proliferation phase of wound healing involves re-epithelialization and granulation tissue formation which take place more or less simultaneously.

Re-epithelialization

Re-epithelialization begins within hours of wounding as a result of keratinocyte migration and proliferation from the wound edges and skin appendages. Cytokines such as epidermal growth factor (EGF), FGF, keratinocyte growth factor (KGF, FGF-7), insulin like growth factor-1 (IGF-1) and TGFα are released by activated fibroblasts and keratinocytes, and stimulate the re-epithelialization process. The mechanisms of keratinocyte migration are not fully understood, although disruption of desmosomes and hemidesmosomes, extracellular matrix contact, formation of cytoplasmic actin filaments and degradation of the fibrin matrix are all likely to be important. There is evidence that keratinocyte expression of matrix metalloproteinases (MMPs) is associated with re-epithelialization. During this phase of cutaneous wound healing, keratinocyte proliferation is thought to be upregulated after migration has started; dividing and migrating cells are found in the first suprabasal as well as basal keratinocyte layers. MMP activity is regulated by the production of tissue inhibitors of MMPs (TIMPs) and a relative imbalance, with upregulation of certain MMPs, may be associated with impaired wound healing. When the denuded wound surface has been covered by a monolayer of keratinocytes, migration ceases. A stratified epidermis with an underlying basal lamina is re-established from the margins of the wound inwards. Anchoring fibrils linking the basal lamina to the underlying connective tissue mark neo-epidermal maturity.

Granulation tissue formation

The term granulation tissue refers to the macroscopic appearance of wound connective tissue, which appears pink and granular. It contains numerous capillaries that invade the initial wound clot and become organized into a microvascular network (angiogenesis), together with the cells and molecules necessary to stimulate neo-matrix deposition. Angiogenesis is a complex process, promoted by dynamic interactions between endothelial cells, angiogenic cytokines (including FGF-2, VEGF (mainly from keratinocytes), PDGF and TGFβ1,2) and the extracellular matrix environment.

Electron microscope studies have shown that the epidermis, basal lamina and papillary dermis all develop on the surface of the granulation tissue. Wounds that fail to granulate do not heal satisfactorily, suggesting that granulation tissue formation is a key aspect of wound repair. Excessive granulation is also associated with delayed re-epithelialization.

Activated fibroblasts in the healing wound proliferate in response to growth factors, notably TGFβ1, IGF-1, PDGF, FGF and EGF. Within 72 hours of injury, these fibroblasts synthesize components of the new extracellular matrix, which are deposited in an orderly sequence. The neo-matrix initially includes fibronectin and hyaluronic acid which form a provisional substratum for cellular migration. Fibronectin acts as an initiation site for collagen fibrillogenesis, and as anchorage for myofibroblasts to effect wound contraction. Hyaluronic acid forms a highly hydrated matrix that is easily penetrated by migrating cells. Ultimately this and other neo-matrix components are replaced, first by collagen type III, and subsequently by collagen type I, which imparts strength to the mature scar (see remodelling, below). Non-structural proteins such as tenascin are also found in the neo-matrix of healing wounds and provide signals that orchestrate the repair process.

Cellularity decreases during the evolution of granulation tissue into a mature scar (and during other phases of wound healing) mainly as a result of apoptosis.

REMODELLING

Remodelling of the extracellular matrix is important throughout the wound healing process and persists for some time after closure of the defect. Fibroblasts are responsible for matrix remodelling as well as deposition. Initially they replace hyaluronic acid in the neo-matrix with sulphated proteoglycans, such as decorin, biglycan, and versican, which contribute to tissue resilience. Increased wound strength coincides with new collagen deposition. Approximately three weeks after injury, collagen breakdown and synthesis equilibrate; subsequent more gradual increases in wound strength reflect collagen remodelling, with the formation of intermolecular cross links and larger collagen bundles. Scar maturation is associated with proportional increases in collagen type I relative to collagen type III. Collagen fibres of the dermis in scars are arranged in an irregular fashion and scarred skin only reaches a maximum tensile strength of about 70% of unwounded skin.

Wound contraction

An important part of remodelling is wound contraction. Once granulation tissue has been laid down, a proportion of activated fibroblasts transform into myofibroblasts, which play a key role in wound contraction: they are thought to generate forces that pull normal dermal and adipose tissue into the wound defect.

SCARLESS WOUND HEALING

Wounds heal with reduced or absent scarring in certain circumstances, notably cutaneous wounds in the early fetus. The development of a major inflammatory response at a wound site appears to be a significant determinant of whether scarring occurs. Scarless fetal wound healing is characterized by fewer inflammatory cells (which are less differentiated than their adult counterparts and which remain in the wound for a shorter time), rapid re-epithelialization, reduced angiogenesis and restoration of the connective tissue architecture in which collagen is arranged in the normal reticular pattern.

An ontogenic transition period, during which cutaneous healing changes from scar-free to scar-forming, has been identified in the third trimester of gestation. Studies of this transition period have led to the identification of molecules of key importance in the scarring process; the most extensively characterized factor to date is TGFβ. Three mammalian TGFβ isoforms have been identified, TGFβ-1, -2 and -3. Comparisons of fetal scar-free and adult scar-forming wounds show that TGFβ-1 and -2 are not present in fetal wounds, suggesting that scarless wound healing is associated with TGFβ-3 activity, rather than TGFβ-1 and -2. The β-1 and -2 isoforms are dominant in fetal, neonatal and adult wounds that form scars. The main sources of TGFβ-3 are fibroblasts and keratinocytes, whilst TGFβ-1, and -2 are produced from degranulating platelets and subsequently from monocytes and macrophages: the low levels of TGFβ-1 seen in fetal wounds have been attributed to a relative lack of platelet de-granulation and fibrin clot formation.

SKIN GRAFTS AND FLAPS

A graft is a piece of tissue which has been detached from its blood supply and therefore needs to regain a blood supply from the bed in which it is placed in order to survive. In contrast, a flap is a piece of tissue which is surgically raised and transferred from one location in the body to another whilst maintaining its blood supply, which enters the base (pedicle) of the flap when it is transplanted.

GRAFTS

Grafts can be composed of skin, fat, fascia or bone, either separately or together as a composite piece of tissue. Skin grafts can be either full thickness grafts or split thickness grafts. Full thickness grafts consist of the epidermis and the full thickness of the dermis. Split thickness grafts consist of the epidermis and a variable quantity of the dermis. An essential difference is that the donor site following the harvest of a full thickness graft has no epidermal elements from which new skin can regenerate. These grafts therefore tend to be taken from sites of the body where the donor defect can be primarily closed. The donor site from split thickness grafting contains adnexal remnants (hair follicles in particular) which have the propensity to divide and regenerate new epidermis and so resurface the donor defect.

Revascularization of grafts is dependent on early and direct connection between host and graft vessels (inosculation), before which graft survival depends on fluid absorption (imbibition). Revascularization, which occurs as early as 48 hours, is by both anastomosis, whereby the severed ends of preexisting graft vessels link up with vessels of the underlying wound bed; and neovascularization, which involves the *de novo* angiogenic ingrowth of vessels from the wound bed into the graft. During the first two weeks, blood vessels from the recipient invade the graft edges along previous vascular channels in the direction of an ischaemic stimulus, whereas native graft vasculature begins to regress. Endothelial progenitor cells appear to play an important role in blood vessel formation, attracted by ischaemic gradients. Inosculation occurs, restoring blood flow to the graft microcirculation. By the start of the third week, complete blood flow in the graft vasculature has been established and in the absence of a continuing ischaemic stimulus, neovascularization ends.

FLAPS

Flaps are named according to the type of tissue transferred, e.g. a fasciocutaneous flap contains skin and fascia, and a musculocutaneous flap contains both muscle and the overlying skin, whereas a skin flap, fascial flap or a muscle flap contain only the separate elements that their names imply. The blood supply to a skin flap can be randomly orientated, which limits the flap length to breadth proportions to no more than 2 : 1 (except on the face, where longer flaps can be raised). Much longer skin flaps can be raised elsewhere if the blood supply to the flap is a direct cutaneous artery and vein: these are called axial pattern flaps.

A free flap (free tissue transfer) is a specific type of flap in which the tissue, whether skin, fascia, muscle, bone or a combination of these, is completely removed from its original location in the body along with a single identifiable artery and vein and transferred to a remote site. The blood vessels in the flap are anastomosed to vessels located in the new site using microsurgical techniques. This often allows for greater flexibility in performing reconstructive surgery. (The arterial perforators in the lower limb are described in Ch. 79.)

REFERENCES

rges AF. Relaxed skin tension lines (RSTL) versus other skin lines. *Plast Reconstr Surg*. 1984;73:144-150.

A mini-review of skin lines which also highlights the shortfalls in using some of these lines when planning elective skin incisions..

rne C, Hardman M, Nield K. Covering the limb – formation of the integument. *J Anat*. 2002;1:113-124. In: Lane EB, Tickle C (eds) Symposium issue: how to make a hand

Current views on the differentiation of skin and its appendages during embryogenesis..

azizadeh S, Taichman LB. Organization of stem cells and their progeny in human epidermis. *J Invest Dermatol*. 2005;124:367-372.

oding CR. Melanocytes: the new black. *Int J Biochem Cell Biol*. 2007;39:275-279.

L-H, Coulombe PA. Keratin function in skin epithelia: a broadening palette with surprising shades. *Curr Op Cell Biol*. 2007;19:13-23.

olbrook KA, Odland GF. Regional development of the human epidermis in the first trimester embryo and the second trimester fetus (ages related to the timing of amniocentesis and fetal biopsy). *J Dermatol*. 1980;4(3):161-168.

vine AD, McLean WHI. Human keratin diseases: increasing spectrum of disease and subtlety of phenotype-genotype correlation. *Br J Dermatol*. 1999;140:815-828.

Reviews the molecular basis of disorders of the skin and other epithelial tissues that are the result of abnormalities in keratin genes..

iller M-C, Nanchahal J. Advances in the modulation of cutaneous wound healing and scarring. *Biodrugs*. 2005;19:363-381.

ontagna W, Kligman AM, Carlisle KS. Atlas of Normal Human Skin. New York: Springer-Verlag, 1992.

emann C, Watt FM. Designer skin: lineage commitment in postnatal epidermis. *Trends Cell Biol*. 2002;12(4):185-192.

Summarizes current understanding of epidermal stem cell biology and commitment to alternative differentiation pathways..

hweizer J, Bowden PE, Coulombe PA, Langbein L, Lane EB, Magin TM, Maltais L, Omary MB, Parry DAD, Rogers MA, Wright MW. New consensus nomenclature for mammalian keratins. *J Cell Biol*. 2006;174:169-174.

eder V, Grim M, Halata Z, Sieber-Blum M. Neural crest origin of mammalian Merkel cells. *Dev Biol*. 2003;253:258-263.

Section 2
EMBRYOGENESIS

CHAPTER 8

Preimplantation development

Understanding the spatial and temporal developmental processes that take place within an embryo as it develops from a single cell into a recognizable human is the challenge of embryology. The control of these processes resides within the genome: fundamental questions remain concerning the genes and interactions involved in development.

STAGING OF EMBRYOS

For the purposes of embryological study, prenatal life is divided into an embryonic period and a fetal period. The embryonic period covers the first 8 weeks of development (weeks following ovulation and fertilization resulting in pregnancy). The ages of early human embryos have previously been estimated by comparing their development with that of monkey embryos of known postovulatory ages. Because embryos develop at different rates and attain different final weights and sizes, a classification of human embryos into 23 stages occurring during the first 8 weeks after ovulation was developed most successfully by Streeter (1942), and the task was continued by O’Rahilly & Müller (1987). An embryo was initially staged by comparing its development with that of other embryos. On the basis of correlating particular maternal menstrual histories and the known developmental ages of monkey embryos, growth tables were constructed so that the size of an embryo (specifically, the greatest length) could be used to predict its presumed age in postovulatory days (synonymous to postfertilizational days). O’Rahilly & Müller (2000) emphasize that the stages are based on external and internal morphological criteria and are not founded on length or age. Ultrasonic examination of embryos *in vivo* has necessitated the revision of some of the ages related to stages, and embryos of stages 6–16 are now thought to be up to 3 to 5 days older than the previously used embryological estimates (O’Rahilly & Müller 1999). Within this staging system, embryonic life commences with fertilization at stage 1; stage 2 encompasses embryos from two cells, through compaction and early segregation, to the appearance of the blastocele. The developmental processes occurring during the first 10 stages of embryonic life are shown in Fig. 8.1.

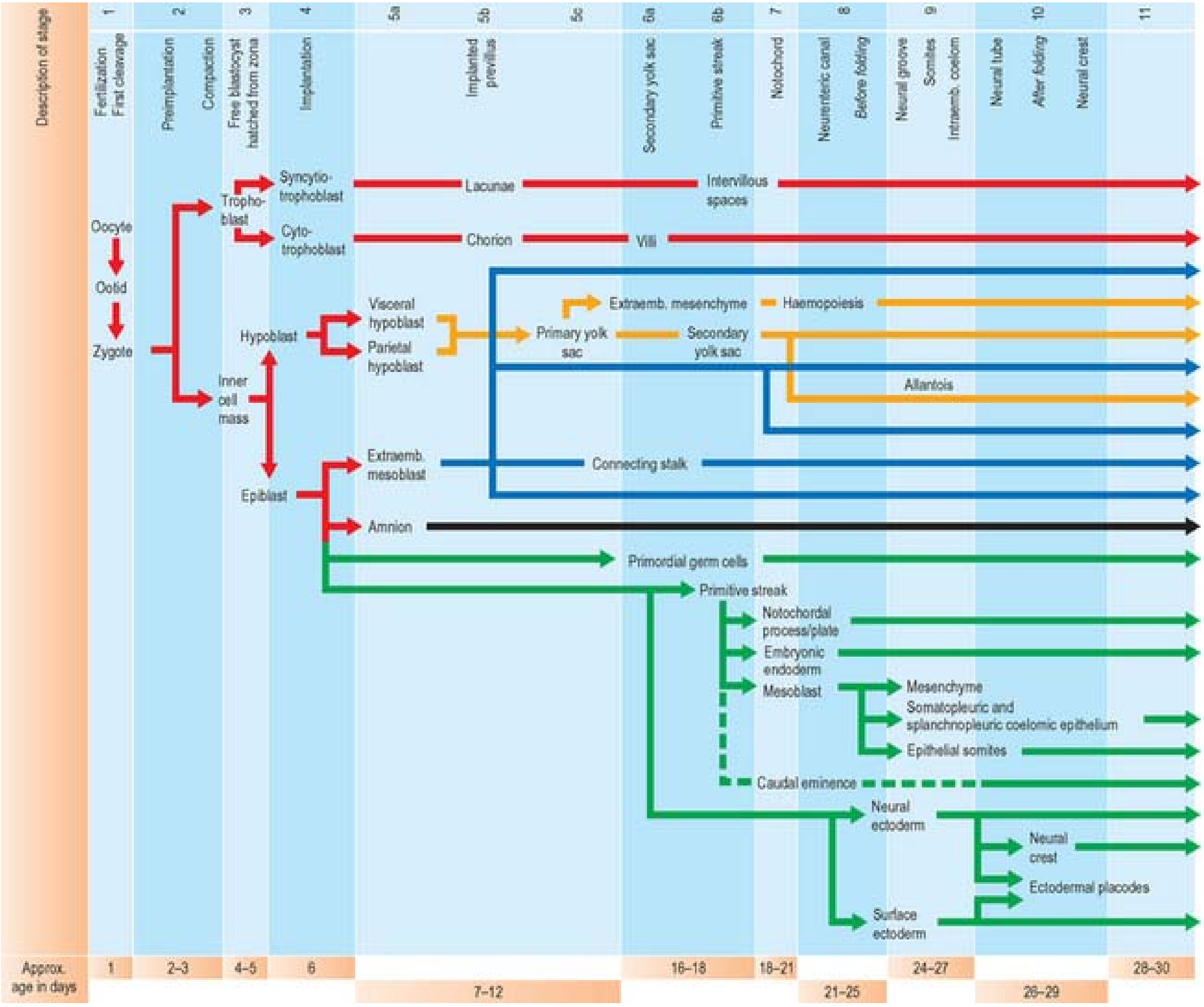
Description of stage
1
Fertilization
First cleavage
2
Preimplantation
Compaction
3
Free blastocyst hatched from zona
4
Implantation
5a
5b
Implanted previllus
5c
6a
Secondary yolk sac
6b
Primitive streak
7
Notochord
8
Neurenteric canal
Before folding
9
Neural groove
Somites
Intraemb. coelom
10
Neural tube
After folding
Neural crest
11
Oocyte
Ootid
Zygote
Tropho-blast
Syncytio-trophoblast
Cyto-trophoblast
Lacunae
Intervillous spaces
Chorion
Villi
Hypoblast
Visceral hypoblast
Parietal hypoblast
Primary yolk sac
Extraemb. mesenchyme
Haemopoiesis
Secondary yolk sac
Allantois
Inner cell mass
Epiblast
Extraemb. mesoblast
Connecting stalk
Amnion
Primordial germ cells
Primitive streak
Notochordal process/plate
Embryonic endoderm
Mesoblast
Mesenchyme
Somatopleuric and splanchnopleuric coelomic epithelium
Epithelial somites
Caudal eminence
Neural ectoderm
Neural crest
Ectodermal placodes
Surface ectoderm
Approx. age in days
1
2–3
4–5
6
7–12
16–18
18–21
21–25
24–27
26–29
28–30

Fig. 8.1 Developmental processes occurring during the first 10 stages of development. In the early stages, a series of binary choices determine the cell lineages. Generally, the earliest stages are concerned with formation of the extraembryonic tissues, whereas the later stages see the formation of embryonic tissues.

Much of our knowledge of the early developmental processes is derived from experimental studies on amniote embryos, particularly the chick, mouse and rat. Figure 8.2 shows the comparative timescales of development of these species and human development up to stage 12. The size and age, in postovulatory days, of human development from stage 10 to stage 23 is given in Fig. 8.3.

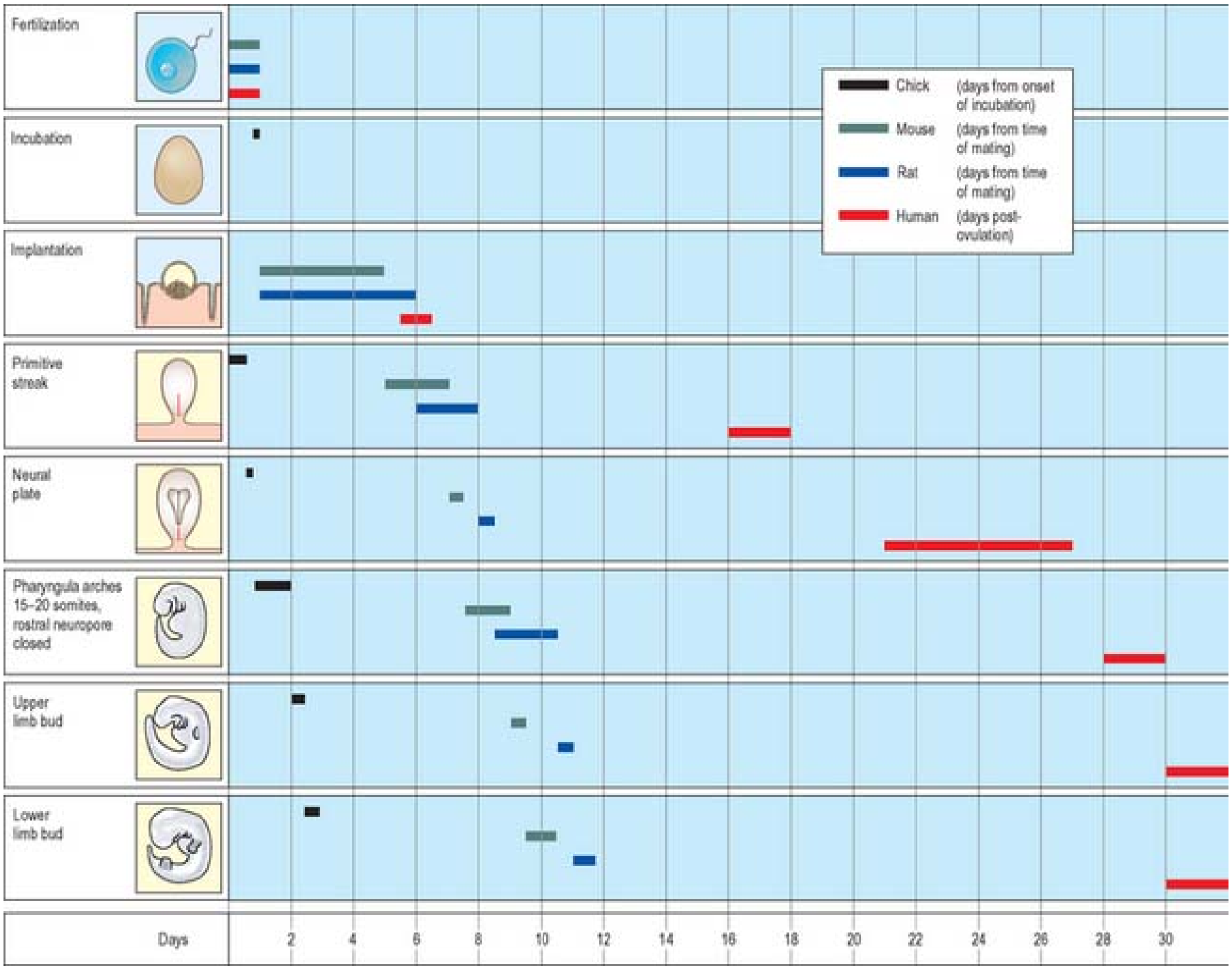

Fig. 8.2 Within developmental biology, evidence concerning the nature of developmental processes has come mainly from studies in vertebrate embryos, most commonly amniote embryos of the chick, mouse and rat. This chart illustrates the comparative timescale of development of these animals and the human.

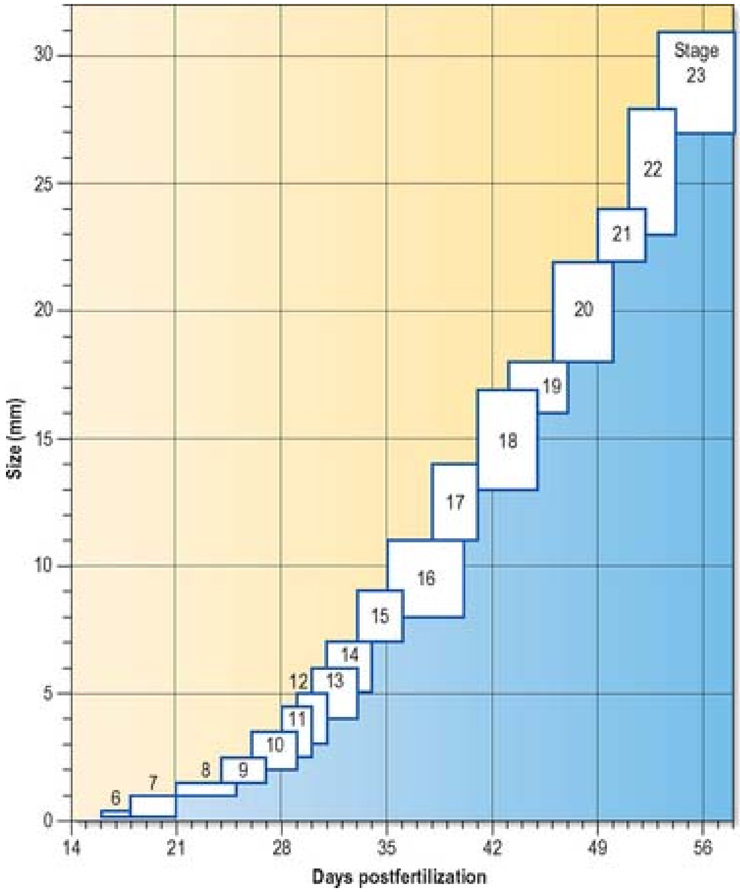

Fig. 8.3 Human developmental stages 10–23. Greatest embryonic length in mm (ordinate) plotted against age in postfertilizational weeks (abscissa) with the stages superimposed according to current information

(Data provided by courtesy of Professor R. O'Rahilly).

Information on developmental age after stage 23 (8 weeks postovulation) is shown in Fig. 14.3, where the developmental staging used throughout this text is juxtaposed with the obstetric estimation of gestation that is used clinically. A critique of staging terminology and the hazards of the concurrent use of gestational age and embryonic age is given in Chapter 14; sizes and ages of fetuses towards the end of gestation are illustrated in Fig. 14.7.

FERTILIZATION

The central feature of reproduction is the fusion of the two gamete pronuclei at fertilization. In humans the male gametes are spermatozoa, which are produced from puberty onwards. Female gametes are released as secondary oocytes in the second meiotic metaphase, usually singly, in a cyclical fashion. The signal for the completion of the second meiotic division is fertilization, which stimulates the cell division cycle to resume, completing meiosis and extruding the second polar body (the second set of redundant meiotic chromosomes).

Fertilization normally occurs in the ampullary region of the uterine tube, probably within 24 hours of ovulation. Very few spermatozoa reach the ampulla to achieve fertilization. They must undergo capacitation, a process which is still incompletely understood, and which may involve modifications of membrane sterols or surface proteins. They traverse the cumulus oophorus and corona radiata, then bind to specific glycoprotein receptors on the zona pellucida, ZP3 and ZP2. Interaction of ZP3 with the sperm head induces the acrosome reaction, in which fusion of membranes on the sperm head releases enzymes, such as acrosin, which help to digest the zona around the sperm head, allowing the sperm to reach the perivitelline space. In the perivitelline space, the spermatozoon fuses with the oocyte microvilli, possibly via two disintegrin peptides in the sperm head and integrin in the oolemma (Fig. 8.4 and Fig. 8.5A).

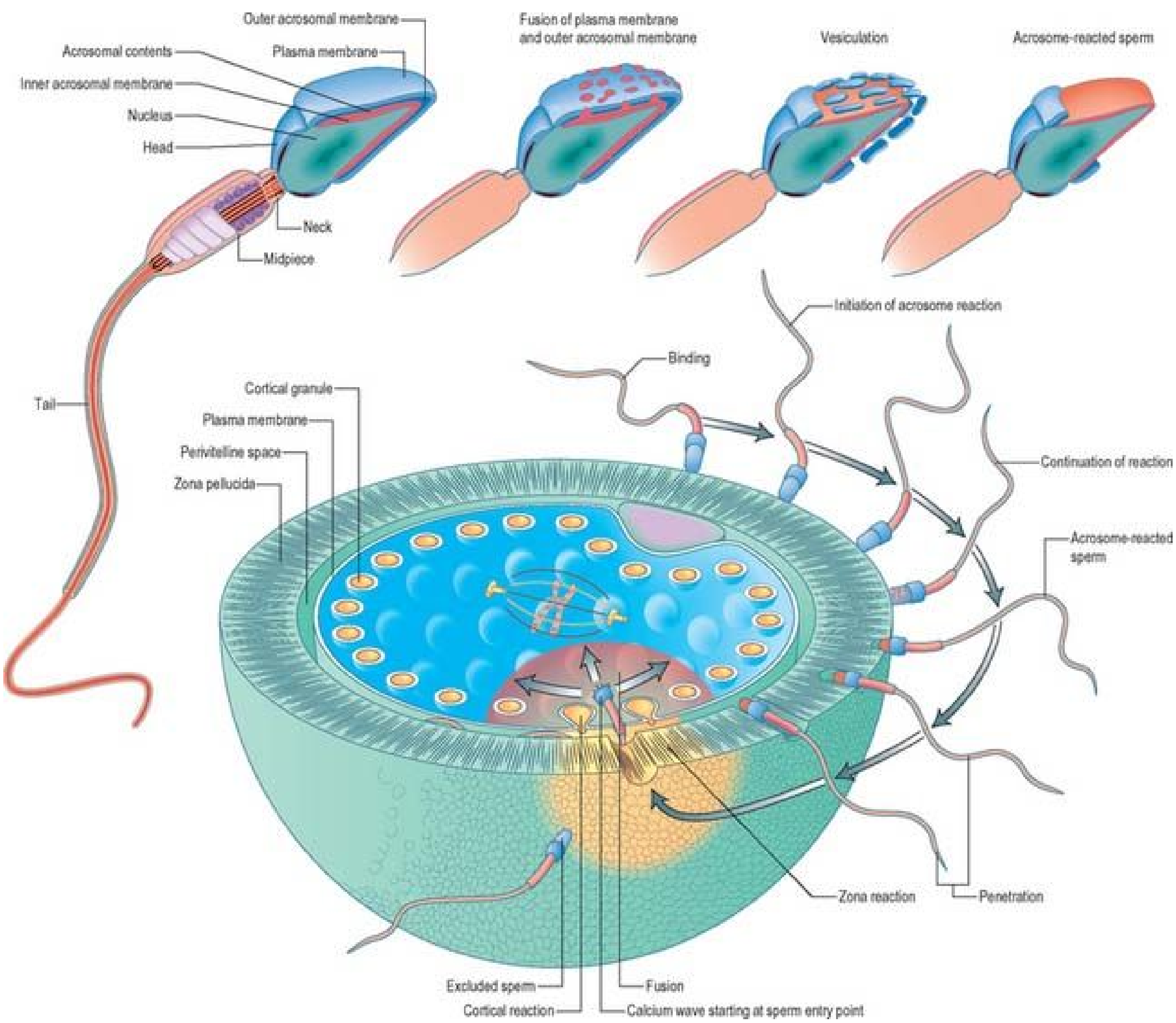
Outer acrosomal membrane
Acrosomal contents
Plasma membrane
Inner acrosomal membrane
Nucleus
Head
Neck
Midpiece
Tail
Fusion of plasma membrane and outer acrosomal membrane
Vesiculation
Acrosome-reacted sperm
Initiation of acrosome reaction
Binding
Cortical granule
Plasma membrane
Perivitelline space
Zona pellucida
Continuation of reaction
Acrosome-reacted sperm
Zona reaction
Penetration
Excluded sperm
Fusion
Cortical reaction
Calcium wave starting at sperm entry point

Fig. 8.4 Fertilization pathway: a succession of steps. After a sperm binds to the zona pellucida, the acrosome reaction takes place (see detail at top). The outer acrosomal membrane (blue), an enzyme-rich organelle in the anterior of the sperm head, fuses at many points with the plasma membrane surrounding the sperm head. Then those fused membranes form vesicles, which are eventually sloughed off from the head, exposing the acrosomal enzymes (red). The enzymes digest a path through the zona pellucida, enabling the sperm to advance. Eventually, the sperm meets and fuses with the secondary oocyte plasma membrane and this triggers cotrical and zona reactions. First, enzyme-rich cortical granules in the oocyte cytoplasm release their contents (yellow) into the zona pellucida, starting at the point of fusion and progressing right and left. Next, in the zona reaction, the

enzymes modify the zona pellucida, transforming it into an impenetrable barrier to sperm as a guard against polyspermy (multiple fertilization).

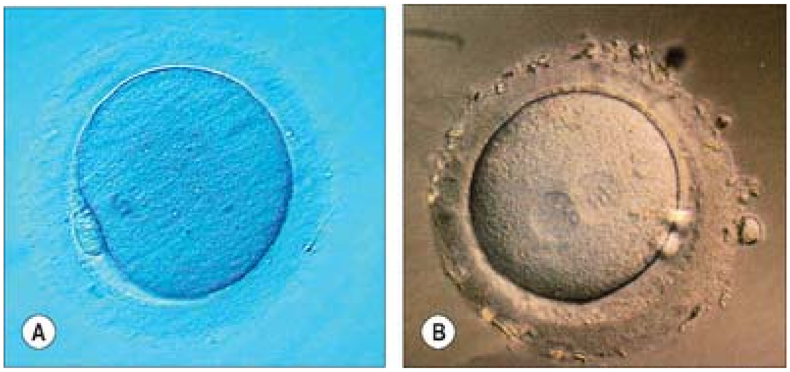

Fig. 8.5 **A**, An unfertilized human secondary oocyte surrounded by the zona pellucida; the first polar body can be seen. Spermatozoa can be seen outside the zona pellucida. **B**, Fertilized human ootid before fusion of the pronuclei. Two polar bodies can be seen beneath the zona pellucida.

Fusion of the sperm with the oolemma causes a weak membrane depolarization and leads to a calcium wave, which is triggered by the sperm at the site of fusion and crosses the egg within 5–20 seconds. The calcium wave amplifies the local signal at the site of sperm–oocyte interaction and distributes it throughout the oocyte cytoplasm. The increase in calcium concentration is the signal that causes the oocyte to resume cell division, initiating the completion of meiosis II and setting off the developmental programme that leads to embryogenesis. The pulses of intracellular calcium that occur every few minutes for the first few hours of development also trigger the fusion of cortical granules with the oolemma. The cortical secretory granules release an enzyme that hydrolyses the ZP3 receptor on the zona pellucida and so prevents other sperm from binding and undergoing the acrosome reaction, thus establishing the block to polyspermy. The same cortical granule secretion may also modify the vitelline layer and oolemma, making them less susceptible to sperm–oocyte fusion and providing a further level of polyspermy block.

The sperm head undergoes its protamine → histone transition as the second polar body is extruded. The two pronuclei grow, move together and condense in preparation for syngamy and cleavage after 24 hours (Fig. 8.5B). Nucleolar rRNA, and perhaps some mRNA, is synthesized in pronuclei. A succeeding series of cleavage divisions produces eight even-sized blastomeres at 2.5 days, when embryonic mRNA is transcribed.

Several examples of cells which contain male and female pronuclei, termed ootids, have been described. Pronuclear fusion as such does not occur: the two pronuclear envelopes disappear and the two chromosome groups move together to assume positions on the first cleavage spindle. No true zygote containing a membrane-bound nucleus is formed.

The presence of the pronuclei from both parental origins is crucial for spatial organization and the controlled growth of cells, tissues and organs. In the mouse, embryos in which the paternal pronucleus has been removed and replaced with a second maternal pronucleus develop to a relatively advanced state (25 somites), but with limited development of the trophoblast and extraembryonic tissues. In contrast, embryos in which the maternal pronucleus has been replaced by a second paternal pronucleus develop very poorly, forming embryos of only six to eight somites, but with extensive trophoblast. Thus it seems that the maternal genome is relatively more important for the development of the embryo, whereas the paternal genome is essential for the development of the extraembryonic tissues that would lead to placental formation.

This functional inequivalence of homologous parental chromosomes is called parental imprinting. The process causes the expression of particular genes to be dependent on their parental origin: some genes are expressed only from the maternally inherited chromosome and others from the paternally inherited chromosome. The genes involved are called imprinted genes. The requirement for both parental genomes is limited to a subset of the chromosomes. Uniparental disomy can arise through meiotic and mitotic non-disjunction events, and results in individuals who are completely disomic or who exhibit mosaicism of disomic and non-disomic cells. If imprinted genes reside on the affected chromosomes, then the uniparental disomic cells will either express a double dose of the gene or have both copies repressed. For example, the gene encoding the embryonal mitogen insulin-like growth factor II is expressed from the paternally inherited chromosome, and repressed when maternally inherited.

In vitro fertilization

Fertilization of human gametes *in vitro* (IVF) is a successful way of overcoming most forms of infertility. Controlled stimulation of the ovaries (e.g. pituitary downregulation using gonadotrophin-releasing hormone superactive analogues, followed by stimulation with purified follicle stimulating hormone or urinary menopausal gonadotrophins) enables many preovulatory oocytes (often 10 or more) to be recruited and matured, and then aspirated either by laparoscopy or transvaginally using ultrasound guidance, 34–38 hours after injection of human chorionic gonadotrophin (which is given to mimic the luteinizing hormone surge). These oocytes are then incubated overnight with motile spermatozoa in a specially formulated culture medium, to achieve successful fertilization *in vitro*. In cases of severe male-factor infertility, in which there are insufficient normal spermatozoa to achieve fertilization *in vitro*, individual spermatozoa can be directly injected into the oocyte in a process known as intracytoplasmic injection of sperm, which is as successful as routine *in vitro* fertilization. In cases in which there are no spermatozoa in the ejaculate, suitable material can sometimes be directly aspirated from the epididymis or surgically retrieved from the testes, and the extracted sperm are then used for intracytoplasmic injection of sperm. It is also now possible, in some cases, to test embryos for the presence of a particular genetic or chromosomal abnormality in a process known as preimplantation genetic diagnosis. A sample (biopsy) is removed from either the oocyte polar body, the embryo itself (a blastomere) or the blastocyst (small piece of trophectoderm), and subjected to a specific genetic test. Unaffected embryos can then be identified for transfer to the patient. Embryos that are surplus to immediate therapeutic requirements can also be cryopreserved in liquid nitrogen for later use. Propanediol or dimethylsulphoxide is used as a cryoprotectant for early embryos, and glycerol is used for blastocysts. Conception rates per cycle using ovarian stimulation, *in vitro* fertilization and successive transfers of fresh and cryopreserved embryos, far outstrip those obtained during non-assisted conception.

PREIMPLANTATION DEVELOPMENT

Cleavage

The first divisions of the zygote are termed cleavage. They distribute the cytoplasm approximately equally among daughter blastomeres, so although the cell number of the preimplantation embryo increases, its total mass actually decreases slightly (Fig. 8.6). The cell cycle is quite long, the first two cell cycles being around 24 hours each, thereafter reducing to 12–18 hours. Cell division is asynchronous and daughter cells may retain a cytoplasmic link through much of the immediately subsequent cell cycle via a midbody, as a result of the delayed completion of cytokinesis. No centrioles are present until 16 to 32 cells are seen, but amorphous pericentriolar material is present and serves to organize the mitotic spindles, which are characteristically more barrel- than spindle-shaped at this time.

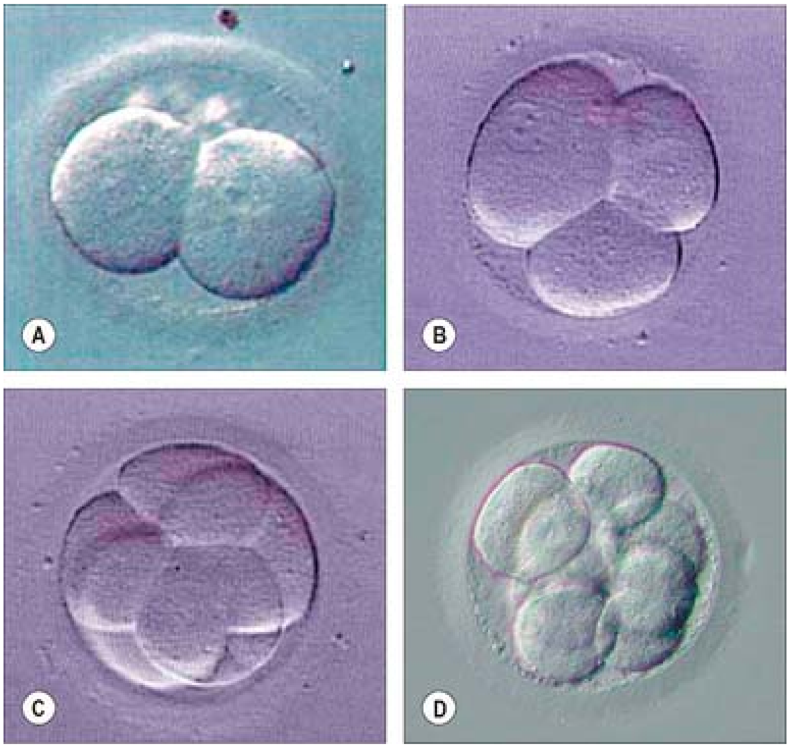

Fig. 8.6 Successive stages of cleavage of a human ootid. **A**, Two-cell stage; **B**, three-cell stage; **C**, five-cell stage; **D**, eight-cell stage.

All cleavage divisions after fertilization are dependent upon continuing protein synthesis. In contrast, passage through the earliest cycles, up to eight cells, is independent of mRNA synthesis. Thereafter, experimental inhibition of transcription blocks further division and development, indicating that activation of the embryonic genome is required. There is also direct evidence for the synthesis of embryonically encoded proteins at this time. As the genes of the embryo first become both active and essential, the previously functional maternally derived mRNA is destroyed. However, protein made on these maternal templates does persist at least during blastocyst growth. Spontaneous developmental arrest of embryo culture *in vitro* seems to occur during the cell cycle of gene activation, but it is not caused by total failure of that activation process. Early cleavage, up to the formation of eight cells, requires pyruvate or lactate as metabolic substrates, but thereafter more glucose is metabolized and may be required.

The earliest time at which different types of cells can be identified within the cleaving embryo is when 8 to 16 cells are present. Up to the formation of eight cells, cells are essentially spherical, touch each other loosely, and have no specialized intercellular junctions or significant extracellular matrix; the cytoplasm in each cell is organized in a radially symmetric manner around a centrally located nucleus. Once eight cells have formed, a process of compaction occurs. Cells flatten on each other to maximize intercellular contact, initiate the formation of gap and focal tight junctions, and radically reorganize their cytoplasmic conformation from a radially symmetric to a highly asymmetric phenotype. This latter process includes the migration of nuclei towards the centre of the embryo, the redistribution of surface microvilli and an underlying mesh of microfilaments and microtubules to the exposed surface, and the localization of endosomes beneath the apical cytoskeletal mesh. As a result of the process of compaction, the embryo forms a primitive protoepithelial cyst, which consists of eight polarized cells, in which the apices face outward and basolateral surfaces face internally. The focal tight junctions, which align to become increasingly linear, are localized to the boundary between the apical and basolateral surfaces. Gap junctions form between apposed basolateral surfaces and become functional.

The process of compaction involves the cell surface and the calcium dependent cell–cell adhesion glycoprotein, E-cadherin (also called L-CAM or uvomorulin). Neutralization of its function disturbs all three elements of compaction. The entire process can function in the absence of both mRNA and protein synthesis. Post-translational controls are sufficient and seem to involve regulation through protein phosphorylation. Significantly, although E-cadherin is not synthesized and present on the surface of cleaving blastomeres, it first becomes phosphorylated when eight cells are visible, at the initiation of compaction.

The process of compaction is important for the generation of cell diversity in the early embryo. As each polarized cell divides, it retains significant elements of its polar organization, so that its daughter cells inherit cytocortical domains, the nature of which reflects their origin and organization in the original parent cell in the eight-celled embryo. Thus, if the axis of division is aligned approximately at right angles to the axis of cell polarity, the more superficially placed daughter cell inherits all the apical cytocortex and some of the basolateral cytocortex and is polar, whereas the more centrally placed cell inherits only basolateral cytocortex and is apolar. In contrast, if the axis of division is aligned approximately along the axis of the cell polarity, two polar daughter cells are formed. In this way, two-cell populations are formed in the 16-cell embryo that differ in phenotype (polar, apolar) and position (superficial, deep). The number of cells in each population in any one embryo will be determined by the ratio of divisions along, and at right angles to, the axis of eight-cell polarity. The theoretical and observed limits of the polar to apolar ratio are 16 : 0 and 8 : 8. The outer polar cells contribute largely to the trophectoderm, whereas the inner apolar cells contribute almost exclusively to the inner cell mass in most embryos.

In cleavage the generation of cell diversity, to either trophectoderm or inner cell mass, occurs in the 16-cell morula and precedes the formation of the blastocyst. During the 16-cell cycle, the outer polar cells continue to differentiate an epithelial phenotype, and display further aspects of polarity and intercellular adhesion typical of epithelial cells, while the inner apolar cells remain symmetrically organized. During the next cell division (16 to 32 cells), a proportion of polar cells again divide differentiatively as in the previous cycle, each yielding one polar and one apolar progeny, which enter the trophectoderm and inner cell mass lineages, respectively. Although differentiative division at this time is less common than at the 8- to 16-cell transition, it has the important function of regulating an appropriate number of cells in the two tissues of the blastocyst. Thus, if differentiative divisions were relatively infrequent at the 8- to 16-cell transition, they will be more frequent at the 16- to 32-cell transition, and *vice versa*.

After division to the 32 cells, the outer polar cells complete their differentiation into a functional epithelium, display structurally complete zonular tight junctions and begin to form desmosomes. The nascent trophectoderm engages in vectorial fluid transport in an apical to basal direction to generate a cavity that expands in size during the 32- to 64-cell cycles and converts the ball of cells, the morula, to a sphere, the blastocyst (Fig. 8.7). Once the blastocyst forms, the diversification of the trophectoderm and inner cell mass lineages is complete, and trophectoderm differentiative divisions no longer occur. In the late blastocyst, the trophectoderm is referred to as the trophoblast, which can be divided into polar trophoblast, which lies in direct contact with the inner cell mass, and mural trophoblast, which surrounds the blastocyst cavity (Fig. 8.8).

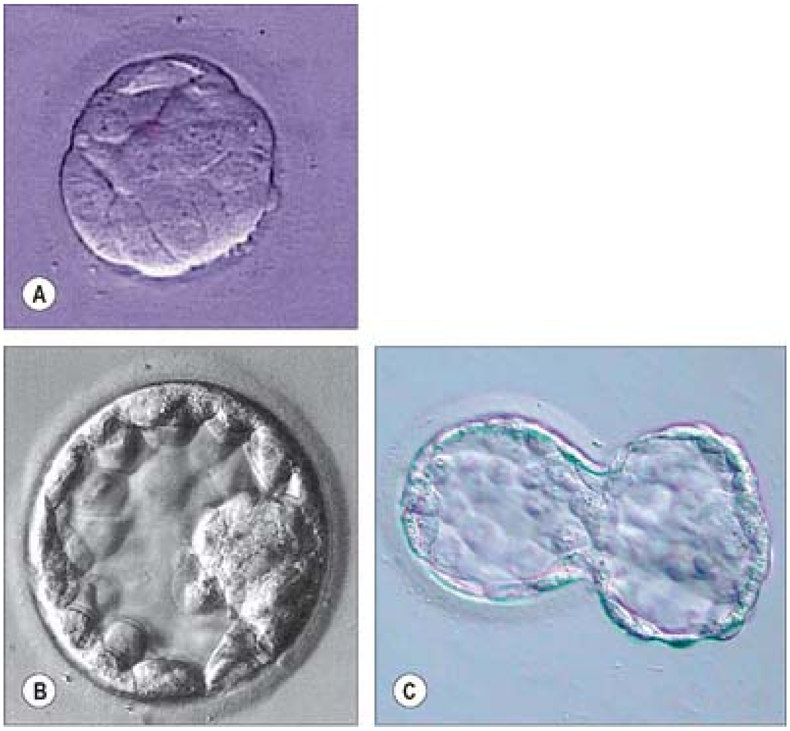

Fig. 8.7 Human embryos. Formation of a morula and blastocyst within the zona pellucida and blastocyst hatching from the zona pellucida. **A**, A ball of cells, the morula, with the cells undergoing compaction; **B**, the blastocyst cavity is developing and the inner cell mass can be seen on one side of the cavity; **C**, the blastocyst is beginning to hatch from the zona pellucida.

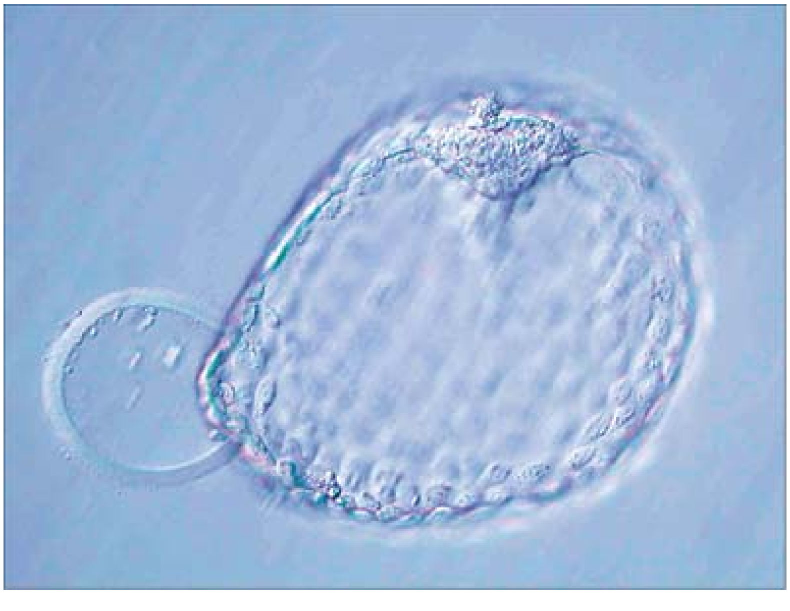

Fig. 8.8 Human blastocyst nearly completely hatched from the zona pellucida. The blastocyst can now expand to its full size.

Blastocyst

The blastocyst ‘hatches’ from its zona pellucida at 6–7 days, possibly assisted by an enzyme similar to trypsin (Figs 8.7C, 8.8). Trophoblast oozes out of a small slit; many embryos form a figure-of-eight shape bisected by the zona pellucida, especially if it has been hardened during oocyte maturation and cleavage. Such half-hatching could result in the formation of identical twins. Hatched blastocysts expand and differentiation of the inner cell mass proceeds (Fig. 8.8).

The outer cells of the blastocyst, the trophoblast or trophectoderm, are flattened polyhedral cells, which possess ultrastructural features typical of a transporting epithelium. The trophoblast covering the inner cell mass is the polar trophoblast and that surrounding the blastocyst cavity is the mural trophoblast. The free, unattached blastocyst is assigned to stage 3 of development at approximately 4 days postovulation, whereas implantation (before villus development) occurs within a period of 7–12 days postovulation and over the next two stages of development. Even at this early stage, cells of the inner cell mass are already arranged into an upper layer (i.e. closest to the polar trophoblast), the epiblast, which will give rise to the embryonic cells, and a lower layer, the hypoblast, which has an extraembryonic fate. Thus the dorsoventral axis of the developing embryo and a bilaminar arrangement of the inner cell mass are both established at or before implantation. (The earliest primordial germ cells may also be defined at this stage.)

Attachment to the uterine wall

On the sixth postovulatory day, the blastocyst adheres to the uterine mucosa and the events leading to the specialized, intimate contact of trophoblast and endometrium begin. Implantation, which is the term used for this complicated process, includes the following stages: dissolution of the zona pellucida; orientation and adhesion of the blastocyst onto the endometrium; trophoblastic penetration into the endometrium; migration of the blastocyst into the endometrium; spread and proliferation of the trophoblast, which envelops and specifically disrupts and invades the maternal tissues.

The site of implantation is normally in the endometrium of the posterior wall of the uterus, nearer to the fundus than to the cervix, and may be in the median plane or to one or other side. Implantation may occur elsewhere in the uterus, or in an extrauterine or ectopic site. Implantation near the internal os results in the condition of placenta praevia, with its attendant risk of severe antepartum haemorrhage.

Ectopic implantation

The conceptus may be arrested at any point during its migration through the uterine tube and implant in its wall. Previous pelvic inflammation damages the tubal epithelium and may predispose to such delay in tubal transport. The presence of an intrauterine contraceptive device or the use of progesterone-based oral contraceptives may also predispose to ectopic pregnancy, probably because of alteration in the normal tubal transport mechanisms.

Nidation of the embryo as an ectopic pregnancy most frequently occurs in the wider ampullary portion of the uterine tube, but may also occur in the narrow intramural part or even in the ovary itself. Most ectopic pregnancies are anembryonic, although the continuing growth of the trophoblast will produce a positive pregnancy test, and may cause rupture of the uterine tube and significant intraperitoneal haemorrhage. Ectopic pregnancies with a live embryo are the most dangerous, because they grow rapidly and may be detected only when they have eroded the uterine tube wall and surrounding blood vessels, as early as 8 weeks of pregnancy. Similarly, cornual ectopics (in the intramural part of the tube) may present with catastrophic haemorrhage, because there is a substantial blood supply in the surrounding muscularis.

Ovarian or abdominal pregnancies are exceptionally rare. Although some are presumed to have been caused by fertilization occurring in the vicinity of the ovary (primary), most are probably caused secondarily and result from an extrusion of the conceptus through the abdominal ostium of the tube.

Apart from their important clinical implications, these conditions emphasize the fact that the conceptus can implant successfully into tissues other than a normal progestational endometrium. Prolonged development can occur in such sites and is usually terminated by a mechanical or vascular accident and not by a fundamental nutritive or endocrine insufficiency or by an immune maternal response. Abdominal implantation may occur on any organ, e.g. bowel, liver, omentum. If such a pregnancy continues, this makes removal of the placenta at delivery or abortion hazardous as a result of haemorrhage, and consequently the placenta is usually left *in situ* to degenerate spontaneously.

Twinning

Spontaneous twinning occurs once in about every 80 births. Monozygotic twins arise from a single ovum fertilized by a single sperm. At some stage up to the establishment of the axis of the embryonic area and the development of the primitive streak, the embryonic cells separate into two parts, each of which gives rise to a complete embryo. The process of hatching of the blastocyst from the zona pellucida may result in constriction of the emerging cells and separation into two discrete entities. There is a gradual decrease in the average thickness of the zona pellucida with increasing maternal age, which may be causally related to the increase in frequency of monozygotic twinning with increased maternal age. The resultant twins have the same genotype, but the description ‘identical twins’ is best avoided, since most monozygotic twins have differences in phenotypes. Late separation of twins from a single conceptus may result in conjoined twins; these may be equal or unequal as in acardia. After twinning, monozygotic embryos enter a period of intense catch-up growth. Despite starting out at half the size, each twin embryo or fetus is of a size comparable to a singleton fetus in the second trimester of pregnancy, but declines in relative size in the last 10 weeks of pregnancy. The sex of monozygotic twins will be the same. Monoamniotic, monochorionic, monozygotic twins are most likely to be female, as are acardiac twins. The male:female ratio for all monozygotic twins is 0.487, and for monoamniotic, monochorionic twins it is 0.231.

Dizygotic twins represent the most frequent form of twinning. They result from multiple ovulations, which can be induced by gonadotrophins or drugs commonly used in patients with infertility. Dizygotic twins may be different sexes; like-sex pairs are more common. The male: female ratio is 0.518. Multiple births greater than twinning, such as triplets or quadruplets, can arise from multiple ovulations, or from a single ovum, or both. It is most likely to be seen in women treated with drugs to stimulate ovulation.

The range of separation of twin embryos is reflected in the separation of the extraembryonic membranes. The types of placentation that can occur are shown in Fig. 8.9. Monoamniotic, monochorionic placentae are associated with the greatest perinatal mortality (50%), caused both by entanglement of the umbilical cords impeding the blood supply and by various vascular shunts between the placentae, which may divert blood from one fetus to the other. Artery–artery anastomoses are the most common, followed by artery–vein anastomoses. If the shunting of blood across the placentae from one twin to the other is balanced by more than one vascular connection, development may proceed unimpaired. However, if this is not the case, one twin may receive blood from the other, leading to cardiac enlargement, increased urination and hydramnios in the recipient, and anaemia, oligohydramnios and atrophy in the donor.

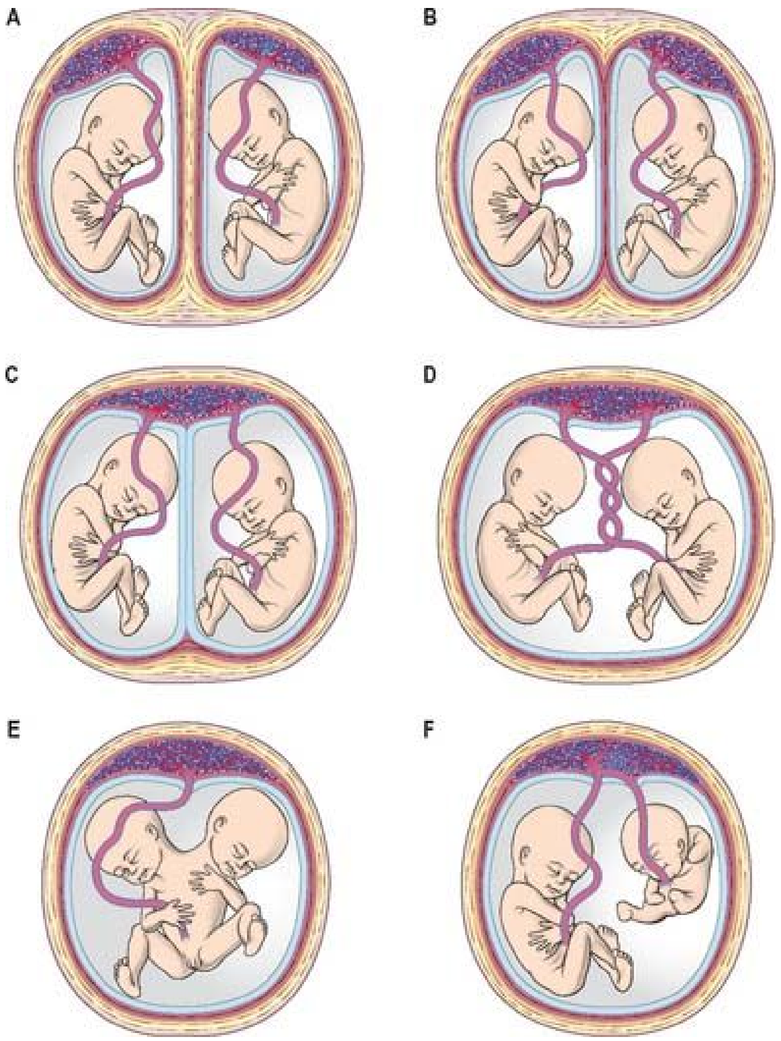

Fig. 8.9 Relationships of the extraembryonic membranes in different types of twinning. **A**, Diamnionic, dichorionic separated; i.e. separation of the first two blastomeres results in separate implantation sites. **B**, Diamnionic, dichorionic fused; here the chorionic membranes are fused, but the fetuses occupy separate choria. **C**, Diamnionic, monochorionic; reduplication of the inner cell mass can result in a single placenta and chorionic sacs, but separate amniotic cavities. **D**, Monoamnionic, monochorionic; duplication of the embryonic axis results in two embryos sharing a single placenta, chorion and amnion. **E**, Incomplete separation of the embryonic axis results in conjoined twins. **F**, Unequal division of the embryonic axis or unequal division of the blood supply may result in an acardiac monster.

Dizygotic twins have either completely separate chorionic sacs or sacs that have fused. Such placentae are separated by four membranes, two amnia and two choria; in addition these placentae have a ridge of firmer tissue at the base of the dividing membranes, caused by the abutting of two expanding placental tissues against each other.

FORMATION OF EXTRAEMBRYONIC TISSUES

The earliest developmental processes in mammalian embryos involve the production of those extraembryonic structures that will support and nourish the embryo during development. Production of these layers begins before implantation is complete. At present it is unclear where the extraembryonic cell lines arise. The trophoblast was considered to be a source, but evidence now points to the inner cell mass as the site of origin. Figure 8.1 shows the sequence of development of various tissues in the early embryo.

Epiblast and amniotic cavity

Epiblast cells, which are closest to the implanting face of the trophoblast, have a definite polarity, being arranged in a radial manner with extensive junctions near the centre of the mass of cells, supported by supranuclear organelles. A few epiblast cells are contiguous with cytotrophoblast cells; apart from this contact a basal lamina surrounds what is initially a spherical cluster of epiblast cells, and isolates them from all other cells. Those epiblast cells adjacent to the hypoblast become taller and more columnar than those adjacent to the trophoblast, and this causes the epiblast sphere to become flattened and the centre of the sphere to be shifted towards the polar trophoblast. Amniotic fluid accumulates at the eccentric centre of the now lenticular epiblast mass, which is bordered by apical junctional complexes and microvilli. As further fluid accumulates, an amniotic cavity forms, roofed by low cuboidal cells that possess irregular microvilli. The cells share short apical junctional complexes and associated desmosomes and rest on an underlying basal lamina. The demarcation between true amnion cells and those of the remaining definitive epiblast is clear. The columnar epiblast cells are arranged as a pseudostratified layer with microvilli, frequently a single cilium, clefted nuclei and large nucleoli; the cells have a distinct, continuous basal lamina. Cell division in the epiblast tends to occur near the apical surface, causing this region to become more crowded than the basal region.

At the margins of the embryonic disc, the amnion cells are contiguous with the epiblast; there is a gradation in cell size from columnar to low cuboidal within a two- to three-cell span (Fig. 8.10; see Fig. 9.1). Further development of the amnion and amniotic fluid is described on pages 180 and 181.

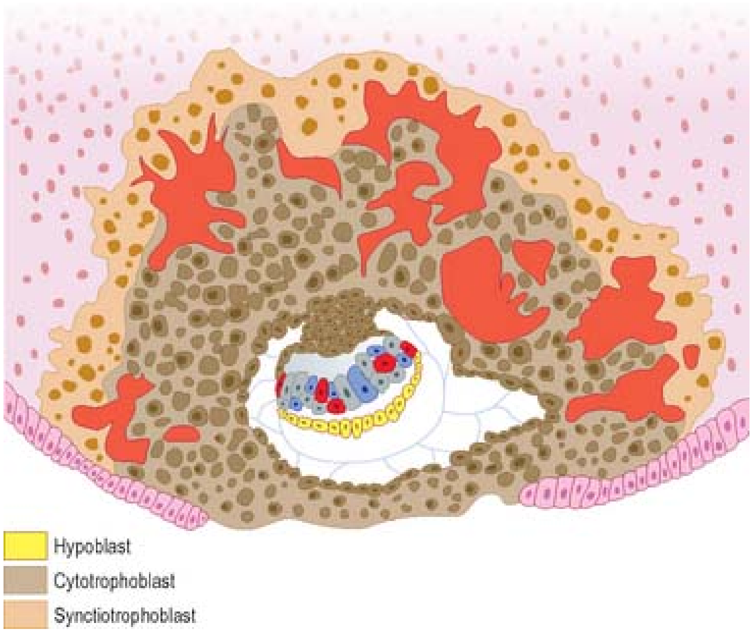

Fig. 8.10 Implanting conceptus at stage 5b. The embryo at this stage is composed only of the abutting epiblast and hypoblast layers. It is suspended within the blastocyst cavity (chorionic cavity) and surrounded by a layer of cytotrophoblast. A large mass of syncytiotrophoblast, with interconnecting lacunae, is penetrating the maternal endometrium.

Hypoblast and yolk sac

Hypoblast is the term used to delineate the lower layer of cells of the early bilaminar disc, most commonly in avian embryos. This layer is also termed anterior, or distal, visceral endoderm in the mouse embryo. Just before implantation, the hypoblast consists of a layer of squamous cells that is only slightly larger in extent than the epiblast. The cells exhibit polarity, with apical microvilli facing the cavity of the blastocyst and apical junctional complexes, but they lack a basal lamina. During early implantation, the hypoblast extends beyond the edges of the epiblast and can now be subdivided into those cells in contact with the epiblast basal lamina, the visceral hypoblast, and those cells in contact with the mural trophoblast, the parietal hypoblast. The parietal hypoblast cells are squamous, they may share adhesion junctions with the mural trophoblast and, rarely, may also share gap junctions. The visceral hypoblast cells are cuboidal; they have a uniform apical surface towards the blastocyst cavity, but irregular basal and lateral regions, with flanges and projections underlying one another and extending into intercellular spaces. There is no basal lamina subjacent to the visceral hypoblast, and the distance between the hypoblast cells and the epiblast basal lamina is variable.

A series of modifications of the original blastocystic cavity develops beneath the hypoblast later than those developing above the epiblast. While the amniotic cavity is enlarging within the sphere of epiblast cells, the parietal hypoblast cells are proliferating and spreading along the mural trophoblast until they extend most of the way around the circumference of the blastocyst, converging towards the abembryonic pole. At the same time, a space appears between the parietal hypoblast and the mural trophoblast that limits the circumference of the hypoblastic cavity. A variety of terms have been applied to the parietal hypoblast layer: extraembryonic hypoblast and later extraembryonic endoderm or the exocoelomic (Heuser’s) membrane. The cavity that the layer initially surrounds is termed the primary yolk sac, or alternatively the primary umbilical vesicle. The resultant smaller cavity lined by hypoblast is termed the secondary yolk sac. It has been suggested that it forms in a variety of ways, including cavitation of visceral hypoblast (a method similar to formation of the amnion), rearrangement of proliferating visceral hypoblast and folding of the parietal layer of the primary yolk sac into the secondary yolk sac. Further development of the yolk sac is described on page 180. The visceral hypoblast cells are now believed to be important in many aspects of the early specification of cell lines. The cells induce the formation of the primitive streak, thus establishing the first axis of the embryonic disc. They are also believed to be necessary for successful induction of the head region and for the successful specification of the primordial germ cells. With the later formation of the embryonic cell layers from the epiblast, the visceral hypoblast appears to be sequestered into the secondary yolk sac wall by the expansion of the newly formed embryonic endoderm beneath the epiblast. Hypoblastic cells remain beneath the primitive streak: their experimental removal causes multiple embryonic axes to form.

After the formation of the secondary yolk sac, a diverticulum of the visceral hypoblast, the allantois, forms towards one end of the embryonic region and extends into the local extraembryonic mesoblast. It passes from the roof of the secondary yolk sac to the same plane as the amnion. Further development of the allantois is described on page 180.

Extraembryonic mesoblast

By definition, extraembryonic tissues encompass all tissues that do not contribute directly to the future body of the definitive embryo and, later, the fetus. At stage 5, blastocysts are implanted but do not yet display trophoblastic villi (Fig. 8.10); they range from 7 to 12 days in age. A feature of this stage is the first formation of extraembryonic mesoblast, which will come to cover the amnion, secondary yolk sac and the internal wall of the mural trophoblast, and will form the connecting stalk of the embryo with its contained allanto-enteric diverticulum. The origin of this first mesoblastic extraembryonic layer is by no means clear, and it may arise from several sources, including the caudal region of the epiblast, the parietal hypoblast and subhypoblastic cells. The trophoblastic origin of extraembryonic mesoblast is questioned, because there is always a complete basal lamina underlying the trophoblast: the migration of cells out of an epithelium is usually associated with previous disruption of the basal lamina. Certainly, the origin of extraembryonic cells will change over time as new germinal populations are established.

The first mesoblastic extraembryonic layer gives rise to the layer known as extraembryonic mesoblast, arranged as a mesothelium with underlying extraembryonic mesenchymal cells; this also appears to form an extracellular structure corresponding to the magma reticulare, between the mural trophoblast and the primary yolk sac in the stage 5 embryo. Later extraembryonic mesoblast populations mushroom beneath the cytotrophoblastic cells at the embryonic pole, forming the cores of the developing villus stems, and villi (see p. 175) and the angioblastic cells that will give rise to the capillaries within them and the earliest blood cells.

Initially, the extraembryonic mesoblast connects the amnion to the chorion over a wide area. Continued development and expansion of the extraembryonic coelom means that this attachment becomes increasingly circumvented to a connecting stalk, which is a permanent connection between the future caudal end of the embryonic disc and the chorion. The connecting stalk forms a pathway along which vascular anastomoses around the allantois establish communication with those of the chorion.

REFERENCES

'Rahilly R, Müller F. Developmental Stages in Human Embryos. Washington: Carnegie Institution, 1987.

'Rahilly R, Müller F. The Embryonic Human Brain. An Atlas of Developmental Stages. 2nd edn.. New York: Wiley-Liss; 1999.

'Rahilly R, Müller F. Minireview: Prenatal ages and stages – measures and errors. *Teratology*. 2000;61:382-384.

reeter GL. Developmental horizons in human embryos. Descriptions of age group XI, 13 to 20 somites, and age group XII, 21 to 29 somites. *Contrib Embryol Carnegie Inst Washington*. 1942;30:211-245.

CHAPTER 9

Implantation and placentation

IMPLANTATION

Implantation involves the initial attachment of the trophoblastic wall of the blastocyst to the endometrial luminal epithelium. The trophoblast lineage gives rise to three main cell types in the human placenta: the syncytiotrophoblast, which forms the epithelial covering of the villous tree and is the main endocrine component of the placenta; the villous cytotrophoblast cells, which represent a germinative population that proliferate throughout pregnancy and fuse to generate the syncytiotrophoblast; and extravillous trophoblast cells, which are non-proliferative and invade the maternal endometrium. The first two cell lines can be seen from stages 4 and 5 onwards. The cytotrophoblast cells that form the mural and polar trophoblast are cuboidal, and covered externally with syncytial trophoblast (syncytiotrophoblast), a multinucleated mass of cytoplasm that forms initially in areas near the inner cell mass after apposition of the blastocyst to the uterine mucosa (see Fig. 8.10).

Preimplantation embryos produce matrix metalloproteinases, which mediate penetration of the maternal subepithelial basal lamina by the syncytiotrophoblast. Trophoblast cells express L-selectin (usually seen as a mediator of neutrophil rolling and tethering in inflamed endothelium), and the maternal epithelium upregulates selectin-oligosaccharide-based ligands. Thus, differentiating cytotrophoblast cells appear to use processes that also occur in vasculogenesis and during leukocyte emigration from the blood into the tissues. Flanges of syncytial trophoblast grow between the cells of the uterine luminal epithelium towards the underlying basal lamina without apparent damage to the maternal cell membranes or disruption of the intercellular junctions. Instead, shared junctions, including tight junctions, are formed with many of the maternal uterine epithelial cells.

Implantation continues with erosion of maternal vascular endothelium and glandular epithelium, and phagocytosis of secretory products, until the blastocyst occupies an uneven implantation cavity in the stroma (interstitial implantation) (Fig. 9.1). In the early postimplantation phase, the maternal surface is resealed by re-epithelialization and the formation of a plug, which may contain fibrin. As the blastocyst burrows more deeply into the endometrium, syncytial trophoblast forms over the mural cytotrophoblast, but never achieves the thickness of the syncytial trophoblast over the embryonic pole.

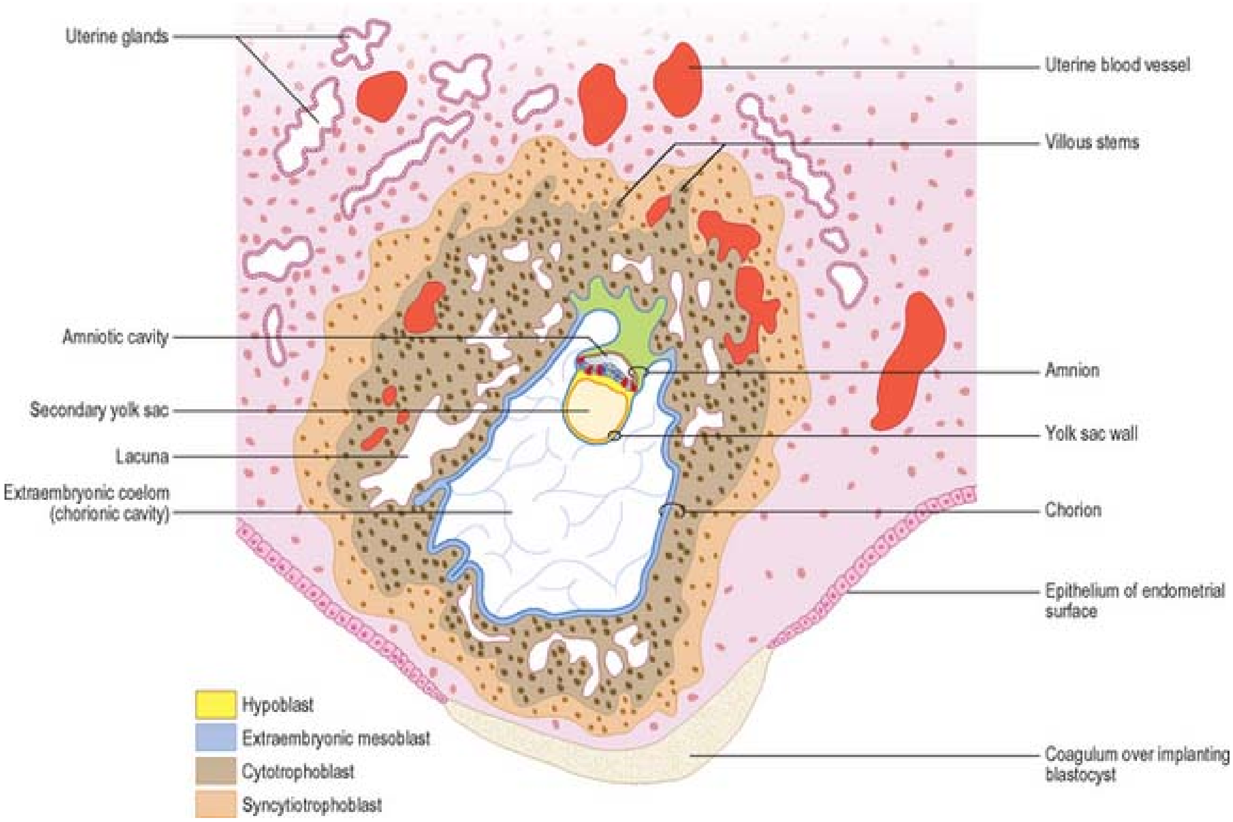
Uterine glands
Uterine blood vessel
Villous stems
Amniotic cavity
Amnion
Secondary yolk sac
Yolk sac wall
Lacuna
Extraembryonic coelom (chorionic cavity)
Chorion
Epithelium of endometrial surface
Hypoblast
Extraembryonic mesoblast
Cytotrophoblast
Syncytiotrophoblast
Coagulum over implanting blastocyst

Fig. 9.1 Implanting conceptus at stage 6. The embryo is composed of epiblast, with the amniotic cavity above it and hypoblast, with the secondary yolk sac below it. Both cavities are covered externally with extraembryonic mesoblast which also lines the larger chorionic cavity. Primary villi cover the outer aspect of the conceptus and extend into the maternal endometrium and in places, maternal blood fills the lacunae.

The syncytiotrophoblast secretes numerous hormones; the most well known, human chorionic gonadotrophin (hCG), can be detected in maternal urine from as early as 10 days after fertilization, and forms the basis for tests for early pregnancy. hCG prolongs the life of the corpus luteum, which continues to secrete progesterone and oestrogens during approximately the first two months of pregnancy. Thereafter, these essential hormones are produced by the placenta.

Menstruation ceases on successful implantation. The endometrium, now known as the decidua in pregnancy, thickens to form a suitable nidus for the conceptus. Decidualization of the endometrial stroma may occur without an intrauterine pregnancy, e.g. in the presence of an ectopic pregnancy, after prolonged treatment with progesterone, and in the late secretory phase of a non-conception cycle.

Decidual differentiation is not evident in the stroma at the earliest stages of implantation, and it may not be until a week later that fully differentiated cells are present. During decidualization the interglandular tissue increases in quantity. It contains a substantial population of leukocytes (large granular lymphocytes, macrophages and T cells) distributed amongst large decidual cells: the most numerous are uterine natural killer (NK) cells which accumulate in the endometrium during the secretory phase of the cycle and persist until mid-pregnancy. Decidual cells are mesenchymally derived stromal cells which contain varying amounts of glycogen, lipid, and vimentin-type intermediate filaments in their cytoplasm. They are generally rounded, but their shape may vary depending on the local packing density. They may contain one, two or sometimes three nuclei and frequently display rows of club-like cytoplasmic protrusions enclosing granules. The cells are associated with a characteristic capsular basal lamina. Decidual cells produce a range of secretory products, including insulin-like growth factor binding protein 1 (IGF-BP1) and prolactin, which may be taken up by the trophoblast. These secretions probably play a role in the maintenance and growth of the conceptus in the early part of postimplantational development, and can be detected in amniotic fluid in the first trimester of pregnancy.

Extracellular matrix, growth factors and protease inhibitors produced by the decidua all probably modulate the degradative activity of the trophoblast and support placental morphogenesis and placental accession to the maternal blood supply. Once implantation is complete, distinctive names are applied to different regions of the decidua (Fig. 9.2). The part covering the conceptus is the decidua capsularis; that between the conceptus and the uterine muscular wall is the decidua basalis (where the placenta subsequently develops); and that which lines the remainder of the body of the uterus is the decidua parietalis. There is no evidence that their respective resident maternal cell populations exhibit site-specific properties.

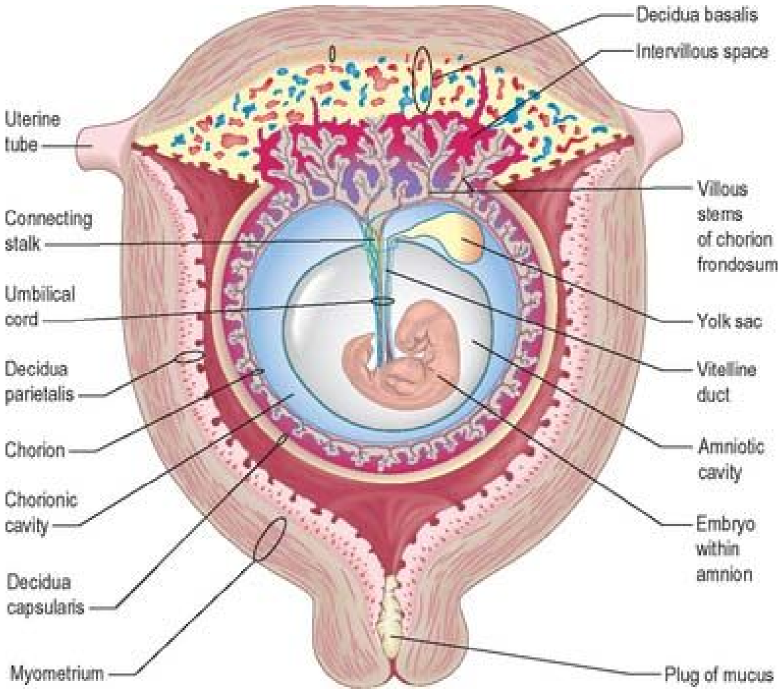
Decidua basalis
Intervillous space
Uterine tube
Villous stems of chorion frondosum
Connecting stalk
Umbilical cord
Yolk sac
Decidua parietalis
Vitelline duct
Chorion
Amniotic cavity
Chorionic cavity
Embryo within amnion
Decidua capsularis
Myometrium
Plug of mucus

Fig. 9.2 The gravid uterus in the second month. A placental site precisely in the uterine fundus as indicated in the plan is rather unusual: the dorsal, ventral or lateral wall of the corpus uteri is more usual. The maternal endometrium is now termed decidua; different regions are distinguished.

DEVELOPMENT OF THE PLACENTA

Formation of the human placenta requires a developmental progression which proceeds in a specific order over time; it is specified by the trophoblast, but dependent on the maternal environment for its correct expression. Immunological rejection of the semi-allogenic conceptus does not occur because the syncytiotrophoblast expresses neither Class I nor Class II MHC antigens. By contrast, the invading extravillous trophoblast expresses human leukocyte antigen-G (HLA-G) and -C, which interact with receptors on the uterine NK cells.

As the blastocyst implants, the syncytiotrophoblast invades the uterine tissues, including the glands and walls of maternal blood vessels (Fig. 9.1), and increases rapidly in thickness over the embryonic pole (Fig. 9.3). A progressively thinner layer covers the rest of the wall towards the abembryonic pole. Microvillus-lined clefts and lacunar spaces develop in the syncytiotrophoblastic envelope (days 9–11 of pregnancy) and establish communications with one another. Initially, many of these spaces contain maternal blood derived from dilated uterine capillaries and veins, as the walls of the vessels are partially destroyed. As the conceptus grows, the lacunar spaces enlarge, and become confluent to form an intervillous space.

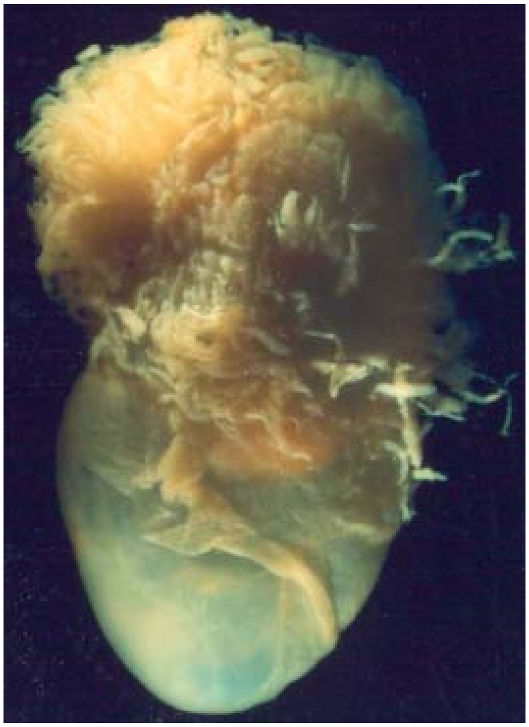

Fig. 9.3 Conceptus at about stage 14. The embryonic pole shows extensive villous formation at the chorion frondosum whereas the abembryonic pole is smooth and villous free at the chorion laevae.

(Photograph by courtesy of P Collins.)

The projections of syncytiotrophoblast into the maternal decidua are called primary villi. They are invaded first with cytotrophoblast and then with extraembryonic mesenchyme (days 13–15) to form secondary placental villi. Fetal capillaries develop in the mesenchymal core of the villi. The cytotrophoblast within the villi continues to grow through the invading syncytiotrophoblast and makes direct contact with the decidua basalis, forming anchoring villi. Further cytotrophoblast proliferation occurs laterally so that neighbouring outgrowths meet to form a spherical cytotrophoblastic shell around the conceptus (Fig. 9.4). Lateral projections from the main stem villus form true and terminal villi.

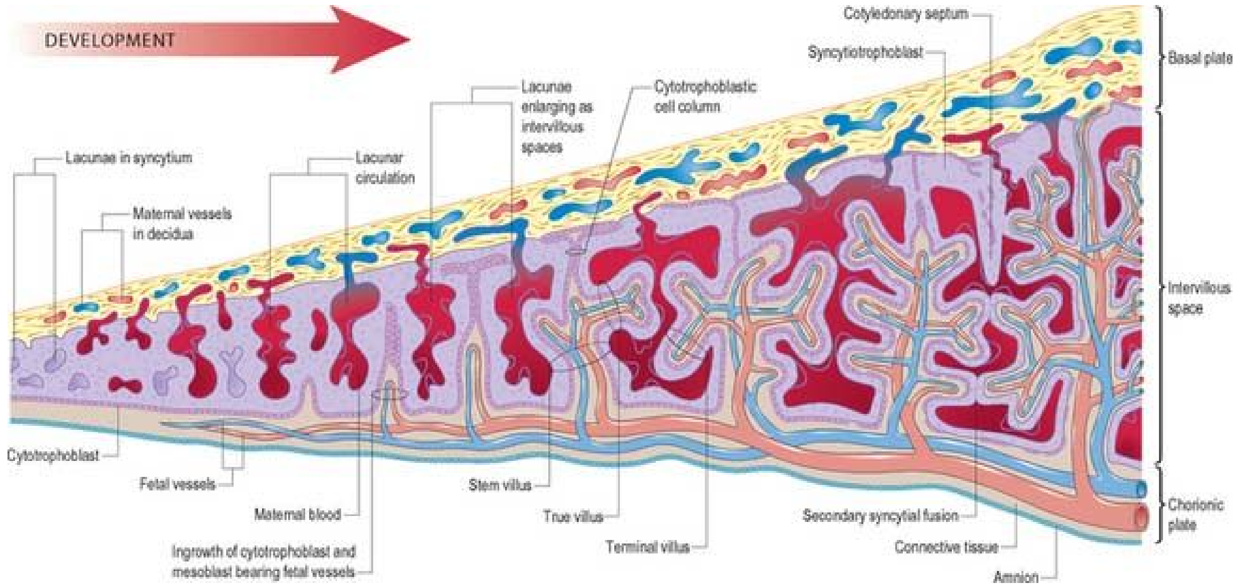
DEVELOPMENT
Cotyledonary septum
Syncytiotrophoblast
Basal plate
Lacunae enlarging as intervillous spaces
Cytotrophoblastic cell column
Lacunae in syncytium
Lacunar circulation
Maternal vessels in decidua
Intervillous space
Cytotrophoblast
Fetal vessels
Maternal blood
Ingrowth of cytotrophoblast and mesoblast bearing fetal vessels
Stem villus
True villus
Terminal villus
Secondary syncytial fusion
Connective tissue
Amnion
Chorionic plate

Fig. 9.4 Placental development is shown from left to right.

As secondary villi form, single mononuclear cells become detached from the distal cytotrophoblast and infiltrate the maternal decidua. These cells are the third line of the original trophoblastic cells. They are found both within and around the spiral arteries in the central area of the placenta and gradually extend laterally, reaching the periphery of the placenta around mid-gestation. They normally extend into the inner third of the uterine myometrium within the central region of the placental bed, but the extent of invasion is progressively shallower towards the periphery. At the same time, cytotrophoblast from the spherical shell penetrates into and migrates along the inner walls of maternal spiral arteries (endovascular extravillous trophoblast) so that by the 18th week it has reached the inner myometrial segments. The interstitially migrating cells invade the spiral arteries from their adventitia. The vessels lose their elastic lamina and consequently their responsiveness to circulating vasoactive compounds. The smooth muscle and associated elastic and collagenous matrix is replaced with non-resistive fibrinoid, an arrangement that permits an expansion of the vessels and as much as a 20-fold increase in the flow of blood into the intervillous space. In normal pregnancies the transformation of spiral arteries into utero-placental arteries is completed around mid gestation. The main aim of these vascular changes appears to be to optimize the distribution of maternal blood into a low-resistance uterine vascular network. Common pregnancy pathologies, including intrauterine growth restriction, pre-eclampsia and spontaneous abortion, are all associated with incomplete vascular remodelling, which probably reflects a failure of penetration by extravillous trophoblast.

With the onset of the embryonic heartbeat, a primitive circulation exists between the embryo and the yolk sac, succeeded later by that between the embryo and the placenta. The formed placenta is composed of a chorionic plate on its fetal aspect and a basal plate on the maternal aspect, and an intervening intervillous space containing villous stems with branches in contact with maternal blood (Fig. 9.4). Since maternal blood bathes the surfaces of the chorion which bound the intervillous space, the human placenta is defined as haemochorial. Different grades of fusion exist between the maternal and fetal tissues in many other mammals (e.g. epitheliochorial, syndesmochorial, endotheliochorial). The chorion is vascularized by the allantoic blood vessels of the body stalk, and so the human placenta is also termed chorio-allantoic (whereas in some mammals a choriovitelline placenta either exists alone or supplements the chorio-allantoic variety). In addition, the human placenta is defined as discoidal (in contrast to other shapes in other mammals) and deciduate because maternal tissue is shed with the placenta and membranes at parturition as part of the afterbirth.

Growth of the placenta

Expansion of the entire conceptus is accompanied by radial growth of the villi and, simultaneously, an integrated tangential growth and expansion of the trophoblastic shell. Eventually each villous stem forms a complex that consists of a single trunk attached by its base to the chorion, from which second and third order branches (intermediate and terminal villi) arise distally. Terminal villi are specialized for exchange between fetal and maternal circulations; each one starts as a syncytial outgrowth and is invaded by cytotrophoblastic cells, which then develop a core of fetal mesenchyme as the villus continues to grow. The core is vascularized by fetal capillaries (i.e. each villus passes through primary, secondary and tertiary grades of histological differentiation). The germinal cytotrophoblast continues to add cells that fuse with the overlying syncytium and so contribute to the expansion of the haemochorial interface. Terminal villi continue to form and branch within the confines of the definitive placenta throughout gestation, projecting in all directions into the intervillous space (Fig. 9.4).

From the third week until about the second month of pregnancy, the entire chorion is covered with villous stems. They are thus continuous peripherally with the trophoblastic shell, which is in close apposition with both the decidua capsularis and the decidua basalis. The villi adjacent to the decidua basalis are stouter, longer and show a greater profusion of terminal villi. As the conceptus continues to expand, the decidua capsularis is progressively compressed and thinned, the circulation through it is gradually reduced, and adjacent villi slowly atrophy and disappear. This process starts at the abembryonic pole, and by the end of the third month, the abembryonic hemisphere of the conceptus is largely denuded. Eventually the whole chorion apposed to the decidua capsularis is smooth and is now termed the chorion laeve. In contrast, the villous stems of the disc-shaped region of chorion apposed to the decidua basalis increase greatly in size and complexity and the region is now termed the chorion frondosum (Fig. 9.3). The chorion frondosum and the decidua basalis constitute the definitive placental site (Fig. 9.2). Abnormalities in this process may account for the persistence of villi at abnormal sites on the chorionic sac and hence the presence of accessory or succenturiate lobes. At term, the placental diameter varies from 200 to 220 mm, the mean placental weight is 470 g, its mean thickness is 25 mm and the total villous surface area is 12–14 m^2.

Coincidentally with the growth of the embryo and the expansion of the amnion, the decidua capsularis is thinned and distended and the space between it and the decidua parietalis is gradually obliterated. By the second month of pregnancy the three endometrial strata recognizable in the premenstrual phase, i.e. compactum, spongiosum and basale, are better differentiated and easily distinguished. The glands in the spongiosum are compressed and appear as oblique slit-like fissures lined by low cuboidal cells. By the beginning of the third month of pregnancy the decidua capsularis and decidua parietalis are in contact, while by the fifth month the decidua capsularis is greatly thinned, and during the succeeding months it virtually disappears.

Chorionic plate

The chorionic plate is covered on its fetal aspect by the amniotic epithelium, on the stromal side of which is a connective tissue layer carrying the main branches of the umbilical vessels (Fig. 9.4 and Fig. 9.5). Subjacent to this is a diminishing layer of cytotrophoblast and then the inner syncytial wall of the intervillous space. The connective tissue layer is formed by fusion between the mesenchyme-covered surfaces of amnion and chorion: it is more fibrous and less cellular than Wharton's jelly (of the umbilical cord), except near the larger vessels. The umbilical vessels radiate and branch from the cord attachment, with variations in the branching pattern, until they reach the bases of the trunks of the villous stems and then arborize within the intermediate and terminal villi. There are no anastomoses between vascular trees of adjacent stems. The two umbilical arteries are normally joined at, or just before they enter, the chorionic plate, by some form of substantial transverse anastomosis (Hyrtl's anastomosis).

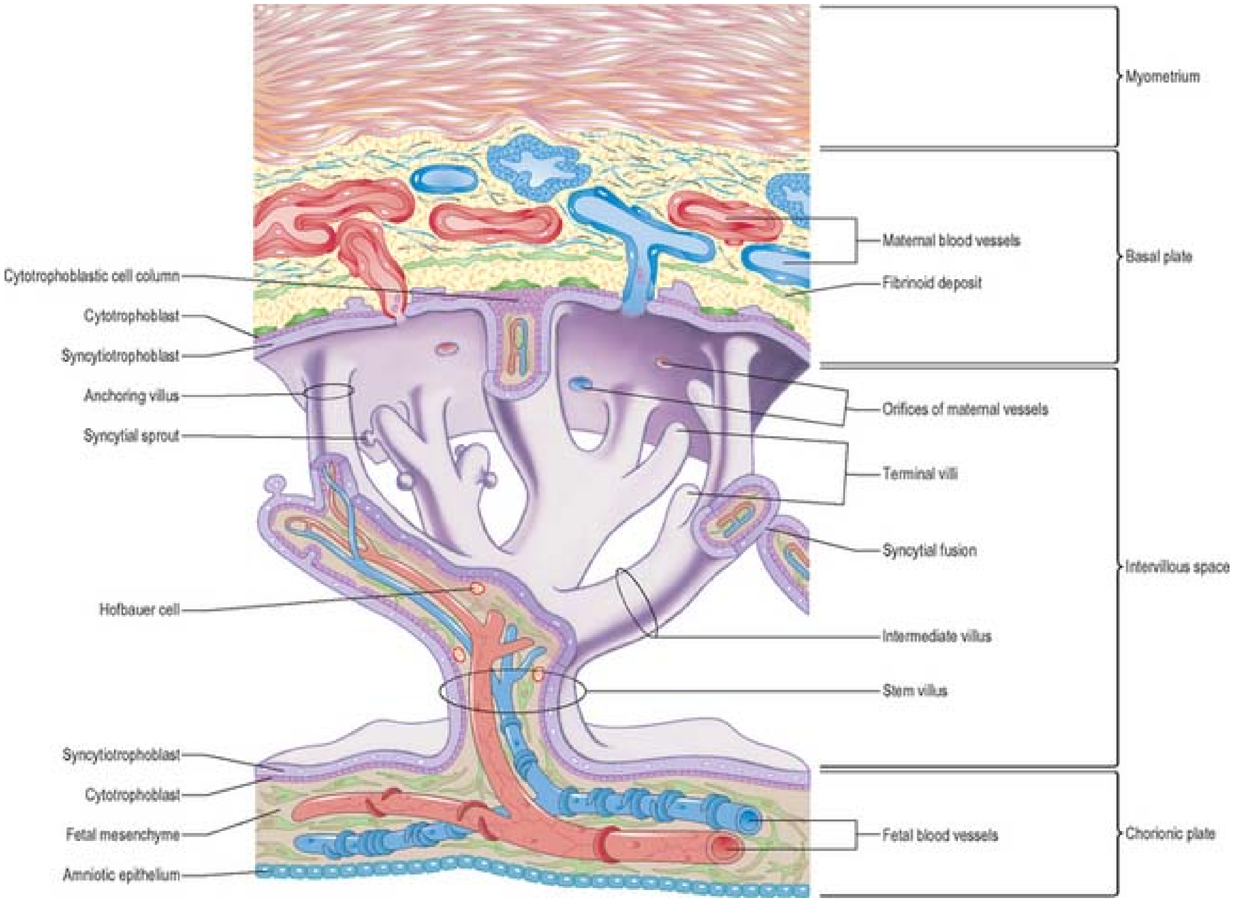
Cytotrophoblastic cell column
Cytotrophoblast
Syncytiotrophoblast
Anchoring villus
Syncytial sprout
Hofbauer cell
Syncytiotrophoblast
Cytotrophoblast
Fetal mesenchyme
Amniotic epithelium
Myometrium
Maternal blood vessels
Fibrinoid deposit
Basal plate
Orifices of maternal vessels
Terminal villi
Syncytial fusion
Intervillous space
Intermediate villus
Stem villus
Fetal blood vessels
Chorionic plate

Fig. 9.5 The arrangement of the placental tissues from the chorionic plate (fetal side) to the basal plate or decidua basalis (maternal side).

Basal plate

The basal plate, from fetal to maternal aspect, forms the outer wall of the intervillous space. The trophoblast and adjacent decidua are enmeshed in layers of fibrinoid and basement membrane-like extracellular matrix to form a complex junctional zone. In different places the basal plate may contain syncytium, cytotrophoblast or fibrinoid matrix, remnants of the cytotrophoblastic shell, and, at the site of implantation, areas of necrotic maternal decidua (the so-called Nitabuch's stria) (Figs 9.4 and 9.5). Nitabuch's stria and the decidua basalis contain cytotrophoblast and multinucleate trophoblast giant cells derived from the mononuclear cytotrophoblast population, which infiltrate the decidua basalis during the first 18 weeks of pregnancy. These cells penetrate as far as the inner one-third of the myometrium, but can often be observed at or near the decidual–myometrial junction. They are not found in the decidua parietalis or the adjacent myometrium, from which it may be inferred that the placental-bed giant cell represents a differentiative end stage in the extravillous trophoblast lineage. The striae of fibrinoid are irregularly interconnected and variable in prominence. Strands pass from Nitabuch’s stria into the adjacent decidua which contains basal remnants of the endometrial glands and large and small decidual cells scattered in a connective tissue framework that supports an extensive venous plexus.

From the third month onwards the basal plate develops placental or cotyledonary septa, which are ingrowths of the cytotrophoblast covered with syncytium that grow toward but do not fuse with the chorionic plate (Fig. 9.4). The septa circumscribe the maternal surface of the placenta into 15–30 lobes, often termed cotyledons. Each cotyledon surrounds a limited portion of the intervillous space associated with a villous trunk from the chorionic plate. From the fourth month these septa are supported by tissue from the decidua basalis. Throughout the second half of pregnancy the basal plate becomes thinned and progressively modified: there is a relative diminution of the decidual elements, increasing deposition of fibrinoid, and admixture of fetal and maternal derivatives.

Intervillous space

The intervillous space contains the main trunks of the villous stems and their arborizations into intermediate and terminal villi (Figs 9.4 and 9.5). A villous trunk and its branches may be regarded as the essential structural, functional and growth unit of the developing placenta.

At term, from the inner myometrium to the intervillous space, the walls of most spiral arteries consist of fibrinoid matrix within which cytotrophoblast is embedded. This arrangement allows expansion of the arterial diameter (and so slows the rate of arterial inflow and reduces the perfusion pressure) independent of the local action of vasoconstrictive agents. Endothelial cells, where present, are often hypertrophic. The veins that drain the blood away from the intervillous space pierce the basal plate and join tributaries of the uterine veins. The presence of a marginal venous sinus, which hitherto has been described as a constant feature occupying the peripheral margin of the placenta and communicating freely with the intervillous space, has not been confirmed.

Recent anatomic and *in vivo* studies have shown that human placentation is in fact not truly haemochorial in early pregnancy (Jauniaux et al 2003). From the time of implantation, the extravillous trophoblast not only invades the uterine tissues but also forms a continuous shell at the level of the decidua. The cells of this shell not only anchor the placenta to the maternal tissue but also form plugs in the tips of the utero-placental arteries (Burton et al 1999). The shell and the plugs act like a labyrinthine interface that filters maternal blood, permitting a slow seepage of plasma but no true blood flow into the intervillous space. This is supplemented by secretions from the uterine glands, which are discharged into the intervillous space until at least 10 weeks (Burton et al 2002). The comparison of these anatomical features with physiological data obtained in utero reveals that the architecture of the human first trimester gestational sac is designed to limit fetal exposure to oxygen to that which is strictly necessary for its development This creates a physiological placental hypoxia which may protect the developing embryo against the deleterious and teratogenic effects of oxygen, and also a uterine O_2 gradient which exerts a regulatory effect on placental tissue development and function. In particular it influences cytotrophoblast proliferation and differentiation along the invasive pathway and villous vasculogenesis. At the end of the first trimester the trophoblastic plugs are progressively dislocated, allowing maternal blood to flow progressively more freely and continuously within the intervillous space. During the transitional phase of 10–14 weeks gestation, two-thirds of the primitive placenta disappears, the chorionic cavity is obliterated by the growth of the amniotic sac, and maternal blood flows progressively throughout the entire placenta (Jauniaux et al 2003). These events bring the maternal blood closer to the fetal tissues, facilitating nutrient and gaseous exchange between the maternal and fetal circulations.

Structure of a placental villus

Chorionic villi are the essential structures involved in exchanges between mother and fetus. The villous tissues separating fetal and maternal blood are therefore of crucial functional importance. From the chorionic plate, progressive branching occurs into the villous tree, as stem villi give way to intermediate and terminal villi. Each villus has a core of connective tissue containing collagen types I, III, V and VI, as well as fibronectin. Cross-banded fibres (30–35 nm) of type I collagen often occur in bundles, whereas type III collagen is present as thinner (10–15 nm) beaded fibres, which form a meshwork that often encases the larger fibres. Collagens V and VI are present as 6–10 nm fibres closely associated with collagens I and III. Laminin and collagen type IV are present in the stroma associated with the basal laminae that surround fetal vessels and also in the trophoblast basal lamina. Overlying this matrix are ensheathing cyto- and syncytiotrophoblast cells bathed by the maternal blood in the intervillous space (Figs 9.4, 9.5 and 9.6). Cohesion between the cells of the cytotrophoblast and also between the cytotrophoblast and the syncytium is provided by numerous desmosomes between the apposed plasma membranes.

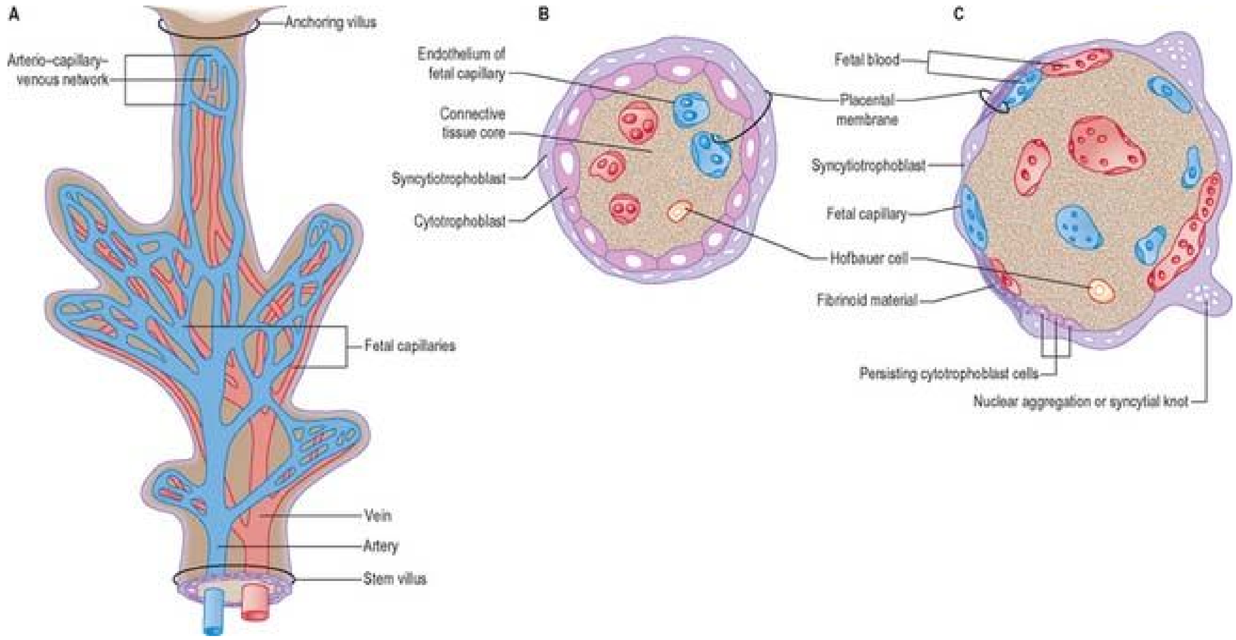
A
Anchoring villus
Arterio–capillary–venous network
Fetal capillaries
Vein
Artery
Stem villus
B
Endothelium of fetal capillary
Connective tissue core
Syncytiotrophoblast
Cytotrophoblast
C
Fetal blood
Placental membrane
Syncytiotrophoblast
Fetal capillary
Hofbauer cell
Fibrinoid material
Persisting cytotrophoblast cells
Nuclear aggregation or syncytial knot

Fig. 9.6 **A**, Chorionic villus and its arterio–capillary–venous system carrying fetal blood. The artery carries deoxygenated blood and waste

products from the fetus and the vein carries oxygenated blood and nutrients to the fetus. Sections through a chorionic villus at 10 weeks, **B**, and at full term, **C**. The villi would be within the intervillous space bathed externally in maternal blood. The placental membrane, composed of fetal tissues, separates the maternal blood from the fetal blood.

In earlier stages, the cytotrophoblast forms an almost continuous layer on the basal lamina. After the fourth month it gradually expends itself producing syncytium, which comes to lie on the basal lamina over an increasingly large area (80% at term), and becomes progressively thinner. Cytotrophoblastic cells persist until term, but because the increase in villous surface area outstrips their proliferation they are usually disposed singly. In the first and second trimester cytotrophoblastic sprouts, covered in syncytium, are present and represent a stage in the development of new villi. Cytotrophoblast columns at the tips of anchoring villi extend from the villous basal lamina to the maternal decidual stroma.

The cells of the villous cytotrophoblast (Langhans cells) are pale-staining with a slight basophilia. Ultrastructurally, they have a rather electron-translucent cytoplasm, and relatively few organelles. They contain intermediate filaments, particularly in association with desmosomes. Between the desmosomes, the membranes of adjacent cells are separated by approximately 20 nm. Sometimes the intercellular gap widens to accommodate microvillous projections from the cell surfaces, and it occasionally contains patches of fibrinoid. A smaller population of intermediate cytotrophoblast may also be found in the chorionic villi. This postmitotic population represents a state of partial differentiation between the cytotrophoblast stem cell and the overlying syncytium.

The syncytium is an intensely active tissue layer across which most transplacental transport must occur. It is a selectively permeable barrier that allows water, oxygen and other nutritive substances and hormones to pass from mother to fetus, and some of the products of excretion to pass from fetus to mother. It secretes a range of placental hormones into the maternal circulation. Syncytial cytoplasm is more strongly basophilic than that of the cytotrophoblastic cells and is packed with organelles consistent with its secretory phenotype. Where the plasma membrane adjoins basal lamina it is often infolded into the cytoplasm, whereas the surface bordering the intervillous space is set with numerous long microvilli, which constitute the brush border seen by light microscopy.

Glycogen is thought to be present in both layers of the trophoblast at all stages, although it is not always possible to demonstrate its presence histochemically. Lipid droplets occur in both layers and are free in the core of the villus. In the trophoblast they are found principally within the cytoplasm, but they also occur in the extracellular space between cytotrophoblast and syncytium, and between the individual cells of the cytotrophoblast. The droplets diminish in number with advancing age and may represent fat in transit from mother to fetus, and/or a pool of precursors for steroid synthesis. Membrane-bound granular bodies of moderate electron density occur in the cytoplasm, particularly in the syncytium, some of which are probably secretion granules. Other membrane-bound bodies, lysosomes and phagosomes, are involved in the degradation of materials engulfed from the intervillous space.

In the immature placenta, syncytial sprouts represent the first stages in the development of new terminal villi, which later become invaded by cytotrophoblast and villous mesenchyme. Occasionally, adjacent syncytial sprouts make contact and fuse to form slender syncytial bridges. The sprouts may become detached, forming maternal syncytial emboli, which pass to the lungs. It has been computed that some 100,000 sprouts pass daily into the maternal circulation. In the lungs they provoke little local reaction and apparently disappear by lysis. However, they may occasionally form foci for neoplastic growth. Syncytial sprouts are present in the term placenta, but are usually degenerating.

Syncytial knots are aggregates of degenerating nuclei, and may represent a sequestration phenomenon by which senescent nuclear material is removed from adjacent metabolically active areas of syncytium. Fibrinoid deposits are frequently found on the villous surface in areas lacking syncytiotrophoblast. They may constitute a repair mechanism in which the fibrinoid forms a wound surface that is subsequently re-epithelialized by trophoblast. The extracellular matrix glycoprotein tenascin has been localized in the stroma adjacent to these sites.

The core of a villus contains small and large reticulum cells, fibroblasts, and macrophages (Hofbauer cells). Early mesenchymal cells probably differentiate into small reticulum cells, which in turn produce fibroblasts or large reticulum cells. The small reticulum cells appear to delimit a collagen-free stromal channel system through which Hofbauer cells migrate. Mesenchymal collagen increases from a network of fine fibres in early mesenchymal villi to a densely fibrous stroma within stem villi in the second and third trimester. After approximately 14 weeks, the stromal channels found in immature intermediate villi are infilled by collagen to give the fibrous stroma characteristic of the stem villus.

Fetal vessels include arterioles and capillaries. Pericytes may be found in close association with the capillary endothelium, and from late first trimester the vessels are surrounded externally by a basal lamina. From the second trimester (and a little later in terminal villi), dilated thin-walled capillaries are found immediately adjacent to the villous trophoblast; their respective basal laminae apparently fuse to produce a vasculo-syncytial interface.

Transport across placental villi

The mechanism of transfer of substances across the placental barrier (membrane) is complex. The volume of maternal blood circulating through the intervillous space has been assessed at 500 ml per minute. Simple diffusion suffices to explain gaseous exchange. Transfer of ions and other water-soluble solutes is by paracellular and transcellular diffusion and transport: the relative importance of each of these for most individual solutes is unknown, and the paracellular pathway is morphologically undefined. Glucose transfer involves facilitated diffusion, while active transport mechanisms carry calcium and at least some amino acids. The fat-soluble and water-soluble vitamins are likely to pass the placental barrier with different degrees of facility. The water-soluble vitamins B and C pass readily. Water is interchanged between fetus and mother (in both directions) at approximately 3.5 litres per hour. The transfer of substances of high molecular weight, such as complex sugars, some lipids and hormonal and non-hormonal proteins, varies greatly in rate and degree, and is not so well understood: energy-dependent selective transport mechanisms including receptor-mediated transcytosis are likely to be involved.

Lipids may be transported unchanged through and between the cells of the trophoblast to the core of the villus. The passage of maternal antibodies (immunoglobulins) across the placental barrier confers some degree of passive immunity on the fetus: it is widely accepted that transfer is by micropinocytosis. Investigation of transplacental mechanisms is complicated by the fact that the trophoblast itself is the site of synthesis and storage of certain substances, e.g. glycogen.

The placenta is an important endocrine organ. Some steroid hormones, various oestrogens, β-endorphins, progesterone, hCG and human chorionic somatomammotropin (hCS), which is also known as placental lactogen (hPL), are synthesized and secreted by the syncytium. The trophoblast also contains enzyme systems that are associated with the synthesis of steroid hormones.

It has been suggested that leukocytes may migrate from the maternal blood through the placental barrier into the fetal capillaries. It has also been shown that some fetal and maternal red blood cells may cross the barrier. The former may have important consequences, e.g. in Rhesus incompatibility.

The majority of drugs are small molecules and are sufficiently lipophilic to pass the placental barrier. Many are tolerated by the fetus, but some may exert grave teratogenic effects on the developing embryo (e.g. thalidomide). A well-documented association exists between maternal alcohol ingestion and fetal abnormalities. Addiction of the fetus can occur to substances of maternal abuse such as cocaine and heroin.

A wide variety of bacteria, spirochaetes, protozoa and viruses, including human immunodeficiency virus (HIV), are known to pass the placental barrier from mother to fetus, although the mechanism of transfer is uncertain.

The presence of maternal rubella in the early months of pregnancy is of especial importance in relation to the production of congenital anomalies.

FETAL MEMBRANES

The implanting conceptus consists initially of three cavities and their surrounding epithelia. The original blastocyst cavity, surrounded by trophoblast, is now termed the chorionic cavity (synonymous with extraembryonic coelom). It is a large cavity containing the much smaller amniotic cavity and secondary yolk sac (see Fig. 9.1). The apposition of the latter two cavities delineates the extent of the early embryo. The chorionic cavity becomes lined with extraembryonic mesoblast which is also reflected over the outer surface of the amnion and yolk sac. A fourth cavity, the allantois, develops later as a caudal hypoblastic diverticulum that becomes embedded within the extraembryonic mesenchyme, forming the connecting stalk of the embryo. It does not have a direct mesothelial covering.

Chorion

The chorion consists of developing trophoblast and extraembryonic mesothelium. It varies in thickness during development both temporally and spatially. It is thickest at the implantation site throughout gestation as the chorion frondosum and then the placenta, and thinner as gestation progresses over the remainder of its surface as the chorion laevae (Fig. 9.3). At term the chorion consists of an inner cellular layer containing fibroblasts and a reticular layer of fibroblasts and Hofbauer cells, which resembles the mesenchyme of an intermediate villus. The outer layer consists of cytotrophoblast 3 to 10 cells deep, resting on a pseudo-basement membrane, which extends beneath and between the cells. Occasional obliterated villi within the trophoblast layer are the remnants of villi present in the chorion frondosum of the first trimester. Although the interface between the trophoblast and decidua parietalis is uneven, no trophoblast infiltration of the decidua parietalis occurs.

Yolk sac

As the secondary yolk sac forms it delineates a cavity lined with parietal, and perhaps visceral, hypoblast, which is continuous with the developing endoderm from the primitive streak (Ch. 10). The secondary yolk sac is the first structure that can be detected ultrasonographically within the chorionic cavity (Jauniaux et al 1991). Its diameter increases slightly between 6 and 10 weeks of gestation, reaching a maximum of 6–7 mm after which its size decreases.

The inner cells of the yolk sac (denoted endoderm in many studies, although this layer is restricted to the embryo itself) display a few short microvilli and are linked by juxtaluminal tight junctions (Jones & Jauniaux 1995). Their cytoplasm contains numerous mitochondria, whorls of rough endoplasmic reticulum, Golgi bodies and secretory droplets, giving them the appearance of being highly active synthetic cells. With further development the epithelium becomes folded to form a series of cyst-like structures or tubules, only some of which communicate with the central cavity. The cells synthesize several serum proteins in common with the fetal liver, such as alpha-fetoprotein (AFP), alpha-1-antitrypsin, albumin, pre-albumin and transferrin (Jauniaux & Gulbis 2000). With rare exceptions, the secretion of most of these proteins is confined to the embryonic compartments.

The yolk sac becomes coated with extraembryonic mesenchyme, which forms mesenchymal and mesothelial layers. A diffuse capillary plexus develops between the mesothelial layer and the underlying secondary yolk sac wall, and subsequently drains through vitelline veins to the developing liver. The mesothelial layer bears a dense covering of microvilli: the presence of numerous coated pits and pinocytotic vesicles gives it the appearance of an absorptive epithelium (Jones & Jauniaux 1995).

The secondary yolk sac plays a major role in the early embryonic development of all mammals. In laboratory rodents it has been demonstrated as one of the initial sites of haematopoiesis. Recent human data indicate that it has an absorptive role for molecules of maternal and placental origin found in the chorionic cavity (Gulbis et al 1998) and mediates the main movement of molecules passing from the chorionic cavity to the yolk sac and subsequently to the embryonic gut and circulation.

After week 9 the cellular components of the wall of the secondary yolk sac start to degenerate, and their function is subsumed into exchanges at the placental chorionic plate. With embryonic development of the midgut, the connection of the yolk sac to the embryo becomes attenuated to a slender and elongated vitelline intestinal duct. Both the yolk sac and its duct remain within the extraembryonic coelom (chorionic cavity) throughout gestation, located between the amnion and chorion as they fuse, near the placental attachment of the umbilical cord.

Allantois

The allantoenteric diverticulum (see Fig. 10.1) arises early in the third week as a solid, endodermal outgrowth from the dorsocaudal part of the yolk sac into the mesenchyme of the connecting stalk. It soon becomes canalized. When the hindgut is developed, the proximal (enteric) part of the diverticulum is incorporated in its ventral wall. The distal (allantoic) part remains as the allantoic duct and is carried ventrally to open into the ventral aspect of the cloaca or terminal part of the hindgut (Fig. 9.7A). The allantois is a site of angiogenesis, giving rise to the umbilical vessels which connect to the placental circulation. The extraembryonic mesenchyme around the allantois forms the connecting stalk, which is later incorporated into the umbilical cord.

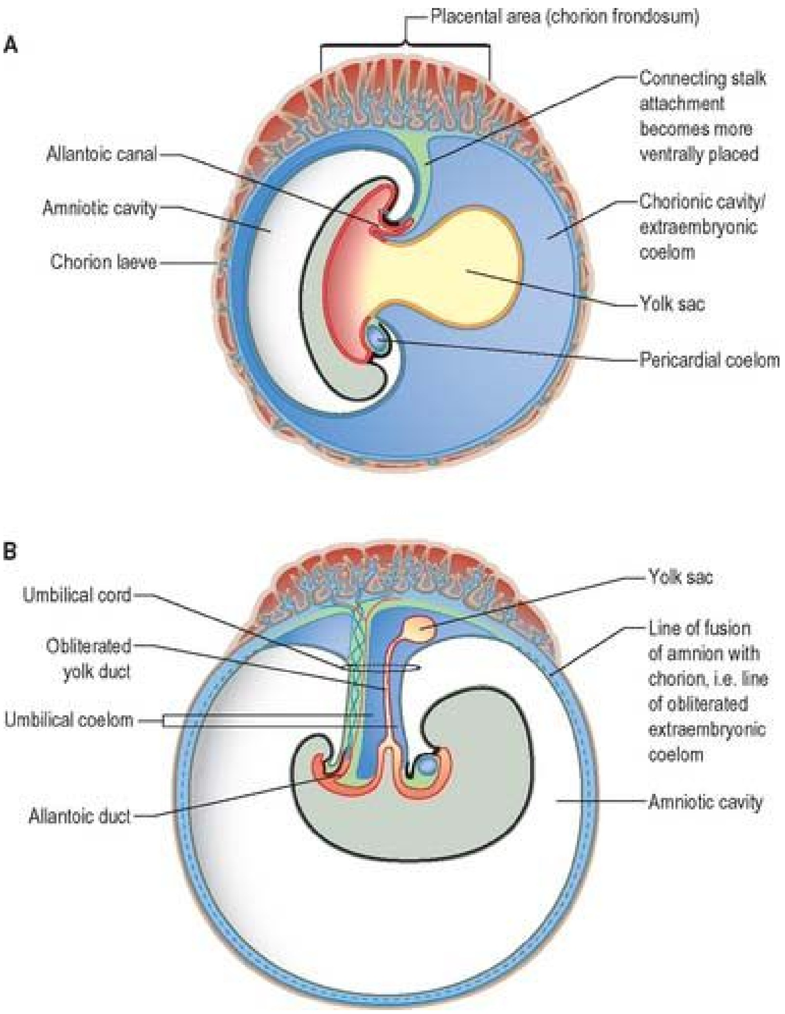
A
Placental area (chorion frondosum)
Connecting stalk attachment becomes more ventrally placed
Allantoic canal
Amniotic cavity
Chorion laeve
Chorionic cavity/ extraembryonic coelom
Yolk sac
Pericardial coelom
B
Umbilical cord
Obliterated yolk duct
Umbilical coelom
Allantoic duct
Yolk sac
Line of fusion of amnion with chorion, i.e. line of obliterated extraembryonic coelom
Amniotic cavity

Fig. 9.7 **A**, Longitudinal section of a conceptus showing the cavities associated with development. The amniotic cavity and yolk sac are both covered with extraembryonic mesoblast. They are contained within the larger chorionic cavity which is lined with extraembryonic mesoblast. The embryo is attached to the chorion frondosum by the connecting stalk into which the allantois projects. **B**, Longitudinal section of conceptus at a later stage showing the diminution of the chorionic cavity, expansion of the amniotic cavity, relative attenuation of the yolk sac and the structures which give rise to the umbilical cord.

In the fetus, the allantoic duct, which is confined to the proximal end of the umbilical cord, elongates and thins. However, it may persist as an interrupted series of epithelial strands at term, in which case the proximal strand is often continuous at the umbilicus with the median intra-abdominal urachus, and this in turn continues into the apex of the bladder.

Amnion (chorio-amnion)

The original amniotic cells develop from the edges of the epiblast of the embryonic disc which ultimately form the interface with the skin at the umbilical region. Between the 10th and 12th weeks of pregnancy the amniotic cavity expands until it makes contact with the chorion to form the chorio-amnion, an avascular membrane which persists to term. The amniotic membrane extends along the connecting stalk and forms the outer covering of the umbilical cord. After birth, the site of this embryonic/extraembryonic junction is important, because the extraembryonic cell lines will die, causing the umbilical cord to degenerate and detach from the body wall. In cases of anomalous development of the ventral body wall, e.g. gastroschisis and exomphalos, the reflections of the amnion along the forming umbilical cord may be incomplete (see below).

The inner surface of the amnion consists of a simple cuboidal epithelium. It has a microvillous apical surface beneath which is a cortical web of intermediate filaments and microfilaments. There are no tight junctional complexes between adjacent cells and cationic dyes penetrate between the cells as far as the basal lamina. The intercellular clefts present scattered desmosomes, but elsewhere the clefts widen and contain interlacing microvilli. These features are consistent with selective permeability properties. The epithelium synthesizes and deposits extracellular matrix into the compact layer of acellular stroma located beneath the basal lamina, as well as the basal lamina itself.

Towards the end of gestation increasing numbers of amniotic cells undergo apoptosis. Apoptotic cells become detached from the amnion and are found in the amniotic cavity at term. The highest incidence is in weeks 40–41, independent of the onset of labour. Apoptosis may play a role in the fragility and rupture of the fetal membranes at term.

Human amniotic epithelial cells are thought to be pluripotent because they arise so early from the conceptus. They can be distinguished from the epiblast cells from day 8. Amniotic cells lack the major histocompatibility complex antigen and so the amnion can be exposed to the maternal immune system without eliciting a maternal immune response. Cultured human amniotic epithelial cells express a range of neural and glial markers, including glial fibrillary acidic protein, myelin basic protein, vimentin and neurofilament proteins, suggesting that these cells may supply neurotrophic factors to the amniotic fluid. They also appear to have a hepatocyte gene expression profile, showing albumin production, glycogen storage and albumin secretion in culture. In organ culture they have been shown to secrete 30-fold larger amounts of albumin than in monolayer culture, and to secrete alpha-1-antitrypsin (Takashima et al 2004). Amnion is used in the repair of corneas after trauma and as a graft material for reconstructing vaginas in women with cloacal abnormalities.

AMNIOTIC FLUID

The amniotic fluid, or liquor amnii, is derived from multiple sources throughout gestation. These include secretions from amniotic epithelium, filtration of fluid from maternal vessels via the parietal decidua and amniochorion, filtration from the fetal vessels via the chorionic plate or the umbilical cord, and fetal urine and fetal lung secretions. In early pregnancy, diffusion from intracorporeal vessels via fetal skin provides another source. Once the gut is formed, fetal swallowing of amniotic fluid is a normal occurrence: the fluid is absorbed into the fetal circulation and passes via the placental barrier into the maternal circulation. There is rapid exchange between the amniotic fluid and maternal and fetal circulations via the placenta and fetal kidneys.

In the early stages amniotic fluid resembles blood plasma in composition and is probably formed largely by transport across the amniotic membrane. As pregnancy advances, it becomes progressively more dilute, partly by the addition of fetal urine. It contains less than 2% of solids, including urea, inorganic salts, a small amount of protein and frequently a trace of sugar. Glycoprotein secretions from amniotic epithelium include fibronectin. Secretory products of the maternal decidua, including prolactin and insulin-like growth factor binding protein 1 (IGF-BP1), are present in the liquor. There is experimental evidence of a considerable and rapid flux of water across the amniotic membrane.

The amount of amniotic fluid increases in quantity up to the sixth or seventh month and then diminishes slightly. At the end of pregnancy it is usually somewhat less than a litre. It provides a buoyant medium which supports the delicate tissues of the young embryo and allows free movement of the fetus during the later stages of pregnancy. It also diminishes the risk to the fetus of injury from without.

A volume of amniotic fluid in excess of 2 litres is generally considered to be abnormal and constitutes polyhydramnios. A deficiency is termed oligohydramnios and absent amniotic fluid is anhydramnios. (For information about amniotic fluid volume and ranges in gestation consult

Brace & Wolf 1989.) Oligohydramnios in the second or third trimester is usually the result of premature rupture of the membranes, uteroplacental insufficiency or urinary tract malformations, e.g. bilateral renal agenesis or obstruction of the lower urinary tract. The major concern with oligohydramnios at less than 20 weeks is the significant risk of pulmonary hypoplasia and neonatal death. The mechanism for the development of pulmonary hypoplasia is poorly understood but loss of lung fluid, and chest compression are contributing factors. Conversely, increased amniotic fluid volume (polyhydramnios) is found essentially in two major circumstances: reduced fetal swallowing or absorption of amniotic fluid and increased fetal urination. Reduced fetal swallowing may be due to congenital malformations e.g. anencephaly, upper intestinal tract obstruction (oesophageal atresia), compressive pulmonary disorders (congenital diaphragmatic hernia) and neuromuscular impairment of swallowing. The cause for abnormal amniotic fluid volume can often be elucidated with detailed prenatal ultrasound examination.

UMBILICAL CORD

The formation of the connecting stalk is described in Chapter 10, and the early formation of the umbilical cord is described on p. 1209. The umbilical cord ultimately consists of an outer covering of flattened amniotic epithelial cells and an interior mass of mesenchyme of diverse origins (Fig. 9.7). It contains two tubes of hypoblastic origin, the vitelline-intestinal and allantoic ducts, and their associated vitelline and allantoic (umbilical) blood vessels. The yolk stalk and continuing duct extend the length of the cord whereas the allantoic duct extends only into its proximal part.

The mesenchymal core is derived from the somatopleuric extraembryonic mesenchyme covering the amniotic folds, splanchnopleuric extraembryonic mesenchyme of the yolk stalk (which carries the vitelline vessels and clothes the yolk duct), and similar allantoic mesenchyme of the connecting stalk (which clothes the allantoic duct and initially carries two umbilical arteries and two umbilical veins). These various mesenchymal compartments fuse and are gradually transformed into the loose connective tissue (Wharton's jelly) that characterizes the more mature cord. The tissue consists of widely spaced elongated fibroblasts separated by a delicate three-dimensional meshwork of fine collagen fibres, which contains a variety of hydrated glycosaminoglycans, and is particularly rich in hyaluronic acid.

The vitelline and allantoic (umbilical) vessels, which are initially symmetrical, become modified as a result of changes in the circulation. The vitelline vessels involute, whereas most of the allantoic (umbilical) vessels persist. The right umbilical vein disappears but the two umbilical arteries normally remain. Occasionally one umbilical artery may disappear; there is some correlation within structural anomalies, most often cardiac, in such cases. The vessels of the umbilical cord are rarely straight, and are usually twisted into either a right- or left-handed cylindrical helix. The number of turns involved ranges from a few to over 300. This conformation may be produced by unequal growth of the vessels, or by torsional forces imposed by fetal movements. Its functional significance is obscure: perhaps the pulsations and contractions of the helical vessels assist the venous return to the fetus in the umbilical vein.

Anomalies of the fetal anterior abdominal wall such as exomphalos and gastroschisis may affect the arrangement of the outer covering of amnion cells along the proximal end of the umbilical cord. Exomphalos arises from a failure of the lateral folds along the ventral surface of the embryo resulting in failure of the normal embryonic regression of the mid-gut from the umbilical stalk into the abdominal cavity. The abdominal contents, including intestines and liver or spleen covered by a sac of parietal peritoneum and amnion, are herniated into the base of the umbilical cord. In gastroschisis, the insertion of the umbilical cord is intact and there is evisceration of the intestine through a small abdominal wall defect usually located to the right of the umbilical cord: this results in free loops of bowel in the amniotic cavity. Theories concerning the aetiology of this defect include abnormal involution of the right umbilical vein or disruption of the omphalo-mesenteric artery by ischaemia.

Mature umbilical vessels, particularly the arteries, have a strong muscular coat which contracts readily in response to mechanical stimuli. The outermost bundles pursue an interlacing spiral course, and when they contract they produce shortening of the vessel and thickening of the media, with folding of the interna and considerable narrowing of the lumen. This action may account for the periodic sharp constrictions of contour, the so-called valves of Hoboken, which often characterize these vessels.

The fully developed umbilical cord is on average some 50 cm long and 1–2 cm in diameter. Its length varies from 20–120 cm: exceptionally short or long cords are associated with fetal problems and complications during labour. A long umbilical cord may prolapse through the cervix into the vagina once the fetal membranes rupture and this may be exacerbated by conditions that prevent the fetal head from fully occupying the maternal pelvis e.g. pelvic tumours (fibroids), ovarian cysts, placenta praevia and prematurity. Compression of the cord by the presenting part of the fetus, or an umbilical artery spasm will lead to fetal hypoxia and death if untreated. The risk of perinatal death rises as the interval from diagnosis to delivery increases. The treatment is either funic replacement (pushing the cord back above the fetal head) or more commonly immediate caesarean section, depending on factors such as the fetal viability.

The distal end of the umbilical cord usually attaches in the central portion of the placenta, but in a minority of cases velamentous insertion is observed (i.e. into the membranes) and this may be associated with vulnerability to injury and fetal haemorrhage. This is especially important if the placenta is low lying and may be associated with vasa praevia in which case fetal blood vessels run across the internal os. Inadvertent rupture of the fetal vessels in spontaneous labour or at the time of amniotomy (artificial rupture of membranes to induce labour) will cause fetal haemorrhage and may prove fatal (see placental variations).

REFERENCES

ace RA, Wolf EJ. Normal amniotic fluid volume changes throughout pregnancy. *Am J Obstet Gynaecol*. 1989;161:382-388.

ırton GJ, Jauniaux E, Watson AL. Maternal arterial connections to the placental intervillous space during the first trimester of human pregnancy; the Boyd Collection revisited. *Am J Obstet Gynecol*. 1999;181:718-724.

ırton GJ, Watson AL, Hempstock J, Skepper JN, Jauniaux E. Uterine glands provide histiotrophic nutrition for the human fetus during the first trimester of pregnancy. *J Clin Endocrinol Metab*. 2002;87:2954-2959.

ılbis B, Jauniaux E, Cotton F, Stordeur P. Protein and enzyme pattern in the fluid cavities of the first trimester human gestational sac: Relevance to the absorptive role of the secondary yolk sac. *Mol Hum Reprod*. 1998;4:857-862.

uniaux E, Gulbis B, Burton GJ. The human first trimester gestational sac limits rather than facilitates oxygen transfer to the foetus: A review. *Placenta-Trophoblast Res*. 2003;24:S86-S93.

uniaux E, Jurkovic D, Henriet Y, Rodesch F, Hustin J. Development of the secondary human yolk sac: Correlation of sonographic and anatomic features. *Hum Reprod*. 1991;6:1160-1166.

uniaux E, Gulbis B. Fluid compartments of the embryonic environment. *Hum Reprod Update*. 2000;6:268-278.

nes CPJ, Jauniaux E. Ultrastructure of the materno-embryonic interface in the first trimester of pregnancy. *Micron*. 1995;2:145-173.

kashina S, Ise H, Zhao P, Akraike T, Nikaido T. Human amniotic epithelial cells possess hepatocyte-like characteristics and functions. *Cell Struct Funct*. 2004;3:13-84.

CHAPTER 10

Cell populations at gastrulation

CONCEPTUS WITH A BILAMINAR EMBRYONIC DISC

At stage 6 the conceptus is composed of the walls of three cavities: the large chorionic cavity is surrounded by a meshwork of trophoblast and developing villi and lined with extraembryonic mesoblast. The chorion, trophoblast and extraembryonic mesoblast enclose the extraembryonic coelom and contain the much smaller amniotic cavity and yolk sac (see Fig. 9.1). These latter cavities abut at the embryonic bilaminar disc where the epithelial epiblast and visceral hypoblast are approximated. A fourth cavity, the allantois, will form as a hypoblastic diverticulum in stage 7. The 'bilaminar disc' commonly referred to in embryology texts does not yet possess the definitive layers of embryonic ectoderm and endoderm that will give rise to embryonic structures. Only the epiblast will give rise to the embryo; all other layers produced so far are extraembryonic. The amnion and chorion (and surrounding mesoblast) are part of the extraembryonic somatopleure, whereas the yolk sac, allantois and surrounding extraembryonic mesoblast constitute extraembryonic splanchnopleure. At the junctional zone surrounding the margins of the embryonic area, where the walls of the amnion and yolk sac converge, the somatopleuric and splanchnopleuric layers of extraembryonic mesoblast are continuous.

The terms epiblast and hypoblast are used to make the distinction between the earliest bilaminar disc layers and the later embryonic layers. Epiblast and hypoblast contain mixed populations of cells with little restriction (see p. 193), which establish the placental structures and extraembryonic tissues before the production of embryonic cell lines at gastrulation. The older terminology depicting three germ layers that give rise to the skin, gut lining and intervening tissues is thus incorrect for the bilaminar and trilaminar embryonic disc. The application and the retention of this aged terminology for the early stages of embryology continues to cause confusion and inhibits the development of more pertinent descriptive language to describe these early events.

At early stage 6, the epiblast is producing extraembryonic mesenchyme from its caudal margin. With the appearance of the primitive streak, a process is begun whereby cells of the epiblast either pass deep to the epiblast layer to form the populations of cells within the embryo, or remain on the dorsal aspect of the embryo to become the embryonic ectoderm. Although human embryos do not form a ‘gastrula’ as such, the term gastrulation is used here to denote an early period of development during which significant rearrangements, migrations and folding of the early embryo occur. The primitive streak is the site of organizer cells analogous to those found in embryos which do undergo gastrulation. The appearance of the primitive streak therefore marks the beginning of a period when gross alterations in morphology and complex rearrangements of cell populations occur. During this time, the epiblast will give rise to a complex multilaminar structure with a defined craniocaudal axis. By the end of gastrulation, cell populations from different, often widely separated, regions of the embryonic disc will become spatially related and the embryonic shape will have been produced.

Primitive streak and node

Seen from the dorsal (epiblastic) aspect, at stage 6, the embryonic disc appears elongated. The primitive streak is first seen in the caudal region of the embryonic disc at this stage as a collection of pluripotent cells, orientated along its long axis in the median position, conferring the future craniocaudal axis of the embryo (Figs 10.1 and 10.2). Although the future cranial and caudal regions of the embryo are well within the boundaries of the embryonic disc, it has become the practice to term the region of the disc closest to the streak ‘caudal’, and the region of the disc furthest from the streak ‘cranial’ or ‘rostral’. With the development of the streak, the terms medial and lateral can be used. The relative dimensions of the primitive streak and the fates of the cells that pass through it change with the developmental stage. Thus the streak extends half way along the disc in the stage 6 embryo, reaches its greatest relative length in stage 7 and its maximum length in stage 8.

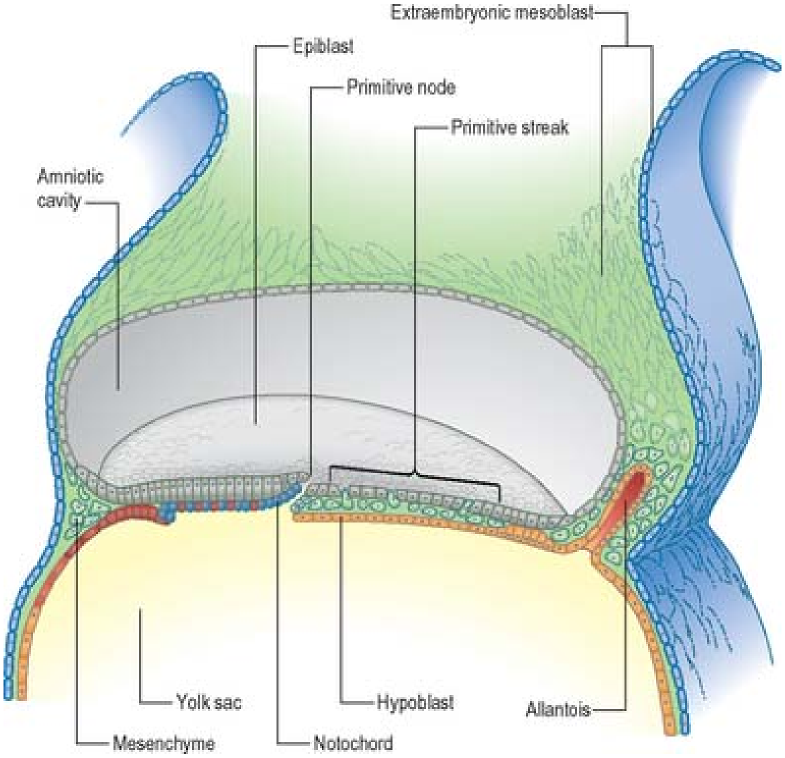
Extraembryonic mesoblast
Epiblast
Primitive node
Primitive streak
Amniotic cavity
Yolk sac
Hypoblast
Allantois
Mesenchyme
Notochord

Fig. 10.1 Longitudinal section through an early conceptus. Ingression of mesoblast is occurring at the primitive streak and the notochord is ingressing via the primitive (Hensen's) node.

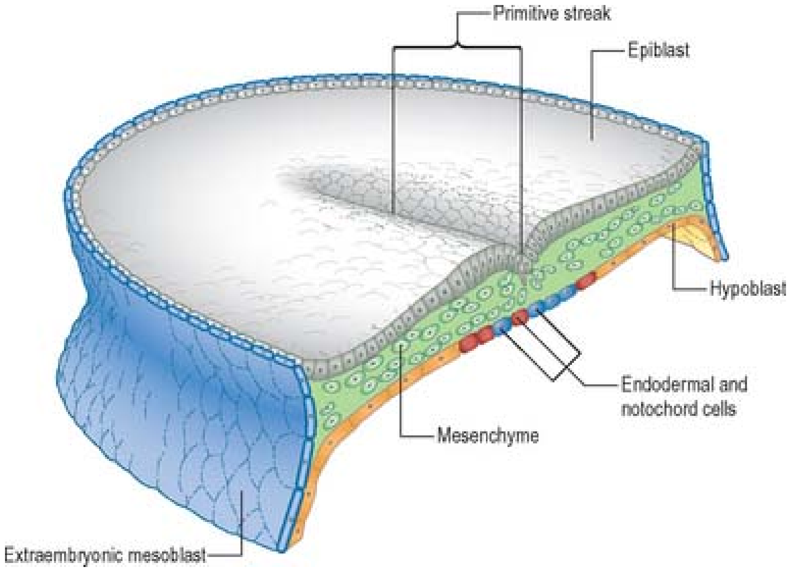
Primitive streak
Epiblast
Hypoblast
Endodermal and notochord cells
Mesenchyme
Extraembryonic mesoblast

Fig. 10.2 Transverse section through the embryonic plate at the level of the primitive streak to show the early movement of mesoblast between the

epiblast and underlying hypoblast.

Formation of the primitive streak is induced by the underlying visceral hypoblast which remains beneath the streak even at later stages. The primitive streak may be considered to be generally homologous with the blastopore of lower vertebrates (e.g. amphibia), with the nodal region corresponding to the dorsal lip. Experiments clearly show the lip of the blastopore to be a dynamic wave front on which cells are carried into the interior to form the roof of the archenteron, a situation analogous to ingression through the node of the prechordal plate and endoderm. The primitive streak similarly may be considered analogous to the coapted, or fused, lateral lips of the blastopore, and the cloacal membrane and its immediate environs are considered analogous to the ventral lip of the blastopore.

At the primitive streak, epiblast cells undergo a period of intense proliferation, the rate of division being much faster than that of blastomeres during cleavage. Streak formation is associated with the local production of several cell layers, extensive disruption of the basal lamina, increase in adhesive plaques and gap junctions, synthesis of vimentin, and loss of cytokeratins by the emerging cells.

As the epiblast cells proliferate, two ridges are formed on each side of the primitive streak, which appears to sink between them. The lower midline portion of the streak is termed the primitive groove. The process by which cells become part of the streak and then migrate away from it beneath the epiblast is termed ingression.

The primitive node, or Hensen’s node, is the most rostral region of the primitive streak. It appears as a curved ridge of cells similar in shape to the top of an old fashioned keyhole. Cells ingressing from the ridge pass into the primitive pit (the most rostral part of the primitive groove), and then migrate rostrally beneath the epiblast. The primitive node has been recorded in all stage 7 human embryos: it produces axial cell populations, the prechordal plate, notochord, embryonic endoderm and the medial halves of the somites.

Experimental removal of the node results in complete absence of the notochord and a failure of neurulation.

Position and time of ingression through the primitive streak

Studies of cell fate have shown that epiblast cells that will pass through the streak are randomly located within the epiblast layer before their ingression, and that epiblast fate is determined at or before the time of ingression through the streak, indicating that passage through the primitive streak is the most important factor for future differentiation.

The position and time of ingression through either streak or node directly affect the developmental fate of cells. Passage through the streak is specified according to position, e.g. via the node, or rostral, middle or caudal regions of the streak. Cells that ingress through the primitive node give rise to the axial cell lines, the prechordal mesenchyme and notochord, and to the endoderm and the medial halves of the somites. The rostral portion of the primitive streak produces cells for the lateral halves of the somites, whereas the middle streak produces the lateral plate mesoblast. The adjacent caudal portion of the streak gives rise to the primordial germ cells, which can be distinguished histologically and histochemically, and the most caudal portion of the streak contributes cells to the extraembryonic mesoblast until the somites are visible. A composite of the information on the position of ingression through the streak and node is shown in Fig. 10.3. The epiblast cells that do not pass through the streak but remain instead within the epiblast population give rise to the neural and surface ectoderm of the embryo.

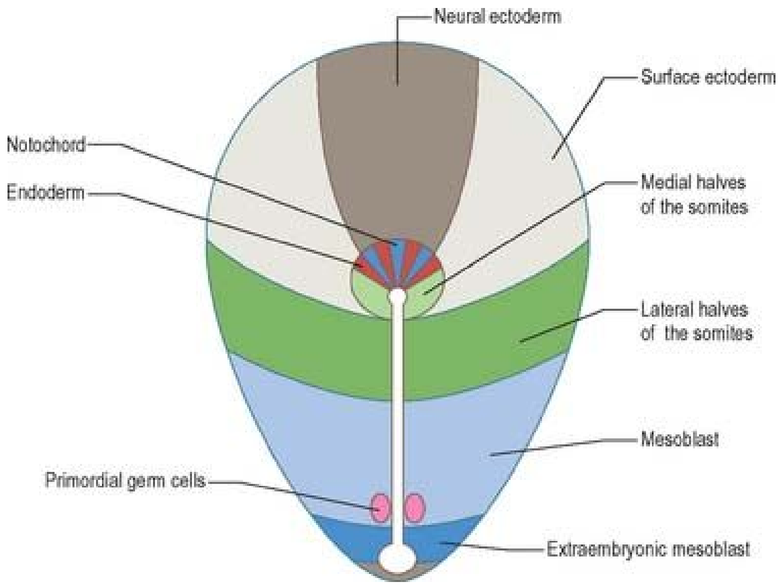
Neural ectoderm
Surface ectoderm
Notochord
Endoderm
Medial halves of the somites
Lateral halves of the somites
Mesoblast
Primordial germ cells
Extraembryonic mesoblast

Fig. 10.3 The predictive fates of the epiblast cell population at the time the primitive streak is present.

Prechordal plate

The earliest cells migrating through the primitive node and streak give rise to both the embryonic endoderm and the notochord. The prechordal plate is first seen at stage 7. It has been defined as a localized thickening of the endoderm rostral to the notochordal process, although it is seen as a highly developed mesenchymal mass in contact with the floor of the neural groove, rostral to the notochordal process, rather than as an epithelial layer. The prechordal plate is a temporary collection of cells which underlies the neural plate during stage 9. It is composed of cells that are similar to, or larger and more spherical than, the ingressing endodermal cells (Müller & O'Rahilly 2003). In stage 8 embryos the prechordal plate is up to eight cells deep and extends along the long axis of the embryonic disc. By stages 9 and 10 the cells at the lateral edge of the plate have begun to migrate laterally as free mesenchymal cells and the plate reduces in height to two cells deep. At stage 11 the migrating prechordal mesenchyme forms bilateral premandibular mesenchymal condensations and is no longer a median structure. The extent of prechordal cells remaining within the endoderm is not clear.

Notochord

The notochord, also called chordamesoderm, the head process or chorda, arises from epiblast cells of the medial part of the primitive node. It passes through several stages during development. The cells of the early notochordal process express myogenic markers transitorily as they migrate beneath the epiblast, but later they become epithelial, forming junctions and a basal lamina. The notochordal cells are intimately mixed with endodermal cells, as both cells lines ingress at the same time (Figs 10.1, 10.2 and 10.4). In the stage 8 embryo, the ingressing notochordal cells remain in the midline along the cephalocaudal axis. They form a rostral part, which is composed of a cell mass continuous with the prechordal mesenchyme, a mid portion in which cells are arranged in a tube with a central notochordal canal, and a caudal epithelial layer of cells, the notochordal plate, which is contiguous with the embryonic endoderm and forms a roof to the secondary yolk sac. There is a transitory opening between the primitive node (and amniotic cavity) and the secondary yolk sac called the neurenteric canal (so named because its upper opening is in the future caudal floor of the neural groove, and its lower opening is into the archenteron, which is the primitive gut); it may still be found at stage 9, and the site of the neurenteric canal can be recognized in stage 10 embryos. The ingression of notochordal cells at the primitive node is matched by specification of the overlying neural ectodermal cells, and the notochordal plate is thus matched in length by the future neural floor plate. Both the notochord and the region of the floor plate of the neural tube may arise from a common progenitor cell. The early notochord is important for the maintenance and subsequent development of the neural floor plate and the induction of motor neurones. Removal of the notochord results in elimination of the neural floor plate and motor neurones, and expression of sensory cells types.

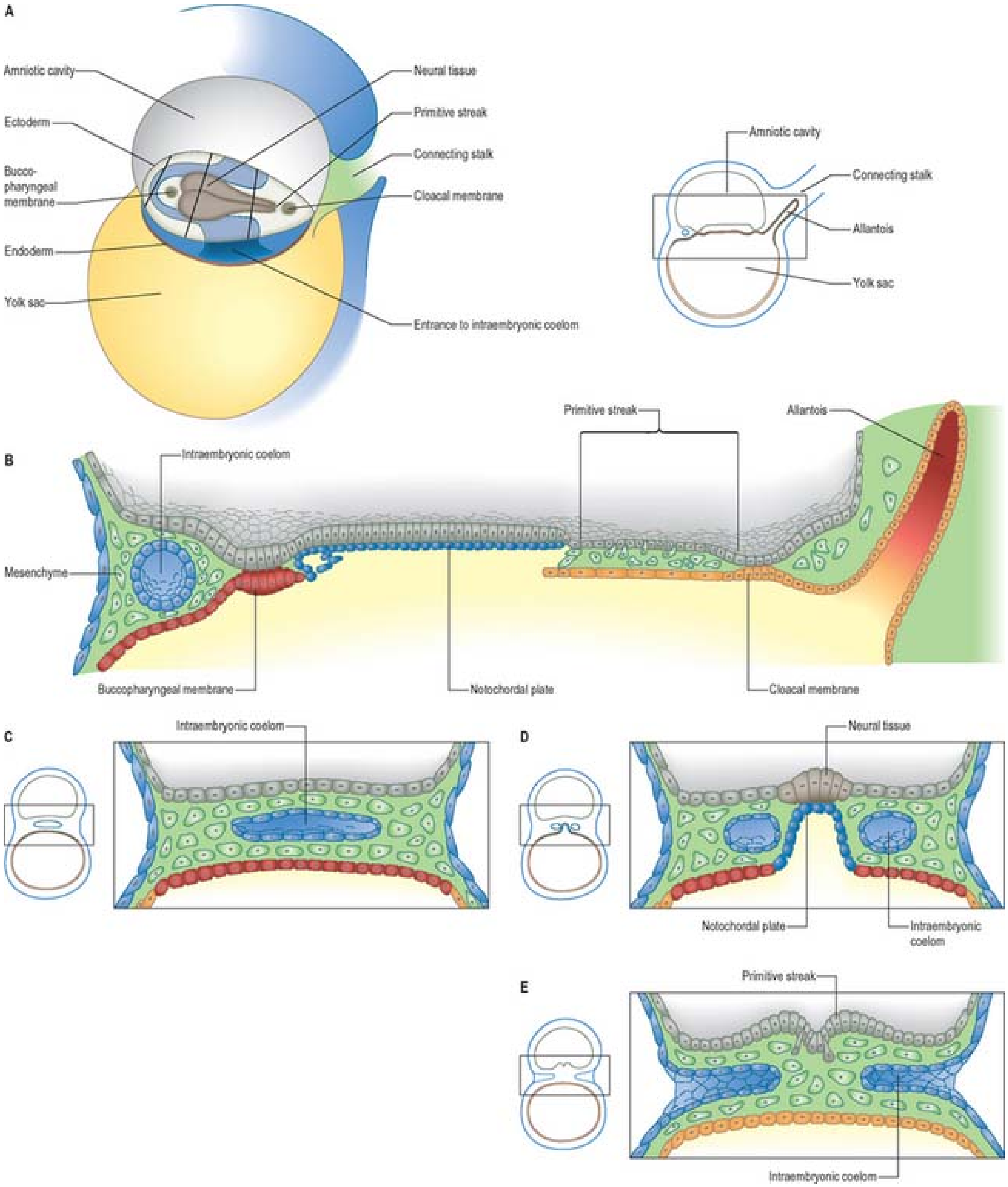
A
Amniotic cavity
Ectoderm
Bucco-
pharyngeal
membrane
Endoderm
Yolk sac
Neural tissue
Primitive streak
Connecting stalk
Cloacal membrane
Entrance to intraembryonic coelom
Amniotic cavity
Connecting stalk
Allantois
Yolk sac
B
Primitive streak
Allantois
Intraembryonic coelom
Mesenchyme
Buccopharyngeal membrane
Notochordal plate
Cloacal membrane
C
Intraembryonic coelom
D
Neural tissue
Notochordal plate
Intraembryonic
coelom
E
Primitive streak
Intraembryonic coelom

Fig. 10.4 **A**, Unfolded embryo, showing the disposition of the intraembryonic coelom within the embryonic disc. The lines across the embryo show the level of transverse sections through the disc. **B**, Longitudinal section through the disc. **C–E**, Transverse sections through the disc at the points indicated in **A**.

Caudal eminence

From stages 9 and 10 the region between the neurenteric canal and the cloacal membrane (see below), including the primitive streak, is termed the caudal eminence. It consists of the caudal region of the trunk composed of mesenchyme derived from the primitive streak and epiblast, covered with surface ectoderm. Whereas ingression of cells through the primitive streak gives rise to the prechordal and notochordal plates, and cells rostral to the neurenteric canal (see below), the cells of the caudal eminence arise from local division of a mesenchymal population positioned caudal to the neurenteric canal. The caudal portions of the notochord, which form later in development when secondary neurulation processes begin, arise from these cell populations, sometimes termed the caudoneural hinge or junction (see p. 361). This tissue is thicker and more advanced in differentiation than the tissues derived from the early primitive streak.

Embryonic endoderm

Before ingression, definitive embryonic endoderm cells are found in the epiblast located at the primitive node and rostral primitive streak. In the mouse, the endodermal cells lie beneaththe epiblast mainly in the midline, interspersed with presumptive notochordal cells, forming the roof of the secondary yolk sac. The ingressing endoderm displaces the visceral hypoblast into the secondary yolk sac wall by a dramatic territorial expansion that is brought about by a change in the morphology of the cells (Figs 10.1, 10.2 and 10.4). The putative endoderm cells are cuboidal epithelial cells within the node, but they become squamous in the endoderm layer; this could result in a four-fold increase in the surface area covered by the cells. A complete replacement of the visceral hypoblast has not yet been confirmed, and there may be a mixed population of cells in the endodermal layer in the early stages. Ingression of cells through the streak and node in the human is apparent at stage 6, and by stage 7 a population of endoderm and notochord cells is present beneath the epiblast (Figs 10.1, 10.2 and 10.4). During stages

6–11, the midline roof of the secondary yolk sac becomes populated mainly by the notochordal plate, which remains in direct lateral continuity with the endodermal cells. It is not until stage 11, after the definitive notochord is formed, that the endoderm cells can join across the midline. For the developmental fate of the embryonic endoderm, see Fig. 12.3.

Intraembryonic mesoblast (mesenchyme)

Epiblast cells ingress through the cranial and middle parts of the streak individually, maintaining their apical epithelial contacts while elongating ventrally. The cells become flask-shaped, with thin attenuated apical necks and broad basal regions. The basal and lateral surfaces form lamellipodia and filopodia and the apical contact is released. The cells are now free mesoblast cells, their fibroblastic, stellate morphology reflecting the release from the epithelial layer. Once through the streak, the cells migrate away from it, using the basal lamina of the overlying epiblast and extracellular matrix as a substratum. The cells contact one another by filopodia and lamellipodia, with which they also contact the basal lamina. Gap junctions have been observed between filopodia and cell bodies. With the appearance of the mesoblast, spaces form between the epiblast and visceral hypoblast that are filled with extracellular matrix rich in glycosaminoglycans. The migrating mesoblast has a leading edge of cells that open up the migration routes, and the following cells seem to be pulled along behind in a coordinated mass movement. Mesoblast formed by cells migrating through the primitive node and rostral primitive streak will form the paraxial mesenchyme, whereas cells migrating through the middle to caudal streak will form the lateral plate mesenchyme (Figs 10.1, 10.2; see Fig. 10.6).

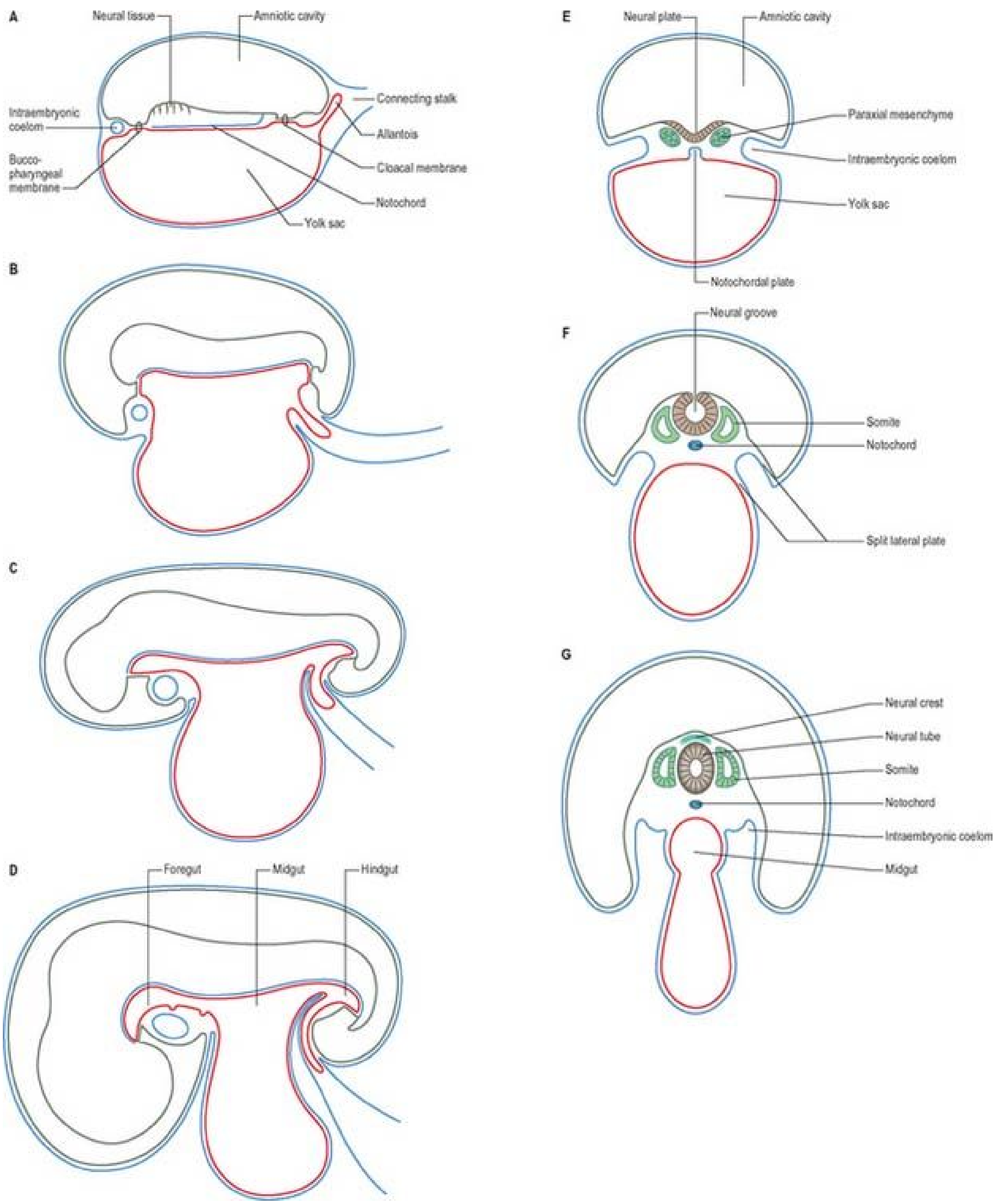
A
Neural tissue
Amniotic cavity
Connecting stalk
Intraembryonic coelom
Allantois
Bucco-pharyngeal membrane
Cloacal membrane
Notochord
Yolk sac
B
C
D
Foregut
Midgut
Hindgut
E
Neural plate
Amniotic cavity
Paraxial mesenchyme
Intraembryonic coelom
Yolk sac
Notochordal plate
F
Neural groove
Somite
Notochord
Split lateral plate
G
Neural crest
Neural tube
Somite
Notochord
Intraembryonic coelom
Midgut

Fig. 10.6 Head and tail folding of the embryo, and lateral folding. **A–D**, Median sagittal (longitudinal or axial) sections through the embryonic disc at successive stages; the relative positions of the buccopharyngeal and cloacal membranes have been maintained, thus the movement of the most

rostral and caudal portions of the disc can be followed. As these portions of the disc move ventrally the initially widely open yolk sac becomes constricted and fore- and hindgut divisions can be seen; the midgut is that region which remains in wide connection to the yolk sac. **E–G**, Transverse sections through the midpoint of the embryonic disc at successive stages to illustrate lateral folding which occurs as neurulation proceeds.

Embryonic ectoderm

When the ingression of cells through the primitive streak is completed, the epithelial cells remaining in the epiblast layer are termed embryonic ectoderm cells. This layer still contains a mixed population, because both surface ectoderm cells and neural ectoderm cells are present. It is believed that these cells were originally in the cranial half of the disc when the primitive streak first appeared, at which time the neural-fated cells were closest to the streak, and the surface ectoderm cells were most cranial (Fig. 10.3). The process of primary neurulation relocates most of the neuroepithelial cells (see below).

Primordial germ cells

Although early studies on human embryos have reported primordial germ cells, and described their development from the early endoderm of the yolk sac and allantois, it is now clear from animal experimentation that the primordial germ cells arise from epiblast ingressing at the caudal end of the primitive streak (Fig. 10.3). It is not known whether these cells originate from rostral regions that migrate to the streak, or from local caudal regions. Extremely early segregation of the germ cells, when the epiblast layer consists of only 10–13 cells, has been demonstrated. It has been suggested that the primordial germ cells remain sequestered in the extraembryonic mesenchyme at the caudal end of the embryo until the embryonic endoderm has been produced and gastrulation completed, and that they start to migrate along the allantoic and hindgut endoderm as the folding of the embryo begins. The formation of the tail fold brings the proximal portion of the allantois within the body, so reducing the final distance over which the cells migrate to the genital ridges. Further development of the germ cells is described on page 1318.

TRILAMINAR DISC

Although the stage 8 embryo is termed a trilaminar disc, the concept of three epithelial layers forming a trilaminar disc is incorrect: the middle, mesoblast, layer is several cells thick with intervening extracellular matrix. The embryo at this stage, approximately 23 days after ovulation, is pear-shaped, and broader cranially than caudally (Fig. 10.5). The upper epiblast cells are tall, and form a pseudostratified columnar epithelial layer with a basal lamina, except at the primitive streak, where the cells are ingressing to form the other layers. The more centrally placed epiblast will give rise to neural ectoderm (neurectoderm) and the more laterally placed epiblast will give rise to surface ectoderm. The future neural ectoderm is seen as a neural plate which matches the length of the notochordal plate directly beneath, being slightly wider near the prechordal plate. The lower embryonic endoderm, a simple squamous layer with a developing basal lamina, is not always complete at this stage, particularly in the midline caudal to the prechordal plate, which is still occupied by the notochordal process or plate.

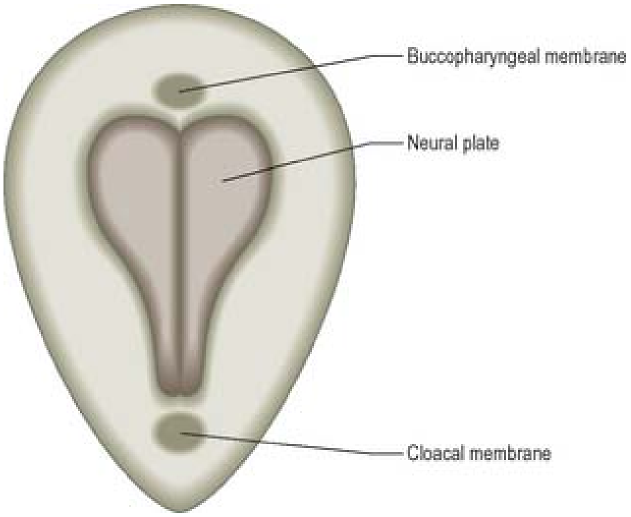

Fig. 10.5 Extent and shape of the neural plate in an unfolded embryo.

The middle, mesoblast, layer is composed of free cells migrating cranially, laterally and caudally from the primitive streak (Fig. 10.4). They produce extracellular matrix, which separates the epiblast and endoderm of the embryonic area and permits their passage. The streams of mesoblast extend between the epiblast and endoderm over all of the disc area except cranially at the buccopharyngeal membrane (where the endoderm and ectoderm become apposed once the prechordal mesenchyme has migrated laterally), and caudally at the cloacal membrane (a patch of thickened endoderm, similar to the buccopharyngeal membrane, caudal to the primitive streak). The mesoblast on each side of the notochord is termed paraxial mesenchyme.

Mesoblast that passes in a cranial direction flanks the notochordal plate and passes around the prechordal plate region, converging medially to fuse in the midline beyond its cephalic border. This transmedian mass, in which the heart and pericardium will develop, is initially termed the cardiogenic mesoblast. It fuses with the junctional zone of extraembryonic mesoblast around the extreme cephalic margin of the embryonic area. This region will eventually form the septum transversum and primitive ventral mesentery of the foregut. Mesoblast passing laterally from the streak soon approaches and becomes confluent with the extraembryonic mesoblast around the margins of the disc, i.e. at the junctional zone where the splanchnic and somatic strata of extraembryonic mesoblast merge. Mesoblast that streams caudally from the primitive streak skirts the margins of the cloacal membrane and then converges towards the caudal midline extremity of the embryonic disc to become continuous with the extraembryonic mesoblast of the connecting stalk. It is unclear if the lower layer of the cloacal membrane consists of visceral hypoblast, like the more cranial primitive streak (the hypoblast is necessary for maintaining the streak), or if it is replaced by migrating embryonic endoderm, or if there is a region for ingression of endoderm at the caudal end of the streak, similar to the node cranially.

Still further caudally, the embryonic disc develops a midline diverticulum adjacent to the cloacal membrane. This diverticulum, the allantois, projects into the extraembryonic connecting stalk (Fig. 10.4, see also Fig. 10.6 and p. 180). There is little information about which cells form the allantois, i.e. whether it is composed of visceral hypoblast, parietal hypoblast or embryonic endoderm. The allantois later develops a rich anastomotic blood supply around it, in the manner of the yolk sac.

The generation of cells at the primitive node produces midline endoderm, notochord and the floor plate of the future neural tube. As the notochord grows and elongates, there is a matched growth of neural floor plate cells until both cell lines extend to the buccopharyngeal membrane. The epiblast lateral to the midline contains both future surface and neural ectoderm. The latter becomes arranged between the primitive node and buccopharyngeal membrane: cells destined to be in the neural plate lie medially, and those destined for the neural crest lie laterally (Fig. 10.5). A smaller subpopulation of neuronal cells, the ectodermal placodes, are arranged either close to the neural crest or within the rostral limit of the neural plate itself.

FOLDING OF THE EMBRYO

In a diagrammatic representation of the trilaminar disc prior to folding and viewed from the ectodermal aspect, all of the future external surface of the body is delimited (see Fig. 10.5). The ends of the gut tube are specified on the ectodermal surface at the buccopharyngeal and cloacal membranes, which are regions where the ectoderm and underlying endoderm are apposed without intervening mesoblast. In the midline between these membranes, proliferation of the neural ectoderm matches the underlying migration of mesoblast from the primitive streak, so that the neural plate covers the paraxial mesenchyme on each side of the notochord (Fig. 10.6E). As the paraxial mesenchyme segments (see p. 763), the formation of the epithelial somites elevates the edges of the neural plate and initiates primary neurulation (Figs 10.6F and 10.8). The neural plate itself undergoes concurrent morphological changes. The most medial cells become wedge-shaped, forming the neural groove. Further elevation of the edges of the neural groove permits fusion of the neuronal populations in the dorsal midline to form the neural tube. The surface ectoderm forms the putative dorsal epidermis (Figs 10.6G and 10.8). Cells at the lateral edge of the neural plate termed neural crest cells remain as a linearly arranged mesenchymal population between these two epithelia. Fusion of the neural tube begins in the future rhombencephalic region of the embryo and proceeds rostrally and caudally to about the level of somite 29. Neurulation is described further in Chapter 24. A population of neural epithelial cells remain within the surface ectoderm; at this stage they are termed ectodermal placodes.

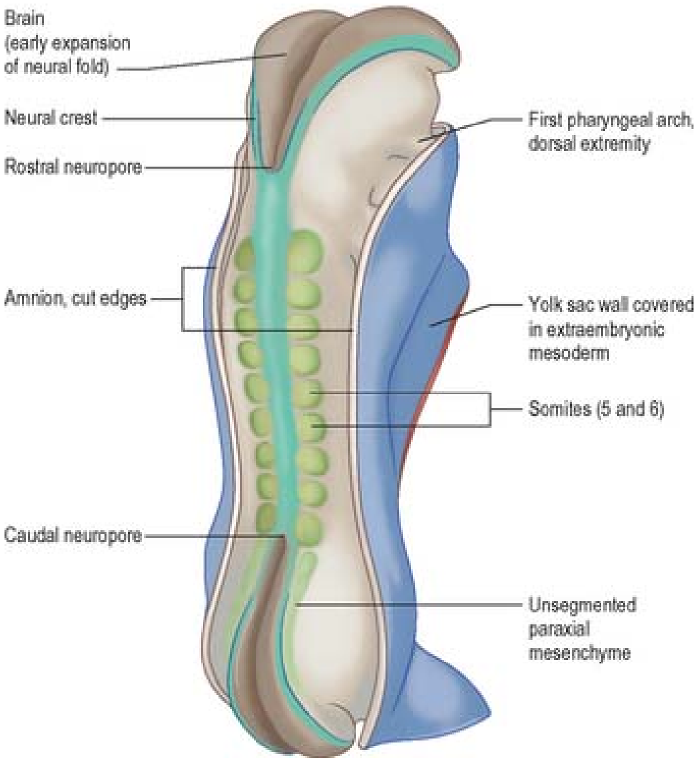
Brain (early expansion of neural fold)
Neural crest
Rostral neuropore
Amnion, cut edges
Caudal neuropore
First pharyngeal arch, dorsal extremity
Yolk sac wall covered in extraembryonic mesoderm
Somites (5 and 6)
Unsegmented paraxial mesenchyme

Fig. 10.8 A human embryo at stage 10, 2.1 mm long, with nine somites: right lateral and dorsal aspects. Nearly all the yolk sac and the caudal amnion have been excised.

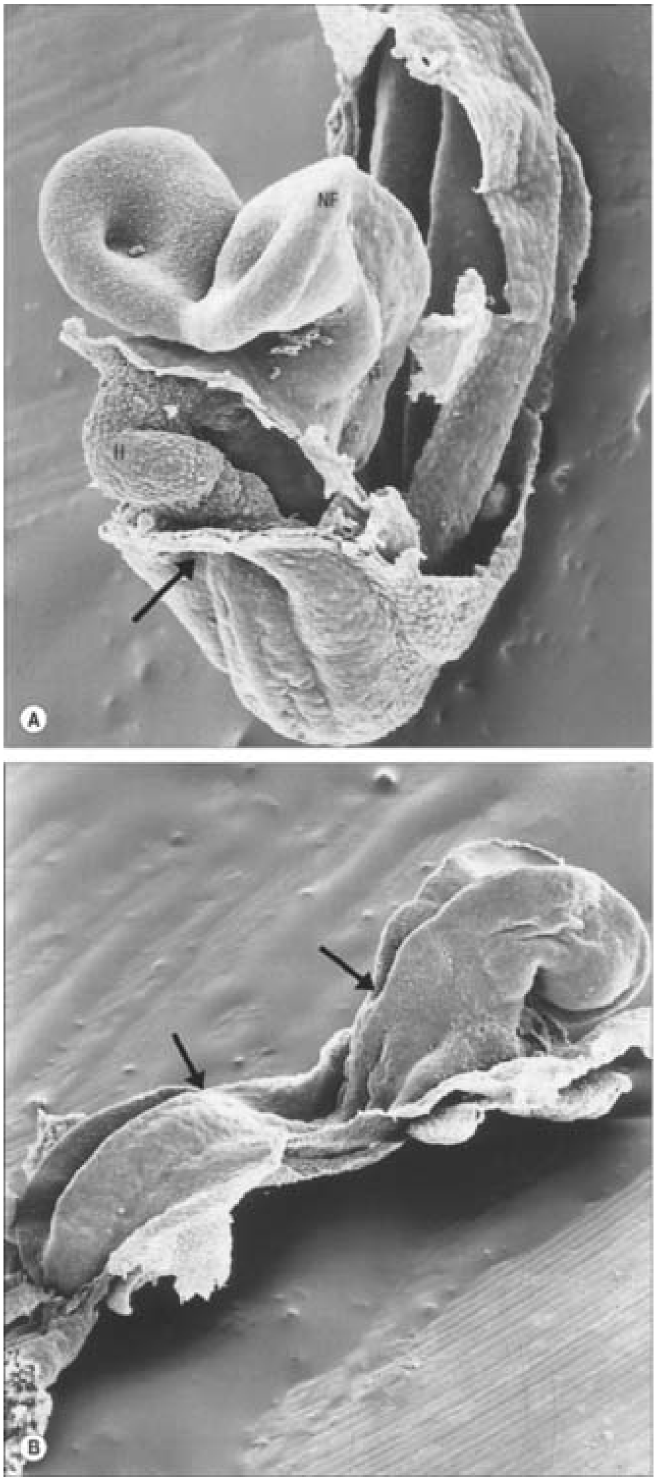

Fig. 10.7 Scanning electron micrographs of rat embryos at the time of neurulation. **A**, Ventral view, showing the neural fold (NF), and the heart (H) with the somatopleuric pericardial membrane and surface ectoderm removed; the arrow indicates the entrance to the foregut via the cranial

intestinal portal. **B**, Dorsolateral view; the arrows indicate the extent of rostral (to the right) and caudal (to the left) neural tube formation.

(Photographs by P Collins; printed by S Cox, Electron Microscopy Unit, Southampton General Hospital.)

The representation of a person on the trilaminar disc (Fig. 10.9) shows, to some extent, the way in which the positions of the main body structures are already specified in the unfolded embryo. The portion of ectoderm lateral to the neural plate and the paraxial mesenchyme will form structures within the back. The portion of the disc between the buccopharyngeal membrane and the edge of the disc will become the ventral thoracic wall and the ventral abdominal wall cranial to the umbilicus. Further caudally, midway along the neural axis, the lateral portions of the disc will become the lateral and ventral abdominal walls of the trunk. The portion of the disc beyond the cloacal membrane will form the ventral abdominal wall caudal to the umbilicus. The circumference of the disc, where the embryonic tissue meets the extraembryonic membranes, will become restricted to the connection between the ventral abdominal wall and the umbilical cord, i.e. the umbilicus.

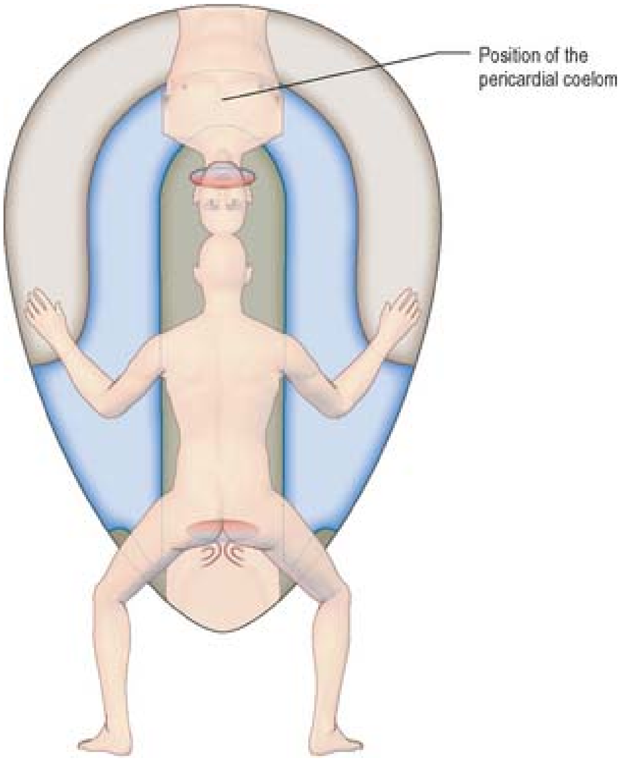

Fig. 10.9 Representation of a person on the flat embryonic disc. The position of the central nervous system has been matched to the dimensions of the neural plate, and the position of the heart in the thorax to the position of the pericardial coelom. The limbs, although represented in this diagram, are not present on the disc at this stage. The usefulness of this diagram lies in its illustration of the extent of the anterior body wall both rostral to the buccopharyngeal membrane and caudal to the cloacal membrane. The future dorsal regions of the body are found medially on the disc, while the ventral regions of the body are situated laterally and peripherally on the disc. After head and tail folding and lateral folding, the peripheral edge of the disc becomes constricted as the edge of the umbilicus.

Head folding begins at stage 9, when the fusing cranial neural plate rises above the surface ectoderm and the portion of the disc rostral to the buccopharyngeal membrane (which contains the cardiogenic mesenchyme) moves to lie ventral to the developing brain (Fig. 10.6). The prosencephalon and buccopharyngeal membrane are now the most rostral structures of the embryo. The previously flat region of endoderm, which may contain cells from the prechordal plate, is now modified into a deep tube, the primitive foregut. Tail folding can be seen in stage 10 embryos, when the entire embryo comes to rise above the level of the yolk sac. Similar movement of the part of the disc caudal to the cloacal membrane results in its repositioning ventral to the neural plate. Generally, as the embryo rises above the edges of the disc, the lateral regions of the disc are drawn ventrally and medially, contributing to the lateral folding of the embryo.

FORMATION OF THE INTRAEMBRYONIC COELOM

At and just before stage 9 (before formation of the head fold), vesicles appear between the mesenchymal cells cranial to the buccopharyngeal membrane and within the cranial lateral plate mesenchyme. At the periphery of the vesicles, the mesenchymal cells develop junctional complexes and apical polarity, and form an epithelium. The vesicles become confluent to form a horse-shoe shaped tube, the intraembryonic coelom, which extends caudally to the level of the first somite and laterally into the lateral plate mesenchyme towards the extraembryonic mesenchyme. The intra- and extra-embryonic coeloms do not communicate at this stage. The lateral plate mesenchyme thus develops somatopleuric coelomic epithelium subjacent to the ectoderm, and a splanchnopleuric coelomic epithelium next to the embryonic endoderm (Fig. 10.4; see also Fig. 12.2C(iv)).

During development of the head fold, the morphological movements that organize the foregut and buccopharyngeal membrane have a similarly profound effect on the shape of the intraembryonic coelom. The midline portion of the originally flat, horse shoe-shaped coelom moves ventrally, leaving the caudal arms of the horse shoe in their original position. In this way the midline part of the coelom, which was originally just rostral to the buccopharyngeal membrane, comes to lie ventral to the foregut (caudal to the buccopharyngeal membrane), and the two lateral extensions of the coelom pass close to the lateral walls of the foregut on each side. The caudal portions of the coelom (the two arms of the horse shoe), which in the unfolded disc communicated laterally with the extraembryonic coelom, turn 90° to lie lateral to the gut, and communicate with the extraembryonic coelom ventrally.

Compartments of the coelom that will later in development give rise to the body cavities can already be seen. The midline ventral portion, caudal to the buccopharyngeal membrane, becomes the pericardial cavity. The canals lateral to the foregut (pericardioperitoneal canals) become the pleural cavities and the uppermost part of the peritoneal cavity. The remaining portion of the coelom becomes the peritoneal cavity. By stage 11, the intraembryonic coelom within the lateral plate mesenchyme extends caudally to the level of the caudal wall of the yolk sac. The intra- and extra-embryonic coeloms communicate widely on each side of the midgut along the length of the embryo from the level of the 4th somite (Fig. 10.10; see also Fig. 12.1).

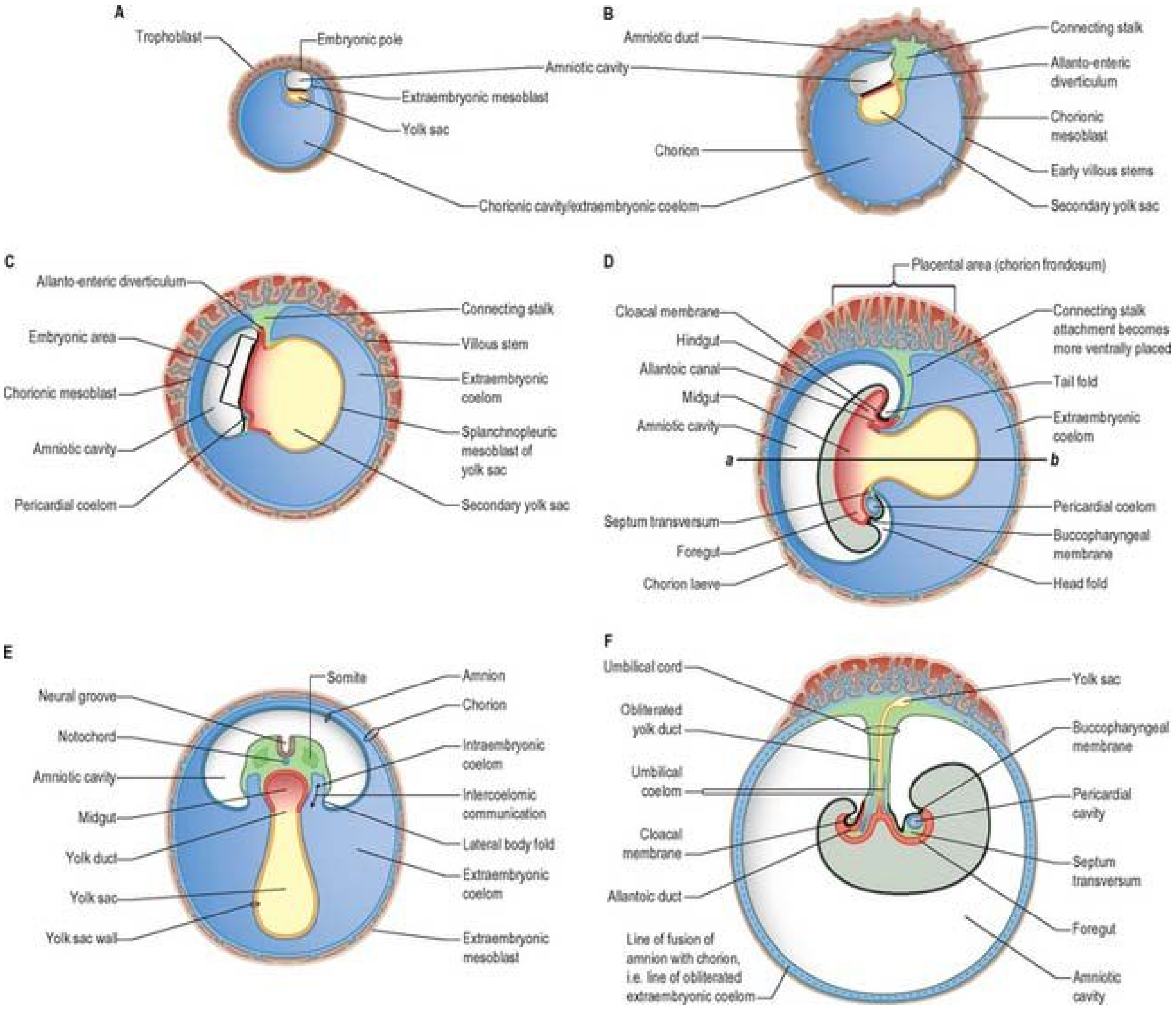
A
Trophoblast
Embryonic pole
Amniotic cavity
Extraembryonic mesoblast
Yolk sac
Chorionic cavity/extraembryonic coelom
B
Amniotic duct
Connecting stalk
Allanto-enteric diverticulum
Chorionic mesoblast
Chorion
Early villous stems
Secondary yolk sac
C
Allanto-enteric diverticulum
Embryonic area
Chorionic mesoblast
Amniotic cavity
Pericardial coelom
Connecting stalk
Villous stem
Extraembryonic coelom
Splanchnopleuric mesoblast of yolk sac
Secondary yolk sac
D
Placental area (chorion frondosum)
Cloacal membrane
Hindgut
Allantoic canal
Midgut
Amniotic cavity
a
b
Septum transversum
Foregut
Chorion laeve
Connecting stalk attachment becomes more ventrally placed
Tail fold
Extraembryonic coelom
Pericardial coelom
Buccopharyngeal membrane
Head fold
E
Neural groove
Notochord
Amniotic cavity
Midgut
Yolk duct
Yolk sac
Yolk sac wall
Somite
Amnion
Chorion
Intraembryonic coelom
Intercoelomic communication
Lateral body fold
Extraembryonic coelom
Extraembryonic mesoblast
F
Umbilical cord
Obliterated yolk duct
Umbilical coelom
Cloacal membrane
Allantoic duct
Line of fusion of amnion with chorion, i.e. line of obliterated extraembryonic coelom
Yolk sac
Buccopharyngeal membrane
Pericardial cavity
Septum transversum
Foregut
Amniotic cavity

Fig. 10.10 **A**, An early stage in development of a human blastocyst. **B**, Blastocyst sectioned through the longitudinal axis of an embryo, showing the early formation of the allantois and the connecting stalk. **C**, Longitudinal section of an embryo at a later stage of development; the pericardial cavity can be seen at the most rostral part of the embryonic area.

D, Longitudinal section of an embryo at a later stage, showing formation of the head and tail folds, the expansion of the amnion and the delimitation of the umbilicus. **E**, Transverse section along the line a–b in **D**; observe that the intraembryonic coelom communicates freely with the extraembryonic coelom. **F**, Longitudinal section of an embryo at a later stage, showing full expansion of the amniotic cavity and the umbilical cord.

In the early embryo, the intraembryonic coelom provides a route for the circulation of coelomic fluid and, with the beating of the heart tube, functions as a primitive circulation that takes nutritive fluid deep into the embryo, until it is superseded by the blood vascular system. The coelomic channel, and the primitive circulation that passes through it, is of paramount importance up to stage 13. Whereas the superficial tissues of the embryo can receive nutrients via the amniotic sac and yolk sac fluids, the deeper tissues are, until the formation of the coelom, under conditions similar to those found in tissue culture. From stage 10, however, exocoelomic fluid, propelled by the first contractions of the developing heart, is brought into contact with the deeply placed mesenchyme. This early ‘circulation’ ensures that an adequate supply of nutrients reaches the rapidly increasing amount of embryonic tissue, and meets most of the requirements of the deeper mesenchymal derivatives. From stage 12 the endothelial system expands and fills rapidly with plasma, which passes across the locally thinned coelomic epithelium into the large hepatocardiac channels that project into the pericardioperitoneal canals at the level of the seventh somite.

In spite of the importance of the coelom in defining the body cavities, and of the coelomic epithelium in the production of the major mesenchymal populations of the trunk (see Fig. 12.2), only a few workers have considered the overall contribution of the coelom and its epithelium to the embryo (Streeter 1942, Langemeijer 1976). The coelom can be described as a single, tubular organ which is comparable to the neural tube, in that it possesses a specialized wall that encloses a cavity. Certainly, the proliferating coelomic epithelium has many similarities to the neural ectoderm. It is pseudostratified columnar epithelium with an inner germinal layer from which cellular progeny migrate. After the germinal phase, both epithelia ultimately form the lining of a cavity, i.e. ependyma for the neural epithelium, and mesothelium for the coelomic epithelium. The coelomic epithelium, like the neural epithelium, produces cells destined for different fates from different sites and at different developmental times. Coelomic cells are like the neural epithelium, in that they have apical epithelial specializations and tapering basal processes that are in direct contact with the underlying mesenchyme, without an intervening basal lamina. The possibility of the tapering processes forming directional signals for migrating progeny, similar to radial glia of the neural tube, has not been examined.

EMBRYONIC CELL POPULATIONS AT GASTRULATION

After gastrulation, the cells of the embryo contribute to two fundamental types of tissue, namely epithelial and mesenchymal. Differentiation of specialized circulating blood cells and other cell types occurs in sequence. Embryonic and fetal cell types are replaced later in development or after birth.

Epithelia

Epithelial populations in the embryo have many of the morphological characteristics of differentiated epithelia, i.e. they are composed of sheets of closely packed cells, with narrow intercellular clefts containing minimal extracellular material, and a developed basal lamina containing specific proteins synthesized by the epithelium itself. The cells usually show juxtaluminal lateral surface specializations such as desmosomes, tight junctions, gap junctions, etc., and specializations of the apical surface, such as microvilli or cilia. Characteristically, epithelia clothe internal and external surfaces as simple or compound cellular sheets that separate phases of differing composition (e.g. the external environment and the subepithelial tissue fluids; intravascular and extravascular fluids, etc.). Traffic of materials in the intercellular clefts is limited. Traffic occurs across the cells because their limiting membranes, which function as energy-dependent selective barriers, enhance the passage of some materials and impede the passage of others.

Embryonic epithelia differ from those in the fetus and adult. Two distinct types can be identified. Early germinal epithelia which give rise to epithelial or mesenchymal populations of the embryo and confer their early patterning are termed organizers, e.g. the primitive streak. Later germinal epithelia give rise to system-specific progenitor populations, e.g. the ventricular zone of the neural tube. All epithelia other than special germinal epithelia divide to produce embryonic growth throughout development and may retain stem cells which will divide throughout life.

Mesenchyme

The terms mesoblast and mesenchyme are used in this text in a specific manner and not interchangeably. Previously, cells forming a population between the epiblast and hypoblast were termed mesoderm and, more recently, mesenchyme. The terms primary and secondary mesenchyme have been used to distinguish between those cells which arise from ingression through the primitive streak and those which arise from neural crest ingression respectively. Primary mesenchymal cells revert to epithelia at their destinations. However, whereas some primary mesenchymal cells may become epithelial within a short time frame, e.g. somites and lateral plate, other cells may transform later, e.g. the epithelium lining blood vessels. To cope with these conflicts in terminology, the mixed population of epiblast cells that ingress through the primitive streak and come to lie between the epiblast and embryonic endoderm is termed mesoblast until the cells have migrated to their final position, at which time the populations of mesenchyme can be identified and their fates inferred.

Mesoblastic and mesenchymal cells have no polarity. They form junctional complexes, which are not exclusively juxtaluminal, and they produce extracellular matrix molecules and fibres from the entire cell surface. Mesenchymal populations are formed from a range of germinal epithelia and by proliferation of mesenchymal cells directly, and occupy all the regions between the various epithelial layers described above. The term mesoderm is reserved for the coelomic epithelia that later form mesothelia.

Mesenchymal cells support epithelia throughout the developing body, both locally where they contribute to the basement membrane and form the lamina propria and smooth muscle of tubes, and generally where they differentiate into connective tissue. Specific mesenchymal populations control the patterning of local regions of epithelium (e.g. the zone of polarizing activity on the postaxial limb border posterior to the apical ectodermal ridge).

Extracellular matrix

The space beneath epithelia and between mesenchyme cells is filled with extracellular matrix: both epithelial and mesenchymal cells synthesize extracellular matrix molecules and their receptors. Epithelial cells produce a two-dimensional basal lamina, which contains a variety of matrix molecules including laminin, fibronectin, type IV collagen and various proteoglycans. The particular molecules can vary during development according to spatial and temporal patterns, resulting in changes in the behaviour of the underlying mesenchymal cells (e.g. in patterning of the basal regions of the skull). Mesenchymal cells produce extracellular matrix molecules in three dimensions. Those adjacent to an epithelial layer will connect with its basal lamina, forming a basement membrane that secures the epithelial layer to the underlying tissue. Cells deep within a mesenchymal population may synthesize matrix molecules (fibrillar or granular) to separate cells locally, open up migration routes or leave information within the matrix to act on cell populations passing at a later time.

Molecules of the extracellular matrix are complex: they include more than 19 individual types of collagen (some of which are capable of being individually spliced to give more than 100 variants), proteoglycans and glycoproteins (which come in a wide variety of forms, with and without binding proteins), and elastic fibres. Hyaluronic acid, a glycosaminoglycan, has a vast capacity to bind water molecules and so create and structure the space between the mesenchymal cells, thereby producing much of the overall shape of an embryo. Experimental removal of hyaluronic acid prevents the formation of cell migration routes, removes the support for overlying epithelia, and disrupts the normal branching of glandular systems.

Fibronectin deposited extracellularly along a migration pathway will affect cells that touch it later, causing realignment of their intracellular actin filaments and thus of their orientation; it also induces cell migration. The receptors for extracellular matrix molecules such as fibronectin and laminin were originally termed integrins because they integrate extracellular proteins and intracellular cytoskeletal elements (via α and β subunits that span the cell membrane), allowing them to act together: the binding preference of integrins depends upon their combination of subunits and environmental conditions.

The extracellular matrix is structured rather than random. Epithelial and mesenchymal cell populations can structure the space around them by secretion of particular matrix molecules or growth factors, which in turn can organize the cells that contact them. Cell–matrix interactions and matrix–cell interactions control the position of migration routes and cellular ‘decisions’ to migrate or to begin to differentiate. Matrix molecules propagate developmental instructions from cell to cell and form a far-reaching four-dimensional (spatial and temporal) mechanism of communication.

Transition between epithelial and mesenchyme states

Transformations of cell morphology from epithelium to mesenchyme, and *vice versa*, occur in specific places and times during development, and can be seen as ways of dispersing germinal centres with increasing restriction. The first epithelial-to-mesenchyme transition occurs at the primitive streak, a germinal epithelium which confers embryonic specification on the resultant mesoblast population. The mesoblast so formed migrates and the cells undergo mesenchyme-to-epithelial transitions when they reach their final destinations. Series of small epithelial germinal centres, the somites, are formed, as are larger, more extensive, germinal epithelial sheets which line the walls of the intraembryonic coelom. The coelomic walls, especially those derived from somatopleure and splanchnopleure, form germinal epithelia which give rise to the major mesenchymal populations that form the viscera. The early epithelial somites undergo further local epithelial-to-mesenchyme transitions to form the sclerotomes, and subsequently form several germinal epithelia in the epithelial plate of each somite. Later mesenchyme-to-epithelium transitions are not associated with the formation of germinal epithelia: the most common involve the transition of mesenchyme into the endothelium of the vascular system (see p. 1017). The nephrons of the mesonephric and metanephric systems also form from mesenchyme-to-epithelial transition (see p. 1308).

REFERENCES

üller F, O’Rahilly R. The prechordal plate, the rostral end of the notochord and nearby median features in staged human embryos. *Cells Tissues Organs*. 2003;173:1-20.

ngemeijer RATM. Le coelome et son revètement comme organoblasteme. *Bull Ass Anat*. 1976;60:547-558.

reeter GL. Developmental horizons in human embryos. Descriptions of age group XI, 13 to 20 somites, and age group XII, 21 to 29 somites. *Contrib Embryol Carnegie Inst Washington*. 1942;30:211-245.

CHAPTER 11

Embryonic induction and cell division

EMBRYONIC INDUCTION AND CELL DIVISION

Cell populations within the embryo interact to provide the developmental integration and fine control necessary to achieve tissue-specific morphogenesis. In the early embryo, such interactions may occur only if particular regions of the embryo are present, e.g. signalling centres or organizers. As the embryo matures, some interactions tend to occur between adjacent cell populations, e.g. epithelium and mesenchyme, and later between adjacent differentiating tissues, e.g. between nerves and muscle, or between muscle and skeletal elements. The interactions between adjacent epithelia and underlying connective tissue continue throughout embryonic and fetal life and extend into postnatal life. In the adult, these interactions also permit the metaplastic changes that tissues can undergo in response to local environmental conditions.

Tissue interactions result in changes or reorganization of one or both tissues, which would not have occurred in the absence of the tissue interactions. The process of tissue interaction is also called induction, i.e. one tissue is said to induce another. The ability of a tissue to respond to inductive signals is called competence, and denotes the ability of a cell population to develop in response to the environments present in the embryo at that particular stage. After a cell population has been induced to develop along a certain pathway, it will lose competence and become restricted. Once restricted, cells are set on a particular pathway of development; after a number of binary choices (further restrictions) they are said to be determined. Determined cells are programmed to follow a process of development that will lead to differentiation. The determined state is a heritable characteristic of cells, and is the final step in restriction. Once a cell has become determined, it will progress to a differentiated phenotype if the environmental factors are suitable.

The process of determination and differentiation within embryonic cell populations is reflected by the ability of these populations to produce specific proteins. Primary proteins (colloquially termed housekeeping proteins) are considered essential for cellular metabolism, whereas proteins synthesized as cells become determined, those specific to the state of determination, are termed secondary proteins; for example, liver and kidney cells, but not muscle cells, produce arginase. Fully differentiated cells produce tertiary proteins, which no other cell line can synthesize, e.g. haemoglobin in erythrocytes.

As populations of cells become progressively determined, they can be described within a hierarchy of cellular development as transiently amplifying cells, progenitor cells, stem cells and terminally differentiated cells.

Transiently amplifying cells

Transiently amplifying cells undergo proliferative cell mitosis and produce cells that are equally determined. At some stage, and as a result of an inductive stimulus, these cells will enter a quantal cycle that culminates in a quantal mitosis. This will result in an increase in the restriction of their progeny, which continue to undergo proliferative mitoses at a progressive level of determination. The quantal mitosis corresponds to the time of binary choice when the commitment of the progeny is different from that of the parent.

Progenitor cells

Progenitor cells are already determined along a particular pathway. They may individually follow that differentiation pathway, or may proliferate and produce large numbers of similarly determined progenitor cells that subsequently differentiate; neuroblasts or myoblasts are examples of progenitor cells.

Stem cells

Either individually or as a population, stem cells can both produce determined progeny and reproduce themselves. It is generally believed that stem cells undergo asymmetric divisions, in which one daughter cell remains as a stem cell, while the other proceeds along a differentiation pathway; in marked contrast, proliferative cell division may be symmetrical, producing derived cells with an identical determination. Human embryonic stem cells (hESC) are pluripotent cells that can be derived from the inner cell mass of human blastocysts *in vitro*; or obtained surplus to *in vitro* fertilization fertility programmes; or created from oocytes donated and fertilized for that purpose. Although not yet achieved, it is hoped that hESCs can be coaxed down particular pathways under appropriate pharmaceutical conditions to produce differentiated cells that will be effective in reversing some degenerative diseases (e.g. dopamine producing neurones for Parkinson's disease, insulin producing islet cells for diabetes), or to replace acutely damaged tissues (e.g. motor neurones for acute spinal cord injury; cardiomyocytes in acute myocardial infarction). Proof of principle has been demonstrated in some animal models, and multipotent haematopoietic progenitor stem cells from human umbilical cord blood are now used as an alternative treatment to bone marrow transplantation for the treatment of some inherited genetic disorders (thalassaemia) and blood malignancies (leukaemias).

Terminally differentiated cells

By virtue of their extreme specialization, terminally differentiated cells can no longer divide, e.g. erythrocytes and neurones. Apoptosis is a particular variety of terminal differentiation in which the final outcome is the death of the individual cells or cell populations. It occurs in the developing limb, where cells die along the pre- and postaxial limits of the apical ectodermal ridge, limiting its extent, and also between the digits, permitting their separation.

Tissue interactions

There are two types of cell and tissue interaction, namely, permissive and instructive.

In a permissive interaction, a signal from an apposing tissue is necessary for the successful self-differentiation of the responding tissue. This means that a particular cell population (or the matrix molecules secreted by the cells that it contains) will maintain mitotic activity in an adjacent cell population.

Since a variety of different cell populations may permit a specific cell population to undergo mitosis and cell differentiation, no specific instruction or signal which may limit the developmental options of the responding tissue is involved: this signal therefore does not influence the developmental pathway selected and there is no restriction. The responding tissue has the intrinsic capacity to develop, and only needs appropriate environmental conditions in order to express this capacity. Permissive interactions often occur later in development, when a tissue whose fate has already been determined is maintained and stabilized by another.

An instructive (directive) interaction (induction) changes the cell type of the responding tissue, so that the cell population becomes restricted. Wessells (1977) proposed four general principles in most instructive interactions:

1 In the presence of tissue A, responding tissue B develops in a certain way.

2 In the absence of tissue A, responding tissue B does not develop in that way.

3 In the absence of tissue A, but in the presence of tissue C, tissue B does not develop in that way.

4 In the presence of tissue A, a tissue D, which would normally develop differently, is changed to develop like tissue B.

Principles 1–4 are exemplified during induction of the lens vesicle by the optic cup (p. 699). An example of principle 4 is the experimental association of chicken flank ectoderm with mouse mammary mesenchyme, which results in the morphogenesis of mammary gland-like structures: chickens do not normally develop mammary glands.

Tissue interactions continue into adult life and are probably responsible for maintaining the functional heterogeneity of adult tissues and organs. This is exemplified by the complex tissue heterogeneity, with sharply compartmentalized boundaries, that occurs in the oral cavity. The junctions between the mucosa of the vestibule and the lip, and between the vermilion border and the facial skin, are distinct boundaries of specific epithelial and mesenchymal differentiation, and are almost certainly maintained by continuing epithelial–mesenchymal interactions in adult life. Perturbation of these interactions throughout the body may underlie a wide variety of adult diseases, including susceptibility to cancer and proliferative disorders.

Signalling between embryonic cells and tissues

Cellular interactions may be signalled by four principal mechanisms: direct cell–cell contact; cell adhesion molecules and their receptors; extracellular matrix molecules and their receptors; growth factors and their receptors. Many of these mechanisms interact, and it is likely that combinations of them are involved in development. Figure 11.1 illustrates diagrammatically some ways by which mesenchymal cells could signal to epithelial cells. An additional set of identical mechanisms could operate for epithelial-to-mesenchymal cell signalling. Clearly, the complexity of these mechanisms will increase in reciprocal interactions; moreover, a single molecule may have different effects on epithelial and mesenchymal cells.

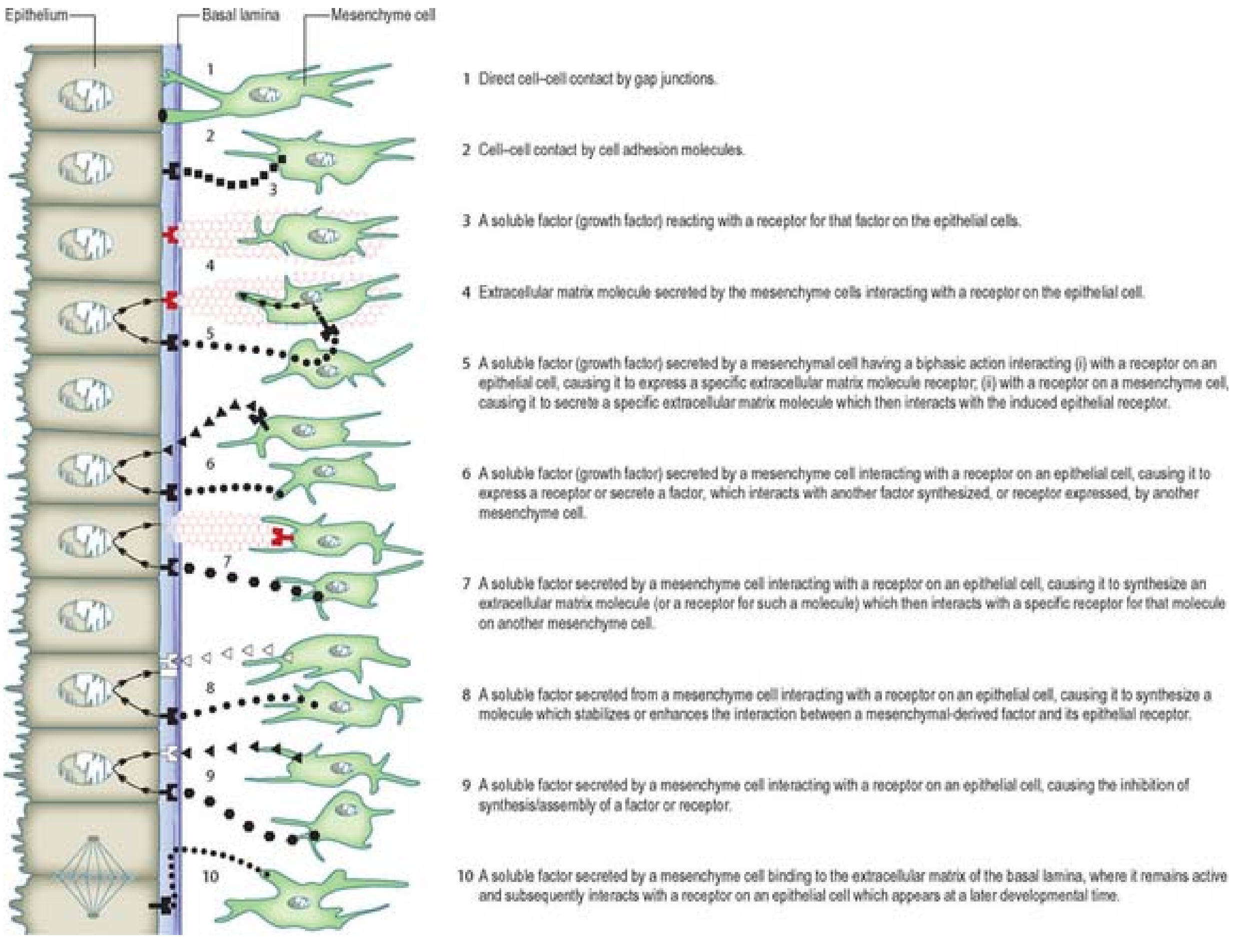

1 Direct cell–cell contact by gap junctions.

2 Cell–cell contact by cell adhesion molecules.

3 A soluble factor (growth factor) reacting with a receptor for that factor on the epithelial cells.

4 Extracellular matrix molecule secreted by the mesenchyme cells interacting with a receptor on the epithelial cell.

5 A soluble factor (growth factor) secreted by a mesenchymal cell having a biphasic action interacting (i) with a receptor on an epithelial cell, causing it to express a specific extracellular matrix molecule receptor; (ii) with a receptor on a mesenchyme cell, causing it to secrete a specific extracellular matrix molecule which then interacts with the induced epithelial receptor.

6 A soluble factor (growth factor) secreted by a mesenchyme cell interacting with a receptor on an epithelial cell, causing it to express a receptor or secrete a factor, which interacts with another factor synthesized, or receptor expressed, by another mesenchyme cell.

7 A soluble factor secreted by a mesenchyme cell interacting with a receptor on an epithelial cell, causing it to synthesize an extracellular matrix molecule (or a receptor for such a molecule) which then interacts with a specific receptor for that molecule on another mesenchyme cell.

8 A soluble factor secreted from a mesenchyme cell interacting with a receptor on an epithelial cell, causing it to synthesize a molecule which stabilizes or enhances the interaction between a mesenchymal-derived factor and its epithelial receptor.

9 A soluble factor secreted by a mesenchyme cell interacting with a receptor on an epithelial cell, causing the inhibition of synthesis/assembly of a factor or receptor.

10 A soluble factor secreted by a mesenchyme cell binding to the extracellular matrix of the basal lamina, where it remains active and subsequently interacts with a receptor on an epithelial cell which appears at a later developmental time.

Fig. 11.1 The many ways by which mesenchyme cells could signal to epithelial cells. Precisely the same mechanisms can operate in reverse, i.e. epithelium to mesenchyme.

Direct cell–cell contact permits the construction of gap junctions, which are important for communication and the transfer of information between cells. The transient production of gap junctions is seen as epithelial somites are formed, between neuroepithelial cells within rhombomeres, and in the tunica media of the outflow tract of the heart. Endogenous electrical fields are also believed to have a role in cell–cell communication. Such fields have been demonstrated in a range of amphibian embryos, and in vertebrate embryos during primitive streak ingression. Neuroepithelial cells are electrically coupled, regardless of their position relative to interrhombomeric boundaries.

The spatial and temporal distribution of a variety of cell adhesion molecules has been localized in the early embryo. The appearance of these molecules correlates with a variety of morphogenetic events that involve cell aggregation or disaggregation, for example, an early response of groups of cells to embryonic inductive influences is the expression of cadherins, calcium-dependent adhesion molecules typically found in epithelial populations. Other molecules found in the extracellular matrix, e.g. fibronectin and laminin, *inter alia* can modulate cell adhesion by their degree of glycosylation. Self-assembly or cross-linking by matrix molecules may affect cell adhesiveness by increasing the availability of binding sites or by obscuring them.

Extracellular matrix molecules include localized molecules of the basal lamina, e.g. laminin, fibronectin, and much larger complex associations of collagen, glycosaminoglycans, proteoglycans and glycoproteins between the mesenchyme cells. Mutations of the genes that code for extracellular matrix molecules give rise to a number of congenital disorders, e.g. mutations in type I collagen produce osteogenesis imperfecta; mutations in type II collagen produce disorders of cartilage; mutations in fibrillin are associated with Marfan's syndrome.

Growth factors are distinguished from extracellular matrix molecules. They can be delivered to, and act upon, cells in a variety of ways, namely endocrine, autocrine, paracrine, intracrine, juxtacrine and matricrine (Fig. 11.2). Many growth factors are secreted in a latent form, e.g. associated with a propeptide (latency-associated peptide) in the case of transforming growth factor β, or attached to a binding protein, in the case of insulin-like growth factors.

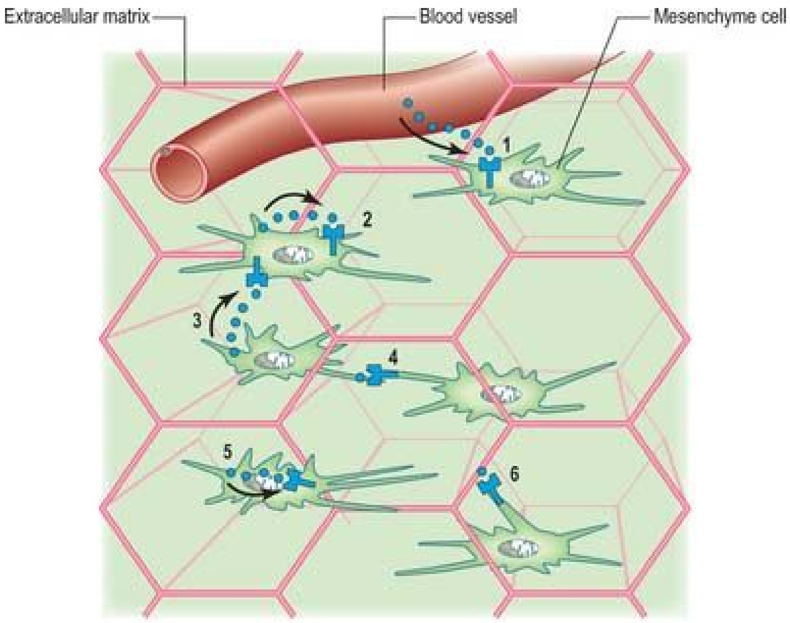

1 **Endocrine** Delivery of growth factor by the bloodstream from a distant biosynthetic site to the target mesenchyme cell.

2 **Autocrine** Synthesis of growth factor by the cell, its secretion, binding and activation of a surface receptor elsewhere on its own surface.

3 **Paracrine** Synthesis of growth factor by the cell, its secretion and diffusion to an adjacent cell (or group of cells) where it binds to and activates a cell surface receptor.

4 **Juxtacrine** Synthesis of growth factor by the cell. The growth factor remains on the cell surface and binds to and activates a receptor on an immediately adjacent cell.

5 **Intracrine** Synthesis of growth factor within the cytoplasm of the cell. The growth factor moves to the nucleus and binds and activates its own nuclear receptors.

6 **Matricrine** Synthesis and export of growth factor from the cell. The growth factor binds to the extracellular matrix where it remains active and subsequently binds to and activates a receptor for that growth factor on the same or a different cell.

Fig. 11.2 Cells can also communicate by the reception, production and secretion of growth factors. A typical embryonic mesenchyme cell could receive and produce growth factors in this way.

MORPHOGENESIS AND PATTERN FORMATION

Morphogenesis may be described as the assumption of form by the whole, or part, of a developing embryo. As a term, it is used to denote the movement of cell populations and the changing shape of an embryo, particularly during early development.

The most obvious examples of morphogenesis are the large migrations that occur during gastrulation; local examples include branching morphogenesis, which occurs e.g. in the developing lungs and kidneys, and in most glandular organs. The development of branches from a tubular duct occur over a period of time. An interaction between the proliferating epithelium of the duct and its surrounding mesenchyme and extracellular matrix results in a series of clefts that produce a characteristic branching pattern (Fig. 11.3). During tubular and acinar development, hyaluronidase secreted by the underlying mesenchymal cells breaks down the basal lamina produced by the epithelial cells; this increases epithelial mitoses locally and results in an expanding acinus. Cleft formation is initiated by the mesenchyme, which produces collagen III fibrils within putative clefts. (If the collagen is removed, no clefts develop, whereas if excess collagen is not removed, supernumerary clefts appear.) The collagen acts to protect the basal lamina from the effects of the hyaluronidase, which means that the overlying epithelia have a locally reduced rate of mitosis. The region of rapid mitoses at the tip of the acinus is therefore split into two, and two branches develop from this point.

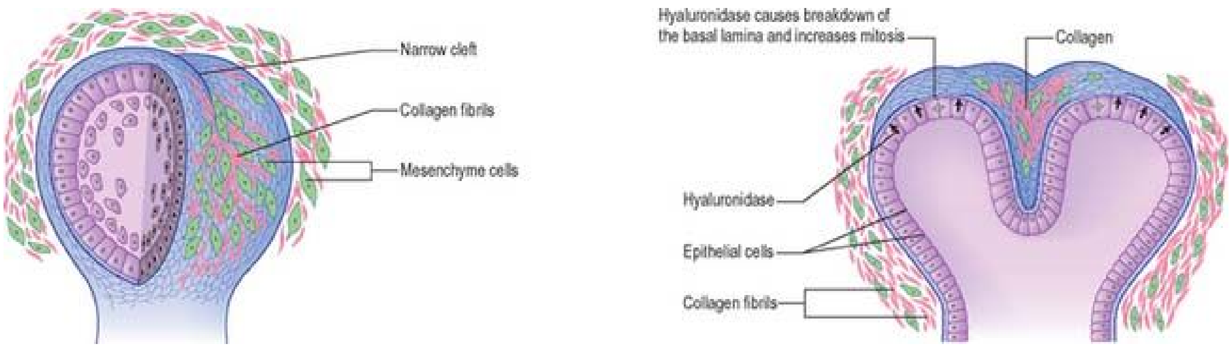
Narrow cleft
Collagen fibrils
Mesenchyme cells
Hyaluronidase causes breakdown of the basal lamina and increases mitosis
Collagen
Hyaluronidase
Epithelial cells
Collagen fibrils

Fig. 11.3 Branching of a tubular duct may occur as a result of an interaction between the proliferating epithelium of the duct and its surrounding mesenchyme and extracellular matrix. Mesenchymal cells initiate cleft formation by producing collagen III fibrils locally within the development clefts and hyaluronidase over other parts of the epithelium. Collagen III prevents local degradation of the epithelial basal lamina by hyaluronidase and slows the rate of mitosis of the overlying epithelial cells. In regions where no collagen III is produced, hyaluronidase breaks down the epithelial basal lamina and locally increases epithelial mitoses, forming an expanded acinus.

(From Gilbert SF 1991 Developmental Biology. Sunderland, MA: Sinauer Associates.)

Pattern formation concerns the processes whereby the individual members of a mass of cells, initially apparently homogeneous, follow a number of different avenues of differentiation which are precisely related to each other in an orderly manner in space and time. The patterns embraced by the term apply not only to regions of regular geometric order, e.g. the crystalline lens, but also to asymmetric structures such as the limb. For such a process to occur, individual cells must be informed of their position within the embryo, and utilize that information for appropriate differentiation. Patterning of regions is seen in: the progress zone and zone of polarizing activity within the limbs; the fates of the medial and lateral and later the cranial and caudal halves of the somites; the neural crest mesenchyme within the pharyngeal arches. For details of patterning in vertebrate development, see Tickle (2003).

Hox genes in development

Two related themes have emerged from experimental studies of development. First, that the control of embryonic morphology has been highly conserved in evolution between vertebrates and invertebrates, and second, that this control involves families of genes coding for proteins that act as transcriptional regulators.

The fruit fly, *Drosophila*, possesses eight homeotic genes that specify the structures developing on each body segment. These genes have been identified in vertebrates, raising the possibility that they have similar functions in development. They are termed homeobox genes, abbreviated to Hox in the mouse and HOX in humans, and are found on four clusters known as A, B, C and D. Individual genes are numbered from 1 to 13: 1 is a cephalic gene and 13 is a more caudally placed gene.

Homeobox genes are believed to be responsible, at least in part, for the evolutionary origin of the embryonic body plan (Robert 2001). Experimental study of transgenic animals in which the homeobox genes have been knocked out provide some evidence of their function: however, because developmental processes permit significant recovery from insult, some of the outcomes cannot be directly interpreted as demonstrating the effect of such gene loss.

Experimental approaches to embryology

One of the most exciting techniques to provide information on cell movements and fates during development is the use of chimeric embryos. Small portions of an embryo are excised and replaced with similar portions of an embryo from a different species at the same stage and the resulting development is then studied. This technique has been particularly effective using chick and quail embryos, because the nucleolus is especially prominent in all quail cells, whereas it is not prominent in chick cells, which means that quail cells may be easily identified within a chick embryo after chimeric transplantation (Le Douarin 1969). The technique has also confirmed the reciprocity of tissue interaction between the embryonic species, a phenomenon that had previously been illustrated, for a limited period, in co-cultures of embryonic avian and mammalian tissues. Somite development and vertebral formation have been studied in mouse–chick chimeras (Fontaine-Pérus 2000). The production in vitro, of human-animal chimeric cell lines is providing new ways of studying cellular pathways, as is the introduction of human artificial chromosome vectors into animal cells to study their interaction.

REFERENCES

ntaine-Pérus J. Mouse-chick chimera: an experimental system for study of somite development. *Curr Top Dev Biol*. 2000;48:269-300.

Douarin NM. Particularités du noyau interphasique chez la Caille japonaise (*Coturnix coturnix japonica*). Utilisation de ces particularités comme ‘marquage biologique’ dans les recherches sur les interactions tissulaires et les migrations cellulaires au cours de l’ontogenèse. *Bull Biol Fr Belg*. 1969;103:435-452.

bert JS. Interpreting the homeobox: metaphors of gene action and activation in development and evolution. *Evol Dev*. 2001;3:287-295.

ckle C. Patterning in Vertebrate Development. Oxford: Oxford University Press, 2003.

essells NK. Tissue Interaction and Development. Menlo Park CA: Benjamin, 1977.

CHAPTER 12

Cell populations at the start of organogenesis

SPECIFICATION OF THE BODY AXES AND THE BODY PLAN

Embryos may be thought of as being constructed with three orthogonal spatial axes (cephalocaudal, dorsoventral and laterolateral), plus a temporal axis. In mammalian embryos, axes cannot be specified at very early stages: embryonic axes can be defined only after the early extraembryonic structures have been formed and the inner cell mass can be seen. The position of the future epiblast can be predicted in human embryos when the hollow blastocyst has formed. The inner cell mass becomes (seemingly) randomly located on the inside of the trophectoderm and forms a population of epiblast cells subjacent to the trophoblast. This region implants first. It is not known whether the trophectoderm in contact with the inner cell mass initiates implantation, so that the future dorsal surface of the embryo is closest to the disrupted maternal vessels at the implantation site, or whether the inner cell mass can travel around the inside of the trophoblast to gain a position subjacent to the implantation site once implantation has started.

Axes may be conferred on the whole embryonic disc, which is initially flat and mainly two-dimensional. However, their subsequent orientation in the folded three-dimensional embryo will be completely different. The dorsal structures of the folded embryo form from a circumscribed central ellipse of the early flat embryonic disc (see Fig. 10.5). Lateral and ventral structures form from the remainder of the disc, and the peripheral edge of the disc eventually becomes constricted at the umbilicus (see Figs 10.9 and 10.10). Although the appearance of part of the epiblast is taken to specify the dorsal surface of the embryo, the inner layer, i.e. the hypoblast, is not by default a ventral embryonic structure.

The primary, cephalocaudal, axis is conferred by the appearance of the primitive streak in the bilaminar disc. The primitive streak patterns cells during ingression, and so also specifies the dorsoventral axis which becomes apparent after embryonic folding. The position of ingression through the streak confers axial, medial or lateral characteristics on the forming mesenchyme cells. The axial and medial populations remain as dorsal structures in the folded embryo, and the surface ectoderm above them will exhibit dorsal characteristics. The lateral plate mesenchyme will assume lateral and ventral positions after embryonic folding, and the surface ectoderm above this population will gain ventral characteristics.

The third and last spatial axis is the bilateral, or laterolateral axis, which appears as a consequence of the development of the former two axes. Initially, the right and left halves of the embryonic body are bilaterally symmetric. Lateral projections, the upper and lower limbs, develop in two places on each side of the body wall (somatopleure).

With the last axis established, the temporal modification of the original embryonic axes can be seen. The segmental arrangement of the cephalocaudal axis is very obvious in the early embryo and is retained in many structures in adult life. Similarly, dorsal embryonic structures remain dorsal and undergo relatively little change. However, structures that were originally midline and ventral, especially those derived from splanchnopleuric mesenchyme, e.g. the cardiovascular system and the gut, are subject to extensive shifts, and change from a bilaterally symmetric arrangement to an entire body that is now chiral, i.e. has distinct left and right sides.

The development of all the body organs and systems, organogenesis, begins after the dramatic events of gastrulation, when the embryo has attained a recognizable body plan. In human embryos this corresponds to the end of stage 10 (Fig. 12.1). The head and tail folds are well formed, with enclosure of the foregut and hindgut (proenteron and metenteron), although the midgut (mesenteron) is only partly constricted from the yolk sac. The forebrain projection dominates the cranial end of the embryo, and the buccopharyngeal membrane and cardiac prominence are caudal and ventral to it. The cardiac prominence contains the transmedian pericardial cavity, which communicates dorsocaudally with right and left pericardioperitoneal canals. These pass dorsally to the transverse septum mesenchyme and open caudally into the extraembryonic coelom on each side of the midgut. The intraembryonic mesenchyme has begun to differentiate and the paraxial mesenchyme is being segmented into somites. Neural groove closure is progressing caudally, so that a neural tube is forming between the newly segmenting somites. Rostrally, the early brain regions, which have not yet fused, can be discerned. The neuroepithelium is separated from the dorsal aspect of the gut by the notochord. The earliest blood vessels have appeared, and a primitive tubular heart occupies the pericardium. The chorionic circulation is soon to be established, after which the embryo rapidly becomes completely dependent upon the maternal bloodstream for its requirements. The embryo is connected to the developing placenta by a mesenchymal connecting stalk in which the umbilical vessels develop, and which also contains the allantois, a hindgut diverticulum. The lateral body walls are still widely separated. The embryo has contact with three different vesicles: the amnion, which is in contact with the surface ectoderm; the yolk sac, which is in contact with the endoderm; and the chorionic cavity, containing the extraembryonic coelom, which is in contact with the intraembryonic coelomic lining (see Fig. 10.10).

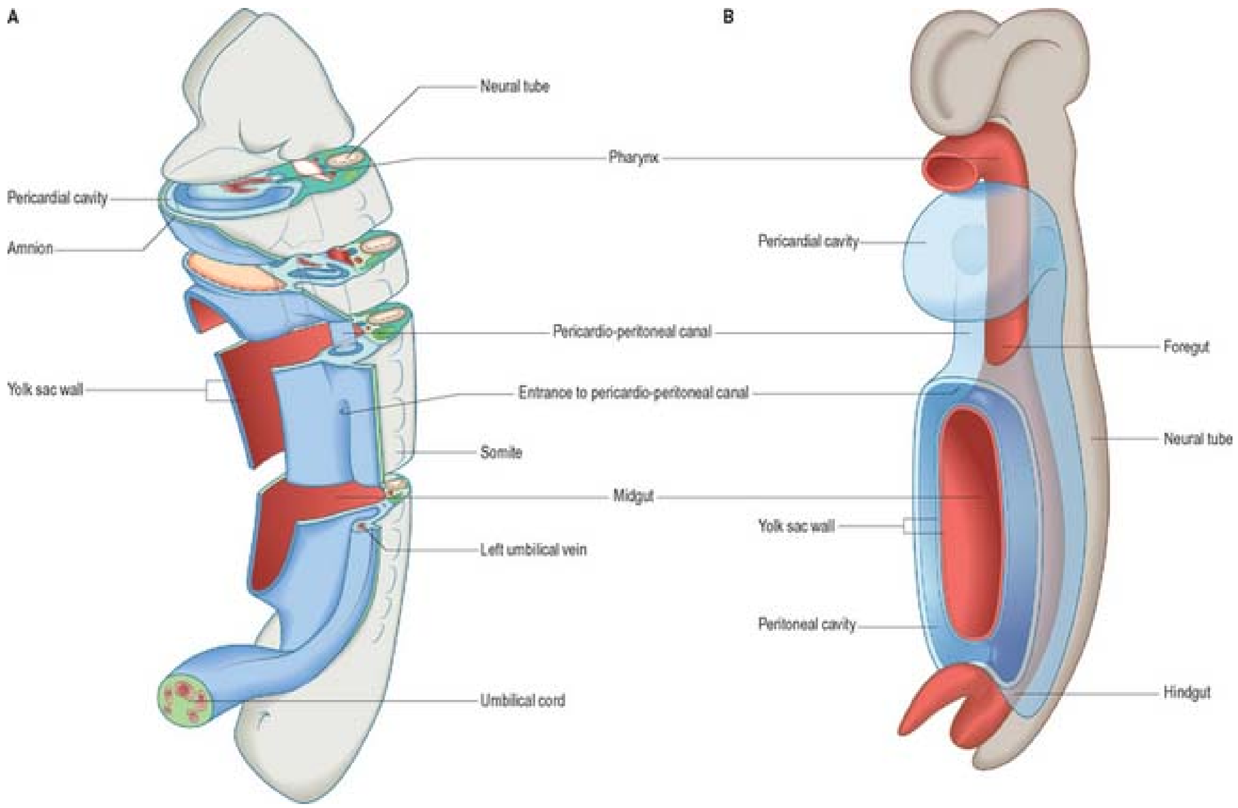
A
B
Neural tube
Pharynx
Pericardial cavity
Amnion
Pericardial cavity
Pericardio-peritoneal canal
Foregut
Yolk sac wall
Entrance to pericardio-peritoneal canal
Neural tube
Somite
Midgut
Yolk sac wall
Left umbilical vein
Peritoneal cavity
Umbilical cord
Hindgut

Fig. 12.1 **A**, Embryo at stage 11, showing the position of the intraembryonic coelom (contained by the walls coloured blue). **B**, The three major epithelial populations within a stage 11 embryo, viewed from a ventrolateral position. The neural tube lies dorsal to the gut; ventrally, the intraembryonic coelom crosses the midline at the level of the foregut and hindgut, but is lateral to the midgut and a portion of the foregut.

The early body plan of the embryo is segmented. The boundaries between the segments are maintained by the differential expression of genes and proteins that restrict cell migration in these regions. Organogenetic processes either retain the segmental plan, e.g. spinal nerves, or replace it locally, e.g. the modifications of somatic intersegmental vessels by the development of longitudinal anastomoses. Abnormalities may result from improper specification of segments along the cephalocaudal axis and may fail to produce the appropriately modified segmental plan.

The degree to which vertebrate embryos are developmentally constrained at this period of development is controversial. Comparative studies on the timing at which specific embryonic structures appear, heterochrony, have shown that other embryonic species do not follow the same developmental sequence as humans (Richardson & Keuck 2002). Although some developmental mechanisms are highly conserved, e.g. the homeobox gene codes, others may have been dissociated and modified in different vertebrate species during evolution.

Organogenesis, the further development of body regions and organs that is described elsewhere in this book, starts from about stage 10 (approximately 28 days). Although it is both conventional and convenient to consider the further development of each body system on an individual basis, not only do all systems develop simultaneously, they also interact and modify each other as they develop. This necessary interdependence is supported by the evidence of experimental embryology and reinforced by the phenomena of growth anomalies, which cut across the artificial boundaries of systems in most instances. For these reasons, it is recommended that the development of an individual system or body region should be studied in relation to others, especially those most closely associated with it, whether spatiotemporally or causally.

EMBRYONIC CELL POPULATIONS AT THE START OF ORGANOGENESIS

The developmental processes operating in the embryo between stages 5 and 9 enabled the construction of the bi- and tri-laminar embryonic disc, the intraembryonic coelom and new proliferative epithelia. From the end of stage 10, a range of local epithelial and mesenchymal populations now interact to produce viscera and appendages. The inductive influences on these tissues and their repertoire of responses are very different from those seen at the onset of gastrulation. The range of tissues present at the start of organogenesis, when the body plan is clear, is given below and shown in Figs 12.1 and 12.2. For a summary of the fates of the embryonic cell populations, see Fig. 12.3.

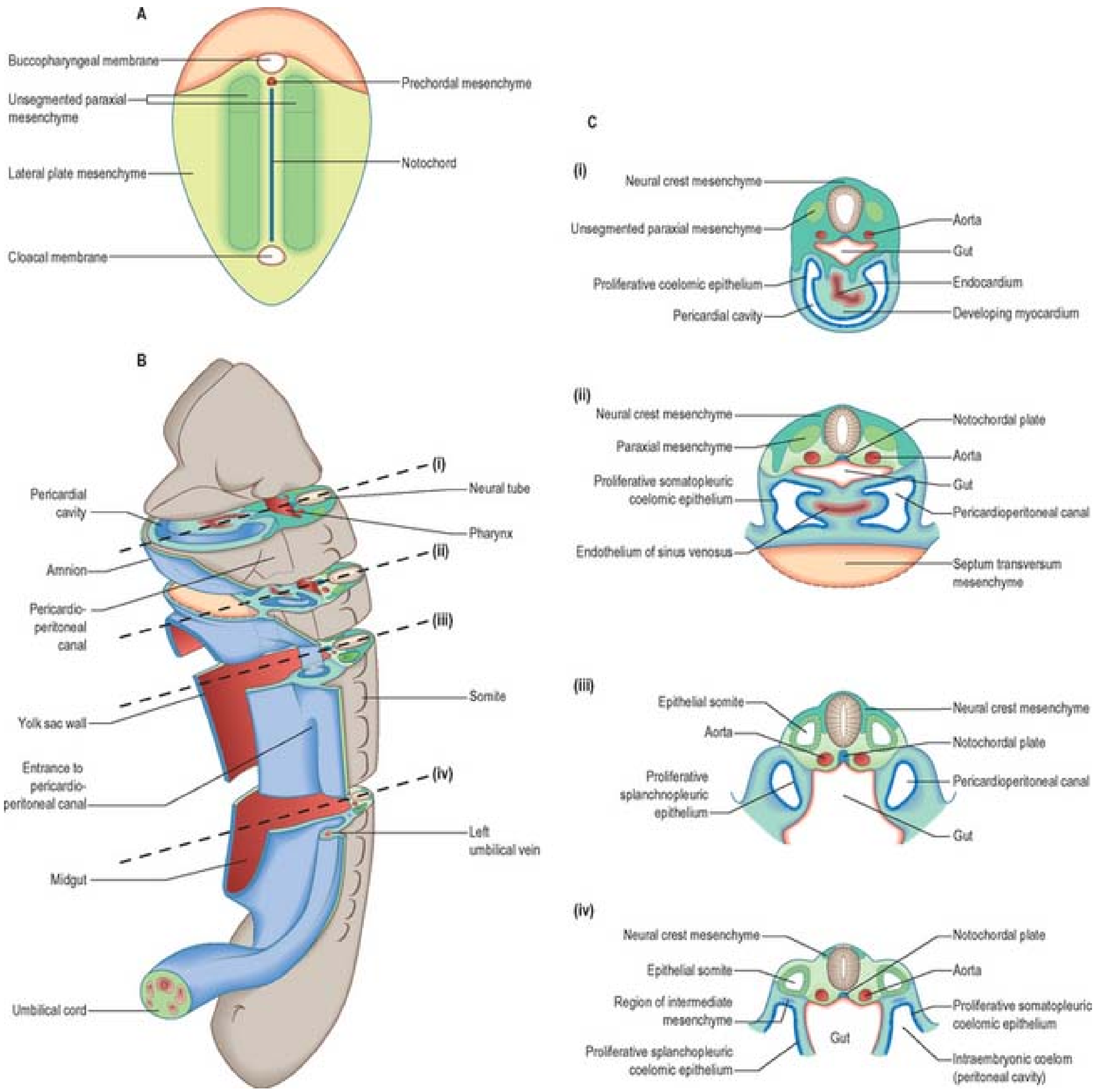
A
Buccopharyngeal membrane
Unsegmented paraxial mesenchyme
Lateral plate mesenchyme
Cloacal membrane
Prechordal mesenchyme
Notochord
B
Pericardial cavity
Amnion
Pericardio-peritoneal canal
Yolk sac wall
Entrance to pericardio-peritoneal canal
Midgut
Umbilical cord
(i)
Neural tube
Pharynx
(ii)
(iii)
Somite
(iv)
Left umbilical vein
C
(i)
Neural crest mesenchyme
Unsegmented paraxial mesenchyme
Proliferative coelomic epithelium
Pericardial cavity
Aorta
Gut
Endocardium
Developing myocardium
(ii)
Neural crest mesenchyme
Paraxial mesenchyme
Proliferative somatopleuric coelomic epithelium
Endothelium of sinus venosus
Notochordal plate
Aorta
Gut
Pericardioperitoneal canal
Septum transversum mesenchyme
(iii)
Epithelial somite
Aorta
Proliferative splanchnopleuric epithelium
Neural crest mesenchyme
Notochordal plate
Pericardioperitoneal canal
Gut
(iv)
Neural crest mesenchyme
Epithelial somite
Region of intermediate mesenchyme
Proliferative splanchnopleuric coelomic epithelium
Gut
Notochordal plate
Aorta
Proliferative somatopleuric coelomic epithelium
Intraembryonic coelom (peritoneal cavity)

Fig. 12.2 **A**, Mesoblast populations within the early embryonic disc. **B**, Stage 11 embryo, showing the position of the intraembryonic coelom (contained by the walls coloured blue) and the positions of the sections (i)–(iv), which are shown in **C**. **C**, Transverse sections, arranged cranial to caudal, from a stage 11 embryo. The populations of mesenchyme and the sites of mesenchymal proliferation are indicated.

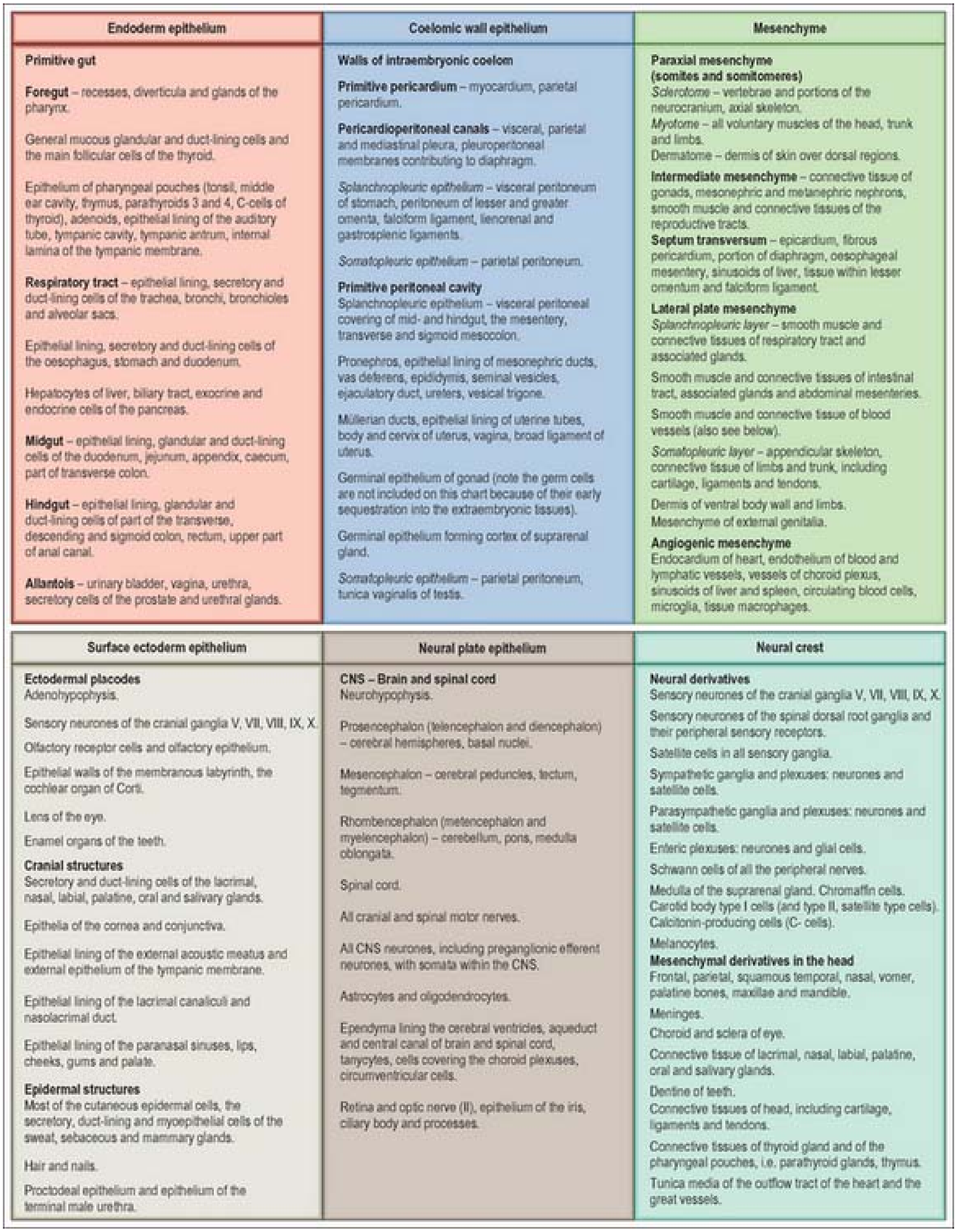

Endoderm epithelium	Coelomic wall epithelium	Mesenchyme
Primitive gut **Foregut** – recesses, diverticula and glands of the pharynx. General mucous glandular and duct-lining cells and the main follicular cells of the thyroid. Epithelium of pharyngeal pouches (tonsil, middle ear cavity, thymus, parathyroids 3 and 4, C-cells of thyroid), adenoids, epithelial lining of the auditory tube, tympanic cavity, tympanic antrum, internal lamina of the tympanic membrane. **Respiratory tract** – epithelial lining, secretory and duct-lining cells of the trachea, bronchi, bronchioles and alveolar sacs. Epithelial lining, secretory and duct-lining cells of the oesophagus, stomach and duodenum. Hepatocytes of liver, biliary tract, exocrine and endocrine cells of the pancreas. **Midgut** – epithelial lining, glandular and duct-lining cells of the duodenum, jejunum, appendix, caecum, part of transverse colon. **Hindgut** – epithelial lining, glandular and duct-lining cells of part of the transverse, descending and sigmoid colon, rectum, upper part of anal canal. **Allantois** – urinary bladder, vagina, urethra, secretory cells of the prostate and urethral glands.	**Walls of intraembryonic coelom** **Primitive pericardium** – myocardium, parietal pericardium. **Pericardioperitoneal canals** – visceral, parietal and mediastinal pleura, pleuroperitoneal membranes contributing to diaphragm. *Splanchnopleuric epithelium* – visceral peritoneum of stomach, peritoneum of lesser and greater omenta, falciform ligament, lienorenal and gastrosplenic ligaments. *Somatopleuric epithelium* – parietal peritoneum. **Primitive peritoneal cavity** Splanchnopleuric epithelium – visceral peritoneal covering of mid- and hindgut, the mesentery, transverse and sigmoid mesocolon. Pronephros, epithelial lining of mesonephric ducts, vas deferens, epididymis, seminal vesicles, ejaculatory duct, ureters, vesical trigone. Müllerian ducts, epithelial lining of uterine tubes, body and cervix of uterus, vagina, broad ligament of uterus. Germinal epithelium of gonad (note the germ cells are not included on this chart because of their early sequestration into the extraembryonic tissues). Germinal epithelium forming cortex of suprarenal gland. *Somatopleuric epithelium* – parietal peritoneum, tunica vaginalis of testis.	**Paraxial mesenchyme (somites and somitomeres)** *Sclerotome* – vertebrae and portions of the neurocranium, axial skeleton. *Myotome* – all voluntary muscles of the head, trunk and limbs. Dermatome – dermis of skin over dorsal regions. **Intermediate mesenchyme** – connective tissue of gonads, mesonephric and metanephric nephrons, smooth muscle and connective tissues of the reproductive tracts. **Septum transversum** – epicardium, fibrous pericardium, portion of diaphragm, oesophageal mesentery, sinusoids of liver, tissue within lesser omentum and falciform ligament. **Lateral plate mesenchyme** *Splanchnopleuric layer* – smooth muscle and connective tissues of respiratory tract and associated glands. Smooth muscle and connective tissues of intestinal tract, associated glands and abdominal mesenteries. Smooth muscle and connective tissue of blood vessels (also see below). *Somatopleuric layer* – appendicular skeleton, connective tissue of limbs and trunk, including cartilage, ligaments and tendons. Dermis of ventral body wall and limbs. Mesenchyme of external genitalia. **Angiogenic mesenchyme** Endocardium of heart, endothelium of blood and lymphatic vessels, vessels of choroid plexus, sinusoids of liver and spleen, circulating blood cells, microglia, tissue macrophages.

Surface ectoderm epithelium	Neural plate epithelium	Neural crest
Ectodermal placodes Adenohypophysis. Sensory neurones of the cranial ganglia V, VII, VIII, IX, X. Olfactory receptor cells and olfactory epithelium. Epithelial walls of the membranous labyrinth, the cochlear organ of Corti. Lens of the eye. Enamel organs of the teeth. **Cranial structures** Secretory and duct-lining cells of the lacrimal, nasal, labial, palatine, oral and salivary glands. Epithelia of the cornea and conjunctiva. Epithelial lining of the external acoustic meatus and external epithelium of the tympanic membrane. Epithelial lining of the lacrimal canaliculi and nasolacrimal duct. Epithelial lining of the paranasal sinuses, lips, cheeks, gums and palate. **Epidermal structures** Most of the cutaneous epidermal cells, the secretory, duct-lining and myoepithelial cells of the sweat, sebaceous and mammary glands. Hair and nails. Proctodeal epithelium and epithelium of the terminal male urethra.	**CNS – Brain and spinal cord** Neurohypophysis. Prosencephalon (telencephalon and diencephalon) – cerebral hemispheres, basal nuclei. Mesencephalon – cerebral peduncles, tectum, tegmentum. Rhombencephalon (metencephalon and myelencephalon) – cerebellum, pons, medulla oblongata. Spinal cord. All cranial and spinal motor nerves. All CNS neurones, including preganglionic efferent neurones, with somata within the CNS. Astrocytes and oligodendrocytes. Ependyma lining the cerebral ventricles, aqueduct and central canal of brain and spinal cord, tanycytes, cells covering the choroid plexuses, circumventricular cells. Retina and optic nerve (II), epithelium of the iris, ciliary body and processes.	**Neural derivatives** Sensory neurones of the cranial ganglia V, VII, VIII, IX, X. Sensory neurones of the spinal dorsal root ganglia and their peripheral sensory receptors. Satellite cells in all sensory ganglia. Sympathetic ganglia and plexuses: neurones and satellite cells. Parasympathetic ganglia and plexuses: neurones and satellite cells. Enteric plexuses: neurones and glial cells. Schwann cells of all the peripheral nerves. Medulla of the suprarenal gland. Chromaffin cells. Carotid body type I cells (and type II, satellite type cells). Calcitonin-producing cells (C- cells). Melanocytes. **Mesenchymal derivatives in the head** Frontal, parietal, squamous temporal, nasal, vomer, palatine bones, maxillae and mandible. Meninges. Choroid and sclera of eye. Connective tissue of lacrimal, nasal, labial, palatine, oral and salivary glands. Dentine of teeth. Connective tissues of head, including cartilage, ligaments and tendons. Connective tissues of thyroid gland and of the pharyngeal pouches, i.e. parathyroid glands, thymus. Tunica media of the outflow tract of the heart and the great vessels.

Fig. 12.3 Structures that will be derived from specific epithelial and mesenchymal populations in the early embryo. CNS, central nervous system.

Epithelial populations in the embryo

Surface ectoderm

During embryogenesis, the surface ectoderm shows regional differences in thickness. Ectoderm over the dorsal region of the head and trunk is thin, as is the pericardial covering; this has been interpreted as a consequence of the expansion of this epithelium over structures that are enlarging rapidly as development proceeds. After the surface ectoderm has completed a number of early interactions it forms the periderm, which remains throughout fetal life and differentiates into epidermis.

Ectodermal ring and ectodermal placodes

The ectoderm on the head and lateral borders of the embryo shows a zone of epithelial thickening, the ectodermal ring, which can be discerned from stage 10 and is completed by stage 12. Rostrally it contains populations of neuroectoderm that remain in the ectoderm after primary neurulation that are termed ectodermal placodes: these placodes may be considered to be neuroepithelial cells that remain within the surface ectoderm until central nervous system development has progressed sufficiently for their inclusion into sensory epithelia and cranial nerve ganglia. The neuronal placodes may invaginate *in toto* to form a vesicle, or remain as a neuronal layer, or contribute individually to neuronal structures with cells of other origins. The midline ectodermal thickening, the adenohypophysial placode, invaginates as Rathke's pouch and forms a vesicle immediately rostral to the buccopharyngeal membrane. The ectodermal ring then passes bilaterally to encompass the olfactory and optic placodes, which give rise to the olfactory sensory epithelium and the lens of the eye respectively. It then overlays the pharyngeal arches where it gives rise to epibranchial placodes which remove themselves individually from the ectoderm at stage 10–11 and become associated with the neural crest cells within the cranial sensory ganglia supplying the arches. It also forms specializations of the ectoderm on the frontonasal, maxillary and mandibular processes which give rise to the tooth buds and the outer coating of the teeth. The paired otic placodes overlying the rhombencephalon at the lateral portion of the second pharyngeal arch invaginate to form the otic vesicles, which give rise to the membranous labyrinth of the ear. The ectodermal ring then passes over the occipital and cervicothoracic parts of the embryo, superficial to the four occipital somites and later to the occipito-cervical junction. Further caudally it is associated with the upper limb field, where it will give rise to the apical ectodermal ridge. O’Rahilly & Müller (1985) have called the portion of the ring between the upper and lower limbs the intermembral part. It overlies the underlying intraembryonic coelom, and later (between stages 12 and 13), the mesonephric duct and ridge. In stages 14 and 15, this portion of the ectodermal ring gives rise to the mammary line. Caudal to the lower limb field, in the unfolded embryo, the ring passes distal to the cloacal membrane. In the folded embryo, this region becomes superior to the cloacal membrane and corresponds to the ectoderm associated with the external genitalia, particularly the genital tubercle and urogenital swellings.

Neural ectoderm

The neuroepithelium at the time of primary neurulation is pseudostratified. It has a midline hinge region which, with concomitant wedging of the cells in the lateral wall of the neural groove, promotes neural tube formation. The processes of the neuroepithelium abut onto internal and external limiting membranes. This epithelium proliferates to form all the cell lines of the central nervous system and, via the production of neural crest, all the cell lines of the peripheral nervous system.

Notochord

During stage 10, the notochordal plate undergoes a process which is similar to, but a mirror image of, neurulation, and forms an epithelial tube from caudal to rostral, ending with the pharynx. The notochordal plate forms a deep groove, the vertical edges of the groove move medially and touch, and then the endodermal epithelium from each side fuses ventral to the notochord. The cells swell and develop an internal pressure (turgor) that confers rigidity on the notochord. The notochord is surrounded by a basal lamina, which is initially referred to as a perinotochordal sheath, but this term is subsequently applied to mesenchymal populations that surround the notochord. After stage 11, the tubular notochord is in contact with the neural tube dorsally and the endoderm ventrally. It is not a proliferative epithelium, but it has inductive effects on the overlying neural tube and the adjacent somites, and later provides a focus for sclerotomal migration.

Endoderm

The craniocaudal progression of development means that the endoderm of the early stomodeum develops ahead of other portions of the endodermal epithelium. The development of the pharyngeal arches and pouches (see Ch. 35) is closely associated with the development of the neural ectoderm and proliferation of the neural crest. The respiratory diverticulum arises slightly later when the postpharyngeal gut may also be distinguished (see pages 1033 and 1203). The endoderm gives rise to the epithelial lining of the respiratory and gastrointestinal tracts, the biliary system (see p. 1207), and the bladder and urethra (see pages 1307, 1310).

Coelomic epithelium

The coelomic epithelium lines the intraembryonic coelom, which is subdivided into a midline pericardial cavity, two bilateral pericardioperitoneal canals, and the initially bilateral peritoneal cavities; the latter are continuous with the extraembryonic coelom. The coelomic epithelium is a germinal epithelium. It produces the myocardium (see p. 189) and connective tissue populations for the viscera (see p. 1033), and also gives rise to the supporting cells for the germ cells (see p. 1314), the epithelial lining of the urogenital tracts (see p. 1313) and the mesothelial lining of the pericardial, pleural (see p. 1013) and peritoneal cavities (see p. 1314).

The relative dispositions of the neural epithelium, endodermal and coelomic epithelia are shown in Fig. 12.1.

Mesenchymal populations in the embryo

In the stage 10 embryo, the major mesenchymal populations are in place. Mesoblast is still being generated at the primitive streak and moving into the presomitic mesenchymal population adjacent to the notochord. Some mesoblast is also contributing to the lateral regions of the embryo. The different mesenchymal populations within the embryo from stage 10 onwards are described below. The relative dispositions of the early mesenchymal populations are shown in Fig. 12.2.

Axial mesenchyme

The first epiblast cells to ingress through the primitive streak form the endoderm and notochord and initially occupy a midline position. The earliest population of endodermal cells rostral to the notochordal plate is termed the prechordal plate. The notochordal cells remain medially and the endodermal cells subsequently flatten and spread laterally. The population of cells that remain mesenchymal in contact with the floor of the neural groove, just rostral to the notochordal plate, is termed prechordal mesenchyme (Fig. 12.4). These axial mesenchyme cells are tightly packed, unlike the more lateral paraxial cells, but unlike the notochord, they are not contained in an extracellular sheath. They are displaced laterally at the time of head flexion and form bilateral premandibular mesenchymal condensations. They become associated with the local paraxial mesenchyme. Orthotopic grafting has demonstrated that these cells leave the edges of the prechordal mesenchyme and migrate laterally into the periocular mesenchyme, where they give rise to all of the extrinsic ocular muscles (see p. 702).

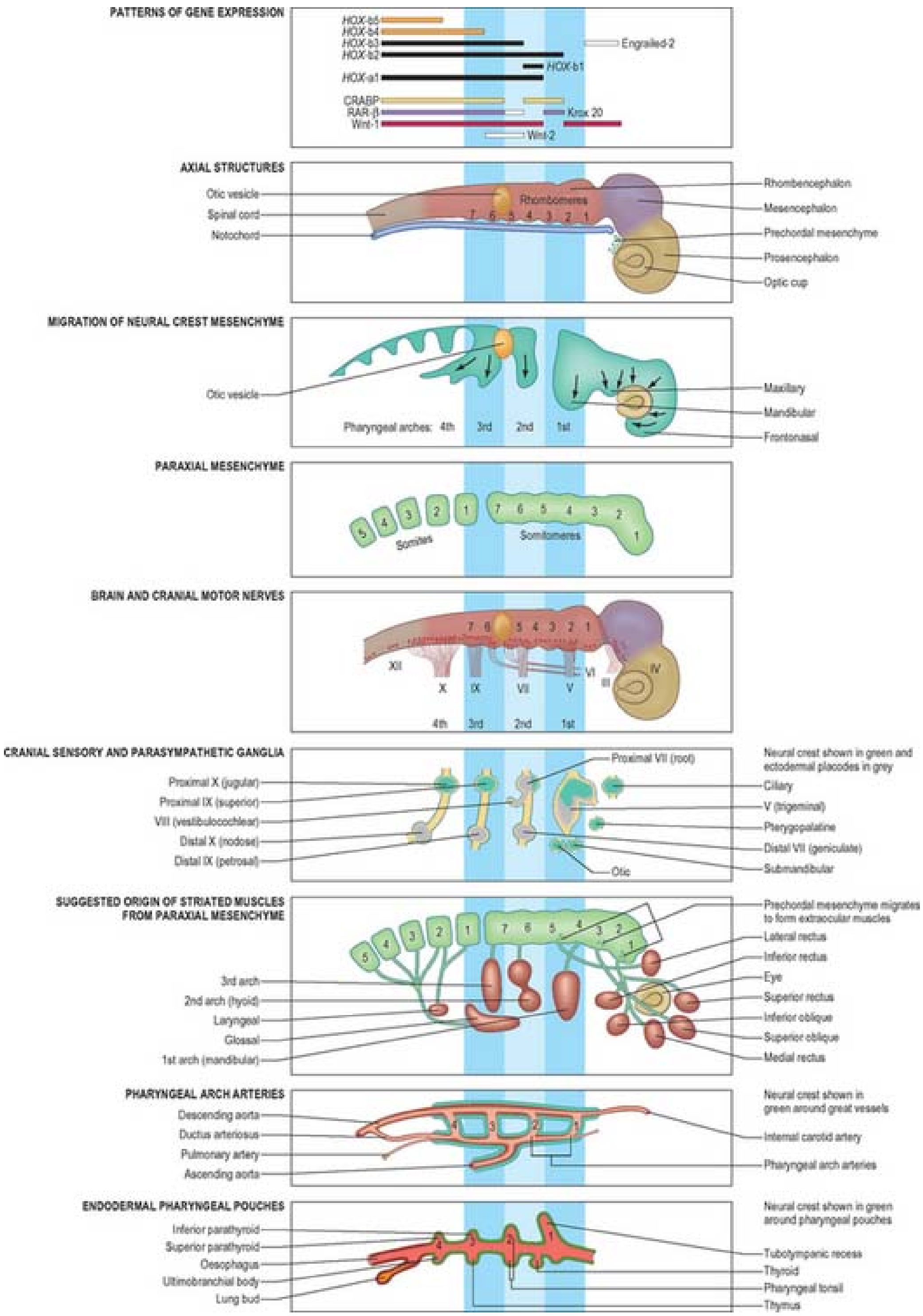
PATTERNS OF GENE EXPRESSION
HOX-b5
HOX-b4
HOX-b3
HOX-b2
HOX-b1
HOX-a1
Engrailed-2
CRABP
RAR-β
Wnt-1
Krox 20
Wnt-2
AXIAL STRUCTURES
Otic vesicle
Spinal cord
Notochord
Rhombomeres
7 6 5 4 3 2 1
Rhombencephalon
Mesencephalon
Prechordal mesenchyme
Prosencephalon
Optic cup
MIGRATION OF NEURAL CREST MESENCHYME
Otic vesicle
Pharyngeal arches: 4th 3rd 2nd 1st
Maxillary
Mandibular
Frontonasal
PARAXIAL MESENCHYME
5 4 3 2 1
Somites
7 6 5 4 3 2 1
Somitomeres
BRAIN AND CRANIAL MOTOR NERVES
7 6 5 4 3 2 1
XII
X
IX
VII
V
VI
III
IV
4th 3rd 2nd 1st
CRANIAL SENSORY AND PARASYMPATHETIC GANGLIA
Proximal X (jugular)
Proximal IX (superior)
VIII (vestibulocochlear)
Distal X (nodose)
Distal IX (petrosal)
Proximal VII (root)
Otic
Neural crest shown in green and ectodermal placodes in grey
Ciliary
V (trigeminal)
Pterygopalatine
Distal VII (geniculate)
Submandibular
SUGGESTED ORIGIN OF STRIATED MUSCLES FROM PARAXIAL MESENCHYME
5 4 3 2 1
7 6 5 4 3 2 1
3rd arch
2nd arch (hyoid)
Laryngeal
Glossal
1st arch (mandibular)
Prechordal mesenchyme migrates to form extraocular muscles
Lateral rectus
Inferior rectus
Eye
Superior rectus
Inferior oblique
Superior oblique
Medial rectus
PHARYNGEAL ARCH ARTERIES
Descending aorta
Ductus arteriosus
Pulmonary artery
Ascending aorta
4 3 2 1
Neural crest shown in green around great vessels
Internal carotid artery
Pharyngeal arch arteries
ENDODERMAL PHARYNGEAL POUCHES
Inferior parathyroid
Superior parathyroid
Oesophagus
Ultimobranchial body
Lung bud
4 3 2 1
Neural crest shown in green around pharyngeal pouches
Tubotympanic recess
Thyroid
Pharyngeal tonsil
Thymus

Fig. 12.4 The organization of the head and pharynx in an embryo at about stage 14. The individual tissue components have been separated but are aligned in register through the numbered zones.

Paraxial mesenchyme

Epiblast cells that migrate through the primitive node and rostral primitive streak during gastrulation form mesoblast cells which migrate to a position lateral to the notochord and beneath the developing neural plate. Cells that ingress through the primitive node form the medial part of this paraxial mesenchyme, and cells that ingress through the rostral streak form the lateral part (see Fig. 10.3). The paraxial mesenchyme extends cranially from the primitive streak to the prechordal plate immediately rostral to the notochord. Before somite formation, this mesenchyme is also termed presomitic or unsegmented mesenchyme in mammals (analogous to the segmental plate in birds). Paraxial mesenchyme rostral to the otic vesicle was previously believed not to segment. However, the mesenchyme in this region shows concentric rings of cell bodies and processes that form paired, bilateral cylinders, termed somitomeres.

Caudal to the otic vesicle, the paraxial mesenchyme on each side of the rhombencephalon segments into somites as the neural folds elevate and neurulation begins: somites are therefore post-otic. During somitogenesis the mesenchyme cells show changes in shape, and in cell–cell adhesion, and become organized into epithelial somites. This process begins at the eighth somitomere, which is just caudal to the midpoint of the notochordal plate. Somite one is also termed the first occipital somite. Somites can be seen on each side of the fusing neural tube in the human embryo from stage 9. Development proceeds in a craniocaudal direction, thus unsegmented paraxial mesenchyme is a transient structure. It forms somites from its cranial end, whilst mesenchyme is added to its caudal end by the regressing primitive streak. Somites give rise to the base of the skull (see p. 610); the vertebral column and ribs (see p. 764); and the skeletal muscle of the body, including that in the limbs (see p. 899).

Septum transversum

Early mesenchyme that invaginates through the middle part of the primitive streak comes to lie rostral to the buccopharyngeal membrane, where the cells form the epithelial wall of the pericardial coelom. As this epithelium proliferates, the visceral pericardial wall gives rise to the myocardium. The parietal pericardial wall forms mesenchyme, initially termed precardiac, or cardiac, mesenchyme, which is able to induce proliferation of hepatic endodermal epithelium. With further proliferation, the precardiac mesenchyme forms a ventral mass caudal to the heart, the septum transversum, which separates the foregut endoderm from the pericardial coelom (Fig. 12.2). By stage 11 the septum transversum extends dorsally on each side of the developing gut, and becomes continuous with the mesenchymal populations that proliferate from the walls of the pericardioperitoneal canals. Cells of the septum transversum give rise to the sinusoids of the liver (see p. 1207), the central portions of the diaphragm (see p. 1014) and the epicardium (see p. 1026).

Neural crest

The neural crest is unique, it gives rise to neural populations in the head and trunk and also provides an extensive mesenchymal population in the head with attributes similar, in terms of patterning, to somatopleuric mesenchyme. Neural crest cells arise from cells that lie initially at the outermost edges of the neural plate, between the presumptive epidermis and the neural tube. The cells are committed to a neural crest lineage before the neural plate begins to fold. After neurulation, neural crest cells form a transient axial population and then disperse, in some cases migrating over considerable distances, to a variety of different developmental fates. Unlike mesoblast, which is produced from the primitive streak, none of the cells that arise from the neural crest become arranged as epithelia. As the development and fate of head and trunk neural crest cells are very different, they will be considered separately.

Trunk neural crest

Trunk neural crest is formed as the neural tube closes cranio-caudally, which means that various stages of crest development can be found in the more caudal regions of an embryo. As the neural tube begins to fuse dorsally in the midline, the neural crest cells lose their epithelial characteristics and junctional connections and form a band of loosely arranged mesenchyme cells immediately dorsal to the neural tube and beneath the ectoderm. Initially, most of the crest cells lie with their long axes perpendicular to the long axis of the neural tube. Later, the cell population expands laterally and around the neural tube as a sheet. Trunk neural crest cells move from their position dorsal to the neural tube via three routes (see Fig. 24.11) dorsolaterally, to form dorsal root ganglia throughout the trunk; ventrally, to form sympathetic ganglia, enteric nerves and the suprarenal medulla; and rostrocaudally along the aorta, to form the preaortic ganglia. In a second migration route, crest cells pass dorsolaterally between the ectoderm and the epithelial plate of the somite into the somatopleure, where they eventually form melanocytes in the skin.

Head neural crest

Unlike its counterpart in the trunk, head neural crest migrates before the neural tube closes. Two populations of crest cells develop. Some cells retain a neuronal lineage and contribute to the somatic sensory and parasympathetic ganglia in the head and neck (see p. 364). Others produce extensive mesenchymal populations: the crest cell population arising from the head is larger than that found at any trunk level. Each brain region has its own crest population that migrates dorsolaterally around the sides of the neural tube to reach the ventral side of the head. Crest cells surround the prosencephalic and optic vesicles and occupy each of the pharyngeal arches (see Ch. 35). They provide mesenchyme cells which will produce the connective tissue in parts of the neuro- and viscero-crania. All cartilage, bone, ligament, tendon, dermal components and glandular stroma in the head are derived from the head neural crest. Head neural crest also contributes to the tunica media of the aortic arch arteries.

Lateral plate

Lateral plate is the term for the early unsegmented mesoblast population lateral to the paraxial mesenchyme. Mesoblastic cells, which arise from the middle of the primitive streak (primary mesenchyme), migrate cranially, laterally and caudally to reach their destinations, where they revert to epithelium and form a continuous layer that adheres to the ectoderm dorsally and the endoderm ventrally. The epithelium faces a new intraembryonic cavity, the intraembryonic coelom, which becomes confluent with the extraembryonic coelom and provides a route for the circulation of coelomic fluid through the embryo. Once formed, the intraembryonic coelomic wall becomes a proliferative epithelium which produces new populations of mesenchymal cells. The mesenchymal population subjacent to the ectoderm is termed somatopleuric mesenchyme, and is produced by the somatopleuric coelomic epithelium. The mesenchymal population surrounding the endoderm is termed splanchnopleuric mesenchyme, and is produced by the splanchnopleuric coelomic epithelium (Fig. 12.2).

It is important to note that these terms are relevant only caudal to the third pharyngeal arch. Rostral to this there is a sparse mesenchymal population between the pharynx and the surface ectoderm prior to migration of the head neural crest, and there are no landmarks with which to demarcate lateral from paraxial mesenchyme. This unsplit lateral plate is believed to contribute to the cricoid and arytenoid cartilages, the tracheal rings and the associated connective tissue.

Somatopleuric mesenchyme

Somatopleuric mesenchyme produces a mixed population of connective tissues and has a significant organizing effect at the level of the developing limbs. The pattern of limb development is controlled by information contained in the somatopleuric mesenchyme. Regions of the limb are specified by interaction between the surface ectoderm (apical ectodermal ridge) and underlying somatopleuric mesenchyme; together these tissues form the progress zone of the limb (see p. 899). The somatopleuric mesenchyme in the limb bud also specifies the postaxial border of the developing limb.

Somatopleuric mesenchyme thus gives rise to the connective tissue elements of the appendicular skeleton, including the pectoral and pelvic girdles and the bones and cartilage of the limbs and their associated ligaments and tendons. It also gives rise to the dermis of the skin of the ventral and lateral body walls and of the limbs.

Muscles of the limbs are derived from paraxially derived somitic precursor muscle cells.

Splanchnopleuric mesenchyme

Splanchnopleuric mesenchyme surrounds the developing gut and respiratory tubes, contributing connective tissue cells to the lamina propria and submucosa, and smooth muscle cells to the muscularis mucosae and muscularis externa. It plays a patterning role in endodermal development, specifying the region and villus type in the gut (see p. 1203), and the branching pattern in the respiratory tract (see p. 1032).

Intermediate mesenchyme

Intermediate mesenchyme is a loose collection of cells found between the somites and the lateral plate (Fig. 12.2). Its development is closely related to the progress of differentiation of the somites and the proliferating coelomic epithelium from which it is derived. Intermediate mesenchyme is not present before somitogenesis or the formation of the eighth somite. In embryos with eight to ten somites, it is present lateral to the sixth somite, but does not extend cranially. The mesenchyme cells are arranged as layers, one continuous with the dorsal side of the paraxial mesenchyme and the somatopleure, the other with the ventral side of the paraxial mesenchyme and the splanchnopleure.

As development proceeds, the intermediate mesenchyme forms a loosely packed dorsolateral cord of cells, which lengthens at the caudal end and ultimately joins the cloaca. It gives rise to the nephric system, gonads and reproductive ducts (see pp. 1305, 1311).

Angioblastic mesenchyme

Mesenchymal cells which give rise to the cellular elements of the blood, and the endothelium and mesenchymal layers of the tunica externa and adventitia of blood and lymphatic vessels, arise from extraembryonic and intraembryonic sources. Evidence suggests that endodermal tissues are necessary for endothelial differentiation. Angioblastic mesenchyme forms early in the third week of development from extraembryonic mesenchyme in the splanchnopleure of the yolk sac, in the body stalk (containing the allantois), and in the somatopleure of the chorion. The peripheral cells flatten as a vascular endothelium, whereas the central cells transform into primitive red blood corpuscles. Later, contiguous islands merge, forming a continuous network of fine vessels. Intraembryonic blood vessels are first seen at the endoderm–mesenchyme interface within the lateral splanchnic mesenchyme at the caudolateral margins of the cranial intestinal portal. Angioblastic competence has been demonstrated within the ventral (splanchnopleuric) mesenchymes with which the endoderm interacts. However, the notochord and prechordal plate do not contain angiogenic cells. Similarly, ectodermal tissues do not appear to give rise to angiogenic cells. Somites, derived from paraxial mesenchyme, have been shown to be a source of angioblasts which either differentiate with the somite derivatives, or migrate to the neural tube, ventrolateral body wall, limb buds, mesonephros and the dorsal part of the aorta.

The earliest angiogenic mesenchymal cells form blood vessels by vasculogenesis, a process in which new vessels (e.g. endothelial heart tubes, dorsal aortae, umbilical and early vitelline vessels) develop *in situ*. Later vessels develop by angiogenesis, sprouting and branching from the endothelium of pre-existing vessels; this process is the means by which most other vessels develop. The ultimate pattern of vessels is controlled by the surrounding, non-angiogenic mesenchyme: vessels become morphologically specific for the organ in which they develop and also immunologically specific, expressing organ-specific proteins.

REFERENCES

'Rahilly R, Müller F. The origin of the ectodermal ring in staged human embryos of the first 5 weeks. *Acta Anat*. 1985;122:145-157.

chardson MK, Keuck G. Haeckel’s ABC of evolution and development. *Biol Rev Camb Philos Soc*. 2002;77:495-528.

CHAPTER 13

Early embryonic circulation

The early embryonic circulation is symmetrical (Fig. 13.1). It is modified throughout development to produce a functioning fetal circulation which is connected to the placenta, and changes rapidly at birth to accommodate disconnection from the placenta and the start of gaseous exchange in the lungs. Major restructuring of early vessels occurs as the embryo grows: anastomoses form and then disappear, capillaries fuse and give rise to arteries or veins, and the direction of blood flow may reverse several times before the final arrangement of vessels is completed.

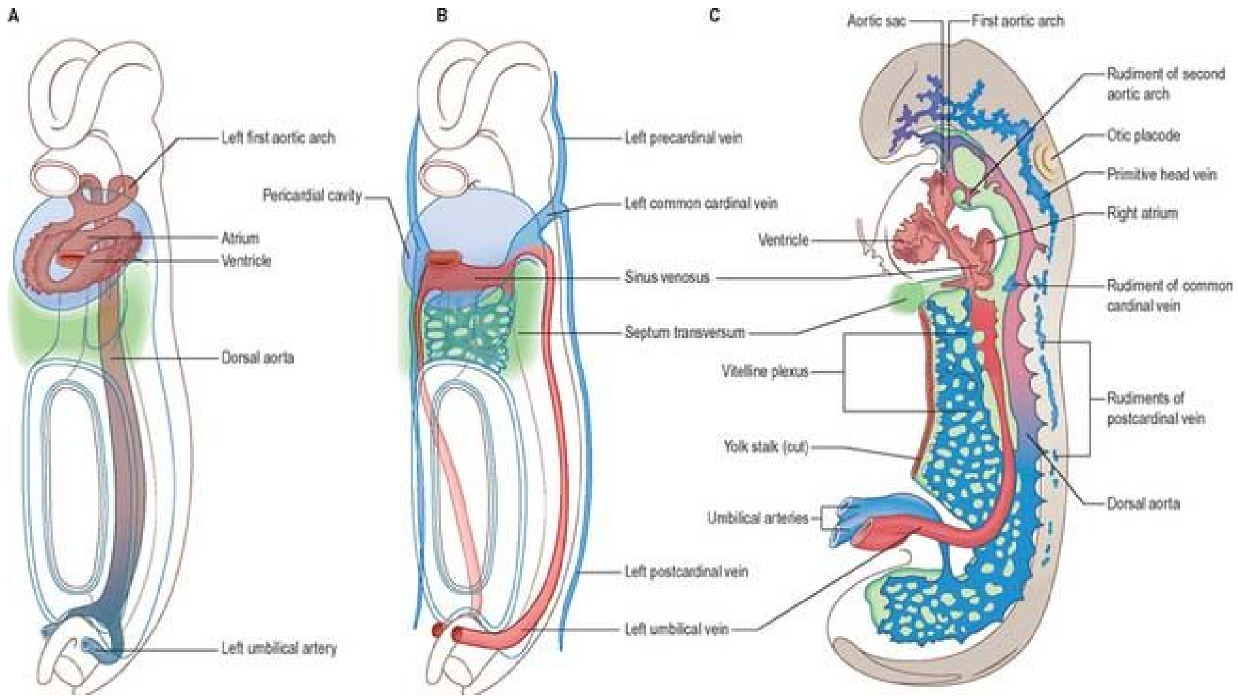
A
Left first aortic arch
Atrium
Ventricle
Dorsal aorta
Left umbilical artery
B
Pericardial cavity
Left precardinal vein
Left common cardinal vein
Sinus venosus
Septum transversum
Left postcardinal vein
Left umbilical vein
C
Aortic sac
First aortic arch
Rudiment of second aortic arch
Otic placode
Primitive head vein
Right atrium
Ventricle
Rudiment of common cardinal vein
Vitelline plexus
Rudiments of postcardinal vein
Yolk stalk (cut)
Dorsal aorta
Umbilical arteries

Fig. 13.1 The early, symmetrical blood vascular system. **A**, Ventrolateral view of the endothelial profile of the heart, the first aortic arch arteries and the dorsal aorta shown in relation to the major epithelial populations. **B**, Ventrolateral view of the main venous channels shown in relation to the major epithelial populations. **C**, Left lateral view of the blood vascular system of a stage 11 human embryo; only the endothelial lining of the heart tube is shown. At this stage the arteries and veins are in the process of development and no true circulation is yet established.

The earliest circulatory components develop by vasculogenesis in the extraembryonic tissues. The endothelial heart tubes, dorsal aortae, umbilical and early vitelline vessels arise by vasculogenesis within the embryo. Further vessel development occurs by a process of angiogenesis in which angioblasts, arising in splanchnic and somitic tissues, add endothelial sprouts and branches to earlier vessels. None of the main vessels of the adult arises as a single trunk in the embryo. A capillary network is first laid down along the course of each vessel; the larger arteries and veins are defined by selection and enlargement of definite paths in this network. Lymphatic vessels develop after the main arteries and veins are formed: they arise initially by angiogenesis from the cardinal veins and subsequently by proliferation of lymphangioblasts to form lymphatic capillaries.

Early blood vessels are initially surrounded by a fibronectin-rich matrix that is later incorporated into the endothelial basal lamina along with laminin, a particularly early constituent. Several layers of fibronectin-expressing cells are seen around larger vessels, such as the dorsal aortae. The endothelium does not synthesize a basal lamina in those regions where remodelling and angiogenesis is active, and the mesenchyme around such endothelium does not express α-actin or laminin until branching has stopped and differentiation of the tunica media begins (after a stable vascular pattern has formed). It is not known how differentiation of pericytes and smooth muscle cells is induced; the majority of arteries accumulate medial smooth muscle from the surrounding mesenchyme.

In early development, the arteries of the embryo are disproportionately large and their walls consist of little more than a single layer of endothelium. The cardiac orifices are also relatively large and the force of the cardiac contraction is weak, and consequently the circulation is sluggish, despite the rapid rate of contraction of the developing heart. However, the tissues are able to draw nourishment not only from the capillaries but also from the large arteries and the intraembryonic coelomic fluid.

It has been suggested that the rapidly expanding cardiovascular system is filled with plasma by the movement of fluid from the intraembryonic coelom to the veins. In general, the wall of the intraembryonic coelom is composed of proliferating cells which produce the splanchnopleuric and somatopleuric mesenchymal populations. However, the walls of a portion of the pericardioperitoneal canals are thinner, and possibly more permeable to coelomic fluid, at the time when the canals surround the hepatocardiac channels (veins). The latter lie between the hepatic plexus and the sinus venosus; the hepatocardiac channel on the right side is more developed and on the left it is more plexiform, with only a transitory connection to the sinus venosus. The differentiation of this specific coelomic region occurs just in advance of the expansion and filling of the right and left atria, at about stage 12.

As the heart muscle thickens, compacts and strengthens, the cardiac orifices become both relatively and absolutely reduced in size, the valves increase their efficiency, and the large arteries acquire their muscular walls and undergo a relative reduction in size. From this time onwards, the embryo is dependent for its nourishment on the expanding capillary beds, and the function of the larger arteries becomes restricted to that of controllable distribution channels to keep the embryonic tissues constantly and appropriately supplied.

The heart starts to beat early, before the development of the conduction system, and a circulation is established before a competent valvular mechanism has formed. Cardiac output increases in proportion with the weight of the embryo and cardiac rate increases with development. However, most of the increase in cardiac output results from a geometric increase in stroke volume. When dorsal aortic blood flow is matched to embryonic weight, blood flow remains constant over a more than 150-fold change in mass of the embryo.

After head folding, the embryo has bilateral primitive aortae, each consisting of ventral and dorsal parts that are continuous through the first embryonic aortic arches (see Ch. 35). The ventral aortae are fused and form a dilated aortic sac. The dorsal aortae run caudally, one on each side of the notochord. In the fourth week they fuse from about the level of the fourth thoracic to that of the fourth lumbar segment to form a single definitive descending aorta (Figs 13.1A,C, 13.2B). In general, more mature endothelial channels are seen in the rostral, more advanced regions of the embryo, whereas more caudally, a changing capillary plexus constantly remodels until it becomes confluent with the vascular channels of the connecting stalk. The dorsal continuation of the primitive dorsal aortae directs blood into an anastomosing network around the allantois which will form the umbilical arteries. Blood is channelled back to the developing heart from the allantois via umbilical veins, from anastomoses in the primitive yolk sac via the vitelline veins, and from the body via pre- and post-cardinal veins that join to form the common cardinal veins (Figs 13.1B,C, 13.2A).

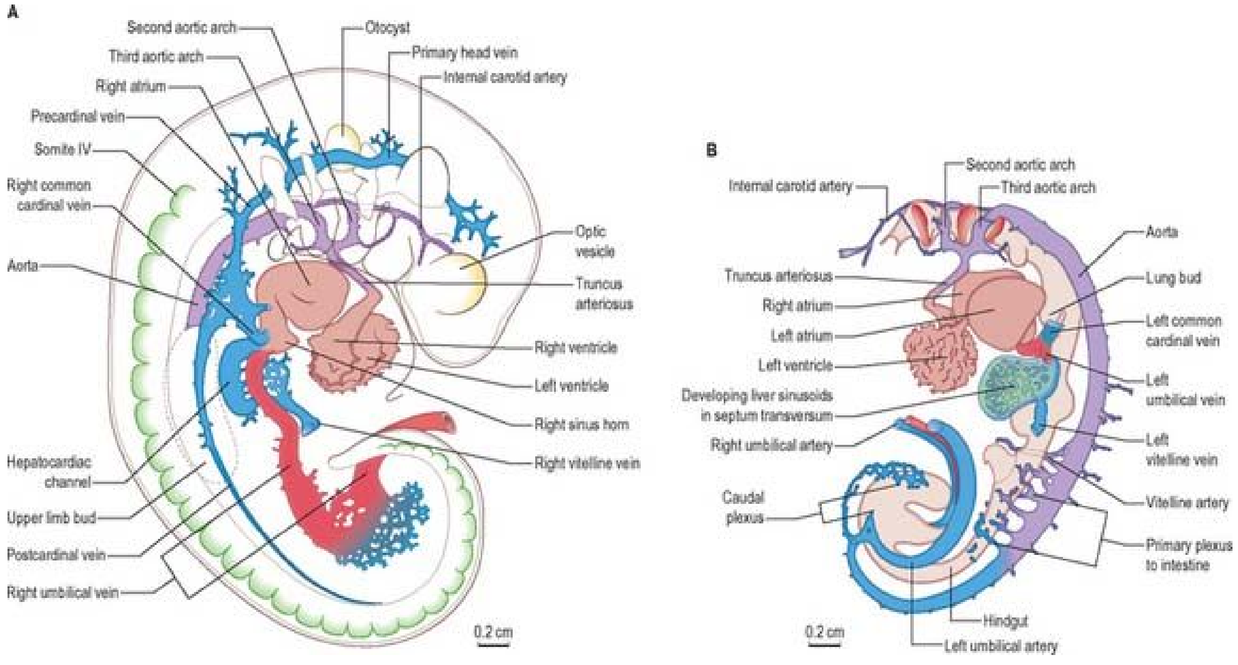
A
Second aortic arch
Third aortic arch
Right atrium
Precardinal vein
Somite IV
Right common cardinal vein
Aorta
Hepatocardiac channel
Upper limb bud
Postcardinal vein
Right umbilical vein
Otocyst
Primary head vein
Internal carotid artery
Optic vesicle
Truncus arteriosus
Right ventricle
Left ventricle
Right sinus horn
Right vitelline vein
0.2 cm
B
Internal carotid artery
Second aortic arch
Third aortic arch
Aorta
Truncus arteriosus
Right atrium
Left atrium
Left ventricle
Developing liver sinusoids in septum transversum
Right umbilical artery
Caudal plexus
Lung bud
Left common cardinal vein
Left umbilical vein
Left vitelline vein
Vitelline artery
Primary plexus to intestine
Hindgut
Left umbilical artery
0.2 cm

Fig. 13.2 Profile reconstructions of the blood vascular system of a stage 13 human embryo. The early circulation is now asymmetrical with the venous vessels enlarging on the right and diminishing on the left. **A**, Right side: the main venous channels to the heart can be seen. **B**, Left side: the aortic arch arteries, the main vessels arising from the dorsal aorta and the umbilical arteries are shown. Note: Only the endothelial lining of the heart chambers is shown and, because the muscular wall has been omitted, the pericardial cavity appears much larger than the contained heart.

EMBRYONIC ARTERIES

Initially the dorsal aortae are the only longitudinal vessels present. Their branches all run at right angles to the long axis of the embryo. Later these transverse arteries become connected by longitudinal anastomosing channels which persist in part, forming arteries such as the vertebral, internal thoracic, superior and inferior epigastric, and gastroepiploic. Each primitive dorsal aorta gives off somatic arteries (intersegmental branches to the body wall), a caudal continuation which passes into the body stalk (the umbilical arteries), lateral splanchnic arteries (paired segmental branches to the mesonephric ridge), and ventral splanchnic arteries (paired segmental branches to the digestive tube).

Somatic arteries

The somatic arteries are intersegmental in position. They persist, almost unchanged, in the thoracic and lumbar regions, as the posterior intercostal, subcostal and lumbar arteries. Each gives off a dorsal ramus, which passes backwards in the intersegmental interval and divides into medial and lateral branches to supply the muscles and superficial tissues of the back (Fig. 13.3). The dorsal ramus also gives off a spinal branch, which enters the vertebral canal and divides into a series of branches that supply the walls and joints of the osteoligamentous canal, and neural branches to the spinal cord and spinal nerve roots. After giving off its dorsal ramus, each intersegmental artery runs ventrally in the body wall, gives off a lateral branch and terminates in muscular and cutaneous rami.

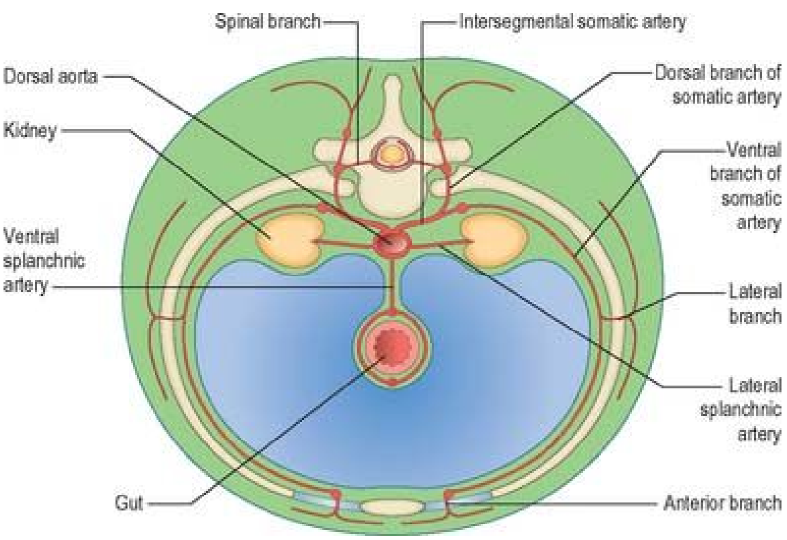
Spinal branch
Intersegmental somatic artery
Dorsal aorta
Dorsal branch of somatic artery
Kidney
Ventral branch of somatic artery
Ventral splanchnic artery
Lateral branch
Lateral splanchnic artery
Gut
Anterior branch

Fig. 13.3 The segmental and intersegmental arteries. Note the positions of the longitudinal anastomoses (small red dilatations).

Early umbilical arteries

Initially, the umbilical arteries are the direct caudal continuation of the primitive dorsal aortae. They are present in the body stalk before any vitelline or visceral branches emerge, indicating the dominance of the allantoic over the vitelline circulation in the human embryo. (On a comparative basis, the umbilical vessels are chorio-allantoic and therefore ‘somatovisceral’.) After the dorsal aortae fuse, the umbilical arteries arise from their ventrolateral aspects and pass medial to the primary excretory duct to the umbilicus. Later, the proximal part of each umbilical artery is joined by a new vessel that leaves the aorta at its termination and passes lateral to the primary excretory duct. This, possibly the fifth lumbar intersegmental artery, constitutes the dorsal root of the umbilical artery (the original stem, the ventral root). The dorsal root gives off the axial artery of the lower limb, branches to the pelvic viscera and, more proximally, the external iliac artery. The ventral root disappears entirely, and the umbilical artery now arises from that part of its dorsal root distal to the external iliac artery, i.e. the internal iliac artery.

Lateral splanchnic arteries

The lateral splanchnic arteries supply, on each side, the mesonephros, metanephros, testis or ovary and the suprarenal gland. All these structures develop, in whole or in part, from the intermediate mesenchyme, later termed the aorta-gonad-mesonephros region. One testicular or ovarian artery and three suprarenal arteries persist on each side. The phrenic artery branches from the most cranial suprarenal artery, and the renal artery arises from the most caudal. Additional renal arteries are frequently present and may be regarded as branches of persistent lateral splanchnic arteries.

Ventral splanchnic arteries

The ventral splanchnic arteries are originally paired vessels distributed to the capillary plexus in the wall of the yolk sac. After fusion of the dorsal aortae, they merge as unpaired trunks that are distributed to the increasingly defined and lengthening primitive digestive tube. Longitudinal anastomotic channels connect these branches along the dorsal and ventral aspects of the tube, forming dorsal and ventral splanchnic anastomoses (Fig. 13.3). These vessels obviate the need for so many ‘subdiaphragmatic’ ventral splanchnic arteries, and these are reduced to three, the coeliac trunk and the superior and inferior mesenteric arteries. As the viscera supplied descend into the abdomen, their origins migrate caudally by differential growth: the origin of the coeliac artery is transferred from the level of the seventh cervical segment to the level of the 12th thoracic; the superior mesenteric from the second thoracic to the first lumbar; and the inferior mesenteric from the twelfth thoracic to the third lumbar. However, above the diaphragm, a variable number of ventral splanchnic arteries persist, usually four or five, supplying the thoracic oesophagus. The dorsal splanchnic anastomosis persists in the gastroepiploic, pancreaticoduodenal and primary branches of the colic arteries, whereas the ventral splanchnic anastomosis forms the right and left gastric and the hepatic arteries.

EMBRYONIC VEINS

The early embryonic veins are often segregated into two groups, visceral and somatic, for convenience and apparent simplicity. The visceral group contains the derivatives of the vitelline and umbilical veins, and the somatic group includes all remaining veins. It should be noted that, with time, embryonic veins change the principal tissues they drain. They may receive radicles from obviously parietal tissues which become confluent with drainage channels that are clearly visceral, and so form a compound vessel. The arrangement of the early embryonic veins is initially symmetrical. The primitive tubular symmetric heart receives its venous return through the right and left sinual horns which are initially embedded in the mesenchyme of the septum transversum. Each horn receives, most medially, the termination of the principal vitelline vein, more laterally, the umbilical vein and, most laterally, having encircled the pleuroperitoneal canal, the common cardinal vein. This symmetric pattern changes as the heart and gut develop and the cardiac return is diverted to the right side of the heart.

Vitelline veins

The vitelline veins drain capillary plexuses developed in the splanchnopleuric mesenchyme of the secondary yolk sac. With head, tail and lateral fold formation, the upper recesses of the yolk sac are enclosed within the embryo as the splanchnopleuric gut tube, which extends from the stomodeal buccopharyngeal membrane to the proctodeal cloacal membrane. Derivatives from all these levels possess a venous drainage that is originally vitelline.

Early umbilical veins

The umbilical veins form by the convergence of venules that drain the splanchnopleure of the extraembryonic allantois. The human endodermal allantois is very small: it projects into the embryonic end of the connecting stalk, which is therefore regarded as precociously formed allantoic mesenchyme, whereas the umbilical vessels are considered to be allantoic.

The peripheral venules drain the mesenchymal cores of the chorionic villous stems and terminal villi (extraembryonic somatopleuric structures). These are the radicles of the vena umbilicalis impar (usually single) which traverses the compacting mixed mesenchyme of the umbilical cord to reach the caudal rim of the umbilicus. Here, the single cordal vein divides into primitive right and left umbilical veins. Each curves rostrally in the somatopleuric lateral border of the umbilicus, i.e. where intraembryonic and extraembryonic or amniotic somatopleure are continuous, lying lateral to the communication between both the intraembryonic and extraembryonic coeloms. Rostrolateral to the umbilicus, the two umbilical veins reach, enter and traverse the junctional mesenchyme of the septum transversum and connect with septal capillary plexuses. They then continue, entering their corresponding cardiac sinual horns lateral to the terminations of the vitelline veins. This early symmetric disposition of the vitelline veins and anastomoses, umbilical and common cardinal veins, and the locus of the hepatic primordial complex are summarized in Figs 13.1B, 13.2A. For further development of the vitelline and umbilical veins see Chapter 73 (Figs 73.8, 73.9).

Cardinal veins and somatic venous complexes

The initial venous channels in the early embryo have traditionally been termed cardinal because of their importance at this stage. The cardinal venous complexes are first represented by two large vessels on each side, the precardinal portion being rostral and the postcardinal, caudal, to the heart. The two veins on each side unite to form a short common cardinal vein, which passes ventrally, lateral to the pleuropericardial canal, to open into the corresponding horn of the sinus venosus (Figs 13.1B, 13.2A, 13.4B). The precardinal veins undergo remodelling as the head develops. The postcardinal veins, which in the early embryo drain the body wall, are insufficient channels for venous return from the developing mesonephros and gonads and for the growing body wall. As the embryo increases in size, they are supplemented by a range of bilateral longitudinal channels that anastomose with the posterior cardinal system and with each other. These channels are the subcardinal, supracardinal, azygos line, subcentral and precostal veins (Fig. 13.4).

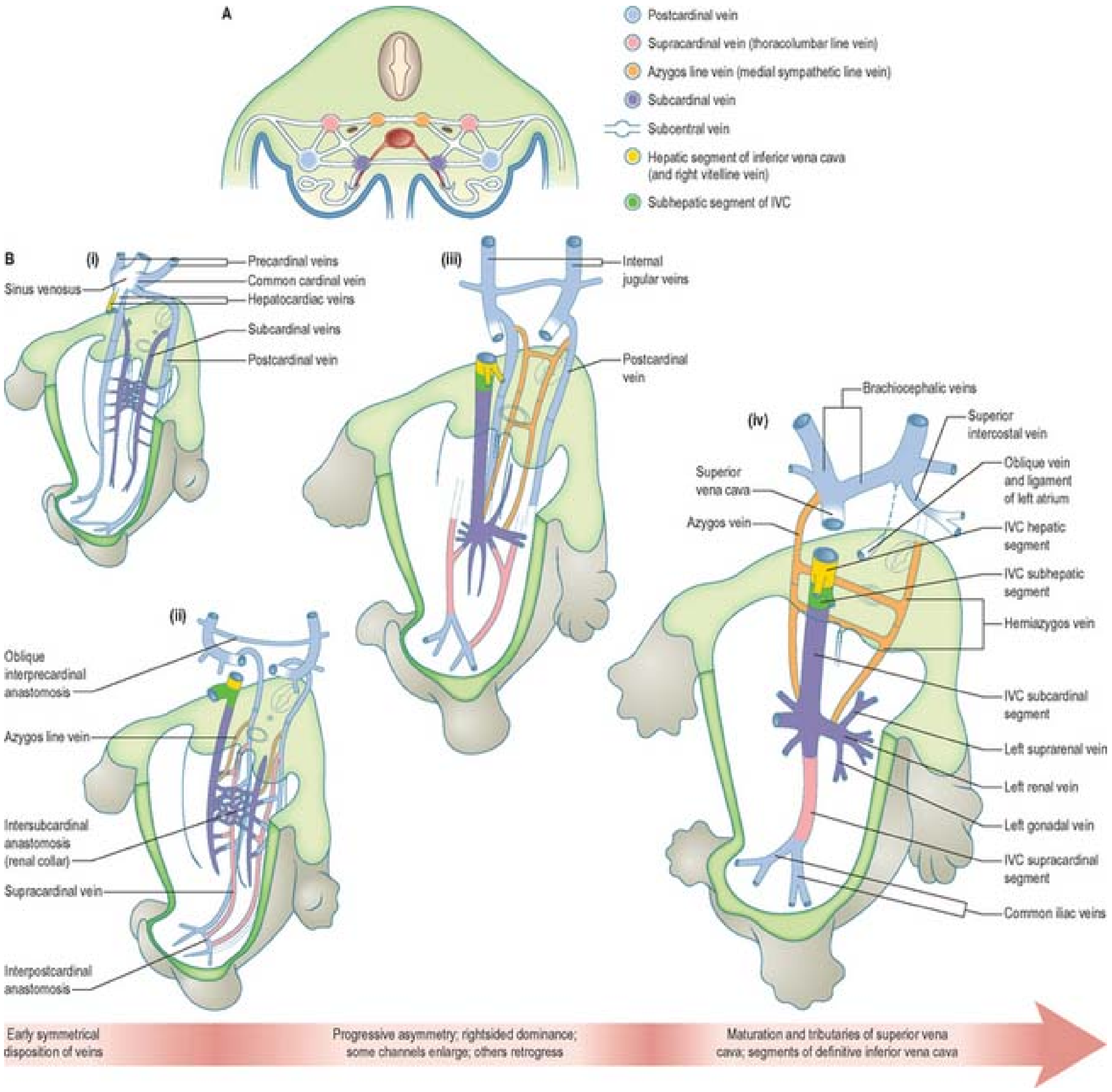
A
Postcardinal vein
Supracardinal vein (thoracolumbar line vein)
Azygos line vein (medial sympathetic line vein)
Subcardinal vein
Subcentral vein
Hepatic segment of inferior vena cava (and right vitelline vein)
Subhepatic segment of IVC
B
(i)
Sinus venosus
Precardinal veins
Common cardinal vein
Hepatocardiac veins
Subcardinal veins
Postcardinal vein
(ii)
Oblique interprecardinal anastomosis
Azygos line vein
Intersubcardinal anastomosis (renal collar)
Supracardinal vein
Interpostcardinal anastomosis
(iii)
Internal jugular veins
Postcardinal vein
(iv)
Brachiocephalic veins
Superior intercostal vein
Superior vena cava
Azygos vein
Oblique vein and ligament of left atrium
IVC hepatic segment
IVC subhepatic segment
Hemiazygos vein
IVC subcardinal segment
Left suprarenal vein
Left renal vein
Left gonadal vein
IVC supracardinal segment
Common iliac veins
Early symmetrical disposition of veins
Progressive asymmetry; rightsided dominance; some channels enlarge; others retrogress
Maturation and tributaries of superior vena cava; segments of definitive inferior vena cava

Fig. 13.4 Somatic venous development. **A**, Schematic section through the embryonic trunk. Principal longitudinal veins are colour-coded. Interconnections and intersegmental veins remain uncoloured. **B**, Plan of development of principal somatic veins from the early symmetric state, through states of increasing asymmetry, to the definitive arrangement.

Subcardinal veins

Subcardinal veins form in the ventromedial parts of the mesonephric ridges and become connected to the postcardinal veins by a number of vessels traversing the medial part of the ridges. The subcardinal veins assume the drainage of the mesonephros, and intercommunicate by a pre-aortic anastomotic plexus, which later constitutes the part of the left renal vein that crosses anterior to the abdominal aorta.

Supracardinal veins

Supracardinal veins form dorsolateral to the aorta and lateral to the sympathetic trunk and take over the intersegmental venous drainage from the posterior cardinal vein. The supracardinal veins are also referred to as the thoracolumbar line or lateral sympathetic line veins.

Azygos line veins

Azygos line veins form dorsolateral to the aorta and medial to the sympathetic trunk. These channels, also referred to as the medial sympathetic line veins, gradually take over the intersegmental venous drainage from the supracardinal veins. The intersegmental veins now reach their longitudinal channel by passing medial to the autonomic trunk, a relationship that the lumbar and intercostal veins subsequently maintain. Cranially, the azygos lines join the persistent cranial ends of the posterior cardinal veins.

Subcentral veins

Subcentral veins form directly dorsal to the aorta in the interval between the origins of the paired intersegmental arteries. These veins communicate freely with each other and with the azygos line veins; these connections ultimately form the retro-aortic parts of the left lumbar veins and of the hemiazygos veins.

A precostal or lumbocostal venous line

A precostal or lumbocostal venous line, anterior to the vertebrocostal element and posterior to the supracardinal, is recognized by some authorities. A possible derivative is the ascending lumbar vein.

Further development of the somatic veins

The supracardinal veins lie lateral to the aorta and the sympathetic trunks, which therefore intervene between them and the azygos lines (Fig. 13.4). They communicate caudally with the iliac veins and cranially with the subcardinal veins in the neighbourhood of the pre-aortic intersubcardinal anastomosis. The supracardinal veins also communicate freely with each other through the medium of the azygos lines and the subcentral veins. The most cranial of these connections, together with the supracardinal–subcardinal and the intersubcardinal anastomoses, complete a venous ring around the aorta below the origin of the superior mesenteric artery, termed the ‘renal collar’.

The ultimate arrangement of these embryonic abdominal and thoracic longitudinal cardinal veins may be summarized as follows. The terminal part of the left postcardinal vein forms the distal part of the left superior intercostal vein. On the right side, its cranial end persists as the terminal part of the azygos vein. The caudal part of the subcardinal vein is in part incorporated in the testicular or ovarian vein and partly disappears. The cranial end of the right subcardinal vein is incorporated into the inferior vena cava and also forms the right suprarenal vein. The left subcardinal vein, cranial to the intersubcardinal anastomosis, is incorporated into the left suprarenal vein. The renal and testicular or ovarian veins on both sides join the supracardinal–subcardinal anastomosis. On the left side, this is connected directly to the part of the inferior vena cava that is of subcardinal status via an intersubcardinal anastomosis. The right supracardinal vein forms much of the postrenal (caudal) segment of the inferior vena cava. The left supracardinal vein disappears entirely. The right azygos line persists in its thoracic part to form all but the terminal part of the azygos vein. Its lumbar part can usually be identified as a small vessel that leaves the vena azygos on the body of the 12th thoracic vertebra and descends on the vertebral column, deep to the right crus of the diaphragm, to join the posterior aspect of the inferior vena cava at the upper end of its postrenal segment. The left azygos line forms the hemiazygos veins. The subcentral veins give rise to the retro-aortic parts of the left lumbar veins and of the hemiazygos veins (Fig. 13.4).

EMBRYONIC LYMPHATIC VESSELS

The earliest lymphatic vessels arise from budding of lymphatic endothelial cells from the cardinal veins to form lymph sacs (Eichman et al 2005). Six early lymph sacs can be identified, two are paired (the jugular and the posterior lymph sacs) and two are unpaired (the retroperitoneal sac and the cisterna chyli). In lower mammals an additional pair (subclavian) is present, but in the human embryo these are merely extensions of the jugular sacs.

The jugular lymph sac is the first to appear, at the junction of the subclavian vein with the precardinal, with later prolongations along the internal and external jugular veins; the posterior lymph sac encircles the left common iliac vein; the retroperitoneal sac appears in the root of the mesentery near the suprarenal glands; and the cisterna chyli appears opposite the third and fourth lumbar vertebrae (Fig. 13.5). The lymph vessels bud out from the lymph sacs along lines that correspond more or less closely with the course of embryonic blood vessels (most commonly veins); many also arise *de novo* in the mesenchyme and establish connections with existing vessels. In the body wall and the wall of the intestine, the deeper plexuses are the first to be developed; the vessels in the superficial layers are gradually formed by continued growth.

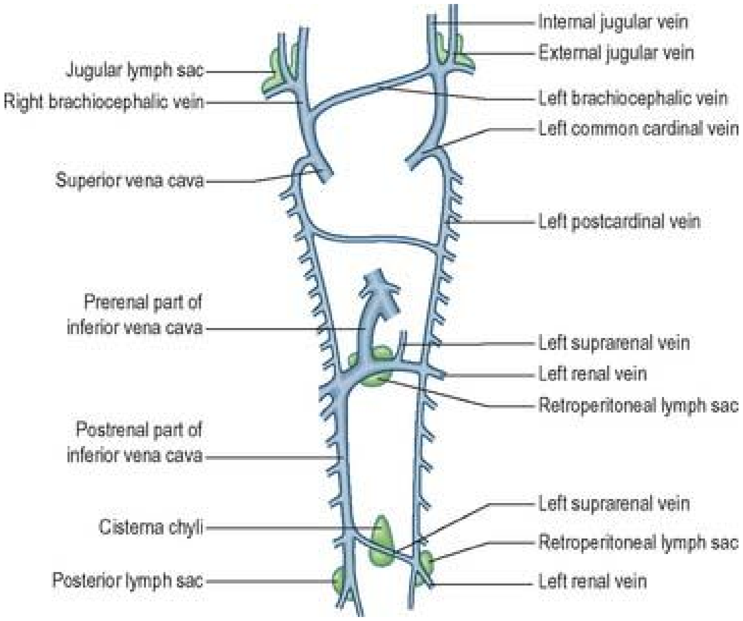
Internal jugular vein
External jugular vein
Jugular lymph sac
Right brachiocephalic vein
Left brachiocephalic vein
Left common cardinal vein
Superior vena cava
Left postcardinal vein
Prerenal part of inferior vena cava
Left suprarenal vein
Left renal vein
Retroperitoneal lymph sac
Postrenal part of inferior vena cava
Left suprarenal vein
Cisterna chyli
Retroperitoneal lymph sac
Posterior lymph sac
Left renal vein

Fig. 13.5 Relative positions of the primary lymph sacs (as originally determined by Sabin, 1912).

LYMPH NODES AND LYMPHOID TISSUES

Lymph vessels can be seen in the embryo in the cervical region from stage 16. Lymph nodes, which provide regional proliferative foci for lymphocytes, have been identified from week 9. Early lymph sacs become infiltrated by lymphoid cells, and the outer portion of each sac becomes the subcapsular sinus of the lymph node. Morphological differentiation of medullary and cortical compartments has not been observed until the end of week 10 (Tonar et al 2001). At the same time as these early lymph nodes are developing, the nasopharyngeal wall is infiltrated by lymphoid cells that are believed to herald the early development of the tubal and pharyngeal tonsils.

In the neonate, a considerable proportion of the total amount of lymphoid tissue is localized in lymph nodes: the subsequent increase in the amount of lymphoid tissues that occurs during childhood reflects the growth of these nodes. Definitive follicles with germinal centres are formed during the first postnatal year. The pharyngeal tonsil reaches its maximal development at 6 years and its subsequent involution is completed by puberty. Details of the development of gut-associated lymphoid tissue are given in Chapter 73.

REFERENCES

chman A, Yuan Li, Moyon D, Lenoble F, Pardanaud L, Bréant C. Vascular development: from precursor cells to branched arterial and venous networks. *Int J Dev Biol*. 2005;49:259-267.

bin FR. On the origin of the abdominal lymphatics in mammals from the vena cava and the renal glands. *Anat Rec*. 1912;6:335-342.

nar Z, Kocova J, Liska V, Slipkja J. Early development of the jugular lymphatics. *Sb Lek*. 2001;102:217-225.

CHAPTER 14

Pre- and postnatal development

PRENATAL STAGES

The absolute size of an embryo or fetus does not afford a reliable indication of either its chronological age or the stage of structural organization, even though graphs based on large numbers of observations have been constructed to provide averages. All such data suffer from the difficulty of timing the moment of conception in humans. It has long been customary to compute the age, whether in a normal birth or an abortion, from the first day of the last menstrual period of the mother but, as ovulation usually occurs near the 14th day of a menstrual cycle, this ‘menstrual age’ is an overestimate of about 2 weeks. Where a single coitus can be held to be responsible for conception, a ‘coital age’ can be established and the ‘fertilization age’ cannot be much less than this, because of the limited viability of both gametes. It is usually held that the difference may be several days, which is a highly significant interval in the earlier stages of embryonic development. Even if the time of ovulation and coitus were known in instances of spontaneous abortion, not only would some uncertainty still persist with regard to the time of fertilization, but there would also remain an indefinable period between the cessation of development and the actual recovery of the conceptus.

To overcome these difficulties, early embryos have been graded or classified into developmental stages or ‘horizons’, on the basis of both internal and external features. The study of the Carnegie collection of embryos by Streeter (1942, 1945, 1948), and the continuation of this work by O’Rahilly & Müller (1987), provided, and continues to provide, a sound foundation for embryonic study and a means of comparing stages of human development with those of the animals routinely used for experimental study, namely the chick, mouse and rat. Recent use of ultrasound for the examination of human embryos and fetuses *in utero* has confirmed much of the staging data.

The development of a human from fertilization to birth is divided into two periods, embryonic and fetal. The embryonic period has been defined by Streeter as 8 weeks postfertilization, or 56 days. This timescale is divided into 23 Carnegie stages, a term introduced by O’Rahilly & Müller (1987) to replace developmental ‘horizons’. The designation of stage is based on external and internal morphological criteria and not on length or age.

Embryonic stages

Embryonic stages 1–10 are shown in detail in Fig. 8.1. It should be noted that estimations of embryonic length may be 1–5 mm less than equivalent *in vivo* estimates, reflecting the shrinkage caused by the fixation procedures that are inevitably used in embryological studies. O’Rahilly & Müller (2000) have revised some of the ages that were previously assigned to early embryonic stages, pointing out that inter-embryonic variation may be greater than had been thought and that consequently some ages may have been underestimated. They note that as a guide, the age of an embryo can reasonably be estimated from the embryonic length within the range 3–30 mm, by adding 27 to the length. Correlating the age of any stage of development to an approximate day may be unreliable, and a generalization using the number of weeks of development might be now more appropriate.

The stages of development encompass all aspects of internal and external morphogenetic change that occur within the embryo within the duration of the stage. They are used to convey a snapshot of the status of the development of all body systems within a particular timeframe. Figure 14.1 shows the external appearance of embryos from stage 6 to stage 23, with details of their size and age in days. The correlation of external appearance of the embryo with internal development is shown in Fig. 14.2.

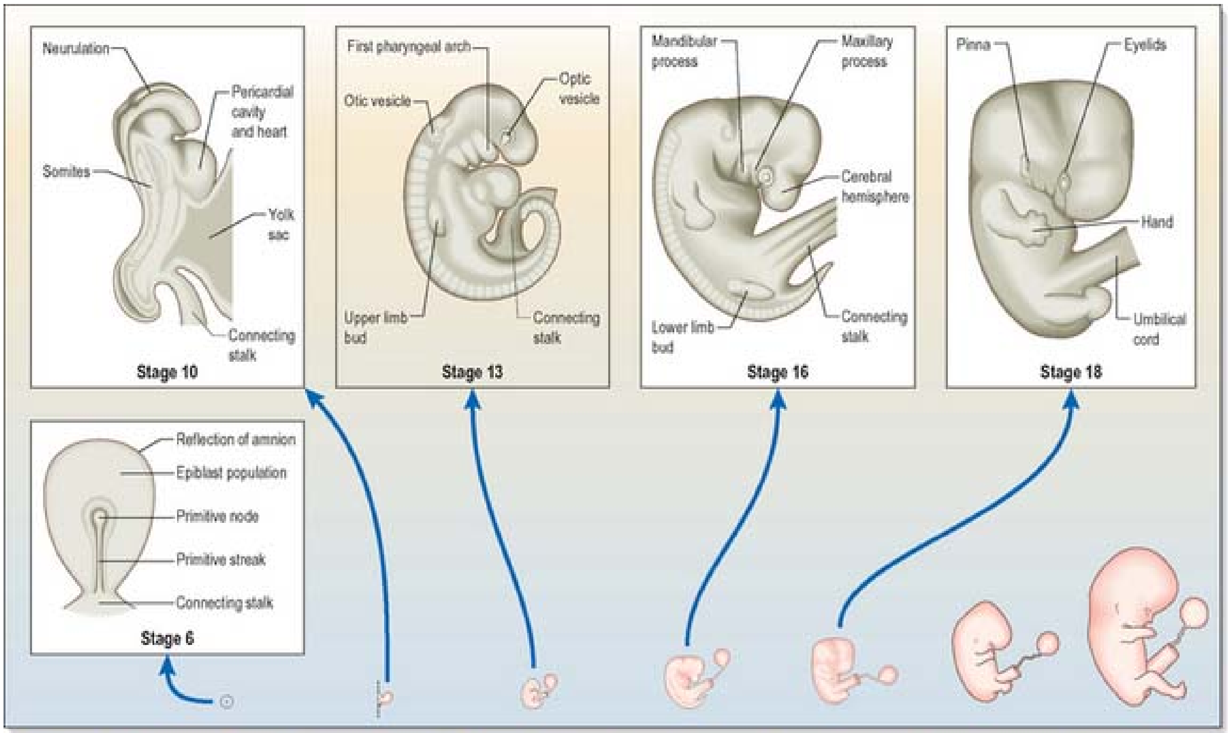
Neurulation
Pericardial cavity and heart
Somites
Yolk sac
Connecting stalk
Stage 10
First pharyngeal arch
Otic vesicle
Optic vesicle
Upper limb bud
Connecting stalk
Stage 13
Mandibular process
Maxillary process
Cerebral hemisphere
Lower limb bud
Connecting stalk
Stage 16
Pinna
Eyelids
Hand
Umbilical cord
Stage 18
Reflection of amnion
Epiblast population
Primitive node
Primitive streak
Connecting stalk
Stage 6

Embryonic stage	6	10	13	16	18	20	23
Size (mm)	0.4	1.5–3	4–6	8–11	13–17	21–23	28–30
Approximate age (days)	16–18	26–29	30–33	35–40	41–45	46–50	53–58

Fig. 14.1 The external appearance and size of embryos between stages 6 and 23. Early in development, external features are used to describe the stage, e.g. somites, pharyngeal arches or limb buds.

(Adapted by permission from Rodeck CH, Whittle MJ 1999 Fetal Medicine. London: Churchill Livingstone.)

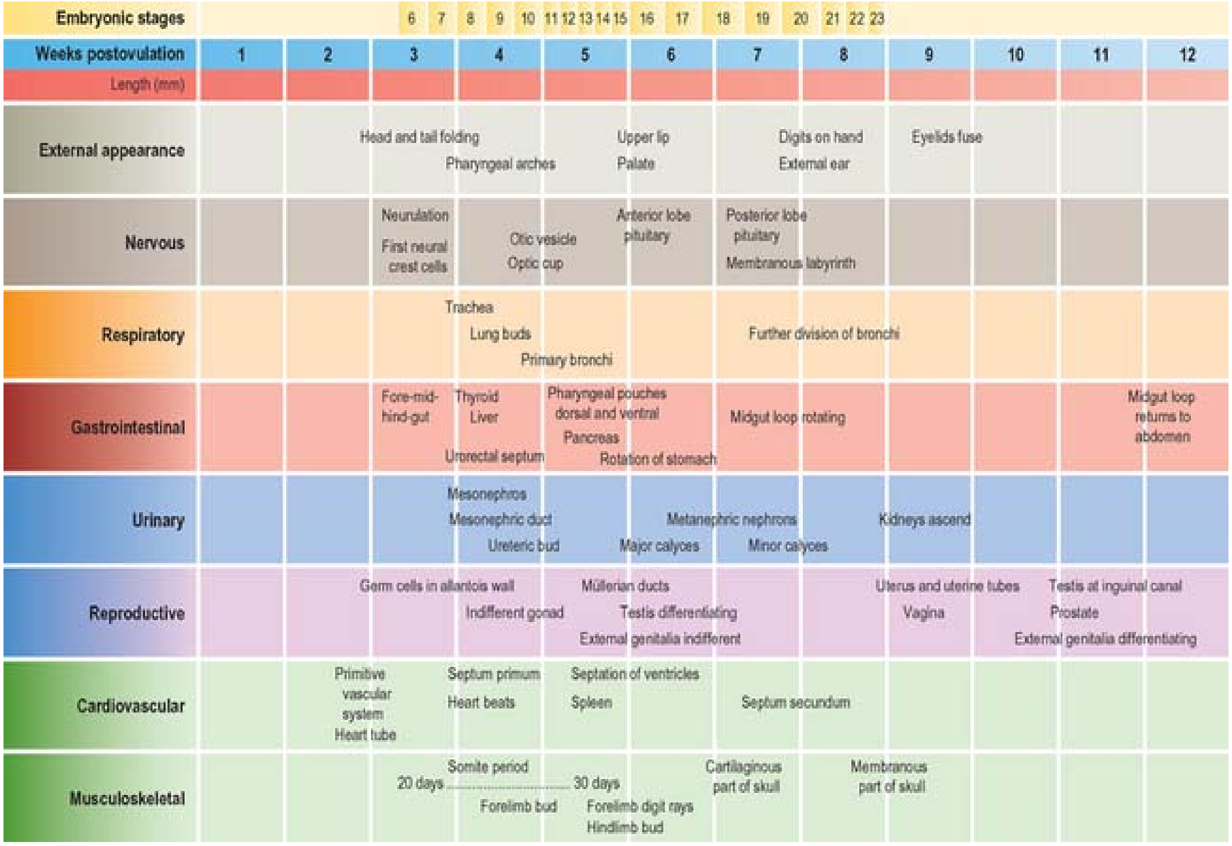

Fig. 14.2 Timetable of development of the body systems. The development of individual systems can be seen progressing from left to right. Embryonic stages, weeks of development and embryo length are shown. Embryonic stages are associated with external and internal morphological features rather than embryonic length. To identify the systems and organs at risk at any time of development, follow a vertical progression from top to bottom.

Obvious external features provide some guidance to the changes occurring within embryos during successive stages. Somite number is related to early embryonic stages and once the number of somites is too great to count with accuracy, the degree of development of the pharyngeal arches is often used. External staging becomes more obvious when the limb buds appear. The upper limb bud is clearly visible at stage 13, and by stage 16 the acquisition of a distal paddle on the upper limb bud is characteristic. At stage 18 the lower limb bud now has a distal paddle, whereas the upper limb bud has digit rays that are beginning to separate. By stage 23, the embryo has a head that is almost erect and rounded, and eyelids are beginning to form. The limbs look far more in proportion and fingers and toes are separate. At this stage the external genitalia are well developed, although they may not be sufficiently developed for the accurate determination of the sex.

Historically, the onset of bone marrow formation in the humerus was used by Streeter to indicate the end of the embryonic and the beginning of the fetal period of prenatal life. The fetal period occupies the remainder of intrauterine life: growth is accentuated, although differentiative processes continue up to and beyond birth. Overall, the fetus increases in length from 30 mm to 500 mm, and increases in weight from 2–3 g to more than 3000 g.

Fetal staging

Currently there is no satisfactory system of morphological staging of the fetal period of development, and the terminology used to describe this time period reflects this confusion. The terms ‘gestation’, ‘gestational age’ and ‘gestational weeks’ are considered ambiguous by O’Rahilly & Müller (2000) who recommend that they should be avoided. However, they are widely used colloquially within obstetric practice. Staging of fetal development and growth is based on an estimate of the duration of a pregnancy. Whereas development of a human from fertilization to full term averages 266 days, or 9.5 lunar months (28 day units), the start of pregnancy is traditionally determined clinically by counting days from the last menstrual period; estimated in this manner, pregnancy averages 280 days, or 10 lunar months (40 weeks). Figure 14.3 shows the embryonic timescale used in all descriptions of embryonic development and the obstetric timescale used to gauge the stage of pregnancy. Studies that discuss fetal development and the gestational age of neonates, particularly those born before 40 weeks’ gestation, use the clinically estimated stages and age unless they specifically correct for this. If a fetal ageing system is used, it must be remembered that the age of the fetus may be 2 weeks more than a comparable fetus that has been aged from postovulatory days.

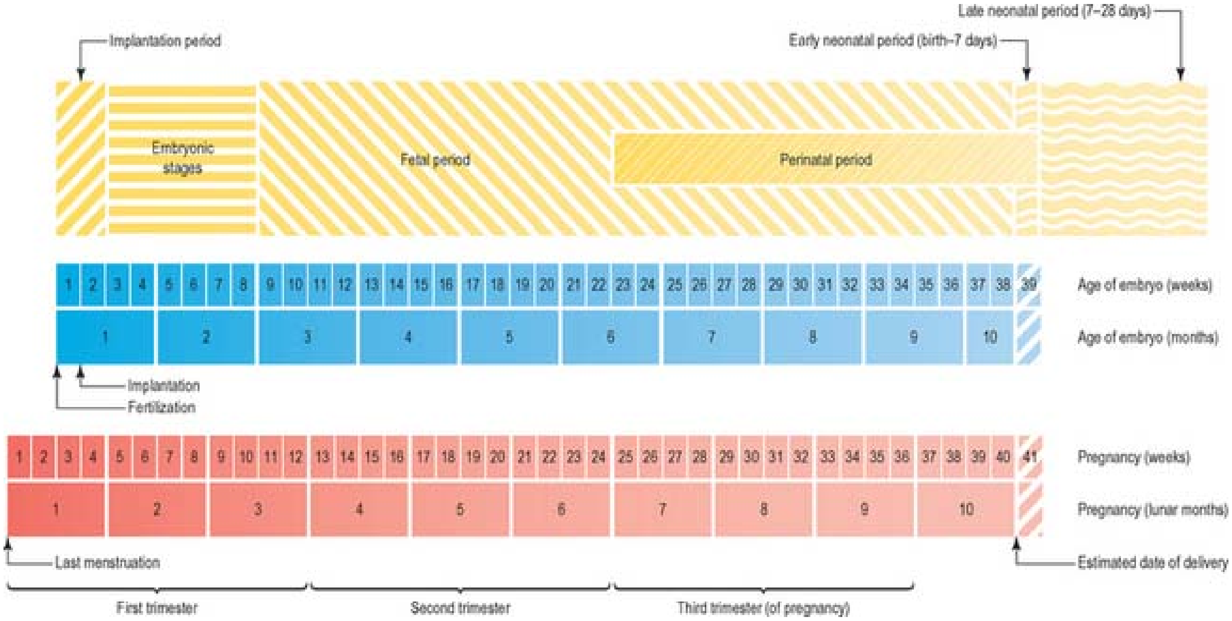
Implantation period
Late neonatal period (7–28 days)
Early neonatal period (birth–7 days)
Embryonic stages
Fetal period
Perinatal period
Age of embryo (weeks)
Age of embryo (months)
Implantation
Fertilization
Pregnancy (weeks)
Pregnancy (lunar months)
Last menstruation
Estimated date of delivery
First trimester
Second trimester
Third trimester (of pregnancy)

Fig. 14.3 The two timescales used to depict human development. Embryonic development, in the upper scale, is counted from fertilization (or from ovulation, i.e. in postovulatory days; see O'Rahilly & Müller 1987). Throughout this book, times given for development are based on this scale. The clinical estimation of pregnancy is counted from the last menstrual period and is shown on the lower scale; throughout this book, fetal ages relating to neonatal anatomy and growth will have been derived from the lower scale. Note that there is a 2-week discrepancy between these scales. The perinatal period is very long, because it includes all preterm deliveries.

The predicted date of full term and delivery is revised after routine ultrasound examination of the fetus. Early ultrasound estimation of gestation increases the rate of reported preterm delivery (delivery at <37 weeks) compared with estimation based on the date of the last menstrual period (Yang et al 2002), possibly because delayed ovulation is more frequent than early ovulation: the predicted age of a fetus estimated from the date of the last menstrual period may differ by more than 2 weeks from estimates of postfertilization days.

A number of biometric indices used to determine fetal growth *in utero* have been evaluated ultrasonographically; the consensus appears to be that some revision of fetal gestational age may be required when using charts based on fetal biometry, and that using fewer biometric variables for the estimation produces a larger standard error. First-trimester growth charts based on biparietal diameter, head circumference and abdominal circumference of normal singleton fetuses correlated against crown–rump length (from 45 to 84 mm) are said to be more accurate than gestational age (Salomon et al 2003). O’Rahilly & Müller (2000) recommend that the term ‘crown–rump length’ should be replaced by greatest length, exclusive of lower limbs in ultrasound examination. Femur length/head circumference ratio may be a more robust ratio to characterize fetal proportions than femur length/biparietal diameter (Johnsen et al 2005), and combining kidney length, biparietal diameter, head circumference and femur length also increases the precision of dating (Konje et al 2002). Johnsen et al (2004) reported that analysis of measurements of biparietal diameter and head circumference at 10–24 weeks gestation gave a gestational age assessment of 3–8 days greater than charts in present use.

Constructions of ultrasound biometry charts for fetal aging now take into account the ethnic population under consideration and it is recommended that locally developed charts specific to the population should be used. The use of these charts means that factors that may influence fetal biometry, including maternal age and nutritional status, can be identified, facilitating accurate prediction of small-for-date and growth-retarded fetuses.

Although accurate morphological stages are not available for the fetal period, the developmental progression is broadly clear. During the fourth and fifth months, the fetus has a head and upper limbs that are still disproportionately large. Although the rates of growth of the trunk and lower limbs increase during the remainder of intra-uterine life, the disproportion is present after birth and, to a diminishing degree, is retained throughout childhood and on into the years of puberty. A covering of primary hair, lanugo, appears. Towards the end of this period, sebaceous glands become active; the sebum that is secreted blends with desquamated epidermal cells to form a cheesy covering over the skin, the vernix caseosa, that is usually considered to protect the skin from maceration by the amniotic fluid. About this time the mother, becomes conscious of fetal movement, formerly termed ‘quickening’.

In the sixth month, the lanugo darkens, the vernix caseosa is more abundant and the skin becomes markedly wrinkled. The eyelids and eyebrows are now well developed. During the seventh month, the hair of the scalp is lengthening and the eyebrow hairs and the eyelashes are well developed. The eyelids themselves separate and the pupillary membrane disappears. The body becomes more plump and rounded in contour and the skin loses its wrinkled appearance as a result of the increased deposition of subcutaneous fat. Fetal length has increased to approximately 350 mm and weight to about 1.5 kg. Towards the end of this month the fetus is viable: if born prematurely it is able to survive without the technological assistance found in Neonatal Intensive Care Units and its postnatal development can proceed normally.

Throughout the remaining lunar months of normal gestation, the covering of vernix caseosa is prominent. There is a progressive loss of lanugo, except for the hairs on the eyelids, eyebrows and scalp. The bodily shape is becoming more infantile but, despite some acceleration in its growth, the leg has not quite equalled the arm in length proportionately, even at the time of birth. The thorax broadens relative to the head, and the infra-umbilical abdominal wall shows a relative increase in area, so that the umbilicus gradually becomes more centrally situated. Average lengths and weights for the eighth, ninth and tenth months are 40, 45 and 50 cm and 2, 2.5 and 3–3.5 kg, respectively. The rate of fetal growth slows from 36 to 40 weeks in response to the physical limitation imposed by the maternal uterus. Birth weight thus reflects the maternal environment more than the genotype of the child. This slowing of the growth rate enables a genetically larger child developing within a small mother to be delivered successfully. After birth, the growth rate of the neonate increases and the rate of weight gain, reaches a peak some 2 months postnatally.

Just before birth, the lanugo almost disappears, the umbilicus is central. The testes, which begin to descend with the processus vaginalis of peritoneum during the seventh month and are approaching the scrotum in the ninth month, are usually scrotal in position. The ovaries are not yet in their final position at birth; although they have attained their final relationship to the uterine folds, they are still above the level of the pelvic brim.

Obstetric stages

In obstetric practice the duration of the period of gestation is regarded as nine calendar months, which is approximately 270 days. The period of pregnancy is divided into thirds, termed trimesters. The first and second trimesters each cover a period of 12 weeks, and the third trimester covers the period from 24 weeks to delivery. Although the expected date of delivery is computed at 40 weeks of pregnancy, the term of the pregnancy, i.e. its completion resulting in delivery, is considered normal between 37 and 42 weeks. Neonates delivered before 37 weeks are called preterm (or premature); those delivered after 42 weeks are post-term. The period from the end of week 24 and up to 7 days after birth, is termed the perinatal period. Fetuses that are delivered and die before 24 weeks are considered to be miscarriages of pregnancy, although technological advances in neonatal care can now assist the delivery and support of infants younger than 24 weeks. Infants born after 24 weeks of pregnancy which subsequently die are classed as stillborn and contribute to the statistics of perinatal mortality.

THE NEONATE

The neonatal period extends from birth to 28 days postnatally, and is divided into an early neonatal period from birth to 7 days, and a late neonatal period from 7 to 28 days.

In Western societies, technological advances have enabled successful management of preterm infants, many at ages that were considered non-viable a decade or two previously. Maturational processes involving local interactions and pattern formation still drive development at local and body-system levels in preterm infants. The sudden release of such fetuses into a gaseous environment, of variable temperature, with full gravity and a range of microorganisms, promotes the rapid maturation of some systems and the compensatory growth (in terms of responses to the effect of gravity or enteral feeding or exposure to microorganisms), of others. To understand the multitude of mechanisms that operate within a newly delivered fetus, as much information as possible concerning normal embryological and fetal development is required.

Details of the relative positions of the viscera and the skeleton in a full term neonate are shown in Figs 14.4-14.6. The newborn infant is not a miniature adult, and extremely preterm infants are not the same as full-term infants. There are immense differences in the relations of some structures between the full-term neonate, child and adult, and there are also major differences between the 20-week gestation fetus and the 40-week fetus, just before birth. The study of fetal anatomy at 20, 25, 30 and 35 weeks is vital for the investigative and life-saving procedures carried out on preterm infants today.

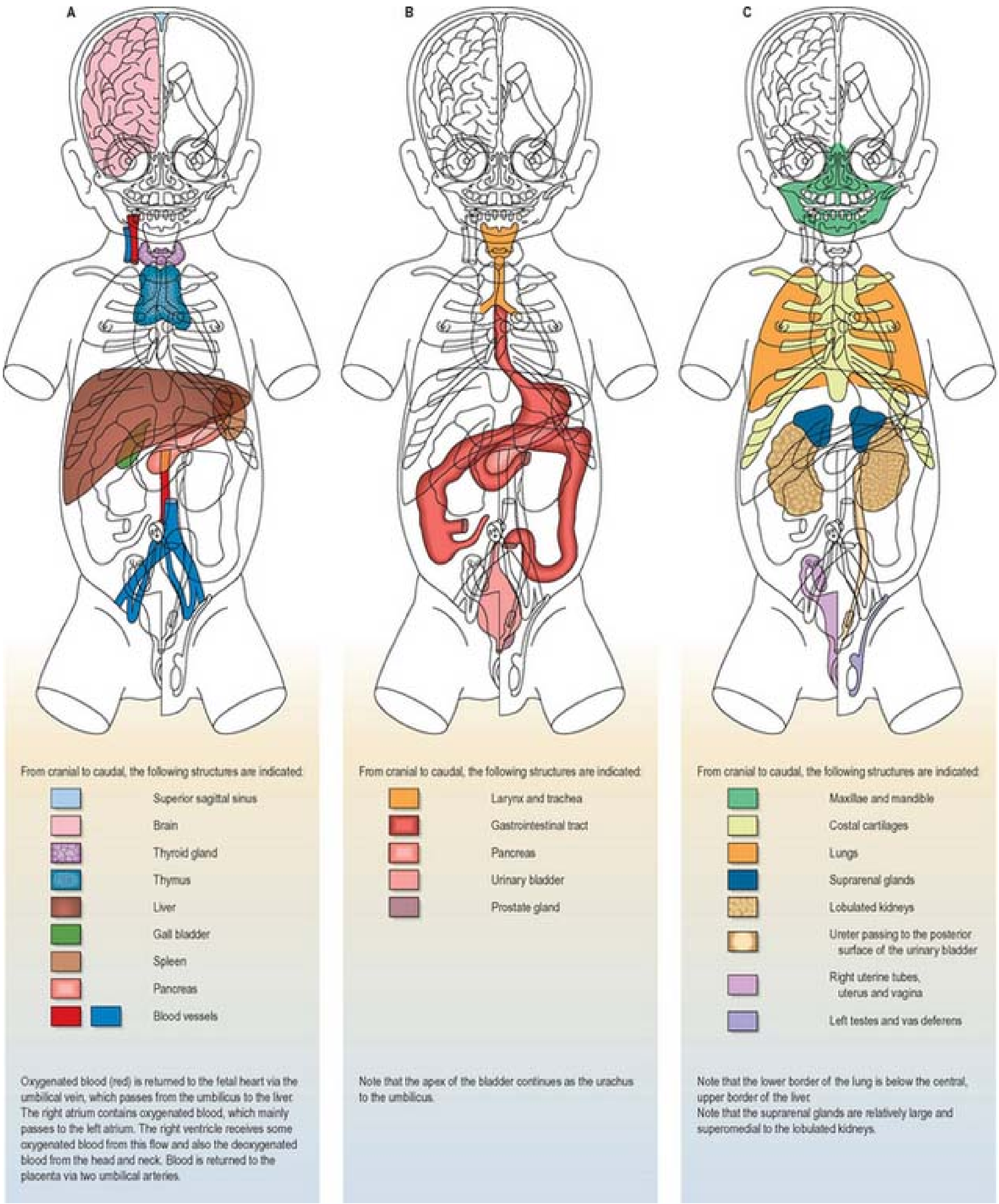

A
B
C
From cranial to caudal, the following structures are indicated:
Superior sagittal sinus
Brain
Thyroid gland
Thymus
Liver
Gall bladder
Spleen
Pancreas
Blood vessels
From cranial to caudal, the following structures are indicated:
Larynx and trachea
Gastrointestinal tract
Pancreas
Urinary bladder
Prostate gland
From cranial to caudal, the following structures are indicated:
Maxillae and mandible
Costal cartilages
Lungs
Suprarenal glands
Lobulated kidneys
Ureter passing to the posterior surface of the urinary bladder
Right uterine tubes, uterus and vagina
Left testes and vas deferens

Oxygenated blood (red) is returned to the fetal heart via the umbilical vein, which passes from the umbilicus to the liver. The right atrium contains oxygenated blood, which mainly passes to the left atrium. The right ventricle receives some oxygenated blood from this flow and also the deoxygenated blood from the head and neck. Blood is returned to the placenta via two umbilical arteries.

Note that the apex of the bladder continues as the urachus to the umbilicus.

Note that the lower border of the lung is below the central, upper border of the liver.
Note that the suprarenal glands are relatively large and superomedial to the lobulated kidneys.

Fig. 14.4 **A–C**, Topographical representation of the anatomy of a full-term neonate. The surface markings of all organs are shown, with some coloured and others only in outline. The female genital tract is shown on the right of the body, with the male tract on the left.

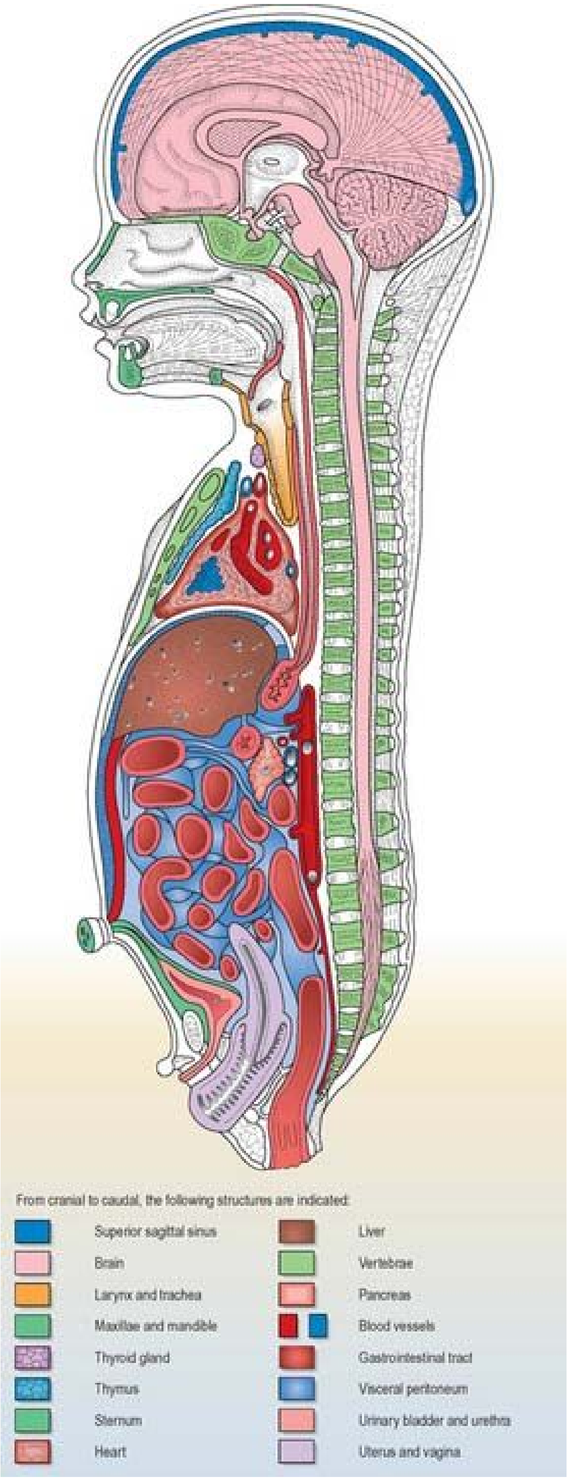
From cranial to caudal, the following structures are indicated:
Superior sagittal sinus
Brain
Larynx and trachea
Maxillae and mandible
Thyroid gland
Thymus
Sternum
Heart
Liver
Vertebrae
Pancreas
Blood vessels
Gastrointestinal tract
Visceral peritoneum
Urinary bladder and urethra
Uterus and vagina

Fig. 14.5 Topographical representation of the anatomy of a full-term female neonate. The cut surfaces of the organs are the same colours as in Fig. 14.4.

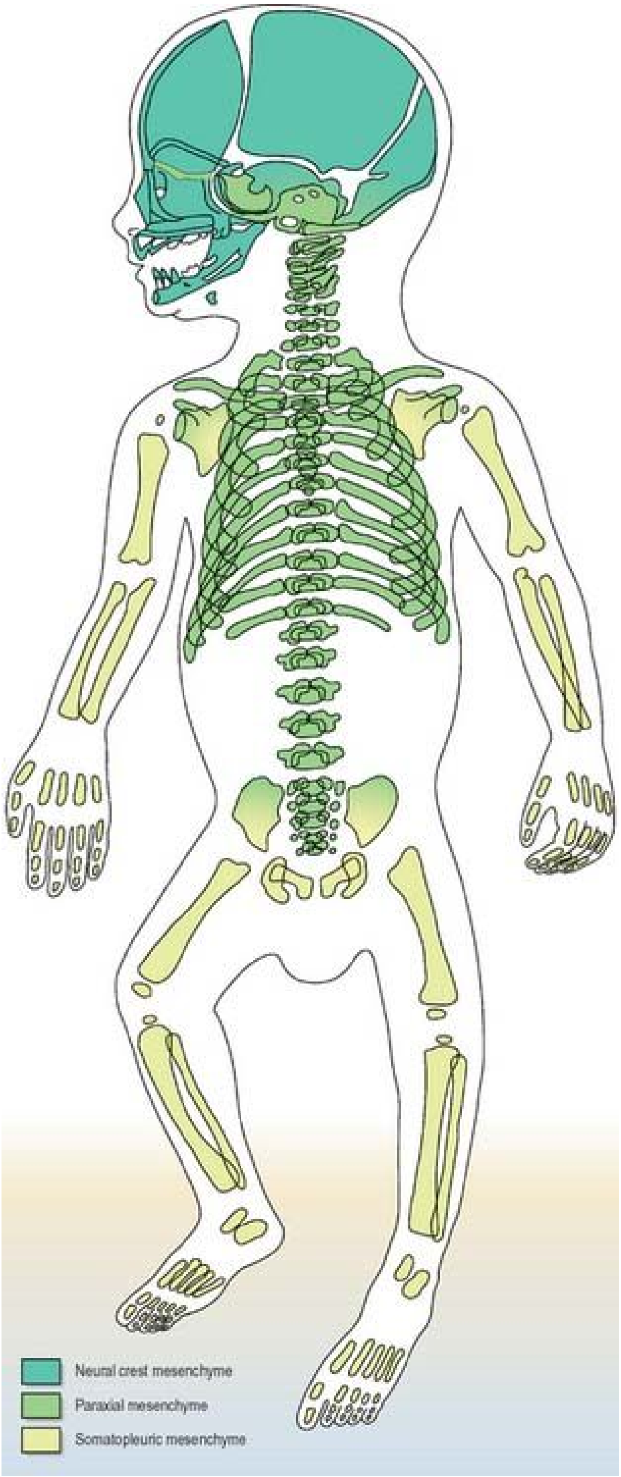
Neural crest mesenchyme
Paraxial mesenchyme
Somatopleuric mesenchyme

Fig. 14.6 The extent of the ossified skeleton in the full term neonate. Note the derivation of the parts of the skeleton: the skull is derived from paraxial mesenchyme and neural crest mesenchyme; the axial skeleton, vertebrae and ribs are derived from paraxial mesenchyme; the skeletal elements in the

limbs are derived from the somatopleuric mesenchyme, which forms the limb buds.

Neonatal measurements and period of time *in utero*

The 10th to 90th centile ranges for length of full-term neonates are 48–53 cm (Fig. 14.7A). Length of the newborn is measured from crown to heel. *In utero*, length has been estimated either from crown–rump length, i.e. the greatest distance between the vertex of the skull and the ischial tuberosities, with the fetus in the natural curved position, or from the greatest length exclusive of the lower limbs. Greatest length is independent of fixed points and thus much simpler to measure. It is generally taken to be the sitting height in postnatal life, and is the measurement recommended by O'Rahilly & Müller (2000) as the standard in ultrasound examination. The 10th to 90th centile ranges for weight of the full-term infant at parturition ranges are 2700–3800 g (Fig. 14.7B), the average being 3400 g; 75–80% of this weight is body water and a further 15–28% is composed of adipose tissue. After birth, there is a general decrease in the total body water, but a relative increase in intracellular fluid. Normally, the newborn loses about 10% of its birth weight by 3–4 days postnatally, because of loss of excess extra-cellular fluid and meconium. By 1 year, total body water makes up 60% of the body weight.

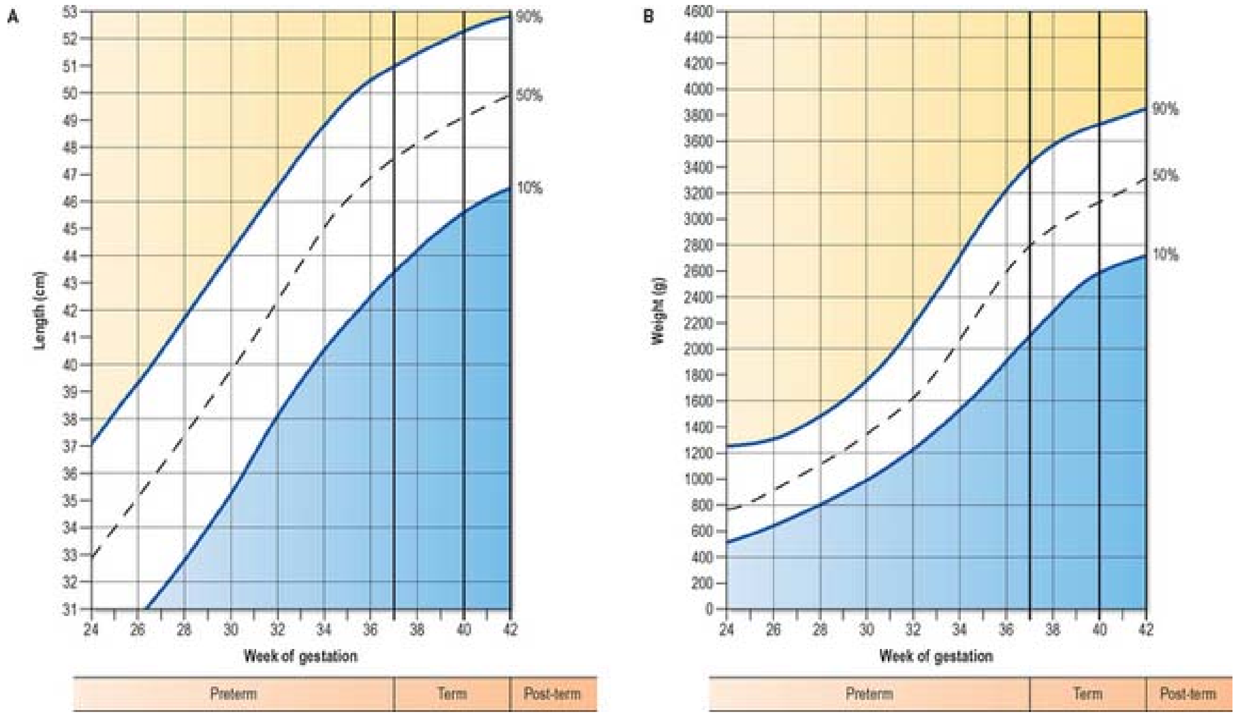

Fig. 14.7 Standardized graphs of (**A**) fetal length and (**B**) weight from 24 weeks of pregnancy, showing the 10th, 50th and 90th centiles.

Low birth weight has been defined as less than 2500 g, very low birth weight as less than 1500 g, and extremely low birth weight as less than 1000 g. Infants may weigh less than 2500 g but not be premature by gestational age. Measurement of the range of weights that fetuses may attain before birth has led to the production of weight charts, which allow babies to be described according to how appropriate their birth weight is for their gestational age, e.g. small for gestational age, appropriate for gestational age or large for gestational age (Fig. 14.8). Small for gestational age infants, also termed ‘small-for-dates’, are often the outcome of intrauterine growth retardation. The causes of growth restriction are many and various and beyond the scope of this text.

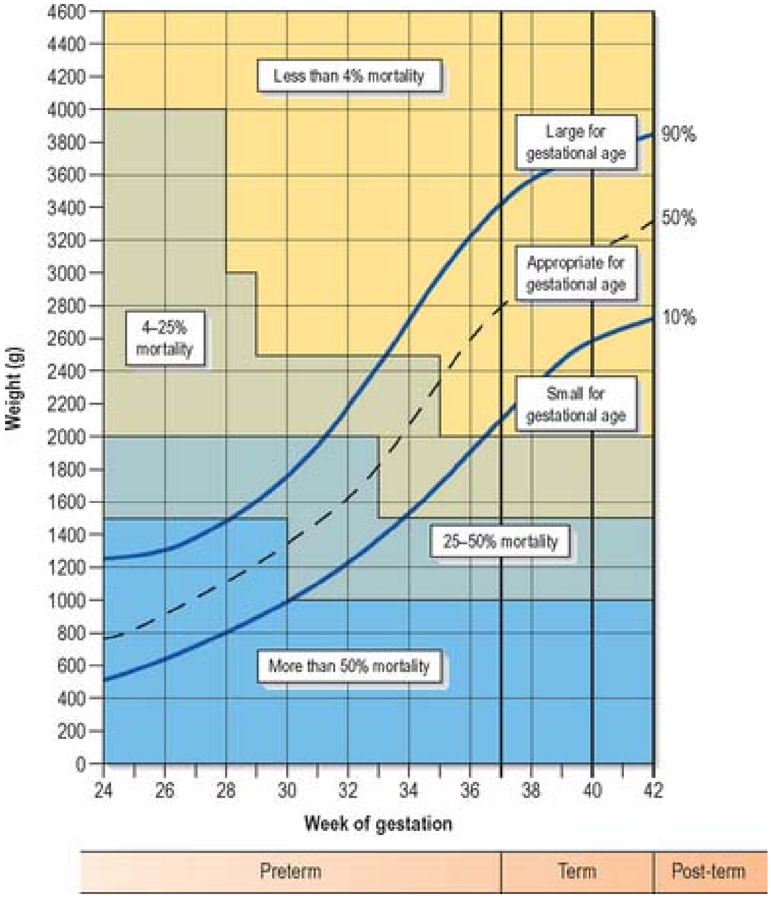

Fig. 14.8 Intrauterine growth status and its appropriateness for gestational age. Gestational age is more closely related to maturity than birth weight. The mortality for the weight ranges is indicated.

For both premature and growth-retarded infants, an assessment of gestational age, which correlates closely with the stage of maturity, is desirable. Gestational age at birth is predicted by its proximity to the estimated date of delivery and the results of ultrasonographic examinations during pregnancy. It is currently assessed in the neonate by evaluation of a number of external physical and neuromuscular signs. Scoring of these signs results in a cumulative score of maturity that is usually within ±2 weeks of the true age of the infant. The scoring scheme has been devised and improved over many years. For an account of methods of assessing gestational age in neonates, consult Gandy (1992).

INTEGRATION OF TYPES OF GROWTH DURING DEVELOPMENT

In the later prenatal months and in the postnatal period, the various types of growth occur in differing patterns. The extent of tissue growth in organs depends on the specific duration of multiplicative growth for the cell types (Fig. 14.9). Different cell populations complete their initial developmental proliferation and become differentiated at different times, the final stage of differentiation usually being cessation of cell division.

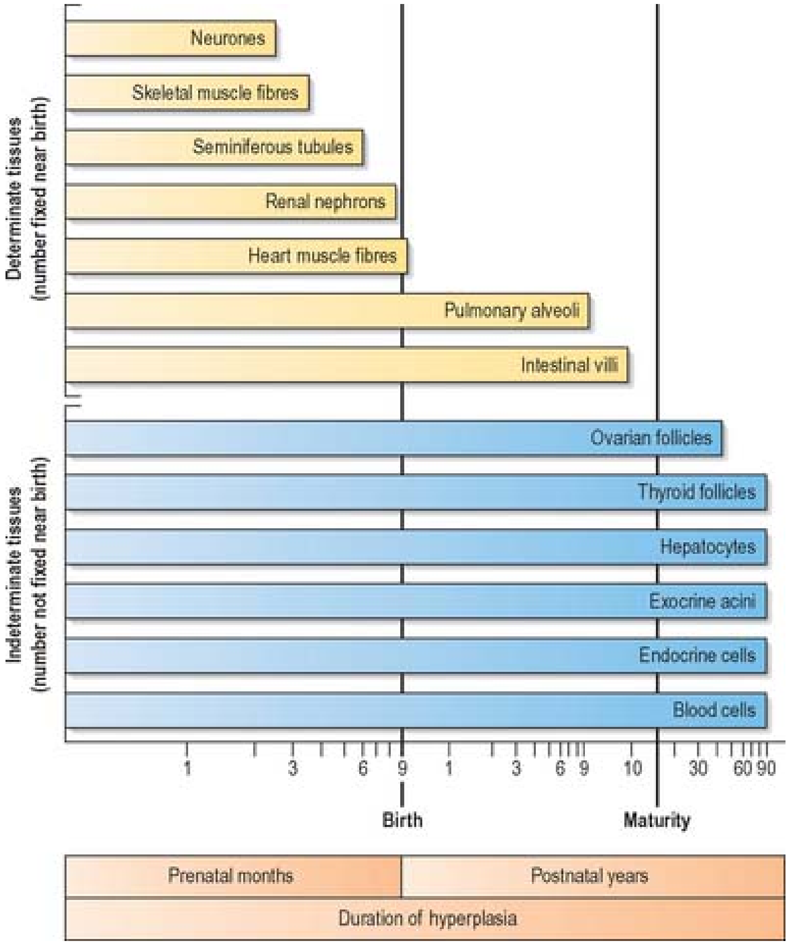

Fig. 14.9 The duration of multiplicative growth for various human tissues.

Growth of a body can be described in two ways, isometric and allometric. Isometric growth implies a progressive proportional increase in all organs and systems with time: it does not occur in the developing embryo, which displays differential rates of growth. Allometric growth describes the differences in the relative rates of growth between one part of the body and another, and is most clearly seen in the changes in body proportion between fetuses, neonates, children and adults. Between 6 and 7 weeks after fertilization, the head is nearly one-half of the total embryonic length. It subsequently grows proportionally more slowly, and at birth it is one-quarter of the entire length. During childhood, this pattern of growth continues with lengthening of the torso and limbs until, in adults, the head is one-eighth the length (Fig. 14.10).

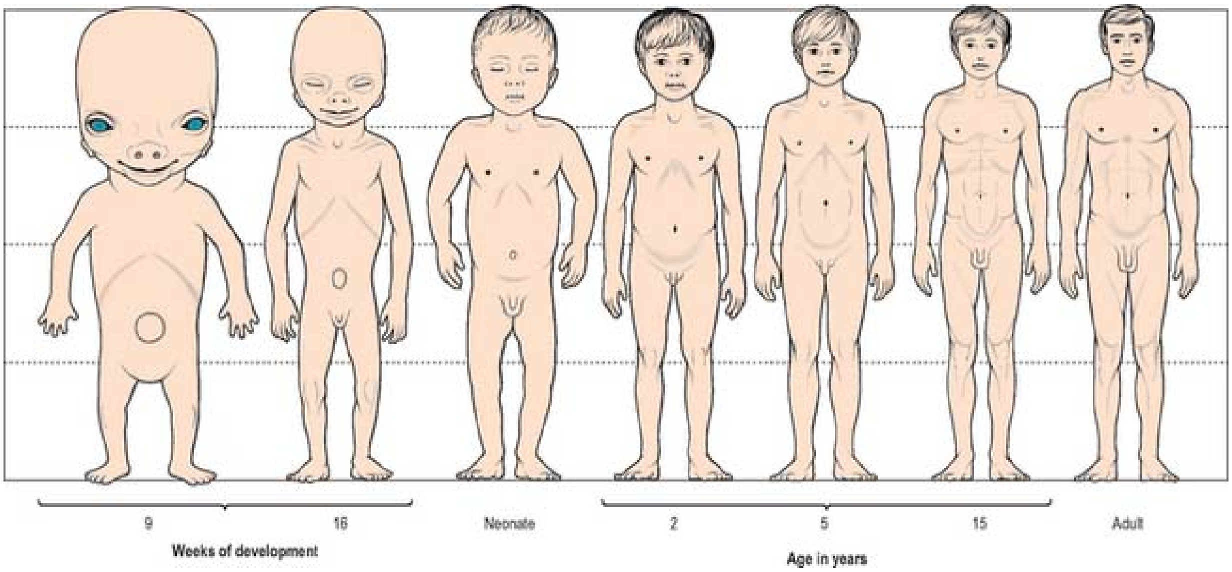

Fig. 14.10 Allometric growth in humans. The head is very large in proportion to the rest of the body during the embryonic period. After this time the head grows more slowly than the torso and limbs and by adulthood the head is only one-eighth of the body length.

Growth of the liver, spleen and kidneys, and skeletal and muscular tissues generally follow pre- and postnatal growth curves given for the entire body. Other tissues have very different growth rates; the brain, skull, lymphoid tissues and reproductive organs all show differing growth rates during childhood and adolescence (Fig. 14.11).

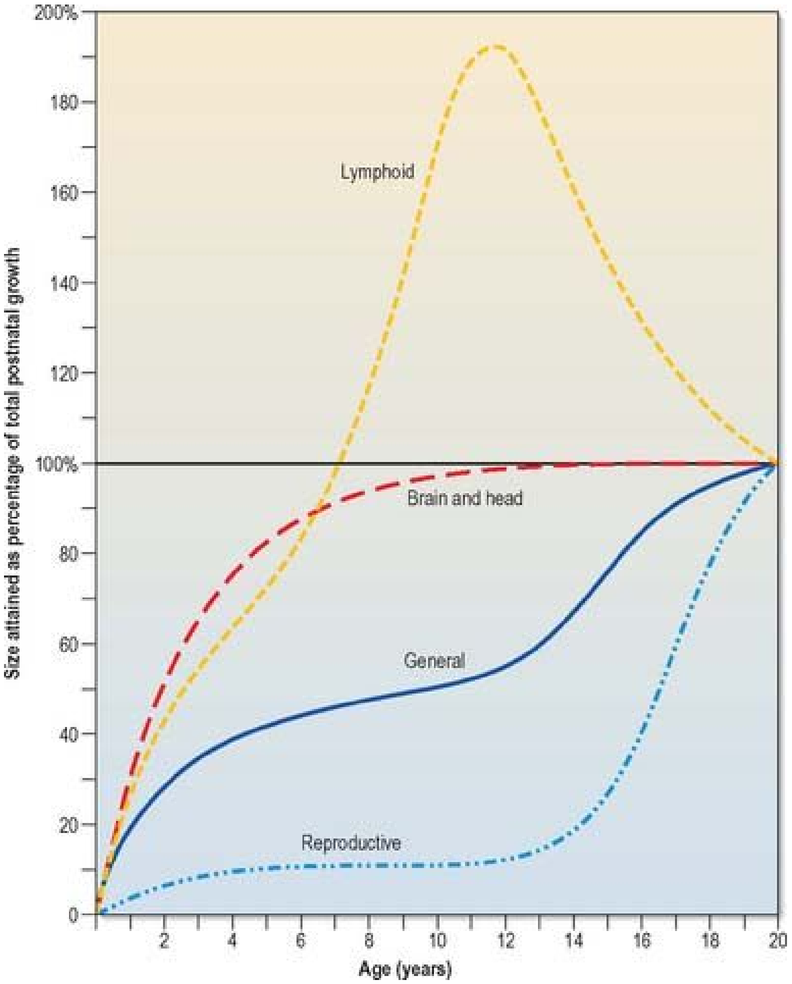

Fig. 14.11 Growth curves of different tissues, regions of the body and systems. Note that the growth of lymphoid tissue, thymus, lymph nodes and intestinal lymph masses decreases after puberty.

(Adapted with permission from Tanner JM 1962 Growth at Adolescence, 2nd edn. Oxford: Blackwell Publishing.)

The amount and distribution of adipose tissue within the body change with age and hormonal status. Subcutaneous fat deposits are estimated by measurements taken by calipers applied to a fold of fat pinched up from the underlying muscles, usually over triceps and beneath the angle of the scapula.

Fat is laid down in the fetus from about 34 weeks, and the amount increases to the 9th postnatal month. After this time subcutaneous fat decreases (i.e. it has a negative growth velocity), until 6–8 years, when it begins to increase again. This early decrease in fat is less marked in girls than in boys so that, after 1 year, girls have more fat than boys. From 7 years the increase in fat occurs in both sexes. At adolescence, the limb fat in boys (triceps measurement) decreases, and is not regained until the late 20s, whereas girls show a slight slowing of the increase in limb fat, but no loss. At this time the trunk fat (subscapular measurement) stops increasing in boys, but shows a steady increase in girls. Postpubertal girls, but not boys, show fat deposits in a secondary sexual distribution, i.e. in the breasts, over the upper arms, lower abdomen and thighs. Adult men are more likely to deposit fat around the anterior abdominal wall.

GROWTH *IN UTERO*

Alterations in the availability of nutrients to the fetus at particular stages of pregnancy elicit adaptive responses by the fetus that ensure fetal coping, but which may result in pathology in adult life: the nutritional status of pregnant women is therefore of fundamental importance for the health of the next generation. For example, poor nutrition at critical stages of fetal life may permanently alter the normal developmental pattern of a range of organs and tissues, e.g. the endocrine pancreas, liver and blood vessels, resulting in their pathological responses to certain conditions in later adult life (Barker et al 1993). An increase in placental size occurs in pregnancy as an adaptive response to both high altitude and mild undernutrition, particularly during mid-pregnancy. However, although a larger placenta may be better able to deliver the full nutritional requirements of the fetus, the perfusion of a larger placenta is not without problems. It may produce changes in fetal blood flow and placental enzymes, and in the normal structure of the fetal vessel wall or of its responses to circulating trophins, e.g. catecholamines or angiotensin II, which will continue into adult life. Undernutrition in later pregnancy does not produce the same sequelae and placental enlargement does not occur. However, fetal growth slows and fetal wasting may occur as oxygen, glucose and amino-acids are redistributed to the placenta to maintain its function.

Maternal starvation during pregnancy decreases fetal IGF-I concentrations, and this may, along with a general hypoglycaemia, impair the development of the fetal β cells of the pancreas. Moreover, fetal undernutrition may induce insulin resistance in the tissues. The coexistence of insulin resistance and impaired β-cell development in the fetus appears to be important in the pathogenesis of non-insulin-dependent diabetes. The risk of developing this ‘type 2’ diabetes is greatest in those individuals with low weight at birth and at 1 year, and who become obese as adults, thus challenging an already impaired glucose–insulin metabolism. Fetal IGF-I concentrations are also lower in infants who are short at birth as a result of a long period of maternal undernutrition: these individuals have an exaggerated responses to growth hormone-releasing factor, which, together with low IGF-I concentrations, suggests a degree of growth hormone resistance.

It is now thought that the balance of hormonal environment in intrauterine and early postnatal life is necessary for future adult health. The presence of altered concentrations of hormones during critical periods of development may act as endogenous functional teratogens (Plagemann 2004).

Different birth phenotypes have been correlated with different pathological sequelae. Infants who are thin at birth, with a low ponderal index (weight/length^3), tend to develop a combination of insulin resistance, hypertension, non-insulin-dependent diabetes and lipid dis-orders, whereas those who are short in relation to head size tend to develop hypertension and high plasma fibrinogen concentrations. These associations have been reported in babies born small for dates, rather than in those born prematurely. Some babies of average weight also develop cardiovascular pathology: they were either small at birth in relation to the size of their placenta, and thin at birth or, although of average weight, were short in relation to head size and had below average weight gain during the first year (Barker et al 1993). For more recent views on this concept the reader is directed to consult Godfrey & Barker (2000) and Gluckman et al (2005).

GROWTH IN CHILDHOOD

The rates of prenatal and postnatal growth can be indicated by increments in body length or weight which, when plotted, form a growth curve (see Fig. 14.7). Growth curves can be plotted for individuals if accurate measurements are taken, preferably by the same person, for the entire period of growth, i.e. a longitudinal study. An alternative method is to collect a series of averages for each year of age obtained from different individuals, i.e. a cross-sectional study. Cross-sectional studies are valuable for the construction of standards for height and weight attained by healthy children at specific ages, and can establish percentile limits of normal growth, but they cannot reveal individual differences in either the rate of growth or the timing of particular phases of growth.

The data from longitudinal and cross-sectional studies can also be used to plot the increments in height or weight from one age to the next. This produces a velocity curve, which reflects a child's state at any particular time much better than the growth curve, in which each point is dependent on the preceding one. The oldest published longitudinal study, still of great value today, was made by Count Philibert de Montbeillard on his son (Fig. 14.12). It shows that the velocity of growth in height decreases from birth onwards, and that a marked acceleration of growth, the adolescent growth spurt, occurs from 13 to 15 years (see below; Fig 14.13).

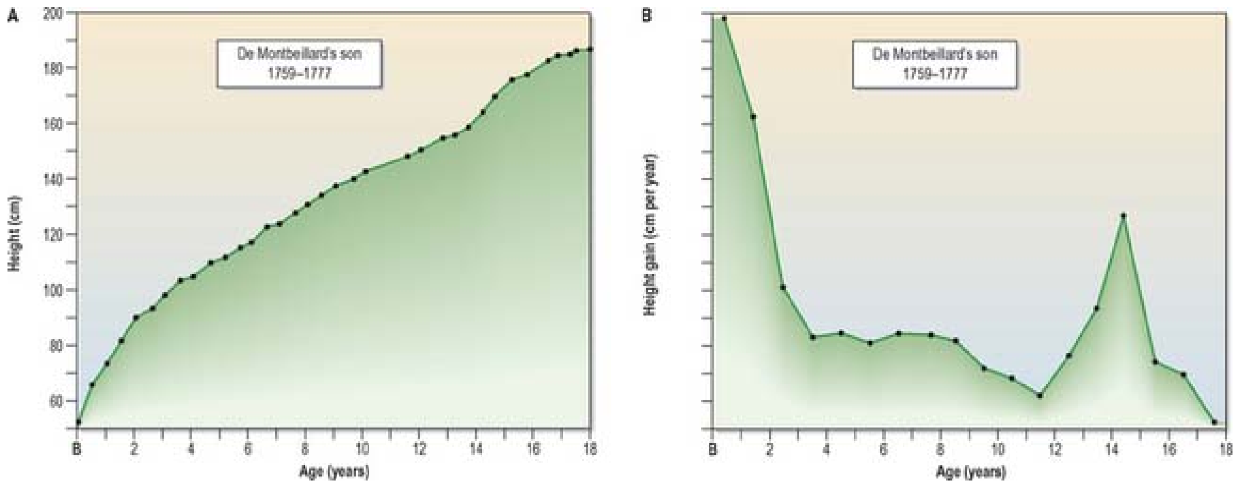

Fig. 14.12 A longitudinal study of growth. **A**, The height of de Montbeillard’s son (1759–1777) from birth to 18 years. **B**, A growth velocity curve, plotting increments in height from year to year.

(After D’Arcy Thompson, On Growth and Form, 1942, Cambridge University Press.)

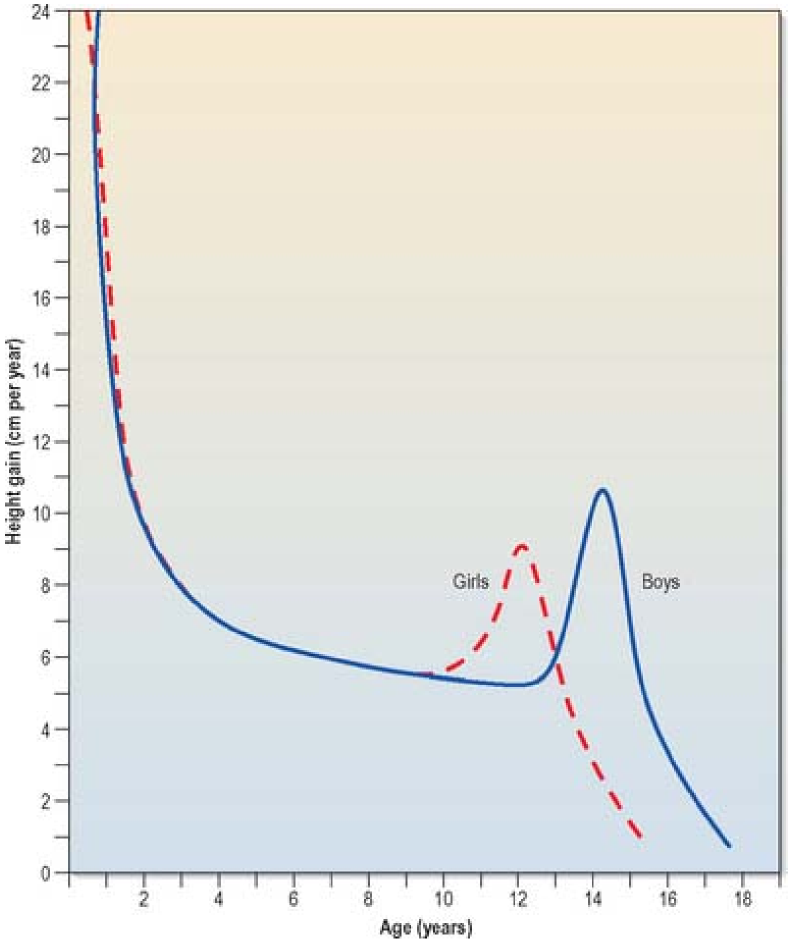

Fig. 14.13 Typical individual velocity curves for height: English boys and girls.

(After Tanner JM, Whitehouse RH, Takaishi IM 1966 Standards from birth to maturity for height, weight, height velocity and weight velocity. Arch Dis Child 41: 454–71, with permission from BMJ Publishing.)

Cross-sectional data permit comparison of prenatal and postnatal growth. Childhood growth charts are used to predict normal childhood development. The velocity curve for the prenatal and postnatal period (Fig. 14.14) shows that the peak velocity for length is reached at about 4 months (note that these prenatal charts use the obstetric measurements of gestational time, in which fetal age is estimated from the last menstrual period, 2 weeks before fertilization). Growth in weight usually reaches its peak velocity after birth.

Rights were not granted to include this figure in electronic media.
Please refer to the printed publication.

Fig. 14.14 Cross-sectional data showing growth in length in the prenatal and early postnatal period (**A**) and the corresponding velocity curve for this period (**B**).

(After D'Arcy Thompson, On Growth and Form, 1942, Cambridge University Press.)

Growth has always been regarded as a regular process. Tanner (in Harrison et al 1964) noted that the more carefully measurements are taken, the more regular is the succession of points on a growth curve. However, a longitudinal study of growth measured weekly, semi-weekly and daily, recorded that growth in length and head circumference occurred by saltatory increments, with a mean amplitude of 1.01 cm for length (Lampl 2002);

growth stasis, steep changes in growth and incremental growth have all been recorded in infancy, childhood and adolescence (Caino et al 2006).

Charts of height and weight correlated to age are compiled from extensive cross-sectional growth studies. Such charts show the mean height or weight attained at each age, termed the 50th centile, and also the centile lines for the 75th, 90th and 97th centiles, in addition to the 25th, 9th and 2nd centiles. The data shown in Fig. 14.15 are derived from United Kingdom cross-sectional references. Any comparison of an individual growth curve with these data must also take into account ethnicity and the nutritional and family history of that individual.

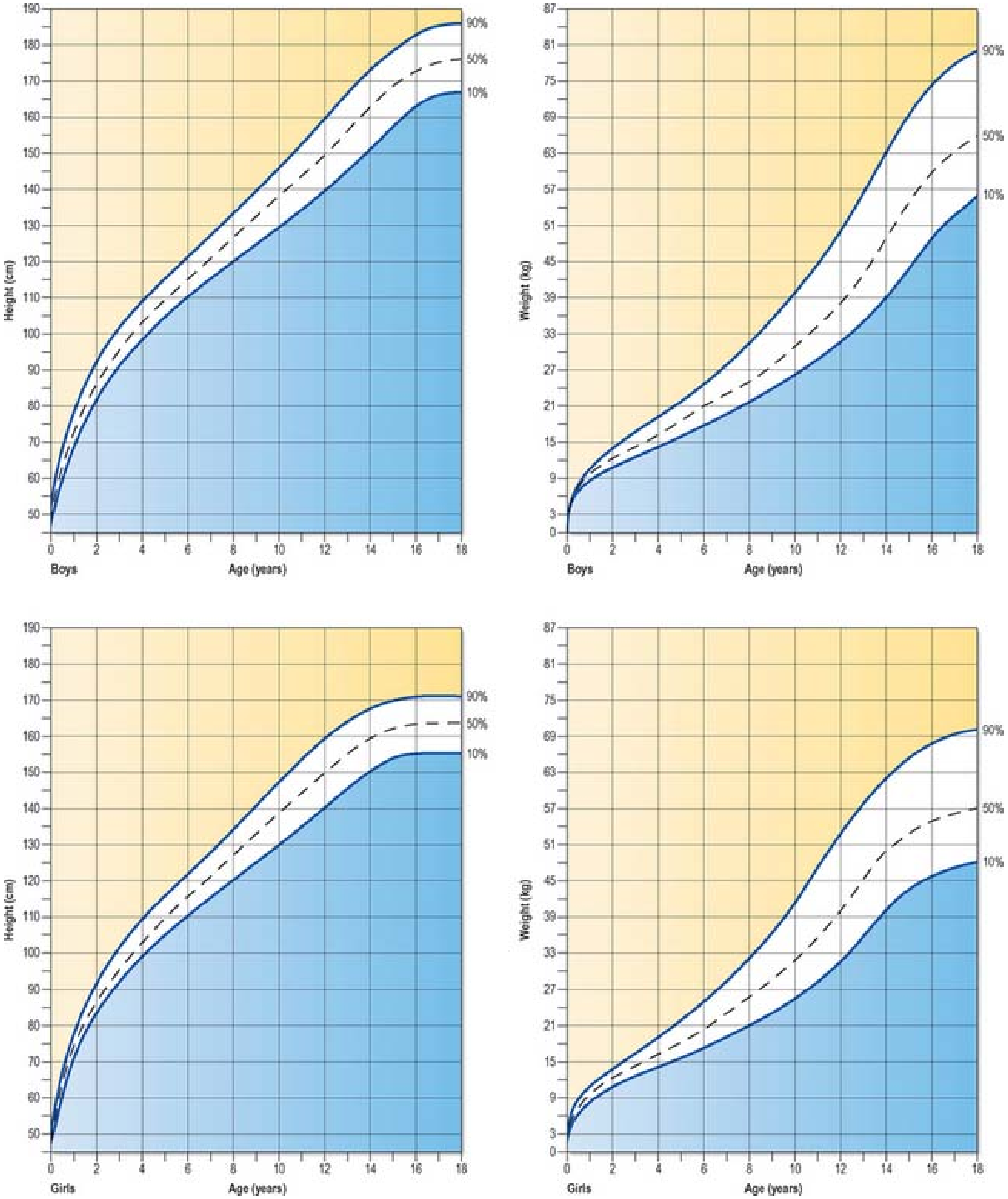

Fig. 14.15 Standard growth charts of boys and girls showing the 90th, 50th and 10th centiles.

(© Child Growth Foundation.)

Plotting the growth of children on such charts provides guidelines for the prediction of normal growth and indicates when investigation of possible growth abnormalities should occur. Children who grow in an environment that does not constrain their growth exhibit a pattern of growth that is mainly parallel to a particular centile, a phenomenon that has been termed homeorhesis or canalization (following the same imaginary ‘canal’ on the growth chart). After deviation from this centile as a consequence of the adolescent growth spurt, most children return to the same centile position in adulthood, a finding that suggests that this pattern is genetically determined within individuals (Cameron 2002). For a comprehensive account on all aspects of postnatal growth the reader is directed to consult Human Growth and Development (Cameron 2002).

ADOLESCENT GROWTH SPURT

Growth charts reveal that body length increases from a neonatal range of 48–53 cm to about 75 cm during the first year after birth, and increases by 12–13 cm in the second year. Thereafter, 5–6 cm is added each year. In individual longitudinal growth curves, an increase in the velocity of growth occurs between 10.5 and 11 years in girls, and 12.5 and 13 years in boys. This rapid increase in growth is the adolescent growth spurt (Figs 14.13 and 14.15). In both sexes it lasts for 2–2.5 years. Girls gain about 16 cm in height during the spurt, with a peak velocity at 12 years of age. Boys gain about 20 cm in height (mostly by growth of the trunk), with a peak velocity at 14 years of age, during which time they may be growing at the rate of 10 cm a year.

Humans seem to be the only species to have a long quiescent interval between the rapid growth that takes place immediately after birth and the adolescent growth spurt. It has been suggested that this period allows the brain to mature, and learning to take place, before individuals pass through puberty and become sexually active.

Growth in height continues at a slower rate after the adolescent growth spurt. Noticeable growth is said to stop at 18 years in females and 20 years in males (longitudinal studies have indicated that an average figure for this is 16.25 years for girls and 17.75 years for boys, with a normal variation of ±2 years (Harrison et al 1964)). After this time, any increments that occur as a result of appositional growth at the cranial and caudal ends of the vertebral bodies and intervening intervertebral discs are so small as to be difficult to measure. There is a loss of height after middle age.

The phenomenal growth rates of adolescence are most obvious in the increase in height. Weight gain is more variable. At birth, weight reflects the maternal environment, the number of conceptuses, the sex of the baby and the parity of the mother. Generally, full-term female babies are lighter than full-term males, twins are lighter than singletons, and later children tend to be heavier than the first-born. Although the birth weight seems to be independent of the maternal diet, unless there has been severe malnutrition, mothers in lower socioeconomic groups have smaller babies than those with a higher rating, and small mothers tend to have small babies.

The birth weight is normally tripled by the end of the first year, and quadrupled by the end of the second year. Thereafter, weight increases by 2.25–2.75 kg annually until the adolescent growth spurt, when boys may add 20 kg to their weight and girls 16 kg. The peak velocity for weight gain lags behind the peak velocity for height by about 3 months. Body weight does not reach adult values until some time after adult height is attained.

REFERENCES

arker DJP, Osmond C, Simmonds SJ, Wield GA. The relation of head size and thinness at birth to death from cardiovascular disease in adult life. *BMJ*. 1993;306:422-426.

Provides evidence for a link between birth weight and size and predictions of later cardiovascular pathology..

aino S, Kelmansky D, Adamo P, Lejarraga H. Short-term growth in healthy infants, schoolchildren and adolescent girls. *Ann Hum Biol*. 2006;33:213-226.

ameron N. Human Growth and Development. New York: Academic Press, 2002.

andy GM. Examination of the neonate including gestational assessment. In: Robertson NRC, editor. *Textbook of Neonatology*. Edinburgh: Churchill Livingstone; 1992:199-215.

Presents the maturation dates of physical characteristics used in the assessment of gestational age of the neonate..

uckman PD, Hanson MA, Morton SM, Pinal CS. Life-long echoes: a critical analysis of the developmental origins of adult disease model. *Biol Neonate*. 2005;87:127-139.

odfrey KM, Barker DJ. Fetal nutrition and adult disease. *Am J Clin Nutr*. 2000;71:1344S-1352S.

arrison GA, Weiner JS, Tanner JM, Barnicot NA. Human Biology. Oxford: Clarendon Press, 1964. Ch. 19.

Presents data on the human growth curve..

hnsen SL, Rasmussen S, Sollien R, Kiserud T. Fetal age assessment based on ultrasound head biometry and the effect of maternal and fetal factors. *Acta Obstet Gynecol Scand*. 2004;83:716-723.

hnsen SL, Rasmussen S, Sollien R, Kiserud T. Fetal age assessment based on femur length at 10–25 weeks of gestation, and reference ranges for femur length to head circumference ratios. *Acta Obstet Gynecol Scand*. 2005;84:725-733.

onje JC, Abrams KR, Bell SC, Talyor DJ. Determination of gestational age after the 24th week of gestation from fetal kidney length measurements. *Ultrasound Obstet Gynecol*. 2002;19:592-597.

mpl M. Saltation and stasis. In: Cameron N, editor. *Human Growth and Development*. New York: Academic Press, 2002. Ch. 12.

Presents the evidence for saltatory growth in humans..

Rahilly R, Müller F. Developmental Stages in Human Embryos. Washington: Carnegie Institution, 1987.

Provides the most comprehensive and detailed morphological account of human development during the first 8 weeks of life, and sets out the basis for the staging system used for human embryos..

Rahilly R, Müller F. The Embryonic Human Brain. An Atlas of Developmental Stages. 2nd edn.. New York: Wiley-Liss; 1999.

Rahilly R, Müller F. Minireview: prenatal ages and stages – measures and errors. *Teratology*. 2000;61:382-384.

agemann A. ‘Fetal programming’ and ‘functional teratogenesis’: on epigenetic mechanisms and prevention of perinatally acquired lasting health risks. *J Perinat Med*. 2004;32:297-305.

lomon LJ, Bernard JP, Duyme M, Dorion A, Ville Y. Revisiting first-trimester fetal biometry. *Ultrasound Obstet Gynecol*. 2003;22:63-66.

reeter GL. Developmental horizons in human embryos. Descriptions of age group XI, 13 to 20 somites, and age group XII, 21 to 29 somites. *Contrib Embryol Carnegie Inst Washington*. 1942;30:211-245.

reeter GL. Developmental horizons in human embryos. Description of age group XIII, embryos of about 4 or 5 millimeters long, and age group XIV, period of indentation of the lens vesicle. *Contrib Embryol Carnegie Inst Washington*. 1945;31:27-63.

reeter GL. Developmental horizons in human embryos. Description of age groups XV, XVI, XVII, and XVIII, being the third issue of a survey of the Carnegie collection. *Contrib Embryol Carnegie Inst Washington*. 1948;32:133-203.

ıng H, Kramer MS, Platt RW, Blondel B, Breat G, Mornin I, Wilkins R, Usher R. How does early ultrasound scan estimation of gestational age lead to higher rates of preterm birth? *Am J Obstet Gynecol*. 2002;186:433-437.

Section 3
NEUROANATOMY

CHAPTER 15

Overview of the nervous system

The human nervous system is the most complex product of biological evolution. The constantly changing patterns of activity of its billions of interactive units represent the fundamental physical basis of every aspect of human behaviour and experience. Many thousands of scientists and clinicians around the world, whether driven by intellectual curiosity or the quest for better methods of disease prevention and treatment, have studied the nervous system over many years. Despite the enormous amount of data available, our understanding of complex neural organization and function is far from complete, as is our ability to deal with its many pathologies. Nevertheless, research on the nervous system is one of the most active areas of contemporary biology and medicine and rapid advances on numerous fronts bring with them the realistic prospect of better prevention and treatment of many neurological disorders in the future.

The functional capabilities of the nervous system are a product of its vast population of intercommunicating nerve cells or neurones, estimated to number in the order of 10^{10} (Ch. 3). In brief, neurones encode information, conduct it, sometimes over considerable distances, and then transmit it to other neurones or to non-neural tissues such as muscles or glandular cells. Most neurones consist of a central mass of cytoplasm within a limiting cell membrane, the cell body or soma, from which extend a number of branched processes, or neurites (Fig. 15.1). One of these, the axon, or nerve fibre, is usually much longer than the others and conducts information away from the cell body. The other processes are termed dendrites and these typically conduct information towards the soma (cell body). The nerve cell membrane is polarized, the inside of the cell being around −70 mV negative with respect to the outside. Information is coded in the form of patterns of transient depolarizations and repolarizations of this membrane potential, known as action potentials or nerve impulses. These are conducted along the axon, which may have collateral branches that permit information to be distributed simultaneously to several targets. Axons possess specialized endings, or axon terminals, which come into close apposition with the membrane of the target cell at synapses, where information passes from one cell to another (Fig. 15.2). Axon terminals may form synaptic contacts with dendrites (axodendritic), cell bodies (axosomatic), other axons (axoaxonic) or non-neural tissue such as muscle cells (neuromuscular junction). Transmission of information to other cells occurs when action potentials cause the release of specific neurotransmitter substances, stored in synaptic vesicles within the presynaptic nerve terminal. The neurotransmitter binds to specialized receptors that are located on the postsynaptic target cell membrane and, depending upon the nature of the chemical and the receptor, either elicits an excitatory (depolarizing) or inhibitory (hyperpolarizing) response, or may modulate intracellular second messenger systems.

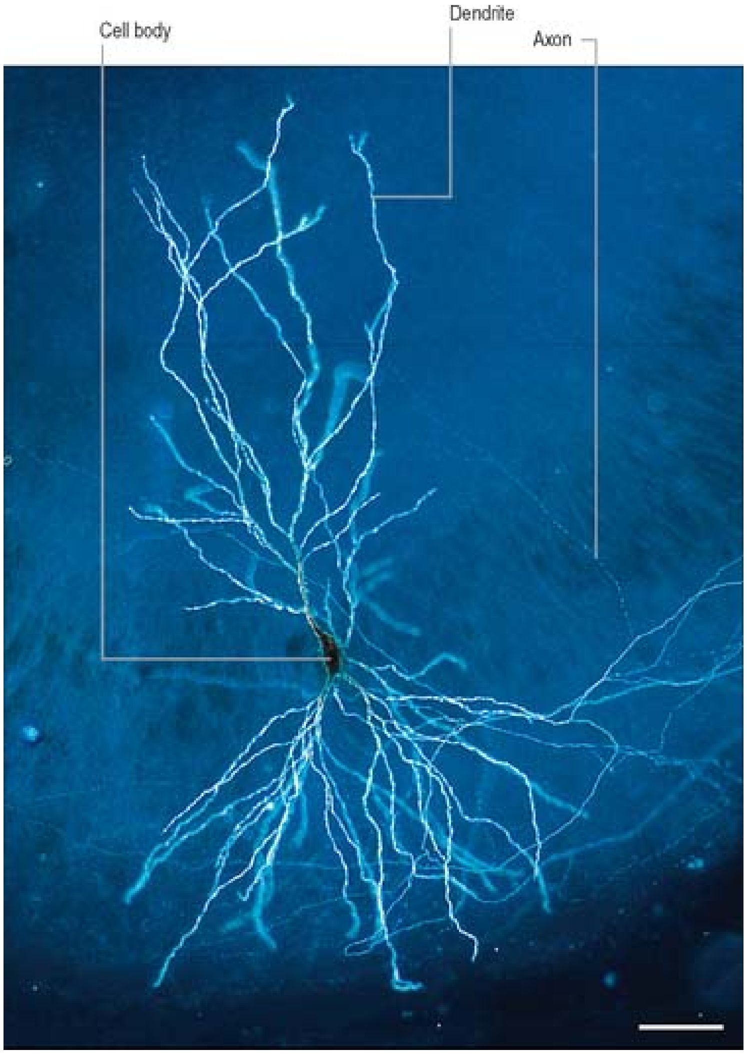

Fig. 15.1 Dark-field photomicrograph of a CA3 pyramidal cell in a hippocampal slice culture, intracellularly injected with the dye biocytin. Scale bar 50 µm.

(Courtesy of Mathias Abegg and R Anne McKinney, Brain Research Institute, University of Zurich.)

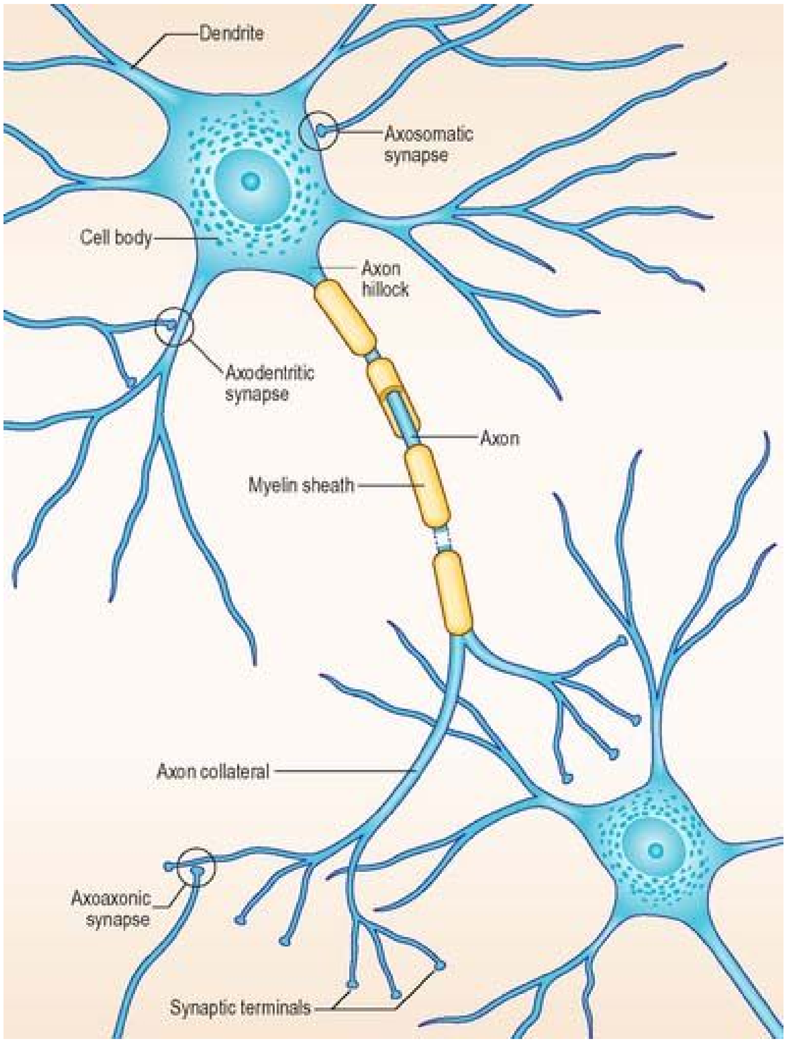
Dendrite
Axosomatic synapse
Cell body
Axon hillock
Axodentritic synapse
Axon
Myelin sheath
Axon collateral
Axoaxonic synapse
Synaptic terminals

Fig. 15.2 Structure of a typical neurone.

The huge complexity of the nervous system reflects the fact that individual neurones may make synaptic contact with hundreds, or even thousands, of other neurones via profuse axonal collateralization and dendritic branching (arborization). The latter is exemplified by the extensive dendritic field of the cerebellar Purkinje cell, which is traversed by thousands of axons, making synaptic contact as they pass. At the level of the individual neurone, competing incoming excitatory and inhibitory synaptic potentials are summated in time (temporal summation) and between synapses (spatial summation). If the postsynaptic neurone is depolarized above a certain threshold it fires action potentials which are conducted along the axon to the next target cells.

The nervous system contains far more supporting cells (neuroglia, glia) than neurones. Glia are responsible for creating and maintaining an appropriate environment in which neurones can operate efficiently. Subsets of glia secrete the myelin sheaths that enwrap axons in many parts of the nervous system. Glia are not electrically excitable in the same way as neurones.

The three basic functional types of neurones in the nervous system, sensory (afferent) and motor (efferent) neurones and interneurones, detect and respond to changes in the internal and external environments of the body. The sensory elements are able to detect a wide range of stimuli: they subserve the general senses (touch, pain, temperature, etc.) and the special senses (vision, hearing, smell, taste, and vestibular sensation). Motor neurones send axons from the central nervous system to effector organs, mainly muscles and glands. Interneurones are confined entirely to the central nervous system and possess neither sensory nor motor terminals: they greatly outnumber sensory and motor neurones and confer on the nervous system its prodigious capacity to analyse, integrate and store information.

The nervous system is conventionally divided into two major parts, the central nervous system (CNS) and the peripheral nervous system (PNS). The CNS consists of the brain and spinal cord. The PNS consists of the cranial and spinal nerves and their ramifications, and certain groupings of cell bodies that constitute the peripheral ganglia. Another convention divides the nervous system into somatic and autonomic components, with elements in both the CNS and PNS. The somatic nervous system controls the contraction of skeletal muscles. The autonomic nervous system, which may be subdivided into sympathetic and parasympathetic components, consists of neurones that innervate secretory glands, cardiac and smooth muscle and are therefore concerned primarily with control of the internal environment. Neurones in the wall of the gastrointestinal tract form the enteric nervous system, and are capable of sustaining local reflex activity that is independent of the CNS (Ch. 73).

CENTRAL NERVOUS SYSTEM

The brain and spinal cord (see Fig. 43.1A) contain the great majority of neuronal cell bodies in the nervous system. In many parts of the CNS, neuronal cell bodies are grouped together and are, more or less, segregated from axons. The generic term for such collections of cell bodies is grey matter. Small aggregations of neuronal cell bodies, which usually share a common functional role, are termed nuclei. Neuronal dendrites and synaptic interactions are mostly confined to grey matter. Axons tend to be grouped together to form white matter, so called because axons are often ensheathed in myelin which confers a paler colouration. Axons that pass between similar origins or destinations within the CNS tend to run together in defined pathways, or tracts. These often cross the midline (decussate), which means that one half of the body is, in many respects, controlled by, and sends information to, the opposite side of the brain.

Some groups of neurones in the spinal cord and brain stem that subserve similar functions are organized into longitudinal columns. The neurones in these columns may be concentrated into discrete, discontinuous nuclei in some areas, e.g. the cranial nerve nuclei of the brain stem, or they may form more or less continuous longitudinal bands, as in much of the spinal cord (Fig. 15.3). Efferent neurones constitute three such columns. The axons of motor neurones in the somatic motor column innervate muscles derived from head somites. The two other columns are related to specialized features of head morphology: neurones in the branchial motor column innervate muscles derived from the wall of the embryonic pharynx (branchial muscles) and the visceral motor column supplies preganglionic parasympathetic fibres to glands and visceral smooth muscle. Four longitudinal cell columns are related to sensory functions. The general somatic sensory column essentially deals with general sensory information from the head; special somatic sensory neurones are related to the special senses and receive vestibular and auditory input; general visceral sensory neurones deal with information from widespread and varied visceral sensory endings; special visceral sensory neurones are related to the special sense of taste.

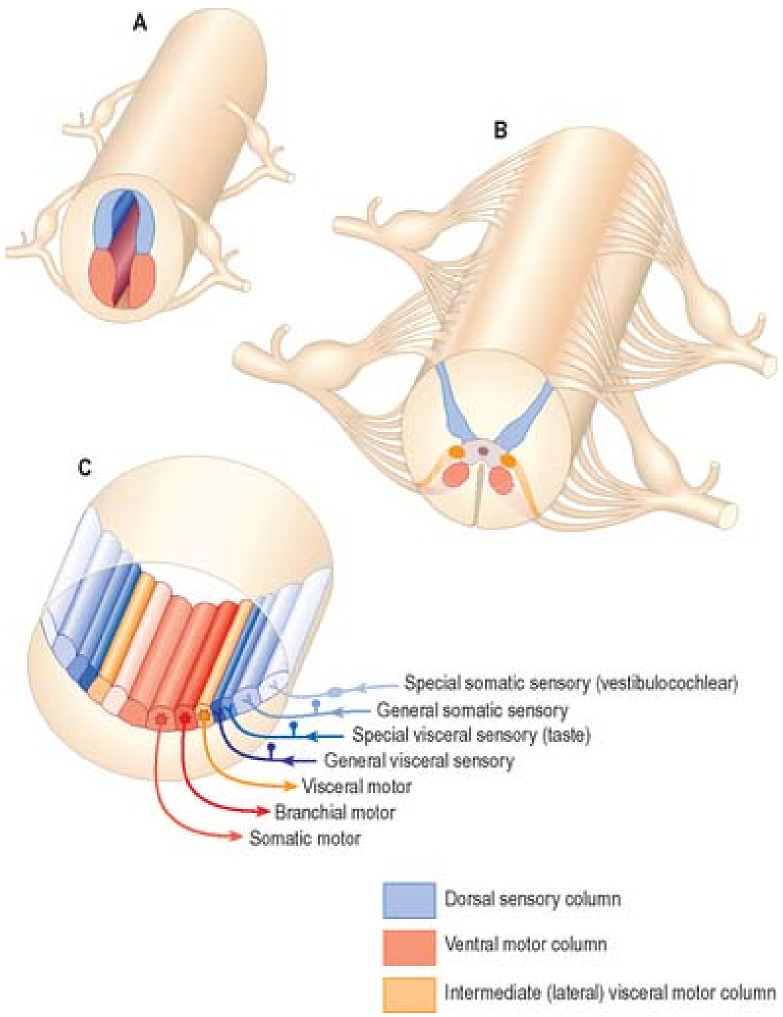
A
B
C
Special somatic sensory (vestibulocochlear)
General somatic sensory
Special visceral sensory (taste)
General visceral sensory
Visceral motor
Branchial motor
Somatic motor
Dorsal sensory column
Ventral motor column
Intermediate (lateral) visceral motor column

Fig. 15.3 Arrangement of sensory and motor cell columns in the spinal cord and brain stem. In each of parts A, B and C, dorsal is towards the top of the diagram. **A** shows the organization of the primitive spinal cord with a dorsal sensory column, a ventral motor column, and segmentally arranged dorsal and ventral nerve roots. **B** depicts the adult thoracic spinal cord with sensory and somatic motor columns and an additional intermediate (lateral) visceral motor column. **C** indicates the arrangement of multiple longitudinal columns in the brain stem, where the motor column is now subdivided into three, and the sensory column into four. For further information about the embryological aspects of the early nervous system consult Ch. 24. Consult also Fig 19.1.

The brain and spinal cord communicate with the rest of the body via the cranial and spinal nerves respectively. These nerves contain afferent fibres that bring information into the CNS from sensory receptors, and efferent fibres that convey instructions from the CNS to peripheral effector organs. The spinal cord and brain stem can control many aspects of bodily function by reflex action mediated via interconnections of varying complexity between the afferent and efferent components of the spinal and cranial nerves. Numerous descending connections from the brain may modulate this activity. Afferent input to the spinal cord and brain stem is channelled into various ascending pathways, some of which eventually impinge upon the cerebral cortex, conferring conscious awareness.

To provide the energy required by constant neuronal activity, the CNS has a high metabolic rate and a rich blood supply (Ch. 17). A blood–brain barrier controls the neuronal environment and imposes severe restrictions on the types of substances that can pass from the bloodstream into nervous tissue (Ch. 3).

SPINAL CORD

The spinal cord lies within the vertebral column, in the upper two-thirds of the vertebral canal, and is continuous rostrally with the medulla oblongata of the brain stem (Ch. 43). For the most part, the spinal cord receives afferent input from, and controls the functions of, the trunk and limbs. Afferent and efferent connections between the periphery and the spinal cord travel in 31 pairs of segmentally arranged spinal nerves that attach to the cord as a linear series of dorsal and ventral rootlets. Adjacent groups of rootlets unite to form dorsal and ventral roots that combine to form the spinal nerves proper (Fig. 15.4). The dorsal and ventral roots are functionally distinct. Dorsal roots carry primary afferent nerve fibres from neuronal cell bodies located in dorsal root ganglia, whereas ventral roots carry efferent fibres from neuronal cell bodies located in the spinal grey matter.

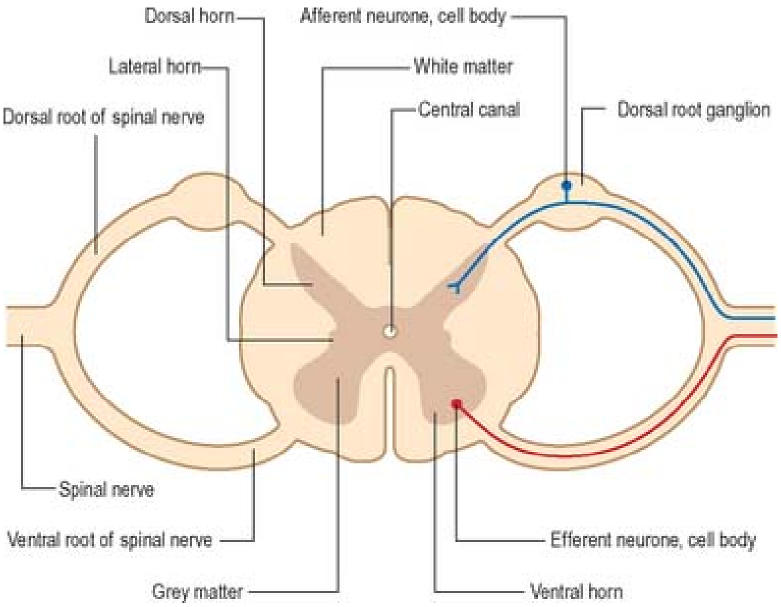
Dorsal horn
Afferent neurone, cell body
Lateral horn
White matter
Dorsal root of spinal nerve
Central canal
Dorsal root ganglion
Spinal nerve
Ventral root of spinal nerve
Efferent neurone, cell body
Grey matter
Ventral horn

Fig. 15.4 Transverse section through the spinal cord illustrating the disposition of grey and white matter and the attachment of dorsal and ventral spinal nerve roots.

Internally, the spinal cord consists of a central core of grey matter surrounded by white matter. The grey matter is configured in a characteristic

H, or butterfly, shape that has projections known as dorsal and ventral horns (Fig. 15.5). In general, neurones situated in the dorsal horn are primarily concerned with sensory functions whilst those in the ventral horn are mostly associated with motor activities. At certain levels of the spinal cord a small lateral horn is additionally present, marking the location of the cell bodies of preganglionic sympathetic neurones. The central canal, a vestigial component of the ventricular system, lies at the centre of the spinal grey matter and runs the length of the cord. The white matter of the spinal cord consists of ascending and descending tracts that link spinal cord segments to one another and the spinal cord to the brain.

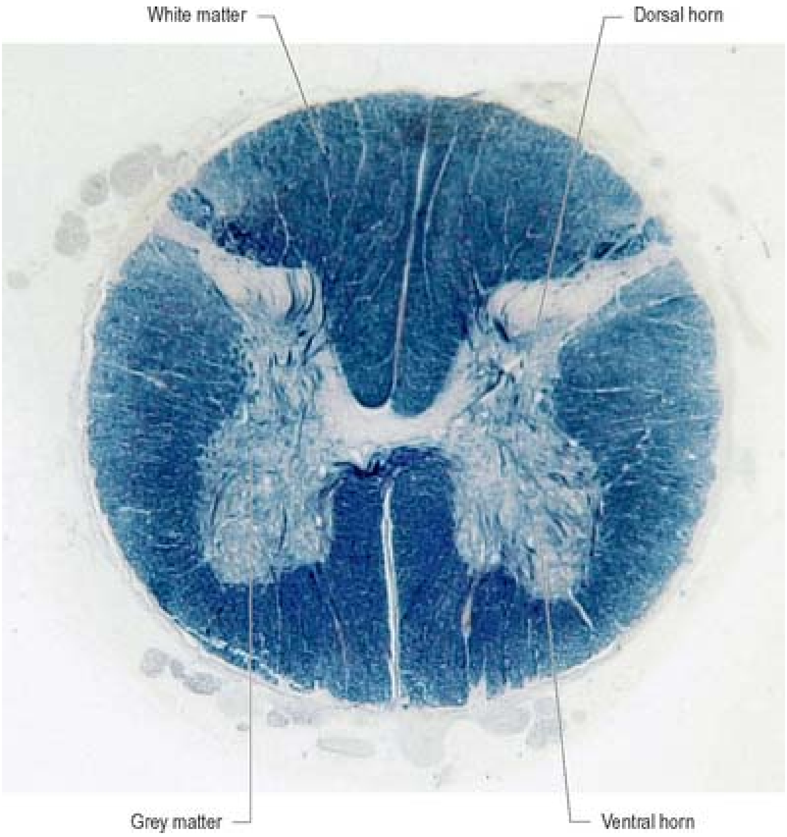

Fig. 15.5 Transverse section through the spinal cord at lumbar level. The section has been stained for nerve fibres, leaving the grey matter relatively unstained. (Figure enhanced by B Crossman.)

BRAIN

The brain (encephalon) lies within the cranium (Ch. 26). The brain receives information from, and controls the activities of, the trunk and limbs mainly through connections with the spinal cord. It also possesses 12 pairs of cranial nerves through which it communicates mostly with structures of the head and neck. The brain is divided into major regions on the basis of ontogenetic growth and phylogenetic principles (Fig. 15.6, Fig. 15.7, Fig. 15.8). Ascending in sequence from the spinal cord, the principal divisions are the rhombencephalon or hindbrain, the mesencephalon or midbrain, and the prosencephalon or forebrain.

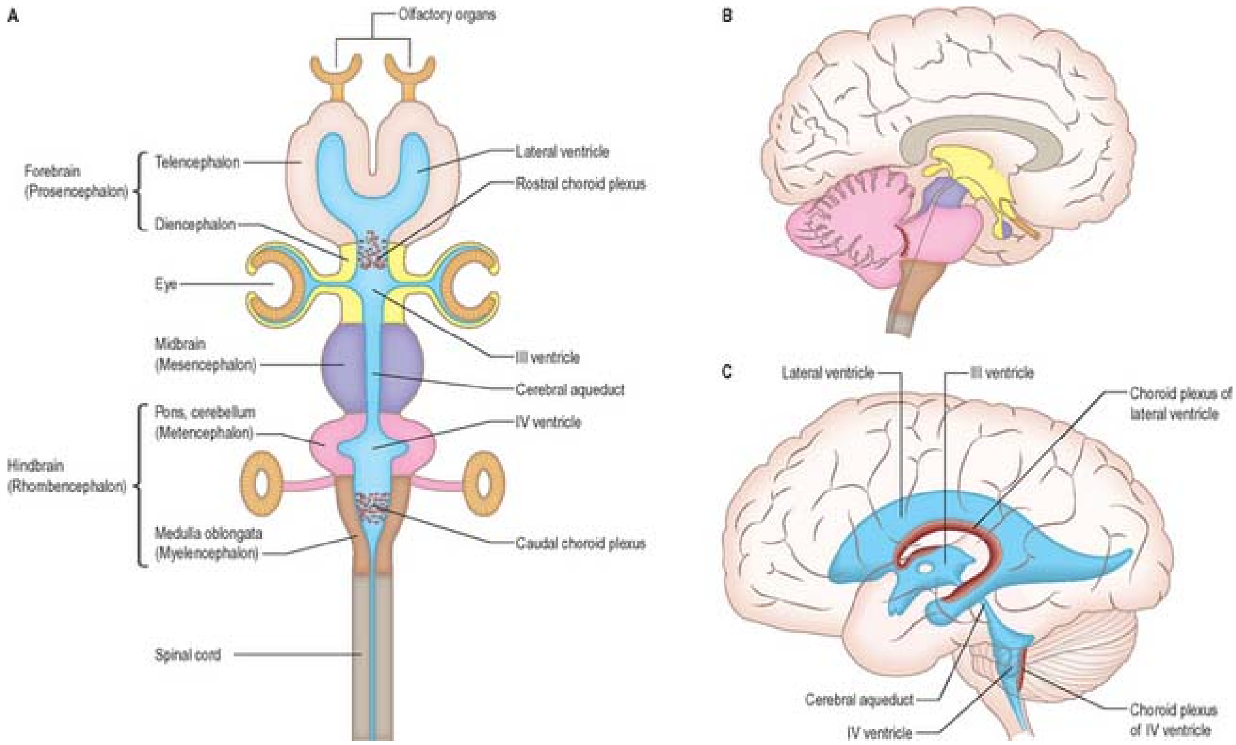
A
Olfactory organs
Forebrain (Prosencephalon)
Telencephalon
Diencephalon
Eye
Midbrain (Mesencephalon)
Pons, cerebellum (Metencephalon)
Hindbrain (Rhombencephalon)
Medulla oblongata (Myelencephalon)
Spinal cord
Lateral ventricle
Rostral choroid plexus
III ventricle
Cerebral aqueduct
IV ventricle
Caudal choroid plexus
B
C
Lateral ventricle
III ventricle
Choroid plexus of lateral ventricle
Cerebral aqueduct
IV ventricle
Choroid plexus of IV ventricle

Fig. 15.6 Nomenclature and arrangement of the major divisions of the brain. **A**, The major features of the basic brain plan, including their relationships to the major special sensory organs of the head. **B**, The corresponding regions in the adult brain, seen in sagittal section. **C**, the organization of the ventricular system in the brain.

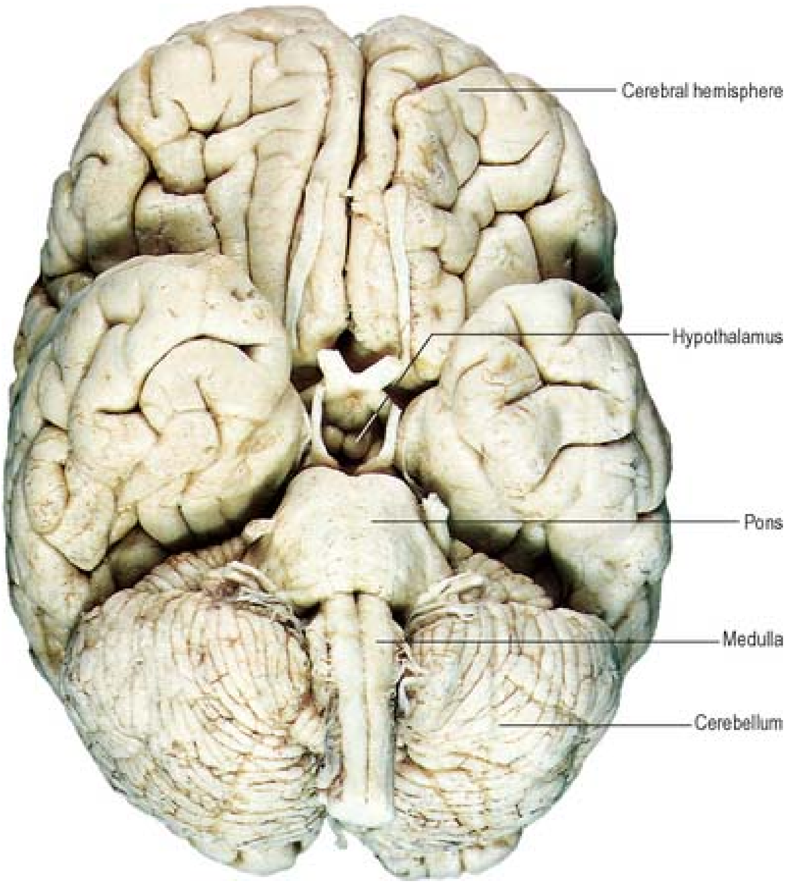
Cerebral hemisphere
Hypothalamus
Pons
Medulla
Cerebellum

Fig. 15.7 Base of the brain, showing major divisions and cranial nerves.

(Figure enhanced by B Crossman, from a photograph by Kevin Fitzpatrick on behalf of GKT School of Medicine, London.)

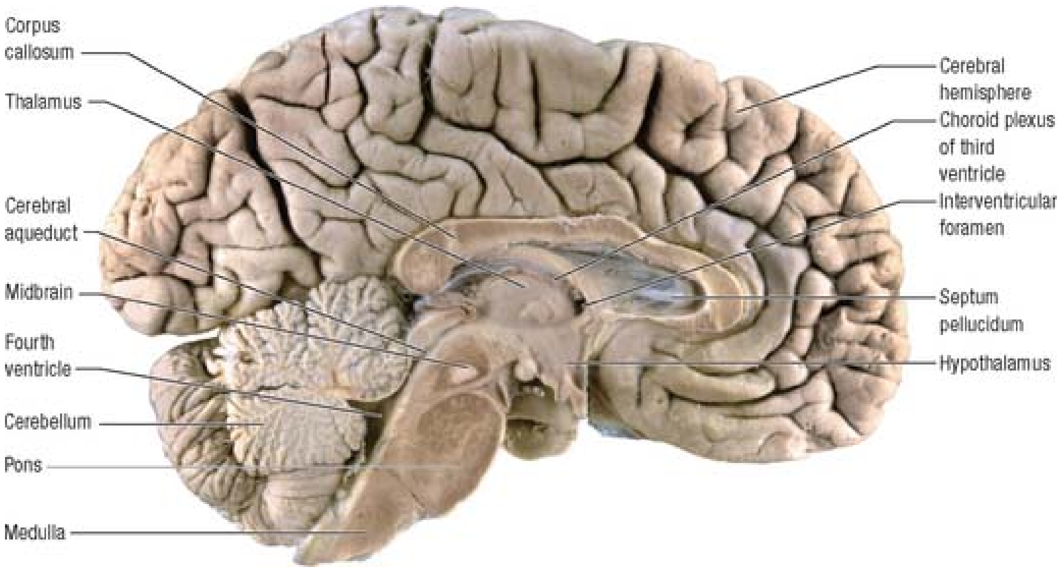
Corpus callosum
Thalamus
Cerebral aqueduct
Midbrain
Fourth ventricle
Cerebellum
Pons
Medulla
Cerebral hemisphere
Choroid plexus of third ventricle
Interventricular foramen
Septum pellucidum
Hypothalamus

Fig. 15.8 Sagittal section of the brain. (Figure enhanced by B Crossman.)

The rhombencephalon is subdivided into the myelencephalon or medulla oblongata, metencephalon or pons, and the cerebellum. The medulla oblongata, pons and midbrain are collectively referred to as the brain stem which lies upon the basal portions of the occipital and sphenoid bones (clivus). The medulla oblongata is the most caudal part of the brain stem and is continuous with the spinal cord below the level of the foramen magnum. The pons lies rostral to the medulla and is distinguished by a mass of transverse nerve fibres which connect it to the cerebellum. The midbrain is a short segment of brain stem, rostral to the pons. The cerebellum consists of paired hemispheres united by a median vermis and lies within the posterior cranial fossa, dorsal to the pons, medulla and caudal midbrain, with all of which it has numerous fibre connections.

The prosencephalon is subdivided into the diencephalon and the telencephalon. The diencephalon equates mostly to the thalamus and hypothalamus, but also includes the smaller epithalamus and subthalamus. The telencephalon is mainly composed of the two cerebral hemispheres or cerebrum. The diencephalon is almost completely embedded in the cerebrum and is therefore largely hidden from the exterior. The human cerebrum constitutes the major part of the brain. It occupies the anterior and middle cranial fossae and is directly related to the cranial vault. It consists of two cerebral hemispheres. The surface of each hemisphere is convoluted into a complex pattern of ridges (gyri) and furrows (sulci). Internally, each hemisphere has an outer layer of grey matter, the cerebral cortex, beneath which lies a thick mass of white matter (Fig. 15.9). One of the most important components of the cerebral white matter, the internal capsule (see Fig. 15.11), contains nerve fibres which pass to and from the cerebral cortex and lower levels of the neuraxis. Several large nuclei of grey matter, usually referred to as the basal ganglia, are partly embedded in the subcortical white matter. Connections between corresponding areas of the two sides of the brain cross the midline within commissures. By far the largest commissure is the corpus callosum, which links corresponding regions of the two cerebral hemispheres.

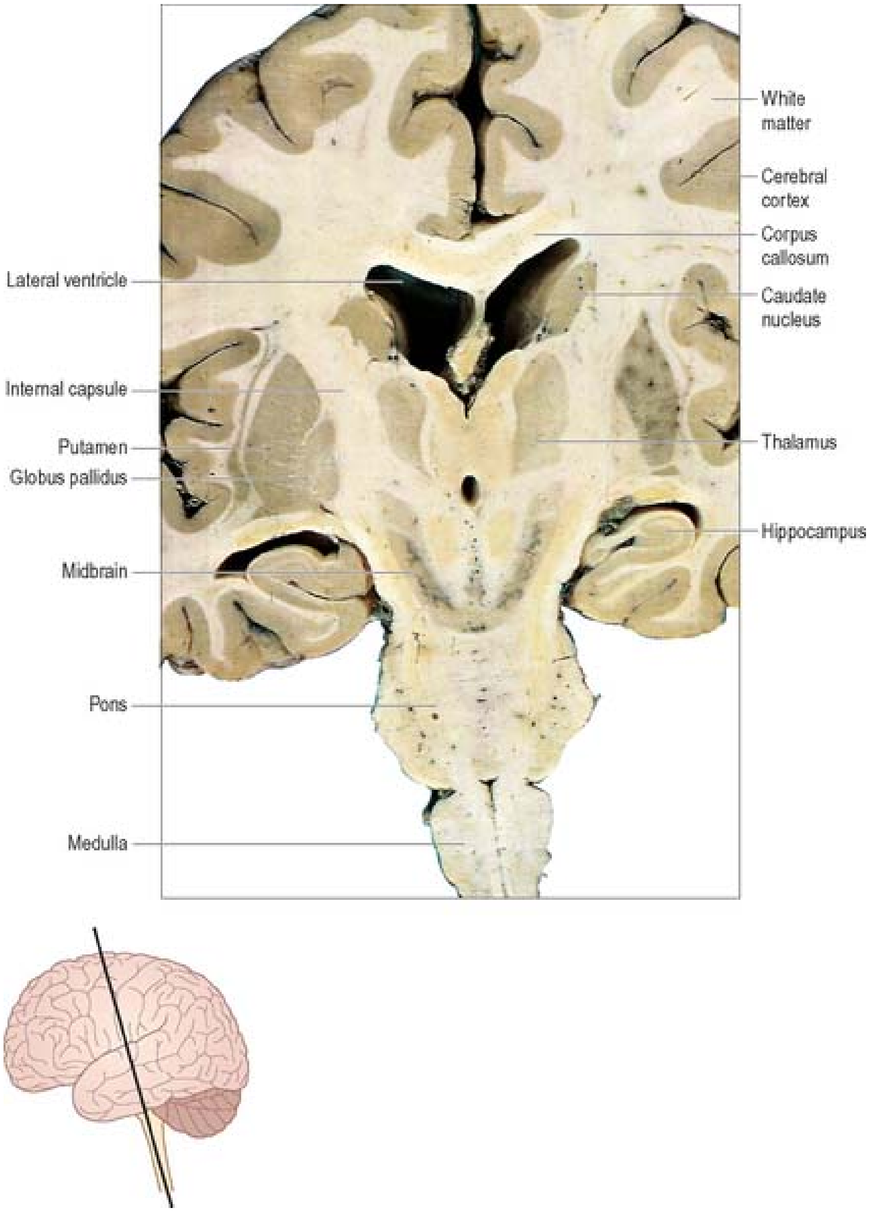
White matter
Cerebral cortex
Corpus callosum
Lateral ventricle
Caudate nucleus
Internal capsule
Putamen
Globus pallidus
Thalamus
Hippocampus
Midbrain
Pons
Medulla

Fig. 15.9 Section through the cerebral hemisphere and brain stem showing the disposition of grey and white matter, the basal ganglia and the internal capsule.

(Photograph by Kevin Fitzpatrick on behalf of GKT School of Medicine, London.)

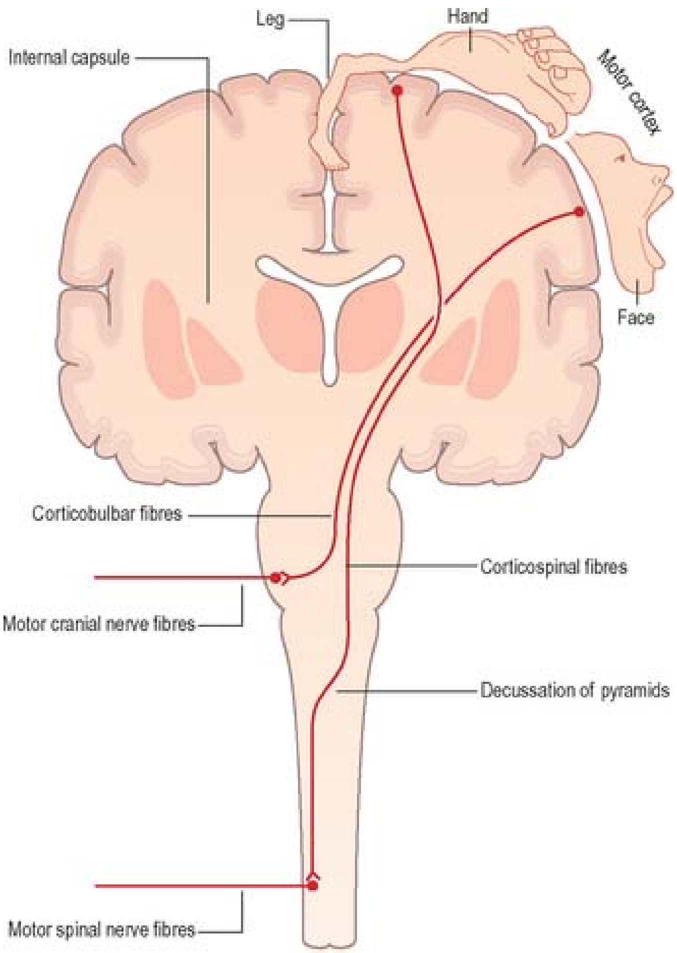
Leg
Hand
Internal capsule
Motor cortex
Face
Corticobulbar fibres
Corticospinal fibres
Motor cranial nerve fibres
Decussation of pyramids
Motor spinal nerve fibres

Fig. 15.11 Corticospinal and corticobulbar tracts.

During prenatal development, the walls of the neural tube thicken greatly, but never completely obliterate the central lumen. Although the latter remains in the spinal cord as the narrow central canal, it becomes greatly expanded in the brain to form a series of interconnected cavities called the ventricular system (Ch. 16). In two regions, the fore- and hindbrains, parts of the roof of the neural tube do not generate nerve cells but become thin, folded sheets of highly vascular secretory tissue, the choroid plexuses. These secrete cerebrospinal fluid which fills the ventricles. The cavity of the rhombencephalon becomes expanded to form the fourth ventricle, which lies dorsal to the pons and upper half of the medulla. Caudally, the fourth ventricle is continuous with a canal in the caudal medulla and, through this, with the central canal of the spinal cord. The fourth ventricle is continuous with the subarachnoid space through three openings in its roof (the foramina of Luschka and of Magendie). At its rostral extent, the fourth ventricle is continuous with a narrow channel, the cerebral aqueduct, which passes through the midbrain. The rostral end of the cerebral aqueduct opens out into the third ventricle, a narrow, slit-like, midline cavity which is bounded laterally by the diencephalon. At the rostral end of the third ventricle, a small aperture on each side leads into the large lateral ventricle which is located within each cerebral hemisphere (see Fig. 15.6C).

OVERVIEW OF ASCENDING SENSORY PATHWAYS

Sensory modalities are conventionally described as being either special senses or general senses. The special senses are olfaction, vision, taste, hearing and vestibular function. Afferent information is encoded by highly specialized sense organs and transmitted to the brain in cranial nerves I, II, VII, VIII and IX (Ch. 25).

The general senses include touch, pressure, vibration, pain, thermal sensation and proprioception (perception of posture and movement). Stimuli from the external and internal environments activate a diverse range of receptors in the skin, viscera, muscles, tendons and joints (Ch. 3). Afferent impulses from the trunk and limbs are conveyed to the spinal cord in spinal nerves whilst those from the head are carried to the brain in cranial nerves. The detailed anatomy of the complex pathways by which the various general senses impinge upon conscious levels is better understood by reference to certain common organizational principles. Whilst undoubtedly oversimplified and subject to exceptions, this schema is helpful in emphasizing the essential similarities that exist between the ascending sensory systems.

In essence, ascending sensory projections related to the general senses consist of a sequence of three neurones that extends from peripheral receptor to contralateral cerebral cortex (Fig. 15.10). These are often referred to as either primary, secondary and tertiary neurones or first-, second- and third-order neurones. Primary afferents have peripherally located sensory endings and cell bodies that lie in dorsal root ganglia or the sensory ganglia associated with certain of the cranial nerves. Their axons enter the CNS through spinal or trigeminal nerves and terminate by synapsing on the cell bodies of ipsilateral second-order neurones: the precise location of this termination depends upon the modality.

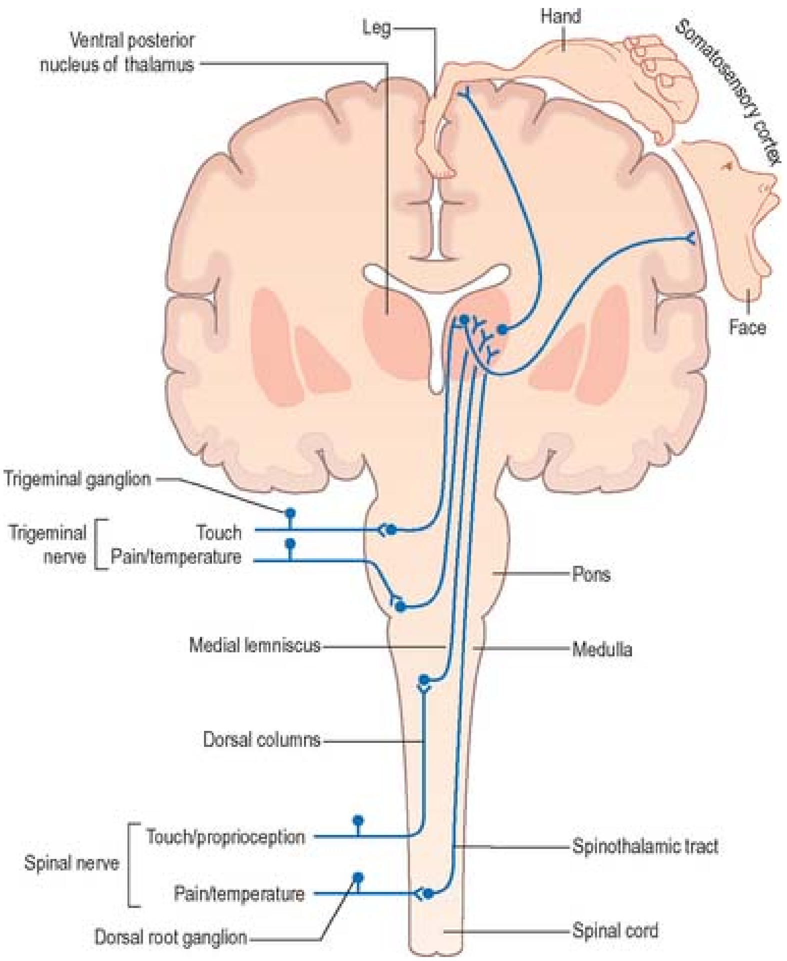
Ventral posterior nucleus of thalamus
Leg
Hand
Somatosensory cortex
Face
Trigeminal ganglion
Trigeminal nerve
Touch
Pain/temperature
Pons
Medial lemniscus
Medulla
Dorsal columns
Spinal nerve
Touch/proprioception
Pain/temperature
Spinothalamic tract
Dorsal root ganglion
Spinal cord

Fig. 15.10 Organization of general sensory pathways showing first-order, second-order and third-order neurones.

Primary afferent fibres carrying pain, temperature and coarse touch/pressure information from the trunk and limbs terminate in the dorsal horn of the spinal grey matter, near their point of entry into the spinal cord. Homologous fibres from the head terminate in the trigeminal sensory nucleus of the brain stem. The cell bodies of second-order neurones are located in either the dorsal horn or the trigeminal sensory nucleus. Their axons decussate and ascend to the ventral posterior nucleus of the contralateral thalamus as the spinothalamic or the trigeminothalamic tract, respectively; they synapse on the cell bodies of third-order neurones in the thalamus. Axons of third-order neurones pass through the internal capsule to reach the cerebral cortex, terminating in the postcentral gyrus of the parietal lobe, which is also known as the primary somatosensory cortex.

Primary afferent fibres carrying proprioceptive information and fine (discriminative) touch from the trunk and limbs ascend ipsilaterally in the spinal cord as the dorsal columns (fasciculus gracilis and fasciculus cuneatus): they end by synapsing on second-order neurones in the dorsal column nuclei (nucleus gracilis and nucleus cuneatus) of the medulla. Axons of second-order neurones decussate in the medulla and then ascend as the medial lemniscus to the ventral posterior nucleus of the contralateral thalamus, where they synapse on the cell bodies of third-order neurones. Axons of third-order neurones pass through the internal capsule to reach the cerebral cortex, terminating in the primary somatosensory cortex. A similar homologous projection exists for afferents derived from the head.

OVERVIEW OF DESCENDING MOTOR PATHWAYS

Corticofugal fibres descend through the internal capsule and pass into the brain stem, where some of them (corticobulbar fibres) terminate. Corticobulbar fibres control the activity of brain stem neurones, including motor neurones within the cranial nerve nuclei. Current neuroanatomical nomenclature does not include a generally accepted term that denotes projections from the cerebral cortex to the brain stem as a whole. Such a term is, however, required in order to draw clinical comparison between the corticospinal system, coursing through the pyramids, and the functionally homologous fibres that terminate in the brain stem. The term 'corticonuclear' is sometimes used, but this implies specific innervation of cranial nerve nuclei and ignores the fact that numerous cortical efferents project to other sites, such as the reticular formation. The term 'corticobulbar' is also sometimes used but this, strictly speaking, refers to projections to the 'bulb', an archaic term for the medulla oblongata. In this text, 'corticobulbar' is used to denote cortical projections to the brain stem as a whole.

Corticospinal fibres (pyramidal tract) originate from widespread regions of the cerebral cortex, including the primary motor cortex of the frontal lobe where the opposite half of the body is represented in a detailed somatotopic fashion. They descend throughout the length of the brain stem; the majority cross to the contralateral side in the decussation of the pyramids in the medulla, subsequently continuing caudally as the lateral corticospinal tract of the spinal cord which terminates in association with interneurones and motor neurones of the spinal grey matter (Fig. 15.11). The principal function of the corticospinal and corticobulbar tracts is the control of fine, fractionated movements, particularly of those parts of the body where delicate muscular control is required. These tracts are particularly important in speech (corticobulbar tract) and movement of the hand (corticospinal tract).

The concept of upper and lower motor neurones is fundamental to the clinical description of the effects of lesions of the motor system. The signs and symptoms of upper and lower motor neurone lesions are very different and are indicative of the anatomical site of the lesion. ‘Lower motor neurones’ are the alpha motor neurones that innervate the extrafusal muscle fibres of skeletal muscle. In theory, the term ‘upper motor neurones’ refers collectively to all the descending pathways that impinge upon the activity of lower motor neurones. In common parlance, however, the term is often equated with the corticospinal tract. The terms upper and lower motor neurone lesion are used clinically to distinguish, for example, between the effects of a stroke in the internal capsule (a typical upper motor neurone lesion) and those of motor neurone disease (a typical lower motor neurone lesion).

Lower motor neurone lesions cause paralysis or paresis of specific muscles because they have lost their direct innervation. There is also loss or reduction of tendon reflex activity and reduced muscle tone. Spontaneous muscular contractions (fasciculation) occur and affected muscles atrophy over time. Upper motor neurone lesions cause paralysis or paresis of movements as a result of loss of higher control. There is increased tendon reflex activity and increased muscle tone but no muscle atrophy occurs. A positive plantar (Babinski) reflex is present. The combination of paralysis, increased tendon reflex activity and hypertonia is referred to as spasticity.

The pathophysiology underlying the symptoms of upper motor neurone lesions is complex. This is because many descending pathways other than the corticospinal tract exist and they also influence lower motor neurone activity. These pathways include corticofugal projections to the brain stem (e.g. corticoreticular and corticopontine) that traverse the internal capsule and numerous pathways that originate within the brain stem itself (e.g. reticulospinal, vestibulospinal). Clearly, these pathways may be compromised to varying extents, depending upon the site of a lesion. Their involvement is believed to be important in the pathophysiological mechanisms that underlie the generation of spasticity. Pure corticospinal tract lesions, which are exceedingly rare in man because corticospinal tract fibres lie in close relationship to other pathways throughout most of their course, are believed specifically to cause deficits in delicate, fractionated movements and to induce the positive plantar reflex.

Two other major systems that contribute to the control of movement are the basal ganglia and the cerebellum. The basal ganglia are a group of large subcortical nuclei, the major components being the caudate nucleus, putamen and globus pallidus (Fig. 15.9; Ch. 22). These structures have important connections with the cerebral cortex, certain nuclei of the thalamus and subthalamus and with the brain stem. They appear to be involved in the selection of appropriate movements and the suppression of inappropriate ones. Disorders of the basal ganglia cause either too little movement (akinesia) or abnormal involuntary movements (dyskinesias) as well as tremor and abnormalities of muscle tone. The basal ganglia are sometimes described as being part of the so-called ‘extrapyramidal (motor) system’. This term is used to distinguish between the effects of basal ganglia disease and those of damage to the ‘pyramidal’ (corticospinal) system. However, the progressive elucidation of the anatomy of the basal ganglia and of the pathophysiology of motor disorders has revealed the close functional interrelationship between the two ‘systems’, and has rendered the terms that distinguish them largely obsolete (Brodal 1981). The cerebellum (Ch. 20) has rich connections with the brain stem, particularly the reticular and vestibular nuclei, and with the thalamus. It is concerned with the coordination of movement: cerebellar disorders cause ataxia, intention tremor and hypotonia.

PERIPHERAL NERVOUS SYSTEM

The PNS is composed mainly of spinal nerves, cranial nerves, their ganglia and their ramifications which carry afferent and efferent neurones between the CNS and the rest of the body. It also includes the peripheral part of the autonomic nervous system, notably the sympathetic trunks and ganglia, and the enteric nervous system which is composed of plexuses of nerve fibres and cell bodies in the wall of the alimentary tract.

SPINAL NERVES

Spinal nerves are the means by which the CNS receives information from, and controls the activities of, the trunk and limbs. Spinal nerves are considered in detail elsewhere on a regional basis (Sections 5, 6, 8 and 9).

In brief, there are 31 pairs of spinal nerves (8 cervical, 12 thoracic, 5 lumbar, 5 sacral, 1 coccygeal) which contain a mixture of sensory and motor fibres. They originate from the spinal cord as continuous series of dorsal and ventral nerve rootlets. Adjacent groups of rootlets fuse to form dorsal and ventral roots which then merge to form the spinal nerves proper. The dorsal roots of spinal nerves contain afferent nerve fibres from cell bodies located in dorsal root ganglia. These cells give off both centrally and peripherally directed processes and do not have synapses on their cell bodies. The ventral roots of spinal nerves contain efferent fibres from cell bodies located in the spinal grey matter. They include motor neurones innervating skeletal muscle and preganglionic autonomic neurones.

Spinal nerves exit from the vertebral canal via their corresponding intervertebral foramina. They then divide to form a large ventral (anterior) ramus and a smaller dorsal (posterior) ramus. In general terms, the ventral ramus innervates the limbs together with the muscles and skin of the anterior part of the trunk. The dorsal ramus innervates the post-vertebral muscles and the skin of the back. The nerve fibres within the ventral rami serving the upper and lower limbs are redistributed within brachial and lumbosacral plexuses, respectively.

CRANIAL NERVES

Cranial nerves are the means by which the brain receives information from, and controls the activities of, the head and neck and to a lesser extent the thoracic and abdominal viscera. The component fibres, their route of exit from the cranial cavity, their subsequent peripheral course and the distribution and functions of the cranial nerves, are considered in detail elsewhere on a regional basis (Sections 4, 7, 8). Their origins, destinations and connections within the CNS are considered in this section.

Briefly, there are 12 pairs of cranial nerves. They are individually named and numbered (Roman numerals) in a rostrocaudal sequence (Table 15.1). Unlike spinal nerves, only some cranial nerves are mixed in function, carrying both sensory and motor fibres. Others are purely sensory or purely motor. The first cranial nerve (I; olfactory) has an ancient lineage and is derived from the forerunner of the cerebral hemisphere. It retains this unique position through the connections of the olfactory bulb, and is the only sensory cranial nerve that projects directly to the cerebral cortex rather than indirectly via the thalamus. The areas of cerebral cortex receiving olfactory input have a primitive cellular organization and are an integral part of the limbic system, which is concerned with the emotional aspects of behaviour (Ch. 23). The second cranial nerve (II; optic) consists of the axons of second order visual neurones and these terminate in the thalamus. The other ten pairs of cranial nerves attach to the brain stem and most of their component fibres originate from, or terminate in, the cranial nerve nuclei of the brain stem (Ch. 19).

Table 15.1 Summary of cranial nerves

No	Name	Components	Cells of origin	Main central connections	Exit from skull	Distribution and function
I	Olfactory	Special somatic afferent	Olfactory receptor cells in nasal mucosa	To olfactory bulb, anterior perforated substance, piriform cortex	Foramena of cribriform plate	Olfaction
II	Optic	Special somatic afferent	Ganglion cells of retina	To lateral geniculate nucleus of thalamus, pretectal area of midbrain	Optic canal	Vision
III	Oculomotor	Somatic efferent	Oculomotor nucleus	From visual cortical areas, medial longitudinal fasciculus	Superior orbital fissure	Motor to medial rectus, inferior rectus, superior rectus, inferior oblique, levator palpebrae superioris
III	Oculomotor	General visceral efferent	Edinger–Westphal nucleus	From pretectal area of midbrain	Superior orbital fissure	Parasympathetic to sphincter pupillae and ciliary muscles, via ciliary ganglion, mediating pupillary constriction and accommodation
IV	Trochlear	Somatic efferent	Trochlear nucleus	From visual cortical areas, medial longitudinal fasciculus	Superior orbital fissure	Motor to superior oblique
V	Trigeminal division:					
	Ophthalmic (V_{I})	General somatic afferent	Trigeminal (semilunar) ganglion	To trigeminal sensory nucleus	Superior orbital fissure	Sensation from forehead, scalp, eyelids, nose and eye, including conjunctiva
	Maxillary (V_{II})	General somatic afferent	Trigeminal (semilunar) ganglion	To trigeminal sensory nucleus	Foramen rotundum	Sensation from mid-face, lower eyelid, nasal cavity and paranasal sinuses, upper lip, maxillary teeth and palate
	Mandibular (V_{III})	General somatic afferent	Trigeminal (semilunar) ganglion	To trigeminal sensory nucleus	Foramen ovale	Sensation from lower face and scalp, tongue and floor of mouth, mandibular teeth and part of external ear
		General somatic afferent	Mesencephalic part of trigeminal sensory nucleus	To trigeminal sensory nucleus, cerebellum	Foramen ovale	Proprioception from muscles of mastication, temporomandibular joint
	Mandibular (V_{III})	Branchial (special visceral) efferent	Trigeminal motor nucleus	From precentral gyrus	Foramen ovale	Motor to muscles of mastication (temporalis, masseter, medial and lateral pterygoids), tensor tympani
VI	Abducens	Somatic efferent	Abducens nucleus	From visual cortical areas, medial longitudinal fasciculus	Superior orbital fissure	Motor to lateral rectus
VII	Facial	General somatic afferent	Geniculate ganglion	To trigeminal sensory nucleus, cerebellum	Internal acoustic meatus	Sensation from part of tympanic membrane, external acoustic meatus and skin behind pinna. Proprioception from facial muscles
VII	Facial	Special visceral afferent	Geniculate ganglion	To nucleus solitarius	Internal acoustic meatus	Taste from anterior two-thirds of tongue
VII	Facial	General visceral efferent	Superior salivatory nucleus	From olfactory areas, nucleus solitarius	Internal acoustic meatus	Parasympathetic to lacrimal gland and mucous membrane of nasal and oral cavities (via pterygopalatine ganglion) and submandibular and sublingual salivary glands (via submandibular ganglion) causing secretion and vasodilatation
VII	Facial	Branchial (special visceral) efferent	Facial nucleus	From precentral gyrus	Internal acoustic meatus	Motor to muscles of facial expression, stapedius, posterior belly of digastric and stylohyoid
VIII	Vestibulocochlear					
	Vestibular division	Special somatic afferent	Vestibular ganglion	To vestibular nuclei, cerebellum	Internal acoustic meatus	Sensations of equilibrium and motion
	Cochlear division	Special somatic afferent	Spiral ganglion	To cochlear nuclei	Internal acoustic meatus	Hearing
IX	Glossopharyngeal	General somatic afferent	Glossopharyngeal ganglia	To trigeminal sensory nucleus	Jugular foramen	General sensation from posterior one-third of tongue, oropharynx and middle ear
IX	Glossopharyngeal	General visceral afferent	Glossopharyngeal ganglia	To nucleus solitarius	Jugular foramen	Sensory from carotid body (chemoreceptors) and carotid sinus (baroreceptors)
IX	Glossopharyngeal	Special visceral afferent	Glossopharyngeal ganglia	To nucleus solitarius	Jugular foramen	Taste from posterior one-third of tongue
IX	Glossopharyngeal	General visceral efferent	Inferior salivatory nucleus	From olfactory areas, nucleus solitarius	Jugular foramen	Parasympathetic to parotid salivary gland (via otic ganglion), causing secretion and vasodilatation
IX	Glossopharyngeal	Branchial (special visceral) efferent	Nucleus ambiguus	From precentral gyrus	Jugular foramen	Motor to stylopharyngeus
X	Vagus	General somatic afferent	Superior (jugular) ganglion	To trigeminal sensory nucleus	Jugular foramen	General sensation from pharynx, larynx, trachea, oesophagus, part of auricle and external auditory meatus
X	Vagus	General visceral afferent	Inferior (nodose) ganglion	To nucleus solitarius	Jugular foramen	Sensory from thoracic and abdominal viscera Sensory from aortic arch (baroreceptors) and aortic bodies (chemoreceptors)
X	Vagus	General visceral efferent	Dorsal motor nucleus of vagus	From hypothalamus, nucleus solitarius	Jugular foramen	Parasympathetic to glands and smooth muscle in the pharynx, larynx; thoracic and

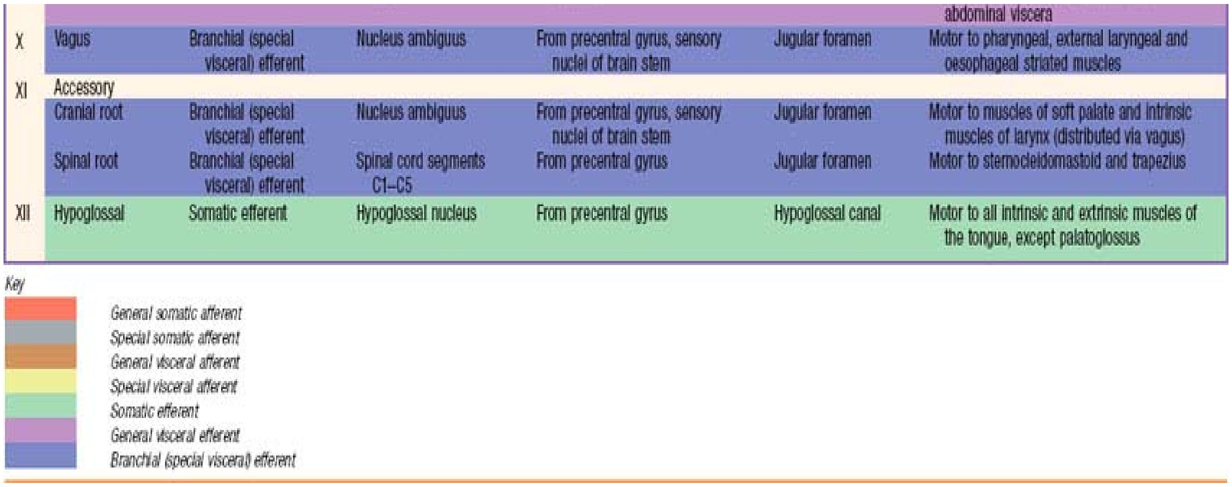

						abdominal viscera
X	Vagus	Branchial (special visceral) efferent	Nucleus ambiguus	From precentral gyrus, sensory nuclei of brain stem	Jugular foramen	Motor to pharyngeal, external laryngeal and oesophageal striated muscles
XI	Accessory					
	Cranial root	Branchial (special visceral) efferent	Nucleus ambiguus	From precentral gyrus, sensory nuclei of brain stem	Jugular foramen	Motor to muscles of soft palate and intrinsic muscles of larynx (distributed via vagus)
	Spinal root	Branchial (special visceral) efferent	Spinal cord segments C1–C5	From precentral gyrus	Jugular foramen	Motor to sternocleidomastoid and trapezius
XII	Hypoglossal	Somatic efferent	Hypoglossal nucleus	From precentral gyrus	Hypoglossal canal	Motor to all intrinsic and extrinsic muscles of the tongue, except palatoglossus

Key

🟥	*General somatic afferent*
▨	*Special somatic afferent*
🟫	*General visceral afferent*
🟨	*Special visceral afferent*
🟩	*Somatic efferent*
🟪	*General visceral efferent*
🟦	*Branchial (special visceral) efferent*

The sensory fibres in individual spinal and cranial nerves have characteristic, but often overlapping, peripheral distributions. As far as the innervation of the body surface is concerned, the area that is supplied by a particular spinal or cranial nerve is referred to as a dermatome. There is marked overlap between dermatomes of adjacent spinal nerves, particularly for the segments least affected by development of the limbs, i.e. the second thoracic to the first lumbar. In some regions, e.g. the upper anterior thoracic wall, the cutaneous nerves that supply adjoining areas are not from consecutive spinal nerves and the overlap is minimal. Maps of dermatome distribution are useful in clinical neurology to identify the location of pathology in patients with peripheral sensory deficits. Dermatome maps are somewhat inconsistently reported by different authors, reflecting the fact that the maps are composite constructs that have been compiled to a large extent by clinical observations on patients with cranial or spinal nerve pathology (Fig. 15.12). Detailed dermatome maps are described on a regional basis (Chs 42, 45, 79). The motor axons of individual spinal and cranial nerves tend to innervate anatomically and functionally related groups of skeletal muscles, that are referred to as myotomes.

Rights were not granted to include this figure in electronic media.
Please refer to the printed publication.

Fig. 15.12 Dermatome maps, illustrating the variation reported by different authors. **A**, Dermatome map based on Keegan JJ, Garrett FD 1948 The segmental distribution of the cutaneous nerves in the limbs of man. Anat Rec 102: 409–439. Mainly used in literature in the USA. **B**, Dermatome map based on Moffat DB 1993 Lecture Notes on Anatomy, 2nd edn. Oxford: Blackwell Scientific. Mainly used in literature in the UK.

AUTONOMIC NERVOUS SYSTEM

The autonomic nervous system represents the visceral component of the nervous system. It consists of neurones located within both the CNS and PNS which are concerned with the control of the internal environment, through the innervation of secretory glands, cardiac and smooth muscle. Its functions are, however, closely integrated with those of the somatic nervous system.

Visceral afferent pathways in many ways resemble somatic afferent pathways. The peripheral processes of visceral afferents run through autonomic ganglia or plexuses, and possibly through somatic nerves. Their cell bodies of origin are unipolar neurones located in either cranial sensory or dorsal root ganglia. Their central processes accompany somatic afferent fibres through cranial nerves or dorsal spinal roots into the CNS where they establish connections that mediate autonomic reflexes and visceral sensation.

Visceral efferent pathways differ from their somatic equivalents in that the former are interrupted by peripheral synapses, there being a sequence of at least two neurones between the CNS and the target structure (Fig. 15.13). These are referred to as preganglionic and postganglionic neurones, respectively. The somata of preganglionic neurones are located in the visceral efferent nuclei of the brain stem and in the lateral grey columns of the spinal cord. Their axons, which are usually finely myelinated, exit from the CNS in certain cranial and spinal nerves and then pass to peripheral ganglia, where they synapse with postganglionic neurones. The axons of postganglionic neurones are usually unmyelinated. Postganglionic neurones are more numerous than preganglionic ones; one preganglionic neurone may synapse with 15 to 20 postganglionic neurones, which permits the wide distribution of many autonomic effects.

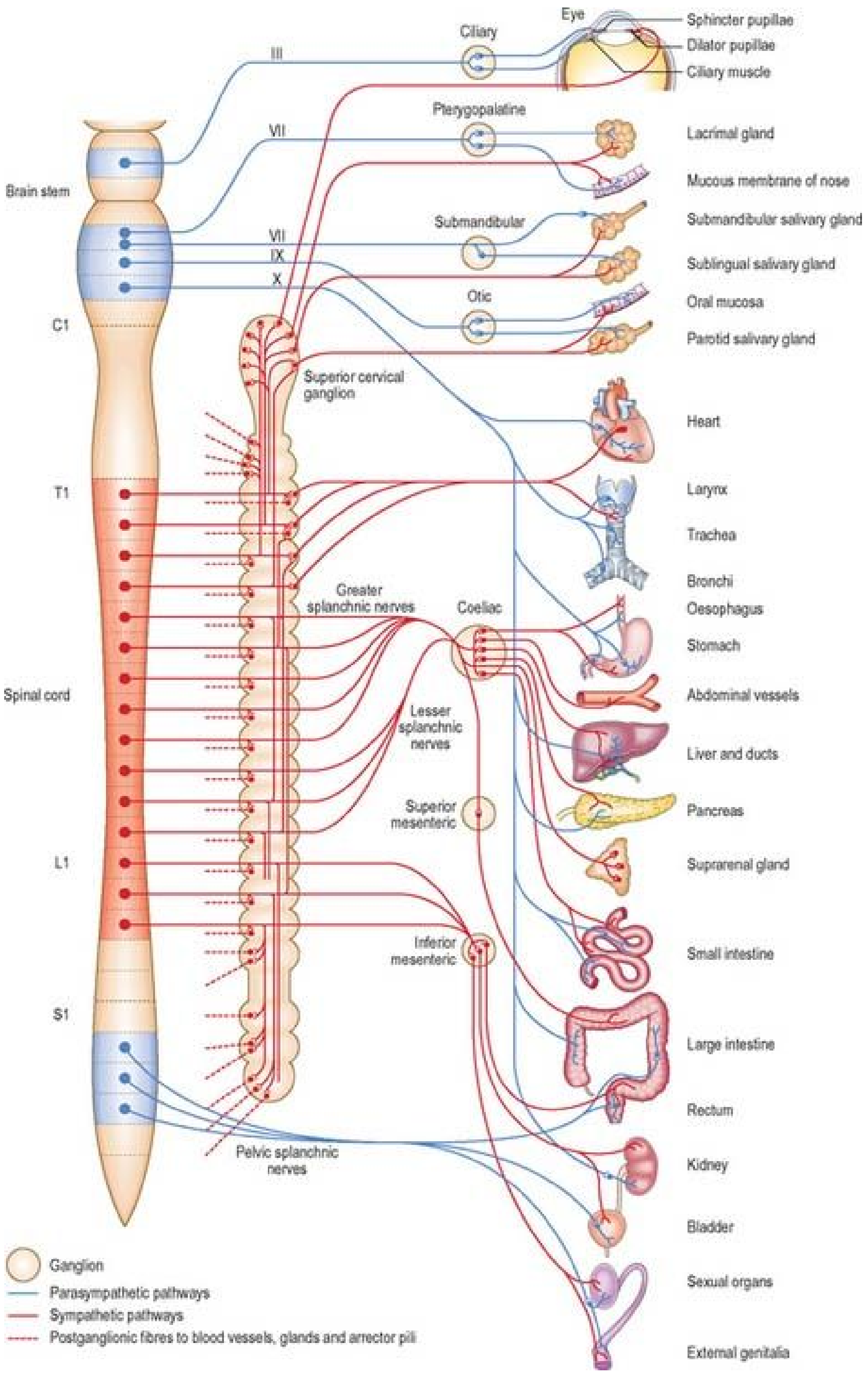
Eye
Sphincter pupillae
Dilator pupillae
Ciliary muscle
Ciliary
III
Pterygopalatine
VII
Lacrimal gland
Mucous membrane of nose
Brain stem
Submandibular
Submandibular salivary gland
VII
IX
X
Sublingual salivary gland
Otic
Oral mucosa
Parotid salivary gland
C1
Superior cervical ganglion
Heart
T1
Larynx
Trachea
Bronchi
Oesophagus
Greater splanchnic nerves
Coeliac
Stomach
Spinal cord
Abdominal vessels
Lesser splanchnic nerves
Liver and ducts
Superior mesenteric
Pancreas
L1
Suprarenal gland
Inferior mesenteric
Small intestine
S1
Large intestine
Rectum
Pelvic splanchnic nerves
Kidney
Bladder
Ganglion
Parasympathetic pathways
Sympathetic pathways
Postganglionic fibres to blood vessels, glands and arrector pili
Sexual organs
External genitalia

Fig. 15.13 Efferent pathways of the autonomic nervous system.

The autonomic nervous system is divided into three major parts: sympathetic, parasympathetic and enteric. These differ in organization and structure but are functionally integrated. Most, but not all, structures innervated by the autonomic nervous system receive both sympathetic and parasympathetic fibres, whereas the enteric nervous system is a network of neurones intrinsic to the wall of the gastrointestinal tract.

Two long-held dogmas are that the sympathetic and parasympathetic nervous systems are functionally antagonistic (because activation of their respective efferents has opposing actions upon target structures) and that sympathetic reactions are mass responses whereas parasympathetic reactions are usually more localized. A better concept is that the two sets of neurones constitute an integrated system for the coordinated neural regulation of visceral and homeostatic functions. Moreover, even though widespread activation of the sympathetic nervous system may occur, e.g. in association with fear or rage, it is recognized that the sympathetic nervous system is also capable of discrete activation. In general, sympathetic activity results in the constriction of cutaneous arteries (increasing blood supply to the heart, muscles and brain), cardiac acceleration, an increase in blood pressure, contraction of sphincters and depression of peristalsis, all of which mobilize body energy stores for dealing with increased activity. Parasympathetic activity results in cardiac slowing and an increase in intestinal glandular and peristaltic activities, which may be considered to conserve body energy stores.

Autonomic activity is not initiated or controlled solely by the reflex connections of general visceral afferent pathways, nor do impulses in these pathways necessarily activate general visceral efferents. For example, in many situations demanding general sympathetic activity the initiator is somatic and typically arises either from the special senses or the skin. Rises in blood pressure and pupillodilatation may result from the stimulation of somatic receptors in the skin and other tissues. Peripheral autonomic activity is integrated at higher levels in the brain stem and cerebrum, including various nuclei of the brain stem reticular formation, thalamus and hypothalamus, the limbic lobe and prefrontal neocortex, together with the ascending and descending pathways which interconnect these regions.

The classical concept of autonomic neurotransmission is that preganglionic neurones of both sympathetic and parasympathetic systems are cholinergic and that postganglionic parasympathetic neurones are also cholinergic while those of the sympathetic nervous system are noradrenergic. The discovery of neurones that do not use either acetylcholine or noradrenaline (norepinephrine) as their primary transmitter, and the recognition of a multiplicity of substances in autonomic nerves which fulfil the criteria for a neurotransmitter or neuromodulator, have greatly complicated neuropharmacological concepts of the autonomic nervous system. Thus, adenosine 5′-triphosphate (ATP), numerous peptides and nitric oxide have all been implicated in the mechanisms of cell signalling in the autonomic nervous system. The principal cotransmitters in sympathetic nerves are ATP and neuropeptide Y, in parasympathetic nerves vasoactive intestinal polypeptide (VIP) and in enteric nerves ATP, VIP and substance P.

SYMPATHETIC NERVOUS SYSTEM

The sympathetic trunks are two ganglionated nerve cords that extend on either side of the vertebral column from the cranial base to the coccyx (Ch. 55). The ganglia are joined to spinal nerves by short connecting nerves called white and grey rami communicantes. Preganglionic axons join the trunk through the white rami communicantes while postganglionic axons leave the trunk in the grey rami. In the neck each sympathetic trunk lies posterior to the carotid sheath and anterior to the transverse processes of the cervical vertebrae. In the thorax the trunks are anterior to the heads of the ribs, in the abdomen they lie anterolateral to the bodies of the lumbar vertebrae, and in the pelvis they are anterior to the sacrum and medial to the anterior sacral foramina. Anterior to the coccyx the two trunks meet in a single, median, terminal ganglion. Cervical sympathetic ganglia are usually reduced to three by fusion. The internal carotid nerve, a continuation of the sympathetic trunk, issues from the cranial pole of the superior ganglion and accompanies the internal carotid artery through its canal into the cranial cavity. There are from 10 to 12 (usually 11) thoracic ganglia, 4 lumbar ganglia and 4 or 5 ganglia in the sacral region.

The cell bodies of preganglionic sympathetic neurones are located in the lateral horn of the spinal grey matter of all thoracic segments and the upper two or three lumbar segments (Fig. 15.14). Their axons are myelinated with diameters of 1.5–4 μm. They leave the cord in the corresponding ventral nerve roots and pass into the spinal nerves, but soon leave in white rami communicantes to join the sympathetic trunk (Fig. 15.15). Neurones like those in the lateral grey column exist at other levels of the cord above and below the thoracolumbar outflow and small numbers of their fibres leave in other ventral roots. Preganglionic sympathetic neurones release acetylcholine as their principal neurotransmitter.

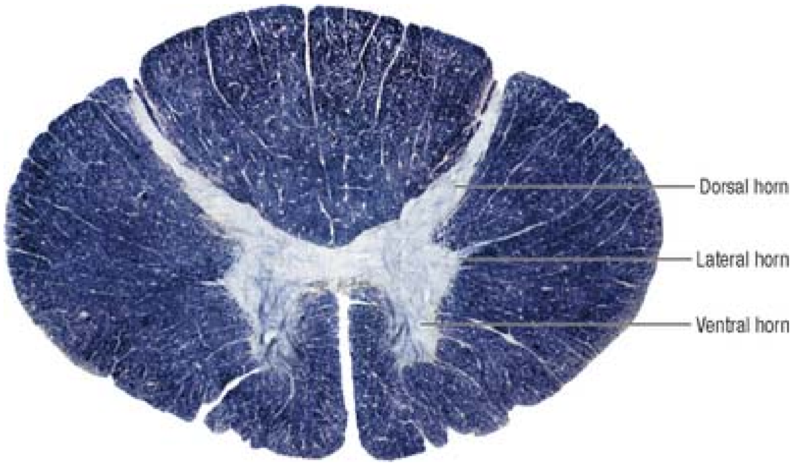
Dorsal horn
Lateral horn
Ventral horn

Fig. 15.14 Transverse section through the thoracic spinal cord showing the lateral horn where preganglionic sympathetic neurones are located. (Figure enhanced by B Crossman.)

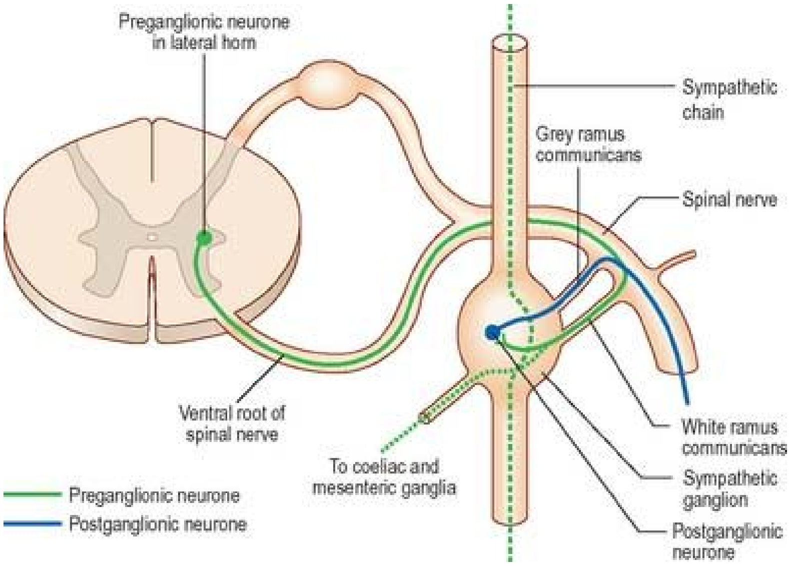
Preganglionic neurone in lateral horn
Sympathetic chain
Grey ramus communicans
Spinal nerve
White ramus communicans
Sympathetic ganglion
Postganglionic neurone
Ventral root of spinal nerve
To coeliac and mesenteric ganglia
Preganglionic neurone
Postganglionic neurone

Fig. 15.15 Relationship between spinal nerves and the sympathetic trunk.

On reaching the sympathetic trunk, preganglionic fibres behave in one of several ways (Fig. 15.15). They may synapse with neurones in the nearest ganglion, or traverse the nearest ganglion and ascend or descend in the sympathetic chain to end in another ganglion. A preganglionic fibre may terminate in a single ganglion or, through collateral branches, synapse with neurones in several ganglia. Preganglionic fibres may traverse the nearest ganglion, ascend or descend and, without synapsing, emerge in one of the medially directed branches of the sympathetic trunk to synapse in the ganglia of autonomic plexuses (mainly situated in the midline, e.g. around the coeliac and mesenteric arteries). More than one preganglionic fibre may synapse with a single postganglionic neurone. Uniquely, the suprarenal gland is innervated directly by preganglionic sympathetic neurones that traverse the sympathetic trunk and coeliac ganglion without synapse.

The somata of sympathetic postganglionic neurones are located mostly in ganglia of the sympathetic trunk or ganglia in more peripheral plexuses. The axons of postganglionic neurones are, therefore, generally longer than those of preganglionic neurones, an exception being some of those that innervate pelvic viscera. The axons of ganglionic cells are unmyelinated. They are distributed to target organs in various ways. Those from a ganglion of the sympathetic trunk may return to the spinal nerve of preganglionic origin through a grey ramus communicans, which usually joins the nerve just proximal to the white ramus, and are then distributed through ventral and dorsal spinal rami to blood vessels, sweat glands, hairs, etc., in their zone of supply. Segmental areas vary in extent and overlap considerably. The extent of innervation of different effector systems, e.g. vasomotor, sudomotor, etc., by a particular nerve may not be the same. Alternatively, postganglionic fibres may pass in a medial branch of a ganglion direct to particular viscera, or innervate adjacent blood vessels, or pass along them externally to their peripheral distribution. They may ascend or descend before leaving the sympathetic trunk as described above. Many fibres are distributed along arteries and ducts as plexuses to distant effectors.

The principal neurotransmitter released by postganglionic sympathetic neurones is noradrenaline. The sympathetic system has a much wider distribution than the parasympathetic. It innervates all sweat glands, the arrector pili muscles, the muscular walls of many blood vessels, the heart, lungs and respiratory tree, the abdominopelvic viscera, the oesophagus, the muscles of the iris, and the non-striated muscle of the urogenital tract, eyelids and elsewhere.

Postganglionic sympathetic fibres that return to the spinal nerves are vasoconstrictor to blood vessels, secretomotor to sweat glands and motor to the arrector pili muscles within their dermatomes. Those that accompany the motor nerves to voluntary muscles are probably only dilatatory. Most, if not all, peripheral nerves contain postganglionic sympathetic fibres. Those reaching the viscera are concerned with general vasoconstriction, bronchial and bronchiolar dilatation, modification of glandular secretion, pupillary dilatation, inhibition of alimentary muscle contraction, etc. A single preganglionic fibre probably synapses with the postganglionic neurones in only one effector system, which means that effects such as sudomotor and vasomotor actions can be separate.

PARASYMPATHETIC NERVOUS SYSTEM

Preganglionic parasympathetic neurone cell bodies are located in certain cranial nerve nuclei of the brain stem (see Fig. 19.1) and in the grey matter of the second to fourth sacral segments of the spinal cord. Efferent fibres, which are myelinated, emerge from the CNS only in cranial nerves III, VII, IX and X and in the second to fourth sacral spinal nerves. Preganglionic parasympathetic neurones are cholinergic.

The cell bodies of postganglionic parasympathetic neurones are mostly sited distant from the CNS, either in discrete ganglia located near the structures innervated, or dispersed in the walls of viscera. In the cranial part of the parasympathetic system there are four small peripheral ganglia, ciliary, pterygopalatine, submandibular and otic, that are all described on a regional basis in Section 4. These are solely efferent parasympathetic ganglia, unlike the trigeminal, facial, glossopharyngeal and vagal ganglia, all of which are concerned exclusively with afferent impulses and contain the cell bodies of sensory neurones. The cranial parasympathetic ganglia are also traversed by afferent fibres, postganglionic sympathetic fibres, and, in the case of the otic ganglion, even by branchial efferent fibres; none of these fibres synapse in the ganglia. Postganglionic parasympathetic fibres are usually unmyelinated and shorter than their counterparts in the sympathetic system, because the ganglia in which the parasympathetic fibres synapse are in or near the viscera they supply. Postganglionic parasympathetic neurones are cholinergic.

ENTERIC NERVOUS SYSTEM AND INTRINSIC NEURONES

Many peripheral autonomic ganglia contain neurones derived from the neural crest during embryonic development that are anatomically distinct from classical sympathetic and parasympathetic neurones. Connections between these intrinsic neurones allow them to sustain and modulate visceral activities by local reflex mechanisms. The enteric nervous system consists of many millions of neurones and enteric glial cells grouped into ganglionated plexuses lying in the wall of the gastrointestinal tract: ganglia containing neuronal cell bodies and glia are connected by bundles of axons to form myenteric and submucous plexi that extend from the oesophagus to the anal sphincter (Chs 3 and 60). This intrinsic circuitry mediates numerous reflex functions including the contractions of the muscular coats of the alimentary tract, secretion of gastric acid, intestinal transport of water and electrolytes and the regulation of mucosal blood flow. Although complex interactions occur between the enteric and sympathetic and parasympathetic nervous systems, the enteric nervous system is capable of sustaining local reflex activity independent of the CNS.

Since intrinsic neurones survive after section of the extrinsic sympathetic and parasympathetic nerves, organs that are transplanted are not truly denervated. Separation from their autonomic input often has no obvious impact on the non-striated muscle or glands innervated by autonomic fibres: contraction may be unaffected and no structural changes ensue. This has been variously attributed to the continued activity of local plexuses or to the intrinsic activity of visceral muscle. In some important instances, however, denervation does result in cessation of activity, e.g. in sweat glands, pilomotor muscle, orbital non-striated muscle and the suprarenal medulla.

VISCERAL AFFERENT PATHWAYS

General visceral afferent fibres from the viscera and blood vessels accompany their efferent counterparts, and are the peripheral processes of unipolar cell bodies located in some cranial nerve and dorsal root ganglia. They are contained in the vagus, glossopharyngeal, and possibly other cranial nerves; the second to fourth sacral spinal nerves, distributed with the pelvic splanchnic nerves; and in thoracic and upper lumbar spinal nerves, distributed through rami communicantes and alongside the efferent sympathetic innervation of viscera and blood vessels.

The cell bodies of vagal general visceral afferent fibres are in the superior and inferior vagal ganglia. Their peripheral processes are distributed to terminals in the pharyngeal and oesophageal walls where, acting synergistically with glossopharyngeal visceral afferents in the pharynx, they are concerned with swallowing reflexes. Vagal afferents are also believed to innervate the thyroid and parathyroid glands. In the heart, vagal afferents innervate the walls of the great vessels, the aortic bodies and pressor receptors, where they are stimulated by raised intravascular pressure. In the lungs they are distributed via the pulmonary plexuses. They supply bronchial mucosa, where they are probably involved in cough reflexes; bronchial muscle, where they encircle myocytes and end in tendrils, which are sometimes regarded as muscle spindles and which are believed to be stimulated by change in the length of myocytes; interalveolar connective tissue, where their knob-like endings, together with terminals on myocytes, may evoke Hering–Breuer reflexes; the adventitia of pulmonary arteries, where they may be pressor receptors; and the intima of pulmonary veins, where they may be chemoreceptors. Vagal visceral afferent fibres also end in the gastric and intestinal walls, digestive glands, and the kidneys. Fibres ending in the gut and its ducts respond to stretch or contraction. Gastric impulses may evoke sensations of hunger and nausea.

The cell bodies of glossopharyngeal general visceral afferents are in the glossopharyngeal ganglia. Their peripheral processes innervate the posterior lingual region, the tonsils and pharynx, but they do not innervate taste buds.

They also innervate the carotid sinus and the carotid body, which contain receptors sensitive to tension and changes in chemical composition of the blood. Impulses from these receptors are essential to circulatory and respiratory reflexes.

Visceral afferents that enter the spinal cord through spinal nerve roots terminate in the spinal grey matter. The central processes of vagal and glossopharyngeal afferent fibres end in the vagal nucleus or the nucleus solitarius of the medulla. Visceral afferents establish connections within the CNS that mediate autonomic reflexes. In addition, afferent impulses probably mediate visceral sensations such as hunger, nausea, sexual excitement, vesical distension, etc. Visceral pain fibres may follow these routes. Although viscera are insensitive to cutting, crushing or burning, excessive tension in smooth muscle and some pathological conditions produce visceral pain. In visceral disease, vague pain may be felt near the viscus itself (visceral pain) or in a cutaneous area or other tissue whose somatic afferents enter spinal segments receiving afferents from the viscus, a phenomenon known as referred pain. If inflammation spreads from a diseased viscus to the adjacent parietal serosa (e.g. the peritoneum), somatic afferents will be stimulated, causing local somatic pain, which is commonly spasmodic. Referred pain is often associated with local cutaneous tenderness.

Afferent fibres in pelvic splanchnic nerves innervate pelvic viscera and the distal part of the colon. Vesical receptors are widespread: those in muscle strata are associated with thickly myelinated fibres and are believed to be stretch receptors, possibly activated by contraction. Pain fibres from the bladder and proximal urethra traverse both the pelvic splanchnic nerves and the inferior hypogastric plexus, hypogastric nerves, superior hypogastric plexus and lumbar splanchnic nerves to reach their cell bodies in ganglia on the lower thoracic and upper lumbar dorsal spinal roots: the significance of this dual sensory pathway is uncertain. Lesions of the cauda equina abolish pain from vesical overdistension, but hypogastric section is ineffective. Pain fibres from the uterus traverse the hypogastric plexus and lumbar splanchnic nerves to reach somata in the lowest thoracic and upper lumbar spinal ganglia, and hypogastric division may relieve dysmenorrhoea. Afferents from the uterine cervix traverse the pelvic splanchnic nerves to reach their somata in the upper sacral spinal ganglia: stretching the cervix uteri causes pain but cauterization and biopsy excisions do not.

In general, afferent fibres that accompany pre- and postganglionic sympathetic fibres have a segmental arrangement and end in spinal cord segments from which preganglionic fibres innervate the region or viscus concerned. General visceral afferents entering thoracic and upper lumbar spinal segments are largely concerned with pain. Nociceptive impulses from the pharynx, oesophagus, stomach, intestines, kidneys, ureter, gallbladder and bile ducts seem to be carried in sympathetic pathways. Cardiac nociceptive impulses enter the spinal cord in the first to fifth thoracic spinal nerves, mainly via the middle and inferior cardiac nerves, but some fibres pass directly to the spinal nerves. It is said that there are no general visceral afferents in the superior cardiac nerves. Peripherally, the fibres pass through the cardiac plexuses and along the coronary arteries. Myocardial anoxia may evoke symptoms of angina pectoris in which pain is typically presternal, and is also referred to much of the left chest, and radiates to the left shoulder, the medial aspect of the left arm, along the left side of the neck to the jaw and occiput, and down to the epigastrium. Cardiac afferents carried in vagal cardiac branches are concerned with the reflex depression of cardiac activity. Ureteric pain fibres, also running with sympathetic fibres, are presumably involved in the agonizing renal colic that follows obstruction by calculi. Afferent fibres from the testis and ovary run through the corresponding plexuses to somata in the tenth and eleventh thoracic dorsal root ganglia.

Certain primary afferent nerve fibres, that have their cell bodies in cranial and dorsal root ganglia, also have an efferent function (so-called sensory–motor nerves). The importance of sensory–motor nerve regulation in many organs, such as the gut, lungs, heart and blood vessels, is now recognized. While most such nerves are, presumably, purely sensory, certain of them have been termed sensory–motor because they release transmitters from their peripheral endings during the axon reflex and have a motor rather than a sensory role. The primary substances released in this way are substance P, calcitonin gene-related peptide (CGRP) and ATP. These act on target cells to produce several biological actions which include vasodilatation, increased venular permeability, changes in smooth muscle contractility, degranulation of mast cells and a variety of effects on leukocytes and fibroblasts, a process collectively known as ‘neurogenic inflammation’. The local release of such substances may play a trophic role in the maintenance of tissue integrity and repair in response to injury.

PARAGANGLIA

Paraganglia are extrasuprarenal aggregations of chromaffin tissue, distributed near to or within the autonomic nervous system (Fig. 15.16). Cells like those in paraganglia also occur in the sympathetic ganglia of various viscera and in a variety of retroperitoneal and mediastinal sites. All are derived from the neural crest, and all synthesize and store catecholamines. Their functions differ with location: some cells act as interneurones, others as sources of neuroendocrine secretion. Paraganglionic catecholamine release occurs mainly in response to chemical rather than to neural stimuli, e.g. in the suprarenal medulla. Extrasuprarenal chromaffin tissue is prominent in the fetus, and acts as the main source of catecholamines while the suprarenal medulla is immature. Although many paraganglia degenerate soon after birth, others persist into adulthood, often as microscopic paraganglia.

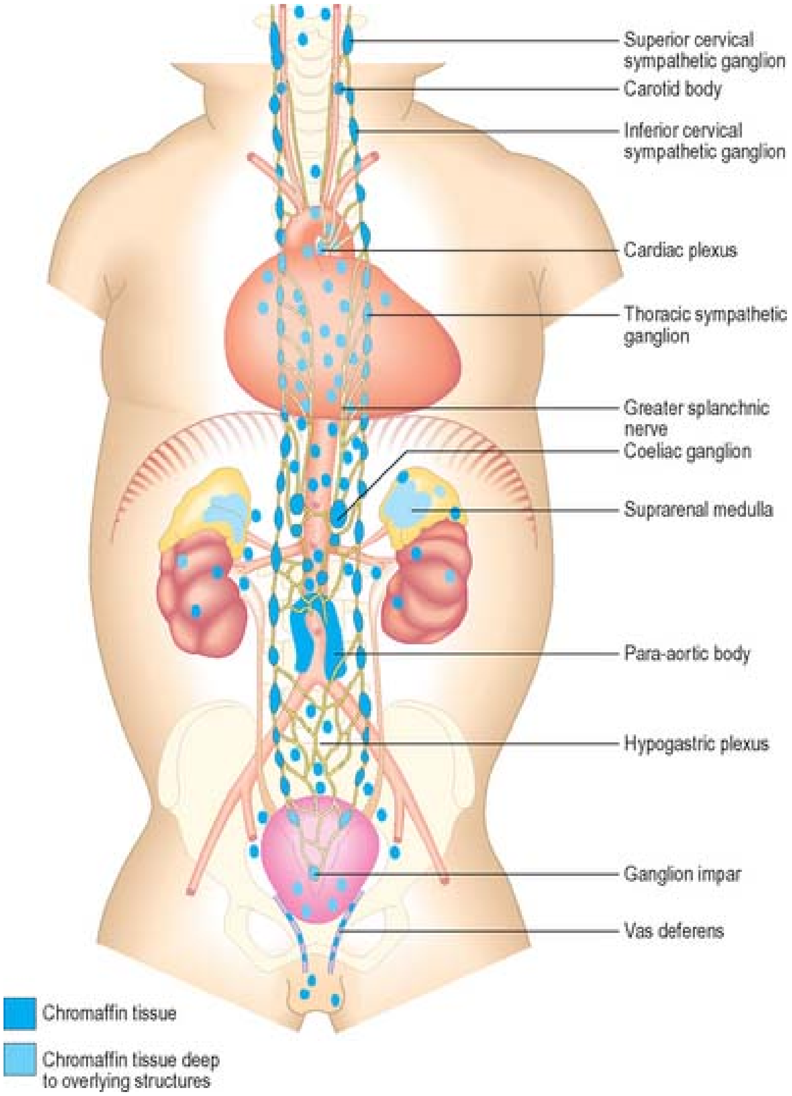
Superior cervical sympathetic ganglion
Carotid body
Inferior cervical sympathetic ganglion
Cardiac plexus
Thoracic sympathetic ganglion
Greater splanchnic nerve
Coeliac ganglion
Suprarenal medulla
Para-aortic body
Hypogastric plexus
Ganglion impar
Vas deferens
Chromaffin tissue
Chromaffin tissue deep to overlying structures

Fig. 15.16 The principal aggregations of ‘classic’ chromaffin tissue in the human neonate. The aggregates in stippled blue lie deep to overlying structures.

Paraganglia are well-vascularized and their secretory cells are usually close to one or more fenestrated capillaries. Most have a sympathetic innervation and act as endocrine organs, e.g. suprarenal medullary chromaffin cells. Others are associated with the parasympathetic system, and their secretions probably have activities on local nerve endings, e.g. the carotid body. Paraganglia produce regulatory peptides, particularly enkephalins, and store them as cytoplasmic granules until stimulated to release them. Their secretions may exert a local paracrine action on nearby cells, in addition to having remote endocrine effects.

REFERENCES

he Peripheral Nervous Systems. Björklund A, Hökfelt T, Owman C, editors. Handbook of Chemical Neuroanatomy, Vol. 6. Amsterdam: Elsevier, 1988.

Description of sensory-motor nerves..

odal A. Neurological Anatomy in Relation to Clinical Medicine, 3rd edn. Oxford: Oxford University Press, 1981.

Unconventional but highly-readable text of neuroanatomy with a strong emphasis on clinical relevance. Contains particularly good account of motor pathways..

rnstock G. Co-transmission. The fifth Heymans lecture. *Arch Int Pharmacodyn Ther*. 1990;304:7-33.

A review of neurotransmission in the autonomic nervous system..

rnstock G, editor. The Autonomic Nervous System, Vols 1–14. Switzerland: Harwood Academic Publishers, 1992–95.

Contains extensive material on the neurotransmitters of the autonomic nervous system..

ossman AR, Neary D. Neuroanatomy. An Illustrated Colour Text. 2nd edn.. Edinburgh: Churchill Livingstone; 2000.

gland MA, Wakely J. A Colour Atlas of the Brain and Spinal Cord. London: Wolfe Publishing, 1991.

eenberg SA. The history of dermatome mapping. *Arch Neurol*. 2003;60:126-131.

ines DE. Neuroanatomy. An Atlas of Structures, Sections and Systems. 5th edn.. Philadelphia: Lippincott Williams & Wilkins; 2000.

aggi CA. The pharmacology of the efferent function of sensory nerves. *J Auton Pharmacol*. 1991;11:173-208.

nken PJ, Bruyn GW. The Autonomic Nervous System. Part 1. Normal Functions. Appenzeller O, volume ed., Amsterdam and London: Elsevier Science, 1999.

nken PJ, Bruyn GW. The Autonomic Nervous System. Part 2. Dysfunctions. Appenzeller O, volume ed., Amsterdam and London: Elsevier Science, 2000.

CHAPTER 16

Ventricular system and subarachnoid space

The cerebral ventricular system consists of a series of interconnecting spaces and channels within the brain (Fig. 16.1) which are derived from the central lumen of the embryonic neural tube and the cerebral vesicles to which it gives rise (Ch. 24). Each cerebral hemisphere contains a large lateral ventricle that communicates near its rostral end with the third ventricle via the interventricular foramen (foramen of Monro). The third ventricle is a midline, slit-like cavity lying between the right and left thalamus and hypothalamus. Caudally, the third ventricle is continuous with the cerebral aqueduct, a narrow tube that passes the length of the midbrain, and which is continuous in turn with the fourth ventricle, a wide tent-shaped cavity lying between the brain stem and cerebellum. The fourth ventricle communicates with the subarachnoid space of the cisterna magna though the foramen of Magendie, and of the cerebellopontine angle through the foramina of Luschka; caudally it is continuous with the vestigial central canal of the spinal cord.

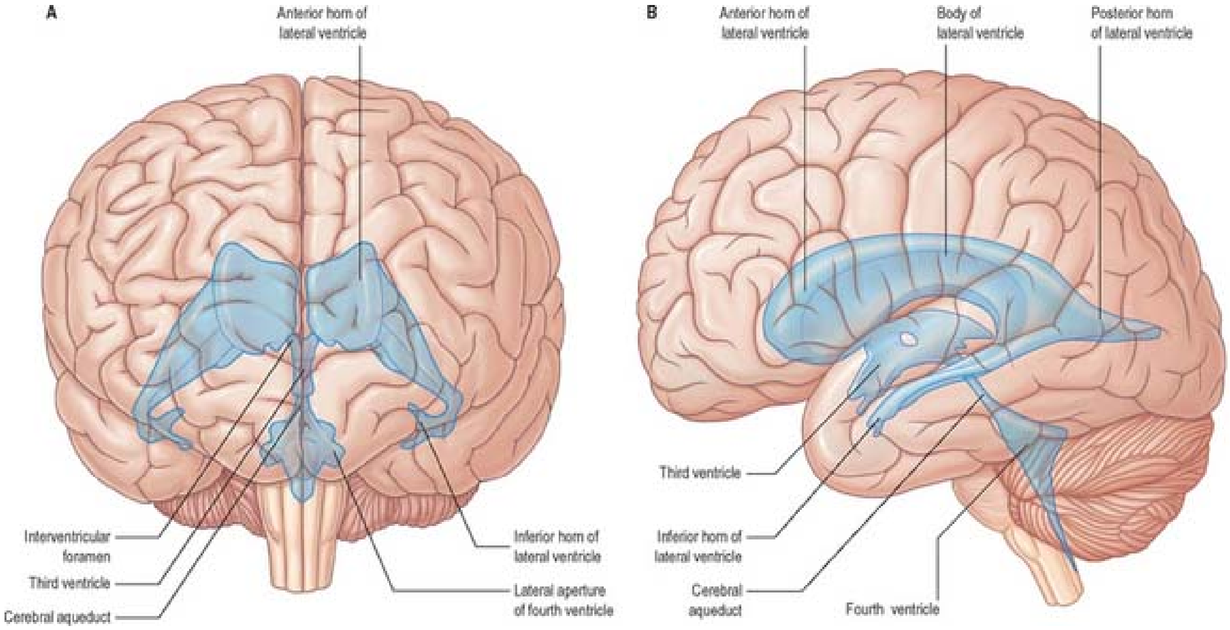
A
Anterior horn of lateral ventricle
Interventricular foramen
Third ventricle
Cerebral aqueduct
Inferior horn of lateral ventricle
Lateral aperture of fourth ventricle
B
Anterior horn of lateral ventricle
Body of lateral ventricle
Posterior horn of lateral ventricle
Third ventricle
Inferior horn of lateral ventricle
Cerebral aqueduct
Fourth ventricle

Fig. 16.1 The ventricular system. **A**, Anterior view; **B**, left lateral view.

The ventricular system contains cerebrospinal fluid (CSF), which is mostly secreted by the choroid plexuses located within the lateral, third and fourth ventricles. CSF flows from the lateral to the third ventricle, then through the cerebral aqueduct and into the fourth ventricle. It leaves the fourth ventricle through the foramen of Magendie and the foramina of Luschka to reach the subarachnoid space surrounding the brain.

TOPOGRAPHY AND RELATIONS OF THE VENTRICULAR SYSTEM

LATERAL VENTRICLE

Viewed from its lateral aspect, the lateral ventricle has a roughly C-shaped profile. The shape is a consequence of the developmental expansion of the frontal, parietal and occipital regions of the hemisphere, which displaces the temporal lobe inferiorly and anteriorly. Both the caudate nucleus and the fornix, which lie in the wall of the ventricle, have adopted a similar morphology, so that the tail of the caudate nucleus encircles the thalamus in a C-shape, and the fornix traces the outline of the ventricle forwards to the interventricular foramen.

The lateral ventricle is customarily divided into a body and anterior (frontal), posterior (occipital) and inferior (temporal) horns. The anterior horn lies within the frontal lobe. It is bounded anteriorly by the posterior aspect of the genu and rostrum of the corpus callosum, and its roof is formed by the anterior part of the body of the corpus callosum. The anterior horns of the two ventricles are separated by the septum pellucidum. The coronal profile of the anterior horn is roughly that of a flattened triangle in which the rounded head of the caudate nucleus forms the lateral wall and floor (Figs 16.2, 16.3). The anterior horn extends back as far as the interventricular foramen. The body lies within the frontal and parietal lobes and extends from the interventricular foramen to the splenium of the corpus callosum. The bodies of the lateral ventricles are separated by the septum pellucidum, which contains the columns of the fornices in its lower edge. The lateral wall of the body of the ventricle is formed by the caudate nucleus superiorly and the thalamus inferiorly. The boundary between the thalamus and caudate nucleus is marked by a groove (Fig. 16.2) which is occupied by a fascicle of nerve fibres, the stria terminalis, and by the thalamostriate vein (see Fig. 22.5). The inferior limit of the body of the ventricle and its medial wall are formed by the body of the fornix (Fig. 16.4). The fornix is separated from the thalamus by the choroidal fissure. The choroid plexus occludes the choroidal fissure and covers part of the thalamus and fornix. The body of the lateral ventricle widens posteriorly to become continuous with the posterior and inferior horns at the collateral trigone or atrium. The posterior horn curves posteromedially into the occipital lobe. It is usually diamond-shaped or square in outline, and the two sides are often asymmetrical. Fibres of the tapetum of the corpus callosum separate the ventricle from the optic radiation, and form the roof and lateral wall of the posterior horn. Fibres of the splenium of the corpus callosum (forceps major) pass medially as they sweep back into the occipital lobe, and produce a rounded elevation in the upper medial wall of the posterior horn. Lower down, a second elevation, the calcar avis, corresponds to the deeply infolded cortex of the anterior part of the calcarine sulcus. The inferior horn is the largest compartment of the lateral ventricle and extends forwards into the temporal lobe. It curves round the posterior aspect of the thalamus (pulvinar), passes downwards and posterolaterally and then curves anteriorly to end within 2.5 cm of the temporal pole, near the uncus. Its position relative to the surface of the hemisphere usually corresponds to the superior temporal sulcus. The roof of the inferior horn is formed mainly by the tapetum of the corpus callosum, but also by the tail of the caudate nucleus and the stria terminalis, which extend forwards in the roof to terminate in the amygdala at the anterior end of the ventricle. The floor of the ventricle consists of the hippocampus medially and the collateral eminence, formed by the infolding of the collateral sulcus, laterally. The inferior part of the choroid fissure lies between the fimbria (a distinct bundle of efferent fibres that leaves the hippocampus) and the stria terminalis in the roof of the temporal horn (Fig. 16.5). The temporal extension of the choroid plexus fills this fissure and covers the outer surface of the hippocampus.

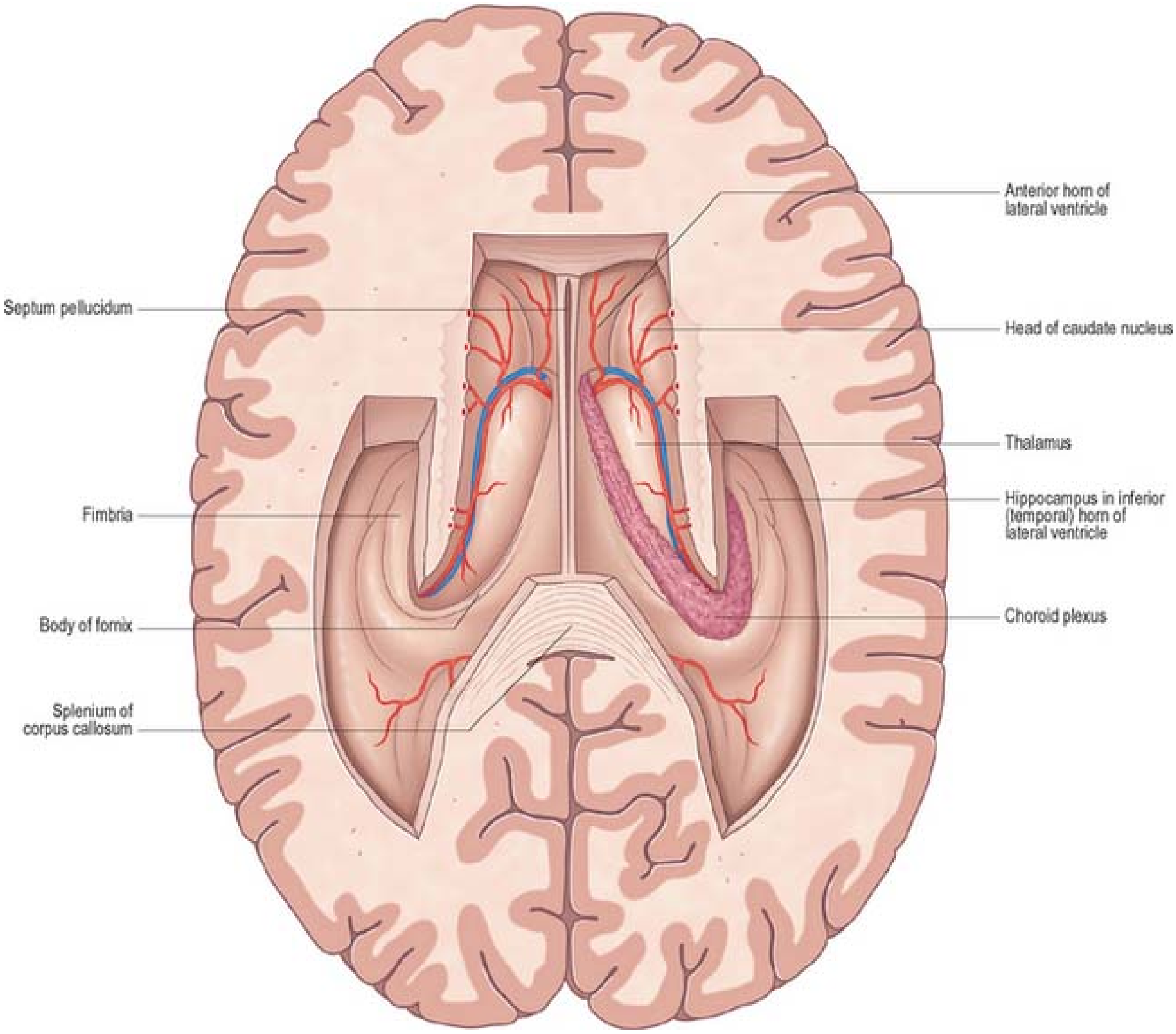
Anterior horn of lateral ventricle
Septum pellucidum
Head of caudate nucleus
Thalamus
Fimbria
Hippocampus in inferior (temporal) horn of lateral ventricle
Body of fornix
Choroid plexus
Splenium of corpus callosum

Fig. 16.2 Horizontal section of the cerebrum dissected to remove the roofs of the lateral ventricles.

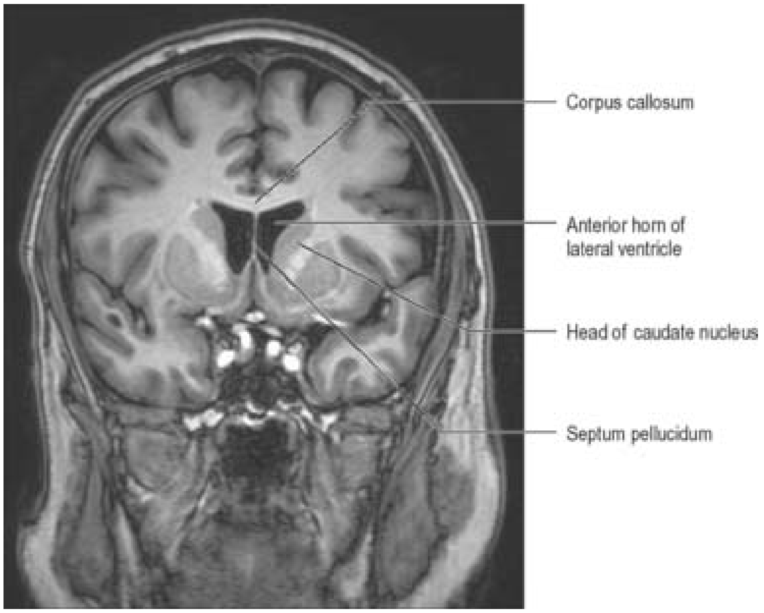
Corpus callosum
Anterior horn of lateral ventricle
Head of caudate nucleus
Septum pellucidum

Fig. 16.3 Coronal MRI scan, at the level of the anterior horn of the lateral ventricle.

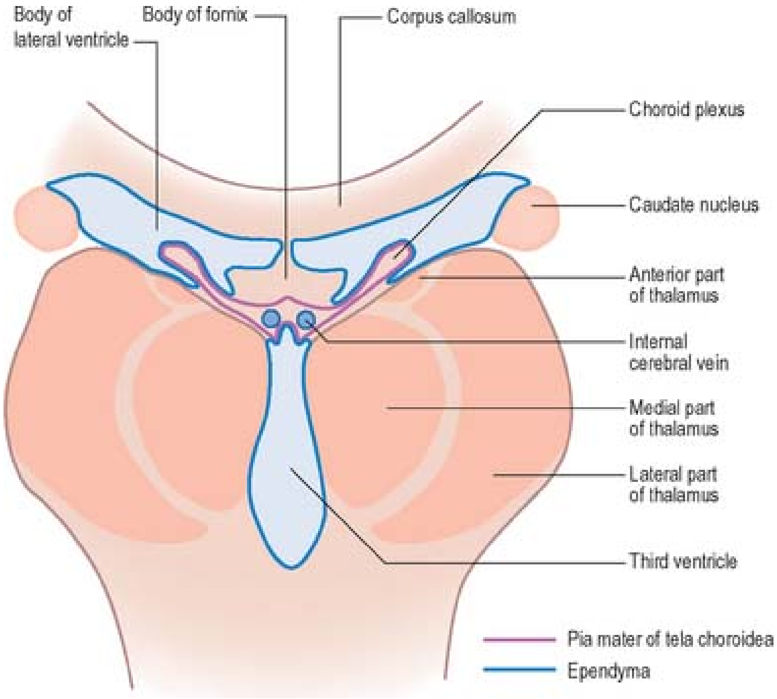
Body of lateral ventricle
Body of fornix
Corpus callosum
Choroid plexus
Caudate nucleus
Anterior part of thalamus
Internal cerebral vein
Medial part of thalamus
Lateral part of thalamus
Third ventricle
Pia mater of tela choroidea
Ependyma

Fig. 16.4 The lateral and third ventricles, coronal section.

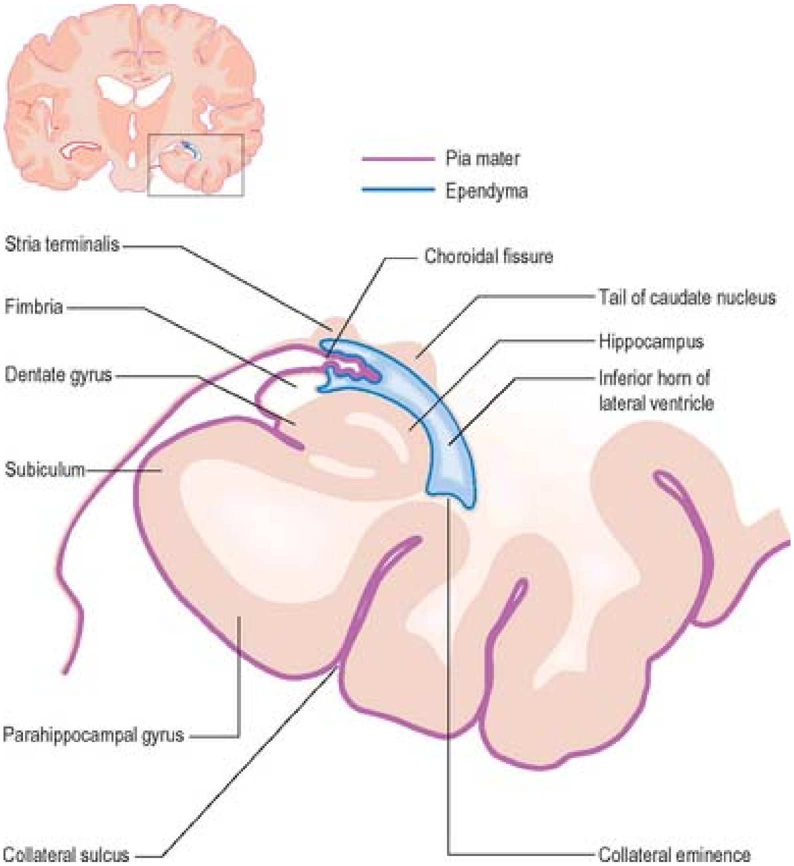
Pia mater
Ependyma
Stria terminalis
Choroidal fissure
Fimbria
Tail of caudate nucleus
Hippocampus
Dentate gyrus
Inferior horn of lateral ventricle
Subiculum
Parahippocampal gyrus
Collateral sulcus
Collateral eminence

Fig. 16.5 The inferior horn of the lateral ventricle, coronal section.

THIRD VENTRICLE

The third ventricle is a midline, slit-like cavity which is derived from the primitive forebrain vesicle (Figs 16.1, 16.4, 16.6, 16.7; see Fig. 15.8). The upper part of the lateral wall of the ventricle is formed by the medial surface of the anterior two-thirds of the thalamus, and the lower part is formed by the hypothalamus anteriorly and the subthalamus posteriorly. An indistinct hypothalamic sulcus extends horizontally on the ventricular wall between the interventricular foramen and the cerebral aqueduct, and marks the boundary between the thalamus and hypothalamus. Dorsally, the lateral wall is limited by a ridge covering the stria medullaris thalami. The lateral walls of the third ventricle are joined by an interthalamic adhesion, or massa intermedia, a band of grey matter which extends from one thalamus to the other.

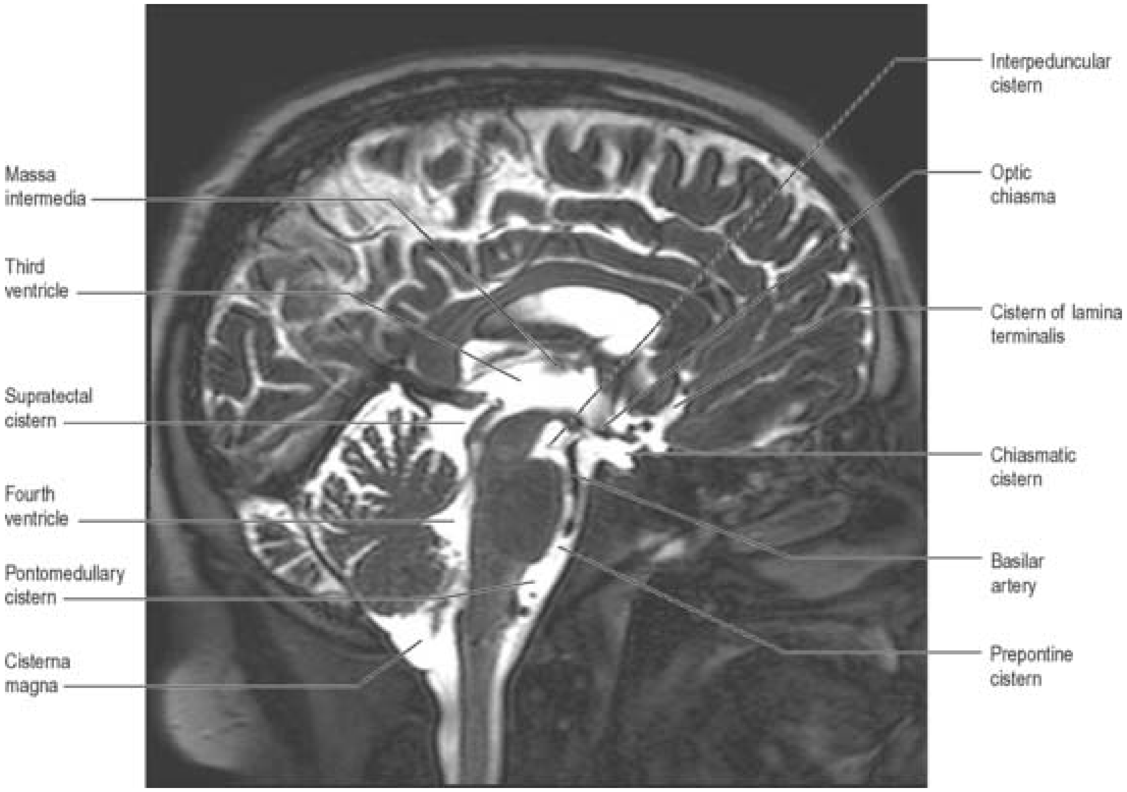
Massa intermedia
Third ventricle
Supratectal cistern
Fourth ventricle
Pontomedullary cistern
Cisterna magna
Interpeduncular cistern
Optic chiasma
Cistern of lamina terminalis
Chiasmatic cistern
Basilar artery
Prepontine cistern

Fig. 16.6 Sagittal MRI scan of the head.

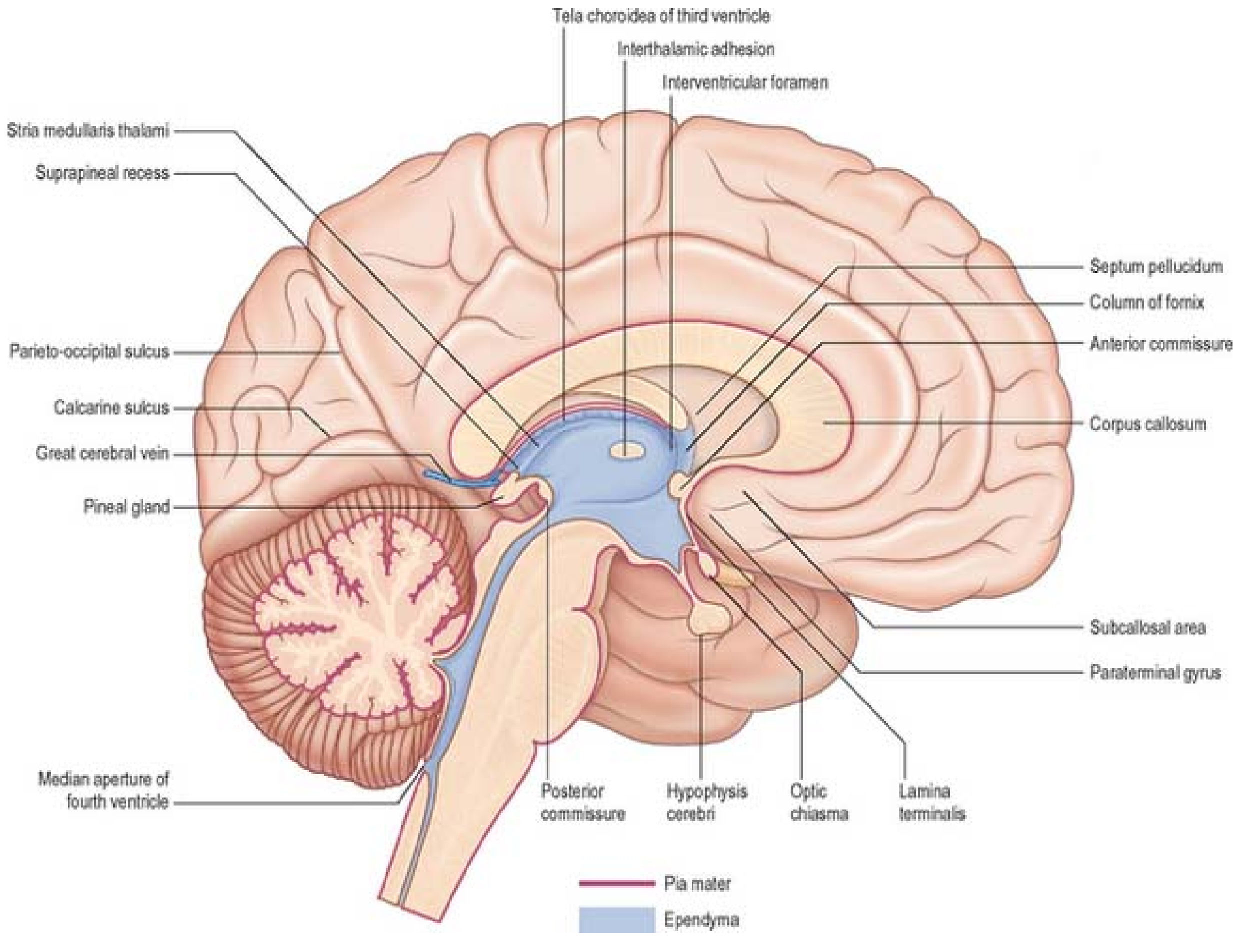
Tela choroidea of third ventricle
Interthalamic adhesion
Interventricular foramen
Stria medullaris thalami
Suprapineal recess
Septum pellucidum
Column of fornix
Anterior commissure
Parieto-occipital sulcus
Calcarine sulcus
Corpus callosum
Great cerebral vein
Pineal gland
Subcallosal area
Paraterminal gyrus
Median aperture of fourth ventricle
Posterior commissure
Hypophysis cerebri
Optic chiasma
Lamina terminalis
Pia mater
Ependyma

Fig. 16.7 The third and fourth ventricles, sagittal hemisection of the brain.

Anteriorly, the third ventricle extends to the lamina terminalis (Fig. 16.7). This thin structure stretches from the optic chiasma to the rostrum of the corpus callosum and represents the rostral boundary of the embryonic neural tube. The lamina terminalis forms the roof of the small virtual cavity lying immediately below the ventricle called the cistern of the lamina terminalis. This is important because it contains the anterior communicating artery and aneurysm formation at this site may cause intraventricular haemorrhage through the thin membrane of the lamina terminalis. Above this, the anterior wall is formed by the diverging columns of the fornices and the transversely orientated anterior commissure, which crosses the midline. The anterior and posterior commissures are important neuroradiological landmarks. Prior to the introduction of modern imaging techniques, the fact that these commissures could be identified by ventriculography led to their use as reference markers for stereotaxic surgical procedures. This convention is now universal: the positions of the anterior and posterior commissures are used as the basic reference points for surgical atlases of brain anatomy. The narrow interventricular foramen is located immediately posterior to the column of the fornix and separates the fornix from the anterior nucleus of the thalamus.

There is a small, angular, optic recess at the base of the lamina terminalis, just dorsal to and extending into the optic chiasma. Behind it, the anterior part of the floor of the third ventricle is formed mainly by hypothalamic structures. Immediately behind the optic chiasma lies the thin infundibular recess, which extends into the pituitary stalk. Behind this recess, the tuber cinereum and the mammillary bodies form the floor of the ventricle.

The roof of the third ventricle is a thin ependymal layer that extends from its lateral walls to the choroid plexus, which spans the choroidal fissure (Fig. 16.4). Above the roof is the body of the fornix. The posterior boundary of the ventricle is marked by a suprapineal recess above the pineal gland, a pineal (epiphysial) recess, which extends into the pineal stalk, and by the posterior commissure. Below the commissure the ventricle is continuous with the cerebral aqueduct of the midbrain.

CEREBRAL AQUEDUCT

The cerebral aqueduct is a small tube, roughly circular in transverse section and 1–2 mm in diameter. It extends throughout the dorsal quarter of the midbrain in the midline and is surrounded by the periaqueductal (central) grey matter (Fig. 16.7; see Fig. 19.19). Rostrally, it commences immediately behind and below the posterior commissure, where it is continuous with the caudal aspect of the third ventricle. Caudally, it is continuous with the lumen of the fourth ventricle at the junction of the midbrain and pons. The superior and inferior colliculi are dorsal to the aqueduct and the midbrain tegmentum is ventral.

FOURTH VENTRICLE

The fourth ventricle lies between the brain stem and the cerebellum (Figs 16.1B, 16.6, 16.7, 16.8; see Fig. 19.3). Rostrally it is continuous with the cerebral aqueduct, and caudally with the central canal of the spinal cord. In sagittal section, the fourth ventricle has a characteristic triangular profile, and the apex of its tented roof protrudes into the inferior aspect of the cerebellum. The ventricle is at its widest at the level of the pontomedullary junction, where a lateral recess on both sides extends to the lateral border of the brain stem. At this point the lateral aperture of the fourth ventricle (foramen of Luschka) provides access to the subarachnoid space at the cerebellopontine angle; CSF flows through it into the lateral extension of the pontine cistern. Occasionally, a lateral recess may not open.

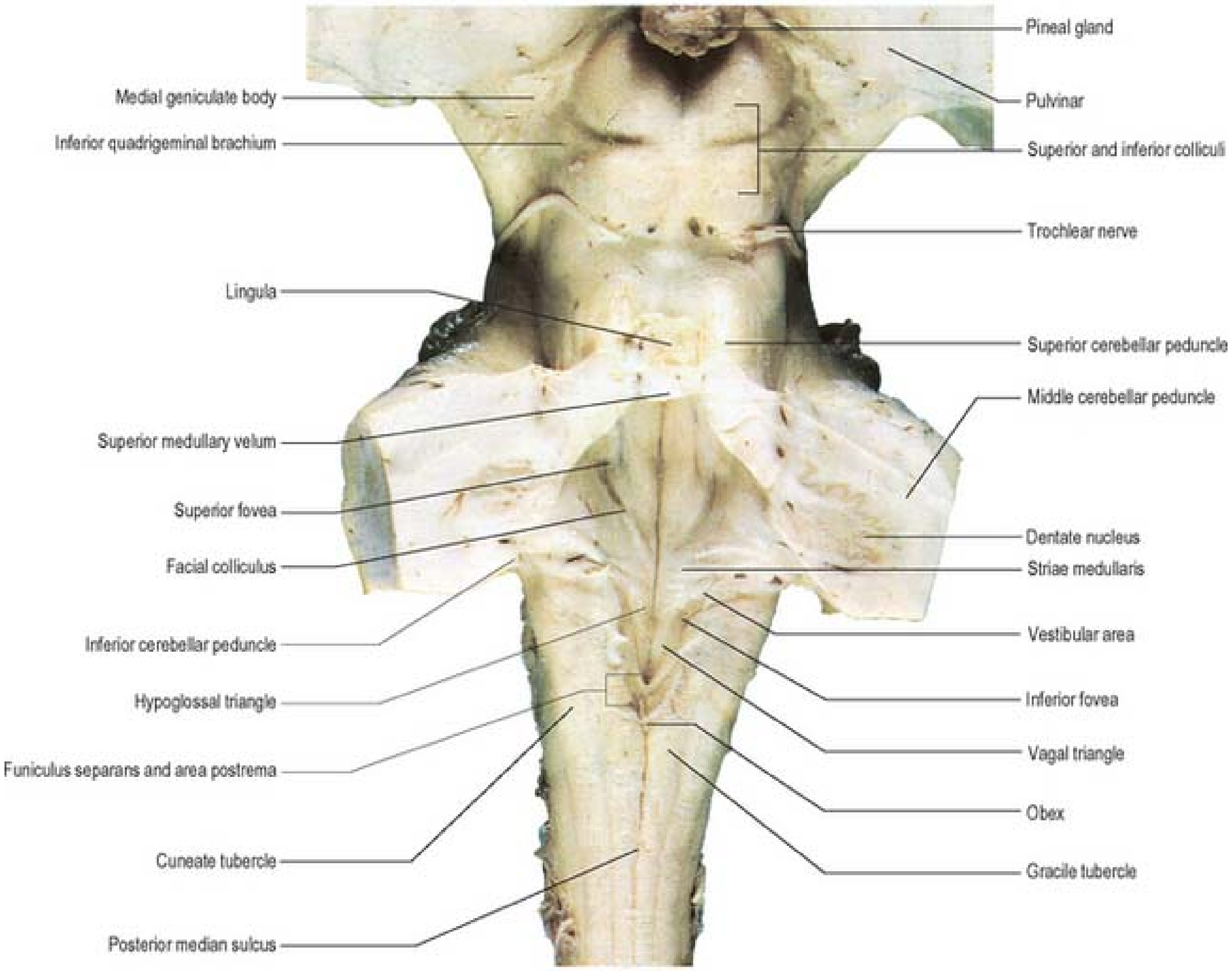

Medial geniculate body
Inferior quadrigeminal brachium
Lingula
Superior medullary velum
Superior fovea
Facial colliculus
Inferior cerebellar peduncle
Hypoglossal triangle
Funiculus separans and area postrema
Cuneate tubercle
Posterior median sulcus
Pineal gland
Pulvinar
Superior and inferior colliculi
Trochlear nerve
Superior cerebellar peduncle
Middle cerebellar peduncle
Dentate nucleus
Striae medullaris
Vestibular area
Inferior fovea
Vagal triangle
Obex
Gracile tubercle

Fig. 16.8 The floor of the fourth ventricle, dorsal aspect of the brain stem.

The floor of the fourth ventricle is a shallow diamond-shaped, or rhomboidal, depression (rhomboid fossa) on the dorsal surfaces of the pons and the rostral half of the medulla. It consists largely of grey matter and contains important cranial nerve nuclei. The precise location of some nuclei is discernible from surface features. The superior part of the ventricular floor is triangular in shape and is limited laterally by the superior cerebellar peduncles as they converge towards the cerebral aqueduct. Its posterior limit is called the obex. The inferior part of the ventricular floor is also triangular in shape and is bounded caudally by the gracile and cuneate tubercles, which contain the dorsal column nuclei, and, more rostrally, by the diverging inferior cerebellar peduncles. A longitudinal median sulcus divides the floor of the fourth ventricle. Each half is itself divided, by an often indistinct sulcus limitans, into a medial region known as the medial eminence and a lateral region known as the vestibular area. The vestibular nuclei lie beneath the vestibular area. In the superior part of the ventricular floor, the medial eminence is represented by the facial colliculus, a small elevation produced by an underlying loop of efferent fibres from the facial nucleus which covers the abducens nucleus. Between the facial colliculus and the vestibular area the sulcus limitans widens into a small depression, the superior fovea. In its upper part, the sulcus limitans constitutes the lateral limit of the floor of the fourth ventricle. Here, a small region of bluish-grey pigmentation denotes the presence of the subjacent locus coeruleus. Inferior to the facial colliculus, at the level of the lateral recess of the ventricle, a variable group of nerve fibre fascicles, known as the striae medullaris, runs transversely across the ventricular floor and passes into the median sulcus. In the inferior area of the floor of the fourth ventricle, the medial eminence is represented by the hypoglossal triangle (trigone), which lies over the hypoglossal nucleus. Laterally, the sulcus limitans widens to produce an indistinct inferior fovea. Caudal to the inferior fovea, between the hypoglossal triangle and the vestibular area, is the vagal triangle (trigone), which covers the dorsal motor nucleus of the vagus. The triangle is crossed below by a narrow translucent ridge, the funiculus separans, which is separated from the gracile tubercle by the small area postrema. The funiculus and area postrema are both covered by thickened ependyma, containing tanycytes; the area postrema also contains neurones. The blood–brain barrier is modified at both sites.

The roof of the fourth ventricle is formed by the superior and inferior medullary veli. Superiorly, a thin sheet of tissue, the superior medullary velum, stretches across the ventricle between the converging superior cerebellar peduncles (Fig. 16.8). The superior medullary velum is continuous with the cerebellar white matter and is covered dorsally by the lingula of the superior vermis. The inferior medullary velum is more complex and is mostly composed of a thin sheet, devoid of neural tissue, formed by ventricular ependyma and the pia mater of the tela choroidea, which covers it dorsally. A large median aperture (foramen of Magendie) is present in the roof of the ventricle as a perforation in the posterior medullary velum, just inferior to the nodule of the cerebellum: CSF flows through the foramen from the ventricle into the cisterna magna.

CIRCUMVENTRICULAR ORGANS

The walls of the ventricular system are lined with ependymal cells covering a subependymal layer of glia. At certain midline sites in the ventricular walls, collectively referred to as circumventricular organs, the blood–brain barrier is absent and specialized ependymal cells called tanycytes are present (Fig. 16.9). The functions of ependyma and tanycytes may include secretion into the CSF; transport of neurochemicals from subjacent neurones, glia or vessels to the CSF; transport of neurochemicals from the CSF to the same subjacent structures; chemoreception. In the adult, the ependymal and subependymal glial cell layers are the source of undifferentiated stem cells that are currently under intensive study for their potential neurorestorative properties.

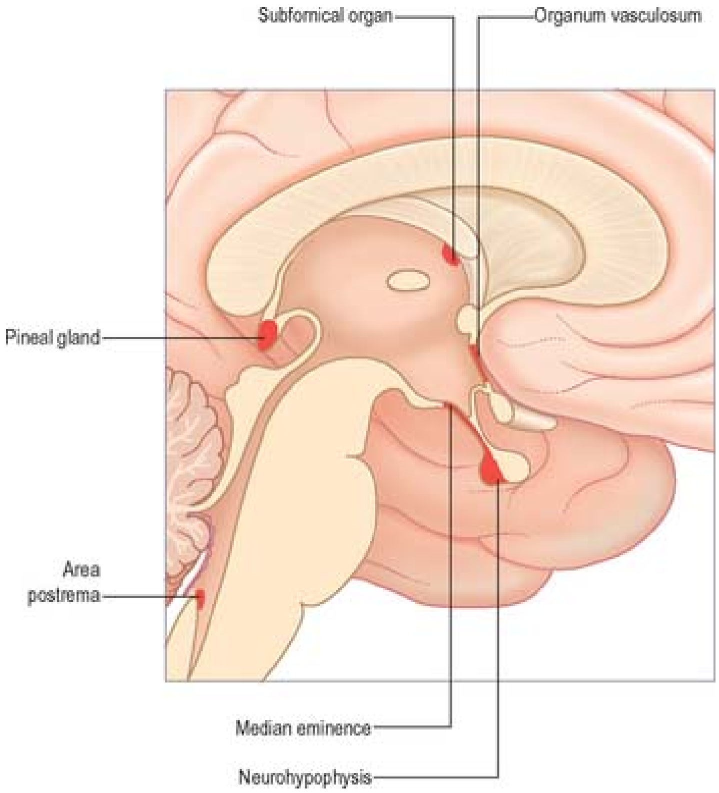
Subfornical organ
Organum vasculosum
Pineal gland
Area postrema
Median eminence
Neurohypophysis

Fig. 16.9 The locations of the circumventricular organs, median sagittal section of the brain.

The circumventricular organs include the vascular organ (organum vasculosum), subfornical organ, neurohypophysis, median eminence, subcommissural organ, pineal gland and area postrema.

The vascular organ lies in the lamina terminalis between the optic chiasma and the anterior commissure. Its external zone contains a richly fenestrated vascular plexus, which covers glia and a network of nerve fibres. The ependymal cells of the vascular organ, like those of other circumventricular organs, are flattened and have few cilia. The major inputs appear to come from the subfornical organ, locus coeruleus and a number of hypothalamic nuclei; the vascular organ projects to the median preoptic and supraoptic nuclei. The vascular organ is involved in the regulation of fluid balance and may also have neuroendocrine functions.

The subfornical organ lies at the level of the interventricular foramen. It contains many neurones, glial cells and a dense fenestrated capillary plexus, and is covered by flattened ependyma. It is believed to have widespread hypothalamic interconnections and to function in the regulation of fluid balance and drinking.

The neurohypophysis (posterior pituitary) is the site of termination of neurosecretory projections from the supraoptic and paraventricular nuclei of the hypothalamus. Neurones in these nuclei release vasopressin and oxytocin respectively into the capillary bed of the neurohypophysis, where the hormones gain access to the general circulation.

The median eminence contains the terminations of axons of hypothalamic neurosecretory cells. Peptides released from these axons control the hormonal secretions of the anterior pituitary via the pituitary portal system of vessels.

The subcommissural organ lies ventral to and below the posterior commissure, near the inferior wall of the pineal recess. The ependymal cells on the dorsal aspect of the cerebral aqueduct are tall, columnar and ciliated, with granular basophilic cytoplasm: they may be involved in the secretion of materials into the CSF from adjoining axonal terminals or capillaries.

The pineal gland (see Ch. 21) is a small structure approximately 8 mm in diameter situated rostro-dorsal to the superior colliculus and behind the stria medullaris. It is part of the epithalamus and consists of internal lobules of pinealocytes and sparse neurones covered by a pial capsule. It secretes melatonin which appears to be involved in the inhibition of puberty in children and in the in the regulation of the sleep–wake cycle in both children and adults.

The area postrema is a bilaterally paired structure, located at the caudal limit of the floor of the fourth ventricle. It is an important chemoreceptive area that triggers vomiting in response to the presence of emetic substances in the blood. The area postrema, along with the nucleus of the solitary tract and the dorsal motor nucleus of the vagus, makes up the so-called dorsal vagal complex, which is the major termination site of vagal afferent nerve fibres.

CHOROID PLEXUS AND CEREBROSPINAL FLUID

CHOROID PLEXUS

The vascular pia mater in the roofs of the third and fourth ventricles, and in the medial wall of the lateral ventricle along the line of the choroid fissure, is closely apposed to the ependymal lining of the ventricles, without any intervening brain tissue. It forms the tela choroidea, which gives rise to the highly vascularized choroid plexuses from which CSF is secreted into the lateral, third and fourth ventricles (Figs 16.2, 16.4, 16.5). The body or stroma of the choroid plexus consists of many capillaries, separated from the subarachnoid space by the pia mater and choroid ependymal cells.

In the lateral ventricle, the choroid plexus extends anteriorly as far as the interventricular foramen, through which it is continuous across the third ventricle with the plexus of the opposite lateral ventricle. From the interventricular foramen, the plexus passes posteriorly, in contact with the thalamus, curving round its posterior aspect to enter the inferior horn of the ventricle and reach the hippocampus. Throughout the body of the ventricle, the choroid fissure lies between the fornix superiorly and the thalamus inferiorly (Fig. 16.4).

From above, the tela choroidea is triangular with a rounded apex between the interventricular foramina, often indented by the anterior columns of the fornices. Its lateral edges are irregular, and contain choroid vascular fringes. At the posterior basal angles of the tela, these fringes continue and curve on into the inferior horn of the ventricle. When the tela is removed, a transverse slit (the transverse fissure) is left between the splenium and the junction of the ventricular roof with the tectum. The transverse fissure contains the roots of the choroid plexus of the third ventricle and of the lateral ventricles.

The choroid plexus of the third ventricle is attached to the tela choroidea which is, in effect, the thin roof of the third ventricle as it develops during fetal life. In coronal sections of the cerebral hemispheres, the choroid plexus of the third ventricle can be seen in continuity with the choroid plexus of the lateral ventricles.

The choroid plexus of the fourth ventricle is similar in structure to that of the lateral and third ventricles. The roof of the inferior part of the fourth ventricle develops as a thin sheet in which the pia mater is in direct contact with the ependymal lining of the ventricle. This thin sheet, the tela choroidea of the fourth ventricle, lies between the cerebellum and the inferior part of the roof of the ventricle. The choroid plexus of the fourth ventricle is T-shaped, with vertical and horizontal limbs but the precise form varies widely from a single vertical limb to an elongated ‘T’ which extends out through the foramina of Luschka into the cerebellopontine angle The vertical (longitudinal) limb is double, flanks the midline and is adherent to the roof of the ventricle. The limbs fuse at the superior margin of the median aperture (foramen of Magendie) and are often prolonged on to the ventral aspect of the cerebellar vermis. The horizontal limbs of the plexus project into the lateral recesses of the ventricle. Small tufts of plexus pass through the lateral apertures (foramina of Luschka) and emerge, still covered by ependyma, in the subarachnoid space of the cerebellopontine angle.

The blood supply of the choroid plexus in the tela choroidea of the lateral and third ventricles is usually via a single vessel from the anterior choroidal branch of the internal carotid artery and several choroidal branches of the posterior cerebral artery; the two sets of vessels anastomose to some extent. Capillaries drain into a rich venous plexus served by a single choroidal vein. The blood supply of the fourth ventricular choroid plexus is from the inferior cerebellar arteries.

CEREBROSPINAL FLUID

CSF is a clear, colourless, liquid. In normal individuals CSF contains a very small amount of protein and differs from blood in its electrolyte content. It is not simply an ultrafiltrate of blood but is actively secreted by the choroid plexus epithelium. Choroid plexus epithelial cells have the characteristics of transport and secretory cells. Their apical surfaces, from which CSF is secreted, possess microvilli, and their basal surfaces exhibit interdigitations and folding. There are tight junctions at the apical ends of the epithelial cells, which are permeable to small molecular weight substances. Fenestrated capillaries in the stroma of the choroid plexus lie just beneath the epithelial cells. A blood–CSF barrier is sited at the choroid plexus epithelium.

Most of the CSF is secreted by the choroid plexuses in the lateral, third and fourth ventricles. However, there is also a small contribution from the ependymal lining of the ventricles and from the extracellular fluid from the brain parenchyma.

SUBARACHNOID SPACE AND CIRCULATION OF CEREBROSPINAL FLUID

SUBARACHNOID SPACE

The subarachnoid space lies between the arachnoid and the pia mater. The cerebral subarachnoid space is connected with the fourth ventricle of the brain by three openings. The median aperture (foramen of Magendie) lies in the median plane in the inferior part of the roof of the fourth ventricle and provides communication with the cisterna magna. The paired lateral apertures (foramina of Luschka) are located at the ends of the lateral recesses of the fourth ventricle, and open into the subarachnoid space at the cerebellopontine angle, behind the upper roots of the glossopharyngeal nerves. The subarachnoid space therefore contains cerebrospinal fluid (CSF); it also contains the larger arteries and veins which traverse the surface of the brain (Fig. 16.10).

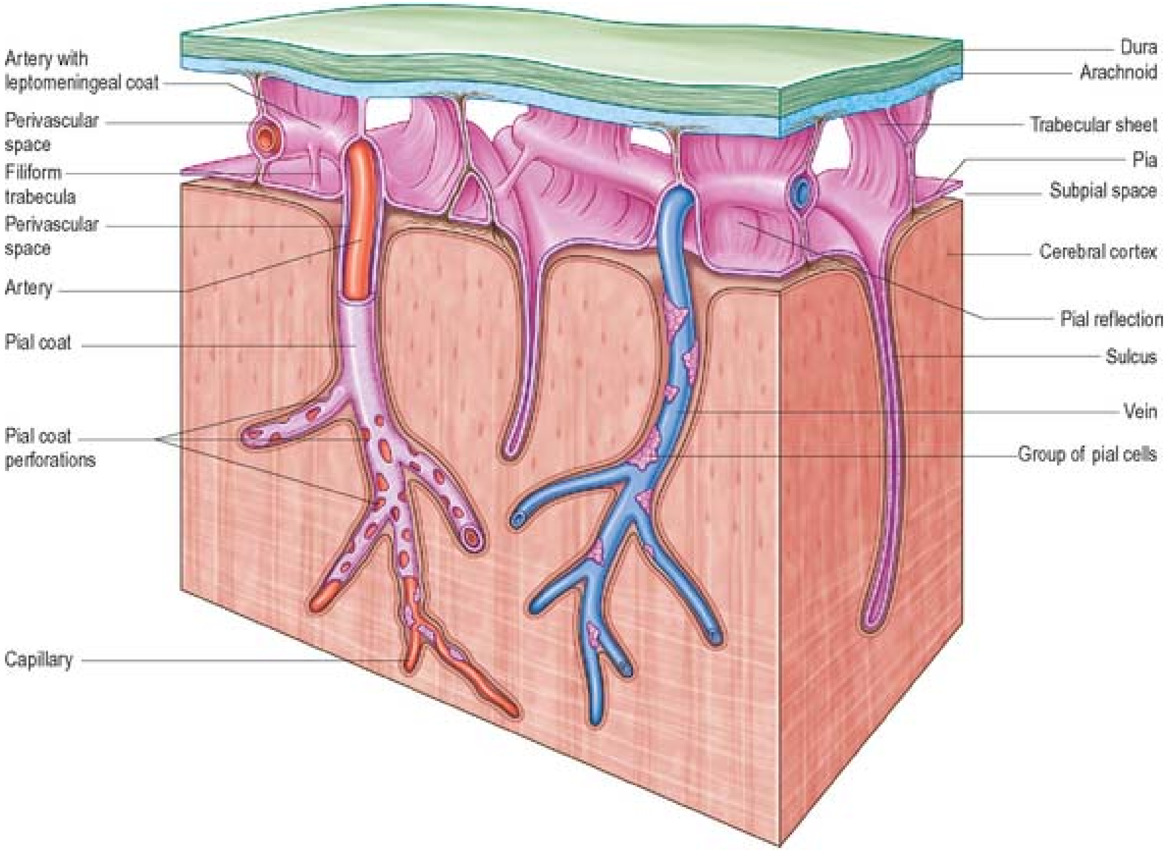
Artery with leptomeningeal coat
Perivascular space
Filiform trabecula
Perivascular space
Artery
Pial coat
Pial coat perforations
Capillary
Dura
Arachnoid
Trabecular sheet
Pia
Subpial space
Cerebral cortex
Pial reflection
Sulcus
Vein
Group of pial cells

Fig. 16.10 The relationships between the dura, the leptomeninges and the blood vessels that enter and leave the cerebral cortex. The subarachnoid

space is divided by trabeculae.

Trabeculae, in the form of sheets or fine filiform structures, traverse the subarachnoid space from the deep layers of the arachnoid mater to the pia mater and are also attached to large blood vessels within the subarachnoid space (Fig. 16.10). Each trabecula has a core of collagen and is coated by leptomeningeal cells. The trabeculae that cross the subarachnoid space may form compartments, particularly in the perivascular regions, which may facilitate directional flow of CSF through the subarachnoid space.

Arteries and veins in the subarachnoid space are coated by a thin layer of leptomeninges, often only one cell thick. Cranial and spinal nerves that traverse the subarachnoid space to pass out of cranial or intervertebral foramina are coated by a thin layer of leptomeninges which fuses with the arachnoid at the exit foramina.

Arachnoid and pia mater are in close apposition over the convexities of the brain, such as the cortical gyri, whereas concavities are followed by the pia but spanned by the arachnoid. This arrangement produces a subarachnoid space of greatly variable depth that is location dependent. The more expansive spaces are identified as subarachnoid cisterns (Fig. 16.11), which are continuous with each other through the general subarachnoid space. Subarachnoid trabeculae that cross the subarachnoid cisterns are long and filamentous.

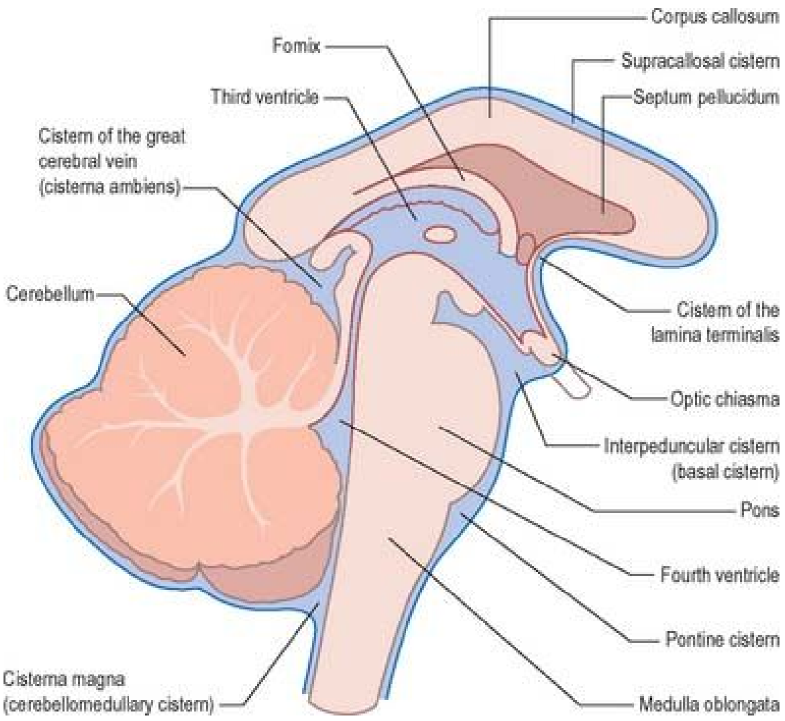
Corpus callosum
Fornix
Supracallosal cistern
Third ventricle
Septum pellucidum
Cistern of the great cerebral vein (cisterna ambiens)
Cerebellum
Cistern of the lamina terminalis
Optic chiasma
Interpeduncular cistern (basal cistern)
Pons
Fourth ventricle
Pontine cistern
Cisterna magna (cerebellomedullary cistern)
Medulla oblongata

Fig. 16.11 The principal subarachnoid cisterns, sagittal section.

The largest cistern, the cisterna magna or cerebellomedullary cistern, is formed where the arachnoid bridges the interval between the medulla oblongata and the inferior surface of the cerebellum. The cistern is continuous above with the lumen of the fourth ventricle through its median aperture, the foramen of Magendie, and below with the subarachnoid space of the spinal cord. The pontine cistern is an extensive space ventral to the pons, that is continuous below with the spinal subarachnoid space, behind with the cisterna magna and, rostral to the pons, with the interpeduncular cistern. The basilar artery runs through the pontine cistern into the interpeduncular cistern. As the arachnoid mater spans between the two temporal lobes it is separated from the cerebral peduncles and structures within the interpeduncular fossa by the interpeduncular cistern, which contains the circulus arteriosus (circle of Willis). Anteriorly, the interpeduncular cistern extends to the optic chiasma. The cistern of the lateral fossa is formed by the arachnoid as it bridges the lateral sulcus between the frontal, parietal and temporal opercula; it contains the middle cerebral artery. The cistern of the great cerebral vein (cisterna ambiens or superior cistern) lies posterior to the brain stem and third ventricle, and occupies the interval between the splenium of the corpus callosum and the superior cerebellar surface. The great cerebral vein traverses this cistern and the pineal gland protrudes into it.

Several smaller cisterns have been described, including the prechiasmatic and postchiasmatic cisterns, which are related to the optic chiasma, and the cistern of the lamina terminalis and the supracallosal cistern, all of which are extensions of the interpeduncular cistern and contain the anterior cerebral arteries. The subarachnoid space also extends through the optic foramen into the orbit where it is bounded by the optic nerve sheath. The latter is formed by fusion of the arachnoid and dura mater, and surrounds the orbital portion of each optic nerve as far as the back of the globe, where the dura fuses with the sclera of the eye.

CIRCULATION OF CEREBROSPINAL FLUID

The total CSF volume is approximately 150 ml, of which 125 ml is intracranial. The ventricles contain about 25 ml, most lying within the lateral ventricles, and the remaining 100 ml is located in the cranial subarachnoid space. CSF is secreted at a rate of 0.35–0.40 ml per minute, which means that normally about 50% of the total volume of CSF is replaced every five to six hours. An effective means of removal from the cranial cavity is thus essential. CSF flows from the lateral ventricles to the third ventricle and then through the cerebral aqueduct to the fourth ventricle. Mixing of CSF from different choroidal sources occurs and is probably assisted by cilia on the ependymal cells lining the ventricles and by arterial pulsations. CSF leaves the fourth ventricle through the medial and lateral apertures to enter the subarachnoid space of the cisterna magna and the subarachnoid cisterns over the front of the pons respectively. The movement of CSF in the subarachnoid space is complex and is characterized by a fast flow component and a much slower bulk flow component. During systole, the major arteries lying in the basal cisterns and other subarachnoid spaces dilate significantly and exert pressure effects on the CSF, causing rapid CSF flow around the brain and out of the cranial cavity into the upper cervical vertebral canal. The pressure wave which causes this outflow of CSF is dispersed through the spinal CSF space, which acts as a capacitance vessel, and is transmitted to the dural venous sinuses through the arachnoid granulations. As the blood within the major arteries passes into the brain in late systole and diastole, CSF re-enters the skull from the spine. This CSF flow occurs at rapid rates and is repeated during every heart cycle. In addition, there is a slow bulk flow of CSF, with a time course measured in hours, which results in circulation of CSF over the cerebral surface in a superolateral direction. CSF is absorbed into the venous system by active diffusion into cerebral capillaries which occurs as a result of the CSF/interstitial pressure differential.

Arachnoid villi and granulations

Arachnoid granulations are focal outpushings of the arachnoid mater and subarachnoid space through the wall of dural venous sinuses, very often close to points where veins enter the sinus: granulations have been reported in the superior sagittal, transverse, superior petrosal and straight sinuses in decreasing frequency. They are most prominent along the margins of the great longitudinal fissure, commonly in the lateral lacunae of the superior sagittal sinus, and also protruding directly into the lumen of the sinus (see Ch. 27). They increase in number and size with increasing age and may appear as focal filling defects in the venous sinuses on angiograms and contrast enhanced CT scans and focal signal alterations in the venous sinuses on MR examination.

Arachnoid villi and arachnoid granulations differ in terms of size and complexity. Villi are microscopic structures that are present in the superior sagittal sinus of the fetus and newborn infant. Granulations are visible to the naked eye by the age of 18 months in the parieto-occipital region of the superior sagittal sinus, and by the age of 3 years in the laterally located sinuses of the posterior fossa; they become more lobulated and complex with increasing age, and may become calcified, when they are known as Pacchionian bodies.

At the base of each arachnoid granulation, a thin neck of arachnoid mater projects through an aperture in the dural lining of the venous sinus and expands to form a core of collagenous trabeculae and interwoven channels (Fig. 16.12). The core is surmounted by an apical cap of arachnoid cells, some 150 μm thick. Channels extend through the cap to reach the subendothelial regions of the granulation. The cap region of each granulation is attached to the endothelium of the sinus over an area some 300 μm in diameter, whereas the rest of the core of the granulation is separated from the endothelium by a fibrous dural cupola.

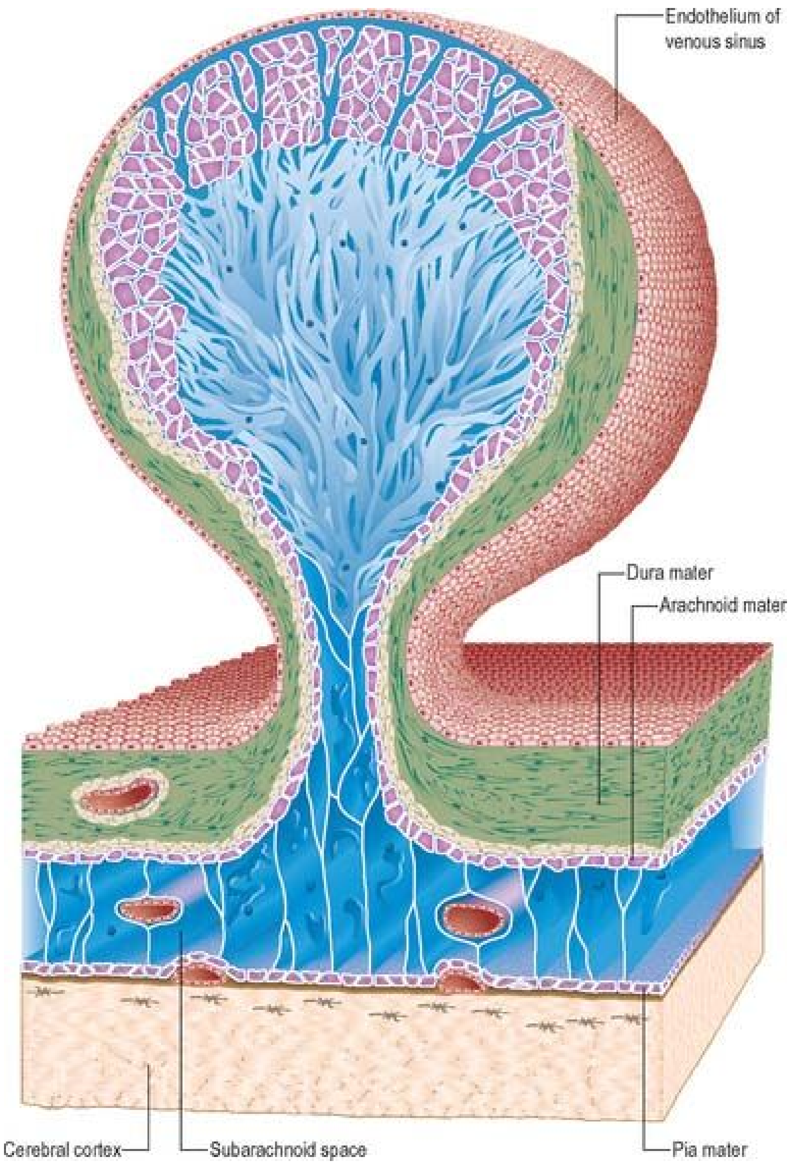
Endothelium of venous sinus
Dura mater
Arachnoid mater
Cerebral cortex
Subarachnoid space
Pia mater

Fig. 16.12 An arachnoid granulation.

(Modified by permission from Springer-Verlag, Principles of Pediatric Neurosurgery, Vol 4: Morphology of CSF drainage pathways in man. Raimondi (ed), Kida and Weller 1994.)

The function of arachnoid granulations remains controversial. It has long been thought that arachnoid villi and arachnoid granulations constitute the major pathway for the resorption of CSF from the subarachnoid space into the blood, although the relative contribution each might make to the process is not known and the exact mechanism of resorption has not been determined. Recent studies using radionuclide cisternography and cardiac gated MRI have shown that CSF may also be resorbed throughout the ventricles and subarachnoid space, through the walls of pial and subarachnoid vessels. Moreover, there is a growing body of experimental evidence that significant volumes of CSF may be absorbed into extracranial lymphatics in animals: radiolabelled proteins injected into the CSF (rabbits, cats), brain parenchyma (rabbits) or ventricles (sheep) have been recovered from cervical lymph, possibly by traveling along extensions of the subarachnoid space that surround the olfactory and optic nerves. It has been suggested that extracranial lymphatics play a major role in CSF reabsorption at relatively low pressures, but that other routes, including arachnoid granulations, become increasingly important as CSF pressure rises. A connection between parenchymal interstitial fluid and extracranial lymphatics in humans has yet to be convincingly demonstrated.

An alternative, and not necessarily mutually exclusive, view of arachnoid granulations is that they are involved in dissipating the pressure wave which occurs in the subarachnoid space during arterial systole (caused by the pulsation of the arterial vessels within the space). Since the dural venous sinuses lie within thick non-compliant dural coverings, pressure changes within them functionally represent the extracranial venous compartment: systolic dilatation of the arachnoid granulations would therefore dissipate intracranial pressure changes into the extracranial venous system.

Hydrocephalus

Obstruction of the circulation of CSF leads to accumulation of fluid within the ventricular system (hydrocephalus), which causes compression of the brain (Fig. 16.13). Within the brain, critical points at which obstruction may occur correspond to the narrow foramina and passages of the ventricular system. Thus, obstruction of the interventricular foramen causes enlargement of the lateral ventricles; obstruction of the cerebral aqueduct leads to enlargement of both the lateral ventricles and the third ventricle; and obstruction or congenital absence of the apertures of the fourth ventricle leads to enlargement of the entire ventricular system. Hydrocephalus may also occur in the presence of intact communications between the ventricular and subarachnoid spaces (communicating hydrocephalus). The conventional view is that obstructions within the subarachnoid space impair CSF circulation and lead to CSF malabsorption, causing either obstructive or communicating hydrocephalus. Analyses of the intracranial hydrodynamics related to the pulse pressure have suggested that this is an oversimplification, and that increased pulse pressure in the brain capillaries maintains the ventricular enlargement in communicating hydrocephalus and chronic obstructive hydrocephalus (see Greitz 2004 for further details of the haemodynamic theory).

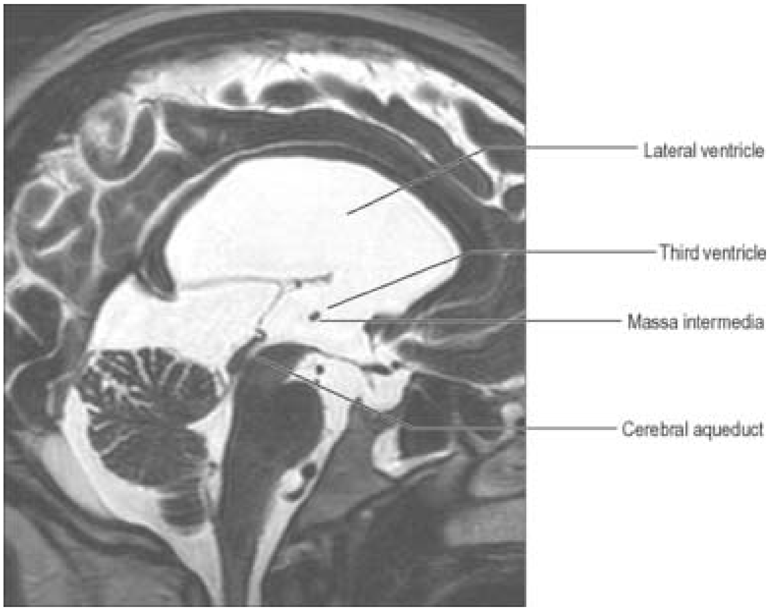

Fig. 16.13 T2 weighted sagittal image of the brain in a patient with obstructive hydrocephalus due to a congenital stenosis of the cerebral aqueduct. The image shows marked dilatation of the third ventricle and proximal aqueduct.

PIA MATER

The pia mater is a delicate membrane which closely invests the surface of the brain, from which it is separated by a microscopic subpial space (Fig. 16.10), and it follows the contours of the brain into concavities and the depths of fissures and sulci. During development, it becomes apposed to the ependyma in the roof of the telencephalon and fourth ventricle to form the stroma of the choroid plexus. The pia mater shares a common embryological origin and structural similarity with the arachnoid mater (see Ch. 27).

Pia mater is formed from a layer of leptomeningeal cells, often only 1 to 2 cells thick, in which the cells are joined by desmosomes and gap junctions but few, if any, tight junctions. The cells are continuous with the coating of the subarachnoid trabeculae and separated from the basal lamina of the glia limitans by bundles of collagen and fibroblast-like cells, and the arteries and veins that lie in the subpial space (Fig. 16.10).

Despite its delicate nature, the pia mater appears to form a regulatory interface between the subarachnoid space and the brain. Pial cells contain enzymes such as catechol-O-methyltransferase and glutamine synthetase (which degrade neurotransmitters), they also exhibit pinocytotic activity and ingest particles up to 1 μm in diameter. Further evidence of the effectiveness of the pia as a barrier is seen in subarachnoid haemorrhage and in subpial haemorrhage in infants, since in neither of these instances do red blood cells penetrate the pia mater.

It was long thought that the subarachnoid space was connected directly with the perivascular spaces (Virchow–Robin spaces) that surround blood vessels in the brain. However, it is now recognized that the pia mater is reflected from the surface of the brain onto the surface of blood vessels in the subarachnoid space, which means that the subarachnoid space is separated by a layer of pia from the subpial and perivascular spaces of the brain.

REFERENCES

eitz D. Radiological assessment of hydrocephalus: new theories and implications for therapy. *Neurosurg Rev*. 2004;27:145-165.

Describes modern theories of CSF production and transport..

da S, Weller RO. Morphology of CSF drainage pathways in man. Raimondi A, editor. Principles of Pediatric Neurosurgery, vol 4. Berlin: Springer, 1994.

Describes the morphology and relationships of the subarachnoid space including the structure of arachnoid granulations..

intworth GK. The ontogeny and growth of the human tentorium cerebelli. *Anat Rec*. 1967;158:433-442.

cKinley MJ, McAllen RM, Davern P, et al. The sensory circumventricular organs of the mammalian brain. *Adv Anat Embryol Cell Biol*. 2003;172:III-XII. 1–122.

ercier F, Kitasako JT, Hatton GI. Anatomy of the brain neurogenic zones revisited: fractones and the fibroblast/macrophage network. *J Comp Neurol*. 2002;451(2):170-188.

Describes the structure and ultrastructure of the basal laminae and subependymal layer..

ulson OB. Blood-brain barrier, brain metabolism and cerebral blood flow. *Eur Neuropsychopharmacol*. 2002;12(6):495-501.

razielle N, Ghersi-Egea JF. Choroid plexus in the central nervous system: biology and physiopathology. *J Neuropathol Exp Neurol*. 2000;59(7):561-574.

Describes choroid plexus functions in brain development, transfer of neurohumoral information, brain/immune system interactions, brain aging, and cerebral pharmacotoxicology..

olburg H, Lippoldt A. Tight junctions of the blood-brain barrier: development, composition and regulation. *Vasc Pharmacol*. 2002;38(6):323-337.

Reviews the molecular properties of the tight junctions between endothelial cells which constitute the blood-brain barrier..

kharov A, Papaiconomou C, Koh L, Djenic J, Bozanovic-Sosic R, Johnston M. Integrating the roles of extracranial lymphatics and intracranial veins in cerebrospinal fluid absorption in sheep. *Microvasc Res*. 2004;67:96-104.

ang ET, Inman CBE, Weller RO. Interrelationships of the pia mater and the perivascular (Virchow-Robin) spaces in the human cerebrum. *J Anat*. 1990;170:111-123.

CHAPTER 17

Vascular supply and drainage of the brain

The brain is a highly vascular organ, its profuse blood supply characterized by a densely branching arterial network. It has a high metabolic rate that reflects the energy requirements of constant neural activity. It receives about 15% of the cardiac output and utilizes 25% of the total oxygen consumption of the body. The brain is supplied by two internal carotid arteries and two vertebral arteries that form a complex anastomosis (circulus arteriosus, circle of Willis) on the base of the brain. Vessels diverge from this anastomosis to supply the various cerebral regions. In general, the internal carotid arteries and the vessels arising from them supply the forebrain, with the exception of the occipital lobe of the cerebral hemisphere, and the vertebral arteries and their branches supply the occipital lobe, the brain stem and the cerebellum. Venous blood from the brain drains into sinuses within the dura mater (see Ch. 27). Acute interruption of the blood supply to the brain for more than a few minutes causes permanent neurological damage. Such ischaemic strokes along with intracranial haemorrhage are major contemporary sources of morbidity and mortality.

ARTERIAL SUPPLY OF THE BRAIN

The arterial supply of the brain is derived from the internal carotid and vertebral arteries, which lie, together with their proximal branches, within the subarachnoid space at the base of the brain.

INTERNAL CAROTID ARTERY

The internal carotid arteries (Fig. 17.1) and their major branches (the internal carotid system or ‘anterior’ circulation) supply blood to the majority of the forebrain. Some parts of the occipital and temporal lobes are supplied by branches of the vertebrobasilar system (see Fig. 17.5).

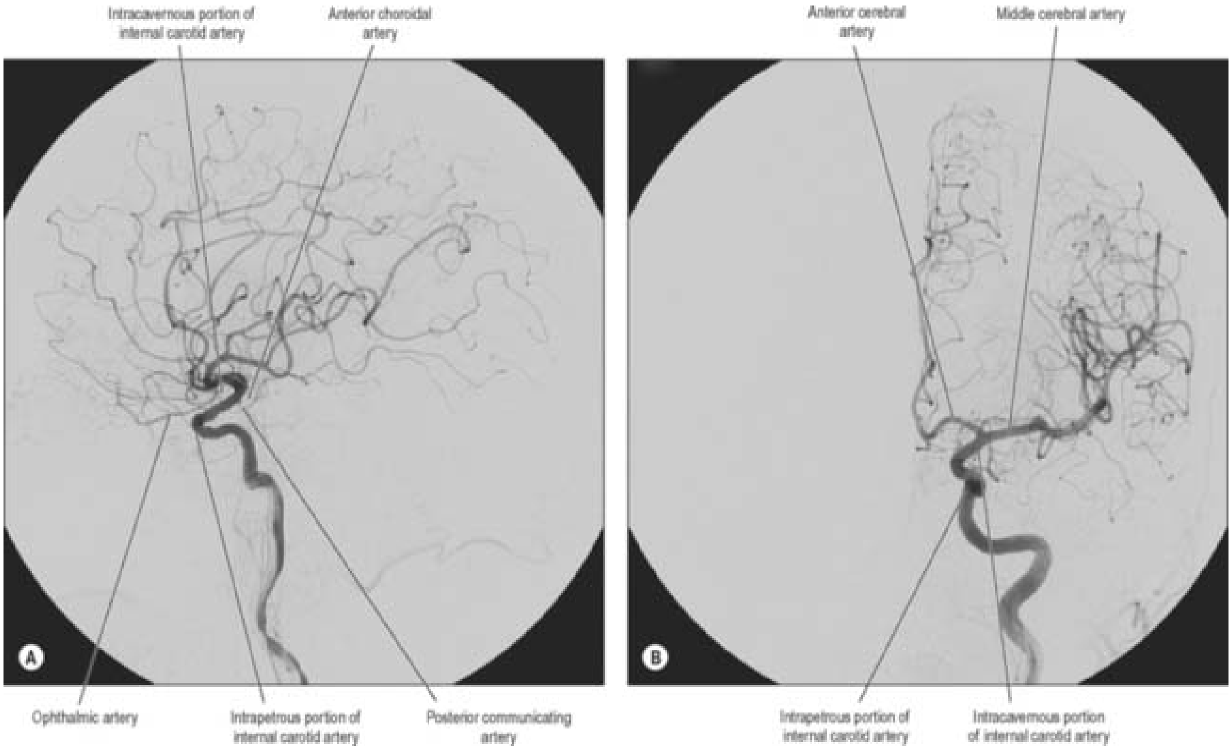
Intracavernous portion of internal carotid artery
Anterior choroidal artery
Anterior cerebral artery
Middle cerebral artery
A
B
Ophthalmic artery
Intrapetrous portion of internal carotid artery
Posterior communicating artery
Intrapetrous portion of internal carotid artery
Intracavernous portion of internal carotid artery

Fig. 17.1 Internal carotid arteriograms. **A**, lateral projection **B**, Towne’s projection.

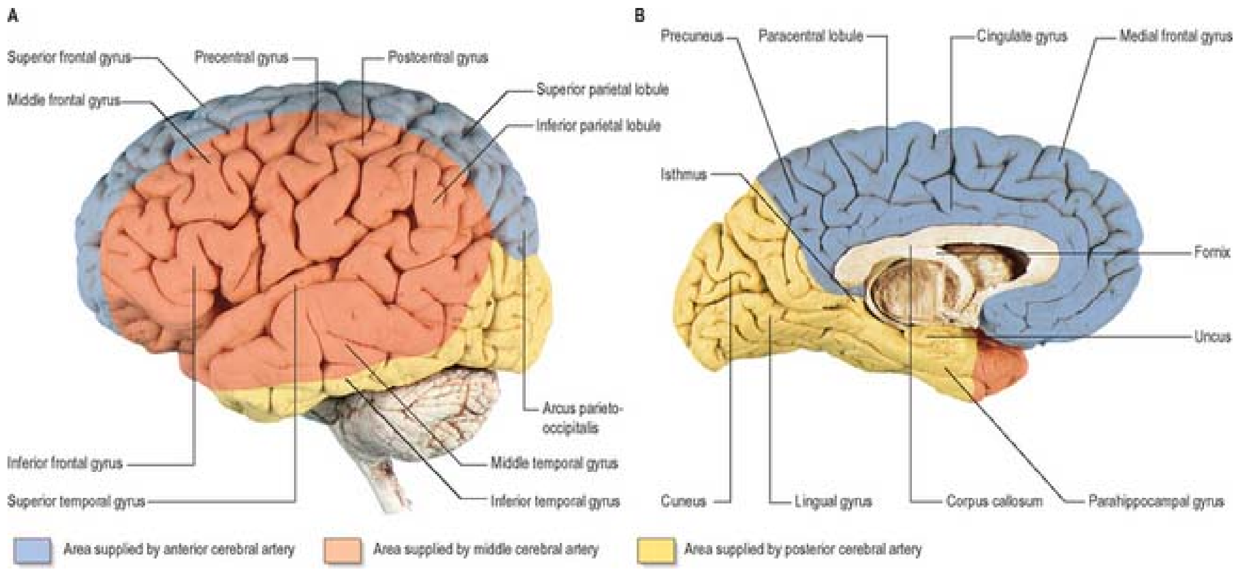
A
Superior frontal gyrus
Precentral gyrus
Postcentral gyrus
Middle frontal gyrus
Superior parietal lobule
Inferior parietal lobule
Arcus parieto-occipitalis
Inferior frontal gyrus
Middle temporal gyrus
Superior temporal gyrus
Inferior temporal gyrus
B
Precuneus
Paracentral lobule
Cingulate gyrus
Medial frontal gyrus
Isthmus
Fornix
Uncus
Cuneus
Lingual gyrus
Corpus callosum
Parahippocampal gyrus
Area supplied by anterior cerebral artery
Area supplied by middle cerebral artery
Area supplied by posterior cerebral artery

Fig. 17.5 The arteries supplying the left cerebral hemispheres. **A**, Lateral surface. **B**, Medial surface.

The internal carotid artery arises from the bifurcation of the common carotid artery, ascends in the neck and enters the carotid canal of the temporal bone. Its subsequent course is said to have petrous, cavernous and intracranial parts.

Petrous part

The petrous part of the internal carotid artery ascends in the carotid canal, curves anteromedially and then superomedially above the cartilage that fills the foramen lacerum, and enters the cranial cavity. It lies at first anterior to the cochlea and tympanic cavity, and is separated from the latter and the pharyngotympanic tube by a thin, bony lamella that is cribriform in the young and partly absorbed in old age. Further anteriorly, it is separated from the trigeminal ganglion by the thin roof of the carotid canal, although this is often deficient. The artery is surrounded by a venous plexus and by the carotid autonomic plexus, derived from the internal carotid branch of the superior cervical ganglion. The petrous part of the artery gives rise to two branches. The caroticotympanic artery is a small, occasionally double, vessel which enters the tympanic cavity by a foramen in the carotid canal and anastomoses with the anterior tympanic branch of the maxillary artery and the stylomastoid artery. The pterygoid artery is inconsistent: when present, it enters the pterygoid canal with the nerve of the same name, and anastomoses with a (recurrent) branch of the greater palatine artery.

Cavernous part

The cavernous part of the internal carotid artery ascends to the posterior clinoid process. It turns anteriorly to the side of the sphenoid within the cavernous sinus and then curves up medial to the anterior clinoid process, to emerge through the dural roof of the sinus. The oculomotor, trochlear, ophthalmic and abducens nerves are lateral to it within the cavernous sinus (see Fig. 27.9). Occasionally, the two clinoid processes form a bony ring round the artery.

This part of the artery gives off a number of small vessels. Cavernous branches supply the trigeminal ganglion, the walls of the cavernous and inferior petrosal sinuses and the nerves contained therein. A minute meningeal branch passes over the lesser wing of the sphenoid to supply the dura mater and bone in the anterior cranial fossa and also anastomoses with a meningeal branch of the posterior ethmoidal artery. Numerous small hypophysial branches supply the neurohypophysis, and are of particular importance because they form the pituitary portal system (Fig. 21.11).

Intracranial part

After piercing the dura mater, the internal carotid artery turns back below the optic nerve to run between it and the oculomotor nerve. It reaches the anterior perforated substance at the medial end of the lateral fissure and terminates by dividing into the anterior and middle cerebral arteries.

Several preterminal vessels leave the cerebral portion of the internal carotid. The ophthalmic artery arises from the anterior part of the internal carotid as it leaves the cavernous sinus, often at the point of piercing the dura, and enters the orbit through the optic canal. The posterior communicating artery (Fig. 17.2, Fig. 17.3) runs back from the internal carotid above the oculomotor nerve, and anastomoses with the posterior cerebral artery (a terminal branch of the basilar artery), thereby contributing to the circulus arteriosus around the interpeduncular fossa. The posterior communicating artery is usually very small. However, sometimes it is so large that the posterior cerebral artery is supplied via the posterior communicating artery rather than from the basilar artery (‘fetal posterior communicating artery’); it is often larger on one side only. Small branches from its posterior half pierce the posterior perforated substance together with branches from the posterior cerebral artery. Collectively they supply the medial thalamic surface and the walls of the third ventricle. The anterior choroidal artery leaves the internal carotid near its posterior communicating branch and passes back above the medial part of the uncus. It crosses the optic tract to reach and supply the crus cerebri of the midbrain, then turns laterally, recrosses the optic tract, and gains the lateral side of the lateral geniculate body, which it supplies with several branches. It finally enters the inferior horn of the lateral ventricle via the choroidal fissure and ends in the choroid plexus. This small, but important, vessel also contributes to the blood supply of the globus pallidus, caudate nucleus, amygdala, hypothalamus, tuber cinereum, red nucleus, substantia nigra, posterior limb of the internal capsule, optic radiation, optic tract, hippocampus and the fimbria of the fornix.

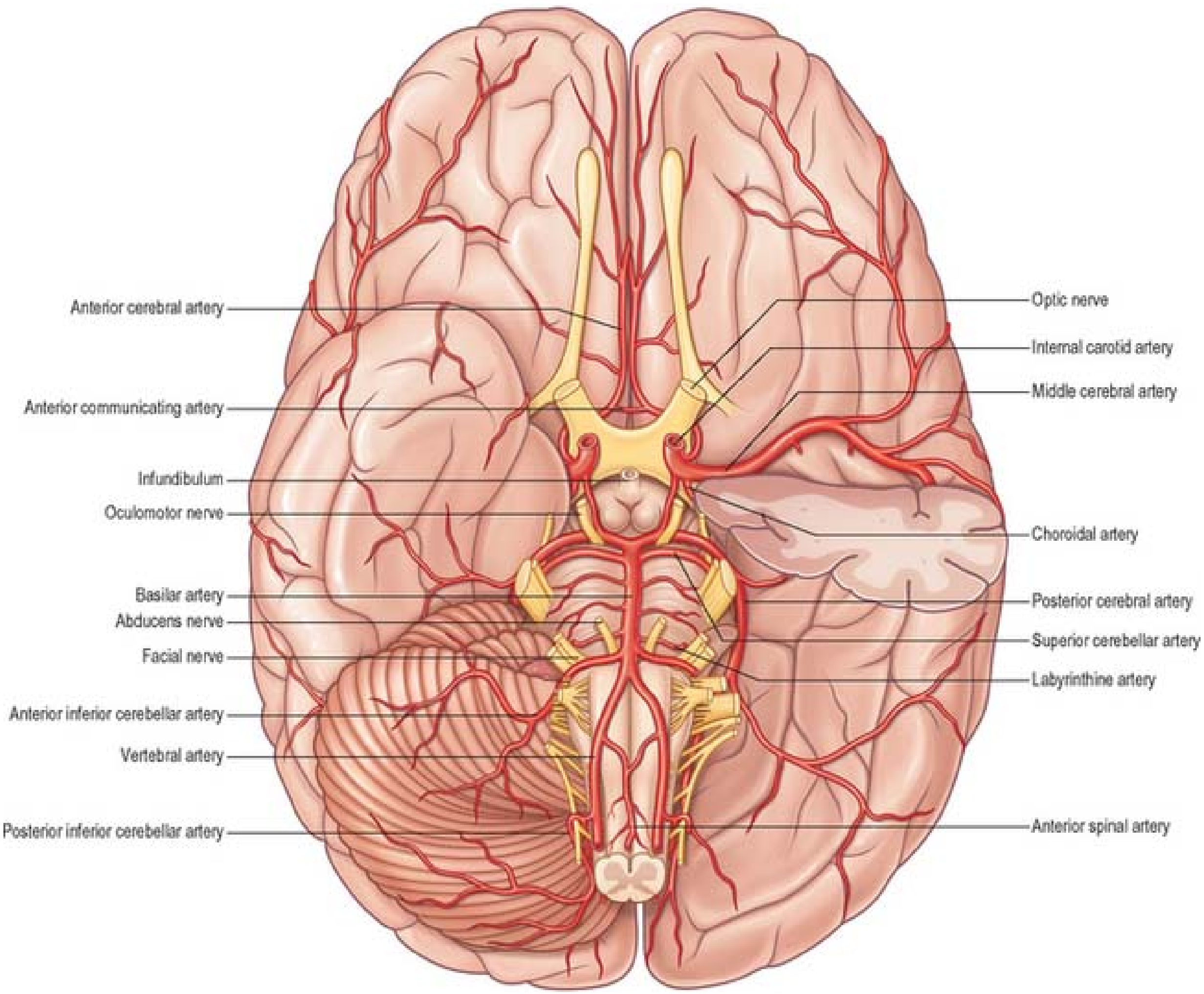
Anterior cerebral artery
Anterior communicating artery
Infundibulum
Oculomotor nerve
Basilar artery
Abducens nerve
Facial nerve
Anterior inferior cerebellar artery
Vertebral artery
Posterior inferior cerebellar artery
Optic nerve
Internal carotid artery
Middle cerebral artery
Choroidal artery
Posterior cerebral artery
Superior cerebellar artery
Labyrinthine artery
Anterior spinal artery

Fig. 17.2 The arteries on the base of the brain. The anterior part of the left temporal lobe has been removed to display the initial course of the middle cerebral artery within the lateral fissure.

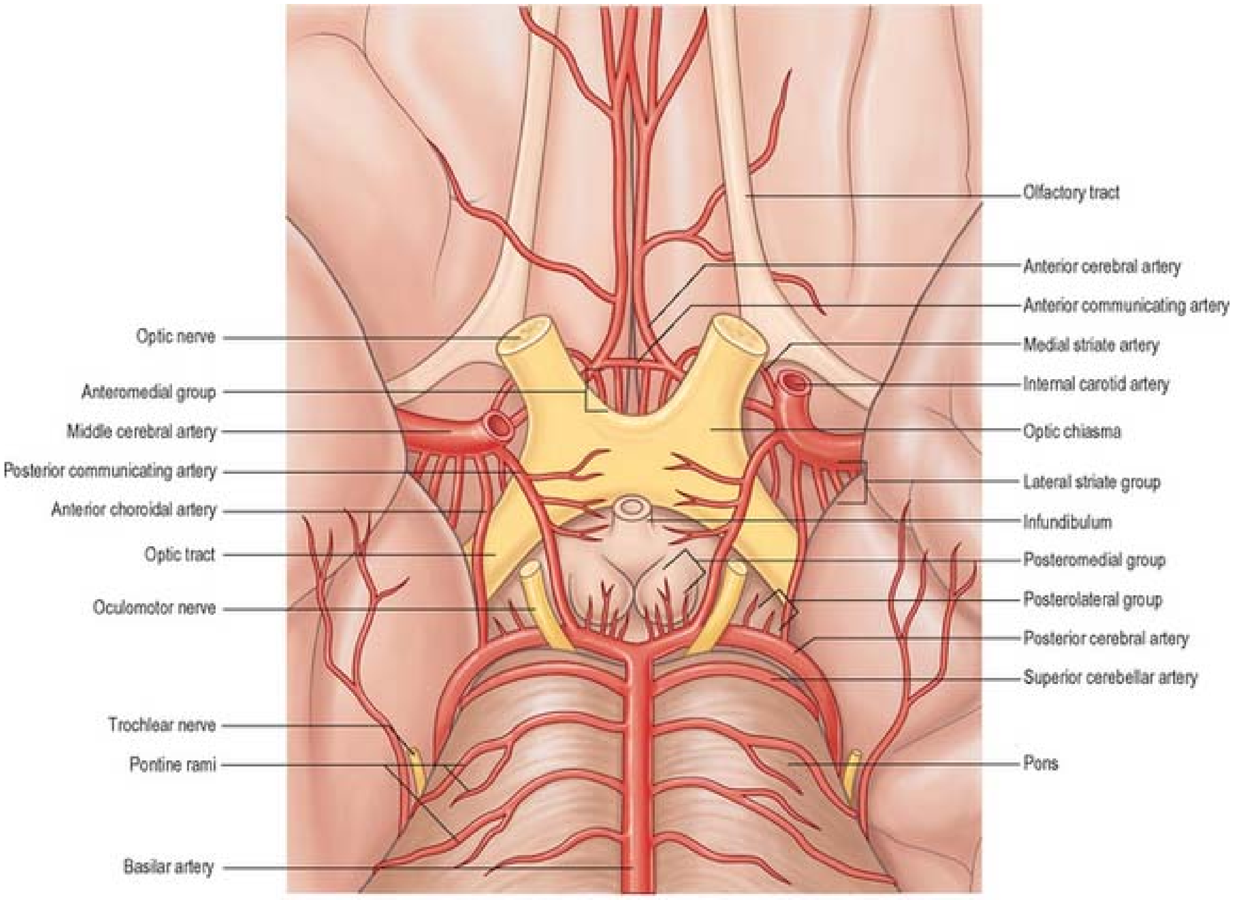
Olfactory tract
Anterior cerebral artery
Anterior communicating artery
Medial striate artery
Internal carotid artery
Optic chiasma
Lateral striate group
Infundibulum
Posteromedial group
Posterolateral group
Posterior cerebral artery
Superior cerebellar artery
Pons
Optic nerve
Anteromedial group
Middle cerebral artery
Posterior communicating artery
Anterior choroidal artery
Optic tract
Oculomotor nerve
Trochlear nerve
Pontine rami
Basilar artery

Fig. 17.3 The circulus arteriosus on the base of the brain showing the distribution of central (perforating or ganglionic) branches.

ANTERIOR CEREBRAL ARTERY

The anterior cerebral artery is the smaller of the two terminal branches of the internal carotid (Fig. 17.3).

Surgical nomenclature divides the vessel into three parts: A_1 – from the termination of the internal carotid artery to the junction with the anterior communicating artery; A_2 – from the junction with the anterior communicating artery to the origin of the callosomarginal artery; and A_3 – distal to the origin of the callosomarginal artery; this segment is also known as the pericallosal artery.

The anterior cerebral artery starts at the medial end of the stem of the lateral fissure. It passes anteromedially above the optic nerve to the great longitudinal fissure where it connects with its fellow by a short transverse anterior communicating artery. The anterior communicating artery is about 4 mm in length and may be double. It gives off numerous anteromedial central branches that supply the optic chiasma, lamina terminalis, hypothalamus, para-olfactory areas, anterior columns of the fornix and the cingulate gyrus.

The two anterior cerebral arteries travel together in the great longitudinal fissure. They pass around the curve of the genu of the corpus callosum and then along its upper surface to its posterior end, where they anastomose with posterior cerebral arteries (Fig. 17.4). They give off cortical and central branches.

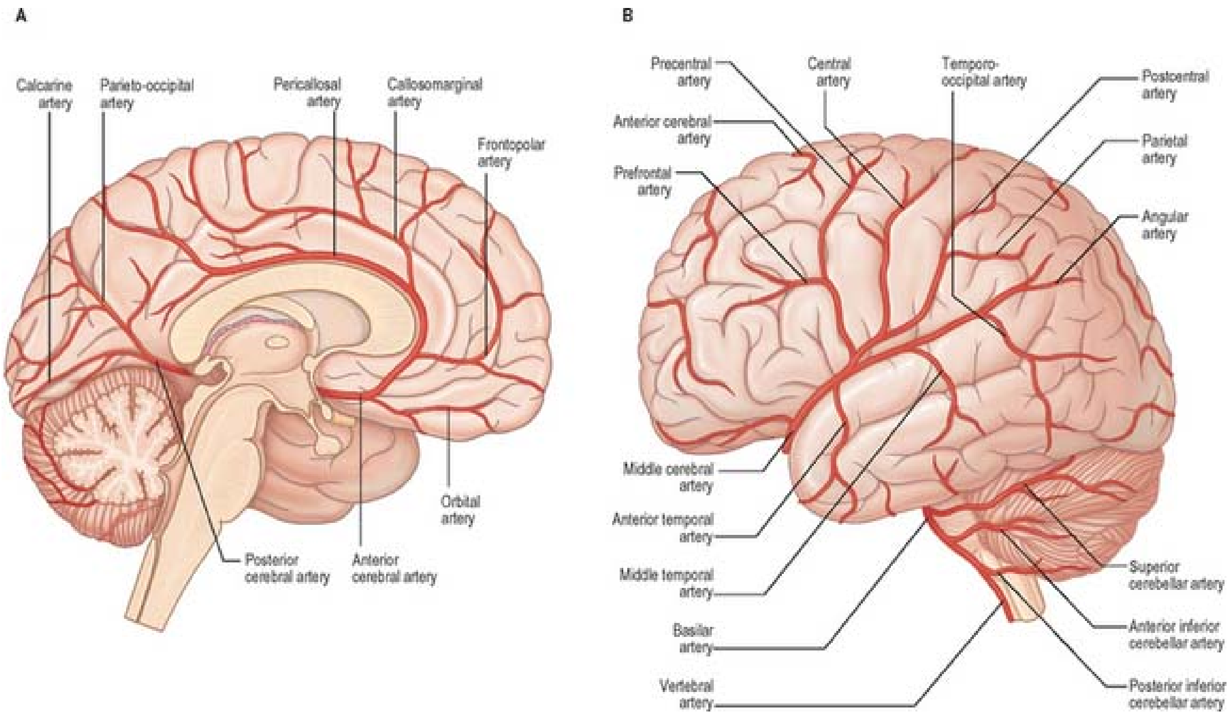
A
Calcarine artery
Parieto-occipital artery
Pericallosal artery
Callosomarginal artery
Frontopolar artery
Orbital artery
Posterior cerebral artery
Anterior cerebral artery
B
Precentral artery
Central artery
Temporo-occipital artery
Postcentral artery
Anterior cerebral artery
Prefrontal artery
Parietal artery
Angular artery
Middle cerebral artery
Anterior temporal artery
Middle temporal artery
Basilar artery
Vertebral artery
Superior cerebellar artery
Anterior inferior cerebellar artery
Posterior inferior cerebellar artery

Fig. 17.4 The major arteries supplying the medial, **A**, and lateral, **B**, aspects of the brain.

The cortical branches of the anterior cerebral artery are named according to their distribution. Two or three orbital branches ramify on the orbital surface of the frontal lobe and supply the olfactory cortex, gyrus rectus and medial orbital gyrus. Frontal branches supply the corpus callosum, cingulate gyrus, medial frontal gyrus and paracentral lobule. Parietal branches supply the precuneus, while the frontal and parietal branches both send twigs over the superomedial border of the hemisphere to supply a strip of territory on the superolateral surface (Fig. 17.5). Cortical branches of the anterior cerebral artery therefore supply the areas of the motor and somatosensory cortices that represent the lower limb.

Central branches of the anterior cerebral artery arise from its proximal portion and enter the anterior perforated substance (Fig. 17.3) and lamina terminalis. Collectively, they supply the rostrum of the corpus callosum, the septum pellucidum, the anterior part of the putamen, the head of the caudate nucleus and adjacent parts of the internal capsule. Immediately proximal or distal to its junction with the anterior communicating artery, the anterior cerebral artery gives rise to the medial striate artery which supplies the anterior part of the head of the caudate nucleus and adjacent regions of the putamen and internal capsule.

MIDDLE CEREBRAL ARTERY

The middle cerebral artery is the larger terminal branch of the internal carotid.

Surgical nomenclature divides the vessel into four parts: M_1 – from the termination of the internal carotid artery to the bi/trifurcation, this segment is also known as the sphenoidal; M_2 – the segment running in the lateral (Sylvian) fissure, also known as the insular; M_3 – coming out of the lateral fissure, also known as the opercular; and M_4 – cortical portions.

The middle cerebral artery runs at first in the lateral fissure, then posterosuperiorly on the insula, and divides into branches distributed to the insula and the adjacent lateral cerebral surface (Fig. 17.3, Fig. 17.4, Fig. 17.5). Like the anterior cerebral artery, it has cortical and central branches.

Cortical branches send orbital vessels to the inferior frontal gyrus and the lateral orbital surface of the frontal lobe. Frontal branches supply the precentral, middle and inferior frontal gyri. Two parietal branches are distributed to the postcentral gyrus, the lower part of the superior parietal lobule and the whole inferior parietal lobule. Two or three temporal branches supply the lateral surface of the temporal lobe. Cortical branches of the middle cerebral artery therefore supply the motor and somatosensory cortices that represent the whole of the body (other than the lower limb), the auditory area and the insula.

Small central branches of the middle cerebral artery, the lateral striate or lenticulostriate arteries, arise at its origin and enter the anterior perforated substance together with the medial striate artery. Lateral striate arteries ascend in the external capsule over the lower lateral aspect of the lentiform complex, then turn medially, traverse the lentiform complex and the internal capsule and extend as far as the caudate nucleus.

VERTEBRAL ARTERY

The vertebral arteries and their major branches (sometimes referred to as the ‘vertebrobasilar system’) essentially supply blood to the upper spinal cord, the brain stem and cerebellum and a significant but variable part of the posterior cerebral hemispheres (Fig. 17.6).

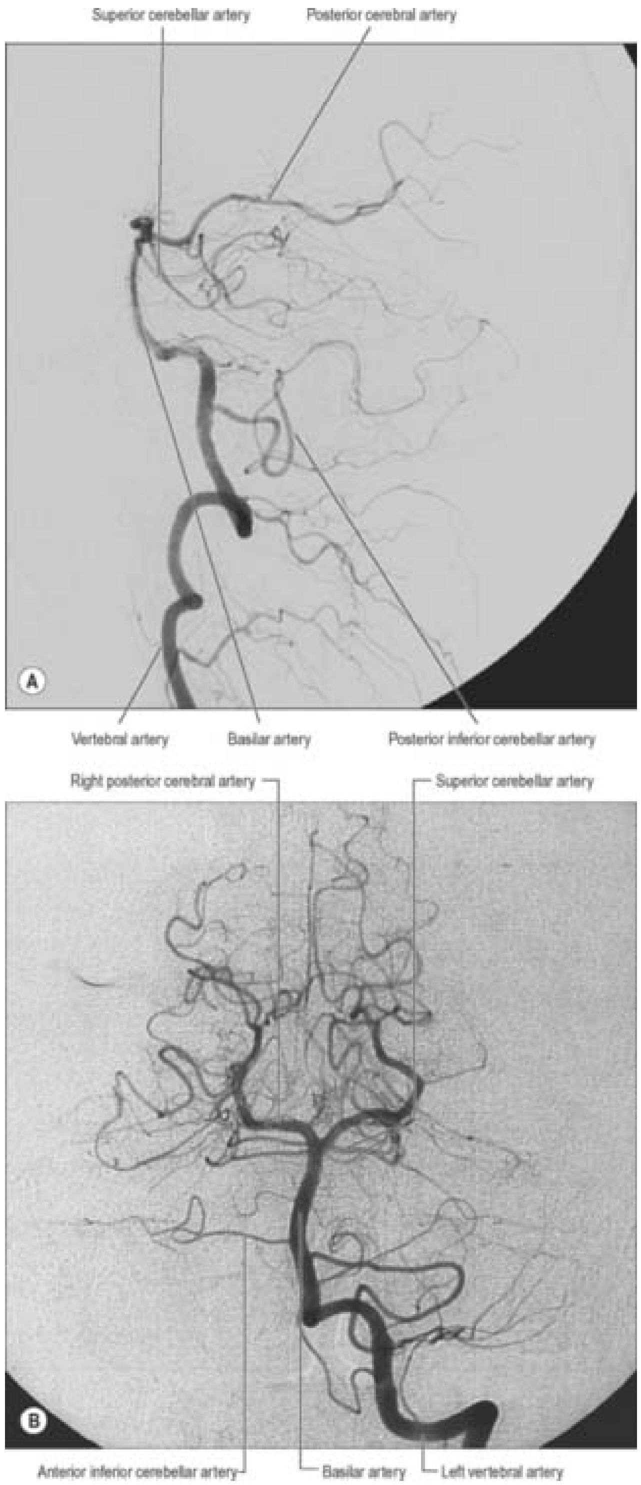
Superior cerebellar artery
Posterior cerebral artery
A
Vertebral artery
Basilar artery
Posterior inferior cerebellar artery
Right posterior cerebral artery
Superior cerebellar artery
B
Anterior inferior cerebellar artery
Basilar artery
Left vertebral artery

Fig. 17.6 Vertebral arteriograms. **A**, lateral projection; **B**, Towne's projection.

The vertebral arteries are derived from the subclavian arteries (see Ch. 30). They ascend through the neck in the foramina transversaria of the upper six cervical vertebrae and enter the cranial cavity through the foramen magnum, close to the anterolateral aspect of the medulla (Fig. 17.2). They converge medially as they ascend the medulla and unite to form the midline basilar artery at approximately the level of the junction between the medulla and pons.

One or two meningeal branches arise from the vertebral artery near the foramen magnum and ramify between the bone and dura mater in the posterior cranial fossa. They supply bone, diploë and the falx cerebelli.

A small anterior spinal artery arises near the end of the vertebral artery, and descends anterior to the medulla oblongata to unite with its fellow from the opposite side at mid-medullary level. The single trunk then descends on the ventral midline of the spinal cord, and is reinforced sequentially by small spinal rami from the vertebral, ascending cervical, posterior intercostal and first lumbar arteries, which all enter the vertebral canal via intervertebral foramina. Branches from the anterior spinal arteries and the beginning of their common trunk are distributed to the medulla oblongata.

The largest branch of the vertebral artery is the posterior inferior cerebellar artery (Fig. 17.6A). It arises near the lower end of the olive and then ascends behind the roots of the glossopharyngeal and vagus nerves to reach the inferior border of the pons. Here it curves and descends along the inferolateral border of the fourth ventricle before it turns laterally into the cerebellar vallecula between the hemispheres, and divides into medial and lateral branches. The medial branch runs back between the cerebellar hemisphere and inferior vermis, and supplies both. The lateral branch supplies the inferior cerebellar surface as far as its lateral border and anastomoses with the anterior inferior and superior cerebellar arteries (from the basilar artery). The trunk of the posterior inferior cerebellar artery supplies the medulla oblongata dorsal to the olivary nucleus and lateral to the hypoglossal nucleus and its emerging nerve roots. It also supplies the choroid plexus of the fourth ventricle and sends a branch lateral to the cerebellar tonsil to supply the dentate nucleus. The posterior inferior cerebellar artery is sometimes absent.

A posterior spinal artery usually arises from the posterior inferior cerebellar artery, but may originate directly from the vertebral artery near the medulla oblongata. It passes posteriorly and descends as two branches which lie anterior and posterior to the dorsal roots of the spinal nerves. These are reinforced by spinal twigs from the vertebral, ascending cervical, posterior intercostal and first lumbar arteries, all of which reach the vertebral canal by the intervertebral foramina, and sustain the posterior spinal arteries to the lower spinal levels.

Minute medullary arteries arise from the vertebral artery and its branches and are distributed widely to the medulla oblongata.

BASILAR ARTERY

The basilar artery is a large median vessel formed by the union of the vertebral arteries at the mid-medullary level (Figs 17.2, 17.3, 17.6). It lies in the pontine cistern, and follows a shallow median groove on the ventral pontine surface, extending to the upper border of the pons. It ends by dividing into two posterior cerebral arteries at a variable level behind the dorsum sellae, usually in the interpeduncular cistern.

Numerous small pontine branches arise from the front and sides of the basilar artery along its course and supply the pons. The long and slender labyrinthine (internal auditory) artery has a variable origin. It usually arises from the anterior inferior cerebellar artery, but variations in its origin include the lower part of the basilar artery, the superior cerebellar artery or, occasionally, the posterior inferior cerebellar artery. The labyrinthine artery accompanies the facial and vestibulocochlear nerves into the internal acoustic meatus and is distributed to the internal ear.

The anterior inferior cerebellar artery (Fig. 17.3) is given off from the lower part of the basilar artery and runs posterolaterally, usually ventral to the abducens, facial and vestibulocochlear nerves. It commonly exhibits a loop into the internal acoustic meatus below the nerves, and when this occurs, the labyrinthine artery may arise from the loop. The anterior inferior cerebellar artery supplies the inferior cerebellar surface anterolaterally and anastomoses with the posterior inferior cerebellar branch of the vertebral artery. A few branches supply the inferolateral parts of the pons and occasionally also supply the upper medulla oblongata.

The superior cerebellar artery (Figs 17.3, 17.6) arises near the distal portion of the basilar artery, immediately before the formation of the posterior cerebral arteries. It passes laterally below the oculomotor nerve, which separates it from the posterior cerebral artery, and curves round the cerebral peduncle below the trochlear nerve to gain the superior cerebellar surface. Here it divides into branches which ramify in the pia mater and supply this aspect of the cerebellum, and also anastomose with branches of the inferior cerebellar arteries. The superior cerebellar artery supplies the pons, pineal body, superior medullary velum and tela choroidea of the third ventricle.

POSTERIOR CEREBRAL ARTERY

The posterior cerebral artery (Figs 17.2, 17.3, 17.4) is a terminal branch of the basilar artery.

Surgical nomenclature divides the vessel into three parts: P_1 – from the basilar bifurcation to the junction with the posterior communicating artery; P_2 – from the junction with the posterior communicating artery to the portion in the perimesencephalic cistern; and P_3 – the portion that runs in the calcarine fissure.

The posterior cerebral artery is larger than the superior cerebellar artery, from which it is separated near its origin by the oculomotor nerve, and, lateral to the midbrain, by the trochlear nerve. It passes laterally, parallel with the superior cerebellar artery, and receives the posterior communicating artery. It then winds round the cerebral peduncle and reaches the tentorial cerebral surface, where it supplies the temporal and occipital lobes. Like the anterior and middle cerebral arteries, the posterior cerebral artery has cortical and central branches.

The cortical branches of the posterior cerebral artery are named according to their distribution. Temporal branches, usually two, are distributed to the uncus, parahippocampal, medial and lateral occipitotemporal gyri. Occipital branches supply the cuneus, lingual gyrus and posterolateral surface of the occipital lobe. Parieto-occipital branches supply the cuneus and precuneus. The posterior cerebral artery supplies the visual areas of the cerebral cortex and other structures in the visual pathway.

The central branches supply subcortical structures. Several small posteromedial central branches arise from the beginning of the posterior cerebral artery (Fig. 17.3) and, together with similar branches from the posterior communicating artery, pierce the posterior perforated substance to supply the anterior thalamus, subthalamus, lateral wall of the third ventricle and globus pallidus. One or more posterior choroidal branches pass over the lateral geniculate body and supply it before entering the posterior part of the inferior horn of the lateral ventricle via the lower part of the choroidal fissure. Branches also curl round the posterior end of the thalamus and pass through the transverse fissure, or go to the choroid plexus of the third ventricle, or traverse the upper choroidal fissure. Collectively these branches supply the choroid plexuses of the third and lateral ventricles and the fornix. Small posterolateral central branches arise from the posterior cerebral artery beyond the cerebral peduncle and supply the peduncle and the posterior thalamus, superior and inferior colliculi, pineal gland and medial geniculate body.

CIRCULUS ARTERIOSUS

The circulus arteriosus (circle of Willis) is a large arterial anastomosis which unites the internal carotid and vertebrobasilar systems (Figs 17.3, 17.6B). It lies in the subarachnoid space within the interpeduncular cistern, and surrounds the optic chiasma and infundibulum. Anteriorly, the anterior cerebral arteries, derived from the internal carotid arteries, are linked by the small anterior communicating artery. Posteriorly, the two posterior cerebral arteries, formed by the division of the basilar artery, are joined to the ipsilateral internal carotid artery by a posterior communicating artery.

There is considerable individual variation in the pattern and calibre of vessels that make up the circulus arteriosus. Although a complete circular channel almost always exists, one vessel is usually sufficiently narrowed to reduce its role as a collateral route and the circle is rarely functionally complete. Cerebral and communicating arteries individually may all be absent, variably hypoplastic, double or even triple. The haemodynamics of the circle are influenced by variations in the calibre of communicating arteries and in the segments of the anterior and posterior cerebral arteries which lie between their origins and their junctions with the corresponding communicating arteries. The greatest variation in calibre between individuals occurs in the posterior communicating artery, which is normally very small, so that only limited flow is possible between the anterior and posterior circulations. Commonly, the diameter of the precommunicating part of the posterior cerebral artery is larger than that of the posterior communicating artery, in which case the blood supply to the occipital lobes is mainly from the vertebrobasilar system. However, sometimes the diameter of the precommunicating part of the posterior cerebral artery is smaller than that of the posterior communicating artery, in which case the blood supply to the occipital lobes is mainly from the internal carotids via the posterior communicating arteries. Since the primary purpose of the vascular circle is to provide anastomotic channels if one vessel is occluded, it is important to note that a normal-sized posterior communicating artery cannot usually fulfil this role. Agenesis or hypoplasia of the initial segment of the anterior cerebral artery are more frequent than anomalies in the anterior communicating artery and contribute to defective circulation in about a third of individuals.

Cerebral aneurysms

Aneurysms are balloon-like swellings which occur on arteries as a result of defects in the vessel wall. They are most commonly found on the vessels of the circulus arteriosus, particularly at or near the junctions of vessels. Aneurysms on the internal carotid artery near its termination may compress the lateral aspect of the optic chiasma, and compromise axons derived from the temporal side of the ipsilateral retina, which causes a defect in the nasal visual field. Aneurysms in the vicinity of the oculomotor nerve, e.g. on the posterior communicating artery, superior cerebellar artery, or the tip of the basilar artery, can cause third nerve palsy by compression (Fig. 17.7).

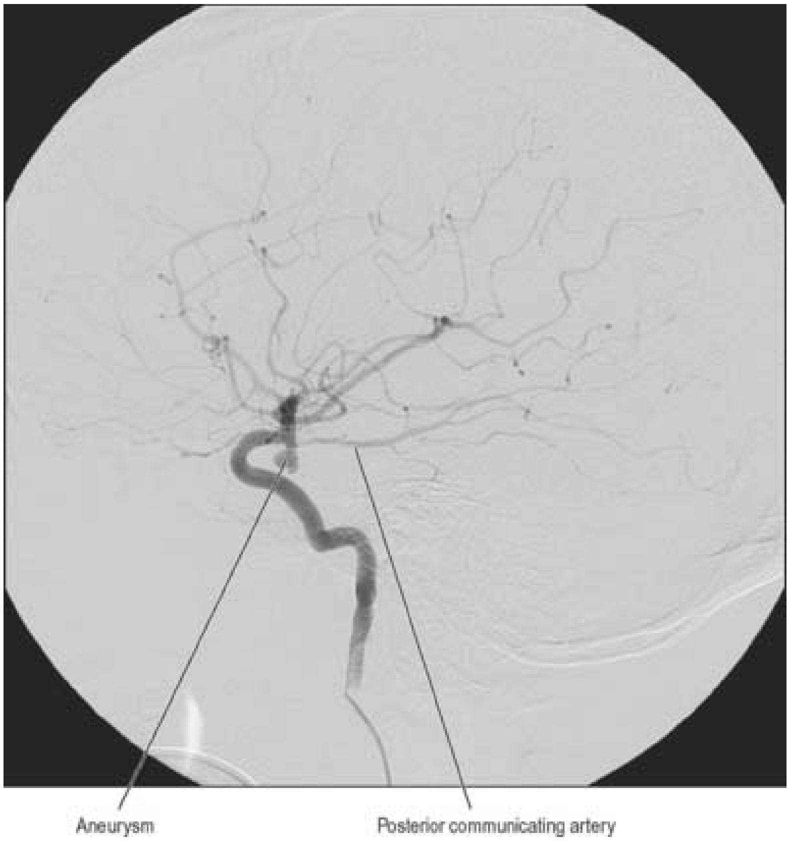

Fig. 17.7 Intra-arterial digital subtraction angiogram of the right internal carotid artery in a patient with a complete right oculomotor nerve palsy. Lateral projection.

Subarachnoid haemorrhage

Bleeding into the subarachnoid compartment, subarachnoid haemorrhage, is the most common pathology that involves the subarachnoid space. There are many causes; in adults the commonest is rupture of an aneurysm of the intracranial vessels that run within the subarachnoid space. A person who has had a subarachnoid haemorrhage usually complains of a very sudden onset of headache that is frequently described as being their 'worst ever headache' or 'like being hit on the head with a hammer'. When this is suspected the first investigation is an X-ray CT examination which has a very high sensitivity for detecting fresh haemorrhage. Blood will be seen in the basal cisterns and entering the depths of the cortical sulci, i.e. delineating the anatomy of the subarachnoid space, a presentation that permits an accurate diagnosis (Fig. 17.8). In marked contrast, the spread of blood in a subdural haemorrhage is limited by the arachnoid mater on its deep surface, and the blood therefore remains on the surface of the brain.

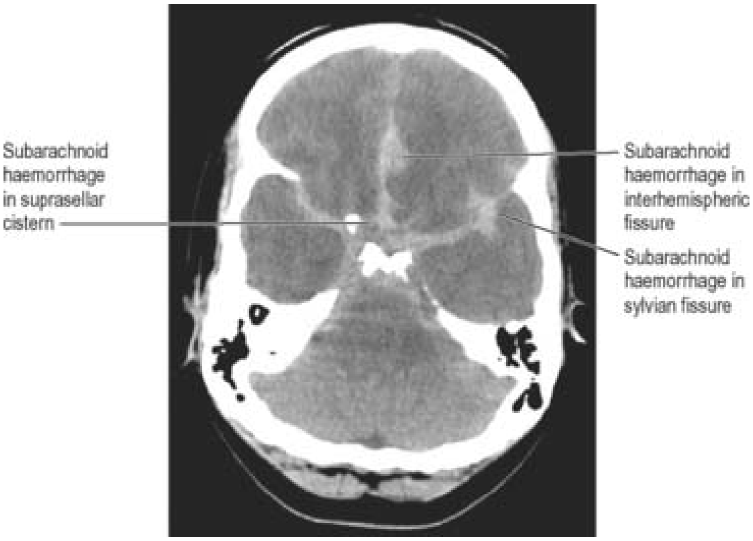
Subarachnoid haemorrhage in suprasellar cistern
Subarachnoid haemorrhage in interhemispheric fissure
Subarachnoid haemorrhage in sylvian fissure

Fig. 17.8 Axial CT image (without intravenous contrast agent) at the level of posterior clinoids. There is abnormally high attenuation in the basal cisterns and subarachnoid space of the interhemispheric fissure, indicating an acute subarachnoid haemorrhage, which was subsequently shown to be due to a ruptured aneurysm on the anterior communicating artery.

CENTRAL OR PERFORATING ARTERIES

Numerous small central (perforating or ganglionic) arteries arise from the circulus arteriosus, or from vessels near it (Fig. 17.3). Many of these enter the brain through the anterior and posterior perforated substances. Central branches supply nearby structures on or near the base of the brain together with the interior of the cerebral hemisphere including the internal capsule, basal ganglia and thalamus. These branches form four principal groups. The anteromedial group arises from the anterior cerebral and anterior communicating arteries and passes through the medial part of the anterior perforated substance. These arteries supply the optic chiasma, lamina terminalis, anterior, preoptic and supraoptic areas of the hypothalamus, septum pellucidum, paraolfactory areas, anterior columns of the fornix, cingulate gyrus, rostrum of the corpus callosum and the anterior part of the putamen and the head of the caudate nucleus. The posteromedial group comes from the entire length of the posterior communicating artery and from the proximal portion of the posterior cerebral artery. Anteriorly, these arteries supply the hypothalamus and pituitary gland, and the anterior and medial parts of the thalamus via thalamoperforating arteries. Caudally, branches of the posteromedial group supply the mammillary bodies, subthalamus, the lateral wall of the third ventricle, including the medial thalamus, and the globus pallidus. The anterolateral group is mostly comprised of branches from the proximal part of the middle cerebral artery that are also known as striate, lateral striate or lenticulostriate arteries. They enter the brain through the anterior perforated substance and supply the posterior striatum, lateral globus pallidus and the anterior limb, genu and posterior limb of the internal capsule. The medial striate artery, derived from the middle or anterior cerebral arteries, supplies the rostral part of the caudate nucleus and putamen and the anterior limb and genu of the internal capsule. The posterolateral group is derived from the posterior cerebral artery distal to its junction with the posterior communicating artery, and supplies the cerebral peduncle, colliculi, pineal gland and, via thalamogeniculate branches, the posterior thalamus and medial geniculate body.

REGIONAL ARTERIAL SUPPLY OF THE BRAIN

Brain stem

The medulla oblongata is supplied by the branches of the vertebral, anterior and posterior spinal, posterior inferior cerebellar and basilar arteries, which enter along the anterior median fissure and the posterior median sulcus. Vessels that supply the central substance enter along the rootlets of the glossopharyngeal, vagus, accessory and hypoglossal nerves. There is an additional supply via a pial plexus from the same main arteries.

The pons is supplied by the basilar artery and the anterior inferior and superior cerebellar arteries. Direct branches from the basilar artery enter the pons along the ventral medial groove (basilar sulcus). Other vessels enter along the trigeminal, abducens, facial and vestibulcochlear nerves and from the pial plexus.

The midbrain is supplied by the posterior cerebral, superior cerebellar and basilar arteries. The crura cerebri are supplied by vessels entering on their medial and lateral sides. The medial vessels enter the medial side of the crus and also supply the superomedial part of the tegmentum, including the oculomotor nucleus, and lateral vessels supply the lateral part of the crus and the tegmentum. The colliculi are supplied by three vessels on each side from the posterior cerebral and superior cerebellar arteries. An additional supply to the crura, and the colliculi and their penduncles, comes from the posterolateral group of central branches of the posterior cerebral artery.

Cerebellum

The cerebellum is supplied by the posterior inferior, anterior inferior and superior cerebellar arteries. The cerebellar arteries form superficial anastomoses on the cortical surface. Anastomoses between deeper, subcortical, branches have been postulated.

The choroid plexus of the fourth ventricle is supplied by the posterior inferior cerebellar arteries.

Optic chiasma, tract and radiation

The blood supplies of the optic chiasma, tract and radiation are of considerable clinical importance. The chiasma is supplied in part by the anterior cerebral arteries but its median zone depends upon rami from the internal carotid arteries reaching it via the stalk of the hypophysis. The anterior choroidal and posterior communicating arteries supply the optic tract, and the optic radiation receives blood through deep branches of the middle and posterior cerebral arteries.

Diencephalon

The thalamus is supplied chiefly by branches of the posterior communicating, posterior cerebral and basilar arteries. A contribution from the anterior choroidal artery is often noted, but this has been disputed. The medial branch of the posterior choroidal artery supplies the posterior commissure, habenular region, pineal gland and medial parts of the thalamus, including the pulvinar. Small central branches, which arise from the circulus arteriosus and its associated vessels, supply the hypothalamus. The pituitary gland is supplied by hypophysial arteries derived from the internal carotid artery and the anterior cerebral and anterior communicating arteries supply the lamina terminalis.

The choroid plexuses of the third and lateral ventricles are supplied by branches of the internal carotid and posterior cerebral arteries.

Basal ganglia

The majority of the arterial supply to the basal ganglia comes from the striate arteries, which are branches from the roots of the anterior and middle cerebral arteries. They enter the brain through the anterior perforated substance and also supply the internal capsule. The caudate nucleus receives blood additionally from the anterior and posterior choroidal arteries. The posteroinferior part of the lentiform complex is supplied by the thalamostriate branches of the posterior cerebral artery. The anterior choroidal artery, a preterminal branch of the internal carotid artery, contributes to the blood supply of both segments of the globus pallidus and the caudate nucleus. Famously, the ligation of this vessel during a neurosurgical procedure on a patient suffering from Parkinson's disease led to alleviation of the Parkinsonian symptoms, presumably as a consequence of infarction of the globus pallidus. This chance observation led to the initiation of pallidal surgery (pallidotomy) for this condition (see also Ch. 22).

Internal capsule

The internal capsule is supplied by central, or perforating, arteries which arise from the circulus arteriosus and its associated vessels. These include the lateral and medial striate arteries which come from the middle and anterior cerebral arteries and which also supply the basal ganglia. The lateral striate arteries supply the anterior limb, genu and much of the posterior limb of the internal capsule and are commonly involved in ischaemic and haemorrhagic stroke. One of the larger striate branches of the middle cerebral artery is known as 'Charcot's artery of cerebral haemorrhage'. The medial striate artery, a branch of the proximal part of either the middle or anterior cerebral artery, supplies the anterior limb and genu of the internal capsule and the basal ganglia. The anterior choroidal artery also contributes to the supply of the ventral part of the posterior limb and the retrolenticular (retrolentiform) part of the internal capsule.

Ischaemic stroke

Stroke refers to the clinical syndrome of a rapidly developing focal neurological deficit that is not due to seizure activity. If the cause is lack of, or reduced, blood supply to a portion of the brain then the term ischaemic stroke (see Fig. 17.9) is used, as opposed to haemorrhagic stroke e.g. subarachnoid haemorrhage. The lack of blood flow can be due to pathology in the vessel lumen, such as thrombosis or embolus (common), pathology outside the blood vessel, such as occlusion from mass effect of a tumour or haematoma (rare), or pathology of the vessel wall, such as inflammatory or infective arteritides (rare). The symptoms and signs of ischaemic stroke depend on the location and extent of the arterial infarction. In certain locations, even a small volume stroke can have devastating effects. For example, the internal capsule and most of the adjacent basal ganglia are supplied by small perforating arteries, which are a common site for ischaemic stroke. Corticobulbar and corticospinal motor pathways and third-order thalamocortical sensory fibres all pass through the internal capsule, so that it is effectively the only route connecting the cerebral cortex with other regions of the neuraxis. The neurological deficits that result from stroke in the internal capsule, therefore, may include contralateral spastic hemiparesis, contralateral hemisensory loss and psychological deficits.

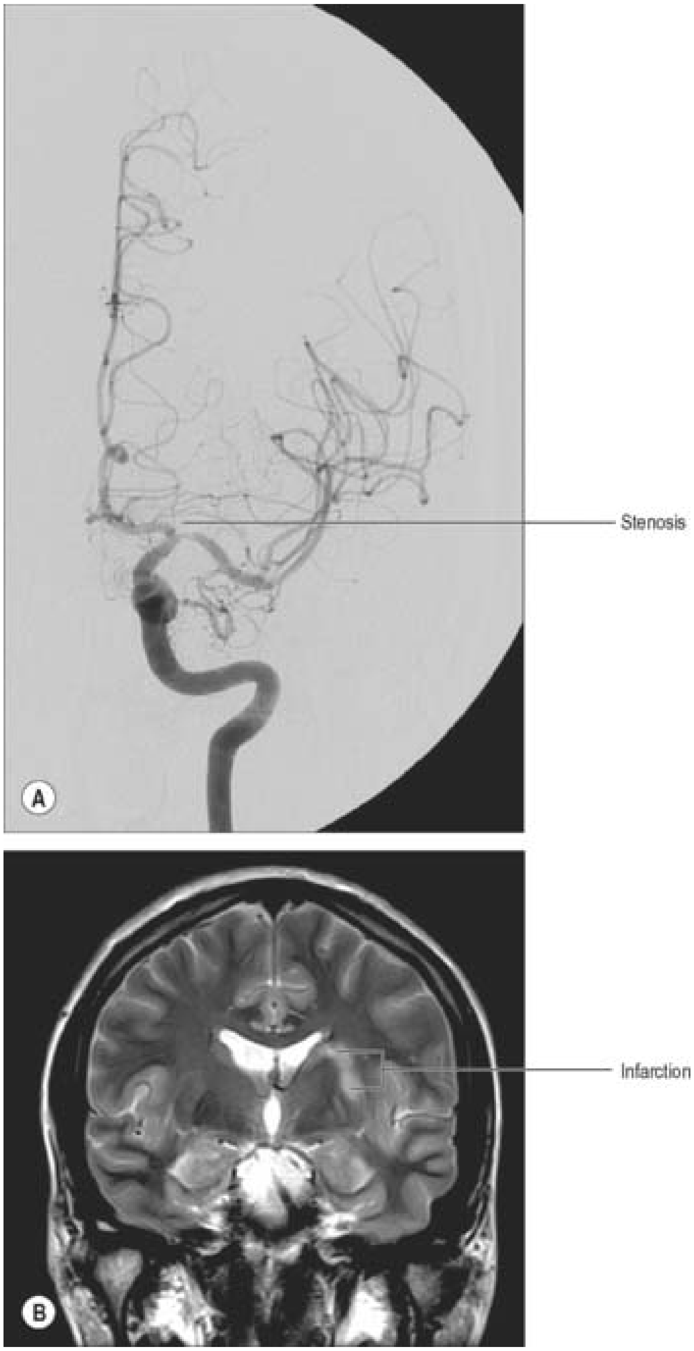

Fig. 17.9 **A**, Frontal projection of a catheter angiogram of the left internal carotid artery, showing a focal narrowing at the termination of the left internal carotid artery and the origin of the left middle cerebral artery. **B**, Coronal T2-weighted image of the brain at the level of the basal ganglia. There is abnormal high signal in the left putamen and adjacent white matter, consistent with infarction. It is likely that the infarction was due to

occlusion of small perforating vessels originating in the area of the stenosis and supplying the basal ganglia.

It is possible for a major vessel, such as the internal carotid artery in the neck, to become occluded and the individual to remain asymptomatic, if an appropriate flow of blood can be recruited to supply the affected brain region from other sources (collateral supply). The primary role of the circle of Willis is to allow for this eventuality by redirecting blood from other sources such as the contralateral internal carotid and vertebrobasilar system in the example given above. If the circle of Willis is complete, two or even three of the four major arteries supplying the brain can occlude without producing an ischaemic stroke. Unfortunately the circle of Willis is rarely complete (a finding in approximately 15% of individuals): ischaemic stroke is therefore often caused because the collateral supply is inadequate. For example, an individual in whom neither anterior nor posterior communicating arteries are patent will suffer an ischaemic stroke if there is occlusion of one internal carotid artery, because the proximal anterior and middle cerebral arteries cannot receive collateral flow from the incomplete circle of Willis. Some collateral flow may be available from anastomoses between distal branches of the external carotid artery (e.g. middle meningeal artery), but invariably this is not sufficient to supply the whole hemisphere.

Somewhat paradoxically, the more distal the occlusion occurs in the cerebral vasculature the more likely it is to cause an ischaemic stroke (although the volume of infarcted tissue will be less). This is because the major capacity to form collateralization is proximal, mainly at the circle of Willis. For example, an embolus formed in the proximal internal carotid artery may travel to the M1 portion of the ipsilateral middle cerebral artery and occlude the vessel. There is very little scope for collateralisation at this site and an ischaemic stroke is unavoidable, unless the embolus can be cleared and flow restored in good time.

Cerebral cortex

The entire blood supply of the cerebral cortex comes from cortical branches of the anterior, middle and posterior cerebral arteries (Fig. 17.4, Fig. 17.5). In general, long branches traverse the cortex and penetrate the subjacent white matter for 3 or 4 cm without communicating. Short branches are confined to the cerebral cortex, and form a compact network in the middle zone of the grey matter, whereas the outer and inner zones are sparingly supplied. Although adjacent vessels anastomose on the surface of the brain, they become end arteries as soon as they enter it. In general, superficial anastomoses only occur between microscopic branches of the cerebral arteries, and there is little evidence that they can provide an effective alternative circulation after the occlusion of larger vessels.

The lateral surface of the hemisphere is mainly supplied by the middle cerebral artery. This includes the territories of the motor and somatosensory cortices which represent the whole of the body, apart from the lower limb, and also the auditory cortex and language areas. The anterior cerebral artery supplies a strip next to the superomedial border of the hemisphere, as far back as the parieto-occipital sulcus. The occipital lobe and most of the inferior temporal gyrus (excluding the temporal pole) are supplied by the posterior cerebral artery.

Medial and inferior surfaces of the hemisphere are supplied by the anterior, middle and posterior cerebral arteries. The area supplied by the anterior cerebral artery is the largest, and extends almost to the parieto-occipital sulcus and includes the medial part of the orbital surface. The rest of the orbital surface and the temporal pole are supplied by the middle cerebral artery, and the remaining medial and inferior surfaces are supplied by the posterior cerebral artery.

Near the occipital pole, the junctional zone between the territories of the middle and posterior cerebral arteries corresponds to the visual (striate) cortex which receives information from the macula. When the posterior cerebral artery is occluded, a phenomenon known as ‘macular sparing’ may occur in which vision with the central part of the retina is preserved. Collateral circulation of blood from branches of the middle cerebral artery into those of the posterior cerebral artery may account for this phenomenon.

In addition, in some individuals, the middle cerebral artery may itself supply the macular area.

Watershed areas

Regions of the brain lying at the extreme edges of the major cerebral arterial territories are called watershed areas: they are the first to be deprived of sufficient blood flow in the event of cerebral hypoperfusion. Ischaemic infarcts of the cortex and adjacent subcortical white matter in the border zones between these territories are known as watershed, boundary zone, or border zone infarcts. There is some evidence that a second arterial border zone, the internal arterial border zone, exists within the white matter of the centrum semiovale and corona radiata (between the lenticulostriate perforators and the deep penetrating branches of the distal middle cerebral artery).

Cerebral blood flow

The brain is devoid of either glucose stores or a means of storing oxygen and is, therefore, dependent minute-by-minute upon an adequate blood supply. It has a high metabolic rate in comparison to other organs, which reflects the metabolic demands of constant neural activity. The blood supply of grey matter is more copious than that of white matter.

Cerebral blood flow in the human brain is approximately 50 ml g^{-1} min^{-1}. Global cerebral blood flow is autoregulated, i.e. it remains constant in normal individuals despite variations in mean arterial blood pressure over a range of 8.7–18.7 kPa (65–140 mmHg). If the blood pressure falls below this range, cerebral blood flow decreases. Alternatively, if the pressure rises above this range, cerebral blood flow may increase. Arterial and arteriolar intraluminal pressure directly control contraction of intramural muscle, so that an increase in arterial pressure, for example, causes arterial constriction, and blood flow remains constant.

Although autoregulation normally ensures that global cerebral blood flow remains constant, regional blood flow varies in response to the level of neural activity and, thus, to local metabolic demand. This has been demonstrated for many brain areas including the motor and sensory cortical regions, areas involved in convulsive activity and even cortical areas involved in complex thought processes. The principal local factors affecting regional blood flow are the local hydrogen ion (H^+) or carbon dioxide concentration, which cause arterial dilatation by both a direct action on the endothelium and through indirect mediators, such as nitric oxide.

Not all substances circulating in arterial blood have access to the brain parenchyma. Particulate matter, such as bacteria, is excluded. In general, lipophilic molecules and small molecules, such as oxygen and carbon dioxide, can cross the blood–brain barrier but hydrophilic ones (excluding glucose) cannot. The cellular basis for the blood–brain barrier is discussed in Chapter 3.

VENOUS DRAINAGE OF THE BRAIN

The venous drainage of the brain occurs through a complex system of deep and superficial veins. These veins possess no valves and have thin walls devoid of muscular tissue. They pierce the arachnoid mater and the inner layer of the dura mater to open into the dural venous sinuses (see Chapter 27).

VENOUS DRAINAGE OF THE POSTERIOR FOSSA

The veins of the brain stem form a superficial venous plexus deep to the arteries.

Veins of the medulla oblongata drain into the veins of the spinal cord or the adjacent dural venous sinuses, or into variable radicular veins which accompany the last four cranial nerves to either the inferior petrosal or occipital sinuses, or to the superior bulb of the jugular vein. Anterior and posterior median medullary veins may run along the anterior median fissure and posterior median sulcus, to become continuous with the spinal veins in corresponding positions. Pontine veins, which may include a median vein and a lateral vein on each side, drain into the basal vein, cerebellar veins, the petrosal sinuses, transverse sinus or the venous plexus of the foramen ovale. Veins of the midbrain join the great cerebral vein or basal vein.

The veins of the cerebellum drain mainly into sinuses adjacent to them or, from the superior surface, into the great cerebral vein. The cerebellar veins course on the cerebellar surface, and consist of superior and inferior groups. Superior cerebellar veins either run anteromedially across the superior vermis to the straight sinus or great cerebral vein, or they run laterally to the transverse and superior petrosal sinuses. Inferior cerebellar veins include a small median vessel that runs backwards on the inferior vermis to enter the straight or sigmoid sinus. Laterally coursing vessels join the inferior petrosal and occipital sinuses.

VENOUS DRAINAGE OF THE CEREBRAL HEMISPHERE

External and internal cerebral veins drain the surfaces and the interior of the cerebral hemisphere (Figs 17.10, 17.11, 17.12, 17.13).

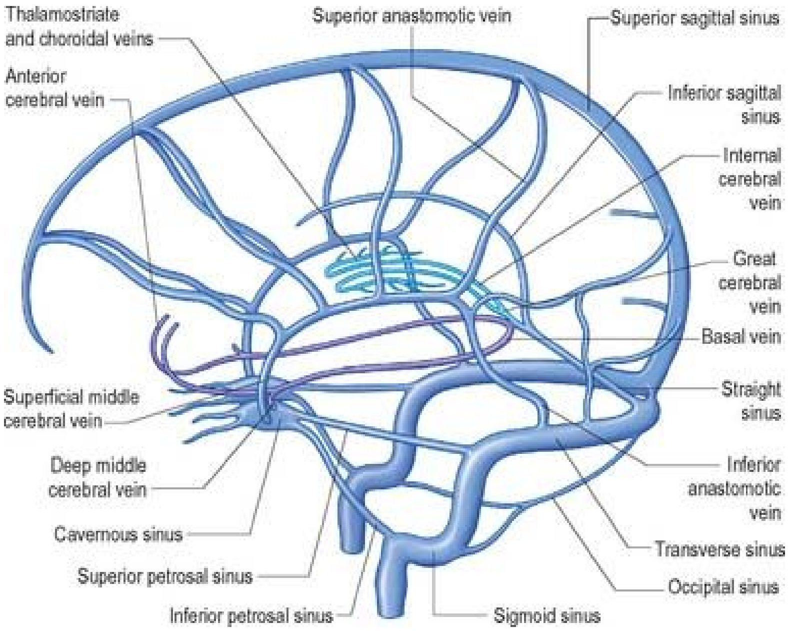
Thalamostriate and choroidal veins
Anterior cerebral vein
Superior anastomotic vein
Superior sagittal sinus
Inferior sagittal sinus
Internal cerebral vein
Great cerebral vein
Basal vein
Straight sinus
Inferior anastomotic vein
Transverse sinus
Occipital sinus
Sigmoid sinus
Inferior petrosal sinus
Superior petrosal sinus
Cavernous sinus
Deep middle cerebral vein
Superficial middle cerebral vein

Fig. 17.10 The cerebral venous system showing the principal superficial and deep veins of the brain and their relationship to the dural venous sinuses, viewed from the left side.

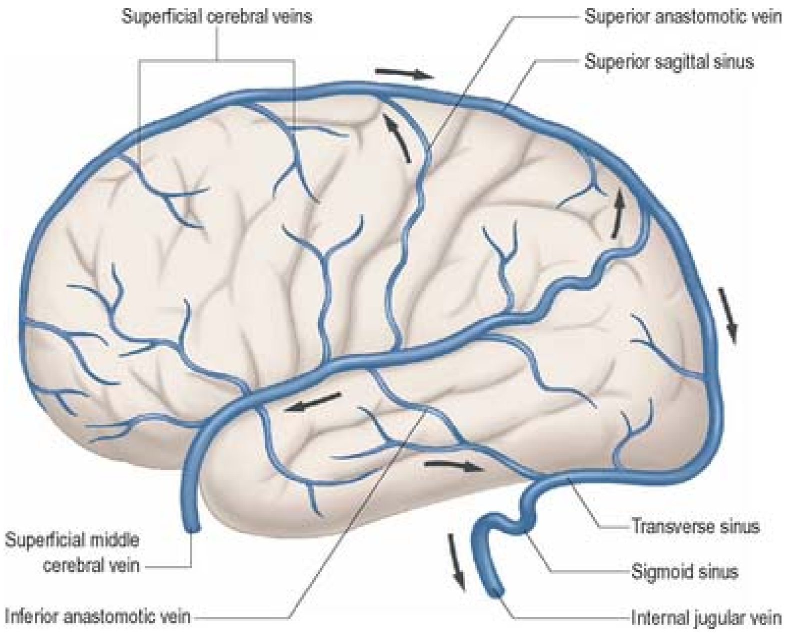
Superficial cerebral veins
Superior anastomotic vein
Superior sagittal sinus
Superficial middle cerebral vein
Inferior anastomotic vein
Transverse sinus
Sigmoid sinus
Internal jugular vein

Fig. 17.11 The external (superficial) cerebral veins of the left hemisphere and their relationship to the dural venous sinuses.

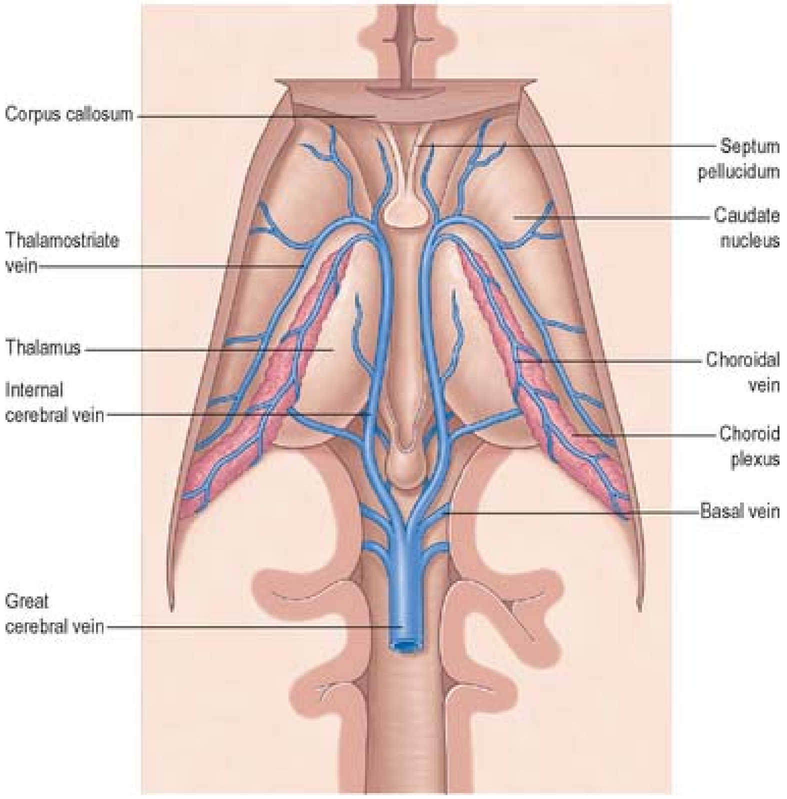
Corpus callosum
Septum pellucidum
Caudate nucleus
Thalamostriate vein
Thalamus
Internal cerebral vein
Choroidal vein
Choroid plexus
Basal vein
Great cerebral vein

Fig. 17.12 The internal (deep) cerebral veins, viewed from above after removal of the central portion of the corpus callosum.

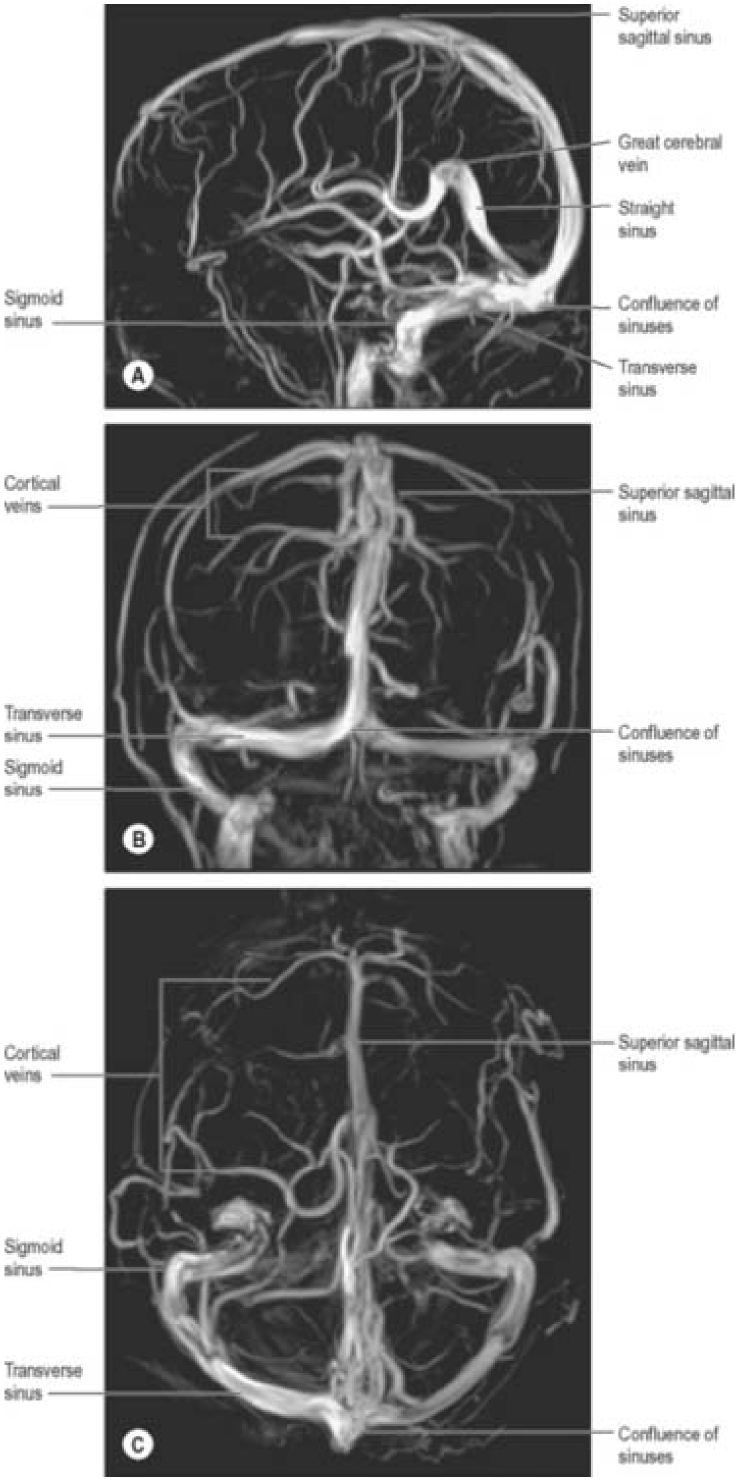
Superior sagittal sinus
Great cerebral vein
Straight sinus
Sigmoid sinus
Confluence of sinuses
Transverse sinus
A
Cortical veins
Superior sagittal sinus
Transverse sinus
Confluence of sinuses
Sigmoid sinus
B
Cortical veins
Superior sagittal sinus
Sigmoid sinus
Transverse sinus
Confluence of sinuses
C

Fig. 17.13 Phase contrast magnetic resonance venograms taken at 3.0T in **A**, lateral; **B**, frontal and **C**, superior projections.

External cerebral veins may be divided into three groups, namely superior, middle and inferior.

Eight to 12 superior cerebral veins drain the superolateral and medial surfaces of each hemisphere. They mainly follow the sulci, although some do pass across gyri. They ascend to the superomedial border of the hemisphere, where they receive small veins from the medial surface, and then open into the superior sagittal sinus. Superior cerebral veins in the anterior part of the hemisphere join the sinus almost at right angles. The larger posterior veins are directed obliquely forwards, against the direction of flow in the sinus, an arrangement which may resist their collapse when intracranial pressure is raised.

The superficial middle cerebral vein drains most of the lateral surface of the hemisphere, and follows the lateral fissure to end in the cavernous sinus. A superior anastomotic vein runs posterosuperiorly between the superficial middle cerebral vein and the superior sagittal sinus, thus connecting the superior sagittal and cavernous sinuses. An inferior anastomotic vein courses over the temporal lobe and connects the superficial middle cerebral vein to the transverse sinus. The deep middle cerebral vein drains the insular region and joins the anterior cerebral and striate veins to form a basal vein. Regions drained by the anterior cerebral and striate veins correspond approximately to those supplied by the anterior cerebral artery and the central branches which enter the anterior perforated substance. The basal veins pass back alongside the interpeduncular fossa and midbrain, receive tributaries from this vicinity and join the great cerebral vein.

Inferior cerebral veins on the orbital surface of the frontal lobe join the superior cerebral veins and thus drain to the superior sagittal sinus. Those on the temporal lobe anastomose with basal veins and middle cerebral veins, and drain to the cavernous, superior petrosal and transverse sinuses.

The basal vein begins at the anterior perforated substance by the union of a small anterior cerebral vein, which accompanies the anterior cerebral artery, a deep middle cerebral vein, which receives tributaries from the insula and neighbouring gyri and runs in the lateral cerebral fissure, and striate veins, which emerge from the anterior perforated substance. The basal vein passes back round the cerebral peduncle to the great cerebral vein and receives tributaries from the interpeduncular fossa, inferior horn of the lateral ventricle, parahippocampal gyrus and midbrain.

The internal cerebral vein drains the deep parts of the hemisphere and the choroid plexuses of the third and lateral ventricles. It is formed near the interventricular foramen, behind the column of the fornix, primarily by union of the thalamostriate and choroidal veins, although numerous smaller veins from surrounding structures also converge here. The thalamostriate vein runs anteriorly, between the caudate nucleus and thalamus, and receives many tributaries from both areas. The choroidal vein runs a convoluted course along the whole choroid plexus, and receives veins from the hippocampus, fornix, corpus callosum and adjacent structures. After their formation, the two internal cerebral veins travel back parallel to one another beneath the splenium of the corpus callosum, where they unite to form the great cerebral vein. The great cerebral vein is a short median vessel which curves sharply up around the splenium of the corpus callosum and opens into the anterior end of the straight sinus after receiving the right and left basal veins.

Intracranial venosinus thrombosis

One of the most potentially serious pathologies affecting the intracranial venous system is venosinus thrombosis. In this condition, blood clots within the dural sinuses and/or intracranial veins, and the resulting obstruction of venous drainage, may produce life-threatening complications. In many cases the cause of the venosinus thrombosis is not found: trauma involving the dural sinuses or infections in the vicinity of the sinuses (e.g. mastoiditis) present significant risk. Conditions that increase the coagulability of the blood, such as the oral contraceptive pill, pregnancy, dehydration and inborn abnormalities of the coagulation pathways, are also risk factors.

At its severest, individuals with intracranial venosinus thrombosis present moribund, in coma or with major seizure activity: in these situations the prognosis is poor. The clot within the dural sinuses and/or cortical veins obstructs the drainage of venous blood from the brain and causes venous hypertension. As the pressure in the venous system approaches the arterial pressure, the blood perfusing the affected parts of the brain decreases. If it decreases below a critical level the brain tissue will become ischaemic and may die (venous infarction). As the arterial supply to the brain is still present, the infarcted areas of the brain frequently undergo major haemorrhage and this is often the factor that kills the patient.

Although they may occur together, clinicians distinguish between thrombosis that affects the ‘superficial’ and ‘deep’ venous systems (Fig. 17.10). Superficial thrombosis usually occurs in the superior sagittal sinus (with or without involvement of the cortical veins), whilst deep intracranial thrombotic disease usually affects the vein of Galen and straight sinus. The parts of the cerebral hemispheres affected are different in the two situations; superficial thrombosis affects the cerebral hemispheres (particularly the white matter) and deep thrombosis affects the thalami and basal ganglia. However, one common feature is the tendency for bilateral involvement, because all of the main draining venous channels are in the midline and accept venous drainage from both hemispheres.

If the extent of the intracranial venosinus thrombosis is less severe, or if alternative venous drainage has been accommodated by reasonable collateral channels, the patient may have more modest symptoms such as headaches or visual disturbance. Those symptoms are due to raised intracranial pressure and if untreated may become chronic.

REFERENCES

deweg J. The anatomy of collateral venous flow from the brain and its value in aetiological interpretation of intracranial pathology. *Neurorad*. 1996;38:621-628.

Includes a brief historical review..

gousslavsky J, Caplan L. Stroke Syndromes, 2nd edn., Cambridge: Cambridge University Press, 2002.

vernoy HM, Delon S, Vannson JL. Cortical blood vessels of the human brain. *Brain Res Bull*. 1981;7:519-579.

vernoy H, Delon S, Vannson JL. The vascularization of the human cerebellar cortex. *Brain Res Bull*. 1983;11:419-480.

aplan HA, Ford DH. The Brain Vascular System. Amsterdam: Elsevier, 1966.

ets C, De Reuck J, Vander Eecken H, Van den Bergh R. The vascularization of the human thalamus. *Acta Neurol Belg*. 1970;70:687-770.

chades-Orts A, Nombela-Gomez M, Ortu-o-Pacheco G. Variation in form of the circle of Willis. Some anatomical and embryological considerations. *Anat Rec*. 1976;185:119-123.

ngupta RP, McAllister VL. Subarachnoid Haemorrhage. Berlin: Springer-Verlag; 1986:9-31.

Includes details on variations of the circle of Willis..

CHAPTER 18

Spinal cord: internal organization

The spinal cord provides innervation for the trunk and limbs via spinal nerves and their peripheral ramifications. It receives primary afferent fibres from peripheral receptors located in widespread somatic and visceral structures, and sends motor axons to skeletal muscle. It also contains the cell bodies of all the preganglionic neurones responsible for the sympathetic innervation of cardiac and smooth muscle and secretory glands, and for the parasympathetic innervation of smooth muscle in the distal part of the hind gut, the pelvic viscera and the erectile tissues of the external genitalia. Many bodily functions are regulated at an unconscious level by intraspinal reflex connections between afferent and efferent neurones. Profuse ascending and descending pathways link the spinal cord with the brain, allowing higher centres to monitor and perceive external and internal stimuli and to modulate and control spinal efferent activity.

EXTERNAL FEATURES AND RELATIONS

The topographical anatomy of the spinal cord, its external features and relations are described in more detail in Chapter 43. In brief, the cord lies within the vertebral canal. It is continuous rostrally with the medulla oblongata, just below the level of the foramen magnum (Fig. 28.11) and it terminates caudally as the conus medullaris, which is continuous with the filum terminale and is anchored to the dorsum of the coccyx. The cord is ensheathed by spinal meninges which are continuous with the cranial meninges through the foramen magnum. Although it is approximately circular in cross-section, the diameter of the spinal cord varies according to level; it bears two enlargements, cervical and lumbar.

The spinal cord is essentially a segmental structure, giving rise to 31 bilaterally-paired spinal nerves. These attach to the cord as linear series of smaller dorsal and ventral nerve rootlets. Dorsal rootlets contain afferent nerve fibres and ventral rootlets contain efferent fibres (see Fig. 15.4). Groups of adjacent rootlets coalesce to form dorsal or ventral nerve roots that cross the subarachnoid space and unite to form functionally mixed spinal nerves as they pass through the intervertebral foramina. The dorsal roots bear dorsal root ganglia that contain the cell bodies of primary afferent neurones.

INTERNAL ORGANIZATION

In transverse section, the spinal cord is incompletely divided into symmetrical halves by a dorsal (posterior) median septum and a ventral (anterior) median sulcus (Fig. 18.1). It consists of an outer layer of white matter and an inner core of grey matter; their relative sizes and configuration vary according to level. The amount of grey matter reflects the number of neurones present; it is proportionately largest in the cervical and lumbar enlargements, which contain the neurones that innervate the limbs. The absolute amount of white matter is greatest at cervical levels, and decreases progressively at lower levels, because descending tracts shed fibres as they descend and ascending tracts accumulate fibres as they ascend.

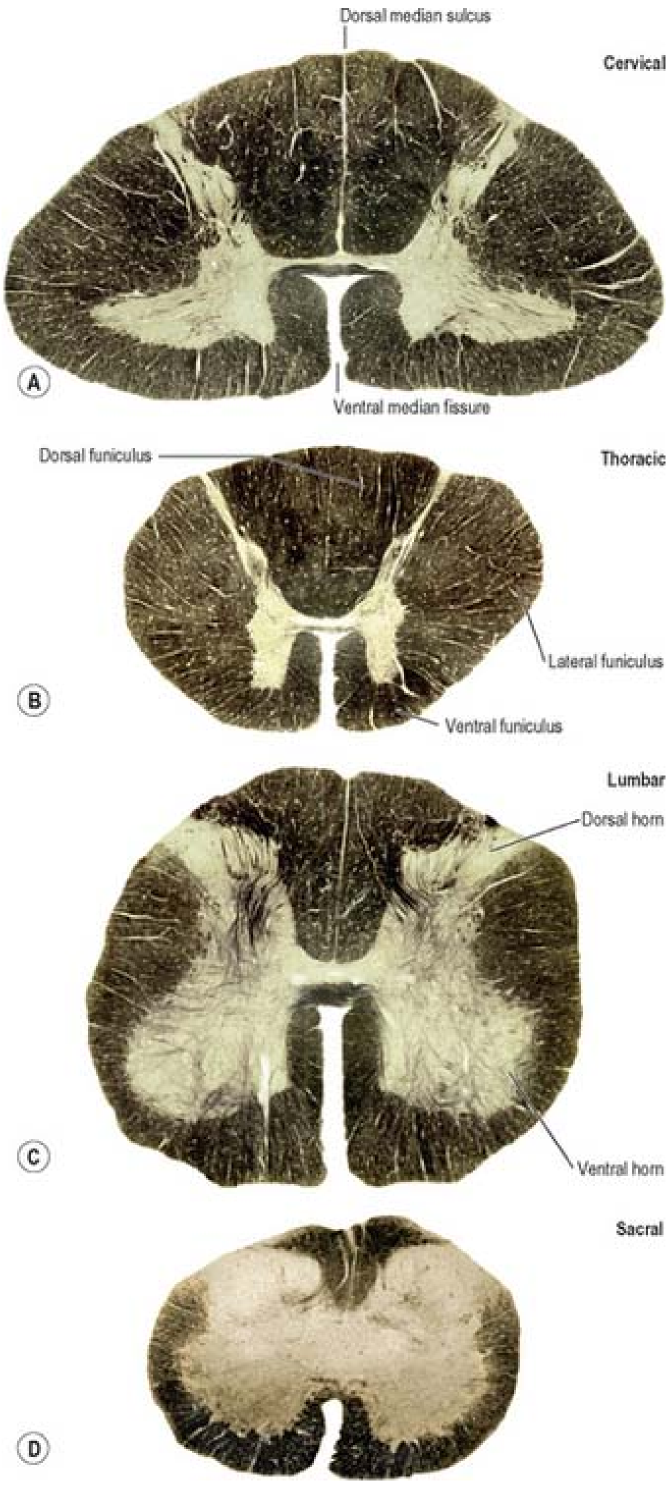
Dorsal median sulcus
Cervical
A
Ventral median fissure
Dorsal funiculus
Thoracic
Lateral funiculus
B
Ventral funiculus
Lumbar
Dorsal horn
C
Ventral horn
Sacral
D

Fig. 18.1 Transverse sections through the spinal cord at representative levels. Approximately ×5. (Figure enhanced by B Crossman.)

A diminutive central canal, lined by columnar, ciliated epithelium (ependyma) and containing cerebrospinal fluid (CSF), extends the whole length of the spinal cord lying in the centre of the spinal grey matter. Rostrally, the central canal extends into the caudal half of the medulla oblongata and then opens into the fourth ventricle.

SPINAL GREY MATTER

In three dimensions, the spinal grey matter is shaped like a fluted column (Fig. 43.1F). In transverse section the column is often described as being ‘butterfly-shaped’ or resembling the letter ‘H’ (Fig. 18.1). It consists of four linked cellular masses, the right and left dorsal and ventral horns, that project dorsolaterally and ventrolaterally towards the surface respectively. The grey matter that immediately surrounds the central canal and unites the two sides constitutes the dorsal and ventral grey commissures. The dorsal horn is the site of termination of the primary afferent fibres that enter the cord via the dorsal roots of spinal nerves. The tip of the dorsal horn is separated from the dorsolateral surface of the cord by a thin fasciculus or tract (of Lissauer) in which primary afferent fibres ascend and descend for a short distance before terminating in the subjacent grey matter. The ventral horn contains efferent neurones whose axons leave the spinal cord in ventral nerve roots. A small intermediate, or lateral, horn is present at thoracic and upper lumbar levels; it contains the cell bodies of preganglionic sympathetic neurones.

Spinal grey matter (Fig. 18.2) is a complex mixture of neuronal cell bodies, their processes and synaptic connections, neuroglia and blood vessels. Neurones in the grey matter are multipolar. They vary in size and features such as the length and the arrangement of their axons and dendrites. Neurones may be intrasegmental, i.e. contained within a single segment, or intersegmental, i.e. their ramifications spread through several segments.

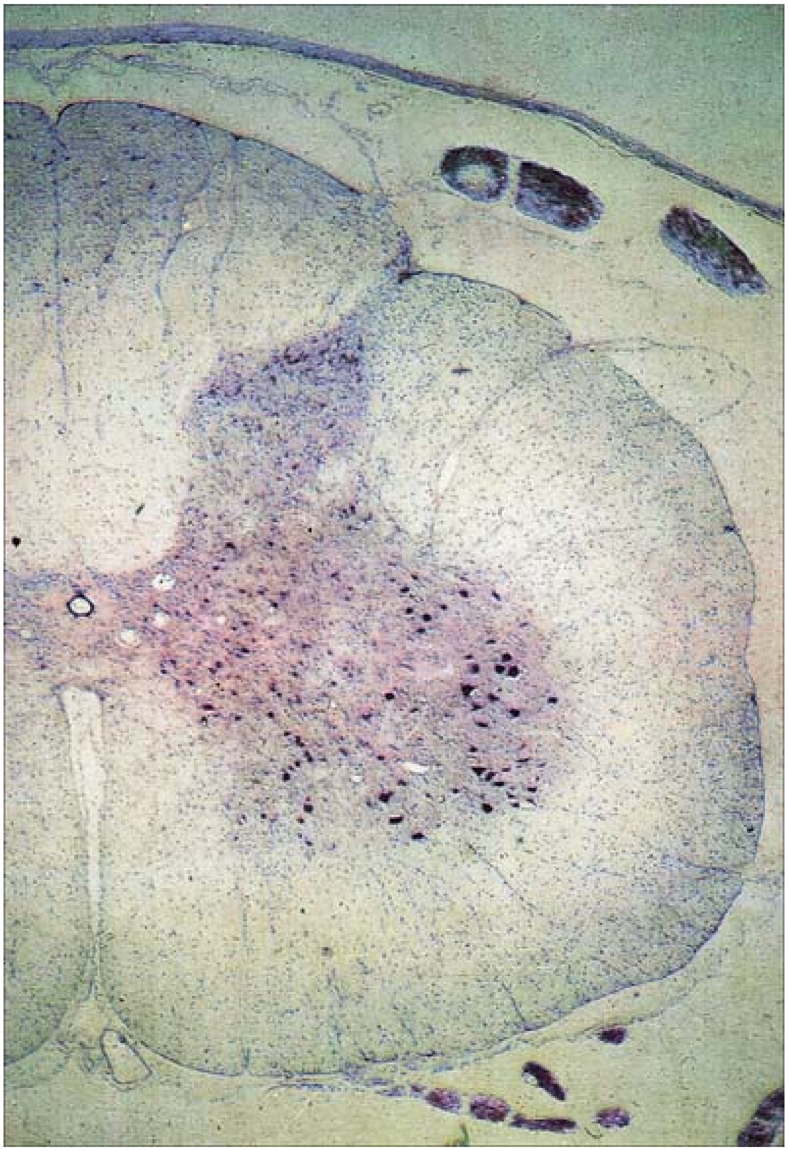

Fig. 18.2 Transverse section of spinal cord at a midlumbar level. The larger motor neurones in the ventral grey column are visibly grouped. Stained with cresyl fast violet.

Neuronal cell groups of the spinal cord

Viewed from the perspective of its longitudinal columnar organization, the grey matter of the spinal cord consists of a series of discontinuous cell groupings associated with their corresponding segmentally arranged spinal nerves. At any particular cross-sectional level these cell groupings are often considered to correspond approximately with one or more of ten cell layers, known as Rexed’s laminae. These laminae are defined on the basis of neuronal size, shape, cytological features and density and are numbered in a dorsoventral sequence.

Laminae I–IV correspond to the dorsal part of the dorsal horn, and are the main site of termination of cutaneous primary afferent terminals and their collaterals. Many complex polysynaptic reflex paths (ipsilateral, contralateral, intrasegmental and intersegmental) start from this region, as also do many long ascending tract fibres which pass to higher levels. Lamina I (lamina marginalis) is a very thin layer with an ill-defined boundary at the dorsolateral tip of the dorsal horn. It has a reticular appearance, reflecting its content of intermingling bundles of coarse and fine nerve fibres. It contains small, intermediate and large neuronal somata, many of which are fusiform in shape. The much larger lamina II consists of densely packed small neurones, responsible for its dark appearance in Nissl-stained sections. With myelin stains, lamina II is characteristically distinguished from adjacent laminae by the almost total lack of myelinated fibres. Lamina II corresponds to the substantia gelatinosa. Lamina III consists of somata which are mostly larger, more variable and less closely packed than those in lamina II. It also contains many myelinated fibres. Some workers consider that the substantia gelatinosa contains part or all of lamina III as well as lamina II. The ill-defined nucleus proprius of the dorsal horn corresponds to some of the cell constituents of laminae III and IV. Lamina IV is a thick, loosely packed, heterogeneous zone permeated by fibres. Its neuronal somata vary considerably in size and shape, from small and round, through intermediate and triangular, to very large and stellate.

Laminae V and VI lie at the base of the dorsal horn. They receive most of the terminals of proprioceptive primary afferents, profuse corticospinal projections from the motor and sensory cortex and input from subcortical levels, suggesting their involvement in the regulation of movement. Lamina V is a thick layer, divisible into a lateral third and medial two-thirds. Both have a mixed cell population but the former contains many prominent well-staining somata interlaced by numerous bundles of transverse, dorsoventral and longitudinal fibres. Lamina VI is most prominent in the limb enlargements. It has a densely staining medial third of small, densely packed neurones and a lateral two-thirds containing larger, more loosely packed, triangular or stellate somata.

Laminae VII–IX show a variety of forms in the limb enlargements. Lamina VII includes much of the intermediate (lateral) horn. It contains prominent neurones of Clarke’s column (nucleus dorsalis, nucleus thoracis, thoracic nucleus) and intermediomedial and intermediolateral cell groupings (Fig. 18.3). The lateral part of lamina VII has extensive ascending and descending connections with the midbrain and cerebellum (via the spinocerebellar, spinotectal, spinoreticular, tectospinal, reticulospinal and rubrospinal tracts) and is thus involved in the regulation of posture and movement. Its medial part has numerous propriospinal reflex connections with the adjacent grey matter and segments concerned both with movement and autonomic functions. Lamina VIII spans the base of the thoracic ventral horn but is restricted to its medial aspect in limb enlargements. Its neurones display a heterogeneous mixture of sizes and shapes from small to moderately large. Lamina VIII is a mass of propriospinal interneurones. It receives terminals from the adjacent laminae, many commissural fibres from the contralateral lamina VIII, and descending connections from the interstitiospinal, reticulospinal and vestibulospinal tracts and the medial longitudinal fasciculus. The axons from these interneurones influence α motor neurone activity bilaterally, perhaps directly but more probably by excitation of small γ motor neurones supplying efferent fibres to muscle spindles. Lamina IX is a complex array of cells consisting of α and γ motor neurones and many interneurones. The large α motor neurones supply motor end-plates of extrafusal muscle fibres in striated muscle. Recording techniques have demonstrated tonic and phasic α motor neurones. The former have a lower rate of firing and lower conduction velocity and tend to innervate type S muscle units. The latter have higher conduction velocity and tend to supply fast twitch (type FR, FF) muscle units. The smaller γ motor neurones give rise to small-diameter efferent axons (fusimotor fibres), which innervate the intrafusal muscle fibres in muscle spindles. There are several functionally distinct types of γ motor neurone. The ‘static’ and ‘dynamic’ responses of muscle spindles have separate controls mediated by static and dynamic fusimotor fibres, which are distributed variously to nuclear chain and nuclear bag fibres.

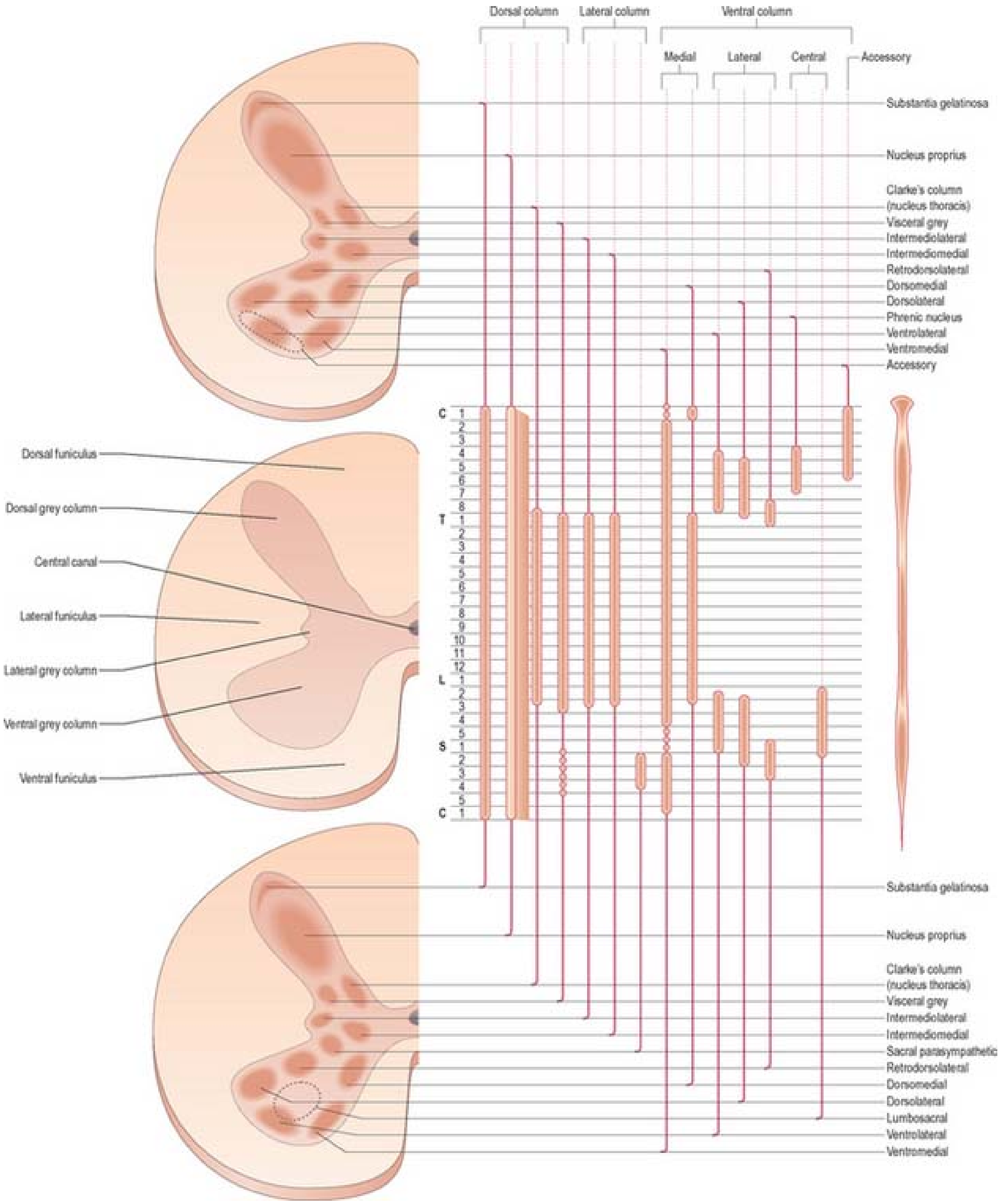

Dorsal column
Lateral column
Ventral column
Medial
Lateral
Central
Accessory
Substantia gelatinosa
Nucleus proprius
Clarke's column (nucleus thoracis)
Visceral grey
Intermediolateral
Intermediomedial
Retrodorsolateral
Dorsomedial
Dorsolateral
Phrenic nucleus
Ventrolateral
Ventromedial
Accessory
Dorsal funiculus
Dorsal grey column
Central canal
Lateral funiculus
Lateral grey column
Ventral grey column
Ventral funiculus
C 1 2 3 4 5 6 7 8
T 1 2 3 4 5 6 7 8 9 10 11 12
L 1 2 3 4 5
S 1 2 3 4 5
C 1
Substantia gelatinosa
Nucleus proprius
Clarke's column (nucleus thoracis)
Visceral grey
Intermediolateral
Intermediomedial
Sacral parasympathetic
Retrodorsolateral
Dorsomedial
Dorsolateral
Lumbosacral
Ventrolateral
Ventromedial

Fig. 18.3 The groups of nerve cells in the grey columns of the spinal cord. The relative positions of these columnar groups and their extent through spinal segments are indicated.

(Modified with the permission of Simon & Schuster from Correlative Anatomy of the Nervous System by E. Crosby, T. Humphrey, E. Lauer. Copyright © 1962 Macmillan Publishing Company.)

Lamina X surrounds the central canal and consists of the dorsal and ventral grey commissures.

Dorsal horn

The dorsal horn is a major zone of termination of primary afferent fibres, which enter the spinal cord through the dorsal roots of spinal nerves. Dorsal root fibres contain numerous molecules, which are either known, or suspected, to fulfil a neurotransmitter or neuromodulator role. These include glutamic acid, substance P, calcitonin gene-related peptide (CGRP), bombesin, vasoactive intestinal polypeptide (VIP), cholecystokinin (CCK), somatostatin, dynorphin and angiotensin II. Dorsal root afferents carry exteroceptive, proprioceptive and interoceptive information. Laminae I–IV are the main cutaneous receptive areas; lamina V receives fine afferents from the skin, muscle and viscera; lamina VI receives proprioceptive and some cutaneous afferents. Most, if not all, primary afferent fibres divide into ascending and descending branches on entering the cord. These then travel for variable distances in the tract of Lissauer, near the surface of the cord, and send collaterals into the subjacent grey matter. The formation, topography and division of dorsal spinal roots have all been confirmed in man.

The lamina marginalis is a thin lamina of neurones at the dorsolateral tip of the dorsal horn, deep to the tract of Lissauer. Beneath it lies the substantia gelatinosa (laminae II and III), which is present at all levels, and consists mostly of small neurones, together with some larger neurones. The substantia gelatinosa receives afferents via the dorsal roots, and its neurones give rise to fibres that form the contralateral spinothalamic tract. The large propriospinal neurones of the nucleus proprius lie ventral to the substantia gelatinosa; they link segments for the mediation of intraspinal coordination (Fig. 18.3).

Clarke’s column lies at the base of the dorsal horn. At most levels, it is near the dorsal white funiculus and may project into it. In the human spinal cord, it can usually be identified from the eighth cervical to the third or fourth lumbar segments. Neurones of Clarke’s column vary in size, but most are large, especially in the lower thoracic and lumbar segments. Some send axons into the dorsal spinocerebellar tracts and others are interneurones.

Lateral horn

The lateral horn is a small lateral projection of grey matter located between the dorsal and ventral horns. It is present from the eighth cervical or first thoracic segment to the second or third lumbar segment. It contains the cell bodies of preganglionic sympathetic neurones. These develop in the embryonic cord dorsolateral to the central canal and migrate laterally, forming intermediomedial and intermediolateral cell columns. Their axons travel via ventral spinal roots and white rami communicantes to the sympathetic trunk. A similar cell group is found in the second to fourth sacral segments, but unlike the thoracolumbar lateral cell column, it does not form a visible lateral projection. It is the source of the sacral outflow of parasympathetic preganglionic nerve fibres.

Ventral horn

Neurones in the ventral horn vary in size. The largest cell bodies, which may exceed 25 μm in diameter, are those of α motor neurones, the axons of which emerge in ventral roots to innervate extrafusal fibres in striated skeletal muscles. Large numbers of smaller neurones, 15–25 μm in diameter, are also present. Some of these are γ motor neurones, which innervate intrafusal fibres of muscle spindles, and the rest are interneurones. Motor neurones utilize acetylcholine as their neurotransmitter.

Considered longitudinally, ventral horn neurones are arranged in elongated groups, and form a number of separate columns, which extend through several segments. These are seen most easily in transverse sections. The ventral horn may be divided into medial, central and lateral cell columns, which all exhibit subdivision at certain levels, usually into dorsal and ventral parts (Fig. 18.3). The medial group extends throughout the cord, but may be absent in the fifth lumbar and first sacral segments. In the thoracic and the upper four lumbar segments, it is subdivided into ventromedial and dorsomedial groups. In segments cranial and caudal to this region, the medial group has only a ventromedial moiety, except in the first cervical segment, where only the dorsomedial group exists.

The central group of cells is the least extensive, and is found only in some cervical and lumbosacral segments. The centrally situated phrenic nucleus, containing the motor neurones that innervate the diaphragm, lies in the third to seventh cervical segments. An irregular accessory group of neurones in the upper five or six cervical segments at the ventral border of the ventral horn give rise to axons that are thought to enter the spinal accessory nerve (Fig. 18.3).

The lateral group of cells in the ventral horn is subdivided into ventral, dorsal and retrodorsal groups, largely confined to the spinal segments which innervate the limbs. The nucleus of Onuf, which is thought to innervate the perineal striated muscles, is a ventrolateral group of cells in the first and second sacral segments.

The motor neurones of the ventral horn are somatotopically organized. The basic arrangement is that medial cell groups innervate the axial musculature, and lateral cell groups innervate the limbs. The basic building block of the somatic motor neuronal populations is represented by a longitudinally disposed group of neurones, which innervate a given muscle, and in which the α and γ motor neurones are intermixed. The various groups innervating different muscles are aggregated into two major longitudinal columns, medial and lateral. In transverse section these form the medial and lateral cell groups in the ventral horn (Fig. 18.4).

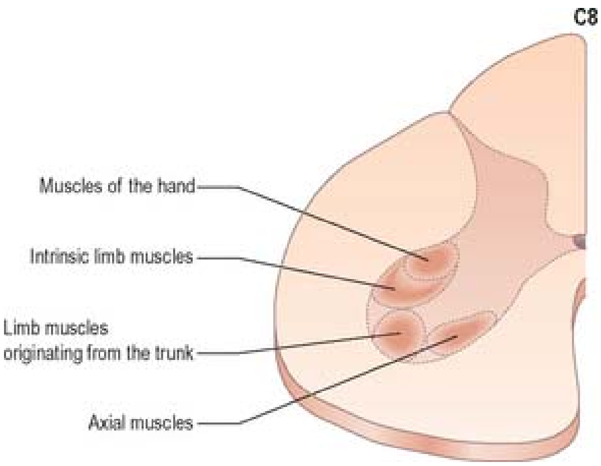

Fig. 18.4 The approximate location of motor cell groups at C8 segmental level of the spinal cord.

The medial longitudinal motor column extends throughout the length of the spinal cord. Its neurones innervate epaxial and hypaxial muscle groups. Basically, epaxial muscles include the erector spinae group (which extend the head and vertebral column), while hypaxial muscles include prevertebral muscles of the neck, intercostal and anterior abdominal wall muscles (which flex the neck and the trunk). The epaxial muscles are innervated by branches of the dorsal primary rami of the spinal nerves, and the hypaxial muscles by branches of the ventral primary rami. In the medial column, motor neurones supplying epaxial muscles are sited ventral to those supplying hypaxial muscles.

The lateral longitudinal motor column is found only in the enlargements of the spinal cord. The motor neurones in this column in the cervical and lumbar enlargements innervate muscles of the upper and lower limbs, respectively. In the cervical enlargement, motor neurones which supply muscles intrinsic to the upper limb are situated dorsally in the ventral grey column, and those innervating the most distal (hand) muscles are sited further dorsally. Motor neurones of the girdle muscles lie in the ventrolateral part of the ventral horn. There is a further somatotopic organization in that the proximal muscles of the limb are supplied from motor cell groups located more rostrally in the enlargement than those supplying the distal muscles. For example, motor neurones innervating intrinsic muscles of the hand are sited in segments C8 and T1, while motor neurones of shoulder muscles are in segments C5 and 6. A similar overall arrangement of motor neurones innervating lower limb muscles applies in the lumbosacral cord (Fig. 18.5).

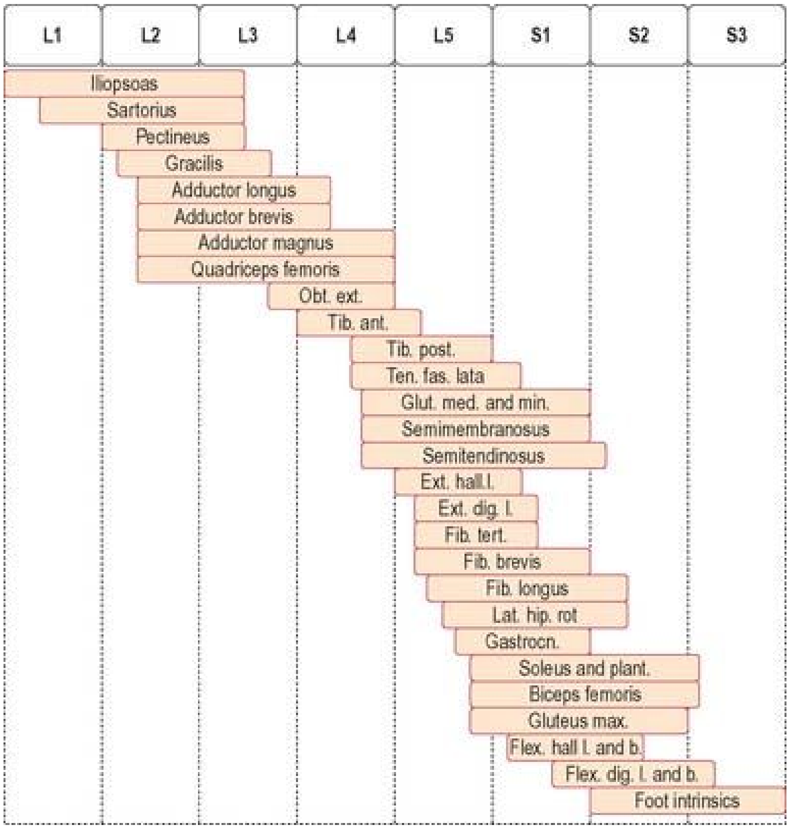

L1
L2
L3
L4
L5
S1
S2
S3
Iliopsoas
Sartorius
Pectineus
Gracilis
Adductor longus
Adductor brevis
Adductor magnus
Quadriceps femoris
Obt. ext.
Tib. ant.
Tib. post.
Ten. fas. lata
Glut. med. and min.
Semimembranosus
Semitendinosus
Ext. hall.l.
Ext. dig. l.
Fib. tert.
Fib. brevis
Fib. longus
Lat. hip. rot
Gastrocn.
Soleus and plant.
Biceps femoris
Gluteus max.
Flex. hall l. and b.
Flex. dig. l. and b.
Foot intrinsics

Fig. 18.5 The segmental arrangement of motor neurones innervating muscles of the lower limb.

The main afferent connections to motor neurones are: direct monosynaptic connections from proprioceptive dorsal root afferents in the same or nearby segments; connections from axonal collaterals of dorsal horn and other interneurones; direct monosynaptic connections from the vestibulospinal and corticospinal tracts.

Spinal reflexes

The intrinsic connections of the spinal cord and brain stem subserve a number of reflexes by which the functions of peripheral structures are modulated in response to afferent information in a relatively automatic or autonomous fashion. The fundamental components of such reflex ‘arcs’ are, thus, an afferent and an efferent neurone. However, in all but the simplest of reflexes, interneurones intervene between the afferent and efferent components, conferring increased versatility and complexity on reflex responses. Reflexes, by their very nature, are relatively fixed and stereotyped in form. Nevertheless, they are strongly influenced and modulated by descending connections. In the case of spinal reflexes these descending controls come from both the brain stem and the cerebral cortex. Pathology of descending supraspinal pathways commonly causes abnormalities of spinal reflex activity, which are routinely tested for in neurological examination. During development, descending control mechanisms suppress what may be regarded as ‘primitive’ spinal reflex responses, such as the extensor plantar reflex and the grasp reflex. When the higher control mechanisms become damaged, these reflexes are released and reappear as a sign of CNS pathology (e.g. the Babinski reflex).

Stretch reflex

The stretch reflex is the mechanism by which stretch applied to a muscle elicits its reflex contraction. It is essential for the maintenance of both muscle tone and an upright stance (via the innervation of the postural muscles of the neck, back and lower limbs). Anatomically it is the simplest of reflexes, since it is mediated solely by an afferent and an efferent neurone. The afferent component arises from stretch receptors associated with intrafusal muscle fibres located within muscle spindles. The primary or annulospiral endings of these receptive cells give rise to primary afferent fibres which enter the spinal cord, where they make excitatory synaptic contact directly onto α motor neurones innervating the same muscle (Fig. 18.6). The α motor neurones of antagonistic muscles are simultaneously inhibited via collateral connections to inhibitory interneurones.

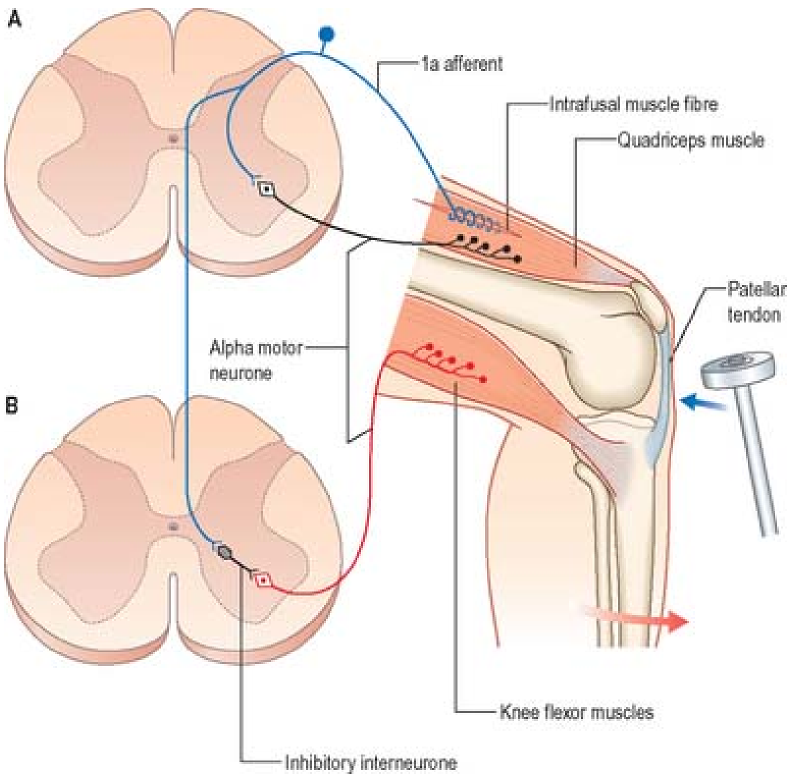
A
1a afferent
Intrafusal muscle fibre
Quadriceps muscle
Patellar tendon
Alpha motor neurone
B
Knee flexor muscles
Inhibitory interneurone

Fig. 18.6 The stretch reflex.

(By permission from Crossman AR, Neary D 2000 Neuroanatomy, 2nd edn. Edinburgh: Churchill Livingstone.)

Gamma reflex

As well as α motor neurones innervating extrafusal muscle fibres, muscles also receive γ motor neurones, which innervate intrafusal muscle fibres. Activation of γ motor neurones increases the sensitivity of the intrafusal fibres to stretch (Fig. 18.7). Therefore, changes in γ activity have a profound effect upon the stretch reflex and upon muscle tone. Like α motor neurones, γ motor neurones are under the influence of descending pathways from the brain stem and cerebral cortex. Changes in the activity of the stretch reflex and of muscle tone are commonly found in disorders of the CNS as well as the PNS.

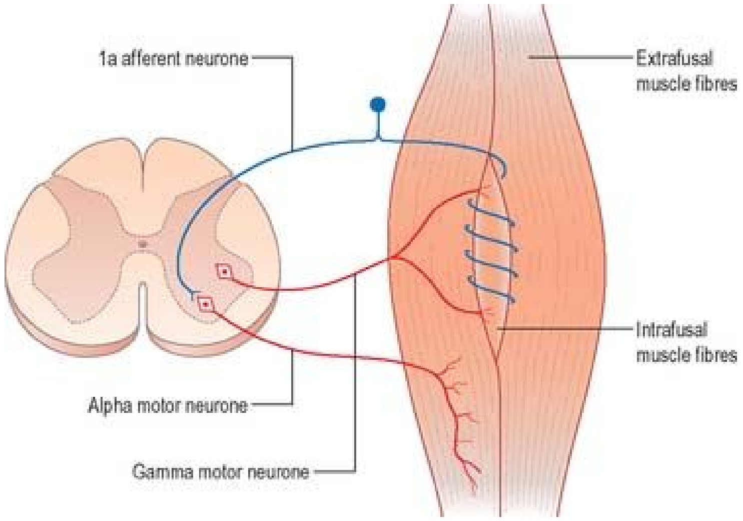

Fig. 18.7 The gamma reflex.

(By permission from Crossman AR, Neary D 2000 Neuroanatomy, 2nd edn. Edinburgh: Churchill Livingstone.)

Flexor reflex

Painful stimulation of the limbs leads to flexion withdrawal, that is mediated by a polysynaptic reflex (Fig. 18.8) in which interneurones link the afferent and efferent neurones. Thus, activation of nociceptive primary afferents indirectly causes activation of limb flexor motor neurones. Collateralization of fibres to nearby spinal segments mediates flexion of a limb at several joints, depending on the intensity of the stimulus. Decussating connections to the contralateral side of the cord activate α motor neurones innervating corresponding extensor muscles, which produces the so-called crossed extensor reflex. In principle, virtually any cutaneous stimulus has the potential to induce a flexor reflex, but, other than in the case of noxious stimuli, this response is normally inhibited by descending pathways. When descending influences are lost, even harmless cutaneous stimulation can elicit flexion of the limbs. The Babinski (extensor plantar) reflex, which is generally regarded as pathognomonic of damage to the corticospinal tract, is part of a flexion withdrawal of the lower limb in response to stimulation of the sole of the foot.

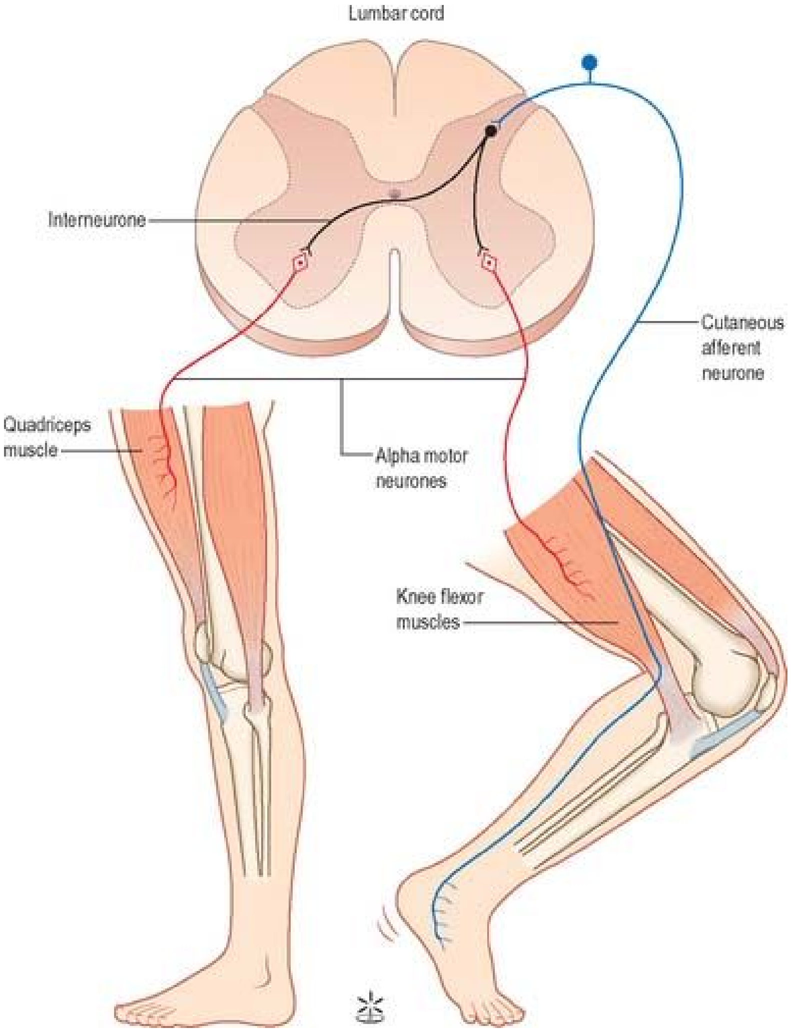
Lumbar cord
Interneurone
Cutaneous afferent neurone
Quadriceps muscle
Alpha motor neurones
Knee flexor muscles

Fig. 18.8 The flexor reflex and crossed extensor reflex.

(By permission from Crossman AR, Neary D 2000 Neuroanatomy, 2nd edn. Edinburgh: Churchill Livingstone.)

SPINAL WHITE MATTER

The spinal white matter surrounds the central core of grey matter. The white matter consists primarily of longitudinally running nerve fibres. Fibres subserving related functions, or those with common origins or destinations, are generally grouped together anatomically to form tracts (fasciculi), which may be ascending, descending and propriospinal. Ascending tracts consist either of primary afferent fibres, that enter the cord via the dorsal roots of spinal nerves, or fibres derived from intrinsic spinal neurones, that carry afferent impulses to supraspinal levels. Descending tracts contain fibres that descend from the cerebral cortex or brain stem nuclei to control the activity of spinal neurones. Propriospinal tracts contain the axons of neurones that are localized entirely to the spinal cord: they contain both ascending and descending components, collectively mediating intersegmental coordination.

The spinal white matter is conventionally described as being arranged into three large, bilaterally paired masses, the dorsal, lateral and ventral funiculi, each of which contains a number of predominantly specific tracts (see Fig. 18.1 and Fig. 18.9). Narrow dorsal and ventral white commissures run between the two halves of the cord.

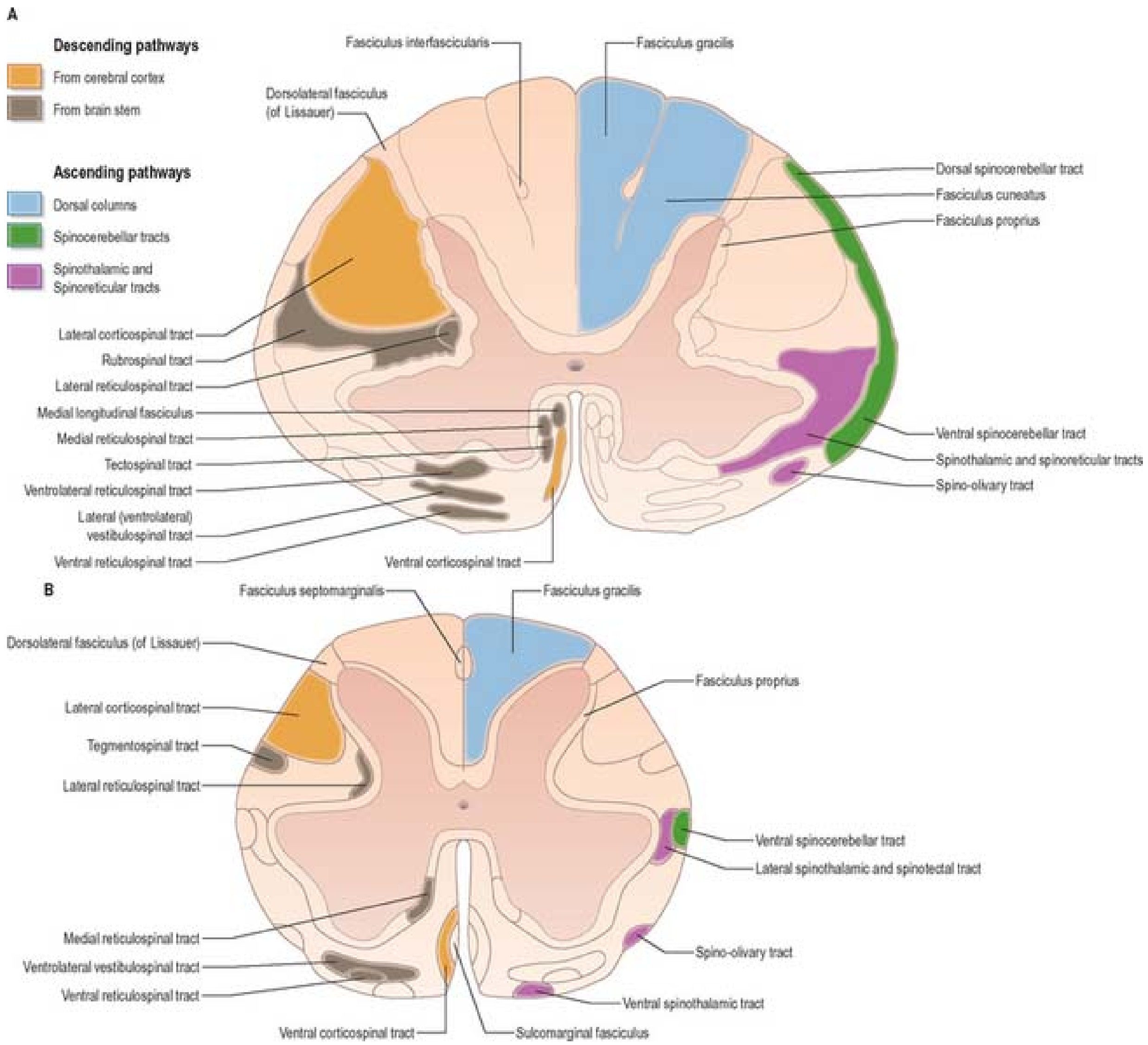
A
Descending pathways
🟧 From cerebral cortex
🟫 From brain stem
Ascending pathways
🟦 Dorsal columns
🟩 Spinocerebellar tracts
🟪 Spinothalamic and Spinoreticular tracts
Fasciculus interfascicularis
Fasciculus gracilis
Dorsolateral fasciculus (of Lissauer)
Dorsal spinocerebellar tract
Fasciculus cuneatus
Fasciculus proprius
Lateral corticospinal tract
Rubrospinal tract
Lateral reticulospinal tract
Medial longitudinal fasciculus
Medial reticulospinal tract
Tectospinal tract
Ventrolateral reticulospinal tract
Lateral (ventrolateral) vestibulospinal tract
Ventral reticulospinal tract
Ventral corticospinal tract
Ventral spinocerebellar tract
Spinothalamic and spinoreticular tracts
Spino-olivary tract
B
Fasciculus septomarginalis
Fasciculus gracilis
Dorsolateral fasciculus (of Lissauer)
Fasciculus proprius
Lateral corticospinal tract
Tegmentospinal tract
Lateral reticulospinal tract
Ventral spinocerebellar tract
Lateral spinothalamic and spinotectal tract
Medial reticulospinal tract
Spino-olivary tract
Ventrolateral vestibulospinal tract
Ventral reticulospinal tract
Ventral spinothalamic tract
Ventral corticospinal tract
Sulcomarginal fasciculus

Fig. 18.9 The approximate positions of nerve fibre tracts in the spinal cord at mid-cervical (**A**) and lumbar (**B**) levels.

Fibres in the spinal white matter vary in calibre. Many are small and lightly, or non-, myelinated. Most regions contain a wide spectrum of fibre diameters, from 1 µm or less to 10 µm. Some tracts typically contain only small fibres, e.g. the dorsolateral tract, fasciculus gracilis and central part of the lateral funiculus. The fasciculus cuneatus, anterior funiculus and peripheral zone of the lateral funiculus all contain many large-diameter fibres.

Whilst the ascending and descending tracts are to a large extent discrete and regularly located, significant overlap between adjacent tracts does occur. Their general disposition is shown in Fig. 18.9.

Ascending pathways

Dorsal columns

The dorsal funiculus consists of two large ascending tracts, the fasciculus gracilis and fasciculus cuneatus (Fig. 18.10), that are also known as the dorsal columns. They are separated by a posterointermediate septum. The dorsal columns contain a high proportion of myelinated fibres carrying proprioceptive (position sense and kinaesthesia), exteroceptive (touch-pressure) and vibratory sensation to higher levels. These fibres come from several sources: long primary afferent fibres which enter the cord in the dorsal roots of spinal nerves and ascend to the dorsal column nuclei in the medulla oblongata; shorter primary afferent fibres projecting to neurones of Clarke’s column and other spinal neurones; axons from secondary neurones of the spinal cord ascending to the dorsal column nuclei. The dorsal columns also contain axons of propriospinal neurones.

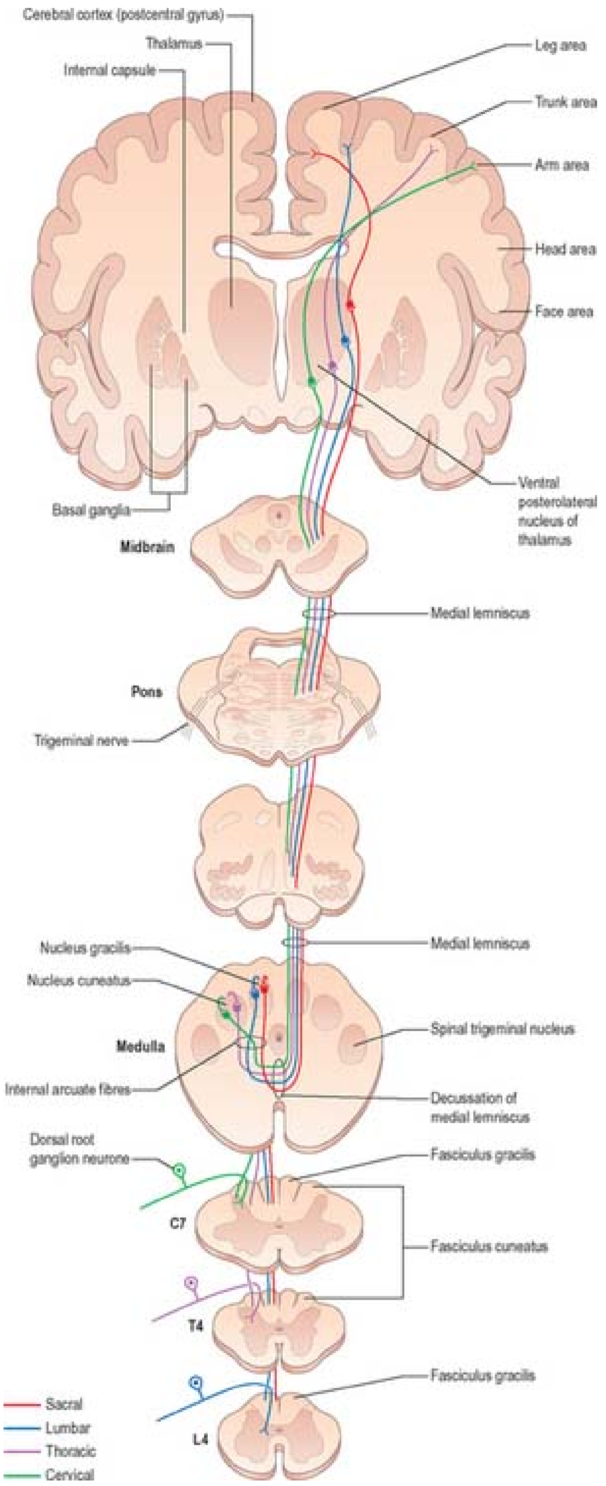
Cerebral cortex (postcentral gyrus)
Thalamus
Internal capsule
Leg area
Trunk area
Arm area
Head area
Face area
Basal ganglia
Ventral posterolateral nucleus of thalamus
Midbrain
Medial lemniscus
Pons
Trigeminal nerve
Medial lemniscus
Nucleus gracilis
Nucleus cuneatus
Medulla
Spinal trigeminal nucleus
Internal arcuate fibres
Decussation of medial lemniscus
Dorsal root ganglion neurone
Fasciculus gracilis
C7
Fasciculus cuneatus
T4
Fasciculus gracilis
L4
Sacral
Lumbar
Thoracic
Cervical

Fig. 18.10 The dorsal columns. Primary afferent fibres from different levels and their associated second- and third-order neurones are depicted in different colours.

The fasciculus gracilis begins at the caudal end of the spinal cord. It contains long ascending branches of primary afferents, which enter the cord through ipsilateral dorsal spinal roots and ascending axons of secondary neurones in laminae IV to VI of the ipsilateral dorsal horn. As the fibres ascend, they are joined by axons of successive dorsal roots. Fibres entering in coccygeal and lower sacral regions are shifted medially by successive additions of fibres entering at higher levels.

The fasciculus gracilis lies medial to the fasciculus cuneatus in the upper spinal cord (Fig. 18.9). At upper cervical levels the fasciculus gracilis contains a larger proportion of afferents from cutaneous receptors than from deep proprioceptors because many of the latter leave the fasciculus at lower segments to synapse in Clarke’s column. Indeed, proprioception from the lower limb mostly reaches the thalamus by relaying in Clarke’s column and then again in nucleus Z (p. 280). Axons of the fasciculus gracilis, from both primary and secondary neurones, terminate in the nucleus gracilis of the dorsal medulla.

The fasciculus cuneatus (Fig. 18.9) begins at midthoracic level and lies lateral to the fasciculus gracilis. It is composed mostly of primary afferent fibres of the upper thoracic and cervical dorsal roots. At upper cervical levels it contains a large population of afferents from both deep and cutaneous receptors of the upper limb. In addition, some of its axons arise from secondary neurones in laminae IV–VI of the ipsilateral dorsal horn. Many axons (both primary and secondary) that ascend in the fasciculus cuneatus terminate in the nucleus cuneatus of the dorsal medulla. Some also end in the lateral (external or accessory) cuneate nucleus; neurones in this nucleus project to the cerebellum via the cuneocerebellar pathway.

Many ascending fibres of the fasciculus gracilis and fasciculus cuneatus terminate by synapsing on neurones of the dorsal column nuclei (nucleus gracilis and nucleus cuneatus, respectively) in the medulla oblongata. (The connections of the dorsal column nuclei are described further with the medulla oblongata, p. 280.) Axons arising from neurones in the dorsal column nuclei arch ventromedially round the central grey matter of the medulla as internal arcuate fibres (Fig. 19.5) and decussate in the great sensory decussation (decussation of the medial lemniscus) to form the medial lemniscus itself. They ascend to the ventral posterolateral nucleus of the thalamus, from where neurones project to the somatosensory cortex in the postcentral gyrus of the parietal lobe (areas 3, 1 and 2). Some neurones of the dorsal column nuclei form posterior external arcuate fibres which enter the cerebellum.

The high degree of somatotopic organization that is present in the dorsal columns is preserved as the pathways ascend through the dorsal column nuclei and thalamus to reach the primary somatosensory cortex. In the dorsal column nuclei, the lower limb is represented in the nucleus gracilis, the upper limb in the nucleus cuneatus, and the trunk is represented in an intermediate position between them. Fibres are also segregated by modality in the dorsal columns: fibres from hair receptors are most superficial, while those from tactile and vibratory receptors lie in deeper layers.

Spinocerebellar tracts

There are two principal spinocerebellar tracts: dorsal (posterior) and ventral (anterior). They occupy the periphery of the lateral aspect of the spinal white matter (Fig. 18.9, Fig. 18.11) and carry proprioceptive and cutaneous information to the cerebellum for the coordination of movement. Both tracts contain large-diameter myelinated fibres, but there are more in the dorsal tract. Finer-calibre fibres are associated with the ventral tract.

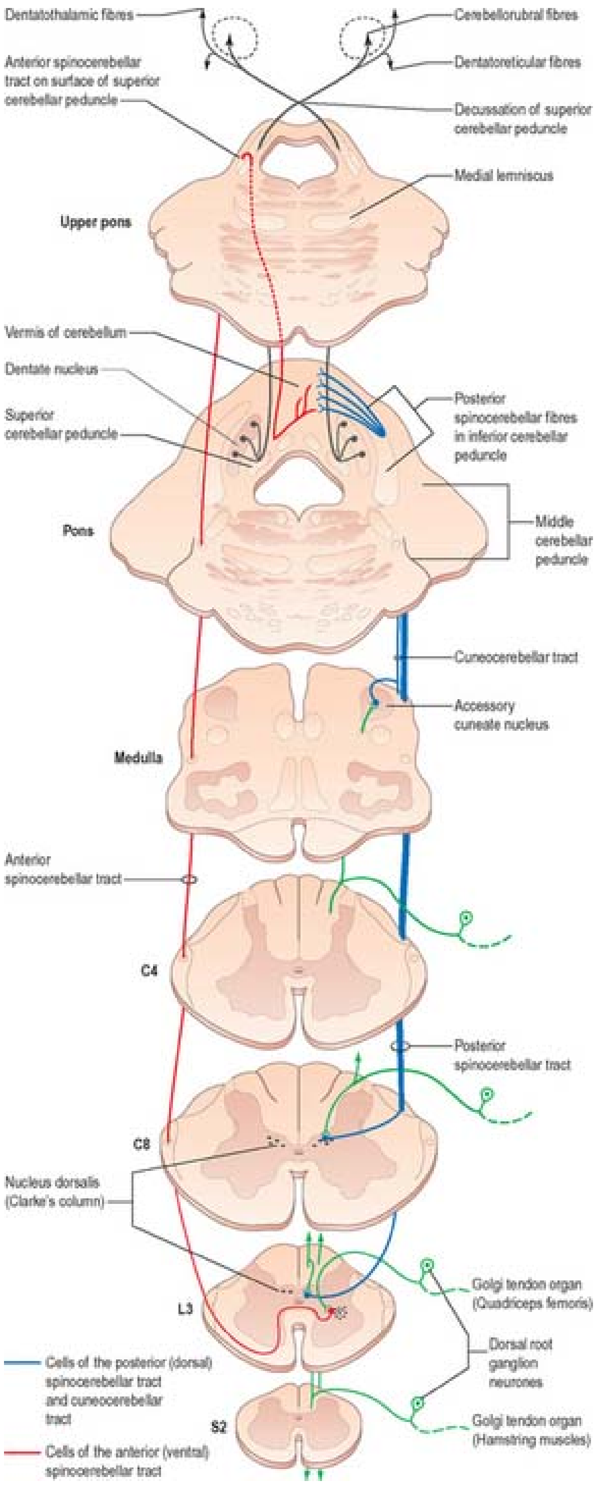
Dentatothalamic fibres
Cerebellorubral fibres
Anterior spinocerebellar tract on surface of superior cerebellar peduncle
Dentatoreticular fibres
Decussation of superior cerebellar peduncle
Medial lemniscus
Upper pons
Vermis of cerebellum
Dentate nucleus
Superior cerebellar peduncle
Posterior spinocerebellar fibres in inferior cerebellar peduncle
Pons
Middle cerebellar peduncle
Cuneocerebellar tract
Accessory cuneate nucleus
Medulla
Anterior spinocerebellar tract
C4
Posterior spinocerebellar tract
C8
Nucleus dorsalis (Clarke's column)
Golgi tendon organ (Quadriceps femoris)
L3
Dorsal root ganglion neurones
Cells of the posterior (dorsal) spinocerebellar tract and cuneocerebellar tract
S2
Golgi tendon organ (Hamstring muscles)
Cells of the anterior (ventral) spinocerebellar tract

Fig. 18.11 The spinocerebellar tracts.

(Redrawn from Carpenter MB 1991 Core Text of Neuroanatomy, 4th edn. Baltimore: Williams and Wilkins, by permission of author and publisher.)

The dorsal spinocerebellar tract lies lateral to the lateral corticospinal tract. It begins about the level of the second or third lumbar segment and enlarges as it ascends. Axons of the tract originate ipsilaterally from the larger neurones of Clarke's column, in lamina VII throughout spinal segments T1–L2. Clarke's column receives input from collaterals of long ascending primary afferents of the dorsal columns and terminals of shorter ascending primary afferents of the dorsal columns. Many of these afferent fibres ascend from segments caudal to L2. In the medulla, the dorsal spinocerebellar tract passes through the inferior cerebellar peduncle to terminate ipsilaterally in the rostral and caudal parts of the cerebellar vermis.

The ventral spinocerebellar tract lies immediately ventral to the dorsal tract. The cells of origin are in laminae V–VII of the lumbosacral cord and the tract carries information from the lower limb. Most of the axons forming the tract decussate, but some remain ipsilateral. The tract begins in the upper lumbar region and ascends through the medulla oblongata to reach the upper pontine level, from where it descends in the dorsal part of the superior cerebellar peduncle to terminate, mainly contralaterally, in the anterior cerebellar vermis.

The spinocerebellar tracts are organized such that fibres from lower spinal segments are most superficial. Both tracts convey proprioceptive and exteroceptive information, but they are functionally different. Neurones of Clarke's column are excited monosynaptically by Ia and Ib primary afferent fibres (from muscle spindles and tendon organs, respectively) and also by group II muscle afferents, and cutaneous touch and pressure afferents. The proprioceptive impulses often arise from a single muscle or from synergistic muscles acting at a common joint. Thus, the dorsal spinocerebellar tract transmits modality-specific and space-specific information that is used in the fine coordination of individual limb muscles. On the other hand, the cells of the ventral tract are activated monosynaptically by Ib afferents and transmit information from large receptive fields that include different segments of a limb. The ventral tract lacks subdivisions for different modalities and transmits information for the coordinated movement and posture of the entire lower limb.

Since Clarke’s column diminishes rostrally (Fig. 18.3) and does not extend above the lowest cervical segment, it follows that the dorsal spinocerebellar tract carries information from the trunk and lower limb. Proprioceptive and exteroceptive information from the upper limb travel in primary afferent fibres of the fasciculus cuneatus. These fibres end somatotopically in the accessory (external or lateral) cuneate nucleus and the adjoining part of the cuneate nucleus situated in the medulla oblongata. Cells of these nuclei give rise to the posterior external arcuate fibres that form the cuneocerebellar tract (Fig. 18.11), which enters the cerebellum via the ipsilateral inferior cerebellar peduncle. The accessory cuneate nucleus and the lateral part of the cuneate nucleus are considered to be homologous to the cells of Clarke’s column. The cuneocerebellar tract is, therefore, functionally allied to the dorsal spinocerebellar tract, and is its upper limb equivalent.

Axons of all the spinocerebellar tracts and the cuneocerebellar tract form part of the ‘mossy-fibre system’. They end in the cerebellar cortex in a highly organized, somatotopical and functional pattern (p. 302).

Spinothalamic tracts

The spinothalamic tracts (Fig. 18.9) consist of second-order neurones which convey pain, temperature, coarse (non-discriminative) touch and pressure information to the somatosensory region of the thalamus. The cells of origin lie in various laminae of all segments of the spinal cord. Fibres decussate in the ventral white commissure to reach the contralateral spinothalamic tracts: pain and temperature fibres do so promptly, within about one segment of their origin, whilst fibres carrying other modalities may ascend for several segments before crossing. Spinothalamic fibres mostly ascend in the white matter ventrolateral to the ventral horn, partly intermingled with ascending spinoreticular fibres and descending reticulospinal fibres. Some authorities describe two spinothalamic tracts (lateral and ventral) with more-or-less distinct anatomical locations and functions. However, physiological studies in animals support the notion that these tracts may be best considered as a structural and functional continuum.

The lateral spinothalamic tract (Fig. 18.12) is sited in the lateral funiculus, lying medial to the ventral spinocerebellar tract. Clinical evidence indicates that it subserves pain and temperature sensations. The ventral spinothalamic tract (Fig. 18.13) lies in the anterior funiculus medial to the point of exit of the ventral spinal nerve roots and dorsal to the vestibulospinal tract, which it overlaps. On the basis of clinical evidence, it subserves coarse tactile and pressure modalities.

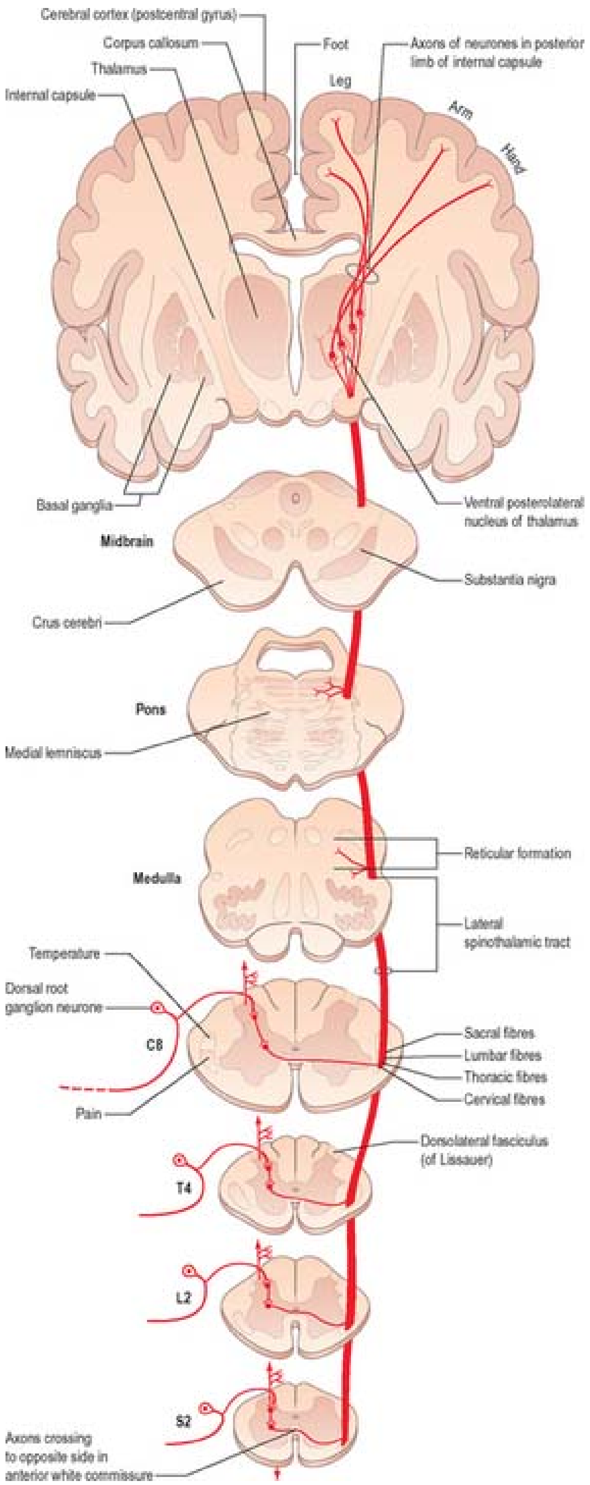
Cerebral cortex (postcentral gyrus)
Corpus callosum
Thalamus
Internal capsule
Foot
Leg
Axons of neurones in posterior limb of internal capsule
Arm
Hand
Basal ganglia
Ventral posterolateral nucleus of thalamus
Midbrain
Substantia nigra
Crus cerebri
Pons
Medial lemniscus
Medulla
Reticular formation
Lateral spinothalamic tract
Temperature
Dorsal root ganglion neurone
C8
Sacral fibres
Lumbar fibres
Thoracic fibres
Cervical fibres
Pain
Dorsolateral fasciculus (of Lissauer)
T4
L2
S2
Axons crossing to opposite side in anterior white commissure

Fig. 18.12 The lateral spinothalamic tract.

(Redrawn from Carpenter MB 1991 Core Text of Neuroanatomy, 4th edn. Baltimore: Williams and Wilkins, by permission of author and publisher.)

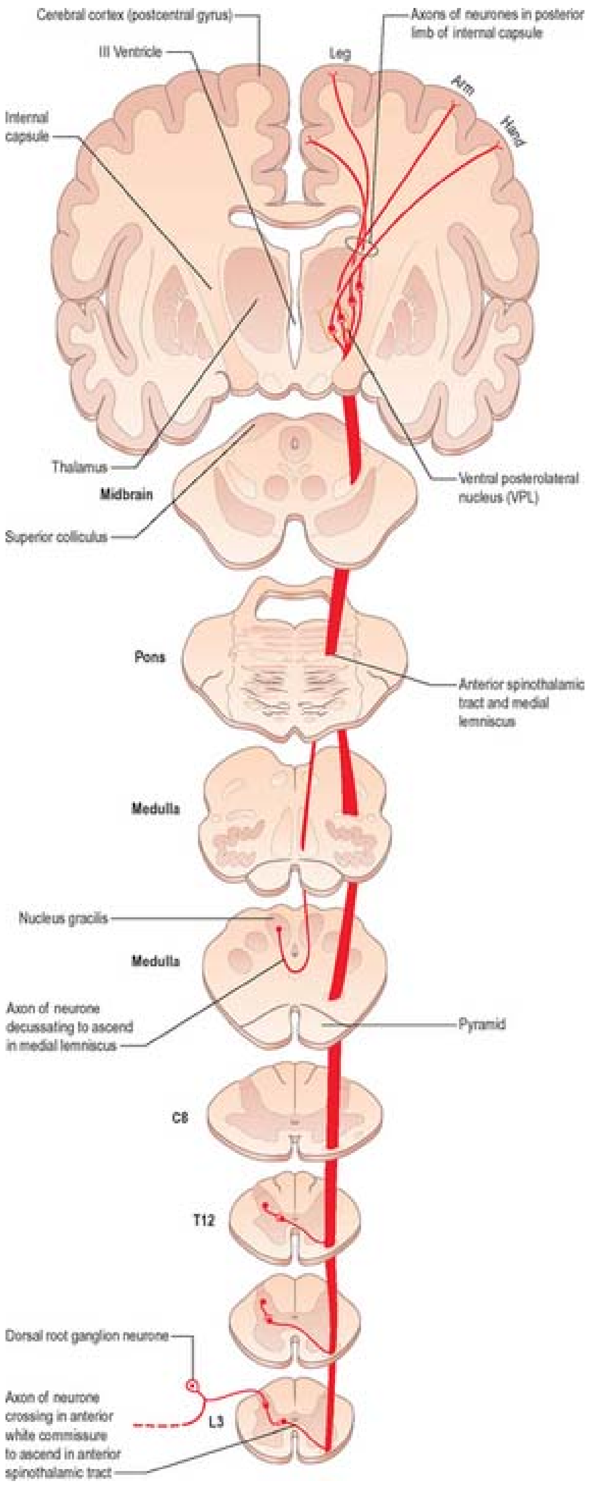
Cerebral cortex (postcentral gyrus)
Axons of neurones in posterior limb of internal capsule
III Ventricle
Leg
Arm
Hand
Internal capsule
Thalamus
Midbrain
Ventral posterolateral nucleus (VPL)
Superior colliculus
Pons
Anterior spinothalamic tract and medial lemniscus
Medulla
Nucleus gracilis
Medulla
Axon of neurone decussating to ascend in medial lemniscus
Pyramid
C8
T12
Dorsal root ganglion neurone
Axon of neurone crossing in anterior white commissure to ascend in anterior spinothalamic tract
L3

Fig. 18.13 The ventral (anterior) spinothalamic tract.

(Redrawn from Carpenter MB 1991 Core Text of Neuroanatomy, 4th edn. Baltimore: Williams and Wilkins, by permission of author and publisher.)

A dorsolateral spinothalamic tract has been described in animals. The axons arise mainly from neurones in lamina I, and cross to ascend in the contralateral dorsolateral funiculus. These neurones respond maximally to noxious, mechanical and thermal cutaneous stimuli. Examples of clinical pain relief following dorsolateral cordotomy suggest that a similar projection exists in man.

On reaching the lower brain stem, spinothalamic tract axons separate. Axons in the ventral tract join the medial lemniscus. Axons in the lateral tract continue as the spinal lemniscus.

There is clear somatotopic organization of the fibres in the spinothalamic tracts throughout their extent. Fibres crossing at any cord level join the deep aspect of those that have already crossed, which means that both tracts are segmentally laminated (Fig. 18.14). Somatotopy is maintained throughout the medulla oblongata and pons. In the midbrain, fibres in the spinal lemniscus conveying pain and temperature sensation from the lower limb extend dorsally, while those from the trunk and upper limb are more ventrally placed. Both lemnisci ascend to end in the thalamus. The major spinothalamic projections in man are to the ventral posterolateral nucleus, and also to the centrolateral intralaminar nucleus.

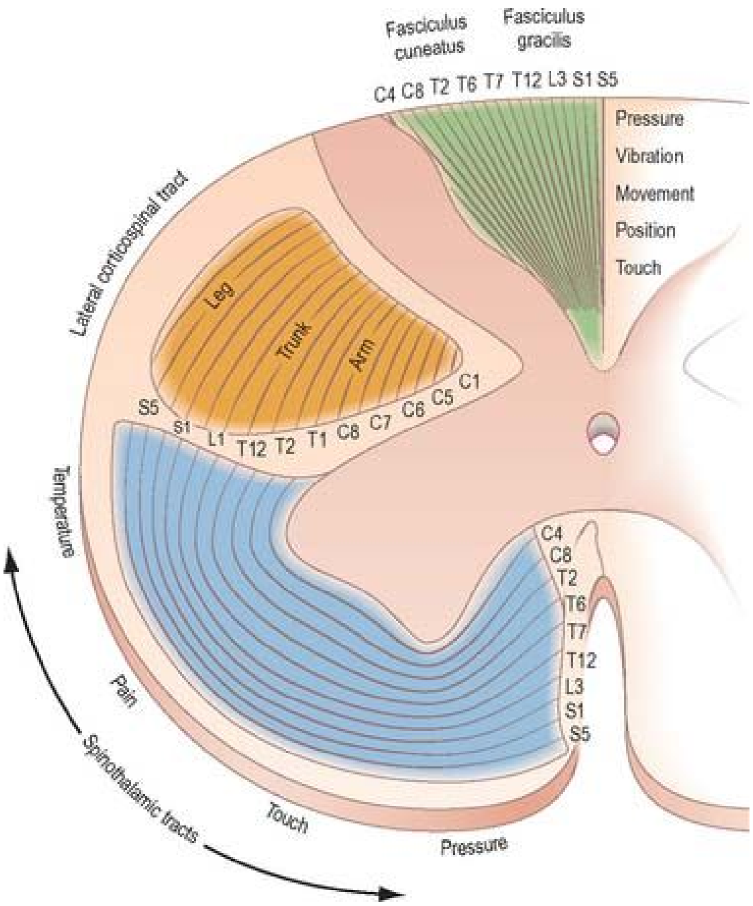
Fasciculus cuneatus
Fasciculus gracilis
C4 C8 T2 T6 T7 T12 L3 S1 S5
Pressure
Vibration
Movement
Position
Touch
Lateral corticospinal tract
Leg
Trunk
Arm
S5 S1 L1 T12 T2 T1 C8 C7 C6 C5 C1
Temperature
C4
C8
T2
T6
T7
T12
L3
S1
S5
Pain
Spinothalamic tracts
Touch
Pressure

Fig. 18.14 General plan of the segmental organization of fibres in the dorsal funiculus, the lateral corticospinal tract and the spinothalamic tracts. The probable cross-sectional areas of these tracts are schematically enlarged. This general plan applies to all segmentally organized tracts whether ascending, descending, ipsilateral or contralateral.

Neurones of the spinothalamic tracts

The specific localization of spinothalamic tract cell bodies is poorly documented in man. In animals, about a third are localized to the upper three cervical segments. About 20% are located in lower cervical segments, 20% in the thoracic region (mostly in segments T1–3), 20% in the lumbar region and 10% in the sacrococcygeal cord. Cells are located in laminae I and IV–VIII, the greatest concentration being in laminae VI and VII. Cell bodies giving rise to spinothalamic tract axons are predominantly contralateral, although a relatively small number (10%), mostly in the upper three cervical segments, are ipsilateral.

Neurones of the spinothalamic tracts have very different receptive fields. Specificity of separate channels, as it exists in the dorsal column nuclei, is absent in the laminae of the cord. Convergence of different functional types of afferent fibres onto an individual tract cell is a common feature in the cord. On the basis of laminar site, functional properties, and specific thalamic termination of their axons, spinothalamic tract neurones may be divided into three separate groups. These are the apical cells of the dorsal grey column (lamina I), deep dorsal column cells (laminae IV–VI), and cells in the ventral grey column (laminae VII, VIII). There are species differences and the description below is derived from studies in non-human primates.

Lamina I cells which project to the thalamus show the following characteristics. In essence they respond maximally to noxious or thermal cutaneous stimulation, and consist mainly of high-threshold, but also some wide-dynamic-range, units. Their receptive fields are usually small, representing a part of a digit or a small area of skin involving several digits. Lamina I spinothalamic tract neurones receive input from Aδ and C fibres, and some respond to convergent input from deep somatic and visceral receptors. Spinothalamic tract cells in the thoracic cord display marked viscerosomatic convergence. Lamina I spinothalamic tract neurones project preferentially to the ventral posterolateral nucleus of the thalamus, with limited projections to the centrolateral and mediodorsal thalamic nuclei. The population of deep dorsal column (laminae IV–VI) spinothalamic neurones of the lumbar cord contains wide-dynamic-range (60%), high-threshold (30%), and low-threshold (10%) type units. They can code accurately both innocuous and noxious cutaneous stimuli. Some cells also respond to input from deep somatic and visceral receptors. In the lumbar cord their receptive fields are small or medium sized; they are larger than the area of the foot, but smaller than the entire leg. In the thoracic cord the fields of these laminar cells are larger, and often include the entire upper limb plus part of the chest. Many of the deep dorsal grey column spinothalamic tract neurones in the thoracic segments receive convergent input from sympathetic afferent fibres. Laminae IV–VI spinothalamic tract units project either to the ventral posterolateral nucleus or to the centrolateral nucleus of the thalamus, and sometimes to both. Units projecting to the ventral posterolateral nucleus receive input from all classes (Aβ, A δ and C) of cutaneous fibres.

Ventral grey column (laminae VII and VIII) spinothalamic tract cells respond mainly to deep somatic (muscle and joint) stimuli, but also to innocuous and/or noxious cutaneous stimuli. In the thoracic regions of the spinal cord they also receive convergent input from visceral sources. The majority of laminae VII and VIII spinothalamic tract neurones have large, complex receptive fields (often bilateral), which encompass widespread areas of the body. Cells of this group, which project exclusively to the medial thalamus, receive input from Aβ, Aδ and C classes of afferent fibres, and many respond to convergent input from receptors of deep structures. This population of neurones contains wide-dynamic-range (25%), high-threshold (63%), and low-threshold (12%) units. Most of the spinothalamic tract cells in the ventral grey column project to the intralaminar nuclei of the thalamus. Wide-dynamic-range type neurones are particularly effective for discriminating between different intensities of painful stimulation.

Pain mechanisms

The ascending connections through which sensory information reaches higher centres are not simple relays, since it is known that they are subject to modulation by intraspinal connections and by descending pathways from the brain stem and cerebral cortex. This is particularly important in relation to the spinothalamic and spinoreticular pathways and the perception of pain.

Presynaptic inhibition influences many, possibly all, primary afferent terminals. A much-investigated site of presynaptic effects is the substantia gelatinosa. It has been proposed that impulses from cutaneous (and other) afferents are here subject to tonic control by presynaptic modulation of primary afferent terminals, mediated by small neurones of the substantia gelatinosa.

The ‘gate control theory’ (Melzack & Wall 1965) proposed a mechanism for the modulation of inflow of information along nociceptive and other afferent pathways (Fig. 18.15). The hypothesis was that large-diameter afferents (e.g. from hairs and touch corpuscles) are excitatory to the large neurones of lamina IV, from which spinothalamic fibres arise, and to interneurones in the substantia gelatinosa. In contrast, fine non-myelinated afferents are excitatory to tract cells but inhibitory to the interneurones. The axons of substantia gelatinosa interneurones are presumed to inhibit presynaptically the terminals of all afferents that synapse with tract cells. In such a system, low activity in the fine afferents inhibits the interneurones, and so prevents them inhibiting tract cells. Hence the ‘gate’ to cells in lamina IV is opened to transmit intermittent, small volleys of impulses from the large fibres. A prolonged high-frequency volley of impulses in the large-diameter afferents would be transmitted to lamina IV tract cells initially, but this would soon cease as activity in the interneurones closed the gate. Conversely, a persistent high activity in the fine afferents would open the gate resulting in massive bombardment of neurones of lamina IV (which include some neurones of high threshold that are only activated by such bombardment). It was assumed that onward transmission in the lateral spinothalamic tract would evoke the perception of pain at supraspinal levels. Pain, therefore, would result from an imbalance between the varieties of afferent impulses when there was a disproportionately large traffic along the fine afferents. In fact, inhibition of spinothalamic tract neurones can be produced by electrical stimulation of peripheral nerves, the most effective being volleys which activate Aδ fibres.

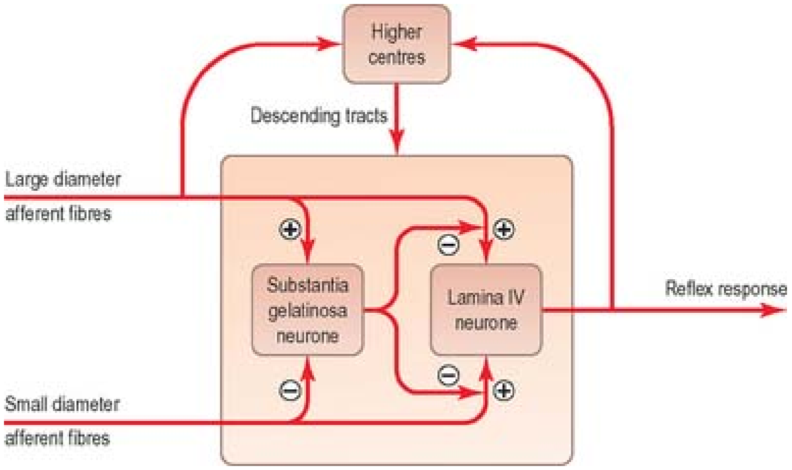
Higher centres
Descending tracts
Large diameter afferent fibres
Substantia gelatinosa neurone
Lamina IV neurone
Reflex response
Small diameter afferent fibres
⊕
⊖

Fig. 18.15 The basic arrangement of the sensory 'gate' mechanism in the dorsal laminae of the grey matter of the spinal cord.

(Redrawn with permission from Melzack R, Wall PD. Pain mechanisms: a new theory. Science 150: 971–979. Copyright 1965 American Association for the Advancement of Science.)

The activity of spinothalamic tract neurones may also be selectively modulated by pathways descending from the brain to the spinal cord. Many studies have shown that the response of spinothalamic tract cells to noxious stimuli is inhibited by stimulation of certain brain regions. This is obviously of considerable clinical interest in the treatment of chronic, intractable, pain.

In the brain stem, the regions inducing such effects correspond to a number of midbrain and rhombencephalic nuclei which, with their connections, constitute an endogenous analgesic system. In the midbrain, these regions are the periaqueductal grey matter, dorsal raphe nucleus and part of the cuneiform nucleus. Neurones in these sites contain serotonin (5-HT), γ-aminobutyric acid (GABA), substance P, CCK, neurotensin, enkephalin and dynorphin. The periaqueductal grey matter receives afferents from the frontal somatosensory and cingulate neocortex, the amygdala, numerous local reticular nuclei and the hypothalamus. Afferents from the latter are separate bundles, which carry histamine, luteinizing hormone-releasing hormone (LHRH), vasopressin, oxytocin, adrenocorticotrophic hormone (ACTH), melanocyte-stimulating hormone (γ-MSH), endorphin, and angiotensin II. Some fibres descend from the periaqueductal grey matter to rhombencephalic centres, others pass directly to the spinal cord.

In the rhombencephalon, the nucleus raphe magnus and the medial reticular column constitute an important multineuromediator centre. Neurones in these sites contain serotonin, substance P, CCK, thyrotrophin-releasing hormone (TRH), enkephalin and dynorphin: some neurones contain two or even three neuromediators. Descending bulbospinal fibres pass to the nucleus of the spinal tract of the trigeminal nerve and its continuation, the substantia gelatinosa. The latter extends throughout the length of the cord and contains populations of neurones that express many different neuromediators, e.g. GABA, substance P, neurotensin, enkephalin and dynorphin. There is abundant physiological and pharmacological evidence that all of these regions are intimately concerned with the control of nociceptive (and probably other modality) inputs.

Stimulation of forebrain sites including the periventricular grey matter, the ventral posterolateral nucleus of the thalamus, and the primary sensory (SI) and posterior parietal cortices, inhibit spinothalamic tract cells. In contrast, some spinothalamic tract cells are excited by stimulation of the medullary reticular formation, and the primary motor cortex (the latter effect probably being mediated by the corticospinal tract).

The perception of pain is further described in Chapter 23.

Spinoreticular pathway

Spinoreticular fibres are intermingled with those of the spinothalamic tracts, and ascend in the ventrolateral quadrant of the spinal cord (Fig. 18.16). Evidence from animal studies suggests that cells of origin occur at all levels of the spinal cord, particularly in the upper cervical segments. Most neurones are in lamina VII, some are in lamina VIII, and others are in the dorsal horn, especially lamina V. Most axons in the lumbar and cervical enlargements cross the midline, but there is a large uncrossed component in cervical regions. Most axons are myelinated. The pattern of anterograde degeneration, in both human postmortem studies and in experimental animals following anterolateral cordotomy, indicates the existence of spinoreticular projections to many nuclei of the medial pontomedullary reticular formation. There is also a projection to the lateral reticular nucleus (a precerebellar relay nucleus). These projections do not appear to be somatotopically organized. Spinoreticular neurones respond to inputs from the skin or deep tissues. Innocuous cutaneous stimuli may inhibit or excite a particular cell, whereas noxious stimuli are often excitatory. A spino-reticulo-thalamo-cortical pathway has been proposed as an important route serving pain perception. Like other ascending pathways, the tract cells are influenced by descending control. For example, electrical stimulation of the periaqueductal grey matter inhibits the responses of certain spinoreticular cells to input from cardiopulmonary afferents. Stimulation of the reticular formation also alters the activity of spinoreticular neurones.

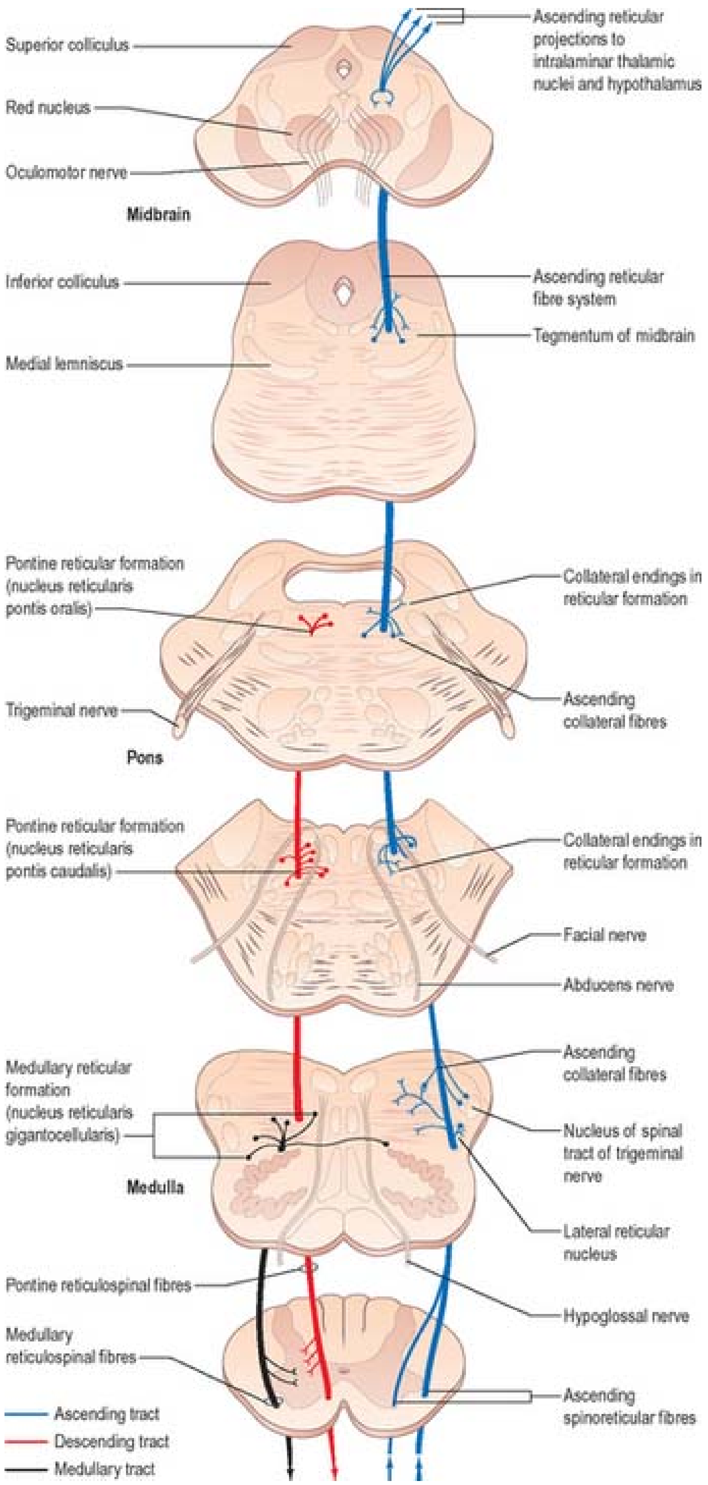
Superior colliculus
Red nucleus
Oculomotor nerve
Midbrain
Ascending reticular projections to intralaminar thalamic nuclei and hypothalamus
Inferior colliculus
Medial lemniscus
Ascending reticular fibre system
Tegmentum of midbrain
Pontine reticular formation (nucleus reticularis pontis oralis)
Trigeminal nerve
Pons
Collateral endings in reticular formation
Ascending collateral fibres
Pontine reticular formation (nucleus reticularis pontis caudalis)
Collateral endings in reticular formation
Facial nerve
Abducens nerve
Medullary reticular formation (nucleus reticularis gigantocellularis)
Medulla
Ascending collateral fibres
Nucleus of spinal tract of trigeminal nerve
Lateral reticular nucleus
Pontine reticulospinal fibres
Medullary reticulospinal fibres
Hypoglossal nerve
Ascending spinoreticular fibres
Ascending tract
Descending tract
Medullary tract

Fig. 18.16 Reticular tracts.

(Redrawn from Carpenter MB 1991 Core Text of Neuroanatomy, 4th edn. Baltimore: Williams and Wilkins, by permission of author and publisher.)

Spinocervicothalamic pathway

The lateral cervical nucleus is small in man. It lies in the lateral funiculus, ventrolateral to the dorsal horn in the upper two cervical segments. In some human cord specimens the nucleus is not distinctly defined, and is possibly incorporated into the dorsal horn. It receives axons from the spinocervical tract, which ascends in the dorsolateral funiculus. The tract cells are found in laminae III–V at all levels of the spinal cord, ipsilateral to the nucleus. Most neurones of the nucleus project to the contralateral thalamus via the medial lemniscus, and some project to the contralateral midbrain. Specific thalamic targets include the ventral posterolateral nucleus and part of the posterior complex. Spinocervical tract neurones respond to hair movement, pressure, pinch and thermal stimuli and to high-threshold muscle input; many also respond to noxious stimuli. Like tract cells of other ascending pathways, they are under tonic descending inhibitory control.

Spinomesencephalic pathway

The spinomesencephalic pathway consists of a number of tracts ascending from the spinal cord to various regions of the midbrain. It includes the spinotectal tract projecting to the superior colliculus, neurones synapsing in the periaqueductal grey matter, and other spinal cord projections which terminate in the parabrachial nucleus, the pretectal nuclei and the nucleus of Darkschewitsch. Cells of origin are located throughout the length of the spinal cord, particularly in the cervical segments and the lumbosacral enlargement, mostly in lamina I, but they are also present in laminae IV–VIII, where they are concentrated in lamina V. Most are contralateral, but a prominent ipsilateral group is also found at upper cervical levels. Spinomesencephalic fibres are mostly myelinated and ascend in the white matter of the ventrolateral quadrant of the spinal cord, in association with the spinothalamic and spinoreticular tracts.

Spinomesencephalic neurones are of low-threshold, wide-dynamic-range, or high-threshold classes. Their receptive fields may be small, or very complex and encompass large surface areas of the body. Many spinomesencephalic cells are nociceptive and are likely to be involved in the motivational–affective component of pain. Electrical stimulation of their site of termination in the periaqueductal grey matter results in severe pain in man. Furthermore, the cells of the deeper layers of the superior colliculus, where spinotectal fibres synapse, are activated by noxious stimuli.

Spino-olivary tract

The spino-olivary tract is described in animals as arising from neurones in the deeper laminae of grey matter. Axons forming the tract cross and then ascend superficially at the junction of the anterior and lateral white funiculi, to end in the dorsal and medial accessory olivary nuclei. The tract carries information from muscle and tendon proprioceptors, and also from cutaneous receptors. A functionally similar route, the dorsal spino-olivary tract, ascends in the dorsal white funiculi, and relays in the dorsal column nuclei to the contralateral inferior olivary nucleus. Information on these tracts in primates is scant, but postmortem evidence following cordotomies in man has revealed degenerating axonal terminals in the inferior olivary nucleus.

Descending tracts

Descending pathways to the spinal cord originate primarily from the cerebral cortex and from numerous sites within the brain stem (Fig. 18.16, Fig. 18.17, Fig. 18.18). They are concerned with the control of movement, muscle tone and posture, the modulation of spinal reflex mechanisms and the transmission of afferent information to higher levels. They also mediate control over spinal autonomic neurones.

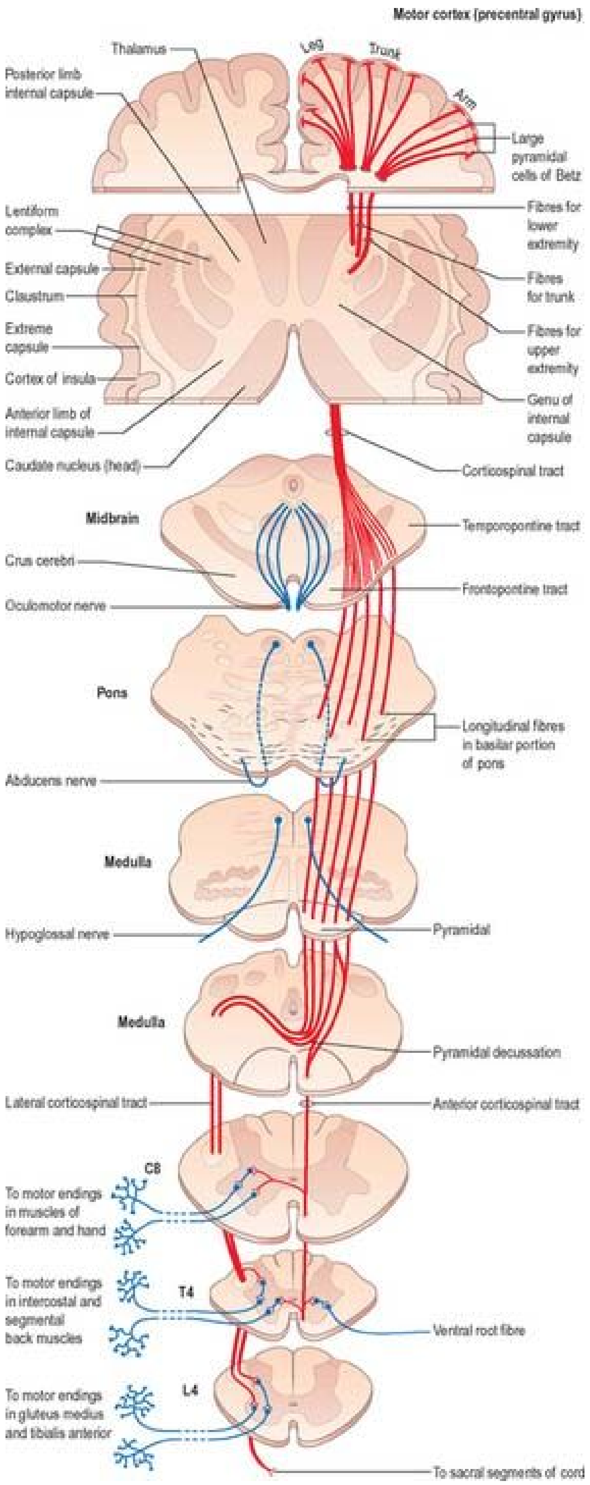
Motor cortex (precentral gyrus)
Leg
Trunk
Arm
Large pyramidal cells of Betz
Thalamus
Posterior limb internal capsule
Lentiform complex
External capsule
Claustrum
Extreme capsule
Cortex of insula
Anterior limb of internal capsule
Caudate nucleus (head)
Fibres for lower extremity
Fibres for trunk
Fibres for upper extremity
Genu of internal capsule
Corticospinal tract
Midbrain
Temporopontine tract
Crus cerebri
Frontopontine tract
Oculomotor nerve
Pons
Longitudinal fibres in basilar portion of pons
Abducens nerve
Medulla
Hypoglossal nerve
Pyramidal
Medulla
Pyramidal decussation
Lateral corticospinal tract
Anterior corticospinal tract
C8
To motor endings in muscles of forearm and hand
T4
To motor endings in intercostal and segmental back muscles
Ventral root fibre
L4
To motor endings in gluteus medius and tibialis anterior
To sacral segments of cord

Fig. 18.17 The corticospinal tracts.

(Redrawn from Carpenter MB 1991 Core Text of Neuroanatomy, 4th edn. Baltimore: Williams and Wilkins, by permission of author and publisher.)

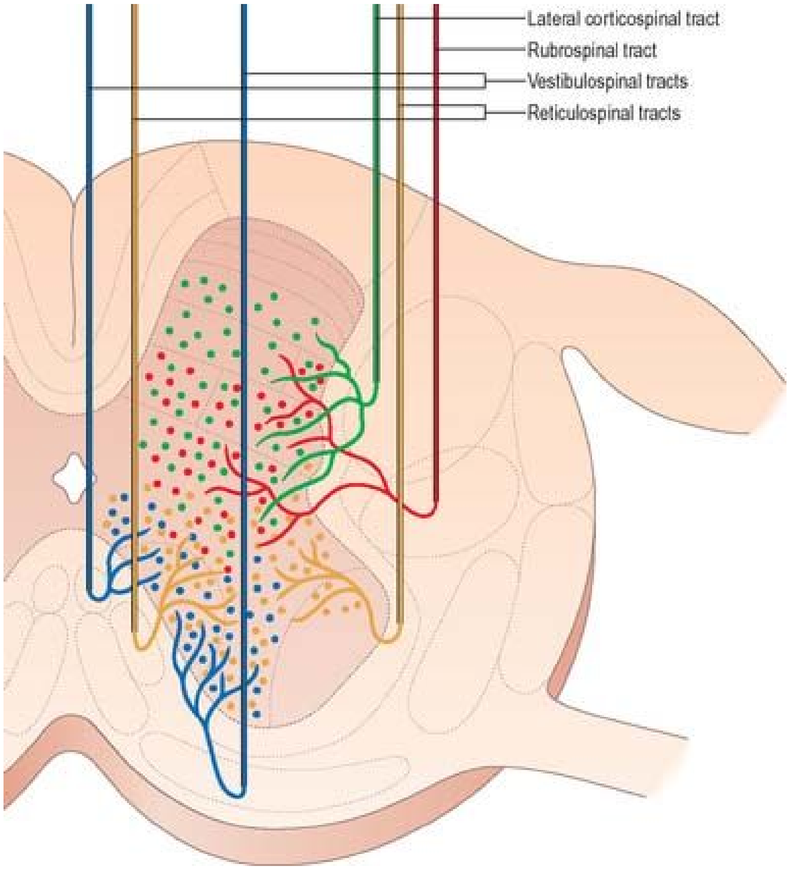

Fig. 18.18 A simplified scheme of some of the major descending pathways of the spinal cord including their overlapping zones of termination in the grey matter. Within the grey matter the dotted lines show the laminar pattern, while within the white matter they are an approximate guide to the topography of the tracts.

Corticospinal and corticobulbar tracts

Corticospinal and corticobulbar fibres arise from neurones in the cerebral cortex. They project, in a somatotopically organized fashion, to neurones that are mostly located in the contralateral side of the spinal cord or brain stem respectively (Fig. 18.17). The majority of corticospinal and corticobulbar fibres arise from cells situated in the primary motor cortex (area 4) and the premotor cortex (area 6). A small contribution comes from cells in the postcentral gyrus (somatosensory cortex; areas 3, 1, and 2) and the adjacent parietal cortex (area 5). In the monkey, 30% of corticospinal fibres arise from area 4, 30% from area 6, and 40% from the parietal regions. Cells of origin of corticospinal and corticobulbar fibres vary in size in the different cortical areas and are clustered into groups or strips. The largest cells (giant pyramidal neurones, or Betz cells) are located in the primary motor cortex of the precentral gyrus.

Corticospinal and corticobulbar fibres descend through the subcortical white matter to enter the genu and posterior limb of the internal capsule. They then pass through the ventral part of the midbrain in the crus cerebri. As they continue caudally through the pons they are separated from its ventral surface, and fragmented into fascicles, by transversely running pontocerebellar fibres. Corticobulbar fibres leave to terminate in association with the cranial nerve motor nuclei of the midbrain, pons and medulla. In the medulla oblongata, the residual corticospinal fibres form a discrete bundle, the pyramid (Fig. 19.2) which forms a prominent longitudinal column on the ventral surface of the medulla. The corticospinal tract is, therefore, also referred to as the pyramidal tract. Each pyramid contains about a million axons of varying diameter. The majority (70%) are myelinated: most (90%) have a diameter of 1–4 μm; 9% have diameters of 5–10 μm; and less than 2% have diameters of 11–22 μm. The largest diameter axons arise from the giant Betz cells.

Just rostral to the level of the spinomedullary junction, approximately 75–90% of the corticospinal fibres in the pyramid cross the median plane in the pyramidal decussation (decussation of the pyramids) and continue caudally as the lateral corticospinal tract. The rest of the fibres continue uncrossed as the ventral corticospinal tract. The lateral tract also contains some uncrossed corticospinal fibres. The lateral corticospinal tract (Fig. 18.17) descends in the lateral funiculus throughout most of the length of the spinal cord. It occupies an oval area, ventrolateral to the dorsal horn and medial to the dorsal spinocerebellar tract (Fig. 18.9). In the lumbar and sacral regions, where the dorsal spinocerebellar tract is absent, the lateral corticospinal tract reaches the dorsolateral surface of the cord. As it descends, the tract diminishes in size as its fibres terminate in progressively lower spinal segments until about the fourth sacral segment: its axons terminate on ipsilateral spinal neurones.

The smaller ventral corticospinal tract (Fig. 18.17) descends in the ventral funiculus. It lies close to the ventral median fissure, and is separated from it by the sulcomarginal fasciculus (Fig. 18.9). The ventral corticospinal tract diminishes as it descends and usually disappears completely at midthoracic cord levels. It may either be absent or, very rarely, contain almost all the corticospinal fibres. Near their termination, most fibres of the tract cross the median plane in the ventral white commissure to synapse on contralateral neurones. The vast majority of corticospinal fibres, irrespective of the tract in which they descend, therefore terminate in the spinal cord on the side contralateral to their cortical origin.

Knowledge of the detailed termination of corticospinal fibres is based largely upon animal studies, but is supplemented by data from postmortem studies on human brains using anterograde degeneration methods. Most corticospinal fibres are believed to terminate contralaterally on interneurones in the lateral parts of laminae IV–VI and both lateral and medial parts of lamina VII. Some are also distributed to lamina VIII bilaterally. Terminals are also associated with contralateral motor neuronal cell groups in lamina IX, in the dorsolateral group and the lateral parts of both central and ventrolateral groups (Fig. 18.18).

Corticospinal fibres from the frontal cortex, including motor and premotor areas 4 and 6, terminate mostly on interneurones in laminae V–VIII, with the densest concentration ending in the lateral part of lamina VI. They influence α and γ motor neurones of lamina IX, via these interneurones. Because the widespread dendrites of multipolar neurones in lamina IX penetrate lamina VII, direct monosynaptic axodendritic contacts also occur on large α motor neurones. Direct termination on motor neurones is most abundant in the spinal enlargements.

Experimental evidence shows that precentral corticospinal axons influence the activities of both α and γ motor neurones, facilitating flexor muscles and inhibiting extensors, which are the opposite effects to those mediated by lateral vestibulospinal fibres. Evidence from animal studies shows that direct projections from the precentral cortical areas to spinal motor neurones are concerned with highly fractionated, precision movements of the limbs. Accordingly, in primates, precentral corticospinal fibres are mainly distributed to motor neurones supplying the distal limb muscles. Corticospinal projections may use glutamate or aspartate, often co-localized, as excitatory neurotransmitters.

Corticospinal fibres from parietal sources end mainly in the contralateral dorsal horn, in the lateral parts of laminae IV–VI and lamina VII. Phylogenetically these fibres represent the oldest part of the corticospinal system. Axons from the sensory cortex terminate chiefly in laminae IV and V. They are concerned with the supraspinal modulation of the transmission of afferent impulses to higher centres, including the motor cortex.

Experimental studies in primates indicate that isolated transection of corticospinal fibres at the level of the pyramid (pyramidotomy) results in flaccid paralysis or paresis of the contralateral limbs and loss of independent hand and finger movements. Destruction of corticospinal fibres at the level of the internal capsule, commonly caused by a cerebral vascular accident or ‘stroke’, results in a contralateral hemiplegia. The paralysis is initially flaccid, but later becomes spastic, and is most marked in the distal muscles of the extremities, especially those concerned with individual movements of the fingers and hand. Associated signs on the paralysed side are: hyperactive deep tendon reflexes; hypertonicity; the loss of superficial abdominal and cremasteric reflexes; and the appearance of dorsiflexion of the toes (Babinski’s sign) in response to stroking the sole of the foot. The latter is usually interpreted as pathognomonic of corticospinal damage, but it is not always present in patients with confirmed corticospinal lesions. Moreover, Babinski’s sign is normally present in human infants up to about 2 years of age – its subsequent disappearance may reflect the completion of myelination of the corticospinal fibres and/or the establishment of direct cortical connections to lower motor neurones.

Some of the sequelae of stroke damage in the internal capsule, in particular hyperreflexia and hypertonia, are due to the involvement of other pathways in addition to the corticospinal tract. These include descending cortical fibres to brain stem nuclei, such as the vestibular and reticular nuclei, that themselves give rise to descending projections which influence motor neurone activity.

Rubrospinal tract

The rubrospinal tract arises from neurones in the caudal magnocellular part of the red nucleus (an ovoid mass of cells situated centrally in the midbrain tegmentum (p. 290)). This part of the nucleus contains some 150–200 large neurones, interspersed with smaller neurones.

The origin, localization, termination and functions of rubrospinal connections are poorly defined in man, and the tract appears to be rudimentary. Rubrospinal fibres cross in the ventral tegmental decussation and descend in the lateral funiculus of the cord, where they lie ventral to, and intermingled with, fibres of the lateral corticospinal tract (Fig. 18.9). In animals, the tract descends as far as lumbosacral levels, whereas in man it appears to project only to the upper three cervical cord segments. Rubrospinal fibres are distributed to the lateral parts of laminae V–VI and the dorsal part of lamina VII of the spinal grey matter. The terminal zones of the tract correspond to those of corticospinal fibres from the motor cortex. Animal studies demonstrate that the effects of rubrospinal fibres on α and γ motor neurones are similar to those of corticospinal fibres.

Tectospinal tract

The tectospinal tract arises from neurones in the intermediate and deep layers of the superior colliculus of the midbrain. It crosses ventral to the periaqueductal grey matter in the dorsal tegmental decussation and descends in the medial part of the ventral funiculus of the spinal cord (Fig. 18.9). Fibres of the tract project only to the upper cervical cord segments, ending in laminae VI–VIII. They make polysynaptic connections with motor neurones serving muscles in the neck, facilitating those that innervate contralateral muscles and inhibiting those that innervate ipsilateral ones. In animals, unilateral electrical stimulation of the superior colliculus causes turning of the head to the contralateral side, an effect mainly mediated through the tectospinal tract.

Vestibulospinal tracts

The vestibular nuclear complex lies in the lateral part of the floor of the fourth ventricle, at the level of the pontomedullary junction. It gives rise to the lateral and medial vestibulospinal tracts, which are functionally and topographically distinct (Fig. 18.19).

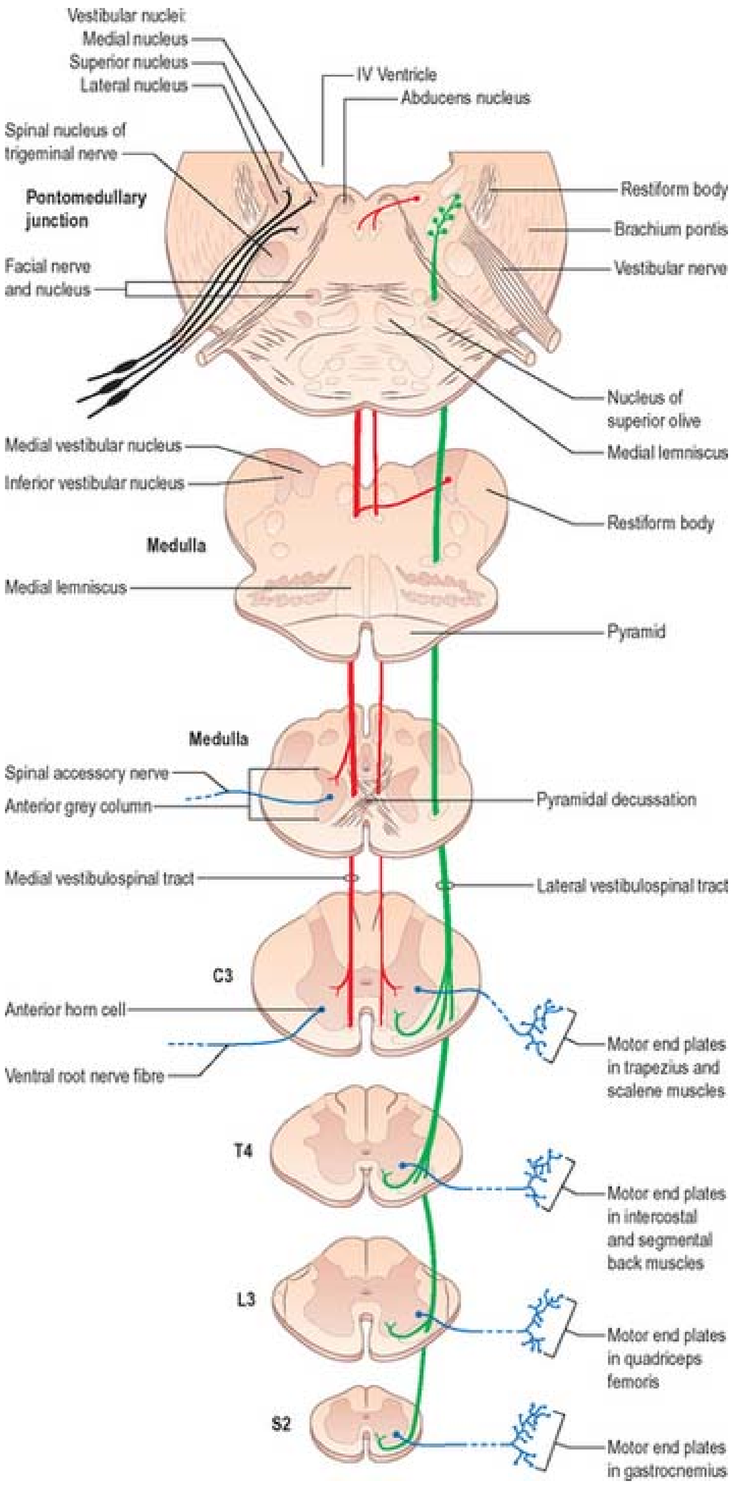
Vestibular nuclei:
Medial nucleus
Superior nucleus
Lateral nucleus
IV Ventricle
Abducens nucleus
Spinal nucleus of trigeminal nerve
Pontomedullary junction
Restiform body
Brachium pontis
Vestibular nerve
Facial nerve and nucleus
Nucleus of superior olive
Medial lemniscus
Medial vestibular nucleus
Inferior vestibular nucleus
Restiform body
Medulla
Medial lemniscus
Pyramid
Medulla
Spinal accessory nerve
Anterior grey column
Pyramidal decussation
Medial vestibulospinal tract
Lateral vestibulospinal tract
C3
Anterior horn cell
Ventral root nerve fibre
Motor end plates in trapezius and scalene muscles
T4
Motor end plates in intercostal and segmental back muscles
L3
Motor end plates in quadriceps femoris
S2
Motor end plates in gastrocnemius

Fig. 18.19 The vestibulospinal tracts.

(Redrawn from Carpenter MB 1991 Core Text of Neuroanatomy, 4th edn. Baltimore: Williams and Wilkins, by permission of author and publisher.)

The lateral vestibulospinal tract arises from small and large neurones of the lateral vestibular nucleus (Deiters' nucleus). It descends ipsilaterally, initially in the periphery of the ventrolateral spinal white matter, but subsequently migrating into the medial part of the ventral funiculus at lower spinal levels. Fibres of this tract are somatotopically organized. Thus, fibres projecting to the cervical, thoracic and lumbosacral segments of the cord arise from neurones in the rostroventral, central and dorsocaudal parts, respectively, of the lateral vestibular nucleus. Lateral vestibulospinal fibres end ipsilaterally, mostly in the medial part of the ventral horn in lamina VIII and the medial part of lamina VII. Axons of the lateral vestibulospinal tract are excitatory to motor neurones of extensor muscles of the neck, back and limbs, through both mono- and polysynaptic connections; γ motor neurones are also probably facilitated. Lateral vestibulospinal tract axons also inhibit motor neurones of flexor limb muscles, via inhibitory interneurones.

The medial vestibulospinal tract (Fig. 18.19) arises mainly from neurones in the medial vestibular nucleus, but some are also located in the inferior and lateral vestibular nuclei. The medial vestibulospinal tract descends in the medial longitudinal fasciculus into the ventral funiculus of the spinal cord where it lies close to the midline in the so-called sulcomarginal fasciculus (Fig. 18.9). Unlike the lateral tract it contains both crossed and uncrossed fibres, and does not extend beyond the midthoracic cord level. Fibres of the medial tract project mainly to the cervical cord segments, ending in lamina VIII and the adjacent dorsal part of lamina VII. Data from stimulation of the vestibular nuclei in animals indicate that axons of the medial tract monosynaptically inhibit the motor neurones that innervate axial muscles of the neck and upper part of the back.

Reticulospinal tracts

The reticulospinal tracts pass from the brain stem reticular formation to the spinal cord. Detailed knowledge of their origins and connections has been obtained mainly from studies in animals.

The medial reticulospinal tract (Fig. 18.16) originates from the medial tegmental fields of the pons and medulla. The main sources are the oral and caudal pontine reticular nuclei and the gigantocellular reticular nucleus in the medulla. Pontine fibres descend, mainly ipsilaterally, in the ventral funiculus of the cord. Medullary fibres descend, both ipsilaterally and contralaterally, in the ventral funiculus and the ventral part of the lateral funiculus. These fibres have many collaterals, and two-thirds of the reticulospinal neurones that reach the cervical cord also descend to lumbosacral levels. The terminals of reticulospinal fibres are distributed to lamina VIII, and the central and medial parts of lamina VII. The medullary reticulospinal terminals are more widely distributed, ending additionally in the lateral parts of laminae VI and VII and also directly on motor neurones. Terminations of reticulospinal fibres that originate in the medulla are, in general, more dorsally placed than those that originate in the pons, although there is considerable overlap.

Both α and γ motor neurones are influenced by reticulospinal fibres, through polysynaptic and monosynaptic connections. Physiological evidence shows that reticulospinal fibres from pontine sources excite motor neurones of axial and limb muscles, while medullary fibres excite, or inhibit motor neurones of cervical muscles and excite motor neurones of axial muscles. Functionally, the medial reticulospinal tract is concerned with posture, the steering of head and trunk movements in response to external stimuli, and crude, stereotyped movements of the limbs.

The lateral reticulospinal tract lies in the lateral funiculus of the spinal cord, closely associated with the rubrospinal and lateral corticospinal tracts (Fig. 18.9). Its fibres arise from neurones of the ventrolateral tegmental field of the pons. The fibres cross in the rostral medulla oblongata and project, with a high degree of collateralization, throughout the length of the spinal cord. Axons of this tract terminate in laminae I, V and VI, and also bilaterally in the lateral cervical nucleus. Evidence suggests that this pathway is involved in the control of pain perception and in motor functions.

Interstitiospinal tract

The interstitiospinal tract arises from neurones in the interstitial nucleus (of Cajal) and the immediate surrounding area, and descends via the medial longitudinal fasciculus into the ventral funiculus of the spinal cord. Its fibres project, mainly ipsilaterally, as far as lumbosacral levels, and are mostly distributed to the dorsal part of lamina VIII and the dorsally adjoining part of lamina VII. They establish some monosynaptic connections with motor neurones supplying neck muscles, but their main connections are disynaptic with motor neurones supplying limb muscles.

Solitariospinal tract

The solitariospinal tract is a small group of mostly crossed fibres which arises from neurones in the ventrolateral part of the nucleus solitarius of the medulla. Descending in the ventral funiculus and ventral part of the lateral funiculus of the cord, these axons terminate on phrenic motor neurones supplying the diaphragm and thoracic motor neurones which innervate intercostal muscles. A pathway with somewhat similar course and terminations to that of the solitariospinal tract originates from the nucleus retroambiguus. Both pathways subserve respiratory activities by driving inspiratory muscles, and some descending axons from the nucleus retroambiguus facilitate expiratory motor neurones. There is clinical evidence that bilateral ventrolateral cordotomy at high cervical levels abolishes rhythmic ventilatory movements.

Hypothalamospinal fibres

Hypothalamospinal fibres exist in animals. They arise from the paraventricular nucleus and other areas of the hypothalamus and descend ipsilaterally, mainly in the dorsolateral region of the cord, to be distributed to sympathetic and parasympathetic preganglionic neurones in the intermediolateral column. Fibres from the paraventricular nucleus show oxytocin and vasopressin immunoreactivity. They are also distributed to laminae I and X. Descending fibres from the dopaminergic cell group (A11) situated in the caudal hypothalamus innervate sympathetic preganglionic neurones and neurones in the dorsal horn. That similar pathways exist in man may be inferred from ipsilateral sympathetic deficits (e.g. Horner’s syndrome), which follow lesions of the hypothalamus, the lateral tegmental brain stem, or the lateral funiculus of the cord.

Monoaminergic spinal pathways

Monoaminergic cell groups utilize dopamine, adrenaline (epinephrine), noradrenaline (norepinephrine) and 5-HT (5-hydroxytryptamine, serotonin) as neurotransmitters. They occur widely throughout the brain stem and in the hypothalamus. They project rostrally to many forebrain areas and caudally to the spinal cord and appear to be concerned with the modulation of sensory transmission, and the control of autonomic and somatic motor neuronal activities.

The projections to the spinal cord arise from several sources. Coeruleospinal projections originate from noradrenergic cell groups A4 and A6 in the locus coeruleus complex in the pons and descend via the ventrolateral white matter to innervate all cord segments bilaterally. They end in the dorsal grey matter (laminae IV–VI) and the intermediate and ventral horns. They also project extensively to preganglionic parasympathetic neurones in the sacral cord. Descending noradrenergic fibres, which arise from the lateral tegmental cell groups A5 and A7 of the pons, travel in the dorsolateral white matter. They are distributed to laminae I–III, and particularly to the intermediate grey horn. Descending fibres from adrenergic cell groups C1 and C3 of the medulla oblongata have been traced into the anterior funiculus of the cord and are extensively distributed to the intermediolateral column. Dopaminergic fibres projecting to the spinal cord travel in the hypothalamospinal pathway.

The raphe nuclei pallidus (B1), obscurus (B2) and magnus (B3) in the brain stem give rise to two serotoninergic descending bundles. The lateral raphe spinal bundle, from B3 neurones, is concerned with the control of nociception. It descends close to the lateral corticospinal tract and ends in the dorsal horn (laminae I, II and V). The ventral bundle, composed mainly of axons from B1 neurones, travels in the medial part of the ventral white column and ends in the ventral horn (laminae VIII and IX). It facilitates extensor and flexor motor neurones. Some descending serotoninergic fibres project to sympathetic preganglionic neurones and are concerned with the central control of cardiovascular function.

Propriospinal pathways

Propriospinal pathways (fasciculi proprii) consist of the ascending and descending fibres of intrinsic spinal neurones. They contact other neurones within the same segment and/or in more distant segments of the spinal cord and so subserve intrasegmental and intersegmental integration and coordination. The majority of spinal neurones are propriospinal neurones, most of which lie in laminae V–VIII. Propriospinal fibres are mainly concentrated around the margins of the grey matter (Fig. 18.9), but are also dispersed diffusely in the white funiculi.

The propriospinal system plays important roles in spinal functions. Descending pathways end on specific subgroups of propriospinal neurones and these, in turn, relay to motor neurones and other spinal neurones. The system mediates all those automatic functions which continue after transection of the spinal cord, e.g. sudomotor and vasomotor activities, bowel and bladder functions.

Some propriospinal axons are very short, and span only one segment, while others run the entire length of the cord. The shortest axons lie immediately adjacent to the grey matter, and the longer ones are situated more peripherally. Propriospinal neurones can be categorized according to the length of their axons as long, intermediate, or short neurones. Long propriospinal neurones distribute their axons throughout the length of the cord, mainly via the ventral and lateral funiculi; their cell bodies are in lamina VIII and the dorsally adjoining part of lamina VII. Axons from the long propriospinal neurones of the cervical cord descend bilaterally, whereas those from the corresponding lumbosacral neurones ascend mainly contralaterally. Most of the fibres are fine (less than 3 µm in diameter). Some are the first spinal tract axons to become myelinated. Intermediate propriospinal neurones occupy the central and medial parts of lamina VII and project mainly ipsilaterally. Short propriospinal neurones are found in the lateral parts of laminae V–VIII and their axons run ipsilaterally in the lateral funiculus.

Propriospinal fibres in the different parts of the white funiculi are distributed preferentially to specific regions of the spinal grey matter. In the spinal enlargements, the propriospinal fibres in the dorsolateral funiculus project to the dorsal and lateral parts of the intermediate zone, and also to spinal motor neurones which supply distal limb muscles, especially those of the hand and the foot. The propriospinal fibres in the ventral part of the ventrolateral funiculus are distributed to the central and medial parts of lamina VII and to motor neurones of proximal limb and girdle muscles. Other propriospinal fibres run in the medial part of the ventral funiculus and travel mainly to the ventromedial part of the intermediate zone, which characteristically contains long propriospinal neurones, and to motor neurones innervating axial and girdle muscles.

The tract of Lissauer

The tract of Lissauer, or the dorsolateral tract, lies between the apex of the dorsal horn and the surface of the spinal cord, where it surrounds the incoming dorsal root fibres. It is present throughout the spinal cord, and is most developed in the upper cervical regions.

The tract consists of fine myelinated and non-myelinated axons. Many are the branches of axons in the lateral bundles of the dorsal roots. These axons bifurcate into ascending and descending branches as they enter the cord. The branches travel in the tract of Lissauer for one or two segments and give off collaterals, which end on and around neurones in the dorsal horn. The tract also contains propriospinal fibres, some of which are short axons of small substantia gelatinosa neurones, which re-enter the dorsal horn.

SPINAL CORD LESIONS

Mechanical compression and secondary ischaemic damage to underlying nervous tissue cause surgically relevant spinal cord disease (myelopathy). The site and the level of damage to the cord determine the particular clinical syndrome, e.g. whether the lesion involves the upper or lower cervical, thoracic or lumbosacral spinal cord. At each of these levels, symptoms and signs are determined by direct destruction of segmental tissue, i.e. transversely distributed damage, and disconnection of suprasegmental ascending and descending tracts above and below the level of a lesion, i.e. longitudinally distributed damage (Fig. 18.20). For example, a lower cervical spinal cord lesion damages the segmental sensory and motor contributions to the nerve roots and brachial plexus causing sensory loss, weakness and wasting of the muscles and loss of tendon reflexes in the upper limbs. Disruption of the ascending sensory pathways in the lateral and dorsal columns of the cervical spinal cord leads to loss of sensation to pain and temperature (lateral spinothalamic tracts) and touch and proprioception (dorsal fasciculi) below the 'sensory level' corresponding to the segment of the spinal cord.

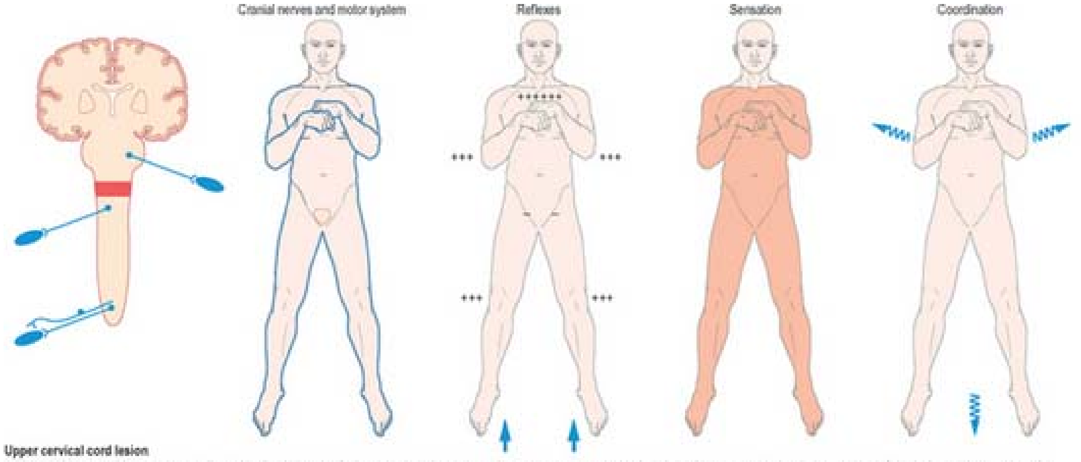
Cranial nerves and motor system
Reflexes
Sensation
Coordination
++++++
+++
+++
– –
+++
+++

Upper cervical cord lesion
A high cervical cord lesion causes spastic tetraplegia with hyperreflexia, extensor plantar responses (upper motor neurone lesion), incontinence, sensory loss below the level of the lesion and 'sensory' ataxia.

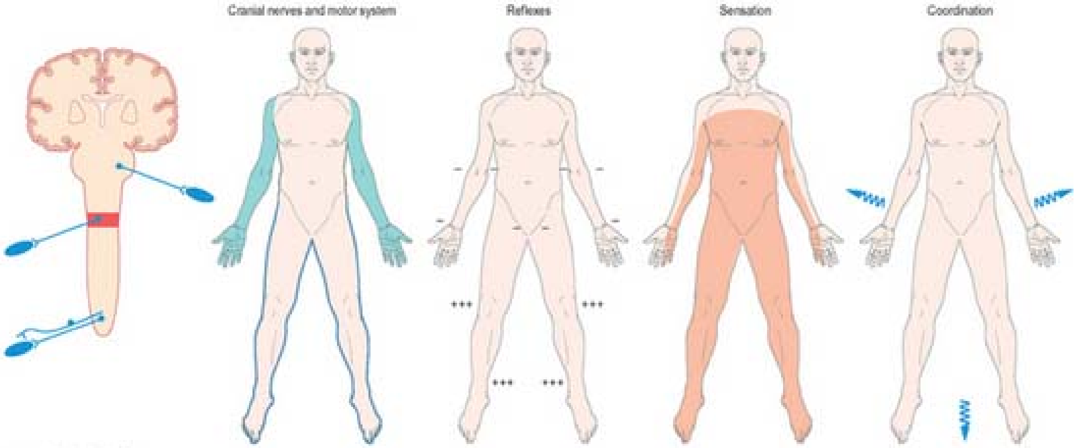
Cranial nerves and motor system
Reflexes
Sensation
Coordination
–
–
–
–
– –
–
–
+++
+++
+++
+++

Lower cervical cord lesion
A lower cervical cord lesion causes weakness, wasting and fasciculation of muscles and areflexia of the upper limbs (lower motor neurone lesion). In addition, there is spastic paraparesis, hyperreflexia and extensor plantar responses (upper motor neurone lesion) in the lower limbs, incontinence, sensory loss below the level of the lesion and 'sensory' ataxia.

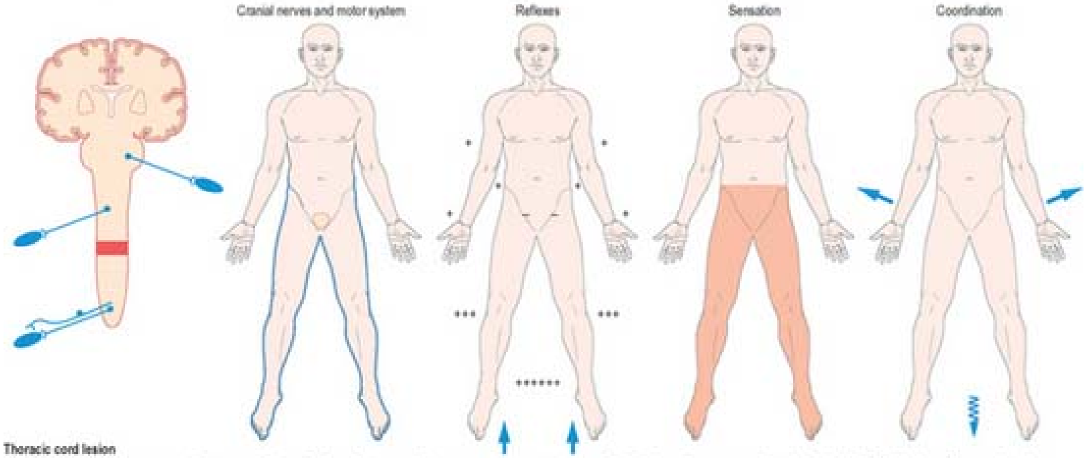
Cranial nerves and motor system
Reflexes
Sensation
Coordination
+
+
+
+
+
+
– –
+++
+++
++++++

Thoracic cord lesion
A thoracic cord lesion causes a spastic paraparesis, hyperreflexia and extensor plantar responses (upper motor neurone lesion), incontinence, sensory loss below the level of the lesion and 'sensory' ataxia.

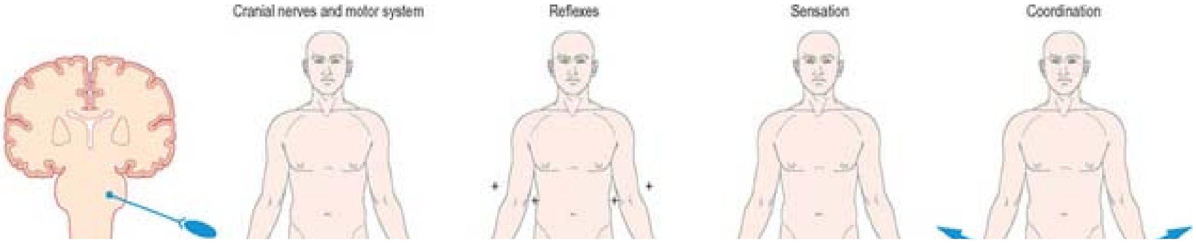
Cranial nerves and motor system
Reflexes
Sensation
Coordination
+
+
+
+

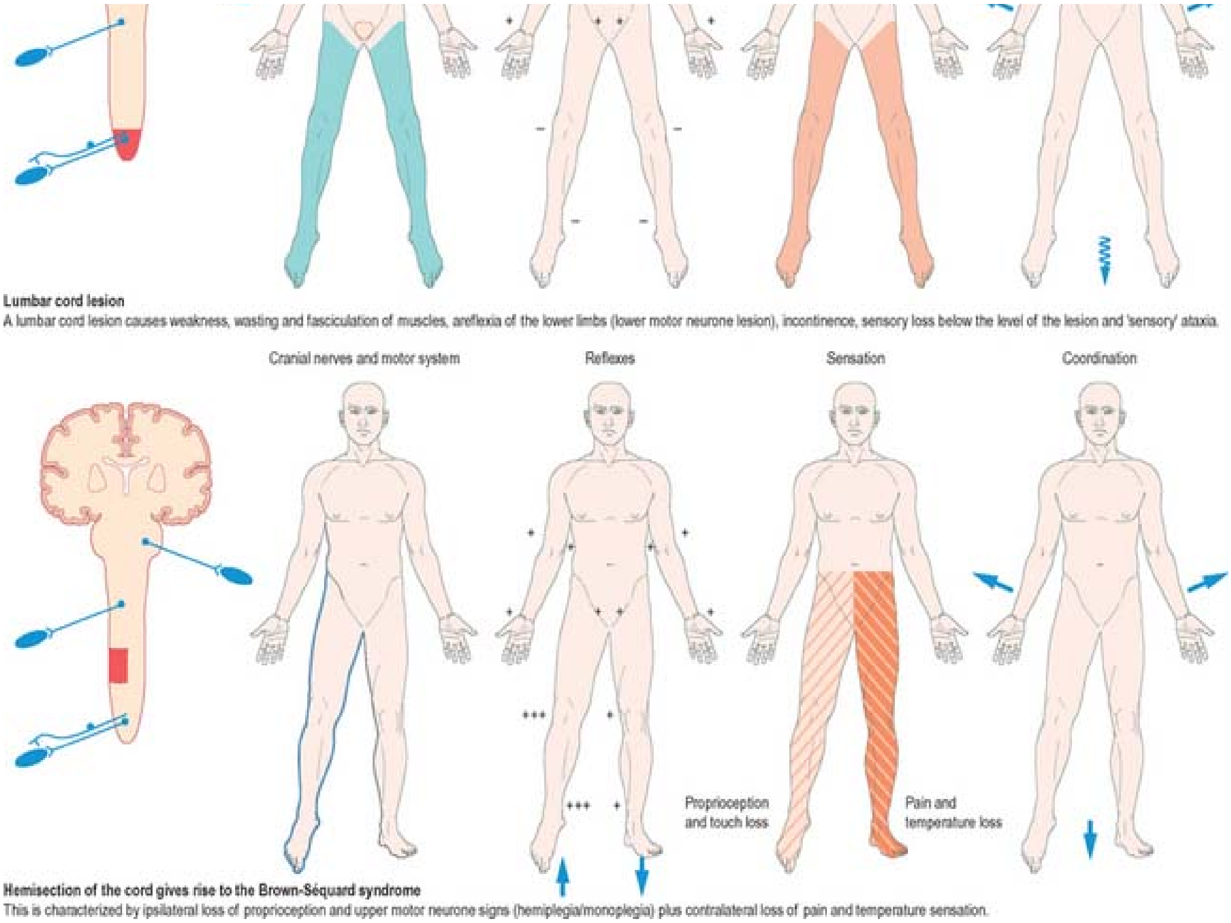

Lumbar cord lesion

A lumbar cord lesion causes weakness, wasting and fasciculation of muscles, areflexia of the lower limbs (lower motor neurone lesion), incontinence, sensory loss below the level of the lesion and 'sensory' ataxia.

Cranial nerves and motor system
Reflexes
Sensation
Coordination
+++
+
Proprioception and touch loss
Pain and temperature loss

Hemisection of the cord gives rise to the Brown-Séquard syndrome

This is characterized by ipsilateral loss of proprioception and upper motor neurone signs (hemiplegia/monoplegia) plus contralateral loss of pain and temperature sensation.

Fig. 18.20 Lesions of the spinal cord.

(By permission from Crossman AR, Neary D 2000 Neuroanatomy, 2nd edn. Edinburgh: Churchill Livingstone.)

Damage to the descending corticospinal tracts in the lateral columns of the spinal cord produces a spastic paraparesis, i.e. increased tone of the muscles, weakness of movements of flexion, exaggerated tendon reflexes and abnormal superficial reflexes, e.g. extensor plantar responses and absent abdominal reflexes. Descending pathways to the bladder are interrupted, and this produces a ‘neurogenic bladder’.

The same principles apply to lesions at other levels of the spinal cord and they are illustrated in diagrammatic form in Fig. 18.20.

The precise clinical syndrome is determined by anatomical site alone and not by pathology. However, it is of practical use to classify lesions on the basis of their anatomical relationship to the spinal cord and meninges, i.e. whether they are extradural, intradural or intramedullary (see table). This anatomic classification provides a guide to the diagnostic probabilities as well as an aid to neuroradiological interpretation prior to neurosurgical intervention. For example, neurofibromas are common in the cervical spinal canal, meningiomas in the thoracic spinal canal, and ependymomas in the lumbosacral spinal canal. Degenerative disease of the vertebral column is common in the cervical and lumbosacral vertebrae, but rare in the thoracic vertebrae. Discrete anterior and central intramedullary lesions, e.g. due to syringomyelia and angiomas respectively, preferentially destroy the spinothalamic pathways in the anterolateral columns and central areas of the spinal cord. This leads to a characteristic ‘dissociated’ sensory loss, i.e. loss of pain and temperature sensation, but with preservation of touch sensation and proprioception at and below the level of the lesion.

Classification of spinal cord lesions

Extradural lesions	A. Disorder of the vertebral column B. Abscess C. Haematoma	Degenerative osteoarthritis (osteophytes and prolapsed intervertebral discs) Tumour (metastatic carcinoma, myeloma, lymphoma, chordoma, sarcoma) (Complication of bleeding, diathesis or anticoagulation)
Intradural lesions		Meningioma, neurofibroma, lipoma, angioma
Intramedullary lesions		Syringomyelia (Arnold–Chiari malformation), angioma, glioma, ependymoma, epidermoid tumour

REFERENCES

yd IA, Gladden MH. The Muscle Spindle. London: Macmillan, 1985.

ypers HGJM. Anatomy of descending pathways. In: Brookhart JM, Mountcastle VB, et al. *Handbook of Physiology, vol 2 Motor Control, pt 1*. Bethesda, MD: Am Physiol Soc; 1981:597-666.

elzack R, Wall PD. Pain mechanisms: a new theory. *Science*. 1965;150:971-979.

xed B. The cytoarchitectonic organization of the spinal cord in the cat. *J Comp Neurol*. 1952;96:415-495.

hoenen J, Faull RLM. Spinal cord: cytoarchitectural, dendroarchitectural and myeloarchitectural organization. In: Paxinos G, editor. *The Human Nervous System*. San Diego, CA: Academic Press; 1990:19-53.

CHAPTER 19

Brain stem

The brain stem consists of the medulla oblongata, pons and midbrain. It is situated in the posterior cranial fossa, and its ventral surface lies on the clivus. It contains numerous intrinsic neuronal cell bodies and their processes, some of which are the brain stem homologues of spinal cell groups. Some brain stem cell groups are the nuclei of cranial nerves III–XII: they are concerned with the sensory, motor and autonomic innervation of the head and neck. Other autonomic fibres that arise from the brain stem are distributed more widely via the vagus nerve. The brain stem also contains a complex and sometimes ill-defined network of neurones, the reticular formation, that extends throughout its length, and is continuous caudally with its spinal counterpart. Some reticular nuclei are referred to as vital centres since they are concerned with regulation of cardiac and respiratory activities; other parts of the reticular formation are essential for cerebral cortical arousal and the maintenance of consciousness, or are involved in the regulation of muscle tone, posture and reflex activities. The brain stem is the site of termination of numerous ascending and descending fibres and is traversed by many others. The spinothalamic tract (spinal lemniscus), medial lemniscus (see Fig. 18.10) and the trigeminothalamic tracts (see Fig. 19.16) all ascend through the brain stem to reach the thalamus Prominent corticospinal projections descend through the brain stem (see Fig. 18.17) and corticobulbar projections end within it.

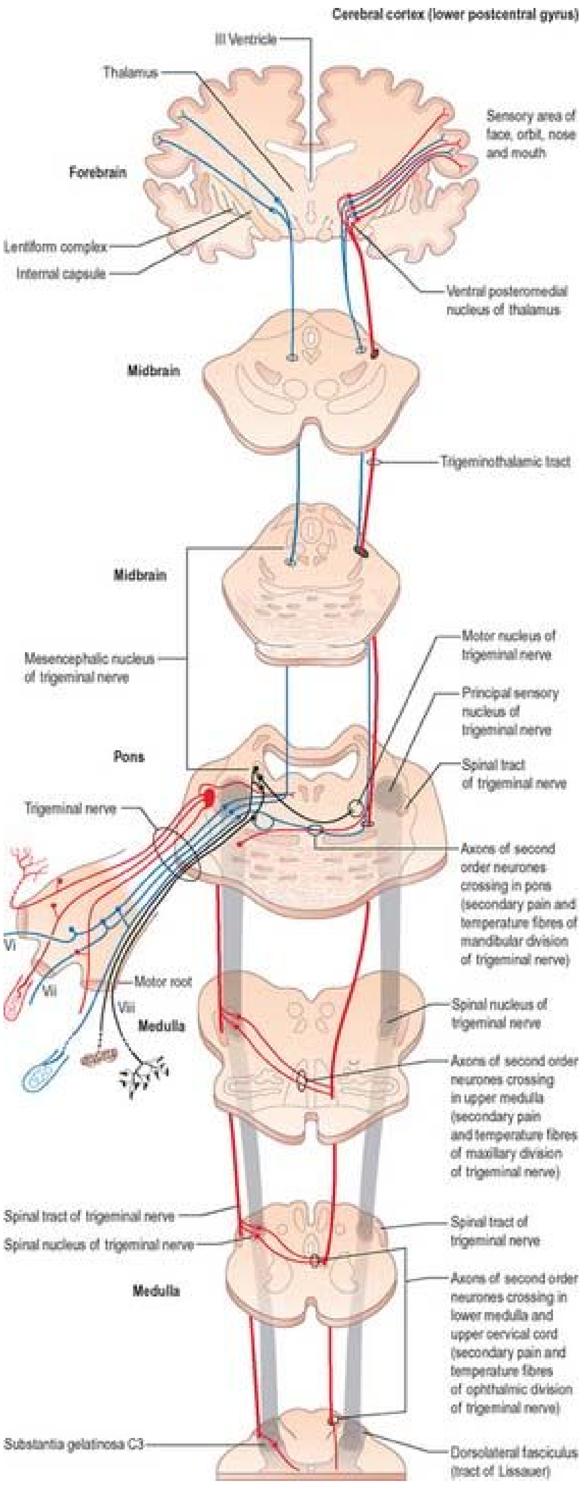
Cerebral cortex (lower postcentral gyrus)
III Ventricle
Thalamus
Sensory area of face, orbit, nose and mouth
Forebrain
Lentiform complex
Internal capsule
Ventral posteromedial nucleus of thalamus
Midbrain
Trigeminothalamic tract
Midbrain
Mesencephalic nucleus of trigeminal nerve
Motor nucleus of trigeminal nerve
Principal sensory nucleus of trigeminal nerve
Pons
Spinal tract of trigeminal nerve
Trigeminal nerve
Axons of second order neurones crossing in pons (secondary pain and temperature fibres of mandibular division of trigeminal nerve)
Vi
Vii
Motor root
Viii
Medulla
Spinal nucleus of trigeminal nerve
Axons of second order neurones crossing in upper medulla (secondary pain and temperature fibres of maxillary division of trigeminal nerve)
Spinal tract of trigeminal nerve
Spinal nucleus of trigeminal nerve
Spinal tract of trigeminal nerve
Medulla
Axons of second order neurones crossing in lower medulla and upper cervical cord (secondary pain and temperature fibres of ophthalmic division of trigeminal nerve)
Substantia gelatinosa C3
Dorsolateral fasciculus (tract of Lissauer)

Fig. 19.16 The trigeminal nerve and its central connections.

Damage to the brain stem is often devastating and life-threatening. This is because it is a structurally and functionally compact region, where even small lesions can destroy vital cardiac and respiratory centres, disconnect forebrain motor areas from brain stem and spinal motor neurones, and sever incoming sensory fibres from higher centres of consciousness, perception and cognition. Irreversible cardiac and respiratory arrest follow complete destruction of the neural respiratory and cardiac centres in the medulla. Clinically, this is called brain stem death, a condition that requires accurate diagnosis since it may occur in patients on life-support machines whose respiratory and cardiac functions can be artificially maintained indefinitely.

OVERVIEW OF CRANIAL NERVES AND CRANIAL NERVE NUCLEI

The cranial nerves are the routes by which the brain receives information directly from, and controls the functions of, structures which are located mainly, although not exclusively, within the head and neck. All but two of the twelve pairs of cranial nerves attach to the brain stem. Below is a brief overview of the cranial nerves (consult also Table 15.1), their associated cranial nerve nuclei, and some of the brain stem reflexes to which they contribute. The cranial nerves are described in detail on a regional basis in appropriate chapters.

The cranial nerves are individually named and numbered (using Roman numerals) in a rostro-caudal sequence, reflecting their order of attachment to the brain. The first cranial nerve (olfactory) terminates directly in cortical and subcortical areas of the frontal and temporal lobes. It is closely associated functionally with the limbic system and is described in that context (Ch. 23). The fibres of the second cranial nerve (optic) pass into the optic chiasma where the centrally located fibres decussate; all of the fibres emerge as the optic tract, which terminates in the lateral geniculate nucleus of the thalamus. Cranial nerves III (oculomotor) and IV (trochlear) attach to the midbrain. Cranial nerve V (trigeminal) attaches to the pons, medial to the middle cerebellar peduncle. Cranial nerves VI (abducens), VII (facial) and VIII (vestibulocochlear) attach to the brain stem at, or close to, the junction of the pons with the medulla. Cranial nerves IX (glossopharyngeal), X (vagus), the cranial part of XI (accessory) and XII (hypoglossal) all attach to the medulla.

Cranial nerves III–XII, which attach to the brain stem, are associated with the brain stem cell groupings referred to collectively as the cranial nerve nuclei (Fig. 19.1). The nuclei are either the origin of efferent cranial nerve fibres or the site of termination of cranial nerve afferents. They are considered to be organized into six discontinuous longitudinal cell columns that correspond to columns that may be identified in the embryo (see Fig. 15.3). Three columns are ‘sensory’ and three are ‘motor’ in function.

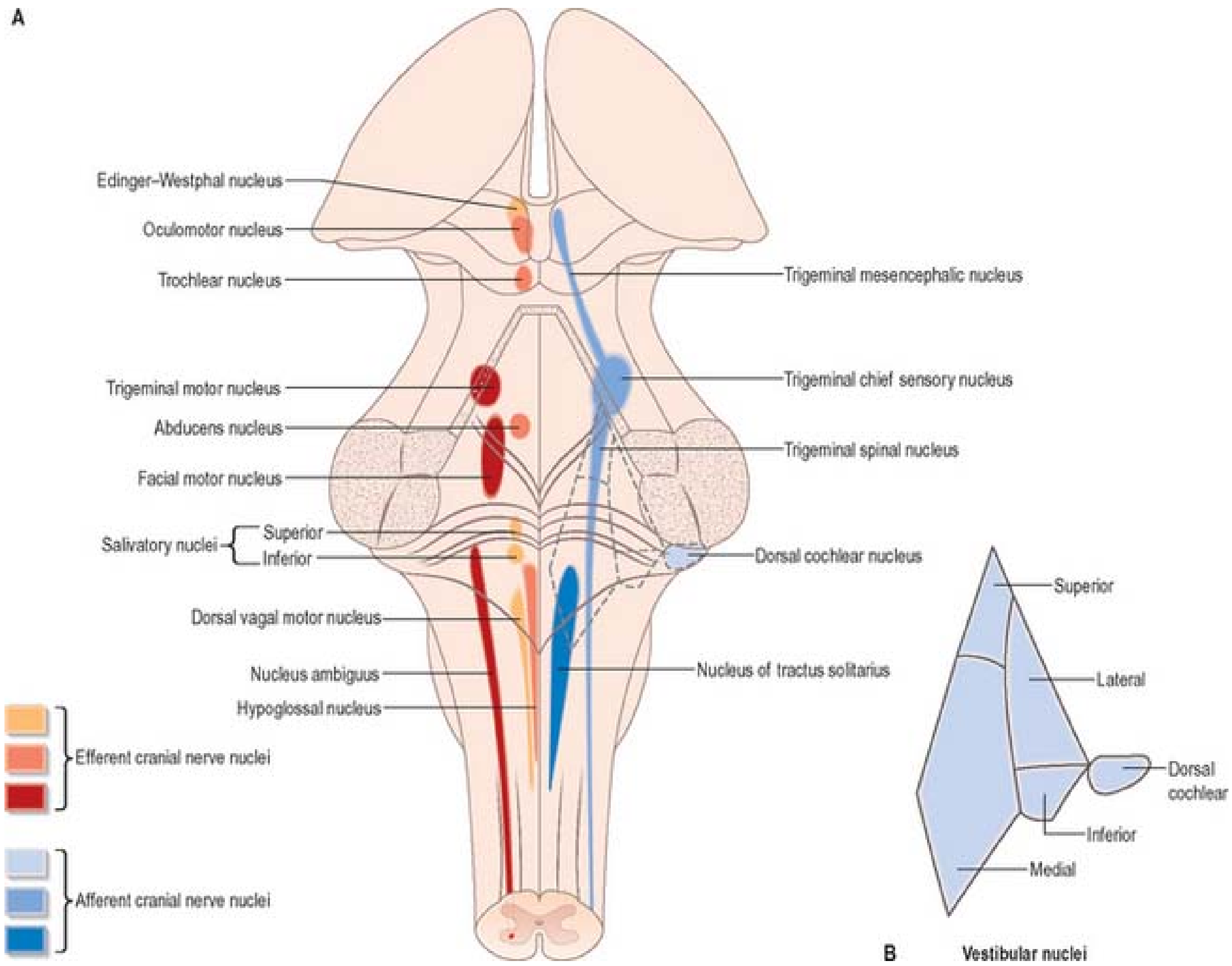
A
Edinger–Westphal nucleus
Oculomotor nucleus
Trochlear nucleus
Trigeminal mesencephalic nucleus
Trigeminal motor nucleus
Abducens nucleus
Facial motor nucleus
Trigeminal chief sensory nucleus
Trigeminal spinal nucleus
Salivatory nuclei
Superior
Inferior
Dorsal cochlear nucleus
Dorsal vagal motor nucleus
Nucleus ambiguus
Hypoglossal nucleus
Nucleus of tractus solitarius
Efferent cranial nerve nuclei
Afferent cranial nerve nuclei
Superior
Lateral
Dorsal cochlear
Inferior
Medial
B
Vestibular nuclei

Fig. 19.1 **A**, The cranial nerve nuclei. The components of the vestibular nuclei are indicated by the dotted lines and shown in more detail in **B**.

The trigeminal sensory nucleus, which extends throughout the length of the brain stem and into the cervical spinal cord, represents a general somatic afferent cell column. Its principal afferents are carried in the trigeminal nerve. General visceral afferents carried by the facial, glossopharyngeal and vagus nerves end in the nucleus solitarius of the medulla. The special somatic afferent column corresponds to the vestibular and cochlear nuclei, which are located beneath the vestibular area of the floor of the fourth ventricle.

The general somatic efferent cell column consists of four nuclei that lie near the midline and give rise to motor fibres which run in nerves of the same name. From rostral to caudal, these are the oculomotor, trochlear and abducens nuclei which innervate the extraocular muscles, and the hypoglossal nucleus, which innervates all but one of the muscles of the tongue. The general visceral efferent, or parasympathetic, cell column is made up of the Edinger–Westphal nucleus of the midbrain, salivary nuclei of the pons, and vagal nucleus of the medulla. Cells in the special visceral efferent column innervate muscles derived from the branchial arches, and lie in the trigeminal motor nucleus, the facial nucleus and the nucleus ambiguus.

MEDULLA OBLONGATA

EXTERNAL FEATURES AND RELATIONS

The medulla oblongata extends from just above the first pair of cervical spinal nerves to the lower border of the pons (Fig. 28.11). It is approximately 3 cm in length and 2 cm in diameter at its widest. The ventral surface of the medulla is separated from the basilar part of the occipital bone and apex of the dens by the meninges and occipito-axial ligaments. Caudally, the dorsal surface of the medulla occupies the midline notch between the cerebellar hemispheres.

The ventral and dorsal surfaces of the medulla (Fig. 19.2, Fig. 19.3) possess a longitudinal median fissure and sulcus, respectively, which are continuous with their spinal counterparts. Caudally, the ventral median fissure is interrupted by the obliquely crossing fascicles of the pyramidal decussation. Rostrally, it ends at the pontine border in a diminutive depression, the foramen caecum. Immediately lateral to the ventral median fissure there is a prominent elongated ridge, the pyramid, which contains descending pyramidal, or corticospinal, axons. The lateral margin of the pyramid is indicated by a shallow ventrolateral sulcus. From this emerges, in line with the ventral spinal nerve roots, a linear series of rootlets which constitute the hypoglossal nerve. The abducens nerve emerges at the slightly narrowed rostral end of the pyramid, where it adjoins the pons. Caudally the pyramid tapers into the spinal ventral funiculus. Lateral to the pyramid and the ventrolateral sulcus there is an oval prominence, the olive (Fig. 19.2), which contains the inferior olivary nucleus. Lateral to the olive is the posterolateral sulcus. The glossopharyngeal, vagus and accessory nerves join the brain stem along the line of this sulcus, in line with the dorsal spinal nerve roots.

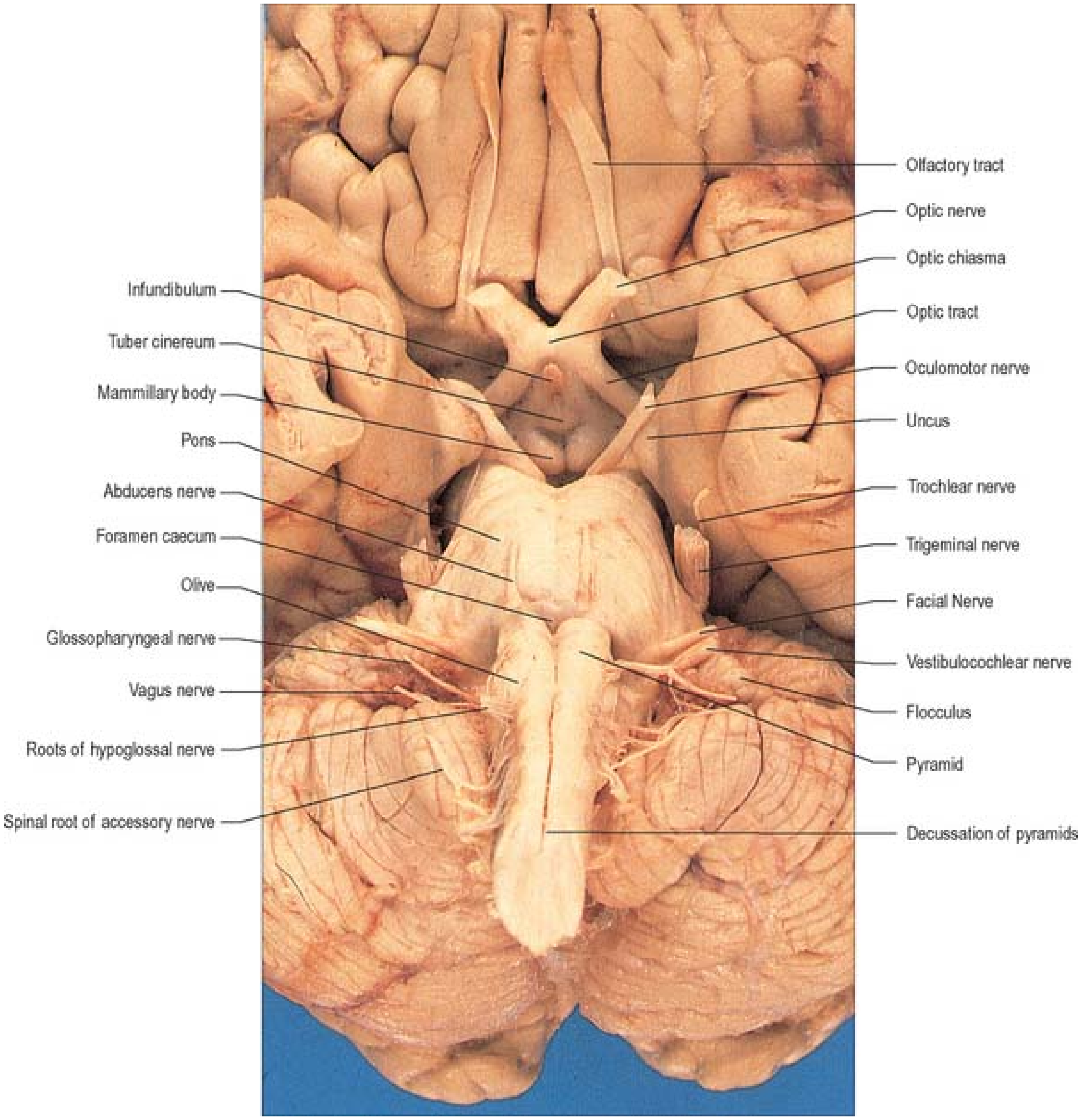
Olfactory tract
Optic nerve
Optic chiasma
Optic tract
Oculomotor nerve
Uncus
Trochlear nerve
Trigeminal nerve
Facial Nerve
Vestibulocochlear nerve
Flocculus
Pyramid
Decussation of pyramids
Infundibulum
Tuber cinereum
Mammillary body
Pons
Abducens nerve
Foramen caecum
Olive
Glossopharyngeal nerve
Vagus nerve
Roots of hypoglossal nerve
Spinal root of accessory nerve

Fig. 19.2 Ventral aspect of the brain stem.

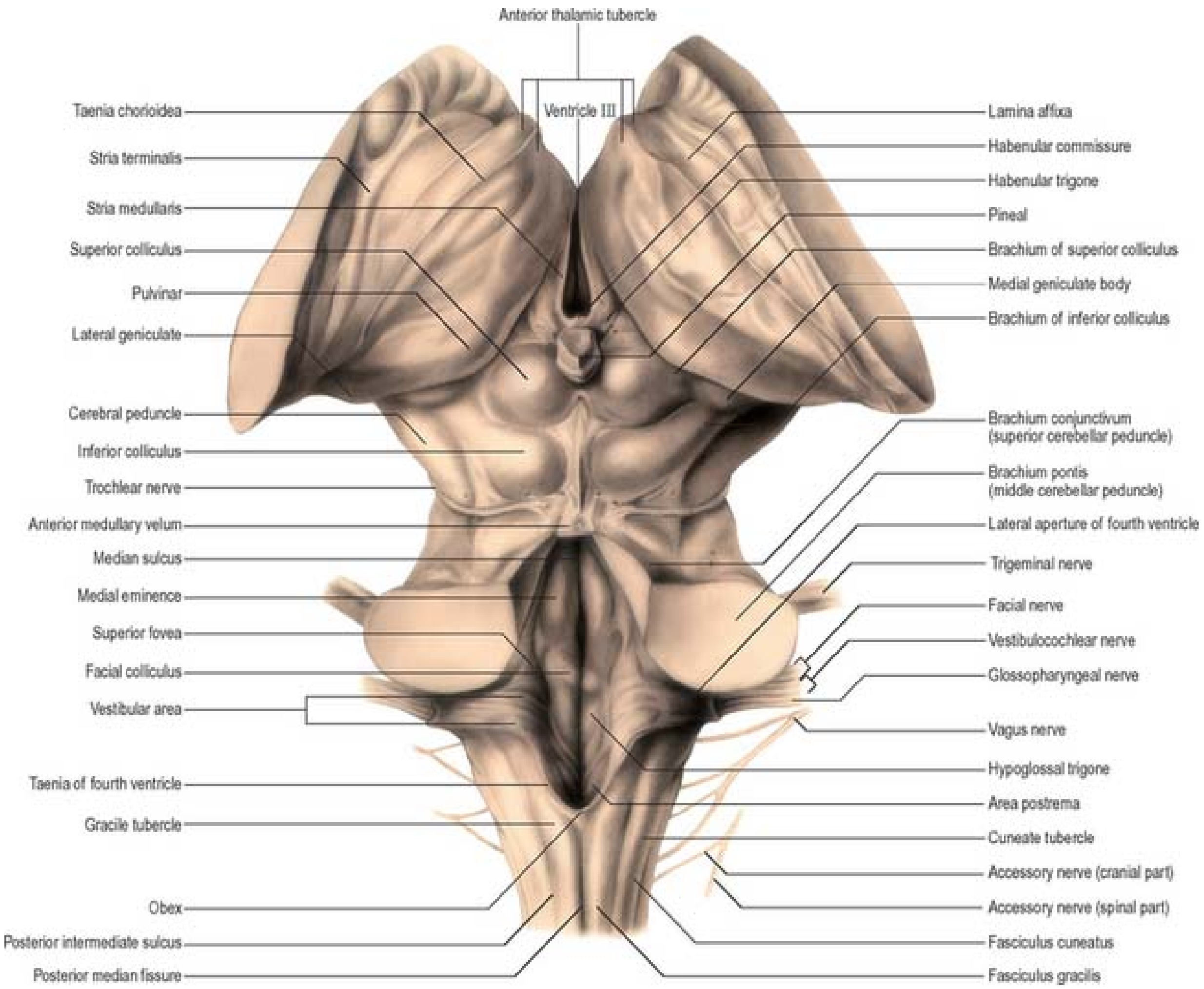
Anterior thalamic tubercle
Ventricle III
Taenia chorioidea
Stria terminalis
Stria medullaris
Superior colliculus
Pulvinar
Lateral geniculate
Cerebral peduncle
Inferior colliculus
Trochlear nerve
Anterior medullary velum
Median sulcus
Medial eminence
Superior fovea
Facial colliculus
Vestibular area
Taenia of fourth ventricle
Gracile tubercle
Obex
Posterior intermediate sulcus
Posterior median fissure
Lamina affixa
Habenular commissure
Habenular trigone
Pineal
Brachium of superior colliculus
Medial geniculate body
Brachium of inferior colliculus
Brachium conjunctivum
(superior cerebellar peduncle)
Brachium pontis
(middle cerebellar peduncle)
Lateral aperture of fourth ventricle
Trigeminal nerve
Facial nerve
Vestibulocochlear nerve
Glossopharyngeal nerve
Vagus nerve
Hypoglossal trigone
Area postrema
Cuneate tubercle
Accessory nerve (cranial part)
Accessory nerve (spinal part)
Fasciculus cuneatus
Fasciculus gracilis

Fig. 19.3 The dorsal aspect of the brain stem. The floor of the fourth ventricle has been exposed by cutting the cerebellar peduncles and removing the cerebellum.

(By permission from Neuroanatomy by FA Mettler (1948) 2nd edn; St Louis: The CV Mosby Company.)

The spinal central canal extends into the caudal half of the medulla, migrating progressively more dorsally until it opens out into the lumen of the fourth ventricle. This divides the medulla into a closed part, which contains the central canal, and an open part, which contains the caudal half of the fourth ventricle (Fig. 19.3).

In the closed part of the medulla, a shallow dorsal intermediate sulcus, on either side of the dorsal median sulcus and continuous with its cervical spinal counterpart, indicates the location of the ascending dorsal columns (fasciculus gracilis and fasciculus cuneatus). The ascending fasciculi are at first parallel to each other, but at the caudal end of the fourth ventricle they diverge, and each develops an elongated swelling, the gracile and cuneate tubercles, produced by the subjacent nuclei gracilis and cuneatus respectively (Fig. 19.3, Fig. 19.4, Fig. 19.5). Most fibres in the fasciculi synapse with neurones in their respective nuclei, and these project to the contralateral thalamus, which, in turn, projects to the primary somaesthetic cortex (see Fig. 18.10). The inferior cerebellar peduncle forms a rounded ridge between the caudal part of the fourth ventricle and the glossopharyngeal and vagal rootlets. The peduncles of the two sides diverge and incline to enter the cerebellar hemispheres, where they are crossed by the striae medullares which run to the dorsal median sulcus of the ventricular floor (Fig. 19.3). Here also the peduncles form the anterior and rostral boundaries of the lateral recess of the fourth ventricle. This becomes continuous with the subarachnoid space through the lateral apertures of the fourth ventricle, or foramina of Luschka. A tuft of choroid plexus, continuous with that of the fourth ventricle, protrudes from the foramina on either side.

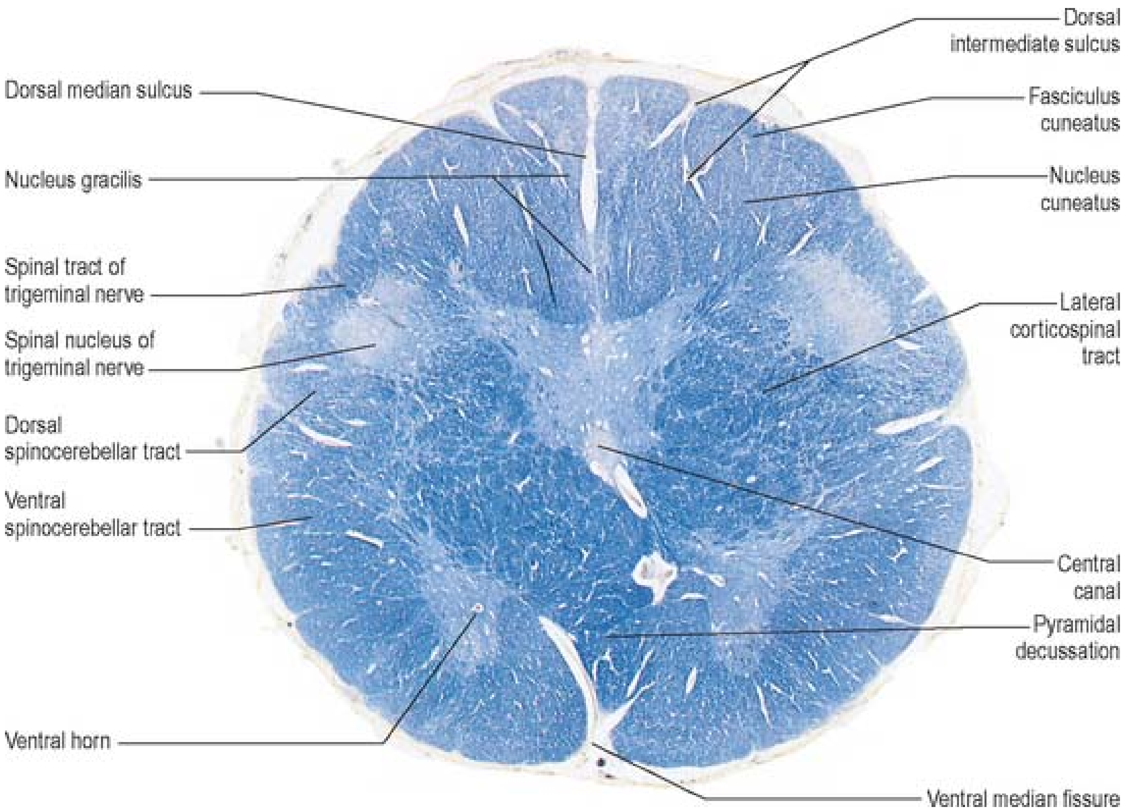
Dorsal median sulcus
Nucleus gracilis
Spinal tract of trigeminal nerve
Spinal nucleus of trigeminal nerve
Dorsal spinocerebellar tract
Ventral spinocerebellar tract
Ventral horn
Dorsal intermediate sulcus
Fasciculus cuneatus
Nucleus cuneatus
Lateral corticospinal tract
Central canal
Pyramidal decussation
Ventral median fissure

Fig. 19.4 Transverse section through the medulla oblongata at the level of the pyramidal decussation. Figs 19.4-19.6, 19.9-19.11, 19.18 and 19.19 are all prepared using a stain for myelinated nerve fibres (blue).

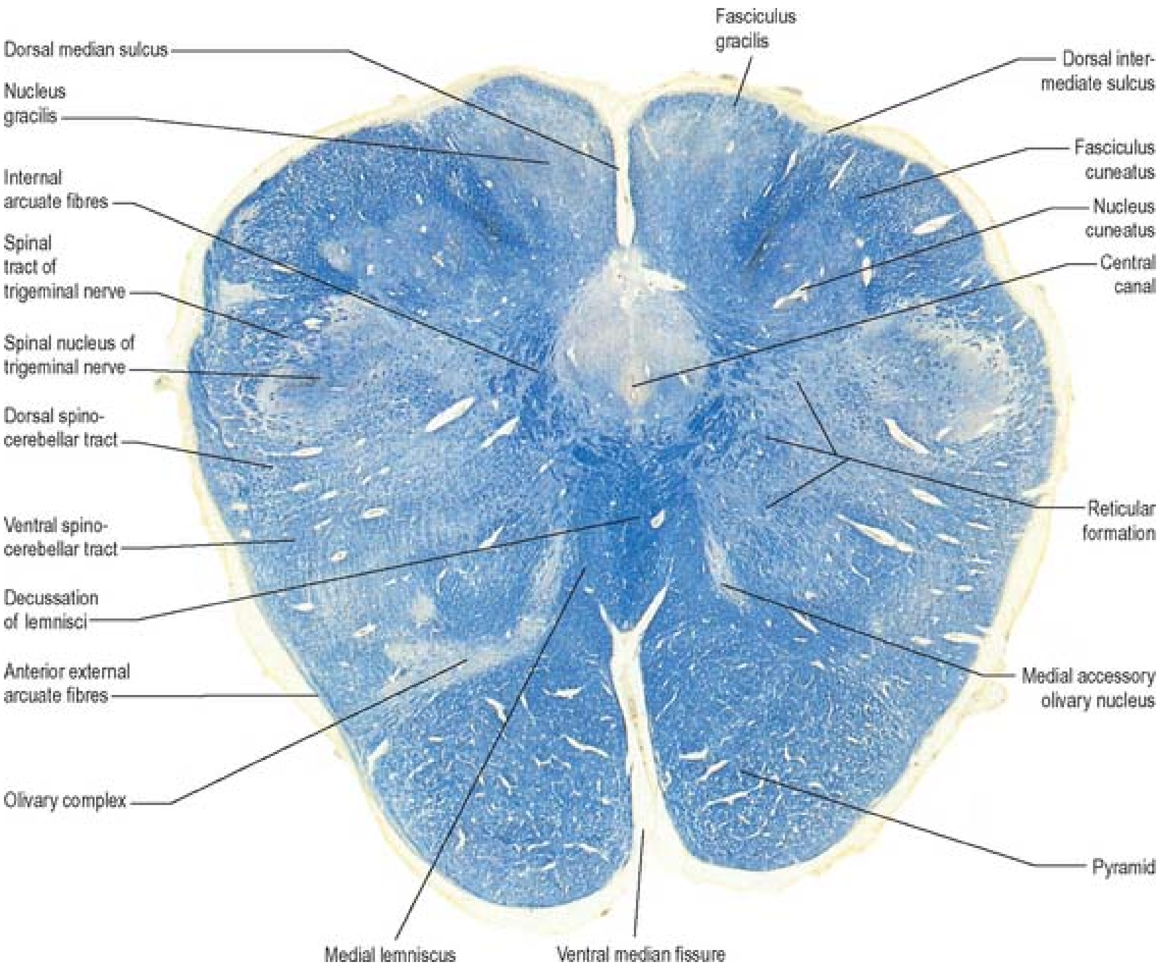
Fasciculus gracilis
Dorsal median sulcus
Dorsal intermediate sulcus
Nucleus gracilis
Fasciculus cuneatus
Internal arcuate fibres
Nucleus cuneatus
Central canal
Spinal tract of trigeminal nerve
Spinal nucleus of trigeminal nerve
Dorsal spinocerebellar tract
Reticular formation
Ventral spinocerebellar tract
Decussation of lemnisci
Medial accessory olivary nucleus
Anterior external arcuate fibres
Olivary complex
Pyramid
Medial lemniscus
Ventral median fissure

Fig. 19.5 Transverse section through the medulla oblongata at the level of the decussation of the medial lemniscus.

INTERNAL STRUCTURE

Transverse section of the medulla at the level of the pyramidal decussation

A transverse section across the lower medulla oblongata (Fig. 19.4) intersects the dorsal, lateral and ventral funiculi, which are continuous with their counterparts in the spinal cord. The ventral funiculi are separated from the central grey matter by corticospinal fibres, which cross in the pyramidal decussation to reach the contralateral lateral funiculi (see Fig. 19.8). The decussation displaces the central grey matter and central canal dorsally. Continuity between the ventral grey column and central grey matter, which is maintained throughout the spinal cord, is lost. The column subdivides into the supraspinal nucleus (continuous above with that of the hypoglossal nerve), which is the efferent source of the first cervical nerve, and the spinal nucleus of the accessory nerve, which provides some spinal accessory fibres and merges rostrally with the nucleus ambiguus.

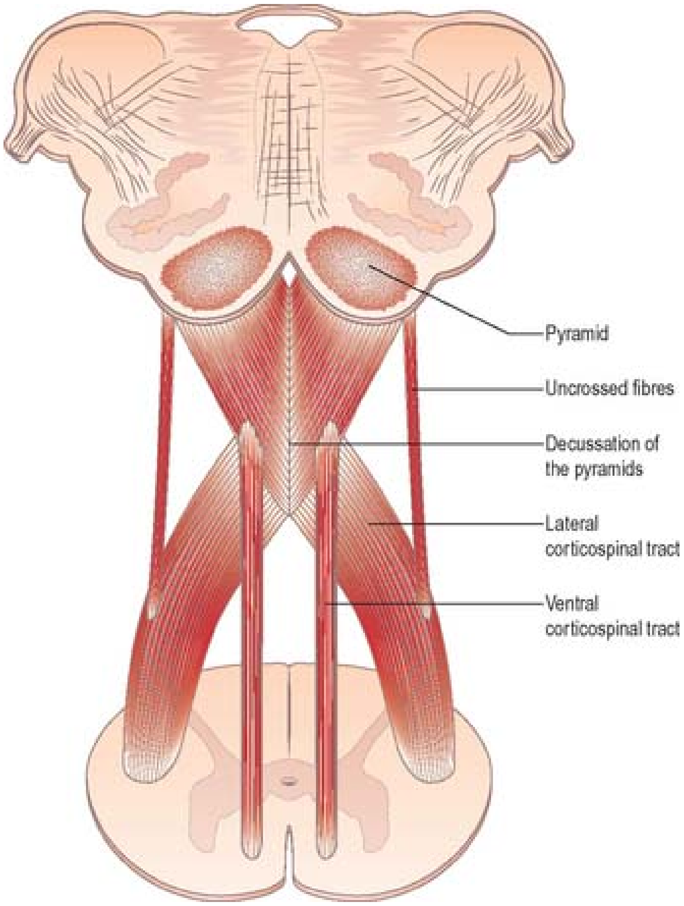
Pyramid
Uncrossed fibres
Decussation of the pyramids
Lateral corticospinal tract
Ventral corticospinal tract

Fig. 19.8 The decussation of the pyramids.

The dorsal grey column is also modified at this level as the nucleus gracilis appears as a grey lamina in the ventral part of the fasciculus gracilis. The nucleus begins caudal to the nucleus cuneatus, which invades the fasciculus cuneatus from its ventral aspect in similar fashion.

The spinal nucleus and spinal tract of the trigeminal nerve are visible ventrolateral to the dorsal columns. They are continuous with the substantia gelatinosa and tract of Lissauer of the spinal cord.

Transverse section of the medulla at the level of the decussation of the medial lemniscus

The medullary white matter is rearranged above the level of the pyramidal decussation (Fig. 19.5). The pyramids form two large ventral bundles flanking the ventral median fissure on the ventral surface of the medulla.

They contain corticospinal fibres of ipsilateral origin. The nucleus gracilis is prominent on the dorsal aspect, with diminishing numbers of fibres of the fasciculus gracilis located on its dorsal, medial and lateral margins. The nucleus cuneatus is well developed. Both nuclei retain continuity with the central grey matter at this level, but this is lost more rostrally. First-order afferent fibres contained within the fasciculi gracilis and cuneatus synapse upon neurones in their respective nuclei. Second-order axons emerge from the nuclei as internal arcuate fibres, at first curving ventrolaterally around the central grey matter and then ventromedially between the spinal tract of the trigeminal nerve and the central grey matter. The fibres decussate in the midline thereafter forming the medial lemniscus which ascends to the thalamus. The decussation of internal arcuate fibres is located dorsal to the pyramids and ventral to the central grey matter, which is therefore more dorsally displaced than in the previous section.

The medial lemniscus ascends from the decussation as a flattened tract, near the median raphe. The pyramidal tract lies ventrally, and the medial longitudinal fasciculus and the tectospinal tract lie dorsally. Decussating lemniscal fibres are rearranged as they cross, so that those derived from the nucleus gracilis come to lie ventral to those from the nucleus cuneatus. Above this level, the medial lemniscus is further rearranged so that ventral (gracile) fibres migrate laterally, whilst dorsal (cuneate) fibres migrate medially. After such rearrangement, the medial lemniscus is somatotopically organized with C1 to S4 spinal segments represented sequentially from medial to lateral.

The nucleus of the spinal tract of the trigeminal nerve is separated from the central grey matter by internal arcuate fibres, and from the lateral medullary surface by the spinal tract of the trigeminal and by some dorsal spinocerebellar tract fibres. The latter progressively incline dorsally, and enter the inferior cerebellar peduncle at a higher level.

Transverse section of the medulla at the caudal end of the fourth ventricle

A transverse section at the lower end of the fourth ventricle (Fig. 19.6) shows some new features together with most of those already described. The total area of grey matter is increased by the presence of the large olivary nuclear complex and nuclei of the vestibulocochlear, glossopharyngeal, vagus and accessory nerves.

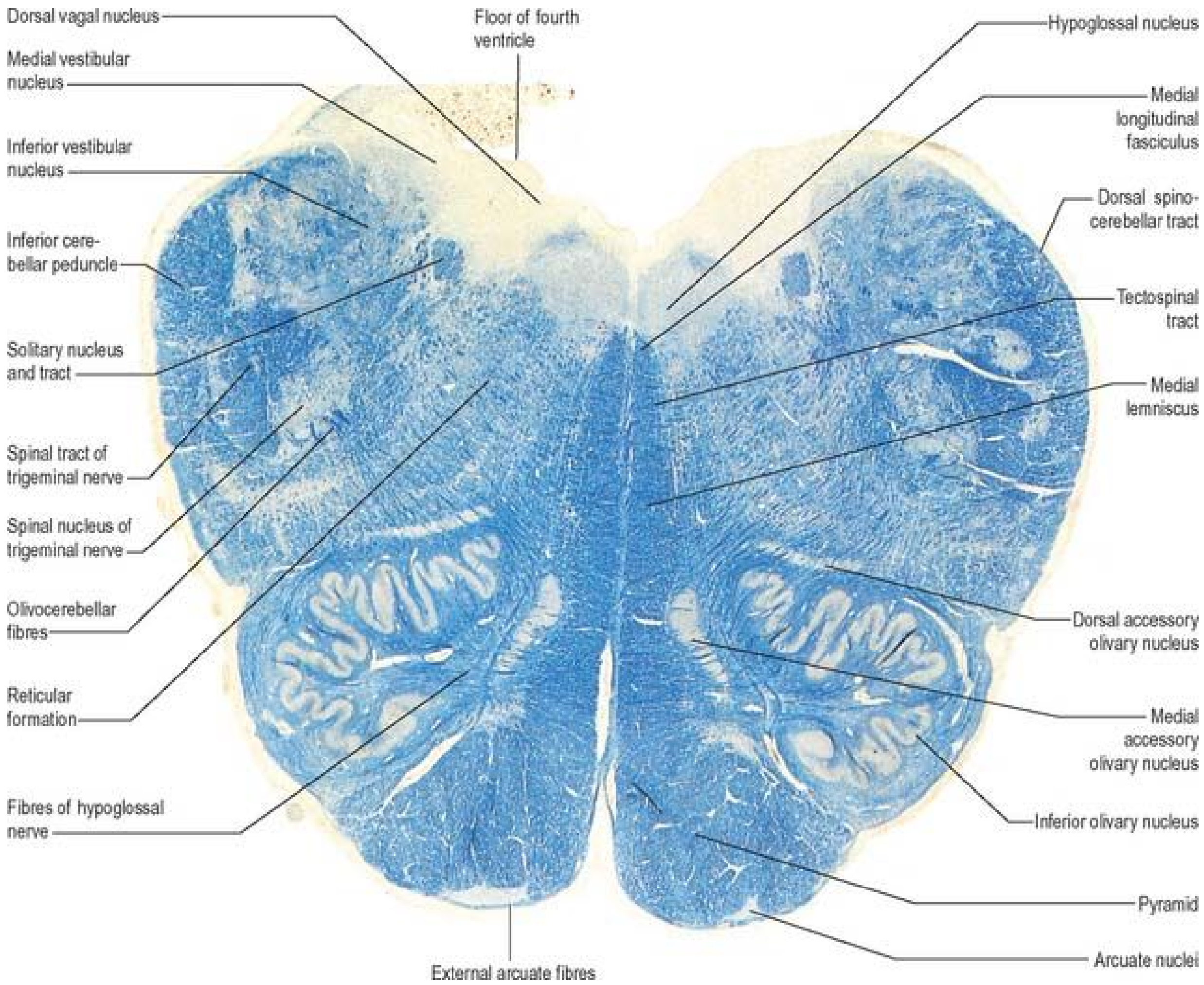
Dorsal vagal nucleus
Medial vestibular nucleus
Inferior vestibular nucleus
Inferior cerebellar peduncle
Solitary nucleus and tract
Spinal tract of trigeminal nerve
Spinal nucleus of trigeminal nerve
Olivocerebellar fibres
Reticular formation
Fibres of hypoglossal nerve
Floor of fourth ventricle
External arcuate fibres
Hypoglossal nucleus
Medial longitudinal fasciculus
Dorsal spinocerebellar tract
Tectospinal tract
Medial lemniscus
Dorsal accessory olivary nucleus
Medial accessory olivary nucleus
Inferior olivary nucleus
Pyramid
Arcuate nuclei

Fig. 19.6 Transverse section through the medulla oblongata at the caudal end of the fourth ventricle.

A smooth, oval elevation, the olive, lies between the ventrolateral and dorsolateral sulci of the medulla. It is formed by the underlying inferior olivary complex of nuclei, and lies lateral to the pyramid, separated from it by the ventrolateral sulcus and emerging hypoglossal nerve fibres. The roots of the facial nerve emerge between its rostral end and the lower pontine border, in the cerebellopontine angle. The arcuate nuclei are curved, interrupted bands, ventral to the pyramids, and are said to be displaced pontine nuclei. Anterior external arcuate fibres and those of the striae medullares are derived from them. They project mainly to the contralateral cerebellum through the inferior cerebellar peduncle (Fig. 19.7).

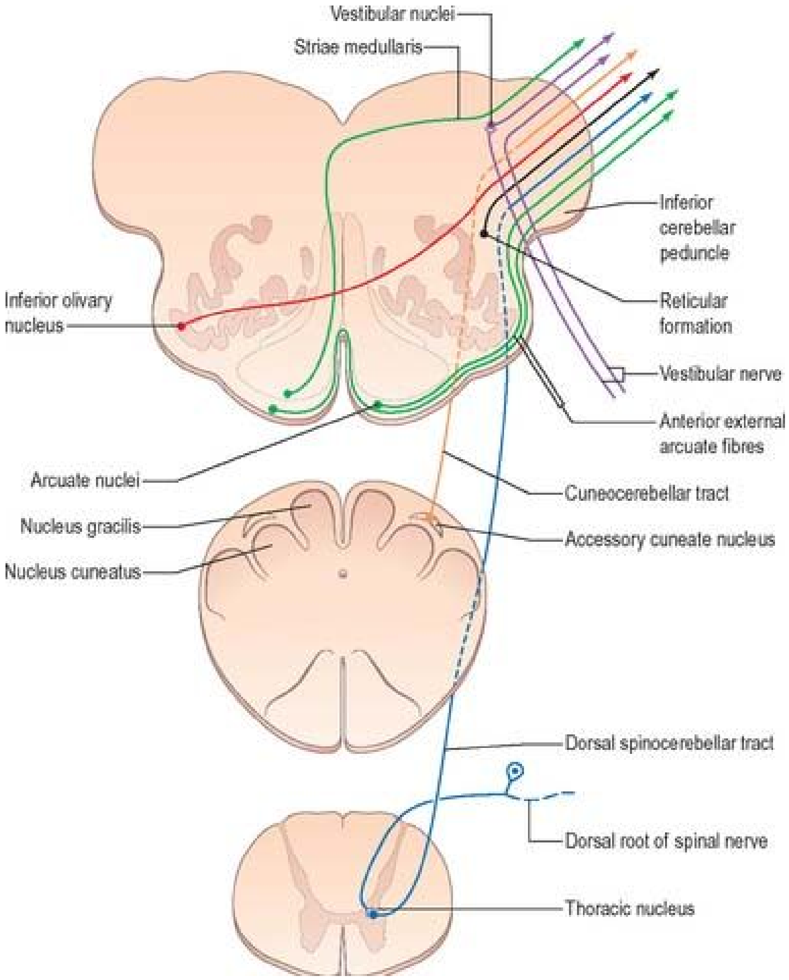
Vestibular nuclei
Striae medullaris
Inferior cerebellar peduncle
Inferior olivary nucleus
Reticular formation
Vestibular nerve
Anterior external arcuate fibres
Arcuate nuclei
Cuneocerebellar tract
Nucleus gracilis
Accessory cuneate nucleus
Nucleus cuneatus
Dorsal spinocerebellar tract
Dorsal root of spinal nerve
Thoracic nucleus

Fig. 19.7 Some of the afferent components of the inferior cerebellar peduncles. The efferent components have been omitted.

The inferior olivary nucleus is an irregularly crenated mass of grey matter with a medially directed hilum, through which numerous fibres enter and leave the nucleus. It has prominent connections with the cerebellum and is described more fully in Chapter 20.

The central grey matter at this level constitutes the ventricular floor. It contains (sequentially from medial to lateral): the hypoglossal nucleus, dorsal motor nucleus of the vagus, nucleus solitarius, and the caudal ends of the inferior and medial vestibular nuclei.

The tractus solitarius and the associated nucleus solitarius extend throughout the length of the medulla. The tract is composed of general visceral afferents from the vagus and glossopharyngeal nerves. The nucleus and its central connections with the reticular formation subserve the reflex control of cardiovascular, respiratory and cardiac functions. The rostral portion of the tract consists of gustatory fibres from the facial, glossopharyngeal and vagal nerves; they project to the rostral pole of the nucleus solitarius, which is sometimes referred to as the gustatory nucleus.

The medial longitudinal fasciculus is a small compact tract near the midline, ventral to the hypoglossal nucleus, that is continuous with the ventral vestibulospinal tract. At this medullary level it is displaced dorsally by the pyramidal and lemniscal decussations. It ascends in the pons and midbrain, maintaining its relationship to the central grey matter and midline, and is therefore near the somatic efferent nuclear column. Fibres from a variety of sources course for short distances in the tract.

The spinocerebellar, spinotectal, vestibulospinal, rubrospinal and lateral spinothalamic (spinal lemniscal) tracts all lie in the ventrolateral area of the medulla at this level. The tracts are limited dorsally by the nucleus of the spinal tract of the trigeminal and ventrally by the pyramid.

Numerous islets of grey matter are scattered centrally in the ventrolateral medulla, an area intersected by nerve fibres that run in all directions. This is the reticular formation, which exists throughout the medulla and extends into the pontine tegmentum and midbrain.

Pyramidal tract

Each pyramid contains descending corticospinal fibres, derived from the ipsilateral cerebral cortex, which have traversed the internal capsule, midbrain and pons (Fig. 19.8). Approximately 70–90% of the axons leave the pyramids in successive bundles, crossing in and deep to the ventral median fissure as the pyramidal decussation. In the rostral medulla fibres cross by inclining ventromedially, whereas more caudally they pass dorsally, decussating ventral to the central grey matter. The decussation is orderly, such that fibres destined to end in the cervical segments cross first. Fibres continue to pass dorsally as they descend, and reach the contralateral spinal lateral funiculus as the crossed lateral corticospinal tract. Most uncrossed corticospinal fibres descend ventromedially in the ipsilateral ventral funiculus, as the ventral corticospinal tract. A minority run dorsolaterally to join the lateral corticospinal tracts as a small uncrossed component. The corticospinal tracts display somatotopy at almost all levels. In the pyramids the arrangement is like that at higher levels, in that the most lateral fibres subserve the most medial arm and neck movements. Similar somatotopy is ascribed to the lateral corticospinal tracts within the spinal cord.

Dorsal column nuclei

The nuclei gracilis and cuneatus are part of the pathway that is the major route for discriminative aspects of tactile and proprioceptive sensation. The upper regions of both nuclei are reticular and contain small and large multipolar neurones with long dendrites. The lower regions contain clusters of large round neurones with short and profusely branching dendrites. Upper and lower zones differ in their connections but both receive terminals from the dorsal spinal roots at all levels. Dorsal funicular fibres from neurones in the spinal grey matter terminate only in the superior, reticular zone. Variable ordering and overlap of terminals, on the basis of spinal root levels, occur in both zones. The lower extremity is represented medially, the trunk ventrally, and the digits dorsally. There is modal specificity, i.e. lower levels respond to low-threshold cutaneous stimuli, and upper reticular levels to inputs from fibres serving receptors in the skin, joints and muscles. The cuneate nucleus is divided into several parts. Its middle zone contains a large pars rotunda, in which rostrocaudally elongated medium-sized neurones are clustered between bundles of densely myelinated fibres. The reticular poles of its rostral and caudal zones contain scattered, but evenly distributed, neurones of various sizes. The pars triangularis is smaller and laterally placed.

There is a somatotopic pattern of termination of cutaneous inputs from the upper limb upon the cell clusters of the pars rotunda. Terminations are diffuse in the reticular poles.

The gracile and cuneate nuclei serve as relays between the spinal cord and higher levels. Primary spinal afferents synapse with multipolar neurones in the nuclei that form the major nuclear efferent projection. The nuclei also contain interneurones, many of which are inhibitory. Descending afferents from the somatosensory cortex reach the nuclei through the corticobulbar tracts, and appear to be restricted to the upper, reticular zones. These afferents both inhibit and enhance activity and are believed to be involved in sensory modulation. The reticular zones also receive connections from the reticular formation.

Neurones of dorsal column nuclei receive terminals of long, uncrossed, primary afferent fibres of the fasciculi gracilis and cuneatus, which carry information concerning deformation of skin, movement of hairs, joint movement and vibration. Unit recording of the neurones in dorsal column nuclei shows that their tactile receptive fields (i.e. the skin area in which a response can be elicited) vary in size, although they are mostly small, and are smallest for the digits. Some fields have excitatory centres and inhibitory surrounds, which means that stimulation just outside its excitatory field inhibits the neurone. Neurones in the nuclei are spatially organized into a somatotopic map of the periphery (in accord with the similar localization in the dorsal columns). In general, specificity is high. Many cells receive input from one or a few specific receptor types, e.g. hair, type I and II slowly adapting receptors and Pacinian corpuscles, and some cells respond to Ia muscle spindle input. However, some neurones receive convergent input from tactile pressure and hair follicle receptors.

A variety of control mechanisms can modulate the transmission of impulses through the dorsal column–medial lemniscus pathway. Concomitant activity in adjacent dorsal column fibres may result in presynaptic inhibition by depolarization of the presynaptic terminals of one of them. Stimulation of the sensory–motor cortex also modulates the transmission of impulses by both pre- and postsynaptic inhibitory mechanisms, and sometimes by facilitation. These descending influences are mediated by the corticospinal tract. Modulation of transmission by inhibition also results from stimulation of the reticular formation, raphe nuclei and other sites.

The accessory cuneate nucleus, dorsolateral to the cuneate nucleus, is part of the spinocerebellar system of precerebellar nuclei (Fig. 19.7). It contains large neurones like those in the spinal thoracic nucleus and receives the lateral fibres of the fasciculus cuneatus, which carry proprioceptive impulses from the upper limb that enter the cervical spinal cord rostral to the thoracic nucleus. The accessory cuneate neurones give rise to the posterior external arcuate fibres that enter the cerebellum by the ipsilateral inferior cerebellar peduncle in the cuneocerebellar tract. A group of neurones, nucleus Z, identified in animals between the upper pole of the nucleus gracilis and the inferior vestibular nucleus, is said to be present in the human medulla. Its input is probably from the dorsal spinocerebellar tract, which carries proprioceptive information from the ipsilateral lower limb, and it projects through internal arcuate fibres to the contralateral medial lemniscus.

Trigeminal sensory nucleus

The trigeminal sensory nucleus receives the primary afferents of the trigeminal nerve. It is a large nucleus, and extends caudally into the cervical spinal cord and rostrally into the midbrain. The principal and largest division of the nucleus is located in the pontine tegmentum.

On entering the pons, the fibres of the sensory root of the trigeminal nerve run dorsomedially towards the principal sensory nucleus, which is situated at this level (Fig. 19.9). Before reaching the nucleus approximately 50% of the fibres divide into ascending and descending branches – the others ascend or descend without division. The descending fibres, of which 90% are less than 4 μm in diameter, form the spinal tract of the trigeminal nerve, which reaches the upper cervical spinal cord. The tract embraces the nucleus of the spinal tract of the trigeminal (spinal trigeminal nucleus; Fig. 19.4, Fig. 19.5, Fig. 19.6, Fig. 19.10, Fig. 19.11). There is a precise somatotopic organization in the tract. Fibres from the ophthalmic division of the trigeminal lie ventrolaterally, those from the mandibular division lie dorsomedially, and the maxillary fibres lie between them. The tract is completed on its dorsal rim by fibres from the sensory roots of the facial, glossopharyngeal and vagus nerves. All of these fibres synapse in the nucleus caudalis.

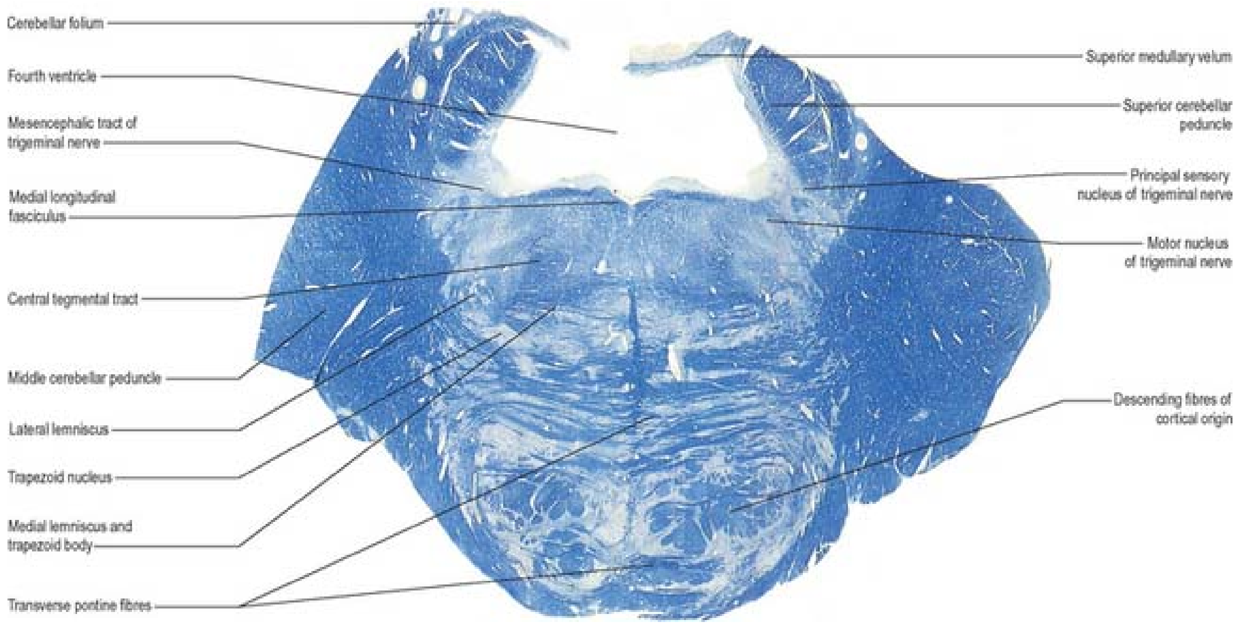
Cerebellar folium
Fourth ventricle
Mesencephalic tract of trigeminal nerve
Medial longitudinal fasciculus
Central tegmental tract
Middle cerebellar peduncle
Lateral lemniscus
Trapezoid nucleus
Medial lemniscus and trapezoid body
Transverse pontine fibres
Superior medullary velum
Superior cerebellar peduncle
Principal sensory nucleus of trigeminal nerve
Motor nucleus of trigeminal nerve
Descending fibres of cortical origin

Fig. 19.9 Transverse section of the pons at the level of the trigeminal nerve.

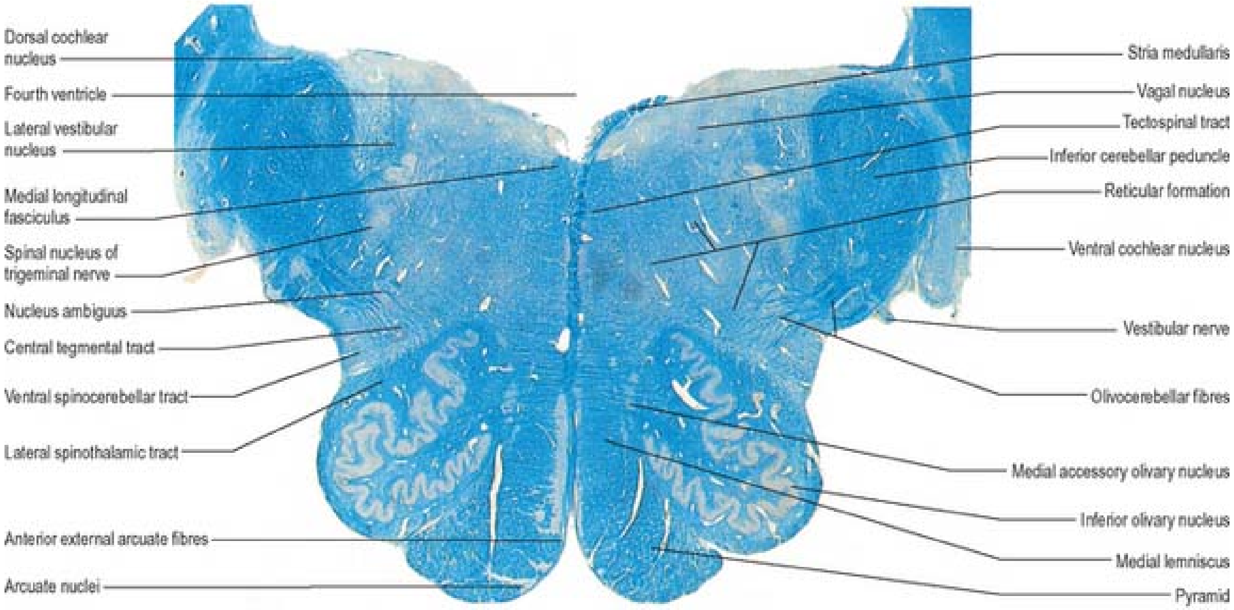
Dorsal cochlear nucleus
Fourth ventricle
Lateral vestibular nucleus
Medial longitudinal fasciculus
Spinal nucleus of trigeminal nerve
Nucleus ambiguus
Central tegmental tract
Ventral spinocerebellar tract
Lateral spinothalamic tract
Anterior external arcuate fibres
Arcuate nuclei
Stria medullaris
Vagal nucleus
Tectospinal tract
Inferior cerebellar peduncle
Reticular formation
Ventral cochlear nucleus
Vestibular nerve
Olivocerebellar fibres
Medial accessory olivary nucleus
Inferior olivary nucleus
Medial lemniscus
Pyramid

Fig. 19.10 Transverse section through the superior half of the medulla oblongata at the level of the inferior olivary nucleus.

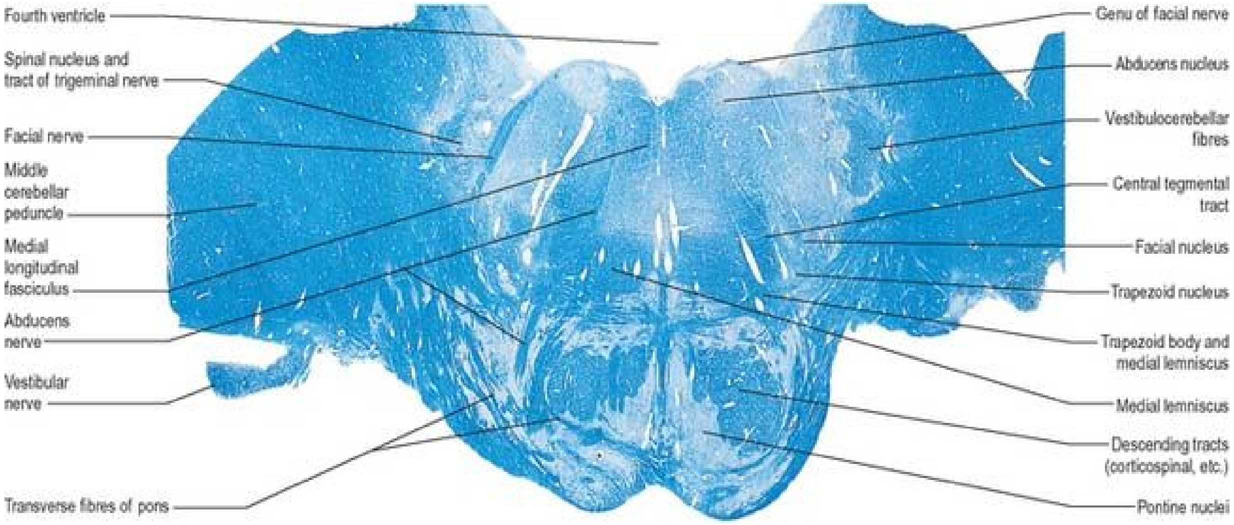
Fourth ventricle
Spinal nucleus and tract of trigeminal nerve
Facial nerve
Middle cerebellar peduncle
Medial longitudinal fasciculus
Abducens nerve
Vestibular nerve
Transverse fibres of pons
Genu of facial nerve
Abducens nucleus
Vestibulocerebellar fibres
Central tegmental tract
Facial nucleus
Trapezoid nucleus
Trapezoid body and medial lemniscus
Medial lemniscus
Descending tracts (corticospinal, etc.)
Pontine nuclei

Fig. 19.11 Transverse section through the pons at the level of the facial colliculus.

The detailed anatomy of the spinal tract of the trigeminal excited early clinical interest because it was recognized that dissociated sensory loss could occur in the trigeminal area. For example, in Wallenberg’s syndrome, occlusion of the posterior inferior cerebellar branch of the vertebral artery leads to loss of pain and temperature sensation in the ipsilateral half of the face with retention of common sensation. Neurosurgery in this region, as early as the 1890s, attempted to alleviate paroxysmal trigeminal neuralgia. The introduction of medullary tractotomy confirmed that dissociated thermoanalgesia of the face was associated with destruction of the tract.

There are conflicting opinions on the pattern of termination of the fibres in the spinal nucleus. It has long been held that fibres are organized rostrocaudally within the tract. According to this view, ophthalmic fibres are ventral and descend to the lower limit of the first cervical spinal segment, maxillary fibres are central and do not extend below the medulla oblongata, whilst mandibular fibres are dorsal and do not extend much below the mid-medullary level. The results of section of the spinal tract in cases of severe trigeminal neuralgia support this distribution. It was found that a section 4 mm below the obex rendered the ophthalmic and maxillary areas analgesic but tactile sensibility, apart from the abolition of ‘tickle’, was much less affected. To include the mandibular area it was necessary to section at the level of the obex. More recently, it has been proposed that fibres are arranged dorsoventrally within the spinal tract. There appear to be sound anatomico-physiological and clinical reasons for believing that all divisions terminate throughout the whole nucleus, although the ophthalmic division may not project fibres as far caudally as the maxillary and mandibular divisions. Fibres from the posterior face (adjacent to C2) terminate in the lower (caudal) part, whilst those from the upper lip, mouth and nasal tip terminate at a higher level. This can give rise to a segmental (cross-divisional) sensory loss in syringobulbia. Tractotomy of the spinal tract, if carried out at a lower level, can spare the perioral region, a finding that would accord with the ‘onion-skin’ pattern of loss of pain sensation. However, in clinical practice, the progression of anaesthesia on the face is most commonly ‘divisional’ rather than onion-skin in distribution.

Fibres of the glossopharyngeal, vagus and facial nerves subserving common sensation (general visceral afferent) form a column dorsally within the spinal tract of the trigeminal nerve and synapse with cells in the lowest part of the spinal trigeminal nucleus. Consequently, operative section of the dorsal part of the spinal tract results in analgesia that extends to the mucosa of the tonsillar sinus, the posterior third of the tongue and adjoining parts of the pharyngeal wall (glossopharyngeal nerve), and the cutaneous area supplied by the auricular branch of the vagus.

Other afferents that reach the spinal nucleus are from the dorsal roots of the upper cervical nerves and from the sensorimotor cortex.

The spinal nucleus is considered to consist of three parts: the subnucleus oralis (which is most rostral and adjoins the principal sensory nucleus); the subnucleus interpolaris; and the subnucleus caudalis (which is the most caudal part and is continuous below with the dorsal grey column of the spinal cord). The structure of the subnucleus caudalis is different from that of the other subnuclei. It has a structure analogous to that of the dorsal horn of the spinal cord, with a similar arrangement of cell laminae, and is involved in trigeminal pain perception. Cutaneous nociceptive afferents and small-diameter muscle afferents terminate in layers I, II, V and VI of the subnucleus caudalis. Low-threshold mechanosensitive afferents of Aβ neurones terminate in layers III and IV of the subnucleus caudalis and rostral (interpolaris, oralis and main sensory) nuclei.

Many of the neurones in the subnucleus caudalis that respond to cutaneous or tooth-pulp stimulation are also excited by stimulation of jaw or tongue muscles. This indicates that convergence of superficial and deep afferent inputs via wide-dynamic-range or nociceptive-specific neurones occurs in the nucleus. Similar convergence of superficial and deep inputs occurs in the rostral nuclei and may account for the poor localization of trigeminal pain, and for the spread of pain, which often makes diagnosis difficult.

There are distinct subtypes of cells in lamina II. Afferents from ‘higher-centres’ arborize within it, as do axons from nociceptive and low-threshold afferents. Descending influences from these higher centres include fibres from the periaqueductal grey matter and from the nucleus raphe magnus and associated reticular formation.

The nucleus raphe magnus projects directly to the subnucleus caudalis, probably via enkephalin, noradrenaline and 5-HT-containing terminals. These fibres directly or indirectly (through local interneurones) influence pain perception. Stimulation of periaqueductal grey matter or nucleus raphe magnus inhibits the jaw opening reflex to nociception, and may induce primary afferent depolarization in tooth-pulp afferents and other nociceptive facial afferents. Neurones in the subnucleus caudalis can be suppressed by stimuli applied outside their receptive field, particularly by noxious stimuli. The subnucleus caudalis is an important site for relay of nociceptive input and functions as part of the pain ‘gate-control’. However, rostral nuclei also have a nociceptive role. Tooth-pulp afferents via wide-dynamic-range and nociceptive-specific neurones may terminate in rostral nuclei, which all project to the subnucleus caudalis.

Most fibres arising in the trigeminal sensory nuclei cross the midline and ascend in the trigeminal lemniscus. They end in the contralateral thalamic nucleus ventralis posterior medialis, from which third-order neurones project to the cortical postcentral gyrus (areas 1, 2 and 3). However, some trigeminal nucleus efferents ascend to the nucleus ventralis posterior medialis of the ipsilateral thalamus.

Fibres from the subnucleus caudalis, especially from laminae I, V and VI, also project to the rostral trigeminal nuclei, cerebellum, periaqueductal grey of the midbrain, parabrachial area of the pons, the brain stem reticular formation and the spinal cord. Fibres from lamina I project to the subnucleus medius of the medial thalamus.

Vagal nucleus

The vagal nucleus (also known as the dorsal motor nucleus of the vagus) lies dorsolateral to the hypoglossal nucleus, from which it is separated by the nucleus intercalatus. It extends caudally to the first cervical spinal segment and rostrally to the open part of the medulla under the vagal triangle of the floor of the fourth ventricle (Fig. 19.6).

The vagal nucleus is a general visceral efferent nucleus and is the largest parasympathetic nucleus in the brain stem. Most (80%) of its neurones give rise to the preganglionic parasympathetic fibres of the vagus nerve. The remainder are interneurones or project centrally. The vagal nucleus controls the non-striated muscle of the viscera of the thorax (heart, bronchi, lungs and oesophagus) and abdomen (stomach, liver, pancreas, spleen, small intestine and proximal part of the colon). Neurones within the nucleus are heterogeneous and can be classified into nine subnuclei, which are regionally grouped into rostral, intermediate and caudal divisions. Topographic maps of visceral representation in animals suggest that the heart and lungs are represented in the caudal and lateral part of the nucleus, the stomach and pancreas in intermediate regions, and the remaining abdominal organs in the rostral and medial part of the nucleus.

There may be a sparse sensory afferent supply, which arises in the nodose ganglion and projects directly to the nucleus and possibly beyond into the nucleus tractus solitarius.

Hypoglossal nucleus

The prominent hypoglossal nucleus lies near the midline in the dorsal medullary grey matter. It is approximately 2 cm long. Its rostral part lies beneath the hypoglossal triangle in the floor of the fourth ventricle (Fig. 19.3) and its caudal part extends into the closed part of the medulla.

The hypoglossal nucleus consists of large motor neurones interspersed with myelinated fibres. It is organized into dorsal and ventral nuclear tiers, each divisible into medial and lateral subnuclei. There is a musculotopic organization of motor neurones within the nuclei that corresponds to the structural and functional divisions of tongue musculature. Thus, motor neurones innervating tongue retrusor muscles are located in dorsal/dorsolateral subnuclei, whereas motor neurones innervating the main tongue protrusor muscle are located in ventral/ventromedial regions of the nucleus. Although relatively little is known about the organization of motor neurones innervating the intrinsic muscles of the tongue, experimental evidence suggests that motor neurones of the medial division of the hypoglossal nucleus innervate tongue muscles that are oriented in planes transverse to the long axis of the tongue (transverse and vertical intrinsics and genioglossus), whereas motor neurones of the lateral division innervate tongue muscles that are oriented parallel to this axis (styloglossus, hyoglossus, superior and inferior longitudinal).

Several smaller groups of cells lie near the hypoglossal nucleus (perihypoglossal nuclei), but none is known for certainty to be connected with the hypoglossal nerve or nucleus. They include the nucleus intercalatus, sublingual nucleus, nucleus prepositus hypoglossi and nucleus paramedianus dorsalis (reticularis). Gustatory and visceral connections are attributed to the nucleus intercalatus.

Hypoglossal fibres emerge ventrally from their nucleus, traverse the reticular formation lateral to the medial lemniscus, pass medial to (sometimes through) the inferior olivary nucleus, and curve laterally to emerge as a linear series of 10–15 rootlets in the ventrolateral sulcus between the pyramid and olive.

The hypoglossal nucleus receives corticobulbar fibres from the precentral gyrus and adjacent areas of (mainly) the contralateral hemisphere. They either synapse on motor neurones of the nucleus directly or on interneurones. Evidence indicates that the most medial hypoglossal subnuclei receive projections from both hemispheres. The nucleus may connect with the cerebellum via adjacent perihypoglossal nuclei, and perhaps also with the medullary reticular formation, the trigeminal sensory nuclei and the solitary nucleus.

Inferior olivary nucleus

The olivary nuclear complex consists of the large inferior olivary nucleus and the much smaller medial accessory and dorsal accessory olivary nuclei (Fig. 19.6). They are the so-called precerebellar nuclei, a group that also includes the pontine, arcuate, vestibular, reticulocerebellar and spinocerebellar nuclei, all of which receive afferents from specific sources and project to the cerebellum. The inferior olivary nucleus contains small neurones, most of which form the olivocerebellar tract, which emerges either from the hilum or through the adjacent grey matter, to run medially and intersect the medial lemniscus (Fig. 19.6). Its fibres cross the midline, and sweep either dorsal to, or through, the opposite olivary nucleus. They intersect the lateral spinothalamic and rubrospinal tracts and the spinal trigeminal nucleus, and enter the contralateral inferior cerebellar peduncle, where they constitute its major component. Fibres from the contralateral inferior olivary complex terminate on Purkinje cells in the cerebellum as climbing fibres – there is a one-to-one relationship between Purkinje cells and neurones in the complex. Afferent connections to the inferior olivary nucleus are both ascending and descending. Ascending fibres, mainly crossed, arrive from all spinal levels in the spino-olivary tracts and via the dorsal columns. Descending ipsilateral fibres come from the cerebral cortex, thalamus, red nucleus and central grey of the midbrain. In part the two latter projections make up the central tegmental tract (fasciculus).

The medial accessory olivary nucleus is a curved grey lamina, concave laterally, between the medial lemniscus and pyramid and the ventromedial aspect of the inferior olivary nucleus. The dorsal accessory olivary nucleus is a similar lamina, dorsomedial to the inferior olivary nucleus. Both nuclei are connected to the cerebellum. The accessory olivary nuclei are phylogenetically older than the inferior olivary nucleus, and they are connected with the paleocerebellum. In all connections, cerebral, spinal and cerebellar, the olivary nuclei display specific topographical organization (Ch. 20).

Nucleus solitarius

The nucleus solitarius (solitary nucleus, nucleus of the solitary tract) lies ventrolateral to the vagal nucleus and is almost coextensive with it. A neuronal group ventrolateral to the nucleus solitarius has been termed the nucleus parasolitarius. The nucleus solitarius is intimately related to, and receives fibres from, the tractus solitarius, which carries afferent fibres from the facial, glossopharyngeal and vagus nerves. These fibres enter the tract in descending order and convey gustatory information from the lingual and palatal mucosa. They may also convey visceral impulses from the pharynx (glossopharyngeal and vagus) and from the oesophagus and abdominal alimentary canal (vagus). There is some overlap in this vertical representation.

Termination of special visceral gustatory afferents within the nucleus shows a viscerotopic pattern, predominantly in the rostral region. Experimental evidence suggests that fibres from the anterior two-thirds of the tongue and the roof of the oral cavity (which travel via the chorda tympani and greater petrosal branches of the facial nerve) terminate in the extreme rostral part of the solitary complex. Those from the circumvallate and foliate papillae of the posterior third of the tongue, tonsils, palate and pharynx (which travel via the lingual branch of the glossopharyngeal nerve) are distributed throughout the rostrocaudal extent of the nucleus, predominantly rostral to the obex. Gustatory afferents from the larynx and epiglottis (which travel via the superior laryngeal branch of the vagus) have a more caudal and lateral distribution. The nucleus solitarius may also receive fibres from the spinal cord, cerebral cortex and cerebellum.

Medial and commissural subnuclei in the caudal part of the nucleus appear to be the primary site of termination for gastrointestinal afferents. Ventral and interstitial subnuclei probably receive tracheal, laryngeal and pulmonary afferents and play an important role in both respiratory control and possibly rhythm generation. The carotid sinus and aortic body nerves terminate in the dorsal and dorsolateral region of the nucleus solitarius, which may be involved in cardiovascular regulation.

The nucleus solitarius is thought to project to the sensory thalamus and thence to the cerebral cortex. It may also project to the upper levels of the spinal cord through a solitariospinal tract. Secondary gustatory axons cross the midline. Many subsequently ascend the brain stem in the dorsomedial part of the medial lemniscus and synapse on the most medial neurones of the thalamic nucleus ventralis posterior medialis (in a region sometimes termed the accessory arcuate nucleus). Axons from the nucleus ventralis posterior medialis radiate through the internal capsule to the anteroinferior area of the sensorimotor cortex and the insula. It is thought that other ascending paths end in a number of the hypothalamic nuclei, and so mediate the route by which gustatory information may reach the limbic system and allow appropriate autonomic reactions to be made.

Swallowing and gag reflexes

During the normal processes of eating and drinking, passage of material to the rear of the mouth stimulates branches of the glossopharyngeal nerve in the oropharynx (Fig. 19.12). This information is relayed via the nucleus solitarius to the nucleus ambiguus, which contains the motor neurones innervating the muscles of the palate, pharynx, and larynx. The nasopharynx is closed off from the oropharynx by elevation of the soft palate. The larynx is raised, its entrance narrowed and the glottis is closed. Peristaltic activity down the oesophagus to the stomach is mediated through the pharyngeal plexus.

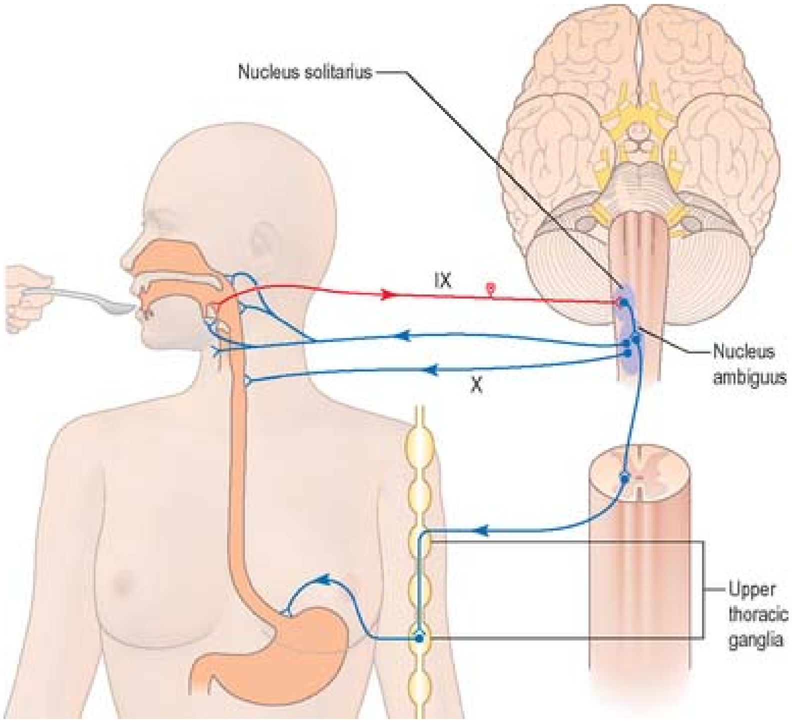

Fig. 19.12 Swallowing and gag reflexes.

If stimulation of the oropharynx occurs, other than during swallowing, the gag reflex may be initiated. There is a reflex contraction of the muscles of the pharynx, soft palate, and fauces that, if extreme, may result in retching and vomiting.

Nucleus ambiguus

The nucleus ambiguus is a group of large motor neurones, situated deep in the medullary reticular formation (see Fig. 19.10). It extends rostrally as far as the upper end of the vagal nucleus while caudally it is continuous with the nucleus of the spinal accessory nerve. Fibres emerging from it pass dorsomedially, then curve laterally. Rostral fibres join the glossopharyngeal nerve. Caudal fibres join the vagus and cranial accessory nerves and are distributed to the pharyngeal constrictors, intrinsic laryngeal muscles and striated muscles of the palate and upper oesophagus.

The nucleus ambiguus contains several cellular subgroups, and some topographical representation of the muscles innervated has been established. Individual laryngeal muscles are innervated by relatively discrete groups of cells in more caudal zones. Neurones that innervate the pharynx lie in the intermediate area, and neurones that innervate the oesophagus and soft palate are rostral.

The nucleus ambiguus receives corticobulbar fibres bilaterally and is connected to many brain stem centres. At its upper end, a small retrofacial nucleus intervenes between it and the facial nucleus. Although the nucleus ambiguus is generally regarded as a special visceral efferent nucleus, it is also a reputed source of general visceral efferent fibres to the vagus.

Cough and sneeze reflexes

Irritation of the larynx or trachea is conveyed via laryngeal branches of the vagus nerve to the trigeminal sensory nucleus of the brain stem. Impulses are relayed to medullary respiratory centres and to the nucleus ambiguus. Forceful exhalation (coughing) occurs, caused by contraction of intercostal and abdominal wall muscles after a build-up of pressure against an initially closed glottis.

A similar mechanism underlies sneezing (Fig. 19.13) except that the stimulus arises from the nasal mucosa and afferent impulses are conveyed by the ophthalmic or maxillary divisions of the trigeminal nerve to the trigeminal sensory nucleus. After sharp inhalation, explosive exhalation occurs with closure of the oropharyngeal isthmus by the action of palatoglossus, which diverts air through the nasal cavity.

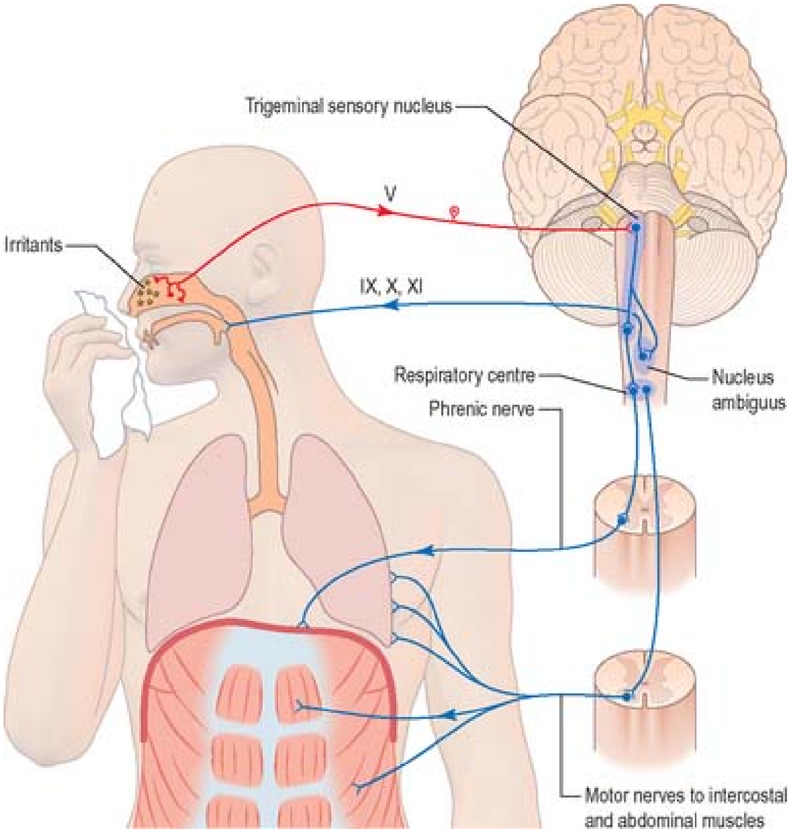
Trigeminal sensory nucleus
V
Irritants
IX, X, XI
Respiratory centre
Phrenic nerve
Nucleus ambiguus
Motor nerves to intercostal and abdominal muscles

Fig. 19.13 Sneeze and cough reflexes.

PONS

EXTERNAL FEATURES AND RELATIONS

The pons lies rostral to the medulla and caudal to the midbrain. On the ventral surface of the brain stem, the transition between medulla and pons is clearly demarcated by a transverse sulcus. Laterally, in a region known as the cerebellopontine angle, the facial, vestibulocochlear and glossopharyngeal nerves emerge. The ventral surface of the pons is separated from the clivus (basisphenoid and dorsum sellae) by the cisterna pontis. It is markedly convex transversely, less so vertically, and grooves the petrous part of the temporal bone laterally up to the internal acoustic meatus. The surface has a shallow median sulcus, in which the basilar artery runs, bounded bilaterally by prominences that are formed partly by underlying corticospinal fibres as they descend through the pons. Bundles of transverse fibres, bridging the midline and originating from nuclei in the basal pons (nuclei pontis, pontine nuclei), converge on each side into the large middle cerebellar peduncle and project to the cerebellum. The trigeminal nerve emerges near the midpontine level. It has a small superomedial motor root and a large inferolateral sensory root.

The dorsal surface of the pons is hidden by the cerebellum which covers the rostral half of the rhomboid fossa, into which the aqueduct of the midbrain empties. The roof of the fossa is formed by a thin sheet of tissue, the superior (anterior) medullary velum, and is overlain by the lingula of the vermis of the cerebellum. The velum is attached on each side to the superior cerebellar peduncles and is enclosed by pia mater above and ependyma below (Fig. 19.3). The trochlear nerves decussate in the velum.

INTERNAL STRUCTURE

Transverse sections of the pons

Transverse sections (Fig. 19.9, Fig. 19.11) reveal that the pons consists of a dorsal tegmentum, which is a continuation of the medulla (excluding the pyramids), and a ventral (basilar) part. The latter contains bundles of longitudinal descending fibres, some of which continue into the pyramids, while others end in the many pontine or medullary nuclei. It also contains numerous transverse fibres and scattered pontine nuclei.

Ventral pons

The ventral pons is similar in structure at all levels. The longitudinal fibres of the corticopontine, corticobulbar and corticospinal tracts descend from the crus cerebri of the midbrain and enter the pons compactly. They rapidly disperse into fascicles, which are separated by the pontine nuclei and transverse pontine fibres. Corticospinal fibres run uninterrupted through the pons to the medullary pyramids, where they again converge into compact tracts. Corticobulbar fibres terminate in contralateral (and some ipsilateral) nuclei of cranial nerves and other nuclei in the pontine tegmentum. Clinical evidence supports the view that the neurones of the facial nucleus, and in particular, those serving the muscles of the upper face, receive bilateral cortical control.

The pontine nuclei (Fig. 19.11) include all the neurones (in man, some 20 million) that are scattered throughout the ventral pons. They are probably all glutamatergic, and most project to the contralateral cerebellar cortex, with some input to the deep cerebellar nuclei. Efferent axons from the pontine nuclei constitute the transverse pontine (pontocerebellar) fibres which decussate and continue as the major constituent of the contralateral middle cerebellar peduncle. All pontocerebellar fibres end as mossy fibres in the cerebellar cortex, and a degree of somatotopy is maintained in these connections.

Corticopontine fibres, from the frontal, temporal, parietal and occipital cortices, end upon neurones in the pontine nuclei. Frontopontine fibres end rostral to the level of the trigeminal nerve, and connect with pontine neurones which project to the contralateral cerebellum in the more rostral transverse pontine fibres. Corticopontine fibres arise mainly from neurones in layer V of the premotor, somatosensory, posterior parietal, extrastriate visual and cingulate neocortices. Projections from prefrontal, temporal and striate cortices are sparse. The terminal fields, although divergent, form topographically segmented patterns resembling overlapping columns, slabs or lamellae within the pons.

Subcortical projections to the pontine nuclei include those from the superior colliculus to the dorsolateral pons, and the medial mammillary nucleus to the rostromedial pons and pretectal nuclei. The lateral geniculate nucleus, dorsal column nuclei, trigeminal nuclei, hypothalamus and intracerebellar nuclei also project to restricted neurones of the pons. Functionally related subcortical and cerebrocortical afferents converge, e.g. those from the somatosensory cortex and dorsal column nuclei. There is also non-specific input from the reticular formation, raphe nuclei, locus coeruleus and paraqueductal grey matter.

Pontine tegmentum

The pontine tegmentum varies in cytoarchitecture at different levels. A transverse section through the lower pontine tegmentum transects the facial colliculus in the floor of the fourth ventricle (Fig. 19.11, Fig. 19.14). The colliculus contains the nucleus of the abducens nerve and the overlying fibres of the facial nerve. More deeply placed are the facial nuclei, the nearby vestibular and cochlear nuclei and other isolated neuronal groups. The vestibular nuclei are laterally placed in the rhomboid fossa of the fourth ventricle, subjacent to the vestibular area, which spans the rostral medulla and caudal pons (Fig. 19.1, Fig. 19.3).

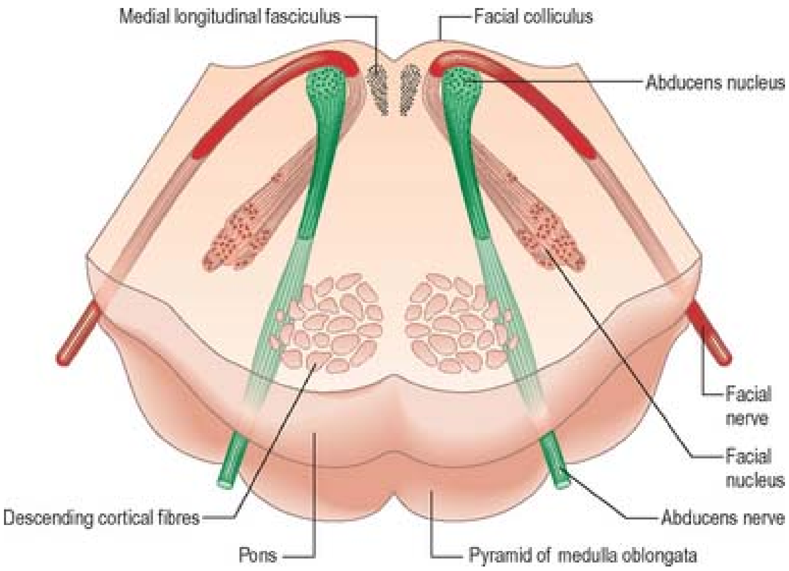
Medial longitudinal fasciculus
Facial colliculus
Abducens nucleus
Facial nerve
Facial nucleus
Abducens nerve
Descending cortical fibres
Pons
Pyramid of medulla oblongata

Fig. 19.14 Transverse section of the pons, viewed from the rostral aspect, showing the central course of fibres of the facial nerve.

The striae medullares of the fourth ventricle (Fig. 19.10) are an aberrant cerebropontocerebellar connection, in which the arcuate nuclei and external arcuate fibres are involved. Axons from arcuate nuclei spread round the medulla, above and below the inferior olive, where they are superficially visible as the circumolivary fasciculus. All these fibres, which collectively are known as the external arcuate fibres, enter the inferior cerebellar peduncle (Fig. 19.7). Some fibres from arcuate nuclei pass dorsally through the medulla near its midline, decussate near the floor of the fourth ventricle, then turn laterally under the ependyma and enter the cerebellum through the inferior peduncle.

In addition to the tracts already noted at lower levels, the lower pontine tegmentum contains the trapezoid body, lateral lemniscus and emerging fibres of the abducens and facial nerves. The medial lemniscus is ventral, its transverse outline now a flat oval. It extends laterally from the median raphe (Fig. 19.9, Fig. 19.11) and is laterally related to the lateral spinothalamic tract and trigeminal lemniscus. The fibres of the latter originate from neurones of the contralateral spinal nucleus, serving pain and thermal sensibility in facial skin and mucosae of the conjunctiva, tongue, mouth, nose, etc. Here the lemnisci together form a transverse band which is composed, in lateral order from the midline, of the medial and trigeminal lemnisci, the lateral spinothalamic tract and the lateral lemniscus.

The trapezoid body contains cochlear fibres, mainly from the ventral cochlear and trapezoid nuclei. They ascend transversely in the ventral tegmentum, pass either through or ventral to the vertical medial lemniscal fibres, and decussate with the contralateral fibres in the median raphe. Below the emerging facial axons, the trapezoid fibres turn up into the lateral lemniscus. As the lateral lemniscus ascends it lies near the dorsolateral surface of the brain stem. Above, its fibres enter the inferior colliculus and medial geniculate body. The ascending auditory pathway is described in detail in Chapter 37.

The medial longitudinal fasciculus is paramedian, ventral to the fourth ventricle, near the abducens nucleus from which it is separated by facial nerve fibres. It is the main intersegmental tract in the brain stem, particularly for interactions between nuclei of cranial nerves innervating the extraocular muscles and the vestibular system. In the lower pons it receives fibres from vestibular, and perhaps dorsal trapezoid, nuclei. Its greater part is formed by vestibular contributions.

A transverse section at an upper pontine tegmental level contains trigeminal elements (Fig. 19.9), but otherwise shows little notable alteration from a section through a lower pontine tegmental level. Its dorsolateral parts are invaded by the superior cerebellar peduncles. The small nucleus of the lateral lemniscus, a relay in the auditory pathway, lies medial to its tract in the upper pons, and receives some lemniscal terminals. Some of its efferent fibres enter the medial longitudinal fasciculus, others return to the lemniscus.

The medial lemniscus (Fig. 19.9, Fig. 19.11) retains its paramedian position in the ventral pontine tegmentum, where it lies a little lateral to the median raphe, and is joined medially by fibres from the principal trigeminal sensory nucleus. The trigeminal lemniscus, lateral spinothalamic tract, and the lateral lemniscus and its nucleus all lie dorsolaterally.

Cochlear nuclei

Fibres of the cochlear division of the vestibulocochlear nerve partially encircle the inferior cerebellar peduncle laterally and end in the dorsal and ventral cochlear nuclei. The dorsal cochlear nucleus forms a bulge, the auditory tubercle, on the posterior surface of the peduncle, and is continuous medially with the vestibular area in the rhomboid fossa. The ventral cochlear nucleus is ventrolateral to the dorsal cochlear nucleus, and lies between the cochlear and vestibular fibres of the vestibulocochlear nerve.

Cochlear nerve fibres, which are derived from neuronal somata in the spiral ganglion, bifurcate on entering the brain stem and terminate in both dorsal and ventral cochlear nuclei (see Fig. 37.20).

The ventral cochlear nucleus has a complex cytoarchitecture. It contains many neuronal types with distinct dendritic field characteristics. Marked topographical order has been demonstrated in cochlear nerve terminals within the nucleus. Different parts of the spiral ganglion and differing stimulation frequencies are related to neurones that are serially arrayed anteroinferiorly in the ventral nucleus. All cochlear nerve fibres enter the nucleus. There are approximately 25,000 axons in the human cochlear nerve, and they project onto a much larger number of neurones in the cochlear nucleus. The number of cochlear fibres in the lateral lemniscus greatly exceeds that in the cochlear nerve. A minor fraction of the cochlear neurones receive terminals from the nerve, though each fibre may connect with several neurones. Terminals are limited to the anteroinferior region of the ventral nucleus, where the neurones are probably mostly local interneurones.

The dorsal cochlear nucleus is almost continuous with the ventral nucleus, from which it is only separated by a thin stratum of nerve fibres. Giant cells predominate, and their dendritic fields are aligned with the incoming auditory fibres.

Though the cellular origins are not precisely known, axons of most neuronal types in the cochlear nuclei leave to end at pontine levels in the superior olivary, trapezoid and lateral lemniscal nuclei (Fig. 19.9). They leave the cochlear nuclei by three routes. The largest group of axons lies ventrally and decussates as the trapezoid body, level with the pontomedullary junction (Fig. 19.9, Fig. 19.11). Most of these axons ascend slightly, decussate and relay in the contralateral nuclei. A few do not cross, and synapse in the ipsilateral superior olivary nuclei. From both nuclei, the next order axons ascend in the corresponding lateral lemniscus. Occasional decussating fibres traverse the contralateral superior olive and enter the lateral lemniscus to relay in lemniscal nuclei.

Some axons from ventral cochlear neurones pass dorsally, superficial to descending trigeminal spinal fibres, cerebellar fibres in the inferior peduncle, and axons of the dorsal cochlear nucleus. This bundle of ventral cochlear fibres is smaller than that of the trapezoid decussation. It swerves ventromedially across the midline, ventral to the medial longitudinal fasciculus, as the intermediate acoustic striae. Its further path is uncertain, but it probably ascends in the contralateral lateral lemniscus.

The most dorsally placed axons issue from the dorsal cochlear nucleus. They curve dorsomedially round the inferior cerebellar peduncle towards the midline as the dorsal acoustic striae, ventral to the striae medullares. They incline ventromedially and cross the midline to ascend in the contralateral lateral lemniscus, probably relaying in its nuclei.

The superior olivary complex is sited in the tegmentum of the caudal pons, lateral in the reticular formation at the level of the pontomedullary junction. The superior complex includes several named nuclei and nameless smaller groups. In humans, the lateral superior olivary nucleus is made up of some six small cellular clusters. The medial (accessory) superior olivary nucleus is large and compact. The trapezoid nucleus is medial. A retro-olivary group, the reputed origin of some efferent cochlear fibres, is dorsal. Some internuclear connections have been described. The medial superior olivary nucleus receives impulses from both spiral organs, and may be involved in sound source localization. The superior olivary complexes and the trapezoid nuclei are relay stations in the ascending auditory projection. These intricate connections have not been well established in man.

The medial nucleus of the trapezoid body is small in man. It has a ventral component, which consists of large neurones scattered among the trapezoid fascicles, and a more compact dorsal nucleus, medial to the superior olivary complex. The nucleus lies at the level of the exiting abducens nerve roots, anterior to the central tegmental tract. It is not known whether the human trapezoid nuclei function in the auditory relay. Some trapezoid axons may enter the medial longitudinal fasciculus, and ascend to end in trigeminal, facial, oculomotor, trochlear and abducens nuclei, where they mediate reflexes involving tensor tympani, stapedius and oculogyric muscles, respectively.

The nucleus of the lateral lemniscus consists of small groups of neurones (counts of 18,000 to 24,000 have been recorded in humans) that lie among the fibres of the lateral lemniscus. Dorsal, ventral and intermediate groups probably receive afferent axons from both cochlear nuclei. Their efferents enter the midbrain along the lateral lemniscus and terminate in the inferior colliculi.

Some efferent axons travel in the cochlear nerves to the spiral organ. Though few in number, they may be involved in hearing, perhaps by modulating sensory transduction through reflexes via cochlear nuclei. The neurones of origin are located at the hilus and along the lateral border of the lateral superior olivary nucleus and lateral edge of the ventral trapezoid nucleus. Fibres from both sides proceed to both cochleae.

Vestibular nuclei

The vestibular complex consist of the medial, lateral (Deiters’ nucleus), superior and inferior vestibular nuclei. The medial vestibular nucleus is the largest. It broadens, then narrows as it ascends from the upper olivary level into the lower pons, where it separates the vagal nucleus from the floor of the fourth ventricle. It is crossed by the striae medullares, running nearer the floor, and is continuous with the nucleus intercalates below. The inferior vestibular nucleus (which is the smallest) lies between the medial vestibular nucleus and inferior cerebellar peduncle, from the level of the upper end of the nucleus gracilis to the pontomedullary junction. It is crossed by descending fibres of the vestibulocochlear nerve and the vestibulospinal tract. The lateral vestibular nucleus lies just above the inferior nucleus and is ventrolateral to the upper part of the medial nucleus. It ascends almost to the level of the abducens nucleus and its rostral end is continuous with the caudal end of the superior nucleus. The lateral vestibular nucleus is composed of large multipolar neurones, which are the main source of the vestibulospinal tract. The superior vestibular nucleus is small and lies above the medial and lateral nuclei. It extends higher into the pons than other subdivisions, and occupies the upper part of the vestibular area.

Through its connections, the vestibular system influences movements of the eyes and head, and of the muscles of the trunk and limbs, in order to maintain equilibrium. The vestibular nuclei receive fibres from the vestibular part of the vestibulocochlear nerve, cerebellum, brain stem reticular formation and spinal cord. They send axons to the cerebellum, medial longitudinal fasciculus, spinal cord and lateral lemniscus. Evidence suggests that the vestibular apparatus is spatially represented in the nuclei. Vestibular fibres of the vestibulocochlear nerve enter the medulla between the inferior cerebellar peduncle and the trigeminal spinal tract, and approach the vestibular area, where they bifurcate into descending and ascending branches. The former descend medial to the inferior cerebellar peduncle and end in medial, lateral and inferior vestibular nuclei, and the latter enter the superior and medial nuclei. A few vestibular fibres enter the cerebellum directly through the inferior peduncle (superficially in the juxtarestiform body), and end in the fastigial nucleus, flocculonodular lobe and uvula.

The vestibular nuclei project extensively to the cerebellum and also receive axons from the cerebellar cortex and the fastigial nuclei. Vestibulocerebellar fibres travel via the inferior cerebellar peduncle mainly to the flocculus and nodule. Cerebellovestibular fibres pass to the nuclei, also through the inferior cerebellar peduncle. They arise mainly in the flocculus and nodule (posterior lobe), but some fibres are derived from the anterior lobe and fastigial nucleus. The vestibular nuclear complex projects to the pontine reticular nuclei and to motor nuclei of the oculogyric muscles in the medial longitudinal fasciculus. The complex also projects to the spinal cord via the vestibulospinal tracts and the medial longitudinal fasciculus (see Fig. 18.19).

Information from the vestibular nuclei also reaches the cerebral cortex by way of the thalamus (probably via posterior parts of the ventroposterior complex and the medial pulvinar). The primary vestibular cortical area is located in the parietal lobe at the junction between the intraparietal and the postcentral sulci, which is adjacent to that portion of the postcentral gyrus where the head is represented. This makes sense functionally because this region of the somatosensory cortex is concerned with conscious appreciation of body position. There may be an additional representation of the vestibular system in the superior temporal gyrus near the auditory cortex.

Abducens nucleus

The abducens nucleus is a group of approximately 6500 neurones, occupying a paramedian position in the central grey matter, in line with the trochlear, oculomotor and hypoglossal nuclei, with which it forms a somatic motor column (Fig. 19.1). It lies ventromedial to the medial longitudinal fasciculus, which is the means by which vestibular, cochlear and other cranial nerve nuclei, especially the oculomotor, connect with the abducens. The abducens nucleus contains large motor neurones and small multipolar interneurones, which are intermixed, although the latter are most heavily concentrated in its lateral and ventral aspects. Axons from the motor neurones cross the midline at the level of the nucleus and ascend in the medial longitudinal fasciculus to all three medial rectus subnuclei of the oculomotor nucleus.

Efferent abducens axons pass ventrally, descend through the reticular formation, trapezoid body and medial lemniscus, and traverse the ventral pons to emerge at its inferior border (Fig. 19.14): they innervate the lateral rectus muscle (see Ch. 39).

The abducens nucleus receives afferent connections from corticobulbar fibres (which are principally contralateral, some of the fibres being aberrant corticospinal fibres that descend from the midbrain to this level in the medial lemniscus); the medial longitudinal fasciculus (by which it is connected to oculomotor, trochlear and vestibular nuclei); the tectobulbar tract (from the deep layers of the superior colliculus); the paramedian pontine reticular formation (which lies rostral and caudal to the nucleus); the nucleus prepositus hypoglossi; and the contralateral medullary reticular formation.

Facial nucleus

The facial (motor) nucleus lies in the caudal pontine reticular formation, posterior to the dorsal trapezoid nucleus and ventromedial to the trigeminal spinal tract and nucleus. Groups of facial neurones form columns, which innervate individual muscles or which correspond to branches of the facial nerve. Neurones innervating muscles in the scalp and upper face are dorsal, and those supplying the lower facial musculature are ventral.

Efferent fibres of the large motor neurones of the facial nucleus form the motor root of the facial nerve. The motor nucleus represents the branchial efferent column, but it lies much more deeply in the pons than might be expected, and its axons have a most unusual course (Fig. 19.14). At first they incline dorsomedially towards the fourth ventricle, below the abducens nucleus, and ascend medial to it, near the medial longitudinal fasciculus. They then curve round the upper pole of the abducens nucleus and descend ventrolaterally through the reticular formation. Finally, they pass between their own nucleus medially and the spinal trigeminal nucleus. They emerge between the olive and the inferior cerebellar peduncle at the cerebellopontine angle.

The facial nucleus receives corticobulbar fibres for volitional control. Neurones that innervate muscles in the scalp and upper face are believed to receive bilateral corticobulbar fibres, while those supplying lower facial musculature only receive a contralateral innervation. Clinically, upper and lower motor neurone lesions of the facial nerve can be differentiated because the former results in paralysis that is confined to the contralateral lower face, whilst the latter results in a complete ipsilateral paralysis (Bell’s palsy).

The facial nucleus also receives ipsilateral afferents from the nucleus solitarius and from the trigeminal sensory nucleus, establishing important reflex connections.

Some efferent fibres of the facial nerve originate from neurones in the superior salivatory nucleus, which is said to be in the reticular formation dorsolateral to the caudal end of the facial nucleus. These preganglionic parasympathetic neurones belong to the general visceral efferent column.

They send fibres into the sensory root of the facial nerve. These travel via the chorda tympani to the submandibular ganglion and via the greater petrosal nerve and the nerve of the pterygoid canal to reach the pterygopalatine ganglion.

Corneal reflex

Touching the cornea or shining a bright light into the eye elicits reflex closure of both eyes. The former action stimulates nasociliary branches of the ophthalmic nerve, and the latter stimulates the retina and optic pathway. In both cases, afferent impulses enter the central nervous system and spread via interneurones to activate neurones in the facial motor nucleus in the pons (Fig. 19.15). Efferent impulses travel in the facial nerve to activate the palpebral component of orbicularis oculi, which contracts, producing a ‘blink’. The sweep of the eyelids carries lacrimal secretions across the eye helping to remove any irritating particles.

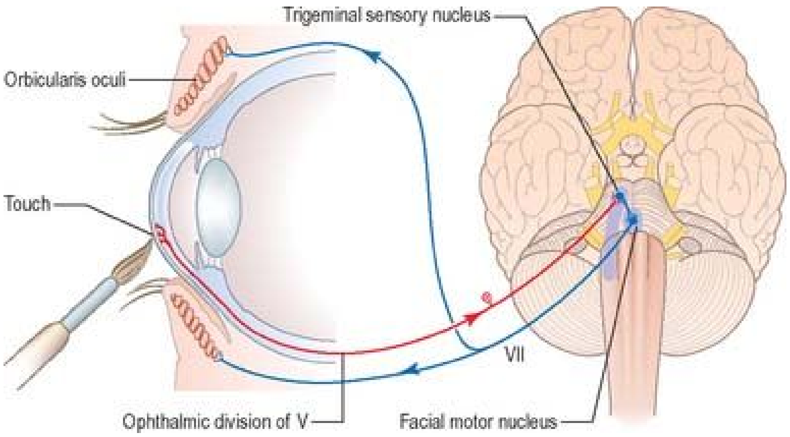

Fig. 19.15 Corneal reflex. Unilateral stimulation of the cornea elicits a bilateral corneal reflex (not illustrated).

Trigeminal sensory nucleus

On entering the pons, the fibres of the sensory root of the trigeminal nerve run dorsomedially towards the principal sensory nucleus (Fig. 19.9). About 50% of the fibres divide into ascending and descending branches; the others ascend or descend without division. The descending fibres form the spinal tract of the trigeminal, which terminates in the subjacent nucleus of the spinal tract (spinal nucleus) of the trigeminal nerve.

Some ascending trigeminal fibres, many of them heavily myelinated, synapse around the small neurones in the principal sensory nucleus (Fig. 19.16), which lies lateral to the motor nucleus and medial to the middle cerebellar peduncle, and is continuous inferiorly with the spinal nucleus. The principal nucleus is considered to be mainly concerned with tactile stimuli.

Other ascending fibres enter the mesencephalic nucleus, a column of unipolar cells whose peripheral branches may convey proprioceptive impulses from the masticatory muscles, and possibly also from the teeth and the facial and oculogyric muscles. Its neurones are unique in being the only primary sensory neurones with somata in the CNS. It is the relay for the ‘jaw jerk’, which is the only significant supraspinal monosynaptic reflex. Nerve fibres that ascend to the mesencephalic nucleus may give collaterals to the motor nucleus of the trigeminal nerve and to the cerebellum.

Jaw jerk reflex

Rapid stretching of the muscles that close the jaw (masseter, temporalis, medial pterygoid) activates muscle spindle afferents, which travel via the mandibular division of the trigeminal nerve to the brain stem (Fig. 19.17). The cell bodies of these primary afferent neurones are located in the mesencephalic nucleus of the trigeminal. Collaterals project monosynaptically to the motor nucleus of the trigeminal nerve in the pons. From here motor axons of the mandibular nerve innervate the muscles that close the jaw.

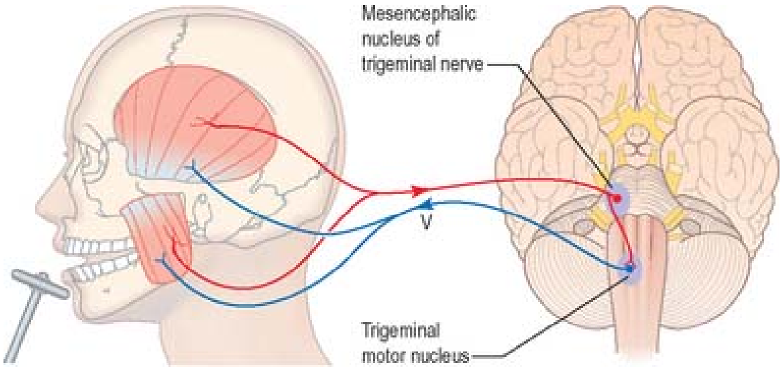

Fig. 19.17 Jaw jerk reflex.

Most fibres that arise in the trigeminal sensory nuclei cross the midline and ascend in the trigeminal lemniscus. They end in the contralateral thalamic nucleus ventralis posterior medialis, from which third-order neurones project to the cortical postcentral gyrus (areas 1, 2 and 3). Some trigeminal nucleus efferents ascend to the nucleus ventralis posterior medialis of the ipsilateral thalamus.

Trigeminal motor nucleus

The trigeminal motor nucleus is ovoid in outline and lies in the upper pontine tegmentum, under the lateral part of the floor of the fourth ventricle (Fig. 19.1). It lies medial to the principal sensory nucleus, and is separated from it by fibres of the trigeminal nerve. It occupies the position of the branchial (special visceral) efferent column.

The motor nucleus contains characteristic large multipolar neurones interspersed with smaller multipolar cells. The neurones are organized into a number of relatively discrete subnuclei, the axons from which innervate individual muscles. It receives fibres from both corticobulbar tracts. These fibres leave the tracts at the nuclear level or higher in the pons (aberrant corticospinal fibres), and descend in the medial lemniscus. They may end on motor neurones or interneurones. The motor nucleus receives afferents from the sensory nuclei of the trigeminal nerve, possibly including some from the mesencephalic nucleus, which form monosynaptic reflex arcs for proprioceptive control of the masticatory muscles. It also receives afferents from the reticular formation, red nucleus and tectum, the medial longitudinal fasciculus and possibly from the locus coeruleus. Collectively these represent pathways by which salivary secretion and mastication may be coordinated.

Tensor tympani and stapedius reflex

Loud sound elicits reflex contraction of tensor tympani and stapedius, which attenuates movement of the tympanic membrane and middle ear ossicles (see Ch. 36). Afferent impulses travel in the cochlear nerve to the cochlear nuclei in the brain stem. Efferent fibres to tensor tympani arise in the trigeminal motor nucleus and travel in the mandibular division of the trigeminal nerve. Efferent fibres to stapedius originate in the facial nucleus and travel in the facial nerve.

Salivatory nucleus

The salivatory (salivary) nucleus is near the upper pole of the vagal nucleus, just above the pontomedullary junction and near the inferior pole of the facial nucleus. It is customarily divided into superior and inferior salivatory nuclei, which send preganglionic parasympathetic fibres into the facial and glossopharyngeal nerves for the control of the salivary and lacrimal glands.

MIDBRAIN

EXTERNAL FEATURES AND RELATIONS

The midbrain traverses the hiatus in the tentorium cerebelli, and connects the pons and cerebellum with the forebrain. It is the shortest brain stem segment, not more than 2 cm in length, and most of it lies in the posterior cranial fossa. Lateral to it are the parahippocampal gyri, which hide its sides when the inferior surface of the brain is examined. For descriptive purposes, the midbrain may be divided into a dorsal tectum and right and left cerebral peduncles, each of which is further divided into a ventral crus cerebri and a dorsal tegmentum by a pigmented lamina, the substantia nigra. The two crura are separate, whereas the tegmental parts are united and traversed by the cerebral aqueduct that connects the third and fourth ventricles. The tectum lies dorsal to the cerebral aqueduct, and consists of the pretectal area and the paired superior and inferior colliculi (corpora quadrigemina).

The crura cerebri are superficially corrugated and emerge from the cerebral hemispheres. They converge as they descend and meet as they enter the pons, where they form the caudolateral boundaries of the interpeduncular fossa (Fig. 19.18, Fig. 19.19). At the level of the tentorial incisure, the basilar artery divides in the interpeduncular fossa into the right and left posterior cerebral arteries. The superior cerebellar arteries branch from the basilar artery immediately before this bifurcation. The posterior cerebral and superior cerebellar arteries both run laterally around the ventral surface of the crus, the former passing above the tentorium cerebelli, the latter passing below. The oculomotor and trochlear nerves lie between the two arteries. The roots of the oculomotor nerve emerge from the medial aspect of the crus (Fig. 15.7). The posterior communicating artery joins the posterior cerebral artery on the medial surface of the peduncle in the interpeduncular fossa. The median caudal part of the interpeduncular fossa constitutes the posterior perforated substance, which is pierced by central (perforating) branches of the posterior cerebral arteries. The optic tract winds dorsolaterally around the crus near where the latter emerges from the cerebral hemispheres.

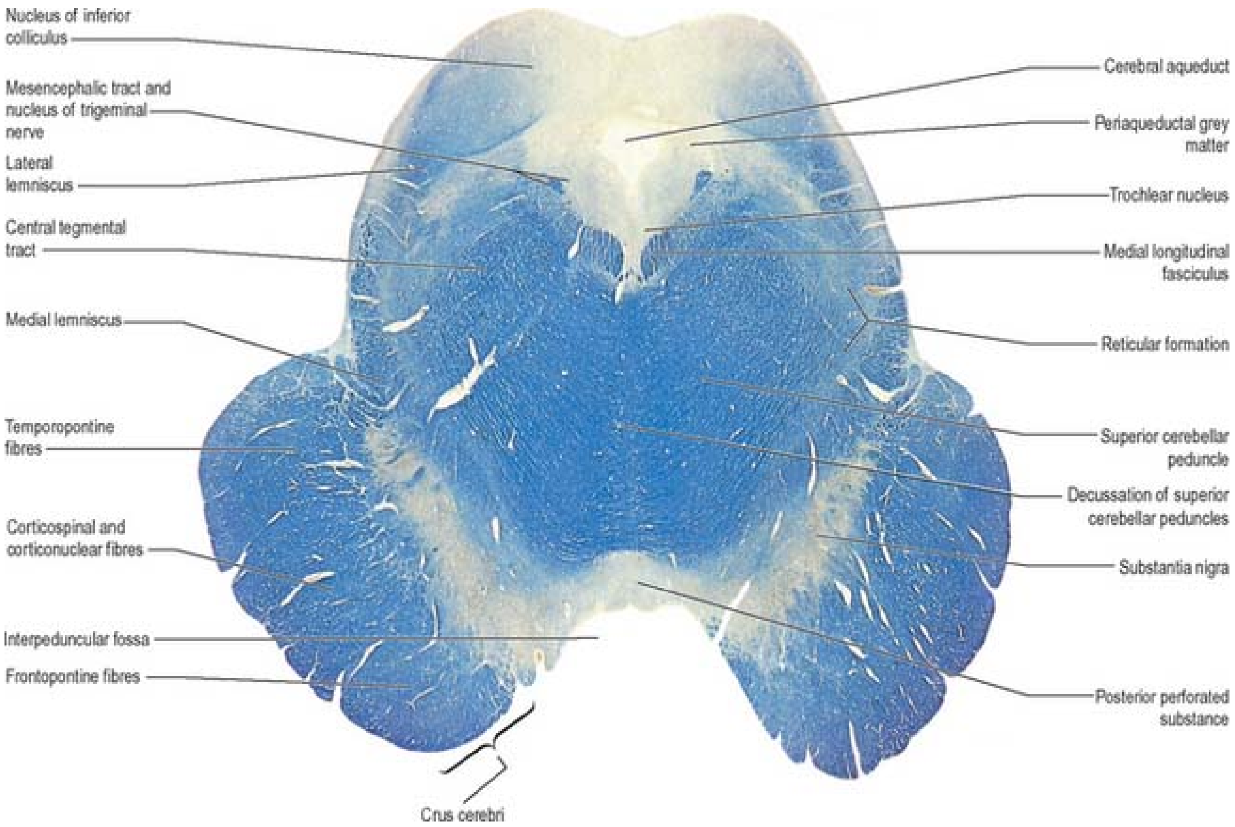
Nucleus of inferior colliculus
Mesencephalic tract and nucleus of trigeminal nerve
Lateral lemniscus
Central tegmental tract
Medial lemniscus
Temporopontine fibres
Corticospinal and corticonuclear fibres
Interpeduncular fossa
Frontopontine fibres
Crus cerebri
Cerebral aqueduct
Periaqueductal grey matter
Trochlear nucleus
Medial longitudinal fasciculus
Reticular formation
Superior cerebellar peduncle
Decussation of superior cerebellar peduncles
Substantia nigra
Posterior perforated substance

Fig. 19.18 Transverse section of the midbrain at the level of the inferior colliculi.

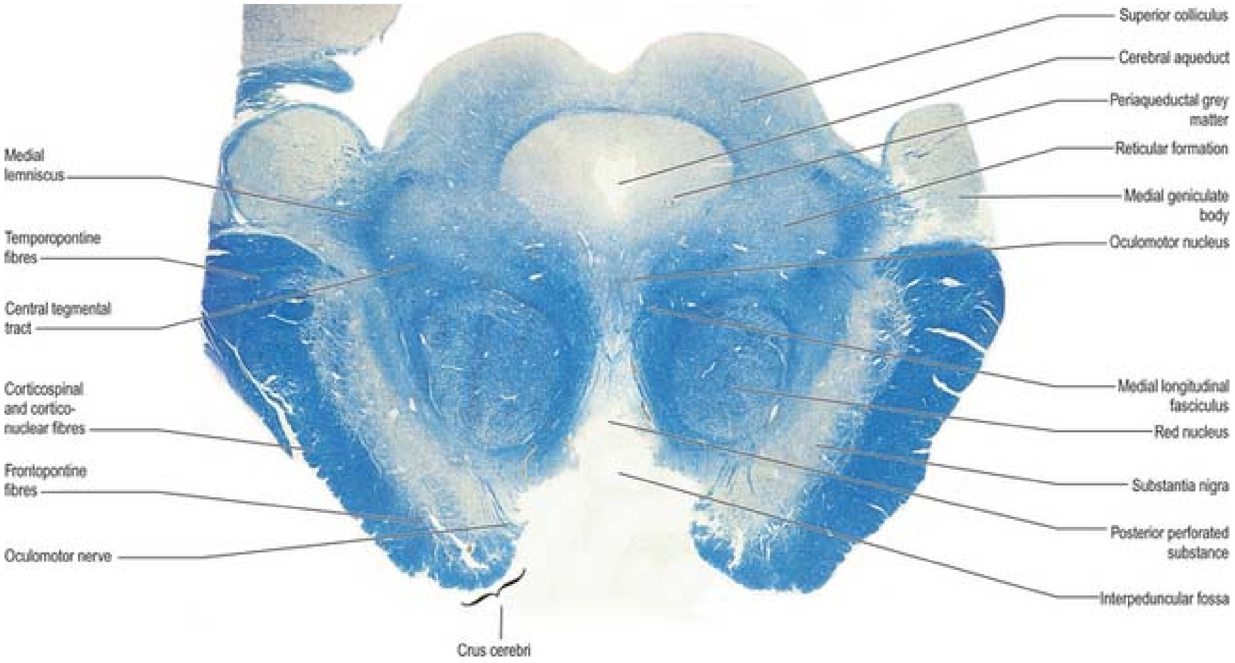
Medial lemniscus
Temporopontine fibres
Central tegmental tract
Corticospinal and cortico-nuclear fibres
Frontopontine fibres
Oculomotor nerve
Crus cerebri
Superior colliculus
Cerebral aqueduct
Periaqueductal grey matter
Reticular formation
Medial geniculate body
Oculomotor nucleus
Medial longitudinal fasciculus
Red nucleus
Substantia nigra
Posterior perforated substance
Interpeduncular fossa

Fig. 19.19 Transverse section of the midbrain at the level of the superior colliculi.

The superior and inferior colliculi are two paired eminences on the dorsal surface of the midbrain (Fig. 19.3). They lie rostral to the superior medullary velum, inferior to the pineal gland and caudal to the posterior commissure. Below the splenium of the corpus callosum, they are partly overlain by the pulvinar of the thalamus. The superior and inferior colliculi are separated by a cruciform sulcus. The upper limit of the sulcus expands into a depression for the pineal gland, and a median frenulum veli is prolonged from its caudal end down over the superior medullary velum. The trochlear nerves emerge lateral to the frenulum, pass ventrally over the lateral aspects of the cerebral peduncles and traverse the interpeduncular cistern to the petrosal end of the cavernous sinus. The superior colliculi, larger than the inferior, are centres for visual reflex responses. The inferior colliculi are a part of the ascending auditory pathway.

A brachium passes ventrolaterally from the lateral aspect of each colliculus (Fig. 19.3). The brachium of the superior colliculus (superior quadrigeminal brachium) passes below the pulvinar, partly overlapping the medial geniculate body, and conveys fibres from the retina to the superior colliculus. The brachium of the inferior colliculus (inferior quadrigeminal brachium) ascends ventrally and conveys fibres from the lateral lemniscus and inferior colliculus to the medial geniculate body.

INTERNAL STRUCTURE

Transverse sections of the midbrain

In transverse section, the cerebral peduncles are seen to be composed of dorsal and ventral regions separated by the substantia nigra (Fig. 19.18, Fig. 19.19). On each side, the dorsal region is the tegmentum and the ventral part is the crus cerebri. The tegmenti are continuous across the midline but the crura are separated.

Crus cerebri

The crus cerebri is approximately semilunar in section, being convex externally and concave internally. It contains corticobulbar and corticospinal fibres. Corticobulbar fibres terminate at various brainstem levels, some in association with the cranial nerve nuclei (corticonuclear fibres). Corticospinal fibres pass uninterrupted through the brainstem to enter the medullary pyramid and, thereafter, form the corticospinal tracts of the spinal cord (Fig. 18.18). Corticonuclear and corticospinal fibres occupy the middle two-thirds of the crus cerebri. Corticopontine fibres arise in the cerebral cortex and form two groups, both of which end in the pontine nuclei. Frontopontine fibres from the frontal lobe, principally areas 6 and 4, traverse the internal capsule and then occupy the medial sixth of the ipsilateral crus cerebri. Temporopontine fibres, which originate largely from the posterior region of the temporal lobe, traverse the internal capsule and then run in the lateral sixth of the ipsilateral crus. Parietopontine and occipitopontine fibres are also described in the crus, lying medial to the temporopontine fibres. There are few fibres from the primary sensory cortex in corticopontine projections.

Mesencephalic tegmentum

The mesencephalic tegmentum is continuous with the pontine tegmentum. At inferior collicular levels, grey matter is restricted to scattered collections of neurones in the reticular formation and a central, periaqueductal region ventral to the cerebral aqueduct. The trochlear nucleus lies in the latter region, near the midline, in a position corresponding to the abducens and hypoglossal nuclei at more caudal levels. It extends through the lower half of the midbrain, just caudal to the oculomotor nucleus and immediately dorsal to the medial longitudinal fasciculus.

The mesencephalic nucleus of the trigeminal nerve occupies a lateral position in the central grey matter (see Fig. 19.2). It ascends from the main trigeminal sensory nucleus in the pons to the level of the superior colliculus in the midbrain. Its large ovoid neurones are unipolar, like those in peripheral sensory ganglia. They are arranged in many small groups which extend as curved laminae on the lateral margins of the periaqueductal grey matter: neurones are most numerous caudally.

Apart from these nuclei, the mesencephalic tegmentum contains many other scattered neurones, most of which are included in the reticular formation.

The white matter of the mesencephalic tegmentum contains the majority of the tracts present in the pontine tegmentum. The decussation of the superior cerebellar peduncles is particularly prominent. Numerous ascending fibres enter the mesencephalic tegmentum from the cerebellum and pass ventromedially, decussating in the midline (Fig. 19.18). Thereafter, ascending fibres encapsulate and penetrate the red nucleus, in which some fibres, or their collaterals, terminate (Fig. 19.19). However, the majority of fibres ascend to terminate in the nucleus ventralis lateralis of the thalamus. A relatively small number of uncrossed fibres are believed to end in the periaqueductal grey matter and reticular formation, the interstitial nucleus and the nucleus of the posterior commissure (nucleus of Darkschewitsch). The latter nucleus may send efferent fibres to the medial longitudinal fasciculus and posterior commissure. Descending fascicles from the superior cerebellar peduncles also apparently end in the pontine and medullary reticular formation, the olivary complex and, possibly, motor cranial nerve nuclei.

The medial longitudinal fasciculus adjoins the somatic efferent cell column, dorsal to the decussating superior cerebellar peduncles (Fig. 19.18). The medial, trigeminal, lateral and spinal lemnisci form a curved band dorsolateral to the substantia nigra. Fibres in the medial, trigeminal and spinal lemnisci continue a rostral course to synapse with neurones in the lateral and medial parts of the ventral posterior nucleus of the thalamus. Some fibres of the lateral lemniscus end in the nucleus of the inferior colliculus, or send collaterals to it. The remaining lateral lemniscal fibres join with fibres originating in the inferior colliculus and enter the inferior quadrigeminal brachium, which carries them to the medial geniculate body.

At the level of the superior colliculus, the tegmentum contains the red nucleus (Fig. 19.19), which extends rostrally into the subthalamic region. The ventromedial central grey matter around the aqueduct contains the elongated oculomotor nucleus, which is adjacent ventrolaterally to the medial longitudinal fasciculus, and caudally reaches the trochlear nucleus. The oculomotor nucleus is divisible into neuronal groups which may be partially correlated with the motor distribution of the oculomotor nerve. A group of preganglionic parasympathetic neurones which control the activity of smooth muscle within the eyeball, the Edinger–Westphal nucleus, lies dorsal to the oculomotor nucleus.

Substantia nigra

The substantia nigra is a large nucleus that extends through the whole length of the midbrain (Fig. 19.18, Fig. 19.19). It has major connections with the basal ganglia and is central to the pathology of Parkinson’s disease (Ch. 22).

The substantia nigra is located between the crus cerebri ventrolaterally and ascending lemniscal fibres dorsomedially. Its medial part is traversed by oculomotor axons passing ventrally to their point of exit in the interpeduncular fossa. The substantia nigra is divided into a dorsal pars compacta and a ventral pars reticulata; the neurones in each part have quite different connections.

The pars compacta consists of darkly pigmented neurones, which contain neuromelanin granules. Their arrangement is irregular and they partially penetrate the subjacent pars reticulata. Pigmentation increases with age, is most abundant in primates, maximal in man, and present even in albinos. The pigmented pars compacta neurones synthesize dopamine as their neurotransmitter and project predominantly to the corpus striatum of the basal ganglia as well as to other sites. The pars compacta corresponds to the dopaminergic cell group A9 (Fig. 22.10). Two other dopaminergic cell groups are found in the ventral tegmentum: cell group A10 in the rostromedial region, which corresponds to the ventral tegmental area (of Tsai), and cell group A8 in the dorsolateral reticular area, which forms the nucleus parabrachialis pigmentosus. The whole ventral tegmental system of dopaminergic neurones appears to act as an integrative centre for adaptive behaviour. It projects via a number of pathways, mainly through ascending fibres in the ipsilateral medial forebrain bundle. These pathways are a mesodiencephalic system, which terminates in thalamic and hypothalamic nuclei; a mesostriatal projection to the caudate nucleus and putamen; a mesolimbic pathway to the nucleus accumbens, olfactory tubercle, lateral septum, interstitial nucleus of the stria terminalis, amygdala and entorhinal cortex; and mesocortical fibres that project to most cortical areas, particularly the prefrontal, orbitofrontal and cingulate cortex.

The pars compacta projects heavily to the caudate nucleus and putamen in a topographically organized fashion (nigrostriatal fibres). Lesser projections end in the globus pallidus and subthalamic nucleus. In Parkinson’s disease, the levels of dopamine in the substantia nigra and striatum decrease dramatically as a result of the degeneration of pars compacta neurones (Ch. 22).

The pars reticulata of the substantia nigra extends rostrally as far as the subthalamic region. It is considered to be a homologue of the medial (internal) segment of the globus pallidus, which it resembles in terms of cell type and connectivity. It consists of clusters of neurones, many of which intermingle with fibres of the crus cerebri. Most pars reticulata neurones are GABAergic and also contain high levels of iron.

There are reciprocal connections between the substantia nigra and the basal ganglia. Efferent fibres from the basal ganglia terminate largely, but not exclusively, in the pars reticulata. Topographically organized striatonigral fibres originate from the caudate nucleus and putamen and project to the pars reticulata. The head of the caudate nucleus projects to the rostral third of the substantia nigra, while the putamen projects to all parts. The fibres end in axodendritic synapses. A small number of GABAergic pallidonigral fibres from the lateral (external) segment of the globus pallidus end mostly in the pars reticulata. The subthalamic nucleus sends an important glutamatergic projection to the pars reticulata and to the globus pallidus. Subthalamonigral and subthalamopallidal projections are important in the pathophysiology of movement disorders such as Parkinson’s disease and dyskinesias (Ch. 22).

GABAergic neurones in the pars reticulata project rostrally to the ventral anterior and dorsomedial thalamic nuclei, and caudally to the pedunculopontine nucleus and reticular formation, whence impulses are relayed to spinal ventral horn neurones. A pars lateralis of the substantia nigra is recognizable, but small, in man. It projects to the ipsilateral superior colliculus, and may be involved in the control of saccadic eye movements.

Some corticonigral fibres appear to exist, passing from precentral and postcentral gyri to neurones in the pars reticulata.

Red nucleus

The red nucleus is a pink, ovoid mass, approximately 5 mm in diameter and lying dorsomedial to the substantia nigra (Fig. 19.19). The tint appears only in fresh material and is caused by a ferric iron pigment in its multipolar neurones. The latter are of varying size and their relative proportions and arrangement vary between species. In primates the magnocellular element is decreased, and there is a reciprocal increase in the size of the parvocellular component. Small multipolar neurones occur in all parts of the nucleus. In man, the larger neurones are restricted to the caudal part of the nucleus and have been estimated to be as few as 200 in number. The magnocellular element is considered phylogenetically old, which accords with the parvocellular predominance in primates. Rostrally, the red nucleus is poorly demarcated, and it blends into the reticular formation and caudal pole of the interstitial nucleus. It is traversed and surrounded by fascicles of nerve fibres, including many from the oculomotor nucleus.

The principal afferent connections of the red nucleus are corticorubral and cerebellorubral fibres. Uncrossed corticorubral fibres originate from primary somatomotor and somatosensory areas. In animals, the red nucleus receives fibres from the contralateral nucleus interpositus (which corresponds to the human globose and emboliform nuclei), and dentate nucleus, via the superior cerebellar peduncle. It has bilateral, probably reciprocal, connections with the superior colliculi. In humans, the rubrospinal tract is small and originates from the caudal magnocellular part of the red nucleus. Few fibres reach the cervical cord. The fibres decussate and then run obliquely laterally in the ventral tegmental decussation, ventral to the tectospinal decussation, and dorsal to the medial lemniscus. On reaching the grey matter ventral to the inferior cerebellar peduncle, the tract turns caudally to enter the lateral part of the lateral lemniscus. It continues descending ventral to the tract and nucleus of the trigeminal nerve throughout the medulla, and enters the upper part of the cervical cord intermingled with fibres of the lateral corticospinal tract. Some efferent axons form a rubrobulbar tract to motor nuclei of the trigeminal, facial, oculomotor, trochlear and abducens nerves.

The largest group of efferents from the red nucleus in man is a descending component of the ipsilateral, central tegmental tract. Initially, this tract lies lateral to the medial longitudinal fasciculus and dorsolateral to both the red nucleus and the decussation of the superior cerebellar peduncles (Fig. 19.9, Fig. 19.10, Fig. 19.11, Fig. 19.18). Most fibres arise from the parvocellular part of the red nucleus and pass to the ipsilateral inferior olivary nucleus in the medulla. Some tract fibres terminate in the brain stem reticular nuclei. Ascending and descending axons from the brain stem reticular formation also run in the central tegmental tract. These axons include dorsal and ventral ascending noradrenergic bundles, a ventral ascending serotoninergic bundle, and some fibres of dorsal and ventral ascending cholinergic bundles.

As mentioned elsewhere (p. 269), lesions of the corticospinal system in man result in permanent paresis or paralysis. In monkeys, although initially complete, the paralysis disappears and good recovery ensues. The explanation for this interprimate variability in recovery from corticospinal lesions appears to lie in the differential capacity of the rubrospinal system to compensate for loss of corticospinal drive. Monkeys never fully recover from combined lesions of both the corticospinal and rubrospinal tracts, which suggests that the two systems are functionally interrelated in the control of movement. Both encode force, velocity and direction parameters, but the rubrospinal system primarily directs activity both during the terminal phase of a movement and preceding a movement. There is, thus, overlap of activity in the two systems for all parameters during movements of limbs and even of individual digits. The corticospinal system is most active during the learning of new movements, whereas the rubrospinal system is most active during the execution of learnt automated movements.

The rubro-olivary projection, which travels in the central tegmental tract, connects the red nucleus indirectly to the contralateral cerebellar cortex. The cerebellum is thought to play a role in motor learning, and so the rubro-olivary system could switch the control of movements from the corticospinal to the rubrospinal system for programmed automation. The relative absence of a rubrospinal system in man could explain the poor recovery of motor function after stroke.

Oculomotor nucleus

The nuclear complex from which the efferent fibres of the oculomotor nerve arise consists of several groups of large motor neurones (collectively, the oculomotor nucleus; Fig. 19.19) and smaller preganglionic parasympathetic neurones (the Edinger–Westphal nucleus). The motor neurone groups of the oculomotor nucleus innervate, in dorsoventral order, the ipsilateral inferior rectus, inferior oblique and medial rectus. A medially placed column of cells innervates the contralateral superior rectus: the axons from this subnucleus decussate in its caudal part. The medial rectus subnucleus consists of three anatomically distinct subpopulations. The ventral portion, which contains the largest number of motor neurones, occupies the rostral two-thirds; a subpopulation of smaller motor neurones lies dorsally throughout the rostral two-thirds of the nucleus and innervates the small orbital fibres of the medial rectus; and another subpopulation lies dorsolaterally in the caudal two-thirds of the nucleus.

A median subnucleus of large neurones, the caudal central nucleus, lies at the caudal pole of the oculomotor nucleus adjacent to the superior rectus and medial rectus subnuclei. In non-human primates, approximately 30% of the motor neurones in this subnucleus innervate levator palpebrae superioris bilaterally, which is unique for paired skeletal muscles.

The Edinger–Westphal nucleus, composed of small, multipolar, preganglionic parasympathetic neurones, lies dorsal to the main oculomotor nucleus. Its neurones give rise to axons that travel in the oculomotor nerve and synapse with postganglionic neurones in the ciliary ganglion.

Fascicles of axons from all of these subnuclei course forward in the midbrain and emerge as the oculomotor nerve in the interpeduncular fossa. The fascicles are most probably arranged from medial to lateral subserving the pupil, inferior rectus, medial rectus, levator palpebrae superioris and superior rectus, and inferior oblique. The human oculomotor nerve contains approximately 15,000 axons.

Afferent inputs to the oculomotor nuclear complex include fibres from the rostral interstitial nucleus of the medial longitudinal fasciculus and the interstitial nucleus of Cajal, both of which are involved in the control of vertical and torsional gaze. Other inputs come, either directly or indirectly, from the nuclei of the posterior commissure, the interstitial nucleus of Cajal, the frontal eye fields, the superior colliculus, the dentate nucleus and other cortical areas. The medial longitudinal fasciculus carries connections from the trochlear, abducens and vestibular nuclei; the medial and lateral vestibular nuclei project to the medial rectus subnucleus.

Afferent inputs to the Edinger–Westphal nucleus come primarily from the pretectal nuclei bilaterally, mediating the pupillary light reflex and from the visual cortex, mediating accommodation.

Trochlear nucleus

The trochlear nucleus lies in the grey matter in the floor of the cerebral aqueduct, level with the upper part of the inferior colliculus (Fig. 19.1, Fig. 19.18). It is in line with the ventromedial part of the oculomotor nucleus, in the position of the somatic efferent column. The medial longitudinal fasciculus is ventral and lateral to it. The oculomotor and trochlear nuclei often overlap slightly but can be distinguished by the smaller size of the trochlear neurones. The afferent inputs to the trochlear nucleus are similar to those described for the oculomotor nucleus. Trochlear efferent fibres pass laterodorsally round the central grey matter, then descend medial to the trigeminal mesencephalic nucleus to reach the upper end of the superior medullary velum, where they decussate and emerge lateral to the frenulum. A few fibres remain ipsilateral.

Medial longitudinal fasciculus

The medial longitudinal fasciculus (Fig. 19.9, Fig. 19.18, Fig. 39.12) is a heavily myelinated composite tract, lying near the midline, ventral to the periaqueductal grey matter. It ascends to the interstitial nucleus of Cajal, which lies in the lateral wall of the third ventricle, just above the cerebral aqueduct. The fasciculus retains its position relative to the central grey matter through the midbrain, pons and upper medulla, but is displaced ventrally by successive decussations of the medial lemnisci and lateral corticospinal tracts. At spinal levels it is synonymous with the medial vestibulospinal tract.

The medial longitudinal fasciculus interconnects the oculomotor, trochlear, abducens, Edinger–Westphal, vestibular, reticular and spinal accessory nuclei, coordinating conjugate eye movements and associated movements of the head and neck. Lesions cause internuclear ophthalmoplegia. All four vestibular nuclei contribute ascending fibres. Those from the superior nucleus remain uncrossed, while the others are partly crossed. Some fibres reach the interstitial and posterior commissural nuclei, and some decussate to the contralateral nuclei. Descending axons, from the medial vestibular nuclei and perhaps the lateral and inferior nuclei, partially decussate and descend in the fasciculus to form the medial vestibulospinal tract (Fig. 18.19). Fibres join the fasciculus from the dorsal trapezoid, lateral lemniscal and posterior commissural nuclei, which means that both the cochlear and vestibular components of the vestibulocochlear nerve may influence movements of the eyes and head via the medial longitudinal fasciculus. Some vestibular fibres may ascend in the medial longitudinal fasciculus as far as the thalamus.

Tectum

Inferior colliculus

The inferior colliculus (Fig. 19.18) is part of the ascending auditory pathway (Ch. 37) and is the principal site of termination of the lateral lemniscus. It has a central, ovoid, main nucleus, which is continuous with the periaqueductal grey matter. It is surrounded by a lamina of nerve fibres, many from the lateral lemniscus, which terminate in it. The central nucleus has dorsomedial and ventrolateral zones, which are covered by a dorsal cortex. In humans, the cortex has four cytoarchitectonic layers: layer I contains small neurones with flattened radial dendritic fields; layer II, medium-sized neurones with ovoid dendritic fields aligned parallel with the collicular surface; layer III, medium-sized neurones with spherical dendritic fields; and layer IV, large neurones with variably shaped dendritic fields. The central nucleus is laminated. Bands of cells with disc-shaped or stellate dendritic fields orthogonally span the fibre layers in which the terminals of lateral lemniscal fibres ramify. The neurones are sharply tuned to frequency, and the laminae may represent the structural basis of tonal discrimination. Experimental studies have found cells driven by low frequencies in the dorsal laminae, and others driven by high frequencies in the ventral laminae. Neurones are broadly frequency-tuned in the dorsal cortex and lateral nucleus.

Most efferent fibres from the inferior colliculus travel via the inferior brachium to the ipsilateral medial geniculate body. Lemniscal fibres relay only in the central nucleus, and some pass without relay to the medial geniculate body. In man, the ventral division of the medial geniculate body receives a topographic projection from the central nucleus and the dorsal division receives a similar projection from the dorsal cortex. Some colliculogeniculate fibres do not relay in the geniculate body, but continue, with those that do, via the auditory radiation to the auditory cortex. A descending projection from the auditory cortex reaches the inferior colliculus via the medial geniculate body. Some fibres may traverse this projection without relay. This descending path may produce effects at levels from the medial geniculate body downwards, and it probably links with efferent cochlear fibres, through the superior olivary and cochlear nuclei.

Inferior collicular projections to the brain stem and spinal cord appear to traverse the superior colliculi before they descend. In this way they connect with the origins of the tectospinal and tectotegmental tracts. These projections are relatively small and probably mediate reflex turning of the head and eyes in response to sounds.

In experimental animals, lesions of either the inferior colliculus or its brachium produce defects in tonal discrimination, sound localization and auditory reflexes. The effects of such lesions are poorly documented in man.

Superior colliculus

The superior colliculus is a laminated structure. At successive depths from the external surface, it may be divided into a stratum zonale, cinereum, opticum and lemnisci. The stratum lemnisci may be subdivided into the stratum griseum medium, album medium, griseum profundum and album profundum. These seven layers have also been termed zonal, superficial grey, optic, intermediate grey, deep grey, deep white and periventricular strata. The two schemes do not completely accord, but, as a generalization, layers may be considered to be composed alternately of neuronal somata or their processes. The zonal layer consists chiefly of myelinated and non-myelinated fibres from the occipital cortex (areas 17, 18 and 19), which arrive as the external corticotectal tract. It also contains a few small neurones, which are horizontally arrayed. The superficial grey layer (stratum cinereum) forms a crescentic lamina over the deeper layers and contains many small multipolar interneurones, on which cortical fibres synapse. The optic layer consists partly of fibres from the optic tract. As they terminate, they permeate the entire anterior–posterior extent of the superficial layers with numerous collateral branches. This arrangement provides a retinotopic map of the contralateral visual field, in which the fovea is represented anterolaterally. Retinal axons terminate in clusters from specific retinotectal neurones and as collaterals of retinogeniculate fibres. The layer also contains some large multipolar neurones. Efferent fibres to the retina are said to start in this layer.

The intermediate grey and white layers collectively constitute the main receptive zone. The main afferent input is the medial corticotectal path from layer V neurones of the ipsilateral occipital cortex (area 18), and from other neocortical areas that are concerned with ocular following movements. Afferent fibres are also received from the contralateral spinal cord (via spinotectal and spinothalamic routes), the inferior colliculus, and the locus coeruleus and raphe nuclei (from noradrenergic and serotoninergic neurones). The deep grey and deep white layers adjacent to the periaqueductal grey matter are collectively called the parabigeminal nucleus. They contain neurones whose dendrites extend into the optic layer, and whose axons of which form many of the collicular efferents.

The superior colliculus receives afferents from many sources including the retina, spinal cord, inferior colliculus and occipital and temporal cortices. The first three of these pathways convey visual, tactile and probably thermal, pain and auditory impulses. Collicular efferents pass to the retina, lateral geniculate nucleus, pretectum, parabigeminal nucleus, the inferior, medial and lateral pulvinar, and to numerous sites in the brain stem and spinal cord. Fibres passing from the pulvinar are relayed to primary and secondary visual cortices and form an extrageniculate retinocortical pathway for visual orientation and attention.

The tectospinal and tectobulbar tracts start from neurones in the superior colliculi. They sweep ventrally round the central grey matter to decussate ventral to the oculomotor nuclei and medial longitudinal fasciculi as part of the dorsal tegmental decussation. The tectospinal tract descends ventral to the medial longitudinal fasciculus as far as the medial lemniscal decussation in the medulla, where it diverges ventrolaterally to reach the spinal ventral white column near the ventral lip of the ventral median fissure. Tectospinal fibres descend to cervical segments. The tectobulbar tract, mainly crossed, descends near the tectospinal tract, and ends in the pontine nuclei and motor nuclei of the cranial nerves, particularly those innervating the oculogyric muscles. It subserves reflex ocular movements. Other tectotegmental fibres reach various tegmental reticular nuclei in the ipsilateral mesencephalic and contralateral pontomedullary reticular formation (gigantocellular reticular, caudal pontine reticular, oral pontine reticular nuclei), and the substantia nigra and red nucleus. Tectopontine fibres, which probably descend with the tectospinal tract, terminate in dorsolateral pontine nuclei, with a relay to the cerebellum. A tecto-olivary projection, from deeper collicular laminae to the upper third of the medial accessory olivary nucleus, exists in primates. It is crossed and links with the posterior vermis.

In animals, central collicular stimulation produces contralateral head movement as well as movements involving the eyes, trunk and limbs, which implicates the superior colliculus in the integration of vision and body movement.

Pretectal nucleus

The pretectal nucleus is a poorly defined mass of neurones at the junction of the mesencephalon and diencephalon. It extends from a position dorsolateral to the posterior commissure caudally towards the superior colliculus, with which it is partly continuous. It receives fibres from the visual cortex via the superior quadrigeminal brachium, from the retina via the lateral root of the optic tract, and from the superior colliculus. Its efferent fibres reach both parasympathetic Edinger–Westphal nuclei. Those which decussate pass ventral to the aqueduct or through the posterior commissure. In this way, sphincter pupillae contract in both eyes in response to impulses from either eye. This bilateral light reflex may not be the sole activity of the pretectal nucleus. Some of its efferents project to the pulvinar and deep laminae of the superior colliculus, and provide another extrageniculate path to the cerebral cortex.

BRAIN STEM RETICULAR FORMATION

The brain stem contains extensive fields of intermingled neuronal cell bodies and nerve fibres, which are collectively termed the reticular formation. The reticular regions are often regarded as phylogenetically ancient, representing a primitive nerve network upon which more anatomically organized, functionally selective, connections have developed during evolution.

Reticular regions tend to be ill-defined collections of neurones with diffuse connections. Their conduction paths are difficult to define, often complex and polysynaptic, and they have ascending and descending components that are partly crossed and uncrossed. Their components subserve somatic and visceral functions. They also include some distinct and important cell groups, which are distinguished on the basis of their neurotransmitter substances. These include dopaminergic and noradrenergic neurones (group A), serotoninergic (group B) adrenergic (group C) and cholinergic (group Ch) neurones.

Studies with the Golgi technique show that few brain stem reticular neurones are classic Golgi type II neurones (i.e. with short axons that branch locally). In contrast, they have long dendrites that spread across the long axis of the brain stem in transverse sheets. These radiating dendrites may spread into 50% of the cross-sectional area of their half of the brain stem, and they are intersected by, and may synapse with, a complex of ascending and descending fibres. Many axons of reticular neurones ascend or descend, or bifurcate to do both. They often travel far, perhaps through the whole brain stem and even beyond. As an example, a bifurcating axon from a cell in the magnocellular medullary nucleus may project rostrally into the upper medulla, pons, midbrain tegmentum, subthalamus, hypothalamus, dorsal thalamus, septum, limbic system and neocortex, while its descending branch innervates the reticular core of the lower medulla and may reach the cervical spinal intermediate grey matter (laminae V and VI). Many reticular neurones have unidirectional, shorter axons which synapse with the radiating dendrites of numerous other neurones *en route*, and give off collaterals which synapse with cells in ‘specific’ brain stem nuclei or cortical formations, such as the cerebellum. Multitudes of afferent fibres converging on individual neurones, and the myriad destinations of efferent fibres, provide the structural basis for considering the reticular formation to be ‘polymodal’, ‘diffuse’ or ‘non-specific’ in function.

A contrasting dendritic form is also found, in which dendrites are short, sinuous or curved, branch profusely and pursue re-entrant courses at the perimeter of a nuclear group, defining a boundary between it and its environs. Neurones with an intermediate dendritic complexity occur in and near such nuclei and vary in density in much of the remaining reticular formation. In different zones, the proportion of different sizes of neuronal somata varies. Some regions contain only small to intermediate multipolar cells (‘parvocellular’ regions). However, there are a few areas where these mingle with large multipolar neurones in ‘gigantocellular’ or ‘magnocellular’ nuclei.

In general terms, the reticular formation is a continuous core that traverses the whole brain stem, and is continuous below with the reticular intermediate spinal grey laminae. It is divisible, on the basis of cytoarchitectonic, chemoarchitectonic and functional criteria, into three bilateral longitudinal columns: median; medial, containing mostly large reticular neurones; and lateral, containing mostly small to intermediate neurones (Fig. 19.20).

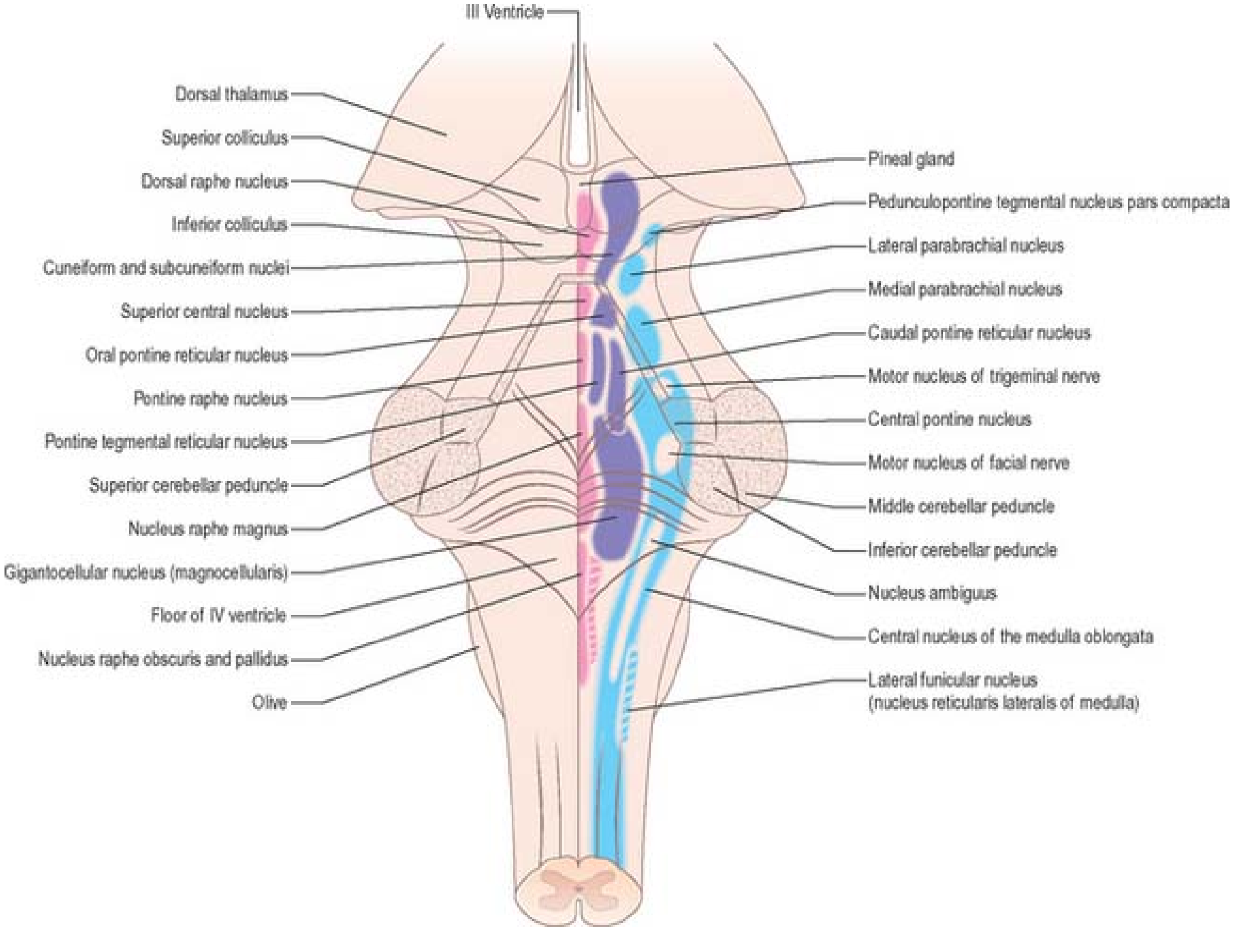
III Ventricle
Dorsal thalamus
Superior colliculus
Dorsal raphe nucleus
Inferior colliculus
Cuneiform and subcuneiform nuclei
Superior central nucleus
Oral pontine reticular nucleus
Pontine raphe nucleus
Pontine tegmental reticular nucleus
Superior cerebellar peduncle
Nucleus raphe magnus
Gigantocellular nucleus (magnocellularis)
Floor of IV ventricle
Nucleus raphe obscuris and pallidus
Olive
Pineal gland
Pedunculopontine tegmental nucleus pars compacta
Lateral parabrachial nucleus
Medial parabrachial nucleus
Caudal pontine reticular nucleus
Motor nucleus of trigeminal nerve
Central pontine nucleus
Motor nucleus of facial nerve
Middle cerebellar peduncle
Inferior cerebellar peduncle
Nucleus ambiguus
Central nucleus of the medulla oblongata
Lateral funicular nucleus
(nucleus reticularis lateralis of medulla)

Fig. 19.20 Dorsal aspect of the brain stem showing the approximate location of nuclei of the reticular formation. Nuclei of the median and paramedian nuclear column: magenta; medial column nuclei: purple, lateral column nuclei: blue.

MEDIAN COLUMN OF RETICULAR NUCLEI

The median column of reticular nuclei extends throughout the medulla, pons and midbrain and contains neurones that are largely aggregated in bilateral, vertical sheets, blended in the midline and occupying the paramedian zones. Collectively they are called the nuclei of the raphe, or raphe nuclei. Many neurones in raphe nuclei are serotoninergic and are grouped into nine clusters, B1–9. The raphe pallidus nucleus and associated raphe obscurus nucleus lie in the upper two-thirds of the medulla and cross the pontomedullary junction. The raphe magnus nucleus, corresponding to many B3 neurones, partly overlaps them, and ascends into the pons. Above it is the pontine raphe nucleus, which is formed by the cell group B5. Also located in the pons is the central superior raphe nucleus, which contains parts of cell groups B6 and B8. The dorsal (rostral) raphe nucleus, approximating to cell group B7, extends through much of the midbrain.

Axons originating from the serotoninergic raphe neurones ramify extensively throughout the CNS. Although many of these fibres are diffusely distributed, others have more specific connections. For example, whereas the central superior raphe nucleus projects divergently to all areas of the cerebral cortex, different neurones in the dorsal raphe nucleus not only project specifically to circumscribed regions of the frontal, parietal and occipital cortices, but also to functionally related regions of the cerebellar cortex. Similarly, the caudate nucleus and putamen receive a preferential input from the dorsal raphe nucleus, whereas the hippocampus, septum and hypothalamus are innervated mainly by cells in the central superior mesencephalic raphe nucleus.

All raphe nuclei provide mainly serotoninergic descending projections, which terminate in the brain stem and spinal cord. Brain stem connections are multiple and complex. For example, the dorsal raphe nucleus, in addition to sending a large number of fibres to the locus coeruleus, projects to the dorsal tegmental nucleus and most of the rhombencephalic reticular formation, together with the central superior, pontine raphe and raphe magnus nuclei.

Raphe spinal serotoninergic axons originate mainly from neurones in the raphe magnus, pallidus and obscurus nuclei. They project as ventral, dorsal and intermediate spinal tracts in the ventral and lateral funiculi, and terminate respectively in the ventral horns and laminae I, II and V of the dorsal horns of all segments, and in the thoracolumbar intermediolateral sympathetic and sacral parasympathetic preganglionic cell columns. The dorsal raphe spinal projections function as a pain control pathway that descends from a mesencephalic pain control centre located in the periaqueductal grey matter, dorsal raphe and cuneiform nuclei (Ch. 18). The intermediate raphe-spinal projection is inhibitory, and, in part, modulates central sympathetic control of cardiovascular function. The ventral raphe spinal system excites ventral horn cells and could function to enhance motor responses to nociceptive stimuli.

Principally, the mesencephalic serotoninergic raphe system is reciprocally interconnected rostrally with the limbic system, septum, prefrontal cortex and hypothalamus. Efferents ascend and form a large ventral and a diminutive dorsal pathway. Both originate from neurones in the dorsal and central superior raphe nuclei. The raphe magnus nucleus also contributes to the dorsal ascending serotoninergic pathway, which is at first incorporated into the dorsal longitudinal fasciculus (of Schütz). A few fibres terminate in the central mesencephalic grey matter and posterior hypothalamus, but most continue into the medial forebrain bundle and merge with the axons of the ventral pathway, which are distributed to the same targets. The fibres of the ventral ascending serotoninergic pathway exit the ventral aspect of the mesencephalic raphe nuclei, and then course rostrally through the ventral tegmentum from where fibres pass to the ventral tegmental area, substantia nigra and interpeduncular nucleus. A large number of fibres then enter the habenulointerpeduncular tract and run rostrally to innervate the habenular nucleus, intralaminar, midline, anterior, ventral and lateral dorsal thalamic nuclei, and the lateral geniculate body. The ventral ascending serotoninergic pathway enters the medial forebrain bundle in the lateral hypothalamic area and splits to pass medially and laterally. The fibres in the medial tract terminate in the mammillary body, dorsomedial, ventromedial, infundibular, anterior and lateral hypothalamic, medial and lateral preoptic and suprachiasmatic nuclei. Those in the lateral tract take the ansa peduncularis–ventral amygdalofugal path to the amygdala, striatum and caudal neocortex. The medial forebrain bundle carries the remaining ventral ascending serotoninergic axons into the medullary stria, stria terminalis, fornix, diagonal band, external capsule, cingulate fasciculus and medial olfactory stria, to terminate in all the structures that these systems interconnect.

Major afferents into the mesencephalic raphe nuclei include those from the interpeduncular nucleus, linking the limbic and serotoninergic systems; from the lateral habenular nucleus, linking the septum, preoptic hypothalamus and prefrontal cortex via the habenulointerpeduncular tract and the medial forebrain bundle; and from the pontine central grey matter.

The ascending raphe system probably functions to moderate forebrain activities, particularly limbic, septal and hypothalamic activities. A degree of region-specific connectivity suggest that it exerts precise, as well as tonal, control.

MEDIAL COLUMN OF RETICULAR NUCLEI

The medial column of reticular nuclei is composed predominantly of neurones of medium size, although very large neurones are found in some regions, and most have processes orientated in the transverse plane. In the lower medulla the column is indistinct, and is perhaps represented by a thin lamina lateral to the raphe nuclei. However, in the upper medulla it expands into the medullary gigantocellular (magnocellular) nucleus, which lies ventrolateral to the hypoglossal nucleus, ventral to the vagal nuclei and dorsal to the inferior olivary complex. Ascending further, the column continues as the pontine gigantocellular (magnocellular) nucleus, which lies medially in the tegmentum. Its neurones suddenly diminish in size to form, in rostral order, the almost coextensive caudal and oral pontine tegmental reticular nuclei. It then expands into the cuneiform nucleus and subcuneiform nucleus, before fading away in the midbrain tegmentum.

Axons of medial reticular column neurones form a multisynaptic ascending and descending system within the column, and ultimately enter the spinal cord and diencephalon. Descending fibres form the pontospinal (lateral reticulospinal), and bulbospinal (medial reticulospinal) tracts. Pontospinal axons arise from neurones in the caudal and oral parts of the pontine reticular nucleus, descend uncrossed in the ventral spinal funiculus, and terminate in spinal cord laminae VII, VIII and IX. Bulbospinal axons descend bilaterally to end in laminae VII, VIII, IX, and X, and ipsilaterally to end in laminae IV, V and VI. The system modulates spinal motor function and segmental nociceptive input.

Afferent components to the medial reticular nuclear column include the spinoreticular projection and collaterals of centrally projecting spinal trigeminal, vestibular and cochlear fibres. Spinoreticular fibres arise from neurones in the intermediate grey matter of the spinal cord. They decussate in the ventral white commissure, ascend in the ventrolateral funiculus, usually via several neurones, and terminate not only at all levels of the medial column of reticular nuclei but also in the intralaminar nuclei of the thalamus. Three areas of the medial reticular zone receive particularly high densities of terminations. These are the combined caudal and rostral ends of the gigantocellular and central nuclei, respectively, and the caudal pontine reticular nucleus and the pontine tegmentum. Retinotectal and tectoreticular fibres relay visual information and the medial forebrain bundle transmits olfactory impulses.

Efferents from the medial column of reticular nuclei project through a multisynaptic pathway within the column to the thalamus. Areas of maximal termination of spinoreticular fibres also project directly to the intralaminar thalamic nuclei. The multisynaptic pathway is integrated into the lateral column of reticular nuclei with cholinergic neurones in the lateral pontine tegmentum. The intralaminar thalamic nuclei project directly to the striatum and neocortex.

LATERAL COLUMN OF RETICULAR NUCLEI

The lateral column of reticular nuclei contains six nuclear groups. These are the parvocellular reticular area, superficial ventrolateral reticular area, lateral pontine tegmental noradrenergic cell groups A1, A2, A4–A7 (A3 is absent in primates), adrenergic cell groups C1–C2 and cholinergic cell groups Ch5–Ch6. The column descends through the lower two-thirds of the lateral pontine tegmentum and upper medulla, where it lies between the gigantocellular nucleus medially, and the sensory trigeminal nuclei laterally. It continues caudally and expands to form most of the reticular formation lateral to the raphe nuclei. It abuts the superficial ventrolateral reticular area, nucleus solitarius, nucleus ambiguus and vagal nucleus, and there contains the adrenergic cell group C2, and the noradrenergic group A2.

The lateral paragigantocellular nucleus lies at the rostral pole of the diffuse superficial ventrolateral reticular area (at the level of the facial nucleus). The zone extends caudally as the nucleus retroambiguus and descends into the spinal cord. It contains noradrenergic cell groups A1, A2, A4 and A5, and the adrenergic cell group C1. The ventrolateral reticular area is involved in cardiovascular, respiratory, vasoreceptor and chemoreceptor reflexes, and in the modulation of nociception. The A2 or noradrenergic dorsal medullary cell group lies in the nucleus of the tractus solitarius, vagal nucleus and adjoining parvocellular reticular area. Adrenergic group C1 lies rostral to the A2 cell group. Noradrenergic cell group A4 extends into the lateral pontine tegmentum, along the subependymal surface of the superior cerebellar peduncle. Noradrenergic group A5 forms part of the paragigantocellular nucleus in the caudolateral pontine tegmentum. Noradrenergic cell group A5 and adrenergic cell group C1 probably function as centres of vasomotor control. The entire region is subdivided into functional areas on the basis of stimulation experiments in animals, in which vasoconstrictor, cardioaccelerator, depressor, inspiratory, expiratory and sudomotor effects have been elicited.

The lateral pontine tegmental reticular grey matter is related to the superior cerebellar peduncle and forms the medial and lateral parabrachial nuclei and the ventral Kölliker–Fuse nucleus, a pneumotaxic centre. The locus coeruleus (noradrenergic cell group A6), area subcoeruleus, noradrenergic cell group A7, and cholinergic group Ch5 in the pedunculopontine tegmental nucleus (nucleus tegmenti pedunculopontinus), are all located in the lateral pontine and mesencephalic tegmental reticular zones. The mesencephalic group Ch5 is continuous caudally with cell group Ch6 in the pontine central grey matter.

Cell group A6 contains all the noradrenergic cells in the central region of the locus coeruleus. Group A6 has ventral (nucleus subcoeruleus, A6 Sc), rostral and caudolateral extensions, the latter merging with the A4 group. The locus coeruleus probably functions as an attention centre, focusing neural functions to prevailing needs. The noradrenergic A7 group occupies the rostroventral part of the pontine tegmentum and is continuous with groups A5 and A1 through the lateral rhombencephalic tegmentum. The A7, A5, A1 complex is also connected by noradrenergic cell clusters with group A2, caudally, and group A6, rostrally. The A5 and A7 groups lie mainly within the medial parabrachial and Kölliker–Fuse nuclei. Reticular neurones in the lateral pontine tegmental reticular area, like those of the ventrolateral zone, function to regulate respiratory, cardiovascular and gastrointestinal activity. Two micturition centres are located in the dorsomedial and ventrolateral parts of the lateral pontine tegmentum.

The connections of the lateral column reticular nuclei are complex. The short ascending and descending axons of the parvocellular reticular area constitute bulbar reflex pathways, which connect all branchiomotor nuclei and the hypoglossal nucleus with central afferent cranial nerve complexes through a propriobulbar system. The area also receives descending afferents from the contralateral motor cortex via the corticotegmental tract, and from the contralateral red nucleus via the rubrospinal tract. The longitudinal catacholamine bundle passes through the parvocellular reticular formation.

The superficial ventrolateral reticular area receives its principal input from the nucleus solitarius, and subserves cardiovascular, baroreceptor, chemoreceptor and respiratory reflexes; it also receives some input from the spinal cord, insular cortex and amygdala. Reticulospinal fibres from the region terminate bilaterally on sympathetic preganglionic neurones in the thoracic spinal cord. Fibres from the pneumotaxic centre project to an inspiratory centre in the ventrolateral part of the nucleus solitarius, and a mixed expiratory–inspiratory centre in the superficial ventrolateral reticular area. Inspiratory neurones in both centres monosynaptically project to the phrenic and intercostal motor neurones. Axons of expiratory neurones terminate on lower motor neurones which innervate intercostal and abdominal musculature.

The superficial ventrolateral area is also the seat of the ‘visceral alerting response’. Fibres from the hypothalamus, periaqueductal grey matter and midbrain tegmentum mediate increased respiratory activity, raised blood pressure, tachycardia, vasodilation in skeletal muscle and renal and gastrointestinal vasoconstriction. Ascending efferents from the superficial ventrolateral area synapse on neurones of the supraoptic and paraventricular hypothalamic nuclei. Excitation of these neurones causes release of vasopressin from the neurohypophysis. Medullary noradrenergic cell groups A1 and A2 also innervate (directly and indirectly) the median eminence, and control the release of growth hormone, luteinizing hormone and adrenocorticotrophic hormone.

The lateral pontine tegmentum, particularly the parabrachial region, is reciprocally connected to the insular cortex. It shares reciprocal projections with the amygdala through the ventral amygdalofugal pathway, medial forebrain bundle and central tegmental tract, and with hypothalamic, median preoptic and paraventricular nuclei, which preferentially project to the lateral parabrachial nucleus and the micturition centres. It also shares reciprocal bulbar projections, many from the pneumotaxic centre, with the nucleus solitarius and superficial ventrolateral reticular area.

Reticulospinal fibres descend from the lateral pontine tegmentum. A mainly ipsilateral subcoeruleospinal pathway is distributed to all spinal segments of the cord through the lateral spinal funiculus. Crossed pontospinal fibres descend from the ventrolateral pontine tegmentum, decussate in the rostral pons and occupy the contralateral dorsolateral spinal funiculus. They terminate in laminae I, II, V and VI of all spinal segments of the cord. Fibres from the pneumotaxic centre innervate the phrenic nucleus and T1–T3 sympathetic preganglionic neurones bilaterally through this projection system.

Bilateral projections from the micturition centres travel in the lateral spinal funiculus. They terminate on preganglionic parasympathetic neurones in the sacral cord (which innervate the detrusor muscle in the urinary bladder), and on neurones in the nucleus of Onuf (which innervate the musculature of the pelvic floor and the anal and urethral sphincters) (Ch. 75).

Descending fibres of the A6 noradrenergic neurones of the locus coeruleus project into the longitudinal dorsal fasciculus (as the caudal limb of the dorsal periventricular pathway), and into the caudal limb of the dorsal noradrenergic bundle (as part of the longitudinal catecholamine bundle). In this way they innervate, mainly ipsilaterally, all other rhombencephalic reticular areas, principal and spinal trigeminal nuclei, pontine nuclei, cochlear nuclei, nuclei of the lateral lemniscus, and bilaterally, all spinal preganglionic autonomic neurones and the ventral region of the dorsal horn in all segments of the spinal cord. Other axons that contribute to the longitudinal catecholamine bundle originate from cell groups C1, A1, A2, A5 and A7. The main projection is a descending one from cell groups C1 and A5, which are sudomotor neural control centres and innervate preganglionic sympathetic neurones.

Most ascending fibres from the locus coeruleus pass in the dorsal noradrenergic (or tegmental) bundle; others run in either the rostral limb of the dorsal periventricular pathway or in the superior cerebellar peduncle. The latter fibres terminate on the deep cerebellar nuclei. The dorsal noradrenergic bundle is large and runs through the ventrolateral periaqueductal grey matter to join the medial forebrain bundle in the hypothalamus, from where fibres continue forward to innervate all rostral areas of the brain. The pathway contains efferent and afferent axons that reciprocally connect the locus coeruleus with adjacent structures along its course, e.g. central mesencephalic grey matter, dorsal raphe nucleus, superior and inferior colliculi, interpeduncular nucleus, epithalamus, dorsal thalamus, habenular nuclei, amygdala, septum, olfactory bulb and anterior olfactory nucleus, the entire hippocampal formation and neocortex. Fibres from the locus coeruleus which travel in the rostral limb of the dorsal periventricular pathway, ascend in the ventromedial periaqueductal grey matter adjacent to the longitudinal dorsal fasciculus and terminate in the parvocellular part of the paraventricular nucleus in the hypothalamus.

The functions of the locus coeruleus and related tegmental noradrenergic cell groups are poorly understood. The diversity of their rostral and caudal projections suggests a widespread role in central processing. In animals, firing rates of locus coeruleus neurones peak during wakefulness and decrease during sleep – they cease almost completely during rapid eye movement (REM) sleep. During wakefulness, firing rates are augmented when novel stimuli are presented. The locus coeruleus may, therefore, function to control the level of attentiveness. Other functions that have been ascribed to the locus coeruleus include control of the wake–sleep cycle, regulation of blood flow, and maintenance of synaptic plasticity.

The A1, A2, A5 and A7 noradrenergic cell groups project rostrally, mainly through the central tegmental tract. Their axons constitute a major longitudinal catecholamine pathway that continues through the medial forebrain bundle and ends in the amygdala, lateral septal nucleus, bed nucleus of the stria terminalis, nucleus of the diagonal band and the hypothalamus. The ascending dorsal periventricular pathway contains a few non-coerulean noradrenergic fibres, which terminate in the periventricular region of the thalamus.

Propriobulbar projections receive a contribution from the diffusely organized dorsal medullary and lateral tegmental noradrenergic cell groups. These interconnect cranial nerve nuclei and other reticular cell groups, particularly those of the vagus, facial and trigeminal nerves, and the rhombencephalic raphe and parabrachial nuclei.

Three precerebellar nuclei, the lateral and paramedian reticular nuclei and the nucleus of the pontine tegmentum, are involved in the relay of spinal information into the vermis and paravermal regions of the ipsilateral cerebellar hemisphere. They receive inputs from the contralateral primary motor and sensory neocortices, and the ipsilateral cerebellar and vestibular nuclei and spinal cord (the latter through the ascending spinoreticular pathway). This system augments the dorsal and ventral spinocerebellar, cuneocerebellar, accessory cuneocerebellar and trigeminocerebellar tracts.

BRAIN STEM LESIONS

Unilateral brain stem lesions (Fig. 19.21, Fig. 19.22) may arise as a result of extrinsic compression of the brain stem by space occupying tumours (e.g. meningioma, acoustic neuroma or metastatic carcinoma) or may be caused by intrinsic disease (e.g. glioma, demyelination or stroke). The clinical syndrome is determined by the neuroanatomical site of the lesion. At the segmental level, an ipsilateral cranial nerve palsy occurs. Below the level of the lesion, there is a contralateral loss of power and sensation in the limbs (corresponding to dysfunction of the decussating corticospinal and ascending sensory pathways), and ipsilateral incoordination of the limbs (as a result of the interruption of efferent and afferent cerebellar connections).

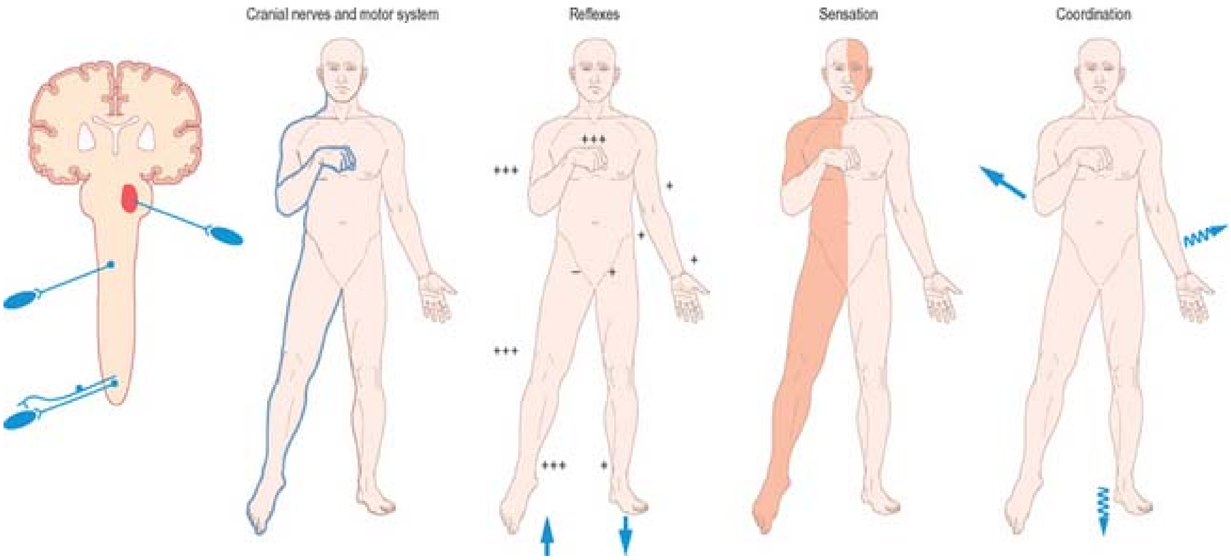

Fig. 19.21 Brain stem lesions.

(By permission from Crossman AR, Neary D 2000 Neuroanatomy, 2nd edn. Edinburgh: Churchill Livingstone.)

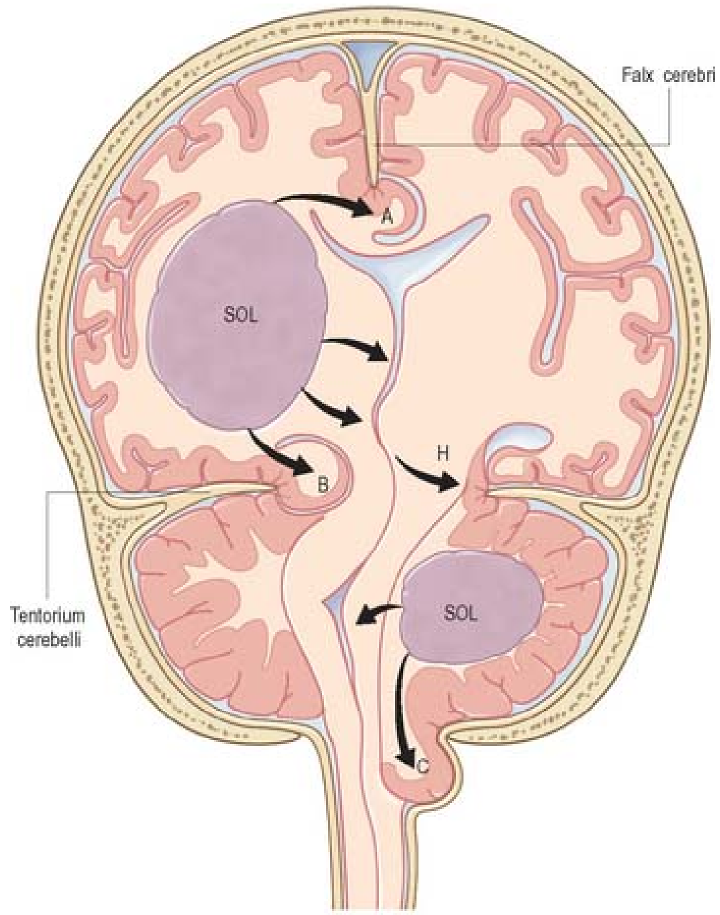

A Herniation of the cingulate gyrus under the falx
B Tentorial herniation of the parahippocampal gyrus
C Herniation of cerebellar tonsils through the foramen magnum
H Haemorrhage into the midbrain: compression of cerebral peduncle against the free edge of the tentorium cerebelli

Fig. 19.22 Consequences of a space-occupying lesion (SOL).

The ipsilateral cranial nerve dysfunction reflects the segmental level of the lesion in the midbrain, pons and medulla. Midbrain lesions cause ophthalmoplegia, pupillary dilatation and ptosis (oculomotor nerve palsy) and impaired upward gaze (e.g. due to a pinealoma). Pontine lesions (e.g. an acoustic neuroma in the cerebellopontine angle) lead to ophthalmoplegia (abducens nerve lesion), loss of facial sensation and weakness of masticatory muscles (trigeminal nerve lesion), weakness of facial muscles (facial nerve lesion), deafness and vertigo (vestibulocochlear nerve lesion). Medullary lesions cause a ‘bulbar palsy’, i.e. dysarthria, dysphagia and dysphonia, with wasting of the hemi-tongue and palate (glossopharyngeal, vagal and hypoglossal nerve lesions) and weakness and wasting of sternocleidomastoid and trapezius (accessory nerve lesion).

In addition to this focal brain stem syndrome, blockage of the outflow of CSF from the fourth ventricle via the foramina of Magendie and Luschka (e.g. by extrinsic tumours) produces hydrocephalus, which is characterized by headache, papilloedema and progressive stupor and coma.

Bilateral destructive lesions of the brain stem are fatal if untreated, because of damage to ‘centres’ in the medulla that control respiration, heart rate and blood pressure. Impairment of the reticular activating system in the core of the brain stem leads to progressive impairment of consciousness, followed by stupor and coma. In this state of ‘brain stem death’, life can only be supported artificially. This is the fate of all untreated expanding space-occupying lesions in the cranium (e.g. haematoma, abscess, tumour, whether extrinsic or intrinsic to the brain, and cerebral oedema). A space-occupying lesion within the unyielding skull raises the intracranial pressure directly and also indirectly by obstruction of CSF flow, which causes headache and papilloedema. The brain is distorted and displaced downward (rostro-caudally) within the skull and meningeal framework. The brain stem is vulnerable to compression at two critical sites, which are determined by the neuroanatomical relationship of the meningeal tentorium and foramen magnum to the cerebral hemisphere (supratentorial) and brain stem (infratentorial). The downward displacement of the cerebral hemisphere leads to herniation of the ipsilateral medial temporal lobe (uncus) through the tentorial notch. There may be direct ipsilateral compression of the midbrain and emergent oculomotor and trochlear cranial nerves or contralateral compression of the upper brain stem by the abutting sharp edge of the tentorium. The ipsilateral posterior cerebral artery is vulnerable to compression at this site. Unilateral herniation is heralded by a progressive oculomotor nerve palsy (ophthalmoplegia, pupillary dilatation and ptosis), contralateral limb weakness, falling level of consciousness, and, if treatment is long delayed, a contralateral homonymous hemianopia. Compression of the contralateral brain stem by the tentorium leads to ipsilateral ‘false localizing’ signs.

Further progressive rostro-caudal displacement of the brain ultimately leads to herniation of the medulla through the foramen magnum and into the spinal canal. This is accompanied by bilateral cranial nerve dysfunction, quadriplegia, deepening coma and finally apnoea, i.e. brain stem death. These neuroanatomical and functional processes underlie the diagnosis and management of the traumatically brain injured patient, and the complications of intracranial haematomas (extradural, subdural and intracerebral) and cerebral oedema.

REFERENCES

odal P, Bjaalie JG. Organization of the pontine nuclei. *Neurosci Res*. 1992;13:83-118.

riello J. Brainstem projections of aortic baroreceptor afferent fibres in the rat. *Neurosci Lett*. 1983;36:37-42.

ahlström A, Fuxe K. Evidence for the existence of monamine-containing neurones in the central nervous system. *Acta Physiol Scand Suppl*. 1964;232:1-55.

ahlström A, Fuxe K. Evidence for the existence of monoamine neurones in the central nervous system. II. Experimentally induced changes in the intraneuronal amine levels of bulbospinal neurone systems. *Acta Physiol Scand Suppl*. 1965;247:1-36.

amilton RB, Norgren R. Central projections of gustatory nerves in the rat. *J Comp Neurol*. 1984;222:560-577.

hnston JB. The morphology of the forebrain vesicle in vertebrates. *J Comp Neurol*. 1909;19:458-539.

illar J, Basbaum AI. Topography of the projection of the body surface of the cat to cuneate and gracile nuclei. *Exp Neurol*. 1975;49(1 pt 1):281-290.

athan PW, Smith MC. The rubrospinal and central tegmental tracts in man. *Brain*. 1982;105:223-269.

euwenhuys R, Voogd J, van Huijzen C. The Human Central Nervous System. A Synopsis and Atlas. 3rd edn.. Berlin: Springer Verlag; 1988.

szewski J. On the anatomical and functional organization of the spinal trigeminal nucleus. *J Comp Neurol*. 1950;92:401-409.

CHAPTER 20

Cerebellum

The cerebellum occupies the posterior cranial fossa, separated from the occipital lobes of the cerebral hemispheres by the tentorium cerebelli. It is the largest part of the hindbrain; in adults the weight ratio of cerebellum to cerebrum is approximately 1 : 10 and in infants 1 : 20. The cerebellum lies dorsal to the pons and medulla, from which it is separated by the fourth ventricle. It is joined to the brain stem by three bilaterally paired cerebellar peduncles, and these contain all the afferent and efferent fibres associated with the cerebellum.

The basic internal organization of the cerebellum is of a superficial cortex overlying a dense core of white matter. The cortex is highly convoluted, forming narrow ridges, or folia, and intervening sulci and fissures. Aggregations of neuronal cell bodies embedded within the white matter constitute the fastigial, globose, emboliform and dentate nuclei – collectively known as the (deep) cerebellar nuclei. In general terms, the majority of afferent input to the cerebellum terminates in the cortex. The output from the cortex is carried by the axons of cortical Purkinje cells; most of these axons terminate in the deep cerebellar nuclei which are themselves the major origin of cerebellar efferent projections.

The cerebellum is an important part of the circuitry that links sensory to motor areas of the brain, and it functions to coordinate movement. It provides corrections during movement, which are the basis for precision and accuracy, and it is critically involved in motor learning and reflex modification. It receives information from peripheral receptors through spinal, trigeminal and vestibulocerebellar pathways and from the cerebral cortex and the tectum, via the intermediary of pontine nuclei. Cerebellar output is directed predominantly to the thalamus and thence to the motor cortex, and also to brain stem centres such as the red nucleus, vestibular nuclei and reticular nuclei that themselves give rise to descending spinal pathways.

EXTERNAL FEATURES AND RELATIONS

The cerebellum consists of two large, laterally located hemispheres which are united by a midline vermis (Figs 20.1, 20.2, 20.3). The superior surface of the cerebellum, which would constitute the anterior part of the unrolled cerebellar cortex, has a flat profile (Fig. 20.3). The paramedian sulci are shallow and the borders between vermis and hemispheres are indicated by kinks in the transverse fissures. The superior surface adjoins the tentorium cerebelli and projects beyond its free edge. The transverse sinus borders the cerebellum at the point where the superior and inferior surfaces meet. The inferior surface is characterized by a massive enlargement of the cerebellar hemispheres, which extend medially to overlie some of the vermis. Deep paramedian sulci demarcate the vermis from the hemispheres. Posteriorly the hemispheres are separated by a deep vallecula, which contains the dural falx cerebelli. The inferior cerebellar surface lies against the occipital squama. The shape of the surface facing the brain stem is irregular and forms the roof of the fourth ventricle and the lateral recesses on each side of it, while the cerebellar peduncles define the diamond shape of the ventricle when viewed from behind. Anterolaterally the cerebellum lies against the posterior surface of the petrous part of the temporal bone.

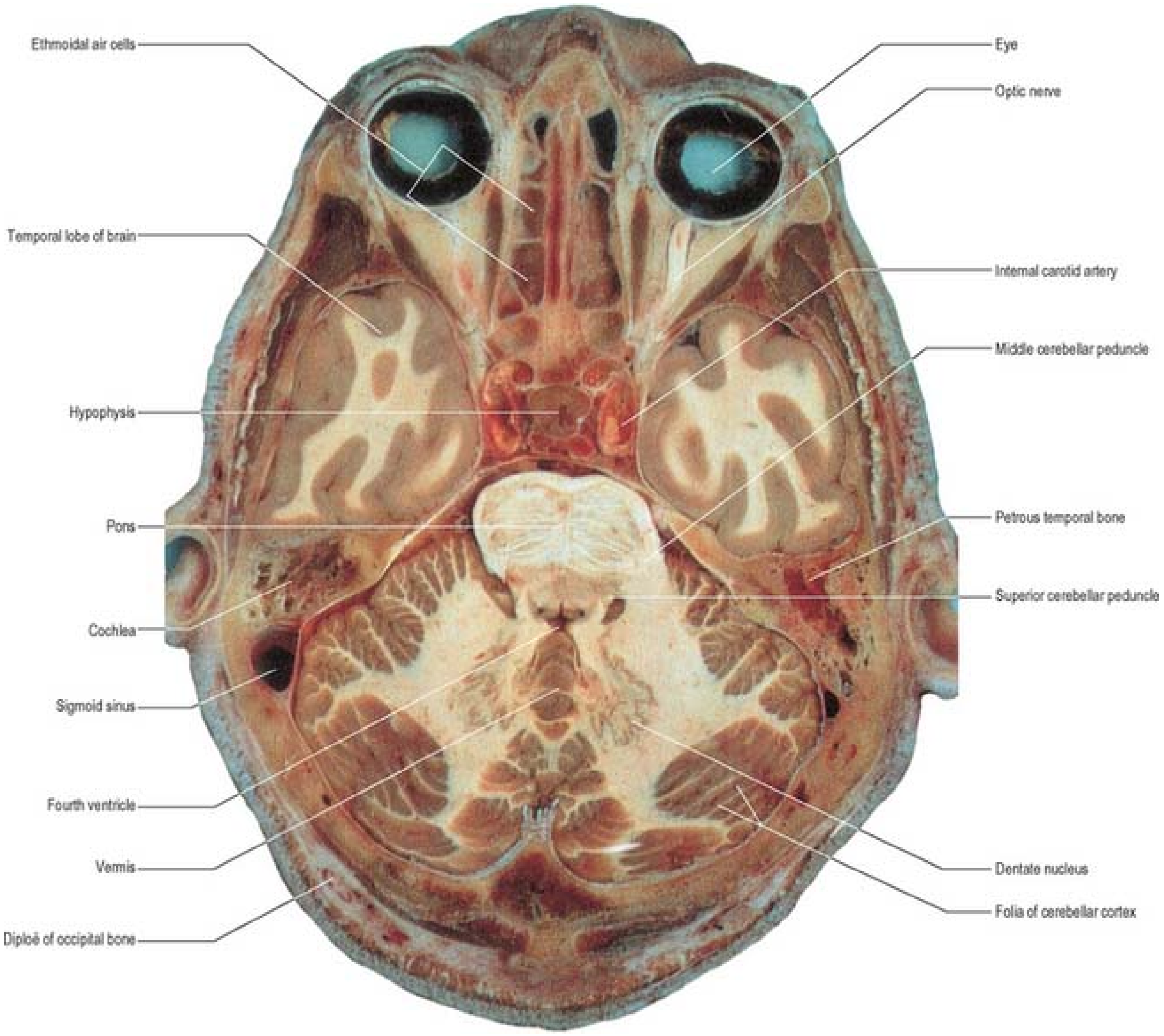
Ethmoidal air cells
Eye
Optic nerve
Temporal lobe of brain
Internal carotid artery
Middle cerebellar peduncle
Hypophysis
Pons
Petrous temporal bone
Superior cerebellar peduncle
Cochlea
Sigmoid sinus
Fourth ventricle
Vermis
Dentate nucleus
Folia of cerebellar cortex
Diploë of occipital bone

Fig. 20.1 Horizontal section through the cerebellum and brain stem.

(By courtesy of Dr GJA Maart.)

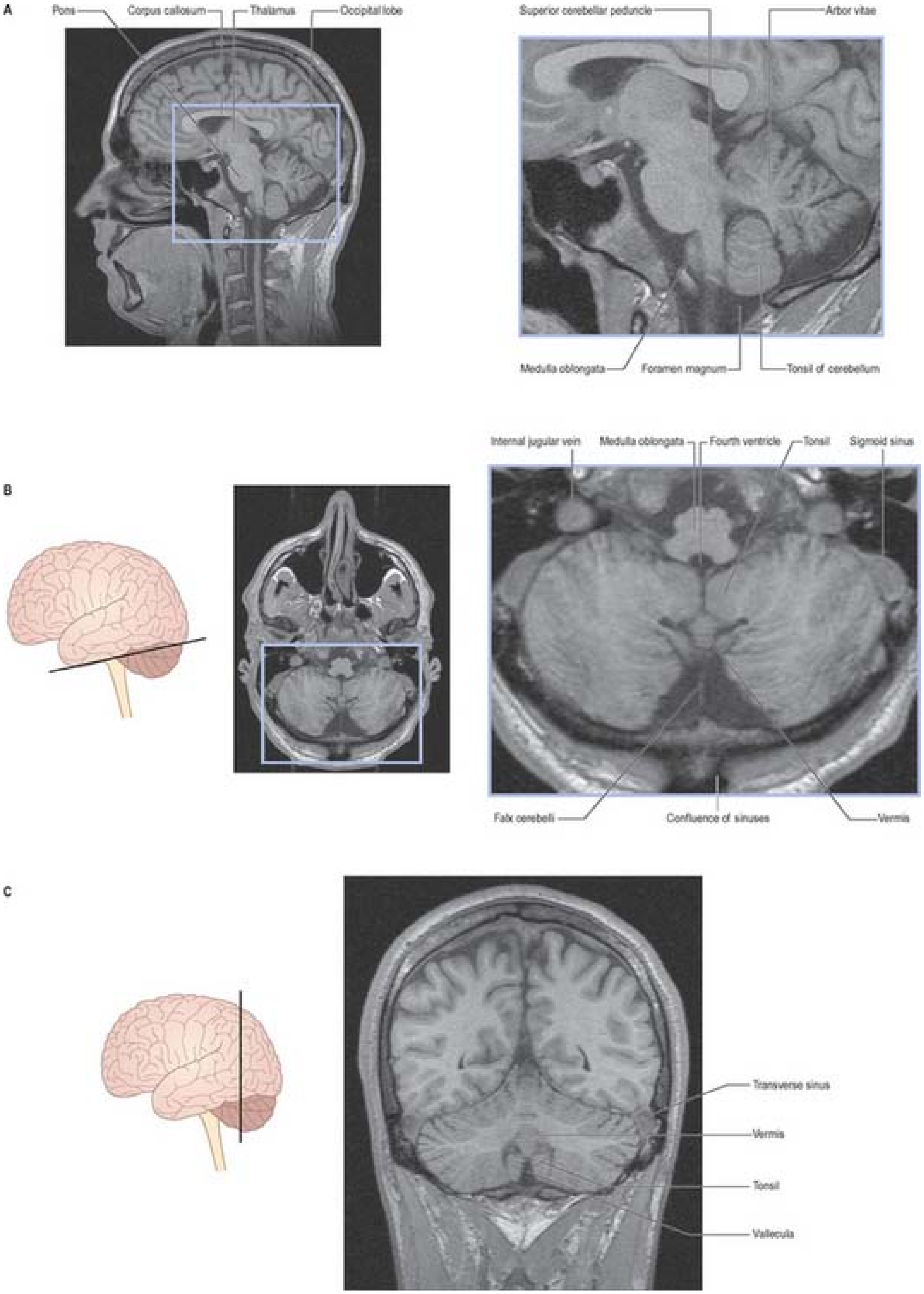
A
Pons
Corpus callosum
Thalamus
Occipital lobe
Superior cerebellar peduncle
Arbor vitae
Medulla oblongata
Foramen magnum
Tonsil of cerebellum
B
Internal jugular vein
Medulla oblongata
Fourth ventricle
Tonsil
Sigmoid sinus
Falx cerebelli
Confluence of sinuses
Vermis
C
Transverse sinus
Vermis
Tonsil
Vallecula

Fig. 20.2 Magnetic resonance images of the cerebellum of a 16-year-old female. **A**, sagittal **B**, axial. **C**, coronal.

(By courtesy of Drs JP Finn and T Parrish, Northwestern University School of Medicine, Chicago.)

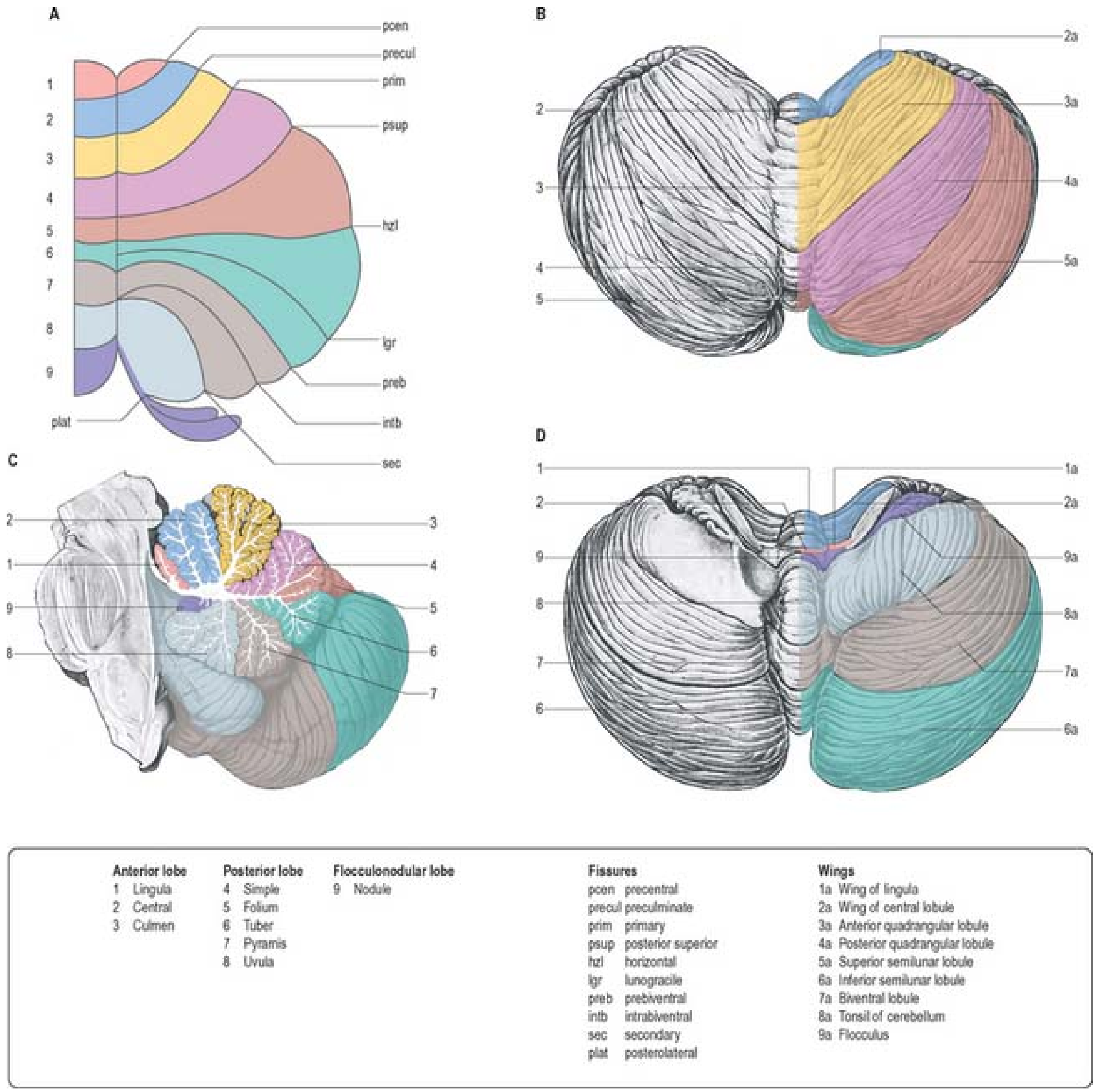
A
pcen
precul
prim
psup
hzl
lgr
preb
intb
sec
plat
1
2
3
4
5
6
7
8
9
B
2a
3a
4a
5a
C
D
1a
9a
8a
7a
6a
Anterior lobe
1 Lingula
2 Central
3 Culmen
Posterior lobe
4 Simple
5 Folium
6 Tuber
7 Pyramis
8 Uvula
Flocculonodular lobe
9 Nodule
Fissures
pcen precentral
precul preculminate
prim primary
psup posterior superior
hzl horizontal
lgr lunogracile
preb prebiventral
intb intrabiventral
sec secondary
plat posterolateral
Wings
1a Wing of lingula
2a Wing of central lobule
3a Anterior quadrangular lobule
4a Posterior quadrangular lobule
5a Superior semilunar lobule
6a Inferior semilunar lobule
7a Biventral lobule
8a Tonsil of cerebellum
9a Flocculus

Fig. 20.3 Terminology of cerebellar lobes and fissures, using a schematic 'unrolled' diagram as a frame of reference. **A**, Unrolled cerebellar cortex. The lobules are labelled by numbers and the fissures between the wings are listed. **B**, Cerebellum viewed from above. **C**, Median sagittal section of cerebellum. The nodules and wings are numbered and listed. **D**, Cerebellum viewed from below.

The cerebellar surface is divided by numerous curved transverse fissures which separate its folia and give it a laminated appearance. The deepest fissures divide it into lobes and lobules. One conspicuous fissure, the horizontal fissure, extends around the dorsolateral border of each hemisphere from the middle cerebellar peduncle to the vallecula, separating the superior and inferior surfaces. Although the horizontal fissure is prominent, it appears relatively late in embryological development and does not mark the boundary between major functional subdivisions of the cortex. The deepest fissure in the vermis is the primary fissure, which curves ventrolaterally around the superior surface of the cerebellum to meet the horizontal fissures; it appears early in embryological development and marks the boundary between the anterior and posterior lobes.

Because the cerebellar cortex has a roughly spherical shape, the true relationships between its parts is somewhat obscure. Thus, the most anterior lobule of the cerebellar vermis, the lingula, lies very close to the most posterior lobule, the nodule. The lobules of the superior vermis that belong to the anterior lobe are the lingula, central lobule and culmen. The lingula is a single lamina of four or five shallow folia. Its white core is continuous with the superior medullary velum, and it is separated from the central lobule by the precentral fissure. The central lobule and culmen are continuous bilaterally with an adjoining lateral extension, or wing, in each hemisphere. The central lobule is separated from the culmen by the preculminary fissure. The culmen (with attached anterior quadrangular lobules) lies between the preculminary and primary fissures.

The simple lobule (with attached posterior quadrangular lobules) and the folium (with attached superior semilunar lobules) lie between the primary and the horizontal fissures: the two lobule sets are separated by the posterior superior fissure.

From the back forward, the inferior vermis is divided into the tuber, pyramis, uvula and nodule, in that order. The tuber is continuous laterally with the inferior semilunar lobules and separated from the pyramis by the lunogracile fissure. The pyramis and attached biventral lobules (containing an intrabiventral fissure) are separated from the uvula and attached cerebellar tonsils by the secondary fissure. Behind the uvula, and separated from it by the median part of the posterolateral fissure, is the nodule. The tonsils are roughly spherical and overhang the foramen magnum on each side of the medulla oblongata.

The nodule and attached flocculi constitute a separate flocculonodular lobe, which is separated from the uvula and tonsils by the deep posterolateral fissure. The flocculonodular lobe is richly interconnected with the vestibular nuclei, which lie at the lateral margin of the fourth ventricle.

FUNCTIONAL DIVISIONS OF THE CEREBELLUM

Functionally speaking, the cerebellum can be divided into a body, with inputs mainly from the spinal cord and pontine nuclei, and a flocculonodular lobe, which has strong afferent and efferent connections with the vestibular nuclei (Fig. 20.4). The body is subdivided into a series of regions dominated by their spinal or pontine inputs. The anterior lobe, simple lobule, pyramis and biventral lobules are the main recipients of spinal and trigeminal cerebellar afferents. Pontocerebellar input dominates in the folium, tuber and uvula, and throughout the entire hemisphere, including those regions that receive afferents from the spinal cord.

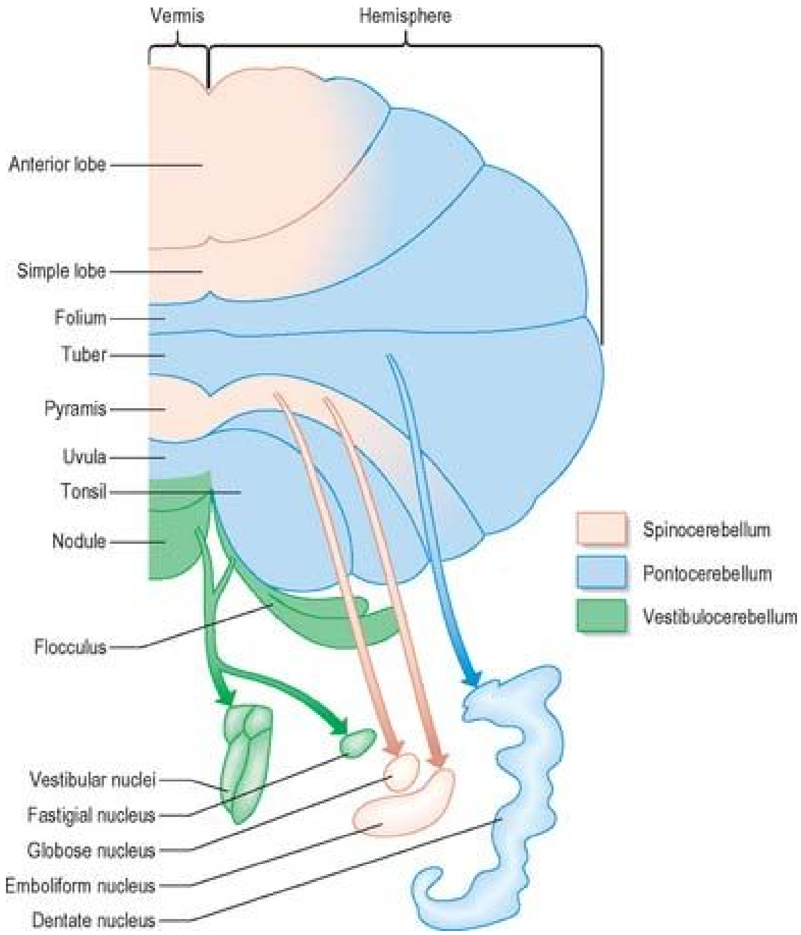
Vermis
Hemisphere
Anterior lobe
Simple lobe
Folium
Tuber
Pyramis
Uvula
Tonsil
Nodule
Flocculus
Vestibular nuclei
Fastigial nucleus
Globose nucleus
Emboliform nucleus
Dentate nucleus
Spinocerebellum
Pontocerebellum
Vestibulocerebellum

Fig. 20.4 The flattened cerebellar surface and cerebellar nuclei. The transverse lobular organization of the afferent spino-, ponto- and vestibulocerebellar connections of the cortex is shown, together with the longitudinal zonal organization of the efferents from vermis and hemispheres to the cerebellar and vestibular nuclei.

The mediolateral subdivision of the cerebellum into vermis and hemispheres represents a functional subdivision that is closely related to its output. In mammals, the increase in the size of the cerebellar hemispheres parallels the development of the cerebral cortex, and reflects the importance of the corticopontocerebellar input and of the efferent projections of the cerebellar hemispheres (through the dentate, emboliform and globose nuclei) to the thalamus and thence to the cerebral cortex.

INTERNAL STRUCTURE

The vast majority of cerebellar neuronal cell bodies are located within the outer, highly convoluted cortical layer. Beneath the cortex, the cerebellar white matter forms an extensive central core from which a characteristic branching pattern of nerve fibres (*arbor vitae*) extends towards the cortical surface. The white matter consists of afferent and efferent fibres travelling to and from the cerebellar cortex. Fibres crossing the midline in the white core of the cerebellum and the anterior medullary velum effectively constitute a cerebellar ‘commissure’; the afferent portion contains fibres of the restiform body and the middle cerebellar peduncle, and the efferent portion contains decussating fibres from the fastigial nucleus.

CEREBELLAR NUCLEI

Laterally, on either side within the white matter core, are four cerebellar nuclei. These are the dentate, emboliform, globose and fastigial nuclei. The dentate nucleus, which is located most laterally and is by far the largest, is the only nucleus easily visible to the naked eye (Fig. 20.1). It has the form of an irregularly folded sheet of neuronal cell bodies, with a medially directed hilum through which pass a mass of fibres mainly derived from dentate neurones and which form the bulk of the superior cerebellar peduncle. The emboliform and globose nuclei lie medial to the dentate and are equated to the nucleus interpositus (interposed nucleus) in lower species; the emboliform and globose nuclei may sometimes be referred to as the anterior and posterior interposed nuclei, respectively. Their efferent fibres join the superior cerebellar peduncle. The fastigial nucleus lies next to the midline, bordering on the roof of the fourth ventricle. A large proportion of the efferent fibres that leave this nucleus decussate within the cerebellar white matter and subsequently constitute the uncinate fasciculus, which passes dorsal to the superior cerebellar peduncle to enter the contralateral vestibular nuclei. Uncrossed fastigiobulbar fibres enter the vestibular nuclei by passing along the lateral angle of the fourth ventricle, and some fibres of the fastigial nucleus ascend in the superior cerebellar peduncle.

CEREBELLAR PEDUNCLES

Three pairs of peduncles connect the cerebellum with the brain stem (see Ch. 19; Fig. 20.5).

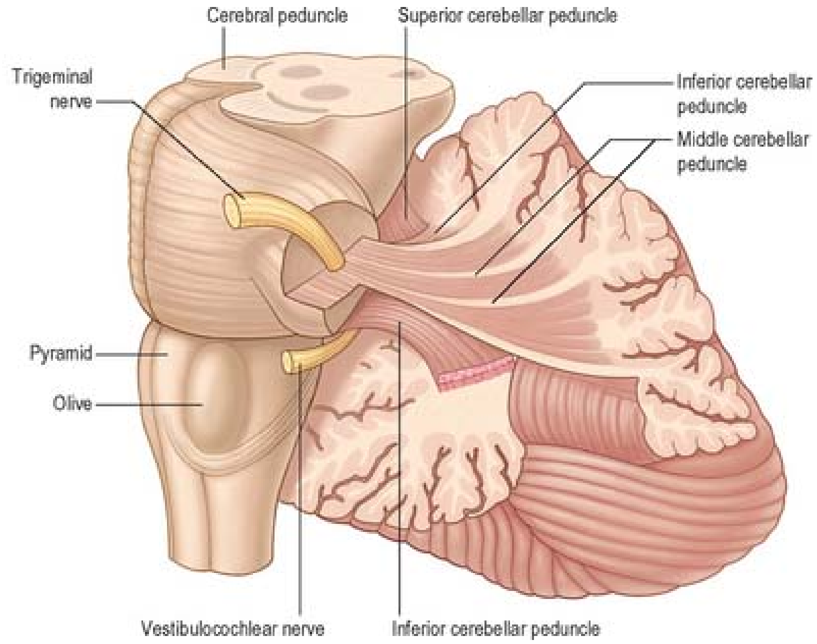
Cerebral peduncle
Superior cerebellar peduncle
Trigeminal nerve
Inferior cerebellar peduncle
Middle cerebellar peduncle
Pyramid
Olive
Vestibulocochlear nerve
Inferior cerebellar peduncle

Fig. 20.5 Dissection of the left cerebellar hemisphere and its peduncles.

The middle cerebellar peduncle is the most lateral and by far the largest of the three. It passes obliquely from the basal pons to the cerebellum and is composed almost entirely of fibres that arise from the contralateral basal pontine nuclei, with a small addition from nuclei in the pontine tegmentum.

The inferior cerebellar peduncle is located medial to the middle peduncle. It consists of an outer, compact fibre tract, the restiform body, and a medial, juxtarestiform body. The restiform body is a purely afferent system; it receives the posterior spinocerebellar tract from the spinal cord and the trigeminocerebellar, cuneocerebellar, reticulocerebellar and olivocerebellar tracts from the medulla oblongata. The juxtarestiform body is mainly an efferent system; it is made up almost entirely of efferent Purkinje cell axons from the vestibulocerebellum, on their way to the vestibular nuclei, and uncrossed fibres from the fastigial nucleus. It also contains primary afferent fibres travelling in the vestibular nerve and secondary afferent fibres from the vestibular nuclei. The crossed fibres from the fastigial nucleus pass dorsal to the superior cerebellar peduncle and enter the brain stem as the uncinate fasciculus at the border of the juxtarestiform and restiform bodies.

The superior cerebellar peduncle contains all of the efferent fibres from the dentate, emboliform and globose nuclei and a small fascicle from the fastigial nucleus. Its fibres decussate in the caudal mesencephalon, on their way to synapse in the contralateral red nucleus and thalamus. The anterior spinocerebellar tract reaches the upper part of the pontine tegmentum before looping down within this peduncle to join the spinocerebellar fibres entering through the restiform body.

CEREBELLAR CORTEX

Although the human cerebellum makes up approximately one-tenth of the entire brain by weight, the surface area of the cerebellar cortex, if unfolded, would be about half that of the cerebral cortex. The great majority of cerebellar neurones are small granule cells, so densely packed that the cerebellar cortex contains many more neurones than the cerebral cortex. Unlike the cerebral cortex, where a large number of diverse cell types are arranged differently in different regions, the cerebellar cortex contains a relatively small number of different cell types, which are interconnected in a highly stereotyped way. As a consequence, all regions of the cerebellar cortex look similar in histological sections.

The elements of the cerebellar cortex possess a precise geometric order, which is arrayed relative to the tangential, longitudinal and transverse planes in individual folia. The cortex contains the terminations of afferent ‘climbing’ and ‘mossy’ fibres, five varieties of neurone (granular, stellate, basket, Golgi and Purkinje), neuroglia and blood vessels.

There are three main layers: molecular, Purkinje cell and granular (Fig. 20.6). The main circuit of the cerebellum involves granule cells, Purkinje cells and neurones in the cerebellar nuclei. Granule cells receive the terminals of the mossy fibre afferents (i.e. all afferent systems except the olivocerebellar fibres). The axons of the granule cells ascend to the molecular layer, where they bifurcate into parallel fibres, which are so called because they are oriented parallel to the transverse fissures and perpendicular to the dendritic trees of the Purkinje cells on which they terminate. Purkinje neurones are large and are the sole output cells of the cerebellar cortex. Their axons terminate in the cerebellar nuclei and in the vestibular nuclei. In addition to the dense array of parallel fibres, the dendritic trees of Purkinje cells receive terminals from climbing fibres which originate from neurones in the inferior olivary nucleus. The cerebellar cortex thus receives two distinct types of input: olivocerebellar climbing fibres, which synapse directly on Purkinje neurones, and mossy fibres, which connect to the Purkinje cells via granular neurones, whose axons are the parallel fibres.

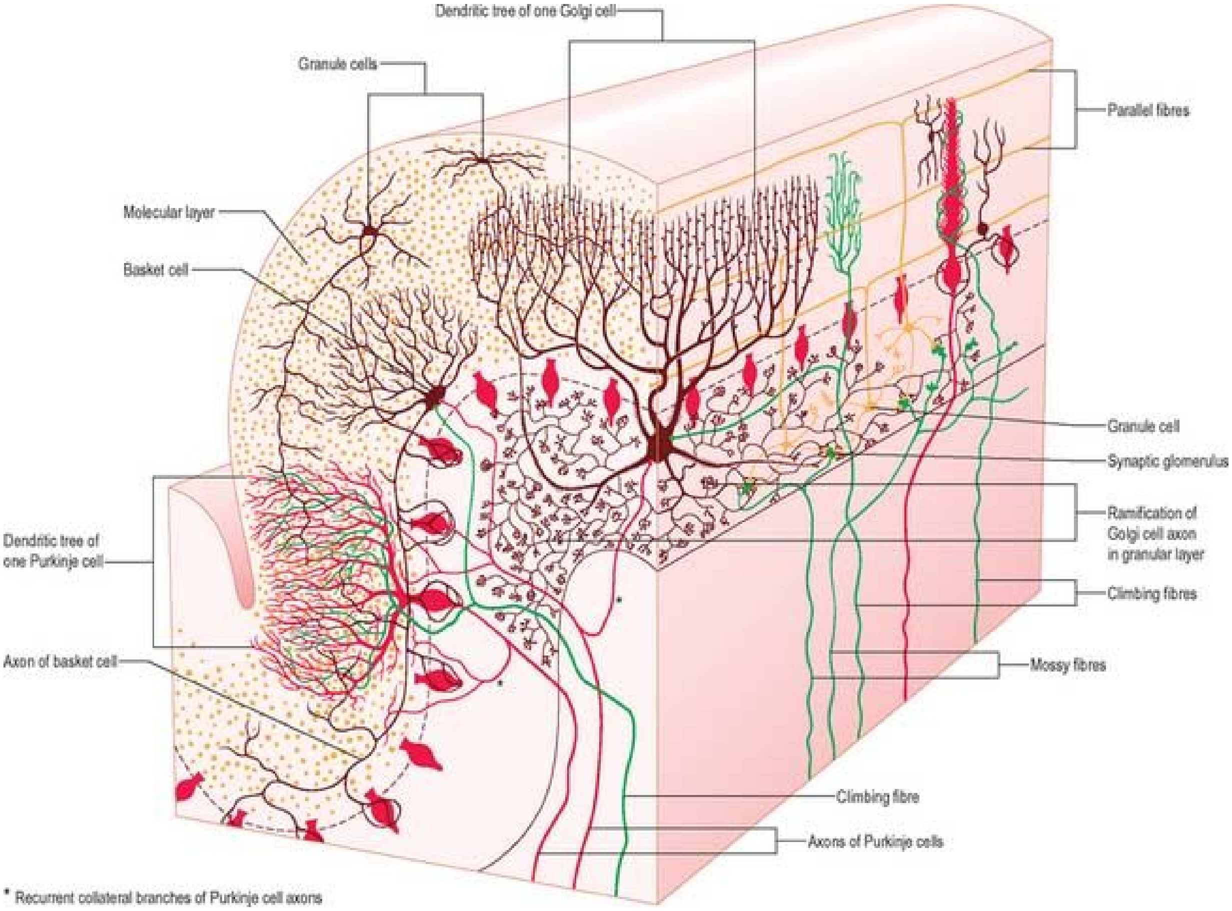
Dendritic tree of one Golgi cell
Granule cells
Parallel fibres
Molecular layer
Basket cell
Granule cell
Synaptic glomerulus
Ramification of Golgi cell axon in granular layer
Dendritic tree of one Purkinje cell
Climbing fibres
Axon of basket cell
Mossy fibres
Climbing fibre
Axons of Purkinje cells

* Recurrent collateral branches of Purkinje cell axons

Fig. 20.6 The general organization of the cerebellar cortex. A single folium has been sectioned vertically, both in its longitudinal axis (right part of diagram) and transversely.

Both parallel and climbing fibres excite the Purkinje cells, but they differ greatly in their firing characteristics and their effect on them. Purkinje cell axons inhibit their target neurones in the cerebellar nuclei; the latter project to motor control centres in the brain stem and cerebrum. The stellate, basket and Golgi cells are inhibitory interneurones and connect the cortical elements in complex geometrical patterns.

The molecular layer is approximately 300–400 µm thick. It contains a sparse population of neurones, dendritic arborizations, non-myelinated axons and radial fibres of neuroglial cells. Purkinje cell dendritic trees extend towards the surface and spread out in a plane perpendicular to the long axis of the cerebellar folia. Purkinje cell dendrites are flattened. The lateral extent of the Purkinje cell dendrites is some 30 times greater in the transverse plane than it is in a plane parallel to the cerebellar folia. Parallel fibres are the axons of granule cells, the stems of which ascend into the molecular layer where they bifurcate at T-shaped branches. The two branches extend in opposite directions as parallel fibres along the axis of a folium. Parallel fibres terminate on the dendrites of the Purkinje cells and Golgi cells, which they pass on their way, and on the basket and stellate cells of the molecular layer. Dendritic trees of Golgi neurones reach towards the surface. Unlike the flattened dendritic tree of the Purkinje cell, Golgi cell dendrites span the territory of many Purkinje neurones longitudinally as well as transversely. These dendrites receive synapses from parallel fibres. Some Golgi cell dendrites enter the granular layer, where they contact mossy fibre terminals. The cell bodies of Golgi neurones lie below, in the superficial part of the granular layer. The molecular layer also contains the somata, dendrites and axons of stellate neurones (which are located superficially within the molecular layer) and of basket cells (whose somata lie deeper within the molecular layer). Climbing fibres, the terminals of olivocerebellar fibres, ascend through the granular layer to contact Purkinje dendrites in the molecular layer. Radiating branches from large epithelial (Bergmann) glial cells give off processes that surround all neuronal elements, except at the synapses. Their conical expansions join to form an external limiting membrane at the surface of the cerebellum.

The Purkinje cell layer contains the large, pear-shaped somata of the Purkinje cells and the smaller somata of Bergmann glia. Clumps of granule cells and occasional Golgi cells penetrate between the Purkinje cell somata.

The granular layer (Fig. 20.6) is about 100 μm thick in the fissures and 400–500 μm on foliar summits. There are approximately 2.7 million granular neurones per cubic millimetre. It has been estimated that the human cerebellum contains a total of 4.6×10^{10} granule cells, and that there are 3000 granule cells for each Purkinje cell.

In summary, the granular layer consists of the somata of granule cells and the initial segment of their axons; dendrites of granule cells; branching terminal axons of afferent mossy fibres; climbing fibres passing through the granular layer *en route* to the molecular layer; and the somata, basal dendrites and complex axonal ramifications of Golgi neurones. Cerebellar glomeruli are synaptic rosettes consisting of a mossy fibre terminal that forms excitatory synapses upon the dendrites of both granule cells and Golgi cells.

Of the five cell types to be described, the first four are inhibitory, liberating γ-aminobutyric acid (GABA), and the fifth is excitatory, liberating L-glutamate. Figure 20.7 summarizes their main connections.

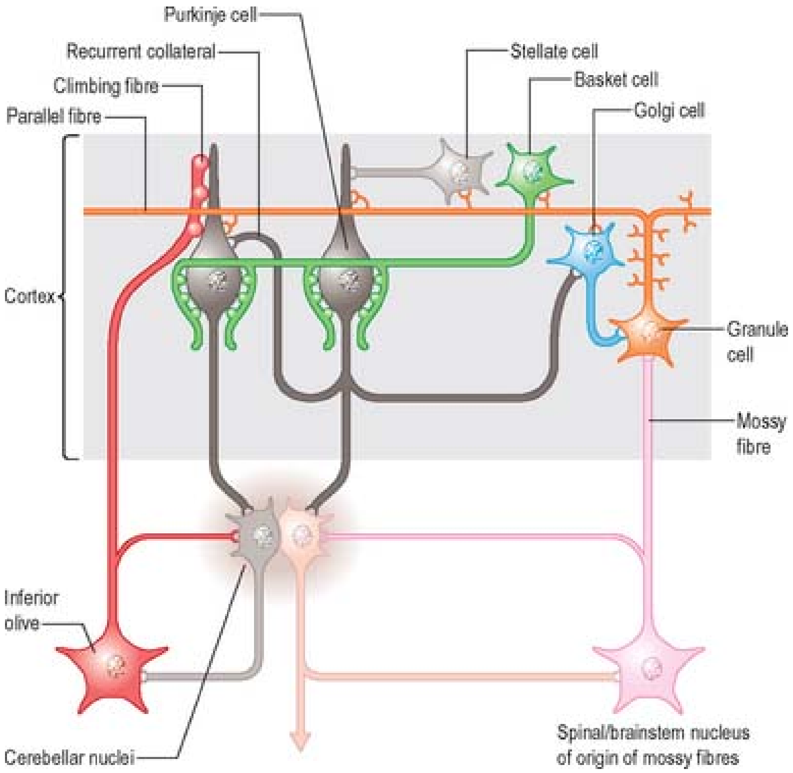
Purkinje cell
Recurrent collateral
Climbing fibre
Parallel fibre
Stellate cell
Basket cell
Golgi cell
Cortex
Granule cell
Mossy fibre
Inferior olive
Cerebellar nuclei
Spinal/brainstem nucleus of origin of mossy fibres

Fig. 20.7 The main intrinsic connections of the cerebellar cortex.

Purkinje cells have a specific geometry, which is conserved in all vertebrate classes (Fig. 20.6). They are arranged in a single layer between the molecular and granular layers. Individual Purkinje cells are separated by about 50 µm transversely and 50–100 µm longitudinally. Their somata measure approximately 50–70 µm vertically and 30–35 µm transversely. The subcellular structure of the Purkinje cell is similar to that of other neurones. One distinguishing feature is subsurface cisterns, often associated with mitochondria, which are present below the plasmalemma of somata and dendrites and may penetrate into the spines. The cisterns are intracellular calcium stores which are important links in the second messenger systems of the cell.

One, sometimes two, large primary dendrites arise from the outer pole of a Purkinje cell. From these an abundant arborization, with several orders of subdivision, extends towards the surface. Branches of each neurone are confined to a narrow sheet in a plane transverse to the long axis of the folium. Proximal first- and second-order dendrites have smooth surfaces with short, stubby spines, and are contacted by climbing fibres. Distal branches show a dense array of dendritic spines, which receive synapses from the terminals of parallel fibres. Inhibitory synapses are received from basket and stellate cells and from the recurrent collaterals of Purkinje cell axons, which contact the shafts of the proximal dendrites. The total number of dendritic spines per Purkinje neurone is in the order of 180,000.

The axon of a Purkinje cell leaves the inner pole of the soma and crosses the granular layer to enter the subjacent white matter. The initial axon segment receives axo-axonic synaptic contacts from distal branches of basket cell axons. Beyond the initial segment, the axon enlarges, becomes myelinated, and gives off collateral branches. The main axon ultimately forms a plexus in one of the cerebellar or vestibular nuclei. The recurrent collateral branches end on other Purkinje cells and on basket and Golgi neurones.

Basket and stellate cells are the neurones of the molecular layer. Their sparsely branched dendritic trees and the ramifications of their axons lie in a plane approximately perpendicular to the long axis of the folium, i.e. in the same plane as the Purkinje cell dendritic tree. Stellate cells are located in the superficial molecular layer and their axons synapse with the shafts of Purkinje cell dendrites. Both stellate and basket cells receive excitatory synapses from parallel fibres passing through their dendritic tree. Basket cells lie in the lower third of the molecular layer. Their somata receive synapses from Purkinje cell recurrent collaterals, climbing and mossy fibres as well as from the parallel fibres. Basket cell axons increase in size away from their somata and run deep in the molecular layer just above the Purkinje cells. Continuing for about 1 mm, each covers the territories of 10 to 12 Purkinje neurones. Collaterals of the basket cell axons ascend along Purkinje cell dendrites, and descend towards Purkinje cell somata and initial axonal segments forming pericellular networks, or ‘baskets’, around them. Branches from each basket cell axon also extend in the direction of the long axis of the folium to a further 3 to 6 rows of Purkinje neurones, flanking the axon. It follows that around 70 Purkinje cell neurones may receive synapses from a single basket neurone.

Most Golgi cell somata occupy the superficial zone of the granular layer, adjoining the Purkinje cell somata. Their dendrites radiate into the molecular layer. Unlike Purkinje cells, the dendritic trees of Golgi cells are not flattened, appearing much the same in transverse and longitudinal foliar section. In both planes they overlap the territories of several neighbouring Purkinje and Golgi cells. Some Golgi dendrites, however, divide in the granular layer and join cerebellar glomeruli, where they receive excitatory synaptic contacts from mossy fibres. The axon of the Golgi cell arises from the base of the cell body or proximal dendrite and immediately divides into a profuse arborization which extends through the entire thickness of the granular layer. The territory occupied by the axonal ramifications is of a volume that corresponds approximately to its dendritic tree in the molecular layer, and which overlaps with the axonal arborizations of adjacent Golgi cells. The main synaptic input to Golgi cell dendrites is from parallel fibres in the molecular layer. Purkinje cell recurrent collaterals and mossy and climbing fibres also terminate on their proximal dendrites and, more sparsely, on their somata.

Each granule cell has a spherical nucleus, 5–8 μm in diameter, with a mere shell of cytoplasm containing a few small mitochondria, ribosomes and a diminutive Golgi complex. Granule cells give rise to 3 to 5 short dendrites, which end in claw-like terminals within the synaptic glomeruli. The fine axons of granule cells enter the molecular layer and branch at a T-junction to form parallel fibres passing in opposite directions over a distance of several millimetres. Terminals located along the parallel fibres give them a beaded appearance and are sites of synapses upon the dendrites of Purkinje, stellate, basket and Golgi cells in the molecular layer. Most numerous are the synapses with Purkinje dendritic spines. It had been estimated that about 250,000 parallel fibres cross a single Purkinje dendritic tree, although every parallel fibre may not synapse with each dendritic tree that it crosses.

Two very different excitatory inputs innervate the cerebellar cortex, namely climbing fibres and mossy fibres.

Climbing fibres arise only from the inferior olivary nucleus. Olivocerebellar fibres cross the white matter and enter the granular layer where they branch to form climbing fibres. Each climbing fibre innervates a single Purkinje cell. There are about ten times as many Purkinje cells as there are cells in the inferior olive and so each olivocerebellar fibre branches into about 10 climbing fibres. Individual climbing fibres pass alongside the soma of a Purkinje cell, and then branch to make numerous synapses on the short, stubby spines that protrude from the proximal segments of Purkinje cell dendrites.

Mossy fibres take their origin from the spinal cord, the trigeminal, dorsal column, and reticular nuclei of the medulla, and the pontine tegmentum and basal pons. Like climbing fibres they are excitatory, but they contrast sharply in their anatomical distribution and physiological properties. As each mossy fibre traverses the white matter its branches diverge to enter several adjacent folia. Within each folium these branches expand into grape-like synaptic terminals (mossy fibre rosettes), which occupy the centre of cerebellar glomeruli.

Noradrenergic and serotoninergic fibres form a rich plexus in all layers of the cerebellar cortex. The aminergic fibres are fine, varicose and form extensive cortical plexuses: their release of noradrenaline and serotonin is assumed to be non-synaptic, and their effects paracrine, involving volumes of tissue. The serotoninergic afferents of the cerebellum take their origin from neurones in the medullary reticular formation, other than the raphe nuclei. The noradrenergic, coeruleocerebellar projection, when active, inhibits Purkinje cell firing not by direct action but via β-adrenergic-receptor-mediated inhibition of adenylate cyclase in the Purkinje cells. Cerebellar afferents have been traced from dopaminergic cells in the ventral tegmental area, and dopamine D2 and D3 receptors are present in the molecular layer. A plexus of thin, ChAT-containing fibres is centred on the Purkinje cell layer. The cells of origin of these cholinergic fibres are not known.

The connections of the cerebellum are organized in two perpendicular planes, corresponding to the planar organization of the cerebellar cortex. Efferent connections of the cortex are disposed in parasagittal sheets or bundles, which connect longitudinal strips of Purkinje cells with specific cerebellar or vestibular nuclei. The climbing fibre afferents to a Purkinje cell zone from the inferior olive display a similar zonal disposition. Cerebellar output is organized in modules, where a module consists of one or more Purkinje cell zones, their cerebellar or vestibular target nucleus, and their olivocerebellar climbing fibre input. Modular function is determined by the brain stem projections of the cerebellar or vestibular target nucleus. A general feature of the modular organization of the cerebellum is that GABAergic neurones in the cerebellar nuclei project to the subnuclei of the contralateral inferior olive, which give rise to their respective climbing fibre afferents. These recurrent connections are known as nucleo-olivary pathways.

Mossy fibre afferent systems from precerebellar nuclei in the spinal cord and the brain stem terminate in the granular layer of certain lobules in transversely oriented terminal fields. The transverse lobular arrangement of the mossy fibre afferents is enforced by the transverse orientation of the parallel fibres, which are axons of the granule cells and constitute the second link in the mossy fibre–parallel fibre input of the Purkinje cells. Parallel fibres cross and terminate on Purkinje cells belonging to several successive modules as they course through the molecular layer.

Purkinje cells can be activated in two different ways. Granule cell activity generates simple spikes, which resemble the response of other neurones in the brain, whereas activation by a climbing fibre produces a prolonged depolarization upon which several spike-like waves are superimposed. The rate of firing of single and complex spikes also differs markedly. While the Purkinje cell may fire simple spikes at a rate of hundreds per second, complex spikes occur at low frequencies, seldom more than three or four per second.

Purkinje cell activity is regulated by local Golgi, basket and stellate cells. Like Purkinje cells, Golgi cells have a rich dendritic tree that extends through the molecular layer. Unlike Purkinje cells, the Golgi cell dendrites are not restricted to a plane transverse to the folia and their axons do not leave the cerebellar cortex. Golgi cells regulate firing by presynaptic inhibition of the mossy fibre afferents, and so act as a governor, or rate limiter, of Purkinje cell activity. Stellate and basket cells synapse directly on Purkinje cells and are powerful inhibitors of their activity.

Structural and functional cerebellar localization

Since the cerebellar cortex is largely uniform in microstructure and microcircuitry, it seems likely that its basic mode of operation is also uniform. The most obvious input for this operation is provided by the mossy fibre afferents, which carry information from all levels of the spinal cord, and specialized sensory and motor information relayed from the cerebral cortex and subcortical motor centres. The most obvious output from the cerebellum is directed at motor systems. Purkinje cells are organized in modules, i.e. discrete, parallel zones that converge upon different cerebellar output nuclei coupled to different motor systems in the brain stem, spinal cord and cerebral cortex. Cerebellar function is therefore determined by temporal and spatial factors, e.g. inhibitory interneurones of the cerebellar cortex, which regulate the access of a particular combination of mossy fibre–parallel fibre inputs to an appropriate output. Plastic changes in the response properties of Purkinje cells, in the form of long-term depression of the parallel fibre–Purkinje cell synapses, may also contribute. Short-term and long-term changes in the response properties of Purkinje cells are under the influence of the climbing fibres.

A double, mirrored, localization exists in the anterior and posterior cerebellum (Fig. 20.8). The anterior lobe, simple lobule, pyramis and the adjoining lobules of the hemisphere of the posterior lobe all receive branches from the same mossy and climbing fibres and project to the same cerebellar nuclei. The efferent pathways of these regions monitor the activity in the corticospinal tract and in the subcortical motor systems descending from the vestibular nuclei and reticular formation. The inputs to the cerebellum and the outputs from it are organized according to the same somatotopical patterns, but the orientation of these patterns is reversed. The representation of the head is found principally in the simple lobule, and caudally in a corresponding region of the posterior lobe. The double representation of the body follows in rough somatotopic order. Vestibular connections of the cerebellum display a similar double representation in the most rostral lobules of the anterior lobe and far caudally in the vestibulocerebellum (Fig. 20.9).

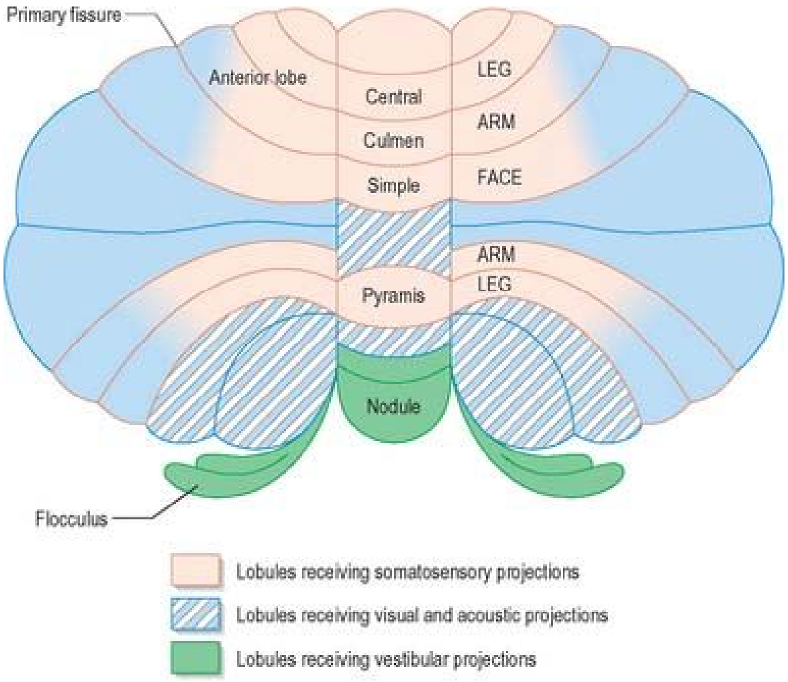
Primary fissure
Anterior lobe
Central
Culmen
Simple
LEG
ARM
FACE
ARM
LEG
Pyramis
Nodule
Flocculus
Lobules receiving somatosensory projections
Lobules receiving visual and acoustic projections
Lobules receiving vestibular projections

Fig. 20.8 Somatotopic localization in the cerebellar cortex.

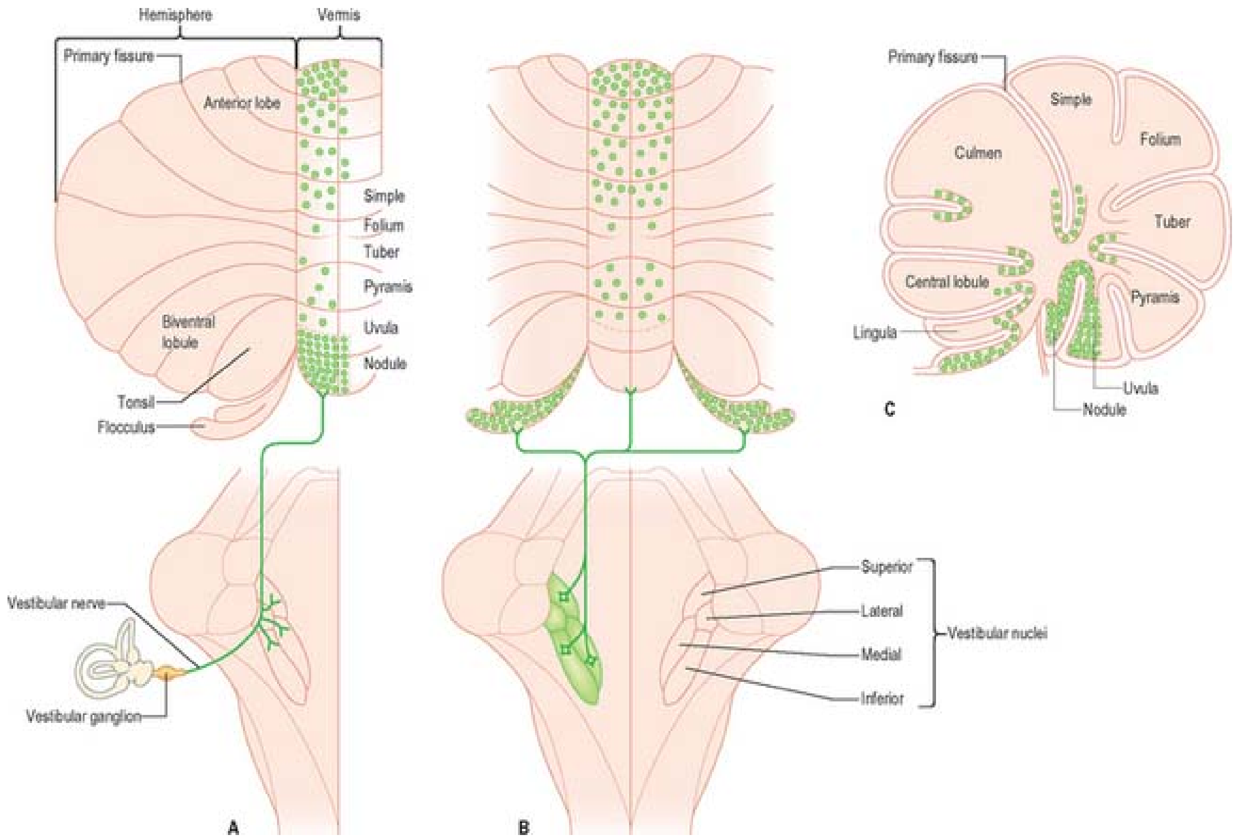
Hemisphere
Vermis
Primary fissure
Anterior lobe
Simple
Folium
Tuber
Pyramis
Biventral lobule
Uvula
Nodule
Tonsil
Flocculus
Vestibular nerve
Vestibular ganglion
A
B
Superior
Lateral
Medial
Inferior
Vestibular nuclei
Primary fissure
Simple
Culmen
Folium
Tuber
Central lobule
Pyramis
Lingula
C
Uvula
Nodule

Fig. 20.9 Vestibulocerebellar mossy fibre projections. **A**, Primary vestibulocerebellar projections from the bipolar neurones of the vestibular ganglion. **B**, Secondary vestibulocerebellar projections from the vestibular nuclei. **C**, Sagittal section showing distribution of both sets of afferents.

The folium, tuber, uvula, tonsil and posterior biventral lobule all receive an almost pure pontine mossy fibre input. Climbing fibres from the inferior olive and mossy fibres from the basilar and tegmental pontine nuclei relay visual and acoustic information from the respective cerebral association areas and midbrain tectum to the folium and tuber thought to represent a vermal visual/acoustic area (Fig. 20.8). The efferent connections of this area travel via the fastigial nucleus to gaze centres in the pons and midbrain.

AFFERENT CONNECTIONS OF THE CEREBELLUM

Mossy fibres and climbing fibres carry the afferent connections of the cerebellum. Mossy fibre systems terminate bilaterally in transversely oriented ‘lobular’ areas; there is considerable overlap amongst the terminations. Climbing fibres from different subnuclei of the inferior olive terminate contralaterally, on discrete longitudinal strips of Purkinje cells. This longitudinal pattern closely corresponds with the zonal arrangement in the corticonuclear projection (Fig. 20.10).

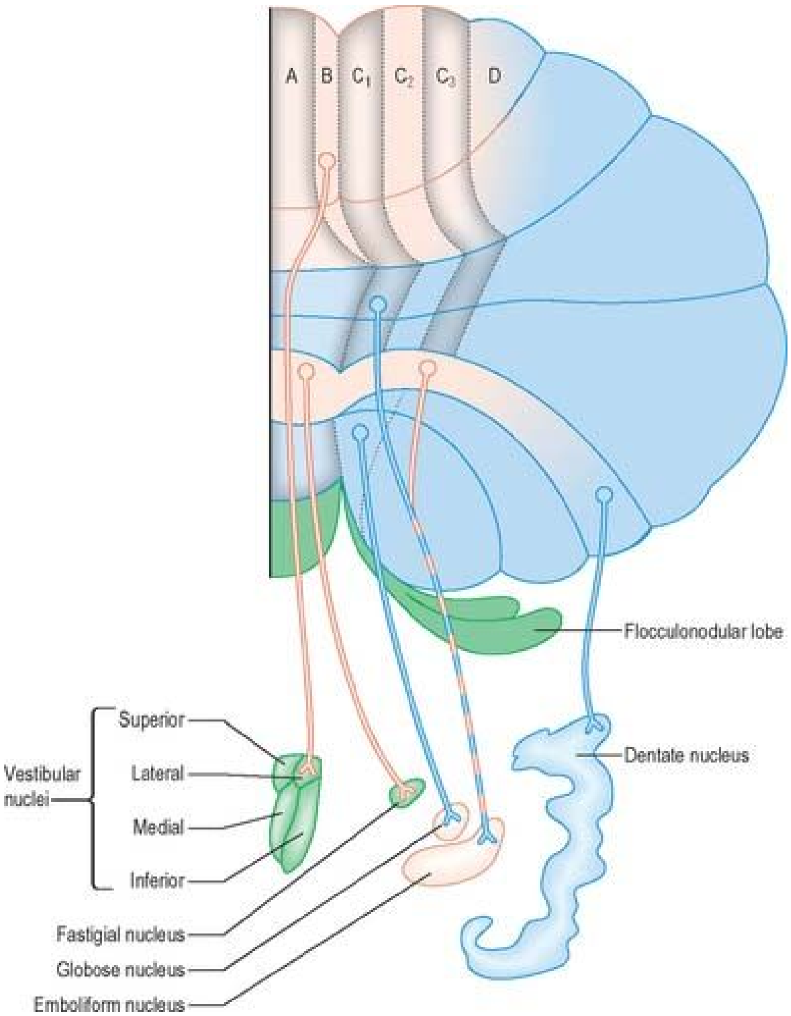
A
B
C_1
C_2
C_3
D
Flocculonodular lobe
Superior
Lateral
Medial
Inferior
Vestibular nuclei
Dentate nucleus
Fastigial nucleus
Globose nucleus
Emboliform nucleus

Fig. 20.10 Cerebellar corticonuclear and corticovestibular projections. The widespread projection from flocculonodular lobe to vestibular nuclei is

not labelled but is indicated in green.

Spinocerebellar and trigeminocerebellar fibres

The spinal cord is connected to the cerebellum through the spinocerebellar and cuneocerebellar tracts and through indirect mossy fibre pathways relayed by the lateral reticular nucleus in the medulla oblongata. These pathways are all excitatory in nature and give collaterals to the interposed and fastigial nuclei before ending on cortical granule cells.

The posterior spinocerebellar tract takes its origin from the cells of Clarke’s column at the base of the dorsal horn in all thoracic segments of the spinal cord (Fig. 20.11). It enters the inferior cerebellar peduncle, gives collaterals to the cerebellar nuclei, and terminates, mainly ipsilaterally, in the vermis and adjoining regions of the anterior lobe and in the pyramis and adjoining lobules of the posterior lobe. Clarke’s column receives primary afferents of all kinds from the muscles and joints of the lower limbs, which reaches the nucleus via the fasciculus gracilis. It also receives collaterals from cutaneous sensory neurones. Accordingly, the tract transmits proprioceptive and exteroceptive information about the ipsilateral lower limb. Very fast conduction is required to keep the cerebellum informed about ongoing movements. The axons in the posterior spinocerebellar tract are the largest in the CNS, measuring 20 μm in diameter. The upper limb equivalent of the posterior spinocerebellar tract is the cuneocerebellar tract.

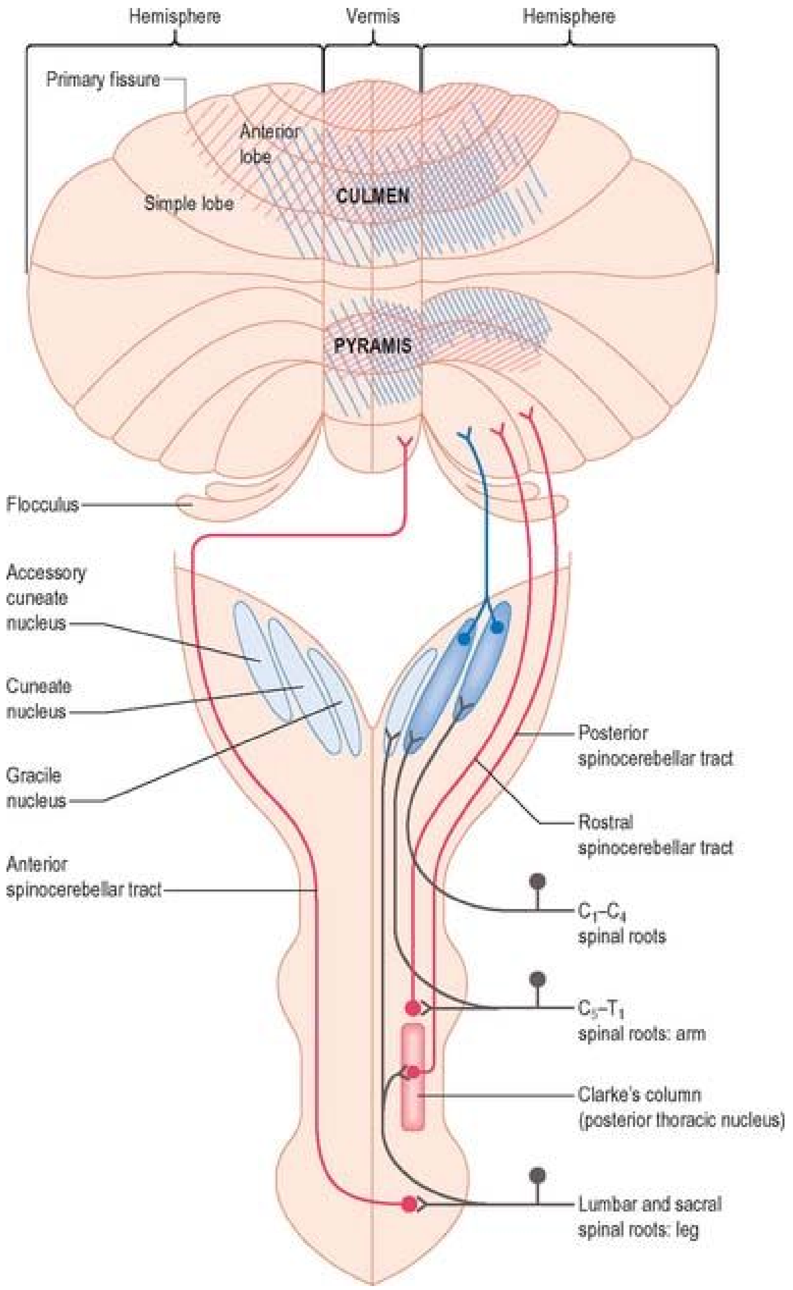
Hemisphere
Vermis
Hemisphere
Primary fissure
Anterior lobe
Simple lobe
CULMEN
PYRAMIS
Flocculus
Accessory cuneate nucleus
Cuneate nucleus
Gracile nucleus
Anterior spinocerebellar tract
Posterior spinocerebellar tract
Rostral spinocerebellar tract
C_1–C_4 spinal roots
C_5–T_1 spinal roots: arm
Clarke's column (posterior thoracic nucleus)
Lumbar and sacral spinal roots: leg

Fig. 20.11 Spinocerebellar and cuneocerebellar mossy fibre projections to the culmen and pyramis and related intermediate areas of the cerebellar cortex.

The anterior spinocerebellar tract is a composite pathway. It informs the cerebellum about the state of activity of spinal reflex arcs related to the lower limb and lower trunk. Its fibres originate in the intermediate grey matter of the lumbar and sacral segments of the spinal cord (Fig. 20.11). They cross near their origin, and ascend close to the surface as far as the lower midbrain before looping down in the superior cerebellar peduncle. Most fibres cross again in the cerebellar white matter. Thus their distributions to the cerebellar nuclei and cortex appear to be the same as those of the posterior tract.

The rostral spinocerebellar tract originates from cell groups of the intermediate zone and horn of the cervical enlargement. Although considered to be the upper limb and upper trunk counterpart of the anterior spinocerebellar tract, most of its fibres remain ipsilateral throughout their course. It enters the inferior cerebellar peduncle and terminates in the same cerebellar nuclei and folia as the cuneocerebellar tract.

The cuneocerebellar tract contains exteroceptive and proprioceptive components which originate from the cuneate and external cuneate nuclei respectively. The primary afferents travel in the fasciculus cuneatus. The tract itself is predominantly uncrossed and ends in the posterior half of the anterior lobe. Exteroceptive and proprioceptive mossy fibre components of the tract terminate differentially in the apical and basal part of the folia. The exteroceptive component overlaps the pontocerebellar mossy fibre projection in the apices of the folia of the anterior lobe.

Comparable sets of ipsilateral proprioceptive and interceptive cerebellar projections exist for the extensive territory of the trigeminal brain stem nuclei. These nuclei also project to the ipsilateral inferior olive, relaying from there to the contralateral cerebellar cortex and deep nuclei. The cortical representation of the head is directly behind the primary fissure.

Olivocerebellar fibres

Localization in the olivocerebellar system: zones and microzones

Climbing fibres originate exclusively from subnuclei of the contralateral inferior olivary complex and terminate on longitudinal strips of Purkinje cells in the cerebellar cortex; their collaterals end on the cerebellar or vestibular target nuclei of these Purkinje cells. A longitudinal zonal arrangement is therefore characteristic of the organization of the olivocerebellar projection. Moreover, the olivocerebellar projection zones correspond precisely to the corticonuclear projection zones already described (Fig. 20.10). Climbing fibres from the inferior olive are able to modify the cerebellar output in such a way that cells within each subnucleus of the inferior olivary complex monitor the output of a single cerebellar module.

The inferior olivary complex and its climbing fibres can be activated by tactile, proprioceptive, visual and vestibular stimulation, and from the sensory, motor and visual cortices and their brain stem relays. A somatotopic arrangement of body parts, matching the olivary projections on to the cerebellar cortex, has been described in animals.

Olivocerebellar climbing fibre connections

The inferior olivary complex can be subdivided into a convoluted principal olivary nucleus, and posterior and medial accessory olivary nuclei. Olivary fibres form the olivocerebellar projection to the contralateral cerebellar cortex, and give off collaterals to the lateral vestibular nucleus and to the cerebellar nuclei. Climbing fibres terminate on longitudinal strips of Purkinje cells. The zonal patterns of the olivocerebellar and Purkinje–nuclear projections correspond precisely. The accessory olivary nuclei project to the vermis and the adjacent hemispheres. The caudal halves of the posterior and medial accessory nuclei innervate the vermis. The caudal part of the posterior accessory nucleus projects to Deiters' nucleus and to the B zone of the anterior vermis. The caudal half of the medial accessory olive gives rise to a projection to the fastigial nucleus and provides climbing fibres to the A zone. The rostral halves of the accessory olives project to the pars intermedia. Climbing fibres from the rostral dorsal accessory olive give collateral projections to the emboliform nucleus and terminate in zones C1 and C3. Zone C2 receives terminals from the rostral medial accessory olive, which provides a collateral projection to the globose nucleus. The principal nucleus projects to the contralateral hemisphere (D zone), and gives collaterals to the dentate nucleus.

The inferior olivary complex receives afferent connections from the spinal cord and from sensory relay nuclei in the brain stem, including the posterior column and sensory trigeminal nuclei. It also receives descending connections from the superior colliculus, parvicellular red nucleus and related nuclei in the midbrain and a GABAergic projection, mainly crossed, from the cerebellar nuclei and certain vestibular nuclei. The latter two connections are topically organized. Thus, the dentate nucleus projects to the principal nucleus, the emboliform nucleus to the rostral posterior accessory nucleus, and the globose nucleus to the rostral medial accessory nucleus. The fastigial nucleus is connected with the caudal medial accessory olive, but the fibres are less numerous. The caudal posterior accessory olive receives a projection from the lateral vestibular nucleus.

The posterior accessory olive and the caudal half of the medial accessory olive receive an input from the spinal cord and sensory relay nuclei. The middle region of the medial accessory olive receives a projection from the superior colliculus and projects to folium and vermis. The parvocellular red nucleus and related nuclei project to the olive through the ipsilateral descending central tegmental tract, which terminates in the rostral half of the medial accessory olive and the principal olive. The parvocellular red nucleus receives converging projections from the cerebellar nuclei and from the motor and premotor cortex. Direct pathways from the cerebral cortex to the inferior olive are sparse. The indirect pathways via the parvicellular red nucleus are much larger.

Climbing fibres that terminate in the vestibulocerebellum (flocculus and nodule) are derived from neurones of the medial accessory olive which receive a strong descending afferent connection from optokinetic centres in the midbrain. Optokinetic information is used by the flocculus in long-term adaptation of compensatory eye movements. Neighbouring neurones are under vestibular control and project to the nodule and the adjoining uvula.

Vestibulocerebellar fibres

Primary vestibulocerebellar mossy fibres are fibres of the vestibular branch of the vestibulocochlear nerve. They enter the cerebellum with the ascending branch of the vestibular nerve, and pass through the superior vestibular nucleus and the juxtarestiform body. They terminate, mainly ipsilaterally, in the granular layer of the nodule, caudal part of the uvula, ventral part of the anterior lobe and bottom of the deep fissures of the vermis (Fig. 20.9A). Secondary vestibulocerebellar mossy fibres arise from the superior vestibular nucleus and the caudal portions of the medial and inferior vestibular nuclei. They terminate bilaterally not only in the same regions that receive primary vestibulocerebellar fibres but also in the flocculus, which lacks a primary vestibulocerebellar projection (Fig. 20.9B). Some of the mossy fibres from the medial and inferior vestibular nuclei are cholinergic.

Reticulocerebellar fibres

The lateral reticular nucleus of the medulla oblongata, and the paramedian reticular and tegmental reticular nuclei of the pons, give rise to mossy fibres. The latter nuclei also supply major collateral projections to the cerebellar nuclei. Spinoreticular fibres terminate in a somatotopical pattern within the entire lateral reticular nucleus, where they overlap with collaterals from the rubrospinal and lateral vestibulospinal tracts and a projection from the cerebral cortex.

The lateral reticular nucleus projects bilaterally to the vermis and hemispheres of the cerebellum. The projection from the dorsal part of the nucleus, which receives collaterals from the rubrospinal tract in addition to spinal afferents, is centred on the ipsilateral hemisphere. The ventral part of the nucleus, which receives a strong projection from the spinal cord and a collateral projection from the lateral vestibulospinal tract, projects bilaterally, mainly to the vermis. The lateral reticular nucleus provides a strong projection to the superior fastigial nucleus, the emboliform nucleus and the medial pole of the globose nucleus.

The paramedian reticular nucleus consists of cell groups at the lateral border of the medial longitudinal fasciculus. It receives fibres from the vestibular nuclei and the interstitiospinal and tectospinal tracts (which descend in the medial longitudinal fasciculus), and from the spinal cord and the cerebral cortex. It projects to the entire cerebellum.

The tegmental reticular nucleus of the pons is located next to the midline in the caudal half of the tegmentum. It receives afferent connections from the cerebral cortex, tectum, nucleus of the optic tract and cerebellar nuclei via the crossed descending branch of the superior cerebellar peduncle. Efferents from the tegmental reticular nucleus reach the cerebellum through the middle cerebellar peduncle. Some terminate superficially in the cortex of the anterior lobe, but many more end in the simple lobule, folium, tuber, vermis and adjoining flocculus. Additional efferents terminate in the caudal fastigial nucleus, dentate nucleus and lateral parts of the globose nucleus.

Pontocerebellar fibres

The cerebral cortex is the largest single source of fibres that project to the pontine nuclei. Fibres from the pontine nuclei access the cerebellum via the middle cerebellar peduncle, which is the largest afferent system of the human cerebellum. Many corticopontine fibres are collaterals of axons that project to other targets in the brain or spinal cord, e.g. it is likely that all corticospinal fibres give off collaterals to the pontine nuclei. Although corticopontine axons arise from lamina V pyramidal cells, the projection from different areas of the cerebral cortex is highly uneven. The areas of cerebral cortex that project to the pontine nuclei are those that are particularly involved in the control of movement. For example, in the case of visual areas, the input arises from extrastriate visual areas in the parietal lobe whose cells are responsive to movement, and function as important links in the visual guidance of movement. Dorsal pontine nuclei receive collateral branches from corticotectal fibres that project to the superior and inferior colliculi from the parietal, temporal and frontal areas of the cerebral cortex, and from tectopontine relays. The onward pontocerebellar projections are to the simple lobule and to the folium and tuber of the vermis.

Fibres of the pontine reticular nuclei are distributed bilaterally, with ipsilateral predominance, to all lobules of the cerebellum other than the lingula and nodule.

More than 90% of fibres in the middle cerebellar peduncle belong to the cortico-ponto-cerebellar pathway. Corticopontine fibres travel in the cerebral peduncle. Fibres from the frontal lobe occupy the medial part of the peduncle, and fibres from the parietal, occipital and temporal lobes occupy the lateral part. They synapse on some 20 million neurones in corresponding regions of the basilar pons. The onward pontocerebellar mossy fibre projection is predominantly to the lateral regions of the posterior and anterior lobes (Fig. 20.4) but collaterals are given off to the dentate nucleus.

EFFERENT CONNECTIONS OF THE CEREBELLUM

The output of the cerebellum consists of the inhibitory projections of the Purkinje cells to the cerebellar and vestibular nuclei, and the efferent connections of the cerebellar nuclei to motor centres in the brain stem and, through the thalamus, the motor cortex. Their effects on movement are always indirect, because there are no direct projections from the cerebellar nuclei to motor neurones. Disynaptic connections of the Purkinje cells in the anterior vermis and vestibulocerebellum with motor neurones controlling oculogyric and proximal limb muscles are mediated by the vestibular nuclei. The vermis also influences these motor neurones bilaterally through multisynaptic pathways that involve the fastigial and vestibular nuclei and the reticular formation (Fig. 20.12). The vermis cannot be considered as a single module. Each half of the vermis is composed of several modules (each made up of a longitudinal Purkinje cell zone and a target nucleus) and their supporting climbing fibre afferent projections.

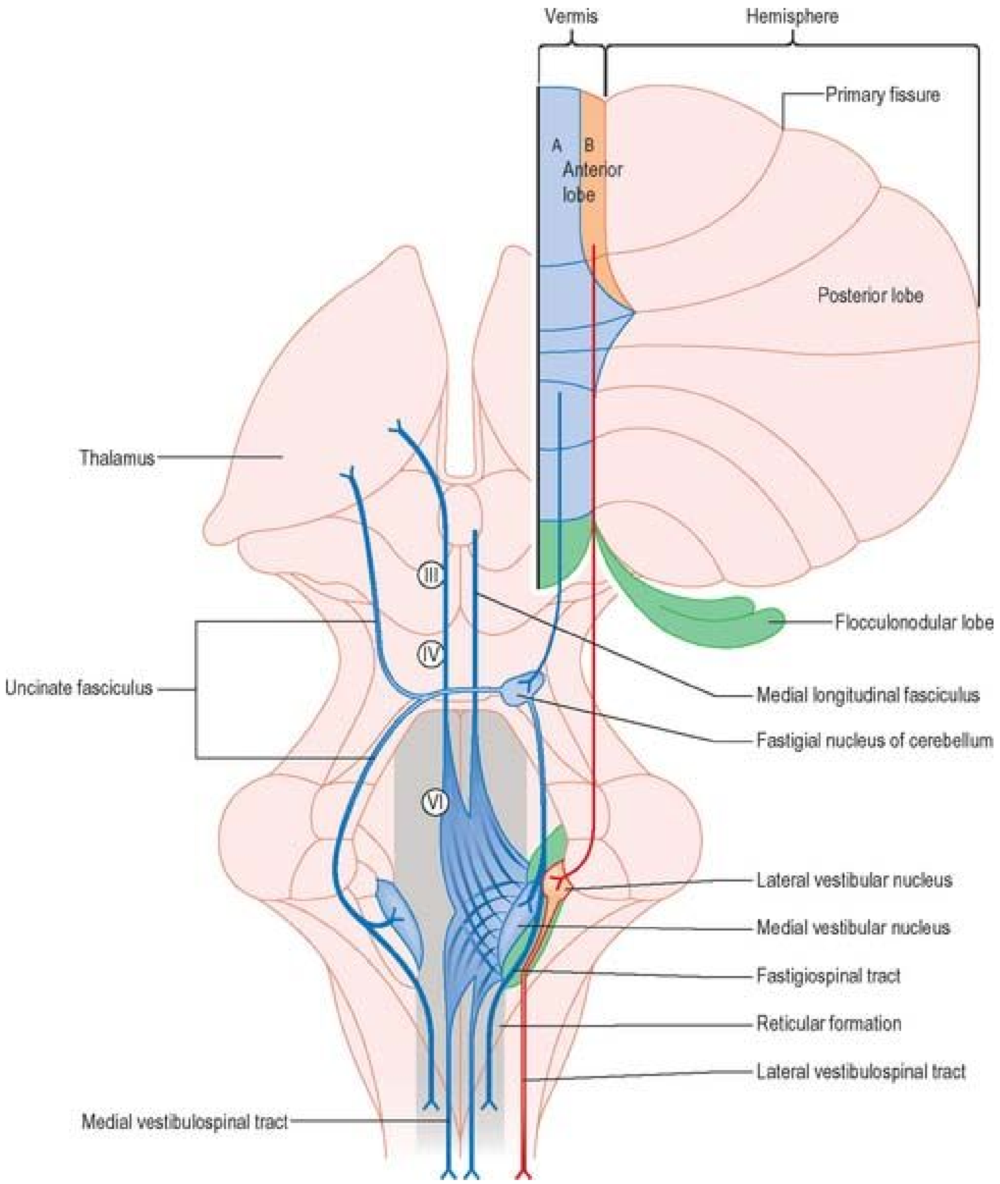
Vermis
Hemisphere
Primary fissure
A
B
Anterior lobe
Posterior lobe
Thalamus
III
IV
VI
Uncinate fasciculus
Flocculonodular lobe
Medial longitudinal fasciculus
Fastigial nucleus of cerebellum
Lateral vestibular nucleus
Medial vestibular nucleus
Fastigiospinal tract
Reticular formation
Lateral vestibulospinal tract
Medial vestibulospinal tract

Fig. 20.12 Efferent connections of the cerebellar vermis. Connections of the A zones of the vermis and flocculonodular lobe with the fastigial nucleus are indicated, also those of the B zone with the lateral vestibular nucleus. Some vestibular efferents ascend bilaterally to the ocular motor nuclei and thalamus, others descend to the spinal cord. Motor nuclei of the 3rd, 4th and 6th cranial nerves: III, IV, VI.

Each cerebellar hemisphere influences movements of the ipsilateral extremities by way of projections to the dentate and interposed (emboliform and globose) nuclei, which in turn project to the contralateral red nucleus, thalamus and motor cortex (Fig. 20.13).

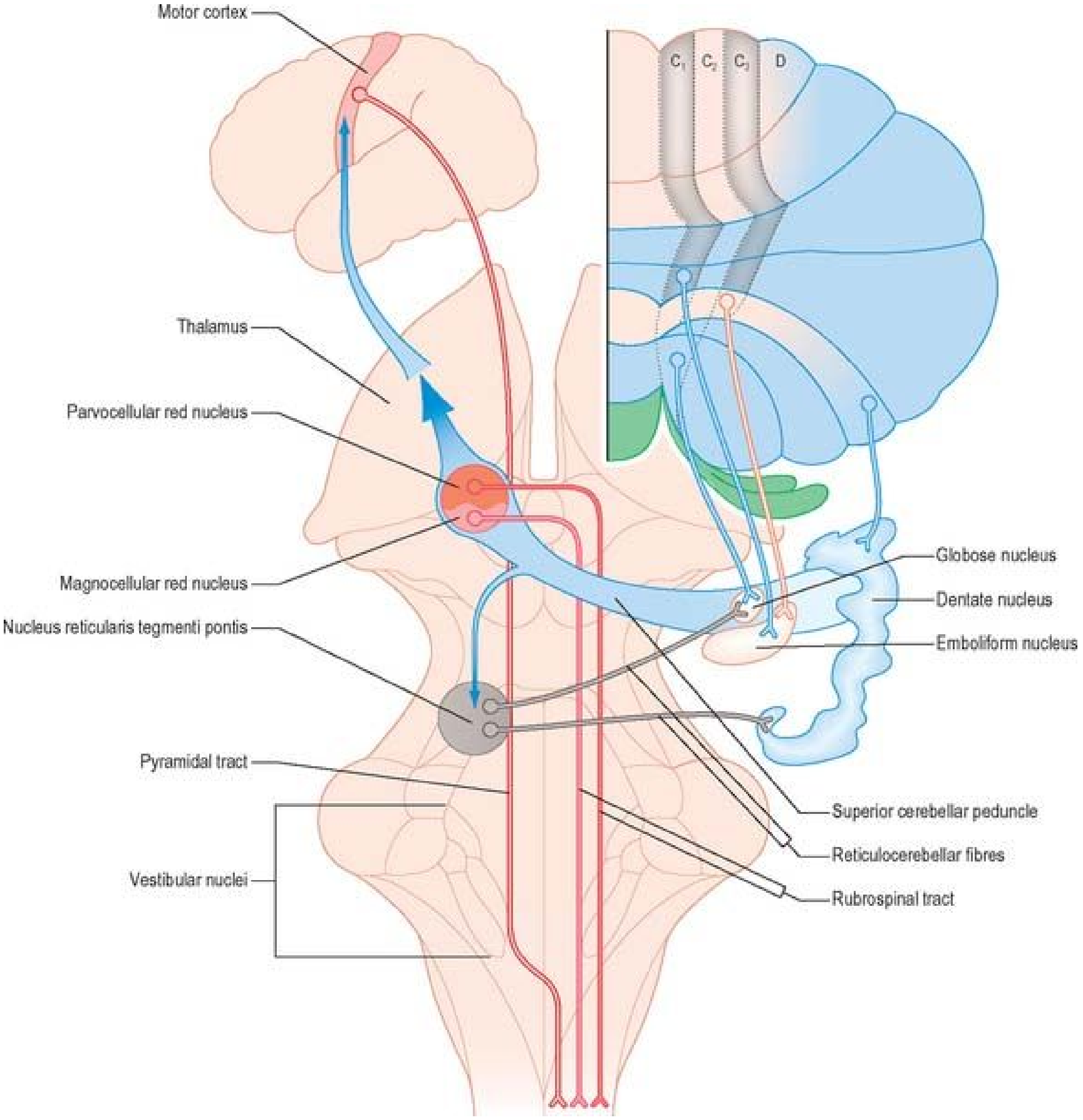
Motor cortex
C1
C2
C3
D
Thalamus
Parvocellular red nucleus
Magnocellular red nucleus
Nucleus reticularis tegmenti pontis
Pyramidal tract
Vestibular nuclei
Globose nucleus
Dentate nucleus
Emboliform nucleus
Superior cerebellar peduncle
Reticulocerebellar fibres
Rubrospinal tract

Fig. 20.13 Efferent connections of the cerebellar hemisphere. Purkinje cell zones and their target nuclei are indicated with the same colours. Efferent fibres from the motor cortex and from the very small magnocellular red nucleus recross and descend to the upper part of the spinal cord.

Corticonuclear and corticovestibular fibres

Purkinje cells of each hemivermis project to the ipsilateral fastigial and vestibular nuclei. Purkinje cells of the hemisphere project to the interposed and dentate nuclei. Although the cerebellar cortex is organized in strips of Purkinje cell zones, which project to different cerebellar and vestibular nuclei, the borders between these strips are not apparent in the structure of the cortex when it is examined histologically using conventional staining methods. The vermis of the anterior lobe and simple lobule consist of two parallel strips, A and B, of Purkinje cells (Figs 20.10, 20.12). The medial strip (A zone) projects to the rostral pole of the fastigial nucleus, and the lateral strip (B zone) projects to the lateral vestibular nucleus. The B zone does not continue beyond the simple lobule. The cortex of the entire caudal vermis, which projects to the fastigial nucleus, is included in the A zone. The folium and tuber, which represent a region of the cerebellum that receives a visual input and which are involved in the accurate calibration of saccades, project to the caudal pole of the fastigial nucleus. The pyramis, uvula and nodule can be subdivided into several Purkinje cell zones. However, the significance of their connections with the cerebellar and vestibular nuclei is not well understood. Corticovestibular projections to the superior, medial and inferior vestibular nuclei, but not to the lateral nucleus, take their origin from the nodule and the adjacent region of the uvula.

The intermediate region consists of two strips of Purkinje cells (C1 and C3 zones), which project to the emboliform (anterior interposed) nucleus. They flank a single zone (C2) that projects to the globose (posterior interposed) nucleus (Figs 20.10, 20.13). The rest of the hemisphere projects to the dentate nucleus. There are indications for a subdivision of the hemisphere into two zones that project to the caudolateral and rostromedial parts of the dentate nucleus, respectively. The neurones of the caudolateral dentate are generally smaller than those of the rostromedial portion and the convolutions are broader. The efferent connections of the flocculus are mainly with the superior, medial and inferior vestibular nuclei and resemble those from the nodule and uvula.

Cerebellovestibular and cerebelloreticular fibres

Efferent connections of the fastigial nucleus

The fastigial nucleus is connected bilaterally with the vestibular nuclei and the medullary and pontine reticular formation (Fig. 20.12). Smaller crossed connections either ascend to the midbrain and diencephalon or descend into the spinal cord. Small GABAergic neurones give rise to fastigio-olivary fibres, which terminate in the medial accessory olive. The uncinate fasciculus is the major efferent pathway of the fastigial nucleus. Its fibres cross in the rostral part of the cerebellar white matter, and pass dorsal to the superior cerebellar peduncle, to enter the vestibular nuclei from their lateral side. Uncrossed fibres enter the vestibular nuclei through the juxtarestiform body. The distribution of the fastigial projection is bilateral, but with a contralateral preponderance. Crossed and uncrossed projections end in the medial and inferior vestibular nuclei, and also traverse these nuclei to terminate in the medial reticular formation. Some crossed fibres can be traced caudally into the spinal cord. A small fascicle of crossed fibres from the fastigial nucleus ascends along the superior cerebellar peduncle and is distributed bilaterally to the dorsal tegmentum, central grey matter and deep layers of the superior colliculus and the nuclei of the posterior commissure. Fibres terminate bilaterally in the ventrolateral nucleus and the intralaminar nuclei of the thalamus.

Cerebellovestibular connections

The relationship between the cerebellum and the vestibular nuclei is complex (Figs 20.9, 20.12). In addition to the vestibulocerebellum (nodule, adjacent folia of the uvula and flocculus), the main vermis and the fastigial nucleus also project to the vestibular nuclei.

The vestibulocerebellum projects to the superior, medial and inferior vestibular nuclei. Neurones of these nuclei, which receive an input from the vestibular nerve and project to the nuclei controlling eye movements (vestibulo-ocular relay cells), are among the main targets of the Purkinje cells of the nodule and flocculus. Through these connections with vestibulo-ocular relay neurones, the flocculus is involved in the long-term adaptation of compensatory eye movements, the generation of smooth eye movements used to pursue an object, and the suppression of the vestibulo-ocular reflex during smooth pursuit. The function of the nodule in the control of eye movement is less well understood.

The vestibular nuclei are the main source of mossy fibre afferents to the nodule; their projection to the flocculus is relatively minor. Most mossy fibres which terminate in the flocculus arise from the reticular formation and relay optokinetic and visual information.

The lateral vestibular nucleus, which lacks an input from the labyrinth and receives Purkinje cell axons from the B zone of the anterior vermis, can be regarded as a displaced cerebellar nucleus. It gives rise to the lateral vestibulospinal tract, which descends to all levels of the spinal cord. It is avoided by the efferent pathways from the fastigial nucleus, which terminate more ventrally on large neurones in the magnocellular part of the medial vestibular nucleus and in the medial reticular formation. The medial and inferior vestibular nuclei receive a major input from the vestibular nerve and give rise to bilaterally ascending and descending tracts that course in the medial longitudinal fasciculus. The ascending tract is composed predominantly of the axons of vestibulo-ocular relay cells. The descending fibres form the medial vestibulospinal tract, which is particularly involved in head righting reflexes when the trunk is tilted.

Fastigial fibres, which terminate in the reticular formation, stimulate the bilaterally descending medullary reticulospinal tracts. The A zone of the vermis exerts a bilateral influence on ventromedially located spinal interneurones and motor neurones that innervate axial, truncal and proximal limb muscles. Some fibres of the uncinate tract descend as far as the cervical cord, where they terminate on the same motor neurones. The B zone exerts an influence on ipsilateral interneurones and motor neurones of the same system through its projection to the lateral vestibular nucleus and the lateral vestibulospinal tract.

The projections of the fastigial nucleus to the thalamus are relatively minor. They are bilateral, because the crossed ascending fibres of the uncinate fasciculus subsequently recross. Their targets include parts of the ventrolateral nucleus and the intralaminar, centrolateral and parafascicular nuclei. Fibres that terminate in the ventrolateral nucleus lie medial to the terminations of fibres from the dentate and interposed nuclei. This region of the ventrolateral nucleus projects to the motor cortex but also sends collaterals to the medullary reticular formation, which influences ventromedial interneurones and motor neurones in lumbar and sacral segments of the spinal cord via the medullary reticulospinal tracts.

The caudal region of the fastigial nucleus receives Purkinje cell axons from the folium and tuber, an area of the vermis that receives visual inputs. It projects to the contralateral horizontal gaze centre (paramedian pontine reticular formation, PPRF), and the vertical gaze centre (rostral interstitial nucleus of the medial longitudinal fasciculus, riMLF), and bilaterally, to deep layers of the superior colliculus. These projections probably mediate the adaptation of saccades by the vermal visual area.

The cerebellum influences visceromotor systems via the projections of the fastigial nucleus to the parasolitary nucleus (a region bordering the viscerosensory nuclei of the solitary tract), the dorsal motor nucleus of the vagus, the central grey matter, the serotoninergic raphe nuclei of the pons and medulla, and the noradrenergic locus coeruleus.

Other pathways from the cerebellar nuclei terminate on precerebellar relay nuclei that give rise to mossy or climbing fibres. Recurrent circuits involving the fastigial nucleus include the nucleus reticularis tegmenti pontis and a projection from the fastigial nucleus to the medial accessory olive. Nucleo-olivary projections arise from all the cerebellar nuclei, are crossed, and contain GABA as a neurotransmitter. The connections of the fastigial nucleus with the reticular nuclei are excitatory.

Cerebellar nuclei also project to the contralateral interstitial nucleus of Darkschewitsch, which lies at the boundary between the midbrain and diencephalon. This nucleus projects to the medial accessory olive via the central tegmental tract. The fastigial nucleus controls the climbing fibre output of the medial accessory olive, both via its nucleo-olivary projection and by its connection to the nucleus of Darkschewitsch.

Cerebellorubral and cerebellothalamic fibres

The axons of neurones in the dentate and interposed nuclei leave the cerebellum in the superior cerebellar peduncle. The superior peduncles, including their nucleo-olivary component, decussate in the caudal midbrain (Fig. 20.13) and each then gives off a small descending branch carrying fibres that terminate in the medial reticular formation of the pons and medulla and the pontine tegmental reticular nucleus. The nucleo-olivary fibres join this descending branch and terminate in the inferior olive in a strictly ordered manner. The ascending branch is distributed to the midbrain and diencephalon, mainly to the red nucleus and thalamus. The emboliform (anterior interposed) nucleus projects to the magnocellular part of the red nucleus. In humans this projection is very small and the target neurones give rise to a relatively trivial rubrospinal tract, which crosses in the caudal midbrain and terminates on lateral medullary interneurones and a small number of motor neurones in the upper cervical spinal cord.

The emboliform (anterior interposed) nucleus projects to lateral parts of the ventrolateral nucleus of the thalamus, which are connected with elements of the motor cortex projecting to axial and proximal limb muscles, and to the reticular formation of the pons and medulla. It also projects to the pontine tegmental reticular nucleus and to basal pontine nuclei, both of which give rise to mossy fibres. Its nucleo-olivary efferents terminate in the rostral half of the dorsal accessory olive.

The projections of the globose (posterior interposed) nucleus are very similar to those of the fastigial nucleus. The two nuclei share projections to the cord, the superior colliculus, the central grey matter and the raphe nuclei. Nucleo-olivary projections from the globose nucleus and the recurrent globose nucleus–interstitial nucleus–inferior olivary nucleus pathway converge upon the rostral half of the medial accessory olive. The thalamic projections overlap those from the fastigial and emboliform nuclei.

The dentate nucleus projects to the contralateral parvicellular red nucleus and the thalamus. The central tegmental tract takes its origin from the parvocellular red nucleus and terminates on the principal nucleus of the olive.

The thalamic projection to the ventrolateral nucleus overlaps those of the other cerebellar nuclei. The inferior and lateral parts of the dentate nucleus project into the most medial region of the ventrolateral nucleus, which in turn projects to the premotor area of the frontal lobe.

The thalamus receives a massive input from other major motor systems, in addition to the input it receives from the cerebellum. In particular, the output of the basal ganglia is relayed to the thalamus by a projection from the globus pallidus (Ch. 22). Available evidence suggests that these two great subcortical motor systems terminate on different regions in the ventral thalamus and project to different targets in the motor and premotor cortex.

CEREBELLAR FUNCTIONS

The vermis of the cerebellum is involved in taking anticipatory action in order to maintain an upright posture when objects are picked up. For example, when a book is taken down from a shelf, the first muscle groups to be activated are not the flexors of shoulder, elbow or fingers, but the plantar flexors of the ankle. Contraction of the ankle flexors causes the forefeet to push the lower limbs and trunk backwards at the moment the hand grasps the book. Once the lift gets under way, the erector spinae muscles correct for the combined weights of the book and the reaching arm, in order to prevent forward sway of the head and trunk. Labyrinthine receptors simultaneously inform the cerebellum of any forward movement of the head, and appropriate antigravity thrust is exerted via one or both lateral vestibulospinal tracts.

The posterolateral region of the cerebellum has a role in postural fixation to prevent oscillation of distal limb parts caused by the viscoelastic properties of the muscles in response to sudden movements. If a volunteer is instructed to exert rapid wrist extension and to maintain the extended posture for two seconds, electromyographic records taken from the prime movers and antagonists reveal that the antagonists begin to contract prior to completion of the movement, and that they continue to contract and relax several times in alternating fashion with the prime movers, although with much less force, during the measured fixation period.

The cerebellum has a role in motor learning. Experimental studies have shown that when a novel motor skill is being learned, the olivocerebellar climbing fibre system becomes active when errors are made. The inferior olivary complex appears to be involved in correction, based on receipt of a copy of the intended movement from collateral branches of the corticospinal tract. Cerebellar output via the superior cerebellar peduncle is also copied on to the parvicellular red nucleus and projected from there to the inferior olive, where it can be compared with the original. Short bursts of climbing fibre activity depress the Purkinje cells responsible for producing the errors.

Many motor skills require precise timing, which involves an extreme degree of cooperation between prime movers and their antagonists. For example, reading a printed page requires that the scanning eyes snap back to the beginning of a line, time after time: even small errors may result in dyslexia, where slight incoordination of eye movements may cause the letters of a word to appear jumbled. Clinical testing of timing can be performed easily by checking the ability to perform rhythmic movements such as repetitive pronation/supination (Fig. 20.14).

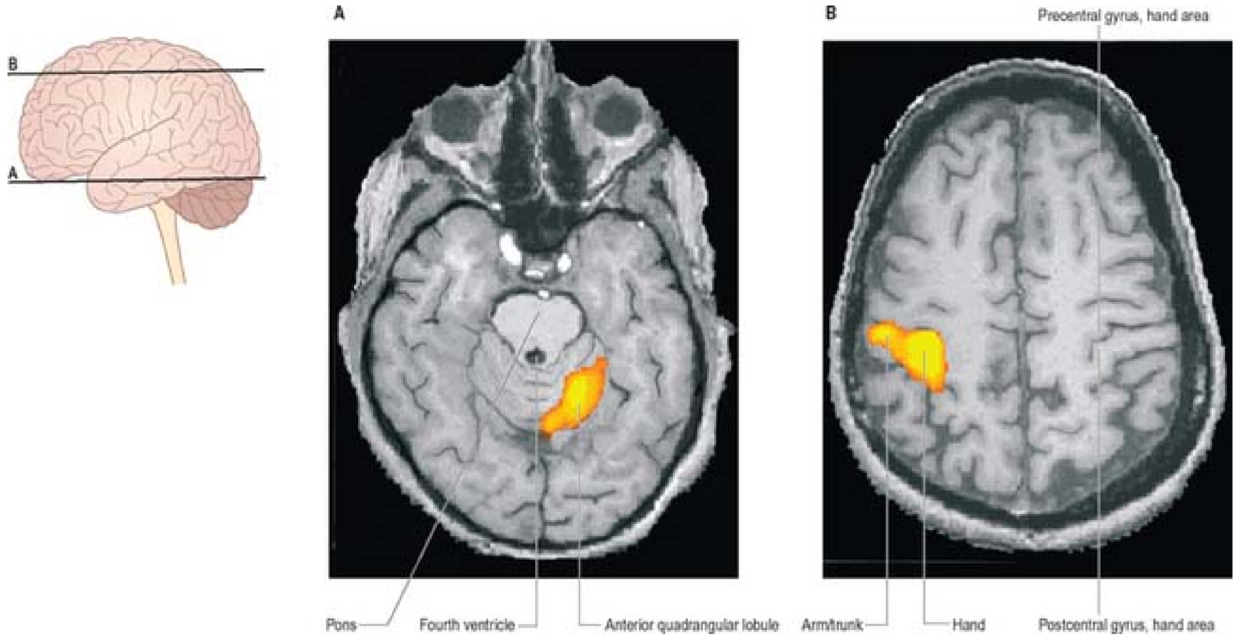
B
A
A
B
Precentral gyrus, hand area
Pons
Fourth ventricle
Anterior quadrangular lobule
Arm/trunk
Hand
Postcentral gyrus, hand area

Fig. 20.14 fMRI (functional magnetic resonance imaging) of a volunteer executing repetitive finger movements of the right hand.

(By courtesy of Drs JP Finn and T Parrish, Northwestern University School of Medicine, Chicago.)

CEREBELLAR LESIONS

Midline cerebellar lesions, e.g. tumours such as medulloblastoma and secondary carcinoma, lead to abnormalities of posture, so that the patient cannot sit or stand, without toppling, usually backwards.

Unilateral lesions in the cerebellar hemispheres, e.g. stroke, produce ipsilateral symptoms and signs. Inco-ordination of eye movements leads to nystagmus, which is most marked when gaze is directed to the side of the lesion. Incoordination of the ipsilateral upper limb is manifested in the finger-nose test. The movements are inaccurate (dysmetria); the limb oscillates to and fro, the amplitude being greater as the target is reached (intention tremor); there is a breakdown of smooth co-operation between muscles controlling the joints of the upper limb (asynergia); alternating hand movements are clumsy (dysdiadochokinesia). When the arm is outstretched, there is a tendency for the limb to hyper-pronate and rise, and when pressure is applied to the extended arm and then released, there is a marked rebound of the limb. Unilateral incoordination of the lower limb is apparent because heel/shin testing is inaccurate.

Bilateral lesions of the cerebellar hemisphere lead to nystagmus and a form of dysarthria in which the syllables are extended and prosody is lost (scanning speech). The gait is wide based, reeling, and incoordinate (ataxia): the ataxia is not made significantly worse on eye closure (negative Romberg’s sign). Bilateral lesions can be acute, as in the encephalitis that follows chicken pox, or chronic, as in alcohol abuse, and the inherited spinocerebellar ataxias. The co-occurrence of nystagmus, scanning speech and intention tremor were held by the 19th century neurologist Charcot to be pathognomonic of multiple sclerosis.

It has been speculated that cerebellar lesions may lead to disorders of higher cortical function and changes in affect, but this has not been substantiated.

REFERENCES

stian AJ, Mugnaini E, Thach WT. Cerebellum. In: Zigmond MJ, Bloom FE, Landis SC, Roberts JL, Squire LR. *Fundamental Neuroscience*. San Diego: Academic Press; 1999:973-992.

eptner M, Kruckenberg M. Anatomic basis of functional magnetic resonance imaging. Motor system. *Neuroimage Clin N Am*. 2001;11:203-219.

e C, Harasty JA, Dzendrowskyj TE, Talcott JB, Simpson JM, Blamire AM, Dixon RM, Lee A, Thompson CH, Styles P, Richardson AJ, Stein JF. Cerebellar morphology in developmental dyslexia. *Neuropsychologia*. 2002;40:1285-1292.

hmahmann JD, Sherman JC. The cerebellar cognitive affective syndrome. *Brain*. 1998;121:561-579.

y RB, Spencer RM, Zelaznik HN, Diedrichsen J. The cerebellum and event timing. *Ann NY Acad Sci*. 2002;978:302-317.

bhart AL, Petersen SE, Thach WT. Role of the posterolateral cerebellum in language. *Ann NY Acad Sci*. 2002;978:318-333.

One of several studies using fMRI which have indicated that the right posterolateral cerebellum is involved during word retrieval and syntax generation..

pka H, Mescheriakov S, Boose A, et al. A cerebellar-like terminal and postural tremor induced in normal man by transcranial magnetic stimulation. *Brain*. 1999;122:1551-1562.

CHAPTER 21

Diencephalon

The diencephalon is part of the prosencephalon (forebrain), which develops from the foremost primary cerebral vesicle and differentiates into a caudal diencephalon and rostral telencephalon. The cerebral hemispheres develop from the sides of the telencephalon, each containing a lateral ventricle. The sites of evagination become the interventricular foramina, through which the two lateral ventricles and midline third ventricle communicate. The diencephalon corresponds largely to the structures that develop lateral to the third ventricle. The lateral walls of the diencephalon form the epithalamus most superiorly, the thalamus centrally and the subthalamus and hypothalamus most inferiorly.

THALAMUS

The thalamus is an ovoid nuclear mass, about 4 cm long, which borders the dorsal part of the third ventricle (Figs 21.1, 21.2). The narrow anterior pole lies close to the midline, and forms the posterior boundary of the interventricular foramen. Posteriorly, an expansion, the pulvinar, extends beyond the third ventricle to overhang the superior colliculus (see Fig. 19.3). The brachium of the superior colliculus (superior quadrigeminal brachium) separates the pulvinar above from the medial geniculate body below. A small oval elevation, the lateral geniculate body, lies lateral to the medial geniculate.

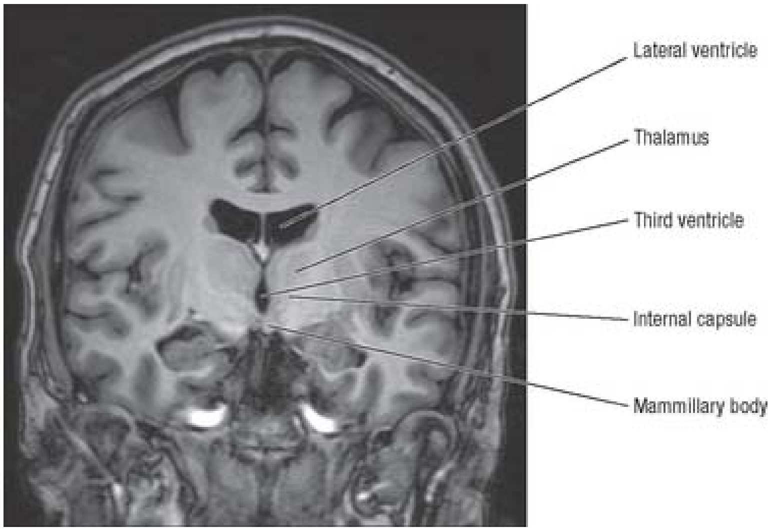

Fig. 21.1 Coronal T1 weighted inversion recovery MRI image at the level of the thalamus and third ventricle in a normal volunteer.

(By courtesy of Professor Alan Jackson, Wolfson Molecular Imaging Centre, The University of Manchester, Manchester, UK.)

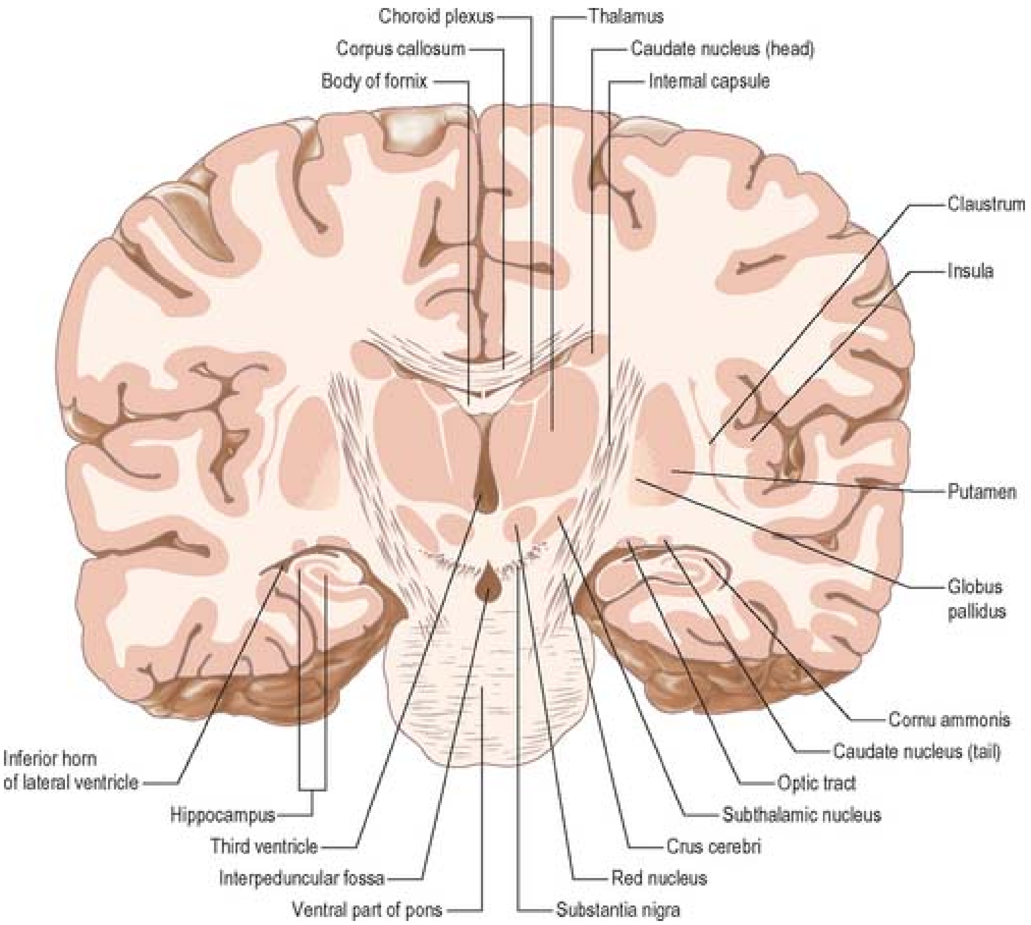
Choroid plexus
Corpus callosum
Body of fornix
Thalamus
Caudate nucleus (head)
Internal capsule
Claustrum
Insula
Putamen
Globus pallidus
Cornu ammonis
Caudate nucleus (tail)
Optic tract
Subthalamic nucleus
Crus cerebri
Red nucleus
Substantia nigra
Inferior horn of lateral ventricle
Hippocampus
Third ventricle
Interpeduncular fossa
Ventral part of pons

Fig. 21.2 The principal parts of the diencephalon and basal ganglia, coronal section.

The superior (dorsal) surface of the thalamus (see Fig. 19.3) is covered by a thin layer of white matter, the stratum zonale. It extends laterally from the line of reflection of the ependyma (taenia thalami), and forms the roof of the third ventricle. This curved surface is separated from the overlying body of the fornix by the choroid fissure with the tela choroidea within it. More laterally, it forms part of the floor of the lateral ventricle. The lateral border of the superior surface of the thalamus is marked by the stria terminalis and overlying thalamostriate vein, which separate the thalamus from the body of the caudate nucleus. Laterally, a slender sheet of white matter, the external medullary lamina, separates the main body of the thalamus from the reticular nucleus. Lateral to this, the thick posterior limb of the internal capsule lies between the thalamus and the lentiform complex.

The medial surface of the thalamus is the superior (dorsal) part of the lateral wall of the third ventricle. It is usually connected to the contralateral thalamus by an interthalamic adhesion behind the interventricular foramina (see Fig. 16.7). The boundary with the hypothalamus is marked by an indistinct hypothalamic sulcus, which curves from the upper end of the cerebral aqueduct to the interventricular foramen. The thalamus is continuous with the midbrain tegmentum, the subthalamus and the hypothalamus.

Internally, the greater part of the thalamus is divided into anterior, medial and lateral nuclear groups by a vertical Y-shaped sheet of white matter, the internal medullary lamina (Figs 21.3, 21.4). In addition, intralaminar nuclei lie embedded within the internal medullary lamina and midline nuclei abut the lateral walls of the third ventricle. The reticular nucleus forms a shell-like lateral covering to the main nuclear mass, separated from it by an external medullary lamina of nerve fibres.

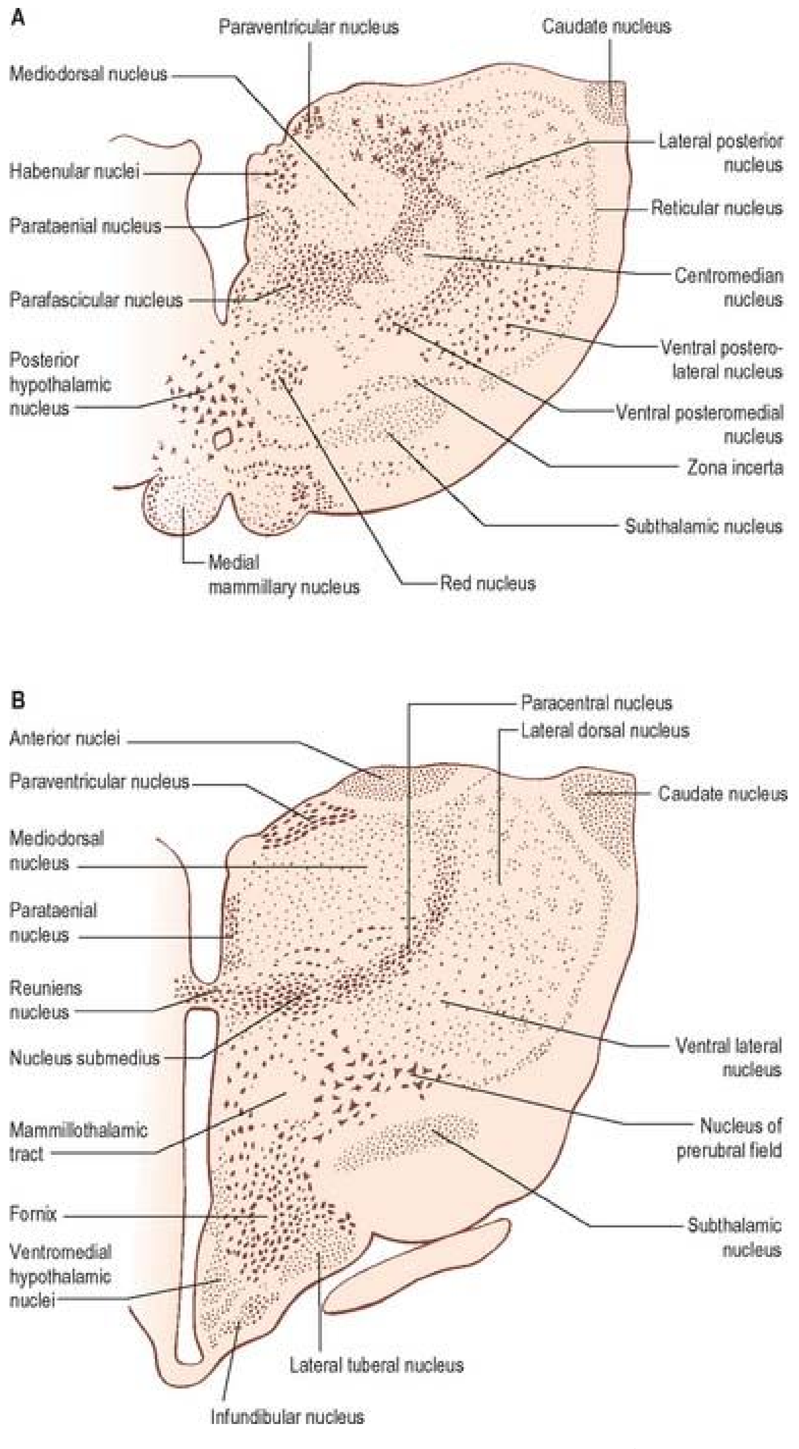
A
Paraventricular nucleus
Caudate nucleus
Mediodorsal nucleus
Lateral posterior nucleus
Habenular nuclei
Reticular nucleus
Parataenial nucleus
Centromedian nucleus
Parafascicular nucleus
Ventral postero-lateral nucleus
Posterior hypothalamic nucleus
Ventral posteromedial nucleus
Zona incerta
Subthalamic nucleus
Medial mammillary nucleus
Red nucleus
B
Paracentral nucleus
Lateral dorsal nucleus
Anterior nuclei
Paraventricular nucleus
Caudate nucleus
Mediodorsal nucleus
Parataenial nucleus
Reuniens nucleus
Nucleus submedius
Ventral lateral nucleus
Mammillothalamic tract
Nucleus of prerubral field
Fornix
Subthalamic nucleus
Ventromedial hypothalamic nuclei
Lateral tuberal nucleus
Infundibular nucleus

Fig. 21.3 The main nuclear aggregations of cell bodies in the diencephalon (coronal sections). **A**, At the level of the mammillary bodies. **B**, At the level of the tuber cinereum. Note the variations in cell size, shape and packing density, which characterize the nuclear masses of the thalamus, subthalamus and hypothalamus at these levels.

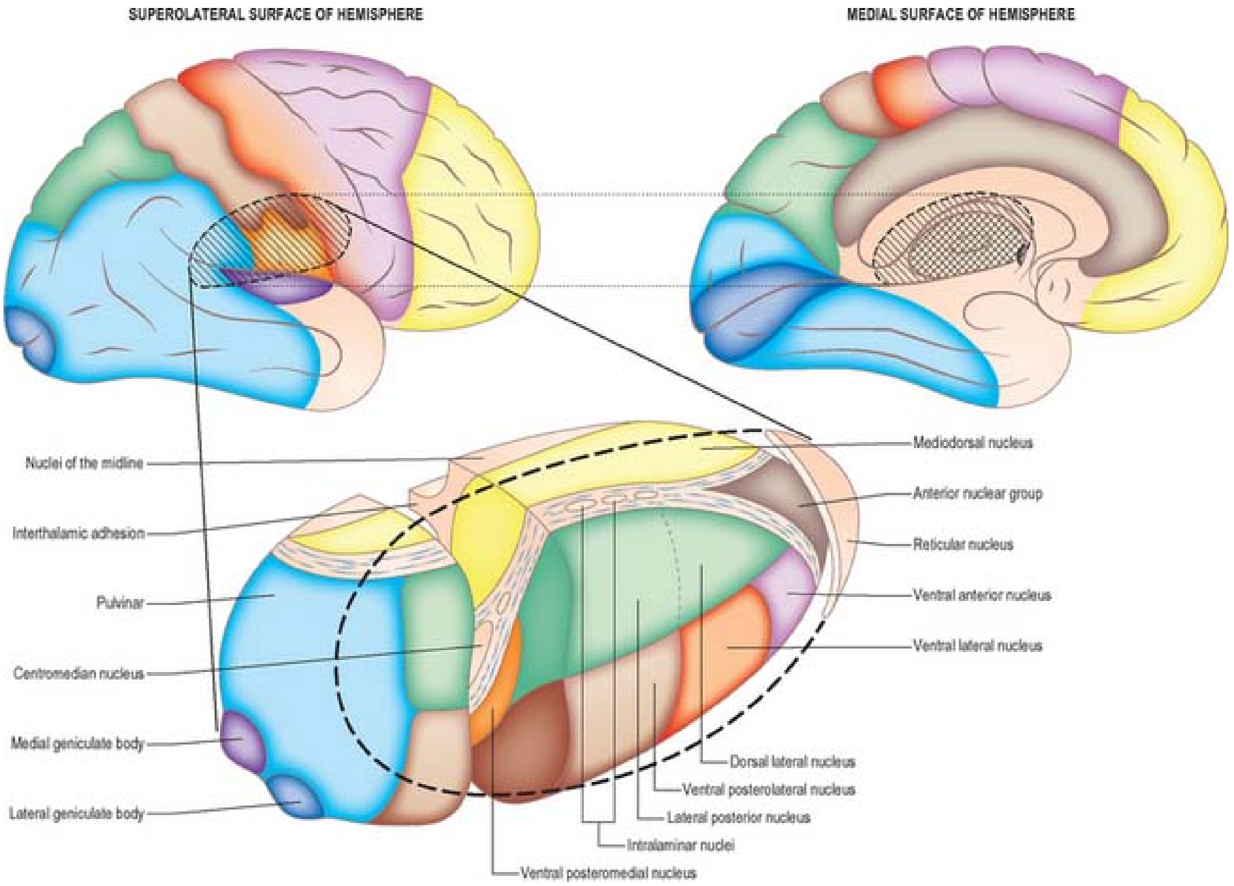
SUPEROLATERAL SURFACE OF HEMISPHERE
MEDIAL SURFACE OF HEMISPHERE
Nuclei of the midline
Interthalamic adhesion
Pulvinar
Centromedian nucleus
Medial geniculate body
Lateral geniculate body
Mediodorsal nucleus
Anterior nuclear group
Reticular nucleus
Ventral anterior nucleus
Ventral lateral nucleus
Dorsal lateral nucleus
Ventral posterolateral nucleus
Lateral posterior nucleus
Intralaminar nuclei
Ventral posteromedial nucleus

Fig. 21.4 The main nuclear masses of the thalamus (viewed from the lateral aspect in the lower illustration) colour coded to indicate the areas of cerebral neocortex with which they are interconnected. The lack of colour in the centromedian, intralaminar and reticular nuclei and in areas of the frontal and temporal lobes is not related to the colour code. The reticular nucleus lies lateral to the main mass of the thalamus. Only the anterior pole of the reticular nucleus is shown, its posterior extent being depicted by the heavy interrupted line.

In general, thalamic nuclei both project to and receive fibres from the cerebral cortex (Fig. 21.4). The whole cerebral cortex, including neocortex, paleocortex of the piriform lobe and archicortex of the hippocampal formation, is reciprocally connected with the thalamus. The thalamus is the major route by which subcortical neuronal activity influences the cerebral cortex, and the greatest input to most thalamic nuclei comes from the cerebral cortex.

The projection to the thalamus from the cortex is precisely reciprocal; each cortical area projects in a topographically organized manner to all sites in the thalamus from which it receives an input. Thalamocortical fibres terminate predominantly in layer IV of the cortex. Corticothalamic fibres which reciprocate ‘specific’ thalamocortical pathways arise from modified pyramidal cells of layer VI, whereas those reciprocating ‘non-specific’ inputs arise from typical pyramidal cells of layer V, and may in part be axon collaterals of other cortico-subcortical pathways.

It is customary to consider thalamic nuclei as either ‘specific’ nuclei, which mediate finely-organized and precisely-transmitted sensory information to discrete cortical sensory areas, or as ‘non-specific’ nuclei, which are part of a general arousal system. The specific nuclei are further subdivided into relay nuclei and association nuclei. However, many nuclei classified as specific may also send non-specific projections to widespread cortical areas. Similarly, the division of thalamic nuclei into relay and association groups rests upon the assumption that relay nuclei receive a major subcortical pathway, whereas association nuclei receive their principal non-cortical input from other thalamic nuclei. There is little evidence of significant intrathalamic connectivity, but increasing indications of non-cortical afferent pathways linked to so-called association nuclei: the extensive connectivity between the reticular nucleus and other thalamic nuclei is a notable exception.

ANTERIOR THALAMIC NUCLEI

The anterior group of nuclei are enclosed between the arms of the Y-shaped internal medullary lamina, and underlie the anterior thalamic tubercle (see Figs 19.3, 21.4). Three subdivisions are recognized: the largest is the anteroventral nucleus, the others being the anteromedial and anterodorsal nuclei.

The anterior nuclei are the principal recipients of the mammillo-thalamic tract, which arises from the mammillary nuclei of the hypothalamus. The mammillary nuclei receive fibres from the hippocampal formation via the fornix. The medial mammillary nucleus projects to the ipsilateral anteroventral and anteromedial thalamic nuclei, and the lateral mammillary nucleus projects bilaterally to the anterodorsal nuclei. The nuclei of the anterior group also receive a prominent cholinergic input from the basal forebrain and the brain stem.

The cortical targets of efferent fibres from the anterior nuclei of the thalamus lie largely on the medial surface of the hemisphere. They include the anterior limbic area (in front of and inferior to the corpus callosum), the cingulate gyrus, and the parahippocampal gyrus (including the medial entorhinal cortex and the pre- and para-subiculum). These thalamocortical pathways are reciprocal. There also appear to be minor connections between the anterior nuclei and the dorsolateral prefrontal and posterior areas of neocortex. The anterior thalamic nuclei are believed to be involved in the regulation of alertness and attention and in the acquisition of memory.

MEDIAL THALAMIC NUCLEI

The single component of this thalamic region is the mediodorsal or dorsomedial nucleus, which is particularly large in man. Laterally, it is limited by the internal medullary lamina and intralaminar nuclei. Medially, it abuts the midline parataenial and reuniens (medioventral) nuclei. It is divided into anteromedial magnocellular, and postero-lateral parvocellular, parts.

The smaller magnocellular division receives olfactory input from the piriform and adjacent cortex, the ventral pallidum, and the amygdala. The mediobasal amygdaloid nucleus projects to the dorsal part of the anteromedial magnocellular nucleus, and the lateral nuclei project to the more central and anteroventral regions. The anteromedial magnocellular nucleus projects to the anterior and medial prefrontal cortex, notably to the lateral posterior and central posterior olfactory areas on the orbital surface of the frontal lobe. In addition, fibres pass to the ventromedial cingulate cortex and some to the inferior parietal cortex and anterior insula. These cortical connections are reciprocal.

The larger, posterolateral parvocellular division connects reciprocally with the dorsolateral and dorsomedial prefrontal cortex, the anterior cingulate gyrus and the supplementary motor area. In addition, efferent fibres pass to the posterior parietal cortex.

The mediodorsal nucleus appears to be involved in a wide variety of higher functions. Damage may lead to a decrease in anxiety, tension, aggression or obsessive thinking. There may also be transient amnesia, with confusion developing particularly over the passage of time. Much of the neuropsychology of medial nuclear damage reflects defects in functions similar to those performed by the prefrontal cortex, with which it is closely linked. The effects of ablation of the mediodorsal nuclei parallel, in part, the results of prefrontal lobotomy.

LATERAL THALAMIC NUCLEI

The lateral nuclear complex, lying lateral to the internal medullary lamina, is the largest division of the thalamus. It is divided into dorsal and ventral tiers of nuclei. The lateral dorsal nucleus, lateral posterior nucleus and the pulvinar all lie dorsally. The lateral and medial geniculate nuclei lie inferior to the pulvinar near the posterior pole of the thalamus. The ventral tier nuclei are the ventral anterior, ventral lateral and ventral posterior nuclei.

Ventral anterior nucleus

The ventral anterior (VA) nuclear complex lies at the anterior pole of the ventral nuclear group. It is limited anteriorly by the reticular nucleus, posteriorly by the ventral lateral nucleus, and lies between the external and internal medullary laminae. It consists of a principal part (VApc) and a magnocellular part (VAmc). The subcortical connections to this region are largely ipsilateral from the internal segment of the globus pallidus and the pars reticulata of the substantia nigra. The terminal fields from these origins do not overlap. Fibres from the globus pallidus end in VApc. The substantia nigra projects to VAmc. Corticothalamic fibres from premotor cortex (area 6) terminate in VApc and fibres from the frontal eye field (area 8) terminate in VAmc. VA thalamus does not appear to receive fibres directly from the motor cortex. The efferent projections from VA are incompletely known. Some pass to intralaminar thalamic nuclei and others project to widespread regions of the frontal lobe and to the anterior parietal cortex. Their functions are unclear. The VA thalamus appears to play a central role in the transmission of the cortical ‘recruiting response’, a phenomenon in which stimulation of the thalamus can initiate long-lasting, high voltage repetitive negative electrical waves over much of the cerebral cortex.

Ventral lateral nucleus

The ventral lateral (VL) nucleus consists of two major divisions with distinctly different connections and functions. The anterior division, or pars oralis (VLo), receives topographically organized fibres from the internal segment of the ipsilateral globus pallidus. The posterior division, or pars caudalis (VLc), receives topographically organized fibres from the contralateral deep cerebellar nuclei. Additional subcortical projections have been reported from the spinothalamic tract and the vestibular nuclei. Numerous cortical afferents to both VLo and VLc originate from precentral motor cortical areas, including both area 4 and area 6.

The VLo nucleus sends efferent fibres to the supplementary motor cortex on the medial surface of the hemisphere and to the lateral premotor cortex. The VLc nucleus projects efferent fibres to the primary motor cortex where they end in a topographically arranged fashion. The head region of area 4 receives fibres from the medial part of VLc, and the leg region receives fibres from lateral VLc.

Approximately 70% of VL neurones are large relay neurones, and the other 30% are local circuit interneurones. Responses can be recorded in VL thalamus during both passive and active movement of the contralateral body. The topography of its connections, and recordings made within the nucleus, suggest that VLc contains a body representation comparable to that in the ventral posterior nucleus. In patients with tremor, clusters of VL neurones fire in bursts that are synchronous with peripheral tremor: these cells have been designated as ‘tremor cells’. Stereotaxic surgery of the ventral lateral nucleus is sometimes used in the treatment of essential tremor. In the past, thalamotomy was used extensively for the treatment of Parkinson’s disease. The internal segment of the globus pallidus and the subthalamic nucleus are now the preferred neurosurgical targets for Parkinson’s disease (see Ch. 22).

Ventral posterior nucleus

The ventral posterior (VP) nucleus is the principal thalamic relay for the somatosensory pathways. It is thought to consist of two major divisions, the ventral posterolateral (VPl) and ventral posteromedial (VPm) nuclei. The VPl nucleus receives the medial lemniscal and spinothalamic pathways, and the VPm nucleus receives the trigeminothalamic pathway. Connections from the vestibular nuclei and lemniscal fibres terminate along the ventral surface of the VP nucleus.

There is a well-ordered topographic representation of the body in the ventral posterior nucleus. The VPl is organized so that sacral segments are represented laterally and cervical segments medially. The latter abut the face area of representation (trigeminal territory) in VPm. Taste fibres synapse most anteriorly and ventromedially within the ventral posterolateral nucleus.

At a more detailed level, single body regions are represented as curved lamellae of neurones, parallel to the lateral border of the ventral posterior nucleus, such that there is a continuous overlapping progression of adjacent receptive fields from dorsolateral to ventromedial. Considerably less change in location of receptive field on the body is seen when passing anteroposteriorly through the nucleus. While not precisely dermatomal in nature, these curvilinear lamellae of cells probably derive from afferents related to a few adjacent spinal segments. There is considerable distortion of the body map within the nucleus, reflecting the differences in the density of peripheral innervation which occur in different body regions, e.g. many more neurones respond to stimulation of the hand than of the trunk. Within a single lamella, neurones in the anterodorsal part of the nucleus respond to deep stimuli, including movement of joints, tendon stretch, and manipulation of muscles. Most ventrally, neurones once again respond to deep stimuli, particularly tapping. Intervening cells within a single lamella respond only to cutaneous stimuli. This organization has been confirmed by recordings made in the human ventral posterior nucleus.

Single lemniscal axons have an extended anteroposterior terminal zone within the nucleus. Rods of cells running the length of the anteroposterior, dorsoventrally oriented, lamellae respond with closely similar receptive field properties and locations, derived from a small bundle of lemniscal afferents. It appears, therefore, that each lamella contains the complete representation of a single body part, e.g. a finger. Lamellae consist of multiple narrow rods of neurones, oriented anteroposteriorly, each of which receives input from the same small region of the body that is represented within the lamella, and from the same type of receptors. These thalamic ‘rods’ form the basis for both the place- and modality-specific input to columns of cells in the somatic sensory cortex. Spinothalamic tract afferents to the ventral posterolateral nucleus terminate throughout the nucleus. The neurones from which these axons originate appear to be mainly of the ‘wide dynamic range’ class, responding to both low threshold mechanoreceptors and high threshold nociceptors; a smaller proportion of neurones respond exclusively to high-threshold nociceptors. Some neurones respond to temperature changes. There is evidence that spinothalamic tract neurones carrying nociceptive and thermal information terminate in a distinct nuclear area, identified as the posterior part of the ventral medial nucleus (VMpo).

The VP nucleus projects to the primary somatic sensory cortex (SI) of the postcentral gyrus and to the second somatic sensory area (SII) in the parietal operculum. VMpo projects to the insular cortex. Within the primary sensory cortex, the central cutaneous core of the VP nucleus projects solely to area 3b; dorsal and ventral to this, a narrow band of cells projects to both 3b and area 1. The most dorsal and ventral deep stimulus receptive cells project to areas 3a and 2. The whole nucleus projects to the second somatic sensory area.

Medial geniculate nucleus

The medial geniculate nucleus, which is a part of the auditory pathway (see Ch. 37), is located within the medial geniculate body, a rounded elevation situated posteriorly on the ventrolateral surface of the thalamus, and separated from the pulvinar by the superior quadrigeminal brachium. It receives fibres travelling in the inferior quadrigeminal brachium. Three major subnuclei, medial, ventral and dorsal, are recognized within it. The inferior brachium separates the medial (magnocellular) nucleus, which consists of sparse, deeply staining neurones, from the lateral nucleus, which is made up of medium-sized, densely packed and darkly staining cells. The dorsal nucleus overlies the ventral nucleus and expands posteriorly; it is, therefore, sometimes known as the posterior nucleus of the medial geniculate. It contains small- to medium-sized, pale-staining cells, which are less densely packed than those of the lateral nucleus. The ventral nucleus receives fibres from the central nucleus of the ipsilateral inferior colliculus via the inferior quadrigeminal brachium and also from the contralateral inferior colliculus.

The nucleus contains a complete tonotopic representation. Low-pitched sounds are represented laterally, and progressively higher-pitched sounds are encountered as the nucleus is traversed from lateral to medial. The dorsal nucleus receives afferents from the pericentral nucleus of the inferior colliculus and from other brain stem nuclei of the auditory pathway. A tonotopic representation has not been described in this subdivision and cells within the dorsal nucleus respond to a broad range of frequencies. The magnocellular medial nucleus receives fibres from the inferior colliculus and from the deep layers of the superior colliculus. Neurones within the magnocellular subdivision may respond to modalities other than sound. However, many cells respond to auditory stimuli, usually to a wider range of frequencies than neurones in the ventral nucleus. Many units show evidence of binaural interaction, with the leading effect arising from stimuli in the contralateral cochlea. The ventral nucleus projects primarily to the primary auditory cortex. The dorsal nucleus projects to auditory areas surrounding the primary auditory cortex. The magnocellular division projects diffusely to auditory areas of the cortex and to adjacent insular and opercular fields.

Lateral geniculate nucleus

The lateral geniculate body, which is part of the visual pathway (see Ch. 40), is a small, ovoid, ventral projection from the posterior thalamus (Fig. 21.5). The superior quadrigeminal brachium enters the posteromedial part of the lateral geniculate body dorsally, lying between the medial geniculate body and the pulvinar.

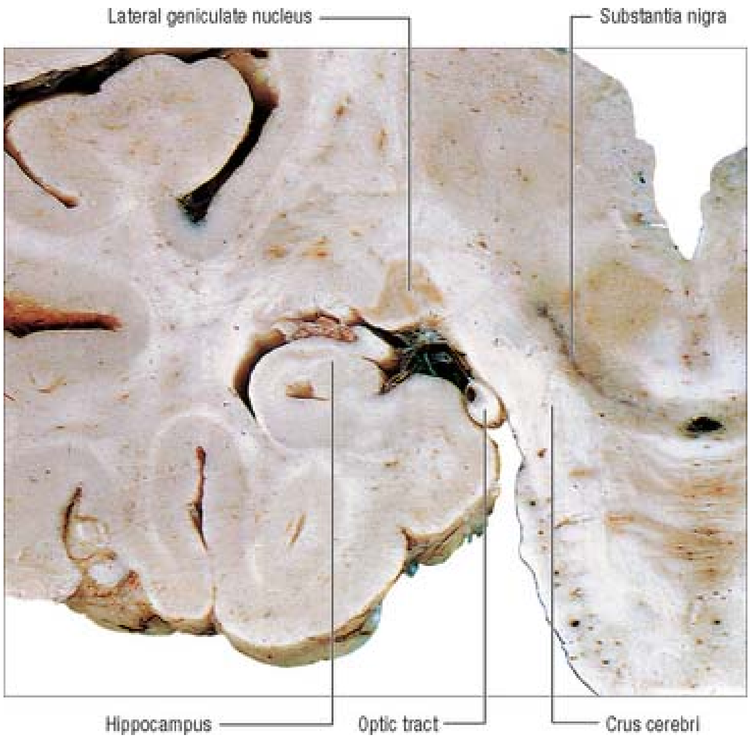
Lateral geniculate nucleus
Substantia nigra
Hippocampus
Optic tract
Crus cerebri

Fig. 21.5 Coronal section through the brain showing the lateral geniculate nucleus.

(Photograph by Kevin Fitzpatrick on behalf of GKT School of Medicine, London.)

The lateral geniculate nucleus is an inverted, somewhat flattened, U-shaped nucleus and is laminated. Its internal organization is usually described on the basis of six laminae, although seven or eight may be present. The laminae are numbered 1 to 6, from the innermost ventral to the outermost dorsal (Fig. 21.6). Laminae 1 and 2 consist of large cells, the magnocellular layers, whereas layers 4 to 6 have smaller neurones, the parvocellular laminae. The apparent gaps between laminae are called the interlaminar zones. Most ventrally an additional superficial, or S, lamina is recognized.

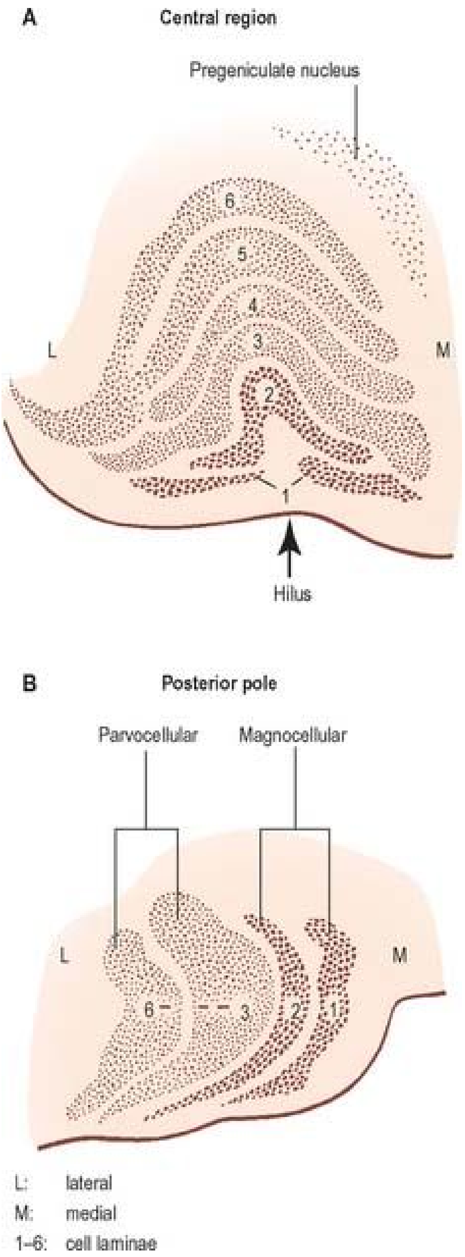
A
Central region
Pregeniculate nucleus
6
5
4
3
L
M
2
1
Hilus
B
Posterior pole
Parvocellular
Magnocellular
L
M
6
3
2
1
L: lateral
M: medial
1–6: cell laminae

Fig. 21.6 Coronal sections through the lateral geniculate nucleus illustrating the laminar arrangement of neurones (**A**) near its central region and (**B**) near its posterior pole.

The lateral geniculate nucleus receives a major afferent input from the retina. The contralateral nasal hemiretina projects to laminae 1, 4 and 6, whereas the ipsilateral temporal hemiretina projects to laminae 2, 3 and 5. The parvocellular laminae receive axons predominantly of X-type retinal ganglion cells, i.e. more slowly conducting cells with sustained responses to visual stimuli. The faster conducting, rapidly adapting Y-type retinal ganglion cells project mainly to the magnocellular laminae 1 and 2, and give off axonal branches to the superior colliculus. A third type of retinal ganglion cell, the W cells, which have large receptive fields and slow responses, project to both the superior colliculus and the lateral geniculate nucleus, where they terminate particularly in the interlaminar zones and in the S lamina.

The lateral geniculate nucleus is organized in a visuotopic manner and it contains a precise map of the contralateral visual field. The vertical meridian is represented posteriorly, the peripheral anteriorly, the upper field laterally, and the lower field medially. Similar precise, point-to-point, representation is also found in the projection of the lateral geniculate nucleus to the visual cortex. Radially arranged inverted pyramids of neurones in all laminae respond to a single, small area of the contralateral visual field and project to a circumscribed area of cortex. The termination of geniculocortical axons in the visual cortex is considered in detail elsewhere (see Ch. 23).

Aside from retinal afferents, the lateral geniculate nucleus receives a major corticothalamic projection, the axons of which ramify densely in the interlaminar zones. The major part of this projection arises from the primary visual cortex, Brodmann’s area 17, but smaller projections from extrastriate visual areas pass to the magnocellular and S laminae. Other afferents include: fibres from the superficial layer of the superior colliculus (which terminate in the interlaminar zone between laminae 1 and 2, 2 and 3, and around lamina S); noradrenergic fibres from the locus coeruleus; serotoninergic afferents from the midbrain raphe nuclei; and cholinergic fibres from the pontine and mesencephalic reticular formation.

The efferent fibres of the lateral geniculate nucleus pass principally to the primary visual cortex (area 17) in the banks of the calcarine sulcus. It is possible that additional small projections pass to extrastriate visual areas in the occipital lobe, possibly arising primarily in the interlaminar zones.

Lateral dorsal nucleus

The lateral dorsal nucleus is the most anterior of the dorsal tier of lateral nuclei. Its anterior pole lies within a splitting of the internal medullary lamina, and posteriorly it merges with the lateral posterior nucleus. Subcortical afferents to the lateral dorsal nucleus are from the pretectum and superior colliculus. It is connected with the cingulate, retrosplenial and posterior parahippocampal cortices, the presubiculum of the hippocampal formation, and the parietal cortex.

Lateral posterior nucleus

The lateral posterior nucleus, which lies dorsal to the ventral posterior nucleus, receives its subcortical afferents from the superior colliculus. It is reciprocally connected with the superior parietal lobe. Additional connections have been reported with the inferior parietal, cingulate and medial parahippocampal cortex.

Pulvinar

The pulvinar corresponds to the posterior expansion of the thalamus, which overhangs the superior colliculus (Fig. 21.4). It has three major subdivisions, which are the medial, lateral and inferior pulvinar nuclei. The medial pulvinar nucleus is dorsomedial and consists of compact, evenly spaced, neurones. The inferior pulvinar nucleus lies laterally and inferiorly, and is traversed by bundles of axons in the mediolateral plane, an arrangement which confers a fragmented appearance of horizontal cords or sheets of cells separated by fibre bundles. The inferior pulvinar nucleus lies most inferiorly and laterally and is a more homogeneous collection of cells.

The subcortical afferents to the pulvinar are uncertain. Medial and lateral pulvinar nuclei may receive fibres from the superior colliculus. It has been suggested that the inferior pulvinar nucleus receives fibres both from the superior colliculus and directly from the retina and that it contains a complete retinotopic representation.

The cortical targets of efferent fibres from the pulvinar are widespread. In essence, the medial pulvinar nucleus projects to association areas of the parietotemporal cortex, whereas lateral and inferior pulvinar nuclei project to visual areas in the occipital and posterior temporal lobes. Thus, the inferior pulvinar nucleus connects with the striate and extrastriate cortex in the occipital lobe, and with visual association areas in the posterior part of the temporal lobe. The lateral pulvinar nucleus connects with extrastriate areas of the occipital cortex, with posterior parts of the temporal association cortex, and with the parietal cortex. The medial pulvinar nucleus connects with the inferior parietal cortex, with the posterior cingulate gyrus and with the widespread areas of the temporal lobe, including the posterior parahippocampal gyrus, perirhinal and entorhinal cortex. It also has extensive connections with prefrontal and orbitofrontal cortices. Similarly, the lateral pulvinar nucleus may also connect with the rostromedial prefrontal cortex.

Little is known of the functions of the pulvinar. The inferior pulvinar nucleus contains a complete retinotopic representation, and lateral and medial pulvinar nuclei also contain visually responsive cells. However, the latter nucleus, at least, is not purely visual – other modality responses can be recorded, and some cells may be polysensory. Given the complexity of functions of the association areas to which they project, particularly in the temporal lobe (e.g. perception, cognition and memory), it is likely that the role of the pulvinar in modulating these functions is equally complex.

Anteriorly, the major subdivisions of the pulvinar blend into a poorly differentiated region, within which several nuclear components have been recognized, including the anterior or oral pulvinar, the suprageniculate-limitans nucleus and the posterior nuclei. The connectivity of this complex is also not well understood. It is recognized that different components receive subcortical afferents from the spinothalamic tract and the superior and inferior colliculi. Cortical connections centre primarily on the insula and adjacent parts of the parietal operculum posteriorly. Stimulation of this region has been reported to elicit pain, and large lesions may alleviate painful conditions. Similarly, excision of its cortical target in the parietal operculum, or small infarcts in this cortical region, may result in hypoalgesia.

INTRALAMINAR NUCLEI

The term intralaminar nuclei refers to collections of neurones within the internal medullary lamina of the thalamus (Fig. 21.4). Two groups of nuclei are recognized. The anterior (rostral) group is subdivided into central medial, paracentral and central lateral nuclei. The posterior (caudal) intralaminar group consists of the centromedian and parafascicular nuclei. The designations central medial and centromedian are open to confusion; however, they are an accepted part of the terminology of thalamic nuclei in common usage. The centromedian nucleus is much larger, is considerably expanded in man in comparison with other species, and is importantly related to the globus pallidus, deep cerebellar nuclei and motor cortex. Anteriorly, the internal medullary lamina separates the mediodorsal nucleus from the ventral lateral complex. It is occupied by the paracentral nucleus laterally, and the central medial nucleus ventromedially, as the two laminae converge towards the midline. A little more posteriorly, the central lateral nucleus appears dorsally in the lamina as the latter splits to enclose the lateral dorsal nucleus. More posteriorly, at the level of the ventral posterior nucleus, the lamina splits to enclose the ovoid centromedian nucleus. The smaller parafascicular nucleus lies more medially.

The anterior intralaminar nuclei, i.e. central medial, paracentral and central lateral, have reciprocal connections with widespread cortical areas. There is some evidence of areal preference: the central lateral nucleus projects mainly to parietal and temporal association areas; the paracentral nucleus to occipitotemporal and prefrontal cortex; and the central medial nucleus to orbitofrontal and prefrontal cortex and to the cortex on the medial surface. In contrast, the posterior nuclei, i.e. centromedian and parafascicular nuclei, have more restricted connections, principally with the motor, premotor and supplementary motor areas. Both anterior and posterior intralaminar nuclei also project to the striatum. Many cells throughout the anterior nuclei have branched axons, which pass to both the cortex and the striatum. Dual projections are less frequent in the posterior nuclei. The thalamostriate projection is topographically organized. The posterior intralaminar nuclei receive a major input from the internal segment of the globus pallidus. Additional afferents come from the pars reticulata of the substantia nigra, the deep cerebellar nuclei, the pedunculopontine nucleus of the midbrain, and possibly the spinothalamic tract. The anterior nuclei have widespread subcortical afferents. The central lateral nucleus receives afferents from the spinothalamic tract, and all component nuclei receive fibres from the brain stem reticular formation, the superior colliculus and several pretectal nuclei. Afferents to all intralaminar nuclei from the brain stem reticular formation include a prominent cholinergic pathway.

The precise functional role of the intralaminar nuclei is unclear. They appear to mediate cortical activation from the brain stem reticular formation and to play a part in sensorimotor integration. Damage to the intralaminar nuclei may contribute to thalamic neglect, i.e. the unilateral neglect of stimuli originating from the contralateral body or extrapersonal space. This may arise particularly from unilateral damage to the centromedian–parafascicular complex. The latter has been targeted in humans for the neurosurgical control of pain and epilepsy. Bilateral injury to the posterior intralaminar nuclei leads to a kinetic mutism with apathy and loss of motivation. A second syndrome associated with damage involving the intralaminar nuclei is that of unilateral motor neglect, in which there is contralateral paucity of spontaneous movement and motor activity.

MIDLINE NUCLEI

There is considerable divergence between different authors as to which elements of the medial diencephalon constitute the nuclei of the midline thalamic group. In the present account, the midline group of nuclei includes those medial thalamic structures ventral to the central medial nucleus, i.e. the rhomboid and reuniens nuclei together with the parataenial nuclei more dorsolaterally.

The midline nuclei receive subcortical afferent fibres from the hypothalamus, the periaqueductal grey matter of the midbrain, the spinothalamic tract and the medullary and pontine reticular formation. They are the major thalamic target of ascending noradrenergic and serotoninergic axons from the locus coeruleus and raphe nuclei respectively, and they also receive a cholinergic input from the midbrain. Efferents from the midline nuclei pass to the hippocampal formation, the amygdala and the nucleus accumbens. Additional thalamocortical axons reach the cingulate, and possibly orbitofrontal, cortex. The dual cortical and basal nuclear relationship of these nuclei has often led to their being considered a part of the intralaminar system. The cortical projections are reciprocal. The relationships of the midline nuclei clearly identify them as part of the limbic system. There is some evidence that they may play a role in memory and arousal, and, pathologically, may be important in the regulation of seizure activity.

RETICULAR NUCLEUS

The reticular nucleus is a curved lamella of large, deeply staining fusiform cells that wraps around the lateral margin of the thalamus, separated from it by the external medullary lamina. Anteriorly, it curves around the rostral pole of the thalamus to lie between it and the prethalamic nuclei, notably the bed nucleus of the stria terminalis. The nucleus is so named because it is criss-crossed by bundles of fibres which, as they pass between thalamus and cortex, produce a reticular appearance.

The nucleus is thought to receive collateral branches of corticothalamic, thalamocortical and probably thalamostriatal and pallidothalamic fibres as they traverse it. It receives an additional, probably cholinergic, afferent pathway from the nucleus cuneiformis of the midbrain. Broadly speaking, the afferents from the cortex and thalamus are topographically arranged. The reticular nucleus contains visual, somatic and auditory regions, each with a crude topographic representation of the sensorium concerned. Cells within these regions respond to visual, somatic or auditory stimuli with a latency suggesting that these properties arise from activation by thalamocortical axon collaterals. Only in areas where representations abut do cells show modality convergence.

The efferent fibres from the reticular nucleus pass into the body of the thalamus and are GABAergic. The projections into the main thalamic nuclei broadly, but not entirely, reciprocate the thalamoreticular connections. There may also be projections to the contralateral dorsal thalamus. The reticular nucleus is believed to function in gating information relayed through the thalamus.

HYPOTHALAMUS

The hypothalamus consists of only 4 cm^3 of neural tissue, or 0.3% of the total brain. Nevertheless, it contains the integrative systems that, via the autonomic and endocrine effector systems, control fluid and electrolyte balance, food ingestion and energy balance, reproduction, thermoregulation, and immune and many emotional responses.

The hypothalamus extends from the lamina terminalis to a vertical plane posterior to the mammillary bodies, and from the hypothalamic sulcus to the base of the brain beneath the third ventricle. It lies beneath the thalamus (Fig. 21.3) and anterior to the tegmental part of the subthalamus and the mesencephalic tegmentum (Figs 21.7, 21.8)). Laterally, it is bordered by the anterior part of the subthalamus, internal capsule and optic tract. Structures in the floor of the third ventricle reach the pial surface in the interpeduncular fossa. From anterior to posterior they are the optic chiasma, the tuber cinereum, tuberal eminences and the infundibular stalk, the mammillary bodies and the posterior perforated substance. The latter lies in the interval between the diverging crura cerebri, and is pierced by small central branches of the posterior cerebral arteries. It contains the small interpeduncular nucleus, which receives terminals of the fasciculus retroflexus of both sides, and has other connections with the mesencephalic reticular formation and mammillary bodies.

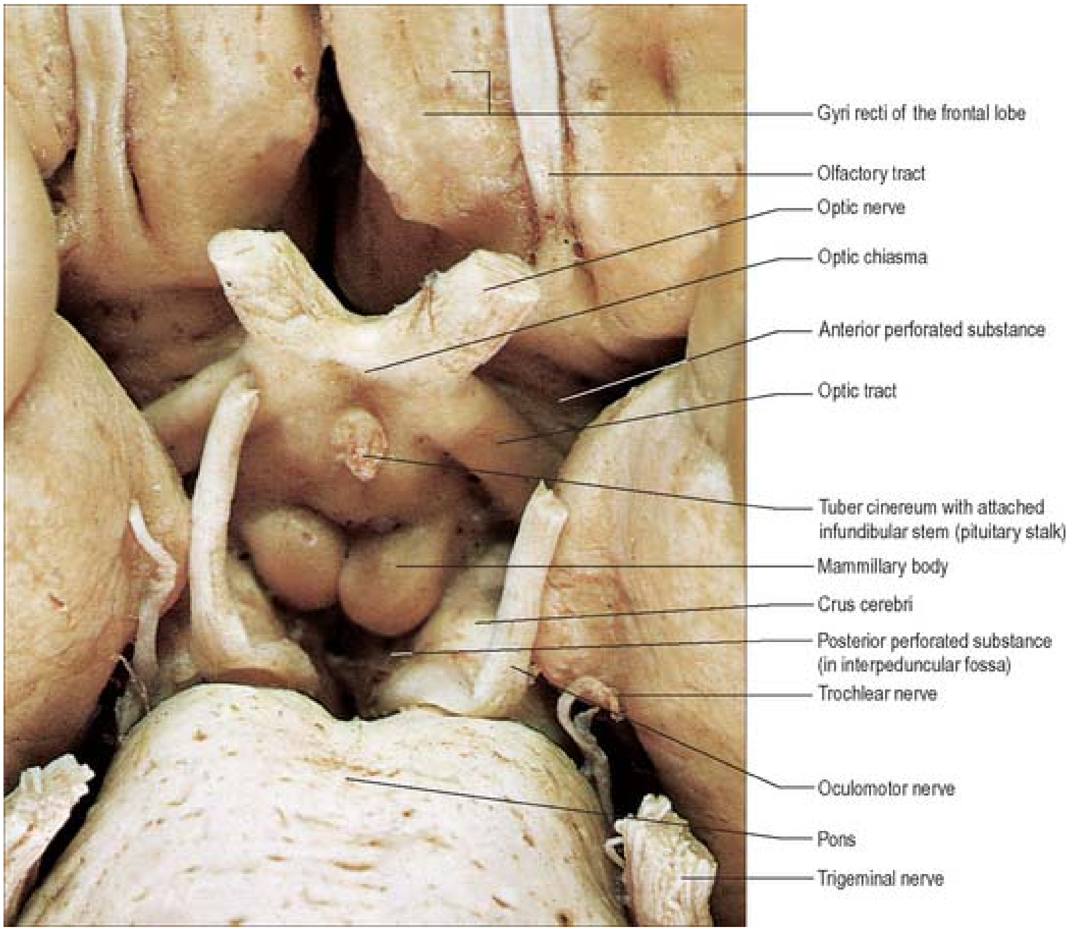
Gyri recti of the frontal lobe
Olfactory tract
Optic nerve
Optic chiasma
Anterior perforated substance
Optic tract
Tuber cinereum with attached infundibular stem (pituitary stalk)
Mammillary body
Crus cerebri
Posterior perforated substance (in interpeduncular fossa)
Trochlear nerve
Oculomotor nerve
Pons
Trigeminal nerve

Fig. 21.7 The inferior aspect of the hypothalamus and surrounding structures.

(Photograph by Kevin Fitzpatrick on behalf of GKT School of Medicine, London.)

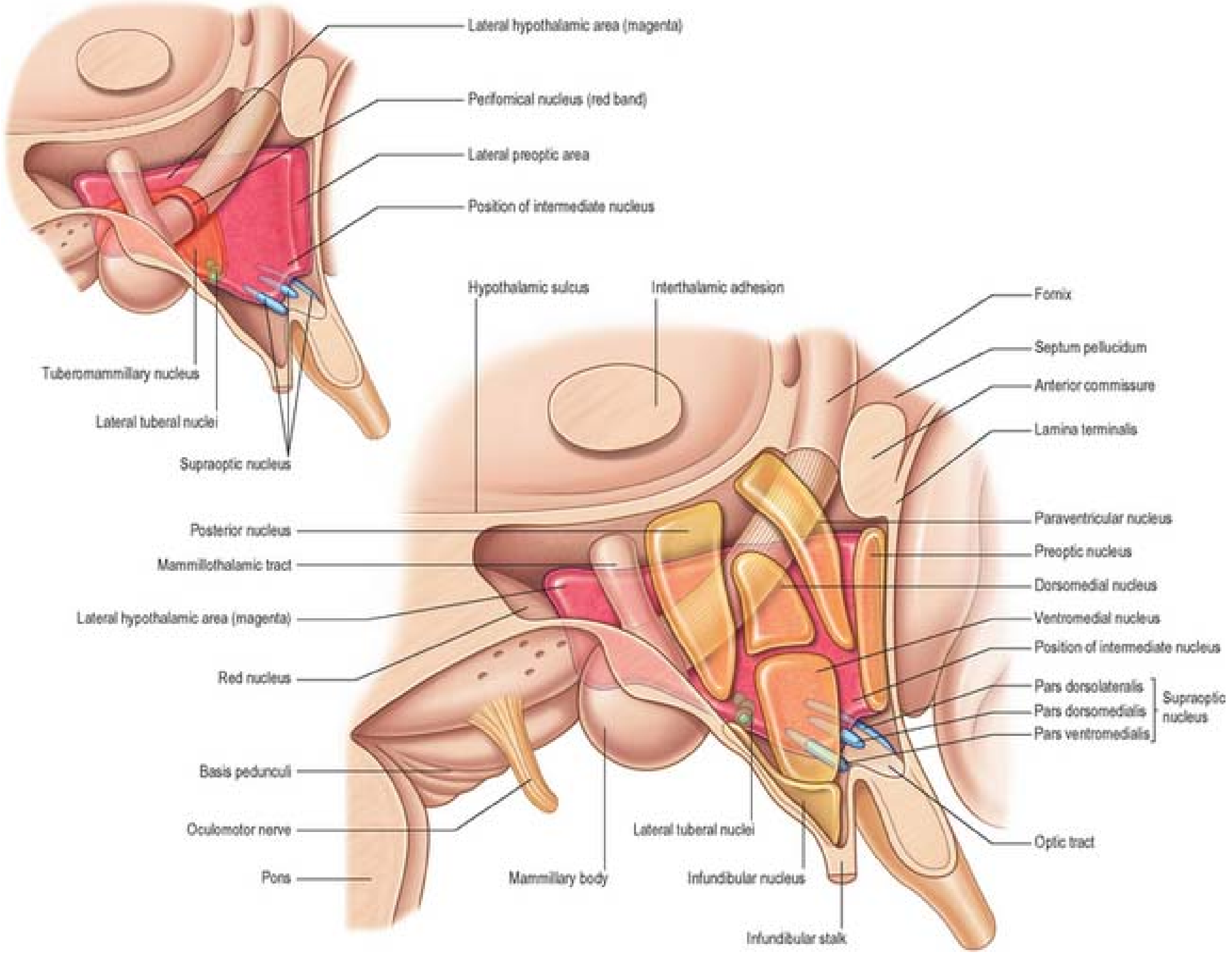
Lateral hypothalamic area (magenta)
Perifornical nucleus (red band)
Lateral preoptic area
Position of intermediate nucleus
Tuberomammillary nucleus
Lateral tuberal nuclei
Supraoptic nucleus
Hypothalamic sulcus
Interthalamic adhesion
Fornix
Septum pellucidum
Anterior commissure
Lamina terminalis
Posterior nucleus
Mammillothalamic tract
Lateral hypothalamic area (magenta)
Red nucleus
Paraventricular nucleus
Preoptic nucleus
Dorsomedial nucleus
Ventromedial nucleus
Position of intermediate nucleus
Pars dorsolateralis
Pars dorsomedialis
Pars ventromedialis
Supraoptic nucleus
Basis pedunculi
Oculomotor nerve
Pons
Mammillary body
Lateral tuberal nuclei
Infundibular nucleus
Infundibular stalk
Optic tract

Fig. 21.8 The hypothalamic region of the left cerebral hemisphere viewed from the medial aspect and dissected to display the major hypothalamic nuclei. In the upper diagram the medially placed nuclear groups have been removed; in the lower diagram both lateral and medial groups are included. Lateral to the fornix and the mammillothalamic tract is the lateral hypothalamic region, in which the tuberomammillary nucleus is situated posteriorly, and the lateral preoptic nucleus rostrally. Surrounding the fornix is the perifornical nucleus, which joins the lateral hypothalamic area with the posterior hypothalamic nucleus. The medially placed nuclei (yellow) fill in much of the region between the mammillothalamic tract and the lamina terminalis, but also project caudal to the tract. The lateral tuberal nuclei are situated ventrally, largely in the lateral hypothalamic area. The supraoptic nucleus may form three rather separate parts. The intermediate nuclei form three groups between the supraoptic and paraventricular nuclei.

(Modified from Nauta WJH, Haymaker W 1969 Hypothalamic nuclei and fibre connections. In: Haymaker W, Anderson E, Nauta WJH (eds) The Hypothalamus, by permission of Charles C Thomas Publisher, Ltd, Springfield, Illinois.)

The mammillary bodies are smooth, hemispherical, pea-sized eminences, lying side by side, anterior to the posterior perforated substance, each with nuclei enclosed in fascicles of fibres derived largely from the fornix. The tuber cinereum, between the mammillary bodies and the optic chiasma, is a convex mass of grey matter. From it, the median, conical, hollow infundibulum becomes continuous ventrally with the posterior lobe of the pituitary. Around the base of the infundibulum is the median eminence, which is demarcated by a shallow tubero-infundibular sulcus.

Hypothalamic lesions have long been linked with widespread and bizarre endocrine syndromes and with metabolic, visceral, motor and emotional disturbances. The hypothalamus has major interactions with the neuroendocrine system and the autonomic nervous system, integrating responses to both internal and external afferent stimuli with the complex analysis of the world provided by the cerebral cortex.

The hypothalamus controls the endocrine system in a variety of ways: through magnocellular neurosecretory projections to the posterior pituitary; through parvocellular neurosecretory projections to the median eminence (these control the endocrine output of the anterior pituitary and thereby the peripheral endocrine organs); and via the autonomic nervous system. The posterior pituitary neurohormones, vasopressin and oxytocin, are primarily involved in the control of osmotic homeostasis and various aspects of reproductive function, respectively. Through its effects on the anterior pituitary, the hypothalamus influences the thyroid gland (thyroid stimulating hormone, TSH), suprarenal cortex (adrenocorticotrophic hormone, ACTH), gonads (luteinizing hormone, LH; follicle stimulating hormone, FSH; prolactin), mammary gland (prolactin), and the processes of growth and metabolic homeostasis (growth hormone, GH).

The hypothalamus influences both parasympathetic and sympathetic divisions of the autonomic nervous system. In general, parasympathetic effects predominate when the anterior hypothalamus is stimulated; sympathetic effects depend more on the posterior hypothalamus.

Stimulation of the anterior hypothalamus and paraventricular nucleus can cause decreased blood pressure and decreased heart rate. Stimulation in the anterior hypothalamus induces sweating and vasodilatation (and thus heat loss) via projections that pass through the medial forebrain bundle to autonomic centres in the brain stem and spinal cord. Damage to the anterior hypothalamus, e.g. during surgery for suprasellar extensions of pituitary tumours, can result in an uncontrollable rise in body temperature. Projections to the ventromedial hypothalamus conjointly regulate food intake. Stimulation in the posterior part of the hypothalamus induces sympathetic arousal which produces vasoconstriction, piloerection, shivering and increased metabolic heat production. Circuitry mediating shivering is located in the dorsomedial posterior hypothalamus. This does not imply the existence of discrete parasympathetic and sympathetic ‘centres’. Stimuli in many different parts of the hypothalamus can cause profound changes in heart rate, cardiac output, vasomotor tone, peripheral resistance, differential blood flow in organs and limbs, the frequency and depth of respiration, motility and secretion in the alimentary tract, erection and ejaculation.

HYPOTHALAMIC NUCLEI

The hypothalamus contains a number of neuronal groups that have been classified on phylogenetic, developmental, cytoarchitectonic, synaptic and histochemical grounds into named nuclei, many of which are not very clearly delimited, especially in the adult. While it contains a few large myelinated tracts, many of the connections are diffuse and unmyelinated, and the precise paths of many afferent, efferent, and intrinsic connections are uncertain.

The hypothalamus can be divided anteroposteriorly into chiasmatic (supraoptic), tuberal (infundibulo-tuberal) and posterior (mammillary) regions, and mediolaterally into periventricular, intermediate (medial), and lateral zones. Between the intermediate and lateral zones is a paramedian plane, which contains the prominent myelinated fibres of the column of the fornix, the mammillothalamic tract and the fasciculus retroflexus. For this reason, some authors group the periventricular and intermediate zones as a single medial zone. These divisions are artificial and functional systems cross them. The main nuclear groups and myelinated tracts are illustrated in Figures 21.8 and 21.9.

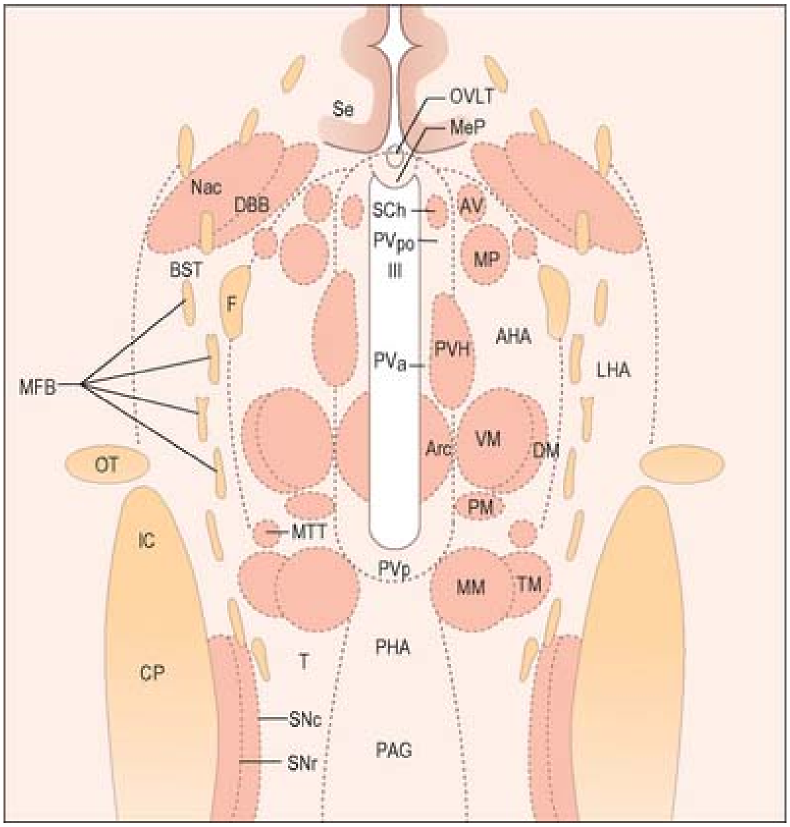

Fig. 21.9 Horizontal section showing the major cell groups and tracts in and around the hypothalamus. Abbreviations: III, third ventricle; AHA, anterior hypothalamic area; Arc, arcuate nucleus; AV, anteroventral preoptic nucleus; BST, bed nucleus of stria terminalis; CP, caudate nucleus and putamen; DBB, nucleus of diagonal band; DM, dorsomedial nucleus; LHA, lateral hypothalamic area; MM, mammillary body (mainly medial mammillary nucleus); MeP, median preoptic nucleus; MP, medial preoptic nucleus; Nac, nucleus accumbens; OVLT, vascular organ of the lamina terminalis; PAG, periaqueductal grey matter; PHA, posterior hypothalamic area; PV, periventricular nucleus (PVpo, preoptic part; PVa, anterior part; PVp, posterior part); PVH, paraventricular (hypothalamic) nucleus; Se, septal cortex; SCh, suprachiasmatic nucleus; T, midbrain tegmentum; TM, tuberomammillary nucleus; VM, ventromedial nucleus; Fibre tracts: CP, cerebral peduncle; F, fornix; IC, internal capsule; MFB, medial forebrain bundle; MTT, mammillothalamic tract; OT, optic tract.

(Modified with permission from Elsevier. Progress in Brain Research, vol 87, Swanson LW, Biochemical switching in hypothalamic circuits mediating responses to stress, pp. 181–200, 1991.)

The periventricular zone of the hypothalamus borders the third ventricle. In the anterior wall of the ventricle is the vascular organ of the lamina terminalis (OVLT, organum vasculosum), which is continuous dorsally with the median preoptic nucleus and subfornical organ. On each side in the chiasmatic region are: part of the preoptic nucleus; the small, sexually dimorphic suprachiasmatic nucleus; periventricular neurones, which are medial to, and blend with, the paraventricular nucleus. In the tuberal region, the periventricular cell group expands around the base of the third ventricle to form the arcuate nucleus, which overlies the median eminence. In the posterior region, the narrow periventricular zone is continuous laterally with the posterior hypothalamic area and behind that with midbrain periaqueductal grey matter. The periventricular zone also contains a prominent periventricular fibre system.

Suprachiasmatic nucleus

Although it contains only a few thousand neurones, the suprachiasmatic nucleus is a remarkable structure. It appears to be the neural substrate for day–night cycles in motor activity, body temperature, plasma concentration of many hormones, renal secretion, sleeping and waking, and many other variables. Lesions of the suprachiasmatic region lead to a disordered sleep–wake cycle.

The suprachiasmatic nucleus has two principal subdivisions, ventrolateral and dorsomedial. Retinal fibres terminate in the ventrolateral subdivision, characterized by neurones immunoreactive for vasoactive intestinal polypeptide (VIP). This appears to be a general input zone, which also receives afferents from the midbrain raphe and parts of the lateral geniculate nucleus of the thalamus. The dorsomedial subdivision has relatively sparse afferent innervation, and characteristically contains parvocellular neurones immunoreactive for arginine vasopressin (AVP). Neurones within the suprachiasmatic nuclei that receive direct retinal input do not respond to pattern, movement or colour. Instead, they operate as luminance detectors, responding to the onset and offset of light, and their firing rates vary in proportion to light intensity, thereby synchronizing to the light–dark cycle.

The suprachiasmatic nucleus receives glutamatergic afferents from retinal ganglion cells that entrain the rhythm to the light–dark cycle, but these are not essential for the production of the rhythm, which persists in the blind. It contains many different neurotransmitters including vasopressin, VIP, neuropeptide Y (NPY) and neurotensin. Axons from the suprachiasmatic nucleus pass to many other hypothalamic nuclei including the paraventricular, ventromedial, dorsomedial and arcuate nuclei.

The suprachiasmatic nucleus also influences the activity of upper spinal preganglionic sympathetic neurones. These neurones in turn project to superior cervical ganglion neurones which project to the pineal gland. In the pineal, which contains modified photoreceptors, circadian variation in the postganglionic sympathetic input causes parallel variation in pineal *N*-acetyltransferase activity and thus pineal melatonin production. The role of the pineal gland in man is uncertain: pineal tumours can influence reproductive development, and administration of melatonin has been advocated to alleviate jet-lag.

Parvocellular neurosecretory neurones lie within the periventricular zone, in particular the medial parvocellular part of the paraventricular nucleus, and the arcuate nucleus. The arcuate nucleus is median in the post-infundibular part of the tuber cinereum. It extends forward into the median eminence and almost encircles the infundibular base, but does not meet anteriorly, where the infundibulum adjoins the median part of the optic chiasma. Its numerous neurones are all small and round in coronal section, and oval or fusiform in sagittal section. No glial layer intervenes between the nucleus and the ependymal tanycytes lining the infundibular recess of the third ventricle. Circadian variation in the secretion of all anterior pituitary hormones suggests that projections from the suprachiasmatic nucleus must reach parvocellular neurosecretory neurones. Afferents from the limbic system probably mediate the widespread effects of stress, and serotonin and noradrenaline from the brain stem influence the output of most anterior pituitary hormones. The axons of parvocellular neurones converge on the infundibulum, forming a tubero-infundibular tract, which ends on the capillary loops that form the hypophysial portal vessels.

Neurones producing growth hormone-releasing hormone (GHRH) are largely restricted to the arcuate nucleus. Some extend dorsally into the periventricular nucleus and laterally into the retrochiasmatic area. Their fibres run through the periventricular region to the neurovascular zone of the median eminence. The neurones receive afferent information from glucose receptors in the ventromedial nucleus. Inputs from the hippocampal–amygdala–septal complex could explain the release of GH during stress. In man, midline defects such as septo-optic dysplasia are associated with defective growth hormone secretion. Dopamine has a stimulatory effect.

Neurones producing somatostatin (growth hormone release-inhibiting hormone) are located in the periventricular nucleus. GHRH and somatostatin are secreted in intermittent (3–5 hour) reciprocal pulses, but the origin of the pulses is unclear. A large pulse of GH is secreted at the onset of slow wave sleep. Somatostatin also inhibits release of pituitary thyroid-stimulating hormone (TSH).

Neurones producing GHRH and projecting to the median eminence are also located in the periventricular and arcuate nuclei. Other GHRH neurones are found in the periventricular preoptic area, but these appear to project to the vascular organ of the lamina terminalis. Luteinizing hormone (LH) and follicle-stimulating hormone (FSH) are secreted in circhoral (hourly) pulses, which are stimulated by GHRH, and are influenced by central monoamine and GABA, by oestrogen and progesterone acting indirectly through other neurones, by corticotrophin-releasing factor, and by endogenous opioids.

Corticotrophin-releasing hormone (CRH) is located primarily in parvocellular paraventricular neurones. They are profoundly stimulated by neurogenic (limbic input) and hypoglycaemic (ventromedial nucleus) stress, and are also controlled by negative feedback by cortisol.

Thyrotrophin-releasing hormone (TRH) neurones are rather more widely distributed in the periventricular, ventromedial and dorsomedial nuclei. TRH release is influenced by core temperature, sensed in the anterior hypothalamus, and by negative feedback of thyroid hormones. It stimulates release of pituitary TSH and also acts to excite cold-sensitive, and to inhibit warm-sensitive neurones in the preoptic area.

Other tubero-infundibular arcuate neurones contain neuropeptide Y (NPY) and neurotensin. Arcuate neurones containing pro-opiomelanocortin peptides project to the periventricular nucleus rather than the median eminence.

In addition to these peptide-containing cells, dopamine neurones in the arcuate nucleus (A12 group) have terminals in the median eminence and infundibulum. Dopamine acts as the principal prolactin-release inhibiting hormone, and also inhibits secretion of TSH (likewise, TSH acts as a prolactin-releasing hormone). Noradrenergic terminals are found in the median eminence, where they may act largely in a paracrine manner.

The intermediate zone of the hypothalamus contains the best differentiated nuclei. These are: the paraventricular and supraoptic nuclei; ‘intermediate’ nuclear groups, which show sexual dimorphism; ventromedial and dorsomedial nuclei; the mammillary body; and tuberomammillary nuclei. Magnocellular neurosecretory neurones are found in the supraoptic nucleus, paraventricular nucleus, and as isolated clusters of cells between them.

Supraoptic and paraventricular nuclei

The supraoptic nucleus, curved over the lateral part of the optic chiasma, contains a uniform population of large neurones. Behind the chiasma, a thin plate of cells in the floor of the brain forms the retrochiasmatic part.

Supraoptic neurones synthesize vasopressin, and they all appear to project to the neurohypophysis. The magnocellular vasopressin neurones detect as little as 1% increase in the osmotic pressure of the blood and stimulate release of vasopressin from the posterior pituitary. A fall in blood volume or blood pressure of greater than 5–10% stimulates the release of vasopressin and the urge to drink. These responses are mediated via volume receptors in the walls of the great veins and atria and baroreceptors in the carotid sinus which all project via the vagus and glossopharyngeal nerves to the nucleus tractus solitarius and thence to the magnocellular nuclei. A biochemical defect in vasopressin production, or interruption of the supraopticohypophysial pathway (e.g. due to a head injury), can cause cranial diabetes insipidus.

The paraventricular nucleus extends from the hypothalamic sulcus downward across the medial aspect of the column of the fornix, its ventrolateral angle reaching towards the supraoptic nucleus. Its neurones are more diverse. Magnocellular neurones, which project to the neurohypophysis, tend to lie laterally; parvocellular neurones, which project to the median eminence and infundibulum, lie more medially; intermediate-sized neurones, which may project caudally, lie posteriorly. The axons of the paraventricular magnocellular neurones pass towards the supraoptic nucleus (paraventriculohypophysial tract), where they join axons of supraoptic neurones to form a supraopticohypophysial tract. This runs down the infundibulum, superficially, and into the neural lobe, where the axons are distended and branch repeatedly around the capillaries. Vasopressin and oxytocin are produced by separate neurones: vasopressin neurones tend to cluster in the ventrolateral part of the paraventricular nucleus and the oxytocin neurones lie around them.

The hypothalamus is essential for the control of pituitary oxytocin, gonadotrophin and prolactin secretion. The release of oxytocin from neurosecretory nerve terminals in the neurohypophysis induces contraction of the uterus and of the myoepithelial cells that surround the mammary gland alveoli. Two neuroendocrine reflexes are involved. Stretching of the cervix of the uterus during childbirth stimulates a multisynaptic afferent pathway that passes via the pelvic plexus, anterolateral column and brain stem to the magnocellular oxytocin neurones (the Ferguson reflex). This is a positive feedback mechanism, which is terminated by the birth of the child. The milk ejection reflex is evoked by suckling of the nipple, which activates intercostal nerves and, thereby, an afferent connection to the hypothalamus. The reflex can be both conditioned to a baby’s cry and inhibited by stress.

At the tuberal level, the ventromedial nucleus is well defined by a surrounding neurone-poor zone, but the dorsomedial nucleus above it is much less distinct. The ventromedial nucleus contains neurones receptive to plasma levels of glucose and other nutrients and receives visceral somatic afferents via the nucleus tractus solitarius. The lateral hypothalamus receives olfactory afferents, which act as important food signals. Both areas receive extensive inputs from limbic structures. Stimulation and lesion experiments, together with human case studies, suggest that the ventromedial nuclei act together as a ‘satiety centre’. Bilateral ventromedial nucleus damage promotes overeating (hyperphagia), and restricting food intake may provoke rage-like outbursts. The resultant obesity is usually coupled with hyposexuality (Fröhlich syndrome). Interestingly, in infants, ventromedial damage can lead to emaciation despite apparent normal feeding. Experimental lesions in the lateral hypothalamus promote hypophagia or aphagia, while stimulation can prolong feeding, supporting the concept of a lateral hypothalamic ‘feeding centre’.

The ventromedial nucleus, lateral hypothalamic area and paraventricular nucleus also influence intermediate metabolism through the autonomic and endocrine systems. These appear to complement the effects on feeding behaviour. Thus, ventromedial stimulation facilitates glucagon release and increases glycogenolysis, gluconeogenesis and lipolysis, whereas lateral hypothalamic stimulation causes insulin release and the opposite metabolic effects. Lesions of the ventromedial nucleus also cause increased vagal and decreased sympathetic tone.

The medial mammillary nuclei, which form the bulk of the mammillary bodies, are very prominent. The distinct existence of a lateral mammillary nucleus is controversial, though a group of larger cells does occur along the lateral border of the medial mammillary nucleus. Lateral to this is the tuberomammillary nucleus, which gives rise to widespread axons that diffusely innervate the entire cerebral cortex, hypothalamus and brain stem.

The lateral zone of the hypothalamus forms a continuum that runs from the preoptic nucleus through the lateral hypothalamic area to the posterior hypothalamus. In the tuberal region, the lateral tuberal nuclei are large and well defined and surrounded by fine fibres.

CONNECTIONS OF THE HYPOTHALAMUS

The hypothalamus has reciprocal interaction with the rest of the body via two (possibly three) quite distinct routes: neural connections, the bloodstream and (probably) the CSF.

Some hypothalamic neurones have specific receptors that sense the temperature, osmolarity, glucose, free fatty acid, and hormone content of the blood. Neurosecretory neurones secrete neurohormones into the blood. These control the anterior pituitary and act on organs such as the kidney, breast, uterus and blood vessels. Some of the neural connections, especially those to the mammillary bodies, form discrete myelinated fascicles, but most are diffuse, unmyelinated and their origin and termination are uncertain. Most pathways are multisynaptic and many of the synapses on hypothalamic neurones are derived from intrinsic interneurones.

Broadly, neural inputs to the hypothalamus are derived from the ascending visceral and somatic sensory systems, the visual and olfactory systems, and numerous tracts from the brain stem, thalamus, ‘limbic’ structures and neocortex. Efferent neural projections are reciprocal to most of these and, in particular, they impinge on and control the central origins of autonomic nerve fibres. The hypothalamus therefore exerts control via the autonomic and endocrine systems and through its connections to the telencephalon.

Afferent connections

The hypothalamus receives visceral, gustatory and somatic sensory information from the spinal cord and brain stem. It receives largely polysynaptic projections from the nucleus tractus solitarius, probably directly and indirectly via the parabrachial nucleus and medullary noradrenergic cell groups (ventral noradrenergic bundle); collaterals of lemniscal somatic afferents (to the lateral hypothalamus); and projections from the dorsal longitudinal reticular formation. Many enter via the medial forebrain bundle (Fig. 21.9) and periventricular fibre system. Others converge in the midbrain tegmentum, forming the mammillary peduncle to the mammillary body.

The major forebrain inputs to the hypothalamus are derived from structures in the limbic system, including the hippocampal formation, amygdala and septum, and from the piriform lobe and adjacent neocortex. These connections, which are reciprocal, form prominent fibre systems, i.e. the fornix, stria terminalis, and ventral amygdalofugal tracts.

The hippocampal formation, in particular the subiculum and CA1, is reciprocally connected to the hypothalamus by the fornix, a complex tract that also contains commissural connections. As the fornix curves ventrally towards the anterior commissure it is joined by fascicles from the cingulate gyrus, indusium griseum and the septal area. It divides around the anterior commissure into pre- and postcommissural parts. The precommissural fornix is distributed to the septum and preoptic hypothalamus, and the septum in turn sends numerous fibres to the hypothalamus. The postcommissural fornix passes ventrally and posteriorly through the hypothalamus to the medial mammillary nucleus. In its course it gives off many fibres to the medial and lateral hypo-thalamic nuclei.

The amygdala innervates most hypothalamic nuclei anterior to the mammillary bodies. Its corticomedial nucleus innervates preoptic and anterior hypothalamic areas and the ventromedial nucleus. The central nuclei project to the lateral hypothalamus. The fibres reach the hypothalamus by two routes. The short ventral amygdalofugal path passes medially over the optic tract, beneath the lentiform complex, to reach the hypothalamus. The long curved stria terminalis runs parallel to the fornix, separated from it by the lateral ventricle, passes through the bed nucleus of the stria terminalis, and is then distributed to the anterior hypothalamus via the medial forebrain bundle.

Olfactory afferents reach the hypothalamus largely via the nucleus accumbens and septal nuclei, and most terminate in the lateral hypothalamus. Visual afferents leave the optic chiasma and pass dorsally into the suprachiasmatic nucleus. No auditory connections have been identified, though it is clear that such stimuli influence hypothalamic activity. However, many hypothalamic neurones respond best to complex sensory stimuli, suggesting that sensory information reaching the neocortex has converged and been processed by the amygdala, hippocampus and neocortex. Neocortical corticohypothalamic afferents to the hypothalamus are poorly defined, but probably arise from frontal and insular cortices. Some may relay in the mediodorsal thalamic nucleus and project into the hypothalamus via the periventricular route. Other direct corticohypothalamic fibres may end in lateral, dorsomedial, mammillary and posterior hypothalamic nuclei, but all these connections are questioned.

Like the rest of the forebrain, the hypothalamus also receives diffuse aminergic inputs from the locus coeruleus and raphe nuclei. In addition, it receives input from the ventral tegmental ascending cholinergic pathway; a noradrenergic input to dorsomedial, periventricular, paraventricular, supraoptic and lateral hypothalamic nuclei from the ventral tegmental noradrenergic bundle, and fibres from the mesolimbic dopaminergic system. Group A11 innervates the medial hypothalamic nuclei, and groups A13 and A14 supply the dorsal and rostral hypothalamic nuclei. Many of these fibres also run in the medial forebrain bundle.

The medial forebrain bundle is a loose grouping of fibre pathways that mostly run longitudinally through the lateral hypothalamus (Fig. 21.9). It connects forebrain autonomic and limbic structures with the hypothalamus and brain stem, receiving and giving small fascicles throughout its course. It contains descending hypothalamic afferents from the septal area and orbitofrontal cortex, ascending afferents from the brain stem, and efferents from the hypothalamus.

Efferent connections

Hypothalamic efferents include reciprocal paths to the limbic system, descending polysynaptic paths to autonomic and somatic motor neurones, and neural and neurovascular links with the pituitary.

Septal areas and the amygdaloid complex have reciprocal hypothalamic connections along the paths described above. The medial pre-optic and anterior hypothalamic areas give short projections to nearby hypothalamic groups. The ventromedial nucleus has more extensive projections that pass via the medial forebrain bundle to the bed nucleus of the stria terminalis, basal nucleus of Meynert, central nucleus of the amygdala, and midbrain reticular formation. The posterior hypothalamus projects largely to the midbrain central grey matter. Some tuberal and posterior lateral hypothalamic neurones project directly to the entire neocortex and appear to be essential for maintaining cortical arousal, but the topography of these projections is unclear.

Hypothalamic neurones projecting to autonomic neurones are found in the paraventricular nucleus (oxytocin and vasopressin neurones), perifornical and dorsomedial nuclei (atrial natriuretic peptide neurones), lateral hypothalamic area (α-melanocyte-stimulating hormone; α-MSH neurones), and zona incerta (dopamine neurones). These fibres run through the medial forebrain bundle into the tegmentum, ventrolateral medulla and dorsal lateral funiculus of the spinal cord. In the brain stem, fibres innervate the parabrachial nucleus, nucleus ambiguus, nucleus of the solitary tract and dorsal motor nucleus of the vagus. In the spinal cord, they end on sympathetic and parasympathetic preganglionic neurones in the intermediolateral column. Both oxytocin- and vasopressin-containing fibres can be traced to the most caudal spinal autonomic neurones.

The medial mammillary nucleus gives rise to a large ascending fibre bundle, which diverges into the mammillothalamic and mammillotegmental tracts (Fig. 21.9). The mammillothalamic tract ascends through the lateral hypothalamus to reach the anterior thalamic nuclei, whence massive projections radiate to the cingulate gyrus. The mammillotegmental tract curves inferiorly into the midbrain ventral to the medial longitudinal fasciculus, and is distributed to tegmental reticular nuclei.

PITUITARY GLAND

The pituitary gland, or hypophysis cerebri (Fig. 21.10; see Fig. 16.7), is a reddish-grey, ovoid body, about 12 mm in transverse and 8 mm in anteroposterior diameter, and with an average adult weight of 500 mg. It is continuous with the infundibulum, a hollow, conical, inferior process from the tuber cinereum of the hypothalamus. It lies within the pituitary fossa of the sphenoid bone, where it is covered superiorly by a circular diaphragma sellae of dura mater. The latter is pierced centrally by an aperture for the infundibulum, and separates the anterior superior aspect of the pituitary from the optic chiasma. Inferiorly, the pituitary is separated from the floor of the fossa by a venous sinus that communicates with the circular sinus. The meninges blend with the pituitary capsule and are not separate layers.

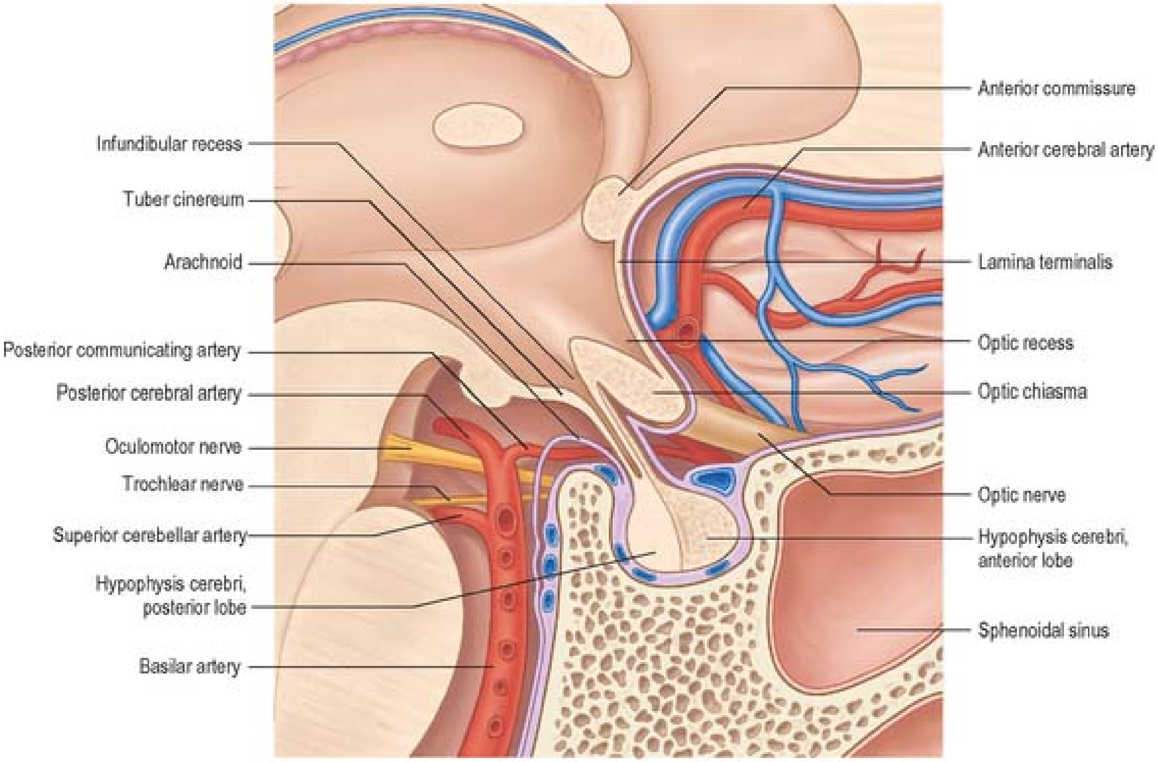
Infundibular recess
Tuber cinereum
Arachnoid
Posterior communicating artery
Posterior cerebral artery
Oculomotor nerve
Trochlear nerve
Superior cerebellar artery
Hypophysis cerebri, posterior lobe
Basilar artery
Anterior commissure
Anterior cerebral artery
Lamina terminalis
Optic recess
Optic chiasma
Optic nerve
Hypophysis cerebri, anterior lobe
Sphenoidal sinus

Fig. 21.10 Median section through the hypophysis cerebri.

The pituitary has two major parts, the neurohypophysis and adenohypophysis, which differ in their origin, structure and function. The neurohypophysis is a diencephalic downgrowth connected with the hypothalamus. The adenohypophysis is an ectodermal derivative of the stomatodeum. Both include parts of the infundibulum (whereas the older terms ‘anterior lobe’ and ‘posterior lobe’ do not). The infundibulum has a central infundibular stem, which contains neural hypophysial connections and is continuous with the median eminence of the tuber cinereum. Thus, the term neurohypophysis includes the median eminence, infundibular stem and neural lobe or pars posterior. Surrounding the infundibular stem is the pars tuberalis, a component of the adenohypophysis. The main mass of the adenohypophysis may be divided into the pars anterior (pars distalis) and the pars intermedia, which are separated in fetal and early postnatal life by the hypophysial cleft, a vestige of Rathke’s pouch, from which it develops. Usually obliterated in childhood, remnants may persist in the form of cystic cavities often present near the adenoneurohypophysial frontier and sometimes invading the neural lobe. The human pars intermedia is rudimentary. It may be partially displaced into the neural lobe, and so it has been included in the anterior and posterior parts by different observers. Apart from this equivocation, which is of little significance, the pars anterior and pars posterior may be equated with the anterior and posterior lobes. When the associated infundibular parts continuous with these lobes are included, the names adenohypophysis and neurohypophysis become appropriate, and will be used here as follows: Neurohypophysis includes the pars posterior (pars nervosa, posterior or neural lobe), infundibular stem and median eminence. Adenohypophysis includes the pars anterior (pars distalis or glandularis), pars intermedia and pars tuberalis.

Neurohypophysis

In early fetal life the neurohypophysis contains a cavity continuous with the third ventricle. Axons arising from groups of hypothalamic neurones (e.g. the magnocellular neurones of the supraoptic and paraventricular nuclei) terminate in the neurohypophysis. The long magnocellular axons pass to the main mass of the neurohypophysis. They form the neurosecretory hypothalamohypophysial tract and terminate near the sinusoids of the posterior lobe. Some smaller parvocellular neurones in the periventricular zone have shorter axons, and end in the median eminence and infundibular stem among the superior capillary beds of the venous portal circulation. These small neurones produce releasing and inhibitory hormones, which control the secretory activities of the adenohypophysis via its portal blood supply.

The neurohormones stored in the main part of the neurohypophysis are vasopressin (antidiuretic hormone; ADH), which controls reabsorption of water by renal tubules (see Ch. 74), and oxytocin, which promotes the contraction of uterine smooth muscle (see Ch. 77) in childbirth and the ejection of milk from the breast during lactation. Storage granules containing active hormone polypeptides bound to a transport glycoprotein, neurophysin, pass down axons from their site of synthesis in the neuronal somata (Fig. 21.11).

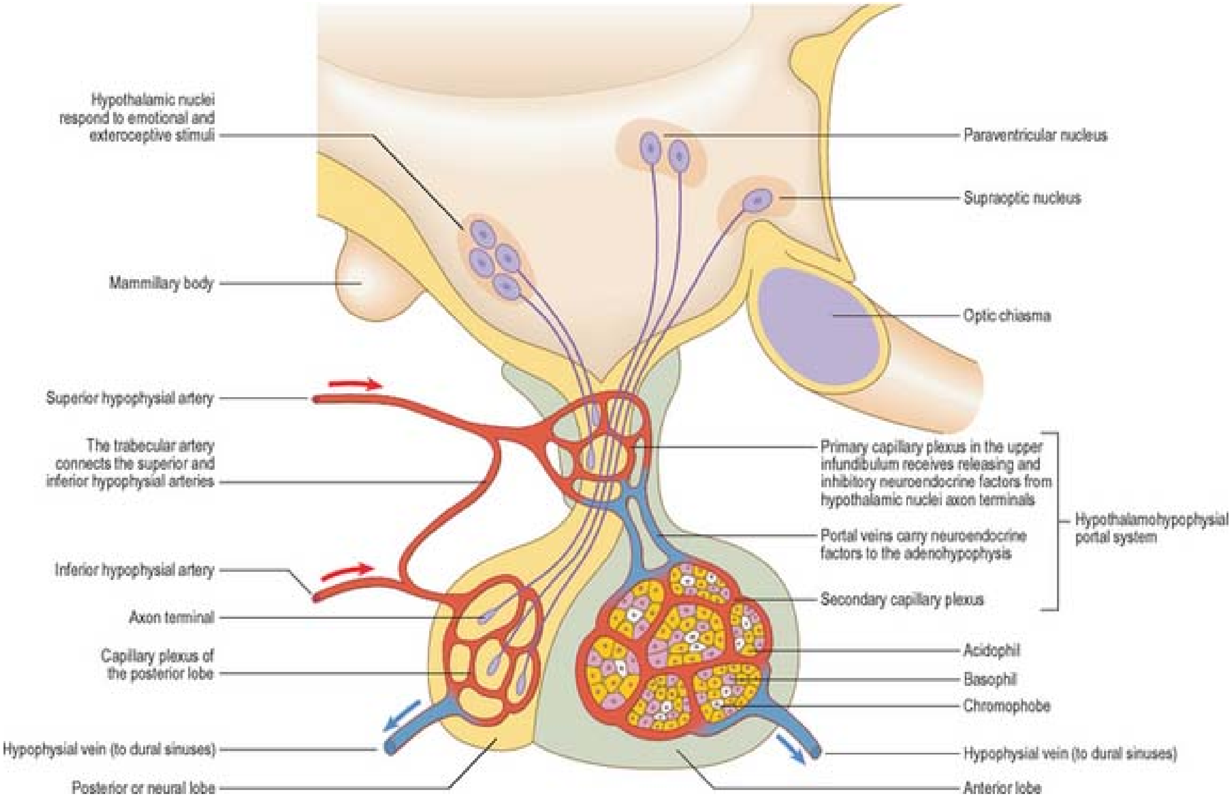
Hypothalamic nuclei respond to emotional and exteroceptive stimuli
Mammillary body
Superior hypophysial artery
The trabecular artery connects the superior and inferior hypophysial arteries
Inferior hypophysial artery
Axon terminal
Capillary plexus of the posterior lobe
Hypophysial vein (to dural sinuses)
Posterior or neural lobe
Paraventricular nucleus
Supraoptic nucleus
Optic chiasma
Primary capillary plexus in the upper infundibulum receives releasing and inhibitory neuroendocrine factors from hypothalamic nuclei axon terminals
Portal veins carry neuroendocrine factors to the adenohypophysis
Secondary capillary plexus
Hypothalamohypophysial portal system
Acidophil
Basophil
Chromophobe
Hypophysial vein (to dural sinuses)
Anterior lobe

Fig. 21.11 The main systems controlling the endocrine secretory activities of the pituitary gland.

The thin, non-myelinated axons of the neurohypophysis are ensheathed by typical astrocytes in the infundibulum (Fig. 21.12). Near the posterior lobe, astrocytes are replaced by pituicytes, which constitute most of the non-excitable tissue in the neurohypophysis. Pituicytes are dendritic neuroglial cells of variable appearance, often with long processes running parallel to adjacent axons. Typically, their cytoplasmic processes end on the walls of capillaries and sinusoids between nerve terminals. Axons also end in perivascular spaces; they lie close to the walls of sinusoids, but remain separated from them by two basal laminae, one around the nerve endings and the other underlying the fenestrated endothelial cells. The spaces between the basal laminae are occupied by fine collagen fibrils.

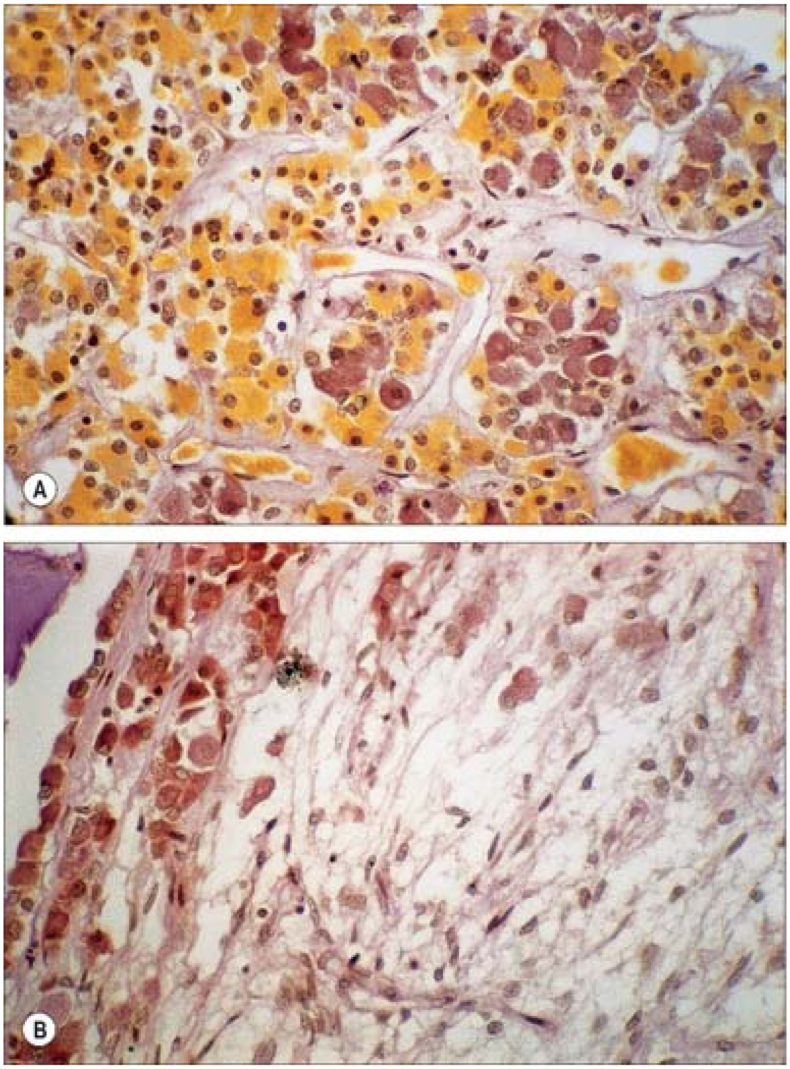

Fig. 21.12 The pituitary gland (trichrome-stained). **A**, The endocrine cells of the adenohypophysis. Chromophils can be distinguished as acidophils (yellow) and basophils (pink). Chromophobes are pale-staining cells. A network of sinusoids is seen between clusters of secretory cells. **B**, The neurohypophysis (right), with nerve fibres and pituicytes. To the left is the pars intermedia with scattered, deeper staining secretory cells and a cyst containing colloid (top left), representing the remnants of Rathke's pouch.

Adenohypophysis

The adenohypophysis is highly vascular. It consists of epithelial cells of varying size and shape arranged in cords or irregular follicles, between which lie thin-walled vascular sinusoids supported by a delicate reticular connective tissue (Figs 21.11, 21.12). Most of the hormones synthesized by the adenohypophysis are trophic. They include the peptides growth hormone (GH), involved in the control of body growth, and prolactin (PRL), which stimulates both growth of breast tissue and milk secretion. Glycoprotein trophic hormones are the large pro-opiomelanocortin precursor of adrenocorticotrophin (ACTH), which controls the secretion of certain suprarenal cortical hormones; thyroid-stimulating hormone (TSH); follicle-stimulating hormone (FSH), which stimulates growth and secretion of oestrogens in ovarian follicles and spermatogenesis (acting on testicular Sertoli cells); and luteinizing hormone (LH), which induces progesterone secretion by the corpus luteum and testosterone synthesis by Leydig cells in the testis. Pro-opiomelanocortin is cleaved into a number of different molecules including ACTH. β-Lipotropin is released from the pituitary, but its lipolytic function in humans is uncertain. β-Endorphin is another cleavage product released from the pituitary.

The epithelial endocrine cells, which secrete the different adenohypophysial hormones, are distinguished in part by their differing affinities for acidic and basic dyes. Cells staining strongly are described as chromophils, those with low affinity for dyes are chromophobes. Chromophils that stain strongly with acidic dyes are classed as acidophils, whereas basophils stain strongly with basic dyes; the latter are more prevalent in the central part of the gland. Classification according to the hormones synthesized divides cells into somatotrophs (GHsecreting acidophils, the most numerous chromophil type); lactotrophs (prolactin-secreting acidophils, which are dominant in pregnancy and hypertrophy during lactation); gonadotrophs (FSH- and LH-secreting basophils); thyrotrophs (TH-secreting basophils); and corticotrophs (ACTH-secreting basophils). Chromophobes are thought to be quiescent or degranulated chromophils, or immature precursor cells; they constitute up to half of the cells of the adenohypophysis.

Neurones that secrete the peptides and amines that control the anterior lobe are widely distributed within the hypothalamus. They are situated mainly in the medial zone, in the arcuate nucleus, medial parvocellular part of the paraventricular nucleus, and periventricular nucleus.

The pars intermedia contains follicles of chromophobe cells that surround cyst-like structures lined by epithelium and filled, to varying degrees, with glycosylated colloidal material. Secretory products of this region may include cleavage products of pro-opiomelanocortin but their functional significance is uncertain. The pars tuberalis contains a large number of blood vessels, between which are cords or clusters of gonadotrophs and undifferentiated cells.

A small collection of adenohypophysial tissue lies in the mucoperiosteum of the human nasopharyngeal roof. By 28 weeks *in utero* it is well vascularized and capable of secretion, receiving blood from the systemic vessels of the nasopharyngeal roof. At this stage it is covered posteriorly by fibrous tissue. This is replaced in the second half of fetal life by venous sinuses, and a trans-sphenoidal portal venous system develops, bringing the nasopharyngeal tissue under the same hypothalamic control as the cranial adenohypophysial tissue. The peripheral vascularity of the pharyngeal hypophysis persists until about the fifth year. The organ is then reinvested by fibrous tissue and presumed to be again controlled by factors present in systemic blood. Though it does not change in size after birth in males, in females it becomes smaller, returning to natal volume during the fifth decade, when once again it may be controlled via a trans-sphenoidal extension of the hypothalamohypophysial portal venous system. The human pharyngeal hypophysis may be a reserve of potential adenohypophysial tissue, which may be stimulated, particularly in females, to synthesize and secrete adenohypophysial hormones in middle age, when intracranial adenohypophysial tissue is beginning to fail.

Vessels of the pituitary

The arteries of the pituitary arise from the internal carotid arteries via a single inferior and several superior hypophysial arteries on each side. The former come from the cavernous part of the internal carotid artery, the latter from its supraclinoid part and from the anterior and posterior cerebral arteries. The inferior hypophysial arteries divide into medial and lateral branches, which anastomose across the midline and form an arterial ring around the infundibulum. Fine branches from this circular anastomosis enter the neurohypophysis to supply its capillary bed. The superior hypophysial arteries supply the median eminence, upper infundibulum and, via arteries of the trabeculae, the lower infundibulum. A confluent capillary net, extending through the neurohypophysis, is supplied by both sets of hypophysial vessels. Reversal of flow can occur in cerebral capillary beds lying between the two supplies.

The arteries of the median eminence and infundibulum end in characteristic sprays of capillaries, which are most complex in the upper infundibulum. In the median eminence these form an external or ‘mantle’ plexus and an internal or ‘deep’ plexus. The external plexus, fed by the superior hypophysial arteries, is continuous with the infundibular plexus and is drained by long portal vessels, which descend to the pars anterior. The internal plexus lies within and is supplied by the external plexus. It is continuous posteriorly with the infundibular capillary bed and, like the external plexus, is drained by long portal vessels. Short portal vessels run from the lower infundibulum to the pars anterior. Both types of portal vessel open into vascular sinusoids, which lie between the secretory cords in the adenohypophysis and provide most of its blood. There is no direct arterial supply. The portal system carries hormone-releasing factors, probably elaborated in parvocellular groups of hypothalamic neurones, and these control the secretory cycles of cells in the pars anterior. The pars intermedia appears to be avascular.

There are three possible routes for venous drainage of the neurohypophysis: to the adenohypophysis, via long and short portal vessels; into the dural venous sinuses, via the large inferior hypophysial veins; and to the hypothalamus, via capillaries passing to the median eminence. The venous drainage carries hypophysial hormones from the gland to their targets and also facilitates feedback control of secretion. However, venous drainage of the adenohypophysis appears restricted: few vessels connect it directly to the systemic veins and so the routes by which blood leaves remain obscure.

SUBTHALAMUS

The subthalamus is a complex region of nuclear groups and fibre tracts (Fig. 22.13). The main nuclear groups are the subthalamic nucleus, the reticular nucleus, the zona incerta, the fields of Forel and the pregeniculate nucleus. The rostral poles of the red nucleus and substantia nigra also extend into this area.

The main subthalamic tracts are: the upper parts of the medial, spinal and trigeminal lemnisci and the solitariothalamic tract, all approaching their terminations in the thalamic nuclei; the dentatothalamic tract from the contralateral superior cerebellar peduncle accompanied by ipsilateral rubrothalamic fibres; the fasciculus retroflexus; the fasciculus lenticularis; the fasciculus subthalamicus; the ansa lenticularis; fascicles from the prerubral field (H field of Forel); the continuation of the fasciculus lenticularis (in the H_2 field of Forel); the fasciculus thalamicus (the H_1 field of Forel).

SUBTHALAMIC NUCLEUS

The subthalamic nucleus is structurally and functionally related to the basal ganglia and is therefore considered with them in Chapter 22.

ZONA INCERTA AND FIELDS OF FOREL

The zona incerta is an aggregation of small cells that lies between the ventral part of the external medullary lamina of the thalamus and the cerebral peduncle. It is linked to the reticular nucleus dorsolaterally. More medially is a scattered group of cells in a matrix of fibres known as the H field of Forel. Field H_1 of Forel consists of the thalamic fasciculus, which lies dorsal to the zona incerta. Field H_2 of Forel contains the fasciculus lenticularis, and lies ventrally, between the zona incerta and the subthalamic nucleus.

The zona incerta receives fibres from the sensorimotor cortex, the pregeniculate nucleus, the deep cerebellar nuclei, the trigeminal nuclear complex and the spinal cord. It projects to the spinal cord and the pretectal region. Its functions are unknown.

The neurones of the H field of Forel receive afferents from, the spinal cord, the reticular formation of the brain stem and possibly the internal segment of the globus pallidus. They may project to the spinal cord. Like the zona incerta, their functions are unknown.

In addition to terminal parts of the lemniscal, dentatothalamic and rubrothalamic tracts, the subthalamus contains massive fibre tracts derived from the globus pallidus. The fasciculus lenticularis is the dorsal component of pallidofugal fibres that traverse the internal capsule. It turns medially near the medial aspect of the capsule, partly intermingled with the dorsal zone of the subthalamic nucleus and the ventral part of the zona incerta, where the fasciculus traverses the H_2 field of Forel. Reaching the medial border of the zona incerta, the fasciculus intermingles with fibres of the ansa lenticularis, scattered elements of the prerubral nucleus, and dentatothalamic and rubrothalamic fibres. This merging of diverse pathways and associated cell groups is variously called the prerubral, tegmental or H field of Forel.

The ansa lenticularis has a complex origin from both parts of the globus pallidus and possibly other adjacent structures. It curves medially round the ventral border of the internal capsule, and continues dorsomedially to mingle with other fibres in the prerubral field. Some fibres in the fasciculus lenticularis and ansa lenticularis synapse in the subthalamic nucleus, prerubral field and zona incerta. The remainder continue laterally, with other fascicles, into the thalamic nuclei, particularly the ventral anterior, ventral lateral and centromedian nuclei.

The thalamic fasciculus extends from the prerubral field, and its territory is termed the H_1 field of Forel. It lies dorsal to, and also partly traverses, the zona incerta, and is related dorsally to the ventral thalamic nuclei. It contains continuations of the fasciculus lenticularis and ansa lenticularis, and dentatothalamic, rubrothalamic and thalamostriate fibres.

The subthalamic fasciculus connects the subthalamic nucleus with the globus pallidus. It contains an abundant two-way array of fibres which traverse the internal capsule, interweaving with it at right angles.

EPITHALAMUS

The epithalamus consists of the anterior and posterior paraventricular nuclei, the medial and lateral habenular nuclei, the stria medullaris thalami, posterior commissure and the pineal body.

HABENULAR NUCLEI AND STRIA MEDULLARIS

The habenular nuclei lie posteriorly at the dorsomedial aspect of the thalamus, immediately deep to the ependyma of the third ventricle, with the stria medullaris thalami above and laterally. The medial habenular nucleus is a densely packed, deeply staining, mass of cholinergic neurones, whereas the lateral nucleus is more dispersed and paler staining. The habenulo-interpenduncular tract, or fasciculus retroflexus, emerges from the ventral margin of the nuclei and courses ventrally, skirts the inferior zone of the thalamic mediodorsal nucleus, and traverses the superomedial region of the red nucleus to reach the interpeduncular nucleus. The habenular nuclear complex is limited laterally by a fibrous lamina, which enters the habenulo-interpeduncular tract. Posteriorly, the nuclei of the two sides and the internal medullary laminae are linked across the midline by the habenular commissure. The tela choroidea of the third ventricle usually arises from the ependyma at the superolateral corner of the medial habenular nucleus.

Afferent fibres to the habenular nuclei travel in the stria medullaris from the prepiriform cortex bilaterally, the basal nucleus of Meynert, and the hypothalamus. Afferents from the internal segment of the globus pallidus ascend through the thalamus, and may be collaterals of pallidothalamic axons. Additional inputs come from the pars compacta of the substantia nigra, the midbrain raphe nuclei and the lateral dorsal tegmental nucleus. The afferent pathways mostly end in the lateral habenular nucleus. The only identified afferent fibres to the medial habenular nucleus come from the septofimbrial nucleus.

The medial habenular nucleus sends efferent fibres to the interpeduncular nucleus of the midbrain. The lateral habenular nucleus sends fibres to the raphe nuclei and the adjacent reticular formation of the midbrain, the pars compacta of the substantia nigra and the ventral tegmental area, and to the hypothalamus and basal forebrain.

The main habenular outflow reaches the interpeduncular nucleus, mediodorsal thalamic nucleus, mesencephalic tectum and reticular formation, the largest component constituting the habenulo-interpeduncular tract to the interpeduncular nucleus. The latter provides relays to the midbrain reticular formation, from which tectotegmentospinal tracts and dorsal longitudinal fasciculi connect with autonomic preganglionic neurones controlling salivation, gastric and intestinal secretory activity and motility, and motor nuclei for mastication and deglutition.

The stria medullaris crosses the superomedial thalamic aspect, skirts medial to the habenular trigone and sends many fibres into the ipsi-lateral habenula. Other fibres cross in the anterior pineal lamina, and decussate, as the habenular commissure, to reach the contralateral habenula. Some fibres are really commissural and interconnect the amygdaloid complexes and hippocampal cortices. They are accompanied by crossed tectohabenular fibres. Serotonin-containing fibres from the ventral ascending tegmental serotoninergic bundle, which join the habenulo-interpeduncular tract to reach the nuclei, may control neurones of the habenulopineal tract, and thus influence innervation of pinealocytes. Similarly, habenular nuclear afferents from the dorsal ascending tegmental noradrenergic bundle may influence pinealocytes.

Little is known of the physiological functions of the habenular nuclei. It has been suggested that they may be involved in the control of sleep mechanisms. Though the human habenula is relatively small, it is a focus of integration of diverse olfactory, visceral and somatic afferent paths. Lesions that include this area of the medial diencephalon indicate that it plays a role in the regulation of visceral and neuroendocrine functions. Ablation of the habenula causes extensive changes in metabolism, and endocrine and thermal regulation.

POSTERIOR COMMISSURE

The posterior commissure, which is of unknown constitution in man, is a small fasciculus that decussates in the inferior pineal lamina. Various small nuclei are associated with it. Among these are the interstitial nuclei of the posterior commissure, the nucleus of Darkschewitscz in the periaqueductal grey matter, and the interstitial nucleus of Cajal near the upper end of the oculomotor complex, closely linked with the medial longitudinal fasciculus. Fibres from all these nuclei and the fasciculus cross in the posterior commissure. It also contains fibres from thalamic and pretectal nuclei and the superior colliculi, together with fibres that connect the tectal and habenular nuclei. The destinations and functions of many of these fibres are obscure.

PINEAL GLAND

The pineal gland or epiphysis cerebri (see Figs 16.7, 19.3) is a small, reddish-grey organ, occupying a depression between the superior colliculi. It is inferior to the splenium of the corpus callosum, from which it is separated by the tela choroidea of the third ventricle and the contained cerebral veins. It is enveloped by the lower layer of the tela, which is reflected from the gland to the tectum. The pineal is about 8 mm long. Its base, directed anteriorly, is attached by a peduncle, which divides into inferior and superior laminae, separated by the pineal recess of the third ventricle, and containing the posterior and habenular commissures respectively. Aberrant commissural fibres may invade the gland but do not terminate near parenchymal cells.

Septa extend into the pineal gland from the surrounding pia mater. They divide the gland into lobules and carry blood vessels and fine unmyelinated sympathetic axons. The gland has a rich blood supply. The pineal arteries are branches of the medial posterior choroidal arteries, which are themselves branches of the posterior cerebral artery. Within the gland, branches of the arteries supply fenestrated capillaries whose endothelial cells rest on a tenuous and sometimes incomplete basal lamina. The capillaries drain into numerous pineal veins, which open into the internal cerebral veins and/or into the great cerebral vein.

Postganglionic adrenergic sympathetic axons (derived from neurones in the superior cervical ganglion) enter the dorsolateral aspect of the gland from the region of the tentorium cerebelli as the nervus conarii, which may be single or paired. The nerve lies deep to the endothelium of the wall of the straight sinus and is associated with blood vessels and parenchymal cells within the pineal.

The pineal gland contains cords and clusters of pinealocytes, associated with astrocyte-like neuroglia. Neuroglia are the main cellular component of the pineal stalk. Pinealocytes are highly modified neurones. They contain multiple synaptic ribbons, randomly distributed between adjacent cells, and are coupled by gap junctions. Two or more processes extend from each cell body and end in bulbous expansions near capillaries or, less frequently, on ependymal cells of the pineal recess. These terminal expansions contain rough endoplasmic reticulum, mitochondria and dense-cored vesicles which store melatonin. Melatonin, and its precursor serotonin, are synthesized from tryptophan by the pinealocytes, and secreted into the surrounding network of fenestrated capillaries.

The pineal is an endocrine gland of major regulatory importance. It modifies the activity of the adenohypophysis, neurohypophysis, endocrine pancreas, parathyroids, adrenal cortex, adrenal medulla and gonads. Its effects are largely inhibitory. Indoleamine and polypeptide hormones secreted by pinealocytes are believed to reduce the synthesis and release of hormones by the pars anterior, either by direct action on its secretory cells or indirectly by inhibiting production of hypothalamic releasing factors. Pineal secretions may reach their target cells via the cerebrospinal fluid or the bloodstream. Some pineal indoleamines, including melatonin and enzymes for their biosynthesis (e.g. serotonin *N*-acetyltransferase) show circadian rhythms in concentration. The level rises during darkness, and falls during the day, when secretion may be inhibited by sympathetic activity. It is thought that the intrinsic rhythmicity of an endogenous circadian oscillator in the suprachiasmatic nucleus of the hypothalamus governs cyclical pineal behaviour (see above).

From the second decade, calcareous deposits accumulate in pineal extracellular matrix, where they are deposited concentrically as corpora arenacea or ‘brain sand’ (Fig. 21.13). Calcification is often detectable in skull radiographs, when it can provide a useful indicator of a space-occupying lesion if the gland is significantly displaced from the midline.

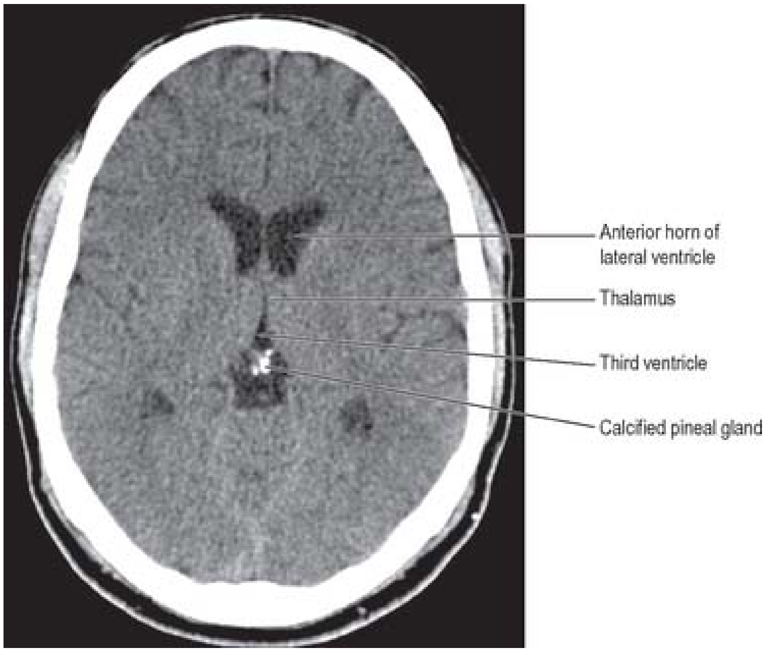
Anterior horn of lateral ventricle
Thalamus
Third ventricle
Calcified pineal gland

Fig. 21.13 Axial CT image of the brain showing calcification of the pineal gland.

REFERENCES

nes EG. The Thalamus. New York: Plenum Press, 1985;403-411.

Describes the nomenclature and connections of thalamic nuclei..

acchi G, Jones EG. Toward an agreement on terminology of nuclear and subnuclear divisions of the motor thalamus. *J Neurosurg*. 1997;86(4):670-685.

Compares the different nomenclatures for motor thalamic nuclei in humans and monkeys and proposes a common terminology..

euwenhuys R. Chemoarchitecture of the Brain. Berlin: Springer-Verlag, 1985.

Describes the connections and neurochemistry of the hypothalamus..

CHAPTER 22

Basal ganglia

The term basal ganglia is used to denote a number of subcortical nuclear masses that lie in the inferior part of the cerebral hemisphere, in close relation with the internal capsule (Figs 22.1, 22.2; see Fig. 23.28). The traditional definition of the basal ganglia included the corpus striatum, claustrum, and amygdaloid complex. The term has now been restricted to the corpus striatum and its associated structures in the diencephalon and midbrain; collectively they form a functional complex involved in the control of movement and motivational aspects of behaviour. The function of the claustrum is unknown; the amygdala is more closely related to the limbic system and is therefore described in that context (see Ch. 23).

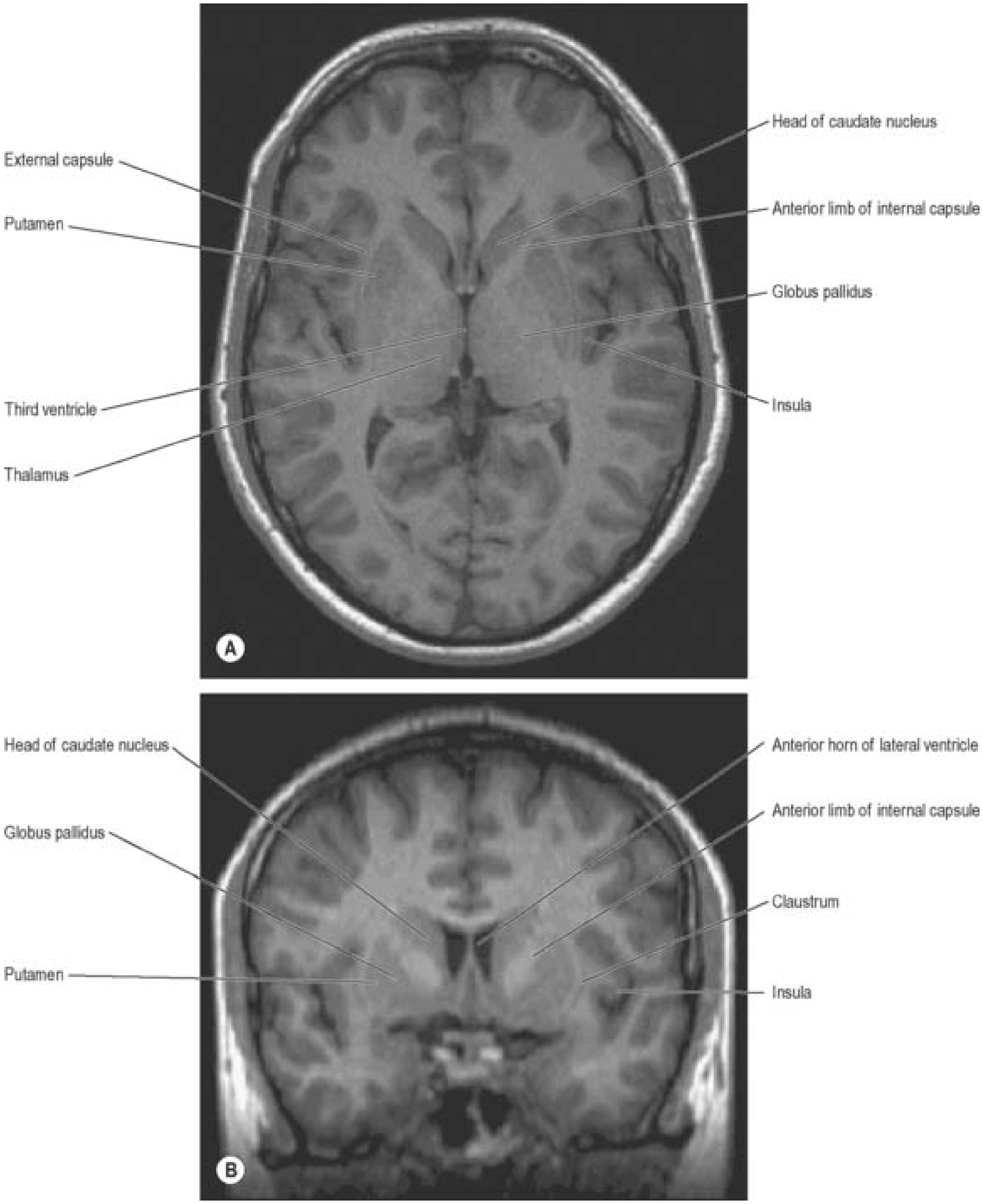
External capsule
Putamen
Third ventricle
Thalamus
Head of caudate nucleus
Anterior limb of internal capsule
Globus pallidus
Insula
A
Head of caudate nucleus
Globus pallidus
Putamen
Anterior horn of lateral ventricle
Anterior limb of internal capsule
Claustrum
Insula
B

Fig. 22.1 Axial (**A**) and coronal (**B**) MR images of the brain.

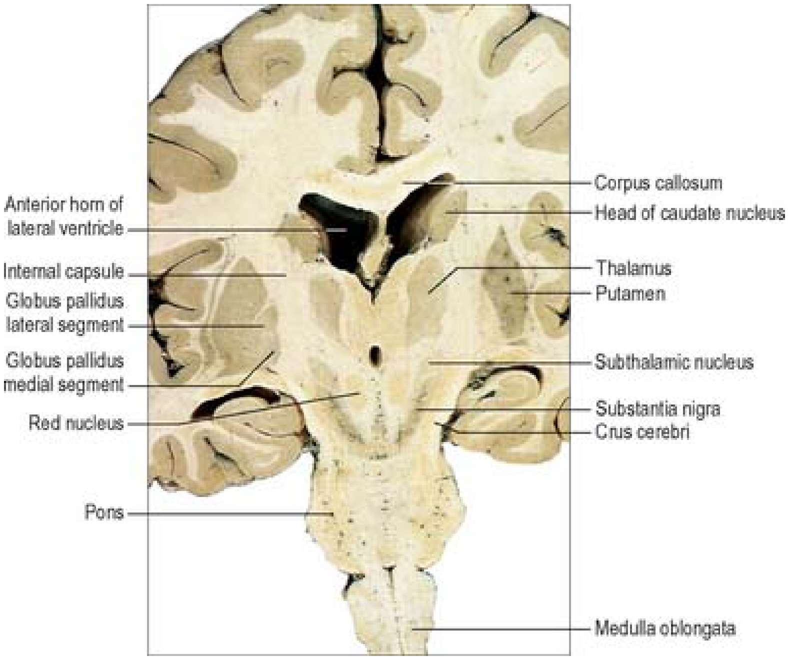
Anterior horn of lateral ventricle
Internal capsule
Globus pallidus lateral segment
Globus pallidus medial segment
Red nucleus
Pons
Corpus callosum
Head of caudate nucleus
Thalamus
Putamen
Subthalamic nucleus
Substantia nigra
Crus cerebri
Medulla oblongata

Fig. 22.2 Oblique coronal section of the brain.

(Dissection by EL Rees; photograph by Kevin Fitzpatrick on behalf of GKT School of Medicine, London.)

The corpus striatum consists of the caudate nucleus, putamen and globus pallidus (Fig. 22.3). Because of their close proximity, the putamen and globus pallidus were once considered as an entity, termed the lentiform (lenticular) complex or nucleus. However, although the name has been retained in gross anatomical terminology and in some compound names (e.g. sublenticular, retrolenticular), it is now known that the putamen and caudate nucleus share a common chemocytoarchitecture and connections, and they are referred to jointly as the neostriatum or simply the striatum.

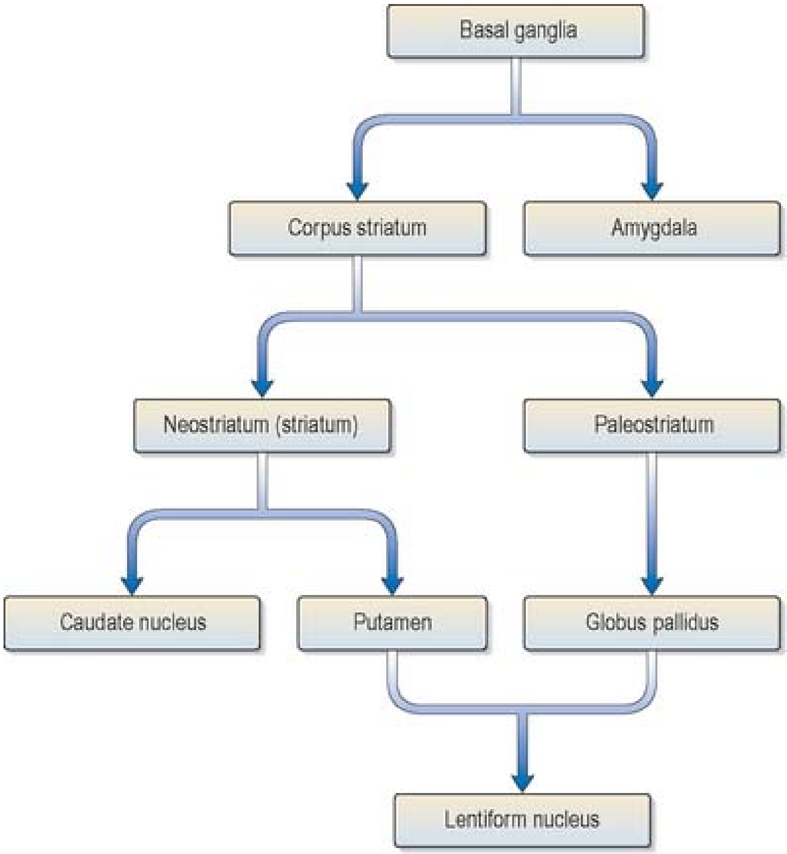
Basal ganglia
Corpus striatum
Amygdala
Neostriatum (striatum)
Paleostriatum
Caudate nucleus
Putamen
Globus pallidus
Lentiform nucleus

Fig. 22.3 Terminology and relationships of structures forming the basal ganglia.

The striatum is considered to be the principal ‘input’ structure of the basal ganglia since it receives the majority of afferents from other parts of the neuraxis. Its principal efferent connections are to the globus pallidus and pars reticulata of the substantia nigra. The globus pallidus and, more particularly, its medial segment, together with the pars reticulata of the substantia nigra is regarded as the main ‘output’ structure because it is the source of basal ganglia efferent fibre projections, mostly directed to the thalamus.

Disorders of the basal ganglia are principally characterized by abnormalities of movement, muscle tone and posture. There is a wide spectrum of clinical presentations ranging from poverty of movement and hypertonia at one extreme (typified by Parkinson’s disease) to abnormal involuntary movements (dyskinesias) at the other. The underlying pathophysiological mechanisms that mediate these disorders have been much studied in recent years and are better understood than for any other type of complex neurological dysfunction. This has led to the introduction of new rational therapeutic strategies for both medical and neurosurgical treatment of movement disorders.

The caudate nucleus is a curved, tadpole-shaped mass. It has a large anterior head, which tapers to a body, and a down-curving tail (Fig. 22.4). The head is covered with ependyma and lies in the floor and lateral wall of the anterior horn of the lateral ventricle, in front of the interventricular foramen. The tapering body is in the floor of the body of the ventricle, and the narrow tail follows the curve of the inferior horn, and so lies in the ventricular roof, in the temporal lobe. Medially, the greater part of the caudate nucleus abuts the thalamus, along a junction that is marked by a groove, the sulcus terminalis. The sulcus contains the stria terminalis, lying deep to the ependyma (Fig. 22.5). The sulcus terminalis is especially prominent anterosuperiorly (because of the large size of the head and body of the caudate nucleus relative to the tail), and here the stria terminalis is accompanied by the thalamostriate vein.

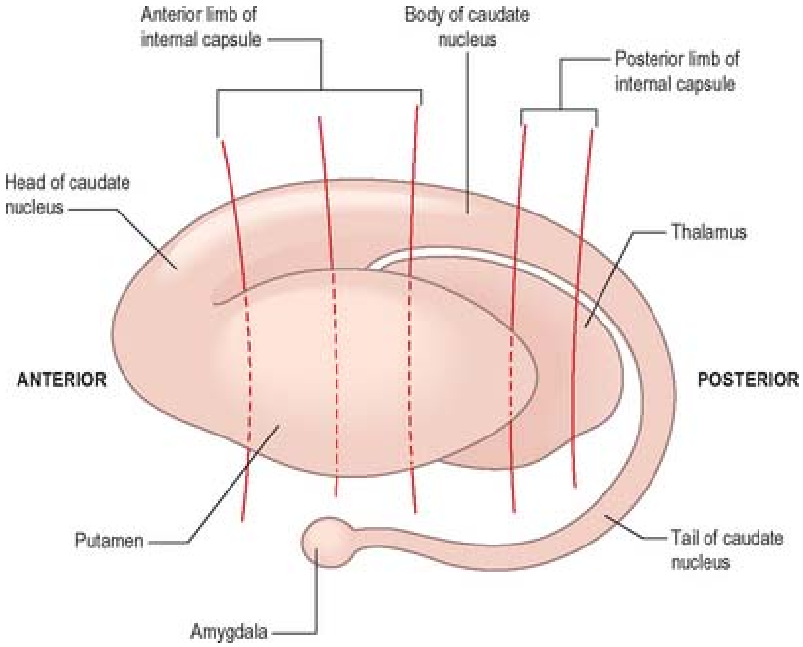
Anterior limb of internal capsule
Body of caudate nucleus
Posterior limb of internal capsule
Head of caudate nucleus
Thalamus
ANTERIOR
POSTERIOR
Putamen
Tail of caudate nucleus
Amygdala

Fig. 22.4 The striatum within the left cerebral hemisphere.

(By permission from Crossman AR, Neary D 2000 Neuroanatomy, 3rd edn. Edinburgh: Churchill Livingstone.)

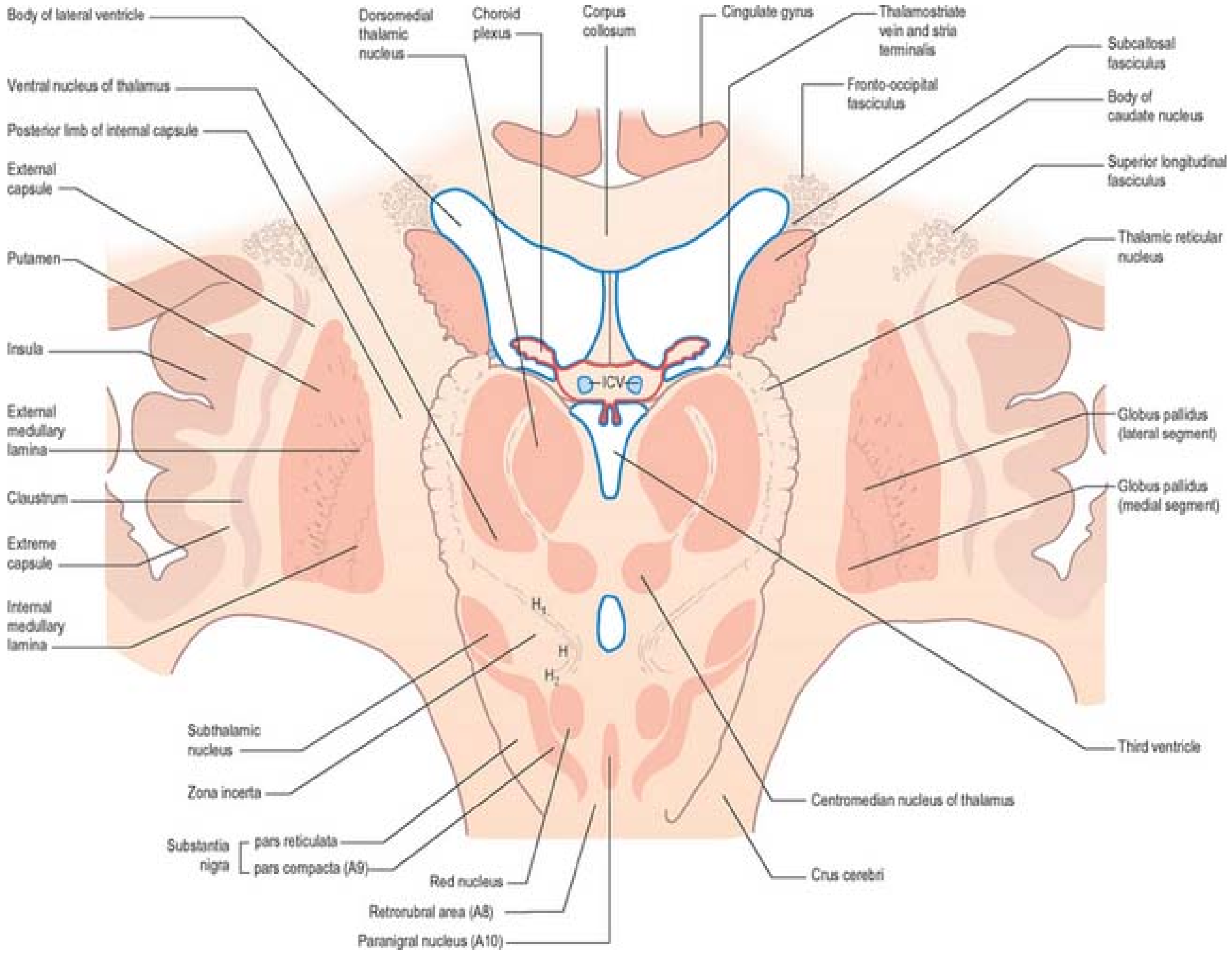

Body of lateral ventricle
Ventral nucleus of thalamus
Posterior limb of internal capsule
External capsule
Putamen
Insula
External medullary lamina
Claustrum
Extreme capsule
Internal medullary lamina
Dorsomedial thalamic nucleus
Choroid plexus
Corpus callosum
Cingulate gyrus
Thalamostriate vein and stria terminalis
Fronto-occipital fasciculus
Subcallosal fasciculus
Body of caudate nucleus
Superior longitudinal fasciculus
Thalamic reticular nucleus
Globus pallidus (lateral segment)
Globus pallidus (medial segment)
ICV
H1
H
H2
Third ventricle
Subthalamic nucleus
Zona incerta
Substantia nigra
pars reticulata
pars compacta (A9)
Red nucleus
Retrorubral area (A8)
Paranigral nucleus (A10)
Centromedian nucleus of thalamus
Crus cerebri

Fig. 22.5 An oblique section through the diencephalon and basal ganglia. ICV, internal cerebral veins; H, H_1, H_2, subthalamic fields of Forel.

The corpus callosum lies above the head and body of the caudate nucleus. The two are separated laterally by the fronto-occipital fasciculus, and medially by the subcallosal fasciculus which caps the nucleus (Figs 22.5, 22.6). The caudate nucleus is largely separated from the lentiform complex by the anterior limb of the internal capsule (Figs 22.1, 22.6 and 22.7). However, the inferior part of the head of the caudate becomes continuous with the most inferior part of the putamen immediately above the anterior perforated substance; this junctional region is sometimes known as the fundus striati (Fig. 22.6). Variable bridges of cells connect the putamen to the caudate nucleus for most of its length. They are most prominent anteriorly, in the region of the fundus striati and the head and body of the caudate nucleus, where they break up the anterior limb of the internal capsule (Fig. 22.7). In the temporal lobe, the anterior part of the tail of the caudate nucleus becomes continuous with the posteroinferior part of the putamen. The vast bulk of the caudate nucleus and putamen are often referred to as the dorsal striatum. A smaller inferomedial part of the rostral striatum is referred to as the ventral striatum, and includes the nucleus accumbens.

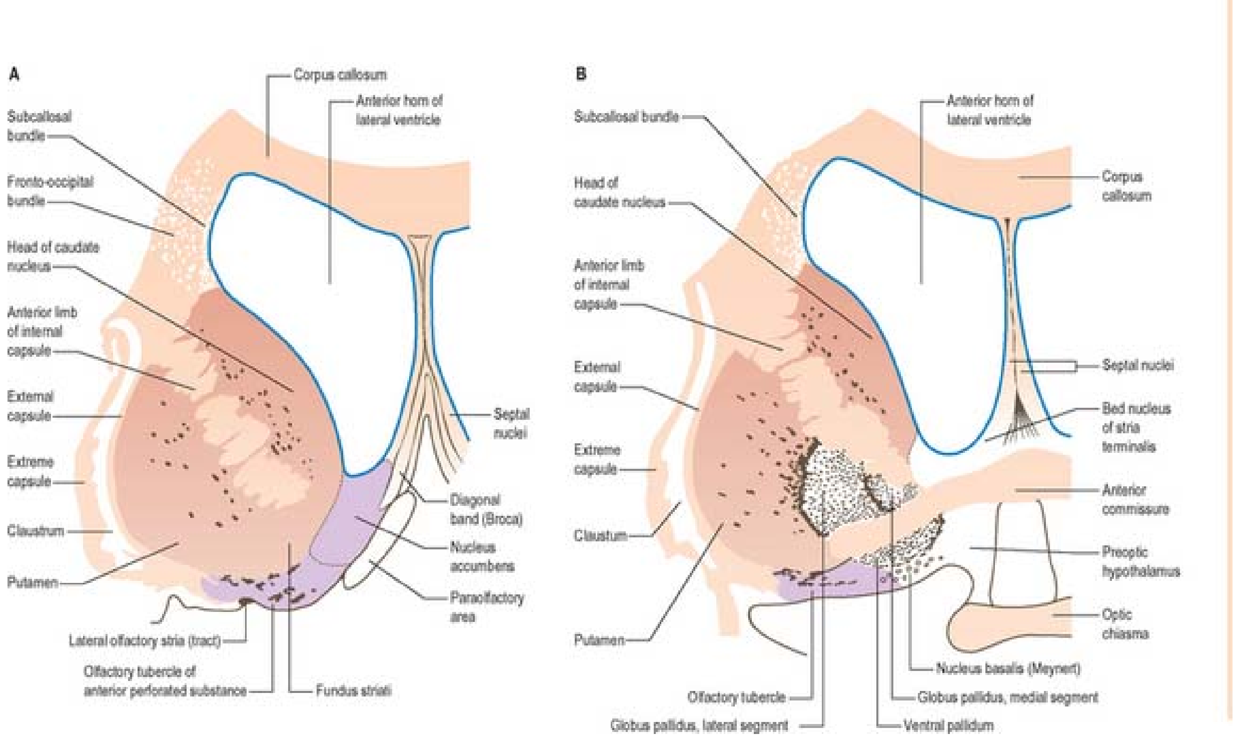
A
Corpus callosum
Anterior horn of lateral ventricle
Subcallosal bundle
Fronto-occipital bundle
Head of caudate nucleus
Anterior limb of internal capsule
External capsule
Extreme capsule
Claustrum
Putamen
Septal nuclei
Diagonal band (Broca)
Nucleus accumbens
Paraolfactory area
Lateral olfactory stria (tract)
Olfactory tubercle of anterior perforated substance
Fundus striati
B
Subcallosal bundle
Head of caudate nucleus
Anterior limb of internal capsule
External capsule
Extreme capsule
Claustum
Putamen
Anterior horn of lateral ventricle
Corpus callosum
Septal nuclei
Bed nucleus of stria terminalis
Anterior commissure
Preoptic hypothalamus
Optic chiasma
Nucleus basalis (Meynert)
Olfactory tubercle
Globus pallidus, medial segment
Globus pallidus, lateral segment
Ventral pallidum

Fig. 22.6 Coronal sections through the corpus striatum and anterior perforated substance. **A** is anterior to **B**.

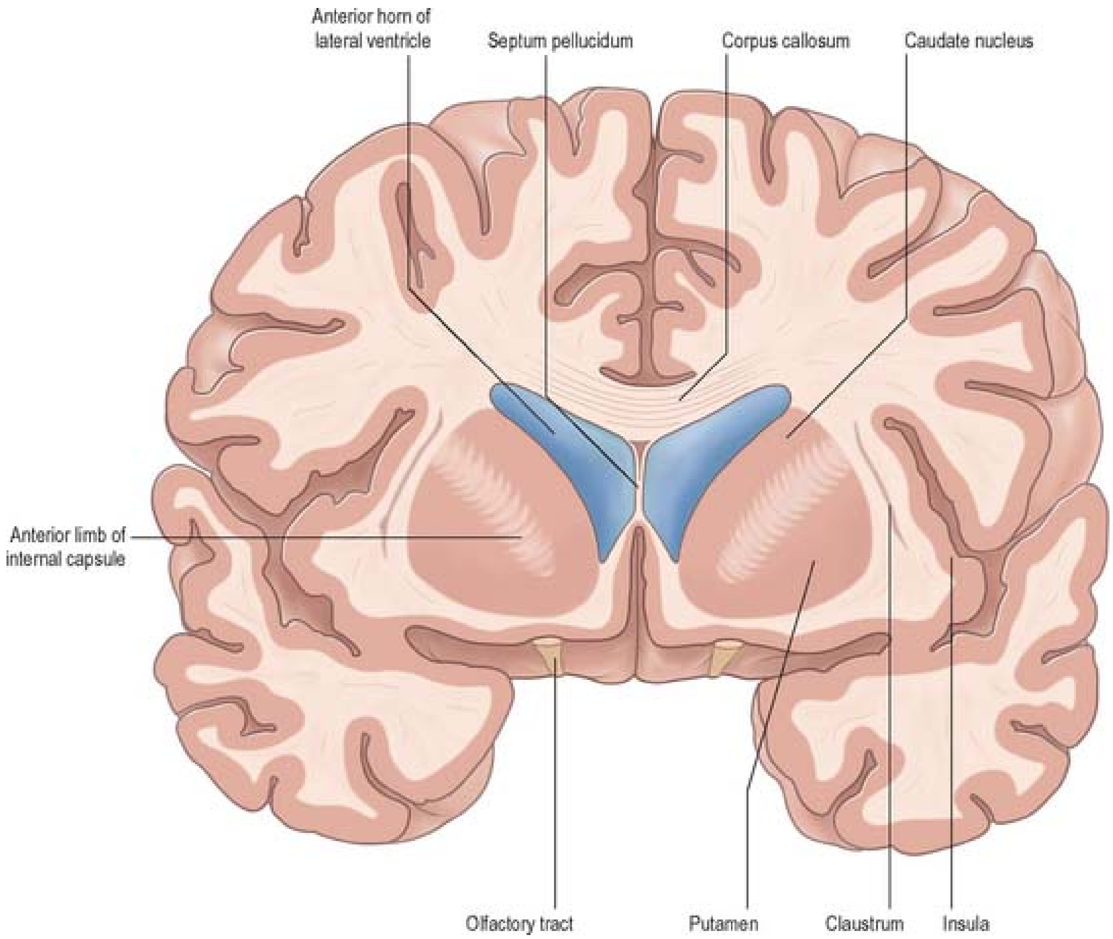
Anterior horn of lateral ventricle
Septum pellucidum
Corpus callosum
Caudate nucleus
Anterior limb of internal capsule
Olfactory tract
Putamen
Claustrum
Insula

Fig. 22.7 Posterior aspect of a coronal section through the anterior horn of the lateral ventricles.

The lentiform complex (Figs 22.1, 22.2, 22.8) lies deep to the insular cortex, with which it is roughly coextensive, although they are separated by a thin layer of white matter and by the claustrum. The latter splits the insular subcortical white matter to create the extreme and external capsules; the external capsule separates the claustrum from the putamen. The internal capsule separates the lentiform complex from the caudate nucleus.

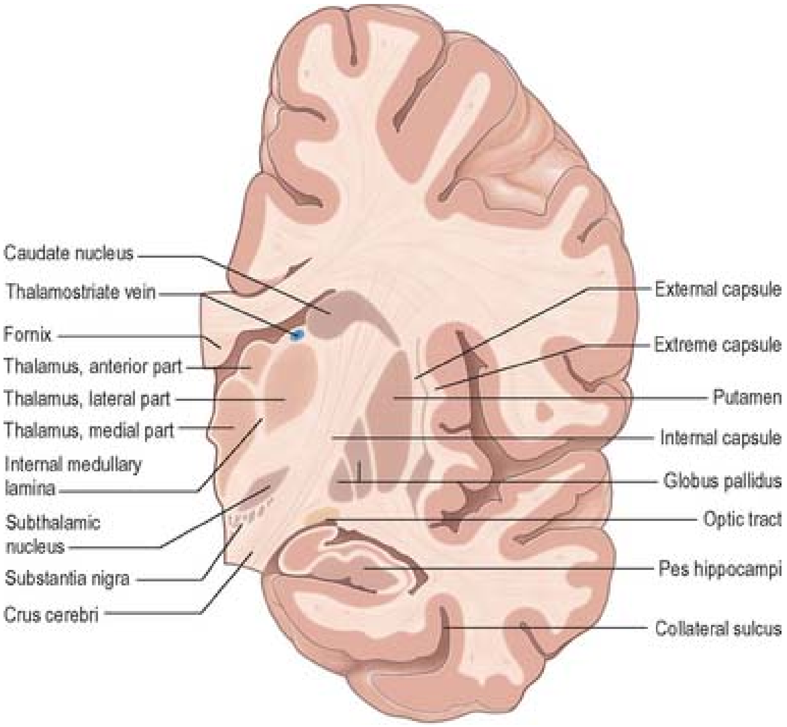
Caudate nucleus
Thalamostriate vein
Fornix
Thalamus, anterior part
Thalamus, lateral part
Thalamus, medial part
Internal medullary lamina
Subthalamic nucleus
Substantia nigra
Crus cerebri
External capsule
Extreme capsule
Putamen
Internal capsule
Globus pallidus
Optic tract
Pes hippocampi
Collateral sulcus

Fig. 22.8 Anterior aspect of a coronal section through the left cerebral hemisphere.

The lentiform complex consists of the laterally placed putamen and the more medial globus pallidus (pallidum), which are separated by a thin layer of fibres, the lateral or external medullary lamina. The globus pallidus is itself divided into two segments, a lateral (or external) segment and a medial (or internal) segment, separated by an internal (or medial) medullary lamina. The two segments have distinct afferent and efferent connections.

Inferiorly, a little behind the fundus striati, the lentiform complex is grooved by the anterior commissure, which connects inferior parts of the temporal lobes and the anterior olfactory cortex of the two sides (Fig. 22.6). The area above the commissure is referred to as the dorsal pallidum, and that below it as the ventral pallidum.

STRIATUM

The striatum consists of the caudate nucleus, putamen and ventral striatum, which are all highly cellular and well vascularized. The caudate and putamen are traversed by numerous small bundles of thinly-myelinated, or non-myelinated, small-diameter axons, which are mostly striatal afferents and efferents. They radiate through the striatal tissue as though converging on, or radiating from, the globus pallidus. The bundles are occasionally referred to by the archaic term ‘Wilson’s pencils’ and they account for the striated appearance of the corpus striatum.

Neurones of both dorsal and ventral striatum are mainly medium-sized multipolar cells. They have round, triangular or fusiform somata, mixed with a smaller number of large multipolar cells. The ratio of medium to large cells is at least 20 : 1. The large neurones have extensive spherical or ovoid dendritic trees up to 60 μm across. The medium-sized neurones also have spherical dendritic trees, approximately 20 μm across, which receive the synaptic terminals of many striatal afferents. The dendrites of both medium and large striatal cells may be either spiny or non-spiny. The most common neurone (usually 75% of the total) is a medium-sized cell with spiny dendrites. These cells utilize γ-aminobutyric acid (GABA) as their transmitter and also express the genes coding for either enkephalin or substance P/dynorphin. Enkephalinergic neurones express D2 dopamine receptors. Substance P/dynorphin neurones express D1 receptors. These neurones are the major, and perhaps exclusive, source of striatal efferents to the pallidum and substantia nigra pars reticulata. The remaining medium-sized striatal neurones are aspiny, and are intrinsic cells that contain acetylcholinesterase (AChE), choline acetyltransferase (CAT) and somatostatin. Large neurones with spiny dendrites contain AChE and CAT; most, perhaps all, are intrinsic neurones. Aspiny large neurones are all intrinsic neurones.

Intrinsic synapses are probably largely asymmetric (type II), while those derived from external sources are symmetric (type I). The aminergic afferents from the substantia nigra, raphe and locus coeruleus all end as profusely branching axons with varicosities, which contain dense-core vesicles (the presumed store of amine transmitters). Many of these varicosities have no conventional synaptic membrane specializations, and may release transmitter in a way analogous to that found in peripheral postsynaptic sympathetic axons.

Neuroactive chemicals, whether intrinsic or derived from afferents, are not distributed uniformly in the striatum. For example, serotonin and glutamic acid decarboxylase (GAD) concentrations are highest caudally, while substance P, acetylcholine (ACh) and dopamine are highest rostrally. However, there is a finer grain neurochemical organization that informs the view of the striatum as a mosaic of islands or striosomes (sometimes referred to as patches), each 0.5–1.5 mm across, packed into a background matrix. Striosomes contain substance P and enkephalin. During development, the first dopamine terminals from the substantia nigra are found in striosomes. Although this exclusivity does not persist after birth, striosomes in the adult caudate nucleus still contain a higher concentration of dopamine than the matrix. The latter contains ACh and somatostatin and is the target of thalamostriate axons. Receptors for at least some neurotransmitters are also differentially distributed. For example, opiate receptors are found almost exclusively within striosomes, and muscarinic receptors predominantly so. Moreover, the distribution of neuroactive substances within the striosomes is not uniform. In humans, the striosome/matrix patchwork is less evident in the putamen, where it appears to consist predominantly of matrix, than it is in the caudate nucleus.

All afferents to the striatum terminate in a mosaic manner. The size of a cluster of terminals is usually 100–200 μm across. Some afferent terminal clusters are not arranged in register with the clear striosome/matrix distributions seen in nigrostriatal and thalamostriatal axons. In general, afferents from neocortex end in striatal matrix and those from allocortex end in striosomes. However, the distinction is not absolute: although afferents from the neocortex arise in layers V and VI, those from the superficial part of layer V end predominantly in striatal matrix, whereas those from deeper neocortex project to striosomes. Striatal cell bodies, which are the sources of efferents, also form clusters, but again are not uniformly related to striosomes. For example, the cell bodies of some striatopallidal and striatonigral axons lie clustered within striosomes, and others lie outside them, but still in clusters. The neurones and neuropil of the ventral striatum are essentially similar to those of the dorsal striatum, but the striosomal/matrix organization is less well-defined, and seems to consist predominantly of striosomes.

The major connections of the striatum are summarized in Fig. 22.9. Although the connections of the dorsal and ventral divisions overlap, the generalization can be made that the dorsal striatum is predominantly connected with motor and associative areas of the cerebral cortex, whilst the ventral striatum is connected with the limbic system and orbitofrontal and temporal cortices. For both dorsal and ventral striatum, the pallidum and substantia nigra pars reticulata are key efferent structures. The fundamental arrangement is the same for both divisions. The cerebral cortex projects to the striatum, which in turn projects to the pallidum and substantia nigra pars reticulata, and efferents from the pallidum and substantia nigra pars reticulata influence the cerebral cortex (either the supplementary motor area or prefrontal and cingulate cortices via the thalamus) and the superior colliculus (see below).

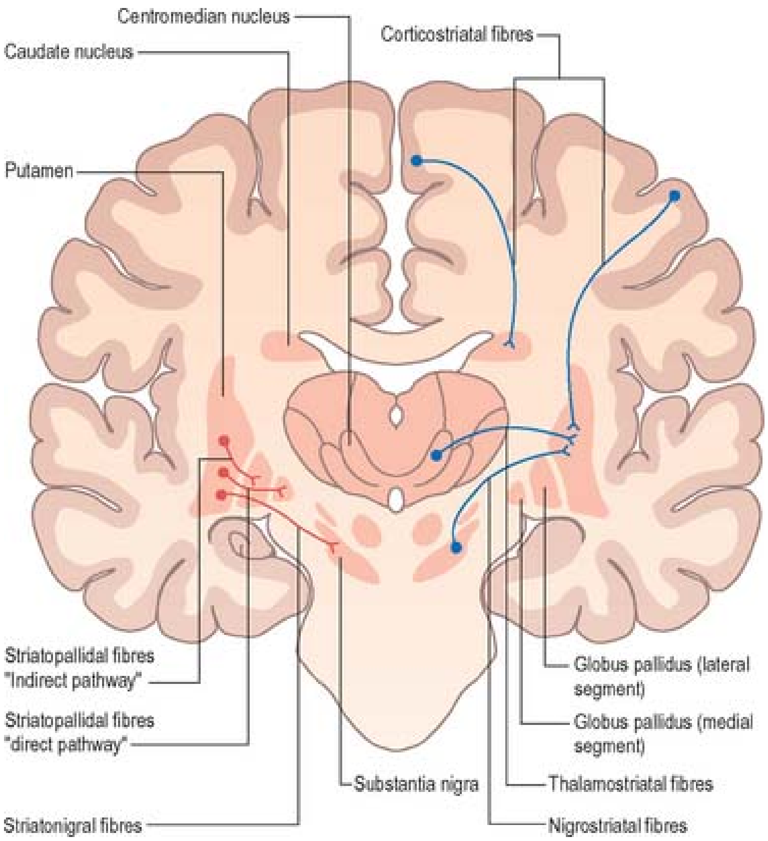
Centromedian nucleus
Caudate nucleus
Corticostriatal fibres
Putamen
Striatopallidal fibres "Indirect pathway"
Striatopallidal fibres "direct pathway"
Striatonigral fibres
Substantia nigra
Globus pallidus (lateral segment)
Globus pallidus (medial segment)
Thalamostriatal fibres
Nigrostriatal fibres

Fig. 22.9 Connections of the striatum. The major afferent projections to the striatum are shown on the right and major efferent projections from the striatum on the left.

The entire neocortex sends glutamatergic axons to the ipsilateral striatum. Previously, these axons were thought to be collaterals of cortical efferents to other regions, but it is now known that they arise exclusively from small pyramidal cells in layers V and VI. It has also been suggested that some of the cells of origin lie in the supragranular 'cortical association' layers II and III. The projection is organized topographically. The greater part of the input from the cerebral cortex to the dorsal striatum is derived from the frontal and parietal lobes, that from the occipitotemporal cortex being relatively small. Thus, the orbitofrontal association cortex projects to the inferior part of the head of the caudate nucleus, which lies next to the ventral striatum. The dorsolateral frontal association cortex and frontal eye fields project to the rest of the head of the caudate nucleus, and much of the parietal lobe projects to the body of the nucleus. The somatosensory and motor cortices project predominantly to the putamen. Their afferents establish a somatotopic pattern, in which the lower body is represented laterally and the upper body is represented medially. The motor cortex is unique in sending axons through the corpus callosum to the opposite putamen, where they end with the same spatial ordering. The occipital and temporal cortices project to the tail of the caudate nucleus and to the inferior putamen.

The striatum also receives afferents, which are more crudely spatially organized, from the polysensory intralaminar thalamus. The cerebello-receptive nucleus centralis lateralis projects to the anterior striatum (especially the caudate nucleus), and the cerebello- and pallidoreceptive centromedian nucleus projects to the putamen.

The aminergic inputs to the caudate and putamen are derived from the substantia nigra pars compacta (dopaminergic group A9; Fig. 22.10), the retrorubral nucleus (dopaminergic group A8), the dorsal raphe nucleus (serotoninergic group B7; Fig. 22.10) and the locus coeruleus (noradrenergic group A6). The nigrostriatal input is sometimes referred to as the ‘mesostriatal’ dopamine pathway. It reaches the striatum by traversing the H fields (of Forel) in the subthalamus and running in the median forebrain bundle. These aminergic inputs appear to modulate the responses of the striatum to cortical and thalamic afferent influences.

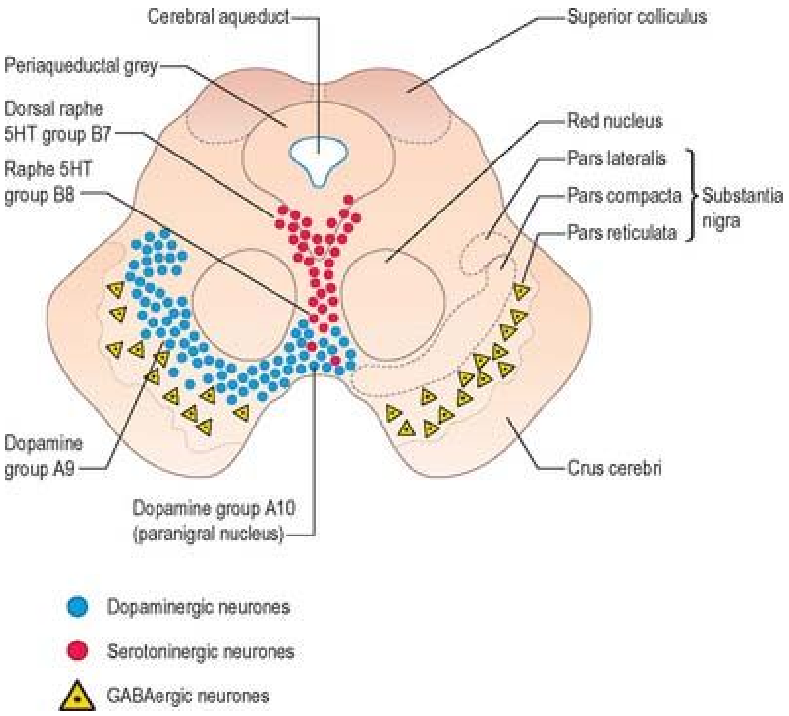
Cerebral aqueduct
Superior colliculus
Periaqueductal grey
Dorsal raphe 5HT group B7
Raphe 5HT group B8
Red nucleus
Pars lateralis
Pars compacta
Pars reticulata
Substantia nigra
Dopamine group A9
Crus cerebri
Dopamine group A10 (paranigral nucleus)
Dopaminergic neurones
Serotoninergic neurones
GABAergic neurones

Fig. 22.10 Transverse section through the midbrain to show the arrangement of dopaminergic cell groups A9 and A10 in the substantia nigra (left) and serotoninergic cell groups B7 and B8 in the raphe.

Efferents from the striatum pass to both segments of the globus pallidus and to the substantia nigra pars reticulata, where they end in a topically ordered fashion. Fibres ending in either the lateral or medial pallidal segment originate from different striatal cells (Fig. 22.9). Those to the lateral pallidum come from neurones which co-localize GABA and enkephalin and give rise to the so-called ‘indirect pathway’. This name refers to the fact that these striatal neurones influence the activity of basal ganglia output neurones in the medial pallidum via the intermediary of the subthalamic nucleus. Other striatal neurones, which co-localize GABA and substance P/dynorphin, project directly to the medial pallidum and are therefore described as the ‘direct pathway’.

A second outflow is established from the striatum to the pars reticulata of the substantia nigra. This also has both direct and indirect components, via the lateral pallidum and subthalamic nucleus (Figs 22.11, 22.12). The axons of the direct striatonigral projection constitute the laterally placed ‘comb’ system, which is spatially quite distinct from the ascending dopaminergic nigrostriatal pathway. Striatonigral fibres end in a spatially ordered way in the pars reticulata.

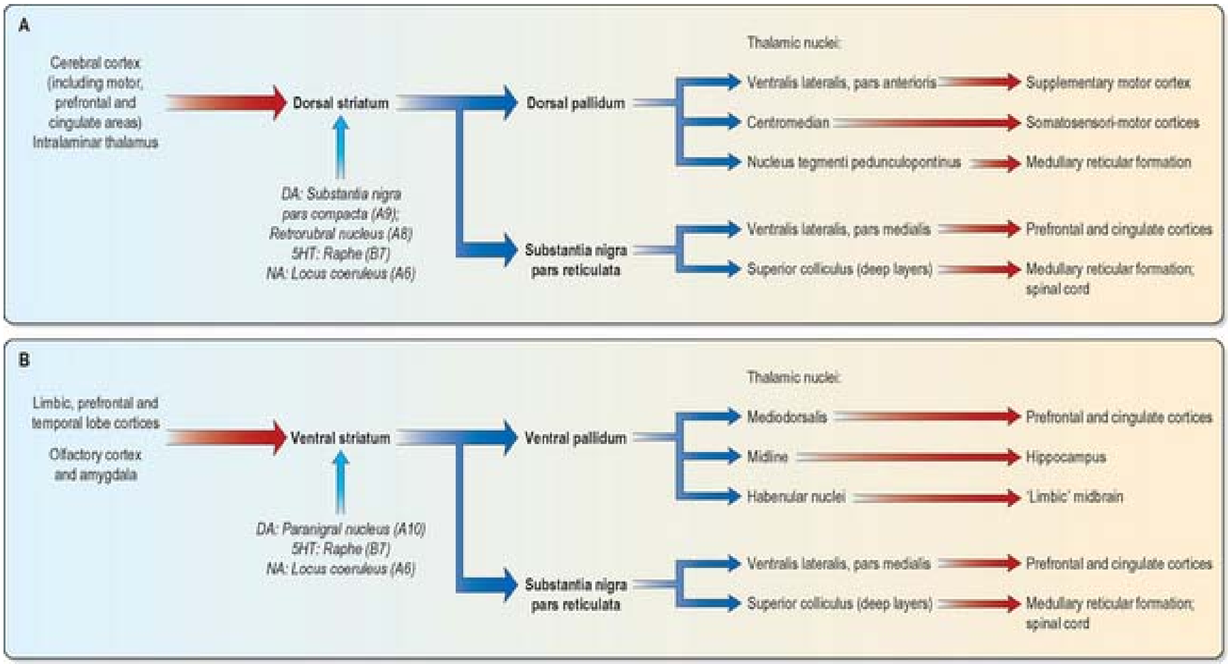
A
Cerebral cortex (including motor, prefrontal and cingulate areas) Intralaminar thalamus
Dorsal striatum
DA: Substantia nigra pars compacta (A9); Retrorubral nucleus (A8)
5HT: Raphe (B7)
NA: Locus coeruleus (A6)
Dorsal pallidum
Substantia nigra pars reticulata
Thalamic nuclei:
Ventralis lateralis, pars anterioris
Centromedian
Nucleus tegmenti pedunculopontinus
Ventralis lateralis, pars medialis
Superior colliculus (deep layers)
Supplementary motor cortex
Somatosensori-motor cortices
Medullary reticular formation
Prefrontal and cingulate cortices
Medullary reticular formation; spinal cord
B
Limbic, prefrontal and temporal lobe cortices
Olfactory cortex and amygdala
Ventral striatum
DA: Paranigral nucleus (A10)
5HT: Raphe (B7)
NA: Locus coeruleus (A6)
Ventral pallidum
Substantia nigra pars reticulata
Thalamic nuclei:
Mediodorsalis
Midline
Habenular nuclei
Ventralis lateralis, pars medialis
Superior colliculus (deep layers)
Prefrontal and cingulate cortices
Hippocampus
'Limbic' midbrain
Prefrontal and cingulate cortices
Medullary reticular formation; spinal cord

Fig. 22.11 The principal output connections of the basal ganglia derived from dorsal (**A**) and ventral (**B**) divisions of the striatum. In each case pathways established through the pallidum are distinguished from those passing through the substantia nigra pars reticulata. DA, dopamine; NA, noradrenaline (norepinephrine); 5HT, 5-hydroxytryptamine.

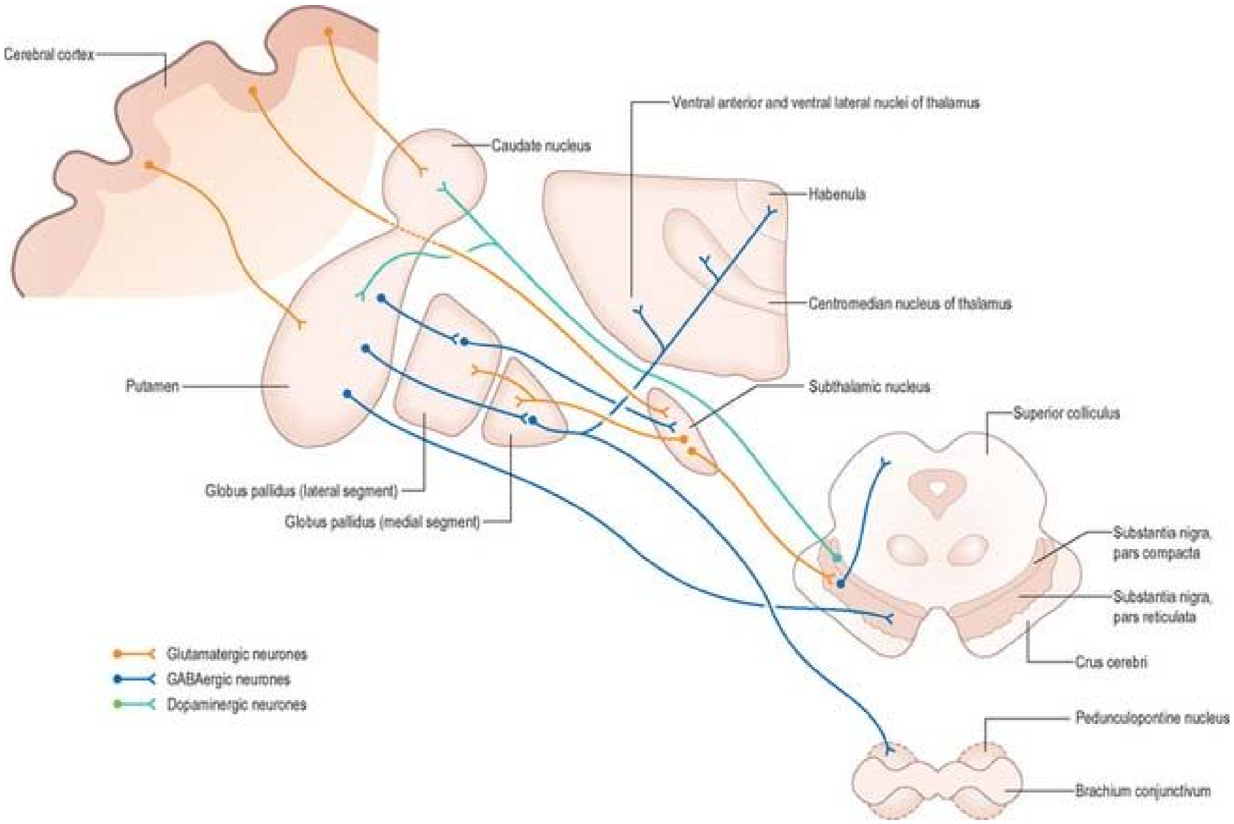
Cerebral cortex
Ventral anterior and ventral lateral nuclei of thalamus
Caudate nucleus
Habenula
Centromedian nucleus of thalamus
Putamen
Subthalamic nucleus
Superior colliculus
Globus pallidus (lateral segment)
Globus pallidus (medial segment)
Substantia nigra, pars compacta
Substantia nigra, pars reticulata
Crus cerebri
Glutamatergic neurones
GABAergic neurones
Dopaminergic neurones
Pedunculopontine nucleus
Brachium conjunctivum

Fig. 22.12 The principal connections of the basal ganglia with the diencephalon and brain stem.

The ventral striatum is the primary target of cortical afferents from limbic cortices, including allocortex, and from limbic associated regions (Fig. 22.11). Thus, the hippocampus (through the fornix) and orbitofrontal cortex (through the internal capsule) project to the nucleus accumbens, and the olfactory, entorhinal, anterior cingulate and temporal visual cortices project to both the nucleus accumbens and olfactory tubercle in varying degrees. The tubercle also receives afferents from the amygdala. The contiguities of the cortical areas, which project to the ventral striatum and neighbouring dorsal striatum, emphasize the imprecise nature of the boundaries between the two divisions. All the cortical regions overlap and abut one another, and they project to neighbouring parts of the dorsal striatum as well as to the ventral striatum. The fundus striati and ventromedial caudate nucleus abut the olfactory tubercle and nucleus accumbens (Fig. 22.6), and receive connections from the orbitofrontal cortex and, to a lesser extent, from the lateral prefrontal and anterior cingulate cortices (which also project to the contiguous head of the caudate nucleus).

This continuity of the ventral and dorsal striata, as revealed by the arrangements of corticostriate projections, is reinforced by consideration of the aminergic inputs to the ventral striatum. They are derived from the dorsal raphe (serotoninergic group B7), the locus coeruleus (noradrenergic group A6) and from the paranigral nucleus (dopamine group A10), as well as the most medial part of the substantia nigra pars compacta (A9) (Fig. 22.10). The dopamine projections constitute the so-called mesolimbic dopamine pathway, which also projects to the septal nuclei, hippocampus and amygdala and prefrontal and cingulate cortices through the medial forebrain bundle. The lateromedial continuity of cell groups A9 and 10 is thus reflected in the relative positions of their ascending fibres in the subthalamus and hypothalamus (the H fields and median forebrain bundle, respectively), as well as in the lateromedial topography of the dorsal and ventral striata (Fig. 22.6), which in turn have contiguous and overlapping sources of cortical afferents.

As with the dorsal striatum, efferents from the ventral striatum project to the pallidum (in this case the ventral pallidum) and the substantia nigra pars reticulata (Figs 22.11, 22.12). In the latter case, the connection is both direct and indirect via the subthalamic nucleus. The projections from the pars reticulata are as described for the dorsal system, but axons from the ventral pallidum reach the thalamic mediodorsal nucleus (which projects to cingulate and prefrontal association cortex) and midline nuclei (which project to the hippocampus). Ventral pallidal axons also reach the habenular complex of the limbic system.

The brain areas beyond the basal nuclei, substantia nigra and subthalamic nucleus, to which both ventral and dorsal systems appear to project, are, therefore, the prefrontal association and cingulate cortices and the deep superior colliculus.

Nucleus accumbens

The ventral striatum consists of the nucleus accumbens and the olfactory tubercle. In front of the anterior commissure, much of the grey matter of the anterior perforated substance, and especially the olfactory tubercle, is indistinguishable from, and continuous with, the fundus striati, in terms of cellular composition, histochemistry and interconnections. The caudate nucleus is continuous medially with the nucleus accumbens (Fig. 22.6), which abuts the nuclei of the septum, close by the paraolfactory area, diagonal band of Broca and the fornix.

The nucleus accumbens receives a dopaminergic innervation from the midbrain ventral tegmental area (cell group A10). It is believed to represent the neural substrate for the rewarding effects of several classes of drugs of abuse and is, therefore, a major determinant of their addictive potential. The experimental observation that the locomotor activating effects of psychomotor stimulant drugs such as amphetamine and cocaine (which act presynaptically on dopaminergic neurones to enhance dopamine release or block its reuptake, respectively) are dependent on dopamine transmission in the nucleus accumbens, led to the hypothesis that the reinforcing or rewarding properties of these drugs are mediated by the mesolimbic dopamine system.

GLOBUS PALLIDUS

The globus pallidus (pallidum) lies medial to the putamen and lateral to the internal capsule. It consists of two segments, lateral (external) and medial (internal), which are separated by an internal medullary lamina, and which have substantially different connections. Both segments receive large numbers of fibres from the striatum and subthalamic nucleus. The lateral segment projects reciprocally to the subthalamic nucleus as part of the ‘indirect pathway’. The medial segment is considered to be a homologue of the pars reticulata of the substantia nigra, with which it shares similar cellular and connectional properties. Together, these segments constitute the main output of the basal ganglia to other levels of the neuraxis, principally to the thalamus and superior colliculus.

The cell density of the globus pallidus is less than one-twentieth of that of the striatum. The morphology of the majority of cells is identical in the two segments. They are large multipolar GABAergic neurones that closely resemble those of the substantia nigra pars reticulata. The dendritic fields are discoid, with planes at right angles to incoming striatopallidal axons, each of which, therefore, potentially contacts many pallidal dendrites *en passant*. This arrangement, coupled with the diameters of the dendritic fields (500 μm), suggests that a precise topographical organization is unlikely within the pallidum.

Striatopallidal fibres are of two main types. They project either to the lateral or the medial pallidal segment. Those projecting to the lateral segment constitute the beginning of the so-called ‘indirect pathway’. They utilize GABA as their primary transmitter and also contain enkephalin. Efferent axons from neurones in the lateral segment pass through the internal capsule in the subthalamic fasciculus, and travel to the subthalamic nucleus (Fig. 22.13).

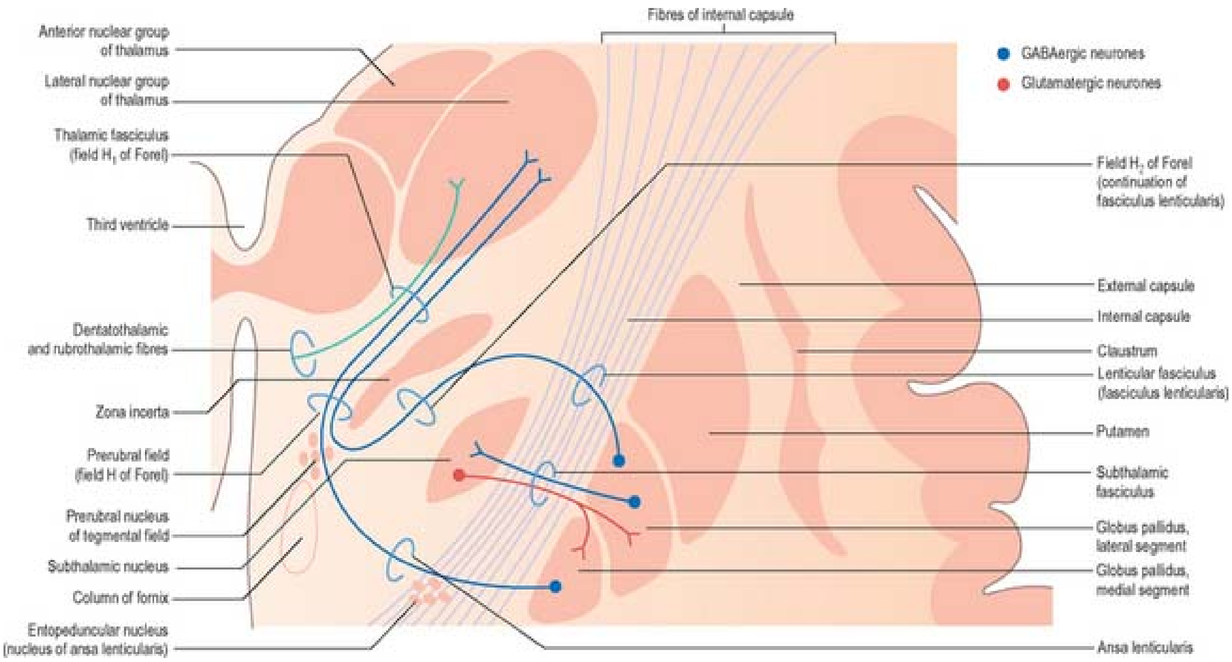
Fibres of internal capsule
Anterior nuclear group of thalamus
Lateral nuclear group of thalamus
Thalamic fasciculus (field H_1 of Forel)
Third ventricle
Dentatothalamic and rubrothalamic fibres
Zona incerta
Prerubral field (field H of Forel)
Prerubral nucleus of tegmental field
Subthalamic nucleus
Column of fornix
Entopeduncular nucleus (nucleus of ansa lenticularis)
● GABAergic neurones
● Glutamatergic neurones
Field H_2 of Forel (continuation of fasciculus lenticularis)
External capsule
Internal capsule
Claustrum
Lenticular fasciculus (fasciculus lenticularis)
Putamen
Subthalamic fasciculus
Globus pallidus, lateral segment
Globus pallidus, medial segment
Ansa lenticularis

Fig. 22.13 Coronal section of the brain showing the major connections of the basal ganglia with the diencephalon.

Striatopallidal axons destined for the medial pallidum constitute the so-called ‘direct pathway’. Like the indirect projection, these also utilize GABA as their primary transmitter but they also contain substance P and dynorphin, rather than enkephalin. Efferent axons from the medial pallidal segment project through the ansa lenticularis and fasciculus lenticularis (Fig. 22.13). The former runs round the anterior border of the internal capsule and the latter penetrates the capsule directly. Having traversed the internal capsule, both pathways unite in the subthalamic region, where they follow a horizontal hairpin trajectory, and turn upwards to enter the thalamus as the thalamic fasciculus. The trajectory circumnavigates the zona incerta and creates the so-called ‘H’ fields of Forel (Figs 22.5, 22.13). Within the thalamus, pallidothalamic fibres end in the ventral anterior and ventral lateral nuclei and in the intralaminar centromedian nucleus. These in turn project excitatory (presumed glutamatergic) fibres primarily to the frontal cortex, including the primary and supplementary motor areas. The medial pallidum also projects fibres caudally to the pedunculopontine nucleus (Fig. 22.12). This lies at the junction of the midbrain and the pons, close to the superior cerebellar peduncle, and corresponds approximately to the physiologically identified ‘mesencephalic locomotor region’.

SUBSTANTIA NIGRA

The substantia nigra is a nuclear complex deep to the crus cerebri in each cerebral peduncle of the midbrain. It consists of a pars compacta, pars reticulata and a smaller pars lateralis (Fig. 22.10). The pars compacta and pars lateralis correspond to the dopaminergic cell group A9. Together with the retrorubral nucleus (A8) they comprise most of the dopaminergic neurone population of the midbrain and are the source of the mesostriatal dopamine system that projects to the striatum. The pars compacta of each side is continuous with its contralateral counterpart through the ventral tegmental dopamine group A10, which is sometimes known as the paranigral nucleus. This is the source of the mesolimbic dopamine system, which supplies the ventral striatum and neighbouring parts of the dorsal striatum, and the prefrontal and anterior cingulate cortices. The dopaminergic neurones of the pars compacta (A9) and paranigral nucleus (ventral tegmental group A10) also contain cholecystokinin (CCK) or somatostatin.

The neurones of the pars reticulata and pallidum collectively constitute the output neurones of the basal ganglia system. The pars reticulata contains large multipolar cells, very similar to those of the pallidum: their disc-like dendritic trees, like those of the pallidum, are orientated at right angles to afferents from the striatum, probably making *en-passant* contacts. Like the striatopallidal axons, of which they may be collaterals, striatonigral axons utilize GABA and substance P or enkephalin. They distribute differentially in the pars reticulata, such that the enkephalinergic axons terminate in the medial part, whereas substance P axons terminate throughout.

The efferent neurones of the pars reticulata are GABAergic. They project to the deep (polysensory) layers of the superior colliculus and to the brain stem reticular formation, including the pedunculopontine nucleus. The pathway from the striatum to the superior colliculus, via the substantia nigra pars reticulata, is thought to function in the control of gaze in a manner analogous to the pathway that initiates general body movement via the pallidum, thalamus and supplementary motor cortex. The uncontrolled or fixed-gaze disturbances of advanced Parkinson’s disease, progressive supranuclear palsy (PSP) and Huntington’s disease tend to support this.

SUBTHALAMIC NUCLEUS

The subthalamic nucleus is a biconvex, lens-shaped nucleus in the subthalamus of the diencephalon. It lies medial to the internal capsule, immediately rostral to the level at which the latter becomes continuous with the crus cerebri of the midbrain (Figs 22.2, 22.5, 22.8). Within the nucleus, small interneurones intermingle with large multipolar cells with dendrites which extend for about one-tenth the diameter of the nucleus. The nucleus is encapsulated dorsally by axons, many of which are derived from the subthalamic fasciculus: they carry a major GABAergic projection from the lateral segment of the globus pallidus as part of the indirect pathway. It also receives afferents from the cerebral cortex. The subthalamic nucleus is unique in the intrinsic circuitry of the basal ganglia in that its cells are glutamatergic and project excitatory axons to both the globus pallidus and substantia nigra pars reticulata. Within the pallidum, subthalamic efferent fibres end predominantly in the medial segment but many also end in the lateral segment.

The subthalamic nucleus plays a central role in the normal function of the basal ganglia and in the pathophysiology of basal ganglia-related disorders. Destruction of the nucleus, which occurs rarely as a result of stroke, results in the appearance of violent, uncontrolled involuntary movements, known as ballism (ballismus). The subthalamic nucleus is also crucially involved in the pathophysiology of Parkinson’s disease and is a target for functional neurosurgical therapy of the condition.

PATHOPHYSIOLOGY OF BASAL GANGLIA DISORDERS

The normal functions of the basal ganglia are difficult to summarize succinctly. As far as their role in movement control is concerned, a reasonable definition is that they function to promote and support patterns of behaviour and movement that are appropriate in the prevailing circumstances and to inhibit unwanted or inappropriate behaviour and movements. This is exemplified by disorders of the basal ganglia, which are characterized, depending on the underlying pathology, by an inability to initiate and execute wanted movements (as in Parkinson's disease) or an inability to prevent unwanted movements (as in Huntington's disease).

Parkinson's disease is the most common pathological condition affecting the basal ganglia. It is characterized by akinesia, muscular rigidity and tremor due to degeneration of the dopaminergic neurones of the substantia nigra pars compacta (which project to the striatum in the nigrostriatal pathway). As a consequence, dopamine terminals are lost in the striatum and dopamine levels are severely depleted. Dopamine receptors, which are located upon medium spiny neurones, and are the target of the nigrostriatal pathway, are spared.

Dopamine appears to have a dual action on medium spiny striatal neurones. It inhibits those of the indirect pathway and excites those of the direct pathway. Consequently, when dopamine is lost from the striatum, the indirect pathway becomes overactive and the direct pathway becomes underactive (Fig. 22.14). Overactivity of the striatal projection to the lateral pallidum results in inhibition of pallidosubthalamic neurones and, consequently, overactivity of the subthalamic nucleus. Subthalamic efferents mediate excessive excitatory drive to the medial globus pallidus and substantia nigra pars reticulata. This is exacerbated by underactivity of the GABAergic, inhibitory direct pathway. Overactivity of basal ganglia output then inhibits the motor thalamus and its excitatory thalamocortical connections. While this description is little more than a first approximation of the underlying pathophysiology, this model of the basis of parkinsonian symptoms has led to the introduction of new neurosurgical approaches to the treatment of Parkinson’s disease, based upon lesioning and deep brain stimulation of the medial globus pallidus and subthalamic nucleus (see below).

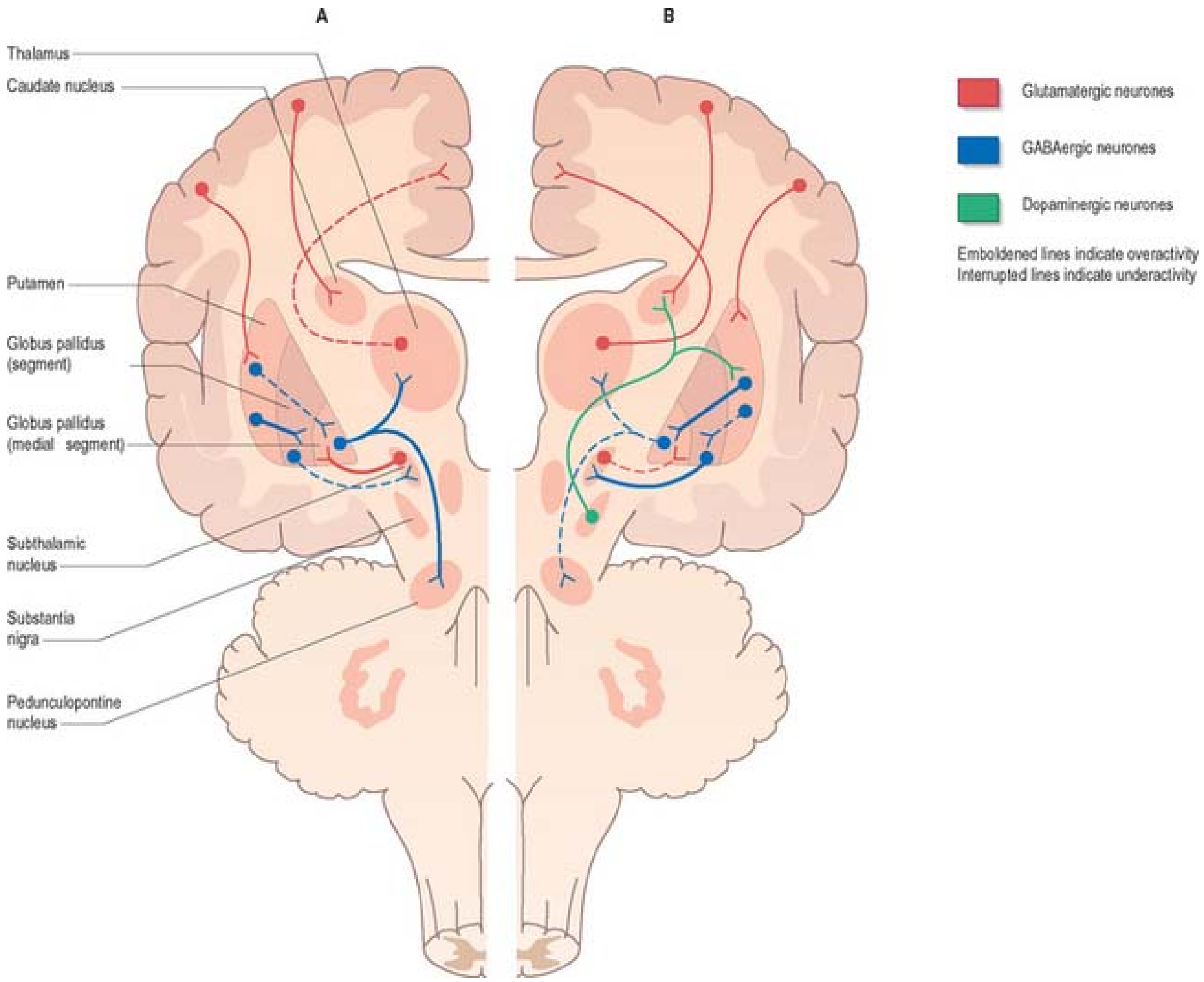
A
B
Thalamus
Caudate nucleus
Putamen
Globus pallidus (segment)
Globus pallidus (medial segment)
Subthalamic nucleus
Substantia nigra
Pedunculopontine nucleus
Glutamatergic neurones
GABAergic neurones
Dopaminergic neurones
Emboldened lines indicate overactivity
Interrupted lines indicate underactivity

Fig. 22.14 Pathophysiology of Parkinson’s disease (**A**) and dyskinesias (**B**).

(Adapted from Crossman AR, Neary D 2000 Neuroanatomy, 2nd edition. Edinburgh: Churchill Livingstone.)

The current medical treatment for Parkinson’s disease relies upon levodopa (L-DOPA; L-dihydroxyphenylalanine), the immediate metabolic precursor of dopamine, or upon dopamine agonists. Whilst these usually provide good symptomatic relief for many years, eventually they lead to the development of side-effects, including dyskinesias. The involuntary movements that occur as a consequence of long-term treatment of Parkinson's disease resemble those seen in Huntington's disease, tardive dyskinesia and ballism. Experimental evidence suggests that these may share a common neural mechanism (Fig. 22.14). Thus, the indirect pathway becomes underactive, e.g. due to the effects of dopaminergic drugs in Parkinson's disease, or the degeneration of the striatopallidal projection to the lateral pallidum in Huntington's disease. This leads to physiological inhibition of the subthalamic nucleus by overactive pallidosubthalamic neurones. The involvement of the subthalamic nucleus explains why the dyskinetic movements of levodopa-induced dyskinesia and Huntington's disease resemble those of ballism produced by lesion of the subthalamic nucleus. Underactivity of the subthalamic nucleus removes the excitatory drive from medial pallidal neurones, which are known to be underactive in dyskinesias. Once again this is an oversimplification. Whilst it is true that underactivity of the medial globus pallidus is associated with dyskinesias, it is also known that lesions of the globus pallidus alleviate them. This suggests that the dynamic aspects of pallidal and nigral efferent activity are important factors in the generation of dyskinesia.

Another manifestation of basal ganglia dysfunction is dystonia, which is characterized by increased muscle tone and abnormal postures. Dystonia may occur as a consequence of levodopa treatment in Parkinson's disease or inherited disease (e.g. early-onset torsion, or Oppenheim's dystonia, an autosomal dominant disorder most commonly associated with a mutation in the *DYT1* gene that encodes torsinA). The pathophysiological basis of dystonia is unclear. Like dyskinesias it is probably caused by underactivity of basal ganglia output, and so deep-brain stimulation of the globus pallidus may be beneficial.

There is evidence that dysfunction of the basal ganglia is involved in other complex, less well-understood, behavioural disorders. In animal experiments, lesions of the basal ganglia, especially of the caudate nucleus, induce uncontrollable hyperactivity (e.g. obstinate progression, incessant pacing and other constantly repeated behaviours). This and other evidence has led to the notion that the corpus striatum enables the individual to make motor choices and to avoid 'stimulus-bound' behaviour. PET scanning studies in man have shown that sufferers from obsessive-compulsive disorder (OCD), which is characterized by repeated ritualistic motor behaviour and intrusive thoughts, exhibit abnormal activity in the prefrontal cortex and caudate nuclei. There are similar suggestive observations in the hyperactive child syndrome. In this respect it may be significant that the basal ganglia, besides receiving connections from the frontal lobe and limbic cortices, also have an ascending influence on the prefrontal and cingulate cortices through the substantia nigra pars reticulata and dorsomedial and ventromedial thalamus (Fig. 22.11).

Before the advent of levodopa therapy, neurosurgery for Parkinson's disease was commonplace. The globus pallidus and thalamus were favoured targets for chemical or thermal lesions. Pallidotomy and thalamotomy often improved rigidity and tremor, but they produced little consistent beneficial effect upon akinesia. With the arrival of levodopa therapy, which has a profound effect upon akinesia, the surgical treatment of Parkinson's disease underwent progressive decline. However, it soon became clear that long-term use of levodopa was associated with a number of side-effects such as dyskinesias, 'wearing-off', and the 'on–off' phenomenon. More recent advances in understanding the pathophysiology of movement disorders, and in particular Parkinson's disease, have stimulated a renaissance in the use of neurosurgery to treat movement disorders.

Lesioning the subthalamic nucleus in experimental primates that had been made parkinsonian with the neurotoxin MPTP dramatically alleviated the parkinsonian symptoms, suggesting that the subthalamic nucleus might be an appropriate clinical target. While therapeutic surgical lesions of the subthalamic nucleus can alleviate tremor, rigidity and bradykinesia in patients with Parkinson's disease, the risk of side-effects is not trivial: the subthalamic nucleus is a small structure wrapped by fibres of passage and close to the hypothalamus and internal capsule. Perhaps not surprisingly, relatively few centres perform this procedure.

In 1992, Laitinen et al reintroduced pallidotomy for the treatment of end-stage Parkinson’s disease, but confined the lesions to the posteroventral part of the medial pallidal segment. These lesions were found to be extremely reliable in abolishing contralateral rigidity and drug-induced dyskinesias, with slightly less efficacy on tremor and bradykinesia.

Implantation of deep-brain electrodes through which high-frequency pulses generated by a pacemaker could inhibit cells in the vicinity has been a concept since the early 1970s, but did not become a widespread reality until the late 1980s, as a result of technological advances. The introduction of the technique of deep brain stimulation (DBS), which avoids making permanent lesions, made bilateral surgery safer. There have been numerous reports of the effectiveness of both bilateral pallidal and subthalamic nucleus stimulation (Figs 22.15, 22.16). Subthalamic nucleus stimulation is favoured by most groups because, unlike pallidal stimulation, it allows patients to reduce their anti-parkinsonian medication.

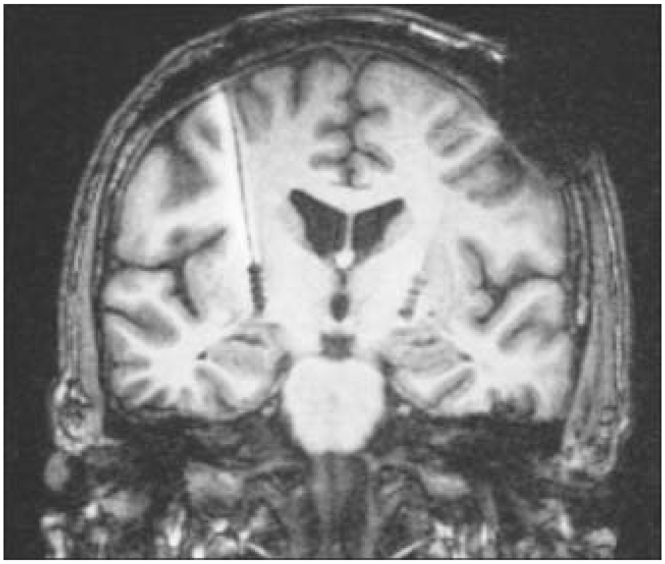

Fig. 22.15 MRI image showing placement of deep brain stimulating electrodes bilaterally in the globus pallidus of a patient with Parkinson’s disease.

(By courtesy of Professor TZ Aziz, Radcliffe Infirmary, Oxford and Charing Cross Hospital, London, UK.)

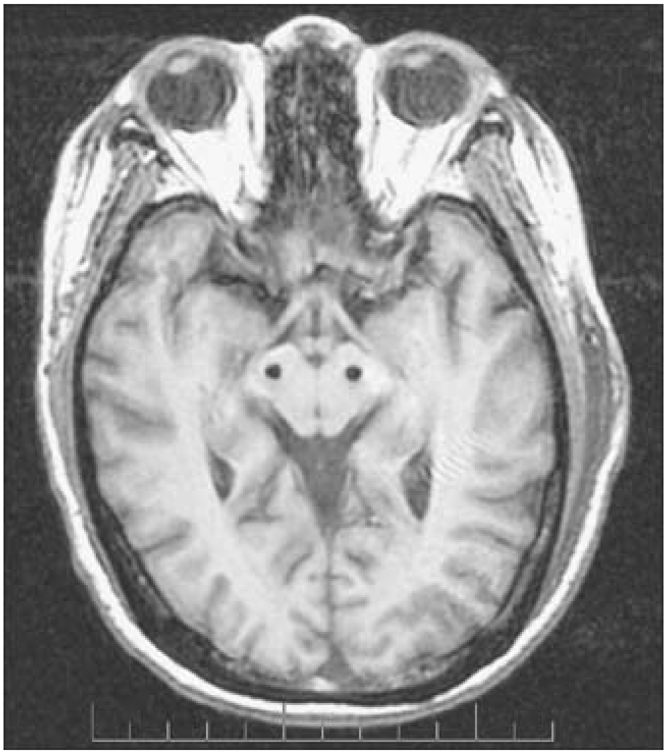

Fig. 22.16 MRI image showing placement of deep brain stimulating electrodes bilaterally in the subthalamic nucleus of a patient with Parkinson's disease.

(By courtesy of Professor AM Lozano, Toronto Western Hospital, Toronto, Canada.)

Serendipity also has a role in such surgery. Clinically, parkinsonian patients can develop painful dystonic posturing of their limbs which responds dramatically to bilateral pallidal stimulation. This has led to preliminary studies of bilateral pallidal stimulation for dystonia with very promising results. Since it is held that in dystonia the pallidal neurones fire at rates below normal, this presents quite a puzzle as it is open to question how stimulation works. It also would appear that the neural mechanism that underlies this therapeutic effect on dystonia may differ from that in Parkinson's disease and tremor, because in dystonia the improvement may take weeks to emerge, whereas it is immediate in the case of Parkinson’s disease.

An even more recent neurosurgical development in the therapy of Parkinson’s disease has involved targeting the pedunculopontine nucleus (nucleus tegmenti pedunculopontinus; PPN). The PPN corresponds approximately to the so-called ‘mesencephalic locomotor region’: stimulation of this region in animals elicits locomotion. The PPN is maximal at the boundary between midbrain and pons, and is bounded laterally by the medial leminiscus and medially by the superior cerebellar peduncle and its decussation. Dorsally it is bounded by the pontine cuneiform and subcuneiform nuclei and ventrally by the pontine reticular formation. Its most caudal pole is adjacent to the locus coeruleus.

The PPN has a caudal pars compacta that consists largely of cholinergic neurones and a rostral pars dissipata that consists largely of glutamatergic neurones. It is known to receive GABAergic efferent fibres from the globus pallidus and substantia nigra. In animal models of Parkinson’s disease these projections are overactive and the PPN is inhibited. Taken in conjunction with other experimental evidence, this suggests the possibility that the PPN is involved in the pathophysiology of disturbances of locomotion, gait and posture in Parkinson’s disease. Recently, DBS of PPN through implanted electrodes has been applied in drug-resistant akinetic parkinsonian patients (Fig. 22.17). Low frequency stimulation alleviates postural instability and on-medication gait freezing, symptoms which conventional medication and surgery fail to improve.

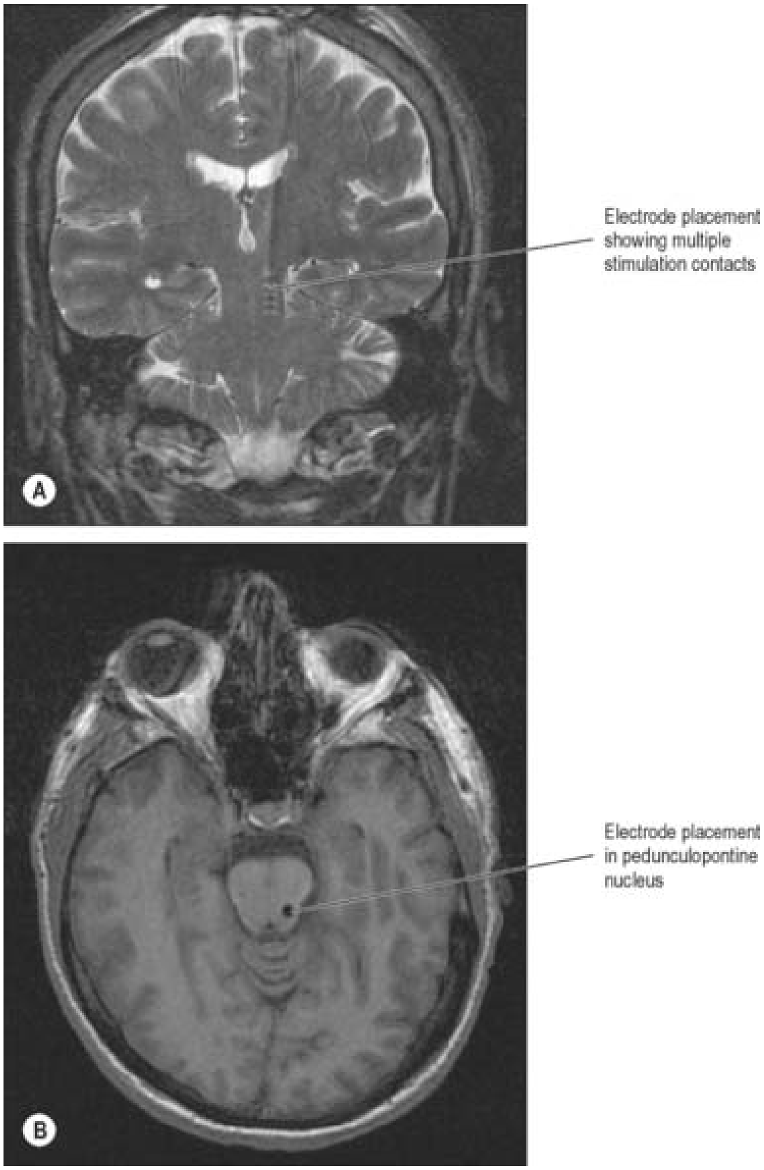
Electrode placement showing multiple stimulation contacts
A
Electrode placement in pedunculopontine nucleus
B

Fig. 22.17 MRI images showing placement of deep brain stimulating electrodes in the pedunculopontine nucleus of a patient with Parkinson's disease. (**A**) Coronal view; (**B**) Axial view.

(By courtesy of Professor AM Lozano, Toronto Western Hospital, Toronto, Canada.)

REFERENCES

exander GE, DeLong MR, Strick PL. Parallel organization of functionally segregated circuits linking basal ganglia and cortex. *Ann Rev Neurosci*. 1986;9:357-382.

A landmark publication setting out a conceptual framework for the way in which the basal ganglia and cerebral cortex process different types of information through largely distinct parallel circuits based upon known anatomical connectivity..

ossman AR. A hypothesis on the pathophysiological mechanisms that underlie levodopa- or dopamine agonist-induced dyskinesia in Parkinson’s disease: implications for future strategies in treatment. *Mov Disord*. 1990;5:100-108.

llett M. Pathophysiology of dystonia. *Neural Transm Suppl*. 2006;70:485-488.

ack P, Batir A, Van Blercom N, et al. Five-year follow-up of bilateral stimulation of the subthalamic nucleus in advanced Parkinson’s disease. *N Engl J Med*. 2003;349:1925-1934.

Reviews the long-term outcome of deep brain stimulation of the subthalamic nucleus in Parkinson’s disease..

itinen LV, Bergenheim AT, Hariz MI. Ventroposterolateral pallidotomy can abolish all Parkinsonian symptoms. *Stereotact Funct Neurosurg*. 1992;58:14-21.

A key paper which ignited widespread interest in functional neurosurgery for Parkinson’s disease..

nney JBJr, Young AB. Striatal inhomogeneities and basal ganglia function. *Mov Disord*. 1986;1:3-15.

A landmark publication, introducing some of the basic concepts behind current models of the pathophysiology of Parkinson’s disease and Huntington’s disease..

CHAPTER 23

Cerebral hemisphere

The two cerebral hemispheres are the largest major divisions of the brain. Each hemisphere consists of an external highly-convoluted cortex, beneath which lies an extensive internal mass of white matter that partly encloses the basal ganglia. Each hemisphere also contains a lateral ventricle that is continuous with the third ventricle through the interventricular foramen. The two hemispheres are linked by the commissural fibres of the corpus callosum.

The cerebral hemisphere contains primary motor and sensory cortical areas. These represent the highest level at which motor activities are controlled and the highest level to which general and special sensory systems project, providing the neural substrate for conscious experience of sensory stimuli. Association areas are modality-specific and also multimodal, and they enable complex analysis of the internal and external environment and the relationship of the individual to the external world. Parts of the hemisphere, termed the limbic system, have an ancient lineage. They are concerned with memory and the emotional aspects of behaviour, and provide an affective overtone to conscious experience as well as interfacing with subcortical areas, such as the hypothalamus, through which widespread physiological activities are integrated. Other cortical areas, primarily within the frontal region, are concerned with the highest aspects of cognitive function, and contribute to personality, foresight and planning.

The cerebral hemispheres are separated by a deep median cleft, the great longitudinal fissure, which contains a crescent-shaped fold of the dura mater, the falx cerebri (see Ch. 27).

Each cerebral hemisphere may be considered to have superolateral, medial and inferior (basal) surfaces or aspects. The superolateral surface follows the concavity of the cranial vault. The medial surface is flat and vertical, separated from the opposite hemisphere by the great longitudinal fissure and falx cerebri. The inferior surface is irregular and divided into orbital and tentorial regions. The orbital part is concave and lies above the orbital and nasal roofs. The tentorial part lies in the middle cranial fossa; posteriorly it lies above the tentorium cerebelli, which separates it from the superior surface of the cerebellum.

GYRI, SULCI AND LOBES

The surface of the cerebral hemisphere shows a complex pattern of convolutions, or gyri, which are separated by furrows of varying depth known as fissures, or sulci (Fig. 23.1, Fig. 23.2). Some of these are consistently located, others less so. They provide part of the basis for the division of the hemisphere into lobes. The frontal, parietal, temporal and occipital lobes approximately correspond in surface extent to the overlying cranial bones from which they take their names. The anterior and posterior extremities of the hemispheres form the frontal and occipital poles respectively, and the temporal pole is the anterior extremity of the temporal lobe.

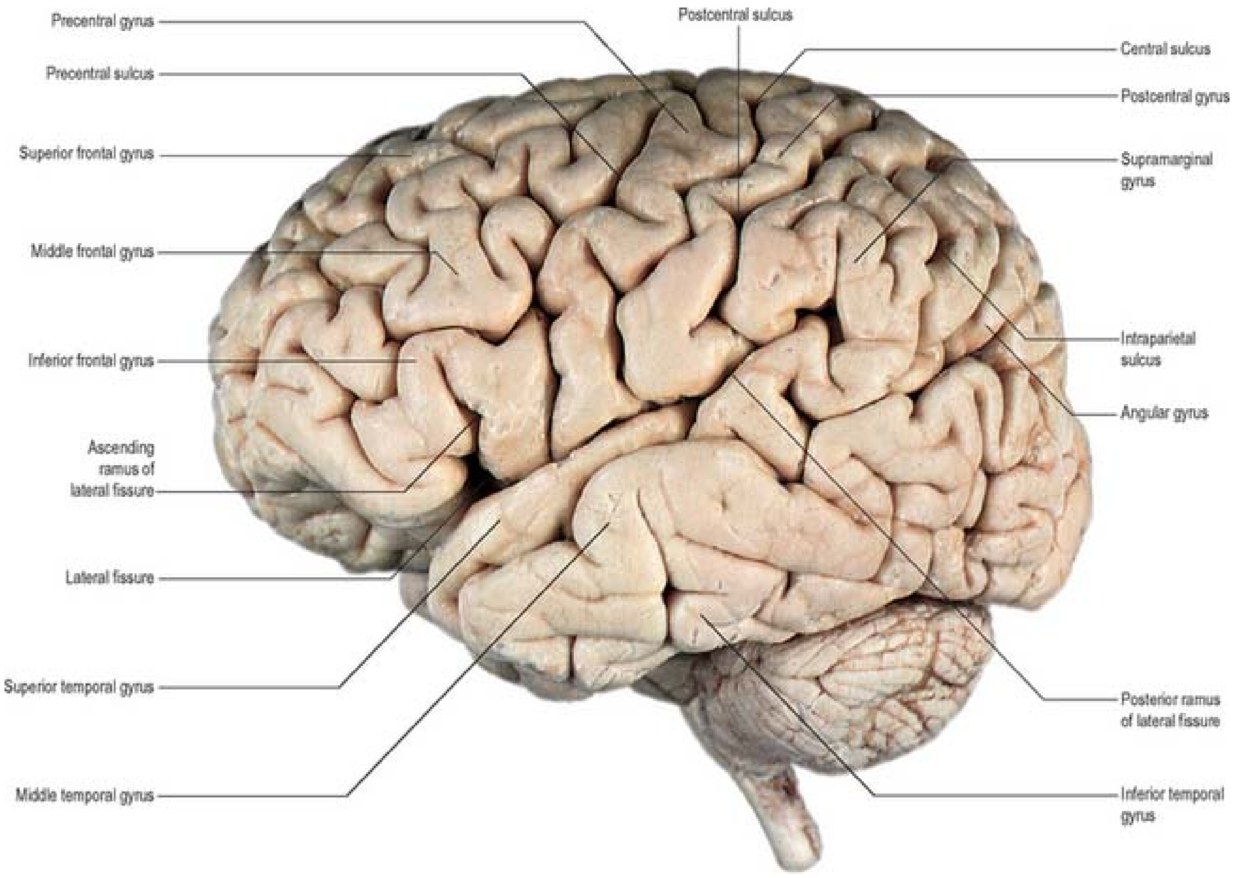
Precentral gyrus
Postcentral sulcus
Central sulcus
Precentral sulcus
Postcentral gyrus
Superior frontal gyrus
Supramarginal gyrus
Middle frontal gyrus
Intraparietal sulcus
Inferior frontal gyrus
Angular gyrus
Ascending ramus of lateral fissure
Lateral fissure
Superior temporal gyrus
Posterior ramus of lateral fissure
Middle temporal gyrus
Inferior temporal gyrus

Fig. 23.1 Lateral aspect of the left cerebral hemisphere indicating the major gyri and sulci.

(Dissection by EL Rees; photograph by Kevin Fitzpatrick on behalf of GKT School of Medicine, London; figure enhanced by B. Crossman.)

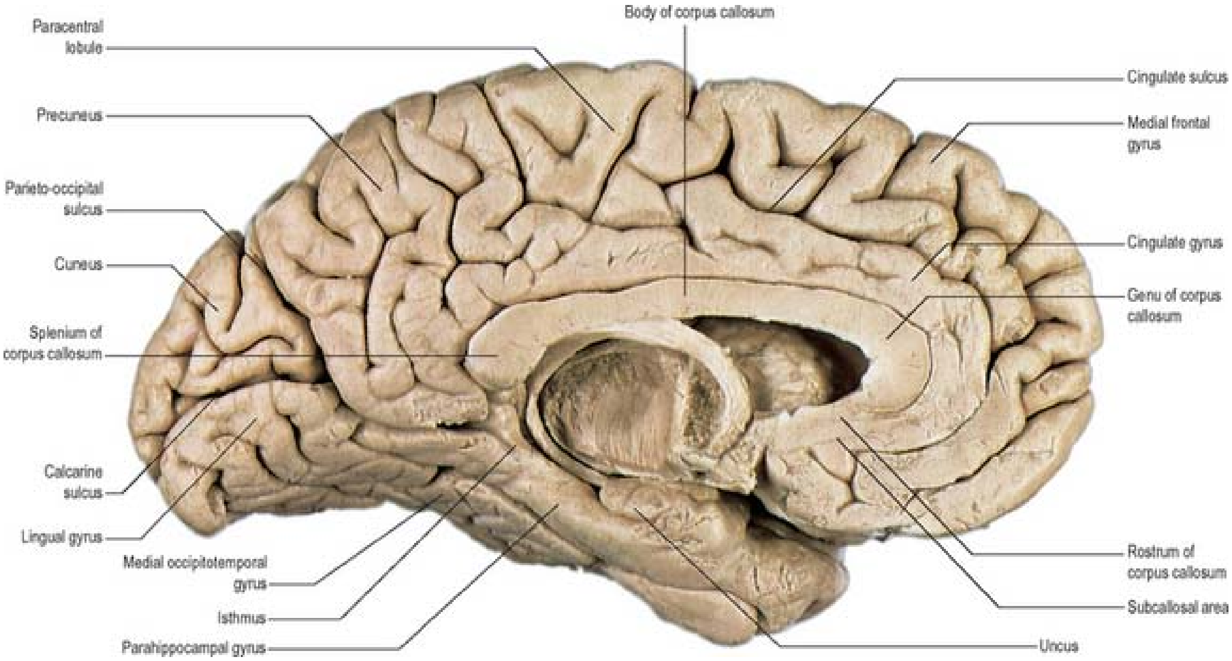
Paracentral lobule
Precuneus
Parieto-occipital sulcus
Cuneus
Splenium of corpus callosum
Calcarine sulcus
Lingual gyrus
Medial occipitotemporal gyrus
Isthmus
Parahippocampal gyrus
Body of corpus callosum
Cingulate sulcus
Medial frontal gyrus
Cingulate gyrus
Genu of corpus callosum
Rostrum of corpus callosum
Subcallosal area
Uncus

Fig. 23.2 Sagittal section of the brain, with the brain stem removed, showing the major gyri and sulci on the medial aspect of the left cerebral hemisphere.

(Photograph by Kevin Fitzpatrick on behalf of GKT School of Medicine, London; figure enhanced by B. Crossman.)

The insula is a cortical region hidden within the depths of the lateral fissure by overhanging parts (opercula) of the frontal, parietal and temporal lobes. A complex of gyri on the medial aspect of the hemisphere makes up the limbic lobe.

The area of the adult cerebral cortex is approximately 2200 cm^2: its convoluted form increases the cortical volume to three times greater than it would be if the surface were smooth.

Two prominent furrows, the lateral (Sylvian) fissure and the central sulcus, are the main features on the superolateral cerebral surface, and they determine its surface divisions.

The lateral fissure is a deep cleft on the lateral and inferior surfaces. It separates the frontal and parietal lobes above from the temporal lobe below and accommodates the middle cerebral vessels. It commences inferiorly at the anterior perforated substance, extending laterally between the orbital surface of the frontal lobe and the anterior pole of the temporal lobe and accommodating the sphenoparietal venous sinus. Reaching the lateral surface of the hemisphere it gives rise to an ascending ramus which runs into the inferior frontal gyrus. The larger posterior ramus runs posteriorly and slightly upwards, across the lateral surface of the hemisphere to end in the parietal lobe. The insula lies in the depths of the lateral fissure.

The central sulcus is the boundary between the frontal and parietal lobes and demarcates the primary motor and somatosensory areas of the cortex, located in the precentral and postcentral gyri, respectively. It starts in or near the superomedial border of the hemisphere, a little behind the midpoint between the frontal and occipital poles. It runs sinuously downwards and forwards to end a little above the posterior ramus of the lateral sulcus.

The superior frontal gyrus, above the superior frontal sulcus, is continuous over the superomedial margin with the medial frontal gyrus and may be incompletely divided. The middle frontal gyrus lies between the superior and inferior frontal sulci. The inferior frontal gyrus lies below the inferior frontal sulcus which is invaded by the ascending ramus of the lateral fissure. In the left hemisphere, the cortical areas around this ramus make up the motor speech area (Broca’s area; areas 44 and 45).

The medial cerebral surface lies within the great longitudinal fissure. The commissural fibres of the corpus callosum lie in the depths of the fissure: the curved anterior part of the corpus callosum, the genu, is continuous below with the rostrum and narrows rapidly as it passes back to the upper end of the lamina terminalis. The cortex immediately below the rostrum is the subcallosal area (parolfactory gyrus). The genu of the corpus callosum continues above into the trunk or body, which arches up and back to a thick, rounded posterior extremity, the splenium. The bilateral vertical laminae of the septum pellucidum are attached to the concave surfaces of the trunk, genu and rostrum, occupying the interval between them and the fornix.

The anterior region of the medial surface of the hemisphere is divided into outer and inner zones by the curved cingulate sulcus, which starts below the rostrum and passes first forwards, then up and finally backwards, conforming to the callosal curvature. Its posterior end turns up to the superomedial margin of the hemisphere approximately 4 cm behind its midpoint, and is posterior to the upper end of the central sulcus. The outer zone, except for its posterior extremity, is part of the frontal lobe, and is subdivided into anterior and posterior areas by a short sulcus, which ascends from the cingulate sulcus above the midpoint of the corpus callosum. The larger anterior area is the medial frontal gyrus; the posterior is the paracentral lobule. The superior end of the central sulcus usually invades the paracentral lobule posteriorly and the precentral gyrus is continuous with the lobule. This area is concerned with movements of the contralateral lower limb and perineal region – clinical evidence suggests that it exercises voluntary control over defaecation and micturition.

The zone under the cingulate sulcus is the cingulate gyrus. Starting below the rostrum, this gyrus follows the callosal curve, separated by the callosal sulcus. It continues round the splenium to the inferior surface, and then into the parahippocampal gyrus, through the narrow isthmus.

The posterior region of the medial surface is traversed by the parieto-occipital and the calcarine sulci. These two deep sulci converge anteriorly to meet a little posterior to the splenium. The parieto-occipital sulcus marks the boundary between parietal and occipital lobes. It starts on the superomedial margin of the hemisphere approximately 5 cm anterior to the occipital pole, sloping down and slightly forwards to the calcarine sulcus. The calcarine sulcus starts near the occipital pole. Though usually restricted to the medial surface, its posterior end may reach the lateral surface. Directed anteriorly, it joins the parieto-occipital sulcus at an acute angle behind the splenium. Continuing forwards, it crosses the inferomedial margin of the hemisphere, and forms the inferior boundary of the isthmus, which connects the cingulate with the parahippocampal gyrus. The visual cortex lies above and below the posterior part of the calcarine sulcus, behind the junction with the parieto-occipital. The calcarine sulcus is deep and produces an elevation, the calcar avis, in the wall of the posterior horn of the lateral ventricle.

The area posterior to the upturned end of the cingulate sulcus, and anterior to the parieto-occipital sulcus, is the precuneus. It forms the medial surface of the parietal lobe with the part of the paracentral lobule behind the central sulcus. The medial surface of the occipital lobe is formed by the cuneus, a wedge of cortex bounded in front by the parieto-occipital sulcus, below by the calcarine sulcus, and above by the superomedial margin.

The inferior cerebral surface is divided by the stem of the lateral fissure into a small anterior and larger posterior part (Fig. 23.3, Fig. 23.4). The anterior part constitutes the orbital region of the frontal lobe. It is concave and lies above the cribriform plate of the ethmoid, the orbital plate of the frontal, and the lesser wing of the sphenoid bone. A rostrocaudal olfactory sulcus traverses it near its medial margin, overlapped by the olfactory bulb and tract. The medial strip thus demarked is the gyrus rectus. The rest of this surface bears irregular orbital sulci, generally H-shaped, which divide it into the anterior, medial, posterior and lateral orbital gyri.

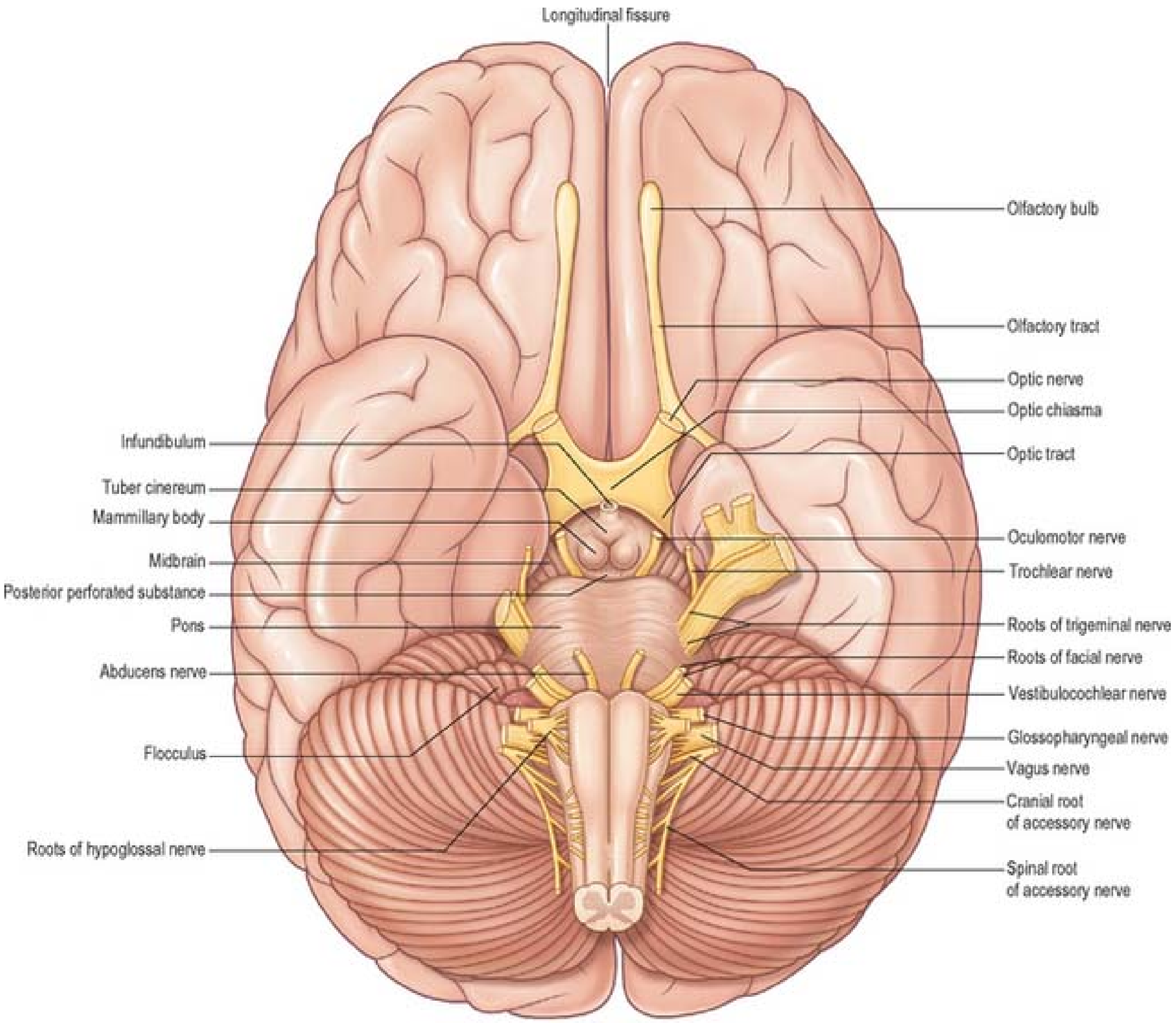
Longitudinal fissure
Olfactory bulb
Olfactory tract
Optic nerve
Optic chiasma
Optic tract
Infundibulum
Tuber cinereum
Mammillary body
Midbrain
Posterior perforated substance
Pons
Abducens nerve
Flocculus
Roots of hypoglossal nerve
Oculomotor nerve
Trochlear nerve
Roots of trigeminal nerve
Roots of facial nerve
Vestibulocochlear nerve
Glossopharyngeal nerve
Vagus nerve
Cranial root of accessory nerve
Spinal root of accessory nerve

Fig. 23.3 Basal aspect of the brain.

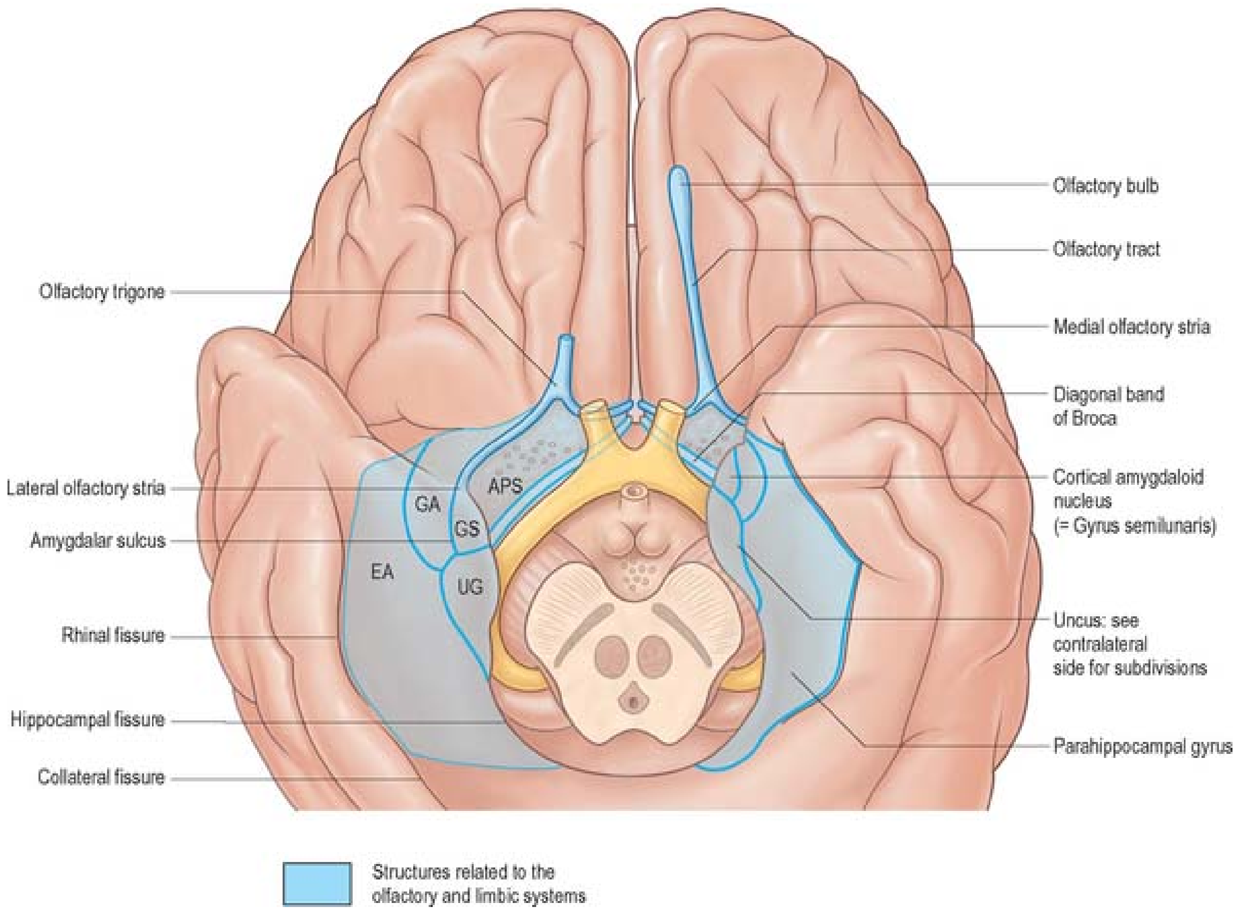
Olfactory bulb
Olfactory tract
Olfactory trigone
Medial olfactory stria
Diagonal band of Broca
Lateral olfactory stria
APS
GA
GS
Cortical amygdaloid nucleus (= Gyrus semilunaris)
Amygdalar sulcus
EA
UG
Uncus: see contralateral side for subdivisions
Rhinal fissure
Hippocampal fissure
Parahippocampal gyrus
Collateral fissure
Structures related to the olfactory and limbic systems

Fig. 23.4 Inferior aspect of the brain with the brain stem removed. The right temporal pole has been displaced laterally to expose underlying structures related to the olfactory and limbic systems. APS, anterior perforated substance; EA, entorhinal area; GA, gyrus ambiens; GS, gyrus semilunaris; UG, uncinate gyrus.

The larger, posterior region of the inferior cerebral surface is partly superior to the tentorium but also to the middle cranial fossa. The collateral sulcus starts near the occipital pole, and extends anteriorly and parallel to the calcarine sulcus, separated from it by the lingual gyrus. The lingual gyrus, between the calcarine and collateral sulci, passes into the parahippocampal gyrus, which begins at the isthmus where it is continuous with the cingulate gyrus. Anteriorly, the parahippocampal gyrus continues into the hook-shaped uncus, which lies lateral to the midbrain and posterolateral to the anterior perforated substance. The uncus is part of the piriform cortex of the olfactory system, phylogenetically one of the oldest parts of the cortex, and is separated from the temporal pole by the rhinal sulcus (fissure) which marks the lateral limit of the entorhinal cortex (area) (Fig. 23.4).

The occipitotemporal sulcus is parallel and lateral to the collateral sulcus, does not usually reach the occipital pole, and is frequently divided. The medial occipitotemporal gyrus extends from the occipital to the temporal pole and is limited medially by the collateral and rhinal sulci and laterally by the occipitotemporal sulcus. The lateral occipitotemporal gyrus is continuous, round the inferolateral margin of the hemisphere, with the inferior temporal gyrus.

CEREBRAL CORTEX

The cerebral cortex is sometimes described as consisting of a phylogenetically old allocortex, which includes archicortex and palaeocortex, and a newer neocortex. These distinctions are reflected in the organizational arrangement of neuronal elements in different regions.

MICROSTRUCTURE

The microscopic structure of the cerebral cortex is an intricate blend of nerve cells and fibres, neuroglia and blood vessels. The neocortex essentially consists of three neuronal cell types. Pyramidal cells are the most abundant. Non-pyramidal cells, also called stellate or granule cells are divided into spiny and non-spiny neurones. All types have been subdivided on the basis of size and shape (Fig. 23.5).

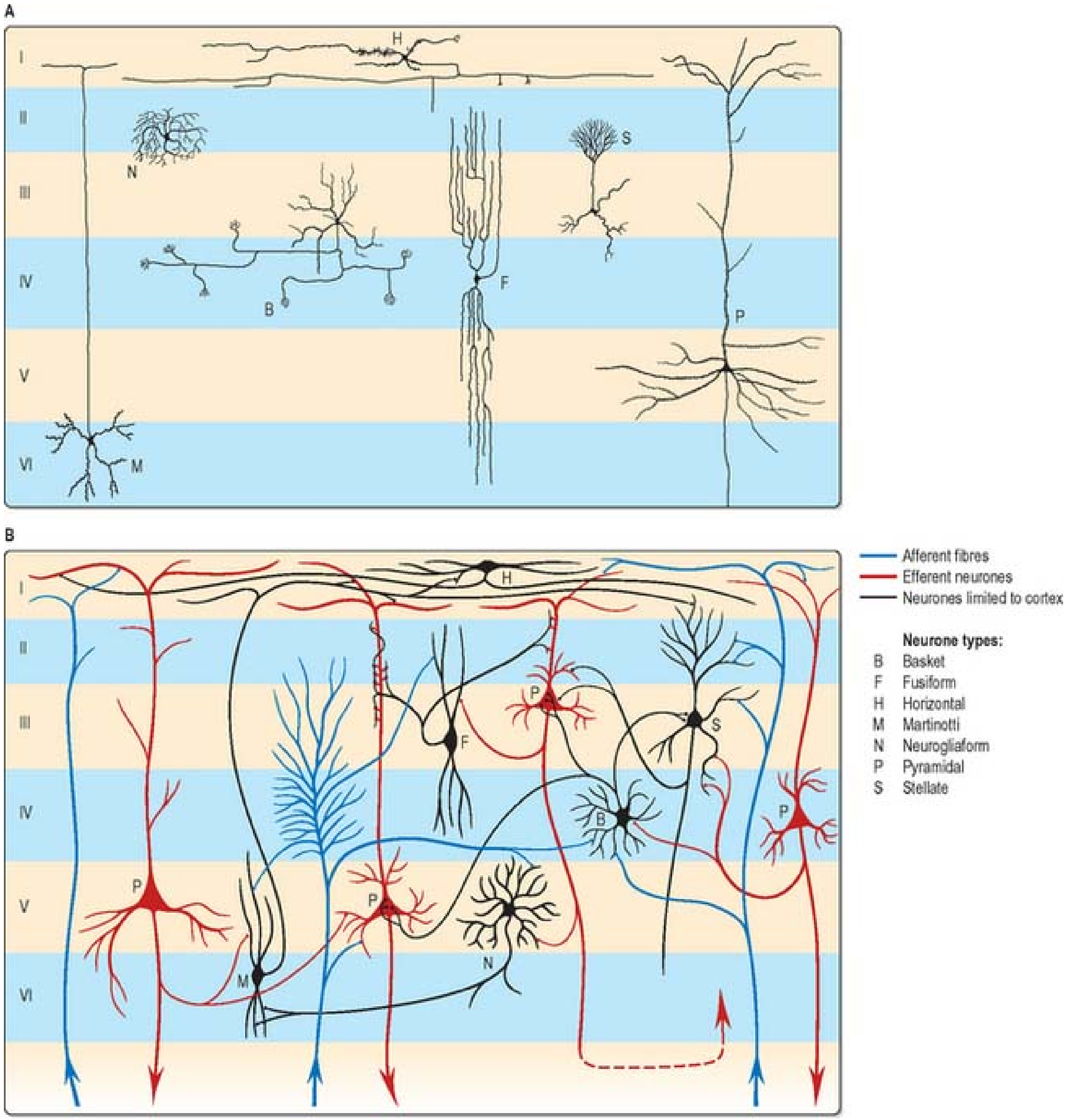
A
I
II
III
IV
V
VI
H
N
S
B
F
P
M
B
I
II
III
IV
V
VI
H
P
F
P
S
B
P
P
N
M
Afferent fibres
Efferent neurones
Neurones limited to cortex
Neurone types:
B Basket
F Fusiform
H Horizontal
M Martinotti
N Neurogliaform
P Pyramidal
S Stellate

Fig. 23.5 **A**, Characteristic neocortical neurones. From left to right are shown Martinotti, neurogliaform, basket, horizontal, fusiform, stellate and pyramidal types of neurone. **B**, The most frequent types of neocortical neurone, showing typical connections with each other and with afferent fibres. The right and left afferent fibres are association or corticocortical connections, the central afferent is a specific sensory fibre. Neurones are shown in their characteristic lamina, but many have somata in more than one layer.

Pyramidal cells have a flask-shaped or triangular cell body ranging from 10 to 80 µm in diameter. The soma gives rise to a single thick apical dendrite and multiple basal dendrites. The apical dendrite ascends towards the cortical surface, tapering and branching, to end in a spray of terminal twigs in the most superficial lamina, the molecular layer. From the basal surface of the cell body, dendrites spread more horizontally, for distances up to 1 mm for the largest pyramidal cells. Like the apical dendrite, the basal dendrites branch profusely along their length. All pyramidal cell dendrites are studded with a myriad of dendritic spines. These become more numerous as distance from the parent cell soma increases. A single slender axon arises from the axon hillock, which is usually situated centrally on the basal surface of the pyramidal neurone. Ultimately, in the vast majority of, if not in all, cases, the axon leaves the cortical grey matter to enter the white matter. Pyramidal cells are thus, perhaps universally, projection neurones. They use an excitatory amino acid, either glutamate or aspartate, as their neurotransmitter.

Spiny stellate cells are the second most numerous cell type in the neocortex and for the most part occupy lamina IV. They have relatively small multipolar cell bodies, commonly 6 to 10 µm in diameter. Several primary dendrites, profusely covered in spines, radiate for variable distances from the cell body. Their axons ramify within the grey matter predominantly in the vertical plane. Spiny stellate cells probably use glutamate as their neurotransmitter.

The smallest group comprises the heterogeneous non-spiny or sparsely spinous stellate cells. All are interneurones, and their axons are confined to grey matter. In morphological terms, this is not a single class of cell, but a multitude of different forms, including basket, chandelier, double bouquet, neurogliaform, bipolar/fusiform and horizontal cells. Various types may have horizontally, vertically or radially ramifying axons.

Neurones with mainly horizontally dispersed axons include basket and horizontal cells. Basket cells have a short, vertical axon, which rapidly divides into horizontal collaterals, and these end in large terminal sprays synapsing with the somata and proximal dendrites of pyramidal cells. The cell bodies of horizontal cells lie mainly at the superficial border of lamina II, occasionally deep in lamina I (the molecular or plexiform layer). They are small and fusiform, and their dendrites spread short distances in two opposite directions in lamina I. Their axons often stem from a dendrite, then divide into two branches, which travel away from each other for great distances in the same layer.

Neurones with an axonal arborization predominantly perpendicular to the pial surface include chandelier, double bouquet and bipolar/fusiform cells. Chandelier cells have a variable morphology, although most are ovoid or fusiform and their dendrites arise from the upper and lower poles of the cell body. The axonal arborization, which emerges from the cell body or a proximal dendrite, is characteristic and identifies these neurones. A few cells in the more superficial laminae (II and IIIa) have descending axons, deeper cells (laminae IIIc and IV) have ascending axons, and intermediate neurones (IIIb) often have both. The axons ramify close to the parent cell body and terminate in numerous vertically oriented strings, which run alongside the axon hillocks of pyramidal cells with which they synapse. Double bouquet (or bitufted) cells are found in laminae II and III and their axons traverse laminae II and V. Generally, these neurones have two or three main dendrites, which give rise to a superficial and deep dendritic tuft. A single axon arises usually from the oval or spindle-shaped cell soma and rapidly divides into an ascending and descending branch. These branches collateralize extensively, but the axonal arbor is confined to a perpendicularly extended, but horizontally confined, cylinder, approximately 50 to 80 μm across. Bipolar cells are ovoid with a single ascending and a single descending dendrite, which arise from the upper and lower poles, respectively. These primary dendrites branch sparsely and their branches run vertically to produce a narrow dendritic tree, rarely more than 10 μm across, which may extend through most of the cortical thickness. Commonly, the axon originates from one of the primary dendrites, and rapidly branches to give a vertically elongated, horizontally confined, axonal arbor, which closely parallels the dendritic tree in extent.

The principal recognizable neuronal type is the neurogliaform or spiderweb cell. These small spherical cells, 10 to 12 μm in diameter, are found mainly in laminae II to IV, depending on cortical area. Seven to ten thin dendrites typically radiate out from the cell soma, some branching once or twice to form a spherical dendritic field of approximately 100 to 150 μm diameter. The slender axon arises from the cell body or a proximal dendrite. Almost immediately, it branches profusely within the vicinity of the dendritic field (and usually somewhat beyond), to give a spherical axonal arbor up to 350 μm in diameter.

The majority of non-spiny or sparsely spinous non-pyramidal cells probably use GABA as their principal neurotransmitter. This is almost certainly the case for basket, chandelier, double bouquet, neurogliaform and bipolar cells. Some are also characterized by the coexistence of one or more neuropeptides, including neuropeptide Y, vasoactive intestinal polypeptide (VIP), cholecystokinin, somatostatin and substance P. Acetylcholine is present in a subpopulation of bipolar cells, which may additionally be GABAergic and contain VIP.

Laminar organization

The most apparent microscopical feature of the neocortex when it has been stained for cell bodies or for fibres is its horizontal lamination. The significance of this for understanding cortical functional organization is debatable, but the use of cytoarchitectonic description to identify regions of cortex is common.

Typical neocortex is described as having six layers or laminae lying parallel to the surface (Fig. 23.6).

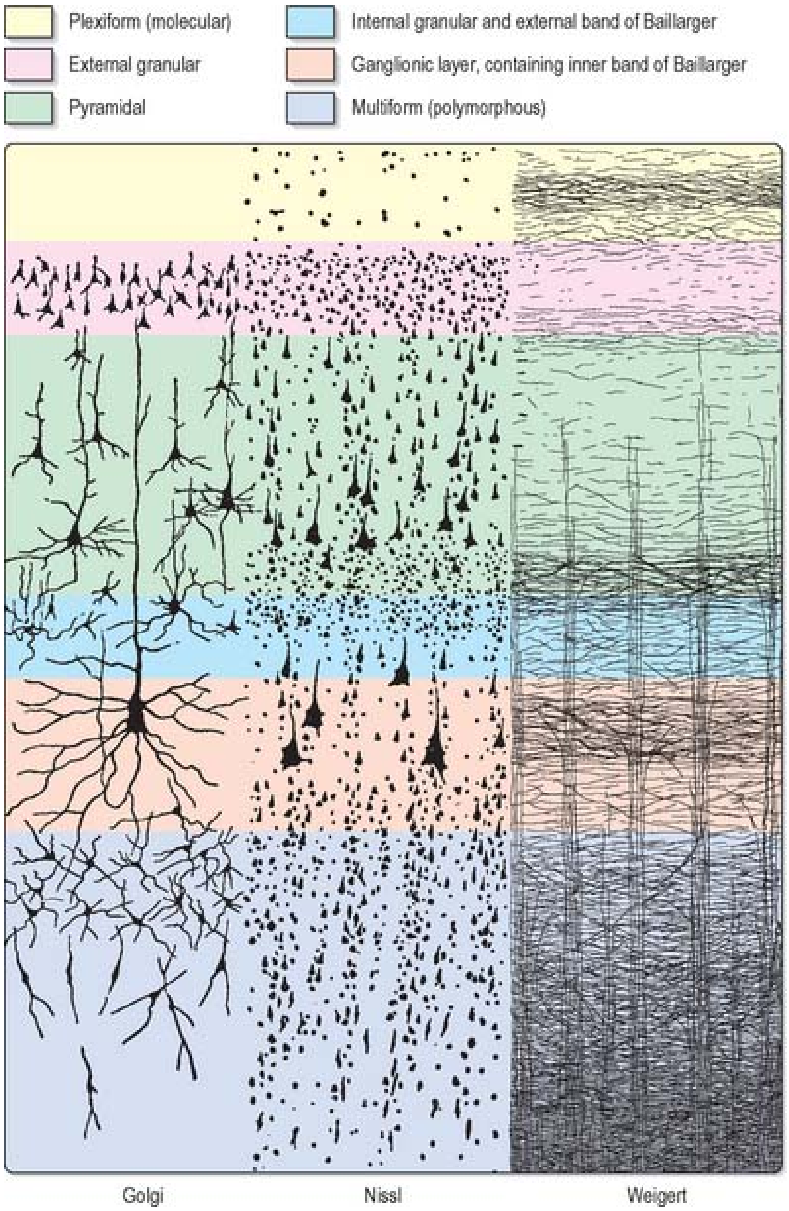
Plexiform (molecular)
External granular
Pyramidal
Internal granular and external band of Baillarger
Ganglionic layer, containing inner band of Baillarger
Multiform (polymorphous)
Golgi
Nissl
Weigert

Fig. 23.6 The layers of the cerebral cortex. The three vertical columns represent the disposition of cellular elements as revealed by the staining techniques of Golgi (impregnating whole neurones), Nissl (staining cell bodies) and Weigert (staining nerve fibres).

I The molecular or plexiform layer is cell sparse, containing only scattered horizontal cells and their processes enmeshed in a compacted mass of tangential, principally horizontal axons and dendrites. These are afferent fibres, which arise from outside the cortical area, together with intrinsic fibres from cortical interneurones, and the apical dendritic arbors of virtually all pyramidal neurones of the cerebral cortex. In histological sections stained to show myelin, layer I appears as a narrow horizontal band of fibres.

II The external granular lamina contains a varying density of small neuronal cell bodies including both small pyramidal and non-pyramidal cells; the latter may predominate. Myelin fibre stains show mainly vertically arranged processes traversing the layer.

III The external pyramidal lamina contains pyramidal cells of varying sizes, together with scattered non-pyramidal neurones. The size of the pyramidal cells is smallest in the most superficial part of the layer and greatest in the deepest part. This lamina is frequently further subdivided into IIIa, IIIb and IIIc, with IIIa most superficial and IIIc deepest. As in layer II, myelin stains reveal a mostly vertical organization of fibres.

IV The internal granular lamina is usually the narrowest of the cellular laminae. It contains densely packed, small, round cell bodies of non-pyramidal cells, notably spiny-stellate cells and some small pyramidal cells. Within the lamina, in myelin stained sections, a prominent band of horizontal fibres (outer band of Baillarger) is seen.

V The internal pyramidal (ganglionic) lamina typically contains the largest pyramidal cells in any cortical area, though actual sizes vary considerably from area to area. Scattered non-pyramidal cells are also present. In myelin stains, the lamina is traversed by ascending and descending vertical fibres, and also contains a prominent central band of horizontal fibres (inner band of Baillarger).

VI The multiform (or fusiform/pleiomorphic) layer consists of neurones with a variety of shapes, including recognizable pyramidal, spindle, ovoid and many other shaped somata. Typically, most cells are small to medium in size. This lamina blends gradually with the underlying white matter, and a clear demarcation of its deeper boundary is not always possible.

Five regional variations are described in neocortical structure (Fig. 23.7). While all are said to develop from the same six-layered pattern, two types, granular and agranular, are regarded as virtually lacking certain laminae, and are referred to as heterotypical. Homotypical variants, in which all six laminae are found, are called frontal, parietal and polar, names that link them with specific cortical regions in a somewhat misleading manner (e.g. the frontal type also occurs in parietal and temporal lobes).

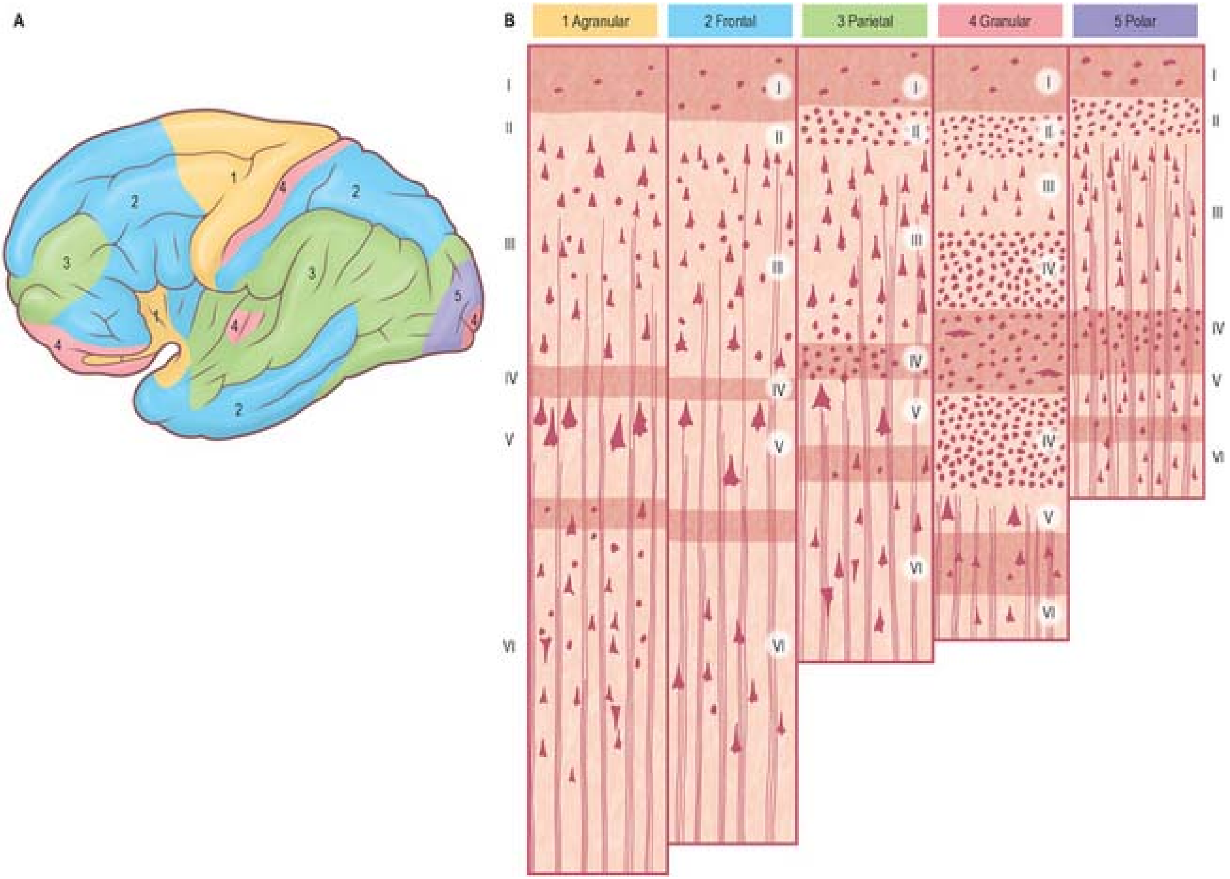

Fig. 23.7 The distribution and characteristics of the five major types of cerebral cortex.

The agranular type is considered to have diminished, or absent, granular laminae (II and IV), but always contains scattered stellate somata. Large pyramidal neurones are found in the greatest densities in agranular cortex, which is typified by the numerous efferent projections of pyramidal cell axons. Although it is often equated with motor cortical areas such as the precentral gyrus (area 4), agranular cortex also occurs elsewhere, e.g. areas 6, 8 and 44 and parts of the limbic system.

In the granular type of cortex the granular layers are maximally developed, and contain densely packed stellate cells, among which small pyramidal neurones are dispersed. Laminae III and IV are poorly developed or unidentifiable. This type of cortex is particularly associated with afferent projections. However, it does receive efferent fibres, derived from the scattered pyramidal cells, although they are less numerous than elsewhere. Granular cortex occurs in the postcentral gyrus (somatosensory area), striate area (visual area) and superior temporal gyrus (acoustic area), and in small areas of the parahippocampal gyrus. Despite its very high density of stellate cells, especially in the striate area, it is almost the thinnest of the five main types. In the striate cortex the external band of Baillarger (lamina IV) is well defined as the stria (white line) of Gennari.

The other three types of cortex are intermediate forms. In the frontal type, large numbers of small- and medium-sized pyramidal neurones appear in laminae III and V, and granular layers (II and IV) are less prominent. The relative prominence of these major forms of neurone vary reciprocally wherever this form of cortex exists.

The parietal type of cortex contains pyramidal cells, which are mostly smaller in size than in the frontal type. In marked contrast, the granular laminae are wider and contain more of the stellate cells: this kind of cortex occupies large areas in the parietal and temporal lobes. The polar type is classically identified with small areas near the frontal and occipital poles and is the thinnest form of cortex. All six laminae are represented, but the pyramidal layer (III) is reduced in thickness and not so extensively invaded by stellate cells as it is in the granular type of cortex. In both polar and granular types, the multiform layer (VI) is more highly organized than in other types.

It is customary to refer to some discrete cortical territories not only by their anatomical location in relation to gyri and sulci, but also in relation to their cytoarchitectonic characteristics (Brodmann’s areas) (Fig. 23.8). Some of the areas so defined, e.g. the primary sensory and motor cortices, have clear relevance in terms of anatomical connections and functional significance, others less so.

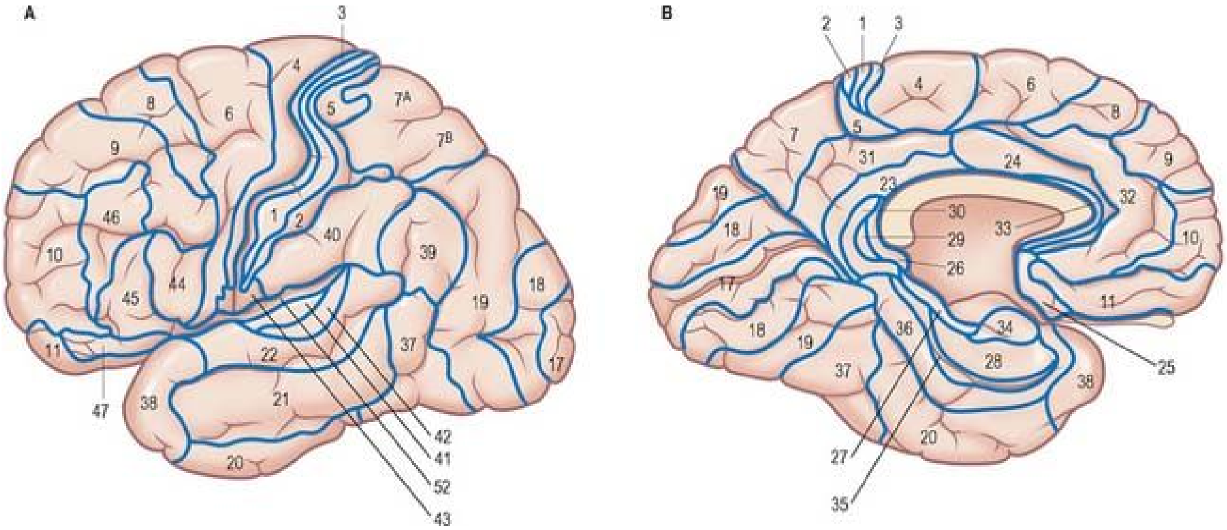
A
3
4
8
6
5
7A
7B
9
46
1
2
40
39
10
44
45
19
18
11
22
37
17
47
38
21
42
41
52
43
20
B
2
1
3
4
6
8
7
5
31
24
9
19
23
30
32
18
29
33
10
26
17
11
36
34
18
19
37
28
25
38
20
27
35

Fig. 23.8 The lateral (**A**) and medial (**B**) surfaces of the left cerebral hemisphere depicting Brodmann's areas.

OVERVIEW OF CORTICAL CONNECTIVITY

All neocortical areas have axonal connections with other cortical areas on the same side (association fibres), the opposite side (commissural fibres), and with subcortical structures (projection fibres).

The primary somatosensory, visual and auditory areas give rise to ipsilateral corticocortical connections to the association areas of the parietal, occipital and temporal lobes, respectively, which then progressively project towards the medial temporal limbic areas, notably the parahippocampal gyrus, entorhinal cortex and hippocampus. Thus, the first (primary) somatic sensory area (SI) projects to the superior parietal cortex (Brodmann’s area 5), which in turn projects to the inferior parietal cortex (area 7). From here connections pass to cortex in the walls of the superior temporal sulcus, and so on to the posterior parahippocampal gyrus, and on into limbic cortex. Similarly, for the visual system, the primary visual cortex (area 17) projects to the parastriate cortex (area 18), which in turn projects to the peristriate region (area 19). Information then flows to inferotemporal cortex (area 20), to cortex in the walls of the superior temporal sulcus, then to medial temporal cortex in the posterior parahippocampal gyrus, and so to limbic areas. The auditory system shows a similar progression from primary auditory cortex to temporal association cortex and so to the medial temporal lobe.

In addition to this stepwise outward progression from sensory areas through posterior association cortex, connections also occur at each stage with parts of the frontal cortex. Thus, taking the somatic sensory system as an example, primary somatic sensory cortex (SI) in the postcentral gyrus is reciprocally connected with the primary motor cortex (area 4) in the precentral gyrus. The next step in the outward progression, the superior parietal lobule (area 5), is interconnected with the premotor cortex (area 6), and this in turn is connected with area 7 in the inferior parietal lobule. This has reciprocal connections with prefrontal association cortex on the lateral surface of the hemisphere (areas 9 and 46), and temporal association areas, which connect with more anterior prefrontal association areas, and, ultimately in the sequence, with orbitofrontal cortex. Similar stepwise links exist between areas on the visual and auditory association pathways in the occipitotemporal lobe and areas of the frontal association cortex. The connections between sensory and association areas are reciprocal.

All neocortical areas are connected with subcortical regions although their density varies between areas. First among these are connections with the thalamus. All areas of the neocortex receive afferents from more than one thalamic nucleus, and all such connections are reciprocal. The vast majority of, if not all, cortical areas project to the striatum, tectum, pons and brain stem reticular formation. Additionally, all cortical areas are reciprocally connected with the claustrum; the frontal cortex connects with the anterior part and the occipital lobe with the posterior part.

All cortical areas receive topographically organized cholinergic projections from the basal forebrain, noradrenergic fibres from the locus coeruleus, serotoninergic fibres from the midbrain raphe nuclei, dopaminergic fibres from the ventral midbrain and histaminergic fibres from the posterior hypothalamus.

Different cortical areas have widely different afferent and efferent connections. Some have connections that are unique, e.g. the corticospinal tract arises from pyramidal cells in a restricted area around the central sulcus.

Widely separated, but functionally interconnected, areas of cortex share common patterns of connections with subcortical nuclei, and within the neocortex. For example, contiguous zones of the striatum, thalamus, claustrum, cholinergic basal forebrain, superior colliculus and pontine nuclei connect with anatomically widely separated areas in the prefrontal and parietal cortex, which are themselves interconnected. In contrast, other functionally distinct cortical regions, e.g. areas in the temporal and parietal cortex, do not share such contiguity in their subcortical connections.

Cortical lamination and cortical connections

The cortical laminae represent, to some extent, horizontal aggregations of neurones with common connections. This is most clearly seen in the lamination of cortical efferent (pyramidal) cells. The internal pyramidal lamina, layer V, gives rise to cortical projection fibres, most notably corticostriate, corticobulbar (including corticopontine) and corticospinal axons. In addition, a significant proportion of feedback corticocortical axons arise from cells in this layer, as do some corticothalamic fibres. Layer VI, the multiform lamina, is the major source of corticothalamic fibres. Supragranular pyramidal cells, predominantly layer III, but also lamina II, give rise primarily to both association and commissural corticocortical pathways. Generally, short corticocortical fibres arise more superficially, and long corticocortical (both association and commissural) axons come from cells in the deeper parts of layer III. Major afferents to a cortical area tend to terminate in layers I, IV and VI. Quantitatively lesser projections end either in the intervening laminae II/III and V, or sparsely throughout the depth of the cortex. Numerically, the largest input to a cortical area tends to terminate mainly in layer IV. This pattern of termination is seen in the major thalamic input to visual and somatic sensory cortex. In general, non-thalamic subcortical afferents to the neocortex, which are shared by widespread areas, tend to terminate throughout all cortical layers, but the laminar pattern of their endings still varies considerably from area to area.

Columns and modules

Experimental physiological and connectional studies have demonstrated an internal organization of the cortex, which is at right angles to the pial surface, with vertical columns or modules running through the depth of the cortex. The term ‘column’ refers to the observation that all cells encountered by a microelectrode penetrating and passing perpendicularly through the cortex respond to a single peripheral stimulus, a phenomenon first identified in the somatosensory cortex. In the visual cortex, narrow (50 µm) vertical strips of neurones respond to a bar stimulus of the same orientation (orientation columns) and wider strips (500 µm) respond preferentially to stimuli detected by one eye (ocular dominance columns). Adjacent orientation columns aggregate within an ocular dominance column to form a hypercolumn, responding to all orientations of stimulus for both eyes for one point in the visual field. Similar functional columnar organization has been described in widespread areas of neocortex, including motor cortex and association areas.

FRONTAL LOBE

The frontal lobe is the rostral region of the hemisphere, anterior to the central sulcus and above the lateral fissure. The precentral gyrus runs parallel to the central sulcus on the superolateral surface and extends onto the medial surface, and is limited anteriorly by the precentral sulcus. The area of the frontal lobe anterior to the precentral sulcus is divided into the superior, middle and inferior frontal gyri (Fig. 23.1). The frontal pole lies in front of these gyri. The ventral surface of the frontal lobe, the orbitofrontal cortex, overlies the bony orbit. The medial surface extends from the frontal pole to the paracentral lobule and consists of the medial frontal cortex and the anterior cingulate cortex.

Primary motor cortex

The primary motor cortex (MI) corresponds to the precentral gyrus (area 4), and is the area of cortex with the lowest threshold for eliciting contralateral muscle contraction by electrical stimulation. It contains a detailed topographically organized map (motor homunculus) of the opposite body half, with the head represented most laterally, and the leg and foot represented on the medial surface of the hemisphere in the paracentral lobule (Fig. 23.9). A striking feature is the disproportionate representation of body parts in relation to their physical size: large areas represent the muscles of the face and hand, which are capable of finely controlled or fractionated movements.

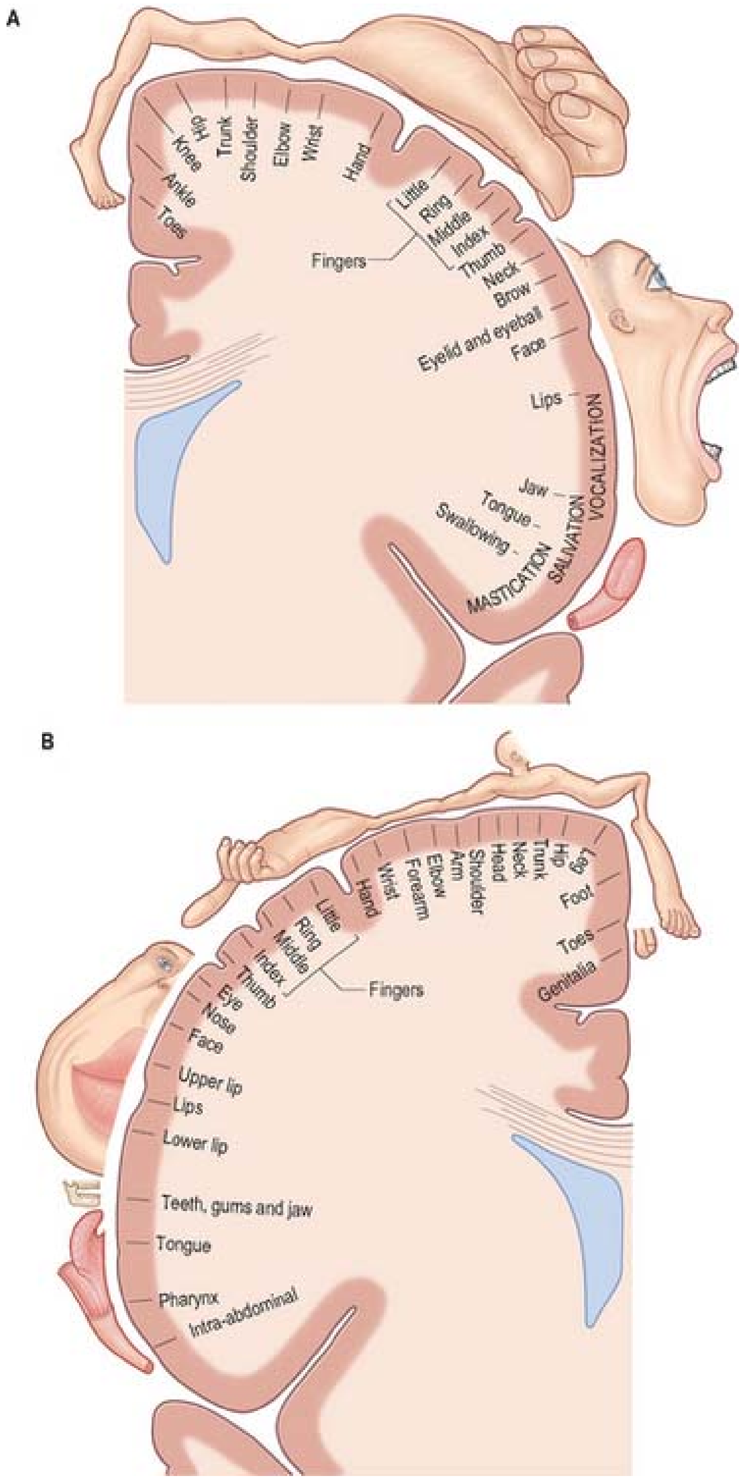
A
Toes
Ankle
Knee
Hip
Trunk
Shoulder
Elbow
Wrist
Hand
Little
Ring
Middle
Index
Thumb
Fingers
Neck
Brow
Eyelid and eyeball
Face
Lips
Jaw
Tongue
Swallowing
MASTICATION
SALIVATION
VOCALIZATION
B
Leg
Hip
Trunk
Neck
Head
Shoulder
Arm
Elbow
Forearm
Wrist
Hand
Little
Ring
Middle
Index
Thumb
Fingers
Eye
Nose
Face
Upper lip
Lips
Lower lip
Teeth, gums and jaw
Tongue
Pharynx
Intra-abdominal
Foot
Toes
Genitalia

Fig. 23.9 **A**, The motor homunculus showing proportional somatotopical representation in the main motor area. **B**, The sensory homunculus showing proportional somatotopical representation in the somaesthetic cortex.

The cortex of area 4 is agranular, and layers II and IV are difficult to identify. The most characteristic feature is the presence in lamina V of some extremely large pyramidal cell bodies, Betz cells, which may approach 80 μm in diameter. These neurones project their axons into the corticospinal and corticobulbar tracts.

The major thalamic connections of area 4 are with the ventral posterolateral nucleus (VPL), which in turn receives afferents from the deep cerebellar nuclei. The VPL nucleus also contains a topographic representation of the contralateral body, which is preserved in its point-to-point projection to area 4, where it terminates largely in lamina IV. Other thalamic connections of area 4 are with the centromedian and parafascicular nuclei. These appear to provide the only route through which output from the basal ganglia, routed via the thalamus, reaches the primary motor cortex, since the projection of the internal segment of the globus pallidus to the ventrolateral nucleus of the thalamus is confined to the anterior division, and there is no overlap with cerebellothalamic territory. The anterior part of the ventrolateral nucleus projects to the premotor and supplementary motor areas of cortex with no projection to area 4.

The ipsilateral somatosensory cortex (SI) projects in a topographically organized way to area 4, and the connection is reciprocal. The projection to the motor cortex arises in areas 1 and 2, with little or no contribution from area 3b. Fibres from SI terminate in layers II and III of area 4, where they contact mainly pyramidal neurones. Evidence suggests that neurones activated monosynaptically by fibres from SI, as well as those activated polysynaptically, make contact with layer V pyramidal cells, including Betz cells, which give rise to corticospinal fibres. Movement-related neurones in the motor cortex which can be activated from SI tend to have a late onset of activity, mainly during the execution of movement. It has been suggested that this pathway plays a role primarily in making motor adjustments during a movement. Additional ipsilateral corticocortical fibres to area 4 from behind the central sulcus come from the second somatic sensory area (SII).

Neurones in area 4 are responsive to peripheral stimulation, and have receptive fields similar to those in the primary sensory cortex. Cells located posteriorly in the motor cortex have cutaneous receptive fields, whereas more anteriorly situated neurones respond to stimulation of deep tissues.

The motor cortex receives major frontal lobe association fibres from the premotor cortex and the supplementary motor area and also fibres from the insula. It is probable that these pathways modulate motor cortical activity in relation to the preparation, guidance and temporal organization of movements. Area 4 sends fibres to, and receives fibres from, its contralateral counterpart, and also projects to the contralateral supplementary motor cortex.

Apart from its contribution to the corticospinal tract, the motor cortex has diverse subcortical projections. The connections to the striatum and pontine nuclei are heavy. It also projects to the subthalamic nucleus. The motor cortex sends projections to all nuclei in the brain stem, which are themselves the origin of descending pathways to the spinal cord, namely the reticular formation, the red nucleus, the superior colliculus, the vestibular nuclei and the inferior olivary nucleus.

Corticospinal tract

The corticospinal or pyramidal tract provides direct control by the cerebral cortex over motor centres of the spinal cord. An homologous pathway to the brain stem, the corticobulbar projection, fulfils a similar function in relation to motor nuclei of the brain stem. The corticospinal tract does not originate solely from the motor cortex, but is conveniently considered in conjunction with it.

The percentage of corticospinal fibres that arise from the primary motor cortex may actually be quite small, probably in the region of 20 to 30%. They arise from pyramidal cells in layer V and give rise to the largest diameter corticospinal axons. There is also a widespread origin from other parts of the frontal lobe, including the premotor cortex and the supplementary motor area. Many axons from the frontal cortex, notably the motor cortex, terminate in the ventral horn of the spinal cord. In cord segments mediating dexterous hand and finger movements they terminate in the lateral part of the ventral horn, in close relationship to motor neuronal groups. A small percentage establish direct monosynaptic connections with α motor neurones.

Between 40 and 60% of pyramidal tract axons arise from parietal areas, including area 3a, area 5 of the superior parietal lobe, and SII in the parietal operculum. The majority of parietal fibres to the spinal cord terminate in the deeper layers of the dorsal horn.

Motor cortical neurones are active in relation to the force of contraction of agonist muscles; their relation to amplitude of movement is less clear. Their activity precedes the onset of electromyographic activity by 50 to 100 milliseconds, suggesting a role for cortical activation in generating rather than monitoring movement.

Premotor cortex

Immediately in front of the primary motor cortex lies Brodmann’s area 6. It extends onto the medial surface, where it becomes contiguous with area 24 in the cingulate gyrus, anterior and inferior to the paracentral lobule. A number of functional motor areas are contained within this cortical region. Lateral area 6, the area over most of the lateral surface of the hemisphere, corresponds to the premotor cortex.

The premotor cortex is divided into a dorsal and a ventral area (PMd and PMv respectively) on functional grounds, and on the basis of ipsilateral corticocortical association connections.

The major thalamic connections of the premotor cortex are with the anterior division of the ventrolateral nucleus and with the centromedian, parafascicular and centrolateral components of the intralaminar nuclei. Subcortical projections to the striatum and pontine nuclei are prominent, and this area also projects to the superior colliculus and the reticular formation. Both dorsal and ventral areas contribute to the corticospinal tract. Commissural connections are with the contralateral premotor, motor and superior parietal (area 5) cortex. Ipsilateral corticocortical connections with area 5 in the superior parietal cortex, and inferior parietal area 7b are common to both dorsal and ventral subdivisions of the premotor cortex, and both send a major projection to the primary motor cortex. The dorsal premotor area also receives fibres from the posterior superior temporal cortex and projects to the supplementary motor cortex. The frontal eye field (area 8) projects to the dorsal subdivision. Perhaps the greatest functionally significant difference in connectivity between the two premotor area subdivisions is that the dorsal premotor area receives fibres from the dorsolateral prefrontal cortex, whereas the ventral subdivision receives fibres from the ventrolateral prefrontal cortex. All of these association connections are likely to be, or are known to be, reciprocal.

Neuronal activity in the premotor cortex in relation to both preparation for movement and movement itself has been extensively studied experimentally. Direction selectivity for movement is a common feature of many premotor neurones. In behavioural tasks, neurones in the dorsal premotor cortex show anticipatory activity and task-related discharge as well as direction selectivity, but little or no stimulus-related changes. The dorsal premotor cortex is probably important in establishing a motor set or intention, contributing to motor preparation in relation to internally guided movement. In contrast, ventral premotor cortex is more related to the execution of externally (especially visually) guided movements in relation to a specific external stimulus.

Frontal eye field

The frontal eye field corresponds to parts of Brodmann’s areas 6, 8 and 9 (Fig. 23.10). It receives its major thalamic projection from the parvocellular mediodorsal nucleus, with additional afferents from the medial pulvinar, the ventral anterior nucleus and the suprageniculate–limitans complex, and connects with the paracentral nucleus of the intralaminar group. The thalamocortical pathways to the frontal eye field form part of a pathway from the superior colliculus, the substantia nigra and the dentate nucleus of the cerebellum. The frontal eye field has extensive ipsilateral corticocortical connections, receiving fibres from several visual areas in the occipital, parietal and temporal lobes, including the medial temporal area (V5) and area 7a. There is also a projection from the superior temporal gyrus, which is auditory rather than visual in function. From within the frontal lobe, the frontal eye field receives fibres from the ventrolateral and dorsolateral prefrontal cortices. It projects to the dorsal and ventral premotor cortices and to the medial motor area, probably to the supplementary eye field adjacent to the supplementary motor area proper. It projects prominently to the superior colliculus, to the pontine gaze centre within the pontine reticular formation, and to other oculomotor related nuclei in the brain stem. As its name implies, it is important in the control of eye movements.

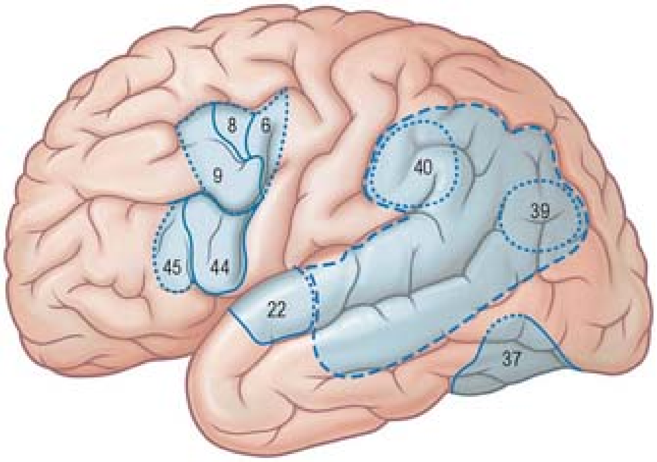

Fig. 23.10 Lateral surface of the left cerebral hemisphere showing the frontal eye field (parts of areas 6, 8, 9), the motor speech (Broca’s) area (areas 44, 45) and Wernicke’s area. The perimeter of these areas is delineated by an interrupted line to indicate uncertainty as to their precise extent. Wernicke’s area is variously depicted by different authorities as encompassing a large parietotemporal area which includes areas 39 and 40. Areas 22 and 37 are considered by some to be respectively auditory and visuo-auditory areas associated with speech and language.

Supplementary motor cortex

The supplementary motor area (SMA; MII) lies medial to area 6, and extends from the most superolateral part to the medial surface of the hemisphere. Area 24 in the cingulate gyrus adjacent to area 6 contains several motor areas, which are termed cingulate motor areas. An additional functional subdivision, the preSMA, lies anterior to the supplementary motor area on the medial surface of the cortex. In the present discussion, these additional medial motor areas are included with the supplementary motor cortex.

The supplementary motor area receives its major thalamic input from the anterior part of the ventral lateral nucleus, which in turn is the major recipient of fibres from the internal segment of the globus pallidus. Additional thalamic afferents are from the ventral anterior nucleus, the intralaminar nuclei, notably the centrolateral and centromedial nuclei, and also from the mediodorsal nucleus. The connections with the thalamus are reciprocal. The supplementary motor cortex receives connections from widespread regions of the ipsilateral frontal lobe, including from the primary motor cortex, the dorsal premotor area, the dorsolateral and ventrolateral prefrontal, medial prefrontal and orbitofrontal cortex and the frontal eye field. These connections are reciprocal, but the major ipsilateral efferent pathway is to the motor cortex. Parietal lobe connections of the supplementary motor cortex are with the superior parietal area 5 and possibly inferior parietal area 7b. Contralateral connections are with the supplementary motor area, and motor and premotor cortices of the contralateral hemisphere. Subcortical connections, other than with the thalamus, pass to the striatum, subthalamic nucleus and pontine nuclei, the brain stem reticular formation and the inferior olivary nucleus. The supplementary motor area makes a substantial contribution to the corticospinal tract, contributing as much as 40% of the fibres from the frontal lobe.

The supplementary motor area contains a representation of the body in which the leg is posterior and the face anterior, with the upper limb between them. Its role in the control of movement is primarily in complex tasks which require temporal organization of sequential movements and in the retrieval of motor memory.

Stimulation of the supplementary motor area in conscious patients has been reported to elicit the sensation of an urge to move, or of anticipation that a movement is about to occur. A region anterior to the supplementary motor area for face representation (areas 44, 45) is important in vocalization and speech production (Fig. 23.10).

Prefrontal cortex

The prefrontal cortex on the lateral surface of the hemisphere comprises predominantly Brodmann's areas 9, 46 and 45 (Fig. 23.8). In non-human primates, two subdivisions of the lateral prefrontal cortex are recognized, a dorsal area equivalent to area 9, and perhaps including the superior part of area 46, and a ventral area, consisting of the inferior part of area 46 and area 45. Areas 44 and 45 are particularly notable in man since, in the dominant hemisphere, they constitute the motor speech area (Broca's area). Both the dorsolateral and ventrolateral prefrontal areas receive their major thalamic afferents from the mediodorsal nucleus, and there are additional contributions from the medial pulvinar, the ventral anterior nucleus and from the paracentral nucleus of the anterior intralaminar group. The dorsolateral area receives long association fibres from the posterior and middle superior temporal gyrus (including auditory association areas), from parietal area 7a, and from much of the middle temporal cortex. From within the frontal lobe it also receives projections from the frontal pole (area 10), and from the medial prefrontal cortex (area 32) on the medial surface of the hemisphere. It projects to the supplementary motor area, the dorsal premotor cortex and the frontal eye field. All these thalamic and corticocortical connections are reciprocal. Commissural connections are with the homologous area, and with the contralateral inferior parietal cortex. The ventrolateral prefrontal area receives long association fibres from both area 7a and area 7b of the parietal lobe, from auditory association areas of the temporal operculum, from the insula and from the anterior part of the lower bank of the superior temporal sulcus. From within the frontal lobe it receives fibres from the anterior orbitofrontal cortex and projects to the frontal eye field and the ventral premotor cortex. It connects with the contralateral homologous area via the corpus callosum. These connections are probably all reciprocal.

The cortex of the frontal pole (area 10) receives thalamic input from the mediodorsal nucleus, the medial pulvinar and the paracentral nucleus. It is reciprocally connected with the cortex of the temporal pole, the anterior orbitofrontal cortex, and the dorsolateral prefrontal cortex. The orbitofrontal cortex connects with the mediodorsal, anteromedial, ventral anterior, medial pulvinar, paracentral and midline nuclei of the thalamus. Cortical association pathways come from the inferotemporal cortex, the anterior superior temporal gyrus and the temporal pole. Within the frontal lobe it has connections with the medial prefrontal cortex, the ventrolateral prefrontal cortex and medial motor areas. Commissural and other connections follow the general pattern for all neocortical areas.

The medial prefrontal cortex is connected with the mediodorsal, ventral anterior, anterior medial pulvinar, paracentral, midline and suprageniculate–limitans nuclei of the thalamus. It receives fibres from the anterior cortex of the superior temporal gyrus. Within the frontal lobe, it has connections with the orbitofrontal cortex, and the medial motor areas of the dorsolateral prefrontal cortex.

PARIETAL LOBE

The parietal lobe lies posterior to the central sulcus. On the medial aspect of the hemisphere its boundary with the occipital lobe is clearly demarcated by the deep parieto-occipital sulcus. On the lateral aspect of the hemisphere its boundaries with the occipital and temporal lobes are less distinct and somewhat arbitrary. The inferior boundary is the posterior ramus of the lateral fissure and its imaginary posterior prolongation.

The lateral aspect of the parietal lobe is divided into three areas by postcentral and intraparietal sulci (Fig. 23.1). The postcentral sulcus, often divided into upper and lower parts, is posterior and parallel to the central sulcus. Inferiorly, it ends above the posterior ramus of the lateral fissure. The postcentral gyrus or primary somatosensory cortex lies between the central and postcentral sulci. Posterior to the postcentral sulcus there is a large area, subdivided by the intraparietal sulcus. It usually starts in the postcentral sulcus near its midpoint and extends posteroinferiorly across the parietal lobe, dividing the latter into superior and inferior parietal lobules.

The superior parietal lobule, between the superomedial margin of the hemisphere and the intraparietal sulcus, is continuous anteriorly with the postcentral gyrus round the upper end of the postcentral sulcus.

The inferior parietal lobule, below the intraparietal sulcus and behind the lower part of the postcentral sulcus, is divided into three. The anterior part is the supramarginal gyrus, which arches over the upturned end of the lateral fissure. It is continuous anteriorly with the lower part of the postcentral gyrus and posteroinferiorly with the superior temporal gyrus. The middle part of the inferior parietal lobule, called the angular gyrus, arches over the end of the superior temporal sulcus and is continuous posteroinferiorly with the middle temporal gyrus. The posterior part of the inferior parietal lobule arches over the upturned end of the inferior temporal sulcus on to the occipital lobe.

Somatosensory cortex

The postcentral gyrus corresponds to the primary somtosensory cortex (SI; Brodmann's areas 3a, 3b, 1 and 2). Area 3a lies most anteriorly, apposing area 4, the primary motor cortex of the frontal lobe; area 3b is buried in the posterior wall of the central sulcus; area 1 lies along the posterior lip of the central sulcus; and area 2 occupies the crown of the postcentral gyrus.

The primary somatosensory cortex contains within it a topographical map of the contralateral half of the body. The face, tongue and lips are represented inferiorly, the trunk and upper limb are represented on the superolateral aspect, and the lower limb on the medial aspect of the hemisphere, giving rise to the familiar 'homunculus' map (Fig. 23.9).

The somatosensory properties of SI depend on its thalamic input from the ventral posterior nucleus of the thalamus, which in turn receives the medial lemniscal, spinothalamic and trigeminothalamic pathways. The nucleus is divided into a ventral posterolateral part, which receives information from the trunk and limbs, and a ventral posteromedial part, in which the head is represented. Within the ventral posterior nucleus, neurones in the central core respond to cutaneous stimuli and those in the most dorsal anterior and posterior parts, which arch as a 'shell' over this central core, respond to deep stimuli. This is reflected in the differential projections to SI: the cutaneous central core projects to 3b, the deep tissue-responsive neurones send fibres to areas 3a and 2, and an intervening zone projects to area 1. Within the ventral posterior nucleus, anteroposterior rods of cells respond with similar modality and somatotopic properties. They appear to project to restricted focal patches in SI of approximately 0.5 mm width, which form narrow strips mediolaterally along SI. The laminar termination of thalamocortical axons from the ventral posterior nucleus is different in the separate cytoarchitectonic subdivisions of SI. In 3a and 3b, these axons terminate mainly in layer IV and the adjacent deep part of layer III, whereas in areas 1 and 2 they end in the deeper half of layer III, avoiding lamina IV. Additional thalamocortical fibres to SI arise from the intralaminar system, notably the centrolateral nucleus.

There is a complex internal connectivity within SI. An apparently stepwise hierarchical progression of information processing occurs from area

3b through area 1 to area 2. Outside the postcentral gyrus, SI has ipsilateral corticocortical association connections with a second somatosensory area (SII); area 5 in the superior parietal lobe; area 4, the motor cortex, in the precentral gyrus; and the supplementary motor cortex in the medial part of area 6 of the frontal lobe.

SI has reciprocal commissural connections with its contralateral homologue, with the exception that the cortices containing the representation of the distal extremities are relatively devoid of such connections. Callosal fibres in SI arise mainly from the deep part of layer III and terminate in layers I to IV. Pyramidal cells contributing callosal projections receive monosynaptic thalamic and commissural connections.

SI has reciprocal subcortical connections with the thalamus and claustrum, and receives afferents from the basal nucleus of Meynert, the locus coeruleus and the midbrain raphe. It has other prominent subcortical projections. Corticostriatal fibres, arising in layer V, pass mainly to the putamen of the same side. Corticopontine and corticotectal fibres from SI arise in layer V. SI projects to the main pontine nuclei, and to the pontine tegmental reticular nucleus. In addition, axons arising in SI pass to the dorsal column nuclei and the spinal cord. Corticospinal pyramidal cells are found in layer V of SI. The topographical representation in the cortex is preserved in terms of the spinal segments to which different parts of the postcentral gyrus project. Thus, the arm representation projects to the cervical enlargement, the leg representation to the lumbosacral enlargement, and so on. Within the grey matter of the spinal cord, fibres from SI terminate in the dorsal horn, in Rexed's laminae 3 to 5: fibres from 3b and 1 end more dorsally, and those from area 2 more ventrally.

The second somatosensory area (SII) lies along the upper bank of the lateral fissure, posterior to the central sulcus. SII contains a somatotopic representation of the body, with the head and face most anteriorly, adjacent to SI, and the sacral regions most posteriorly. SII is reciprocally connected with the ventral posterior nucleus of the thalamus in a topographically organized fashion. Some thalamic neurones probably project to both SI and SII via axon collaterals. Other thalamic connections of SII are with the posterior group of nuclei and with the intralaminar central lateral nucleus. SII also projects to laminae IV to VII of the dorsal horn of the cervical and thoracic spinal cord, the dorsal column nuclei, the principal trigeminal nucleus, and the periaqueductal grey matter of the midbrain.

Within the cortex, SII is reciprocally connected with SI in a topographically organized manner, and projects to the primary motor cortex. SII also projects in a topographically organized way to the lateral part of area 7 (area 7b) in the superior parietal lobe, and makes connections with the posterior cingulate gyrus. Both right and left SII areas are interconnected across the corpus callosum, although distal limb representations are probably excluded. There are additional callosal projections to SI and area 7b.

Experimental studies show that neurones in SII respond particularly to transient cutaneous stimuli, e.g. brush strokes or tapping, which are characteristic of the responses of Pacinian corpuscles in the periphery. They show little response to maintained stimuli.

Superior and inferior parietal lobules

Posterior to the postcentral gyrus, the superior part of the parietal lobe is composed of areas 5, 7a and 7b (Fig. 23.8). Area 5 receives a dense feedforward projection from all cytoarchitectonic areas of SI in a topographically organized manner. The thalamic afferents to this area come from the lateral posterior nucleus and from the central lateral nucleus of the intralaminar group. Ipsilateral corticocortical fibres from area 5 go to area 7, the premotor and supplementary motor cortices, the posterior cingulate gyrus, and the insular granular cortex. Commissural connections between area 5 on both sides tend to avoid the areas of representation of the distal limbs. The response properties of cells in area 5 are more complex than in SI, with larger receptive fields and evidence of submodality convergence. Area 5 contributes to the corticospinal tract.

In non-human primates, the inferior parietal lobe is area 7. In man, this area is more superior, and areas 39 and 40 intervene inferiorly. The counterparts for the latter areas in monkeys are unclear and little experimental evidence is available on their connections and functions. Their role in human cerebral processing is discussed below. In the monkey, area 7b receives somatosensory inputs from area 5 and SII. Connections pass to the posterior cingulate gyrus (area 23), insula and temporal cortex. Area 7b is reciprocally connected with area 46 in the prefrontal cortex and the lateral part of the premotor cortex. Commissural connections of area 7b are with the contralateral homologous area, and with SII, the insular granular cortex and area 5. Thalamic connections are with the medial pulvinar nucleus and the intralaminar paracentral nucleus.

In monkeys, area 7a is not related to the cortical pathways for somatosensory processing, but instead forms part of a dorsal cortical pathway for spatial vision. The major ipsilateral corticocortical connections to area 7a are derived from visual areas in the occipital and temporal lobes. In the ipsilateral hemisphere, area 7a has connections with the posterior cingulate cortex (area 24) and with areas 8 and 46 of the frontal lobe. Commissural connections are with its contralateral homologue. Area 7a is connected with the medial pulvinar and intralaminar paracentral nuclei of the thalamus. In experimental studies, neurones within area 7a are visually responsive: they relate largely to peripheral vision, respond to stimulus movement, and are modulated by eye movement.

TEMPORAL LOBE

The temporal lobe is inferior to the lateral fissure. It is limited behind by an arbitrary line from the preoccipital incisure to the parieto-occipital sulcus which meets the superomedial margin of the hemisphere approximately 5 cm from the occipital pole. Its lateral surface is divided into three parallel gyri by the superior and inferior temporal sulci.

The superior temporal sulcus begins near the temporal pole and slopes slightly up and backwards parallel to the posterior ramus of the lateral sulcus. Its end curves up into the parietal lobe. The inferior temporal sulcus is subjacent and parallel to the superior and is often broken into two or three short sulci. Its posterior end also ascends into the parietal lobe, posterior and parallel to the upturned end of the superior sulcus.

The three parallel gyri on the lateral surface of the temporal lobe are the superior (area 22); middle (area 21); and inferior (area 20) temporal gyri. The temporal pole (area 38) lies in front of the termination of these gyri. Along its superior margin the superior temporal gyrus is continuous with gyri in the floor of the posterior ramus of the lateral sulcus. These vary in number, and extend obliquely anterolaterally from the circular sulcus around the insula as the transverse temporal gyri of Heschl (Fig. 23.11). The anterior transverse temporal gyrus and adjoining part of the superior temporal gyrus are auditory in function, and are considered to be Brodmann’s area 42. The anterior gyrus is approximately area 41.

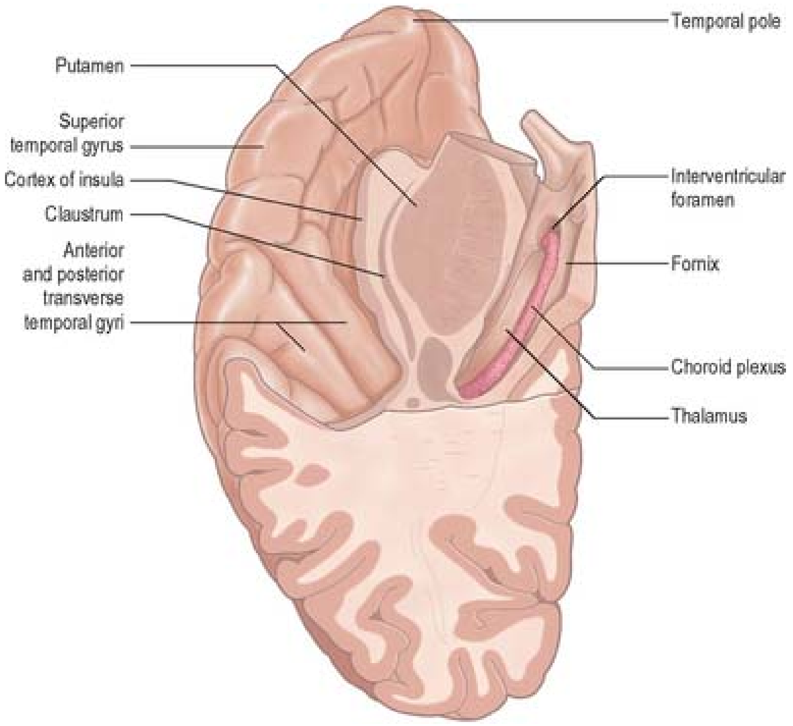
Temporal pole
Putamen
Superior temporal gyrus
Cortex of insula
Claustrum
Anterior and posterior transverse temporal gyri
Interventricular foramen
Fornix
Choroid plexus
Thalamus

Fig. 23.11 Horizontal section showing the left temporal lobe, viewed from above.

The cortex of the medial temporal lobe includes major subdivisions of the limbic system, such as the hippocampus and entorhinal cortex. Areas of neocortex adjacent to these limbic regions are grouped together as medial temporal association cortex. The temporal and frontal lobes are expanded enormously in man, which poses a problem when relating physiological and anatomical studies of non-human primates to human brain topography. In general, the commonly studied old world monkeys lack a middle temporal gyrus.

Auditory cortex

The temporal operculum houses the primary auditory cortex, AI. This is coextensive with the granular area 41 in the transverse temporal gyri. Surrounding areas constitute auditory association cortex. The primary auditory cortex is reciprocally connected with all subdivisions of the medial geniculate nucleus, and may receive additional thalamocortical projections from the medial pulvinar. The geniculocortical fibres terminate densely in layer IV. AI contains a tonotopic representation of the cochlea in which high frequencies are represented posteriorly, and low frequencies anteriorly. Single-cell responses are to single tones of a narrow frequency band. Cells in single vertical electrode penetrations share an optimum frequency response.

The auditory cortex interconnects with prefrontal cortex, though the projections from AI are small. In general, posterior parts of the operculum project to areas 8 and 9. Central parts project to areas 8, 9 and 46. More anterior regions project to areas 9 and 46, to area 12 on the orbital surface of the hemisphere, and to the anterior cingulate gyrus on the medial surface. Contralateral corticocortical connections are with the same and adjacent regions in the other hemisphere. Onward connections of the auditory association pathway converge with those of the other sensory association pathways in cortical regions within the superior temporal sulcus.

Evidence suggests that area 21, the middle temporal cortex, is polysensory in man, and that it connects with auditory, somatosensory and visual cortical association pathways. The auditory association areas of the superior temporal gyrus project in a complex ordered fashion to the middle temporal gyrus, as does the parietal cortex. The middle temporal gyrus connects with the frontal lobe: the most posterior parts project to posterior prefrontal cortex, areas 8 and 9, while intermediate regions connect more anteriorly with areas 19 and 46. Further forwards, the middle temporal region has connections with anterior prefrontal areas 10 and 46, and with anterior orbitofrontal areas 11 and 14. The most anterior middle temporal cortex is connected with the posterior orbitofrontal cortex, area 12, and with the medial surface of the frontal pole. Further forwards, this middle temporal region projects to the temporal pole and the entorhinal cortex. Thalamic connections are with the pulvinar nuclei and the intralaminar group. Other subcortical connections follow the general pattern for all cortical areas. Some projections (e.g. to the pons), particularly from anteriorly in the temporal lobe, are minimal. Physiological responses of cells in this middle temporal region show convergence of different sensory modalities, and many neurones respond to faces.

The inferior temporal cortex, area 20, is a higher visual association area. The posterior inferior temporal cortex receives major ipsilateral corticocortical fibres from occipitotemporal visual areas, notably V4. It contains a coarse retinotopic representation of the contralateral visual field, and sends a major feedforward pathway to the anterior part of the inferior temporal cortex. The anterior inferior temporal cortex projects onto the temporal pole and to paralimbic areas on the medial surface of the temporal lobe. Additional ipsilateral association connections of the inferior temporal cortex are with the anterior middle temporal cortex, in the walls of the superior temporal gyrus, and with visual areas of the parietotemporal cortex. Frontal lobe connections are with area 46 in the dorsolateral prefrontal cortex (posterior inferior temporal), and with the orbitofrontal cortex (anterior inferior temporal). The posterior area also connects with the frontal eye field. Reciprocal thalamic connections are with the pulvinar nuclei; the posterior part is related mainly to the inferior and lateral nuclei, and the anterior part to the medial and adjacent lateral pulvinar. Intralaminar connections are with the paracentral and central medial nuclei. Other subcortical connections conform to the general pattern of all cortical regions. Callosal connections are between corresponding areas and the adjacent visual association areas of each hemisphere.

The cortex of the temporal pole receives feedforward projections from widespread areas of temporal association cortex which are immediately posterior to it. The dorsal part receives predominantly auditory input from the anterior part of the superior temporal gyrus. The inferior part receives visual input from the anterior area of the inferior temporal cortex. Other ipsilateral connections are with the anterior insular, the posterior and medial orbitofrontal, and the medial prefrontal cortices. The temporal pole projects onwards into limbic and paralimbic areas. Thalamic connections are mainly with the medial pulvinar nucleus, and with intralaminar and midline nuclei. Other subcortical connections are as for the cortex in general, although some projections, such as that to the pontine nuclei, are very small. Physiological responses of cells in this and more medial temporal cortex correspond particularly to behavioural performance and to the recognition of high-level aspects of social stimuli.

Nuclei of the amygdala project to, and receive fibres from, neocortical areas, predominantly of the temporal lobe, and possibly inferior parietal cortex. The density of these pathways increases towards the temporal pole.

INSULA

The insula (Fig. 23.12) lies deep in the floor of the lateral fissure, almost surrounded by a circular sulcus, and overlapped by adjacent cortical areas, the opercula. The frontal operculum is between the anterior and ascending rami of the lateral fissure, forming a triangular division of the inferior frontal gyrus. The frontoparietal operculum, between ascending and posterior rami of the lateral fissure, consists of the posterior part of the inferior frontal gyrus, the lower ends of the precentral and postcentral gyri, and the lower end of the anterior part of the inferior parietal lobule. The temporal operculum, below the posterior ramus of the lateral fissure, is formed by superior temporal and transverse temporal gyri. Anteriorly, the inferior region of the insula adjoins the orbital part of the inferior frontal gyrus.

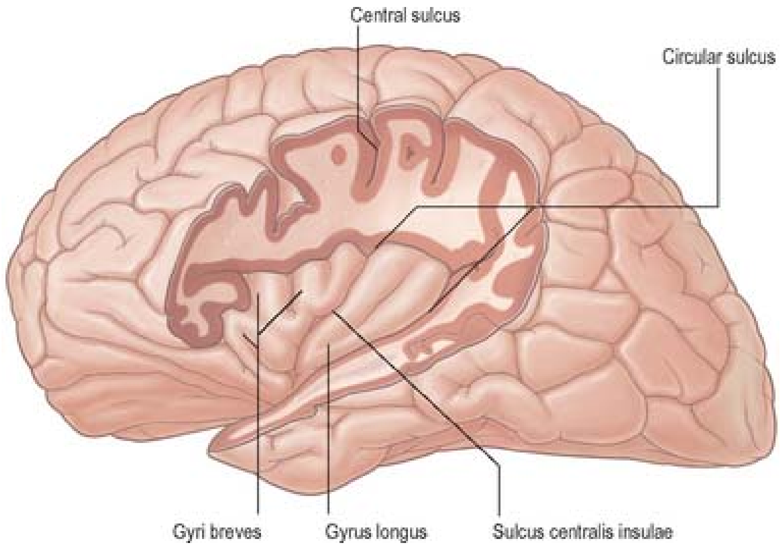

Fig. 23.12 The insula, exposed by removal of the opercula.

When the opercula are removed, the insula appears as a pyramidal area, its apex beneath and near the anterior perforated substance, where the circular sulcus is deficient. The medial part of the apex is termed the limen insulae (gyrus ambiens). A central insular sulcus, which slants posterosuperiorly from the apex, divides the insular surface into a large anterior and a small posterior part. The anterior part is divided by shallow sulci into three or four short gyri, whereas the posterior part is one long gyrus, often divided at its upper end. The cortex of the insula is continuous with that of its opercula in the circular sulcus. The insula is approximately coextensive with the subjacent claustrum and putamen.

Cytoarchitectonically, three zones are recognized within the insula. Anteriorly, and extending caudally into the central insula, the cortex is agranular. It is surrounded by a belt of dysgranular cortex, in which laminae II and III can be recognized, and this in turn is surrounded by an outer zone of homotypical granular cortex which extends to the caudal limit of the insula.

Thalamic afferents to the insula come from subdivisions of the ventral posterior nucleus and of the medial geniculate body, from the oral and medial parts of the pulvinar, the suprageniculate/nucleus limitans complex, the mediodorsal nucleus and the nuclei of the intralaminar and midline groups. It appears that the anterior (agranular) cortex is connected predominantly with the mediodorsal and ventroposterior nuclei, while the posterior (granular) cortex is connected predominantly with the pulvinar and the ventral posterior nuclei. The other nuclear groups appear to connect with all areas.

Ipsilateral cortical connections of the insula are diverse. Somatosensory connections are with SI, SII and surrounding areas, area 5 of the superior parietal lobe and area 7b of the inferior parietal lobe. The insular cortex also has connections with the orbitofrontal cortex. Several auditory regions in the temporal lobe interconnect with the posterior granular insula and the dysgranular cortex more anteriorly. Connections with visual areas are virtually absent. The anterior agranular cortex of the insula appears to have connections primarily with olfactory, limbic and paralimbic structures, including, most prominently, the amygdala. Little is known about the functions of the human insula other than that the anterior insular cortex appears to have a role in olfaction and taste and the posterior part in somatosensory functions. The latter has also been implicated in language functions, which resonates with the possibility that higher order auditory association pathways may pass via areas in the insula.

Claustrum

The claustrum (see Fig. 23.27) is a thin sheet of grey matter lying deep to the insula. It is approximately coextensive with the insula, from which it is separated by the extreme capsule. Medially, the claustrum is separated from the putamen by the external capsule. It is thickest anteriorly and inferiorly, where it becomes continuous with the anterior perforated substance, amygdala and prepiriform cortex. In animals, it has reciprocal, topographically organized, connections with many regions of the neocortex. Little is known about the connections and functional significance of the claustrum in the human brain.

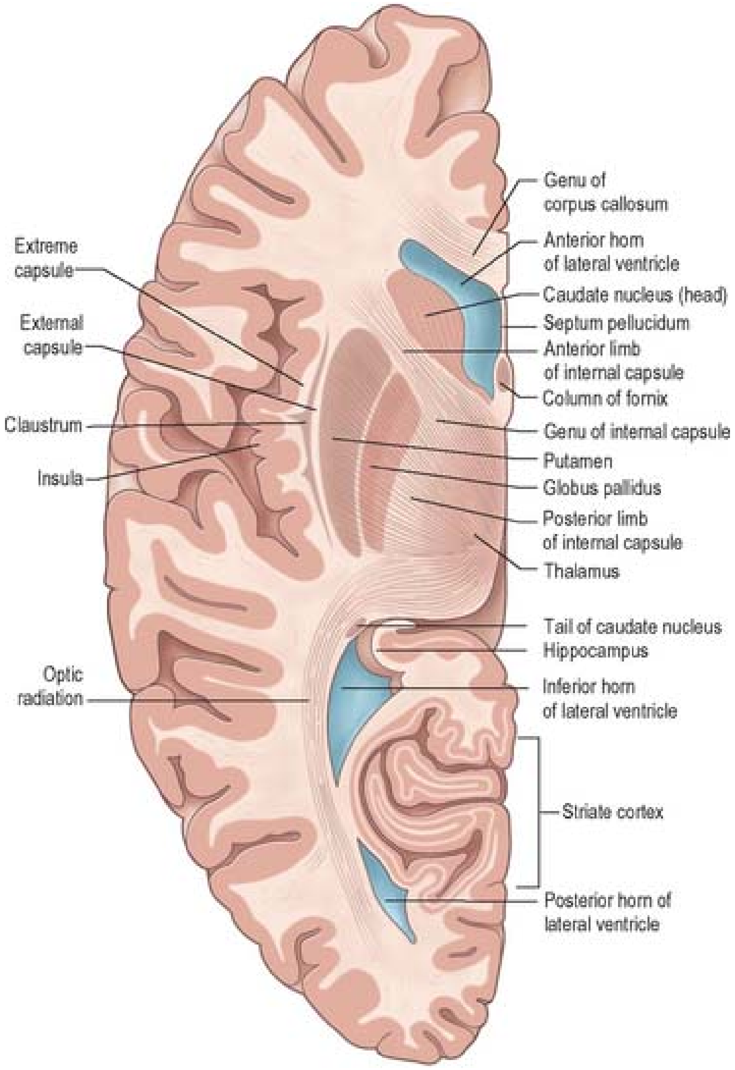
Extreme capsule
External capsule
Claustrum
Insula
Optic radiation
Genu of corpus callosum
Anterior horn of lateral ventricle
Caudate nucleus (head)
Septum pellucidum
Anterior limb of internal capsule
Column of fornix
Genu of internal capsule
Putamen
Globus pallidus
Posterior limb of internal capsule
Thalamus
Tail of caudate nucleus
Hippocampus
Inferior horn of lateral ventricle
Striate cortex
Posterior horn of lateral ventricle

Fig. 23.27 Superior aspect of a horizontal section through the left cerebral hemisphere.

OCCIPITAL LOBE

The occipital lobe lies behind an arbitrary line joining the preoccipital incisure and the parieto-occipital sulcus (Fig. 23.1, Fig. 23.2) and is comprised almost entirely of Brodmann’s areas 17, 18 and 19. Area 17, the striate cortex, is the primary visual cortex (VI). A host of other distinct visual areas reside in the occipital and temporal cortex. Functional subdivisions V2, V3 (dorsal and ventral) and V3A lie within Brodmann’s area 18. Other functional areas at the junction of the occipital cortex with the parietal or temporal lobes lie wholly or partly in area 19.

The primary visual cortex is mostly located on the medial aspect of the occipital lobe, and is coextensive with the subcortical nerve fibre stria of Gennari in layer IV; hence its alternative name, the striate cortex. It occupies the upper and lower lips and depths of the posterior part of the calcarine sulcus and extends into the cuneus and lingual gyrus.

The primary visual cortex receives afferent fibres from the lateral geniculate nucleus via the optic radiation (see Fig. 23.27). The latter curves posteriorly and spreads through the white matter of the occipital lobe. Its fibres terminate in strict point-to-point fashion in the striate area. The cortex of each hemisphere receives impulses from two hemi-retinae, which represent the contralateral half of the binocular visual field. Superior and inferior retinal quadrants are connected with corresponding areas of the striate cortex. Thus, the superior retinal quadrants (representing the inferior half of the visual field) are connected with the visual cortex above the calcarine sulcus, and the inferior retinal quadrants (representing the upper half of the visual field) are connected with the visual cortex below the calcarine sulcus. The peripheral parts of the retinae activate the most anterior parts in the visual cortex. The macula impinges upon a disproportionately large posterior part around the occipital pole.

The striate cortex is granular. Layer IV, bearing the stria of Gennari, is commonly divided into three sublayers. Passing from superficial to deep, these are IVA, IVB (which contains the stria), and IVC. The densely cellular IVC is further subdivided into a superficial IVCα and a deep IVCβ. Layer

IVB contains only sparse, mainly non-pyramidal, neurones. The input to area 17 from the lateral geniculate nucleus terminates predominantly in layers IVA and IVC. Other thalamic afferents, from the inferior pulvinar nucleus and the intralaminar group, pass to layers I and VI. Geniculocortical fibres terminate in alternating bands. Axons from geniculate laminae which receive information from the ipsilateral eye (laminae 2, 3 and 5), are segregated from those of laminae which receive input from the contralateral eye (laminae 1, 4 and 6). Neurones within layer IVC are monocular, i.e. they respond to stimulation of either the ipsilateral or contralateral eye, but not both. This horizontal segregation forms the anatomical basis of the ocular dominance column in that neurones encountered in a vertical strip from pia to white matter, although binocular outside layer IV, exhibit a preference for stimulation of one or other eye. The other major functional basis for visual cortical columnar organization is the orientation column. This describes the observation that an electrode passing through the depth of the cortex at right angles to the plane from pia to white matter, encounters neurones that all respond preferentially to either a stationary or a moving straight line of a given orientation within the visual field. Cells with simple, complex and hypercomplex receptive fields occur in area 17. Simple cells respond optimally to lines in a narrowly defined position. Complex cells respond to a line anywhere within a receptive field, but with a specific orientation. Hypercomplex cells are similar to complex cells except that the length of the line or bar stimulus is also critical for an optimal response. There is a relationship between the complexity of response and the position of cells in relation to the cortical laminae. Simple cells are mainly in layer IV and complex and hypercomplex cells predominate in either layers II and III or layers V and VI.

Ipsilateral corticocortical fibres pass from area 17 to a variety of functional areas in areas 18 and 19 and in the parietal and temporal cortices. Fibres from area 17 pass to area 18 (which contains visual areas V2, V3 and V3a); area 19 (which contains V4); the posterior intraparietal and the parieto-occipital areas; and to parts of the posterior temporal lobe, the middle temporal area and the medial superior temporal area. Subcortical efferents of the striate cortex pass to the superior colliculus, pretectum and parts of the brain stem reticular formation. Projections to the striatum (notably the tail of the caudate nucleus), and to the pontine nuclei, are sparse. Geniculo- and claustrocortical projections are reciprocated by prominent descending projections, which arise in layer VI.

The second visual area (V2) occupies much of area 18 but is not coextensive with it. It contains a complete retinotopic representation of the visual hemifield, which is a mirror image of that in area 17, with the vertical meridian represented most posteriorly along the border between areas 17 and 18. The major ipsilateral corticocortical feedforward projection to V2 comes from V1. Feedforward projections from V2 pass to several other visual areas (and are reciprocated by feedback connections) including the third visual area (V3) and its various subdivisions (V3/V3d; VP/V3v; V3a); the fourth visual area (V4); areas in the temporal and parietal association cortices; and the frontal eye field. Thalamic afferents to V2 come from the lateral geniculate nucleus, the inferior and lateral pulvinar nuclei and parts of the intralaminar group of nuclei. Additional subcortical afferents are as for cortical areas in general. Subcortical efferents arise predominantly in layers V and VI. They pass to the thalamus, claustrum, superior colliculus, pretectum, brain stem reticular formation, striatum and pons. As for area 17, the callosal connections of V2 are restricted predominantly to the cortex, which contains the representation of the vertical meridian.

The third visual area (V3) is a narrow strip adjoining the anterior margin of V2, probably still within area 18 of Brodmann. V3 has been subdivided into dorsal (V3/V3d) and ventral (VP/V3v) regions on the basis of its afferents from area V1, myeloarchitecture, callosal and association connections, and receptive field properties. The dorsal subdivision receives from V1, whereas the ventral does not. Functionally, the dorsal part shows less wavelength selectivity, greater direction selectivity and smaller receptive fields than does the ventral subdivision. Both areas receive a feedforward projection from V2, and are interconnected by association fibres. A further visual area, area V3a, lies anterior to the dorsal subdivision of V3. It receives afferent association connections from V1, V2, V3/V3d and VP/V3v, and has a complex and irregular topographic organization. All subdivisions project to diverse visual areas in the parietal, occipital and temporal cortices, including V4, and to the frontal eye fields.

The fourth visual area, V4, lies within area 19 anterior to the V3 complex. It receives a major ipsilateral feedforward projection from V2. Colour selectivity as well as orientation selectivity may be transmitted to V4 and bilateral damage causes achromatopsia. V4 is more complex than a simple colour discrimination area because it is also involved in the discrimination of orientation, form and movement. It sends a feedforward projection to the inferior temporal cortex and receives a feedback projection. It also connects with other visual areas that lie more dorsally in the temporal lobe, and in the parietal lobe. Thalamocortical connections are with the lateral and inferior pulvinar and the intralaminar nuclei. Other subcortical connections conform to the general pattern for all cortical areas. Callosal connections are with the contralateral V4 and other occipital visual areas.

A fifth visual area, V5 or the middle temporal area, is found in non-human primates towards the posterior end of the superior temporal sulcus. It receives ipsilateral association connections from areas VI, V2, V3 and V4, in a topographically organized way. Other lesser projections are received from widespread visual areas in the temporal and parieto-occipital lobes and from the frontal eye fields. V5 is primarily a movement detection or discrimination area, and contains a high proportion of movement-sensitive, direction-selective, cells. Feedforward projections go to surrounding temporal and parietal areas, and to the frontal eye field. Thalamic connections are with the lateral and inferior pulvinar and intralaminar group of nuclei. Other connections follow the general pattern of all neocortical areas.

Current concepts of visual processing in inferior temporal and temporoparietal cortices suggest that two parallel pathways (dorsal and ventral) emanate from the occipital lobe. The dorsal pathway, concerned primarily with visuospatial discrimination, projects from V1 and V2 to the superior temporal and surrounding parietotemporal areas and ultimately to area 7a of the parietal cortex. The fourth visual area, V4, is a key relay station for the ventral pathway, which is related to perception and object recognition. Its connections pass sequentially along the inferior temporal gyrus in a feedforward manner, from V4 to posterior, intermediate and then anterior, inferior temporal cortices. Ultimately they feed into the temporal polar and medial temporal areas and so interface with the limbic system.

LIMBIC LOBE

The limbic lobe (Fig. 23.13) includes large parts of the cortex on the medial wall of the hemisphere, principally the subcallosal, cingulate and parahippocampal gyri. It also includes the hippocampal formation, which consists of the hippocampus proper (Ammon's horn or 'cornu ammonis'), the dentate gyrus, the subicular complex (subiculum, presubiculum, parasubiculum) and the entorhinal cortex (area 28). There is a close relationship between these phylogenetically old cortical structures and the termination of the olfactory tract in the frontal and medial temporal lobes.

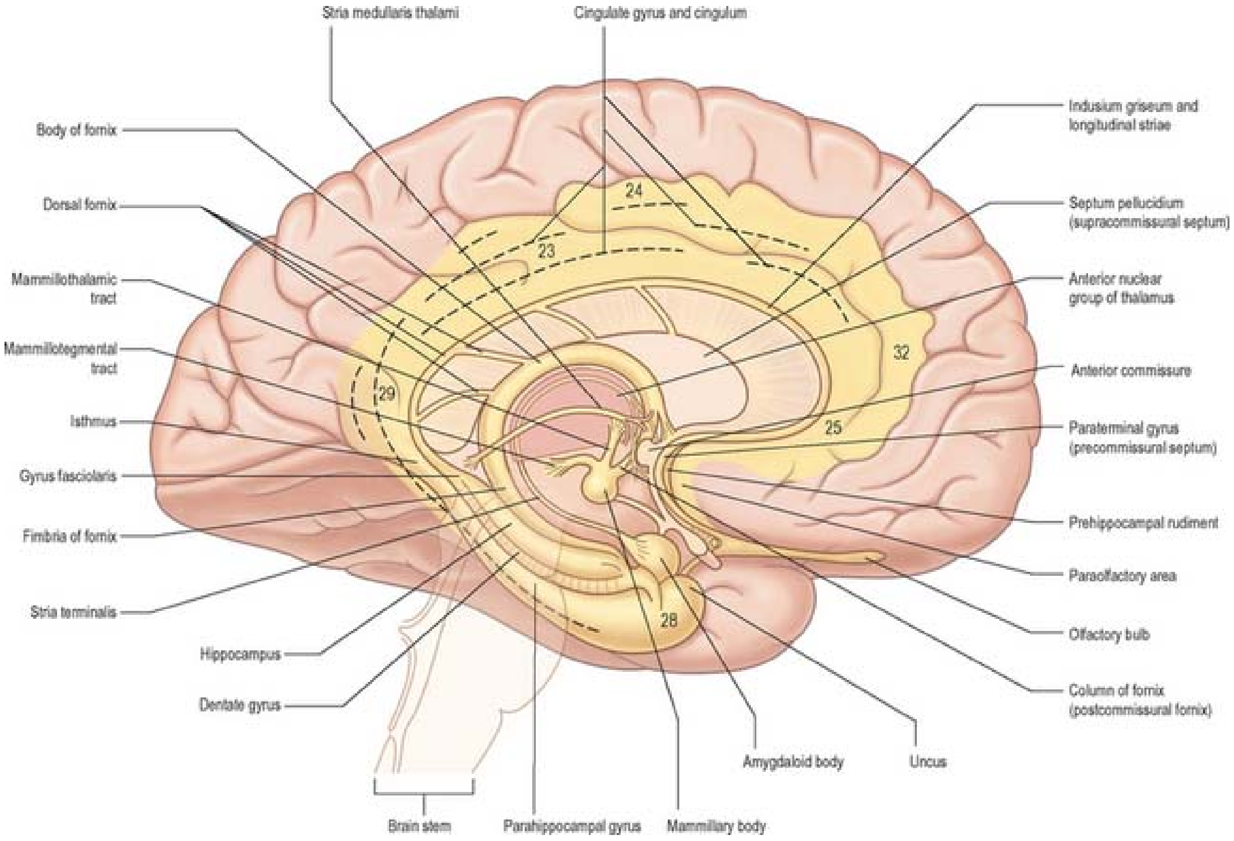
Stria medullaris thalami
Cingulate gyrus and cingulum
Body of fornix
Dorsal fornix
Mammillothalamic tract
Mammillotegmental tract
Isthmus
Gyrus fasciolaris
Fimbria of fornix
Stria terminalis
Hippocampus
Dentate gyrus
Brain stem
Parahippocampal gyrus
Mammillary body
Amygdaloid body
Uncus
Indusium griseum and longitudinal striae
Septum pellucidum (supracommissural septum)
Anterior nuclear group of thalamus
Anterior commissure
Paraterminal gyrus (precommissural septum)
Prehippocampal rudiment
Paraolfactory area
Olfactory bulb
Column of fornix (postcommissural fornix)
24
23
32
29
25
28

Fig. 23.13 Components of the limbic system (yellow). Medial aspect of the left cerebral hemisphere. The approximate locations of some Brodmann's areas are indicated.

On the basis of emotional disturbances displayed by patients who presented with damage to the hippocampus and cingulate gyrus, Papez (1937) described a closed circuit (the Papez circuit), which linked the hippocampus with the cingulate cortex, via the mammillary bodies and anterior thalamus. He proposed that emotional expression is organized in the hippocampus, experienced in the cingulate gyrus and expressed via the mammillary bodies. The hypothalamus was considered to be the site where hippocampal processes gain access to the autonomic outflow that controls the peripheral expression of emotional states. The Papez circuit is now widely accepted to be involved with cognitive processes, including mnemonic functions and spatial short-term memory.

Later the term ‘limbic system’ became popular to describe the limbic lobe, together with closely associated subcortical nuclei including the amygdala, septum, hypothalamus, habenula, anterior thalamic nuclei and parts of the basal ganglia.

The cingulate gyrus may be divided rostrocaudally into several cytoarchitectonically discrete areas. These are the prelimbic (area 32) and infralimbic (area 25) cortices, the anterior cingulate cortex (areas 23 and 24) and part of the posterior cingulate or retrosplenial cortex (area 29).

The cingulate gyrus, which is related to the medial surfaces of the frontal lobe, contains specific motor areas, and has extensive connections with neocortical areas of the frontal lobe. The cingulate gyrus on the medial surface of the parietal lobe has equally extensive connections with somatosensory and visual-association areas of the parietal, occipital and temporal lobes. These afferents to the cingulate gyrus are predominantly from neocortical areas on the lateral surface of the hemisphere. Within the cingulate cortex, most projections pass caudally, ultimately into the posterior parahippocampal gyrus. Through this system, afferents from widespread areas of association cortex converge upon the medial temporal lobe and hippocampal formation. There are other parallel stepwise routes to these targets through cortical areas on the lateral surface.

The cingulate gyrus is the area that shows the most consistent pain-evoked changes in synaptic activity related to regional cerebral blood flow (rCBF) as measured by either positron emission tomography (PET) or functional magnetic resonance imaging (fMRI) (Derbyshire et al 1997). It must be remembered that pain evokes a multidimensional response in the brain including cognitive, emotional, autonomic and motor components, and so it is not always possible to assign specific functions to parts of the brain that generate PET or fMRI signals in response to pain (Peyron et al 2000). However, in many experimental paradigms, a combination of signals from the cingulate gyrus, somatosensory area SII and the insula appears to be involved in the conscious appreciation of nociception and neuropathic pain.

The parahippocampal gyrus includes areas 27, 28 (entorhinal cortex), 35, 36, 48, 49 and temporal cortical fields. It has complex interconnections with the cingulate cortex and with the hippocampal formation. In monkeys, the infralimbic cortex (area 25) has been shown to project to areas 24a and 24b. Area 25 also has reciprocal connections with the entorhinal cortex. Projections between the paralimbic area 32 and the limbic cortex (anterior, retrosplenial and entorhinal cortex) are somewhat less prominent. Areas 24 and 29 are connected with the paralimbic posterior cingulate area 23. A pattern of cortical connections running outwards from the hippocampus, via the entorhinal cortex to the perirhinal cortex, caudal parahippocampal gyrus and posterior cingulate gyrus, is considered to be of great functional importance so far as the hippocampus is concerned. The parahippocampal gyrus projects to virtually all association areas of the cortex in primates and also provides the major funnel through which polymodal sensory inputs converge on the hippocampus.

Olfactory pathways

The organization of the olfactory system reflects its phylogenetically ancient lineage: afferent olfactory pathways proceed directly to the cerebral cortex, bypassing the thalamus, and its terminal fields are primitive cortical areas that are considered to be parts of the limbic system. Details of the relationship between the olfactory pathways and the limbic system are shown in Fig. 23.4.

The olfactory nerves arise from olfactory receptor neurones in the olfactory mucosa (see Ch. 32). The axons collect into numerous small bundles ensheathed by a population of unique glia and surrounded by layers of meninges, and enter the anterior cranial fossa by passing through the foramina in the cribriform plate of the ethmoid bone. They attach to the inferior surface of the olfactory bulb, which is situated at the anterior end of the olfactory sulcus on the orbital surface of the frontal lobe, and terminate in the bulb. Olfactory receptor neurones are continually replaced throughout life by differentiation of stem cells in the olfactory mucosa. The olfactory bulb is continuous posteriorly with the olfactory tract, through which the output of the bulb passes directly to the olfactory cortex.

There is a clear laminar structure in the olfactory bulb (Fig. 23.14). From the surface inwards the laminae are the olfactory nerve layer, glomerular layer, external plexiform layer, mitral cell layer, internal plexiform layer and granule cell layer. The olfactory nerve layer consists of the unmyelinated axons of the olfactory neurones. The continuous turnover of receptor cells means that axons in this layer are at different stages of growth, maturity or degeneration. The glomerular layer consists of a thin sheet of glomeruli where the incoming olfactory axons divide and synapse on terminal dendrites of secondary olfactory neurones, i.e. mitral, tufted and periglomerular cells. The external plexiform layer contains the principal and secondary dendrites of mitral and tufted cells. The mitral cell layer is a thin sheet composed of the cell bodies of mitral cells, each of which sends a single principal dendrite to a glomerulus, secondary dendrites to the external plexiform layer, and a single axon to the olfactory tract. It also contains a few granule cell bodies. The internal plexiform layer contains axons, recurrent and deep collaterals of mitral and tufted cells, and granule cell bodies. The granule cell layer contains the majority of the granule cells and their superficial and deep processes, together with numerous centripetal and centrifugal nerve fibres which pass through the layer.

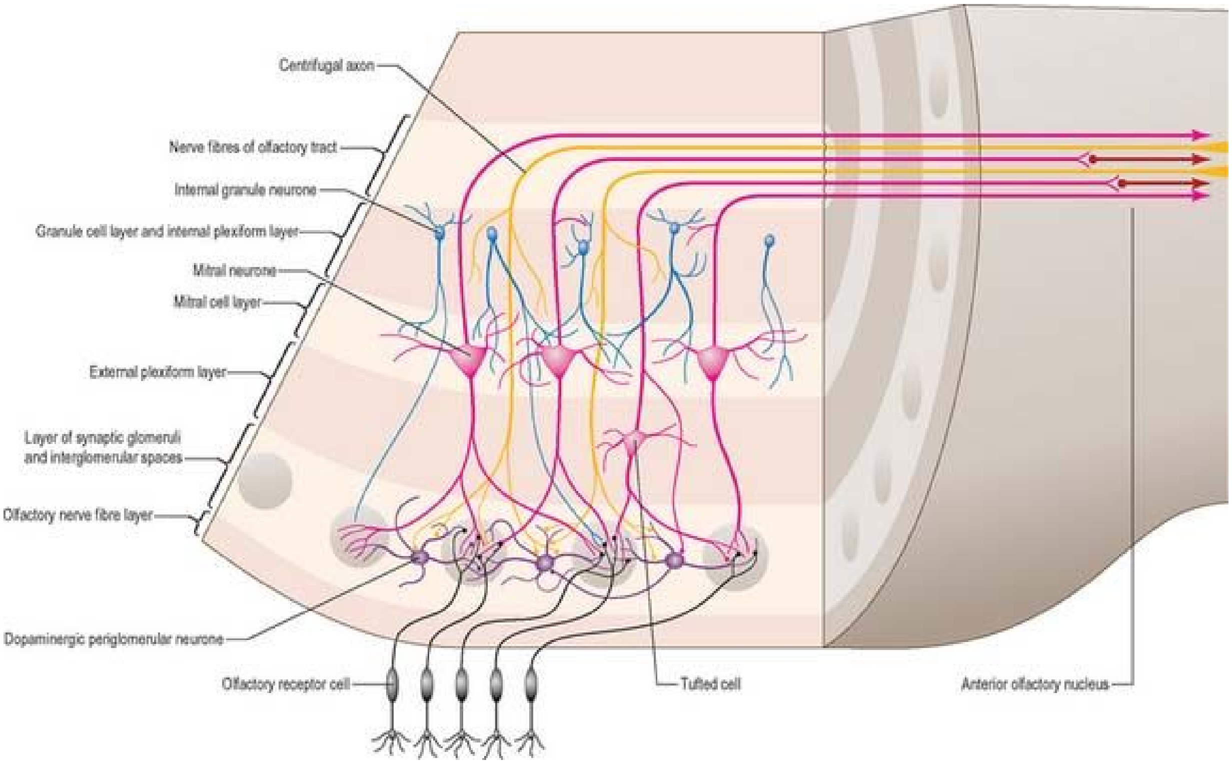
Centrifugal axon
Nerve fibres of olfactory tract
Internal granule neurone
Granule cell layer and internal plexiform layer
Mitral neurone
Mitral cell layer
External plexiform layer
Layer of synaptic glomeruli
and interglomerular spaces
Olfactory nerve fibre layer
Dopaminergic periglomerular neurone
Olfactory receptor cell
Tufted cell
Anterior olfactory nucleus

Fig. 23.14 Organization of the olfactory bulb.

The principal neurones in the olfactory bulb are the mitral and tufted cells: their axons form its output via the olfactory tract. These cells are morphologically similar and most use an excitatory amino acid, probably glutamate or aspartate, as their neurotransmitter. The mitral cell spans the layers of the bulb, and receives the sensory input superficially at its glomerular tuft. The axons of mitral and tufted cells appear to be parallel output pathways from the olfactory bulb.

The main types of interneurones in the olfactory bulb are the periglomerular cells and granule cells. The majority of periglomerular cells are dopaminergic (cell group A15), but some are GABAergic: their axons are distributed laterally and terminate within extraglomerular regions. Granule cells are similar in size to periglomerular cells. Their most characteristic feature is the absence of an axon, and they therefore resemble amacrine cells in the retina. Granule cells have two principal spine-bearing dendrites which pass radially in the bulb: they appear to be GABAergic. The granule cell is likely to be a powerful inhibitory influence on the output neurones of the olfactory bulb.

Centrifugal inputs to the olfactory bulb arise from a variety of central sites. Neurones of the anterior olfactory nucleus and collaterals of pyramidal neurones in the olfactory cortex project to the granule cells of the olfactory bulb. Cholinergic neurones in the horizontal limb nucleus of the diagonal band of Broca, part of the basal forebrain cholinergic system, project to the granule cell layer and also to the glomerular layer. Other afferents to the granule cell layer and the glomeruli arise from the pontine locus coeruleus and the mesencephalic raphe nucleus.

The granule cell layer of the bulb is extended into the olfactory tract as scattered medium-sized multipolar neurones that constitute the anterior olfactory nucleus. Many centripetal axons from mitral and tufted cells relay in, or give collaterals to, the anterior olfactory nucleus; the axons from the nucleus continue with the remaining direct fibres from the bulb into the olfactory striae.

As the olfactory tract approaches the anterior perforated substance it flattens and splays out as the olfactory trigone. Fibres of the tract continue from the caudal angles of the trigone as diverging medial and lateral olfactory striae, which border the anterior perforated substance. The lateral olfactory stria follows the anterolateral margin of the anterior perforated substance to the limen insulae, where it bends posteromedially to merge with an elevated region, the gyrus semilunaris, at the rostral margin of the uncus in the temporal lobe. The lateral olfactory gyrus forms a tenuous grey layer covering the lateral olfactory stria: it merges laterally with the gyrus ambiens, part of the limen insulae. The lateral olfactory gyrus and gyrus ambiens form the prepiriform region of the cortex, passing caudally into the entorhinal area of the parahippocampal gyrus. The prepiriform and periamygdaloid regions and the entorhinal area (area 28) together make up the piriform cortex. The medial olfactory stria passes medially along the rostral boundary of the anterior perforated substance towards the medial continuation of the diagonal band of Broca. Together, they curve up on the medial aspect of the hemisphere, anterior to the attachment of the lamina terminalis.

The olfactory cortex receives a direct input from the olfactory bulb which arrives via the olfactory tract without relay in the thalamus. The largest cortical olfactory area is the piriform cortex. The anterior olfactory nucleus, olfactory tubercle, regions of the entorhinal and insular cortex and amygdala also receive direct projections from the olfactory bulb.

The entorhinal cortex (Brodmann’s area 28) is the most posterior part of the piriform cortex, and is divided into medial and lateral areas (areas 28a and 28b). The lateral parts receive fibres mainly from the olfactory bulb, and also from the piriform and periamygdaloid cortices.

Projections from the piriform olfactory cortex are widespread, and include the neocortex (especially the orbitofrontal cortex), thalamus (especially the medial dorsal thalamic nucleus), hypothalamus, amygdala and hippocampal formation.

Hippocampal formation

The hippocampal formation includes the dentate gyrus, hippocampus, subicular complex and entorhinal cortex.

The hippocampus lies above the subiculum and medial parahippocampal gyrus, forming a curved elevation, approximately 5 cm long, along the floor of the inferior horn of the lateral ventricle (Fig. 23.15). Its anterior end is expanded, and here its margin may present two or three shallow grooves that give a paw-like appearance, the pes hippocampi. The ventricular aspect is convex. It is covered by ependyma, beneath which fibres of the alveus converge medially on a longitudinal bundle of fibres, the fimbria of the fornix. Passing medially from the collateral sulcus, the neocortex of the parahippocampal gyrus merges with the transitional juxtallocortex of the subiculum (Fig. 23.16). The latter curves superomedially to the inferior surface of the dentate gyrus, then laterally to the laminae of the hippocampus. This curvature continues, first superiorly, then medially above the dentate gyrus, and ends pointing towards the centre of the superior surface of the dentate gyrus. The dentate gyrus is a crenated strip of cortex related inferiorly to the subiculum, laterally to the hippocampus and, more medially, to the fimbria of the fornix (Fig. 23.16, Fig. 23.17). The form of the fimbria is quite variable, but medially it is separated from the crenated medial margin of the dentate gyrus by the fimbriodentate sulcus (Fig. 23.18). The hippocampal sulcus, of variable depth, lies between the dentate gyrus and the subicular extension of the parahippocampal gyrus. Posteriorly, the dentate gyrus is continuous with the gyrus fasciolaris and thus with the indusium griseum. Anteriorly, it is continued into the notch of the uncus, turning medially across its inferior surface, as the tail of the dentate gyrus (band of Giacomini), and vanishes on the medial aspect of the uncus (Fig. 23.17). The tail separates the inferior surface of the uncus into an anterior uncinate gyrus and posterior intralimbic gyrus.

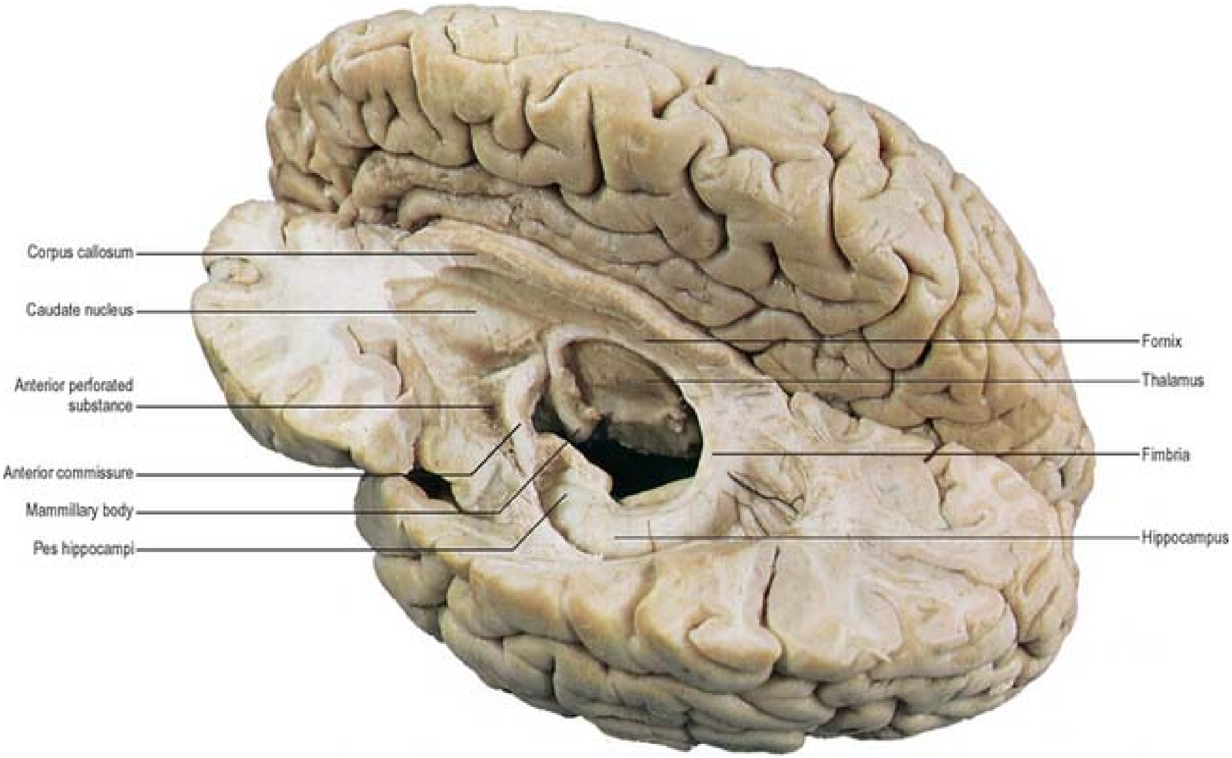
Corpus callosum
Caudate nucleus
Anterior perforated substance
Anterior commissure
Mammillary body
Pes hippocampi
Fornix
Thalamus
Fimbria
Hippocampus

Fig. 23.15 Dissection of the left cerebral hemisphere demonstrating structures of the limbic system. The body of the corpus callosum has been divided sagitally. The frontal, temporal and occipital lobes have been sectioned horizontally and their superior parts removed. The left lentiform complex and thalamus have been removed and the floor of the inferior horn of the lateral ventricle opened.

(Dissection by AM Seal; photograph by Kevin Fitzpatrick on behalf of GKT School of Medicine, London; figure enhanced by B. Crossman.)

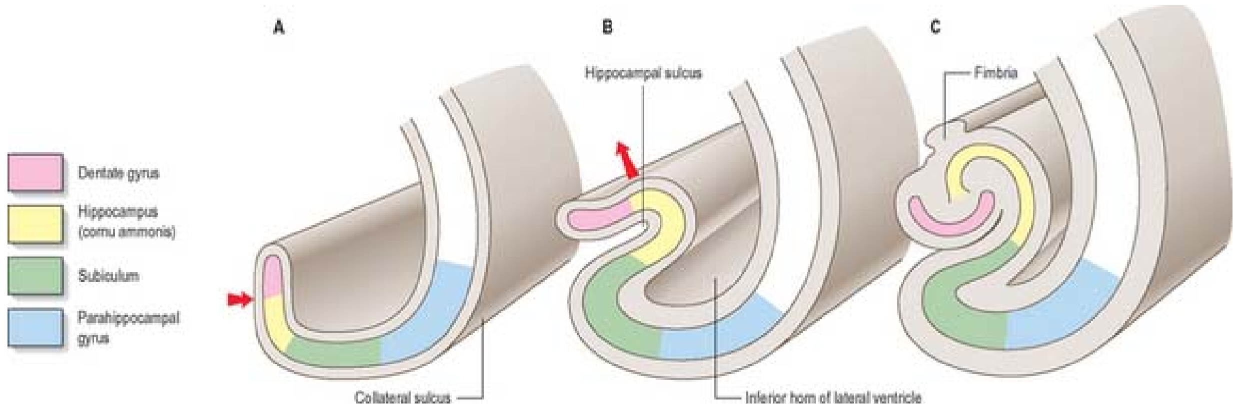
A
B
C
Hippocampal sulcus
Fimbria
Dentate gyrus
Hippocampus (cornu ammonis)
Subiculum
Parahippocampal gyrus
Collateral sulcus
Inferior horn of lateral ventricle

Fig. 23.16 Series of coronal sections of the temporal lobe and inferior horn of the lateral ventricle illustrating the relationships between the components of the hippocampal formation.

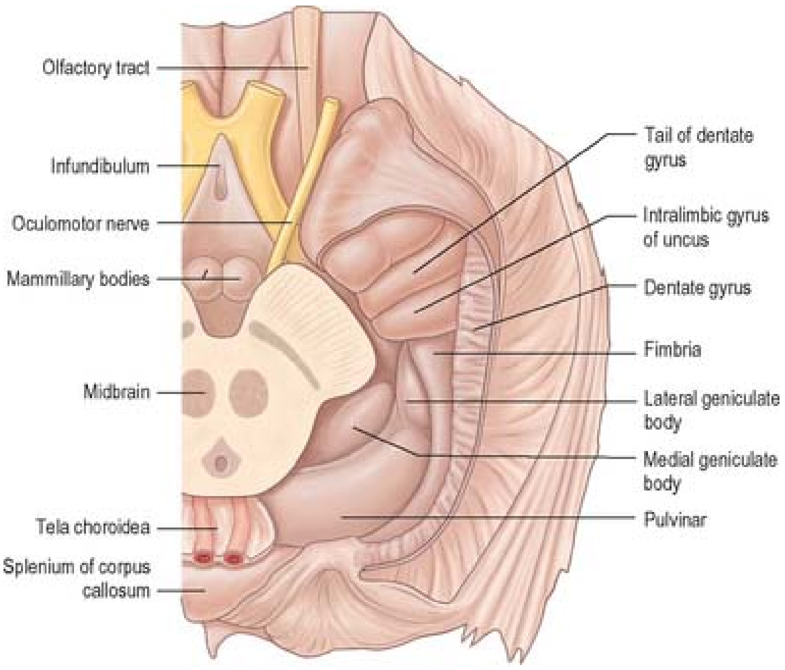
Olfactory tract
Infundibulum
Oculomotor nerve
Mammillary bodies
Midbrain
Tela choroidea
Splenium of corpus callosum
Tail of dentate gyrus
Intralimbic gyrus of uncus
Dentate gyrus
Fimbria
Lateral geniculate body
Medial geniculate body
Pulvinar

Fig. 23.17 Basal aspect of the brain dissected to display the dentate gyrus, uncus and fimbria on the left.

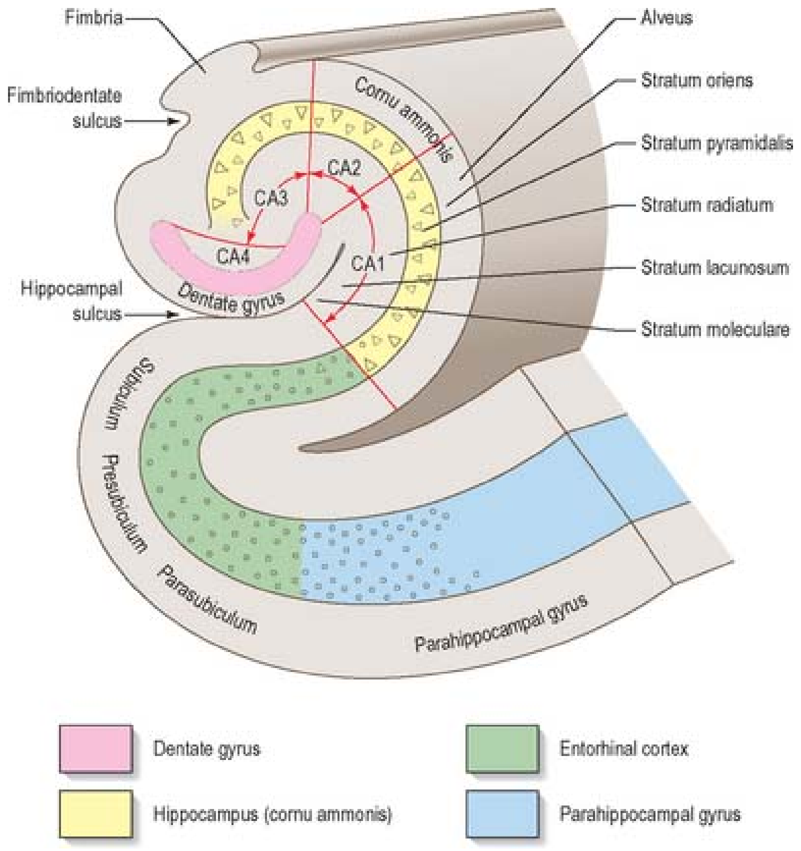
Fimbria
Fimbriodentate sulcus
Hippocampal sulcus
Cornu ammonis
CA2
CA3
CA4
CA1
Dentate gyrus
Subiculum
Presubiculum
Parasubiculum
Parahippocampal gyrus
Alveus
Stratum oriens
Stratum pyramidalis
Stratum radiatum
Stratum lacunosum
Stratum moleculare
Dentate gyrus
Hippocampus (cornu ammonis)
Entorhinal cortex
Parahippocampal gyrus

Fig. 23.18 The hippocampal formation showing the disposition of the various cell fields.

The trilaminar cortex of the dentate gyrus is the least complex of the hippocampal fields (Fig. 23.19). Its major cell type is the granule cell, found in the dense granule cell layer. Granule cells have unipolar dendrites that extend into the overlying molecular layer. The latter receives most of the afferent projections to the dentate gyrus, primarily from the entorhinal cortex (Fig. 23.20). The granule cell and molecular layers are sometimes referred to as the fascia dentata. The polymorphic layer, or hilus of the dentate gyrus, contains cells that give rise primarily to ipsilateral association fibres. They remain within the dentate gyrus and do not extend into other hippocampal fields.

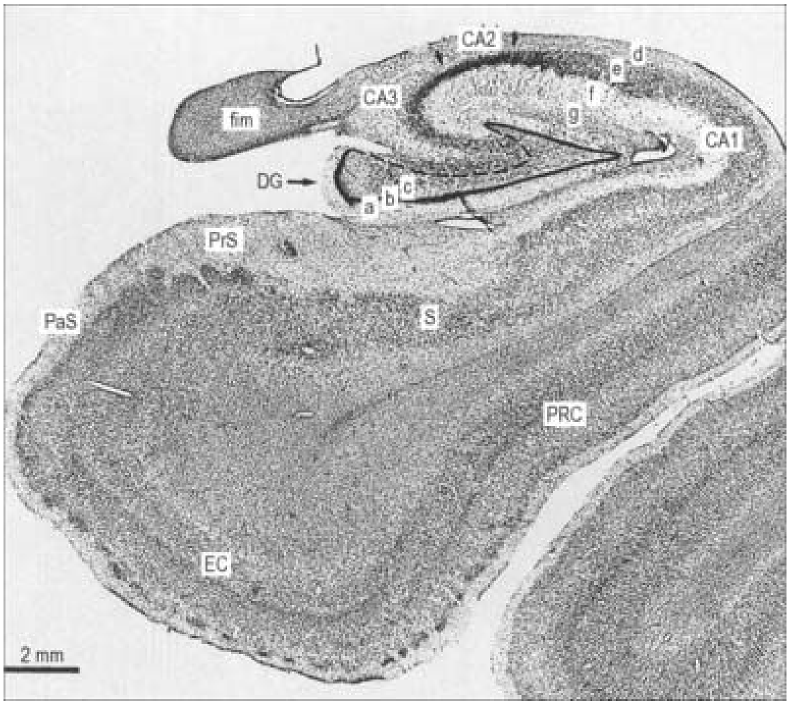

Fig. 23.19 Coronal, thionin-stained section of the human hippocampal formation. Abbreviations: a, molecular layer of the dentate gyrus; b, granule cell layer of the dentate gyrus; c, plexiform layer of the dentate gyrus; CA1–3, fields of the hippocampus; d, stratum oriens layer of the hippocampus; DG, dentate gyrus; e, pyramidal cell layer of the hippocampus; EC, entorhinal cortex; f, stratum radiatum of the hippocampus; fim, fimbria; g, stratum lacunosum-molecular of the hippocampus; PaS, parasubiculum; PRC, perirhinal cortex; PrS, presubiculum; S, subiculum.

(By courtesy of D. Amaral.).

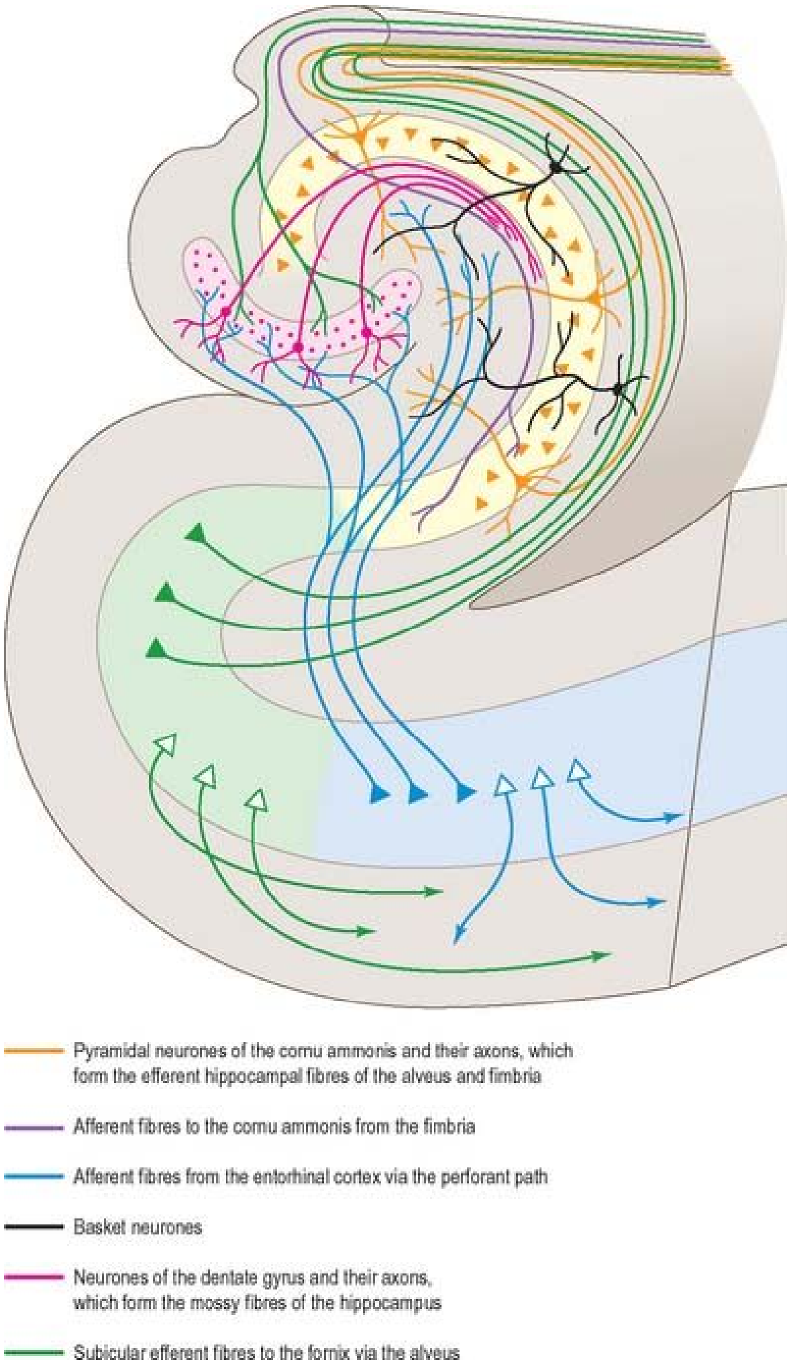
Pyramidal neurones of the cornu ammonis and their axons, which form the efferent hippocampal fibres of the alveus and fimbria
Afferent fibres to the cornu ammonis from the fimbria
Afferent fibres from the entorhinal cortex via the perforant path
Basket neurones
Neurones of the dentate gyrus and their axons, which form the mossy fibres of the hippocampus
Subicular efferent fibres to the fornix via the alveus

Fig. 23.20 Neuronal organization and connections of the dentate gyrus, hippocampus (cornu ammonis), subiculum and parahippocampal gyrus.

The hippocampus is trilaminar archicortex. It consists of a single pyramidal cell layer, with plexiform layers above and below it. It may best be divided into three distinct fields, CA1, CA2 and CA3 (Fig. 23.18, Fig.

23.19). Field CA3 borders the hilus of the dentate gyrus at one end, and field CA2 at the other. Field CA3 pyramidal cells are the largest in the hippocampus and receive the mossy fibre input from dentate granule cells on their proximal dendrites. The whole pyramidal cell layer in this field is about 10 cells thick. The border between CA3 and CA2 is not well marked. The CA2 field has the most compact layer of pyramidal cells. It completely lacks a mossy fibre input from dentate granule cells and receives a major input from the supramammillary region of the hypothalamus. Field CA1 is usually described as the most complex of the hippocampal subdivisions and its appearance varies along its transverse and rostrocaudal axes. The CA1/CA2 border is not sharp, and at its other end CA1 overlaps the subiculum for some distance. Approximately 10% of neurones in this field are interneurones.

It is common to describe several strata within the layers of the hippocampus. Starting from the ventricular aspect, these are the alveus (contains subicular and hippocampal pyramidal cell axons converging on the fimbria of the fornix); stratum oriens (mainly the basal dendrites of pyramidal cells and some interneurones); stratum pyramidalis; stratum lucidum (contains mossy fibres which make contact with the proximal dendrites of pyramidal cells in field CA3); and the stratum radiatum and stratum lacunosum-moleculare. The stratum lucidum is not as prominent in man as it is in other primates, and is not present in fields CA1 and CA2.

In the stratum radiatum and stratum oriens, CA3 and CA2 cells receive associational connections from other rostrocaudal levels of the hippocampus, as well as afferents from subcortical structures, e.g. the septal nuclei and supramammillary region. The projections from pyramidal cells of fields CA3 and CA2 to CA1, often called Schaffer collaterals, also terminate in the stratum radiatum and stratum oriens. The projections from the entorhinal cortex to the dentate gyrus (the perforant pathway) travel in the stratum lacunosum-moleculare, where they make synaptic contact *en passant* with the distal apical dendrites of hippocampal pyramidal cells.

The subicular complex is generally subdivided into subiculum, presubiculum and parasubiculum. The major subcortical projections of the hippocampal formation (to the septal nuclei, mammillary nuclei, nucleus accumbens and anterior thalamus), and to the entorhinal cortex, all arise from pyramidal neurones of the subicular complex. The subiculum consists of a superficial molecular layer containing apical dendrites of subicular pyramidal cells, a pyramidal cell layer, and a deep polymorphic layer. The presubiculum is medial to the subiculum and is distinguished by a densely packed superficial layer of pyramidal cells. It forms the boundary between the subicular complex as a whole and the entorhinal cortex. The cell layers deep to the parasubiculum are indistinguishable from the deep layers of the entorhinal cortex.

The entorhinal cortex (Brodmann's area 28, Fig. 23.19) extends rostrally to the anterior limit of the amygdala. Caudally it overlaps a portion of the hippocampal fields. The more primitive levels of the entorhinal cortex (below the amygdala) receive projections from the olfactory bulb. More caudal regions do not generally receive primary olfactory inputs. The entorhinal cortex is divisible into six layers and is quite distinct from other neocortical regions. Layer I is acellular and plexiform. Layer II is a narrow cellular layer, which consists of islands of large pyramidal and stellate cells. These cell islands are a distinguishing feature of the entorhinal cortex. They form small bumps on the surface of the brain that can be seen by the naked eye (verrucae hippocampae), and provide an indication of the boundaries of the entorhinal cortex. Layer III consists of medium-sized pyramidal cells. There is no internal granular layer (another classic feature of entorhinal cortex); in its place is an acellular region of dense fibres called the lamina dissecans, which is sometimes called layer IV. Layers III and V are apposed in regions where the lamina dissecans is absent. Layer V consists of large pyramidal cells five or six deep. Layer VI is only readily distinguishable from layer V close to the border with the perirhinal cortex. Its cells continue around the angular bundle (subcortical white matter deep to the subicular complex made up largely of perforant path axons) to lie beneath the pre- and parasubiculum.

Glutamate and/or aspartate appears to be the major excitatory transmitter in three pathways in the hippocampal formation, namely the perforant pathway (which arises in the entorhinal cortex and terminates primarily in the dentate gyrus); the mossy fibres, which run from the dentate granule cells to the pyramidal cells of the CA3 field; and in the Schaffer collaterals of CA3 pyramidal cells, which terminate on CA1 pyramidal cells.

GABAergic neurones are found in the deep portions of the granule cell layer in the dentate gyrus (basket cells). The highest concentration of GABA receptors is found in the molecular layer of the dentate gyrus. In the hippocampus proper, GABAergic cells are found mostly in the stratum oriens, but also in the pyramidal cell layer and stratum radiatum.

There are many peptide-containing neurones in the hippocampal formation. Granule cells in the dentate gyrus appear to contain the opioid peptide dynorphin, which is also present in mossy fibres running to the CA3 field. Enkephalin, or a related peptide, may be present in fibres arising in the entorhinal cortex. There is a dense plexus of somatostatin-immunoreactive fibres in the molecular layer of the dentate gyrus and also in the stratum lacunosum-moleculare of the hippocampus. The polymorphic layer of the dentate gyrus, stratum oriens of the hippocampus and the deep layers of the entorhinal cortex, all contain somatostatin-immunoreactive neurones. Vasoactive intestinal polypeptide (VIP)-immunoreactive neurones are plentiful in many hippocampal fields, especially in the superficial layers of the entorhinal cortex. Cells containing cholecystokinin (CCK)-immunoreactivity are found in the hilar region of the dentate gyrus, in all layers of the hippocampus, especially in the pyramidal cell layer, and also throughout the subicular complex and entorhinal cortex. There are also substantial plexuses of CCK-immunoreactive fibres in the stratum lacunosum-moleculare, subicular complex and entorhinal cortex. Hippocampal CCK-immunoreactive cells may give rise to extrinsic projections, e.g. to the lateral septum and medial mammillary nucleus, because CCK-immunoreactive fibres are found in the fimbria/fornix.

The medial septal complex and the supramammillary area of the posterior hypothalamus are the two major sources of subcortical afferents to the hippocampal formation. There are also projections from the amygdaloid complex and claustrum (to the subicular complex and entorhinal cortex), as well as monoaminergic projections from the ventral tegmental area, the mesencephalic raphe nuclei and the locus coeruleus. The noradrenergic and serotoninergic projections reach all hippocampal fields, but are especially dense in the dentate gyrus.

The projections from the septal complex arise in the medial septal and vertical limb nuclei of the diagonal band. They travel via the dorsal fornix, fimbria, supracallosal striae and a ventral route through the amygdaloid complex. While these projections reach all hippocampal fields, the most prominent terminations are in the dentate gyrus, field CA3, presubiculum, parasubiculum and entorhinal cortex. Many of these medial septal/diagonal band neurones are GABAergic or cholinergic, and they form part of the topographically organized basal forebrain cholinergic system (cell groups Ch1 and Ch2).

Neurones in the supramammillary area also provide a significant innervation of the hippocampal formation. They arrive partly through the fornix and partly through a ventral route, and terminate most heavily in the dentate gyrus, and fields CA2 and CA3 of the cornu ammonis.

All divisions of the anterior thalamic nuclear complex and associated lateral dorsal nucleus project to the hippocampal formation, and are directed predominantly to the subicular complex. Some midline thalamic nuclei, particularly the parataenial, central medial and reuniens nuclei, also project to the hippocampal formation, especially to the entorhinal cortex.

The human fornix contains more than a million fibres. Cells in the CA3 field project bilaterally to the lateral nucleus of the septal complex, via the precommissural fornix. They give rise to the Schaffer collaterals to CA1 cells and to the commissural projections to the contralateral hippocampus. Neurones in the subicular complex and entorhinal cortex give rise to projections to the nucleus accumbens and to parts of the caudate nucleus and putamen. The subicular complex gives rise to the major, postcommissural fibre system of the fornix. The presubiculum, in particular, projects to the anterior thalamic nuclear complex (anteromedial, anteroventral and laterodorsal nuclei). Both the subiculum and presubiculum provide the major extrinsic input to the mammillary complex. Both the lateral and the medial mammillary nuclei receive afferents from the subicular complex.

Several fields in the temporal lobe neocortex, especially the parahippocampal gyrus, the dorsal bank of the superior temporal gyrus, the perirhinal cortex (Brodmann’s area 35) and the temporal polar cortex, together with the agranular insular cortex and posterior orbitofrontal cortex, project to the entorhinal cortex. Projections to the entorhinal cortex also arise from the dorsolateral prefrontal cortex (Brodmann’s areas 9, 10, 46), the medial frontal cortex (Brodmann’s areas 25, 32), the cingulate cortex (Brodmann’s areas 23, 24), and retrosplenial cortex. The subicular complex receives direct cortical inputs, e.g. from the temporal polar cortex, perirhinal cortex, parahippocampal gyrus, superior temporal gyrus and dorsolateral prefrontal cortex. The entorhinal cortex projects to the perirhinal cortex as well as to temporal polar cortex, caudal parahippocampal and cingulate gyri. In monkeys, the subicular complex also projects to a number of cortical areas, including perirhinal cortex, parahippocampal gyrus, caudal cingulate gyrus, medial frontal and medial orbitofrontal cortex.

Septum

The septum is a midline and paramedian structure (Fig. 23.13, Fig. 22.6). Its upper portion corresponds largely to the bilateral laminae of fibres, sparse grey matter and neuroglia, known as the septum pellucidum, which separates the lateral ventricles. Below this, the septal region is made up of four main nuclear groups: dorsal, ventral, medial and caudal. The dorsal group is essentially the dorsal septal nucleus, the ventral group consists of the lateral septal nucleus, the medial group contains the medial septal nucleus and the nucleus of the diagonal band of Broca, and the caudal group contains the fimbrial and triangular septal nuclei.

The major afferents to the region terminate primarily in the lateral septal nucleus. They include fibres carried in the fornix that arise from hippocampal fields CA3 and CA1 and the subiculum. There are also afferents arising from the preoptic area, anterior, paraventricular and ventromedial hypothalamic nuclei and the lateral hypothalamic area. The lateral septum receives a rich monaminergic innervation, including noradrenergic afferents from the locus coeruleus and medullary cell groups (A1, A2). It also receives serotoninergic afferents from the midbrain raphe nuclei and dopaminergic afferents from the ventral tegmental area (A10).

Projections from the lateral septum run to the medial and lateral preoptic areas, anterior hypothalamus, supramammillary and midbrain ventral tegmental area, via the medial forebrain bundle. There is also a projection to the medial habenular nucleus and some midline thalamic nuclei via the stria medullaris thalami, which runs on the dorsomedial wall of the third ventricle. The projections from the habenula via the fasciculus retroflexus to the interpeduncular nucleus and adjacent ventral tegmental area in the midbrain provide a route through which forebrain limbic structures can influence midbrain nuclear groups.

A large proportion of the medial septal/diagonal band neurones are cholinergic or GABAergic. They project to the hippocampal formation and cingulate cortex.

Amygdala

The amygdala (amygdaloid nuclear complex) consists of lateral, central and basal nuclei that lie in the dorsomedial temporal pole, anterior to the hippocampus, close to the tail of the caudate nucleus (Fig. 23.13) and partly deep to the gyrus semilunaris, gyrus ambiens and uncinate gyrus (Fig. 23.4). Collectively the nuclei form the ventral, superior and medial walls of the tip of the inferior horn of the lateral ventricle. The amygdala is partly continuous above with the inferomedial margin of the claustrum. Fibres of the external capsule and substriatal grey matter, including the cholinergic magnocellular nucleus basalis (of Meynert), incompletely separate it from the putamen and globus pallidus. Laterally, it is close to the optic tract.

The lateral nucleus has dorsomedial and ventrolateral subnuclei. The central nucleus has medial and lateral subdivisions. The basal nucleus is commonly divided into a dorsal magnocellular basal nucleus, an intermediate parvicellular basal nucleus, and a ventral band of darkly staining cells usually referred to as the paralaminar basal nucleus, because it borders the white matter ventral to the amygdaloid complex. The accessory basal nucleus lies medial to the basal nuclear divisions and is usually divided into dorsal, magnocellular, and ventral, parvicellular, parts. The lateral and basal nuclei are often referred to collectively as the basolateral area (nuclear group) of the amygdaloid complex.

It has been suggested that the basolateral complex of nuclei (lateral, basal, accessory basal) shares several characteristics with the cortex, and that it may be considered as a quasi-cortical structure. Although it lacks a laminar structure, it has direct, often reciprocal, connections with adjacent temporal and other areas of cortex, and it projects to the motor or premotor cortex. It receives a direct cholinergic and non-cholinergic input from the magnocellular corticopetal system in the basal forebrain, and has reciprocal connections with the mediodorsal thalamus. The distribution of small peptidergic neurones in the basolateral nuclear complex, e.g. those containing neuropeptide-Y (NY), somatostatin (SOM) and CCK, are also similar in form and density to those found in the adjacent temporal lobe cortex. Projection neurones from this part of the amygdala appear to utilize, at least in part, the excitatory amino acids glutamate or aspartate as a transmitter. Moreover, they project to the ventral striatum rather than to hypothalamic and brain stem sites. Thus, it may be appropriate to consider this part of the amygdaloid complex as a polymodal cortex-like area, separated from the cerebral cortex by fibres of the external capsule.

The central nucleus is present through the caudal half of the amygdaloid complex. It lies dorsomedial to the basal nucleus and is divided into medial and lateral parts. The medial part, which contains larger cells than the lateral part, resembles the adjacent putamen. The medial and central nuclei appear to have an extension across the basal forebrain, as well as within the stria terminalis, which merges with the bed nucleus of the stria terminalis. This extensive nuclear complex is sometimes referred to as the ‘extended amygdala’ (Fig. 23.21). It can be considered as a macrostructure formed by the centromedial amygdaloid complex (medial nucleus, medial and lateral parts of the central nucleus), the medial bed nucleus of the stria terminalis, and the cell columns that traverse the sublenticular substantia innominata, which lies between them. It has been suggested that portions of the medial nucleus accumbens may be included in the extended amygdala.

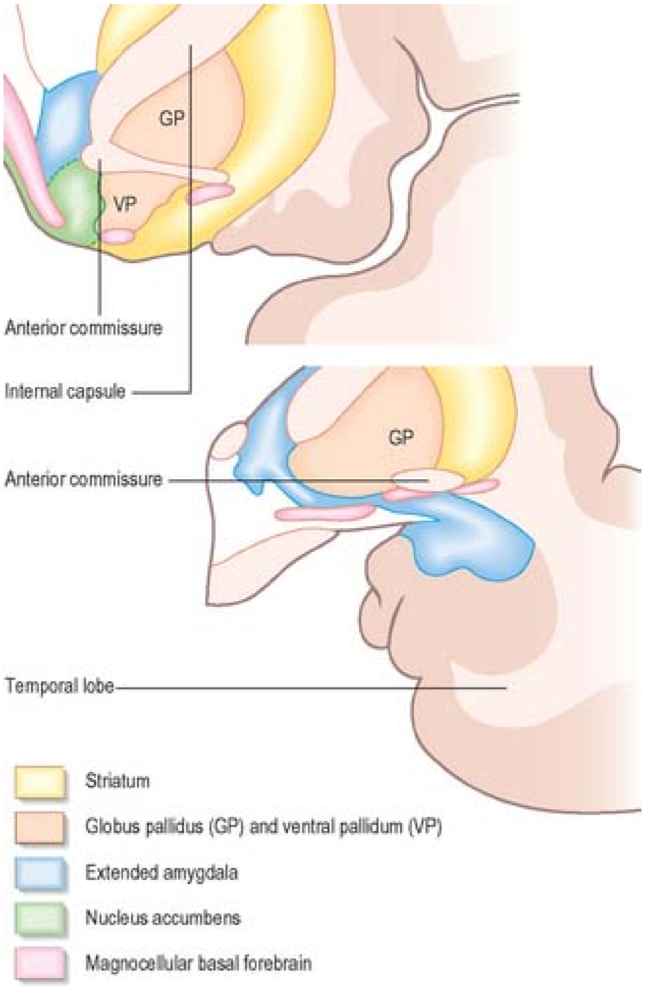
GP
VP
Anterior commissure
Internal capsule
GP
Anterior commissure
Temporal lobe
Striatum
Globus pallidus (GP) and ventral pallidum (VP)
Extended amygdala
Nucleus accumbens
Magnocellular basal forebrain

Fig. 23.21 Coronal section through the basal forebrain and temporal pole, illustrating the relationship between the striatum, nucleus accumbens, globus pallidus, ventral pallidum, extended amygdala and magnocellular basal forebrain system.

A consistent feature of the intrinsic connections among amygdaloid nuclei is that they arise primarily in lateral and basal nuclei, and terminate in the central and medial nuclei, which suggests a largely unidirectional flow of information. In brief, the lateral nucleus projects to all divisions of the basal nucleus, accessory basal nucleus, paralaminar and anterior cortical nuclei, and less heavily to the central nucleus: it receives few afferents from other nuclei. The magnocellular, parvicellular and intermediate parts of the basal nucleus project to the accessory basal, central (especially the medial part) and medial nuclei, as well as to the periamygdaloid cortex and the amygdalohippocampal area. The accessory basal nucleus projects densely to the central nucleus, especially its medial division, as well as to the medial and cortical nuclei. Its major intra-amygdaloid afferents arise from the lateral nucleus. The medial nucleus projects to the accessory basal, anterior cortical and central nuclei as well as to the periamygdaloid cortex and amygdalohippocampal area, while afferents arise especially from the lateral nucleus. The intrinsic connections of the cortical nucleus are not very well understood. The posterior part of the cortical nucleus projects to the medial nucleus, but it has been difficult to differentiate this projection from that arising in the amygdalohippocampal area. The central nucleus projects to the anterior cortical nucleus and the various cortical transition zones. It forms an important focus for afferents from many of the amygdaloid nuclei, especially the basal and accessory basal nuclei, and it has major extrinsic connections.

The organization of the extensive subcortical and cortical connections of the amygdala are consistent with a role in emotional behaviour. It receives highly processed unimodal and multimodal sensory information from the thalamus, sensory and association cortices; olfactory information from the olfactory bulb and piriform cortex; visceral and gustatory information relayed via brain stem structures and the thalamus. Its projections reach widespread areas of the brain, including the endocrine and autonomic domains of the hypothalamus and brain stem.

Afferent connections

The heaviest brain stem projection to the amygdala arises in the peripeduncular nucleus. The parabrachial nuclei also project to the central nucleus. The amygdala receives a rich monoaminergic innervation. The noradrenergic projection arises primarily from the locus coeruleus, serotonergic fibres arise from the dorsal and, to some extent the median, raphe nuclei, and the dopaminergic innervation arises primarily in the midbrain ventral tegmental area (A10). The basal and parvicellular accessory basal nuclei, the amygdalohippocampal area and nucleus of the lateral olfactory tract receive a very dense cholinergic innervation arising from the magnocellular nucleus basalis of Meynert.

The amygdala has rich interconnections with allocortical, juxtallocortical and, especially, neocortical areas. In addition to direct projections from the olfactory bulb to the nucleus of the lateral olfactory tract, anterior cortical nucleus and the periamygdaloid cortex (piriform cortex), there are also associational connections between all parts of the primary olfactory cortex and these same superficial amygdaloid structures. The amygdaloid complex has particularly extensive and rich connections with many areas of the neocortex in unimodal and polymodal regions of the frontal, cingulate, insular and temporal neocortices.

The anterior temporal lobe provides the largest proportion of the cortical input to the amygdala, predominantly to the lateral nucleus. Rostral parts of the superior temporal gyrus, which may represent unimodal auditory association cortex, project to the lateral nucleus. There are also projections from polymodal sensory association cortices of the temporal lobe, including perirhinal cortex (areas 35 and 36), the caudal half of the parahippocampal gyrus, the dorsal bank of the superior temporal sulcus, and both the medial and lateral areas of the cortex of the temporal pole.

The CA1 field of the hippocampus and adjacent subiculum, and possibly the entorhinal cortex, project to the amygdala, mainly to the parvicellular basal nucleus.

The rostral insula projects heavily to the lateral, parvicellular basal and medial nuclei. The caudal insula, which is reciprocally connected with the second somatosensory cortex, also projects to the lateral nucleus, thus providing a route by which somatosensory information reaches the amygdala. The caudal orbital cortex projects to the basal, magnocellular accessory basal and lateral nuclei. The medial prefrontal cortex projects to the magnocellular divisions of the accessory and basal nuclei.

Efferent connections

The central nucleus provides the major relay for projections from the amygdala to the brain stem and receives many of the return projections. It projects to the periaqueductal grey matter, ventral tegmental area, substantia nigra pars compacta, peripeduncular nucleus and tegmental reticular formation (midbrain); the parabrachial nuclei (pons); the nucleus of the solitary tract and the dorsal motor nucleus of the vagus (medulla).

The central nucleus is the major relay for amygdaloid projections to the hypothalamus. Amygdaloid fibres reach the bed nucleus of the stria terminalis primarily via the stria terminalis, but also via the ventral amygdalofugal pathway. In general, central and basal nuclei project to the lateral part of the bed nucleus, while medial and posterior cortical nuclei project to the medial bed nucleus. Anterior cortical and medial nuclei project largely to the medial preoptic area and anterior medial hypothalamus, including the paraventricular and supraoptic nuclei. There is a particularly prominent projection to the ventromedial and premammillary nuclei. The amygdala projects to the rostrocaudal extent of the lateral hypothalamus. The majority of the fibres originate in the central nucleus and run principally in the ventral amygdalofugal pathway and medial forebrain bundle.

There is a rich projection to the mediodorsal nucleus of the thalamus, which gives access to the prefrontal cortex, and also complements direct projections from the amygdala to the same cortical domain. The projection to the mediodorsal nucleus arises from most amygdaloid nuclei, but particularly from the lateral, basal and accessory basal nuclei and the periamygdaloid cortex. The major termination of amygdaloid afferents is in the medial, magnocellular part of the mediodorsal nucleus, especially rostrally. This part of the mediodorsal nucleus projects to the identical medial and orbital prefrontal cortical areas that receive amygdaloid afferents directly. However, this projection to the mediodorsal nucleus is not reciprocated. The central and medial nuclei do not project to the mediodorsal nucleus, but to the midline nuclei, especially the nucleus centralis and nucleus reuniens.

The parvicellular division of the basal nucleus, magnocellular accessory basal nucleus (but not the magnocellular basal nucleus), and the central nucleus all project to basal forebrain cholinergic cell groups, notably the nucleus basalis of Meynert and the horizontal limb nucleus of the diagonal band.

The striatum, and particularly the nucleus accumbens, receives prominent projections from the amygdaloid complex. The basal and accessory basal nuclei are the most important contributors to this projection. The ventral striatum sends many fibres to the ventral pallidum, which in its turn projects to the mediodorsal nucleus of the thalamus. Thus, the ventral striatopallidal system provides a second route through which the amygdala can influence mediodorsal thalamic–prefrontal cortical processes.

The lateral, magnocellular accessory basal and parvicellular basal nuclei contribute the largest proportion of efferents to the hippocampal formation. The main projection is from the lateral nucleus to the rostral entorhinal cortex, but many fibres also terminate in the hippocampus proper and the subiculum. There appears to be marked polarity in amygdalohippocampal connections – the amygdala has a greater influence on hippocampal processes than vice versa.

The amgygdaloid nuclear complex projects to widely dispersed neocortical fields. Amygdalocortical projections principally originate in the basal nucleus, and to a smaller extent in the lateral and cortical nuclei.

The amygdala projects to virtually all levels of the visual cortex in both temporal and occipital lobes. The largest component of these projections arises from the magnocellular basal nucleus. The amygdala also reciprocates projections to the auditory cortex in the rostral half of the superior temporal gyrus. Projections to the polymodal sensory areas of the temporal lobe generally reciprocate the amygdalopetal projections. Efferents from the lateral and accessory basal nuclei are directed to the temporal pole, particularly the medial perirhinal area.

The insular cortex is heavily innervated by the amygdaloid medial and anterior cortical nuclei. The orbital cortex and medial frontal cortical areas 24, 25 and 32, including parts of the anterior cingulate gyrus, also receive a heavy projection. Areas 8, 9, 45 and 46 of the dorsolateral prefrontal cortex, as well as the premotor cortex (area 6), receive a patchy innervation. The basal nucleus is an important source of these projections, which are augmented by contributions from the accessory basal (magnocellular and parvicellular divisions) and lateral nuclei.

WHITE MATTER OF CEREBRAL HEMISPHERE

The nerve fibres which make up the white matter of the cerebral hemispheres are categorized on the basis of their course and connections. They are either association fibres, which link different cortical areas in the same hemisphere; commissural fibres, which link corresponding cortical areas in the two hemispheres; or projection fibres, which connect the cerebral cortex with the corpus striatum, diencephalon, brain stem and the spinal cord.

ASSOCIATION FIBRES

Association fibres (Fig. 23.22, Fig. 23.23) may be either short association (arcuate or 'U') fibres, which link adjacent gyri, or long association fibres, which connect more widely separated gyri.

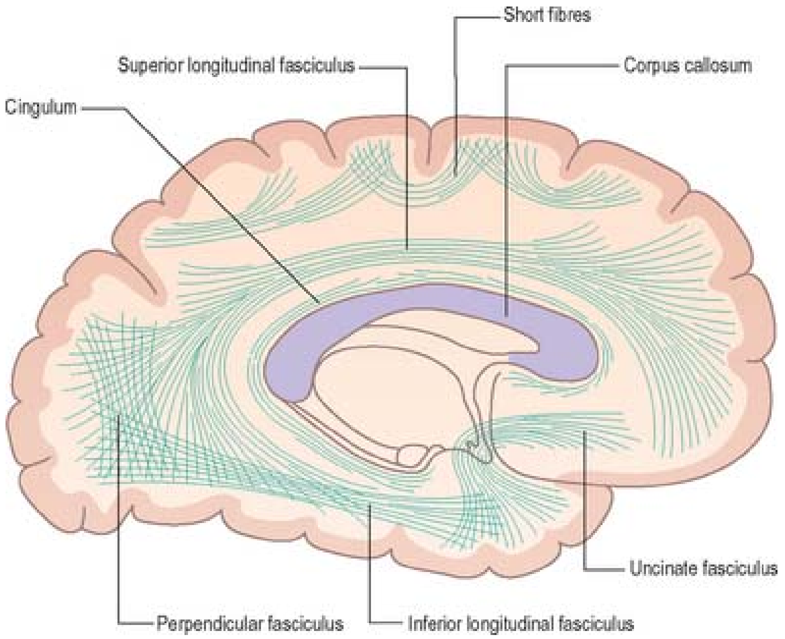
Short fibres
Superior longitudinal fasciculus
Corpus callosum
Cingulum
Uncinate fasciculus
Perpendicular fasciculus
Inferior longitudinal fasciculus

Fig. 23.22 The organization of the principal association fibres projected upon a sagittal section of the left cerebral hemisphere.

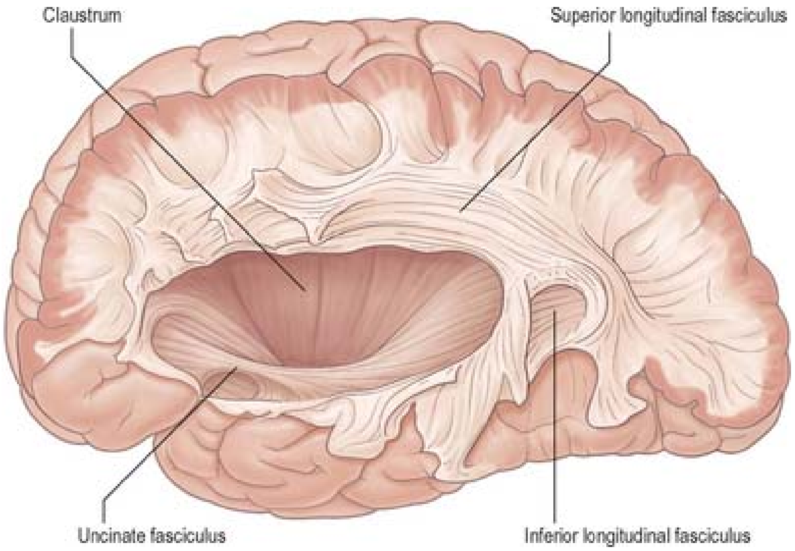
Claustrum
Superior longitudinal fasciculus
Uncinate fasciculus
Inferior longitudinal fasciculus

Fig. 23.23 Some of the long association fasciculi of the left cerebral hemisphere.

Short association fibres may be entirely intracortical. Many pass subcortically between adjacent gyri, some merely pass from one wall of a sulcus to the other.

Long association fibres are grouped into bundles, e.g. uncinate fasciculus, cingulum, superior longitudinal fasciculus, inferior longitudinal fasciculus and fronto-occipital fasciculus.

The uncinate fasciculus connects the motor speech (Broca’s) area and orbital gyri of the frontal lobe with the cortex in the temporal pole. The fibres follow a sharply curved course across the stem of the lateral sulcus, near the anteroinferior part of the insula. The cingulum is a long, curved fasciculus, which lies deep to the cingulate gyrus. It starts in the medial cortex below the rostrum of the corpus callosum, follows the curve of the cingulate gyrus, enters the parahippocampal gyrus and spreads into the adjoining temporal lobe. The superior longitudinal fasciculus is the largest of the long association fasciculi. It starts in the anterior frontal region and arches back, above the insular area, contributing fibres to the occipital cortex (areas 18 and 19). It curves down and forwards, behind the insular area, to spread out in the temporal lobe. The inferior longitudinal fasciculus starts near the occipital pole. Its fibres, probably derived mostly from areas 18 and 19, sweep forwards, separated from the posterior horn of the lateral ventricle by the optic radiation and tapetal commissural fibres, and are distributed throughout the temporal lobe. The fronto-occipital fasciculus starts at the frontal pole. It passes back deep to the superior longitudinal fasciculus, separated from it by the projection fibres in the corona radiata. It lies lateral to the caudate nucleus near the central part of the lateral ventricle. Posteriorly, it fans out into the occipital and temporal lobes, lateral to the posterior and inferior horns of the lateral ventricle.

COMMISSURAL FIBRES

Commissural fibres cross the midline, many linking corresponding areas in the two cerebral hemispheres. By far the largest commissure is the corpus callosum. Others include the anterior, posterior and habenular commissures, and the commissure of the fornix.

Corpus callosum

The corpus callosum (Fig. 23.2, Fig. 23.24, Fig. 23.25; see Fig. 22.2) is the largest fibre pathway of the brain. It links the cerebral cortex of the two cerebral hemispheres, and it roofs much of the lateral ventricles. It forms an arch approximately 10 cm long, with an anterior end approximately 4 cm from the frontal poles and a posterior end approximately 6 cm from the occipital poles. Its anterior portion is known as the genu. This recurves posteroinferiorly in front of the septum pellucidum, then diminishes rapidly in thickness and is prolonged to the upper end of the lamina terminalis as the rostrum. The trunk of the corpus callosum arches back and is convex above. It ends posteriorly in the expanded splenium, which is its thickest part.

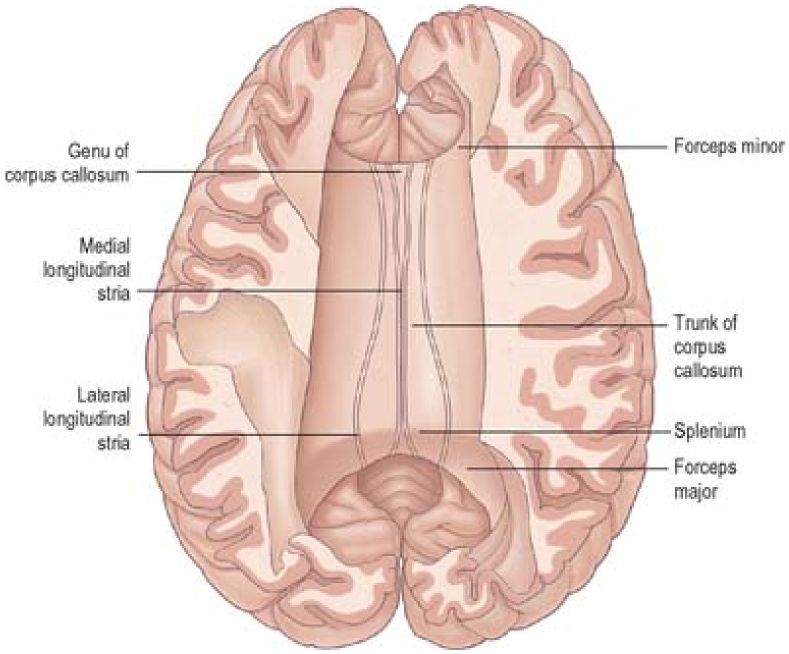
Genu of corpus callosum
Medial longitudinal stria
Lateral longitudinal stria
Forceps minor
Trunk of corpus callosum
Splenium
Forceps major

Fig. 23.24 The superior aspect of the corpus callosum revealed by partial removal of the cerebral hemispheres.

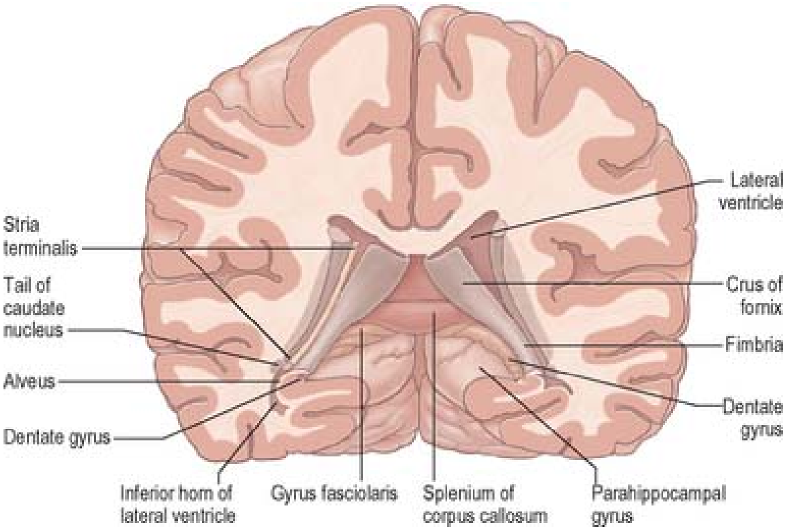
Stria terminalis
Tail of caudate nucleus
Alveus
Dentate gyrus
Inferior horn of lateral ventricle
Gyrus fasciolaris
Splenium of corpus callosum
Parahippocampal gyrus
Lateral ventricle
Crus of fornix
Fimbria
Dentate gyrus

Fig. 23.25 Anterior aspect of a coronal section of the cerebrum. The posterior parts of the thalami have been removed to reveal the splenium of the corpus callosum.

The median region of the trunk of the corpus callosum forms the floor of the great longitudinal fissure. Here, it lies close to the anterior cerebral arteries and the lower border of the falx cerebri, which may contact it behind. On each side, the trunk is overlapped by the cingulate gyrus, from which it is separated by the callosal sulcus. The inferior surface of the corpus callosum is concave in its long axis: it is attached to the septum pellucidum anteriorly and fused with the fornix and its commissure posteriorly.

The superior surface of the callosal trunk (Fig. 23.24) is covered by a thin layer of grey matter, the indusium griseum. This extends anteriorly around the genu and then continues into the paraterminal gyrus on the inferior aspect of the rostrum. It contains narrow longitudinal bundles of fibres on each side, the medial and lateral longitudinal striae. Posteriorly, the indusium griseum is continuous with the dentate gyrus and hippocampus through the gyrus fasciolaris (Fig. 23.25).

The splenium of the corpus callosum overhangs the posterior ends of the thalami, the pineal gland and tectum, but is separated from them by several structures. On each side the crus of the fornix and gyrus fasciolaris curve up to the splenium. The crus continues forwards on the inferior surface of the callosal trunk, but the gyrus fasciolaris skirts above the splenium, then rapidly diminishes into the indusium griseum. The tela choroidea of the third ventricle advances below the splenium through the transverse fissure, and the internal cerebral veins emerge between its two layers to form the great cerebral vein. Posteriorly the splenium is near the tentorium cerebelli, great cerebral vein and the start of the straight sinus.

Nerve fibres of the corpus callosum radiate into the white matter core of each hemisphere, thereafter dispersing to the cerebral cortex. Commissural fibres forming the rostrum extend laterally, below the anterior horn of the lateral ventricle, connecting the orbital surfaces of the frontal lobes. Fibres in the genu curve forwards, as the forceps minor, to connect the lateral and medial surfaces of the frontal lobes. Fibres of the trunk pass laterally, intersecting with the projection fibres of the corona radiata to connect wide neocortical areas of the hemispheres. Fibres of the trunk and splenium, which form the roof and lateral wall of the posterior horn and the lateral wall of the inferior horn of the lateral ventricle, constitute the tapetum. The remaining fibres of the splenium curve back into the occipital lobes as the forceps major.

Interhemispheric connections through the corpus callosum do not all represent a simple linking of loci in one hemisphere with the same loci in the other. In areas containing a clear representation of a contralateral sensorium (e.g. body surface, visual field), only those areas that are functionally related to midline representation are linked to the contralateral hemisphere. This is most clearly seen for the visual areas, where the cortex containing the representation of each midline retinal zone is linked to its counterpart on the contralateral side. A similar arrangement is seen in somatic areas, where the trunk representation is callosally linked, but the peripheral limb areas (hand and foot) are not.

Connections that link the same, or similar, areas on each side are termed homotopic connections. The corpus callosum also interconnects heterogeneous cortical areas on the two sides (heterotopic connections). These may serve to connect functionally similar, but anatomically different, loci in the two hemispheres, and/or to connect functional areas in one hemisphere with regions that are specialized for a unilaterally confined function in the other.

Anterior commissure

The anterior commissure is a compact bundle of myelinated nerve fibres which crosses anterior to the columns of the fornix and is embedded in the lamina terminalis, where it is part of the anterior wall of the third ventricle (Fig. 23.13). In sagittal section it is oval, its long (vertical) diameter is approximately 1.5 mm. Laterally it splits into anterior and posterior bundles. The smaller anterior bundle curves forwards on each side to the anterior perforated substance and olfactory tract. The posterior bundle curves posterolaterally on each side in a deep groove on the anteroinferior aspect of the lentiform complex, and subsequently fans out into the anterior part of the temporal lobe, including the parahippocampal gyrus. Areas thought to be connected via commissural fibres include: the olfactory bulb and anterior olfactory nucleus; the anterior perforated substance, olfactory tubercle and diagonal band of Broca; the prepiriform cortex; the entorhinal area and adjacent parts of the parahippocampal gyrus; part of the amygdaloid complex (especially the nucleus of the lateral olfactory stria); the bed nucleus of the stria terminalis and the nucleus accumbens; the anterior regions of the middle and inferior temporal gyri.

PROJECTION FIBRES

Projection fibres connect the cerebral cortex with lower levels in the brain and spinal cord. They include large numbers of both corticofugal and corticopetal projections. Corticofugal projection fibres converge from all directions to form the dense subcortical white matter mass of the corona radiata (Fig. 23.26). Large numbers of fibres pass to the corpus striatum and the thalamus, intersecting commissural fibres of the corpus callosum en route. The corona radiata is continuous with the internal capsule, which contains the majority of the cortical projection fibres.

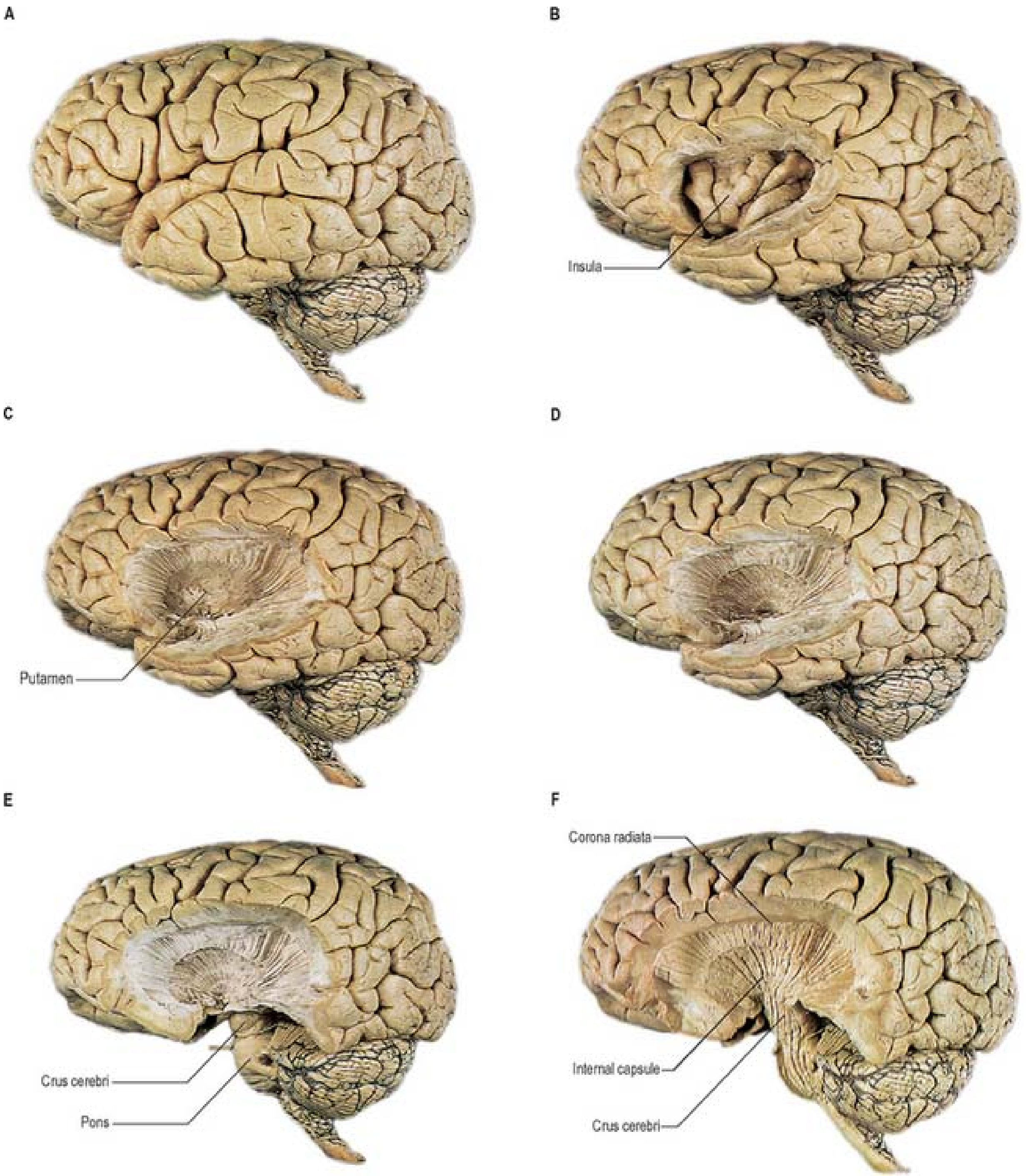
A
B
Insula
C
D
Putamen
E
F
Corona radiata
Crus cerebri
Pons
Internal capsule
Crus cerebri

Fig. 23.26 A series of dissections of the left cerebral hemisphere at progressively deeper levels to demonstrate the relationships of the internal capsule. **A**, intact brain; **B**, cortical gyri of the insula exposed by removal of the frontal, temporal and parietal opercula; **C**, removal of the insular cortex, extreme capsule, claustrum and external capsule to expose the lateral aspect

of the putamen; **D**, removal of the lentiform complex to display fibres of the internal capsule; **E**, removal of part of the temporal lobe to show the internal capsule fibres converging on the crus cerebri of the midbrain; **F**, removal of the optic tract, and superficial dissection of the pons and upper medulla, emphasizing the continuity of the corona radiata, internal capsule, crus cerebri, longitudinal pontine fibres and the medullary pyramid.

(Dissection by E.L. Rees; photograph by Kevin Fitzpatrick on behalf of GKT School of Medicine, London; figure enhanced by B. Crossman.)

Internal capsule

In horizontal cerebral sections the internal capsule appears as a broad white band, with a lateral concavity, which accommodates the lentiform complex (Fig. 23.27, Fig. 23.28, Fig. 23.29). It has an anterior limb, genu, posterior limb, and retrolenticular (retrolentiform) and sublenticular (sublentiform) parts. Both anterior and posterior limbs are medial to the lentiform complex. The head of the caudate nucleus is medial to the anterior limb, and the thalamus is medial to the posterior limb. Cortical efferent fibres of the internal capsule continue to converge as they descend. Fibres derived from the frontal lobe tend to pass posteromedially, while temporal and occipital fibres pass anterolaterally. Many, but not all, corticofugal fibres pass into the crus cerebri of the ventral midbrain. Here, corticospinal and corticobulbar fibres are located in the middle half of the crus. Frontopontine fibres are located medially, whereas corticopontine fibres from temporal, parietal and occipital cortices are found laterally.

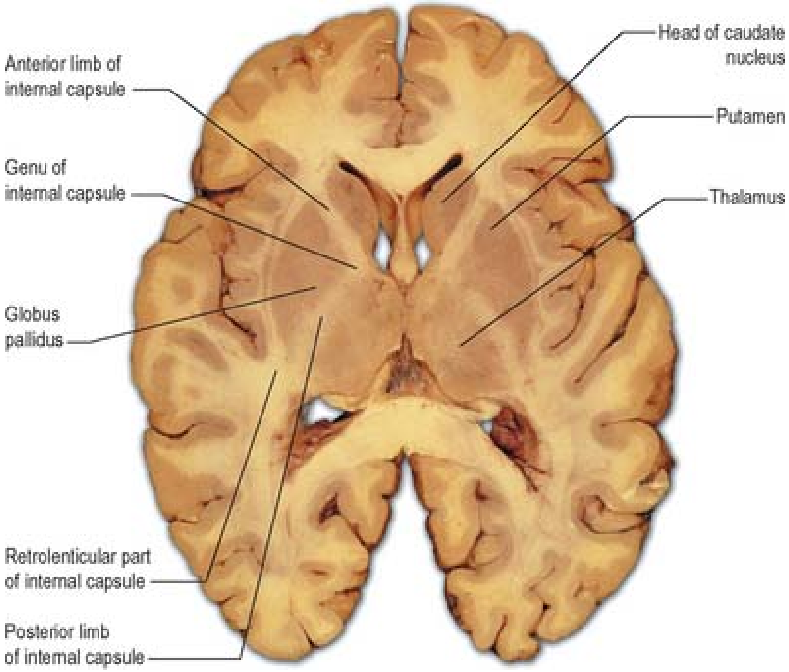
Anterior limb of internal capsule
Genu of internal capsule
Globus pallidus
Retrolenticular part of internal capsule
Posterior limb of internal capsule
Head of caudate nucleus
Putamen
Thalamus

Fig. 23.28 Horizontal section of the brain through the frontal and occipital poles of the cerebral hemispheres. (Figure enhanced by B. Crossman.)

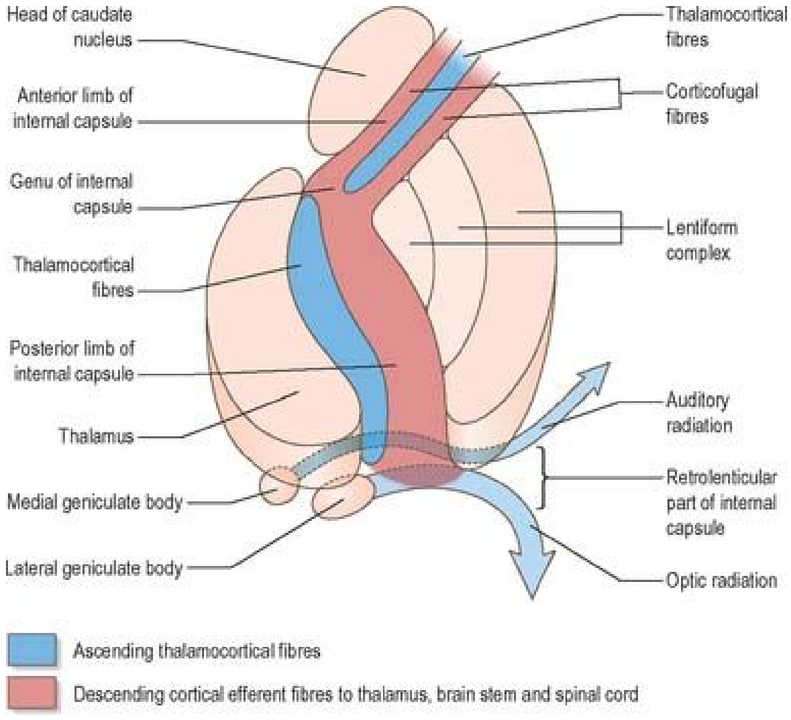
Head of caudate nucleus
Anterior limb of internal capsule
Genu of internal capsule
Thalamocortical fibres
Posterior limb of internal capsule
Thalamus
Medial geniculate body
Lateral geniculate body
Thalamocortical fibres
Corticofugal fibres
Lentiform complex
Auditory radiation
Retrolenticular part of internal capsule
Optic radiation
🟦 Ascending thalamocortical fibres
🟥 Descending cortical efferent fibres to thalamus, brain stem and spinal cord

Fig. 23.29 Horizontal section through the internal capsule illustrating its main fibre components.

The anterior limb of the internal capsule contains frontopontine fibres, which arise from the cortex in the frontal lobe. They synapse with cells in the pontine nuclei. Axons of these cells enter the opposite cerebellar hemisphere through the middle cerebellar peduncle. Anterior thalamic radiations interconnect the medial and anterior thalamic nuclei and various hypothalamic nuclei and limbic structures with the frontal cortex.

The genu of the internal capsule is usually regarded as containing corticobulbar fibres, which are mainly derived from area 4 and terminate mostly in the contralateral motor nuclei of cranial nerves. Anterior fibres of the superior thalamic radiation, between the thalamus and cortex, also extend into the genu.

The posterior limb of the internal capsule includes the corticospinal tract. The fibres concerned with the upper limb are anterior. More posterior regions contain fibres representing the trunk and lower limbs. Other descending axons include frontopontine fibres, particularly from areas 4 and 6, and corticorubral fibres, which connect the frontal lobe to the red nucleus. Most of the posterior limb also contains fibres of the superior thalamic radiation (the somaesthetic radiation) ascending to the postcentral gyrus.

The retrolenticular part of the internal capsule contains parietopontine, occipitopontine, and occipitotectal fibres. It also includes the posterior thalamic radiation and the optic radiation, and interconnections between the occipital and parietal lobes and caudal parts of the thalamus, especially the pulvinar.

The optic radiation arises in the lateral geniculate body. It sweeps backwards, intimately related to the superolateral aspect of the inferior horn and the lateral aspect of the posterior horn of the lateral ventricle, from which it is separated by the tapetum.

The sublenticular part of the internal capsule contains temporopontine and some parietopontine fibres, the auditory radiation from the medial geniculate body to the superior temporal and transverse temporal gyri (areas 41 and 42), and a few fibres that connect the thalamus with the temporal lobe and insula. Fibres of the auditory radiation sweep anterolaterally below and behind the lentiform complex to reach the cortex.

CEREBRAL ASYMMETRY

The two human cerebral hemispheres are not simply mirror images of each other. Much information on the lateralization of cerebral function has come from studying patients in whom the corpus callosum had been divided (commissurotomy) as a treatment for intractable epilepsy, and from those rare individuals who lack part, or all, of their corpus callosum. Commissurotomy produces the ‘split-brain’ syndrome, which has provided evidence supporting the notion that abilities or functions are predominantly associated with one or other hemisphere. Knowledge of such lateralization of function has been advanced more recently by functional brain imaging techniques such as positron emission tomography (PET).

The left hemisphere usually prevails for verbal and linguistic functions, for mathematical skills and for analytical thinking. The right hemisphere is mostly non-verbal. It is more involved in spatial and holistic or ‘Gestalt’ thinking, in many aspects of musical appreciation, and in some emotions. Memory also shows lateralization. Thus, verbal memory is primarily a left hemisphere function, while non-verbal memory is represented in the right hemisphere. These asymmetries are relative, not absolute, and vary in degree according to the function and individual concerned. Moreover, they apply primarily to right-handed men. Those men with left-hand preference, or mixed handedness, make up a heterogeneous group, which (as an approximation) shows reduced or anomalous lateralization, rather than a simple reversal of the situation in right-handers. For example, speech representation can occur in either or both hemispheres. Women show less functional asymmetry, on average, than men.

Certain cerebral anatomical asymmetries are apparent at both the macroscopic and histological levels. One of the most notable is in the planum temporale, which is usually larger on the left than the right side. Subtle asymmetries in the superior temporal lobe have been demonstrated in terms of overall size and shape, sulcal pattern, cytoarchitecture and at the neuronal level. It seems reasonable to assume that these differences underlie some of the functional asymmetry for language representation.

Asymmetries in areal size, cytoarchitecture or neurocytology occur elsewhere in the cerebral cortex as well as subcortically. For example, many brains have a wider right frontal pole and a wider left occipital pole. Brodmann’s area 45 in the inferior frontal lobe, corresponding to Broca’s area, contains a population of large pyramidal neurones that are found only on the left side. The cortical surface surrounding the central sulcus is larger in the left hemisphere, especially in the areas containing the primary somatosensory and motor maps of the arm, suggesting that one cerebral manifestation of hand preference is a larger amount of neural circuitry in the relevant parts of the cortex. Histological asymmetries are also found in areas that are not usually considered to be closely related either to language or handedness. The left entorhinal cortex has significantly more neurones than the right.

NEUROPSYCHOLOGICAL FUNCTIONS

The neuropsychological functions of perception, spatial analysis, learned skilled movement, language, memory, problem solving (all executive functions) and emotion, are organized within the cerebral hemispheres (Fig. 23.30).

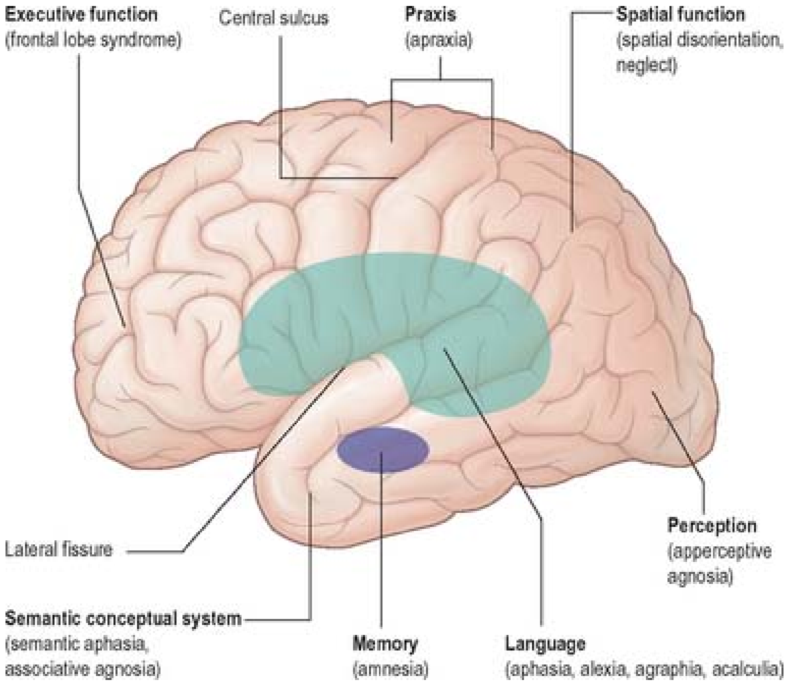
Executive function
(frontal lobe syndrome)
Central sulcus
Praxis
(apraxia)
Spatial function
(spatial disorientation, neglect)
Lateral fissure
Perception
(apperceptive agnosia)
Semantic conceptual system
(semantic aphasia, associative agnosia)
Memory
(amnesia)
Language
(aphasia, alexia, agraphia, acalculia)

Fig. 23.30 Regional localization of cognitive function (dysfunction) in the cerebral hemisphere.

The organization of neuropsychological functions is highly localized and involves the association areas of the neocortex and the limbic system. The parietal association areas are concerned with the perceptual recognition of objects by kinaesthetic and visual stimuli, and the visuo-spatial orientation of the body and its parts in space. Large focal lesions (particularly of the right cerebral hemisphere) and bilateral lesions (e.g. in Alzheimer’s disease), lead to visual disorientation in space, with an inability to navigate the environment, locate objects, and dress in relationship to body parts. Acute focal lesions (especially of the right cerebral hemisphere) lead to neglect of the body and space in the opposite side of corporeal and visual space (neglect). Failure of recognition of objects by touch or vision, represents tactile or visual agnosia. The parietal-temporal cortical connections are particularly important for visual object recognition and lesions lead to an inability to identify, copy, or match, objects (apperceptive visual agnosia). The anterior superior parietal lobes and the related connections with the pre-motor areas, including the supplementary motor areas, are concerned in the execution of skilled movements through development and experience (praxis). Lesions of these areas lead to contralateral loss of skilled movements of the face, mouth and limbs (ideomotor apraxia).

The anterior temporal neocortex (middle and inferior temporal gyri) is concerned in ascribing meaning to perceptual stimuli. Bilateral lesions of these areas (e.g. in semantic dementia) leads to loss of recognition of words and percepts. Unilateral lesions in the left hemisphere particularly affect word meaning and naming (semantic or trans-cortical aphasia), whereas lesions of the right hemisphere lead primarily to loss of recognition of visual percepts (associative visual agnosia) and faces (prosopagnosia), and objects can be copied or matched but not identified for meaning or name.

The pre-motor areas (frontal association cortex, parietal and temporal association cortex) combine to form the ‘language area’ in the cortex that surrounds the lateral fissure in the left dominant hemisphere. Focal lesions of the language area lead to breakdown in verbal communication (aphasia) and loss of the ability to read (alexia), write (agraphia), and calculate (acalculia). The aphasic syndromes of Broca, conduction and Wernicke, correspond to lesions within the frontal, parietal, and temporal cortical areas, respectively. Lesions of the parietal cortex immediately posterior to the language area (angular gyrus) can lead to alexia, agraphia and acalculia, in the absence of aphasia.

The pre-frontal association cortex and its connections with the limbic system, and in particular, with the amygdala, are essential for problem solving behaviour (executive functions) and the affective motivational aspects of behaviour. Bilateral lesions of these areas (e.g. in frontotemporal dementia) lead to the ‘frontal lobe syndrome’, in which there is a radical change in personality, with loss of reason, judgement, and insight, together with loss of personal and social feelings (sympathy and empathy). The restricted involvement of the orbital frontal areas and limbic connections leads to over-activity and disinhibition (pseudo psychopathic behaviour). Spread of lesions into the dorsolateral surface of the pre-frontal area leads to an inert, apathetic, state (pseudo depression). Unilateral focal lesions of the pre-frontal areas are not usually associated with obvious cognitive or behavioural change.

The limbic allocortex and its connections comprising the Papez circuit (hippocampus, mammillary body, anterior nucleus of the thalamus, and cingulate gyrus) are responsible for the laying down of autobiographical (episodic) memory. Bilateral lesions (e.g. in Alzheimer's disease) or following alcoholic encephalopathy (Korsakoff psychosis) lead to the loss of ability to learn new information (anterograde amnesia) or remember experiences in the relatively recent past (retrograde amnesia). However, perceptual information about the world and language (semantic memory) are preserved, because the temporal neocortical association areas are spared.

Patients with chronic epilepsy, who have undergone surgical section of the corpus callosum in order to relieve their seizures, portray few difficulties under normal circumstances. However, when these 'split brain' patients undergo psychological testing, the two halves of the brain appear to behave relatively autonomously, e.g. visual information directed to the right cerebral hemisphere alone does not evoke a verbal response, and consequently individuals cannot name objects or read words solely presented to the left visual field. Destruction of the splenium of the corpus callosum and its connections to the left occipital cortex, either by stroke or tumour, leads to the posterior disconnection syndrome of 'alexia without agraphia'. Such individuals speak and write without difficulty but cannot understand written material (alexia). Disconnection of visual processes in the right hemisphere from the verbal processes of the dominant left cerebral hemisphere is thought to explain the syndrome.

REFERENCES

heid GF, Heimer L. New perspectives in basal forebrain organization of special relevance for neuropsychiatric disorders: the striatopallidal, amygdaloid and corticopetal components of the substantia innominata. *Neuroscience*. 1988;27:1-39.

Provides evidence that the region of the 'substantia innominata' in the basal forebrain is composed of parts of three forebrain structures: the ventral striatopallidal system; the extended amygdala; and the magnocellular corticopetal system..

erbyshire SW, Jones AK, Gyulai F, Clark S, Townsend D, Firestone LL. Pain processing during three levels of noxious stimulation produces differential patterns of central activity. *Pain*. 1997;73:431-445.

pez JW. A proposed mechanism of emotion. *Arch Neurol Psychiat*. 1937;38:725-743.

The classic description of the mechanism of emotion in man..

ssingham RE. The Frontal Lobes and Voluntary Action. Oxford: Oxford University Press, 1993.

nfield W, Rasmussen T. The Cerebral Cortex of Man. New York: Macmillan, 1950.

The classic description of the organization of sensory and motor homunculi in the human cerebral cortex..

yron R, Laurent B, Garcia-Larrea L. Functional imaging of brain responses to pain. A review and meta-analysis. *Neurophysiol Clin*. 2000;30:263-288.

erry RW. Lateral specialization in the surgically separated hemisphere. In: Schmidt FO, Worden FG. *The Neurosciences. Third study program*. Cambridge, Mass: MIT Press; 1974:5-19.

erry RW. Consciousness, personal identity and the divided brain. *Neuropsychologia*. 1984;17:153-166.

ga AW, Thompson PM, Mori S, Amunts K, Zilles K. Towards multimodal atlases of the human brain. *Nature Rev Neurosci*. 2006;7:952-966.

CHAPTER 24

Development of the nervous system

The entire nervous system and the special sense organs originate from three sources, each derived from specific cell populations of the early epiblast termed neural ectoderm. The first source to be clearly delineated is the neural plate, which gives rise to the central nervous system, the somatic motor nerves and the preganglionic autonomic nerves. The second source is from cells at the perimeter of the neural plate, neural crest cells, which remove themselves by epithelial/mesenchymal transition from the plate and migrate away just prior to its fusion into a neural tube. These cells give rise to the majority of the neurones and glia of the peripheral nervous system, i.e. the somatic sensory nerves, the somatic and autonomic ganglia, postganglionic autonomic nerves and suprarenal and chromaffin cells. They also give rise to significant mesenchymal populations in the head. The third source is from ectodermal placodes, which are focal thickening of the ectoderm covering the embryonic head. They contribute cells to the cranial sensory neurones, and form the olfactory epithelia, the epithelia of the inner ear and, by a non-neuronal contribution, the lens of the eye.

NEURULATION

Primary neurulation begins at stage 9 and is completed during stage 12 (Fig. 24.1). The process, although continuous spatially and temporally, has been envisaged as four stages. It begins with local elongation of the ectoderm cells in a midline zone of the embryonic disc and their reorganization into a pseudostratified epithelium, the neural plate. This is followed by reshaping and bending of the neural plate into a neural groove which subsequently closes to form into a neural tube bidirectionally from the midportion to its cranial and caudal ends. A continuous surface ectoderm forms dorsal to the tube.

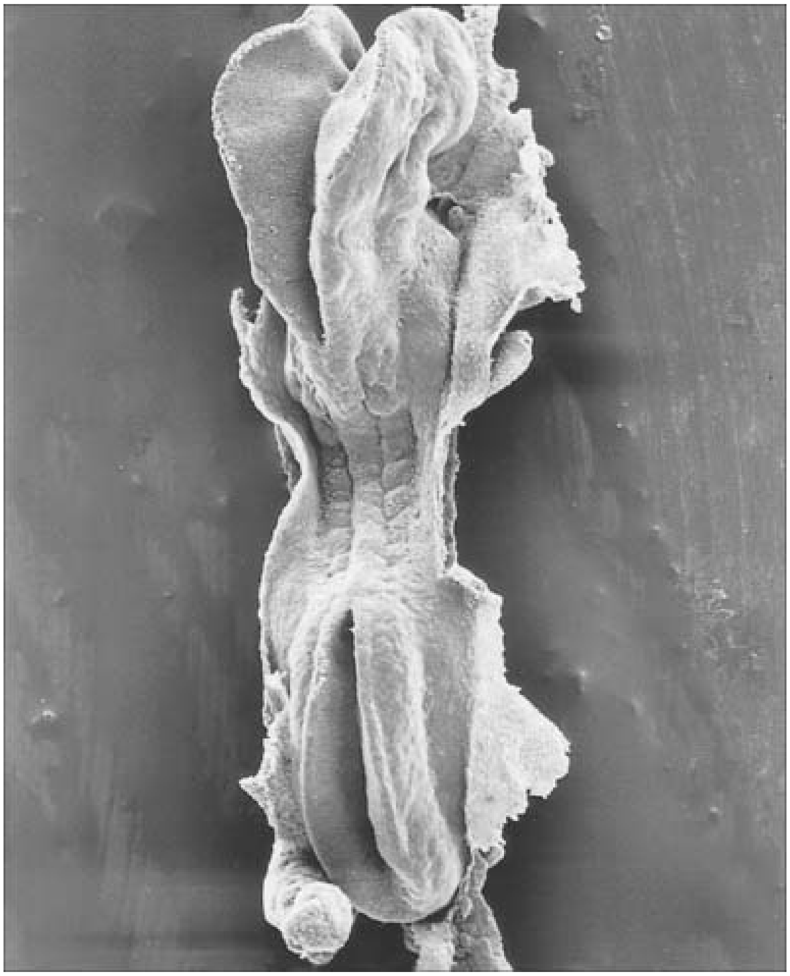

Fig. 24.1 Scanning electron micrograph of a neurulating rat embryo comparable to a stage-10 human embryo (22–24 days). The expanded brain

region can be seen at the top of the image with somite formation occurring centrally as neurulation proceeds caudally. Caudally the ridge of underlying neural crest cells can be seen medial to the unsegmented paraxial mesenchyme.

(Photograph by P Collins; printed by S Cox, Electron Microscopy Unit, Southampton General Hospital.)

Primary neurulation depends on cellular changes within the neural plate: in the trunk it may also involve movements of the paraxial mesenchyme. There is fusion initially of the surface ectoderm followed by fusion of the neural ectoderm. The neural ectodermal cells become elongated and then wedge-shaped. It has been suggested that the forces needed to shape the neural tube are intrinsic to the cells of the neurectoderm. When the neural tube is closing, its walls consist of a single layer of columnar neural epithelial cells, whose extremities abut on internal and external limiting membranes. The columnar cells increase in length and develop numerous longitudinally disposed microtubules. The borders of their luminal ends are firmly attached to adjacent cells by junctional complexes, and the cytoplasmic aspect of the complexes are associated with a dense paraluminal web of microfilaments. The nuclei assume basal positions which, together with the disposition of organelles, impart a slight wedge conformation on some of the cells, and create a hinge point.

The position of hinge points within the neural plate confers different characteristics on the formed neural tube. With a median hinge point, the neural folds remain relatively straight and the tube in this position has a slit-shaped lumen: this can be seen from the initial region of fusion rostralward. If dorsolateral hinge points are added, the resulting neural tube is rhombic, and the hinge points describe the position of the sulcus limitans. If all the neuroepithelial cells exhibit some apical narrowing, then the resulting tube has a circular lumen. The rostral slit-shaped profile of the neural tube may depend more on support from adjacent tissues than the caudal end of the tube, where neurulation is generated by the neuroepithelium. The transition from primary to secondary neurulation (see below) continues the production of a neural tube with a circular lumen.

Fusion of the neural tube starts in embryos with 4–6 somites, at the level of somites 1 and 2, forming the future rhombencephalon. The tube closes caudally and rostrally, forming sequentially cervical and thoracic cord regions, then mesencephalic and prosencephalic brain regions. Rostrally two sites of fusion can be seen. The initial fusion termed α, or the dorsal lip of the rostral neuropore, proceeds caudorostrally. A second site, termed β, or the terminal lip of the rostral neuropore, closes from the rostral end of the neural plate and proceeds rostrocaudally (O’Rahilly & Müller 2002). Closure of these lips of the rostral neuropore is completed when 19–20 pairs of somites are present. Caudal neuropore closure starts when approximately 29 somites are present and the site of closure corresponds to the level of the future somite 31 (the level of the future second sacral vertebra) (O’Rahilly & Müller 2004).

Secondary neurulation starts from the closure of the caudal neuropore at stage 12 and ends at about stage 17; it is the process by which the caudal portion of the neural tube is formed in the absence of a neural plate. At the time of caudal neuropore closure, the caudal midline cells are generically termed the caudal eminence. A specific population of mesenchymal cells, the caudoneural hinge or junction, shares the same molecular markers as the primitive node. These cells aggregate at the midline and undergo mesenchymal/epithelial transformation, producing a cellular cylinder that is contiguous with the caudal end of the neural tube. Further elongation of the caudal neural tube involves cavitation of the neural cylinder. Neural crest cells delaminate from the dorsal surface of the cylinder in a rostrocaudal direction and concurrently, the paraxial mesenchyme undergoes somitogenesis.

EARLY BRAIN REGIONS

Prior to the closure of the neural tube, the neural folds become considerably expanded in the head region; the first indication of a brain and its major divisions can be seen at stage 10 (Fig. 24.2). Regional expansions, prosencephalon (forebrain), mesencephalon (midbrain), and rhombencephalon (hindbrain), have been called the three primary cerebral vesicles, although the term ‘vesicle’ in this context has been considered inappropriate to describe localized accelerations of growth in the wall of the brain. As the neural tube closes, the neural wall appears to form a series of ridges and depressions perpendicular to its long axis. These transient repeating segments are termed primary neuromeres, and initially six can be identified: the prosencephalon, mesencephalon and four subdivisions of the rhombencephalon, rhombomeres A, B, C and D. The primary neuromeres themselves become subdivided during stages 10, 11 and 12 and a total of 16 secondary neuromeres have been identified. The prosencephalon gives rise to the telencephalon, diencephalon 1 (D1) and diencephalon 2 (D2), which has three subdivisions. The mesencephalon is subdivided into mesencephalon 1 (M1) and mesencephalon 2 (M2). The rhombencephalon is subdivided into the isthmus rhombencephali and rhombomeres 1–8; the original rhombomere A gives rise to secondary rhombomeres 1, 2 and 3; rhombomere B gives rise to secondary rhombomere 4; rhombomere C gives rise to secondary rhombomeres 5, 6 and 7; and rhombomere D gives rise to secondary rhombomere 8 (O’Rahilly & Müller 1999). As the rhombencephalon grows the rhombomeric boundaries become less distinct. With the early appearance of the cerebellum from the isthmus rhombencephali and rhombomere 1, the rhombocephalon is traditionally divided into the metencephalon, which extends to about rhombomere 3, and the myelencephalon, which extends to the spinomedullary junction. A summary of the derivative of the cerebral regions is given in Table 24.1 on page 376.

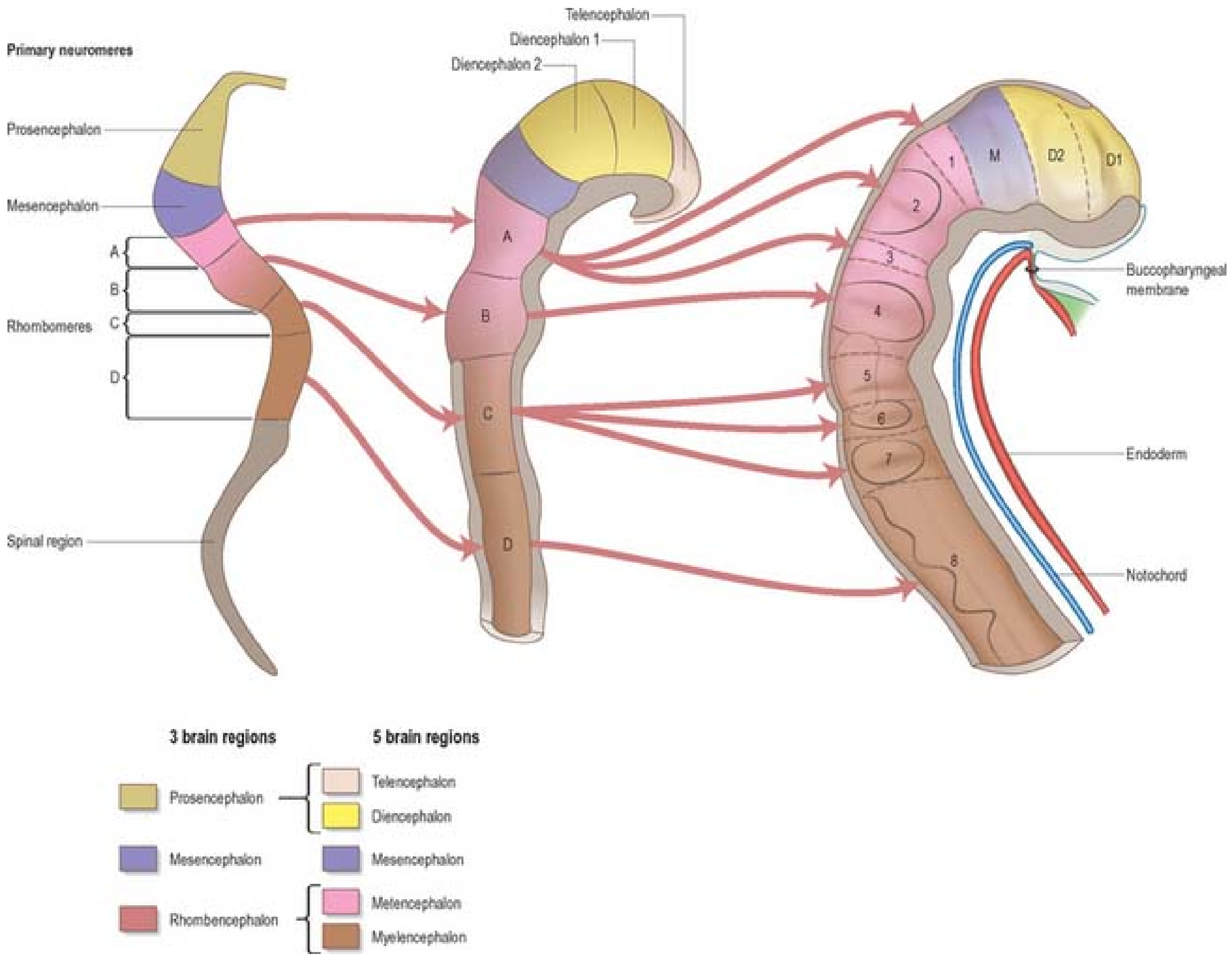
Primary neuromeres
Prosencephalon
Mesencephalon
A
B
Rhombomeres
C
D
Spinal region
Telencephalon
Diencephalon 1
Diencephalon 2
A
B
C
D
1
2
3
4
5
6
7
8
M
D2
D1
Buccopharyngeal membrane
Endoderm
Notochord
3 brain regions
5 brain regions
Prosencephalon
Mesencephalon
Rhombencephalon
Telencephalon
Diencephalon
Mesencephalon
Metencephalon
Myelencephalon

Fig. 24.2 The primary brain regions, neuromeres, and their expansion during neurulation.

Table 24.1 Derivatives of the cerebral regions from caudal to rostral

Rhombencephalon (or hindbrain)	
1. Myelencephalon	Medulla oblongata Caudal part of the 4th ventricle Inferior cerebellar peduncles
2. Metencephalon	Pons Cerebellum

	Middle part of the 4th ventricle Middle cerebellar peduncles
3. Isthmus rhombencephali	Superior medullary velum Superior cerebellar peduncles
Mesencephalon (or midbrain)	
	Cerebral peduncles Tegmentum Tectum Aqueduct
Prosencephalon (or forebrain)	
1. Diencephalon	Thalamus Metathalamus Subthalamus Epithalamus Caudal part of the hypothalamus Caudal part of the 3rd ventricle
2. Telencephalon	Rostral part of the hypothalamus Rostral part of the 3rd ventricle Cerebral hemispheres Lateral ventricles Cortex (archaeocortex, palaeocortex, neocortex) Corpus striatum

The elongation of the brain occurs at the same time as the appearance of three flexures, which also appear prior to the closure of the neural tube; two are concave ventrally and one concave dorsally. During stages 13 and 14 the brain bends at the mesencephalon (mesencephalic flexure) so that the prosencephalon bends in a ventral direction around the cephalic end of the notochord and foregut until its floor lies almost parallel with that of the rhombencephalon (Fig. 24.3). A bend also appears at the junction of the rhombencephalon and spinal cord (cervical flexure). This increases from the fifth to the end of the seventh week, by which time the rhombencephalon forms nearly a right angle to the spinal cord. However, after the seventh week, extension of the head takes place and the cervical flexure diminishes and eventually disappears. The third bend, the pontine flexure, is directed ventrally between the metencephalon and myelencephalon. It does not substantially affect the outline of the head. In this region, the roof plate thins until it is composed only of a single layer of cells and pia mater, the tela choroidea. The flexure of the neural tube at this point produces a rhombic shape in the roof which later forms the medullary velum.

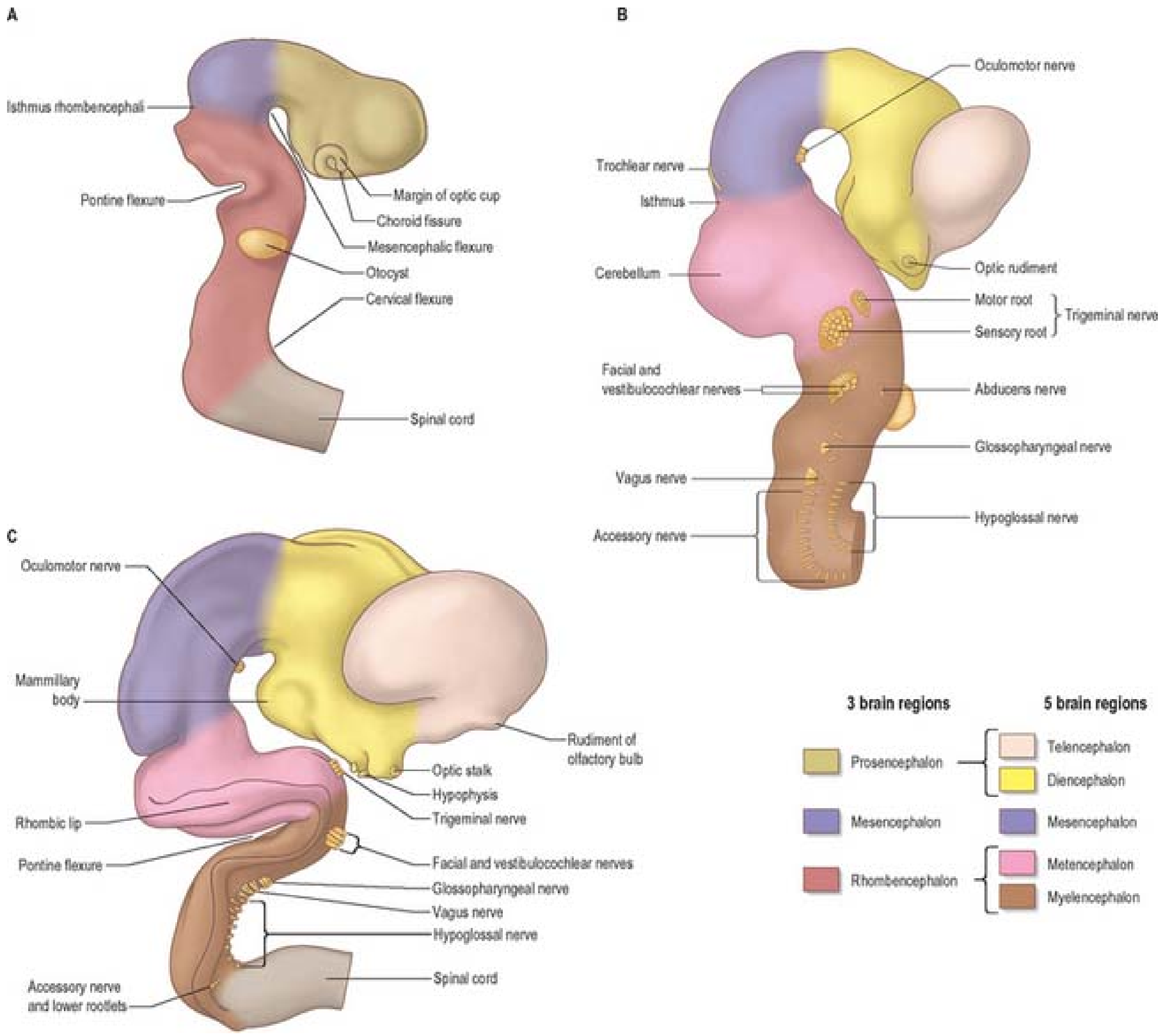
A
Isthmus rhombencephali
Pontine flexure
Margin of optic cup
Choroid fissure
Mesencephalic flexure
Otocyst
Cervical flexure
Spinal cord
B
Oculomotor nerve
Trochlear nerve
Isthmus
Cerebellum
Optic rudiment
Motor root
Sensory root
Trigeminal nerve
Facial and vestibulocochlear nerves
Abducens nerve
Glossopharyngeal nerve
Vagus nerve
Hypoglossal nerve
Accessory nerve
C
Oculomotor nerve
Mammillary body
Rudiment of olfactory bulb
Optic stalk
Hypophysis
Trigeminal nerve
Rhombic lip
Pontine flexure
Facial and vestibulocochlear nerves
Glossopharyngeal nerve
Vagus nerve
Hypoglossal nerve
Spinal cord
Accessory nerve and lower rootlets
3 brain regions
5 brain regions
Prosencephalon
Telencephalon
Diencephalon
Mesencephalon
Mesencephalon
Rhombencephalon
Metencephalon
Myelencephalon

Fig. 24.3 Developing human brains indicating formation of the mesencephalic, cervical and pontine flexures, lateral views. **A**, Human embryo, 9 mm long. **B**, Human embryo, approximately 10.2 mm long. **C**, Human embryo, 13.6 mm long. The roof of the rhombencephalon has been removed in each case.

EARLY CELLULAR ARRANGEMENT OF THE NEURAL TUBE

Histologically the early neural tube is composed of a pseudostratified neuroepithelium. It extends from the inner aspect of the tube to the outer limiting basal lamina and the surrounding pia mater. The epithelium contains stem cells which will give rise to populations of neuroblasts and glioblasts. A population of radial glia differentiates very early and provides a scaffold for later cells to follow. As development proceeds, three zones or layers develop (Figs 24.4-24.6). These are an internal ventricular zone (variously termed the germinal, primitive ependymal or matrix layer), in which mitosis occurs, and which contains the nucleated parts of the columnar cells and rounded cells undergoing mitosis; a middle, mantle zone (also termed the intermediate zone) which contains the migrant cells from the divisions occurring in the ventricular zone; and an outer, marginal zone, which initially consists of the external cytoplasmic processes of the radial glia. The latter is soon invaded by tracts of axonal processes which grow from neuroblasts developing in the mantle zone, together with varieties of non-neuronal cells (glial cells and later vascular endothelium and perivascular mesenchyme). For further development of these layers see pages 368–369.

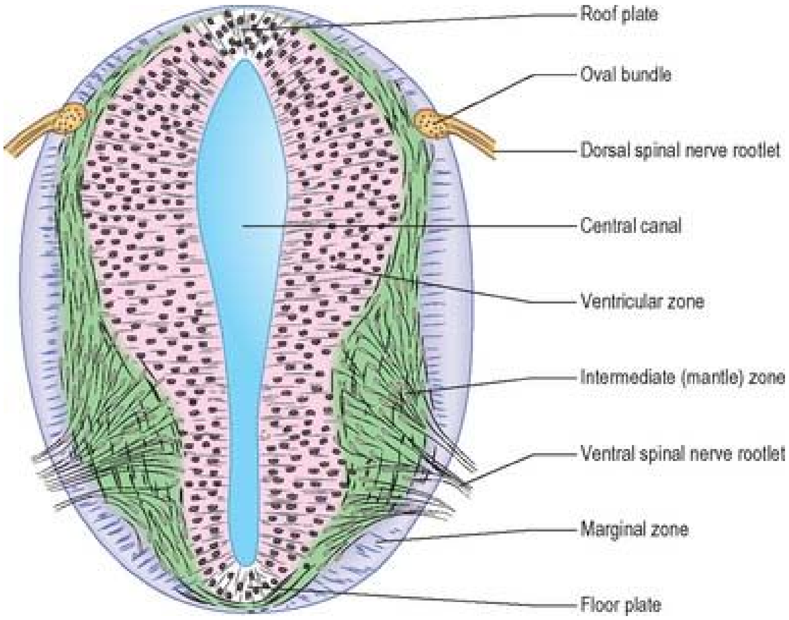
Roof plate
Oval bundle
Dorsal spinal nerve rootlet
Central canal
Ventricular zone
Intermediate (mantle) zone
Ventral spinal nerve rootlet
Marginal zone
Floor plate

Fig. 24.4 Transverse section through the developing spinal cord of a 4-week-old human embryo.

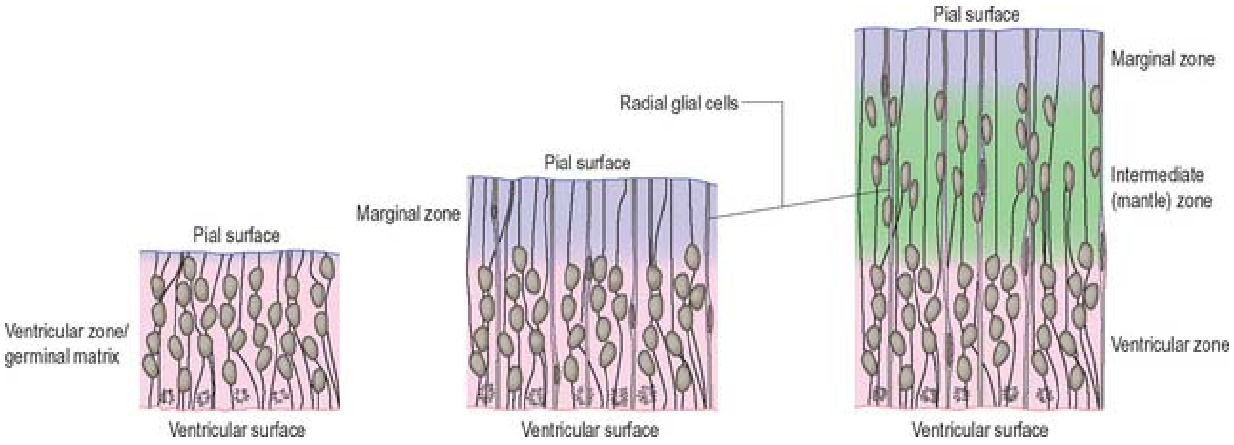
Pial surface
Ventricular zone/
germinal matrix
Ventricular surface
Pial surface
Marginal zone
Ventricular surface
Radial glial cells
Pial surface
Marginal zone
Intermediate
(mantle) zone
Ventricular zone
Ventricular surface

Fig. 24.5 Early development of the neural tube: three layers can be delineated in the spinal cord and brain stem.

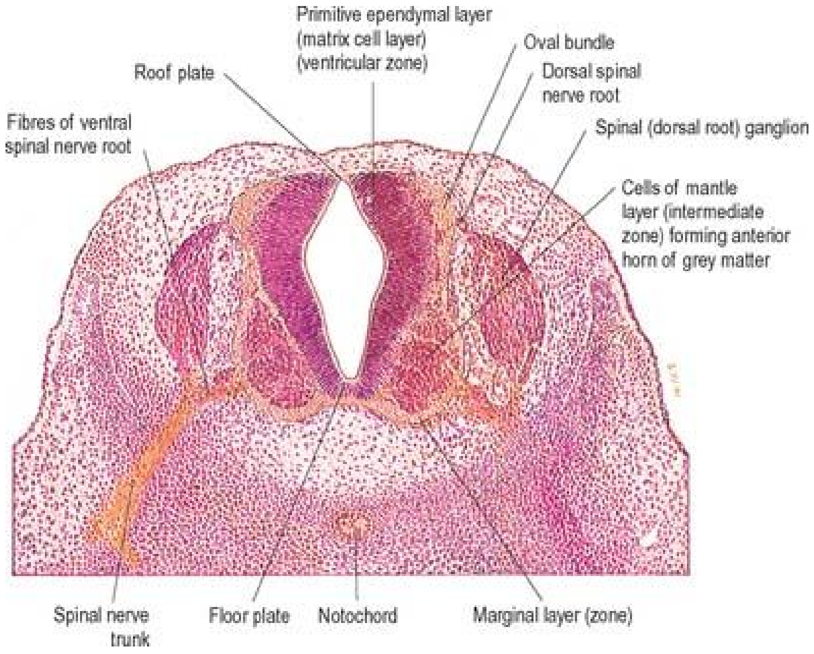
Primitive ependymal layer
(matrix cell layer)
(ventricular zone)
Roof plate
Oval bundle
Dorsal spinal
nerve root
Fibres of ventral
spinal nerve root
Spinal (dorsal root) ganglion
Cells of mantle
layer (intermediate
zone) forming anterior
horn of grey matter
Spinal nerve
trunk
Floor plate
Notochord
Marginal layer (zone)

Fig. 24.6 The developing spinal cord in the cervical region of a human embryo early in the sixth week; CR length 8 mm. Transverse section.

At first the neural tube caudal to the brain is oval in transverse section and its lumen is narrow and slit-like (Fig. 24.4). The original floor plate and the dorsal site of fusion of the tube initially contain non-neural cells. With cellular proliferation, the lateral walls thicken and the lumen, now the central canal, widens in its dorsal part and is somewhat diamond-shaped on cross-section (Fig. 24.6). The widening of the canal is associated with the development of a longitudinal sulcus limitans on each side which divides the ventricular and mantle (intermediate) zones in each lateral wall into a ventrolateral lamina or basal plate and a dorsolateral lamina or alar plate respectively. This separation underlies a fundamental functional difference.

Throughout the neural tube there is a generic pattern in the position of the neurones which is specified by the juxtaposition of the notochord to the neural tube. Experimental lateral or dorsal grafting of a notochord results in the induction of a floor plate overlying the grafted notochord and the induction of ectopic motor neurones dorsally. Similarly, lateral or dorsal grafts of a floor plate also result in the induction of a new floor plate overlying the graft and the induction of ectopic dorsal motor neurones. Removal of the notochord results in the elimination of the floor plate and the motor neurones and the differentiation of dorsal cell types in the ventral region of the cord (Fig. 24.7).

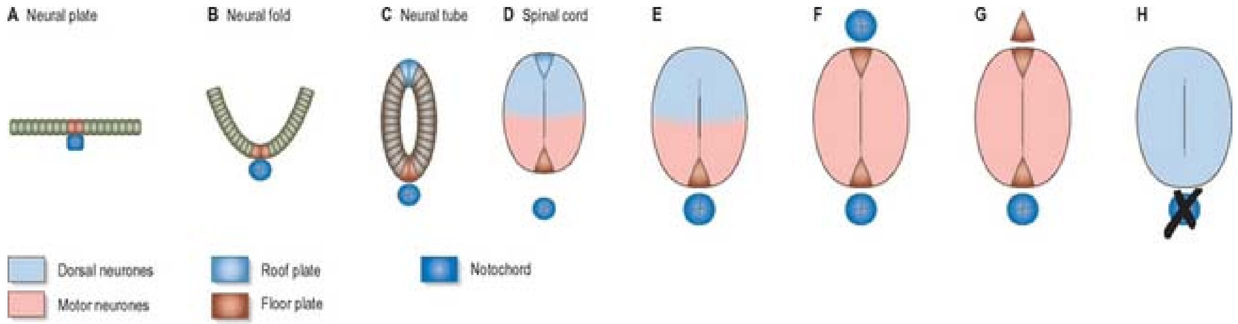

Fig. 24.7 **A–B**, Successive stages in the development of the neural tube and spinal cord. **A**, The neural plate consists of epithelial cells. Cells in the midline of the neural plate are contacted directly by the notochord. More lateral regions of the neural plate overlie the paraxial mesenchyme (not shown). **B**, During neurulation, the neural plate bends at its midline and this

elevates the lateral edges of the plate as the neural folds. Contact between the midline of the neural plate and the notochord is maintained at this stage. **C**, The neural tube is formed when the dorsal tips of the neural folds fuse. Cells in the region of fusion form the roof plate which is a specialized group of dorsal midline cells. **D**, Cells at the ventral midline of the neural tube retain proximity to the notochord and differentiate into the floor plate. After neural tube closure neuroepithelial cells continue to proliferate and eventually differentiate into defined classes of neurones at different dorsoventral positions within the spinal cord. For example, sensory relay, commissural and other classes of dorsal neurones differentiate near to the roof plate, and motor neurones differentiate ventrally near the floor plate, which by this time is no longer in contact with the notochord. **E–H**, A summary of the results obtained from experiments in chick embryos in which a notochord or floor plate is grafted to the dorsal midline of the neural tube or where the notochord is removed before neural tube closure. **E**, The normal condition, showing the ventral location of motor neurones and the dorsal location of sensory relay neurones. **F**, Dorsal grafts of a notochord result in the induction of a floor plate in the dorsal midline and ectopic dorsal motor neurones. **G**, Dorsal grafts of a floor plate induce a new floor plate in the dorsal midline and ectopic dorsal motor neurones. **H**, Removal of the notochord results in the elimination of the floor plate and the motor neurones and the expression of dorsal cells types in the ventral region of the spinal cord.

The basal plate is normally concerned predominantly with motor function, and contains the cell bodies of motor neurones of the future anterior and lateral grey columns. The alar plate receives sensory inflow from external dorsal root ganglia. Motor and sensory axons combine to form the mixed nerves.

FAILURE OF NEURULATION

Failure of neurulation produces the conditions of craniorachischisis totalis (where the entire neural tube is unfused in the dorsal midline), cranioschisis or anencephaly (where the neural tube is fused dorsally to form the spinal cord but is not fused dorsally in the brain), and spina bifida (where local regions of the spinal neural tube are unfused, or there is failure of formation of the vertebral neural arches). (Fig. 24.8; see also Ch. 44). Anencephalic fetuses display severe disturbances in the shape, position and ossification of the basichondrocranium and in the course of the intracranial notochord and so the condition is more complicated than ‘simply’ a failure of neural tube fusion.

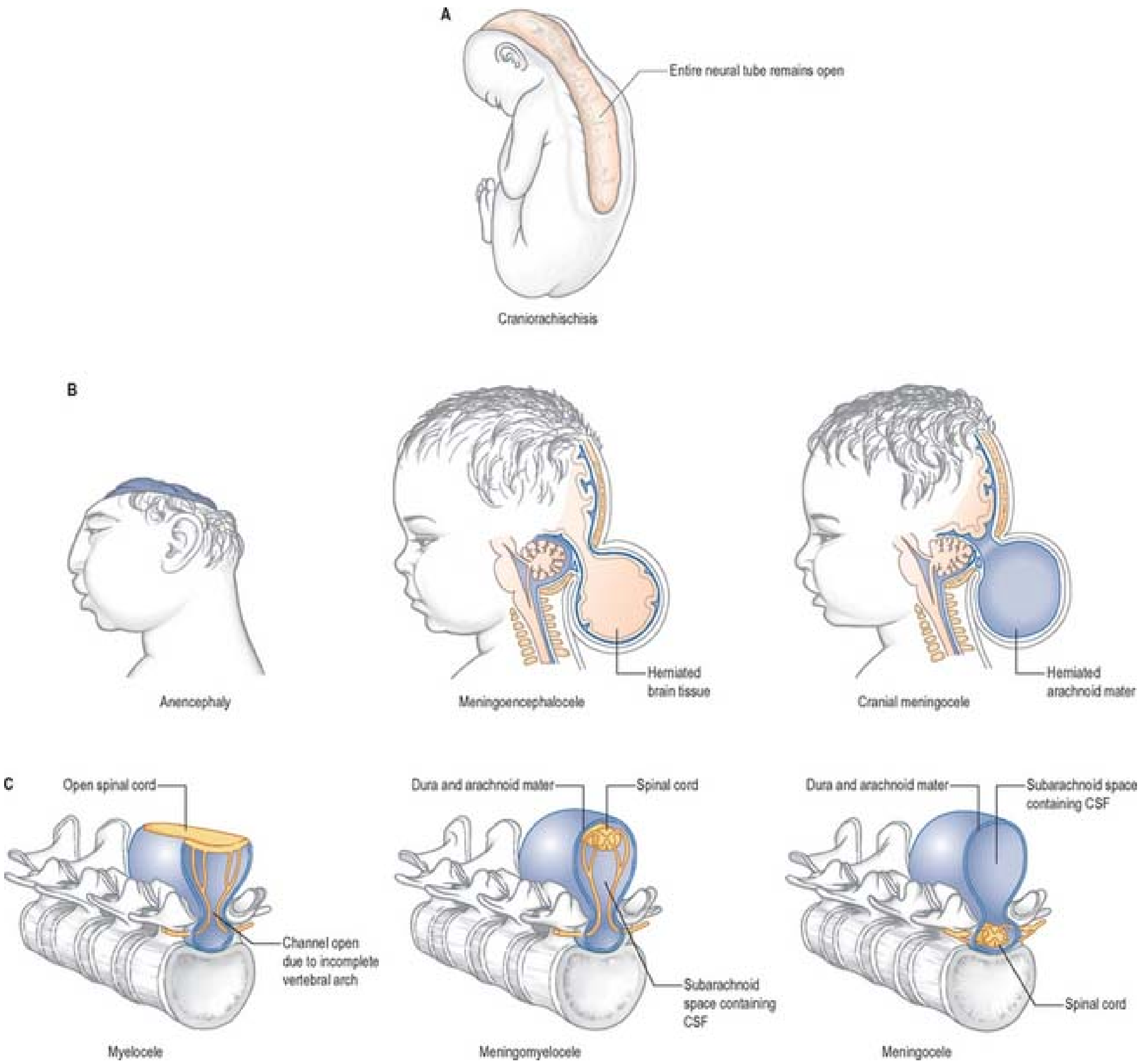
A
Entire neural tube remains open
Craniorachischisis
B
Anencephaly
Meningoencephalocele
Herniated brain tissue
Cranial meningocele
Herniated arachnoid mater
C
Open spinal cord
Channel open due to incomplete vertebral arch
Myelocele
Dura and arachnoid mater
Spinal cord
Subarachnoid space containing CSF
Meningomyelocele
Dura and arachnoid mater
Subarachnoid space containing CSF
Spinal cord
Meningocele

Fig. 24.8 Defects caused by failure of neural tube formation. **A**, Total failure of neurulation. **B**, Failure of rostral neurulation. **C**, Failure of caudal neurulation.

NEURAL CREST

The neuronal populations of the early epiblast become arranged in the medial region of the embryonic disc as the neural plate. Laterally, neural folds or crests indicate the transitional region between neural and surface ectoderm. Along most of the neuraxis the cells at the tips of the neural folds undergo an epithelial/mesenchyme transformation. They acquire migratory properties and leave the epithelium just prior to its fusion with the contralateral fold in the dorsal midline. The migratory cells so formed are collectively termed the neural crest. Cells within the rostral prosencephalic neural fold and smaller populations of cells in bilateral sites lateral to the early brain do not form migratory neural crest cells but remain within the surface epithelium as ectodermal placodes.

Neural crest populations arise from the neural folds as primary neurulation proceeds and simultaneously progresses rostrally and caudally. Crest cells migrate from the neural folds of the brain prior to tube closure. Caudally, from approximately somite 29, secondary neurulation processes produce the most caudal neural crest. Two distinct populations of neural crest cells are formed: a neuronal population produced throughout the brain and spinal cord which gives rise to sensory and autonomic neurones and glia, and a non-neuronal mesenchymal population which arises only from the brain (Figs 24.9 and 24.10). Melanocytes develop from a subpopulation of neural crest cells derived from both the head and trunk. They form one of the three pigment cell types (the others being retinal pigment epithelium and the pigment cells of the pineal organ, which both originate from the diencephalon).

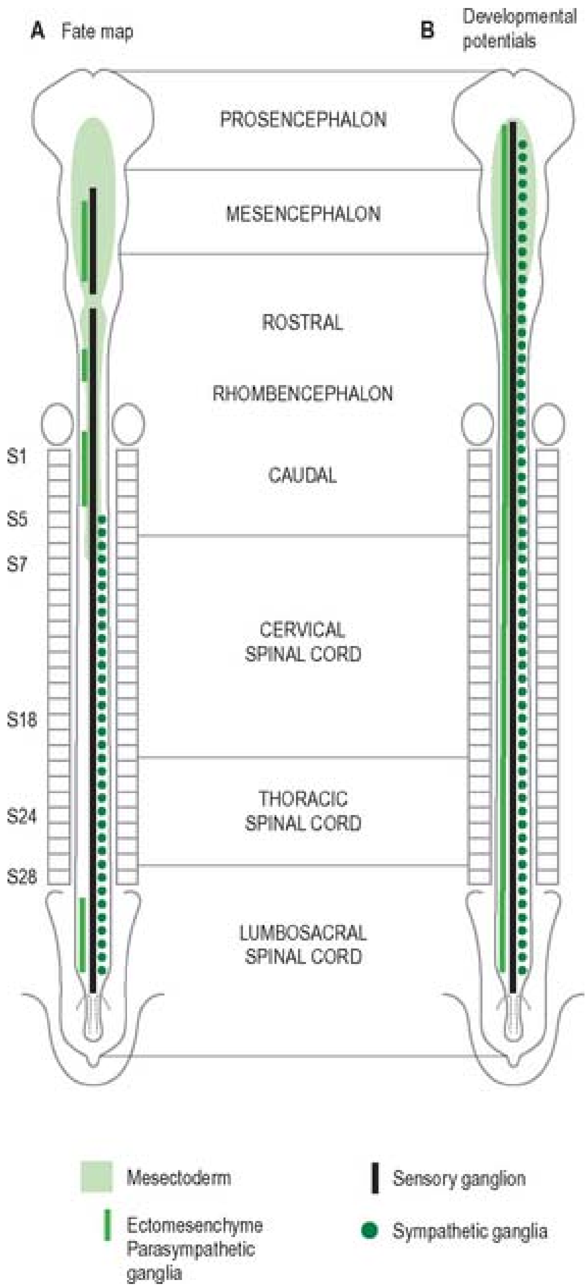
A Fate map
B Developmental potentials
PROSENCEPHALON
MESENCEPHALON
ROSTRAL
RHOMBENCEPHALON
CAUDAL
CERVICAL SPINAL CORD
THORACIC SPINAL CORD
LUMBOSACRAL SPINAL CORD
S1
S5
S7
S18
S24
S28
Mesectoderm
Ectomesenchyme Parasympathetic ganglia
Sensory ganglion
Sympathetic ganglia

Fig. 24.9 **A**, Fate map along the neural crest of the presumptive territories which yield the ectomesenchyme, the sensory, parasympathetic and sympathetic ganglia and neural crest derived mesenchyme in normal development. **B**, Developmental potentials for the same cell types. If neural crest cells from any level of the neural axis are implanted into the appropriate sites of a host embryo, they can give rise to almost all the cell types forming the various kinds of PNS ganglia. This is not true for the

neural crest derived mesenchyme whose precursors are confined to the cephalic area of the crest down to the level of somite 5. S, somite.

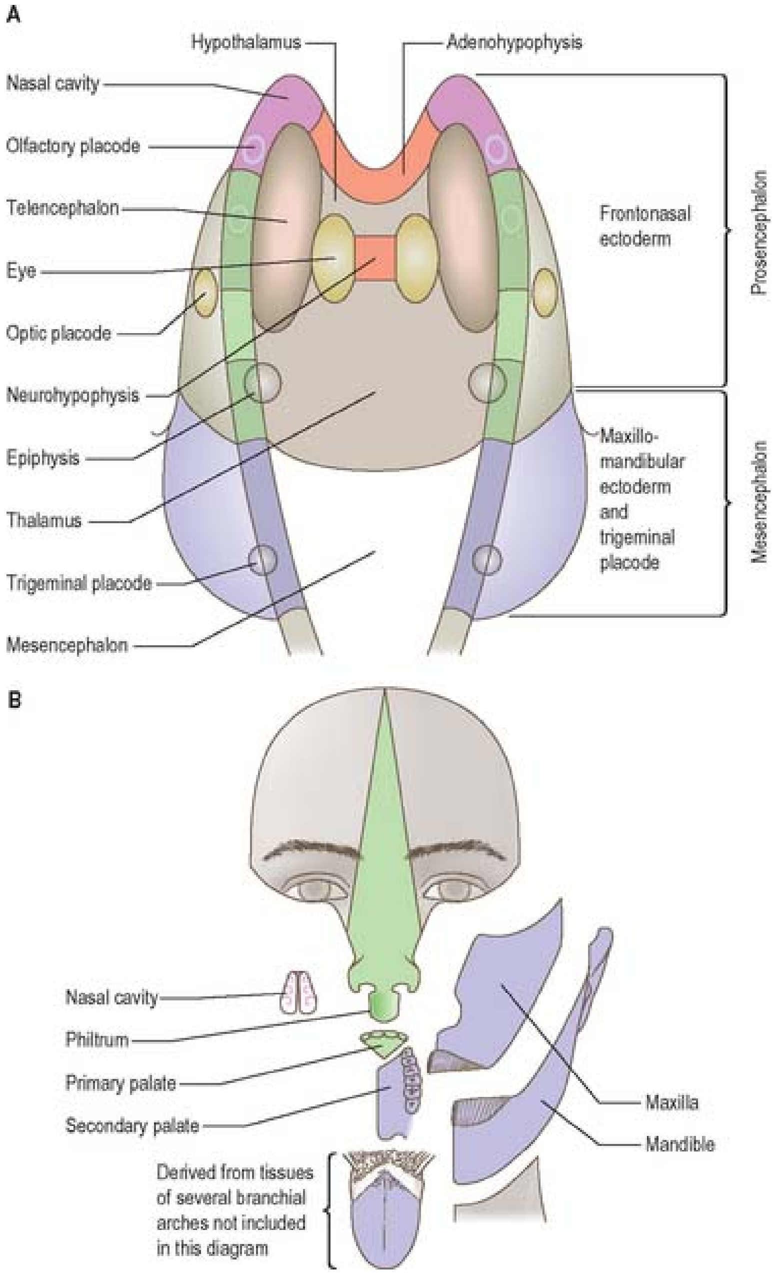
A
Hypothalamus
Adenohypophysis
Nasal cavity
Olfactory placode
Telencephalon
Eye
Optic placode
Neurohypophysis
Epiphysis
Thalamus
Trigeminal placode
Mesencephalon
Frontonasal ectoderm
Prosencephalon
Maxillo-mandibular ectoderm and trigeminal placode
Mesencephalon
B
Nasal cavity
Philtrum
Primary palate
Secondary palate
Derived from tissues of several branchial arches not included in this diagram
Maxilla
Mandible

Fig. 24.10 Fate map of the rostral region of the neural primordium as established by the quail–chick chimera system. **A**, The various territories yielding rostral head are indicated on the neural plate and neural fold of a 1–3 somite embryo. **B**, The results obtained in the avian embryo have been

extrapolated to the human head. Thus, the neural fold area coloured green in **A** yields the epithelium of the nose, philtrum and primary palate.

In the trunk the migration patterns of neural crest cells is channelled by the somites. As the crest cells move laterally and ventrally they can pass between the somites and within the rostral sclerotomal half of each somite, but they cannot penetrate the caudal moiety of the sclerotomal mesenchyme. Thus the segmental distribution of the spinal and sympathetic ganglia is imposed on the neural crest cells by a prepattern that exists within the somitic paraxial mesenchyme (Fig. 24.11). The origin of the cranial-caudal patterning of the ventral neural crest cells is not clear.

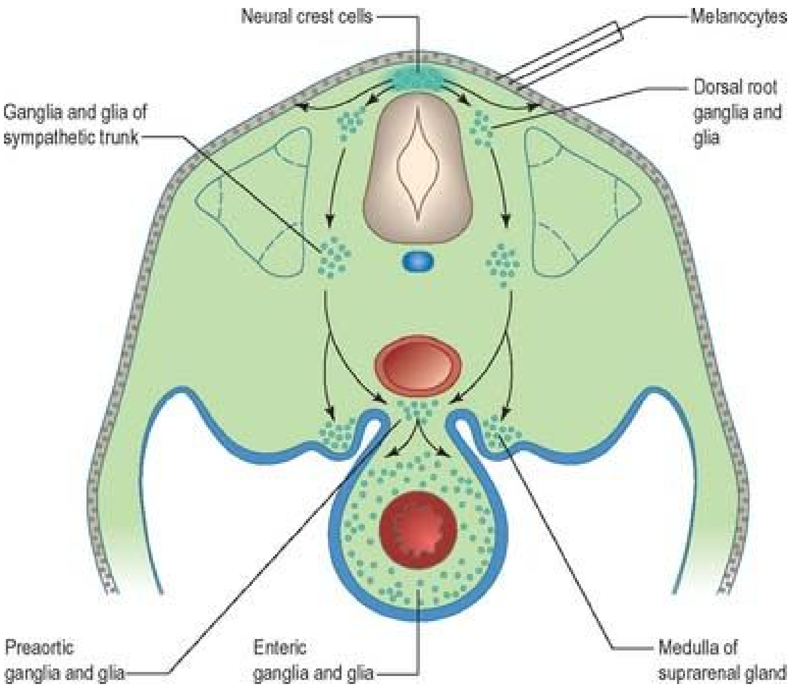
Neural crest cells
Melanocytes
Dorsal root ganglia and glia
Ganglia and glia of sympathetic trunk
Preaortic ganglia and glia
Enteric ganglia and glia
Medulla of suprarenal gland

Fig. 24.11 The migration routes taken by neural crest cells in the trunk.

Rostral to the otic vesicle, neural crest cells arise from specific regions of the brain. Early in development, a number of transverse subdivisions perpendicular to the long axis of the brain can be seen within the rhombencephalon, dividing it into segments termed rhombomeres (Müller & O’Rahilly 1997). Eight main rhombomeres extend from the midbrain–

hindbrain boundary rostrally to the spinal cord caudally (Fig. 24.2). Rhombomeres 8 and 7 give rise to neural crest cells which migrate into the fourth and sixth pharyngeal arches; rhombomere 6 crest cells invade pharyngeal arch three. Rhombomere 4 crest cells migrate into arch 2, whereas rhombomeres 5 and 3 give rise to a very small number of neural crest cells which migrate rostrally and caudally to enter the adjacent even-numbered neighbours. Rhombomeres 1 and 2 produce crest cells which invade the first pharyngeal arch. In each rhombomere, mesenchymal populations and the sensory and autonomic ganglia are formed from the crest cells (see Fig. 12.4).

Further rostrally, neural crest from the mesencephalon migrates into the first arch maxillary and mandibular processes. Crest cells are produced from the diencephalon up to the level of the epiphysis. Neural crest cells which are produced from this rostral portion of the brain contribute mesenchymal populations to the frontonasal process. The most rostral prosencephalic neural fold does not give rise to neural crest.

ECTODERMAL PLACODES

Prior to neural tube closure, the elevating neural folds contain two distinctive neuronal populations. The larger population of neural crest cells migrates from the neural epithelium prior to neural tube fusion. A smaller population of neuroepithelial cells becomes incorporated into the surface ectoderm after neural tube closure. These areas of neuroepithelium within the surface ectoderm have been termed ectodermal placodes. Although the majority of the ectodermal placodes form nervous tissue, non-neurogenic placodes also occur (Begbie & Graham 2001). After an appropriate inductive stimulus, the placodes thicken and either generate migratory neuronal cells that will contribute to the cranial sensory ganglia, or the whole placodal region invaginates to form a vesicle beneath the remaining surface ectoderm. Neurogenic placodes undergo both processes. Paired non-neurogenic placodes invaginate to form the lens vesicles under the inductive influence of the optic vesicles (see Ch. 41).

The neural folds meet in the rostral midline adjacent to the buccopharyngeal membrane. This rostral neural fold does not generate neural crest but gives rise to the hypophysial placode, i.e. the future Rathke’s pouch, which remains within the surface ectoderm directly rostral to the buccopharyngeal membrane. The rostral neural fold also gives rise to the olfactory placodes, which remain as paired, laterally placed placodes, and to the epithelium of the nasal cavity (Fig. 24.10).

Further caudally, similar neurogenic placodes can be identified and divided into three categories, namely the epibranchial, otic and trigeminal placodes (Fig. 24.12). The epibranchial placodes appear in the surface ectoderm immediately dorsal to the area of pharyngeal (branchial) cleft formation. The first epibranchial placode is located at the level of the first pharyngeal groove and contributes cells to the distal (geniculate) ganglion of the facial nerve, the second and third epibranchial placodes contribute cells to the distal ganglia of the glossopharyngeal (petrosal) and vagus (nodose) nerves respectively. These placodes thicken and cells begin to detach from their epithelium soon after the pharyngeal pouches have contacted the overlying ectoderm. Concurrently the neural crest cells reach and move beyond these lateral extensions of the pharynx. Neurones migrate from the epibranchial placodes internally to the sites of ganglion formation, where they show signs of early differentiation into neurones, including the formation of neurites.

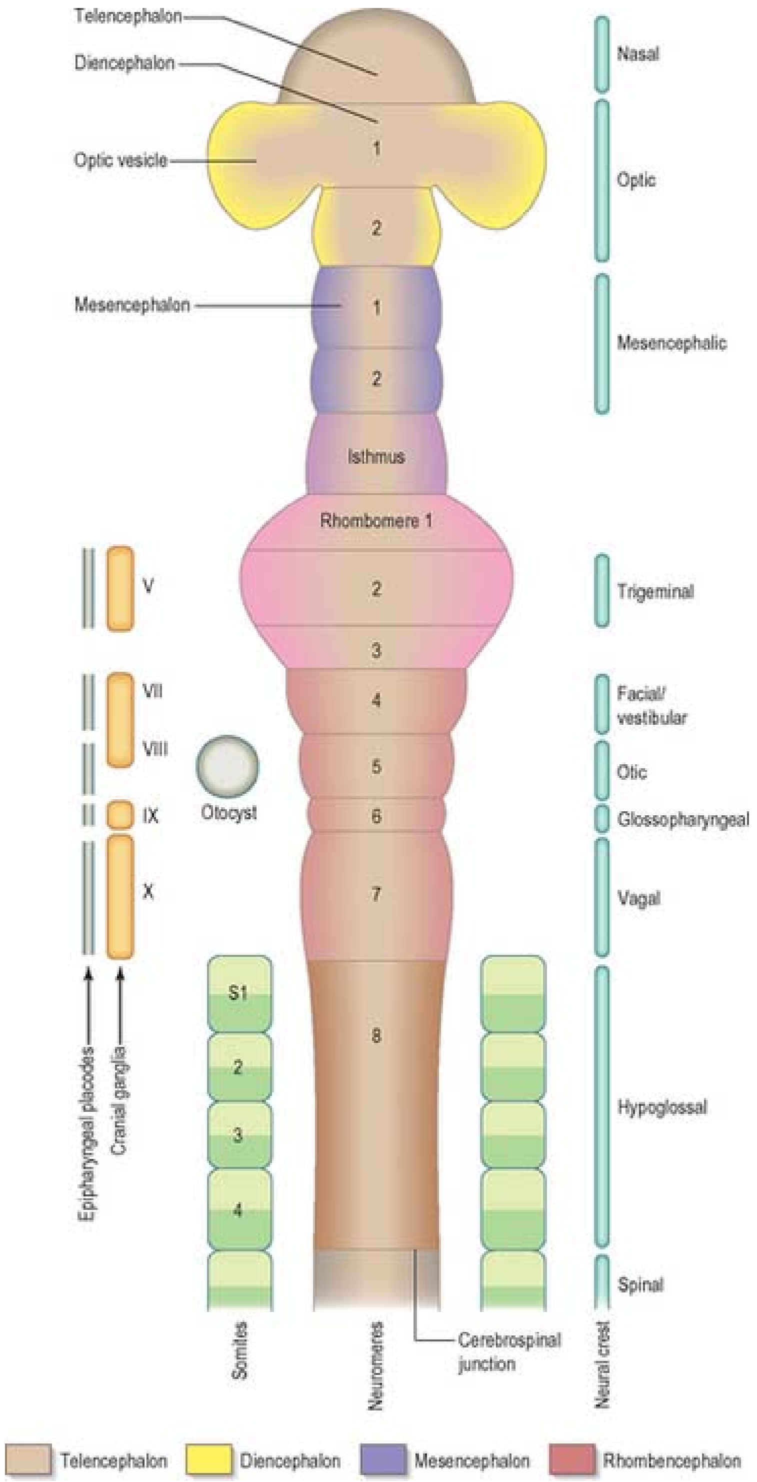
Telencephalon
Diencephalon
Optic vesicle
1
2
Mesencephalon
1
2
Isthmus
Rhombomere 1
2
3
4
5
6
7
8
Nasal
Optic
Mesencephalic
Trigeminal
Facial/ vestibular
Otic
Glossopharyngeal
Vagal
Hypoglossal
Spinal
V
VII
VIII
IX
X
Otocyst
S1
2
3
4
Epipharyngeal placodes
Cranial ganglia
Somites
Neuromeres
Cerebrospinal junction
Neural crest
Telencephalon
Diencephalon
Mesencephalon
Rhombencephalon

Fig. 24.12 Scheme of a human embryo of stage 13 (4 mm, 32 somites), rendered flat to eliminate the cerebral flexures. The cranial sensory ganglia and otocyst, derived from the epibranchial placodes are shown on the left. The levels of origin of the neural crest which contributes to the cranial

sensory ganglia and mesenchymal populations in the head on the right is indicated. This arrangement may vary in other species. (Provided by Professor R O’Rahilly and Dr F Müller.)

The otic placodes, located lateral to the myelencephalon, invaginate to form otic vesicles from which the membranous labyrinth of the ear develops. Neurones of the vestibulocochlear nerve ganglia arise from neurones that bud off the ventromedial aspect of the otic cup, after which they can be distinguished in the acoustic and vestibular ganglia (see Ch. 38).

The profundal and maxillomandibular trigeminal placodes, which fuse in man to form a single entity, lie rostral of the otic placodes, alongside the mesencephalic–rhombencephalic junction. Prospective neuroblasts migrate from foci dispersed throughout the surface ectoderm lateral and ventrolateral to the caudal mesencephalon and metencephalon to contribute to the distal portions of the trigeminal ganglia.

PITUITARY GLAND (HYPOPHYSIS CEREBRI)

The hypophysis cerebri consists of the adenohypophysis and the neurohypophysis. Prior to neurulation the cell populations which give rise to these two portions of the pituitary gland are found next to each other within the rostral portion of the floor of the neural plate and the contiguous midline neural fold. As neurulation proceeds the future neurohypophysis remains within the floor of the prosencephalon. The cells of the future adenohypophysis are displaced into the surface ectoderm, where they form the hypophysial placode in close apposition and adherent to the overlying prosencephalon.

The most rostral portion of the neural plate, which will form the hypothalamus, is in contact rostrally with the future adenohypophysis in the rostral neural ridge, and caudally with the neurohypophysis, in the floor of the neural plate (Fig. 24.10). After neurulation the cells of the rostral neural ridge remain in the surface ectoderm and form the hypophysial placode which is in close apposition and adherent to the overlying prosencephalon.

Neural crest mesenchyme later moves between the prosencephalon and surface ectoderm except at the region of the placode. Before rupture of the buccopharyngeal membrane, proliferation of the periplacodal mesenchyme means that the placode forms the roof and walls of a saccular depression. This hypophysial recess (pouch of Rathke, Figs 24.13 and 24.14) is the rudiment of the adenohypophysis. It lies immediately ventral to the dorsal border of the buccopharyngeal membrane, extending in front of the rostral tip of the notochord, and retaining contact with the ventral surface of the prosencephalon. It is constricted by continued proliferation of the surrounding mesenchyme to form a closed vesicle, but remains for a time connected to the ectoderm of the stomodeum by a solid cord of cells, which can be traced down the posterior edge of the nasal septum. Masses of epithelial cells form mainly on each side and in the ventral wall of the vesicle, and the development of the adenohypophysis progresses by the ingrowth of a mesenchymal stroma. Differentiation of epithelial cells into stem cells and three differentiating types is said to be apparent during the early months of fetal development. It has been suggested that different types of cells arise in succession, and that they may be derived in differing proportions from different parts of the hypophysial recess. A craniopharyngeal canal, which sometimes runs from the rostral part of the hypophysial fossa of the sphenoid to the exterior of the skull, is often said to mark the original position of the hypophysial recess. Traces of the stomodeal end of the recess are usually present at the junction of the septum of the nose with the palate. Others have claimed that the craniopharyngeal canal itself is a secondary formation caused by the growth of blood vessels, and is quite unconnected with the stalk of the adenohypophysis.

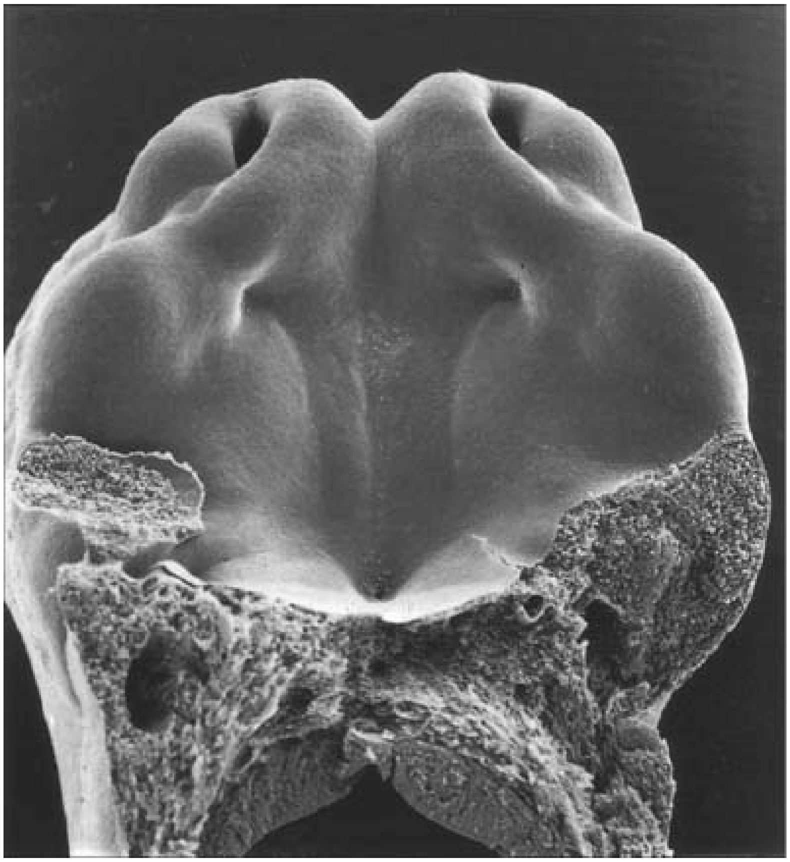

Fig. 24.13 Scanning electron micrograph of the roof of the pharynx showing the invagination of placodal ectoderm to form the adenohypophysis (Rathke’s pouch).

(Photograph by P Collins; printed by S Cox, Electron Microscopy Unit, Southampton General Hospital.)

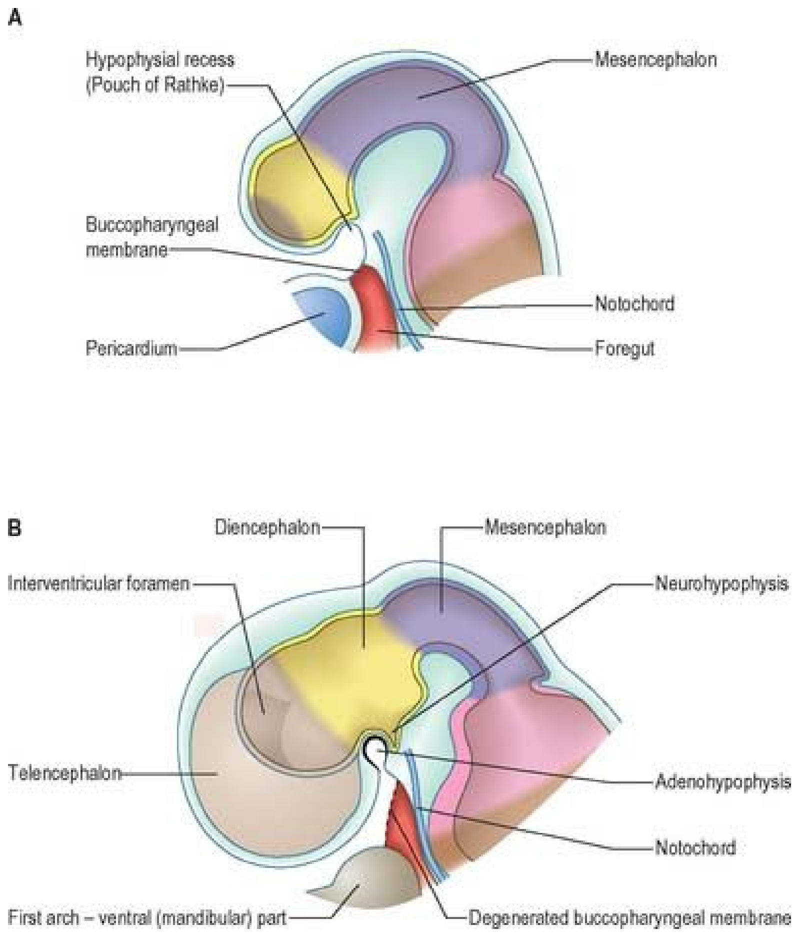
A
Hypophysial recess
(Pouch of Rathke)
Mesencephalon
Buccopharyngeal
membrane
Notochord
Pericardium
Foregut
B
Diencephalon
Mesencephalon
Interventricular foramen
Neurohypophysis
Telencephalon
Adenohypophysis
Notochord
First arch – ventral (mandibular) part
Degenerated buccopharyngeal membrane

Fig. 24.14 **A**, **B**, Sagittal sections of heads of early embryos showing initial stages in the development of the hypophysis.

A small endodermal diverticulum, named Seessel's pouch, projects towards the brain from the cranial end of the foregut, immediately caudal to the buccopharyngeal membrane. In some marsupials this pouch forms a part of the hypophysis, but in man it is not well defined and disappears entirely.

Just caudal to, but in contact with, the adenohypophysial recess, a hollow diverticulum elongates towards the stomodeum from the floor of the neural plate just caudal to the hypothalamus (Fig. 24.14B); this region of neural outgrowth is the neurohypophysis. It forms an infundibular sac, the walls of which increase in thickness until the contained cavity is obliterated except at its upper end, where it persists as the infundibular recess of the third ventricle. The neurohypophysis becomes invested by the adenohypophysis, which extends dorsally on each side of it. The adenohypophysis gives off two processes from its ventral wall which grow along the infundibulum and fuse to surround it, coming into relation with the tuber cinereum and forming the tuberal portion of the hypophysis. The original cavity of Rathke’s pouch remains first as a cleft, and later as scattered vesicles, and can be identified readily in sagittal sections through the mature gland. The dorsal wall of Rathke’s pouch remains thin and fuses with the adjoining part of the neurohypophysis as the pars intermedia.

At birth the hypophysis is about one-sixth the weight of the adult gland: it increases in weight to become about one-half the weight of the adult gland at 7 years, and attains adult weight at puberty. Throughout postnatal life the gland appears larger in females, in both size and weight.

NEUROGLIA

Glial cells which support neurones in the CNS and PNS are derived from three lineages, namely, neuroectoderm, neural crest and angioblastic mesenchyme. In the CNS, cells of the proliferating ventricular zone give rise to astrocytes and oligodendrocytes. After the proliferative phase the cells remaining at the ventricular surface differentiate into ependymal cells, which are specialized in many regions of the ventricular system as circumventricular organs. In the PNS, neural crest cells produce Schwann cells and astrocyte-like support cells in the enteric nervous system. Angioblastic mesenchyme gives rise to a variety of blood cell types including circulating monocytes which infiltrate the brain as microglial cells later in development.

The ventricular zone lining the early central canal of the spinal cord and the cavities of the brain gives rise to neurones and glial cells (Figs 24.4 and 24.5). One specialized form of glial cell is the radial glial cell, whose radial processes extend both outwards to form the outer limiting membrane deep to the pia mater, and inwards, to form the inner limiting membrane around the central cavity. The geometry of these cells may provide contact guidance paths for cell migrations, both neuronic and glioblastic. A secondary radial glial scaffold is formed in the late developing cerebellum and dentate gyrus and serves to translocate neurones, formed in secondary germinal centres, to their definitive adult locations. Radial glia eventually lose their connections with both inner and outer limiting membranes, except those persisting in the retina as Müller cells, in the cerebellum as Bergmann glia and in the hypothalamus as tanycytes. They can differentiate into neurones as well as astrocytes. They may partially clothe the somata of neighbouring developing neurones (between presumptive synaptic contacts), or similarly enwrap the intersynaptic surfaces of their neurites. Glial processes may expand around intraneural capillaries as perivascular end-feet. Other glioblasts retain an attachment (or form new expansions) to the pia mater, the innermost stratum of the meninges, as pial end-feet. Glioblasts also line the central canal and cavities of the brain as generalized or specialized ependymal cells, but lose their peripheral attachments. In some situations, as in the anterior median fissure of the spinal cord, ependymal cells retain their attachments to both the inner and outer limiting membranes. Thus, glia function as perineuronal satellites, and provide cellular channels interconnecting extracerebral and intraventricular cerebrospinal fluid, the cerebral vascular bed, the intercellular crevices of the neuropil and the cytoplasm of all neural cell varieties.

Microglia appear in the CNS after it has been penetrated by blood vessels and invade it in large numbers from certain restricted regions, whence they spread in what have picturesquely been called ‘fountains of microglia’, to extend deeply among the nervous elements.

MECHANISMS OF NEURAL DEVELOPMENT

For more than a century the mechanisms that operate during the development of the nervous system have been studied experimentally. While much has been established, answers to many fundamental questions still remain obscure. In recent years, significant advances in our understanding of the development of vertebrates have come from work on amphibian, chicken, mouse and fish embryos, using a combination of genetic, embryological, biochemical and molecular techniques to elucidate the mechanisms that regulate the behaviour of early neural populations.

The CNS has a fundamental structure of layers and cells, which are all derived from a pluripotential neuroepithelium. Developing neurones produce axons which traverse great distances to reach their target organs. Within the CNS, they form myriad connections with other neurons in response to locally secreted cues.

HISTOGENESIS OF THE NEURAL TUBE

The wall of the early neural tube consists of an internal ventricular zone (sometimes termed the germinal matrix) abutting the central lumen. It contains the nucleated parts of the pseudostratified columnar neuroepithelial cells and rounded cells undergoing mitosis. The early ventricular zone also contains a population of radial glial cells whose processes pass from the ventricular surface to the pial surface, thus forming the internal and external glia limitans (glial limiting membrane). As development proceeds the early pseudostratified epithelium proliferates and an outer layer, the marginal zone, devoid of nuclei but containing the external cytoplasmic processes of cells, is delineated. Subsequently a middle, mantle layer (intermediate zone) forms as the newly formed neurones migrate ventriculofugally from the ventricular zone (see Fig. 24.5).

Most CNS cells are produced in the proliferative zone adjacent to the future ventricular system, and in some regions this area is the only actively mitotic zone. According to the monophyletic theory of neurogenesis it is assumed to produce all cell types. The early neural epithelium, including the deeply placed ventricular mitotic zone, consists of a homogeneous population of pluripotent cells whose varying appearances reflect different phases in a proliferative cycle. The ventricular zone is considered to be populated by a single basic type of progenitor cell and to exhibit three phases. The cells show an ‘elevator movement’ as they pass through a complete mitotic cycle, progressively approaching and then receding from the internal limiting membrane (Fig. 24.15). DNA replication occurs while the cells are extended and their nuclei approach the pial surface; they then enter a premitotic resting period while the cells shorten and their nuclei pass back towards the ventricular surface. The cells now become rounded close to the internal limiting membrane and undergo mitosis. They then elongate and their nuclei move towards the outer edge during the postmitotic resting period, after which DNA synthesis commences once more and the cycle is repeated. The cells so formed may then either start another proliferative cycle or migrate outwards (i.e. radially) and differentiate into neurones as they approach and enter the adjacent stratum. This differentiation may be initiated as they pass outwards during the postmitotic resting period. The proliferative cycle continues with the production of clones of neurones and glioblasts. This sequence of events has been called inter-kinetic nuclear migration: it eventually declines. At the last division two postmitotic daughter cells are produced and they differentiate at the ventricular surface into ependyma.

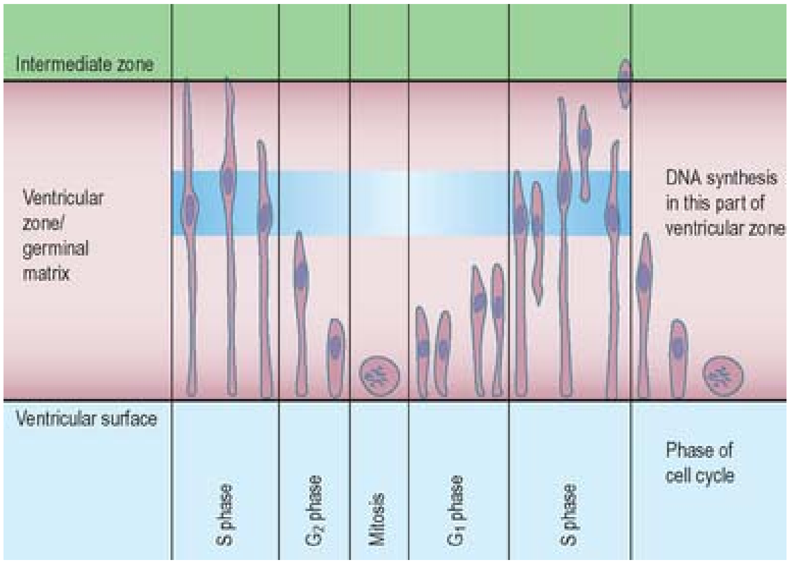
Intermediate zone
Ventricular zone/ germinal matrix
DNA synthesis in this part of ventricular zone
Ventricular surface
Phase of cell cycle
S phase
G_2 phase
Mitosis
G_1 phase
S phase

Fig. 24.15 The cell cycle in the ventricular zone of the developing neural tube. The nuclei of the proliferating stem cells show interkinetic migration.

(From Journal of Comparative Neurology 120: 37–42, S Fujita, 1963. Reprinted by permission from Wiley-Liss.)

The progeny of some of these divisions move away from the ventricular zone to form an intermediate zone of neurones. The early spinal cord and much of the brain stem shows only these three main layers, i.e. ventricular, intermediate and marginal zones. However, in the telencephalon the region of cellular proliferation extends deeper than the ventricular zone where the escalator movement of interkinetic migration is seen, and a subventricular zone appears between the ventricular and intermediate layers (Fig. 24.15). Here cells continue to multiply to provide further generations of neurones and glia which subsequently migrate into the intermediate and marginal zones. In some regions of the nervous system (e.g. the cerebellar cortex) some mitotic subventricular stem cells migrate across the entire neural wall to form a subpial population, and establish a new zone of cell division and differentiation. Many cells formed in this site remain subpial in position, but others migrate back towards the ventricle through the developing nervous tissue, and finish their migrations in various definitive sites where they differentiate into neurones or macroglial cells. In the cerebral hemispheres, a zone termed the cortical plate is formed outside the intermediate zone by radially migrating cells from the ventricular zone. The most recently formed cells migrate to the outermost layers of the cortical plate, so that earlier formed and migrating cells become subjacent to those migrating later. In the forebrain there is an additional transient stratum deep to the early cortical plate, the subplate zone.

LINEAGE AND GROWTH IN THE NERVOUS SYSTEM

Neurones come from three embryonic sources: CNS neurones originate from the pluripotential neural plate and tube, whereas ganglionic neurones originate from the neural crest and ectodermal placodes. The neural plate also provides ependymal and macroglial cells. Peripheral Schwann cells and chromaffin cells arise from the neural crest. The origins and lineages of cells in the nervous system have been determined experimentally by the use of autoradiography, microinjection or retroviral labelling of progenitor cells, and in cell culture.

During development, neurones are formed before glial cells. The timing of events differs in various parts of the CNS and between species. Most neurones are formed prenatally in mammals but some postnatal neurogenesis does occur, e.g. the small granular cells of the cerebellum, olfactory bulb and hippocampus, and neurones of the cerebral cortex. Gliogenesis continues after birth in periventricular and other sites. Autoradiographic studies have shown that different classes of neurones develop at specific times. Large neurones such as principal projection neurones tend to differentiate before small ones such as local circuit neurones. However, their subsequent migration appears to be independent of the times of their initial formation. Neurones can migrate extensively through populations of maturing, relatively static cells, to reach their destination, e.g. cerebellar granule cells pass through a layer of Purkinje cells en route from the external pial layer to their final central position. Later, the final form of their projections, cell volume and indeed their continuing survival, depend on the establishment of patterns of functional connection.

Initially immature neurones are rotund or fusiform. Their cytoplasm contains a prominent Golgi apparatus, many lysosomes, glycogen and numerous unattached ribosomes. As maturation proceeds, cells send out fine cytoplasmic processes which contain neurofilaments, microtubules and other structures, often including centrioles at their bases where microtubules form. Internally, endoplasmic reticulum cisternae appear and attached ribosomes and mitochondria proliferate, whereas the glycogen content progressively diminishes. One process becomes the axon and other processes establish a dendritic tree. Axonal growth, studied in tissue culture, may be as much as 1 mm per day.

Growth cones

Ramón y Cajal (1890) was the first to recognize that the expanded end of an axon, the growth cone, is the principal sensory organ of the neurone. Classically, the growth cone is described as an expanded region that is constantly active, changing shape, extending and withdrawing small filopodia and lamellipodia that apparently ‘explore’ the local environment for a suitable surface along which extension may occur. These processes are stabilized in one direction, determining the direction of future growth, and following consolidation of the growth cone, the exploratory behaviour recommences. This continuous cycle resembles the behaviour at the leading edge of migratory cells such as fibroblasts and neutrophils. The molecular basis of this behaviour is the transmission of signals external to the growth cone via cell surface receptors to the scaffolding of microtubules and neurofilaments within the axon. Growing neuroblasts have a cortex rich in actin associated with the plasma membrane, and a core of centrally located micro-tubules and sometimes neurofilaments. The assembly of these components, along with the synthesis of new membrane, occurs in segments distal to the cell body and behind the growth cone, though some assembly of microtubules may take place near the cell body.

The driving force of growth cone extension is uncertain. One possible mechanism is that tension applied to objects by the leading edge of the growth cone is mediated by actin, and that local accumulations of F-actin redirect the extension of microtubules. Under some culture conditions, growth cones can develop mechanical tension, pulling against other axons or the substratum to which they are attached. Possibly, tension in the growth cone acts as a messenger to mediate the assembly of cytoskeletal components. Adhesion to the substratum appears to be important for consolidation of the growth cone and elaboration of the cytoskeleton in that direction.

During development, the growing axons of neuroblasts navigate with precision over considerable distances, often pursuing complex courses to reach their targets. Eventually they make functional contact with their appropriate end organs (neuromuscular endings, secreto-motor terminals, sensory corpuscles or synapses with other neurones). During the outgrowth of axonal processes the earliest nerve fibres are known to traverse appreciable distances over an apparently virgin landscape, often occupied by loose mesenchyme. A central problem for neurobiologists, therefore, has been understanding the mechanisms of axon guidance (Gordon-Weeks 2000). Axon guidance is thought to involve short-range, local guidance cues and long-range diffusible cues, any of which can be either attractive and permissive for growth, or repellent and hence inhibitory. Short-range cues require factors which are displayed on cell surfaces or in the extracellular matrix, e.g. axon extension requires a permissive, physical substrate, the molecules of which are actively recognized by the growth cone. They also require negative cues which inhibit the progress of the growth cone. Long-range cues come from gradients of specific factors diffusing from distant targets, which cause neurones to turn their axons towards the source of the attractive signal. The evidence for this has come from *in vitro* co-culture studies. The floor plate of the developing spinal cord exerts a chemotropic effect on commissural axons that later cross it, whereas there is chemorepulsion of developing motor axons from the floor plate. These forces are thought to act *in vivo* in concert in a dynamic process to ensure the correct passage of axons to their final destinations and to mediate their correct bundling together en route.

Dendritic tree

Once growth cones have arrived in their general target area, they then have to form terminals and synapses. In recent years, much emphasis has been placed on the idea that patterns of connectivity depend on the death of inappropriate cells. Programmed cell death or apoptosis occurs during the period of synaptogenesis if neurones fail to acquire sufficient amounts of specific neurotrophic factors. Coincident firing of neighbouring neurones that have found the appropriate target region might be involved in eliciting release of factor(s), thus reinforcing correct connections. Such mechanisms may explain the numerical correspondence between neurones in a motor pool and the muscle fibres innervated. On a subtler level, pruning of collaterals may give rise to mature neuronal architecture. The projections of pyramidal neurones from the motor and visual cortex, for example, start out with similar architecture: the mature repertoire of targets is produced by the pruning of collaterals leading to loss of projections to some targets.

The final growth of dendritic trees is also influenced by patterns of afferent connections and their activity. If deprived of afferents experimentally, dendrites fail to develop fully and, after a critical period, may become permanently affected even if functional inputs are restored, e.g. in the visual systems of young animals which have been visually deprived. This is analogous to the results of untreated amblyopia in infants. Metabolic factors also affect the final branching patterns of dendrites, e.g. thyroid deficiency in perinatal rats results in a small size and restricted branching of cortical neurones. This may be analogous to the mental retardation of cretinism.

Once established, dendritic trees appear remarkably stable and partial deafferentation affects only dendritic spines or similar small details. As development proceeds plasticity is lost, and soon after birth a neuron is a stable structure with a reduced rate of growth.

Neurotrophins

If neurones lose all afferent connections or are totally deprived of sensory input, there is atrophy of much of the dendritic tree and even the whole soma. Different regions of the nervous system vary quantitatively in their response to such anterograde transneuronal degeneration. Similar effects occur in retrograde transneuronal degeneration. Thus neurones are dependent on peripheral structures for their survival. Loss of muscles or sensory nerve endings, e.g. in the developing limb, will result in reduction in numbers of motor and sensory neurones. Specific factors which these target organs produce, such as the neurotrophins, are taken into nerve endings and transported back to the neuronal somata: they are necessary for the survival of many types of neurone during early development, and for the growth of their axons and dendrites, and also promote the synthesis of neurotransmitters and enzymes.

The neurotrophins, nerve growth factor (NGF), brain derived neurotrophic factor (BDNF), neurotrophin 3 (NT-3) and NT-4/5 exert their survival effects selectively on particular subsets of neurones. NGF is specific to sensory ganglion cells from the neural crest, sympathetic postganglionic neurones and basal forebrain cholinergic neurones. BDNF promotes the survival of retinal ganglion cells, motor neurones, and some placode-derived neurones, such as those of the nodose ganglion, that are unresponsive to NGF. NT-3 has effects on motor neurones, limb proprioceptive neurones and both placode and neural crest-derived sensory neurones. Other growth factors found to influence the growth and survival of neural cells include the fibroblast growth factors (FGFs) and ciliary neurotrophic factor (CNTF), all of which are unrelated in sequence to the NGF family. Members of the FGF family support the survival of embryonic neurones from many regions of the CNS. CNTF may control the proliferation and differentiation of sympathetic ganglion cells and astrocytes.

Each of the neurotrophins binds specifically to certain receptors on the cell surface. The receptor termed $p75^{NTR}$ binds all the neurotrophins with similar affinity. By contrast, members of the family of receptor tyrosine kinases (Trks) bind with higher affinity and display binding preferences for particular neurotrophins. However, the presence of a Trk receptor seems to be required for $p75^{NTR}$ function.

Nervous tissue influences the metabolism of its target tissues. If during development a nerve fails to connect with its muscle, both degenerate. If the innervation of slow (red) or fast (white) skeletal muscle is exchanged, the muscles change structure and properties to reflect the new innervation, indicating that the nerve determines muscle type and not vice versa.

INDUCTION AND PATTERNING OF THE BRAIN AND SPINAL CORD

The generation of neural tissue involves an inductive signal from the underlying chordamesoderm (notochord), termed the ‘organizer’. The observation by Spemann in 1925 that, in intact amphibian embryos, the presence of an organizer caused ectodermal cells to form nervous tissue, whereas in its absence they formed epidermis, led to the discovery of neural induction. However, experiments performed much later in the century revealed that when ectodermal cells were dissociated they also gave rise to neural tissue. The paradox was resolved by the finding that intact ectodermal tissue is prevented from becoming neural by an inhibitory signal(s) that is diluted out when cells are dissociated. Many lines of evidence now indicate that this inhibitory signal is mediated by members of a family of secreted proteins, the bone morphogenetic proteins (BMP). These molecules are found throughout ectodermal tissue during early development, and their inhibitory effect is antagonized by several neural inducers which are present within the organizer, i.e. noggin, chordin and follistatin. Each of these factors is capable of blocking BMP signalling, in some cases by preventing it from binding to its receptor(s).

The regional pattern of the nervous system is induced before and during neural tube closure. Early concepts about regional patterning envisaged that regionalization within mesenchymal populations which transmit inductive signals to the ectoderm impose a similar mosaic of positional values on the overlying neural plate. For example, transplantation of caudal mesenchyme beneath the neural plate in Amphibia induced spinal cord, whereas rostral mesenchyme induced brain, as assessed by the morphology of the neuroepithelial vesicles. However, later work indicated a more complex scenario in which organizer grafts from early embryos induced mainly head structures, while later grafts induced mainly trunk structures. Subsequent molecular data have tended to support a model in which neural-inducing factors released by the organizer such as noggin, chordin and follistatin, neuralize the ectoderm and promote a mainly rostral neural identity. Later secreted signals then act to caudalize this rostral neural tissue, setting up an entire array of axial values along the neural tube. Candidates for these later, caudalizing, signals have been shown to be retinoic acid, fibroblast growth factors and the WNT secreted proteins, which are present in the paraxial mesenchyme and later in its derivatives, the somites. This combination of signals does not seem to be sufficient to produce the most rostral, forebrain structures. Other secreted proteins resident in the rostralmost part of the earliest ingressing axial populations of endoderm and mesenchyme are also capable of inducing markers of forebrain identity from ectodermal cells (Withington, Beddington & Cooke 2001).

As the neural tube grows and is modified in shape, a number of mechanisms refine the crude rostrocaudal pattern which has been imposed during neurulation. Molecules which diffuse from tissues adjacent to the neural tube such as the somites have patterning influences. The neural tube possesses a number of intrinsic signalling centres, such as the midbrain–hindbrain boundary, which produce diffusible molecules capable of influencing tissue development at a distance. In this way extrinsic and intrinsic factors serve to subdivide the neural tube into a number of fairly large domains, on which local influences can then act. Domains are distinguished by their expression of particular transcription factors, which in many cases have been causally related to the development of particular regions. Examples of such genes are the *Hox* family which are expressed in the spinal cord and hindbrain, and the *Dlx*, *Emx* and *Otx* families of genes which are expressed in various regions of the forebrain. All of these are developmental control genes which lie high up in the hierarchy, and are capable of initiating cascades of expression of other genes to create a more fine-grained pattern of cellular differentiation. In contrast to the aforementioned secreted molecules, these genes encode proteins which are retained in the cell nucleus, and so can act on DNA to induce or repress further gene expression.

Segmentation in the neural tube

The early neural tube is visibly divided into segments, termed neuromeres, by shallow transverse folds which extend perpendicular to its long axis. Primary neuromeres can be identified at stage 9, and 16 secondary neuromeres are present at stage 14. They are especially noted in the rhombencephalon, where they are termed rhombomeres; they have now been shown to constitute crucial units of pattern formation. Domains of expression of developmental control genes abut rhombomere boundaries; single cell labelling experiments have revealed that cells within rhombomeres form segregated non-mixing populations (Fig. 24.16). The neural crest also shows intrinsic segmentation in the rhombencephalon, and is segregated into streams at its point of origin in the dorsal neural tube. This may represent a mechanism whereby morphogenetic specification of the premigratory neural crest cells is conveyed to the pharyngeal arches (see Fig. 12.4). Although these segmental units lose their morphological prominence with subsequent development, they represent the fundamental ground plan of this part of the neuraxis, creating a series of semi-autonomous units within which local variations in patterning can then develop. The consequences of early segmentation for events later in development, such as the formation of definitive neuronal nuclei within the brain stem, and of peripheral axonal projections remain to be explored.

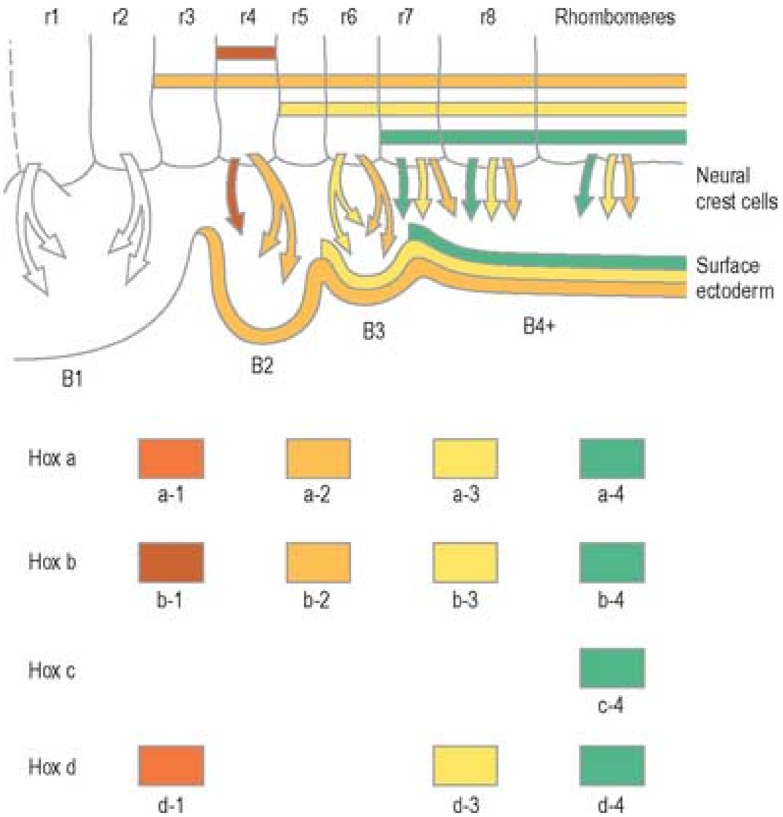
r1
r2
r3
r4
r5
r6
r7
r8
Rhombomeres
Neural crest cells
Surface ectoderm
B1
B2
B3
B4+
Hox a
a-1
a-2
a-3
a-4
Hox b
b-1
b-2
b-3
b-4
Hox c
c-4
Hox d
d-1
d-3
d-4

Fig. 24.16 *Hox* gene expression domains in the branchiorhombomeric area in the mouse embryo at E9.5. The arrows indicate neural crest cells migrating from the rhombencephalon and midbrain. At the former level they are shaded to indicate the *Hox* genes they express. The same combination of *Hox* genes is expressed in the rhombomeres and in the superficial ectoderm of the pharyngeal arches at the corresponding rostrocaudal levels. The four *Hox* clusters are represented below.

(Modified by permission from the Annual Review of Cell and Developmental Biology, Volume 8, 1992 by Annual Reviews www.annualreviews.org.)

Other brain regions are not segmented in quite the same way as the hindbrain. However, morphological boundaries, domains of cell lineage restriction and of cell mixing, and regions of gene expression that abut sharp boundaries, are found in the diencephalon and telencephalon. It is thus likely that compartmentation of cell groups with some, if not all, the features of rhombomeres plays an important role in the formation of various brain regions.

The significance of intrinsic segmentation in the hindbrain is underlined by the absence of overt segmentation of the adjacent paraxial mesenchyme. There is no firm evidence for intrinsic segmentation in the spinal cord. Instead, segmentation of the neural crest, motor axons, and thus eventually the spinal nerves, is dependent on the segmentation of the neighbouring somites. Both neural crest cell migration and motor axon outgrowth occur through only the rostral and not the caudal sclerotome of each somite, so that dorsal root ganglia form only at intervals. The caudal sclerotome possesses inhibitory properties that deter neural crest cells and motor axons from entering. This illustrates the general principle that the nervous system is closely interlocked, in terms of morphogenesis, with the ‘periphery’, i.e. surrounding non-nervous structures, and each is dependent upon the other for its effective structural and functional maturation.

Genes such as the *Hox* and *Pax* gene families, which encode transcription factor proteins, show intriguing expression patterns within the nervous system. Genes of the *Hox-b* cluster, for example, are expressed throughout the caudal neural tube, and up to discrete limits in the hindbrain that coincide with rhombomere boundaries. The ordering of these genes within a cluster on the chromosome (5′-3′) is the same as the caudal to rostral limits of expression of consecutive genes. This characteristic pattern is surprisingly similar in fish, frogs, birds and mammals. *Hox* genes play a role in patterning not only of the neural tube but also of much of the head region, consistent with their expression in neural crest cells, and within the pharyngeal arches. Disruption of *Hox a-3* gene in mice mimics DiGeorge’s syndrome, a congenital human disorder characterized by the absence (or near absence) of the thymus, parathyroid and thyroid glands, by the hypotrophy of the walls of the arteries derived from the aortic arches, and by subsequent conotruncal cardiac malformations. Some *Pax* genes are expressed in different dorsoventral domains within the neural tube. *Pax-3* is expressed in the alar lamina, including the neural crest, while *Pax-6* is expressed in the intermediate plate. The *Pax-3* gene has the same chromosomal localization as the mouse mutation Splotch and the affected locus in the human Waardenburg's syndrome, both of which are characterized by neural crest disturbances with pigmentation disorders and occasional neural tube defects. Both *Hox* and *Pax* genes have restricted expression patterns with respect to the rostrocaudal and the dorsoventral axes of the neural tube, consistent with roles in positional specification. (For reviews of the expression patterns of these genes see Krumlauf et al 1993.)

While craniocaudal positional values are probably conferred on the neuroepithelium at the neural plate or early neural tube stage, dorsoventral positional values may become fixed later. The development of the dorsoventral axis is heavily influenced by the presence of the underlying notochord. The notochord induces the ventral midline of the neural tube, the floor plate. This specialized region consists of a strip of non-neural cells with distinctive adhesive and functional properties. Notochord and floor plate together participate in inducing the differentiation of the motor columns. Motor neurone differentiation occurs early, giving some grounds for the idea of a ventral to dorsal wave of differentiation. The notochord/floor plate complex may also be responsible for allotting the values of more dorsal cell types within the tube (Fig. 24.7). For example, the dorsal domain of expression of *Pax-3* extends more ventrally in embryos experimentally deprived of notochord and floor plate, while grafting an extra notochord adjacent to the dorsal neural tube leads to a repression of *Pax-3* expression.

PERIPHERAL NERVOUS SYSTEM

SOMATIC NERVES

Spinal nerves

Each spinal nerve is connected to the spinal cord by a ventral root and a dorsal root (Fig. 24.17). The fibres of the ventral roots grow out from cell bodies in the anterior and lateral parts of the intermediate zone. These pass through the overlying marginal zone and external limiting membrane. Some enter the myotomes of the somites, and some penetrate the somites, reaching the adjacent somatopleure, and in both sites they ultimately form the α-, β- and γ-efferents. At appropriate levels these are accompanied by the outgrowing axons of preganglionic sympathetic neuroblasts (segments T1–L2), or preganglionic parasympathetic neuroblasts (S2–S4).

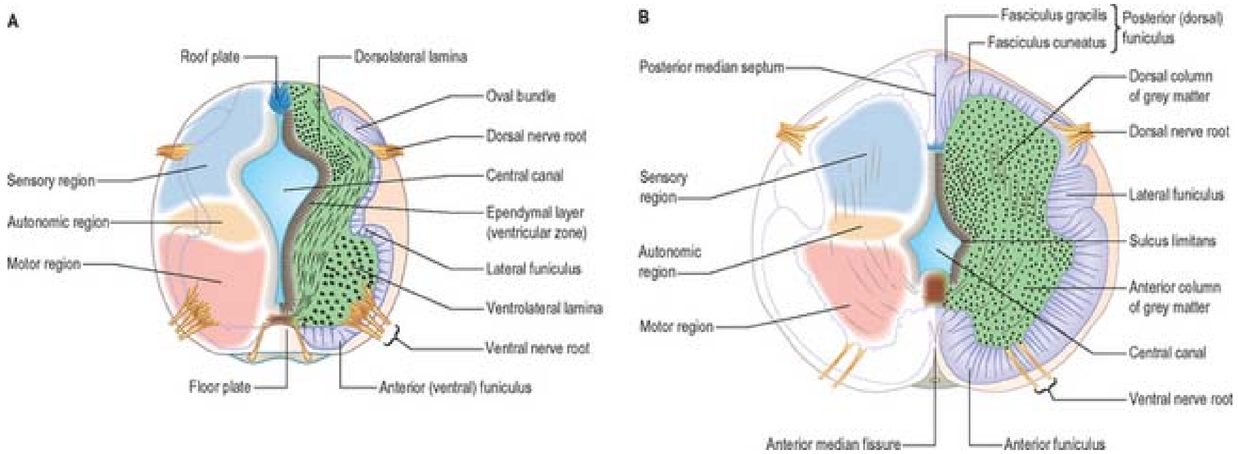
A
Roof plate
Dorsolateral lamina
Oval bundle
Dorsal nerve root
Central canal
Ependymal layer (ventricular zone)
Lateral funiculus
Ventrolateral lamina
Ventral nerve root
Anterior (ventral) funiculus
Floor plate
Sensory region
Autonomic region
Motor region
B
Fasciculus gracilis
Fasciculus cuneatus
Posterior (dorsal) funiculus
Posterior median septum
Dorsal column of grey matter
Dorsal nerve root
Lateral funiculus
Sulcus limitans
Anterior column of grey matter
Central canal
Ventral nerve root
Anterior funiculus
Anterior median fissure
Sensory region
Autonomic region
Motor region

Fig. 24.17 The developing spinal cord of human embryos: **A**, approximately 6 weeks; **B**, approximately 3 months. Transverse sections.

The fibres of the dorsal roots extend from cell somata in dorsal root ganglia (DRG) into the spinal cord and also extend into the periphery. Neural crest cells are produced continuously along the length of the spinal cord, but gangliogenic cells migrate only into the rostral part of each somitic sclerotome where they condense and proliferate to form a bilateral series of oval-shaped primordial spinal ganglia (dorsal root ganglia) (Fig. 24.11). Negative factors in the caudal sclerotome deter neural crest from entering.

The rostral sclerotome has a mitogenic effect on the crest cells that settle within it. From the ventral region of each ganglion a small part separates to form sympathochromaffin cells, while the remainder becomes a definitive spinal ganglion (dorsal root ganglion). The spinal ganglia are arranged symmetrically at the sides of the neural tube and, except in the caudal region, are equal in number to the somites. The cells of the ganglia, like the cells of the intermediate zone of the early neural tube, are glial and neuronal precursors. The glial precursors develop into satellite cells (which become closely applied to the ganglionic nerve cell somata), Schwann cells, and possibly other cells. The neuroblasts, at first round or oval, soon become fusiform, and their extremities gradually elongate into central and peripheral processes. The central processes grow into the neural tube as the fibres of dorsal nerve roots, while the peripheral processes grow ventrolaterally to mingle with the fibres of the ventral root, thus forming a mixed spinal nerve. As development proceeds the original bipolar form of the cells in the spinal ganglia changes and the two processes become approximated until they ultimately arise from a single stem to form a unipolar cell. The bipolar form is retained in the ganglion of the vestibulocochlear nerve.

Cranial nerves

Cranial nerves may contain motor, sensory or both types of fibres. With the exception of the olfactory and optic nerves, the cranial nerves develop in a manner similar in some respects to components of the spinal nerves. The somata of motor neuroblasts originate within the neuroepithelium, while those of sensory neuroblasts are derived from the neural crest with the addition in the head of contributions from ectodermal placodes (Fig. 24.18; see Fig. 12.4).

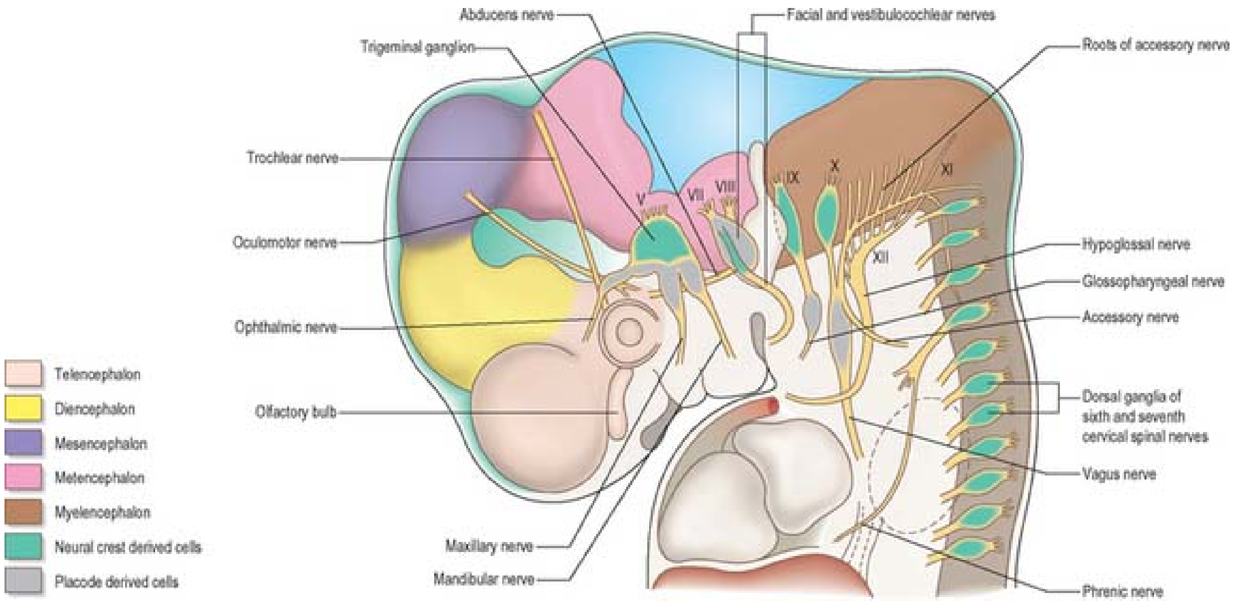
Abducens nerve
Trigeminal ganglion
Facial and vestibulocochlear nerves
Roots of accessory nerve
Trochlear nerve
Oculomotor nerve
Ophthalmic nerve
Olfactory bulb
Maxillary nerve
Mandibular nerve
V
VII
VIII
IX
X
XI
XII
Hypoglossal nerve
Glossopharyngeal nerve
Accessory nerve
Dorsal ganglia of sixth and seventh cervical spinal nerves
Vagus nerve
Phrenic nerve
Telencephalon
Diencephalon
Mesencephalon
Metencephalon
Myelencephalon
Neural crest derived cells
Placode derived cells

Fig. 24.18 The brain and cranial nerves of a human embryo, 10.2 mm long. Note the derivation of the ganglia associated with the trigeminal, facial, vestibulocochlear, glossopharyngeal, vagus and spinal accessory nerves.

The motor fibres of the cranial nerves which project to striated muscle are the axons of cells originating in the basal plate of the midbrain and hindbrain. The functional and morphological distinction between the neurones within these various nerves is based on the types of muscle innervated. In the trunk, the motor roots of the spinal nerves all emerge from the spinal cord close to the ventral midline to supply the muscles derived from the somites.

In the head the motor outflow is traditionally segregated into two pathways (Figs 24.3B and 24.18). General somatic efferent neurones exit ventrally in a similar manner to those of the spinal cord. Thus the oculomotor, trochlear, abducens and hypoglossal nerves parallel the organization of the somatic motor neurones in the spinal cord. The second motor component, special branchial efferent, consists of the motor parts of the trigeminal, facial, glossopharyngeal and vagus nerves which supply the pharyngeal (branchial) arches, and the accessory nerve. These nerves all have nerve exit points more dorsally placed than the somatic motor system.

The cranial nerves also contain general visceral efferent neurones (parasympathetic preganglionic) which travel in the oculomotor, facial, glossopharyngeal and vagus nerves and leave the hindbrain via the same exit points as the special branchial efferent fibres. All three categories of motor neurones probably originate from the same region of the basal plate, adjacent to the floor plate. The definitive arrangement of nuclei reflects the differential migration of neuronal somata. It is not known whether all these cell types share a common precursor within the rhombencephalon, however, in the spinal cord somatic motor and preganglionic autonomic neurones are linearly related.

These motor neurone types have been designated according to the types of muscles or structures they innervate. General somatic efferent nerves supply striated muscle derived from the cranial (occipital) somites and prechordal mesenchyme. Myogenic cells from the ventrolateral edge of the epithelial plate of occipital somites give rise to the intrinsic muscles of the tongue, while the prechordal mesenchyme gives rise to the extrinsic ocular muscles. Special branchial efferent nerves supply the striated muscles developing within the pharyngeal (branchial) arches (see Fig. 12.4) which are derived from parachordal mesenchyme between the occipital somites and the prechordal mesenchyme. All the voluntary muscles of the head originate from axial (prechordal) or paraxial mesenchyme which renders the distinction between somatic efferent supply and branchial efferent supply somewhat artificial. However, the obviously special nature of the arch musculature, its patterning by the neural crest cells, its particularly rich innervation for both voluntary and reflex activity, and the different origins from the basal plate of the branchial efferent nerves compared to the somatic efferent nerves, make the retention of a distinction between the two of some value.

General visceral efferent neurones (parasympathetic preganglionic) innervate glands of the head, the sphincter pupillae and ciliary muscles, and the thoracic and abdominal viscera.

The cranial sensory ganglia are derived in part from the neural crest, and in part from cells of the ectodermal placodes (Figs 24.12 and 24.18).

Generally, neurones distal to the brain are derived from placodes while proximal ones are derived from the neural crest (Fig. 24.18). Supporting cells of all sensory ganglia arise from the neural crest. The most rostral sensory ganglion, the trigeminal, contains both neural crest and placode-derived neurones that mediate general somatic afferent functions. In the case of more caudal cranial nerves (the facial, glossopharyngeal and vagus), the same applies, but the two cell populations form separate ganglia in the case of each nerve. The proximal series of ganglia is neural crest derived (forming the proximal ganglion of the facial nerve, the superior ganglion of the glossopharyngeal nerve and the jugular ganglion of the vagus) while the distal series is derived from placodal cells (forming the geniculate ganglion of the facial nerve, the petrosal ganglion of the glossopharyngeal nerve and the nodose ganglion of the vagus). These ganglia contain neurones that mediate special, general visceral and somatic afferent functions. The vestibular ganglion contains both crest and placodal cells and the acoustic ganglion contains only placodal neurones: the axons from these cells are special somatic afferents and they all travel in the vestibulocochlear nerve.

The neurones and supporting cells of the cranial autonomic ganglia in the head and the trunk originate from neural crest cells. Caudal to the vagal ganglion, the occipital region of the neural crest is concerned with the ‘ganglia’ of the accessory and hypoglossal nerves. Rudimentary ganglion cells may occur along the hypoglossal nerve in the human embryo, but they subsequently regress. Ganglion cells are found on the developing spinal root of the accessory nerve and are believed to persist in the adult. The central processes of the cells of these various ganglia, where they persist, enter the alar lamina of the hindbrain. Their peripheral processes join the efferent components of the nerve to be distributed to the various tissues innervated. Some incoming fibres from the facial, glossopharyngeal and vagus nerves collect to form an oval bundle, the tractus solitarius, on the lateral aspect of the myelencephalon. This bundle is the homologue of the oval bundle of the spinal cord, but in the hindbrain it becomes more deeply placed by the overgrowth, folding and subsequent fusion of tissue derived from the rhombic lip on the external aspect of the bundle.

AUTONOMIC NERVOUS SYSTEM

Autonomic nerves, apart from the preganglionic motor axons arising from the CNS, are formed by the neural crest. The autonomic nervous system includes the sympathetic and parasympathetic neurones in the peripheral ganglia and their accompanying glia, the enteric nervous system and glia, and the suprarenal medulla.

In the trunk at neurulation, neural crest cells migrate from the neural epithelium to lie transitorily on the fused neural tube. Thereafter crest cells migrate laterally and then ventrally to their respective destinations (Fig. 24.11). Within the head the neural crest cells migrate prior to neural fusion, producing a vast mesenchymal population as well as autonomic neurones.

The four major regions of neural crest cell distribution to the autonomic nervous system are cranial, vagal, trunk and lumbosacral. The cranial neural crest gives rise to the cranial parasympathetic ganglia, whereas the vagal neural crest gives rise to the thoracic parasympathetic ganglia. The trunk neural crest gives rise to the sympathetic ganglia, mainly the paravertebral ganglia, and suprarenomedullary cells. This category is often referred to as the sympathosuprarenal lineage.

Neurones of the enteric nervous system are described as arising from the vagal crest, i.e. neural crest derived from somite levels 1–7, and the sacral crest, caudal to the 28th somite. At all of these levels the crest cells also differentiate into glial-like support cells alongside the neurones (Fig. 24.19).

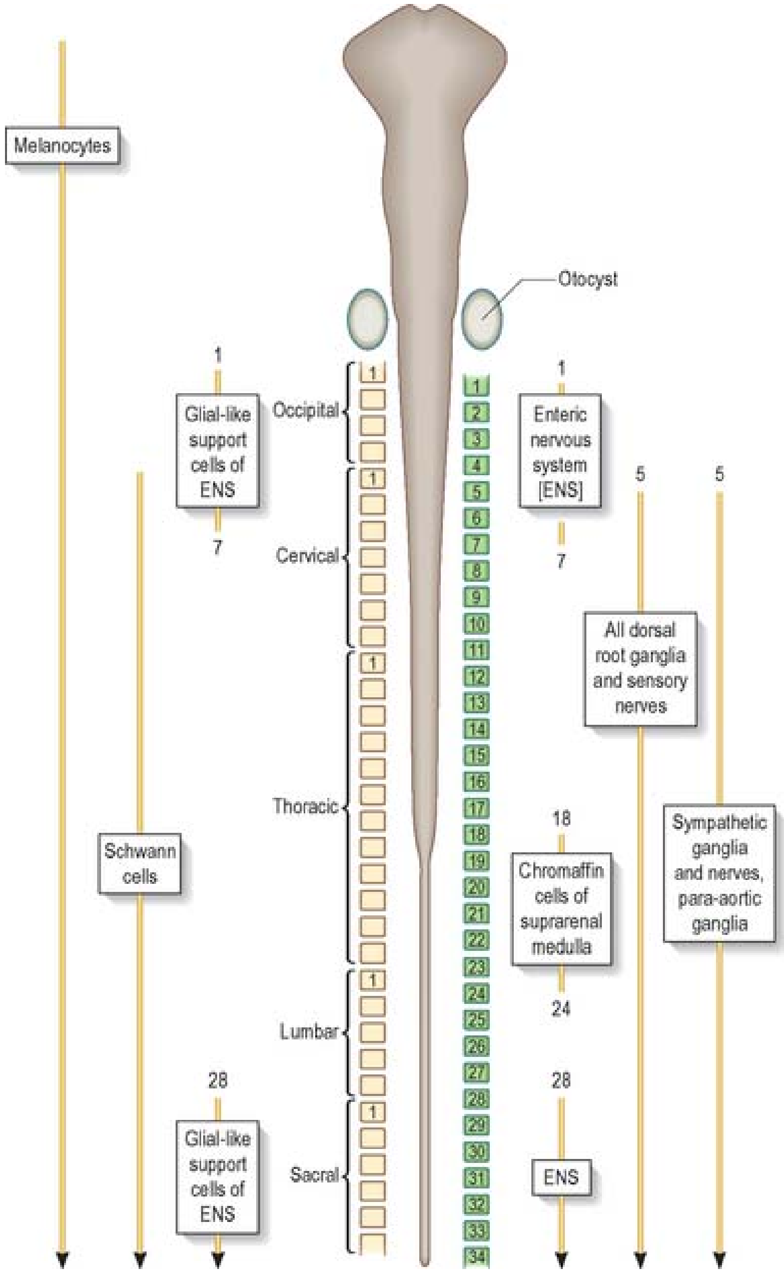
Melanocytes
Otocyst
1
Glial-like support cells of ENS
7
Occipital
Cervical
Thoracic
Lumbar
Sacral
1
Enteric nervous system [ENS]
7
5
5
All dorsal root ganglia and sensory nerves
18
Chromaffin cells of suprarenal medulla
24
Sympathetic ganglia and nerves, para-aortic ganglia
Schwann cells
28
Glial-like support cells of ENS
28
ENS
1 2 3 4 5 6 7 8 9 10 11 12 13 14 15 16 17 18 19 20 21 22 23 24 25 26 27 28 29 30 31 32 33 34

Fig. 24.19 The derivatives of neural crest cells in the trunk. The fate of crest cells arising at particular somite levels is shown.

Parasympathetic ganglia

Neural crest cells migrate from the region of the mesencephalon and rhombencephalon prior to neural tube closure. From rostral to caudal, three populations of neural crest have been noted: cranial neural crest, cardiac neural crest and vagal neural crest. The migration of the sacral neural crest and the formation of the caudal parasympathetic ganglia have attracted little research interest.

Neural crest cells from the caudal third of the mesencephalon and the rostral metencephalon migrate along or close to the ophthalmic branch of the trigeminal nerve and give rise to the ciliary ganglion. Cells migrating from the nucleus of the oculomotor nerve may also contribute to the ganglion; a few scattered cells are always demonstrable in postnatal life along the course of this nerve. Preotic myelencephalic neural crest cells give rise to the pterygopalatine ganglion, which may also receive contributions from the ganglia of the trigeminal and facial nerves. The otic and submandibular ganglia are also derived from myelencephalic neural crest and may receive contributions from the glossopharyngeal and facial cranial nerves respectively (see Fig. 12.4).

Neural crest from the region located between the otic placode and the caudal limit of somite 3 has been termed cardiac neural crest. Cells derived from these levels migrate through pharyngeal arches 3, 4, and 6 where they provide, inter alia, support for the embryonic aortic arch arteries, cells of the aorticopulmonary septum and truncus arteriosus. Some of these neural crest cells also differentiate into the neural anlage of the parasympathetic ganglia of the heart. Sensory innervation of the heart is from the inferior ganglion of the vagus, which is derived from the nodose placodes. Neural crest cells migrating from the level of somites 1–7 are collectively termed vagal neural crest; they migrate to the gut along with sacral neural crest.

Sympathetic ganglia

Neural crest cells migrate ventrally within the body segments, penetrate the underlying somites and continue to the region of the future paravertebral and prevertebral plexuses, where they form the sympathetic chain of ganglia and the major ganglia around the ventral visceral branches of the abdominal aorta (Figs 24.11 and 24.19). Neural crest cells are induced to differentiate into sympathetic neurones by the dorsal aorta through the actions of the signaling molecules, Bmp-4 and Bmp-7.

There is cell specific recognition of postganglionic neurones and the growth cones of sympathetic preganglionic neurones. They meet during their growth, and this may be important in guidance to their appropriate target. The position of postganglionic neurones, and the exit point from the spinal cord of preganglionic neurones, may influence the types of synaptic connections made, and the affinity for particular postganglionic neurones. When a postganglionic neuroblast is in place it extends axons and dendrites and synaptogenesis occurs. The earliest axonal outgrowths from the superior cervical ganglion occur at about stage 14: although the axon is the first cell process to appear, the position of the neurones does not apparently influence the appearance of the cell processes.

The local environment plays a major role in controlling the appropriate differentiation of the presumptive autonomic ganglion neurones. The identity of the factors responsible for subsequent adrenergic, cholinergic or peptidergic phenotype has yet to be elucidated: it has been proposed that fibronectin and basal lamina components initiate adrenergic phenotypic expression at the expense of melanocyte numbers. Cholinergic characteristics are acquired relatively early and the appropriate phenotypic expression may be promoted by cholinergic differentiation factor and ciliary neurotrophic factor.

Neuropeptides are expressed by autonomic neurones *in vitro* and may be stimulated by various target tissue factors in sympathetic and parasympathetic neurones. Some neuropeptides are expressed more intensely during early stages of ganglion formation.

Enteric nervous system

The enteric nervous system is different from the other components of the autonomic nervous system because it can mediate reflex activity independently of control by the brain and spinal cord. The number of enteric neurones that develop is believed to be of the same magnitude as the number of neurones in the spinal cord, whereas the number of preganglionic fibres that supply the intestine, and therefore modulate the enteric neurones, is much fewer.

The enteric nervous system is derived from the neural crest. The axial levels of crest origin are shown in Fig. 24.19. Premigratory neural crest cells are not prepatterned for specific axial levels, rather they attain their axial value as they leave the neuraxis. Once within the gut wall there is a regionally specific pattern of enteric ganglia formation which may be controlled by the local splanchnopleuric mesenchyme. Cranial neural crest from somite levels 1–7 contributes to the enteric nervous system, forming both neuroblasts and glial support cells.

The most caudal derivatives of neural crest cells, from the lumbosacral region, somites 28 onwards, form components of the pelvic plexus after migrating through the somites towards the level of the colon, rectum and cloaca. Initially the cells come to lie within the developing mesentery, then transiently between the layers of the differentiating muscularis externa, before finally forming a more substantial intramural plexus characteristic of the adult enteric nervous system.

Of the neural crest cells that colonize the bowel, some in the foregut may acquire the ability to migrate outwards and colonize the developing pancreas.

Hirschsprung’s disease appears to result from a failure of neural crest cells to colonize the gut wall appropriately. The condition is characterized by a dilated segment of colon proximally and lack of peristalsis in the segment distal to the dilatation. Infants with Hirschsprung’s disease show delay in the passage of meconium, constipation, vomiting and abdominal distension. In humans, Hirschsprung’s disease is often seen associated with other defects of neural crest development, e.g. Waardenburg type II syndrome, which includes deafness and facial clefts with megacolon.

CHROMAFFIN CELLS

Chromaffin cells are derived from the neural crest and found at numerous sites throughout the body. They are the classic chromaffin cells of the suprarenal medulla, bronchial neuroepithelial cells, dispersed epithelial endocrine cells of the gut (formerly known as argentaffin cells), carotid body cells, and the paraganglia.

The sympathetic ganglia, suprarenal medulla and chromaffin cells are all derived from the cells of the sympathosuprarenal lineage. In the suprarenal medulla these cells differentiate into a number of types consisting of small and intermediate-sized neuroblasts or sympathoblasts and larger, initially rounded phaeochromocytoblasts.

Large cells with pale nuclei, thought to be the progenitors of chromaffin cells, can be detected from 9 weeks in human fetuses, and clusters of small neurones are evident from 14 weeks.

Intermediate-sized neuroblasts differentiate into the typical multipolar postganglionic sympathetic neurones (which secrete noradrenaline at their terminals) of classic autonomic neuroanatomy. The smaller neuroblasts have been equated with the small intensely fluorescent (SIF) cells, types I and II, which store and secrete dopamine type I and are thought to function as true interneurones, synapsing with the principal postganglionic neurones. Type II probably operate as local neuroendocrine cells, secreting dopamine into the ganglionic microcirculation. Both types of SIF cells can modulate preganglionic/postganglionic synaptic transmission in the ganglionic neurones. The large cells differentiate into masses of columnar or polyhedral phaeochromocytes (classic chromaffin cells) which secrete either adrenaline (epinephrine) or noradrenaline (norepinephrine). These cell masses are termed paraganglia and may be situated near, on the surface of, or embedded in, the capsules of the ganglia of the sympathetic chain, or in some of the large autonomic plexuses. The largest members of the latter are the para-aortic bodies which lie along the sides of the abdominal aorta in relation to the inferior mesenteric artery. During childhood the para-aortic bodies and the paraganglia of the sympathetic chain partly degenerate and can no longer be isolated by gross dissection, but even in the adult, chromaffin tissue can still be recognized microscopically in these various sites. Both phaeochromocytes and SIF cells belong to the amine precursor uptake and decarboxylation (APUD) series of cells and are paraneuronal in nature.

CENTRAL NERVOUS SYSTEM

SPINAL CORD

In the future spinal cord the median roof plate (dorsal lamina) and floor plate (ventral lamina) of the neural tube do not participate in the cellular proliferation which occurs in the lateral walls and so remain thin. Their cells contribute largely to the formation of the ependyma.

The neuroblasts of the lateral walls of the tube are large and at first round or oval (apolar). Soon they develop processes at opposite poles and become bipolar neurons. However, one process is withdrawn and the neuroblast becomes unipolar, although this is not invariably so in the case of the spinal cord. Further differentiation leads to the development of dendritic processes and the cells become typical multipolar neurones. In the developing cord they occur in small clusters representing clones of neurones. The development of a longitudinal sulcus limitans on each side of the central canal of the cord divides the ventricular and intermediate zones in each lateral wall into a basal (ventrolateral) plate or lamina and an alar (dorsolateral) plate or lamina (Fig. 24.17). This separation indicates a fundamental functional difference. Neural precursors in the basal plate include the motor cells of the anterior (ventral) and lateral grey columns, while those of the alar plate exclusively form ‘interneurones’ (which possess both short and long axons), some of which receive the terminals of primary sensory neurones. Caudally the central canal of the cord ends as a fusiform dilatation, the terminal ventricle.

Anterior (ventral) grey column

The cells of the ventricular zone are closely packed at this stage and arranged in radial columns (Fig. 24.6). Their disposition may be determined in part by contact guidance along the earliest radial array of glial fibres which cross the full thickness of the early neuroepithelium. The cells of the intermediate zone are more loosely packed. They increase in number initially in the region of the basal plate. This enlargement outlines the anterior (ventral) column of the grey matter and causes a ventral projection on each side of the median plane: the floor plate remains at the bottom of the shallow groove so produced. As growth proceeds these enlargements, which are further increased by the development of the anterior funiculi (tracts of axons passing to and from the brain), encroach on the groove until it becomes converted into the slit-like anterior median fissure of the adult spinal cord (Fig. 24.17). The axons of some of the neuroblasts in the anterior grey column cross the marginal zone and emerge as bundles of ventral spinal nerve rootlets on the anterolateral aspect of the spinal cord. These constitute, eventually, both the α-efferents which establish motor end plates on extrafusal striated muscle fibres and the γ-efferents which innervate the contractile polar regions of the intrafusal muscle fibres of the muscle spindles.

Lateral grey column

In the thoracic and upper lumbar regions some intermediate zone neuroblasts in the dorsal part of the basal plate outline a lateral column. Their axons join the emerging ventral nerve roots and pass as preganglionic fibres to the ganglia of the sympathetic trunk or related ganglia, the majority eventually myelinating to form white rami communicantes. The axons within the rami synapse on the autonomic ganglionic neurones, and axons of some of the latter pass as postganglionic fibres to innervate smooth muscle cells, adipose tissue or glandular cells. Other preganglionic sympathetic efferent axons pass to the cells of the suprarenal medulla. An autonomic lateral column is also laid down in the midsacral region. It gives origin to the preganglionic parasympathetic fibres which run in the pelvic splanchnic nerves.

The anterior region of each basal plate initially forms a continuous column of cells throughout the length of the developing cord. This soon develops into two columns (on each side): one is medially placed and concerned with innervation of axial musculature, and the other is laterally placed and innervates the limbs. At limb levels the lateral column enlarges enormously, but regresses at other levels.

Axons arising from ventral horn neurones, i.e. α-, β- and γ-efferent fibres, are accompanied at thoracic, upper lumbar and midsacral levels by preganglionic autonomic efferents from neuroblasts of the developing lateral horn. Numerous interneurones develop in these sites (including Renshaw cells): it is uncertain how many of these differentiate directly from ventrolateral lamina (basal plate) neuroblasts and how many migrate to their final positions from the dorsolateral lamina (alar plate).

In the human embryo, the definitive grouping of the ventral column cells, which characterizes the mature cord, occurs early, and by the 14th week (80 mm) all the major groups can be recognized. As the anterior and lateral grey columns assume their final form the germinal cells in the ventral part of the ventricular zone gradually stop dividing. The layer becomes reduced in thickness until ultimately it forms the single-layered ependyma which lines the ventral part of the central canal of the spinal cord.

Posterior (dorsal) grey column

The posterior (dorsal) column develops later; consequently the ventricular zone is for a time much thicker in the dorsolateral lamina (alar plate) than it is in the ventrolateral lamina (basal plate) (Fig. 24.6).

While the columns of grey matter are being defined, the dorsal region of the central canal becomes narrow and slit-like, and its walls come into apposition and fuse with each other (Fig. 24.17). In this way the central canal becomes relatively reduced in size and somewhat triangular in outline.

About the end of the fourth week advancing axonal sprouts invade the marginal zone. The first to develop are those destined to become short intersegmental fibres from the neuroblasts in the intermediate zone, and fibres of dorsal roots of spinal nerves which pass into the spinal cord from neuroblasts of the early spinal ganglia. The earlier dorsal root fibres that invade the dorsal marginal zone arise from small dorsal root ganglionic neuroblasts. By the sixth week they form a well-defined oval bundle near the peripheral part of the dorsolateral lamina (Figs 24.6 and 24.7). This bundle increases in size and, spreading towards the median plane, forms the primitive posterior funiculus of fine calibre. Later, fibres derived from new populations of large dorsal root ganglionic neuroblasts join the dorsal root: they are destined to become fibres of much larger calibre. As the posterior funiculi increase in thickness, their medial surfaces come into contact separated only by the posterior medial septum, which is ependymal in origin and neuroglial in nature. It is thought that the displaced primitive posterior funiculus may form the basis of the dorsolateral tract or fasciculus (of Lissauer).

Maturation of the spinal cord

Long intersegmental fibres begin to appear at about the third month and corticospinal fibres are seen at about the fifth month. All nerve fibres at first lack myelin sheaths. Myelination starts in different groups at different times, e.g. the ventral and dorsal nerve roots about the fifth month, the corticospinal fibres after the ninth month. In peripheral nerves the myelin is formed by Schwann cells (derived from neural crest cells) and in the CNS by oligodendrocytes (which develop from the ventricular zone of the neural tube). Myelination persists until overall growth of the CNS and PNS has ceased. In many sites, slow growth continues for long periods, even into the postpubertal years.

The cervical and lumbar enlargements appear at the time of the development of their respective limb buds.

In early embryonic life, the spinal cord occupies the entire length of the vertebral canal and the spinal nerves pass at right angles to the cord. After the embryo has attained a length of 30 mm the vertebral column begins to grow more rapidly than the spinal cord and the caudal end of the cord gradually becomes more cranial in the vertebral canal. Most of this relative rostral migration occurs during the first half of intrauterine life. By the 25th week the terminal ventricle of the spinal cord has altered in level from the second coccygeal vertebra to the third lumbar, a distance of nine segments. As the change in level begins rostrally, the caudal end of the terminal ventricle, which is adherent to the overlying ectoderm, remains *in situ*, and the walls of the intermediate part of the ventricle and its covering pia mater become drawn out to form a delicate filament, the filum terminale. The separated portion of the terminal ventricle persists for a time, but it usually disappears before birth. It does, however, occasionally give rise to congenital cysts in the neighbourhood of the coccyx. In the definitive state, the upper cervical spinal nerves retain their position roughly at right angles to the cord. Proceeding caudally, the nerve roots lengthen and become progressively more oblique.

During gestation the relationship between the conus medullaris and the vertebral column changes, such that the conus medullaris gradually ascends to lie at higher vertebral levels. By 19 weeks of gestation the conus is adjacent to the fourth lumbar vertebra, and by full term (40 weeks) it is at the level of the second lumbar vertebra. By 2 months postnatally the conus medullaris has usually reached its permanent position at the level of the body of the first lumbar vertebra.

BRAIN

A summary of the derivatives of the cerebral regions from caudal to rostral is given in Table 24.1.

Rhombencephalon

By the time the midbrain flexure appears, the length of the rhombencephalon is greater than that of the combined extent of the mesencephalon and prosencephalon. Rostrally it exhibits a constriction, the isthmus rhombencephali (Fig. 24.3B), best viewed from the dorsal aspect. Ventrally the hindbrain is separated from the dorsal wall of the primitive pharynx only by the notochord, the two dorsal aortae and a small amount of mesenchyme; on each side it is closely related to the dorsal ends of the pharyngeal arches.

The pontine flexure appears to ‘stretch’ the thin, epithelial roof plate which becomes widened. The greatest increase in width corresponds to the region of maximum convexity, so that the outline of the roof plate becomes rhomboidal. By the same change the lateral walls become separated, particularly dorsally, and the cavity of the hindbrain, subsequently the fourth ventricle, becomes flattened and somewhat triangular in cross-section. The pontine flexure becomes increasingly acute until, at the end of the second month, the laminae of its cranial (metencephalic) and caudal (myelencephalic) slopes are opposed to each other (see Fig. 24.21) and, at the same time, the lateral angles of the cavity extend to form the lateral recesses of the fourth ventricle.

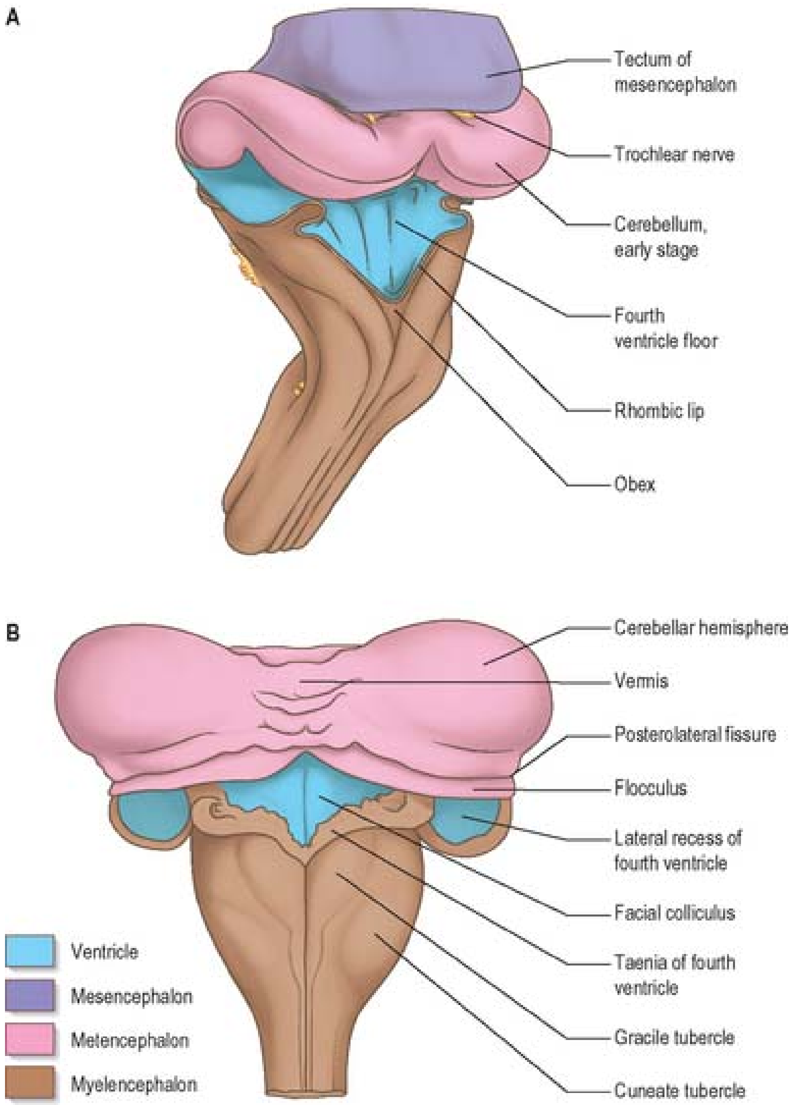
A
Tectum of mesencephalon
Trochlear nerve
Cerebellum, early stage
Fourth ventricle floor
Rhombic lip
Obex
B
Cerebellar hemisphere
Vermis
Posterolateral fissure
Flocculus
Lateral recess of fourth ventricle
Facial colliculus
Taenia of fourth ventricle
Gracile tubercle
Cuneate tubercle
Ventricle
Mesencephalon
Metencephalon
Myelencephalon

Fig. 24.21 **A**, The developing brainstem of a human fetus approximately 3 months, left dorsolateral aspect. **B**, The developing cerebellum in the fifth month, dorsal aspect.

At about four and a half weeks of development, when the pontine flexure is first discernible, the association between the rhombomeres and the underlying motor nuclei of certain cranial nerves can be seen. The general pattern of distribution of motor nuclei is as follows: rhombomere 1 contains the trochlear nucleus, rhombomeres 2 and 3 contain the trigeminal nucleus, rhombomeres 4 and 5 contain the facial nucleus, rhombomere 5 contains the abducens nucleus, rhombomeres 6 and 7 contain the glossopharyngeal nucleus, and rhombomeres 7 and 8 contain the vagal, accessory and hypoglossal nuclei. Rhombomeric segmentation represents the ground plan of development in this region of the brain stem and is pivotal for the development of regional identity (see Fig. 12.4). However, with further morphogenesis the obvious constrictions of the rhombomere boundaries disappear, and the medulla once again assumes a smooth contour. The differentiation of the lateral walls of the hindbrain into basal (ventrolateral) and alar (dorsolateral) plates has a similar significance to the corresponding differentiation in the lateral wall of the spinal cord, and ventricular, intermediate and marginal zones are formed in the same way.

Cells of the basal plate (ventrolateral lamina)

Cells of the basal plate form three elongated, discontinuous, columns that are positioned ventrally and dorsally with an intermediate column between (Fig. 24.20).

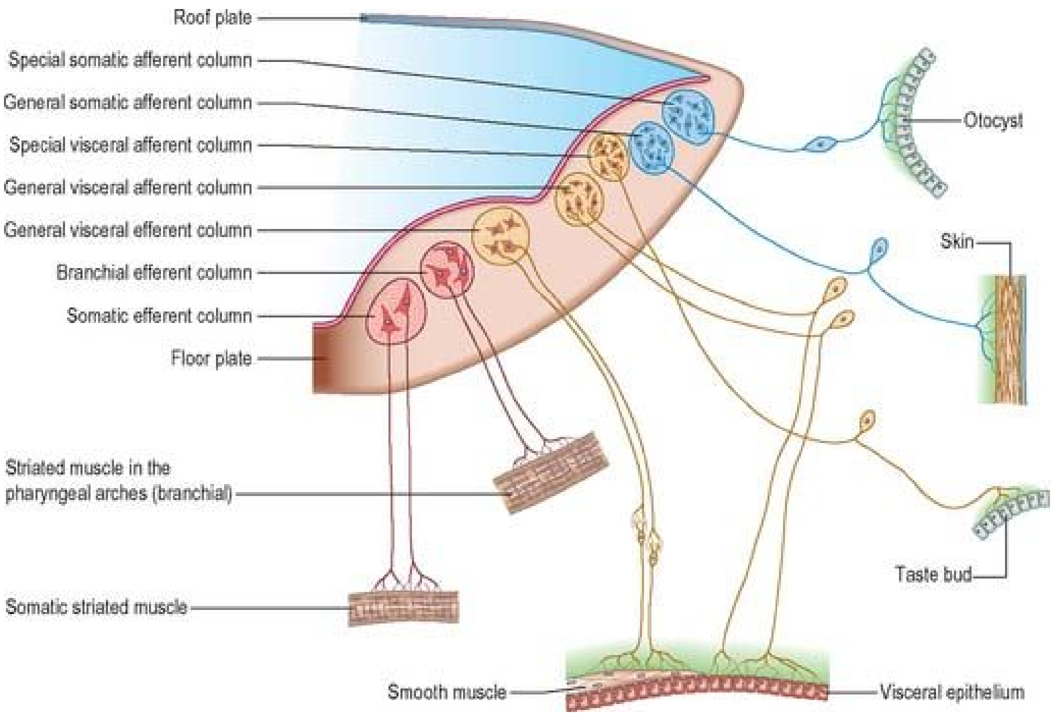
Roof plate
Special somatic afferent column
General somatic afferent column
Special visceral afferent column
General visceral afferent column
General visceral efferent column
Branchial efferent column
Somatic efferent column
Floor plate
Striated muscle in the pharyngeal arches (branchial)
Somatic striated muscle
Smooth muscle
Visceral epithelium
Taste bud
Skin
Otocyst

Fig. 24.20 Transverse section through the developing hindbrain of a human embryo 10.5 mm long, showing the relative positions of the columns of grey matter from which the nuclei associated with the different varieties

of nerve components are derived. Postganglionic neurones are associated with the general visceral efferent column, bipolar neurones are associated with the otocyst and unipolar afferent neurones are associated with the other alar plate columns.

The most ventral column is continuous with the anterior grey column of the spinal cord and will supply muscles considered ‘myotomic’ in origin. It is represented in the caudal part of the hindbrain by the hypoglossal nucleus, and it reappears at a higher level as the nuclei of the abducens, trochlear and oculomotor nerves (somatic efferent nuclei). The intermediate column is represented in the upper part of the spinal cord and caudal brainstem (medulla oblongata and pons) and its neurones supply branchial (pharyngeal) and postbranchial musculature. It is discontinuous, forming the elongated nucleus ambiguus in the caudal brainstem, which gives fibres to the ninth, tenth and eleventh cranial nerves, and continues into the cervical spinal cord as the origin of the spinal accessory nerve. At higher levels, parts of this column give origin to the motor nuclei of the facial and trigeminal nerves. The nucleus ambiguus and the facial and trigeminal motor nuclei are termed branchial (special visceral) efferent nuclei. Neurones in the most dorsal column of the basal plate (represented in the spinal cord by the lateral grey column) innervate viscera. The column is discontinuous, its large caudal part forms some of the dorsal nucleus of the vagus and its cranial part forms the salivatory nucleus. These nuclei are termed general visceral (general splanchnic) efferent nuclei, and their neurones give rise to preganglionic, parasympathetic nerve fibres.

It should be noted that the neurones of the basal plate and their three columnar derivatives are only motor in the sense that some of their number form either motor neurones or preganglionic parasympathetic neurones. The remainder, which greatly outnumber the former, differentiate into functionally related interneurones and, in some loci, into neuroendocrine cells.

Cell columns of the alar plate (dorsolateral lamina)

Cell columns of the alar plate are discontinuous and give rise to general visceral (general splanchnic) afferent, special visceral (special splanchnic) afferent, general somatic afferent, and special somatic afferent nuclei (their relative positions, in simplified transverse section, are shown in Fig. 24.20). The general visceral afferent column is represented by a part of the dorsal nucleus of the vagus, the special visceral afferent column by the nucleus of the tractus solitarius, the general somatic afferent column by the afferent nuclei of the trigeminal nerve and the special somatic afferent column by the nuclei of the vestibulocochlear nerve. (The relatively simple functional independence of these afferent columns implied by the foregoing classification is, in the main, an aid to elementary learning. The emergent neurobiological mechanisms are in fact much more complex and less well understood.) Although they tend to retain their primitive positions, some of these nuclei are later displaced by differential growth patterns and by the appearance and growth of neighbouring fibre tracts, and possibly by active migration.

It has been suggested that a neurone tends to remain as near as possible to its predominant source of stimulation, and that to achieve this aim it will migrate around intervening structures, towards the greatest density of stimuli. The curious paths of the axons arising from the facial nucleus and the nucleus ambiguus have been regarded as exemplars of this phenomenon of neurobiotaxis. In a 10 mm embryo, the facial nucleus lies in the floor of the fourth ventricle, occupying the position of the special visceral efferent column, and it is placed at a higher level than the abducens nucleus. As growth proceeds, the facial nucleus migrates at first caudally and dorsally, relative to the abducens nucleus, and then ventrally to reach its adult position. As it migrates, the axons to which its somata give rise elongate and their subsequent course is assumed to map out the pathway along which the facial nucleus has travelled. Similarly the nucleus ambiguus arises initially immediately deep to the ventricular floor, but in the adult it is more deeply placed and its efferent fibres pass first dorsally and medially before curving laterally to emerge at the surface of the medulla oblongata.

Myelencephalon

The caudal slope of the embryonic hindbrain constitutes the myelencephalon, which develops into the medulla oblongata (Fig. 24.2). The nuclei of the ninth, tenth, 11th and 12th cranial nerves develop in the positions already indicated and afferent fibres from the ganglia of the ninth and tenth nerves form an oval marginal bundle in the region overlying the alar (dorsolateral) lamina. Throughout the rhombencephalon, the dorsal edge of this lamina is attached to the thin expanded roof plate and is termed the rhombic lip. (The inferior rhombic lip is confined to the myelencephalon; the superior rhombic lip to the metencephalon.) As the walls of the rhombencephalon spread outwards, the rhombic lip protrudes as a lateral edge which becomes folded over the adjoining area. The rhombic lip may later become adherent to this area, and its cells migrate actively into the marginal zone of the basal plate. In this way the oval bundle which forms the tractus solitarius becomes buried. Alar plate cells which migrate from the rhombic lip are believed to give rise to the olivary and arcuate nuclei and the scattered grey matter of the nuclei pontis. While this migration is in progress, the floor plate is invaded by fibres which cross the median plane (accompanied by neurones that cluster in and near this plane), and it becomes thickened to form the median raphe. Some of the migrating cells from the rhombic lip in this region do not reach the basal plate and form an oblique ridge, the corpus pontobulbare (nucleus of the circumolivary bundle), across the dorsolateral aspect of the inferior cerebellar peduncle.

The lower (caudal half) part of the myelencephalon takes no part in the formation of the fourth ventricle and, in its development, it closely resembles the spinal cord. The gracile and cuneate nuclei, and some reticular nuclei, are derived from the alar plate, and their efferent arcuate fibres and interspersed neurones play a large part in the formation of the median raphe.

At about the fourth month the descending corticospinal fibres invade the ventral part of the medulla oblongata to initiate formation of the pyramids. Contemporaneously, dorsally, the inferior cerebellar peduncle is formed by ascending fibres from the spinal cord, and by olivocerebellar and parolivocerebellar fibres, external arcuate fibres, and two-way reticulocerebellar and vestibulocerebellar interconnections. (The reticular nuclei of the lower medulla probably have a dual origin from both basal and alar plates.) In the neonate the brain stem is more oblique and has a distinct bend as it passes through the foramen magnum to become the spinal cord.

Metencephalon

The rostral slope of the embryonic hindbrain is the metencephalon, from which both the cerebellum and pons develop. Before formation of the pontine flexure, the dorsolateral laminae of the metencephalon are parallel with one another. After its formation the roof plate of the hindbrain becomes rhomboidal and the dorsal laminae of the metencephalon lie obliquely. They are close at the cranial end of the fourth ventricle, but widely separated at the level of its lateral angles (see Fig. 24.21). Accentuation of the flexure approximates the cranial angle of the ventricle to the caudal, and the alar plates of the metencephalon now lie almost horizontally.

The basal plate of the metencephalon becomes the pons. Ventricular, intermediate and marginal zones are formed in the usual way, and the nuclei of the trigeminal, abducens and facial nerves develop in the intermediate layer. It is possible that the grey matter of the formatio-reticularis is derived from the basal plate and that of the nuclei pontis from the alar plate by the active migration of cells from the rhombic lip. However, about the fourth month the pons is invaded by corticopontine, corticobulbar and corticospinal fibres, becomes proportionately thicker, and takes on its adult appearance: it is relatively smaller in the full-term neonate.

The region of the isthmus rhombencephali undergoes a series of changes that are notoriously difficult to interpret, but which result in the incorporation of the greater part of the region into the caudal end of the midbrain. Only the roof plate, in which the superior medullary velum is formed, and the dorsal part of the alar plate, which becomes invaded by converging fibres of the superior cerebellar peduncles, remain as recognizable derivatives in the adult. Early in development, the decussation of the trochlear nerves is caudal to the isthmus, but as growth changes occur it is displaced rostrally until it reaches its adult position.

Fourth ventricle and choroid plexus

Caudal to the developing cerebellum the roof of the fourth ventricle remains epithelial, and covers an approximately triangular zone from the lateral angles of the rhomboid fossa to the median obex (see Fig. 24.21). Nervous tissue fails to develop over this region and vascular pia mater is closely applied to the subjacent ependyma. At each lateral angle and in the midline caudally the membranes break through forming the lateral (Luschka) and median (Magendie) apertures of the roof of the fourth ventricle. These become the principal routes by which cerebrospinal fluid, produced in the ventricles, escapes into the subarachnoid space. The vascular pia mater (tela choroidea), in an inverted V formation cranial to the apertures, invaginates the ependyma to form vascular fringes which become the vertical and horizontal parts of the choroid plexuses of the fourth ventricle.

Cerebellum

The cerebellum develops from the rhombic lip, the dorsal part of the alar plate of the metencephalon, which constitutes the rostral margin of the diamond-shaped fourth ventricle. Two rounded swellings develop which at first project partly into the ventricle (Fig. 24.21), forming the rudimentary cerebellar hemispheres. The most rostral part of the roof of the metencephalon originally separates the two swellings, but it becomes invaded by cells derived from the alar plate, which form the rudiments of the vermis. At a later stage, extroversion of the cerebellum occurs, its intraventricular projection is reduced and the dorsal extraventricular prominence increases. The cerebellum now consists of a bilobar (dumb-bell shaped) swelling stretched across the rostral part of the fourth ventricle (Fig. 24.21). It is continuous rostrally with the superior medullary velum, formed from the isthmus rhombencephali, and caudally with the epithelial roof of the myelencephalon. With growth, a number of transverse grooves appear on the dorsal aspects of the cerebellar rudiment: these are the precursors of the numerous fissures which characterize the surface of the mature cerebellum (Fig. 24.22).

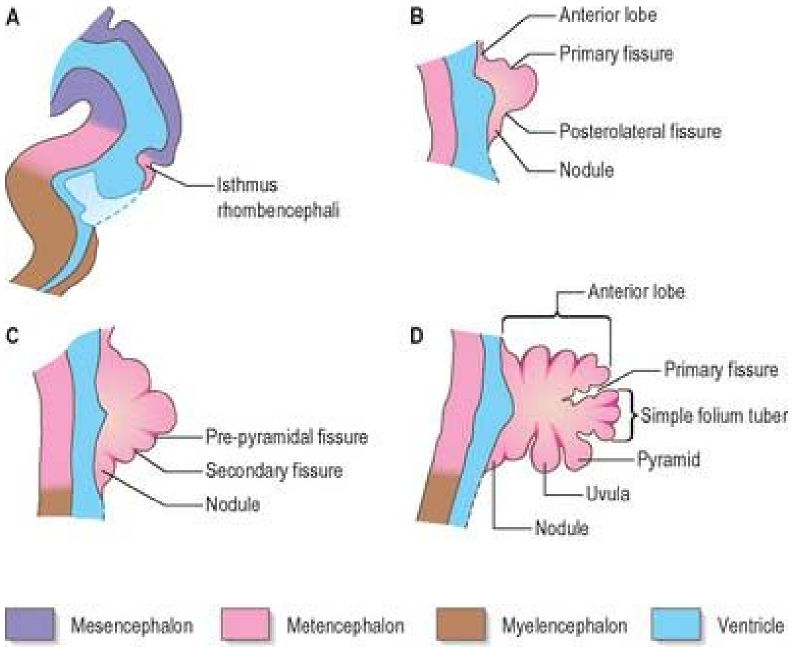
A
Isthmus rhombencephali
B
Anterior lobe
Primary fissure
Posterolateral fissure
Nodule
C
Pre-pyramidal fissure
Secondary fissure
Nodule
D
Anterior lobe
Primary fissure
Simple folium tuber
Pyramid
Uvula
Nodule
Mesencephalon
Metencephalon
Myelencephalon
Ventricle

Fig. 24.22 Median sagittal sections through the developing cerebellum, at four chronologically later stages.

The first fissure to appear on the cerebellar surface (Fig. 24.22) is the lateral part of the posterolateral fissure which forms the border of a caudal region corresponding to the flocculi of the adult. The right and left parts of this fissure subsequently meet in the midline, where they form the boundary between the most caudal vermian lobule, the nodule, and the rest of the vermis. The flocculonodular lobe can now be recognized as the most caudal cerebellar subdivision at this stage and it serves as the attachment of the epithelial roof of the fourth ventricle. Because of the expansion of the other divisions of the cerebellum, the flocculonodular lobe comes to occupy an anteroinferior position in adults. At the end of the third month a transverse sulcus appears on the rostral slope of the cerebellar rudiment and deepens to form the fissura prima. This cuts into the vermis and both hemispheres, and forms the border between the anterior and posterior lobes. Contemporaneously, two short transverse grooves appear in the caudal vermis. The first is the fissura secunda (postpyramidal fissure), which forms the rostral border of the uvula; the second, the prepyramidal fissure, demarcates the pyramid (Fig. 24.22). The cerebellum now grows dorsally, rostrally, caudally and laterally, and the hemispheres expand much more than the inferior vermis, which therefore becomes buried at the bottom of a deep hollow, the vallecula. Numerous other transverse grooves develop, the most extensive being the horizontal fissure.

Cellular development of the cerebellum

The cerebellum consists of a cortex beneath which are buried a series of deep nuclei. The organization of the cerebellar cortex is similar to that of the cerebral cortex, except that the latter has six layers, while the former has only three. However, whereas in the cerebral cortex neuroblasts originate from the ventricular zone and migrate ventriculofugally towards the pial surface (in an ‘inside-out’ fashion), early in cerebellar development a layer of cells derived exclusively from the metencephalic rhombic lip initially migrates ventriculofugally to form a layer beneath the glia limitans over the surface of the developing cerebellum. These cells form the external germinative layer and later in development their progeny will migrate ventriculopetally (in an ‘outside-in’ manner), into the cerebellum. Thus, the cerebellum has an intraventricular portion (cells proliferating from the ventricular zone) and an extraventricular portion (cells proliferating from the external germinative layer) during development. The extraventricular portion becomes larger at the expense of the intraventricular part, the so-called extroversion of the cerebellum. Before the end of the third month the main mass of the cerebellum is extraventricular.

The developed cerebellar cortex contains three layers, namely the molecular layer, the Purkinje layer, and the granular layer. The early bilateral expansion of the ventricular surface reflects the production, by the metencephalic alar plate ventricular epithelium, of neuroblasts which will give rise to the radial glia, cerebellar nuclei, and efferent neurones of the cerebellar cortex (the Purkinje cells) (Fig. 24.23). The radial glia play a role in guiding the Purkinje cells to the meningeal surface of the cerebellar anlage. During this early stage of cerebellar development, which is dominated by the production and migration of efferent cerebellar neurones, the surface of the cerebellar anlage remains smooth. The extroversion of the cerebellum begins later when cells of the external germinative layer, also termed the superficial matrix, begin proliferation and migration. These cells produce the granule cells, which migrate inward along the radial glia, through the layers of Purkinje cells, settling deep to them in the granular layer. This stage coincides with the emergences of the transverse folial pattern. Proliferation and migration of granule cells leads to a great rostrocaudal expansion of the meningeal surface of the cerebellum, forming the transverse fissures and transforming the multicellular layer of Purkinje cells into a monolayer. Purkinje cells and nuclear cells are formed prior to the granule cells, and granule cells serve as the recipient of the main afferent (mossy fibre) system of the cerebellum. Thus the development of the efferent neurones of the cerebellar cortex and nuclei precedes the development of its afferent organization.

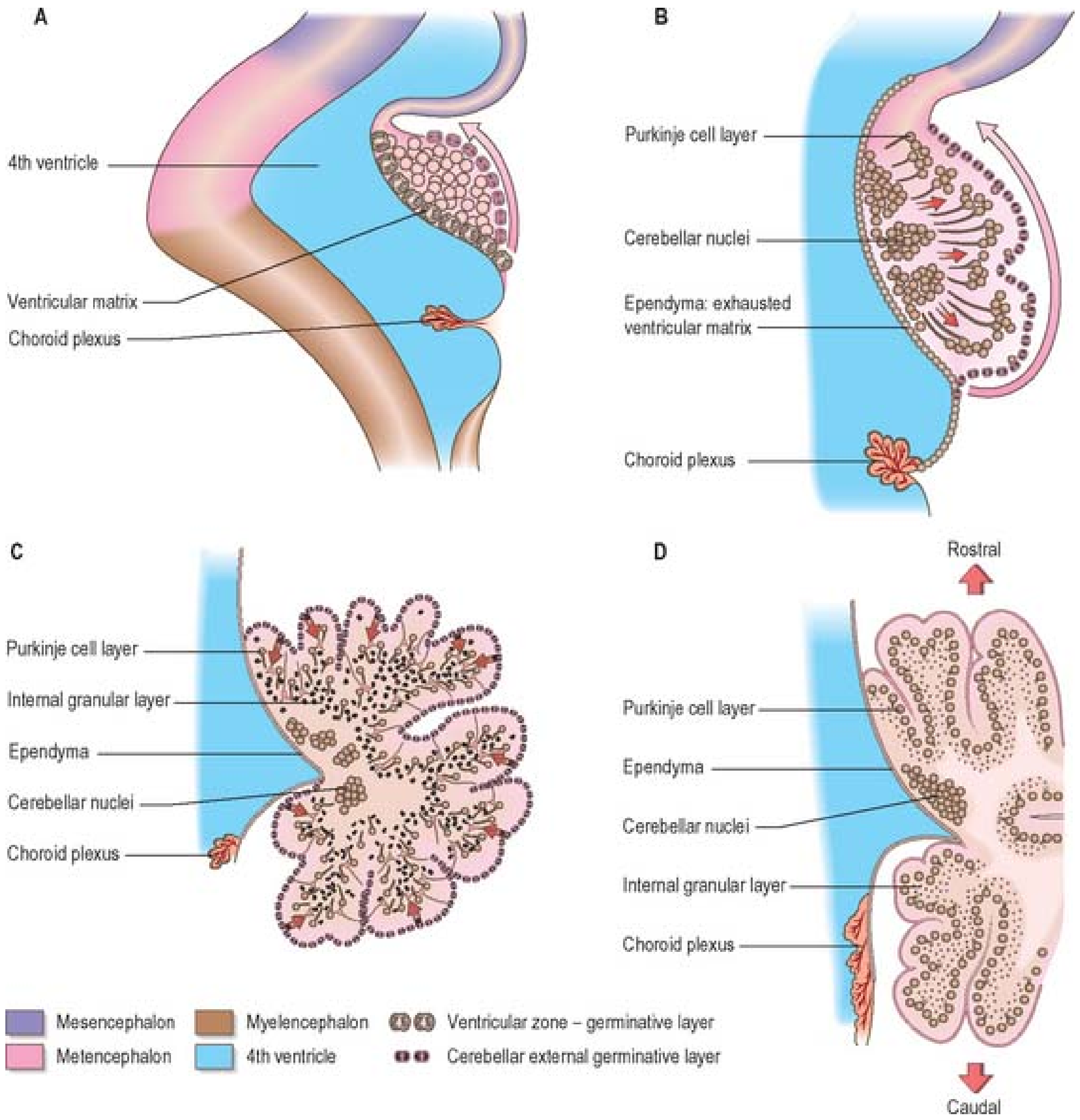
A
4th ventricle
Ventricular matrix
Choroid plexus
B
Purkinje cell layer
Cerebellar nuclei
Ependyma: exhausted ventricular matrix
Choroid plexus
C
Purkinje cell layer
Internal granular layer
Ependyma
Cerebellar nuclei
Choroid plexus
D
Rostral
Purkinje cell layer
Ependyma
Cerebellar nuclei
Internal granular layer
Choroid plexus
Caudal
Mesencephalon
Metencephalon
Myelencephalon
4th ventricle
Ventricular zone – germinative layer
Cerebellar external germinative layer

Fig. 24.23 The histogenesis of the cerebellar cortex and the cerebellar nuclei. **A**, Purkinje cells and cells of the cerebellar nuclei are produced by the ventricular zone and migrate to their future positions. The cells of the superficial matrix (the external granular layer) take their origin from the ventricular epithelium at the caudal pole of the cerebellar anlage and migrate rostrally over its surface. **B**, After migration the Purkinje cells constitute a multicellular layer beneath the external germinative layer. Cell production in the ventricular epithelium has stopped. The remaining cells transform into ependymal cells. **C**, Granule cells produced by the external germinative layer migrate inwards through the Purkinje cell layer to their

position in the internal granular layer. Purkinje cells spread into a monolayer. **D**, Adult position of cortical and nuclear neurones.

The early bilateral cerebellar anlage is changed into a unitary structure by fusion of the bilateral intraventricular bulges and the disappearance of the ependyma at this site, the merging of the left and right primitive cerebellar cortex over the midline, and the development of the cerebellar commissure by ingrowth of afferent fibres and outgrowth of efferent axons of the medial cerebellar nucleus.

When the external germinative layer is initially formed, the multicellular Purkinje cell layer beneath is not uniform, but subdivided into clusters which form rostrocaudally extending columns (Fig. 24.24). The medial Purkinje cell clusters develop into the future vermis. These Purkinje cells will grow axons which connect to neurones in the vestibular nuclei and the fastigial nucleus. The lateral clusters belong to the future hemispheres and will grow axons terminating in the interposed and dentate nuclei. The sharp border in the efferent projections from the vermis and hemispheres is thus established at an early age. These clusters will give rise to Purkinje cell zones in the adult cerebellum which project to a single vestibular or cerebellar nucleus.

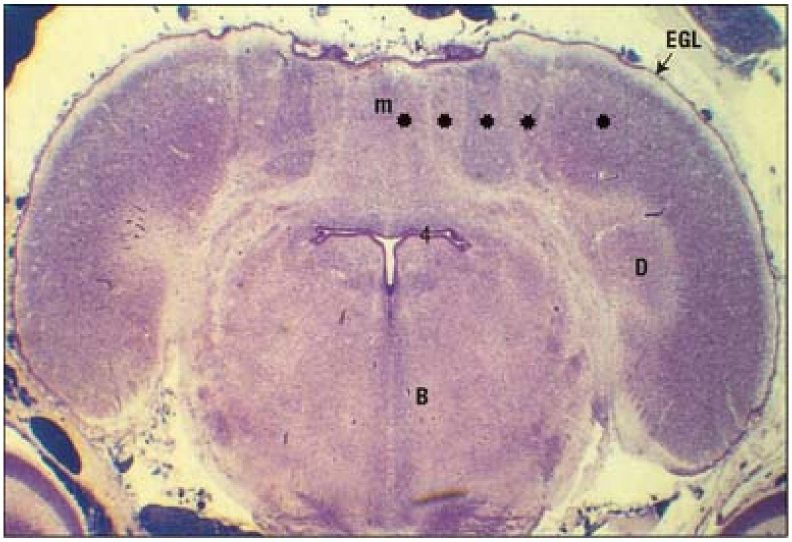

Fig. 24.24 Coronal section through the cerebellum and the brain stem of 65 mm human fetus. The Purkinje cells are located in five multicellular

clusters (stars) on both sides of the midline. The anlage of the dentate nucleus occupies the centre of the most lateral Purkinje cell cluster. Abbreviations: B, brain stem; D, dentate nucleus; EGL, external granular layer; m, midline; 4, fourth ventricle.

(By courtesy of the Schenk Collection, Dr Johan M Kros, Division of Neuropathology, Department of Pathology, Erasmus Medical Centre, Rotterdam, The Netherlands.)

In the developing human brain only the external germinative layer can be seen at 17–18 weeks; the Purkinje cells become apparent between 20–23 weeks. After 30 weeks four layers can be recognized, the extermal germinative layer (external granular layer) is formed by 6–8 rows of densely packed small round cells; the Purkinje cell layer is formed by 5–6 layers of larger, round immature neurones external to the internal granular layer; the molecular layer contains cells resembling external granular layer cells in migration (Lavezzi et al 2006). The external granular layer involutes between 5 and 7 months after birth: it is only a discontinuous layer at 10 months, and is totally absent by 12 months, after which time the cerebellar cortex shows a three-layered structure. From 5 to 7 months the Purkinje cells are reduced in number, more widely spaced and display mature polygonal somata with evident axon and dendrites.

Mesencephalon

The mesencephalon or midbrain is subdivided early in development into two neuromeres, mesencephalon 1 and mesencephalon 2. It persists for a time as a thin-walled tube enclosing a cavity of some size, separated from that of the prosencephalon by a slight constriction and from the rhombencephalon by the isthmus rhombencephali (Figs 24.2 and 24.25). Later, its cavity becomes relatively reduced in diameter, and in the adult brain it forms the cerebral aqueduct. The basal (ventrolateral) plate of the midbrain increases in thickness to form the cerebral peduncles, which are at first of small size, but enlarge rapidly after the fourth month, when their numerous fibre tracts begin to appear in the marginal zone. The neuroblasts of the basal plate of mesencephalon 2 give rise to the nuclei of the oculomotor nerve and some grey masses of the tegmentum, while the nucleus of the trochlear nerve remains in the region of the isthmus rhombencephali. The cells which give rise to the trigeminal mesencephalic nucleus arise either side of the dorsal midline, from the isthmus rhobencephali rostrally across the roof of the mesencephalon. Recent studies have shown that the progenitors of these cells do not express neural crest cell markers.

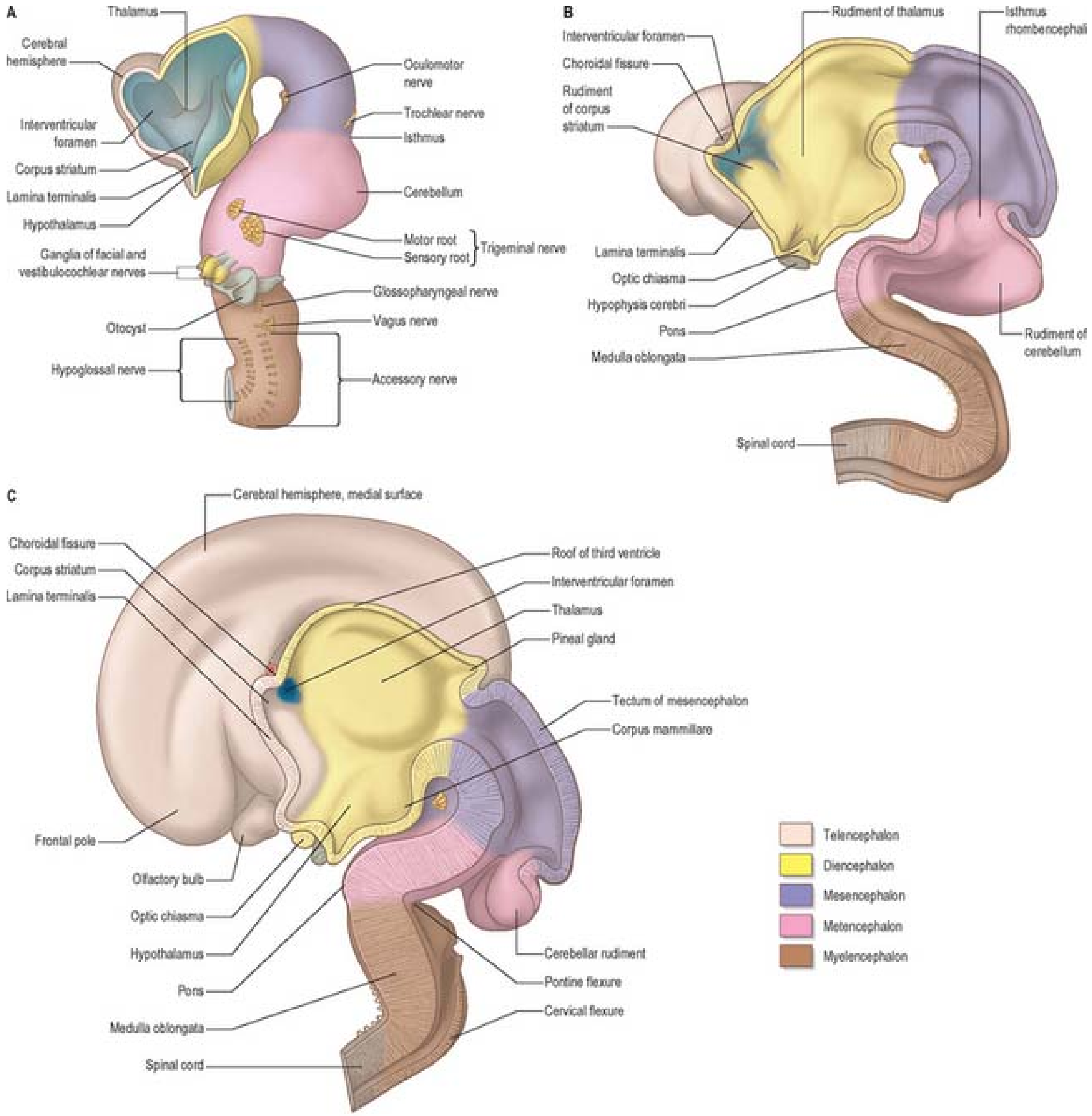
A
Thalamus
Cerebral hemisphere
Interventricular foramen
Corpus striatum
Lamina terminalis
Hypothalamus
Ganglia of facial and vestibulocochlear nerves
Otocyst
Hypoglossal nerve
Oculomotor nerve
Trochlear nerve
Isthmus
Cerebellum
Motor root
Sensory root
Trigeminal nerve
Glossopharyngeal nerve
Vagus nerve
Accessory nerve
B
Interventricular foramen
Choroidal fissure
Rudiment of corpus striatum
Rudiment of thalamus
Isthmus rhombencephali
Lamina terminalis
Optic chiasma
Hypophysis cerebri
Pons
Medulla oblongata
Rudiment of cerebellum
Spinal cord
C
Cerebral hemisphere, medial surface
Choroidal fissure
Corpus striatum
Lamina terminalis
Roof of third ventricle
Interventricular foramen
Thalamus
Pineal gland
Tectum of mesencephalon
Corpus mammillare
Frontal pole
Olfactory bulb
Optic chiasma
Hypothalamus
Pons
Medulla oblongata
Spinal cord
Cerebellar rudiment
Pontine flexure
Cervical flexure
Telencephalon
Diencephalon
Mesencephalon
Metencephalon
Myelencephalon

Fig. 24.25 The shape of the developing ventricular system and the expansion of the medial portion of the telencephalon. **A**, Human embryo, approximately 10.2 mm long, left lateral surface of the diencephalon and telencephalon removed. **B**, Human embryo 13.6 mm long, median section. **C**, Human fetus, approximately 3 months old, median section. The roof of the metencephalon and myelencephalon has been removed in each case.

The cells of the dorsal part of the alar (dorsolateral) plates proliferate and invade the roof plate, which therefore thickens and is later divided into corpora bigemina by a median groove. Caudally this groove becomes a median ridge, which persists in the adult as the frenulum veli. The corpora bigemina are later subdivided into the superior and inferior colliculi by a transverse furrow. The red nucleus, substantia nigra and reticular nuclei of the midbrain tegmentum may first be defined at the end of the third month. Their origins are probably mixed from neuroblasts of both basal and alar plates.

The detailed histogenesis of the tectum and its main derivatives, the colliculi, will not be followed here, but in general the principles outlined for the cerebellar cortex, the palaeopallium and neopallium also apply to this region. A high degree of geometric order exists in the developing retinotectal projection (the equivalent of the retinogeniculate projection), and in the tectospinal projection.

Prosencephalon

At an early stage, a transverse section through the forebrain shows the same parts as are displayed in similar sections of the spinal cord and medulla oblongata, i.e. thick lateral walls connected by thin floor and roof plates. Moreover, each lateral wall is divided into a dorsal area and a ventral area separated internally by the hypothalamic sulcus (Fig. 24.25). This sulcus ends rostrally at the medial end of the optic stalk. In the fully developed brain it persists as a slight groove extending from the interventricular foramen to the cerebral aqueduct. It is analogous to, if not the homologue of, the sulcus limitans. The thin roof plate remains epithelial, but invaginated by vascular mesenchyme, the tela choroidea of the choroid plexuses of the third ventricle. Later, the lateral margins of the tela undergo a similar invagination into the medial walls of the cerebral hemispheres. The floor plate thickens as the nuclear masses of the hypothalamus and subthalamus develop.

At a very early period, before the closure of the rostral neuropore, the subdivision of the prosencephalon into the most rostral telencephalon and two subdivisions of the diencephalon, D1 and D2, is heralded (Fig. 24.2). At this early time two eye fields are separated by the future neurohypophysis in the floor of the future D1. After head folding, the eye fields expand as two lateral optic evaginations which become optic vesicles, one on each side of the early brain. For a time they communicate with the cavity of the prosencephalon by relatively wide openings. The distal parts of the optic vesicles expand, while the proximal parts become the tubular optic stalks. The optic vesicles (which are described with the development of the eye in Ch. 41) are thus derived from the lateral walls of the D1 subdivision of the prosencephalon before the telencephalon can be clearly identified. The optic chiasma is often regarded as the boundary between diencephalon and telencephalon.

As the most rostral portion of the prosencephalon enlarges it curves ventrally, and two further diverticula expand rapidly from it, one on each side. These diverticula, which are rostrolateral to the optic stalks, subsequently form the cerebral hemispheres. Their cavities are the rudiments of the lateral ventricles and they communicate with the median part of the forebrain cavity by relatively wide openings which ultimately become the interventricular foramina. The rostral limit of the median part of the forebrain consists of a thin sheet, the lamina terminalis (Fig. 24.25A–C), which stretches from the interventricular foramina to the recess at the base of the optic stalks. The rostral part of the forebrain, including the rudiments of the cerebral hemispheres, consists of the telencephalon and the caudal part of the diencephalon: both contribute to the formation of the third ventricle, although the latter predominates. The fate of the lamina terminalis is described below.

Diencephalon

The diencephalon, D2, is broadly divided by the hypothalamic sulcus into dorsal (pars dorsalis diencephali) and ventral (pars ventralis diencephali) parts: each contributes to diverse neural structures. The dorsal part develops into the (dorsal) thalamus and metathalamus along the immediate suprasulcal area of its lateral wall, while the highest dorsocaudal lateral wall and roof form the epithalamus. The thalamus (Fig. 24.25A–C) is first visible as a thickening that involves the rostral part of the dorsal area. Caudal to the thalamus, the lateral and medial geniculate bodies, or metathalamus, are recognizable at first as surface depressions on the internal aspect and as elevations on the external aspect of the lateral wall. As the thalami enlarge as smooth ovoid masses, the wide interval between them gradually narrows into a vertically compressed cavity which forms the greater part of the third ventricle. After a time these medial surfaces may come into contact and become adherent over a variable area, the connection (single or multiple) constituting the interthalamic adhesion or massa intermedia. The caudal growth of the thalamus excludes the geniculate bodies from the lateral wall of the third ventricle.

At first the lateral aspect of the developing thalamus is separated from the medial aspect of the cerebral hemisphere by a cleft, but with growth the cleft becomes obliterated (Fig. 24.26) as the thalamus fuses with the part of the hemisphere in which the corpus striatum is developing. Later, with the development of the projection fibres (corticofugal and corticopetal) of the neocortex, the thalamus becomes related to the internal capsule, which intervenes between it and the lateral part of the corpus striatum (lentiform nucleus). Ventral to the hypothalamic sulcus, the lateral wall of the diencephalon, in addition to median derivatives of its floor plate, forms a large part of the hypothalamus and subthalamus.

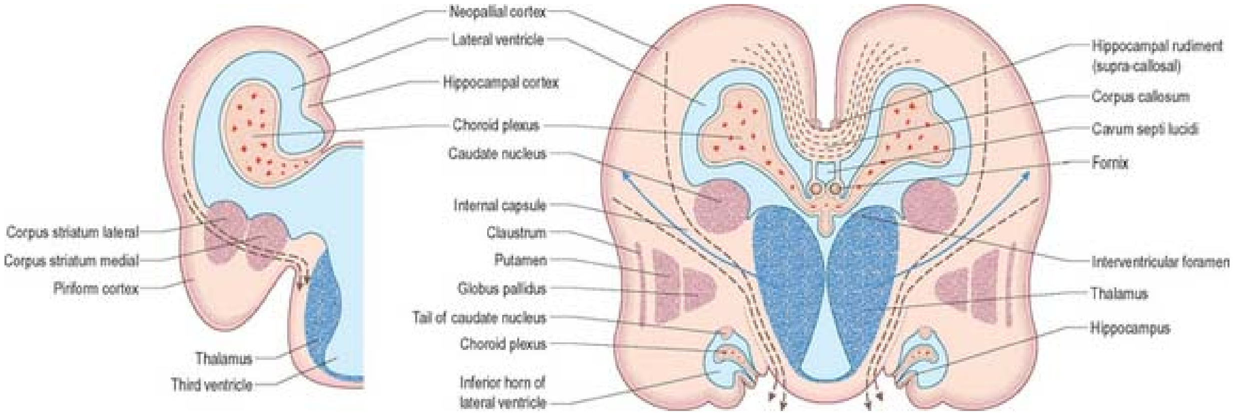

Neopallial cortex
Lateral ventricle
Hippocampal cortex
Choroid plexus
Caudate nucleus
Corpus striatum lateral
Corpus striatum medial
Piriform cortex
Thalamus
Third ventricle
Internal capsule
Claustrum
Putamen
Globus pallidus
Tail of caudate nucleus
Choroid plexus
Inferior horn of lateral ventricle
Hippocampal rudiment (supra-callosal)
Corpus callosum
Cavum septi lucidi
Fornix
Interventricular foramen
Thalamus
Hippocampus

Fig. 24.26 The development of the basal nuclei and internal capsule, coronal views

(Redrawn by permission from Hamilton WJ, Boyd JD, Mossman HW 1972 Human Embryology: Prenatal Development of Form and Function. Baltimore: Williams and Wilkins.)

The epithalamus, which includes the pineal gland, the posterior and habenular commissures and the trigonum habenulae, develops in association with the caudal part of the roof plate and the adjoining regions of the lateral walls of the diencephalon. At an early period (12–20 mm CR length), the epithalamus in the lateral wall projects into the third ventricle as a smooth ellipsoid mass, larger than the adjacent mass of the (dorsal) thalamus and separated from it by a well-defined epithalamic sulcus. In subsequent months, growth of the thalamus rapidly overtakes that of the epithalamus and the intervening sulcus is obliterated. Thus, structures of epithalamic origin are ultimately topographically relatively diminutive.

The pineal gland arises as a hollow outgrowth from the roof plate, immediately adjoining the mesencephalon. Its distal part becomes solid by cellular proliferation, but its proximal stalk remains hollow, containing the pineal recess of the third ventricle. In many reptiles the pineal outgrowth consists of a rostral outgrowth (parapineal organ) that develops into the pineal or parietal eye and a glandular caudal outgrowth: the caudal outgrowth is homologous with the pineal gland in man. The rostral outgrowth also develops in the human embryo but soon disappears entirely.

The nucleus habenulae, which is the most important constituent of the trigonum habenulae, develops in the lateral wall of the diencephalon and is at first in close relationship with the geniculate bodies, from which it becomes separated by the dorsal growth of the thalamus. The habenular commissure develops in the cranial wall of the pineal recess. The posterior commissure is formed by fibres which invade the caudal wall of the pineal recess from both sides.

The ventral part of the diencephalon forms the subsulcal lateral walls of the third ventricle and takes part in the formation of the hypothalamus, including the mammillary bodies, the tuber cinereum and infundibulum of the hypophysis. The mammillary bodies arise as a single thickening which becomes divided by a median furrow during the third month. The tuber cinereum develops rostral to the mammillary bodies as a cellular proliferation that extends forwards as far as the infundibulum. In front of the tuber cinereum, a wide-mouthed diverticulum forms in the floor of the diencephalon, grows towards the stomodeal roof and comes into contact with the posterior aspect of a dorsally directed ingrowth from the stomodeum (Rathke’s pouch). These two diverticula together form the hypophysis cerebri (Fig. 24.14). An extension of the third ventricle persists in the base of the neural outgrowth as the infundibular recess. The remaining caudolateral walls and floor of the ventral diencephalon are an extension of the midbrain tegmentum, the subthalamus. This forms the rostral limits of the red nucleus, substantia nigra, numerous reticular nuclei and a wealth of interweaving, ascending, descending and oblique nerve fibre bundles, which have many origins and destinations.

Third ventricle and choroid plexus

The roof plate of the diencephalon rostral to the pineal gland, and continuing over the median telencephalon, remains thin and epithelial in character and is invaginated by the choroid plexuses of the third ventricle (Fig. 24.27). Before the development of the corpus callosum and the fornix it lies at the bottom of the longitudinal fissure, between and reaching the two cerebral hemispheres. It extends as far rostrally as the interventricular foramina and lamina terminalis. Here, and elsewhere, choroid plexuses develop by the close apposition of vascular pia mater and ependyma without intervening nervous tissue. With development, the vascular layer is infolded into the ventricular cavity and develops a series of small villous projections, each covered by a cuboidal epithelium derived from the ependyma. The cuboidal cells display numerous microvilli on their ventricular surfaces and complex folding of their basal plasma membranes. The early choroid plexuses secrete a protein-rich cerebrospinal fluid into the ventricular system which may provide a nutritive medium for the developing epithelial neural tissues. As the latter become increasingly vascularized the histochemical reactions of the cuboidal cells and the character of the fluid change to the adult type. Many regions of the lining of the third ventricle become highly specialized, and develop concentrations of tanycytes or other modified cells that are collectively termed the circumventricular organs, e.g. the subfornical organ, the organum vasculosum (intercolumnar tubercle) of the lamina terminalis, the subcommissural organ and the linings of the pineal, suprapineal, and infundibular recesses.

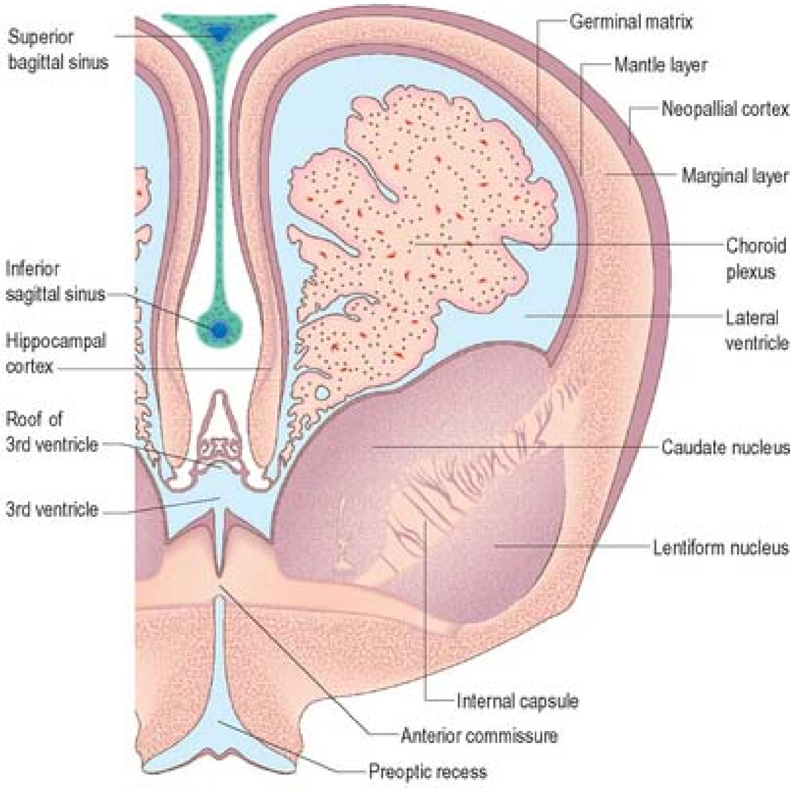
Superior
bagittal sinus
Inferior
sagittal sinus
Hippocampal
cortex
Roof of
3rd ventricle
3rd ventricle
Germinal matrix
Mantle layer
Neopallial cortex
Marginal layer
Choroid
plexus
Lateral
ventricle
Caudate nucleus
Lentiform nucleus
Internal capsule
Anterior commissure
Preoptic recess

Fig. 24.27 Coronal section of the left cerebral hemisphere in a 73 mm fetus.

(Redrawn by permission from Hamilton WJ, Boyd JD, Mossman HW 1972 Human Embryology: Prenatal Development of Form and Function. Baltimore: Williams and Wilkins.)

Telencephalon

The telencephalon consists of two lateral diverticula connected by a median region, the telencephalon impar. The rostral part of the third ventricle develops from the impar, and is closed below and in front by the lamina terminalis. The lateral diverticula are outpouchings of the lateral walls of the telencephalon, which may correspond to the alar lamina, although this is uncertain. Their cavities are the future lateral ventricles, and their walls are formed by the presumptive nervous tissue of the cerebral hemispheres. The roof plate of the median part of the telencephalon remains thin and is continuous behind with the roof plate of the diencephalon (Fig. 24.25). The rostral parts of the hypothalamus, which include the optic chiasma, optic recess and related nuclei, develop in the floor plate and lateral walls of the prosencephalon, ventral to the primitive interventricular foramina. The chiasma is formed by the meeting, and partial decussation, of the optic nerves in the ventral part of the lamina terminalis. The optic tracts subsequently grow backwards from the chiasma to end in the diencephalon and midbrain.

Cerebral hemispheres

The cerebral hemispheres arise as diverticula of the lateral walls of the telencephalon, with which they remain in continuity around the margins of initially relatively large interventricular foramina, except caudally, where they are continuous with the rostral part of the lateral wall of the diencephalon (Figs 24.2 and 24.25). As growth proceeds each hemisphere enlarges forwards, upwards and backwards and acquires an oval outline, medial and superolateral walls, and a floor. As a result the medial surfaces approach, but are separated by, a vascularized mesenchyme and pia mater which fills the median longitudinal fissure (Fig. 24.27). At this stage the floor of the fissure is the epithelial roof plate of the telencephalon, which is directly continuous caudally with the epithelial roof plate of the diencephalons.

At the early oval stage of hemispheric development, regions are named according to their future principal derivatives. The rostromedial and ventral floor becomes linked with the forming olfactory apparatus and is termed the primitive olfactory lobe. The floor (ventral wall, or base) of the remainder of each hemisphere forms the anlage of the primitive corpus striatum and amygdaloid complex, including its associated rim of lateral and medial walls (the striate part of the hemisphere). The rest of the hemisphere i.e. the medial, lateral, dorsal and caudal regions, is the suprastriate part of the hemisphere. Although it is the largest in terms of surface area, initially it possesses comparatively thin walls. The rostral end of each oval hemisphere becomes the definitive frontal pole. As the hemisphere expands, its original posterior pole moves relatively in a caudoventral and lateral direction, following a curve like a ram’s horn: it curves towards the orbit in association with the growth of the caudate nucleus and other structures to form the definitive temporal pole. A new posterior part persists as the definitive occipital pole of the mature brain (Fig. 24.28).

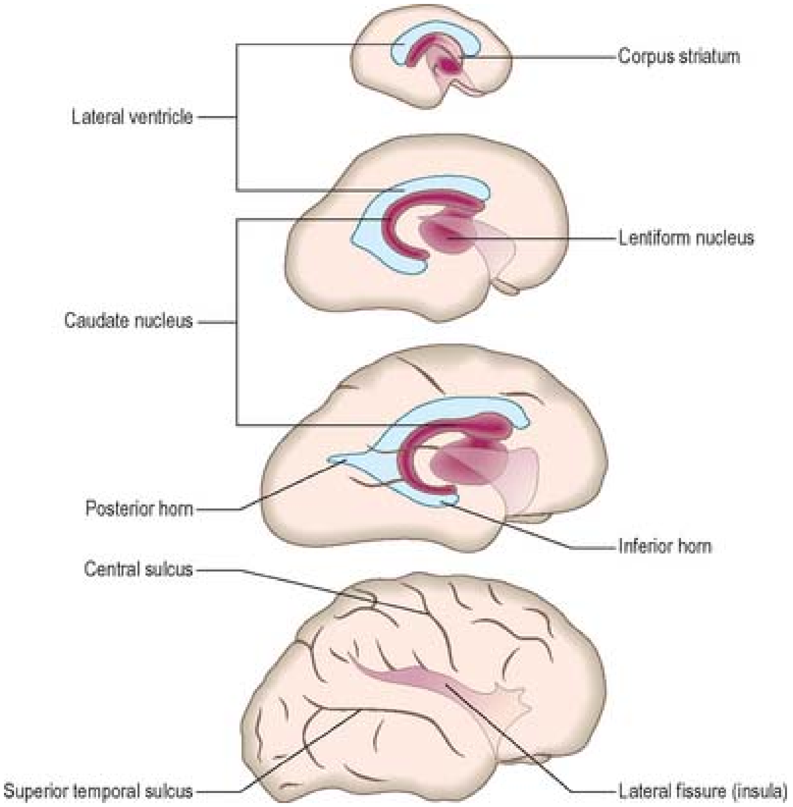
Corpus striatum
Lateral ventricle
Lentiform nucleus
Caudate nucleus
Posterior horn
Inferior horn
Central sulcus
Superior temporal sulcus
Lateral fissure (insula)

Fig. 24.28 Lateral views of developing brains show the formation of the basal nuclei and lateral ventricles as the telencephalon develops.

(Redrawn by permission from Hamilton WJ, Boyd JD, Mossman HW 1972 Human Embryology: Prenatal Development of Form and Function. Baltimore: Williams and Wilkins.)

The migration and differentiation of neural progenitors to form nuclei is either minimal or limited throughout the brain stem and spinal cord: the progeny of these progenitors remain immediately extra-ependymal or partially displaced towards the pial exterior, and are arrested deeply embedded in the myelinated fibre ‘white matter’ of the region. In marked contrast, proliferation and migration of neuroblasts in the cerebral hemispheres produces a superficial layer of grey matter in both the striate and suprastriate regions, but not in the central areas of the original medial wall (where secondary fusion with the diencephalon occurs). The superficial layer of grey matter consists of neuronal somata, dendrites, the terminations of incoming (afferent) axons, the stems of (or the whole of) efferent axons, and glial cells and endothelial cells. Successive generations of neuroblasts migrate through the layers of earlier generations to attain subpial positions (see below),which means that the surface of the cerebral hemispheres expands at a rate greater than that of the hemispheres as a whole: the great expansion of the cerebral hemispheres is characteristic of mammals and especially of man. Neuroblast differentiation produces a highly organized subpial surface coat of grey matter termed the cortex or pallium. The growing hemispheres subsequently overlap, successively, the diencephalon and the mesencephalon, and then meet the rostral surface of the cerebellum. The temporal lobes embrace the flanks of the brain stem.

The terminology used to describe regions of the cortex is based on evolutionary concepts. The oldest portions of cortex receive information concerned with olfaction; they are termed the archicortex (archipallium) and paleocortex (paleopallium), and both are subdivisions of an overall allocortex. The archicortex is the forerunner of the hippocampal lobe, and the paleocortex gives rise to the piriform area. The remaining cortical surface expands greatly in mammals forming the neocortex (young cortex) which displaces the earlier cortices so that they come to lie partially internally in each hemisphere.

Olfactory bulb

A longitudinal groove appears in the anteromedial part of the floor of each developing lateral ventricle about the fifth week of embryonic development. It deepens and forms a hollow diverticulum which is continuous with the hemisphere by a short stalk. The diverticulum becomes connected on its ventral or inferior surface to the olfactory placode. Placodal cells give rise to afferent axons which terminate in the walls of the diverticulum. As the head increases in size, the diverticulum grows forwards, loses its cavity and becomes converted into the solid olfactory bulb. The forward growth of the bulb is accompanied by elongation of its stalk, which forms the olfactory tract. The part of the floor of the hemisphere to which the tract is attached constitutes the piriform area.

Lateral ventricles and choroid plexus

The early diverticulum or anlage of the cerebral hemisphere initially contains a simple spheroidal lateral ventricle which is continuous with the third ventricle via the interventricular foramen. The rim of the foramen is the site of the original evagination. The expanding ventricle develops the ram’s horn shape of the surrounding hemisphere, becoming first roughly ellipsoid and then a curved cylinder which is convex dorsally (Fig. 24.28). The ends of the cylinder expand towards, but do not reach, the frontal and (temporary) occipital poles; differentiating and thickening neural tissues separate the ventricular cavities and pial surfaces at all points, except along the line of the choroidal fissure. Pronounced changes in ventricular form accompany the emergence of a temporal pole. The original caudal end of the curved cylinder expands within its substance and the temporal extensions in each hemisphere pass ventrolaterally to encircle both sides of the upper brain stem. Another extension may develop from the root of the temporal extension in the substance of the definitive occipital pole and pass caudomedially; it is quite variable in size, often asymmetrical on the two sides, and one or both may be absent. Although the lateral ventricle is a continuous system of cavities, specific parts are now given regional names. The central part (body) extends from the interventricular foramen to the level of the posterior edge (splenium) of the corpus callosum. Three cornua (horns) diverge from the body: anterior towards the frontal pole, posterior towards the occipital pole, and inferior towards the temporal pole.

At these early stages of hemispheric development the term pole is preferred, in most instances, to lobe. Lobes are defined by specific surface topographical features which will appear over several months, and differential growth patterns persist for a considerable period.

The pia mater which covers the epithelial roof of the third ventricle at this stage is itself covered with loosely arranged mesenchyme and developing blood vessels. These vessels subsequently invaginate the roof of the third ventricle on each side of the median plane to form its choroid plexuses. The lower part of the medial wall of the cerebral hemisphere, which immediately adjoins the epithelial roof of the interventricular foramen and the rostral extremity of the diencephalon, also remains epithelial. It consists of ependyma and pia mater; elsewhere the walls of the hemispheres are thickening to form the pallium. The thin part of the medial wall of the hemisphere is invaginated by vascular tissue which is continuous in front with the choroid plexus of the third ventricle and constitutes the choroid plexus of the lateral ventricle. This invagination occurs along a line which arches upwards and backwards, parallel with and initially limited to, the rostral and upper boundaries of the interventricular foramen. This curved indentation of the ventricular wall, where no nervous tissue develops between ependyma and pia mater, is termed the choroidal fissure (Figs 24.25C and 24.26). The subsequent assumption of the definitive form of the choroidal fissure depends on related growth patterns in neighbouring structures. Of particular importance are the relatively slow growth of the interventricular foramen, the secondary 'fusion' between the lateral diencephalon and medial hemisphere walls, the encompassing of the upper brain stem by the forward growth of the temporal lobe and its pole towards the apex of the orbit, and the massive expansion of two great cerebral commissures (the fornix and corpus callosum). The choroidal fissure is now clearly a caudal extension of the much reduced interventricular foramen, which arches above the thalamus and is here only a few millimetres from the median plane. Near the caudal end of the thalamus it diverges ventrolaterally, its curve reaching and continuing in the medial wall of the temporal lobe over much of its length (i.e. to the tip of the inferior horn of the lateral ventricle). The upper part of the arch will be overhung by the corpus callosum and, throughout its convexity, it is bordered by the fornix and its derivatives.

Basal nuclei

At first growth proceeds more actively in the floor and the adjoining part of the lateral wall of the developing hemisphere, and elevations formed by the rudimentary corpus striatum encroach on the cavity of the lateral ventricle

(Figs 24.25 and 24.26). The head of the caudate nucleus appears as three successive parts, medial, lateral and intermediate, which produce elevations in the floor of the lateral ventricle. Caudally these merge to form the tail of the caudate nucleus and the amygdaloid complex, which both remain close to the temporal pole of the hemisphere. When the occipital pole grows backwards, and the general enlargement of the hemisphere carries the temporal pole downwards and forwards, the tail of the caudate is continued from the floor of the central part (body) of the ventricle into the roof of its temporal extension, the future inferior horn. The amygdaloid complex encapsulates its tip. Rostrally the head of the caudate nucleus extends forwards to the floor of the interventricular foramen, where it is separated from the developing rostral end of the thalamus by a groove; later, the head expands in the floor of the anterior horn of the lateral ventricle. The lentiform nucleus develops from two laminae of cells, medial and lateral, which are continuous with both the medial and lateral parts of the caudate nucleus. The internal capsule appears first in the medial lamina and extends laterally through the outer lamina to the cortex. It divides the laminae into two, the internal parts join the caudate nucleus and the external parts form the lentiform nucleus. In the latter, the remaining medial lamina cells give rise mainly to the globus pallidus and the lateral lamina cells to the putamen. The putamen subsequently expands concurrently with the intermediate part of the caudate nucleus.

Fusion of diencephalic and telencephalic walls

As the hemisphere enlarges, the caudal part of its medial surface overlaps and hides the lateral surface of the diencephalon (thalamic part), from which it is separated by a narrow cleft occupied by vascular connective tissue. At this stage (about the end of the second month) a transverse section made caudal to the interventricular foramen would pass from the third ventricular cavity successively through the developing thalamus, the narrow cleft just mentioned, the thin medial wall of the hemisphere, and the cavity of the lateral ventricle, with the corpus striatum in its floor and lateral wall (Fig. 24.26).

As the thalamus increases in extent it acquires a superior surface in addition to medial and lateral surfaces. The lateral part of its superior surface fuses with the thin medial wall of the hemisphere so that this part of the thalamus is finally covered with the ependyma of the lateral ventricle immediately ventral to the choroidal fissure. As a result the corpus striatum is approximated to the thalamus and is separated from it only by a deep groove which becomes obliterated by increased growth along the line of contact. The lateral aspect of the thalamus is now in continuity with the medial aspect of the corpus striatum so that a secondary union between the diencephalon and the telencephalon is affected over a wide area, providing a route for the subsequent passage of projection fibres to and from the cortex (Fig. 24.26).

Formation of the insula

At the end of the third month, while the corpus striatum is developing, there is a relative restriction of growth between the frontal and temporal lobes. The region lateral to the striatum becomes depressed to form a lateral cerebral fossa with a portion of cortex, the insula, at its base (Fig. 24.28). As the temporal lobe continues to protrude towards the orbit, and with more rapid growth of the temporal and frontal cortices, the surface of the hemisphere expands at a rate greater than the hemisphere as a whole and the cortical areas become folded, forming gyri and sulci. The insula is gradually overgrown by these adjacent cortical regions, and they overlap it forming the opercula, the free margins of which form the anterior part of the lateral fissure. This process is not completed until after birth. The lentiform nucleus remains deep to and coextensive with the insula.

Olfactory nerve, limbic lobe and hippocampus

The growth changes in the temporal lobe which help to submerge the insula produce important changes in the olfactory and neighbouring limbic areas. As it approaches the hemispheric floor, the olfactory tract diverges into lateral, medial and (variable) intermediate striae. The medial stria is clothed with a thin archaeocortical medial olfactory gyrus. This curves up into further archaeocortical areas rostral to the lamina terminalis (paraterminal gyrus, prehippocampal rudiment, parolfactory gyrus, septal nuclei) and these continue into the indusium griseum. The lateral stria, clothed by the lateral olfactory gyrus, and the intermediate stria (when present), terminate in the rostral parts of the piriform area, including the olfactory trigone and tubercle, anterior perforated substance, uncus and entorhinal area of the anterior part of the future parahippocampal gyrus. The lateral limit of the lateral stria is indicated by the rhinal sulcus. The forward growth of the temporal pole and the general expansion of the neocortex cause the lateral olfactory gyrus to bend laterally, the summit of the convexity lying at the anteroinferior corner of the developing insula (Fig. 24.29). During the fourth and fifth months, much of the piriform area becomes submerged by the adjoining neocortex and in the adult only a part of it remains visible on the inferior aspect of the cerebrum.

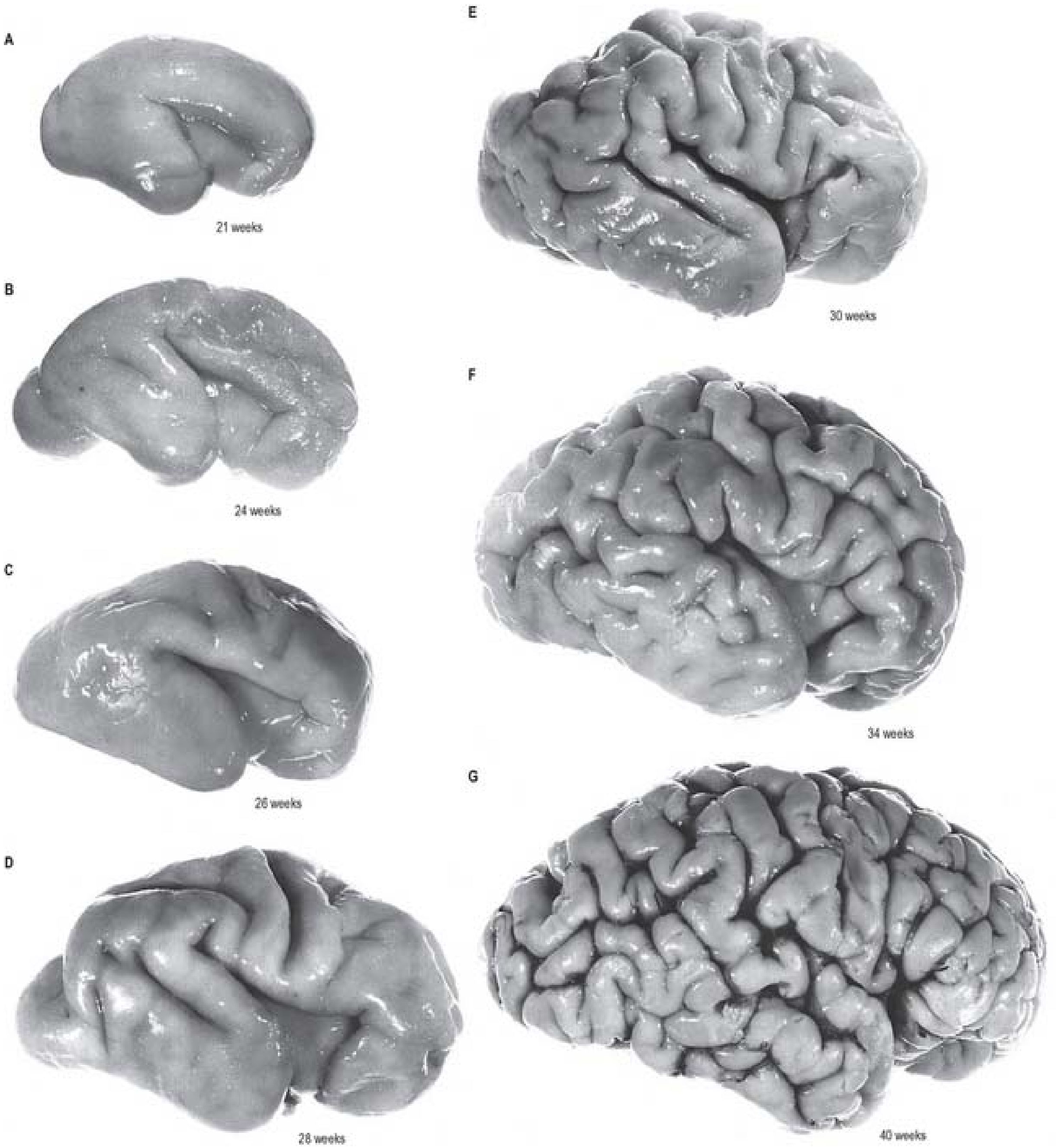
A
21 weeks
B
24 weeks
C
26 weeks
D
28 weeks
E
30 weeks
F
34 weeks
G
40 weeks

Fig. 24.29 **A–G**, The superolateral surfaces of human fetal cerebral hemispheres at the ages indicated, showing the changes in size, profile and the emerging pattern of cerebral sulci with increasing maturation. Note the changing prominence and relative positions of the frontal, occipital and particularly the temporal pole of the hemisphere. At the earliest stage (**A**) the lateral cerebral fossa is already obvious; its floor covers the developing corpus striatum in the depths of the hemisphere and progressively matures

into the cortex of the insula. The fossa is bounded by overgrowing cortical regions, the frontal, temporal and parietal opercula, which gradually converge to bury the insula; their approximation forms the lateral cerebral sulcus. By the sixth month the central, pre- and postcentral, superior temporal, intraparietal and parieto-occipital sulci are all clearly visible. In the subsequent stages shown all the remaining principal and subsidiary sulci rapidly appear and by 40 weeks all the features which characterize the adult hemisphere in terms of surface topography are present in miniature.

(Photographs provided by Dr Sabina Strick, The Maudsley Hospital, London.)

The limbic lobe is the first part of the cortex to differentiate and at first it forms a continuous, almost circular strip on the medial and inferior aspects of the hemisphere. Below and in front, where the stalk of the olfactory tract is attached, it constitutes a part of the piriform area. The portion outside the curve of the choroid fissure (Fig. 24.30) constitutes the hippocampal formation. In this region the neural progenitors of the developing cortex proliferate and migrate. The wall of the hemisphere thickens, producing an elevation that projects into the medial side of the ventricle. The elevation is the hippocampus; it appears first on the medial wall of the hemisphere in the area above and in front of the lamina terminalis (paraterminal area) and gradually extends backwards, curving into the region of the temporal pole where it adjoins the piriform area. The marginal zone in the neighbourhood of the hippocampus is invaded by neurones to form the dentate gyrus. Both extend from the paraterminal area backwards above the choroid fissure and follow its curve downwards and forwards towards the temporal pole, where they continue into the piriform area. A shallow groove, the hippocampal sulcus, crosses the medial surface of the hemisphere throughout the hippocampal formation. The efferent fibres from the cells of the hippocampus collect along its medial edge and run forwards immediately above the choroid fissure. Rostrally they turn ventrally and enter the lateral part of the lamina terminalis to gain the hypothalamus, where they end in and around the mammillary body and neighbouring nuclei. These efferent hippocampal fibres form the fimbria hippocampi and the fornix.

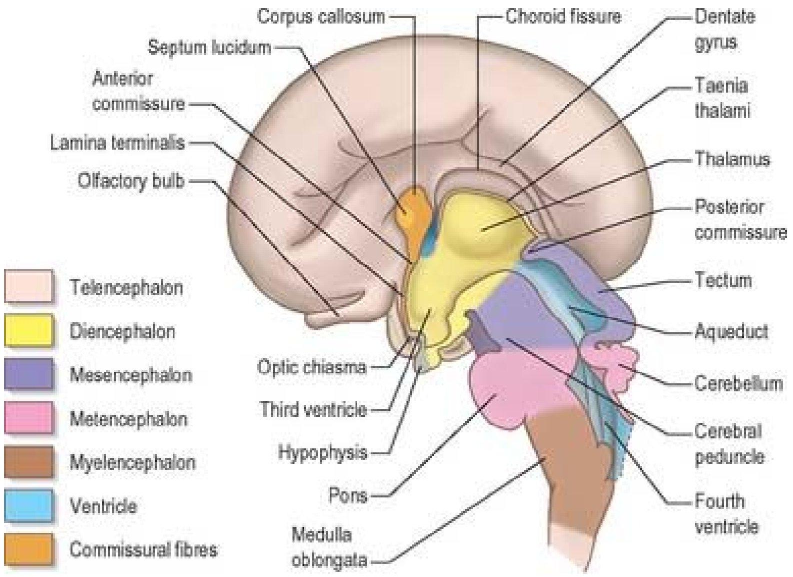
Corpus callosum
Septum lucidum
Anterior commissure
Lamina terminalis
Olfactory bulb
Choroid fissure
Dentate gyrus
Taenia thalami
Thalamus
Posterior commissure
Tectum
Aqueduct
Cerebellum
Cerebral peduncle
Fourth ventricle
Optic chiasma
Third ventricle
Hypophysis
Pons
Medulla oblongata
Telencephalon
Diencephalon
Mesencephalon
Metencephalon
Myelencephalon
Ventricle
Commissural fibres

Fig. 24.30 The anterior and posterior commissures in the brain of a 16 week human fetus; medial aspect of left half of the brain.

Projection fibres, internal capsule

The growth of the neocortex, and its enormous expansion during the latter part of the third month, is associated with the initial appearance of corticofugal and corticopetal projection fibres and the internal capsule. The fibres follow the route provided by the apposition of the lateral aspect of the thalamus with the medial aspect of the corpus striatum. They divide the latter, almost completely, into a lateral part, the lentiform nucleus, and a medial part, the caudate nucleus: these two nuclei remain confluent only in their anteroinferior regions (Figs 24.26 and 24.28). The corticospinal tracts begin to develop in the ninth week of fetal life and reach their caudal limits by the twenty-ninth week. The fibres destined for the cervical and upper thoracic regions, which innervate the upper limbs, are in advance of those which innervate the lower limbs, and these, in turn, are in advance of fibres that innervate the face: the timing of the appearance of reflexes associated with these three parts of the body is similarly staggered.

The majority of subcortical nuclear masses receive terminals from descending fibres of cortical origin. These are joined by thalamocortical, hypothalamocortical and other afferent ascending bundles. The internal capsular fibres pass lateral to the head and body of the caudate nucleus, the anterior cornu and central part of the lateral ventricle, the rostroventral extensions and body of the fornix, the dorsal thalamus and dorsal choroidal fissure, and medial to the lentiform nucleus (Fig. 24.26).

Formation of gyri and sulci

Apart from the shallow hippocampal sulcus and the lateral cerebral fossa, the surfaces of the hemisphere remain smooth and uninterrupted until early in the fourth month (Fig. 24.29). The parieto-occipital sulcus appears about that time on the medial aspect of the hemisphere. Its appearance seems associated with an increase in the number of splenial fibres in the corpus callosum. Over the same period the posterior part of the calcarine sulcus appears as a shallow groove extending forwards from a region near the occipital pole. It is a true infolding of the cortex in the long axis of the striate area and produces an elevation, the calcar avis, on the medial wall of the posterior horn of the ventricle.

During the fifth month the cingulate sulcus appears on the medial aspect of the hemisphere, and sulci appear on the inferior and superolateral aspects in the sixth month. The central, precentral and postcentral sulci appear, each in two parts, upper and lower, which usually coalesce shortly afterwards, although they may remain discontinuous. The superior and inferior frontal, the intraparietal, occipital, superior and inferior temporal, occipitotemporal, collateral and rhinal sulci all make their appearance during the same period. By the end of the eighth month all the important sulci can be recognized (Fig. 24.29).

Development of commissures

The development of the commissures causes a very profound alteration of the medial wall of the hemisphere. At the time of their appearance the two hemispheres are connected to each other by the median part of the telencephalon. The roof plate of this area remains epithelial, while its floor becomes invaded by the decussating fibres of the optic nerves and developing hypothalamic nuclei. These two routes are thus not available for the passage of commissural fibres passing from hemisphere to hemisphere across the median plane, and these fibres therefore pass through the rostral wall of the interventricular foramen, i.e. the lamina terminalis. The first commissures to develop are those associated with the palaeocortex and archicortex. Fibres of the olfactory tracts cross in the ventral or lower part of the lamina terminalis and, together with fibres from the piriform and prepiriform areas and the amygdaloid bodies, form the rostral part of the anterior commissure (Figs 24.30 and 24.31). In addition the two hippocampi become interconnected by transverse fibres which cross from fornix to fornix in the upper part of the lamina terminalis as the commissure of the fornix (hippocampal commissure). Various other decussating fibre bundles (known as the supraoptic commissures, although they are not true commissures) develop in the lamina terminalis immediately dorsal to the optic chiasma, between it and the anterior commissure.

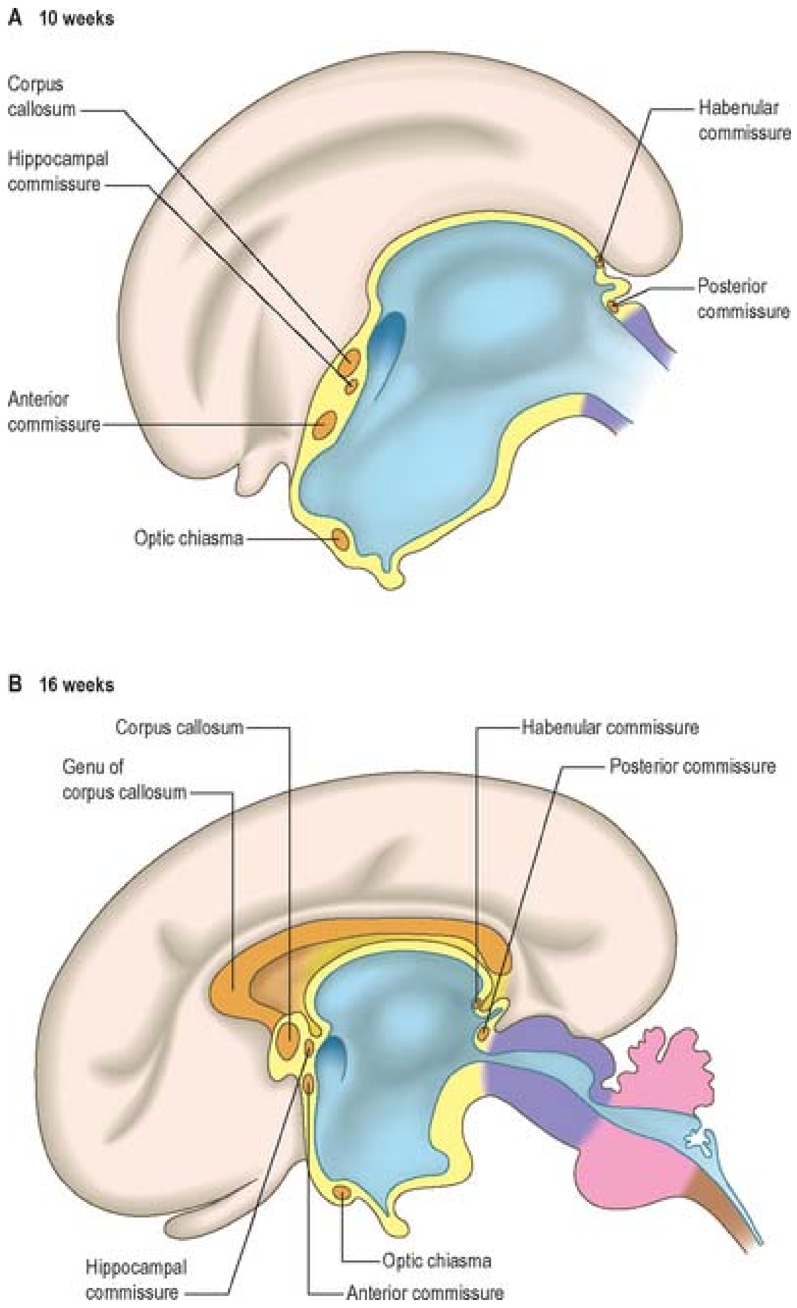
A 10 weeks
Corpus callosum
Hippocampal commissure
Anterior commissure
Optic chiasma
Habenular commissure
Posterior commissure
B 16 weeks
Corpus callosum
Genu of corpus callosum
Habenular commissure
Posterior commissure
Hippocampal commissure
Optic chiasma
Anterior commissure

Fig. 24.31 Median sections showing formation of the commissures. The telencephalon gives rise to commissural tracts that integrate the activities of the left and right cerebral hemispheres. Tracts include the anterior and hippocampal commissures and the corpus callosum. The small posterior and habenular commissures arise from the epithalamus.

The commissures of the neocortex develop later and follow the pathways already established by the commissures of the limbic system. Fibres from the tentorial surface of the hemisphere join the anterior commissure and constitute its larger posterior part. All the other commissural fibres of the neocortex associate themselves closely with the commissure of the fornix and lie on its dorsal surface. These fibres increase enormously in number and the bundle rapidly outgrows its neighbours to form the corpus callosum (Figs 24.30 and 24.31).

The corpus callosum originates as a thick mass connecting the two cerebral hemispheres around and above the anterior commissure. (This site has been called the precommissural area, but this use has been rejected here because of the increasing use of the adjective precommissural to denote the position of parts of the limbic lobe, i.e. prehippocampal rudiment, septal areas and nuclei and strands of the fornix, in relation to the anterior commissure of the mature brain.) The upper end of this neocortical commissural area extends backwards to form the trunk of the corpus callosum. The rostrum of the corpus callosum develops later and separates some of the rostral end of the limbic area from the remainder of the cerebral hemisphere. Further backward growth of the trunk of the corpus callosum then results in the entrapped part of the limbic area becoming stretched out to form the bilateral septum pellucidum. As the corpus callosum grows backwards it extends above the choroidal fissure, carrying the commissure of the fornix on its under surface. In this way a new floor is formed for the longitudinal fissure, and additional structures come to lie above the epithelial roof of the third ventricle. In its backward growth the corpus callosum invades the area hitherto occupied by the upper part of the archaeo-cortical hippocampal formation, and the corresponding parts of the dentate gyrus and hippocampus are reduced to vestiges, the indusium griseum and the longitudinal striae. However, the posteroinferior (temporal) archaeocortical regions of both dentate gyrus and hippocampus persist and enlarge.

Cellular development of the cerebrum

The wall of the earliest cerebral hemisphere consists of a pseudostratified epithelium, whose cells exhibit interkinetic nuclear migration as they proliferate to form clones of germinal cells. The columnar cells elongate and their non-nucleated peripheral processes now constitute a marginal zone (but see Fig. 24.32A legend), while their nucleated, paraluminal and mitosing regions constitute the ventricular zone. Some of their progeny leave the ventricular zone and migrate to occupy an intermediate zone. The proliferative phase continues for a considerable period of fetal life. Ultimately, groups of progenitor cells form, at first, generations of definitive neurones and, later, glial cells which migrate to, and mature in, their final positions. These phases of proliferation, migration, differentiation and maturation overlap each other in space and time, and are not precisely sequential.

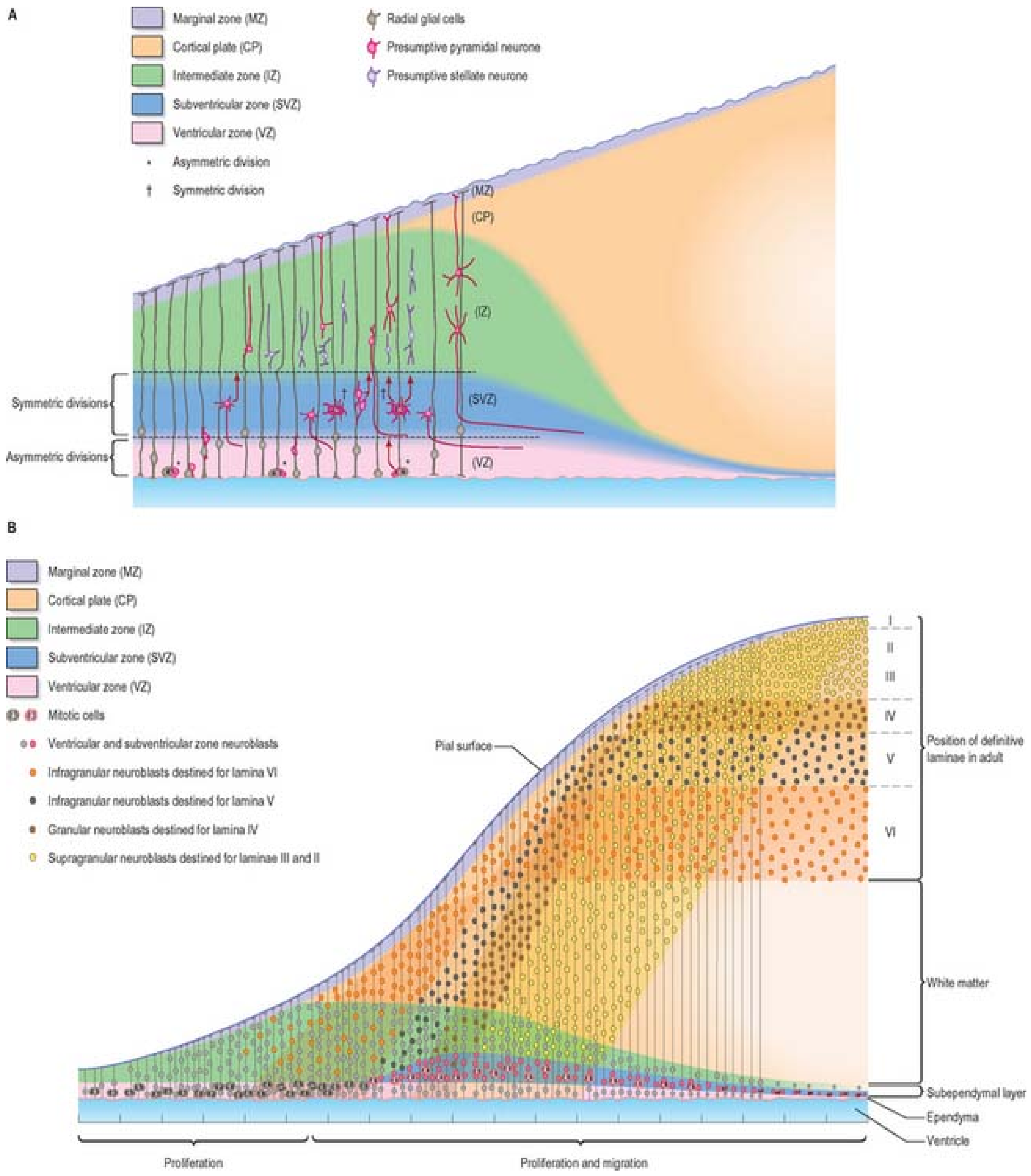
A
Marginal zone (MZ)
Cortical plate (CP)
Intermediate zone (IZ)
Subventricular zone (SVZ)
Ventricular zone (VZ)
Asymmetric division
Symmetric division
Radial glial cells
Presumptive pyramidal neurone
Presumptive stellate neurone
(MZ)
(CP)
(IZ)
(SVZ)
(VZ)
Symmetric divisions
Asymmetric divisions
B
Marginal zone (MZ)
Cortical plate (CP)
Intermediate zone (IZ)
Subventricular zone (SVZ)
Ventricular zone (VZ)
Mitotic cells
Ventricular and subventricular zone neuroblasts
Infragranular neuroblasts destined for lamina VI
Infragranular neuroblasts destined for lamina V
Granular neuroblasts destined for lamina IV
Supragranular neuroblasts destined for laminae III and II
Pial surface
I
II
III
IV
V
VI
Position of definitive laminae in adult
White matter
Subependymal layer
Ependyma
Ventricle
Proliferation
Proliferation and migration

Fig. 24.32 **A**, Two distinct programmes of cell division are observed in the ventricular zone. Asymmetric division where radial glia give rise to neurones directly; symmetric division where neurones arise via intermediate progenitors after arrest in the subventricular zone. **B**, The dynamics of neuroblast proliferation and successive migrations to form the cerebral neocortex. Cells divide initially in the ventricular and subventricular zones

and successive progeny migrate towards the pia. The first cells to migrate form deep cortical laminae; later cells pass through these layers to form successively superficial laminae. The following revisions to the 1970 Bolder Committee nomenclature for development of the human cerebral cortex given by Bystron, Blakemore and Rakic (2008) are included here, although not shown on the above diagram. Within the developing cerebral cortex: there is no distinct marginal zone beneath the pial layer before the cortical plate forms; the subventricular zone appears as a distinct proliferative layer before the cortical plate forms; a transient preplate layer forms before the cortical plate appears; the intermediate zone denotes a heterogenous compartment lying between the proliferative layers (ventricular and subventricular zones) and the postmigratory cells above; there is a transient subplate zone directly below the cortical plate.

(Adapted from Noctor et al 2004.)

The migration of neuronal precursors from the ventricular and intermediate zones occurs radially towards the pial surface Radial glial cells are now considered as neural progenitors (Kriegstein & Gotz 2003). Some early progeny from the ventricular zone form a primordial plexiform layer, or preplate. Their somata become arranged as a transient dense cortical plate from which subsequently generated cortical plate cells arise to form a subplate region. At later stages a considerable proportion of cortical progenitors divide in a subventricular zone (Fig. 24.32A). Proliferation in the ventricular zone, which produces excitatory pyramidal neurones of the infragranular layers of the cortex, wanes, whereas in the subventricular zone proliferation persists for a considerable period: the symmetrical terminal division of these cells gives rise to neurones which migrate to form the supragranular layers of the cortex (Kriegstein & Noctor 2004). From the pial surface inwards, the following zones may be defined: marginal, cortical plate, subplate, intermediate, subventricular and ventricular (Fig. 24.32B). (For a review of the nomenclature of the developing zones see Bystron et al 2008.) The marginal zone, the outermost layer of the developing cerebral cortex, will form layer 1, and the neurones of the cortical plate and subplate form the neurones of the remaining (2–6) cortical laminae, the complexity varying in different locations and with further additions of neurones from the deeper zones. The intermediate zone gradually transforms into the white matter of the hemisphere. Meanwhile other deep progenitor cells produce generations of glioblasts which also migrate into the more superficial layers. As proliferation wanes and finally ceases in the ventricular and subventricular zones, their remaining cells differentiate into general or specialized ependymal cells, tanycytes or subependymal glial cells.

The time of the proliferation of different cortical neurones vary according to their laminar destination and cell type. The first groups of cells to migrate are destined for the deep cortical laminae and later groups pass through them to more superficial regions. The subplate zone, a transient feature containing some of the earliest generated cortical neurones is most prominent during mid-gestation. It contains neurones surrounded by a dense neuropil and is the site of the most intense synaptogenesis in the embryonic cortex. The cumulative effect of this radial and tangential growth is evident in a marked increase in cortical thickness and surface area.

In the pallial walls of the mammalian cerebral hemisphere, the phylogenetically oldest regions, which are the first to differentiate during ontogeny, are those that border the interventricular foramen and its extension the choroidal fissure, the lamina terminalis and the piriform lobe. The pallidum also contributes interneurones to the formation of the cerebral cortex. A large portion of GABAergic inhibitory (nonpyramidal) cells are not generated in the cortical ventricular zone, but migrate tangentially through the striatocortical junction to reach the cortex (Wonders & Anderson 2006; Metin et al 2006; Fig. 24.33). An increasingly complex level of organization, from three to six tangential laminae, is encountered in passing from the dentate gyrus and cornu ammonis through the subiculum to the general neocortex. (Many investigators find the simple progression from three to six major laminae a gross oversimplification, and numerous subdivisions have been proposed.)

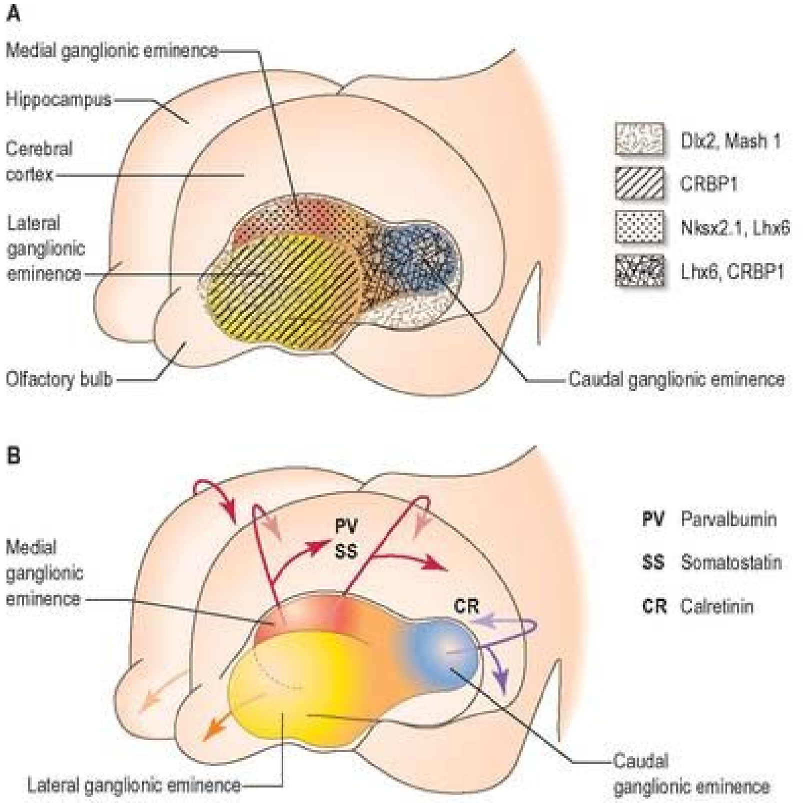
A
Medial ganglionic eminence
Hippocampus
Cerebral cortex
Lateral ganglionic eminence
Olfactory bulb
Caudal ganglionic eminence
Dlx2, Mash 1
CRBP1
Nksx2.1, Lhx6
Lhx6, CRBP1
B
Medial ganglionic eminence
PV
SS
CR
Lateral ganglionic eminence
Caudal ganglionic eminence
PV Parvalbumin
SS Somatostatin
CR Calretinin

Fig. 24.33 (**A**) The ganglionic eminence (GE) of the subpallium is subdivided into three regions: lateral (LGE), medial (MGE), and caudal (CGE) according to the expression patterns of various transcription factors (Dlx2, Mash1, Nksx2.1 and Lhx6) and of the cellular retinol-binding protein 1 (CRBP1). (**B**) Main migratory paths of interneurones derived from the three subdivisions of the GE. MGE cells tend to migrate laterally and spread throughout the cortex, CGE cells migrate predominantly towards the caudal telencephalon, whereas LGE cells migrate rostrally and contribute to interneurones in the olfactory bulb. It has been suggested that most MGE cells differentiate into parvalbumin (PV)- and somatostatin (SS)-immunoreactive interneurones, whereas most CGE cells differentiate into calretinin (CR) immunoreactive interneurones.

Mechanisms of cortical development

Rakic (1971) initially demonstrated the migration of neurones along radial glial processes, and this has subsequently been seen to occur in three phases. First, the neurones become apposed to the radial glial cells and establish an axis of polarity away from the ventricular surface. Next, they are propelled along the glial surface until they ‘recognize’ their final destination, whereupon they cease locomotion and detach from the glial processes. They then continue to differentiate according to their final position, and later-born neurones migrate past them towards the pial surface (Fig. 24.5). Cortical neurones or cerebellar granule cells appear equally capable of migrating on hippocampal or cerebellar Bergmann glia, indicating conservation of migration mechanisms in different brain regions. These observations are still valid, although it is now recognized that radial glia represent the major neuronal progenitor population of the cortex.

Various lines of evidence support the proposal that the laminar fate of neurones is determined prior to migration. In the mutant reeler mouse, laminar formation is inverted so that layers form in outside-in rather than inside-out array, yet axonal connections and neuronal properties appear normal, suggesting that the cells differentiate according to their time of origin rather than their location. Likewise, the prevention of neuronal migration by irradiation leads to the production of cells which remain apposed to the ventricular surface but which develop an appropriate phenotype and efferent projections. Transplantation of labelled cells has suggested that commitment to a particular cortical lamina occurs shortly after S-phase. Neurones of pre-existing laminae that have begun axonogenesis may provide a feedback on the forming cortical layers, providing a sort of developmental clock for histogenesis.

In a plane perpendicular to its laminae, i.e. tangentially/circumferentially, the cortex is divided up into a number of areas, displaying a hierarchy of organization (see Ch. 23). These include primary areas, such as the motor cortex, unimodal association areas concerned with the integration of information from one of the primary areas, and multimodal association areas that integrate information from more than one modality. There are also the areas concerned with functions that are even less understood, such as the frontal lobes, concerned with goal-orientation, responsibility and long-term planning. The primary areas are further divided into somatotopic maps. At the finest level, the cortex is known to consist of a series of ‘columns’, 50–500 μm wide, within which cells on a vertical traverse display common features of modality and electrophysiological responses to stimuli, e.g. the ocular dominance columns of the visual cortex. Despite the precise stacking of neurones in these columns, only 80–85% of cells are thought to migrate radially along the glial cells: a subpopulation is thought to move tangentially in the intermediate zone (O’Rourke et al 1995). Moreover, some neurones may also migrate tangentially on the radial glial cells, as a result of glial cell branching in the cortical plate. The ventricular zone is not the only source of cortical neurones, because striatal and GABAergic neurones are known to migrate from the medial, lateral and caudal ganglionic eminences into the developing cortex. The proportion of locally generated and tangentially migrating GABAergic neurones it believed to be 65–35% in human and 5–95% in mouse.

Two models have been proposed to explain the development of the complexity of cortical organization. The ‘protocortex’ model assumes that the proliferative ventricular epithelium is a ‘tabula rasa’ generating homogeneous layers of neurones that are patterned solely by their future connectivity, especially by the ingrowth of processes from the thalamus. The ‘protomap’ hypothesis proposes that the intrinsic differences between the different areas are specified prior to cell generation and migration (Rakic 1988, 2003). The radial glial cells translate this map from the ventricular zone to the cortical plate where the pattern is refined by innervating axons. In this ‘radial unit’ model, the tangential co-ordinates of the different areas are determined by the position of their ventricular ancestors, whereas their radial position is determined by their time of birth and rate of migration.

But what would constitute such a ‘protomap’? The investigation of gene expression patterns shows that the early cortex is not homogeneous, and that it expresses some markers that are transient and some that persist into the adult. For example, the mouse gene *Id2* marks the transition between the motor and somatosensory cortices in the embryo, whereas limbic associated membrane protein (LAMP) delineates the limbic cortex throughout life. LAMP expression is regulated by transforming growth factor-α, which is expressed by the lateral ganglionic eminence at the lateral edge of the cortex, whereas the medial edge or cortical hem expresses signalling molecules of the Wnt and BMP families. Any, if not all, of these may be the components of short range signalling centres along the edges of the cortex (e.g. FGF8) (Fig. 24.34). Coupled with the gradients of transcription factors such as Emx2 and Lhx2, there is therefore evidence to support the ‘protomap’ hypothesis (Donoghue & Rakic 1999). The challenge is to relate the gradients of gene expression patterns to formation of sharp cytoarchitectonic boundaries.

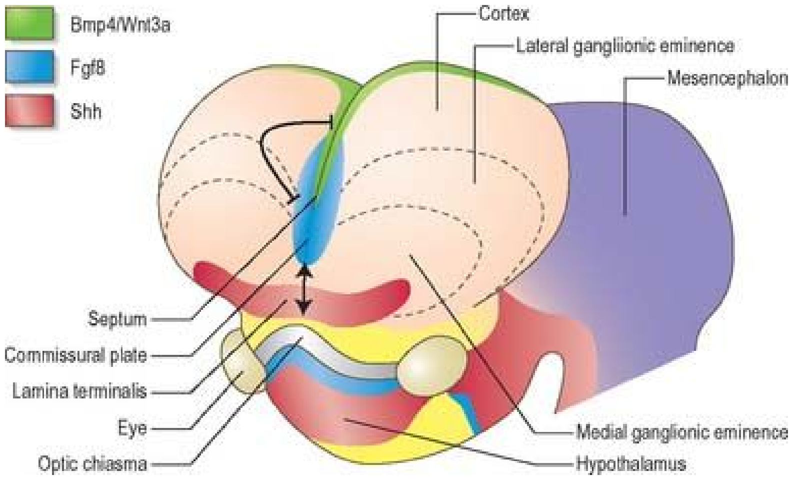
Bmp4/Wnt3a
Fgf8
Shh
Cortex
Lateral gangliionic eminence
Mesencephalon
Septum
Commissural plate
Lamina terminalis
Eye
Optic chiasma
Medial ganglionic eminence
Hypothalamus

Fig. 24.34 Frontolateral view of the telencephalon showing the patterning centres as marked by expression of the genes indicated in the key, the cross regulation between the *Fgf8* and *Bmp4*/*Wnt3a*-expressing centres, and the positive interactions between the *Fgf8* and *Shh*-expressing domains.

However, studies of cell migration are consistent with the idea that cortical areas might not be rigidly determined. Experimental manipulations of the developing cortex by deafferentation or manipulation of inputs give some indication of the state of commitment of cortical areas. In two independent sets of experiments, somatosensory or auditory cortex was induced to process visual information by misrouting retinal axons to somatosensory thalamus or auditory thalamus (von Melchner, Pallas & Sur 2000). When the lateral geniculate nucleus and the visual cortex were ablated and space was created in the medial geniculate by ablating the inferior colliculus, cells in the somatosensory or auditory cortex were visually driven due to the subcortical rewiring, and receptive field and response properties resembled those typical of the visual cortex. These results suggest that the modality of a sensory thalamic nucleus or cortical area can be specified by inputs during development.

The development of cortical projections has been investigated both in terms of laminar and area-specific connectivity. Recently, attention has focused on the idea that connections might be influenced by the existence of a transient population of subplate neurones, which later dies. The cortex develops within a preplate, consisting of corticopetal nerve fibres and the earliest generated neurones. This zone is then split into two zones, the subplate underneath the cortical plate, and the marginal zone at the pial surface, by the arrival of cortical neurones. Subplate neurones integrate into the intra- and extra-cortical circuitry, they extend axons via the internal capsule towards the thalamus and superior colliculus at times before other cortical neurones have been born.

How are region-specific projections generated? Layer 5 neurones in various cortical areas extend axons to different repertoires of targets. For instance, layer 5 neurones of the visual cortex project to the tectum, pons and mesencephalic nuclei, while those in the motor cortex project to mesencephalic and pontine targets, the inferior olive and dorsal column nuclei and the spinal cord. An interesting feature of these cortical projections is that they arise by collateral formation rather than by projection of the primary axon, or by growth cone bifurcation. In the case of the corticopontine projection, collaterals are elicited by a diffusible, chemotrophic agent. Retrograde labelling of layer 5 neurones at various times in development has shown that rather than being generated *de novo*, these patterns seem to arise by pruning of collaterals from a more widespread projection. Visual cortical neurones possess a projection to the spinal cord early in development, which is later eliminated. This late emergence of the specificity of projections could be driven by intrinsic programming of the neurones to be pruned, or a response to position-dependent factors. There is evidence that the latter is the case. When pieces of visual cortex were transplanted into motor areas, and the resulting layer 5 projections labelled at later times in development, projections to the spinal cord persisted, rather than being eliminated as in normal development. Thus position plays an important role in the modelling of cortical projections, implying that the same classes of neurones exist in different tangential regions of the cortex. Regressive events such as axon and synapse elimination and neuronal death thus play an important part in modelling the cortex. For example in rodents approximately 30% of cortical neurones die, and the number of cells in layer 4 is governed by thalamic input.

Human cortical malformations are thought to arise as neuronal migration disorders (NMDs). A broad class of NMDs is lissencephaly, in which the cortex has a normal thickness, but a decreased number of neurones and a smoothened surface with a decreased number of gyri. The mutated protein in some forms of the disorder, LIS-1, is expressed in the ventricular neuroepithelium and is responsible for regulating the levels of the lipid messenger platelet activating factor (PAF). How this translates into a cell migration defect remains as yet obscure. Conversely, polymicrogyria manifests as a highly convoluted cerebrum, with a nearly normal surface area but a thinner cortex. It is thought that the normal number of proliferative units and thus ontogenetic columns are established, but each column contains fewer neurones, implying either a reduced rate of proliferation and/or cell migration, or an enhanced level of cell death.

Neonatal brain and reflexes

The brain of the full-term neonate ranges from 300–400 g with an average of 350 g; the brains of neonatal males are slightly heavier than those of females. Because the head is large at birth, measuring one quarter the total body length, the brain is also proportionally larger, and constitutes 10% of the body weight compared with 2% in the adult. At birth the volume of the brain is 25% of its volume in adult life. The greater part of the increase occurs during the first year, at the end of which the volume of the brain has increased to 75% of its adult volume. The growth can be accounted for partly by increase in the size of nerve cell somata, the profusion and dimensions of their dendritic trees, axons and collaterals, and by the growth of the neuroglial cells and cerebral blood vessels, but mostly it reflects the myelination of many of the axons: the sensory pathways, visual, auditory and somatic, myelinate first, and the motor fibres later. During the second and subsequent years, growth proceeds much more slowly. The brain reaches 90% of its adult size by the fifth year, 95% by 10 years, and attains adult size by the 17th or 18th year, largely as a result of the continuing myelination of various groups of nerve fibres.

The sulci of the cerebral hemispheres appear from the fourth month of gestation (Fig. 24.29). At full term, the general arrangement of sulci and gyri is present, but the insula is not completely covered, the central sulcus is situated further rostrally, and the lateral sulcus is more oblique than in the adult. Most of the developmental stages of sulci and gyri have been identified in the brains of premature infants. Of the cranial nerves, the olfactory nerve and the optic nerve at the chiasma are much larger than in the adult, whereas the roots of the other nerves are relatively smaller.

The brain occupies 97.5% of the cranial cavity from birth to 6 years of age, after which the space between the brain and skull increases in volume until the adult brain occupies only 92.5% of the cranial cavity. The cerebral ventricles are larger in the neonatal brain than they are in the adult. The newborn has a total of 10–15 ml of cerebrospinal fluid when delivered vaginally and 30 ml when delivered by Caesarean section. As the head moves down the birth canal and is compressed, the cerebrospinal fluid is pushed out into the venous sinuses; this does not happen in a Caesarean delivery.

Myelination

Myelination occurs over a protracted period that starts during the second trimester in the peripheral nervous system (PNS). Motor roots start to myelinate before sensory roots in the PNS, whereas sensory nerves start to myelinate before motor nerves. The cranial nerves of the midbrain, pons and medulla oblongata begin to myelinate at about 6 months’ gestation. Myelination is not complete at birth; its most rapid phase occurs during the first 6 months of postnatal life, after which it continues at a slower rate up to puberty and beyond. The sequence of myelination of the motor pathways may explain, at least partially, the order of development of muscle tone and posture in the premature infant and neonate. Myelination of the various subcorticospinal pathways, i.e. vestibulospinal, reticulospinal, olivospinal and tectospinal (often grouped as bulbospinal tracts) starts at 24–30 weeks' gestation for the medial groups, and at 28–34 weeks' gestation for the lateral groups. Myelination of the corticospinal tracts starts some 10–14 days after birth in the internal capsule and cerebral peduncles, and then proceeds simultaneously in both tracts. Myelination appears to start first around longer axons. Thus, in the preterm infant, axial extension precedes flexion, whereas finger flexion precedes extension. By term the neonate at rest has a strong flexor tone accompanied by adduction of all limbs. Neonates also display a distinct preference for a head position facing to the right, which appears to be independent of handling practices and may reflect the normal asymmetry of cerebral function at this age.

Reflexes present at birth

A number of reflexes are present at birth and their demonstration is used to indicate normal development of the nervous system and responding muscles. Five tests of neurological development are most useful in determining gestational age. The pupillary reflex is consistently absent before 29 weeks' gestation and present after 31 weeks; the glabellar tap, a blink in response to a tap on the glabella, is absent before 32 weeks and present after 34 weeks; the neck righting reflex appears between 34 and 37 weeks; the traction response, where flexion of the neck or arms occurs when the baby is pulled up by the wrists from the supine position appears after 33 weeks; head turning in response to light appears between 32 and 36 weeks. The spinal reflex arc is fully developed by the eighth week of gestation and lower limb flexor tone is detectable from about 29 weeks. The Babinski response, which involves extension of the great toe with spreading of the remaining toes in response to stimulation of the lateral aspect of the sole of the foot, is elicited frequently in neonates; it reflects poor cortical control of motor function by the immature brain. Generally reflexes develop as muscles gain tone. They appear in a sequential manner from caudal to cephalic, i.e. in the lower limb before the upper, and centripetally, i.e. distal reflexes appear before proximal ones (Allen & Capute 1990).

The usual reflexes that can be elicited in the neonate include Moro, asymmetric tonic neck response, rooting–sucking, grasp, placing (contacting the dorsum of the foot with the edge of a table produces a ‘stepping over the edge’ response), stepping, and trunk incurvation (elicited by stroking down the paravertebral area with the infant in the prone position). Examination of the motor system and evaluation of these reflexes allows assessment of the nervous system in relation to gestational age. The neonate also exhibits complex reflexes such as nasal reflexes and sucking and swallowing.

Nasal reflexes produce apnoea via the diving reflex, sneezing, sniffing, and both somatic and autonomic reflexes. Stimulation of the face or nasal cavity with water or local irritants produces apnoea in neonates. Breathing stops in expiration, with laryngeal closure, and infants exhibit bradycardia and a lowering of cardiac output. Blood flow to the skin, splanchnic areas, muscles and kidneys decreases, whereas flow to the heart and brain is protected. Different fluids produce different effects when introduced into the pharynx of preterm infants. A comparison of the effects of water and saline in the pharynx showed that apnoea, airway obstruction, and swallowing occur far more frequently with water than with saline, suggesting the presence of an upper airway chemoreflex. Reflex responses to the temperature of the face and nasopharynx are necessary to start pulmonary ventilation. Midwives have for many years blown on the faces of neonates to induce the first breath.

Sucking and swallowing are a particularly complex set of reflexes, partly conscious and partly unconscious. As a combined reflex sucking and swallowing require the coordination of several of the 12 cranial nerves. The neonate can, within the first couple of feeds, suck at the rate of once per second, swallow after five or six sucks, and breathe during every second or third suck. Air moves in and out of the lungs via the nasopharynx, and milk crosses the pharynx en route to the oesophagus without apparent interruption of breathing and swallowing, or significant misdirection of air into the stomach or fluids in the trachea.

Swallowing movements are first noted at about 11 weeks' gestation; *in utero* fetuses swallow 450 ml of amniotic fluid per day. Sucking and swallowing in premature infants (1700 g) is not associated with primary peristaltic waves in the intestine; however, in older babies and full-term neonates, at least 90% of swallows will initiate primary peristaltic waves.

Sucking develops, generally, slightly later than swallowing, although mouthing movements have been detected in premature babies as early as 18–24 weeks' gestation, and infants delivered at 29–30 weeks' gestation make sucking movements a few days after birth. Coordinated activities are not noted before 33–34 weeks. The concept of nonnutritive and nutritive sucking has been introduced to account for the different rates of sucking seen in the neonate. Non-nutritive sucking, when rhythmic negative intraoral pressures are initiated which do not result in the delivery of milk, can be spontaneous or stimulated by an object in the mouth. This type of sucking tends to be twice as fast as nutritive sucking: the sucking frequency for non-nutritive sucking is 1.7 sucks/second in 37–38 week premature babies, two sucks/second in term neonates, and 2.7 sucks/second at 7–9 months postnatally. Corresponding times for nutritive sucking are about one suck/second in term neonates, increasing to 1.5 sucks/second by 7 months postnatally.

The taste of the fluid as well as nutrient content affects the efficiency of nutritive sucking in the early neonatal period. There is more sucking with milk than with 5% dextrose; however, sucking activities increase with solutions that are determined to be sweet by adult appraisal.

In full-term neonates, the placing of a spoon or food onto the anterior part of the tongue elicits an extrusion reflex: the lips are pursed and the tongue pushes vigorously against the object. By 4–6 months the reflex changes and food deposited on the anterior part of the tongue is moved to the back of the tongue, into the pharynx, and swallowed (see Ch. 33 for a description of swallowing in the adult). Rhythmic biting movements occur by 7–9 months postnatally, even in the absence of teeth.

Difficulties in sucking and swallowing in infancy may be an early indication of disturbed nervous system function. There is an interesting correlation between feeding styles of neonates and later eating habits. Children who were obese at 1 and 2 years of age, as measured by triceps skin-fold thickness, had a feeding pattern in the first month of life that was characterized by sucking more rapidly, producing higher pressures during prolonged bursts of sucking, and having shorter periods between bursts of sucking. Fewer feeds and higher sucking pressure seem to be associated with greater adiposity.

MENINGES

The meningeal layers originate from paraxial mesenchyme in the trunk and caudal regions of the head and from neural crest in regions rostral to the mesencephalon (the prechordal plate has also been suggested to make a contribution). Those skull bones that are formed from neural crest, i.e. the base of the skull rostral to the sella turcica, and the frontal, parietal and squamous temporal bones, overlie meninges that are also formed from crest cells.

The meninges may be divided in development into the pachymeninx (dura mater) and leptomeninges (arachnoid mater, subarachnoid space with arachnoid cells and fibres, and pia mater). All meningeal layers are derived from loose mesenchyme which surrounds the developing neural tube, termed meninx primitiva, or primary meninx. (For a detailed account of the development of the meninges in the human consult O'Rahilly & Müller 1986.)

The first indication of pia mater, containing a plexus of blood vessels which forms on the neural surface, is seen at stage 11 (24 days), around the caudal-most part of the medulla; this extends to the mesencephalic level by stage 12. Mesenchymal cells projecting from the rostral end of the notochord, and those in the region of the prechordal plate, extend rostrally into the mesencephalic flexure and form the earliest cells of the tentorium cerebelli; at the beginning of its development the medial part of the tentorium is predominantly leptomeningeal. By stage 17 (41 days) dura mater can be seen in the basal areas where the future chondrocranium is also developing. The precursors of the venous sinuses lie within the pachymeninx at stage 19 (48 days), and by stage 20, cell populations in the region of the future falx cerebri are proliferating, although the dorsal regions of the brain are not yet covered with putative meninges.

By stage 23 (57 days) the dura is almost complete over the rhombencephalon and mesencephalon, but is only present laterally around the prosencephalon. Subarachnoid spaces and most of the cisternae are present from this time, after the arachnoid mater becomes separated from the primitive dura mater by the accumulation of cerebrospinal fluid (which now has a net movement out of the ventricular system). The medial part of the tentorium is becoming thinner. A dural component of the tentorium is seen from stage 19. The earlier medial portion disappears leaving an incomplete partition which separates a subarachnoid area containing the telencephalon and diencephalon from one containing the cerebellum and rhombencephalon.

There is a very close relationship, during development, between the mesenchyme from which the cranial dura mater is formed and that which is either chondrified and ossified, or ossified directly, to form the skull. These layers are only clearly differentiated as the venous sinuses develop. The relationship between the developing skull and the underlying dura mater continues during postnatal life while the bones of the calvaria are still growing.

The growth of the cranial vault is initiated from ossification centres within the desmocranial mesenchyme. A wave of osteodifferentiation moves radially outward from these centres stopping when adjacent bones meet at regions where sutures are induced to form. Once sutures are formed, a second phase of development occurs in which growth of the cranial bones occurs at the sutural margins. This growth forms most of the skull (see Ch. 35). A number of hypotheses have been generated to explain the process of sutural morphogenesis. It has been suggested that the dura mater contains fibre tracts which extend from fixed positions in the cranial base to sites of dural reflection underlying each of the cranial sutures, and that the tensional forces so generated dictate the position of the sutures and locally inhibit precocious ossification. Other hypotheses support the concept of local factors in the calvaria which regulate suture morphogenesis. Following removal of the entire calvaria, the skull regenerates and sutures and bones develop in anatomically correct positions, suggesting that the dura can dictate suture position at least in regeneration of the neonatal calvaria. In transplants of sutures in which the fetal dura mater was left intact, a continuous fibrous suture remained between developing vault bones, whereas bony fusion occurred in transplants in which the fetal dura mater was removed (Opperman et al 1993).

The presence of fetal dura is not required for initial suture morphogenesis, which appears to be controlled by mesenchymal cell proliferation and fibrous extracellular matrix synthesis induced by the overlapping of the advancing osteoinductive fronts of the calvarial bones. It is thought that following overlap of the bone fronts, a signal is transferred to the underlying dura which induces changes in localized regions beneath the sutures. Once a suture has formed, it serves as a primary site for cranial bone growth; constant interaction with the dura is required to avoid ossiferous obliteration.

VASCULAR SUPPLY

ARTERIES

Cranial arteries

The internal carotid artery is formed progressively from the third arch artery is the dorsal aorta cranial to this, and a further forward continuation which differentiates, at the time of regression of the first and second aortic arches, from the capillary plexus extending to the walls of the forebrain and midbrain. At its anterior extremity this primitive internal carotid artery divides into cranial and caudal divisions. The former terminates as the primitive olfactory artery, and supplies the developing regions implied (see Fig. 35.8). The latter sweeps caudally to reach the ventral aspect of the midbrain, its terminal branches are the primitive mesencephalic arteries. Simultaneously bilateral longitudinal channels differentiate along the ventral surface of the hindbrain from a plexus fed by intersegmental and transitory presegmental branches of the dorsal aorta and its forward continuation. The most important of the presegmental branches is closely related to the fifth nerve, the primitive trigeminal artery. Otic and hypoglossal presegmental arteries occur and may persist. The longitudinal channels later connect cranially with the caudal divisions of the internal carotid arteries (each of which gives rise to an anterior choroidal artery supplying branches to the diencephalon, including the telae choroideae and midbrain) and caudally with the vertebral arteries through the first cervical intersegmental arteries. Fusion of the longitudinal channels results in the formation of the basilar artery, while the caudal division of the internal carotid artery becomes the posterior communicating artery and the stem of the posterior cerebral artery. The remainder of the posterior cerebral artery develops comparatively late, probably from the stem of the posterior choroidal artery which is annexed by the caudally expanding cerebral hemisphere, its distal portion becoming a choroidal branch of the posterior cerebral artery. The posterior choroidal artery supplies the tela choroidea at the future temporal end of the choroidal fissure; its rami advance through the tela to become confluent with branches of the anterior choroidal artery. The cranial division of the internal carotid artery gives rise to anterior choroidal, middle cerebral and anterior cerebral arteries. The stem of the primitive olfactory artery remains as a small medial striate branch of the anterior cerebral artery. The cerebellar arteries, of which the superior is the first to differentiate, emerge from the capillary plexus on the wall of the rhombencephalon.

The source of the blood supply to the territory of the trigeminal nerve varies at different stages in development. When the first and second aortic arch arteries begin to regress, the supply to the corresponding arches is derived from a transient ventral pharyngeal artery, which grows from the aortic sac. It terminates by dividing into mandibular and maxillary branches.

Leptomeningeal arteries

At stage 20–23 (7–8 weeks), further expansion of the cerebral hemispheres produces the completion of the circle of Willis; the anterior communicating arteries develop by 8 weeks' gestation. An anular network of leptomeningeal arteries originating mainly from each middle cerebral artery passes over each developing cerebral hemisphere. Caudally, similar meningeal branches arise from the vertebral and basilar arteries and embrace the cerebellum and brain stem. The further development of the telencephalon somewhat obscures this early pattern over the cerebrum.

The meningeal arteries so formed have been classified into three groups, namely paramedian, short circumferential and long circumferential arteries. They can be described both supratentorially and infra-tentorially, and all give off fine side branches and end as penetrating arteries. Of the supratentorial vessels, the paramedian arteries have a short course prior to penetrating the cerebral neuropil (e.g. branches of the anterior cerebral artery); the short circumferential arteries have a slightly longer course before becoming penetrating arteries (e.g. the striate artery); and the long circumferential arteries reach the dorsal surface of the hemispheres. Infratentorial meningeal arteries are very variable. The paramedian arteries, after arising from the basilar or vertebral arteries, penetrate the brain stem directly. The short circumferential arteries end at the lateral surface of the brain before penetration and the long circumferential arteries later form the range of cerebellar arteries. These vessels, arranged as a series of loops over the brain, arise from the circle of Willis and brain stem vessels on the base of the brain.

At 16 weeks' gestation, the anterior, middle and posterior cerebral arteries that contribute to the formation of the circle of Willis are well established. The leptomeningeal arteries arising from them display a simple pattern with little tortuosity and very few branches. With the increasing age of the fetus and acquisition of the gyral pattern on the surface of the brain, their tortuosity, diameter and number of branches all increase. The branching pattern is completed by 28 weeks' gestation and the number of branches does not increase further. Numerous anastomoses (varying in size from 200–760 μm) occur between the meningeal arteries in the depths of the developing sulci, nearly always in the cortical boundary zones of the three main cerebral arteries supplying each hemisphere. The number, diameter and location of these anastomoses change as fetal growth progresses, reflecting the regression and simplification of the complex embryonic cerebral vascular system. The boundary zones between the cerebral arteries may be the sites of inadequate perfusion in the premature infant.

Vascularization of the brain

The brain becomes vascularized by angiogenesis (angiotrophic vasculogenesis) rather than by direct invasion by angioblasts. Blood vessels form by sprouting from vessels in the pial plexus that surrounds the neural tube from an early stage. These sprouts form branches that elongate at the junction between the ventricular and marginal zones; the branches project laterally within the inter-rhombomeric boundaries and longitudinally adjacent to the median floorplate. Subsequently, additional sprouts penetrate the inter-rhombomeric regions on the walls and floor of the hindbrain. Branches from the latter elongate towards and join the branches in the inter-rhombomeric junctions, forming primary vascular channels between rhombomeres and longitudinally on each side of the median floorplate. Later additional sprouts invade the hindbrain within the rhombomeres, anastomosing in all directions.

The leptomeningeal perforating branches pass into the brain parenchyma as cortical, medullary and striate branches (Fig. 24.35). The cortical vessels supply the cortex via short branches which may form precapillary anastomoses, whereas the medullary branches supply the white matter. The latter converge towards the ventricle but rarely reach it; they often follow a tortuous course as they pass around bundles of nerves. The striate branches which penetrate into the brain through the anterior perforated substance, supply the basal nuclei and internal capsule via a sinuous course: they are larger than the medullary branches and the longest of them reach close to the ventricle. The periventricular region and basal nuclei are also supplied by branches from the tela choroidea, which develops from the early pial plexus but becomes medially and deeply placed as the telencephalon enlarges.

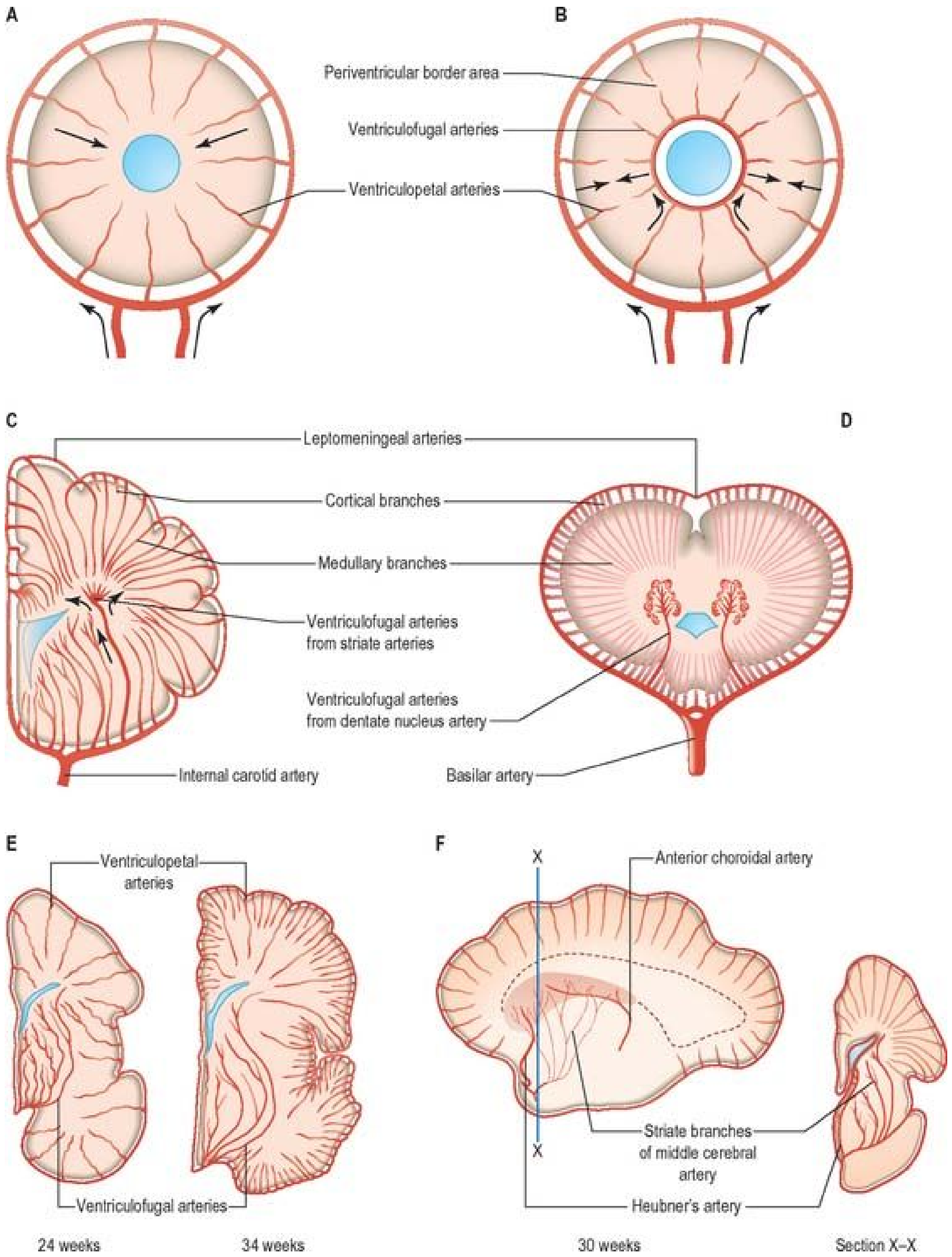
A
B
Periventricular border area
Ventriculofugal arteries
Ventriculopetal arteries
C
D
Leptomeningeal arteries
Cortical branches
Medullary branches
Ventriculofugal arteries from striate arteries
Ventriculofugal arteries from dentate nucleus artery
Internal carotid artery
Basilar artery
E
F
Ventriculopetal arteries
Ventriculofugal arteries
X
X
Anterior choroidal artery
Striate branches of middle cerebral artery
Heubner's artery
24 weeks
34 weeks
30 weeks
Section X–X

Fig. 24.35 Development of cerebral blood vessels. **A**, The brain is surrounded by a system of leptomeningeal arteries from afferent trunks at its base. Intracerebral arteries arise from this system and converge (ventriculopetally) towards the ventricle (the inner circle in this diagram).

B, A few deep penetrating vessels supply the brain close to the ventricle and send ventriculofugal arteries towards the ventriculopetal vessels without making anastomoses. **C**, The arrangement of ventriculopetal and ventriculofugal vessels around a cerebral hemisphere. **D**, The similar arrangement of vessels around the cerebellum. **E**, Changes in the arterial pattern of the human cerebrum between 24 and 34 weeks' gestation. **F**, Arterial supply to the basal nuclei at 30 weeks' gestation.

*(**A–D**, by permission from Van den Bergh R, Van der Eecken H 1968 Anatomy and embryology of cerebral circulation. Prog Brain Res 30: 1–25; **E** and **F**, by permission from the BMJ Publishing Group from Hambleton G, Wigglesworth J S 1976 Origin of intraventricular haemorrhage in the preterm infant. Arch Dis Child 51: 651–659.)*

The cortical and medullary branches irrigate a series of corticosubcortical cone-shaped areas, each centred around a sulcus containing an artery. They supply a peripheral portion of the cerebrum and are grouped as ventriculopetal arteries. In contrast, striate branches arborize close to the ventricle and supply a more central portion of the cerebrum; together with branches from the tela choroidea, they give rise to ventriculofugal arteries which supply the ventricular zone (germinal matrix of the brain) and send branches towards the cortex. The ventriculopetal and ventriculofugal arteries run towards each other but they do not make any connections or anastomoses: the ventriculopetal arteries form networks of small arterioles (Fig. 24.35). The ventriculopetal vessels supply relatively more mature regions of the brain compared to the ventriculofugal vessels, which are subject to constant remodelling and do not develop tunicae mediae until ventricular zone proliferation is completed. The boundary zone between these two systems (an outer centripetal and inner centrifugal) has practical implications related to the location of ischaemic lesions (periventricular leukomalacia, PVL) in the white matter of premature infant brains. Although it was thought that the distribution of ischaemic lesions in PVL coincided with the demarcation zone between the centrifugal and centripetal vascular arterial systems, this is now not thought to provide the complete answer. Three major interacting factors contribute to the pathology seen in PVL: the incomplete state of development of the vasculature in the ventricular zone, the maturation-dependent impairment of cerebral blood flow regulation in premature infants, and the vulnerability of oligodendroblasts in the periventricular region (which are particularly affected by swings in cerebral ischaemia and reperfusion) (Volpe 2001).

The same pattern of centripetal and centrifugal arteries develops around the fourth ventricle. The ventriculofugal circulation is more extensive in the cerebellum than in the telencephalon. The arteries arise from the various cerebellar arteries and course, with the cerebellar peduncles, directly to the centre of the cerebellum, by-passing the cortex. The ventriculopetal arteries are derived from the meningeal vessels over the cerebellar surface, and most terminate in the white matter.

At 24 weeks' gestation, the blood supply to the basal nuclei and internal capsule is relatively well-developed, via a prominent Heubner's artery (arteria recurrens anterior), a branch of the anterior cerebral artery. In contrast, the cortex and the white matter regions are rather poorly vascularized at this stage. The distribution of arteries and veins on the lateral aspect of the cerebral hemispheres is affected by the formation of the lateral fissure and development of cerebral sulci and gyri. Between 12 and 20 weeks' gestation the middle cerebral artery and its branches are relatively straight, branching in an open-fan pattern. At the end of 20 weeks, the arteries become more curved as the opercula begin to appear and submerge the insular cortex. The area supplied by the middle cerebral artery becomes dominant when compared to the territories supplied by the anterior and posterior cerebral arteries. Early arterial anastomoses appear around 16 weeks of gestation and increase in size with advancing age. The sites of anastomoses between the middle and anterior cerebral arteries move from the convexity of the brain towards the superior sagittal sinus. Anastomotic connections between the middle and posterior cerebral arteries shift towards the basal aspect of the brain.

By 32–34 weeks, marked involution of the ventricular zone (germinal matrix) has occurred and the cortex acquires its complex gyral pattern and an increased vascular supply. Ventricular zone capillaries are gradually remodelled to blend with the capillaries of the caudate nucleus. Heubner's artery eventually supplies only a small area at the medial aspect of the head of the caudate nucleus. In the cortex there is progressive elaboration of cortical blood vessels (Fig. 24.35) and towards the end of the third trimester the balance of cerebral circulation shifts from one which is central and basal nuclei-oriented, to one which predominantly serves the cortex and white matter. These changes in the pattern of cerebral circulation are of major significance in the pathogenesis and distribution of hypoxic/ischaemic lesions in the developing human brain. In a premature brain, the majority of ischaemic lesions occur in the boundary zone between the centripetal and centrifugal arteries, i.e. in the periventricular white matter, whereas in a full-term infant the cortical boundary zones and watershed areas between different arterial blood supplies are similar to those in adults and so presumably are the risks of ischaemic lesion.

Vessels of the ventricular zone (germinal matrix)

The germinal matrix (ventricular zone) is the end zone or border zone between the cerebral arteries and the collection zone of the deep cerebral veins. The germinal matrix is probably particularly prone to ischaemic injury in the immature infant because of its unusual vascular architecture. The subependymal veins (septal, choroidal, thalamostriate and posterior terminal) flow towards the interventricular foramen. There is a sudden change of flow at the level of the foramen, and the veins recurve at an acute angle to form the paired internal cerebral veins. The capillary channels in the germinal matrix open at right angles directly into the veins, and it has been postulated that these small vessels may be points of vascular rupture and the site of subependymal haemorrhage.

The capillary bed in the ventricular zone is supplied mainly by Heubner's artery and terminal branches of the lateral striate arteries from the middle cerebral artery. The highly cellular structure of the ventricular zone is a temporary feature, and the vascular supply to this area displays some primitive features: it has the capacity to remodel when the ventricular zone cells migrate and the remaining cells differentiate as ependyma towards the end of gestation.

Vessel density is relatively low in the ventricular zone, suggesting that this area may normally have a relatively low blood flow. Immature vessels, without a complex basal lamina or glial sheet, have been described up to 26 weeks' gestation in the zone: the endothelium of these vessels is apparently thinner than in the cortical vessels. In infants of less than 30 weeks' gestation, the vessels in the ventricular zone contain no smooth muscle, collagen or elastic fibres. Collagen and smooth muscle are seen in other regions after 30 weeks, but are not detected in the remains of the germinal matrix. The lack of these components could make the vessels in this zone vulnerable to changes in intraluminal pressure, and the lack of smooth muscle would preclude them from participating in autoregulatory processes. Cerebral vessels in premature infants lack elastic fibres and have a disproportionately small number of reticulin fibres. Comparison of the cortical and ventricular zone blood vessels shows that in infants of between 25 and 32 weeks' gestation the walls of vessels in the germinal matrix consist commonly of 1–2 endothelial cells with an occasional pericyte, and the capillary lumina are larger than those of the vessels in the cortex. In more mature infants the basal lamina surrounding germinal matrix vessels is thicker and more irregular when compared to cortical vessels.

Glial fibrillary acidic protein positive cells have been detected around blood vessels in the germinal matrix from 23 weeks' gestation. Glial cells may contribute to changes in the nature of endothelial intercellular junctions in brain capillaries.

VEINS

Cerebral veins

From 16 weeks onwards, cerebral veins can be identified. The superior, middle, inferior, anterior and posterior cerebral veins appear more tortuous than meningeal arteries. Veins draining the cortex, white matter and deeper structures are recognized in the midtrimester. Subcortical veins drain the deep white matter, deep cortical and subcortical superficial tissue: they terminate together with cortical veins which drain the cortex in the meningeal veins. The deep white matter and central nuclei are drained by longer veins which meet and join subependymal veins from the ventricular zone. Anastomoses between various groups of cortical veins can be recognized by 16 weeks' gestation. The inferior anastomotic vein (of Labbé), an anastomosis between the middle cerebral and inferior cerebral veins, becomes recognizable at 20 weeks, but the superior anastomotic vein (of Trolard), connecting the superior and middle cerebral veins, does not appear before the end of 30 weeks.

Rapid cortical development is correlated with the regression of the middle cerebral vein and its tributaries, and development of ascending and descending cortical veins and intraparenchymal (medullary) arteries and veins.

Cerebral venous drainage in a full-term baby is essentially composed of two principal venous arrays, the superficial veins and the deep Galenic venous system: anastomoses between these two systems persist into adult life.

Veins of the head

The earliest vessels form a transitory primordial hindbrain channel which drains into the precardinal vein. This is soon replaced by the primary head vein which runs caudally from the medial side of the trigeminal ganglion, lateral to the facial and vestibulocochlear nerves and otocyst, and then medial to the vagus nerve, to become continuous with the precardinal vein. An anastomosis to other more lateral venous channels developing over the hindbrain ultimately brings the primary head vein lateral to the vagus nerve. The cranial part of the precardinal vein forms the internal jugular vein.

The primary capillary plexus of the head is separated into three fairly distinct strata by the differentiation of the skull and meninges. The superficial vessels drain the skin and underlying soft parts, and eventually discharge in large part into the external jugular system, although they retain some connections with the deeper veins through so-called emissary veins. The next layer of vessels is the venous plexus of the dura mater, from which the dural venous sinuses differentiate: vessels from the plexus converge on each side into anterior, middle and posterior dural stems (Fig. 24.36). The anterior stem drains the prosencephalon and mesencephalon and enters the primary head vein rostral to the trigeminal ganglion. The middle stem drains the metencephalon and empties into the primary head vein caudal to the trigeminal ganglion, and the posterior stem drains the myelencephalon into the start of the precardinal vein. The deepest capillary stratum is the pial plexus from which the veins of the brain differentiate. It drains at the dorsolateral aspect of the neural tube into the adjacent dural venous plexus. The primary head vein also receives, at its cranial end, the primitive maxillary vein which drains the maxillary prominence and region of the optic vesicle.

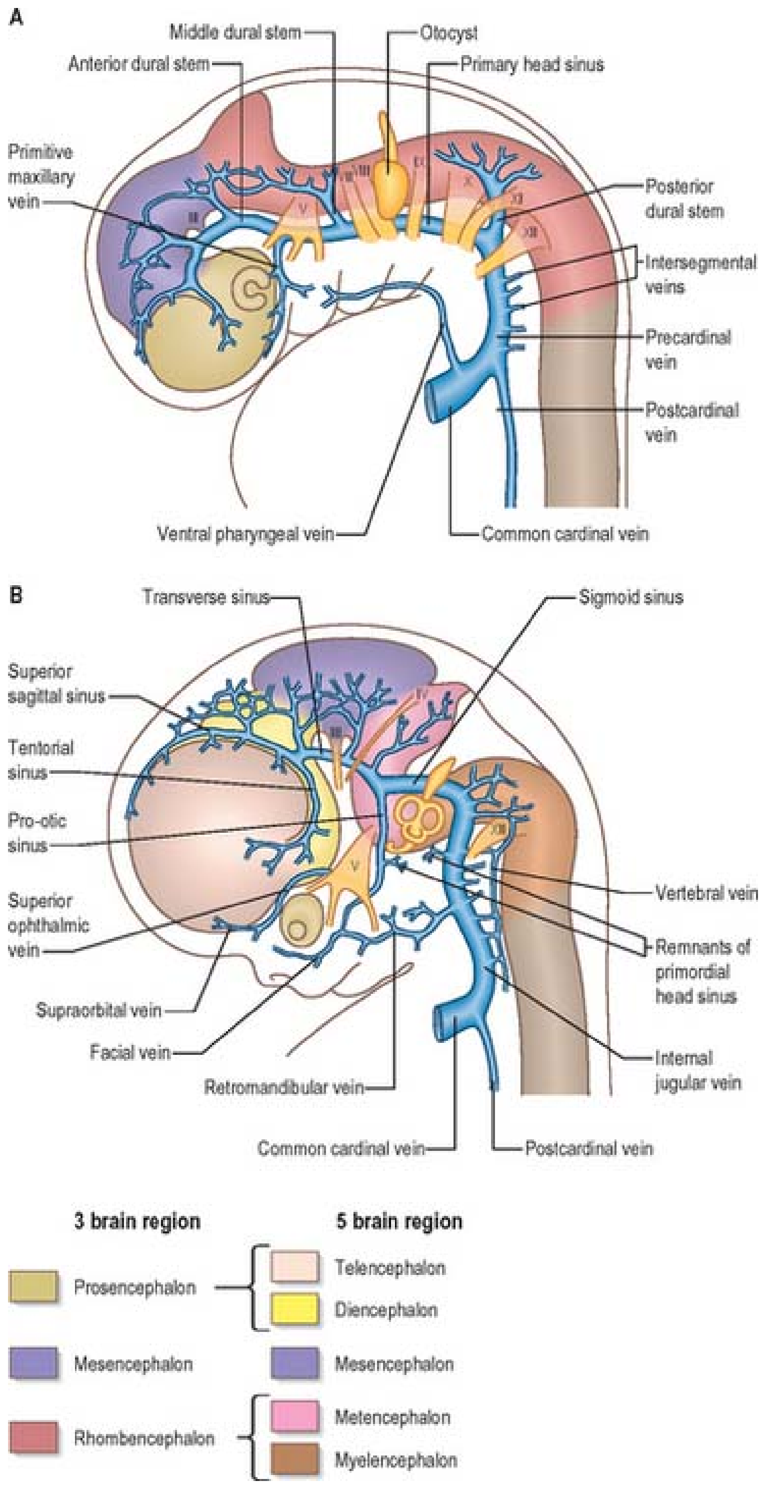
A
Middle dural stem
Otocyst
Anterior dural stem
Primary head sinus
Primitive maxillary vein
Posterior dural stem
Intersegmental veins
Precardinal vein
Postcardinal vein
Ventral pharyngeal vein
Common cardinal vein
B
Transverse sinus
Sigmoid sinus
Superior sagittal sinus
Tentorial sinus
Pro-otic sinus
Superior ophthalmic vein
Vertebral vein
Remnants of primordial head sinus
Supraorbital vein
Facial vein
Retromandibular vein
Internal jugular vein
Common cardinal vein
Postcardinal vein
3 brain region
5 brain region
Prosencephalon
Telencephalon
Diencephalon
Mesencephalon
Mesencephalon
Rhombencephalon
Metencephalon
Myelencephalon

Fig. 24.36 Successive stages in the development of the veins of the head and neck. **A**, At approximately 8 mm CR length; **B**, at approximately 24 mm CR length.

The vessels of the dural plexus undergo profound changes, largely accommodating the growth of the cartilaginous otic capsule of the membranous labyrinth and the expansion of the cerebral hemispheres. As the otic capsule grows, the primary head vein is gradually reduced and a new channel joining anterior, middle and posterior dural stems appears dorsal to the cranial nerve ganglia and the capsule. The adult sigmoid sinus is formed where this channel joins the middle and posterior stems, together with the posterior dural stem itself (Fig. 24.36B).

A curtain of capillary veins, the sagittal plexus, forms between the growing cerebral hemispheres and along the dorsal margins of the anterior and middle plexuses, in the position of the future falx cerebri. Rostrodorsally this plexus forms the superior sagittal sinus. It is continuous behind with the anastomosis between the anterior and middle dural stems, which forms most of the transverse sinus. Ventrally the sagittal plexus differentiates into the inferior sagittal and straight sinuses and the great cerebral vein: it commonly drains into the left transverse sinus.

The vessels along the ventrolateral edge of the developing cerebral hemisphere form the transitory tentorial sinus, which drains the convex surface of the cerebral hemisphere and basal ganglia, and the ventral aspect of the diencephalon, into the transverse sinus. With expansions of the cerebral hemispheres, and in particular the emergence of the temporal lobe, the tentorial sinus becomes elongated, attenuated and eventually disappears; its territory is drained by enlarging anastomoses of pial vessels which become the basal veins, radicles of the great cerebral vein.

The anterior dural stem disappears and the caudal part of the primary head vein dwindles: it is represented in the adult by the inferior petrosal sinus. The cranial part of the primary head vein, medial to the trigeminal ganglion, persists and still receives the stem of the primitive maxillary vein. The latter has now lost most of its tributaries to the anterior facial vein, and its stem becomes the main trunk of the primitive supraorbital vein, which will form the superior ophthalmic vein of the adult. The main venous drainage of the orbit and its contents is now carried via the augmented middle dural stem, the pro-otic sinus, into the transverse sinus and, at a later stage, into the cavernous sinus. The cavernous sinus is formed from a secondary plexus derived from the primary head vein and lying between the otic and basioccipital cartilages. The plexus forms the inferior petrosal sinus which drains through the primordial hindbrain channel into the internal jugular vein. The superior petrosal sinus arises later from a ventral metencephalic tributary of the pro-otic sinus and it communicates secondarily with the cavernous sinus. The pro-otic sinus meanwhile has developed a new and more caudally situated stem, the petrosquamosal sinus, which drains into the sigmoid sinus. With progressive ossification of the skull, the pro-otic sinus becomes diploic in position.

The development of the venous drainage and portal system of the hypophysis cerebri is closely associated with that of the venous sinuses.

REFERENCES

len MC, Capute AJ. Tone and reflex development before term. *J Pediatrics*. 1990;85:393-399.

Provides details of the development of reflexes in extremely premature infants..

gbie J, Graham A. The ectodermal placodes: a dysfunctional family. *Phil Trans R Soc Lond B Biol Sci*. 2001;356:1655-1660.

Challenges the view of ectodermal placodes as a coherent group and discusses their early development, induction and evolution..

own M, Keynes R, Lumsden A. The Developing Brain. Oxford: Oxford University Press, 2001.

Covers the main mechanisms of neural development from neurulation to synaptic reorganization..

stron I, Blakemore C, Rakic P. Development of the human cerebral cortex: Boulder Committee revisited. *Nat Rev Neurosci*. 2008;9:110-122.

Reviews current data on the development of the human cerebral cortex and updates the classical model..

noghue MJ, Rakic P. Molecular gradients and compartments in the embryonic primate cerebral cortex. *Cereb Cortex*. 1999;9:586-600.

Presents evidence for the existence of an intrinsic protomap which predicts the functional map of the mature cerebral cortex..

ordon-Weeks PR. Neuronal Growth Cones. Cambridge: Cambridge University Press, 2000.

iegstein AR, Gotz M. *Radial glia diversity: a matter of cell fate Glia*. 2003;43(1):37-43.

iegstein AR, Noctor SC. Patterns of neuronal migration in the embryonic cortex. *Trends Neurosci*. 2004;27(7):392-399.

umlauf R, Marshall H, Studer M, Nonchev S, Sham MH, Lumsden A. Hox homeobox genes and regionalisation of the nervous system. *J Neurobiol*. 1993;24:1328-1340.

Discusses the influence of the Hox family of homeobox-containing genes on the patterning of rhombomeres and neural crest..

vezzi AM, Ottavianni G, Terni L, Matturri L. Histological and biological developmental characterization of the human cerebellar cortex. *Int J Dev Neurosci*. 2006;24:365-371.

etin C, Baudoin JP, Rakic S, Parnavelas JG. Cell and molecular mechanisms involved in the migration of cortical interneurones. *Eur J Neurosci*. 2006;23(4):894-900.

üller F, O’Rahilly R. The timing and sequence of appearance of neuromeres and their derivatives in staged human embryos. *Acta Anat (Basel)*. 1997;158:83-99.

octor SC, Martinez-Cerdeno V, Ivic L, Kriegstein AR. Cortical neurones arise in symmetric and asymmetric division zones and migrate through specific phases. *Nat Neurosci*. 2004;7(2):136-144.

pperman LA, Sweeney TM, Redmon J, Persing JA, Ogle RC. Tissue interactions with underlying dura mater inhibit osseous obliteration of developing cranial sutures. *Dev Dynam*. 1993;198:312-322.

Examines the role of the dura mater in the development of the skull bones and sutures..

Rahilly R, Müller F. The meninges in human development. *J Neuropath Exp Neurol*. 1986;45:588-608.

Rahilly R, Müller F. The Embryonic Human Brain. An Atlas of Developmental Stages. 2nd edition.. Chichester: Wiley-Liss; 1999.

Rahilly R, Müller F. The two sites of fusion of the neural folds and the two neuropores in the human embryo. *Teratology*. 2002;65:162-170.

Rahilly R, Müller F. The primitive streak, the caudal eminence and related structures in staged human embryos. *Cells Tissues Organs*. 2004;117:2-20.

Rourke NA, Sullivan DP, Kaznowski CE, Jacobs AA, McConnell SK. Tangential migration of neurones in the developing cerebral cortex. *Development*. 1995;121:2165-2176.

kic P. Specification of cerebral cortical areas. *Science*. 1988;241:170-176.

Discusses the radial unit hypothesis as a framework for exploring cerebral evolution and the causes of some cortical disorders in humans..

kic P. Developmental and evolutionary adaptations of cortical radial glia. *Cereb Cortex*. 2003;13:541-549.

Discusses cortical development and evolution and the pathogenesis of some genetic and acquired cortical anomalies..

e Boulder Committee. Embryonic vertebrate central nervous system: revised terminology. *Anat Rec*. 1970;166(2):257-261.

orm EE, Garel S, Borello U, Hebert JM, Martinez S, McConnell SK, Martin GR, Rubenstein JL. Dose-dependent functions of Fgf8 in regulating telencephalic patterning centers. *Development*. 2006;133(9):1831-1844.

lpe JJ. Neurobiology of periventricular leukomalacia in the premature infant. *Pediatr Res*. 2001;50:553-562.

n Melchner L, Pallas SL, Sur M. Visual behaviour mediated by retinal projections directed to the auditory pathway. *Nature*. 2000;404:820-821.

Describes the consequences of successful routing of visual projections into non-visual structures in the brain..

ithington S, Beddington R, Cooke J. Foregut endoderm is required at head process stage for anteriormost neural patterning in chick. *Development*. 2001;128:309-320.

Presents evidence for an early system of neuroepithelial patterning by the most rostral endoderm, the region of the prechordal plate..

onders CP, Anderson SA. The origin and specification of cortical interneurones. *Nat Rev Neurosci*. 2006;7(9):687-696.

Section 4
HEAD AND NECK

CHAPTER 25

Head and neck: overview and surface anatomy

This chapter contains an overview of the topographical anatomy of the head and neck described in detail in Chapters 26–34 Chapter 27 Chapter 28 Chapter 29 Chapter 30 Chapter 31 Chapter 32 Chapter 33 Chapter 34, and an account of the clinically relevant surface anatomy.

SKIN AND FASCIA

FACE AND SCALP

The superficial fascia of the scalp is firm, dense and fibroadipose, and closely adherent to the skin and to the underlying muscle, epicranius, and the epicranial aponeurosis. Posteriorly, the fascia is continuous with the superficial fascia of the back of the neck, and laterally it is prolonged into the temporal region, where it is looser in texture. Three fascial layers (a subcutaneous fibroadipose tissue, a superficial musculo-aponeurotic system, SMAS, and the parotid–masseteric fascia), are recognized on the face superficial to the plane of the facial nerve and its branches. On the lateral side of the head, above the zygomatic arch, the temporo-parietal fascia lies in the same plane as, but does not blend with, the SMAS. It is superficial to the temporal fascia and blends superiorly with the epicranial aponeurosis. The parotid gland is surrounded by a fibrous capsule derived from the deep cervical fascia.

NECK

The superficial cervical fascia contains a variable amount of adipose tissue and platysma. The deep cervical fascia is conventionally subdivided into three sheets (investing, pretracheal and prevertebral layers) that surround the muscles and viscera of the neck to varying degrees, and the carotid sheath, a condensation of deep fascia around the common and internal carotid arteries, internal jugular vein, vagus and ansa cervicalis (see Ch. 28). The fascial layers of the neck define a number of potential tissue ‘spaces’ above and below the hyoid bone. In health, the tissues within these spaces are either closely applied to each other or are filled with relatively loose connective tissue. However, they offer potential routes by which unchecked infection may spread within the head and neck, and between the tissue spaces of the face and the mediastinum. They also offer convenient planes for intraoperative dissection during surgery.

BONES AND JOINTS

SKULL AND MANDIBLE

The skull is composed of 28 separate bones, most of them paired (Ch. 26). It can be divided into a robust calvarium that surrounds and protects the brain, and a delicate facial skeleton composed mainly of thin-walled bones, some of which contain air-filled cavities known collectively as the paranasal sinuses. The cranial cavity contains the brain and the intracranial portions of the cranial and spinal nerves; the blood vessels that supply and drain the brain and the haemopoietic marrow of the overlying bones; the meninges (dura, arachnoid and pia mater) and the cerebrospinal fluid (Ch. 27). The cavity is incompletely divided by dural partitions, notably the falx cerebri, lying between the cerebral hemispheres, and the tentorium cerebelli, lying between the cerebellum and occipital lobes. Almost all of the venous blood from the brain and cranial bones drains via sinuses lying between the endosteal and meningeal layers of the dura mater into the internal jugular vein (Ch. 27). Internally, the cranial base is divided into anterior, middle and posterior cranial fossae, which contain the frontal and temporal lobes of the cerebral hemispheres and the cerebellum respectively. Foramina in the bones of the skull base and facial skeleton transmit neurovascular bundles which may be compromised at these sites by pathology or trauma.

The skull provides attachments for numerous muscles. The craniofacial muscles arise from the bones of the facial skeleton, whereas the extrinsic muscles of the tongue, the muscles that act on the temporomandibular joint, the superior constrictor of the pharynx and the muscles of the soft palate all arise from sites on the cranial base. Movements of the mandible, which typically occur during mastication and articulation, take place at the temporomandibular joints (see Ch. 31). Movements of the skull on the cervical vertebrae occur at the atlanto-occipital joints (see Ch. 42).

CERVICAL VERTEBRAE

There are seven cervical vertebrae (see Ch. 42). They are the smallest of the movable vertebrae, and are characterized by a foramen in each transverse process, the foramen transversarium, and a disproportionately large vertebral canal. The first (atlas), second (axis) and seventh (vertebra prominens) cervical vertebrae are atypical.

HYOID BONE AND LARYNGEAL CARTILAGES

The hyoid bone (see Ch. 28) lies in the midline at the front of the neck at the level of the third cervical vertebra. It is suspended from the styloid processes by the stylohyoid ligaments and gives attachment to the supra- and infrahyoid groups of muscles. The skeletal framework of the larynx is formed by a series of cartilages interconnected by ligaments and fibrous membranes, and moved by a number of muscles (Ch. 34). The laryngeal cartilages are the single cricoid, thyroid and epiglottic cartilages, and the paired arytenoid, cuneiform, corniculate and tritiate cartilages.

MUSCLES

The striated muscles of the head and neck produce the movements of the facial soft tissues that animate so many aspects of communication (Ch. 29); the movements at the temporomandibular joint that occur during mastication and speech (Ch. 31); the conjugate movements of the eyeballs (Ch. 39); and the co-ordinated movements that occur during activities such as swallowing, speaking and turning the head in response to visual and/or auditory stimuli. The ‘extrinsic’ muscles that run between the axial skeleton and upper limb act on the scapula and humerus (Ch. 46).

Smooth muscle occurs in the superior tarsal muscle, the sphincter and dilator pupillae and the ciliary muscle (Chs 39 and 40).

VASCULAR SUPPLY AND LYMPHATIC DRAINAGE

ARTERIAL SUPPLY

The main arterial supply of the head and neck is derived from branches of the carotid and subclavian arteries (Figs 25.1, 25.2). Branches of the internal carotid and vertebral arteries anastomose in the circle of Willis within the interpeduncular cistern on the ventral aspect of the brain (see Ch. 17).

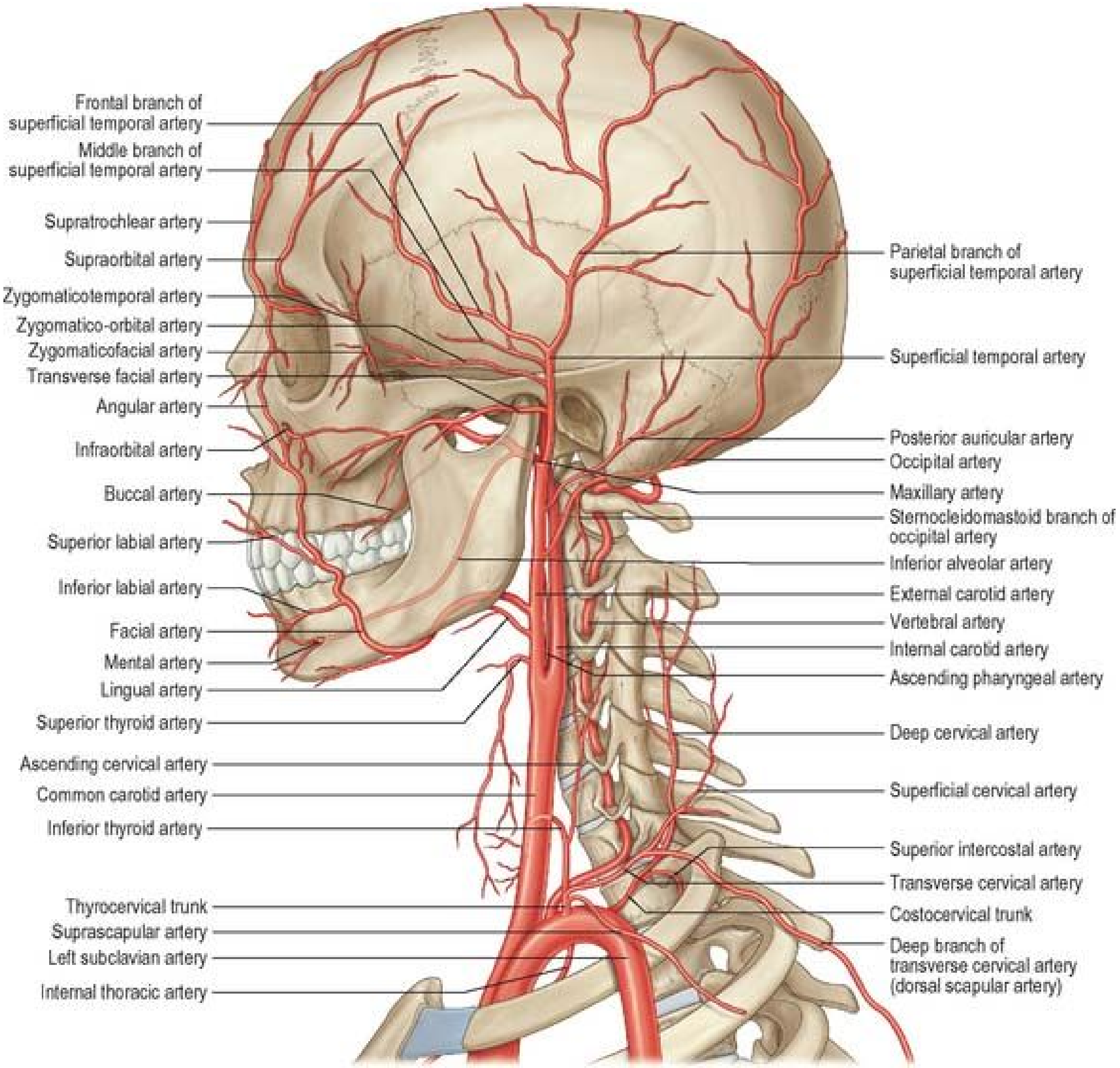
Frontal branch of superficial temporal artery
Middle branch of superficial temporal artery
Supratrochlear artery
Supraorbital artery
Zygomaticotemporal artery
Zygomatico-orbital artery
Zygomaticofacial artery
Transverse facial artery
Angular artery
Infraorbital artery
Buccal artery
Superior labial artery
Inferior labial artery
Facial artery
Mental artery
Lingual artery
Superior thyroid artery
Ascending cervical artery
Common carotid artery
Inferior thyroid artery
Thyrocervical trunk
Suprascapular artery
Left subclavian artery
Internal thoracic artery
Parietal branch of superficial temporal artery
Superficial temporal artery
Posterior auricular artery
Occipital artery
Maxillary artery
Sternocleidomastoid branch of occipital artery
Inferior alveolar artery
External carotid artery
Vertebral artery
Internal carotid artery
Ascending pharyngeal artery
Deep cervical artery
Superficial cervical artery
Superior intercostal artery
Transverse cervical artery
Costocervical trunk
Deep branch of transverse cervical artery (dorsal scapular artery)

Fig. 25.1 Overview of the superficial arteries of the head and neck.

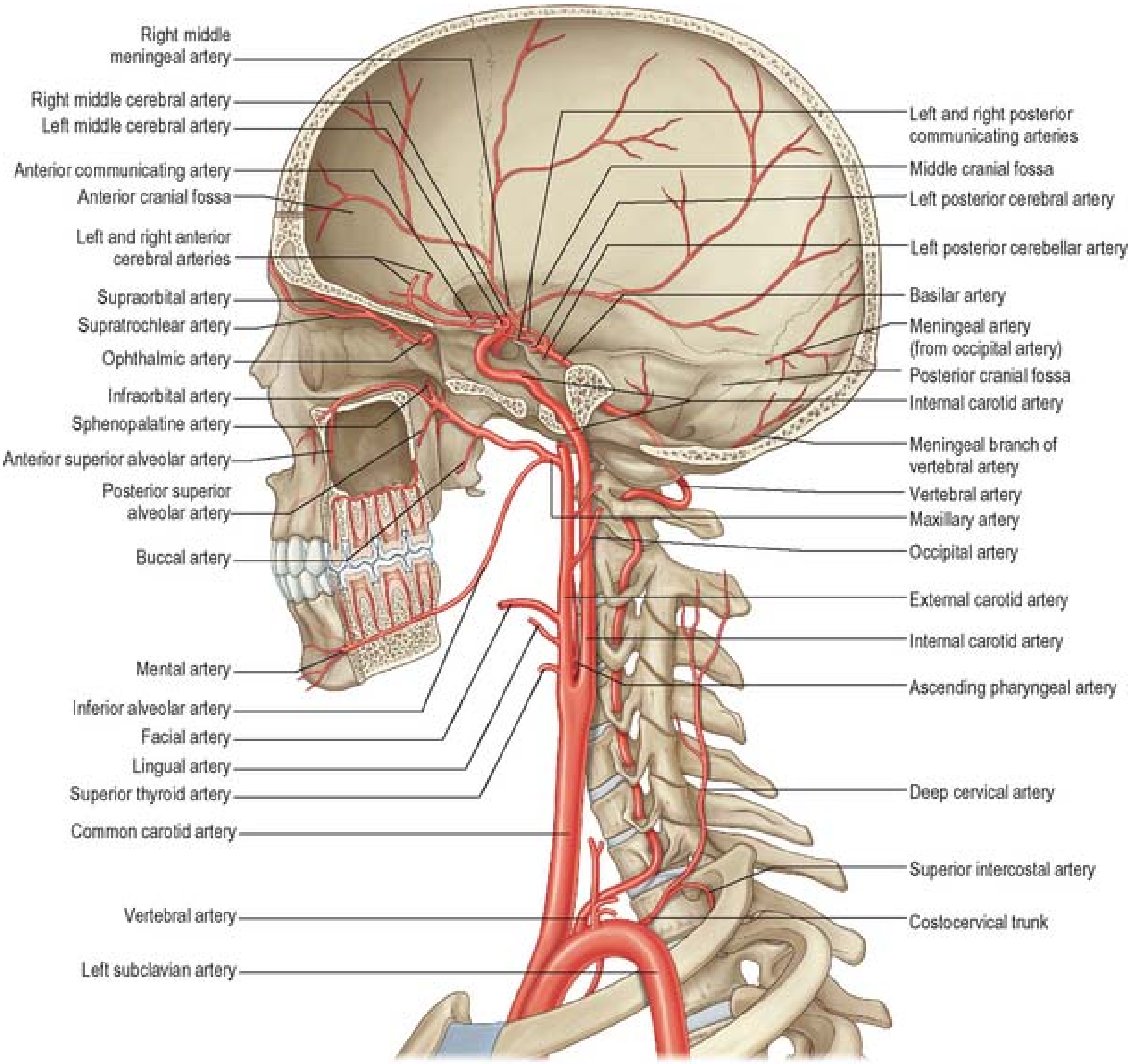
Right middle meningeal artery
Right middle cerebral artery
Left middle cerebral artery
Anterior communicating artery
Anterior cranial fossa
Left and right anterior cerebral arteries
Supraorbital artery
Supratrochlear artery
Ophthalmic artery
Infraorbital artery
Sphenopalatine artery
Anterior superior alveolar artery
Posterior superior alveolar artery
Buccal artery
Mental artery
Inferior alveolar artery
Facial artery
Lingual artery
Superior thyroid artery
Common carotid artery
Vertebral artery
Left subclavian artery
Left and right posterior communicating arteries
Middle cranial fossa
Left posterior cerebral artery
Left posterior cerebellar artery
Basilar artery
Meningeal artery (from occipital artery)
Posterior cranial fossa
Internal carotid artery
Meningeal branch of vertebral artery
Vertebral artery
Maxillary artery
Occipital artery
External carotid artery
Internal carotid artery
Ascending pharyngeal artery
Deep cervical artery
Superior intercostal artery
Costocervical trunk

Fig. 25.2 Overview of the deep arteries of the head and neck.

Carotid system

The cervical portion of the common carotid artery is similar on both sides. Each lies within the carotid sheath of deep cervical fascia, together with the internal jugular vein and vagus nerve. In the lower part of the neck the arteries are separated by a narrow gap which contains the trachea, and higher up they are separated by the thyroid gland, larynx and pharynx. At the level of the upper border of the thyroid cartilage (C4), the common carotid artery bifurcates into external and internal carotid arteries (see below). The external carotid artery passes upwards on either side of the neck, inclined at first slightly forwards and then backwards and a little laterally. It usually gives off the ascending pharyngeal, superior thyroid, lingual, facial, occipital and posterior auricular arteries, and then enters the parotid salivary gland where it divides into its terminal branches, the superficial temporal and maxillary arteries. The branches of the external carotid artery supply the face, scalp, tongue, upper and lower teeth and gingivae, palatine tonsil, paranasal sinuses and nasopharyngeal tube, external and middle ears, pharynx, larynx and superior pole of the thyroid gland. They also anastomose with branches of the internal carotid arteries on the scalp, forehead and face, and in the orbit, nasopharynx and nasal cavity, and with branches of the subclavian artery in the pharynx, larynx and thyroid glands.

The internal carotid artery supplies most of the ipsilateral cerebral hemisphere, eye and accessory organs, forehead and, in part, the external nose, nasal cavity and paranasal sinuses. It passes up the neck anterior to the transverse processes of the upper three cervical vertebrae and enters the cranial cavity via the carotid canal in the petrous part of the temporal bone. The artery has no branches in the neck and so is easily distinguishable from the external carotid artery, should the latter require ligation, e.g. to control haemorrhage from a penetrating injury to the neck.

Subclavian artery

The subclavian arteries give off several branches that supply structures in the head and neck. The vertebral arteries supply the upper spinal cord, brain stem, cerebellum and occipital lobe of the cerebrum. They pass through the foramena transversaria of the first six cervical vertebrae, enter the cranial cavity through the foramen magnum and unite at the lower border of the pons to form the basilar artery (hence this system is often called the vertebrobasilar system). Branches from the thyrocervical trunk supply the inferior poles of the thyroid gland and the parathyroid glands, the larynx and pharynx, and branches from the costocervical trunks supply deep cervical muscles.

VENOUS DRAINAGE

Veins of the neck lie superficial or deep to the deep investing fascia. Superficial veins ultimately drain into either the external, anterior or posterior external jugular veins, and drain a much smaller volume of tissue than the deep veins. Deep veins tend to drain into either the internal jugular vein or the subclavian vein. The internal jugular vein drains blood from the skull, brain, superficial face and much of the neck. It descends in the neck within the carotid sheath and unites with the subclavian vein behind the sternal end of the clavicle to form the brachiocephalic vein (Figs 25.3, 25.4). At its junction with the internal jugular vein, the left subclavian vein usually receives the thoracic duct and the right subclavian vein receives the right lymphatic duct.

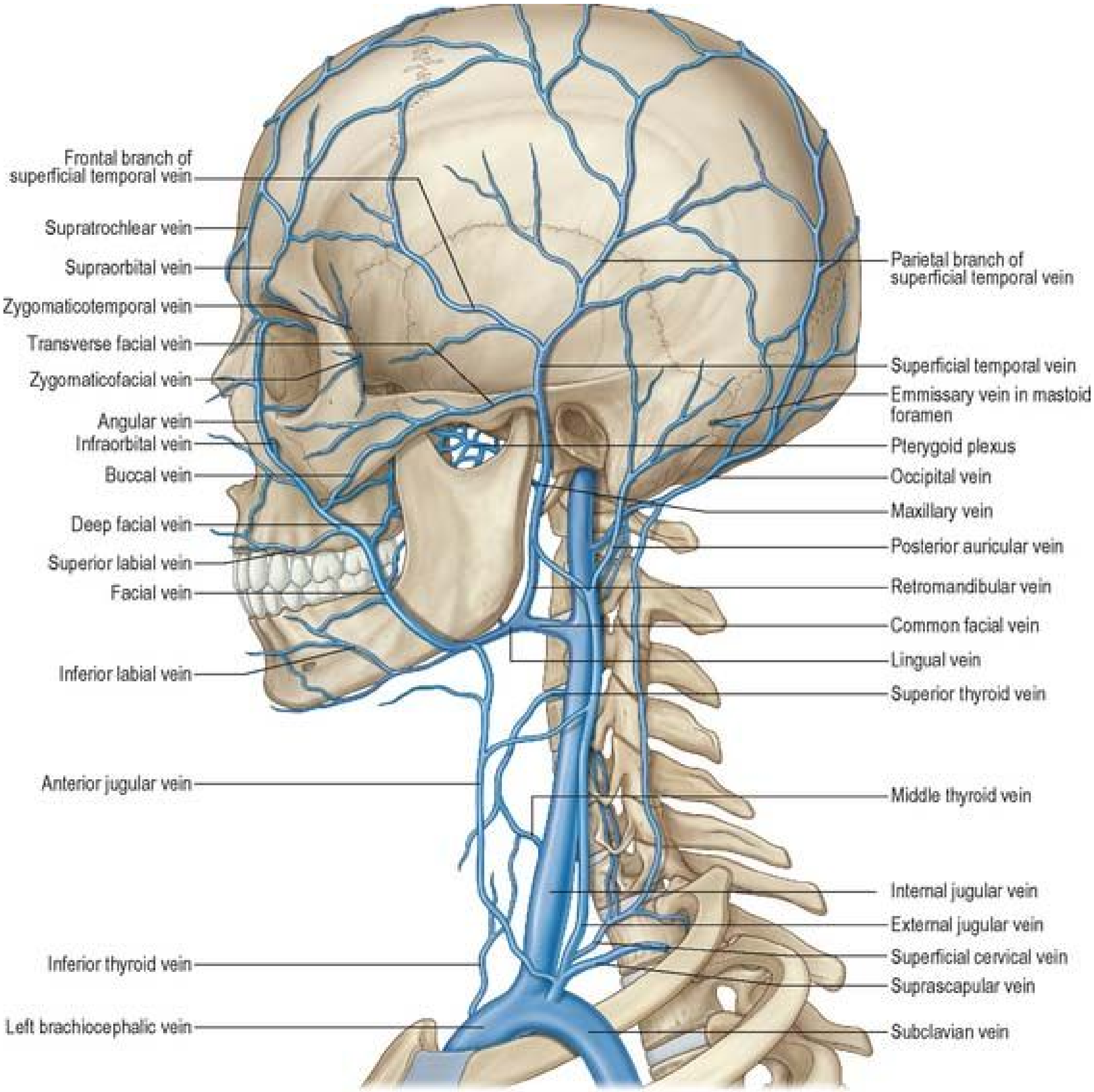
Frontal branch of superficial temporal vein
Supratrochlear vein
Supraorbital vein
Zygomaticotemporal vein
Transverse facial vein
Zygomaticofacial vein
Angular vein
Infraorbital vein
Buccal vein
Deep facial vein
Superior labial vein
Facial vein
Inferior labial vein
Anterior jugular vein
Inferior thyroid vein
Left brachiocephalic vein
Parietal branch of superficial temporal vein
Superficial temporal vein
Emmissary vein in mastoid foramen
Pterygoid plexus
Occipital vein
Maxillary vein
Posterior auricular vein
Retromandibular vein
Common facial vein
Lingual vein
Superior thyroid vein
Middle thyroid vein
Internal jugular vein
External jugular vein
Superficial cervical vein
Suprascapular vein
Subclavian vein

Fig. 25.3 Overview of the superficial veins of the head and neck.

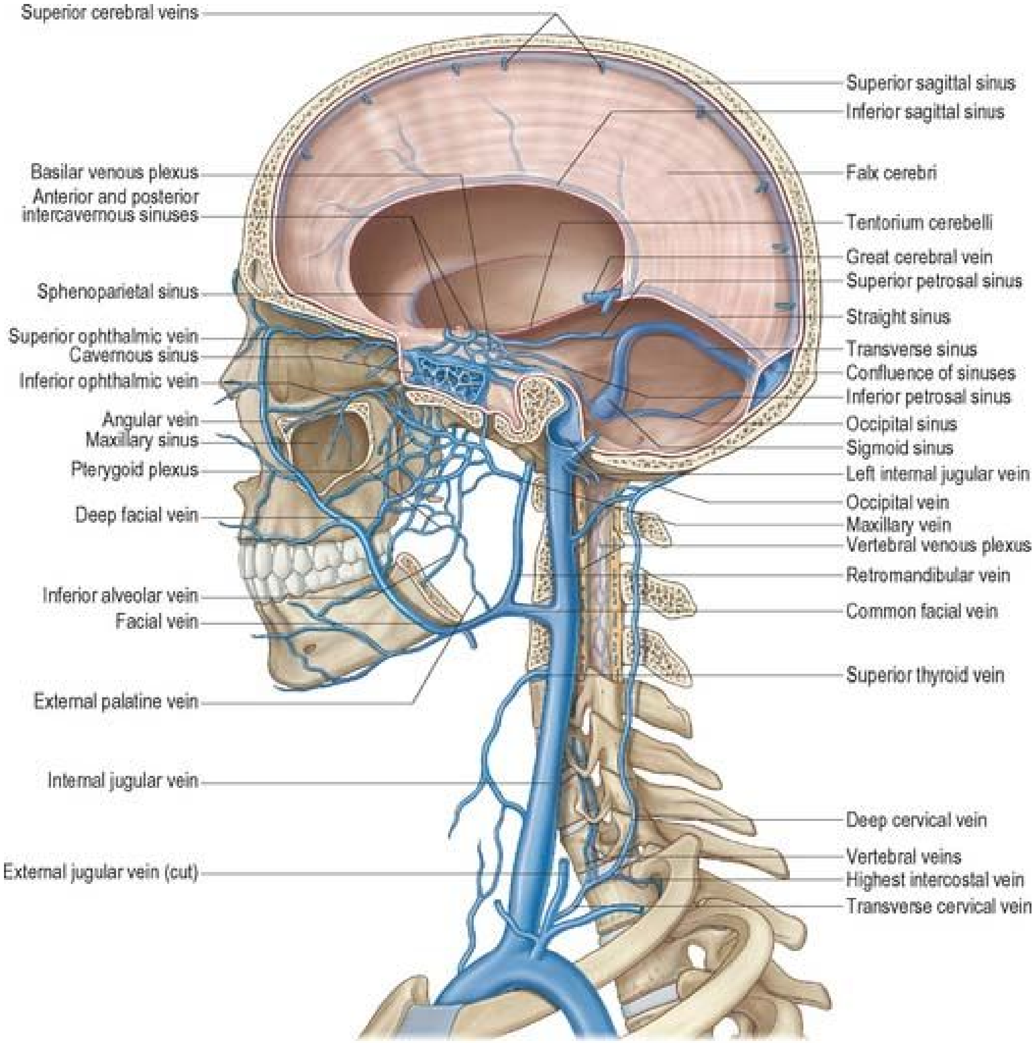
Superior cerebral veins
Superior sagittal sinus
Inferior sagittal sinus
Falx cerebri
Basilar venous plexus
Anterior and posterior intercavernous sinuses
Tentorium cerebelli
Great cerebral vein
Superior petrosal sinus
Sphenoparietal sinus
Straight sinus
Superior ophthalmic vein
Cavernous sinus
Transverse sinus
Confluence of sinuses
Inferior ophthalmic vein
Inferior petrosal sinus
Angular vein
Occipital sinus
Maxillary sinus
Sigmoid sinus
Pterygoid plexus
Left internal jugular vein
Occipital vein
Deep facial vein
Maxillary vein
Vertebral venous plexus
Retromandibular vein
Inferior alveolar vein
Facial vein
Common facial vein
Superior thyroid vein
External palatine vein
Internal jugular vein
Deep cervical vein
Vertebral veins
External jugular vein (cut)
Highest intercostal vein
Transverse cervical vein

Fig. 25.4 Overview of the deep veins of the head and neck.

LYMPHATIC DRAINAGE

Lymph nodes in the head and neck are arranged in two horizontal rings and two vertical chains on either side of the neck (Fig. 25.5). The outer, superficial, ring consists of the occipital, preauricular (parotid), submandibular and submental nodes, and the inner, deep, ring is formed by clumps of mucosa associated lymphoid tissue (MALT) located primarily in the naso- and oro-pharynx (Waldeyer's ring). The vertical chain consists of superior and inferior groups of nodes related to the carotid sheath. All lymph vessels of the head and neck drain into the deep cervical nodes, either directly from the tissues or indirectly via nodes in outlying groups. Lymph is returned to the systemic venous circulation via either the right lymphatic duct or the thoracic duct.

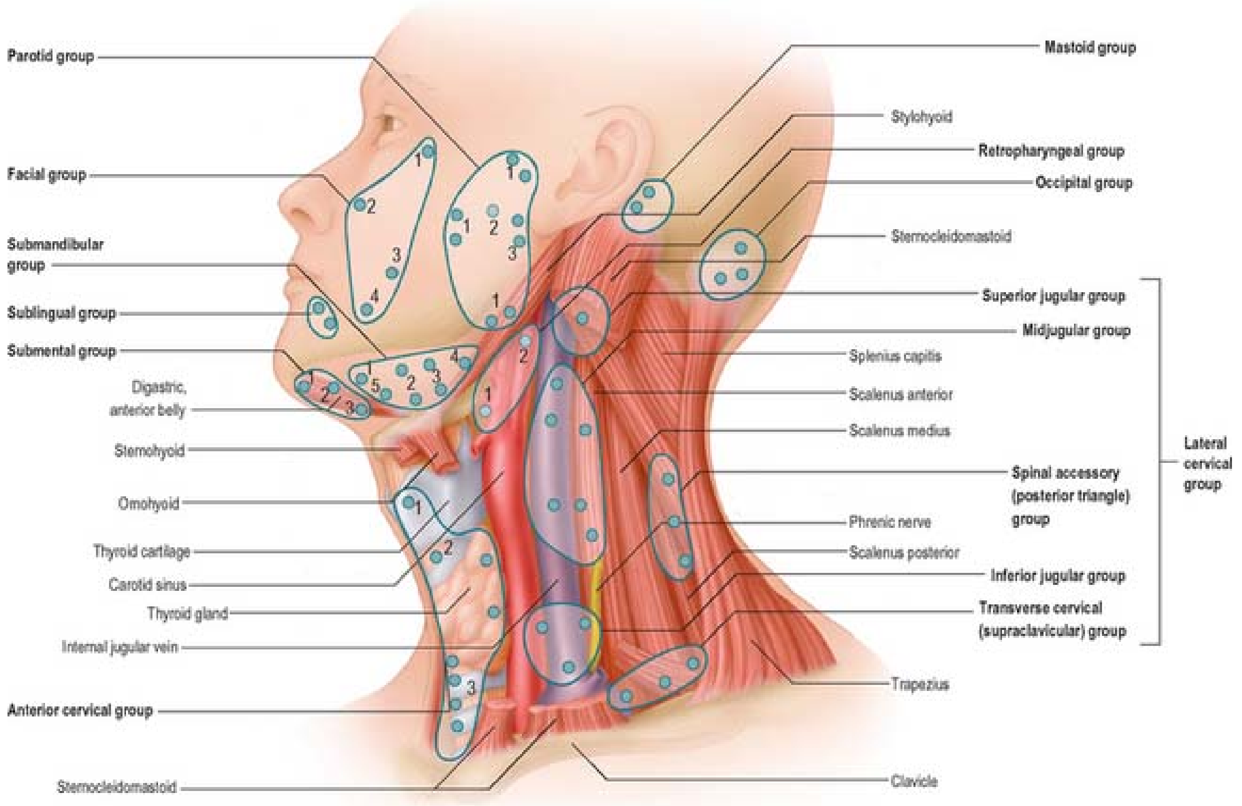
Parotid group
Facial group
Submandibular group
Sublingual group
Submental group
Digastric, anterior belly
Sternohyoid
Omohyoid
Thyroid cartilage
Carotid sinus
Thyroid gland
Internal jugular vein
Anterior cervical group
Sternocleidomastoid
Mastoid group
Stylohyoid
Retropharyngeal group
Occipital group
Sternocleidomastoid
Superior jugular group
Midjugular group
Splenius capitis
Scalenus anterior
Scalenus medius
Spinal accessory (posterior triangle) group
Phrenic nerve
Scalenus posterior
Inferior jugular group
Transverse cervical (supraclavicular) group
Lateral cervical group
Trapezius
Clavicle
1
2
3
4
1
2
3
1
1
2
3
4
5
1
2
3
1
2
1
2
1
2
3

Facial group	1. Malar 2. Infraorbital 3. Buccinator 4. Inferior maxillary	**Submandibular group**	1. Preglandular 2. Prevascular 3. Retrovascular 4. Retroglandular 5. Intracapsular	**Retropharyngeal group**	1. Lateral 2. Medial
Parotid group	1. Subfacial, extraglandular 2. Deep intraglandular 3. Suprafacial	**Submental group**	1. Anterior 2. Middle 3. Posterior	**Anterior cervical group**	1. Superficial anterior jugular chain 2. Prelaryngeal 3. Pretracheal

Fig. 25.5 Overview of the lymph nodes of the head and neck.

INNERVATION

CRANIAL NERVES

There are 12 pairs of cranial nerves. They are individually named and numbered (using Roman numerals) in a rostrocaudal sequence (see **Table 15.1**). Some are functionally mixed, others are either purely motor or purely sensory, and some also carry pre- or post-ganglionic parasympathetic fibres that are secretomotor to the salivary and lacrimal glands or motor to some of the smooth muscle within the eyeball. Branches of the oculomotor, trochlear, trigeminal, abducens, facial, glossopharyngeal, vagus, accessory and hypoglossal nerves supply muscle groups within the eyeball, face, pharynx, larynx and tongue. Branches of the trigeminal, glossopharyngeal and vagus nerves transmit general sensory information from the skin of the face and part of the scalp; the epithelium lining the oral and nasal cavities, the paranasal sinuses, middle ear, pharynx and larynx, and the dorsal surface of the tongue and the cornea; the intracranial meninges; the periosteum and bones of the skull. Branches of the trigeminal nerve innervate the temporomandibular joint. The olfactory, optic, trigeminal, facial, vestibulocochlear and vagus contain axons that transmit the special sensations of olfaction, vision, hearing, balance, and taste. The olfactory nerve is the only sensory cranial nerve that projects directly to the cerebral cortex rather than indirectly via the thalamus. The optic nerve terminates in the thalamus. The other ten pairs of cranial nerves are attached to the brainstem; their component fibres arise from or terminate in named cranial nerve nuclei (Ch. 19). The cranial nerves pass through named foramina in the skull, often with named vessels.

With one exception, all of the cranial nerves are confined to the head and neck. The exception is the vagus, which travels through the neck and thorax and enters the abdominal cavity by passing through the diaphragm with the oesophagus.

Reflexes

A number of reflexes involving structures in the head and neck are mediated by sensory and motor branches of certain of the cranial nerves, co-ordinated via appropriate nuclei in the brain stem. They include swallowing, gagging, retching and vomiting (Fig. 19.12); sneezing and coughing (Fig. 19.13); lacrimation (Fig. 39.25); jaw jerk (Fig. 19.17); visual reflexes (pupillary light reflex and accommodation) (see Ch. 40); corneal ‘blink’ reflex (Fig. 19.15); stapedial reflex (see p. 628, Ch. 36). Reflexes that involve energetic exhalation, e.g. sneezing and coughing, also involve the recruitment of cervical and thoracic spinal neurones to mediate the co-ordinated contraction of intercostal and abdominal wall muscles this activity requires.

SPINAL NERVES

There are eight pairs of cervical spinal nerves (Fig. 25.6). Cutaneous branches of the dorsal rami of the second, third, fourth and fifth cervical nerves innervate the scalp and the skin over the back of the neck, and motor branches of all of the cervical dorsal rami supply cervical postvertebral muscles. All of the cervical ventral rami supply anterior and lateral groups of prevertebral muscles. The upper four cervical ventral rami form the cervical plexus whose branches collectively innervate the infrahyoid strap muscles and the diaphragm, and the skin covering the lateral and anterior parts of the neck, and the angle of the mandible. The lower four cervical ventral rami, together with most of the first thoracic ventral ramus, form the brachial plexus.

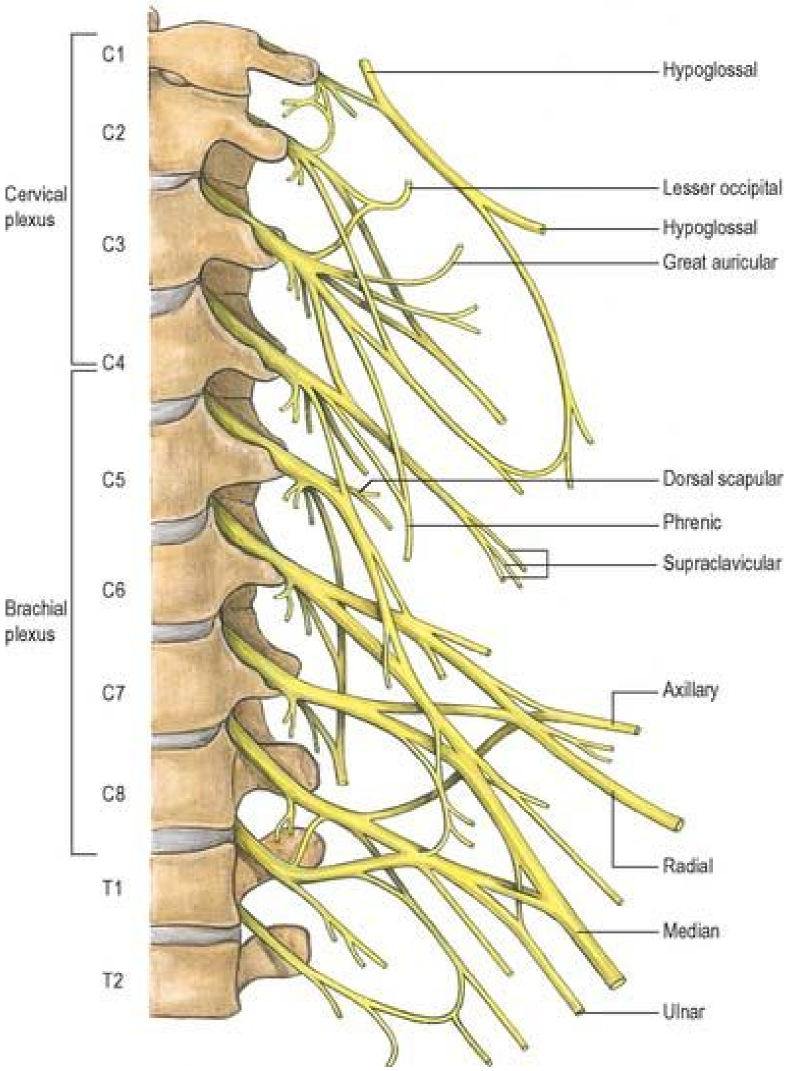
C1
C2
Cervical plexus
C3
C4
C5
Brachial plexus
C6
C7
C8
T1
T2
Hypoglossal
Lesser occipital
Hypoglossal
Great auricular
Dorsal scapular
Phrenic
Supraclavicular
Axillary
Radial
Median
Ulnar

Fig. 25.6 Overview of the nerves forming the cervical and brachial plexuses.

(From Sobotta 2006.)

PARASYMPATHETIC NERVES

In the head and neck, the parasympathetic system innervates the salivary and lacrimal glands, the mucous glands of the oral and nasal cavities and the sphincter pupillae and ciliary muscles in the eyeball. Many thousands of preganglionic parasympathetic axons travel in the vagus nerve from the vagal nucleus (dorsal motor nucleus of the vagus) in the medulla. Although they travel through the neck in the right and left vagi, they are destined for pulmonary, cardiac, oesophageal, gastric and intestinal targets: they synapse in minute ganglia in the walls of the viscera and do not innervate structures in the head and neck.

There are four pairs of parasympathetic ganglia in the head, named ciliary, pterygopalatine, otic and submandibular (Fig. 25.7).

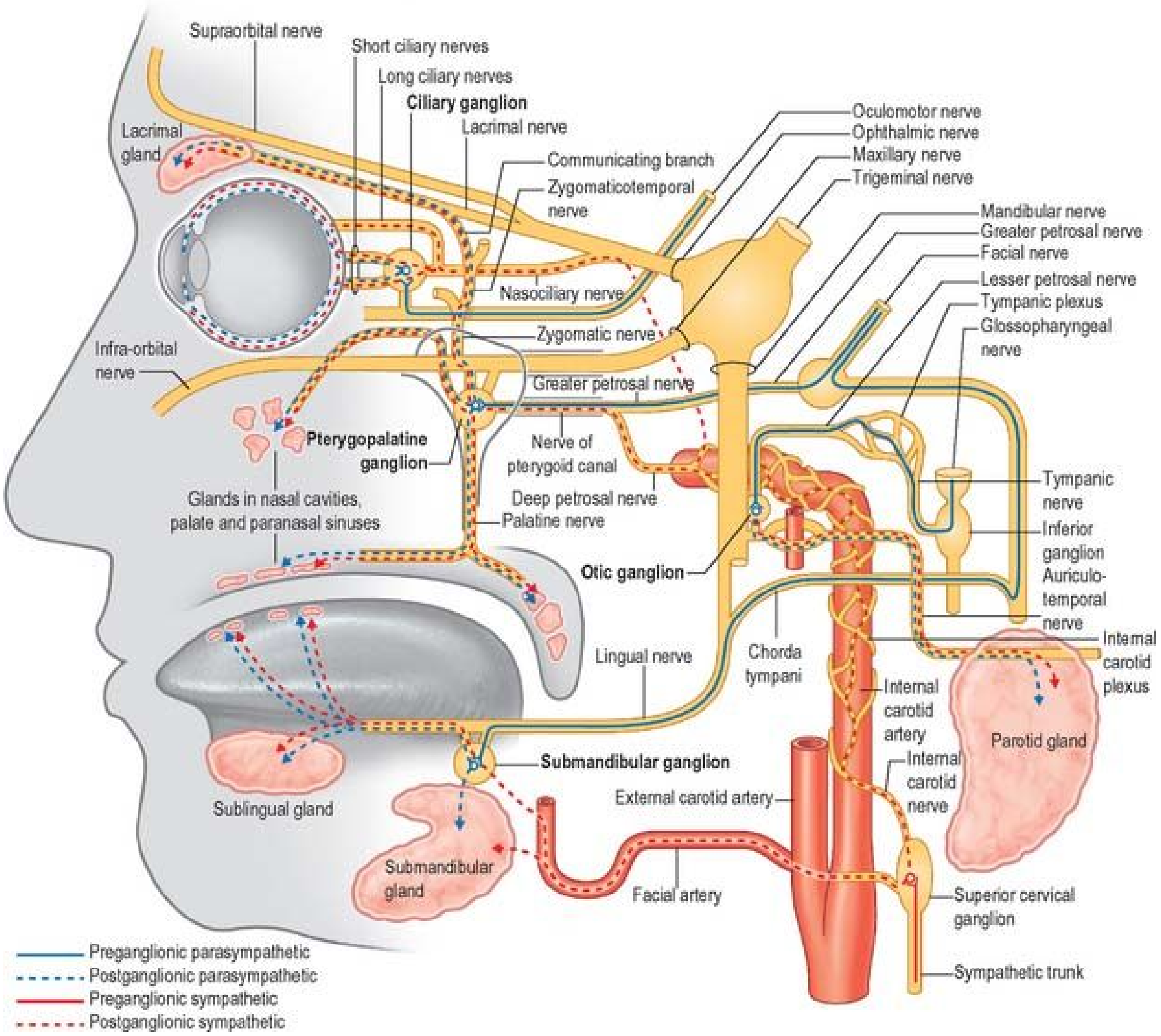
Supraorbital nerve
Short ciliary nerves
Long ciliary nerves
Ciliary ganglion
Lacrimal nerve
Lacrimal gland
Communicating branch
Zygomaticotemporal nerve
Nasociliary nerve
Zygomatic nerve
Greater petrosal nerve
Infra-orbital nerve
Pterygopalatine ganglion
Nerve of pterygoid canal
Deep petrosal nerve
Palatine nerve
Glands in nasal cavities, palate and paranasal sinuses
Otic ganglion
Lingual nerve
Chorda tympani
Submandibular ganglion
Sublingual gland
External carotid artery
Submandibular gland
Facial artery
Oculomotor nerve
Ophthalmic nerve
Maxillary nerve
Trigeminal nerve
Mandibular nerve
Greater petrosal nerve
Facial nerve
Lesser petrosal nerve
Tympanic plexus
Glossopharyngeal nerve
Tympanic nerve
Inferior ganglion
Auriculo-temporal nerve
Internal carotid plexus
Internal carotid artery
Internal carotid nerve
Parotid gland
Superior cervical ganglion
Sympathetic trunk
Preganglionic parasympathetic
Postganglionic parasympathetic
Preganglionic sympathetic
Postganglionic sympathetic

Fig. 25.7 Overview of the visceral efferent pathways in the head.

(Adapted from Drake, Vogl, Mitchell et al 2007.)

Ciliary ganglion

Preganglionic axons originate in the Edinger–Westphal nucleus of the midbrain. They travel via a branch of the oculomotor nerve (nerve to the inferior oblique) to the ciliary ganglion where they synapse. Postganglionic fibres travel in the short ciliary nerves which pierce the scleral coat of the eyeball and run forwards in the perichoroidal space to enter the ciliary muscle and the sphincter pupillae. Their activation mediates accommodation of the eye to near objects and pupillary constriction.

Submandibular ganglion

Preganglionic axons originate in the superior salivatory nucleus. They emerge from the brain stem in the nervus intermedius and leave the main facial nerve trunk in the middle ear to join the chorda tympani, which subsequently joins the lingual nerve. In this way, they reach the submandibular ganglion, where they synapse. Postganglionic fibres innervate the submandibular and sublingual salivary glands and are said to travel in the lingual nerve. Some preganglionic fibres may synapse around cells in the hilum of the submandibular gland. Stimulation of the chorda tympani dilates the arterioles in both glands as well as having a direct secretomotor effect.

Pterygopalatine ganglion

Preganglionic axons travel in the greater petrosal branch of the facial nerve and the nerve of the pterygoid canal, and relay in the pterygopalatine ganglion. Postganglionic secretomotor axons are thought to travel to the lacrimal gland via the zygomatic branches of the maxillary division of the trigeminal nerve and by ganglionic branches to the nasal and palatal mucous glands.

Otic ganglion

Preganglionic axons originate in the inferior salivatory nucleus and travel in the glossopharyngeal nerve and its tympanic branch. They traverse the tympanic plexus and lesser petrosal nerve to reach the otic ganglion where they synapse. Postganglionic fibres pass by communicating branches to the auriculotemporal nerve, which conveys them to the parotid gland. Stimulation of the lesser petrosal nerve produces vasodilator and secretomotor effects.

SYMPATHETIC SYSTEM

In the neck the sympathetic trunk lies behind and medial to the carotid sheath and anterior to the transverse processes of the cervical vertebrae and the prevertebral muscles. There are usually three cervical ganglia on each side, superior, middle and inferior (cervicothoracic); they may be connected by a solid trunk or by two or three fibrous strands. The ganglia receive preganglionic fibres from neurones whose cell bodies lie in the intermediolateral column of the upper thoracic spinal cord: there is no preganglionic output from the cervical spinal cord. Postganglionic fibres reach their target tissues in the head and neck via the cervical spinal nerves and perivascular nerve plexuses distributed along the carotid and vertebral arteries (Fig. 25.7).

SURFACE ANATOMY

SURFACE ANATOMY OF THE HEAD

Skeletal landmarks

The palpable bony landmarks of the head can be examined from the back, sides and front (Figs 25.8, 25.9).

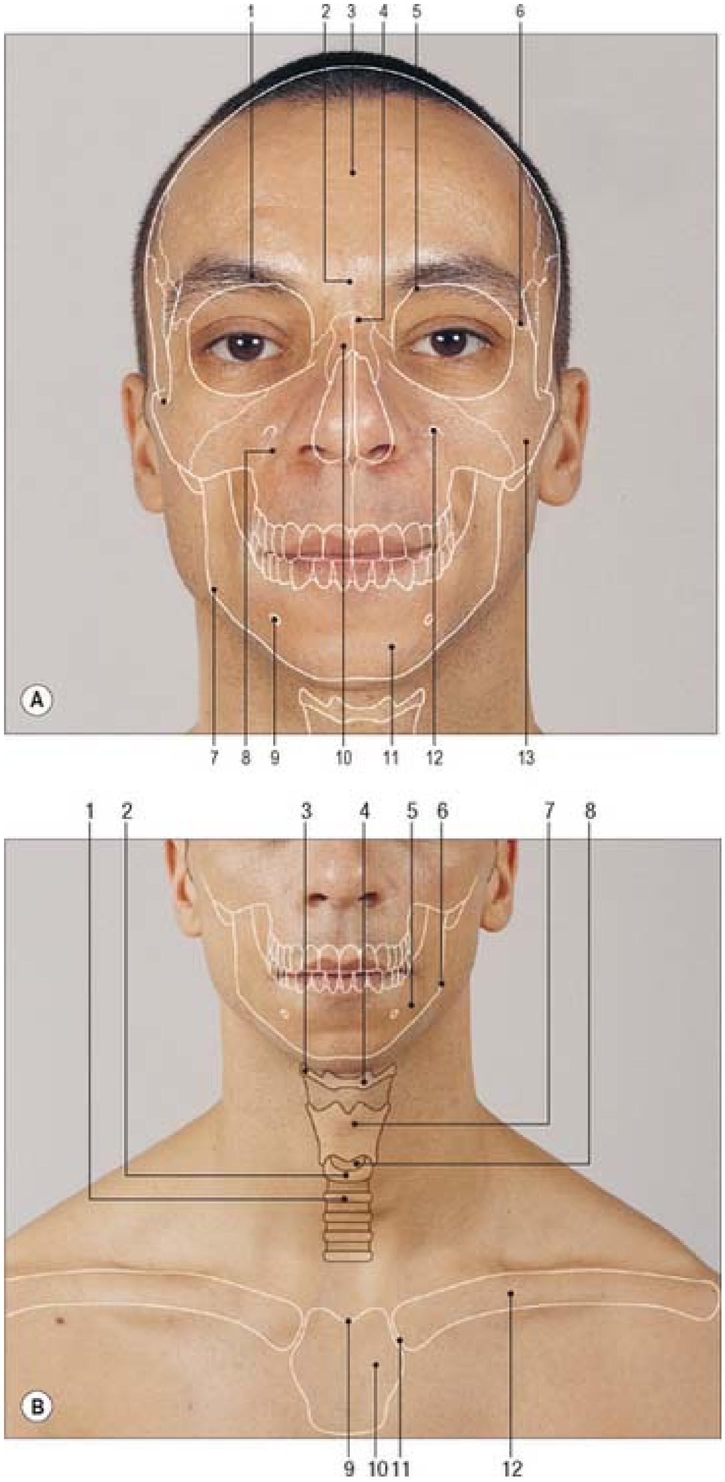
1
2
3
4
5
6
7
8
9
10
11
12
13
A
1
2
3
4
5
6
7
8
9
10
11
12
B

Fig. 25.8 **A**, Anterior aspect of the head: bones. **1**. Superciliary arch. **2**. Glabella. **3**. Frontal bone. **4**. Nasion. **5**. Supraorbital notch. **6**. Frontozygomatic suture. **7**. Angle of mandible. **8**. Maxilla. **9**. Mental foramen. **10**. Nasal bone. **11**. Body of mandible. **12**. Infraorbital foramen.

13. Zygomatic bone. **B**, Anterior aspect of the neck: bones and cartilage. **1**. First tracheal ring. **2**. Cricoid cartilage. **3**. Greater horn of hyoid bone. **4**. Body of hyoid bone. **5**. Body of mandible. **6**. Angle of mandible. **7**. Thyroid cartilage. **8**. Anterior (median) cricothyroid ligament. **9**. Sternal notch. **10**. Manubrium. **11**. Sternoclavicular joint. **12**. Clavicle.

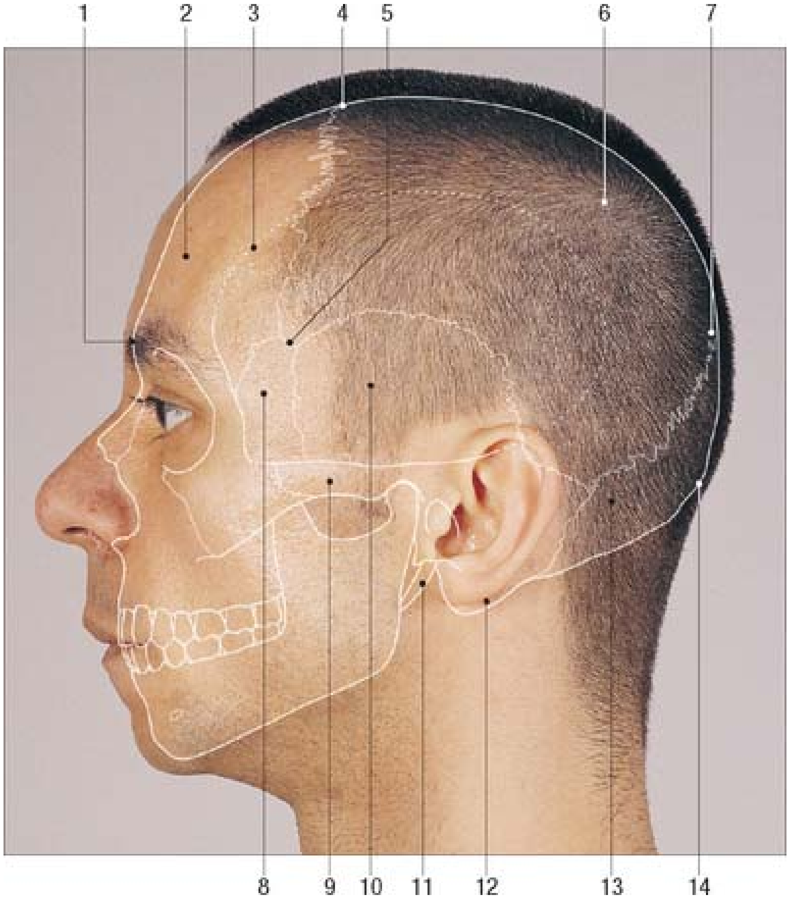

Fig. 25.9 Lateral aspect of the head. **1**. Glabella. **2**. Frontal bone. **3**. Temporal line. **4**. Bregma (anterior fontanelle). **5**. Pterion. **6**. Parietal bone. **7**. Lambda (posterior fontanelle). **8**. Greater wing of sphenoid. **9**. Zygomatic arch. **10**. Squamous temporal. **11**. Styloid process. **12**. Mastoid process. **13**. Occipital bone. **14**. External occipital protuberance.

Skull and mandible

Calvarial landmarks are visible in bald people but more commonly they have to be palpated through the hair. The anterior fontanelle, at the junction of the coronal and sagittal sutures, may be palpated until approximately 18 months after birth (Ch. 26).

Most of the superficial aspect of the skull is covered by skin, subcutaneous tissue and thin muscles, and this means that the bony prominences and surfaces are relatively easy to feel. The pericraniocervical line, which demarcates the head from the neck, runs from the midpoint of the chin anteriorly to the external occipital protuberance posteriorly. Starting anteriorly from the midline, where the mental tubercles may be felt, the lower border of the body of the mandible may be traced to the mandibular angle (C2 level). An oblique line, the external oblique ridge, joins the mental tubercle to the lower end of the anterior border of the ramus of the mandible. The mental foramen, which transmits the mental nerve and vessels, lies below the apices of the lower pre-molar teeth, about two fingers' breadth from the median plane and about one finger's breadth above the lower border of the mandible. The supraorbital, infraorbital and mental foramina all lie in approximately the same vertical plane.

The ramus of the mandible, although largely covered by masseter, is easily palpable. Its posterior border may be palpated up to the neck of the condylar process, which lies just under the lobule of the ear. As the mouth is opened, the coronoid process can be felt to move from its resting position under the zygomatic arch. A finger probing inwards just behind the condylar process enters the small retromandibular fossa which is bordered anteriorly by the mandibular neck and superiorly by the inferior wall of the external acoustic meatus (Ch. 30). The latter is bounded anteriorly by the tragus, a small curved flap of cartilage, covered by skin, that partly projects over the orifice of the meatus. Articulation at the temporomandibular joint may be appreciated by palpating anterior to the tragus for the head of the condyle during mouth opening and closure.

Palpating behind the meatus, first the anterolateral aspect and tip of the mastoid process, and, on deeper palpation, a somewhat indistinct resistance offered by the styloid process and its attached structures, will be encountered.

If the examining finger is then taken posteriorly over the convexity of the mastoid process, the lateral part of the superior nuchal line is felt. This curves upwards to meet the contralateral superior nuchal line at a bony midline prominence, the external occipital protuberance, an important surface marking for the confluence of the underlying dural venous sinuses.

Face

The lateral aspect of the face, from above downwards, consists of the temporal region, cheek and lower jaw (Ch. 29). The temporal region lies in front of the external ear and above the zygomatic arch. It is demarcated superiorly by the superior and inferior temporal lines, and inferiorly and laterally by the zygomatic arch. (The arch is formed by the zygomatic process of the temporal bone posteriorly and the temporal process of the zygomatic bone anteriorly, the two bones articulating at the zygomaticotemporal suture.) The variable prominence of the ‘cheekbone’ (zygoma) is largely attributable to the shape of the body of the underlying zygomatic bone. If the sharp posterior margin of the frontal process of the zygomatic bone is followed upwards, its fusion with the zygomatic process of the frontal bone at the zygomaticofrontal suture may be detected. Continuing posteriorly, in the line of a gentle arch, the temporal lines may be palpated. The lower temporal line terminates by curving downwards and forwards to end just above the root of the mastoid process as the supramastoid crest on the squamous part of the temporal bone. The suprameatal triangle, which lies above and behind the external acoustic meatus, overlies the lateral wall of the mastoid (tympanic) antrum. It is bounded above by the supramastoid crest, in front by the posterosuperior margin of the meatus, and behind by a vertical tangent to the posterior border of the meatus. The pterion is a small circular area within the temporal fossa which contains the junction of the frontal, sphenoid, parietal and temporal sutures. It usually lies 4 cm above the zygomatic arch and 3.5 cm behind the frontozygomatic suture, and marks the anterior (frontal) branch of the middle meningeal artery (Ch. 27) and the Sylvian point of the brain. Its position can be estimated roughly by a shallow palpable hollow, approximately 3.5 cm above the centre of the zygomatic bone. A knowledge of the surface anatomy of the middle meningeal artery is important for accurate positioning of burr-holes to evacuate extradural haematomas. The posterior (parietal) branch runs backwards and parallel with the upper border of the zygomatic arch and is usually exposed vertically above the mastoid process on a level horizontal with the upper margin of the orbit. The asterion is a craniometric point at the site of the postero-lateral, or mastoid, fontanelle. It is found at the junction of the lambdoid, occipitomastoid and parietomastoid sutures, and has been used as a landmark in lateral approaches to the posterior fossa. However, its reliability is questionable: burr holes placed at the asterion may often open the bone directly over the transverse-sigmoid sinus complex (Day & Tschabitscher 1998).

The forehead extends from the hair margin of the scalp to the eyebrows. The rounded frontal tuberosity may be felt approximately 3 cm above the midpoint of each supraorbital margin. The superciliary arch is usually palpable above the orbit and is better marked in the male than the female. The glabella, a small horizontal ridge, is easily palpable between the superciliary arches. Below the glabella the nasal bones meet the frontal bone in a small depression, the nasion, at the root of the nose. With a little finger inserted into the nostril, the bony margins of the anterior nasal aperture can be felt: they are formed by the inferior border of the nasal bone, the sharp margins of the nasal notch, and the coapted nasal spines of the maxillae (Ch. 32).

The orbital opening is somewhat quadrangular (Ch. 39). The supraorbital margin is formed entirely by the frontal bone and is easily palpable. At the junction of its sharp lateral two-thirds and rounded medial third (about two fingers’ breadth from the median plane) the supraorbital notch, if present, may be felt. This notch transmits the supraorbital nerve and vessels, and pressure exerted here with the fingernail can be painful. A frontal notch may also be found towards the bridge of the nose and is associated with the supratrochlear neurovascular bundle.

The lateral margin of the orbit consists of the frontal process of the zygomatic bone and the zygomatic process of the frontal bone. The frontozygomatic suture between them may be felt as a palpable depression. Approximately 1 cm below this suture a tubercle (Whitnall’s tubercle) may be palpated within the orbital opening: it gives attachment to the lateral palpebral and check ligaments. The inferior border of the orbit is formed by the zygomatic bone laterally and the maxilla medially. It blends into the medial margin which is less obvious, and is formed above by the frontal bone and below by the lacrimal crest of the frontal process of the maxilla. A shallow fossa behind the lower part of the medial wall houses the lacrimal sac. The anterior lacrimal crest is a guide to the location of the anterior ethmoidal artery, which may occasionally require ligation to control severe epistaxis, and which lies approximately 2.4 cm posterior to the crest. The optic foramen lies approximately 4.5 cm posterior to the infraorbital margin (approximately 4.2 cm from the anterior lacrimal crest): these distances are important in orbital floor exploration in order to avoid injury to the optic nerve. The inferior orbital fissure lies approximately 2 cm posterolateral to the infraorbital margin: it does not contain any important anatomical structures, which means that surgery can be performed safely in this region. The infraorbital foramen, which transmits the infraorbital nerve and vessels, lies approximately 0.5 cm below the middle of the infraorbital margin.

The anterior surface of the maxilla is extensive and may be palpated between the infraorbital margin and the alveolar processes that bear the upper teeth (when present). The canine eminence overlies the roots of the canine tooth and separates the incisive fossa anteriorly from the deeper canine fossa posteriorly. The bone in the canine fossa is thin and may be removed easily to access the maxillary sinus via an intraoral approach as part of a Caldwell–Luc procedure, e.g. to remove a tooth fragment that has been accidentally dislodged into the sinus during the attempted extraction of a posterior maxillary tooth in close proximity to the sinus. The palatine process of the maxilla, which forms the greater part of the roof of the mouth, is easily palpable within the mouth (Ch. 30).

Soft tissues and viscera

The muscular, fatty and cutaneous features which so clearly differentiate individuals are readily apparent on inspection. The external features of the eyelids and eyebrows are described in (Ch. 39). The tympanic membrane may be examined under direct vision using an auroscope and is described in (Ch. 36). The retinal vascular supply may be examined directly by ophthalmoscopy (Ch. 40).

Temporalis is palpable if the flat of the hand is placed on the side of the head and the jaw is clenched and unclenched, and the anterior border of masseter is prominent when the jaw is clenched. With the mouth open, it is possible to examine all the teeth and the palatine tonsils (when present), and to inspect and palpate the orifices of the parotid ducts. The palatine tonsil lies between the anterior and posterior pillars of the fauces (palatoglossus and palatopharyngeus respectively). Patients with a peritonsillar abscess (quinsy) present with ispilateral enlargement of the tonsil with displacement of the uvula to the contralateral side. The tongue may be examined for its general appearance and any abnormalities of movement, which may reflect neuronal damage. Deviation of the protruded tongue to the affected side, muscle wasting and fasciculation may occur following hypoglossal nerve injury.

Parotid gland

The parotid gland is soft and indistinct and lies largely below the external acoustic meatus, wedged between the ramus of the mandible, the mastoid process and sternocleidomastoid (Ch. 29). The anterior border of the gland is represented by a line descending from the mandibular condyle to a point just above the middle of masseter and then to a point approximately 2 cm below and behind the angle of the mandible. Its concave upper border corresponds to a curve traced from the mandibular condyle across the lobule of the ear to the mastoid process. The posterior border corresponds to a line drawn between the posterior ends of the anterior and upper borders. A large tumour of the deep lobe of the parotid may present as an intraoral mass. The parotid duct arises from the gland just above half-way along its anterior margin. It runs over masseter to its anterior border where it bends sharply and pierces the underlying buccinator opposite the upper second permanent molar. The orifice of the duct is visible as a small papilla within the cheek opposite the second upper molar tooth. Cannulation of the duct is integral to the procedures of sialography, ductal dilatation and basket retrieval of ductal stones (sialoliths). The duct can be palpated on the face at the anterior border of the clenched masseter, and its course can be represented by the middle third of a line drawn from the lower border of the tragus of the auricle to the midpoint of the philtrum of the upper lip.

Pulses

Facial pulse

The facial pulse can be felt as the facial artery crosses the lower border of the mandible immediately in front of masseter, approximately 1 cm lateral to the angle of the mouth.

Superficial temporal artery pulse

The superficial temporal artery may be palpated immediately in front of the tragus of the auricle. This is of particular relevance during anaesthesia, when access to the patient is frequently restricted to the head. The artery divides into frontal and parietal branches approximately 2.5 cm above the zygomatic arch.

Nerves

Facial nerve

The facial nerve may be injured in its extratemporal course as a result of facial trauma and laceration, or iatrogenically during surgery involving the parotid or submandibular glands or the temporomandibular joint, or during facelift procedures. Knowledge of the topographical and surgical landmarks that aid location of its branches is therefore essential if the nerve is to be preserved during surgery.

The nerve exits the skull at the stylomastoid foramen and so is initially deep to the posterior margin of the external acoustic meatus: the nerve trunk lies approximately 1 cm deep and inferior to the tragal point. It usually divides within the substance of the parotid gland into superior (temporofacial) and inferior (cervicofacial) trunks which collectively give off five main peripheral branches that radiate out across the face (Fig. 25.10; see Fig. 29.17). Cadaveric and intra-operative microdissection studies have revealed that the distribution of the rami that are given off from these branches is highly variable: the use of surface anatomical coordinates alone to locate them is therefore unreliable, and can only give an approximation of their underlying trajectory. The course of the temporal branch(es) corresponds to a line extending anteriorly and superiorly from the attachment of the lobule (approximately 0.5 cm below the tragus) to a point 1.5 cm above the lateral aspect of the ipsilateral eyebrow. This branch is particularly vulnerable to damage as it runs over the zygomatic arch, and to a lesser extent in the lateral brow: it may be injured in facial rhytidectomy or with coronal or endoscopic brow lifting. The buccal branches have been described as running both above and below the parotid duct. The marginal mandibular nerve lies either along the body of the mandible (80%) or it may briefly enter the neck, where it lies within 1.2 cm of the lower border of the body (20%). Branches that enter the neck curve upwards and re-enter the face by crossing the lower border of the mandible at the anterior border of masseter. As they do so, they also cross the facial artery and vein. Incisions to access the submandibular region of the neck are therefore usually made at least 1.5 cm (two fingers' breadth) below the lower border of the mandible in order to avoid damaging the marginal mandibular branch: injury results in ipsilateral paralysis of depressor anguli oris and depressor labii inferioris and produces a characteristic deformity.

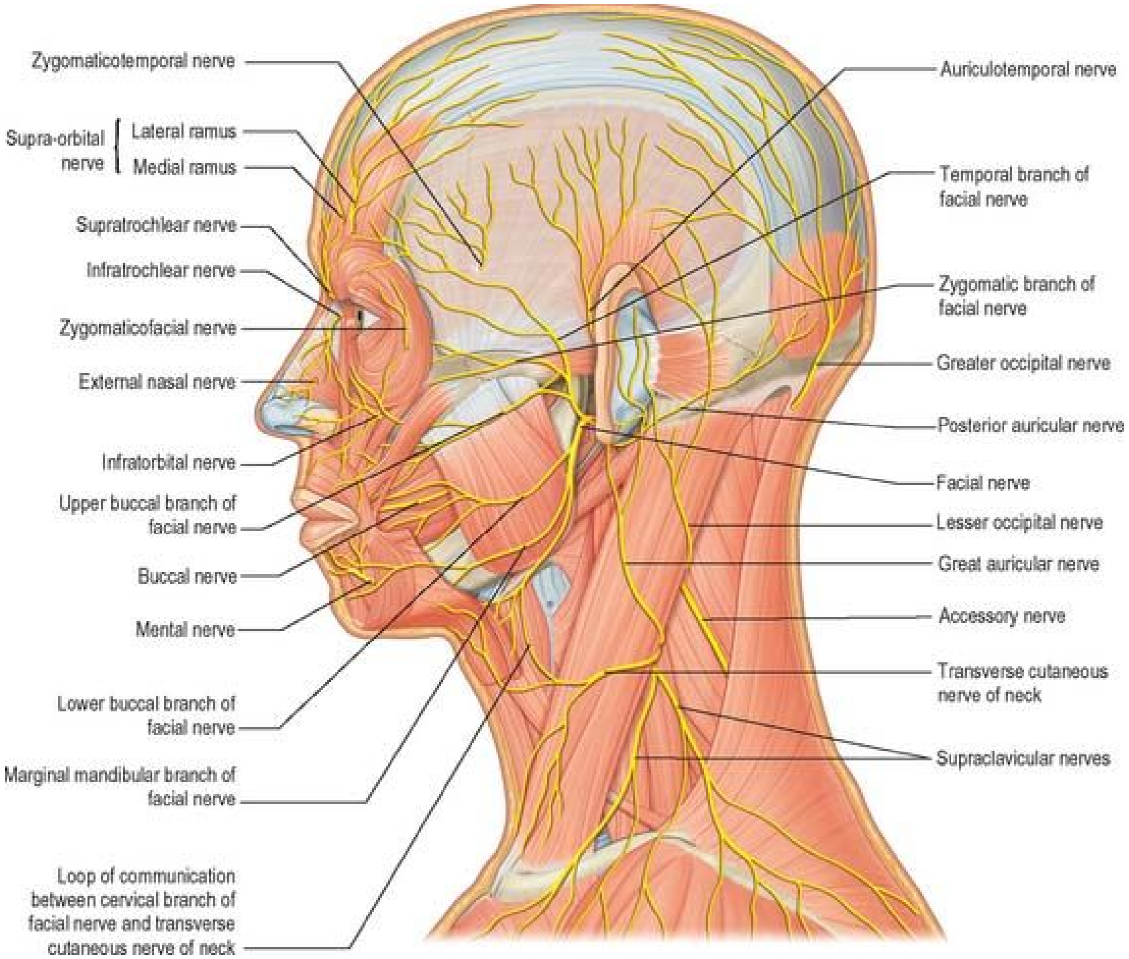
Zygomaticotemporal nerve
Supra-orbital nerve
Lateral ramus
Medial ramus
Supratrochlear nerve
Infratrochlear nerve
Zygomaticofacial nerve
External nasal nerve
Infraorbital nerve
Upper buccal branch of facial nerve
Buccal nerve
Mental nerve
Lower buccal branch of facial nerve
Marginal mandibular branch of facial nerve
Loop of communication between cervical branch of facial nerve and transverse cutaneous nerve of neck
Auriculotemporal nerve
Temporal branch of facial nerve
Zygomatic branch of facial nerve
Greater occipital nerve
Posterior auricular nerve
Facial nerve
Lesser occipital nerve
Great auricular nerve
Accessory nerve
Transverse cutaneous nerve of neck
Supraclavicular nerves

Fig. 25.10 Distribution of the cutaneous branches of the trigeminal nerve and of the cervical plexus, and the motor branches of the facial nerve in the face and neck.

Dermatomes

Our knowledge of the extent of individual dermatomes is largely based on clinical evidence. The dermatomes of the face arise mainly from cutaneous branches of the three major divisions of the trigeminal nerve (Fig. 25.10). The skin covering the front and sides of the neck, and over the angle of the mandible, and of the lateral scalp and posterior aspect of the pinna, is supplied by branches of the cervical plexus (C2–C4), and the skin over the back of the head is supplied by the greater occipital nerve (C2, posterior primary ramus) (see Fig. 25.10, and Figs 29.15 and 42.3).

SURFACE ANATOMY OF THE NECK

Skeletal landmarks

The head and neck are extremely mobile. The following account therefore assumes, unless otherwise stated, that the head is held in the anatomical position. The superior limit of the neck is the pericraniocervical line. Inferiorly the neck blends with the thorax and upper limb at the level of the clavicle and scapula. Several skeletal features are easily palpable. At the back of the neck the cervical vertebrae may be felt in the midline. The transverse process of the first cervical vertebra (atlas) may be palpated in the uppermost part of the neck, in the hollow between the mastoid process of the temporal bone and the external ear. Just below, the transverse process of the second cervical vertebra (axis) can be felt on deep palpation. Inferiorly the spine of the seventh cervical vertebra (vertebra prominens) is especially prominent along the midline posteriorly, particularly when the neck is flexed. The remaining cervical spines are indistinct because they are covered by the ligamentum nuchae, which separates the postvertebral musculature on both sides. However, the spines of the second, fifth and sixth cervical vertebrae may be felt on deeper palpation.

The hyoid bone may be felt a few centimetres below and behind the chin, especially if the neck is extended. It may be palpated between finger and thumb and moved from side to side. The hyoid bone lies approximately at the level of the third cervical vertebra. The most obvious palpable feature in the front of the neck below the hyoid bone is the thyroid cartilage, and the prominent midline subcutaneous laryngeal prominence or Adam’s apple, which indicates the line of fusion of the two thyroid laminae. In the male, the prominence is usually clearly visible, whereas in the female it is not usually apparent, even when the neck is viewed from the side. The curved upper border of the thyroid cartilage and the thyroid notch are easily palpable. The thyroid cartilage lies at the level of the fourth and fifth cervical vertebrae. The anterior arch of the cricoid cartilage can be felt below the inferior border of the thyroid cartilage. The cricoid cartilage lies at the level of the sixth cervical vertebra. The groove between the thyroid and cricoid cartilages, filled by the anterior (median) cricothyroid ligament, is a useful site for emergency access to the airway if there is obstruction at or above the vocal cords (cricothyroid puncture or cricothyroidotomy). In the child the laryngeal structures lie at a higher level. The trachea can be palpated inferior to the cricoid cartilage. It normally lies in the midline but may be deviated by disease, e.g. tension pneumothorax, cardiac tamponade. The upper tracheal cartilages may be impalpable if they are covered by the thyroid isthmus, which joins the two lobes of the gland across the midline of the neck. Confirmation of the surface anatomy of the hyoid bone, thyroid and cricoid cartilages and suprasternal notch is helpful prior to performing a tracheostomy.

The clavicle is a sigmoid-shaped bone which is easily visible in thin people and palpable in all except the morbidly obese. Its medial two-thirds are rounded and convex forwards and the lateral third is flat and concave forwards. The suprasternal (jugular) notch lies between the medial expanded ends of the clavicles: its inferior border is the superior edge of the manubrium sterni. For much of its length the clavicle may be almost encircled by two fingers, but medially its massive ligamentous attachments make definition more difficult. The posterior end of the first rib may sometimes be felt rather indistinctly as it lies in the supraclavicular fossa in the root of the neck, between sternocleido-mastoid and trapezius and above the clavicle.

Soft tissues and viscera

Triangles of the neck

From the front and side the neck is obviously divided into anterior and posterior triangles by sternocleidomastoid (Fig. 25.11). In prosected cadaveric specimens, the anterior triangle may be further subdivided into submental, muscular, carotid and digastric triangles, and the posterior cervical triangle may be partitioned into occipital and supraclavicular triangles. It should be noted that the structures that form the boundaries of some of these lesser triangles are not readily palpable or visible.

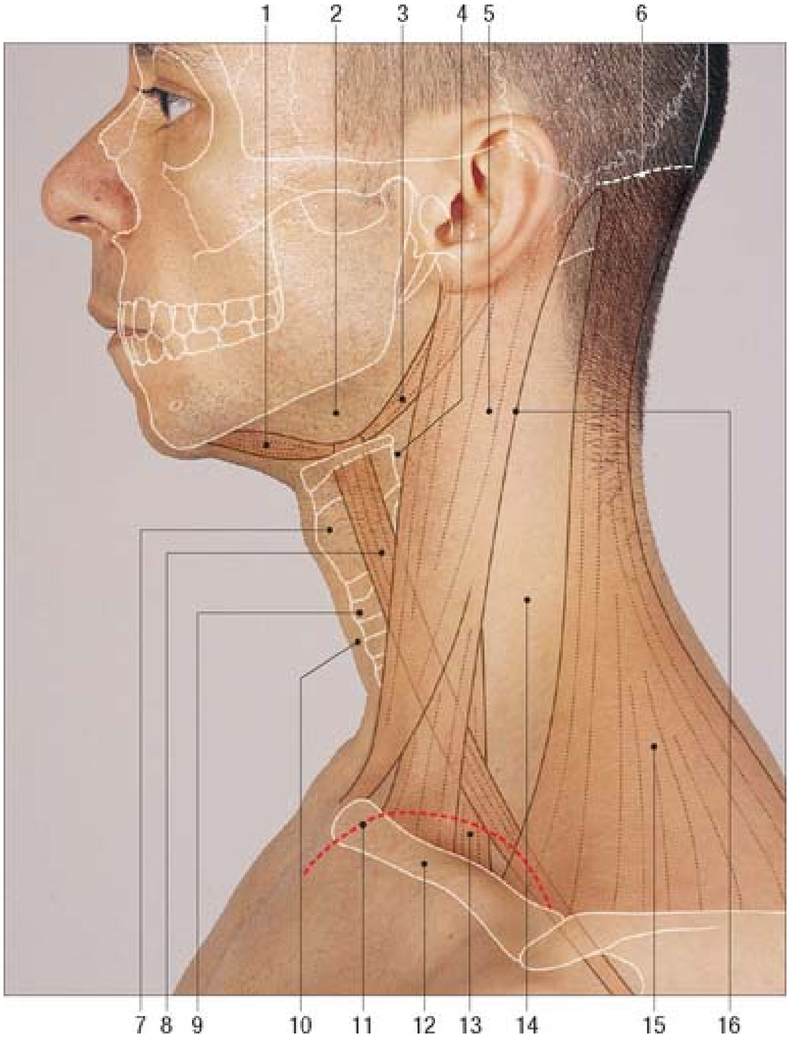

Fig. 25.11 Anterior and posterior triangles of the neck. **1**. Anterior belly of digastric. **2**. Digastric triangle. **3**. Posterior belly of digastric. **4**. Carotid triangle. **5**. Sternocleidomastoid. **6**. Superior nuchal line. **7**. Thyroid cartilage. **8**. Omohyoid. **9**. Cricoid cartilage. **10**. Muscular triangle. **11**. Apex of lung. **12**. Clavicle. **13**. Scalenus anterior. **14**. Posterior triangle. **15**. Trapezius **16**. Erb’s point.

Anterior triangle

The base of the anterior triangle is formed by the base of the mandible and a line from its angle to the mastoid process, and the sides are formed by the midline anteriorly and the anterior edge of sternocleidomastoid laterally. The triangle is inspected from the front, but best examined bimanually with the examiner standing behind the subject and using the fingers of both hands to examine the structures within the triangle. Inspection reveals the rounded tendinous oblique head of sternocleidomastoid, which arises from the superolateral angle of the manubrium, and the more vertical muscular portion, which arises from the upper surface of the medial third of the clavicle. Between these two heads there is usually a hollow which contains the internal jugular vein just before it joins the subclavian vein posterior to the clavicle.

The trachea and its cartilaginous ‘rings’ can be palpated inferior to the cricoid cartilage. If the examining finger is moved laterally, the lobes of the thyroid gland may be felt, particularly if the subject is asked to swallow. The thyroid gland consists of two lobes lying either side of the thyroid cartilage and joined in the midline of the neck by an isthmus. The upper border of each lobe lies alongside the lower half of the lamina of the cartilage. The lower border reaches towards the sternal end of the clavicle. The isthmus, approximately 2 cm wide, lies in front of the trachea just below the cricoid cartilage and usually overlies the second and third tracheal ‘rings’.

Taken superiorly, an examining finger will enter either the submental or submandibular triangle, in which enlarged lymph nodes or salivary glands may be felt. The submandibular gland extends approximately 2 cm beneath the lower border of the mandible and reaches the approximate level of the hyoid bone. Its posterior border is level with the angle of the mandible; its anterior border extends forwards approximately 4 cm.

It should be noted that above the hyoid bone the musculature runs in a predominantly horizontal or oblique direction, and below the hyoid it runs in a vertical direction. Lymph nodes above the hyoid bone tend to be disposed in a horizontal plane and lie mainly just below the pericraniocervical line, whereas the deep cervical nodes run vertically and are related to the internal jugular vein. Apart from a few retrovisceral nodes and some nodes deep to sternocleidomastoid, members of all of the groups of lymph nodes in the head and neck are clinically palpable when enlarged.

Posterior triangle

The boundaries of the posterior triangle are the posterior border of sternocleidomastoid, the middle third of the superior surface of the clavicle, which forms the base, and the anterior margin of trapezius. The apex is the point where sternocleidomastoid and trapezius approximate to each other at the superior nuchal line. The lower portion of the posterior triangle forms the supraclavicular fossa, a very important clinical area, which lies just above and behind the clavicle at the confluence of the thoracic inlet and the aditus to the axilla and arm. It is better inspected from in front, but palpated from behind, when a right-handed examiner stands behind and to the right of the subject.

When inspecting the supraclavicular fossa, the pulsation of the great veins may be seen if the central venous pressure is raised. The external jugular vein, a prominent feature, may be distended due to kinking, raised venous pressure or obstruction (see below). The supraclavicular fossa is a common site in which to feel pathologically enlarged lymph nodes. In particular, cancers of the upper gastrointestinal tract and of the lung frequently spread to the supraclavicular group of nodes. The posterior end of the first rib may be felt as a fullness in the posterior aspect of the fossa. The subclavian artery can be felt pulsating as it crosses the first rib, and the trunks of the brachial plexus may be felt above and behind it. A point approximately 2.5 cm above the middle of the medial third of the clavicle marks the level of the neck of the first rib and thus the surface marking for the apex of the dome of the cervical pleura and lung: any penetrating injury (iatrogenic or otherwise) in this region will run the risk of creating a pneumothorax.

Root of the neck

The root of the neck (Ch. 28) is the transitional zone between the neck, thorax and both upper limbs. It contains numerous important structures, including the oesophagus and trachea in the midline, and the apices of the lungs covered by apical pleura, the common carotid and subclavian arteries and the branches of the thyrocervical trunks, the internal jugular veins, the phrenic and vagus nerves and cervical sympathetic trunks, and the roots of the brachial plexus on both sides, and the terminations of the thoracic and right lymphatic ducts on the left and right sides respectively.

Course of vessels

Carotid arteries

In the neck, the common carotid artery and its continuation, the internal carotid artery, may be represented by a more or less straight line from the sternoclavicular joint to a point just behind the condyle of the mandible. At the level of the upper border of the thyroid cartilage (approximately at a level between the third and fourth cervical vertebrae) the common carotid artery divides into the external and internal carotid arteries. The common carotid artery may be compressed against the prominent transverse process of the sixth cervical vertebra (Chassaignac’s or carotid tubercle). Above this level the artery is superficial and its pulsation can be readily felt beneath the anterior border of sternocleidomastoid. The pulse is produced as much by the roots of the main branches as it is by the internal and external carotid arteries themselves, and this is therefore one of the prime sites in the body to feel for a pulse.

Subclavian artery

The subclavian artery enters the root of the neck behind the sternoclavicular joint. It arches upwards to reach a point approximately 2 cm above the clavicle deep to the posterior border of sternocleidomastoid, and then passes across the upper surface of the first rib behind the middle region of the clavicle. The subclavian pulse may therefore be located behind the clavicle at the lateral border of sternocleidomastoid or where the artery crosses the first rib.

Anterior jugular vein

The anterior jugular vein runs downwards beneath the chin approximately a finger's breadth from the midline. It turns laterally approximately 2.5 cm from the sternal end of the clavicle and passes beneath sternocleidomastoid to drain into the external jugular vein. The veins of each side join to form a jugular arch just above the manubrium sterni. The vein may be encountered if the operator drifts laterally while creating a surgical airway.

External jugular vein

The external jugular vein lies superficial to sternocleidomastoid and can be represented by a line which starts just below and behind the angle of the mandible and runs down to the clavicle near the posterior border of sternocleidomastoid (Fig. 25.3). It drains into the subclavian vein after penetrating the investing layer of deep cervical fascia and may be kinked at this point. If the proximal part of the vein is damaged it may be held open by the surrounding fascia: air can then be sucked in, resulting in an air embolus. The external jugular vein can be distended if venous pressure is raised, e.g. by performing Valsalva's manoeuvre (forced expiration against a closed mouth and blocked nostrils) or by supraclavicular digital pressure.

Internal jugular vein

The internal jugular vein runs in the carotid sheath, lying just lateral to the arteries. It therefore has similar surface markings to those described for the common and internal carotid arteries and is represented in surface projection by a broad band from the lobule of the ear to the medial end of the clavicle, where it joins the subclavian vein. The inferior bulb of the internal jugular vein lies in the lesser supraclavicular fossa (the depression between the sternal and clavicular heads of sternocleidomastoid): this site is one of several at which the internal jugular vein may be accessed for central vein cannulation (see Ch. 28). The jugular venous pulse reflects the jugular venous pressure (central venous pressure) and is a measure of cardiac function. Pulsation of the great veins may be seen in this region if the central venous pressure is raised (e.g. right-sided heart failure). Internal jugular vein cannulation is described in Chapter 28.

Subclavian vein

The subclavian vein runs just below the subclavian artery. Subclavian vein cannulation is described in Chapter 28.

Course of nerves

Spinal accessory nerve

The course of the spinal accessory nerve can be indicated by a line that crosses the floor of the posterior triangle passing from the junction of the upper third and middle thirds of the posterior border of sternocleidomastoid (Erb's point; see Fig. 25.11) to the junction of the lower and middle thirds of the anterior border of trapezius. The course of the nerve may also be represented by a line joining the palpable transverse process of the atlas (approximately 1 cm below the mastoid process) to the anterior border of trapezius 5 cm above the clavicle.

Cervical plexus

The cutaneous branches of the cervical plexus emerge from behind the posterior border of sternocleidomastoid just below the spinal accessory nerve (Fig. 25.10).

Brachial plexus

The roots and trunks of the brachial plexus can be represented by a line passing between the middle of the posterior border of sternocleido-mastoid and the middle of the clavicle. In thin individuals, the scalene muscles are visible when the head is laterally flexed to the contralateral side, and the roots are palpable behind scalenus anterior. The trunks lie in the posterior triangle of the neck, and the divisions lie behind the clavicle near the lateral border of the first rib. The cords enter the axilla above the first part of the subclavian artery, embrace its second part and give off branches around the third part.

Cervical sympathetic ganglia

The superior cervical ganglion lies slightly anterior to the (palpable) transverse process of the second cervical vertebra, while the middle cervical ganglion, when present, lies just in front of the transverse process of the sixth cervical vertebra (which is difficult to palpate). The inferior cervical ganglion may be fused with the first thoracic cervical ganglion, forming the stellate or cervicothoracic ganglion. Stellate ganglion block is often employed to perform a sympathetic nerve block to the head and neck, or to the arm: the surface marking is approximately at the level of the transverse process of the seventh cervical vertebra (situated two finger's breadths above the sterno-clavicular joint when the neck is fully extended) (Ellis et al 1997).

REFERENCES

ay JD, Tschabitscher M. Anatomic position of the asterion. *Neurosurgery*. 1998;42:198-199.

lis H, Feldman S, Lawson S. Anatomy for Anaesthetists, 7th edn. Oxford: Blackwell Science, 1997.

CHAPTER 26

External skull

The skull is the bony skeleton of the head. It shields the brain, the organs of special sense and the cranial parts of the respiratory and digestive systems, and provides attachments for many of the muscles of the head and neck. Movement of the lower jaw (mandible) occurs at the temporomandibular joint.

The skull without the mandible is called the cranium, and may be subdivided into two regions. The cranial vault or neurocranium encloses the brain, cranial meninges and cerebrospinal fluid, while the facial skeleton or viscerocranium hangs down from the front of the neurocranium and houses the organs of special sense.

The skull is the most complex osseous structure in the body: the young adult skull is composed of an average of 28 separate bones, many of which are paired, although some in the median plane are single. Most of the vault bones are flat, and consist of two tables or plates of compact bone enclosing a narrow layer of relatively dense cancellous marrow (diploic bone). The marrow within the skull bones is a site of haemopoiesis, at least in the young individual. These bones form by intramembranous ossification of a highly vascular connective tissue membrane and have often been referred to as ‘dermal’ in deference to their alleged ancient phylogenetic origin. The inner table is thinner and more brittle while the outer tends to be thicker and more resilient: this is important to remember when examining fractures to the skull caused by either blunt or sharp trauma. The skull bones vary in thickness in different regions, tending to be thinner where they are covered by muscles, e.g. in the temporal region, and thicker where muscles attach, e.g. in the occipital region. The thinner regions are more prone to fracture.

The majority of bones in the skull are held together firmly by fibrous joints termed sutures: in the developing skull sutures allow for growth. The three main sutural morphologies are dependent upon the magnitude of strains placed upon them. Thus the margins of adjacent bones of a suture may be smooth and meet end-to-end, giving a simple (butt-end) suture (e.g. median palatine suture); bevelled, so that the border of one bone overlaps the other (e.g. parietotemporal suture); or present numerous projections that interlock, giving a serrated appearance (e.g. sagittal suture). The complexity of serrated sutures increases from the inner to the outer surface. Fusion across sutures (synostosis) can start early in the third decade, although its variability precludes using this information to assess age at death in skulls with any degree of accuracy. The process of fusion starts on the internal surface of the cranium first and proceeds externally; the sagittal suture is often one of the first affected. By middle age, many of the larger sutures will show evidence of synostoses, although there are some which rarely show fusion, e.g. the zygomaticofacial. Premature fusion of sutures during the early growth phase of the skull will result in various abnormalities.

The bones forming the base of the skull develop mainly via endochondral ossification, and also play an important part in the overall growth of the face and the neurocranium. The joints between bones in the skull base are primary cartilaginous. One of the most important is the spheno-occipital synchondrosis between the body of the sphenoid anteriorly and the basilar part of the occipital bone posteriorly: fusion is completed between 13 and 18 years of age.

There are only two sites of synovial articulation associated with the exterior of the skull – the temporomandibular joint with the mandible and the atlanto-occipital joint between the condyles of the occipital bone and the superior articular facets of the atlas. Rotation of the skull does not directly involve any joints of the skull, but occurs at the atlanto-axial joint between the first and second cervical vertebrae.

Many important nerves and vessels pass in and out of the skull via openings (foramina). The skull is a prime site for fractures resulting from trauma, which means that these structures can be damaged as a result of head injury. In addition to main foramina, irregular emissary foramina allow veins situated externally on the face and scalp to communicate with those lying intracranially. The spread of infection along these routes can have serious clinical consequences.

In the account of the skull that follows, only generalized standard views of the skull will be considered. A more detailed account of each individual bone will be found associated with the relevant regional text.

FRONTAL (ANTERIOR) VIEW

Viewed from the front, the skull is generally ovoid in shape and is wider above than below (Fig. 26.1). The upper part is formed by the frontal bone which underlies the forehead region above the orbits. Superomedial to each orbit is a rounded superciliary arch (more pronounced in males) between which there may be a median elevation, the glabella. The glabella may show the remains of the inter-frontal (metopic) suture, which is present in about 9% of adult skulls. Above each superciliary arch is a slightly elevated frontal tuber or eminence which is generally more obvious in the female. Below, where the nasal bones meet the frontal bone, is a depression marking the root of the nose. The frontal bone articulates with the two nasal bones at the frontonasal sutures; the point at which the frontonasal and internasal sutures meet is the anthropometric landmark known as the nasion.

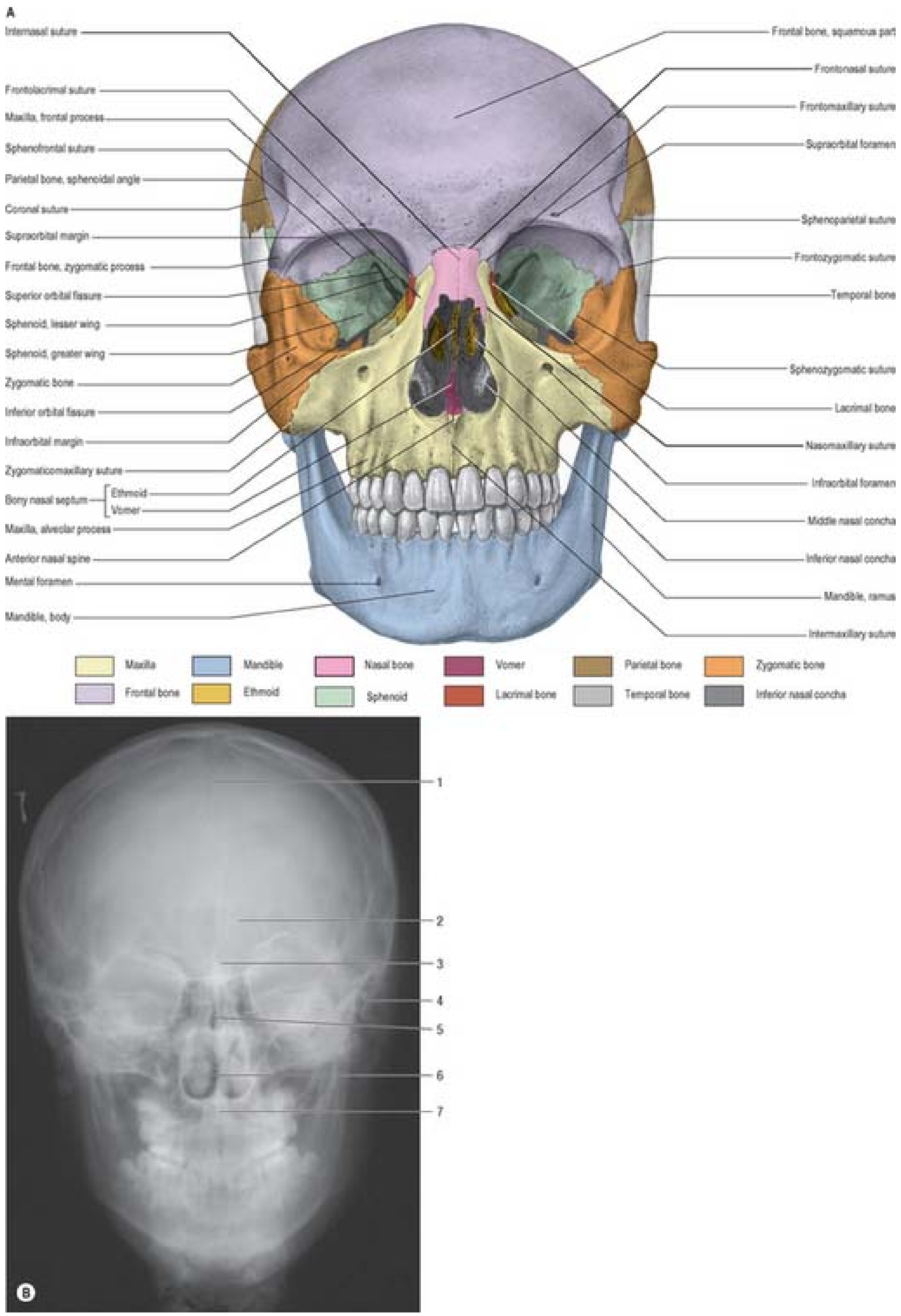
A
Internasal suture
Frontolacrimal suture
Maxilla, frontal process
Sphenofrontal suture
Parietal bone, sphenoidal angle
Coronal suture
Supraorbital margin
Frontal bone, zygomatic process
Superior orbital fissure
Sphenoid, lesser wing
Sphenoid, greater wing
Zygomatic bone
Inferior orbital fissure
Infraorbital margin
Zygomaticomaxillary suture
Bony nasal septum
Ethmoid
Vomer
Maxilla, alveolar process
Anterior nasal spine
Mental foramen
Mandible, body
Frontal bone, squamous part
Frontonasal suture
Frontomaxillary suture
Supraorbital foramen
Sphenoparietal suture
Frontozygomatic suture
Temporal bone
Sphenozygomatic suture
Lacrimal bone
Nasomaxillary suture
Infraorbital foramen
Middle nasal concha
Inferior nasal concha
Mandible, ramus
Intermaxillary suture
Maxilla
Frontal bone
Mandible
Ethmoid
Nasal bone
Sphenoid
Vomer
Lacrimal bone
Parietal bone
Temporal bone
Zygomatic bone
Inferior nasal concha
1
2
3
4
5
6
7
B

Fig. 26.1 **A**, Bones of the adult skull, frontal aspect. **B**, Anteroposterior view of the skull and upper cervical spine, young adult. **1**. Sagittal suture. **2**. Frontal sinus. **3**. Crista galli. **4**. Mastoid air cells. **5**. Nasal septum. **6**. Inferior concha. **7**. Dens of axis.

***A** (From Sobotta 2006.) (**B** by courtesy of Mr Eric Whaites, Dental Institute, King’s College, London.)*

The upper part of the face is occupied by the orbits and the bridge of the nose. Each orbital opening is approximately quadrangular (see Ch. 39). The upper, supraorbital, margin is formed entirely by the frontal bone, interrupted at the junction of its sharp lateral two-thirds and rounded medial third by the supraorbital notch or foramen, which transmits the supraorbital vessels and nerve. The lateral margin of the orbit is formed largely by the frontal process of the zygomatic bone and is completed above by the zygomatic process of the frontal bone; the suture between them lies in a palpable depression. The infraorbital margin is formed by the zygomatic bone laterally and maxilla medially. Both lateral and infraorbital margins are sharp and palpable. The medial margin of the orbit is formed above by the frontal bone and below by the lacrimal crest of the frontal process of the maxilla.

The central part of the face is occupied mainly by the two maxillae, separated by the anterior nasal aperture. Each maxilla contributes to the upper jaw, the floor of the orbital cavity, the lateral wall of the nose, the floor of the nasal aperture and the bone of the cheek. Medially, the maxilla forms the nasal notch which is the floor and inferolateral border of the anterior nasal aperture. The prominent anterior nasal spine surmounts the intermaxillary suture at the lower margin of the anterior nasal aperture and is palpable in the nasal septum. The infraorbital foramen, which transmits the infraorbital vessels and nerve, lies about 1 cm below the infraorbital margin. The maxillary alveolar process bears the upper teeth. The short, thick zygomatic process of the maxilla has an oblique upper surface that articulates with the zygomatic bone at the zygomaticomaxillary suture. The frontal process of the maxilla ascends posterolateral to the nasal bone to articulate with the frontal bone.

The anterior nasal aperture is piriform in shape, and is wider below than above and bounded by the nasal bones and maxillae. The upper boundary of the aperture is formed by the nasal bones while the remainder is formed by the maxillae. In life, various cartilages (septal, lateral nasal, major and minor alar) help to delineate two nasal cavities (see Ch. 32). The defleshed skull presents a single anterior nasal aperture because these cartilages are lost during preparation or decomposition. However, the shape of these bones can be used quite successfully to predict the shape of the cartilaginous nose.

The lower part of the face, below the nose, is formed from the alveolar arch of the maxillae and the upper dentition, and the body of the mandible, the alveolar process of the mandible and the lower dentition. In the midline the mental protuberance produces the characteristic prominence of the chin. The mental foramen, which transmits the mental nerve and accompanying vessels, lies in the same vertical plane as the supraorbital and infraorbital foramina.

AP radiographs of the skull clearly show the central location of the paranasal air sinuses in the frontal bone, the maxilla and the ethmoid. These can be particularly useful indicators of identity when postmortem images are compared with premortem clinical films.

POSTERIOR VIEW

The parietal, temporal and occipital bones form the entirety of the posterior view (Fig. 26.2). The superolateral region is occupied by the parietal bones, the mastoid part of the temporal bones comprises the inferolateral regions and the central portion is occupied by the occipital bone, which is why this aspect is also referred to as the occipital view. The parietal bones articulate with the occipital bone at the lambdoid suture and extend inferiorly into the occipitomastoid and the parietomastoid sutures behind and above the mastoid process respectively. Sutural or wormian bones are islands of bone that are commonly found within the lambdoid suture. They may arise from separate centres of ossification and they appear to have no clinical significance, being of genetic rather than pathological aetiology. A large interparietal bone is not uncommon and is sometimes referred to as an Inca bone (Fig. 26.2).

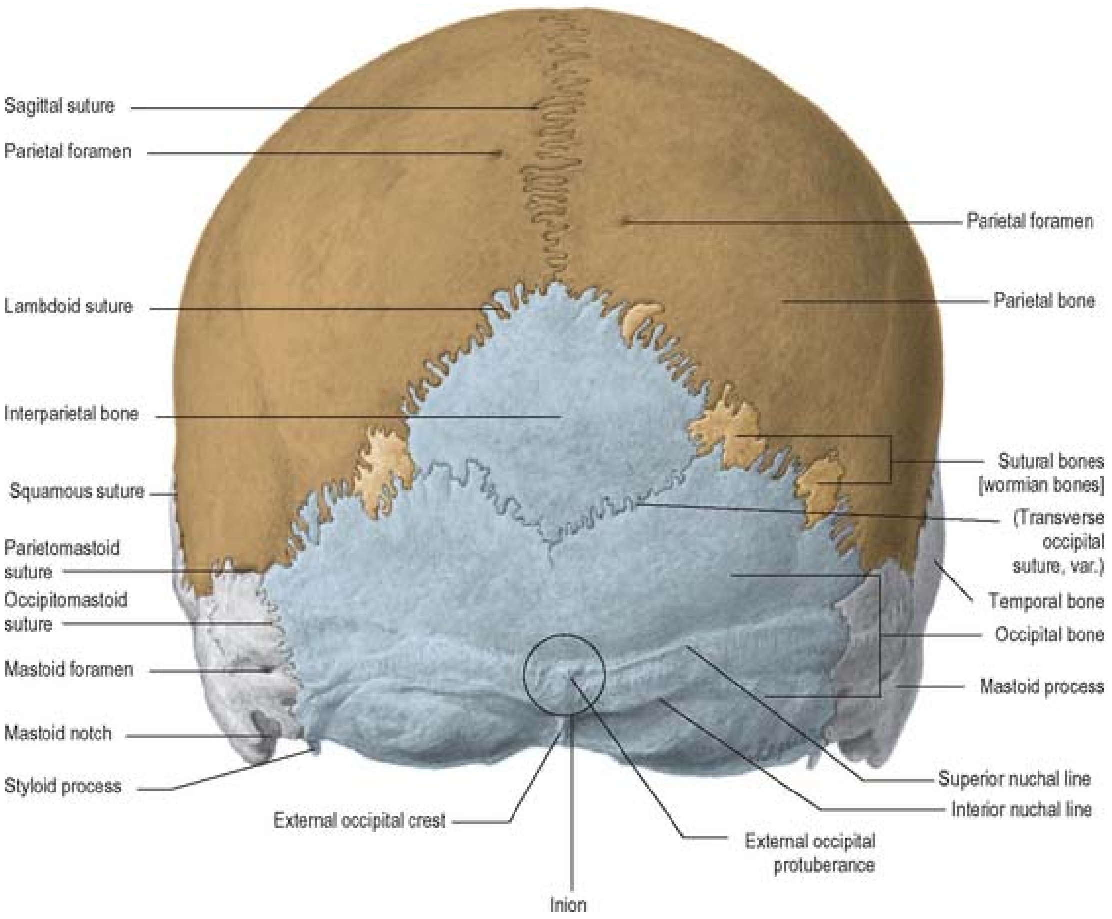
Sagittal suture
Parietal foramen
Lambdoid suture
Interparietal bone
Squamous suture
Parietomastoid suture
Occipitomastoid suture
Mastoid foramen
Mastoid notch
Styloid process
External occipital crest
Inion
External occipital protuberance
Parietal foramen
Parietal bone
Sutural bones [wormian bones]
(Transverse occipital suture, var.)
Temporal bone
Occipital bone
Mastoid process
Superior nuchal line
Inferior nuchal line

Fig. 26.2 Bones of the adult skull, posterior aspect.

(From Sobotta 2006.)

The external occipital protuberance is a midline ridge or a distinct process on the occipital bone which can become particularly well developed in the male. Superior nuchal lines extend laterally from the protuberance and represent the boundary between the scalp and the neck. Inferior nuchal lines run parallel to, and below, the superior nuchal lines; a set of highest nuchal lines may sometimes occur above the superior lines. The external occipital protuberance, nuchal lines and roughened external surface of the occipital bone between the nuchal lines, all afford attachment to muscles of the neck.

SUPERIOR VIEW

Seen from above, the contour of the cranial vault varies greatly but is usually ellipsoid, or more strictly, a modified ovoid with its greatest width lying nearer to the occipital pole (Fig. 26.3). Four bones constitute this view and articulate via three well-defined sutures. The squamous part of the frontal bone is anterior, the squamous part of the occipital bone is posterior and the two parietal bones meet in the midline and separate the frontal from the occipital bone. The maximal parietal convexity on each site is palpable at the parietal tuber or eminence: it is most conspicuous in the female who ostensibly retains a paedomorphic appearance. The superior and inferior temporal lines run close to the parietal eminence but are best seen in a lateral view.

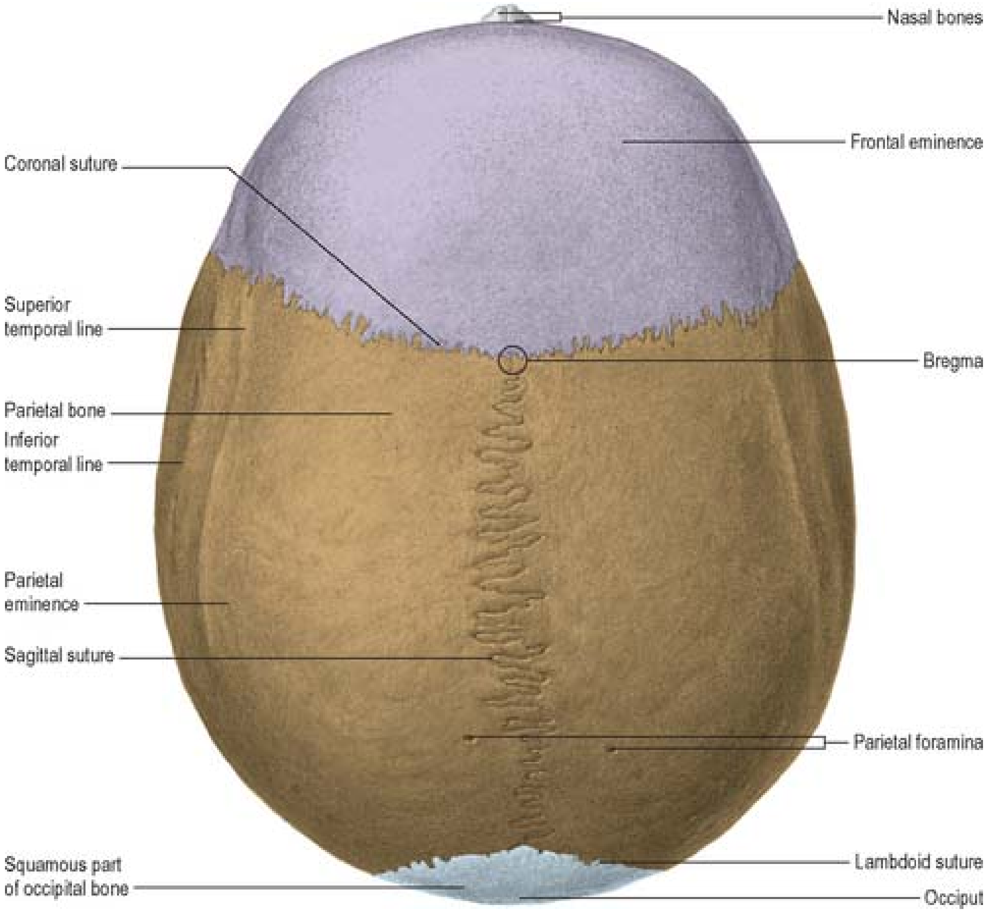
Nasal bones
Frontal eminence
Coronal suture
Superior temporal line
Bregma
Parietal bone
Inferior temporal line
Parietal eminence
Sagittal suture
Parietal foramina
Squamous part of occipital bone
Lambdoid suture
Occiput

Fig. 26.3 Bones of the adult skull, superior aspect.

(From Sobotta 2006.)

The coronal suture marks the articulation between the posterior margin of the frontal bone and the anterior margins of the two parietal bones. It descends across the cranial vault and projects inferiorly until it meets the junction between the greater wing of the sphenoid and the squamous temporal bone at the pterion. The sagittal suture runs in the midline between the two parietal bones and extends from the bregma anteriorly to the lambda posteriorly. The lambdoid suture delineates the articulation between the posterior borders of the right and left parietal bones and the superior border of the occipital bone.

The bregma represents the position of the fetal anterior fontanelle and is the junction between the coronal and sagittal sutures. The anterior fontanelle is a diamond-shaped membrane-filled space located between the two frontal and two parietal bones of the developing fetal skull and persists until approximately 18 months after birth. The lambda, at the junction of the sagittal and lambdoid sutures, is the site of the posterior fontanelle, which persists for the first 2–3 months after birth.

A parietal foramen may pierce either or both parietal bones near the sagittal suture about 3.5 cm anterior to the lambda. It transmits a small emissary vein from the superior sagittal sinus. The vertex is the highest point on the skull and it usually occupies a position in the middle third of the sagittal suture.

LATERAL VIEW

The skull, viewed from the side, can be subdivided into three zones: face (anterior); temporal region (middle); occipital region (posterior) (Fig. 26.4). The face has been considered in the section on the anterior view of the skull.

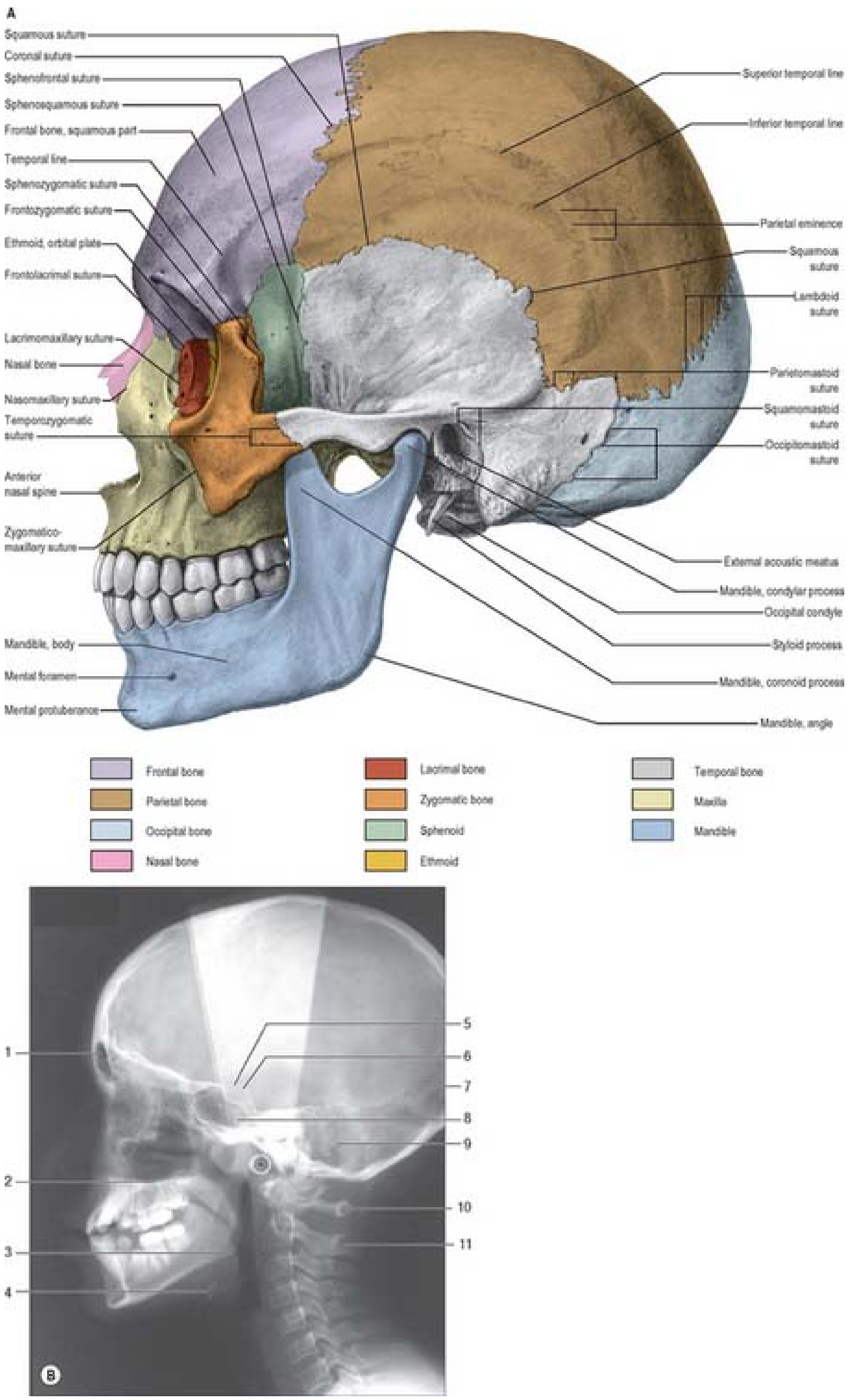
A
Squamous suture
Coronal suture
Sphenofrontal suture
Sphenosquamous suture
Frontal bone, squamous part
Temporal line
Sphenozygomatic suture
Frontozygomatic suture
Ethmoid, orbital plate
Frontolacrimal suture
Lacrimomaxillary suture
Nasal bone
Nasomaxillary suture
Temporozygomatic suture
Anterior nasal spine
Zygomatico-maxillary suture
Mandible, body
Mental foramen
Mental protuberance
Superior temporal line
Inferior temporal line
Parietal eminence
Squamous suture
Lambdoid suture
Parietomastoid suture
Squamomastoid suture
Occipitomastoid suture
External acoustic meatus
Mandible, condylar process
Occipital condyle
Styloid process
Mandible, coronoid process
Mandible, angle
Frontal bone
Parietal bone
Occipital bone
Nasal bone
Lacrimal bone
Zygomatic bone
Sphenoid
Ethmoid
Temporal bone
Maxilla
Mandible
B
1
2
3
4
5
6
7
8
9
10
11

Fig. 26.4 **A**, Bones of the adult skull, lateral aspect. **B**, True cephalometric lateral skull and cervical spine, young adult. Head is held in a cephalostat to obtain true lateral view. The concentric circle is the ear rod placed in the external auditory meatus (bilaterally) and the brighter area

over the middle third of the skull is the head band. The soft tissues of the face can just be discerned. **1**. Frontal sinus. **2**. Hard palate. **3**. Angle of mandible. **4**. Hyoid bone. **5**. Pituitary fossa. **6**. Posterior clinoid process. **7**. Lambdoid suture. **8**. Sphenoidal sinus. **9**. Mastoid air cells. **10**. Posterior tubercle of atlas. **11**. Spinous process of axis.

***A** (From Sobotta 2006.) (**B** by courtesy of Mr Eric Whaites, Dental Institute, King's College, London.)*

The temporal region can be divided into an upper temporal fossa and a lower infratemporal fossa, separated by the zygomatic arch. The temporal fossa is bounded inferiorly by the zygomatic arch, superiorly and posteriorly by the temporal lines and anteriorly by the frontal process of the zygomatic bone, and is continuous inferiorly with the infratemporal fossa deep to the zygomatic arch. The temporal lines often present anteriorly as distinct ridges, but become much less prominent as they arch posteriorly across the parietal bone. Indeed, the superior line may become quite indistinct posteriorly. The inferior temporal line becomes more prominent as it curves down the posterior part of the squamous temporal bone, forming a supramastoid crest at the base of the mastoid process. The superior temporal line gives attachment to the temporal fascia while the inferior temporal line provides attachment for temporalis.

The floor of the temporal fossa is formed by the frontal and parietal bones superiorly and the greater wing of the sphenoid and squamous temporal inferiorly. All four bones of one side meet at an H-shaped sutural junction termed the pterion. This is an important anthropometric landmark as it overlies both the anterior branch of the middle meningeal artery and the lateral fissure of the cerebral hemisphere. The pterion corresponds to the site of the anterolateral (sphenoidal) fontanelle of the neonatal skull which closes in the third month after birth.

The vertical suture between the sphenoid and temporal bones, the sphenosquamosal suture, is formed by articulation between the posterior border of the greater wing of the sphenoid and the anterior border of the squamous part of the temporal bone.

The lateral surface of the ramus of the mandible will be described briefly here as its position lies within the middle region of this view of the skull (see Ch. 31). The ramus is a plate of bone projecting upwards from the back of the body of the mandible; its lateral surface gives attachment to masseter. The ramus bears two prominent processes superiorly, the coronoid process anteriorly and condylar process posteriorly, separated by the mandibular notch. The coronoid process is the site of insertion of temporalis and the condylar process articulates with the mandibular fossa of the temporal bone at the temporomandibular joint. The inferior and posterior borders of the mandible meet at the angle, which is often splayed in the male because of the larger site of muscle attachment for medial pterygoid on the internal surface.

The zygomatic arch stands clear of the rest of the skull, and the temporal and infratemporal fossae communicate via the gap thus created. In life, this space is largely filled by temporalis. The zygomatic bone is the principal bone of the cheek together with the zygomatic processes of the maxillae and temporal bones. The term ‘zygomatic arch’ is generally restricted to the temporal process of the zygomatic bone and the zygomatic process of the temporal bone, which articulate at the zygomaticotemporal suture. The suture between the zygomatic process of the frontal bone and the frontal process of the zygomatic bone is the frontozygomatic suture, that between the maxillary margin of the zygomatic bone and the zygomatic process of the maxillary bone is the zygomaticomaxillary suture, and between the sphenoid and zygomatic is the sphenozygomatic suture. As the zygomatic process of the temporal bone passes posteriorly, it becomes associated with the articular tubercle of the mandibular fossa anteriorly and the supramastoid crest posteriorly.

The temporal bone is a prominent structure on the lateral aspect of the skull. Its squamous part lies in the floor of the temporal fossa and its zygomatic process contributes to the structure of the cheek. Additional components visible in the lateral view of the skull are the mandibular fossa and its articular eminence (tubercle), the tympanic plate, the external acoustic meatus, and the mastoid and styloid processes.

The mandibular (glenoid) fossa is the part of the temporomandibular joint with which the condylar process of the mandible articulates. It is bounded in front by the articular eminence and behind by the tympanic plate. The articular eminence provides a surface over which the mandibular condyle glides during mandibular movements (see Ch. 31).

The tympanic plate of the temporal bone contributes most of the margin of the external acoustic (auditory) meatus, and the squamous part forms the posterosuperior region (see Ch. 36). The external margin is roughened to provide an attachment for the cartilaginous part of the meatus. A small depression, the suprameatal triangle, lies above and behind the meatus and is related to the lateral wall of the mastoid antrum.

The mastoid process is a small inferior projection of the temporal bone, lying posteroinferior to the external acoustic meatus and is the site of attachment of sternocleidomastoid. It is in contact behind with the posteroinferior angle of the parietal bone at the parietomastoid suture and with the squamous part of the occipital bone at the occipitomastoid suture. These two sutures meet the lateral end of the lambdoid suture at the asterion, which coincides with the site of the posterolateral fontanelle in the neonatal skull and which closes during the second year. A mastoid foramen may be found near or in the occipitomastoid suture and transmits an emissary vein from the sigmoid sinus. Sutural bones may appear in the parietomastoid suture.

The styloid process lies anterior and medial to the mastoid process and gives attachment to several muscles and ligaments. Its base is partly ensheathed by the tympanic plate and it descends anteromedially, its tip usually reaching a point medial to the posterior margin of the mandibular ramus. However, the styloid process is very variably developed, and ranges in length from a few millimetres to a few centimetres.

The infratemporal fossa is an irregular postmaxillary space located deep to the ramus of the mandible; it communicates with the temporal fossa deep to the zygomatic arch (see Ch. 31). It is best visualized, therefore, when the mandible is removed but, for completeness, is considered here. Its roof is the infratemporal surface of the greater wing of the sphenoid. The lateral pterygoid plate lies medial to the fossa and the ramus of the mandible and styloid process lie laterally and posteriorly respectively. The infratemporal fossa has no anatomical floor. Its anterior and medial walls are separated above by the pterygomaxillary fissure lying between the lateral pterygoid plate and the posterior wall of the maxilla. The infratemporal fossa communicates with the pterygopalatine fossa through the pterygomaxillary fissure.

INFERIOR (BASAL) VIEW

The inferior surface of the skull, the base of the cranium, is complex: it extends from the upper incisor teeth anteriorly to the superior nuchal lines of the occipital bone posteriorly (Fig. 26.5). The region contains many of the foramina through which structures enter and exit the cranial cavity. The inferior surface can be conveniently subdivided into anterior, middle, posterior and lateral parts. The anterior part contains the hard palate and the dentition of the upper jaw and lies at a lower level than the rest of the cranial base. The middle and posterior parts can be arbitrarily divided by a transverse plane passing through the anterior margin of the foramen magnum. The middle part is occupied mainly by the base of the sphenoid bone, the apices of the petrous processes of the temporal bones and the basilar part of the occipital bone. The lateral part contains the zygomatic arches, mandibular fossa, tympanic plate and the styloid and mastoid processes. The posterior part lies in the midline and is exclusively formed from the occipital bone. Whereas the middle and posterior parts are directly related to the cranial cavity (the middle and posterior cranial fossae), the anterior part (the palate) is some distance from the anterior cranial fossa, being separated from it by the nasal cavities.

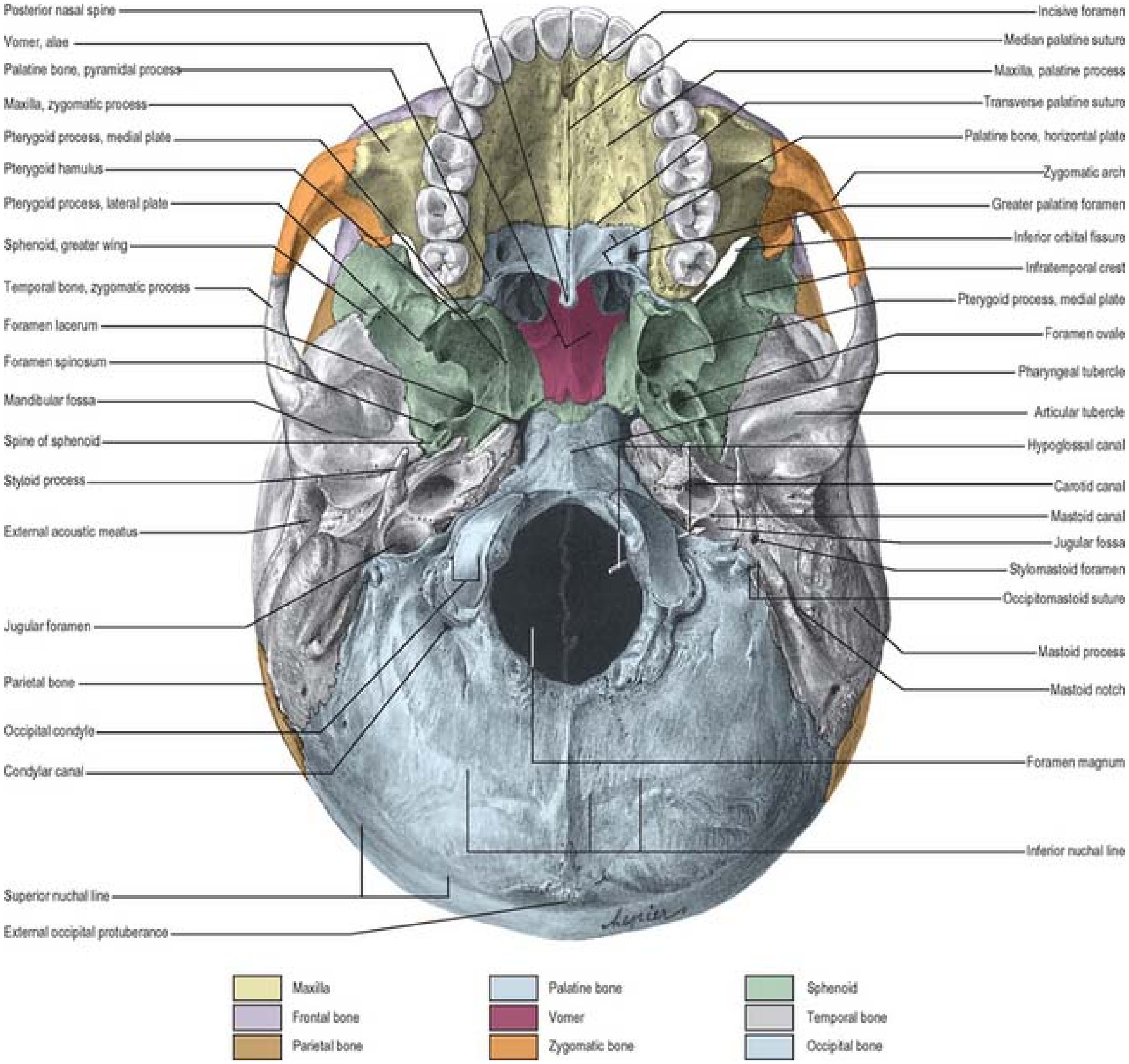
Posterior nasal spine
Vomer, alae
Palatine bone, pyramidal process
Maxilla, zygomatic process
Pterygoid process, medial plate
Pterygoid hamulus
Pterygoid process, lateral plate
Sphenoid, greater wing
Temporal bone, zygomatic process
Foramen lacerum
Foramen spinosum
Mandibular fossa
Spine of sphenoid
Styloid process
External acoustic meatus
Jugular foramen
Parietal bone
Occipital condyle
Condylar canal
Superior nuchal line
External occipital protuberance
Incisive foramen
Median palatine suture
Maxilla, palatine process
Transverse palatine suture
Palatine bone, horizontal plate
Zygomatic arch
Greater palatine foramen
Inferior orbital fissure
Infratemporal crest
Pterygoid process, medial plate
Foramen ovale
Pharyngeal tubercle
Articular tubercle
Hypoglossal canal
Carotid canal
Mastoid canal
Jugular fossa
Stylomastoid foramen
Occipitomastoid suture
Mastoid process
Mastoid notch
Foramen magnum
Inferior nuchal line
Maxilla
Frontal bone
Parietal bone
Palatine bone
Vomer
Zygomatic bone
Sphenoid
Temporal bone
Occipital bone

Fig. 26.5 External surface of the base of the adult skull.

(From Sobotta 2006.)

ANTERIOR PART OF CRANIAL BASE

The bony palate within the superior alveolar arch is formed by the palatine processes of the maxillae anteriorly and the horizontal plates of the palatine bones posteriorly, all meeting at a cruciform system of sutures (Fig. 26.5). The median palatine suture runs anteroposteriorly and divides the palate into right and left halves. This suture is continuous with the intermaxillary suture between the maxillary central incisor teeth. The transverse palatine (palatomaxillary) sutures run transversely across the palate between the maxillae and the palatine bones. The palate is arched sagittally and transversely: its depth and breadth are variable but are always greatest in the molar region. The incisive fossa lies behind the central incisor teeth, and the lateral incisive foramina, through which incisive canals pass to the nasal cavity, lie in its lateral walls. Median incisive foramina are present in some skulls and open onto the anterior and posterior walls of the fossa. The incisive fossa transmits the nasopalatine nerve and the termination of the greater palatine vessels. When median incisive foramina occur, the left nasopalatine nerve usually traverses the anterior foramen and the right nerve traverses the posterior foramen. The greater palatine foramen lies near the lateral palatal border of the transverse palatine suture; a vascular groove, deeper behind and shallower in front, leads forwards from the foramen. The lesser palatine foramina, usually two, lie behind the greater palatine foramen and pierce the pyramidal process of the palatine bone which is wedged between the lower ends of the medial and lateral pterygoid plates. The palate is pierced by many other small foramina and is marked by pits for palatine glands. Variably prominent palatine crests extend medially from behind the greater palatine foramina. The posterior border projects back as the posterior nasal spine. In the adult, the alveolar arch bears a maximum of 16 sockets or alveoli for the teeth: the sockets vary in size and depth, some are single and some are subdivided by septa, according to the morphology of the dental roots.

The nasal fossae lie above the hard palate and are separated by the nasal septum in the midline. The nasal septum is formed from the perpendicular plate of the ethmoid superiorly and the vomer inferiorly. The upper border of the vomer approximates to the inferior aspect of the body of the sphenoid, where it expands into an ala on each side. The two posterior nasal apertures (choanae) are located where the nasal fossae end: they are separated by the free posterior border of the vomer, and bounded below by the posterior border of the horizontal plate of the palatine bones, above by the sphenoid and laterally by the medial pterygoid plates.

MIDDLE PART OF CRANIAL BASE

The middle part of the cranial base is made up from the body of the sphenoid, the petrous temporal bones and the basiocciput (Fig. 26.5). It extends from the posterior nares anteriorly to an artificial line drawn transversely through the anterior margin of the foramen magnum posteriorly. In the adult, the body of the sphenoid fuses with the basiocciput to form a midline bar of bone that extends posteriorly to the foramen magnum. The basilar part of the occipital bone bears a small midline pharyngeal tubercle, which gives attachment to the pharyngeal raphe and the highest attachment of the superior pharyngeal constrictor.

The middle part of the cranial base is completed by the petrous processes of the two temporal bones, which pass from the lateral sides of the base of the skull and fill the triangular space between the greater wing of the sphenoid anteriorly and the lateral margins of the basiocciput posteriorly. Each petrous process meets the basilar part of the occipital bone at a petro-occipital suture, which is deficient posteriorly at the jugular foramen. The petrosphenoidal suture and the groove for the pharyngotympanic tube lie between the petrous process and the infratemporal surface of the greater wing of the sphenoid. The apex of the petrous process does not meet the spheno-occipital suture, and the deficit so produced forms the foramen lacerum.

Pterygoid processes descend from the junction between the greater wing and body of the sphenoid bone. Each separates into two laminae, the medial and lateral pterygoid plates, which are separated by a pterygoid fossa. Anteriorly the plates are fused, except inferiorly, where they are separated by the pyramidal process of the palatine bone. Sutures are usually discernible at this site. Laterally the pterygoid plates are separated from the posterior maxillary surface by the pterygomaxillary fissure, which leads into the pterygopalatine fossa. The posterior border of the medial pterygoid plate is sharp, and bears a small projection near the midpoint, above which it is curved and attached to the pharyngeal end of the pharyngotympanic tube. Above, the medial pterygoid plate divides to enclose the scaphoid fossa, while below it projects as a slender pterygoid hamulus, which curves laterally and is grooved anteriorly by the tendon of tensor veli palatini. The pterygoid hamulus gives origin to the pterygomandibular raphe. The lateral pterygoid plate projects posterolaterally and its lateral surface forms the medial wall of the infratemporal fossa. Superiorly and laterally the pterygoid process is continuous with the infratemporal surface of the greater wing of the sphenoid bone which forms part of the roof of the infratemporal fossa. This surface forms the posterolateral border of the inferior orbital fissure and bears an infratemporal crest associated with the origin of the upper part of lateral pterygoid. The infraorbital and zygomatic branches of the maxillary nerve and accompanying vessels pass through the inferior orbital fissure. Laterally the greater wing of the sphenoid articulates with the squamous part of the temporal bone.

The medial aspect of the greater wing of the sphenoid presents a crescent of foramina of which only the most posterior two, foramen ovale and foramen spinosum, can be viewed on the basal aspect. The foramen ovale lies medial to the foramen spinosum and lateral to the foramen lacerum on the infratemporal surface of the greater wing of the sphenoid bone. It transmits the mandibular division of the trigeminal nerve, the lesser petrosal nerve, the accessory meningeal branch of the maxillary artery and an emissary vein which connects the cavernous venous sinus to the pterygoid venous plexus in the infratemporal fossa. Posterolaterally, the smaller and rounder foramen spinosum transmits the middle meningeal artery and a recurrent meningeal branch of the mandibular nerve. The irregular spine of the sphenoid projects posterolateral to the foramen spinosum. The medial surface of the spine is flat and, with the adjoining posterior border of the greater wing of the sphenoid, forms the anterolateral wall of a groove that is completed posteromedially by the petrous part of the temporal bone. This groove contains the cartilaginous pharyngotympanic tube which leads posterolaterally into the bony portion of the tube that lies within the petrous part of the temporal bone. Occasionally the foramen ovale and foramen spinosum are confluent or the posterior edge of the foramen spinosum may be defective. A small foramen, the sphenoidal emissary foramen (of Vesalius), is sometimes found between the foramen ovale and scaphoid fossa.

When present, it contains an emissary vein linking the pterygoid venous plexus in the infratemporal fossa with the cavernous sinus in the middle cranial fossa.

The foramen lacerum is bounded in front by the body and adjoining roots of the pterygoid process and greater wing of the sphenoid bone, posterolaterally by the apex of the petrous part of the temporal bone and medially by the basilar part of the occipital bone. Although it is nearly 1 cm long, it is not traversed by any major structure. The almost circular carotid canal lies behind and posterolateral to the foramen lacerum in the petrous part of the temporal bone. The internal carotid artery enters the skull through this foramen, ascends in the carotid canal, and turns anteromedially to reach the posterior wall of the foramen lacerum. It ascends through the upper end of the foramen lacerum accompanied by venous and sympathetic nerve plexuses. Meningeal branches of the ascending pharyngeal artery and emissary veins from the cavernous sinus also traverse the foramen lacerum. In life, the lower part of the foramen lacerum is partially occluded by cartilaginous remnants of the embryological chondrocranium. The pterygoid canal can be seen on the base of the skull at the anterior margin of the foramen lacerum, above and between the pterygoid plates of the sphenoid bone. It leads into the pterygopalatine fossa and transmits the nerve of the pterygoid canal and accompanying blood vessels.

POSTERIOR PART OF CRANIAL BASE

The posterior part of the cranial base is largely formed by the occipital bone (Fig. 26.5). Prominent features are the foramen magnum and associated occipital condyles, jugular foramen, mastoid notch and squamous part of the occipital bone up to the external occipital protuberance and the superior nuchal lines, hypoglossal canals (anterior condylar canals) and condylar canals (posterior condylar canals).

The foramen magnum lies in an anteromedian position and leads into the posterior cranial fossa. It is oval and wider behind, with its greatest diameter being anteroposterior. It contains the lower end of the medulla oblongata, meninges, vertebral arteries and spinal accessory nerve: the apical ligament of the dens and the tectorial membrane pass through it to attach to the internal basiocciput. Anteriorly, the margin of the foramen magnum is slightly overlapped by the occipital condyles which project down to articulate with the superior articular facets on the lateral masses of the atlas. Each occipital condyle is oval in outline and oriented obliquely so that its anterior end lies nearer the midline than its posterior end. It is markedly convex anteroposteriorly, less so transversely, and its medial aspect is roughened by ligamentous attachments. The hypoglossal canal, directed laterally and slightly forwards, traverses deep to each condyle and transmits the hypoglossal nerve, a meningeal branch of the ascending pharyngeal artery and an emissary vein from the basilar plexus. A depression, the condylar fossa, lies immediately posterior to the condyle and sometimes contains a (posterior) condylar canal for an emissary vein from the sigmoid sinus. This fossa accommodates the posterior margin of the atlas when the head is fully extended. A jugular process articulates with the petrous part of the temporal bone lateral to each condyle and its anterior free border forms the posterior boundary of the jugular foramen.

Laterally, the occipital bone articulates with the petrous part of the temporal bone anteriorly at the petro-occipital suture, and the mastoid process of the temporal bone more posteriorly at the petromastoid suture. The jugular foramen, a large irregular hiatus, lies at the posterior end of the petro-occipital suture between the jugular process of the occipital bone and the jugular fossa of the petrous part of the temporal bone. A number of important structures pass through this foramen: inferior petrosal sinus (anterior); glossopharyngeal, vagus and accessory cranial nerves (middle); internal jugular vein (posterior). A mastoid canaliculus runs through the lateral wall of the jugular fossa and transmits the auricular branch of the vagus nerve. The canaliculus for the tympanic nerve branch of the glossopharyngeal nerve lies on the ridge between the jugular fossa and the opening of the carotid canal. A small notch, related to the inferior glossopharyngeal ganglion, may be found medially, on the upper boundary of the jugular foramen (it is more easily identified internally). The orifice of the cochlear canaliculus may be found at the apex of the notch.

The squamous part of the occipital bone exhibits the external occipital protuberance, supreme, superior and inferior nuchal lines, and the external occipital crest, all of which lie in the midline, posterior to the foramen magnum. The region is roughened for the attachment of muscles whose primary function is extension of the skull (see Ch. 42).

LATERAL PART OF CRANIAL BASE

The lateral part of the cranial base consists of the zygomatic arch and infratemporal fossa anteriorly and the mandibular fossa, tympanic plate and styloid and mastoid processes posteriorly (Fig. 26.5) – the anterior structures have been considered earlier in this chapter.

A thin-walled depression in the temporal bone, the mandibular fossa, may be most easily inspected when the mandible is removed. The zygomatic arch extends laterally in front of the fossa and a distinct ridge, the articular eminence, lies anterior to the fossa. Three fissures can be distinguished behind the mandibular fossa. The squamotympanic fissure extends from the spine of the sphenoid, between the mandibular fossa and the tympanic plate of the temporal bone, and curves up the anterior margin of the external acoustic meatus. A thin wedge of bone forming the inferior margin of the tegmen tympani lies within the fissure and divides the squamotympanic fissure into petrotympanic and petrosquamous fissures. The petrotympanic fissure transmits the chorda tympani branch of the facial nerve from the intracranial cavity into the infratemporal fossa. The tympanic plate forms the floor of the external auditory meatus.

The stylomastoid foramen lies between the mastoid and styloid processes on the lateral aspect of the temporal bone. It transmits the facial nerve and the stylomastoid artery. A groove, the mastoid notch, lies medial to the mastoid process and gives origin to the posterior belly of digastric. A groove related to the occipital artery often lies medial to the mastoid notch. A mastoid foramen may be present near or in the occipitomastoid suture; when present, it transmits an emissary vein from the sigmoid sinus. The external acoustic meatus lies in front of the mastoid process. It is surrounded inferiorly by the tympanic plate which partly ensheathes the base of the styloid process as the vaginal process.

CRANIAL FOSSAE (ANTERIOR, MIDDLE, POSTERIOR)

The cranial fossae are described in Chapter 27.

DISARTICULATED INDIVIDUAL BONES

Individual bones are described in appropriate chapters. The bones of the facial skeleton and cranial vault are described in the chapters on the face and scalp (29), nose and paranasal sinuses (32), external and middle ear (35) and orbit (39). The sphenoid and mandible are described in the chapter on the infratemporal fossa and the occipital bone is described in the chapter on the neck.

JOINTS

The general characteristics of cranial sutures and the detailed anatomy of the temporomandibular joint and the atlanto-occipital joints are described in Chapters 5, 31 and 42, respectively. Sutural bones are described below on page 418.

NEONATAL, PAEDIATRIC AND SENESCENT ANATOMY

THE SKULL AT BIRTH

At birth the skull is large in proportion to other skeletal parts; the facial region is relatively small and constitutes only about one-eighth of the neonatal cranium, compared with half in adult life (Fig. 26.6). Smallness of the face at birth is largely due to the rudimentary stage of development of the mandible and maxillae because the teeth are unerupted. The nose lies almost entirely between the orbits, and the lower border of the nasal aperture is only slightly lower in position than the orbital floors. The large size of the calvaria, especially the neurocranium, reflects precocious cerebral maturation. Bones of the cranial vault are unilaminar and lack diploë. Frontal and parietal tuberosities are prominent; in the frontal view, the greatest width occurs between the parietal tuberosities. The glabella, superciliary arches and mastoid processes are not developed and the cranial base is relatively short and narrow.

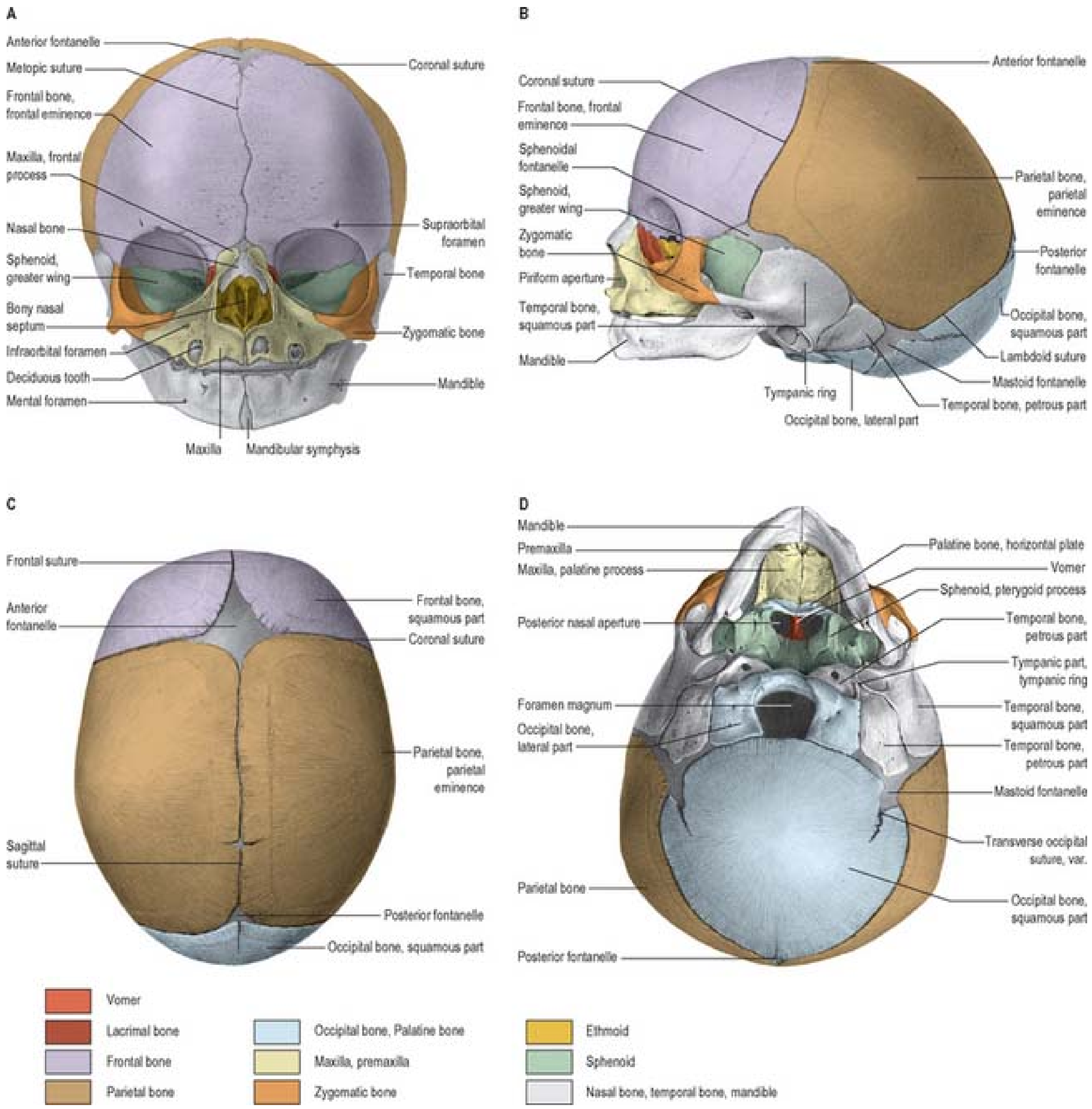
A
Anterior fontanelle
Metopic suture
Frontal bone, frontal eminence
Maxilla, frontal process
Nasal bone
Sphenoid, greater wing
Bony nasal septum
Infraorbital foramen
Deciduous tooth
Mental foramen
Maxilla
Mandibular symphysis
Coronal suture
Supraorbital foramen
Temporal bone
Zygomatic bone
Mandible
B
Coronal suture
Frontal bone, frontal eminence
Sphenoidal fontanelle
Sphenoid, greater wing
Zygomatic bone
Piriform aperture
Temporal bone, squamous part
Mandible
Tympanic ring
Occipital bone, lateral part
Anterior fontanelle
Parietal bone, parietal eminence
Posterior fontanelle
Occipital bone, squamous part
Lambdoid suture
Mastoid fontanelle
Temporal bone, petrous part
C
Frontal suture
Anterior fontanelle
Sagittal suture
Frontal bone, squamous part
Coronal suture
Parietal bone, parietal eminence
Posterior fontanelle
Occipital bone, squamous part
D
Mandible
Premaxilla
Maxilla, palatine process
Posterior nasal aperture
Foramen magnum
Occipital bone, lateral part
Parietal bone
Posterior fontanelle
Palatine bone, horizontal plate
Vomer
Sphenoid, pterygoid process
Temporal bone, petrous part
Tympanic part, tympanic ring
Temporal bone, squamous part
Temporal bone, petrous part
Mastoid fontanelle
Transverse occipital suture, var.
Occipital bone, squamous part
Vomer
Lacrimal bone
Frontal bone
Parietal bone
Occipital bone, Palatine bone
Maxilla, premaxilla
Zygomatic bone
Ethmoid
Sphenoid
Nasal bone, temporal bone, mandible

Fig. 26.6 **A–D**, Neonatal skull. **A**, frontal aspect; **B**, lateral aspect; **C**, superior aspect; **D**, basal aspect.

(From Sobotta 2006.)

Ossification is incomplete, and many bones are still in several elements united by fibrous tissue or cartilage. The ‘os incisivum’ is continuous with the maxilla; pre- and postsphenoids have just united, but the two halves of the frontal bone and mandible, and the squamous, lateral and basilar parts of the occipital bone are all separate. A second styloid centre (stylohyal) has not appeared, and parts of the temporal bones are separate except that fusion of the tympanic with the petrous and squamous parts has started. The fibrous membrane that forms the cranial vault before ossification is unossified at the angles of the parietal bones, producing six fontanelles: two median (anterior and posterior) and two lateral pairs (sphenoidal/anterolateral and mastoid/posterolateral). The anterior fontanelle is the largest and measures approximately 4 cm in anteroposterior and 2.5 cm in transverse dimensions. It occupies the junction between the sagittal, coronal and frontal sutures and is therefore rhomboid in shape. The posterior fontanelle lies at the junction between the sagittal and lambdoid sutures and is therefore triangular. The sphenoidal (anterolateral) and mastoid (posterolateral) fontanelles are small, irregular and occur at the sphenoidal and mastoid angles of the parietal bones respectively.

At birth the orbits appear relatively large. The developing tooth germs are generally contained within the alveolar crypts, although eruption of the upper central incisor teeth can occur prior to, or shortly after, birth. Temporal bones differ greatly from their adult form. The internal ear, tympanic cavity, auditory ossicles and mastoid antrum are all almost adult in size, the tympanic plate is an incomplete ring which has usually started to fuse with the squamous part, and the mastoid process is absent. The external acoustic meatus is short, straight and wholly cartilaginous. The external aspect of the tympanic membrane faces more inferiorly than laterally, in accord with the basal cranial contour. The stylomastoid foramen is exposed on the lateral surface of the skull, the styloid process has not fused with the temporal bone, the mandibular fossa is flat and more lateral, and its articular tubercle is undeveloped. The paranasal sinuses are rudimentary or absent and only the maxillary sinuses are usually identifiable.

During birth the skull is moulded by slow compression. That part of the scalp which is more central in the birth canal is often temporarily oedematous as a result of interference with venous return, and is called the caput succedaneum. Fontanelles and the openness and width of the sutures allow bones of the cranial vault some overlap. The skull is compressed in one plane with compensatory orthogonal elongation. These effects disappear within the first week after birth.

POSTNATAL GROWTH

Although postnatal growth of the vault and facial skeleton usually proceeds in a co-ordinated fashion, these regions exhibit different rates and temporal periods of expression. In general, early growth of the vault is largely influenced by cerebral maturation while growth of the facial skeleton responds to spatial requirement for the development of the teeth and the muscles of mastication. Growth of the cranial base is largely independent of both vault and facial development and therefore the three regions must be considered separately.

Growth of the vault

Growth of the vault is rapid during the first year and then continues at a slower rate until the seventh year, when it has reached almost adult dimensions. For most of this period, expansion is largely concentric; overall form is determined early in the first year and remains largely unaltered thereafter. However, the shape of the vault is not solely related to cerebral growth, but is also influenced by genetic factors that manifest in an extensive range of shapes and sizes that may be sufficient to allow a reliable evaluation of racial origin. During the first and early second year, growth of the vault occurs primarily through ossification at apposed margins of bones (which possess an osteogenic layer) accompanied by some accretion and absorption of bone at surfaces in order to adapt to continually altering curvatures. Growth in breadth is said to occur at the sagittal, sphenofrontal, sphenotemporal, occipitomastoid and petro-occipital junctions, while growth in height is said to occur at the frontozygomatic and squamosal sutures, pterion and asterion. During this period, fontanelles are closed by progressive ossification of the bones around them, but separate rogue centres of ossification may develop into sutural bones. The sphenoidal and posterior fontanelles ossify within 2 or 3 months of birth, the mastoid fontanelles usually ossify near the end of the first year and the anterior fontanelle ossifies around the middle of the second year. Those fontanelles which close first are most likely to show sutural bones.

Early in the first years the calvarial bones commence interlocking at sutural junctions. Further expansion of the vault is largely achieved by accretion and absorption on external and internal bone surfaces respectively. At the same time the bones also thicken, although this is not a uniform process. At birth the vault is unilaminar but the tabular structure with intervening diploë is generally apparent by about the fourth year. Thickening of the vault and development of external muscular markings reflect the influences of musculoskeletal maturation. The mastoid processes do not develop until the second year and they are invaded by air cells (pneumatized) in the sixth year.

Growth of the base

Growth in the cranial base is largely responsible for much of the cranial lengthening: it occurs at the cartilaginous joints between the sphenoid and ethmoid anteriorly, and especially between the sphenoid and occipital bones posteriorly. Largely independent of cerebral growth, it continues at the spheno-occipital synchondrosis until the 18th year. The prolonged period of continued expansion reflects a significant delaying mechanism to allow continued and relatively late eruption of the permanent dentition. There is some evidence that growth may cease at about 15 years following eruption of the second molars, which can often lead to insufficient space for growth of the third molars. A pubertal growth spurt has been ascribed to both sexes; it tends to occur some 2 years earlier in females and is likely to continue until the 18th year in the male.

Growth of the face

Growth of the facial skeleton occurs over a longer time period than is witnessed for the calvaria. The ethmoid and the orbital and upper nasal cavities have almost completed growth by the seventh year. Orbital and upper nasal growth is achieved by sutural accretion, with deposition of bone preferentially occurring on the facial aspects of the sutural junctions. The maxilla is carried downwards and forwards by expansion of the orbits and nasal septum and by sutural growth, especially at the fontanelles and zygomaticomaxillary and pterygomaxillary sutures. In the first year, growth in width occurs at the symphysis menti and midpalatal, internasal and frontal sutures: such growth diminishes or even ceases when the symphysis menti and frontal suture close during the first few years, even though the midpalatal suture persists until mature years. Facial growth continues up to puberty and shows a period of expansion that is linked to the growth spurt and hormonal influences of secondary sexual alteration. After sutural growth, near the end of the second year, expansion of the facial skeleton occurs by surface accretion on the face, alveolar processes and palate, and resorption in the walls of the maxillary sinuses, the upper surface of the hard palate and the labial aspect of the alveolar process. Co-ordinated growth and divergence of the pterygoid processes reflects deposition and resorption of bone on appropriate surfaces.

Obliteration of the calvarial sutures progresses with age, starting between 20 and 30 years internally, and somewhat later on the exterior. Closure times vary greatly. Obliteration usually begins in the coronal suture and then extends into the sagittal and lambdoid sutures, in that order. The most striking senile feature is diminution in size of the mandible and maxillae following the loss of teeth and absorption of alveolar bone; this reduces the vertical depth of the face and increases the mandibular angles.

Sutural bones

Additional ossification centres may occur in or near sutures, giving rise to isolated sutural bones (also called Wormian bones, Fig. 26.2). Usually irregular in size and shape, and most frequent in the lambdoid suture, they frequently occur at fontanelles, especially the posterior fontanelle. They may represent a pre-interparietal element, a true interparietal, or some composite. An isolated bone at the lambda is sometimes referred to as an Inca bone or Goethe’s ossicle. One or more pterion ossicles or epipteric bones may appear between the sphenoidal angle of the parietal and the greater wing of the sphenoid; they vary greatly in size but are more or less symmetrical. Sutural bones usually have little morphological significance. However, they appear in great numbers in hydrocephalic skulls (Fig. 26.7), and they have therefore been linked with rapid cranial expansion. For a detailed analysis of these and other epigenetic variations in adult crania, consult Berry & Berry (1967) and Berry (1975).

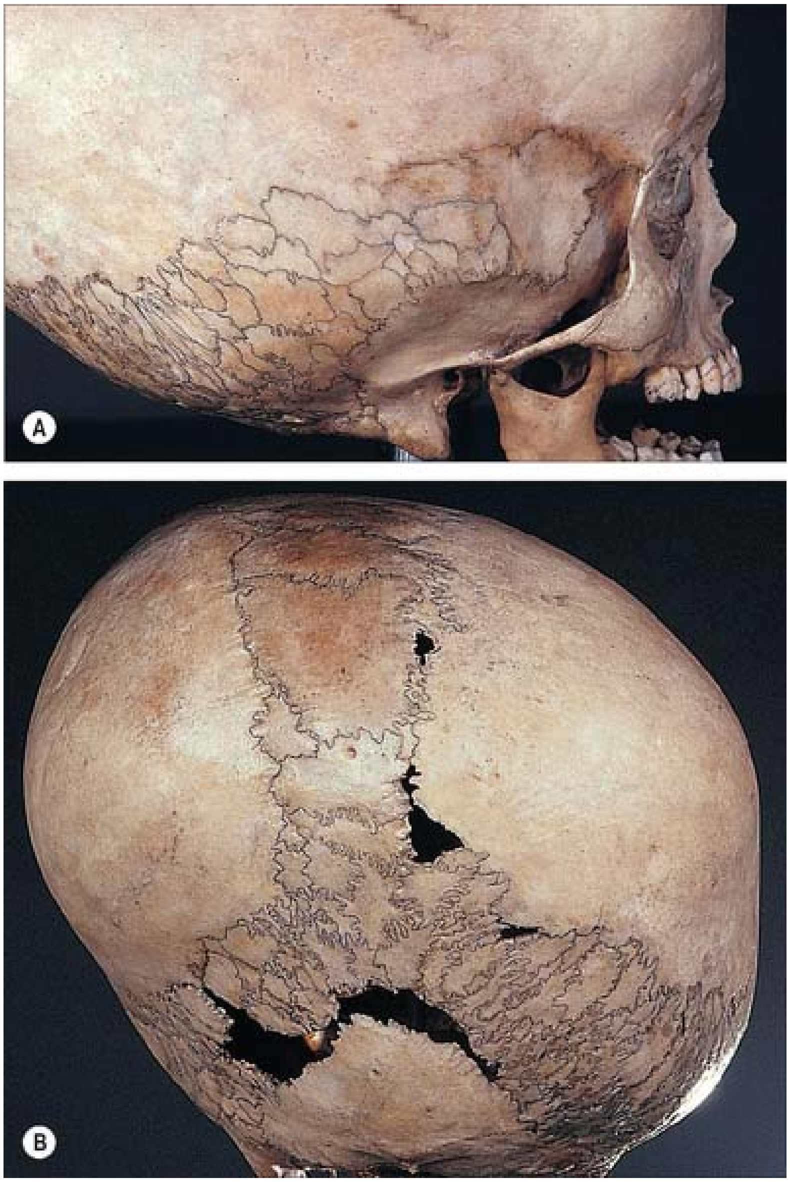

Fig. 26.7 Lateral (**A**) and posterior (**B**) views of the hydrocephalic skull of a 25-year-old male showing numerous sutural bones.

(By courtesy of the Museum of the Royal College of Surgeons of England. Photograph by Mr J Carr.)

Craniosynostosis

Sutural growth makes an important contribution to growth of the skull, especially during the first few years of life. The reasons for premature fusion of sutures (synostosis) are varied, but many occur as a result of small brain size or failure of the development of dural bands between the sutures. Premature fusion may occur in one or more of the cranial sutures: when the sutures around the skull base are involved, severe limitation of facial bone growth will occur. Metabolic disorders such as rickets and familial hypophosphatasia can also result in synostosis. Raised intracranial pressure with or without hydrocephalus, visual deterioration and mental retardation may result. Scaphocephaly (sagittal craniosynostosis) is the commonest and leads to lengthening of the vault in an anteroposterior direction. It also occurs in conjunction with other sutures, e.g. Crouzon's syndrome. Coronal synostosis, either unilateral (plagiocephaly) or bilateral (brachycephaly/oxycephaly) is the next most frequently seen and results in reduced anteroposterior development with marked supraorbital recession. When it is unilateral the face develops asymmetrically and is rotated away from the side with premature fusion. Metopic craniosynostosis (trigonocephaly) and pansynostosis (turricephaly, where both the coronal and sphenofrontal sutures are involved) are much less common.

Treatment of these premature sutural fusions is critical to prevent abnormalities of skull growth and to relieve raised intracranial pressure. It is usually carried out between 3–6 months of age. Treatment consists of release of the sutures involved and the prevention of refusion, which is usually achieved by covering the bone edges with silastic sheeting after the radical removal of bone from either side of the suture line. Simultaneous expansion and reshaping of the skull is often required, particularly if diagnosis has been delayed. It is usually necessary to advance the supraorbital ridge and to straighten it if there is asymmetrical growth (as seen in plagiocephaly).

The craniofacial dysostosis syndromes such as Crouzon's, Apert's, Saethre–Chotzen, Pfeiffer's and Carpenter's, show varying degrees of calvarial synostoses which are usually accompanied by a significant lack of growth in the mid-face. Early release of the calvarial synostoses does not result in normal facial growth, and a midfacial osteotomy at the Le Fort III level is usually required later in life. When significant orbital hypertelorism develops, a transcranial bipartitioning procedure is needed in order to bring the two orbits together.

Skull deformities can also be derived deliberately by affecting sutural growth using binding and other pressure, as has been practiced in certain cultures of the world (Fig. 26.8).

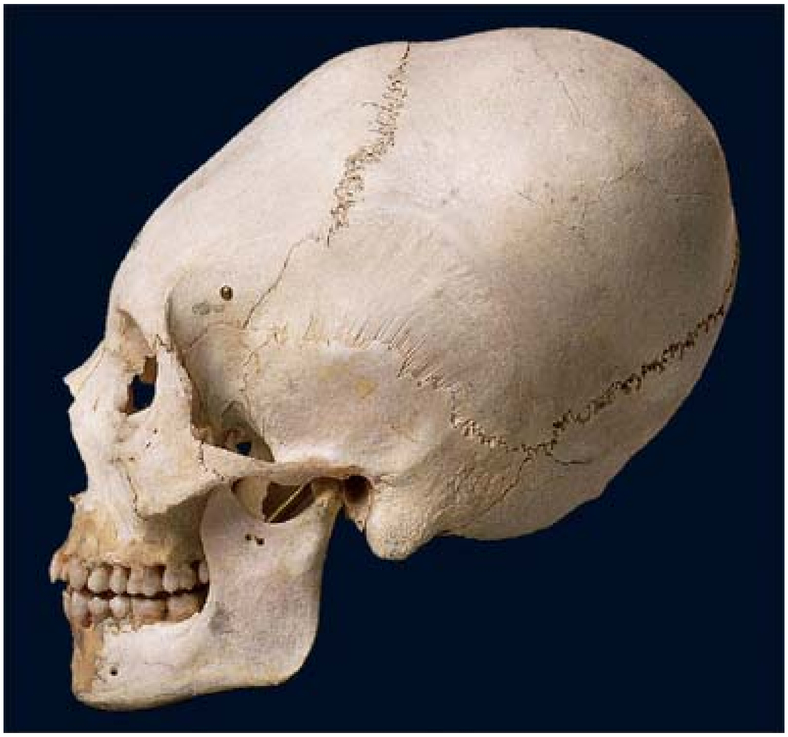

Fig. 26.8 Skull binding. Egyptian Copts.

(By courtesy of John Langdon.)

Congenital anomalies affecting the skull

A large number of malformations and anomalies affect the bones and associated soft tissue structures of the skull and are the result of a localized error of morphogenesis during embryological development. Many are recognized patterns of malformation which are presumed to have the same aetiology. They do not arise as the result of just one isolated error in morphogenesis, and are described as syndromes.

Hemifacial microsomia (Goldenhar syndrome)

These patients present with unilateral microtia, macrostomia and varying degrees of failure of formation of the mandibular ramus and condyle. Vertebral anomalies and epibulbar dermoids are common. Most cases are sporadic, but familial instances have been described. The facies are strikingly asymmetric as a result of hypoplasia or displacement of the ear. The ear deformities vary from complete aplasia to minor distortions of the pinna, which is displaced anteriorly and inferiorly. Absence of the external auditory meatus is common, as are middle ear deficiencies, which result in conduction deafness. Supernumerary ear tags are present and occur anywhere along a line from the tragus to the angle of the mouth.

The maxilla, temporal and zygomatic bones show varying degrees of hypoplasia on the affected side. The mandible shows varying degrees of hypoplasia ranging from mild asymmetry to major failure of development of the ramus and condyle. The mastoid process also shows degrees of hypoplasia. Often there is frontal bossing. Ten per cent of cases are bilateral, but invariably one side is more severely affected.

There is concomitant hypoplasia of the main masticatory muscles on the affected side, and occasionally the muscles of facial expression are involved. In 10% of cases there is a lower motor neurone weakness of the facial nerve. Epibulbar dermoids occur and are usually located at the limbus or lower outer quadrant. A coloboma of the upper lid is present in most cases. Unilateral microphthalmia or anophthalmia can occur and is associated with mental retardation, however mental retardation is unusual. Vertebral anomalies are common and include occipitalization of the atlas, cuneiform vertebrae, and fusion of several adjacent vertebrae. A variety of cardiac anomalies have been described ranging from ventricular septal defects to Fallot’s tetralogy. Pulmonary hypoplasia and renal anomalies have also been recorded.

Mandibulofacial dysostosis (Treacher Collins syndrome)

Mandibulofacial dysostosis mainly involves structures derived from the first branchial arch, groove and pouch. It is inherited as an autosomal dominant trait with variable penetration. The facial appearance is characteristic: downward sloping palpebral fissures, depressed cheek prominences, deformed ears, mandibular hypoplasia and a large fishlike mouth. The hairline often shows a tongue-shaped extension toward the cheek.

Clinically the skull vault appears normal, but on imaging it is seen that the supraorbital ridges are poorly developed and despite normal sutural development there may be increased digital markings (copper beating) on the inner table. The zygomatic bones may be totally absent, or more frequently are grossly deficient in a symmetrical manner with failure of fusion of the zygomatic arches. The mastoid processes are not pneumatized and may be sclerotic. The paranasal sinuses are frequently abnormally small or even absent. The infraorbital rims are also poorly developed.

There may be various eye anomalies, including colobomas affecting the lateral third of the lower eyelid (75% of cases) and microphthalmia. The ears are usually severely deformed, have a crumpled appearance and are often wrongly positioned. In a third of patients the external auditory meatus is absent, and there may be ossicular defects which result in conduction deafness. Additional ear tags and blind fistulae may be present anywhere between the tragus and the angle of the mouth. The nasofrontal angle is usually obliterated and the bridge of the nose elevated. The alar cartilages are hypoplastic and there may be choanal atresia. The mandible is almost always hypoplastic, the angle is obtuse and the ramus deficient. The coronoid and condylar processes may also be hypoplastic. A cleft palate is present in 30% of cases and there is a high arched palate. Mental retardation is common.

Distraction osteogenesis

The pioneering Russian orthopaedic surgeon Ilizarov demonstrated that long bones could be lengthened by performing osteotomies in the axial plane and then slowly separating (distracting) the two ends of the bone. This stimulates release of bone morphogenetic proteins and new bone is formed between the sectioned bone ends: when the desired length has been achieved, the long bone is immobilized in its desired position. After a period of a few weeks the initial woven bone is replaced by normal mature bone and the resulting lengthened bone is stable and functional.

These techniques are now applied to the bones of the skull. Mandibular distraction is commonly used, particularly to treat asymmetry of the mandible, e.g. in hemifacial microsomia. By performing the osteotomies at the angles of the mandible, and using carefully adjusted distraction devices, the mandible can be lengthened in the vertical and anteroposterior planes. Distraction is usually performed at a rate of one millimetre per day; the jaw can be lengthened indefinitely until the distraction is stopped and the callus allowed to mature and unite.

Distraction techniques have now been applied to the middle third of the facial skeleton, using complicated frames bolted onto the skull vault. The technique is particularly useful for the management of the craniofacial syndromes such as Crouzon’s, where the facial bones which articulate with the sphenoid fail to develop normally. If the facial bones can be released at an early age, and the mobilized bones distracted, the facial profile can develop normally.

IDENTIFICATION FROM THE SKULL

There are many ways of identifying an individual: in physical and forensic anthropology the most important concern biological and personal identity. Biological identity pertains to those features that allow an individual to be classified in relation to features present in other individuals e.g. sex, age, race and stature, whereas personal identity establishes criteria that are characteristic and discriminatory for a particular individual e.g. DNA, fingerprints and dental information. The skull is a useful source of information for the establishment of both biological and personal identity. It is probably the most studied aspect of the skeleton. The foundation of this obsession has many historical roots, but fundamentally it has arisen from the importance that humans place in the concept that the skull is the repository of ‘self’, and that it is the means by which interpersonal communication is effected. Our face is our primary means of recognition and communication and therefore it plays a pivotal role in establishing and reconstructing the identity of an individual.

SEX

The determination of sex from a juvenile skull is notoriously unreliable. While sexual differences have been detected in measurements of the mandible, orbits, tooth size and pattern of dental eruption, they do not reach a level of discrimination that will allow accurate and reliable assessment. It is equally difficult to assign sex to the face of a child because the faces of prepubertal boys and girls are comparable: perceivable sexual dimorphism is not manifest until secondary sexual changes are completed. Growth in the female face ceases in advance of the male, and consequently female sex-related characteristics are more paedomorphic. The defining characteristics of sex in an adult skull are therefore male in orientation and reflect the effects of the increased mass of the muscles of mastication, which attach to the mandible, and the muscles associated with maintaining the erect head. It is reported that using the skull alone, sex can be predicted with over 80% accuracy in the adult. This is extremely encouraging because research has shown that the correct sex can usually be predicted from the adult living face with around 96% accuracy.

Generally speaking, the male skull is more robust and the female more gracile, although there are obvious genetic, and therefore racial, variations which must be considered when attempting to assign sex from a skull. The female forehead is generally higher, more vertical and more rounded than the male, and there is a clear retention of the frontal eminences in the female. The male mandible is more robust and larger than that of the female: it generally displays a greater height in the region of the symphysis menti, the chin is more square, the condyles are larger, the muscle attachments are more pronounced and the gonial angle is generally less than 125°. A male skull has thicker and more rounded orbital margins, pronounced supra-orbital ridges, and often a well-defined glabella that occupies the midline above the root of the nose. The temporal lines are more pronounced in the male and the supramastoid crest generally extends posterior to the external auditory meatus.

Other sites of muscle attachment on the skull reflect the biomechanical requirement to keep the more robust male head erect. They include the mastoid process for sternocleidomastoid, which is generally more robust in the male and more gracile in the female, and the nuchal lines, especially the external occipital protuberance for the attachment of the ligamentum nuchae. The cranial base in the male is generally more robust and the bone is thicker, which means that this area of the skull survives inhumation particularly well and is therefore of great value in sex identification from fragmentary remains.

AGE DETERMINATION

Age is a continuous variable: to establish chronological age from a skull requires that structures change with age at a relatively constant and predictable rate. The relationship between chronological age and skeletal maturity is closest in the juvenile years, and therefore greater accuracy is achieved in the prediction of age from the juvenile than from the adult skull.

The neonatal skull has been described above. Examples of additional features that allow reliable age determination throughout the subadult years are: development of the nasal spine (by year 3), completion of the hypoglossal canal (by year 4), formation of the foramen of Huschke (by year 5), ossification of the dorsum sellae (by year 5) and fusion of the different parts of the occipital bone (by year 7). The fontanelles are usually all closed by the middle of the second year: the posterolateral is the first to close in the first two months after birth, and the anterior fontanelle is the last to close around the middle of the second year. The mastoid process appears in the second year and the metopic suture between the two frontal bones will close by year 4. The spheno-occipital synchondrosis will fuse between 11 and 16 years in the female and 13 and 18 years in the male, while the vomer and the ethmoid will fuse between 20 and 30 years of age. The last part of the skull to show active age-related growth is the jugular growth plate, a small triangular area sited posterolateral to the jugular foramen in the occipitotemporal suture. Fusion here does not begin until 22 years of age, and bilateral fusion may not be completed before 34 years; in a small proportion of individuals, the plate may remain unfused beyond 50 years. Closure of the cranial sutures is age-related but the correlation is not strong and displays strong genetic variation. Thus, while it can be said that suture closure may begin in the early part of the third decade, and it is likely that many of the sutures will be obliterated with advancing age, it is not a reliable means of establishing the age of an individual.

The most accurate means for determining age from the skull (of both a living and a deceased individual) is by assessment of dental maturation. Tooth development can be studied throughout the entire juvenile age span (from the early embryo to the adolescent), and importantly dental age and chronological age have been shown to exhibit a stronger correlation than skeletal and chronological age. Further, the teeth tend to survive inhumation successfully and are remarkably resilient to fire and explosion, ensuring their value in forensic investigations.

The chronological pattern of dental maturation is well documented and is an extremely important tool for age evaluation. Tooth development can be separated into a number of well defined stages: deciduous mineralization (crown and root), deciduous emergence and maturation, deciduous root resorption, shedding of deciduous teeth, mineralization (crown and root) of permanent dentition, emergence and maturation of deciduous dentition and attrition of permanent crowns (see Ch. 30). These stages do not occur in a linear fashion: while some of the deciduous teeth are emerging, permanent teeth are already being formed. For example, mineralization of the deciduous central incisor commences around the 15th week post fertilization, and this is the first tooth to emerge within the first 5 months after birth. All deciduous teeth are in occlusion by around 3 years of age. The first deciduous teeth to be shed are generally the central and lateral incisors around 7 years of age, when the permanent incisors emerge. The last deciduous tooth to be shed is generally the second molar in the 10th year. The first permanent tooth to show mineralization is the first molar, which occurs around the time of birth (sometimes earlier and sometimes later): it is also the first permanent tooth to emerge at around 6 years of age, and it will reach occlusion by the end of the 7th year. The last permanent tooth to emerge is the third molar: the variability of this occurrence makes it of restricted value for age prediction.

While the patterns of mineralization, emergence and shedding are extremely useful, there are other methods available for determining age from the dentition. These include tooth length, cementum apposition, secondary dentine formation, incremental enamel lines, attrition rates, root translucency and dentine transparency.

RACE DETERMINATION

The determination of racial or genetic origin is particularly difficult to achieve although it is something that both physical and forensic anthropologists insist on trying to do. The traditional view of race is that it is ‘one of the major zoological subdivisions of mankind, regarded as having a common origin and exhibiting a relatively constant set of physical traits’ (Bamshad & Olson 2003). Classifying groups on this basis is rather restrictive and, in our migrant modern world, somewhat artificial. It is still useful to be able to attempt to assign a ‘most likely’ racial group, especially when dealing with unidentified forensic remains, but there are enormous areas of overlap between the characteristics, and within any racial group there is often a full spectrum of representation. Yet we persist in classification on the basis of visual characteristics, and the area of the body that is most often analysed in this way is the skull.

Early anthropologists classified man largely through geographical origins and recognized physical traits. The four traditional races of man were: (1) Caucasoid – geographically from Europe, North Africa, Middle East, Indian subcontinent and parts of Central Asia. Classically the Caucasoid skull has a rounded to long shape (dolicocephalic) with a narrow nasal aperture, moderately developed supraorbital ridging, a prominent nasal spine, a steeple shaped nasal root, little prognathism and a narrow interorbital distance. The forehead is steep, the chin is prominent, the palate is long and narrow, the cheek bones are not overly prominent and there is a tendency to maxillary protrusion or mandibular retrusion. (2) Negroid – geographically represented by sub-Saharan and West African groups. The Negroid skull is also long with a wide nasal aperture, strong alveolar prognathism, low nasal root, guttering of the nasal aperture and a wide interorbital distance. The forehead is rounder, the palate is wider and the teeth are larger. (3) Mongoloid – geographically represented by groups in East Asia, South East Asia, Central Asia, Americas, Greenland, Inuit, Polynesia, South Asia and Eastern Europe. The Mongoloid skull is generally described as round with a nasal aperture of medium width, well developed and high cheek bones, moderate prognathism, a tented nasal root, short nasal spine and shovel shaped incisors. The palate is foreshortened, the forehead is vertical, the nasal bridge is low and there is a tendency for a forward rotation of the mandible. (4) Australoid – geographically represented by Australian Aborigines, Maori, Pacific Islanders, Fijians and Papuans. This skull of this rather heterogeneous group is generally represented by a broad nasal aperture, well developed supraorbital ridging and glabella, and a wide palate with large teeth.

There is a current resurgence in research into racial determination which is largely centred on genetic markers: skeletal indicators now play a significantly reduced role in this task.

FACIAL APPROXIMATION (RECONSTRUCTION)

Once the biological identity of an individual has been established (i.e. sex, age, stature and race) an attempt to establish personal identity may be necessary, particularly in relation to a forensic investigation. Achieving a possible name for a victim is necessary before comparison of antemortem and postmortem data can be achieved and a positive identity established. One of the accepted ways to achieve this is to reconstruct the face from the skull, thereby producing a facial approximation that can be released to the community or the public at large in an attempt to identify the victim. Experts in this discipline utilize the many variations in the skull to reconstruct individual possible representations of the face from the material available. Biological variation will dictate the appropriate data used for tissue thickness that are applied to the skeletal scaffold.

There are fundamentally two approaches to facial reconstruction: (1) Computer reconstruction – the skull is usually scanned by a laser 3-D scanner and an ‘average’ virtual face is wrapped around the skeletal scaffold. This approach is largely automated and requires limited training and expertise. It is rapid to achieve and relatively inexpensive, but relies on a large data set to ensure that the ‘average’ face utilized is appropriate. (2) Modelled reconstruction – the skull is usually cast, and pegs are inserted into the cast at the appropriate tissue depth requirements. In the ‘American’ approach a skin of clay is then moulded over the pegs to approximate the face. In the ‘Manchester’ method each sequential muscle and soft tissue layer is built up around the pegs before a clay skin is moulded over the underlying structures. The modelling approach is clearly more dependent upon experience, takes longer to achieve and is more costly.

There is great debate over which approach is the most accurate and, as yet, no agreement has been reached. Most practitioners state that the process achieves an approximation of one of the potential faces for the deceased and does not purport to reconstruct the actual face. The rationale is to produce an image that will jog the memory of the public and provide some possible names that will allow comparison of antemortem and postmortem identity data.

FACIAL SUPERIMPOSITION

Once a possible name has been derived it may be necessary to compare the skull with photographs of the suspected individual. In these circumstances an image of the skull is superimposed onto an image of the face of the missing person (Fig. 26.9). This relies on achieving a live capture image of the skull so that it can be rotated and manipulated into an identical position and to an identical size as the photograph. Features that do not change are lined up: a photograph that shows teeth is ideal because teeth can be lined up with the dentition on the skull. The image of the skull and photograph can then be faded in and out: if this is undertaken at speed, any discrepancies will show up on the image as distortion.

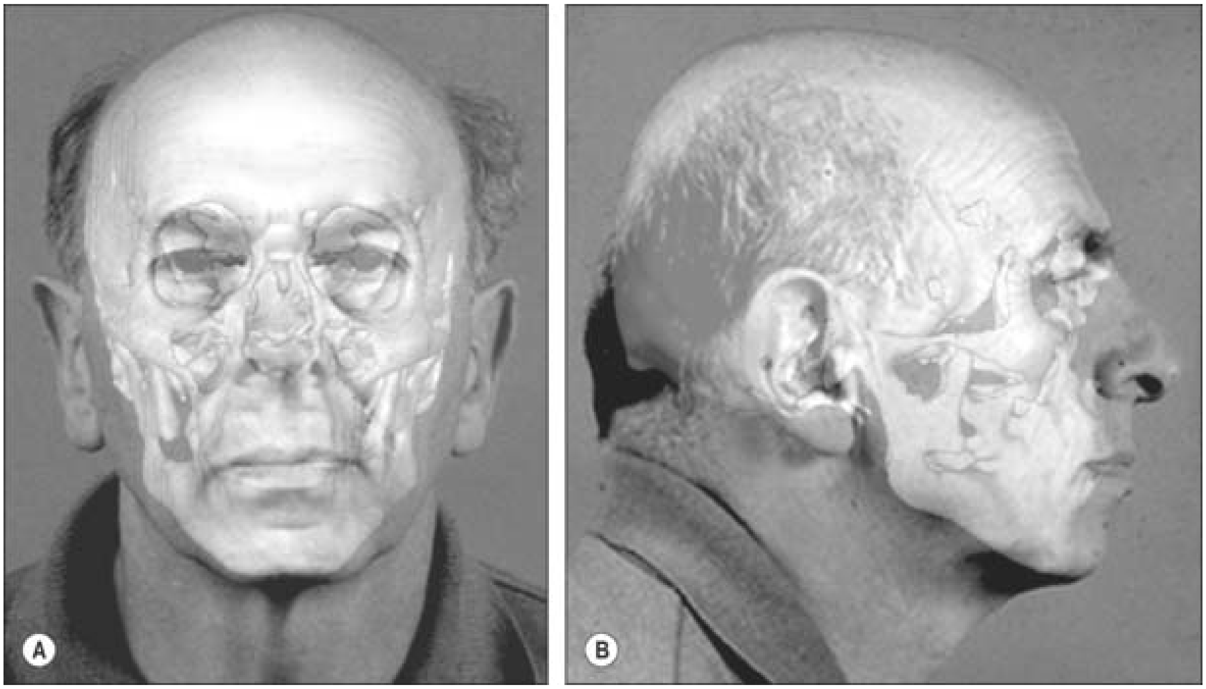

Fig. 26.9 Facial superimposition: a live capture image of the skull has been manipulated into the identical position and size of the face in the photograph.

(By courtesy of Dr Caroline Wilkinson and Professor Sue Black, Centre for Anatomy and Human Identification, College of Life Sciences, University of Dundee.)

REFERENCES

ımshad M, Olson S. Does race exist? *Sci Am*. 2003;289:78-85.

ərkovitz BKB, Moxham BJ. Color Atlas of the Skull. London: Mosby-Wolfe, 1994.

ərry AC. Factors affecting the incidence of non-metrical skeletal variants. *J Anat*. 1975;120:519-535.

ərry AC, Berry RJ. Epigenetic variation in the human cranium. *J Anat*. 1967;101:361-380.

uce V, Burton AM, Hanna E, Healey P, Mason O, Coombes A, Fright R, Linney A. Sex discrimination: how do we tell the difference between male and female faces? *Perception*. 1993;22:131-152.

ll GW, Rhine S. Skeletal Attribution of Race: Methods for Forensic Anthropology. New Mexico: Maxwell Museum of Anthropology, 2004.

zarov GA, Ledyaev VI. The replacement of long tubular bone defects by lengthening distraction osteotomy of one of the fragments. *Clin Orthopaed Relat Res*. 1992;280:7-10.

ıhr MM. The Evolution of Modern Human Diversity: A Study of Cranial Variation. Cambridge: Cambridge University Press, 1996.

ele S, Richtsmeier JT. Euclidean distance matrix analysis: a coordinate-free approach for comparing biological shapes using landmark data. *Am J Phys Anthropol*. 1991;86:415-427.

eberman DE, McCarthy RC. The ontogeny of cranial base angulation in humans and chimpanzees and its implications for reconstructing pharyngeal dimensions. *J Hum Evol*. 1999;36:487-517.

eberman DE, Pearson OM, Mowbray KM. Basicranial influence on overall cranial shape. *J Hum Evol*. 2000;38:291-315.

versidge H. The dentition. In: Scheuer L, Black S. *The Juvenile Skeleton*. London: Elsevier, 2004.

aat GJR, Mastwijk RW. Ossification status of the jugular growth plate. An aid for age at death determination. *Int J Osteoarch*. 1995;5:163-168.

:heuer L, Black S. Developmental Juvenile Osteology. London: Academic Press, 2000.

›erber GH. Craniofacial Development, 4th edn. Ontario: BC Decker, 2001.

darsdottir US, O'Higgins P, Stringer C. A geometric morphometric study of regional differences in the ontogeny of the modern human facial skeleton. *J Anat*. 2002;201:211-229.

hittaker DK, MacDonald DG. A Colour Atlas of Forensic Dentistry. London: Wolfe, 1989.

ilkinson C. Forensic Facial Reconstruction. Cambridge: Cambridge University Press, 2004.

CHAPTER 27

Intracranial region

The cranial cavity contains the brain, the intracranial portions of cranial and spinal nerves, blood vessels, meninges and cerebrospinal fluid. Its walls are formed by parts of the frontal, ethmoid, parietal, sphenoid, temporal and occipital bones.

INTERNAL SURFACE OF CRANIAL VAULT

The internal surface of the cranial vault is deeply concave. It includes most of the frontal and parietal bones and the squamous part of the occipital bone, variously united at the coronal, sagittal and lambdoid sutures (Fig. 27.1). With increasing age, these sutures become obliterated by a gradual process that begins on their intracranial surfaces. Inconstant foramina may occur in the parietal bones near the sagittal sulcus and anterior to the lambdoid suture: they admit emissary veins associated with the superior sagittal sinus. The internal surfaces of the frontal and parietal bones are grooved by furrows that house the frontal and parietal branches of the middle meningeal vessels; the grooves contain the openings of minute channels that admit perforating vessels to the haemopoietic marrow within the diploic bone. Impressions for cerebral gyri are less distinct on the vault than they are on the cranial base.

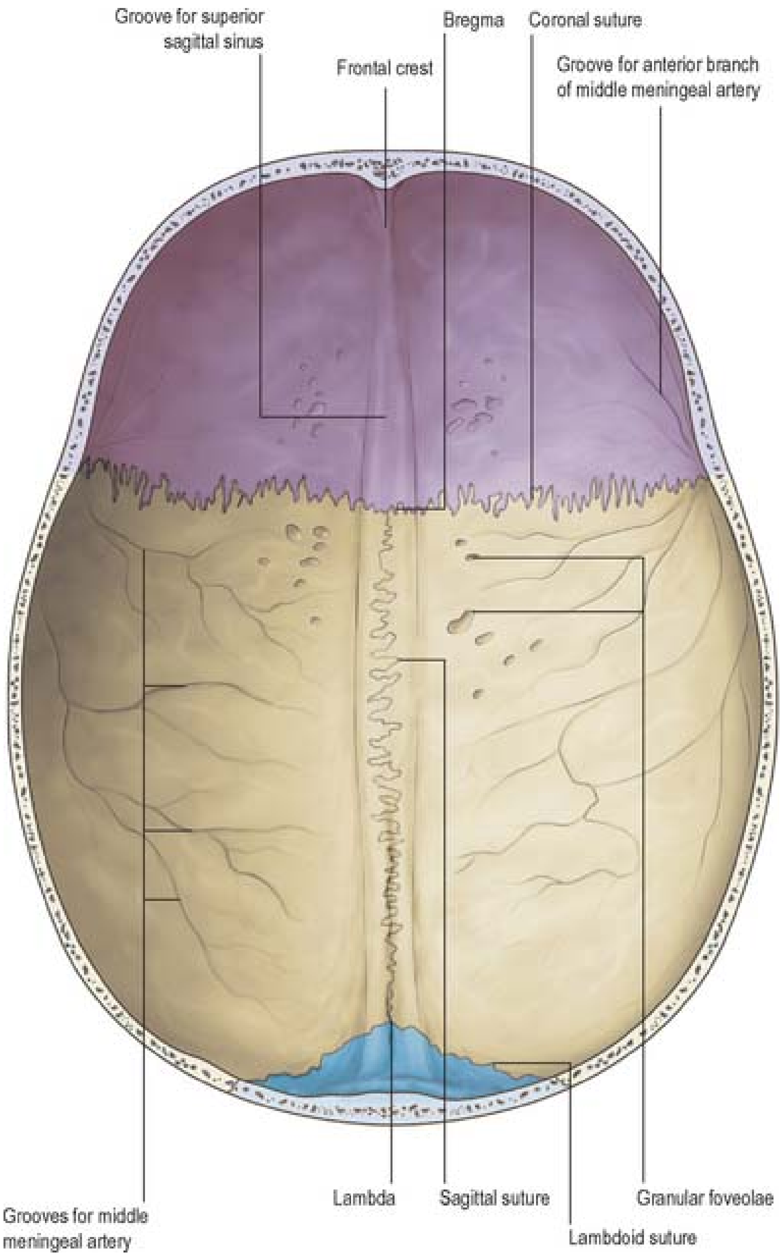
Groove for superior sagittal sinus
Bregma
Coronal suture
Frontal crest
Groove for anterior branch of middle meningeal artery
Lambda
Sagittal suture
Granular foveolae
Grooves for middle meningeal artery
Lambdoid suture

Fig. 27.1 Internal surface of the cranial vault.

(From Drake, Vogl and Mitchell 2005.)

The falx cerebri, a dural partition that passes between the two cerebral hemispheres of the brain, is attached anteriorly to a backward projecting anteromedian frontal crest. The crest exhibits a groove that widens as it passes back below the sagittal suture and becomes continuous with the sagittal sulcus which houses the superior sagittal sinus. Irregular depressions, granular foveolae, which become larger and more numerous with age, lie on either side of the sulcus and usually house arachnoid granulations.

CRANIAL FOSSAE (ANTERIOR, MIDDLE, POSTERIOR)

The base of the cranial cavity is divided into three distinct fossae, the anterior, middle and posterior cranial fossae (Fig. 27.2). The floor of the anterior cranial fossa is at the highest level and the floor of the posterior fossa is at the lowest.

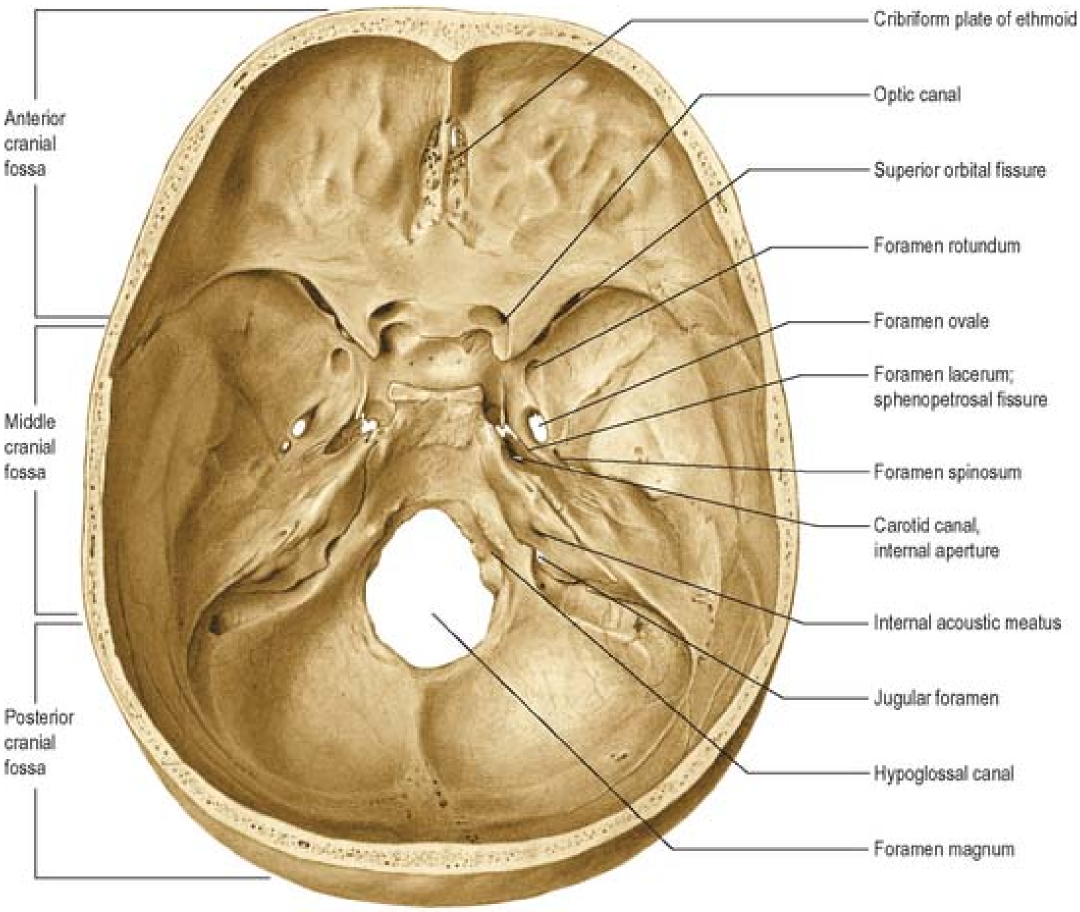
Anterior cranial fossa
Middle cranial fossa
Posterior cranial fossa
Cribriform plate of ethmoid
Optic canal
Superior orbital fissure
Foramen rotundum
Foramen ovale
Foramen lacerum; sphenopetrosal fissure
Foramen spinosum
Carotid canal, internal aperture
Internal acoustic meatus
Jugular foramen
Hypoglossal canal
Foramen magnum

Fig. 27.2 Floor of cranial cavity showing the cranial fossae.

(From Sobotta 2006.)

Detailed descriptions of the microsurgical anatomy of each region of the cranial base are beyond the scope of this book, and the interested reader is directed in the first instance to Rhoton (2002).

ANTERIOR CRANIAL FOSSA

The anterior cranial fossa is formed at the front and sides by the frontal bone. Its floor is composed of the orbital plate of the frontal bone, the cribriform plate and crista galli of the ethmoid bone, and the lesser wings and anterior part of the body of the sphenoid. Unlike the other cranial fossae, it does not directly communicate with the inferior surface of the cranium.

A perforated plate of bone, the cribriform plate of the ethmoid bone, spreads across the midline between the orbital plates of the frontal bone, and is depressed below them, forming part of the roof of the nasal cavity. Olfactory nerves pass from the nasal mucosa to the olfactory bulb of the brain through numerous small foramina in the cribriform plate. Anteriorly a spur of bone, the crista galli, projects upwards between the cerebral hemispheres. A depression between the crista galli and the crest of the frontal bone is crossed by the fronto-ethmoidal suture. It bears the foramen caecum, which is usually a small blind-ended depression, but which occasionally accommodates a vein draining from the nasal mucosa to the superior sagittal sinus. The anterior ethmoidal nerve enters the cranial cavity where the cribriform plate meets the orbital part of the frontal bone and then passes into the roof of the nose via a small foramen by the side of the crista galli: the nerve grooves the crista galli. The anterior ethmoidal vessels accompany the nerve. The posterior ethmoidal canal, which transmits the posterior ethmoidal nerve and vessels, opens at the posterolateral corner of the cribriform plate and is overhung by the sphenoid bone.

The convex cranial surface of the frontal bone separates the brain from the orbit and bears impressions of cerebral gyri and small grooves for meningeal vessels. Posteriorly, it articulates with the anterior border of the lesser wing of the sphenoid bone which forms the posterior boundary of the anterior cranial fossa. The medial end of the lesser wing constitutes the anterior clinoid process. The lesser wing joins the body of the sphenoid body by two roots which are separated by the optic canal. The anterior root, broad and flat, is continuous with the jugum sphenoidale, while the smaller and thicker posterior root joins the body of the sphenoid bone near the posterior bank of the sulcus chiasmatis. The frontosphenoid and sphenoethmoidal sutures divide the sphenoid from the adjacent bones.

The posterior border of each lesser wing fits the stem of the lateral cerebral sulcus and may be grooved by the sphenoparietal sinus. Above lies the inferior surface of the frontal lobe of the cerebral hemisphere and the anterior perforated substance lies medially. Inferiorly the lesser wing bounds the superior orbital fissure, and completes the orbital roof. Each anterior clinoid process gives attachment to the free margin of the tentorium cerebelli and is grooved medially by the internal carotid artery as it leaves the cavernous sinus. The anterior and middle clinoid processes may be connected by a thin osseous bar, formed by ossification either of the carotico-clinoid ligament or of a dural fold extending between the processes: the resulting carotico-clinoid foramen surrounds the artery.

MIDDLE CRANIAL FOSSA

The middle cranial fossa is deeper and more extensive than the anterior fossa, particularly laterally, where it supports the temporal lobes of the cerebral hemispheres. It is bounded in front by the lesser wings and part of the body of the sphenoid, behind by the superior borders of the petrous part of the temporal bone and the dorsum sellae of the sphenoid, and laterally by the squamous parts of the temporal bone, parietal bone and greater wings of the sphenoid. The region corresponds with the middle part of the cranial base.

The middle cranial fossa communicates with the orbits by the superior orbital fissures, each bounded above by a lesser wing, below by a greater wing, and medially by the body of the sphenoid bone. The fissures are wider medially, and each has a long axis sloping inferomedially and forwards. They are the major gateways into the orbit from the cranial cavity and contain the oculomotor, trochlear and abducens nerves, and the lacrimal, frontal and nasociliary branches of the ophthalmic division of the trigeminal nerve, together with filaments from the internal carotid plexus (sympathetic), the ophthalmic veins, the orbital branch of the middle meningeal artery, and the recurrent branch of the lacrimal artery (see Ch. 39).

Centrally the floor of the fossa is narrower and formed by the body of the sphenoid bone which contains the sphenoidal sinuses (see Ch. 32). The roof of the sinus is deeply concave and houses the pituitary gland (hypophysis): it is therefore termed the pituitary (hypophysial) fossa, also known as the sella turcica because it resembles the shape of a Turkish saddle. The anterior edge of the pituitary fossa is completed laterally by a middle clinoid process, the floor forms the roof of the sphenoidal air sinuses, and the posterior boundary presents a vertical pillar of bone, the dorsum sellae. The superolateral angles of the dorsum are expanded as the posterior clinoid processes. A fold of dura, the diaphragma sella, is attached to the anterior and posterior clinoid processes and roofs over the pituitary fossa. The smooth upper part of the anterior wall of the fossa, the jugum sphenoidale, is bounded behind by the anterior border of the grooved sulcus chiasmatis which leads laterally into the optic canals. Each canal transmits the optic nerve and ophthalmic artery. The optic chiasma usually lies posterosuperior to the sulcus chiasmatis, the tuberculum sellae lies below the sulcus. The cavernous sinus lies lateral to the pituitary fossa. The lateral wall of the body of the sphenoid contains a shallow carotid groove related to the internal carotid artery as it ascends from the carotid canal and runs through the cavernous sinus. Posterolaterally the groove may be deepened by a small projecting lingula.

The greater wing of the sphenoid bone contains three consistent foramina and other small variable foramina. The foramen rotundum, situated just below and behind the medial end of the superior orbital fissure, leads forwards into the pterygopalatine fossa, and contains the maxillary nerve. Behind the foramen rotundum is the foramen ovale which transmits the mandibular nerve: it is occasionally divided into two or three components. Accessory named foramina, the foramen of Vesalius and the cavernous foramen, may occur close to the foramen ovale. The small foramen of Vesalius occurs in some 20% of skulls: it is consistently symmetrical and lies anteromedial to the foramen ovale and lateral to the foramen rotundum and vidian canal. It transmits an emissary vein through which the cavernous sinus and pterygoid plexus communicate. The foramen spinosum lies posterolateral to the foramen ovale and transmits the middle meningeal artery and veins. The vessels groove the floor and lateral wall of the middle cranial fossa. The foramen ovale and foramen spinosum open into the underlying infratemporal fossa.

The foramen lacerum is situated at the posterior end of the carotid groove, posteromedial to the foramen ovale. It is bounded in front by the body and adjoining roots of the pterygoid process and greater wing of the sphenoid bone, posterolaterally by the apex of the petrous part of the temporal bone, and medially by the basilar part of the occipital bone. A small emissary sphenoidal foramen may occur at the root of the greater wing of the sphenoid medial to the foramen lacerum; when present it transmits a vein from the cavernous sinus.

The trigeminal impression, which accommodates the trigeminal ganglion, is situated posterior to the foramen lacerum on the anterior surface of the petrous part of the temporal bone near its apex. Its depth is variable. Posterolateral to the impression is a small, shallow, pit, limited posteriorly by a rounded arcuate eminence (produced by the underlying anterior semicircular canal). Lateral to the impression a narrow groove passes posterolaterally into the hiatus for the greater petrosal nerve, and even further laterally is the hiatus for the lesser petrosal nerve. A smooth trigeminal notch leads into the impression. It lies on the upper border of the petrous temporal, anteromedial to the groove for the superior petrosal sinus; at this point, the trigeminal nerve separates the sinus from bone. At the anterior end of the trigeminal notch is the petrosphenoidal ligament (of Gruber), attached to a minute bony spicule, directed anteromedially. The abducens nerve bends sharply across the upper petrous border, and passes between the ligament and the dorsum sellae anterior to the petrosphenoidal ligament (for a detailed analysis of the course of the abducens nerve in the petroclival region see Ozveren et al 2002).

The anterior surface of the petrous part of the temporal bone is formed by the tegmen tympani, a thin osseous lamina in the roof of the tympanic cavity, which extends anteromedially above the pharyngotympanic tube, anterolateral to the arcuate eminence. The posterior part of the tegmen tympani roofs the mastoid antrum, lateral to the eminence. The superior border of the petrous part of the temporal bone separates the middle and the posterior cranial fossae, and is grooved by the superior petrosal sinus. In young skulls, a petrosquamous suture may be visible at the lateral limit of the tegmen tympani but it is obliterated in adults. The tegmen tympani then turns down as the lateral wall of the osseous portion of the pharyngotympanic tube and its lower border may appear in the squamotympanic fissure. Lateral to the anterior part of the tegmen tympani, the squamous part of the temporal bone is thinned over a small area that coincides with the deepest part of the mandibular fossa.

POSTERIOR CRANIAL FOSSA

The posterior cranial fossa, the largest and deepest of the cranial fossae, contains the cerebellum, pons and medulla oblongata. It is bounded in front by the dorsum sellae, posterior aspects of the body of the sphenoid and the basilar part of occipital bone; behind by the squamous part of the occipital bone; laterally by the petrous and mastoid parts of the temporal bone and by the lateral parts of the occipital bone; and above and behind by the mastoid angles of the parietal bones. The region corresponds extracranially with the posterior part of the cranial base.

The most prominent feature in the floor of the posterior cranial fossa is the foramen magnum in the occipital bone. A sloping surface, the clivus, formed successively by the basilar part of the occipital bone, the posterior part of the body and then the dorsum sellae of the sphenoid bone, lies anterior to the foramen magnum. The clivus is gently concave from side to side. On each side it is separated from the petrous part of the temporal bone by a petro-occipital fissure, which is filled by a thin plate of cartilage and limited behind by the jugular foramen. Its margins are grooved by the inferior petrosal sinus. The spheno-occipital synchondrosis is evident on the clivus of a growing child.

The jugular foramen is a large opening sited at the posterior end of the petro-occipital fissure, above and lateral to the foramen magnum. Its upper border is sharp and irregular, and contains a notch for the glossopharyngeal nerve. The cochlear canaliculus, which contains the perilymphatic ‘duct’, is sited in the deepest part of the notch. The lower border of the jugular foramen is smooth. Posteriorly it is grooved by the sigmoid sinus which continues into the foramen as the internal jugular vein. The accessory, vagus and glossopharyngeal nerves pass through the anterior part of the jugular foramen from behind forwards, and may groove the jugular tubercle as they enter the foramen. They lie between the inferior petrosal sinus (accompanied by a meningeal branch of the ascending pharyngeal artery) and the sigmoid sinus (accompanied by a meningeal branch of the occipital artery).

The hypoglossal (anterior condylar) canal lies medial to and below the lower border of the jugular foramen, at the junction of the basilar and lateral parts of the occipital bone. It transmits the hypoglossal nerve and its recurrent branch together with the meningeal branch of the ascending pharyngeal artery and an emissary vein which links the (intracranial) basilar plexus with the (extracranial) internal jugular vein. When a posterior condylar canal is present behind the occipital condyle, its internal orifice is posterolateral to that of the hypoglossal canal and it contains a sigmoid emissary vein (associated with the occipital veins) and a meningeal branch of the occipital artery. The occipital condyles lie within the anterior aspect of the foramen magnum: their medial aspects are roughened for the attachments of the alar ligaments associated with the atlanto-axial joints.

The posterior surface of the petrous part of the temporal bone forms much of the anterolateral wall of the posterior cranial fossa. It contains the internal acoustic meatus, which lies anterosuperior to the jugular foramen, and transmits the facial and vestibulocochlear nerves, the nervus intermedius, and labyrinthine vessels.

The mastoid part of the temporal bone lies behind the petrous part of the temporal bone in the lateral wall of the posterior cranial fossa. Anteriorly it is grooved by a wide sigmoid sulcus which runs forwards and downwards, then downwards and medially, and finally forwards to the jugular foramen: it contains the sigmoid sinus. Superiorly, where the groove touches the mastoid angle of the parietal bone, it becomes continuous with a groove that transmits the transverse sinus, and then crosses the parietomastoid suture and descends behind the mastoid antrum. A mastoid foramen which transmits an emissary vein from the sigmoid sinus and a meningeal branch of the occipital artery, sometimes large enough to groove the squamous part of the occipital bone, may be sited here. The lowest part of the sigmoid sulcus crosses the occipitomastoid suture and grooves the jugular process of the occipital bone. The right sigmoid sulcus is usually larger than the left.

A thin plate with an irregularly curved margin projects back behind the internal acoustic meatus. It bounds a slit that contains the opening of the vestibular aqueduct (which houses the saccus and ductus endolymphaticus and a small artery and vein). A small subarcuate fossa lined with dura mater lies between the internal acoustic meatus and the aqueductal opening. Near the superior border of the petrous part of the temporal bone the fossa is pierced by a small vein. In infants the fossa is a relatively large blind tunnel under the anterior semicircular canal.

The squamous part of the occipital bone displays a median internal occipital crest. This runs posteriorly from the foramen magnum to an internal occipital protuberance, gives attachment to the falx cerebelli, and may be grooved by the occipital sinus. The internal occipital protuberance is close to the confluence of the sinuses. It is grooved bilaterally by the transverse sinuses which curve laterally with an upward convexity to the mastoid angles of the parietal bones. The groove for the transverse sinus is usually deeper on the right, where it is generally a continuation of the superior sagittal sinus, while on the left it is frequently a continuation of the straight sinus. On both sides the transverse sulcus is continuous with the sigmoid sulcus. Below the transverse sulcus, the internal occipital crest separates two shallow fossae which house the cerebellar hemispheres. The posterior clinoid process and the margins of the grooves for the transverse and superior petrosal sinuses all provide anchorage for the attached margin of the tentorium cerebelli.

MENINGES

Three concentric membranes, the meninges, envelop the brain and spinal cord. They provide support and protection for the delicate tissues they surround. The individual layers, in order from outside to inside, are the dura mater (pachymeninx), arachnoid mater and pia mater. The dura is an opaque, tough, fibrous coat which incompletely divides the cranial cavity into compartments and accommodates the dural venous sinuses. The arachnoid is much thinner than the dura and is mostly translucent. It surrounds the brain loosely, spanning over depressions and concavities. The pia mater is a transparent, microscopically thin, membrane which follows the contours of the brain and is closely adherent to its surface.

The dura is separated from the arachnoid by a narrow subdural space. The arachnoid is separated from the pia by the subarachnoid space, which varies greatly in depth; the larger expanses are termed subarachnoid cisterns. The subarachnoid space contains cerebrospinal fluid, CSF, which is secreted by the choroid plexuses of the cerebroventricular system. CSF circulates within the subarachnoid space and is reabsorbed into the venous system through arachnoid villi and granulations associated with the dural venous sinuses.

Cranial and spinal meninges are continuous through the foramen magnum. The cranial meninges are described in this section and the spinal meninges are described on p. 751).

DURA MATER

Dura mater is thick, dense and fibrous. It is predominantly acellular, and consists mainly of densely packed fascicles of collagen fibres arranged in laminae. The fascicles run in different directions in adjacent laminae, producing a lattice-like appearance which is particularly obvious in the tentorium cerebelli and around the defects or perforations that sometimes occur in the anterior portion of the falx cerebri.

The cranial dura, which lines the cranial cavity, differs from the spinal dura mainly in its relationship to the surrounding bones. It has an inner, or meningeal, layer and an outer, or endosteal, layer. These layers are united except where they separate to enclose the venous sinuses that drain blood from the brain. There is little histological difference between the endosteal and meningeal layers. Both contain fibroblasts, and the endosteal layer also contains osteoblasts. Focal calcification may occur in the falx cerebri.

The dura mater adheres to the internal surfaces of the cranial bones, particularly at the sutures, the cranial base and around the foramen magnum. Fibrous bands pass from the dura into the bones, and it is difficult to remove the dura from the suture lines in young skulls. However, as the suture lines fuse the dura becomes separated from them. It also becomes thicker, less pliable, and more firmly adherent to the inner surface of the skull, particularly that of the calvaria, with increasing age. The endosteal layer of the dura is continuous with the pericranium through the cranial sutures and foramina and with the orbital periosteum through the superior orbital fissure. The meningeal layer provides tubular sheaths for the cranial nerves as they pass out through the cranial foramina, and these sheaths fuse with the epineurium as the nerves emerge from the skull. The dural sheath of the optic nerve is continuous with the ocular sclera. The dura fuses with the adventitia of major vessels, such as the internal carotid and vertebral arteries, at sites where they pierce it to enter the cranial cavity.

The inner aspect of the dura mater is closely applied to the arachnoid mater over the surface of the brain. However the two membranes are physically joined only at sites where either veins pass from the brain into venous sinuses, e.g. the superior sagittal sinus, or where they connect the brain to the dura, e.g. at the anterior pole of the temporal lobe.

Extradural haematoma

The anatomical organization of the dura, and its relationships to the major venous sinuses, sutures and blood vessels, is clinically significant. Separation of the dura from the underlying periosteum requires significant force, and consequently occurs only when high-pressure arterial bleeding occurs into the virtual space. This can result from damage to any arterial vessel, commonly following skull fracture. The classic site for such injury is along the course of the middle meningeal artery, where a direct blow causing a bone fracture can rupture the artery and cause rapid collection of an extradural haematoma. The haematoma is under considerable pressure because of the arterial blood pressure feeding it and the resistance offered by the strong adhesion between dura and periosteum. An extradural haematoma therefore acts as a rapidly expanding intracranial mass lesion: it is a classic medical emergency that requires immediate diagnosis and surgery.

Dural partitions

The meningeal layer of the dura is reflected inwards to form four septa, namely the falx cerebri, falx cerebelli, diaphragma sellae and tentorium cerebelli that partially divide the cranial cavity into compartments.

Falx cerebri

The falx cerebri is a strong, crescent-shaped sheet that lies in the sagittal plane and occupies the longitudinal fissure between the two cerebral hemispheres (Fig. 27.3). The crescent is narrow in front, where the falx is fixed to the crista galli, and broad behind, where it blends with the tentorium cerebelli: the straight sinus runs along this line of attachment (Fig. 27.3). The anterior part of the falx is thin and may have a number of irregular perforations. Its convex upper margin is attached to the internal cranial surface on each side of the midline, as far back as the internal occipital protuberance. The superior sagittal sinus runs in a cranial groove within the dura along this margin: the falx is attached to the lips of this groove. The lower edge of the falx is free and concave and contains the inferior sagittal sinus.

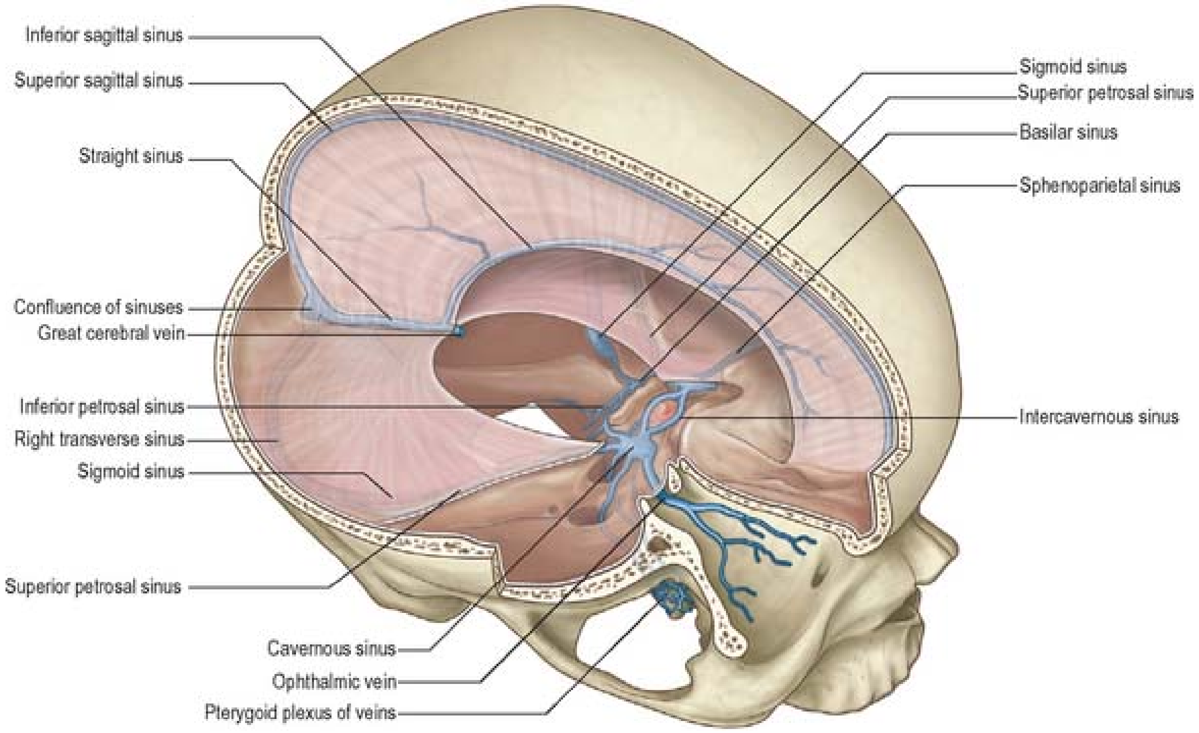
Inferior sagittal sinus
Superior sagittal sinus
Straight sinus
Confluence of sinuses
Great cerebral vein
Inferior petrosal sinus
Right transverse sinus
Sigmoid sinus
Superior petrosal sinus
Cavernous sinus
Ophthalmic vein
Pterygoid plexus of veins
Sigmoid sinus
Superior petrosal sinus
Basilar sinus
Sphenoparietal sinus
Intercavernous sinus

Fig. 27.3 The cerebral dura mater, its reflections and associated major venous sinuses.

(Adapted from Drake, Vogl and Mitchell 2005.)

Falx cerebelli

The falx cerebelli is a small midline fold of dura mater that lies below the tentorium cerebelli and projects forward into the posterior cerebellar notch between the cerebellar hemispheres. Its base is directed upwards and is attached to the posterior part of the inferior surface of the tentorium cerebelli in the midline. Its posterior margin contains the occipital sinus and is attached to the internal occipital crest. The apex of the falx cerebelli frequently divides into two small folds, which disappear at the sides of the foramen magnum. The falx cerebelli is often double.

Diaphragma sellae

The diaphragma sellae is a small, circular, horizontal sheet of dura mater. It forms a roof over the sella turcica and often almost completely covers the pituitary gland. The infundibulum and pituitary stalk pass into the pituitary fossa through a central opening in the diaphragma. There is wide individual variation in the size of this opening. In the past, the diaphragma sellae was an important landmark structure in pituitary surgery, because extension of a pituitary tumour above it was an indication for a subfrontal approach through a craniotomy. However, a transsphenoidal approach is currently the first preferred option, irrespective of whether there is suprasellar extension.

Tentorium cerebelli

The shape of the tentorium cerebelli (Fig. 27.3) is reminiscent of a single-poled tent, from which its name is derived. It lies between the cerebellum and the occipital lobes of the cerebral hemispheres and divides the cranial cavity into supratentorial and infratentorial compartments, which contain the forebrain and hindbrain respectively. Its concave anterior edge is free and separated from the dorsum sellae of the sphenoid bone by a large curved hiatus, the tentorial incisure or notch, which is filled by the midbrain and the anterior part of the superior aspect of the cerebellar vermis. The convex outer limit of the tentorium is attached posteriorly to the lips of the transverse sulci of the occipital bone and to the posterior-inferior angles of the parietal bones, where it encloses the transverse sinuses. Laterally, it is attached to the superior borders of the petrous parts of the temporal bones, where it contains the superior petrosal sinuses. On each side, near the apex of the petrous temporal bone, the lower layer of the tentorium is evaginated anterolaterally under the superior petrosal sinus to form a recess between the endosteal and meningeal layers in the middle cranial fossa. The recess contains the roots and ganglion of the trigeminal nerve; the evaginated meningeal layer fuses in front with the anterior part of the ganglion.

The arrangement of the dura mater in the central part of the middle cranial fossa is complex. The tentorium forms a large part of the floor of the middle cranial fossa, and fills much of the gap between the ridges of the petrous temporal bones. On both sides, the rim of the tentorial incisure is attached to the apex of the petrous temporal bone and continues forward as a ridge of dura mater to attach to the anterior clinoid process. This ridge marks the junction of the roof and the lateral part of the cavernous sinus. The periphery of the tentorium cerebelli (attached to the superior border of the petrous temporal bone), crosses under the free border of the tentorial incisure at the apex of the petrous temporal bone, and continues forward to the posterior clinoid processes as a rounded, indefinite ridge of the dura mater. The angular depression between the anterior parts of the peripheral attachment of the tentorium and the free border of the tentorial incisure is part of the roof of the cavernous sinus. It is pierced in front by the oculomotor and behind by the trochlear nerves, which proceed anteroinferiorly into the lateral wall of the cavernous sinus. In the anteromedial part of the middle cranial fossa the dura ascends as the lateral wall of the cavernous sinus, reaches the ridge produced by the anterior continuation of the free border of the tentorium, and runs medially as the roof of the cavernous sinus, where it is pierced by the internal carotid artery. Medially, the roof of the sinus is continuous with the upper layer of the diaphragma sellae. At, or just below, the opening in the diaphragma for the infundibulum and pituitary stalk, the dura, arachnoid and pia mater blend with each other and with the capsule of the pituitary gland. The layers of the meninges cannot be distinguished within the sella turcica, and the subarachnoid space is obliterated.

Transtentorial coning

Normally, the arrangement of dural partitions such as the falx cerebri and tentorium cerebelli may help to stabilize the brain within the cranial cavity. However, when there is focal brain swelling or a focal space-occupying lesion within the brain or cranial cavity, raised intracranial pressure may cause the brain to herniate under the falx cerebri or, more significantly, through the tentorial incisure, which will compress the oculomotor nerve, midbrain and arteries on the inferior medial surface of the temporal lobe.

This process of transtentorial coning is particularly dangerous because of the risk of secondary vascular compression; it often represents the terminal event in patients with supratentorial space-occupying lesions. Similarly, space-occupying lesions in the small infratentorial compartment may cause upward herniation through the tentorial hiatus or downward herniation through the foramen magnum (see Fig. 19.22).

Dural venous sinuses

Dural venous sinuses form a complex network of venous channels which drain blood from the brain and cranial bones (Fig. 27.4, see Fig. 17.10). They lie between the endosteal and meningeal layers of dura mater, are lined by endothelium, have no valves, and their walls are devoid of muscular tissue. They develop initially as venous plexuses, and most adult sinuses preserve a plexiform arrangement (to a variable degree), rather than being simple vessels with a single lumen. Plexiform arrays of small veins adjoin the sagittal superior and inferior sagittal and straight sinuses and, less frequently, the transverse sinuses, and ridges of ‘spongy’ venous tissue often project into the lumina of the superior sagittal and transverse sinuses (Browder & Kaplan 1976; Kaplan & Browder 1976).

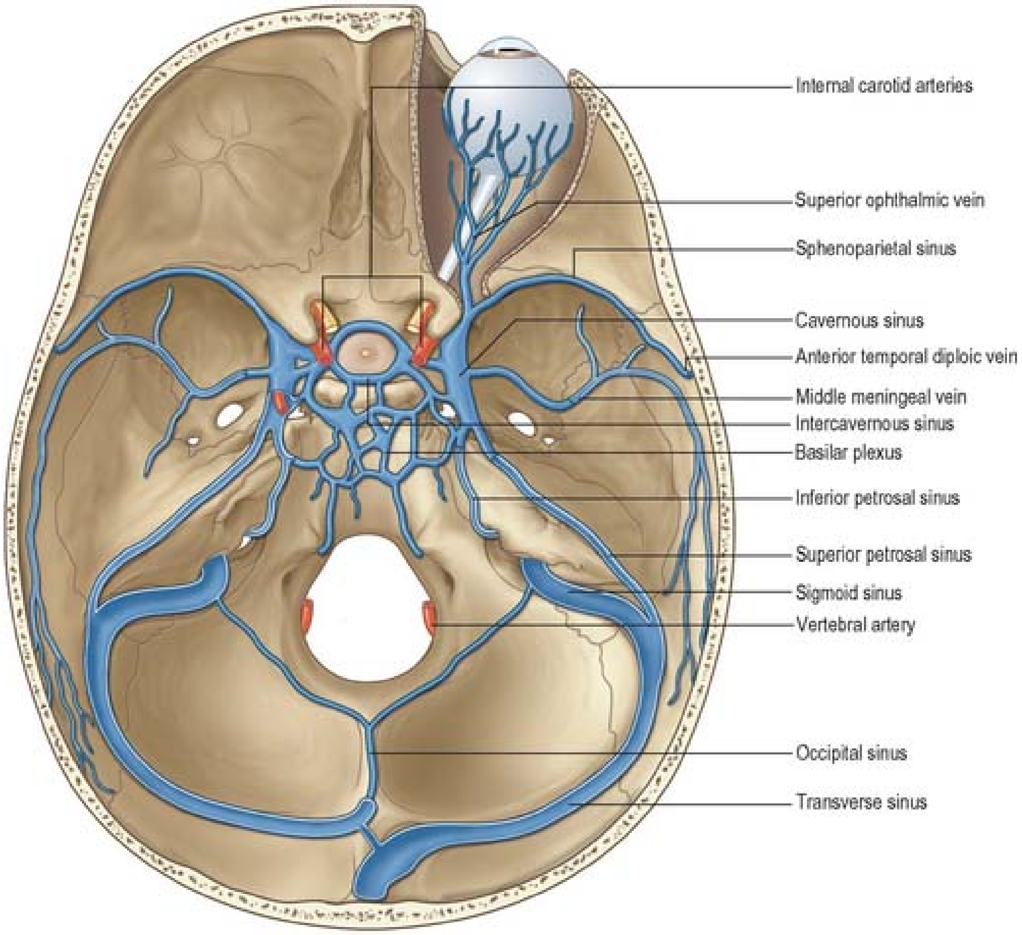
Internal carotid arteries
Superior ophthalmic vein
Sphenoparietal sinus
Cavernous sinus
Anterior temporal diploic vein
Middle meningeal vein
Intercavernous sinus
Basilar plexus
Inferior petrosal sinus
Superior petrosal sinus
Sigmoid sinus
Vertebral artery
Occipital sinus
Transverse sinus

Fig. 27.4 The major venous sinuses at the base of the skull. The sinuses coloured dark blue have been opened up.

The structure of cranial venous sinuses, their plexiform nature and wide connections with cerebral and cerebellar veins, vary considerably, particularly in earlier years, e.g. in infancy the falx cerebelli may contain large plexiform channels and venous lacunae that augment the occipital sinus. These variations cannot be detailed in a general text but must be established for the individual by angiography when clinical necessity arises. There is experimental evidence that parts of sinuses (and even diploic veins) can be filled by forcible internal carotid injection, from which it has been inferred that arteriovenous shunts may exist (Browder & Kaplan 1976). A connection between the middle meningeal arteries and the superior sagittal sinus has been demonstrated in this way, although the sites of communication are unknown. Dural arteriovenous fistulas are thought to be acquired lesions that form in an area of thrombosis within a sinus. If the sinus remains completely thrombosed, venous drainage from these lesions occurs through cortical veins, or, if the sinus is open, venous drainage is usually into the involved sinus.

The named sinuses are the superior and inferior sagittal, straight, transverse, petrosquamous, sigmoid, occipital, cavernous, intercavernous, superior and inferior petrosal, sphenoparietal, basilar and marginal.

Superior sagittal sinus

The superior sagittal sinus runs in the attached convex margin of the falx cerebri. It grooves the internal surface of the frontal bone, the adjacent margins of the two parietal bones and the squamous part of the occipital bone (Fig. 27.3, Fig. 27.5, see Fig. 17.10). It begins near the crista galli, a few millimetres posterior to the foramen caecum, and receives primary tributaries from cortical veins of the frontal lobes, the ascending frontal veins. The sinus is triangular in cross-section and invaded, in its intermediate third, by variable bands and projections from its dural walls, which may extend as horizontal shelves that divide its lumen into superior and inferior channels. It is narrow anteriorly, and widens gradually to approximately 1 cm diameter as it runs backwards. At its posterior end, the sinus enters the confluence of the sinuses (Fig. 27.4) which is situated to one side (usually the right) of the internal occipital protruberance. At the confluence the superior sagittal sinus usually deviates to become continuous with the right transverse sinus, but it also usually connects with the occipital and contralateral transverse sinuses. The size and degree of communication of the channels meeting at the confluence are highly variable: any sinus involved may be duplicated, narrowed, or widened near the confluence. In more than half of subjects all venous channels that converge towards the occiput interconnect, including the straight and occipital sinuses, but communication between channels may be absent or tenuous.

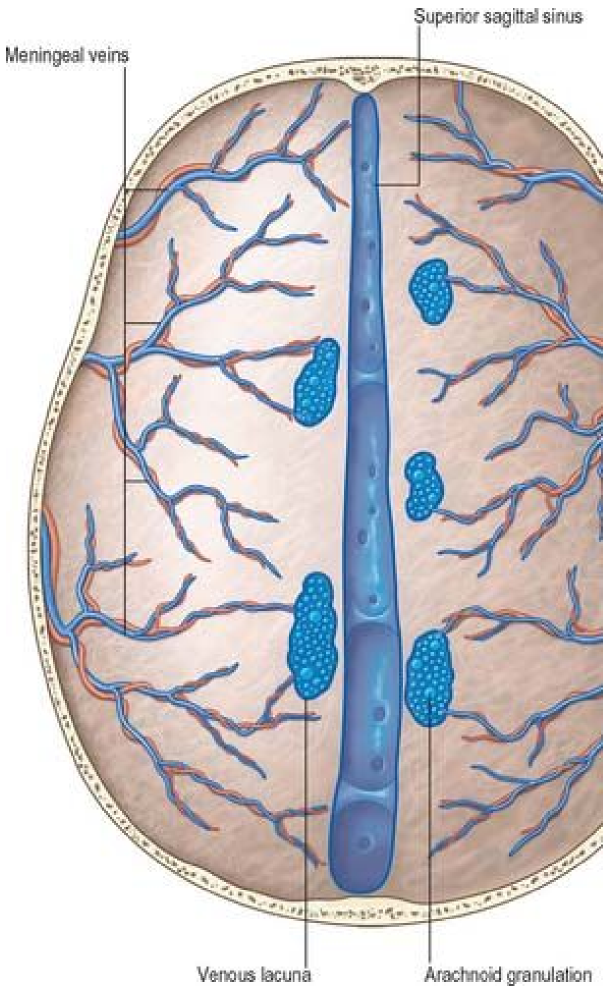

Fig. 27.5 The superior sagittal sinus opened up after removal of the cranial vault. Note the fibrous bands that cross the sinus from two of the venous lacunae.

The superior sagittal sinus receives the superior cerebral veins and communicates by small orifices with irregular venous lacunae which lie near it in the dura mater. There are usually two or three lateral lacunae on each side of the midline, named frontal (small), parietal (large) and occipital (intermediate) lacunae: they tend to become confluent in the elderly, producing a single elongated lacuna on each side. These venous spaces are often so complex as to be almost plexiform. Fine fibrous bands cross the lacunae, and numerous arachnoid granulations project into them (Fig. 27.5, Fig. 27.6). The lacunae drain diploic and meningeal veins. Near its posterior end, the superior sagittal sinus receives veins from the pericranium which pass through parietal foramina.

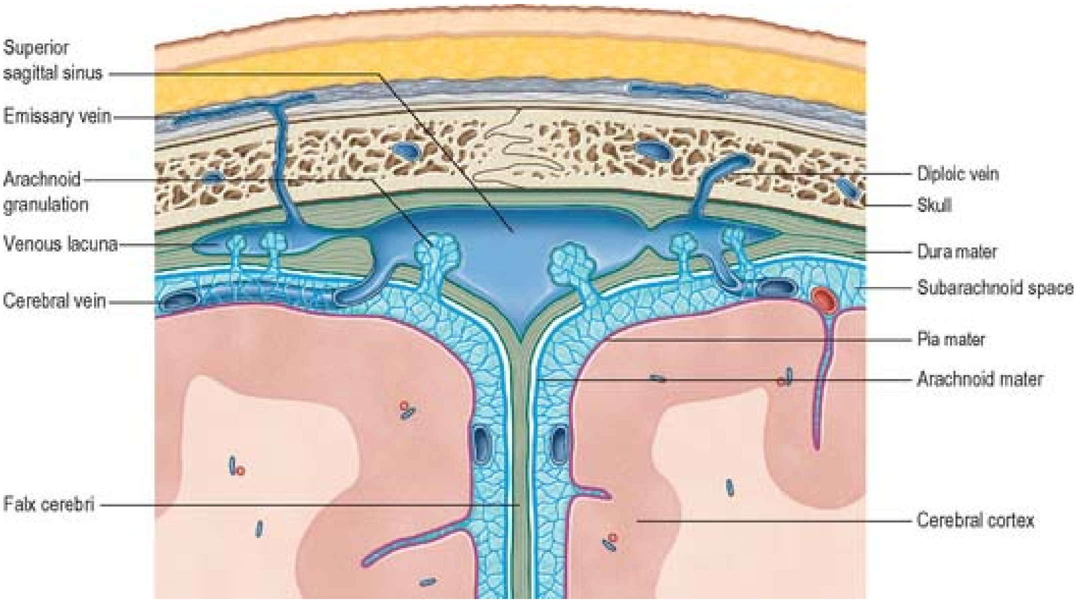
Superior sagittal sinus
Emissary vein
Arachnoid granulation
Venous lacuna
Cerebral vein
Falx cerebri
Diploic vein
Skull
Dura mater
Subarachnoid space
Pia mater
Arachnoid mater
Cerebral cortex

Fig. 27.6 Coronal section through the vertex of the skull to show the relationships between the superior sagittal sinus, meninges and arachnoid granulations.

(Adapted from Drake, Vogl and Mitchell 2005.)

Inferior sagittal sinus

The inferior sagittal sinus is located in the posterior half or two-thirds of the free margin of the falx cerebri (Fig. 27.3). It increases in size posteriorly, ends in the straight sinus and receives veins from the falx and sometimes from the medial surfaces of the cerebral hemispheres.

Straight sinus

The straight sinus lies in the junction of the falx cerebri with the tentorium cerebelli (Fig. 27.3, see Fig. 17.10). It runs posteroinferiorly as a continuation of the inferior sagittal sinus and drains into the transverse sinus. It is not (or only tenuously) continuous with the superior sagittal sinus. Its tributaries include the great cerebral vein and some superior cerebellar veins. It is triangular in cross-section.

Transverse sinus

The transverse sinuses begin at the internal occipital protuberance (Fig. 27.3, Fig. 27.4). One, usually the right, is directly continuous with the superior sagittal sinus, the other with the straight sinus. On both sides the sinuses run in the attached margin of the tentorium cerebelli, first on the squama of the occipital bone, then on the mastoid angle of the parietal bone. Each follows a gentle anterolateral curve, increasing in size as it does so, to the posterolateral part of the petrous temporal bone. Here it turns down as a sigmoid sinus, which ultimately becomes continuous with the internal jugular vein. Transverse sinuses are triangular in section and usually unequal in size; the one draining the superior sagittal sinus is the larger. They receive the inferior cerebral, inferior cerebellar, diploic and inferior anastomotic veins, and are joined by the superior petrosal sinuses where they continue as sigmoid sinuses.

Petrosquamous sinus

The petrosquamous sinus runs back in a groove, which posteriorly sometimes becomes a canal, along the junction of the squamous and petrous parts of the temporal bone, and opens behind into the transverse sinus. Anteriorly it connects with the retromandibular vein through a postglenoid or squamous foramen. The sinus may be absent or it may drain entirely into the retromandibular vein.

Sigmoid sinus

The sigmoid sinuses are continuations of the transverse sinuses, beginning where these leave the tentorium cerebelli (Fig. 27.4, Fig. 27.7). Each sigmoid sinus curves inferomedially in a groove on the mastoid process of the temporal bone, crosses the jugular process of the occipital bone and turns forward to the superior jugular bulb, lying posterior in the jugular foramen.

Anteriorly, a thin plate of bone separates its upper part from the mastoid antrum and air cells. It connects with pericranial veins via mastoid and condylar emissary veins.

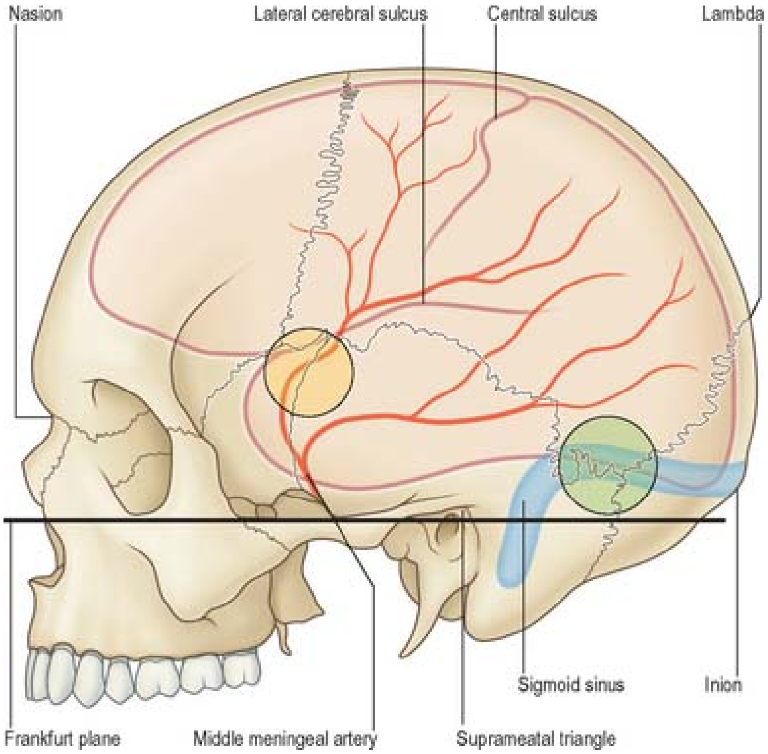
Nasion
Lateral cerebral sulcus
Central sulcus
Lambda
Sigmoid sinus
Inion
Frankfurt plane
Middle meningeal artery
Suprameatal triangle

Fig. 27.7 The relations of the brain, the middle meningeal artery and the transverse and sigmoid sinuses to the surface of the skull. Area enclosed in yellow circle (including the pterion) for trephining over the frontal branch of the middle meningeal artery and lateral Sylvian fissure; area enclosed in green circle for trephining over the transverse sinus.

Occipital sinus

The occipital sinus is the smallest of the sinuses. It lies in the attached margin of the falx cerebelli (Fig. 27.4) and is occasionally paired. It commences near the foramen magnum in several small channels, one joining the end of the sigmoid sinus, and connects with the internal vertebral plexuses. It ends in the confluence of the sinuses.

Cavernous sinus

The cavernous sinuses are two large venous plexuses that lie on either side of the body of the sphenoid bone, extending from the superior orbital fissure to the apex of the petrous temporal bone, with an average length of 2 cm and width of 1 cm. Each sinus contains the cavernous portions of the internal carotid artery, associated with a perivascular sympathetic plexus that can be seen with the naked eye, and several cranial nerves which run forward through the sinus to access the orbit via the superior orbital fissure (Fig. 27.4, Fig. 27.8, Fig. 27.9). Three major venous spaces have been described within the sinus, posterosuperior, anteroinferior, and medial to the cavernous portion of the carotid artery (Harris & Rhoton 1976). The sphenoidal air sinus and pituitary gland are medial relations and the uncus of the temporal lobe is lateral to the sinus. The trigeminal cave is near the inferoposterior part of its lateral wall, and extends posteriorly beyond it to enclose the trigeminal ganglion.

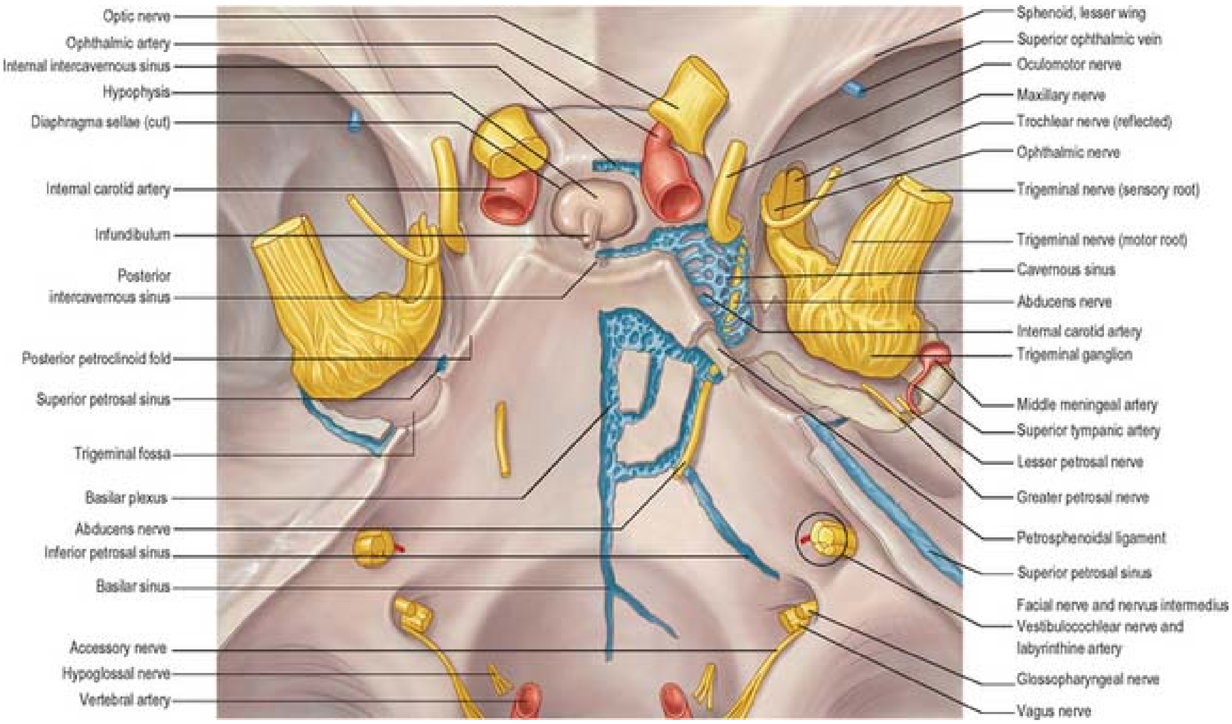
Optic nerve
Ophthalmic artery
Internal intercavernous sinus
Hypophysis
Diaphragma sellae (cut)
Internal carotid artery
Infundibulum
Posterior intercavernous sinus
Posterior petroclinoid fold
Superior petrosal sinus
Trigeminal fossa
Basilar plexus
Abducens nerve
Inferior petrosal sinus
Basilar sinus
Accessory nerve
Hypoglossal nerve
Vertebral artery
Sphenoid, lesser wing
Superior ophthalmic vein
Oculomotor nerve
Maxillary nerve
Trochlear nerve (reflected)
Ophthalmic nerve
Trigeminal nerve (sensory root)
Trigeminal nerve (motor root)
Cavernous sinus
Abducens nerve
Internal carotid artery
Trigeminal ganglion
Middle meningeal artery
Superior tympanic artery
Lesser petrosal nerve
Greater petrosal nerve
Petrosphenoidal ligament
Superior petrosal sinus
Facial nerve and nervus intermedius
Vestibulocochlear nerve and labyrinthine artery
Glossopharyngeal nerve
Vagus nerve

Fig. 27.8 The middle cranial fossa, viewed from above, to show the cavernous sinuses, their contents and immediate relations, exposed by

partial removal of the dura mater. The trigeminal, trochlear and oculomotor nerves have been reflected forwards on both sides.

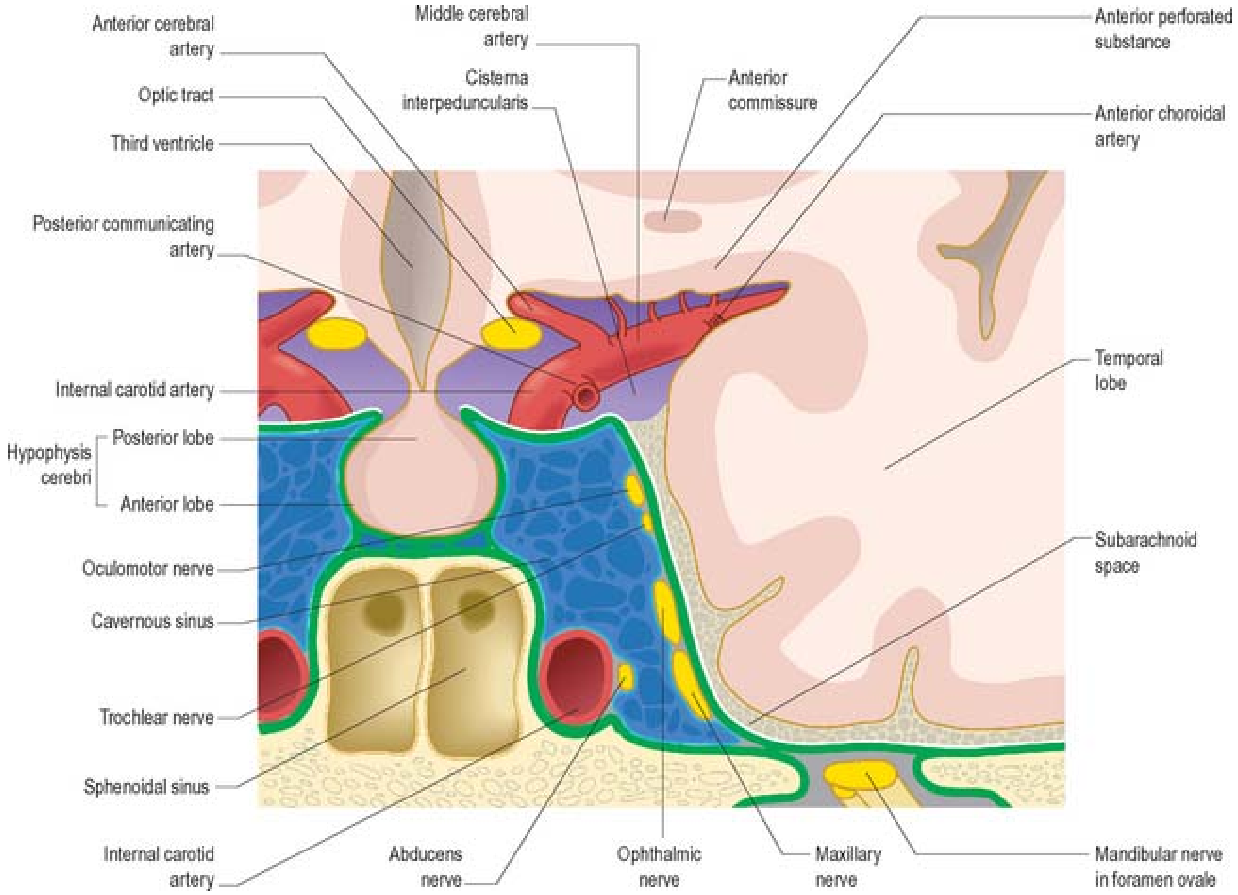
Anterior cerebral artery
Optic tract
Third ventricle
Posterior communicating artery
Internal carotid artery
Hypophysis cerebri
Posterior lobe
Anterior lobe
Oculomotor nerve
Cavernous sinus
Trochlear nerve
Sphenoidal sinus
Internal carotid artery
Middle cerebral artery
Cisterna interpeduncularis
Anterior commissure
Anterior perforated substance
Anterior choroidal artery
Temporal lobe
Subarachnoid space
Abducens nerve
Ophthalmic nerve
Maxillary nerve
Mandibular nerve in foramen ovale

Fig. 27.9 Coronal, slightly oblique section through the middle cranial fossa, showing the cavernous and cerebral portions of the internal carotid artery and the cavernous sinus. The carotid artery and abducens nerve are within the cavernous sinus but outside the endothelial lining of the sinus. Pia mater: pale brown; arachnoid mater: white; layers of dura mater (the mesothelium of the dura mater is not indicated): green; endothelium of cavernous sinus: blue.

The oculomotor and trochlear nerves and the ophthalmic and maxillary divisions of the trigeminal nerve all lie in the lateral wall of the sinus. They project into the lumen and are usually covered medially by little more than endothelium. The abducens nerve pierces the dura close to the upper border of the apex of the petrous part of the temporal bone and enters the cavernous sinus by passing below the petrosphenoid ligament within a dural tunnel (Dorello's canal). The abducens lies on the lateral side of the internal carotid artery, medial to the ophthalmic nerve, and below and medial to the nasociliary nerve. Numerous branches from the cavernous portion of the internal carotid artery, especially from the meningohypophysial and inferolateral trunks, supply the cavernous portions of all of the nerves that pass through the sinus. The preservation of these vessels during cavernous sinus surgery is important in preventing or minimizing postoperative cranial nerve deficits. (For more detailed descriptions of these branches, including their main variations, see Tran-Dinh 1987; Krisht et al 1994; Reisch et al 1996; Tekdemir et al 1998). Propulsion of blood in the cavernous sinus is partly due to pulsation of the internal carotid artery, but it is also influenced by gravity, and hence by the position of the head.

Tributaries of the cavernous sinus are the superior ophthalmic vein, inferior ophthalmic vein (either a branch or the whole vessel), superficial middle cerebral vein, inferior cerebral veins and sphenoparietal sinus. Less frequently, the central retinal vein and frontal tributary of the middle meningeal vein drain into it. The cavernous sinus drains to the transverse sinus via the superior petrosal sinus; to the internal jugular vein via the inferior petrosal sinus and a plexus of veins associated with the internal carotid artery; to the pterygoid plexus by veins traversing the emissary sphenoidal foramen, foramen ovale and foramen lacerum; and to the facial vein via the superior ophthalmic vein.

For more detailed descriptions of the microsurgical anatomy of the cavernous sinus, see Umansky et al 1994; Seoane et al 1998; Yasuda et al 2004.

Caroticocavernous sinus fistula and cavernous sinus thrombosis

Direct communication between the intracavernous portion of the internal carotid artery and the cavernous sinus, creating a caroticocavernous sinus fistula (CCF), occurs occasionally, either as a result of severe head trauma or degenerative or aneurysmal vessel disease. The classic signs are ptosis, proptosis (which may be pulsatile), chemosis, eyelid edema, peri-orbital edema and extra-ocular dysmotility caused by combinations of third, fourth and sixth cranial nerve palsies. Hypo- or hyperesthesia of the ophthalmic and maxillary divisions of the fifth cranial nerve and a decreased corneal reflex may also be detected. There may be evidence of dilated, tortuous retinal veins and papilloedema. These changes can cause permanent blindness. CCFs are most commonly treated by passing a catheter up the carotid into the fistula, and then occluding it with dilatable balloons or flexible metal coils. Any spreading infection involving the upper nasal cavities, paranasal sinuses, cheek (especially near the medial canthus), upper lip, anterior nares or even an upper incisor or canine tooth, may very rarely lead to septic thrombosis of the cavernous sinuses: infected thrombi pass from the facial vein or pterygoid venous complex into the sinus via either ophthalmic veins or emissary veins that enter the cranial cavity through the foramen ovale. This is a critical medical emergency with a high risk of disseminated cerebritis and cerebral venous thrombosis.

Middle fossa triangles and the cavernous sinus

Parkinson described a triangle within the lateral wall of the cavernous sinus through which the cavernous portion of the carotid artery could be exposed for the surgical treatment of carotid-cavernous fistulae. At least ten triangles, formed by the convergence or divergence of the cranial nerves that lie either in the middle cranial fossa or in the cavernous sinus, have now been described. They may be used as intra-operative landmarks in approaching cavernous sinus lesions or in gaining access to the posterior cranial fossa from the middle cranial fossa (Watanabe et al 2003). The middle fossa triangles are formed as the three main divisions of the trigeminal nerve diverge from the trigeminal ganglion and head towards their exit foramina. The cavernous sinus triangles are formed as the optic, oculomotor, trochlear, and ophthalmic nerves converge on the optic canal and on the superior orbital fissure.

Intercavernous sinuses

The two cavernous sinuses are connected by anterior and posterior intercavernous sinuses and the basilar plexus (Fig. 27.4, Fig. 27.8). The intercavernous sinuses lie in the anterior and posterior attached borders of the diaphragma sellae and they thus form a complete circular venous sinus. All connections are valveless and the direction of flow in them is reversible. Small irregular sinuses inferior to the pituitary gland drain into the intercavernous sinuses. The inferior intercavernous sinuses are plexiform in nature and important in a surgical transnasal approach to the pituitary gland.

Superior petrosal sinus

This small narrow sinus drains the cavernous sinus into the transverse sinus on either side (Fig. 27.4, Fig. 27.8). It leaves the posterosuperior part of the cavernous sinus and runs posterolaterally in the attached margin of the tentorium cerebelli. It then crosses above the trigeminal nerve to lie in a groove on the superior border of the petrous part of the temporal bone and ends by joining a transverse sinus at the point where this curves down to become the sigmoid sinus. The superior petrosal sinus receives cerebellar, inferior cerebral and tympanic veins, and connects with the inferior petrosal sinus and the basilar plexus.

Inferior petrosal sinus

The inferior petrosal sinus drains the cavernous sinus into the internal jugular vein (Fig. 27.4, Fig. 27.8, see Fig. 17.10). It begins at the posteroinferior aspect of the cavernous sinus and runs back in a groove between the petrous temporal and basilar occipital bones. It next passes through the anteromedial part of the jugular foramen, accompanied by a meningeal branch of the ascending pharyngeal artery, and descends obliquely backwards to drain into the superior jugular bulb. It sometimes drains by a vein in the hypoglossal canal to the suboccipital vertebral plexus.

The sinus is often plexiform. It receives labyrinthine veins via the cochlear canaliculus and the vestibular aqueduct, and tributaries from the medulla oblongata, pons and inferior cerebellar surface. The venous spaces in the sphenopetroclival area, which are filled anteriorly by blood from the lateral sellar compartment of the cavernous sinus, medially by blood from the basilar plexus, and laterally by blood from the superior petrosal sinus, typically drain into the inferior petrosal sinus (Iaconetta et al 2003).

Sphenoparietal sinus

Understanding the venous anatomy related to the lesser wing of the sphenoid is of clinical importance in the diagnosis, classification, and treatment of dural arteriovenous fistulas in this region. The classic description of the sphenoparietal sinus is that it is a dural venous channel under the lesser wing of the sphenoid bone, lying near its posterior edge (Fig. 27.4). It curves medially to open into the anterior part of the cavernous sinus and receives small veins from the adjacent dura mater and sometimes the frontal ramus of the middle meningeal vein. It may also receive connecting rami, in its middle course, from the superficial middle cerebral vein, and veins from the temporal lobe and the anterior temporal diploic vein. When these connections are well developed, the sphenoparietal sinus is a large channel. It has recently been suggested that the term sphenoparietal sinus should be abandoned on the basis that it is not an anatomical entity, but an artificial combination of two independent meningeal vessels, namely the parietal portion of the anterior branch of the middle meningeal veins and the sinus of the lesser wing of the sphenoid (see Ruiz et al 2004).

Basilar sinus and plexus

The basilar sinus and plexus consist of interconnecting channels between layers of dura mater on the clivus (Fig. 27.4, Fig. 27.8). The basilar venous plexus interconnects the inferior petrosal sinuses and joins the internal vertebral venous plexus. It also usually connects with the cavernous and superior petrosal sinuses at its anterior end.

Marginal sinus

The marginal sinus encircles the foramen magnum. It communicates anteriorly with the basilar plexus and with the occipital sinus posteriorly. It typically drains to the sigmoid sinus or jugular bulb by small sinuses and may connect extracranially to the internal vertebral venous plexus, paravertebral or deep cervical veins in the suboccipital region.

Arterial supply and venous drainage of the cranial dura mater

Despite their names, the cranial meningeal arteries are predominantly periosteal (Fig. 27.10A). Their main targets are bone and haemopoietic marrow, and only very fine arterial branches are distributed to the cranial dura mater *per se*.

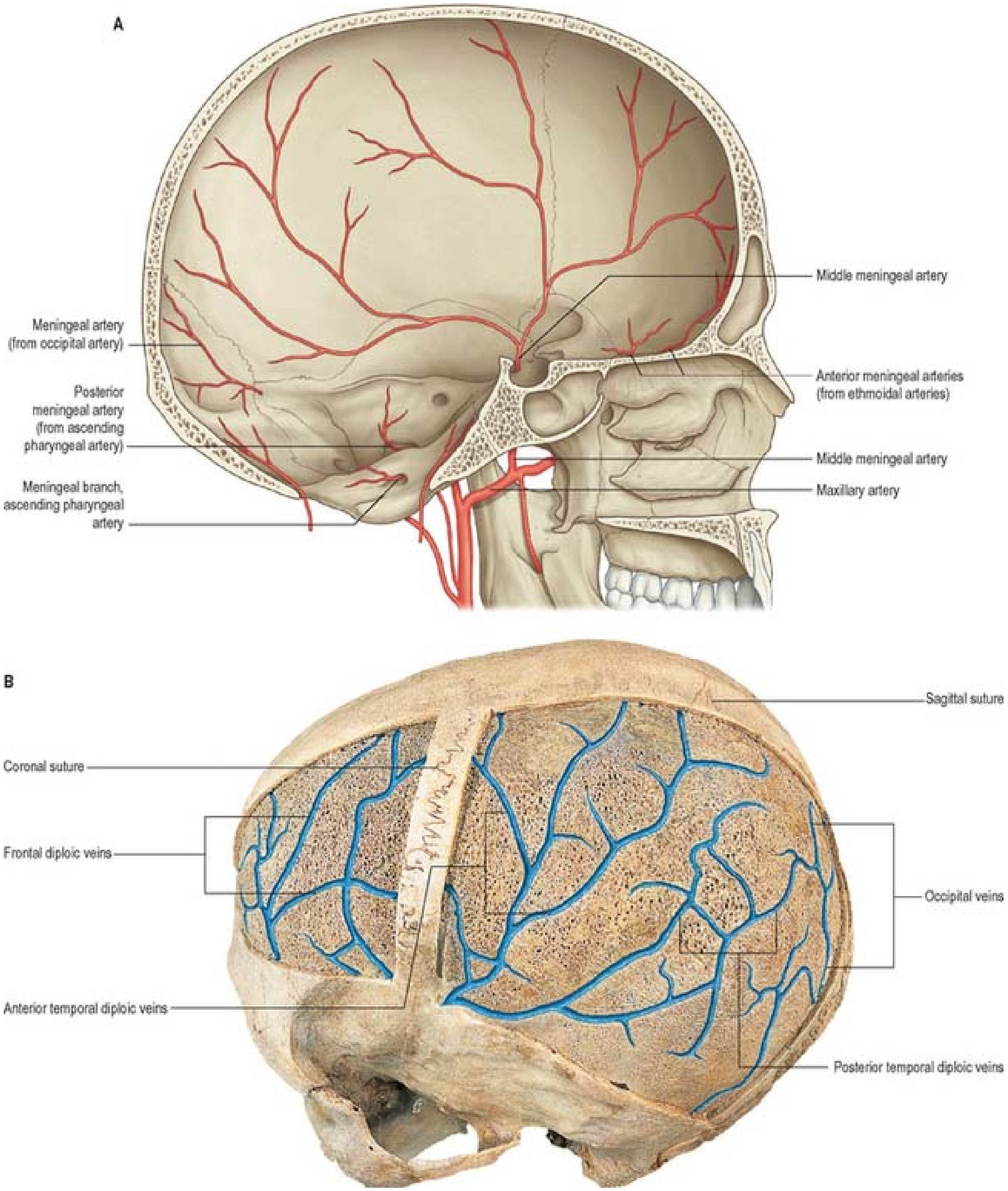
A
Middle meningeal artery
Meningeal artery (from occipital artery)
Anterior meningeal arteries (from ethmoidal arteries)
Posterior meningeal artery (from ascending pharyngeal artery)
Middle meningeal artery
Meningeal branch, ascending pharyngeal artery
Maxillary artery
B
Sagittal suture
Coronal suture
Frontal diploic veins
Occipital veins
Anterior temporal diploic veins
Posterior temporal diploic veins

Fig. 27.10 **A**, The meningeal arteries. **B**, Diploic canals and veins after removal of the external table of calvarium.

(A, Adapted from Drake, Vogl and Mitchell 2005. B, From Sobotta 2006.)

The smaller branches of the meningeal vessels lie mainly in the endosteal layer of dura. In the anterior cranial fossa, the dura is supplied by the anterior meningeal branches of the anterior and posterior ethmoidal and internal carotid arteries and a branch of the middle meningeal artery. In the middle cranial fossa, it is supplied by the middle and accessory meningeal branches of the maxillary artery, a branch of the ascending pharyngeal artery (entering via the foramen lacerum), branches of the internal carotid and a recurrent branch of the lacrimal artery. In the posterior fossa, the dura is supplied by the meningeal branches of the occipital artery (one enters the skull by the jugular foramen and another by the mastoid foramen), the posterior meningeal branches of the vertebral artery and occasional small branches of the ascending pharyngeal artery, which enter by the jugular foramen and hypoglossal canal.

Middle meningeal artery

The middle meningeal artery is the largest of the meningeal arteries. It arises from the first part of the maxillary artery and passes between the roots of the auriculotemporal nerve. It may lie lateral to tensor veli palatini, then enters the cranial cavity through the foramen spinosum and runs in an anterolateral groove on the squamous part of the temporal bone, dividing into frontal and parietal branches. The larger frontal (anterior) branch crosses the greater wing of the sphenoid and enters a groove or canal in the sphenoidal angle of the parietal bone (the sphenoparietal canal). It divides into branches between the dura mater and cranium; some branches ascend to the vertex, others to the occipital region. One ascending branch grooves the parietal bone approximately 15 mm behind the coronal suture, and corresponds approximately to the precentral sulcus (Fig. 27.7). The parietal (posterior) branch curves back on the squamous temporal bone, reaches the lower border of the parietal bone anterior to its mastoid angle and divides to supply the posterior parts of the dura mater and cranium. These branches anastomose with their fellows and with the anterior and posterior meningeal arteries.

Ganglionic branches supply the trigeminal ganglion and associated roots. The petrosal branch enters the hiatus for the greater petrosal nerve, supplies the facial nerve, geniculate ganglion and tympanic cavity, and anastomoses with the stylomastoid artery. The superior tympanic artery runs in the canal for tensor tympani and supplies the muscle and the mucosa that lines the canal. Temporal branches traverse minute foramina in the greater wing of the sphenoid and anastomose with deep temporal arteries. An anastomotic branch enters the orbit laterally in the superior orbital fissure, and anastomoses with a recurrent branch of the lacrimal artery: enlargement of this anastomosis is believed to account for the occasional origin of the lacrimal artery from the middle meningeal artery.

Accessory meningeal artery

The accessory meningeal artery may arise from the maxillary or the middle meningeal artery. It enters the cranial cavity through the foramen ovale, and supplies the trigeminal ganglion, dura mater and bone. Its main distribution is extracranial, principally to medial pterygoid, lateral pterygoid (upper head), tensor veli palatini, the greater wing and pterygoid processes of the sphenoid bone, the mandibular nerve and otic ganglion. It is sometimes replaced by separate small arteries.

Meningeal veins

Meningeal veins begin from plexiform vessels in the dura mater and drain into efferent vessels in the outer dural layer which connect with lacunae associated with some of the cranial sinuses. They include the middle meningeal and the diploic veins. Intracranial veins also communicate with extracranial vessels via emissary veins.

Middle meningeal vein (sinus)

The frontal (anterior) branch of the middle meningeal vein crosses the floor of the middle cranial fossa, from either foramen ovale or foramen spinosum, to the pterion, usually in the form of two parallel channels that accompany the middle meningeal artery. The vein subsequently passes cranially along the anterior margin of the parietal squama to empty into the venous lakes of the superior sagittal sinus. As they course under the most lateral aspect of the lesser sphenoid wing, the anterior branches of the middle meningeal vessels are contained for a short distance within a bony canal, the sphenoparietal canal (of Trolard), which they leave to enter a groove on the internal surface of the parietal squama. The veins lie closer to the bone than the artery, and sometimes occupy separate grooves: they are particularly liable to tear in cranial fractures. Before entering the sphenoparietal canal, the anterior branch of the middle meningeal vein usually connects with the sinus of the lesser sphenoid wing. The latter is connected medially with the anterior and superior aspect of the cavernous sinus by a channel that crosses over the superior ophthalmic vein to reach the cavernous sinus.

The parietal (posterior) trunk of the middle meningeal vein may traverse the foramen spinosum to end in the pterygoid venous plexus. The frontal trunk may also reach this plexus via the foramen ovale, or it may end in the sphenoparietal or cavernous sinus (Fig. 27.4). The middle meningeal vein receives meningeal tributaries and small inferior cerebral veins, and connects with the diploic and superficial middle cerebral veins. It frequently bears arachnoid granulations.

Diploic veins

The diploic veins are large, thin-walled vessels that occupy channels in the diploë of the cranial bones (Fig. 27.10B). Four main trunks are usually described; these are the frontal, anterior and posterior temporal, and occipital diploic veins. The frontal opens into the supraorbital vein and the superior sagittal sinus; the anterior temporal is mainly confined to the frontal bone, and opens into the sphenoparietal sinus, and one of the deep temporal veins through an aperture in the great wing of the sphenoid; the posterior temporal is situated in the parietal bone, and empties into the transverse sinus either through an opening at the mastoid angle of the parietal bone or through the mastoid foramen; and the occipital, the largest of the four, is confined to the occipital bone, and may open externally into the occipital vein, or internally into either the transverse sinus or the confluence of the sinuses.

Sinus pericranii

Sinus pericranii is a rare condition involving congenital or acquired anomalous connections between an extracranial blood-filled nodule and an intracranial dural venous sinus via dilated diploic and/or emissary veins of the skull (Sheu et al 2002).

Emissary veins

Emissary veins traverse cranial apertures and make connections between intracranial venous sinuses and extracranial veins. Some are relatively constant, others may be absent. These connections are of clinical significance in determining the spread of infection from extracranial foci to venous sinuses, for example, the spread of infection from the mastoid to the venous sinuses or from the paranasal sinuses to the cavernous sinus.

The following emissary veins have been recognized. A mastoid emissary vein in the mastoid foramen connects the sigmoid sinus with the posterior auricular or occipital veins. A parietal emissary vein in the parietal foramen connects the superior sagittal sinus with the veins of the scalp (these veins are usually minute and do not appear to connect with veins of the scalp in corrosion casts). The venous plexus of the hypoglossal canal, which is occasionally a single vein, connects the sigmoid sinus and the internal jugular vein. A (posterior) condylar emissary vein connects the sigmoid sinus and veins in the suboccipital triangle via the (posterior) condylar canal. A plexus of emissary veins (venous plexus of foramen ovale) connects the cavernous sinus to the pterygoid plexus via the foramen ovale. Two or three small veins which traverse the foramen lacerum and connect the cavernous sinus and the pharyngeal veins and pterygoid plexus. A vein in the emissary sphenoidal foramen (of Vesalius) connects the cavernous sinus with the pharyngeal veins and pterygoid plexus. The internal carotid venous plexus, which passes through the carotid canal, connects the cavernous sinus and the internal jugular vein. The petrosquamous sinus connects the transverse sinus with the external jugular vein. A vein may traverse the foramen caecum (which is patent in about 1% of adult skulls) and connect nasal veins with the superior sagittal sinus. An occipital emissary vein usually connects the confluence of sinuses with the occipital vein through the occipital protuberance, and also receives the occipital diploic vein. The occipital sinus connects with variably developed veins around the foramen magnum (so-called marginal sinuses) and thus with the vertebral venous plexuses; this pathway provides an alternative venous drainage when the jugular vein is blocked or tied. The ophthalmic veins are potentially emissary, because they connect intracranial to extracranial veins.

Innervation of the cranial dura mater

The innervation of the cranial dura mater is derived mainly from the three divisions of the trigeminal nerve, the second and third cervical spinal nerves, and the cervical sympathetic trunk (Fig. 27.11). Less well-established meningeal branches have been described arising from the vagus and hypoglossal nerves and possibly from the facial and glossopharyngeal nerves.

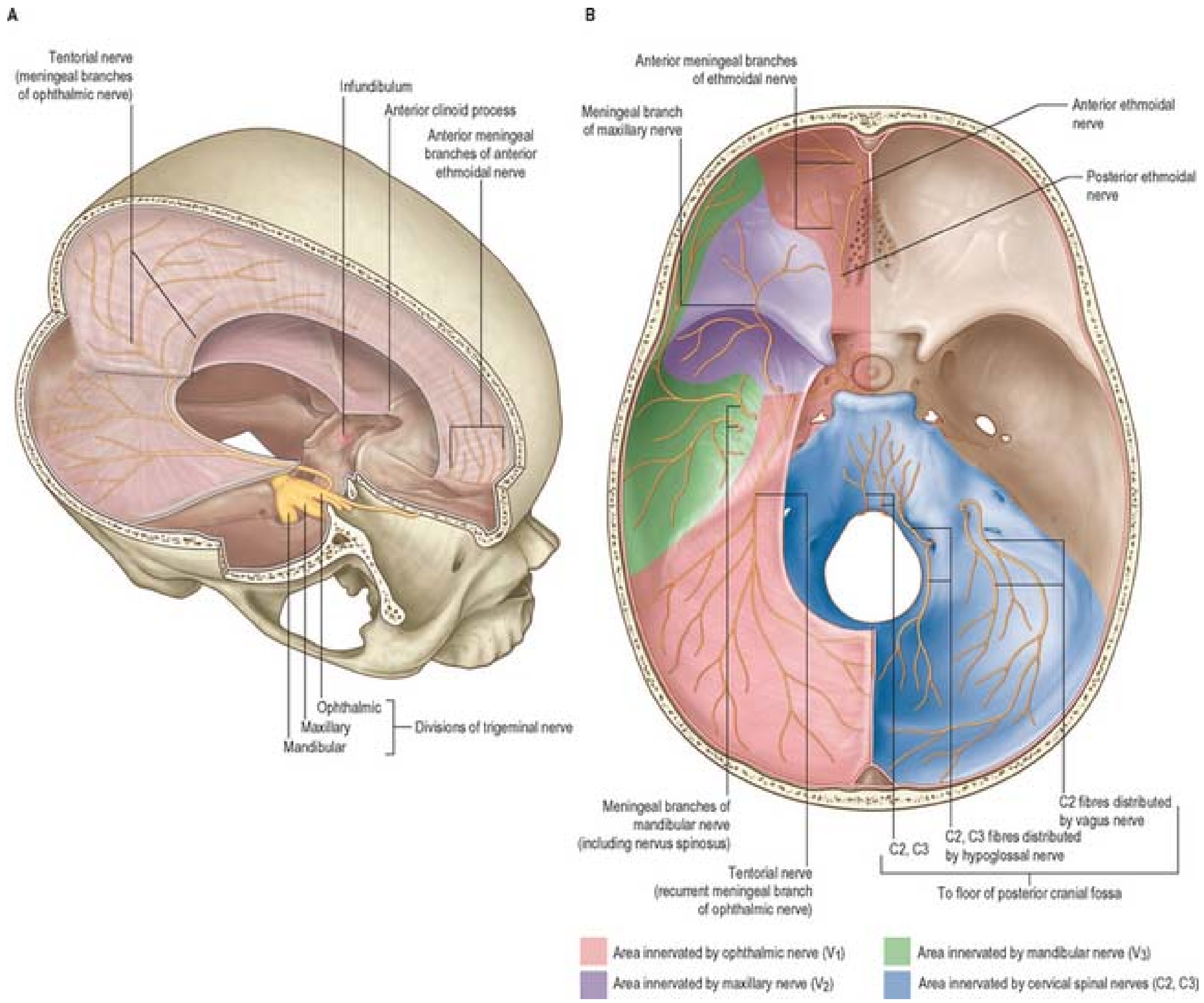
A
Tentorial nerve (meningeal branches of ophthalmic nerve)
Infundibulum
Anterior clinoid process
Anterior meningeal branches of anterior ethmoidal nerve
Ophthalmic
Maxillary
Mandibular
Divisions of trigeminal nerve
B
Anterior meningeal branches of ethmoidal nerve
Meningeal branch of maxillary nerve
Anterior ethmoidal nerve
Posterior ethmoidal nerve
Meningeal branches of mandibular nerve (including nervus spinosus)
Tentorial nerve (recurrent meningeal branch of ophthalmic nerve)
C2, C3
C2, C3 fibres distributed by hypoglossal nerve
C2 fibres distributed by vagus nerve
To floor of posterior cranial fossa
Area innervated by ophthalmic nerve (V1)
Area innervated by maxillary nerve (V2)
Area innervated by mandibular nerve (V3)
Area innervated by cervical spinal nerves (C2, C3)

Fig. 27.11 The innervation of the cranial meninges.

In the anterior cranial fossa, the dura is innervated by meningeal branches of the anterior and posterior ethmoidal nerves and anterior filaments of the meningeal rami of the maxillary (nervus meningeus medius) and mandibular (nervus spinosus) divisions of the trigeminal nerve. Nervi meningeus medius and spinosus are, however, largely distributed to the dura of the middle cranial fossa, which also receives filaments from the trigeminal ganglion. The nervus spinosus re-enters the cranium through the foramen spinosum with the middle meningeal artery, and divides into anterior and posterior branches which accompany the main divisions of the artery and supply the dura mater in the middle cranial fossa and, to a lesser extent, the anterior fossa and calvarium. The anterior branch communicates with the meningeal branch of the maxillary nerve; the posterior branch also supplies the mucous lining of the mastoid air cells. The nervus spinosus contains sympathetic postganglionic fibres from the middle meningeal plexus. The nervus tentorii, a recurrent branch of the intracranial portion of the ophthalmic division of the trigeminal supplies the supratentorial falx cerebri and the tentorium cerebelli. Intraoperative mechanical stimulation of the falx may trigger the trigeminocardiac reflex (Bauer et al 2005). The dura in the posterior cranial fossa is innervated by ascending meningeal branches of the upper cervical nerves which enter through the anterior part of the foramen magnum (second and third cervical nerves) and through the hypoglossal canal and jugular foramen (first and second cervical nerves).

Meningeal branches from the vagus and hypoglossal nerves have been described. Those from the vagus apparently start from the superior vagal ganglion and are distributed to the dura mater in the posterior cranial fossa. Those from the hypoglossal leave the nerve in its canal and supply the diploë of the occipital bone, the dural walls of the occipital and inferior petrosal sinuses, and much of the floor and anterior wall of the posterior cranial fossa. These meningeal rami may not contain vagal or hypoglossal fibres but ascending, mixed sensory and sympathetic fibres from the upper cervical nerves and superior cervical sympathetic ganglion. All meningeal nerves contain a postganglionic sympathetic component, either from the superior cervical sympathetic ganglion or by communication with its perivascular intracranial extensions. The role of the autonomic nerve supply of the cranial dura mater is uncertain.

Sensory nerve endings are restricted to the dura mater and cerebral blood vessels, and are not found in either the brain itself, or in the arachnoid or pia mater. Stimulation of these nerve endings causes pain and is the basis of certain forms of headache.

Arachnoid and pia mater

The arachnoid mater and the pia mater together are sometimes referred to as the leptomeninges. They are separated by the subarachnoid space and joined by trabeculae. They are composed of cells that share a common embryological origin from the mesenchyme that surrounds the developing nervous system. The cells are flattened or cuboidal and each has an oval nucleus, usually with a single small but prominent nucleolus. The outer layer of the arachnoid, the dura–arachnoid interface, is formed from five or six layers of cells joined by numerous desmosomes and tight junctions. This layer forms a barrier that normally prevents permeation of CSF through the arachnoid into the subdural space. The central portion of the arachnoid is closely apposed to the outer layer, and is formed from tightly packed polygonal cells joined by desmosomes and gap junctions. The cells are more loosely packed in the inner layer of the arachnoid, where they intermingle with bundles of collagen continuous with the trabeculae that cross the subarachnoid space. The leptomeningeal cells are not surrounded by basement membrane, except where they are in contact with collagen in the inner layers of the arachnoid and on the deep aspects of the pia mater.

The anatomical relationships of the arachnoid and pia differ to some extent in the cerebral and spinal regions. The cerebral part of the arachnoid mater invests the brain loosely. It does not enter the sulci or fissures, other than the great longitudinal fissure between the cerebral hemispheres, and it coats the superior surface of the pituitary fossa. It is thicker on the basal aspect of the brain and is also slightly opaque where it extends between the temporal lobes and the front of the pons, and produces a large subarachnoid cistern between the arachnoid and underlying pia mater. The arachnoid is easily separated from the dura over the surface of the brain, but adherent to the adventitia of the internal carotid and the vertebral arteries where they enter the subarachnoid space. It is reflected onto the surface of blood vessels in the subarachnoid space and is eventually continuous with the pia mater. In the young, the arachnoid on the upper surface of the brain is transparent, but with age it may become white and opaque, particularly near the midline.

Subdural haematoma

Separation of the arachnoid and dura mater requires little physical force, which means that damage to small bridging veins in the space can result in subdural haematoma after even relatively mild head trauma. The characteristics of a subdural haematoma differ from the extradural haematoma described above. Clinically the accumulation is often of relatively low pressure and seldom presents as a medical emergency: even sizeable accumulations may be tolerated on a chronic basis with mild or no symptoms. In many cases there is some predisposing factor, such as cerebral atrophy or increased size of the underlying subarachnoid space. The distinction between subdural and extradural haematoma on a CT scan relies on the anatomical features of the space. Extradural collections tend to be lentiform in shape reflecting the pressure required to separate the dura and periosteum. They will pass deep to any major dural sinus and cannot extend along the falx cerebri or tentorium cerebelli. In contrast, subdural haematomas tend to be biconcave in shape and more extensive: they often follow the line of the dura along the falx or tentorium and always lie superficial to the deep venous sinuses.

REFERENCES

uer DF, Youkilis A, Schenck C, Turner CR, Thompson BG. The falcine trigeminocardiac reflex: case report and review of the literature. *Surg Neurol*. 2005;63:143-148.

owder J, Kaplan HA. Cerebral Dural Sinuses and their Tributaries. Springfield, Illinois: Thomas, 1976.

Describes variations in the form of the superior sagittal and other venous sinuses..

rris FS, Rhoton AL. Anatomy of the cavernous sinus. A microsurgical study. *J Neurosurg*. 1976;45:169-180.

onetta G, Fusco M, Samii M. The sphenopetroclival venous gulf: a microanatomical study. *J Neurosurg*. 2003;99:366-375.

plan HA, Browder J. Neurosurgical consideration of some features of the cerebral dural sinuses and their tributaries. *Clin Neurosurg*. 1976;23:155-169.

da S, Weller RO. Morphology of CSF drainage pathways in man. Raimondi A, editor. Principles of Pediatric Neurosurgery, vol 4. Berlin: Springer, 1994.

Describes the morphology and relationships of the subarachnoid space including the structure of arachnoid granulations..

intworth GK. The ontogeny and growth of the human tentorium cerebelli. *Anat Rec*. 1967;158:433-442.

isht A, Barnett DW, Barrow DL, Bonner G. The blood supply of the intracavernous cranial nerves: an anatomic study. *Neurosurgery*. 1994;34:275-279.

zveren MF, Uchida K, Aiso S, Kawase T. Meningovenous structures of the petroclival region: clinical importance for surgery and intravascular surgery. *Neurosurgery*. 2002;50:829-836.

isch R, Vutskits L, Patonay L, Fries G. The meningohypophyseal trunk and its blood supply to different intracranial structures. An anatomical study. *Minim Invasive Neurosurg*. 1996;39:78-81.

ïz DSM, Fasel JHD, Rüfenacht DA, Gailloud P. The sphenoparietal sinus of Breschet: Does it exist? An anatomic study. *Am J Neuroradiol*. 2004;25:112-120.

oane E, Rhoton ALJr, de Oliveira E. Microsurgical anatomy of the dural collar (carotid collar) and rings around the clinoid segment of the internal carotid artery. *Neurosurgery*. 1998;42:869-884.

eu M, Fauteux G, Chang H, Taylor W, Stopa E, Robinson-Bostom L. Sinus pericranii: dermatologic considerations and literature review. *J Am Acad Dermatol*. 2002;46:934-941.

kdemir I, Tuccar E, Aslan A, et al. The jugular foramen. A comparative radioanatomic study. *Surg Neurol*. 1998;50:557-562.

kdemir I, Tuccar E, Cubuk HE, Ersoy M, Elhan A, Deda H. Branches of the intracavernous internal carotid artery and the blood supply of the intracavernous cranial nerves. *Ann Anat*. 1998;180:343-348.

nansky F, Valarezo A, Elidan J. The superior wall of the cavernous sinus: a microanatomical study. *J Neurosurg*. 1994;81:914-920.

atanabe A, Nagaseki Y, Ohkubo S, Ohhashi Y, Horikoshi T, Nishigaya K, Nukui H. Anatomical variations of the ten triangles around the cavernous sinus. *Clin Anat*. 2003;16:9-14.

illiams JL. Rowe and Williams' Maxillofacial Injuries. Edinburgh: Churchill Livingstone, 1994.

ısuda A, Campero A, Martins C, Rhoton ALJr, Ribas GC. The medial wall of the cavernous sinus: microsurgical anatomy. *Neurosurgery*. 2004;55:179-189.

ıang ET, Inman CBE, Weller RO. Interrelationships of the pia mater and the perivascular (Virchow-Robin) spaces in the human cerebrum. *J Anat*. 1990;170:111-123.

CHAPTER 28

Neck

The neck extends from the base of the cranium and the inferior border of the mandible to the thoracic inlet.

SKIN

The skin in the neck is normally under tension. The direction in which this is greatest varies regionally; in the living face these lines often coincide with wrinkle lines. Lines of greatest tension have been termed ‘relaxed skin tension lines’, and surgical incisions made along these lines are said to heal with minimal postoperative scarring. Susceptible individuals are more prone to keloid scarring in the head and neck region.

Cutaneous vascular supply and lymphatic drainage

The blood vessels supplying the skin of the neck are derived principally from the facial, occipital, posterior auricular and subclavian arteries. They form a rich network within platysma and in the subdermal plexus, and account for the viability of the various skin flaps raised during block dissection of the neck, irrespective of whether they include platysma: the latter is usually elevated in extensive incisions.

The anterior cervical skin is supplied mainly by the superior thyroid artery and the transverse cervical branch of the subclavian artery. The posterior skin is supplied by branches from the occipital artery and the deep cervical and transverse cervical branches of the subclavian artery. The superior skin is supplied by the occipital artery and its upper sternocleidomastoid branch, and the submandibular and submental branches of the facial artery. Inferiorly, the skin is supplied by the transverse cervical and/or suprascapular branches of the subclavian artery.

The pattern of venous drainage of the skin of the neck mirrors the arterial supply: the veins drain into the jugular and facial veins.

Many lymphatic vessels draining the superficial cervical tissues skirt the borders of sternocleidomastoid to reach the superior or inferior deep cervical nodes. Some pass over sternocleidomastoid and the posterior triangle to drain into the superficial cervical and occipital nodes (see Fig. 28.15). Lymph from the superior region of the anterior triangle drains to the submandibular and submental nodes. Vessels from the anterior cervical skin inferior to the hyoid bone pass to the anterior cervical lymph nodes near the anterior jugular veins, and their efferents go to the deep cervical nodes of both sides, including the infrahyoid, prelaryngeal and pretracheal groups. An anterior cervical node often occupies the suprasternal space.

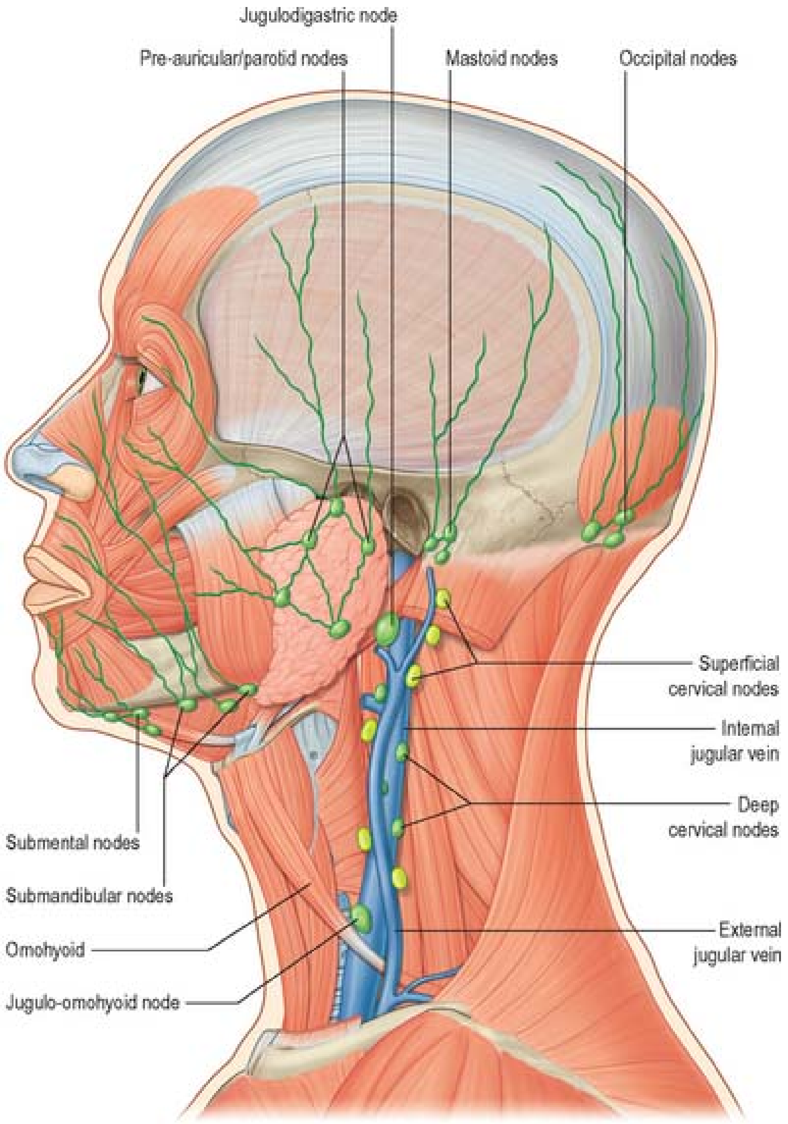
Jugulodigastric node
Pre-auricular/parotid nodes
Mastoid nodes
Occipital nodes
Superficial cervical nodes
Internal jugular vein
Deep cervical nodes
External jugular vein
Submental nodes
Submandibular nodes
Omohyoid
Jugulo-omohyoid node

Fig. 28.15 Superficial lymphatic system in the head and neck: the nodes are organized into a superficial group around the head, superficial cervical nodes along the external jugular vein, and deep cervical nodes along the internal jugular vein.

(From Drake, Vogl and Mitchell 2005.)

Cutaneous innervation

The cervical skin is innervated by branches of cervical spinal nerves, via both dorsal and ventral rami (see Fig. 43.6). The dorsal rami supply skin over the back of the neck and scalp, and the ventral rami supply skin covering the lateral and anterior portions of the neck, and the angle of the mandible (Fig. 28.1). The dorsal rami of the first, sixth, seventh and eighth cervical nerves have no cutaneous distribution in the neck. The greater occipital nerve mainly supplies the scalp; it comes from the medial branch of the dorsal ramus of the second cervical nerve. The medial branches of the dorsal rami of the third, fourth and fifth cervical nerves pierce trapezius to supply skin over the back of the neck sequentially. The ventral rami of the second, third and fourth cervical nerves supply named cutaneous branches (the lesser occipital, great auricular, transverse cutaneous and supraclavicular nerves), via the cervical plexus (Fig. 28.1) (see p. 456 for details of the motor branches of the cervical plexus).

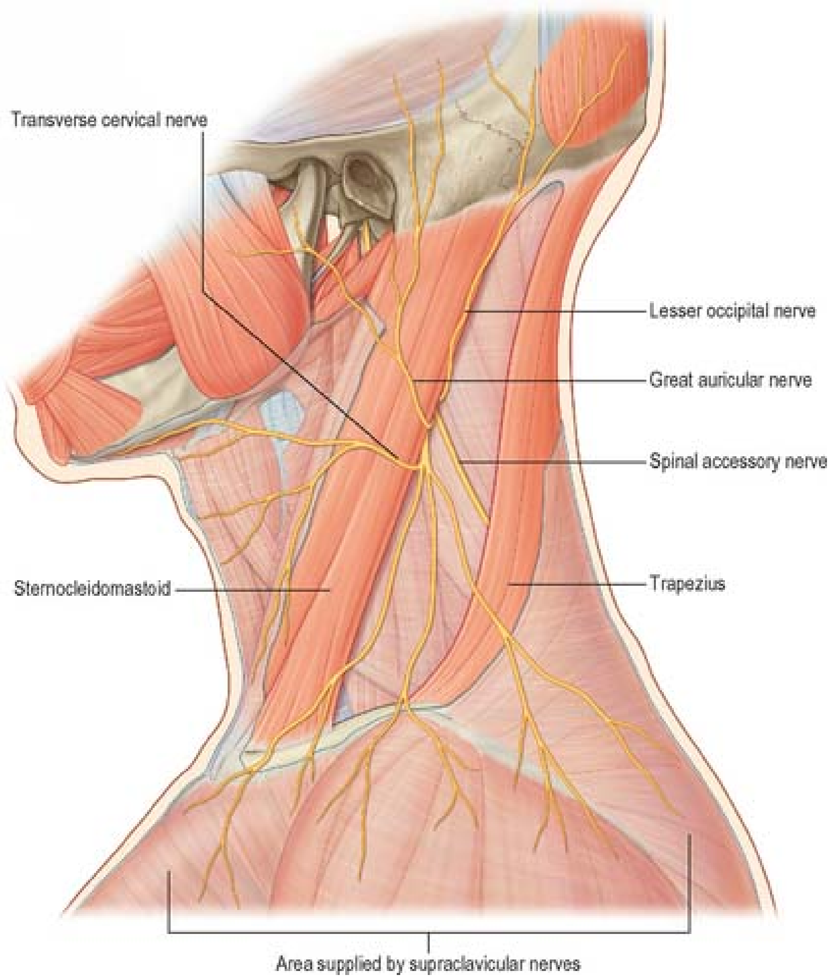
Transverse cervical nerve
Lesser occipital nerve
Great auricular nerve
Spinal accessory nerve
Sternocleidomastoid
Trapezius
Area supplied by supraclavicular nerves

Fig. 28.1 The cutaneous branches of the cervical plexus. The spinal part of the accessory nerve that supplies trapezius is also shown as it crosses the posterior triangle. Note that the interval between the upper attachments of sternocleidomastoid and trapezius is not normally as extensive as shown here.

(Adapted from Drake, Vogl and Mitchell 2005.)

Lesser occipital nerve

The lesser occipital nerve is derived mainly from the second cervical nerve (although fibres from the third cervical nerve may sometimes contribute). It passes first anterior to the plane of the spinal accessory nerve before winding around it and becoming anterior to it. It next ascends along the posterior margin of sternocleidomastoid. Near the cranium it perforates the deep fascia and passes up onto the scalp behind the auricle to supply the skin and connect with the great auricular and greater occipital nerves and the auricular branch of the facial nerve. Its auricular branch supplies the skin on the upper third of the medial aspect of the auricle and connects with the posterior branch of the great auricular nerve. The auricular branch is occasionally derived from the greater occipital nerve. It has been suggested that compression or stretching of the lesser occipital nerve contributes to cervicogenic headache.

Great auricular nerve

The great auricular nerve is the largest ascending branch of the cervical plexus. It arises from the second and third cervical rami, encircles the posterior border of sternocleidomastoid, perforates the deep fascia and ascends on the muscle beneath platysma with the external jugular vein. On reaching the parotid gland, it divides into anterior and posterior branches. The anterior branch is distributed to the facial skin over the parotid gland and connects in the gland with the facial nerve. This cross innervation between somatic sensory supply (great auricular) and parasympathetic secretomotor fibres to the parotid is considered to be part of the anatomical basis for the phenomenon of gustatory sweating (Frey’s syndrome) seen after parotid surgery, when the nerve is at risk of injury. The posterior branch supplies the skin over the mastoid process and on the back of the auricle (except its upper part); a filament pierces the auricle to reach the lateral surface where it is distributed to the lobule and concha. The posterior branch communicates with the lesser occipital nerve, the auricular branch of the vagus and the posterior auricular branch of the facial nerve.

Transverse cervical cutaneous nerve

The transverse cervical cutaneous nerve arises from the second and third cervical rami. It curves round the posterior border of sternocleidomastoid near its midpoint and runs obliquely forwards, deep to the external jugular vein, to the anterior border of the muscle. It perforates the deep cervical fascia, and divides under platysma into ascending and descending branches that are distributed to the anterolateral areas of the neck. The ascending branches ascend to the submandibular region, forming a plexus with the cervical branch of the facial nerve beneath platysma. Some branches pierce platysma and are distributed to the skin of the upper anterior areas of the neck. The descending branches pierce platysma and are distributed anterolaterally to the skin of the neck, as low as the sternum.

Supraclavicular nerves

The supraclavicular nerves arise from a common trunk formed from rami from the third and fourth cervical nerves and emerge at the posterior border of sternocleidomastoid. Descending under platysma and the deep cervical fascia, the trunk divides into medial, intermediate and lateral (posterior) branches, which diverge to pierce the deep fascia a little above the clavicle. The medial supraclavicular nerves run inferomedially across the external jugular vein and the clavicular and sternal heads of sternocleidomastoid to supply the skin as far as the midline and as low as the second rib. They also supply the sternoclavicular joint. The intermediate supraclavicular nerves cross the clavicle to supply the skin over pectoralis major and deltoid down to the level of the second rib, next to the area of supply of the second thoracic nerve. Overlap between these nerves is minimal. The lateral supraclavicular nerves descend superficially across trapezius and the acromion, supplying the skin of the upper and posterior parts of the shoulder.

BONES, JOINTS AND CARTILAGES

The bones and cartilages of the neck are the cervical vertebrae and the hyoid bone, and the cartilages of the upper respiratory tract, including the larynx. The cervical vertebrae, occipital bone and the atlantooccipital and atlanto-axial joints are described in Chapter 42, and the laryngeal cartilages are described in Chapter 34.

HYOID BONE

The U-shaped hyoid bone (Fig. 28.2) is suspended from the tips of the styloid processes by the stylohyoid ligaments. It has a body, two greater and two lesser horns, or cornua.

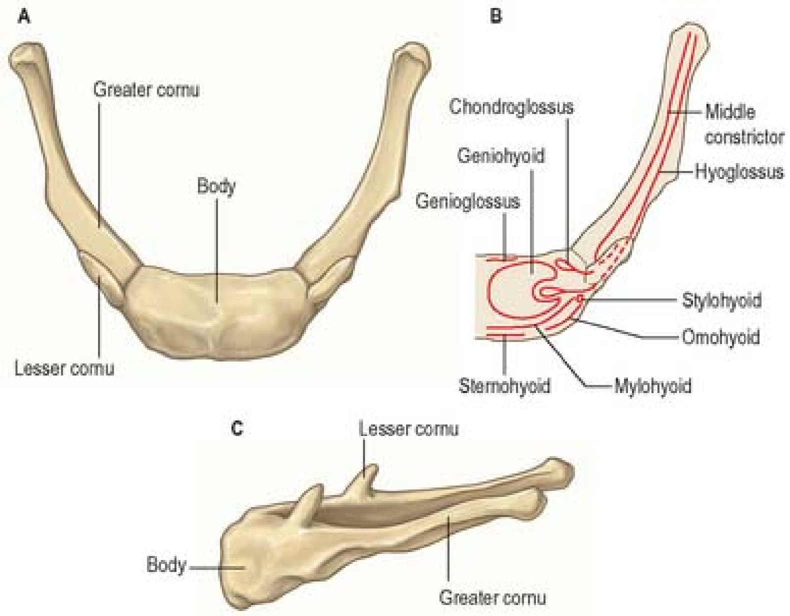
A
Greater cornu
Body
Lesser cornu
B
Chondroglossus
Geniohyoid
Genioglossus
Middle constrictor
Hyoglossus
Stylohyoid
Omohyoid
Sternohyoid
Mylohyoid
C
Lesser cornu
Body
Greater cornu

Fig. 28.2 The hyoid bone: **A**, **B**, anterosuperior aspect; **C**, lateral aspect. **B** shows the positions of muscular attachments.

Body

The body is irregular, elongated and quadrilateral. Its anterior surface is convex, faces anterosuperiorly, and is crossed by a transverse ridge with a slight downward convexity. A vertical median ridge often bisects the upper part of the body, but rarely extends to the lower part. The posterior surface is smooth, concave, faces posteroinferiorly, and is separated from the epiglottis by the thyrohyoid membrane and loose areolar tissue. There is a bursa between the hyoid bone and the membrane.

Geniohyoid is attached to most of the anterior surface of the body, above and below the transverse ridge; the medial part of hyoglossus invades the lateral geniohyoid area. The lower anterior surface gives attachment to mylohyoid, the line of attachment lying above sternohyoid medially and omohyoid laterally. The lowest fibres of genioglossus, the hyoepiglottic ligament and (most posteriorly) the thyrohyoid membrane are all attached to the rounded superior border. Sternohyoid is attached to the inferior border medially and omohyoid is attached laterally. Occasionally the medial fibres of thyrohyoid and, when present, of levator glandulae thyroideae, are attached along the inferior border.

Greater cornua

In early life, the greater cornua are connected to the body by cartilage, but after middle age they are usually united by bone. They project backwards (curving posterolaterally) from the lateral ends of the body. They are horizontally flattened, taper posteriorly, and each ends in a tubercle. When the throat is gripped between finger and thumb above the thyroid cartilage, the greater cornua can be identified and the bone can be moved from side to side.

The middle pharyngeal constrictor and, more laterally (i.e. superficially), hyoglossus, are attached along the whole length of the upper surface of each greater cornu. Stylohyoid is attached near the junction of the cornu with the body. The fibrous loop for the digastric tendon is attached lateral and a little posterior to hyoglossus. The thyrohyoid membrane is attached to the medial border and thyrohyoid is attached to the lateral border. The oblique inferior surface is separated from the thyrohyoid membrane by fibroareolar tissue.

Lesser cornua

The lesser cornua are two small conical projections at the junctions of the body and greater cornua. At its base, each is connected to the body by fibrous tissue and occasionally to the greater cornu by a synovial joint which occasionally becomes ankylosed.

The middle pharyngeal constrictors are attached to the posterior and lateral aspects of the lesser cornua. The stylohyoid ligaments are attached to their apices and are often partly calcified, and the chondroglossi are attached to the medial aspects of their bases.

Ossification

The hyoid bone develops from cartilages of the second and third pharyngeal arches, the lesser cornua from the second, the greater cornua from the third and the body from the fused ventral ends of both. Chondrification begins in the fifth fetal week in these elements, and is completed in the third and fourth months. Ossification proceeds from six centres, i.e. a pair for the body and one for each cornu. Ossification begins in the greater cornua towards the end of intrauterine life, in the body shortly before or after birth, and in the lesser cornua around puberty. The greater cornual apices remain cartilaginous until the third decade and epiphyses may occur here. They fuse with the body. Synovial joints between the greater and lesser cornua may be obliterated by ossification in later decades.

JOINTS

The atlanto-occipital and atlanto-axial joints are described on pages 733–734.

TRIANGLES OF THE NECK

Anterolaterally the neck appears as a somewhat quadrilateral area, limited superiorly by the base of the mandible and a line continued from the angle of the mandible to the mastoid process, inferiorly by the upper border of the clavicle, anteriorly by the anterior median line, and posteriorly by the anterior margin of trapezius. This quadrilateral area can be further divided into anterior and posterior triangles by sternocleidomastoid, which passes obliquely from the sternum and clavicle to the mastoid process and occipital bone (Fig. 28.3). It is true that these triangles and their subdivisions are somewhat arbitrary, because many major structures – arteries, veins, lymphatics, nerves, and some viscera – transgress their boundaries without interruption, nevertheless they have a topographical value in description. Moreover, some of their subdivisions are easily identified by inspection and palpation and provide invaluable assistance in surface anatomical and clinical examination.

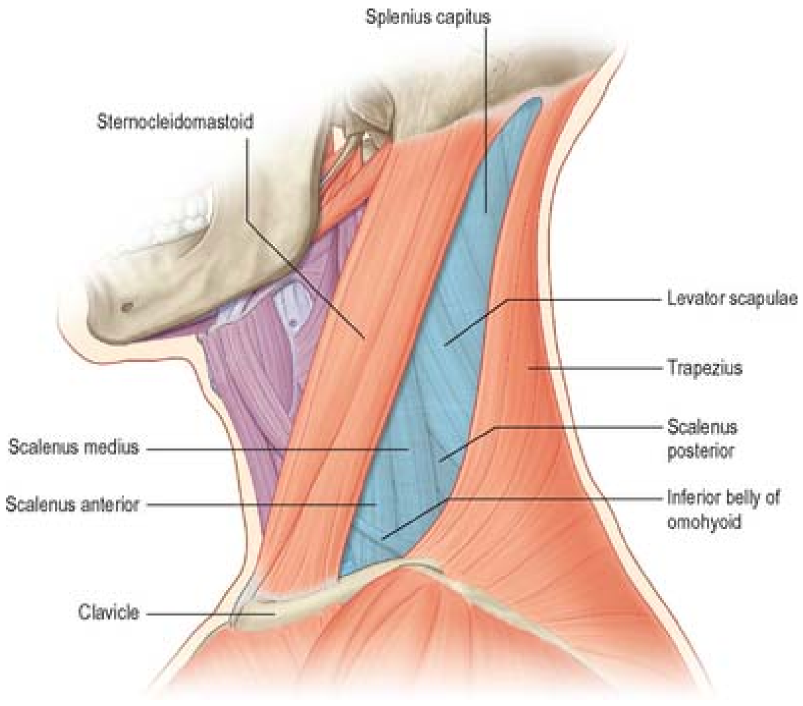
Splenius capitus
Sternocleidomastoid
Levator scapulae
Trapezius
Scalenus medius
Scalenus posterior
Scalenus anterior
Inferior belly of omohyoid
Clavicle

Fig. 28.3 The anterior and posterior triangles of the neck, left lateral aspect. See note in caption for **Fig. 28.1**

(Adapted from Drake, Vogl and Mitchell 2005.)

ANTERIOR TRIANGLE OF THE NECK

The anterior triangle of the neck is bounded anteriorly by the median line of the neck and posteriorly by the anterior margin of sternocleidomastoid. Its base is the inferior border of the mandible and its projection to the mastoid process, and its apex is at the manubrium sterni. It can be subdivided into suprahyoid and infrahyoid areas above and below the hyoid bone, and into digastric, submental, muscular and carotid triangles by the passage of digastric and omohyoid across the anterior triangle (see Fig. 28.5).

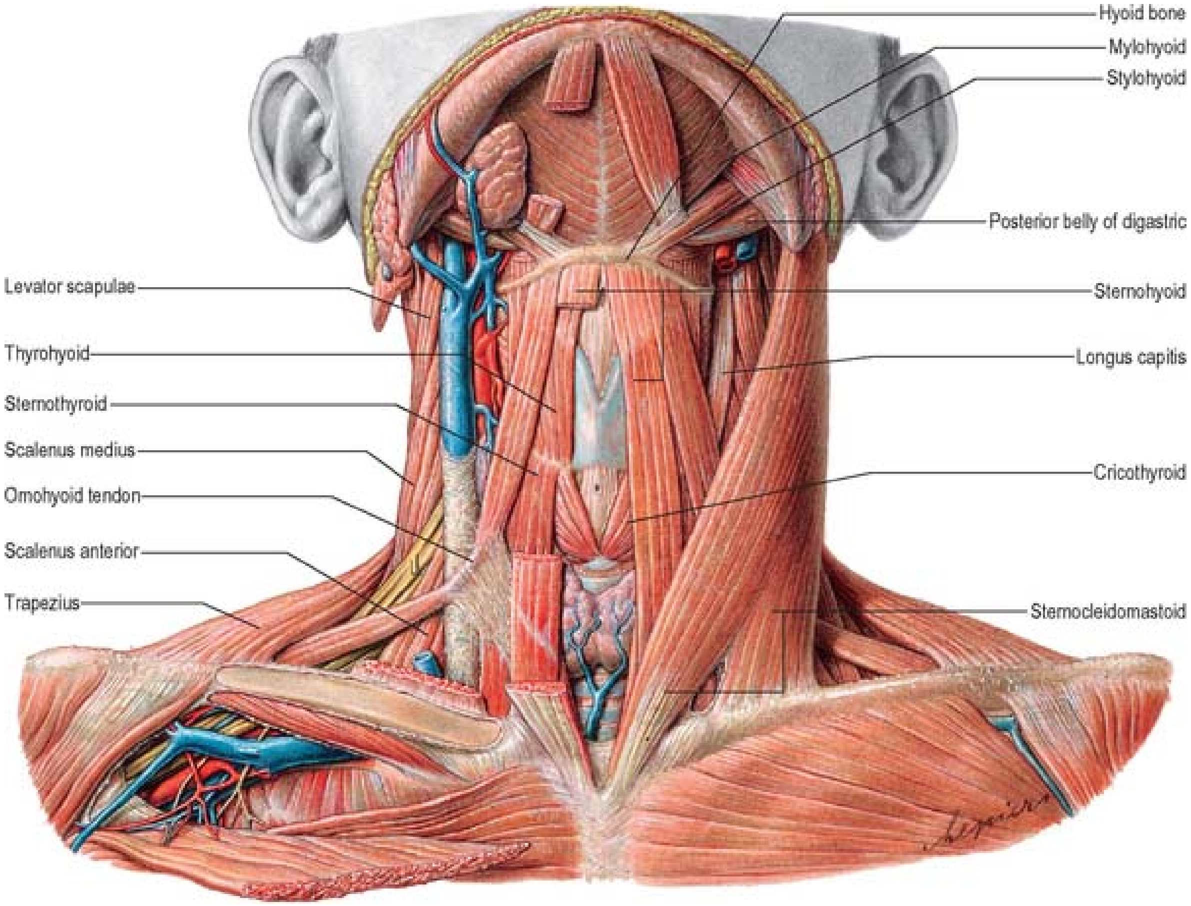
Hyoid bone
Mylohyoid
Stylohyoid
Posterior belly of digastric
Levator scapulae
Sternohyoid
Thyrohyoid
Longus capitis
Sternothyroid
Scalenus medius
Cricothyroid
Omohyoid tendon
Scalenus anterior
Trapezius
Sternocleidomastoid

Fig. 28.5 Muscles of the neck: note that the head is slightly extended in order to expose the suprahyoid muscles.

(From Sobotta 2006.)

Digastric triangle

The digastric triangle is bordered above by the base of the mandible and its projection to the mastoid process, posteroinferiorly by the posterior belly of digastric and by stylohyoid, and anteroinferiorly by the anterior belly of digastric. It is covered by the skin, superficial fascia, platysma and deep fascia, which contain branches of the facial and transverse cutaneous cervical nerves. Its floor is formed by mylohyoid and hyoglossus. The anterior region of the digastric triangle contains the submandibular gland, which has the facial vein superficial to it and the facial artery deep to it. The submental and mylohyoid arteries and nerves lie on mylohyoid. The submandibular lymph nodes are variably related to the submandibular gland. The posterior region of the digastric triangle contains the lower part of the parotid gland. The external carotid artery, passing deep to stylohyoid, curves above the muscle, and overlaps its superficial surface as it ascends deep to the parotid gland before entering it. The internal carotid artery, internal jugular vein and vagus nerve lie deeper and are separated from the external carotid artery by styloglossus, stylopharyngeus and the glossopharyngeal nerve.

Submental triangle

The single submental triangle is demarcated by the anterior bellies of both digastric muscles. Its apex is at the chin, its base is the body of the hyoid bone and its floor is formed by both mylohyoid muscles. It contains lymph nodes and small veins that unite to form the anterior jugular vein. The structures within the digastric and submental triangles are described in more detail with the floor of the mouth (on p. 501).

Muscular triangle

The muscular triangle is bounded anteriorly by the median line of the neck from the hyoid bone to the sternum, inferoposteriorly by the anterior margin of sternocleidomastoid and posterosuperiorly by the superior belly of omohyoid. The triangle contains omohyoid, sternohyoid, sternothyroid and thyrohyoid.

Carotid triangle

The carotid triangle is limited posteriorly by sternocleidomastoid, anteroinferiorly by the superior belly of omohyoid and superiorly by stylohyoid and the posterior belly of digastric. In the living (except the obese) the triangle is usually a small visible triangular depression, sometimes best seen with the head and cervical vertebral column slightly extended and the head contralaterally rotated. The carotid triangle is covered by the skin, superficial fascia, platysma and deep fascia containing branches of the facial and cutaneous cervical nerves. The hyoid bone forms its anterior angle and adjacent floor and can be located on simple inspection, verified by palpation. Parts of thyrohyoid, hyoglossus and inferior and middle pharyngeal constrictor muscles form its floor. The carotid triangle contains the upper part of the common carotid artery and its division into external and internal carotid arteries. Overlapped by the anterior margin of sternocleidomastoid, the external carotid artery is first anteromedial, then anterior to the internal carotid artery. Branches of the external carotid artery are encountered in the carotid triangle. Thus the superior thyroid artery runs anteroinferiorly, the lingual artery anteriorly with a characteristic upward loop, the facial artery anterosuperiorly, the occipital artery posterosuperiorly and the ascending pharyngeal artery medial to the internal carotid artery. Arterial pulsation greets the examining finger. The superior thyroid, lingual, facial, ascending pharyngeal and sometimes the occipital, veins, correspond to the branches of the external carotid artery, and all drain into the internal jugular vein. The hypoglossal nerve crosses the external and internal carotid arteries. It curves round the origin of the lower sternocleidomastoid branch of the occipital artery, and at this point the superior root of the ansa cervicalis leaves it to descend anteriorly in the carotid sheath. The internal laryngeal nerve and, below it, the external laryngeal nerve, lie medial to the external carotid artery below the hyoid bone. Many structures in this region, such as all or part of the internal jugular vein, associated deep cervical lymph nodes, and the vagus nerve, may be variably obscured by sternocleidomastoid, and, pedantically, are thus ‘outside the triangle’.

POSTERIOR TRIANGLE OF THE NECK

The posterior triangle is delimited anteriorly by the posterior edge of sternocleidomastoid, posteriorly by the anterior edge of trapezius, and inferiorly by the middle third of the clavicle (Fig. 28.3). Its apex is between the attachments of sternocleidomastoid and trapezius to the occiput and is often blunted, so that the ‘triangle’ becomes quadrilateral. The roof of the posterior triangle is formed by the investing layer of the deep cervical fascia. The floor of the triangle is formed by the prevertebral fascia overlying splenius capitis, levator scapulae and the scalene muscles. It is crossed, approximately 2.5 cm above the clavicle, by the inferior belly of omohyoid, which subdivides it into occipital and supraclavicular triangles. The contents of the posterior triangle include fat, lymph nodes (level V – see later), spinal accessory nerve, cutaneous branches of the cervical plexus, inferior belly of omohyoid, branches of the thyrocervical trunk (transverse cervical and suprascapular arteries), the third part of the subclavian artery, and the external jugular vein. The anterior and lateral groups of prevertebral muscles form the floor of the posterior triangle.

Occipital triangle

The occipital triangle constitutes the upper and larger part of the posterior triangle, with which it shares the same borders, except that inferiorly it is limited by the inferior belly of omohyoid. Its floor, from above down, is formed by splenius capitis, levator scapulae, and scaleni medius and posterior; semispinalis capitis occasionally appears at the apex. The triangle is covered by skin, superficial and deep fasciae and inferiorly by platysma. The spinal accessory nerve pierces sternocleidomastoid and crosses levator scapulae obliquely downwards and backwards to reach the deep surface of trapezius. The surface marking of its course is in a line from the junction of the superior one-third and inferior two-thirds of sternocleidomastoid, to the junction of the inferior one-third and superior two-thirds of trapezius. Cutaneous and muscular branches of the cervical plexus emerge at the posterior border of sternocleidomastoid. Inferiorly, supraclavicular nerves, transverse cervical vessels and the uppermost part of the brachial plexus cross the triangle. Lymph nodes lie along the posterior border of sternocleidomastoid from the mastoid process to the root of the neck.

Supraclavicular triangle

The supraclavicular triangle is the lower and smaller division of the posterior triangle, with which it shares the same boundaries, except that superiorly it is limited by omohyoid. It corresponds in the living neck with the lower part of a deep, prominent hollow, namely, the greater supraclavicular fossa. Its floor contains the first rib, scalenus medius and the first slip of serratus anterior. Its size varies with the extent of the clavicular attachments of sternocleidomastoid and trapezius and also the level of the inferior belly of omohyoid. The triangle is covered by skin, superficial and deep fasciae and platysma and crossed by the supraclavicular nerves. Just above the clavicle, the third part of the subclavian artery curves inferolaterally from the lateral margin of scalenus anterior across the first rib to the axilla. The subclavian vein is behind the clavicle and is not usually in the triangle; but it may rise as high as the artery and even accompany it behind scalenus anterior. The brachial plexus is partly superior, and partly posterior to the artery and is always closely related to it. The trunks of the brachial plexus may easily be palpated here if the neck is contralaterally flexed and the examining finger is drawn across the trunks at right angles to their length. With the musculature relaxed, pulsation of the subclavian artery may be felt and the arterial flow can be controlled by retroclavicular compression against the first rib. The suprascapular vessels pass transversely behind the clavicle, below the transverse cervical artery and vein. The external jugular vein descends behind the posterior border of sternocleidomastoid to end in the subclavian vein. It receives the transverse cervical and suprascapular veins, which form a plexus in front of the third part of the subclavian artery; occasionally it is joined by a small vein that crosses the clavicle anteriorly from the cephalic vein. Other structures within the triangle include the nerve to subclavius, which crosses the triangle, and lymph nodes.

CERVICAL FASCIA

SUPERFICIAL CERVICAL FASCIA

The superficial cervical fascia is usually a thin lamina covering platysma and is hardly demonstrable as a separate layer. It may, however, contain considerable amounts of adipose tissue, especially in females. Like all superficial fascia it is not a separate stratum, but merely a zone of loose connective tissue between dermis and deep fascia, and is joined to both. In the lower cervical region, aponeurotic fibres of platysma gradually fan out in the superficial fascia: they either become skin ligaments or continue into the fascia covering pectoralis major and deltoid. These aponeurotic fibres cover the anterior and lateral cervical regions and often mimic the investing layer of deep cervical fascia, forming a tissue barrier (Nash et al 2005).

DEEP CERVICAL FASCIA

Descriptions of the organization of the deep cervical fascia are largely based on the classic work of Grodinsky & Holyoke in 1938. However recent anatomical studies using techniques such as sheet plastination and confocal microscopy have indicated that the arrangement of the deep cervical fascia is more complicated than was previously thought (Zhang & Lee 2002, Nash et al 2005) (Fig. 28.4).

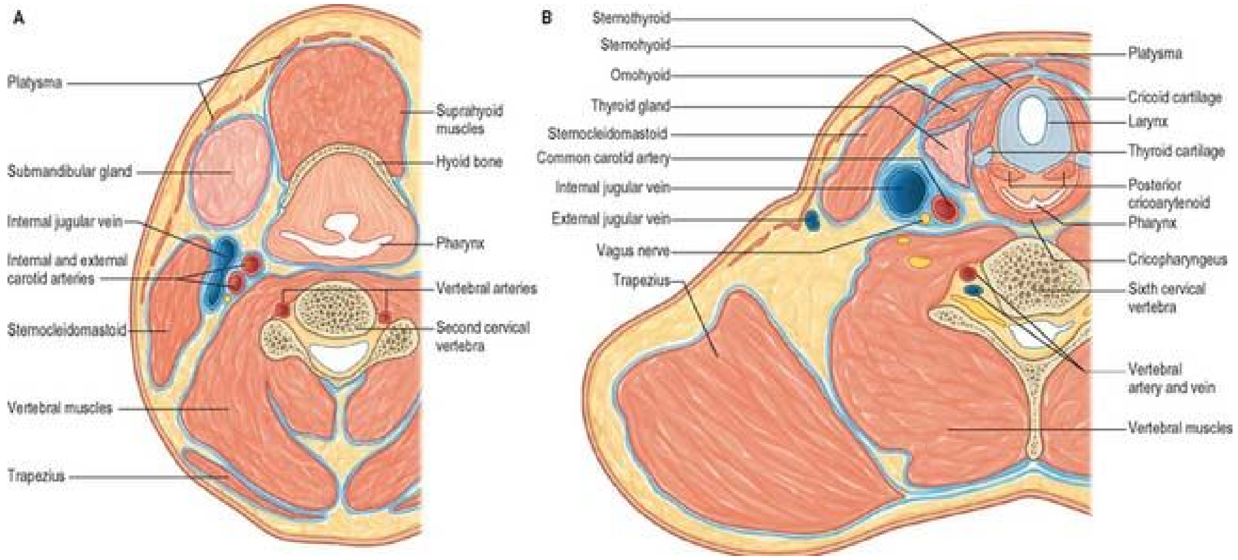
A
Platysma
Submandibular gland
Internal jugular vein
Internal and external carotid arteries
Sternocleidomastoid
Vertebral muscles
Trapezius
Suprahyoid muscles
Hyoid bone
Pharynx
Vertebral arteries
Second cervical vertebra
B
Sternothyroid
Sternohyoid
Omohyoid
Thyroid gland
Sternocleidomastoid
Common carotid artery
Internal jugular vein
External jugular vein
Vagus nerve
Trapezius
Platysma
Cricoid cartilage
Larynx
Thyroid cartilage
Posterior cricoarytenoid
Pharynx
Cricopharyngeus
Sixth cervical vertebra
Vertebral artery and vein
Vertebral muscles

Fig. 28.4 Transverse sections through the neck at the levels of the second (**A**) and sixth (**B**) cervical vertebrae, showing the arrangement of the deep cervical fascia, much of which has been coloured blue. Diagrams are based on plastinated sections: note that many muscles have not been individually delineated.

(By courtesy of Dr M Zhang and Mr Robbie McPhee.)

Deep fascia in the neck is conventionally divided into an investing layer, pretracheal fascia, and prevertebral fascia.

Investing layer

The investing layer of the deep cervical fascia is continuous posteriorly with the corresponding fascia from the opposite side. It forms a thin covering for trapezius and encloses sternocleidomastoid. The portions between trapezius and sternocleidomastoid and in the anterior triangle of the neck are formed of areolar tissue, indistinguishable from that in the superficial cervical fascia and deep potential tissue spaces. Superiorly, the deep fascia fuses with periosteum along the superior nuchal line of the occipital bone, over the mastoid process and along the entire base of the mandible. Between the angle of the mandible and the anterior edge of sternocleidomastoid it is particularly strong. Between the mandible and the mastoid process it is related to the parotid gland, extending beneath it to become attached to the zygomatic arch. From this region the strong stylomandibular ligament ascends to the styloid process. Inferiorly, along trapezius and sternocleidomastoid, the investing layer of the deep cervical fascia is attached to the acromion, clavicle and manubrium sterni, fusing with their periostea. A short distance above the manubrium, the investing layer interweaves with aponeurotic fibres of platysma and the fascia investing the strap muscles. It is organized into superficial and deep layers which are attached to the anterior border of the manubrium, and to the posterior border and the interclavicular ligament respectively. Between these two layers a slit-like interval, the suprasternal space, contains a small amount of areolar tissue, the lower parts of the anterior jugular veins and the jugular venous arch, the sternal heads of the sternocleidomastoid muscles and sometimes a lymph node.

Pretracheal fascia

The pretracheal layer of the deep cervical fascia is very thin. It provides fascial sheaths for the thyroid gland, larynx, pharynx, trachea, oesophagus and the infrahyoid strap muscles. Superiorly, it is attached to the hyoid bone; inferiorly, it continues into the superior mediastinum along the great vessels and merges with the fibrous pericardium; laterally, it merges with the investing layer of deep cervical fascia and with the carotid sheath.

Prevertebral fascia

The prevertebral layer of the deep cervical fascia covers the anterior vertebral muscles and extends laterally on scalenus anterior, scalenus medius and levator scapulae, forming a fascial floor for the posterior triangle of the neck. As the subclavian artery and the brachial plexus emerge from behind scalenus anterior they carry the prevertebral fascia downwards and laterally behind the clavicle as the axillary sheath.

The prevertebral fascia is particularly prominent in front of the vertebral column, where there may be two distinct layers of fascia. The space created by the splitting of the anterior prevertebral fascia, the danger space, is a part of the prevertebral space. Traced laterally, the prevertebral fascia becomes thin and areolar. Superiorly it is attached to the base of the skull. Inferiorly it descends in front of longus colli into the superior mediastinum, where it blends with the anterior longitudinal ligament. Anteriorly the prevertebral fascia is separated from the pharynx and its covering buccopharyngeal fascia by a loose areolar zone, the retropharyngeal space. Laterally this loose tissue connects the prevertebral fascia to the carotid sheath and the fascia on the deep surface of sternocleidomastoid. All the ventral rami of the cervical nerves are initially behind the prevertebral fascia. The nerves to the rhomboids and serratus anterior and the phrenic nerve retain this position throughout their course in the neck, but the accessory nerve lies superficial to the prevertebral fascia.

Carotid sheath

The carotid sheath is a condensation of deep cervical fascia around the common and internal carotid arteries, the internal jugular vein, the vagus nerve and the constituents of the ansa cervicalis. It is thicker around the arteries than the vein, an arrangement that allows the vein to expand. Peripherally the carotid sheath is connected to adjacent fascial layers by loose areolar tissue.

Tissue spaces and the spread of infection and injectate

The fascial layers of the neck define a number of potential tissue ‘spaces’ above and below the hyoid bone. In health, the tissues within these spaces are closely applied to each other or are filled with relatively loose connective tissue. However, infections arising superiorly, such as dental, tonsillar, vertebral or intervertebral disc-related infections, can alter these relationships. The organisms responsible are often betahaemolytic streptococci or a variety of anaerobes. Streptococci produce proteolytic enzymes which digest the loose connective tissue and so open up the tissue spaces. Since there are no tissue barriers running horizontally in the neck, infections which are not treated promptly can rapidly spread from the infratemporal fossa down to the mediastinum below (see Ch. 55), cross the midline through the sublingual and submental spaces and even track into the axilla.

Understanding the configuration of the cervical fasciae and spaces is essential for the placement of local anaesthetic cervical plexus blocks in the neck to facilitate operations such as thyroidectomy, parathyroidectomy and carotid endarterectomy (Pandit et al 2000). For example, injection of local anaesthetic either in the superficial fascial plane or under the investing fascia of the posterior triangle can provide a similarly effective cervical plexus block (Pandit et al 2003), presumably because the investing fascia between sternocleidomastoid and trapezius is not a well-defined fascial sheet and is indistinguishable from the surrounding loose connective tissue (Zhang & Lee 2002).

The tissue spaces above the hyoid bone are the submandibular and submental spaces beneath the inferior border of the mandible; the pharyngeal spaces; and the prevertebral space near the base of the skull. These spaces are described on pages 524 and 568. Tissue spaces around the larynx are described on page 584.

Tissue spaces below the hyoid bone are the pretracheal and retrovisceral tissue spaces in the visceral compartment of the neck; the prevertebral space in front of the vertebral column; and a space associated with the carotid sheath.

Pretracheal space

The pretracheal tissue space lies behind the pretracheal fascia and the strap muscles, and in front of the anterior wall of the oesophagus, and therefore immediately surrounds the trachea. It is bounded superiorly by the attachments of the strap muscles to the thyroid cartilage of the larynx. Inferiorly, it extends down into the anterior portion of the superior mediastinum. Infection usually spreads into the pretracheal space either by perforating the anterior wall of the oesophagus or from the retrovisceral space.

Radiologically, the portion of the pretracheal space between the strap fascia and the fascia of the thyroid gland is referred as the anterior cervical space. The posterolateral border of the space is the carotid sheath or the fascia of sternocleidomastoid. The anterior cervical space often provides a symmetric landmark on transverse imaging (Smoker & Harnsberger 1991).

Retrovisceral space

The retrovisceral space is continuous superiorly with the retropharyngeal space. It is situated between the posterior wall of the oesophagus and the prevertebral fascia. Inferiorly, the retrovisceral space extends into the superior mediastinum. Should the prevertebral fascia merge with the connective tissue on the posterior surface of the oesophagus – usually at the level of the fourth thoracic vertebra – the retrovisceral space then has a distinct inferior boundary.

Prevertebral space

The prevertebral tissue space has been variously described as the potential space lying between the prevertebral fascia and the vertebral column, and as the space between the two layers of the prevertebral fascia, the so-called danger space. Infection usually spreads into the space via its fascial walls from the retrovisceral area because it is closed superiorly and laterally. Inferiorly, it extends into the posterior mediastinum. Clinically, however, the danger space and the retropharyngeal or retrovisceral space are often considered together because they cannot be differentiated radiologically.

Carotid space

The carotid sheath is a layer of loose connective tissue demarcated by adjacent portions of the investing layer of deep cervical fascia, the pretracheal fascia, and the prevertebral fascia. It delineates a potential space into which infections from the visceral spaces may track. Infections around the carotid sheath may be restricted because superiorly (near the hyoid bone) and inferiorly (near the root of the neck) the connective tissues adhere to the vessels.

Cellulitis in the neck

The main cause of cellulitis of the neck is infection arising from the region of the mandibular molar teeth. Several fascial spaces are accessible from this area, and several anatomical factors contribute to the spread of infection. Thus, the apices of the second and, more especially, the third, mandibular molar teeth are often close to the lingual surface of the mandible. The apices of the roots of the third mandibular molars are usually, and the second molars are often below the attachment of mylohyoid on the inner aspect of the mandible and so drain directly into the submandibular tissue space. The posterior free border of mylohyoid is close to the sockets of the third mandibular molars, and at this point, the floor of the mouth consists only of mucous membrane covering part of the submandibular salivary gland. Any virulent periapical infection of the mandibular third molar teeth may therefore penetrate the lingual plate of the mandible and is then at the entrance to the submandibular and sublingual spaces anteriorly, and the parapharyngeal and pterygoid spaces posteriorly. Infection in this area may also spread from an acute pericoronitis, particularly when the deeper tissues are opened to infection by extraction of the tooth during the acute phase.

In general, cellulitis around the jaw is only likely to develop when the tissues are infected by virulent and invasive organisms at a point where there is access to the fascial spaces: the predisposing causes do not often coincide, and cellulitis is therefore uncommon. Cellulitis in the region of the maxilla is even more uncommon, but fascial space infections may develop in various sites as the result of infected local anaesthetic needles. Since there are no barriers running horizontally with respect to the tissue spaces in the neck, infection entering in this site can rapidly spread more or less unhindered down the neck and may enter the mediastinum (see Ch. 55).

All forms of cellulitides of the neck or deep neck space infections are potentially serious. Narrowing of the upper airway can occur as a result of inflammation and oedema, leading to dyspnoea or obstruction of the upper airway (with stridor) and reduced oxygenation of the lungs. This situation can be extremely difficult to manage by conventional techniques. The increased rigidity and reduced compliance of the tissues mean that manoeuvres such as manual anterior jaw thrust or laryngoscopy may fail to re-open the airway. Specialized techniques, e.g. flexible fibreoptic-assisted tracheal intubation or surgical tracheostomy under local anaesthesia, may be required to provide general anaesthesia to facilitate the surgical drainage and treatment of the cellulitis or deep space abscess.

MUSCLES

The superficial muscles of the neck are platysma, which lies in the subcutaneous tissue of the neck, and sternocleidomastoid and trapezius. Sternocleidomastoid is a key landmark because it divides the neck into anterior and lateral regions (anterior and posterior triangles respectively); the anterior region may be further subdivided into several smaller named triangles (see above). Muscles in the anterior region are organized into supra- and infra-hyoid groups, and with one exception are all attached to the hyoid bone. The supra-hyoid muscles, which connect the hyoid bone to the mandible and the base of the skull, include mylohyoid, geniohyoid, stylohyoid and digastric. The infrahyoid (strap) muscles, which connect the hyoid, sternum, clavicle and scapula, are arranged in two planes, a superficial plane consisting of sternohyoid and omohyoid and a deep plane consisting of sternothyroid and thyrohyoid.

The muscles that form part of the musculoskeletal column in the neck are described in Chapter 42. They can be considered in three groups, anterior, lateral and posterior; very broadly speaking, the muscles in these groups lie anterior, lateral or posterior to the cervical vertebrae. The anterior and lateral groups include longi colli and capitis; recti capitis anterior and lateralis; scaleni anterior, medius, posterior and minimi (when present). The posterior muscle group is composed of the cervical components of the intrinsic muscles of the back, overlaid by some of the extrinsic ‘immigrant’ muscles of the back that run between the upper limb and the axial skeleton (trapezius, levator scapulae, see Ch. 42). The intrinsic muscles are arranged in superficial and deep layers. The superficial layer contains splenius capitis and cervicis. The deeper layers include the transversospinal group (semispinales cervicis and capitis, multifidus and rotatores cervicis), interspinales and intertransversarii, and the suboccipital group (recti capitis posterior major and minor and obliquus capitis superior and inferior).

The muscles associated with the pharynx and larynx are described in Chapters 33 and 34 respectively.

Platysma

Platysma is a broad sheet of muscle of varying prominence which arises from the fascia covering the upper parts of pectoralis major and deltoid. Its fibres cross the clavicle and ascend medially in the side of the neck. Anterior fibres interlace across the midline with the fibres of the contralateral muscle, below and behind the symphysis menti. Other fibres attach to the lower border of the mandible or to the lower lip or cross the mandible to attach to skin and subcutaneous tissue of the lower face. Careful elevation of a myocutaneous flap in the subplatysmal plane as part of a neck dissection will include this muscle and its associated blood supply, thereby minimizing the risk of skin necrosis and wound breakdown.

Vascular supply

Platysma is supplied by the submental branch of the facial artery and by the suprascapular artery (from the thyrocervical trunk of the subclavian artery).

Innervation

Platysma is innervated by the cervical branch of the facial nerve which descends on the deep surface of the muscle close to the angle of the mandible.

Actions

Contraction diminishes the concavity between the jaw and the side of the neck and produces tense oblique ridges in the skin of the neck. Platysma may assist in depressing the mandible, and via its labial and modiolar attachments it can draw down the lower lip and corners of the mouth in expressions of horror or surprise.

Sternocleidomastoid

Sternocleidomastoid (Fig. 28.5) descends obliquely across the side of the neck and forms a prominent surface landmark, especially when contracted. It is thick and narrow centrally, and broader and thinner at each end. The muscle is attached inferiorly by two heads. The medial or sternal head is rounded and tendinous, arises from the upper part of the anterior surface of the manubrium and sterni and ascends posterolaterally. The lateral or clavicular head, which is variable in width and contains muscular and fibrous elements, ascends almost vertically from the superior surface of the medial third of the clavicle. The two heads are separated near their attachments by a triangular interval which corresponds to a surface depression, the lesser supraclavicular fossa. As they ascend, the clavicular head spirals behind the sternal head and blends with its deep surface below the middle of the neck, forming a thick, rounded belly. Sternocleidomastoid inserts superiorly by a strong tendon into the lateral surface of the mastoid process from its apex to its superior border, and by a thin aponeurosis into the lateral half of the superior nuchal line. The clavicular fibres are directed mainly to the mastoid process; the sternal fibres are more oblique and superficial, and extend to the occiput. The direction of pull of the two heads is therefore different, and the muscle may be classed as ‘cruciate’ and slightly ‘spiralized’.

Relations

The superficial surface of sternocleidomastoid is covered by skin and platysma, between which lie the external jugular vein, the great auricular and transverse cervical nerves and the superficial lamina of the deep cervical fascia. Near its insertion the muscle is overlapped by a small part of the parotid gland. The deep surface of the muscle near its origin is related to the sternoclavicular joint and sternohyoid, sternothyroid and omohyoid. The anterior jugular vein crosses deep to it, but superficial to the infrahyoid muscles, immediately above the clavicle. The carotid sheath and the subclavian artery are deep to these muscles. Between omohyoid and the posterior belly of digastric, the anterior part of sternocleidomastoid lies superficial to the common, internal and external carotid arteries, the internal jugular, facial and lingual veins, the deep cervical lymph nodes, the vagus nerve and the rami of the ansa cervicalis. The sternocleidomastoid branch of the superior thyroid artery crosses deep to the muscle at the upper border of omohyoid. The posterior part of sternocleidomastoid is related on its internal surface to splenius capitis, levator scapulae and the scalene muscles, the cervical plexus, the upper part of the brachial plexus, the phrenic nerve and the transverse cervical and suprascapular arteries. The occipital artery crosses deep to the muscle at, or under cover of, the lower border of the posterior belly of digastric. At this point the accessory nerve passes deep to sternocleidomastoid, then pierces and supplies the muscle, before it reappears just above the middle of the posterior border. At its insertion the muscle lies superficial to the mastoid process, splenius capitis, longissimus capitis and the posterior belly of digastric.

Vascular supply

Sternocleidomastoid receives its blood supply from branches of the occipital and posterior auricular arteries (upper part of muscle), the superior thyroid artery (middle part of muscle), and the suprascapular artery (lower part of muscle). A superiorly based flap can be raised on sternocleidomastoid to include a paddle of skin supplied by perforator vessels. This flap has been used to reconstruct the lips, floor of mouth and inner aspect of the cheeks, however its use has been superseded by microvascular free transfer flaps or by conventional myocutaneous flaps such as the pectoralis major flap.

Innervation

Sternocleidomastoid is supplied by the spinal part of the accessory nerve. Branches from the ventral rami of the second, third, and sometimes fourth, cervical spinal nerves also enter the muscle. Although these cervical rami were believed to be solely proprioceptive, clinical evidence suggests that some of their fibres are motor.

Actions

Acting alone, each sternocleidomastoid will tilt the head towards the ipsilateral shoulder, simultaneously rotating the head so as to turn the face towards the opposite side. This movement occurs in an upward, sideways glance. A more common visual movement is a level rotation from side to side, and this probably represents the most frequent use of the sternocleidomastoids. Acting together from below, the muscles draw the head forwards and so help longi colli to flex the cervical part of the vertebral column, which is a common movement in feeding. The two sternocleidomastoids are also used to raise the head when the body is supine, and when the head is fixed, they help to elevate the thorax in forced inspiration.

Branchial cysts and fistulae

Branchial cysts usually present in the upper neck in early adulthood as fluctuant swellings at the junction of the upper and middle thirds of the anterior border of sternocleidomastoid. The cyst typically passes backwards and upwards through the carotid bifurcation and ends at the pharyngeal constrictor muscles, a course which brings it into intimate association with the hypoglossal, glossopharyngeal and spinal accessory nerves. Great care must be taken to avoid damage to these nerves during surgical removal of a branchial cyst.

Branchial fistulae represent a persistent connection between the second branchial pouch and the cervical sinus. The fistula typically presents as a small pit adjacent to the anterior border of the lower third of sternocleidomastoid, which may weep saliva and become intermittently infected. Excision involves following the tract of the fistula up the neck – often through the carotid bifurcation – and into the distal tonsillar fossa where it opens into the pharynx.

Branchial cysts, sinuses and fistulae are thought to arise from inclusions of salivary gland tissue in lymph nodes: they may also occur around the parotid gland.

MUSCLES OF THE ANTERIOR TRIANGLE OF THE NECK

Apart from the superficial neck muscles already described, the anterior triangle contains two of the suprahyoid muscles, namely digastric and stylohyoid, and the four infrahyoid strap muscles (Fig. 28.5). The other suprahyoid muscles, namely mylohyoid and geniohyoid, are described with the floor of the mouth on page 501.

Digastric

Digastric has two bellies and lies below the mandible, extending from the mastoid process to the chin (Fig. 28.5). The posterior belly, which is longer than the anterior, is attached in the mastoid notch of the temporal bone, and passes downwards and forwards. The anterior belly is attached to the digastric fossa on the base of the mandible near the midline, and slopes downwards and backwards. The two bellies meet in an intermediate tendon which perforates stylohyoid and runs in a fibrous sling attached to the body and greater cornu of the hyoid bone and is sometimes lined by a synovial sheath. The two bellies of digastric mark out the borders of the submandibular triangle.

Variations

Digastric may lack the intermediate tendon and is then attached midway along the body of the mandible. The posterior belly may be augmented by a slip from the styloid process or arise wholly from it. The anterior belly may cross the midline and it is not uncommon for it to fuse with mylohyoid.

Relations

Superficial to digastric are platysma, sternocleidomastoid, splenius capitis, longissimus capitis and stylohyoid, the mastoid process, the retromandibular vein and the parotid and submandibular salivary glands. Mylohyoid is medial to the anterior belly, and hyoglossus, superior oblique and rectus capitis lateralis, the transverse process of the atlas vertebra, the accessory nerve, internal jugular vein, occipital artery, hypoglossal nerve, internal and external carotid, facial and lingual arteries are all medial to the posterior belly.

Vascular supply

The posterior belly is supplied by the posterior auricular and occipital arteries. The anterior belly of digastric receives its blood supply chiefly from the submental branch of the facial artery.

Innervation

The anterior belly of digastric is supplied by the mylohyoid branch of the inferior alveolar nerve, and the posterior belly is supplied by the facial nerve. The different innervation of the two parts reflects their separate derivations from the mesenchyme of the first and second branchial arches.

Actions

Digastric depresses the mandible and can elevate the hyoid bone. The posterior bellies are especially active during swallowing and chewing.

Stylohyoid

Stylohyoid arises by a small tendon from the posterior surface of the styloid process, near its base. Passing downwards and forwards, it inserts into the body of the hyoid bone at its junction with the greater cornu (and just above the attachment of the superior belly of omohyoid). It is perforated near its insertion by the intermediate tendon of digastric (Fig. 28.5). The muscle may be absent or double. It may lie medial to the external carotid artery and may end in the suprahyoid or infrahyoid muscles.

Vascular supply

Stylohyoid receives its blood supply from branches of the facial, posterior auricular and occipital arteries.

Innervation

Stylohyoid is innervated by the stylohyoid branch of the facial nerve, which frequently arises with the digastric branch, and enters the middle part of the muscle.

Actions

Stylohyoid elevates the hyoid bone and draws it backwards, elongating the floor of the mouth.

Stylohyoid ligament

The stylohyoid ligament is a fibrous cord extending from the tip of the styloid process to the lesser cornu of the hyoid bone. It gives attachment to the highest fibres of the middle pharyngeal constrictor and is intimately related to the lateral wall of the oropharynx. Below, it is overlapped by hyoglossus. The ligament is derived from the cartilage of the second branchial arch, and may be partially calcified.

INFRAHYOID MUSCLES

The infrahyoid muscles are organized so that sternohyoid and omohyoid lie superficially and sternothyroid and thyrohyoid lie more deeply (Fig. 28.5). The muscles are involved in movements of the hyoid bone and thyroid cartilage during vocalization, swallowing and mastication and are mainly innervated from the ansa cervicalis.

Sternohyoid

Sternohyoid is a thin, narrow strap muscle that arises from the posterior surface of the medial end of the clavicle, the posterior sternoclavicular ligament and the upper posterior aspect of the manubrium (Fig. 28.5). It ascends medially and is attached to the inferior border of the body of the hyoid bone. Inferiorly, there is a considerable gap between the muscle and its contralateral fellow, but the two usually come together in the middle of their course, and are contiguous above this. Sternohyoid may be absent or double, augmented by a clavicular slip (cleidohyoid), or interrupted by a tendinous intersection.

Vascular supply

Sternohyoid is supplied by branches from the superior thyroid artery.

Innervation

Sternohyoid is innervated by branches from the ansa cervicalis (C1, 2, 3).

Action

Sternohyoid depresses the hyoid bone after it has been elevated.

Omohyoid

Omohyoid consists of two bellies united at an angle by an intermediate tendon (Fig. 28.5). The inferior belly is a flat, narrow band, which inclines forwards and slightly upwards across the lower part of the neck. It arises from the upper border of the scapula, near the scapular notch, and occasionally from the superior transverse scapular ligament. It then passes behind sternocleidomastoid and ends there in the intermediate tendon. The superior belly begins at the intermediate tendon, passes almost vertically upwards near the lateral border of sternohyoid and is attached to the lower border of the body of the hyoid bone lateral to the insertion of sternohyoid. The length and form of the intermediate tendon varies, although it usually lies adjacent to the internal jugular vein at the level of the arch of the cricoid cartilage. The angulated course of the muscle is maintained by a band of deep cervical fascia, attached below to the clavicle and the first rib, which ensheathes the tendon. A variable amount of skeletal muscle may be present in the fascial band; either belly may be absent or double; the inferior belly may be attached directly to the clavicle and the superior is sometimes fused with sternohyoid.

Vascular supply

Omohyoid is supplied by branches from the superior thyroid and lingual arteries.

Innervation

The superior belly of omohyoid is innervated by branches from the superior ramus of the ansa cervicalis (C1). The inferior belly is innervated from the ansa cervicalis itself (C1, 2 and 3).

Actions

Omohyoid depresses the hyoid bone after it has been elevated. It has been speculated that the muscle tenses the lower part of the deep cervical fascia in prolonged inspiratory efforts, reducing the tendency for soft parts to be sucked inward.

Sternothyroid

Sternothyroid is shorter and wider than sternohyoid, and lies deep and partly medial to it (Fig. 28.5). It arises from the posterior surface of the manubrium sterni inferior to the origin of sternohyoid and from the posterior edge of the cartilage of the first rib. It is attached above to the oblique line on the lamina of the thyroid cartilage, where it delineates the upward extent of the thyroid gland. In the lower part of the neck the muscle is in contact with its contralateral fellow, but the two diverge as they ascend.

Vascular supply

Sternothyroid is supplied by branches from the superior thyroid and lingual arteries.

Innervation

Sternothyroid is innervated by branches from the ansa cervicalis (C1, 2 and 3).

Action

Sternothyroid draws the larynx downwards after it has been elevated by swallowing or vocal movements. In the singing of low notes, this downward traction would be exerted with the hyoid bone relatively fixed.

Thyrohyoid

Thyrohyoid is a small, quadrilateral muscle that may be regarded as an upward continuation of sternothyroid (Fig. 28.5). It arises from the oblique line on the lamina of the thyroid cartilage, and passes upwards to attach to the lower border of the greater cornu and adjacent part of the body of the hyoid bone.

Vascular supply

Thyrohyoid is supplied by branches from the superior thyroid and lingual arteries.

Innervation

Unlike the other infrahyoid muscles, thyrohyoid is not innervated by the ansa cervicalis. In common with geniohyoid, it is supplied by fibres from the first cervical spinal nerve which branch off from the hypoglossal nerve beyond the descendens hypoglossi.

Actions

Thyrohyoid depresses the hyoid bone. With the hyoid bone stabilized, it pulls the larynx upwards, e.g. when high notes are sung.

ANTERIOR VERTEBRAL MUSCLES

The anterior vertebral group of muscles are longi colli and capitis, and recti capitis anterior and lateralis (Fig. 28.6), all of which are flexors of the head and neck to varying degrees. Together with the lateral vertebral muscles they form the prevertebral muscle group.

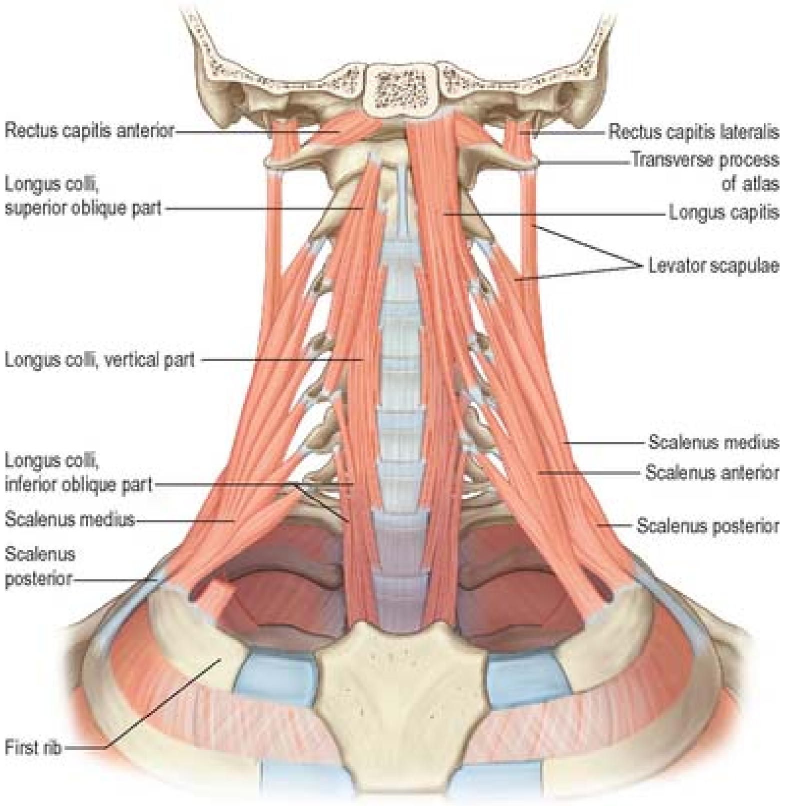
Rectus capitis anterior
Longus colli, superior oblique part
Longus colli, vertical part
Longus colli, inferior oblique part
Scalenus medius
Scalenus posterior
First rib
Rectus capitis lateralis
Transverse process of atlas
Longus capitis
Levator scapulae
Scalenus medius
Scalenus anterior
Scalenus posterior

Fig. 28.6 The anterior and lateral vertebral muscles. Scalenus anterior and longus capitis have been removed on the right side.

Rectus capitis anterior

Rectus capitis anterior is a short, flat muscle situated behind the upper part of longus capitis. It arises from the anterior surface of the lateral mass of the atlas and the root of its transverse process, and ascends almost vertically to the inferior surface of the basilar part of the occipital bone immediately anterior to the occipital condyle.

Vascular supply

Rectus capitis anterior is supplied by branches from the vertebral and ascending pharyngeal arteries.

Innervation

Rectus capitis anterior is innervated by branches from the loop between the ventral rami of the first and second cervical spinal nerves.

Actions

Rectus capitis anterior flexes the head at the atlanto-occipital joints.

Rectus capitis lateralis

Rectus capitis lateralis is a short, flat muscle that arises from the upper surface of the transverse process of the atlas and inserts into the inferior surface of the jugular process of the occipital bone. In view of its attachments and its relation to the ventral ramus of the first spinal nerve, rectus capitis lateralis is regarded as homologous with the posterior intertransverse muscles.

Vascular supply

Rectus capitis lateralis is supplied by branches from the vertebral, occipital and ascending pharyngeal arteries.

Innervation

Rectus capitis lateralis is innervated by branches from the loop between the ventral rami of the first and second cervical spinal nerves.

Actions

Rectus capitis lateralis flexes the head laterally to the same side.

Longus capitis

Longus capitis (Fig. 28.6) has a narrow origin from tendinous slips from the anterior tubercles of the transverse processes of the third, fourth, fifth and sixth cervical vertebrae and becomes broad and thick above, where it is inserted into the inferior surface of the basilar part of the occipital bone.

Vascular supply

Longus capitis is supplied by the ascending pharyngeal, ascending cervical branch of the inferior thyroid and the vertebral arteries.

Innervation

Longus capitis is innervated by branches from the ventral rami of the first, second and third cervical spinal nerves.

Actions

Longus capitis flexes the head.

Longus colli

Longus colli (Fig. 28.6) is applied to the anterior surface of the vertebral column, between the atlas and the third thoracic vertebra. It can be divided into three parts which all arise by tendinous slips. The inferior oblique part is the smallest, running upwards and laterally from the fronts of the bodies of the first two or three thoracic vertebrae to the anterior tubercles of the transverse processes of the fifth and sixth cervical vertebrae. The superior oblique part passes upwards and medially from the anterior tubercles of the transverse processes of the third, fourth and fifth cervical vertebrae to be attached by a narrow tendon to the anterolateral surface of the tubercle on the anterior arch of the atlas. The vertical intermediate part ascends from the fronts of the bodies of the upper three thoracic and lower three cervical vertebrae to the fronts of the bodies of the second, third and fourth cervical vertebrae.

Vascular supply

Longus colli is supplied by branches from the vertebral, inferior thyroid and ascending pharyngeal arteries.

Innervation

Longus colli is innervated by branches from the ventral rami of the second, third, fourth, fifth and sixth cervical spinal nerves.

Actions

Longus colli flexes the neck forwards. In addition, the oblique parts may flex it laterally, and the inferior oblique part rotates it to the opposite side. Its main antagonist is longissimus cervicis.

LATERAL VERTEBRAL MUSCLES

Scaleni anterior, medius and posterior extend obliquely between the upper two ribs and the cervical transverse processes. Scalenus minimus (pleuralis) is associated with the suprapleural membrane and cervical pleura, and is described in Chapter 57.

Scalenus anterior

Scalenus anterior lies at the side of the neck deep (posteromedial) to sternocleidomastoid (Fig. 28.5; see also Fig. 28.18). Above, it is attached by musculotendinous fascicles to the anterior tubercles of the transverse processes of the third, fourth, fifth and sixth cervical vertebrae. These converge, blend and descend almost vertically, to be attached by a narrow, flat tendon to the scalene tubercle on the inner border of the first rib, and to a ridge on the upper surface of the rib anterior to the groove for the subclavian artery.

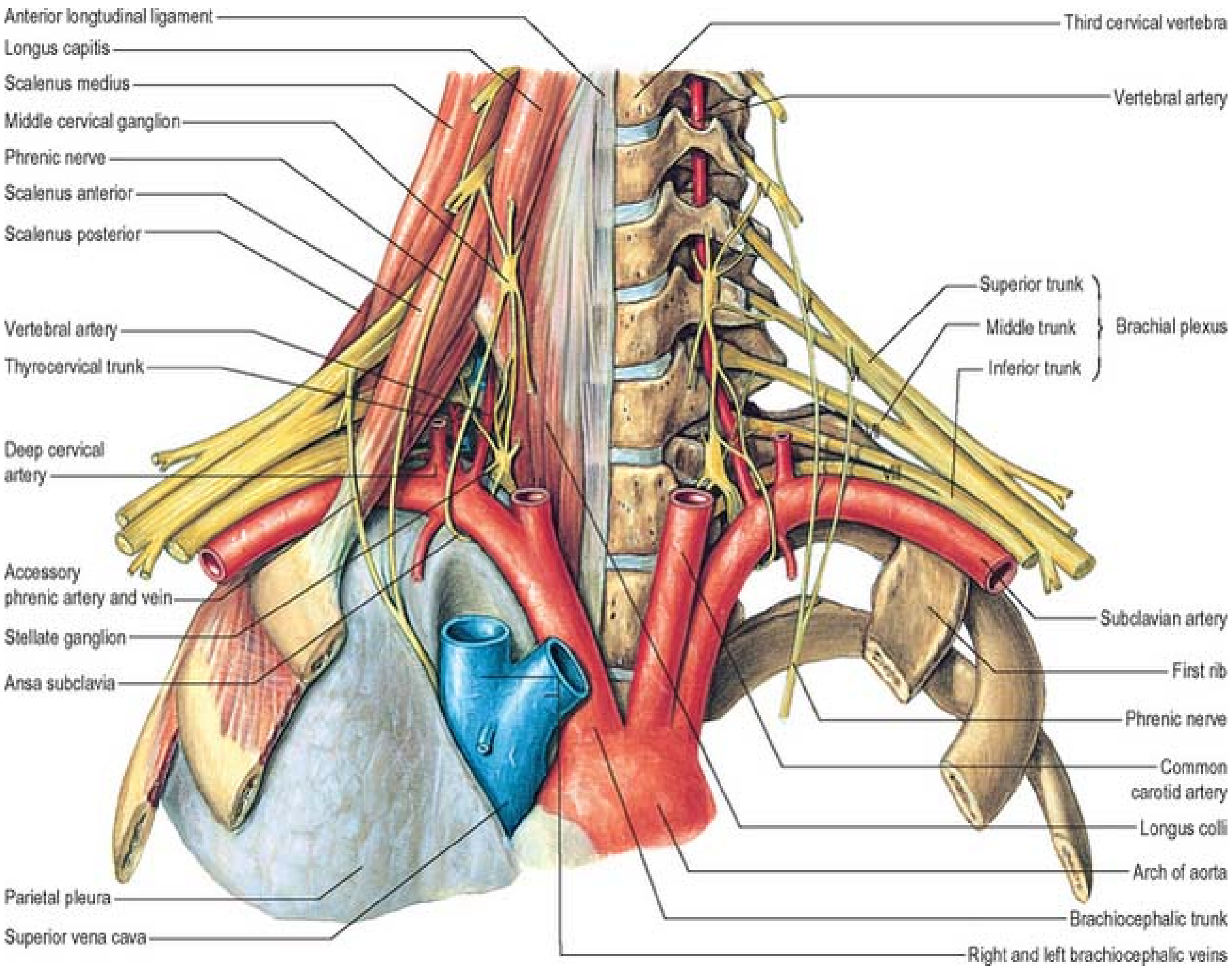
Anterior longtudinal ligament
Longus capitis
Scalenus medius
Middle cervical ganglion
Phrenic nerve
Scalenus anterior
Scalenus posterior
Vertebral artery
Thyrocervical trunk
Deep cervical artery
Accessory phrenic artery and vein
Stellate ganglion
Ansa subclavia
Parietal pleura
Superior vena cava
Third cervical vertebra
Vertebral artery
Superior trunk
Middle trunk
Inferior trunk
Brachial plexus
Subclavian artery
First rib
Phrenic nerve
Common carotid artery
Longus colli
Arch of aorta
Brachiocephalic trunk
Right and left brachiocephalic veins

Fig. 28.18 The root of the neck. Note the sympathetic chain, the middle and inferior cervical sympathetic ganglia, the trunks of the brachial plexus, the phrenic nerve and the vertebral artery.

(From Sobotta 2006.)

Relations

Scalenus anterior forms an important landmark in the root of the neck, because the phrenic nerve passes anterior to it, the subclavian artery posterior to it, and the brachial plexus lies at its lateral border. The clavicle, subclavius, sternocleidomastoid and omohyoid, lateral part of the carotid sheath, transverse cervical, suprascapular and ascending cervical arteries, subclavian vein, prevertebral fascia and phrenic nerve are all anterior to scalenus anterior. Posteriorly are the suprapleural membrane, pleura, roots of the brachial plexus and the subclavian artery: the latter two separate scalenus anterior from scalenus medius. The proximity of the muscle to the brachial plexus, subclavian artery and vein can give rise to compression syndromes. Below its attachment to the sixth cervical vertebra, the medial border of the muscle is separated from longus colli by an angular interval in which the vertebral artery and vein pass to and from the foramen transversarium of the sixth cervical vertebra. The inferior thyroid artery crosses this interval from the lateral to the medial side near its apex. The sympathetic trunk and its cervicothoracic ganglion are closely related to the posteromedial side of this part of the vertebral artery. On the left side the thoracic duct crosses the triangular interval at the level of the seventh cervical vertebra and usually comes into contact with the medial edge of scalenus anterior. The musculotendinous attachments of scalenus anterior to anterior tubercles are separated from those of longus capitis by the ascending cervical branch of the inferior thyroid artery.

Innervation

Scalenus anterior is innervated by branches from the ventral rami of the fourth, fifth and sixth cervical spinal nerves.

Actions

Acting from below, scalenus anterior bends the cervical portion of the vertebral column forwards and laterally and rotates it towards the opposite side. Acting from above, the muscle helps to elevate the first rib.

Scalenus medius

Scalenus medius, the largest and longest of the scaleni, is attached above to the transverse process of the axis and the front of the posterior tubercles of the transverse processes of the lower five cervical vertebrae (Fig. 28.6). It frequently extends upwards to the transverse process of the atlas. Below it is attached to the upper surface of the first rib between the tubercle of the rib and the groove for the subclavian artery.

Relations

The anterolateral surface of the muscle is related to sternocleidomastoid (Fig. 28.5). It is crossed anteriorly by the clavicle and omohyoid, and it is separated from scalenus anterior by the subclavian artery and ventral rami of the cervical spinal nerves. Levator scapulae and scalenus posterior lie posterolateral to it. The upper two roots of the nerve to serratus anterior and the dorsal scapular nerve (to the rhomboids) pierce the muscle and appear on its lateral surface.

Innervation

Scalenus medius is supplied by branches from the ventral rami of the third to eighth cervical spinal nerves.

Actions

Acting from below, scalenus medius bends the cervical part of the vertebral column to the same side. Acting from above, it helps to raise the first rib. The scalene muscles, particularly scalenus medius, are active during inspiration, even during quiet breathing in the erect attitude.

Scalenus posterior

Scalenus posterior is the smallest and most deeply situated of the scalene muscles (Fig. 28.6). It passes from the posterior tubercles of the transverse processes of the fourth, fifth, and sixth cervical vertebrae to the outer surface of the second rib, behind the tubercle for serratus anterior, where it is attached by a thin tendon.

Scalenus posterior is occasionally blended with scalenus medius. The scalene muscles vary a little in the number of vertebrae to which they are attached, in their degree of separation, and their segmental innervation.

Vascular supply

All the scalene muscles are chiefly supplied by the ascending cervical branch of the inferior thyroid artery. Scalenus posterior receives an additional supply from the superficial cervical artery.

Innervation

Scalenus posterior is innervated by branches from the ventral rami of the lower three cervical spinal nerves.

Actions

When the second rib is fixed, scalenus posterior bends the lower end of the cervical part of the vertebral column to the same side. When its upper attachment is fixed, it helps to elevate the second rib.

POSTERIOR VERTEBRAL MUSCLES

Splenius capitis and splenius cervicis are described in Chapter 42.

VASCULAR SUPPLY AND LYMPHATIC DRAINAGE

ARTERIES OF THE NECK

The common carotid, internal carotid, and external carotid arteries provide the major source of blood to the head and neck (Figs 28.7A, 28.8). Additional arteries arise from branches of the subclavian artery, particularly the vertebral artery.

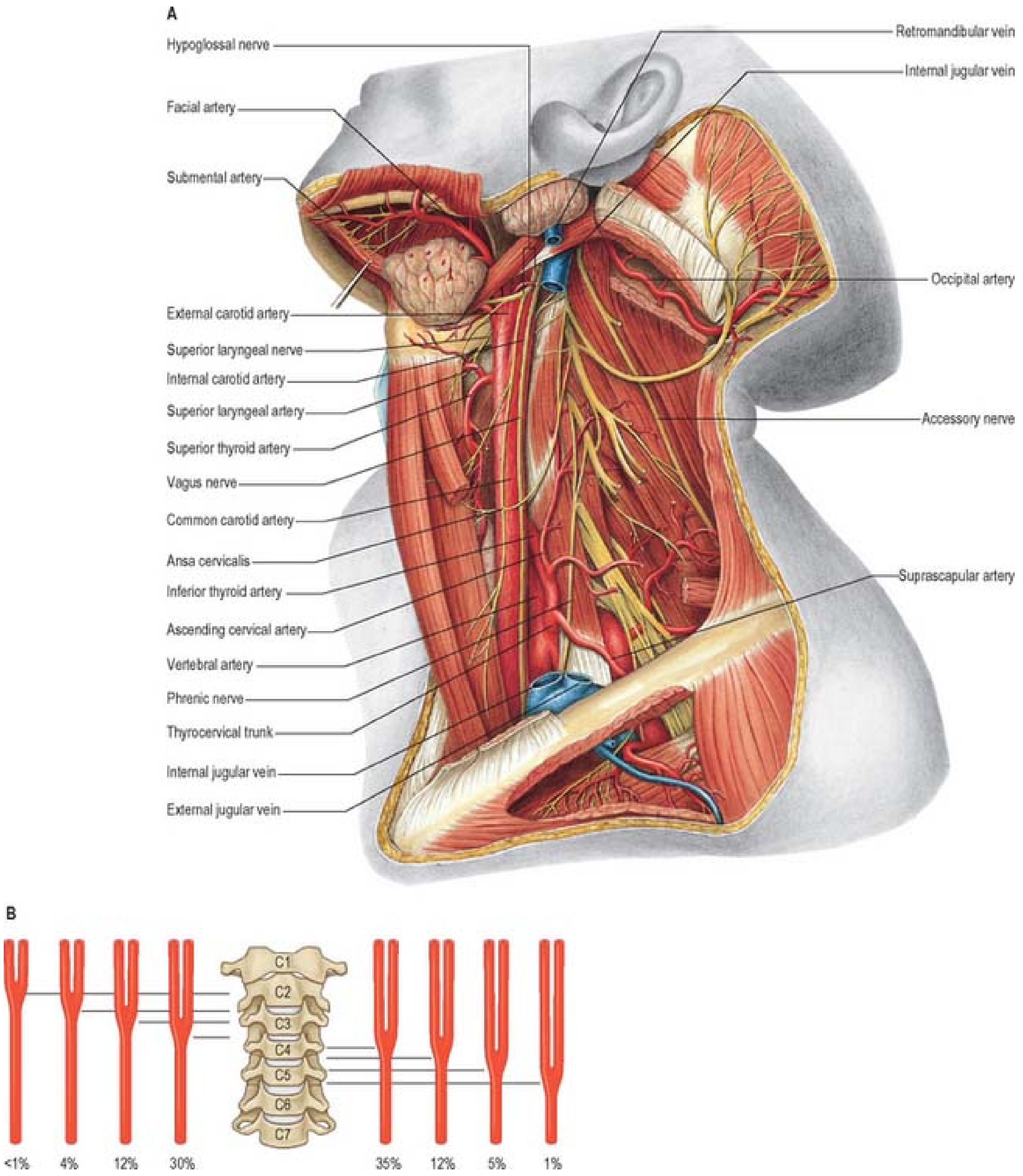
A
Hypoglossal nerve
Facial artery
Submental artery
External carotid artery
Superior laryngeal nerve
Internal carotid artery
Superior laryngeal artery
Superior thyroid artery
Vagus nerve
Common carotid artery
Ansa cervicalis
Inferior thyroid artery
Ascending cervical artery
Vertebral artery
Phrenic nerve
Thyrocervical trunk
Internal jugular vein
External jugular vein
Retromandibular vein
Internal jugular vein
Occipital artery
Accessory nerve
Suprascapular artery
B
C1
C2
C3
C4
C5
C6
C7
<1%
4%
12%
30%
35%
12%
5%
1%

Fig. 28.7 **A**, Vessels and nerves of the neck, left lateral view: sternocleidomastoid and the greater part of omohyoid and the internal jugular vein have been removed. Compare with **Fig. 28.17**, which shows a deeper level of dissection. **B**, Variation in levels of bifurcation of the common carotid artery, related to the cervical vertebrae.

(A, From Sobotta 2006.) (Redrawn with permission from Sobatta 2006.)

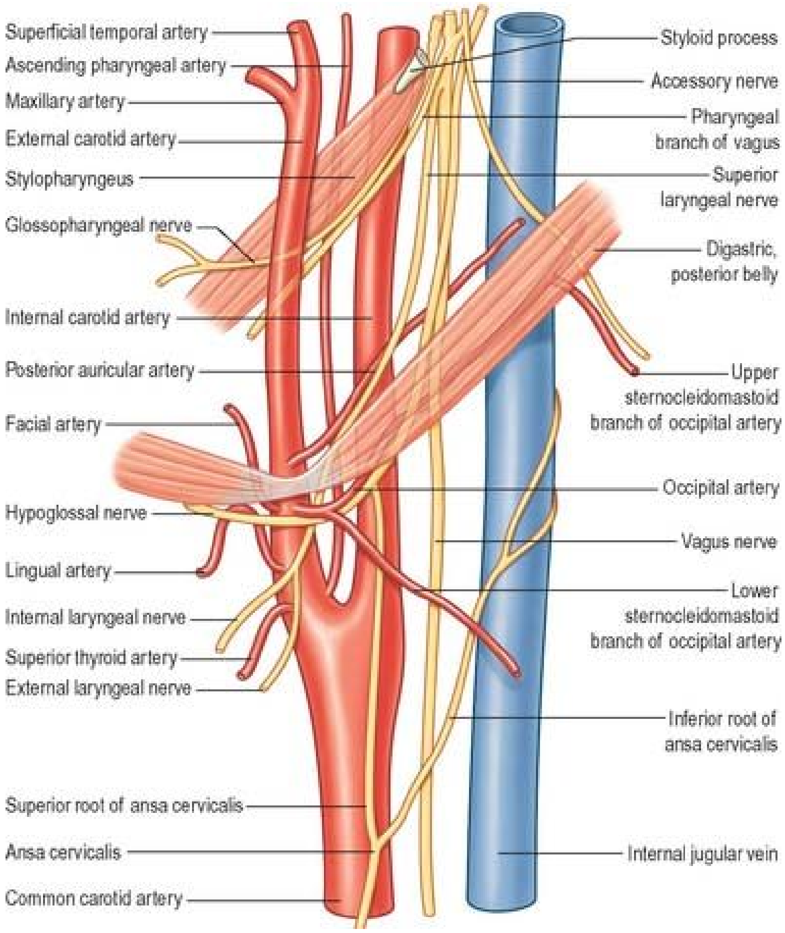
Superficial temporal artery
Ascending pharyngeal artery
Maxillary artery
External carotid artery
Stylopharyngeus
Glossopharyngeal nerve
Internal carotid artery
Posterior auricular artery
Facial artery
Hypoglossal nerve
Lingual artery
Internal laryngeal nerve
Superior thyroid artery
External laryngeal nerve
Superior root of ansa cervicalis
Ansa cervicalis
Common carotid artery
Styloid process
Accessory nerve
Pharyngeal branch of vagus
Superior laryngeal nerve
Digastric, posterior belly
Upper sternocleidomastoid branch of occipital artery
Occipital artery
Vagus nerve
Lower sternocleidomastoid branch of occipital artery
Inferior root of ansa cervicalis
Internal jugular vein

Fig. 28.8 The branches of the external carotid artery. Note the structures that either cross the internal jugular vein and the carotid arteries or intervene between the external and internal carotid arteries.

The common, internal and external carotid arteries and accompanying veins and nerves, all lie in a cleft that is bound posteriorly by the transverse processes of cervical vertebrae and attached muscles, medially by the trachea, oesophagus, thyroid gland, larynx and pharyngeal constrictors, and anterolaterally by sternocleidomastoid and, at different levels, omohyoid, sternohyoid, sternothyroid, digastric and stylohyoid muscles. The common and internal carotid arteries lie within the carotid sheath, accompanied by the internal jugular vein and the vagus nerve.

Common carotid artery

The common carotid arteries differ on the right and left sides with respect to their origins. On the right, the common carotid arises from the brachiocephalic artery as it passes behind the sternoclavicular joint. On the left, the common carotid artery comes directly from the arch of the aorta in the superior mediastinum. The right common carotid has, therefore, only a cervical part whereas the left common carotid has cervical and thoracic parts. Following a similar course on both sides, the common carotid artery ascends, diverging laterally from behind the sternoclavicular joint to the level of the upper border of the thyroid cartilage of the larynx (C3–4 junction), where it divides into external and internal carotid arteries. This bifurcation can sometimes be at a higher level. The artery may be compressed against the prominent transverse process of the sixth cervical vertebra (Chassaignac's tubercle), and above this level it is superficial and its pulsation can be easily felt.

Relations

In the lower part of the neck the common carotid arteries are separated by a narrow gap which contains the trachea. Above this, the arteries are separated by the thyroid gland, larynx and pharynx. Each artery is contained within the carotid sheath of deep cervical fascia, which also encloses the internal jugular vein and vagus nerve. The vein lies lateral to the artery, and the nerve lies between them and posterior to both.

The artery is crossed anterolaterally, at the level of the cricoid cartilage, by the intermediate tendon – sometimes the superior belly – of omohyoid. Below omohyoid it is sited deeply, covered by skin, superficial fascia, platysma, deep cervical fascia, and sternocleidomastoid, sternohyoid and sternothyroid. Above omohyoid it is more superficial, covered merely by skin, superficial fascia, platysma, deep cervical fascia and the medial margin of sternocleidomastoid, and it is crossed obliquely from its medial to lateral side by the sternocleidomastoid branch of the superior thyroid artery. The superior root of the ansa cervicalis, joined by its inferior root from the second and third cervical spinal nerves, lies anterior to, or embedded within, the carotid sheath as it crosses it obliquely. The superior thyroid vein usually crosses near the upper border of the thyroid cartilage, and the middle thyroid vein crosses a little below the level of the cricoid cartilage. The anterior jugular vein crosses the common carotid artery above the clavicle, separated from it by sternohyoid and sternothyroid. Posterior to the carotid sheath are the transverse processes of the fourth to sixth cervical vertebrae, to which are attached longus colli, longus capitis and tendinous slips of scalenus anterior. The sympathetic trunk and ascending cervical branch of the inferior thyroid artery lie between the common carotid artery and the muscles. Below the level of the sixth cervical vertebra the artery is in an angle between scalenus anterior and longus colli, anterior to the vertebral vessels, inferior thyroid and subclavian arteries, sympathetic trunk and, on the left, the thoracic duct. The oesophagus, trachea, inferior thyroid artery and recurrent laryngeal nerve and, at a higher level, the larynx and pharynx are medial to the sheath and its contents. The thyroid gland overlaps it anteromedially. The internal jugular vein lies lateral, and, in the lower neck also anterior, to the artery, while the vagus nerve lies posterolaterally in the angle between artery and vein.

On the right side, low in the neck, the recurrent laryngeal nerve crosses obliquely behind the artery. The right internal jugular vein diverges from it below but the left vein approaches and often overlaps its artery.

In 12% of cases the right common carotid artery arises above the level of the sternoclavicular joint, or it may be a separate branch from the aorta. The left common carotid artery varies in origin more than the right and may arise with the brachiocephalic artery. Division of the common carotid may occur higher, near the level of the hyoid bone, or, more rarely, at a lower level alongside the larynx. Very rarely it ascends without division, so that either the external or internal carotid is absent, or it may be replaced by separate external and internal carotid arteries which arise directly from the aorta, on one side, or bilaterally.

Although the common carotid artery usually has no branches, it may occasionally give rise to the vertebral, superior thyroid, superior laryngeal, ascending pharyngeal, inferior thyroid or occipital arteries.

External carotid artery

The external carotid artery (Figs 28.7A, 28.8) begins lateral to the upper border of the thyroid cartilage, level with the intervertebral disc between the third and fourth cervical vertebrae. A little curved and with a gentle spiral, it first ascends slightly forwards and then inclines backwards and a little laterally, to pass midway between the tip of the mastoid process and the angle of the mandible. Here, in the substance of the parotid gland behind the neck of the mandible, it divides into its terminal branches, the superficial temporal and maxillary arteries. As it ascends, it gives off several large branches, and diminishes rapidly in calibre. In children the external carotid is smaller than the internal carotid, but in adults the two are of almost equal size. At its origin, it is in the carotid triangle and lies anteromedial to the internal carotid artery. It later becomes anterior, then lateral, to the internal carotid as it ascends. At mandibular levels the styloid process and its attached structures intervene between the vessels: the internal carotid is deep, and the external carotid superficial, to the styloid process. A fingertip placed in the carotid triangle perceives a powerful arterial pulsation, which represents the termination of the common carotid, the origins of external and internal carotids and the stems of the initial branches of the external carotid.

Relations

The skin and superficial fascia, the loop between the cervical branch of the facial nerve and the transverse cutaneous nerve of the neck, the deep cervical fascia and the anterior margin of sternocleidomastoid all lie superficial to the external carotid artery in the carotid triangle. The artery is crossed by the hypoglossal nerve and its vena comitans and by the lingual, facial and, sometimes, the superior thyroid veins. Leaving the carotid triangle, the external carotid artery is crossed by the posterior belly of digastric and by stylohyoid, and ascends between these muscles and the posteromedial surface of the parotid gland, which it next enters. Within the parotid, the artery lies medial to the facial nerve and the junction of the superficial temporal and maxillary veins. The pharyngeal wall, superior laryngeal nerve and ascending pharyngeal artery are the initial medial relations of the artery. At a higher level, it is separated from the internal carotid artery by the styloid process, styloglossus and stylopharyngeus, glossopharyngeal nerve, pharyngeal branch of vagus nerve and part of the parotid gland. The artery is equally likely to lie medial to the parotid gland, or within it.

The external carotid artery has eight named branches distributed to the head and neck. The superior thyroid, lingual and facial arteries arise from its anterior surface, the occipital and posterior auricular arteries arise from its posterior surface and the ascending pharyngeal artery arises from its medial surface. The maxillary and superficial temporal arteries are its terminal branches within the parotid gland.

Superior thyroid artery

The superior thyroid artery is the first branch of the external carotid artery, and arises from the anterior surface of the external carotid just below the level of the greater cornu of the hyoid bone (Figs 28.7A, 28.8). It descends along the lateral border of thyrohyoid to reach the apex of the lobe of the thyroid gland. Lying medially are the inferior constrictor muscle and the external laryngeal nerve: the nerve is often posteromedial, and therefore at risk when the artery is being ligatured. Occasionally it may issue directly from the common carotid.

Branches

The superior thyroid artery supplies the thyroid gland and some adjacent skin. Glandular branches are: anterior, which runs along the medial side of the upper pole of the lateral lobe to supply mainly the anterior surface; a branch which crosses above the isthmus to anastomose with its fellow of the opposite side; and posterior, which descends on the posterior border to supply the medial and lateral surfaces and anastomoses with the inferior thyroid artery. Sometimes a lateral branch supplies the lateral surface. The artery also has the following named branches: infrahyoid, superior laryngeal, sternocleidomastoid and cricothyroid.

Infrahyoid artery

The infrahyoid artery is a small branch which runs along the lower border of the hyoid bone deep to thyrohyoid and anastomoses with its fellow of the opposite side to supply the infrahyoid strap muscles.

Superior laryngeal artery

The superior laryngeal artery accompanies the internal laryngeal nerve. Deep to thyrohyoid it pierces the lower part of the thyrohyoid membrane to supply the tissues of the upper part of the larynx. It anastomoses with its fellow of the opposite side and with the inferior laryngeal branch of the inferior thyroid artery.

Sternocleidomastoid artery

The sternocleidomastoid artery descends laterally across the carotid sheath and supplies the middle region of sternocleidomastoid. Like the parent artery itself, it may arise directly from the external carotid artery.

Cricothyroid artery

The cricothyroid artery crosses high on the anterior cricothyroid ligament, anastomoses with its fellow of the opposite side and supplies cricothyroid.

Ascending pharyngeal artery

The ascending pharyngeal artery is the smallest branch of the external carotid. It is a long, slender vessel which arises from the medial (deep) surface of the external carotid artery near the origin of that artery. It ascends between the internal carotid artery and the pharynx to the base of the cranium. The ascending pharyngeal artery is crossed by styloglossus and stylopharyngeus, and longus capitis lies posterior to it. It gives off numerous small branches to supply longus capitis and longus colli, the sympathetic trunk, the hypoglossal, glossopharyngeal and vagus nerves and some of the cervical lymph nodes. It anastomoses with the ascending palatine branch of the facial artery and the ascending cervical branch of the vertebral artery. Its named branches are the pharyngeal, inferior tympanic and meningeal arteries.

Pharyngeal artery

The pharyngeal artery gives off three or four branches to supply the constrictor muscles of the pharynx and stylopharyngeus. A variable ramus supplies the palate, and may replace the ascending palatine branch of the facial artery. The artery descends forwards between the superior border of the superior constrictor and levator veli palatini to the soft palate, and also supplies a branch to the palatine tonsil and the pharyngotympanic tube.

Inferior tympanic artery

The inferior tympanic artery is a small branch which traverses the temporal canaliculus with the tympanic branch of the glossopharyngeal nerve and supplies the medial wall of the tympanic cavity.

Meningeal branches

The meningeal branches are small vessels which supply the nerves that traverse the foramen lacerum, jugular foramen and hypoglossal canal, and the associated dura mater and adjoining bone. One branch, the posterior meningeal artery, reaches the cerebellar fossa via the jugular foramen, and is usually regarded as the terminal branch of the ascending pharyngeal artery.

Lingual artery

The lingual artery provides the chief blood supply to the tongue and the floor of the mouth (Fig. 28.8; see Ch. 30). It arises anteromedially from the external carotid artery opposite the tip of the greater cornu of the hyoid bone, between the superior thyroid and facial arteries. It often arises with the facial or, less often, with the superior thyroid artery. It may be replaced by a ramus of the maxillary artery. Ascending medially at first, it loops down and forwards, passes medial to the posterior border of hyoglossus and then runs horizontally forwards deep to it. The lingual artery next ascends again almost vertically, and courses sinuously forwards on the inferior surface of the tongue as far as its tip. The further course of the lingual artery is described on page 505.

Relations

Its relationship to hyoglossus naturally divides the lingual artery into descriptive ‘thirds’. In its first part the lingual artery is in the carotid triangle. Skin, fascia and platysma are superficial to it, while the middle pharyngeal constrictor muscle is medial. The artery ascends a little medially, then descends to the level of the hyoid bone, and the loop so formed is crossed externally by the hypoglossal nerve. The second part passes along the upper border of the hyoid bone, deep to hyoglossus, the tendons of digastric and stylohyoid, the lower part of the submandibular gland and the posterior part of mylohyoid. Hyoglossus separates it from the hypoglossal nerve and its vena comitans. Here its medial aspect adjoins the middle constrictor muscle and it crosses the stylohyoid ligament accompanied by lingual veins. The third part is the arteria profunda linguae which turns upward near the anterior border of hyoglossus and then passes forwards close to the inferior lingual surface near the frenulum, accompanied by the lingual nerve. Genioglossus is a medial relation, and the inferior longitudinal muscle of the tongue lies lateral to it below the lingual mucous membrane. Near the tip of the tongue the lingual artery anastomoses with its fellow of the opposite side. Its named branches are the suprahyoid, dorsal lingual and sublingual arteries.

Suprahyoid artery

The suprahyoid artery is a small branch which runs along the upper border of the hyoid bone to anastomose with the contralateral artery. It supplies adjacent structures.

Dorsal lingual arteries

The dorsal lingual arteries are described on page 505.

Sublingual artery

The sublingual artery is described on page 505.

Facial artery

The facial artery (Figs 28.7, 28.8; see Figs 29.13, 29.18) arises anteriorly from the external carotid in the carotid triangle, above the lingual artery and immediately above the greater cornu of the hyoid bone. In the neck, at its origin, it is covered only by the skin, platysma, fasciae and often by the hypoglossal nerve. It runs up and forwards, deep to digastric and stylohyoid. At first on the middle pharyngeal constrictor, it may reach the lateral surface of styloglossus, separated there from the palatine tonsil only by this muscle and the lingual fibres of the superior constrictor. Medial to the mandibular ramus it arches upwards and grooves the posterior aspect of the submandibular gland. It then turns down and descends to the lower border of the mandible in a lateral groove on the submandibular gland, between the gland and medial pterygoid. Reaching the surface of the mandible, the facial artery curves round its inferior border, anterior to masseter, to enter the face: its further course is described on page 490. The artery is very sinuous throughout its extent. In the neck this may be so that the artery is able to adapt to the movements of the pharynx during deglutition, and similarly on the face, so that the artery can adapt to movements of the mandible, lips and cheeks. Facial artery pulsation is most palpable where the artery crosses the mandibular base, and again near the corner of the mouth. Its branches in the neck are the ascending palatine, tonsillar, submental and glandular arteries.

Ascending palatine artery

The ascending palatine artery arises close to the origin of the facial artery. It passes up between styloglossus and stylopharyngeus to reach the side of the pharynx, along which it ascends between the superior constrictor of the pharynx and medial pterygoid towards the cranial base. It bifurcates near levator veli palatini. One branch follows this muscle, winding over the upper border of the superior constrictor of the pharynx to supply the soft palate and to anastomose with its fellow of the opposite side and the greater palatine branch of the maxillary artery. The other branch pierces the superior constrictor muscle to supply the tonsil and pharyngotympanic tube and to anastomose with the tonsillar and ascending pharyngeal arteries.

Tonsillar artery

The tonsillar artery provides the main blood supply to the palatine tonsil. It ascends between medial pterygoid and styloglossus, penetrates the superior constrictor of the pharynx at the upper border of styloglossus, and enters the inferior pole of the tonsil. Its branches ramify in the tonsil and in the musculature of the posterior part of the tongue. The tonsillar artery may sometimes arise from the ascending palatine artery.

Submental artery

The submental artery is the largest cervical branch of the facial artery (Fig. 28.7). It arises as the facial artery separates from the submandibular gland and turns forwards on mylohyoid below the mandible. It supplies the overlying skin and muscles, and anastomoses with a sublingual branch of the lingual and mylohyoid branch of the inferior alveolar artery. At the chin it ascends over the mandible, and divides into superficial and deep branches, which anastomose with the inferior labial and mental arteries to supply the chin and lower lip.

Glandular branches

Three or four large vessels supply the submandibular salivary gland and associated lymph nodes, adjacent muscles and skin.

Occipital artery

The occipital artery arises posteriorly from the external carotid artery, approximately 2 cm from its origin (Figs 28.7A, 28.8). At its origin, the artery is crossed superficially by the hypoglossal nerve, which winds round it from behind. The artery next passes backwards, up and deep to the posterior belly of digastric, and crosses the internal carotid artery, internal jugular vein, hypoglossal, vagus and accessory nerves. Between the transverse process of the atlas and the mastoid process, the occipital artery reaches the lateral border of rectus capitis lateralis. It then runs in the occipital groove of the temporal bone, medial to the mastoid process and attachments of sternocleidomastoid, splenius capitis, longissimus capitis and digastric, and lies successively on rectus capitis lateralis, obliquus superior and semispinalis capitis. Finally, accompanied by the greater occipital nerve, it turns upwards to pierce the investing layer of the deep cervical fascia connecting the cranial attachments of trapezius and sternocleidomastoid, and ascends tortuously in the dense superficial fascia of the scalp where it divides into many branches.

The occipital artery has two main branches (upper and lower) to the upper part of sternocleidomastoid in the neck. The lower branch arises near the origin of the occipital artery, and may sometimes arise directly from the external carotid artery. It descends backwards over the hypoglossal nerve and internal jugular vein, enters sternocleidomastoid and anastomoses with the sternocleidomastoid branch of the superior thyroid artery. The upper branch arises as the occipital artery crosses the accessory nerve, and runs down and backwards superficial to the internal jugular vein. It enters the deep surface of sternocleidomastoid with the accessory nerve.

Posterior auricular artery

The posterior auricular artery is a small vessel which branches posteriorly from the external carotid just above digastric and stylohyoid. It ascends between the parotid gland and the styloid process to the groove between the auricular cartilage and mastoid process, and divides into auricular and occipital branches which are described with the face on page 491. In the neck, it provides branches to supply digastric, stylohyoid, sternocleidomastoid and the parotid gland. It also gives origin to the stylomastoid artery – described as an indirect branch of the posterior auricular artery in about a third of subjects – which enters the stylomastoid foramen to supply the facial nerve, tympanic cavity, mastoid antrum air cells and semicircular canals. In the young, its posterior tympanic ramus forms a circular anastomosis with the anterior tympanic branch of the maxillary artery.

Internal carotid artery

The internal carotid artery supplies most of the ipsilateral cerebral hemisphere, eye and accessory organs, forehead and, in part, the nose. From its origin at the carotid bifurcation (Fig. 28.8) (where it usually has a carotid sinus), it ascends in front of the transverse processes of the upper three cervical vertebrae to the inferior aperture of the carotid canal in the petrous part of the temporal bone. Here it enters the cranial cavity and turns anteriorly through the cavernous sinus in the carotid groove on the side of the body of the sphenoid bone. It terminates below the anterior perforated substance by division into the anterior and middle cerebral arteries. It may be divided conveniently into cervical, petrous, cavernous and cerebral parts.

Relations

The internal carotid artery is initially superficial in the carotid triangle, then passes deeper, medial to the posterior belly of digastric. Except near the skull, the internal jugular vein and vagus nerve are lateral to it within the carotid sheath. The external carotid artery is first anteromedial, but then curves back to lie superficial. Posteriorly the internal carotid adjoins longus capitis, and the superior cervical sympathetic ganglion lies between them. The superior laryngeal nerve crosses obliquely behind it. The pharyngeal wall lies medial to the artery, which is separated by fat and pharyngeal veins from the ascending pharyngeal artery and superior laryngeal nerve. Anterolaterally the internal carotid artery is covered by sternocleidomastoid. Below the posterior belly of digastric, the hypoglossal nerve and superior root of the ansa cervicalis and the lingual and facial veins are superficial to the artery. At the level of the digastric, the internal carotid is crossed by stylohyoid and the occipital and posterior auricular arteries. Above the digastric it is separated from the external carotid artery by the styloid process, styloglossus and stylopharyngeus, the glossopharyngeal nerve and the pharyngeal branch of the vagus, and the deeper part of the parotid gland. At the base of the skull the glossopharyngeal, vagus, accessory and hypoglossal nerves lies between the internal carotid artery and the internal jugular vein, which here has become posterior. The length of the artery varies with the length of the neck and the point of the carotid bifurcation. It may arise from the aortic arch in which case it lies medial to the external carotid as far as the larynx, where it crosses behind it. The cervical portion is normally straight but may be very tortuous, when it lies closer to the pharynx than usual, very near the tonsil. The internal carotid artery enters the cranium without giving off any branches. It may occasionally be absent.

Occlusive atherosclerotic disease within either the internal carotid or common carotid artery may cause strokes or transient ischaemic attacks (TIAs) characterized by weakness of the contralateral side. It may also result in visual disturbances characterized classically as a ‘curtain’ falling down over the visual field (amaurosis fugax). These episodes will be experienced in the ipsilateral eye.

Carotid sinus and carotid body

The common carotid artery shows two specialized organs near its bifurcation, the carotid sinus and the carotid body. They relay information concerning the pressure and chemical composition of the arterial blood respectively, and are innervated principally by carotid branch(es) of the glossopharyngeal nerve, with small contributions from the cervical sympathetic trunk and the vagus nerve.

The carotid sinus usually appears as a dilation of the lower end of the internal carotid, and functions as a baroreceptor.

The carotid body is a reddish-brown, oval structure, 5–7 mm in height and 2.5–4 mm in width. It lies either posterior to the carotid bifurcation or between its branches, and is attached to, or sometimes partly embedded in, their adventitia. Occasionally it takes the form of a group of separate nodules. Aberrant miniature carotid bodies, microstructurally similar but with diameters of 600 μm or less, may appear in the adventitia and adipose tissue near the carotid sinus.

The carotid body is surrounded by a fibrous capsule from which septa divide the enclosed tissue into lobules. Each lobule contains glomus (type I) cells which are separated from an extensive network of fenestrated sinusoids by sustentacular (type II) cells (Fig. 28.9). Glomus cells store a number of peptides, particularly enkephalins, bombesin and neurotensin, and amines including dopamine, serotonin, adrenaline (epinephrine) and noradrenaline (norepinephrine), and are therefore regarded as paraneurones. Unmyelinated axons lie in a collagenous matrix between the sustentacular cells and the sinusoidal endothelium, and many synapse on the glomus cells. They are visceral afferents which travel in the carotid sinus nerve to join the glossopharyngeal nerve. Preganglionic sympathetic axons and fibres from the carotid sinus synapse on parasympathetic and sympathetic ganglion cells, which lie either in isolation or in small groups near the surface of each carotid body. Postganglionic axons travel to local blood vessels: the parasympathetic efferent fibres are probably vasodilatory and the sympathetic ones are vasoconstrictor.

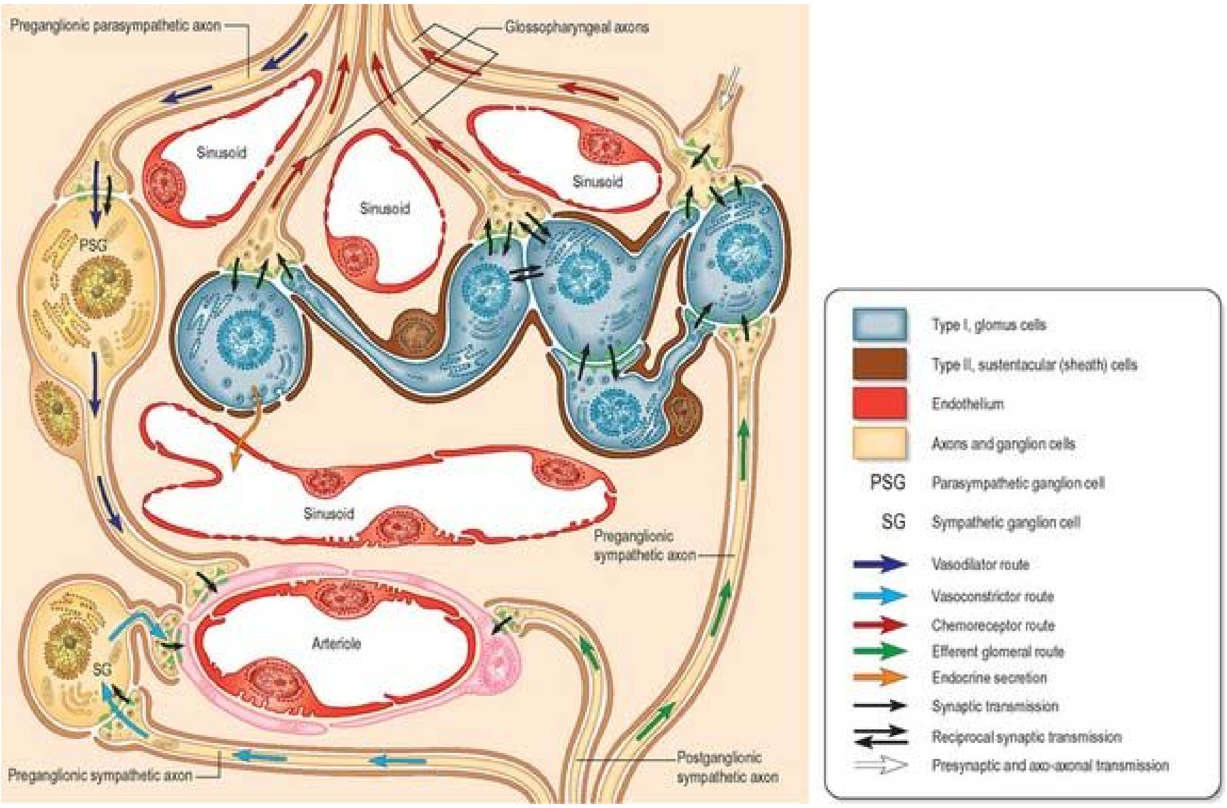
Preganglionic parasympathetic axon
Glossopharyngeal axons
Sinusoid
Sinusoid
Sinusoid
PSG
Sinusoid
Preganglionic sympathetic axon
Arteriole
SG
Preganglionic sympathetic axon
Postganglionic sympathetic axon
Type I, glomus cells
Type II, sustentacular (sheath) cells
Endothelium
Axons and ganglion cells
PSG Parasympathetic ganglion cell
SG Sympathetic ganglion cell
Vasodilator route
Vasoconstrictor route
Chemoreceptor route
Efferent glomeral route
Endocrine secretion
Synaptic transmission
Reciprocal synaptic transmission
Presynaptic and axo-axonal transmission

Fig. 28.9 The cellular, neural and vascular architecture of the carotid body: functional pathways are indicated.

The carotid body receives a rich blood supply from branches of the adjacent external carotid artery, which is consistent with its role as an arterial chemoreceptor. When stimulated by hypoxia, hypercapnia or increased hydrogen ion concentration (low pH) in the blood flowing through it, it elicits reflex increases in the rate and volume of ventilation via connections with brain stem respiratory centres. The bodies are most prominent in children and normally involute in older age, when they are infiltrated by lymphocytes and fibrous tissue. Individuals with chronic hypoxia, or who live at high altitude or suffer from lung disease, may have enlarged carotid bodies as a result of hyperplasia.

Other small bodies, resembling carotid bodies, and also considered to be chemoreceptors, occur near the arteries of the fourth and sixth pharyngeal arches and hence are found near the aortic arch, ligamentum arteriosum and right subclavian artery, and are supplied by the vagus nerve.

Subclavian artery

The right subclavian artery arises from the brachiocephalic trunk, the left from the aortic arch (see Figs 28.14, 28.18). For description, each is divided into a first part, from its origin to the medial border of scalenus anterior, a second part behind this muscle and a third part from the lateral margin of scalenus anterior to the outer border of the first rib, where the artery becomes the axillary artery. Each subclavian artery arches over the cervical pleura and pulmonary apex. Their first parts differ, whereas the second and third parts are almost identical.

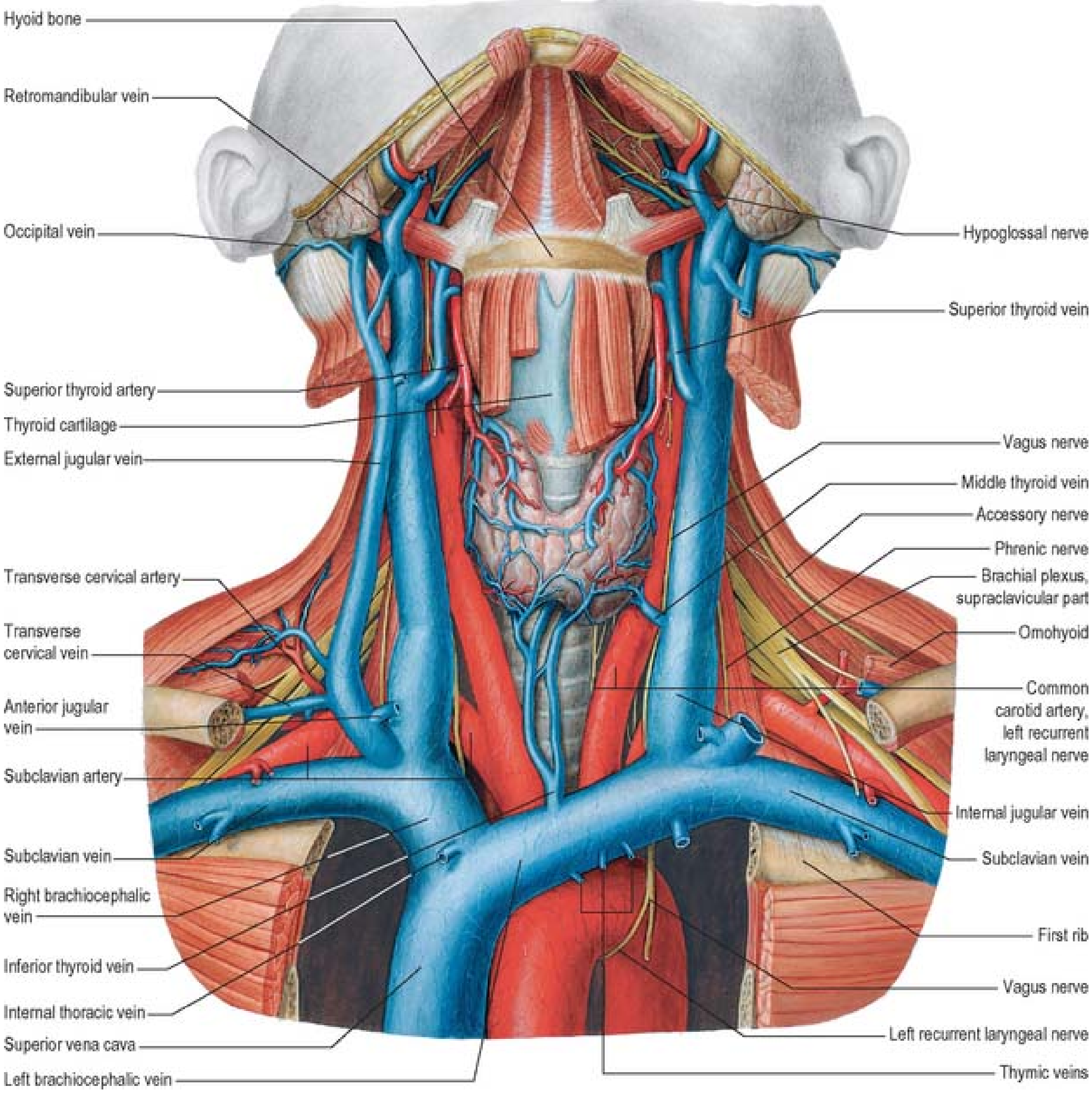
Hyoid bone
Retromandibular vein
Occipital vein
Superior thyroid artery
Thyroid cartilage
External jugular vein
Transverse cervical artery
Transverse cervical vein
Anterior jugular vein
Subclavian artery
Subclavian vein
Right brachiocephalic vein
Inferior thyroid vein
Internal thoracic vein
Superior vena cava
Left brachiocephalic vein
Hypoglossal nerve
Superior thyroid vein
Vagus nerve
Middle thyroid vein
Accessory nerve
Phrenic nerve
Brachial plexus, supraclavicular part
Omohyoid
Common carotid artery, left recurrent laryngeal nerve
Internal jugular vein
Subclavian vein
First rib
Vagus nerve
Left recurrent laryngeal nerve
Thymic veins

Fig. 28.14 The veins of the neck, seen from the front and at a deeper level than Fig. 28.13. Both sternocleidomastoids have been removed and additional dissection has exposed the thyroid gland and some of the structures that pass through the upper thoracic aperture.

(From Sobotta 2006.)

Parts of the subclavian arteries

First part of right subclavian artery

The right subclavian artery branches from the brachiocephalic trunk behind the upper border of the right sternoclavicular joint, and passes superolaterally to the medial margin of scalenus anterior. It usually ascends 2 cm above the clavicle, but this varies.

Relations

The artery is deep to the skin, superficial fascia, platysma, supraclavicular nerves, deep fascia, clavicular attachment of sternocleidomastoid, sternohyoid and sternothyroid. It is at first behind the origin of the right common carotid artery; more laterally it is crossed by the vagus nerve, the cardiac branches of the vagus and the sympathetic chain and by internal jugular and vertebral veins; the subclavian sympathetic loop encircles it. The anterior jugular vein diverges laterally in front of it, separated by sternohyoid and sternothyroid. Below and behind the artery are the pleura and pulmonary apex: they are separated from the artery by the suprapleural membrane, the ansa subclavia, a small accessory vertebral vein and the right recurrent laryngeal nerve which winds round the lower and posterior part of the vessel.

First part of left subclavian artery

The first part of the left subclavian artery springs from the aortic arch, behind the left common carotid, level with the disc between the third and fourth thoracic vertebrae. It ascends into the neck, then arches laterally to the medial border of scalenus anterior.

Relations

In the neck, near the medial border of scalenus anterior, the artery is crossed anteriorly by the left phrenic nerve and the termination of the thoracic duct. Otherwise anterior relations are the same as those of the first part of the right subclavian artery. Posteriorly and inferiorly, the relations of both vessels are identical but the left recurrent laryngeal nerve, medial to the left subclavian artery in the thorax, is not directly related to its cervical part.

Second part of subclavian artery

The second part of the subclavian artery lies behind scalenus anterior; it is short and the highest part of the vessel (see Fig. 28.18).

Relations

The skin, superficial fascia, platysma, deep cervical fascia, sternocleidomastoid and scalenus anterior are anterior. The right phrenic nerve is often described as being separated from the second part of the subclavian artery by scalenus anterior, whereas it crosses the first part of the left subclavian artery. However, both nerves may sometimes lie anterior to the muscle. The suprapleural membrane, pleura and lung and the lower trunk of the brachial plexus are posteroinferior; the upper and middle trunks of the plexus are superior; the subclavian vein is anteroinferior, separated by scalenus anterior.

Third part of subclavian artery

The third part of the subclavian artery descends laterally from the lateral margin of scalenus anterior to the outer border of the first rib, where it becomes the axillary artery. It is the most superficial part of the artery and lies partly in the supraclavicular triangle, where its pulsations may be felt and it may be compressed. The third part of the subclavian artery is the most accessible segment of the artery. Since the line of the posterior border of sternocleidomastoid approximates to the (deeper) lateral border of scalenus anterior, the artery can be felt in the anteroinferior angle of the posterior triangle. It can only be effectively compressed against the first rib: with the shoulder depressed, pressure is exerted down, back and medially in the angle between sternocleidomastoid and the clavicle. The palpable trunks of the brachial plexus may be injected with local anaesthetic allowing major surgical procedures to the arm.

Relations

The skin, superficial fascia, platysma, supraclavicular nerves and deep cervical fascia are anterior. The external jugular vein crosses its medial end and here receives the suprascapular, transverse cervical and anterior jugular veins, which collectively often form a venous plexus. The nerve to subclavius descends between the veins and the artery; the latter is terminally behind the clavicle and subclavius, where it is crossed by the suprascapular vessels. The subclavian vein is anteroinferior and the lower trunk of the brachial plexus is posteroinferior, between the subclavian artery and the scalenus medius (and on the first rib). The upper and middle trunks of the brachial plexus (which are palpable here) and the inferior belly of omohyoid are superolateral. The first rib is inferior.

The right subclavian artery may arise above or below sternoclavicular level; it may be a separate aortic branch and be the first or last branch of the arch. When it is the first branch, it is in the position of a brachiocephalic trunk. When it is the last branch, it arises from the left end of the arch, and ascends obliquely to the right behind the trachea, oesophagus and right common carotid to the first rib. When this occurs, the right recurrent laryngeal nerve hooks round the common carotid artery. Sometimes, when the right subclavian artery is the last aortic branch, it passes between the trachea and oesophagus and can cause dysphagia, a condition known as dysphagia lusoria. It may perforate scalenus anterior, and very rarely may pass anterior to it. Sometimes the subclavian vein accompanies the artery behind scalenus anterior. The artery may ascend as high as 4 cm above the clavicle or it may reach only its upper border. The left subclavian artery is occasionally combined at its origin with the left common carotid artery.

Vertebral artery

The vertebral artery arises from the superoposterior aspect of the first part of the subclavian artery. It passes through the foramina in the transverse processes of all of the cervical vertebrae except the seventh, curves medially behind the lateral mass of the atlas and enters the cranium via the foramen magnum (Fig. 28.11). At the lower pontine border it joins its fellow to form the basilar artery. Occasionally it may enter the cervical vertebral column via the fourth, fifth or seventh cervical vertebra (Fig. 28.10).

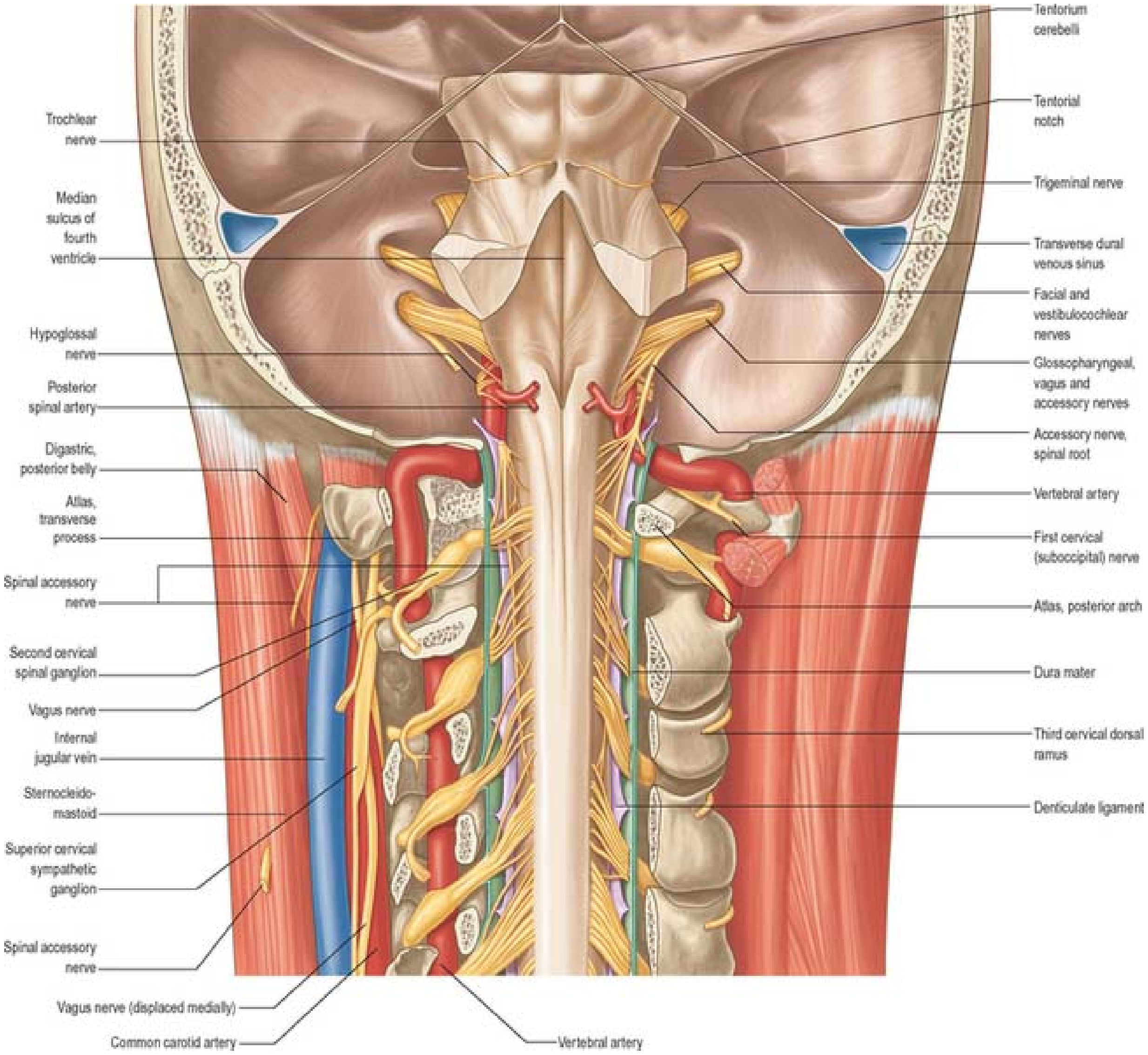
Tentorium cerebelli
Tentorial notch
Trochlear nerve
Trigeminal nerve
Median sulcus of fourth ventricle
Transverse dural venous sinus
Facial and vestibulocochlear nerves
Hypoglossal nerve
Glossopharyngeal, vagus and accessory nerves
Posterior spinal artery
Accessory nerve, spinal root
Digastric, posterior belly
Vertebral artery
Atlas, transverse process
First cervical (suboccipital) nerve
Spinal accessory nerve
Atlas, posterior arch
Second cervical spinal ganglion
Dura mater
Vagus nerve
Internal jugular vein
Third cervical dorsal ramus
Sternocleido-mastoid
Denticulate ligament
Superior cervical sympathetic ganglion
Spinal accessory nerve
Vagus nerve (displaced medially)
Common carotid artery
Vertebral artery

Fig. 28.11 A dissection of the brain stem and the upper part of the spinal cord after removal of large portions of the occipital and parietal bones, the cerebellum and the roof of the fourth ventricle. On the left side, the foramina transversaria of the atlas and the third, fourth and fifth cervical vertebrae have been opened to expose the vertebral artery. On the right side the posterior arch of the atlas and the laminae of the succeeding cervical vertebrae have been divided and have been removed together with the vertebral spines and the contralateral laminae. The tentorium cerebelli and the transverse sinuses have been divided and their posterior portions removed.

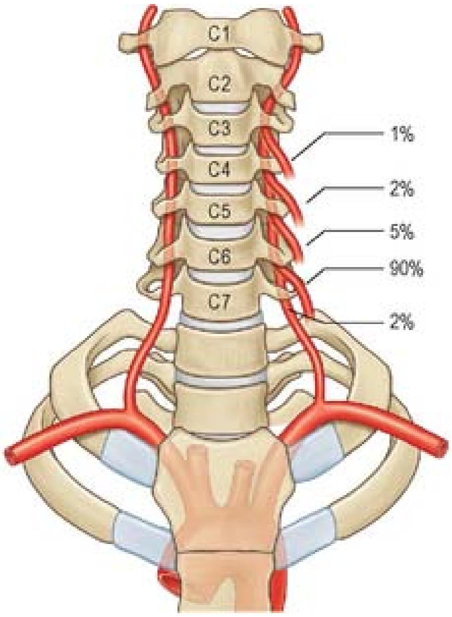

Fig. 28.10 The level of entry of the vertebral artery into the foramina transversaria of the cervical vertebrae. Note that 90% enter at the level of the sixth cervical vertebra.

(Redrawn with permission from Sobotta 2006.)

Relations

The first part passes back and upwards between longus colli and scalenus anterior, behind the common carotid artery and the vertebral vein. It is crossed by the inferior thyroid artery, and by the thoracic duct on the left side and the right lymphatic duct on the right side. The seventh cervical transverse process, the inferior cervical ganglion and ventral rami of the seventh and eighth cervical spinal nerves lie posterior to the artery. The second part ascends through the transverse foramina of the remaining cervical vertebrae, accompanied by a large branch from the inferior cervical ganglion and a plexus of veins which form the vertebral vein low in the neck. It lies anterior to the ventral rami of the cervical spinal nerves (C.2–C.6), and ascends almost vertically to pass through the transverse process of the axis, where it turns laterally to gain access to the transverse foramen of the atlas (Fig. 28.11). The third part issues medial to rectus capitis lateralis, and curves backwards and medially behind the lateral mass of the atlas, with the first cervical ventral spinal ramus lying on its medial side. In this position it lies in a groove on the upper surface of the posterior arch of the atlas, and it enters the vertebral canal below the inferior border of the posterior atlanto-occipital membrane. This part of the artery, covered by semispinalis capitis, lies in the suboccipital triangle. The first cervical dorsal spinal ramus separates the artery from the posterior arch. The fourth part pierces the dura and arachnoid mater, and ascends anterior to the hypoglossal roots. It inclines anterior to the medulla oblongata and unites with its contralateral fellow to form the midline basilar artery at the lower border of the pons.

Cervical branches of the vertebral artery

Spinal branches

The spinal branches enter the vertebral canal via the intervertebral foramina, and supply the spinal cord and its membranes. They fork into ascending and descending rami, which unite with those above and below, to form two lateral anastomotic chains on the posterior surfaces of the vertebral bodies near the attachment of their pedicles. Branches from these chains supply the periosteum and vertebral bodies, and others communicate with similar branches across the midline; from these connections small rami join similar ones above and below, to form a median anastomotic chain on the posterior surfaces of the vertebral bodies.

Muscular branches

Muscular branches arise from the vertebral artery as it curves round the lateral mass of the atlas. They supply the deep muscles of the suboccipital region and anastomose with the occipital, ascending and deep cervical arteries.

Internal thoracic artery

The internal thoracic artery arises inferiorly from the first part of the subclavian artery, 2 cm above the sternal end of the clavicle, opposite the root of the thyrocervical trunk.

Thyrocervical trunk

The thyrocervical trunk is a short wide artery which arises from the front of the first part of the subclavian artery near the medial border of scalenus anterior, and divides almost at once into the inferior thyroid, suprascapular and superficial cervical arteries.

Inferior thyroid artery

The inferior thyroid artery loops upwards anterior to the medial border of the scalenus anterior, turns medially just below the sixth cervical transverse process, then descends on longus colli to the lower border of the thyroid gland (Figs 28.7A, 28.17). It passes anterior to the vertebral vessels and posterior to the carotid sheath and its contents (and usually the sympathetic trunk, whose middle cervical ganglion frequently adjoins the vessel). On the left, near its origin, the artery is crossed anteriorly by the thoracic duct as the latter curves inferolaterally to its termination. Relations between the terminal branches of the artery and recurrent laryngeal nerve are very variable and of considerable surgical importance. The artery usually passes behind the nerve as it nears the gland. However, very close to the gland, the right nerve is equally likely to be anterior, posterior or amongst, the branches of the artery, and the left nerve is usually posterior. The artery is not accompanied by the inferior thyroid vein.

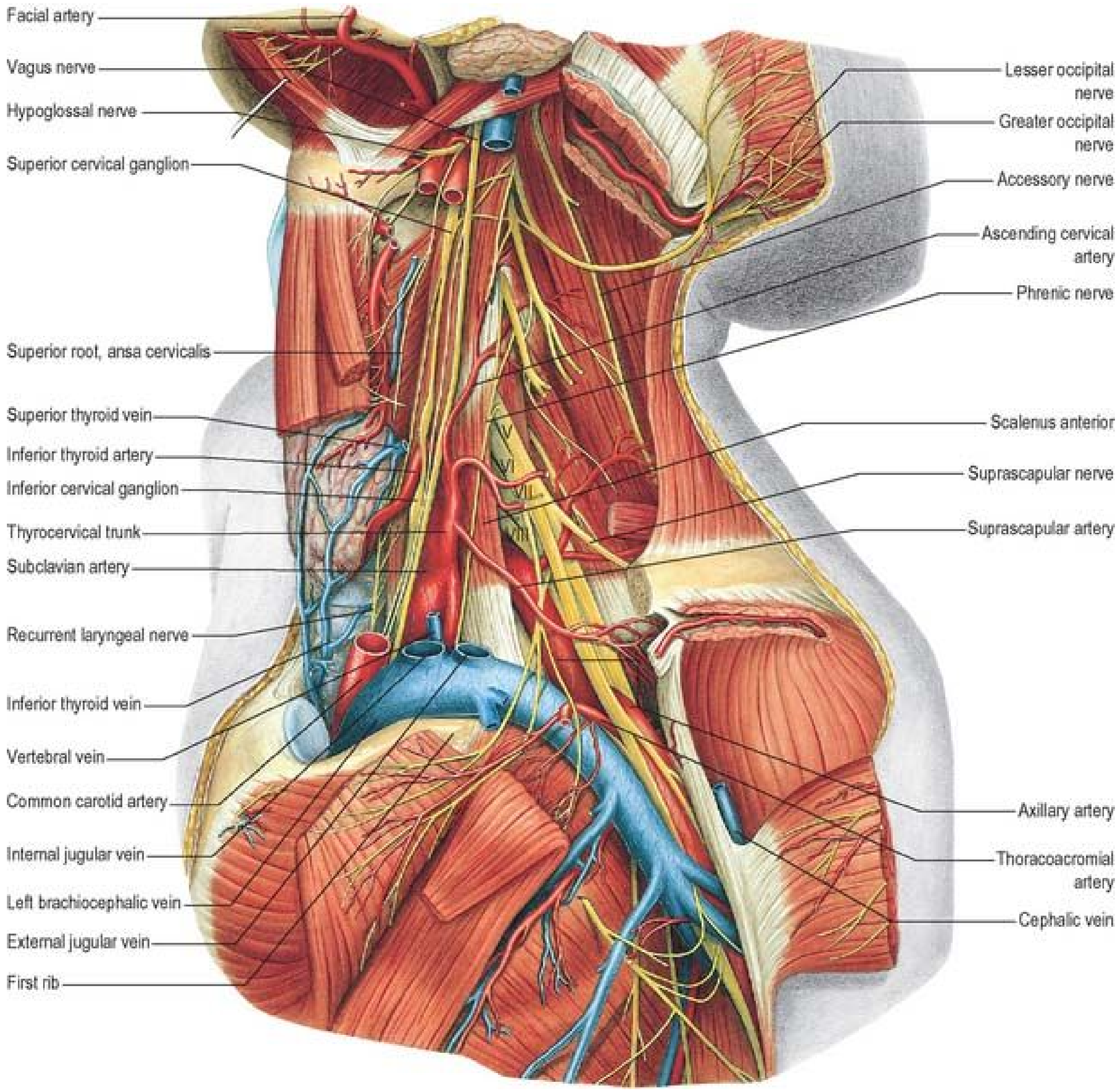
Facial artery
Vagus nerve
Hypoglossal nerve
Superior cervical ganglion
Superior root, ansa cervicalis
Superior thyroid vein
Inferior thyroid artery
Inferior cervical ganglion
Thyrocervical trunk
Subclavian artery
Recurrent laryngeal nerve
Inferior thyroid vein
Vertebral vein
Common carotid artery
Internal jugular vein
Left brachiocephalic vein
External jugular vein
First rib
Lesser occipital nerve
Greater occipital nerve
Accessory nerve
Ascending cervical artery
Phrenic nerve
Scalenus anterior
Suprascapular nerve
Suprascapular artery
Axillary artery
Thoracoacromial artery
Cephalic vein
V
VI
VII
VIII

Fig. 28.17 Vessels and nerves of the neck, left lateral view. The left sternocleidomastoid, the greater part of the infrahyoid group of muscles and numerous vessels have been removed in order to expose deeper structures. Compare with **Fig. 28.7A**, which shows a more superficial level of dissection. V, VI, VII, VIII refer to the anterior primary rami of C5, C6, C7, and C8, respectively.

(From Sobotta 2006.)

Muscular branches

These supply the infrahyoid muscles, longus colli, scalenus anterior and the inferior pharyngeal constrictor.

Ascending cervical artery

The ascending cervical artery is a small branch which arises as the inferior thyroid turns medially behind the carotid sheath and ascends on the anterior tubercles of the cervical transverse processes between scalenus anterior and longus capitis. It supplies the adjacent muscles and gives off one or two spinal branches which enter the vertebral canal through the intervertebral foramina to supply the spinal cord and membranes and vertebral bodies, and thereby supplement the spinal branches of the vertebral artery. The ascending cervical artery anastomoses with the vertebral, ascending pharyngeal, occipital and deep cervical arteries.

Inferior laryngeal

The inferior laryngeal artery ascends on the trachea with the recurrent laryngeal nerve, enters the larynx at the lower border of the inferior constrictor and supplies the laryngeal muscles and mucosa. It anastomoses with its contralateral fellow, and with the superior laryngeal branch of the superior thyroid artery.

Pharyngeal branches

These supply the lower part of the pharynx. Tracheal branches supply the trachea and anastomose with the bronchial arteries; oesophageal branches supply the oesophagus and anastomose with the oesophageal branches of the thoracic aorta; inferior and ascending glandular branches supply the posterior and inferior regions of the thyroid gland, and anastomose with the contralateral inferior and ipsilateral superior thyroid arteries. The ascending branch also supplies the parathyroid glands.

Suprascapular artery

The suprascapular artery descends laterally across scalenus anterior and the phrenic nerve, posterior to the internal jugular vein and sternocleidomastoid (Fig. 28.7A). It then crosses anterior to the subclavian artery and brachial plexus, posterior to, and parallel with, the clavicle, subclavius and the inferior belly of omohyoid, to reach the superior scapular border.

Superficial cervical artery

The superficial cervical artery is given off at a higher level than the suprascapular artery. It crosses anterior to the phrenic nerve, scalenus anterior and the brachial plexus and is covered by the internal jugular vein, sternocleidomastoid and platysma. It crosses the floor of the posterior triangle to reach the anterior margin of levator scapulae, and ascends deep to the anterior part of the trapezius, which it supplies, together with the adjoining muscles and the cervical lymph nodes. It anastomoses with the superficial ramus of the descending branch of the occipital artery. About a third of the superficial cervical and dorsal scapular arteries arise in common from the thyrocervical trunk, with a superficial (superficial cervical artery) and a deep (dorsal scapular artery) branch (see Figs 25.1, 25.2 and 46.26). The latter passes laterally anterior to the brachial plexus and then posterior to levator scapulae.

Costocervical trunk

On the right, this short vessel arises posteriorly from the second part of the subclavian artery, and, on the left, from its first part. It arches back above the cervical pleura to the neck of the first rib, where it divides into superior intercostal and deep cervical branches.

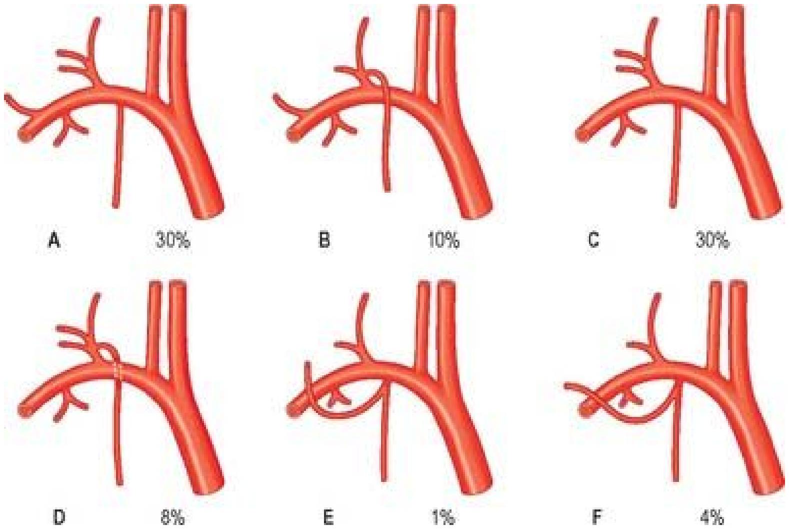

Fig. 28.12 Variations in the origins of the inferior thyroid, suprascapular, transverse cervical and internal thoracic arteries.

(Redrawn with permission from Sobotta 2006.)

Deep cervical artery

The deep cervical artery usually arises from the costocervical trunk (see Fig. 25.1). It is analogous in its first segment to a posterior branch of a posterior intercostal artery, and occasionally is a separate branch of the subclavian artery. It passes back above the eighth cervical spinal nerve between the transverse process of the seventh cervical vertebra and the neck of the first rib (sometimes between the transverse processes of the sixth and seventh cervical vertebrae). It then ascends between semispinales capitis and cervicis to the level of the second cervical vertebra. It supplies adjacent muscles and anastomoses with the deep branch of the descending branch of the occipital artery and branches of the vertebral artery. A spinal branch enters the vertebral canal between the seventh cervical and first thoracic vertebrae.

Dorsal scapular artery

The dorsal scapular artery arises from the third, or less often the second, part of the subclavian artery. It gives off a small branch (which sometimes arises directly from the subclavian artery), to scalenus anterior. It passes laterally through the brachial plexus in front of scalenus medius and then deep to levator scapulae to the superior scapular angle.

VEINS OF THE NECK

Veins in the neck show considerable variation. They are superficial or deep to the deep fascia but are not entirely separate systems. Superficial veins are tributaries, some with specific names, given below, of the anterior, external and posterior jugular veins (Figs 28.13, 28.14). They drain a much smaller volume of tissue than the deep veins. The latter drain all but the subcutaneous structures, mostly into the internal jugular vein and also into the subclavian vein.

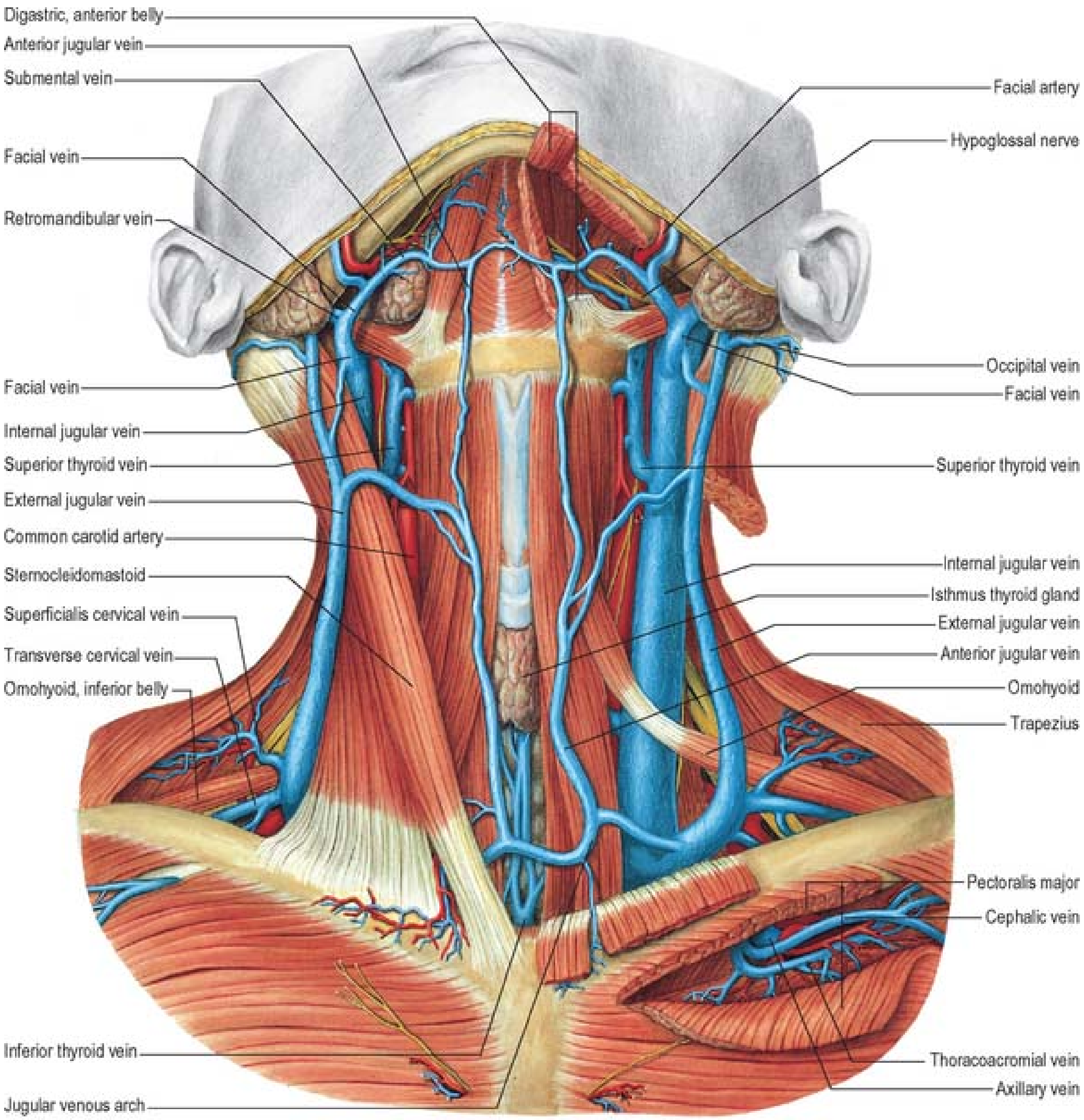
Digastric, anterior belly
Anterior jugular vein
Submental vein
Facial vein
Retromandibular vein
Facial vein
Internal jugular vein
Superior thyroid vein
External jugular vein
Common carotid artery
Sternocleidomastoid
Superficialis cervical vein
Transverse cervical vein
Omohyoid, inferior belly
Inferior thyroid vein
Jugular venous arch
Facial artery
Hypoglossal nerve
Occipital vein
Facial vein
Superior thyroid vein
Internal jugular vein
Isthmus thyroid gland
External jugular vein
Anterior jugular vein
Omohyoid
Trapezius
Pectoralis major
Cephalic vein
Thoracoacromial vein
Axillary vein

Fig. 28.13 The veins of the neck, seen from the front. The greater part of sternocleidomastoid has been removed on the left side and the cut lower edges have been reflected over the clavicle.

(From Sobotta 2006.)

External jugular vein

The external jugular vein mainly drains the scalp and face, although it also drains some deeper parts. The vein is formed by the union of the posterior division of the retromandibular vein with the posterior auricular vein and begins near the mandibular angle just below or in the parotid gland (see Fig. 25.3). It descends from the angle to the midclavicle, running obliquely, superficial to sternocleidomastoid, to the root of the neck. Here it crosses the deep fascia and ends in the subclavian vein, lateral or anterior to scalenus anterior. There are valves at its entrance into the subclavian, but they do not prevent regurgitation. Its wall is adherent to the rim of the fascial opening. It is covered by platysma, superficial fascia and skin, and is separated from sternocleidomastoid by deep cervical fascia. The vein crosses the transverse cutaneous nerve and lies parallel with the great auricular nerve, posterior to its upper half. In size the external jugular vein is inversely proportional to the other veins in the neck, and may be double. Between the entrance into the subclavian vein and a point approximately 4 cm above the clavicle, the vein is often dilated, producing a so-called sinus.

Tributaries

In addition to formative tributaries, the external jugular receives the posterior external jugular and, near its end, transverse cervical, suprascapular and anterior jugular veins. In the parotid gland it is often joined by a branch from the internal jugular. The occipital vein occasionally joins it.

Posterior external jugular vein

The posterior external jugular vein begins in the occipital scalp, and drains the skin and the superficial muscles which lie posterosuperior in the neck. It usually joins the middle part of the external jugular vein.

Anterior jugular vein

The anterior jugular vein arises near the hyoid bone from the confluence of the superficial submandibular veins. It descends between the midline and the anterior border of sternocleidomastoid. Turning laterally, low in the neck, deep to sternocleidomastoid but superficial to the infrahyoid strap muscles, it joins either the end of the external jugular vein or may enter the subclavian vein directly. In size it is usually inverse to the external jugular vein. It communicates with the internal jugular vein, and receives the laryngeal veins and sometimes a small thyroid vein. There are usually two anterior jugular veins, united just above the manubrium by a large transverse jugular arch, receiving the inferior thyroid tributaries. They have no valves and may be replaced by a midline trunk.

Internal jugular vein

The internal jugular vein collects blood from the skull, brain, superficial parts of face and much of the neck. It begins at the cranial base in the posterior compartment of the jugular foramen, where it is continuous with the sigmoid sinus. At its origin it is dilated as the superior bulb, which lies below the posterior part of the tympanic floor. The internal jugular vein descends in the carotid sheath, and unites with the subclavian vein, posterior to the sternal end of the clavicle, to form the brachiocephalic vein (Fig. 28.14). Near its termination the vein dilates into the inferior bulb, above which is a pair of valves.

Relations

From above, rectus capitis lateralis, the transverse process of the atlas, levator scapulae, scalenus medius, scalenus anterior, the cervical plexus, the phrenic nerve, thyrocervical trunk, vertebral vein and the first part of the subclavian artery all lie posterior to the vein. On the left, the internal jugular crosses anterior to the thoracic duct. The internal and common carotid arteries and the vagus nerve are medial to the vein: the nerve lies between vein and arteries but posterior to them. Superficially the internal jugular vein is overlapped above, then covered below, by sternocleidomastoid and is crossed by the posterior belly of digastric and the superior belly of omohyoid. Superior to digastric the parotid gland, styloid process, accessory nerve, and posterior auricular and occipital arteries cross the vein. Between digastric and omohyoid, the sternocleidomastoid arteries and inferior root of the ansa cervicalis cross it, although the nerve often passes between the vein and the common carotid artery. Below omohyoid, the vein is covered by the infrahyoid muscles and sternocleidomastoid and is crossed by the anterior jugular vein. Deep cervical lymph nodes lie along the internal jugular, mainly on its superficial aspect. At the root of the neck the right internal jugular vein is separated from the common carotid artery, but the left usually overlaps its artery. At the base of the skull the internal carotid artery is anterior to the vein, separated from it by the ninth to 12th cranial nerves.

Tributaries

The inferior petrosal sinus, facial, lingual, pharyngeal, superior and middle thyroid veins, and occasionally the occipital vein, are all tributaries of the internal jugular vein. The internal jugular vein may communicate with the external jugular vein. The thoracic duct opens near the union of the left subclavian and internal jugular veins, and the right lymphatic duct opens at the same site on the right.

Inferior petrosal sinus

The inferior petrosal sinus leaves the skull through the anterior part of the jugular foramen, crosses lateral or medial to the ninth to eleventh cranial nerves and joins the superior jugular bulb.

Facial vein

The initial part of the facial vein as it lies on the face is described on page 492. From the face it passes over the surface of masseter, crosses the body of the mandible and enters the neck where it runs obliquely back under platysma. Here it lies superficial to the submandibular gland, digastric and stylohyoid (Fig. 28.14). Just anteroinferior to the mandibular angle it is joined by the anterior division of the retromandibular vein, and then descends superficial to the loop of the lingual artery, the hypoglossal nerve and external and internal carotid arteries, to enter the internal jugular near the greater cornu of the hyoid bone, i.e. in the upper angle of the carotid triangle. Near its end a large branch often descends along the anterior border of sternocleidomastoid to the anterior jugular vein. Its uppermost segment, above its junction with the superior labial vein, is often termed the angular vein.

Tributaries

Submental, tonsillar, external palatine (paratonsillar), submandibular, vena comitans of the hypoglossal nerve (sometimes), pharyngeal and superior thyroid veins are all tributaries of the portion of the facial vein that lies below the mandible.

Lingual vein

The lingual veins follow two routes. The dorsal lingual veins drain the dorsum and sides of the tongue, join the lingual veins accompanying the lingual artery between hyoglossus and genioglossus and enter the internal jugular near the greater cornu of the hyoid bone. The deep lingual vein begins near the tip of the tongue and runs back, lying near the mucous membrane on the inferior surface of the tongue. Near the anterior border of hyoglossus it joins a sublingual vein, from the sublingual salivary gland, to form the vena comitans nervi hypoglossi which runs back between mylohyoid and hyoglossus with the hypoglossal nerve to join the facial, internal jugular or lingual vein.

Pharyngeal veins

The pharyngeal veins begin in a pharyngeal plexus external to the pharynx. They receive meningeal veins and a vein from the pterygoid canal, and usually end in the internal jugular vein, but may sometimes end in the facial, lingual or superior thyroid vein.

Superior thyroid vein

The superior thyroid vein is formed by deep and superficial tributaries corresponding to the arterial branches in the upper part of the thyroid gland (Figs 28.13, 28.14). It accompanies the superior thyroid artery, receives the superior laryngeal and cricothyroid veins, and ends in the internal jugular or facial vein.

Middle thyroid vein

The middle thyroid vein drains the lower part of the gland and also receives veins from the larynx and trachea. It crosses anterior to the common carotid artery to join the internal jugular vein behind the superior belly of omohyoid.

Tympanic body

The tympanic body (glomus jugulare) is ovoid, 0.5 mm long and 0.25 mm broad, and lies in the adventitia of the upper part of the superior bulb of the internal jugular vein. It is similar in structure to the carotid body and is presumed to have a similar function. The predominant cell type has morphological similarities to adrenal chromaffin cells, and is derived from the neural crest. Cells obtained from glomus jugulare paragangliomas show spontaneous neurite outgrowth in culture, and have vasoactive intestinal peptide (VIP)-like activity. The tympanic body may be present as two or more parts near the tympanic branch of the glossopharyngeal nerve or the auricular branch of the vagus as they lie within their canals in the petrous part of the temporal bone. Tumours of tympanic bodies may involve the adjacent cranial nerves and the middle ear.

Subclavian vein

The subclavian vein is a continuation of the axillary vein and extends from the outer border of the first rib to the medial border of scalenus anterior, where it joins the internal jugular vein to form the brachiocephalic vein (Fig. 28.14). The clavicle and subclavius lie anterior to it, the subclavian artery is posterosuperior, separated by scalenus anterior and the phrenic nerve, and the first rib and pleura are inferior. The vein usually has a pair of valves 2 cm from its end. Its tributaries are the external jugular, dorsal scapular and sometimes the anterior jugular vein. At its junction with the internal jugular, the left subclavian vein receives the thoracic duct, and the right subclavian vein receives the right lymphatic duct.

Vertebral vein

Numerous small tributaries from internal vertebral plexuses leave the vertebral canal above the posterior arch of the atlas and join small veins from local deep muscles in the suboccipital triangle. Their union produces a vessel which enters the foramen in the transverse process of the atlas and forms a plexus around the vertebral artery. It descends through successive transverse foramina and ends as the vertebral vein. The vein emerges from the sixth cervical transverse foramen, whence it descends, at first anterior, then anterolateral, to the vertebral artery, to open superoposteriorly into the brachiocephalic vein: the opening has a paired valve. As it descends it passes behind the internal jugular vein and in front of the first part of the subclavian artery. A small accessory vertebral vein usually descends from the vertebral plexus, traverses the seventh cervical transverse foramen and turns forwards between the subclavian artery and the cervical pleura to join the brachiocephalic vein.

Tributaries

The vertebral vein connects with the sigmoid sinus by a vessel in the posterior condylar canal, when this exists. It also receives branches from the occipital vein, prevertebral muscles, internal and external vertebral plexuses. It is joined by anterior vertebral and deep cervical veins (see below) and, sometimes near its end, by the first intercostal vein.

Anterior vertebral vein

The anterior vertebral vein starts in a plexus around the upper cervical transverse processes, descends near the ascending cervical artery between attachments of scalenus anterior and longus capitis, and opens into the end of the vertebral vein.

Deep cervical vein

The deep cervical vein accompanies its artery between semispinales capitis and cervicis. It is formed in the suboccipital region by the union of communicating branches of the occipital vein; veins from suboccipital muscles; and veins from plexuses around the cervical spines. It passes forwards between the seventh cervical transverse process and the neck of the first rib to end in the lower part of the vertebral vein.

Central venous access

Central venous cannulation permits monitoring of the central venous pressure and the administration of drugs directly into the central circulation.

Internal jugular vein cannulation

The patient is placed in the supine position with the head turned slightly towards the contralateral side. The key anatomical landmarks are the two inferior heads of sternocleidomastoid, which form two sides of a triangle with the clavicle as its base. The internal jugular vein lies between the two heads of the muscle, slightly lateral and anterior to the common carotid artery. After the skin has been prepared, local anaesthetic is injected around the apex of the triangle. With one hand palpating the carotid artery, the physician inserts a needle at the apex of the triangle and the tip is directed lateral to the midpoint of the triangle, with a downward angulation of 30°. From a high internal jugular approach, the needle is inserted at the midpoint of the medial border of sternocleidomastoid and directed towards the ipsilateral nipple with a downward angulation of 30–45°. When the left internal jugular vein is cannulated, additional care must be taken to avoid the thoracic duct and the cupula of the pleura, which is higher than on the right side, an arrangement which increases the risk of accidental pneumothorax. The left internal jugular vein is often smaller in diameter than the right.

Subclavian vein cannulation

Subclavian vein cannulation is performed with the patient supine, the head turned slightly to the opposite side, and the arms placed by the side. The bed is tilted down by 10° and a small bedroll may be placed between the shoulder blades in order to ensure that the infraclavicular area is more prominent. The skin is cleaned and local anaesthetic injected into the skin 3 cm lateral to the midpoint of the clavicle. The central venous needle is then inserted from the inferior edge of the clavicle towards the suprasternal notch. The needle is directed so that it passes just below the posterior border of the clavicle; care must be taken to avoid downward direction of the needle, which may cause a pneumothorax. Gentle aspiration of the syringe is performed whilst the needle is being advanced until the subclavian vein is punctured.

CERVICAL GROUPS OF LYMPH NODES

Lymph nodes in the head and neck are distributed in terminal and outlying groups (Fig. 28.15; see Fig. 25.5). The terminal group is related to the carotid sheath and the nodes it contains are the deep cervical lymph nodes. All lymph vessels of the head and neck drain into this group, either directly from tissues or indirectly through nodes in the outlying groups. Efferents of the deep cervical nodes form the jugular trunk. The right jugular trunk collects lymph from the right arm and right half of the thorax and the right head and neck and may end in the jugulosubclavian junction or the right lymphatic duct. The left jugular trunk usually enters the thoracic duct, but it may join the internal jugular or subclavian vein.

Lymphatic drainage of the neck

Many vessels draining the superficial cervical tissues skirt the borders of sternocleidomastoid to reach the superior or inferior deep cervical nodes. Others pass to the superficial cervical and occipital nodes. Lymph from the superior region of the anterior triangle drains to the submandibular and submental nodes. Vessels from the anterior cervical skin inferior to the hyoid bone pass to the anterior cervical lymph nodes near the anterior jugular veins. Their efferents go to the deep cervical nodes of both sides, including the infrahyoid, prelaryngeal and pretracheal groups. An anterior cervical node often occupies the suprasternal space. Lymph from tissues of the head and neck internal to the deep fascia drains to the deep cervical nodes directly or through outlying groups that include the retropharyngeal, paratracheal, lingual, infrahyoid, prelaryngeal and pretracheal groups. The lymphatic drainage associated with the nasal region, larynx and oral cavity is described in the appropriate regions. The deep cervical lymphatic nodes lie alongside the carotid sheath, and form superior and inferior groups.

Superior deep cervical nodes

The superior deep cervical nodes adjoin the upper part of the internal jugular vein. Most are deep to sternocleidomastoid, but a few extend beyond it. One subgroup, consisting of one large and several small nodes, is in a triangular region bounded by the posterior belly of digastric and the facial and internal jugular veins, and is known as the jugulodigastric group. It is concerned specially with drainage of the tongue. Efferents from the upper deep cervical nodes drain either to the lower group or direct to the jugular trunk.

Inferior deep cervical nodes

The inferior deep cervical nodes are partly deep to the sternocleidomastoid, and are particularly related to the lower part of the internal jugular vein. Some are closely related to the brachial plexus and subclavian vessels. The jugulo-omohyoid node lies on, or just above, the intermediate tendon of omohyoid, and is concerned especially with lymphatic drainage from the tongue. Efferents from this lower group join the jugular lymph trunk.

Retropharyngeal nodes

Retropharyngeal nodes lie between the pharyngeal and prevertebral fasciae and form a median and two lateral groups, the latter anterior to the lateral masses of the atlas along the lateral borders of longus capitis. The nodes receive afferents from the nasopharynx, pharyngotympanic tube and atlanto-occipital and atlanto-axial joints and drain to the upper deep cervical nodes.

Paratracheal nodes

The paratracheal nodes flank both trachea and oesophagus along the recurrent laryngeal nerves. Efferents pass to the corresponding deep cervical nodes.

Infrahyoid, prelaryngeal and pretracheal nodes

The infrahyoid, prelaryngeal and pretracheal nodes lie beneath the deep cervical fascia. They drain afferents from the anterior cervical nodes, and their efferents join the deep cervical nodes. Infrahyoid nodes are anterior to the thyrohyoid membrane, prelaryngeal nodes lie on the cricovocal membrane, and pretracheal nodes lie anterior to the trachea near the inferior thyroid veins.

Lingual nodes

Lingual nodes are small and inconstant, and are situated on the external surface of hyoglossus and also between the genioglossi. They drain to the upper deep cervical nodes.

Spread of malignant disease in the neck

Cancers arising in the head and neck from regions such as the thyroid gland, larynx, oral cavity and oropharynx, nasopharynx and paranasal sinuses have predictable patterns of spread through the chains of lymph nodes in the neck. When operating on malignant disease in this region it is vitally important to understand these patterns of spread so that for any individual cancer the appropriate operation is undertaken. Clinical experience has shown that the lymph nodes in the neck fall into five distinct groups (see Fig. 25.5). Level I nodes lie in the submandibular triangle bounded by the anterior and posterior bellies of digastric and the lower border of the mandible above. Level II (upper jugular) nodes lie around the upper portion of the internal jugular vein and the upper part of the spinal accessory nerve. They extend from the skull base to the bifurcation of the common carotid artery or the hyoid bone. Level III (middle jugular) nodes lie around the middle third of the internal jugular vein from the inferior border of level II to the superior belly of omohyoid or cricothyroid membrane. Level IV (lower jugular) nodes lie around the lower third of the internal jugular vein from the inferior border of level III to the clavicle. The anterior and posterior borders for levels II, III and IV are the lateral border of sternohyoid and the posterior border of sternocleidomastoid respectively. Level V (posterior triangle) nodes lie around the lower part of the spinal accessory nerve and the transverse cervical vessels.

Knowing which levels of nodes are likely to be involved in the metastatic spread of a particular cancer arising in the head and neck means that appropriate nodal clearance can be undertaken. The classic radical neck dissection first described by Crile in 1906 involves a thorough clearance of levels I to V including the sacrifice of sternocleidomastoid, the internal jugular vein and the spinal accessory nerve. Modified radical neck dissections (so-called functional neck dissections) still remove level I to V nodes, but spare either or all of sternocleidomastoid, the internal jugular vein and the spinal accessory. Selective neck dissections remove selected groups of nodes, e.g. the supraomohyoid neck dissection removes level I to III nodes, the lateral neck dissection removes level II to IV nodes, and the posterolateral neck dissection removes level II to V nodes.

Cervical lymphovenous portals

Lymph is returned to the systemic venous circulation via right and left lymphovenous portals sited at, or near, the junctions of the internal jugular and subclavian veins (Fig. 28.16). The arrangement of these terminations is variable. Usually, three small lymph trunks converge towards their venous junctions on either side of the body, and they are joined, on the left side only, by the larger thoracic duct.

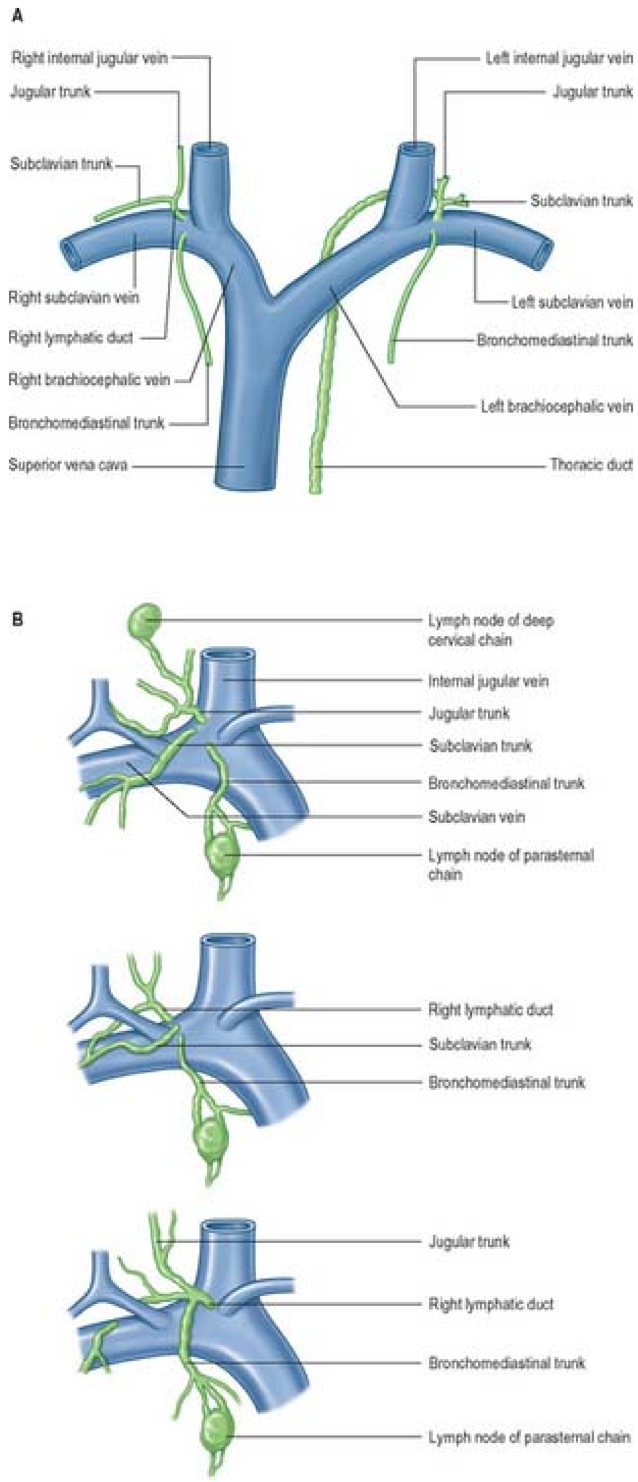
A
Right internal jugular vein
Jugular trunk
Subclavian trunk
Right subclavian vein
Right lymphatic duct
Right brachiocephalic vein
Bronchomediastinal trunk
Superior vena cava
Left internal jugular vein
Jugular trunk
Subclavian trunk
Left subclavian vein
Bronchomediastinal trunk
Left brachiocephalic vein
Thoracic duct
B
Lymph node of deep cervical chain
Internal jugular vein
Jugular trunk
Subclavian trunk
Bronchomediastinal trunk
Subclavian vein
Lymph node of parasternal chain
Right lymphatic duct
Subclavian trunk
Bronchomediastinal trunk
Jugular trunk
Right lymphatic duct
Bronchomediastinal trunk
Lymph node of parasternal chain

Fig. 28.16 **A**, The termination of the right lymphatic trunk and the thoracic duct.

(From Drake, Vogl and Mitchell 2005.) ***B***, *Variations in the terminal lymphatic trunks nodes of the right side.*

On the right side, the three trunks are the right jugular, right subclavian and right bronchomediastinal. The right jugular trunk extends from the terminal lower deep cervical nodes along the ventrolateral aspect of the internal jugular vein, and conveys all the lymph from the right half of the head and neck. The right subclavian trunk drains from the terminal apical axillary group. It extends along the axillary and subclavian veins, and conveys lymph from the right upper limb and superficial tissues of the right half of the thoracoabdominal wall, down to the umbilicus anteriorly and iliac crest posteriorly (and includes much of the breast). The right bronchomediastinal trunk, ascends over the trachea towards the lymphovenous portal and conveys lymph from the thoracic walls, the right cupola of the diaphragm and subjacent liver, the right lung, bronchi and trachea, the greater part of the 'right heart' – of clinical parlance, not the geometric right half – and a proportionately small drainage from the thoracic oesophagus.

The three right lymphatic trunks usually open independently (Fig. 28.16B). Their orifices are clustered either on the ventral aspect of the jugulo/subclavian junction, or in the nearby wall of either of the great veins. Sometimes one or more of the trunks may bifurcate (or even trifurcate) preterminally and then terminate via multiple orifices. Rarely, the three trunks fuse to form a short, single, right lymphatic duct (about 1 cm long) that inclines across the medial border of scalenus anterior at the root of the neck to reach the ventral aspect of the venous junction, where its orifice is guarded by a bicuspid semilunar valve. An incomplete right lymphatic duct may be present if the subclavian and jugular trunks, or any combination of their terminals, are fused. When this occurs, the bronchomediastinal trunk almost invariably opens separately.

On the left, the four trunks that converge on the left lymphovenous portal are the left jugular and left subclavian trunks, which have a disposition corresponding to that of their counterparts on the right; the left bronchomediastinal trunk, which has a drainage similar to the right trunk, but which drains more of the heart – the 'left' and part of the 'right' hearts of clinical parlance – and more of the oesophagus; and the thoracic duct, which drains all of the rest of the body (Fig. 28.16A).

INNERVATION

The skin, joints, viscera and muscles of the neck are innervated by branches of the glossopharyngeal, vagus and spinal accessory nerves, the cervical spinal nerves and the cervical sympathetic trunk.

The first and second cervical dorsal root ganglia lie on the vertebral arches of the atlas and axis respectively. The first cervical ganglion may be absent. Smaller aberrant ganglia sometimes occur on the upper cervical dorsal roots between the ganglia and cord. The upper four cervical roots are small, the lower four are large. In general, cervical dorsal roots have a thickness ratio to the ventral roots of three to one, which is greater than is seen in other regions. The first dorsal root is an exception, being smaller than the ventral, and in 8% cases it is absent. The first and second cervical roots are short, and run almost horizontally to their exit from the vertebral canal. From the third to the eighth cervical they slope obliquely down. Obliquity and length increase successively, however the distance between spinal attachment and vertebral exit never exceeds the height of one vertebra.

CERVICAL VENTRAL RAMI

Cervical ventral rami, except the first, appear between the anterior and posterior intertransverse muscles. The upper four form the cervical plexus, and the lower four, together with most of the first thoracic ventral ramus, form the brachial plexus. Each receives at least one grey ramus communicans, the upper four from the superior cervical sympathetic ganglion, the fifth and sixth from the middle ganglion and the seventh and eighth from the cervicothoracic ganglion.

The first cervical ventral ramus, the suboccipital nerve, emerges above the posterior arch of the atlas, passes forwards lateral to its lateral mass and medial to the vertebral artery. It supplies rectus capitis lateralis, emerges medial to it, descends anterior to the transverse process of the atlas and posterior to the internal jugular vein and joins the ascending branch of the second cervical ventral ramus.

The second cervical ventral ramus issues between the vertebral arches of the atlas and axis. It ascends between their transverse processes, passes anterior to the first posterior intertransverse muscle and emerges lateral to the vertebral artery generally between longus capitis and levator scapulae. The ramus divides into an ascending branch which joins the first cervical nerve and a descending branch which joins the ascending branch of the third cervical ventral ramus.

The third cervical ventral ramus appears between longus capitis and scalenus medius. The remaining ventral rami emerge between scalenus anterior and the scalenus medius.

Cervical plexus

The cervical plexus is formed by the ventral rami of the upper four cervical nerves, and supplies some neck muscles and the diaphragm, and areas of skin on the head, neck and chest (Fig. 28.1). It is situated in the neck opposite a line drawn down the side of the neck from the root of the auricle to the level of the upper border of the thyroid cartilage. It lies deep to the internal jugular vein, the deep fascia and sternocleidomastoid, and anterior to scalenus medius and levator scapulae. Each ramus, except the first, divides into ascending and descending parts, which unite in communicating loops. From the first loop (C2 and 3) superficial branches supply the head and neck; cutaneous nerves of the shoulder and chest arise from the second loop (C3 and 4). Muscular and communicating branches arise from the same nerves. The branches are superficial or deep. The superficial branches perforate the cervical fascia to supply the skin while the deep branches in general supply muscles. The superficial branches either ascend (the lesser occipital, great auricular and the transverse cutaneous nerves) or descend (supraclavicular nerves). These nerves are described in detail in this chapter on page 435. The deep branches form medial and lateral series.

Deep branches – medial series

Communicating branches

Communicating branches pass from the loop between the first and second cervical rami to the vagus and hypoglossal nerves and to the sympathetic trunk. The hypoglossal branch later leaves the hypoglossal nerve as a series of branches, viz. the meningeal, superior root of ansa cervicalis, nerves to thyrohyoid and to geniohyoid. A branch also connects the fourth and fifth cervical rami. The first four cervical ventral rami each receive a grey ramus communicans from the superior cervical sympathetic ganglion.

The superior root of the ansa cervicalis (descendens hypoglossi) (Figs 28.7A, 28.8) leaves the hypoglossal nerve where it curves round the occipital artery and then descends anterior to or in the carotid sheath. It contains only fibres from the first cervical spinal nerve. After giving a branch to the superior belly of omohyoid, it is joined by the inferior root of the ansa from the second and third cervical spinal nerves. The two roots form the ansa cervicalis (ansa hypoglossi), from which branches supply sternohyoid, sternothyroid and the inferior belly of omohyoid. Another branch is said to descend anterior to the vessels into the thorax to join the cardiac and phrenic nerves.

Muscular branches

Muscular branches supply rectus capitis lateralis (C1), rectus capitis anterior (C1, 2), longus capitis (C1–3) and longus colli (C2–4). The inferior root of the ansa cervicalis and the phrenic nerve are additional muscular branches.

The inferior root of the ansa cervicalis (nervus descendens cervicalis) (Figs 28.7A, 28.8) is formed by the union of a branch from the second with another from the third cervical ramus. It descends on the lateral side of the internal jugular vein, crosses it a little below the middle of the neck, and continues forwards to join the superior root anterior to the common carotid artery, forming the ansa cervicalis (ansa hypoglossi), from which all infrahyoid muscles except thyrohyoid are supplied. The inferior root comes from the second and third cervical ventral rami in 75% cases, from the second to fourth in 15%, from the third alone in 5%. Occasionally it may be derived from either the second alone or from the first to third.

Phrenic nerve

The phrenic nerve arises chiefly from the fourth cervical ventral ramus, but also has contributions from the third and fifth. It is formed at the upper part of the lateral border of scalenus anterior and descends almost vertically across its anterior surface behind the prevertebral fascia (Figs 28.7A, 28.17, 28.18). It descends posterior to sternocleidomastoid, the inferior belly of omohyoid (near its intermediate tendon), the internal jugular vein, transverse cervical and suprascapular arteries and, on the left, the thoracic duct. At the root of the neck, it runs anterior to the second part of the subclavian artery, from which it is separated by the scalenus anterior (some accounts state that on the left side the nerve passes anterior to the first part of the subclavian artery), and posterior to the subclavian vein. The phrenic nerve enters the thorax by crossing medially in front of the internal thoracic artery.

In the neck, each nerve receives variable filaments from the cervical sympathetic ganglia or their branches and may also connect with internal thoracic sympathetic plexuses.

Accessory phrenic nerve

The accessory phrenic nerve is composed of fibres from the fifth cervical ventral ramus which run in a branch of the nerve to subclavius. This lies lateral to the phrenic nerve and descends posterior (occasionally anterior) to the subclavian vein. The accessory phrenic nerve usually joins the phrenic nerve near the first rib, but may not do so until near the pulmonary hilum or beyond. The accessory phrenic nerve may be derived from the fourth or sixth cervical ventral rami or from the ansa cervicalis.

Deep branches – lateral series

Communicating branches

Lateral deep branches of the cervical plexus (C2, 3, 4) may connect with the spinal accessory nerve within sternocleidomastoid, the posterior triangle or beneath trapezius.

Muscular branches

Muscular branches are distributed to sternocleidomastoid (C2, 3, 4), trapezius (C2 and possibly C3), levator scapulae (C3, 4) and scalenus medius (C3, 4). Branches to trapezius cross the posterior triangle obliquely below the spinal accessory nerve.

Brachial plexus

The brachial plexus is formed by the union of the ventral rami of the lower four cervical nerves and the greater part of the ventral ramus of the first thoracic ventral ramus. It may also receive contributions from the fourth cervical and second thoracic spinal nerves. As its name suggests, its branches supply the muscles, joints and skin of the upper limb. The relations and distribution of the brachial plexus are described in detail in Section 6. However, it is also mentioned here because, at its origin, the brachial plexus lies in the posterior triangle of the neck, in the angle between the clavicle and the lower posterior border of sternocleidomastoid. It emerges between the scaleni anterior and medius, superior to the third part of the subclavian artery, and is covered by platysma, deep fascia and skin, through which it is palpable

(Fig. 28.17). It is crossed by the supraclavicular nerves, the nerve to subclavius, the inferior belly of omohyoid, the external jugular vein and the superficial ramus of the transverse cervical artery. The plexus passes posterior to the medial two-thirds of the clavicle, subclavius and the suprascapular vessels, and lies on the first digitation of serratus anterior and on subscapularis.

CERVICAL DORSAL RAMI

Each cervical spinal dorsal ramus except the first divides into medial and lateral branches, and all innervate muscles. In general, only medial branches of the second to fourth, and usually the fifth, supply skin. Except for the first (sometimes called the suboccipital nerve) and second, each dorsal ramus passes back medial to a posterior intertransverse muscle, curving round the articular process into the interval between semispinalis capitis and semispinalis cervicis. The cervical dorsal rami are described in detail on pages 755–756.

CRANIAL NERVES

Glossopharyngeal nerve

The glossopharyngeal nerve (Figs 28.8, 28.11, 28.19) supplies motor fibres to stylopharyngeus, parasympathetic secretomotor fibres to the parotid gland (derived from the inferior salivatory nucleus), sensory fibres to the tympanic cavity, pharyngotympanic tube, fauces, tonsils, nasopharynx, uvula and posterior (postsulcal) third of the tongue, and gustatory fibres for the postsulcal part of the tongue.

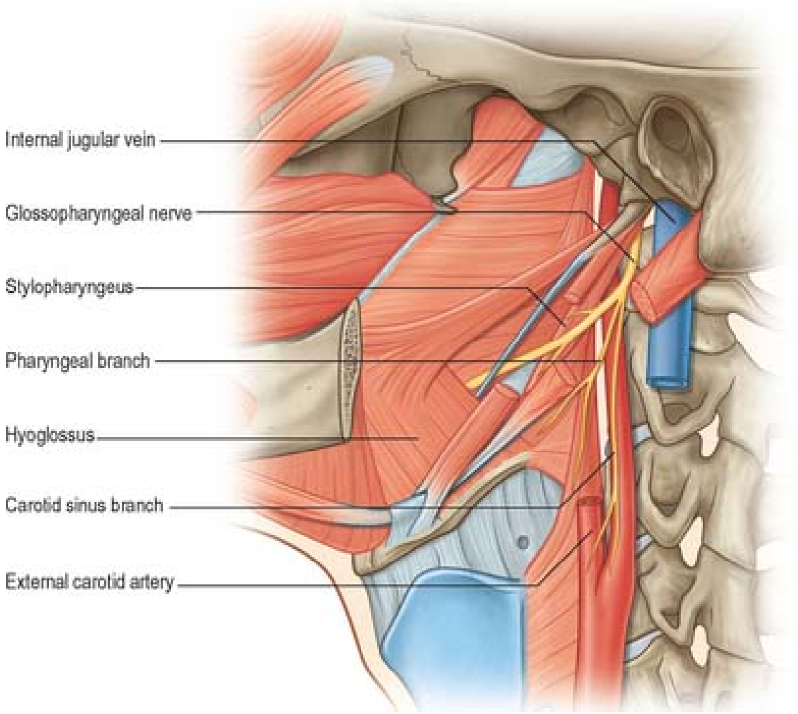
Internal jugular vein
Glossopharyngeal nerve
Stylopharyngeus
Pharyngeal branch
Hyoglossus
Carotid sinus branch
External carotid artery

Fig. 28.19 Glossopharyngeal nerve in the anterior triangle of the neck.

(From Drake, Vogl and Mitchell 2005.)

The nerve leaves the skull through the anteromedial part of the jugular foramen, anterior to the vagus and accessory nerves, and in a separate dural sheath. In the foramen it is lodged in a deep groove leading from the cochlear aqueductal depression, and is separated by the inferior petrosal sinus from the vagus and accessory nerves. The groove is bridged by fibrous tissue, which is calcified in 25% of skulls. After leaving the foramen, the nerve passes forwards between the internal jugular vein and internal carotid artery and then descends anterior to the latter, deep to the styloid process and its attached muscles, to reach the posterior border of stylopharyngeus. It curves forwards on stylopharyngeus and either pierces the lower fibres of the superior pharyngeal constrictor or passes between it and the middle constrictor to be distributed to the tonsil, the mucosae of the pharynx and postsulcal part of the tongue, the vallate papillae, and oral mucous glands.

Two ganglia, superior and inferior, are situated on the glossopharyngeal nerve as it traverses the jugular foramen. The superior ganglion is in the upper part of the groove occupied by the nerve in the jugular foramen. It is small, has no branches and is usually regarded as a detached part of the inferior ganglion. The inferior ganglion is larger and lies in a notch in the lower border of the petrous part of the temporal bone. Its cells are typical unipolar neurones, whose peripheral branches convey gustatory and tactile signals from the mucosa of the tongue (posterior third including the sulcus terminalis and vallate papillae) and general sensation from the oropharynx, where it is responsible for initiating the gag reflex.

Communicating branches

The glossopharyngeal nerve communicates with the sympathetic trunk, vagus and facial nerves. Its inferior ganglion is connected with the superior cervical sympathetic ganglion. Two filaments from the inferior ganglion pass to the vagus, one to its auricular branch and the other to its superior ganglion. A branch to the facial nerve arises from the glossopharyngeal nerve below the inferior ganglion, and perforates the posterior belly of digastric to join the facial nerve near the stylomastoid foramen.

Branches of distribution

The glossopharyngeal nerve has tympanic, carotid, pharyngeal, muscular, tonsillar and lingual branches.

Tympanic nerve

The tympanic nerve leaves the inferior ganglion, ascends to the tympanic cavity through the inferior tympanic canaliculus and divides into branches that contribute to the tympanic plexus. The lesser petrosal nerve is derived from the tympanic plexus.

Carotid branch

The carotid branch is often double. It arises just below the jugular foramen and descends on the internal carotid artery to the wall of the carotid sinus and to the carotid body. The nerve contains primary afferent fibres from chemoreceptors in the carotid body and from the baroreceptors lying in the carotid sinus wall. It may communicate with the inferior ganglion of the vagus, or with one of its branches, and with a sympathetic branch from the superior cervical ganglion.

Pharyngeal branches

The pharyngeal branches are three or four filaments which unite with the pharyngeal branch of the vagus and the layngopharyngeal branches of the sympathetic trunk to form the pharyngeal plexus near the middle pharyngeal constrictor. They constitute the route by which the glossopharyngeal nerve supplies sensory fibres to the mucosa of the pharynx.

Muscular branch

The muscular branch supplies stylopharyngeus.

Tonsillar, lingual and lesser petrosal branches

The tonsillar, lingual and lesser petrosal branches are described on pages 565, 506 and 543 respectively.

Lesions of the glossopharyngeal nerve

Damage to the glossopharyngeal nerve rarely occurs without involvement of other lower cranial nerves. Transient or sustained hypertension may follow surgical section of the nerve, and indicates involvement of the carotid branch.

Isolated lesions of the glossopharyngeal nerve lead to loss of sensation over the ipsilateral soft palate, fauces, pharynx and posterior third of the tongue, although this is difficult to assess clinically and confirmation requires galvanic stimulation. The palatal and pharyngeal (gag) reflexes are reduced or absent and salivary secretion from the parotid gland may also be reduced. Weakness of stylopharyngeus cannot be tested individually. Glossopharyngeal neuralgia consists of episodic brief but severe pain, often precipitated by swallowing, and experienced in the throat, behind the angle of the jaw and within the ear. Superior jugular bulb thromboses (e.g. in otitis media) and jugular foramen syndrome (associated with nasopharyngeal carcinoma or a glomus tumour) may cause lesions of the adjacent glossopharyngeal, vagus and accessory nerves, with associated weakness in the muscles supplied in the pharynx and larynx.

Vagus nerve

The vagus is a large mixed nerve. It has a more extensive course and distribution than any other cranial nerve, and runs through the neck, thorax and abdomen. Its central connections are described in Chapter 19.

The vagus exits the skull through the jugular foramen accompanied by the accessory nerve, with which it shares an arachnoid and a dural sheath. Both nerves lie anterior to a fibrous septum that separates them from the glossopharyngeal nerve. The vagus descends vertically in the neck in the carotid sheath, between the internal jugular vein and the internal carotid artery, to the upper border of the thyroid cartilage, and then passes between the vein and the common carotid artery to the root of the neck. Its relationships in this part of its course are therefore similar to those described for these structures (Figs 28.7A, 28.8, 28.17). Its further course differs on the two sides. The right vagus descends posterior to the internal jugular vein to cross the first part of the subclavian artery and enter the thorax. The left vagus enters the thorax between the left common carotid and subclavian arteries and behind the left brachiocephalic vein.

After emerging from the jugular foramen, the vagus bears two marked enlargements, a small, round, superior ganglion and a larger inferior ganglion.

Superior (jugular) ganglion

The superior ganglion is greyish, spherical and approximately 4 mm in diameter. It is connected to the cranial root of the accessory nerve, the inferior glossopharyngeal ganglion, and the sympathetic trunk, the latter by a filament from the superior cervical ganglion. The significance of these connections is not entirely clear, but the first probably contains aberrant motor fibres from the nucleus ambiguus which issue in the accessory nerve, to be distributed to the palatal, pharyngeal, laryngeal and upper oesophageal musculature via the vagus.

Inferior (nodose) ganglion

The inferior or nodose ganglion is larger than the superior ganglion, and is elongated and cylindrical in shape with a length of 25 mm and a maximum breadth of 5 mm. It is connected with the hypoglossal nerve, the loop between the first and second cervical spinal nerves, and with the superior cervical sympathetic ganglion. Just above the ganglion the cranial accessory blends with the vagus nerve, its fibres being distributed mainly in pharyngeal and recurrent laryngeal vagal branches. Most visceral afferent fibres have their cell bodies in the nodose ganglion.

Both vagal ganglia are exclusively sensory, and contain somatic, special visceral and general visceral afferent neurones. The superior ganglion is chiefly somatic, and most of its neurones enter the auricular nerve, whilst neurones in the inferior ganglion are concerned with visceral sensation from the heart, larynx, lungs and the alimentary tract from the pharynx to the transverse colon. Some fibres transmit impulses from taste endings in the vallecula and epiglottis. Large afferent fibres are derived from muscle spindles in the laryngeal muscles. Vagal sensory neurones in the nodose ganglion may show some somatotopic organization. Both ganglia are traversed by parasympathetic, and perhaps some sympathetic fibres, but there is no evidence that vagal parasympathetic components relay in the inferior ganglion. Preganglionic motor fibres from the dorsal vagal nucleus and the special visceral efferents from the nucleus ambiguus, which descend to the inferior vagal ganglion, commonly form a visible band, skirting the ganglion in some mammals. These larger fibres probably provide motor innervation to the larynx in the recurrent laryngeal nerve, together with some contribution to the superior laryngeal nerve supplying cricothyroid.

Branches in the neck

The branches of the vagus in the neck are the meningeal, auricular, pharyngeal, carotid body, superior and recurrent laryngeal nerves and cardiac branches.

Meningeal branch(es)

Meningeal branches appear to start from the superior vagal ganglion and pass through the jugular foramen to be distributed to the dura mater in the posterior cranial fossa.

Auricular branch

The auricular branch arises from the superior vagal ganglion and is joined by a branch from the inferior ganglion of the glossopharyngeal nerve. It passes behind the internal jugular vein and enters the mastoid canaliculus on the lateral wall of the jugular fossa. Traversing the temporal bone, it crosses the facial canal approximately 4 mm above the stylomastoid foramen and here supplies an ascending branch to the facial nerve. Fibres of the nervus intermedius may pass to the auricular branch at this point, which may explain the cutaneous vesiculation in the auricle that sometimes accompanies geniculate herpes. The auricular branch then traverses the tympanomastoid fissure, and divides into two rami. One ramus joins the posterior auricular nerve and the other is distributed to the skin of part of the ear and to the external acoustic meatus.

Pharyngeal branch

The pharyngeal branch of the vagus is the main motor nerve of the pharynx. It emerges from the upper part of the inferior vagal ganglion and consists chiefly of filaments from the cranial accessory nerve. It passes between the external and internal carotid arteries to the upper border of the middle pharyngeal constrictor, and divides into numerous filaments which join rami of the sympathetic trunk and glossopharyngeal nerve to form a pharyngeal plexus. A minute filament, the ramus lingualis vagi, joins the hypoglossal nerve as it curves round the occipital artery.

Branches to the carotid body

Branches to the carotid body are variable in number. They may arise from the inferior ganglion or travel in the pharyngeal branch, and sometimes in the superior laryngeal nerve. They form a plexus with the glossopharyngeal rami and branches of the cervical sympathetic trunk.

Superior laryngeal nerve

The superior laryngeal nerve is larger than the pharyngeal branch, and issues from the middle of the inferior vagal ganglion. It receives a branch from the superior cervical sympathetic ganglion and descends alongside the pharynx, at first posterior, then medial, to the internal carotid artery, and divides into the internal and external laryngeal nerves.

The internal laryngeal nerve is sensory to the laryngeal mucosa down to the level of the vocal folds. It also carries afferent fibres from the laryngeal neuromuscular spindles and other stretch receptors. It descends to the thyrohyoid membrane, pierces it above the superior laryngeal artery and divides into an upper and lower branch. The upper branch is horizontal and supplies the mucosa of the pharynx, the epiglottis, vallecula and laryngeal vestibule. The lower branch descends in the medial wall of the piriform recess, supplies the aryepiglottic fold, the mucosa on the back of the arytenoid cartilage and one or two branches to transverse arytenoid (the latter unite with twigs from the recurrent laryngeal to supply the same muscle). The internal laryngeal nerve ends by piercing the inferior pharyngeal constrictor to unite with an ascending branch from the recurrent laryngeal nerve. As it ascends in the neck it supplies branches, more numerous on the left, to the mucosa and tunica muscularis of the oesophagus and trachea and to the inferior constrictor.

The external laryngeal nerve, smaller than the internal, descends behind sternohyoid with the superior thyroid artery, but on a deeper plane. It lies first on the inferior pharyngeal constrictor, then pierces it to curve round the inferior thyroid tubercle and reach cricothyroid, which it supplies. The nerve also gives branches to the pharyngeal plexus and the inferior constrictor. Behind the common carotid artery, the external laryngeal nerve communicates with the superior cardiac nerve and superior cervical sympathetic ganglion.

Recurrent laryngeal nerve

The recurrent laryngeal nerve differs, in origin and course, on the two sides. On the right it arises from the vagus anterior to the first part of the subclavian artery, and curves backwards below and then behind it to ascend obliquely to the side of the trachea behind the common carotid artery. Near the lower pole of the lateral lobe of the thyroid gland it is closely related to the inferior thyroid artery, and crosses either in front of, behind, or between, its branches. On the left, the nerve arises from the vagus on the left of the aortic arch, curves below it immediately behind the attachment of the ligamentum arteriosum to the concavity of the aortic arch and ascends to the side of the trachea. As the recurrent laryngeal nerve curves round the subclavian artery, or the aortic arch, it gives cardiac filaments to the deep cardiac plexus. On both sides the recurrent laryngeal nerve ascends in or near a groove between the trachea and oesophagus. It is closely related to the medial surface of the thyroid gland before it passes under the lower border of the inferior constrictor, and it enters the larynx behind the articulation of the inferior thyroid cornu with the cricoid cartilage. The recurrent laryngeal nerve supplies all laryngeal muscles, except the cricothyroid, and it communicates with the internal laryngeal nerve, supplying sensory filaments to the laryngeal mucosa below the vocal folds. It also carries afferent fibres from laryngeal stretch receptors. The recurrent laryngeal nerve is described further with the larynx (p. 589).

Accessory nerve

The accessory nerve (Figs 28.7A, 28.11, 28.17) is conventionally described as a single entity, even though its two components, which join for a relatively short part of its course, are of quite separate origin.

Cranial root

The cranial root of the accessory nerve is smaller than the spinal root. It exits the skull through the jugular foramen, and unites for a short distance with the spinal root. It is also connected to the superior vagal ganglion. After traversing the foramen, the cranial root separates from the spinal part and immediately joins the vagus nerve superior to the inferior vagal ganglion. Those of its fibres that are distributed in the pharyngeal branches of the vagus are derived from the nucleus ambiguus, and probably innervate the pharyngeal and palatal muscles except tensor veli palatini. Other fibres enter the recurrent laryngeal nerve to supply the adductor muscles of the vocal cords, thyroarytenoid and lateral cricoarytenoid.

The status of the cranial root of the accessory nerve continues to excite debate. Cadaveric dissection studies have revealed wide variation in the patterns of anastomosis between the intracranial branches of the lower four cranial nerves (glossopharyngeal, vagus, accessory and hypoglossal) in the posterior cranial fossa: a separate cranial root of the accessory cannot always be demonstrated.

Spinal root

The spinal root arises from an elongated nucleus of motor cells situated in the lateral aspect of the ventral horn which extends from the junction of the spinal cord and medulla to the sixth cervical segment (Fig. 28.11). Some rootlets emerge directly, others turn cranially before exiting. Their line of exit is irregular rather than linear, and the spinal root usually passes through the first cervical dorsal root ganglion. The rootlets form a trunk which ascends between the ligamentum denticulatum and the dorsal roots of the spinal nerves and enters the skull via the foramen magnum, behind the vertebral artery. It then turns upwards and passes laterally to reach the jugular foramen, which it traverses in a common dural sheath with the vagus, but separated from that nerve by a fold of arachnoid mater. As the spinal root exits the jugular foramen it runs posterolaterally and passes either medial or lateral to the internal jugular vein. Occasionally it passes through the vein. The nerve then crosses the transverse process of the atlas and is itself crossed by the occipital artery. It descends obliquely, medial to the styloid process, stylohyoid and the posterior belly of the digastric. Running with the superior sternocleidomastoid branch of the occipital artery, it reaches the upper part of sternocleidomastoid and enters its deep surface, to form an anastomosis with fibres from C2 alone, C3 alone, or C2 and C3, the ansa of Maubrac. It may also communicate with the anterior root of the first cervical nerve (McKenzie branch).

The accessory nerve occasionally terminates in sternocleidomastoid. More commonly it emerges a little above the midpoint of the posterior border of sternocleidomastoid, generally above the emergence of the great auricular nerve (usually within 2 cm of it) and between 4–6 cm from the tip of the mastoid process. However, the point of emergence is very variable. The nerve then crosses the posterior triangle on levator scapulae (Fig. 28.7A), separated from it by the prevertebral layer of deep cervical fascia and adipose tissue. Here the nerve is relatively superficial and related to the superficial cervical lymph nodes. About 3–5 cm above the clavicle it passes behind the anterior border of trapezius, often dividing to form a plexus on its deep surface which receives contributions from C3 and C4, or C4 alone. It then enters the deep surface of the muscle.

The cervical course of the nerve follows a line from the lower anterior part of the tragus to the tip of the transverse process of the atlas and then across the sternocleidomastoid and the posterior triangle to a point on the anterior border of the trapezius 3–5 cm above the clavicle.

Conventionally, the spinal root is thought to provide the sole motor supply to sternocleidomastoid, and the second and third cervical nerves are believed to carry proprioceptive fibres from it. The supranuclear pathway of fibres destined for sternocleidomastoid is not simple: fibres may undergo a double decussation in the brainstem and/or there may be a bilateral projection to the muscle from each hemisphere. The motor supply to the upper and middle portions of trapezius is primarily from the spinal accessory nerve. However, the lower two-thirds of the muscle, in 75% of subjects, receives an innervation from the cervical plexus. On the basis of the incomplete denervation of the muscle that sometimes occurs following sacrifice of both the accessory nerve and the cervical plexus, it has been suggested that the trapezius receives a partial motor supply from other sources, possibly via thoracic roots. In addition to their motor contribution, C3 and 4 carry proprioceptive fibres from trapezius. In 25% of subjects the spinal accessory nerve receives no fibres from the cervical plexus. (For a detailed review of the applied surgical anatomy of the spinal accessory nerve plexus, see Brown 2002.)

Sensory ganglia have been described along the course of the spinal root.

Lesions affecting the accessory nerve

Lesions of the accessory nerve may occur centrally; at its exit from the skull; in the neck. The supranuclear fibres which influence motor neurones innervating sternocleidomastoid decussate twice, therefore a lesion of the pyramidal system above the pons produces weakness of the ipsilateral sternocleidomastoid and contralateral trapezius. Episodic contraction of sternocleidomastoid and trapezius, often accompanied by contraction of other muscle groups, e.g. splenius capitis, occurs in spasmodic torticollis, a focal dystonia. In jugular foramen syndrome, caused by pathologies including nasopharyngeal carcinoma or a glomus tumour, lesions of the glossopharyngeal, vagus and accessory nerves coexist. The accessory nerve can be injured more distally in the neck by trauma or by surgical exploration in the posterior triangle. If the accessory nerve is sacrificed as part of a radical neck dissection, and the innervation of trapezius is lost, the patient develops intractable neuralgia due to traction on the brachial plexus caused by the unsupported weight of the shoulder and arm.

Hypoglossal nerve

The hypoglossal nerve is motor to all the muscles of the tongue, except palatoglossus. The hypoglossal rootlets run laterally behind the vertebral artery, collected into two bundles which perforate the dura mater separately opposite the hypoglossal canal in the occipital bone, and unite after traversing it. The canal is sometimes divided by a spicule of bone. The nerve emerges from the canal in a plane medial to the internal jugular vein, internal carotid artery, ninth, tenth and eleventh cranial nerves, and passes inferolaterally behind the internal carotid artery and glossopharyngeal and vagus nerves to the interval between the artery and the internal jugular vein (Fig. 28.8). Here it makes a half-spiral turn round the inferior vagal ganglion, and is united with it by connective tissue. It then descends almost vertically between the vessels and anterior to the vagus to a point level with the angle of the mandible, becoming superficial below the posterior belly of digastric and emerging between the internal jugular vein and internal carotid artery. It loops round the inferior sternocleidomastoid branch of the occipital artery, crosses lateral to both internal and external carotid arteries and the loop of the lingual artery a little above the tip of the greater cornu of the hyoid, and is itself crossed by the facial vein (Figs 28.7A, 28.8, 28.17). Its course is described further on page 506.

Communications

The hypoglossal nerve communicates with the sympathetic trunk, vagus, first and second cervical nerves and lingual nerve. Near the atlas it is joined by branches from the superior cervical sympathetic ganglion and by a filament from the loop between the first and second cervical nerves which leaves the hypoglossal as the upper root of the ansa cervicalis. The vagal connections occur close to the skull, and numerous filaments pass between the hypoglossal nerve and the inferior vagal ganglion in the connective tissue uniting them. As the hypoglossal nerve curves round the occipital artery it receives the ramus lingualis vagi from the pharyngeal plexus. Near the anterior border of hyoglossus it is connected with the lingual nerve by many filaments which ascend on the muscle.

Branches of distribution

The branches of distribution of the hypoglossal nerve are meningeal, descending, thyrohyoid and muscular nerves.

Meningeal branches

Meningeal branches leave the nerve in the hypoglossal canal and return through it to supply the diploë of the occipital bone, the dural walls of the occipital and inferior petrosal sinuses and much of the floor of the anterior wall of the posterior cranial fossa, probably through pathways other than that of the hypoglossal nerve, e.g. upper cervical spinal nerves.

Descending branch

The descending branch (descendens hypoglossi) contains fibres from the first cervical spinal nerve. It leaves the hypoglossal nerve when it curves around the occipital artery, and runs down on the carotid sheath. It provides a branch to the superior belly of omohyoid before joining with the descendens cervicalis to form the ansa cervicalis (Figs 28.7A, 28.8).

Nerves to thyrohyoid and geniohyoid

The nerves to thyrohyoid and geniohyoid arise near the posterior border of hyoglossus. They represent the remaining fibres from the first cervical spinal nerves.

Lesions of the hypoglossal nerve

The hypoglossal nerve may be damaged during neck dissection. Complete hypoglossal division causes unilateral lingual paralysis and eventual hemiatrophy; the protruded tongue deviates to the paralysed side, and, on retraction, the wasted and paralysed side rises higher than the unaffected side. The larynx may deviate towards the active side in swallowing, due to unilateral paralysis of the hyoid depressors associated with loss of the first cervical spinal nerve which runs with the hypoglossal nerve. If paralysis is bilateral, the tongue is motionless. Taste and tactile sensibility are unaffected but articulation is slow and swallowing very difficult.

CERVICAL SYMPATHETIC TRUNK

The cervical sympathetic trunk lies on the prevertebral fascia behind the carotid sheath and contains three interconnected ganglia, the superior, middle and inferior (stellate or cervicothoracic) (Figs 28.17, 28.18). However there may occasionally be two or four ganglia. The cervical sympathetic ganglia send grey rami communicantes to all the cervical spinal nerves but receive no white rami communicantes from them. Their spinal preganglionic fibres emerge in the white rami communicantes of the upper five thoracic spinal nerves (mainly the upper three), and ascend in the sympathetic trunk to synapse in the cervical ganglia. In their course, the grey rami communicantes may pierce longus capitis or scalenus anterior.

Superior cervical ganglion

The superior cervical ganglion is the largest of the three ganglia (Fig. 28.17). It lies on the transverse processes of the second and third cervical vertebrae and is probably formed from four fused ganglia judging by its grey rami to C1–4. The internal carotid artery within the carotid sheath is anterior, and longus capitis is posterior. The lower end of the ganglion is united by a connecting trunk to the middle cervical ganglion. Postganglionic branches are distributed in the internal carotid nerve, which ascends with the internal carotid artery into the carotid canal to enter the cranial cavity, and in lateral, medial and anterior branches. They supply vasoconstrictor and sudomotor nerves to the face and neck, dilator pupillae and smooth muscle in the eyelids and orbitalis.

Lateral branches

The lateral branches are grey rami communicantes to the upper four cervical spinal nerves and to some of the cranial nerves. Branches pass to the inferior vagal ganglion, the hypoglossal nerve, the superior jugular bulb and associated jugular glomus or glomera, and to the meninges in the posterior cranial fossa. Another branch, the jugular nerve, ascends to the cranial base and divides into two; one part joins the inferior glossopharyngeal ganglion and the other joins the superior vagal ganglion.

Medial branches

The medial branches of the superior cervical ganglion are the laryngopharyngeal and cardiac. The laryngopharyngeal branches supply the carotid body and pass to the side of the pharynx, joining glossopharyngeal and vagal rami to form the pharyngeal plexus. A cardiac branch arises by two or more filaments from the lower part of the superior cervical ganglion and occasionally receives a twig from the trunk between the superior and middle cervical ganglia. It is thought to contain only efferent fibres, the preganglionic outflow being from the upper thoracic segments of the spinal cord, and to be devoid of pain fibres from the heart. It descends behind the common carotid artery, in front of longus colli, and crosses anterior to the inferior thyroid artery and recurrent laryngeal nerve. The courses on the two sides then differ. The right cardiac branch usually passes behind, but sometimes in front of, the subclavian artery and runs posterolateral to the brachiocephalic trunk to join the deep (dorsal) part of the cardiac plexus behind the aortic arch. It has other sympathetic connections. About midneck it receives filaments from the external laryngeal nerve. Inferiorly, one or two vagal cardiac branches join it. As it enters the thorax it is joined by a filament from the recurrent laryngeal nerve. Filaments from the nerve also communicate with the thyroid branches of the middle cervical ganglion. The left cardiac branch, in the thorax, is anterior to the left common carotid artery and crosses in front of the left side of the aortic arch to reach the superficial (ventral) part of the cardiac plexus. Sometimes it descends on the right of the aorta to end in the deep (dorsal) part of the cardiac plexus. It communicates with the cardiac branches of the middle and inferior cervical sympathetic ganglia and sometimes with the inferior cervical cardiac branches of the left vagus, and branches from these mixed nerves form a plexus on the ascending aorta.

Anterior branches

The anterior branches of the superior cervical ganglion ramify on the common and external carotid arteries and the branches of the external carotid, and form a delicate plexus around each in which small ganglia are occasionally found. The plexus around the facial artery supplies a filament to the submandibular ganglion; the plexus on the middle meningeal artery sends one ramus to the otic ganglion and another, the external petrosal nerve, to the facial ganglion. Many of the fibres coursing along the external carotid and its branches ultimately leave them to travel to facial sweat glands via branches of the trigeminal nerve.

Middle cervical ganglion

The middle cervical ganglion is the smallest of the three, and is occasionally absent, in which case it may be replaced by minute ganglia in the sympathetic trunk or may be fused with the superior ganglion. It is usually found at the level of the sixth cervical vertebra, anterior or just superior to the inferior thyroid artery, or it may adjoin the inferior cervical ganglion. It probably represents a coalescence of the ganglia of the fifth and sixth cervical segments, judging by its postganglionic rami, which join the fifth and sixth cervical spinal nerves (but sometimes also the fourth and seventh). It is connected to the inferior cervical ganglion by two or more very variable cords. The posterior cord usually splits to enclose the vertebral artery, while the anterior cord loops down anterior to, and then below, the first part of the subclavian artery, medial to the origin of its internal thoracic branch, and supplies rami to it. This loop is the ansa subclavia and is frequently multiple, lies closely in contact with the cervical pleura and typically connects with the phrenic nerve, and sometimes with the vagus (Fig. 28.18).

The middle cervical ganglion gives off thyroid and cardiac branches. The thyroid branches accompany the inferior thyroid artery to the thyroid gland. They communicate with the superior cardiac, external laryngeal and recurrent laryngeal nerves, and send branches to the parathyroid glands. Fibres to both glands are largely vasomotor but some reach the secretory cells. The cardiac branch, the largest sympathetic cardiac nerve, either arises from the ganglion itself or more often from the sympathetic trunk cranial or caudal to it. On the right side it descends behind the common carotid artery, in front of or behind the subclavian artery, to the trachea where it receives a few filaments from the recurrent laryngeal nerve before joining the right half of the deep (dorsal) part of the cardiac plexus. In the neck, it connects with the superior cardiac and recurrent laryngeal nerves. On the left side the cardiac nerve enters the thorax between the left common carotid and subclavian arteries to join the left half of the deep (dorsal) part of the cardiac plexus. Fine branches from the middle cervical ganglion also pass to the trachea and oesophagus.

Inferior (or cervicothoracic/stellate) ganglion

The inferior cervical ganglion (cervicothoracic/stellate) is irregular in shape and much larger than the middle cervical ganglion (Fig. 28.18). It is probably formed by a fusion of the lower two cervical and first thoracic segmental ganglia, sometimes including the second and even third and fourth thoracic ganglia. The first thoracic ganglion may be separate, leaving an inferior cervical ganglion above it. The sympathetic trunk turns backwards at the junction of the neck and thorax and so the long axis of the cervicothoracic ganglion becomes almost anteroposterior. The ganglion lies on or just lateral to the lateral border of longus colli between the base of the seventh cervical transverse process and the neck of the first rib (which are both posterior to it). The vertebral vessels are anterior, and the ganglion is separated from the posterior aspect of the cervical pleura inferiorly by the suprapleural membrane. The costocervical trunk of the subclavian artery branches near the lower pole of the ganglion, and the superior intercostal artery is lateral.

A small vertebral ganglion may be present on the sympathetic trunk anterior or anteromedial to the origin of the vertebral artery and directly above the subclavian artery. When present, it may provide the ansa subclavia and is also joined to the inferior cervical ganglion by fibres enclosing the vertebral artery. It is usually regarded as a detached part of the middle cervical or inferior cervical ganglion. Like the middle cervical ganglion it may supply grey rami communicantes to the fourth and fifth cervical spinal nerves. The inferior cervical ganglion sends grey rami communicantes to the seventh and eighth cervical and first thoracic spinal nerves, and gives off a cardiac branch, branches to nearby vessels and sometimes a branch to the vagus nerve.

The grey rami communicantes to the seventh cervical spinal nerve vary from one to five (two being the usual number). A third often ascends medial to the vertebral artery in front of the seventh cervical transverse process. It connects with the seventh cervical nerve, and sends a filament upwards through the sixth cervical transverse foramen in company with the vertebral vessels to join the sixth cervical spinal nerve as it emerges from the intervertebral foramen. An inconstant ramus may traverse the seventh cervical transverse foramen. Grey rami to the eighth cervical spinal nerve vary from three to six in number.

The cardiac branch descends behind the subclavian artery and along the front of the trachea to the deep cardiac plexus. Behind the artery it connects with the recurrent laryngeal nerve and the cardiac branch of the middle cervical ganglion (the latter is often replaced by fine branches of the inferior cervical ganglion and ansa subclavia).

The branches to blood vessels form plexuses on the subclavian artery and its branches. The subclavian supply is derived from the inferior cervical ganglion and ansa subclavia, and typically extends to the first part of the axillary artery, although a few fibres may extend further. An extension of the subclavian plexus to the internal thoracic artery may be joined by a branch of the phrenic nerve.

Within the foramina transversaria and intertransverse spaces, the cervical grey rami communicantes form intersegmental arcades as they communicate with one another and the ventral rami of the upper five or six cervical spinal nerves. These arcades accompany the second part of the vertebral artery and create the appearance of a long nerve known as the vertebral nerve. Fine filaments from this nerve and the grey rami communicantes form the vertebral plexus on the surface of the vertebral artery. This plexus contains not only sympathetic efferent fibres but also somatic sensory fibres from the adventitia of the artery, whose cell bodies are located in the cervical dorsal root ganglia. The vertebral nerve sends filaments to the posterolateral corners of the cervical intervertebral discs (Bogduk et al 1988), and gives rise to the meningeal branches (sinuvertebral nerves) at each cervical segment. The vertebral plexus, which contains some neuronal cell bodies, continues into the skull along the vertebral and basilar arteries and their branches as far as the posterior cerebral artery, where it meets a plexus from the internal carotid artery. The plexus on the inferior thyroid artery reaches the thyroid gland, and connects with the recurrent and external laryngeal nerves, the cardiac branch of the superior cervical ganglion, and the common carotid plexus.

Horner’s syndrome

Any condition or injury that destroys the sympathetic trunk ascending from the thorax through the neck into the face results in Horner’s syndrome, characterized by a drooping eyelid (ptosis), sunken globe (enophthalmos), narrow palpebral fissure, contracted pupil (meiosis), vasodilatation and lack of thermal sweating (anhydrosis) on the affected side. This occurs classically when a bronchial carcinoma invades the sympathetic trunk. It also occurs as a complication of cervical sympathectomy or a radical neck dissection. Avulsion of the first thoracic nerve from the spinal cord may be diagnosed by development of the syndrome after closed traction lesion of the supraclavicular brachial plexus.

VISCERA

The main cervical viscera are the submandibular salivary glands, the thyroid and parathyroid glands and the cervical portions of the trachea and oesophagus.

SUBMANDIBULAR SALIVARY GLAND

Each submandibular salivary gland is situated behind and below the ramus of the mandible, in the region of the submandibular triangle, between the anterior and posterior bellies of digastric (Fig. 28.7A). The gland is described in detail on page 520.

THYROID GLAND

The thyroid gland, brownish-red and highly vascular, is placed anteriorly in the lower neck, level with the fifth cervical to the first thoracic vertebrae (Figs 28.4, 28.17). It is ensheathed by the pretracheal layer of deep cervical fascia and consists of right and left lobes connected by a narrow, median isthmus. It usually weighs 25 g, but this varies. The gland is slightly heavier in females, and enlarges during menstruation and pregnancy. Estimation of the size of the thyroid gland is clinically important in the evaluation and management of thyroid disorders and can be achieved non-invasively by means of diagnostic ultrasound. No significant difference in thyroid gland volume has been observed between males and females from 8 months to 15 years.

The lobes of the thyroid gland are approximately conical. Their ascending apices diverge laterally to the level of the oblique lines on the laminae of the thyroid cartilage, and their bases are level with the fourth or fifth tracheal cartilages. Each lobe is usually 5 cm long, its greatest transverse and anteroposterior extents being 3 cm and 2 cm respectively. The posteromedial aspects of the lobes are attached to the side of the cricoid cartilage by a lateral thyroid ligament.

The isthmus connects the lower parts of the two lobes, although occasionally it may be absent. It measures 1.25 cm transversely and vertically, and is usually anterior to the second and third tracheal cartilages, though often higher or sometimes lower because its site and size vary greatly.

A conical pyramidal lobe often ascends towards the hyoid bone from the isthmus or the adjacent part of either lobe (more often the left). It is occasionally detached or in two or more parts. A fibrous or fibromuscular band, the levator of the thyroid gland, musculus levator glandulae thyroideae, sometimes descends from the body of the hyoid to the isthmus or pyramidal lobe. Small detached masses of thyroid tissue may occur above the lobes or isthmus as accessory thyroid glands. Vestiges of the thyroglossal duct may persist between the isthmus and the foramen caecum of the tongue, sometimes as accessory nodules or cysts of thyroid tissue near the midline or even in the tongue.

Surfaces and relations

The convex lateral (superficial) surface is covered by sternothyroid, whose attachment to the oblique thyroid line prevents the upper pole of the gland from extending on to thyrohyoid. More anteriorly lie sternohyoid and the superior belly of omohyoid, overlapped inferiorly by the anterior border of sternocleidomastoid. The medial surface of the gland is adapted to the larynx and trachea; its superior pole contacts the inferior pharyngeal constrictor and the posterior part of cricothyroid, which separate it from the posterior part of the thyroid lamina and the side of the cricoid cartilage. The external laryngeal nerve is medial to this part of the gland as it passes to supply cricothyroid. Inferiorly, the trachea and, more posteriorly, the recurrent laryngeal nerve and oesophagus (which is closer on the left), are medial relations. The posterolateral surface of the thyroid gland is close to the carotid sheath, and overlaps the common carotid artery.

The anterior border of the gland is thin, and near the anterior branch of the superior thyroid artery it slants down medially. The posterior border is rounded and related inferiorly to the inferior thyroid artery and its anastomosis with the posterior branch of the superior thyroid artery. On the left side, the lower end of the posterior border lies near the thoracic duct. The parathyroid glands are usually related to the posterior border.

The isthmus is covered by sternothyoid, from which it is separated by pretracheal fascia. More superficially it is covered by sternohyoid, the anterior jugular veins, fascia and skin. The superior thyroid arteries anastomose along its upper border and the inferior thyroid veins leave the gland at its lower border.

Vascular supply and lymphatic drainage

Arteries

The thyroid gland is supplied by the superior and inferior thyroid arteries and sometimes by an arteria thyroidea ima from the brachiocephalic trunk or aortic arch (Figs 28.14, 28.17). The arteries are large and their branches anastomose frequently both on and in the gland, ipsilaterally and contralaterally. The superior thyroid artery, which is closely related to the external laryngeal nerve, pierces the thyroid fascia and then divides into anterior and posterior branches. The anterior branch supplies the anterior surface of the gland, and the posterior branch supplies the lateral and medial surfaces. The inferior thyroid artery approaches the base of the thyroid gland and divides into superior (ascending) and inferior thyroid branches to supply the inferior and posterior surfaces of the gland. The superior branch also supplies the parathyroid glands. The relationship between the inferior thyroid artery and the recurrent laryngeal nerve is highly variable and of considerable clinical importance: iatrogenic injury to the nerves that supply the larynx represents a major complication of thyroid surgery (Yalcxin 2006). The recurrent laryngeal nerve is usually related to the posterior branch of the inferior thyroid artery, which may be replaced by a vascular network (Moreau et al 1998).

Veins

The venous drainage of the thyroid gland is usually via superior, middle, and inferior thyroid veins (Figs 28.13, 28.14). The superior thyroid vein emerges from the upper part of the gland and runs with the superior thyroid artery towards the carotid sheath: it drains into the internal jugular vein. The middle thyroid vein collects blood from the lower part of the gland: it emerges from the lateral surface of the gland and drains into the internal jugular vein. The inferior thyroid veins arise in a glandular venous plexus, which also connects with the middle and superior thyroid veins. These veins form a pretracheal plexus, from which the left inferior vein descends to join the left brachiocephalic vein and the right descends obliquely across the brachiocephalic artery to join the right brachiocephalic vein at its junction with the superior vena cava. The inferior thyroid veins often open via a common trunk into the superior vena cava or left brachiocephalic vein. They drain the oesophageal, tracheal and inferior laryngeal veins and have valves at their terminations.

Lymphatics

Thyroid lymphatic vessels communicate with the tracheal plexus, and pass to the prelaryngeal nodes just above the thyroid isthmus and to the pretracheal and paratracheal nodes; some may also drain into the brachiocephalic nodes related to the thymus in the superior mediastinum. Laterally the gland is drained by vessels lying along the superior thyroid veins to the deep cervical nodes. Thyroid lymphatics may drain directly, with no intervening node, to the thoracic duct.

Innervation

The thyroid gland receives its innervation from the superior, middle and inferior cervical sympathetic ganglia. Postganglionic fibres from the inferior cervical ganglion form a plexus on the inferior thyroid artery which accompanies the artery to the thyroid gland, and communicates with the recurrent and external laryngeal nerves, with the superior cardiac nerve, and with the plexus on the common carotid artery.

Imaging

The follicular nature of the thyroid gland is not resolved by current imaging techniques and thus presents a homogeneous texture on cross-sectional imaging (US, CT, MRI). Its superficial location makes the thyroid an ideal organ for sonographic examination (Fig. 28.20). The thyroid gland is highly vascular and demonstrates intense contrast enhancement and increased signal on T_2-weighted MRI (Fig. 28.21). Radionuclide imaging of the thyroid may be performed with technetium (Tc^{99m}) pertechnetate. This readily available radionuclide is trapped by the thyroid in the same way as iodine, but is not organified. It yields morphological information and will reveal the presence of ectopic thyroid tissue. Functional data can be obtained with the use of ^{131}iodine which is trapped and organified.

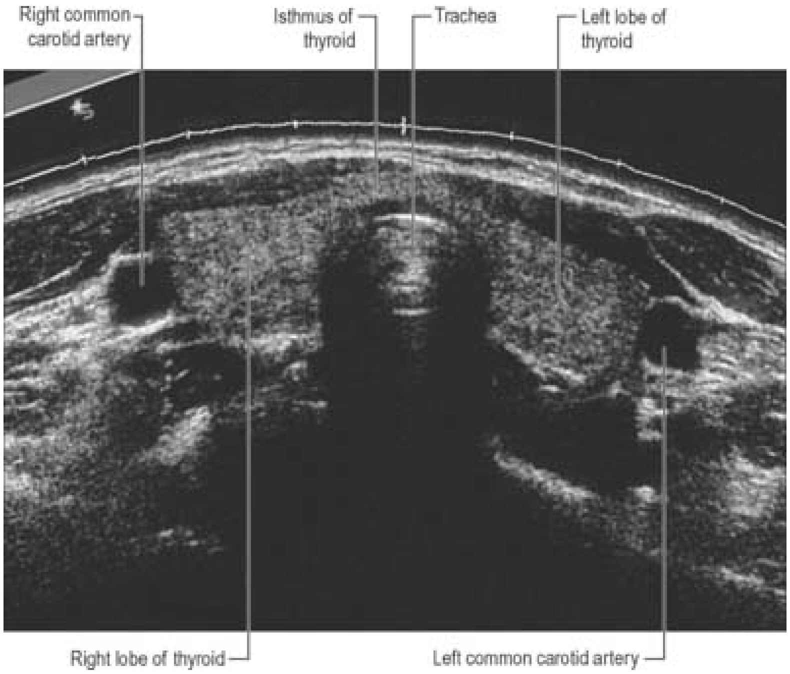
Right common carotid artery
Isthmus of thyroid
Trachea
Left lobe of thyroid
Right lobe of thyroid
Left common carotid artery

Fig. 28.20 Thyroid sonogram.

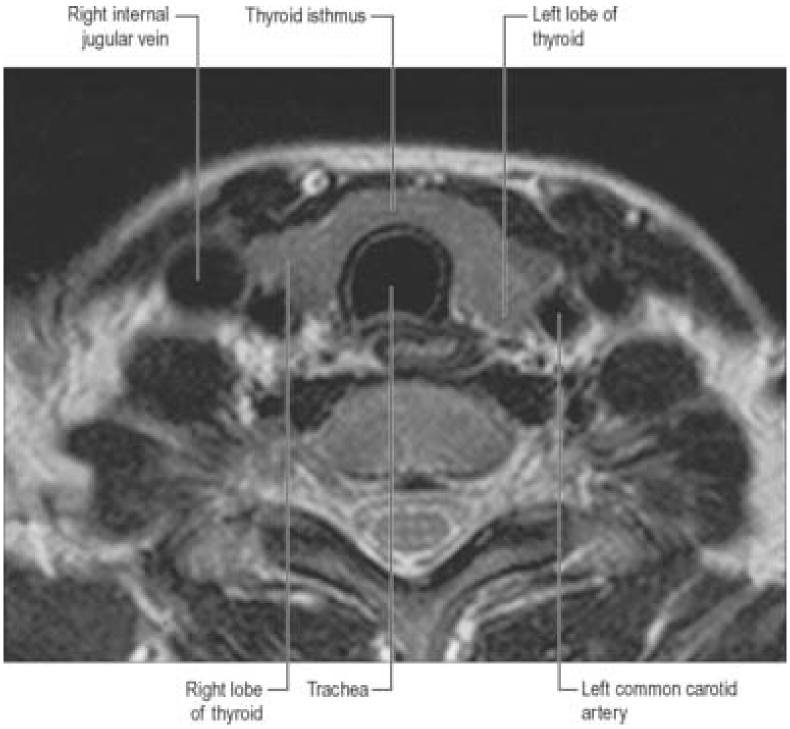
Right internal jugular vein
Thyroid isthmus
Left lobe of thyroid
Right lobe of thyroid
Trachea
Left common carotid artery

Fig. 28.21 T_2-weighted MRI at the level of the thyroid isthmus: compare with **Fig. 28.20**.

Microstructure

The thyroid gland has a thin capsule of connective tissue, which extends into the glandular parenchyma and divides each lobe into irregularly shaped and sized lobules. The functional units of the thyroid are follicles, which are spherical and cyst-like, between 0.02 and 0.9 mm in diameter. Follicles consist of a central colloid core surrounded by a single-layered epithelium resting on a basal lamina (Fig. 28.22). Colloid consists almost entirely of an iodinated glycoprotein, iodothyroglobulin, which is the inactive, stored form of the active thyroid hormones, tri-iodothyronine (T_3) and tetraiodothyronine or thyroxine (T_4), and is produced by the follicular epithelial cells. Sufficient iodothyroglobulin is stored extracellularly within follicles to regulate the metabolic activity of the body for up to three months. Follicles are surrounded by a delicate connective tissue stroma, containing dense plexuses of fenestrated capillaries, extensive lymphatic networks and sympathetic nerve fibres which supply the arterioles and capillaries. Some nerve fibres end close to the follicular epithelial cells.

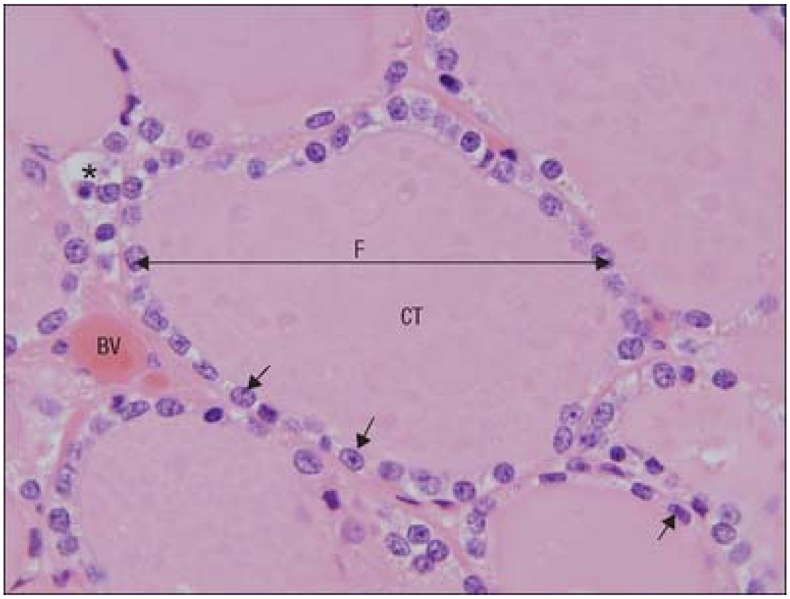

Fig. 28.22 A section through parts of several human thyroid follicles, one of which is labelled (F), showing the follicular epithelium (arrows) enclosing a lumen filled with colloidal thyroglobulin (CT). Calcitonin-secreting C cells are not readily identifiable in routine preparations of

human tissue, where they appear as poorly-staining (clear) cells within follicles; an example is indicated by the asterisk. A network of blood vessels (BV) within connective tissue septa surrounds the follicles.

(By courtesy of Mr Peter Helliwell and Dr Joseph Mathew, Department of Histopathology, Royal Cornwall Hospitals Trust, UK.)

Follicular cells

Follicular cells vary from squamous or low cuboidal to columnar, depending on their level of activity, which is controlled mainly by circulating hypophysial thyroid-stimulating hormone (TSH, thyrotropin). Resting follicles are large and lined by squamous or low cuboidal epithelium with abundant luminal colloid. Apical microvilli are short in resting cells, but elongate and often branch on stimulation by TSH. Follicles showing differing levels of activity may co-exist.

Active follicular cells are highly polarized functionally. The secretion of TSH leads to endocytosis of colloidal droplets at the luminal epithelium (Fig. 28.22). The hormone provokes the cells to extend cytoplasmic processes into the luminal colloid and sequester droplets of colloid. The iodinated thyroglobulin in the intracellular colloid droplets is then degraded by follicular cell lysosomes, liberating T_3 and T_4 which pass to the base of the cell, where they are released. They are exported from the thyroid mainly via the blood capillaries and lymphatics. Prolonged high levels of circulating TSH induce follicular cell hypertrophy, progressive resorption of colloid and increased stromal vascularity.

C cells

Thyroid parenchyma also contains C (clear) cells, so-called because they have pale-staining cytoplasm, which is more pronounced in some species than in the human thyroid. C cells are members of the amine precursor uptake and decarboxylation (APUD) system of dispersed neuroendocrine cells. They produce the peptide hormone calcitonin (thyrocalcitonin) which lowers blood calcium by inhibiting bone resorption and calcium recovery from renal tubule ultrafiltrate. C cells populate the middle third of each lateral lobe of the thyroid and are typically found scattered within thyroid follicles, lying inside the basal lamina but not reaching the follicle lumen. Occasionally they occur in clusters in the interfollicular stroma, which is why they are also called parafollicular cells.

Thyroidectomy

Apart from variable enlargement during menstruation and pregnancy, any thyroid swelling is a goitre, which may press on related structures. Symptoms most commonly are the consequence of pressure on the trachea or on the recurrent laryngeal nerves, and there may also be venous engorgement. During thyroidectomy, care must be taken when tying off the superior and inferior thyroid arteries to avoid damage to adjacent nerves. The external laryngeal nerve runs close to the superior thyroid artery and the recurrent laryngeal nerve runs close to the inferior thyroid artery. Partial thyroidectomy is often necessary in the treatment of hyperthyroidism and thyroid enlargement: the posterior parts of both lobes are left intact to preserve the parathyroid glands.

PARATHYROID GLANDS

The parathyroid glands are small, yellowish-brown, ovoid or lentiform structures, usually lying between the posterior lobar borders of the thyroid gland and its capsule. They are commonly 6 mm long, 3–4 mm across, and 1–2 mm from back to front, each weighing about 50 mg. Typically there are two on each side, superior and inferior, but there may be more or there may be only three or many minute parathyroid islands scattered in connective tissue near the usual sites. Very occasionally an occult gland may follow a blood vessel into a groove on the surface of the thyroid. Normally the inferior parathyroids migrate only to the inferior thyroid poles, but they may descend with the thymus into the thorax or they may be sessile and remain above their normal level near the carotid bifurcation. The anastomotic connection between the superior and inferior thyroid arteries that occurs along the posterior border of the thyroid gland usually passes very close to the parathyroids, and is a useful aid to their identification.

The superior parathyroid glands are more constant in location than the inferior and are usually to be found midway along the posterior borders of the thyroid gland, although they may be higher. The inferior pair are more variably situated (related to their embryological development) and may be within the fascial thyroid sheath, below the inferior thyroid arteries and near the inferior lobar poles; or outside the sheath, immediately above an inferior thyroid artery; or in the thyroid gland near its inferior pole. These variations are surgically important (Fig. 28.23). A tumour of the inferior parathyroid situated within the fascial thyroid sheath may descend along the inferior thyroid veins anterior to the trachea into the superior mediastinum, whereas if it is outside the sheath it may extend posteroinferiorly behind the oesophagus into the posterior mediastinum. The superior parathyroids are usually dorsal, and the inferior parathyroids ventral, to the recurrent laryngeal nerves.

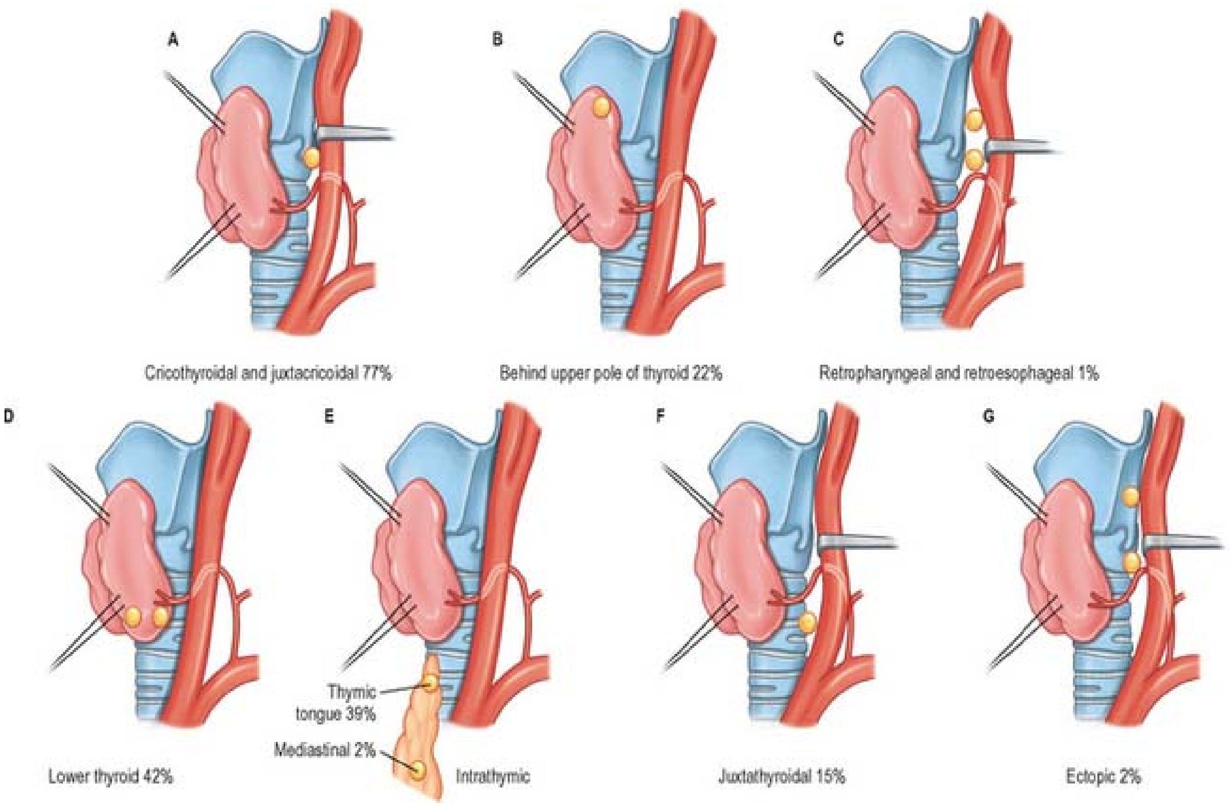
A
Cricothyroidal and juxtacricoidal 77%
B
Behind upper pole of thyroid 22%
C
Retropharyngeal and retroesophageal 1%
D
Lower thyroid 42%
E
Thymic tongue 39%
Mediastinal 2%
Intrathymic
F
Juxtathyroidal 15%
G
Ectopic 2%

Fig. 28.23 Distribution of superior (**A–C**) and inferior (**D–G**) parathyroid glands. **A**, Cricothyroidal and juxtathyroidal; **B**, Behind upper pole of thyroid; **C**, Retropharyngeal and retroesophageal; **D**, Lower thyroid; **E**, Intrathymic; **F**, Juxtathyroidal; **G**, Ectopic.

The parathyroid glands are very flattened in cross-section and are not normally visible by current imaging methods, including scintigraphy.

Vascular supply and lymphatic drainage

Both superior and inferior parathyroid glands are usually supplied by the inferior thyroid arteries; the superior thyroid may be supplied by the superior thyroid artery or from anastomoses between the superior and inferior thyroid arteries in 10–15% cases. The glands drain into the plexus of veins on the anterior surface of the thyroid. Lymph vessels are numerous and associated with those of the thyroid and thymus glands.

Innervation

The nerve supply is sympathetic, either direct from the superior or middle cervical ganglia or via a plexus in the fascia on the posterior lobar aspects. Parathyroid activity is controlled by variations in blood calcium level: it is inhibited by a rise and stimulated by a fall. The nerves are believed to be vasomotor but not secretomotor.

Microstructure

Each parathyroid gland has a thin connective tissue capsule with intraglandular septa but lacks distinct lobules. The parathyroids synthesize and secrete parathyroid hormone (PTH, parathormone), a single-chain polypeptide of 84 amino-acid residues concerned with the control of the level and distribution of calcium and phosphorus. In childhood, the gland consists of wide, irregular, interconnecting columns of chief or principal cells separated by a dense plexus of fenestrated sinusoidal capillaries. After puberty, adipose tissue accumulates in the stroma and typically accounts for about one third of the adult tissue mass, increasing further with age.

Chief cells differ ultrastructurally according to their level of activity: active chief cells have large Golgi complexes with numerous vesicles and small membrane-bound granules. Glycogen granules are most abundant in inactive cells, which have few of the cytoplasmic features of synthetic or secretory activity, and appear histologically as ‘clear’ cells. In normal human parathyroid glands, inactive chief cells outnumber active cells in a ratio of 3–5 : 1 (Fig. 28.24). In contrast to the thyroid, where the activities of adjacent follicular cells are coordinated, individual chief cells of the parathyroid glands go through cycles of secretory activity and rest independently, according to serum calcium levels.

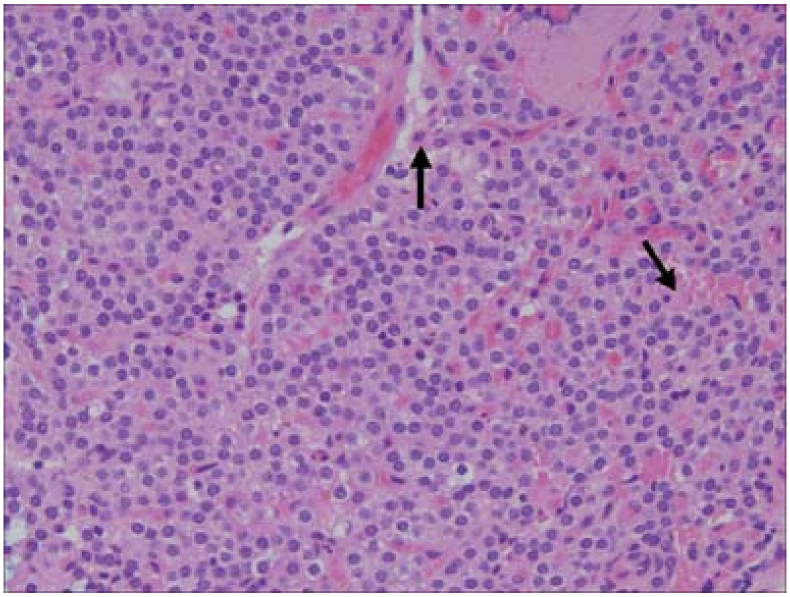

Fig. 28.24 Parathyroid gland, showing clusters and cords of small, tightly packed chief cells surrounded by vascular sinusoids. Scattered oxyphil cells (arrowed) are generally larger and more eosinophilic.

(By courtesy of Mr Peter Helliwell and Dr Joseph Mathew, Department of Histopathology, Royal Cornwall Hospitals Trust, UK.)

A second cell type, the oxyphil (eosinophil) cell, appears just before puberty and increases in number with age. Oxyphil cells are larger than chief cells and contain more cytoplasm, which stains deeply with eosin. Their nuclei are smaller and more darkly staining than those of chief cells, and their cytoplasm is unusually rich in mitochondria. The functional significance of oxyphil cells and their relationship to chief cells are uncertain.

ROOT OF THE NECK

The root of the neck is a zone of transition between four discrete anatomical spaces: the neck, the thorax and both upper limbs (Fig. 28.18). It contains the subclavian vessels; common carotid artery; trunks of the brachial plexus; sympathetic trunk; phrenic, vagus and recurrent laryngeal nerves (all bilaterally); the terminal portion of the thoracic duct (on the left side only); the terminal portion of the right lymphatic duct (on the right side only); and the oesophagus and trachea (in the midline). The brachiocephalic veins are formed by the union of the internal jugular and subclavian veins at the junction of the neck and thorax, behind the head of the clavicle.

The essential anatomical landmark in orienting and understanding the root of the neck is scalenus anterior, covered by the prevertebral layer of deep cervical fascia. Anteriorly lie sternocleidomastoid and subclavius, the intermediate tendon of omohyoid, the subclavian vein, branches from the thyrocervical trunk of the first part of the subclavian artery (transverse cervical, suprascapular and ascending cervical arteries), and the phrenic nerve. The nerve lies on the surface of scalenus anterior in the root of the neck, before passing between it and the subclavian vein to enter the superior mediastinum, and is the anatomical key to identifying the muscle intra-operatively. Posteriorly, the roots of the brachial plexus and the second part of the subclavian artery separate scalenus anterior from scalenus medius. Pathologies that cause impingement upon either brachial plexus or subclavian artery may present clinically as an upper limb compression syndrome. The suprapleural membrane and pleura are intimate posterior relations of scalenus anterior. On each side, the apical (cervical) pleura and the apex of the lung bulge up into the root of the neck. The height to which the apical pleura rises – with reference to the first pair of ribs and costal cartilages – varies in different individuals according to the obliquity of the thoracic inlet. Posteriorly, the apical pleura typically reaches the level of the neck of the first rib; it forms a domed roof over each side of the thoracic cavity that is strengthened by the suprapleural membrane. Scalenus anterior covers the anterolateral part of the dome of the pleura, and separates it from the subclavian vein. The subclavian artery crosses the dome below its summit, immediately above the vein. The costocervical trunk arches backwards from the subclavian artery and crosses the summit of the dome: its superior intercostal branch descends behind the dome, between the first intercostal nerve laterally and the first thoracic sympathetic ganglion medially.

Medial relations of scalenus anterior are longus colli and the inferior thyroid artery. The two muscles are separated by an angular interval through which the vertebral artery and vein pass to gain access to the foramen transversarium of the sixth cervical vertebra, and more anteriorly the inferior thyroid artery arches from lateral to medial on its way to the thyroid gland. The cervical sympathetic chain and the inferior cervical ganglion lie close to the posteromedial aspect of the vertebral artery here. The internal thoracic artery descends from the first part of the subclavian artery: it passes behind the brachiocephalic vein and, on the right side, is crossed by the phrenic nerve. The vagus descends anterior to the first part of the subclavian artery; on the right side only its recurrent laryngeal branch usually turns around the lower border of the artery. The terminal portions of the thoracic duct and the right lymphatic duct, on the left and right sides respectively, cross the triangular interval at the level of the seventh cervical vertebra, coming into contact with the medial edge of scalenus anterior.

The axillary sheath, an extension of the prevertebral fascia that accompanies the axillary artery and trunks of the brachial plexus, lies lateral to scalenus anterior.

Cervical rib

A small extra rib (cervical rib) may develop in the root of the neck in association with the seventh cervical vertebra. It is often fibrous in nature, although in some cases it may have undergone ossification. A cervical rib may cause compression of the subclavian artery and the lower roots of the brachial plexus. Should this occur, affected individuals will complain of pain, paraesthesia and even pallor of the affected upper limb, a condition known as thoracic outlet syndrome.

OESOPHAGUS – CERVICAL PORTION

The oesophagus is a muscular tube approximately 25 cm long, connecting the pharynx to the stomach. It begins in the neck, level with the lower border of the cricoid cartilage and the sixth cervical vertebra. It descends, largely anterior to the vertebral column, into the superior mediastinum. Generally vertical and median, it inclines to the left as far as the root of the neck, and also bends in an anteroposterior plane to follow the cervical curvature of the vertebral column.

Relations

The trachea lies anterior to the oesophagus, attached to it by loose connective tissue. The vertebral column, longus colli and prevertebral layer of deep cervical fascia are posterior, and the common carotid artery and posterior part of the thyroid gland are lateral on each side. In the lower neck, where the oesophagus deviates to the left, it becomes closer to the left carotid sheath and thyroid gland than it is on the right. The thoracic duct ascends for a short distance along its left side. The recurrent laryngeal nerves ascend on each side in or near the groove between the trachea and the oesophagus.

Vascular supply and lymphatic drainage

The cervical part of the oesophagus is mainly supplied by branches from the inferior thyroid arteries. The oesophageal veins drain into the brachiocephalic veins, and lymphatic vessels pass to retropharyngeal, paratracheal, or deep cervical lymph nodes.

Innervation

The cervical part of the oesophagus is innervated by the recurrent laryngeal nerves and by the sympathetic plexus around the inferior thyroid artery.

TRACHEA – CERVICAL PORTION

The trachea is a tube 10–11 cm long, formed of cartilage and fibromuscular membrane. It descends from the larynx, and extends from the level of the sixth cervical vertebra to the upper border of the fifth thoracic vertebra (Figs 28.14, 28.17). It lies approximately in the sagittal plane but its point of bifurcation is usually a little to the right. The trachea is flexible and can rapidly alter in length. It is flattened posteriorly so that in transverse section it is shaped, with some individual variation, like a letter D. Its external transverse diameter is 2 cm in adult males, and 1.5 cm in adult females. The lumen in live adults is 1.2 cm in transverse diameter. In children the trachea is smaller, more deeply placed and more mobile. Tracheal diameter does not exceed 3 mm in the first postnatal year: during later childhood its diameter in millimetres is about equal to age in years.

Relations

The relationships of the trachea to other cervical structures is of clinical significance: tracheostomy is not an uncommon clinical procedure (see below). Anteriorly the cervical part of the trachea is crossed by skin and by the superficial and deep fasciae. It is also crossed by the jugular arch and overlapped by sternohyoid and sternothyroid. The second to fourth tracheal cartilages are crossed by the isthmus of the thyroid gland, above which an anastomotic artery connects the bilateral superior thyroid arteries. Below and in front are the pretracheal fascia, inferior thyroid veins, thymic remnants and the arteria thyroidea ima (when it exists). In children the brachiocephalic artery crosses obliquely in front of the trachea at or a little above the upper border of the manubrium. The left brachiocephalic vein may also rise a little above this level. The oesophagus lies posterior to the trachea, and separates it from the vertebral column. The paired lobes of the thyroid gland, which descend to the fifth or sixth tracheal cartilage, and the common carotid and inferior thyroid arteries, all lie lateral to the trachea. The recurrent laryngeal nerves ascend on each side, in or near the grooves between the sides of the trachea and oesophagus.

Vascular supply and lymphatic drainage

The cervical part of the trachea is mainly supplied by branches from the inferior thyroid arteries. The tracheal veins drain into the bracheocephalic veins via the inferior thyroid plexus, and lymphatic vessels drain into the pretracheal and paratracheal nodes.

Innervation

The trachea is innervated by branches from the vagi, recurrent laryngeal nerves and sympathetic trunks.

Surgical airway

The trachea may be accessed directly in the neck via cricothyroidotomy or tracheostomy. There are numerous indications for performing an elective tracheostomy. They include: the need to provide prolonged intubation, manage acute airway obstruction from supraglottic or glottic pathology or trauma (for example, midface, mandibular or laryngeal fractures).

For detailed descriptions of the operative procedures, appropriate surgical texts should be consulted. However, it is worth emphasizing here the importance of understanding the relevant regional anatomy. In creating a surgical airway, potential hazards can be avoided by dissecting in the midline. Dissections that stray laterally, which are a real risk in pediatric patients or in those who are obese, can result in pneumothorax, pneumomediastinum and damage to paratracheal structures (the carotid sheath and its contents, and the recurrent laryngeal nerves and inferior thyroid veins lying in the tracheo-oesophageal groove). In the midline, the isthmus of the thyroid gland, which overlies the 2nd and 3rd tracheal rings, must be divided. Careful haemostasis of the divided stumps, and secure transfixion of the thyroidea ima artery and inferior thyroid vein, minimize the risk of catastrophic post-operative bleeding. A high bifurcation of the brachiocephalic trunk, or aberrant anterior jugular veins (which usually lie between the midline and anterior border of sternocleidomastoid), are additional anatomical complications.

Cricothyroidotomy endangers the cricothyroid artery (a branch of the superior thyroid artery), which is usually found close to the midline, and which reaches the median cricothyroid ligament close to the thyroid cartilage.

REFERENCES

rkovitz BKB, Kirsch C, Moxham BJ, Alusi G, Cheeseman T. Interactive Head and Neck. London: Primal Pictures, 2002.

gduk N, Windsor M, Inglis A. The innervation of the cervical intervertebral discs. *Spine*. 1988;13:2-8.

own H. Anatomy of the spinal accessory nerve plexus: relevance to head and neck cancer and atherosclerosis. *Exp Biol Med*. 2002;227:570-578.

dy B, Rossi RL. Surgery of the Thyroid and Parathyroid Glands. Philadelphia: Saunders, 1991.

ile G. Excision of cancer of the head and neck with special reference to the plan of dissection based on one hundred and thirty two operations. *J Am Med Assoc*. 1906;47:1780-1786.

Seminal paper which considers the surgical anatomy of radical neck dissection..

oes LB, De Tolosa EMC, Camargo RDC, Pompeu E, Liberti EA. Blood supply to the human sternocleidomastoid muscle by the sternocleidomastoid branch of the occipital artery. *Clin Anat*. 1999;12:412-416.

r R, Evans JT. Tracheostomy: an anatomico-clinical review. *Clin Anat*. 1993;6:337-341.

rvis JF. Displaced brachiocephalic artery: a potential hazard in tracheostomy. *S Afr Med J*. 1966;40:396-397.

pandji IA. The Physiology of Joints. Ediburgh: Churchill Livingstone, 1975.

ngeman RE. Surgical anatomy. Cummings CW, et al, editors. Otolaryngology, Head and Neck Surgery, 3rd edn., vol. 2. St Louis: Mosby, 1998;1673-1685.

cas GDA, Laudanna A, Chopard RP, Raffaelli EJr. Anatomy of the lesser occipital nerve in relation to cervicogenic headache. *Clin Anat*. 1994;7:90-96.

atthers LHJr, Smith DW, Frankel L. Anatomical considerations in placement of central venous catheters. *Clin Anat*. 1992;5:89-106.

oreau S, de Rugy MG, Babin E, Salame E, Delmas P, Valdazo A. The recurrent laryngeal nerve: related vascular anatomy. *Laryngoscope*. 1998;108:1351-1355.

ash L, Nicholson HD, Zhang M. Does the investing layer of the deep cervical fascia exist? *Anesthesiology*. 2005;103:962-968.

ndit JJ, Dutta D, Morris JF. Spread of injectate with superficial cervical plexus block in humans: an anatomical study. *Br J Anaesth*. 2003;91:733-735.

acic G, Matulic J, Roje Z, Dogas Z, Vilovic K. Abnormally high bifurcation of the brachiocephalic trunk as a potential operative hazard: case report. *Otolaryngol Head Neck Surg*. 2005;133:811-813.

obbins KT. Neck dissection. Cummings CW, et al, editors. Otolaryngology, Head and Neck Surgery, 3rd edn., vol. 2. St Louis: Mosby, 1998;1787-1819.

ah JP, Patel SJ. Cervical lymph nodes. In *Head and Neck Surgery and Oncology*, 3rd edn., Edinburgh: Mosby; 2003:353-394.

noker WRK, Harnsberger HR. Differential diagnosis of head and neck lesions based on their space of origin. 2. The infrahyoid portion of the neck. *Am J Roentgenol*. 1991;157:155-159.

ilson-Pauwels L, Akesson EJ, Stewart PA. Cranial Nerves: Anatomy and Clinical Comments. Toronto: Decker, 1998.

lcxin B. Anatomic configurations of the recurrent laryngeal nerve and inferior thyroid artery. *Surgery*. 2006;139:181-187.

ang M, Lee ASJ. The investing layer of the deep cervical fascia does not exist between the sternocleidomastoid and trapezius muscles. *Otolaryngol Head Neck Surg*. 2002;127:452-457.

CHAPTER 29

Face and scalp

SKIN

The scalp and buccolabial tissues are described here. The structure of the eyelids is described in Chapter 39.

SCALP

The scalp extends from the top of the forehead in front to the superior nuchal line behind. Laterally it projects down to the zygomatic arch and external acoustic meatus. It consists of five layers: skin, subcutaneous tissue, occipitofrontalis (epicranius) and its aponeurosis, subaponeurotic loose areolar tissue and periosteum of the skull (pericranium).

The skin of the scalp is hairy and rich in sebaceous glands: it is the commonest site for sebaceous cysts. The dense subcutaneous connective tissue has the richest cutaneous blood supply in the body. The anterior and posterior muscular bellies of occipitofrontalis are connected by a tough, fibrous, epicranial aponeurosis, and this layer is therefore often called the aponeurotic layer (galea aponeurotica). These three upper layers of the scalp can easily slide on the underling layer of loose connective tissue. A scalp flap can be raised within the plane between the galea and the pericranium without compromising either the blood or nerve supply of the scalp, because all of these structures lie in the subcutaneous layer (superficial fascia). Anteriorly based subgaleal scalp flaps (bicoronal) provide excellent access to the craniofacial skeleton for the correction of congenital deformity such as craniosynostoses; treatment of craniofacial fractures involving the frontal bone, nasoethmoid complex, orbit or zygomatic arch; skull base surgery or craniotomies. Pericranial flaps can be used to separate the frontal sinus floor from the nasal cavity in the management of fractures of the posterior wall of the frontal sinus (frontal sinus cranialization). Traumatic scalp avulsion may occur if hair becomes trapped in moving machinery or a shearing force is applied in the subgaleal plane during a road traffic accident or fall injury.

The arterial blood supply to the scalp is particularly rich, and there are free anastomoses between branches of the occipital and superficial temporal vessels. Scalp lacerations continue to bleed profusely because the elastic fibres of the underlying galea aponeurotica prevent initial vessel retraction. Their repair requires a two-layer closure technique to approximate the galea aponeurotica and skin layers. The pericranial layer, if involved, cannot usually be closed because it retracts.

EYEBROWS

The eyebrows are two arched eminences of skin which surmount the orbits. Numerous short, thick hairs are set obliquely in them. Fibres of orbicularis oculi, corrugator and the frontal part of occipitofrontalis, are inserted into the dermis of the eyebrows.

BUCCOLABIAL TISSUE

Cheeks

The cheeks are continuous in front with the lips. The external junction is indicated by the nasolabial groove (sulcus) and further laterally by the nasolabial fold, which descends from the side of the nose to the angle of the mouth. The cheek is covered on the outer surface by skin and on the inner surface by mucosa. Each cheek contains the buccinator muscle, and a variable, but usually considerable, amount of adipose tissue which is often encapsulated to form a biconcave mass, the buccal fat pad (of Bichat), particularly evident in infants. The walls of the cheek also contain fibrous connective tissue, vessels, nerves and numerous small buccal mucous (salivary) glands. The buccal fat pad can be used to reconstruct small intraoral defects of the palate, buccal and retromolar regions following surgery.

Lips

The lips are two fleshy folds surrounding the oral orifice. The centre of each lip contains a thick fibrous strand, consisting of parallel bundles of skeletal muscle fibres (orbicularis oris, together with incisivus superior and inferior, and the direct labial tractors), and their attachments to skin, mucosa or other muscle fibres. The free external surface of each lip is covered by a thin keratinized epidermis, and is continuous with the mucosa at the vermilion (red) zone of the lip. The dermis is well vascularized and contains numerous hair follicles (many of them large in the male), sebaceous glands (Fordyce spots) and sweat glands. Subcutaneous adipose tissue is scanty. The internal mucous surfaces are lined with a thick non-keratinizing stratified squamous epithelium. The submucosa is well vascularized and contains numerous minor salivary glands, which may be harvested for histological confirmation of Sjögren’s connective tissue disease.

Between the skin and mucosa, the vermilion zone is covered with a specialized keratinized stratified squamous epithelium which is thin near the skin, increases in thickness slightly as the mucosa is approached, and then thickens abruptly when true mucosa is reached. The epithelium is covered with transparent, dead squames and its deep surface is highly convoluted, interdigitating with abundant long dermal papillae. The latter carry a rich capillary plexus which imparts a dusky red colour. These surfaces are hairless, their dermis lacks sebaceous, sweat or mucous glands, and they are moistened with saliva by the tip of the tongue. The dense innervation of the lips is reflected in their acute sensitivity to light touch sensation, attributable mainly to the increased density of Meissner's corpuscles in the dermal papillae.

The size and curvature of the exposed red lip surfaces is subject to considerable individual, gender, and ethnic variation. The line of contact between the lips, the oral fissure, lies just above the incisal edges of the anterior maxillary teeth. On each side a labial commissure forms the angle (corner) of the mouth, usually near the first premolar tooth. The labial epithelia and internal tissues radiate over the boundaries of the commissure to become continuous with those of the cheek. With age, buccolabial (labiomarginal) grooves appear at the corners of the mouth. On each side, the upper lip is separated from the cheek laterally by the nasolabial groove and is continuous above the nasal ala with the circumalar groove (sulcus). The lower lip is separated from the chin by the mentolabial groove (sulcus).

Externally, the central region of the upper lip presents a shallow vertical groove, the philtrum, which is limited above by its attachment to the columella of the nose, and ends below in a slight tubercle limited by lateral ridges. The lower lip shows a small depression in the midline that corresponds to the tubercle. The junction between the external, hair-bearing skin and the red, hairless surface of the upper lip almost invariably takes the form of a double-curved Cupid's bow. From the centre it rises rapidly on each side to an apex that corresponds to the lower end of each ridge of the philtrum, and then slopes gently downwards towards the angle of the mouth. The line of contact between the red lip surfaces is typically almost horizontal. The Cupid's bow is interrupted in cleft lip anomalies.

In the upper lip, a narrow band of smooth tissue related to the subnasal maxillae marks the point at which labial mucosa becomes continuous with gingival mucosa. The corresponding reflexion in the lower lip coincides approximately with the mentolabial sulcus, and here the lip is continuous with mental tissues. The upper and lower lips differ in cross-sectional profile in that neither is a simple fold of uniform thickness. The upper lip has a bulbous asymmetrical profile: the skin and red-lip have a slight external convexity, and the adjoining red-lip and mucosa a pronounced internal convexity, creating a mucosal ridge or shelf that can be wrapped around the incisal edges of the parted teeth. The lower lip is on a more posterior plane than the upper lip. In the position of neutral lip contact, the external surface of the lower lip is concave, and there is little or no elevation of the internal mucosal surface. The profile of the lips can be modified by muscular activity.

RELAXED SKIN TENSION LINES AND SKIN FLAPS ON THE FACE

The direction in which facial skin tension is greatest varies regionally. Skin tension lines which follow the furrows formed when the skin is relaxed are known as ‘relaxed skin tension lines’ (Borges & Alexander 1962). In the living face, these lines frequently (but not always) coincide with wrinkle lines (Fig. 29.1) and can therefore act as a guide in planning elective incisions.

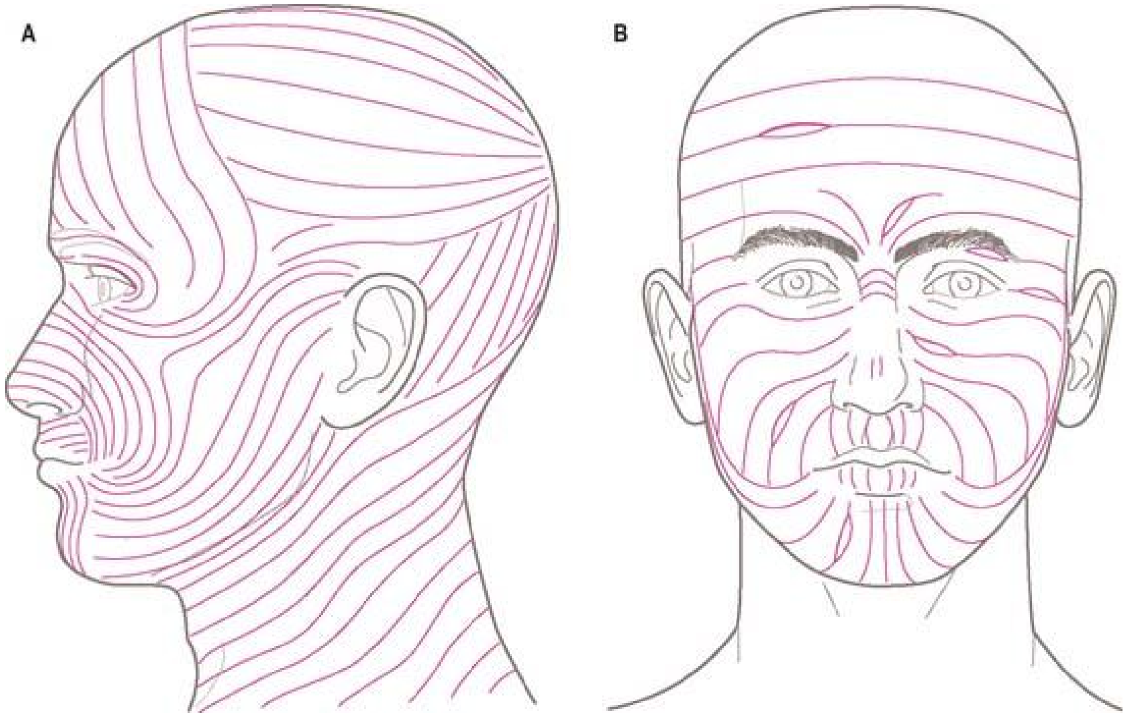

Fig. 29.1 **A**, Distribution of relaxed skin tension lines (Kraissl’s lines) lateral view. **B**, Anterior view.

When lesions on the face such as scars, pigmented lesions and skin cancers are excised, the dimensions of these lesions often require excision as an ellipse, so that the resulting defect can be closed as a straight line. If the resulting scar is to be aesthetically acceptable it is important to make the long axis of the ellipse parallel to the natural relaxed skin tension lines, so that the scar will look like a natural skin crease. If the excision line runs contrary to the skin tension lines, the scar may be more conspicuous and will tend to stretch transversely as a result of natural expressive facial movements.

When larger lesions are excised it may be necessary to advance or rotate adjacent soft tissue to fill the defect. The ability to raise these skin flaps is entirely dependent on the regional blood supply and both random pattern and axial pattern skin flaps are used surgically. Because of the richness of the subdermal plexus in the face, random pattern flaps can be raised with a greater length : breadth ratio than in any other area of the body.

The following are examples of axial pattern flaps that can be used to reconstruct defects on the face and scalp. Supratrochlear/supraorbital arteries support forehead flaps that are useful for nasal reconstruction: there is usually enough skin laxity to allow the majority of the donor site to be closed directly. The frontal branch of the superficial temporal artery anastomoses in the midline with its opposite number, and consequently the entire forehead skin can be raised on a narrow pedicle based on just one of the superficial temporal arteries. These flaps can be used to repair many facial defects and also intraoral defects, but the donor site defect cannot be closed directly and must be covered by a skin graft. The parietal branch of the superficial temporal artery and the occipital artery can support hair-bearing flaps from the scalp which are useful for reconstructing defects involving the scalp. The nasolabial flap utilizes the lax skin just lateral to the nasolabial groove. It is not supplied by a named axial artery but rather its blood supply is provided by many small branches from the underlying facial artery. These branches run perpendicular to the skin surface. Nasolabial flaps can be either superiorly or inferiorly based.

SOFT TISSUE

FASCIAL LAYERS

Fascia of scalp

The superficial fascia of the scalp is firm, dense and fibroadipose, and adheres closely to both skin and the underlying epicranius and its aponeurosis. Posteriorly it is continuous with the superficial fascia of the back of the neck, and laterally it is prolonged into the temporal region, where it is looser in texture.

Fascial layers and tissue planes in the face

On the basis of gross dissection and complementary histological studies, four distinct tissue planes are recognized on the face superficial to the plane of the facial nerve and its branches. From superficial to deep, these layers are the skin; a subcutaneous layer of fibro-adipose tissue; the superficial musculo-aponeurotic system (SMAS); and the parotid–masseteric fascia.

Subcutaneous fibroadipose tissue

This homogeneous layer is present throughout the face, although the degree of adiposity varies in different parts of the face and with age. Anteriorly, it crosses the nasolabial fold onto the lip, and superiorly it crosses the zygomatic arch. In both locations the layer is more fascial than fatty. The fat content of the subcutaneous tissue in the cheek accounts for the cheek mass: part of the subcutaneous adipose tissue is the malar fat pad, a more or less discrete aggregation of fatty tissue inferolateral to the orbital margin.

Superficial musculo-aponeurotic system (SMAS)

This is described as a single tissue plane in the face. In some areas it is composed of muscle fibres, and elsewhere it is composed of fibrous or fibroaponeurotic tissue: it is not directly attached to bone. When traced below the level of the lower border of the mandible it becomes continuous with platysma in the neck. Microdissection has revealed that the SMAS becomes indistinct on the lateral aspect of the face approximately 1 cm below the level of the zygomatic arch. Anteromedially, the SMAS layer becomes continuous with some of the mimetic muscles including zygomaticus major, frontalis and the peri-orbital fibres of orbicularis oculi.

In most areas of the face, a distinct sub-SMAS plane can be defined deep to SMAS. It is continuous with the plane between platysma and the underlying investing layer of deep cervical fascia in the neck. However, where it overlies the parotid gland, the SMAS is firmly blended with the superficial layer of the parotid fascia, which means that a clear sub-SMAS plane is difficult, if not impossible, to define in the region of the parotid.

Parotid–masseteric fascia

This is a filmy areolar layer that overlies the filamentous branches of the facial nerve and the parotid duct as these structures lie on the surface of masseter. Further anteriorly the parotid–masseteric fascia overlies the buccal fat pad which lies superficial to buccinator. Having crossed the surface of the buccal fat pad, the fascia blends with the epimysium on the surface of buccinator. Below the lower border of the mandible, it is continuous with the investing layer of deep cervical fascia.

Parotid fascia (capsule)

The parotid gland is surrounded by a fibrous capsule called the parotid fascia or capsule. Traditionally this has been described as an upward continuation of the investing layer of deep cervical fascia in the neck which splits to enclose the gland within a superficial and a deep layer. The superficial layer is attached above to the zygomatic process of the temporal bone, the cartilaginous part of the external acoustic meatus, and the mastoid process. The deep layer is attached to the mandible, and to the tympanic plate, styloid and mastoid processes of the temporal bone. The prevailing view is that the deep layer of the parotid gland is derived from the deep cervical fascia. However, the superficial layer of the parotid capsule appears to be continuous with the fascia associated with platysma, and is now regarded as a component of the SMAS (Mitz & Peyronie 1976; Wassef 1987; Gosain et al 1993). It varies in thickness from a thick fibrous layer anteriorly to a thin translucent membrane posteriorly. It may be traced forwards as a separate layer which passes over the masseteric fascia (itself derived from the deep cervical fascia), separated from it by a cellular layer which contains branches of the facial nerve and the parotid duct. Histologically, the parotid fascia is atypical in that it contains muscle fibres which parallel those of platysma, especially in the lower part of the parotid capsule. Although thin fibrous septa may be seen in the subcutaneous layer at the histological level, macroscopically there is little evidence of a distinct layer of superficial fascia.

The deep fascia covering the muscles forming the parotid bed (digastric and styloid group of muscles) contains the stylomandibular and mandibulostylohyoid ligaments. The stylomandibular ligament passes from the styloid process to the angle of the mandible. The more extensive mandibulostylohyoid ligament (angular tract) passes between the angle of the mandible and the stylohyoid ligament for varying distances, generally reaching the hyoid bone. It is thick posteriorly but thins anteriorly in the region of the angle of the mandible. There is some dispute as to whether the mandibulostylohyoid ligament is part of the deep cervical fascia (Ziarah & Atkinson 1981), or lies deep to it (Shimada & Gasser 1988). The stylomandibular and mandibulostylohyoid ligaments separate the parotid gland region from the superficial part of the submandibular gland, and so are landmarks of surgical interest.

Temporo-parietal and temporal fasciae

Above the level of the zygomatic arch, on the lateral side of the head, the temporo-parietal fascia (superficial temporal fascia) constitutes a fascial layer which lies in the same plane as, but is not continuous with, the SMAS. It is quite separate from, and superficial to, the temporal fascia (deep temporal fascia). More superiorly, it blends with the galea aponeurotica. The plane between the temporo-parietal fascia and the underlying deep temporal fascia contains loose areolar tissue and a small amount of fat. This tissue plane, the temporo-parietal fat pad, is continuous superiorly with the subgaleal plane of loose areolar tissue in the scalp. Running superiorly in the temporo-parietal fascia or just deep to it are the superficial temporal vessels, the auriculotemporal nerve and its branches, and the temporal branches of the facial nerve. When raising a bicoronal flap, identification of the temporoparietal fat pad helps to separate these two fascial layers; subsequent dissection in a plane deep to the temporoparietal fascia protects the temporal branch of the facial nerve. The temporal fascia is a dense aponeurotic layer which lies deep to the temporo-parietal fat pad and covers temporalis: the deep surface of the fascia affords attachment to the superficial fibres of temporalis. Above, it is a single layer attached along the length of the superior temporal line, blending with the periosteum. Below, at approximately the level of the superior orbital rim, it splits into superficial and deep laminae which run downwards to attach to the lateral and medial margins of the upper surface of the zygomatic arch respectively. These fascial attachments have a clinical application in the reduction of fractures of the zygomatic complex via a Gillies approach: an instrument is inserted deep to the deep lamina of temporalis fascia through a scalp incision and used to elevate depressed zygomatic complex fractures. The fat enclosed between these two layers is termed the superficial temporal fat pad; it contains the zygomatico-orbital branch of the superficial temporal artery and a cutaneous nerve, the zygomatico-temporal branch of the maxillary nerve. The temporal fascia is overlapped by auriculares anterior and superior, the epicranial aponeurosis and part of orbicularis oculi, and the superficial temporal vessels and auriculotemporal nerve ascend over it.

Buccopharyngeal fascia

Buccinator is covered by a thin layer of fascia, the buccopharyngeal fascia, which also covers the superior constrictor of the pharynx.

Retaining ligaments of the face

These ligaments are fascial bands at specific sites which serve to anchor the skin to the underlying bone. The general cutaneous laxity that attends the ageing process renders facial skin subject to gravitational pull. However, at sites where retaining ligaments are present, the effect of gravitational pull is resisted. When performing facelift procedures, these ligaments must be surgically divided in order to facilitate redraping of facial skin. Examples of retaining ligaments in the face are the zygomatic ligament (also known as McGregor’s patch) and the mandibular ligament.

Fascial spaces

Two tissue spaces on the face may be involved in spread of odontogenic infection. They are the buccal tissue space, lying between the skin and surface of buccinator, and the infraorbital tissue space, lying between the bony attachments of levator labii superioris and levator anguli oris.

BONES OF THE FACIAL SKELETON AND CRANIAL VAULT

The skull consists of the facial skeleton and cranial vault (calvarium) attached at the skull base. The cranial vault encloses and protects the brain. The facial skeleton is the anterior part of the skull and includes the mandible. The bones of the nasoethmoidal and zygomaticomaxillary complexes are described here. The mandible is described in Chapter 30.

PARIETAL BONE

The two parietal bones form most of the cranial roof and sides of the skull. Each is irregularly quadrilateral and has two surfaces, four borders and four angles (Fig. 29.2).

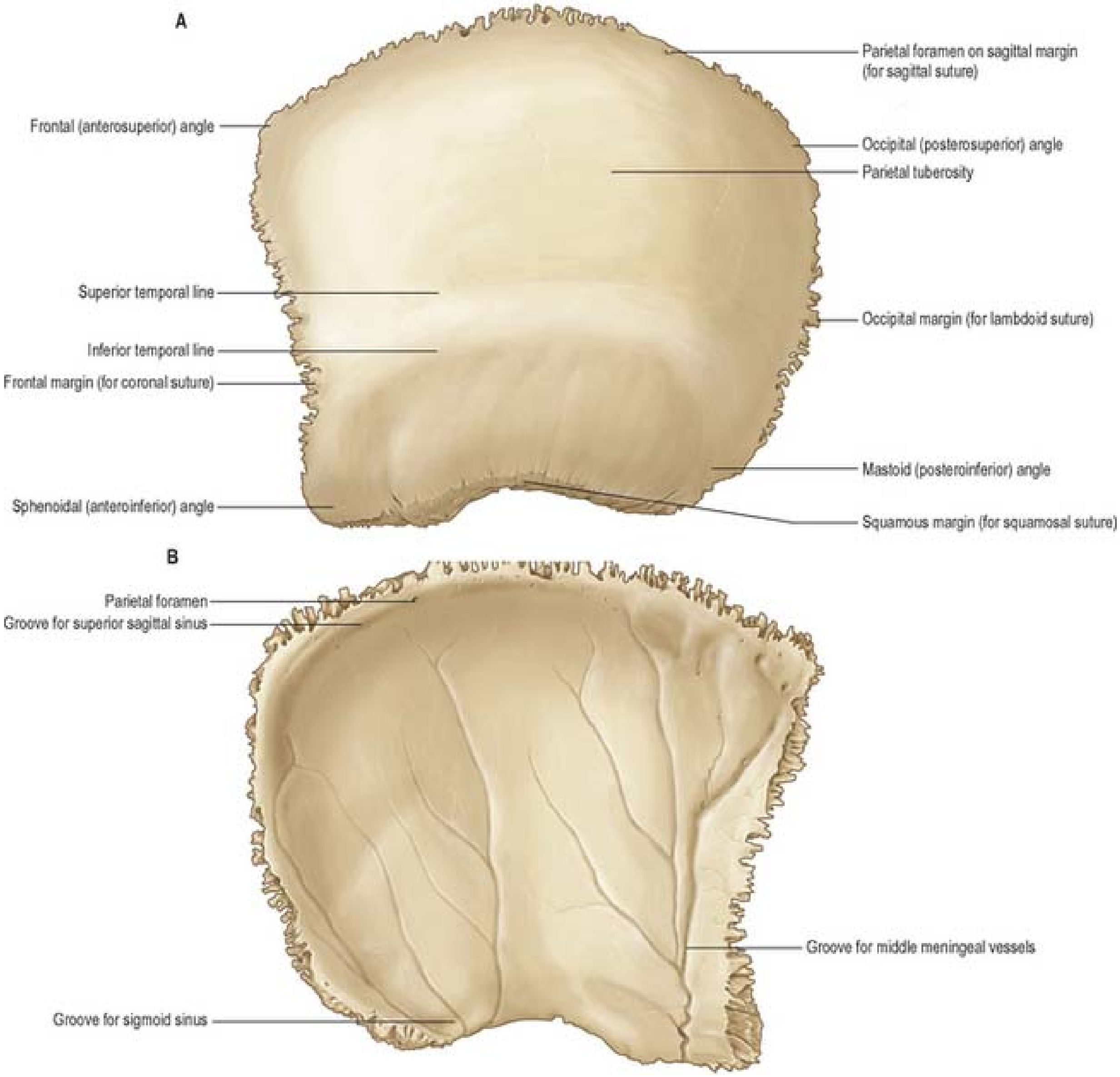
A
Parietal foramen on sagittal margin (for sagittal suture)
Frontal (anterosuperior) angle
Occipital (posterosuperior) angle
Parietal tuberosity
Superior temporal line
Occipital margin (for lambdoid suture)
Inferior temporal line
Frontal margin (for coronal suture)
Mastoid (posteroinferior) angle
Sphenoidal (anteroinferior) angle
Squamous margin (for squamosal suture)
B
Parietal foramen
Groove for superior sagittal sinus
Groove for middle meningeal vessels
Groove for sigmoid sinus

Fig. 29.2 Left parietal bone. **A**, External view; **B**, Internal view.

The external surface is convex and smooth, with a central parietal tuber (tuberosity). Curved superior and inferior temporal lines cross it and form posterosuperior arches. The temporal fascia is attached to the superior line or arch and temporalis is attached to the inferior line or arch. The epicranial aponeurosis lies above these lines, and part of the temporal fossa lies below. Posteriorly, close to the sagittal (superior) border, an inconstant parietal foramen transmits a vein from the superior sagittal sinus and sometimes a branch of the occipital artery.

The internal surface is concave and marked by impressions of cerebral gyri and by grooves for the middle meningeal vessels. The latter ascend, inclining backwards, from the sphenoidal (anteroinferior) angle and posterior half (or more) of its inferior border. A groove for the superior sagittal sinus lies along the sagittal border, and is completed by the groove on the opposite parietal bone. The falx cerebri is attached to the edges of the groove. Granular foveolae for arachnoid granulations flank the sagittal sulcus, and are most pronounced in old age.

The dentated sagittal border, longest and thickest, articulates with the opposite parietal bone at the sagittal suture. The anterior part of the squamosal (inferior) border is short, thin and truncated, bevelled externally and overlapped by the greater wing of the sphenoid. The middle part of the inferior border is arched, bevelled externally and overlapped by the squamous part of the temporal bone. The posterior part of the inferior border is short, thick and serrated for articulation with the mastoid part.

The frontal border is deeply serrated, bevelled externally above, internally below, and articulates with the frontal bone to form one half of the coronal suture. The occipital border, deeply dentated, articulates with the occipital bone, forming one half of the lambdoid suture.

The frontal (anterosuperior) angle, which is approximately 90°, is at the bregma, where sagittal and coronal sutures meet, and marks the site of the anterior fontanelle in the neonatal skull. The sphenoidal (anteroinferior) angle lies between the frontal bone and greater wing of the sphenoid. Its internal surface is marked by a deep groove or canal that carries the frontal branches of the middle meningeal vessels. The frontal, parietal, sphenoid and temporal bones usually meet at the pterion, which marks the site of the sphenoidal fontanelle in the embryonic skull. The frontal bone sometimes meets the squamous part of the temporal bone, in which case the parietal bone fails to reach the greater wing of the sphenoid bone. The rounded occipital (posterosuperior) angle is at the lambda, the meeting of the sagittal and lambdoid sutures, which marks the site of the posterior fontanelle in the neonatal skull. The blunt mastoid (posteroinferior) angle articulates with the occipital bone and the mastoid portion of the temporal bones at the asterion. Internally it bears a broad, shallow groove for the junction of the transverse and sigmoid sinuses.

Ossification

Each parietal bone is ossified from two centres which appear in dense mesenchyme near the tuberosity, one above the other, at about the seventh week *in utero*. These two centres unite early and ossification subsequently radiates from them towards the margins. The angles are therefore the last parts to be ossified, and fontanelles occur at these sites. At birth the temporal lines are low down; they only reach their final position after the eruption of the molar teeth. Occasionally the parietal bone is divided by an anteroposterior suture.

FRONTAL BONE

The frontal bone is like half a shallow, irregular cap forming the forehead or frons (Fig. 29.3). It has three parts, and contains two cavities, the frontal sinuses.

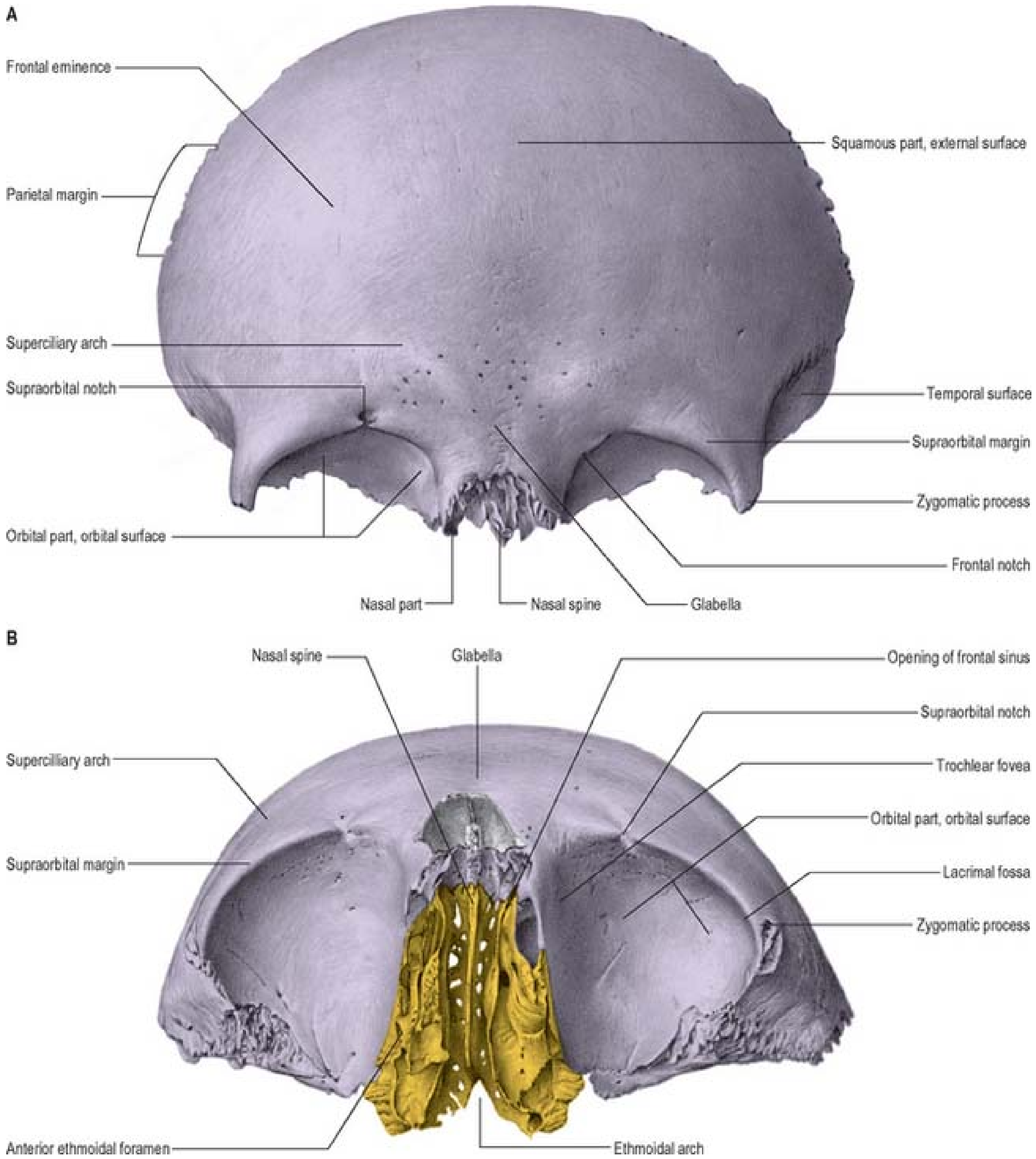

A
Frontal eminence
Parietal margin
Superciliary arch
Supraorbital notch
Orbital part, orbital surface
Squamous part, external surface
Temporal surface
Supraorbital margin
Zygomatic process
Frontal notch
Nasal part
Nasal spine
Glabella
B
Nasal spine
Glabella
Supercilliary arch
Supraorbital margin
Opening of frontal sinus
Supraorbital notch
Trochlear fovea
Orbital part, orbital surface
Lacrimal fossa
Zygomatic process
Anterior ethmoidal foramen
Ethmoidal arch

Fig. 29.3 Frontal bone. **A**, anterior view; **B**, inferior view, including the articulations between the frontal, ethmoid and nasal bones.

(From Sobotta 2006.)

Squamous part

The squamous part forms the major portion of the frontal bone. Its external surface has a rounded frontal tuber (tuberosity) approximately 3 cm above the midpoint of each supraorbital margin. These tubera vary, but are especially prominent in young skulls and more so in adult females than males. Below them and separated by a shallow groove, are two curved superciliary arches, medially prominent and joined by a smooth median elevated glabella. The arches are more prominent in males; prominence depends partly on the size of the frontal sinuses, but is occasionally associated with small sinuses. The curved supraorbital margins of the orbital openings lie inferior to the superciliary arches. The lateral two-thirds of each margin are sharp, the medial third rounded; a supraorbital notch or foramen, which transmits the supraorbital vessels and nerve, lies at the junction between them. A small frontal notch or foramen lies medial to the supraorbital notch in 50% of skulls. Both features show sexual dimorphism. The supraorbital margin ends laterally in a strong, prominent zygomatic process that articulates with the zygomatic bone. A line curves posterosuperiorly from the process and divides into superior and inferior temporal lines, which are continued on the squamous part of the temporal bone. The area of the frontal bone below and behind the temporal lines is known as the temporal surface and forms the anterior part of the temporal fossa. The parietal (posterior) margin is thick, deeply serrated, and bevelled internally above and externally below. Inferiorly it becomes a rough, triangular surface that articulates with the greater wing of the sphenoid.

The internal surface of the frontal bone is concave. Its upper, median, part displays a vertical sulcus whose edges unite below as the frontal crest. The sulcus contains the anterior part of the superior sagittal sinus. The crest ends in a small notch which is completed by the ethmoid bone to form a foramen caecum. The anterior portion of the falx cerebri is attached to the margins of the sulcus and to the frontal crest. The internal surface shows impressions of cerebral gyri, small furrows for meningeal vessels, and granular foveolae for arachnoid granulations near the sagittal sulcus.

Nasal part

The nasal part of the frontal bone lies between the supraorbital margins. A serrated nasal notch articulates with the nasal bones inferiorly and with the frontal processes of the maxillae and the lacrimal bones laterally. From the centre of the notch posteriorly the bone projects anteroinferiorly behind the nasal bones and the frontal processes of the maxillae, and supports the nasal bridge. The region ends in a sharp nasal spine, on each side of which a small grooved surface partly roofs the ipsilateral nasal cavity. The nasal spine makes a very small contribution to the nasal septum: it articulates anteriorly with the crest of the nasal bones and posteriorly with the perpendicular plate of the ethmoid bone.

Orbital parts

Most of the frontal bone is thick, and consists of trabecular tissue lying between two compact laminae. In contrast, the orbital plates consist entirely of compact bone and are thin and often translucent posteriorly, indeed they may be partly absorbed in old age.

The orbital plates form the largest part of the orbital roofs and are two thin, curved, triangular laminae separated by a wide ethmoidal notch. The orbital surface of each plate is smooth and concave, and bears a shallow anterolateral fossa for the lacrimal gland. The trochlear fovea (or spine) for attachment of a fibrocartilaginous trochlea through which the tendon of superior oblique plays, lies below and behind the medial end of the supraorbital margin, midway between the supraorbital notch and frontolacrimal suture. The convex cerebral surface is marked by frontal gyri and faint grooves for meningeal vessels.

The quadrilateral ethmoidal notch is occupied by the cribriform plate of the ethmoid bone. Inferior to its lateral margins, the bone articulates with the labyrinths of the ethmoid bone and impressions of the ethmoidal air cells can be seen on this surface. Two transverse grooves across each margin are converted into anterior and posterior ethmoidal canals by articulation with the ethmoid bone: these canals open on the medial orbital wall and transmit the anterior and posterior ethmoidal nerves and vessels. The posterior borders of the orbital plates are thin and serrated and articulate with the lesser wings of the sphenoid; their lateral parts usually appear in the middle cranial fossa between the greater and lesser wings of the sphenoid.

The frontal sinuses are two irregular cavities that ascend posterolaterally for a variable distance between the frontal laminae. They are separated by a thin septum and usually deflected from the median plane, which means that they are rarely symmetrical. The sinuses are variable in size and usually larger in males. Their openings lie anterior to the ethmoidal notch and lateral to the nasal spine, and each communicates with the middle meatus in the ipsilateral nasal cavity by a frontonasal canal.

The frontal sinuses are rudimentary at birth and can barely be distinguished. They show a primary expansion with eruption of the first deciduous molars at about 18 months, and again when the permanent molars begin to appear in the sixth year. Growth is slow in the early years but it can be detected radiographically by 6 years. They reach full size after puberty, although with advancing age osseous absorption may lead to further enlargement. Their degree of development appears to be linked to the prominence of the superciliary arches, which is thought to be a response to masticatory stresses. The frontal sinuses are described in Chapter 32.

Ossification

The frontal bone is ossified in fibrous mesenchyme from two primary centres that appear in the eighth week *in utero*, one near each frontal tuber. Ossification extends superiorly to form half of the main part of the bone; posteriorly to form the orbital part, and inferiorly to form nasal parts. Two secondary centres for the nasal spine appear about the tenth year. At birth the bone consists of two halves. The median suture usually disappears by about 8 years, but may persist as the metopic suture. Metopism has been assessed at 0–7.4% of individuals in various ethnic groups.

ETHMOID BONE

The ethmoid bone is cuboidal and fragile (Fig. 29.3B, Fig. 29.4, Fig. 29.5, Fig. 29.6). It lies anteriorly in the cranial base and contributes to the medial walls of the orbit, the nasal septum and the roof and lateral walls of the nasal cavity. It has a horizontal perforated cribriform plate, a median perpendicular plate, and two lateral labyrinths that contain the ethmoidal air cells.

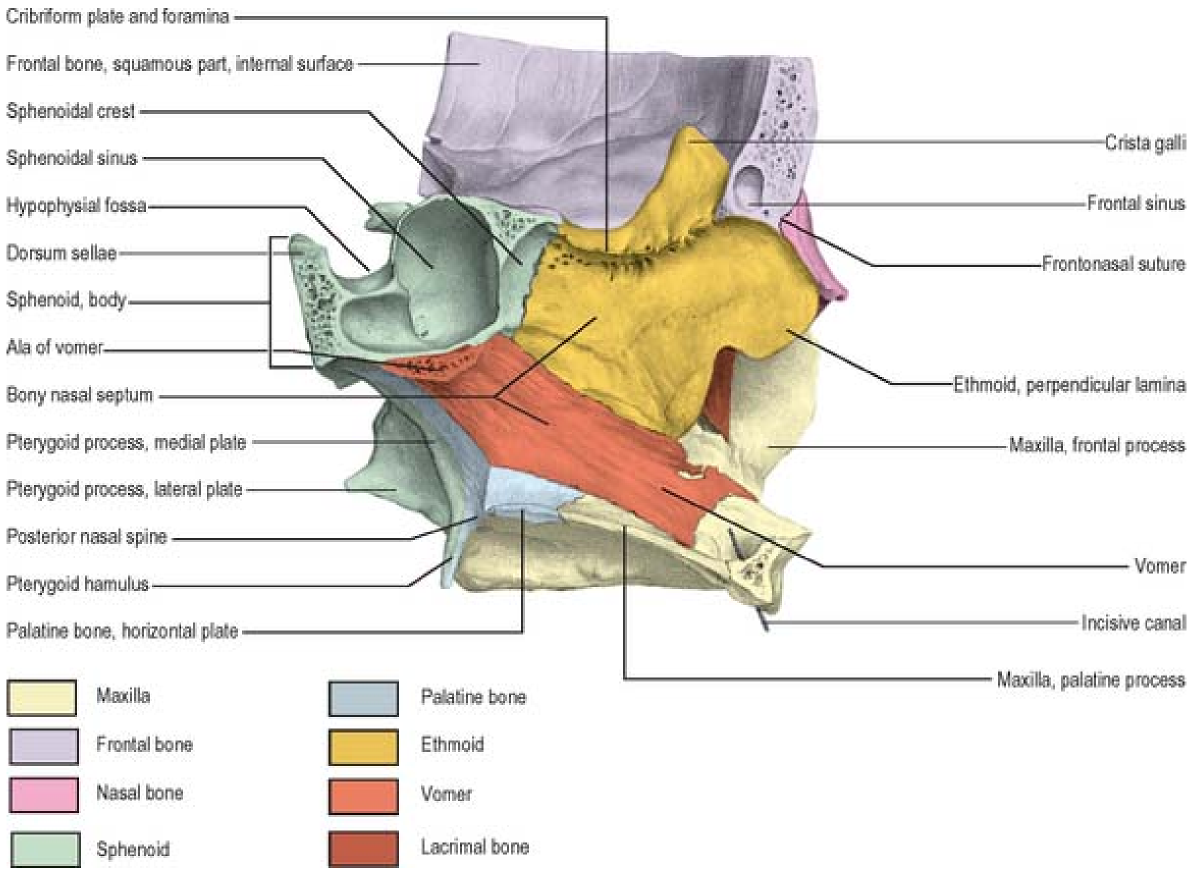
Cribriform plate and foramina
Frontal bone, squamous part, internal surface
Sphenoidal crest
Sphenoidal sinus
Hypophysial fossa
Dorsum sellae
Sphenoid, body
Ala of vomer
Bony nasal septum
Pterygoid process, medial plate
Pterygoid process, lateral plate
Posterior nasal spine
Pterygoid hamulus
Palatine bone, horizontal plate
Crista galli
Frontal sinus
Frontonasal suture
Ethmoid, perpendicular lamina
Maxilla, frontal process
Vomer
Incisive canal
Maxilla, palatine process
Maxilla
Frontal bone
Nasal bone
Sphenoid
Palatine bone
Ethmoid
Vomer
Lacrimal bone

Fig. 29.4 Sagittal view of the facial skeleton, viewed from the right side of the nasal septum, looking towards the left.

(From Sobotta 2006.)

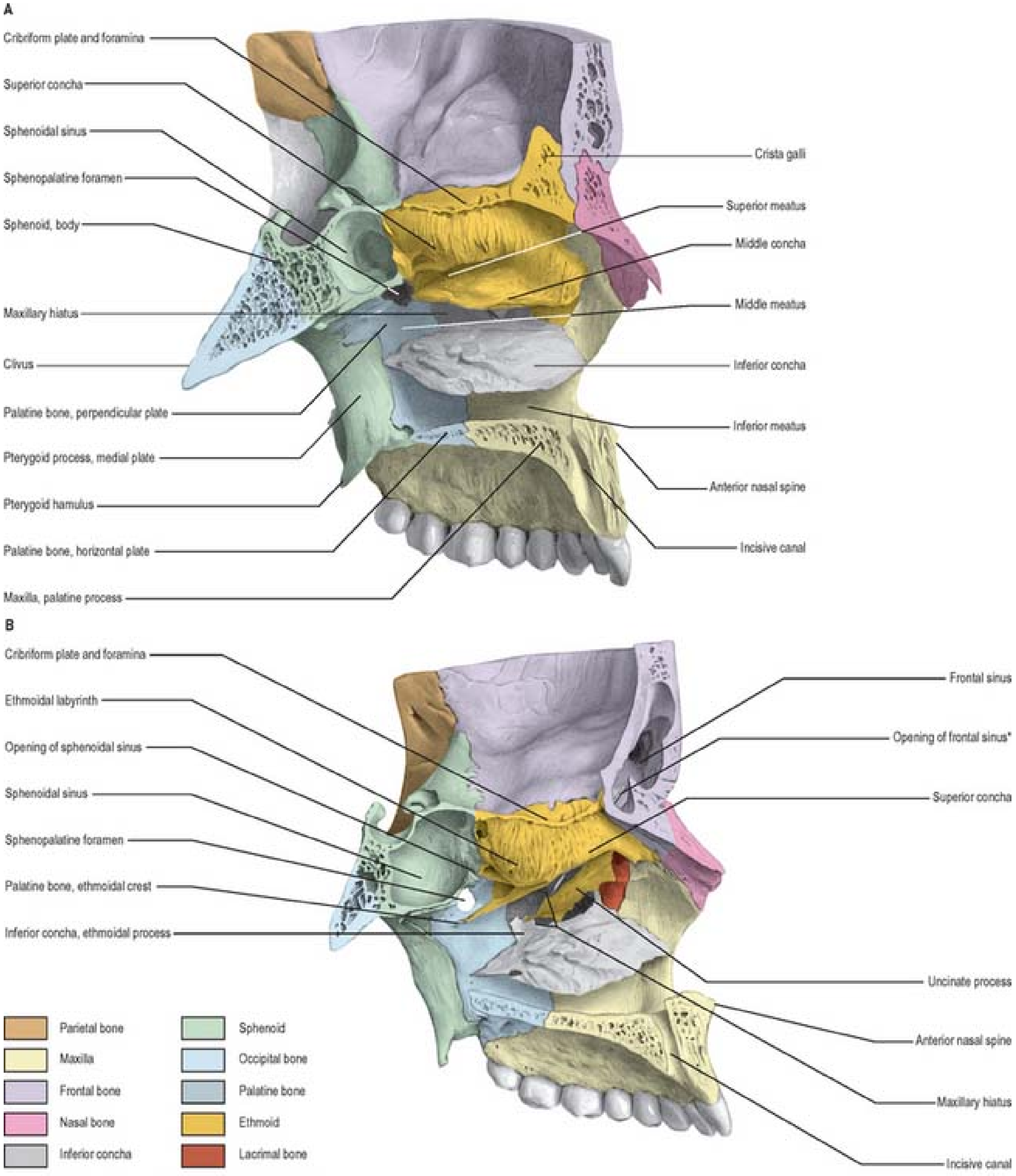
A
Cribriform plate and foramina
Superior concha
Sphenoidal sinus
Sphenopalatine foramen
Sphenoid, body
Maxillary hiatus
Clivus
Palatine bone, perpendicular plate
Pterygoid process, medial plate
Pterygoid hamulus
Palatine bone, horizontal plate
Maxilla, palatine process
Crista galli
Superior meatus
Middle concha
Middle meatus
Inferior concha
Inferior meatus
Anterior nasal spine
Incisive canal
B
Cribriform plate and foramina
Ethmoidal labyrinth
Opening of sphenoidal sinus
Sphenoidal sinus
Sphenopalatine foramen
Palatine bone, ethmoidal crest
Inferior concha, ethmoidal process
Frontal sinus
Opening of frontal sinus*
Superior concha
Uncinate process
Anterior nasal spine
Maxillary hiatus
Incisive canal
Parietal bone
Maxilla
Frontal bone
Nasal bone
Inferior concha
Sphenoid
Occipital bone
Palatine bone
Ethmoid
Lacrimal bone

* Probe located in the passage from the frontal sinus to the middle meatus

Fig. 29.5 **A**, **B** Sagittal view of the facial skeleton, showing the floor of the anterior cranial fossa, the lateral wall of the nasal cavity, the hard palate and the sphenoidal air sinus. In B, the middle concha in the lateral wall of the nasal cavity has been removed to reveal the uncinate process.

(From Sobotta 2006.)

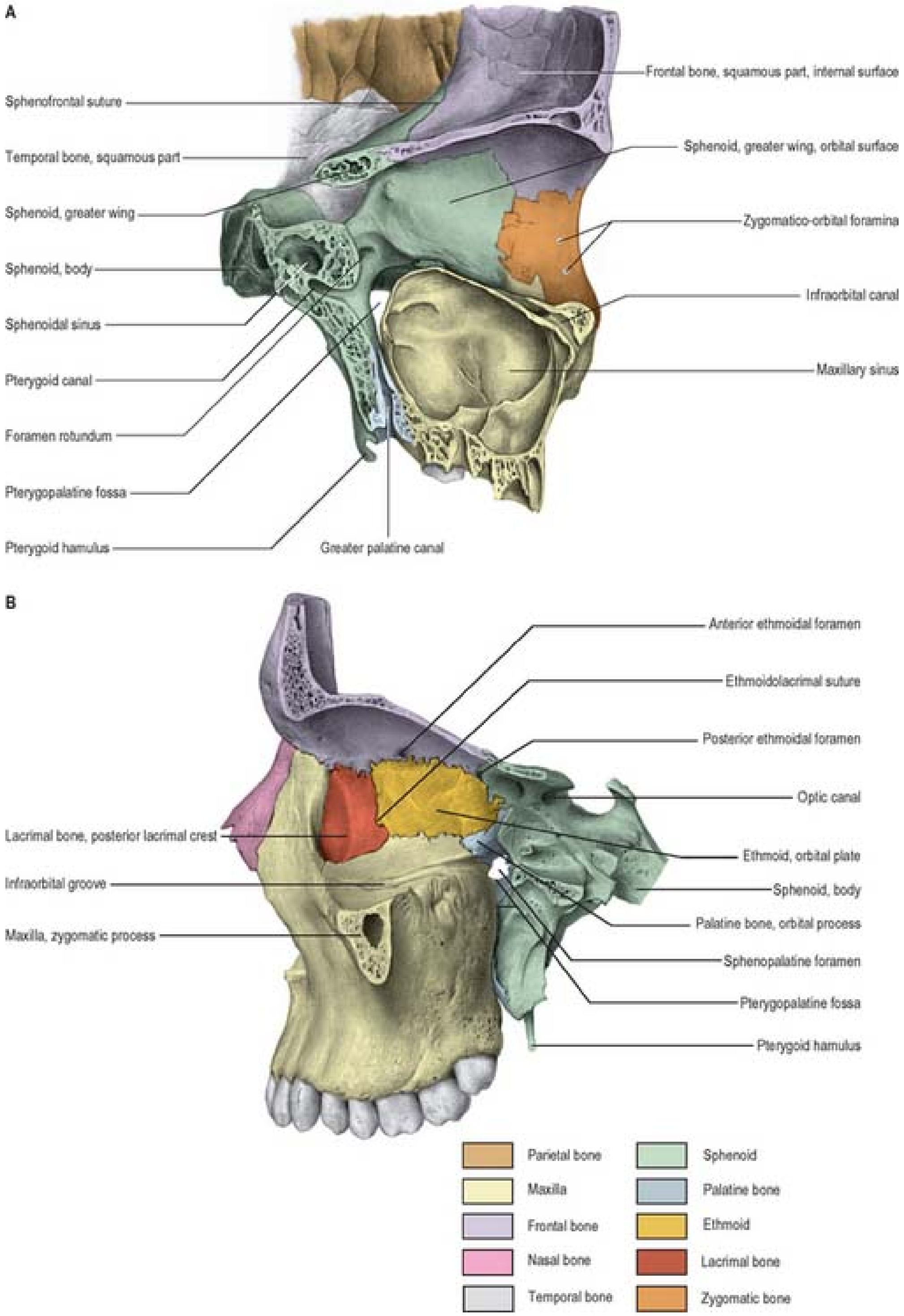
A
Sphenofrontal suture
Temporal bone, squamous part
Sphenoid, greater wing
Sphenoid, body
Sphenoidal sinus
Pterygoid canal
Foramen rotundum
Pterygopalatine fossa
Pterygoid hamulus
Greater palatine canal
Frontal bone, squamous part, internal surface
Sphenoid, greater wing, orbital surface
Zygomatico-orbital foramina
Infraorbital canal
Maxillary sinus
B
Anterior ethmoidal foramen
Ethmoidolacrimal suture
Posterior ethmoidal foramen
Optic canal
Lacrimal bone, posterior lacrimal crest
Ethmoid, orbital plate
Infraorbital groove
Sphenoid, body
Maxilla, zygomatic process
Palatine bone, orbital process
Sphenopalatine foramen
Pterygopalatine fossa
Pterygoid hamulus
Parietal bone
Maxilla
Frontal bone
Nasal bone
Temporal bone
Sphenoid
Palatine bone
Ethmoid
Lacrimal bone
Zygomatic bone

Fig. 29.6 **A**, Sagittal view of the facial skeleton, showing the bones forming the lateral wall of the left orbit and the maxillary air sinus. **B**, The

bones forming the medial wall and the floor of the left orbit.

(From Sobotta 2006.)

Cribriform plate and crista galli

The cribriform plate fills the ethmoidal notch of the frontal bone and forms a large part of the nasal roof. It derives its name from the fact that it is penetrated by numerous foramina that transmit branches of the olfactory nerves and their associated meninges. A thick, smooth, triangular, median process, the crista galli, projects upwards from the centre of the cribriform plate. The falx cerebri is attached to its thin and curved posterior border, while its shorter, thick, anterior border articulates with the frontal bone by two small alae, so completing the foramen caecum. Its sides are generally smooth, but may show slight bulges that are related to underlying ethmoidal air cells. On both sides of the crista galli, the cribriform plate is narrow and depressed and is related to the gyrus rectus and the olfactory bulb which lie above it. On each side of the crista anteriorly there is a small slit occupied by dura mater. Just anterolateral to the slit, a foramen transmits the anterior ethmoidal nerve and vessels to the nasal cavity. A groove runs forwards to the foramen caecum from the anterior ethmoidal canal.

Perpendicular plate

The perpendicular plate is thin, flat, quadrilateral and median. It descends from the cribriform plate to form the upper part of the nasal septum, usually deviating slightly from the midline. Its anterior border articulates with the nasal spine of the frontal bone and the crests of the nasal bones, and its posterior border articulates with the crest of the body of the sphenoid bone above and the vomer below. The thick inferior border is attached to the nasal septal cartilage. Its surfaces are smooth except above, where numerous grooves and canals that transmit filaments of the olfactory nerves lead to medial foramina in the cribriform plate.

Ethmoidal labyrinths

The ethmoidal labyrinths consist of thin-walled ethmoidal air cells between two vertical plates. The lateral surface (orbital plate) of the labyrinth is part of the medial orbital wall. The air cells are arranged in anterior, middle and posterior groups. On average there are 11 anterior ethmoidal air cells, three middle, and six posterior. In the disarticulated bone, many air cells are open, but in life, and in the articulated skull, they are closed by proximity to adjoining bones, except where they open into the nasal cavity. The superior surface is crossed by two grooves that are converted into the anterior and posterior ethmoidal canals by the frontal bone; it shows open-air cells that are covered by the edges of the ethmoidal notch of the frontal bone. On the posterior surface open air cells are covered by the sphenoidal conchae and the orbital process of the palatine bone. The middle and posterior ethmoidal air cells are covered by a thin, smooth, oblong orbital plate that articulates superiorly with the orbital plate of the frontal bone, inferiorly with the maxilla and orbital process of the palatine bone, anteriorly with the lacrimal bone and posteriorly with the sphenoid bone. The walls of the air cells lying anterior to the orbital plate are completed by the lacrimal bone and frontal process of the maxilla.

A thin, curved uncinate process, variable in size, projects posteroinferiorly from the labyrinth. The upper edge of this process is a medial boundary of the hiatus semilunaris in the middle meatus. The uncinate process appears in the medial wall of the maxillary sinus as it crosses the ostium of the maxillary sinus to join the ethmoidal process of the inferior nasal concha.

The medial surface of the labyrinth forms part of the lateral nasal wall. It appears as a thin lamella that descends from the inferior surface of the cribriform plate and ends as the convoluted middle nasal concha. Superiorly the surface contains numerous vertical grooves that transmit bundles of olfactory nerves. Posteriorly it is divided by the narrow, oblique superior meatus, bounded above by the thin, curved superior nasal concha. Posterior ethmoidal air cells open into the superior meatus. The convex surface of the middle nasal concha extends along the entire medial surface of the labyrinth, anteroinferior to the superior meatus. Its lower edge is thick and its lateral surface is concave and forms part of the middle meatus. Middle ethmoidal air cells produce a swelling, the bulla ethmoidalis, on the lateral wall of the middle meatus, and open into the meatus, either on the bulla or above it. A curved infundibulum extends up and forwards from the middle meatus and communicates with the anterior ethmoidal sinuses. In more than 50% of crania it continues up as the frontonasal duct to include the drainage point for the frontal sinus. (The ethmoidal air cells are described further in Chapter 32.)

Ossification

The ethmoid bone ossifies in the cartilaginous nasal capsule from three centres, one in the perpendicular plate, and one in each labyrinth. The latter two appear in the orbital plates between the fourth and fifth months *in utero*, and extend into the ethmoid conchae. At birth, the labyrinths, although ill-developed, are partially ossified, and the remainder are cartilaginous. The perpendicular plate begins to ossify from the median centre during the first year, and fuses with the labyrinths early in the second year. The cribriform plate is ossified partly from the perpendicular plate, and partly from the labyrinths. The crista galli ossifies during the second year. The parts of the ethmoid bone unite to form a single bone at around 3 years of age. Ethmoidal air cells begin to develop at about 3 months *in utero*, and are therefore present at birth, however, they are difficult to visualize radiographically until the end of the first year. They grow slowly and have almost reached adult size by the age of 12 years.

INFERIOR NASAL CONCHA

The inferior nasal conchae are curved horizontal laminae in the lateral nasal walls (Fig. 29.5) (see also Ch. 32). Each has two surfaces (medial and lateral), two borders (superior and inferior) and two ends (anterior and posterior). The medial surface is convex, much perforated, and longitudinally grooved by vessels. The lateral surface is concave and part of the inferior meatus. The superior border, thin and irregular, may be divided into three regions: an anterior region articulating with the conchal crest of the maxilla; a posterior region articulating with the conchal crest of the palatine bone; and a middle region with three processes, which are variable in size and form. The lacrimal process is small and pointed and lies towards the front. It articulates apically with a descending process from the lacrimal bone, and at its margins with the edges of the nasolacrimal groove on the medial surface of the maxilla, thereby helping to complete the nasolacrimal canal. Most posteriorly, a thin ethmoidal process ascends to meet the uncinate process of the ethmoid bone. An intermediate thin maxillary process curves inferolaterally to articulate with the medial surface of the maxilla at the opening of the maxillary sinus. The inferior border is thick and spongiose, especially in its midpart. Both the anterior and posterior ends of the inferior nasal concha are more or less tapered, the posterior more than the anterior.

Ossification

Ossification is from one centre which appears at about the fifth month *in utero* in the incurved lower border of the cartilaginous lateral wall of the nasal capsule. The inferior concha loses continuity with the nasal capsule during ossification.

LACRIMAL BONE

The lacrimal bones are the smallest and most fragile of the cranial bones and lie anteriorly in the medial walls of the orbits (Fig. 29.5B). Each has two surfaces (medial and lateral) and four borders (anterior, posterior, superior and inferior). The lateral (orbital) surface is divided by a vertical posterior lacrimal crest. Anterior to the crest is a vertical groove whose anterior edge meets the posterior border of the frontal process of the maxilla to complete the fossa that houses the lacrimal sac. The medial wall of the groove is prolonged by a descending process that contributes to the formation of the nasolacrimal canal by joining the lips of the nasolacrimal groove of the maxilla and the lacrimal process of the inferior nasal concha. A smooth part of the medial orbital wall lies behind the posterior lacrimal crest: the lacrimal part of orbicularis oculi is attached to this surface and crest. The surface ends below in the lacrimal hamulus which, together with the maxilla, completes the upper opening of the nasolacrimal canal. The hamulus may appear as a separate lesser lacrimal bone. The anteroinferior region of the medial (nasal) surface is part of the middle meatus. Its posterosuperior part meets the ethmoid to complete some of the anterior ethmoidal air cells. The anterior border of the lacrimal bone articulates with the frontal process of the maxilla, the posterior border with the orbital plate of the ethmoid bone, the superior border with the frontal bone, and the inferior border with the orbital surface of the maxilla.

Ossification

Ossification is from a centre that appears at about the 12th week *in utero* in mesenchyme around the nasal capsule. In later life the lacrimal bone is subject to patchy erosion.

NASAL BONE

The nasal bones are small, oblong, variable in size and form, and placed side by side between the frontal processes of the maxillae (Fig. 29.4, Fig. 29.5, Fig. 29.6B). They jointly form the nasal bridge. Each nasal bone has two surfaces (external and internal) and four borders (superior, inferior, lateral and mesial). The external surface has a descending concavo-convex profile and is transversely convex. It is covered by procerus and nasalis and perforated centrally by a small foramen that transmits a vein. The internal surface, transversely concave, bears a longitudinal groove that houses the anterior ethmoidal nerve. The superior border, thick and serrated, articulates with the nasal part of the frontal bone. The inferior border, thin and notched, is continuous with the lateral nasal cartilage. The lateral border articulates with the frontal process of the maxilla. The medial border, thicker above, articulates with its fellow and projects behind as a vertical crest, thereby forming a small part of the nasal septum. It articulates from above with the nasal spine of the frontal bone, the perpendicular plate of the ethmoid bone, and the nasal septal cartilage.

Ossification

Ossification is from a centre that appears early in the third month *in utero* in the mesenchyme overlying the cartilaginous anterior part of the nasal capsule.

VOMER

The vomer is thin, flat, and almost trapezoid (Fig. 29.4). It forms the posteroinferior part of the nasal septum and presents two surfaces and four borders. Both surfaces are marked by grooves for nerves and vessels. A prominent groove for the nasopalatine nerve and vessels lies obliquely in an anteroinferior plane. The superior border is thickest, and possesses a deep furrow between projecting alae which fits the rostrum of the body of the sphenoid bone. The alae articulate with the sphenoidal conchae, the vaginal processes of the medial pterygoid plates of the sphenoid bone, and the sphenoidal processes of the palatine bones. Where each ala lies between the body of the sphenoid and the vaginal process, its inferior surface helps to form the vomerovaginal canal. The inferior border articulates with the median nasal crests of the maxilla and palatine bones. The anterior border is the longest, and articulates in its upper half with the perpendicular plate of the ethmoid bone. Its lower half is cleft to receive the inferior margin of the nasal septal cartilage (see Ch. 32). The concave posterior border is thick and bifid above and thin below: it separates the posterior nasal apertures. The anterior extremity of the vomer articulates with the posterior margin of the maxillary incisor crest and descends between the incisive canals.

Ossification

The nasal septum is at first a plate of cartilage, part of which is ossified above to form the perpendicular plate of the ethmoid. Its anteroinferior region persists as septal cartilage. The vomer is ossified in a layer of connective tissue which covers the cartilage posteroinferiorly on each aspect. About the eighth week *in utero*, two centres appear flanking the midline, and in the twelfth week these unite below the cartilage, to form a deep groove for the nasal septal cartilage. Union of the bony lamellae progresses anterosuperiorly while the intervening cartilage is absorbed. By puberty the lamellae are almost united, but evidence of their bilaminar origin remains in the everted alae and anterior marginal groove.

ZYGOMATIC BONE

Each zygomatic bone forms the prominence of a cheek, contributes to the floor and lateral wall of the orbit and the walls of the temporal and infratemporal fossae, and completes the zygomatic arch. Each is roughly quadrangular and is described as having three surfaces, five borders and two processes (Fig. 29.7).

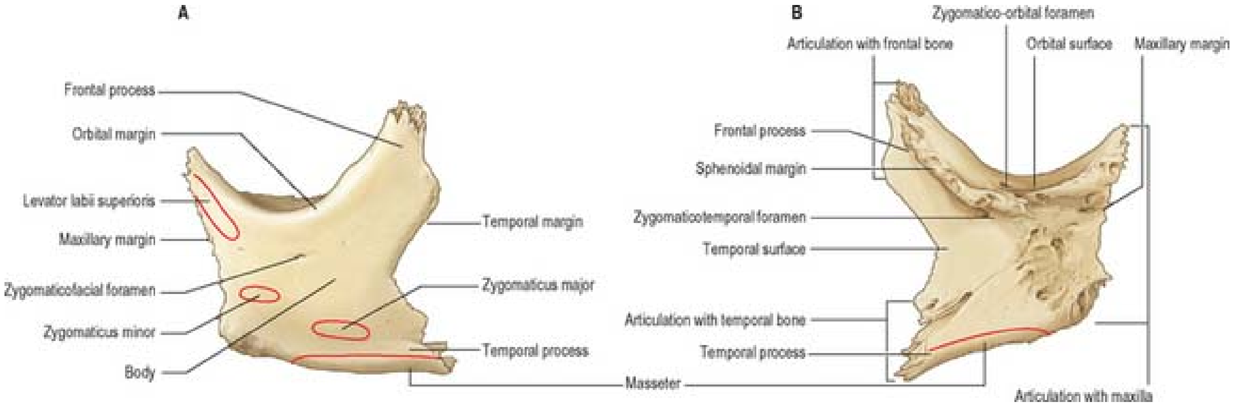
A
Frontal process
Orbital margin
Levator labii superioris
Maxillary margin
Zygomaticofacial foramen
Zygomaticus minor
Body
Temporal margin
Zygomaticus major
Temporal process
Masseter
B
Zygomatico-orbital foramen
Articulation with frontal bone
Orbital surface
Maxillary margin
Frontal process
Sphenoidal margin
Zygomaticotemporal foramen
Temporal surface
Articulation with temporal bone
Temporal process
Articulation with maxilla

Fig. 29.7 Zygomatic bone. **A**, Anterolateral aspect. **B**, Posterolateral aspect. Muscle attachments shown in A.

The lateral (facial) surface is convex and is pierced near its orbital border by the zygomaticofacial foramen, which is often double and occasionally absent, and transmits the zygomaticofacial nerve and vessels. This surface gives attachment to zygomaticus major posteriorly and zygomaticus minor anteriorly. The posteromedial (temporal) surface has a rough anterior area for articulation with the zygomatic process of the maxilla, and a smooth, concave posterior area that extends up posteriorly on its frontal process as the anterior aspect of the temporal fossa. It also extends back on the medial aspect of the temporal process as an incomplete lateral wall for the infratemporal fossa. The zygomaticotemporal foramen pierces this surface near the base of the frontal process. The smooth and concave orbital surface forms the anterolateral part of the floor and adjoining lateral wall of the orbit, and extends up on the medial aspect of its frontal process. It usually bears zygomatico-orbital foramina which represent the openings of canals leading to the zygomaticofacial and zygomaticotemporal foramina.

The smoothly concave anterosuperior (orbital) border forms the inferolateral circumference of the orbital opening, and separates the orbital and lateral surfaces of the bone. The anteroinferior (maxillary) border articulates with the maxilla. Its medial end tapers to a point above the infraorbital foramen. A part of levator labii superioris is attached at this surface. The posterosuperior (temporal) border is sinuous, convex above and concave below, and is continuous with the posterior border of the frontal process and upper border of the zygomatic arch. The temporal fascia is attached to this border. There is often a small, easily palpable, marginal tubercle below the frontozygomatic suture. The posteroinferior border is roughened for the attachment of masseter. The serrated posteromedial border articulates with the greater wing of the sphenoid bone above, and the orbital surface of the maxilla below. Between these serrated regions a short, concave, non-articular part usually forms the lateral edge of the inferior orbital fissure. Occasionally absent, the fissure is then completed by the articulation of the maxilla and sphenoid (or with a small sutural bone between them).

The frontal process, thick and serrated, articulates above with the zygomatic process of the frontal bone and behind with the greater wing of the sphenoid bone. A tubercle of varying size and form, Whitnall’s tubercle, is usually present on its orbital aspect, within the orbital opening and about 1 cm below the frontozygomatic suture. This tubercle provides attachment for the lateral palpebral ligament, the suspensory ligament of the eye, and part of the aponeurosis of levator palpebrae superioris. The temporal process, directed backwards, has an oblique, serrated end that articulates with the zygomatic process of the temporal bone to complete the zygomatic arch.

Ossification

Ossification is from one centre, which appears in fibrous tissue about the eighth week *in utero*. The bone is sometimes divided by a horizontal suture into a larger upper and smaller lower part.

MAXILLA

The maxillae are the largest of the facial bones, other than the mandible, and jointly form the whole of the upper jaw. Each bone forms the greater part of the floor and lateral wall of the nasal cavity, and of the floor of the orbit, contributes to the infratemporal and pterygopalatine fossae, and bounds the inferior orbital and pterygomaxillary fissures. Each maxilla has a body and four processes, namely the zygomatic, frontal, alveolar and palatine processes (Fig. 29.6, Fig. 29.8).

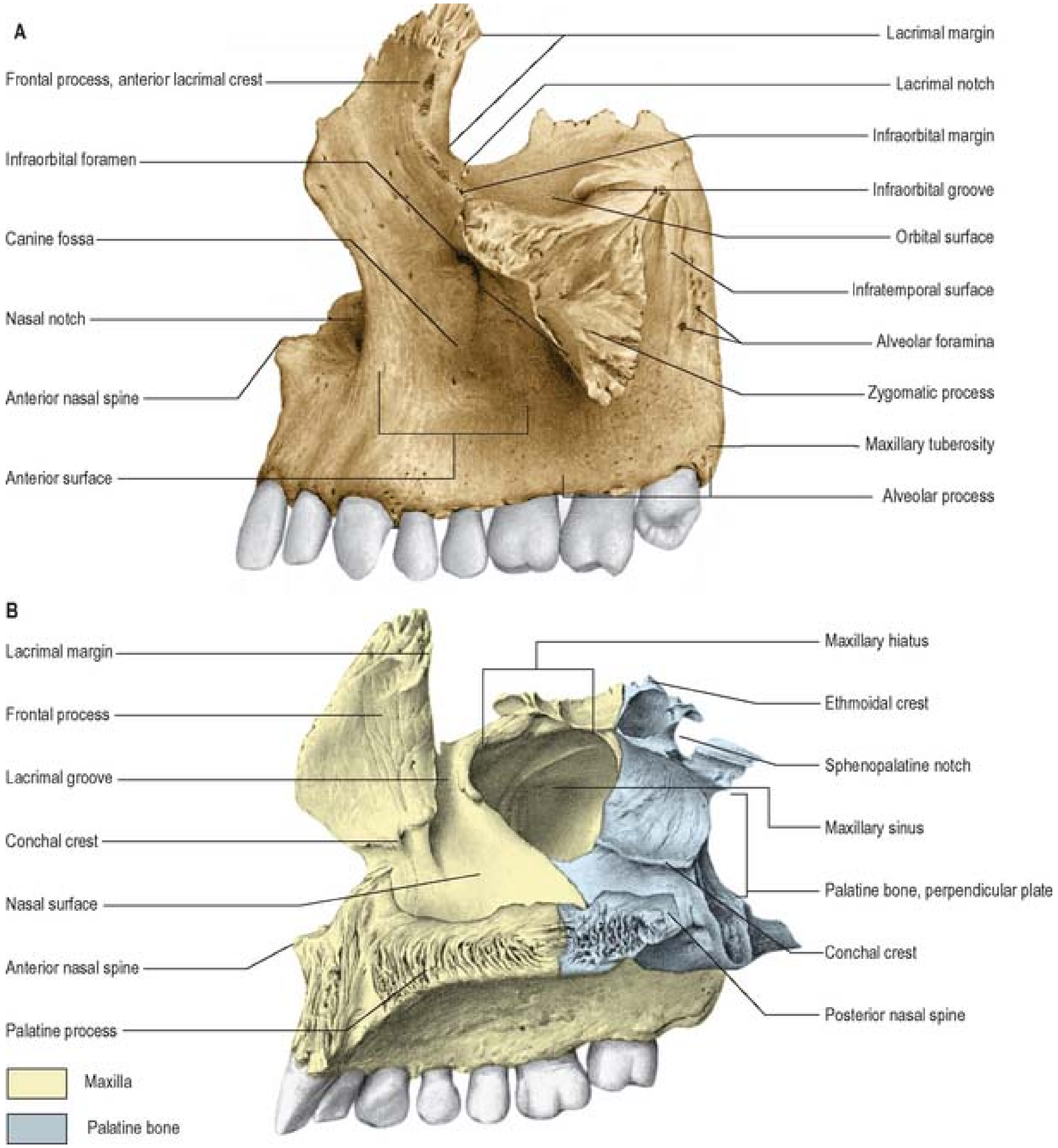
A
Frontal process, anterior lacrimal crest
Infraorbital foramen
Canine fossa
Nasal notch
Anterior nasal spine
Anterior surface
Lacrimal margin
Lacrimal notch
Infraorbital margin
Infraorbital groove
Orbital surface
Infratemporal surface
Alveolar foramina
Zygomatic process
Maxillary tuberosity
Alveolar process
B
Lacrimal margin
Frontal process
Lacrimal groove
Conchal crest
Nasal surface
Anterior nasal spine
Palatine process
Maxilla
Palatine bone
Maxillary hiatus
Ethmoidal crest
Sphenopalatine notch
Maxillary sinus
Palatine bone, perpendicular plate
Conchal crest
Posterior nasal spine

Fig. 29.8 Maxilla and palatine bone. **A**, Maxilla. **B**, Maxilla and palatine bone.

(From Sobotta 2006.)

Body

The body of the maxilla is roughly pyramidal, and has anterior, infratemporal (posterior), orbital and nasal surfaces that enclose the maxillary sinus.

Anterior surface

This surface faces anterolaterally and displays inferior elevations overlying the roots of teeth. There is a shallow incisive fossa above the incisors to which depressor septi is attached. A slip of orbicularis oris is attached to the alveolar border below this fossa, and nasalis is attached superolateral to it. Lateral to the incisive fossa is a larger, deeper canine fossa: levator anguli oris is attached to the bone of this fossa. The incisive and canine fossae are separated by the canine eminence, which overlies the socket of the canine tooth. The infraorbital foramen lies above the fossa and transmits the infraorbital vessels and nerve. Above the foramen a sharp border separates the anterior and orbital surfaces of the bone and contributes to the infraorbital margin. Levator labii superioris is attached here above the infraorbital foramen and levator anguli oris below it. Medially the anterior surface ends at a deeply concave nasal notch, terminating in a pointed process which, with its contralateral fellow, forms the anterior nasal spine. Nasalis and depressor septi are attached to the anterior surface near the notch.

Infratemporal surface

This surface is concave and faces posterolaterally, forming the anterior wall of the infratemporal fossa. It is separated from the anterior surface by the zygomatic process and a ridge (jugal crest) that ascends to it from the first molar socket. Near its centre are the openings of two or three alveolar canals which transmit posterior superior alveolar vessels and nerves. Posteroinferior is the maxillary tuberosity, roughened superomedially where it articulates with the pyramidal process of the palatine bone. A few fibres of medial pterygoid are attached here. Above the tuberosity the smooth anterior boundary of the pterygopalatine fossa is grooved by the maxillary nerve as it passes laterally and slightly upwards into the infraorbital groove on the orbital surface.

Orbital surface

This surface is smooth and triangular, and forms most of the floor of the orbit. Anteriorly its medial border bears a lacrimal notch, behind which it articulates with the lacrimal bone, the orbital plate of the ethmoid and, posteriorly, with the orbital process of the palatine bone. Its posterior border is smoothly rounded, and forms most of the anterior edge of the inferior orbital fissure. The infraorbital groove lies centrally. The anterior border is part of the orbital margin, and is continuous medially with the lacrimal crest of the frontal process of the maxilla. The infraorbital groove transmits the infraorbital vessels and nerve, and begins midway on the posterior border, where it is continuous with a groove on the posterior surface. It passes forwards into the infraorbital canal which opens on the anterior surface below the infraorbital margin. Near its midpoint, the infraorbital canal gives off a small lateral branch, the canalis sinuosus, that transmits the anterior superior alveolar nerve and vessels. The canalis sinuosus descends in the orbital floor lateral to the infraorbital canal, curves medially in the anterior wall of the maxillary sinus, and then passes below the infraorbital foramen to the margin of the anterior nasal aperture in front of the anterior end of the inferior concha. It follows the lower margin of the aperture and opens near the nasal septum in front of the incisive canal. The site of the attachment of inferior oblique may be indicated by a small depression in the bone at the anteromedial corner of the orbital surface, lateral to the lacrimal groove.

Nasal surface

This surface displays posterosuperiorly a large, irregular maxillary hiatus that leads into the maxillary sinus. Parts of air sinuses that are completed by articulation with the ethmoid and lacrimal bones lie at the upper border of the hiatus. The smooth concave surface below the hiatus is part of the inferior meatus. Posteriorly, the surface is roughened where it articulates with the perpendicular plate of the palatine bone. This surface is traversed by a groove which descends forwards from the midposterior border, and is converted into a greater palatine canal by the perpendicular plate. Anterior to the hiatus, a deep nasolacrimal groove, continuous above with the lacrimal groove, makes up about two-thirds of the circumference of the nasolacrimal canal. The rest is contributed by the descending part of the lacrimal bone and the lacrimal process of the inferior nasal concha. This canal conveys the nasolacrimal duct to the inferior meatus. More anteriorly, an oblique conchal crest articulates with the inferior nasal concha. The concavity below it is part of the inferior meatus, while the surface above it is part of the atrium of the middle meatus.

Zygomatic process

Anterior, infratemporal and orbital surfaces of the maxilla converge at a pyramidal projection, the zygomatic process. Anteriorly, the process merges into the facial surface of the body of the maxilla. Posteriorly, it is concave and continuous with the infratemporal surface. Superiorly, it is roughly serrated for articulation with the zygomatic bone. Inferiorly, a bony arched ridge, the zygomaticoalveolar ridge or jugal crest, separates the facial (anterior) and infratemporal surfaces.

Frontal process

The frontal process projects posterosuperiorly between the nasal and lacrimal bones. Its lateral surface is divided by a vertical anterior lacrimal crest which gives attachment to the medial palpebral ligament and is continuous below with the infraorbital margin. A small palpable tubercle at the junction of the crest and orbital surface is a guide to the lacrimal sac. The smooth area anterior to the lacrimal crest merges below with the anterior surface of the body of the maxilla. Parts of orbicularis oculi and levator labii superioris alaeque nasi are attached here. Behind the crest, a vertical groove combines with a groove on the lacrimal bone to complete the lacrimal fossa. The medial surface is part of the lateral nasal wall. A rough subapical area articulates with the ethmoid, and closes anterior ethmoidal air cells. Below this an oblique ethmoidal crest articulates posteriorly with the middle nasal concha, and anteriorly underlies the agger nasi, a ridge anterior to the concha on the lateral nasal wall. The ethmoidal crest forms the upper limit of the atrium of the middle meatus. The frontal process articulates above with the nasal part of the frontal bone. Its anterior border articulates with the nasal bone and its posterior border articulates with the lacrimal bone.

Alveolar process

The alveolar process is thick and arched, wide behind, and socketed for the roots of the upper teeth. The eight sockets on each side vary according to the tooth type. The socket for the canine is deepest, the sockets for the molars are widest and subdivided into three by septa, those for the incisors and second premolar are single, and that for the first premolar usually double. Buccinator is attached to the external alveolar aspect as far forwards as the first molar. In articulated maxillae the processes form the alveolar arch. Occasionally a variably prominent maxillary torus is present in the midline of the palate.

Palatine process

The palatine process, thick and horizontal, projects medially from the lowest part of the medial aspect of the maxilla. It forms a large part of the nasal floor and hard palate and is much thicker in front. Its inferior surface is concave and uneven, and with its contralateral fellow it forms the anterior three-fourths of the osseous (hard) palate. The palatine process displays numerous vascular foramina and depressions for palatine glands and, posterolaterally, two grooves that transmit the greater palatine vessels and nerves. The infundibular incisive fossa is placed between the two maxillae, behind the incisor teeth. The median intermaxillary palatal suture runs posterior to the fossa, and although a little uneven, is usually relatively flat on its oral aspect. Its bony margins are sometimes raised into a prominent longitudinal palatine torus. Two lateral incisive canals, each ascending into its half of the nasal cavity, open in the incisive fossa: they transmit the terminations of the greater palatine artery and nasopalatine nerve. Two additional median openings, anterior and posterior incisive foramina, are occasionally present: they transmit the nasopalatine nerves, the left usually passing through the anterior, and the right through the posterior foramen. On the inferior palatine surface a fine groove, sometimes termed the incisive suture, and prominent in young skulls, may be observed in adults. It extends anterolaterally from the incisive fossa to the interval between the lateral incisor and canine teeth. The superior surface of the palatine process is smooth, concave transversely, and forms most of the nasal floor. The incisive canal lies anteriorly, near its median margin. The lateral border is continuous with the body of the maxilla. The medial border, thicker in front, is raised into a nasal crest that, with its contralateral fellow, forms a groove for the vomer. The front of this ridge rises higher as an incisor crest, prolonged forwards into a sharp process which, with its fellow, forms an anterior nasal spine. The posterior border is serrated for articulation with the horizontal plate of the palatine bone.

Maxillary sinus

The maxillary sinus is the largest of the paranasal sinuses and is situated in the body of the maxilla. It is described in detail in Chapter 32.

Ossification

The maxilla ossifies from a single centre in a sheet of mesenchyme that appears above the canine fossa at about the sixth week *in utero* and spreads into the rest of the maxilla and its processes. The pattern of spread of ossification may initially leave an unmineralized zone roughly corresponding to a site where a premaxillary suture may occur. However, this deficiency is soon ossified; there is no evidence of a separate centre of ossification for the incisor-bearing portion of the maxilla (i.e. premaxilla).

The maxillary sinus appears as a shallow groove on the nasal aspect at about the fourth month *in utero*. Though small at birth, the sinus is identifiable radiologically. After birth it enlarges with the growing maxilla, though it is only fully developed following the eruption of the permanent dentition. The infraorbital vessels and nerve are for a time in an open groove in the orbital floor; the anterior part of the groove is subsequently converted into a canal by a lamina that grows in from the lateral side.

At birth the transverse and sagittal maxillary dimensions are greater than the vertical. The frontal process is prominent, but the body is little more than an alveolar process, because the alveoli reach almost to the orbital floor. In adults the vertical dimension is the greatest, reflecting the development of the alveolar process and enlargement of the sinus. When teeth are lost, the bone reverts towards its infantile shape: its height diminishes, the alveolar process is absorbed, and the lower parts of the bone contract and become reduced in thickness at the expense of the labial wall.

PALATINE BONE

The palatine bones are posteriorly placed in the nasal cavity, between the maxillae and the pterygoid processes of the sphenoid bones. They contribute to the floor and lateral walls of the nose, to the floor of the orbit and the hard palate, to the pterygopalatine and pterygoid fossae, and to the inferior orbital fissures. Each has two plates (horizontal and perpendicular) arranged as an L-shape, and three processes (pyramidal, orbital and sphenoidal) (Fig. 29.9).

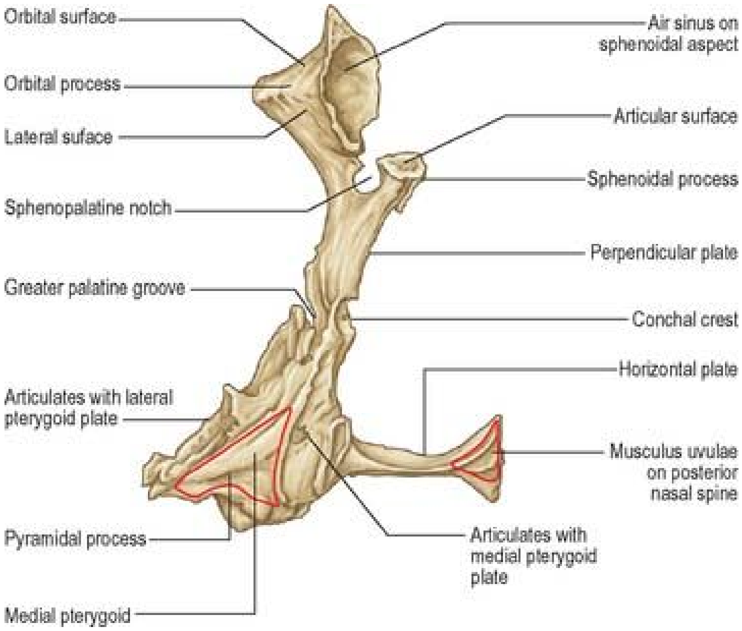
Orbital surface
Orbital process
Lateral suface
Sphenopalatine notch
Greater palatine groove
Articulates with lateral pterygoid plate
Pyramidal process
Medial pterygoid
Air sinus on sphenoidal aspect
Articular surface
Sphenoidal process
Perpendicular plate
Conchal crest
Horizontal plate
Musculus uvulae on posterior nasal spine
Articulates with medial pterygoid plate

Fig. 29.9 Palatine bone, posterior view.

Horizontal plate

The horizontal plate is quadrilateral, with two surfaces (nasal and palatine) and four borders (anterior, posterior, lateral and medial). The nasal surface, transversely concave, forms the posterior nasal floor. The palatine surface forms the posterior quarter of the bony palate with its contralateral fellow. There is often a curved palatine crest near its posterior margin. The posterior border is thin and concave: the expanded tendon of tensor veli palatini is attached to it and to its adjacent surface behind the palatine crest. Medially, with its contralateral fellow, the posterior border forms a median posterior nasal spine to which the uvular muscle is attached. The anterior border is serrated and articulates with the palatine process of the maxilla. The lateral border is continuous with the perpendicular plate of the palatine bone and is marked by a greater palatine groove. The medial border is thick and serrated and articulates with its contralateral fellow in the midline, forming the posterior part of the nasal crest which articulates with the posterior part of the lower edge of the vomer.

Perpendicular plate

The perpendicular plate is thin and oblong, and has two surfaces (nasal and maxillary) and four borders (anterior, posterior, superior and inferior). The nasal surface bears two crests (conchal and ethmoidal) and shows areas which contribute to the inferior, middle and superior meatuses. Inferiorly, the nasal surface is concave where it contributes to part of the inferior meatus. Above this is a horizontal conchal crest that articulates with the inferior concha. Above the conchal crest the surface presents a shallow depression that forms part of the middle meatus; it is limited above by an ethmoidal crest for the middle nasal concha, above which a narrow, horizontal groove forms part of the superior meatus.

The maxillary surface is largely rough and irregular and articulates with the nasal surface of the maxilla. Posterosuperiorly it forms a smooth medial wall to the pterygopalatine fossa. Its anterior area, also smooth, overlaps the maxillary hiatus from behind to form a posterior part of the medial wall of the maxillary sinus. A deep, obliquely descending greater palatine groove (converted into a canal by the maxilla) lies posteriorly on this maxillary surface: it transmits the greater palatine vessels and nerve.

The anterior border is thin and irregular. Level with the conchal crest, a pointed lamina projects below and behind the maxillary process of the inferior concha: it articulates with it and so appears in the medial wall of the maxillary sinus. The posterior border articulates via a serrated suture with the medial pterygoid plate. It is continuous above with the sphenoidal process of the palatine bone and expands below into its pyramidal process. Orbital and sphenoidal processes project from the superior border, and are separated by the sphenopalatine notch, which is converted into a foramen by articulation with the body of the sphenoid. This foramen connects the pterygopalatine fossa to the posterior part of the superior meatus, and transmits sphenopalatine vessels and the posterior superior nasal nerves. The inferior border is continuous with the lateral border of the horizontal plate and bears the lower end of the greater palatine groove in front of the pyramidal process.

Pyramidal process

The pyramidal process slopes down posterolaterally from the junction of the horizontal and perpendicular palatine plates into the angle between the pterygoid plates of the sphenoid bone. On its posterior surface a smooth, grooved triangular area, limited on each side by rough articular furrows which articulate with the pterygoid plates, completes the lower part of the pterygoid fossa. Anteriorly the lateral surface articulates with the maxillary tuberosity. This area gives attachment to fibres of the superficial head of medial pterygoid. Posteriorly a smooth triangular area appears low in the infratemporal fossa between the tuberosity and the lateral pterygoid plate. The inferior surface, near its union with the horizontal plate, bears the lesser palatine foramina which transmit the lesser palatine nerves and vessels.

Orbital process

The orbital process is directed superolaterally from in front of the perpendicular plate, and has a constricted “neck”. It encloses an air sinus and presents three articular and two non-articular surfaces. Of the articular surfaces, the oblong anterior (maxillary) surface faces down and anterolaterally and articulates with the maxilla. The posterior (sphenoidal) surface is directed up and posteromedially, and bears the opening of an air sinus. It usually communicates with the sphenoidal sinus, and is completed by a sphenoidal concha. The medial (ethmoidal) surface faces anteromedially and articulates with the labyrinth of the ethmoid bone. The sinus of the orbital process sometimes opens on the surface, and communicates with the posterior ethmoidal air cells. More rarely it opens on both the ethmoidal and sphenoidal surfaces, and communicates with both posterior ethmoidal air cells and the sphenoidal sinus.

Of the non-articular surfaces, the triangular superior (orbital) surface is directed superolaterally to the posterior part of the orbital floor. The lateral surface is oblong, faces the pterygopalatine fossa and is separated from the orbital surface by a rounded border that forms a medial part of the lower margin of the inferior orbital fissure. This surface may present a groove, directed superolaterally, for the maxillary nerve, and is continuous with the groove on the upper posterior surface of the maxilla. The border between the lateral and posterior surfaces descends anterior to the sphenopalatine notch.

Sphenoidal process

The sphenoidal process is a thin plate that is smaller and lower than the orbital process, and is directed superomedially. Its superior surface articulates with the sphenoidal concha and, above it, with the root of the medial pterygoid plate. It carries a groove that contributes to the formation of the palatovaginal canal. The concave inferomedial surface forms part of the roof and lateral wall of the nose. Posteriorly the lateral surface articulates with the medial pterygoid plate, while its smooth anterior region forms part of the medial wall of the pterygopalatine fossa. The posterior border articulates with the vaginal process of the medial pterygoid plate. The anterior border is the posterior edge of the sphenopalatine notch. The medial border articulates with the ala of the vomer. The sphenopalatine notch, between the two processes, is converted into a foramen by articulation with the body of the sphenoid bone.

Ossification

Ossification is in mesenchyme from one centre in the perpendicular plate that appears during the eighth week *in utero*. From this centre, ossification spreads into all parts. At birth, the height of the perpendicular plate equals the width of the horizontal plate, but in adults it is almost twice as great, a change in proportions that accords with those that occur in the maxilla.

FRACTURES OF THE FACIAL SKELETON

Fractures affecting the facial bones are common. They occur in road traffic accidents, sports injuries, accidents at work and, increasingly, as a consequence of interpersonal violence, often alcohol-related. Given that most people are right-handed, fractures resulting from assault occur more commonly on the left side of the facial skeleton. Skull fractures tend to adopt well-recognized patterns reflecting the shape and structure of the facial bones, local anatomical factors, and stress points which constitute sites of weakness.

Frequently these fractures do not occur as bilateral symmetrical fractures but occur in various combinations, e.g. both together, on the same side, and involving both sides. Typically these fractures arise from force applied anteriorly over a wide area. Such injuries are seen in road traffic accidents where, e.g. a driver or passenger is thrown forwards on to the steering wheel or dashboard. The direction of the applied force determines the displacement of these fractures. With the possible exception of the relatively weak lateral pterygoids, muscle pull plays a relatively small role. As the fractures are generally displaced backwards, because of the angulation of the strong skull base, there is also a downward component, which results clinically in a lengthening of the face and a dished-in appearance. There may be airway obstruction if this downwards and backwards displacement is severe.

Although the fractures that occur in severe injuries are often complex, it is convenient to describe them as arising in the upper, middle and lower thirds of the face, even though fractures may involve one or more of these areas. Upper third fractures involve the frontal bones. Middle third fractures involve the nasoethmoidal complex, orbit, zygomatic complex and maxilla. Lower third fractures correspond to fractures of the mandible.

Upper third of face

Fractures in the upper third of the face are almost invariably comminuted and are often associated with fractures of the middle third of the face. Fractures of the frontal bone may involve the frontal sinuses and/or orbital roof. If the frontonasal duct is traumatized its drainage may be impaired, which predisposes to ascending intracranial infection and mucocele development within the frontal sinuses. This risk may be minimized with frontonasal stents or frontonasal duct and frontal sinus obliteration with autogenous bone graft (see Ch. 32). Fractures that involve both the anterior and posterior walls of the frontal sinus also carry a risk of early and delayed intracranial infection, and often it is necessary to obliterate the frontal sinuses or cranialize the frontal sinuses in order to prevent this complication. Cranialization of the frontal sinuses involves the removal of the posterior wall and all frontal sinus mucosa, typically through a frontal craniotomy approach. Fractures of the posterior wall of the frontal sinus may be associated with dural tears (and cerebrospinal rhinorrhoea) which must be repaired at the same time. Fractures involving the orbital roof may be associated with displacement of the globe of the eye, diplopia and supraorbital nerve injury.

Middle third of the face

The middle third of the face is defined as that area bounded above by a transverse line connecting the two zygomaticofrontal sutures, passing through the frontomaxillary and frontonasal sutures, and limited below by the occlusal plane of the maxillary teeth. Posteriorly the region is limited by the sphenoethmoidal junction, but it includes the free margins of the pterygoid plates inferiorly. Fractures of the middle third of the facial skeleton may involve the maxillae, palatine bones, zygomatic bones, zygomatic processes of the temporal bones, nasal bones, vomer, ethmoid bone together with its nasal conchae, and the body and greater and lesser wings of the sphenoid bone. They are subdivided into fractures involving the central block and fractures involving the lateral middle thirds.

Central middle third of the face

The majority of the skeleton of the central middle third is composed of wafer thin sheets of cortical bone with stronger reinforcements, i.e. the palate and alveolar process; the lateral rim of the piriform aperture extending upwards (via the canine fossa) to the medial orbital rim, and finally to the glabella; the zygomatic buttress and its connections to the inferior and lateral orbital margins and the zygomatic arch; the orbital rims and the pterygoid plates. The strength lies in the facial surface of the skeleton which, although thin in most areas, is cross-braced. The design is ideally suited to transmit occlusal forces vertically to the skull base.

Central middle third fractures may involve the nasoethmoidal complex in isolation or as part of a more complex Le Fort pattern of injury. Le Fort I, II or III fractures inevitably involve the infratemporal fossa. The bones of the midface transmit the forces of impact directly to the cranium. The most important strut related to the infratemporal and pterygopalatine fossae is the pterygomaxillary strut. Fractures involving this strut may extend elsewhere to involve the cranial base and orbit. The associated soft tissue damage which accompanies these fractures may damage nerves, blood vessels and muscles. Injuries to the second or third divisions of the trigeminal nerve or the chorda tympani nerve result in altered sensation to the oral cavity, face and jaws, including impaired taste; fractures extending into the orbit may result in decreased visual acuity and ophthalmoplegia and neural damage to motor nerves or direct damage to muscles may result in problems with chewing, swallowing, speech, middle ear function and eye movements; injuries involving the pterygopalatine or otic ganglia interfere with lacrimation, nasal secretions and salivation.

Nasoethmoidal complex

Fractures may involve the osteocartilaginous framework of the nose in isolation or as part of complex injuries that also involve the paranasal sinuses and/or the orbits.

Simple fractures involve the nasal bones and/or frontal process of the maxilla. Only if there is displacement of the bones is a closed reduction of the fracture required. The terminal branch of the anterior ethmoidal nerve and its accompanying vessels are at risk when injuries involve the dorsum of the nose.

Complex nasal injuries may include nasofrontal suture disjunction, nasolacrimal and frontonasal duct injury and fracture of the ethmoid complex. The skeletal foundation of the nasoethmoidal complex consists of a strong triangular-shaped frame. However, all these structures are fragile and any force sufficient to fracture the frame results in severe comminution and displacement. The ethmoid air cells act as a crumple zone protecting the skull base from mechanical forces. A severe impact delivered to the midface, particularly over the bridge of the nose, may result in these structures being driven backwards between the orbits. This may result in traumatic hypertelorism, producing an increase in distance between the pupils. Associated displacement of the medial canthal ligaments results in traumatic telecanthus. Increased intercanthal distance (normal range 24–39 mm in Caucasians) may be corrected using microplates, stainless steel wire and acrylic canthal splints. Damage to the lacrimal system requires approximation of the severed canalicular ends or dacrocystorhinostomy. Comminution of the cribriform plates of the ethmoid may result in dural tears and cerebrospinal rhinorrhoea. Often nasoethmoidal fractures are combined with more extensive fractures of the frontal bone. The complexity of the injury has implications for subsequent facial reconstruction.

Le Fort I fractures (Guerin’s fracture)

Le Fort I fractures consist of a horizontal fracture line above the level of the floor of the nose involving the lower third of the nasal septum. The mobile segment consists of the palate, the alveolar process and the lower thirds of the pterygoid plates.

Le Fort II fractures (pyramidal fracture)

Le Fort II fractures are pyramidal fractures involving the maxillary bones. From the nasal bridge, the fracture enters the medial wall of the orbit to involve the lacrimal bone and then crosses the inferior orbital rim, usually at the junction of the medial one-third and lateral two-thirds, and often involves the infraorbital foramen. The fracture line then runs beneath the zygomaticomaxillary suture, traversing the lateral wall of the maxillary sinus to extend posteriorly and horizontally across the pterygoid plates. The zygomatic bones and arches remain attached to the skull base.

Le Fort III fractures

Le Fort III fractures run parallel with the base of the skull, separating the entire mid-facial skeleton from the cranial base. The fracture extends through the nasal base and continues posteriorly across the ethmoid bone. The fracture then crosses the lesser wing of the sphenoid and, on occasion, involves the optic foramen. Usually, however, it slopes down medially passing below the optic foramen to reach the pterygomaxillary fissure and pterygopalatine fossa. From the base of the inferior orbital fissure the fracture runs laterally and upwards, separating the greater wing of the sphenoid from the zygomatic bone, to reach the frontozygomatic suture. It also extends downwards and backwards across the pterygopalatine fossa to involve the root of the pterygoid plates. The zygomatic arch is usually fractured at the zygomaticotemporal suture.

Lateral middle third of the face

Fractures of the lateral middle third involve the zygomaticomaxillary complex. The zygomatic bone forms the prominence of the cheek. Since the most common cause of a zygomatic fracture is a blow from a fist, depressed fractures of the zygomaticomaxillary complex are a common injury. These injuries may occur in isolation or in association with orbital blow-out fractures. Isolated fractures of the zygomatic arch are relatively unusual.

Classic zygomatic complex fractures involve the zygomaticomaxillary, zygomaticotemporal and zygomaticofrontal sutures. The fracture line extends from the lateral wall of the orbit laterally into the infratemporal fossa at the zygomaticofrontal suture. From this point the fracture line extends inferiorly to join the most lateral aspect of the inferior orbital fissure, continues inferiorly along the posterior surface of the zygomatic buttress – where it communicates with the lateral bulge of the maxillary antrum – and runs around the zygomatic buttress, high in the buccal sulcus in the upper molar region, and then extends upwards towards the infraorbital foramen. It finally runs laterally along the floor of the orbit to reach the lateral extension of the inferior orbital fissure. Clinical signs may include facial asymmetry, infraorbital nerve paraesthesia/anaesthesia, limitation of mouth opening (if there is impingement of the coronoid process by a depressed arch fracture) and signs of orbital blow-out fracture (see below).

As zygomatic fractures involve the maxillary sinus (the lateral wall of which is frequently comminuted) and the infratemporal fossa, there is potential for spread of infection between these structures and then via foraminae in the skull base to the middle cranial fossa. Patients with zygomatic complex fractures must be advised to refrain from sneezing or nose-blowing which may force air from the antrum into the surrounding tissues (surgical emphysema) or into the orbit, resulting in proptosis of the eye.

Orbital fractures

The orbit is invariably involved in fractures of the zygomatic bone and in Le Fort II and III fractures. The orbit may also be involved in fractures of the frontal bone and extensive nasal complex injuries. Direct blunt trauma to the globe may result in displacement of the globe and fracture of the thin orbital floor (or medial wall) without associated rim involvement and is known as a ‘blow-out’ fracture. This protective mechanism of injury helps to maintain the integrity of the globe itself in preference to the orbital walls. There may be associated herniation of periorbital fat and/or inferior rectus muscle resulting in restriction of eye movement, diplopia, ipsilateral lowering of pupillary height, and enophthalmos (due to increased orbital volume). Fortunately the optic foramen which is situated within the lesser wing of the sphenoid bone is surrounded by dense bone and is only rarely involved in fractures. Direct injury to the optic nerve is therefore unusual.

Lower third of face (mandible)

The mandible is essentially a tubular bone bent into a blunt V-shape (see Ch. 30). This basic configuration is modified by sites of muscle attachment, principally masseter and medial pterygoid at the angle, and temporalis at the coronoid process. The presence of teeth, particularly those with long roots such as the canines, or of unerupted teeth, produces lines of weakness in the mandible. When the teeth are lost, or fail to develop, the subsequent progressive resorption of the alveolar bone means that the mandible reverts to its underlying tubular structure. Like all tubular bones, the strength of the mandible resides in a dense cortical plate, thickened anteriorly and at its lower border: it follows that the mandible is strongest anteriorly in the midline and is progressively weaker posteriorly towards the condylar processes. Again, like all tubular bones, the mandible has great resistance to compressive forces, but fractures at sites of tensile strain. It is liable to particular patterns of distribution of tensile strain when forces are applied to it. Anterior forces applied to the mental symphysis, or over the body of the mandible, lead to strain at the condylar necks and also along the lingual cortical plates on the contralateral side in the molar region. The mandible therefore often fractures at two sites and isolated fractures are relatively unusual. In order of frequency, fractures occur most commonly at the neck of the condyle, the angle, the parasymphysial region and the body of the mandible.

Condylar process

The condyle is protected from direct injury by the zygomatic arches. Fractures occur usually by the transmission of force following a blow to the front of the mandible or to the contralateral body. Except in children, most condylar fractures are not intracapsular, and occur in the neck. They usually run obliquely downwards and backwards from the mandibular notch. The condyle is usually displaced anteromedially (because of the attachment of lateral pterygoid to the temporomandibular joint disc, capsule and anterior border of the neck of the condyle).

Angle of the mandible

The majority of fractures of the mandible run posteriorly and inferiorly from the alveolar bone to the angle. The presence of a third molar tooth produces a line of weakness and a fracture line will pass through its socket. The unopposed pull of the powerful elevator muscles (masseter, medial pterygoid and temporalis) will typically displace the posterior fragment superiorly, anteriorly and medially.

Ramus and coronoid process

Fractures at the ramus exhibit very little displacement as a consequence of the splinting activity of medial pterygoid medially and masseter laterally, the pterygo-masseteric sling: their wide attachments to the ramus extend across the fracture lines. Similarly the coronoid process is rarely significantly displaced because it is splinted by the tendinous insertion of temporalis.

Body of the mandible

Most fractures of the body of the mandible occur as the result of direct trauma and tend to be concentrated in the first molar or canine region. The more anterior the site of the fracture, the more the upward displacement of the elevators is counteracted by the downward pull of geniohyoid and the anterior belly of digastric. When teeth are present displacement is limited by the dental occlusion (i.e. further displacement is resisted by the lower and upper teeth), whereas displacement may be considerable in an edentulous patient.

Campbell’s lines

Campbell’s lines are five lines that are systematically traced when assessing maxillofacial radiographs. Line 1 joins the two zygomaticofrontal sutures: it runs along the superior orbital margins and crosses the midline in the region of the glabella. Line 2 runs along the zygomatic bone and the inferior orbital margin, crosses the frontal process of the maxilla and lateral wall of the nose, then passes through the nasal septum to follow a similar course to the contralateral zygomatic bone. Line 3 begins at the condyle of the mandible, passes across the mandibular notch and coronoid process of the mandible, then crosses the maxillary sinus from its lateral to medial walls and continues through the lateral wall of the nose at the level of the nasal floor; it follows a similar course on the contralateral side. Line 4 follows the occlusal plane of the upper and lower teeth, and line 5 follows the lower border of the mandible.

Cranial base

The cranial base, namely the frontal, ethmoid, sphenoid and occipital bones, is a relatively solid platform inclined at an angle of 45° to the maxillary occlusal plane. Fractures of the cranial base are not readily visible on normal radiographs and are best detected on CT scans. They result in bleeding in the floor of the middle cranial fossa which often presents as bruising over the mastoid process (Battle’s sign). These fractures may be associated with dural tears and escape of cerebrospinal fluid from the nose (rhinorrhoea) or ruptured tympanic membrane (otorrhoea). Alternatively, if this membrane remains intact it may be seen as blue and bulging, haemotympanum.

SKELETAL ACCESS SURGERY

The craniofacial skeleton has an excellent blood supply, and so can be dismantled as a series of osteoplastic flaps. The surgical disarticulation of the craniofacial skeleton has been used to gain access to otherwise inaccessible sites in order to allow the surgeon to attend to pathology in the skull base, cervical spine and anterior and posterior cranial fossae. The aim is to provide increased and more direct exposure of both the pathology and the adjacent vital structures without the need to resect uninvolved structures. The craniofacial skeleton can be divided into a series of modular osteotomies, which permit both independent and conjoined mobilization.

The zygomatic and nasal bones and the maxilla may be exposed and mobilized, pedicled on the overlying soft tissues either unilaterally or bilaterally. These approaches improve access to the nasal cavity, maxillary, ethmoid and sphenoid sinuses, the soft palate and nasopharynx, and the infratemporal fossa and pharyngeal space. The exposures may be extended to gain access to the anterior and middle cranial fossae, cavernous sinus, clivus, craniocervical junction and upper cervical vertebrae.

A variety of different access osteotomies have been described and found to be useful in specific clinical situations. Most of the osteotomies described follow the conventional patterns of facial fractures described above. The entire hemimaxilla and zygoma can be mobilized, and pedicled on the soft tissues of the face by making bone cuts that follow the lines of a Le Fort II fracture on one side. The osteotomy is completed by dividing the upper alveolus and palate just to the side of the nasal septum and perpendicular plate of the vomer. The maxilla may be mobilized at the Le Fort I level and downfractured, pedicled on the palatoglossal muscles and soft tissue attachments. This gives good access to the nasopharynx, clivus and upper cervical spine, particularly if the palate is divided in the midline.

Lateral zygomatic osteotomies may be performed to gain access to the orbital apex and infratemporal fossa. The surgical approach is from behind using a hemi- or bicoronal flap. The zygomatic complex is mobilized inferiorly pedicled on masseter. When combined with a mandibular ramus osteotomy, access is gained to the retromaxillary area and pterygoid space as well as to the infratemporal fossa. In combination with a frontotemporal craniotomy, the zygomatic osteotomy has been used for access to the middle cranial fossa, cavernous sinus, apex of the petrous temporal bone and the interpeduncular cistern.

Dividing the lower lip in the midline, and dividing the mandible either in the midline or just in front of the mental foramen, allows the hemimandible to be swung laterally. The technique is used to give improved access to the floor of the mouth, the base of the tongue, tonsillar fossa, soft palate, oropharynx, posterior pharyngeal wall, supraglottic larynx and pterygomandibular region. By extending the dissection laterally access is gained to the pterygoid space, infratemporal fossa and parapharyngeal space. By dissecting more medially access is gained to the nasopharynx, lower part of the clivus and all seven of the cervical vertebrae. A modification of the mandibular swing procedure increases access up to the skull base, by combining the classic mandibular swing with a horizontal osteotomy of the mandibular ramus above the level of the lingula.

MUSCLES OF THE FACE

Craniofacial muscles are associated with the orbital margins and eyelids, external nose and nostrils, lips, cheeks and mouth, pinna, scalp and cervical skin, and collectively are often called, not very accurately, ‘muscles of facial expression’ (Fig. 29.10). Their organization differs from that of muscles in most other regions of the body because there is no deep membranous fascia beneath the skin of the face, and many small slips of muscle that are attached to the facial skeleton insert directly into the skin.

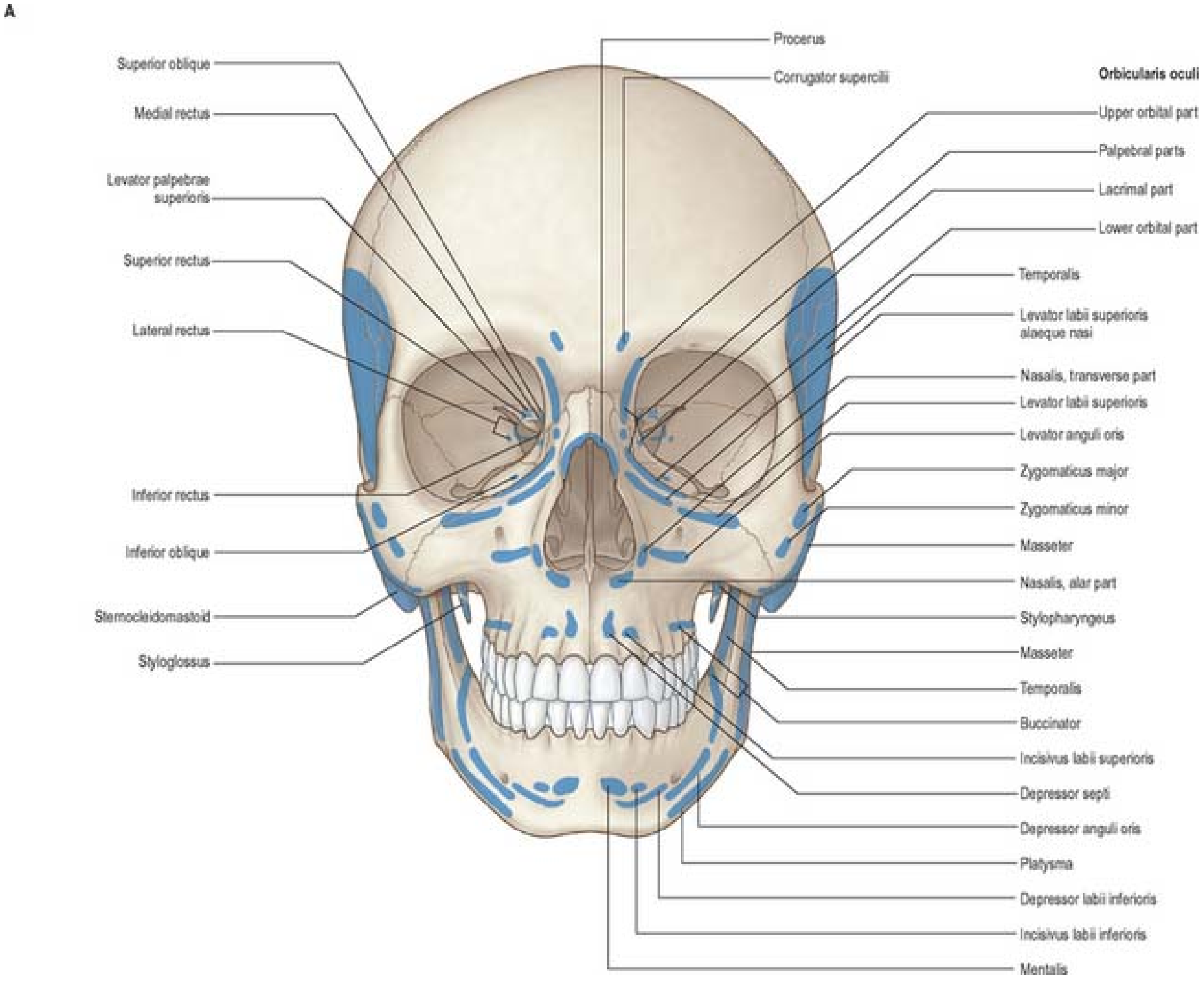
A
Superior oblique
Medial rectus
Levator palpebrae superioris
Superior rectus
Lateral rectus
Inferior rectus
Inferior oblique
Sternocleidomastoid
Styloglossus
Procerus
Corrugator supercilii
Orbicularis oculi
Upper orbital part
Palpebral parts
Lacrimal part
Lower orbital part
Temporalis
Levator labii superioris alaeque nasi
Nasalis, transverse part
Levator labii superioris
Levator anguli oris
Zygomaticus major
Zygomaticus minor
Masseter
Nasalis, alar part
Stylopharyngeus
Masseter
Temporalis
Buccinator
Incisivus labii superioris
Depressor septi
Depressor anguli oris
Platysma
Depressor labii inferioris
Incisivus labii inferioris
Mentalis

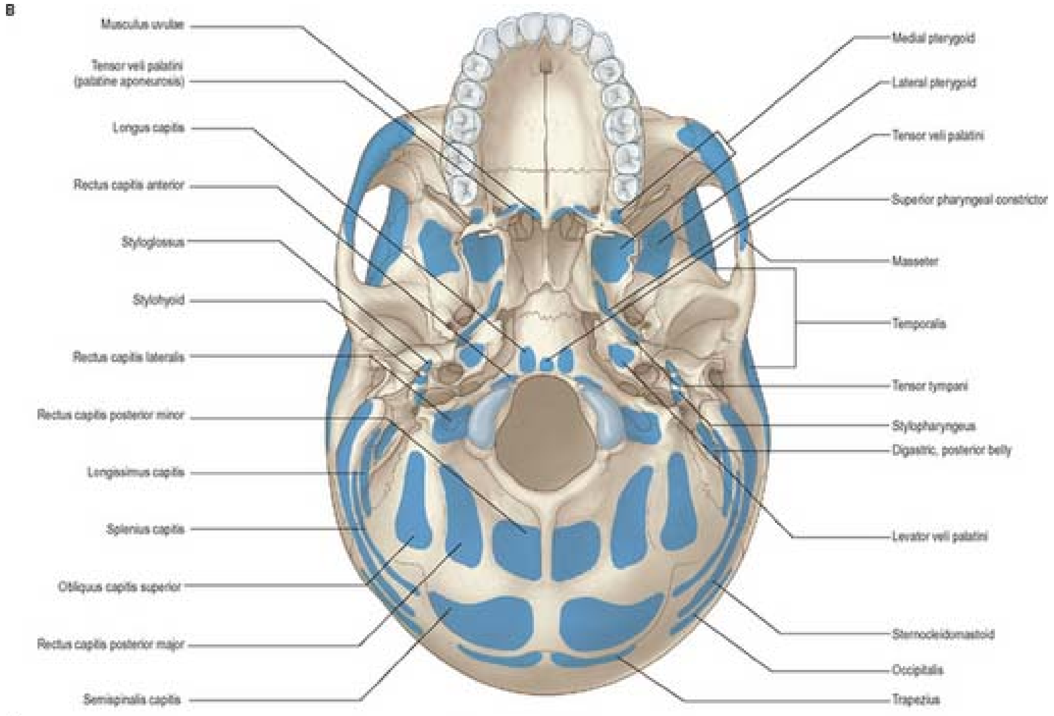
B
Musculus uvulae
Tensor veli palatini (palatine aponeurosis)
Longus capitis
Rectus capitis anterior
Styloglossus
Stylohyoid
Rectus capitis lateralis
Rectus capitis posterior minor
Longissimus capitis
Splenius capitis
Obliquus capitis superior
Rectus capitis posterior major
Semispinalis capitis
Medial pterygoid
Lateral pterygoid
Tensor veli palatini
Superior pharyngeal constrictor
Masseter
Temporalis
Tensor tympani
Stylopharyngeus
Digastric, posterior belly
Levator veli palatini
Sternocleidomastoid
Occipitalis
Trapezius

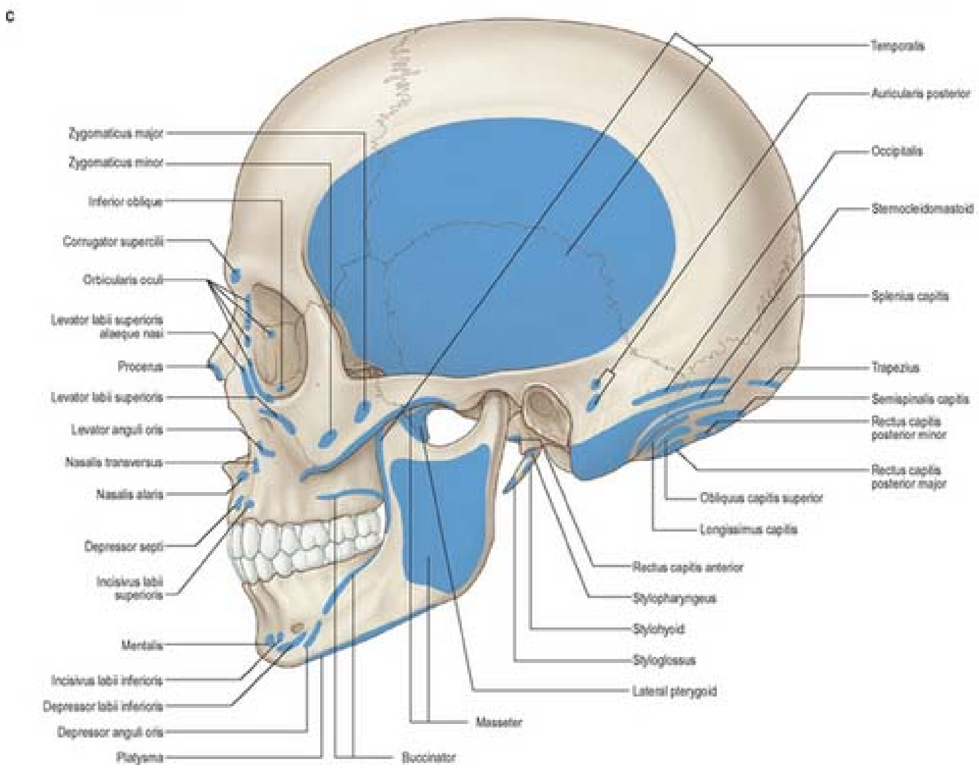
C
Zygomaticus major
Zygomaticus minor
Inferior oblique
Corrugator supercilii
Orbicularis oculi
Levator labii superioris alaeque nasi
Procerus
Levator labii superioris
Levator anguli oris
Nasalis transversus
Nasalis alaris
Depressor septi
Incisivus labii superioris
Mentalis
Incisivus labii inferioris
Depressor labii inferioris
Depressor anguli oris
Platysma
Temporalis
Auricularis posterior
Occipitalis
Sternocleidomastoid
Splenius capitis
Trapezius
Semispinalis capitis
Rectus capitis posterior minor
Rectus capitis posterior major
Obliquus capitis superior
Longissimus capitis
Rectus capitis anterior
Stylopharyngeus
Stylohyoid
Styloglossus
Lateral pterygoid
Masseter
Buccinator

Fig. 29.10 **A**, Anterior view of the skull, showing muscle attachments. **B**, Basal view of the skull, showing muscle attachments. **C**, Lateral view of the skull, showing muscle attachments.

Although these muscles produce movements of the facial skin that reflect emotions, it is usually argued that their primary function is to act as sphincters and dilators of the facial orifices and that the function of facial expression has developed secondarily. Embryologically, they are derived from the mesenchyme of the second branchial arch and so are innervated by the facial nerve. Topographically and functionally the muscles of facial expression may be subdivided into epicranial, circumorbital and palpebral, nasal, and buccolabial groups (Fig. 29.11).

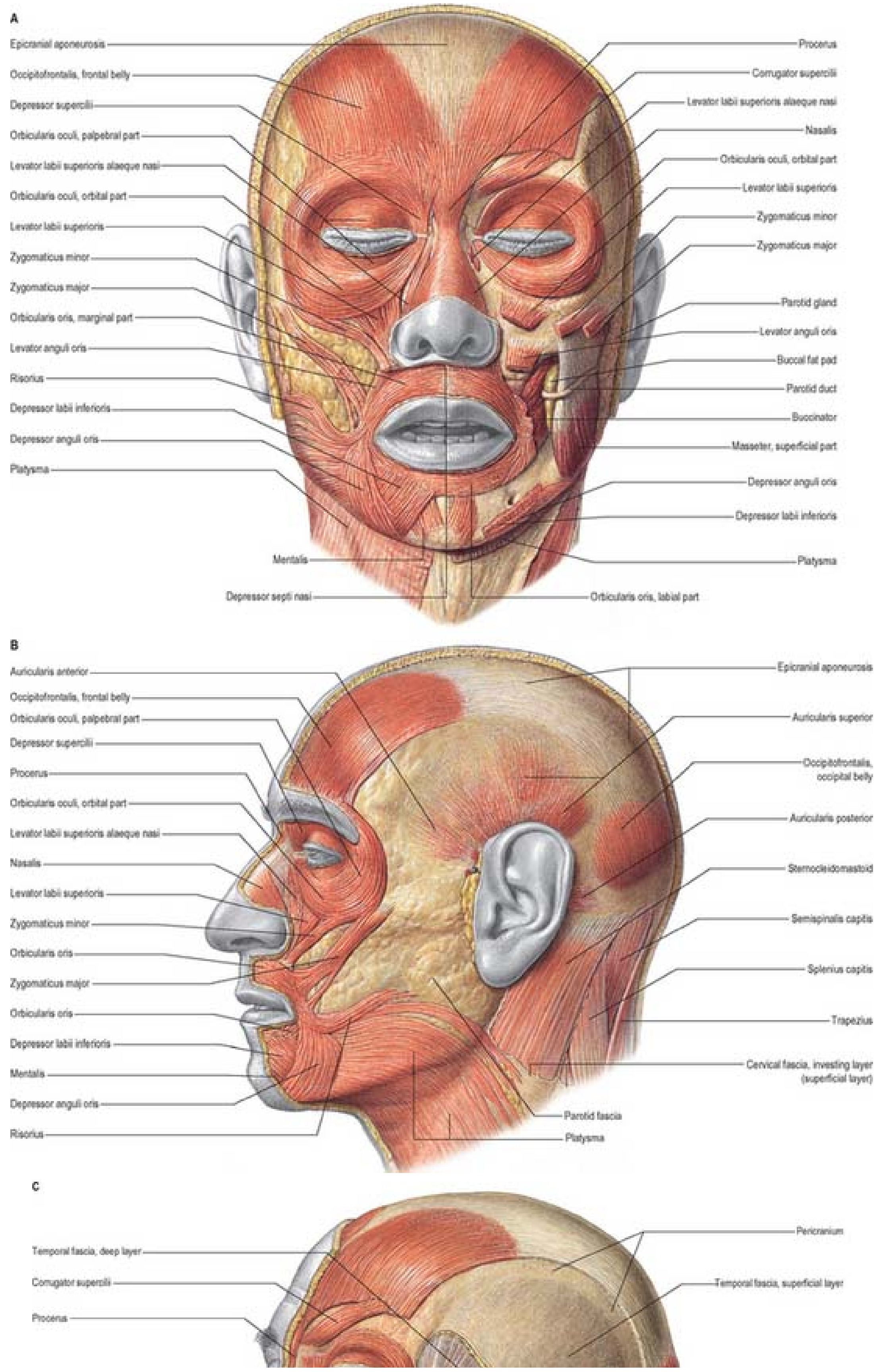
A
Epicranial aponeurosis
Occipitofrontalis, frontal belly
Depressor supercilii
Orbicularis oculi, palpebral part
Levator labii superioris alaeque nasi
Orbicularis oculi, orbital part
Levator labii superioris
Zygomaticus minor
Zygomaticus major
Orbicularis oris, marginal part
Levator anguli oris
Risorius
Depressor labii inferioris
Depressor anguli oris
Platysma
Mentalis
Depressor septi nasi
Orbicularis oris, labial part
Procerus
Corrugator supercilii
Levator labii superioris alaeque nasi
Nasalis
Orbicularis oculi, orbital part
Levator labii superioris
Zygomaticus minor
Zygomaticus major
Parotid gland
Levator anguli oris
Buccal fat pad
Parotid duct
Buccinator
Masseter, superficial part
Depressor anguli oris
Depressor labii inferioris
Platysma
B
Auricularis anterior
Occipitofrontalis, frontal belly
Orbicularis oculi, palpebral part
Depressor supercilii
Procerus
Orbicularis oculi, orbital part
Levator labii superioris alaeque nasi
Nasalis
Levator labii superioris
Zygomaticus minor
Orbicularis oris
Zygomaticus major
Orbicularis oris
Depressor labii inferioris
Mentalis
Depressor anguli oris
Risorius
Epicranial aponeurosis
Auricularis superior
Occipitofrontalis, occipital belly
Auricularis posterior
Sternocleidomastoid
Semispinalis capitis
Splenius capitis
Trapezius
Cervical fascia, investing layer (superficial layer)
Parotid fascia
Platysma
C
Temporal fascia, deep layer
Corrugator supercilii
Procerus
Pericranium
Temporal fascia, superficial layer

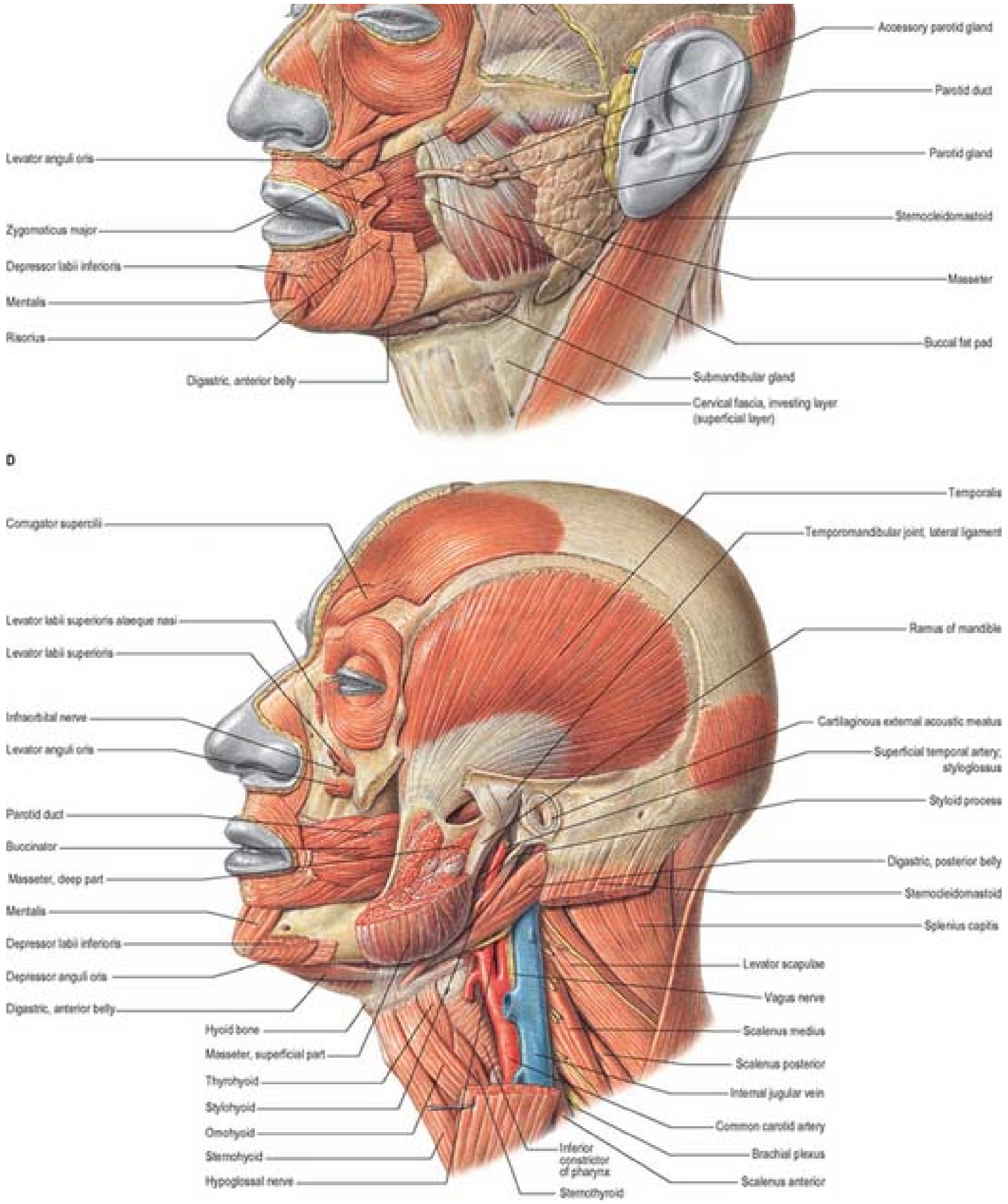
Accessory parotid gland
Parotid duct
Parotid gland
Sternocleidomastoid
Masseter
Buccal fat pad
Submandibular gland
Cervical fascia, investing layer (superficial layer)
Levator anguli oris
Zygomaticus major
Depressor labii inferioris
Mentalis
Risorius
Digastric, anterior belly
D
Temporalis
Temporomandibular joint, lateral ligament
Ramus of mandible
Cartilaginous external acoustic meatus
Superficial temporal artery; styloglossus
Styloid process
Digastric, posterior belly
Sternocleidomastoid
Splenius capitis
Levator scapulae
Vagus nerve
Scalenus medius
Scalenus posterior
Internal jugular vein
Common carotid artery
Brachial plexus
Scalenus anterior
Corrugator supercilii
Levator labii superioris alaeque nasi
Levator labii superioris
Infraorbital nerve
Levator anguli oris
Parotid duct
Buccinator
Masseter, deep part
Mentalis
Depressor labii inferioris
Depressor anguli oris
Digastric, anterior belly
Hyoid bone
Masseter, superficial part
Thyrohyoid
Stylohyoid
Omohyoid
Sternohyoid
Hypoglossal nerve
Inferior constrictor of pharynx
Sternothyroid

Fig. 29.11 The superficial muscles of the head and neck. **A**, frontal view; **B–D** show the muscles of the left lateral side of the head and upper part of the neck at progressively deeper levels.

(From Sobotta 2006.)

EPICRANIAL MUSCLE GROUP

Epicranius

Epicranius consists of occipitofrontalis and temporoparietalis.

Occipitofrontalis

Occipitofrontalis covers the dome of the skull from the highest nuchal lines to the eyebrows. It is a broad, musculofibrous layer and consists of four thin, muscular quadrilateral parts, two occipital and two frontal, connected by the epicranial aponeurosis. Each occipital part (occipitalis) arises by tendinous fibres from the lateral two-thirds of the highest nuchal line of the occipital bone and the adjacent region of the mastoid part of the temporal bone, and extends forwards to join the aponeurosis. The gap between the two occipital parts is occupied by an extension of the epicranial aponeurosis. Each frontal part (frontalis) is adherent to the superficial fascia, particularly of the eyebrows. Although frontalis has no bony attachments of its own, its fibres blend with those of adjacent muscles – procerus, corrugator supercilii and orbicularis oculi – and ascend to join the epicranial aponeurosis in front of the coronal suture.

Vascular supply

Occipitofrontalis is supplied by branches of the superficial temporal, ophthalmic, posterior auricular and occipital arteries.

Innervation

The occipital part of occipitofrontalis is supplied by the posterior auricular branch of the facial nerve and the frontal part is supplied by the temporal branches of the facial nerve.

Actions

Acting from above, the frontal parts raise the eyebrows and the skin over the root of the nose (e.g. as in expressions of surprise or horror). Acting from below, the frontal parts draw the scalp forwards, throwing the forehead into transverse wrinkles. The occipital parts draw the scalp backwards. Acting alternately, the occipital and frontal parts can move the entire scalp backwards and forwards.

Variations

A thin muscular slip, transversus nuchae, is present in 25% of people. It arises from the external occipital protuberance or from the superior nuchal line, either superficial or deep to trapezius. It is frequently inserted with auricularis posterior, but may blend with the posterior edge of sternocleidomastoid.

Epicranial aponeurosis

The epicranial aponeurosis covers the upper part of the cranium and, with the epicranial muscle, forms a continuous fibromuscular sheet that extends from the occiput to the eyebrows. Posteriorly, between the occipital parts of occipitofrontalis, it is attached to the external protuberance and highest nuchal line of the occipital bone. Anteriorly it splits to enclose the frontal parts and sends a short narrow prolongation between them. Laterally, the anterior and superior auricular muscles are attached to it; the aponeurosis is thinner, and continues over the temporal fascia to the zygomatic arch. It is united to the skin lying over the cranial vault by fibrous superficial fascia, but it is connected more loosely to the underlying pericranium by areolar tissue, an arrangement that allows it to move freely, carrying with it the skin of the scalp.

Temporoparietalis

Temporoparietalis is a variably developed sheet of muscle which lies between the frontal parts of occipitofrontalis and the anterior and superior auricular muscles.

CIRCUMORBITAL AND PALPEBRAL MUSCLE GROUP

The circumorbital and palpebral group of muscles are orbicularis oculi, corrugator supercilii and levator palpebrae superioris. The first two are described here; levator palpebrae superioris is described in Chapter 39.

Orbicularis oculi

Orbicularis oculi is a broad, flat, elliptical muscle which surrounds the circumference of the orbit and spreads into the adjacent regions of the eyelids, anterior temporal region, infraorbital cheek and superciliary region. It has orbital, palpebral and lacrimal parts and a small ciliary bundle.

The orbital part arises from the nasal component of the frontal bone, the frontal process of the maxilla and from the medial palpebral ligament. The fibres form complete ellipses, without interruption on the lateral side, where there is no bony attachment. The upper orbital fibres blend with the frontal part of occipitofrontalis and corrugator supercilii. Many of them are inserted into the skin and subcutaneous tissue of the eyebrow and constitute depressor supercilii. Inferiorly and medially, the ellipses overlap or blend to some extent with adjacent muscles (levator labii superioris alaeque nasi, levator labii superioris and zygomaticus minor). At the extreme periphery, sectors of complete, and sometimes incomplete, ellipses have a loose areolar connection with the temporal extension of the epicranial aponeurosis.

The palpebral part arises from the medial palpebral ligament, mainly from its superficial surface, and from the bone immediately above and below the ligament. The fibres sweep across the eyelids anterior to the orbital septum, interlacing at the lateral commissure to form the lateral palpebral raphe. A small group of fine fibres, close to the margin of each eyelid behind the eyelashes, constitutes the ciliary bundle.

The lacrimal part arises from the upper part of the lacrimal crest, and the adjacent lateral surface, of the lacrimal bone. It passes laterally behind the nasolacrimal sac (where some fibres are inserted into the associated fascia), and divides into upper and lower slips. Some fibres are inserted into the tarsi of the eyelids close to the lacrimal canaliculi, but most continue across in front of the tarsi and interlace in the lateral palpebral raphe.

Vascular supply

Orbicularis oculi is supplied by branches of the facial, superficial temporal, maxillary and ophthalmic arteries.

Innervation

Orbicularis oculi is supplied by temporal and zygomatic branches of the facial nerve.

Actions

Orbicularis oculi is the sphincter muscle of the eyelids and plays an important role in facial expression and various ocular reflexes. The orbital portion is usually activated under voluntary control. Contraction of the upper orbital fibres produces vertical furrowing above the bridge of the nose, narrowing of the palpebral fissure, and bunching and protrusion of the eyebrows, which reduces the amount of light entering the eyes. Eye closure is largely affected by lowering of the upper eyelid, but there is also considerable elevation of the lower eyelid. The palpebral portion can be contracted voluntarily, to close the lids gently as in sleep, or reflexly, to close the lids protectively in blinking. The palpebral part has upper depressor and lower elevator fascicles. The lacrimal part of the muscle draws the eyelids and the lacrimal papillae medially, thereby exerting traction on the lacrimal fascia, and may aid drainage of tears by dilating the lacrimal sac. It may also influence pressure gradients within the lacrimal gland and ducts. This activity may assist in the sinuous flow of tears across the cornea, direct the lacrimal punctum into the lacus lacrimalis, and express secretions of the ciliary and tarsal glands. When the entire orbicularis oculi muscle contracts, the skin is thrown into folds which radiate from the lateral angle of the eyelids. Such folds, when permanent, cause wrinkles in middle age (the so-called ‘crow’s feet’).

Corrugator supercilii

Corrugator supercilii is a small pyramidal muscle located at the medial end of each eyebrow, lying deep to the frontal part of occipitofrontalis and orbicularis oculi, with which it is partially blended. It arises from bone at the medial end of the superciliary arch and its fibres pass laterally and slightly upwards to exert traction on the skin above the middle of the supraorbital margin.

Vascular supply

Corrugator supercilii is supplied by branches from adjacent arteries, mainly from the superficial temporal and ophthalmic arteries.

Innervation

Corrugator supercilii is innervated by temporal branches of the facial nerve.

Actions

Corrugator supercilii cooperates with orbicularis oculi to draw the eyebrows medially and downwards to shield the eyes in bright sunlight. It is also involved in frowning. The combined action of the two muscles produces mainly vertical wrinkles on the supranasal strip of the forehead.

NASAL MUSCLE GROUP

The nasal muscle group, which consists of procerus, nasalis and depressor septi, is described in Chapter 32.

BUCCOLABIAL MUSCLE GROUP

The shape of the mouth and the posture of the lips are controlled by a complex three-dimensional assembly of muscular slips. These include elevators, retractors and evertors of the upper lip (levator labii superioris alaeque nasi, levator labii superioris, zygomaticus major and minor, levator anguli oris and risorius); depressors, retractors and evertors of the lower lip (depressor labii inferioris, depressor anguli oris, and mentalis); a compound sphincter (orbicularis oris, incisivus superior and inferior); and buccinator.

Levator labii superioris alaequae nasi

Levator labii superioris alaequae nasi is described in Chapter 32.

Levator labii superioris

Levator labii superioris arises from the maxilla and zygomatic bone above the infraorbital foramen. Its fibres converge into the muscular substance of the upper lip between the lateral slip of levator labii superioris alaequae nasi and zygomaticus minor.

Vascular supply

Levator labii superioris is supplied by the facial artery and the infraorbital branch of the maxillary artery.

Innervation

Levator labii superioris is innervated by the zygomatic and buccal branches of the facial nerve.

Actions

Levator labii superioris elevates and everts the upper lip. Acting with other muscles, it modifies the nasolabial furrow. In some faces, this furrow is a highly characteristic feature and it is often deepened in expressions of sadness or seriousness.

Zygomaticus major

Zygomaticus major arises from the zygomatic bone, just in front of the zygomaticotemporal suture, and passes to the angle of the mouth where it blends with the fibres of levator anguli oris, orbicularis oris and more deeply placed muscular bands.

Vascular supply

Zygomaticus major is supplied by the superior labial branch of the facial artery.

Innervation

Zygomaticus major is innervated by the zygomatic and buccal branches of the facial nerve.

Actions

Zygomaticus major draws the angle of the mouth upwards and laterally as in laughing.

Zygomaticus minor

Zygomaticus minor arises from the lateral surface of the zygomatic bone immediately behind the zygomaticomaxillary suture, and passes downwards and medially into the muscular substance of the upper lip. Superiorly it is separated from levator labii superioris by a narrow triangular interval, and inferiorly it blends with this muscle.

Vascular supply

Zygomaticus minor is supplied by the superior labial branch of the facial artery.

Innervation

Zygomaticus minor is innervated by the zygomatic and buccal branches of the facial nerve.

Actions

Zygomaticus minor elevates the upper lip, exposing the maxillary teeth. It also assists in deepening and elevating the nasolabial furrow. Acting together, the main elevators of the lip – levator labii superioris alaequae nasi, levator labii superioris and zygomaticus minor – curl the upper lip in smiling, and in expressing smugness, contempt or disdain.

Levator anguli oris

Levator anguli oris arises from the canine fossa of the maxilla, just below the infraorbital foramen and inserts into and below the angle of the mouth. Its fibres mingle there with other muscle fibres (zygomaticus major, depressor anguli oris, orbicularis oris). Some superficial fibres curve anteriorly and attach to the dermal floor of the lower part of the nasolabial furrow. The infraorbital nerve and accompanying vessels enter the face via the infraorbital foramen between the origins of levator anguli oris and levator labii superioris.

Vascular supply

Levator anguli oris is supplied by the superior labial branch of the facial artery and the infraorbital branch of the maxillary artery.

Innervation

Levator anguli oris is innervated by the zygomatic and buccal branches of the facial nerve.

Actions

Levator anguli oris raises the angle of the mouth in smiling, and contributes to the depth and contour of the nasolabial furrow.

Malaris

Malaris is a thin sheet of muscle that is sometimes found covering and blending with zygomaticus major and minor and levator labii superioris. It is subject to considerable variation. When present, it is continuous with the inferior limit of orbicularis oculi, from which it is possibly derived. Its fibres incline medially and downwards. Some of its superficial fascicles have a dermal attachment to the nasolabial ridge and sulcus, and others pass directly to the angle of the mouth and to the outer third of the upper lip to intersect with bundles of orbicularis oris.

Mentalis

Mentalis is a conical fasciculus lying at the side of the frenulum of the lower lip. The fibres arise from the incisive fossa of the mandible and descend to attach to the skin of the chin.

Vascular supply

Mentalis is supplied by the inferior labial branch of the facial artery and the mental branch of the maxillary artery.

Innervation

Mentalis is innervated by the mandibular branch of the facial nerve.

Actions

Mentalis raises the lower lip, wrinkling the skin of the chin. It raises the base of the lower lip and therefore helps in protruding and everting the lower lip in drinking and also in expressing doubt or disdain.

Depressor labii inferioris

Depressor labii inferioris is a quadrilateral muscle that arises from the oblique line of the mandible, between the symphysis menti and the mental foramen. It passes upwards and medially into the skin and mucosa of the lower lip, blending with its contralateral fellow and with orbicularis oris. Below and laterally it is continuous with platysma.

Vascular supply

Depressor labii inferioris is supplied by the inferior labial branch of the facial artery and the mental branch of the maxillary artery.

Innervation

Depressor labii inferioris is innervated by the mandibular branch of the facial nerve.

Actions

Depressor labii inferioris draws the lower lip downwards and a little laterally in masticatory activity, and may assist in eversion of the lower lip. It contributes to the expressions of irony, sorrow, melancholy and doubt.

Depressor anguli oris

Depressor anguli oris has a long, linear origin from the mental tubercle of the mandible and its continuation, the oblique line, below and lateral to depressor labii inferioris. It converges into a narrow fasciculus that blends at the angle of the mouth with orbicularis oris and risorius, and some fibres continue into levator anguli oris. Depressor anguli oris is continuous below with platysma and cervical fasciae. Some of its fibres may pass below the mental tubercle and cross the midline to interlace with their contralateral fellows, thereby forming transversus menti (the ‘mental sling’).

Vascular supply

Depressor anguli oris is supplied by the inferior labial branch of the facial artery and the mental branch of the maxillary artery.

Innervation

Depressor anguli oris is innervated by the buccal and mandibular branches of the facial nerve.

Actions

Depressor anguli oris draws the angle of the mouth downwards and laterally in opening the mouth and in expressing sadness. During opening of the mouth the mentolabial sulcus becomes more horizontal and its central part deepens.

Buccinator

The muscle of the cheek, buccinator, is a thin quadrilateral muscle which occupies the interval between the maxilla and the mandible. Its upper and lower boundaries are attached to the outer surfaces of the alveolar processes of the maxilla and mandible respectively opposite the molar teeth, and its posterior border is attached to the anterior margin of the pterygomandibular raphe. In addition, a few fibres spring from a fine tendinous band that bridges the interval between the maxilla and the pterygoid hamulus, between the tuberosity of the maxilla and the upper end of the pterygomandibular raphe. On its way to the soft palate the tendon of tensor veli palatini pierces the pharyngeal wall in the small gap that lies behind this tendinous band. The posterior part of buccinator is deeply placed, internal to the mandibular ramus and in the plane of the medial pterygoid plate. Its anterior component curves out behind the third molar tooth to lie in the submucosa of the cheek and lips. The fibres of buccinator converge towards the modiolus near the angle of the mouth. Here the central (pterygomandibular) fibres intersect, those from below cross to the upper part of orbicularis oris, and those from above cross to the lower part. The highest (maxillary) and lowest (mandibular) fibres of buccinator continue forward to enter their corresponding lips without decussation. As buccinator courses through the cheek and modiolus substantial numbers of its fibres are diverted internally to attach to submucosa.

Relations

Posteriorly, buccinator lies in the same plane as the superior pharyngeal constrictor, which arises from the posterior margin of the pterygomandibular raphe, and is covered there by the buccopharyngeal fascia. Superficially, the buccal pad of fat separates the posterior part of buccinator from the ramus of the mandible, masseter and part of temporalis. Anteriorly, the superficial surface of buccinator is related to zygomaticus major, risorius, levator and depressor anguli oris, and the parotid duct. It is crossed by the facial artery, facial vein and branches of the facial and buccal nerves. The deep surface of buccinator is related to the buccal glands and mucous membrane of the mouth. The parotid duct pierces buccinator opposite the third upper molar tooth, and lies on the deep surface of the muscle before opening into the mouth opposite the maxillary second molar tooth.

Vascular supply

Buccinator is supplied by branches from the facial artery and the buccal branch of the maxillary artery.

Innervation

Buccinator is supplied by the buccal branch of the facial nerve.

Actions

Buccinator compresses the cheek against the teeth and gums during mastication, and assists the tongue in directing food between the teeth. As the mouth closes, the teeth glide over the buccolabial mucosa, which must be retracted progressively from their occlusal surfaces by buccinator and other submucosally attached muscles. When the cheeks have been distended with air, the buccinators expel it between the lips, an activity important when playing wind instruments, and which accounts for the name of the muscle (Latin *buccinators* = trumpeter).

Pterygomandibular raphe

The pterygomandibular raphe is a thin band of tendinous fibres that stretches from the hamulus of the medial pterygoid plate down to the posterior end of the mylohyoid line of the mandible. It is easily palpated medially, where it is covered by the mucous membrane of the mouth, and laterally it is separated from the ramus of the mandible by a quantity of adipose tissue. It gives attachment posteriorly to the superior constrictor of the pharynx, and anteriorly to the central part of buccinator. The pterygomandibular raphe is a useful anatomical landmark for the administration of inferior alveolar nerve blocks because the nerve lies lateral to it.

Orbicularis oris

Orbicularis oris is so named because it was once assumed that the oral fissure was surrounded by a series of complete ellipses of striated muscle which acted together in the manner of a sphincter. However, it is now recognized that the muscle actually consists of four substantially independent quadrants (upper, lower, left and right), each of which contains a larger pars peripheralis and a smaller pars marginalis. Marginal and peripheral parts are apposed along lines that correspond externally to the lines of junction between the vermilion zone of the lip and the skin. Thus, orbicularis oris is composed of eight segments, each of which is named systematically according to its location. Each segment resembles a fan that has its stem at the modiolus and is open in peripheral segments and almost closed in marginal segments.

Pars peripheralis

Pars peripheralis has, in each quadrant, a lateral stem attached to the labial side of the modiolus over its full thickness, from apex to base, including the corresponding upper or lower cornu. Most of these stem fibres are thought to originate within the modiolus (although it is possible that some are direct continuations from the other modiolar muscles). The consensus view is that stem fibres are reinforced directly by fibres from buccinator (upper fibres and decussating lower central fibres), levator anguli oris and the superficial part of zygomaticus major in the upper lip, and from buccinator (lower fibres and decussating upper central fibres), and depressor anguli oris in the lower lip.

The fibres of orbicularis oris enter their respective superior and inferior labial areas and diverge to form triangular muscular sheets. These are thickest at the junctions between skin and the vermilion zone and become progressively thinner as they reach the limits of the labial region (as defined above). The greater part of each sheet enters the free lip, where its fibres aggregate into cylindrical bundles orientated parallel to the vermilion zone. Fibres of the direct labial tractors pass to their submucosal attachments between these cylindrical bundles and between pars peripheralis and pars marginalis. In the upper lip, the highest fibres run near the nasolabial sulcus, a few fibres attach to the sulcus, and a few to the nasal ala and septum. In the lower lip, the lowest fibres reach and attach to the mentolabial sulcus. A small proportion of the main body of fibres is thought to end in the labial connective tissue, dermis or submucosa as it traverses its quadrant of free lip. Most fibres continue towards the median plane and cross some 5 mm into the opposite half-lip. At this point the fibres from the two sides interlace on their way to their dermal insertions, creating the ridges of the philtrum of the upper lip and the less marked corresponding depression in the lower lip.

Pars marginalis

Pars marginalis of orbicularis oris is developed to a unique extent in human lips and is closely associated with speech and the production of some kinds of musical tone. In each quadrant the pars marginalis consists of a single (occasionally double) band of narrow diameter muscle fibres lodged within the tissues of each vermilion zone. At their medial end, the marginal fibres meet and interlace with their contralateral fellows and then attach to the dermis of the vermilion zone a few millimetres beyond the median plane in a manner similar to pars peripheralis. At their lateral ends, the fibres converge and attach to the deepest part of the modiolar base along a horizontal strip level with the buccal angle.

The relations between pars marginalis and pars peripheralis are complex. In a full thickness section of an upper lip at right angles to the vermilion zone, the cylindrical bundles of peripheralis fibres form an S-shape, with an external convexity above, and an internal convexity below: the classic analogy is to the shank and initial curved part of a hook. Beyond peripheralis, the hook-shape is completed by the blunted triangular profile of marginalis, which occupies the core of the vermilion zone with its base adjacent to peripheralis and its apex reaching upwards and anteriorly towards the junction between vermilion zone and skin. In a similar section through the lower lip, peripheralis bundles form a continuous curve that is concave towards the external surface. This is surmounted by the flattened triangular profile of marginalis, which curves anteriorly, its apex again nearing the vermilion/cutaneous junction. Thus, throughout the vermilion zones of both lips, marginalis lies substantially anterior to the adjacent bundles of peripheralis. However, as the muscles are traced laterally beyond the vermilion zone and across the buccal angle, this relationship alters and marginalis becomes inverted as it wraps progressively around the adjacent edge of peripheralis to reach its deep (submucosal) surface, and maintains this position up to its attachment at the modiolar base.

Vascular supply

Orbicularis oris is supplied mainly by the superior and inferior labial branches of the facial artery, the mental and infraorbital branches of the maxillary artery and the transverse facial branch of the superficial temporal artery.

Nerve supply

Orbicularis oris is supplied by the buccal and mandibular branches of the facial nerve.

Actions

The actions of orbicularis oris are considered in detail in the next section.

Incisivus labii superioris

Incisivus labii superioris has a bony origin from the floor of the incisive fossa of the maxilla above the eminence of the lateral incisor tooth. Initially it lies deep to orbicularis oris pars peripheralis superior. Arching laterally, its fibre bundles become intercalated between, and parallel to, the orbicular bundles. Approaching the modiolus, it segregates into superficial and deep parts: the former blends partially with levator anguli oris and attaches to the body and apex of the modiolus and the latter is attached to the superior cornu and base of the modiolus.

Incisivus labii inferioris

Incisivus labii inferioris, an accessory muscle of the orbicularis oris muscle complex, has many features in common with incisivus labii superioris. Its osseous attachment is to the floor of the incisive fossa of the mandible, lateral to mentalis and below the eminence of the lateral incisor tooth. Curving laterally and upwards, it blends to some extent with orbicularis oris pars peripheralis inferior before reaching the modiolus, where superficial bundles attach to the apex and body, and deep bundles attach to the base and inferior cornu.

Platysma

Platysma is described as a muscle of the neck (see Ch. 28) but it is considered here as a contributor to the orbicularis oris muscle complex. It has mandibular, labial and modiolar parts. Pars mandibularis attaches to the lower border of the body of the mandible. Posterior to this attachment, a substantial flattened bundle separates and passes superomedially to the lateral border of depressor anguli oris, where a few fibres join this muscle. The remainder continue deep to depressor anguli oris and reappear at its medial border. Here they continue within the tissue of the lateral half of the lower lip, as a direct labial tractor, platysma pars labialis. Pars labialis occupies the interval between depressor anguli oris and depressor labii inferioris and is in the same plane as these muscles. The adjacent margins of all three muscles blend and they have similar labial attachments. Platysma pars modiolaris constitutes all the remaining bundles posterior to pars labialis, other than a few fine fascicles that end directly in buccal dermis or submucosa. Pars modiolaris is posterolateral to depressor anguli oris and passes superomedially, deep to risorius, to apical and subapical modiolar attachments.

Risorius

Risorius is a highly variable muscle that ranges from one or more slender fascicles to a wide, thin superficial fan. Its peripheral attachments may include some or all of the following: the zygomatic arch, parotid fascia, fascia over the masseter anterior to the parotid, fascia enclosing platysma pars modiolaris, and fascia over the mastoid process. Its fibres converge to apical and subapical attachments at the modiolus.

Vascular supply

Risorius is supplied mainly by the superior labial branch of the facial artery.

Nerve supply

Risorius is supplied by buccal branches of the facial nerve.

Actions

Risorius pulls the corner of the mouth laterally in numerous facial activities, including grinning and laughing.

MOVEMENTS OF THE FACE AND LIPS

Direct labial tractors

Direct labial tractors, as their name suggests, pass directly into the tissues of the lips and not via the modioli. In broad terms, the force exerted by tractors is directed vertically at an approximate right angle to the oral fissure. Their action will therefore elevate and/or evert the whole, or part, of the upper lip and depress and/or evert the whole, or part, of the lower lip. The tractors are, from medial to lateral, the labial part of levator labii superioris alaequae nasi; levator labii superioris and zygomaticus minor in the upper lip; depressor labii inferioris and platysma pars labialis in the lower lip.

In both upper and lower lips the tractors blend into a continuous sheet that divides into a series of superimposed coronal sheets which are anterior to the muscle bundles of pars peripheralis orbicularis oris as they enter the free lip. The sheets may be divided into three groups at increasing depths from the skin surface, each with a distinct zone of attachment (Fig. 29.12). The superficial group comprises a succession of fine fibre bundles which curve anteriorly a short distance before attaching in a series of horizontal rows to the dermis between the hair follicles, sebaceous glands and sweat glands. The intermediate group attaches to the dermis of the vermilion zone, which they reach by two routes: the more superficial bundles continue past the skin/vermilion junction, then curve posteriorly over pars marginalis orbicularis oris to punctate attachments on the ventral half of the dermis of the vermilion zone, while the deeper bundles first pass posteriorly between pars peripheralis and pars marginalis, then curve anteriorly to punctate attachments on the dorsal half of the dermis of the vermilion zone. The deep group is closely applied to the anterior surface of pars peripheralis orbicularis oris, and sends fine tractor fibres between its parallel bundles to attach posteriorly into the submucosa and periglandular connective tissue.

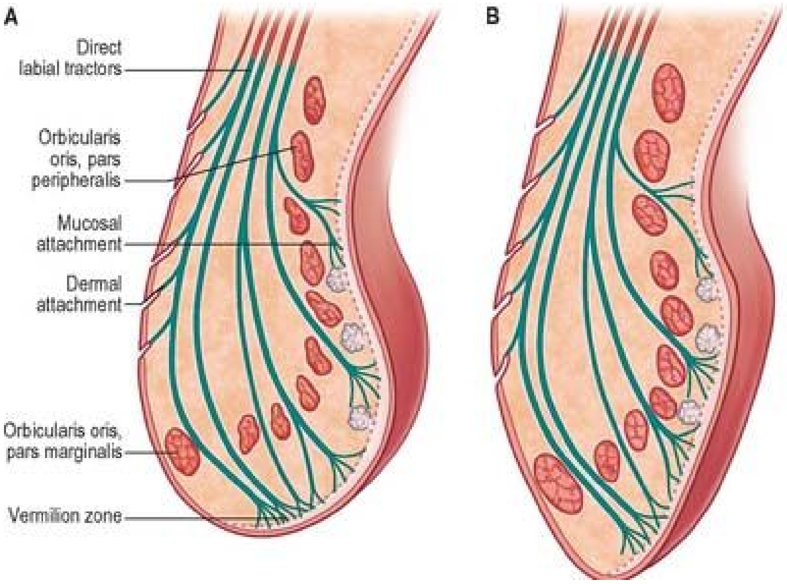

Fig. 29.12 **A**, Sagittal section of the upper lip in repose. On the left is thin skin with oblique hair follicles; on the right is thick mucosa with mucous glands and mucosal shelf; between them is the vermilion zone. **B**, as **A** but slightly contracted, forming a narrowed profile (labial cord).

Movements of the lips

The various groups of direct labial tractors may act together or individually, and their effects may involve a complete labial quadrant, or be restricted to a short segment. For example, partial contraction of the superior labial tractors can result in localized elevation of a segment of the upper lip, in a postural expression reminiscent of the ‘canine snarl’. Normally, however, the activity of the tractors is modified by the superimposed activity of orbicularis oris and the modiolar muscles. The resultant actions range from delicate adjustments of the tension and profile of the lip margins to large increases of the oral fissure with eversion of the lips.

Lip protrusion is passive in its initial stages. It may be suppressed by powerful contraction of the whole of orbicularis oris or enhanced by selective activation of parts of the direct labial tractors. However, lip movements must accommodate separation of the teeth brought about by mandibular depression at the temporomandibular joints. Beyond a certain range of mouth opening, labial movements are almost completely dominated by mandibular movements. Thus over the last 2.5–3 cm interincisal distance of wide jaw separation, strong contraction of orbicularis oris cannot effect lip contact, and instead it causes full-thickness inflection of upper and lower lips, including the vermilion zone, towards the oral cavity, wrapping them around the incisal edges, canine cusps and premolar occlusal surfaces. The involvement of the lips in speech is described in Chapter 34, but some aspects relevant to the actions of orbicularis oris pars marginalis will be described here. Contraction of marginalis is considered to alter the cross-sectional profile of the free margin of the vermilion zone such that both the gentle bulbous profile of the upper lip and the smooth posterosuperior convexity of the lower lip change to a narrow, symmetrical triangular profile. The transformed rims, whose length and tension can be delicately controlled, have been named labial cords. They are known to be involved in the production of some consonantal (labial) sounds. A labial cord may also function as a ‘vibrating reed’ in whistling or playing a wind instrument such as the trumpet.

The modiolus and its role in facial movements

On each side of the face a number of muscles converge towards a focus just lateral to the buccal angle, where they interlace to form a dense, compact, mobile, fibromuscular mass called the modiolus. This can be palpated most effectively by using the opposed thumb and index finger to compress the mucosa and skin simultaneously. At least nine muscles, depending on the classification employed, are attached to each modiolus. Moreover, the muscles lie in different planes, their modiolar stems are often spiralized, and most divide into two bundles, some into three or four, each of them interlacing and attaching in a distinctive way. Not surprisingly, therefore, the three-dimensional organization of the modiolus has proved difficult to analyse.

The shape and dimensions of the modiolus are given approximately because they are subject to individual, age, sexual and ethnic variation. Furthermore the modiolus has no precise histological boundaries, and is an irregular zone where dense, compact interlacing tissue grades into the stems of individually recognizable muscles. The modiolus has the rough form of a blunt cone. The base of the cone (basis moduli) is adjacent and adherent to the mucosa. It is roughly elliptical in outline and extends vertically 20 mm above and 20 mm below a horizontal line through the buccal angle. It also extends laterally a similar distance from the angle. The blunt apex of the cone (apex moduli) is 4 mm across, and is centred approximately 12 mm lateral to the buccal angle. From mucosa to dermis the thickness of the mass is usually 10 mm, divided approximately equally into basal, central and apical parts. The central body has an oblique fibrous cleft or channel that transmits the facial artery, an arrangement that may limit the extent to which it is compressed by contraction of the buccolabial musculature. The cone shape is modified by two round-edged flanges (or cornua) that extend into the lateral free lip tissues above and below the corner of the mouth. The tip of the superior cornu extends 5.5 mm medial to the buccal angle, the tip of the inferior cornu only 3.5 mm. With these additions, the modiolar base becomes kidney-shaped, with the buccal angle projecting towards the hilum.

The apex of the modiolus is deep and adherent to the panniculus carnosus, which extends posteromedially as a thin sloping sheet down to the buccal angle. There, its free border forms a crescentic, narrow, flexible, subcutaneous fibroelastic cord that accommodates the varying postures of the modioli, lips, mouth and jaws.

Controlled three-dimensional mobility of the modioli enables them to integrate the activities of the cheeks, lips and oral fissure, the oral vestibule and the jaws. Such activities include biting, chewing, drinking, sucking, swallowing, changes in vestibular contents and pressure, the innumerable subtle variations involved in speech, the modulation (and occasional generation) of musical tones, production of harsher sounds in shouting and screaming, crying, and all the permutations of facial expression, ranging from mere hints to gross distortion, symmetrical or asymmetrical. Major modiolar movements appear to involve many, if not all, of its associated muscles, and there is little value in considering the actions of the individual muscles in isolation. While the most obvious determinant of modiolar position and mobility is the balance between the forces exerted by muscles that are directly attached to it, another influential factor is the degree of separation or ‘gape’ between the upper and lower teeth. Starting from the occlusal position, and with the lips maintained in contact, the teeth can be separated by approximately 1.25 cm near the midline, and the mentolabial sulcus descends by a similar distance. With further separation the lips part, and as gape increases to its maximum, interlabial and interdental distances approach 4 cm, at which point the mentolabial sulcus has descended a further 2 cm. In this posture the modiolus has descended about 1 cm to lie over the interdental space, into which its basal and surrounding buccal mucosa projects a few millimetres, and its cornua diverge into their respective lips at an obtuse angle to each other, the dispositions of the modiolar muscles being correspondingly modified. The general hexagonal shape of the labial area changes as the mouth and jaws open progressively. In maximal opening, the distance between the superior and inferior boundaries has increased by 3–3.5 cm at the centre; the transverse distance between its lateral angles has decreased by 1 cm and the angles are obtuse; the nasolabial sulci are longer, straighter and more vertical; and the inferior buccolabial sulci are less deep and curved. These soft tissue changes radiate from the bilateral modioli.

With the lips in contact and the teeth in tight occlusion, the modiolus can move a few millimetres in all directions. However, mobility is maximal when there is 2–3 mm clearance between the teeth: the apex of the modiolus may then move vertically upwards 10 mm, downwards 5 mm, posterolaterally 10 mm, and anteromedially 10 mm, these movements occurring in the curved planes of the cheek and lips. Specific movements of the modiolus may occur to any point, and along any path, within the boundaries of the envelope of movement thus defined. When the mouth is opened wide, the modiolus becomes immobile. From the neutral position the modiolus may be displaced superficially along its apicobasal axis for up to 5–10 mm by liquids or solids in the vestibule, or by an increase in air pressure that ‘balloons’ the cheeks and lips.

Many activities take place in three phases. Initially, a particular modiolar muscle group becomes dominant over its antagonists and the modiolus is rapidly relocated. Next, the modiolus is transiently fixed in this new site by simultaneous contraction of modiolar muscles, principally zygomaticus major, levator anguli oris, depressor anguli oris, platysma pars modiolaris, and this provides a fixed base from which the main physiological effectors, buccinator and orbicularis oris, carry out their specific actions. These actions are usually integrated with partial separation or closure of the jaws, and with varying degrees of activity in the direct labial tractors. All these factors combine to determine the positions of the lips and oral fissure from moment to moment. Modiolar movements may be bilaterally symmetrical, unilateral or asymmetrical.

MUSCLES OF MASTICATION

Masseter and temporalis, two of the muscles of mastication, are seen on the face. Masseter covers the ramus of the mandible, and temporalis lies over the temporal fossa. These muscles are described in detail with the other main muscles of mastication in Chapter 31.

VASCULAR SUPPLY AND LYMPHATIC DRAINAGE

ARTERIAL SUPPLY TO THE FACE

The main arterial supply to the face is derived from the facial and superficial temporal arteries, with additional supply from branches of the maxillary and ophthalmic arteries. The back of the scalp is supplied by the posterior auricular and occipital arteries. There are numerous anastomoses between the branches.

Facial artery

The facial artery arises in the neck from the external carotid artery (see Ch. 28). It initially lies beneath platysma, passing onto the face at the anteroinferior border of masseter, where its pulse can be felt as it crosses the mandible. The artery is deep to skin, the fat of the cheek and, near the angle of the mouth, zygomaticus major and risorius, and superficial to buccinator and levator anguli oris. It may pass over or through levator labii superioris, and pursues a tortuous course along the side of the nose towards the medial corner of the eye. At its termination it is embedded in levator labii superioris alaequae nasi.

Occasionally, the facial artery barely extends beyond the angle of the mouth, in which case its normal territory beyond this region is taken over by an enlarged transverse facial branch from the superficial temporal artery and by branches from the contralateral facial artery. The facial vein is posterior to the artery, and runs a more direct course across the face. At the anterior border of masseter, the two vessels are in contact, whereas in the neck the vein is superficial to the artery.

The facial artery supplies branches to the muscles and skin of the face (Fig. 29.13). Its named branches on the face are the premasseteric artery, the superior and inferior labial arteries and the lateral nasal artery. The part of the artery distal to its terminal branch is called the angular artery.

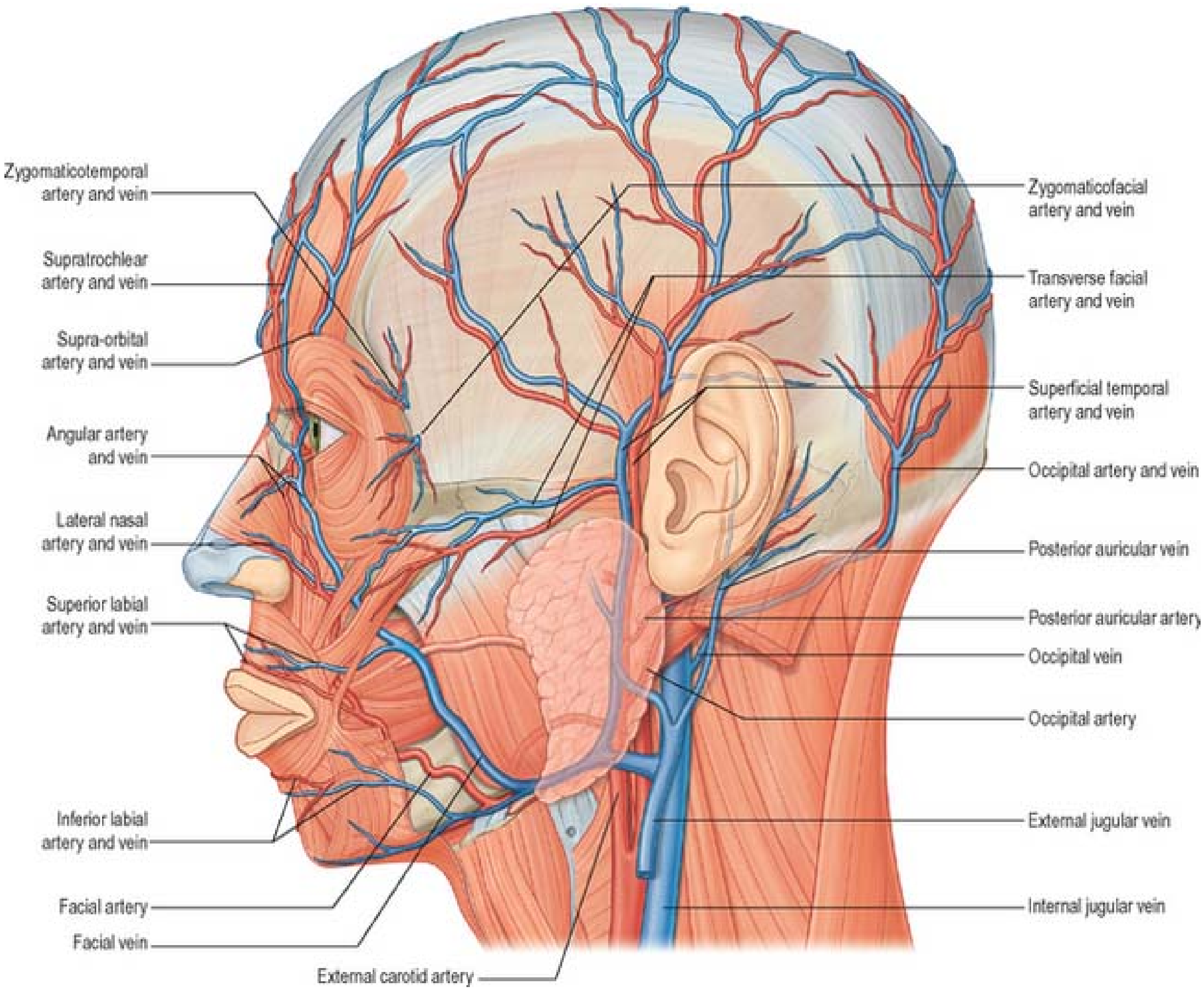
Zygomaticotemporal artery and vein
Supratrochlear artery and vein
Supra-orbital artery and vein
Angular artery and vein
Lateral nasal artery and vein
Superior labial artery and vein
Inferior labial artery and vein
Facial artery
Facial vein
External carotid artery
Zygomaticofacial artery and vein
Transverse facial artery and vein
Superficial temporal artery and vein
Occipital artery and vein
Posterior auricular vein
Posterior auricular artery
Occipital vein
Occipital artery
External jugular vein
Internal jugular vein

Fig. 29.13 The arteries and veins of the left side of the face, head and neck and their main branches. The infraorbital artery is shown in Fig. 25.1.

Premasseteric artery

The premasseteric artery is small and inconstant. When present, it passes upwards along the anterior border of masseter and supplies the surrounding tissues.

Inferior labial artery

The inferior labial artery arises near the angle of the mouth, passes upwards and forwards under depressor anguli oris, then penetrates orbicularis oris to run sinuously near the margin of the lower lip, between the muscle and the mucous membrane. It supplies the inferior labial glands, mucous membrane and muscles, and anastomoses with its contralateral fellow and with the mental branch of the inferior alveolar artery.

Superior labial artery

The superior labial artery is larger and more tortuous than the inferior labial artery. It pursues a similar course along the superior labial margin, between the mucous membrane and orbicularis oris, anastomoses with its contralateral fellow, and supplies the upper lip. It gives off an alar branch and a septal branch, which ramifies anteroinferiorly in the nasal septum.

Lateral nasal artery

The lateral nasal artery is given off by the side of the nose, supplies the dorsum and alae of nose, and anastomoses with its contralateral fellow. The lateral nasal artery may be replaced by a branch from the superior labial artery.

Superficial temporal artery

The superficial temporal artery is the smaller terminal branch of the external carotid artery. It arises in the parotid gland behind the neck of the mandible, where it is crossed by temporal and zygomatic branches of the facial nerve. Initially deep, it becomes superficial as it passes over the posterior root of the zygomatic process of the temporal bone, where its pulse can be felt. It then runs up the scalp for approximately 4 cm and divides into frontal (anterior) and parietal (posterior) branches. The artery is accompanied by corresponding veins, and by the auriculotemporal nerve which lies just posterior to it.

The superficial temporal artery supplies the skin and muscles at the side of the face and in the scalp, the parotid gland and the temporomandibular joint. It is occasionally biopsied when a histological diagnosis of giant cell arteritis is required. The named branches of the superficial temporal artery are the transverse facial, auricular, zygomatico-orbital, middle temporal, frontal and parietal arteries. The relative sizes of the frontal, parietal and transverse facial branches vary; the frontal and parietal branches may be absent, and the transverse facial may replace a shortened transverse facial artery.

Transverse facial artery

The transverse facial artery arises before the superficial temporal artery emerges from the parotid gland. It traverses the gland, crosses masseter between the parotid duct and the zygomatic arch (accompanied by one or two facial nerve branches) and divides into numerous branches that supply the parotid gland and duct, masseter and adjacent skin. The branches anastomose with the facial, masseteric, buccal, lacrimal and infraorbital arteries, and may have a direct origin from the external carotid artery.

Auricular artery

The branches of the auricular artery are distributed to the lobule and lateral surface of the auricle and to the external acoustic meatus.

Zygomatico-orbital artery

The zygomatico-orbital artery may arise independently from the superficial temporal artery or from its middle temporal or parietal branches. It runs close to the upper border of the zygomatic arch, between the two layers of temporal fascia, to the lateral orbital angle. It supplies orbicularis oculi and anastomoses with the lacrimal and palpebral branches of the ophthalmic artery. A well-developed zygomatico-orbital artery is associated with a delayed division into frontal and parietal branches.

Middle temporal artery

The middle temporal artery arises just above the zygomatic arch and perforates the temporal fascia to supply temporalis. It anastomoses with the deep temporal branches of the maxillary artery.

Frontal (anterior) branch

The frontal branch passes upwards towards the frontal tuberosity and supplies the muscles, skin and pericranium in this region. It anastomoses with its contralateral fellow and with the supraorbital and supratrochlear branches of the ophthalmic artery.

Parietal (posterior) branch

The parietal branch is larger than the frontal branch of the superficial temporal artery. It curves upwards and backwards, remains superficial to the temporal fascia, and anastomoses with its contralateral fellow and with the posterior auricular and occipital arteries.

Facial branches of the maxillary artery

The maxillary artery is the larger of the two terminal branches of the external carotid artery, and has three branches that supply the face, namely the mental, buccal and infraorbital arteries.

Mental artery

The mental artery arises from the first part of the maxillary artery as a terminal branch of the inferior alveolar artery. It emerges onto the face from the mandibular canal at the mental foramen, supplies muscles and skin in the chin region, and anastomoses with the inferior labial and submental arteries.

Buccal artery

The buccal artery is a branch of the second part of the maxillary artery. It emerges onto the face from the infratemporal fossa, crosses buccinator to supply the cheek, and anastomoses with the infraorbital artery and with branches of the facial artery.

Infraorbital artery

The infraorbital artery arises from the third part of the maxillary artery. It runs through the infraorbital foramen and onto the face, supplying the lower eyelid, the lateral aspect of the nose and the upper lip. The infraorbital artery has extensive anastomoses with the transverse facial and buccal arteries and with branches of the ophthalmic and facial arteries.

Facial branches of the ophthalmic artery

The ophthalmic artery is a branch of the internal carotid artery. Its supratrochlear, supraorbital, lacrimal, medial palpebral, dorsal nasal and external nasal branches supply the face.

Supratrochlear artery

The supratrochlear artery emerges from the orbit onto the face at the frontal notch. It supplies the medial parts of the upper eyelid, forehead and scalp, and anastomoses with the supraorbital artery and with its contralateral fellow.

Supraorbital artery

The supraorbital artery leaves the orbit through the supraorbital notch or foramen. It divides into superficial and deep branches that supply the skin and muscle of the upper eyelid, forehead and scalp. It anastomoses with the supratrochlear artery, frontal branch of the superficial temporal and its contralateral fellow. At the supraorbital margin it often sends a branch to the diploë of the frontal bone and may also supply the mucoperiosteum in the frontal sinus.

Lacrimal artery

The lacrimal artery appears on the face at the upper lateral corner of the orbit and supplies the lateral part of the eyelids. Within the orbit, it gives off a zygomatic artery which subdivides into zygomaticofacial and zygomaticotemporal arteries. The zygomaticofacial artery passes through the lateral wall of the orbit to emerge onto the face at the zygomaticofacial foramen, and supplies the region overlying the prominence of the cheek. The zygomaticotemporal artery also passes through the lateral wall of the orbit, via the zygomaticotemporal foramen, and supplies the skin over the non-beard part of the temple. The lacrimal artery anastomoses with the deep temporal branch of the maxillary artery and the transverse facial branch of the superficial temporal artery.

Medial palpebral arteries

Superior and inferior medial palpebral arteries arise from the ophthalmic artery below the trochlea. They descend behind the nasolacrimal sac to enter the eyelids where each divides into two branches that course laterally along the edges of the tarsal plates, forming the superior and inferior arches and supplying the eyelids. They anastomose with branches of the supraorbital, zygomatico-orbital and lacrimal arteries. The inferior arch also anastomoses with the facial artery.

External (dorsal) nasal artery

The external nasal artery is a terminal branch of the anterior ethmoidal artery which arises from the ophthalmic artery. It emerges at the junction of the nasal bone and the lateral nasal cartilage and supplies the skin covering the external nose.

Occipital artery

The occipital artery arises in the neck from the external carotid artery (see Ch. 28). It runs in a groove on the temporal bone, medial to the mastoid process. Accompanied by the greater occipital nerve, the occipital artery enters the back of the scalp by piercing the investing layer of deep cervical fascia that connects the cranial attachments of trapezius and sternocleidomastoid. Tortuous branches run between the skin and the occipital belly of occipitofrontalis, anastomosing with the opposite occipital, posterior auricular and superficial temporal arteries as well as with the transverse cervical branch of the subclavian artery. These branches supply the occipital belly of occipitofrontalis and the skin and pericranium associated with the scalp as far forward as the vertex. The artery may give off a meningeal branch which traverses the parietal foramen.

Posterior auricular artery

The posterior auricular artery arises in the neck from the external carotid artery, and ascends between the auricle and mastoid process. It supplies the cranial surface of the auricle via its auricular branch, and the occipital belly of occipitofrontalis and the scalp behind and above the auricle via its occipital branch. The posterior auricular artery anastomoses with the occipital artery.

VEINS OF THE FACE

The veins of the face are subject to considerable variations: the following description concerns those that are relatively constant (Fig. 29.13).

Supratrochlear vein

The supratrochlear vein starts on the forehead from a venous network connected to the frontal tributaries of the superficial temporal vein. Veins from this network form a single trunk that descends to the bridge of the nose, near the midline and parallel with its contralateral fellow. The veins are joined by a nasal arch across the nose. They then diverge, each joining a supraorbital vein to form the facial vein near the medial canthus of the eye.

Supraorbital vein

The supraorbital vein begins near the zygomatic process of the frontal bone, connecting with branches of the superficial and middle temporal veins. It passes medially above the orbital opening, pierces orbicularis oculi and unites with the supratrochlear vein near the medial canthus of the eye to form the facial vein. A branch passes through the supraorbital notch, where it receives veins from the frontal sinus and frontal diploë, and subsequently connects with the superior ophthalmic vein.

Facial vein

The facial vein is the main vein of the face. After receiving the supratrochlear and supraorbital veins, it travels obliquely downwards by the side of the nose, passes under zygomaticus major, risorius and platysma, descends to the anterior border and then passes over the surface of masseter. It crosses the body of the mandible, and runs down in the neck to drain into the internal jugular vein. The facial vein initially lies behind the more tortuous facial artery, but crosses the artery at the lower border of the mandible. The uppermost segment of the facial vein, above its junction with the superior labial vein, is also called the angular vein: any infection of the mouth or face can spread via the angular veins to the cavernous sinuses resulting in thrombosis (see Ch. 27).

Tributaries

Near its origin, the facial vein connects with the superior ophthalmic vein, both directly and via the supraorbital vein, and so is linked to the cavernous sinus. The facial vein receives tributaries from the side of the nose and, below this, an important deep facial vein from the pterygoid venous plexus. It also receives the inferior palpebral, superior and inferior labial, buccinator, parotid and masseteric veins, and other tributaries which join it below the mandible.

Superficial temporal vein

A widespread venous network across the scalp receives branches from the supratrochlear, supraorbital, posterior auricular and occipital veins. Anterior and posterior tributaries from this network unite above the zygomatic arch to form the superficial temporal vein on each side. The vein accompanies its artery, usually lying behind it, crosses the posterior root of the zygoma, and enters the parotid gland where it joins the maxillary vein to form the retromandibular vein.

Tributaries

The tributaries are the parotid veins, rami draining the temporomandibular joint, anterior auricular, transverse facial and middle temporal veins. The middle temporal vein receives the orbital vein (formed by the lateral palpebral veins), pierces the temporal fascia and then passes back between the layers of the fascia to join the superficial temporal vein just above the level of the zygomatic arch.

Buccal, mental and infraorbital veins

The buccal, mental and infraorbital veins drain the cheek and chin regions and pass into the pterygoid venous plexus.

Posterior auricular and occipital veins

The posterior auricular vein arises in a parieto-occipital network that also drains into tributaries of the occipital and superficial temporal veins. It descends behind the auricle to join the posterior division of the retromandibular vein in, or just below, the parotid gland, to form the external jugular vein. It receives a stylomastoid vein and tributaries from the cranial surface of the auricle, drains the region of the scalp behind the ear and drains into the external jugular vein. The occipital vein begins in a posterior network in the scalp, pierces the cranial attachment of trapezius, turns into the suboccipital triangle and joins the deep cervical and vertebral veins. It may be joined by a vein draining the diploë in the occipital bone and then passes to either the internal jugular, posterior auricular, deep cervical or vertebral veins. Emissary veins connect the occipital vein to the intracranial venous sinuses via the mastoid and parietal foramina and through the posterior condylar canal and occipital protuberances.

LYMPHATIC DRAINAGE OF THE FACE AND SCALP

Lymph vessels from the frontal region above the root of the nose drain to the submandibular nodes (Fig. 29.14; see Fig. 28.15). Vessels from the rest of the forehead, temporal region, upper half of the lateral auricular aspect and anterior wall of the external acoustic meatus drain to the superficial parotid nodes, which lie just anterior to the tragus, either on or deep to the parotid fascia. These nodes also drain lateral vessels from the eyelids and skin of the zygomatic region, and their efferent vessels pass to the upper deep cervical nodes. A strip of scalp above the auricle, the upper half of the cranial aspect and margin of the auricle, and the posterior wall of the external acoustic meatus all drain to the upper deep cervical and posterior auricular nodes. The posterior auricular nodes are superficial to the mastoid attachment of sternocleidomastoid and deep to auricularis posterior, and drain to the upper deep cervical nodes. The auricular lobule, floor of the external acoustic meatus and skin over the mandibular angle and lower parotid region all drain to the superficial cervical or upper deep cervical nodes. Superficial cervical nodes lie along the external jugular vein superficial to sternocleidomastoid. Some efferents pass round the anterior border of sternocleidomastoid to the upper deep cervical nodes, others follow the external jugular vein to the lower deep cervical nodes in the subclavian triangle.

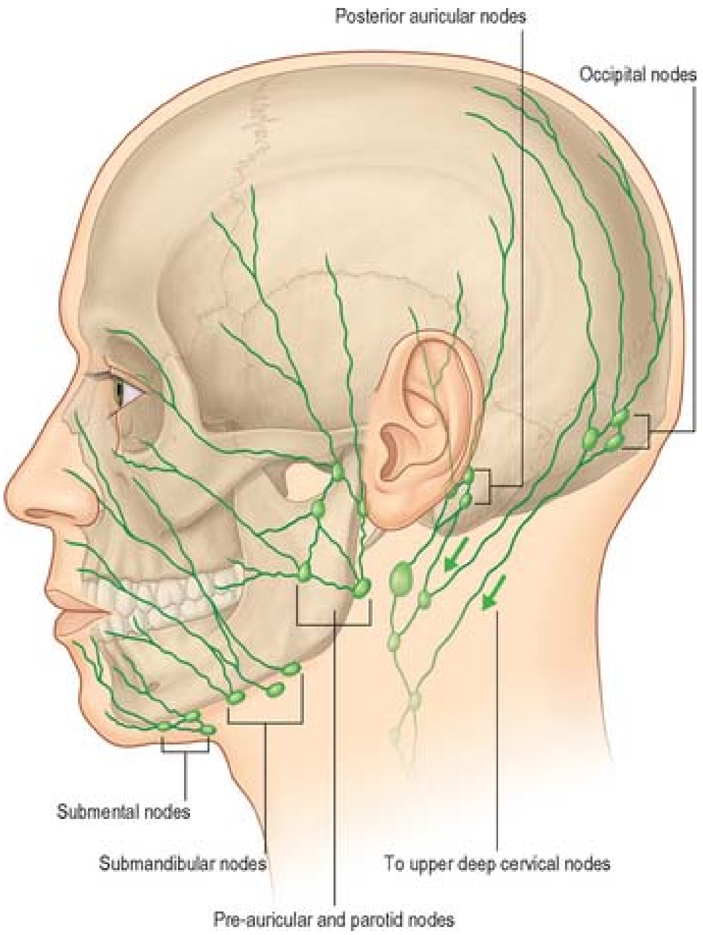
Posterior auricular nodes
Occipital nodes
Submental nodes
Submandibular nodes
To upper deep cervical nodes
Pre-auricular and parotid nodes

Fig. 29.14 The lymphatic drainage of the face and scalp. Arrows indicate direction of flow.

(From Drake, Vogl and Mitchell 2005.)

The occipital region of the scalp drains partly to the occipital nodes, and partly by a vessel that runs along the posterior border of sternocleidomastoid to the lower deep cervical nodes. Occipital nodes are commonly superficial to the upper attachment of trapezius, but occasionally lie in the superior angle of the posterior triangle.

There are usually three submandibular nodes, internal to the deep cervical fascia in the submandibular triangle. One lies at the anterior pole of the submandibular gland, and two flank the facial artery as it reaches the mandible. Other nodes are often embedded in the gland or deep to it. Submandibular nodes drain a wide area, including vessels from the submental, buccal and lingual groups of nodes, and their efferents pass to the upper and lower deep cervical nodes. The external nose, cheek, upper lip and lateral parts of the lower lip drain directly to the submandibular nodes; the afferent vessels may have a few buccal nodes along their course and near the facial vein. The mucous membrane of the lips and cheek drains to the submandibular nodes and the lateral part of the cheek drains to the parotid nodes. The central part of the lower lip, buccal floor and tip of the tongue all drain to the submental nodes which lie on mylohyoid between the anterior bellies of the digastric muscles. These nodes receive afferents bilaterally, some decussating across the chin; their efferents pass to the submandibular and jugulo-omohyoid nodes.

INNERVATION

The numerous muscles of facial expression are supplied by the facial nerve, while the two muscles of mastication that relate to the face are innervated by the mandibular division of the trigeminal nerve. The sensory innervation is primarily from the three divisions of the trigeminal nerve, with smaller contributions from the cervical spinal nerves. The detailed innervation of the auricle is considered on p. 620.

TRIGEMINAL NERVE

Three large areas of the face can be mapped out to indicate the peripheral nerve fields associated with the three divisions of the trigeminal nerve. The fields are not horizontal but curve upwards (Fig. 29.15), apparently because the facial skin moves upwards with growth of the brain and skull. Embryologically, each division of the trigeminal nerve is associated with a developing facial process which gives rise to a specific area of the adult face: the ophthalmic nerve is associated with the frontonasal process, the maxillary nerve with the maxillary process, and the mandibular nerve with the mandibular process.

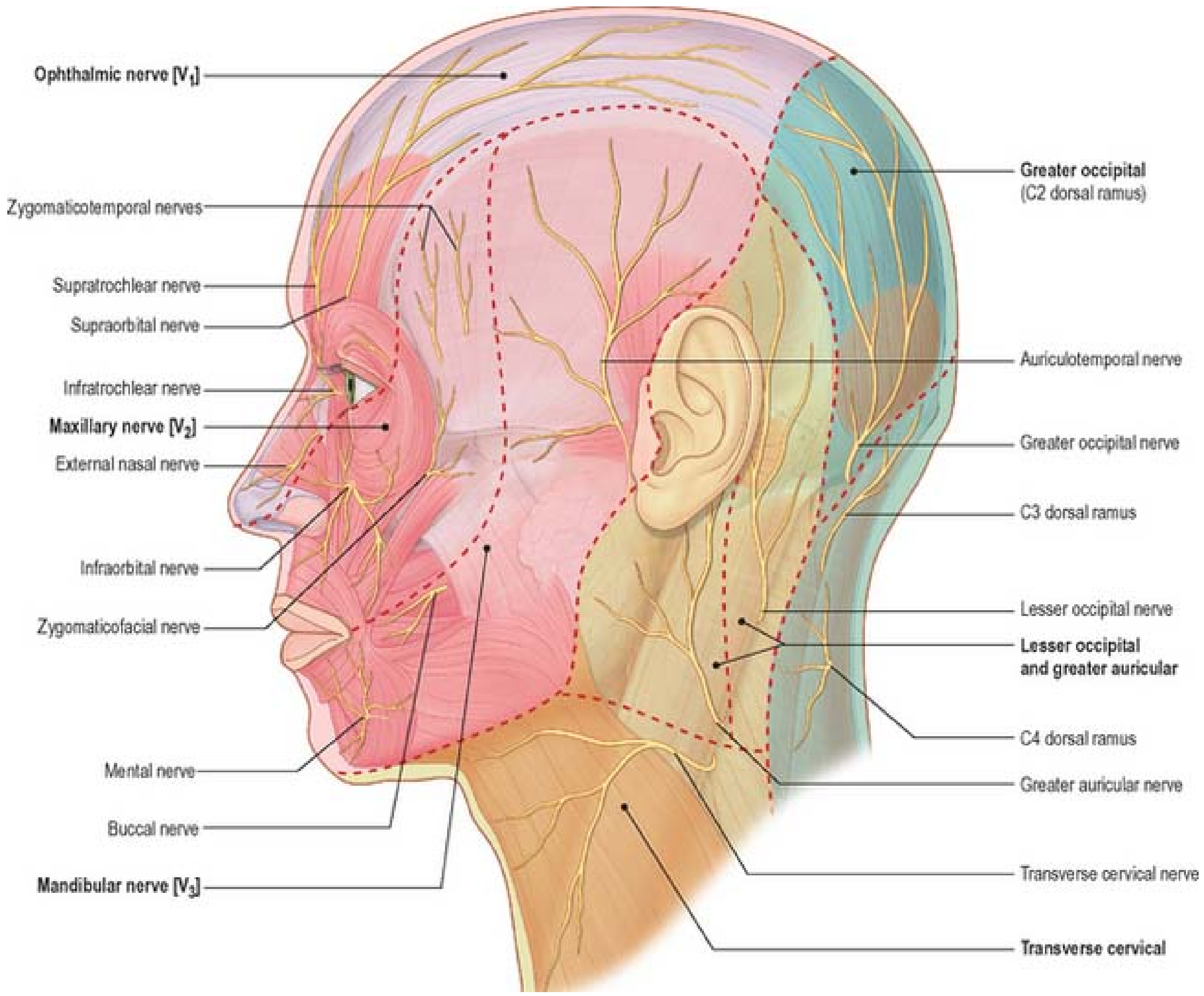
Ophthalmic nerve [V$_1$]
Zygomaticotemporal nerves
Supratrochlear nerve
Supraorbital nerve
Infratrochlear nerve
Maxillary nerve [V$_2$]
External nasal nerve
Infraorbital nerve
Zygomaticofacial nerve
Mental nerve
Buccal nerve
Mandibular nerve [V$_3$]
Greater occipital
(C2 dorsal ramus)
Auriculotemporal nerve
Greater occipital nerve
C3 dorsal ramus
Lesser occipital nerve
Lesser occipital and greater auricular
C4 dorsal ramus
Greater auricular nerve
Transverse cervical nerve
Transverse cervical

Fig. 29.15 Cutaneous innervation of the face and neck, showing dermatomes (in bold).

(Adapted from Drake, Vogl and Mitchell 2005.)

Ophthalmic nerve

The cutaneous branches of the ophthalmic nerve supply the conjunctiva, skin over the forehead, upper eyelid and much of the external surface of the nose.

Supratrochlear nerve

The supratrochlear nerve is the smaller terminal branch of the frontal nerve. It runs anteromedially in the roof of the orbit, passes above the trochlea, and supplies a descending filament to the infratrochlear branch of the nasociliary nerve. The nerve emerges between the trochlea and the supraorbital foramen at the frontal notch, curves up on the forehead close to the bone with the supratrochlear artery and supplies the conjunctiva and the skin of the upper eyelid. It then ascends beneath the corrugator and the frontal belly of occipitofrontalis before dividing into branches which pierce these muscles to supply the skin of the lower forehead near the midline.

Supraorbital nerve

The supraorbital nerve is the larger terminal branch of the frontal nerve. It traverses the supraorbital notch or foramen and supplies palpebral filaments to the upper eyelid and conjunctiva. It ascends on the forehead with the supraorbital artery, and divides into medial and lateral branches which supply the skin of the scalp nearly as far back as the lambdoid suture. These branches are at first deep to the frontal belly of occipitofrontalis. The medial branch perforates the muscle to reach the skin, while the lateral branch pierces the epicranial aponeurosis.

Lacrimal nerve

The lacrimal nerve is the smallest of the main ophthalmic branches and pierces the orbital septum to end in the lateral region of the upper eyelid, which it supplies. It anastomoses with filaments of the facial nerve. Occasionally it is absent, in which case it is replaced by the zygomaticotemporal nerve: the relationship is reciprocal, and when the zygomaticotemporal nerve is absent it is replaced by a branch of the lacrimal nerve.

Infratrochlear nerve

The infratrochlear nerve branches from the nasociliary nerve. It leaves the orbit below the trochlea and supplies the skin of the eyelids, the conjunctiva, lacrimal sac, lacrimal caruncle and the side of the nose above the medial canthus.

External nasal nerve

The external nasal nerve is the terminal branch of the anterior ethmoidal nerve. It descends through the lateral wall of the nose, and supplies the skin of the nose below the nasal bones, excluding the alar portion around the external nares.

Maxillary nerve

The maxillary nerve passes through the orbit to supply the skin of the lower eyelid, the prominence of the cheek, the alar part of the nose, part of the temple, and the upper lip. It has three cutaneous branches, the zygomaticotemporal, zygomaticofacial and infraorbital nerves.

Zygomaticotemporal nerve

The zygomaticotemporal nerve traverses a canal in the zygomatic bone and emerges into the anterior part of the temporal fossa, where it ascends between the bone and temporalis before piercing the temporal fascia about 2 cm above the zygomatic arch to supply the skin of the temple. It communicates with the facial and auriculotemporal nerves. As it pierces the deep layer of the temporal fascia it sends a slender twig between the two layers of the fascia towards the lateral angle of the eye: the branch carries parasympathetic postganglionic fibres from the pterygopalatine ganglion to the lacrimal gland.

Zygomaticofacial nerve

The zygomaticofacial nerve traverses the inferolateral angle of the orbit, and emerges on the face through a foramen in the zygomatic bone. It perforates orbicularis oculi to supply the skin on the prominence of the cheek and forms a plexus with zygomatic branches of the facial nerve and palpebral branches of the maxillary nerve. Occasionally the nerve is absent.

Infraorbital nerve

The infraorbital nerve emerges onto the face at the infraorbital foramen, where it lies between levator labii superioris and levator anguli oris. It gives off palpebral, nasal and superior labial branches. The palpebral branches ascend deep to orbicularis oculi, pierce the muscle to supply the skin in the lower eyelid and join with the facial and zygomaticofacial nerves near the lateral canthus. Nasal branches supply the skin of the side of the nose and of the movable part of the nasal septum, and join the external nasal branch of the anterior ethmoidal nerve. Superior labial branches, which are large and numerous, descend behind levator labii superioris to supply the skin of the anterior part of the cheek and upper lip. They are joined by branches from the facial nerve to form the infraorbital plexus. The infraorbital nerve is commonly implicated in trigeminal neuralgia, and is amenable to cryotherapy where medical therapy fails.

Mandibular nerve

The mandibular nerve supplies skin over the mandible, the lower lip, the fleshy part of the cheek, part of the auricle of the ear and part of the temple via the buccal, mental and auriculotemporal nerves.

Buccal nerve

The buccal nerve emerges onto the face from behind the ramus of the mandible and passes laterally in front of masseter to unite with the buccal branches of the facial nerve. It supplies the skin over the anterior part of buccinator.

Mental nerve

The mental nerve is the terminal branch of the inferior alveolar nerve (see Ch. 30). It enters the face through the mental foramen, where it is directed backwards, and supplies the skin of the lower lip and labial gingivae. Occasionally the mental nerve is important aetiologically in the pain of trigeminal neuralgia, and it is amenable to cryotherapy surgery.

Auriculotemporal nerve

The auriculotemporal nerve emerges onto the face behind the temporomandibular joint within the superior surface of the parotid gland. It ascends posterior to the superficial temporal vessels, passes over the posterior root of the zygoma, and divides into superficial temporal branches. The cutaneous branches of the auriculotemporal nerve supply the tragus and part of the adjoining auricle of the ear and the posterior part of the temple. The nerve may be damaged during parotid gland surgery resulting in impaired sensation of the tragus and temple. It communicates with the temporofacial division of the facial nerve, usually by two rami that pass anterolaterally behind the neck of the mandible. These communications anchor the facial nerve close to the lateral surface of the condylar process of the mandible, and limit its mobility during surgery. Communications with the temporal and zygomatic branches of the facial nerve loop around the transverse facial and superficial temporal vessels.

FACIAL NERVE

The facial nerve emerges from the base of the skull at the stylomastoid foramen and almost immediately gives off the nerves to the posterior belly of digastric and stylohyoid, and the posterior auricular nerve, which supplies the occipital belly of occipitofrontalis and some of the auricular muscles (Fig. 29.16A).

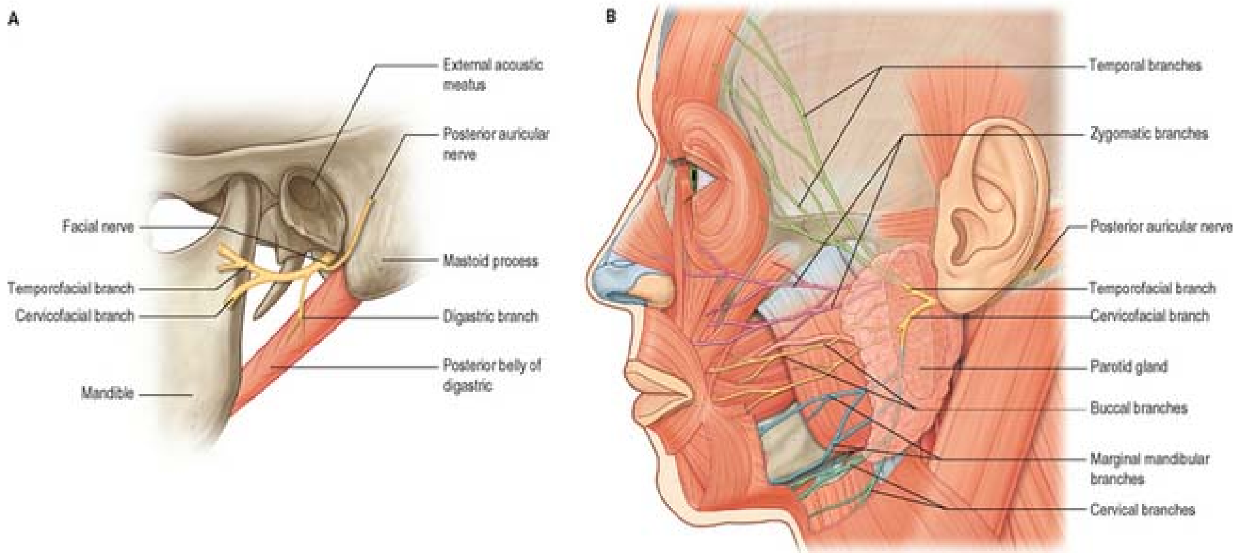
A
External acoustic meatus
Posterior auricular nerve
Facial nerve
Mastoid process
Temporofacial branch
Cervicofacial branch
Digastric branch
Posterior belly of digastric
Mandible
B
Temporal branches
Zygomatic branches
Posterior auricular nerve
Temporofacial branch
Cervicofacial branch
Parotid gland
Buccal branches
Marginal mandibular branches
Cervical branches

Fig. 29.16 Distribution of the facial nerve. **A**, The branches given off immediately after the nerve exits the stylomastoid foramen. **B**, The branches of the nerve on the face.

(From Drake, Vogl and Mitchell 2005.)

The nerve next enters the parotid gland high up on its posteromedial surface and passes forwards and downwards behind the mandibular ramus. Within the substance of the gland it branches into superior (temporofacial) and inferior (cervicofacial) trunks, usually just behind and superficial to the retromandibular vein. The trunks branch further to form a parotid plexus (pes anserinus). Five main terminal branches arise from the plexus, they diverge within the gland and leave by its anteromedial surface, medial to its anterior margin, to supply the muscles of facial expression (Fig. 29.16B). Six distinctive anastomotic patterns were originally classified by Davis et al (1956) and these are illustrated in Fig. 29.17. Numerous microdissection studies have demonstrated that branching patterns and anastomoses between branches, both within the parotid and on the face, exhibit considerable individual variation (e.g. Lineaweaver et al 1997; Kwak et al 2004): the account that follows is therefore an overview. In surgical terms these anastomoses are important, and presumably explain why accidental or deliberate division of a small branch often fails to result in the expected facial nerve weakness. The surface anatomy of the facial nerve is described in Chapter 25.

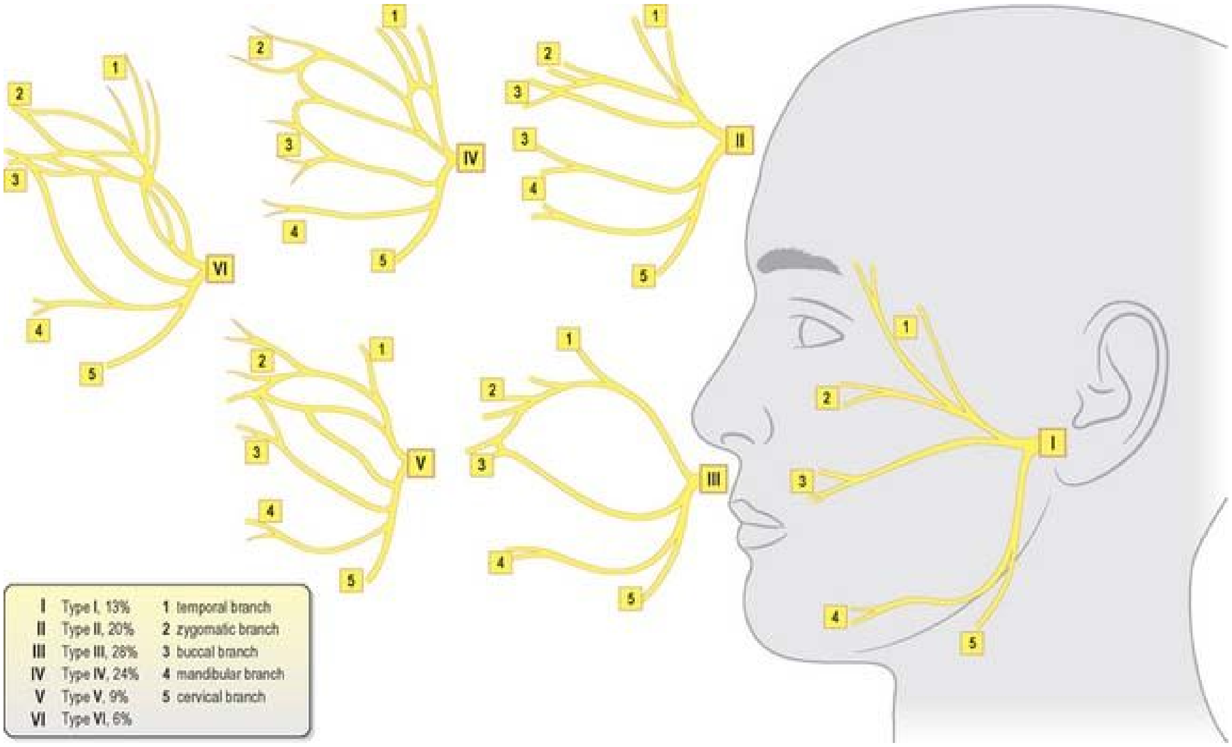
VI
IV
II
V
III
I
1
2
3
4
5
I Type I, 13%
II Type II, 20%
III Type III, 28%
IV Type IV, 24%
V Type V, 9%
VI Type VI, 6%
1 temporal branch
2 zygomatic branch
3 buccal branch
4 mandibular branch
5 cervical branch

Fig. 29.17 Pattern of branching of the facial nerve.

(Modified with permission from Berkovitz BKB, Moxham BJ 2002 Head and Neck Anatomy. London: Martin Dunitz, and from Davis RA, Anson BJ, Budinger JM, Kurth IE 1956 Surgical anatomy of the facial nerve and parotid gland based upon a study of 350 cervicofacial halves. Surg Gynecol Obstet 102: 385–412, with permission from the American College of Surgeons.)

The temporal branch usually divides into anterior and posterior rami soon after piercing the parotidomasseteric fascia below the zygomatic arch; there is often a middle (frontal) ramus. These rami cross the arch in subcutaneous tissue and above the arch lie in the subgaleal space, where their course is extremely variable. Twigs supply intrinsic muscles on the lateral surface of the auricle, and the anterior and superior auricular muscles, and communicate with the zygomaticotemporal branch of the maxillary nerve and the auriculotemporal branch of the mandibular nerve. The more anterior branches supply the frontal belly of occipitofrontalis, orbicularis oculi and corrugator, and join the supraorbital and lacrimal branches of the ophthalmic nerve.

Zygomatic branches are generally multiple. They cross the zygomatic bone to the lateral canthus of the eye and supply orbicularis oculi: they may also supply muscles innervated by the buccal branch. Twigs communicate with filaments of the lacrimal nerve and the zygomaticofacial branch of the maxillary nerve.

The buccal branch is usually single. It has a close relationship to the parotid duct for about 2.5 cm after emerging from the parotid gland, and typically lies below the duct. Superficial branches run beneath the subcutaneous fat and superficial musculo-aponeurotic system (SMAS). Some branches pass deep to procerus and join the infratrochlear and external nasal nerves. Upper deep branches supply zygomaticus major and levator labii superioris, and form an infraorbital plexus with the superior labial branches of the infraorbital nerve. They also supply levator anguli oris, zygomaticus minor, levator labii superioris alaequae nasi and the small nasal muscles: these branches are sometimes described as lower zygomatic branches. Lower deep branches supply buccinator and orbicularis oris; they communicate with filaments of the buccal branch of the mandibular nerve.

There are usually two marginal mandibular branches. They run forwards towards the angle of the mandible under platysma, then turn upwards across the body of the mandible to pass under depressor anguli oris. The branches supply risorius and the muscles of the lower lip and chin, and filaments communicate with the mental nerve. The marginal mandibular branch has an important surgical relationship with the lower border of the mandible (see Ch. 25).

The cervical branch emerges from the lower part of the parotid gland and runs anteroinferiorly under platysma to the front of the neck. Typically single, it supplies platysma and communicates with the transverse cutaneous cervical nerve.

Cutaneous branches of the facial nerve accompany the auricular branch of the vagus; they are believed to innervate the skin on both auricular aspects, in the conchal depression and over its eminence.

Facial nerve lesions

Facial paralysis may be due to an upper motor neurone lesion (when frontalis is partially spared due to the bilateral innervation of the muscle of the upper part of the face), or a lower motor neurone lesion (when all branches may be involved). Ipsilateral lower motor neurone facial paralysis occurs in Bell's palsy and Ramsay Hunt syndrome, and may be the consequence of an acoustic neuroma, a malignant parotid tumour or, more commonly, cheek laceration. Only those muscles innervated by degenerating or demyelinating branches of the facial nerve become weak.

The facial nerve is routinely isolated as part of a superficial parotidectomy operation – typically in the treatment of parotid tumours – when that part of the gland lying superficial to the plane of the facial nerve is removed. Although all branches of the facial nerve are preserved, there is often some postoperative facial weakness caused by bruising and ischaemia of the nerve which may result in temporary demyelination of the nerve fibres. Although this can affect all the branches of the facial nerve, the weakness is often confined to the territory innervated by the marginal mandibular branch and is manifested by a weakness of the lower lip on the affected side. This is because anastomotic arcades between the marginal mandibular branch and other branches of the facial nerve are relatively rare, whereas they are plentiful between the various branches of the temporofacial division and the buccal branch of the cervicofacial division of the facial nerve.

Cervical spinal nerves

Cervical spinal nerves have cutaneous branches which supply areas of skin in the face and scalp (Fig. 29.15). The named branches are the great auricular and lesser occipital nerves, which are part of the cervical plexus, and are described on page 435 (see Fig. 28.1) and the greater occipital nerve which is described on page 755 (see Fig. 42.52, Fig. 43.6).

PAROTID SALIVARY GLAND

The paired parotid glands are the largest of the salivary glands. Each has an average weight of 25 g and is an irregular, lobulated, yellowish mass, lying largely below the external acoustic meatus between the mandible and sternocleidomastoid. The gland also projects forwards onto the surface of masseter (Fig. 29.16B). In 20% of cases, a small, usually detached, part called the accessory parotid gland (pars accessoria or socia parotidis) lies between the zygomatic arch above and the parotid duct below. The overall shape of the parotid gland is variable. Viewed laterally, in 50% of cases it is roughly triangular in outline. However in 30% of cases the gland is more or less of even width throughout, and the upper and lower poles are rounded.

In its usual inverted pyramidal form, the parotid gland presents a small superior surface, and superficial, anteromedial and posteromedial surfaces. It tapers inferiorly to a blunt apex. The concave superior surface is related to the cartilaginous part of the external acoustic meatus and posterior aspect of the temporomandibular joint. Here the auriculotemporal nerve curves round the neck of the mandible, embedded in the capsule of the gland. The apex overlaps the posterior belly of digastric and the carotid triangle to a variable extent.

The superficial surface is covered by skin and superficial fascia, which contains the facial branches of the great auricular nerve, superficial parotid lymph nodes and the posterior border of platysma. It extends upwards to the zygomatic arch, backwards to overlap sternocleidomastoid, downwards to its apex posteroinferior to the mandibular angle, and forwards to lie on masseter below the parotid duct.

The anteromedial surface is grooved by the posterior border of the mandibular ramus. It covers the posteroinferior part of masseter, the lateral aspect of the temporomandibular joint and the adjoining part of the mandibular ramus. It passes forwards, medial to the ramus of the mandible, to reach medial pterygoid. The gland may therefore be subdivided into a larger superficial part and a smaller part, the deep ‘lobe’, deep to the ramus, the two being joined by an isthmus. Branches of the facial nerve emerge on the face from the anterior margin of this surface.

The posteromedial surface is moulded to the mastoid process, sternocleidomastoid, posterior belly of the digastric, and the styloid process and its associated muscles. The external carotid artery grooves this surface before entering the gland, and the internal carotid artery and internal jugular vein are separated from the gland by the styloid process and its associated muscles (Fig. 29.18). The anteromedial and posteromedial surfaces meet at a medial margin that may project so deeply that it contacts the lateral wall of the pharynx.

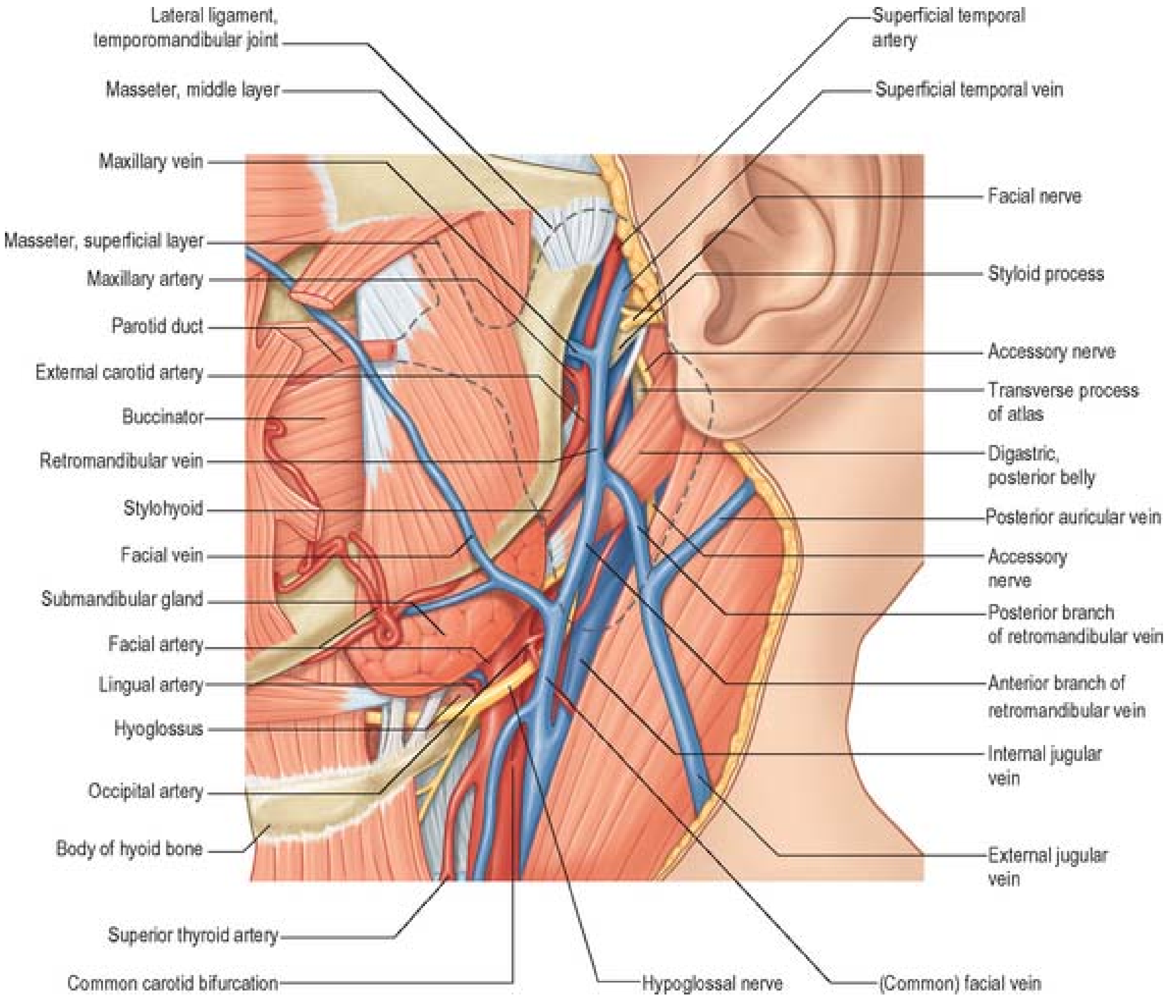
Lateral ligament, temporomandibular joint
Masseter, middle layer
Maxillary vein
Masseter, superficial layer
Maxillary artery
Parotid duct
External carotid artery
Buccinator
Retromandibular vein
Stylohyoid
Facial vein
Submandibular gland
Facial artery
Lingual artery
Hyoglossus
Occipital artery
Body of hyoid bone
Superior thyroid artery
Common carotid bifurcation
Hypoglossal nerve
(Common) facial vein
Superficial temporal artery
Superficial temporal vein
Facial nerve
Styloid process
Accessory nerve
Transverse process of atlas
Digastric, posterior belly
Posterior auricular vein
Accessory nerve
Posterior branch of retromandibular vein
Anterior branch of retromandibular vein
Internal jugular vein
External jugular vein

Fig. 29.18 The principal immediate deep relations of the parotid gland. The outline of the parotid gland is indicated by the interrupted black line.

Deep lobe tumours

The deep ‘lobe’ of the gland extends behind the mandibular ramus, where its deep surface lies immediately lateral to the superior constrictor of the pharynx. When a parotid tumour, either benign or malignant, occurs in the deep ‘lobe’, the mass presents as a swelling in the lateral wall of the pharynx and not as a facial swelling, which means that it is important to examine the oropharynx when following-up a patient who has undergone parotid surgery for the removal of a tumour.

STRUCTURES WITHIN THE PAROTID GLAND

The external carotid artery, retromandibular vein and facial nerve, either in part or in whole, traverse the gland and branch within it. The external carotid artery enters the posteromedial surface, and divides into the maxillary artery, which emerges from the anteromedial surface, and the superficial temporal artery, which gives off its transverse facial branch in the gland and ascends to leave its upper limit (Fig. 29.16). The posterior auricular artery may also branch from the external carotid artery within the gland, leaving by its posteromedial surface.

The retromandibular vein, formed by the union of the maxillary and superficial temporal veins (which enter near the points of exit of the corresponding arteries), is superficial to the external carotid artery. It descends in the parotid gland and emerges behind the apex of the gland, where it usually divides into an anterior branch, which passes forwards to join the facial vein, and a posterior branch, which joins the posterior auricular vein to form the external jugular vein. Occasionally it is not connected to the external jugular vein, which is then small, and the anterior jugular vein is enlarged.

PAROTID CAPSULE

The parotid gland is enclosed within an unyielding parotid capsule derived from the investing layer of deep cervical fascia. Acute inflammation of the parotid gland (acute sialadenitis) may cause exquisite pain in the preauricular region as a result of stretching of the capsule and stimulation of the great auricular nerve. The pain is usually exacerbated at mealtimes when the gustatory stimulus to the gland results in further turgor within the capsule. Causes of acute sialadenitis include parotid duct obstruction (calculus, mucus plug and duct stricture) and mumps.

PAROTID DUCT

The average dimensions of the parotid duct are 5 cm long and 3 mm wide (although it is narrower at its oral orifice). It begins by the confluence of two main tributaries within the anterior part of the parotid gland: the duct appears at the anterior border of the upper part of the gland and passes horizontally across masseter, approximately midway between the angle of the mouth and the zygomatic arch (Fig. 29.16). If the duct arises lower down, it may run obliquely upwards. It crosses masseter, turns medially at its anterior border at almost a right angle, and traverses the buccal fat pad and buccinator opposite the crown of the upper third molar tooth. The duct then runs obliquely forwards for a short distance between buccinator and the oral mucosa before it opens upon a small papilla opposite the second upper molar crown. The submucosal passage of the duct serves as a valvular mechanism preventing inflation of the gland with raised intraoral pressures. While crossing masseter, the duct lies between the upper and lower buccal branches of the facial nerve, and may receive the accessory parotid duct.

The accessory part of the gland and the transverse facial artery lie above the parotid duct; the buccal branch of the mandibular nerve, emerging from beneath temporalis and masseter, lies just below, at the anterior border of masseter. The parotid duct may be crossed by anastomosing branches between the zygomatic and buccal branches of the facial nerve.

The ramifications of the ductal systems, and their patterns and calibres, can be demonstrated radiographically by injecting a radio-opaque substance into the parotid duct via a cannula. In a lateral parotid sialogram the main duct can be seen to be formed near the centre of the posterior border of the mandibular ramus by the union of two or three ducts which ascend or descend respectively at right angles to the main duct. As it crosses the face, the main duct also receives from above five or six ductules from the accessory parotid gland (Fig. 29.19). As it curves round the anterior border of masseter it is often compressed and its shadow is attenuated. Deep lacerations of the cheek where the integrity of the parotid duct is in doubt should be explored and repaired using microsurgical techniques, to prevent saliva leaking into the soft tissues of the cheek and subsequent sialocele formation.

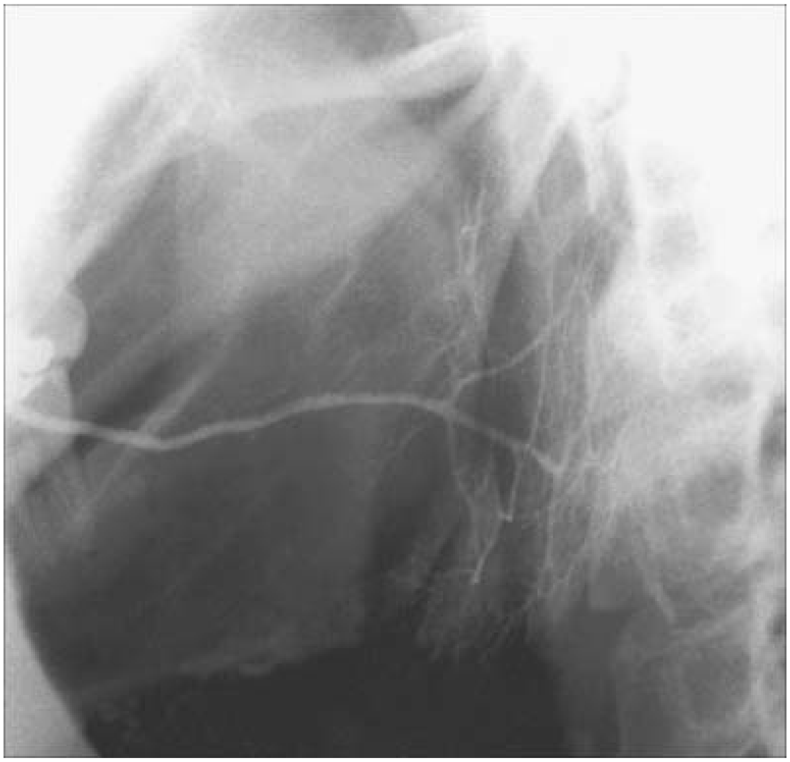

Fig. 29.19 Oblique lateral radiograph showing normal parotid duct outlined after injection of radiopaque contrast medium (sialogram). Note that here the main duct is formed by the union of three smaller ducts at the posterior border of the ramus of the mandible.

(By courtesy of Dr N Drage.)

VASCULAR SUPPLY AND LYMPHATIC DRAINAGE

The parotid gland receives its arterial supply from the external carotid artery and its branches within and near the gland. The veins drain to the external jugular vein via local tributaries.

Lymph nodes occur in the skin overlying the parotid gland (preauricular nodes) and in the substance of the gland. There are usually 10 lymph nodes present in the gland, the majority lie in the superficial part of the gland above the plane related to the facial nerve. Lymph from the parotid gland drains to the upper deep cervical lymph nodes.

INNERVATION

Preganglionic nerves travel in the lesser petrosal branch of the glossopharyngeal nerve and synapse in the otic ganglion. Postganglionic secretomotor fibres reach the gland via the auriculotemporal nerve.

Gustatory sweating (Frey's syndrome or auriculotemporal syndrome)

Gustatory sweating (auriculotemporal syndrome) commonly occurs following parotid surgery or other surgery or trauma that results in opening of the parotid capsule. It is thought to reflect aberrant innervation of sweat glands on the face by regrowing parasympathetic secretomotor axons that would previously have innervated the parotid gland. Frey's syndrome is characterized by sweating, warmth and redness of the face as a result of salivary stimulation by the smell or taste of food. The management of Frey's syndrome is difficult. Denervation by tympanic neurectomy or auriculotemporal nerve avulsion have been advocated, but are often not curative. The symptoms can be managed by the subcutaneous infiltration of purified botulinum toxin into the affected area, and use of antiperspirant.

REFERENCES

ɔrges AF, Alexander JE. Relaxed skin tension lines, Z-plasties on scars, and fusiform excision of lesions. *Br J Plast Surg*. 1962;15:242-254.

ıvis RA, Anson BJ, Budinger JM, Kurth LE. Surgical anatomy of the facial nerve and parotid gland based upon a study of 350 cervicofacial halves. *Surg Gynecol Obstet*. 1956;102:385-412.

omer J. The human accessory parotid gland: its incidence, nature and significance. *Oral Surg Oral Med Oral Pathol*. 1977;43:671-676.

ɔsain AK, Yousif NJ, Madiedo G, Larson DL, Matloub HS, Sanger JR. Surgical anatomy of the SMAS: a reinvestigation. *Plast Reconstruct Surg*. 1993;92:1254-1263.

wak HH, Park HD, Youn KH, Hu KS, Koh KS, Han SH, Kim HJ. Branching patterns of the facial nerve and its communication with the auriculotemporal nerve. *Surg Radiol Anat*. 2004;26:494-500.

neaweaver W, Rhoton A, Habal MB. Microsurgical anatomy of the facial nerve. *Craniofac Surg*. 1997;8:6-10.

ngdon JD. Parotid surgery. In: Langdon JD, Patel MF. *Operative Maxillofacial Surgery*. London: Chapman and Hall; 1998:381-390.

A detailed account of the procedures for the safe dissection of the intraparotid part of the facial nerve..

arkus AF, Delaire J, Smith WP. Facial balance in cleft lip and palate II. Cleft lip and palate and secondary deformities. *Br J Oral Maxillofac Surg*. 1992;30:296-304.

Discusses the anatomical basis for the repair of cleft lip and palate deformities..

itz V, Peyronie M. The superficial musculo-aponeurotic system (SMAS) in the parotid and cheek area. *Plast Reconstruct Surg*. 1976;58:80-88.

yint K, Azian AL, Khairul FA. The clinical significance of the branching pattern of the facial nerve in Malaysian subjects. *Med J Malaysia*. 1992;47:114-121.

Norman JE, McGurk M. Color Atlas and Text of the Salivary Glands. London: Mosby-Wolfe, 1995.

rk IY, Lee ME. A morphological study of the parotid gland and the peripheral part of the facial nerve in Koreans. *Yonsei Med J*. 1977;18:45-51.

imada K, Gasser RF. Morphology of the mandibulo-stylohyoid ligament in human adults. *Anat Rec*. 1988;222:207-210.

assef M. Superficial fascial and muscular layers in the face and neck: a histological study. *Aesth Plast Surg*. 1987;11:171-176.

usif NJ, Mendelson BC. Anatomy of the midface. *Clin Plast Surg*. 1995;22:227-240.

arah HA, Atkinson ME. The surgical anatomy of the mandibular distribution of the facial nerve. *Br J Oral Surg*. 1981;19:159-170.

CHAPTER 30

Oral cavity

The mouth or oral cavity extends from the lips and cheeks externally to the anterior pillars of the fauces internally, where it continues into the oropharynx (Fig. 30.1). The mouth can be subdivided into the vestibule external to the teeth and the oral cavity proper internal to the teeth. The palate forms the roof of the mouth and separates the oral and nasal cavities. The floor of the mouth is formed by the mylohyoid muscles and is occupied mainly by the tongue. The lateral walls of the mouth are defined by the cheeks and retromolar regions. Three pairs of major salivary glands (parotid, submandibular and sublingual) and numerous minor salivary glands (labial, buccal, palatal, lingual) open into the mouth. The muscles in the oral cavity are associated with the lips, cheeks, floor of the mouth and tongue. The muscles of the lips and cheeks are described with the face in Chapter 29. The muscles of the soft palate are described with the pharynx in Chapter 33.

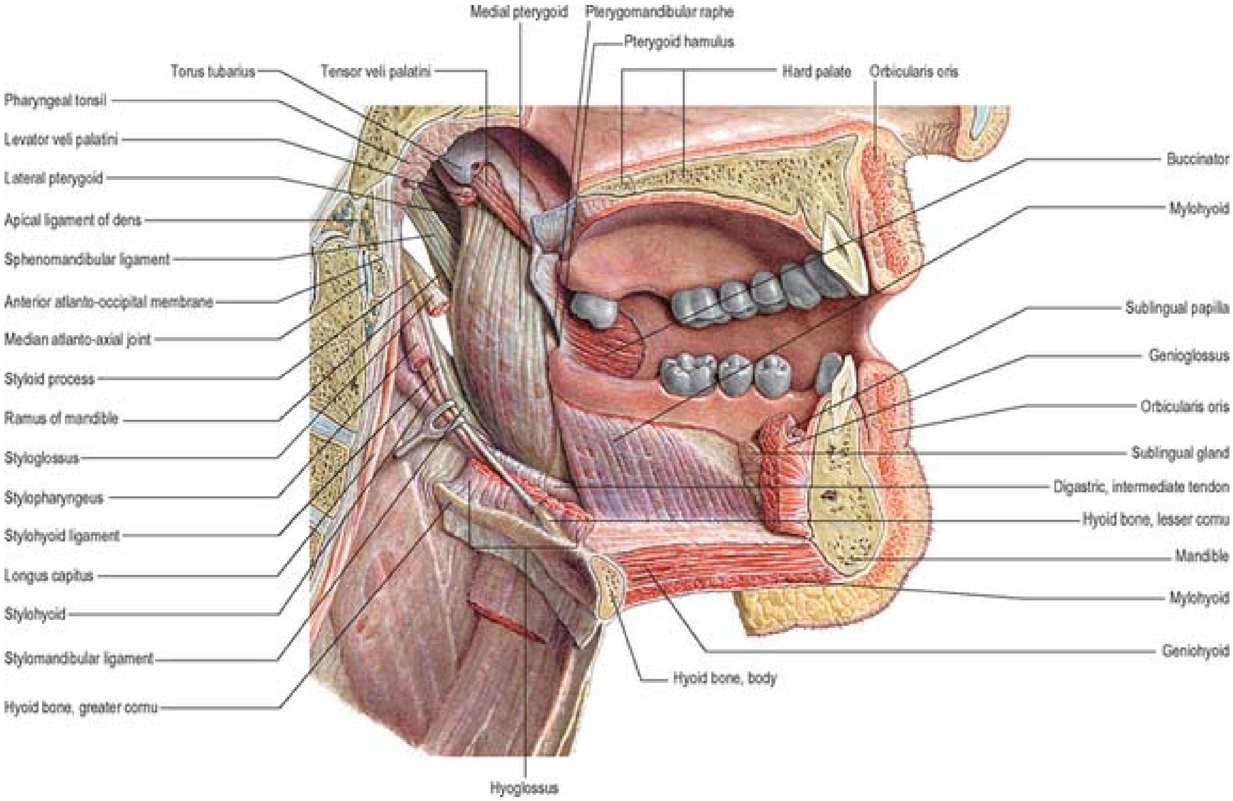
Medial pterygoid
Pterygomandibular raphe
Pterygoid hamulus
Torus tubarius
Tensor veli palatini
Hard palate
Orbicularis oris
Pharyngeal tonsil
Levator veli palatini
Lateral pterygoid
Apical ligament of dens
Sphenomandibular ligament
Anterior atlanto-occipital membrane
Median atlanto-axial joint
Styloid process
Ramus of mandible
Styloglossus
Stylopharyngeus
Stylohyoid ligament
Longus capitus
Stylohyoid
Stylomandibular ligament
Hyoid bone, greater cornu
Buccinator
Mylohyoid
Sublingual papilla
Genioglossus
Orbicularis oris
Sublingual gland
Digastric, intermediate tendon
Hyoid bone, lesser cornu
Mandible
Mylohyoid
Geniohyoid
Hyoid bone, body
Hyoglossus

Fig. 30.1 Oral cavity. The tongue and soft palate have been removed.

(From Sobotta 2006.)

The mouth is concerned primarily with the ingestion and mastication of food, which is mainly the function of the teeth. The mouth is also associated with phonation and ventilation.

CHEEKS

The external features of the cheeks are described in Chapter 29. Internally, the mucosa of the cheek is tightly adherent to buccinator and is thus stretched when the mouth is opened and wrinkled when closed. Ectopic sebaceous glands may be evident as yellow patches (Fordyce’s spots). Their numbers increase in puberty and in later life.

Few structural landmarks are visible. The parotid duct drains into the cheek opposite the maxillary second molar tooth at a small parotid papilla. A hyperkeratinized line (the linea alba) may be seen at a position related to the occlusal plane of the teeth. In the retromolar region, a fold of mucosa containing the pterygomandibular raphe extends from the upper to the lower alveolus. The entrance to the pterygomandibular space (which contains the lingual and inferior alveolar nerves) lies lateral to this fold and medial to the ridge produced by the anterior border of the ramus of the mandible: this is the site for injection for an inferior alveolar nerve block, commonly used to anaesthetize the ipsilateral lower teeth and gums.

Vascular supply and innervation

The cheek receives its arterial blood supply principally from the buccal branch of the maxillary artery, and is innervated by cutaneous branches of the maxillary division of the trigeminal nerve, via the zygomaticofacial and infraorbital nerves, and by the buccal branch of the mandibular division of the trigeminal nerve.

LIPS

The external features of the lips are described in Chapter 29. The central part of the lips contains orbicularis oris. Internally, the labial mucosa is smooth and shiny and shows small elevations caused by underlying mucous glands.

The position and activity of the lips are important in controlling the degree of protrusion of the incisors. With normal (competent) lips, the tips of the maxillary incisors lie below the upper border of the lower lip, and this arrangement helps to maintain the ‘normal’ inclination of the incisors. When the lips are incompetent, the maxillary incisors may not be so controlled and the lower lip may even lie behind them, thus producing an exaggerated proclination of these teeth. A tight, or overactive, lip musculature may be associated with retroclined maxillary incisors. The lips are kept moist both by tongue deposition of saliva and by numerous minor salivary glands within them. These glands are liable to trauma by the teeth, particularly in the lower lip: this can produce a mucocele as a result of either extravasation of saliva into the submucosal tissues or retention of saliva within the gland or its duct.

Vascular supply and innervation

The lips are mainly supplied by the superior and inferior labial branches of the facial artery. The upper lip is innervated by superior labial branches of the infraorbital nerve and the lower lip is innervated by the mental branch of the mandibular division of the trigeminal.

ORAL VESTIBULE

The oral vestibule is a slit-like space between the lips or cheeks on one side and the teeth on the other. When the teeth occlude, the vestibule is a closed space that only communicates with the oral cavity proper in the retromolar regions behind the last molar tooth on each side. Where the mucosa that covers the alveolus of the jaw is reflected onto the lips and cheeks, a trough or sulcus is formed which is called the fornix vestibuli. A variable number of sickle-shaped folds containing loose connective tissue run across the fornix vestibuli. In the midline these are the upper and lower labial frena (or frenula). Other folds may traverse the fornix near the canines or premolars. The folds in the lower fornix are said to be more pronounced than those in the upper fornix (Fig. 30.2).

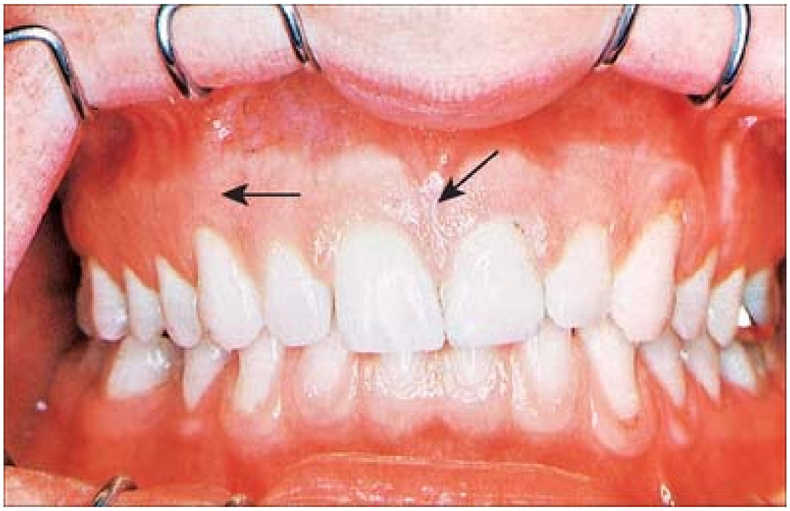

Fig. 30.2 Anterior view of the dentition in centric occlusion, with the lips retracted. Note the pale pink, stippled gingivae and the red, shiny, smooth alveolar mucosa. The degree of overbite is rather pronounced and the gingiva and its epithelial attachment have receded onto the root of the upper left canine. Note frena (arrows).

The upper labial frenulum is normally attached well below the alveolar crest. A large frenulum with an attachment near or on the crest may be associated with a midline gap (diastema) between the maxillary first incisors. This can be corrected by simple surgical removal of the frenulum (frenulectomy), because it contains no structures of clinical importance. Prominent frena may compromise the stability of dentures.

ORAL MUCOSA

The oral mucosa is continuous with the skin at the labial margins (vermilion border) and with the pharyngeal mucosa at the oropharyngeal isthmus. It varies in structure, function and appearance in different regions of the oral cavity and is traditionally divided into lining, masticatory and specialized mucosae.

LINING MUCOSA

The lining mucosa is red in colour, and covers the soft palate, ventral surface of the tongue, floor of the mouth, alveolar processes excluding the gingivae, and the internal surfaces of the lips and cheeks. It has a non-keratinized stratified squamous epithelium which overlies a loosely fibrous lamina propria, and the submucosa contains some fat deposits and collections of minor mucous salivary glands. The oral mucosa covering the alveolar bone – which supports the roots of the teeth – and the necks (cervical region) of the teeth is divided into two main components. That portion lining the lower part of the alveolus is loosely attached to the periosteum via a diffuse submucosa and is termed the alveolar mucosa. It is delineated from the masticatory gingival mucosa, which covers the upper part of the alveolar bone and the necks of the teeth, by a well-defined junction, the mucogingival junction. The alveolar mucosa appears dark red; the gingival appears pale pink. These colour differences relate to differences in the type of keratinization and the proximity to the surface of underlying small blood vessels which may sometimes be seen coursing beneath the alveolar mucosa.

MASTICATORY MUCOSA AND THE GINGIVAE

Masticatory mucosa, i.e. mucosa that is subjected to masticatory stress, is bound firmly to underlying bone or to the necks of the teeth, and forms a mucoperiosteum in the gingivae and palatine raphe. Gingival, palatal and dorsal lingual mucosae are keratinized or parakeratinized.

The gingivae may be further subdivided into the attached gingivae and the free gingivae. Attached gingivae are firmly bound to the periosteum of the alveolus and to the teeth, whereas free gingivae, which constitute approximately a 1 mm margin of the gingivae, lie unattached around the cervical region of each tooth. The free gingival groove between the free and attached gingivae corresponds roughly to the floor of the gingival sulcus which separates the inner surface of the attached gingivae from the enamel. The interdental papilla is that part of the gingivae which fills the space between adjacent teeth. The surface of the attached gingivae is characteristically stippled, although there is considerable interindividual variation in the degree of stippling, and variation according to age, sex and the health of the gingivae. The free gingivae are not stippled. A mucogingival line delineates the attached gingivae on the lingual surface of the lower jaw from the alveolar mucosa towards the floor of the mouth. There is no corresponding obvious division between the attached gingivae and the remainder of the palatal mucosa because this whole surface is orthokeratinized masticatory mucosa, which is pink.

A submucosa is absent from the gingivae and the midline palatine raphe, but is present over the rest of the hard palate. Posterolaterally it is thick where it contains mucous salivary glands and the greater palatine nerves and vessels, and it is anchored to the periosteum of the maxillae and palatine bones by collagenous septa.

Vascular supply and lymphatic drainage

The gingival tissues derive their blood supply from the maxillary and lingual arteries. The buccal gingivae around the maxillary cheek teeth are supplied by gingival and perforating branches from the posterior superior alveolar artery and by the buccal branch of the maxillary artery. The labial gingivae of anterior teeth are supplied by labial branches of the infraorbital artery and by perforating branches of the anterior superior alveolar artery. The palatal gingivae are supplied primarily by branches of the greater palatine artery.

The buccal gingivae associated with the mandibular cheek teeth are supplied by the buccal branch of the maxillary artery and by perforating branches from the inferior alveolar artery. The labial gingivae around the anterior teeth are supplied by the mental artery and by perforating branches of the incisive artery. The lingual gingivae are supplied by perforating branches from the inferior alveolar artery and by its lingual branch, and by the main lingual artery, a branch of the external carotid artery.

No accurate description is available concerning the venous drainage of the gingivae, although it may be assumed that buccal, lingual, greater palatine and nasopalatine veins are involved. These veins run into the pterygoid plexuses (apart from the lingual veins, which may pass directly into the internal jugular veins).

The lymph vessels of the labial and buccal gingivae of the maxillary and mandibular teeth unite to drain into the submandibular nodes, though in the labial region of the mandibular incisors they may drain into the submental lymph nodes. The lingual and palatal gingivae drain into the jugulodigastric group of nodes, either directly or indirectly through the submandibular nodes.

Innervation

The nerves supplying the gingivae in the upper jaw come from the maxillary nerve via its greater palatine, nasopalatine, and anterior, middle and posterior superior alveolar branches (see Table 30.2). Surgical division of the nasopalatine nerve, for example during the removal of an ectopic canine tooth, causes no obvious sensory deficit in the anterior part of the palate, which suggests that the territory of the greater palatine nerve reaches as far forwards as the gingivae lingual to the incisor teeth or the nerve has large regenerative potential. The mandibular nerve innervates the gingivae in the lower jaw by its inferior alveolar, lingual and buccal branches.

Table 30.2 Nerve supply to the teeth and gingivae.

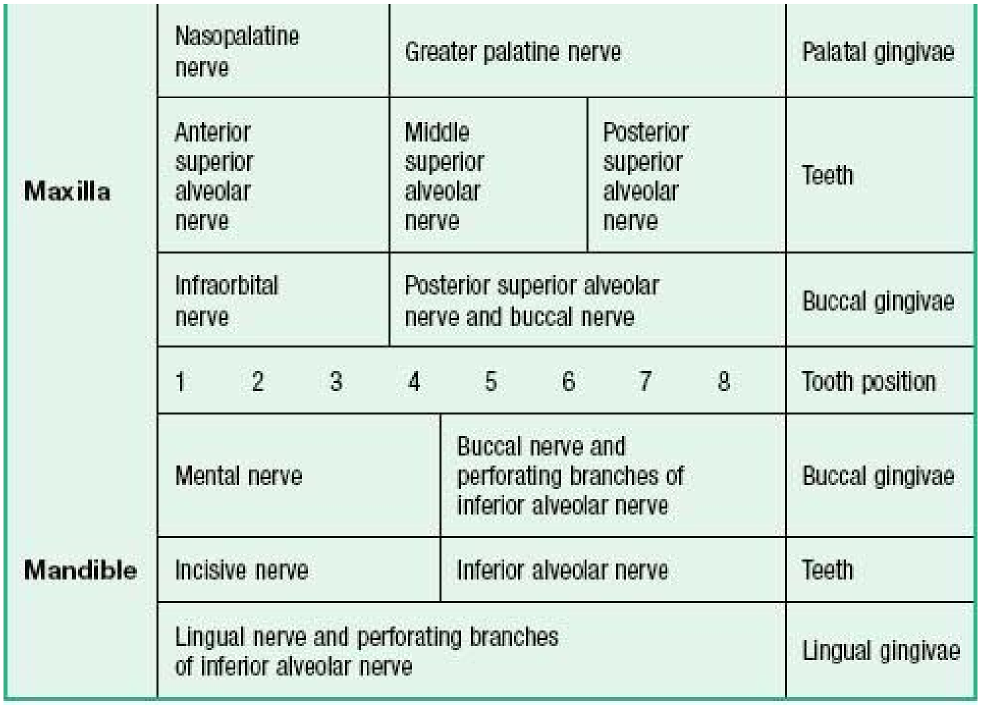

Maxilla	Nasopalatine nerve			Greater palatine nerve					Palatal gingivae
	Anterior superior alveolar nerve			Middle superior alveolar nerve		Posterior superior alveolar nerve			Teeth
	Infraorbital nerve			Posterior superior alveolar nerve and buccal nerve					Buccal gingivae
	1	2	3	4	5	6	7	8	Tooth position
Mandible	Mental nerve				Buccal nerve and perforating branches of inferior alveolar nerve				Buccal gingivae
	Incisive nerve				Inferior alveolar nerve				Teeth
	Lingual nerve and perforating branches of inferior alveolar nerve								Lingual gingivae

(By permission from Berkovitz BKB, Holland GR, Moxham BJ 2002 Oral Anatomy, Embryology and Histology, 3rd edn. Edinburgh: Mosby.)

SPECIALIZED ORAL MUCOSA

The specialized mucosa covering the anterior two-thirds of the dorsum of the tongue is described on page 507.

OROPHARYNGEAL ISTHMUS

The oropharyngeal isthmus lies between the soft palate and the dorsum of the tongue, and is bounded on both sides by the palatoglossal arches. Each palatoglossal arch runs downwards, laterally and forwards, from the soft palate to the side of the tongue and consists of palatoglossus and its covering mucous membrane (Fig. 30.3). The approximation of the arches shuts off the mouth from the oropharynx, and is essential to deglutition (see Ch. 33).

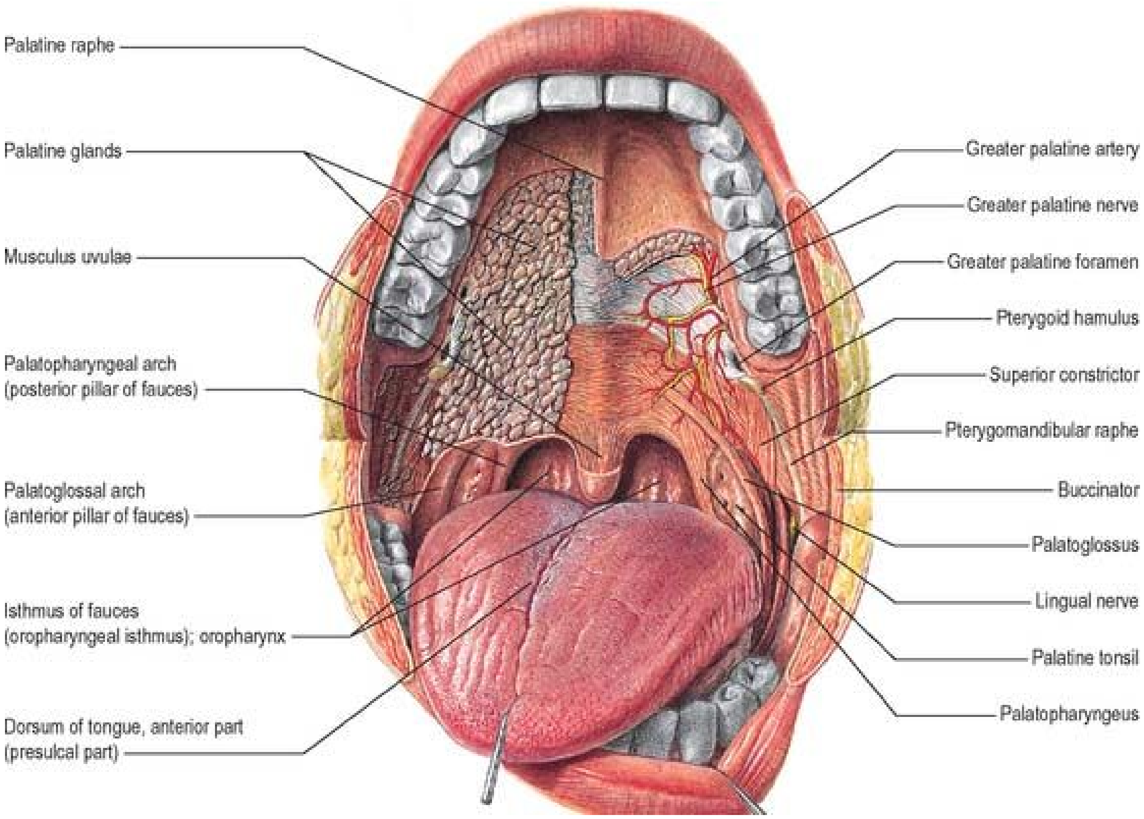
Palatine raphe
Palatine glands
Musculus uvulae
Palatopharyngeal arch (posterior pillar of fauces)
Palatoglossal arch (anterior pillar of fauces)
Isthmus of fauces (oropharyngeal isthmus); oropharynx
Dorsum of tongue, anterior part (presulcal part)
Greater palatine artery
Greater palatine nerve
Greater palatine foramen
Pterygoid hamulus
Superior constrictor
Pterygomandibular raphe
Buccinator
Palatoglossus
Lingual nerve
Palatine tonsil
Palatopharyngeus

Fig. 30.3 Oral cavity, oropharyngeal isthmus and muscles of the palate.

(From Sobotta 2006.)

FLOOR OF THE MOUTH

The floor of the mouth is a small horseshoe-shaped region situated beneath the movable part of the tongue and above the muscular diaphragm formed by the mylohyoid muscles (Fig. 30.4, see Fig. 30.7). A fold of tissue, the lingual frenulum, extends onto the inferior surface of the tongue from near the base of the tongue. It occasionally extends across the floor of the mouth to be attached onto the mandibular alveolus, known colloquially as a 'tongue tie'; historically, this has been removed to aid speech, but the evidence for this is scanty. The submandibular salivary ducts open into the mouth at the sublingual papilla (caruncle), which is a large centrally positioned protuberance at the base of the tongue.

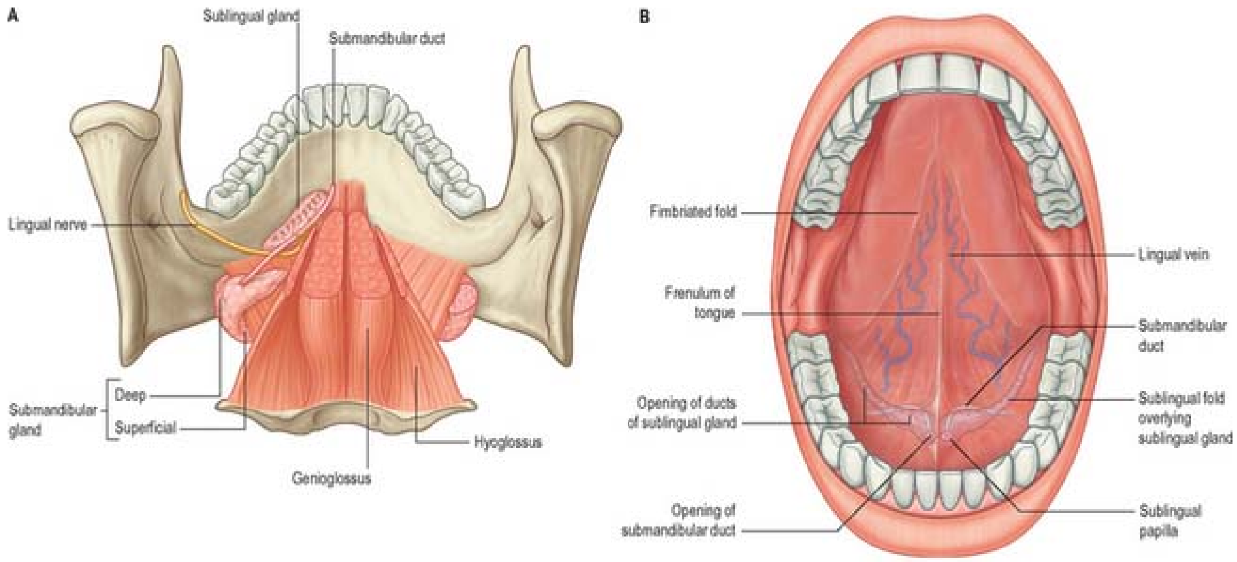
A
Sublingual gland
Submandibular duct
Lingual nerve
Submandibular gland
Deep
Superficial
Genioglossus
Hyoglossus
B
Fimbriated fold
Frenulum of tongue
Opening of ducts of sublingual gland
Opening of submandibular duct
Lingual vein
Submandibular duct
Sublingual fold overlying sublingual gland
Sublingual papilla

Fig. 30.4 Floor of the mouth. **A**, Viewed from above when the bulk of the tongue musculature has been removed. Note the relationships between the lingual nerve and the submandibular duct, and between the submandibular and sublingual salivary glands. **B**, The ventral surface of the tongue visible when the tip of the tongue is turned upwards.

(From Drake, Vogl and Mitchell 2005.)

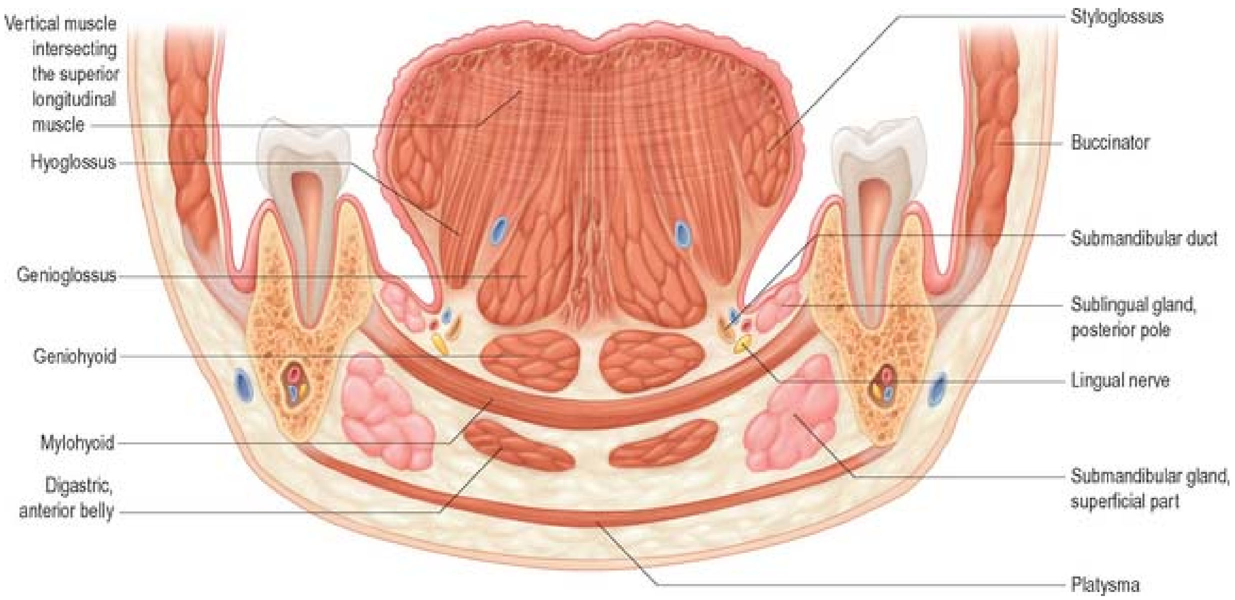
Vertical muscle intersecting the superior longitudinal muscle
Hyoglossus
Genioglossus
Geniohyoid
Mylohyoid
Digastric, anterior belly
Styloglossus
Buccinator
Submandibular duct
Sublingual gland, posterior pole
Lingual nerve
Submandibular gland, superficial part
Platysma

Fig. 30.7 Coronal section through the tongue, the mouth and the body of the mandible opposite the first molar tooth.

The sublingual folds lie on either side of the sublingual papilla and cover the underlying submandibular ducts and sublingual salivary glands. The blood supply of the floor of the mouth is described with the blood supply of the tongue (see p. 505). The main muscle forming the floor of the mouth is mylohyoid, with geniohyoid lying immediately above it.

Mylohyoid

Mylohyoid lies superior to the anterior belly of digastric and, with its contralateral fellow, forms a muscular floor for the oral cavity. It is a flat, triangular sheet attached to the whole length of the mylohyoid line of the mandible (Fig. 30.4A, see Fig. 30.7). The mylohyoid line is of variable length, sometimes ending before the lower third molar (wisdom) tooth. The posterior fibres of mylohyoid pass medially and slightly downwards to the front of the body of the hyoid bone near its lower border. The middle and anterior fibres from each side decussate in a median fibrous raphe that stretches from the symphysis menti to the hyoid bone. The median raphe is sometimes absent, in which case the two muscles form a continuous sheet, or it may be fused with the anterior belly of digastric. In about one-third of subjects there is a hiatus in the muscle through which a process of the sublingual gland protrudes.

Relations

The inferior (external) surface is related to platysma, the anterior belly of digastric, the superficial part of the submandibular gland, the facial and submental vessels, and the mylohyoid vessels and nerve. The superior (internal) surface is related to geniohyoid, part of hyoglossus and styloglossus, the hypoglossal and lingual nerves, the submandibular ganglion, the sublingual gland, the deep part of the submandibular gland and its duct, the lingual and sublingual vessels, and, posteriorly, the mucous membrane of the mouth.

Vascular supply

Mylohyoid receives its arterial supply from the sublingual branch of the lingual artery, the maxillary artery, via the mylohyoid branch of the inferior alveolar artery, and the submental branch of the facial artery.

Innervation

Mylohyoid is supplied by the mylohyoid branch of the inferior alveolar nerve, which can sometimes also supply accessory innervation to the posterior mandibular teeth.

Actions

Mylohyoid elevates the floor of the mouth in the first stage of deglutition. It may also elevate the hyoid bone or depress the mandible.

Geniohyoid

Geniohyoid is a narrow muscle which lies above the medial part of mylohyoid (see Figs 30.6, 30.10). It arises from the inferior mental spine (genial tubercle) on the back of the symphysis menti, and runs backwards and slightly downwards to attach to the anterior surface of the body of the hyoid bone. The paired muscles are contiguous and may occasionally fuse with each other or with genioglossus.

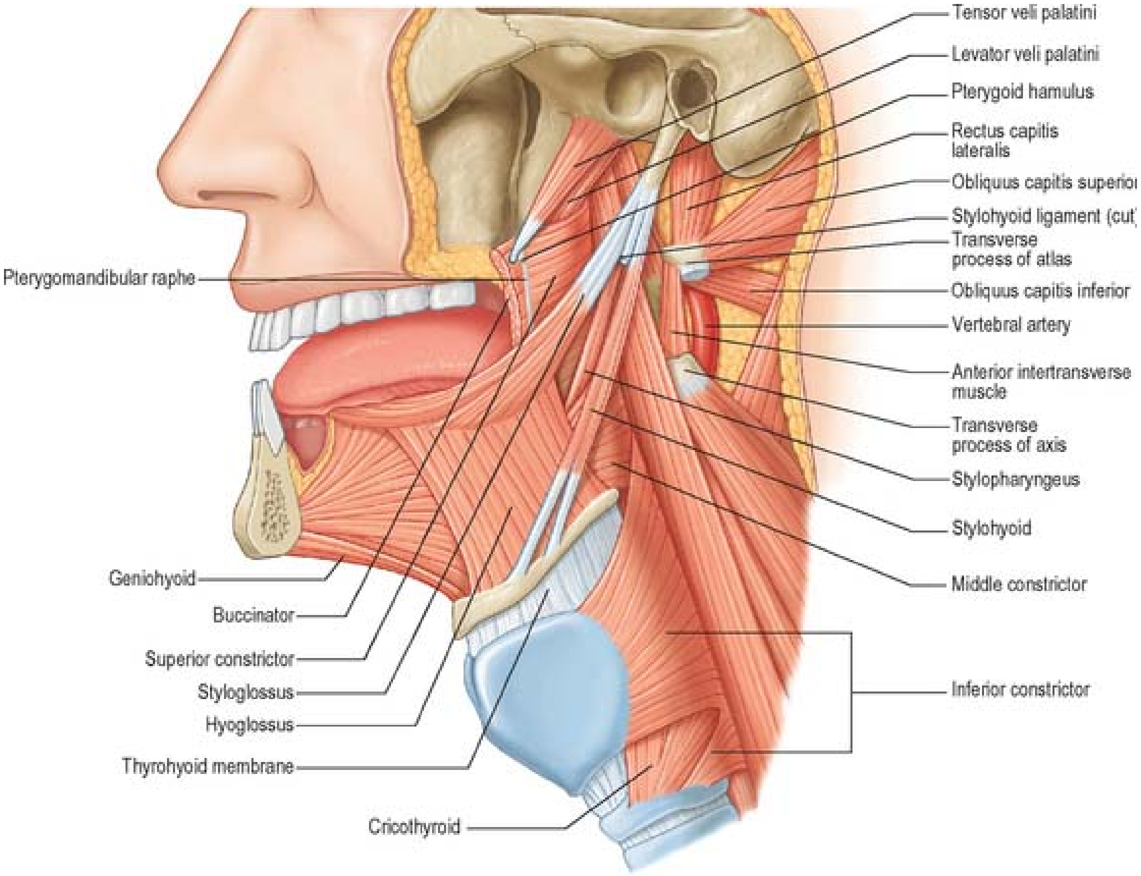
Tensor veli palatini
Levator veli palatini
Pterygoid hamulus
Rectus capitis lateralis
Obliquus capitis superior
Stylohyoid ligament (cut)
Transverse process of atlas
Pterygomandibular raphe
Obliquus capitis inferior
Vertebral artery
Anterior intertransverse muscle
Transverse process of axis
Stylopharyngeus
Stylohyoid
Middle constrictor
Geniohyoid
Buccinator
Superior constrictor
Styloglossus
Hyoglossus
Thyrohyoid membrane
Inferior constrictor
Cricothyroid

Fig. 30.6 Muscles of the tongue and pharynx. Palatoglossus is not shown here, but is depicted in **Fig. 33.4**.

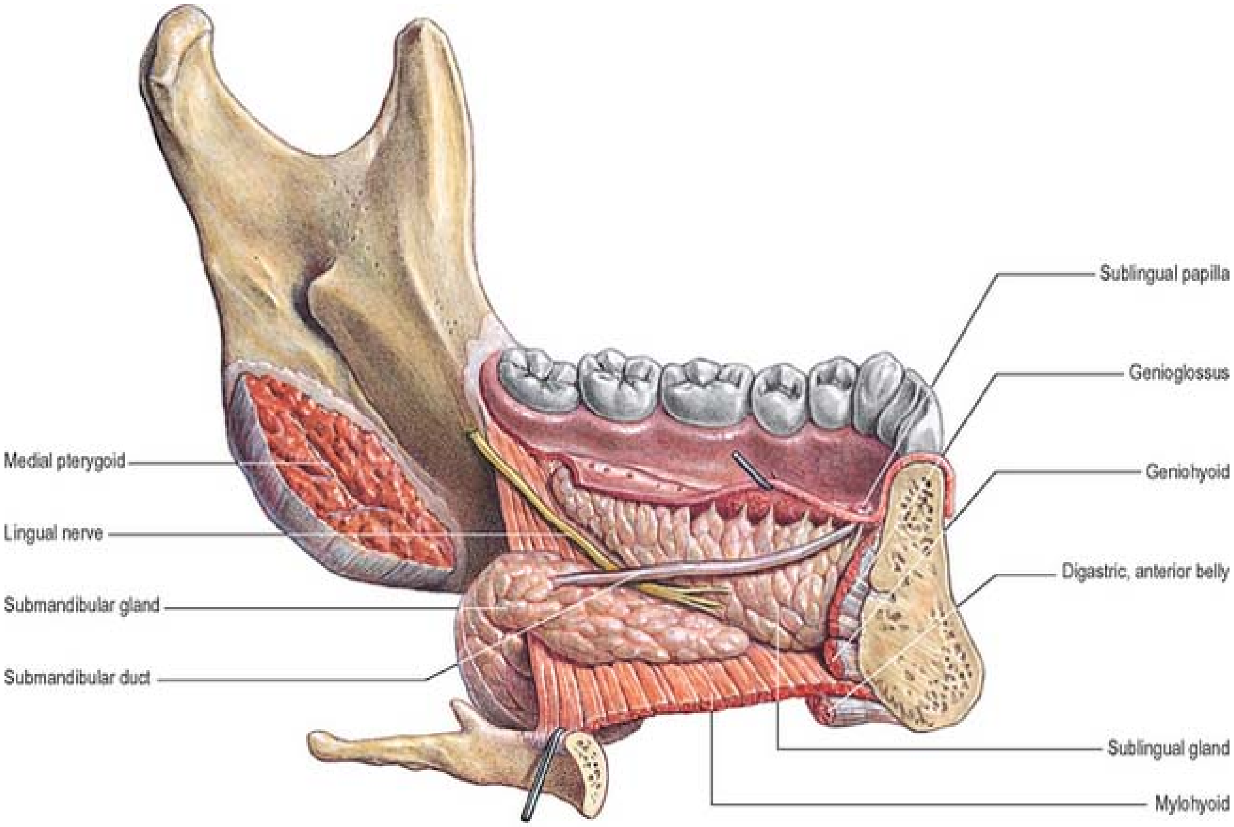
Medial pterygoid
Lingual nerve
Submandibular gland
Submandibular duct
Sublingual papilla
Genioglossus
Geniohyoid
Digastric, anterior belly
Sublingual gland
Mylohyoid

Fig. 30.10 Lingual nerve, submandibular duct, and submandibular and sublingual salivary glands in the floor of the mouth. Lingual aspect, left side.

(From Sobotta 2006.)

Vascular supply

The blood supply to geniohyoid is derived from the lingual artery (sublingual branch).

Innervation

Geniohyoid is supplied by the first cervical spinal nerve, through the hypoglossal nerve.

Actions

Geniohyoid elevates the hyoid bone and draws it forwards, and therefore acts partly as an antagonist to stylohyoid. When the hyoid bone is fixed, geniohyoid depresses the mandible.

PALATE

The palate forms the roof of the mouth and is divisible into two regions, namely the hard palate in front and soft palate behind.

SOFT PALATE

The soft palate is described with the pharynx in Chapter 33.

HARD PALATE

The hard palate is formed by the palatine processes of the maxillae and the horizontal plates of the palatine bones (see Fig. 30.14A). The hard palate is bounded in front and at the sides by the tooth-bearing alveolus of the upper jaw and is continuous posteriorly with the soft palate. It is covered by a thick mucosa bound tightly to the underlying periosteum. In its more lateral regions it also possesses a submucosa containing the main neurovascular bundle. The mucosa is covered by keratinized stratified squamous epithelium which shows regional variations and may be ortho- or parakeratinized.

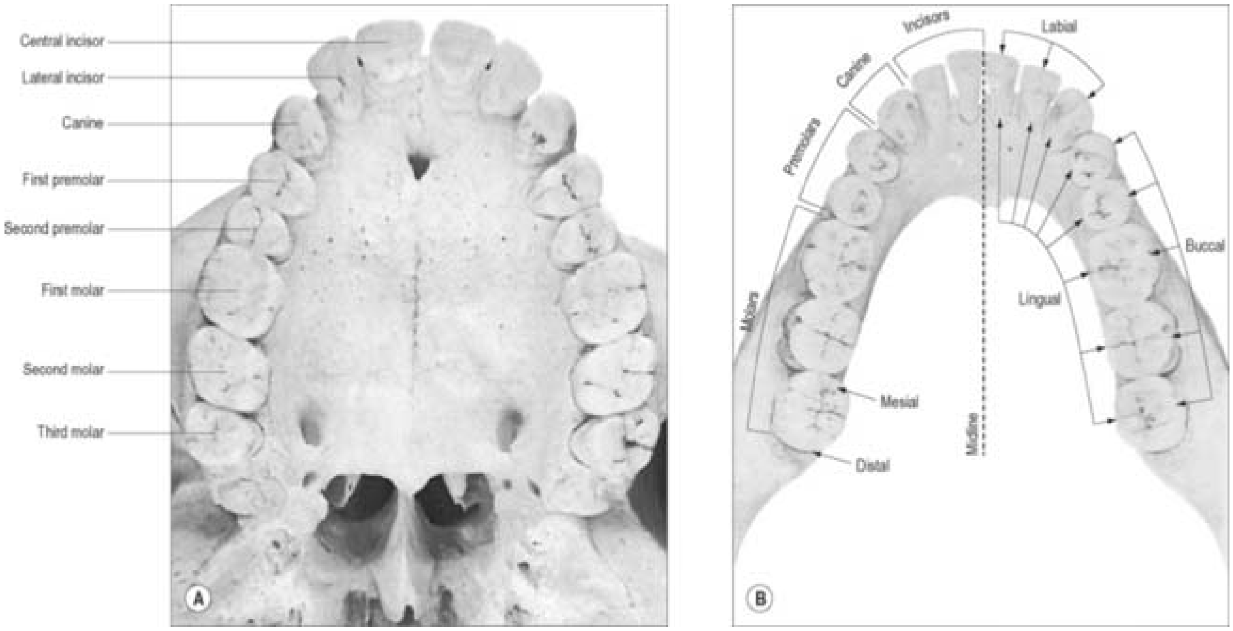
Central incisor
Lateral incisor
Canine
First premolar
Second premolar
First molar
Second molar
Third molar
A
Incisors
Labial
Canine
Premolars
Buccal
Lingual
Molars
Mesial
Distal
Midline
B

Fig. 30.14 The permanent teeth: occlusal aspect. **A** Upper dental arch. **B**, Lower dental arch. The terminology employed for the identification of teeth according to their location is shown in the lower jaw: the same terminology is used to describe the teeth in the upper jaw.

The periphery of the hard palate consists of gingivae. A narrow ridge, the palatine raphe, devoid of submucosa, runs anteroposteriorly in the midline. An oval prominence, the incisive papilla, lies at the anterior extremity of the raphe. It covers the incisive fossa at the oral opening of the incisive canal and also marks the position of the fetal nasopalatine canal. Irregular transverse ridges or rugae, each containing a core of dense connective tissue, radiate outwards from the palatine raphe in the anterior half of the hard palate: their pattern is unique.

The submucosa in the posterior half of the hard palate contains minor mucous-type salivary glands (Fig. 30.3). They secrete via numerous small ducts which often drain into a larger duct that opens bilaterally at the paired palatine foveae. These depressions, sometimes a few millimetres deep, flank the midline raphe at the posterior border of the hard palate. They provide a useful landmark for the extent of an upper denture; if not observed during construction of the denture they cause the denture to become unstable when the soft palate moves during deglutition and mastication. The upper surface of the hard palate is the floor of the nasal cavity and is covered by ciliated respiratory epithelium.

Vascular supply and lymphatic drainage of the hard palate

The palate derives its blood supply principally from the greater palatine artery, a branch of the third part of the maxillary artery. The greater palatine artery descends with its accompanying nerve in the palatine canal, where it gives off two or three lesser palatine arteries which are transmitted through lesser palatine canals to supply the soft palate and tonsil, and anastomose with the ascending palatine branch of the facial artery. The greater palatine artery emerges onto the oral surface of the palate at the greater palatine foramen adjacent to the second maxillary molar and runs in a curved groove near the alveolar border of the hard palate to the incisive canal. It ascends this canal and anastomoses with septal branches of the nasopalatine artery to supply the gingivae, palatine glands and mucous membrane.

The veins of the hard palate accompany the arteries and drain largely to the pterygoid plexus.

Innervation of the hard palate

The sensory nerves of the hard palate are the greater palatine and nasopalatine branches of the maxillary nerve, which all pass through the pterygopalatine ganglion. The greater palatine nerve descends through the greater palatine canal, emerges on the hard palate from the greater palatine foramen, runs forwards in a groove on the inferior surface of the bony palate almost to the incisor teeth and supplies the gums and the mucosa and glands of the hard palate (Fig. 30.3). It also communicates with the terminal filaments of the nasopalatine nerve. As it leaves the greater palatine canal, it supplies palatine branches to both surfaces of the soft palate. The lesser (middle and posterior) palatine nerves, which are much smaller, descend through the greater palatine canal and emerge through the lesser palatine foramina in the tubercle of the palatine bone to supply the uvula, tonsil and soft palate. The nasopalatine nerves enter the palate at the incisive foramen and are branches of the maxillary nerve which pass through the pterygopalatine ganglion to supply the anterior part of the hard palate behind the incisor teeth.

Fibres conveying taste impulses from the palate probably pass via the palatine nerves to the pterygopalatine ganglion, and travel through it without synapsing to join the nerve of the pterygoid canal and the greater petrosal nerve to the facial ganglion, where their cell bodies are situated. The central processes of these neurones traverse the sensory root of the facial nerve (nervus intermedius) to pass to the gustatory nucleus in the nucleus of the tractus solitarius. Parasympathetic postganglionic secretomotor fibres from the pterygopalatine ganglion run with the nerves to supply the palatine mucous glands.

TONGUE

The tongue is a highly muscular organ of deglutition, taste and speech. It is partly oral and partly pharyngeal in position, and is attached by its muscles to the hyoid bone, mandible, styloid processes, soft palate and the pharyngeal wall. It has a root, an apex, a curved dorsum and an inferior surface. Its mucosa is normally pink and moist, and is attached closely to the underlying muscles. The dorsal mucosa is covered by numerous papillae, some of which bear taste buds. Intrinsic muscle fibres are arranged in a complex interlacing pattern of longitudinal, transverse, vertical and horizontal fasciculi and this allows great mobility. Fasciculi are separated by a variable amount of adipose tissue which increases posteriorly. The root of the tongue is attached to the hyoid bone and mandible, and between them it is in contact inferiorly with geniohyoid and mylohyoid. The dorsum (posterosuperior surface) is generally convex in all directions at rest. It is divided by a V-shaped sulcus terminalis into an anterior, oral (presulcal) part which faces upwards, and a posterior, pharyngeal (postsulcal) part which faces posteriorly. The anterior part forms about two-thirds of the length of the tongue. The two limbs of the sulcus terminalis run anterolaterally to the palatoglossal arches from a median depression, the foramen caecum, which marks the site of the upper end of the embryonic thyroid diverticulum (thyroglossal duct). The oral and pharyngeal parts of the tongue differ in their mucosa, innervation and developmental origins.

ORAL (PRESULCAL) PART

The presulcal part of the tongue is located in the floor of the oral cavity. It has an apex touching the incisor teeth, a margin in contact with the gums and teeth, and a superior surface (dorsum) related to the hard and soft palates. On each side, in front of the palatoglossal arch, there are four or five vertical folds, the foliate papillae, which represent vestiges of larger papillae found in many other mammals. The dorsal mucosa has a longitudinal median sulcus and is covered by filiform, fungiform and circumvallate papillae (Fig. 30.5). The mucosa on the inferior (ventral) surface is smooth, purplish and reflected onto the oral floor and gums: it is connected to the oral floor anteriorly by the lingual frenulum. The deep lingual vein, which is visible, lies lateral to the frenulum on either side. The plica fimbriata (fimbriated fold), a fringed mucosal ridge directed anteromedially towards the apex of the tongue, lies lateral to the vein. This part of the tongue develops from the lingual swellings of the mandibular arch and from the tuberculum impar, and this embryological derivation explains its sensory innervation.

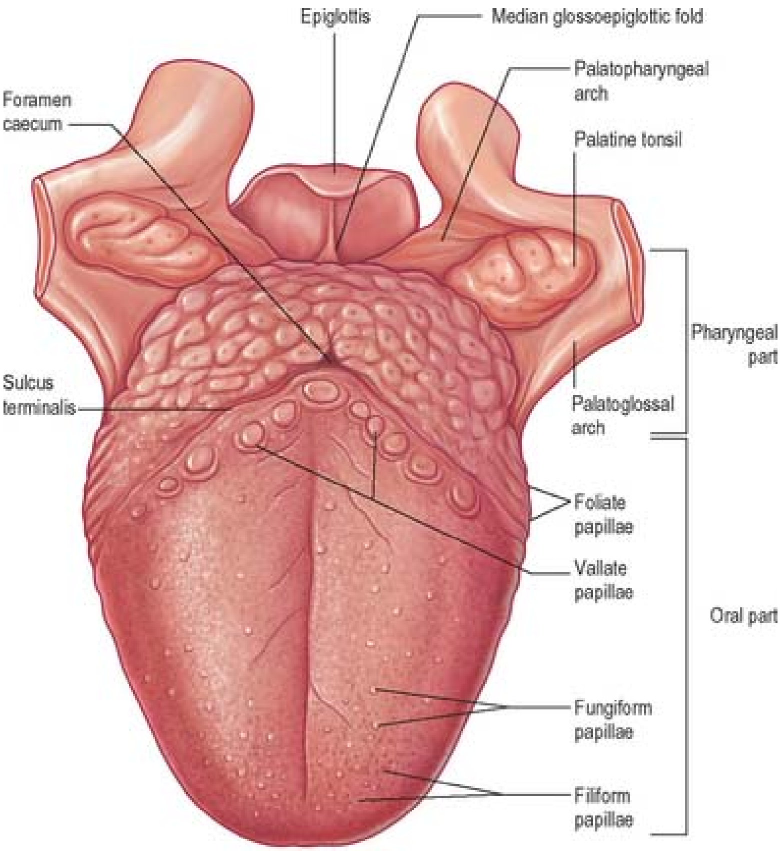
Epiglottis
Median glossoepiglottic fold
Palatopharyngeal arch
Foramen caecum
Palatine tonsil
Pharyngeal part
Sulcus terminalis
Palatoglossal arch
Foliate papillae
Vallate papillae
Oral part
Fungiform papillae
Filiform papillae

Fig. 30.5 Dorsum of the tongue, adjoining palatoglossal and palatopharyngeal arches, and epiglottis. The palatine tonsils lie in the tonsillar recesses between the palatoglossal and palatopharyngeal arches.

PHARYNGEAL (POSTSULCAL) PART

The postsulcal part of the tongue constitutes its base and lies posterior to the palatoglossal arches. Although it forms the anterior wall of the oropharynx, it is described here for convenience. Its mucosa is reflected laterally onto the palatine tonsils and pharyngeal wall, and posteriorly onto the epiglottis by a median and two lateral glossoepiglottic folds which surround two depressions or valleculae. The pharyngeal part of the tongue is devoid of papillae, and exhibits low elevations. There are underlying lymphoid nodules which are embedded in the submucosa and collectively termed the lingual tonsil. The ducts of small seromucous glands open on the apices of these elevations. The postsulcal part of the tongue develops from the hypobranchial eminence. On the rare occasions that the thyroid gland fails to migrate away from the tongue during development, it remains in the postsulcal part of the tongue as a functioning lingual thyroid gland.

MUSCLES OF THE TONGUE

The tongue is divided by a median fibrous septum, attached to the body of the hyoid bone. There are extrinsic and intrinsic muscles in each half, the former extending outside the tongue and moving it bodily, the latter wholly within it and altering its shape. The extrinsic musculature consists of four pairs of muscles, namely genioglossus, hyoglossus, styloglossus (and chondroglossus) and palatoglossus.

Genioglossus

Genioglossus is triangular in sagittal section, lying near and parallel to the midline. It arises from a short tendon attached to the superior genial tubercle behind the mandibular symphysis, above the origin of geniohyoid. From this point it fans out backwards and upwards (Fig. 30.6). The inferior fibres of genioglossus are attached by a thin aponeurosis to the upper anterior surface of the hyoid body near the midline (a few fasciculi passing between hyoglossus and chondroglossus to blend with the middle constrictor of the pharynx). Intermediate fibres pass backwards into the posterior part of the tongue, and superior fibres ascend forwards to enter the whole length of the ventral surface of the tongue from root to apex, intermingling with the intrinsic muscles. The muscles of opposite sides are separated posteriorly by the lingual septum. Anteriorly they are variably blended by decussation of fasciculi across the midline. The attachment of the genioglossi to the genial tubercles prevents the tongue from sinking back and obstructing respiration, therefore anaesthetists pull the mandible forward to obtain the full benefit of this connection.

Vascular supply

Genioglossus is supplied by the sublingual branch of the lingual artery and the submental branch of the facial artery.

Innervation

Genioglossus is innervated by the hypoglossal nerve.

Actions

Genioglossus brings about the forward traction of the tongue to protrude its apex from the mouth. Acting bilaterally, the two muscles depress the central part of the tongue, making it concave from side to side. Acting unilaterally, the tongue diverges to the opposite side.

Hyoglossus

Hyoglossus is thin and quadrilateral, and arises from the whole length of the greater cornu and the front of the body of the hyoid bone (Fig. 30.6). It passes vertically up to enter the side of the tongue between styloglossus laterally and the inferior longitudinal muscle medially. Fibres arising from the body of the hyoid overlap those from the greater cornu.

Relations

Hyoglossus is related at its superficial surface to the digastric tendon, stylohyoid, styloglossus and mylohyoid, the lingual nerve and submandibular ganglion, the sublingual gland, the deep part of the submandibular gland and duct, the hypoglossal nerve and the deep lingual vein. By its deep surface it is related to the stylohyoid ligament, genioglossus, the middle constrictor and the inferior longitudinal muscle of the tongue, and the glossopharyngeal nerve. Posteroinferiorly it is separated from the middle constrictor by the lingual artery. This part of the muscle is in the lateral wall of the pharynx, below the palatine tonsil. Passing deep to the posterior border of hyoglossus are, in descending order: the glossopharyngeal nerve, stylohyoid ligament and lingual artery.

Vascular supply

Hyoglossus is supplied by the sublingual branch of the lingual artery and the submental branch of the facial artery.

Innervation

Hyoglossus is innervated by the hypoglossal nerve.

Action

Hyoglossus depresses the tongue.

Chondroglossus

Sometimes described as a part of hyoglossus, this muscle is separated from it by some fibres of genioglossus, which pass to the side of the pharynx. It is about 2 cm long, and arises from the medial side and base of the lesser cornu and the adjoining part of the body of the hyoid. It ascends to merge into the intrinsic musculature between hyoglossus and genioglossus. A small slip occasionally springs from the cartilago triticea and enters the tongue with the posterior fibres of hyoglossus.

Vascular supply, innervation and action

These are similar to those described for hyoglossus.

Styloglossus

Styloglossus is the shortest and smallest of the three styloid muscles (Fig. 30.6). It arises from the anterolateral aspect of the styloid process near its apex, and from the styloid end of the stylomandibular ligament. Passing downwards and forwards, it divides at the side of the tongue into a longitudinal part, which enters the tongue dorsolaterally to blend with the inferior longitudinal muscle in front of hyoglossus, and an oblique part, overlapping hyoglossus and decussating with it.

Vascular supply

Styloglossus is supplied by the sublingual branch of the lingual artery.

Innervation

Styloglossus is innervated by the hypoglossal nerve.

Action

Styloglossus draws the tongue up and backwards.

Stylohyoid ligament

The stylohyoid ligament is a fibrous cord which extends from the tip of the styloid process to the lesser cornu of the hyoid bone (Fig. 30.6). It gives attachment to some fibres of styloglossus and the middle constrictor of the pharynx and is closely related to the lateral wall of the oropharynx. Below it is overlapped by hyoglossus. The ligament is derived embryologically from the second branchial arch. It may be partially calcified.

Palatoglossus

Palatoglossus is closely associated with the soft palate in function and innervation, and is described with the other palatal muscles (see Ch. 33).

Intrinsic muscles

The intrinsic muscles are the bilateral superior and inferior longitudinal, the transverse and the vertical (Fig. 30.7).

Superior longitudinal

The superior longitudinal muscle constitutes a thin stratum of oblique and longitudinal fibres lying beneath the mucosa of the dorsum of the tongue. It extends forwards from the submucous fibrous tissue near the epiglottis and from the median lingual septum to the lingual margins. Some fibres are inserted into the mucous membrane.

Inferior longitudinal

The inferior longitudinal muscle is a narrow band of muscle close to the inferior lingual surface between genioglossus and hyoglossus. It extends from the root of the tongue to the apex. Some of its posterior fibres are connected to the body of the hyoid bone. Anteriorly it blends with styloglossus.

Transverse

The transverse muscles pass laterally from the median fibrous septum to the submucous fibrous tissue at the lingual margin, blending with palatopharyngeus.

Vertical

The vertical muscles extend from the dorsal to the ventral aspects of the tongue in the anterior borders.

Vascular supply

The intrinsic muscles are supplied by the lingual artery.

Innervation

All intrinsic lingual muscles are innervated by the hypoglossal nerve.

Actions

The intrinsic muscles alter the shape of the tongue. Thus, contraction of the superior and inferior longitudinal muscles tend to shorten the tongue, but the former also turns the apex and sides upwards to make the dorsum concave, while the latter pulls the apex down to make the dorsum convex. The transverse muscle narrows and elongates the tongue, while the vertical muscle makes it flatter and wider. Acting alone or in pairs and in endless combination, the intrinsic muscles give the tongue precise and highly varied mobility, important not only in alimentary function but also in speech.

VASCULAR SUPPLY AND LYMPHATIC DRAINAGE OF THE TONGUE

Lingual artery

The tongue and the floor of the mouth are supplied chiefly by the lingual artery, which arises from the anterior surface of the external carotid artery. It passes between hyoglossus and the middle constrictor of the pharynx to reach the floor of the mouth accompanied by the lingual veins and the glossopharyngeal nerve. At the anterior border of hyoglossus, the lingual artery bends sharply upwards (Fig. 30.8). It is covered by the mucosa of the tongue and lies between genioglossus medially and the inferior longitudinal muscle laterally. Near the tip of the tongue, it anastomoses with its contralateral fellow; this contribution is important in maintaining the blood supply to the tongue in any surgical resection of the tongue. The branches of the lingual artery form a rich anastomotic network, which supplies the musculature of the tongue, and a very dense submucosal plexus. Named branches of the lingual artery in the floor of the mouth are the dorsal lingual, sublingual and deep lingual arteries.

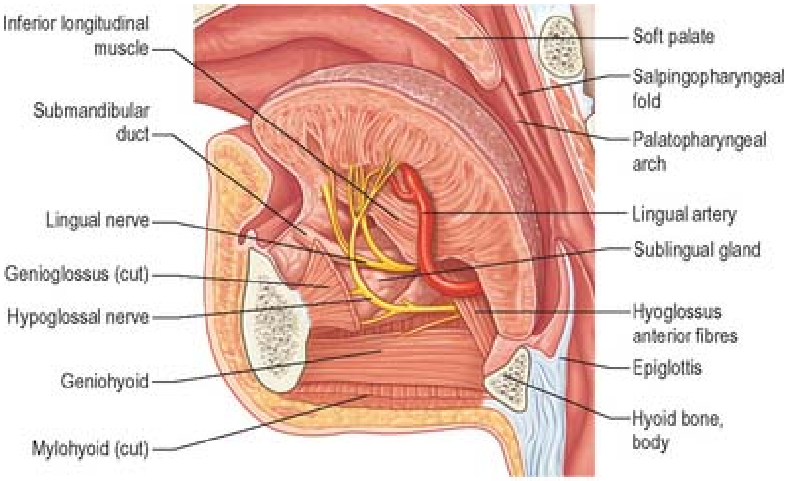
Inferior longitudinal muscle
Submandibular duct
Lingual nerve
Genioglossus (cut)
Hypoglossal nerve
Geniohyoid
Mylohyoid (cut)
Soft palate
Salpingopharyngeal fold
Palatopharyngeal arch
Lingual artery
Sublingual gland
Hyoglossus anterior fibres
Epiglottis
Hyoid bone, body

Fig. 30.8 Left half of the tongue, viewed from the medial side, showing the lingual artery and ramifications of the hypoglossal and lingual nerves.

Dorsal lingual arteries

The dorsal lingual arteries are usually two or three small vessels. They arise medial to hyoglossus and ascend to the posterior part of the dorsum of the tongue. The vessels supply its mucous membrane, and the palatoglossal arch, tonsil, soft palate and epiglottis. They anastomose with their contralateral fellows.

Sublingual artery

The sublingual artery arises at the anterior margin of hyoglossus. It passes forward between genioglossus and mylohyoid to the sublingual gland, and supplies the gland, mylohyoid and the buccal and gingival mucous membranes. One branch pierces mylohyoid and joins the submental branches of the facial artery. Another branch courses through the mandibular gingivae to anastomose with its contralateral fellow. A single artery arises from this anastomosis and enters a small foramen (lingual foramen) on the mandible, situated in the midline on the posterior aspect of the symphysis immediately above the genial tubercles.

Deep lingual artery

The deep lingual artery is the terminal part of the lingual artery and is found on the inferior surface of the tongue near the lingual frenulum.

In addition to the lingual artery, the tonsillar and ascending palatine branches of the facial and ascending pharyngeal arteries also supply tissue in the root of the tongue. In the region of the valleculae, epiglottic branches of the superior laryngeal artery anastomose with the inferior dorsal branches of the lingual artery.

Lingual veins

The lingual veins are formed from the union of the dorsal lingual and deep lingual veins and the vena comitans of the hypoglossal nerve. The veins draining the tongue follow two routes. Dorsal lingual veins drain the dorsum and sides of the tongue, join the lingual veins accompanying the lingual artery between hyoglossus and genioglossus, and empty into the internal jugular vein near the greater cornu of the hyoid bone. The deep lingual vein begins near the tip of the tongue and runs back just beneath the mucous membrane on the inferior surface of the tongue. It joins a sublingual vein from the sublingual salivary gland near the anterior border of hyoglossus and forms the vena comitans nervi hypoglossi, which run back with the hypoglossal nerve between mylohyoid and hyoglossus to join the facial, internal jugular or lingual vein. The lingual veins usually join the facial and retromandibular veins (anterior division) to form the common facial vein, which drains into the internal jugular vein.

Lymphatic drainage

The mucosa of the pharyngeal part of the dorsal surface of the tongue contains many lymphoid follicles aggregated into dome-shaped groups, the lingual tonsils. Each group is arranged around a central deep crypt, or invagination, which opens onto the surface epithelium. The ducts of mucous glands open into the bases of the crypts. Small isolated follicles also occur beneath the lingual mucosa. The lymphatic drainage of the tongue can be divided into three main regions, marginal, central and dorsal. The anterior region of the tongue drains into marginal and central vessels, and the posterior part of the tongue behind the circumvallate papillae drains into the dorsal lymph vessels. The more central regions may drain bilaterally, and this must be borne in mind when planning to remove malignant tumours of the tongue that are approaching the midline. If the tumour has a propensity for lymphatic spread, both cervical chains may be involved.

Marginal vessels

Marginal vessels from the apex of the tongue and the lingual frenulum area descend under the mucosa to widely distributed nodes. Some vessels pierce mylohyoid as it contacts the mandibular periosteum to enter either the submental or anterior or middle submandibular nodes, or else to pass anterior to the hyoid bone to the jugulo-omohyoid node. Vessels arising in the plexus on one side may cross under the frenulum to end in contralateral nodes.

Efferent vessels of median submental nodes pass bilaterally. Some vessels pass inferior to the sublingual gland and accompany the companion vein of the hypoglossal nerve to end in jugulodigastric nodes. One vessel often descends further to reach the jugulo-omohyoid node, and passes either superficial or deep to the intermediate tendon of digastric.

Vessels from the lateral margin of the tongue cross the sublingual gland, pierce mylohyoid and end in the submandibular nodes. Others end in the jugulodigastric or jugulo-omohyoid nodes. Vessels from the posterior part of the lingual margin traverse the pharyngeal wall to the jugulodigastric lymph nodes (Fig. 30.9).

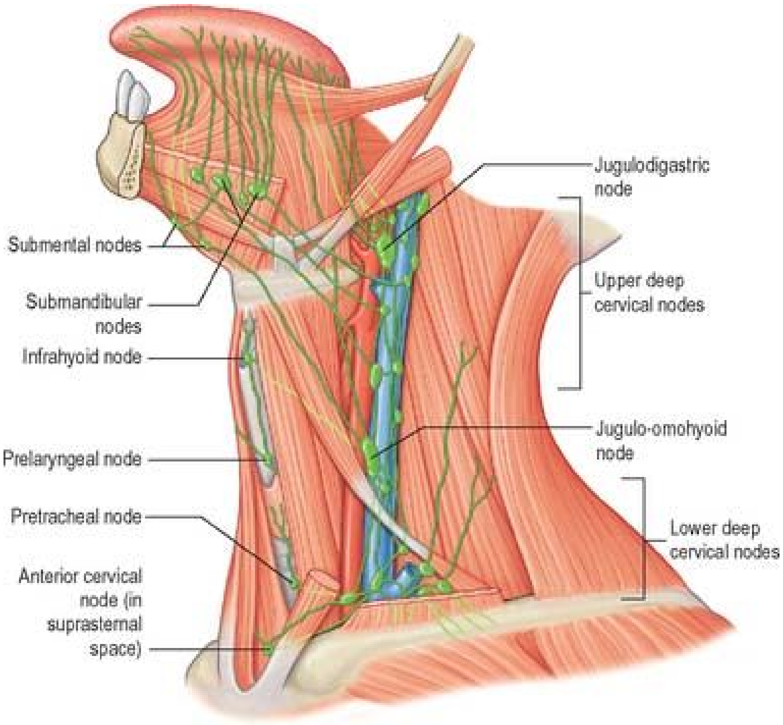
Jugulodigastric node
Upper deep cervical nodes
Jugulo-omohyoid node
Lower deep cervical nodes
Submental nodes
Submandibular nodes
Infrahyoid node
Prelaryngeal node
Pretracheal node
Anterior cervical node (in suprasternal space)

Fig. 30.9 Lymphatic drainage of the tongue. Removal of sternocleidomastoid has exposed the whole chain of deep cervical lymph nodes.

Central vessels

The regions of the lingual surface draining into the marginal or central vessels are not distinct. Central lymphatic vessels ascend between the fibres of the two genioglossi; most pass between the muscles and diverge to the right or left to follow the lingual veins to the deep cervical nodes, especially the jugulodigastric and jugulo-omohyoid nodes. Some pierce mylohyoid to enter the submandibular nodes.

Dorsal vessels

Vessels draining the postsulcal region and the circumvallate papillae run posteroinferiorly. Those near the median plane may pass bilaterally. They turn laterally, join the marginal vessels and all pierce the pharyngeal wall, passing around the external carotid arteries to reach the jugulodigastric and jugulo-omohyoid lymph nodes. One vessel may descend posterior to the hyoid bone, perforating the thyrohyoid membrane to end in the jugulo-omohyoid node.

INNERVATION OF THE TONGUE

The muscles of the tongue, with the exception of palatoglossus, are supplied by the hypoglossal nerve. Palatoglossus is supplied via the pharyngeal plexus (see Ch. 33). The pathways for proprioception associated with the tongue musculature are unknown, but presumably may involve the lingual, glossopharyngeal or hypoglossal nerves, and the cervical spinal nerves which communicate with the hypoglossal nerve.

The sensory innervation of the tongue reflects its embryological development: the anterior two-thirds is derived from first-arch mesenchyme and the posterior one-third from third-arch mesenchyme. The nerve of general sensation to the anterior two-thirds is the lingual nerve, which also carries taste sensation derived from the chorda tympani branch of the facial nerve. The nerve supplying both general and taste sensation to the posterior one-third is the glossopharyngeal nerve. An additional area in the region of the valleculae is supplied by the internal laryngeal branch of the vagus nerve.

Lingual nerve

The lingual nerve is sensory to the mucosa of the floor of the mouth, mandibular lingual gingivae and mucosa of the presulcal part of the tongue (excluding the circumvallate papillae). It also carries postganglionic parasympathetic fibres from the submandibular ganglion to the sublingual and anterior lingual glands.

The lingual nerve arises from the posterior trunk of the mandibular nerve in the infratemporal fossa (see Fig. 31.13A) where it is joined by the chorda tympani branch of the facial nerve and often by a branch of the inferior alveolar nerve. It then passes below the mandibular attachment of the superior pharyngeal constrictor and pterygomandibular raphe, closely applied to the periosteum of the medial surface of the mandible, until it lies opposite the distal (posterior) root of the third molar tooth, where it is covered only by the gingival mucoperiosteum. At this point it can contact the lingual cortical plate and may be at the level of, or higher than, the alveolar bone crest. It next passes medial to the mandibular attachment of mylohyoid, which carries it progressively away from the mandible, and separates it from the alveolar bone covering the mesial root of the third molar tooth, and then passes downward and forward on the deep surface of mylohyoid (i.e. the surface nearer the mucosa covering the floor of the mouth), crossing the lingual sulcus beneath the mucosa. In this position it lies on the deep portion of the submandibular gland which bulges over the top of the posterior border of mylohyoid. It passes below the submandibular duct which crosses it from medial to lateral, and curves upward, forward and medially to enter the tongue (Figs 30.8, 30.10). Within the tongue the lingual nerve lies first on styloglossus and then the lateral surface of hyoglossus and genioglossus, before dividing into terminal branches that supply the overlying lingual mucosa. The lingual nerve is connected to the submandibular ganglion (see Fig. 31.15) by two or three branches, and also forms connecting loops with twigs of the hypoglossal nerve at the anterior margin of hyoglossus.

The lingual nerve is at risk during surgical removal of (impacted) lower third molars, and, after such operations, up to 0.8% of patients may develop lingual sensory disturbance, which may persist in 0.3% (Robinson & Smith 1996). The nerve is also at risk during operations to remove the submandibular salivary gland, because the duct must be dissected from the lingual nerve, and because its connection to the submandibular ganglion pulls it into the operating field.

Glossopharyngeal nerve

The glossopharyngeal nerve is distributed to the posterior one-third of the tongue and the circumvallate papillae. It communicates with the lingual nerve. The course of the glossopharyngeal nerve in the neck is described in Chapter 28.

Hypoglossal nerve

The course of the hypoglossal nerve in the neck is described in Chapter 28. After crossing the loop of the lingual artery a little above the tip of the greater cornu of the hyoid, it inclines upwards and forwards on hyoglossus, passing deep to stylohyoid, the tendon of digastric and the posterior border of mylohyoid. Between mylohyoid and hyoglossus the hypoglossal nerve lies below the deep part of the submandibular gland, the submandibular duct and the lingual nerve, with which it communicates. It then passes onto the lateral aspect of genioglossus, continuing forwards in its substance as far as the tip of the tongue (Fig. 30.8). It distributes fibres to styloglossus, hyoglossus and genioglossus and to the intrinsic muscles of the tongue. If the nerve suffers either iatrogenic or pathological damage, the tongue, on protrusion, will deviate towards the unaffected side and there may be wasting of the affected side.

Special sensory innervation of the tongue

The sense of taste is dependent on scattered groups of sensory cells, the taste buds, which occur in the oral cavity and pharynx and are particularly plentiful on the lingual papillae of the dorsal lingual mucosa.

Dorsal lingual mucosa

The dorsal mucosa is somewhat thicker than the ventral and lateral mucosae, is directly adherent to underlying muscular tissue with no discernible submucosa, and is covered by numerous papillae. The dorsal epithelium consists of a superficial stratified squamous epithelium, which varies from non-keratinized stratified squamous epithelium posteriorly, to fully keratinized epithelium overlying the filiform papillae more anteriorly. These features probably reflect the fact that the apex of the tongue is subject to greater dehydration than the posterior and ventral parts and is subject to more abrasion during mastication. The underlying lamina propria is a dense fibrous connective tissue, with numerous elastic fibres, and is continuous with similar tissue extending between the lingual muscle fasciculi. It contains numerous vessels and nerves from which the papillae are supplied, and also large lymph plexuses and lingual glands.

Lingual papillae

Lingual papillae are projections of the mucosa covering the dorsal surface of the tongue (Fig. 30.5). They are limited to the presulcal part of the tongue, produce its characteristic roughness and increase the area of contact between the tongue and the contents of the mouth. There are four principal types, named filiform, fungiform, foliate and circumvallate papillae, and all except the filiform papillae bear taste buds. Papillae are more visible in the living when the tongue is dry.

Filiform papillae

Filiform papillae are minute, conical or cylindrical projections which cover most of the presulcal dorsal area, and are arranged in diagonal rows that extend anterolaterally, parallel with the sulcus terminalis, except at the lingual apex, where they are transverse. They have irregular cores of connective tissue and their epithelium, which is keratinized, may split into whitish fine secondary processes (Fig. 30.11). They appear to function to increase the friction between the tongue and food, and facilitate the movement of particles by the tongue within the oral cavity.

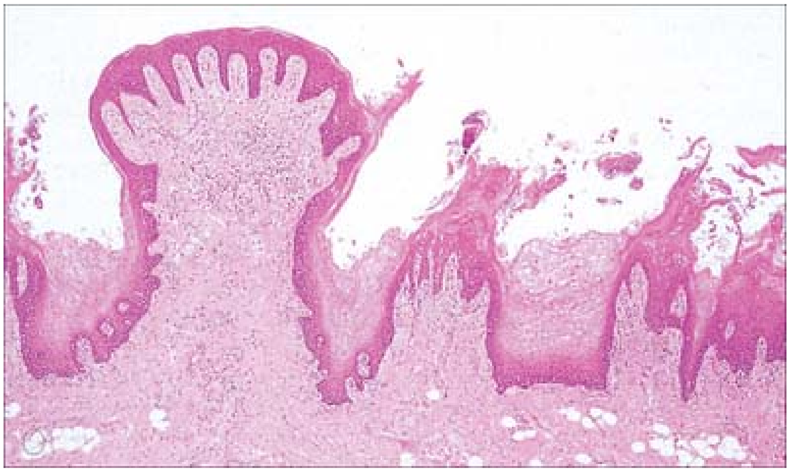

Fig. 30.11 Dorsal surface of the anterior tongue showing non-keratinized fungiform (left) and two keratinized filiform papillae (centre and right) with non-keratinized regions between.

(By permission from Young B, Heath JW 2000 Wheater's Functional Histology. Edinburgh: Churchill Livingstone.)

Fungiform papillae

Fungiform papillae occur mainly on the lingual margin but also irregularly on the dorsal surface, where they may occasionally be numerous (Fig. 30.11). They differ from filiform papillae because they are larger, rounded and deep red in colour, this last reflecting their thin, non-keratinized epithelium and highly vascular connective tissue core. Each usually bears one or more taste buds on its apical surface.

Foliate papillae

Foliate papillae lie bilaterally in two zones at the sides of the tongue near the sulcus terminalis, each formed by a series of red, leaf-like mucosal ridges, covered by a non-keratinized epithelium. They bear numerous taste buds.

Circumvallate papillae

Circumvallate papillae are large cylindrical structures, varying in number from 8 to 12, which form a V-shaped row immediately in front of the sulcus terminalis on the dorsal surface of the tongue. Each papilla, 1–2 mm in diameter, is surrounded by a slight circular mucosal elevation (vallum or wall) which is separated from the papilla by a circular sulcus (Figs 30.12, 30.13). The papilla is narrower at its base than its apex and the entire structure is generally covered with non-keratinized stratified squamous epithelium. Numerous taste buds are scattered in both walls of the sulcus, and small serous glands (of von Ebner) open into the sulcal base.

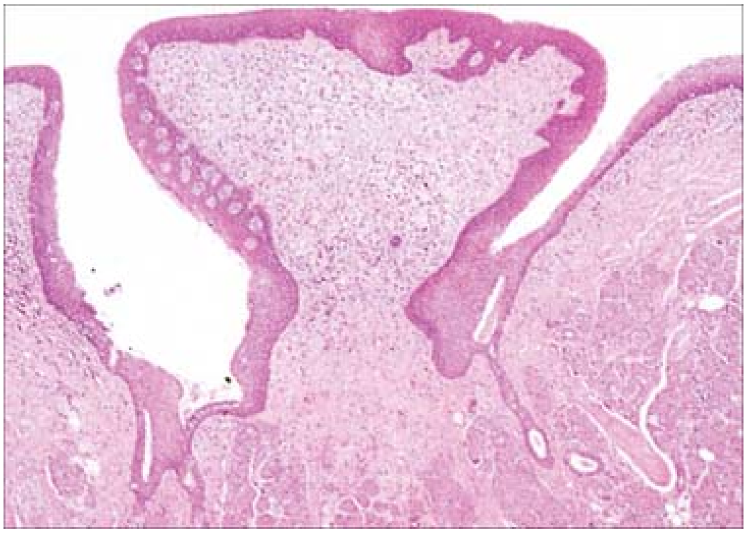

Fig. 30.12 Section through a circumvallate papilla. Serous glands (of von Ebner) empty via ducts into the base of the trench and numerous taste buds are contained within the stratified epithelium of the papillary wall (pale structures on the inner wall of the cleft, left side).

(By permission from Young B, Heath JW 2000 Wheater's Functional Histology. Edinburgh: Churchill Livingstone.)

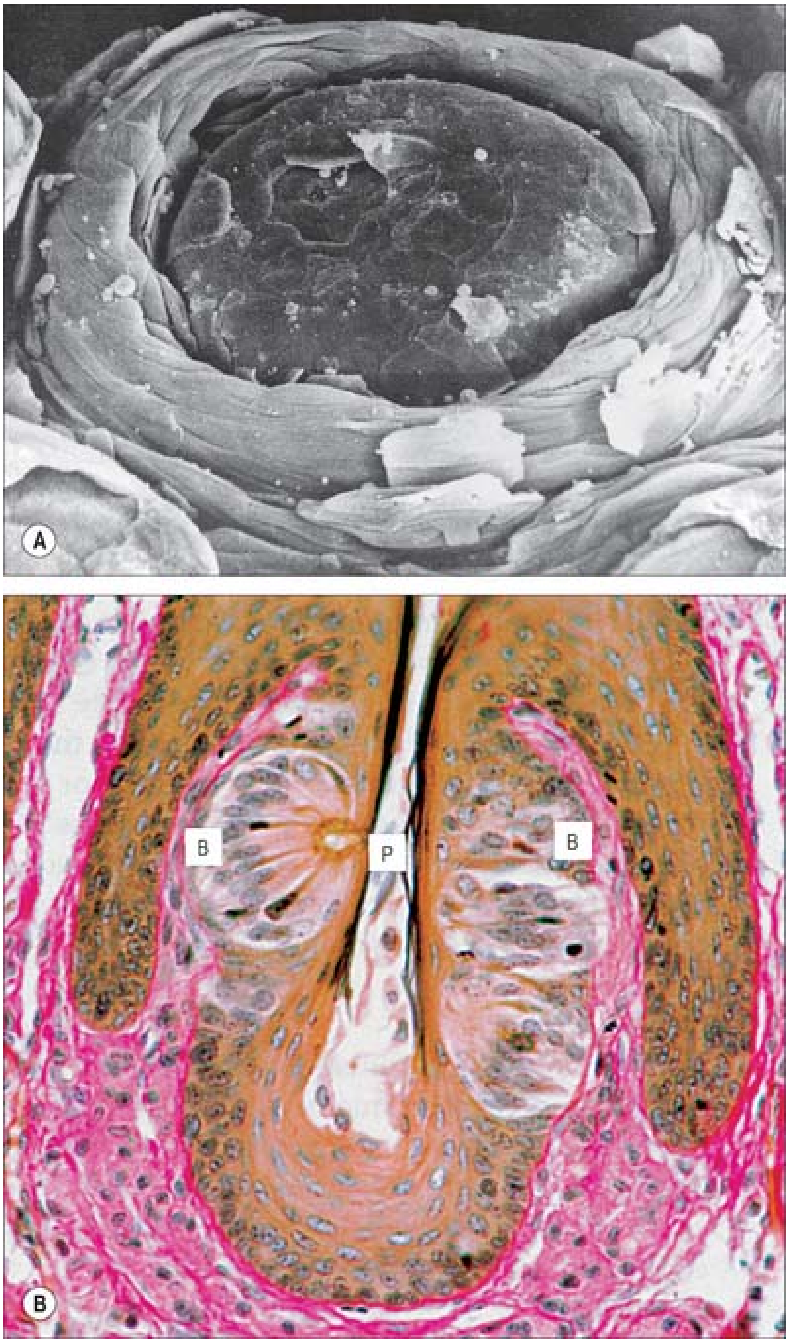

Fig. 30.13 Circumvallate papilla. **A**, Scanning electron micrograph showing a circumvallate papilla surrounded by a trench. **B**, Section of circumvallate papilla showing pale barrel-shaped taste buds (B) in its walls. P, apical pore.

*(**A**, By courtesy of S Franey and by permission from Berkovitz BKB, Holland GR, Moxham BJ 2002 Oral Anatomy, Embryology and Histology, 3rd edn. Edinburgh: Mosby; **B**, by permission from Dr JB*

Kerr, Monash University, from Kerr JB 1999 Atlas of Functional Histology. London: Mosby.)

Taste buds

Taste buds are microscopic barrel-shaped epithelial structures which contain chemosensory cells in synaptic contact with the terminals of gustatory nerves. They are numerous on all types of lingual papillae (except filiform papillae), particularly on their lateral aspects. Taste buds are not restricted to the papillae, and are scattered over almost the entire dorsal and lateral surfaces of the tongue and, rarely, on the epiglottis and lingual aspect of the soft palate. Each taste bud is linked by synapses at its base to one of three cranial nerves which carry taste, i.e. the facial, glossopharyngeal or vagus. They share some physiological features with neurones, for example action potential generation and synaptic transmission, and are therefore often referred to as paraneurones.

There is considerable individual variation in the distribution of taste buds in humans. They are most abundant on the posterior parts of the tongue, especially around the walls of the circumvallate papillae and their surrounding sulci, where there is an average of 250 taste buds for each of the 8–12 papillae. Over 1000 taste buds are distributed over the sides of the tongue, particularly over the more posterior folds of the two foliate papillae, whereas they are rare, and sometimes even absent, on fungiform papillae (≤3 per papilla). Taste buds have been described on the fetal epiglottis and soft palate but most disappear from these sites during postnatal development.

Microstructure of taste buds

Each taste bud is a barrel-shaped cluster of 50–150 fusiform cells which lies within an oval cavity in the epithelium and converges apically on a gustatory pore, a 2 μm wide opening on the mucosal surface. The whole structure is about 70 μm in height by 40 μm across and is separated by a basal lamina from the underlying lamina propria. A small fasciculus of afferent nerve fibres penetrates the basal lamina and spirals around the sensory cells. Chemical substances dissolved in the oral saliva diffuse through the gustatory pores of the taste buds to reach the taste receptor cell membranes, where they cause membrane depolarization.

Innervation of taste buds

Individual nerve fibres branch to give a complex distribution of taste bud innervation. Each fibre may have many terminals, which may spread to innervate widely separated taste buds or may innervate more than one sensory cell in each bud. Conversely, individual buds may receive the terminals of several different nerve fibres. These convergent and divergent patterns of innervation may be of considerable functional importance.

The gustatory nerve for the anterior part of the tongue, excluding the circumvallate papillae, is the chorda tympani, which travels via the lingual nerve. In most individuals, taste fibres run in the chorda tympani to cell bodies in the facial ganglion, but occasionally they diverge to the otic ganglion, which they reach via the greater petrosal nerve. Taste buds in the inferior surface of the soft palate are supplied mainly by the facial nerve, through the greater petrosal nerve, pterygopalatine ganglion and lesser palatine nerve: they may also be supplied by the glossopharyngeal nerve. Taste buds in the circumvallate papillae, postsulcal part of the tongue and in the palatoglossal arches and the oropharynx are innervated by the glossopharyngeal nerve, and those in the extreme pharyngeal part of the tongue and epiglottis receive fibres from the internal laryngeal branch of the vagus.

Each taste bud receives two distinct classes of fibre: one branches in the periphery of the bud to form a perigemmal plexus, the other forms an intragemmal plexus within the bud itself which innervates the bases of the receptor cells. The perigemmal fibres contain various neuropeptides including calcitonin gene-related peptide (CGRP) and substance P, and appear to represent free sensory endings. Intragemmal fibres branch within the taste bud and each forms a series of synapses.

Central connections

On entering the brainstem, gustatory afferents constitute the tractus solitarius and terminate in the rostral third of the nucleus solitarius of the medulla (see Ch. 19).

Taste discrimination

Gustatory receptors detect four main categories of taste sensation, classified as salty, sweet, sour and bitter; other taste qualities have been suggested, including metallic and umami (Japanese: taste typified by monosodium glutamate). Although it is commonly stated that particular areas of the tongue are specialized to detect these different tastes, evidence indicates that all areas of the tongue are responsive to all taste stimuli. Each afferent nerve fibre is connected to widely separated taste buds and may respond to several different chemical stimuli. Some respond to all four classic categories, others to fewer or only one. Within a particular class of tastes, receptors are also differentially sensitive to a wide range of similar chemicals. Moreover, taste buds alone are able to detect only a rather restricted range of chemical substances in aqueous solution. It is difficult to separate the perceptions of taste and smell, because the oral and nasal cavities are continuous. Indeed, much of what is perceived as taste is the result of airborne odorants from the oral cavity which pass through the nasopharynx to the olfactory area above it.

Perceived sensations of taste are the results of the processing (presumably central) of a complex pattern of responses from particular areas of the tongue.

Autonomic innervation of the tongue

The parasympathetic innervation of the various glands of the tongue is from the chorda tympani branch of the facial nerve which synapses in the submandibular ganglion: postganglionic branches are distributed to the lingual mucosa via the lingual nerve. The postganglionic sympathetic supply to lingual glands and vessels arises from the carotid plexus and enters the tongue through plexuses around the lingual arteries. Isolated nerve cells, perhaps postganglionic parasympathetic neurones, have been reported in the postsulcal region: presumably they innervate glandular tissue and vascular smooth muscle.

TEETH

INTRODUCTION AND TERMINOLOGY

Humans have two generations of teeth: the deciduous (primary) dentition and the permanent (secondary) dentition. The first deciduous teeth erupt into the mouth at about 6 months after birth and all of the deciduous teeth have erupted by 3 years of age. The first permanent molar erupts at or around 6 years, and thence the deciduous teeth are exfoliated one by one to be replaced by their permanent successors. A complete permanent dentition is present when the third molars erupt at or around the age of 18–21 years. In the complete deciduous dentition there are 20 teeth, five in each jaw quadrant. In the complete permanent dentition there are 32 teeth, eight in each jaw quadrant.

There are three basic tooth forms in both dentitions: incisiform, caniniform and molariform. Incisiform teeth (incisors) are cutting teeth, and have thin, blade-like crowns. Caniniform teeth (canines) are piercing or tearing teeth, and have a single, stout, pointed, cone-shaped crown. Molariform teeth (molars and premolars) are grinding teeth and possess a number of cusps on an otherwise flattened biting surface. Premolars are bicuspid teeth that are restricted to the permanent dentition and replace the deciduous molars.

The tooth-bearing region of the jaws can be divided into four quadrants, the right and left maxillary and mandibular quadrants. A tooth may thus be identified according to the quadrant in which it is located (e.g. a right maxillary tooth or a left mandibular tooth). In both the deciduous and permanent dentitions, the incisors may be distinguished according to their relationship to the midline. Thus, the incisor nearest the midline is the central (first) incisor and the incisor that is more laterally positioned is termed the lateral (second) incisor. The permanent premolars and the permanent and deciduous molars can also be distinguished according to their mesiodistal relationships. The molar most mesially positioned is designated the first molar, and the one behind it is the second molar. In the permanent dentition, the tooth most distally positioned is the third molar. The mesial premolar is the first premolar, and the premolar behind it is the second premolar.

The terminology used to indicate tooth surfaces is shown in Fig. 30.14B. The aspect of teeth adjacent to the lips or cheeks is termed labial or buccal, that adjacent to the tongue being lingual (or palatal in the maxilla). Labial and lingual surfaces of an incisor meet medially at a mesial surface and laterally at a distal surface, terms which are also used to describe the equivalent surfaces of premolar and molar (postcanine) teeth. On account of the curvature of the dental arch, mesial surfaces of postcanine teeth are directed anteriorly and distal surfaces are directed posteriorly. Thus, the point of contact between the central incisors is the datum point for mesial and distal. The biting or occlusal surfaces of postcanine teeth are tuberculated by cusps which are separated by fissures forming a pattern characteristic of each tooth. The biting surface of an incisor is the incisal edge.

TOOTH MORPHOLOGY

There are two incisors, a central and a lateral, in each half jaw or quadrant (Figs 30.14, 30.15). In labial view, the crowns are trapezoid, the maxillary incisors (particularly the central) are larger than the mandibular. The biting or incisal edges initially have three tubercles or mamelons, which are rapidly removed by wear. In mesial or distal view, their labial profiles are convex while their lingual surfaces are concavo-convex (the convexity near the cervical margin is caused by a low ridge or cingulum, which is prominent only on upper incisors). The roots of incisors are single and rounded in maxillary teeth, but flattened mesiodistally in mandibular teeth. The upper lateral incisor may be congenitally absent or may have a reduced form (peg-shaped lateral incisor).

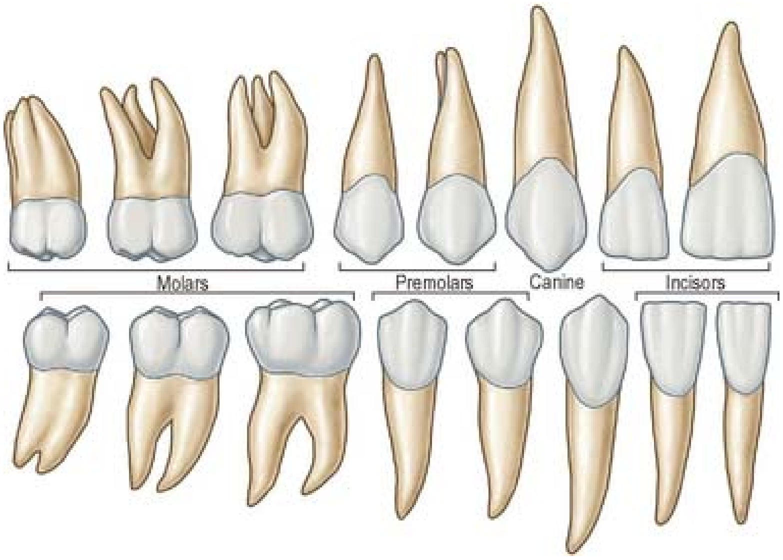

Fig. 30.15 The permanent upper and lower teeth of the right side: labial and buccal surfaces.

Behind each lateral incisor is a canine tooth with a single cusp (hence the American term cuspid) instead of an incisal edge. The maxillary canine is stouter and more pointed than the mandibular canine whose cusp tip is inclined lingually. The canine root, which is the longest of any tooth, produces a bulge (canine eminence) on the alveolar bone externally, particularly in the upper jaw. Although canines usually have single roots, those of the lower jaw may sometimes be bifid.

Distal to the canines are two premolars, each with a buccal and lingual cusp (hence the term bicuspid). The occlusal surfaces of the maxillary premolars are oval (the long axis is buccopalatal) and a mesiodistal fissure separates the two cusps. In buccal view, premolars resemble the canines but are smaller. The maxillary first premolar can have two roots (one buccal, one palatal) but may have one, and very rarely three, roots (two buccal and one palatal) and this makes the tooth more likely to fracture on removal. The maxillary second premolar usually has one root. The occlusal surfaces of the mandibular premolars are more circular or squarer than those of the upper premolars. The buccal cusp of the mandibular first premolar towers above a diminutive lingual cusp to which it is connected by a ridge separating the mesial and distal occlusal pits. In the mandibular second premolar a mesiodistal fissure usually separates a buccal from two smaller lingual cusps. Each lower premolar has one root, but very rarely the root of the first is bifid. Lower second premolars fail to develop in about 2% of individuals.

Posterior to the premolars are three molars whose size decreases distally. Each has a large rhomboid (upper jaw) or rectangular (lower jaw) occlusal surface with four or five cusps. The maxillary first molar has a cusp at each corner of its occlusal surface and the mesiopalatal cusp is connected to the distobuccal by an oblique ridge. A smaller cusplet or tubercle (cusplet of Carabelli) usually appears on the mesiopalatal cusp (most commonly in Caucasian races). The tooth has three widely separated roots, two buccal, of which the mesiobuccal is larger and broader and the distobuccal is rounder and smaller, and one large palatal: their proximity to the maxillary air sinus is thought to be the reason first molar roots are wide apart and second and third molar roots are converged. The smaller maxillary second molar has a reduced or occasionally absent distopalatal cusp. Its three roots show varying degrees of fusion. The maxillary third molar, the smallest, is very variable in form. It usually has three cusps (the distopalatal being absent) and commonly the three roots are fused.

The mandibular first molar has three buccal and two lingual cusps on its rectangular occlusal surface, the smallest cusp being distal. The cusps of this tooth are all separated by fissures. It has two widely separated roots, one mesial and one distal. The smaller mandibular second molar is like the first, but has only four cusps (it lacks the distal cusp of the first molar) and its two roots are closer together. The mandibular third molar is smaller still and, like the upper third molar, is variable in form. Its crown may resemble that of the lower first or second molar and its roots are frequently fused. As it erupts anterosuperiorly, the third molar is often impacted against the second molar, producing food packing which subsequently causes inflammation. The maxillary third molar erupts posteroinferiorly and is rarely impacted. One or more third molars (upper or lower) fail to develop in up to 30% of individuals.

Impacted mandibular third molars

In many subjects there is a disproportion between the size of the teeth and the size of the jaws such that there is insufficient space for all the teeth to erupt. As the third mandibular molar teeth (the wisdom teeth) are the last to erupt, they are often impeded in their eruption and either become impacted or remain unerupted deeply within the jaw bone. If the tooth is completely covered by bone and mucosa, it is very unlikely to cause any symptoms, and the subject remains unaware of its presence unless the tooth is seen on a routine dental radiograph. Very rarely, the surrounding dental follicle may undergo cystic degeneration which can ‘hollow out’ the jaw, usually the mandible, to a considerable degree. The developing cyst may displace the tooth as it expands and the tooth may end up as far away as the condylar neck or coronoid process.

More commonly, the erupting wisdom tooth erupts partially before impacting against the distal aspect of the second molar. When this occurs, symptoms are common due to recurrent soft tissue inflammation and infection around the partially erupted tooth. This condition is known as pericoronitis and if the infecting organism is virulent, the infection may rapidly spread into the adjacent tissue spaces as described elsewhere. The tooth only merits surgical removal if the patient suffers a severe bout or multiple bouts of pericoronitis. Surgery is not immediately indicated because it is associated with a degree of morbidity: the lingual and inferior alveolar nerves, which are often in close proximity to the tooth, may be damaged during its removal. The lingual nerve passes across the surface of the periosteum lingually to the lower wisdom tooth, separated from the tooth only by a cortical plate of bone no thicker than an egg shell. Damage to this nerve results in altered sensation to the ipsilateral side of the tongue. The root apices of the impacted tooth often lie immediately above the mandibular canal, and removal of the tooth can result in damage to the underlying neurovascular bundle, causing altered sensation in its dermatome. Maxillary third molars are only rarely impacted.

Deciduous teeth

The incisors, canine and premolars of the permanent dentition replace two deciduous incisors, a deciduous canine and two deciduous molars in each jaw quadrant (Figs 30.16, 30.17). The deciduous incisors and canine are shaped like their successors but are smaller and whiter and become extremely worn in older children. The deciduous second molars resemble the first permanent molars rather than their successors, the premolars. The upper first deciduous molar has a triangular occlusal surface (its rounded ‘apex’ is palatal) and a fissure separates a double buccal cusp from the palatal cusp. The lower first deciduous molar is long and narrow; its two buccal cusps are separated from its two lingual cusps by a zigzagging mesiodistal fissure. Both deciduous molars have large buccal protuberances on their mesial aspect. Upper deciduous molars have three roots (fusion of the palatal and distobuccal root is commonplace), and lower deciduous molars have two roots. These roots diverge more than those of permanent teeth because each developing premolar tooth crown is accommodated directly under the crown of its deciduous predecessor. The roots of deciduous teeth are progressively resorbed by osteoclast-like cells (odontoclasts) prior to being shed.

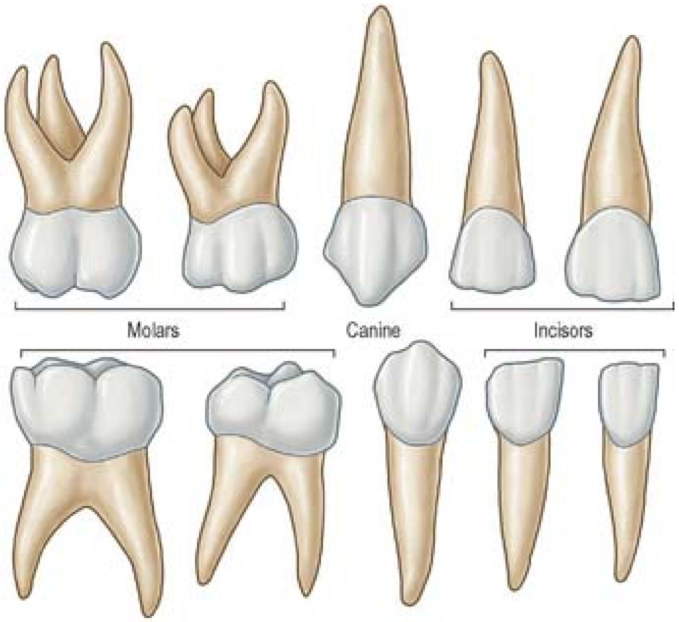
Molars
Canine
Incisors

Fig. 30.16 The deciduous upper and lower teeth of the right side: labial and buccal surfaces.

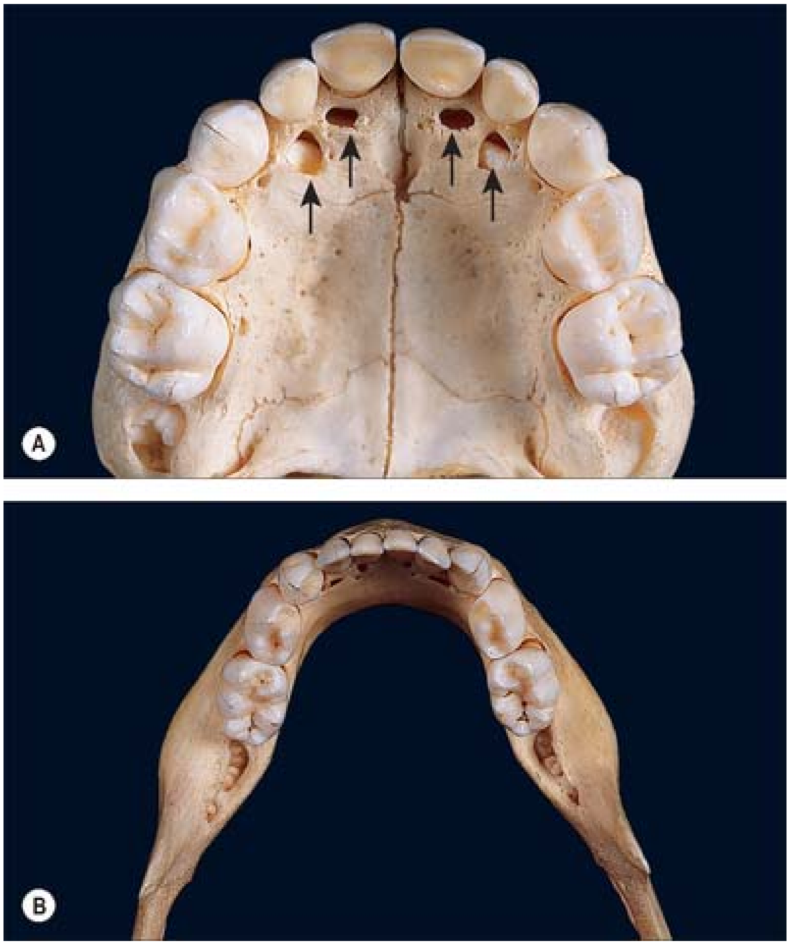

Fig. 30.17 **A**, The upper deciduous dentition. Note the channels (arrows) leading to the developing permanent teeth. **B**, The lower deciduous dentition.

(By permission from Berkovitz BKB, Moxham BJ 1994 Color Atlas of the Skull. London: Mosby.)

Eruption of teeth

Information on the sequence of development and eruption of teeth into the oral cavity (Fig. 30.18) is important in clinical practice and also in forensic medicine and archaeology. The tabulated data provided in Table 30.2 are largely based on European-derived populations and there is evidence of ethnic variation. When a permanent tooth erupts, about two-thirds of the root is formed and it takes about another 3 years for the root to be completed. For deciduous teeth, root completion is more rapid (Table 30.1). The developmental stages of initial calcification and crown completion are less affected by environmental influences than is eruption, the timing of which may be modified by several factors such as early tooth loss and severe malnutrition.

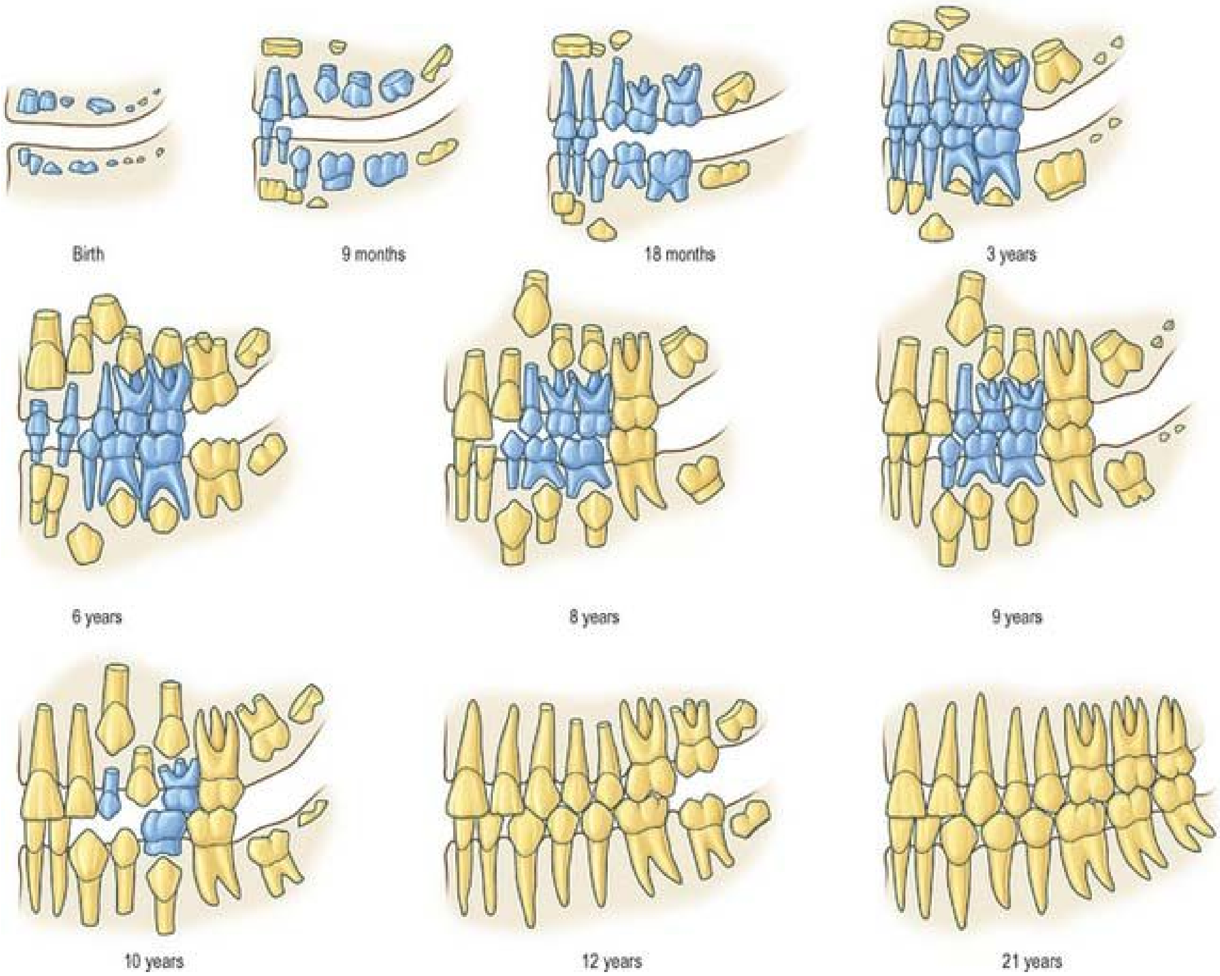
Birth
9 months
18 months
3 years
6 years
8 years
9 years
10 years
12 years
21 years

Fig. 30.18 Development of the deciduous (blue) and permanent (yellow) teeth.

(Modified with permission from Schour I, Massler M 1941 The development of the human dentition. J Am Dent Assoc 28: 1153–1160.)

Table 30.1 Chronology of the human dentition.

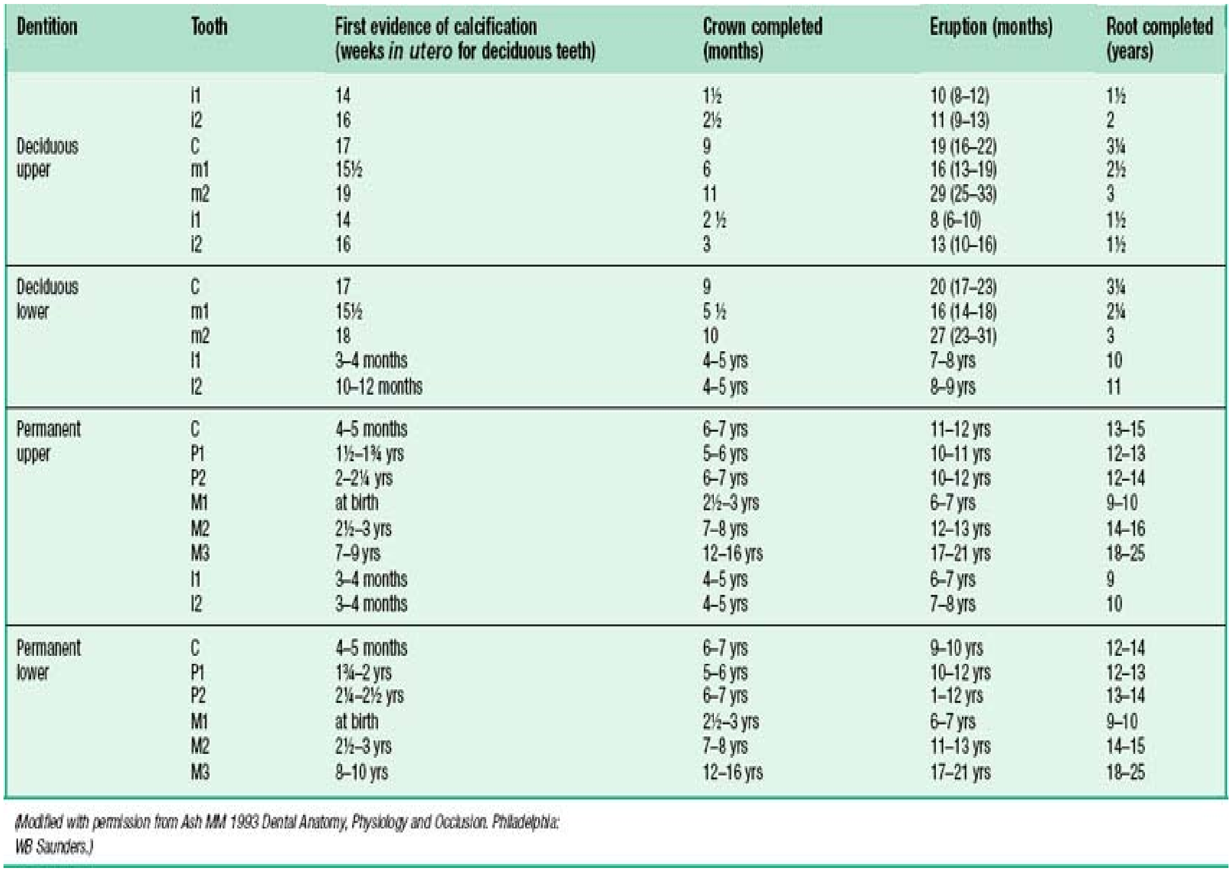

Dentition	Tooth	First evidence of calcification (weeks *in utero* for deciduous teeth)	Crown completed (months)	Eruption (months)	Root completed (years)
Deciduous upper	i1	14	1½	10 (8–12)	1½
	i2	16	2½	11 (9–13)	2
	C	17	9	19 (16–22)	3¼
	m1	15½	6	16 (13–19)	2½
	m2	19	11	29 (25–33)	3
	i1	14	2 ½	8 (6–10)	1½
	i2	16	3	13 (10–16)	1½
Deciduous lower	C	17	9	20 (17–23)	3¼
	m1	15½	5 ½	16 (14–18)	2¼
	m2	18	10	27 (23–31)	3
	I1	3–4 months	4–5 yrs	7–8 yrs	10
	I2	10–12 months	4–5 yrs	8–9 yrs	11
Permanent upper	C	4–5 months	6–7 yrs	11–12 yrs	13–15
	P1	1½–1¾ yrs	5–6 yrs	10–11 yrs	12–13
	P2	2–2¼ yrs	6–7 yrs	10–12 yrs	12–14
	M1	at birth	2½–3 yrs	6–7 yrs	9–10
	M2	2½–3 yrs	7–8 yrs	12–13 yrs	14–16
	M3	7–9 yrs	12–16 yrs	17–21 yrs	18–25
	I1	3–4 months	4–5 yrs	6–7 yrs	9
	I2	3–4 months	4–5 yrs	7–8 yrs	10
Permanent lower	C	4–5 months	6–7 yrs	9–10 yrs	12–14
	P1	1¾–2 yrs	5–6 yrs	10–12 yrs	12–13
	P2	2¼–2½ yrs	6–7 yrs	1–12 yrs	13–14
	M1	at birth	2½–3 yrs	6–7 yrs	9–10
	M2	2½–3 yrs	7–8 yrs	11–13 yrs	14–15
	M3	8–10 yrs	12–16 yrs	17–21 yrs	18–25

(Modified with permission from Ash MM 1993 Dental Anatomy, Physiology and Occlusion. Philadelphia: WB Saunders.)

Fig. 30.19 shows the panoramic appearance of the dentition seen with orthopantomograms at the time of birth, 2½, 6½, 10 and 16 years of age.

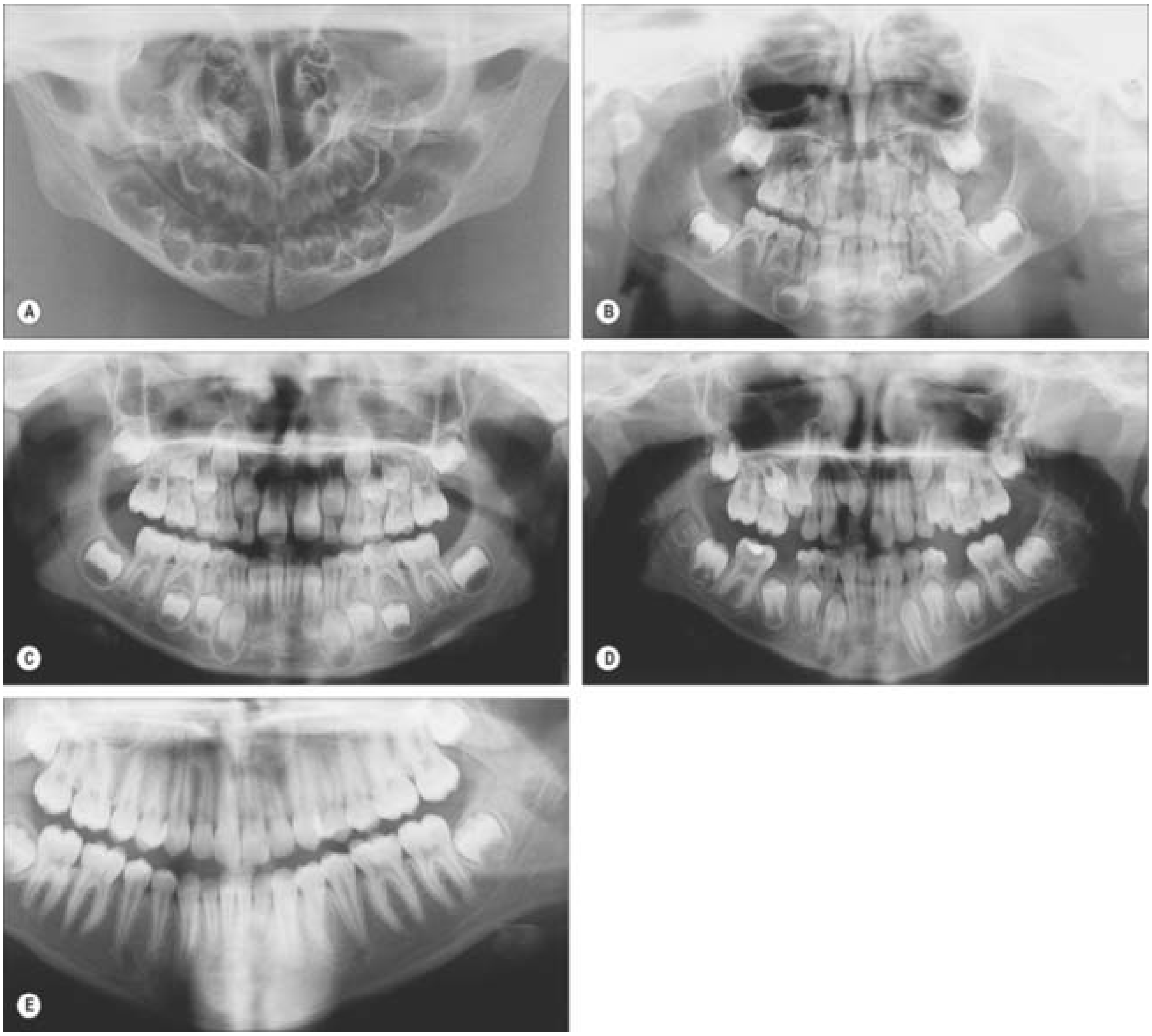

Fig. 30.19 Orthopantomograms of the dentition at birth (**A**), 2½ years (**B**), 6½ years (**C**), 10 years (**D**) and 16 years (**E**).

*(**B–E**, By permission from Berkovitz BKB, Holland GR, Moxham BJ 2002 Oral Anatomy, Embryology and Histology, 3rd edn. Edinburgh: Mosby; **D** and **E**, also by courtesy of Dr Eric Whaites.)*

Dental alignment and occlusion

It is possible to bring the jaws together so that the teeth meet or occlude in many positions. When opposing occlusal surfaces meet with maximal ‘intercuspation’ (i.e. maximum contact), the teeth are said to be in centric occlusion. In this position the lower teeth are normally opposed symmetrically and lingually with respect to the upper. Some important features of centric occlusion in a normal (idealized) dentition may be noted. Each lower postcanine tooth is slightly in front of its upper equivalent and the lower canine occludes in front of the upper. Buccal cusps of the lower postcanine teeth lie between the buccal and palatal cusps of the upper teeth. Thus, the lower postcanine teeth are slightly lingual and mesial to their upper equivalents. Lower incisors bite against the palatal surfaces of upper incisors, the latter normally obscuring about one-third of the crowns of the lower. This vertical overlap of incisors in centric occlusion is the overbite. The extent to which upper incisors are anterior to lowers is termed the overjet. In the most habitual jaw position, the resting posture, the teeth are slightly apart, the gap between them being the freeway space or interocclusal clearance. During mastication, especially with lateral jaw movements, the food is comminuted, which facilitates the early stages of digestion.

The ideal occlusion is a rather subjective concept. If there is an ideal occlusion, it can only presently be defined in broad functional terms. Therefore, the occlusion can be considered ‘ideal’ when the teeth are aligned such that the masticatory loads are within physiological range and act through the long axes of as many teeth in the arch as possible; mastication involves alternating bilateral jaw movements (and not habitual, unilateral biting preferences as a result of adaptation to occlusal interference); lateral jaw movements occur without undue mechanical interference; in the rest position of the jaw, the gap between teeth (the freeway space) is correct for the individual concerned; the tooth alignment is aesthetically pleasing to its possessor.

Variations from the ideal occlusion may be termed malocclusions (although these could be regarded as normal, since they are more commonly found in the population: 75% of the population in the USA has some degree of occlusal ‘disharmony’). However, the majority of malocclusions should be regarded as anatomical variations rather than abnormalities, as they are rarely involved in masticatory dysfunction or pain, although they may be aesthetically displeasing.

Variations in tooth number, size and form

The incidence of variation in number and form, which is often related to race, is rare in deciduous teeth but not uncommon in the permanent dentition. One or more teeth may fail to develop, a condition known as hypodontia. Conversely, additional or supernumerary teeth may form, producing hyperdontia. The third permanent molar is the most frequently missing tooth: in one study, one or more third molars failed to form in 32% of Chinese, 24% of English Caucasians and 2.5% of West Africans. In declining order of incidence, other missing teeth are maxillary lateral incisors, maxillary or mandibular second premolars, mandibular central incisors and maxillary first premolars.

Hyperdontia affects the maxillary arch much more commonly than the mandibular dentition. The extra teeth are usually situated on the palatal aspect of the permanent incisors or distal to the molars. More rarely, additional premolars develop. Supernumerary teeth in the incisor region can often impede the eruption of the permanent teeth and indeed this is often the first indication of their presence. A supernumerary tooth situated between the central incisors is known as a mesiodens. Teeth may be unusually large (macrodontia) or small (microdontia). For example, the crowns of maxillary central incisors may be abnormally wide mesiodistally; in contrast, a common variant of the maxillary lateral incisor has a small, peg-shaped crown. Epidemiological studies reveal that hyperdontia tends to be associated with macrodontia and hypodontia with microdontia, the most severely affected individuals representing the extremes of a continuum of variation. Together with family studies, this indicates that the causation is multifactorial, combining polygenic and environmental influences.

Some variations in the form of teeth, being characteristic of race, are of anthropological and forensic interest. Mongoloid dentitions tend to have shovel-shaped maxillary incisors with enlarged palatal marginal ridges. The additional cusp of Carabelli is commonly found on the mesiopalatal aspect of maxillary first permanent or second deciduous molars in Caucasian but rarely in Mongoloid dentitions. In African races, the mandibular second permanent molar often has five rather than four cusps.

General arrangement of dental tissues

A tooth consists of a crown covered by very hard translucent enamel and a root covered by yellowish bone-like cementum (Fig. 30.20A). These meet at the neck or cervical margin. A longitudinal ground section (Fig. 30.20B) reveals that the body of a tooth is mostly dentine (ivory) with an enamel covering up to about 2 mm thick, while the cementum is much thinner. The dentine surrounds a central pulp cavity, expanded at its coronal end into a pulp chamber and narrowed in the root as a pulp canal, opening at or near its tip by an apical foramen, occasionally multiple. The pulp is a connective tissue, continuous with the periodontal ligament via the apical foramen. It contains vessels for the support of the dentine and sensory nerves.

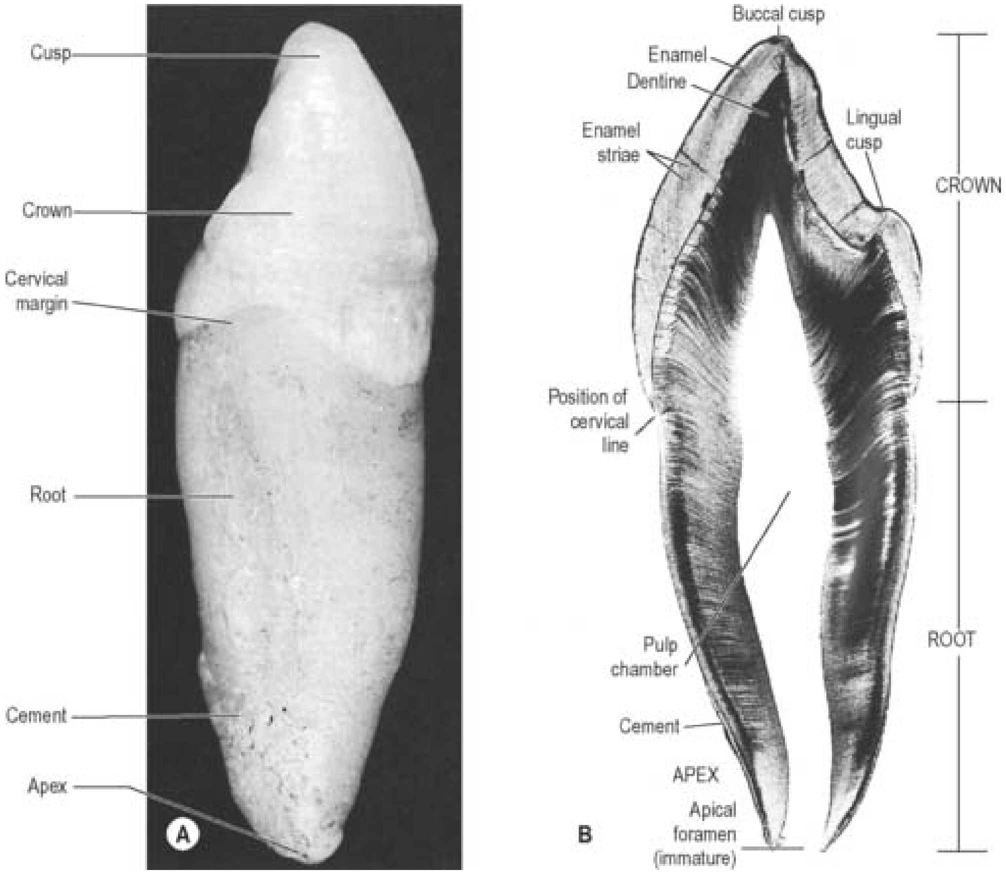
Cusp
Crown
Cervical margin
Root
Cement
Apex
A
Buccal cusp
Enamel
Dentine
Enamel striae
Lingual cusp
CROWN
Position of cervical line
Pulp chamber
ROOT
Cement
APEX
Apical foramen (immature)
B

Fig. 30.20 The principal parts of a tooth. **A**, An extracted upper right canine tooth viewed from its mesial aspect. The root is covered by cement (partially removed), and the curved cervical margin is convex towards the cusp of the tooth. **B**, A ground section of a young (permanent) lower first premolar tooth sectioned in the buccolingual longitudinal plane, photographed with transmitted light. The enamel striae are incremental lines of enamel growth (compare with **Fig. 30.24**). Within the dentine the lines of the dentinal tubules are visible, forming S-shaped curves in the apical region but straighter in the root.

The root is surrounded by alveolar bone, its cementum separated from the osseous socket (alveolus) by the connective tissue of the periodontal ligament, approximately 0.2 mm thick (Fig. 30.21). Coarse bundles of collagen fibres, embedded at one end in cementum, cross the periodontal ligament to enter the osseous alveolar wall, these bundles of collagen being termed Sharpey’s fibres. Near the cervical margin, the tooth, periodontal ligament and adjacent bone are covered by the gingiva. On its internal surface the gingiva is attached to the tooth surface by the junctional epithelium, a zone of profound clinical importance because just above it is a slight recess, the gingival sulcus. As the sulcus is not necessarily self-cleansing, dental plaque may accumulate in it and this predisposes to periodontal disease.

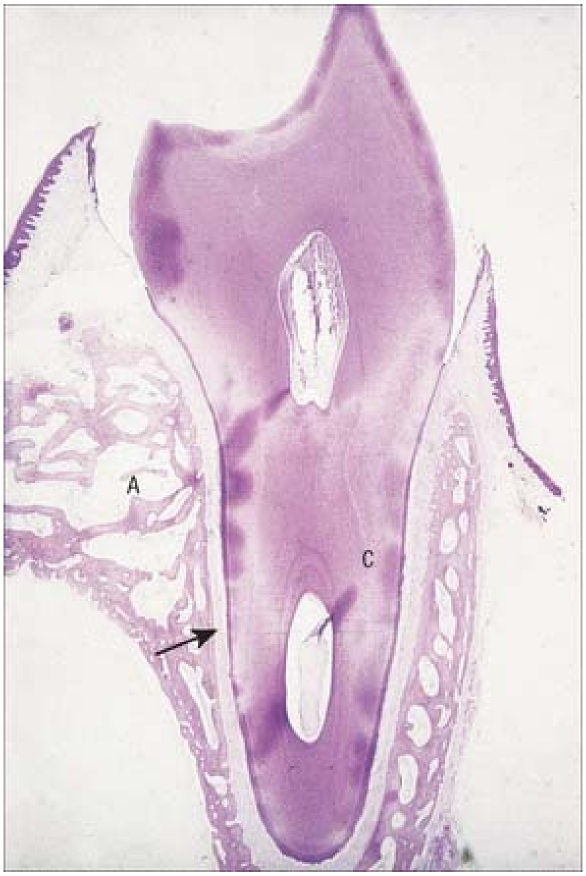

Fig. 30.21 Demineralized section of a tooth with its root attached to the surrounding bone by the periodontal ligament. A, alveolar bone; C, root of tooth lined by cementum; arrow indicates periodontal space.

(By courtesy of Dr D Lunt.)

Enamel

Enamel is an extremely hard and rigid material which covers the crowns of teeth. It is a heavily mineralized epithelial cell secretion, containing 95–96% by weight crystalline apatites (88% by volume) and less than 1% organic matrix. The organic matrix comprises mainly unique enamel proteins, amelogenins and non-amelogenins such as enamelins, tuftelins. Although comprising a very small percentage of the weight and volume of enamel, the organic matrix permeates the whole of enamel. As its formative cells are lost from the surface during tooth eruption, enamel is incapable of further growth. Repair is limited to the remineralization of minute carious lesions.

Enamel reaches a maximum thickness of 2.5 mm over cusps and thins at the cervical margins. It is composed of closely packed enamel prisms or rods. In longitudinal section, enamel prisms extend from close to the enamel–dentine junction to within 20 μm of the surface, where they are generally replaced by prismless (non-prismatic, aprismatic) enamel (Fig. 30.22A). In cross-section the prisms are mainly horseshoe-shaped and are arranged in rows that are staggered such that the tails of the prisms in one row lie between the heads of the prism in the row above (prism pattern 3) (Fig. 30.22B) and the tails are directed rootwards. The appearance of prism boundaries results from sudden changes in crystallite orientation. Prisms have a diameter of approximately 5 μm, and are packed with flattened hexagonal hydroxyapatite crystals, far larger than those found in collagen-based mineralized tissues.

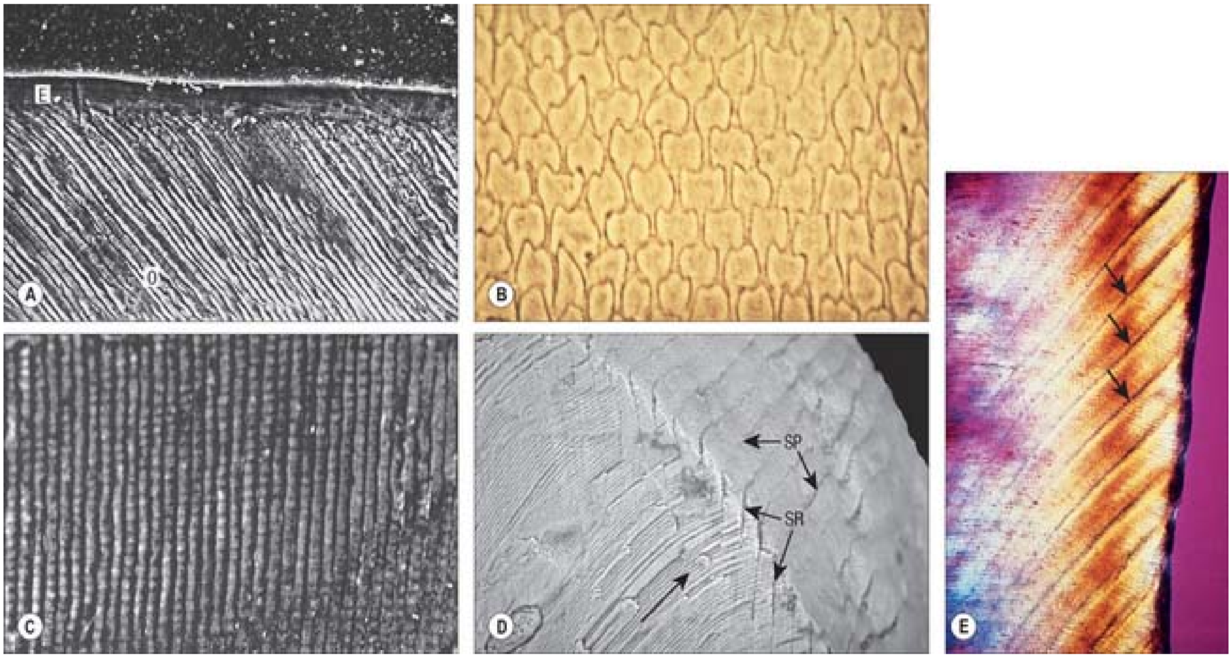

Fig. 30.22 Enamel. **A**, Scanning electron micrograph of acid-etched outer enamel (O) showing enamel prisms, approximately 5 μm wide. A layer of prismless enamel (E) is evident on the surface. **B**, Ground cross-section showing cross-sectional keyhole (fish scale) appearance of enamel prisms (pattern 3). **C**, Ground longitudinal section viewed with phase contrast showing prisms (vertical lines) and cross-striations (horizontal lines). **D**,

Low-power scanning electron micrograph illustrating the relationship of enamel prism direction (long arrow), striae of Retzius (SR) and surface perikymata (SP). **E**, Ground longitudinal section showing enamel striae (arrows). Viewed between crossed polarizing filters.

*(**A**, by courtesy of Professor D Whittaker; **B**, by permission from Berkovitz BKB, Holland GR, Moxham BJ 2002 Oral Anatomy, Embryology and Histology, 3rd edn. Edinburgh: Mosby; **C**, by permission from Berkovitz BKB, Holland GR, Moxham BJ 2002 Oral Anatomy, Embryology and Histology, 3rd edn. Edinburgh: Mosby; **D**, by permission from: Kelley J, Smith TM. Age at first molar emergence in early Miocene Afropithecus turkanensis and life-history evolution in the Hominoidea. Journal of Human Evolution 2003; 44:307–329; **E**, by courtesy of Dr AD Beynon)*

Two types of incremental lines are visible in enamel, short-term and long-term. At intervals that average 4 µm – with a range of 2–3 µm at the enamel dentine junction and 4–6 µm in outer enamel – along its length, each prism is crossed by a line, probably reflecting diurnal swelling and shrinking in diameter during its growth. This short-term daily growth line is known as a cross-striation (Fig. 30.22C). The longer-term incremental lines pass from the enamel–dentine junction obliquely to the surface, where they end in shallow furrows, perikymata, visible on newly erupted teeth (Fig. 30.22D). Each line, known as an enamel stria of Retzius, represents a period that ranges between 6 and 12 days of enamel growth with a modal value of 9 days. This is known as an individual's periodicity and it is constant in all teeth from the same individual but varies considerably between individuals (Reid & Dean 2006) (Fig. 30.22E). A prominent striation, the neonatal line, is formed in teeth whose mineralization spans birth. Neonatal lines are present in the enamel and dentine of teeth mineralizing at the time of birth (all the deciduous teeth and the first permanent molars; see Fig. 30.14) and are therefore of forensic importance, indicating that an infant has survived for a few days after birth. They reflect a disturbance in mineralization during the first few days after birth. Other accentuated lines can be observed throughout enamel growth; these are generally reflections in disturbances in ameloblast secretion caused by illness or nutritional deficiencies. In serious cases these disturbances will manifest as hypoplasia (enamel thinning on the tooth surface).

Dentine

Dentine is a yellowish avascular tissue which forms the bulk of a tooth. It is a tough and compliant composite material, with a mineral content of 70% dry weight (largely crystalline hydroxyapatite with some calcium carbonate) and 20% organic matrix (type I collagen, glycosaminoglycans and phosphoproteins). Its conspicuous feature is the regular pattern of microscopic dentinal tubules, 3 μm in diameter, which extend from the pulpal surface to the enamel–dentine junction. The tubules show lateral and terminal branching near the enamel–dentine junction (Fig. 30.23A) and may project a short distance into the enamel (enamel spindles). Each tubule encloses a single cytoplasmic process of an odontoblast whose cell body lies in a pseudostratified layer which lines the pulpal surface. Processes are believed to extend the full thickness of dentine in newly erupted teeth, but in older teeth they may be partly withdrawn and occupy only the pulpal third, while the outer regions contain probably only extracellular fluid. The diameter of the dentine tubule is narrowed by deposition of peritubular dentine. This is different from normal dentine (intertubular dentine) because it is more highly mineralized and lacks a collagenous matrix. Peritubular dentine can therefore be identified by microradiography (Fig. 30.23B). In time, it may completely fill the tubule, a process which gives rise to translucent dentine and which commences in the apical region of the root.

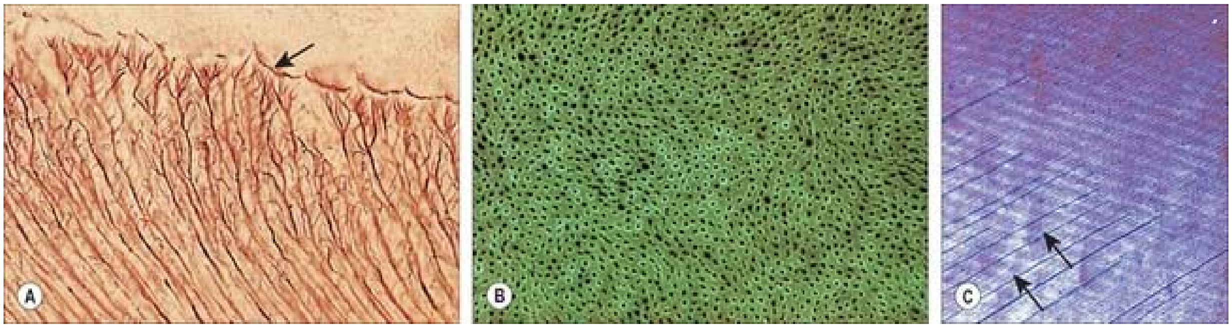

Fig. 30.23 Dentine. **A**, Ground longitudinal section showing branching of dentine tubules near the enamel–dentine junction (arrow). **B**, Microradiograph of transversely sectioned dentinal tubules surrounded by a more radiopaque and therefore more mineralized zone of peritubular

dentine. **C**, Ground longitudinal section viewed in polarized light showing alternate light and dark bands representing long-period incremental lines (Andresen lines). The bands are approximately orientated at right angles to the direction of the dentinal tubules (arrows).

(By permission from Berkovitz BKB, Holland GR, Moxham BJ 2002 Oral Anatomy, Embryology and Histology, 3rd edn. Edinburgh: Mosby.)

The outermost zone (10–20 μm) of dentine differs in the crown and the root. In the crown it is referred to as mantle dentine and differs in the orientation of its collagen fibres. In the root, the peripheral zone presents a granular layer – with less overall mineral – beyond which is a hyaline layer which lacks a tubular structure and may function to produce a good bond between the cementum and dentine.

Dentine is formed slowly throughout life, and so there is always an unmineralized zone of predentine at the surface of the mineralized dentine, adjacent to the odontoblast layer at the periphery of the pulp. Biochemical changes within the mineralizing matrix mean that preentine stains differently to the matrix of the mineralized dentine. The predentine–dentine border is generally scalloped, because dentine mineralizes both linearly and as microscopic spherical aggregates of crystals (calcospherites). Dentine, like enamel, is deposited incrementally, and exhibits both short- and long-term incremental lines. Long-term lines are known as Andresen lines and in the mid-axial region are approximately 20 μm apart: they represent increments of about 6–12 days (Fig. 30.23C). Daily incremental lines (von Ebner lines) in the mid-axial plane are typically 4 μm apart; they are considerably closer together (1–2 μm apart) at the enamel–dentine junction and in root dentine. Where mineralization spans birth (i.e. all deciduous teeth and usually the first permanent molars) a neonatal line is formed in dentine similar to that which is seen in enamel, and it signals the abrupt change in both environment and nutrition which occurs at birth. As with enamel, disturbances in growth of dentine will exhibit as accentuated lines, commonly called contour lines of Owen.

Primary dentine formation proceeds at a steady but declining rate as first the crown and then the root is completed. A slow and intermittent deposition of dentine (regular secondary dentine) continues throughout life and further reduces the size of the pulp chamber; it is distinguished from primary dentine by the reduction and haphazard arrangement of dentinal tubules within it. The presence of the odontoblast process means that dentine is a vital tissue. It responds to adverse external stimuli – such as rapidly advancing caries, excessive wear or tooth breakage – by forming poorly mineralized dead tracts, in which the odontoblasts of the affected region die and the tubules remain empty (tertiary dentine). A dead tract may be sealed from the pulp by a thin zone of sclerosed dentine and the deposition of irregular (tertiary) dentine by newly differentiated pulp cells (Fig. 30.24).

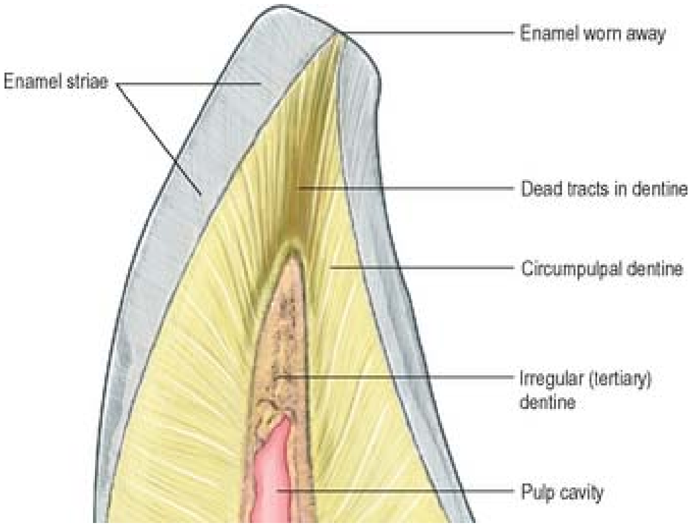

Fig. 30.24 Longitudinal ground section of an incisor tooth.

Dental pulp

Dental pulp provides the nutritive support for the synthetic activity of the odontoblast layer. It is a well-vascularized, loose connective tissue, enclosed by dentine and continuous with the periodontal ligament via apical and accessory foramina. Several thin-walled arterioles enter by the apical foramen and run longitudinally within the pulp to an extensive subodontoblastic plexus. Blood flow rate per unit volume of tissue is greater in the pulp than in other oral tissues, and tissue fluid pressures within the pulp appear to be unusually high.

As well as typical connective tissue cells, pulp uniquely contains the cell bodies of odontoblasts whose long processes occupy the dentinal tubules. Pulp also has dendritic antigen-presenting cells. Approximately 60% of pulpal collagen is type I, and the bulk of the remainder is type III. As dentine deposition increases with age, the pulp recedes until the whole of the crown may be removed without accessing the pulp.

Dental pulp is extensively innervated by unmyelinated postganglionic vasoconstrictor sympathetic nerve fibres from the superior cervical ganglion, which enter with the arterioles, and by myelinated (Aδ) and unmyelinated (C) sensory nerve fibres from the trigeminal ganglion, which traverse the pulp longitudinally and ramify as a plexus (Raschkow’s plexus) beneath the odontoblast layer (Figs 30.25, 30.26). Here, any myelinated nerve fibres lose their myelin sheaths and continue into the odontoblast layer, and some enter the dentinal tubules, especially the region beneath the cusps. Stimulation of dentine, whether by thermal, mechanical or osmotic means, evokes a pain response. Pulp nerves release numerous neuropeptides.

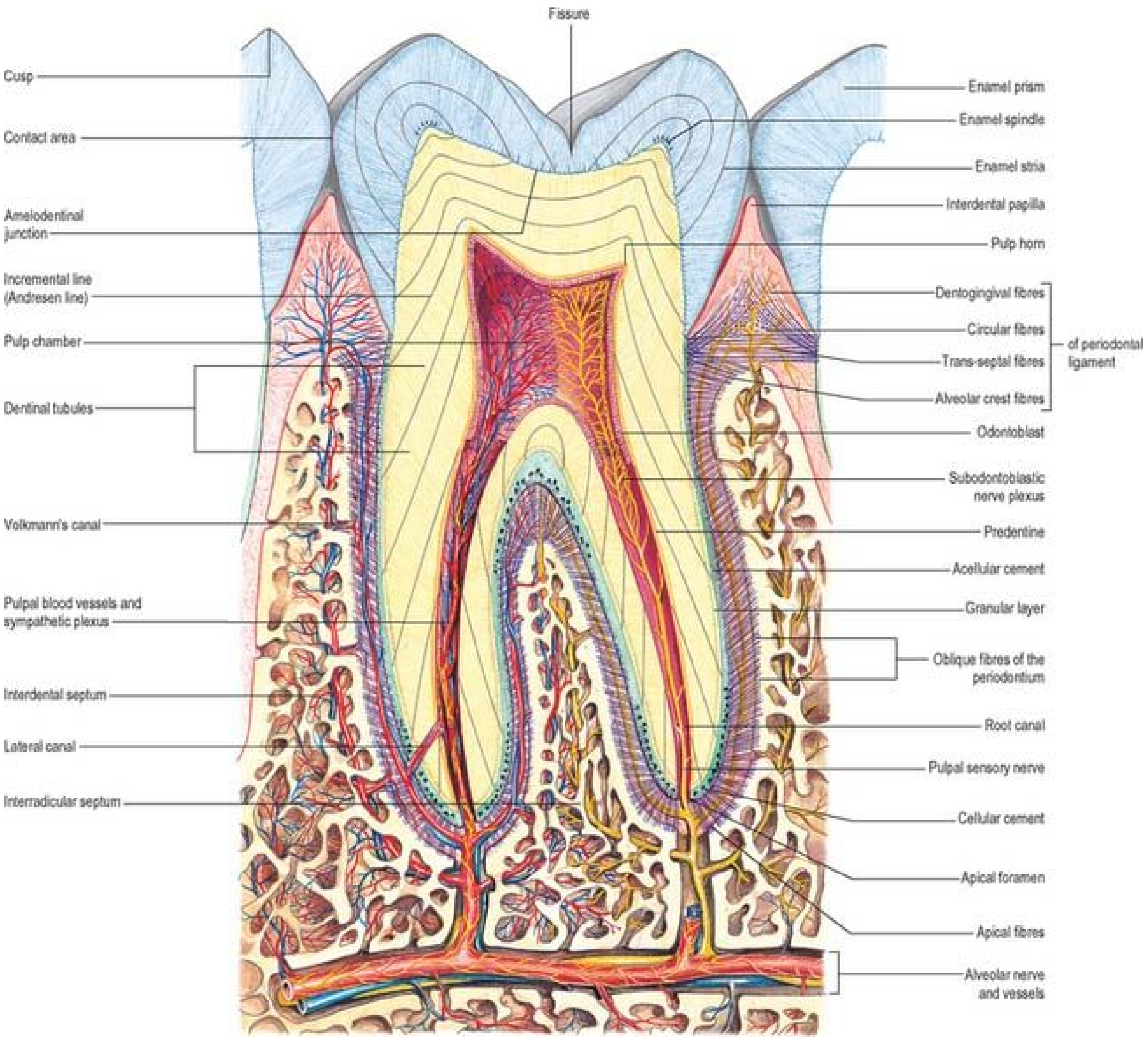
Fissure
Cusp
Contact area
Amelodentinal junction
Incremental line (Andresen line)
Pulp chamber
Dentinal tubules
Volkmann's canal
Pulpal blood vessels and sympathetic plexus
Interdental septum
Lateral canal
Interradicular septum
Enamel prism
Enamel spindle
Enamel stria
Interdental papilla
Pulp horn
Dentogingival fibres
Circular fibres
Trans-septal fibres
Alveolar crest fibres
of periodontal ligament
Odontoblast
Subodontoblastic nerve plexus
Predentine
Acellular cement
Granular layer
Oblique fibres of the periodontium
Root canal
Pulpal sensory nerve
Cellular cement
Apical foramen
Apical fibres
Alveolar nerve and vessels

Fig. 30.25 Longitudinal section of a tooth and its surrounding tissues.

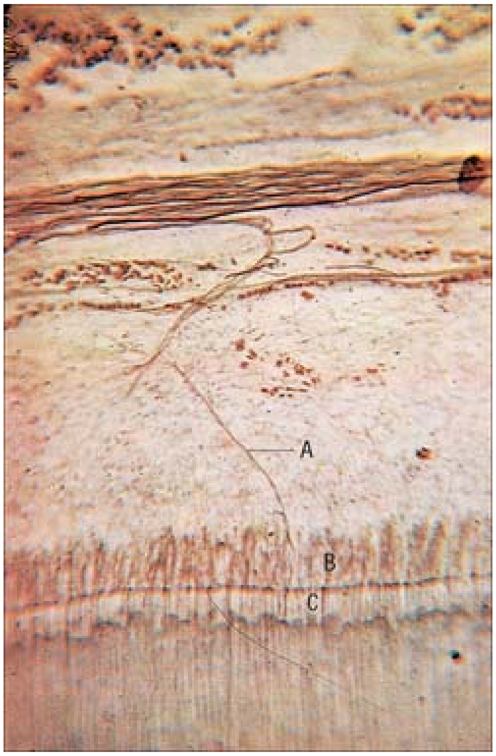

Fig. 30.26 Longitudinal demineralized section of a tooth stained with a silver impregnation technique. Note the small bundle of nerves within the pulp (top); one of the fine axons from the bundle (A) passes between the odontoblasts (B) lining the surface of the predentine (C).

Cementum

Cementum is a bone-like tissue which covers the dental roots, and is 50% by weight mineralized (mainly hydroxyapatite crystals). However, unlike bone, cementum is avascular and lacks nerves. The cementum generally overlaps the enamel slightly, although it may meet it end on. Occasionally, the two tissues may fail to meet, in which case dentine is exposed in the mouth. If the exposed dentinal tubules remain patent, then the teeth may be sensitive to stimuli such as cold water. In older teeth, the root may become exposed in the mouth as a consequence of occlusal drift and gingival recession, and cementum is often abraded away by incorrect tooth brushing and dentine exposed.

Like bone, cementum is perforated by Sharpey's fibres, which represent the attachment bundles of collagen fibres in the periodontal ligament (extrinsic fibres). New layers of cementum, which are deposited incrementally throughout life to compensate for tooth movements, incorporate new Sharpey's fibres. Incremental lines are irregularly spaced. The first cement to be formed is thin (up to 200 μm), acellular and contains only extrinsic fibres. Cementum formed later towards the root apex is produced more rapidly and contains cementocytes lying in lacunae joined by canaliculi. The latter are mainly directed towards their source of nutrients from the periodontal ligament. This cementum contains both extrinsic fibres derived from the periodontal ligament and intrinsic fibres of cementoblastic origin which lie parallel to the surface. Varying arrangements of layering between cellular and acellular cement occur. With increasing age, cellular cement may reach a thickness of a millimetre or more around the apices and at the branching of the roots, where it compensates for the loss of enamel by attrition. Cementum is not remodelled but small areas of resorption with evidence of repair may be seen.

Forensic anatomy of teeth

In forensic medicine, dental evidence is valuable in identification of individuals, especially following mass disasters; estimation of age at death of skeletonized remains; and establishing guilt in cases of criminal injury by biting.

If teeth have been restored, extracted or replaced by a denture, an individual will have a virtually unique dentition which may have been recorded by the dentist in the form of charts, radiographs or plaster casts. Teeth are the most indestructible bodily structures and can provide identification when trauma or fire has rendered the face unrecognizable. Moreover, the chronology of crown development, eruption and root formation can be used to estimate age until the third molar is completed at about 21 years. The method is even applicable to the fetus because the weight of mineralized tissue in teeth is closely related to age from about 22 weeks' gestation until birth. The time taken for a crown to form can be calculated from ground sections with considerable accuracy by counting the number of daily cross-striations from the neonatal line. For permanent teeth, the time taken for the crown to form can be calculated by counting the number of the enamel striae and multiplying by the individual's periodicity. The age of adult teeth can be estimated from factors such as wear of the crown, reduction in size of the pulp and increase in thickness of cement in the apical half of the root. However, probably the most useful single characteristic is the amount of translucent dentine in the root, which is proportional to age. Such estimations are within 5–7 years of the chronological age and likely to be closer to the true age than those derived from skeletal changes.

Periodontal ligament

The principal functions of the periodontal ligament are to support the teeth, generate the force of tooth eruption and provide sensory information about tooth position and forces to facilitate reflex jaw activity. The periodontal ligament is a dense fibrous connective tissue 0.2 mm wide which contains cells associated with the development and maintenance of alveolar bone (osteoblasts and osteoclasts) and of cementum (cementoblasts and odontoclasts). It also contains a network of epithelial cells (epithelial cell rests of Malassez) which are embryological remnants of an epithelial root sheath. They have no evident function but may give rise to dental cysts.

The majority of collagen fibres of the periodontal ligament are arranged as variously oriented dense fibre bundles that connect alveolar bone and cementum and which may help to resist movement in specific directions (Fig. 30.27). About 80% of the collagen in the periodontal ligament is type I, most of the remainder is type III. The rate of turnover of collagen is probably the highest of any site in the body, for reasons which are as yet unclear. A very small volume of fibres are oxytalan fibres.

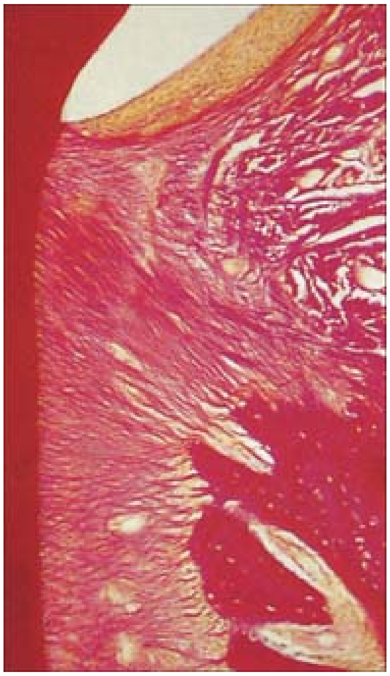

Fig. 30.27 Decalcified longitudinal section of a tooth showing groups of periodontal ligament fibres (the alveolar crest fibres and the horizontal fibres) in the region of the alveolar crest. van Gieson stain.

(By permission from Berkovitz BKB, Holland GR, Moxham BJ 2002 Oral Anatomy, Embryology and Histology, 3rd edn. Edinburgh: Mosby.)

The periodontal ligament has a rich nerve and blood supply. The nerves are both autonomic (for the vasculature) and sensory (for pain and proprioception). The majority of proprioceptive nerve endings appear to be Ruffini-like endings. The blood vessels tend to lie towards the bone side of the periodontal ligament and the capillaries are fenestrated. Tissue fluid pressures appear to be high.

Alveolar bone

That part of the maxilla or mandible which supports and protects the teeth is known as alveolar bone. An arbitrary boundary at the level of the root apices of the teeth separates the alveolar processes from the body of the mandible or the maxilla (Fig. 30.28). Like bone in other sites, alveolar bone functions as a mineralized supporting tissue, gives attachment to muscles, provides a framework for bone marrow and acts as a reservoir for ions, especially calcium. It is dependent on the presence of teeth for its development and maintenance, and requires functional stimuli to maintain bone mass. Where teeth are congenitally absent, as for example in anodontia, it is poorly developed, and it atrophies after tooth extraction, which can cause difficulties in the prosthodontic rehabilitation of patients.

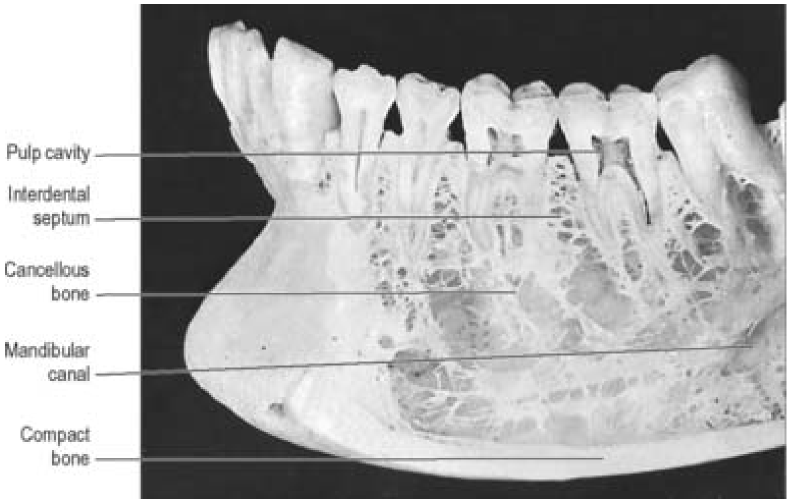

Fig. 30.28 Anterior part of the left side of the mandible, with superficial bone removed on the buccal side to show roots of a number of teeth, some of which have also been sectioned vertically. Note the cortical plate of compact bone lining the sockets of the teeth (the lamina dura of radiographs: see Fig. 30.30), and the flat table of bone surmounting the interdental bone septa. In this specimen the mandibular canal is widely separated from the roots of the teeth, a variable condition.

The alveolar tooth-bearing portion of the jaws consists of outer and inner alveolar plates. The individual sockets are separated by plates of bone termed the interdental septa, while the roots of multi-rooted teeth are divided by interradicular septa. The compact layer of bone which lines the tooth socket has been called either the cribriform plate, on account of its content of vascular (Volkmann's) canals which pass from the alveolar bone into the periodontal ligament, or bundle bone, because numerous bundles of Sharpey's fibres pass into it from the periodontal ligament (Fig. 30.29).

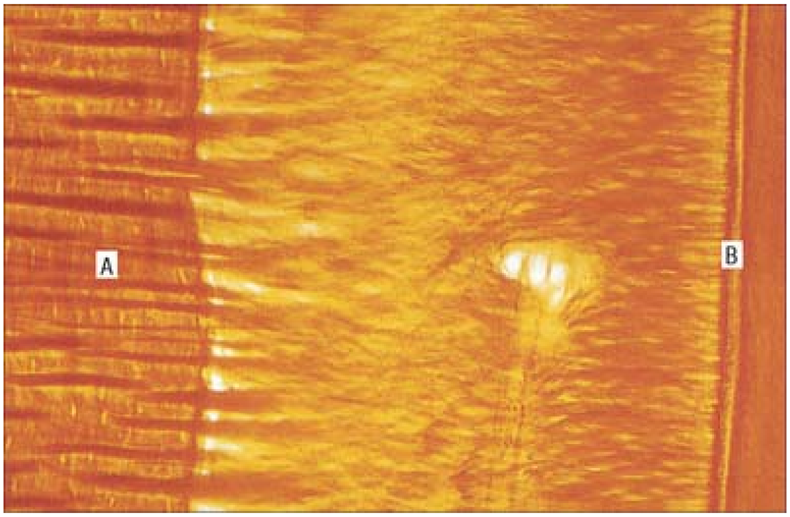

Fig. 30.29 Decalcified section of a root of a tooth showing Sharpey's fibres from the periodontal ligament entering alveolar bone (A). The Sharpey's fibres in bone are seen to be thicker, but less numerous, than those entering the cementum (B) on the tooth surface. van Gieson stain.

(By permission from Berkovitz BKB, Holland GR, Moxham BJ 2002 Oral Anatomy, Embryology and Histology, 3rd edn. Edinburgh: Mosby.)

In clinical radiographs, the bone lining the alveolus commonly appears as a continuous dense white line about 0.5–1 mm thick, the lamina dura (Fig. 30.30). However, this appearance gives a misleading impression of the density of alveolar bone: the X-ray beam passes tangentially through the socket wall, and so the radiopacity of the lamina dura is an indication of the quantity of bone the beam has passed through, rather than the degree of mineralization of the bone. Superimposition also obscures the Volkmann's canals. Chronic infections of the dental pulp spread into the periodontal ligament, which leads to resorption of the lamina dura around the root apex. The presence of a continuous lamina dura around the apex of a tooth therefore usually indicates a healthy apical region (except in acute infections where resorption of bone has not yet begun).

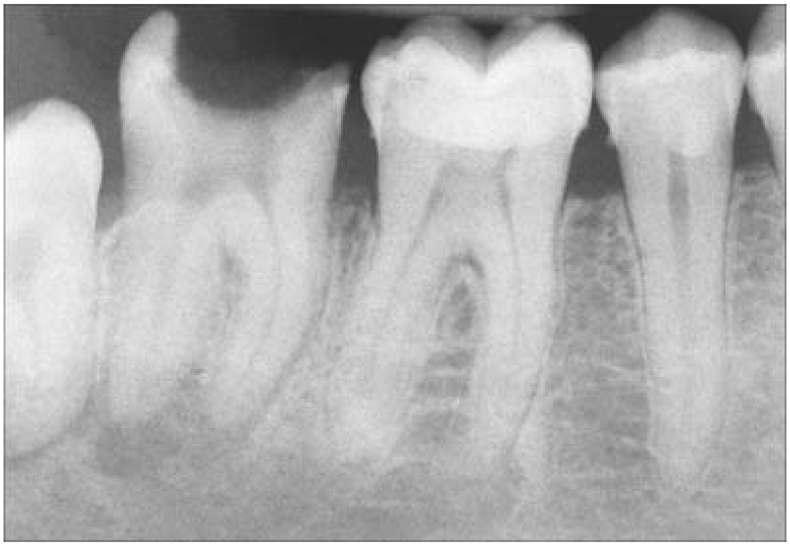

Fig. 30.30 Bite-wing radiograph of teeth and surrounding bone. Note the different radiopacities of enamel and dentine. In a healthy tooth, such as the first molar illustrated here, the lamina dura is complete and appears as a radiopaque line. In the case of the adjacent second molar tooth in which the bulk of the crown has been lost due to dental caries, an abscess has formed at the base of the tooth and as a result the lamina dura has lost its continuity.

(By courtesy of Ms Nadine White.)

On the labial and buccal aspects of upper teeth, the two cortical plates usually fuse, and there is very little trabecular bone between them, except where the buccal bone thickens over the molar teeth near the root of the zygomatic arch. It is easier and more convenient to extract upper and lower teeth by widening the tooth socket in a buccal direction due to its thinness. Anteriorly in the lower jaw, labial and lingual plates are thin, but in the molar region the buccal plate is thickened as the external oblique line. Near the lower third molar, the lingual bone is much thinner than the buccal and it is important to realize that the lingual nerve is easily damaged by poor technique.

VASCULAR SUPPLY AND LYMPHATIC DRAINAGE OF THE TEETH AND SUPPORTING STRUCTURES

The main arteries to the teeth and their supporting structures are derived from the maxillary artery, one of the two terminal branches of the external carotid artery. The upper teeth are supplied by branches from the superior alveolar arteries and the lower teeth by branches from the inferior alveolar arteries.

Superior alveolar arteries

The upper jaw is supplied by posterior, middle and anterior superior alveolar (dental) arteries. The posterior superior alveolar artery usually arises from the third part of the maxillary artery in the pterygopalatine fossa. It descends on the infratemporal surface of the maxilla, and divides to give branches that enter the alveolar canals to supply molar and premolar teeth, adjacent bone and the maxillary sinus, and other branches that continue over the alveolar process to supply the gingivae. The middle and anterior superior alveolar arteries are branches from the infraorbital artery.

The infraorbital artery often arises with the posterior superior alveolar artery. It enters the orbit posteriorly through the inferior orbital fissure and runs in the infraorbital groove and canal with the infraorbital nerve. When the small middle superior alveolar artery is present, it runs down the lateral wall of the maxillary sinus and forms anastomotic arcades with the anterior and posterior vessels, terminating near the canine tooth. The anterior superior alveolar artery curves through the canalis sinuosus to supply the upper incisor and canine teeth and the mucous membrane in the maxillary sinus. The canalis sinuosus swerves laterally from the infraorbital canal and inferomedially below it in the wall of the maxillary sinus, following the rim of the anterior nasal aperture, between the alveoli of canine and incisor teeth and the nasal cavity. It ends near the nasal septum where its terminal branch emerges. The canal may be up to 55 mm long.

Inferior alveolar artery

The inferior alveolar (dental) artery, a branch of the maxillary artery, descends in the infratemporal fossa posterior to the inferior alveolar nerve. Here, it lies between bone laterally and the sphenomandibular ligament medially. Before entering the mandibular foramen it gives off a mylohyoid branch, which pierces the sphenomandibular ligament to descend with the mylohyoid nerve in its groove on the inner surface of the ramus of the mandible. The mylohyoid artery ramifies superficially on the muscle and anastomoses with the submental branch of the facial artery. The inferior alveolar artery then traverses the mandibular canal with the inferior alveolar nerve to supply the mandibular molars and premolars and divides into the incisive and mental branches near the first premolar.

The incisive branch continues below the incisor teeth (which it supplies) to the midline, where it anastomoses with its fellow, although few anastomotic vessels cross the midline. In the canal the arteries supply the mandible, tooth sockets and teeth via branches which enter the minute hole at the apex of each root to supply the pulp. The mental artery leaves the mental foramen and supplies the chin and anastomoses with the submental and inferior labial arteries. Near its origin the inferior alveolar artery has a lingual branch, which descends with the lingual nerve to supply the lingual mucous membrane. The pattern of branching of the inferior alveolar artery reflects that of the nerves of the same name.

Arterial supply of periodontal ligaments

The periodontal ligaments supporting the teeth are supplied by dental branches of alveolar arteries. One branch enters the alveolus apically and sends two or three small rami into the dental pulp through the apical foramen, and other rami into the periodontal ligament. Interdental arteries ascend in the interdental septa, sending branches at right angles into the periodontal ligament, and terminate by communicating with gingival vessels that also supply the cervical part of the ligament. The periodontal ligament therefore receives its blood from three sources: from the apical region; ascending interdental arteries; and descending vessels from the gingivae. These vessels anastomose with each other, which means that when the pulp of a tooth is removed during endodontic treatment, the attachment tissues of the tooth remain vital.

Venous drainage of the teeth

Veins accompanying the superior alveolar arteries drain the upper jaw and teeth anteriorly into the facial vein, or posteriorly into the pterygoid venous plexus. Veins from the lower jaw and teeth collect either into larger vessels in the interdental septa or into plexuses around the root apices and thence into several inferior alveolar veins. Some of these veins drain through the mental foramen to the facial vein; others drain via the mandibular foramen to the pterygoid venous plexus.

Lymphatic drainage of the teeth

The lymph vessels from the teeth usually run directly into the ipsilateral submandibular lymph nodes. Lymph from the mandibular incisors, however, drains into the submental lymph nodes. Occasionally, lymph from the molars may pass directly into the jugulodigastric group of nodes.

INNERVATION OF THE TEETH

The regional innervation of the teeth and gingivae is shown in Table 30.2. The teeth in the upper jaw are supplied by the superior alveolar nerves, while those in the lower jaw are supplied by the inferior alveolar nerve.

Superior alveolar nerves

The teeth in the upper jaw are supplied by the three superior alveolar (dental) nerves which arise from the maxillary nerve in the pterygopalatine fossa or in the infraorbital groove and canal. The posterior superior alveolar (dental) nerve leaves the maxillary nerve in the pterygopalatine fossa and runs anteroinferiorly to pierce the infratemporal surface of the maxilla, at which point it is possible to perform a local anaesthetic block which will anaesthetize the pulps of the premolar and molar ipsilateral teeth, and then descends under the mucosa of the maxillary sinus. After supplying the lining of the sinus the nerve divides into small branches which link up as the molar part of the superior alveolar plexus, supplying twigs to the molar teeth. It also supplies a branch to the upper gingivae and the adjoining part of the cheek.

The middle superior alveolar (dental) nerve arises from the infraorbital nerve as it runs in the infraorbital groove, and runs downwards and forwards in the lateral wall of the maxillary sinus. It ends in small branches which link up with the superior dental plexus, supplying small rami to the upper premolar teeth. This nerve is variable, and it may be duplicated or triplicated or absent.

The anterior superior alveolar (dental) nerve leaves the lateral side of the infraorbital nerve near the midpoint of its canal and traverses the canalis sinuosus in the anterior wall of the maxillary sinus. It curves first under the infraorbital foramen, then passes medially towards the nose and finally turns downwards and divides into branches to supply the incisor and canine teeth. It assists in the formation of the superior dental plexus and it gives off a nasal branch, which passes through a minute canal in the lateral wall of the inferior meatus to supply the mucous membrane of the anterior area of the lateral wall as high as the opening of the maxillary sinus, and the floor of the nasal cavity. It communicates with the nasal branches of the pterygopalatine ganglion and finally emerges near the root of the anterior nasal spine to supply the adjoining part of the nasal septum.

Inferior alveolar (dental) nerve

The course of the inferior alveolar nerve in the infratemporal fossa is described in Chapter 31. Just before entering the mandibular canal the inferior alveolar nerve gives off a small mylohyoid branch which pierces the sphenomandibular ligament and enters a shallow groove on the medial surface of the mandible, following a course roughly parallel to its parent nerve. It passes below the origin of mylohyoid to lie on the superficial surface of the muscle, between it and the anterior belly of digastric, both of which it supplies. It gives a few filaments to supply the skin over the point of the chin.

In the mandibular canal, the inferior alveolar nerve runs downward and forward, generally below the apices of the teeth until below the first and second premolars where it divides into terminal incisive and mental branches. The incisive branch continues forward in a bony canal or in a plexiform arrangement, giving off branches to the first premolar, canine and incisor teeth, and the associated labial gingivae. The lower central incisor teeth receive a bilateral innervation, fibres probably crossing the midline within the periosteum to re-enter the bone via numerous canals in the labial cortical plate.

The mental nerve passes upward, backward and outward to emerge from the mandible via the mental foramen between and just below the apices of the premolar teeth. It immediately divides into three branches, two of which pass upward and forward to form an incisor plexus labial to the teeth, supplying the gingiva (and probably the periosteum). From this plexus and the dental branches, fibres turn downwards and then lingually to emerge on the lingual surface of the mandible on the posterior aspect of the symphysis or opposite the premolar teeth, probably communicating with the lingual or mylohyoid nerve. The third branch of the mental nerve passes through the intermingled fibres of depressor anguli oris and platysma to supply the skin of the lower lip and chin. Branches of the mental nerve also communicate with terminal filaments of the mandibular branch of the facial nerve.

Variations in the fascicular organization of the inferior alveolar nerve are clinically important when extracting impacted third molars. The nerve may appear as a single bundle lying a few millimetres below the roots of the teeth, or it may lie much lower and almost reach the lower border of the bone, so that it gives off a variable number of large rami which pass anterosuperiorly towards the roots before dividing to supply the teeth and interdental septa. Only rarely is it plexiform. The nerve may lie on the lingual or buccal side of the mandible (slightly more commonly on the buccal side). Even when the third molar tooth is in a normal position, the nerve may be so intimately related to it that it grooves its root. Exceptionally the nerve may be similarly related to the second molar.

Nerves may pass from the substance of temporalis to enter the mandible through the retromolar fossa or the condylar head, where they communicate with branches of the inferior alveolar nerve. Foramina occur in some 10% of retromolar fossae and infiltration in this region can abolish the sensation which occasionally remains after an inferior alveolar nerve block. Similarly, branches from the buccal, mylohyoid and lingual nerves may enter the mandible and provide additional routes of sensory transmission from the teeth. Thus, even when the inferior alveolar nerve has been anaesthetized correctly, pain may still be experienced by a patient when undergoing dental cavity preparation.

Pain sensation in teeth

The teeth are supplied by nociceptors that generate pain sensation of a very high order. The mechanism underlying this sensitivity is of considerable clinical significance and is controversial. Currently, the most widely accepted view is that fluid movements through the dentine tubules stimulate nerve endings at the periphery of the dental pulp (hydrodynamic hypothesis).

Local analgesia

It is technically possible to achieve profound regional anaesthesia by depositing local anaesthetic solution adjacent to the trigeminal nerve trunks or their branches within the infratemporal fossa. These injections can either be performed transorally – posterior superior alveolar nerve block, maxillary nerve block, inferior alveolar nerve block, lingual nerve block and mandibular nerve block – or more rarely by an external route through the skin of the face – maxillary nerve block, inferior alveolar nerve block and mandibular nerve block.

In the case of the mandible, the anterior teeth can be anaesthetized by simple diffusion techniques as the bone is relatively thin. However, this is not adequate for the cheek teeth due to the increased thickness of the bone. In this case, the inferior alveolar nerve has to be anaesthetized before it enters the inferior alveolar canal. The needle has to be placed within the pterygomandibular space to achieve a successful inferior alveolar nerve block. The lingual nerve is also usually blocked, as it lies close to the inferior alveolar nerve. Because of the other structures within the infratemporal fossa, it is vitally important that the operator has a detailed knowledge of the anatomy in this region to understand, and therefore try to avoid, the complications that may arise. Any damage to blood vessels in the infratemporal fossa, generally the pterygoid venous plexus, can lead to haematoma formation. In extreme cases, bleeding can track through the inferior orbital fissure resulting in a retrobulbar haematoma, which can result in loss of visual acuity or blindness. Intravascular injection of local anaesthetic solution (which usually contains adrenaline [epinephrine]) can have profound systemic effects and for this reason an aspirating syringe is always used to check that the needle has not entered a vessel prior to injection (vessels in this area that theoretically may be entered include the maxillary and internal carotid arteries). If the needle is placed too medially, it may enter medial pterygoid, while if directed too laterally, it may penetrate temporalis. In either case, there will be lack of anaesthesia followed later by trismus. If the needle is placed too deeply, anaesthetic solution may cause a temporary facial nerve palsy due to loss of conduction from the facial nerve in the region of the parotid gland.

SALIVARY GLANDS

Salivary glands are compound, tubuloacinar exocrine glands whose ducts open into the oral cavity. They secrete saliva, a fluid which lubricates food to assist deglutition, moistens the buccal mucosa, which is important for speech, and provides an aqueous solvent necessary for taste and a fluid seal for sucking and suckling. They also secrete digestive enzymes, e.g. salivary amylase, and antimicrobial agents, e.g. immunoglobulin A (IgA), lysozyme and lactoferrin, into saliva. Conditions where there is a significant decrease in the production of saliva (xerostomia) may result in periodontal inflammation and dental caries. An illustration of the position of the major salivary glands and their ducts is shown in Fig. 30.31.

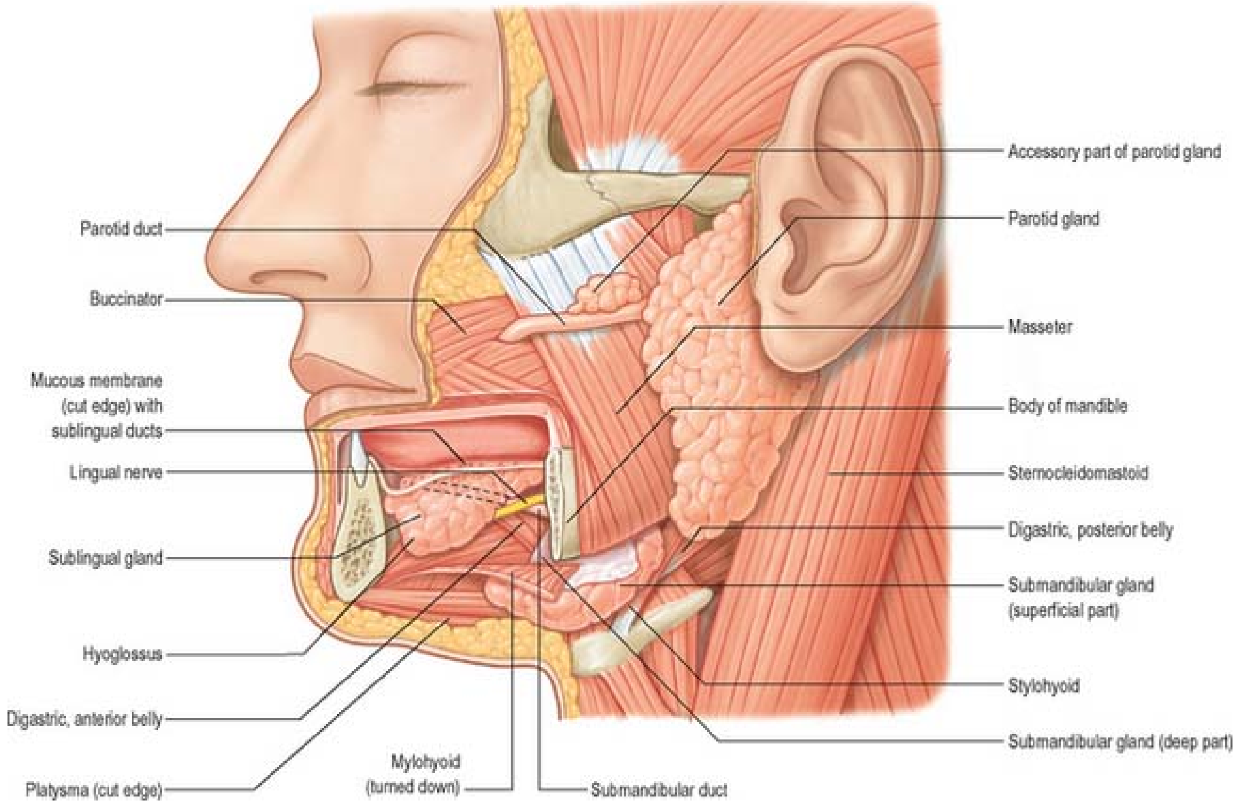
Parotid duct
Buccinator
Mucous membrane (cut edge) with sublingual ducts
Lingual nerve
Sublingual gland
Hyoglossus
Digastric, anterior belly
Platysma (cut edge)
Mylohyoid (turned down)
Submandibular duct
Accessory part of parotid gland
Parotid gland
Masseter
Body of mandible
Sternocleidomastoid
Digastric, posterior belly
Submandibular gland (superficial part)
Stylohyoid
Submandibular gland (deep part)

Fig. 30.31 The salivary glands of the left side. The cranial region of the superficial part of the submandibular gland has been excised and mylohyoid

has been cut and turned down to expose a portion of the deep part of the gland.

The major salivary glands are the paired parotid, submandibular and sublingual glands. In addition, there are numerous minor salivary glands scattered throughout the oral mucosa and submucosa.

Approximately 0.5 L of saliva is secreted per day. Salivary flow rates are typically 0.3 mL/min when unstimulated, and rise to 1.5–2 mL/min when stimulated. Flow rate is negligible during sleep. In the unstimulated state, the parotid gland contributes 20%, the submandibular gland 65%, and the sublingual and minor salivary glands 15% of the daily output of saliva. When stimulated, the parotid contribution rises to 50%.

PAROTID GLAND

The parotid gland is the largest salivary gland. It is almost entirely serous. The parotid duct runs through the cheek and drains into the mouth opposite the maxillary second permanent molar tooth. The parotid gland is situated in front of the external ear and is described in detail in relation to the face (see Ch. 29).

SUBMANDIBULAR SALIVARY GLAND

The submandibular gland is irregular in shape and about the size of a walnut. It consists of a larger superficial and a smaller deep part, continuous with each other around the posterior border of mylohyoid. It is a seromucous (but predominantly serous) gland.

Superficial part of the submandibular gland

The superficial part of the gland is situated in the digastric triangle where it reaches forward to the anterior belly of digastric and back to the stylomandibular ligament, by which it is separated from the parotid gland. Above, it extends medial to the body of the mandible. Below, it usually overlaps the intermediate tendon of digastric and the insertion of stylohyoid. This part of the submandibular gland presents inferior, lateral and medial surfaces, and is partially enclosed between two layers of deep cervical fascia that extend from the greater cornu of the hyoid bone. The superficial layer is attached to the lower border of the mandible and covers the inferior surface of the gland. The deep layer is attached to the mylohyoid line on the medial surface of the mandible and covers the medial surface of the gland.

The inferior surface, covered by skin, platysma and deep fascia, is crossed by the facial vein and the cervical branch of the facial nerve. Near the mandible the submandibular lymph nodes are in contact with the gland and some may be embedded within it.

The lateral surface is related to the submandibular fossa on the medial surface of the body of the mandible and the mandibular attachment of medial pterygoid. The facial artery grooves its posterosuperior part, lies at first deep to the gland and then emerges between its lateral surface and the mandibular attachment of the medial pterygoid to reach the lower border of the mandible.

The medial surface is related anteriorly to mylohyoid, from which it is separated by the mylohyoid nerve and vessels and branches of the submental vessels. More posteriorly, it is related to styloglossus, the stylohyoid ligament and the glossopharyngeal nerve, which separate it from the pharynx. In its intermediate part the medial surface is related to hyoglossus, from which it is separated by styloglossus, the lingual nerve, submandibular ganglion, hypoglossal nerve and deep lingual vein (sequentially from above down). Below, the medial surface is related to the stylohyoid muscle and the posterior belly of digastric.

Deep part of the submandibular gland

The deep part of the gland extends forwards to the posterior end of the sublingual gland. It lies between mylohyoid inferolaterally, hyoglossus and styloglossus medially, the lingual nerve superiorly, and the hypoglossal nerve and deep lingual vein inferiorly (Fig. 30.10).

Vascular supply and lymphatic drainage

The arteries supplying the gland are branches of the facial and lingual arteries. The lymph vessels drain into the deep cervical group of lymph nodes (particularly the jugulo-omohyoid node), interrupted by the submandibular nodes.

Innervation

The secretomotor supply to the submandibular gland is derived from the submandibular ganglion. This is a small, fusiform body which lies on the upper part of hyoglossus. There are additional ganglion cells in the hilum of the gland. Like the ciliary, pterygopalatine and otic ganglia, the submandibular is a peripheral parasympathetic ganglion. It is superior to the deep part of the submandibular gland and inferior to the lingual nerve, and is suspended from the latter by anterior and posterior filaments. Though related to the lingual nerve, the ganglion is connected functionally with the facial nerve and its chorda tympani branch.

As with the other cranial parasympathetic ganglia, there are three roots associated with the submandibular ganglion. The motor, parasympathetic root is the posterior filament which connects it to the lingual nerve. This conveys preganglionic fibres from the superior salivatory nucleus which travel in the facial, chorda tympani and lingual nerves to the ganglion, where they synapse. The postganglionic fibres are secretomotor to the submandibular and sublingual salivary glands. Some fibres may also reach the parotid gland. The sympathetic root is derived from the plexus on the facial artery. It consists of postganglionic fibres from the superior cervical ganglion which traverse the submandibular ganglion without synapsing. They are vasomotor to the blood vessels of the submandibular and sublingual glands. Five or six branches from the ganglion supply the submandibular gland and its duct. Other fibres pass through the anterior filament that connects the submandibular gland to the lingual nerve and are carried to the sublingual and anterior lingual glands. Sensory fibres are derived from the lingual nerve.

Submandibular duct

The submandibular duct is usually 5 cm long and has a thinner wall than the parotid duct. It begins from numerous tributaries in the superficial part of the gland and emerges from the medial surface of this part of the gland behind the posterior border of mylohyoid. It traverses the deep part of the gland, and then passes at first up and slightly back for approximately 5 mm, this sharp bend over the free edge of mylohyoid being known as the genu of the duct. It then runs forwards between mylohyoid and hyoglossus passing between the sublingual gland and genioglossus to open in the floor of the mouth on the summit of the sublingual papilla at the side of the frenulum of the tongue (Figs 30.4, 30.10). It lies between the lingual and hypoglossal nerves on hyoglossus, but, at the anterior border of the muscle, it is crossed laterally by the lingual nerve, terminal branches of which ascend on its medial side. As the duct traverses the deep part of the gland it receives small tributaries draining this part of the gland. It has been suggested previously that the genu of the duct predisposes to the stasis of saliva and thereby encourages salivary stone (sialolith) formation, but this is somewhat controversial and largely unproven.

Like the parotid gland, the duct system of the submandibular gland can be visualized by sialography (Fig. 30.32).

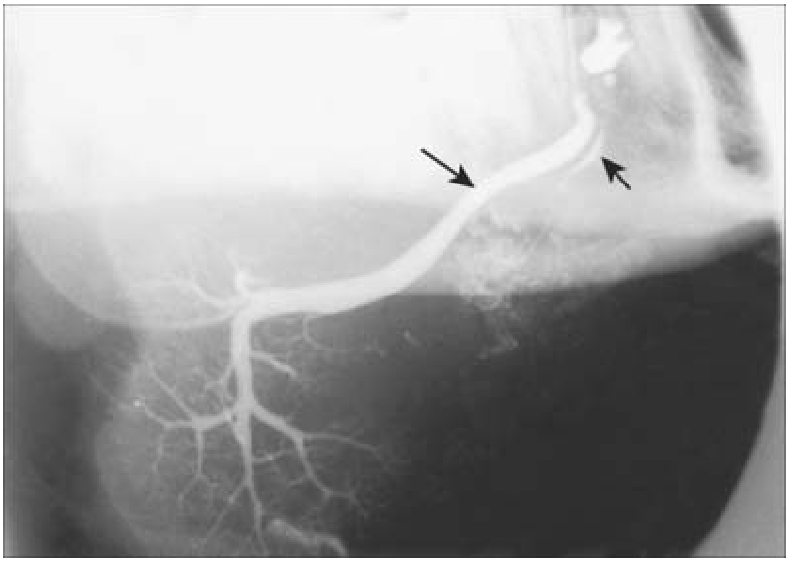

Fig. 30.32 Sialogram showing a normal submandibular duct (long arrow). Unusually, a sublingual duct is also evident (short arrow).

(By courtesy of Dr N. Drage.)

SUBLINGUAL SALIVARY GLAND

The sublingual gland is the smallest of the main salivary glands: each gland is narrow, flat, shaped like an almond, and weighs approximately 4 g. The sublingual gland lies on mylohyoid, and is covered by the mucosa of the floor of the mouth, which is raised as a sublingual fold (Fig. 30.4). The anterior end of the contralateral sublingual gland lies in front, and the deep part of the submandibular gland lies behind. The mandible above the anterior part of the mylohyoid line, the sublingual fossa, is lateral, and genioglossus is medial, separated from the gland by the lingual nerve and submandibular duct.

The sublingual glands are seromucous, but predominantly mucous.

Vascular supply, innervation and lymphatic drainage

The arterial supply is from the sublingual branch of the lingual artery and the submental branch of the facial artery. Innervation is via the submandibular ganglion. Lymphatic drainage is to the submental nodes.

Sublingual ducts

The sublingual gland has 8–20 excretory ducts (Fig. 30.10). Smaller sublingual ducts open, usually separately, from the posterior part of the gland onto the summit of the sublingual fold (a few sometimes open into the submandibular duct). Small rami from the anterior part of the gland sometimes form a major sublingual duct (Bartholin's duct), which opens with, or near to, the orifice of the submandibular duct. This duct may be visualized occasionally in a submandibular sialogram (Fig. 30.32).

Ranula

If the ducts draining any salivary gland become obstructed, the gland itself is at risk of developing a retention cyst where the retained secretions dilate the gland itself rather like a balloon. This phenomenon is seen mostly in the minor salivary glands which line the lips and oral cavity, where it is known as a mucocele. Trauma such as persistent lip biting results in scarring of the overlying oral mucosa and obstruction of the small drainage duct. When trauma occurs in the floor of the mouth and obstructs the drainage duct/s of the sublingual gland, the resulting retention cyst is known as a ranula. (Ranula is the Latin name for a frog and is used here because the tense cystic swelling is said to resemble the throat of a croaking frog.)

A ranula usually presents as a large tense bluish swelling anteriorly in the floor of the mouth just to one side of the midline, which often displaces the tongue. Occasionally the developing retention cyst herniates through a midline dehiscence where the two mylohyoid muscles fail to meet in the midline anteriorly, and then the ranula may present as a submental swelling or as a combined submental and floor of mouth swelling, a ‘plunging’ ranula. The treatment of a ranula is excision of the sublingual gland responsible.

MINOR SALIVARY GLANDS

The minor salivary glands of the mouth include the labial, buccal, palatoglossal, palatal and lingual glands. The labial and buccal glands contain both mucous and serous elements. The palatoglossal glands are mucous glands and are located around the pharyngeal isthmus. The palatal glands are mucous glands and occur in both the soft and hard palates. The anterior and posterior lingual glands are mainly mucous. The anterior glands are embedded within muscle near the ventral surface of the tongue and open by means of four or five ducts near the lingual frenulum and the posterior glands are located in the root of the tongue. The deep posterior lingual glands are predominantly serous. Serous glands (of von Ebner) occur around the circumvallate papillae, their secretion is watery, and they probably assist in gustation by spreading taste stimuli over the taste buds and then washing them away.

MICROSTRUCTURE

Salivary glands have numerous lobes composed of smaller lobules separated by dense connective tissue which is continuous with the capsule of the gland, and contains excretory (collecting) ducts, blood vessels, lymph vessels, nerve fibres and small ganglia. Each lobule has a single duct, whose branches terminate at dilated secretory ‘endpieces’, which are tubular or acinar in shape (Fig. 30.33). Their primary secretion is modified as it flows through intercalated, striated and excretory ducts into one or more main ducts which discharge saliva into the oral cavity. They contain a variable amount of intralobular adipose tissue: adipocytes are particularly numerous in the parotid gland.

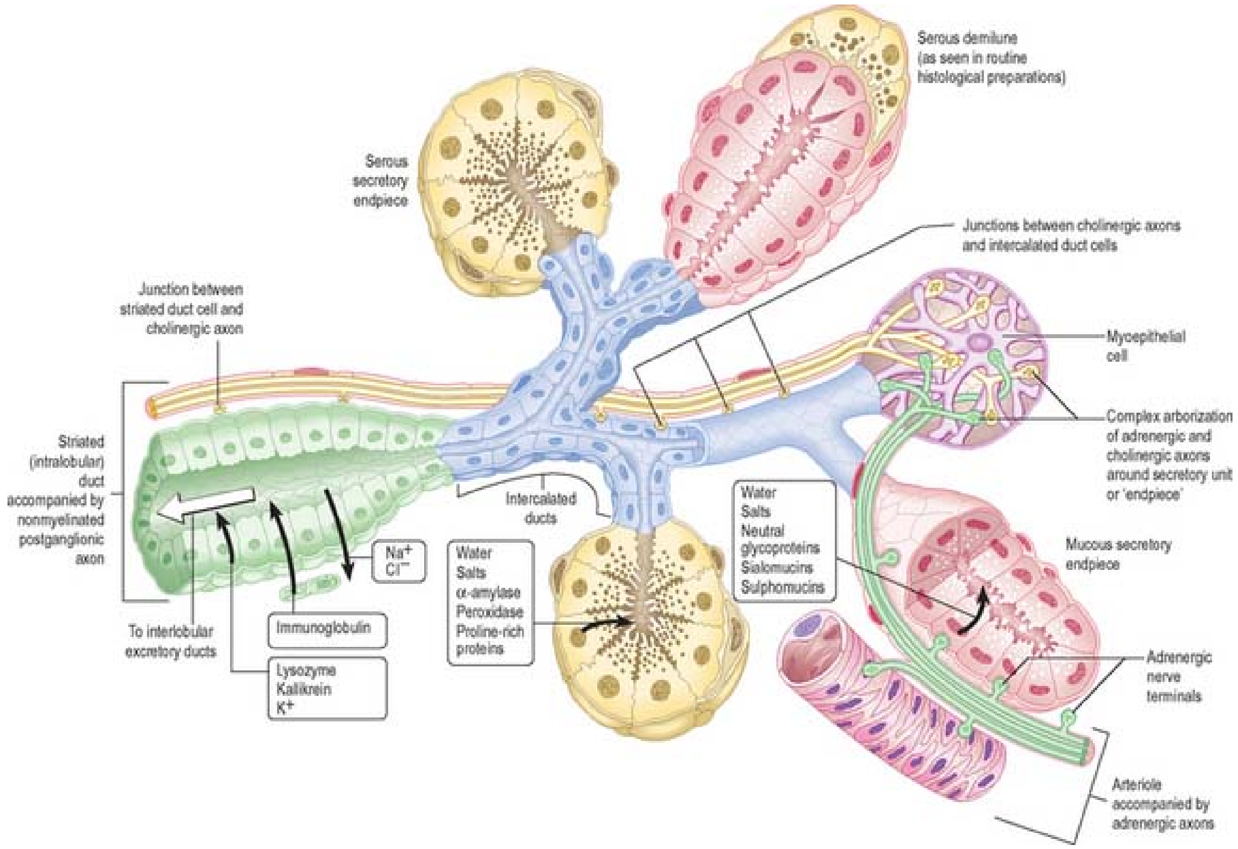
Serous demilune (as seen in routine histological preparations)
Serous secretory endpiece
Junctions between cholinergic axons and intercalated duct cells
Junction between striated duct cell and cholinergic axon
Myoepithelial cell
Complex arborization of adrenergic and cholinergic axons around secretory unit or 'endpiece'
Striated (intralobular) duct accompanied by nonmyelinated postganglionic axon
Intercalated ducts
Na^+ Cl^-
Water Salts α-amylase Peroxidase Proline-rich proteins
Water Salts Neutral glycoproteins Sialomucins Sulphomucins
Mucous secretory endpiece
To interlobular excretory ducts
Immunoglobulin
Lysozyme Kallikrein K^+
Adrenergic nerve terminals
Arteriole accompanied by adrenergic axons

Fig. 30.33 Architecture of a generalized salivary gland. Solid black arrows indicate the direction of transport of salivary components and the

open white arrow the direction of salivary flow. The innervation of the ducts, secretory units and arterioles is shown.

The secretory endpieces of the human parotid gland are almost exclusively serous acini (Fig. 30.34A): mucous tubules or acini are rare. In the submandibular gland, secretory units are predominantly serous acini, with some mucous tubules and acini (Fig. 30.34B). Mucous tubules are often associated with groups of serous cells at their blind ends, appearing as crescent-shaped serous demilunes in routine histological preparations. However, this appears to be a fixation artefact, as tissue prepared by rapid freezing methods lacks serous demilunes and the serous secretory cells align with mucous cells around a common lumen. In the sublingual gland, mucous tubules and acini predominate (Fig. 30.34C), but serous cells also occur, as acini or as serous demilunes.

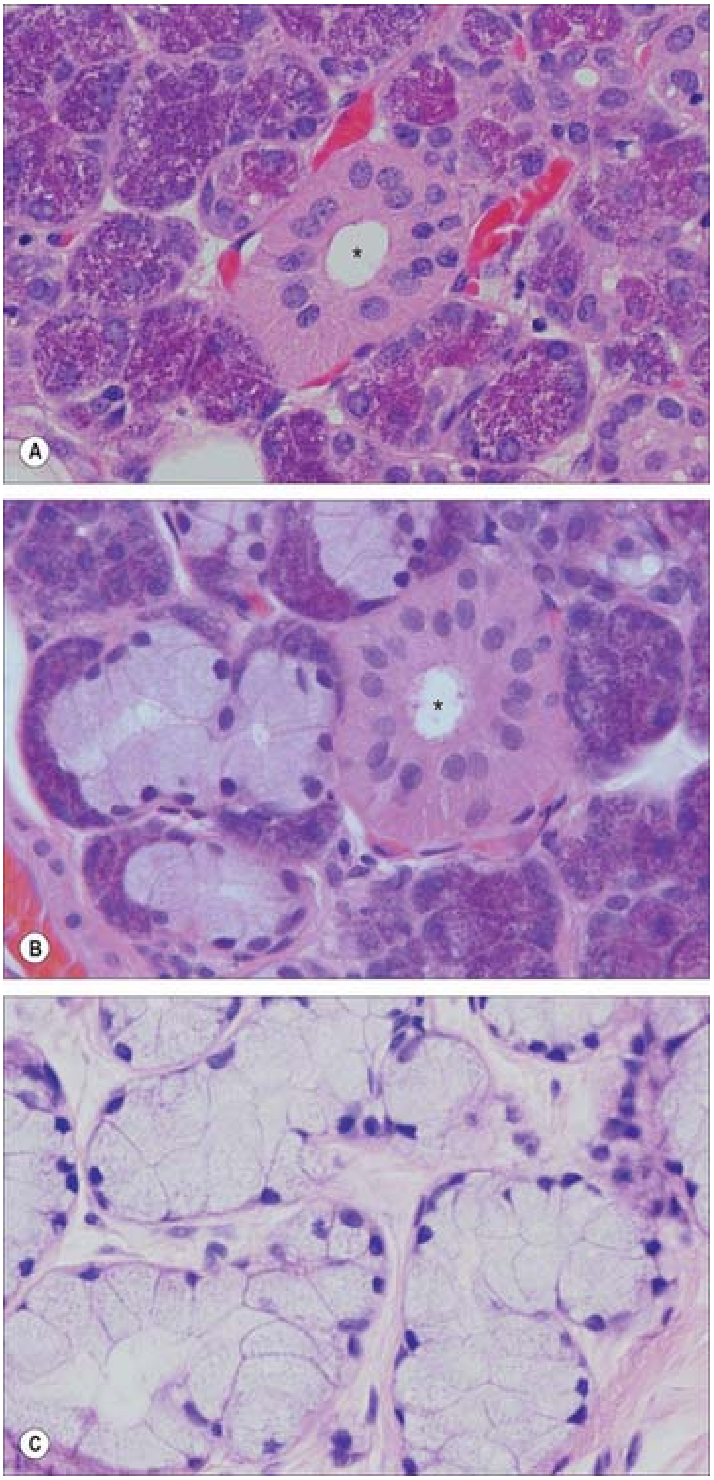

Fig. 30.34 The microstructure of the salivary glands. **A**, Parotid gland; **B**, mixed secretory units of the submandibular gland; **C**, mucous acini in the sublingual gland. Asterisks indicate the lumen of a striated duct.

(By courtesy of Mr Peter Helliwell and Dr Joseph Mathew, Department of Histopathology, Royal Cornwall Hospitals Trust, UK.)

Serous cells are approximately pyramidal in shape. Their nuclei vary in shape and position, but are more rounded and situated less basally than in mucous cells. Apically, the cytoplasm is filled by proteinaceous secretory (zymogen) granules with high amylase activity. Additionally, serous cells secrete kallikrein, lactoferrin and lysozyme, an antibacterial enzyme whose synthesis has been localized in particular to the serous demilunes of the submandibular and sublingual glands, and which is important in the defence against oral pathogens. In the human parotid and submandibular glands, zymogen granules also show a positive periodic acid–Schiff staining reaction, which indicates the presence of polysaccharides, and some texts refer to these cells as seromucous. Mucous cells are cylindrical and have flattened, basal nuclei. Their apical cytoplasm is typically packed with large, pale-staining and electron-translucent secretory droplets.

Ducts

Intercalated, striated (both intralobular) and extralobular collecting ducts lead consecutively from the secretory endpieces. The lining cells of intercalated ducts are flat nearest the secretory endpiece, but become cuboidal. Intercalated ducts function primarily as a conduit for saliva but, together with the striated ducts, may also modify its content of electrolytes and secrete IgA. Striated ducts are lined by a low columnar epithelium and are so called because their lining cells have characteristic basal striations. The latter are regions of highly infolded basal plasma membrane, between which lie columns of vertically aligned mitochondria. The nuclei are consequently displaced by the basal striations from a typical ductal basal position to a central or even apical location (Fig. 30.34). Infolding of the basal plasma membrane, and local abundance of mitochondria, are typical features of epithelial cells which actively transport electrolytes. Here, the cells transport potassium and bicarbonate into saliva: they produce a hypotonic saliva by reabsorbing sodium and chloride ions in excess of water. Striated ducts modify electrolyte composition and secrete IgA, lysozyme and kallikrein. IgA is produced by subepithelial plasma cells and transported transcytotically across the epithelial barrier to be secreted, once it has been dimerized by epithelial secretory component, into the saliva. This is also a function of serous acinar cells and other secretory epithelia, notably the lactating breast (see Ch. 54). The intralobular ductal system of the sublingual gland is less well developed than that of the parotid and submandibular glands.

Collecting ducts are metabolically relatively inert conduits which run within interlobular connective tissue septa in the glands. They transport saliva to the main duct which opens onto the mucosal surface of the buccal cavity. The lining epithelium of collecting ducts varies. It may be pseudostratified columnar, stratified cuboidal or columnar in the larger ducts, and has a distinct basal layer. It becomes a stratified squamous epithelium near the buccal orifice.

Myoepithelial cells

Myoepithelial cells (Fig. 30.33) are contractile cells (see Ch. 2) associated with secretory endpieces and with much of the ductal system. They lie between the basal lamina and the epithelial cells proper. They extend numerous cytoplasmic processes around serous acini and are often termed basket cells. Myoepithelial cells associated with ducts are more fusiform in shape, and are aligned along the length of the duct. Their cytoplasm contains abundant actin microfilaments which mediate contraction under the control of both sympathetic and parasympathetic stimulation. The outflow of saliva is thus accelerated through reduction in the luminal volume of secretory endpieces and ducts, contributing to the secretory pressure.

CONTROL OF SALIVARY GLAND ACTIVITY

The observed wide and rapid variation in the composition, quantity and rate of salivary secretion in response to various stimuli suggests an elaborate control mechanism. Secretion may be continuous, but at a low resting level, and may also occur spontaneously. It is mainly a response to the drying of the oral and pharyngeal mucosae. A rapid increase can be superimposed on the resting level, e.g. during mastication or when stimulated by the autonomic innervation. The controlled variation in the activity of the many types of salivary effector cells (serous, seromucous and mucous secretory cells, myoepithelial cells, epithelial cells of all the ductal elements and the smooth muscle of local blood vessels) affects the quantity and quality of saliva. There is no clear evidence that circulating hormones evoke secretion directly at physiological levels, but they may alter the response of glandular cells to neural stimuli.

The control of salivation depends on reflex nerve impulses. The afferent inputs to the reflex arc pass to brainstem salivatory centres, especially from taste and mechanoreceptors in the mouth. A variety of other sensory modalities in and around the mouth are also involved, e.g. smell, for certain aspects of submandibular secretion in man. The afferent input is integrated centrally by the salivatory centres, which are themselves influenced by higher centres. The latter may provide facilitatory or inhibitory influences, which presumably explains why the mouth becomes dry under stress. The efferent drive to the glands passes via parasympathetic and sympathetic outputs from the centres. Relatively little is known about the connections of the preganglionic parasympathetic neurones in the salivatory centres, and virtually nothing is known about either the central location of the sympathetic preganglionic neurones, or the output pathways. No peripheral inhibitory mechanisms exist in the glands.

The typical pattern of innervation is shown in Fig. 30.33, but details vary in different glands, and with age. Only the more constant features are illustrated and described here. Cholinergic nerves often accompany ducts and arborize freely around secretory endpieces, but adrenergic nerves usually enter glands along arteries and ramify with them. The main secretomotor nerves are predominantly non-myelinated axons: the few myelinated axons that have been seen are presumably either preganglionic efferent or visceral afferent. Within the glands the nerve fibres intermingle, such that cholinergic and adrenergic axons often lie in adjacent invaginations of one Schwann cell. Secretion and vasoconstriction are mediated via separate sympathetic axons. A single parasympathetic axon may, through serial en passant terminals, induce vasodilatation, secretion and myoepithelial contraction.

Secretory endpieces are usually the most densely innervated structures in the gland: individual cells often have both cholinergic and adrenergic innervation. Secretion of water and electrolytes, which creates the foundation for the volume of saliva secreted, is the outcome of a complex set of processes which is largely induced by parasympathetic impulses. Secretion of protein is an ongoing constitutive process wherever it occurs. The regulated exocytosis of pre-packaged proteins, which is the principal source of protein secretion into saliva, depends on the relative levels of activity in sympathetic and parasympathetic fibres.

The ductal elements of salivary glands can markedly modify the composition of saliva. They are less densely innervated than secretory endpieces but their activity is also under neural control. Adrenal aldosterone promotes resorption of sodium and release of potassium into saliva by striated ductal cells, as it does in kidney tubules. Myoepithelial contraction is stimulated mainly by adrenergic innervation, but there may be an additional role for cholinergic axons.

TISSUE SPACES AROUND THE JAWS

The dissemination of infection in soft tissues is influenced by the natural barriers presented by bone, muscle and fascia. However, the tissue spaces around the jaws are primarily defined by muscles, principally mylohyoid, buccinator, masseter, medial pterygoid, superior constrictor and orbicularis oris (Fig. 30.35). None of these ‘spaces’ is actually empty and they should merely be regarded as potential spaces that are normally occupied by loose connective tissue. It is only when inflammatory products such as hyaluronase destroy the loose connective tissue that a definable space is produced.

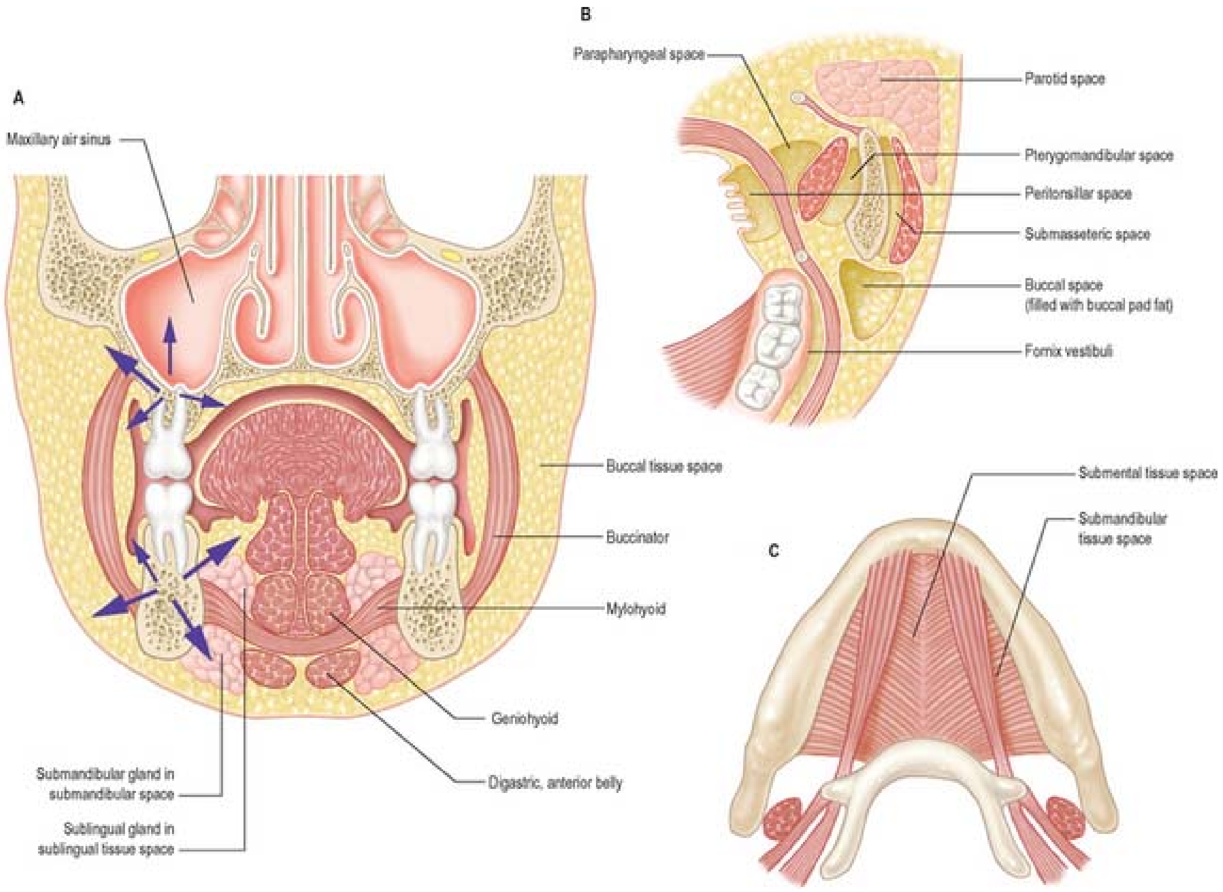
B
Parapharyngeal space
Parotid space
Pterygomandibular space
Peritonsillar space
Submasseteric space
Buccal space
(filled with buccal pad fat)
Fornix vestibuli
A
Maxillary air sinus
Buccal tissue space
Buccinator
Mylohyoid
Geniohyoid
Digastric, anterior belly
Submandibular gland in
submandibular space
Sublingual gland in
sublingual tissue space
C
Submental tissue space
Submandibular
tissue space

Fig. 30.35 Potential tissue spaces around the jaws. **A**, Coronal section showing the sublingual and submandibular spaces in the floor of the mouth and the possible routes for the spread of infections from periapical dental abscesses (left). **B**, Horizontal section through the mandibular molar region

showing the associated tissue spaces. **C**, Inferior view of the floor of the mouth (suprahyoid region of the neck) showing the position of the submandibular and sublingual tissue spaces.

*(**B** and **C**, By permission from Berkovitz BKB, Moxham BJ 2002 Head and Neck Anatomy. London: Martin Dunitz.)*

The spaces are paired except for the submental, sublingual and palatal spaces.

POTENTIAL TISSUE SPACES AROUND THE LOWER JAW

The important potential tissue spaces of the lower jaw are the submental, submandibular, sublingual, buccal, submasseteric, parotid, pterygomandibular, peritonsillar, parapharyngeal and retropharyngeal spaces (Fig. 30.35).

The submental and submandibular spaces are located below the inferior border of the mandible beneath mylohyoid, in the suprahyoid region of the neck. The submental space lies beneath the chin in the midline, between the mylohyoid muscles and the investing layer of deep cervical fascia. It is bounded laterally by the two anterior bellies of the digastric muscles. The submental space communicates posteriorly with the two submandibular spaces. The submandibular space is situated between the anterior and posterior bellies of the digastric muscle and communicates with the sublingual space around the posterior free border of mylohyoid. The sublingual space lies in the floor of the mouth, above the mylohyoid muscles, and is continuous across the midline: it communicates with the submandibular spaces over the posterior free borders of the mylohyoid muscles, helped by the submandibular gland's slight extension over this edge.

The remaining tissue spaces are illustrated in Fig. 30.35B. The buccal space is located in the cheek, on the lateral side of buccinator. The submasseteric spaces are a series of spaces between the lateral surface of the ramus of the mandible and masseter: they are formed because the fibres of masseter have multiple insertions onto most of the lateral surface of the ramus. The pterygomandibular space lies between the medial surface of the ramus of the mandible and medial pterygoid, and the parotid space lies behind the ramus of the mandible, in and around the parotid gland. The parapharyngeal space is bounded by the superior constrictor of the pharynx and the medial surface of medial pterygoid. It is restricted to the infratemporal region of the head and the suprahyoid region of the neck and communicates with the retropharyngeal space, which itself extends into the retrovisceral space in the lower part of the neck (the tissue spaces of the neck are described in Chapter 28, and of the pharynx in Chapter 33). The peritonsillar space lies around the palatine tonsil between the pillars of the fauces, and is part of the intrapharyngeal space. It is bounded by the medial surface of the superior constrictor of the pharynx and its mucosa.

POTENTIAL TISSUE SPACES AROUND THE UPPER JAW

The tissue spaces of the upper jaw are usually associated with spread of infection from the teeth. They are the canine (infraorbital), palatal and infratemporal spaces. The canine (infraorbital) space associated with the canine fossa lies between the levator labii superioris and zygomaticus muscles. The palatal space is not truly a tissue space in the hard palate, as the mucosa there is firmly bound to the periosteum. However, inflammation can strip away some of this periosteum to produce a well-circumscribed abscess. The infratemporal space is the upper extremity of the pterygomandibular space. It is closely related to the maxillary tuberosity and therefore the upper molars.

DENTAL ABSCESS

Abscesses developing in relation to the apices of roots ultimately penetrate the surrounding bone where it is thinnest. The position of the resultant swelling in the soft tissues is largely determined by the relationship between muscle attachments and the sinus (the path taken by the infected material) in the bone. Thus, in the lower incisor region, because the labial bone is thin, abscesses generally appear as a swelling in the labial sulcus, above the attachment of mentalis. The abscess may open below mentalis, when it will point beneath the chin. If an abscess from a lower postcanine tooth opens below the attachment of buccinator, the swelling is in the neck; if it opens above, the swelling is in the buccal sulcus. If an abscess opens lingually above mylohyoid, the swelling is in the lingual sulcus; if it is below, the swelling is in the neck. Third molar abscesses tend to track into the neck rather than the mouth, because mylohyoid ascends posteriorly and the termination of its attachment is variable, sometimes terminating before the position of the third molar, thereby allowing relatively unhindered access into the tissue spaces of the neck.

Apart from canine teeth, which have long roots, abscesses on upper teeth usually open buccally below, rather than above, the attachment of buccinator. Because its root apex is occasionally curved towards the palate, abscesses of the upper lateral incisors may track into the palatal submucosa. Abscesses of upper canines often open facially just below the orbit. Here, the swelling may obstruct drainage in the angular part of the facial vein which has no valves, and it is therefore possible for infected material to travel via the angular and ophthalmic veins into the cavernous sinus, potentially causing a cavernous sinus thrombosis. Abscesses on the palatal roots of upper molars usually open on the palate.

The superficial lamina of deep cervical fascia opposes the spread of abscesses towards the surface, and pus beneath it tends to migrate laterally. If the pus is in the anterior triangle, it may find its way into the mediastinum, anterior to the pretracheal lamina, but because the fascia here is so thin, it more often approaches the surface and ‘points’ above the sternum. Pus behind the prevertebral lamina may extend laterally and point in the posterior triangle, or it may perforate the lamina and the buccopharyngeal fascia to bulge into the pharynx as a retropharyngeal abscess.

Upper second premolars and first and second molars are related to the maxillary sinus. When this is large, the root apices of these teeth may be separated from its cavity solely by the lining mucosa. Sinus infections may stimulate the nerves entering the teeth, simulating toothache in the ipsilateral premolars and molars; this phenomenon is known as referred pain. Upper first premolars and third molars may be closely related to the maxillary sinus. With loss of teeth, alveolar bone is extensively resorbed. Thus, in the edentulous mandible, the mental nerve, originally inferior to premolar roots, may lie near the crest of the bone. In the edentulous maxilla, the sinus may enlarge to approach the oral surface of the bone. Both of these facts are of importance when planning surgery in this area. Occasional bony prominences, termed the torus mandibularis, torus maxillaris and torus palatinus, may lie lingual to the lower premolars or molars, or the upper molars. They lie in the midline of the palate and may need surgical removal before satisfactory dentures can be fitted.

Severe systemic infections during the time the teeth are developing may lead to faults in enamel, which are visible as horizontal lines (cf. Harris's growth lines).

REFERENCES

eid DJ, Dean CM. Variation in modern human enamel formation times. *J Hum Evol*. 2006;50:329-346.

obinson PP, Smith KG. Lingual nerve damage during third lower molar removal: a comparison of two surgical methods. *Br Dent J*. 1996;180:456-461.

CHAPTER 31

Infratemporal and pterygopalatine fossae and temporomandibular joint

INFRATEMPORAL FOSSA

The infratemporal fossa lies deep to the ramus of the mandible. It communicates with the temporal fossa deep to the zygomatic arch and the pterygopalatine fossa through the pterygomaxillary fissure. The major structures that occupy the infratemporal fossa are the lateral and medial pterygoid muscles, the mandibular division of the trigeminal nerve, the chorda tympani branch of the facial nerve, the otic parasympathetic ganglion, the maxillary artery and the pterygoid venous plexus.

The infratemporal fossa has a roof, and lateral and medial walls, and is open to the neck posteroinferiorly, i.e. the fossa has no anatomical floor. The roof is formed by the infratemporal surfaces of the temporal bone and of the greater wing of the sphenoid, and contains the foramena ovale and spinosum and the petrotympanic fissure: it is open superiorly to the temporal fossa. The medial wall is formed anteriorly by the lateral pterygoid plate of the pterygoid process of the sphenoid, and more postero-medially by the pharynx and tensor and levator veli palatini. It contains the pterygomaxillary fissure across which structures pass between the infratemporal and pterygopalatine fossae (Fig. 31.1). The lateral wall is formed by the medial surface of the ramus of the mandible.

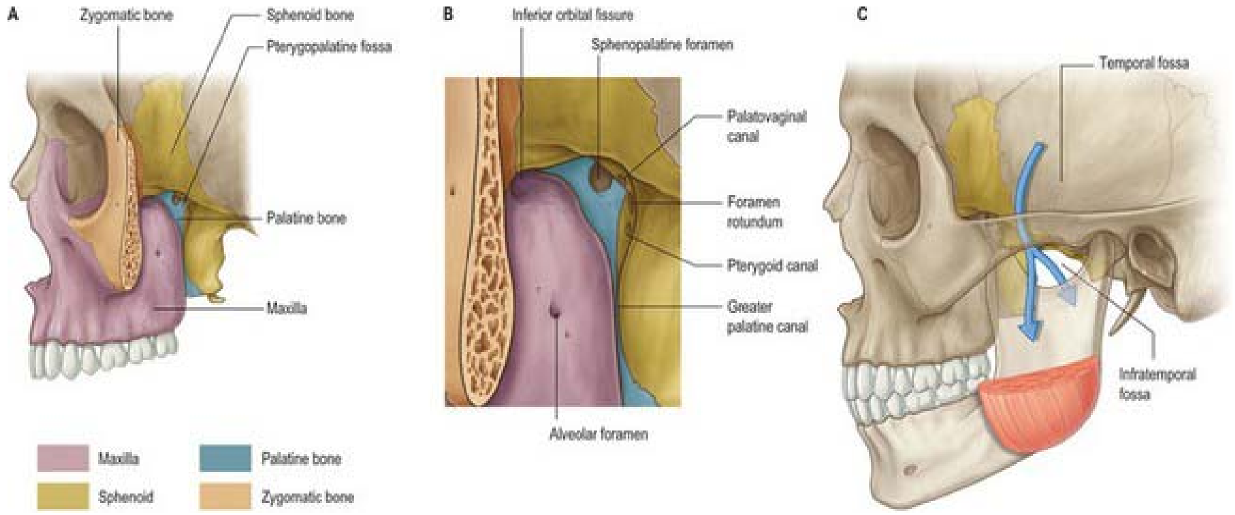
A
Zygomatic bone
Sphenoid bone
Pterygopalatine fossa
Palatine bone
Maxilla
Maxilla
Palatine bone
Sphenoid
Zygomatic bone
B
Inferior orbital fissure
Sphenopalatine foramen
Palatovaginal canal
Foramen rotundum
Pterygoid canal
Greater palatine canal
Alveolar foramen
C
Temporal fossa
Infratemporal fossa

Fig. 31.1 **A**, Pterygopalatine fossa after detachment of the mandible and removal of the zygomatic arch; **B**, anteromedial view; **C**, lateral view; arrows show that the floor of the temporal fossa is open medially to the infratemporal fossa and laterally to the region containing the masseter.

(From Drake, Vogl and Mitchell 2005.)

Lateral pterygoid provides a key to understanding the relationships of structures within the infratemporal fossa. This muscle lies in the roof of the fossa and runs anteroposteriorly in a more or less horizontal plane from the region of the pterygoid plates to the mandibular condyle (Fig. 31.1). Branches of the mandibular nerve and the main origin of medial pterygoid are deep relations and the maxillary artery is superficial. The buccal branch of the mandibular nerve passes between the two heads of lateral pterygoid. Medial pterygoid and the lingual and inferior alveolar nerves emerge below its inferior border and the deep temporal nerves and vessels emerge from its upper border. A venous network, the pterygoid venous plexus, lies around and within lateral pterygoid and is important in the spread of infection.

BONES

The sphenoid bone, the paired maxillae and temporal bones, and the mandible, collectively provide the skeletal framework to the infratemporal and pterygopalatine regions. The mandible and the two temporal bones articulate at the right and left temporomandibular joints. The disarticulated maxilla is described in Chapter 29, the temporal bone is described in Chapter 36, and the sphenoid and mandible are described here.

Sphenoid bone

The sphenoid bone lies in the base of the skull between the frontal, temporal and occipital bones. It has a central body, paired greater and lesser wings that spread laterally from the body, and two pterygoid processes that descend from the junction of the body and greater wings (Fig. 31.2).

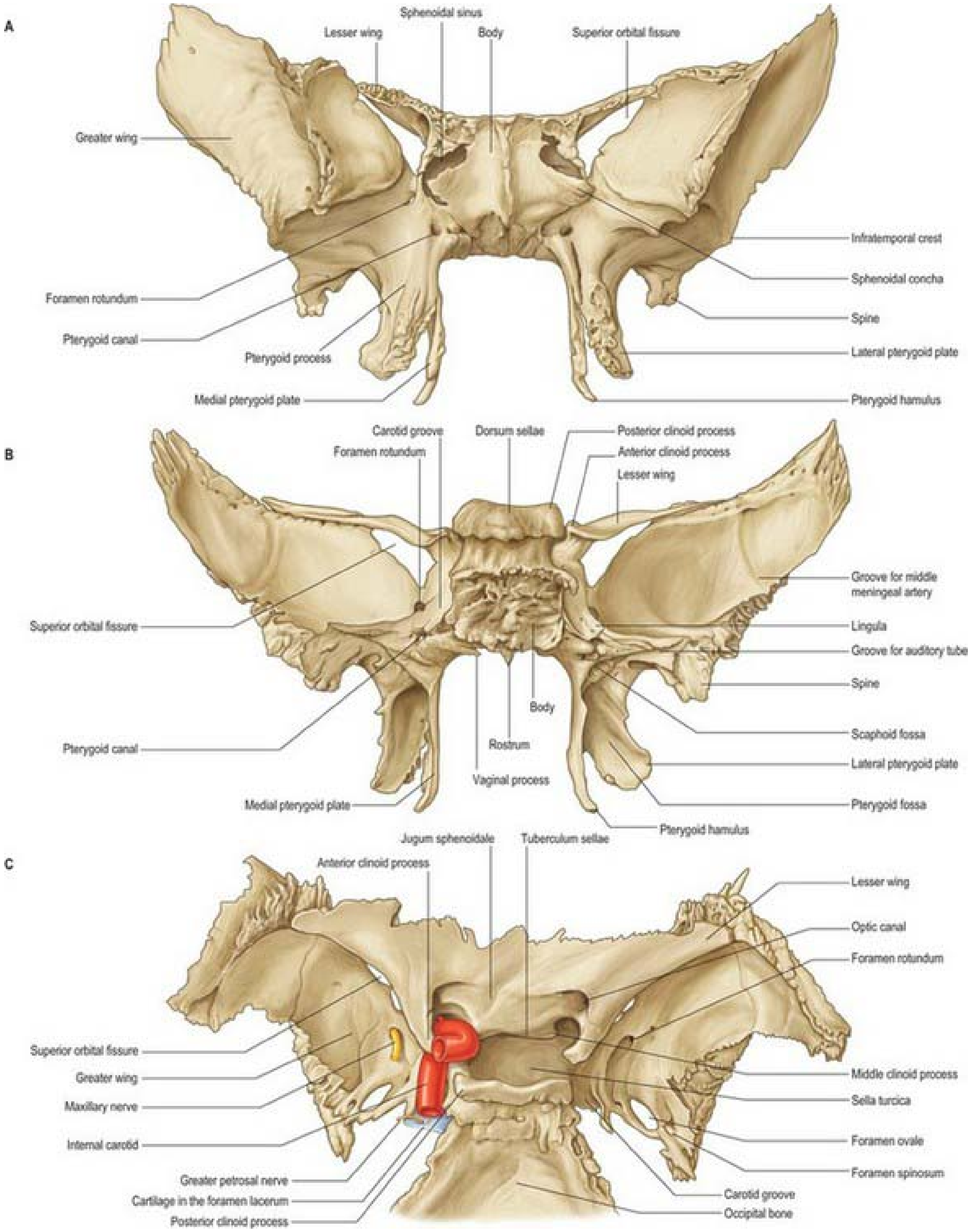
A
Sphenoidal sinus
Lesser wing
Body
Superior orbital fissure
Greater wing
Infratemporal crest
Sphenoidal concha
Foramen rotundum
Spine
Pterygoid canal
Pterygoid process
Lateral pterygoid plate
Medial pterygoid plate
Pterygoid hamulus
B
Carotid groove
Foramen rotundum
Dorsum sellae
Posterior clinoid process
Anterior clinoid process
Lesser wing
Groove for middle meningeal artery
Superior orbital fissure
Lingula
Groove for auditory tube
Spine
Body
Pterygoid canal
Scaphoid fossa
Rostrum
Lateral pterygoid plate
Vaginal process
Medial pterygoid plate
Pterygoid fossa
Pterygoid hamulus
C
Jugum sphenoidale
Tuberculum sellae
Anterior clinoid process
Lesser wing
Optic canal
Foramen rotundum
Superior orbital fissure
Middle clinoid process
Greater wing
Sella turcica
Maxillary nerve
Internal carotid
Foramen ovale
Foramen spinosum
Greater petrosal nerve
Carotid groove
Cartilage in the foramen lacerum
Occipital bone
Posterior clinoid process

Fig. 31.2 Sphenoid bone. **A**, anterior view; **B**, posterior view; **C**, superior view.

(From Sobotta 2006.)

Body

The body of the sphenoid is cuboidal. It contains two air sinuses, separated by a septum (see Ch. 32). Its cerebral (superior) surface articulates in front with the cribriform plate of the ethmoid bone. Anteriorly is the smooth jugum sphenoidale, which is related to the gyri recti and olfactory tracts. The jugum is bounded behind by the anterior border of the sulcus chiasmatis, which leads laterally to the optic canals. Posteriorly is the tuberculum sellae, behind which is the deeply concave sella turcica. In life the sella contains the hypophysis cerebri in the hypophysial fossa. Its anterior edge is completed laterally by two middle clinoid processes, while posteriorly the sella turcica is bounded by a square dorsum sellae, the superior angles of which bear variable posterior clinoid processes. The diaphragma sella and the tentorium cerebelli are attached to the clinoid processes (see Ch. 27). On each side, below the dorsum sellae, a small petrosal process articulates with the apex of the petrous part of the temporal bone. The body of the sphenoid slopes directly into the basilar part of the occipital bone posterior to the dorsum sellae, together these bones form the clivus. In the growing child this is the site of the spheno-occipital synchondrosis: premature closure of this joint gives rise to the skull appearances seen in achondroplasia.

The lateral surfaces of the body are united with the greater wings and the medial pterygoid plates. A broad carotid sulcus accommodates both the internal carotid artery and the cranial nerves associated with the cavernous sinus above the root of each wing (see Ch. 27). The sulcus is deepest posteriorly. It is overhung medially by the petrosal part of the temporal bone and has a sharp lateral margin, the lingula, which continues back over the posterior opening of the pterygoid canal.

A median triangular, bilaminar sphenoidal crest on the anterior surface of the body of the sphenoid makes a small contribution to the nasal septum. The anterior border of the crest joins the perpendicular plate of the ethmoid bone, and a sphenoidal sinus opens on each side of it (see Ch. 32). In the articulated state the sphenoidal sinuses are closed anteroinferiorly by the sphenoidal conchae, which are largely destroyed when disarticulating a skull.

Each half of the anterior surface of the body of the sphenoid possesses a superolateral depressed area joined to the ethmoid labyrinth which completes the posterior ethmoidal sinuses; a lateral margin which articulates with the orbital plate of the ethmoid above and the orbital process of the palatine bone below; and an inferomedial, smooth, triangular area, which forms the posterior nasal roof, and near whose superior angle lies the orifice of a sphenoidal sinus.

The inferior surface of the body of the sphenoid bears a median triangular sphenoidal rostrum, embraced above by the diverging lower margins of the sphenoidal crest. The narrow anterior end of the rostrum fits into a fissure between the anterior parts of the alae of the vomer, and the posterior ends of the sphenoidal conchae flank the rostrum, articulating with its alae. A thin vaginal process projects medially from the base of the medial pterygoid plate on each side of the posterior part of the rostrum, behind the apex of the sphenoidal concha.

Greater wings

The greater wings of the sphenoid curve broadly superolaterally from the body. Posteriorly each is triangular, fitting the angle between the petrous and squamous parts of the temporal bone at a sphenosquamosal suture. The cerebral surface contributes to the anterior part of the middle cranial fossa. Deeply concave, its undulating surface is adapted to the anterior gyri of the temporal lobe of the cerebral hemisphere. The foramen rotundum lies anteromedially and transmits the maxillary nerve. Posterolateral to the foramen rotundum is the foramen ovale, which transmits the mandibular nerve, accessory meningeal artery and sometimes the lesser petrosal nerve, although the latter nerve may have its own canaliculus innominatus medial to the foramen spinosum. A small emissary sphenoidal foramen, which transmits a small vein from the cavernous sinus, lies medial to the foramen ovale (on one or both sides) in approximately 40% of skulls. The foramen spinosum, which transmits the middle meningeal artery and meningeal branch of the mandibular nerve, lies behind the foramen ovale.

The lateral surface is vertically convex and divided by a transverse infratemporal crest into temporal (upper) and infratemporal (lower) surfaces. Temporalis is attached to the temporal surface. The infratemporal surface is directed downwards and, with the infratemporal crest, is the site of attachment of the upper fibres of lateral pterygoid. It contains the foramen ovale and foramen spinosum. The small downward projecting spine of the sphenoid lies posterior to the foramen spinosum; the sphenomandibular ligament is attached to its tip. The medial side of the spine bears a faint anteroinferior groove for the chorda tympani nerve and appears in the lateral wall of the sulcus for the pharyngotympanic (auditory) tube. Medial to the anterior end of the infratemporal crest, a ridge passes downwards to the front of the lateral pterygoid plate, thereby forming a posterior boundary of the pterygomaxillary fissure.

The quadrilateral orbital surface of the greater wing faces anteromedially, and forms the posterior part of the lateral wall of the orbit. It has a serrated upper edge which articulates with the orbital plate of the frontal bone, and a serrated lateral margin which articulates with the zygomatic bone. Its smooth inferior border is the posterolateral edge of the inferior orbital fissure, and its sharp medial margin forms the inferolateral edge of the superior orbital fissure, on which a small tubercle gives partial attachment to the common anular ocular tendon. Below the medial end of the superior orbital fissure a grooved area forms the posterior wall of the pterygopalatine fossa; the latter is pierced by the foramen rotundum.

The irregular margin of the greater wing, from the body of the sphenoid to the spine, is an anterior limit of the medial half of the foramen lacerum. It also displays the posterior aperture of the pterygoid canal. Its lateral half articulates with the petrous part of the temporal bone at a sphenopetrosal synchondrosis. Inferior to this, the sulcus tubae contains the cartilaginous pharyngotympanic (auditory) tube. Anterior to the spine of the sphenoid the concave squamosal margin is serrated – bevelled internally below, externally above – for articulation with the squamous part of the temporal bone. The tip of the greater wing, bevelled internally, articulates with the sphenoidal angle of the parietal bone at the pterion. Medial to this, a triangular rough area articulates with the frontal bone: its medial angle is continuous with the inferior boundary of the superior orbital fissure, and its anterior angle joins the zygomatic bone by a serrated articulation.

Lesser wings

The lesser wings of the sphenoid are triangular pointed plates that protrude laterally from the anterosuperior regions of the body. The superior surface of each wing is smooth and related to the frontal lobe of the cerebral hemisphere. The inferior surface is a posterior part of the orbital roof and upper boundary of the superior orbital fissure, and overhangs the middle cranial fossa. The posterior border projects into the lateral fissure of the cerebral hemisphere. The medial end of the lesser wing forms the anterior clinoid process. The anterior and middle clinoid processes are sometimes united to form a caroticoclinoid foramen. The lesser wing is connected to the body by a thin flat anterior root and a thick triangular posterior root, between which lies the optic canal. Growth of the posterior root is closely associated with variations in the geometry of the canal. The cranial opening of the canal may be duplicated, or more commonly, the division is incomplete.

Superior orbital fissure

The superior orbital fissure connects the cranial cavity with the orbit. It is bounded medially by the body of the sphenoid, above by the lesser wing of the sphenoid, below by the medial margin of the orbital surface of the greater wing, and laterally, between the greater and lesser wings, by the frontal bone. The contents of the superior orbital fissure are described in Chapter 39.

Pterygoid processes

The pterygoid processes descend perpendicularly from the junctions of the greater wings and body. Each consists of a medial and lateral plate, whose upper parts are fused anteriorly. The plates are separated below by the angular pterygoid fissure, whose margins articulate with the pyramidal process of the palatine bone, and diverge behind. Medial pterygoid and tensor veli palatini lie in the cuneiform pterygoid fossa between the plates. Above is the small, oval, shallow scaphoid fossa, which is formed by division of the upper posterior border of the medial plate. Part of tensor veli palatini is attached to the fossa. The anterior surface of the root of the pterygoid process is broad and triangular and forms the posterior wall of the pterygopalatine fossa: it is pierced by the anterior opening of the pterygoid canal.

Lateral pterygoid plate

The lateral pterygoid plate is broad, thin and everted. The lateral surface forms part of the medial wall of the infratemporal fossa; the lower part of lateral pterygoid is attached to it. The medial surface is the lateral wall of the pterygoid fossa; most of the deep head of medial pterygoid is attached to it. The upper part of its anterior border is a posterior boundary of the pterygomaxillary fissure, and the lower part articulates with the palatine bone. The posterior border is free.

Medial pterygoid plate

The medial pterygoid plate is narrower and longer than the lateral. Its lower end is continued into an unciform projection, the pterygoid hamulus, which curves laterally. The pterygomandibular raphe is attached to the hamulus and the tendon of tensor veli palatini winds around the hamulus. The lateral surface forms the medial wall of the pterygoid fossa and the medial surface provides a lateral boundary of the posterior nasal aperture. The medial plate is prolonged above on the inferior aspect of the body of the sphenoid as a thin vaginal process that articulates anteriorly with the sphenoidal process of the palatine bone and medially with the ala of the vomer. The plate articulates with the posterior border of the perpendicular plate of the palatine bone in the lower part of its anterior margin. Inferiorly it bears a furrow, which is converted anteriorly into the palatovaginal canal by the sphenoidal process of the palatine bone. The palatovaginal canal transmits pharyngeal branches of the maxillary artery and pterygopalatine ganglion. The pharyngobasilar fascia is attached to the whole of the posterior margin of the medial plate, and the superior pharyngeal constrictor is attached to its lower end. The small pterygoid tubercle is found at the upper end of the plate, just below the posterior opening of the pterygoid canal. The processus tubarius, which supports the cartilaginous pharyngeal end of the pharyngotympanic tube, projects back near the midpoint of the margin of the medial pterygoid plate.

Midface fractures

Midface fractures at Le Fort I, II and III levels invariably involve the pterygoid plates; displacement of the outlines of these bones radiographically confirms the diagnosis.

Sphenoidal conchae

The sphenoidal conchae are two thin, curved small plates, attached anteroinferiorly to the body of the sphenoid bone. The superior concave surface of each forms the anterior wall and part of the floor of a sphenoidal sinus. *In situ*, each has vertical quadrilateral anterior and horizontal triangular posterior parts. The anterior part consists of a superolateral depressed area, which completes the posterior ethmoidal sinuses and joins below with the orbital process of a palatine bone, and a smooth and triangular inferomedial area, which forms part of the nasal roof and is perforated above by the round opening connecting the sphenoidal sinus and sphenoethmoidal recess.

Anterior parts of the two bones meet in the midline, and protrude as the sphenoidal crest. The horizontal part appears in the nasal roof and completes the sphenopalatine foramen. Its medial edge articulates with the rostrum of the sphenoid and the ala of the vomer. Its apex, directed posteriorly, is superomedial to the vaginal process of the medial pterygoid plate and joins the posterior part of the ala. A small conchal part sometimes appears in the medial wall of the orbit, lying between the orbital plate of the ethmoid in front, the orbital process of the palatine bone below and the frontal bone above.

Ossification

Until the seventh or eighth month *in utero* the sphenoid body has a presphenoidal part, anterior to the tuberculum sellae, with which the lesser wings are continuous, and a postsphenoidal part, consisting of the sella turcica and dorsum sellae, and integral with the greater wings and pterygoid processes. Much of the bone is preformed in cartilage. There are six ossification centres for the presphenoidal parts, and eight for the postsphenoidal parts.

Presphenoidal part

About the ninth week of fetal life, a centre appears in each wing, lateral to the optic canal, and a little later two bilateral centres appear in the presphenoidal body. Each sphenoidal concha has a centre, appearing superoposteriorly in the nasal capsule in the fifth month *in utero*. As this enlarges it partly surrounds a posterosuperior expansion of the nasal cavity, which becomes the sphenoidal sinus. The posterior conchal wall is absorbed and the sinus invades the presphenoid component. In the fourth year the concha fuses with the ethmoidal labyrinth and before puberty it fuses with the sphenoid and palatine bones. Its anterior deficiency persists as an opening for the sphenoidal sinus.

Postsphenoidal part

The first centres appear in the greater wings about the eighth week of fetal life, one in the basal cartilage of each wing below the foramen rotundum. These centres only contribute to the root of the greater wing (near the foramen rotundum and pterygoid canal). The remainder of the greater wing and the lateral pterygoid plate are ossified in mesenchyme. About the fourth month of fetal life two centres appear, flanking the sella turcica, and soon fuse. The medial pterygoid plates are also ossified in ‘membrane’, a centre in each probably appearing about the ninth or tenth week. The hamulus is chondrified during the third fetal month and at once begins to ossify. Medial and lateral pterygoid plates join about the sixth fetal month. During the fourth month, a centre appears for each lingula, soon joining the body. The optic canal in the neonate is relatively large and has a keyhole or ‘figure of eight’ shape rather than the circular profile seen in the adult.

Postnatal details

Presphenoidal and postsphenoidal parts fuse about the eighth month *in utero*, but an unciform cartilage persists after birth in lower parts of the junction. At birth the bone is tripartite and consists of a central part (body and lesser wings) and two lateral parts (each consisting of a greater wing and pterygoid process). During the first year the greater wings and body unite around the pterygoid canals and the lesser wings extend medially above the anterior part of the body, meeting to form the smooth, elevated jugum sphenoidale. By the 25th year, sphenoid and occipital bones are completely fused. An occasional vascular foramen, often erroneously termed the craniopharyngeal canal, is occasionally seen in the anterior part of the hypophysial fossa. Although the sphenoidal sinus can be identified in the fourth month of fetal life as an evagination of the posterior part of the nasal capsule, by birth it represents an outgrowth of the sphenoethmoidal recess. Pneumatization of the body of the sphenoid commences in the second or third year and spreads first into the presphenoid, and later invades the postsphenoid, part. It reaches full size in adolescence, but often enlarges further by absorption of its walls as age advances.

Certain parts of the sphenoid are connected by ligaments that may occasionally ossify, e.g. the pterygospinous ligament between the sphenoid spine and upper part of lateral pterygoid plate; the interclinoid ligament joining the anterior to the posterior clinoid process; and the caroticoclinoid ligament that connects the anterior to the middle clinoid process.

Premature synostosis of the junction between pre- and post-sphenoidal parts, or of the spheno-occipital suture, produces a characteristic appearance, obvious in profile, of an abnormal depression of the nasal bridge (hypertelorism).

Mandible

The mandible is the largest, strongest and lowest bone in the face. It has a horizontally curved body that is convex forwards, and two broad rami that ascend posteriorly (Fig. 31.3). The body of the mandible supports the mandibular teeth within the alveolar process. The rami bear the coronoid and condylar processes. Each condyle articulates with the adjacent temporal bone at the temporomandibular joint.

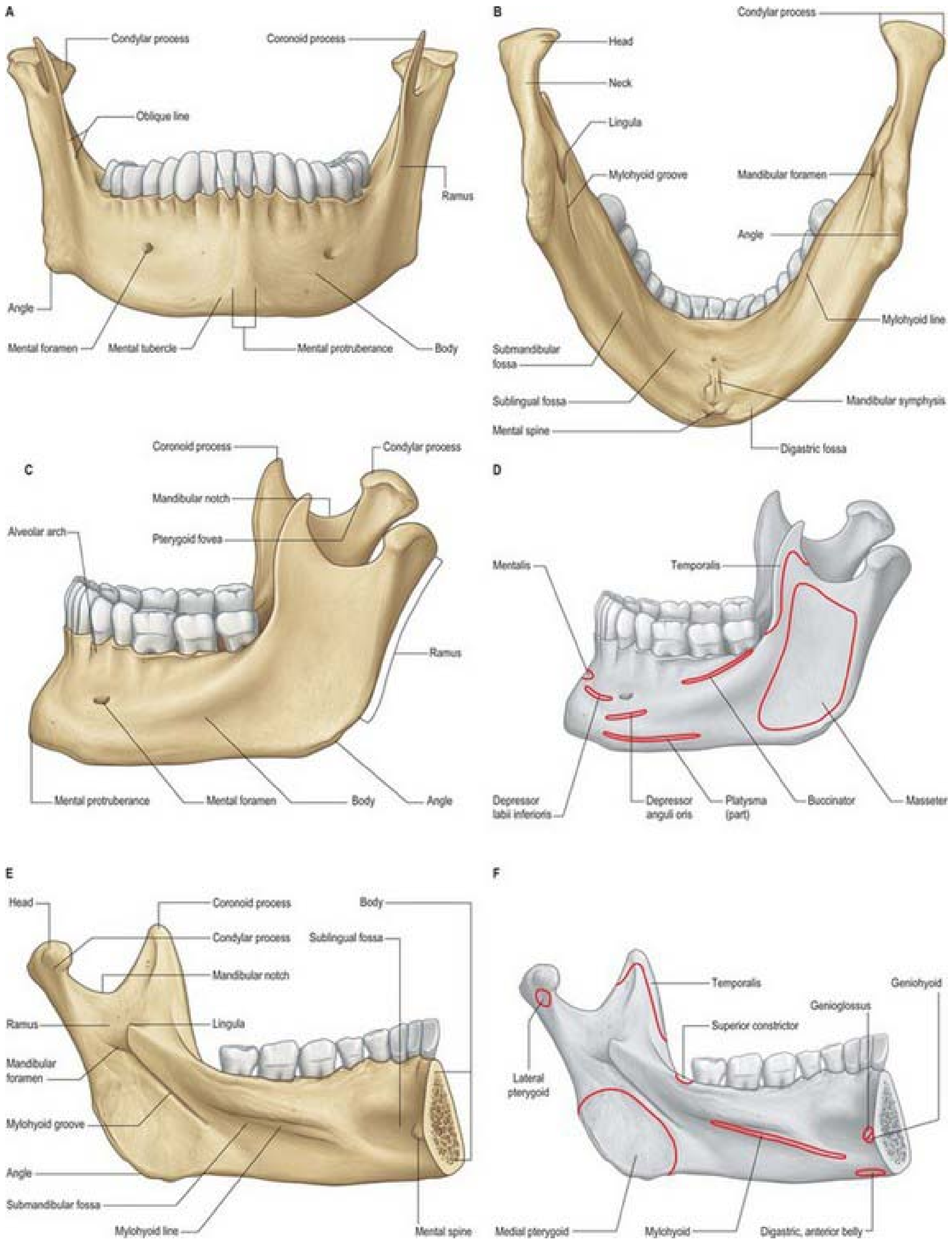
A
Condylar process
Coronoid process
Oblique line
Ramus
Angle
Mental foramen
Mental tubercle
Mental protruberance
Body
B
Head
Neck
Lingula
Mylohyoid groove
Condylar process
Mandibular foramen
Angle
Mylohyoid line
Submandibular fossa
Sublingual fossa
Mental spine
Mandibular symphysis
Digastric fossa
C
Coronoid process
Condylar process
Mandibular notch
Alveolar arch
Pterygoid fovea
Ramus
Mental protruberance
Mental foramen
Body
Angle
D
Mentalis
Temporalis
Depressor labii inferioris
Depressor anguli oris
Platysma (part)
Buccinator
Masseter
E
Head
Coronoid process
Body
Condylar process
Sublingual fossa
Mandibular notch
Ramus
Lingula
Mandibular foramen
Mylohyoid groove
Angle
Submandibular fossa
Mylohyoid line
Mental spine
F
Temporalis
Geniohyoid
Genioglossus
Superior constrictor
Lateral pterygoid
Medial pterygoid
Mylohyoid
Digastric, anterior belly

Fig. 31.3 Adult mandible. **A**, anterior view; **B**, inferior view; **C**, lateral view (with muscle attachments in **D**); **E**, internal view (with muscle attachments in **F**).

(Redrawn with permission from Sobotta 2006.)

Body

The body is somewhat U-shaped. It has external and internal surfaces separated by upper and lower borders. Anteriorly, the upper external surface shows an inconstant faint median ridge indicating the site of the fused symphysis menti. Inferiorly this ridge divides to enclose a triangular mental protuberance; its base is centrally depressed but raised on each side as a mental tubercle. The mental protuberance and mental tubercles constitute the chin. The mental foramen, from which the mental neurovascular bundle emerges, lies below either the interval between the premolar teeth, or the second premolar tooth, midway between the upper and lower borders of the body. The posterior border of the foramen is smooth, and accommodates the nerve as it emerges posterolaterally. A faint external oblique line ascends backwards from each mental tubercle, and sweeps below the mental foramen; it becomes more marked as it continues into the anterior border of the ramus.

The lower border of the body, the base, extends posterolaterally from the mandibular symphysis into the lower border of the ramus behind the third molar tooth. Near the midline on each side there is a rough digastric fossa which gives attachment to the anterior belly of digastric. Behind the fossa the base is thick and rounded: it has a slight anteroposterior convexity which changes to a gentle concavity as the ramus is approached, and so the base has an overall sinuous profile.

The upper border, the alveolar part, contains 16 alveoli for the roots of the lower teeth. It consists of buccal and lingual plates of bone joined by interdental and inter-radicular septa. Near the second and third molar teeth the external oblique line is superimposed upon the buccal plate. Like the maxilla, the form and depth of the tooth sockets is related to the morphology of the roots of the mandibular teeth. The sockets of the incisor, canine and premolar teeth usually contain a single root, while those for the three molar teeth each contain two or three roots. The third molar is variable in its position and root presentation. It may be impacted vertically, horizontally, mesially or distally, and its roots may be bulbous, hooked, divergent or convergent, and occasionally embrace the mandibular (inferior dental) canal (see Ch. 30). The internal surface of the mandible is divided by an oblique mylohyoid line that gives attachment to mylohyoid (and, above its posterior end, to the superior pharyngeal constrictor, some retromolar fascicles of buccinator, and the pterygomandibular raphe behind the third molar). The mylohyoid line extends from a point approximately 1 cm from the upper border behind the third molar as far forwards as the mental symphysis; it is sharp and distinct near the molars, but faint further forwards. The mylohyoid groove extends downwards and forwards from the ramus below the posterior part of the mylohyoid line and contains the mylohyoid neurovascular bundle. The area below the line is a slightly concave submandibular fossa and is related to the submandibular gland. The area above the line widens anteriorly into a triangular sublingual fossa and is related to the sublingual gland: the bone is covered by oral mucosa above the sublingual fossa as far back as the third molar. In an edentulous subject it may be necessary to reduce any ridge-like prominence of the mylohyoid line in order that dentures may fit without traumatizing the overlying oral mucosa.

Above the anterior ends of the mylohyoid lines, the posterior symphysial aspect bears a small elevation, often divided into upper and lower parts, the mental spines (genial tubercles). The spines are sometimes fused to form a single eminence, or they may be absent, in which case their position is indicated merely by an irregularity of the surface. The upper part gives attachment to genioglossus, the lower part to geniohyoid. Above the mental spines, most mandibles display a lingual (genial) foramen which opens into a canal that traverses the bone to 50% of the buccomandibular dimension of the mandible, and which contains a branch of the lingual artery. A rounded torus mandibularis sometimes occurs above the mylohyoid line, medial to the molar roots: it is only of clinical significance if repeatedly traumatized.

Ramus

The mandibular ramus is quadrilateral, and has two surfaces (lateral and medial), four borders (superior, inferior, anterior and posterior) and two processes (coronoid and condylar). The lateral surface is relatively featureless and bears the (external) oblique ridge in its lower part. The medial surface presents, a little above centre, the mandibular foramen, through which the inferior alveolar neurovascular bundle passes to gain access to the mandibular canal (see below). Anteromedially, the mandibular foramen is overlapped by a thin, sharp triangular spine, the lingula, to which the sphenomandibular ligament is attached, and which is also the landmark for an inferior alveolar local anaesthetic block injection. Below and behind the foramen, the mylohyoid groove runs obliquely downward and forward.

The inferior border is continuous with the mandibular base and meets the posterior border at the angle, which is typically everted in males, but frequently inverted in females. The thin superior border bounds the mandibular incisure, which is surmounted in front by the somewhat triangular, flat, coronoid process and behind by the condylar process. The thick, rounded posterior border extends from the condyle to the angle, and is gently convex backwards above, and concave below. The anterior border is thin above, where it is continuous with the edge of the coronoid process, and thicker below where it is continuous with the external oblique line. The temporal crest is a ridge that descends on the medial side of the coronoid process from its tip to the bone just behind the third molar tooth. The triangular depression between the temporal crest and the anterior border of the ramus is the retromolar fossa.

The ramus and its processes provide attachment for the four primary muscles of mastication. Masseter is attached to the lateral surface, medial pterygoid is attached to the medial surface, temporalis is inserted into the coronoid process and lateral pterygoid is attached to the condyle.

Mandibular canal

The mandibular foramen leads into the mandibular canal, which runs obliquely downward and forward within the ramus, and then horizontally forward within the body under the roots of the molar teeth, with which it communicates by small openings. The canal is not always easy to define, especially anterior to the mental foramen. Its walls may be formed either by a thin layer of cortical bone or, more frequently, by trabecular bone. Although the buccal-lingual and superior-inferior positions of the canal vary considerably between mandibles, in general, the mandibular canal is situated nearer the lingual cortical plate in the posterior two-thirds of the bone, and closer to the labial cortical plate in the anterior third. Bilateral symmetry (location of the canal in each half of the mandible) is reported to be common. Near the mental foramen the inferior alveolar nerve branches into the mental nerve, which ultimately leaves the mandible via the mental foramen, and the incisive nerve, which remains within the bone and supplies the anterior teeth. The mental nerve may extend anteriorly for 2–3 mm within the mandible before curving back to the mental foramen (the ‘anterior loop’ of the mental nerve). The intra osseous anatomy of the mental nerve is of particular importance in dental implant surgery: the nerve may be damaged if the interforaminal area of the mandible is invaded during surgery or while harvesting block grafts from the symphysial region.

Coronoid process

The coronoid process projects upwards and slightly forwards as a triangular plate of bone. Its posterior border bounds the mandibular incisure, and its anterior border continues into that of the ramus.

Condylar process

The mandibular condyle varies considerably both in size and shape. When viewed from above, the condyle is roughly ovoid in outline, its anteroposterior dimension (approximately 1 cm) being roughly half its mediolateral dimension. The medial aspect of the condyle is wider than the lateral. The long axis of the condyle is not at right angles to the ramus, but diverges posteriorly from a strictly coronal plane. Thus, the lateral pole of the condyle lies slightly anterior to the medial, and if the long axes of the two condyles are extended, they meet at an obtuse angle (approximately 145°) at the anterior border of the foramen magnum. The articular head of the condyle joins the ramus through a thin bony projection, the neck of the condyle. The pterygoid fovea, a small depression situated on the anterior surface of the neck below the articular surface, receives part of the attachment of lateral pterygoid.

The condyle consists of a core of cancellous bone covered by a thin outer layer of compact bone whose intra-articular aspect is covered by layers of fibrocartilage. The condyle is the commonest site of mandibular fractures.

Accessory foramina of the mandible

These are usually unnamed and infrequently described, yet they are numerous. They may transmit auxiliary nerves to the teeth (from facial, mylohyoid, buccal, transverse cervical cutaneous and other nerves), and their occurrence is significant in dental anaesthetic blocking techniques.

Ossification

The mandible forms in dense fibromembranous tissue lateral to the inferior alveolar nerve and its incisive branch, and also in the lower parts of Meckel’s cartilage (first branchial arch). Each half is ossified from a centre that appears near the mental foramen about the sixth week *in utero*. From this site, ossification spreads medially and posterocranially to form the body and ramus, first below, and then around, the inferior alveolar nerve and its incisive branch. Ossification then spreads upwards, initially forming a trough, and later crypts, for the developing teeth. By the tenth week, Meckel’s cartilage below the incisor rudiments is surrounded and invaded by bone. Secondary cartilages appear later (Fig. 31.4): a conical mass, the condylar cartilage, extends from the mandibular head downwards and forwards in the ramus, and contributes to its growth in height. Although it is largely replaced by bone by midfetal life, its proximal end persists as proliferating cartilage under the fibrous articular lining until about the third decade. Another secondary cartilage, which soon ossifies, appears along the anterior coronoid border, and disappears before birth. One or two cartilaginous nodules also occur at the symphysis menti. At about the seventh month *in utero* these may ossify as variable mental ossicles in symphysial fibrous tissue: they unite with adjacent bone before the end of the first postnatal year.

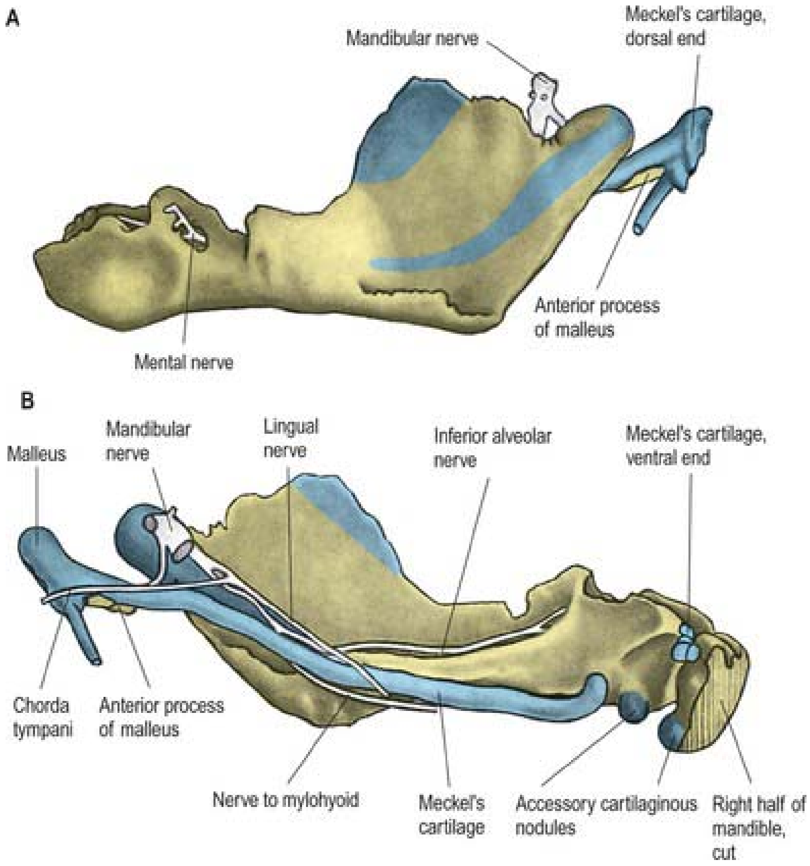
A
Mandibular nerve
Meckel's cartilage, dorsal end
Anterior process of malleus
Mental nerve
B
Malleus
Mandibular nerve
Lingual nerve
Inferior alveolar nerve
Meckel's cartilage, ventral end
Chorda tympani
Anterior process of malleus
Nerve to mylohyoid
Meckel's cartilage
Accessory cartilaginous nodules
Right half of mandible, cut

Fig. 31.4 The left half of a mandible of a human embryo, 95 mm long. **A**, Lateral aspect; **B**, Medial aspect. Blue: cartilage; yellow: bone.

(By courtesy of A. Low.)

Age changes in the mandible

At birth the two halves of the mandible are united by a fibrous symphysis menti (Fig. 31.5). The anterior ends of both rudiments are covered by cartilage, separated only by a symphysis. Until fusion occurs, new cells are added to each cartilage from symphysial fibrous tissue, and ossification on its mandibular side proceeds towards the midline. When the latter process overtakes the former, and ossification extends into median fibrous tissue, the symphysis fuses. At this stage the body is a mere shell which encloses the imperfectly separated sockets of deciduous teeth. The mandibular canal is near the lower border, and the mental foramen opens below the first deciduous molar and is directed forwards. The coronoid process projects above the condyle.

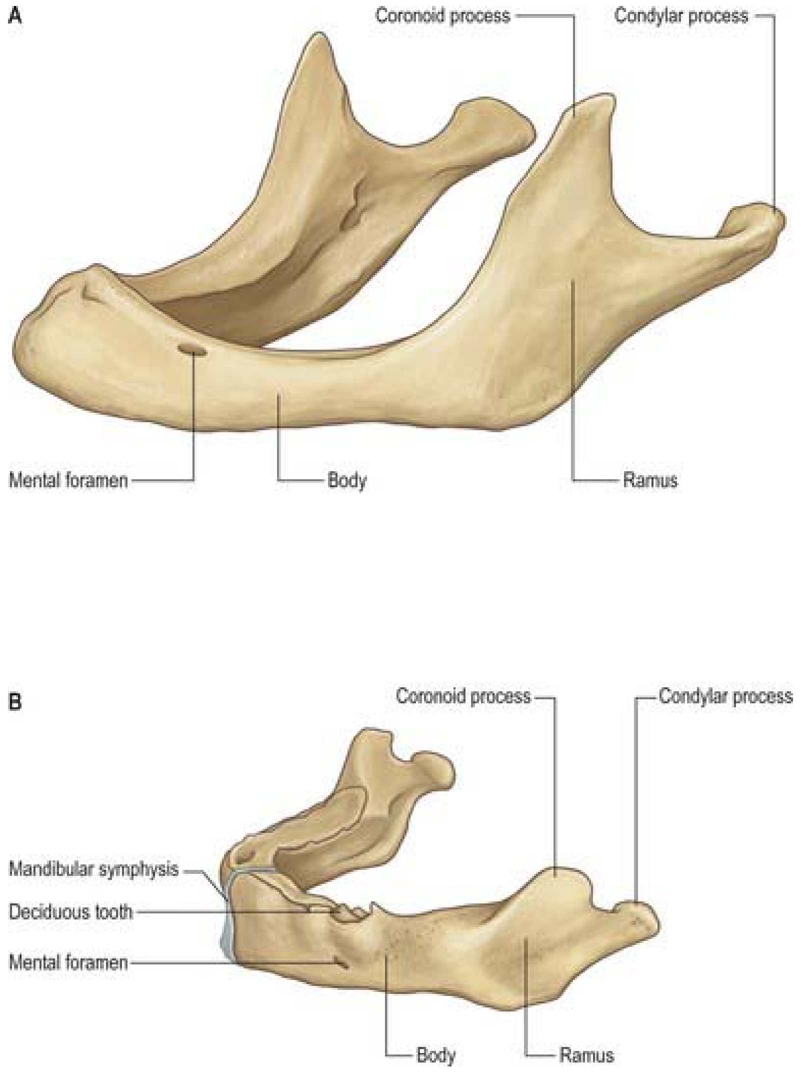
A
Coronoid process
Condylar process
Mental foramen
Body
Ramus
B
Coronoid process
Condylar process
Mandibular symphysis
Deciduous tooth
Mental foramen
Body
Ramus

Fig. 31.5 **A**, Edentulous mandible; note position of mental foramen; **B**, Neonatal mandible.

(Redrawn with permission from Sobotta 2006.)

During the first three postnatal years, the two halves join at their symphysis from below upwards, although separation near the alveolar margin may persist into the second year. The body elongates, especially behind the mental foramen, providing space for three additional teeth. During the first and second years, as a chin develops, the mental foramen alters direction: it no longer faces forwards but now faces backwards, as in the adult mandible, and accommodates the changing direction of the emerging mental nerve.

In general terms, increase in height of the body of the mandible is achieved primarily by formation of alveolar bone associated with the developing and erupting teeth, although some bone is also deposited on the lower border. Increase in length of the mandible is accomplished by deposition of bone on the posterior surface of the ramus and concomitant compensatory resorption on the anterior surface (accompanied by deposition of bone on the posterior surface of the coronoid process and resorption on the anterior surface of the condylar process). Increase in width of the mandible is produced by deposition of bone on the outer surface of the mandible and resorption on the inner surface. An increase in the comparative size of the ramus compared with the body of the mandible occurs during postnatal growth and tooth eruption.

The role of the condylar cartilages in mandibular growth remains controversial. One view states that continued proliferation of this cartilage is primarily responsible for the increase in both the mandibular length and the height of the ramus. Alternatively, there is persuasive experimental evidence that proliferation of the condylar cartilage is an adaptive response to function, rather than being genetically determined. Condylar growth and remodeling has been shown to be influenced significantly by local factors, notably movement and loading of the temporomandibular joint, and to be relatively immune to systemic influences such as vitamin C and D deficiency. Considering the changes that occur in the dentition throughout life, continuous adaptation of the temporomandibular articulation is required in order to maintain functional occlusal alignment between the upper and lower arches of teeth: this adaptation is thought to be largely the result of ongoing condylar remodelling.

In adults, alveolar and subalveolar regions are about equal in depth, and the mental foramen appears midway between the upper and lower borders. If teeth are lost, alveolar bone is resorbed, which means that the mandibular canal (which runs parallel to the mylohyoid line) and the mental foramen come to lie much nearer to the superior border (Fig. 31.5), indeed, sometimes they may both disappear, so that the nerves lie just beneath the oral mucosa.

TEMPOROMANDIBULAR JOINT

The temporomandibular joint is a synovial joint between the articular fossa (also known as the mandibular fossa or glenoid fossa) of the temporal bone above and the mandibular condyle. It is unusual in that its articular surfaces are lined by fibro-cartilage (rather than hyaline cartilage) and its joint cavity is divided into two by an articular disc.

The articular eminence, a transversely elliptical region sinuously curved in the sagittal plane and tilted downwards anteriorly at approximately 25° to the occlusal plane, forms most of the articular surface of the mandibular fossa. Its steepness is variable, and it becomes flatter in the edentulous subject. Its anterior limit is the summit of the articular eminence, a transverse ridge that extends laterally out to the zygomatic arch as far as the articular tubercle. Articular tissue extends anteriorly beyond the articular summit and on to the preglenoid plane. Posteriorly it extends behind the depth of the fossa as far as the squamotympanic fissure. A postglenoid tubercle (at the root of the zygomatic arch, just anterior to the fissure) is usually poorly developed in human skulls.

The articular surface of the mandibular condyle is slightly curved and tilted forward at approximately 25° to the occlusal plane. Like the articular eminence, its slope is variable. In the coronal plane its shape varies from that of a gable (particularly marked in those whose diet is hard), to roughly horizontal in the edentulous.

It is probably impossible to measure the pressure developed on the articular surfaces of the human jaw joint when biting, however direct measurement of loads across the joint in animals has demonstrated significant intermittent loading during mastication. There is also irrefutable theoretical evidence based on Newtonian mechanics that the jaw joint is a weight-bearing joint. With a vertical bite force of 500 N on the left first molar, the right condyle must support a load of well over 300 N (Osborn 1995a). The non-working condyle is more loaded than the condyle on the working side, which may help explain why patients with a fractured condyle choose to bite on the side of the fracture.

Fibrous capsule

The lower part of the joint is surrounded by tight fibres which attach the condyle of the mandible to the disc. The upper part of the joint is surrounded by loose fibres which attach the disc to the temporal bone (Fig. 31.6). Thus the articular disc is attached separately to the temporal bone and to the mandibular condyle forming what could be considered two joint capsules. Longer fibres joining the condyle directly to the temporal bone may be regarded as reinforcing. The capsule is attached above to the anterior edge of the preglenoid plane, posteriorly to the lips of the squamotympanic fissure, between these to the edges of the articular fossa, and below to the periphery of the neck of the mandible.

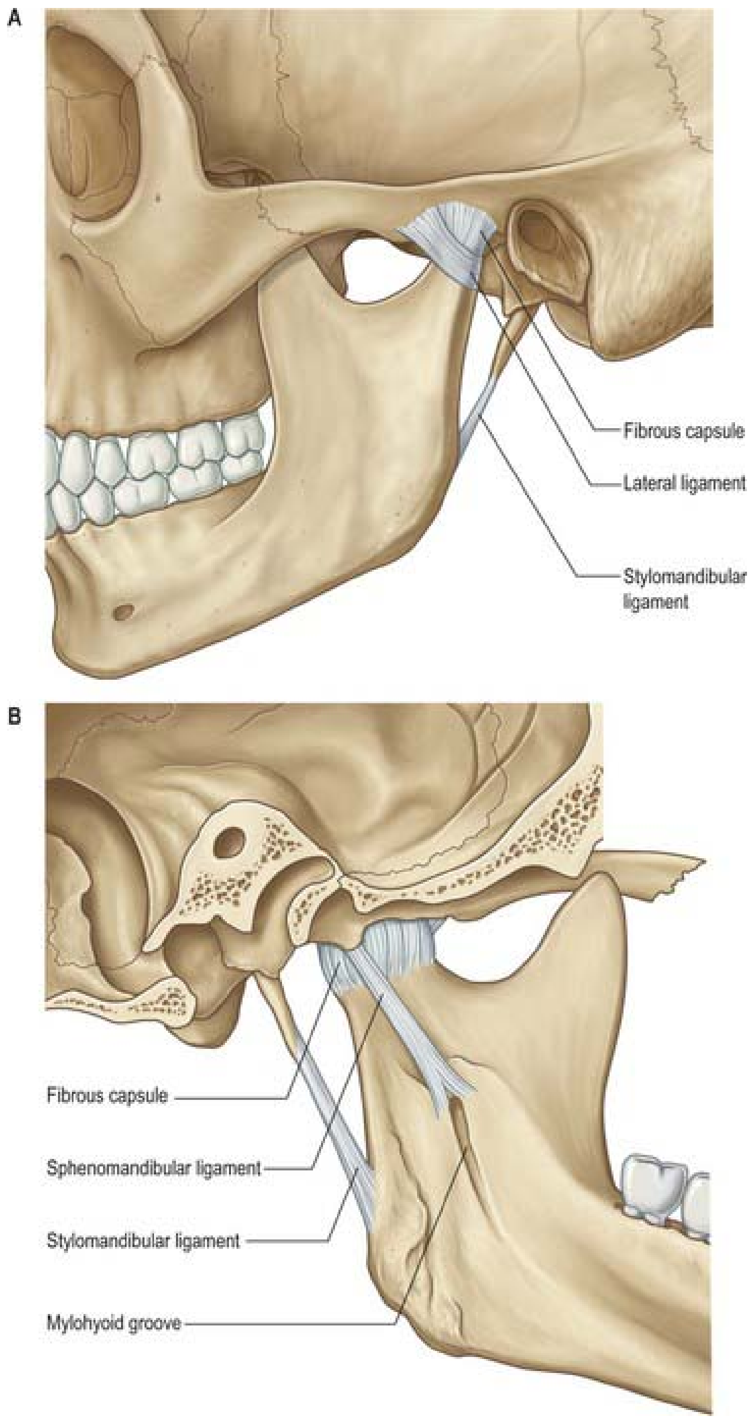
A
Fibrous capsule
Lateral ligament
Stylomandibular ligament
B
Fibrous capsule
Sphenomandibular ligament
Stylomandibular ligament
Mylohyoid groove

Fig. 31.6 The left temporomandibular joint. **A**, lateral aspect; **B**, medial aspect.

Ligaments

Sphenomandibular ligament

The sphenomandibular ligament is medial to, and normally separate from, the capsule (Fig. 31.6). It is a flat, thin band that descends from the spine of the sphenoid and widens as it reaches the lingula of the mandibular foramen. Some fibres traverse the medial end of the petrotympanic fissure and attach to the anterior malleolar process. This part is a vestige of the dorsal end of Meckel's cartilage.

With the jaw closed, there is approximately 5 mm slack within the ligament, but it becomes taut when the jaw is about half open. Lateral pterygoid and the auriculotemporal nerve are lateral relations, the chorda tympani nerve lies medial near its upper end and medial pterygoid is an inferomedial relation. The sphenomandibular ligament is separated from the neck of the mandible below lateral pterygoid by the maxillary artery and from the ramus of the mandible by the inferior alveolar vessels and nerve and a parotid lobule. At this point the vessels and nerve to mylohyoid pierce the ligament. It is separated from the pharynx by fat and a pharyngeal vein.

Stylomandibular ligament

The stylomandibular ligament is a thickened band of deep cervical fascia that stretches from the apex and adjacent anterior aspect of the styloid process to the angle and posterior border of the mandible (Fig. 31.6). Its position and orientation indicate that it cannot mechanically constrain any normal movements of the mandible and does not seem to warrant the status of a ligament of the joint.

Temporomandibular (lateral) ligament

The broad temporomandibular ligament is attached above to the articular tubercle on the root of the zygomatic process of the temporal bone (Fig. 31.6). It extends downwards and backwards at an angle of approximately 45° to the horizontal, to attach to the lateral surface and posterior border of the neck of the condyle, deep to the parotid gland. A short, almost horizontal, band of collagen connects the articular tubercle in front to the lateral pole of the condyle behind. It may function to prevent posterior displacement of the resting condyle.

Synovial membrane

The synovial membrane lines the inside of the capsule of the joint but does not extend to cover the disc or the articular surfaces.

Development of the temporomandibular joint

The bony components of the secondary jaw joint develop in membrane as two separate ectomesenchymal condensations between the 8th and 12th week *in utero*. This arrangement is different from that seen with most synovial joints, where a single blastema cavitates to form a joint space and the articulating bones are derived from the same condensation of tissue (see Ch. 51). The separate development of the temporal and condylar parts of the temporomandibular joint means that the articular surface of each bone is covered by a persisting layer of proliferative cells that is continuous with the periosteum surrounding each separate bony component (Fig. 31.7).

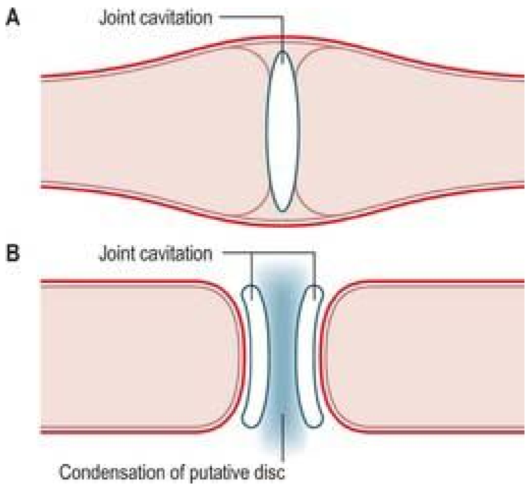

Fig. 31.7 **A,B**, Development of the temporomandibular joint; the temporal and condylar components of the joint develop from two separate condensations of ectomesenchyme.

Articular surfaces

The fibrocartilaginous covering of the condyle is composed of four distinct layers (De Bont et al 1984). The most superficial layer consists of densely packed fibres of type I collagen that are arranged mostly parallel to the articular surface. This covers a thin cellular layer, the proliferative zone, that is continuous with the cambial layer of the periosteum beyond the margins of the joint. The third layer, of hypertrophic cartilage, is rich in intercellular matrix: it contains chondrocytes scattered throughout its depth, and randomly oriented fibres of collagen type II. The fourth layer, immediately above the subchondral bone, is the zone of calcification. Although the number of chondrocytes within the hypertrophic zone decreases with age, undifferentiated mesenchymal cells have been identified in post mortem specimens of all ages (Hansson 1977). This indicates that a capacity for proliferation persists in condylar cartilage, and may be the reason why condylar remodeling occurs throughout life (Robinson 1993, Toller 1974).

Articular disc

The transversely oval articular disc is composed predominantly of dense fibrous connective tissue with some chondrification in areas of maximum loading (Fig. 31.8). It has a thick margin which forms a peripheral anulus and a central depression in its lower surface that accommodates the articular surface of the mandibular condyle. The depression probably develops as a mechanical response to pressure from the condyle as it rotates inside the anulus. The disc is stabilized on the condyle in three ways. Its edges are fused with the part of the capsular ligament that tightly surrounds the lower joint compartment and is attached around the neck of the condyle; well-defined bands in the capsular ligament attach the disc to the medial and lateral poles of the condyle, and additionally, the thick anulus prevents the disc sliding off the condyle, provided that the condyle and disc are firmly lodged against the articular fossa (as is normally the case).

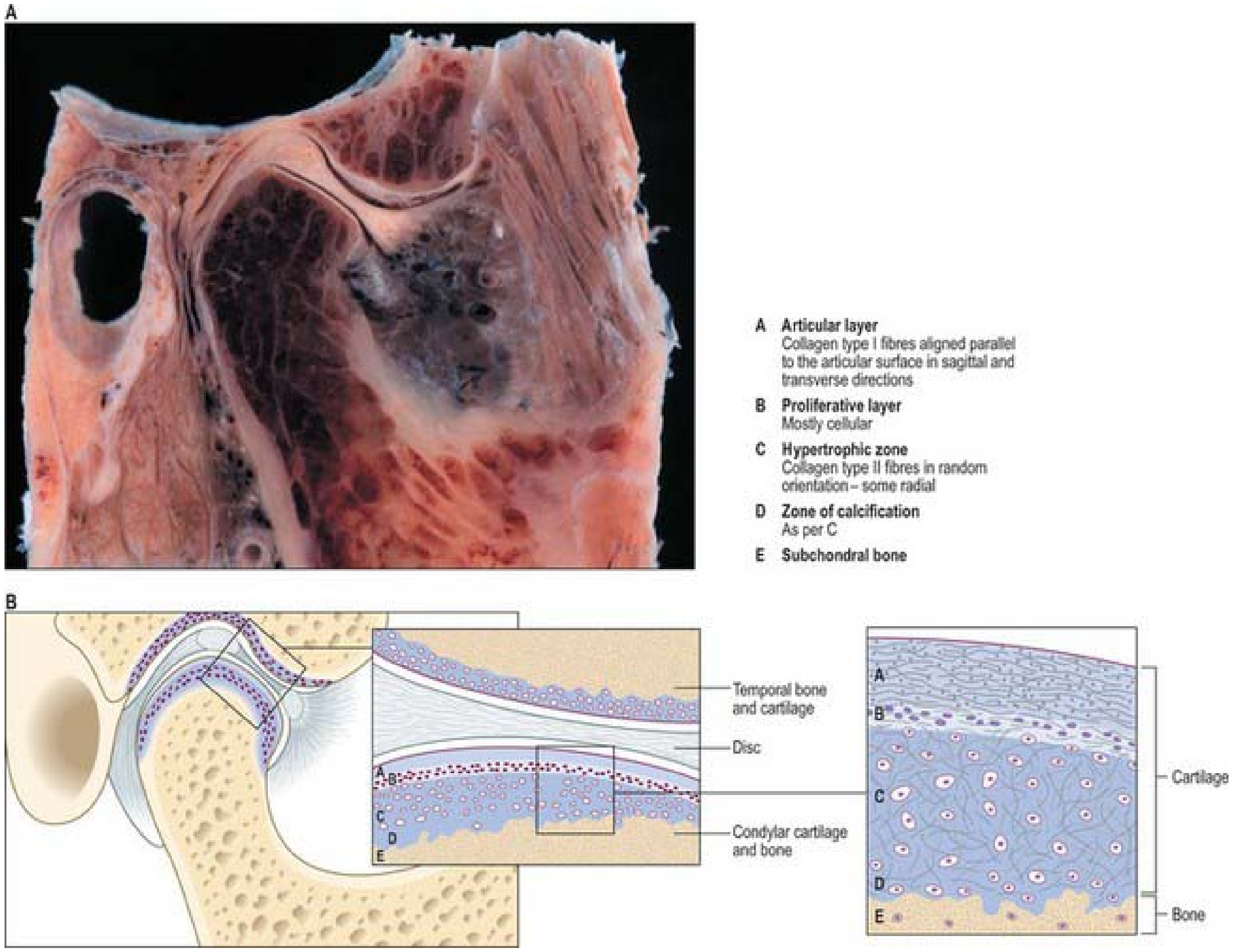
A
A Articular layer
Collagen type I fibres aligned parallel to the articular surface in sagittal and transverse directions
B Proliferative layer
Mostly cellular
C Hypertrophic zone
Collagen type II fibres in random orientation – some radial
D Zone of calcification
As per C
E Subchondral bone
B
Temporal bone and cartilage
Disc
Condylar cartilage and bone
A
B
C
D
E
A
B
C
D
E
Cartilage
Bone

Fig. 31.8 **A,B**, Sagittal sections through the right temporomandibular joint. **A**, Note the relationship of the external auditory meatus and articular disc to the mandibular condyle. **B**, The microstructure of condylar cartilage.

(By courtesy of Professor Cristina Manzanares Céspedes, Anatomy and Human Embryology Unit, Bellvitge Campus, University of Barcelona.)

In sagittal section, the disc appears to possess a thin intermediate zone and thickened anterior and posterior bands, and its upper surface appears concavo-convex where it fits against the convex articular eminence and the concavity of the articular fossa. Posteriorly the disc is attached to a region of loose vascular and nervous tissue which splits into two laminae, the bilaminar region: unlike the rest of the disc, its normal function is to provide attachment rather than intra-articular support. The upper lamina, composed of fibroelastic tissue, is attached to the squamotympanic fissure, and the lower lamina, composed of fibrous non-elastic tissue, is attached to the back of the condyle. The bilaminar region contains a venous plexus, but the central part of the disc is avascular. Cells in the disc also secrete chondroitin sulphate (a glycosaminoglycan found in cartilage) which is most heavily concentrated in the centre of the disc and which probably gives the disc some of the resilience and compressive strength of cartilage. The amount increases in response to load and to age, and by the fifth decade the disc shows signs of ageing including fraying, thinning and perforation.

Functions of the articular disc

The functions of the articular disc remain controversial. It is generally believed that the disc helps to stabilize the condyle within the temporomandibular joint (although see below). The articulating surfaces of the mandibular condyle and the articular fossa fit together poorly and so are separated by an irregular space. Muscle forces control the position of the mandible, and therefore of the condyle, in relation to the articular eminence, and these in turn determine the shape and thickness of the irregular space. The position of the disc is controlled by neuromuscular forces: the upper head of lateral pterygoid anteriorly, and the elastic tissue in the bilaminar region posteriorly, together pull the disc forward or backward to keep the joint space filled and thereby stabilize the condyle.

The presence of an articular disc may also reduce wear, because the frictional force on the condyle and the articular eminence is halved by separating slide and rotation into different joint compartments, and may aid lubrication of the joint by storing fluid squeezed out from loaded areas to create a weeping lubricant.

There is an alternative view that a slippery articular disc doubles the number of virtually friction-free sliding surfaces, and so destabilizes the condyle in the same way that stepping on a banana skin destabilizes the foot. All other joints are most heavily loaded when their articular surfaces are closely fitted together, creating a large area of contact, and braced to prevent further movement. However the condyle of the mandible is most heavily loaded when it is required to move, sliding backward during the buccal phase of the power stroke of a masticatory cycle on the opposite side of the jaw.

Relations

Superiorly a thin plate of temporal bone (2–3 mm) separates the upper joint space from the middle cranial fossa. This bony partition is occasionally breached inadvertently during surgery to the joint, particularly for release of ankylosis, or rarely by the condyle being driven superiorly by violent trauma to the mandible. The maxillary artery and its proximal branches, most notably the middle meningeal artery, lie medially, just beyond the joint capsule. The uppermost part of the parotid capsule enclosing the branches of the facial nerve that supply the muscles of the upper face, including obicularis oculi, are lateral to the joint capsule: the thread-like nerves are at risk during surgical approach to the joint. The upper part of the infratemporal space, which contains the two heads of lateral pterygoid, is anterior to the condyle (Fig. 31.9). It is into this space anterior to the articular eminence that the condyle is displaced in cases of dislocation of the TMJ or fracture dislocation of the condylar head. Posteriorly is the tegmen tympani and behind it the middle ear cavity. Perforation through this thin bony wall into the middle ear is a recognized complication of TMJ arthroscopy. Just below the joint, the maxillary artery winds around the posterior aspect of the condylar neck.

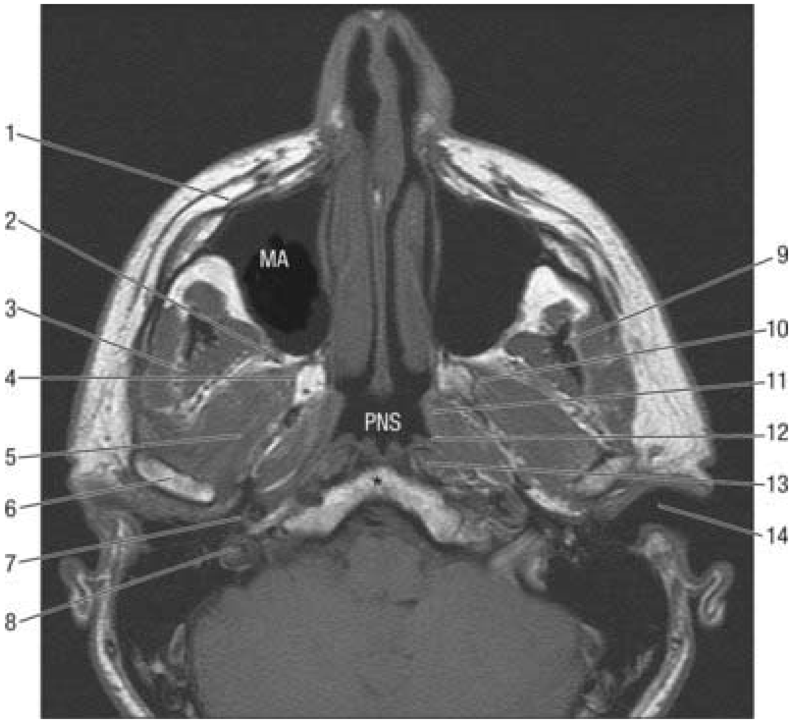

Fig. 31.9 Axial MRI at level of external acoustic meatus: **1**. Body of zygoma; **2**. Pterygopalatine fossa; **3**. Temporalis; **4**. Medial pterygoid plate; **5**. Lateral pterygoid; **6**. Condylar head; **7**. Internal carotid artery; **8**. Jugular bulb/foramen; **9**. Coronoid process; **10**. Lateral pterygoid plate; **11**. Torus tubarius; **12**. Fossa of Rosenmüller; **13**. Longus colli; **14**. External auditory meatus. MA, Maxillary antrum; PNS, Postnasal space. *, Anterior arch of atlas.

Vascular supply and innervation

The articular tissues and the dense part of the articular disc have no nerve supply. Branches of the auriculotemporal and masseteric nerves and postganglionic sympathetic nerves supply the tissues associated with the capsular ligament and the looser posterior bilaminar extension of the disc. The temporomandibular joint capsule, lateral ligament and retroarticular tissue contain mechanoreceptors and nociceptors. The input from mechanoreceptors provides a source of proprioceptive sensation that helps control mandibular posture and movement.

The joint derives its arterial supply from the superficial temporal artery laterally and the maxillary artery medially. Penetrating vessels that supply lateral pterygoid may also supply the condyle. Veins drain the anterior aspect of the joint and associated tissues into the plexus surrounding lateral pterygoid, and posteriorly they drain into the vascular region that separates the two laminae of the bilaminar region of the disc. Pressure produced by forward and backward movement of the condyle shunts blood between these regions. Lymphatics drain deeply to the upper cervical lymph nodes surrounding the internal jugular vein.

Jaw movements

Movements of the condyle in the temporomandibular joint

The major function of the mandible is to exert, via the teeth, the force necessary to break down food into smaller particles and so facilitate digestion. Pure vertical movements of the lower teeth create a crushing force that is ineffective in breaking up tough fibrous food. Man uses a lateral movement of the lower jaw to create a shear component of force that enhances the effectiveness of the power stroke of mastication. Bodily lateral movement of the whole jaw, the Bennett shift, is insignificant. Extensive lateral movement is only possible when the jaw is rotated horizontally about one condyle while the other condyle slides backward and forward.

The temporomandibular joint is structurally adapted to accommodate both sliding and rotation in a parasagittal plane. Sliding occurs because the capsular ligament which surrounds the upper joint compartment is loose, whereas the capsular ligament which encloses the lower joint compartment is tight, and only allows the condyle to rotate over the depression inside the anulus of the articular disc. The normal range of maximum mouth opening measured between the upper and lower incisor tips is 35–50 mm. The adult range of movements is reached at around 10 years in females and 15 years in males. Lateral excursions of the chin can normally achieve 8–12 mm of movement at the lower incisors.

Symmetrical opening

Symmetrical jaw opening is associated with preparation for incising. At the start, each mandibular condyle rotates in the lower joint compartment inside the anulus of its disc. After a few degrees of opening, the condyle continues rotating inside its disc, and, in addition, both slide forward down the articular eminence of the upper joint compartment. Without this forward slide, it becomes impossible to continue opening the jaw beyond a gape of approximately 25 mm.

There are conflicting views about the reason why forward slide occurs, probably because direct experimental testing is not possible. No other animal has an articular eminence constraint and ligaments comparable to man, which means that most supporting evidence for any theory is based on analyses of human joint dysfunction. It has been argued that a sensory input from the rotary movement, possibly from either the joint capsule or the jaw muscles, initiates a response that reflexly activates muscles that cause the slide. The fact that the condyle in a cadaver still slides forward when the jaw is rotated open suggests that it is not a neuromuscular response, but that it is the mechanical result of physical constraints. When the jaw is rotated open the temporomandibular ligament rapidly becomes taut (Osborn 1995b). The taut ligament acts as a constraint that allows the mandible only two rotary movements: it can swing about the upper attachment of the ligament and rotate about the lower attachment. The lower end of the taut ligament acts as a moving fulcrum that converts the downward and backward pull of the opening rotary force (created at the front by digastric and geniohyoid) into one that drives the condyle upward and forward into the concavity of the overlying articular disc. This now pushes the disc forward. Swing about the upper attachment creates space above for the disc to slide further forward which is possible because the upper part of the capsular ligament is loose. The two movements, rotation and swing, are inextricably linked by the taut ligament and, via the condyle, combine to keep the disc in firm contact with the articular eminence while the jaw is opened. The disc is stabilized by its tight attachment to the condyle and by the thickened margins of its anulus that prevent it sliding through the thinner compressed region between the centre of the condyle and the articular eminence.

As forward slide of the condyle continues, the controlling influence exerted by the temporomandibular ligament diminishes. The lingula of the mandible moves away from the spine of the sphenoid, tautening the originally slack sphenomandibular ligament, which now acts in the same way as the temporomandibular ligament, to maintain the condyle against the articular eminence. Symmetrical opening thus appears to consist of at least three separate phases: an early phase controlled by the temporomandibular ligament and articular eminence; a short middle phase in which either both, or neither, temporomandibular and sphenomandibular ligaments act to constrain movements; and a late phase controlled by the sphenomandibular ligament and articular eminence.

Changes in disc position during movement

With the teeth in occlusion, the condyle is in the glenoid fossa and the intra-articular disc sits on the condylar head; its posterior band above the summit of the condyle (Fig. 31.10A). As mouth opening begins (Fig. 31.10B), the condyle rotates within the lower joint space and the disc remains stationary. At about mid-opening, the condyle and disc begin to move forward together so that their relative position is maintained (Fig. 31.10C). At maximum gape (Fig. 31.10D) the condylar head slides further anteriorly than the disc so that the anterior band of the articular disc is above the summit of the condyle. Mouth closure involves the disc moving back in tandem with the condyle (Fig. 31.10E) which also reverses its angular rotation (Fig. 31.10F) to reassume the starting position of the cycle.

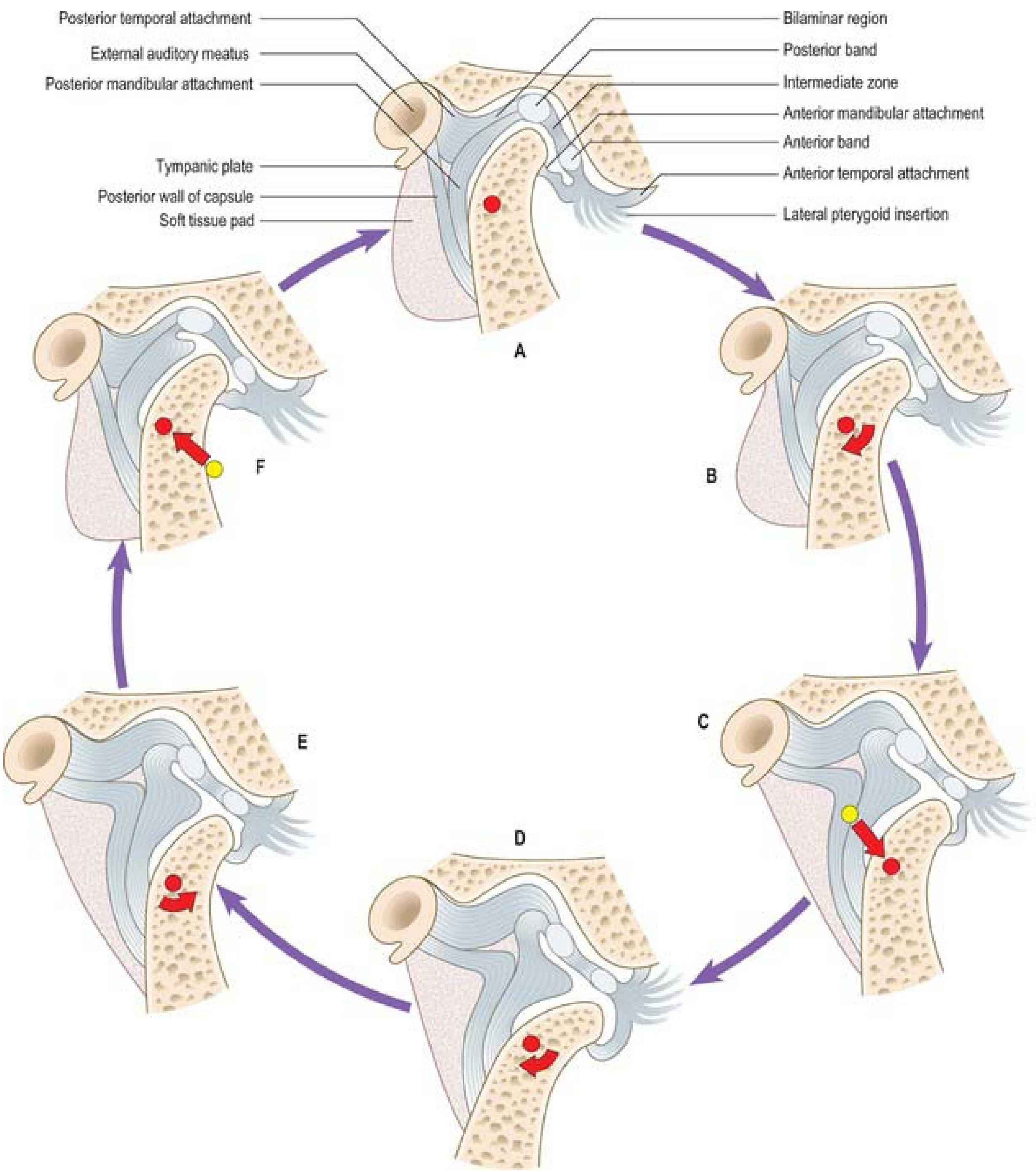
Posterior temporal attachment
External auditory meatus
Posterior mandibular attachment
Tympanic plate
Posterior wall of capsule
Soft tissue pad
Bilaminar region
Posterior band
Intermediate zone
Anterior mandibular attachment
Anterior band
Anterior temporal attachment
Lateral pterygoid insertion
A
B
C
D
E
F

Fig. 31.10 Changing relationships of the condyle of the mandible, the articular disc and the articular surface of the temporal bone during one complete opening (A → D) and closing (D → A) cycle of the mouth.

Commonly, the shifts in disc position become out of phase with those of the condyle, which causes obstruction to smooth jaw movement. The disc is typically pulled anteromedially by lateral pterygoid, so preventing forward translation of the condyle. As the force from the condyle on the disc increases, the elastic posterior attachments of the disc are stretched until the resistance to movement is overcome and the energy that had been stored is then released with an audible click (audible to the patient, and occasionally to others). The normal disc–condyle relation is then reestablished and the mouth is free to achieve maximum gape (Fig. 31.10C,D). The disc may then snap back in front of the condyle on mouth closure. This phenomenon is called reciprocal clicking or disc displacement with reduction.

If the disc is pulled completely anterior to the condylar head, so that it is not reduced during opening, the condyle is prevented from any forward translation and mouth opening is limited to the rotational component and therefore a maximum gape of 25 mm. This is also a common clinical condition and is known appropriately as closed lock or disc displacement without reduction.

Eccentric jaw opening

Eccentric jaw opening is associated with preparing for the power stroke of mastication. The mandibular condyle on the non-working side slides back and forth during lateral movements associated with the power stroke on the working side. Although the jaw muscles now have the major control over mandibular movements, the temporomandibular and sphenomandibular ligaments keep the condyle firmly against its articular eminence during opening.

Eccentric and symmetrical jaw closing

The resultant of the jaw closing muscles of the mandible has a component that forces the joint surfaces together. This compresses the joint tissues and potentially shortens the ligaments so that they no longer constrain jaw movements. Under these conditions, jaw movements and the positions of the condyles are controlled by neuromuscular processes (within the limits of constraints imposed by the articular eminence, the occluding surfaces of the teeth and the presence of food between them). Note that the non-working condyle moves the furthest, and is the most heavily loaded, during the power stroke of mastication. The loads on each joint, balancing and working, drive each condyle more forcefully into its articular eminence.

The envelope of motion

The envelope of motion is the volume of space within which all movements of a point on the mandible have to occur because the limits are set by anatomical features, i.e. by the shape or size of the upper and lower jaws, by tooth contacts, and by the attachment of muscle and ligaments.

In consciously controlled movement of the jaw from the rest position to the fully opened position, the trajectory of the mandibular incisal edge is two-phased. The first phase is a hinge-like movement during which the condyles are retruded within the mandibular fossae. When the teeth are opened by approximately 25 mm, the second phase of opening occurs by anterior movement or protrusion of the condyles down the articular eminences with further rotation.

If conscious effort is used, a closure path can then be followed in which the jaw is closed to an extreme protruded tooth contact position after which it has to be retruded to the starting position. The free, habitual, unconscious movement during both jaw opening and closing has a significantly more limited trajectory. Similar considerations apply to lateral movements: mandibular rotation around a retruding condyle and the protraction of the opposite condyle are anatomically limiting factors that are again rarely encountered in normal function.

Imaging of the temporomandibular joint

Magnetic resonance imaging (MRI) and arthrography have enriched the information available about pathological changes that can occur in all components of the joint, particularly the disc. It is of interest that the advent of these techniques has coincided with a significant reduction in numbers of open surgical operations for abnormality of disc position (collectively known as internal derangements). MRI has shown that although disc position and clinical symptoms are often linked, a significant proportion of subjects with no TMJ abnormality in terms of function have grossly abnormal disc movements, and that patients who have undergone disc repositioning procedures often show functional improvement despite persistent displacement of their intra-articular disc. It would appear that the adaptive remodeling capacity of the joint, especially of the mandibular condyle, is an important mechanism for maintaining function of the TMJ.

MUSCLES

The four principal muscles of mastication are medial and lateral pterygoid, temporalis and masseter: their actions produce movements of the mandible at the temporomandibular joints. The infratemporal fossa contains medial and lateral pterygoid and the tendon of temporalis. Masseter lies on the face, on the lateral surface of the ramus of the mandible, but will be considered here.

Masseter

Masseter (Fig. 31.11) consists of three layers which blend anteriorly. The superficial layer is the largest. It arises by a thick aponeurosis from the maxillary process of the zygomatic bone and from the anterior two-thirds of the inferior border of the zygomatic arch. Its fibres pass downwards and backwards, to insert into the angle and lower posterior half of the lateral surface of the mandibular ramus. Intramuscular tendinous septa in this layer are responsible for the ridges on the surface of the ramus. The middle layer of masseter arises from the medial aspect of the anterior two-thirds of the zygomatic arch and from the lower border of the posterior third of this arch. It inserts into the central part of the ramus of the mandible. The deep layer arises from the deep surface of the zygomatic arch and inserts into the upper part of the mandibular ramus and into its coronoid process. There is still debate as to whether fibres of masseter are attached to the anterolateral part of the articular disc of the temporomandibular joint. Masseteric hypertrophy, e.g. in response to excessive use of masseter, may be treated by surgical reduction from the deep aspect of masseter or injections of botulinus toxin to paralyse the motor nerves.

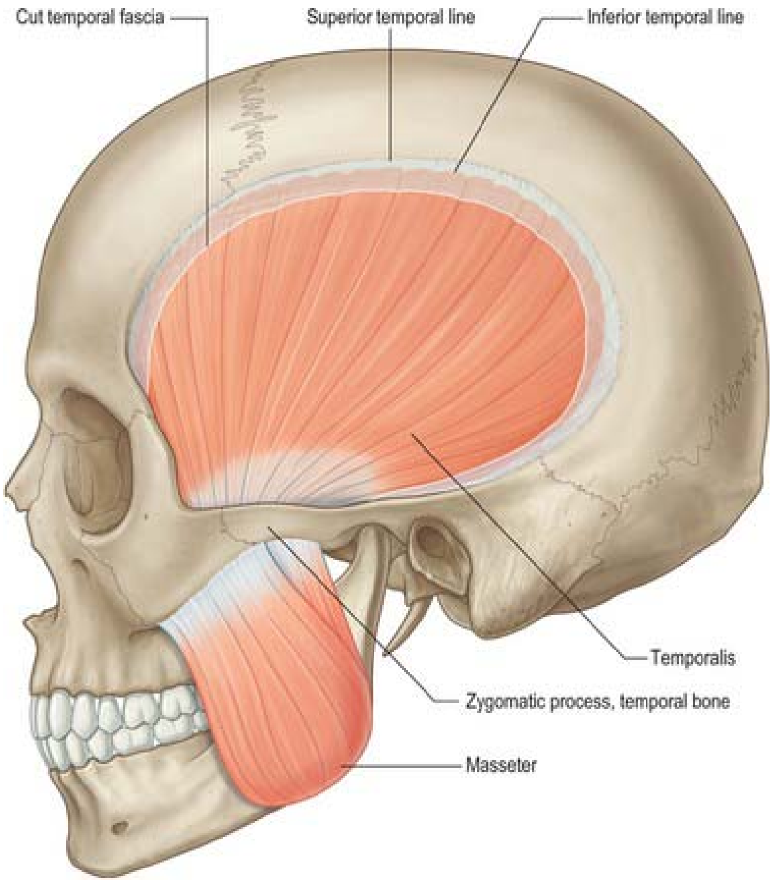
Cut temporal fascia
Superior temporal line
Inferior temporal line
Temporalis
Zygomatic process, temporal bone
Masseter

Fig. 31.11 Masseter and temporalis muscles.

(Adapted from Drake, Vogl and Mitchell 2005.)

Relations

Skin, platysma, risorius, zygomaticus major, the parotid gland and duct, branches of the facial nerve and the transverse facial branches of the superficial temporal vessels are all superficial relations. Temporalis and the ramus of the mandible lie deep to masseter. The anterior margin of masseter is separated from buccinator and the buccal branch of the mandibular nerve by a buccal pad of fat and crossed by the facial vein. The posterior margin of the muscle is overlapped by the parotid gland. The masseteric nerve and artery reach the deep surface of masseter by passing over the mandibular incisure (mandibular notch).

Vascular supply

Masseter is supplied by the masseteric branch of the maxillary artery, the facial artery and the transverse facial branch of the superficial temporal artery.

Innervation

Masseter is supplied by the masseteric branch of the anterior trunk of the mandibular nerve.

Actions

Masseter elevates the mandible to occlude the teeth in mastication and has a small effect in side-to-side movements, protraction and retraction. Its electrical activity in the resting position of the mandible is minimal.

Submasseteric space infections

Sometimes infection around a mandibular third molar tooth tracks backwards, lateral to the mandibular ramus and pus localizes deep to the attachment of masseter in the submasseteric tissue space. Such an abscess, lying deep to this thick muscle produces little visible swelling, but is accompanied by profound muscle spasm and severe limitation of jaw opening (trismus).

Temporalis

Temporalis (Fig. 31.11) arises from the whole of the temporal fossa up to the inferior temporal line – except the part formed by the zygomatic bone – and from the deep surface of the temporal fascia. Its fibres converge and descend into a tendon which passes through the gap between the zygomatic arch and the side of the skull. A plane exists beneath the temporal fascia, which is attached to the superior surface of the zygomatic arch, and the muscle, which passes beneath the arch. An elevator introduced into this plane through an incision above the hairline may therefore be placed beneath a fractured zygomatic arch or bone in order to reduce the fracture (Gillies approach). Temporalis is attached to the medial surface, apex, anterior and posterior borders of the coronoid process and to the anterior border of the mandibular ramus almost up to the third molar tooth. Its anterior fibres are orientated vertically, the most posterior fibres almost horizontally, and the intervening fibres with intermediate degrees of obliquity, in the manner of a fan. Fibres of temporalis may occasionally gain attachment to the articular disc.

Relations

Skin, auriculares anterior and superior, temporal fascia, superficial temporal vessels, the auriculotemporal nerve, temporal branches of the facial nerve, the zygomaticotemporal nerve, the epicranial aponeurosis, the zygomatic arch and the masseter muscle are all superficial relations. Posterior relations of temporalis are the temporal fossa above and the major components of the infratemporal fossa below. Behind the tendon of the muscle, the masseteric nerve and vessels traverse the mandibular notch. The anterior border is separated from the zygomatic bone by a mass of fat.

Vascular supply

Temporalis is supplied by the deep temporal branches from the second part of the maxillary artery. The anterior deep temporal artery supplies 20% of the muscle anteriorly, the posterior deep temporal supplies 40% of the muscle in the posterior region and the middle temporal artery supplies 40% of the muscle in its mid-region.

Innervation

Temporalis is supplied by the deep temporal branches of the anterior trunk of the mandibular nerve.

Actions

Temporalis elevates the mandible and so closes the mouth and approximates the teeth. This movement requires both the upward pull of the anterior fibres and the backward pull of the posterior fibres, because the head of the mandibular condyle rests on the articular eminence when the mouth is open. The muscle also contributes to side-to-side grinding movements. The posterior fibres retract the mandible after it has been protruded.

Lateral pterygoid

Lateral pterygoid (Fig. 31.12) is a short, thick muscle consisting of two parts. The upper head arises from the infratemporal surface and infratemporal crest of the greater wing of the sphenoid bone. The lower head arises from the lateral surface of the lateral pterygoid plate. From the two origins, the fibres converge, and pass backwards and laterally, to be inserted into a depression on the front of the neck of the mandible (the pterygoid fovea). A part of the upper head may be attached to the capsule of the temporomandibular joint and to the anterior and medial borders of its articular disc. Unlike the other muscles of mastication, lateral pterygoid is not pennate, nor does it have a significant number of Golgi tendon organs associated with its attachments.

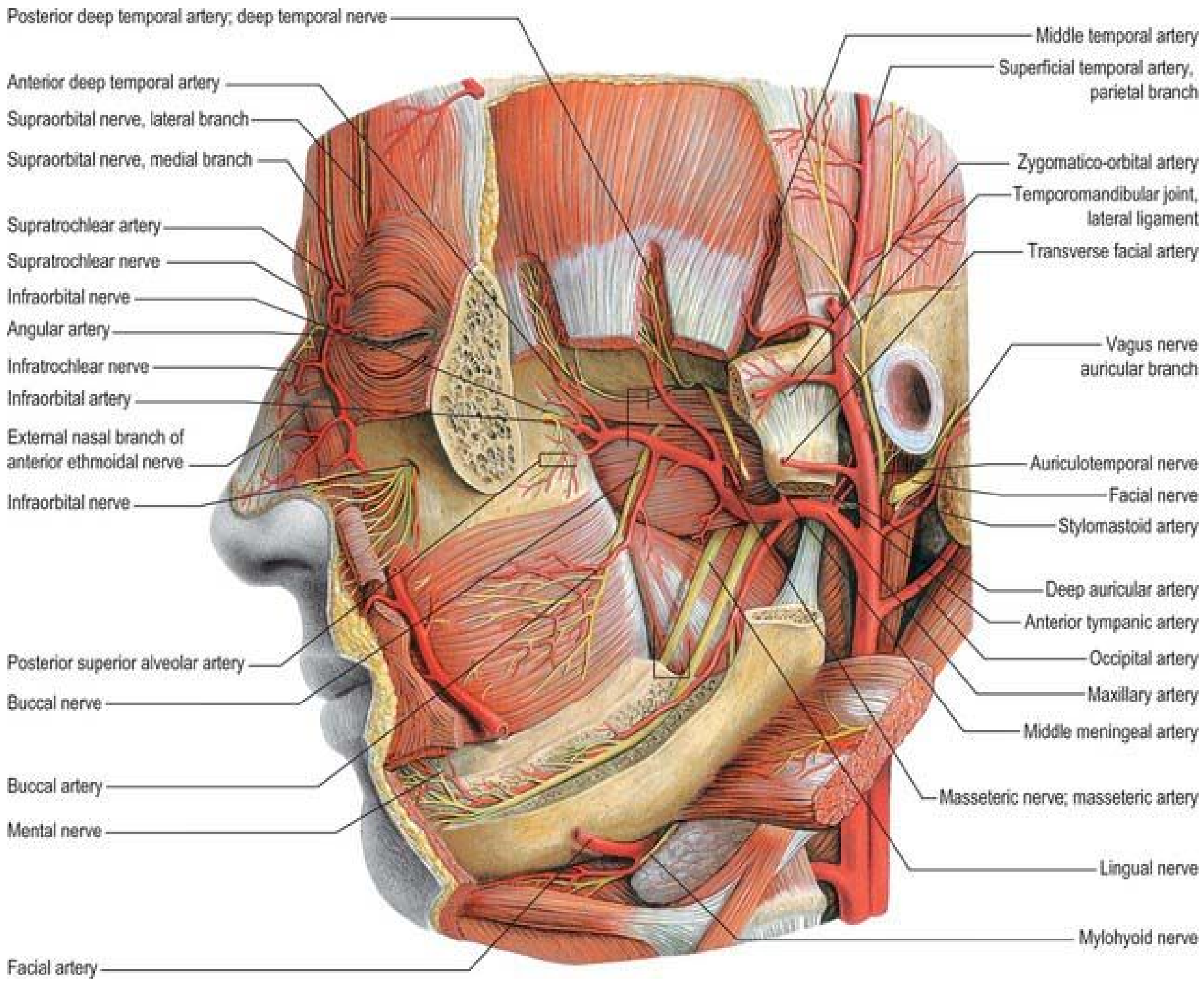
Posterior deep temporal artery; deep temporal nerve
Anterior deep temporal artery
Supraorbital nerve, lateral branch
Supraorbital nerve, medial branch
Supratrochlear artery
Supratrochlear nerve
Infraorbital nerve
Angular artery
Infratrochlear nerve
Infraorbital artery
External nasal branch of
anterior ethmoidal nerve
Infraorbital nerve
Posterior superior alveolar artery
Buccal nerve
Buccal artery
Mental nerve
Facial artery
Middle temporal artery
Superficial temporal artery,
parietal branch
Zygomatico-orbital artery
Temporomandibular joint,
lateral ligament
Transverse facial artery
Vagus nerve
auricular branch
Auriculotemporal nerve
Facial nerve
Stylomastoid artery
Deep auricular artery
Anterior tympanic artery
Occipital artery
Maxillary artery
Middle meningeal artery
Masseteric nerve; masseteric artery
Lingual nerve
Mylohyoid nerve

Fig. 31.12 Arteries and nerves of the head; deeper lateral regions. Most of the zygomatic arch and the ramus and body of the mandible have been removed; masseter has been cut and reflected laterally.

(From Sobotta 2006.)

Relations

The mandibular ramus and masseter, the maxillary artery – which crosses either deep or superficial to the muscle – and the superficial head of medial pterygoid and the tendon of temporalis, are all superficial relations. Deep to the muscle are the deep head of medial pterygoid, the sphenomandibular ligament, the middle meningeal artery, and the mandibular nerve. The upper border is related to the temporal and masseteric branches of the mandibular nerve and the lower border is related to the lingual and inferior alveolar nerves. A deeply placed posterior superior alveolar nerve block has been known to also anaesthetize the lingual nerve. The buccal nerve and the maxillary artery pass between the two heads of the muscles. In temporomandibular joint dysfunction syndrome, spasm of lateral pterygoid can give rise to tenderness when palpating behind the maxillary tuberosity high in the buccal sulcus (the pterygoid sign).

Vascular supply

Lateral pterygoid is supplied by pterygoid branches from the maxillary artery which are given off as the artery crosses the muscle and from the ascending palatine branch of the facial artery.

Innervation

The nerves to lateral pterygoid (one for each head) arise from the anterior trunk of the mandibular nerve, deep to the muscle. The upper head and the lateral part of the lower head receive their innervation from a branch given off from the buccal nerve. However, the medial part of the lower head has a branch arising directly from the anterior trunk of the mandibular nerve.

Actions

When left and right muscles contract together the condyle is pulled forward and slightly downward. This protrusive movement alone has little or no function except to assist opening the jaw. Digastric and geniohyoid are the main jaw opening muscles: unlike lateral pterygoid, when acting alone they rotate the jaw open, provided other muscles attached to the hyoid prevent if from being pulled forward. If only one lateral pterygoid contracts, the jaw rotates about a vertical axis passing roughly through the opposite condyle and is pulled medially toward the opposite side. This contraction together with that of the adjacent medial pterygoid (both attached to the lateral pterygoid plate) provides most of the strong medially directed component of the force used when grinding food between teeth of the same side. It is arguably the most important function of the inferior head of lateral pterygoid. It is often stated that the upper head is used to pull the articular disc forward when the jaw is opened. But electromyography studies have proved that the upper head is inactive during jaw opening and most active when the jaws are clenched. An explanation for this surprising activity is as follows (Osborn 1995a). Most of the power of a clenching force is due to contractions of masseter and temporalis. The associated backward pull of temporalis is greater than the associated forward pull of (superficial) masseter, and so their combined jaw closing action potentially pulls the condyle backward. This is prevented by the simultaneous contraction of the upper head of lateral pterygoid.

Medial pterygoid

Medial pterygoid (Fig. 31.12) is a thick, quadrilateral muscle with two heads of origin. The major component is the deep head which arises from the medial surface of the lateral pterygoid plate of the sphenoid bone and is therefore deep to the lower head of lateral pterygoid. The small, superficial head arises from the maxillary tuberosity and the pyramidal process of the palatine bone, and therefore lies on the lower head of lateral pterygoid. The fibres of medial pterygoid descend posterolaterally and are attached by a strong tendinous lamina to the posteroinferior part of the medial surface of the ramus and angle of the mandible, as high as the mandibular foramen and almost as far forwards as the mylohyoid groove. This area of attachment is often ridged. Inferior alveolar nerve block injection can occasionally cause haemorrhage into the muscle, which may give rise to painful trismus.

Relations

The lateral surface of medial pterygoid is related to the mandibular ramus, from which it is separated above its insertion by lateral pterygoid, the sphenomandibular ligament, the maxillary artery, the inferior alveolar vessels and nerve, the lingual nerve and a process of the parotid gland. The medial surface is related to tensor veli palatini and is separated from the superior pharyngeal constrictor by styloglossus and stylopharyngeus and by some areolar tissue.

Vascular supply

Medial pterygoid derives its main arterial supply from the pterygoid branches of the maxillary artery.

Innervation

Medial pterygoid is innervated by the medial pterygoid branch of the mandibular nerve.

Actions

The medial pterygoid muscles assist in elevating the mandible. Acting with the lateral pterygoids they protrude it. When the medial and lateral pterygoids of one side act together, the corresponding side of the mandible is rotated forwards and to the opposite side, with the opposite mandibular head as a vertical axis. Alternating activity in the left and right sets of muscles produces side-to-side movements, which are used to triturate food.

Pterygospinous ligament

The pterygospinous ligament, which is occasionally replaced by muscle fibres, stretches between the spine of the sphenoid bone and the posterior border of the lateral pterygoid plate near its upper end. It is sometimes ossified, and then completes a foramen which transmits the branches of the mandibular nerve to temporalis, masseter and lateral pterygoid.

VASCULAR SUPPLY AND LYMPHATIC DRAINAGE

Maxillary artery

The maxillary artery, the larger terminal branch of the external carotid artery, arises behind the neck of the mandible, and is at first embedded in the parotid gland (see Ch. 29). It then crosses the infratemporal fossa to enter the pterygopalatine fossa through the pterygomaxillary fissure. The artery is widely distributed to the mandible, maxilla, teeth, muscles of mastication, palate, nose and cranial dura mater (Figs 31.12, 31.13). It will be described in three parts, mandibular, pterygoid and pterygopalatine.

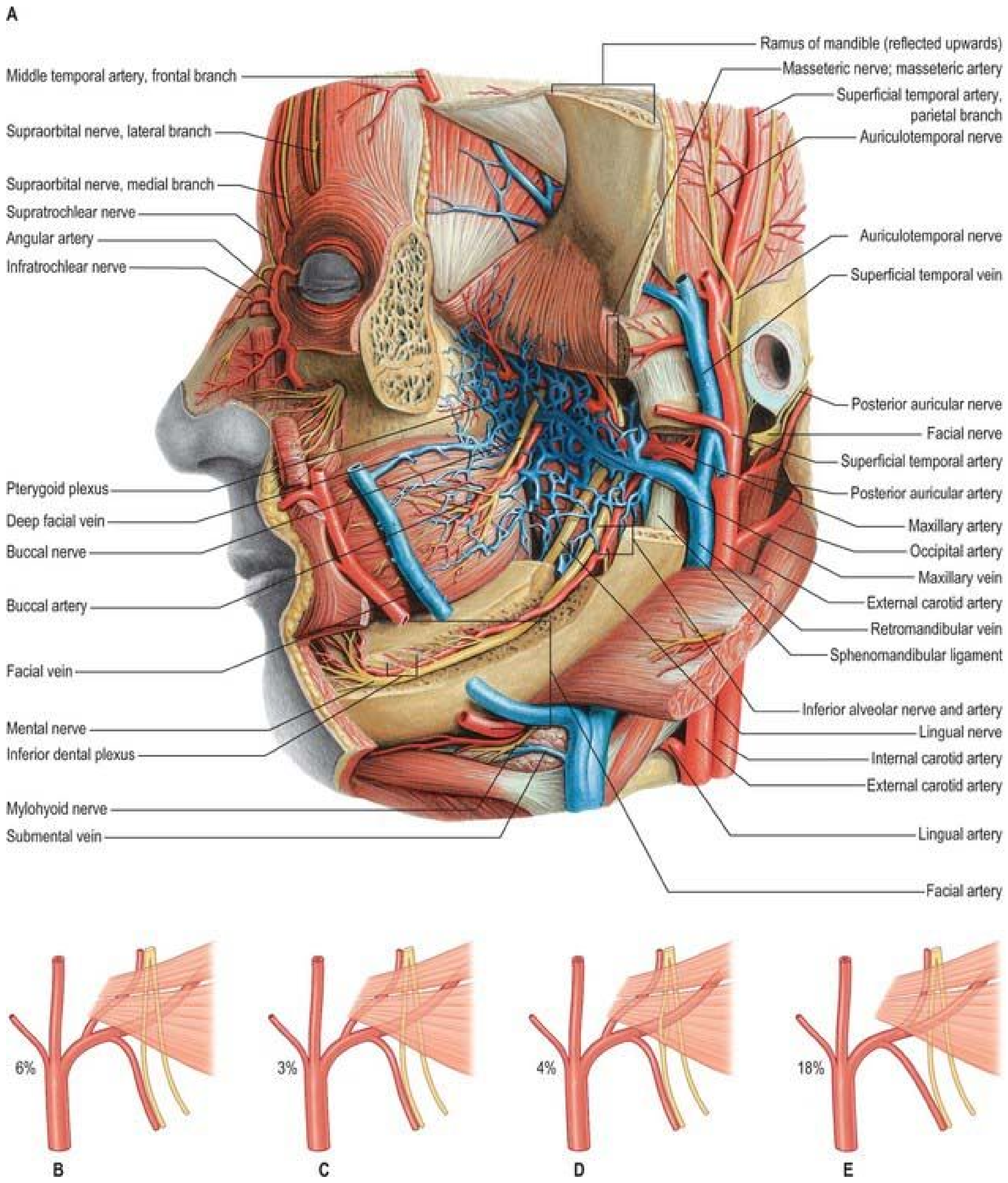
A
Middle temporal artery, frontal branch
Supraorbital nerve, lateral branch
Supraorbital nerve, medial branch
Supratrochlear nerve
Angular artery
Infratrochlear nerve
Pterygoid plexus
Deep facial vein
Buccal nerve
Buccal artery
Facial vein
Mental nerve
Inferior dental plexus
Mylohyoid nerve
Submental vein
Ramus of mandible (reflected upwards)
Masseteric nerve; masseteric artery
Superficial temporal artery, parietal branch
Auriculotemporal nerve
Auriculotemporal nerve
Superficial temporal vein
Posterior auricular nerve
Facial nerve
Superficial temporal artery
Posterior auricular artery
Maxillary artery
Occipital artery
Maxillary vein
External carotid artery
Retromandibular vein
Sphenomandibular ligament
Inferior alveolar nerve and artery
Lingual nerve
Internal carotid artery
External carotid artery
Lingual artery
Facial artery
6%
B
3%
C
4%
D
18%
E

Fig. 31.13 **A**, Vessels and nerves of the head, exposed at a level deeper than that shown in Fig. 31.12 Note the pterygoid venous plexus. **B–E**, Variations in the course of the maxillary artery. In **B**, the maxillary artery passes medial to lateral pterygoid, and to the lingual and inferior alveolar nerves; in **C**, the artery passes between the lingual and inferior alveolar

nerves; in **D**, the artery passes through a loop formed by the inferior alveolar nerve; in **E**, the middle meningeal artery branches off distal to the inferior alveolar artery.

(From Sobotta 2006.)

The mandibular part runs horizontally by the medial surface of the ramus. It passes between the neck of the mandible and the sphenomandibular ligament, parallel with and slightly below the auriculotemporal nerve. It next crosses the inferior alveolar nerve and skirts the lower border of lateral pterygoid. The pterygoid part ascends obliquely forwards medial to temporalis and in 60% of cases is superficial to the lower head of lateral pterygoid. When it runs deep to lateral pterygoid it lies between the muscle and branches of the mandibular nerve, and may project as a lateral loop between the two parts of lateral pterygoid. Asymmetry in this pattern of distribution may occur between the right and left infratemporal fossae and ethnic differences have been reported. Where the maxillary artery runs superficial to the lower head of lateral pterygoid, the commonest pattern is that the artery passes lateral to the inferior alveolar, lingual and buccal nerves. Less frequently, only the buccal nerve crosses the artery laterally, and rarely the artery passes deep to all the branches of the mandibular nerve. The pterygopalatine part passes between the two heads of lateral pterygoid to reach the pterygomaxillary fissure before it passes into the pterygopalatine fossa, where it terminates as the third part of the maxillary artery.

The mandibular part of the maxillary artery has five branches which all enter bone, namely, deep auricular, anterior tympanic, middle meningeal, accessory meningeal and inferior alveolar arteries. The pterygoid part of the maxillary artery has five branches that do not enter bone, but supply muscle, and include deep temporal, pterygoid, masseteric and buccal arteries. The branches of the pterygopalatine part of the artery accompany similarly named branches of the maxillary nerve (including those associated with the pterygopalatine ganglion) and are described in Chapter 32.

Deep auricular artery

The deep auricular artery pierces the osseous or cartilaginous wall of the external acoustic meatus and supplies the skin of the external acoustic meatus and part of the tympanic membrane. A small branch contributes to the arterial supply of the temporomandibular joint.

Anterior tympanic artery

The anterior tympanic artery passes through the petrotympanic fissure to supply part of the lining of the middle ear and accompanies the chorda tympani nerve.

Middle meningeal artery

The middle meningeal artery is the main source of blood to the bones of the vault of the skull (Fig. 31.14). It may arise either directly from the first part of the maxillary artery or from a common trunk with the inferior alveolar artery. When the maxillary artery lies superficial to lateral pterygoid, the middle meningeal artery is usually the first branch of the maxillary artery. However, when the maxillary artery takes a deep course in relation to the muscle this is not usually the case. The middle meningeal artery ascends between the sphenomandibular ligament and lateral pterygoid, passes between the two roots of the auriculotemporal nerve and leaves the infratemporal fossa through the foramen spinosum to enter the cranial cavity medial to the midpoint of the zygomatic bone. Its further course is described in Chapter 27.

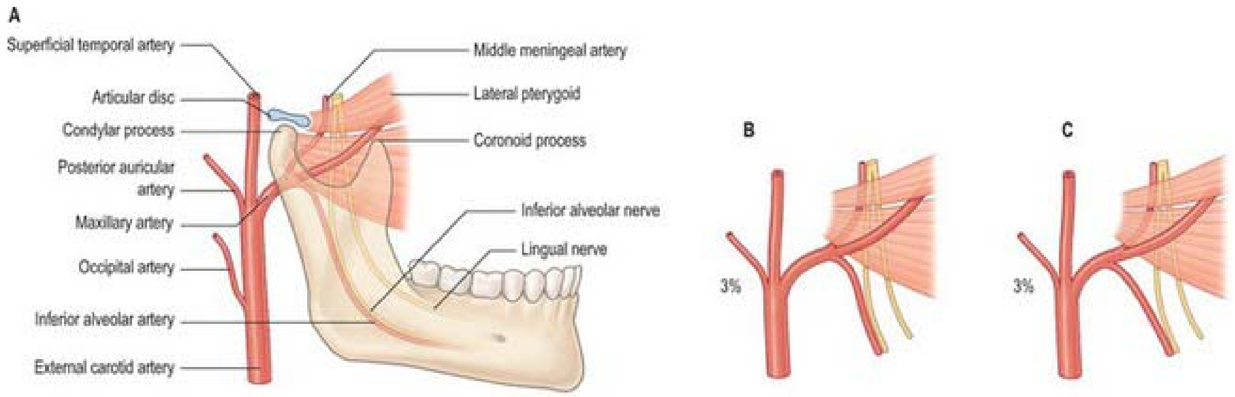
A
Superficial temporal artery
Articular disc
Condylar process
Posterior auricular artery
Maxillary artery
Occipital artery
Inferior alveolar artery
External carotid artery
Middle meningeal artery
Lateral pterygoid
Coronoid process
Inferior alveolar nerve
Lingual nerve
B
3%
C
3%

Fig. 31.14 Variations in the origin of the middle meningeal artery. In **A**, the middle meningeal artery branches off proximal to the inferior alveolar artery; in **B**, the artery branches off opposite the inferior alveolar artery; in **C**, the artery branches off distal to the inferior alveolar artery.

(From Sobotta 2006.)

Accessory meningeal artery

The accessory meningeal artery runs through the foramen ovale into the middle cranial fossa and may arise directly from the maxillary artery or as a branch of the middle meningeal artery itself. In its course in the infratemporal fossa, the accessory meningeal artery is closely related to tensor and levator veli palatini and usually runs deep to the mandibular nerve. Although it runs intracranially, its main distribution is extracranial, principally to medial pterygoid, lateral pterygoid (upper head), tensor veli palatini, the greater wing and pterygoid processes of the sphenoid, branches of the mandibular nerve and the otic ganglion. The accessory meningeal artery is sometimes replaced by separate small arteries.

Deep temporal arteries

The anterior, middle and posterior branches of the deep temporal arteries pass between temporalis and the pericranium, producing shallow grooves in the bone. They anastomose with the middle temporal branch of the superficial temporal artery. The anterior deep temporal artery connects with the lacrimal artery by small branches which perforate the zygomatic bone and greater wing of the sphenoid.

Masseteric artery

The masseteric artery, which is small, accompanies the masseteric nerve as it passes behind the tendon of temporalis through the mandibular incisure (notch) to enter the deep surface of masseter. Its branches can also supply the temporomandibular joint. The masseteric artery anastomoses with the masseteric branches of the facial artery and with the transverse facial branch of the superficial temporal artery.

Pterygoid arteries

The pterygoid arteries are irregular in number and origin, and are distributed to lateral and medial pterygoid.

Buccal artery

The buccal artery runs obliquely forwards between medial pterygoid and the attachment of temporalis and supplies the skin and mucosa over buccinator, accompanying the lower part of the buccal branch of the mandibular nerve. It anastomoses with branches of the facial and infraorbital arteries. A small lingual branch may be given off to accompany the lingual nerve and supply structures in the floor of the mouth.

Maxillary veins and the pterygoid venous plexus

Maxillary vein

The maxillary vein is a short trunk which accompanies the first part of the maxillary artery (Fig. 31.13A). It is formed from the confluence of veins from the pterygoid plexus and passes back between the sphenomandibular ligament and the neck of the mandible, to enter the parotid gland. It unites within the substance of the gland with the superficial temporal vein to form the retromandibular vein.

Pterygoid venous plexus

The pterygoid plexus of veins is found partly between temporalis and lateral pterygoid and partly between the two pterygoid muscles. Sphenopalatine, deep temporal, pterygoid, masseteric, buccal, alveolar (dental), greater palatine and middle meningeal veins and a branch or branches from the inferior ophthalmic vein are all tributaries. The plexus connects with the facial vein via the deep facial vein and with the cavernous sinus through veins that pass through the sphenoidal emissary foramen, foramen ovale and foramen lacerum. Its deep temporal tributaries often connect with tributaries of the anterior diploic veins and thus with the middle meningeal veins.

INNERVATION

The infratemporal fossa contains the major subdivisions of the mandibular branch of the trigeminal nerve, together with the chorda tympani, which enters the fossa and joins the lingual nerve, and the otic ganglion, which is functionally related to the parotid gland. The main sensory branches of the mandibular nerve extend beyond the infratemporal fossa and their distribution to the face is described in Chapter 29.

Mandibular nerve

The mandibular nerve is the largest trigeminal division and is a mixed nerve. Its sensory branches supply the teeth and gums of the mandible, the skin in the temporal region, part of the auricle – including the external meatus and tympanic membrane – and the lower lip, the lower part of the face and the mucosa of the anterior two-thirds (presulcal part) of the tongue and the floor of the oral cavity (Figs 31.12, 31.13A, 31.15). The motor branches innervate the muscles of mastication. The large sensory root emerges from the lateral part of the trigeminal ganglion and exits the cranial cavity through the foramen ovale. The small motor root passes under the ganglion and through the foramen ovale to unite with the sensory root just outside the skull. As it descends from the foramen ovale, the nerve is usually around 4 cm from the surface and a little anterior to the neck of the mandible. The mandibular nerve immediately passes between tensor veli palatini, which is medial, and lateral pterygoid, which is lateral, and gives off a meningeal branch and the nerve to medial pterygoid from its medial side. The nerve then divides into a small anterior and large posterior trunk. The anterior division gives off branches to the four main muscles of mastication and a buccal branch which is sensory to the cheek. The posterior division gives off three main sensory branches, the auriculotemporal, lingual and inferior alveolar nerves, and motor fibres to supply mylohyoid and the anterior belly of digastric.

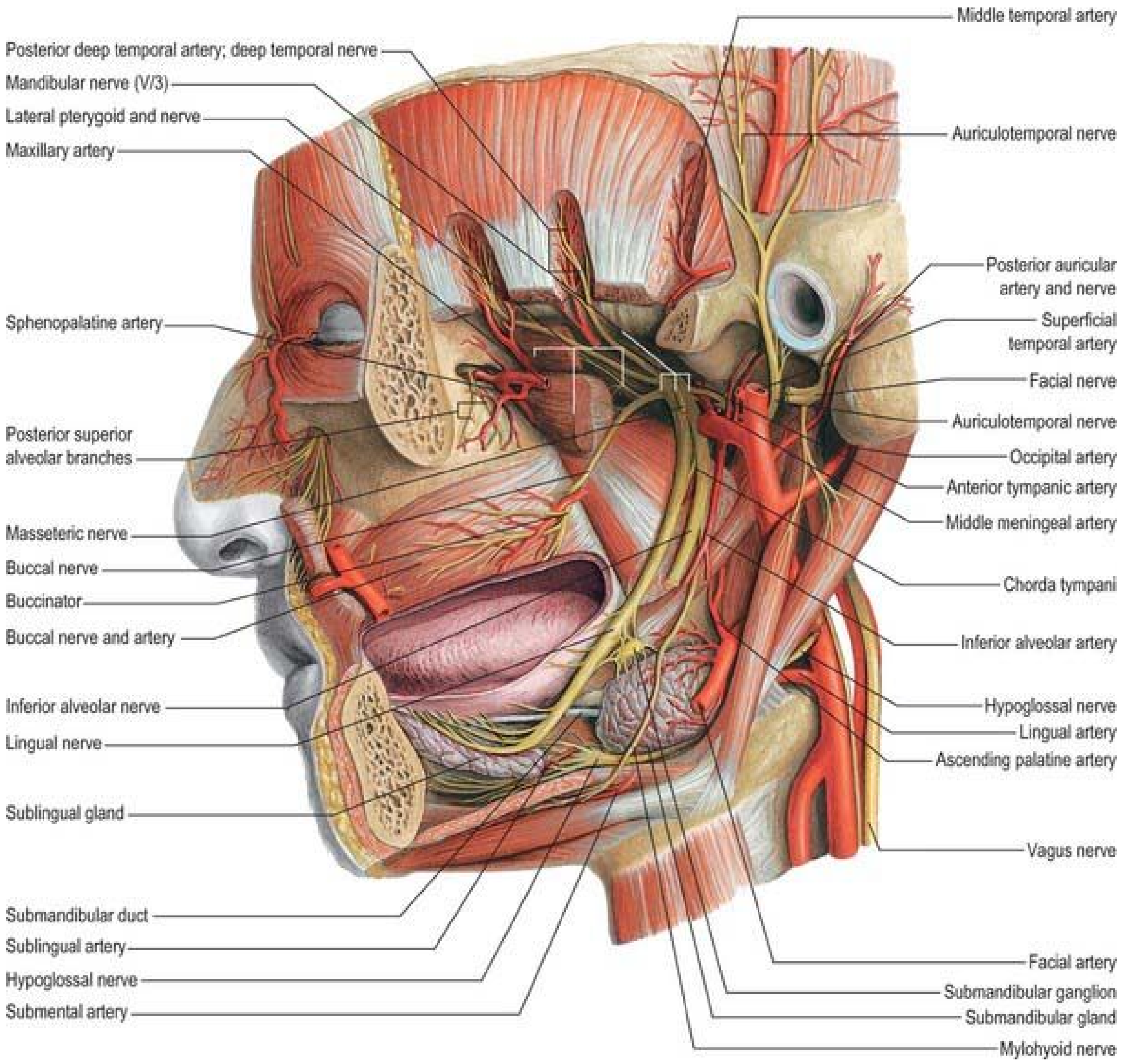
Middle temporal artery
Posterior deep temporal artery; deep temporal nerve
Mandibular nerve (V/3)
Lateral pterygoid and nerve
Maxillary artery
Auriculotemporal nerve
Posterior auricular artery and nerve
Sphenopalatine artery
Superficial temporal artery
Facial nerve
Auriculotemporal nerve
Posterior superior alveolar branches
Occipital artery
Anterior tympanic artery
Middle meningeal artery
Masseteric nerve
Buccal nerve
Buccinator
Chorda tympani
Buccal nerve and artery
Inferior alveolar artery
Inferior alveolar nerve
Hypoglossal nerve
Lingual nerve
Lingual artery
Ascending palatine artery
Sublingual gland
Vagus nerve
Submandibular duct
Sublingual artery
Hypoglossal nerve
Submental artery
Facial artery
Submandibular ganglion
Submandibular gland
Mylohyoid nerve

Fig. 31.15 Arteries and nerves of the head, deepest lateral regions. Compare with **Figs 31.12** and **31.13A**.

(From Sobotta 2006.)

Meningeal branch (nervus spinosus)

The meningeal branch re-enters the cranium through the foramen spinosum with the middle meningeal artery. It divides into anterior and posterior branches which accompany the main divisions of the middle meningeal artery and supply the dura mater in the middle cranial fossa and, to a lesser extent, in the anterior fossa and calvarium.

Nerve to medial pterygoid

The nerve to medial pterygoid is a slender ramus which enters the deep aspect of the muscle. It supplies one or two filaments that pass through the otic ganglion without interruption to supply tensor tympani and tensor veli palatini.

Anterior trunk of mandibular nerve

The anterior trunk of the mandibular nerve gives rise to the buccal nerve, which is sensory, and the masseteric, deep temporal and lateral pterygoid nerves, which are all motor.

Buccal nerve

The buccal nerve passes between the two heads of lateral pterygoid. It descends deep to the tendon of temporalis, passes laterally in front of masseter, and anastomoses with the buccal branches of the facial nerve. It carries the motor fibres to lateral pterygoid, and these are given off as the buccal nerve passes through the muscle. It may also give off the anterior deep temporal nerve. The buccal nerve supplies sensation to the skin over the anterior part of buccinator and the buccal mucous membrane, together with the posterior part of the buccal gingivae adjacent to the second and third molar teeth.

Nerve to masseter

The nerve to masseter passes laterally above lateral pterygoid, on to the skull base, anterior to the temporomandibular joint and posterior to the tendon of temporalis. It crosses the posterior part of the mandibular notch with the masseteric artery and ramifies on and enters the deep surface of masseter. It also provides articular branches which supply the temporomandibular joint.

Deep temporal nerves

The deep temporal nerves usually consist of two branches, anterior and posterior, although there may be a middle branch. They pass above lateral pterygoid to enter the deep surface of temporalis. The anterior nerve frequently arises as a branch of the buccal nerve. The small posterior nerve sometimes arises in common with the nerve to masseter.

Nerve to lateral pterygoid

The nerve to lateral pterygoid enters the deep surface of the muscle. It may arise separately from the anterior division of the mandibular nerve or from the buccal nerve.

Posterior trunk of mandibular nerve

The posterior trunk of the mandibular nerve is larger than the anterior and is mainly sensory, although it receives fibres from the motor root for the nerve to mylohyoid. It divides into auriculotemporal, lingual and inferior alveolar (dental) nerves.

Auriculotemporal nerve

The auriculotemporal nerve usually has two roots which encircle the middle meningeal artery. It runs back under lateral pterygoid on the surface of tensor veli palatini, passes between the sphenomandibular ligament and the neck of the mandible, and then runs laterally behind the temporomandibular joint related to the upper part of the parotid gland. Emerging from behind the joint, it ascends over the posterior root of the zygoma, posterior to the superficial temporal vessels, and divides into superficial temporal branches. It communicates with the facial nerve and otic ganglion. The rami to the facial nerve, usually two, pass anterolaterally behind the neck of the mandible to join the facial nerve at the posterior border of masseter. Filaments from the otic ganglion join the roots of the auriculotemporal nerve close to their origin. The sensory distribution of the auriculotemporal nerve on the face is described in Chapter 29.

Lingual nerve

The lingual nerve is sensory to the mucosa of the anterior two-thirds of the tongue, the floor of the mouth and the mandibular lingual gingivae. It arises from the posterior trunk of the mandibular nerve and at first runs beneath lateral pterygoid and superficial to tensor veli palatini, where it is joined by the chorda tympani branch of the facial nerve, and often by a branch of the inferior alveolar nerve. Emerging from under cover of lateral pterygoid, the lingual nerve then runs downwards and forwards on the surface of medial pterygoid, and is thus carried progressively closer to the medial surface of the mandibular ramus. It becomes intimately related to the bone a few millimetres below and behind the junction of the vertical ramus and horizontal body of the mandible. Here it lies anterior to, and slightly deeper than, the inferior alveolar (dental) nerve. It next passes below the mandibular attachment of the superior pharyngeal constrictor and pterygomandibular raphe, closely applied to the periosteum of the medial surface of the mandible, until it lies opposite the posterior root of the third molar tooth, where it is covered only by the gingival mucoperiosteum. At this point it usually lies 2–3 mm below the alveolar crest and 0.6 mm from the bone, however in 5% of cases it lies above the alveolar crest. It next passes medial to the mandibular origin of mylohyoid, and this carries it progressively away from the mandible, and separates it from the alveolar bone covering the mesial root of the third molar tooth. The rest of the nerve is described with the mouth and oral cavity in Chapter 30.

Inferior alveolar (dental) nerve

The inferior alveolar nerve descends behind lateral pterygoid. At the lower border of the muscle the nerve passes between the sphenomandibular ligament and the mandibular ramus and enters the mandibular canal via the mandibular foramen. Below lateral pterygoid it is accompanied by the inferior alveolar artery, a branch of the first part of the maxillary artery, which also enters the canal with associated veins. The subsequent course of the inferior alveolar nerve is described in Chapter 30.

Otic ganglion

This is a small, oval, flat reddish-grey ganglion situated just below the foramen ovale. It is a peripheral parasympathetic ganglion related topographically to the mandibular nerve, but connected functionally with the glossopharyngeal nerve. Near its junction with the trigeminal motor root, the mandibular nerve lies lateral to the ganglion; tensor veli palatini lies medially, separating the ganglion from the cartilaginous part of the pharyngotympanic tube, and the middle meningeal artery is posterior to the ganglion. The otic ganglion usually surrounds the origin of the nerve to medial pterygoid.

Like all parasympathetic ganglia, there are three roots, motor, sympathetic and sensory. Only the parasympathetic fibres relay in the ganglion. The motor, parasympathetic, root of the otic ganglion is the lesser petrosal nerve, conveying preganglionic fibres from the glossopharyngeal nerve which originate from neurones in the inferior salivatory nucleus. The lesser petrosal nerve runs intracranially in the middle cranial fossa on the anterior surface of the petrous bone before passing through the foramen ovale to join the otic ganglion. The nerve synapses in the otic ganglion, and postganglionic fibres pass by a communicating branch to the auriculotemporal nerve and so to the parotid gland. The sympathetic root is from a plexus on the middle meningeal artery. It contains postganglionic fibres from the superior cervical sympathetic ganglion which traverse the otic ganglion without relay and emerge with parasympathetic fibres in the connection with the auriculotemporal nerve to supply blood vessels in the parotid gland. The sensory fibres from the gland are derived from the auriculotemporal nerve. Clinical observations suggest that in humans the gland also receives secretomotor fibres through the chorda tympani.

Branches

A branch connects the otic ganglion to the chorda tympani nerve, while another ramus ascends to join the nerve of the pterygoid canal. These branches may form an additional pathway by which gustatory fibres from the anterior two-thirds of the tongue may reach the facial ganglion without traversing the middle ear, and they do not synapse in the otic ganglion. Motor branches to tensor veli palatini and tensor tympani, derived from the nerve to medial pterygoid, also pass through the ganglion without synapsing.

Chorda tympani

The chorda tympani nerve enters the infratemporal fossa region by passing through the medial end of the petrotympanic fissure behind the capsule of the temporomandibular joint. The nerve descends medial to the spine of the sphenoid bone – which it sometimes grooves – lying posterolateral to tensor veli palatini. It is crossed medially by the middle meningeal artery, the roots of the auriculotemporal nerve and by the inferior alveolar nerve (Fig. 31.15). The chorda tympani joins the posterior aspect of the lingual nerve at an acute angle. It carries taste fibres for the anterior two-thirds of the tongue and efferent preganglionic parasympathetic (secretomotor) fibres destined for the submandibular ganglion in the floor of the mouth.

SPREAD OF INFECTION FROM THE INFRATEMPORAL FOSSA

Infections from most teeth in the upper jaw or the front of the lower jaw usually drain harmlessly into the oral cavity, either via the vestibule buccally, or via the palate or mouth lingually. In contrast, a pericoronitis that affects a mandibular third molar tooth which communicates with the oral cavity, or, less commonly, either a dental abscess associated with this tooth, or a postoperative infection, may spread along tissue planes. Spread may be buccal, submasseteric, parapharyngeal, submandibular, or, more rarely, infratemporal. The main symptom caused by infection of the pterygomandibular region is trismus (painful reflex muscle spasm) which usually affects medial pterygoid. When the submandibular, sublingual and submental areas are primarily affected (Ludwig's angina), there is a risk that the airway may become obstructed. Infection may (potentially) spread further, either along the tissue spaces of the neck below or the tissue planes of the face above, when it may even reach the orbit via the inferior orbital fissure. Once in the orbit, further spread directly through the superior orbital fissure into the cranial cavity, resulting in a life threatening cavernous sinus thrombosis, remains a remote possibility. Infection may also spread to the cavernous sinus from the pterygoid plexus and ophthalmic veins.

PTERYGOPALATINE FOSSA

The pterygopalatine fossa is a small pyramidal space below the apex of the orbit on the lateral side of the skull. The posterior boundary is the root of the pterygoid process and adjoining anterior surface of the greater wing of the sphenoid, and the anterior boundary is the superomedial part of the infratemporal surface of the maxilla. The perpendicular plate of the palatine bone, with its orbital and sphenoidal processes forms the medial boundary, and the pterygomaxillary fissure is the lateral boundary. The fossa communicates with the nasal cavity via the sphenopalatine foramen, with the orbit via the medial end of the inferior orbital fissure, and with the infratemporal fossa via the pterygomaxillary fissure, which lies between the back of the maxilla and the pterygoid process of the sphenoid and transmits the maxillary artery. It also communicates with the oral cavity via the greater palatine canal, which opens in the posterolateral aspect of the hard palate. There are two openings in the posterior wall of the pterygopalatine fossa, the foramen rotundum, which transmits the maxillary nerve, and the pterygoid canal, which transmits the nerve of the pterygoid canal (Vidian nerve). When the anterior aspect of the pterygoid plate is examined in a disarticulated sphenoid, the foramen rotundum is seen to lie above and lateral to the pterygoid canal (see Fig. 31.2).

The main contents of the pterygopalatine fossa are the third part of the maxillary artery, the maxillary nerve and many of its branches, and the pterygopalatine ganglion.

Maxillary artery

The maxillary artery passes through the pterygomaxillary fissure from the infratemporal fossa into the pterygopalatine fossa, where it terminates as the third part of the maxillary artery. It gives off numerous branches including the posterior superior alveolar, infraorbital, sphenopalatine and greater palatine arteries.

Posterior superior alveolar artery

The posterior superior alveolar artery arises from the maxillary artery within the pterygopalatine fossa and runs through the pterygomaxillary fissure onto the maxillary tuberosity. It gives off branches which penetrate the bone here to supply the maxillary molar and premolar teeth and the maxillary air sinus, and other branches that supply the buccal mucosa. Occasionally the posterior superior alveolar artery arises from the infraorbital artery.

Infraorbital artery

The infraorbital artery enters the orbit through the inferior orbital fissure. It runs on the floor of the orbit in the infraorbital groove and infraorbital canal and emerges onto the face at the infraorbital foramen to supply the lower eyelid, part of the cheek, the side of the external nose, and the upper lip. While within the infraorbital canal it gives off the anterior superior alveolar artery which runs downwards to supply the anterior teeth and the anterior part of the maxillary sinus. A middle superior alveolar artery is also often described. When present, it branches from the infraorbital artery within the infraorbital canal and runs inferiorly along the lateral wall of the maxillary sinus toward the region of the canine and lateral incisor teeth and anastomoses with the anterior and posterior superior alveolar arteries.

Artery of the pterygoid canal

The artery of the pterygoid canal (Vidian artery) arises as a branch of either the distal part of the maxillary artery (70%) or the petrous segment of the internal carotid artery (30%). It passes through the pterygoid canal and anastomoses with the pharyngeal, ethmoidal and sphenopalatine arteries in the pterygopalatine fossa and with the ascending pharyngeal, accessory meningeal, ascending palatine and descending palatine (occasionally) arteries in the oropharynx and around the pharyngotympanic tube. Through these complex anastomoses, the artery of the pterygoid canal contributes to the supply of part of the pharyngotympanic tube, the tympanic cavity, and the upper part of the pharynx. It may also anastomose with the artery of the foramen rotundum, and so communicate with branches of the cavernous portion of the internal carotid artery.

Pharyngeal artery

The pharyngeal branch of the maxillary artery passes through the palatovaginal canal, accompanying the nerve of the same name, and is distributed to the mucosa of the nasal roof, nasopharynx, sphenoidal air sinus and pharyngotympanic tube.

Greater (descending) palatine artery

The greater palatine artery leaves the pterygopalatine fossa through the greater (anterior) palatine canal, within which it gives off two or three lesser palatine arteries. The greater palatine artery supplies the inferior meatus of the nose, then passes onto the roof of the hard palate at the greater (anterior) palatine foramen and runs forwards to supply the hard palate and the palatal gingivae of the maxillary teeth. It gives off a branch that runs up into the incisive canal to anastomose with the sphenopalatine artery, and so contribute to the arterial supply of the nasal septum. The lesser palatine arteries emerge onto the palate through the lesser (posterior) palatine foramen, or foramina, and supply the soft palate.

Sphenopalatine artery

The sphenopalatine branch of the maxillary artery passes through the sphenopalatine foramen and enters the nasal cavity posterior to the superior meatus. From here its posterior lateral nasal branches ramify over the conchae and meatuses, anastomosing with the ethmoidal arteries and nasal branches of the greater palatine artery to supply the frontal, maxillary, ethmoidal and sphenoidal air sinuses. The sphenopalatine artery next crosses anteriorly on the inferior surface of the sphenoid and ends on the nasal septum in a series of posterior septal branches which anastomose with the ethmoidal arteries. A branch descends on the vomer to the incisive canal to anastomose with the greater palatine artery and the septal branch of the superior labial artery.

Maxillary nerve

The maxillary division of the trigeminal nerve is wholly sensory (Fig. 31.16). It leaves the skull via the foramen rotundum, which leads directly into the posterior wall of the pterygopalatine fossa. Crossing the upper part of the pterygopalatine fossa, the nerve gives off two large ganglionic branches which contain fibres destined for the nose, palate and pharynx, and these pass through the pterygopalatine ganglion without synapsing. It then inclines sharply laterally on the posterior surface of the orbital process of the palatine bone and on the upper part of the posterior surface of the maxilla in the inferior orbital fissure (which is continuous posteriorly with the pterygopalatine fossa): it lies outside the orbital periosteum, and gives off its zygomatic, and then posterior superior alveolar branches. About halfway between the orbital apex and the orbital rim the maxillary nerve turns medially to enter the infraorbital canal as the infraorbital nerve. The subsequent course of the maxillary nerve is described in Chapter 29.

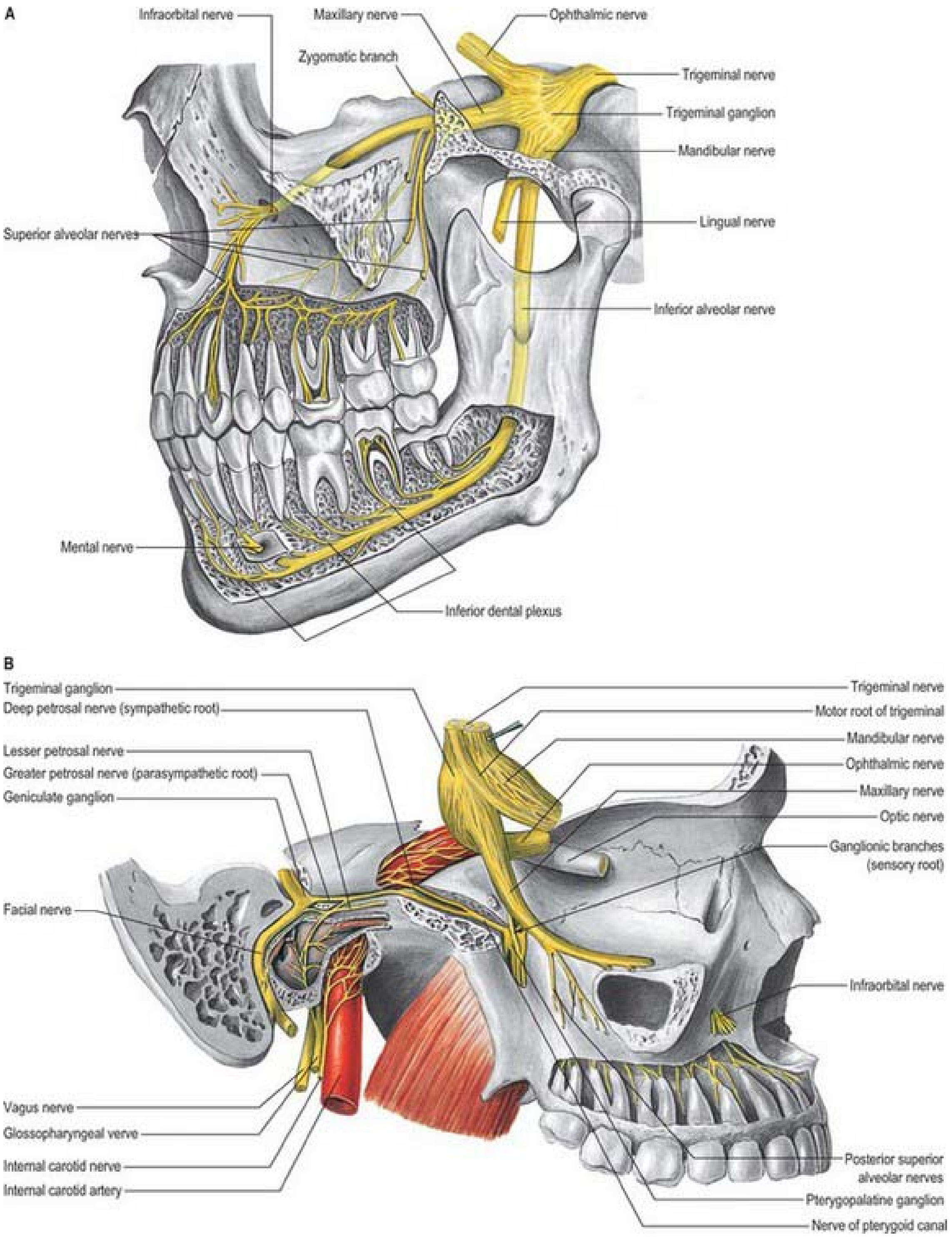
A
Infraorbital nerve
Maxillary nerve
Ophthalmic nerve
Zygomatic branch
Trigeminal nerve
Trigeminal ganglion
Mandibular nerve
Lingual nerve
Superior alveolar nerves
Inferior alveolar nerve
Mental nerve
Inferior dental plexus
B
Trigeminal ganglion
Deep petrosal nerve (sympathetic root)
Lesser petrosal nerve
Greater petrosal nerve (parasympathetic root)
Geniculate ganglion
Facial nerve
Vagus nerve
Glossopharyngeal verve
Internal carotid nerve
Internal carotid artery
Trigeminal nerve
Motor root of trigeminal
Mandibular nerve
Ophthalmic nerve
Maxillary nerve
Optic nerve
Ganglionic branches (sensory root)
Infraorbital nerve
Posterior superior alveolar nerves
Pterygopalatine ganglion
Nerve of pterygoid canal

Fig. 31.16 **A**, Maxillary and mandibular nerves; **B**, Pterygopalatine ganglion, showing its connections with the nerve of the pterygoid canal and the maxillary division of the trigeminal. The trigeminal ganglion has been

lifted forwards out of the trigeminal impression. Note the sympathetic plexus on the internal carotid artery.

(From Sobotta 2006.)

The maxillary nerve gives off many of its branches in the pterygopalatine fossa. They can be subdivided into those that come directly from the nerve, and those that are associated with the pterygopalatine parasympathetic ganglion. Named branches from the main trunk are meningeal, ganglionic, zygomatic, posterior, middle and anterior superior alveolar and infraorbital nerves. Named branches from the pterygopalatine ganglion are orbital, nasopalatine, posterior superior nasal, greater (anterior) palatine, lesser (posterior) palatine and pharyngeal.

Meningeal nerve

The meningeal branch of the maxillary nerve arises within the middle cranial fossa and runs with the middle meningeal vessels. It contributes to the innervation of the dura mater.

Ganglionic branches

There are usually two ganglionic branches that connect the maxillary nerve to the pterygopalatine ganglion.

Zygomatic nerve

The zygomatic branch of the maxillary nerve leaves the pterygopalatine fossa through the inferior orbital fissure together with the maxillary nerve. Its subsequent course is described in Chapter 29.

Posterior superior alveolar nerve

The posterior superior alveolar nerve leaves the maxillary nerve in the pterygopalatine fossa. Its subsequent course and distribution is described in detail in Chapter 30.

Infraorbital nerve

The infraorbital nerve can be regarded as the terminal branch of the maxillary nerve. It leaves the pterygopalatine fossa to enter the orbit at the inferior orbital fissure, and its subsequent course and distribution are described in Chapter 29.

Pterygopalatine ganglion

The pterygopalatine ganglion is the largest of the peripheral parasympathetic ganglia. It is placed deeply in the pterygopalatine fossa, near the sphenopalatine foramen, and anterior to the pterygoid canal and foramen rotundum (Fig. 31.16B). It is flattened, reddish-grey in colour, and lies just below the maxillary nerve as it crosses the pterygopalatine fossa. The majority of the ‘branches’ of the ganglion are connected with it morphologically, but not functionally, because they are primarily sensory branches of the maxillary nerve. Thus they pass through the ganglion without synapsing, and enter the maxillary nerve through its ganglionic branches, but they convey some parasympathetic fibres to the palatine, pharyngeal and nasal mucous glands.

Preganglionic parasympathetic fibres destined for the pterygopalatine ganglion run initially in the greater petrosal branch of the facial nerve, and then in the nerve of the pterygoid canal (Vidian nerve), after the greater petrosal unites with the deep petrosal nerve. The nerve of the pterygoid canal enters the ganglion posteriorly. Postganglionic parasympathetic fibres leave the ganglion and join the maxillary nerve via a ganglionic branch, then travel via the zygomatic and zygomaticotemporal branches of the maxillary nerve to the lacrimal gland. Preganglionic secretomotor fibres of uncertain origin also travel in the nerve of the pterygoid canal. They synapse in the pterygopalatine ganglion, and postganglionic fibres are distributed to palatine, pharyngeal and nasal mucous glands via palatine and nasal branches of the maxillary nerve.

Postganglionic sympathetic fibres pass through the ganglion without synapsing and supply blood vessels and orbitalis. They arise in the superior cervical ganglion and travel via the internal carotid plexus and deep petrosal nerve to enter the pterygopalatine ganglion within the nerve of the pterygoid canal.

General sensory fibres destined for distribution via orbital, nasopalatine, superior alveolar, palatine and pharyngeal branches of the maxillary division of the trigeminal nerve run through the ganglion without synapsing.

Orbital branches

Fine orbital branches enter the orbit through the inferior orbital fissure and supply orbital periosteum. Some fibres also pass through the posterior ethmoidal foramen to supply the sphenoidal and ethmoidal sinuses. The orbital branches probably join branches of the internal carotid nerve to form a ‘retro-orbital’ plexus from which orbital structures such as the lacrimal gland and orbitalis receive an autonomic innervation.

Nasopalatine nerve

The nasopalatine nerve leaves the pterygopalatine fossa through the sphenopalatine foramen and enters the nasal cavity. It passes across the cavity to the back of the nasal septum, runs downwards and forwards on the septum in a groove in the vomer, and then turns down through the incisive fossa in the anterior part of the hard palate to enter the roof of the mouth. When an anterior and a posterior incisive foramen exist in this fossa, the left nasopalatine nerve passes through the anterior foramen, and the right nerve passes through the posterior foramen. The nasopalatine nerve supplies the lower part of the nasal septum and the anterior part of the hard palate, where it communicates with the greater palatine nerve.

Posterior superior nasal nerves (lateral and medial)

The posterior superior alveolar nerves enter the back of the nasal cavity through the sphenopalatine foramen. Lateral posterior superior nasal nerves (about 6) innervate the mucosa lining the posterior part of the superior and middle nasal conchae and the posterior ethmoidal sinuses. Two or three medial posterior superior nasal nerves cross the nasal roof below the opening of the sphenoidal sinus to supply the mucosa of the posterior part of the roof and of the nasal septum.

Palatine nerves (greater and lesser)

The greater and lesser palatine nerves pass downwards from the pterygopalatine ganglion through the greater palatine canal. The greater palatine nerve descends through the greater palatine canal, emerges on the hard palate from the greater palatine foramen and runs forwards in a groove on the inferior surface of the bony palate almost to the incisor teeth. It supplies the gingivae, mucosa and glands of the hard palate and also communicates with the terminal filaments of the nasopalatine nerve. In the greater palatine canal it gives off posterior inferior nasal branches that emerge through the perpendicular plate of the palatine bone and ramify over the inferior nasal concha and walls of the middle and inferior meatuses. As it leaves the greater palatine canal, it gives off branches which are distributed to both surfaces of the adjacent part of the soft palate.

The lesser (middle and posterior) palatine nerves are much smaller than the greater palatine nerve. They descend through the greater palatine canal, from which they diverge low down to emerge through the lesser palatine foramina in the tubercle or pyramidal process of the palatine bone. They innervate the uvula, tonsil and soft palate.

Fibres conveying taste impulses from the palate probably pass via the palatine nerves to the pterygopalatine ganglion. They pass through the ganglion without synapsing, and leave via the greater petrosal nerve. Their cell bodies are located in the facial ganglion and their central processes pass via the sensory root of the facial nerve (nervus intermedius) to the gustatory nucleus in the nucleus of the tractus solitarius.

Pharyngeal nerve

The pharyngeal branch of the maxillary nerve leaves the pterygopalatine ganglion posteriorly. It passes through the palatovaginal canal with the pharyngeal branch of the maxillary artery and supplies the mucosa of the nasopharynx behind the pharyngotympanic tube.

REFERENCES

rker BCW, Davies PL. The applied anatomy of the pterygomandibular space. *Br J Surg*. 1972;10:43-55.

Describes the relationships of the structures within the pterygomandibular space, with particular reference to anaesthesia associated with an inferior alveolar nerve block..

rtilsson O, Strom D. A literature survey of a hundred years of anatomic and functional lateral pterygoid muscle research. *J Orofac Pain*. 1995;9:17-23.

Bont LGM, Boering G, Havinga P, Liem RSB. Spacial arrangement of collagen fibrils in the articular cartilage of the mandibular condyle. *J Oral Maxillofac Surg*. 1984;42:306-313.

nsson T, Oberg T, Carlsson GE, Kopp S. Thickness of the soft tissue layers and the articular disc in the temporomandibular joint. *Acta Odont Scand*. 1977;35:77-83.

llingshead WH. The Head and Neck. 2nd edn. *Anatomy for Surgeons*. vol. 1. New York: Harper & Row; 1968.

ng J. Clinical Anatomy of the Masticatory Apparatus and Peripharyngeal Spaces. New York: Thième Medical Publishers, 1995.

Provides detailed anatomical information (including quantitation) of the infratemporal fossa, relating such information to the clinic..

ngdon JD, Patel MF. Operative Maxillofacial Surgery. London: Chapman and Hall, 1998.

ngdon JD, Berkovitz BKB, Moxham BJ. The Surgical Anatomy of the Infratemporal Fossa. London: Dunitz, 2002.

chardson R, Cadden W. Mastication. Linden RWA, editor. The Scientific Basis of Eating. Taste and Smell, Salivation. Mastication and Swallowing and their Dysfunctions. Frontiers of Oral Biology Series Vol 9. Basel: Karger; 1998:76-121

sborn JW. Internal derangement and the accessory ligaments around the temporomandibular joint. *J Oral Rehab*. 1995;22:731-740.

Analyses of the anatomy of the ligaments associated with the jaw joint and how they control the movements of the condyle during border movements of the jaw associated with jaw opening and the aetiology of jaw dislocation and disc displacement..

grel MA, Renaut A, Schmidt B, Ammar A. The relationship of the lingual nerve to the mandibular third molar region. *J Oral Maxillofac Surg*. 1995;53:1178-1181.

binson PD. Articular cartilage of the temporomandibular joint – can it regenerate? *Ann R Coll Surg Engl*. 1993;75:231-236.

ller PA. Temporomandibular arthropathy. *Proc Roy Soc Med*. 1974;67:153-159.

rker KS. Reflex control of human jaw muscles. *Crit Rev Oral Biol Med*. 2002;13:85-104.

CHAPTER 32

Nose, nasal cavity and paranasal sinuses

The nose is the first part of the upper respiratory tract, and is responsible for warming, humidifying, and, to some extent, filtering inspired air. It also houses the olfactory epithelium which contains olfactory receptor neurones responsible for detecting airborne odorant molecules.

The nose may be subdivided into an external nose, which opens anteriorly onto the face through the nostrils or nares, and an internal chamber, divided sagittally by a septum into right and left cavities which open posteriorly into the nasopharynx through the posterior nasal apertures or choanae. The nasal cavities are housed in a supporting framework composed of bone and fibro-elastic cartilages. The larger bones in this framework contain air-filled spaces lined with respiratory epithelium, described collectively as the paranasal sinuses. The sinuses and the nasolacrimal ducts drain into the nasal cavity via openings in its lateral walls (Fig. 32.1).

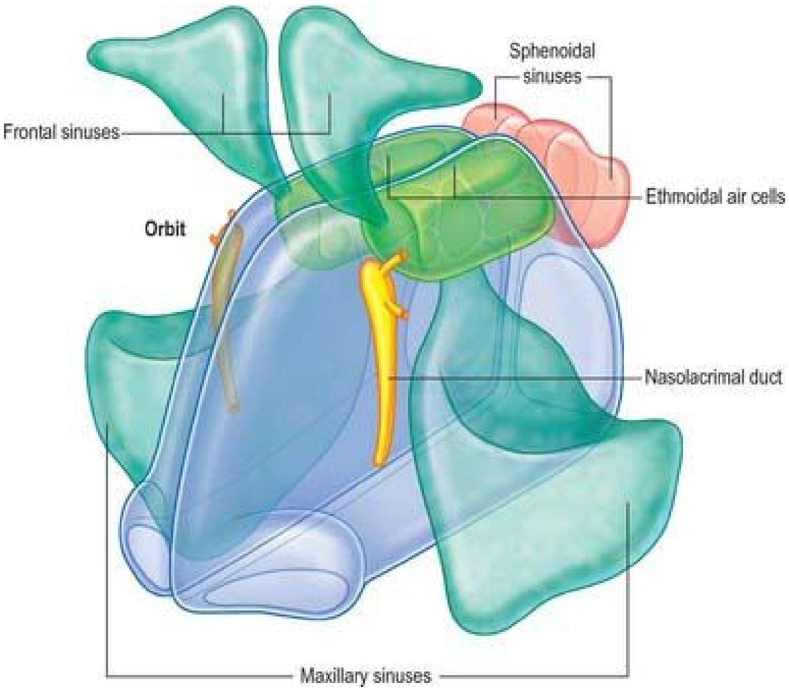
Frontal sinuses
Sphenoidal sinuses
Orbit
Ethmoidal air cells
Nasolacrimal duct
Maxillary sinuses

Fig. 32.1 Overview of spatial relationships between the nasal cavity, paranasal sinuses and nasolacrimal ducts.

(From Drake, Vogl and Mitchell 2005.)

EXTERNAL NOSE

The proportions of the nose and face, both from in front and the side, are of enormous significance to the rhinoplastic surgeon.

The shape of the external nose varies considerably between individuals. It is a pyramidal structure located in the midline of the midface and attached to the facial skeleton. Its upper angle or root is continuous with the forehead, and its free tip forms the apex which projects anteriorly. Its base contains two ellipsoidal apertures, the external nares or nostrils, which open onto its inferior surface, separated by the nasal septum and columella. The overall shape of the external nares is very variable. They usually measure 1.5–2 cm anteroposteriorly and 0.5–1 cm transversely and are narrower in front. The lateral surfaces of the nose unite in the median plane to form the dorsum. The alar sulcus is a groove in the skin bounding the nasal alae above and joining the nasiolabial sulcus. Below it curves towards the tip of the nose but does not reach it.

SKIN AND SOFT TISSUE

The skin and soft tissue covering the dorsum of the nose is usually thin, especially at the osseo-cartilaginous junction, and loosely connected to the nasal aponeurosis and the muscle fibres that fan out within it. Over the tip the skin is often thicker in men and has numerous large sebaceous glands but this varies considerably. These variations affect the final nasal contour and profile after nasal augmentation.

BONE AND CARTILAGE

Bony skeleton of the external nose

The piriform aperture has sharp edges. It is bounded below and laterally by the maxilla and above by the nasal bones (Fig. 32.2). The lateral part of the inferior edge of the piriform aperture merges into its lateral wall, which is formed by the frontal process of the maxilla. It is bounded above by the nasal part of the frontal bone and superomedially by the lateral edge of the nasal bone. The bony nasal septum articulates with the undersurface of the nasal bones and provides support to the dorsum of the nose. The nasal bones vary in thickness and width, which is of significance in planning osteotomies. They are thick and widest at the nasofrontal suture, narrow at the nasofrontal angle before they widen, and become thinner 9–12 mm below the nasofrontal angle.

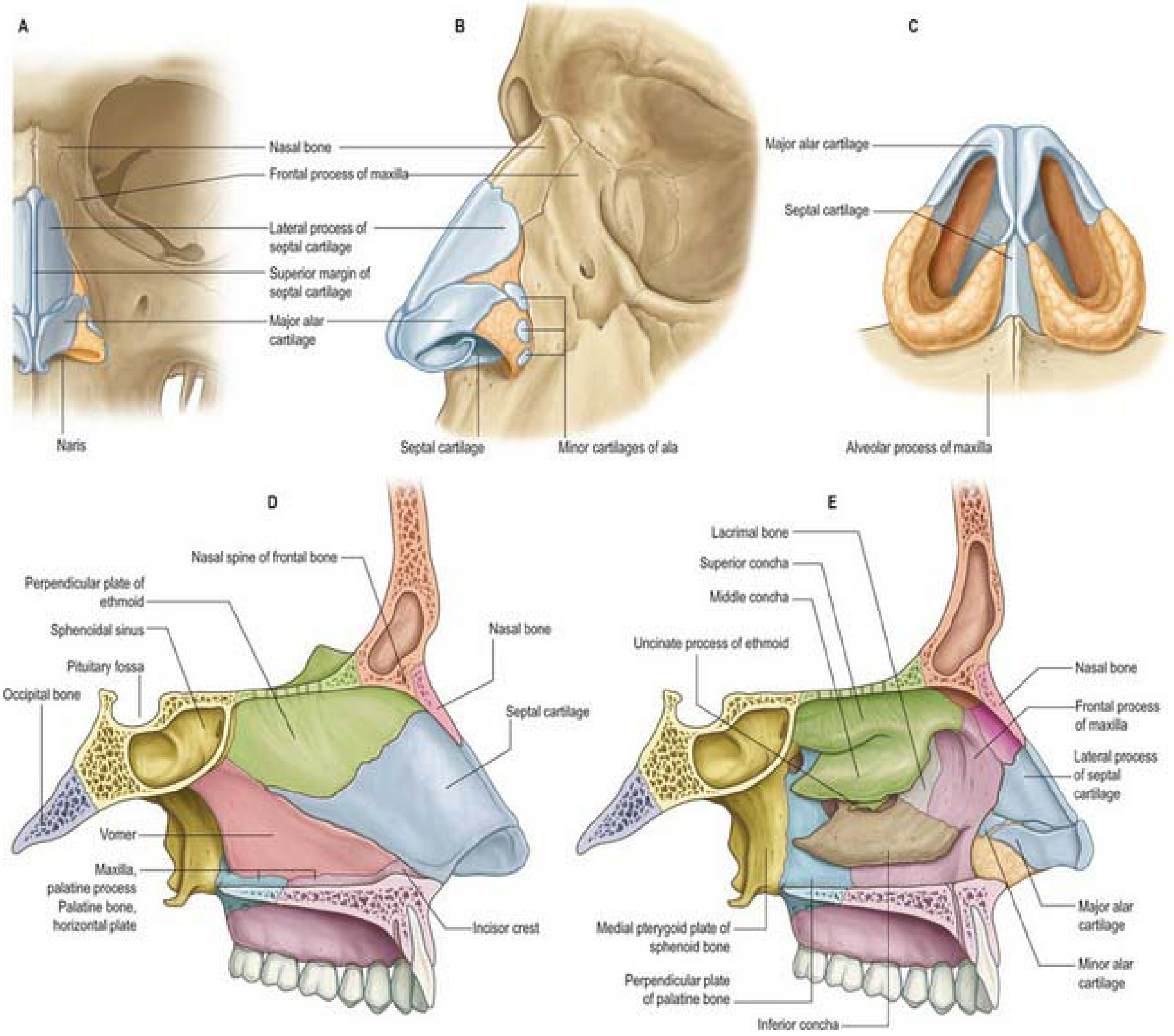
A
B
C
Nasal bone
Frontal process of maxilla
Lateral process of septal cartilage
Superior margin of septal cartilage
Major alar cartilage
Naris
Septal cartilage
Minor cartilages of ala
Major alar cartilage
Septal cartilage
Alveolar process of maxilla
D
Nasal spine of frontal bone
Perpendicular plate of ethmoid
Sphenoidal sinus
Pituitary fossa
Occipital bone
Nasal bone
Septal cartilage
Vomer
Maxilla, palatine process
Palatine bone, horizontal plate
Incisor crest
E
Lacrimal bone
Superior concha
Middle concha
Uncinate process of ethmoid
Nasal bone
Frontal process of maxilla
Lateral process of septal cartilage
Major alar cartilage
Minor alar cartilage
Medial pterygoid plate of sphenoid bone
Perpendicular plate of palatine bone
Inferior concha

Fig. 32.2 The bony and cartilaginous skeletons of the nose. **A**, External nose, frontal view; **B**, External nose, lateral view; **C**, Inferior view of cartilages; **D**, Nasal cavity, medial wall; **E**, Nasal cavity, lateral wall (left side).

Fractures of the nasal bones

The commonest injury of the facial skeleton is a fracture of the nasal bones. In simple fractures the break usually occurs in the frontal process of the maxilla rather than at the nasofrontal suture. The terminal branch of the anterior ethmoidal nerve and its accompanying vessels are at risk when injuries involve the dorsum of the nose

Cartilaginous skeleton of the external nose

The cartilaginous framework consists of the paired lateral and major cartilages and several minor alar nasal cartilages (Fig. 32.2).

Lateral (superior) nasal cartilage

The lateral nasal cartilage is triangular, and its anterior margin is thicker than the posterior margin. The upper part is continuous with the septal cartilage, but anteroinferiorly it may be separated from it by a narrow fissure. The superior margin of the lateral nasal cartilage is attached to the nasal bone and frontal process of the maxilla, and the inferior margin is connected by fibrous tissue to the lateral crus of the major alar cartilage.

Major alar cartilage

The major alar cartilage is a thin flexible plate. It lies below the upper lateral cartilage and curves acutely around the anterior part of its naris. The medial part, the narrow medial crus (septal process), is loosely connected by fibrous tissue to its contralateral counterpart and to the anteroinferior part of the septal cartilage. The intermediate crus forms the margin of the apex of the nostril. The lateral crus lies lateral to the naris and runs superolaterally away from the margin of the nasal ala. The upper border of the lateral crus of the major alar cartilage is attached by fibrous tissue to the lower border of the lateral nasal cartilage. Its lateral border is connected to the frontal process of the maxilla by a tough fibrous membrane containing three or four minor alar cartilages. The junction between the lateral crura of the major alar and lateral cartilages is variable: the two edges may abut or overlap, in which case the lateral crus is then the more lateral at the junction. The lateral crus of the major alar cartilage is shorter than the lateral margin of the naris and runs away from the margin of the ala nasi. The lateral part of the margin of the ala nasi is fibroadipose tissue covered by skin. In front, the angulations or ‘domes’ between the medial and lateral crurae of the major alar cartilages are separated by a notch palpable at the tip of the nose.

MUSCLES

The nasal muscle group includes procerus, nasalis, dilator naris anterior, depressor septi and levator labii superioris alaequae nasi (Fig. 32.3). These muscles are involved in respiration, facial expression and in the production of some sounds during speech, when their activity is dependent upon the activity of orbicularis oris and the type of sound (see Clark et al 1998). Any or all of these muscles may be absent in cleft lip deformities with corresponding functional and aesthetic consequences.

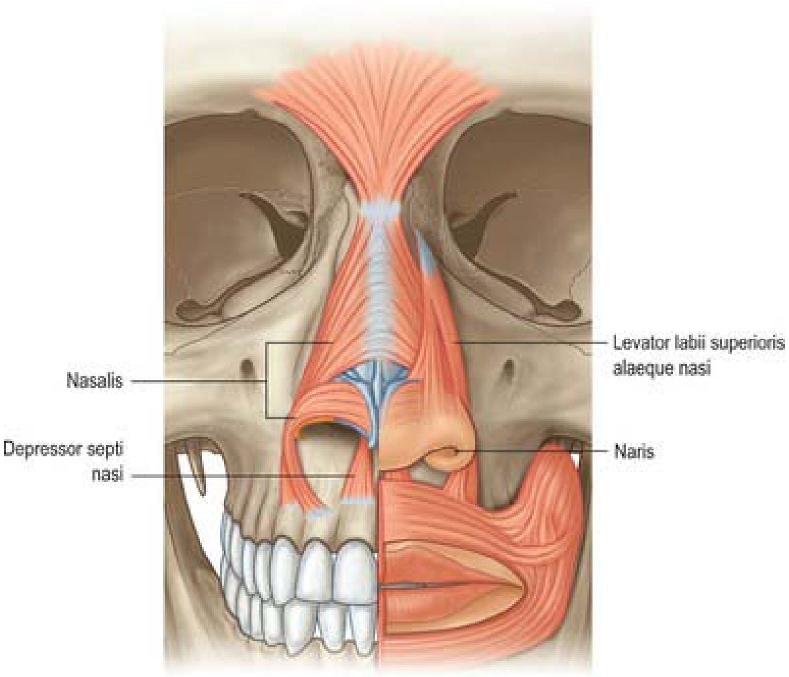

Fig. 32.3 The nasal musculature.

(From Drake, Vogl and Mitchell 2005.)

Procerus

Procerus is a small pyramidal muscle that lies close to, and is often partially blended with, the medial side of the frontal part of occipitofrontalis. It arises from a fascial aponeurosis attached to the periosteum covering the lower part of the nasal bone, the perichondrium covering the upper part of the lateral nasal cartilage and the aponeurosis of the transverse part of nasalis. It is inserted into the glabellar skin over the lower part of the forehead between the eyebrows.

Vascular supply

Procerus is supplied mainly by branches from the facial artery.

Innervation

Procerus is supplied by temporal and lower zygomatic branches from the facial nerve (a supply from the buccal branch has been described).

Actions

Procerus draws down the medial angle of the eyebrow and produces transverse wrinkles over the bridge of the nose. It is active in frowning and ‘concentration’, and helps to reduce the glare of bright sunlight.

Nasalis

Nasalis consists of transverse and alar components. The transverse part (compressor naris) is attached to the maxilla above and lateral to the incisive fossa, and lateral to the alar part. Its fibres pass upwards and medially and expand into a thin aponeurosis which merges with its counterpart across the bridge of the nose. The merged aponeuroses blend with the aponeuroses of procerus and with fibres from levator labii superioris alaequae nasi. Fibres from the transverse part may also blend with the skin of the nasolabial and alar folds. The alar part (pars alaris or dilator naris posterior) is attached to the maxilla above the lateral incisor and canine, lateral to the bony attachment of depressor septi, and medial to the transverse part, with which it partly merges. Its fibres pass upwards and anteriorly and are attached to the skin of the ala above the lateral crus of the lower lateral cartilage, and to the posterior part of the mobile septum. The pars alaris helps to produce the upper ridge of the philtrum.

Vascular supply

Nasalis is supplied by branches from the facial artery and from the infraorbital branch of the maxillary artery.

Innervation

Nasalis is supplied by the buccal branch of the facial nerve. It may also be supplied by the zygomatic branch of the facial nerve.

Actions

The transverse part compresses the nasal aperture at the junction of the vestibule and the nasal cavity. The alar parts draw the alae and posterior part of the columella downwards and laterally and so assist in widening the nares and in elongating the nose. They are active immediately before inspiration.

Dilator naris anterior

Dilator naris anterior (also known as apicis nasi or the small dilator muscle of the nose) is a very small muscle attached to the upper lateral cartilage and the alar part of nasalis, and to the caudal margin of the lateral crus and the lateral alar crus. It encircles the naris and acts as a primary dilator of the nostril.

Dilator naris anterior and the alar part of nasalis (dilator naris posterior) probably function to prevent collapse of the nasal valve during inspiration. Their EMG activity is directly proportional to ventilatory resistance and is modified by signals that travel from pulmonary mechano- and pressure receptors via afferent vagal pathways to the brainstem respiratory centre: the efferent limb of the reflex arc runs in the facial nerve.

Depressor septi

Depressor septi lies immediately deep to the mucous membrane of the upper lip. It is usually attached to the periosteum covering the maxilla above the central and lateral incisors and the anterior nasal spine, and to the fibres of orbicularis oris above the central incisor. Its fibres pass to the columella, the mobile part of the nasal septum and the base of the medial crus of the nasal cartilage. A few muscle slips may pass between the medial crura into the nasal tip. Depressor septi may be absent or rudimentary.

Vascular supply

Depressor septi is supplied by the superior labial branch of the facial artery.

Innervation

Depressor septi is innervated by the buccal branch, and sometimes by the zygomatic branch, of the facial nerve.

Actions

Depressor septi pulls the columella, the tip of the nose and the nasal septum downwards. It tenses the nasal septum at the start of nasal inspiration, and, with the alar part of nasalis, widens the nasal aperture as well as causing the nose to ‘dip’ when some people smile.

Levator labii superioris alaequae nasi

Levator labii superioris alaequae nasi arises from the upper part of the frontal process of the maxilla and, passing obliquely downwards and laterally, divides into medial and lateral slips. The medial slip blends into the perichondrium of the lateral crus of the major alar cartilage of the nose and the skin over it. The lateral slip is prolonged into the lateral part of the upper lip, where it blends with levator labii superioris and orbicularis oris. Superficial fibres of the lateral slip curve laterally across the front of levator labii superioris and attach along the floor of the dermis at the upper part of the nasolabial furrow and ridge.

Vascular supply

Levator labii superioris alaequae nasi is supplied by the facial artery and the infraorbital branch of the maxillary artery.

Innervation

Levator labii superioris alaequae nasi is innervated by zygomatic and superior buccal branches of the facial nerve.

Actions

The lateral slip raises and everts the upper lip and raises, deepens and increases the curvature of the top of the nasolabial furrow. The medial slip pulls the lateral crus superiorly, displaces the circumalar furrow laterally, and modifies its curvature: it is a dilator of the naris. Depressor septi and the medial slip of levator labii superioris alaequae nasi are sometimes described as secondary nasal dilators: there is little evidence that either of these muscles has any direct influence on the nasal valve.

Anomalous nasal muscles

Anomalous, inconstant, nasal muscles have been described. They include anomalous nasi, attached to the frontal process of the maxilla, procerus, transverse part of nasalis and the upper lateral cartilage (i.e. in a region normally devoid of muscle) and compressor narium minor, which passes between the anterior part of the lower lateral cartilage and the skin near the margins of the nares. The existence of a small levator septi nasi has been questioned.

CUTANEOUS VASCULAR SUPPLY AND LYMPHATIC DRAINAGE

Nasal skin receives its blood supply from branches of the facial, ophthalmic and infraorbital arteries. The alae and lower part of the nasal septum are supplied by lateral nasal and septal branches of the facial artery and the lateral aspects and dorsum of the nose are supplied by the dorsal nasal branch of the ophthalmic artery and the infraorbital branch of the maxillary artery. The venous networks draining the external nose do not run parallel to the arteries but correspond to arteriovenous territories of the face. The frontomedian region of the face, including the nose, drains to the facial vein, and the orbitopalpebral area of the face, including the root of the nose, drains to the ophthalmic veins. The connections of the veins of the nose, upper lip and cheek with the drainage area of the ophthalmic veins are clinically significant because they can be the route which spreads infection and initiates thrombosis of the major intracranial sinuses. Lymph drainage is primarily to the submandibular group of nodes although lymph draining from the root of the nose drains to superficial parotid nodes. There is experimental evidence that nasal lymphatics might play a major role in CSF transport in animals such as the sheep: there is currently very little evidence that a similar pathway exists in humans (but see Johnston et al 2004).

CUTANEOUS INNERVATION

Nasal skin is innervated by the infratrochlear and external nasal branches of the nasociliary nerve, and by the nasal branch of the infraorbital nerve.

NASAL CAVITY

The nasal cavity is an irregular space between the roof of the mouth and the cranial base. It is wider below than above, and widest and vertically deepest in its central region, where it is divided by a vertical osseocartilaginous septum that is approximately median in position. The bony part of the septum reaches the posterior limit of the cavity.

The nasal cavity communicates with the frontal, ethmoidal, maxillary and sphenoidal paranasal sinuses and opens into the nasopharynx through a pair of oval openings, the posterior nasal apertures or choanae. The latter are separated by the posterior border of the vomer, and each is limited above by the vaginal process of the medial pterygoid plates, laterally by the perpendicular plate of the palatine bone and the medial pterygoid plate, and below by the horizontal plate of the palatine bone (Fig. 32.4). The adult choana typically measures 2.5 cm in vertical height and 1.3 cm transversely: size is not usually affected by deviations of the nasal septum. The vomerovaginal and palatovaginal canals are found in the roof of this region.

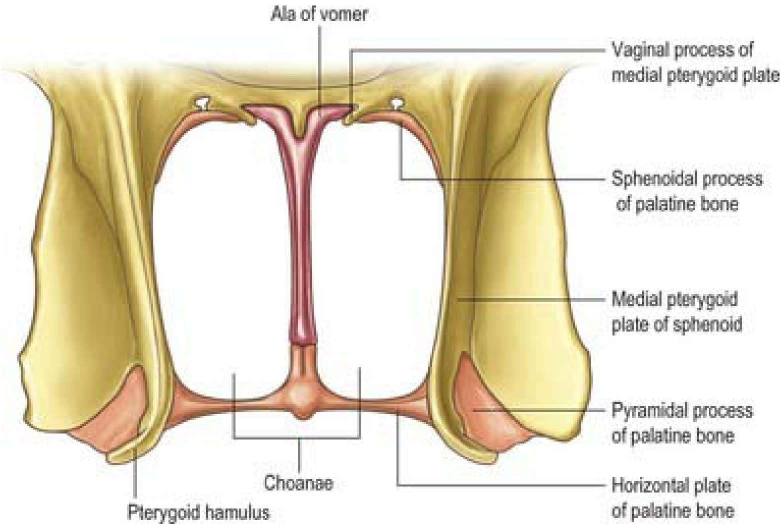
Ala of vomer
Vaginal process of medial pterygoid plate
Sphenoidal process of palatine bone
Medial pterygoid plate of sphenoid
Pyramidal process of palatine bone
Horizontal plate of palatine bone
Choanae
Pterygoid hamulus

Fig. 32.4 Posterior view of the choanae.

Each half of the nasal cavity has a roof, floor, medial (septal) and lateral walls and a vestibule.

ROOF

The roof is horizontal in its central part and slopes downwards in front and behind (Fig. 32.3). The anterior slope is formed by the nasal spine of the frontal bones and by the nasal bones. The central region is formed by the cribriform plate of the ethmoid bone which separates the nasal cavity from the floor of the anterior cranial fossa. It contains numerous small perforations which transmit the olfactory nerves and their ensheathing meningeal layers, and a separate anterior foramen which transmits the anterior ethmoidal nerve and vessels. The posterior slope is formed by the anterior aspect of the body of the sphenoid, interrupted on each side by an opening of a sphenoidal sinus, and the sphenoidal conchae or superior conchae.

FLOOR

The floor of the nasal cavity is smooth and concave transversely, and slopes up from anterior to posterior apertures. The greater part is formed by the palatine processes of the maxillae which articulate posteriorly with the horizontal plates of the palatine bones at the palatomaxillary suture. Anteriorly, near the septum, a small infundibular opening in the bone of the nasal floor leads into the incisive canals that descend to the incisive fossa: this opening is marked by a slight depression in the overlying mucosa.

The floor of the nose may be deficient as a result of congenital clefting of the hard and/or soft palate.

MEDIAL WALL

The medial wall of each nasal cavity is the nasal septum, a thin sheet of bone (posteriorly) and cartilage (anteriorly), that lies between the roof and floor of the cavity (Fig. 32.2D).

Bony septum

The septum is usually relatively featureless but sometimes exhibits ridges or bony spurs. The posterosuperior part of the septum and its posterior border are formed by the vomer, which extends from the body of the sphenoid to the hard palate (for more details, see Chapter 29). Its surface is grooved by the nasopalatine nerves and vessels. The anterosuperior part of the septum is formed by the perpendicular plate of the ethmoid which is continuous above with the cribriform plate. Other bones which make minor contributions to the septum at the upper and lower limits of the medial wall are the nasal bones and the nasal spine of the frontal bones (anterosuperior), the rostrum and crest of the sphenoid (posterosuperior), and the nasal crests of the maxilla and palatine bones (inferior).

Cartilaginous septum

The septal cartilage is almost quadrilateral and may extend back (especially in children) for some distance between the vomer and the perpendicular plate of the ethmoid. Its anterosuperior margin is connected above to the posterior border of the internasal suture, and the distal end of its superior portion is continuous with the upper lateral cartilages. The anteroinferior border is connected by fibrous tissue on each side to the medial crurae of the major alar cartilage. The posterosuperior border joins the perpendicular plate of the ethmoid, while the posteroinferior border is attached to the vomer and anterior to that to the nasal crest and anterior nasal spine of the maxilla. The anteroinferior part of the nasal septum between the nares is devoid of cartilage and is therefore called the membranous septum: it is continuous with the columella anteriorly.

Above the incisive canals, at the lower edge of the septal cartilage, a depression pointing downwards and forwards is all that remains of the nasopalatine canal which connected the nasal and buccal cavities in early fetal life. Near this recess, a minute orifice leads back into a blind tubule, 2–6 mm long, which lies on each side of the septum and houses remnants of the vomeronasal organ.

Vomeronasal organ

In most amphibia, reptiles and mammals, the vomeronasal organ is the peripheral sensory organ of the accessory olfactory system. In these animals, paired vomeronasal organs are located either at the base of the nasal septum or in the roof of the mouth, and are involved in chemical communication that often, but not exclusively, is mediated via pheromones. In many macrosomatic animals the vomeronasal organ consists of a vomeronasal duct which contains chemosensory cells, and a vomeronasal nerve which terminates in the accessory olfactory bulb in the CNS. Whether adult humans possess a vomeronasal organ remains controversial; it is claimed that the duct sometimes persists beyond the embryonic stage (for detailed reviews, see Meredith 2001, Witt & Hummel 2006) but no neural connection appears to be present in humans after birth.

LATERAL WALL

The lateral wall of the nasal cavity is formed anteroinferiorly by the maxilla and its anterior and posterior fontanelles (bony deficiencies in the medial wall of the maxilla which are obliterated to varying degrees by fibrous tissue); posteriorly by the perpendicular plate of the palatine bone; and superiorly by the labyrinth of the ethmoid bone. It contains three projections of variable size, the inferior, middle and superior nasal conchae (turbinates) (Figs 32.2E, 32.5). The conchae curve generally inferomedially, each roofing a groove, or meatus, which is open to the nasal cavity. The middle conchae may also curve inferolaterally, or may be expanded by an enclosed air cell to form a so called ‘concha bullosa’ (30% of individuals) or have a concave medial surface, known as a paradoxical turbinate (10% of individuals).

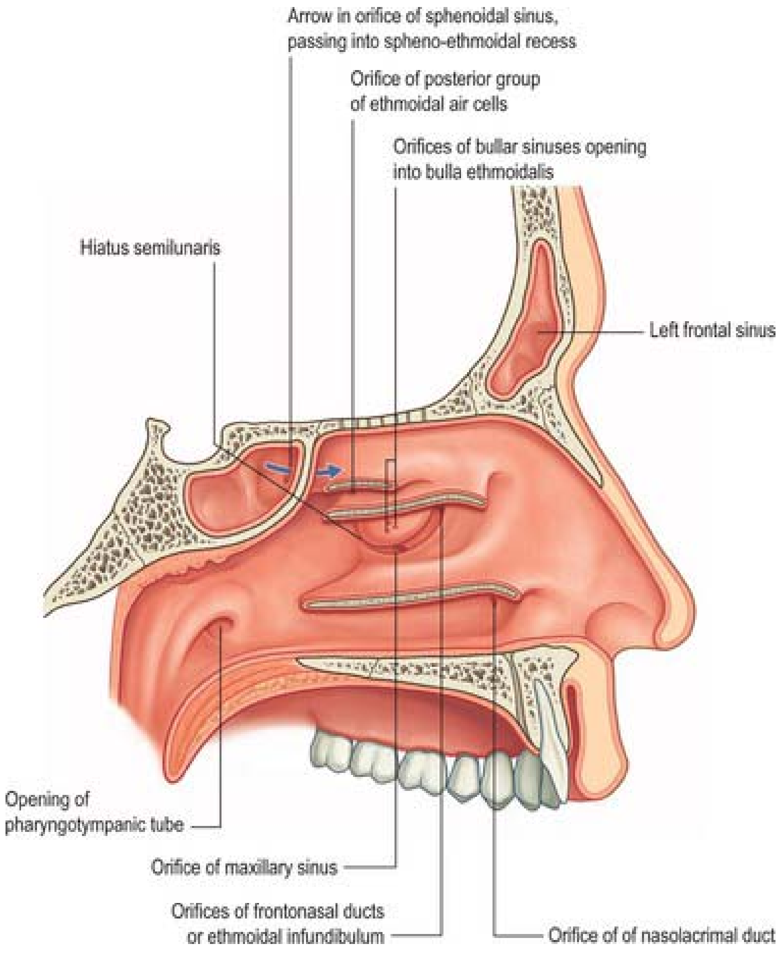
Arrow in orifice of sphenoidal sinus, passing into spheno-ethmoidal recess
Orifice of posterior group of ethmoidal air cells
Orifices of bullar sinuses opening into bulla ethmoidalis
Hiatus semilunaris
Left frontal sinus
Opening of pharyngotympanic tube
Orifice of maxillary sinus
Orifices of frontonasal ducts or ethmoidal infundibulum
Orifice of of nasolacrimal duct

Fig. 32.5 Lateral wall of the nasal cavity. The conchae have been removed to show the positions of the ostia of the paranasal sinuses and the nasolacrimal duct.

(From Drake, Vogl and Mitchell 2005.)

Inferior concha and inferior meatus

The inferior concha is a thin, curved, independent bone (for more details, see Chapter 29). It articulates with the nasal surface of the maxilla and the perpendicular plate of the palatine bone. Its free lower border is gently curved and the subjacent inferior meatus reaches the nasal floor. The inferior meatus is the largest meatus, and it extends along almost all of the lateral nasal wall. It is deepest at the junction of its anterior and middle thirds, where it admits the inferior opening of the nasolacrimal canal (see Ch. 39). The canal is formed by the articulations between the lacrimal groove of the maxilla, the descending process of the lacrimal bone and the lacrimal process of the inferior concha. During postnatal development, the ostium of the nasolacrimal duct moves upwards and is increasingly hidden under the over-arching inferior concha.

Middle concha and middle meatus

The middle concha is a medial process of the ethmoidal labyrinth and may be pneumatized (conchal sinus). It extends back to articulate with the perpendicular plate of the palatine bone. The region beneath it is the middle meatus, which is deeper in front than behind, lies below and lateral to the middle concha, and continues anteriorly into a shallow fossa above the vestibule, termed the atrium of the middle meatus.

The main features of the lateral nasal wall are a rounded elevation, the bulla ethmoidalis, and a curved cleft, the hiatus semilunaris, formed by the posterior edge of the uncinate process, which constitutes the medial limit of the ethmoid infundibulum, a slit-like space that leads towards the maxillary ostium. The maxillary ostium is normally found lateral to the antero-inferior aspect of the uncinate process. The latter can be attached to the lateral nasal wall (50%), the anterior cranial fossa (25%) or the middle concha (25%). Where the uncinate process is attached determines whether the frontal sinus drains lateral to the ethmoid infundibulum or into it; if the uncinate process is attached to the lateral wall, the frontal sinus will drain into the middle meatus and not into the ethmoid infundibulum, but with the other configurations the sinus will drain into the infundibulum, and thus near or into the maxillary ostium. Agger nasi air cells are the name given to anterior ethmoid air cells that lie anterior to the ethmoid bulla (Fig. 32.5; see Fig. 32.12). The posterior fontanelle lies posterior to the uncinate process where there is no bone in the medial wall of the maxillary sinus, inferoposterior to the hiatus; it frequently has an accessory opening.

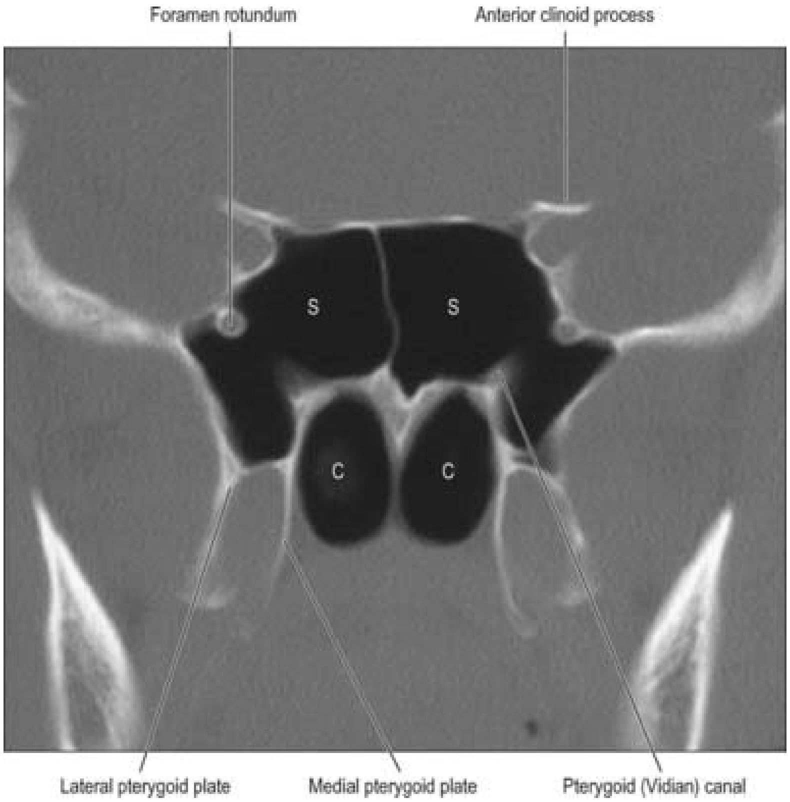
Foramen rotundum
Anterior clinoid process
S
S
C
C
Lateral pterygoid plate
Medial pterygoid plate
Pterygoid (Vidian) canal

Fig. 32.12 Coronal CT scan showing the sphenoidal air sinus. S, Sphenoid sinus; C, Posterior choanae.

Sphenopalatine foramen

The sphenopalatine foramen, which is really a fissure, can be approached surgically through the middle meatus. It is posterior to the middle meatus and transmits the sphenopalatine artery and nasopalatine and superior nasal nerves from the pterygopalatine fossa (see Ch. 31). It is bounded above by the body and concha of the sphenoid, below by the superior border of the perpendicular plate of the palatine bone, and in front and behind by the orbital and sphenoidal processes of the palatine bone respectively.

Superior concha and superior meatus

The superior concha is a medial process of the ethmoidal labyrinth and presents as a small curved lamina, posterosuperior to the middle concha. It roofs the superior meatus and is the shortest and shallowest of the three conchae. Above the superior concha, the sphenoidal sinus opens into the triangular sphenoethmoidal recess which separates the superior concha and anterior aspect of the body of the sphenoid. The superior meatus is a short oblique passage extending about halfway along the upper border of the middle concha. The posterior ethmoidal sinuses open, via a variable number of apertures, into its anterior part.

Highest (supreme) nasal concha

Occasionally a fourth concha, the highest or supreme nasal concha, appears on the lateral wall of the sphenoethmoidal recess. The passage immediately below it is called the supreme nasal meatus; it may contain an opening for the posterior ethmoidal sinus.

Nasal vestibule

The nasal vestibule lies just inside the naris. It is limited above and behind by a curved ridge, the limen nasi, raised where the greater ala of the lateral cartilaginous crus overlaps the lower edge of the lateral nasal cartilage on each side. On the septal side of the nasal cavity the superior edge of the medial crus of the major alar cartilage (the medial intumescence) marks the boundary between the nasal vestibule and the nasal cavity. The medial wall of the vestibule is formed by a mobile septum consisting of the columella (which does not contain cartilage) and the underlying medial crura of the alar cartilages.

Nasal obstruction

The septum may be displaced by injury or by disproportionate growth of the cartilage that may cause it to bend; sometimes the deviation may cause unilateral nasal obstruction. Variations in the anatomy of the lateral nasal wall, usually associated with variations in the size and position of the anterior ethmoidal cells, may obstruct frontal or maxillary sinus drainage, e.g. frontal cells, supraorbital ethmoid cells and infraorbital or Haller’s cells, which represent an extension of anterior ethmoidal pneumatization along the infraorbital margin, sometimes within the roof of the maxillary sinus (see below).

NASAL AND OLFACTORY MUCOSAE

Nasal mucosa

The lining of the anterior part of the nasal cavity and vestibule is continuous with the skin, and consists of keratinized stratified squamous epithelium overlying a connective tissue lamina propria. Inferiorly the skin bears coarse hairs (vibrissae) which curve towards the naris and help to arrest the passage of particles in inspired air. In males, after middle age, these hairs increase considerably in size. Further posteriorly, at the limen nasi, this grades into a mucosa which is lined initially by non-keratinizing stratified squamous epithelium, and then by pseudostratified ciliated (respiratory) epithelium rich in goblet cells. Respiratory epithelium forms most of the surface of the nasal cavity, i.e. it covers the conchae, meati, septum, floor and roof, except superiorly in the olfactory cleft, where the olfactory epithelium is present. It is adherent to the periosteum or perichondrium of the neighbouring skeletal structures. In some areas, cells of the respiratory epithelium may be low columnar or cuboidal, and the proportion of ciliated to non-ciliated cells is variable.

There are numerous seromucous glands within the lamina propria of the nasal mucosa. Their secretions make the surface sticky so that it traps particles in the inspired air. The mucous film is continually moved by ciliary action (the mucociliary escalator or rejection current) posteriorly into the nasopharynx at a rate of 6 mm per minute. Palatal movements transfer the mucus and its entrapped particles to the oropharynx for swallowing, but some also enters the nasal vestibule anteriorly. The secretions of the nasal mucosa contain the bacteriocides lysozyme, β-defensin and lactoferrin, and also secretory immunoglobulins (IgA). The mucosa is continuous with the nasopharyngeal mucosa through the posterior nasal apertures, the conjunctiva through the nasolacrimal duct and lacrimal canaliculi, and the mucosa of the sphenoidal, ethmoidal, frontal and maxillary sinuses through their openings into the meati.

The mucosa is thickest and most vascular over the conchae, especially at their extremities, and also on the anterior and posterior parts of the nasal septum and between the conchae. The mucosa is very thin in the meati, on the nasal floor and in the paranasal sinuses. Its thickness reduces the volume of the nasal cavity and its apertures significantly. The lamina propria contains cavernous vascular tissue with large venous sinusoids.

Olfactory mucosa

Olfactory mucosa (Fig. 32.6) covers approximately 5 cm^2 of the posterior upper parts of the lateral nasal wall, including the upper part of the vertical portion of the middle concha (where it is interspersed with respiratory epithelium in a checkerboard fashion) and the opposite part of the nasal septum, the superior concha, the sphenoethmoidal recess, the upper part of the perpendicular plate of the ethmoid and the portion of the roof of the nose that arches between the septum and lateral wall, including the underside of the cribriform plate (constituting the olfactory cleft or groove). It consists of a yellowish brown pigmented pseudostratified epithelium, containing olfactory receptor neurones, sustentacular cells and two classes of basal cell, lying on a subepithelial lamina propria containing subepithelial olfactory glands (of Bowman) and bundles of axons derived from the olfactory receptor neurones which course through the mucosa on their way to the cribriform plate. The glands secrete a predominantly serous fluid through ducts which open onto the epithelial surface. These secretions form a thin fluid layer in which sensory cilia and the microvilli of the sustentacular cells are embedded.

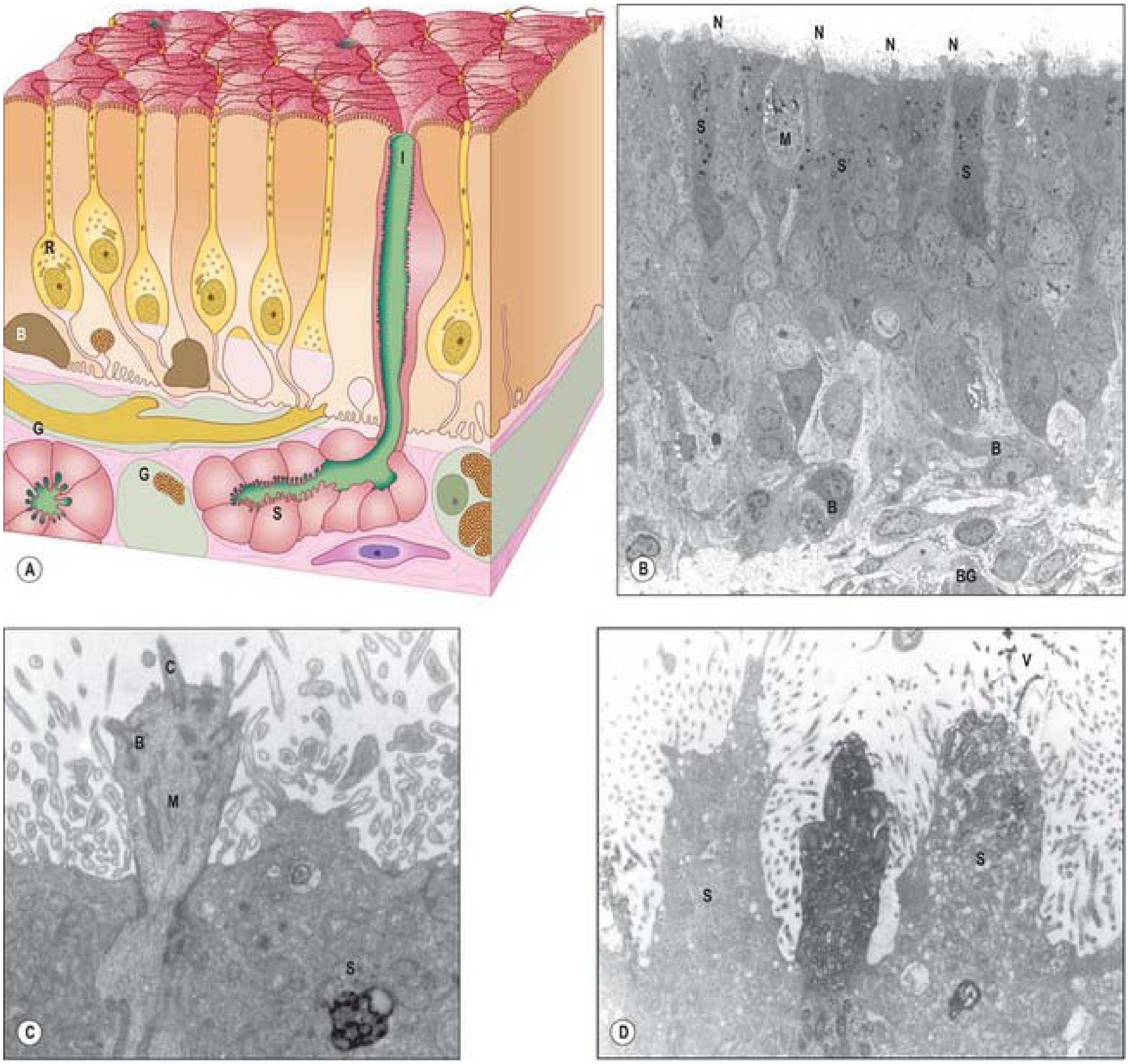

Fig. 32.6 **A**, The chief cytological features of the olfactory epithelium. Receptor cells (neurones) (R) are situated among columnar sustentacular cells. The axons of the receptor cells emerge from the epithelium in bundles enclosed by ensheathing glial cells (G). Rounded globose basal cells (B) and flattened horizontal basal cells (not shown) lie on the basal lamina and the subepithelial glands (of Bowman) (S) open on to the surface via their intraepithelial ducts (I). At the surface are cilia of the receptor cells and microvilli of the supporting cells. **B**, **C** and **D** are longitudinal sections through human olfactory epithelium: **B**, Ciliated olfactory receptor neurones with characteristic expanded ends (N) project into the nasal lumen. M,

microvillar cell; S, supporting or sustentacular cells containing electron dense material; B, basal cells resting upon the basal lamina. The edge of a Bowman's gland (BG) lies deeper in the lamina propria. **C**, Higher power view of the expanded end of an olfactory receptor neurone. The electron dense, osmiophilic material within the adjacent supporting cell (S) is thought to contribute to the pigmentation of the olfactory epithelium. C, olfactory cilium; B, basal body with projecting 'feet'. **D**, Section of human olfactory epithelium immunostained with anti-OMP (olfactory marker protein): an immunopositive olfactory receptor neurone lies between two unstained supporting cells (S). V, microvilli.

*(Parts **B**, **C** and **D** by courtesy of Professor Bruce Jafek, Department of Otolaryngology, University of Colorado, Denver, USA.)*

Olfactory receptor neurones

Olfactory receptor neurones are bipolar. Their cell bodies and nuclei are located in the middle zone of the olfactory epithelium. Each neurone has a single unbranched apical dendrite, 2 μm diameter, which extends to the epithelial surface, and a basally directed unmyelinated axon, 0.2 μm diameter, which passes in the opposite direction, penetrates the basal lamina and enters the lamina propria. The tips of the dendrites project into the overlying secretory fluid and are expanded into characteristic endings (knobs) (Fig. 32.6B). Groups of up to 20 cilia radiate from the circumference of each ending and extend for long distances parallel to the epithelial surface. Internally, the short proximal part of each cilium has the '9 + 2′ pattern of microtubules typical of motile cilia, while the longer distal trailing end contains only the central pair of microtubules. The olfactory cilia lack dynein arms and are thought to be non-motile; their primary purpose is to increase the surface area of sensory receptor membrane available for the efficient detection of odorant molecules transferred across the mucous layer by odorant binding proteins. Mature olfactory neurones express olfactory marker protein (OMP), an abundant cytoplasmic protein involved in olfactory signal transduction (Fig. 32.6D). Each olfactory receptor neurone expresses receptors for a single (or very few) odorant molecules. In humans, over 1000 genes code for functional odorant receptors; the number of functional genes is much higher in macrosmotic animals (Buck & Axel 1991). Although neurones with the same receptor specificity are randomly distributed within anatomical zones of the epithelium, their axons all converge on the same glomerulus in the olfactory bulb. Specific odours activate a unique spectrum of receptor neurones which in turn activate restricted groups of glomeruli and their second order neurones.

The axons form small intraepithelial fascicles among the processes of sustentacular and basal cells. The fascicles penetrate the basal lamina, and are immediately surrounded by olfactory ensheathing cells. Groups of up to 50 such fascicles join to form larger olfactory nerve rootlets which pass through the cribriform plate of the ethmoid bone, wrapped in meningeal sheaths. They immediately enter the overlying olfactory bulbs, where they synapse in glomeruli with mitral cells and, to a lesser extent, with smaller tufted cells.

Microvillar cells

Microvillar cells occupy a superficial position in the olfactory epithelium. They are flask-shaped and electron-lucent, and the apical end of each cell gives rise to a tuft of microvilli that project into the mucus layer lining the nasal cavity (Fig. 32.6B). Cell counts in longitudinal sections reveal that microvillar cells occur with a density that is approximately one tenth of the density of ciliated olfactory neurones: their function and origin has yet to be determined.

Sustentacular cells

Sustentacular, or supporting, cells are columnar cells that separate and partially ensheathe the olfactory receptor neurones. Their large nuclei form a layer superficial to the neuronal nuclei within the epithelium. The cells are capped by numerous long, irregular, microvilli which lie in the secretory fluid layer that covers the surface of the epithelium, intermingled with the trailing ends of the cilia on the olfactory receptor endings. Their expanded bases contain numerous lamellated dense bodies, which are the remnants of secondary lysosomes, and which contribute significantly to the pigmentation of the olfactory area (Fig. 32.6B,C). The granules gradually accumulate with age, and because these cells are long-lived, the intensity of pigmentation also increases with age. Neighbouring sustentacular cells are linked by desmosomes close to the epithelial surface, an arrangement that helps to stabilize the epithelium mechanically. Sustentacular cells and olfactory receptor neurones are linked by tight junctions at the level of the epithelial surface.

Basal cells

There are horizontal and globose basal cells. Horizontal basal cells are flattened against the basal lamina. Their nuclei are condensed and their darkly staining cytoplasm contains numerous intermediate filaments of the cytokeratin family, inserted into desmosomes between the basal cells and surrounding sustentacular cells. Globose cells are rounded or elliptical in shape, and have pale, euchromatic nuclei, and pale cytoplasm. They form a distinct zone that is slightly internal to the basal surface of the epithelium and characterized by mitotic figures: globose basal cells are the immediate source of new olfactory receptor neurones.

Olfactory ensheathing cells

Olfactory ensheathing cells share properties with astrocytes and non-myelinating Schwann cells, but also possess distinctive features that indicate they are a separate class of glia. Developmentally they are derived from the olfactory placode rather than the neural crest. They ensheath olfactory axons in a unique manner throughout their entire course, and accompany them into the olfactory bulb, where they contribute to the glia limitans. In recent years, olfactory ensheathing cells have been the focus of intense experimental scrutiny in the search for a source of transplantable glia capable of supporting neuronal regeneration within the CNS, possibly in the treatment of paraplegia.

Olfactory glands

Olfactory (Bowman's) glands are branched tubuloalveolar structures that lie beneath the olfactory epithelium and secrete their products onto the epithelial surface through narrow, vertical ducts. Their secretions, which include defensive substances, lysozyme, lactoferrin, IgA and sulphated proteoglycans, together with odorant-binding proteins which increase the efficiency of odour detection, bathe the dendritic endings and cilia of the olfactory receptors. The fluid acts as a solvent for odorant molecules, allowing their diffusion to the sensory receptors.

Turnover of olfactory receptor neurones

Olfactory receptor neurones are lost and replaced throughout life. Individual receptor cells have a variable lifespan, thought to average 1–3 months. Stem cells situated near the base of the epithelium undergo periodic mitotic division throughout life, giving rise to new olfactory receptor neurones which then grow a dendrite to the olfactory surface and an axon to the olfactory bulb. The cell bodies of these new receptor neurones gradually move apically until they reach the region just below the supporting cell nuclei. When they degenerate, dead neurones are either shed from the epithelium or are phagocytosed by sustentacular cells. The rate of receptor cell loss and replacement increases after exposure to damaging stimuli, but declines slowly with age, a phenomenon that presumably contributes to diminishing olfactory sensory function in old age. Biopsy specimens from normosmic adults have revealed that patchy replacement of olfactory with respiratory epithelium occurs even in young healthy adults (Paik et al 1992, Holbrook et al 2005).

VASCULAR SUPPLY AND LYMPHATIC DRAINAGE OF THE NASAL CAVITY

Many of the vessels and nerves supplying the nasal cavities arise within the pterygopalatine fossa and these origins are described in Chapter 31.

Arteries

Branches of the ophthalmic, maxillary and facial arteries supply different territories within the walls, floor and roof of the nose (Fig. 32.7A,B). They ramify to form anastomotic plexuses within and deep to the nasal mucosa. Anastomoses also occur between some larger arterial branches. The anterior and posterior ethmoidal branches of the ophthalmic artery supply the ethmoidal and frontal sinuses and the roof of the nose (including the septum). The anterior ethmoidal artery usually runs within the bone of the anterior skull base unless this is well pneumatized with a supraorbital cell, in which case the artery is more likely to be positioned away from the skull base and to be more prone to surgical damage. The sphenopalatine branch of the maxillary artery supplies the mucosa of the conchae, meati and posteroinferior part of the nasal septum, i.e. it is the principal vessel supplying the nasal mucosa. The artery comes out of a fissure (erroneously termed a foramen), and normally divides before it enters the nasal cavity behind the crista ethmoidalis. The number and distribution of its branches show great variation. The greater palatine branch of the maxillary artery supplies the region of the inferior meatus. Its terminal part ascends through the incisive canal to anastomose on the septum with branches of the sphenopalatine and anterior ethmoidal arteries and with the septal branch of the superior labial artery. This septal region (Little’s area) is a common site of bleeding from the nose. The infraorbital artery and the superior, anterior, and posterior alveolar branches of the maxillary artery supply the mucosa of the maxillary sinus. The pharyngeal branch of the maxillary artery supplies the sphenoidal sinus.

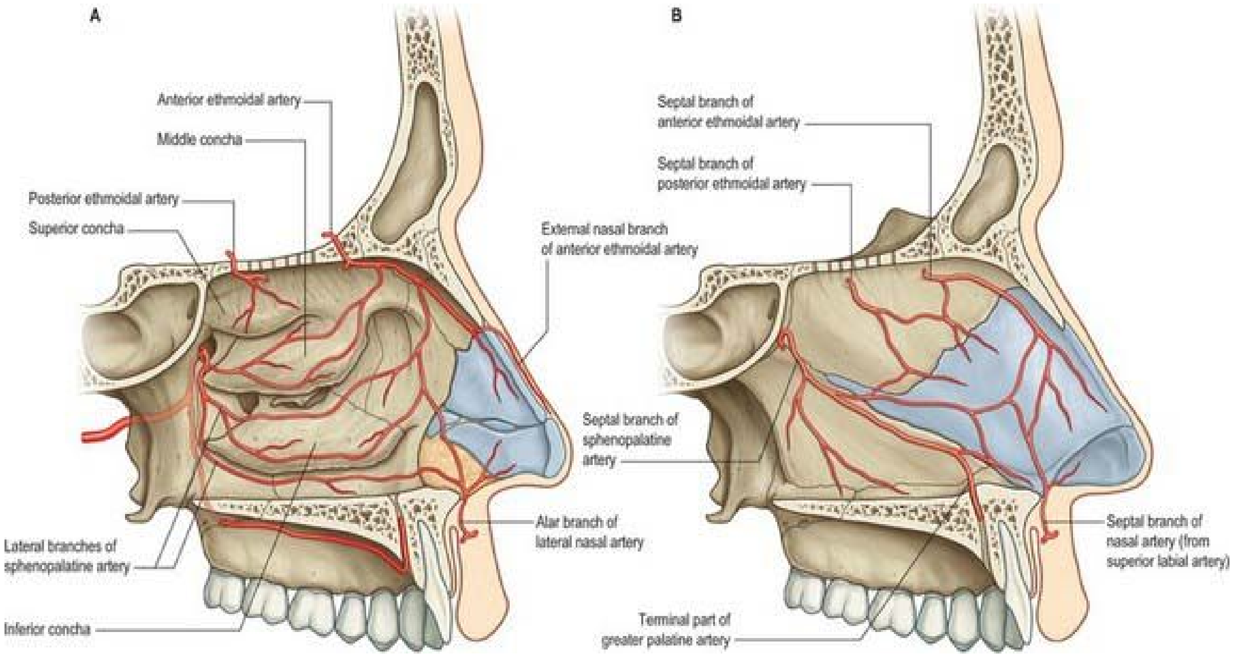
A
Anterior ethmoidal artery
Middle concha
Posterior ethmoidal artery
Superior concha
External nasal branch of anterior ethmoidal artery
Septal branch of sphenopalatine artery
Alar branch of lateral nasal artery
Lateral branches of sphenopalatine artery
Inferior concha
B
Septal branch of anterior ethmoidal artery
Septal branch of posterior ethmoidal artery
Septal branch of nasal artery (from superior labial artery)
Terminal part of greater palatine artery

Fig. 32.7 The arterial supply of the nasal cavity. **A**, Lateral wall of the left nasal cavity; **B**, Medial wall of the left nasal cavity.

(From Drake, Vogl and Mitchell 2005.)

Veins

A rich submucosal cavernous plexus is especially dense in the posterior part of the septum and in the middle and inferior conchae (Fig. 32.8). Numerous arteriovenous anastomoses are present in the deep layer of the mucosa and around the mucosal glands. The cavernous conchal plexuses resemble those in erectile tissue: the nasal cavity is susceptible to blockage should they become engorged. Veins from the posterior part of the nose generally pass to the sphenopalatine vein that runs back through the sphenopalatine foramen to drain into the pterygoid venous plexus. The anterior part of the nose is drained mainly through veins accompanying the anterior ethmoidal arteries, and these veins subsequently pass into the ophthalmic or facial veins. A few veins pass through the cribriform plate to connect with those on the orbital surface of the frontal lobes of the brain. When the foramen caecum is patent, it transmits a vein from the nasal cavity to the superior sagittal sinus.

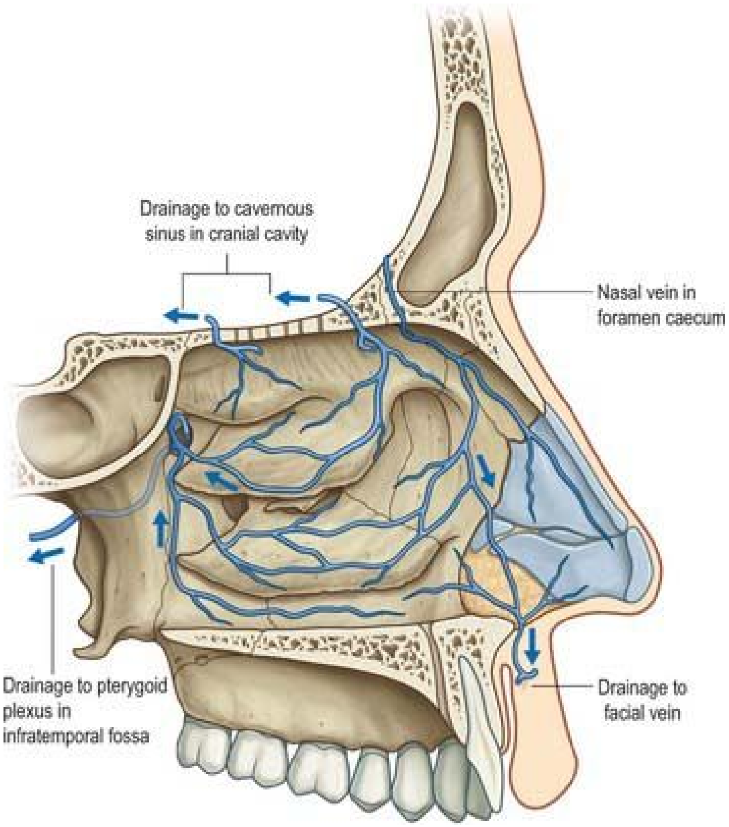
Drainage to cavernous sinus in cranial cavity
Nasal vein in foramen caecum
Drainage to pterygoid plexus in infratemporal fossa
Drainage to facial vein

Fig. 32.8 Venous drainage of the nasal cavity: lateral wall of the left nasal cavity.

(From Drake, Vogl and Mitchell 2005.)

Nose bleeds

The vast majority of nosebleeds, particularly in children, occur as a result of digital trauma to the anastomosis of arterioles and veins in Little's area (Kiesselbach's plexus), on the nasal septum just inside the nasal vestibule. In older patients brisker bleeding may occur as a result of the spontaneous rupture of arteries further back in the nose. These may be controlled by applying pressure with a nasal pack but where this fails, knowledge of the pattern of arterial blood supply to the nasal cavity permits interruption of the appropriate blood supply by ligation or embolization of the feeding vessel. The sphenopalatine artery may be ligated under endoscopic visualization as it enters the nose. The ethmoidal arteries may be exposed within the orbit and ligated to arrest bleeding high up in the nasal cavity. The maxillary artery may be exposed surgically behind the posterior wall of the maxillary sinus and ligated, or alternatively it may be identified radiologically, using a radio-opaque dye, so that it may be blocked by embolization.

Lymphatic drainage

Lymph vessels from the anterior region of the nasal cavity pass superficially to join those draining the external nasal skin, and end in the submandibular nodes. The rest of the nasal cavity, paranasal sinuses, nasopharynx and pharyngeal end of the pharyngotympanic tube, all drain to the upper deep cervical nodes either directly or through the retropharyngeal nodes. The posterior nasal floor probably drains to the parotid nodes.

INNERVATION OF THE NASAL CAVITY

Olfaction is mediated via the olfactory nerves. General sensation (touch, pain and temperature) from the nasal mucosa is carried by branches of the ophthalmic and maxillary divisions of the trigeminal nerves (Fig. 32.9). Trigeminal fibres close to, and within, the epithelial layer are sensitive to noxious chemicals, e.g. ammonia and sulphur dioxide. Autonomic fibres innervate mucous glands and control cyclical and reactive vasomotor activity.

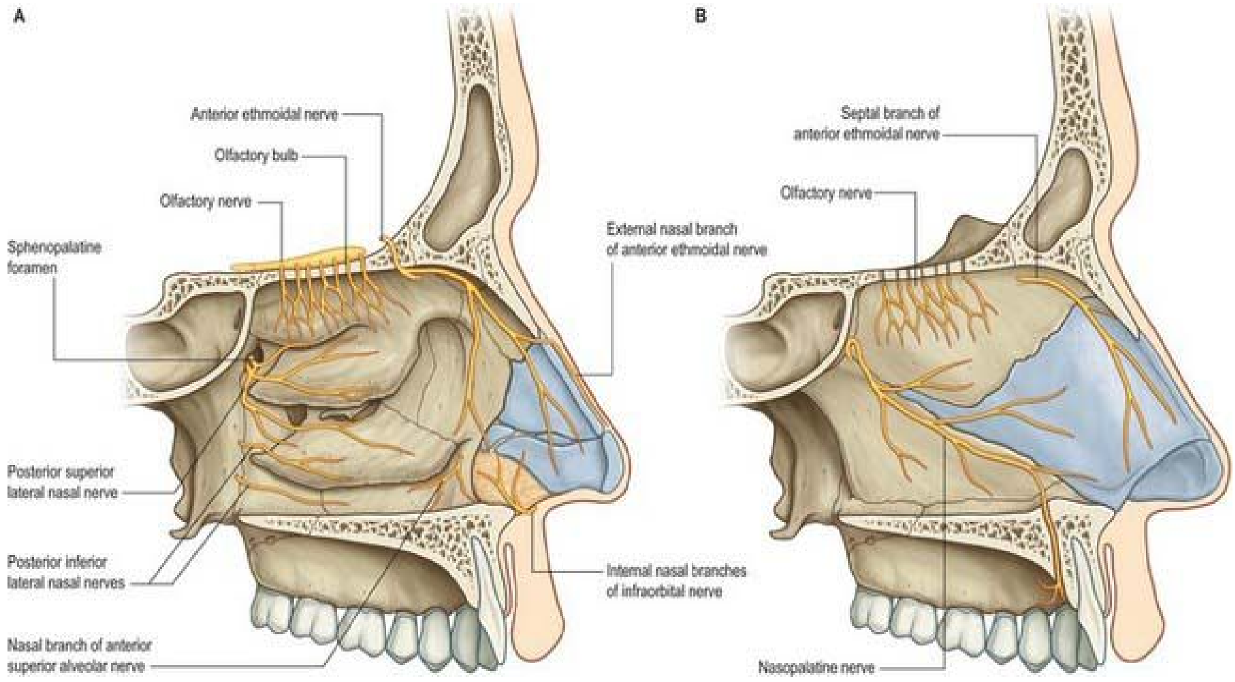
A
Anterior ethmoidal nerve
Olfactory bulb
Olfactory nerve
Sphenopalatine foramen
Posterior superior lateral nasal nerve
Posterior inferior lateral nasal nerves
Nasal branch of anterior superior alveolar nerve
External nasal branch of anterior ethmoidal nerve
Internal nasal branches of infraorbital nerve
B
Septal branch of anterior ethmoidal nerve
Olfactory nerve
Nasopalatine nerve

Fig. 32.9 The innervation of the nasal cavity. **A**, Lateral wall of the left nasal cavity. **B**, Medial wall of the left nasal cavity.

(From Drake, Vogl and Mitchell 2005.)

Trigeminal innervation

The anterior ethmoidal branch of the nasociliary nerve leaves the cranial cavity through a small slit near the crista galli and enters the roof of the nasal cavity where it runs in a groove on the inner surface of the nasal bone, supplying the roof of the nasal cavity. It gives off a lateral internal branch to supply the anterior part of the lateral wall and a medial internal branch to the anterior and upper parts of the septum, before emerging at the inferior margin of the nasal bone as the external nasal nerve to supply the skin of the external nose to the nasal tip. The infraorbital nerve supplies the nasal vestibule. The anterior superior alveolar nerve supplies part of the septum, the floor near the anterior nasal spine and the anterior part of the lateral wall as high as the opening of the maxillary sinus; the lateral posterior superior nasal and the posterior inferior nasal branches of the greater palatine nerve together supply the posterior three-quarters of the lateral wall, roof and floor; the medial posterior superior nasal nerves and the nasopalatine nerve supply the inferior part of the nasal septum; and branches from the nerve of the pterygoid canal supply the upper and posterior part of the roof and septum.

Autonomic innervation

Sympathetic postganglionic vasomotor fibres are distributed to the nasal blood vessels. Postganglionic parasympathetic fibres derived from the pterygopalatine ganglion provide the secretomotor supply to the nasal mucous glands, and are distributed via branches of the maxillary nerves.

Olfactory nerves

Olfactory nerves are bundles of very small axons derived from olfactory receptor neurons in the olfactory mucosa. The axons are unmyelinated, and in varying stages of maturity, reflecting the constant turnover of olfactory neurones that takes place in the olfactory epithelium. Bundles of axons surrounded by olfactory ensheathing cells form a plexiform network in the subepithelial lamina propria of the mucosa. The bundles unite into as many as 20 branches that cross the cribriform plate in lateral and medial groups, and enter the overlying olfactory bulb where they end in glomeruli. Each branch is ensheathed by dura mater and pia-arachnoid as it passes through the cribriform plate. The dura subsequently becomes continuous with the nasal periosteum, and the pia-arachnoid merges with the connective tissue sheaths surrounding the nerve bundles, an arrangement that may favour the spread of infection into the cranial cavity from the nasal cavity.

In severe injuries involving the anterior cranial fossa, the olfactory bulb may be separated from the olfactory nerves or the nerves may be torn, producing anosmia, i.e. loss of olfaction. Fractures may involve the meninges, so that cerebrospinal fluid may leak into the nose resulting in cerebrospinal rhinorrhoea. Such injuries open up avenues for intracranial infection from the nasal cavity.

NASAL AIRFLOW AND THE NASAL CYCLE

The paired nasal valves are critical regulators of nasal airflow and resistance. Each is divided into external and internal portions, although often only the internal portion is regarded as the ‘nasal valve’ or flow limiting segment. The external valve is made of the ala, the skin of the vestibule, the nasal sill and the contour of the medial crus of the lower lateral cartilage. The external valve has a tendency to collapse at high flow rates even in normal individuals.

The upper lateral cartilages are in continuity with the superior border of the nasal septum. A valve-like mechanism exists at its distal end that regulates nasal airflow. The nasal valve area and internal nasal valve are two entities that should not be confused. The nasal valve area is the narrowest portion of the nasal passage. It is bounded medially by the septum and the tuberculum of Zukerkandl, superiorly and laterally by the caudal margin of the upper lateral cartilages, its fibro-adipose attachment to the pyriform aperture, the anterior end of the inferior turbinate and inferiorly it is made of the floor of the pyriform aperture.

The entire nasal valve area averages 55 mm^2 and 64 mm. The nasal valve, on the other hand, is the specific slit-like segment between the caudal margin of the upper lateral cartilage and the septum. It is measured in degrees and normally ranges between 10 and 15°. The dialator naris anterior muscle and the alar part of nasalis muscle support the nasal valves.

Airflow dynamics are recognized as playing a key role in conditioning (i.e. warming, humidifying and filtering) inspired air, however these dynamics are still poorly understood (Churchill et al 2004, Boyce & Eccles 2006). It is generally agreed that airflow within the nose is both laminar and turbulent. Inspired air is forced to pass through the nasal valve, and then expands as it passes further into the nasal cavity which offers little airflow resistance. This sudden change in speed and pressure produces turbulence and eddies. These currents allow adequate contact of inspired air with respiratory epithelium and facilitate odorant transport to the olfactory area.

Chewing also affects nasal airflow: pulses of aroma-laden air are pumped out of the mouth into the retronasal region with each chew.

The cross sectional area of the nasal airway depends on the dimensions of the septal partition and inferior conchae, which are modulated by changes in the dimensions of the erectile tissue that covers them, and on the stability of the lateral nasal walls during breathing. The nasal cycle is an alternating fluctuation of nasal engorgement and airflow through the nasal passages, with period lengths ranging from approximately 1 to 5 hours. The mechanism involves changes in sympathetic tone to the venous erectile tissue of the nasal mucosa; increased sympathetic vasoconstriction causes resistance to fall. These alterations in the thickness and contours of the mucosal surfaces are visible as a swelling or shrinkage of the nasal lining, and may serve to protect the mucosae from desiccation. The pacemaker for the cycle is believed to lie within the suprachiasmatic nucleus. The rhythmicity of the cycle decreases with age.

Disturbances of the normal airflow pattern, whether produced by mucocutaneous or skeletal changes within the nose, affect normal nasal breathing and are usually perceived as some form of nasal obstruction.

PARANASAL SINUSES

The paranasal sinuses are the frontal, ethmoidal, sphenoidal and maxillary sinuses, housed within the bones of the same name (Figs 32.1, 32.10-32.13). They all open into the lateral wall of the nasal cavity by small apertures that permit both the equilibration of air between the various air spaces and the clearance of mucus from the sinuses into the nose via a mucociliary escalator. The detailed position of these apertures, and the precise form and size of each of the sinuses, varies enormously between individuals. Respiratory epithelium extends through the apertures of the paranasal sinuses to line their cavities, a feature that unfortunately favours the spread of infections. Sinus mucosa is thinner, less vascular and has fewer goblet cells than nasal mucosa. Cilia are always present in the mucosa near the apertures but less evenly distributed elsewhere within the sinuses.

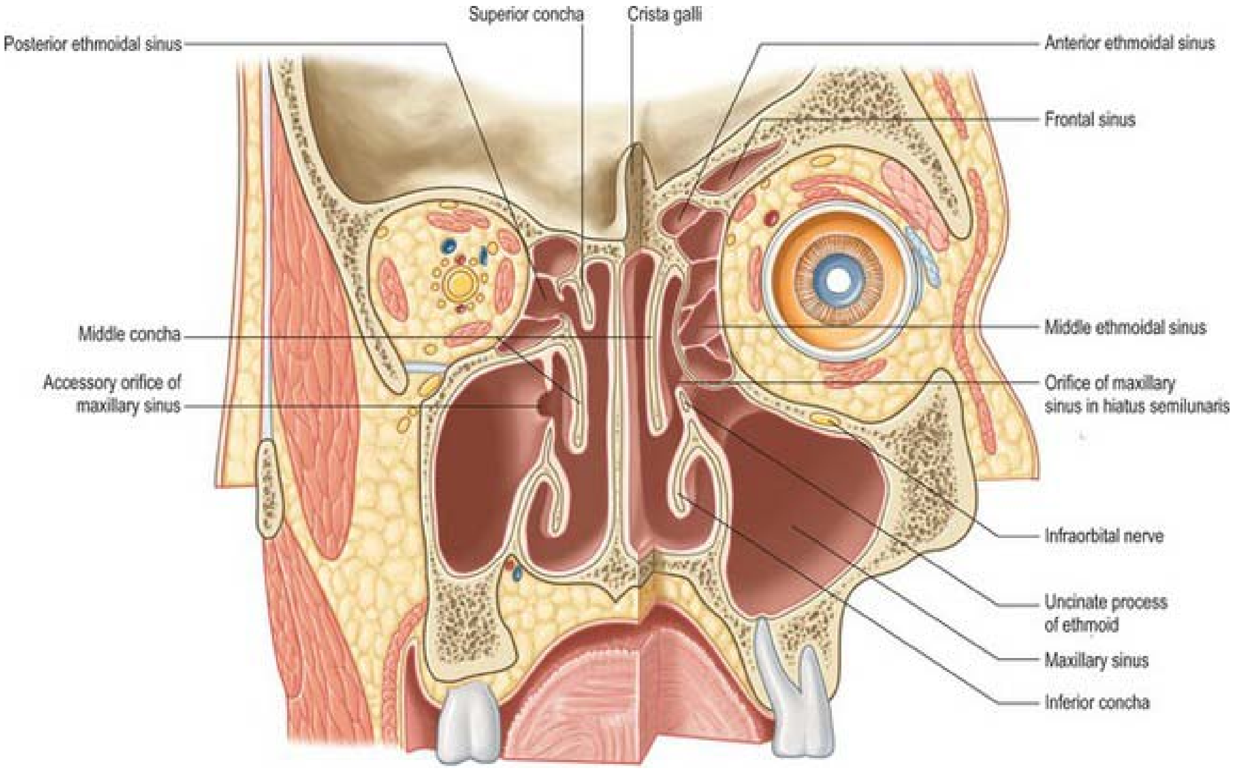
Superior concha
Crista galli
Posterior ethmoidal sinus
Anterior ethmoidal sinus
Frontal sinus
Middle concha
Middle ethmoidal sinus
Accessory orifice of maxillary sinus
Orifice of maxillary sinus in hiatus semilunaris
Infraorbital nerve
Uncinate process of ethmoid
Maxillary sinus
Inferior concha

Fig. 32.10 A coronal section through the nasal cavity, viewed from the posterior aspect. The plane of the section on the right side is more anterior.

The normal orifice of the maxillary sinus is shown on the right side and an accessory orifice on the left side.

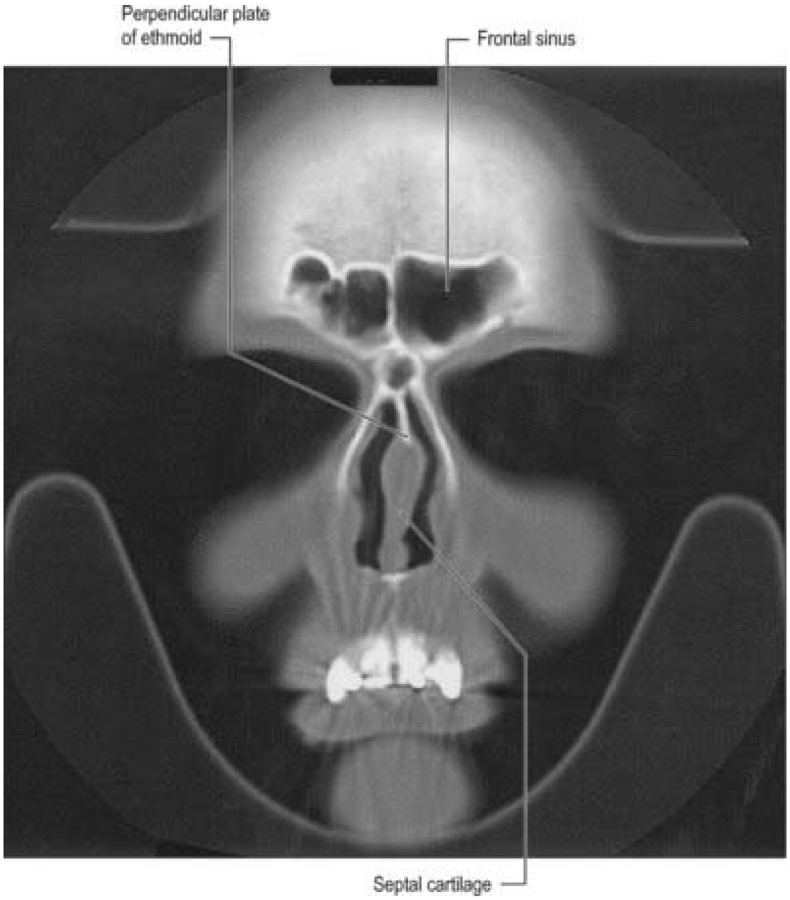
Perpendicular plate of ethmoid
Frontal sinus
Septal cartilage

Fig. 32.11 Coronal CT scan showing the frontal sinus.

(By courtesy of Dr N Drage.)

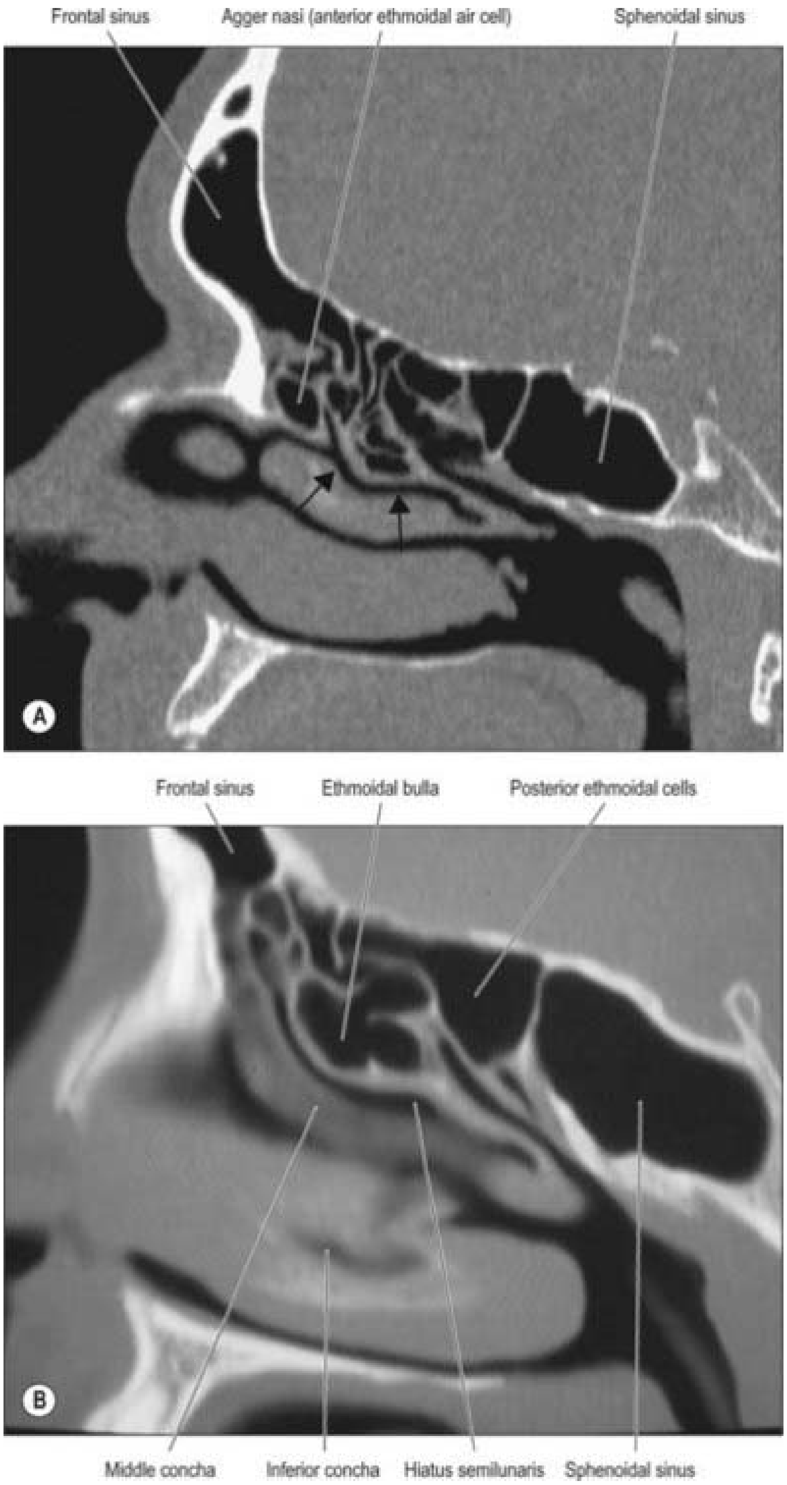
Frontal sinus
Agger nasi (anterior ethmoidal air cell)
Sphenoidal sinus
A
Frontal sinus
Ethmoidal bulla
Posterior ethmoidal cells
B
Middle concha
Inferior concha
Hiatus semilunaris
Sphenoidal sinus

Fig. 32.13 **A** and **B**, Sagittal CT scans showing the frontal, ethmoidal and sphenoidal sinuses. Arrows indicate the hiatus semilunaris in **A**.

*(**A** by courtesy of Professor D Bell.)*

Most sinuses are rudimentary or absent at birth, but enlarge appreciably during the eruption of the permanent teeth and after puberty, events that significantly alter the size and shape of the face.

The functions of the paranasal sinuses remain speculative. They clearly add some resonance to the voice, and also allow the enlargement of local areas of the skull while minimizing a corresponding increase in bony mass. It is likely that such growth-related changes serve to strengthen particular regions, e.g. the alveolar process of the maxilla when the secondary dentition erupts, but they may also function in contouring the head to provide visual signals indicating the individual’s status in a social context (e.g. gender, sexual maturity and group identity).

FRONTAL SINUS

The paired frontal sinuses are posterior to the superciliary arches, between the outer and inner tables of the frontal bone (Figs 32.10, 32.11, 32.13A). Each usually underlies a triangular area on the surface of the face, its angles formed by the nasion, a point 3 cm above the nasion and the junction of the medial one-third and lateral two-thirds of the supraorbital margin. The two sinuses are rarely symmetrical, since the septum between them usually deviates from the median plane. Each sinus may be further divided into a number of communicating recesses by incomplete bony septa.

The average dimensions of an adult frontal sinus are: height 3.2 cm; breadth 2.6 cm; depth 1.8 cm. Each usually has a frontal portion that extends upwards above the medial part of the eyebrow, and an orbital portion that extends back into the medial part of the roof of the orbit. In 4% one or both sinuses may be hypoplastic or even absent; racial differences have been reported. The prominence of the superciliary arches is no indication of the presence or size of the frontal sinuses. A frontal sinus may extend posteriorly as far as the lesser wing of the sphenoid bone but does not invade it. The morphology of the frontal sinus may be specific enough to allow identification of individuals from radiological evidence for forensic purposes.

The aperture of each frontal sinus either opens into the anterior part of the corresponding middle meatus by the ethmoidal infundibulum either as a frontonasal recess (rather than a duct) or medial to the hiatus semilunaris if the uncinate process is attached to the lateral nasal wall or an agger nasi cell.

The frontal sinuses are rudimentary or absent at birth, generally well developed between the seventh and eighth years, but reach full size only after puberty. They are more prominent in males, and lend the forehead an obliquity that contrasts with the vertical or convex profile typical of children and females. In the presence of a persistent metopic suture, the frontal sinuses develop separately on either side of the suture, which can be helpful in excluding frontal fractures. (The frontal bone is described in Chapter 29.)

Vascular supply, lymphatic drainage and innervation

The frontal sinuses receive their arterial supply from the supraorbital and anterior ethmoidal arteries. The veins drain into an anastomotic vein in the supraorbital notch that connects the supraorbital and superior ophthalmic veins. Lymphatic drainage is to the submandibular nodes. The sinuses are innervated by branches of the supraorbital nerves (general sensation), and the orbital branches of the pterygopalatine ganglia (parasympathetic secretomotor fibres).

SPHENOIDAL SINUS

The sphenoidal sinuses are two large irregular cavities within the body of the sphenoid and therefore lie posterior to the upper part of the nasal cavity (Figs 32.12-32.15). Each opens into the corresponding sphenoethmoidal recess via an aperture high on the anterior wall of the sinus. At birth the sinuses are minute cavities, and their main development occurs after puberty. The average adult dimensions are: vertical height 2 cm; transverse breadth 1.8 cm; anteroposterior depth 2.1 cm. The sinuses are usually separated by a septum that deviates from the midline in 75%, so that they are unequal in size and form. Their lumina may be further partially divided by bony laminae, accessory septa, especially in the region of former synchondroses. Occasionally one sinus overlaps the other above and, rarely, they intercommunicate. Bony ridges, produced by the internal carotid artery, pterygoid canal, maxillary branch of trigeminal and, in 15% of individuals, the optic nerve, may project into the sinuses from their lateral walls. Dehiscences in the osseous walls of either sinus may occasionally leave their mucosa in contact with the overlying dura mater.

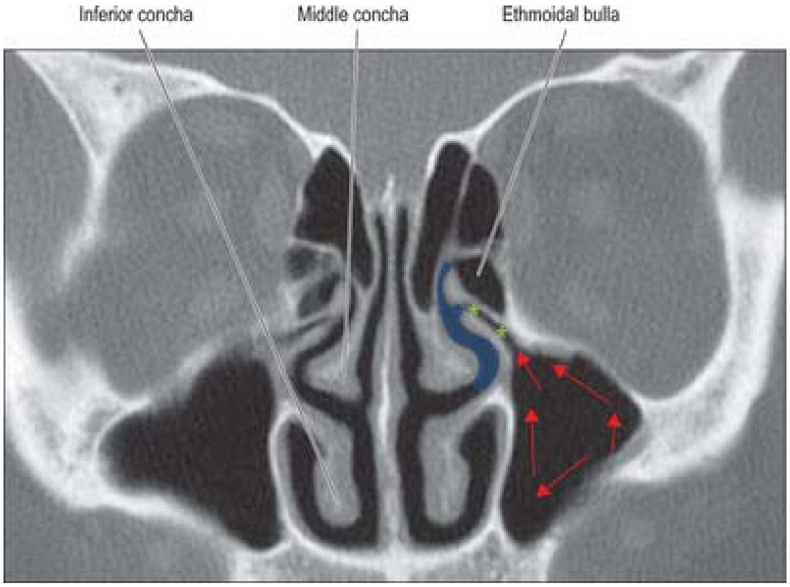

Fig. 32.14 Coronal CT scan through the ostiomeatal complex. Red arrows, direction of mucociliary flow; blue area, middle meatus; green stars, infundibulum.

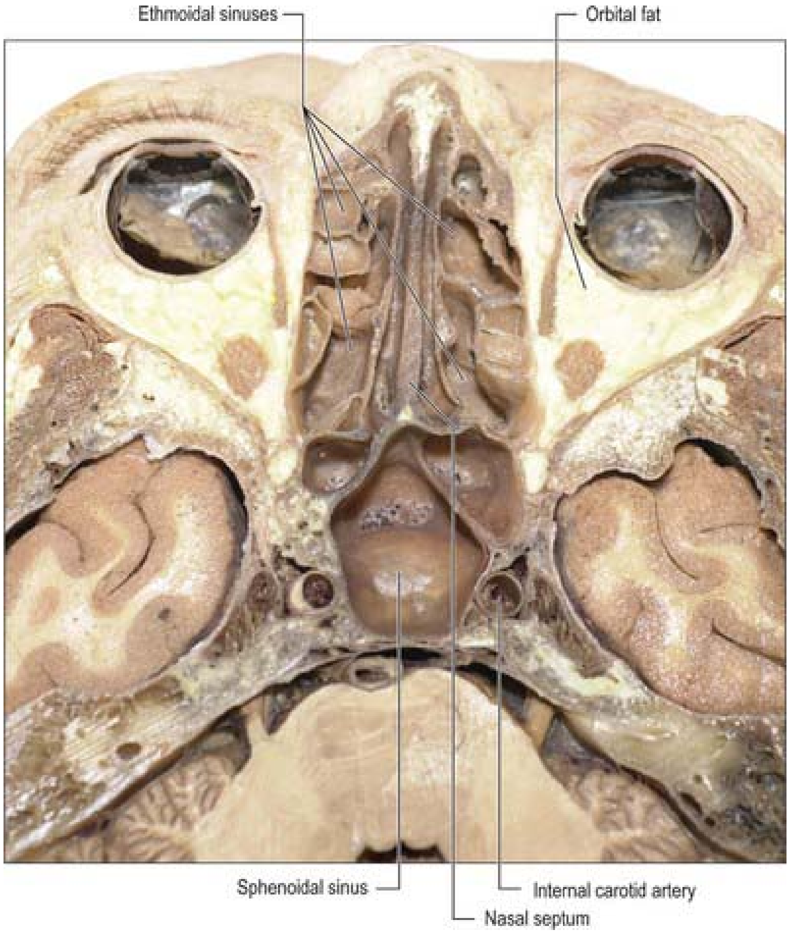
Ethmoidal sinuses
Orbital fat
Sphenoidal sinus
Internal carotid artery
Nasal septum

Fig. 32.15 Horizontal section of the head showing the ethmoidal and sphenoidal sinuses.

(By permission from Berkovitz BKB, Moxham BJ 2002 Head and Neck Anatomy. London: Martin Dunitz.)

The extent of pneumatization of surrounding bone is highly variable. In nearly 50% of skulls, a lateral recess may extend into the greater and lesser wings of the sphenoid or the pterygoid processes, and may even invade the basilar part of the occipital bone almost to the foramen magnum. A posterior ethmoidal sinus may extend posterosuperior to the relatively smaller sphenoidal sinuses. The sphenoidal sinuses are related above to the optic chiasma and hypophysis cerebri and on each side to the internal carotid artery and cavernous sinus (see Ch. 27). One or both sinuses may partially encircle the optic canal.

The shape and position of the sphenoidal sinus is of clinical importance in the trans-sphenoidal surgical approach to the hypophysis cerebri. The sinuses may be classified into three main types: sellar, the commonest type, where the sinus extends for a variable distance beyond the tuberculum sellae; presellar, where the sinus occasionally extends posteriorly towards, but not beyond, the tuberculum sellae; conchal, the rarest type, where a small sinus is separated from the sella turcica by 10 mm of trabecular bone. The anterior midline septum often becomes deviated to one side posteriorly: identification of this septation is important prior to surgery.

Vascular supply, lymphatic drainage and innervation

The sphenoidal sinuses receive their arterial supply from the posterior ethmoidal branches of the ophthalmic arteries and nasal branches of the sphenopalatine arteries. Venous drainage is through the posterior ethmoidal veins draining into the superior ophthalmic veins. Lymph drainage is to the retropharyngeal nodes. The sinuses are innervated by the posterior ethmoidal branches of the ophthalmic nerves (general sensation), and the orbital branches of the pterygopalatine ganglia (parasympathetic secretomotor fibres).

ETHMOIDAL SINUSES

The ethmoidal sinuses differ from the other paranasal sinuses in that they are formed of multiple thin-walled cavities in the ethmoidal labyrinth (Figs 32.10, 32.13-32.15) (for more details, see Chapter 29). The number and size of the cavities varies, from three large to 18 small sinuses on each side. They lie between the upper part of the nasal cavity and the orbit, and are separated from the latter by the paper-thin lamina papyracea or orbital plate of the ethmoid (this presents a poor barrier to infection which may therefore spread into the orbit). Pneumatization may extend into the middle concha, or into the body and wings of the sphenoid bone lateral to the sphenoid sinus.

The ethmoidal sinuses are divided clinically into anterior and posterior groups on each side, distinguished by their sites of communication with the nasal cavity. (Cells previously designated as belonging to a middle group are now included with the anterior group.) The anterior and posterior groups are separated from each other by the basal lamella of the middle concha; this may be indented by cells from either group and therefore it forms a rather tortuous barrier between them. In each group the sinuses are only partially separated by incomplete bony septa. The sinuses are of clinical significance at birth because they are susceptible to inflammation. They grow rapidly between the ages of 6 and 8 years and after puberty.

Anterior group

Peri-infundibular sinuses (anterior ethmoidal air cells)

Up to 11 anterior ethmoidal air cells drain into either the ethmoidal infundibulum or the frontonasal duct by one or more orifices. The most anterior group, agger nasi cells, are medial relations of the lacrimal sac and duct and invaginate beneath the agger nasi on the lateral wall of the nasal cavity anteriorly. Larger anterior and middle cells, Haller’s cells, may develop medially beneath the orbital floor. The most anterior supraorbital ethmoidal sinus cells may encroach on the frontal sinus.

Bullar sinuses (middle ethmoidal air cells)

There are usually less than three middle ethmoidal air cells. They open into the middle meatus by one or more orifices on or above the ethmoidal bulla.

Posterior group

Up to seven posterior ethmoidal air cells usually drain by a single orifice into the superior meatus; one may drain into the supreme meatus when present, and one or more into the sphenoidal sinus. The posterior group lies very close to the optic canal and optic nerve: optic nerve injury is a devastating potential complication of endoscopic sinus surgery, particularly if a spheno-ethmoid or Onodi cell is present. The reported incidence of an Onodi cell varies widely (3.5 to 51%), according to racial group: it is more common in non-Caucasians. The Onodi cell is usually regarded as the most posterior ethmoid cell that pneumatizes lateral and superior to the sphenoid sinus and is intimately associated with the optic nerve: it may contain a tuberculum nervi optici, where the optic canal bulges into the wall of the cell.

Vascular supply and innervation

The ethmoidal sinuses receive their arterial supply from nasal branches of the sphenopalatine artery and the anterior and posterior ethmoidal branches of the ophthalmic artery. Venous drainage is by the corresponding veins. The lymphatics of the anterior group drain to the submandibular nodes, and those of the posterior group to the retropharyngeal nodes. The sinuses are innervated by the anterior and posterior ethmoidal branches of the ophthalmic nerves (general sensation), and the orbital branches of the pterygopalatine ganglia (parasympathetic secretomotor fibres).

MAXILLARY SINUS

The maxillary sinus (maxillary antrum), is the largest of the paranasal sinuses. It fills the body of the maxilla (Chapter 29) and is pyramidal in shape (Fig. 32.10, Fig. 32.14). The base is medial and forms much of the lateral wall of the nasal cavity. The floor, which often lies below the nasal floor, is formed by the alveolar process and part of the palatine process of the maxilla. It is related to the roots of the teeth, especially the second premolar and first molar, but may extend posteriorly to the third molar tooth and/or anteriorly to incorporate the first premolar, and sometimes the canine. Defects in the bone overlying the roots are not uncommon. The roof of the sinus forms the major part of the floor of the orbit. It contains the infraorbital canal which may exhibit dehiscences. The lateral truncated apex of the pyramid extends into the zygomatic process of the maxilla, and may reach the zygomatic bone, in which case it forms the zygomatic recess which throws a V-shaped shadow over the antrum on a lateral radiograph.

The facial surface of the maxilla forms its anterior wall, and is grooved internally by a delicate canal (canalis sinuosus) which houses the anterior superior alveolar nerve and vessels as they pass forwards from the infraorbital canal. The posterior wall is formed by the infratemporal surface of the maxilla: it contains alveolar canals that may produce ridges in the sinus and that also conduct the posterior superior alveolar vessels and nerves to the molar teeth. The medial wall is deficient posterosuperiorly at the maxillary hiatus, a large opening which is partially closed in an articulated skull by portions of the perpendicular plate of the palatine bone, the uncinate process of the ethmoid bone, the inferior nasal concha, the lacrimal bone, and the overlying nasal mucosa, to form an ostium and anterior and posterior fontanelles. The ostium usually opens into the inferior part of the ethmoidal infundibulum, and thence into the middle meatus, via the hiatus semilunaris (the hiatus forms the area above the superior edge of the uncinate process). The fontanelles are covered only by periosteum and mucosa and may contain accessory ostia which may be visible on CT. All of the openings are nearer the roof than the floor of the sinus which means that the natural drainage of the maxillary sinus is reliant on an intact mucociliary escalator: the cilia of the sinus mucoperiosteum normally beat towards the ostium.

The maxillary sinus may be incompletely divided by septa; complete septa are very rare. The thinness of its walls is clinically significant in determining the spread of tumours from the maxillary sinus. A tumour may push up the orbital floor and displace the eyeball; project into the nasal cavity, causing nasal obstruction and bleeding; protrude onto the cheek, causing swelling and numbness if the infraorbital nerve is damaged; spread back into the infratemporal fossa, causing restriction of mouth opening due to pterygoid muscle damage and pain; or spread down into the mouth, loosening teeth and causing malocclusion. Extraction of molar teeth may damage the floor, and impact may fracture its walls. Hypoplasia of one maxillary antrum is present in up to 0.3% of the population.

Ostiomeatal complex

The term ostiomeatal complex, or ostiomeatal unit, refers to the area that includes the maxillary sinus ostium, ethmoid infundibulum and the hiatus semilunaris (Fig. 32.14). It is the common pathway for drainage of secretions from the maxillary and anterior group of ethmoidal sinuses; where the uncinate process attaches to the lateral nasal wall the complex also drains the frontal sinus.

Vascular supply, lymphatic drainage and innervation

The arterial supply of the maxilla is derived mainly from the maxillary arteries via the superior anterior, middle and posterior alveolar branches and from the infraorbital and greater palatine arteries. Branches of the posterior superior alveolar artery and the infraorbital artery form an anastomosis in the bony wall of the sinus, which also supplies the mucous membrane that lines the nasal chambers. An extraosseous anastomosis frequently exists between the posterior superior alveolar artery and the infraorbital artery. The intra- and extra-osseous anastomoses form a double arterial arcade which supplies the lateral antral wall and, partly, the alveolar process.

Veins corresponding to the arteries drain into the facial vein or pterygoid venous plexus on either side. Lymph drainage is to the submandibular nodes. The sinuses are innervated by the infraorbital and anterior, middle and posterior superior alveolar branches of the maxillary nerves (general sensation), and nasal branches of the pterygopalatine ganglia (parasympathetic secretomotor fibres).

For further details concerning the dimensions of the various air sinuses and the size and positions of their openings the reader is referred to Lang (1989).

IMAGING OF THE PARANASAL SINUSES

Standard radiological images are no longer recommended in the diagnosis of rhinosinusitis because of their poor specificity and sensitivity, although they may be used to confirm the presence of acute frontal or maxillary sinusitis that has failed to respond to medical treatment and requires urgent drainage. CT defines anatomical variations but should not be used in isolation for diagnosis because 1 in 3 asymptomatic individuals show incidental mucosal changes. Spiral CT provides good quality axial, coronal and sagittal images that facilitate an appreciation of the size and relationship of the paranasal sinuses.

SPREAD OF INFECTION TO CRANIAL CAVITY

The state of health of the paranasal sinuses depends on immunity, mucociliary clearance and aeration of the sinuses. The middle meatus forms the common drainage pathway for the anterior ethmoidal, frontal and maxillary sinuses, and can be readily examined with a fibreoptic endoscope (Simmen & Jones 2005). The posterior ethmoidal and sphenoidal sinuses drain into the superior meatus and sphenoethmoidal recess. Endoscopic examination will usually show infected mucus draining from these areas. Maxillary sinus infection may also spread from infected teeth.

REFERENCES

yce J, Eccles R. Do chronic changes in nasal airflow have any physiological or pathological effect on the nose and paranasal sinuses? A systematic review. *Clin Otolaryngol*. 2006;31:15-19.

ck L, Axel R. A novel multigene family may encode odorant receptors: a molecular basis for odor recognition. *Cell*. 1991;65:175-187.

The 2004 Nobel Prize in Physiology or Medicine was awarded to Axel and Buck for their discoveries of the genetic determinants of the olfactory receptors and the organization of the olfactory system in humans..

urchill SE, Shackelford LL, Georgi JN, Black MT. Morphological variation and airflow dynamics in the human nose. *Am J Hum Biol*. 2004;16:625-638.

ig TN, McDonald SW, McGregor OA. Possible routes of spread of carcinoma of the maxillary sinus to the oral cavity. *Clin Anat*. 1998;11:149-156.

nanuel JM. Epistaxis. Cummings CW, et al, editors. Otolaryngology Head and Neck Surgery, 3rd edn., vol. 2. St Louis: Mosby, 1998;852-865.

Describes the blood supply to the nose and the surgical approaches to control epistaxis..

lbrook EH, Leopold DA, Schwob JE. Abnormalities of axon growth in human olfactory mucosa. *Laryngoscope*. 2005;115:2144-2154.

fek BW. Ultrastructure of human nasal mucosa. *Laryngoscope*. 1983;93:1576-1599.

hnston M, Zakharov A, Papaiconomou C, Salmasi G, Armstrong D. Evidence of connections between cerebrospinal fluid and nasal lymphatic vessels in humans, non-human primates and other mammalian species. *Cerebrospinal Fluid Res*. 2004;1:2.

ng J. Clinical Anatomy of the Nose, Nasal Cavity and Paranasal Sinuses. Stuttgart: Thième, 1989.

cGowan DA, Baxter PW, James J. The Maxillary Sinus. Oxford: Wright, 1993.

eredith M. Human vomeronasal organ function: a critical review of best and worst cases. *Chem Senses*. 2001;26:433-445.

avarro JAC. The Nasal Cavity and Paranasal Sinuses: Surgical Anatomy. Berlin: Springer, 1997.

ik SI, Lehman MN, Seiden AM, Duncan HJ, Smith DV. Human olfactory biopsy. The influence of age and receptor distribution. *Arch Otolaryngol Head Neck Surg*. 1992;118:731-738.

mmen D, Jones N. Manual of endoscopic sinus surgery and its extended applications. Stuttgart: Thieme, 2005.

ammberger H, Kennedy DW. Paranasal sinuses: anatomic terminology and nomenclature. *Ann Otol Rhinol Laryngol*. 1995;104(Suppl 167):7-16. (10) Part 2

axler H, Windisch A, Geyerhofer U, Surd R, Solar P, Firbas W. Arterial blood supply of the maxillary sinus. *Clin Anat*. 1999;12:417-421.

itt M, Hummel T. Vomeronasal versus olfactory epithelium: is there a cellular basis for human vomeronasal perception? *Internat Rev Cytol*. 2006;248:209-259.

CHAPTER 33

Pharynx

The pharynx is a 12–14 cm long musculomembranous tube shaped like an inverted cone. It extends from the cranial base to the lower border of the cricoid cartilage (the level of the sixth cervical vertebra), where it becomes continuous with the oesophagus. The width of the pharynx varies constantly because it is dependent on muscle tone, especially of the constrictors: at rest the pharyngo-oesophageal junction is closed as a result of tonic closure of the upper oesophageal sphincter, and during sleep muscle tone is low and the dimensions of the pharynx are markedly decreased (which may give rise to snoring and sleep apnoea). The pharynx is limited above by the posterior part of the body of the sphenoid and the basilar part of the occipital bone, and it is continuous with the oesophagus below. Behind, it is separated from the cervical part of the vertebral column and the prevertebral fascia which covers longus colli and longus capitis by loose connective tissue in the retropharyngeal space above and the retrovisceral space below.

The muscles of the pharynx are three circular constrictors and three longitudinal elevators. The constrictors may be thought of as three overlapping cones which arise from structures at the sides of the head and neck and pass posteriorly to insert into a midline fibrous band, the pharyngeal raphe. The arterial supply to the pharynx is derived from branches of the external carotid artery, particularly the ascending pharyngeal artery, but also from the ascending palatine and tonsillar branches of the facial artery, the maxillary artery (greater palatine and pharyngeal arteries and the artery of the pterygoid canal) and dorsal lingual branches of the lingual artery. The pharyngeal veins begin in a plexus external to the pharynx, receive meningeal veins and a vein from the pterygoid canal, and usually end in the internal jugular vein. Lymphatic vessels from the pharynx and cervical oesophagus pass to the deep cervical nodes, either directly or through the retropharyngeal or paratracheal nodes. The motor and sensory innervation is principally via branches of the pharyngeal plexus.

The pharynx lies behind, and communicates with, the nasal, oral and laryngeal cavities via the nasopharynx, oropharynx and laryngopharynx respectively (Figs 33.1, 33.2). Its lining mucosa is continuous with that lining the pharyngotympanic tubes, nasal cavity, mouth and larynx.

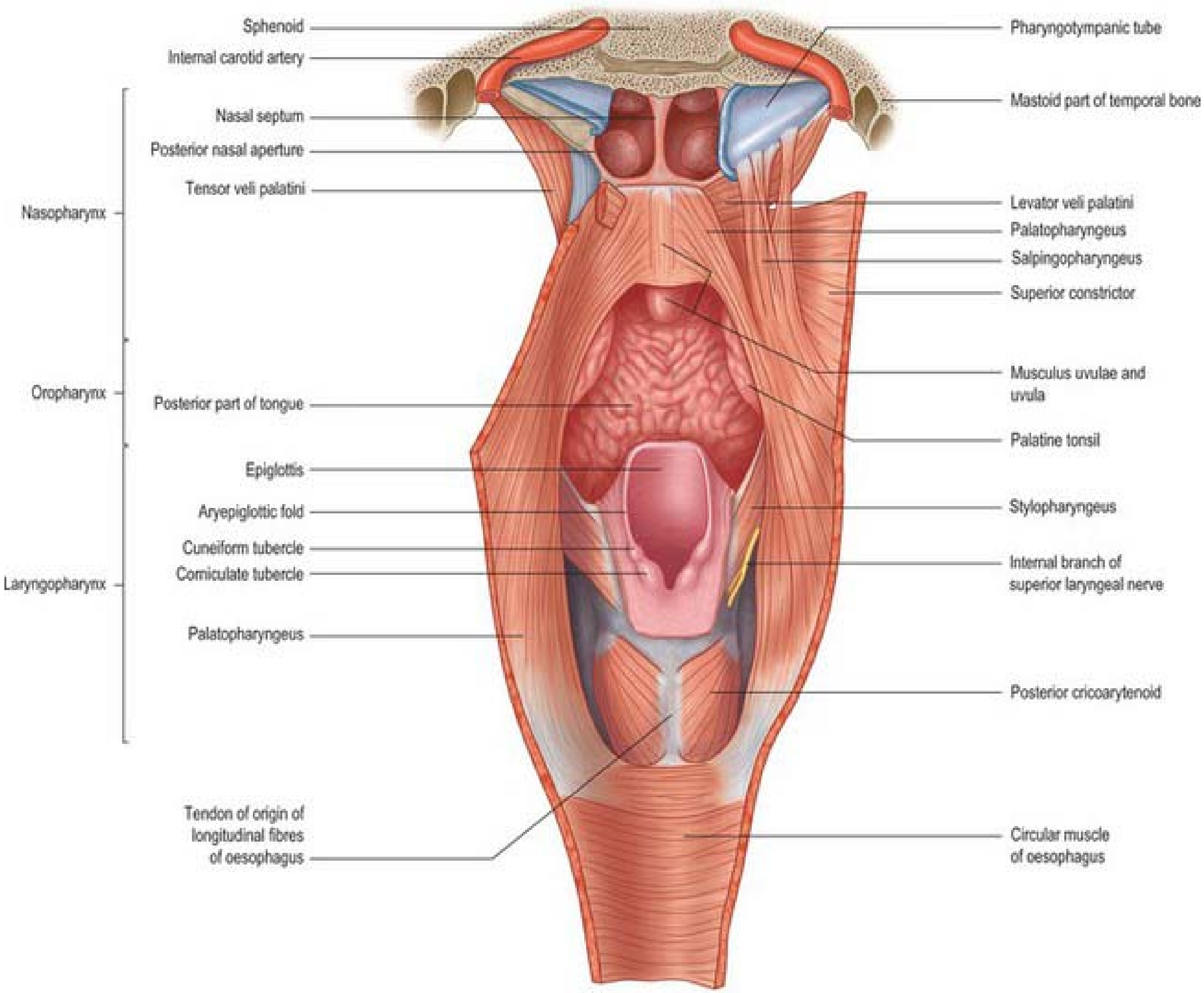
Sphenoid
Internal carotid artery
Nasal septum
Posterior nasal aperture
Tensor veli palatini
Nasopharynx
Oropharynx
Posterior part of tongue
Epiglottis
Aryepiglottic fold
Cuneiform tubercle
Corniculate tubercle
Laryngopharynx
Palatopharyngeus
Tendon of origin of longitudinal fibres of oesophagus
Pharyngotympanic tube
Mastoid part of temporal bone
Levator veli palatini
Palatopharyngeus
Salpingopharyngeus
Superior constrictor
Musculus uvulae and uvula
Palatine tonsil
Stylopharyngeus
Internal branch of superior laryngeal nerve
Posterior cricoarytenoid
Circular muscle of oesophagus

Fig. 33.1 The nasopharynx, oropharynx and laryngopharynx, exposed by cutting the median pharyngeal raphe and reflecting the constrictor muscles laterally on either side, posterior view.

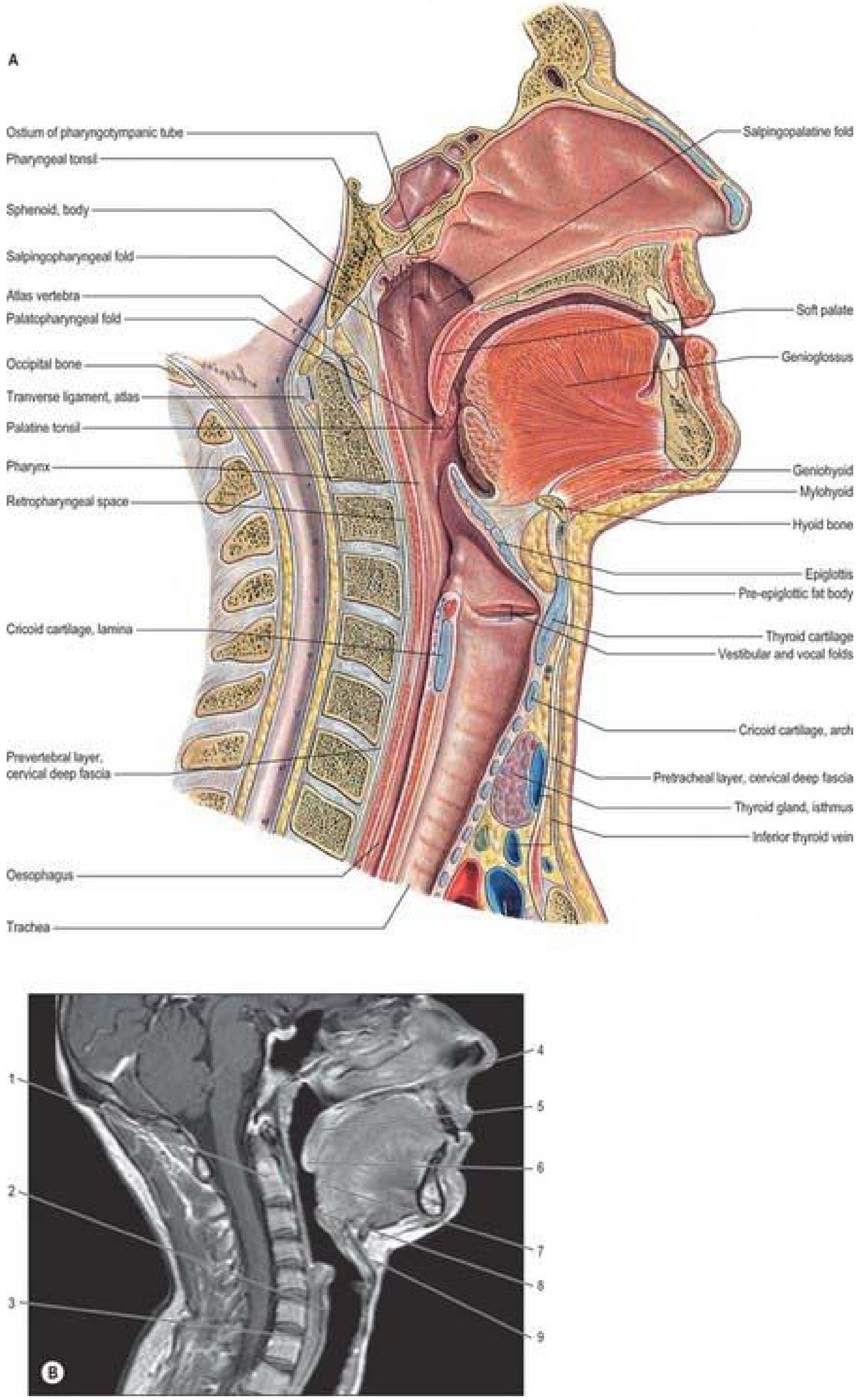
A
Ostium of pharyngotympanic tube
Pharyngeal tonsil
Sphenoid, body
Salpingopharyngeal fold
Atlas vertebra
Palatopharyngeal fold
Occipital bone
Tranverse ligament, atlas
Palatine tonsil
Pharynx
Retropharyngeal space
Cricoid cartilage, lamina
Prevertebral layer, cervical deep fascia
Oesophagus
Trachea
Salpingopalatine fold
Soft palate
Genioglossus
Geniohyoid
Mylohyoid
Hyoid bone
Epiglottis
Pre-epiglottic fat body
Thyroid cartilage
Vestibular and vocal folds
Cricoid cartilage, arch
Pretracheal layer, cervical deep fascia
Thyroid gland, isthmus
Inferior thyroid vein
1
2
3
4
5
6
7
8
9
B

Fig. 33.2 **A**, Sagittal section through the head and neck, including the nasal and oral cavities but excluding the intracranial region (from Sobotta 2006). **B**, Corresponding MRI, also includes the posterior cranial fossa,

cerebellum and cervical spinal cord. **1**. Dens of axis. **2**. Lamina of cricoid cartilage. **3**. Oesophagus. **4**. Hard palate. **5**. Soft palate. **6**. Uvula. **7**. Pharyngeal part of tongue. **8**. Epiglottis. **9**. Hyoid bone.

*(**B** by courtesy of Dr Roger JS Chinn.)*

NASOPHARYNX

BOUNDARIES

The nasopharynx lies above the soft palate and behind the posterior nares, which allow free respiratory passage between the nasal cavities and the nasopharynx (Figs 33.1, 33.2). The nasal septum separates the two posterior nares, each of which measures approximately 25 mm vertically and 12 mm transversely. Just within these openings lie the posterior ends of the inferior and middle nasal conchae. The nasopharynx has a roof, a posterior wall, two lateral walls and a floor. These are rigid (except for the floor, which can be raised or lowered by the soft palate) and the cavity of the nasopharynx is therefore never obliterated by muscle action, unlike the cavities of the oro- and laryngopharynx. The nasal and oral parts of the pharynx communicate through the pharyngeal isthmus which lies between the posterior border of the soft palate and the posterior pharyngeal wall. Elevation of the soft palate and constriction of the palatopharyngeal sphincter close the isthmus during swallowing.

The roof and posterior wall form a continuous concave slope that leads down from the nasal septum to the oropharynx. It is bounded above by mucosa overlying the posterior part of the body of the sphenoid, and further back by the basilar part of the occipital bone as far as the pharyngeal tubercle. Further down, the mucosa overlies the pharyngobasilar fascia and the upper fibres of the superior constrictor, and behind these, the anterior arch of the atlas. A lymphoid mass, the adenoid, lies in the mucosa of the upper part of the roof and posterior wall in the midline.

The lateral walls of the nasopharynx display a number of important surface features. On either side each receives the opening of the pharyngotympanic tube (also termed the auditory or Eustachian tube), situated 10–12 mm behind and a little below the level of the posterior end of the inferior nasal concha (Fig. 33.2). The tubal aperture is approximately triangular in shape, and is bounded above and behind by the tubal elevation which consists of mucosa overlying the protruding pharyngeal end of the cartilage of the pharyngotympanic tube. A vertical mucosal fold, the salpingopharyngeal fold, descends from the tubal elevation behind the aperture (Fig. 33.2) and covers salpingopharyngeus in the wall of the pharynx (see Fig. 33.4); a smaller salpingopalatine fold extends from the anterosuperior angle of the tubal elevation to the soft palate in front of the aperture. As levator veli palatini enters the soft palate it produces an elevation of the mucosa immediately around the tubal opening (see Fig. 33.4). A small variable mass of lymphoid tissue, the tubal tonsil, lies in the mucosa immediately behind the opening of the pharyngotympanic tube, and further behind the tubal elevation there is a variable depression in the lateral wall, the lateral pharyngeal recess (fossa of Rosenmüller). The floor of the nasopharynx is formed by the nasal, upper surface of the soft palate.

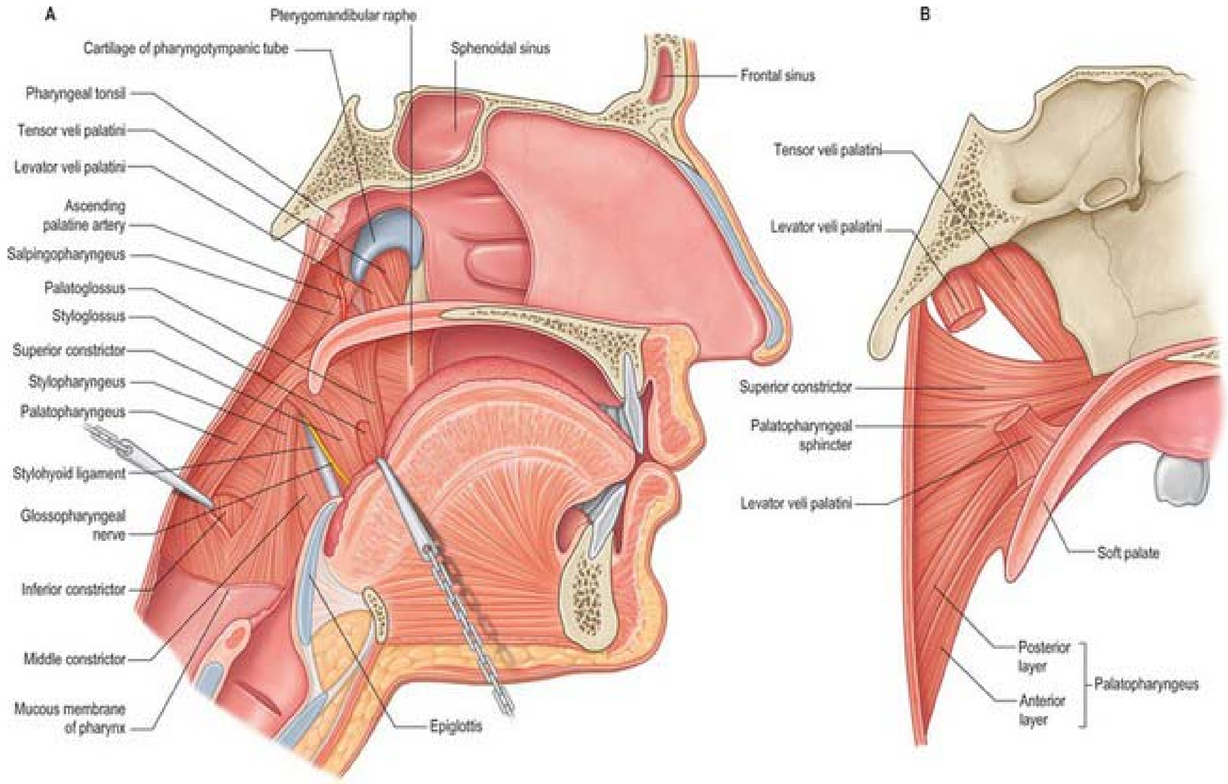
A
Pterygomandibular raphe
Cartilage of pharyngotympanic tube
Sphenoidal sinus
Frontal sinus
Pharyngeal tonsil
Tensor veli palatini
Levator veli palatini
Ascending palatine artery
Salpingopharyngeus
Palatoglossus
Styloglossus
Superior constrictor
Stylopharyngeus
Palatopharyngeus
Stylohyoid ligament
Glossopharyngeal nerve
Inferior constrictor
Middle constrictor
Mucous membrane of pharynx
Epiglottis
B
Tensor veli palatini
Levator veli palatini
Superior constrictor
Palatopharyngeal sphincter
Levator veli palatini
Soft palate
Posterior layer
Anterior layer
Palatopharyngeus

Fig. 33.4 **A**, Interior of the pharynx, exposed by removal of the mucous membrane, sagittal section. The bodies of the cervical vertebrae have been removed, the cut posterior wall of the pharynx retracted dorsolaterally and palatopharyngeus reflected dorsally to show the cranial fibres of the inferior constrictor. The dorsum of the tongue has been pulled ventrally to display a part of styloglossus in the angular interval between the mandibular and the

lingual fibres of origin of the superior constrictor. **B**, Muscles of the left half of the soft palate and adjoining part of the pharyngeal wall, sagittal section.

MICROSTRUCTURE OF NON-TONSILLAR NASOPHARYNX

The nasopharyngeal epithelium anteriorly is ciliated, pseudostratified respiratory in type with goblet cells (see Fig. 2.2). The ducts of mucosal and submucosal seromucous glands open onto its surface. Posteriorly, the respiratory epithelium changes to non-keratinized stratified squamous epithelium which continues into the oropharynx and laryngopharynx. The transitional zone between the two types of epithelium consists of columnar epithelium with short microvilli instead of cilia. Superiorly, this zone meets the nasal septum; laterally, it crosses the orifice of the pharyngotympanic tube; and it passes posteriorly at the union of the soft palate and the lateral wall. Numerous mucous glands surround the tubal orifices.

INNERVATION

Much of the mucosa of the nasopharynx behind the pharyngotympanic tube is supplied by the pharyngeal branch of the pterygopalatine ganglion which traverses the palatovaginal canal with a pharyngeal branch of the maxillary artery.

ADENOID OR PHARYNGEAL TONSIL

The adenoid, or pharyngeal tonsil, is a median mass of mucosa-associated lymphoid tissue (MALT) situated in the roof and posterior wall of the nasopharynx (Fig. 33.3). At its maximal size (during the early years of life) it is shaped like a truncated pyramid, often with a vertically oriented median cleft, so that its apex points towards the nasal septum and its base to the junction of the roof and posterior wall of the nasopharynx.

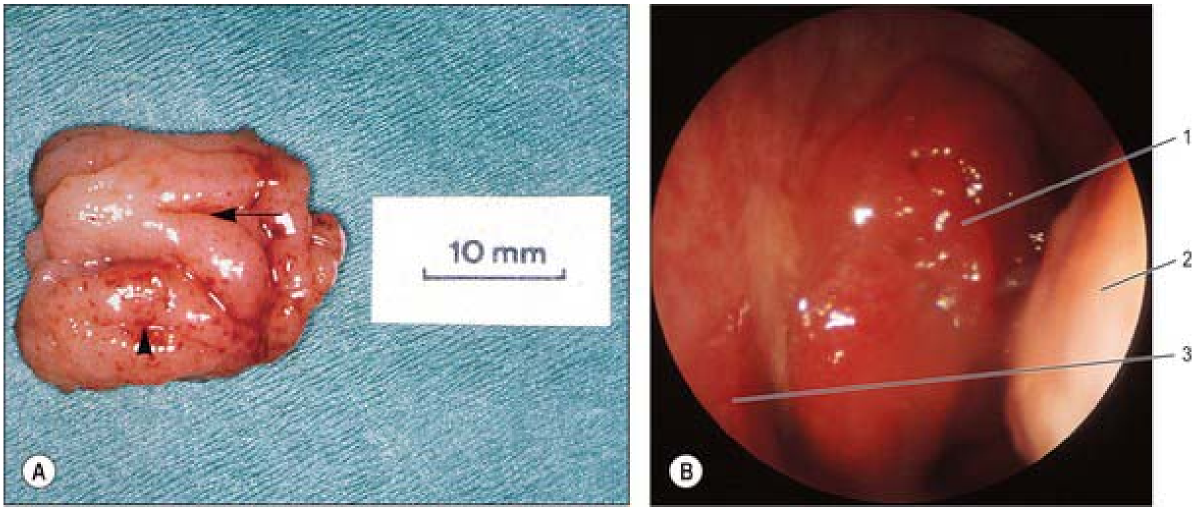

Fig. 33.3 **A**, Nasopharyngeal tonsil following adenoidectomy by curettage. The rostral surface is to the left; surface folds radiate forwards from a median recess (arrow). In this example, the impression left by contact with the left Eustachian cushion is evident laterally (arrowhead). **B**, Transnasal endoscopic view of adenoid. **1**. Adenoid (in posterior naris). **2**. Inferior concha (posterior view). **3**. Posterior end of nasal septum.

*(**A**, Specimen provided by Professor MJ Gleeson, School of Medicine, King's College London; **B**, by courtesy of Mr Simon A Hickey.)*

The free surface of the pharyngeal tonsil is marked by folds that radiate forwards and laterally from a median blind recess, the pharyngeal bursa (bursa of Luschka), which extends backwards and up. The recess is present in the fetus and the young, but only occasionally present in the adult, and marks the rostral end of the embryological notochord. The number and position of the folds and of the deep fissures which separate them vary. A median fold may pass forwards from the pharyngeal bursa towards the nasal septum, or instead a fissure may extend forwards from the bursa, dividing the nasopharyngeal tonsil into two distinct halves which reflect its paired developmental origins (Fig. 33.3).

The prenatal origins of the nasopharyngeal tonsil are described on page 604. After birth it initially grows rapidly, but usually undergoes a degree of involution and atrophy from the age of 8–10 years (although hypoplasia may still occur in adults up to the seventh decade). Relative to the volume of the nasopharynx, the size of the tonsil is largest at 5 years, which may account for the frequency of nasal breathing problems in preschool children, and the incidence of adenoidectomy in this age group.

Vascular supply and lymphatic drainage

The arterial supply of the pharyngeal tonsil is derived from the ascending pharyngeal and ascending palatine arteries, the tonsillar branches of the facial artery, the pharyngeal branch of the maxillary artery and the artery of the pterygoid canal (see Figs 33.5, 33.6). In addition, a nutrient or emissary vessel to the neighbouring bone, the basisphenoid artery, which is a branch of the inferior hypophysial arteries, supplies the bed of the pharyngeal tonsil and is a possible cause of persistent postadenoidectomy haemorrhage in some patients.

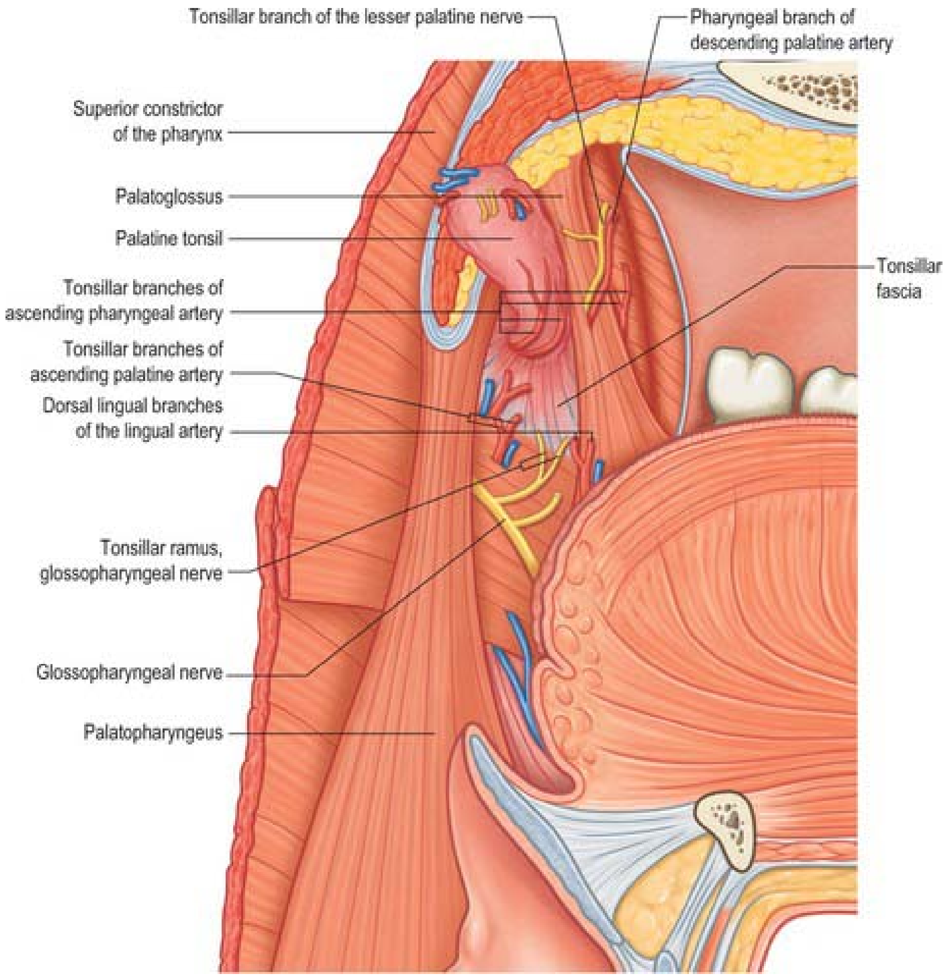
Tonsillar branch of the lesser palatine nerve
Pharyngeal branch of descending palatine artery
Superior constrictor of the pharynx
Palatoglossus
Palatine tonsil
Tonsillar fascia
Tonsillar branches of ascending pharyngeal artery
Tonsillar branches of ascending palatine artery
Dorsal lingual branches of the lingual artery
Tonsillar ramus, glossopharyngeal nerve
Glossopharyngeal nerve
Palatopharyngeus

Fig. 33.5 The tonsillar bed, sagittal section.

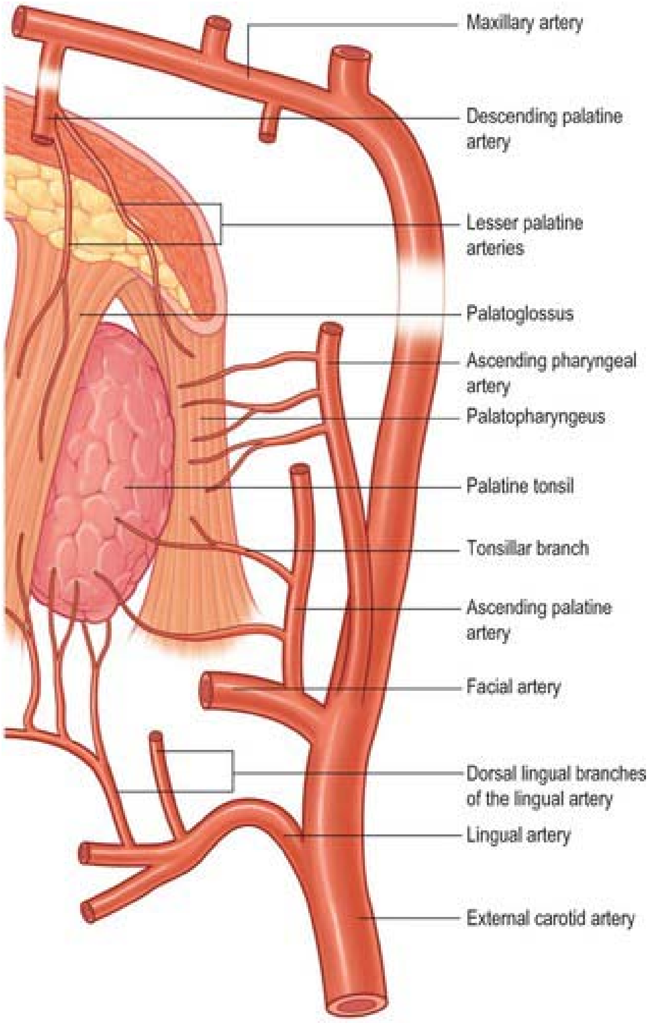
Maxillary artery
Descending palatine artery
Lesser palatine arteries
Palatoglossus
Ascending pharyngeal artery
Palatopharyngeus
Palatine tonsil
Tonsillar branch
Ascending palatine artery
Facial artery
Dorsal lingual branches of the lingual artery
Lingual artery
External carotid artery

Fig. 33.6 Arterial supply to the palatine tonsil.

Numerous communicating veins drain the pharyngeal tonsil into the internal submucous and external pharyngeal venous plexuses. They emerge from the deep lateral surface of the tonsil and join the external palatine (paratonsillar) veins, and pierce the superior constrictor either to join the pharyngeal venous plexus, or to unite to form a single vessel that enters the facial or internal jugular vein; they may also connect with the pterygoid venous plexus.

Microstructure of the pharyngeal tonsil

The adenoid is covered laterally and inferiorly mainly by ciliated respiratory epithelium which contains scattered small patches of non-keratinized stratified squamous epithelium. Its superior surface is separated from the periosteum of the sphenoid and occipital bones by a connective tissue hemicapsule. The fibrous framework of the tonsil, consisting of a mesh of collagen type III (reticular) fibres supporting a lymphoid parenchyma similar to that in the palatine tonsil, is anchored to the hemicapsule.

The nasopharyngeal epithelium lines a series of mucosal folds around which the lymphoid parenchyma is organized into follicles and extrafollicular areas. Internally, the tonsil is subdivided into four to six lobes by connective tissue septa, which arise from the hemicapsule and penetrate the lymphoid parenchyma. Seromucous glands lie within the connective tissue, and their ducts extend through the parenchyma to reach the nasopharyngeal surface.

Functions of the pharyngeal tonsil

The pharyngeal tonsil forms part of the circumpharyngeal lymphoid ring (Waldeyer’s ring), and therefore presumably contributes to the defence of the upper respiratory tract. The territories served by its lymphocytes are uncertain, but may include the nasal cavities, nasopharynx, pharyngotympanic tubes and the middle and inner ears.

Adenoidectomy

Surgical removal of the adenoid is commonly performed to clear nasopharyngeal obstruction and as part of the treatment of chronic secretory otitis media. A variety of methods are employed, including suction diathermy, suction microdebridement and, most commonly, blind curettage. When using the latter, it is important to avoid hyperextension of the cervical spine as this throws the arch of the atlas into prominence and may result in damage to the prevertebral fascia and anterior spinal ligaments, with resultant infection and cervical instability. Extreme lateral curettage can result in damage to the tubal orifice and excessive bleeding because the vasculature is denser laterally. Removal of the adenoid in children can result in an impairment in the ability of the soft palate to close the pharyngeal isthmus fully (velopharyngeal insufficiency, VPI), causing excessive nasality of speech.

PHARYNGOTYMPANIC TUBE

The pharyngotympanic tube (see Fig. 36.7) connects the tympanic cavity to the nasopharynx and allows the passage of air between these spaces in order to equalize the air pressure on both aspects of the tympanic membrane. It is about 36 mm long and descends anteromedially from the tympanic cavity to the nasopharynx at an angle of approximately 45° with the sagittal plane and 30° with the horizontal (these angles increase with age and elongation of the skull base). It is formed partly by cartilage and fibrous tissue and partly by bone.

The cartilaginous part, which is approximately 24 mm long, is formed by a triangular plate of cartilage, the greater part of which is in the posteromedial wall of the tube. Its apex is attached by fibrous tissue to the circumference of the jagged rim of the bony part of the tube, and its base is directly under the mucosa of the lateral nasopharyngeal wall, forming a tubal elevation (torus tubarius; Eustachian cushion) behind the pharyngeal orifice of the tube (Fig. 33.2; see Fig. 30.1). The upper part of the cartilage is bent laterally and downwards, producing a broad medial lamina and narrow lateral lamina. In transverse section it is hook-like and incomplete below and laterally, where the canal is composed of fibrous tissue. The cartilage is fixed to the cranial base in the groove between the petrous part of the temporal bone and the greater wing of the sphenoid, and ends near the root of the medial pterygoid plate. The cartilaginous and bony parts of the tube are not in the same plane, the former descending a little more steeply than the latter. The diameter of the tube is greatest at the pharyngeal orifice, least at the junction of the two parts (the isthmus), and increases again towards the tympanic cavity.

The bony part, approximately 12 mm long, is oblong in transverse section, with its greater dimension in the horizontal plane. It starts from the anterior tympanic wall and gradually narrows to end at the junction of the squamous and petrous parts of the temporal bone, where it has a jagged margin for the attachment of the cartilaginous part. The carotid canal lies medially.

The mucosa of the pharyngotympanic tube is continuous with the nasopharyngeal and tympanic mucosae. It is lined by a ciliated columnar epithelium and is thin in the osseous part but thickened by mucous glands in the cartilaginous part. Near the pharyngeal orifice there is a variable, but sometimes considerable, lymphoid mass called the tubal tonsil.

At birth the pharyngotympanic tube is about half its adult length, it is more horizontal and its bony part is relatively shorter but much wider. The pharyngeal orifice is a narrow slit, level with the palate and without a tubal elevation.

Relations

Salpingopharyngeus is attached to the inferior part of the cartilaginous tube near its pharyngeal opening. Posteromedially are the petrous part of the temporal bone and levator veli palatini, which arises partly from the medial lamina of the tube. Anterolaterally, tensor veli palatini separates the tube from the otic ganglion, the mandibular nerve and its branches, the chorda tympani nerve and the middle meningeal artery. Some fibres of tensor veli palatini are attached to the lateral lamina of the cartilage and to the fibrous part, and these fibres are sometimes referred to as dilator tubae. The pharyngotympanic tube is opened during deglutition but the mechanism is uncertain: dilator tubae, aided by salpingopharyngeus, may be responsible. Levator veli palatini elevates the cartilaginous part of the pharyngotympanic tube, and so might allow passive opening by releasing tension on the cartilage.

Vascular supply

Arteries to the pharyngotympanic tube arise from the ascending pharyngeal branch of the external carotid artery, and from the middle meningeal artery and the artery of the pterygoid canal, which are both branches of the maxillary artery. The veins of the pharyngotympanic tube usually drain to the pterygoid venous plexus.

Innervation

The pharyngotympanic tube is innervated by filaments from the tympanic plexus and from the pharyngeal branch of the pterygopalatine ganglion. The tympanic plexus ramifies on the promontory in the middle ear cavity and is formed by the tympanic branch of the glossopharyngeal nerve and caroticotympanic nerves of sympathetic origin (see also Ch. 36).

OROPHARYNX

BOUNDARIES

The oropharynx extends from below the soft palate to the upper border of the epiglottis (Figs 33.1, 33.2). It opens into the mouth through the oropharyngeal isthmus, demarcated by the palatoglossal arch, and faces the pharyngeal aspect of the tongue. Its lateral wall consists of the palatopharyngeal arch and palatine tonsil (see Fig. 30.3). Posteriorly, it is level with the bodies of the second, and upper part of the third, cervical vertebrae (Fig. 33.2).

SOFT PALATE

The soft palate is a mobile flap suspended from the posterior border of the hard palate, sloping down and back between the oral and nasal parts of the pharynx (Figs 33.2, 33.4). The boundary between the hard and soft palate is readily palpable and may be distinguished by a change in colour, the soft palate being a darker red with a yellowish tint. The soft palate is a thick fold of mucosa enclosing an aponeurosis, muscular tissue, vessels, nerves, lymphoid tissue and mucous glands; almost half its thickness is represented by numerous mucous glands which lie between the muscles and the oral surface of the soft palate. The latter is covered by a stratified squamous epithelium, while the nasal surface is covered with a ciliated columnar epithelium. In most individuals, two small pits, the fovea palatini, may be seen, one on each side of the midline: they represent the orifices of ducts from some of the minor mucous glands of the palate. In its usual relaxed and pendant position, the anterior (oral) surface of the soft palate is concave, and has a median raphe. The posterior aspect is convex and continuous with the nasal floor, the anterosuperior border is attached to the posterior margin of the hard palate, and the sides blend with the pharyngeal wall. The inferior border is free, and hangs between the mouth and pharynx. A median conical process, the uvula, projects downwards from its posterior border (see Fig. 30.3). Taste buds are found on the oral aspect of the soft palate.

The anterior third of the soft palate contains little muscle and consists mainly of the palatine aponeurosis. This region is less mobile and more horizontal than the rest of the soft palate and is the chief area acted upon by tensor veli palatini.

A small bony prominence, produced by the pterygoid hamulus, can be felt just behind and medial to each upper alveolar process, in the lateral part of the anterior region of the soft palate. The pterygomandibular raphe (a tendinous band between buccinator and the superior constrictor) passes downwards and outwards from the hamulus to the posterior end of the mylohyoid line. When the mouth is opened wide, this raphe raises a fold of mucosa that indicates the internal, posterior boundary of the cheek; it is an important landmark for an inferior alveolar nerve block.

Palatine aponeurosis

A thin, fibrous, palatine aponeurosis composed of the expanded tendons of the tensor veli palatini muscles strengthens the soft palate. It is attached to the posterior border and inferior surface of the hard palate behind any palatine crests, and extends medially from behind the greater palatine foramina. It is thick in the anterior two-thirds of the soft palate but very thin further back. Near the midline it encloses the musculus uvulae. All the other palatine muscles are attached to the aponeurosis.

Palatoglossal and palatopharyngeal arches

The lateral wall of the oropharynx presents two prominent folds, the palatoglossal and palatopharyngeal folds (anterior and posterior pillars of the fauces respectively) (see Fig. 30.3). The palatoglossal arch, the anterior fold, runs from the soft palate to the side of the tongue and contains palatoglossus. The palatopharyngeal arch, the posterior fold, projects more medially and passes from the soft palate to merge with the lateral wall of the pharynx; it contains palatopharyngeus. A triangular tonsillar fossa (tonsillar sinus), lies on each side of the oropharynx between the diverging palatopharyngeal and palatoglossal arches, and contains the palatine tonsil.

Vascular supply

The arterial supply of the soft palate is usually derived from the ascending palatine branch of the facial artery. Sometimes this is replaced or supplemented by a branch of the ascending pharyngeal artery which descends forwards between the superior border of the superior constrictor and levator veli palatini, and accompanies the latter to the soft palate. The veins of the soft palate usually drain to the pterygoid venous plexus.

Innervation

General sensation from most of the soft palate is carried by branches of the lesser palatine nerve (a branch of the maxillary nerve) and from the posterior part of the palate by pharyngeal branches from the glossopharyngeal nerve and from the plexus around the tonsil (formed by tonsillar branches of the glossopharyngeal and lesser palatine nerves). The special sensation of taste from taste buds in the oral surface of the soft palate is carried in the lesser palatine nerve: the taste fibres initially travel in the greater petrosal nerve (a branch of the facial nerve) and pass through the pterygopalatine ganglion without synapsing. The lesser palatine nerve also carries the secretomotor supply to most of the mucosa of the soft palate, via postganglionic branches from the pterygopalatine ganglion. Postganglionic secretomotor parasympathetic fibres may pass to the posterior parts of the soft palate from the otic ganglion (which receives preganglionic fibres via the lesser petrosal branch of the glossopharyngeal nerve). Postganglionic sympathetic fibres run from the carotid plexus along arterial branches supplying the palate.

Uvulopalatopharyngoplasty

The pharyngeal airway is kept patent in the patient who is awake by the combined dilating action of genioglossus, tensor veli palatini, geniohyoid and stylohyoid, which act to counter the negative pressure generated in the lumen of the pharynx during inspiration. The tone in the muscles is reduced during sleep, and is also affected by alcohol and other sedatives, hypothyroidism and a variety of neurological disorders. If the dilator muscle tone is insufficient, the walls of the pharynx may become apposed. Intermittent pharyngeal obstruction may cause snoring, and complete obstruction may cause apnoea, hypoxia and hypercarbia which lead to arousal and sleep disturbance.

Surgical techniques involving reduction in the length of the soft palate, removal of the tonsils and plicating of the tonsillar pillars can be used to raise the intrinsic dilating tone in the pharyngeal wall and to reduce the bulk of (and to stiffen) the soft palate. This will reduce the tendency of the soft palate to vibrate and generate noise during periods of incipient collapse of the pharynx. An alternative treatment is to deliver air to the pharynx at above atmospheric pressure via a closely fitting facemask, thus inflating the pharynx and countering its tendency to collapse.

PALATINE TONSIL

The right and left palatine tonsils form part of the circumpharyngeal lymphoid ring. Each tonsil is an ovoid mass of lymphoid tissue situated in the lateral wall of the oropharynx (Fig. 33.5; see Figs 30.3, 30.5). Size varies according to age, individuality and pathological status (tonsils may be hypertrophied and/or inflamed). It is therefore difficult to define the normal appearance of the palatine tonsil. For the first 5 or 6 years of life the tonsils increase rapidly in size. They usually reach a maximum at puberty, when they average 20–25 mm in vertical, and 10–15 mm in transverse, diameters, and they project conspicuously into the oropharynx. Tonsillar involution begins at puberty, when the reactive lymphoid tissue begins to atrophy, and by old age only a little tonsillar lymphoid tissue remains.

The long axis of the tonsil is directed from above, downwards and backwards. Its medial, free, surface usually presents a pitted appearance. The pits, 10–20 in number, lead into a system of blind-ending, often highly branching, crypts which extend through the whole thickness of the tonsil and almost reach the connective tissue hemicapsule. In a healthy tonsil the openings of the crypts are fissure-like and the walls of the crypt lumina are collapsed so that they are in contact with each other. The human tonsil is polycryptic. The branching crypt system reaches its maximum size and complexity during childhood. The mouth of a deep tonsillar cleft (intratonsillar cleft, recessus palatinus) opens in the upper part of the medial surface of the tonsil. It is often erroneously called the supratonsillar fossa, and yet it is not situated above the tonsil but within its substance. The mouth of the cleft is semilunar, curving parallel to the convex dorsum of the tongue in the sagittal plane. The upper wall of the recess contains lymphoid tissue which extends into the soft palate as the pars palatina of the palatine tonsil. After the age of 5 years this embedded part of the tonsil diminishes in size. There is a tendency for the whole tonsil to involute from the age of 14 years, and for the tonsillar bed to flatten out. During young adult life, a mucosal fold, the plica triangularis, stretches back from the palatoglossal arch down to the tongue. It is infiltrated by lymphoid tissue and frequently represents the most prominent (anteroinferior) portion of the tonsil. It rarely persists into middle age.

The lateral or deep surface of the tonsil spreads downwards, upwards and forwards. Inferiorly, it invades the dorsum of the tongue, superiorly, the soft palate, and, anteriorly, it may extend for some distance under the palatoglossal arch. This deep, lateral aspect is covered by a layer of fibrous tissue, the tonsillar hemicapsule. The latter is separable with ease for most of its extent from the underlying muscular wall of the pharynx, which is formed here by the superior constrictor, and sometimes by the anterior fibres of palatopharyngeus, with styloglossus on its lateral side (Fig. 33.5). Anteroinferiorly, the hemicapsule adheres to the side of the tongue and to palatoglossus and palatopharyngeus. In this region, the tonsillar artery, a branch of the facial artery, pierces the superior constrictor to enter the tonsil, accompanied by venae comitantes (Fig. 33.5). An important and sometimes large vein, the external palatine or paratonsillar vein, descends from the soft palate lateral to the tonsillar hemicapsule before piercing the pharyngeal wall. Haemorrhage from this vessel from the upper angle of the tonsillar fossa may complicate tonsillectomy. The muscular wall of the tonsillar fossa separates the tonsil from the ascending palatine artery, and, occasionally, from the tortuous facial artery itself, which may lie near the pharyngeal wall at the lower tonsillar level. The glossopharyngeal nerve lies immediately lateral to the muscular wall of the tonsillar fossa (Figs 33.4A, 33.5): it is at risk if the wall is pierced, and is commonly temporarily affected by oedema following tonsillectomy. The internal carotid artery lies approximately 25 mm behind and lateral to the tonsil. In some individuals the styloid process may be elongated and deviate towards the tonsillar bed.

Microstructure of the palatine tonsil

Each tonsil is a mass of lymphoid tissue associated with the oropharyngeal mucosa and fixed in its position, unlike most other examples of mucosa-associated lymphoid tissue. It is covered on its oropharyngeal aspect by non-keratinized stratified squamous epithelium. The whole of the tonsil is supported internally by a delicate meshwork of fine collagen type III (reticulin) fibres which are condensed in places to form more robust connective tissue septa that also contain elastin. These septa partition the tonsillar parenchyma, and merge at their ends with the dense irregular fibrous hemicapsule on the deep aspect of the tonsil and with the lamina propria on the pharyngeal surface. Blood vessels, lymphatics and nerves branch or join within the connective tissue condensations. The hemicapsule forms its lateral boundary with the oropharyngeal wall, and with the mucosa which covers its highly invaginated free surface.

The 10–20 crypts formed by invagination of the free surface mucosa are narrow tubular epithelial diverticula which often branch within the tonsil and frequently are packed with plugs of shed epithelial cells, lymphocytes and bacteria, which may calcify. The epithelium lining the crypts is mostly similar to that of the oropharyngeal surface, i.e. stratified squamous, but there are also patches of reticulated epithelium, which is much thinner, and which has a complex structure that is of great importance in the immunological function of the tonsil.

Reticulated epithelium

Reticulated epithelium lacks the orderly laminar structure of stratified squamous epithelium. Its base is deeply invaginated in a complex manner so that the epithelial cells, with their slender branched cytoplasmic processes, provide a coarse mesh to accommodate the infiltrating lymphocytes and macrophages. The basal lamina of this epithelium is discontinuous. Although the oropharyngeal surface is unbroken, the epithelium may become exceedingly thin in places, so that only a tenuous cytoplasmic layer separates the pharyngeal lumen from the underlying lymphocytes. Epithelial cells are held together by small desmosomes, anchored into bundles of keratin filaments. Interdigitating dendritic cells (antigen-presenting cells, APCs) are also present. The intimate association of epithelial cells and lymphocytes facilitates the direct transport of antigen from the external environment to the tonsillar lymphoid cells, i.e. reticulated epithelial cells are functionally similar to the microfold (M) cells of the gut. The total surface area of the reticulated epithelium is very large because of the complex branched nature of the tonsillar crypts, and has been estimated at 295 cm^2 for an average palatine tonsil.

Tonsillar lymphoid tissue

There are four lymphoid compartments in the palatine tonsils. Lymphoid follicles, many with germinal centres, are arranged in rows roughly parallel to neighbouring connective tissue septa. Their size and cellular content varies in proportion to the immunological activity of the tonsil. The mantle zones of the follicles, each with closely packed small lymphocytes, form a dense cap, always situated on the side of the follicle nearest to the mucosal surface. These cells are the products of B-lymphocyte proliferation within the germinal centres. Extrafollicular, or T-lymphocyte, areas contain a specialized microvasculature including high endothelial venules (HEVs), through which circulating lymphocytes enter the tonsillar parenchyma. The lymphoid tissue of the reticulated crypt epithelium contains predominantly IgG- and IgA-producing B lymphocytes (including some mature plasma cells), T lymphocytes and antigen-presenting cells. There are numerous capillary loops in this subsurface region.

Vascular supply and lymphatic drainage

The arterial blood supply to the palatine tonsil is derived from branches of the external carotid artery (Figs 33.5, 33.6). Three arteries enter the tonsil at its lower pole. The largest is the tonsillar artery, which is a branch of the facial, or sometimes the ascending palatine, artery. It ascends between medial pterygoid and styloglossus, perforates the superior constrictor at the upper border of styloglossus, and ramifies in the tonsil and posterior lingual musculature (Figs 35.5, 33.6). The other arteries found at the lower pole are the dorsal lingual branches of the lingual artery, which enter anteriorly, and a branch from the ascending palatine artery, which enters posteriorly to supply the lower part of the palatine tonsil. The upper pole of the tonsil also receives branches from the ascending pharyngeal artery, which enter the tonsil posteriorly, and from the descending palatine artery and its branches, the greater and lesser palatine arteries. All of these arteries enter the deep surface of the tonsil, branch within the connective tissue septa, narrow to become arterioles and then give off capillary loops into the follicles, interfollicular areas and the cavities within the base of the reticulated epithelium. The capillaries rejoin to form venules, many with high endothelia, and the veins return within the septal tissues to the hemicapsule as tributaries of the pharyngeal drainage. The tonsillar artery and its venae comitantes often lie within the palatoglossal fold, and may haemorrhage if this fold is damaged during surgery.

Unlike lymph nodes, the palatine tonsils do not possess afferent lymphatics or lymph sinuses. Instead, dense plexuses of fine lymphatic vessels surround each follicle and form efferent lymphatics which pass towards the hemicapsule, pierce the superior constrictor, and drain to the upper deep cervical lymph nodes directly (especially the jugulodigastric nodes) or indirectly through the retropharyngeal lymph nodes. The jugulodigastric nodes are typically enlarged in tonsillitis, when they project beyond the anterior border of sternocleidomastoid and are palpable superficially 1–2 cm below the angle of the mandible: when enlarged, they represent the most common swelling in the neck.

Innervation

The tonsillar region is innervated by tonsillar branches of the maxillary and glossopharyngeal nerves (Fig. 33.5). The fibres from the maxillary nerve pass through, but do not synapse in, the pterygopalatine ganglion; they are distributed through the lesser palatine nerves and form a plexus (the circulus tonsillaris) around the tonsil together with the tonsillar branches of the glossopharyngeal nerve. Nerve fibres from this plexus are also distributed to the soft palate and the region of the oropharyngeal isthmus. The tympanic branch of the glossopharyngeal nerve supplies the mucous membrane lining the tympanic cavity. Infection, malignancy and postoperative inflammation of the tonsil and tonsillar fossa may therefore be accompanied by pain referred to the ear.

Tonsillectomy

Surgical removal of the pharyngeal tonsils is commonly performed to prevent recurrent acute tonsillitis or to treat airway obstruction by hypertrophied or inflamed palatine tonsils. Occasionally, the tonsil may be removed to treat an acute peritonsillar abscess, which is a collection of pus between the superior constrictor and the tonsillar hemicapsule. Many methods have been employed, the commonest being dissection in the plane of the fibrous hemicapsule followed by ligation or electrocautery to the vessels divided during the dissection. The nerve supply to the tonsil is so diffuse that tonsillectomy under local anaesthesia is performed successfully by local infiltration rather than by blocking the main nerves. Surgical access to the glossopharyngeal nerve may be achieved by separating the fibres of superior constrictor.

Waldeyer’s ring

Waldeyer’s ring is a circumpharyngeal ring of mucosa-associated lymphoid tissue which surrounds the openings into the digestive and respiratory tracts. It is made up anteroinferiorly by the lingual tonsil, laterally by the palatine and tubal tonsils, and posterosuperiorly by the nasopharyngeal tonsil and smaller collections of lymphoid tissue in the inter-tonsillar intervals.

LARYNGOPHARYNX

BOUNDARIES

The laryngopharynx is situated behind the entire length of the larynx (known clinically as the hypopharynx) and extends from the superior border of the epiglottis, where it is delineated from the oropharynx by the lateral glossoepiglottic folds, to the inferior border of the cricoid cartilage, where it becomes continuous with the oesophagus (Figs 33.1, 33.2). The laryngeal inlet lies in the upper part of its incomplete anterior wall, and the posterior surfaces of the arytenoid and cricoid cartilages lie below this opening.

Piriform fossa

A small piriform fossa lies on each side of the laryngeal inlet, bounded medially by the aryepiglottic fold and laterally by the thyroid cartilage and thyrohyoid membrane. Branches of the internal laryngeal nerve lie beneath its mucous membrane. At rest, the laryngopharynx extends posteriorly from the lower part of the third cervical vertebral body to the upper part of the sixth. During deglutition it may be elevated considerably by the hyoid elevators.

Inlet of larynx

The obliquely sloping inlet of the larynx lies in the anterior part of the laryngopharynx and is bounded above by the epiglottis, below by the arytenoid cartilages of the larynx, and laterally by the aryepiglottic folds (Fig. 33.1). Below the inlet, the anterior wall of the laryngopharynx is formed by the posterior surface of the cricoid cartilage.

PHARYNGEAL FASCIA

The two named layers of fascia in the pharynx are the pharyngobasilar and buccopharyngeal fascia. The fibrous layer that supports the pharyngeal mucosa is thickened above the superior constrictor to form the pharyngobasilar fascia (see Fig. 33.9). It is attached to the basilar part of the occipital bone and the petrous part of the temporal bone medial to the pharyngotympanic tube, and to the posterior border of the medial pterygoid plate and the pterygomandibular raphe. Inferiorly, it diminishes in thickness, but is strengthened posteriorly by a fibrous band attached to the pharyngeal tubercle of the occipital bone which descends as the median pharyngeal raphe of the constrictors. This fibrous layer is really the internal epimysial covering of the muscles and their aponeurotic attachment to the base of the skull. The thinner, external part of the epimysium is the buccopharyngeal fascia, which covers the superior constrictor and passes forwards over the pterygomandibular raphe to cover buccinator.

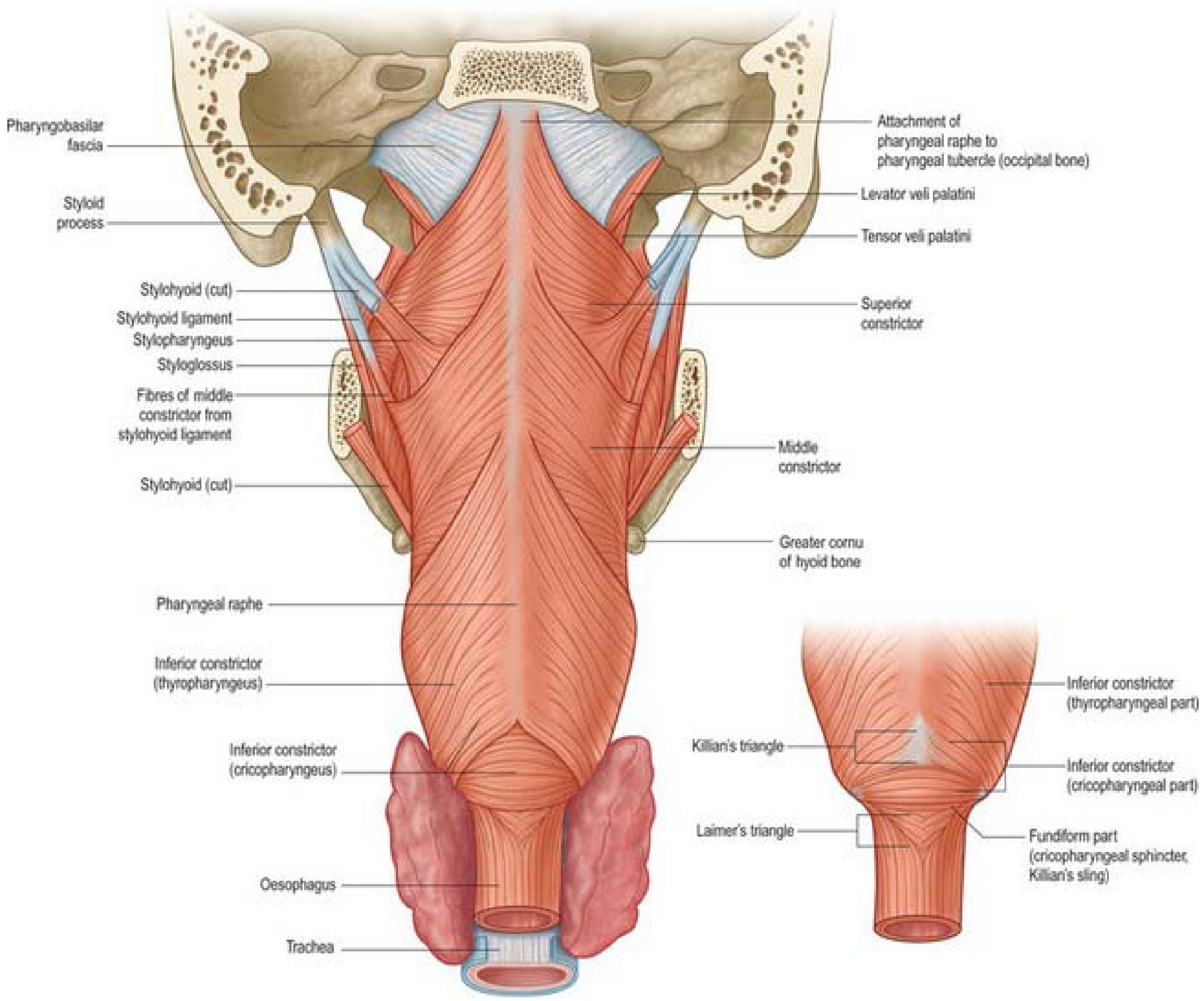
Pharyngobasilar fascia
Styloid process
Stylohyoid (cut)
Stylohyoid ligament
Stylopharyngeus
Styloglossus
Fibres of middle constrictor from stylohyoid ligament
Stylohyoid (cut)
Pharyngeal raphe
Inferior constrictor (thyropharyngeus)
Inferior constrictor (cricopharyngeus)
Oesophagus
Trachea
Attachment of pharyngeal raphe to pharyngeal tubercle (occipital bone)
Levator veli palatini
Tensor veli palatini
Superior constrictor
Middle constrictor
Greater cornu of hyoid bone
Inferior constrictor (thyropharyngeal part)
Killian's triangle
Inferior constrictor (cricopharyngeal part)
Laimer's triangle
Fundiform part (cricopharyngeal sphincter, Killian's sling)

Fig. 33.9 The muscles of the pharynx and the pharyngobasilar fascia, posterior view.

PHARYNGEAL TISSUE SPACES

Pharyngeal tissue spaces can be subdivided into peripharyngeal and intrapharyngeal spaces. The anterior part of the peripharyngeal space is formed by the submandibular and submental spaces, posteriorly by the retropharyngeal space and laterally by the parapharyngeal spaces. The retropharyngeal space is an area of loose connective tissue which lies behind the pharynx and anterior to the prevertebral fascia, extending upwards to the base of the skull and downwards to the retrovisceral space in the infrahyoid part of the neck. Each parapharyngeal space passes laterally around the pharynx and is continuous with the retropharyngeal space. However, unlike the retropharyngeal space, it is a space which is restricted to the suprahyoid region. It is bounded medially by the pharynx, laterally by the pterygoid muscles (where it is part of the infratemporal fossa) and by the sheath of the parotid gland, superiorly by the base of the skull, and inferiorly by suprahyoid structures, particularly the sheath of the submandibular gland. An intrapharyngeal space potentially exits between the inner surface of the constrictor muscles and the pharyngeal mucosa. Infections in this space are either restricted locally or spread through the pharynx into the retropharyngeal or parapharyngeal spaces. The peritonsillar space is an important part of the intrapharyngeal space: it lies around the palatine tonsil between the pillars of the fauces. Infections in the intratonsillar space usually spread up or down the intrapharyngeal space, or through the pharynx into the parapharyngeal space.

Tissue spaces between the layers of cervical fascia are described in Chapter 28: tissue spaces around the larynx are described in Chapter 34.

SPREAD OF INFECTION

Infection that spreads into the parapharyngeal space will produce pain and trismus. There may be swelling in the oropharynx which extends up to the uvula, displacing it to the contralateral side, and dysphagia. Posterior spread from the parapharyngeal space into the retropharyngeal space will produce bulging of the posterior pharyngeal wall, dyspnoea and nuchal rigidity. Involvement of the carotid sheath may produce symptoms caused by thrombosis of the internal jugular vein and cranial nerve symptoms involving the glossopharyngeal, vagus, cranial accessory and hypoglossal nerves. If the infection continues to spread unchecked, mediastinitis will ensue. A virulent infection in the retropharyngeal space may spread through the prevertebral fascia into the underlying prevertebral space: infection in this tissue space may descend into the thorax and even below the diaphragm, and results in chest pain, severe dyspnoea and retrosternal discomfort.

Pharyngeal infection from mucosa-associated lymph tissues such as the palatine tonsil, or as a result of a penetrating injury (e.g. from an ingested foreign body), may result in the spread of infection into the tissue spaces of the neck adjacent to the pharynx. This is an extremely dangerous situation because there is potential for rapid spread throughout the neck and, more dangerously, to the superior mediastinum, to cause overwhelming life-threatening infection.

PARAPHARYNGEAL SPACE TUMOURS

Tumours that develop in the parapharyngeal tissue space may remain asymptomatic for some time. When they do present, it may be with a diffuse pattern of symptoms, reflecting the effects of compression on the lower cranial nerves, e.g. dysarthria, resulting from impairment of tongue movements secondary to hypoglossal nerve damage; dysphagia, with overspill and aspiration of ingested material into the airway, resulting from loss of sensory information from the territory of the pharyngeal plexus nerves; motor dysfunction of the pharynx and larynx, resulting from loss of motor innervation via the pharyngeal plexus and the recurrent laryngeal branch of the vagus to the intrinsic muscles of the larynx.

MUSCLES OF THE SOFT PALATE AND PHARYNX

The muscles of the soft palate and pharynx are levator veli palatini, tensor veli palatini, palatoglossus, palatopharyngeus, musculus uvulae, salpingopharyngeus, stylopharyngeus, and the superior, middle and inferior constrictors.

Levator veli palatini

Levator veli palatini arises by a small tendon from a quadrilateral roughened area on the medial end of the inferior surface of the petrous part of the temporal bone, in front of the lower opening of the carotid canal (Figs 33.4, 33.7, 33.8, 33.9). Additional fibres arise from the inferior aspect of the cartilaginous part of the pharyngotympanic tube and from the vaginal process of the sphenoid bone. At its origin the muscle is inferior rather than medial to the pharyngotympanic tube and only crosses medial to it at the level of the medial pterygoid plate. It passes medial to the upper margin of the superior constrictor and anterior to salpingopharyngeus. Its fibres spread in the medial third of the soft palate between the two strands of palatopharyngeus to attach to the upper surface of the palatine aponeurosis as far as the midline, where they interlace with those of the contralateral muscle. Thus, the two levator muscles form a sling above and just behind the palatine aponeurosis.

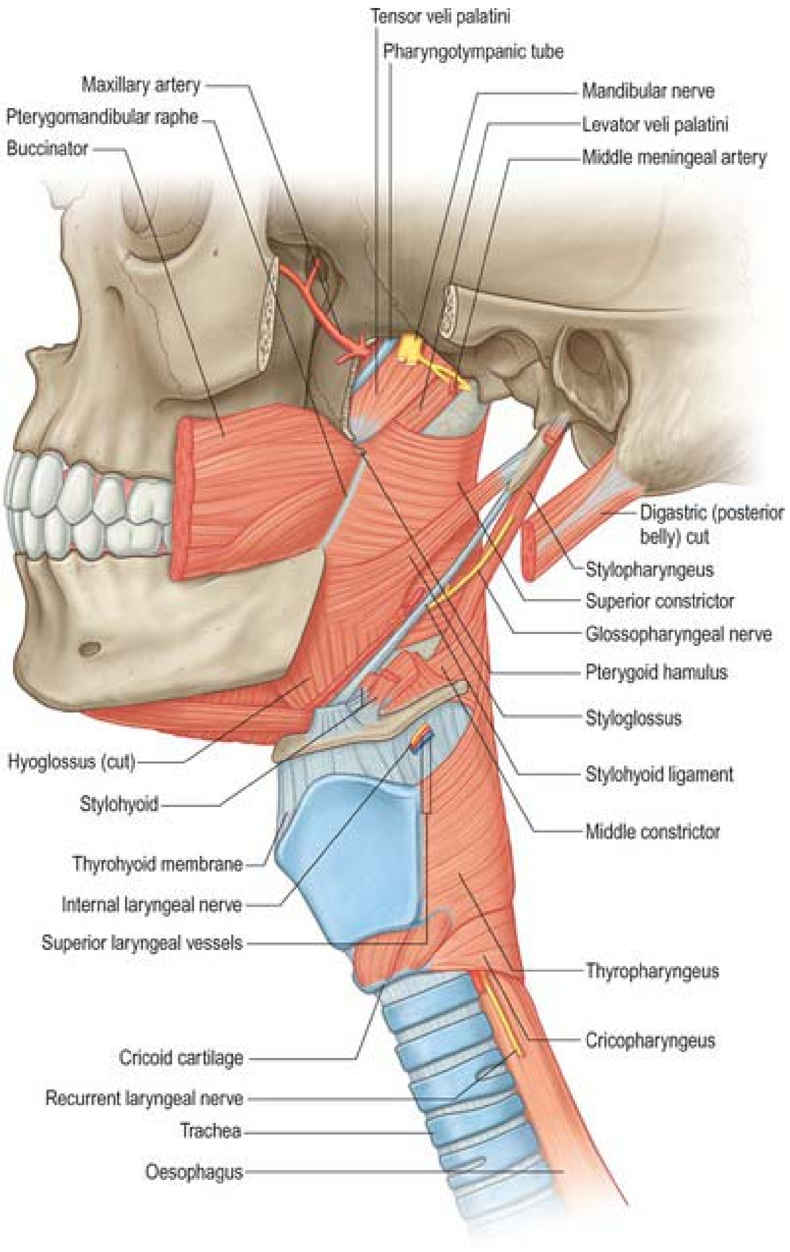
Tensor veli palatini
Pharyngotympanic tube
Maxillary artery
Pterygomandibular raphe
Buccinator
Mandibular nerve
Levator veli palatini
Middle meningeal artery
Digastric (posterior belly) cut
Stylopharyngeus
Superior constrictor
Glossopharyngeal nerve
Pterygoid hamulus
Styloglossus
Stylohyoid ligament
Middle constrictor
Hyoglossus (cut)
Stylohyoid
Thyrohyoid membrane
Internal laryngeal nerve
Superior laryngeal vessels
Thyropharyngeus
Cricopharyngeus
Cricoid cartilage
Recurrent laryngeal nerve
Trachea
Oesophagus

Fig. 33.7 Muscles of the pharynx, lateral view.

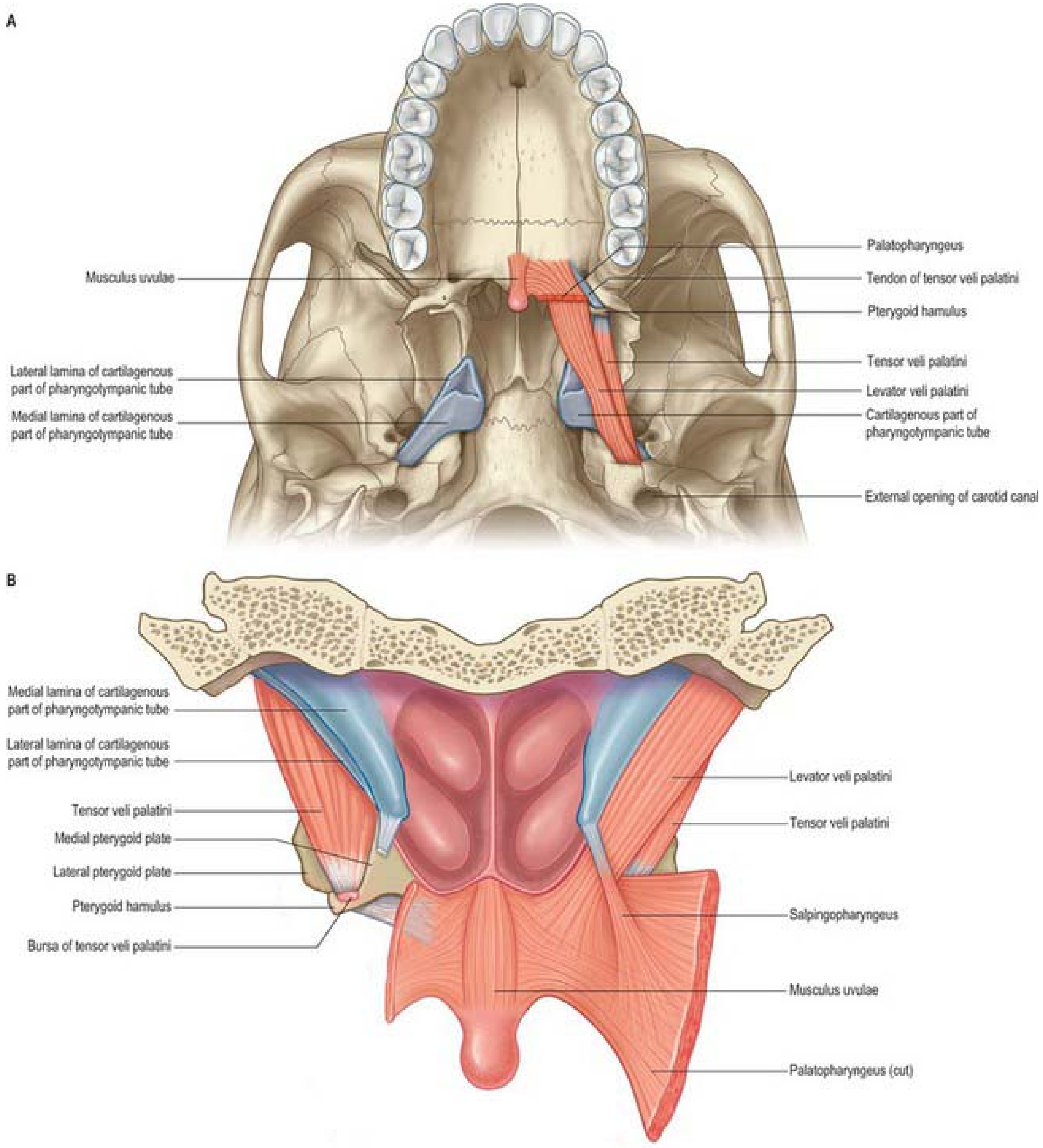
A
Musculus uvulae
Lateral lamina of cartilagenous part of pharyngotympanic tube
Medial lamina of cartilagenous part of pharyngotympanic tube
Palatopharyngeus
Tendon of tensor veli palatini
Pterygoid hamulus
Tensor veli palatini
Levator veli palatini
Cartilagenous part of pharyngotympanic tube
External opening of carotid canal
B
Medial lamina of cartilagenous part of pharyngotympanic tube
Lateral lamina of cartilagenous part of pharyngotympanic tube
Tensor veli palatini
Medial pterygoid plate
Lateral pterygoid plate
Pterygoid hamulus
Bursa of tensor veli palatini
Levator veli palatini
Tensor veli palatini
Salpingopharyngeus
Musculus uvulae
Palatopharyngeus (cut)

Fig. 33.8 Muscles of the soft palate. **A**, Inferior view. **B**, Superior view.

Vascular supply

The blood supply of levator veli palatini is derived from the ascending palatine branch of the facial artery and the greater palatine branch of the maxillary artery.

Innervation

Levator veli palatini is innervated from the cranial part of the accessory nerve via the pharyngeal plexus.

Actions

The primary role of the levator veli palatini muscles is to elevate the almost vertical posterior part of the soft palate and pull it slightly backwards: during swallowing, the soft palate is elevated so that it touches the posterior wall of the pharynx, separating the nasopharynx from the oropharynx. By additionally pulling on the lateral walls of the nasopharynx posteriorly and medially, the levator veli palatini muscles also narrow that space. The muscle has little or no effect on the pharyngotympanic tube, although it might allow passive opening.

Tensor veli palatini

Tensor veli palatini arises from the scaphoid fossa of the pterygoid process and posteriorly from the medial aspect of the spine of the sphenoid bone (Figs 33.4, 33.7, 33.8, 33.9; see Fig. 30.6). Between these two sites it is attached to the anterolateral membranous wall of the pharyngotympanic tube (including its narrow isthmus where the cartilaginous medial two-thirds meets the bony lateral one-third). Some fibres may be continuous with those of tensor tympani. Inferiorly, the fibres converge on a delicate tendon that turns medially around the pterygoid hamulus to pass through the attachment of buccinator to the palatine aponeurosis and the osseous surface behind the palatine crest on the horizontal plate of the palatine bone. There is a small bursa between the tendon and the pterygoid hamulus.

The muscle is thin and triangular and lieslateral to the medial pterygoid plate, pharyngotympanic tube and levator veli palatini. Its lateral surface contacts the upper and anterior part of medial pterygoid, the mandibular, auriculotemporal and chorda tympani nerves, the otic ganglion and the middle meningeal artery.

Vascular supply

The blood supply of tensor veli palatini is derived from the ascending palatine branch of the facial artery and the greater palatine branch of the maxillary artery.

Innervation

The motor innervation of tensor veli palatini is derived from the mandibular nerve via the nerve to medial pterygoid, and reflects the development of the muscle from the first branchial arch.

Actions

Acting together, the tensor veli palatini muscles tauten the soft palate, principally its anterior part, and depress it by flattening its arch. Acting unilaterally, the muscle pulls the soft palate to one side. Although contraction of both muscles will slightly depress the anterior part of the soft palate, it is often assumed that the increased rigidity aids palatopharyngeal closure. However, it is now believed that a primary role of the tensor is to open the pharyngotympanic tube, for example during deglutition and yawning. In this way, the muscle equalizes air pressure between the middle ear and nasopharynx.

Palatoglossus

Palatoglossus is narrower at its middle than at its ends (Fig. 33.4). Together with its overlying mucosa it forms the palatoglossal arch or fold (see Fig. 30.3). It arises from the oral surface of the palatine aponeurosis where it is continuous with its contralateral fellow. It extends forwards, downwards and laterally in front of the palatine tonsil to the side of the tongue. Some of its fibres spread over the dorsum of the tongue, others pass deeply into its substance to intermingle with fibres of the intrinsic transverse muscle.

Vascular supply

Palatoglossus receives its blood supply from the ascending palatine branch of the facial artery and from the ascending pharyngeal artery.

Innervation

Palatoglossus is supplied by the cranial part of the accessory nerve via the pharyngeal plexus, and is therefore unlike all the other muscles of the tongue, which are supplied by the hypoglossal nerve.

Actions

Palatoglossus elevates the root of the tongue and approximates the palatoglossal arch to its contralateral fellow, thus shutting off the oral cavity from the oropharynx.

Palatopharyngeus

Palatopharyngeus and its overlying mucosa form the palatopharyngeal arch (see Fig. 30.3). Within the soft palate, palatopharyngeus is composed of two fasciculi that are attached to the upper surface of the palatine aponeurosis; they lie in the same plane but are separated from each other by levator veli palatini (Figs 33.4, 33.8). The thicker, anterior fasciculus arises from the posterior border of the hard palate as well as the palatine aponeurosis, where some fibres interdigitate across the midline. The posterior fasciculus is in contact with the mucosa of the pharyngeal aspect of the palate, and joins the posterior band of the contralateral muscle in the midline. The two layers unite at the posterolateral border of the soft palate, and are joined by fibres of salpingopharyngeus. Passing laterally and downwards behind the tonsil, palatopharyngeus descends posteromedial to and in close contact with stylopharyngeus, to be attached with it to the posterior border of the thyroid cartilage. Some fibres end on the side of the pharynx, attached to pharyngeal fibrous tissue, and others cross the midline posteriorly, decussating with those of the contralateral muscle. Palatopharyngeus thus forms an incomplete internal longitudinal muscular layer in the wall of the pharynx.

Passavant’s muscle (palatopharyngeal sphincter)

The existence of Passavant’s muscle remains controversial. It has been described as a part of the superior constrictor and palatopharyngeus muscles. An alternative view holds that it is a distinct palatine muscle that arises from the anterior and lateral parts of the upper surface of the palatine aponeurosis, lies lateral to levator veli palatini, blends internally with the upper border of the superior constrictor, and encircles the pharynx as a sphincter-like muscle (Figs 33.4, 33.8). Whatever its origin, when it contracts, it forms a ridge (Passavant's ridge) when the soft palate is elevated. The change from columnar, ciliated, 'respiratory' epithelium to stratified, squamous epithelium that takes place on the superior aspect of the soft palate occurs along the line of attachment of the palatopharyngeal sphincter to the palate. The muscle is hypertrophied in cases of complete cleft palate.

Vascular supply

Palatopharyngeus receives its arterial supply from the ascending palatine branch of the facial artery, the greater palatine branch of the maxillary artery and the pharyngeal branch of the ascending pharyngeal artery.

Innervation

Palatopharyngeus is innervated by the cranial part of the accessory nerve via the pharyngeal plexus.

Actions

Acting together, the palatopharyngei pull the pharynx up, forwards and medially, and thus shorten it during swallowing. They also approximate the palatopharyngeal arches and draw them forwards.

Musculus uvulae

Musculus uvulae arises from the posterior nasal spine of the palatine bone and the superior surface of the palatine aponeurosis, and lies between the two laminae of the aponeurosis (Figs 33.1, 33.8). It runs posteriorly above the sling formed by levator veli palatini and inserts beneath the mucosa of the uvula. The two sides of the muscle are united along most of its length.

Vascular supply

The blood supply of musculus uvulae is derived from the ascending palatine branch of the facial artery and the descending palatine branch of the maxillary artery.

Innervation

The nerve supply to musculus uvulae is derived from the cranial part of the accessory nerve via the pharyngeal plexus.

Actions

By retracting the uvular mass and thickening the middle third of the soft palate, musculus uvulae aids levator veli palatini in palatopharyngeal closure. The two muscles run at right angles to each other and their contraction raises a ‘levator eminence’ which helps seals off the nasopharynx.

Salpingopharyngeus

Salpingopharyngeus arises from the inferior part of the cartilage of the pharyngotympanic tube near its pharyngeal opening and passes downwards within the salpingopharyngeal fold to blend with palatopharyngeus (Figs 33.1, 33.4A, 33.8).

Vascular supply

Salpingopharyngeus receives its arterial supply from the ascending palatine branch of the facial artery, the greater palatine branch of the maxillary artery and the pharyngeal branch of the ascending pharyngeal artery.

Innervation

Salpinopharyngeus is innervated through the cranial part of the accessory nerve from the pharyngeal plexus.

Actions

Salpingopharyngeus elevates the pharynx, and may also assist tensor veli palatini to open the cartilaginous end of the pharyngotympanic tube during swallowing.

Stylopharyngeus

Stylopharyngeus is a long slender muscle, cylindrical above and flat below. It arises from the medial side of the base of the styloid process, descends along the side of the pharynx, and passes between the superior and middle constrictors to spread out beneath the mucous membrane (Figs 33.4, 33.9; see Fig. 30.6). Some fibres merge into the constrictors and the lateral glossoepiglottic fold, while others join fibres of palatopharyngeus and are attached to the posterior border of the thyroid cartilage. The glossopharyngeal nerve curves round the posterior border and the lateral side of stylopharyngeus, and passes between the superior and middle constrictors to reach the tongue.

Vascular supply

Stylopharyngeus receives its arterial supply from the pharyngeal branch of the ascending pharyngeal artery.

Innervation

Stylopharyngeus is innervated by the glossopharyngeal nerve.

Actions

Stylopharyngeus elevates the pharynx and larynx.

Superior constrictor

The superior constrictor is a quadrilateral sheet of muscle and is thinner than the other two constrictors. It is attached anteriorly to the pterygoid hamulus (and sometimes to the adjoining posterior margin of the medial pterygoid plate), the posterior border of the pterygomandibular raphe, the posterior end of the mylohyoid line of the mandible, and, by a few fibres, to the side of the tongue (Figs 33.1, 33.4, 33.5, 33.7, 33.9; see Fig. 30.6). The fibres curve back into a median pharyngeal raphe which is attached superiorly to the pharyngeal tubercle on the basilar part of the occipital bone.

Relations

The upper border of the superior constrictor is separated from the cranial base by a crescentic interval which contains levator veli palatini, the pharyngotympanic tube and an upward projection of pharyngobasilar fascia. The lower border is separated from the middle constrictor by stylopharyngeus and the glossopharyngeal nerve (Fig. 33.8). Anteriorly, the pterygomandibular raphe separates the superior constrictor from buccinator, and, posteriorly, the superior constrictor lies on the prevertebral muscles and fascia, from which it is separated by the retropharyngeal space. The ascending pharyngeal artery, pharyngeal venous plexus, glossopharyngeal and lingual nerves, styloglossus, middle constrictor, medial pterygoid, stylopharyngeus and the stylohyoid ligament all lie laterally, and palatopharyngeus, the tonsillar capsule and the pharyngobasilar fascia lie internally.

Vascular supply

The arterial supply of the superior constrictor is derived mainly from the pharyngeal branch of the ascending pharyngeal artery and the tonsillar branch of the facial artery.

Innervation

The superior constrictor is innervated by the cranial part of the accessory nerve from the pharyngeal plexus.

Actions

The superior constrictor constricts the upper part of the pharynx.

Middle constrictor

The middle constrictor is a fan-shaped sheet attached anteriorly to the lesser cornu of the hyoid and the lower part of the stylohyoid ligament (the chondropharyngeal part of the muscle), and to the whole of the upper border of the greater cornu of the hyoid (the ceratopharyngeal part) (Figs 33.4A, 33.7, 33.9; see Fig. 30.6). The lower fibres descend deep to the inferior constrictor to reach the lower end of the pharynx; the middle fibres pass transversely and the superior fibres ascend and overlap the superior constrictor. All fibres insert posteriorly into the median pharyngeal raphe.

Relations

The glossopharyngeal nerve and stylopharyngeus pass through a small gap between the middle and superior constrictors, and the internal laryngeal nerve and the laryngeal branch of the superior thyroid artery pass between the middle and inferior constrictors. The prevertebral fascia and longus colli and longus capitis are posterior, the superior constrictor, stylopharyngeus and palatopharyngeus are internal, and the carotid vessels, pharyngeal plexus of nerves and some lymph nodes are lateral. Near its hyoid attachment, the middle constrictor lies deep to hyoglossus, from which it is separated by the lingual artery.

Vascular supply

The arterial supply of the middle constrictor is derived mainly from the pharyngeal branch of the ascending pharyngeal artery and the tonsillar branch of the facial artery.

Innervation

The middle constrictor is innervated by the cranial part of the accessory nerve from the pharyngeal plexus.

Actions

The middle constrictor constricts the middle part of the pharynx during swallowing.

Inferior constrictor

The inferior constrictor is the thickest of the three constrictor muscles, and is usually described in two parts, thyropharyngeus and cricopharyngeus (Figs 33.4A, 33.7, 33.9; see Fig. 30.6). Thyropharyngeus arises from the oblique line of the thyroid lamina, a strip of the lamina behind this, and by a small slip from the inferior cornu. Some additional fibres arise from a tendinous cord that loops over cricothyroid. Cricopharyngeus arises from the side of the cricoid cartilage between the attachment of cricothyroid and the articular facet for the inferior thyroid cornu. Some authors have described cricopharyngeus as consisting of a superficial upper oblique portion, the pars oblique, and a lower, deeper, transverse portion, the pars fundiformis. The upper part attaches to the median raphe while the lower part forms a circular band that lacks a median raphe. The area demarcated by the pars oblique and pars fundiformis of cricopharyngeus is termed Killian’s dehiscence (or Killian’s triangle). A second triangular area, Laimer’s triangle, can be identified beneath cricopharyngeus between the longitudinal fibres of the oesophagus as they pass laterally on either side to attach to the cricoid cartilage: only the circular muscle of the oesophagus forms the wall here. Both triangles are postulated to be sites of weakness in the wall of the pharynx and oesophagus, and are therefore areas where diverticula could potentially form. Both cricopharyngeus and thyropharyngeus spread posteromedially to join the contralateral muscle. Thyropharyngeus is inserted into the median pharyngeal raphe, and its upper fibres ascend obliquely to overlap the middle constrictor; however, cricopharyngeus blends with the circular oesophageal fibres around the narrowest part of the pharynx.

Relations

The buccopharyngeal fascia is external, the prevertebral fascia and muscles are posterior, the thyroid gland, common carotid artery and sternothyroid are lateral, and the middle constrictor, stylopharyngeus, palatopharyngeus and the fibrous lamina are internal. The internal laryngeal nerve and laryngeal branch of the superior thyroid artery reach the thyrohyoid membrane by passing between the inferior and middle constrictors. The external laryngeal nerve descends on the superficial surface of the muscle, just behind its thyroid attachment, and pierces its lower part. The recurrent laryngeal nerve and the laryngeal branch of the inferior thyroid artery ascend deep to its lower border to enter the larynx.

Vascular supply

The arterial supply of the inferior constrictor is derived mainly from the pharyngeal branch of the ascending pharyngeal artery and the muscular branches of the inferior thyroid artery.

Innervation

Both parts of the inferior constrictor are usually supplied by the cranial part of the accessory nerve from the pharyngeal plexus. Although controversial, available evidence in humans suggests that cricopharyngeus is also supplied by the recurrent laryngeal nerve and the external branch of the superior laryngeal nerve.

Actions

Thyropharyngeus constricts the lower part of the pharynx. Cricopharyngeus is the main component of the upper oesophageal sphincter, or pharyngoesophageal high-pressure zone, the other parts being thyropharyngeus and the proximal cervical oesophagus. (The extent to which the lower fibres of thyropharyngeus and the upper fibres of the oesophageal musculature are involved in closing the upper end of the oesophagus appears to depend on the physiological state, whereas cricopharyngeus always participates in closure.) The upper oesophageal sphincter is defined manometrically as a region of elevated intraluminal pressure, 2–4 cm long, located at the junction of the hypopharynx and cervical oesophagus.

Cricopharyngeus contains about 40% of endomysial connective tissue, much of which is elastic, but it lacks muscle spindles. It contains both slow-twitch type I and fast-twitch type II fibres, a structural arrangement that underpins the various functions of the upper oesophageal sphincter, i.e. maintaining constant basal tone, yet being able to relax and contract rapidly during swallowing, belching and vomiting. The tonic activity of cricopharyngeus between swallows prevents influx of air during inspiration and tracheobronchial aspiration and pharyngeal reflux of oesophageal contents during oesophageal peristalsis. For further reading, see Lang and Shaker (2000).

Hypopharyngeal diverticula

The pharyngeal mucosa that lies between cricopharyngeus and thyropharyngeus is relatively unsupported by pharyngeal muscles and is called the dehiscence of Killian. A delay in the relaxation of cricopharyngeus, which can occur when the swallowing mechanism becomes discoordinated, generates a zone of elevated pressure adjacent to the mucosa in the dehiscence. The result is the development of a pulsion diverticulum (a pouch of prolapsing mucosa), which breaches the thin muscle wall adjacent to the sixth cervical vertebra and expands, usually a little to the left side, into the parapharyngeal potential space. This may trap portions (or all) of the passing food bolus, resulting in regurgitation of old food, aspiration pneumonia, halitosis and weight loss. Treatment may involve open excision or inversion of the pouch to prevent it filling, coupled with division of the circular fibres of cricopharyngeus, to prevent the build-up of pressure in the region and recurrence of the pouch.

PHARYNGEAL PLEXUS

Almost all of the nerve supply to the pharynx, whether motor or sensory, is derived from the pharyngeal plexus, which is formed by the pharyngeal branches of the glossopharyngeal and vagus nerves with contributions from the superior cervical sympathetic ganglion. The plexus lies on the external surface of the pharynx, especially on the middle constrictor. Filaments from the plexus ascend or descend external to the superior and inferior constrictors before branching within the muscular layer and mucosa of the pharynx.

The pharyngeal branch of the vagus supplies all the muscles of the pharynx (excluding stylopharyngeus, which is supplied by the glossopharyngeal nerve) and of the soft palate (excluding tensor veli palatini, which is supplied by the mandibular division of the trigeminal via the nerve to medial pterygoid). It emerges from the upper part of the inferior vagal ganglion and consists mainly of filaments derived from the cranial accessory nerve: almost all the neuronal cell bodies are in the nucleus ambiguus. The nerve passes between the external and internal carotid arteries to reach the upper border of the middle pharyngeal constrictor, and subsequently divides into numerous filaments which contribute to the pharyngeal plexus. It also gives off a minute filament, the ramus lingualis vagi, which joins the hypoglossal nerve as it curves round the occipital artery.

ANATOMY OF SWALLOWING (DEGLUTITION)

Swallowing involves a series of activities that occur within a matter of seconds. Traditionally described as a reflex, the process is more properly regarded as a programmed motor behaviour. Swallowing is initiated when food or liquid stimulates sensory nerves in the oropharynx. In a 24-hour period, an average person will swallow between 600 and 1000 times, but, of these, only some 150 will relate to feeding; the remainder occur to clear continuously produced saliva and are less frequent at night.

Eating and drinking are basic human pleasures, and problems associated with swallowing can impact dramatically upon the quality of life. Swallowing disorders are usually symptoms of other complex diseases: an inability to swallow may adversely affect nutritional status and therefore indirectly exacerbate the underlying disease. Aside from the risk of asphyxiation through choking, swallowing disorders can also be a direct cause of morbidity and mortality as a result of aspiration of food, liquid or possibly refluxed gastric acid contents, causing bacterial infection or tissue damage.

Swallowing in the adult human has traditionally been studied in relation to swallowing solid or liquid food carried out on command. For descriptive purposes, the process has been divided into four phases: oral preparatory, oral transit/transfer, pharyngeal and oesophageal. However, the boundaries between these phases are not entirely clear, thus, for example, the demarcation between the first and second phases is defined primarily by convention. Moreover, although it has long been thought that the oral and pharyngeal stages of swallowing were clearly separated, some authors consider that the initiation of the swallow entails both oral and pharyngeal movements, especially when swallowing solid food rather than saliva or other liquids.

Food is reduced in the mouth to a consistency suitable for swallowing and is formed into a cohesive bolus (oral preparatory phase). The bolus is delivered to the oropharynx (oral transit/transfer phase), transported down the pharynx past the airways and through the upper oesophageal sphincter (pharyngeal phase), and then transported down the oesophagus to the stomach (oesophageal phase). The oral preparatory and oral transit/transfer phases are voluntary and under cortical control, whereas the pharyngeal and oesophageal phases are involuntary and controlled by the brainstem. Airway protection is vital during the pharyngeal phase.

ORAL PREPARATORY PHASE

In the oral preparatory phase, the essential action is chewing: the mandible is moved by the action of the jaw elevators and depressors (see Ch. 31), and the food is reduced by the grinding action of the teeth and simultaneously mixed with saliva. The lips are maintained as a tight labial seal by the contraction of orbicularis oris: buccinator performs a similar function for the cheeks. In this way, the sulci are closed, the vestibule normally remains empty, and any food that enters the vestibule is returned to the oral cavity proper. Buccinator also keeps the cheeks taut, ensuring that they are kept clear of the occlusal surfaces of the teeth during chewing: loss of the nerve supply to buccinator as a result of damage to the facial nerve results in painful and repeated lacerations of the cheeks.

The soft palate is depressed during this phase and premature spillage of food is common. Spillage occurs because the soft palate is not in continuous contact with the posterior part of the tongue, as was once thought (Hiiemae & Palmer 1999). Bolus formation appears to involve several cycles of food being transported from the anterior to the posterior part of the tongue through the palatoglossal and palatopharyngeal arches until a bolus accumulates on the oropharyngeal surface of the tongue (retrolingual loading). Throughout this phase, the lateral and rotatory tongue movements that deliver the food to the teeth for grinding and reduction are crucial for normal bolus formation. If effective tongue movements do not occur, chewing will be compromised. The end of this phase of swallowing is marked by the tongue holding the bolus of food that has been formed against the hard palate in readiness for transport to the posterior part of the oral cavity.

ORAL TRANSIT/TRANSFER PHASE

In the oral transit/transfer phase, the bolus formed in the oral preparatory stage is finally transported through the palatoglossal and palatopharyngeal arches into the oropharynx.

Genioglossus raises both the tongue tip and the part of the tongue immediately behind the tip. The soft palate is then fully lowered by contraction of palatoglossus and palatopharyngeus, and the posterior part of the tongue is simultaneously elevated: the apposed soft palate and tongue form a tight seal that helps to prevent premature entry of the bolus into the pharynx. Orbicularis oris and buccinator remain contracted, so keeping the lips and cheeks taut and the bolus of food central in the oral cavity. The bolus is accommodated in a shallow midline gutter that forms along the dorsum of the tongue, probably as a result of the co-contraction of the styloglossi and the genioglossi, aided by the superior longitudinal and transverse fibres of the intrinsic muscles.

The mandible is elevated and the mouth is closed. The floor of the mouth and the anterior and middle portions of the tongue are elevated, by co-contraction of the suprahyoid group of muscles (mylohyoid, digastric, geniohyoid and stylohyoid): the effectiveness of the suprahyoid muscles is increased as they contract against a fixed mandible (the mouth does not have to be closed to swallow, but it is much harder to swallow if it is open). Contraction of stylohyoid elevates the more posterior parts of the tongue and empties the longitudinal gutter. At the same time, the tongue flattens, probably as a result of the contraction of hyoglossus and some of the intrinsic lingual muscles, especially the vertical fibres. The elevated, flattened tongue pushes the bolus against the hard palate, and the sides of the tongue seal against the maxillary alveolar processes, helping to move the bolus further posteriorly. Contraction of styloglossus and mylohyoid completes the elevation of the posterior part of the tongue. At the same time, the posterior oral seal relaxes and the posterior tongue moves forward: the overall effect is of a cam-like action of the tongue, sweeping or squeezing the bolus towards the pillars of the fauces, finally delivering it to the oropharynx where the pharyngeal aperture is initially increased and then closed.

PHARYNGEAL PHASE

The delivery of the bolus to the oropharynx triggers the pharyngeal phase of the swallow. This phase, which is involuntary and the most critical stage of swallowing, involves the pharynx changing from being an air channel (between the posterior nares and laryngeal inlet) to a food channel (from the fauces to the upper end of the oesophagus). The airway is protected from aspiration during swallowing by hyolaryngeal elevation, and by resetting respiratory rhythm so that airflow ceases briefly as the bolus passes through the hypopharynx: the total time that elapses from the bolus triggering the pharyngeal phase to the re-establishment of the airway is barely 1 second.

The nasopharynx is sealed off from the oropharynx by activation of the superior pharyngeal constrictor and contraction of a subset of palatopharyngeal fibres to form a variable, ridge-like structure (Passavant's ridge) against which the soft palate is elevated. From an evolutionary perspective, this ridge represents the remnant of a sphincter which encircled a more highly placed larynx: a high laryngeal position is the norm in other mammals and in the human infant (see below), but not in the human adult. Interestingly, the pharyngeal ridge becomes hypertrophic in an infant with a cleft palate, presumably in an attempt to produce a seal to the nasal airway. Ineffective velopharyngeal closure may result in nasal regurgitation of food.

The airway is sealed at the laryngeal inlet by closure of the glottis (see Ch. 34), and the epiglottis is retroflexed over the laryngeal aditus as a result of passive pressure from the base of the tongue and active contraction of the aryepiglottic muscles. The conventional view that laryngeal closure during swallowing occurs from inferior to superior, i.e the vocal folds adduct first and the epiglottis covers the arytenoids and glottis last, has been challenged by studies using simultaneous electromyography and fibreoptic endoscopic evaluation of swallowing, FEES, which have reported that the aryepiglottic folds close before vocal fold adduction during a swallow. It is probably reasonable to assume that the sequence of events that close the glottis may alter according to the type of swallow and consistency of the bolus. What is not in dispute is that the hyoid bone and larynx are raised and pulled anteriorly by the suprahyoid muscles and the longitudinal muscles of the pharynx, so that the laryngeal inlet is brought forward under the bulge of the posterior tongue, i.e. out of the path of the bolus. This action helps expand the hypopharyngeal space and relax the upper oesophageal sphincter, which is also raised by several centimetres. The bolus passes over the reflected anterior surface of the epiglottis and is swept through the laryngopharynx to the upper oesophageal sphincter.

The sequential contraction of the three pharyngeal constrictor muscles is often assumed to be the driving force propelling the bolus towards the oesophagus. However, evidence that the head of the bolus moves faster than the wave of pharyngeal contraction suggests that, at least in some situations, the kinetic energy imparted to the bolus as it is expelled from the mouth into the oropharynx may be sufficient to carry it through the pharynx. This energy is generated by pressure gradients created within the pharynx by the tongue driving force, the hypopharyngeal suction pump, and the ‘stripping action’ of the pharyngeal constrictors.

The tongue driving force, or the tongue thrust pressure force, is a positive pressure that squeezes the bolus towards the laryngopharynx. It is generated by the upward movement of the tongue pressing the bolus against the contracting pharyngeal wall and requires a tight nasopharyngeal seal (created by elevation of the soft palate). There is a view that the tongue driving force is the most important factor responsible for moving the bolus down the pharynx. The hypopharyngeal suction pump is caused by the elevation and anterior movement of the hyoid and larynx, which creates a negative pressure in the laryngopharynx, drawing the bolus towards the oesophagus, aided by a more negative pressure inside the oesophagus. The pharyngeal constrictors generate a positive pressure wave behind the bolus. Their sequential contraction may facilitate clearance (‘stripping’) of the pharyngeal walls and piriform sinuses: if this is so, residues that remain in the valleculae must reflect inadequate tongue force generation at the end of the oral phase of swallowing.

Gag reflex

Traditionally, the stimulus for triggering a swallow has been regarded as contact with the posterior wall of the pharynx, since this is usually where the gag reflex is triggered (see p. 283 and Fig. 19.12). However, it has become clear that many regions of the oropharynx, when appropriately stimulated by the presence of food or liquid, are capable of triggering a swallow, although some regions are more sensitive than others, e.g. the area over the palatoglossal arches. Moreover, there appears to be little relationship between a functioning gag reflex and the ability to swallow normally. Individuals with a reduced or absent gag reflex can swallow safely; conversely, the presence of a brisk and clear gag reflex is not always associated with the ability to swallow normally.

OESOPHAGEAL PHASE

The third, or oesophageal, stage begins after the relaxation of the upper oesophageal sphincter has allowed the bolus to enter the oesophagus. Sequential waves of contractions of the oesophageal musculature subsequently propel the bolus down to the lower oesophageal sphincter, which opens momentarily to admit the bolus to the stomach. The oesophageal phase of swallowing is much more variable than the other phases, and lasts between 8 and 20 seconds.

SWALLOWING PATTERN GENERATOR

The patterning and timing of striated muscle contraction during swallowing are generated at a brainstem level in a network of neural circuits which collectively form a central swallowing pattern generator (SPG). Experimental neurophysiological and tracer studies in animals have shown that the SPG includes several brainstem motor nuclei and two groups of interneurones in the dorsal and ventral medulla, a dorsal swallowing group (DSG) and a ventral swallowing group (VSG). The DSG is located in the nucleus of the solitary tract and possibly in the adjacent reticular formation, and contains neurones that generate the swallowing pattern, probably triggered by convergent information from both cortical and peripheral inputs. The afferent feedback from the branches of the superior laryngeal nerve which innervate the valleculae, epiglottis and supraglottic part of the larynx, and which relay through the nucleus of the solitary tract, facilitates laryngeal closure during swallowing (Jafari et al 2003). The VSG is in the ventrolateral medulla above the nucleus ambiguus and contains neurones that act as ‘switches’, distributing the swallowing drive to motoneurone pools in the trigeminal, facial and hypoglossal nuclei and in the nucleus ambiguus.

The patterns of activation in the smooth muscle of the lower part of the oesophagus are generated locally in intramural plexuses driven by vagal autonomics.

Supramedullary influence on swallowing

Techniques including transcranial magnetic stimulation, cortical evoked potentials, positron emission tomography and functional magnetic resonance imaging (fMRI) have all been exploited in the study of volitional swallowing in humans. Thus far, these studies have shown that numerous cortical and subcortical regions are recruited in swallowing, although, as yet, the functional contributions made by each region have not been established, and it is not known how they influence the SPG. The most consistent cortical activation occurs in the primary motor and somatosensory cortices. Perhaps not surprisingly, the greatest area of fMRI activation in the primary motor cortex occurs over the portion of the precentral gyrus where the face, tongue and pharynx are represented: there is evidence for functional asymmetry between the right and left oral sensorimotor cortices (Martin et al 2004). The activity of the SPG is coordinated with other medullary reflexes, e.g. it is difficult to elicit a swallow when the cortical masticatory centres are stimulated.

SWALLOWING IN THE NEONATE

In the adult, the tip of the epiglottis is significantly lower than the inferior edge of the soft palate. In the neonate, the larynx is high in the neck and the epiglottis may extend above the soft palate so that the laryngeal airway is in direct continuity with the posterior nares (Fig. 33.10): a potential space is therefore formed between the soft palate above, the epiglottis behind and the tongue anteroinferiorly. In other mammals with an oropharyngeal anatomy similar to that of the human infant, up to 14 cycles of tongue movement or oral phases cause the accumulation of food in this space. Subsequent emptying of the space is a single event followed by movement of the bolus down the oesophagus. The ratio of accumulation cycles to swallow events in the human neonate is approximately 1.5 : 1, which is lower than in other mammals, but still implies some temporary accumulation. In the case of a liquid bolus, accumulated material may be passed laterally to the epiglottis through the piriform fossae rather than over the flexed epiglottis, although it is not known whether this happens in the human infant.

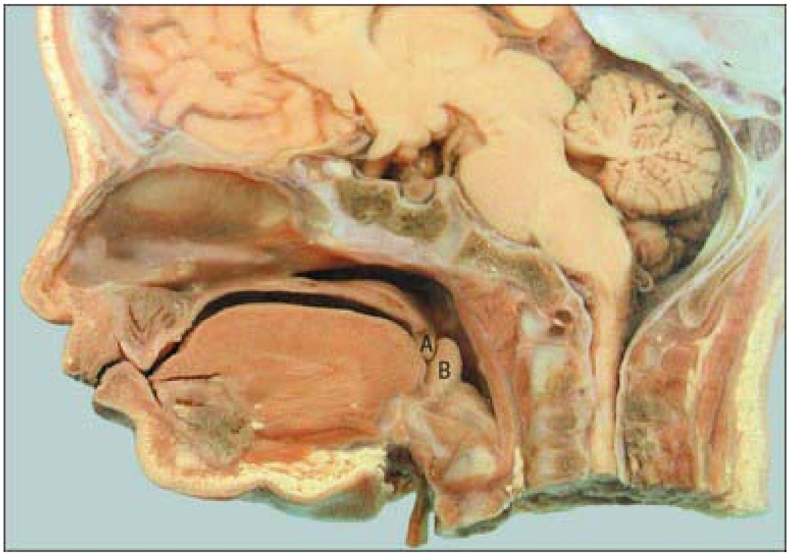

Fig. 33.10 Sagittal section of the head of a neonate. Note the relatively high position of the larynx, the opening being at the level of the soft palate **A**, **B**, epiglottis.

(By permission from Berkovitz BKB, Holland GR, Moxham BJ 2002 Oral Anatomy, Embryology and Histology, 3rd edn. Edinburgh: Mosby.)

Swallow safety is critical at all ages. In the neonate, where coordination of suckling, swallowing and breathing is not fully developed, the potential risk of airway obstruction and/or aspiration of ingested milk or other material during swallowing is reduced because the intranarial larynx prevents the bolus from entering the larynx before and after a swallow (see Ch. 34). The change towards adult anatomy and coordination of the phases of swallowing starts a few months after birth. Differential growth in length of the human pharynx causes the larynx to take up its low adult position and the epiglottis to lose contact with the soft palate: the larynx reaches its final position around the time of puberty. The adult anatomy does not allow any significant accumulation of food to occur immediately anterior to the epiglottis, which means that the transport of food through the fauces has to bear a 1 : 1 relationship to pharyngeal and oesophageal transit. Moreover, the lowered larynx compromises the previously protected airway: the hyoid and larynx are therefore raised and pulled forwards during a swallow in order to minimize the risk of deglutitive aspiration.

PHARYNGOSTOMY AND EPIGLOTTOPEXY

Loss of control of the pharyngeal phase of swallowing, e.g. due to neurological disease or ablative head and neck surgery, may result in aspiration of food, especially fluids, leading to pneumonia. This problem may be addressed surgically by pharyngostomy or epiglottopexy. In pharyngostomy, a fine bore feeding tube is passed into the lower oesophagus or stomach via the nose or anterior abdominal wall. Alternatively, a tube may be passed through the cervical skin, fascia and platysma directly into the piriform fossa. This is achieved by passing a curved forcep into the piriform fossa and pushing it laterally, displacing the contents of the carotid sheath and tenting up the platysma and cervical skin from the inside. By cutting down on to the forcep, it is possible to grasp the feeding tube and pull it into the piriform fossa prior to feeding it on into the oesophagus. The tract formed by such a puncture epithelializes and may be used for long-term alimentation. In epiglottopexy, the neck and the pharynx are opened to expose the laryngeal inlet, the aryepiglottic folds are denuded of mucosa to encourage their adhesion, and the epiglottis is sutured down to the aryepiglottic folds to shield the laryngeal inlet. The resultant compromise of the airway can be offset by the creation of an alternative airway via a tracheostomy. The pharyngeal wall and cervical skin are reconstituted by suturing.

REFERENCES

uestone CD. Anatomy and physiology of the Eustachian tube. Cummings CW, et al, editors. Otolaryngology: Head and Neck Surgery, 3rd edn., vol 4. St Louis: Mosby, 1998;3003-3025.

onnington A, Mahon M, Whitmore I. A histological study of the cricopharyngeus muscle in man. *J Anat*. 1988;156:27-37.

ownlow H, Whitmore I, Willan PLT. A quantitative study of the histochemical and morphometric characteristics of the human cricopharyngeus muscle. *J Anat*. 1989;166:67-75.

The above two references provide an account of the detailed anatomy of cricopharyngeus in relation to its function as the main part of the upper oesophageal sphincter..

eelander E. Blood supply of the human levator and tensor veli palatini muscles. *Clin Anat*. 1992;5:34-44.

aney DO, Retruzzelli GJ, Myers EW. Anatomy. Cummings CW, et al, editors. Otolaryngology: Head and Neck Surgery, 3rd edn., vol 2. St Louis: Mosby, 1998;1327-1348.

Provides a concise account of the anatomy of the pharynx, highlighting features of clinical relevance..

ay SD, Pinborough-Zimmerman J. Velopharyngeal incompetence. In: Cummings CW, et al. *Otolaryngology: Head and Neck Surgery, vol 5: Pediatric Otolaryngology*. 3rd edn. St Louis: Mosby; 1998:174-187.

arris ML, Julyan P, Kulkarni B, et al. Mapping metabolic brain activation during human volitional swallowing: a positron emission tomography study using [18F]fluorodeoxyglucose. *J Cereb Blood Flow Metab*. 2005;25:520-526.

iemae KM, Palmer JB. Food transport and bolus formation during complete feeding sequences on foods of different initial consistency. *Dysphagia*. 1999;14:31-42.

fari S, Prince RA, Kim DY, Paydarfar D. Sensory regulation of swallowing and airway protection: a role for the internal superior laryngeal nerve in humans. *J Physiol*. 2003;550:287-304.

ng IM, Shaker R. An overview of the upper esophageal sphincter. *Curr Gastroenterol Rep*. 2000;2:185-190.

artin RE, MacIntosh BJ, Smith RC, et al. Cerebral areas processing swallowing and tongue movement are overlapping but distinct: a functional magnetic resonance imaging study. *J Neurophysiol*. 2004;92:2428-2443.

de J, editor. Basic Aspects of the Eustachian Tube and Middle Ear Disease. Geneva: Kugler & Ghedini, 1989.

exton A. Some aspects of swallowing. In: Harris M, Edgar M, Meghji S. *Clinical Oral Science*. Oxford: Wright; 1998:150-166.

exton AJ, Crompton AW. The control of swallowing. Linden RWA, editor. The Scientific Basis of Eating. Taste and Smell, Salivation, Mastication and Swallowing and their Dysfunctions. Frontiers of Oral Biology Series vol 9. Basel: Karger; 1998:168-222.

ood-Jones I. The nature of the soft palate. *J Anat*. 1940;77:147-170.

Describes the structure of the soft palate and its movements during swallowing..

CHAPTER 34

Larynx

The larynx is an air passage, a sphincter and an organ of phonation, and extends from the tongue to the trachea. It projects ventrally between the great vessels of the neck and is covered anteriorly by skin, fasciae and the hyoid depressor muscles. Above, it opens into the laryngopharynx and forms its anterior wall; below, it continues into the trachea (see Fig. 33.2). It is mobile on deglutition. At rest, the larynx lies opposite the third to sixth cervical vertebrae in adult males; it is somewhat higher in children and adult females. In infants between 6 and 12 months, the tip of the epiglottis (the highest part of the larynx) lies a little above the junction of the dens and body of the axis vertebra. Until puberty, male and female larynges are similar in size. After puberty, the male larynx enlarges considerably in comparison with that of the female: all the cartilages increase in both size and weight, the thyroid cartilage projects in the anterior midline of the neck, and its sagittal diameter nearly doubles. The male thyroid cartilage continues to increase in size until 40 years of age, after which no further growth occurs.

SKELETON OF THE LARYNX

The skeletal framework of the larynx is formed by a series of cartilages interconnected by ligaments and fibrous membranes, and moved by a number of muscles (Figs 34.1-34.3). The hyoid bone is attached to the larynx: it is usually regarded as a separate structure with distinctive functional roles, and is described on page 436. The laryngeal cartilages are the single thyroid, cricoid and epiglottic cartilages, and the paired arytenoid, cuneiform, corniculate and tritiate cartilages.

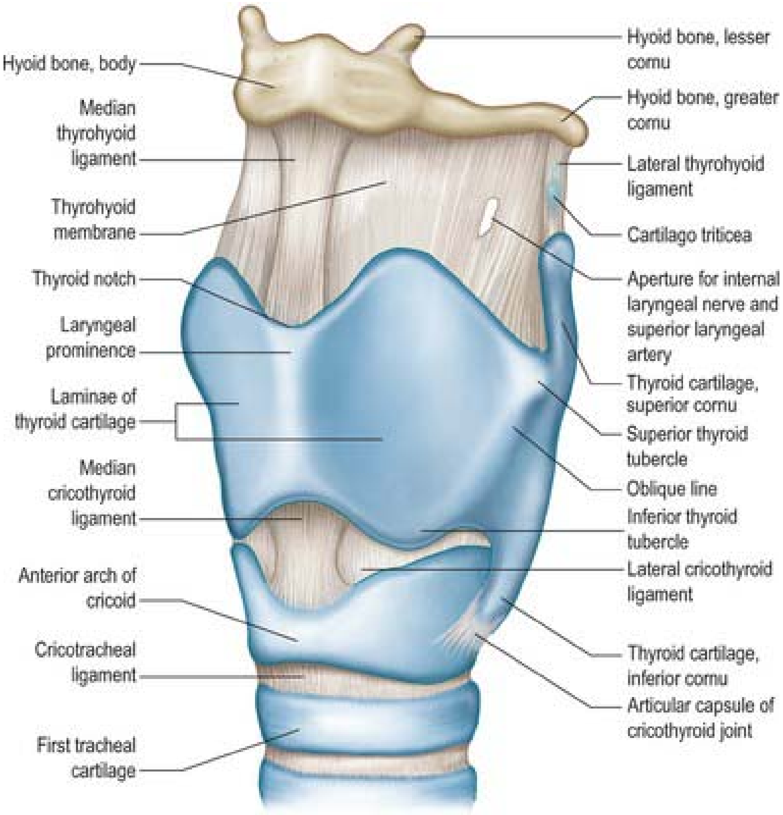
Hyoid bone, body
Median thyrohyoid ligament
Thyrohyoid membrane
Thyroid notch
Laryngeal prominence
Laminae of thyroid cartilage
Median cricothyroid ligament
Anterior arch of cricoid
Cricotracheal ligament
First tracheal cartilage
Hyoid bone, lesser cornu
Hyoid bone, greater cornu
Lateral thyrohyoid ligament
Cartilago triticea
Aperture for internal laryngeal nerve and superior laryngeal artery
Thyroid cartilage, superior cornu
Superior thyroid tubercle
Oblique line
Inferior thyroid tubercle
Lateral cricothyroid ligament
Thyroid cartilage, inferior cornu
Articular capsule of cricothyroid joint

Fig. 34.1 Anterolateral view of the laryngeal cartilages and ligaments.

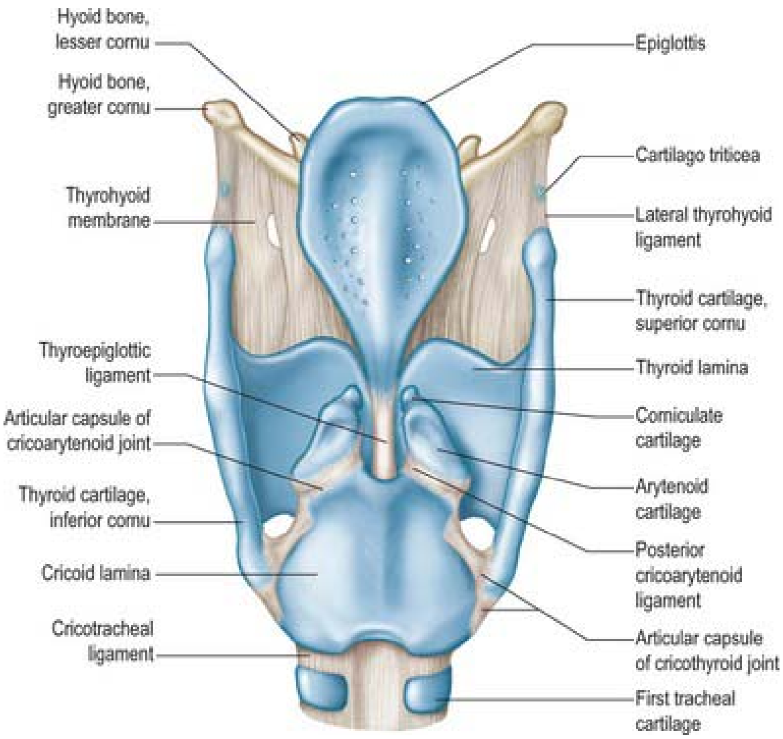
Hyoid bone, lesser cornu
Hyoid bone, greater cornu
Thyrohyoid membrane
Thyroepiglottic ligament
Articular capsule of cricoarytenoid joint
Thyroid cartilage, inferior cornu
Cricoid lamina
Cricotracheal ligament
Epiglottis
Cartilago triticea
Lateral thyrohyoid ligament
Thyroid cartilage, superior cornu
Thyroid lamina
Corniculate cartilage
Arytenoid cartilage
Posterior cricoarytenoid ligament
Articular capsule of cricothyroid joint
First tracheal cartilage

Fig. 34.2 Posterior view of the laryngeal cartilages and ligaments.

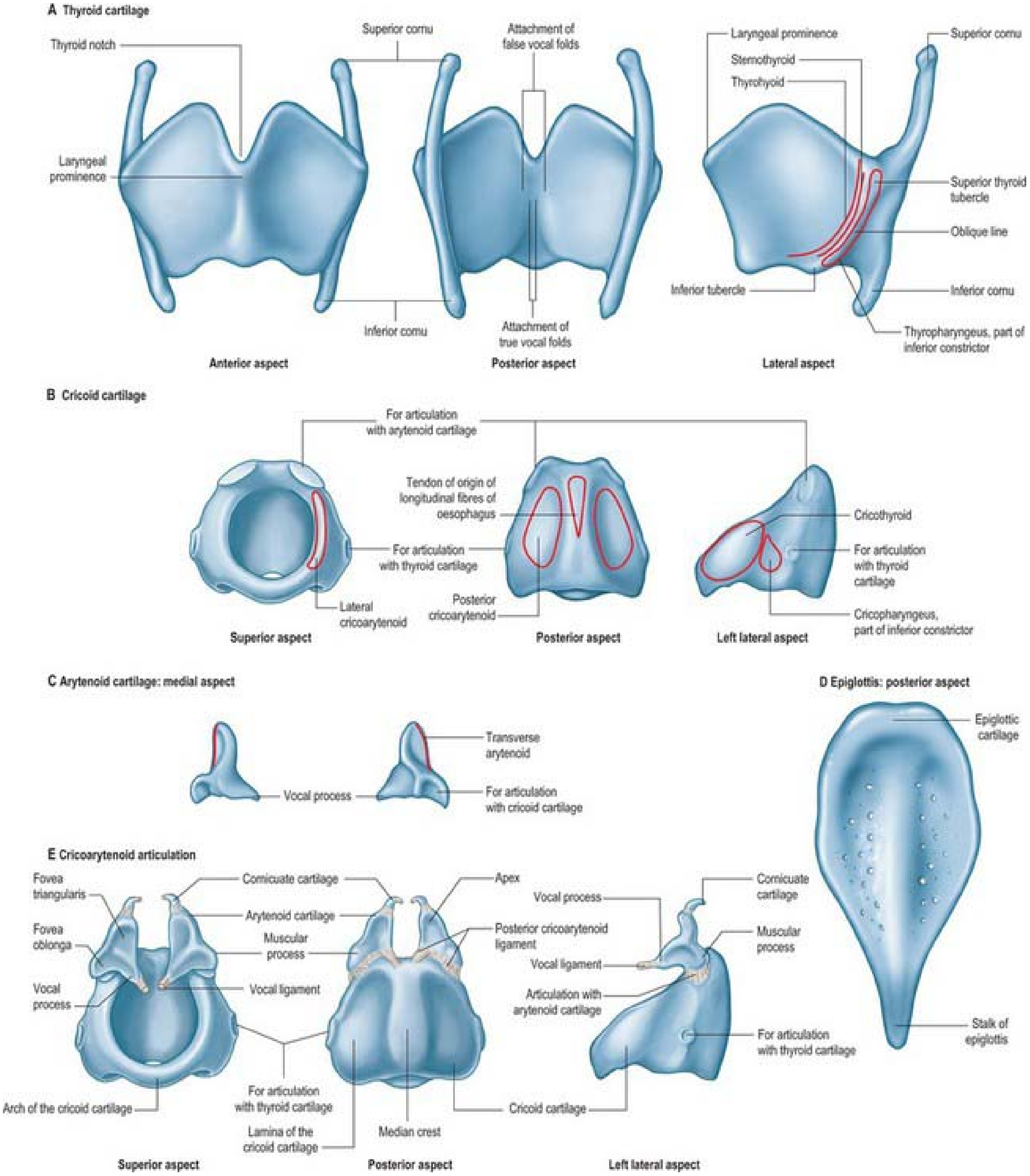
A Thyroid cartilage
Thyroid notch
Superior cornu
Attachment of false vocal folds
Laryngeal prominence
Sternothyroid
Thyrohyoid
Superior cornu
Laryngeal prominence
Superior thyroid tubercle
Oblique line
Inferior tubercle
Inferior cornu
Inferior cornu
Attachment of true vocal folds
Thyropharyngeus, part of inferior constrictor
Anterior aspect
Posterior aspect
Lateral aspect
B Cricoid cartilage
For articulation with arytenoid cartilage
Tendon of origin of longitudinal fibres of oesophagus
Cricothyroid
For articulation with thyroid cartilage
For articulation with thyroid cartilage
Lateral cricoarytenoid
Posterior cricoarytenoid
Cricopharyngeus, part of inferior constrictor
Superior aspect
Posterior aspect
Left lateral aspect
C Arytenoid cartilage: medial aspect
D Epiglottis: posterior aspect
Epiglottic cartilage
Transverse arytenoid
Vocal process
For articulation with cricoid cartilage
E Cricoarytenoid articulation
Fovea triangularis
Corniculate cartilage
Apex
Corniculate cartilage
Vocal process
Arytenoid cartilage
Fovea oblonga
Muscular process
Posterior cricoarytenoid ligament
Muscular process
Vocal ligament
Vocal process
Vocal ligament
Articulation with arytenoid cartilage
Stalk of epiglottis
For articulation with thyroid cartilage
Arch of the cricoid cartilage
For articulation with thyroid cartilage
Cricoid cartilage
Lamina of the cricoid cartilage
Median crest
Superior aspect
Posterior aspect
Left lateral aspect

Fig. 34.3 Cartilages of the larynx: thyroid (**A**), cricoid (**B**), arytenoid (**C**), epiglottis (**D**), cricoarytenoid joint (**E**). The attachments of the false vocal folds (vestibular ligaments) (above) and the true vocal folds (vocal ligaments) (below) are shown in **A**, posterior aspect. Note the pitted surface of the epiglottis (**D**).

In relation to the surface anatomy of the larynx, the levels of the laryngeal cartilages worth noting are: C3 (level of body of hyoid and its greater cornu); C3–4 junction (level of upper border of thyroid cartilage and bifurcation of common carotid artery); C4–5 junction (level of thyroid cartilage); C6 (level of cricoid cartilage).

The corniculate, cuneiform, tritiate and epiglottic cartilages and the apices of the arytenoid are composed of elastic fibrocartilage, with little tendency to calcify. The thyroid, cricoid and the greater part of the arytenoid cartilages consist of hyaline cartilage and may undergo mottled calcification as age advances, starting about the 25th year in the thyroid cartilage and somewhat later in the cricoid and arytenoids. By the 65th year, these cartilages commonly appear patchily dense in radiographs.

EPIGLOTTIS

The epiglottis is a thin leaf-like plate of elastic fibrocartilage which projects obliquely upwards behind the tongue and hyoid body, and in front of the laryngeal inlet (Figs 34.2, 34.3; see Fig. 34.5). Its free end, which is broad and round, and occasionally notched in the midline, is directed upwards. Its attached part, or stalk (petiolus), is long and narrow and is connected by the elastic thyroepiglottic ligament to the back of the laryngeal prominence of the thyroid cartilage just below the thyroid notch. Its sides are attached to the arytenoid cartilages by aryepiglottic folds (which contain the aryepiglottic muscle). Its free upper anterior, or lingual, surface is covered by mucosa (the epithelium is non-keratinized stratified squamous), which is reflected onto the pharyngeal aspect of the tongue and the lateral pharyngeal walls as a median glossoepiglottic, and two lateral glossoepiglottic, folds. There is a depression, the vallecula, on each side of the median fold. The lower part of its anterior surface, behind the hyoid bone and thyrohyoid membrane, is connected to the upper border of the hyoid by an elastic hyoepiglottic ligament, and separated from the thyrohyoid membrane by adipose tissue, which constitutes the clinically important preepiglottic space. The smooth posterior, or laryngeal, surface is transversely concave and vertically concavo-convex, and is covered by ciliated respiratory mucosa: its lower projecting part is called the tubercle. This surface forms the oblique anterior wall of the laryngeal vestibule. The cartilage is posteriorly pitted by small mucous glands (Fig. 34.3D) and is perforated by branches of the internal laryngeal nerve and fibrous tissue, which means that the posterior surface of the epiglottis is in continuity through these perforations with the pre-epiglottic space.

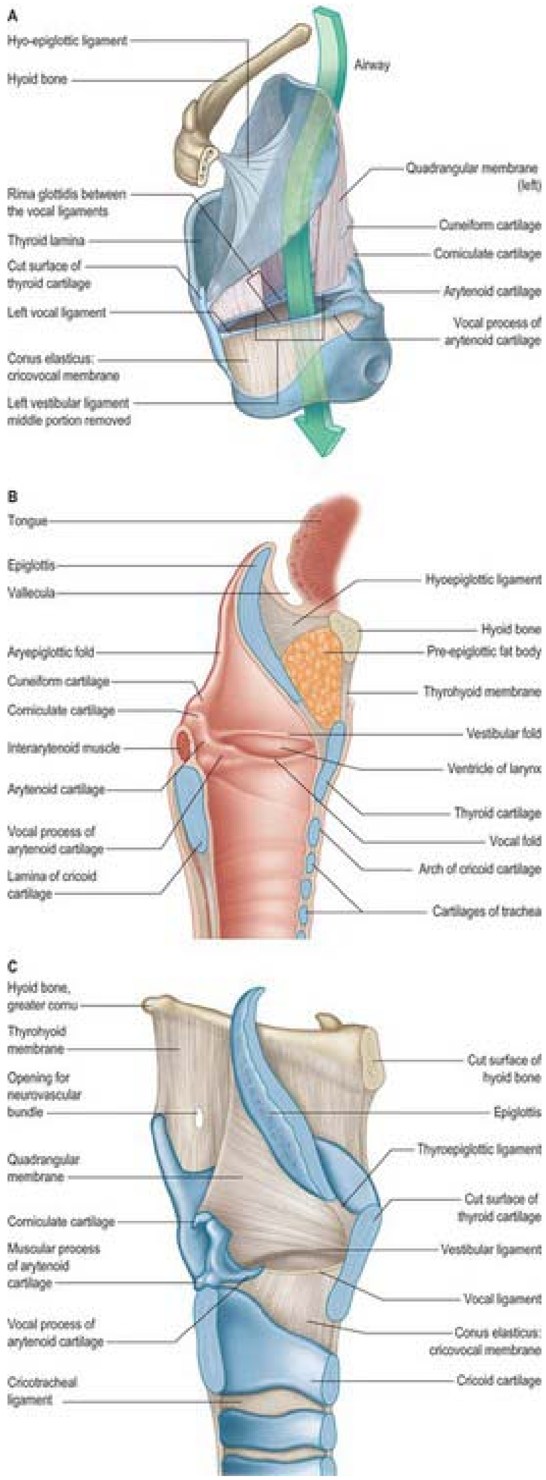
A
Hyo-epiglottic ligament
Hyoid bone
Airway
Quadrangular membrane (left)
Rima glottidis between the vocal ligaments
Thyroid lamina
Cut surface of thyroid cartilage
Cuneiform cartilage
Corniculate cartilage
Arytenoid cartilage
Left vocal ligament
Vocal process of arytenoid cartilage
Conus elasticus: cricovocal membrane
Left vestibular ligament middle portion removed
B
Tongue
Epiglottis
Vallecula
Hyoepiglottic ligament
Hyoid bone
Aryepiglottic fold
Pre-epiglottic fat body
Cuneiform cartilage
Thyrohyoid membrane
Corniculate cartilage
Interarytenoid muscle
Vestibular fold
Ventricle of larynx
Arytenoid cartilage
Thyroid cartilage
Vocal process of arytenoid cartilage
Vocal fold
Lamina of cricoid cartilage
Arch of cricoid cartilage
Cartilages of trachea
C
Hyoid bone, greater cornu
Thyrohyoid membrane
Cut surface of hyoid bone
Opening for neurovascular bundle
Epiglottis
Thyroepiglottic ligament
Quadrangular membrane
Cut surface of thyroid cartilage
Corniculate cartilage
Vestibular ligament
Muscular process of arytenoid cartilage
Vocal ligament
Vocal process of arytenoid cartilage
Conus elasticus: cricovocal membrane
Cricoid cartilage
Cricotracheal ligament

Fig. 34.5 **A** and **B**, Sagittal sections of the left side of the larynx, showing the laryngeal membranes (**A**) and the interior aspect (**B**) of the left half of the larynx. **C**, The quadrangular membrane viewed from the left side.

*(**A**, From Drake, Vogl and Mitchell 2005.)*

Functions of the epiglottis

During swallowing, the hyoid bone moves upwards and forwards, and the epiglottis is bent posteriorly as a result of passive pressure from the base of the tongue and active contraction of the aryepiglottic muscles. Though the epiglottis is not essential to swallowing, which can occur with minimal aspiration even if the epiglottis is destroyed by disease, it diverts food and liquids away from the laryngeal inlet and into the lateral food channels. It is not essential for respiration or phonation.

THYROID CARTILAGE

The thyroid cartilage is the largest of the laryngeal cartilages (Figs 34.1-34.3). It consists of two quadrilateral laminae with anterior borders that fuse along their inferior two-thirds at a median angle to form the subcutaneous laryngeal prominence (‘Adam’s apple’). This projection is most distinct at its upper end, and is well marked in men but scarcely visible in women. Above, the laminae are separated by a V-shaped superior thyroid notch or incisure. Posteriorly, the laminae diverge, and their posterior borders are prolonged as slender horns, the superior and inferior cornua. A shallow ridge, the oblique line, curves downwards and forwards on the external surface of each lamina: it runs from the superior thyroid tubercle lying a little anterior to the root of the superior cornu, to the inferior thyroid tubercle on the inferior border of the lamina. Sternothyroid, thyrohyoid and thyropharyngeus (part of the inferior pharyngeal constrictor) are attached to the oblique line, usually as little more than a tendon (Fig. 34.3A).

The internal surface of the lamina is smooth. Above and behind, it is slightly concave and covered by mucosa. The thyroepiglottic ligament, the paired vestibular and vocal ligaments, the thyroarytenoid, thyroepiglottic and vocalis muscles, and the stalk of the epiglottis are all attached to the inner surface of the cartilage, in the angle between the laminae. The true vocal folds lie 6–9 mm below the median thyroid notch. The superior border of each lamina is concave behind and convex in front, and the thyrohyoid membrane is attached along this edge (Figs 34.1, 34.2). The inferior border of each lamina is concave behind and nearly straight in front, and the two parts are separated by the inferior thyroid tubercle. Anteriorly, the thyroid cartilage is connected to the cricoid cartilage by the anterior (median) cricothyroid ligament, which is a thickened portion of the cricothyroid membrane.

The anterior border of each thyroid lamina fuses with its partner at an angle of approximately 90° in men and approximately 120° in women. The shallower angle in men is associated with the larger laryngeal prominence, the greater length of the vocal cords, and the resultant deeper pitch of the voice. The posterior border is thick and rounded and receives fibres of stylopharyngeus and palatopharyngeus. The superior cornu, which is long and narrow, curves upwards, backwards and medially, and ends in a conical apex to which the lateral thyrohyoid ligament is attached. The inferior cornu is short and thick, and curves down and slightly anteromedially. On the medial surface of its lower end there is a small oval facet for articulation with the side of the cricoid cartilage: this facet is variable and is well defined only sometimes.

During infancy, a narrow, rhomboidal, flexible strip, the intra-thyroid cartilage, lies between the two laminae, and is joined to them by fibrous tissue.

CRICOID CARTILAGE

The cricoid cartilage is attached below to the trachea, and articulates with the thyroid cartilage and the two arytenoid cartilages by synovial joints. It forms a complete ring around the airway, the only laryngeal cartilage to do so (Fig. 34.3B). It is smaller, but thicker and stronger, than the thyroid cartilage, and has a narrow curved anterior arch, and a broad, flatter posterior lamina.

Cricoid arch

The cricoid arch is vertically narrow in front (5–7 mm in height), and widens posteriorly towards the lamina. Cricothyroid is attached to the external aspect of its front and sides, and cricopharyngeus (part of the inferior pharyngeal constrictor) is attached behind cricothyroid. The arch is palpable below the laryngeal prominence, from which it is separated by a depression containing the resilient cricothyroid membrane. The inferior border of the cartilage is nearly horizontal and is circular in outline, whereas the upper border is more elliptical.

Cricoid lamina

The cricoid lamina is approximately quadrilateral in outline, and 2–3 cm in vertical dimension. It bears a posterior median vertical ridge that creates posterior concavities on either side. The two fasciculi of the longitudinal layer of oesophageal muscle fibres (muscularis externa) are attached by a tendon to the upper part of the ridge. Posterior cricoarytenoid attaches to a shallow depression on either side of the ridge.

A discernible circular synovial facet, facing posterolaterally, sometimes marks the junction of the lamina and arch: it indicates the site where the cricoid articulates with the inferior thyroid cornu. The inferior border of the cricoid is horizontal, and joined to the first tracheal cartilage by the cricotracheal ligament (Fig. 34.1). The superior border runs obliquely up and back, and gives attachment anteriorly to the thick median part of the cricothyroid membrane, and laterally to the membranous parts of the cricothyroid membrane (Fig. 34.1) and lateral cricoarytenoid. The posterosuperior aspect of the lamina presents a shallow median notch, on each side of which is a smooth, oval, convex facet, directed upwards and laterally, for articulation with the base of an arytenoid cartilage.

The internal surface of the cricoid cartilage is smooth and lined by mucosa.

Subglottic stenosis

Congenital malformation of the cricoid cartilage may result in severe narrowing of the subglottic airway and respiratory obstruction, which, in severe cases, is present from birth. It is the third most common congenital disorder of the larynx. Acquired subglottic stenosis is more common and is the result of trauma and scarring following prolonged endotracheal intubation for the purposes of ventilation of premature babies on intensive care units.

ARYTENOID CARTILAGE

The paired arytenoid cartilages articulate with the lateral parts of the superior border of the cricoid lamina (Figs 34.2, 34.3). Each is pyramidal, and has three surfaces, two processes, a base and an apex. The posterior surface, which is triangular, smooth and concave, is covered by transverse arytenoid. The anterolateral surface is convex and rough, and bears, near the apex of the cartilage, an elevation from which a crest curves back, down and then forwards to the vocal process. The lower part of this arcuate crest separates two depressions (foveae). The upper is triangular (fovea triangularis), and the vestibular ligament is attached to it. The lower is oblong (fovea oblonga), and vocalis and lateral cricoarytenoid are attached to it. The medial surface is narrow, smooth and flat, and is covered by mucosa: its lower edge forms the lateral boundary of the intercartilaginous part of the rima glottidis. The base is concave, with a smooth surface for articulation with the lateral part of the upper border of the cricoid lamina. Its round, prominent lateral angle, or muscular process, projects backwards and laterally: it gives attachment to posterior cricoarytenoid behind, and lateral cricoarytenoid in front. The vocal ligament is attached to its pointed anterior angle (vocal process), which projects horizontally forward. The apex curves backwards and medially and articulates with the corniculate cartilage.

CORNICULATE CARTILAGES

The corniculate cartilages are two conical nodules of elastic fibrocartilage which articulate with the apices of the arytenoid cartilages, prolonging them posteromedially (Fig. 34.3E). They lie in the posterior parts of the aryepiglottic mucosal folds, and are sometimes fused with the arytenoid cartilages.

CUNEIFORM CARTILAGES

The cuneiform cartilages are two small, elongated, club-like nodules of elastic fibrocartilage, one in each aryepiglottic fold anterosuperior to the corniculate cartilages, and are visible as whitish elevations through the mucosa (see Fig. 34.5).

TRITIATE CARTILAGES (CARTILAGO TRITICEA)

The tritiate cartilages are two small nodules of elastic cartilage, situated one on either side above the larynx within the posterior free edge of the thyrohyoid membrane, about halfway between the superior cornu of the thyroid cartilage and the tip of the greater cornu of the hyoid bone (Figs 34.1, 34.2). Their functions are unknown, although they may serve to strengthen this connection.

CALCIFICATION OF LARYNGEAL CARTILAGES

The thyroid, cricoid, and most of the arytenoid cartilages consist of hyaline cartilage, and may therefore become calcified. This process normally starts at about 18 years of age. Initially it involves the lower and posterior part of the thyroid cartilage, and subsequently spreads to involve the remaining cartilages, calcification of the arytenoid cartilage starting at its base. The degree and frequency of calcification of the thyroid and cricoid cartilages appear to be less in females. There is some evidence to suggest that a predilection for tumour invasion may be enhanced by calcification of the laryngeal cartilages.

The tip and upper portion of the vocal process of the arytenoid cartilage consists of non-calcifying, elastic cartilage. This may have considerable functional significance: the vocal process may bend at the elastic cartilage during adduction and abduction, and the two arytenoid cartilages will contact mainly at their ‘elastic’ superior portions during adduction.

JOINTS

CRICOTHYROID JOINT

The joints between the inferior cornua of the thyroid cartilage and the sides of the cricoid cartilage are synovial. Each is enveloped by a capsular ligament strengthened posteriorly by fibrous bands (Figs 34.1, 34.2, 34.4). Both capsule and ligaments are rich in elastin fibres. The primary movement at the joint is rotation around a transverse axis which passes transversely through both cricothyroid joints. The effect of this rotation is to move the cricoid and thyroid cartilages relative to one another in such a way as to bring together the lamina of the thyroid cartilage and the arch of the cricoid cartilage (‘closing the visor’). There is some controversy as to which cartilage moves, but it seems most likely that the cricoid cartilage rotates to a greater extent. When the joint is in a neutral position, the ligaments are slack and the cricoid can glide, to a limited extent, in different directions on the thyroid cornua. The effect of these movements is to lengthen the vocal folds, provided the arytenoid cartilages are stabilized at the cricoarytenoid joint. This may also increase vocal fold tension.

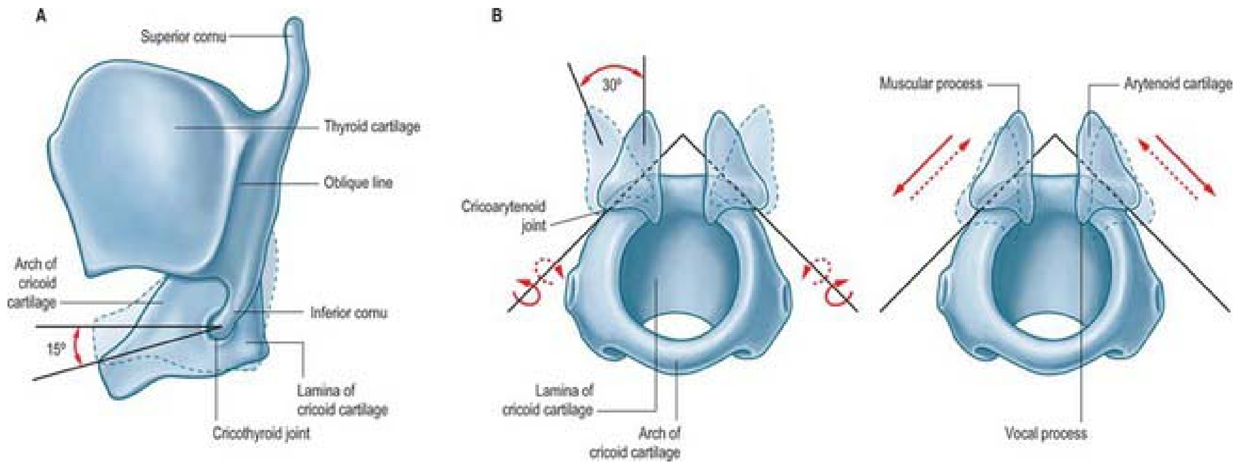
A
Superior cornu
Thyroid cartilage
Oblique line
Arch of cricoid cartilage
Inferior cornu
15°
Lamina of cricoid cartilage
Cricothyroid joint
B
30°
Muscular process
Arytenoid cartilage
Cricoarytenoid joint
Lamina of cricoid cartilage
Arch of cricoid cartilage
Vocal process

Fig. 34.4 **A**, Lateral view of the cricothyroid joint. **B**, Anterosuperior view of the cricoarytenoid joint.

CRICOARYTENOID JOINT

The cricoarytenoid joints are a pair of synovial joints between the facets on the lateral parts of the upper border of the lamina of the cricoid cartilage and the bases of the arytenoids. Each joint is enclosed by a capsular ligament and strengthened by a ligament that, although traditionally called the posterior cricoarytenoid ligament, is largely medial in position (Figs 34.1-34.4).

The cricoid facets are elliptical, convex and obliquely directed laterally, anteriorly and downwards. The long axes of the two facets intersect posteriorly at an angle of about 50°. Two movements occur at this joint. The first is rotation of the arytenoid cartilages at right angle to the long axis of the cricoid facet (dorso-medio-cranial to ventro-latero-caudal), which, because of its obliquity, causes each vocal process to swing laterally or medially, thereby increasing or decreasing the width of the rima glottidis. This movement is sometimes referred to as a rocking movement of the arytenoid cartilages. There is also a gliding movement, by which the arytenoids approach or recede from one another, the direction and slope of their articular surfaces imposing a forward and downward movement on lateral gliding. The movements of gliding and rotation are associated, i.e. medial gliding occurs with medial rotation and lateral gliding with lateral rotation, resulting in adduction or abduction of the vocal folds respectively. When viewed from above, foreshortening can give the illusion that the arytenoid cartilages are rotating about their vertical axes, but the shape of the facets prevents such movement occurring. The posterior cricoarytenoid ligaments limit forward movements of the arytenoid cartilages on the cricoid cartilage. It has been suggested that the ‘rest’ position of the cricoarytenoid ligament is a major determinant of the position of a denervated vocal cord.

ARYTENOCORNICULATE JOINTS

Synovial or cartilaginous joints link the arytenoid and corniculate cartilages.

INNERVATION OF THE CRICOTHYROID, CRICOARYTENOID AND ARYTENOCORNICULATE JOINTS

The cricothyroid, cricoarytenoid and arytenocorniculate joints are innervated by branches of the recurrent laryngeal nerves, which arise either independently or from branches of the nerve to the laryngeal muscles. The capsules of the laryngeal joints contain numerous lamellated (Pacinian) corpuscles, Ruffini corpuscles and free nerve endings.

SOFT TISSUES

The skeletal framework of the larynx is joined to surrounding structures by extrinsic membranes. It is also interconnected by intrinsic ligaments and fibroelastic membranes, of which the thyrohyoid, quadrangular and cricothyroid membranes and the conus elasticus are the most significant. The thyrohyoid membrane is external to the larynx, whereas the paired quadrangular membranes, the cricothyroid membrane and the conus elasticus are internal. The named ligaments are the median (anterior) cricothyroid ligament, the hyoepiglottic and thyroepiglottic ligaments and the cricotracheal ligament.

EXTRINSIC LIGAMENTS AND MEMBRANES

Thyrohyoid membrane

The thyrohyoid membrane is a broad, fibroelastic layer attached below to the superior border of the thyroid cartilage lamina and the front of its superior cornua, and above to the superior margin of the body and greater cornua of the hyoid (Figs 34.1, 34.2, 34.5). It thus ascends behind the concave posterior surface of the hyoid, separated from its body by a bursa which facilitates the ascent of the larynx during swallowing. Its thicker part is the median thyrohyoid ligament. The more lateral, thinner, parts are pierced by the superior laryngeal vessels and internal laryngeal nerves (Fig. 34.1). Externally, it is in contact with thyrohyoid and omohyoid and the body of the hyoid bone. Its inner surface is related to the lingual surface of the epiglottis and the piriform fossae of the pharynx. The round, cord-like, elastic lateral thyrohyoid ligaments form the posterior borders of the thyrohyoid membrane, and connect the tips of the superior thyroid cornua to the posterior ends of the greater hyoid cornua (Fig. 34.1).

Hyo- and thyroepiglottic ligaments

The epiglottis is attached to the hyoid bone and thyroid cartilage by the extrinsic hyoepiglottic and intrinsic thyroepiglottic ligaments respectively.

Cricotracheal ligament

The cricotracheal ligament unites the lower border of the cricoid to the first tracheal cartilage, and is thus continuous with the perichondrium of the trachea (Fig. 34.1).

INTRINSIC LIGAMENTS AND MEMBRANES

The fibroelastic membrane of the larynx lies within the cartilaginous skeleton of the larynx, beneath the laryngeal mucosa (Fig. 34.5). It forms a discontinuous sheet separated on both sides of the larynx by a horizontal cleft between the vestibular and vocal ligaments. Its upper part, the quadrangular membrane, extends between the arytenoid cartilages and the sides of the epiglottis. Its lower part, the cricothyroid membrane and conus elasticus, connects the thyroid, cricoid and arytenoid cartilages.

Quadrangular membrane

Each quadrangular membrane passes from the lateral margin of the epiglottis to the ipsilateral arytenoid cartilage. It is often poorly defined, especially in its upper portion. The upper and lower borders of the membrane are free. The upper border slopes posteriorly to form the aryepiglottic ligament, which constitutes the central component of the aryepiglottic fold. Posteriorly, it passes through the fascial plane of the oesophageal suspensory ligament, and helps to form the median corniculopharyngeal ligament which extends into the submucosa adjacent to the cricoid cartilage. This ligament may exert vertical traction on the tissues of the laryngopharynx. The cuneiform cartilages lie within the aryepiglottic folds. The lower border of the quadrangular membrane forms the vestibular fold.

Cricothyroid membrane and the conus elasticus

The cricothyroid ligament is composed mainly of elastic tissue. It consists of two parts: the cricothyroid membrane below and the conus elasticus above.

Cricothyroid membrane and median (anterior) cricothyroid ligament

The cricothyroid membrane passes upwards from the upper border of the cricoid cartilage to the lower border of the thyroid cartilage. Anteriorly, it is thickened to form the median (anterior) cricothyroid ligament, which is broader below and narrower above.

Conus elasticus

In part or in whole, the conus elasticus has been variously described as the cricovocal membrane, cricothyroid ligament or lateral cricothyroid ligament. The conus elasticus is thinner than the anterior cricothyroid ligament. It arises beneath the cricothyroid membrane on both sides from the inner surface of the cricoid cartilage, near its lower margin, and passes upwards beneath the lower border of the thyroid cartilage. It is attached anteriorly to the inner surface of the angle of the thyroid cartilage (just below its midpoint) and posteriorly to the tip of the vocal process of the arytenoid cartilage. Between these attachments, the upper edge of the conus elasticus is free, horizontally aligned and thickened to form the vocal ligament, which lies within the mucosa-covered vocal fold. It is covered internally by mucosa and externally by lateral cricoarytenoid and thyroarytenoid. The conus elasticus derives its name from the cone or funnel shape produced by the superior and medial curving of its walls between its inferior and superior attachments. This is said to maximize efficient flow of air towards the rima glottidis during phonation.

LARYNGEAL CAVITY

The laryngeal cavity extends from the laryngeal inlet (from the pharynx) down to the lower border of the cricoid cartilage, where it continues into the trachea (Figs 34.5, 34.6). The walls of the cavity are formed of the fibroelastic membranes described above and are lined with mucous membrane which folds over the free edges of these fibroelastic membranes within the larynx. On either side, the continuity of the fibroelastic membrane is interrupted between the upper and lower folds.

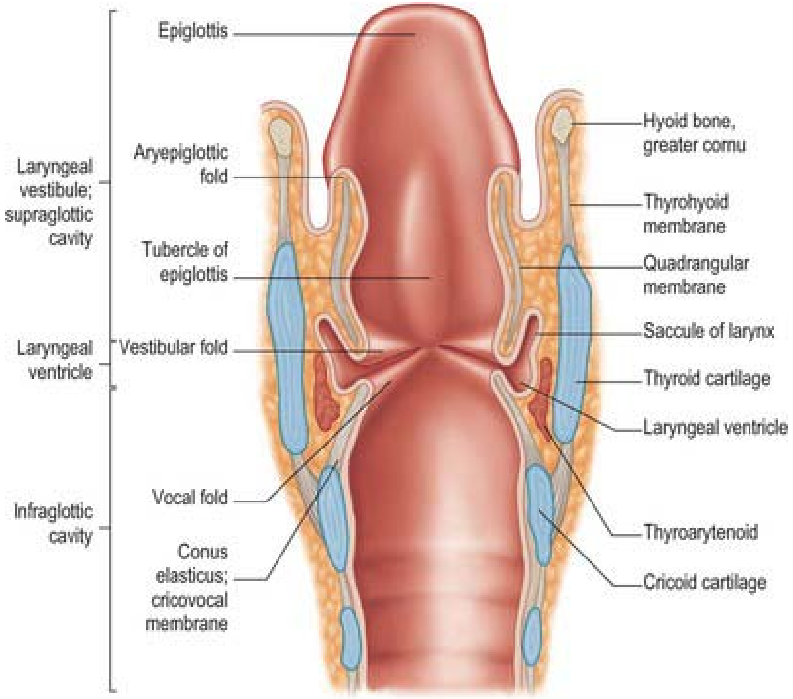
Laryngeal vestibule; supraglottic cavity
Laryngeal ventricle
Infraglottic cavity
Epiglottis
Aryepiglottic fold
Tubercle of epiglottis
Vestibular fold
Vocal fold
Conus elasticus; cricovocal membrane
Hyoid bone, greater cornu
Thyrohyoid membrane
Quadrangular membrane
Saccule of larynx
Thyroid cartilage
Laryngeal ventricle
Thyroarytenoid
Cricoid cartilage

Fig. 34.6 Coronal section through the larynx and the cranial end of the trachea: posterior aspect.

The folds project into the lumen of the cavity and divide it into upper and lower parts, separated by a middle portion between the two sets of folds leading into the laryngeal ventricle. The upper folds are the vestibular (ventricular or false vocal) folds; the median aperture which they guard is the rima vestibuli. The lower pair are the (true) vocal folds (or vocal cords), and the fissure between them is the rima glottidis or glottis. The true vocal folds are the primary source of phonation, whereas the vestibular folds normally do not contribute directly to sound production. The clinical term supraglottis refers to the part of the larynx that lies above the glottis and comprises the laryngeal inlet formed of the laryngeal surface of the epiglottis and arytenoid cartilages and the laryngeal aspects of the aryepiglottic folds, the laryngeal vestibule (introitus) and the vestibular folds.

MICROSTRUCTURE OF THE LARYNX

The laryngeal mucosa is continuous with that of the pharynx above and the trachea below. It lines the entire inner surface of the larynx, including the ventricle and saccule, and is thickened over the vestibular folds, where it is the chief component. Over the vocal folds it is thinner, and is firmly attached to the underlying vocal ligaments. It is loosely adherent to the anterior surface of the epiglottis, but firmly attached to its anterior surface and the floor of the valleculae. On the aryepiglottic folds it is reinforced by a considerable amount of fibrous connective tissue, and it adheres closely to the laryngeal surfaces of the cuneiform and arytenoid cartilages.

The laryngeal epithelium is mainly a ciliated, pseudostratified respiratory epithelium where it covers the inner aspects of the larynx, including the posterior, laryngeal surface of the epiglottis, and it provides a mucociliary clearance mechanism shared with most of the respiratory tract (see Ch. 57). However, the vocal folds are covered by non-keratinized, stratified squamous epithelium where they contact each other: this important variation protects the tissue from the effects of the considerable mechanical stresses that act on the surfaces of the vocal folds. The exterior surfaces of the larynx, which merge with the laryngopharynx and oropharynx (including the anterior, lingual surface of the epiglottis and the aryepiglottic folds), are subject to the abrasive effects of swallowed food, and are therefore covered by non-keratinized, stratified squamous epithelium.

The laryngeal mucosa has numerous mucous glands, especially over the epiglottis, where they pit the cartilage, and along the margins of the aryepiglottic folds anterior to the arytenoid cartilages, where they are known as the arytenoid glands. Many large glands in the saccules of the larynx secrete periodically over the vocal folds during phonation. The free edges of these folds are devoid of glands, and their stratified epithelium is vulnerable to drying and requires the secretions of neighbouring glands: hoarseness as a result of excessive speaking is due to partial temporary failure of this secretion. The epithelial surfaces are ridged and this may help retain the lubricating secretions over the surfaces of the edges of the folds. Poorly lubricated folds offer increased resistance to airflow, which means that higher subglottal pressures are needed to initiate phonation. Taste buds, like those in the tongue, occur on the posterior epiglottic surface, aryepiglottic folds and less often in other laryngeal regions.

UPPER PART

The upper part of the laryngeal cavity contains the laryngeal inlet (aditus), the aryepiglottic fold and the laryngeal vestibule (introitus).

Laryngeal inlet (aditus)

The upper part of the laryngeal cavity is entered by the laryngeal inlet (aditus laryngis), the aperture between the larynx and pharynx. This faces backwards and somewhat upwards, because the anterior wall of the larynx is much longer than the posterior (and slopes downwards and forwards in its upper part because of the oblique inclination of the epiglottis). The inlet is bounded anteriorly by the upper edge of the epiglottis, posteriorly by the transverse mucosal fold between the two arytenoids (posterior commissure), and on each side by the edge of a mucosal ridge, the aryepiglottic fold, that runs between the side of the epiglottis and the apex of the arytenoid cartilage. The midline groove between the two corniculate tubercles is termed the interarytenoid notch.

Aryepiglottic fold

The aryepiglottic fold contains ligamentous and muscular fibres. The ligamentous fibres represent the free upper border of the quadrangular membrane (Fig. 34.5). The muscle fibres are continuations of the oblique arytenoids. The posterior part of the aryepiglottic fold contains two oval swellings, one above and in front, the other behind and below, that mark the positions of the underlying cuneiform and corniculate cartilages respectively. They are separated by a shallow vertical furrow which is continuous below with the opening of the laryngeal ventricle.

Laryngeal vestibule (introitus)

Vestibule is a clinical term that denotes the space between the laryngeal inlet and vestibular folds. It is wide above, narrow below, and higher anteriorly than posteriorly. Its anterior wall is formed by the posterior surface of the epiglottis, the lower part of which (epiglottic tubercle) bulges backwards a little. Its lateral walls, which are higher in front and shallow behind, are formed by the medial surfaces of the aryepiglottic folds. Its posterior wall consists of the interarytenoid mucosa above the ventricular folds.

MIDDLE PART

The middle part of the laryngeal cavity is the smallest, and extends from the rima vestibuli above to the rima glottidis below. On each side it contains the vestibular folds, the ventricle and the saccule of the larynx.

Vestibular folds and ligaments

The narrow vestibular ligament represents the thickened lower border of the quadrangular membrane (Fig. 34.5). It is fixed in front to the thyroid angle below the epiglottic cartilage and behind to the anterolateral surface of the arytenoid cartilage above its vocal process. With its covering of mucosa, it is termed the vestibular (ventricular or false vocal) fold (Figs 34.5, 34.6). The presence of a loose vascular mucosa lends the vestibular folds a pink appearance *in vivo*, as they lie above and lateral to the vocal cords.

Ventricle (sinus) of the larynx

The laryngeal ventricle is a slit between the vestibular and vocal cords (Figs 34.5, 34.6). It opens into a fusiform recess on each side of the larynx and extends upwards into the laryngeal wall lateral to the vestibular fold, opening into the saccule.

Saccule of the larynx

The saccule is a pouch which ascends forwards from the ventricle, between the vestibular fold and thyroid cartilage, and occasionally reaches the upper border of the cartilage (Fig. 34.6). It is conical, and curves slightly backwards; 60–70 mucous glands, sited in the submucosa, open onto its luminal surface. The orifice of the saccule is guarded by a delicate fold of mucosa, the ventriculosaccular fold.

The saccule has a fibrous capsule that is continuous below with the vestibular ligament. It is covered medially by a few muscular fasciculi from the apex of the arytenoid cartilage which pass forwards between the saccule and vestibular mucosa into the aryepiglottic fold, and laterally it is separated from the thyroid cartilage by the thyroepiglottic muscle. The latter compresses the saccule, expressing its secretion onto the vocal cords, which lack glands, to lubricate and protect them against desiccation and infection. Saccules occasionally protrude through the thyrohyoid membrane.

Laryngoceles and saccular cysts

Laryngoceles and saccular cysts are air- or fluid-filled enlargements of the saccule. A laryngocele is a herniation of the saccular mucosa. The aetiology is uncertain: repeated sustained high transglottal pressures (such as in trumpet playing) may be a possible cause of acquired symptoms, and some cases may be the result of congenital enlargement of the saccule. Growth of a laryngocele is constrained by the surrounding tissues, and so it expands upwards into the paraglottic space anterior to the piriform fossa, and superiorly to expand the aryepiglottic fold and reach the vallecula (internal laryngocele). It can extend to the thyrohyoid membrane, which it may pierce to form an external laryngocele, and where it may be palpable in the neck. Symptoms include hoarseness, stridor and dysphagia. The laryngeal saccule can also become pathologically enlarged as a result of obstruction of the ventricular aditus by inflammation, scarring, or compression by a tumour: an expanding mucus-filled cyst forms as the glandular secretions accumulate. These fluid-filled saccular cysts can expand in a similar direction to a laryngocele and may also pierce the thyrohyoid membrane. In addition to hoarseness and stridor, acute respiratory obstruction may occur, especially in the young, if the contents of the cyst become infected.

Vocal folds (cords) and ligaments

The free thickened upper edge of the conus elasticus forms the vocal ligament. It stretches back on either side from the mid level of the thyroid angle to the vocal processes of the arytenoids. When covered by mucosa, it is termed the vocal fold or vocal cord (cord is the preferred clinical term) (Figs 34.5, 34.6). The vocal folds form the anterolateral edges of the rima glottidis and are concerned with sound production. Each fold consists of five layers, namely mucosa, lamina propria (three layers) and the vocalis muscle (Fig. 34.7).

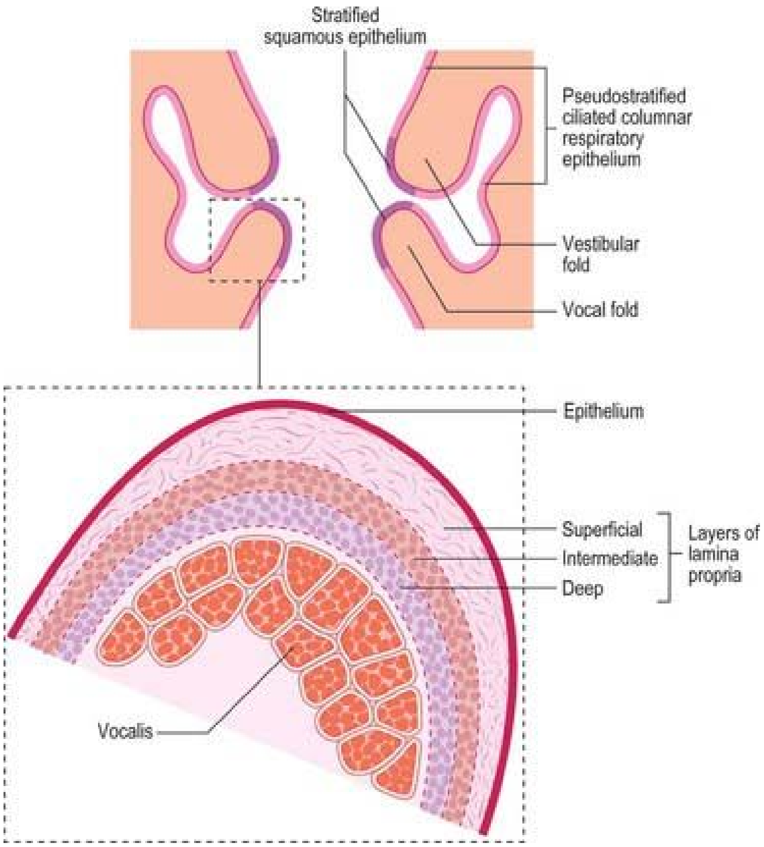
Stratified squamous epithelium
Pseudostratified ciliated columnar respiratory epithelium
Vestibular fold
Vocal fold
Epithelium
Superficial
Intermediate
Deep
Layers of lamina propria
Vocalis

Fig. 34.7 Coronal view of the laryngeal cavity, showing the distribution of the mucous membrane in the laryngeal cavity; the inset shows the structure of the true vocal folds.

The mucosa overlying the vocal ligament is thin and attached to the underlying lamina propria by a basement membrane. It lies directly on the ligament, and so the vocal fold appears pearly white *in vivo*. The lamina propria consists of three layers. The most superficial consists of loose collagen and elastic fibres, and is only loosely attached to the underlying vocal ligament, an arrangement that produces a potential space (Reinke’s space) that extends along the length of the free margin of the vocal ligament and a little way onto the superior surface of the cord: oedema fluid readily collects here in disease. The intermediate layer consists of elastic fibres, and the deep layer is formed of collagen fibres; these two layers collectively form the vocal ligament. Fibres of the vocalis muscle form the fifth layer of the vocal folds. The site where the vocal folds meet anteriorly is known as the anterior commissure, and is the region where fibres of the vocal ligament pass through the thyroid cartilage to blend with the overlying perichondrium, forming Broyle’s ligament. Since Broyle’s ligament contains blood vessels and lymphatics, it represents a potential route for the escape of malignant tumours from the larynx.

Reinke’s oedema

The mucous membrane is loosely attached throughout the larynx, and can accommodate considerable swelling which may compromise the airway in acute infections. At the edge of the true vocal folds the mucosal covering is tightly bound to the underlying ligament so that oedema fluid does not pass between the upper and lower compartments of the vocal cord mucosa. Any tissue swelling above the vocal cord exaggerates the potential space deep to the mucosa (Reinke’s space), causing accumulation of extracellular fluid and flabby swelling of the vocal cords (Reinke’s oedema). The oedema can persist because of the poor lymphatic drainage in this region of the larynx. Vocal abuse may initiate such changes, but the condition is nearly always confined to smokers.

Vocal cord nodules

Vocal fold nodules are chronic lesions of the vocal folds and develop most commonly as the result of persistent overuse of the voice which has caused an increase in vocal fold tension and a more forceful adduction. They normally develop at the point of maximum contact of the vocal folds, i.e. at the junction of the anterior third and the posterior two-thirds of the vocal ligament. Excessive trauma at this point, for example when singing with poor technique or forcing the voice, initially produces subepithelial haemorrhage or bruising; in time this results in pathological changes such as subepithelial scarring (‘singer’s nodes’ or ‘clergyman’s nodes’). Nodules increase vocal fold mass and affect vocal fold closure: the persistent posterior glottal opening causes hoarseness, a breathy voice, reduced vocal intensity and an inability to produce higher frequencies of vibration. These changes can cause a cycle in which increasing vocal effort is required by way of compensation, and this exacerbates the problem.

Rima glottidis

The rima glottidis or glottis is the fissure between the vocal cords anteriorly and the arytenoid cartilages posteriorly (see Figs 34.8, 34.9). It is bounded behind by the mucosa that passes between the arytenoid cartilages at the level of the vocal cords. The glottis is customarily divided into two regions, an anterior intermembranous part, which makes up about three-fifths of its anteroposterior length and is formed by the underlying vocal ligament, and a posterior intercartilaginous part formed by the vocal processes of the arytenoid cartilages. It is the narrowest part of the larynx, having an average sagittal diameter in adult males of 23 mm, and in adult females of 17 mm: its width and shape vary with the movements of the vocal cords and arytenoid cartilages during respiration and phonation (see p. 590).

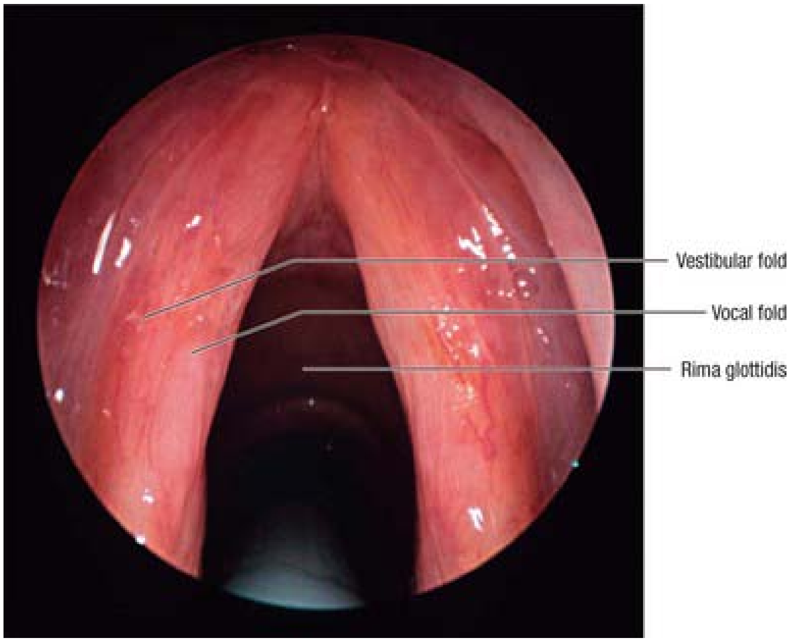

Fig. 34.8 The true vocal folds viewed through a fibre endoscope.

(By permission from Berkovitz BKB, Moxham BJ 2002. Head and Neck Anatomy. London: Martin Dunitz.)

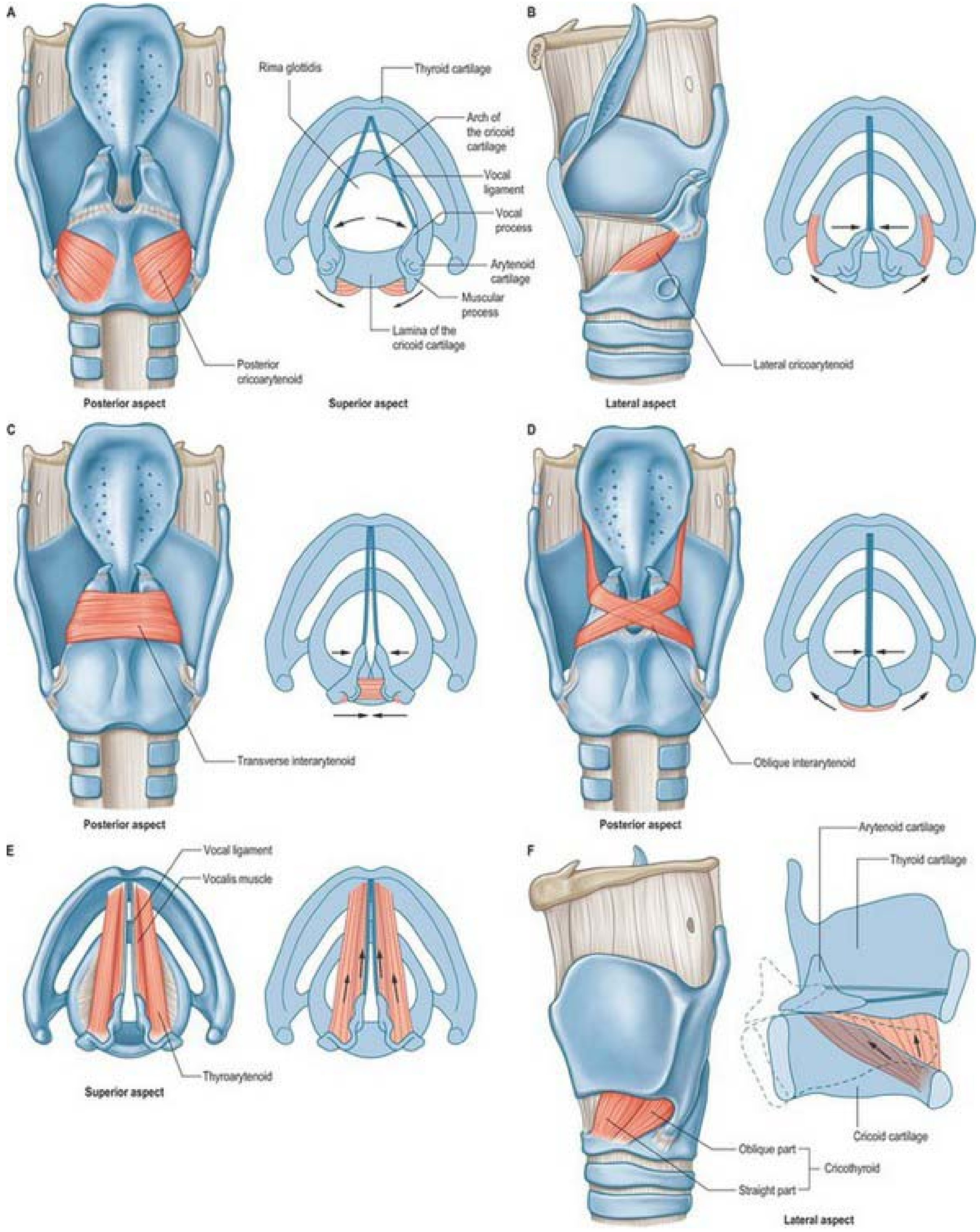
A
Rima glottidis
Thyroid cartilage
Arch of the cricoid cartilage
Vocal ligament
Vocal process
Arytenoid cartilage
Muscular process
Lamina of the cricoid cartilage
Posterior cricoarytenoid
Posterior aspect
Superior aspect
B
Lateral cricoarytenoid
Lateral aspect
C
Transverse interarytenoid
Posterior aspect
D
Oblique interarytenoid
Posterior aspect
E
Vocal ligament
Vocalis muscle
Thyroarytenoid
Superior aspect
F
Arytenoid cartilage
Thyroid cartilage
Cricoid cartilage
Oblique part
Straight part
Cricothyroid
Lateral aspect

Fig. 34.9 Intrinsic muscles of the larynx in posterior or lateral views with their actions shown alongside in a superior view. The arrows indicate the direction of movement of the cartilage in each case.

LOWER PART

The lower part of the laryngeal cavity, the subglottis or infraglottic cavity, extends from the vocal cords to the lower border of the cricoid. In transverse section it is elliptical above and wider and circular below, and is continuous with the trachea. Its walls are lined by respiratory mucosa, and supported by the cricothyroid ligament above and the cricoid cartilage below. The walls of this part of the laryngeal cavity are said to be exponentially curved, a feature that may serve to accelerate the airflow towards the glottis with the minimum loss of energy.

LARYNGOSCOPIC EXAMINATION

The laryngeal inlet, the structures around it, and the cavity of the larynx can all be inspected using fibreoptic endoscopy, through either the mouth or nasopharynx. The epiglottis is seen foreshortened, but its tubercle is visible. From the epiglottic margins the aryepiglottic folds can be traced posteromedially and the cuneiform and corniculate elevations recognized. The pink vestibular folds and pearly white vocal cords are visible and, when the rima glottidis is wide open, the anterior arch of the cricoid cartilage, the tracheal mucosa and cartilages may be seen (Fig. 34.8). The piriform fossae can also be inspected.

LARYNGEAL OBSTRUCTION AND TRAUMA

The mucosa of the upper larynx is highly sensitive, and contact with foreign bodies excites immediate coughing. Large foreign bodies may obstruct the laryngeal inlet or rima glottidis and suffocation may ensue. Smaller articles may enter the trachea or bronchi, or lodge in the laryng-eal ventricle and cause reflex closure of the glottis with subsequent suffocation. Inflammation of the upper larynx, e.g. secondary to infection or the effects of smoke inhalation, may swell the mucosa by effusion of fluid into the loose submucous tissue (oedema of the supraglottis). The effusion neither involves nor extends below the vocal cords, because the mucosa here is bound directly to the vocal ligaments and there is no submucous tissue. Laryngotomy below the vocal cords through the cricothyroid ligament, or tracheotomy below the cricoid cartilage, may be necessary to restore a free airway.

Suicidal wounds are usually made through the thyrohyoid membrane, damaging the epiglottis, superior thyroid vessels, external and internal carotid arteries and internal jugular veins. Less frequently, these wounds are inflicted above the hyoid, so that the lingual muscles and lingual and facial vessels are damaged.

THE INFANT LARYNX

The infant larynx differs markedly from its adult counterpart. Although it is about one-third adult size, it is proportionately larger. Its lumen is short and funnel-shaped and disproportionately narrower than that of the adult. It lies higher in the neck than the adult larynx (see Fig. 33.10). At rest, the upper border of the infant epiglottis is at the level of the second or third cervical vertebra; when the larynx is elevated, it reaches the level of the first cervical vertebra. This high position enables an infant to use its nasal airway to breathe while suckling. The epiglottis is X-shaped, with a furled petiole, and the laryngeal cartilages are softer and more pliable than in the adult larynx (which may predispose to airway collapse in inspiration, leading to the clinical picture of laryngomalacia). The thyroid cartilage is shorter and broader and lies closer to the hyoid bone in the neonate, which means that the thyrohyoid ligament is relatively short. Neither the superior notch nor the laryngeal prominence are as marked as they are in the adult. The cricoid cartilage is the same shape as in the adult. The arytenoid cartilages are more prominent and the aryepiglottic folds are disproportionally large. The vocal cords are 4–4.5 mm long, which is relatively shorter than in either childhood or the adult. The ventricle of the larynx is small, whereas the saccule of the larynx is often considerably larger than it is in adult life.

The mucosa of the supraglottis is more loosely attached than it is in the adult larynx and it exhibits multiple submucosal glands. Inflammation of the supraglottis will therefore rapidly result in gross oedema. The mucosa is also lax in the subglottis, the narrowest part of the infant larynx (3.5 mm in diameter in neonates). Swelling at this point rapidly results in severe respiratory obstruction because of the disproportionally narrower lumen. Unlike in the adult, the neonatal subglottic cavity extends posteriorly as well as inferiorly, which is an important consideration when passing an endotracheal tube.

By about the third year, sexual differences become apparent: the larynx is larger in boys, although the angle between the thyroid laminae is more pronounced in girls. At puberty these changes increase, and there is greater enlargement of the male larynx.

PARALUMENAL SPACES

A number of potential spaces lie between the laryngeal cartilages and the ligaments and membranes that support them. The three main spaces are the pre-epiglottic, the paraglottic and the subglottic spaces. Their precise definition, and the extent to which they communicate with one another, remain controversial. They are not closed compartments and so their existence does not preclude the spread of tumours. An awareness of the anatomy of these spaces, and the potential pathways of spread of tumours from them, has significantly influenced the surgical approach to disease in this region.

PRE-EPIGLOTTIC SPACE

Its name implies that the pre-epiglottic space lies anterior to the epiglottis; in reality, it also extends beyond the lateral margins of the epiglottis, an arrangement that gives it the form of a horseshoe. The space is primarily filled with adipose tissue and does not appear to contain any lymph nodes.

The upper boundary is formed by the weak hyoepiglottic membrane, strengthened medially as the median hyoepiglottic ligament. The anterior boundary is the thyrohyoid membrane, strengthened medially as the median thyrohyoid ligament, and the lower boundary is the thyroepiglottic ligament, continuous laterally with the quadrangular membrane behind. The greater cornu of the hyoid bone forms its upper lateral border. Inferolaterally, the pre-epiglottic space is in continuity with the paraglottic space, from where it is often invaded by the laryng-eal saccule. It is also in continuity with the mucosa of the laryngeal surface of the epiglottis via multiple perforations in the cartilage of the epiglottis. Malignancies of the laryngeal surface of the epiglottis may invade the fat and areolar tissue of the pre-epiglottic space through these perforations.

PARAGLOTTIC SPACE

The paraglottic space is a region of adipose tissue that contains the internal laryngeal nerve, the laryngeal ventricle, and all or part of the laryngeal saccule. It is bounded laterally by the thyroid cartilage and thyrohyoid membrane, superomedially by the quadrangular membrane, inferomedially by the conus elasticus, and posteriorly by the piriform fossa. The lower border of the thyroid cartilage is inferior, and the paraglottic space is continuous inferiorly with the space between the cricoid and thyroid cartilages. Anteroinferiorly, there are deficiencies in the paramedian gap at the side of the anterior cricothyroid ligament, and posteroinferiorly, adipose tissue extends towards the cricothyroid joint. Some authorities exclude thyroarytenoid from the paraglottic space. Superiorly, the space is usually continuous with the pre-epiglottic space, although the two spaces may be separated by a fibrous septum.

Supraglottic tumours may spread into the paraglottic space and reach the subglottis, or extend beyond the limits of the larynx. Ventricular tumours may obstruct mucus outflow from the saccule and cause its expansion within the paraglottic space to form a saccular cyst: the tumour itself may also spread transglottically, and thereby fix the vocal cord either by invasion of the cricoarytenoid joint or by damaging the recurrent laryngeal nerve. Fixation of the vocal cord is a good indicator of a tumour within the paraglottic space. The proximity of the mucosa at the piriform fossa makes its removal in surgery mandatory for such disease.

SUBGLOTTIC SPACE

The subglottic space is bounded laterally by the cricovocal membrane, medially by the mucosa of the subglottic region, and above by the undersurface of Broyle’s ligament in the midline. It is continuous below with the inner surface of the cricoid cartilage and its mucosa.

MUSCLES

The muscles of the larynx may be divided into extrinsic and intrinsic groups. The extrinsic muscles connect the larynx to neighbouring structures and are responsible for moving it vertically during phonation and swallowing. They include the infrahyoid strap muscles, thyrohyoid, sternothyroid and sternohyoid, and the inferior constrictor muscle of the pharynx. Two of the three elevator muscles of the pharynx, stylopharyngeus and palatopharyngeus, are also connected directly to the thyroid cartilage, mainly to the posterior aspect of the thyroid laminae and cornua.

The role of the extrinsic muscles during respiration appears to be variable: the larynx has been seen to rise, descend or barely move during inspiration. The extrinsic muscles can affect the pitch and the quality of the voice by raising or lowering the larynx, and geniohyoid elevates and anteriorly displaces the larynx, particularly during deglutition.

The intrinsic muscles are the cricothyroid, posterior and lateral cricoarytenoid, transverse and oblique arytenoid, aryepiglotticus, thyroarytenoid and its subsidiary part, vocalis, and thyroepiglotticus: all are confined to the larynx in their attachments, and all but the transverse arytenoid are paired (Fig. 34.9). Whereas most of the intrinsic muscles lie internally, under cover of the thyroid cartilage or the mucosa, the cricothyroids appear on the outer aspect of the larynx.

The intrinsic laryngeal muscles may be placed in three groups according to their main actions. The posterior and lateral cricoarytenoids and oblique and transverse arytenoids vary the dimensions of the rima glottidis. The cricothyroids, posterior cricoarytenoids, thyroarytenoids and vocales regulate the tension of the vocal ligaments. In reality, the obliquity of the cricoarytenoid facets means that some functional overlap between these two muscle groups is inevitable. Thus, alterations in the dimensions of the rima glottidis will produce small changes in vocal fold length, and shortening the vocal folds will also result in a degree of adduction. The oblique arytenoids, aryepiglottic and thyroepiglottic muscles modify the laryngeal inlet. Bilateral pairs of muscles usually act in concert with each other.

Neuromuscular spindles have been found in all human laryngeal muscles, the maximum number (23) being found in the transverse arytenoid. The control of phonation requires very considerable neuromuscular coordination, and effective proprioception would appear to be essential to this capacity. The mass of muscle related to adduction far outweighs that related to abduction. In this context, it is of interest to note that histological examination of normal larynges revealed evidence of some degenerative changes in posterior cricoarytenoid, the single muscle associated with abduction, but none in the remaining muscles.

INTRINSIC MUSCLES

Oblique arytenoid and aryepiglotticus

The oblique arytenoids lie superficial to the transverse arytenoid, and are sometimes considered to be part of it. They cross each other obliquely at the back of the larynx, each extending from the back of the muscular process of one arytenoid cartilage to the apex of the opposite one. Some fibres continue laterally round the arytenoid apex into the aryepiglottic fold, forming the aryepiglottic muscle.

Vascular supply

Oblique arytenoid receives its blood supply from the laryngeal branches of the superior and inferior thyroid arteries.

INNERVATION

Oblique arytenoid is innervated by the recurrent laryngeal nerve.

Actions

The oblique arytenoids and aryepiglottic muscles act as a sphincter of the laryngeal inlet by adducting the aryepiglottic folds, and approximating the arytenoid cartilages to the tubercle of the epiglottis. Their poor development limits their capacity to act as a sphincter of the inlet. The oblique interarytenoids are weak adductors of the vocal folds, and may be more effective in this action than the transverse interarytenoids because of the superior mechanical advantage.

Transverse (inter) arytenoid

Transverse arytenoid is a single, unpaired muscle deep to the oblique interarytenoids (Fig. 34.9C). It bridges the gap at the back of the larynx between the two arytenoid cartilages and fills their posterior concave surfaces. It is attached to the back of the muscular process and adjacent lateral border of both arytenoids.

Vascular supply

Transverse arytenoid receives its blood supply from the laryngeal branches of the superior and inferior thyroid arteries.

Innervation

Transverse arytenoid is innervated by the recurrent laryngeal nerves. It also receives branches from the internal laryngeal nerve, although there is debate as to whether these branches contain any distinct motor input. The nerves form a dense, but highly variable, plexus.

Actions

Transverse arytenoid pulls the arytenoid cartilages towards each other, closing the posterior, intercartilaginous, part of the rima glottidis, such as occurs during a whisper (Fig. 34.9C). This action is accomplished by drawing the arytenoids upwards to slide along the sloping shoulders of the cricoid lamina, without rotation.

Posterior cricoarytenoid

Posterior cricoarytenoid arises from the posterior surface of the cricoid lamina (Fig. 34.9A). Its fibres ascend laterally and converge to insert on the upper and posterior surfaces of the muscular process of the ipsilateral arytenoid cartilage. The highest fibres run almost horizontally, the middle obliquely, and the lowest are almost vertical: some reach the anterolateral surface of the arytenoid cartilage. An additional strip of muscle, ceratocricoid, is occasionally seen in relation to the lower border of posterior cricoarytenoid, arising from the cricoid cartilage and inserting onto the posterior aspect of the inferior cornu of the thyroid cartilage.

Vascular supply

Posterior cricoarytenoid receives its blood supply from the laryngeal branches of the superior and inferior thyroid arteries.

Innervation

Posterior cricoarytenoid is innervated by the recurrent laryngeal branch of the vagus.

Actions

The posterior cricoarytenoids are the only laryngeal muscles that open the glottis. They rotate the arytenoid cartilages laterally around an axis that passes through the cricoarytenoid joints, producing separation of the vocal processes and the attached vocal cords (Fig. 34.9A). They also pull the arytenoids backwards, assisting the cricothyroids to lengthen the vocal cords. The most lateral fibres draw the arytenoid cartilages laterally, and so the rima glottidis becomes triangular when the posterior cricoarytenoid muscles contract. The posterior cricoarytenoids are active in the production of unvoiced sounds.

Lateral cricoarytenoid

Lateral cricoarytenoid is attached anteriorly to the upper border of the cricoid arch. It ascends obliquely backwards to be attached to the front of the muscular process of the ipsilateral arytenoid cartilage (Fig. 34.9B).

Vascular supply

Lateral cricoarytenoid receives its blood supply from the laryngeal branches of the superior and inferior thyroid arteries.

Innervation

Lateral cricoarytenoid is innervated by one to six branches of the anterior terminal division of the recurrent laryngeal nerve, with the most frequent pattern consisting of three branches. In the majority of cases, these branches arise over the muscle itself.

Actions

Lateral cricoarytenoid rotates the arytenoid cartilage in a direction opposite to that of posterior cricoarytenoid, and so closes the rima glottidis (Fig. 34.9B). As it does so, it brings the tips of the vocal processes together, closing the ligamentous part of the rima glottidis, an action known as medial compression. The action of lateral cricoarytenoid in adducting the vocal folds is therefore distinct and complementary to that of the interarytenoid muscles. Contraction of lateral cricoarytenoid also results in shortening and relaxing of the vocal folds.

Cricothyroid

Cricothyroid is attached anteriorly to the external aspect of the arch of the cricoid cartilage (Fig. 34.9F). Its fibres pass backwards and diverge into two groups, a lower 'oblique' part which slants backwards and laterally to the anterior border of the inferior cornu of the thyroid, and a superior 'straight' part which ascends more steeply backwards to the posterior part of the lower border of the thyroid lamina. The medial borders of the paired cricothyroids are separated anteriorly by a triangular gap occupied by the median cricothyroid ligament.

Vascular supply

Cricothyroid is supplied by the cricothyroid artery, a branch of the superior thyroid artery, which crosses high on the cricothyroid ligament to communicate with its contralateral fellow.

Innervation

Unlike the other intrinsic muscles of the larynx, cricothyroid is innervated by the external branch of the superior laryngeal nerve, and not by the recurrent laryngeal nerve.

Actions

Cricothyroid lengthens and affects tension in the vocal folds. It does this by shortening the space between the inferior border of the thyroid cartilage and the cricoid cartilage, an action that increases the distance between the tip of the vocal process of the arytenoid cartilage and the posterior surface of the thyroid lamina. Rotation occurs at the cricothyroid joint: it remains unclear which cartilage rotates to a greater extent, although the consensus appears to be that the predominant rotation is by the cricoid. At the same time, the posterior part of cricothyroid pulls the thyroid cartilage forwards, and this gliding action also lengthens the vocal folds.

Thyroarytenoid and vocalis

Thyroarytenoid is a broad, thin muscle, lying lateral to the vocal fold, conus elasticus, laryngeal ventricle and saccule (Fig. 34.9E). It is attached anteriorly to the lower half of the angle of the thyroid cartilage, and to the cricothyroid ligament. Its fibres pass backwards, laterally and upwards to the anterolateral surface of the arytenoid cartilage. The lower and deeper fibres form a band which, in coronal section, appears as a triangular bundle attached to the lateral surface of the vocal process and to the inferior impression on the anterolateral surface of the arytenoid cartilage. This bundle, the vocalis muscle, is parallel with, and just lateral to, the vocal ligament. It is said to be thicker behind than in front, because many deeper fibres start from the vocal ligament and do not extend to the thyroid cartilage. (An alternative view is that all its fibres loop and intertwine as they pass from the thyroid to the arytenoid cartilage.) A few fibres extend along the wall of the ventricle from the lateral margin of the arytenoid cartilage to the side of the epiglottis. Superior thyroarytenoid, an inconstant small muscle, lies on the lateral surface of the main mass of thyroarytenoid; when present, it extends obliquely from the thyroid angle to the muscular process of the arytenoid cartilage.

Vascular supply

Thyroarytenoid receives its arterial blood supply from the laryngeal branches of the superior and inferior thyroid arteries.

Innervation

All parts of thyroarytenoid are supplied by the recurrent laryngeal nerve. It also receives a communicating branch from the external laryngeal nerve, although it is not clear whether such branches carry motor or sensory fibres.

Actions

The thyroarytenoids draw the arytenoid cartilages towards the thyroid cartilage, thereby shortening and relaxing the vocal ligaments. At the same time, they rotate the arytenoids medially to approximate the vocal folds and so aid closure of the rima glottidis. Relaxation of the posterior parts of the vocal ligaments by the vocalis muscles, combined with tension in the anterior parts of the ligaments, is responsible for raising the pitch of the voice. Vocalis can change the timbre of the voice by affecting the mass of the vocal cords.

Thyroepiglotticus

Many of the fibres of thyroarytenoid are prolonged into the aryepiglottic fold, where some terminate, and others continue to the epiglottic margin as thyroepiglotticus. The thyroepiglottics can widen the inlet of the larynx by their action on the aryepiglottic folds.

VASCULAR SUPPLY AND LYMPHATIC DRAINAGE

The blood supply of the larynx is derived mainly from the superior and inferior laryngeal arteries (Fig. 34.10). Rich anastomoses exist between the corresponding contralateral laryngeal arteries and between the ipsilateral laryngeal arteries. The superior laryngeal arteries supply the greater part of the tissues of the larynx, from the epiglottis down to the level of the vocal cords, including the majority of the laryngeal musculature. The inferior laryngeal artery supplies the region around cricothyroid, while its posterior laryngeal branch supplies the tissue around posterior cricoarytenoid.

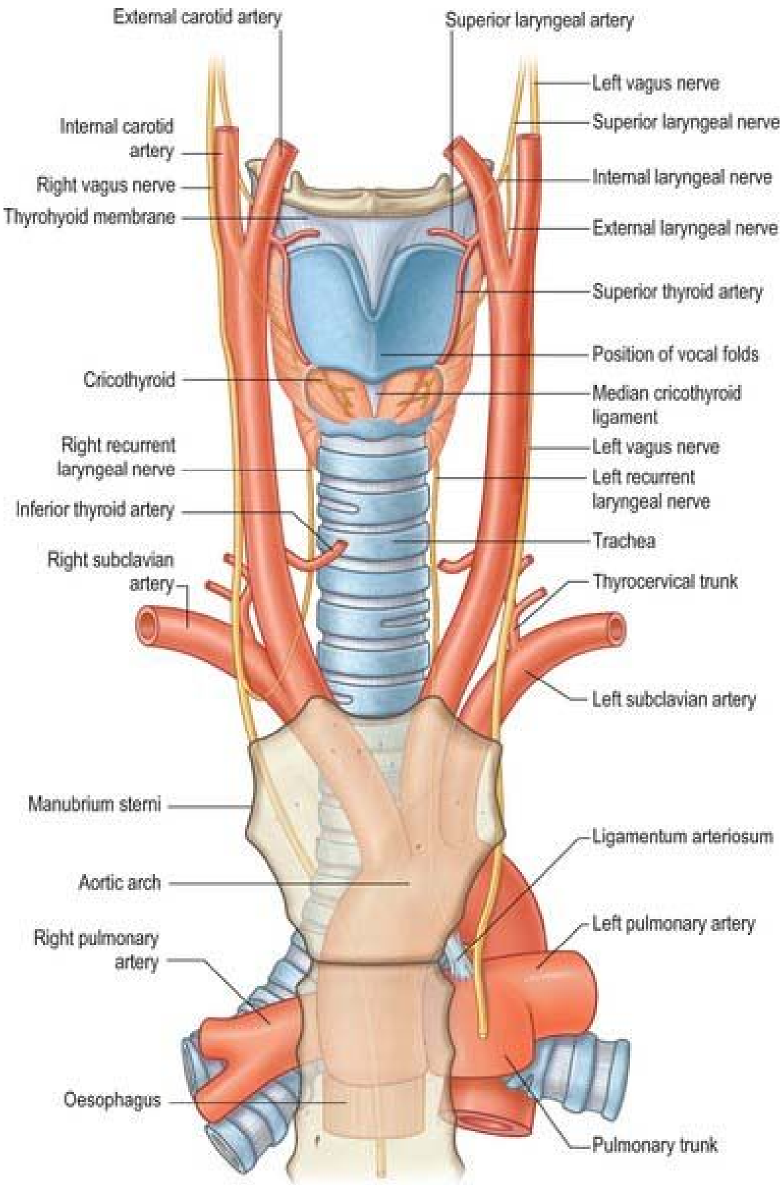
External carotid artery
Superior laryngeal artery
Left vagus nerve
Superior laryngeal nerve
Internal carotid artery
Right vagus nerve
Internal laryngeal nerve
Thyrohyoid membrane
External laryngeal nerve
Superior thyroid artery
Position of vocal folds
Cricothyroid
Median cricothyroid ligament
Right recurrent laryngeal nerve
Left vagus nerve
Left recurrent laryngeal nerve
Inferior thyroid artery
Trachea
Right subclavian artery
Thyrocervical trunk
Left subclavian artery
Manubrium sterni
Ligamentum arteriosum
Aortic arch
Left pulmonary artery
Right pulmonary artery
Oesophagus
Pulmonary trunk

Fig. 34.10 Anterior view of the blood supply and innervation of the larynx.

(From Drake, Vogl and Mitchell 2005.)

Superior laryngeal artery

The superior laryngeal artery is normally derived from the superior thyroid artery, a branch of the external carotid artery, as this artery passes down towards the upper pole of the thyroid gland. However, sometimes it arises directly from the external carotid artery between the origins of the superior thyroid and lingual arteries. The superior laryngeal artery runs down towards the larynx, with the internal branch of the superior laryngeal nerve lying above it. It enters the larynx by penetrating the thyrohyoid membrane and divides into a number of branches which supply the larynx from the tip of the epiglottis down to the inferior margin of thyroarytenoid. It anastomoses with its contralateral fellow and with the inferior laryngeal branch of the inferior thyroid artery.

Cricothyroid artery

The cricothyroid artery arises from the superior thyroid artery and may contribute to the supply of the larynx. It follows a variable course either superficial or deep to sternothyroid. If superficial, it may be accompanied by branches of the ansa cervicalis, and if deep, it may be related to the external laryngeal nerve. It can anastomose with the artery of the opposite side and with the laryngeal arteries.

Inferior laryngeal artery

The inferior laryngeal artery is smaller than the superior laryngeal artery. It is a branch of the inferior thyroid artery, which arises from the thyrocervical trunk of the subclavian artery. It ascends on the trachea with the recurrent laryngeal nerve, enters the larynx at the lower border of the inferior constrictor, just behind the cricothyroid articulation, and supplies the laryngeal muscles and mucosa. The inferior laryngeal artery anastomoses with its contralateral fellow and with the superior laryngeal branch of the superior thyroid artery.

A posterior laryngeal artery of variable size has been described as a regular feature that arises as an internal branch of the inferior thyroid artery.

Superior and inferior laryngeal veins

Venous return from the larynx occurs via superior and inferior laryngeal veins which run parallel to the laryngeal arteries and are tributaries of the superior and inferior thyroid veins respectively. The superior thyroid vein drains into the internal jugular vein, and the inferior thyroid vein usually into the left brachiocephalic vein.

LYMPHATIC DRAINAGE

The vocal cords, with their firmly bound mucosa and paucity of lymphatics, provide a clear demarcation between the upper and lower areas of the larynx. Above the vocal cords, the lymph vessels draining the supraglottic part of the larynx accompany the superior laryngeal artery, pierce the thyrohyoid membrane, and end in the upper deep cervical lymph nodes, often bilaterally. The supraglottic lymphatics also communicate with those at the base of the tongue. Below the vocal cords, some of the lymph vessels pass through the conus elasticus to reach the prelaryngeal (Delphian) and/or pretracheal and paratracheal lymph nodes, while others accompany the inferior laryngeal artery and join the lower deep cervical nodes.

Spread of supra- and subglottic tumours

The upper deep cervical lymph nodes act as pathways of spread for malignant tumours of the supraglottic larynx: up to 40% of these tumours will have undergone such spread at the time of clinical presentation. The glottis is very poorly endowed with lymphatic vessels: 95% of malignant tumours confined to the glottis will present with a change in voice or airway obstruction but will not show signs of spread to adjacent lymph nodes at presentation. Tumours of the subglottic larynx will often spread to the paratracheal lymph node chain prior to clinical presentation. However, the presenting symptoms may be voice change and airway obstruction rather than a mass in the neck, because the paratracheal lymph nodes occupy a deep-seated position in the root of the neck and so their enlargement may remain occult.

INNERVATION

The larynx is innervated by the internal and external branches of the superior laryngeal nerve, the recurrent laryngeal nerve and sympathetic nerves (Figs 34.10, 34.11). Conventionally, the internal laryngeal nerve is described as sensory, the external laryngeal nerve as motor, and the recurrent laryngeal nerve as mixed. The internal laryngeal nerve is sensory down to the vocal cords, the recurrent laryngeal nerve is sensory below the vocal cords, and there is overlap between the territories innervated by the two nerves at the vocal cords themselves. All the intrinsic muscles of the larynx are supplied by the recurrent laryngeal nerve except for cricothyroid, which is supplied by the external laryngeal nerve. However, a number of anastomoses between these three nerves have been described, with varying estimates of their incidence. The majority occur on the posterior surface of the larynx, forming what has been described as a laryngeal plexus to parallel the pharyngeal plexus. Their precise nature and function is unclear, but since some are thought to convey motor fibres, it is reasonable to assume that functions commonly ascribed to the three laryngeal nerves may be more complex than the conventional descriptions imply, and this may have potential clinical implications.

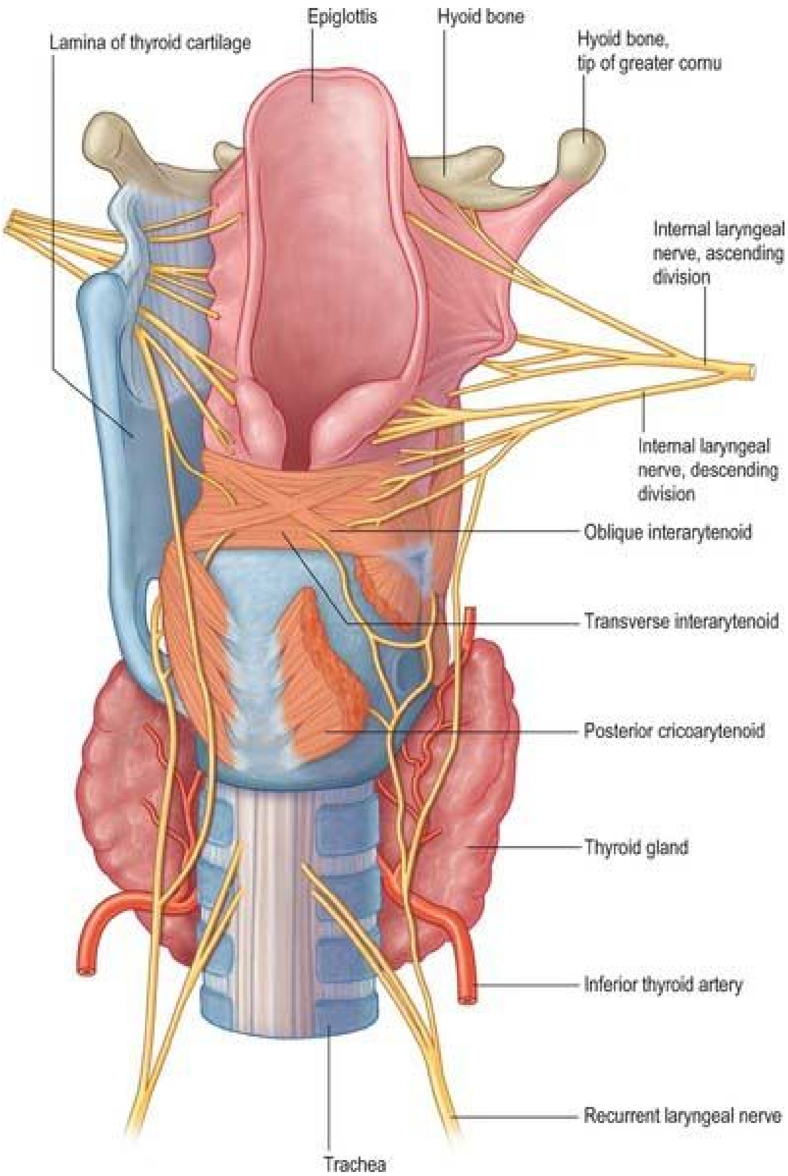
Lamina of thyroid cartilage
Epiglottis
Hyoid bone
Hyoid bone, tip of greater cornu
Internal laryngeal nerve, ascending division
Internal laryngeal nerve, descending division
Oblique interarytenoid
Transverse interarytenoid
Posterior cricoarytenoid
Thyroid gland
Inferior thyroid artery
Recurrent laryngeal nerve
Trachea

Fig. 34.11 Posterior view of the laryngeal innervation.

The detailed course of the vagus in the neck is described on page 458.

Superior laryngeal nerve

The superior laryngeal nerve arises from the middle of the inferior vagal ganglion, and in its course receives one or more communications from the superior cervical sympathetic ganglion: most frequently, the connection is with the external laryngeal nerve. The superior laryngeal nerve divides into two branches – a smaller, external and a larger, internal branch – approximately 1.5 cm below the ganglion: rarely, both branches may arise from the ganglion.

Internal laryngeal nerve

The internal laryngeal nerve passes forwards approximately 7 mm before piercing the thyrohyoid membrane, usually at a higher level than the superior thyroid artery. It splits into superior, middle and inferior branches on entering the larynx. The superior branch supplies the mucosa of the piriform fossa. The large middle branch is distributed to the mucosa of the ventricle, specifically the quadrangular membrane, and therefore probably conveys the afferent component of the cough reflex. The inferior ramus is mainly distributed to the mucosa of the ventricle and subglottic cavity. On the medial wall of the piriform fossa, descending branches give twigs to the interarytenoid muscle and share a number of communicating branches with the recurrent laryngeal nerve.

External laryngeal nerve

The external laryngeal nerve continues downwards and forwards on the lateral surface of the inferior constrictor, to which it contributes some small branches. Indeed, in approximately 30% of cases, the nerve is located within the fibres of the constrictor muscle. It passes beneath the attachment of sternothyroid to the oblique line of the thyroid cartilage and supplies cricothyroid. A communicating nerve continues from the posterior surface of cricothyroid, crosses the piriform fossa and enters thyroarytenoid, where it anastomoses with branches from the recurrent laryngeal nerve. It has been suggested that these communicating branches may provide both additional motor components to thyroarytenoid and sensory fibres to the mucosa in the region of the subglottis. An anastomosis between the external and internal laryngeal nerves has also been described in some cases.

The close relationship of the external laryngeal nerve to the superior thyroid artery puts the nerve at potential risk when the artery is clamped during thyroid lobectomy. The external laryngeal nerve is potentially at risk where it is either particularly close to the artery (in some 20% of cases), or where, instead of crossing the superior thyroid vessels approximately 1 cm or more above the superior pole of the gland, it actually passes below this point (in some 20% of cases).

Recurrent laryngeal nerve

The upper part of the recurrent laryngeal nerve has a close but variable relationship to the inferior thyroid artery: it may pass in front of, behind, or parallel to, the artery. The nerve enters the larynx by passing either deep to (two-thirds of cases) or between (one-third of cases) the fibres of cricopharyngeus at its attachment to the lateral aspect of the cricoid cartilage. It supplies cricopharyngeus as it passes. At this point, the nerve is in intimate proximity to the posteromedial aspect of the thyroid gland. The main trunk divides into two or more branches, usually below the lower border of the inferior constrictor, although branching may occur higher up. The anterior branch is mainly motor and is sometimes called the inferior laryngeal nerve (although this term is best avoided), while the posterior branch is mainly sensory. The anterior branch of the recurrent laryngeal nerve ascends posterior to the cricothyroid joint and its ligament, and is usually covered by fibres of posterior cricoarytenoid at this point. It bends over the joint, continuing forward over the lateral cricoarytenoid muscle before terminating within thyroarytenoid.

The anterior branch of the recurrent laryngeal nerve first innervates posterior cricoarytenoid by one or more branches, then innervates interarytenoid and lateral cricoarytenoid, and terminates in thyroarytenoid, which it also supplies.

The recurrent laryngeal nerve forms several anastomoses with the superior laryngeal nerves (Fig. 34.11). The posterior branch of the recurrent laryngeal nerve ascends deep to posterior cricoarytenoid to join the descending branch of the internal laryngeal nerve. In addition, the ansa Galeni that lies on the interarytenoid muscles forms a direct connection between the recurrent and internal laryngeal nerves (Fig. 34.11), while there is also a complex anastomosis within and over the posterior surface of the interarytenoid muscles; and, less frequently, anastomoses on the cricoid lamina and thyroarytenoid that also form connections with the internal laryngeal nerve.

The recurrent laryngeal nerve does not always lie in a protected position in the tracheo-oesophageal groove, but may be slightly anterior to it (more often on the right), and it may be markedly lateral to the trachea at the level of the lower part of the thyroid gland. On the right the nerve is as often anterior to, or posterior to, or intermingled with, the terminal branches of the inferior thyroid artery. On the left the nerve is usually posterior to the artery, though occasionally it lies anterior to it. The nerve may supply extralaryngeal branches to the larynx which arise before it passes behind the inferior thyroid cornu.

Outside its capsule the thyroid gland has a distinct covering of pretracheal fascia which splits into two layers at the posterior border of the gland. One layer covers the entire medial surface of its lobe; at, or just above, the isthmus it is conspicuously thickened to form the lateral ligament of the thyroid gland, which attaches the gland to the trachea and the lower part of the cricoid cartilage. The other layer is posterior; it passes behind the oesophagus and pharynx and is attached to the prevertebral fascia (p. 439). In this way, a compartment is formed on each side of the midline, lateral to the trachea and oesophagus: the recurrent laryngeal nerve and terminal parts of the inferior thyroid artery lie in the fat of this compartment. The nerve may be lateral or medial to the lateral ligament of the thyroid gland, and sometimes may be embedded in it.

An very rare anomaly that is of relevance to laryngeal pathology and surgery is the so-called ‘non-recurrent’ laryngeal nerve, where the right recurrent laryngeal nerve arises directly from the vagus nerve trunk high up in the neck and enters the larynx close to the inferior pole of the thyroid gland. Only the right side is affected, and it is always associated with an abnormal origin of the right subclavian artery from the aortic arch on the left side. If unrecognized, a non-recurrent laryngeal nerve may be susceptible to injury during surgery. It may also potentially be compressed by small tumours of the thyroid gland (p. 462).

Vagal nerve lesions and recurrent laryngeal nerve paralysis

Unilateral complete palsy of the recurrent laryngeal nerve is more common on the left side, presumably because the nerve is longer on this side. There is isolated paralysis of all the laryngeal muscles on the affected side except cricothyroid, which is innervated by the external laryngeal nerve. The patient may be asymptomatic or have a hoarse, breathy voice and there will be a loss of ability to manipulate pitch. The hoarseness may be permanent or may become less severe with time as the contralateral cord develops the ability to hyperadduct and appose the paralysed cord and thus close the glottis during phonation and coughing, although this is seldom enough to restore full voice quality.

Clinically, the position of the vocal cord in the acute phase after section of the recurrent laryngeal nerve is very variable. Stridor is more common after bilateral lesions, but by no means the rule; indeed, the cords may be sufficiently abducted that there is little problem with airway obstruction, although the voice is always weaker in this situation. The cords are more widely separated in chronic lesions, which means that the voice is weaker but the upper airway is more secure. Atrophy and fibrosis of paraglottic muscles probably affect the position of paralysed vocal cords in chronic lesions to a greater degree than variations in the strength of the apposing adductor and abductor muscle groups.

For many years the conventional wisdom was that movements of abduction were affected to a greater degree than those of adduction when the recurrent laryngeal nerve was partially lesioned (Semon’s law). This was attributed to the presumed segregation of the axons supplying the laryngeal abductor muscles within the recurrent laryngeal nerve. However, studies of human nerves have failed to support this idea, and have shown that axons destined for particular laryngeal muscles are randomly distributed within the recurrent laryngeal nerve. It seems more likely that the relative sparing of abduction in these lesions is a consequence of the weak abduction produced by crico-thyroid, which is spared. The difficulty of predicting the effect of partial lesions of the recurrent laryngeal nerve may reflect the variable patterns of anastomosis between the laryngeal nerves.

Paralysis of all laryngeal musculature (including cricothyroid) suggests a lesion proximal to the inferior (nodose) ganglion that involves the superior laryngeal nerve as well as the recurrent laryngeal nerve. The affected cord is paralysed and lies in the so-called ‘cadaveric’ position halfway between abduction and adduction. If the lesion is unilateral, the voice is weak and hoarse, but if it is bilateral, phonation is almost absent, the vocal pitch cannot be altered, and the cough is weak and ineffective.

There is debate as to the effect of lesions of the external laryngeal nerve. Complete section is most likely during the ligation of the vessels forming the vascular pedicle of the thyroid gland during thyroid lobectomy, and characteristically causes breathiness and mild hoarseness accompanied by reduced pitch and loudness in bilateral lesions; these effects may not be noticeable when lesions are unilateral.

Damage to the internal laryngeal nerve causes loss of mechanoreceptive and proprioceptive sensation from the larynx. Unilaterally, this produces a feeling that something is stuck in the throat. Bilaterally, it will result in aspiration and can cause dysphagia, with a risk of choking.

Autonomic innervation

Parasympathetic secretomotor fibres run with both the superior and recurrent laryngeal nerves to mucous glands throughout the larynx. Postganglionic sympathetic fibres run to the larynx with its blood supply; they originate in the superior and middle cervical ganglia.

ANATOMY OF SPEECH

The principal biological function of the larynx is to act as a sphincter controlling the entry of foreign bodies into the airways and regulate airflow during ventilation. Thus, the larynx is opened widely during ventilation and is closed tightly during swallowing. The larynx can also close tightly during exertion, effort closure, to regulate thoracic and abdominal pressure during activities such as defecation or parturition, or to fix the thorax to increase mechanical advantage when using the arms to lift objects. The importance of the latter activity should not be underestimated: one of the many problems reported by patients who have undergone a laryngectomy is a loss of power in their arms when trying to lift heavy objects.

The larynx is much more than a simple valve that opens and closes. In addition to its sphincteric functions, its location means that it is perfectly placed to act as a sound source, or voice, that forms the basis of nearly all sounds in human speech. The musculoskeletal structure of the larynx is under exquisite neuromuscular control, allowing it to modify the expiratory stream to produce highly complex patterns of sound of varying loudness, frequency and duration. The ability to execute these complex movements depends largely on specific areas of the cerebral hemispheres which are involved in the motor aspects of language, such as speech and writing, and sensory manifestations of language, including reading and understanding the spoken word.

OVERVIEW OF SPEECH PRODUCTION

All speech requires an input of energy. For all sounds in Western European languages, and most sounds in other languages, this energy takes the form of a pulmonary expiration. This continuous airflow is converted into a vibration within the larynx by a mechanism called phonation, in which the vocal folds vibrate periodically, interrupting the column of air as it leaves the lungs and converting it into a series of discrete puffs of air. Speech sounds that are produced by vocal fold vibration in this way are said to be voiced. Speech sounds that are produced without vocal fold vibration are termed unvoiced sounds.

The larynx is an inadequate sound source: the laryngeal ‘buzz’ that is produced by phonation is very quiet and cannot be varied sufficiently to produce the complex range of sounds that is human speech. Amplification and modification of the sound occur in the supralaryngeal vocal tract, which may be considered as a 17 cm long tube, narrow at the larynx and broadening out proximally as it passes through the pharynx, and oral and nasal cavities. This tube acts as a passive amplifier of the sound. (The analogy here is of a megaphone: cupping the hands round the lips lengthens the vocal tract and increases the volume of speech.) The supralaryngeal vocal tract modifies the basic vibration of the larynx by altering its geometry, length and calibre: it provides a series of resonators that can dampen or amplify certain sound frequencies and can transiently interrupt the exhaled air flow and modify it to produce speech. This process is known as articulation. The range of sounds that the human vocal tract is capable of producing is very wide, although any one human language will employ a subset of these sounds to convey meaning.

MUSCULAR CONTROL OF THE AIRSTREAM

Normal vegetative ventilation involves rhythmic movements of the thoracic cage that are produced by intercostal muscles and the diaphragm and a number of accessory muscles in the neck, arm and abdomen that have one attachment to some part of the thoracic cage. The thorax is capable of responding mechanically to widely varying demands for oxygen. From a tidal volume at rest of 500 mL and a respiratory rate of 12 per min, ventilation can increase in fit individuals during vigorous exercise to tidal volumes of 4.5 L and respiratory rates of 20–25.

Normal ventilatory patterns are considerably modified during speech, reflecting the special demands that speech places upon ventilation. The main source of energy for the production of speech sounds is a pulmonary expiration, although other mechanisms are possible. In order that speech is produced, sufficient pressure has to be generated beneath the vocal folds. This subglottal pressure (the difference between the air pressures above and below the vocal folds) has to be sustained above a minimum level throughout an utterance. It sets the vocal folds into vibration if the sound is to be voiced or generates airflow for an unvoiced sound. The minimum subglottal pressure needed for speech production is 7 cmH_2O, and this increases when loud sounds are produced or when sounds are stressed.

The need to generate sufficient sustained pressure means that speech ventilation is markedly non-rhythmical. At the onset of an utterance, inspiration is typically 1.5 L, which is deeper than for normal quiet ventilation, ensuring that sufficient air is taken in to maintain adequate subglottal pressure for the duration of the utterance. Inspiration is also quicker, 0.5 sec rather than 2–3 sec. Expiration is much longer than normal, perhaps lasting up to 30 sec, reflecting the fact that the vocal tract is more constricted at the larynx to ensure that pauses for further inspirations are made at suitable points in an utterance. At the end of the first inspiration during running speech, lung volumes do not fully return to resting levels. Conversational speech normally takes place at a higher range of lung capacities than operate in normal quiet ventilation.

The non-rhythmical pattern during speech requires greater inspiratory effort, and for most people it involves a greater use of the diaphragm, usually in combination with the abdominal muscles that are attached to the lower ribs (they stabilize the costal attachments of the diaphragm and increase the effectiveness of its action) (see p. 1011). However, the main differences are seen in expiration. Speech takes place at higher lung volumes, which means that greater recoil forces are stored in the elastic tissues of the lungs and the ribcage. The generation of subglottal pressure is the product of these elastic recoil forces and the muscular forces generated by the expiratory muscles. At the onset of an utterance, unrestrained recoil forces would generate excessive subglottal pressures that would be wasteful of air, and hence energy, and would affect the loudness of speech. Conversely, towards the end of an utterance, as recoil forces decline, subglottal pressure would fall without additional muscular exertion. Therefore, early in an utterance, inspiratory muscles, particularly the external intercostals and parasternal parts of the internal intercostals, continue to contract, relaxing slowly to counteract the effects of excessive passive elastic recoil. As the recoil forces decline below the point where they can maintain the minimum subglottal pressure needed for phonation, expiratory muscles contract to maintain subglottal pressure as lung air volume nears its resting expiratory level. The main muscles involved are the costal parts of the internal intercostals and the subcostal and transversus thoracis muscles. Their actions are aided by contraction of the anterior abdominal muscles to compress the abdomen. Accessory muscles such as latissimus dorsi may also come into play, but normally these accessory muscles are only active at the end of a very long or loud utterance, or in patients whose ventilatory function is compromised.

Though subglottal pressure tends to remain fairly constant during an utterance, it rises when sounds are stressed, and falls during the production of unvoiced sounds when the larynx is less constricted. At these times, compensatory mechanisms to ensure that pressure is maintained are required: the precise mechanisms have yet to be elucidated, but the internal intercostal muscles have been implicated. The anterior abdominal muscles are also active in singing, shouting and in attempts to speak without the pause necessary for inspiration. Contrary to popular belief, the diaphragm plays little part in the regulation of expiratory force. Unlike the intercostal muscles, the diaphragmatic musculature is sparsely supplied with muscle spindles, and therefore control of the diaphragm is poorly regulated: minute changes can be effected more successfully using the intercostal and anterior abdominal muscles.

Though the expiratory airflow from the lungs is the source of energy for most speech sounds, other sources of airflow are also used. The larynx can be used to generate airflow. The sound /p/ is produced by closing the larynx and then raising it with the lips closed, using the larynx like a piston. Opening the lips then releases a puff of air. This is called an ejective, and is an example of egressive glottalic airflow. Ingressive glottalic airflow is also possible, though less effective; examples are not found in English, but do occur in some African and native American languages. A third kind of airflow is velaric, in which the back of the tongue is raised against a lowered soft palate and the vocal tract is closed anterior to that point, either at the lips or with the tongue against the hard palate. This produces a click and is rare. A non-linguistic example in English is the sound made in encouraging a horse. Ingressive pulmonary airflow, such as is found in a groan or a gasp, is theoretically possible, but none of the world's languages employ this as a source of airflow.

After removal of the larynx, e.g. following laryngeal cancer, patients can be taught to swallow air, store it in a segment of the oesophagus and then use it as the energy source to produce egressive oesophageal airflow (oesophageal speech). Speech in these circumstances tends to have a belching quality and may be badly phrased. Laryngectomy patients always produce phrases that are shorter than normal, and so prostheses incorporating valves and surgical shunts are often inserted to provide a larger egressive airstream by diverting air from the respiratory tract into the oesophagus.

PHONATION

The default position of the rima glottidis is open, to maintain patency of the airway during respiration. In quiet respiration, the anterior intermembranous part of the rima glottidis is triangular when viewed from above. Its apex is anterior and its base posterior, and it is represented by an imaginary line approximately 8 mm long connecting the anterior ends of the arytenoid vocal processes. The intercartilaginous part between the medial surfaces of the arytenoids is rectangular as the two vocal processes lie parallel to each other. During forced respiration, the rima glottidis is widened and the vocal cords are fully abducted to increase the airway. The arytenoid cartilages rotate laterally, and this moves their vocal processes apart, and converts the rima glottidis into a diamond shape in which both intermembranous and intercartilaginous parts are triangular. The greatest width of the rima glottidis is at the point of the attachments of the vocal cords to the vocal processes.

During speech the true vocal folds vibrate to act as a source of sound for subsequent speech. There have been a number of theories to explain the mechanism that produces this vibration, but these are now only of historic interest. The aerodynamic–myoelastic theory is generally accepted as the mechanism underlying vocal fold vibration, although it does not account for all aspects of phonation.

At the onset of an utterance, during an expiration, the true vocal folds are adducted: the lateral cricoarytenoids and interarytenoids bring together both the intermembranous and intercartilaginous parts of the glottis, actions which either close the glottis completely or reduce the space between the vocal folds to a linear chink. The mucous membrane covering the interarytenoid muscles, the interarytenoid fold, intrudes into the larynx when these muscles adduct the arytenoids, and so aids closure of the intercartilaginous part of the rima glottidis. The vocal cords are also tensed, an essential prerequisite for vibration. These actions cause a build-up of subglottal pressure that continues until a point is reached when the muscular force of adduction is no longer sufficient to resist the rising pressure, and the vocal folds are forced open a little, releasing air into the supralaryngeal vocal tract. The subglottal pressure falls when the subglottic and supraglottic cavities become continuous and the vocal folds begin to close. Two mechanisms bring about closure. If adductive tension is sustained, then the vocal folds will close. In addition, rapid closure is aided by a physical process, the Bernoulli effect. The forcing of air from a region of high to low pressure through a narrow space causes an increase in the kinetic energy of the molecules at the edge of the space. The effect of this is to lower pressure in the space between the folds at the level of the folds themselves, and this negative pressure simply sucks the folds together because they are mobile. This causes a rise once more in the subglottal pressure and the cycle is repeated. The effect is to cause the release of a series of puffs of air into the supralaryngeal vocal tract at a frequency of many times per second, which is perceived as a sound of a particular frequency (Figs 34.12, 34.13).

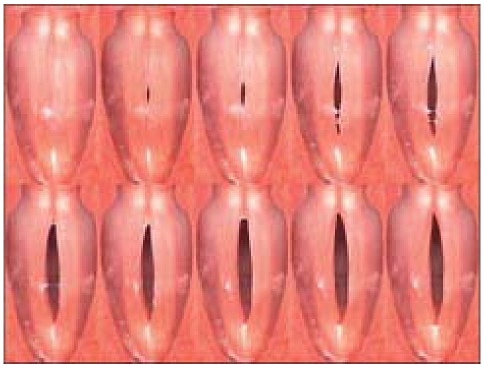

Fig. 34.12 Video montage of the normal phonatory cycle, obtained using a rigid fibre endoscope with stroboscopic illumination.

(By courtesy of Professor Paul Carding.)

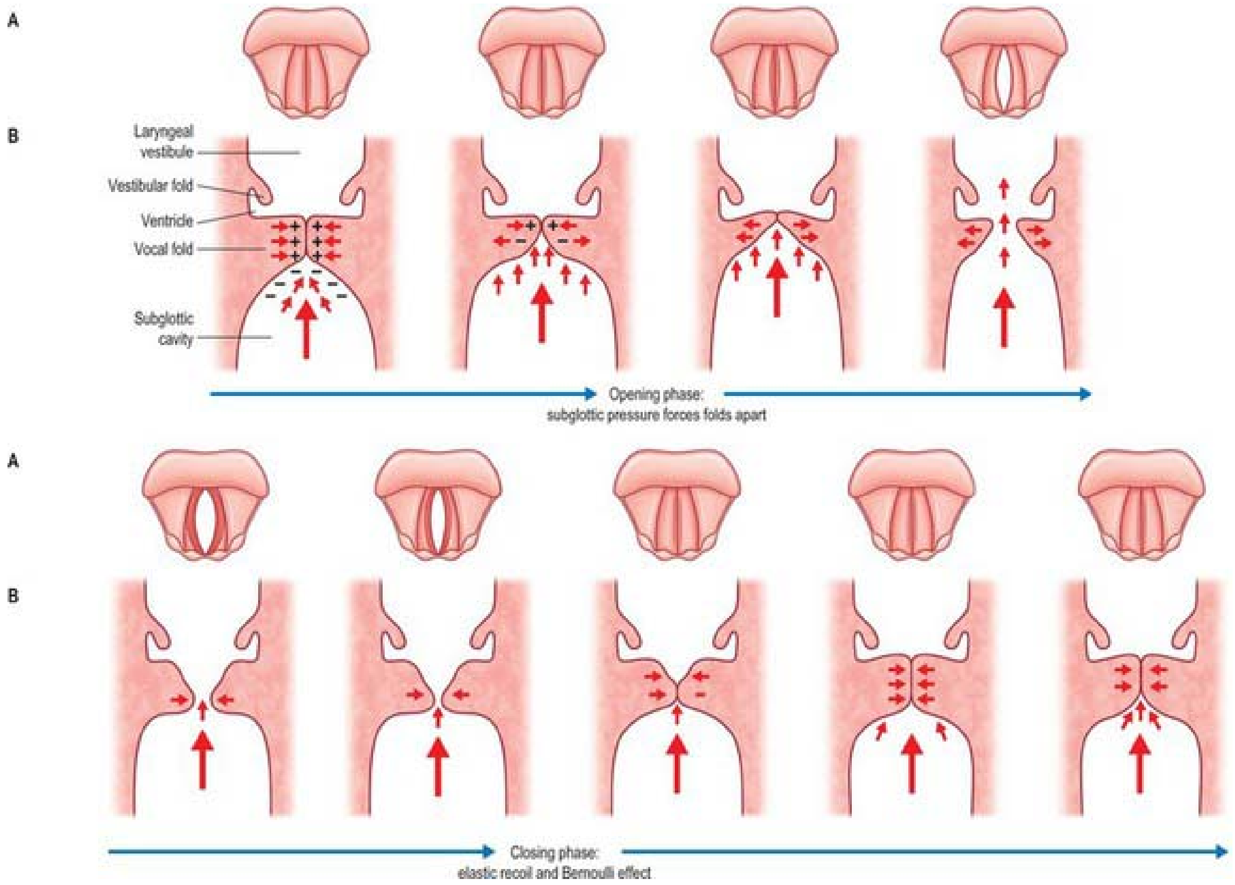
A
B
Laryngeal vestibule
Vestibular fold
Ventricle
Vocal fold
Subglottic cavity
Opening phase:
subglottic pressure forces folds apart
A
B
Closing phase:
elastic recoil and Bernoulli effect

Fig. 34.13 Position of the vocal folds during a cycle of vocal fold vibration (phonatory cycle) in superior (**A**) and coronal (**B**) views.

The source of energy for the vibration does not come from the larynx itself. The vocal folds do not behave like the prongs of a tuning fork: their predominant motion is in the horizontal plane at right angles to the movement of the air column, and there is little vertical movement. The energy is derived from the motion of the air generated by the muscular and recoil forces in the thorax, and the larynx is simply chopping that column into a series of segments.

The aerodynamic–myoelastic theory does not explain how vocal fold vibration is sustained, nor does it account for the very obvious muco-undulatory component of vocal fold vibration that is visible when the larynx is viewed stroboscopically. Without further input of energy the vibration of the vocal folds as described above would not be sustained but would be damped and gradually diminish. For vibration to continue there has to be additional energy input. The analogy here is with a child on a swing. For the motion to continue either the parent has to push the child at an appropriate point in the cycle, or the child has to sustain the motion for themselves by swinging their legs at the crucial point in the swing cycle. In the case of phonation, the source of this additional energy is unclear. It may come from the inertia of the air column itself, i.e. once the vocal folds close, the air column will continue moving upwards because inertia creates a negative pressure above the folds. Alternatively, the energy could come from the manner in which the folds open and close. As the subglottal pressure rises, the lower portion of the fold opens first and the upper edge of the fold is last to open, and when the subglottal pressure falls, the folds close from the bottom edge. It has been suggested that this non-uniform closure creates different shapes within the glottis that may result in differing negative pressures at different phases of the cycle. It also produces a vertical wave-like motion in the folds, termed the muco-undulatory component. The analogy here is with a flag blowing in the wind, and it reflects the differing stiffnesses of the various layers of the vocal folds described above. This vertical component will impart a negligible amount of energy to the air column, but it is likely to impart harmonics to the basic laryngeal vibration.

The sound that results from the process of phonation has three characteristics: a frequency that is perceived as pitch, an intensity that is perceived as loudness, and a timbre perceived as voice quality.

The fundamental frequency of the human voice is determined by the resting length of the vocal cords and varies with age and sex. The frequency range of human speech is from 60 to 500 Hz, with an average of approximately 120 Hz in males, 200 Hz in females and 270 Hz in children. The mechanism of frequency alteration is not entirely clear. An increase in subglottal pressure will cause the frequency of phonation to rise. However, during an utterance, subglottal pressure appears to remain fairly constant, which suggests that the mechanism of frequency alteration resides in intrinsic changes within the vocal folds. Variations in frequency (pitch changes) during an utterance are determined by the complex interrelationships between length, tension and thickness of the vocal cords: one of these variables cannot be altered without affecting the other two parameters to some extent. Gross changes to the vocal cords demonstrate the effects of these variables. Inflamed and swollen vocal cords are much thicker than normal and result in a hoarse voice. At puberty, growth of the thyroid cartilage in males lengthens the vocal cords and lowers the fundamental frequency, and the voice ‘breaks’ as a result. During panic, the vocal cords may be tensed, which means that the cry for help is a high-pitched squeak.

Pitch is increased by increasing the length of the vocal folds, as may be confirmed during direct endoscopic examination of the larynx. At first sight this may seem counterintuitive, but, as the vocal cords are lengthened, there will be a consequent thinning and change in tension. Although an analogy is often drawn between the vocal cords and vibrating strings, a better analogy is a rubber band: if a rubber band is lengthened, the tension will increase, but the thickness will decrease. The vocal cords may be lengthened by up to 50% of their resting length. It is likely that the initial pitch setting is achieved by action of the cricothyroids, and that fine adjustments can then be made using the vocales. Paralysis of both cricothyroids, which is usually associated with loss of the neurones that are distributed via the superior laryngeal nerve (as a result of damage to the vagal nuclei in brainstem stroke), results in permanent hoarseness and inability to vary the pitch of the voice. It is important to remember that once the vocal cords are set in motion they will deviate from their original setting as they vibrate. Auditory feedback of the sounds produced is used to make minute compensatory adjustments to length, tension and thickness in order to maintain a constant pitch.

Any lengthening of the vocal cords tends to thin them. The thickness can be increased by the vocalis part of thyroarytenoid: as vocalis shortens, it will relax the vocal cords and at the same time increase their thickness. Changes in the tension of the vocal cords are produced by the same muscles that change their length, namely cricothyroid, posterior cricoarytenoid and vocalis, probably acting isometrically.

The mechanism by which loudness is increased is the subject of less debate. Loud sounds are produced by increasing subglottal pressure. This is achieved, in turn, by changing the opening quotient of the glottis (the ratio of the time spent in the open phase of the cycle to the total cycle time). In normal speech, this ratio is usually around 0.5, but in very loud speech it can fall to 0.3.

Timbre or voice quality refers to the harsh or mellow quality of the voice. At high volume the voice tends to be harsher, especially in untrained voices: higher-frequency components predominate because higher subglottal pressures are needed to sustain the increased volume. This can be overcome to an extent by increasing the airflow rather than the pressure.

A fundamental distinction in speech needs to be made between voiced and unvoiced sounds: nearly all languages make this distinction. Voicing has been described above. In unvoiced sounds, the vocal folds are not vibrating and will usually be opened under the action of posterior cricoarytenoid. The energy from the airstream is then used by other parts of the vocal tract to generate sound, normally by constricting or stopping the airflow. However, phonation is not an all-or-nothing process, but is subject to considerable modification and adjustment. In modal voice, i.e. speaking using habitual pitch, forces acting on the vocal folds are moderate, pressures are sustained, and air is conserved. However, phonation can occur when the vocal folds are more open than usual, resulting in breathy phonation with more air escaping per phonatory cycle than usual. Some languages in South Asia exploit the difference between breathy and non-breathy sounds, whereas in spoken English, a breathy voice is simply recognized as a feature of some speakers. At the other end of the spectrum is vocal creak, in which the vocal folds are more closed than normal. Different speakers will habitually employ different laryngeal settings which contribute to their particular voiced quality. In whispering, the intramembranous part of the glottis is closed, but the intercartilaginous part remains open, which produces a characteristic Y-shaped glottis and a greater loss of air at each phonatory cycle.

The main function of the larynx is to act as a sound source, but it can also function in speech as an airstream generator and as an articulator.

ARTICULATION

The sound produced by the phonation is not a pure tone because several harmonics at multiples of the fundamental frequency are also generated. Harmonics give a note of a particular frequency its defining characteristics. An ‘A’ played on an oboe or violin is immediately recognizable because of the different harmonics generated by the design of the instrument. The harmonic spectra of individual voices differ and will also vary depending upon the mode of phonation adopted. In the human vocal tract, the fundamental frequency and its harmonics are transmitted to the column of air which extends from the vocal cords to the exterior, mainly through the mouth. Part of the airstream can also be diverted through the nasal cavities when the soft palate is depressed to allow air into the nasopharynx. The supralaryngeal vocal tract acts as a selective resonator whose length, shape and volume can be varied by the actions of the muscles of the pharynx, soft palate, fauces, tongue, cheeks and lips; the relative positions of the upper and lower teeth, which are determined by the degree of opening and protrusion or retraction of the mandible; and alterations in the tension of the walls of the column, especially in the pharynx. Thus, the fundamental frequency (pitch) and harmonics produced by the passage of air through the glottis are modified by changes in the supralaryngeal vocal tract.

Harmonics may be amplified, or dampened. The fundamental frequency and its associated harmonics may also be raised or lowered by appropriate elevation or depression respectively of the hyoid bone and the larynx as a unit by the selective actions of the extrinsic laryngeal muscles. Effectively, these movements shorten or lengthen the resonating column, and to some extent also alter the geometry of the walls of the air passages. Analysis of the human voice shows that it has a very similar pattern of harmonics for all fundamental frequencies, determined by the vocal tract acting as a selective filter and resonator. This maintains a constant quality of voice without which intelligibility would be lost (recorded speech played back without its harmonics is completely unintelligible). Each human voice is unique: it has been suggested that the unique frequency spectrum of each individual voice could be used for personal identification.

During articulation the egressive airstream is given a rapidly changing specific quality by the articulatory organs, the lips, oral cavity, tongue, teeth, palate, pharynx, and nasal cavity. The discipline of phonetics primarily deals with the way in which speech sounds are produced, and consequently with the analysis of the mode of production of speech sounds by the vocal apparatus. In order to analyse the way in which the articulators are used in different speech sounds, words are broken down into units called phonemes, which are defined as the minimal sequential contrastive units used in any language.

The human vocal tract can produce many more phonemes than are employed in any one language. Not all languages have the same phonemes, and within the same language, the phonemes can vary in different parts of the same country and in other countries where that language is also spoken. Reproducing phonemes that are not used in native speech is difficult because such phonemes require unfamiliar positioning of the speech organs. A native speaker of any language can quickly recognize the origins of anyone attempting to use their language as a second language. The second-language speaker will usually speak it with an accent characteristic of their own first language because they are using the familiar configurations of their vocal tract for each phoneme instead of the correct positioning.

PRODUCTION OF VOWELS

All vowel sounds require phonation by vibration of the vocal cords. Each vowel sound has its own characteristic higher harmonics (frequency spectrum) that exhibit peaks of energy at certain frequencies. These energy peaks are always higher multiples of the fundamental frequencies and are called formants. Formants are the result of the combined effects of phonation, selective resonance of the vocal tract, and the properties of the head as a radiator of sound. The sounds of the different vowels are determined by the shape and size of the mouth, and the positions of the tongue and lips are the most important variables. The tongue may be placed high or low (close and open vowels), or further forwards or back (front and back vowels) and the lips may be rounded or spread.

PRODUCTION OF CONSONANTS

The production of consonants always involves some degree of constriction of the vocal tract. There are many more consonants than vowels, and, in general, consonants cannot be combined to produce syllables. The classification of consonants is complex and beyond the remit of this book: what follows is a summary (for fuller details, a textbook of phonetics should be consulted).

Consonants may be classified of the basis of where the constriction occurs, termed the place of articulation; the degree or extent of constriction, termed the manner of articulation; the shape of the constriction, termed the stricture; and whether or not there is vibration of the vocal folds, when consonants are described as voiced or unvoiced respectively.

Consonants may also be classified as labial, dental, alveolar, velar, uvular, pharyngeal or glottic, depending upon whether the point of maximum constriction occurs at the level of the lips, teeth, bony ridge behind the teeth, palate, uvula or pharynx (Fig. 34.14). Different parts of the tongue can be used in combination with the above places of articulation. Phoneticians divide the tongue into the tip, anterior edge, the front part of the dorsum, the centre and back parts of the remaining dorsum, and a most posterior part (the root). These divisions bear no obvious relationship to the anatomical landmarks on the tongue, but they are useful in describing the part of the dorsum of the tongue that contacts other areas of the mouth. Similarly, the manner of articulation can vary from a complete closure to a slight narrowing. An actual closure of the vocal tract is called a stop. A narrowing that is sufficient to produce turbulence of the air in the vocal tract, and which is perceived as a rustling sound, is termed a fricative. Approximants involve a degree of closure insufficient to produce turbulence but with closure greater than that for a vowel. Nasals involve a stoppage in the oral cavity with the soft palate lowered to allow airflow through the nose, and, unlike stops, they can be sustained. Stricture describes the shape of the constriction, e.g. a lateral consonant involves depression of the sides of the tongue, while a grooved consonant is produced by grooving the dorsum of the tongue.

Consonants can be produced with the vocal folds vibrating, when they are termed voiced, or without vocal fold vibration, in which case they are termed unvoiced.

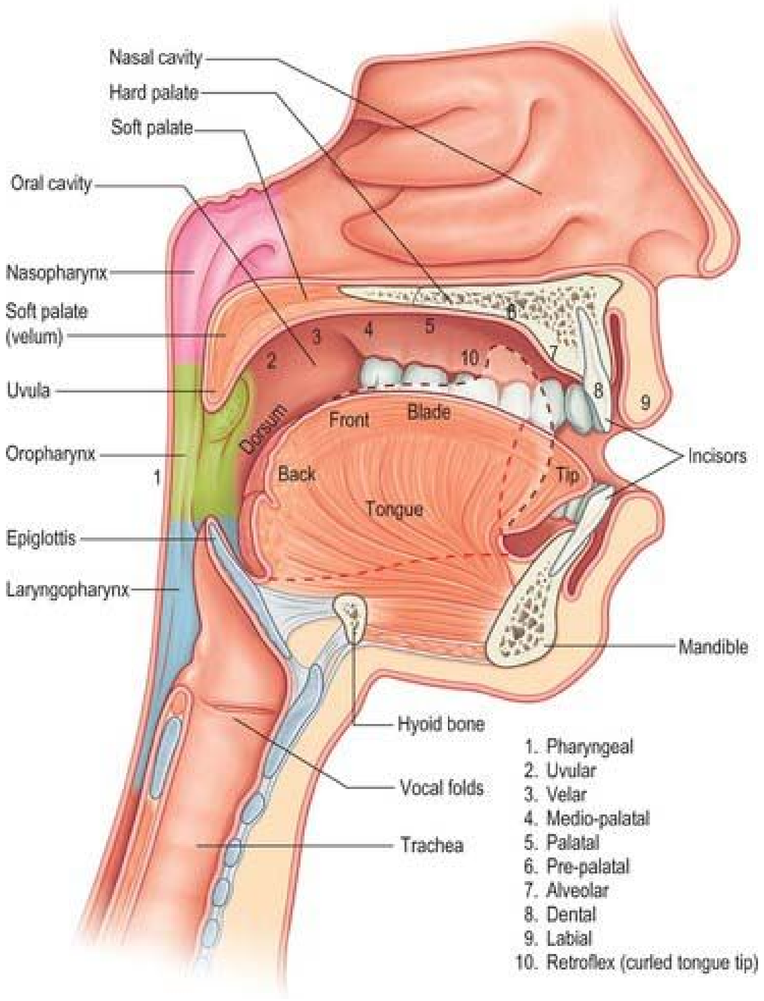
Nasal cavity
Hard palate
Soft palate
Oral cavity
Nasopharynx
Soft palate (velum)
Uvula
Oropharynx
1
Epiglottis
Laryngopharynx
2
3
4
5
6
7
8
9
10
Dorsum
Front
Blade
Back
Tongue
Tip
Incisors
Mandible
Hyoid bone
Vocal folds
Trachea
1. Pharyngeal
2. Uvular
3. Velar
4. Medio-palatal
5. Palatal
6. Pre-palatal
7. Alveolar
8. Dental
9. Labial
10. Retroflex (curled tongue tip)

Fig. 34.14 Sagittal view of the left side of the head, showing the supralaryngeal vocal tract, the articulators and places of articulation. The broken line indicates the tongue position during retroflexion (10).

The best way to illustrate these classificatory systems in operation is by contrasting the production of different consonant pairs in which only one or two parameters have been changed. The /p/ of peat, the /b/ of beat and the /m/ of meat are all bilabial stops, meaning that they are produced by bringing together the lips. The /b/ and the /m/ are voiced but the /p/ is not. The contrast between the /b/ and the /p/ is in the differing way in which the airstreams are produced. The /b/ is produced with an egressive pulmonary airflow, while the /p/ is produced with the glottis closed, hence unvoiced, and the glottis is then raised using the larynx as a piston to compress the air in the supra-laryngeal vocal tract prior to the stop being released. The /m/ differs from the other two stops in being a nasal in which the soft palate is lowered to allow air to escape through the nasal cavity, and unlike the other two stops it can be sustained as in a sound of approval, e.g. encouraging a horse to move. Bilabial stops can be contrasted with the labiodental fricatives /f/ of feet and the /v/ of veal, both of which are produced by retracting the lower lip beneath the upper teeth. Neither involves a complete closure but both produce a significant constriction of the vocal tract with audible turbulence: the /f/ is unvoiced, while the /v/ is voiced. The sh sound (/ʃ/) in ship is also a fricative involving a grooving of the tongue and is associated with significant audible turbulence; it may be contrasted with the lateral approximant /l/ in law, in which the sides of the tongue are lowered. In this case it is the nature of the stricture which is different and the degree of closure, e.g. in the case of the approximant /l/, closure is insufficient to produce turbulence. The sh sound in ship can be compared to the /k/ in keen, where the position of the tongue is different: in /k/ the tongue blade contacts the soft palate, while in sh the tongue tip or the blade contact the postalveolar region. The most dramatic example of the difference between voiced and unvoiced sounds may be appreciated if the /s/ sound in sip is compared with the /z/ in zip. If the larynx is loosely palpated while making a sustained unvoiced ‘ssssss’ sound, no vibration is felt, but if the ‘ssssss’ is commuted into a prolonged voiced ‘zzzzzz’, then vibration in the larynx should be readily detectable. The position of the tongue and other articulators is exactly the same for both /s/ and /z/, the difference between them is the presence or absence of phonation.

REFERENCES

kinson M, McHanwell S. Basic Medical Science for Speech & Language Therapy Students. London: Whurr Publishers, 2002.

rkovitz BKB, Moxham BJ, Hickey S. The anatomy of the larynx. In: Ferlito A, editor. *Diseases of the Larynx*. London: Chapman & Hall; 2000:25-44.

sma JF, Bartner MA. Ligaments of the larynx and the adjacent pharynx and esophagus. *Dysphagia*. 1993;8:23-28.

ark J, Yallop C. An Introduction to Phonetics and Phonology, 2nd edn. Oxford: Blackwell, 1995.

A comprehensive introduction to all aspects of phonetics and phonology..

rham FC, Harrison TS. The surgical anatomy of the superior laryngeal nerve. *Surg Gynecol Obstet*. 1962;118:33-44.

kki A, Pitkanen R, Suominen H. Observations on the structure and the biomechanics of the cricothyroid articulation. *Acta Otolaryngol (Stockh)*. 1987;103:117-126.

iedman M, Toriumi DM, Grybauskas V, Katz A. Nonrecurrent laryngeal nerves and their clinical significance. *Laryngoscope*. 1986;96:87-90.

rchner JA, Carter D. Intralaryngeal barriers to the spread of cancer. *Acta Otolaryngol (Stockh)*. 1987;103:503-513.

aranillo E, Leon X, Orus C, Quer M, Sanudo J-R. Variability in nerve patterns of the adductor muscle group supplied by the recurrent laryngeal nerve. *Laryngoscope*. 2005;115:358-362.

This paper and that by Sanudo et al (1999) below describe variations in the innervation of the human larynx and discuss the possible functions and clinical significance of the variations described..

unir Turk L, Hogg DA. Age changes in the human laryngeal cartilages. *Clin Anat*. 1993;6:154-162.

Provides data concerning the distribution of areas of calcification that occur with age within the cartilages of the larynx..

acy R. The infant larynx. *J Laryngol Otol*. 1983;97:933-947.

Draws attention to features that differ from the adult condition and that may have clinical significance..

idenbach MM. Normal topography of the conus elasticus. Anatomical bases for the spread of laryngeal cancer. *Surg Radiol Anat*. 1995;17:107-111.

eidenbach MM. The periepiglottic space: topographic relations and histological organisation. *J Anat*. 1996;188:173-182.

eidenbach MM. The paraglottic space and transglottic cancer: anatomic considerations. *Clin Anat*. 1996;9:244-251.

eidenbach MM. Subglottic region: normal topography and possible clinical implications. *Clin Anat*. 1998;11:9-21.

The four papers by Reidenbach are based on serial reconstruction of sections derived from plastinated material..

nudo J-R, Maranillo E, León X, Mirapeix R-M, Orús C, Quer M. An anatomical study of anastomoses between the laryngeal nerves. *Laryngoscope*. 1999;109:983-987.

to I, Shimada K. Arborization of the inferior laryngeal nerve and internal nerve on the posterior surface of the larynx. *Clin Anat*. 1995;8:379-387.

Discusses the possible clinical significance of connections between the inferior (recurrent) laryngeal nerve and the internal laryngeal nerve..

elsh LW, Welsh JJ, Rizzo TA. Laryngeal spaces and lymphatics: current anatomic concepts. *Ann Otol Rhinol Laryngol Suppl*. 1983;105:19-31.

Describes the ‘tissue spaces’ and lymphatic drainage of the larynx and their importance in determining the route of spread of tumours..

CHAPTER 35

Development of the head and neck

Head development is distinct from that of the trunk, utilizing region-specific genes, signalling mechanisms and morphogenetic processes. This chapter will provide a description of head and neck development based primarily on data from studies on human embryos. Since this information is necessarily purely descriptive, it will be supplemented by observations from lineage and genetic studies in mouse embryos, where the results are likely to be valid for all mammals, including human. Human studies are taken from the following sources, which incorporate primary data by the authors as well as references to older primary source material: O'Rahilly and Müller (1987, 2001); Hinrichsen (1990). References to experimental studies in the mouse are provided in the text.

Evolution of the vertebrate head was made possible by the origin of a novel cell population, the neural crest. Neural crest cells have the potential to form connective and skeletal tissues in the head, and they make major contributions to the skull. In mammalian embryos, cranial neural crest cells emigrate from the edges of the still unfused cranial neural folds, unlike trunk neural crest cells and the cranial crest of other vertebrates, which begin migration only after neural tube closure. Figure 35.1 shows stylized views of human embryos at an early stage of neural crest migration (A) and at the end of the crest migration (B). N.B. These views do not show the neural crest cells themselves and not by a specific staining procedure.

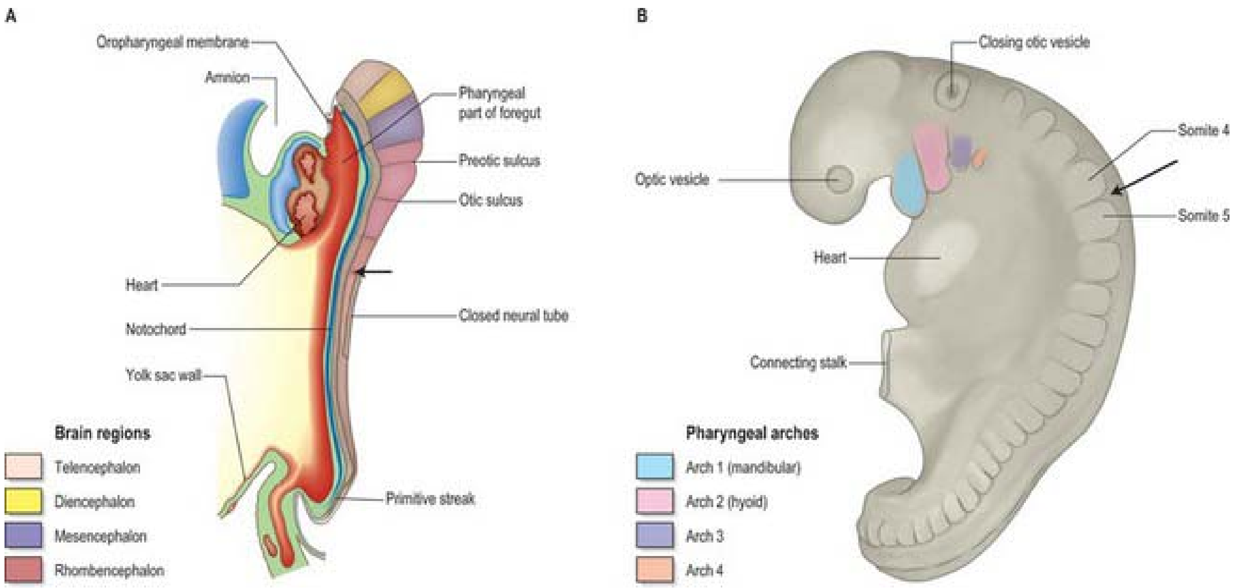
A
Oropharyngeal membrane
Amnion
Pharyngeal part of foregut
Preotic sulcus
Otic sulcus
Heart
Notochord
Closed neural tube
Yolk sac wall
Primitive streak
Brain regions
Telencephalon
Diencephalon
Mesencephalon
Rhombencephalon
B
Closing otic vesicle
Somite 4
Optic vesicle
Somite 5
Heart
Connecting stalk
Pharyngeal arches
Arch 1 (mandibular)
Arch 2 (hyoid)
Arch 3
Arch 4

Fig. 35.1 Human embryos during early stages of head development. The occipital–cervical boundary is indicated by an arrow. **A**. Sagittal section of a stage 10 embryo in which neural tube closure has begun in the future occipito-cervical region. **B**. Lateral view of a stage 12 embryo; the occipital/cervical boundary between somites 4 and 5 is indicated by an arrow. (See also fig 24.2).

In the mouse, a lineage marker has enabled neural crest cells to be traced from the stage at which they leave the neural epithelium to their locations in adult tissues. These studies show three separate populations of neural crest cells migrating from the cranial neural folds which give rise to neuronal and non-neuronal progeny (Fig. 35.2). The first of these populations (trigeminal) originates from the diencephalic region of the forebrain, the midbrain, and prorhombomere A of the hindbrain, which subsequently divides to form the first two rhombomeres (Fig. 35.2A,B; see also Fig. 24.2). Those neural crest cells with a neuronal fate contribute to the trigeminal ganglion (Jiang et al 2002). The non-neuronal mesenchymal crest cells migrate extensively to surround the telencephalon and part of the diencephalon, forming the frontonasal mesenchymal populations; they also migrate lateral to the rhombencephalon to form the mesenchyme of the maxillary and mandibular regions of the first arch (Fig. 35.2C,D). The second (hyoid) population gives rise to the otic ganglion and then migrates from prorhombomere B (which forms rhombomeres 3 and 4), into the second pharyngeal arch. The third (vagal) population has a more extensive origin, from the neural folds caudal to the otocyst, i.e. prorhombomere C. These cells will contribute to the ganglia of the glossopharyngeal and vagal nerves, with the non-neuronal vagal crest cells migrating into pharyngeal arches 3, 4 and 6, some of them continuing into the heart to contribute to the division of the cardiac outflow tract. The neural crest also gives rise to the parasympathetic ganglia and parasympathetic postganglionic nerves in the head and neck. For a full account of the neuronal contribution of neural crest cells, see Chapter 24. In human embryos, histological methods have revealed equivalent cranial neural crest cell origins and migration routes to those of the mouse, except that no emigration from the diencephalon has been detected (O'Rahilly & Müller 2007).

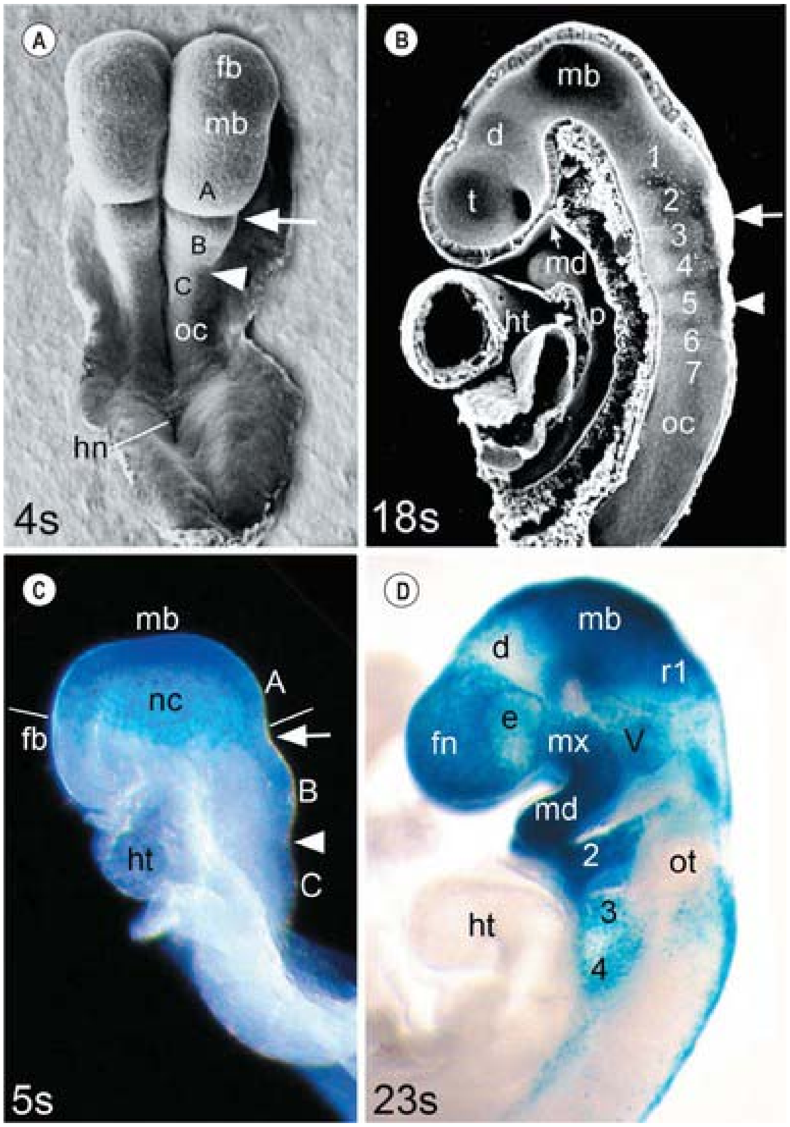
A
fb
mb
A
B
C
oc
hn
4s
B
mb
d
t
1
2
3
4
5
6
7
md
ht
p
oc
18s
C
mb
nc
A
fb
B
ht
C
5s
D
mb
d
r1
e
fn
mx
V
md
2
ot
ht
3
4
23s

Fig. 35.2 Mouse embryo heads during the period of cranial neural crest cell migration. **A** and **B**, Scanning electron micrographs (**A**, dorsal view; **B**, median section) of embryos near the start (4 somite pairs) and end (18 somite pairs, interior view) of the period of neural crest cell migration. At the 4-somite stage the neural folds are convex and the hindbrain is divided into prorhombomeres A, B and C by the preotic (arrow) and otic (arrowhead) sulci; at the 18-somite stage the neural tube is closed and the hindbrain is divided into seven rhombomeres (numbered) and the unsegmented occipital region (oc). **C** and **D**, Lateral views of 5- and 23-somite stage embryos carrying a permanent marker for neural crest cells and the neural epithelium from which the trigeminal crest cells originate (blue

stain). Neural crest cells (nc) migrate as a veil-like mass beneath the surface ectoderm, originating as a continuous group from prorhombomere A, the midbrain and the caudal diencephalic region of the forebrain, into the frontonasal region (fn) and the first arch (lines indicate the level of the migrating edge). After migration, frontonasal neural crest cells (fn) cover the telencephalon and rostral diencephalon, surrounding the eye (e); maxillary (mx) and mandibular (md) neural crest populates the first pharyngeal arch; the trigeminal ganglion primordium (V) is also present. Crest cells from prorhombomere B have populated the hyoid arch and the primordium of ganglion VII/VIII, rostral to the otocyst (ot); crest cells from prorhombomere C are migrating into arches 3 and 4 and starting to form the primordia of cranial ganglia IX and X, caudal to the otocyst. d, diencephalon; fb, forebrain; hn, Hensen's node; ht, heart; mb, midbrain; oc, occipital region of neural fold/tube; p, pharynx; r1, rhombomere 1 of the hindbrain; t, telencephalon; Rathke's pouch is indicated by a small arrow on **B**. (**A** and **B**, From Morriss-Kay and Wilkie 2005; **C** and **D**, from Jiang et al 2002.)

Caudal to the segmented region of the neural tube, neural crest cells from rhombomere 8 migrate with the occipital myotome-derived mesenchyme to form the hypoglossal cord, eventually differentiating to form the connective tissue (neural crest) and musculature of the tongue. No sensory ganglia are formed from the occipital neural crest in human embryos. The origin of the rhombomeres and brain regions in human embryos is given in Figures 24.2 and 24.12.

Ectodermal placodes also make important contributions to the developing head. There is good evidence to suggest that all cranial placodes originate from a continuous pre-placodal territory, the ectodermal ring, around the periphery of the early neural plate, distinct from neural and neural crest cell precursors; this territory is then subdivided into separate placodes, each with its distinct developmental fate (Bailey & Streit 2006). During neurulation the placodes are segregated into the surface ectoderm, moving within the epithelium to their final positions.

Ectodermal placodes appear as patches of columnar or pseudostratified epithelium within the otherwise squamous epithelium of the surface ectoderm. They contribute to the paired sensory organs, forming the olfactory epithelium, the lens and the otocyst, undergoing morphogenesis to form a pit and then (for the lens and otic pits) a closed cyst (vesicle). Epipharyngeal placodes are situated within the dorsal ectoderm of pharyngeal arches 2, 3 and 4: some of their cells undergo epithelial–mesenchymal transformation, joining the underlying neural crest cell condensations to form the sensory neuroblasts in the cranial sensory ganglia. Some cells from the otocyst similarly delaminate to contribute to the ganglion of cranial nerve VIII.

The epithelial-to-mesenchymal transformation of some cells from ectodermal placodes contributes a third component to the cranial mesenchyme. It important to note that the term mesenchyme simply describes a loose cellular organization with a rich extracellular matrix, in contrast to the sheets of simple epithelial tissue that form the outer ectodermal and inner endodermal layers of early embryos. Prior to the migration of neural crest cells from the edges of the cranial neural folds to their final destinations, the only mesenchyme in the embryonic head is ‘primary mesenchyme’, i.e. mesenchymal cells formed by epithelial-mesenchymal transformation in the primitive streak. In the head, all of the primary mesenchyme is paraxial mesoderm. Cranial mesenchyme derived from placodal, mesodermal and neural crest sources have specific distributions and specific derivatives, and are not interchangeable.

The first transverse division to form in the early embryonic brain is the preotic sulcus (Figs 35.1A, 35.2A), which defines the boundary between prorhombomeres A and B. This early division is of major functional and organizational significance, since it separates the regions of origin of the skeletogenic neural crest populations that make a major contribution to the skull from those that form skeletal structures in the neck (hyoid bone and larynx). During cranial neurulation the prorhombomeres undergo subdivision so that by the time the brain region of the neural tube closes, seven rhombomeres can be clearly distinguished; the occipital region (adjacent to the four occipital somites) remains unsegmented (Fig. 35.2B). By analogy with the segmented rhombencephalon, it is also referred to as prorhombomere D/rhombomere A. The segmental organization of the embryonic head caudal to prorhombomere A is related to the expression of evolutionarily conserved *HOX* genes (written *Hox* in the mouse) that have their rostral boundaries at specific rhombomere divisions; they are also expressed in the corresponding neural crest cells (reviewed by Santagati & Rijli 2003; see also Fig. 24.16). Genetic experiments in the mouse and other vertebrates have shown that skeletal patterning of the pharyngeal arch neural crest cells depends on the absence of *Hox* gene expression in the cells migrating into the first arch, and the expression of *Hoxa2* in the second arch crest cells. Investigation of *Hox* gene functions in arches 3–6 has not revealed clear skeletal patterning functions.

EMBRYONIC PHARYNX AND PHARYNGEAL ARCHES

The most cranial portion of the foregut, the embryonic pharynx, is the scaffolding around which the face, palate and anterior neck structures are built. The development of this region from neural crest, surface ectoderm and foregut endoderm involves spatio-temporal integration of cell movement, tissue growth and tissue interactions. As successive populations of neural crest cells migrate around the pharynx at progressively more caudal levels, five pairs of pharyngeal arches are formed (numbered 1, 2, 3, 4, 6 for comparative anatomy reasons). This process is complete by the stages 10–13. Depressions between the arches externally, paired pharyngeal grooves or clefts, are matched internally by paired internal depressions, the pharyngeal pouches. The pharyngeal arches are also known as branchial arches because of their evolutionary origin supporting the gills in the earliest vertebrates. Many of the changes seen during development of the mammalian pharynx reflect the functional evolutionary origins of this region. Since the term ‘branchial’ means ‘of the gills’, the term ‘pharyngeal arch’ will be used in the following account of human embryology.

Each pharyngeal arch consists of an epithelial covering, ectoderm and endoderm, filled with mesenchyme which is mainly of neural crest origin, with some contribution from mesoderm (primitive streak-derived mesenchyme) (Fig. 35.3A,B; Table 35.1). The neural crest cells of each arch form a skeletal element and associated connective tissue; they also give rise to the walls of an aortic arch blood vessel which is lined with endothelium derived from angiogenic mesenchyme. Paraxial mesoderm forms the muscle associated with each pharyngeal arch and motor and sensory innervation derives from arch-specific cranial nerves. For an overview of the organization of these tissues in the pharynx, see Fig. 12.4; for their fate, see Figs 35.3, 35.5-35.8. Since the organization of the embryonic pharynx and related structures is similar in all vertebrate embryos, this phase has been termed ‘pharyngula’.

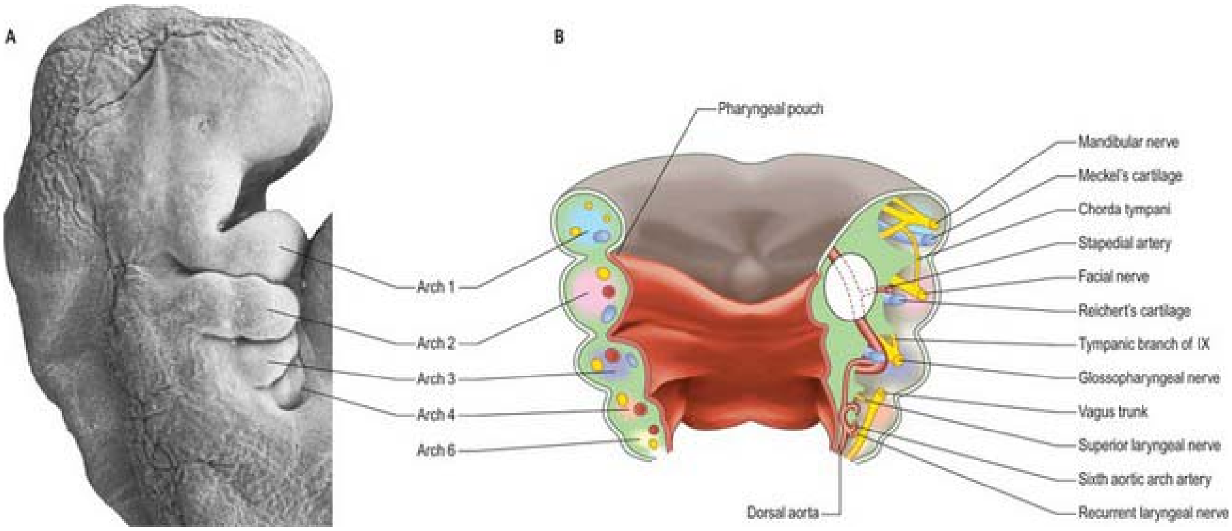
A
B
Pharyngeal pouch
Arch 1
Arch 2
Arch 3
Arch 4
Arch 6
Dorsal aorta
Mandibular nerve
Meckel's cartilage
Chorda tympani
Stapedial artery
Facial nerve
Reichert's cartilage
Tympanic branch of IX
Glossopharyngeal nerve
Vagus trunk
Superior laryngeal nerve
Sixth aortic arch artery
Recurrent laryngeal nerve

Fig. 35.3 Pharyngeal arch development. **A**. SEM of a human embryo (stage 14/15) showing the right lateral aspect of the pharyngeal arches; auricular hillocks are visible on arch two. **B**. Diagrammatic representation of the pharyngeal region (stage 15) viewed from the dorsal aspect. The whole left side and part of the right side of the endodermal roof of the pharynx has been removed to show the grooves in its lateral walls and floor and the nerves, arteries and cartilages of the arches. The position of the right otocyst is shown as a clear oval. (Based on a reconstruction of a 6.3 mm embryo by Blechschmidt.)

(Courtesy of Prof G Steding, Georg-August-University of Göttingen, Göttingen, Germany.)

Table 35.1 Chart of derivatives of the pharyngeal arches

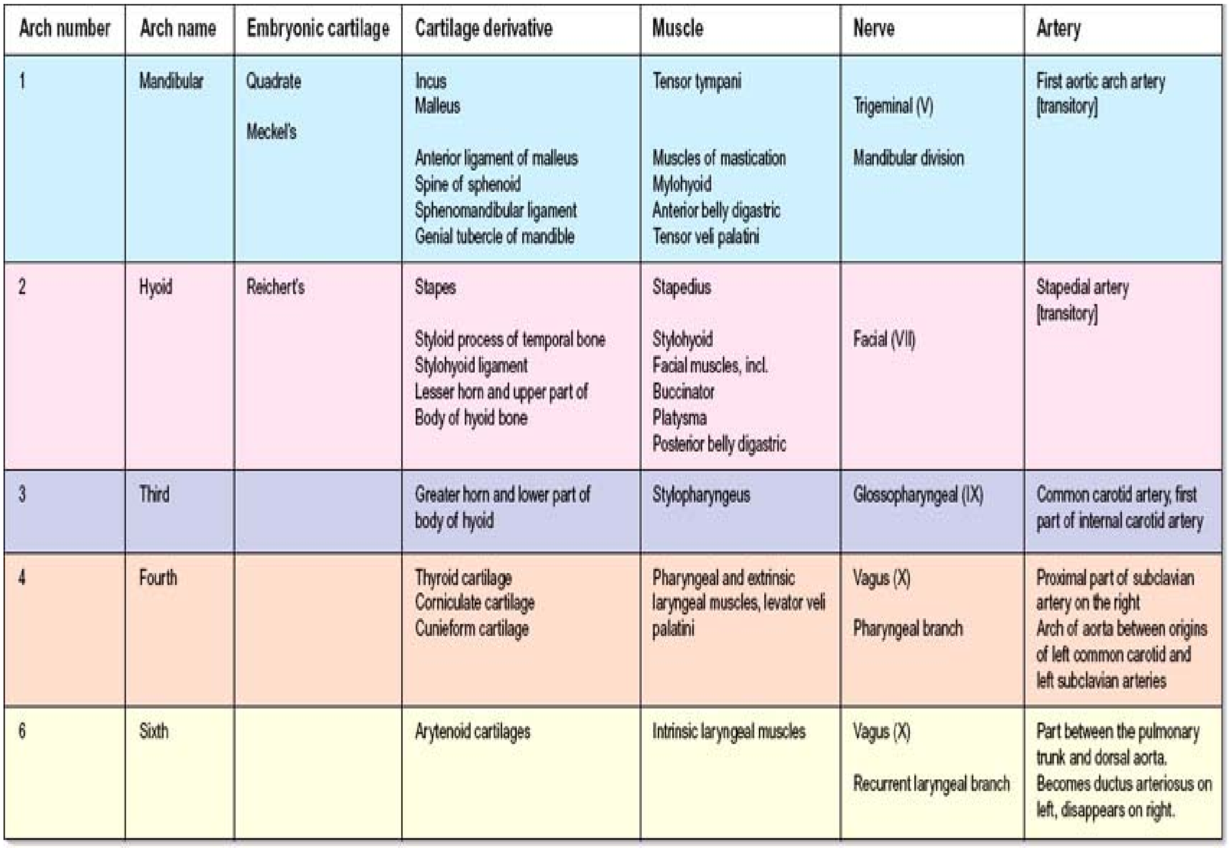

Arch number	Arch name	Embryonic cartilage	Cartilage derivative	Muscle	Nerve	Artery
1	Mandibular	Quadrate Meckel's	Incus Malleus Anterior ligament of malleus Spine of sphenoid Sphenomandibular ligament Genial tubercle of mandible	Tensor tympani Muscles of mastication Mylohyoid Anterior belly digastric Tensor veli palatini	Trigeminal (V) Mandibular division	First aortic arch artery [transitory]
2	Hyoid	Reichert's	Stapes Styloid process of temporal bone Stylohyoid ligament Lesser horn and upper part of Body of hyoid bone	Stapedius Stylohyoid Facial muscles, incl. Buccinator Platysma Posterior belly digastric	Facial (VII)	Stapedial artery [transitory]
3	Third		Greater horn and lower part of body of hyoid	Stylopharyngeus	Glossopharyngeal (IX)	Common carotid artery, first part of internal carotid artery
4	Fourth		Thyroid cartilage Corniculate cartilage Cunieform cartilage	Pharyngeal and extrinsic laryngeal muscles, levator veli palatini	Vagus (X) Pharyngeal branch	Proximal part of subclavian artery on the right Arch of aorta between origins of left common carotid and left subclavian arteries
6	Sixth		Arytenoid cartilages	Intrinsic laryngeal muscles	Vagus (X) Recurrent laryngeal branch	Part between the pulmonary trunk and dorsal aorta. Becomes ductus arteriosus on left, disappears on right.

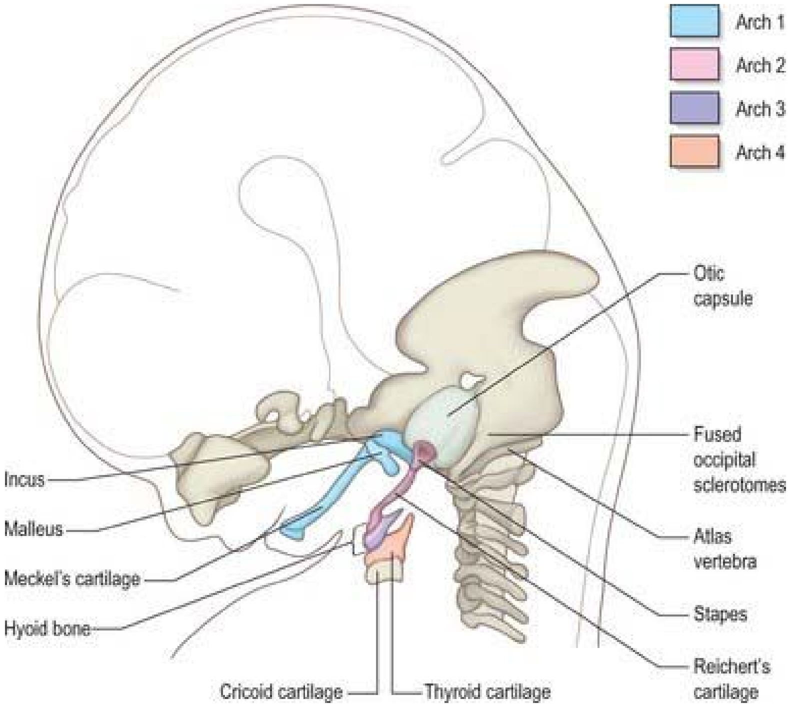
Arch 1
Arch 2
Arch 3
Arch 4
Otic capsule
Fused occipital sclerotomes
Atlas vertebra
Stapes
Reichert's cartilage
Incus
Malleus
Meckel's cartilage
Hyoid bone
Cricoid cartilage
Thyroid cartilage

Fig. 35.5 Chondrocranium and arch cartilage derivatives, 7 weeks (stage 20).

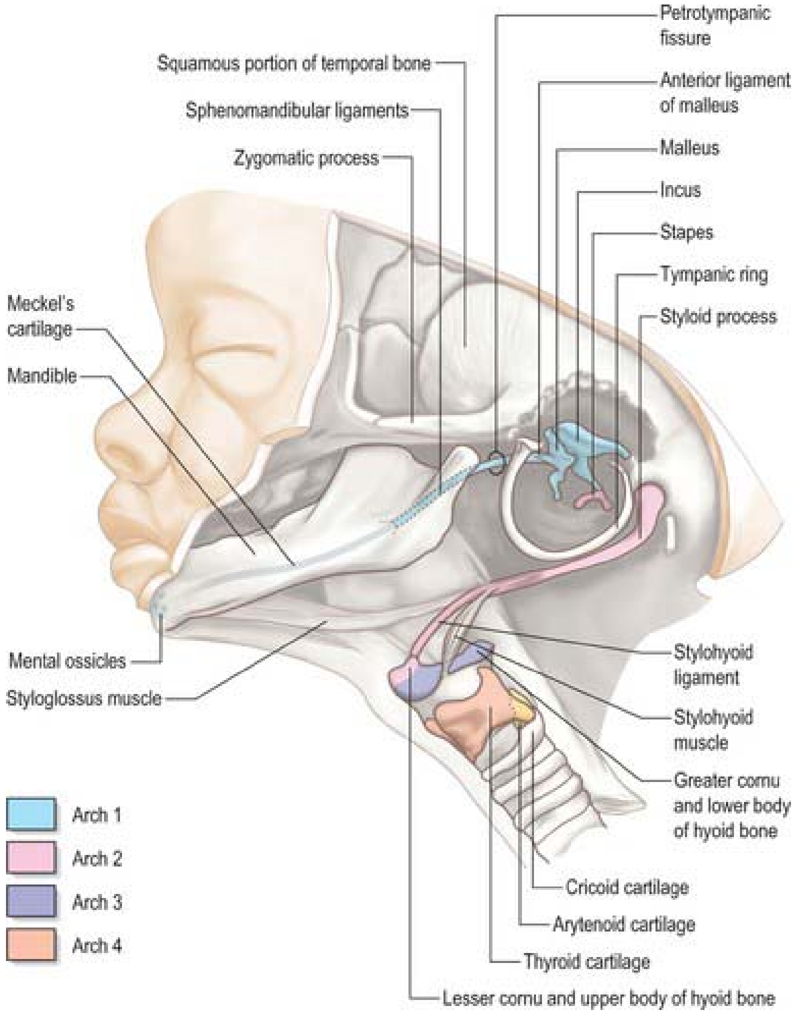
Petrotympanic fissure
Squamous portion of temporal bone
Anterior ligament of malleus
Sphenomandibular ligaments
Malleus
Zygomatic process
Incus
Stapes
Tympanic ring
Meckel's cartilage
Styloid process
Mandible
Mental ossicles
Styloglossus muscle
Stylohyoid ligament
Stylohyoid muscle
Greater cornu and lower body of hyoid bone
Arch 1
Arch 2
Arch 3
Arch 4
Cricoid cartilage
Arytenoid cartilage
Thyroid cartilage
Lesser cornu and upper body of hyoid bone

Fig. 35.6 Derivatives of the pharyngeal arch cartilages in a fetus.

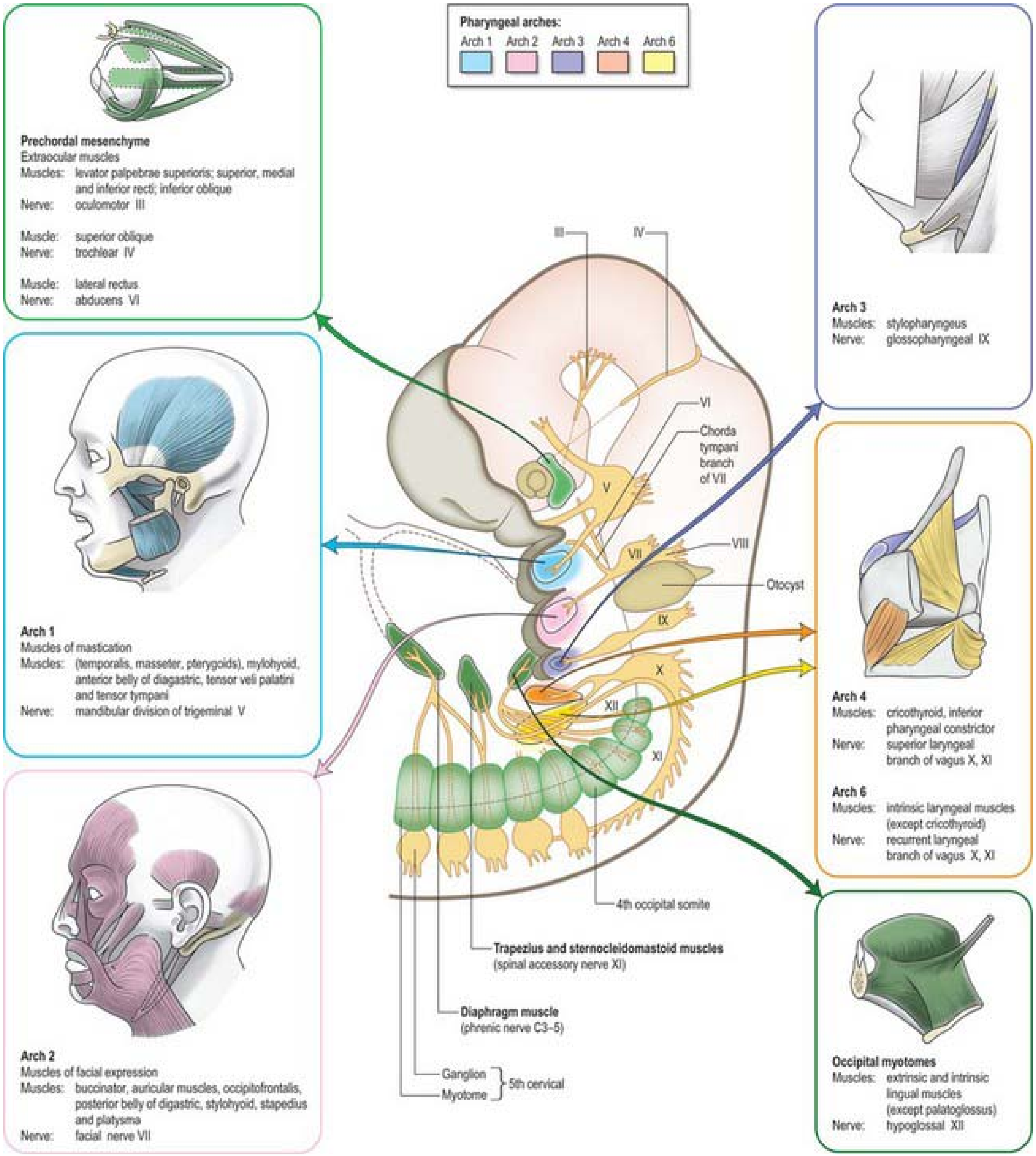
Pharyngeal arches:
Arch 1
Arch 2
Arch 3
Arch 4
Arch 6
Prechordal mesenchyme
Extraocular muscles
Muscles: levator palpebrae superioris; superior, medial and inferior recti; inferior oblique
Nerve: oculomotor III
Muscle: superior oblique
Nerve: trochlear IV
Muscle: lateral rectus
Nerve: abducens VI
Arch 1
Muscles of mastication
Muscles: (temporalis, masseter, pterygoids), mylohyoid, anterior belly of diagastric, tensor veli palatini and tensor tympani
Nerve: mandibular division of trigeminal V
Arch 2
Muscles of facial expression
Muscles: buccinator, auricular muscles, occipitofrontalis, posterior belly of digastric, stylohyoid, stapedius and platysma
Nerve: facial nerve VII
III
IV
VI
Chorda tympani branch of VII
V
VII
VIII
Otocyst
IX
X
XII
XI
4th occipital somite
Trapezius and sternocleidomastoid muscles
(spinal accessory nerve XI)
Diaphragm muscle
(phrenic nerve C3–5)
Ganglion
Myotome
5th cervical
Arch 3
Muscles: stylopharyngeus
Nerve: glossopharyngeal IX
Arch 4
Muscles: cricothyroid, inferior pharyngeal constrictor
Nerve: superior laryngeal branch of vagus X, XI
Arch 6
Muscles: intrinsic laryngeal muscles (except cricothyroid)
Nerve: recurrent laryngeal branch of vagus X, XI
Occipital myotomes
Muscles: extrinsic and intrinsic lingual muscles (except palatoglossus)
Nerve: hypoglossal XII

Fig. 35.7 The muscular derivatives of the prechordal mesenchyme, unsegmented paraxial mesenchyme and rostral somites.

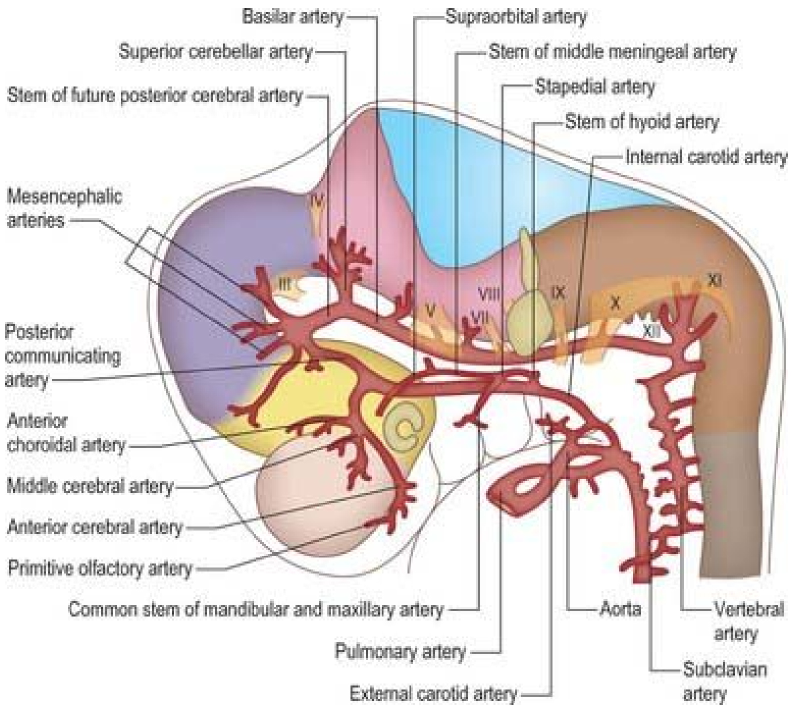
Basilar artery
Superior cerebellar artery
Stem of future posterior cerebral artery
Mesencephalic arteries
Posterior communicating artery
Anterior choroidal artery
Middle cerebral artery
Anterior cerebral artery
Primitive olfactory artery
Common stem of mandibular and maxillary artery
Pulmonary artery
External carotid artery
Supraorbital artery
Stem of middle meningeal artery
Stapedial artery
Stem of hyoid artery
Internal carotid artery
Aorta
Vertebral artery
Subclavian artery
IV
III
V
VIII
VII
IX
X
XI
XII

Fig. 35.8 The arterial system of the head at stage 17 (approx 40 days).

The first pharyngeal arch, unlike the other arches, possesses dorsal and ventral processes and appears C-shaped in lateral view. It is also termed the ‘mandibular arch’; however, this is not entirely appropriate because its proximal (dorsal) end also contributes to maxillofacial and palatopharyngeal structures and to the middle ear. The second pharyngeal arch is termed the hyoid arch because of its contribution to the hyoid bone (and to other parts of the hyomandibular apparatus in fishes). Arches 3, 4 and 6 are not named.

The mandibular arches, first seen at stage 10, grow ventromedially in the floor of the pharynx to meet in the median plane, forming the ventral border of the early mouth above the cardiac (pericardial) prominence. The maxillary processes are not clearly visible as surface structures until stage 13: their enlargement coincides with the proliferation of the frontonasal mesenchyme to form the nasal swellings. The hyoid arches appear at stage 11, the third arches at stage 12 and the fourth arches by stage 13. The sixth arch cannot be recognized externally and can only be identified by the arrangement of the arch arteries and nerves, and by a slight projection on the pharyngeal aspect. The floor of the pharynx is formed mainly by ventral apposition of the arches.

SKELETAL ELEMENTS OF THE PHARYNGEAL ARCHES

The skeletal elements of each arch are formed by condensation of neural crest-derived mesenchyme, which subsequently chondrifies in part or all of its length. Where chondrogenesis is complete (first and second arch cartilages), the element extends dorsally until it comes into contact with the cranial base lateral to the hindbrain (Fig. 35.5). An arch cartilage may remain as cartilage, undergo endochondral ossification, or become ligamentous, or a combination of these (Fig. 35.6).

The first arch cartilage, Meckel's cartilage, forms the embryonic jaw skeleton. After the mandible forms by intramembranous ossification of the neural crest-derived mesenchyme lateral to it, Meckel's cartilage degenerates but its sheath persists as the anterior malleolar and sphenomandibular ligaments. Its proximal end undergoes endochondral ossification to form two of the middle ear bones, the incus and malleus. These are homologous with the quadrate and articular bones of reptiles, and the joint between them is evolutionarily derived from the reptilian jaw articulation. In reptiles, the quadrate forms from the caudal end of the palatopterygoquadrate cartilage; the mammalian evolutionary derivatives of the palatopterygoquadrate are thought to include part of the greater wing of the sphenoid bone and the roots of its pterygoid plates, in addition to the incus. The portion of Meckel's cartilage that extends from the mental foramen almost to the site of the future mandibular symphysis probably becomes ossified and incorporated into the intramembranous mandibular bone, and the remainder of the cartilage is ultimately absorbed.

The second arch cartilage, Reichert's cartilage, extends from the proximity of the otic capsule dorsally to the median plane ventrally. It ossifies to form the upper part of the body and lesser cornua of the hyoid bone distally, and the styloid process proximally; between these two bones it becomes ligamentous to form the stylohyoid ligament. It also gives rise to the most ancient of the three auditory ossicles, the stapes (homologous with the rod-shaped columella auris of reptiles and birds). The cartilages of arches 3 and 4 form only anterior neck skeletal structures: the lower part of the body and greater cornua of the hyoid bone (arch 3) and the thyroid cartilage of the larynx (arch 4). Neural crest cells also give rise to ligaments, tendons and connective tissue in the arches. The cricoid and arytenoid cartilages are mesodermal.

MUSCLES OF THE PHARYNGEAL ARCHES

The striated muscle of each arch (sometimes termed branchiomeric) is derived from the rostral continuation of the paraxial mesoderm. The paraxial mesoderm of the head rostral to the occipital region is unsegmented, and the suggestion that a segmental pattern of seven cranial somitomeres exists is not generally accepted today. In the occipital region of the head, epithelialization takes place to form four pairs of somites; these are similar to those of the trunk. Myoblasts migrate from the paraxial mesoderm to sites of future muscle differentiation and form premuscle condensations prior to the development of any skeletal elements. The pattern of primary myotube alignment for any one muscle is specified by the surrounding neural crest-derived mesenchyme and is not related to the source of the myoblasts. The rate and pattern of muscle maturation are closely associated with the development of the skeletal elements but remain unattached until an appropriate time. Figs 35.3 and 35.7 show the muscle masses of each arch, their innervation and their derivatives in the adult.

The muscle mass of the mandibular part of the first arch forms tensor tympani, tensor veli palatini, mylohyoid, anterior belly of digastric, and the masticatory muscles (Fig. 35.7). Tensor tympani retains its connection with the skeletal element of the arch through its attachments to the malleus, and tensor veli palatini remains attached to the base of the medial pterygoid process – which may be derived from the dorsal cartilage of the first arch. However, the masticatory muscles become attached to the mandible, which is mainly a dermal bone. All of these muscles are supplied by the mandibular nerve, the mixed nerve of the first arch.

The muscles of the second arch migrate widely, but retain their original nerve supply from the facial nerve: migration is facilitated by the early obliteration of some of the first groove (cleft) and pouch. Stapedius, stylohyoid and posterior belly of digastric remain attached to the hyoid skeleton, but the facial musculature, platysma, auricular muscles and epicranius all lose connection with it (Fig. 35.7).

The muscle masses from arches 3 and 4 are adapted to form the musculature of the pharynx, larynx and soft palate. Stylopharyngeus is a third arch muscle, cricothyroid develops in the fourth arch (Fig. 35.7), and the rest of the laryngeal muscles are derived from the sixth arch. The precise origin of the remaining palatal muscles and the pharyngeal constrictors is uncertain. Palatoglossus, a muscle of the palate, is innervated by the cranial part of the accessory nerve and may derive from the lower arches.

NERVES OF THE PHARYNGEAL ARCHES

The nerves associated with each arch arise from the adjacent hindbrain (Fig. 35.7; see also Figs 12.4, 24.18). They are cranial nerves V (trigeminal), VII (facial), IX (glossopharyngeal), X (vagal) and XI (accessory). The motor nerves extend from the basal plate of the hindbrain to innervate the striated muscle of the arches: they are termed special branchial (visceral) efferent nerves because they innervate pharyngeal (branchiomeric) musculature. Sensory nerves extend peripherally and centrally from cranial ganglia that are formed partly from neural crest and partly from cells that delaminate from epipharyngeal placodes; they convey general and special somatic afferent axons. Each arch is innervated by a mixed nerve, but the nerves of arches 1–3 also have a purely sensory branch that innervates the arch rostral to its 'own' arch; this sensory nerve is called the pretrematic branch, because it extends rostral to the cleft or trema between the two arches (Figs 35.3, 35.7). Hence, the nerves to the mandibular arch include the mandibular division of the trigeminal nerve, which is mixed, and the chorda tympani and greater petrosal nerves, purely sensory pretrematic branches of the facial nerve. The maxillary branch of the trigeminal and the tympanic branch of the glossopharyngeal are also considered to be pretrematic nerves. The ophthalmic branch of the trigeminal nerve, which supplies the frontonasal area, is not an arch nerve; in fishes its ganglion is separate from the first arch nerve ganglion.

The vagus nerve, together with some fibres from the cranial part of the accessory nerve, supplies arches 3 (pharyngeal muscles), 4 and 6 (Fig. 35.7). The recurrent laryngeal branch initially loops under the sixth arch artery on both sides, but the asymmetric changes to the vascular system affect the symmetry of this nerve. On the right, where the sixth aortic arch disappears beyond the right pulmonary artery, the recurrent laryngeal nerve loops under the fourth arch-derived subclavian artery; on the left it loops round the ductus arteriosus (ligamentum arteriosum in the adult). Hence, the right and left branches of this nerve have asymmetric courses in the adult. Further details of cranial nerve development and composition are provided in Chapter 24.

BLOOD VESSELS OF THE PHARYNGEAL ARCHES

The aortic arches initially develop by vasculogenesis, soon after neural crest cells have invaded the early pharyngeal arches. Angiogenic mesenchyme forms the endothelial lining of the vessels and neural crest contributes to the outer layers of the walls (Jiang et al, 2000). The first aortic arch artery is part of the original vascular circuit that links the truncus arteriosus of the heart to the paired dorsal aortae, blood returning to the heart via the allantoic, vitelline and common cardinal veins (see Figs 13.1, 59.8). As the heart descends relative to the forebrain and other rostral structures, the aortic sac gives rise to paired aortic arches at successively more caudal levels, each of which passes laterally on each side of the pharynx to join the dorsal aortae. The dorsal aortae are not invested by neural crest cells, and nor are the more distal (cranial) parts of the carotid arteries, which form by angiogenesis. The whole complement of aortic arches never coexists – the first aortic arch degenerates through remodelling of the cranial arteries before the sixth is formed.

When the first and second aortic arch arteries begin to regress, the supply to the corresponding pharyngeal arches is derived from a transient ventral pharyngeal artery which terminates by dividing into mandibular and maxillary branches. The second aortic arch artery also degenerates, remaining only as the stem of the stapedial artery. The early vessel anastomoses with the ventral pharyngeal artery passing as it does through the mesenchyme of the stapedial cartilage, which condenses around it, forming the foramen of the stapes. The fully developed stapedial artery possesses three branches, mandibular, maxillary and supraorbital, which follow the divisions of the trigeminal nerve (Fig. 35.8). The mandibular and maxillary branches diverge from a common stem.

Further development of the third, fourth and sixth aortic arches (Fig. 35.9) produces the main arteries to the head and the great vessels arising from the heart. The external carotid artery first appears as a sprout, which extends cranially from the aortic sac close to the ventral end of the third arch artery. The common carotid arises from an elongation of the adjacent part of the aortic sac, and the third arch artery becomes the proximal part of the internal carotid artery. The fourth aortic arch on the right forms the proximal part of the right subclavian artery, whereas the corresponding vessel on the left constitutes the arch of the definitive aorta between the origins of the left common carotid and left subclavian arteries.

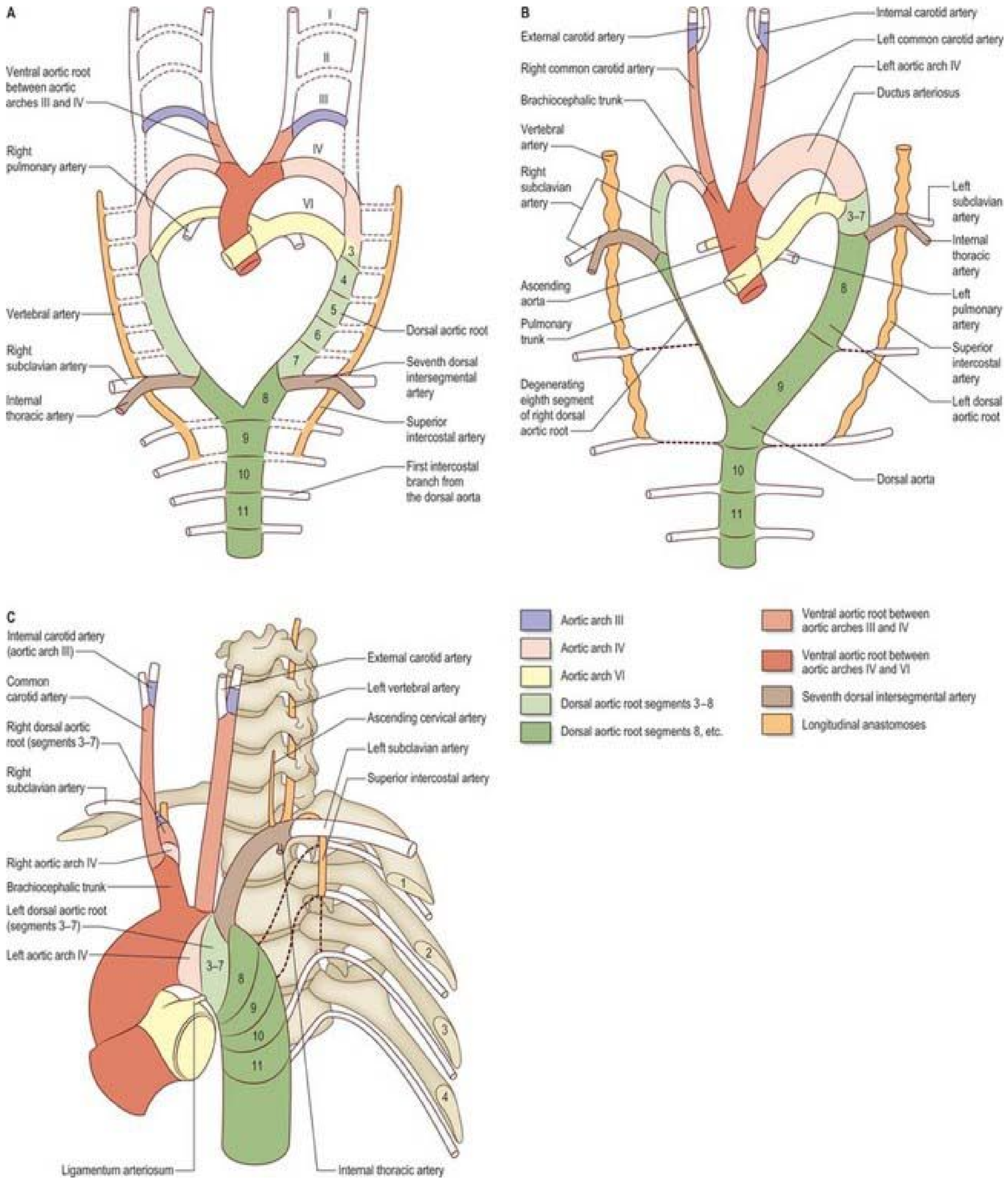
A
I
II
III
IV
VI
Ventral aortic root between aortic arches III and IV
Right pulmonary artery
Vertebral artery
Right subclavian artery
Internal thoracic artery
3
4
5
6
7
8
9
10
11
Dorsal aortic root
Seventh dorsal intersegmental artery
Superior intercostal artery
First intercostal branch from the dorsal aorta
B
External carotid artery
Right common carotid artery
Brachiocephalic trunk
Vertebral artery
Right subclavian artery
Ascending aorta
Pulmonary trunk
Degenerating eighth segment of right dorsal aortic root
Internal carotid artery
Left common carotid artery
Left aortic arch IV
Ductus arteriosus
3–7
Left subclavian artery
Internal thoracic artery
Left pulmonary artery
Superior intercostal artery
Left dorsal aortic root
Dorsal aorta
C
Internal carotid artery (aortic arch III)
Common carotid artery
Right dorsal aortic root (segments 3–7)
Right subclavian artery
Right aortic arch IV
Brachiocephalic trunk
Left dorsal aortic root (segments 3–7)
Left aortic arch IV
Ligamentum arteriosum
External carotid artery
Left vertebral artery
Ascending cervical artery
Left subclavian artery
Superior intercostal artery
Internal thoracic artery
1
2
3
4
Aortic arch III
Aortic arch IV
Aortic arch VI
Dorsal aortic root segments 3–8
Dorsal aortic root segments 8, etc.
Ventral aortic root between aortic arches III and IV
Ventral aortic root between aortic arches IV and VI
Seventh dorsal intersegmental artery
Longitudinal anastomoses

Fig. 35.9 Aortic arch arteries and their derivatives.

When the external carotid artery emerges from the base of the third arch, it incorporates the stem of the ventral pharyngeal artery, and its maxillary branch communicates with the common trunk of origin of the maxillary and mandibular branches of the stapedial artery and annexes these vessels. The proximal part of the common trunk persists as the root of the middle meningeal artery. More distally, the meningeal artery is derived from the proximal part of the supraorbital artery. The maxillary branch becomes the infraorbital artery and the mandibular branch forms the inferior alveolar artery.

When the definitive ophthalmic artery differentiates as a branch from the terminal part of the internal carotid artery, it communicates with the supraorbital branch of the stapedial artery which distally becomes the lacrimal artery. The latter retains an anastomotic connection with the middle meningeal artery. The dorsal stem of the original second arch artery remains as one or more caroticotympanic branches of the internal carotid artery.

From its inception, the sixth aortic arch is associated with the developing lung buds. Initially, each bud is supplied by a capillary plexus from the aortic sac; as the sixth aortic arch develops, it becomes the channel for blood from the aortic sac to the developing lung buds as well as to the corresponding dorsal aorta, the latter being the main channel. Soon after formation of the sixth aortic arch, the outflow tract of the heart is divided by an influx of neural crest cells which form the spiral aorticopulmonary septum (Jiang et al 2000) which separates the aortic sac into the pulmonary trunk and ascending aorta; the pulmonary trunk attains alignment with the left sixth aortic arch (see p. 1025). The part of the sixth aortic arch between the pulmonary trunk and the dorsal aorta becomes the main vascular channel on the left, and is defined as the ductus arteriosus when the equivalent vessel on the right side is lost. Loss of the right sixth aortic arch may be related to the changes in blood flow dynamics consequent on division of the outflow tract. The caudal part of the right dorsal aorta (close to its conjunction with the left) also degenerates, separating the definitive aorta from the developing subclavian artery (Fig. 35.9B). The ductus arteriosus remains the main channel for blood to pass from the right ventricle to the descending aorta until the lungs and their associated blood vessels expand at birth. After birth, the ductus arteriosus is functionally closed by contraction of the circular muscle of the tunica media (see Ch. 59) (Fig. 35.9C).

PHARYNGEAL ECTODERM AND CLEFTS

Surface ectoderm lines the roof of the embryonic pharynx up to and including the adenohypophysial pouch (for the early development of the pituitary gland, see page 367 of Chapter 24). It also completely clothes the first arch covering the lateral walls and floor of the pharynx, unlike the more caudal arches which are dependent on the proximity of pharyngeal endoderm for their development. The external surface ectoderm of the first arch ultimately produces the keratinized stratified squamous epithelium of the epidermis including hair follicles, sweat and sebaceous glands, and the specialized epithelium of the vermilion of the lip. The first pharyngeal cleft is obliterated ventrally; its dorsal end deepens to form the external acoustic meatus and the external surface of the tympanic membrane (Fig. 35.4B,C); the ectoderm giving rise to the lining epidermis and ceruminous glands. The ectodermal covering of the oral aspect of the first arch forms the mucous membranes of the palate, oral cavity and anterior part of the tongue and the ectodermal components of the teeth, salivary and mucous glands. Three auricular hillocks form on arches 1 and 2, each side of the first pharyngeal groove beginning at stage 15; they form the auricle of the external ear (see Ch. 38).

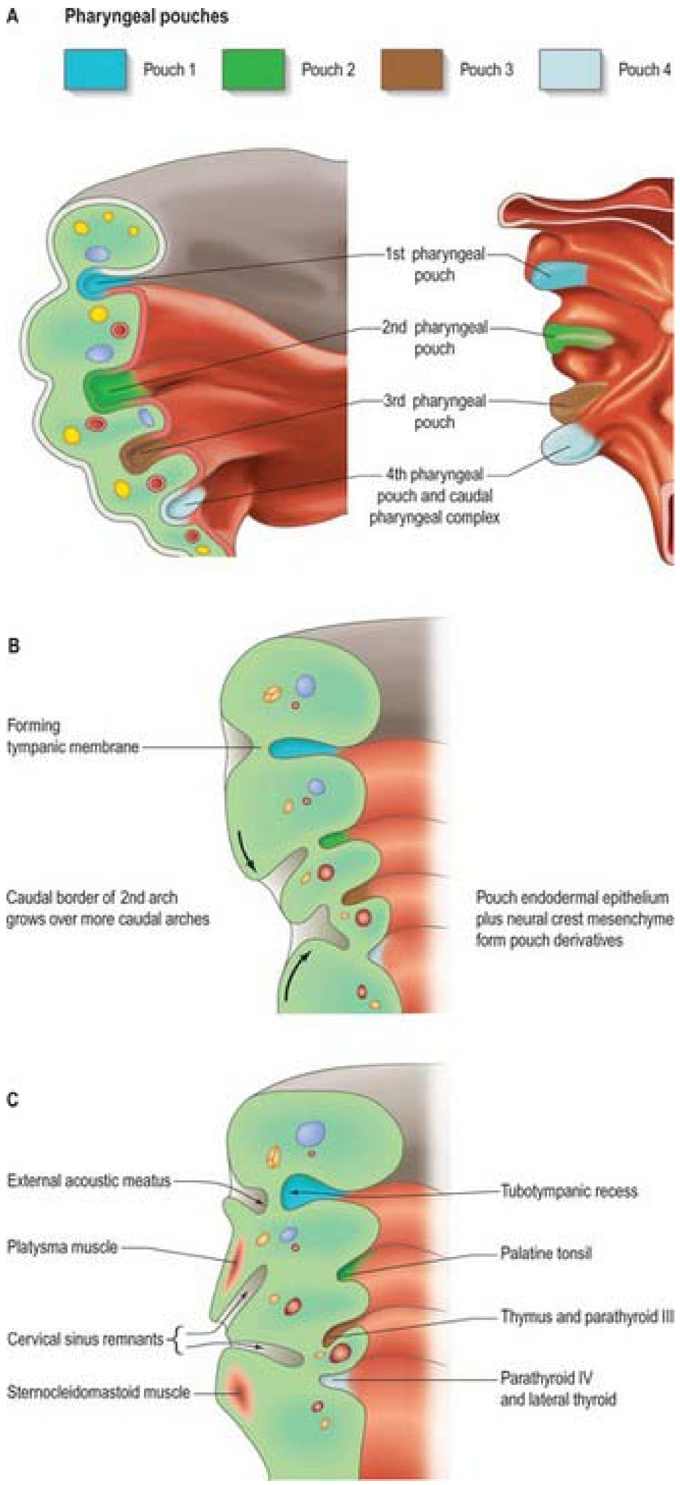
A
Pharyngeal pouches
Pouch 1
Pouch 2
Pouch 3
Pouch 4
1st pharyngeal pouch
2nd pharyngeal pouch
3rd pharyngeal pouch
4th pharyngeal pouch and caudal pharyngeal complex
B
Forming tympanic membrane
Caudal border of 2nd arch grows over more caudal arches
Pouch endodermal epithelium plus neural crest mesenchyme form pouch derivatives
C
External acoustic meatus
Platysma muscle
Cervical sinus remnants
Sternocleidomastoid muscle
Tubotympanic recess
Palatine tonsil
Thymus and parathyroid III
Parathyroid IV and lateral thyroid

Fig. 35.4 Pharyngeal pouch development. **A**. The arrangement of the early pharyngeal pouches: on the left, the internal aspect of the pharyngeal floor viewed from above; on the right, the external aspect of the pharyngeal floor viewed from below. **B**. Coronal section of the left side of the pharynx

at stage 18, showing changes to the pharyngeal pouches internally and pharyngeal clefts externally. **C**. Coronal section of the left side of the pharynx at stage 19. See also **Fig 35.18** for further development.

The external contours of the arches and clefts are modified as the skeletal and muscular elements develop. During the fifth week, pharyngeal clefts 2 and 3+4 form the rostral and caudal parts of a retrohyoid depression, the cervical sinus (Fig. 35.4C). Cranially, the sinus is bounded by the hyoid arch; dorsally, by a ridge produced by ventral extensions from the occipital myotomes and by mesenchyme that develops into the sternocleidomastoid and trapezius muscles. Caudally, the smaller epipericardial ridge separates the sinus from the pericardium. Fusion of the hyoid arch with the cardiac elevation covers the cervical sinus, excluding the arches 3–6 from contributing to the skin of the neck; it also results in platysma muscle, bounded both superficially and deep with superficial fascia, passing along the neck to the anterior thoracic wall.

Thickened patches of ectoderm, the epibranchial placodes, appear at the dorsal ends of the pharyngeal grooves. They are closely related to the developing ganglia of the facial, glossopharyngeal and vagus nerves, to which they contribute. Together with dorsolateral and suprabranchial placodal cells, the epibranchial placodes also contribute to the trigeminal and vestibulocochlear ganglia (see Figs 12.4, 24.18).

PHARYNGEAL ENDODERM AND POUCHES

The first four pharyngeal pouches appear in sequence craniocaudally during stages 10–13. The rostral pharynx is broad and dorsoventrally compressed (see Fig. 35.18). Laterally, the endoderm of the pouches approaches the ectoderm of the pharyngeal clefts to form thin closing membranes (Fig. 35.4). The approximating ectoderm and endoderm between the first cleft and pouch form the outer and inner surfaces of the tympanic membrane. The ventral end of the first pouch is obliterated, but its dorsal end persists and expands as the head enlarges. This, together with the adjoining lateral part of the pharynx and possibly with a contribution from the dorsal part of the second pharyngeal pouch, constitutes the tubotympanic recess. The recess forms the middle ear cavity, the pharyngotympanic tube and their extensions. Expansion of the middle ear cavity around the ear ossicles occurs late during fetal life, by breakdown of the mesenchyme around the ossicles so that the cavity comes to surround them except at their attachments to the tympanic membrane and fenestra ovalis (fenestra vestibuli, oval window).

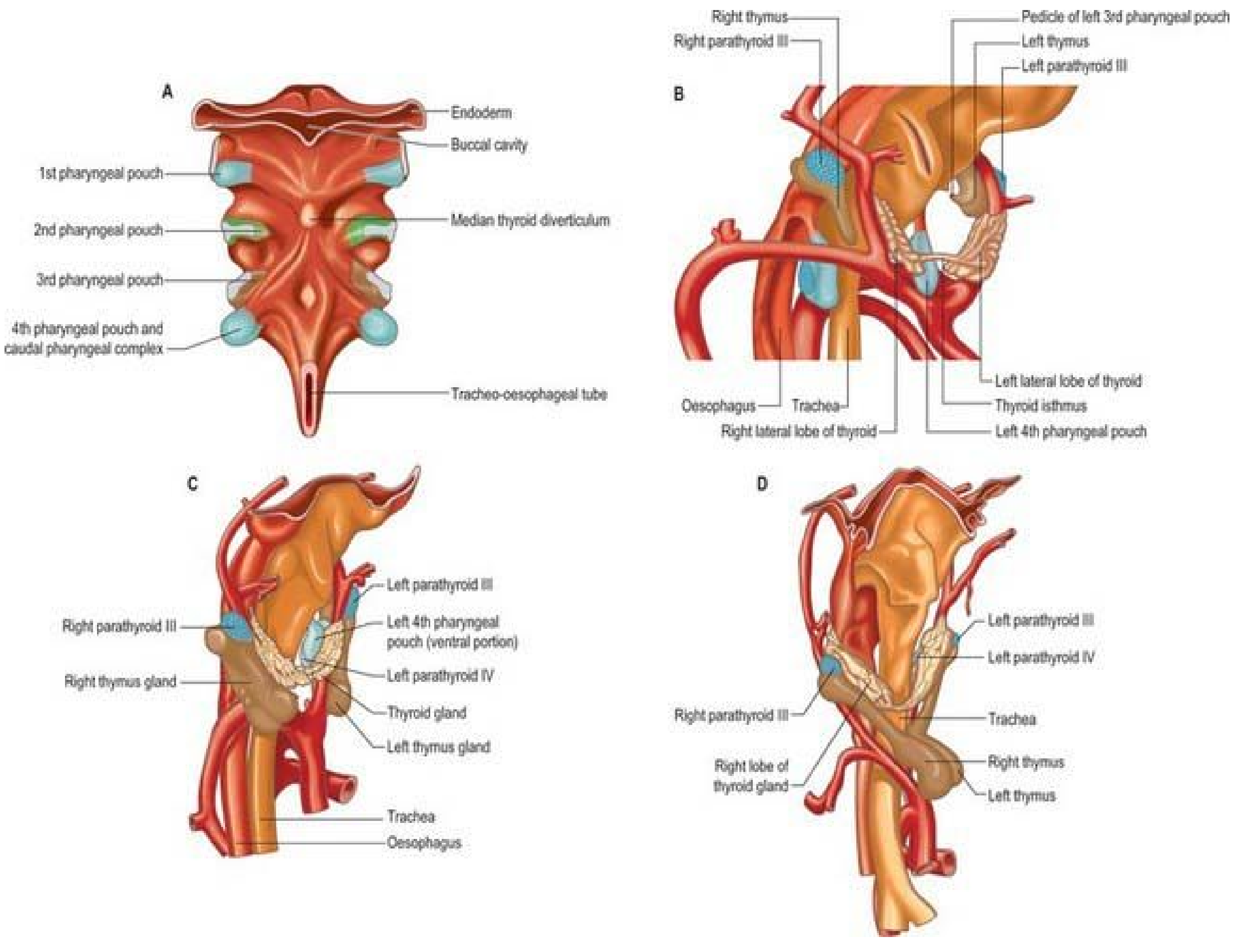
A
Endoderm
Buccal cavity
1st pharyngeal pouch
2nd pharyngeal pouch
Median thyroid diverticulum
3rd pharyngeal pouch
4th pharyngeal pouch and caudal pharyngeal complex
Tracheo-oesophageal tube
B
Right thymus
Right parathyroid III
Pedicle of left 3rd pharyngeal pouch
Left thymus
Left parathyroid III
Oesophagus
Trachea
Right lateral lobe of thyroid
Left lateral lobe of thyroid
Thyroid isthmus
Left 4th pharyngeal pouch
C
Left parathyroid III
Right parathyroid III
Left 4th pharyngeal pouch (ventral portion)
Right thymus gland
Left parathyroid IV
Thyroid gland
Left thymus gland
Trachea
Oesophagus
D
Left parathyroid III
Left parathyroid IV
Right parathyroid III
Trachea
Right lobe of thyroid gland
Right thymus
Left thymus

Fig. 35.18 **A**, Ventral aspect of the endoderm of the pharynx. showing the pharyngeal pouches. The areas of contact of the pharyngeal endoderm with the surface ectoderm are shown as flattened surfaces. Note the colours of the pharyngeal pouches and the median thyroid diverticulum are retained in **B**, **C** and **D**. **B**, Ventral and dorsal diverticuli of the third and fourth pharyngeal pouches and midline thyroid gland at 6 weeks. **C**, Thymus, thyroid and parathyroid glands at 7 weeks. **D**, Thymus, thyroid and parathyroid glands at 7½ weeks.

(Redrawn by permission from Hamilton WJ, Boyd JD, Mossman HW 1962 Human Embryology: Prenatal Development of Form and Function. Cambridge: W Heffer & Sons.)

The ectoderm of the pharyngeal clefts and the endoderm of the pouches become increasingly separated by mesenchyme. The blind recesses of the second, third and fourth pouches are prolonged dorsally and ventrally as angular, wing-like diverticula (see Fig. 35.18); the pouch endoderm thickens and evaginates into localized neural crest-derived mesenchymal condensations. The ventral part of the second pouch is the focus of lymphoid development as the palatine tonsil. A generalized ring of lymphoid tissue, the lymphatic ring, develops in this region. The third pouch gives rise to the thymus ventrally and the parathyroid III dorsally, whereas the fourth pouch produces the parathyroid IV and an ultimobranchial body. The dorsal and ventral portions of the fourth pouch, together with the lower ultimobranchial body, are collectively termed the caudal pharyngeal complex.

Rarely, failure of normal modification of the pharyngeal clefts and pouches may lead to the formation of fistulae, external or internal sinuses, and cysts. Lateral cervical cysts are now considered to be lymphoepithelial in origin.

FACE, NASAL CAVITIES AND PALATE, ORAL CAVITY AND TONGUE

FACE

By stage 12, migration of the most rostral neural crest cell population is complete and the sequence of morphogenetic changes that will form the face begins (Fig. 35.10). Neural crest cells have populated the mandibular arch and its dorsal maxillary extension, and formed the frontonasal mesenchyme that covers the telencephalon and caudal diencephalon. They also contribute to the primordium of the trigeminal nerve, whose first fibres develop at stage 13. The three divisions of the trigeminal nerve will provide sensory innervation to the frontonasal, maxillary and mandibular parts of the face. All of the mesenchyme of the facial region is neural crest-derived, except for the angiogenic mesenchyme, which has migrated from the cranial paraxial mesoderm to form the facial blood vessels. There are no muscle cells in this region during the morphogenetic period of facial development.

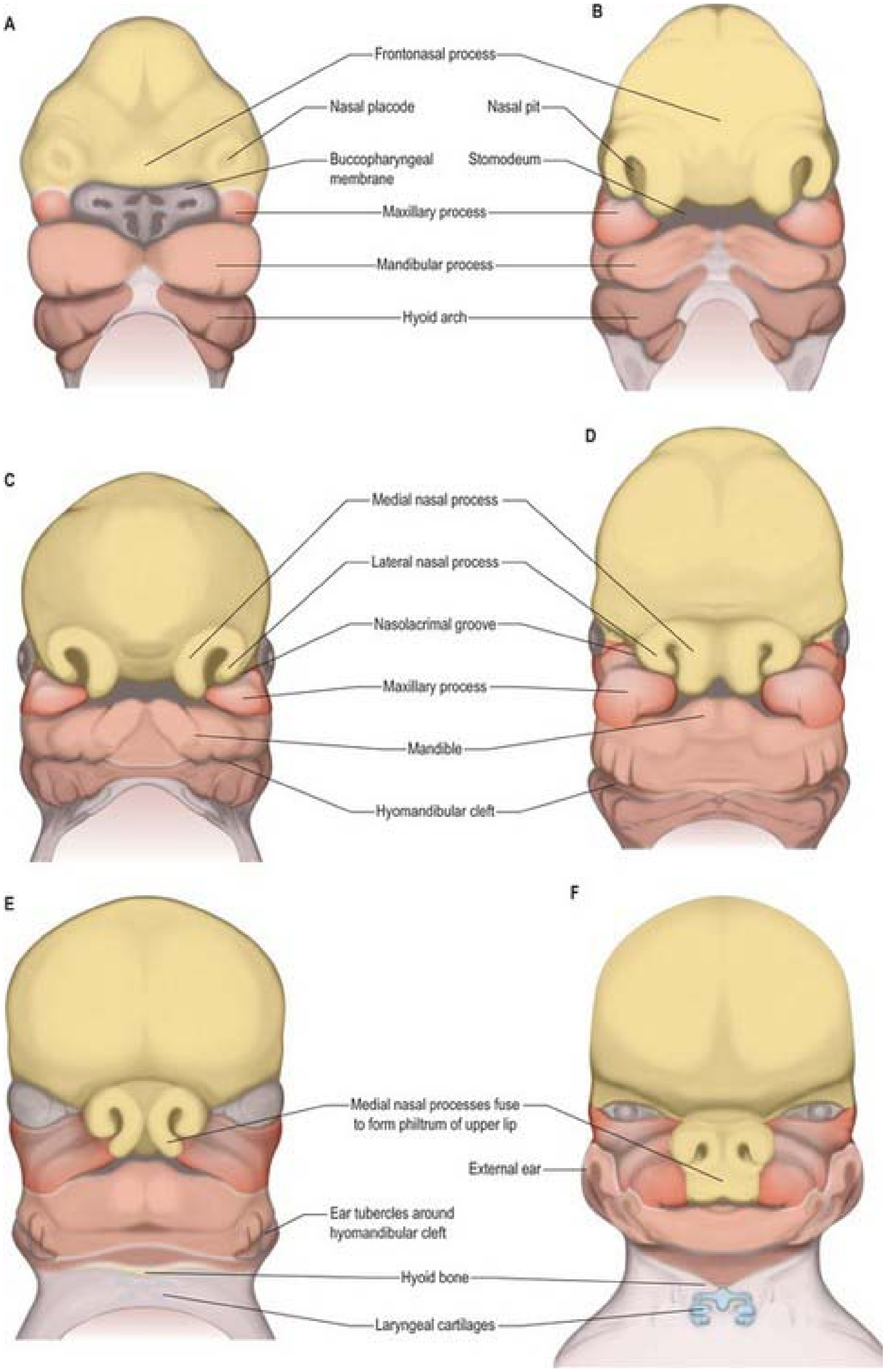
A
B
Frontonasal process
Nasal placode
Nasal pit
Buccopharyngeal membrane
Stomodeum
Maxillary process
Mandibular process
Hyoid arch
C
D
Medial nasal process
Lateral nasal process
Nasolacrimal groove
Maxillary process
Mandible
Hyomandibular cleft
E
F
Medial nasal processes fuse to form philtrum of upper lip
External ear
Ear tubercles around hyomandibular cleft
Hyoid bone
Laryngeal cartilages

Fig. 35.10 Development of the face during stages 12–18. **A**, 4 weeks (3.5 mm); **B**, 5 weeks (6.5 mm); **C**, 5½ weeks (9 mm); **D**, 6 weeks (12 mm); **E**, 7 weeks (19 mm); **F**, 8 weeks (28 mm).

Localized mesenchymal proliferation results in the formation of four paired processes: the medial and lateral nasal, maxillary and mandibular processes. The lateral and medial nasal processes surround the nasal placodes, causing them to sink deep to the surface within the nasal pits. Below the developing nasal region, the median tissue forms the premaxillary component of the upper lip and jaw, and the primary palate. Concomitant with formation of the nasal processes, proliferation of the maxillary mesenchyme forms the maxillary processes. These make contact with the medial and lateral nasal processes at stage 16–17. Fusion of the maxillary processes with the medial nasal processes unites the premaxillary and maxillary parts of the upper jaw and lip; failure of this process on one or both sides causes unilateral or bilateral cleft lip (see Fig. 35.17). Superiorly, this fusion closes the cleft at the lower edge of the nasal pits, completing the future nostrils. Fusion of the maxillary with the lateral nasal processes is a much simpler process and rarely gives rise to abnormality. At stage 16, the epithelium of the groove between them thickens to form the lacrimal lamina, the primordium of the lacrimal system. At stage 19, it separates from the surface ectoderm, forming the lacrimal cord beneath the surface. The cord becomes canalized to form the nasolacrimal duct in the tenth week (de la Cuadra-Blanco et al 2006). The original site of the lacrimal lamina marks the lateral division between frontonasal and maxillary contributions to the face, the territories whose sensory nerve supply is respectively from the ophthalmic and maxillary divisions of the trigeminal nerve (Fig. 35.11).

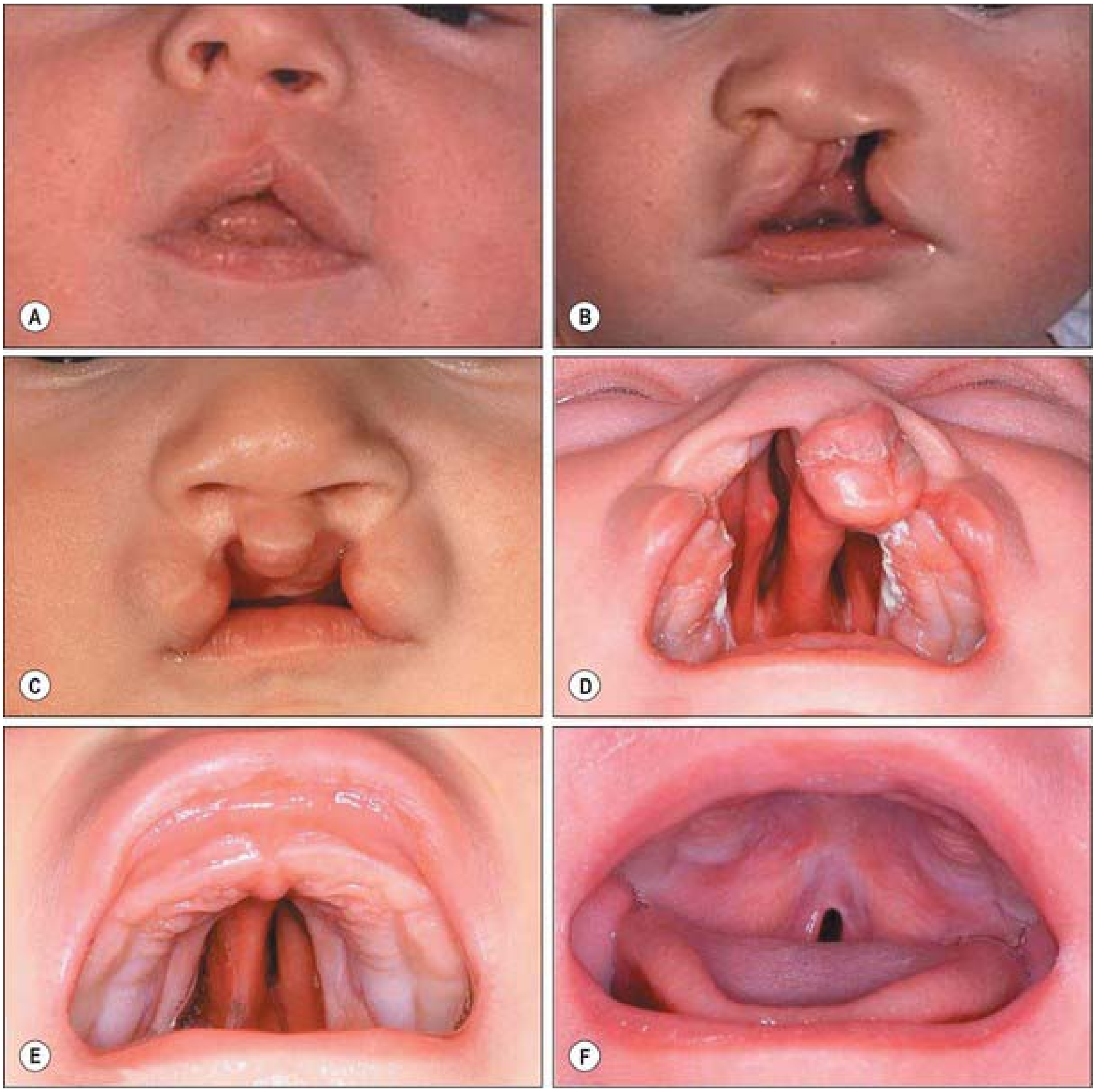

Fig. 35.17 Cleft lip and cleft palate. **A**, incomplete unilateral cleft lip; **B**, complete unilateral cleft lip; **C**, incomplete bilateral cleft lip; **D**, complete bilateral cleft lip and cleft palate (the nasal septum and both inferior nasal conchae can be seen); **E**, cleft palate (the nasal septum and left inferior nasal concha can be seen); **F**, cleft of the soft palate.

(Courtesy of Mr T Goodacre and Oxford Radcliffe Hospitals NHS Trust.)

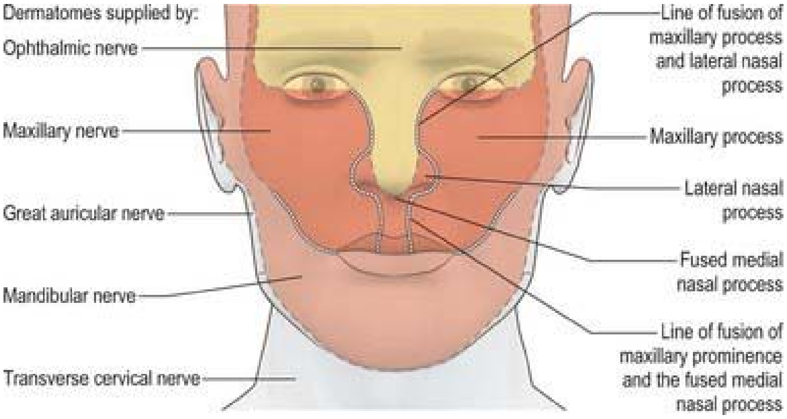
Dermatomes supplied by:
Ophthalmic nerve
Maxillary nerve
Great auricular nerve
Mandibular nerve
Transverse cervical nerve
Line of fusion of maxillary process and lateral nasal process
Maxillary process
Lateral nasal process
Fused medial nasal process
Line of fusion of maxillary prominence and the fused medial nasal process

Fig. 35.11 The parts of the adult face derived from the ophthalmic (frontonasal), maxillary and mandibular divisions of the skin of the face, showing the lines of fusion and definitive innervation.

At the start of facial development, the stomodeal opening extends across the whole width of the embryonic head. A wide mouth is maintained until differential growth brings the eyes and the lateral parts of the maxillary–mandibular structures from the sides to the front of the face (stage 18 to stage 23, 7–8 weeks). Although differential growth makes the mouth opening proportionately smaller, progressive fusion of the lateral regions of the maxillary and mandibular processes also makes an important contribution to decreasing the width of the mouth and to formation of the cheeks. Differences in mouth width within the human population are mainly due to variation in the extent of maxillomandibular fusion. The period from 7 to 8 weeks is the final period of facial development. In addition to formation of the mouth and cheeks, it is marked by further narrowing of the nasal region and philtrum and ascent of the ears. By stage 20, the face is recognizably human, although differential growth will continue to bring about changes in proportion and relative position of the features.

The contribution made by the frontonasal process to surface epithelial derivatives extends from the skin of the forehead, over the supraorbital and glabellar regions including the upper eyelid and conjunctiva, to the external aspect of the nose and philtrum of the upper lip. During later development, the maxillary nerve invades the skin of the philtrum and nasal alae (Fig.

35.11; see Fig. 24.10). Internally, the epithelial contribution to mucous membrane includes the nasal vestibule, the nasal mucosa of the conchae and paranasal sinuses, the olfactory epithelium, the mucosa of the philtrum, gums and primary palate.

NASAL CAVITIES AND PALATE

After formation of the nasal pits, the olfactory placodal cells differentiate into olfactory neuroblasts, supporting (sustentacular) cells and stem cells. Neurites begin to extend from the olfactory neuroblasts, reaching the olfactory region of the telencephalon by stage 16 (sixth week). The earliest pioneer neurites cross a mesenchyme-filled gap between the placode and the brain. The remaining placodal cells differentiate into columnar supporting (sustentacular) cells, rounded basal cells and, by invagination, the flattened duct-lining and polyhedral acinar cells of the glands of Bowman. Basal infiltration by lymphocytes is a relatively late event.

Once the nasal cavities have formed, the roof of the oral cavity is regarded as the primitive palate (not to be confused with the primary palate). Each nasal cavity has an arcuate shape, extending upwards to the olfactory epithelium and then down again towards the oral cavity, from which it is separated by the thin epithelial choanal membrane. Towards the end of stage 18, the choanal membranes degenerate to form the choanae; the nasal cavites are now a duct from the external environment to the oral cavity. The triangular wedge of tissue between the left and right nasal cavities and the oral cavity comprises the primitive palate below and the nasal septum above. Caudal to the primary palate, the internal aspect of each maxillary process bulges into the oral cavity as a palatal process: the palatal processes (first detectable at stage 17) are the primordia of the secondary palate. The tongue is already well developed, and its domed form fills the space between the nascent palatal shelves laterally, and the primitive palate above. The mandible is at this stage short relative to the maxillary region and does not extend as far as the primary palate. Further growth brings the mandibular region and tongue forwards, to a position below the primary palate. At the same time, the (secondary) palatal processes continue to grow, projecting vertically downwards on either side of the tongue. At stage 23 (56–57 days), the tongue descends and the palatal shelves rotate, bringing the shelves to a horizontal position above the tongue (Fig. 35.12). The rapidity of the process of shelf elevation is caused at least in part by swelling of the palatal mesenchyme due to accumulation and hydration of hyaluronan (Ferguson 1991). This occurs during a period of continuous growth in head height but almost no growth in head width. This latter factor is important, because if palatal shelf elevation is delayed so that it occurs during a period of growth in facial width, the unfused processes may be unable to touch physically, resulting in a cleft palate. Other factors affecting palatal closure are the growth in length of Meckel's cartilages, which allows the tongue to descend, and the change in position of the maxillae relative to the anterior cranial base, which has the effect of lifting the head and upper jaw away from the mandible during weeks 9 and 10, facilitating withdrawal of the tongue from between the palatal shelves and creating space for their elevation. Mouth opening, tongue protrusion and hiccup movements have also been noted at this time, and it may be that these movements and their associated pressure changes assist palatal shelf elevation. Generally, in female embryos palatal shelf elevation occurs 7 days later than in males, and congenital cleft palate is more common in females.

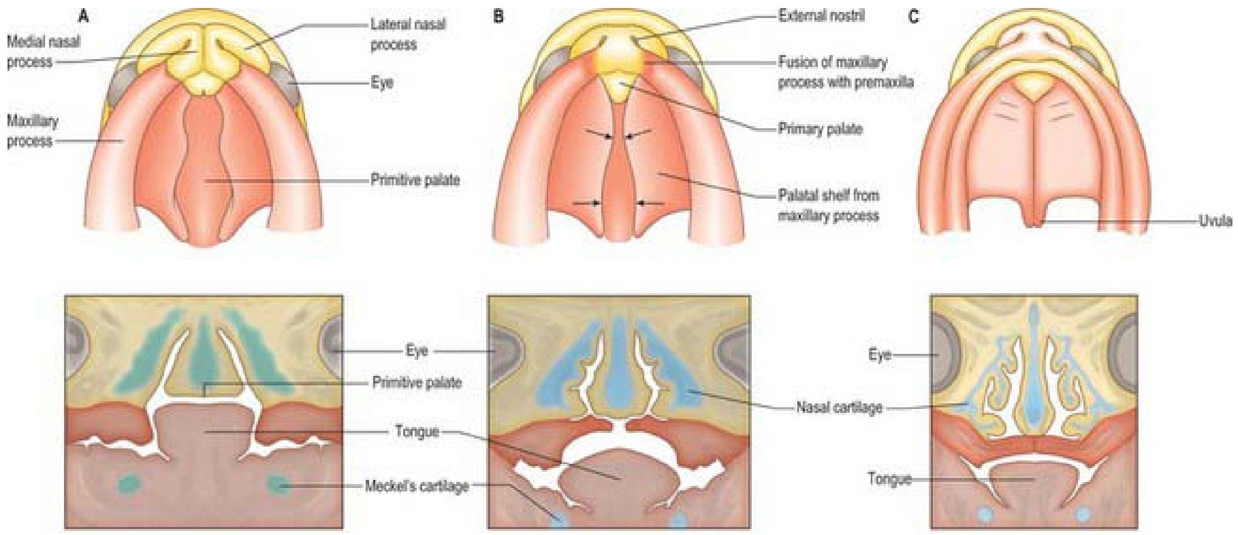
A
Medial nasal process
Lateral nasal process
Eye
Maxillary process
Primitive palate
B
External nostril
Fusion of maxillary process with premaxilla
Primary palate
Palatal shelf from maxillary process
C
Uvula
Eye
Primitive palate
Tongue
Meckel's cartilage
Eye
Nasal cartilage
Tongue

Fig. 35.12 Development of the palate. **A–C** show developmental progression over weeks 7–8. Ventral view (top row) and coronal section (bottom row).

Midline fusion of the two palatal shelves involves adherence and breakdown (by apoptosis) of the apposed epithelial surfaces. They also fuse with the posterior border of the primary palate, except over a small median area where a nasopalatine canal maintains connection between the nasal and oral cavities for some time and marks the future position of the incisive fossa. During the period of palatal shelf development, a median downgrowth from the primitive palate forms the definitive nasal septum; it is supported by cartilage. The fusing medial edges of the elevated palatal shelves also fuse with the free edge of the nasal septum, forming separate right and left nasal cavities above the secondary palate. Bone forms by intramembranous ossification within the palatal mesenchyme, and by endochondral ossification of the cartilaginous nasal septum. At this time, the free (caudal) edge of the palatal shelves lies directly below the former position of the attachment of the adenohypophysial pouch to the roof of the oral cavity. Caudal to the hard palate, its free edges grow (especially medially) to form the soft palate and uvula, which extend into the oropharynx. Myogenic mesenchyme from the first (tensor palati only) and third pharyngeal arches migrates into the soft palate and around the caudal margins of the pharyngotympanic tube. Separation of the definitive nasal and oral cavities is now complete. A number of elevations appear on the lateral wall of each nasal cavity: the superior, middle and inferior conchae.

Within the nasal septum, on either side of the septal cartilage, the ectoderm is invaginated to form a pair of small diverticula; these are the vomeronasal organs, auxiliary olfactory organs derived from the olfactory placodes. Their openings are close to the junction between the premaxilla and maxillae on each side. Their function in humans is not clear; but their cells differentiate to form neurones that project to the olfactory area of the brain, and may function in pheromone-related olfactory communication.

Bilateral dorsal expansions of the first, second and possibly third pharyngeal pouches form the tubotympanic recesses, which will become the tympanic cavities and pharyngotympanic tubes. The latter open into the lateral wall of the nasopharynx, above the soft palate. A number of focal proliferations of nasopharyngeal endoderm become invaded by lymphoid tissue. The adenoid or pharyngeal tonsil develops in the posterior midline of the nasopharynx, and the tubal tonsil develops close to the pharyngeal opening of the pharyngotympanic tube.

ORAL CAVITY

In the fifth week (stage 12), the oropharyngeal membrane breaks down so that communication is established between the stomodeum and the cranial end of the foregut (future naso- and oropharynx respectively). Formation of the hard and soft palates separates the cranial foregut into the nasal cavity and nasopharynx above and the definitive oral cavity below. The oral cavity is demarcated from the oropharynx posteriorly by the free edge of the soft palate and uvula above, and the palatoglossal arch laterally, which demarcates the oropharyngeal isthmus.

Tongue

Because the mandibular arch grows more rapidly than the others, this component of the pharyngeal floor is longer craniocaudally than that of the other arches. By stage 14, three swellings are apparent on its surface: a small median elevation, the tuberculum impar or median tongue bud, and paired mandibular (lingual) swellings. The mandibular swellings fuse with each other and with the tuberculum impar to form the anterior two-thirds of the tongue (Fig. 35.13). A sulcus forms along the ventral and lateral margins of this elevation and deepens, internal to the future alveolar process of the mandible, to form the linguogingival groove, while the elevation constitutes the anterior or oral (presulcal) part of the tongue. Caudal to the tuberculum impar, the copula and the hypobranchial (hypopharyngeal) eminence, form in the pharyngeal floor, and the ventral ends of the second, third and fourth pharyngeal arches converge onto them. The third arch component of the hypopharyngeal eminence grows over the second arch and approaches the anterior tongue rudiment; the two parts fuse along a V-shaped line corresponding later to the sulcus terminalis. Another transverse groove separates its caudal (fourth arch) part to delineate the epiglottis.

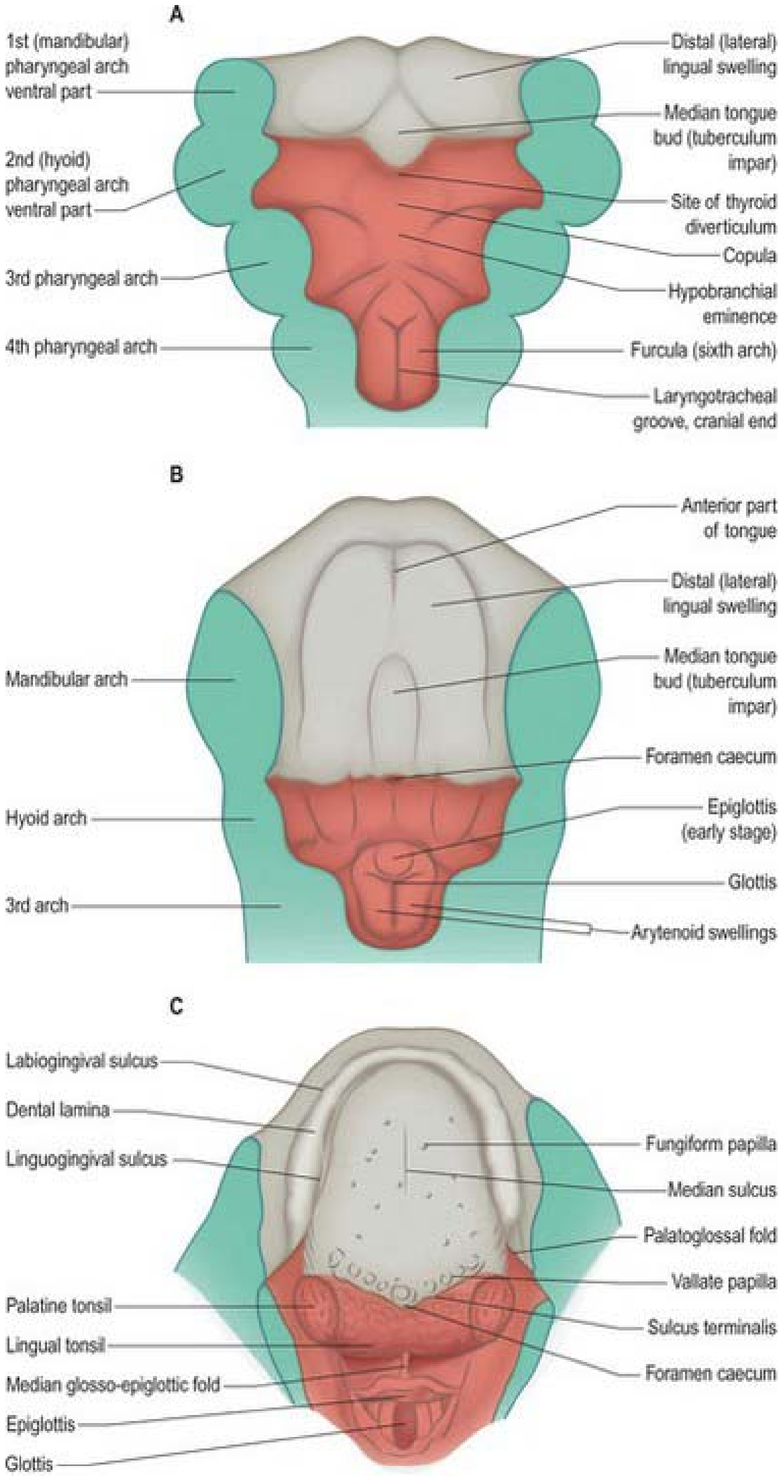
A
1st (mandibular) pharyngeal arch ventral part
2nd (hyoid) pharyngeal arch ventral part
3rd pharyngeal arch
4th pharyngeal arch
Distal (lateral) lingual swelling
Median tongue bud (tuberculum impar)
Site of thyroid diverticulum
Copula
Hypobranchial eminence
Furcula (sixth arch)
Laryngotracheal groove, cranial end
B
Anterior part of tongue
Distal (lateral) lingual swelling
Mandibular arch
Median tongue bud (tuberculum impar)
Foramen caecum
Hyoid arch
Epiglottis (early stage)
Glottis
3rd arch
Arytenoid swellings
C
Labiogingival sulcus
Dental lamina
Linguogingival sulcus
Fungiform papilla
Median sulcus
Palatoglossal fold
Vallate papilla
Palatine tonsil
Sulcus terminalis
Lingual tonsil
Foramen caecum
Median glosso-epiglottic fold
Epiglottis
Glottis

Fig. 35.13 Development of the pharyngeal floor and tongue. **A**, Stage 14, showing median and lateral swellings in the floor of the first arch; **B**, after fusion of the swellings; **C**, the tongue and oropharynx at birth.

During this sequence of events, the second arch is excluded from the tongue. The sulcus terminalis has its apex at the foramen caecum: this is a small median diverticulum that forms at the time of fusion of the constituent parts of the tongue, and is the site of downgrowth of the median rudiment of the thyroid gland. Failure of downgrowth of all or part of the thyroid gland from this site results in ectopic thyroid tissue within the tongue (lingual thyroid), between the foramen caecum and the epiglottis. The tongue primordia fuse at stage 17 (15 mm), and the sulcus terminalis is formed by the line of fusion. The vallate papillae appear around 10 weeks (52 mm), and increase in number until the end of the second trimester. Serial reconstructions suggest that the territory of the glossopharyngeal nerve extends considerably beyond these papillae. However, in general the composite character of the mucous membrane of the tongue is reflected by its sensory innervation. The anterior, oral part is innervated by the lingual branch of the mandibular nerve, and by the chorda tympani of the facial nerve. The posterior, pharyngeal part of the tongue is innervated by the glossopharyngeal, the nerve of the third arch, and the root of the tongue, near the epiglottis, is innervated by the vagus. During stages 14 and 15, the mesenchyme of the tongue is invaded by cells from the occipital myotomes which migrate from the lateral aspects of the myelencephalon. They pass ventrally round the pharynx to reach its floor accompanied by the hypoglossal nerves. The posterior parts of the tongue and epiglottis, i.e. the embryonic pharyngeal floor derivatives of the third, fourth and sixth arches, lie within the oropharynx. Striations appear on the surface of the tongue early in the fetal period. The tongue is short and broad, and its entire surface lies within the oral cavity (see Fig. 14.5). The posterior third of the tongue descends as the hyoid bone and larynx descend during the first postnatal year, and by the fourth or fifth year it forms part of the anterior wall of the oropharynx.

Salivary glands

The salivary glands arise bilaterally as the result of epithelial–mesenchymal interactions between the ectodermal epithelial lining of the oral cavity and the subjacent neural crest-derived mesenchyme. They form as solid diverticula that undergo branching morphogenesis, the whole tree-like structure later acquiring a lumen. The blind ends of the branches form acini, whose cells differentiate firstly to form serous cells and, postnatally, mucus-secreting cells (except for the parotid gland, which remains mainly or entirely serous).

The parotid gland can be recognized at stage 15 (8 mm) as an elongated furrow running dorsally from the angle of the mouth between the mandibular and maxillary prominences. The groove, which is converted into a tube, loses its connection with the epithelium of the oral cavity, except at its ventral end, and grows dorsally into the soft tissue of the cheek. The tube persists as the parotid duct. After fusion of the lateral parts of the maxillary and mandibular prominences, the parotid duct opens on the inside of the cheek at some distance from the angle of the mouth. As the gland develops, its branches interweave with the branches of the facial nerve. In the neonate, the parotid gland is rounded and lies between masseter and the ear. During infancy and early childhood, the growing gland covers the parotid duct.

The submandibular gland is identifiable at stage 18 as an epithelial diverticulum into the mesenchyme from the floor of the caudal part of the linguogingival groove. It increases rapidly in size and branches several times. At first the connection of the submandibular gland with the floor of the mouth lies at the side of the tongue, but as the edges of the linguogingival groove come together, from behind forwards, the tubular part of the submandibular duct forms. As a result, the orifice of the duct is shifted forwards until it is below the tip of the tongue, close to the median plane. The sublingual gland arises at stage 20 as a number of small epithelial thickenings in the linguogingival groove and on the lateral side of the groove. Each thickening canalizes separately, so multiple sublingual ducts open separately on the summit of the sublingual fold, while others join the submandibular duct.

The minor salivary glands, which are distributed throughout the wall of the oral cavity except the gingiva and hard palate, form in a similar manner to the major glands but undergo very little branching and remain within the submucosa.

Lymphoid tissues

Tonsils form at several sites around the oral cavity and pharynx, where focal proliferations of endoderm become invaded by lymphoid tissue. The endodermal epithelial lining grows into the surrounding mesenchyme as a number of solid buds, which are excavated by degeneration and shedding of their central cells, forming tonsillar fossae and crypts. Lymphoid cells accumulate around the crypts and become grouped as lymphoid follicles; T- and B-cell regions can be identified. The palatine tonsils develop from the ventral parts of the second pharyngeal pouches (Fig. 35.4; see Fig. 35.18). A slit-like intratonsillar cleft extends into the upper part of the tonsil and is possibly a remnant of the second pharyngeal pouch. Lymphoid tissue similar to that of the palatine tonsils usually develops on the surface of the posterior part of the tongue, forming the lingual tonsil.

Teeth and gums

Demarcation of the lips begins after fusion of the facial primordia at stage 18, during the period of secondary palatal development. Two parallel epithelial thickenings, an outer labiogingival lamina (vestibular band) and an inner dental lamina, form around the interior border of the mouth in both upper and lower jaws (Fig. 35.13; see Fig. 35.15). The linguogingival groove (sulcus) is formed as an indentation between the dental lamina and the tongue. At stage 22, each labiogingival lamina indents the underlying mesenchyme to form a shallow groove that deepens to form the vestibule between the lips and gums. The lining of the oral cavity between the vestibular epithelium of the upper and lower jaws forms the inner aspect of the cheeks. The dental lamina gives rise to the epithelial component of the teeth.

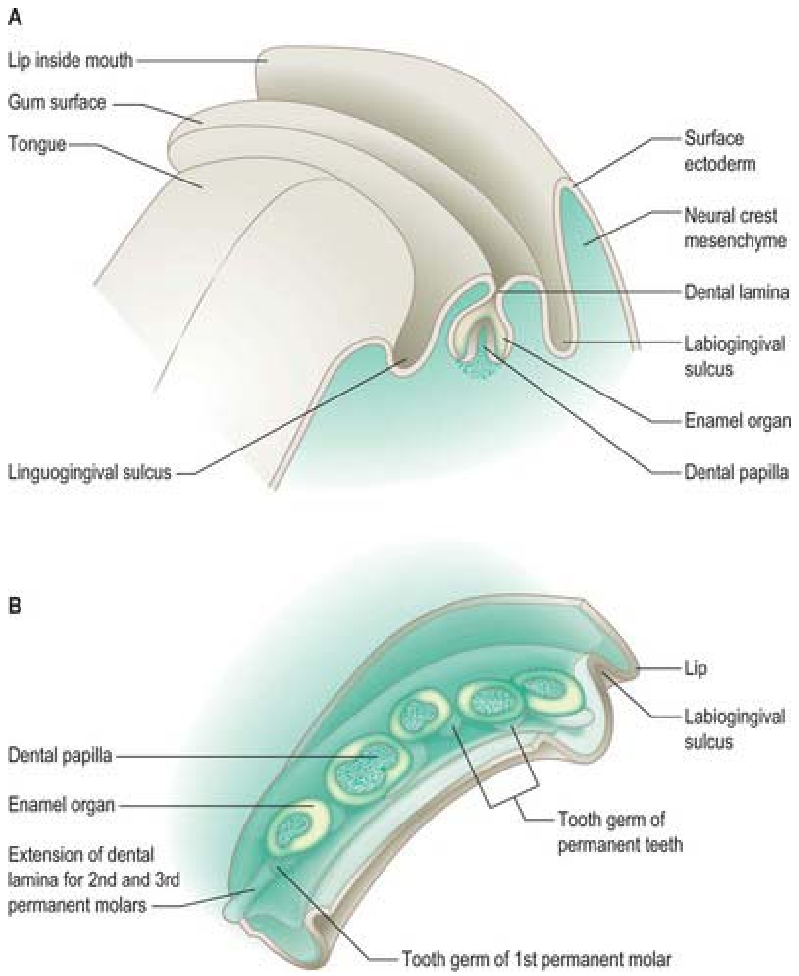
A
Lip inside mouth
Gum surface
Tongue
Surface ectoderm
Neural crest mesenchyme
Dental lamina
Labiogingival sulcus
Enamel organ
Dental papilla
Linguogingival sulcus
B
Lip
Labiogingival sulcus
Dental papilla
Enamel organ
Tooth germ of permanent teeth
Extension of dental lamina for 2nd and 3rd permanent molars
Tooth germ of 1st permanent molar

Fig. 35.15 Development of the lip, gums and teeth. A. oral view. B. the right half of the lower jaw viewed from below.

Tooth formation involves a sequence of epithelial–mesenchymal interactions along the dental lamina (Fig. 35.14). These interactions are controlled by a large number of genetic factors, and the extracellular matrix (particularly of the basement membranes) is of major importance (Thesleff 2000, Fukumoto & Yamada 2005). In 25 mm embryos, 10 localized thickenings of the upper and lower dental laminae initiate formation of the dental epithelial components of the tooth primordia (Figs 35.14, 35.15). They expand into dental sacs surrounded by vascular mesenchyme. The epithelium proliferates and indents to form an enamel organ which by 10 weeks forms a cap over a mesenchymal condensation, the dental papilla: collectively this unit constitutes a tooth bud or germ. The enamel organ becomes bell-shaped and differentiates into two layers, the internal and external enamel epithelia; these are separated by a glycosaminoglycan-rich stellate reticulum. The cells of the internal epithelium differentiate into ameloblasts, and the underlying layer of mesenchymal cells differentiates into odontoblasts. The odontoblasts produce and secrete dentine, which influences the ameloblasts to form enamel; this is laid down in successive layers, and after mineralization is the hardest tissue in the body. Enamel and dentine production from the bell-shaped tooth germ both begin at 24 weeks. The dental papilla mesenchyme below the odontoblast layer forms the pulp, which becomes vascularized and innervated. Experimental studies in mice (which have only incisors and molars) have revealed that regional differences in gene expression within the maxillary and mandibular mesenchymes govern the type of tooth produced. Fibronectin is present in the basement membrane of the internal enamel epithelium during the bell phase; it assists attachment of the preodontoblasts and is essential for their differentiation; it becomes progressively more abundant during the later fetal period. Collagen I is the major supportive extracellular scaffold in the maturing dental papilla and stellate reticulum.

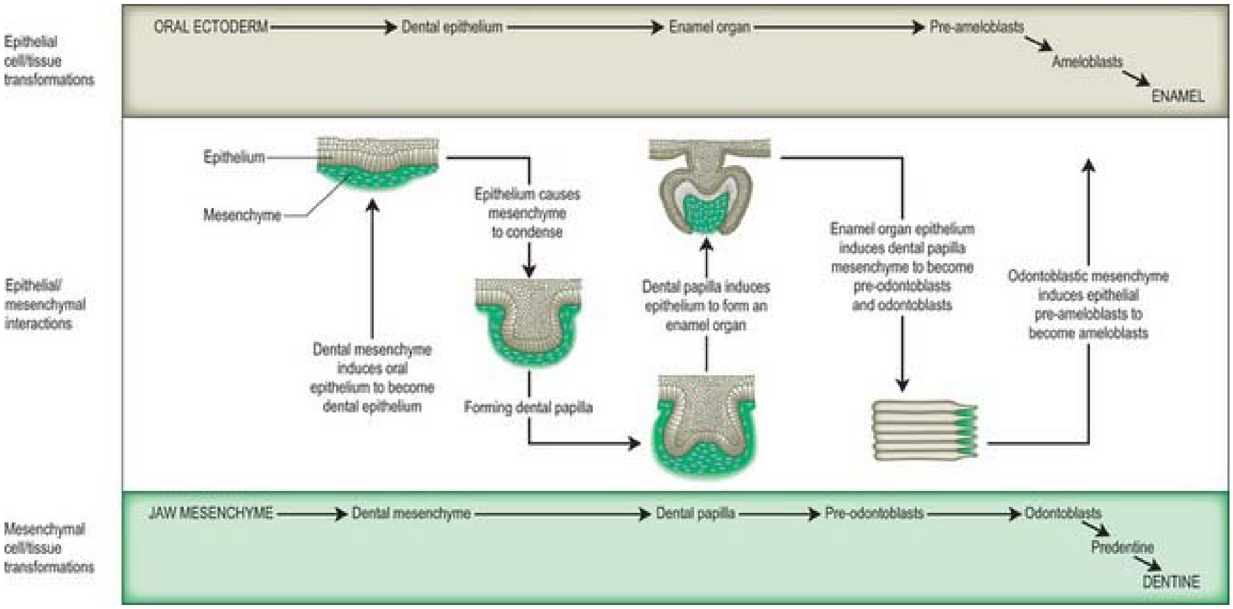
Epithelial cell/tissue transformations
ORAL ECTODERM
Dental epithelium
Enamel organ
Pre-ameloblasts
Ameloblasts
ENAMEL
Epithelium
Mesenchyme
Epithelium causes mesenchyme to condense
Enamel organ epithelium induces dental papilla mesenchyme to become pre-odontoblasts and odontoblasts
Epithelial/ mesenchymal interactions
Dental papilla induces epithelium to form an enamel organ
Odontoblastic mesenchyme induces epithelial pre-ameloblasts to become ameloblasts
Dental mesenchyme induces oral epithelium to become dental epithelium
Forming dental papilla
Mesenchymal cell/tissue transformations
JAW MESENCHYME
Dental mesenchyme
Dental papilla
Pre-odontoblasts
Odontoblasts
Predentine
DENTINE

Fig. 35.14 A summary of the epithelial–mesenchymal interactions during tooth development.

At birth, each quadrant of the jaws has the five deciduous tooth germs and the germ of the first permanent molar. The timing of eruption of the teeth, beginning with the lower middle incisors, is variable. Permanent teeth develop in accessional positions from the lingual aspects of the deciduous tooth germs, and, for the 12 permanent molar teeth, from posterior extensions of the dental laminae on each side of both jaws. Mineralization begins in both deciduous and permanent teeth before birth. The deciduous teeth have well-developed crowns by full term, and eruption through the gingiva (gum) begins with the lower incisors between 3 and 6 months after birth. After eruption, the gingiva remains attached to the neck of each tooth by the upper part of the periodontal ligament, whose major part attaches the tooth root to the bone of the tooth socket.

The oral cavity after birth

In the neonate, the oral cavity is only potential with the mouth closed. Three spaces are formed in the oral cavity during suckling. The median space between the tongue and hard palate that is occupied by the nipple bifurcates posteriorly to produce channels on each side of the approximated soft palate and epiglottis. The hard palate is only slightly arched and its mucous membrane is corrugated by five or six irregular transverse folds (rugae) which assist with gripping of the nipple. Two lateral spaces, the lateral arcuate cavities, are formed between the tongue medially and the cheeks laterally; the upper and lower gums situated within these spaces do not touch during suckling. Each cheek is supported by a mass of subcutaneous fat, the suctorial pad, which lies between buccinator and masseter. The epiglottis is high and makes direct contact with the soft palate (see Fig. 14.15). The larynx is elevated so that its opening is directed into the nasopharynx, i.e. above the level of the spaces, as milk passes on either side of it to the pharynx. This ensures that babies can breathe while suckling.

ANOMALIES OF FACIAL DEVELOPMENT

Malformations involving the neural crest

Congenital malformations of the face may be initiated early, and related to abnormal migration, proliferation and/or apoptosis of neural crest cells, or later, during the morphogenetic phase of facial development. Craniofrontonasal syndrome is characterized by a broad forehead and hypertelorism, premature fusion of one or both coronal sutures, a central nasal groove, and sometimes cleft lip and palate; there are also extracranial features. It is caused by deletions of the gene *EFNB1*, which is known to play essential roles in boundary formation between tissues, including those between neural crest and adjacent non-crest cells. Mandibulofacial dysostosis (Treacher Collins syndrome) is characterized by incomplete orbits, reduced jaws and auditory ossicles (hence conductive deafness), abnormal external ears and fistulae or cysts, suggesting involvement of all levels of the cranial neural crest. It is caused by haploinsufficiency of the gene *TCOF1*. Hemifacial microsomia (Goldenhaar syndrome) affects only one side of the face and comprises a small mandible (sometimes with absence of the temporomandibular joint), malformed or absent ears with accessory ear tags, and facial clefts. Experimental evidence in animals suggests that it is due to haemorrhage of the stapedial artery, which may have a genetic basis. Deficient growth of the mandible (micrognathia) is usually associated with other defects. In Pierre Robin sequence (Fig. 35.16), the small size of the mandible obstructs descent of the tongue, resulting in a U-shaped cleft palate; a conotruncal septum defect is present in one-quarter of cases, suggesting possible involvement of the cardiac neural crest. Further details and references for facial malformations may be found in Gorlin et al (2001), Wilkie and Morriss-Kay (2001), and Morriss-Kay and Wilkie (2005).

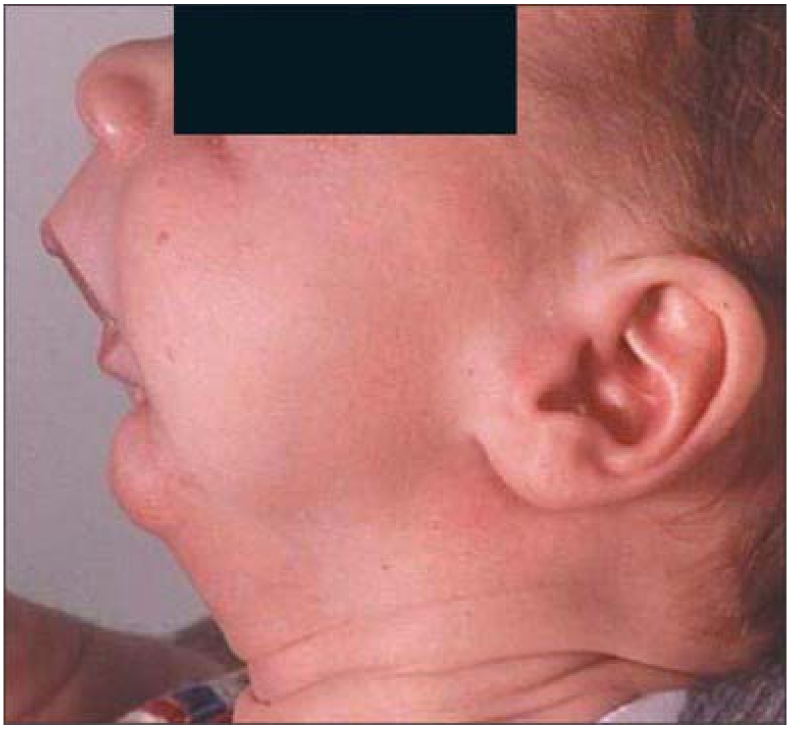

Fig. 35.16 Pierre Robin sequence.

(Courtesy of Mr T Goodacre and Oxford Radcliffe Hospitals NHS Trust.)

Clefts of the face and palate

Cleft lip occurs when one or both medial nasal processes fail to fuse with the corresponding maxillary process(es). The severity of clefting varies from a small notch in the upper lip to a double cleft extending into both nostrils (Fig. 35.17). In a unilateral cleft lip, the nasal septum deviates to the non-cleft side due to absence of the correct insertion of the transverse muscles of the nose and of orbicularis oris on the medial aspect of the cleft onto the tissues around the anterior nasal spine and nasal septum and, most importantly, to the contralateral muscles (Fig. 35.17B). The three functional groups of superficial facial muscles – nasolabial (transverse nasalis, levator labii superioris and levator labii superioris alequae nasi), bilabial (orbicularis oris) and labiomental (depressor anguli oris) – are all displaced inferiorly. A further consequence is the underdevelopment of the incisor-bearing part of the maxilla. These abnormalities, in turn, influence the mucocutaneous tissues, which results in the displacement of the skin of the nostril to the upper part of the lip, retraction of the labial skin and abnormalities of the soft tissues on either side of the mucocutaneous junction.

A narrow or incomplete cleft of the hard palate is likely to be due to a growth defect in the palatal shelves and/or a delay in shelf elevation, and/or to failure of fusion of the apposed palatal shelves. Broader clefts (Fig. 35.17D,E), in which the tongue lies between the still-vertical shelves, are caused by a greater developmental delay that may be associated with abnormality of other structures in the face and elsewhere in the body. In the mildest forms of cleft palate, only the soft palate, and sometimes just the uvula, is cleft (Fig. 35.17F). A submucous cleft can cause speech difficulties; it may be detected as a median V-shaped notch of the soft palate. Very rarely, palatopharyngeal incompetence is due to muscle hypoplasia, particularly of the musculus uvulae.

Cleft lip with or without cleft palate (CL/P) appears to be multigenic or multifactorial in origin, with both genetic and environmental components (Gorlin et al 2001). CL/P has a frequency of 0.5–3.6/1000 live births, with a 2 : 1 male : female ratio. Isolated cleft palate is genetically unrelated to CL/P, and has a frequency of 0.4/1000; it is more common in females. Clefts of the face are rare (1/50,000–1/175,000 births); they are mainly caused by pressure from amniotic bands rather than from dysmorphogenesis, although a morphogenetic component cannot be ruled out when the cleft is along a line of fusion, e.g. maxillary–mandibular. Median cleft lip (true hare lip) is also rare, since this is not a line of morphogenetic fusion. Median grooving of the nose occurs with hypertelorism in various frontonasal dysplasias, suggesting an early broadening of the median region of the face.

FORMATION OF THE NECK

By the time the facial swellings have merged to form a recognizably human face (stage 20), Meckel's cartilage has grown sufficiently to project outwards as a potential chin, but the face is still orientated towards, and close to, the cardiac prominence. Formation of the posterior part of the neck is by this time well advanced, with cartilaginous cervical vertebrae, muscles, nerves and blood vessels. The anterior neck forms gradually, as relatively rapid growth of the anterior structures, including the trachea, oesophagus, common carotid arteries and jugular veins, and an increase in the angle between the spinal cord and brainstem take place. Other contributory changes include growth of the first pharyngeal arch at a more rapid rate than the others, so that Meckel's cartilage and the developing membrane bone of the mandible project further forwards, while the hyoid bone primordium remains small, defining the future angle between the anterior neck with the jaw. Myoblasts derived from paraxial mesenchyme invading the second pharyngeal arch are present in the superficial connective tissue beneath the anterior neck skin; these spread out to populate this layer from the underside of the chin to the upper thorax and differentiate to form the platysma (this is the main human remnant of the panniculus carnosus, the muscle that is present throughout the skin of many mammals).

The interface between cranial nerve-innervated pharyngeal arch muscles and spinal nerve-innervated trunk muscles occurs at the lower neck and the upper parts of the pectoral girdle. Both the proximal and distal connections of the trapezius muscle, at the nuchal line of the occipital bone and the attachment to the spine of the scapula, are formed from post-otic neural crest cells (Matsuoka et al 2005). The neural crest generates areas of endochondral ossification in the cervical vertebral column and scapula associated with trapezius attachment. This observation has promoted the conception of a 'muscle scaffold model' of development to replace the older 'ossification model', to explain the types of ossification seen associated with the accessory nerve-innervated trapezius and sternocleidomastoid muscles. It is suggested that defects in the fate choices of neural crest cells could explain a number of syndromes which have pharyngeal, laryngeal, occipital, cervical and shoulder dysmorphologies and co-occurrence of swallowing problems; related syndromes include Klippel–Feil, Sprengel’s deformity and cleidocranial dysplasia (Matsuoka et al 2005).

GLANDS OF THE NECK

The development of the pharyngeal floor and lower pharyngeal pouches gives rise to glands finally disposed in the neck and anterior mediastinum.

Thyroid gland

The thyroid gland is a midline derivative of the pharynx. It is first identifiable in embryos of approximately 20 somites as a median thickening of endoderm lying in the floor of the pharynx between the first and second pharyngeal pouches and immediately dorsal to the aortic sac. This area is later invaginated to form a median diverticulum which appears late in the fourth week in the furrow immediately caudal to the median tongue bud (Fig. 35.18). It grows caudally as a tubular duct. The tip of the duct bifurcates and the tissue mass subsequently divides into a series of double cellular plates, from which the isthmus and the lateral lobes of the thyroid gland are developed. The primary thyroid follicles differentiate by reorganization and proliferation of the cells of these plates. Secondary follicles subsequently arise by budding and subdivision. These primary and secondary endodermal cells are the progenitors of the follicular parenchyma proper. The parafollicular or C cells of the thyroid gland are derived from the ultimobranchial body.

The original diverticulum, its bifurcation and generations of follicles invade the cardiac neural crest mesenchyme. The latter gives rise to the connective tissue capsule, interlobular septa and perifollicular investments which carry the main neurovascular and lymphatic supply to the gland.

The median diverticulum is connected to the pharynx by the thyroglossal duct. The site of its initial connection with the endodermal floor of the mouth is marked by the foramen caecum, whence it extends caudally in the midline ventral to the primordium of the hyoid bone (behind which it later forms a recurrent loop). The distal part of the duct may differentiate into the pyramidal lobe and levator muscle – or suspensory fibrous band – of the thyroid. The remainder becomes fragmented and disappears, although the lingual part is often identifiable until late in fetal life. Occasionally, parts of the midline thyroglossal duct persist and may occur in lingual, suprahyoid, retrohyoid or infrahyoid positions. They may form aberrant masses of thyroid tissue, cysts, fistulae or sinuses, usually in the midline. A lingual thyroid situated at the junction of the buccal and pharyngeal parts of the tongue is not uncommon, but nodules of glandular tissue may also be found other than in the midline, e.g. laterally placed posterior to sternocleidomastoid, and, on occasion, below the level of the thyroid isthmus.

The thyroid gland is relatively large in the neonate (see Fig. 14.4), where it has a long narrow isthmus connecting lobes which do not yet contact the upper part of the trachea. The gland attains half the adult size by 2 years postnatally. Colloid is present in the gland from 3 months' gestation and thyroxin is present by 4.5 months' gestation.

Parathyroid glands

The parathyroid glands develop from interactions between the third and fourth pharyngeal pouch endoderm and local cranial (vagal) neural crest mesenchyme. The third pharyngeal pouch has dorsal and ventral sites of proliferation (Fig. 35.18). Bilaterally, the epithelium on the dorsal aspect of the pouch and in the region of its duct-like connection with the cavity of the pharynx becomes differentiated as the primordium of the inferior parathyroid glands (parathyroid III). Although the connection between the pouches and the pharynx is soon lost, the connection between the dorsal parathyroids III and the ventral thymic rudiments persists for some time, and the former passes caudally with the developing thymus. The superior parathyroid glands (parathyroid IV) develop from the dorsal recess of the fourth pharyngeal pouches. They come into relation with, and appear to be anchored by, the lateral lobes of the thyroid gland and thus remain cranial to the parathyroid glands derived from the third pouches. The cardiac neural crest mesenchyme provides the connective tissue elements, whereas invading angiogenic mesenchyme gives rise to the vasculature which includes fenestrated capillaries and lymphatics. In the neonate the parathyroid glands are as variable in size and position as they are in the adult. They double in size between birth and puberty. Parathyroid hormone is produced from the 12th week of development.

Thymus

The thymus gland is formed from the ventral part of the third pharyngeal pouch on each side (Fig. 35.18). It cannot be recognized prior to the differentiation of the inferior parathyroid glands at stage 16, but thereafter it is represented by two elongated diverticula which soon become solid cellular masses and grow caudally into the surrounding cardiac (vagal) neural crest mesenchyme. Ventral to the aortic sac the two thymic rudiments meet but do not fuse, and they are subsequently united by connective tissue only. The thymus gland becomes located in the anterior mediastinum of the thorax once the neck is fully developed and the heart has descended. The connection with the third pouch is soon lost, but the stalk may persist for some time as a solid, cellular cord.

As the thymus proliferates and descends, the local cardiac (vagal) neural crest mesenchyme controls the pattern and development of the gland. Defective development of the cardiac neural crest which affects the heart and peripheral neural ganglia also results in thymic deficiencies as seen in the DiGeorge and Pierre Robin syndromes. Crest mesenchyme forms connective tissue septa which produce the lobulated architecture of the gland. Angiogenic mesenchyme, including lymphoid stem cells, invades this local mesenchyme, and, by 10 weeks, over 95% of the cells in the gland belong to the T-cell lineage, with a few developing erythroblasts and B lymphocytes. Hassall’s corpuscles are also present. By 12 weeks, the mesenchymal septa, blood vessels and nerves have reached the newly differentiating medulla, which allows the entry of macrophage lineage precursors. Macrophages and interdigitating cells are first seen at 14 weeks. Granulopoiesis occurs in the perivascular spaces. By 17 weeks, the thymus appears fully differentiated, and after this time it produces the main type of thymocyte that is present throughout life (designated TdT+).

Caudal pharyngeal complex

The most caudal endodermal invaginations of the pharynx are the fourth pharyngeal pouch and elements of the transitory fifth pharyngeal pouch (the ultimobranchial body). Collectively these diverticuli are termed the caudal pharyngeal complex (Fig. 35.18), and they are connected to the pharynx via the pharyngobranchial duct. They are surrounded by cardiac (vagal) neural crest and by the tissues of the developing thyroid gland. The cells of the ultimobranchial body, the lowest of the pharyngeal pouches, become incorporated into the lateral thyroid lobes, and may give rise to the ‘C’ or parafollicular cells of the thyroid gland. C-cell hyperplasia is associated with medullary carcinoma, and has been reported within the neck in what are presumed to be remnants of the ultimobranchial body.

PHARYNX, LARYNX, OESOPHAGUS AND TRACHEA

The larynx forms at the cranial end of the laryngotracheal groove, where it is bounded laterally by the ventral ends of the sixth arches and ventrally by the caudal part of the hypobranchial eminence (Figs 35.5, 35.6, 35.13). The thyroid cartilage develops from the ventral ends of the cartilages of the fourth, or fourth and sixth, pharyngeal arches. The cartilage appears as two lateral plates, each chondrified from two centres and united in the midventral line by a fibrous membrane within which an additional centre of chondrification develops. The cricoid cartilage arises from two cartilaginous centres, which soon unite ventrally, gradually extend, and ultimately fuse on the dorsal surface of the tube as the cricoid lamina. Paired arytenoid swellings appear in the ventral ends of the sixth arches from stage 14, one on each side of the cranial end of the groove. As they enlarge, they approximate to each other and to the caudal part of the hypobranchial eminence where the epiglottis develops. The opening into the larynx, at first a vertical slit, is converted into a T-shaped cleft by the enlargement of the arytenoid swellings. The vertical limb of the T lies between the two swellings, and its horizontal limb lies between them and the epiglottis. The arytenoid swellings differentiate into the arytenoid and corniculate cartilages (Fig. 35.6), and the ridges that join them to the epiglottis become the definitive aryepiglottic folds within which the cuneiform cartilages differentiate from the epiglottis. After the caudal part of the hypobranchial eminence has separated from the pharyngeal (posterior) part of the tongue (Fig. 35.13), it is in continuity with two linear ridges which appear in the ventral wall of the pharynx. The ridges are the sixth arches, which are placed very obliquely owing to the shortness of the pharyngeal floor compared with the greater extent of the roof. They are carried downwards on the ventral wall of the foregut and bound the median laryngotracheal groove, from which the lower part of the larynx, the trachea, bronchi and lungs are developed (see Ch. 59).

From stage 12, the early pharyngeal foregut develops a ventral endodermal outgrowth into the mesenchyme surrounding the sinus venosus and inflow tract of the heart (see Figs 59.1, 73.3). This initiates the separation of the respiratory and alimentary tubes. The point at which the original respiratory diverticulum buds from the foregut, the laryngotracheal groove, remains at a constant level during the embryonic period, and the trachea lengthens distally as the bifurcation point descends. The cells of the splanchnopleuric mesenchyme that surrounds the developing trachea and oesophagus are sufficiently diverged in their inductive ability to promote the characteristics of the two different tubes. The respiratory diverticulum becomes surrounded by angiogenic mesenchyme that connects to the developing sixth aortic arch artery. By stage 17, the mesenchyme around the trachea is beginning to condense to form C-shaped cartilages, whereas that around the oesophagus has a wide submucosal zone and muscular coats can be distinguished.

For details of early development of the trachea see p. 1033, and early development of the oesophagus see p. 1203.

In the neonate the pharynx is one-third of the relative length in the adult. The nasopharynx is a narrow tube which curves gradually to join the oropharynx without any sharp junctional demarcation. An oblique angle is formed at this junction by 5 years of age and in the adult the nasopharynx and oropharynx join at almost a right angle. The oesophagus in the newborn commences and ends one to two vertebrae higher than in the adult, extending from between the fourth and sixth cervical vertebrae to the level of the ninth thoracic vertebra. The narrowest constriction is at its junction with the pharynx, where the inferior pharyngeal constrictor functions to constrict the lumen, and in this region it may be traumatized with instruments or catheters.

In the normal neonate the hyoid bone and larynx are relatively high in the neck; both descend during infancy, and the trachea is relatively small in relation to the larynx (see Fig. 14.4). The walls of the trachea are relatively thick and the tracheal cartilages are relatively closer together than in the adult. The trachea commences at the upper border of the sixth cervical vertebra, a relationship that is conserved with growth, and it bifurcates at the level of the third or fourth thoracic vertebra.

BLOOD VESSELS IN THE NECK

With elongation of the neck and the appearance of the major conducting vessels from the aortic arch arteries, longitudinal anastomoses in the cervical region link intersegmental arteries and their branches and direct blood flow to the developing brain in the vertebral arteries, in parallel with the internal carotid arteries (see Figs 35.8, 35.9).

The primary blood vessels of the head and neck consist of a close-meshed capillary plexus drained on each side by the precardinal vein, which is at first continuous cranially with a transitory primordial hindbrain channel that lies on the neural tube medial to the cranial nerve roots (see Figs 13.1, 13.2). This is soon replaced by the primary head vein which runs caudally from the medial side of the trigeminal ganglion, lateral to the facial and vestibulocochlear nerves and the otocyst, then medial to the vagus nerve, to become continuous with the precardinal vein. A lateral anastomosis subsequently brings it lateral to the vagus nerve.

The ventral pharyngeal vein drains the mandibular and hyoid arches into the common cardinal vein (see Fig. 24.36A). As the neck elongates, its termination is transferred to the cranial part of the precardinal vein which later becomes the internal jugular vein (see Fig. 24.36B). The ventral pharyngeal vein receives tributaries from the face and tongue and becomes the linguofacial vein. As the face develops, the primitive maxillary vein extends its drainage into the territories of supply of the ophthalmic and mandibular divisions of the trigeminal nerve, including the pterygoid and temporal muscles, and it anastomoses with the linguofacial vein over the lower jaw. This anastomosis becomes the facial vein which receives a strong retromandibular vein from the temporal region, and drains through the linguofacial vein into the internal jugular. The stem of the linguofacial vein is now the lower part of the facial vein, whilst the dwindling connection of the facial with the primitive maxillary becomes the deep facial vein. The external jugular vein develops from a tributary of the cephalic vein from the tissues of the neck; it anastomoses secondarily with the anterior facial vein. At this stage the cephalic vein forms a venous ring around the clavicle by which it is connected with the caudal part of the precardinal vein. The deep segment of the venous ring forms the subclavian vein and receives the definitive external jugular vein. The superficial segment of the venous ring dwindles, but may persist in adult life. The deep aspects of the maxillomandibular facial prominences, retrogingival oral cavity, the pharyngeal walls and their lymphoid and endocrine derivatives, and the cervicothoracic oesophagus, thus all have drainage channels that connect with the precardinal complex. Laryngeal and tracheobronchial veins also drain to the precardinal complex, whilst the capillary plexuses, developed in the (splanchnopleuric) walls of the fine terminal respiratory passages and alveoli, converge on pulmonary veins of increasing calibre, finally making secondary connections with the left atrium of the heart, and may be grouped with the vitelline systems.

SKULL

The skull has two major functional and anatomical components: the neurocranium and viscerocranium. The neurocranium is composed of the skull vault and skull base; it surrounds and protects the brain and the special sense organs of olfaction, vision, hearing and balance. The viscerocranium forms the skeleton of the face, palate and pharynx, and mediates the functions of feeding, breathing and facial expression; it also protects the tongue and forms the middle ear and the bony external acoustic meatus. The most rostral neural crest cell population (see introductory section) makes a major contribution to the skull, forming the whole viscerocranium and the rostral part of the neurocranium (Fig. 35.19). The boundary between neural crest and cranial mesoderm lies between the frontal and parietal bones (coronal suture) of the skull vault; the skull base is formed by neural crest rostral to the tip of the notochord, and is sclerotome-derived (i.e. mesodermal) in the notochordal region. The bones of the skull base are formed by endochondral ossification, whereas those of the skull vault and face ossify directly from mesenchymal condensations (intramembranous ossification). Several bones are of compound structure with respect to their tissue origins and/or type of ossification: the occipital, temporal and sphenoid bones, and the mandible. The following account is based largely on descriptive studies on human embryos and fetuses (O’Rahilly & Müller 1987, 2001, 2007), with some details on cell lineage based on investigations in the mouse.

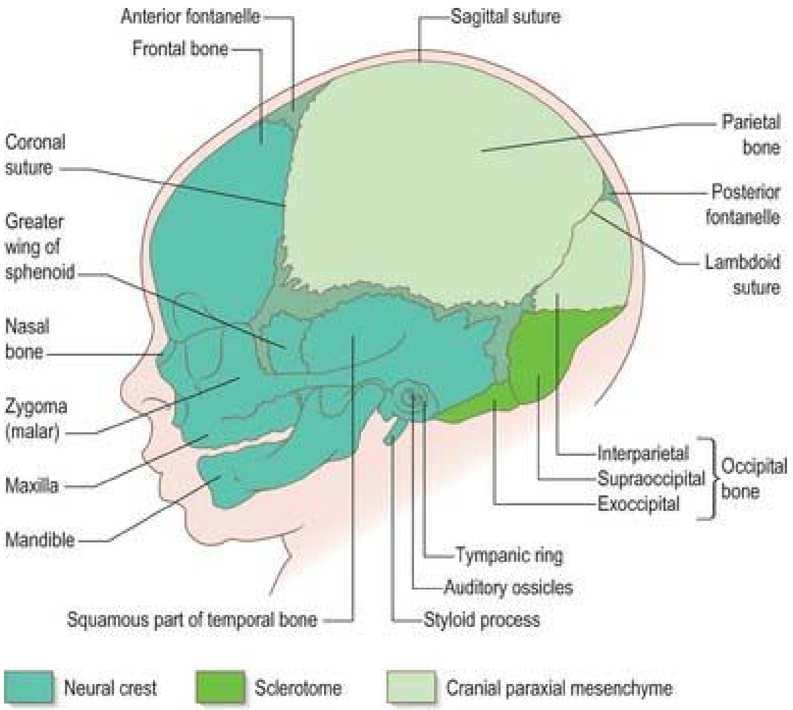
Anterior fontanelle
Frontal bone
Sagittal suture
Coronal suture
Parietal bone
Posterior fontanelle
Greater wing of sphenoid
Lambdoid suture
Nasal bone
Zygoma (malar)
Maxilla
Mandible
Interparietal
Supraoccipital
Exoccipital
Occipital bone
Tympanic ring
Auditory ossicles
Styloid process
Squamous part of temporal bone
Neural crest
Sclerotome
Cranial paraxial mesenchyme

Fig. 35.19 Newborn skull, showing tissue origins of the bones (based on combined mouse and human data).

CHONDROCRANIUM

The first cranial skeletal structures to differentiate are the cartilages of the skull base, sensory capsules, viscerocranium and occiput (Figs 35.5, 35.20B). Development of the pharyngeal arch-related cartilages of the viscerocranium and ear ossicles has been described in the pharynx section above. Before any mesenchyme condenses to initiate the formation of cranial cartilage, the major cranial nerves and blood vessels are already in place – hence, the foramina of the skull are specified before the bones are formed. The adenohypophysial pouch is still connected to the roof of the oral cavity as the skull base cartilage forms, but already lies adjacent to the diencephalon-derived neurohypophysis to form the downwardly projecting pituitary gland (hypophysis) at the base of the caudal diencephalon.

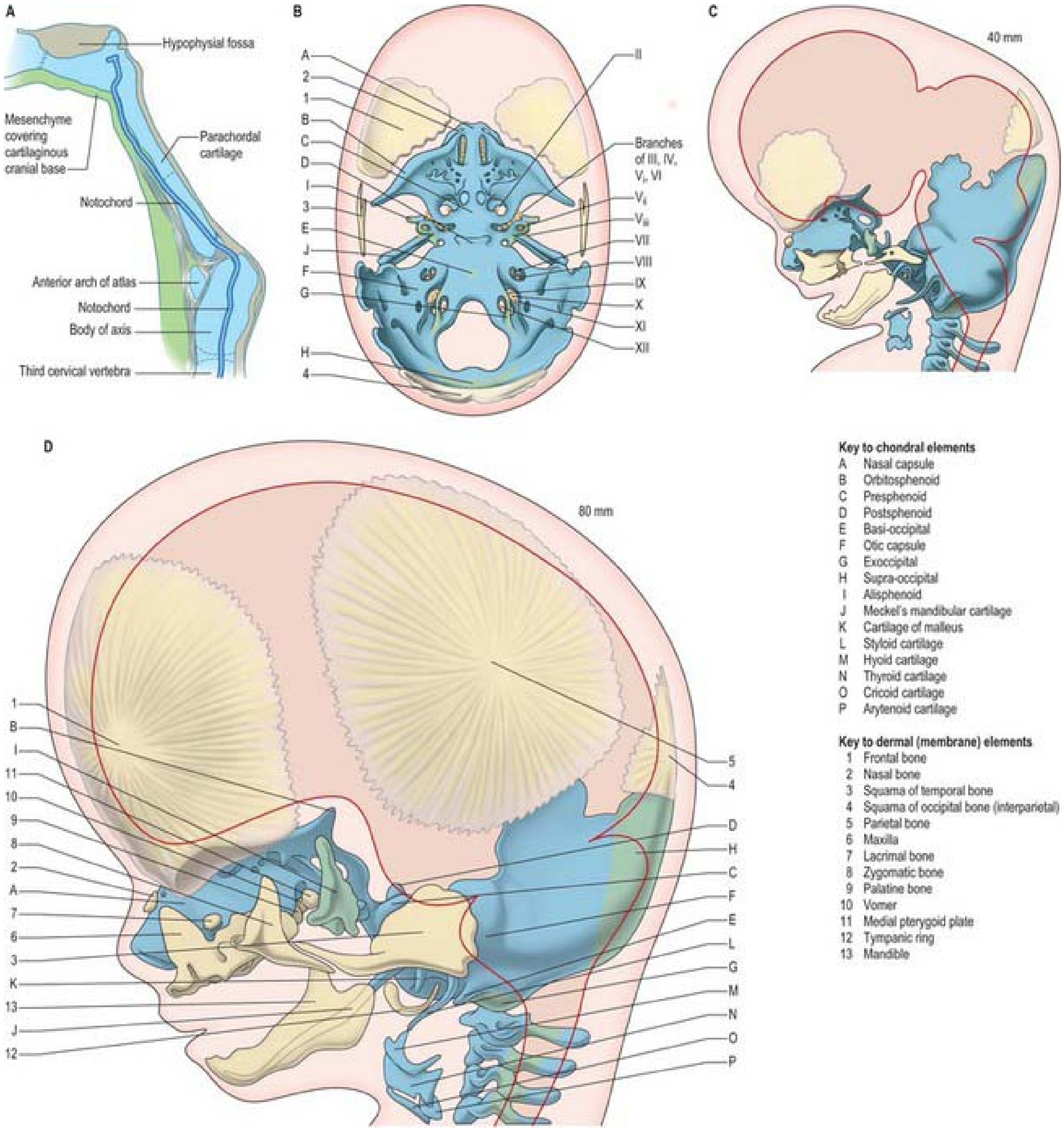
A
Hypophysial fossa
Mesenchyme covering cartilaginous cranial base
Parachordal cartilage
Notochord
Anterior arch of atlas
Notochord
Body of axis
Third cervical vertebra
B
A
2
1
B
C
D
I
3
E
J
F
G
H
4
II
Branches of III, IV, V1, VI
V2
V3
VII
VIII
IX
X
XI
XII
C
40 mm
D
80 mm
1
B
I
11
10
9
8
2
A
7
6
3
K
13
J
12
5
4
D
H
C
F
E
L
G
M
N
O
P
Key to chondral elements
A Nasal capsule
B Orbitosphenoid
C Presphenoid
D Postsphenoid
E Basi-occipital
F Otic capsule
G Exoccipital
H Supra-occipital
I Alisphenoid
J Meckel's mandibular cartilage
K Cartilage of malleus
L Styloid cartilage
M Hyoid cartilage
N Thyroid cartilage
O Cricoid cartilage
P Arytenoid cartilage
Key to dermal (membrane) elements
1 Frontal bone
2 Nasal bone
3 Squama of temporal bone
4 Squama of occipital bone (interparietal)
5 Parietal bone
6 Maxilla
7 Lacrimal bone
8 Zygomatic bone
9 Palatine bone
10 Vomer
11 Medial pterygoid plate
12 Tympanic ring
13 Mandible

Fig. 35.20 Representative stages in the development of the cranium. In all the diagrams, the chondrocranium and cartilaginous stages of vertebrae are shown in blue, except where ossification is occurring and here the colour is green. The desmocranium, consisting of elements ossifying directly in mesenchyme, is shown in yellow. Cranial nerves are indicated by the appropriate Roman numeral. **A**, Sagittal section through the cranial end of the developing axial skeleton in an early human embryo of approximately

10 mm, showing the extent of the notochord. **B**, Superior aspect of cranium of human embryo at 40 mm. **C**, Lateral aspect of **B**. **D**, Lateral aspect of cranium of human embryo at 80 mm.

The rostral tip of the notochord extends to a position just caudal to the hypophysis (Fig. 35.20A). Its sheath is rich in sulphated glycosaminoglycans, which play a role in inducing condensation and chondrification of the occipital sclerotome-derived mesenchyme on either side of it.

The central regions of all four occipital sclerotomes contribute to the parachordal cartilage, which surrounds the notochord and extends as a flat plate on either side of it by the end of the seventh week, forming the basioccipital component of the occipital bone. The exoccipital components (derived from sclerotomes 3 and 4) chondrify soon afterwards; they border the rostral half of the foramen magnum, forming the occipital arch, which is developmentally equivalent to the neural arch components of vertebrae. Roots of the hypoglossal nerve run between the parachordal and exoccipital cartilages, so that when the exoccipital and parachordal components fuse, they leave foramina for these nerve roots. The supraoccipital part of the occipital cartilage (tectum posterius, which is not sclerotome-derived) extends from the exoccipital cartilage around the foramen magnum, completing it. After formation of the exoccipital cartilages, differentiation also extends further rostrally in the medial part of the skull base, with formation of the hypophysial cartilages on either side of the stalk of the hypophysial pouch; they unite in the median plane to form the primordium of the postsphenoid, cradling the hypophysis and retaining a perforation for the hypophysial stalk until the third month. This part of the basisphenoid cartilage will form the sella turcica with its hypophysial fossa. The presphenoid cartilages, rostral to it, form the jugum of the sphenoid body. This is the last part of the medial part of the cranial base to differentiate as cartilage, bridging the gap between the postsphenoid and the cartilaginous nasal capsule.

At stage 17, mesenchyme begins to condense and later to chondrify around the nasal pits at the same time as the polar cartilages, forming the outer part of the nasal capsule and the nasal septum; the roof of each nasal capsule is completed slightly later, when cartilage differentiates around the olfactory nerve bundles to form the cribriform plates of the ethmoid bone. During the third month, cartilaginous conchae form. The whole nasal capsule is well developed by the end of the third month, and consists of a common median septal part – sometimes initially termed the interorbitonasal septum or mesethmoid – and the outer ectethmoid. The conchae ossify during the fifth month; the superior and middle conchae form part of the ethmoid bone, and the inferior pair become separate elements. Each lateral part of the nasal capsule becomes ossified as the orbital plate and ethmoidal labyrinth, whose spaces (‘cells’) communicate with the nasal cavity and become filled with air after birth. Part of the capsule remains cartilaginous as the septal and alar cartilages of the nose, and part is replaced by the intramembranous vomer and nasal bones.

Orbital cartilages surround the eye, but do not undergo ossification in their entirety. The most rostral of them becomes continuous with the presphenoid cartilage by differentiation of a cartilaginous bridge that forms the caudal boundary of the optic foramen, enclosing the optic nerve: this later ossifies to form the lesser wing of the sphenoid bone (orbitosphenoid). The greater wing of the sphenoid (alisphenoid) has both intramembranous and endochondral components; the endochondral part initially differentiates as a cartilage surrounding the mandibular branch of the trigeminal nerve, forming the foramen ovale. This condensation extends medially to join the rostral edge of the polar cartilage on each side. It also expands rostrally, coming to surround the maxillary branch of the trigeminal nerve to form the foramen rotundum. Lastly it extends laterally to join the intramembranous part of the bone, which replaces the caudal part of the orbital cartilage. The greater and lesser wings of the sphenoid are separated by the oculomotor, trochlear and abducent nerves and by the first (ophthalmic) division of the trigeminal nerve.

The otic capsule differentiates from a mesenchymal condensation around the otocyst, after its morphogenesis to form the cochlea and semicircular canals. Differentiation of cartilage begins laterally, at the same time as the polar cartilages are first detectable; it is complete by stage 20. Chondrogenesis around the point of exit of the vestibulocochlear nerve creates the internal acoustic meatus. Chondrogenesis of mesenchyme around the carotid arteries joins each polar cartilage to the otic capsule, forming the carotid canals. A gap occupied by the jugular vein remains between each otic capsule and the parachordal cartilage: this is the jugular foramen. Chondrogenesis of the mesenchyme between the separate cartilages completes formation of the cartilaginous skull base and sensory capsules, which together form a continuous framework around the pre-existing blood vessels and cranial nerves by 9 weeks (40 mm) (Fig. 35.20B).

The process of endochondral ossification in the skull is essentially the same as that of the long bones except that each ossification centre is equivalent to a primary centre, and follows a specific programme of growth and patterning. Growth takes place in the unossified cartilage between adjacent ossification centres; these joints are termed synchondroses. The first ossification centres to appear are those of the lesser and greater wings of the sphenoid, at 8 and 9 weeks respectively. A single basisphenoid ossification centre appears at 11 weeks; three presphenoid and four postsphenoid ossification centres appear at 16 weeks. Bone replaces most of the cartilage until only the major synchondroses remain; these enable the endochondral skull base and sense capsules to continue growing until they reach their final size at puberty or earlier. At birth, unossified chondrocranium persists in the alae, lateral nasal cartilage and septum of the nose, the sphenoethmoidal junction, the spheno-occipital and sphenopetrous junctions, the apex of the petrous temporal bone (foramen lacerum), and between ossification centres of the sphenoid and occipital bones. As indicated above, parts of the chondrocranium do not ossify, but are replaced by adjacent intramembranous bone. In general, endochondral ossification centres form later than intramembranous ossification sites, which first appear during the seventh and eighth weeks.

SKULL VAULT

The bones of the skull vault or calvaria (roof and lateral walls of the neurocranium) are formed entirely by intramembranous ossification. They are also described as dermal bones, since they are considered to be the evolutionary descendants of dermal plates formed as a protective cover for the brain in fishes. In humans, as in all mammals, the major part of the skull vault is formed by paired frontal and parietal bones and the unpaired interparietal (membranous part of the occipital bone). The squamous part of the temporal bones and the membranous part of the alisphenoid contribute to the lateral walls. Lineage data from mouse studies indicates that the frontal and squamous temporal bones are of neural crest origin and the parietals are of mesodermal origin; the interparietal is mixed (Jiang et al 2002). The coronal suture thus forms at the neural crest–mesoderm interface, as does the sagittal suture, due to a small tongue of neural crest tissue lying between the two developing bones. These tissue interfaces may be significant for initiating the molecular signalling system that governs growth of the skull vault. Growth at the borders of adjacent bone, i.e. in the sutures, is the major mechanism of skull vault growth. A sequence of events that maintains a balance between cell proliferation and osteogenic differentiation is mediated by an intercellular signalling system that includes the transcription factor TWIST and ligand–receptor interactions between fibroblast growth factors (FGFs) and their receptors (FGFRs). Mutations in the genes encoding these proteins cause premature fusion of the cranial sutures (craniosynostosis) (for further details and references for this and related descriptions in this section, see Morriss-Kay & Wilkie 2005). In addition to the expansion-related growth that takes place in the sutures, appositional growth, in which bone is laid down on, and resorbed from, the bone surfaces, plays an important role in remodelling the calvarial bones to maintain a degree of curvature that matches the curved surface of the growing brain.

The frontal and parietal bones are initiated as basolateral mesenchymal primordia which extend upwards between the dermal connective tissue and the mesenchymal dura mater. They do not, as previously thought, differentiate within the mesenchyme of an ‘ectomeninx’ that surrounds the brain. As the frontal and then the parietal primordia extend upwards, the differentiating osteoblasts secrete osteoid which then undergoes mineralization. Only the mineralized parts of the bones are detected in Alizarin-stained specimens and X-rays. Clear frontal bone primordia are detectable in the superciliary arch region of Alizarin-stained human embryos by the eighth week. As they become mineralized above this level, the parietal bone primordia can also be seen. The two bones appear to be separated by a wide gap at the coronal suture; in fact, this gap only shows the separation of the mineralized parts of the bone – the unmineralized edge of the parietal bone actually overlaps the caudal edge of the frontal bone. After the upgrowth phase, mineralization takes place centrifugally from the central points of the frontal and parietal bones, which by this time form convex plates over the curvature of the underlying brain.

During birth, the overlap of the frontal and parietal bones enables them to slide over each other; during the neonatal period, when the baby cries and intracranial pressure rises, the overlapping bones slide apart, increasing the fronto-occipital diameter of the skull. Growth at the coronal suture provides the major increase of the fronto-occipital plane of the skull vault. Premature synostosis of the coronal sutures restricts growth in this plane, causing brachycephaly; unilateral coronal synostosis leads to plagiocephaly, in which one side of the skull fails to grow in the fronto-occipital plane. Uni- and bilateral coronal synostosis comprises 20–25% of all forms of craniosynostosis.

The metopic and sagittal sutures are formed when the upwardly extending frontal and parietal bones (respectively) reach the vertex of the skull and abut in the median plane. Growth in these sutures increases the breadth of the skull. The metopic suture fuses at around 18 months after birth, by which time most of the increase in breadth of the forehead is complete; further growth of the frontal bones is mediated by appositional growth. The sagittal suture continues as an active growth centre until puberty, when growth of the brain is complete. Premature fusion results in the formation of a narrow, elongated skull. Sagittal synostosis is the most common form of craniosynostosis (40–55%).

The interparietal bone (supranuchal squamous portion of the occipital bone) forms from two ossification centres that appear in the eighth week. These are considered to be homologous with the paired postparietal bones of reptiles. The fact that they unite to form a single bone in mammals may be due to the interpolation of a small area of neural crest that migrates from the hindbrain after neural tube closure (Jiang et al 2002). Two further ossification centres develop laterally at 12 weeks. There is at first a wide gap occupied by cartilage between the interparietal and parietal bones, which disappears as the membrane bones grow towards each other, forming the lambdoid suture when they abut. The cartilage is in a deeper tissue layer than the intramembranous bone, reflecting the dermal origins of the latter. The lambdoid suture contributes growth to the caudal border of the parietal bones and to the upper part of the occipital bone. Synostosis of this suture is relatively rare (0–5% of craniosynostosis cases) and has a less severe effect on overall skull growth than coronal and median fusions. Posteriorly, between the interparietal bone and the foramen magnum, the skull vault is not formed by membrane bones but by endochondral ossification of the supraoccipital component of the occipital bone.

In addition to the sutures that are formed where two membrane bones abut, fontanelles are formed where three or four bones meet. In the median plane these are the anterior fontanelle, at the junction of the metopic and sagittal sutures, and the posterior fontanelle, at the junction of the sagittal and lambdoid sutures. Laterally, the anterolateral fontanelle lies between the frontal, parietal, greater wing of the sphenoid and squamous temporal bones; its site after closure is called the pterion. The posterolateral fontanelle lies between the parietal, petrous temporal, exoccipital and basioccipital bones; after closure its site is called the asterion. The size of the fontanelles at birth, and the timing of their closure, are highly variable. Delayed growth of the skull bones causes ossification defects including cranium bifidum and parietal foramina, for which several genetic defects have been identified. Cleidocranial dysplasia is a defect of ossification affecting the intramembranous part of the clavicle as well as the skull vault; it is caused by haploinsufficiency of the bone master gene *RUNX2*.

MEMBRANE BONES OF THE FACE AND VISCEROCRANIUM

The face and viscerocranium are formed from neural crest-derived membrane bones. The facial skeleton includes, from forehead to chin, the frontal bones, the orbital bones (frontal, lacrimal and zygomatic), the nasal bones and vomer, the maxilla and mandible. The maxilla and mandible are also classed as part of the membranous viscerocranium since they form from first arch mesenchyme; this category also includes the medial pterygoid plates of the sphenoid bone, the palatine and the tympanic bones. These components are considered together in this section.

During migration, the trigeminal neural crest cells divide into a frontonasal population that migrates superior to the eye, a mandibular population that migrates into the first pharyngeal arch, and a maxillary population closely associated with the proximal end of the first arch (Fig. 35.2). The frontal, lacrimal, nasal bones, the vomer and the premaxillary (incisor tooth-bearing) part of the maxilla are derived from the frontonasal mesenchyme; the maxilla and zygoma are derived from the maxillary mesenchyme; the mandible and tympanic bone are derived from the mandibular mesenchyme. The mandible is the first membrane bone to begin ossification: its single ossification centre appears in the seventh week. The maxilla and premaxilla have primary ossification centres by 7 weeks, and three further ossification centres form in the maxillary mesenchyme at 8 weeks; all of these components fuse to form a single bone, in contrast to some mammals in which the premaxilla remains separate. In the neonatal skull, the suture between the primary and secondary parts of the palate is still patent, indicating the premaxillary contribution here. By 8 embryonic weeks, ossification centres for most of the facial and viscerocranial bones are present, except for the tympanic ring, for which four ossification centres appear at 12 weeks. They fuse to form the sickle-shaped bone that supports the tympanic membrane.

The mandible is a developmentally complex bone. Although the body of the bone is formed by intramembranous ossification, the coronoid region and condyle are formed by endochondral ossification in cartilage that develops after formation of the membrane bone. These secondary ossification centres form at 10–14 weeks. Distal cartilage forms secondary ossification centres, the mental ossicles, at 7 months. This complex system enables the mandible to grow at both proximal and distal ends, analogous to a long bone.

Growth of the face occurs in the sutures between the membrane bones in a similar manner to that of the skull vault sutures, but the amount of growth is proportionately less than in the skull vault, reflecting the dominant influence of brain growth in the latter.

POSTNATAL GROWTH OF THE SKULL

Postnatal growth of the skull is characterized by changing proportions of its components. Growth of the brain continues to be extremely rapid in the first 2 years; in addition to continuing growth of the frontal and parietal bones, the squamous temporal bone increases in size so that it contributes a greater proportion of the skull vault in the adult than in the neonate (Fig. 35.21). The inner ear and the petrous temporal bone around it grow very little after birth, so the increasing breadth of the skull draws the petrous temporal bone out laterally, creating the bony external acoustic meatus. The tympanic ring (with the tympanic membrane) lies at the surface of the meatus in the neonatal skull; it remains at the proximal end of the deepening canal. Use of the sternocleidomastoid muscle to lift the head results in formation of the mastoid process of the temporal bone, which develops air-filled spaces that are continuous with the middle ear cavity. The paranasal sinuses begin to form in late fetal life as diverticula from the nasal cavity which gradually invade the maxilla, frontal, ethmoid and sphenoid bones. At birth they fill with air when the amniotic fluid drains from them. Thickening of the skull bones is accompanied by increasing size of the sinuses, and by a change in form of the sutures, from straight to wavy lines and finally to the complex interdigitations seen in the adult. After growth ceases, the skull sutures contain inert connective tissue and some cartilage; in old age some of them are completely replaced by bone (natural synostosis).

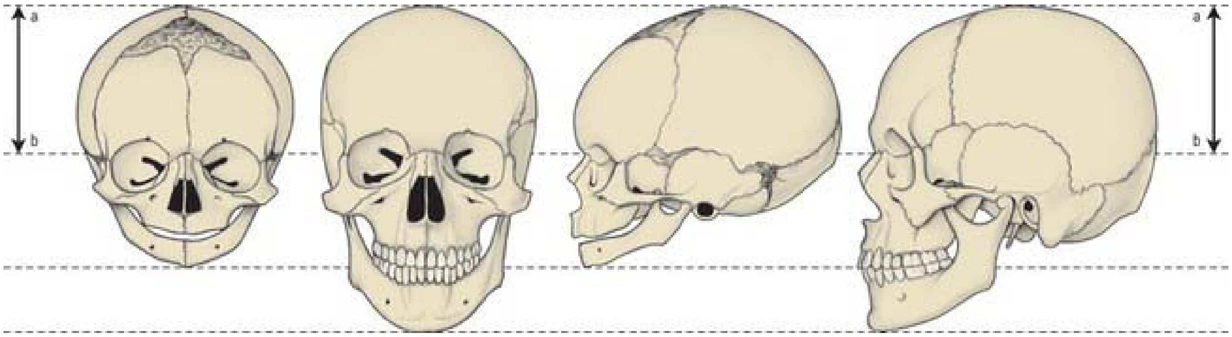

Fig. 35.21 Much of the postnatal growth of the skull is concerned with development of the viscerocranium. This diagram shows that with the

height of the cranial vault expressed as similar in newborn and adult skulls (lines a↔b), the facial skeleton increases particularly during childhood and puberty.

REFERENCES

iley AP, Streit A. Sensory organs: making and breaking the pre-placodal region. *Curr Top Dev Biol*. 2006;72:167-204.

rry A. The aortic arch derivatives in the human adult. *Anat Rec*. 1951;III:221-238.

echschmidt E. The Stages of Human Development Before Birth. Philadelphia: WB Saunders, 1961.

la Cuadra-Blanco C, Peces-Peña MD, Jáñez-Escalada L, Mérida-Velasco JR. Morphogenesis of the human excretory lacrimal system. *J Anat*. 2006;209:127-135.

rguson MWF. The orofacial region. In: Wigglesworth JS, Singer DB. *Textbook of Fetal and Perinatal Pathology*. Oxford: Blackwell Scientific, 1991. Chapter 22.

kumoto S, Yamada Y. Extracellular matrix regulates tooth morphogenesis. *Connect Tissue Res*. 2005;46:220-226.

rlin RJ, Cohen MM, Hennekam RCM. Syndromes of the Head and Neck. 4th edn.. New York: Oxford University Press; 2001.

milton WJ, Mossman HW. Human Embryology. Cambridge: Heffer, 1972.

nrichsen KV, editor. Human-Embryologie. Berlin: Springer-Verlag, 1990.

ng X, Iseki S, Maxson RE, Sucov HM, Morriss-Kay GM. Tissue origins and interactions in the mammalian skull vault. *Dev Biol*. 2002;241:106-116.

ng X, Rowitch DH, Soriano P, McMahon AP, Sucov HM. Fate of the mammalian cardiac neural crest. *Development*. 2000;127:1607-1616.

atsuoka T, Ahlberg PE, Kessaris N, et al. Neural crest origins of the neck and shoulder. *Nature*. 2005;436:347-355.

orriss-Kay GM, Wilkie AOMW. Growth of the normal skull vault and its alteration in craniosynostosis. *J Anat*. 2005;207:637-653.

'Rahilly R, Müller F 1987 Developmental Stages in Human Embryos. Carnegie Institution of Washington Publication 637.

'Rahilly R, Müller F. Human Embryology and Teratology. 3rd edn.. New York: Wiley-Liss; 2001.

'Rahilly R, Müller F. The development of the neural crest in the human. *J Anat*. 2007;211:335-351.

tten BM. Human Embryology. 3rd edn.. New York: Blakiston; 1968.

ntagati F, Rijli FM. Cranial neural crest and the building of the vertebrate head. *Nat Rev Neurosci*. 2003;4:806-820.

esleff I. Genetic basis of tooth development and dental defects. *Acta Odontol Scand*. 2000;58:191-194.

ilkie AOMW, Morriss-Kay GM. Genetics of craniofacial development and malformation. *Nat Rev Genet*. 2001;2:458-468.

CHAPTER 36

External and middle ear

By convention, the ear is subdivided into three parts, the external, middle and inner ear. It is largely, but not entirely, contained within the temporal bone. The ears not only receive, modulate, conduct, amplify and discriminately analyse the complex pressure waves that are sound, but also contain the end organs of balance.

TEMPORAL BONE

Each temporal bone consists of four components: the squamous, petromastoid and tympanic parts and the styloid process (Fig. 36.1). The squamous part has a shallow mandibular fossa associated with the temporomandibular joint (Ch. 31). The petromastoid part is relatively large: its petrous portion houses the auditory apparatus and is formed of compact bone. In contrast, the mastoid process is trabecular and variably pneumatized. The tympanic part has the form of a thin and incomplete ring whose ends are fused with the squamous part. The styloid process gives attachment to the styloid group of muscles. Two canals are associated with the temporal bone. The external acoustic meatus, visible on the lateral surface, conveys sound waves to the tympanic membrane. The internal acoustic meatus, evident on the medial surface, conveys the facial and vestibulocochlear nerves.

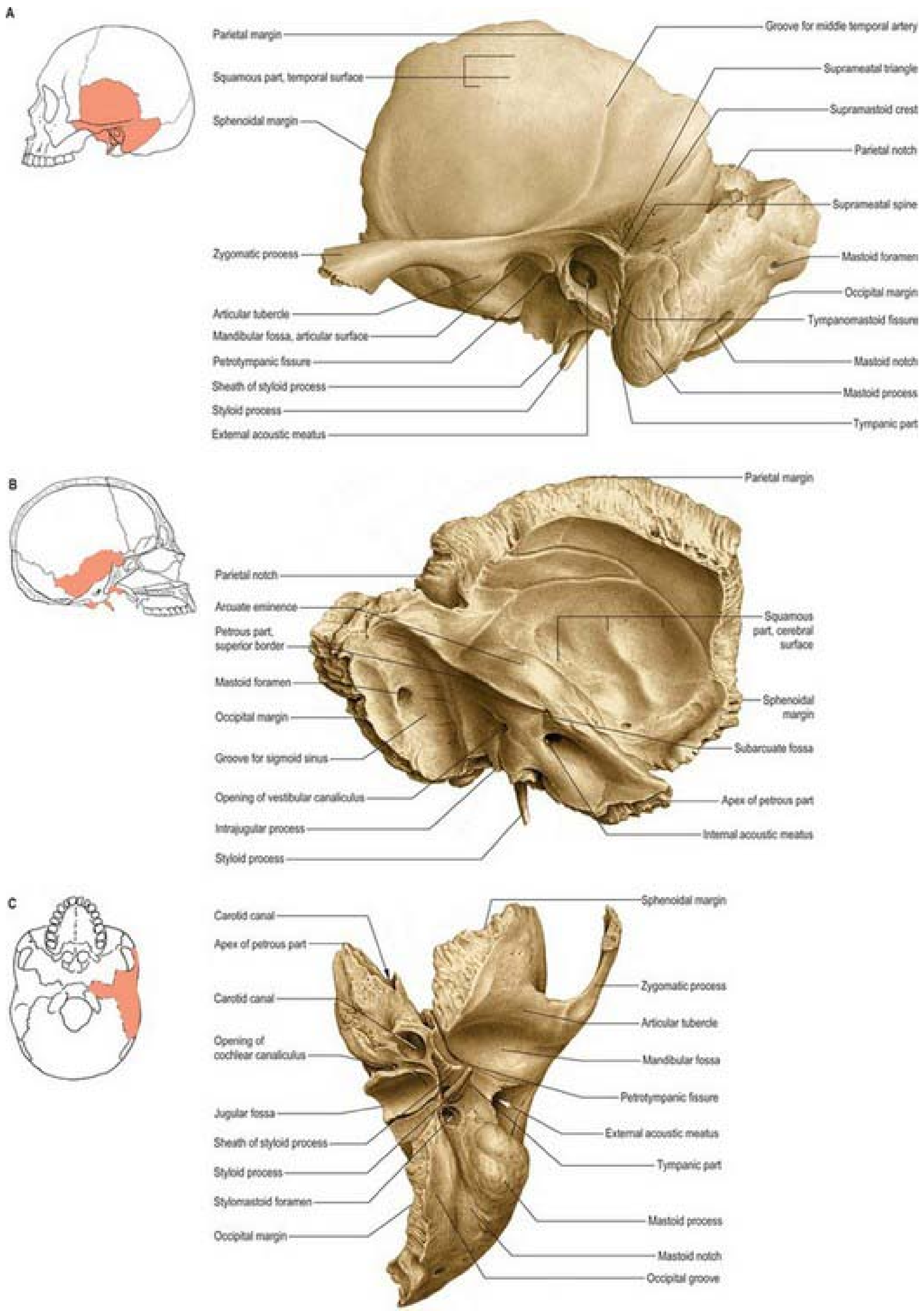
A
Parietal margin
Squamous part, temporal surface
Sphenoidal margin
Zygomatic process
Articular tubercle
Mandibular fossa, articular surface
Petrotympanic fissure
Sheath of styloid process
Styloid process
External acoustic meatus
Groove for middle temporal artery
Suprameatal triangle
Supramastoid crest
Parietal notch
Suprameatal spine
Mastoid foramen
Occipital margin
Tympanomastoid fissure
Mastoid notch
Mastoid process
Tympanic part
B
Parietal margin
Parietal notch
Arcuate eminence
Petrous part, superior border
Mastoid foramen
Occipital margin
Groove for sigmoid sinus
Opening of vestibular canaliculus
Intrajugular process
Styloid process
Squamous part, cerebral surface
Sphenoidal margin
Subarcuate fossa
Apex of petrous part
Internal acoustic meatus
C
Carotid canal
Apex of petrous part
Carotid canal
Opening of cochlear canaliculus
Jugular fossa
Sheath of styloid process
Styloid process
Stylomastoid foramen
Occipital margin
Sphenoidal margin
Zygomatic process
Articular tubercle
Mandibular fossa
Petrotympanic fissure
External acoustic meatus
Tympanic part
Mastoid process
Mastoid notch
Occipital groove

Fig. 36.1 Left temporal bone. **A**, Lateral aspect. **B**, Medial aspect. **C**, Inferior aspect.

(From Sobotta 2006.)

Squamous part

The squamous part lies anterosuperiorly and is thin and partly translucent. Its external temporal surface is smooth, slightly convex, and forms part of the temporal fossa to which temporalis is attached. Above the external acoustic meatus, it is grooved vertically by the middle temporal artery. The supramastoid crest curves backwards and upwards across its posterior part and gives attachment to the temporal fascia. The junction between the squamous and mastoid parts is approximately 1.5 cm below this crest, and traces of the squamomastoid suture may persist. The suprameatal triangle, a depression marking the position of the mastoid antrum (which is medial to the triangle at a depth of approximately 1.25 cm), lies between the anterior end of the supramastoid crest and the posterosuperior quadrant of the external acoustic meatus. The triangle usually contains a small suprameatal spine anteriorly.

The internal cerebral surface of the squamous part is concave and contains depressions which correspond to convolutions of the temporal lobe of the cerebral hemisphere. This surface is grooved by the middle meningeal vessels. Its lower border is fused to the anterior region of the petrous part, but traces of a petrosquamosal suture often appear in adult bones. The superior border is thin, bevelled internally and overlaps the inferior border of the parietal bone at the squamosal suture. Posteriorly it forms an angle with the mastoid element. The anteroinferior border, thin above and thick below, meets the greater wing of the sphenoid bone: it is bevelled internally above, and bevelled externally below.

The squamous part has a zygomatic process and a mandibular fossa.

Zygomatic process

The zygomatic process juts forwards from the lower region of the squamous part. Its triangular posterior part has a broad base that is directed laterally, presenting superior and inferior surfaces. The zygomatic process then twists anteromedially, so that its surfaces become medial and lateral.

The superior surface of the posterior part is concave. The inferior surface is bounded by anterior and posterior roots, converging into the anterior part of the process. The tubercle of the zygomatic root gives attachment to the lateral temporomandibular ligament at the junction of the roots. The posterior root is prolonged forwards above the external acoustic meatus, its upper border continuing into the supramastoid crest. Very rarely, the squamous part is perforated above the posterior root by a squamosal foramen, which transmits the petrosquamous sinus. The anterior root juts almost horizontally from the squamous part. Its inferior surface, with an anteroposterior convexity, forms a short semi-cylindrical articular tubercle and comes into contact with the articular disc of the temporomandibular joint. The tubercle forms the anterior limit of the mandibular fossa.

The anterior part of the zygomatic process is thin and flat and the temporal fascia is attached to its superior border. The inferior border is short and arched and gives origin to some fibres of masseter. The lateral surface is convex. The medial surface is concave and provides further attachment for part of masseter. The anterior end is deeply serrated and slopes obliquely posteroinferiorly to articulate with the temporal process of the zygomatic bone, forming the zygomatic arch. Anterior to the articular tubercle, a small triangular area forms part of the roof of the infratemporal fossa: it is continuous behind with the anterior root and in front with the infratemporal crest of the greater wing of the sphenoid.

Mandibular fossa

The mandibular fossa is limited in front by the articular eminence of the zygomatic process. It presents an anterior articular area, formed by the squamous part, and a posterior non-articular area, formed by the tympanic element. The articular surface is smooth, oval and concave, and contacts the articular disc of the temporomandibular joint (Ch. 31). Unlike most other synovial joints, it is lined by fibrous tissue rather than hyaline cartilage, reflecting its intramembranous development. The non-articular area sometimes contains part of the parotid gland. A small, conical postglenoid tubercle separates the articular surface laterally from the tympanic plate.

Posteriorly, the mandibular fossa is separated from the tympanic part by the squamotympanic fissure. Rarely, a postglenoid foramen exists anterior to the external acoustic meatus in the line of fusion of the squamous and tympanic parts. When present, it replaces the squamosal foramen noted above and transmits the petrosquamous sinus. Medially, a projection from the petrous part of the temporal bone (tegmen tympani) comes to lie within the squamotympanic fissure, further dividing it into petrotympanic and petrosquamous fissures. The petrotympanic fissure leads into the tympanic cavity and contains an anterior malleolar ligament and the anterior tympanic branch of the maxillary artery. The anterior opening of the anterior canaliculus for the chorda tympani nerve lies at the medial end of the fissure.

Petromastoid part

The petromastoid part of the temporal bone, although morphologically one element, is more conveniently described as two parts, namely mastoid and petrous parts.

Mastoid part

The mastoid part is the posterior region of the temporal bone and has an outer surface roughened by the attachments of the occipital belly of occipitofrontalis and auricularis posterior. A mastoid foramen, of variable size and position, and traversed by a vein from the sigmoid sinus and a small dural branch of the occipital artery, frequently lies near its posterior border. The foramen may be in the occipital or occipitotemporal suture; it may be parasutural (40–50% of crania); or may be absent.

The mastoid part projects down as the conical mastoid process, and is larger in adult males. Sternocleidomastoid, splenius capitis and longissimus capitis are all attached to its lateral surface, and the posterior belly of digastric is attached to a deep mastoid notch on its medial aspect. The occipital artery runs in a shallow occipital groove which lies medial to the mastoid notch. The internal surface of the mastoid process bears a deep, curved sigmoid sulcus for the sigmoid venous sinus: the sulcus is separated from the underlying innermost mastoid air cells by a thin lamina of bone.

The superior border of the mastoid part is thick and serrated for articulation with the mastoid angle of the parietal bone. The posterior border is also serrated and articulates with the inferior border of the occipital bone between its lateral angle and jugular process. The mastoid element is fused with the descending process of the squamous part: below, it appears in the posterior wall of the tympanic cavity.

Petrous part

The petrous part is a mass of bone that is wedged between the sphenoid and occipital bones in the cranial base: it contains the acoustic labyrinth. It is inclined superiorly and anteromedially, and has a base, apex, three surfaces (anterior, posterior and inferior) and three borders (superior, posterior and anterior).

The base would correspond to the part that lies on the base of the skull and is separated from the squamous part by a suture. However, this suture disappears soon after birth. The subsequent development of the mastoid processes means that the precise boundaries of the base are no longer identifiable.

The apex, blunt and irregular, is angled between the posterior border of the greater wing of the sphenoid and the basilar part of the occipital bone. It contains the anterior opening of the carotid canal and limits the foramen lacerum posterolaterally.

The anterior surface contributes to the floor of the middle cranial fossa (Ch. 27) and is continuous with the cerebral surface of the squamous part (although the petrosquamosal suture often persists late in life). The whole surface is adapted to the inferior temporal gyri. Behind the apex is a trigeminal impression for the trigeminal ganglion. Bone anterolateral to this impression roofs the anterior part of the carotid canal, but is often deficient. A ridge separates the trigeminal impression from another hollow behind which partly roofs the internal acoustic meatus and cochlea. This, in turn, is limited behind by the arcuate eminence which is raised by the superior (anterior) semicircular canal. Laterally, the anterior surface roofs the vestibule and, partly, the facial canal. Between the squamous part laterally and the arcuate eminence and the hollows just described medially, the anterior surface is formed by the tegmen tympani, a thin plate of bone which forms the roof of the mastoid antrum, and extends forwards above the tympanic cavity and the canal for tensor tympani. The lateral margin of the tegmen tympani meets the squamous part at the petrosquamosal suture, turning down in front as the lateral wall of the canal for tensor tympani and the osseous part of the pharyngotympanic tube: its lower edge is in the squamotympanic fissure. Anteriorly the tegmen bears a narrow groove related to the greater petrosal nerve (which passes posterolaterally to enter the bone by a hiatus anterior to the arcuate eminence). The groove passes forwards to the foramen lacerum. A smaller and similar hiatus and groove may be found more laterally: they are related to the lesser petrosal nerve (which runs to the foramen ovale). The posterior slope of the arcuate eminence overlies the posterior and lateral semicircular canals. Lateral to the eminence, the posterior part of the tegmen tympani roofs the mastoid antrum.

The posterior surface contributes to the anterior part of the posterior cranial fossa and is continuous with the internal surface of the mastoid part. The opening of the internal acoustic meatus lies near its centre. A small slit leading to the vestibular aqueduct lies behind the opening of the meatus, almost hidden by a thin plate of bone. This contains the saccus and ductus endolymphaticus together with a small artery and vein. The terminal half of the saccus endolymphaticus protrudes through the slit between the periosteum and dura mater. The subarcuate fossa lies above these openings.

The irregular inferior surface is part of the exterior of the cranial base. Near the apex of the petrous part, a quadrilateral area is partly associated with the attachment of levator veli palatini and the cartilaginous pharyngotympanic tube, and partly connected to the basilar part of the occipital bone by dense fibrocartilage. Behind this region is the large, circular opening of the carotid canal, and behind the opening of the canal is the jugular fossa, which is of variable depth and size and contains the superior jugular bulb. The inferior ganglion of the glossopharyngeal nerve lies in a triangular depression anteromedial to the jugular fossa (below the internal acoustic meatus). At its apex is a small opening into the cochlear canaliculus, occupied by the perilymphatic duct (a tube of dura mater) and a vein draining from the cochlea to the internal jugular vein. A canaliculus for the tympanic nerve from the glossopharyngeal nerve lies on the ridge between the carotid canal and the jugular fossa. The mastoid canaliculus for the auricular branch of the vagus nerve is laterally positioned in the jugular fossa. Behind the jugular fossa, the rough quadrilateral jugular surface is covered by cartilage which joins it to the jugular process of the occipital bone.

The superior border, the longest, is grooved by the superior petrosal sinus. The attached margin of the tentorium cerebelli is fixed to the edges of the groove except at its medial end, where it is crossed by the roots of the trigeminal nerve. The posterior border, intermediate in length, bears a sulcus medially which forms, together with the occipital bone, a gutter for the inferior petrosal sinus. Behind this, the jugular fossa contributes (together with the occipital bone) to the jugular foramen and is notched by the glossopharyngeal nerve. Bone on either or both sides of the jugular notch may meet the occipital bone and divide the jugular foramen into two or three parts. The anterior border is joined laterally to the squamous part of the temporal bone at the petrosquamosal suture; medially it articulates with the greater wing of the sphenoid bone.

Two canals exist at the junction of the petrous and squamous parts, one above the other, separated by a thin osseous plate and both leading to the tympanic cavity: the upper canal contains tensor tympani, the lower canal is the pharyngotympanic tube.

Tympanic part

The tympanic part of the temporal bone is a curved plate below the squamous part and anterior to the mastoid process. Internally it fuses with the petrous part and appears between this and the squamous part, where it is inferolateral to the auditory orifice. Behind, it fuses with the squamous part and mastoid process and is the anterior limit of the tympanomastoid fissure. Its concave posterior surface forms the anterior wall, floor and part of the posterior wall of the external acoustic meatus. The tympanic membrane is attached to a narrow tympanic sulcus on its medial surface. The quadrilateral concave anterior surface is the posterior wall of the mandibular fossa and may contact the parotid gland. Its rough lateral border forms most of the margin of the osseous part of the external acoustic meatus and is continuous with its cartilaginous part. Laterally the upper border is fused with the back of the postglenoid tubercle; medially it forms the posterior edge of the petrotympanic fissure. The inferior border is sharp, and splits laterally to form, at its root, the sheath of the styloid process (vaginal process). Centrally the tympanic part is thin, and is often perforated. The stylomastoid foramen lies between the styloid and mastoid processes: it represents the external end of the facial canal and transmits the facial nerve and stylomastoid artery.

Styloid process

The styloid process is slender, pointed and projects anteroinferiorly from the inferior aspect of the temporal bone. Its length varies, ranging from a few millimetres to an average of 2.5 cm. Often almost straight, it can show a curvature, an anteromedial concavity being most common. Its proximal part (tympanohyal) is ensheathed by the tympanic plate, especially anterolaterally, while muscles and ligaments are attached to its distal part (stylohyal). *In vivo*, its relationships are important. The styloid process is covered laterally by the parotid gland; the facial nerve crosses its base; the external carotid artery crosses its tip, embedded in the parotid; and medially the process is separated from the beginning of the internal jugular vein by the attachment of stylopharyngeus.

External acoustic meatus

The temporal bone contains the bony (osseous) part of the external acoustic meatus (see p. 620).

Ossification

The four temporal components ossify independently (Fig. 36.2). The squamous part is ossified in a sheet of condensed mesenchyme from a single centre near the zygomatic roots, which appear in the seventh or eighth week *in utero*. The petromastoid part has several centres which appear in the cartilaginous otic capsule during the fifth month: as many as 14 have been described. These centres vary in order of appearance. Several are small and inconstant, soon fusing with others. The otic capsule is almost fully ossified by the end of the sixth month. The tympanic part is also ossified in mesenchyme from a centre identifiable about the third month; at birth it is an incomplete tympanic ring, deficient above, its concavity grooved by a tympanic sulcus for the tympanic membrane. The malleolar sulcus for the anterior malleolar process, chorda tympani and anterior tympanic artery inclines obliquely downwards and forwards across the medial aspect of the anterior part of the ring. The styloid process develops from two centres at the cranial end of cartilage in the second visceral or hyoid arch: a proximal centre for the tympanohyal appears before birth, and another, for the distal stylohyal, appears after birth. The tympanic ring unites with the squamous part shortly before birth, and the petromastoid fuses with it and the tympanohyal during the first year. The stylohyal does not unite with the rest of the process until after puberty and may never do so.

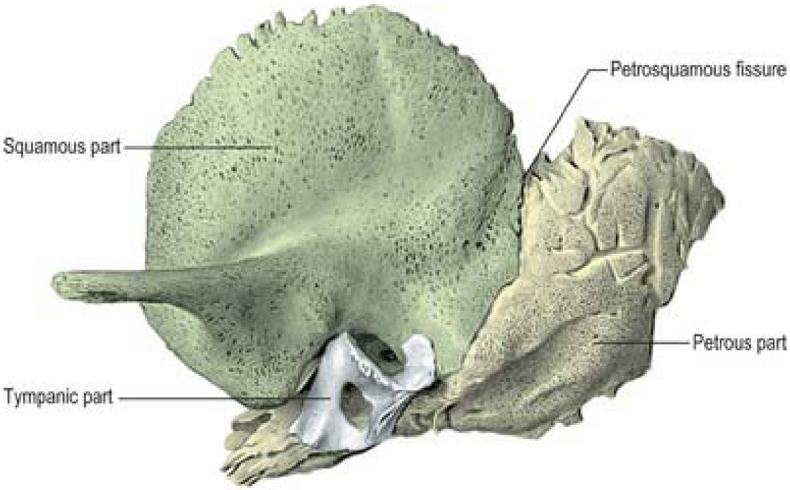

Fig. 36.2 Left temporal bone at birth.

(From Sobotta 2006.)

Once ossified, the tympanic cavity, mastoid antrum and the posterior end of the pharyngotympanic tube become surrounded by bone. The petrous part forms the roof, floor and medial wall of the cavity, while the squamous and tympanic parts, together with the tympanic membrane, form its lateral wall. At birth the middle and inner ears are adult size, and the tympanic cavity, mastoid antrum, tympanic membrane and auditory ossicles are all almost adult size. The anterior process does not join the malleus until 6 months later. The internal acoustic meatus is approximately 6 mm in horizontal diameter, 4 mm in vertical diameter and 7 mm in length at birth, and the adult diameters are 7.7 mm and 11 mm respectively.

After birth and apart from general growth, the tympanic ring extends posterolaterally to become cylindrical, growing into a fibrocartilaginous tympanic plate, which forms the adjacent part of the external acoustic meatus at this stage. This growth is not equal but is rapid in the anterior and posterior regions, which meet and blend. Thus, for a time, an opening (foramen of Huschke) exists in the floor: it usually closes at about the fifth year, but is sometimes permanent (in 5–46% of adult crania from ancient and modern populations). The external acoustic meatus is relatively as long in children as it is in adults, but the canal is fibrocartilaginous, whereas its medial two-thirds are osseous in adults. Surgical access to the tympanic cavity is via the mastoid antrum, and in children it is necessary to remove only a thin scale of bone in the suprameatal triangle to reach the antrum. The tympanic plate ensheathes the styloid process by posterior extension, and extends medially over the petrous bone to the carotid canal.

Initially, the mandibular fossa is shallow, facing more laterally, but it then deepens and ultimately faces downwards. Posteroinferiorly, the squamous part grows down behind the tympanic ring to form the lateral wall of the mastoid antrum. The mastoid part is at first flat, so that the stylomastoid foramen and rudimentary styloid process are immediately behind the tympanic ring. The mastoid part becomes invaded by air cells, especially at puberty. The lateral mastoid region grows downwards and forwards to form the mastoid process, which means that the styloid process and stylomastoid foramen become inferior. Descent of the foramen lengthens the facial canal. The mastoid process is not perceptible until late in the second year. The subarcuate fossa gradually fills and is almost obliterated.

In the neonate, the petrous and squamous parts of the temporal bone are usually partially separated by the petrosquamous fissure which opens directly into the mastoid antrum of the middle ear. The fissure closes in 4% of infants during the first year, but it remains unclosed in 20–40% up to the age of 19 years: it is a route for the spread of infection from the middle ear to the meninges. The neonatal internal acoustic meatus is about half the length of its adult counterpart. Its opening from the middle ear cavity is as large as it is in the adult, but the pharyngeal opening in the nasal part of the pharynx is relatively smaller. The course of the pharyngotympanic tube is horizontal in the newborn, whereas in the adult it passes from the middle ear downward, forward and medially.

EXTERNAL EAR

The external ear is not simply an ear-trumpet but the first of a series of stimulus modifiers in the auditory apparatus. It consists of the auricle, or pinna, and the external acoustic meatus. The auricle projects to a variable and individual degree from the side of the head and collects sound waves, which it conducts along the external auditory canal inwards to the eardrum, the tympanic membrane.

AURICLE (PINNA)

The lateral surface of the auricle is irregularly concave, faces slightly forwards, and displays numerous eminences and depressions (Fig. 36.3). It has a prominent curved rim, the helix. This usually bears a small tubercle posterosuperiorly, Darwin's tubercle, which is quite pronounced around the sixth month of intrauterine life. The antihelix is a curved prominence, parallel and anterior to the posterior part of the helix: it divides above into two crura which flank a depressed triangular fossa. The curved depression between the helix and antihelix is the scaphoid fossa. The antihelix encircles the deep, capacious concha of the auricle, which is incompletely divided by the crus or anterior end of the helix. The conchal area above this, the cymba conchae, overlies the suprameatal triangle of the temporal bone, which can be felt through it, and which overlies the mastoid antrum. The tragus is a small curved flap below the crus of the helix and in front of the concha: it projects posteriorly, partly overlapping the meatal orifice. The antitragus is a small tubercle opposite the tragus and separated from it by the intertragic incisure or notch. Below it is the lobule, composed of fibrous and adipose tissues. It is soft, unlike the majority of the auricle which is supported by elastic cartilage and is firm. The cranial surface of the auricle presents elevations which correspond to the depressions on its lateral surface, and after which they are named (e.g. eminentia conchae, eminentia fossae triangularis).

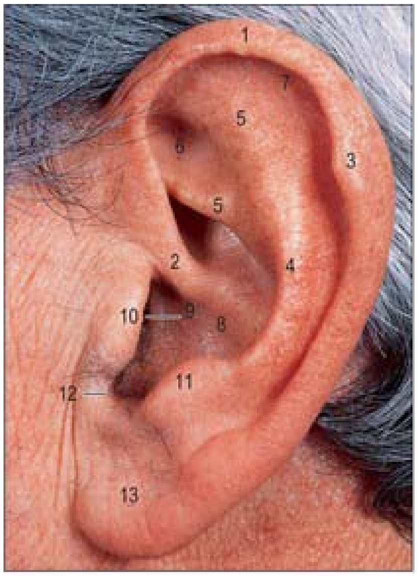

1. Helix. 2. Crus of helix 3. Auricular tubercle. 4. Antihelix. 5. Crura of antihelix. 6. Triangular fossa. 7. Scaphoid fossa. 8. Concha of auricle. 9. External acoustic meatus. 10. Tragus. 11. Antitragus. 12. Intertragic notch. 13. Lobule of auricle.

Fig. 36.3 Lateral surface of the left auricle.

(By permission from Berkovitz BKB, Moxham BJ 2002 Head and Neck Anatomy. London: Martin Dunitz.)

A number of common abnormalities have been recognized and carry descriptive names or eponyms (Porter & Tan 2005).

Anotia

Anotia is complete absence of the external ear, and is most likely caused by a developmental disturbance between the seventh and eighth gestational week.

Cryptotia

Cryptotia (hidden or pocket ear) is an abnormality of the auricle where the upper pole is buried beneath the temporal skin. It can be restored to a more normal form by a sequence of surgical procedures that involve the use of splints to create a new scaphoid fossa and grafts or local flaps to release the cartilage from the side of the head.

Microtia

Microtia (diminutive ear) is usually an isolated congenital abnormality, but is sometimes associated with recognized syndromes, e.g. fetal alcohol syndrome, maternal diabetic syndrome, thalidomide and isotretinoin exposure.

Polyotia

Polyotia (also known as mirror ear) is caused by persistence of pre-auricular tissue that would normally be included in the pinna, but instead lies in front of the tragus in the posterior aspect of the cheek.

Stahl’s bar

Stahl’s bar (also known as Satiro’s ears) is a common congenital deformity of the auricle where the helix is flattened and the upper crus of the antihelix is duplicated, producing a ridge of cartilage running from the antihelix to the rim of the helix. This causes a pointing of the ear and a reversal of the normal concavity of the scaphoid fossa. Occasionally, the upper part of the pinna flops over to produce an appearance known as ‘lop ear’. A variety of surgical procedures have been designed to correct this deformity using external moulds etc. Attempts at correction are made in the neonatal period while the cartilage is soft and pliable: delay until such time as the cartilage has become stiff may jeopardize a good outcome.

Prominent ears

Prominent ears (also known as ‘bat’ ears) are caused by the absence or inadequacy of an antihelical fold.

Pre-auricular sinus

Six auricular hillocks, the embryological precursors of the auricle, form round the margins of the dorsal portion of the first pharyngeal cleft, three on the caudal edge of the first pharyngeal arch and three on the cranial edge of the second pharyngeal arch (see Ch. 40). They fuse to form the auricle and surround the dorsal end of the first branchial cleft from which the external acoustic meatus arises. Sinuses and cysts are often found just anterior to the root of the helix, near to the point of fusion of the hillocks derived from the first branchial arch and those derived from the second branchial arch. There is debate as to whether the abnormalities are epithelial inclusions between the hillocks or remnants of the first branchial cleft. The sinuses may be simple pits or complex branching sinuses that occasionally extend deeply towards the external acoustic meatus so that they lie close to the facial nerve. Clinically they may become chronically infected and require surgical excision: this may be technically demanding surgery given the close proximity to the facial nerve.

Skin

The skin of the auricle continues into the external auditory meatus to cover the outer surface of the tympanic membrane. It is thin, has no dermal papillae, and is closely adherent to the cartilaginous and osseous parts of the canal (inflammation of the canal skin is very painful because of this attachment to the underlying structures). The thick subcutaneous tissue of the cartilaginous part of the meatus contains numerous ceruminous glands that secrete wax, or cerumen. Their coiled tubular structure resembles that of sweat glands. The secretory cells are columnar when active, but cuboidal when quiescent; they are covered externally by myoepithelial cells. Ducts open either onto the epithelial surface or into the nearby sebaceous gland of a hair follicle. Cerumen prevents the maceration of meatal skin by trapped water. Antibacterial properties have been attributed to cerumen, but the evidence for this is lacking (Campos et al 2000, Pata et al 2003).

Two types of wax, wet and dry, are recognized. They are genetically determined. Dry wax is common in East Asians, while the wet type is more common in other ethnic groups (Yoshiura et al 2006). Overproduction, accumulation or impaction of wax may completely occlude the meatus, thereby hindering sound from reaching the tympanic membrane and also restricting the natural vibration of the drum. Although ceruminous glands and hair follicles are largely limited to the cartilaginous meatus, a few small glands and fine hairs are also present in the roof of the lateral part of the osseous part of the canal. The warm, humid environment of the relatively enclosed meatal air aids the mechanical responses of the tympanic membrane.

Cartilaginous framework

The auricle is a single thin plate of elastic fibrocartilage covered by skin, its surface moulded by eminences and depressions (Fig. 36.4). It is connected to the surrounding parts by ligaments and muscles, and is continuous with the cartilage of the external acoustic meatus. There is no cartilage in the lobule or between the tragus and the crus of the helix, where the gap is filled by dense fibrous tissue. Anteriorly, where the helix curves upwards, there is a small cartilaginous projection, the spine of the helix. Its other extremity is prolonged inferiorly as the tail of the helix and it is separated from the antihelix by the fissura antitragohelicina. The cranial aspect of the cartilage bears the eminentia conchae and eminentia scaphae, which correspond to the depressions on the lateral surface. The two eminences are separated by a transverse furrow, the sulcus antihelicis transversus, which corresponds to the inferior crus of the antihelix on the lateral surface. The eminentia conchae is crossed by an oblique ridge, the ponticulus, for the attachment of auricularis posterior. There are two fissures in the auricular cartilage, one behind the crus of the helix and another in the tragus.

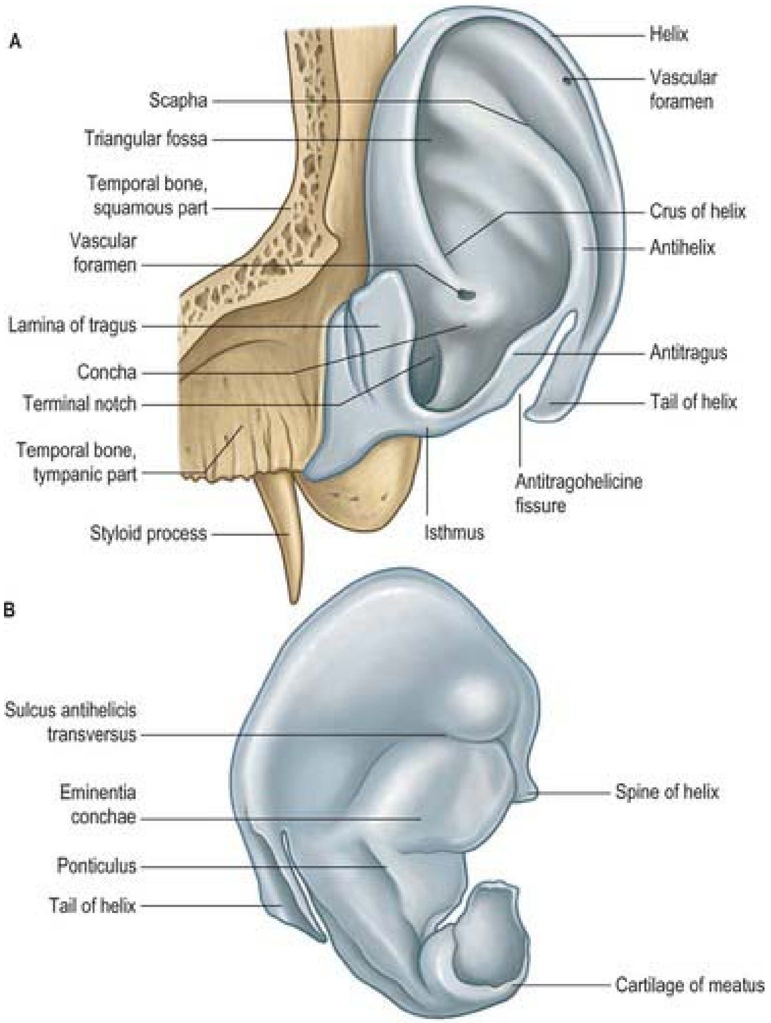
A
Scapha
Triangular fossa
Temporal bone, squamous part
Vascular foramen
Lamina of tragus
Concha
Terminal notch
Temporal bone, tympanic part
Styloid process
Helix
Vascular foramen
Crus of helix
Antihelix
Antitragus
Tail of helix
Antitragohelicine fissure
Isthmus
B
Sulcus antihelicis transversus
Eminentia conchae
Ponticulus
Tail of helix
Spine of helix
Cartilage of meatus

Fig. 36.4 The auricular cartilages of the left ear. **A**, Lateral surface. **B**, Medial surface.

Ligaments

Anterior and posterior extrinsic ligaments connect the auricle with the temporal bone. The anterior ligament extends from the tragus and the spine of the helix to the root of the zygomatic process of the temporal bone. The posterior ligament passes from the posterior surface of the concha to the lateral surface of the mastoid process. Two main intrinsic ligaments connect individual auricular cartilages: a strong fibrous band passes from the tragus to the helix, thereby completing the meatus anteriorly and forming part of the boundary of the concha; and another band passes between the antihelix and the tail of the helix. Less prominent bands exist on the cranial aspect of the auricle.

Auricular muscles

Extrinsic auricular muscles connect the auricle to the skull and scalp and move the auricle as a whole. Intrinsic auricular muscles connect the different parts of the auricle.

Extrinsic muscles

The extrinsic auricular muscles are the auriculares anterior, superior and posterior. The smallest of the three is auricularis anterior, a thin fan of pale fibres which arise from the lateral edge of the epicranial aponeurosis and converge to attach to the spine of the helix. The largest of the three, auricularis superior, is also thin and fan-shaped and converges from the epicranial aponeurosis via a thin, flat tendon to attach to the upper part of the cranial surface of the auricle. The auricularis posterior consists of two or three fleshy fasciculi which arise by short aponeurotic fibres from the mastoid part of the temporal bone and insert into the ponticulus on the eminentia conchae.

Vascular supply

The arterial supply of the extrinsic auricular muscles is derived mainly from the posterior auricular artery.

Innervation

Auriculares anterior and superior are supplied by temporal branches of the facial nerve and auricularis posterior is supplied by the posterior auricular branch of the facial nerve.

Actions

In man these muscles have very little obvious effect. However, despite the paucity of auricular movement, auditory stimuli may evoke patterned responses from these small muscles and electromyography can detect the ‘crossed acoustic response’, used to determine auditory threshold levels and brainstem latencies, which is elicited by this means in investigative clinical neurology.

Intrinsic muscles

The intrinsic auricular muscles are helicis major and minor, tragicus, antitragicus, transversus auriculae and obliquus auriculae (Fig. 36.5). Helicis major is a narrow vertical band on the anterior margin of the helix, passing from its spine to its anterior border, where the helix is about to curve back. Helicis minor is an oblique fasciculus covering the crus of the helix. Tragicus is a short, flattened, vertical band on the lateral aspect of the tragus. Antitragicus passes from the outer part of the antitragus to the tail of the helix and the antihelix. Transversus auriculae, located on the cranial aspect of the auricle, consists of scattered fibres, partly tendinous, partly muscular, which extend between the eminentia conchae and the eminentia scaphae. Obliquus auriculae, also located on the cranial aspect of the auricle, consists of a few fibres which extend from the upper and posterior parts of the eminentia conchae to the eminentia scaphae.

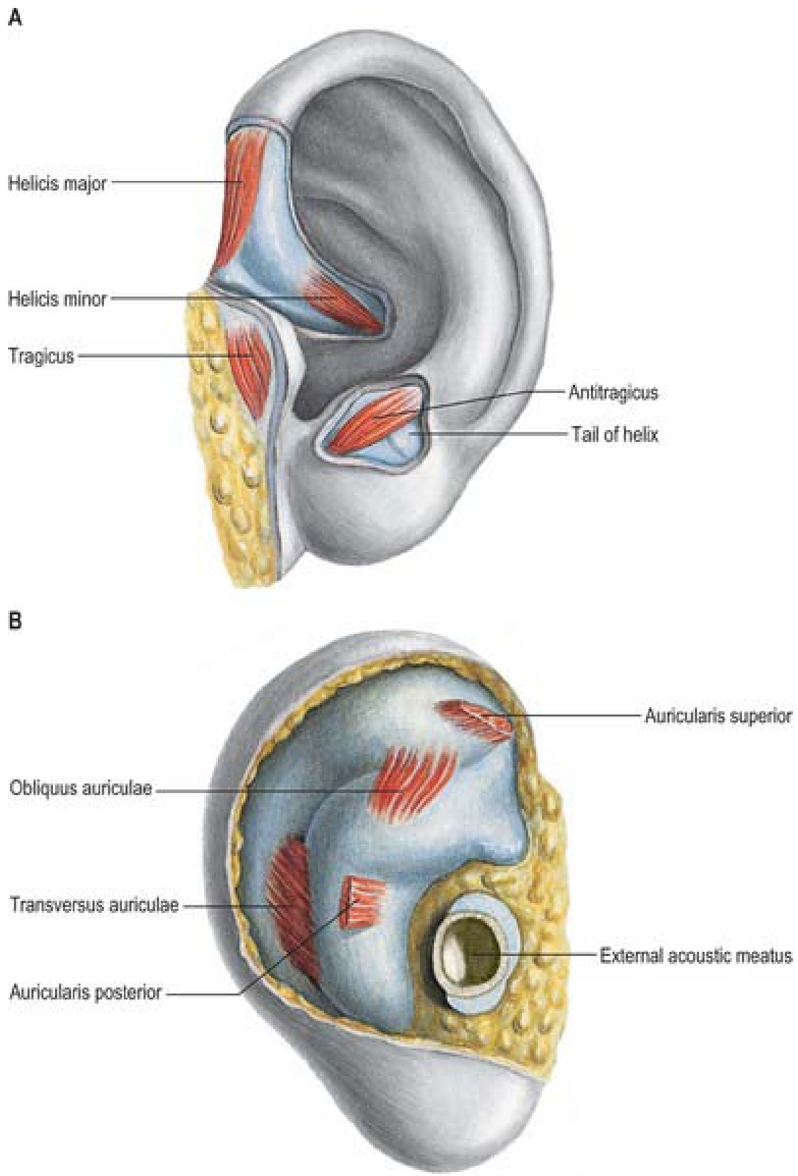
A
Helicis major
Helicis minor
Tragicus
Antitragicus
Tail of helix
B
Auricularis superior
Obliquus auriculae
Transversus auriculae
Auricularis posterior
External acoustic meatus

Fig. 36.5 Auricular muscles of the left ear.

(From Sobotta 2006.)

Vascular supply

The intrinsic auricular muscles are supplied by branches of the posterior auricular and superficial temporal arteries.

Innervation

The intrinsic auricular muscles on the lateral aspect of the auricle are innervated by the temporal branches of the facial nerve, and those on the cranial aspect of the auricle are innervated by the posterior auricular branch of the facial nerve.

Actions

The intrinsic muscles modify auricular shape minimally, if at all, in most human ears: helicis major can draw the auricle forwards and upwards. Rare individuals can modify the shape and position of their external ears.

Vascular supply and lymphatic drainage

Arteries

The posterior auricular branch of the external carotid artery is the dominant blood supply (Imanishi et al 1997). It supplies three or four branches to the cranial surface of the auricle: twigs from these arteries reach the lateral surface, some through fissures in the cartilage, others round the margin of the helix. The posterior auricular artery ascends between the parotid gland and the styloid process to the groove between the auricular cartilage and mastoid process. The superior auricular artery has a constant course and connects the superior temporal artery and the posterior auricular arterial network: this branch can provide a reliable vascular pedicle for retro-auricular flaps (Moschella et al 2003) The auricle is also supplied by anterior auricular branches of the superficial temporal artery, which are distributed to its lateral surface, and by a branch from the occipital artery.

Veins

Auricular veins correspond to the arteries of the auricle. Arteriovenous anastomoses are numerous in the skin of the auricle and are thought to be important in the regulation of core temperature.

Lymphatic drainage

The posterior aspect of the pinna drains to nodes at the mastoid tip. The tragus and upper part of the pinna drain into pre-auricular nodes, while the remainder of the pinna drains to upper deep cervical lymph nodes.

Innervation

The sensory innervation of the auricle is complex and not fully determined. This is perhaps because the external ear represents an area where skin originally derived from a branchial region meets skin originally derived from a postbranchial region. The sensory nerves involved are the great auricular nerve, which supplies most of the cranial surface and the posterior part of the lateral surface (helix, antihelix, lobule); the lesser occipital nerve, which supplies the upper part of the cranial surface; the auricular branch of the vagus, which supplies the concavity of the concha and posterior part of the eminentia; the auriculotemporal nerve, which supplies the tragus, crus of the helix and the adjacent part of the helix; and the facial nerve, which together with the auricular branch of the vagus probably supplies small areas on both aspects of the auricle, in the depression of the concha, and over its eminence. The details of the cutaneous innervation derived from the facial nerve require further clarification. It is possible that as the auricular branch of the vagus traverses the temporal bone and crosses the facial canal, approximately 4 mm above the stylomastoid foramen, it contributes an ascending branch to the facial nerve, and that in this way fibres of the vagus are carried via the facial nerve to the pinna (see p. 494).

EXTERNAL ACOUSTIC MEATUS

The external acoustic meatus extends from the concha to the tympanic membrane: it is approximately 2.5 cm from the floor of the concha and approximately 4 cm from the tragus. It has two structurally different parts: its lateral third is cartilaginous and its medial two-thirds is osseous (Figs 36.6A, 36.7, 36.8). It forms an S-shaped curve, directed at first medially, anteriorly and slightly up (pars externa), then posteromedially and up (pars media), and lastly anteromedially and slightly down (pars interna). It is oval in section, its greatest diameter is obliquely inclined posteroinferiorly at the external orifice, but is nearly horizontal at its medial end. There are two constrictions, one near the medial end of the cartilaginous part, the other, the isthmus, in the osseous part about 2 cm from the bottom of the concha. The tympanic membrane, which closes its medial end, is obliquely set, which means that the floor and the anterior wall of the meatus are longer than its roof and posterior wall.

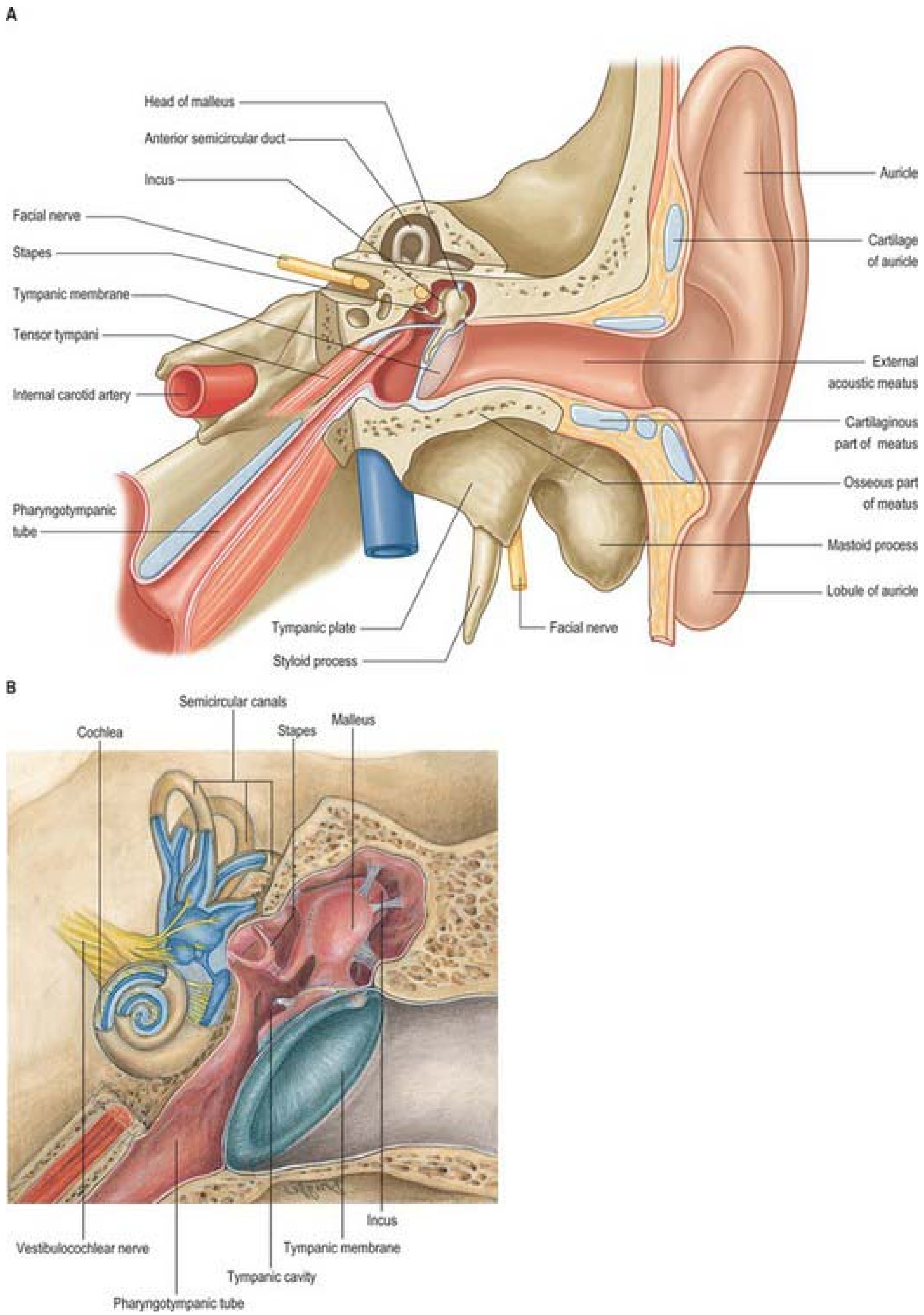
A
Head of malleus
Anterior semicircular duct
Incus
Facial nerve
Stapes
Tympanic membrane
Tensor tympani
Internal carotid artery
Pharyngotympanic tube
Auricle
Cartilage of auricle
External acoustic meatus
Cartilaginous part of meatus
Osseous part of meatus
Mastoid process
Lobule of auricle
Tympanic plate
Styloid process
Facial nerve
B
Semicircular canals
Cochlea
Stapes
Malleus
Incus
Vestibulocochlear nerve
Tympanic membrane
Tympanic cavity
Pharyngotympanic tube

Fig. 36.6 The external, middle and inner regions of the left ear. **A**, Anterior aspect. **B**, A more detailed view of the relationships of structures in the middle and inner ear. (**B**, From Sobotta 2006.)

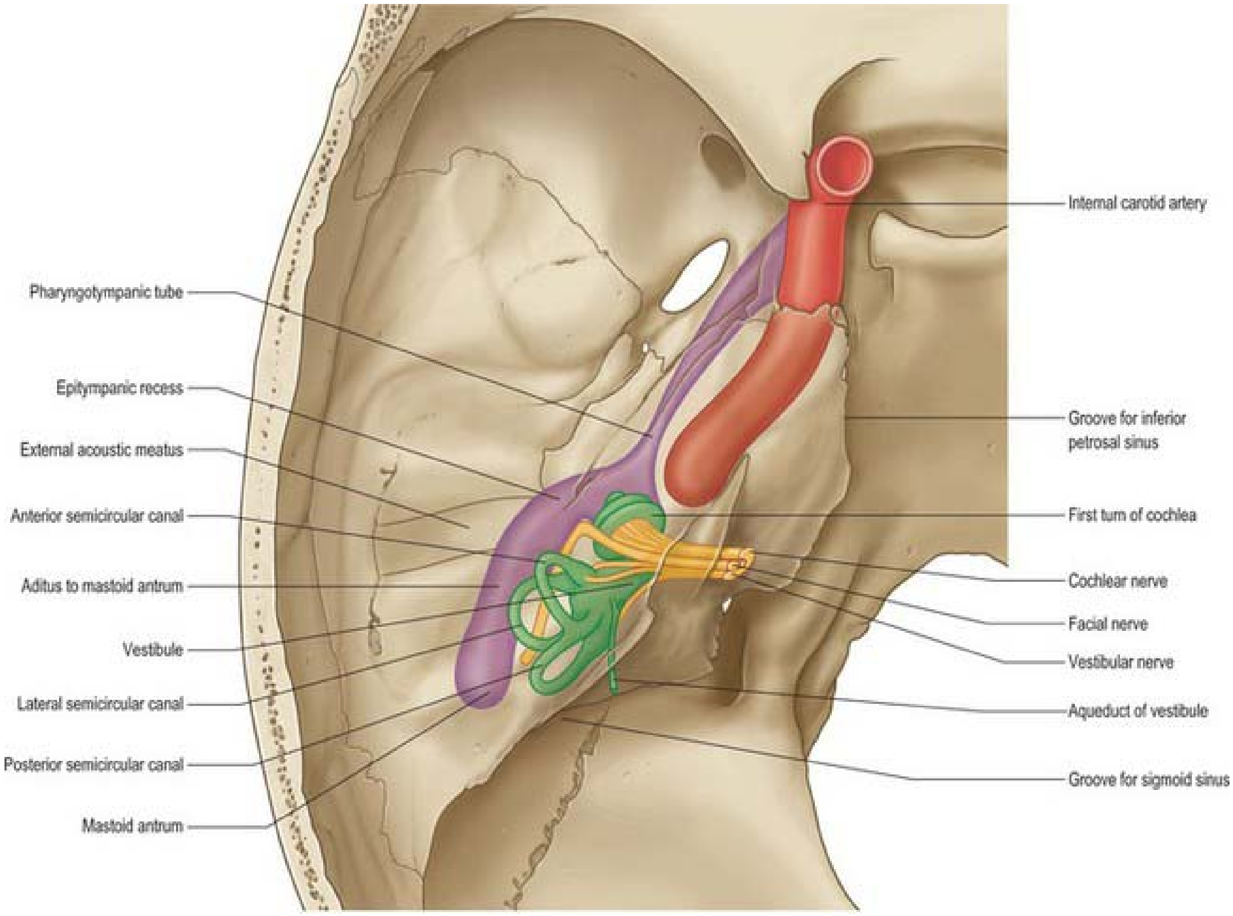
Internal carotid artery
Pharyngotympanic tube
Epitympanic recess
External acoustic meatus
Anterior semicircular canal
Aditus to mastoid antrum
Vestibule
Lateral semicircular canal
Posterior semicircular canal
Mastoid antrum
Groove for inferior petrosal sinus
First turn of cochlea
Cochlear nerve
Facial nerve
Vestibular nerve
Aqueduct of vestibule
Groove for sigmoid sinus

Fig. 36.7 The left auditory apparatus as if viewed through a semi-transparent temporal bone. Note the genu in the facial nerve at the site of the geniculate ganglion.

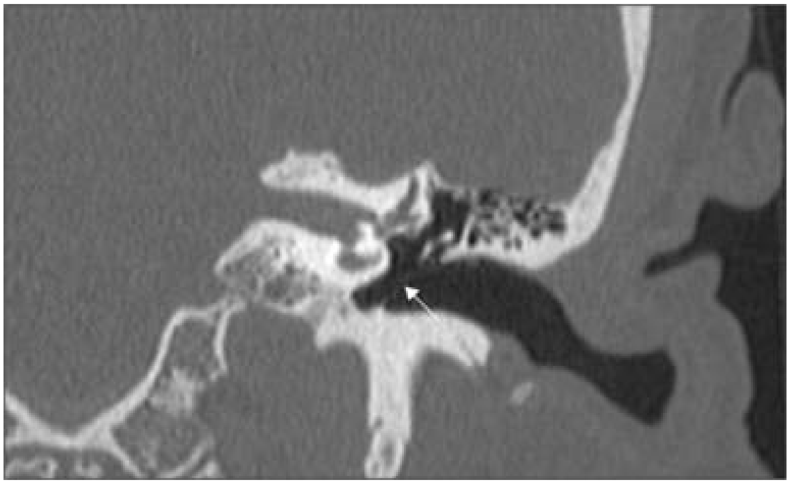

Fig. 36.8 Bone-windowed, coronal CT scan of external ear canal and middle ear showing the curvature of the floor and roof, and the obliquity of the tympanic membrane (arrow) at the medial end of the external auditory meatus.

(By courtesy of Dr Steven Connor.)

The lateral, cartilaginous part is approximately 8 mm long. It is continuous with the auricular cartilage and attached by fibrous tissue to the circumference of the osseous part. The meatal cartilage is deficient posterosuperiorly, and the gap is occupied by a sheet of collagen. Two or three deep fissures (of Santorini) exist in its anterior part: tumours of the external acoustic meatus escape the confines of the canal through these fissures and spread into the adjacent soft tissues.

The osseous part is approximately 16 mm long, and is narrower than the cartilaginous part. In sagittal section it is oval or elliptical and it is directed anteromedially and slightly downwards, with a slight posterosuperior convexity. Its medial end is smaller than the lateral end and it terminates obliquely. The anterior wall projects medially approximately 4 mm beyond the posterior and is marked, except above, by a narrow tympanic sulcus or anulus, to which the perimeter of the tympanic membrane is attached. Its lateral end is dilated and mostly rough for the attachment of the meatal cartilage. The anterior, inferior, and most of the posterior, parts of the osseous meatus are formed by the tympanic plate of the temporal bone, which in the fetus is only a tympanic ring. The posterosuperior region is formed by the squamous part of the temporal bone. The outer wall of the meatus is bounded above by the posterior zygomatic root, below which there may be a suprameatal spine.

Relations of the meatus

The condylar process of the mandible lies anterior to the meatus and is partially separated from the cartilaginous part by a small portion of the parotid gland. A blow on the chin may cause the condyle to break into the meatus. The middle cranial fossa lies above the osseous meatus and the mastoid air cells are posterior to it, separated from the meatus only by a thin layer of bone. Its deepest part is situated below the epitympanic recess, and is anteroinferior to the mastoid antrum: the lamina of bone which separates it from the antrum is only 1–2 mm thick and provides the ‘transmeatal approach’ of aural surgery.

Vasculature and lymphatic drainage

The arterial supply of the external acoustic meatus is derived from the posterior auricular artery, the deep auricular branch of the maxillary artery and the auricular branches of the superficial temporal artery. Associated veins drain into the external jugular and maxillary veins and the pterygoid plexus. The lymphatics drain into those associated with the pinna.

Innervation

The sensory innervation of the external acoustic meatus is derived from the auriculotemporal branch of the mandibular nerve, which supplies the anterior and superior walls, and the auricular branch of the vagus, which supplies the posterior and inferior walls. The facial nerve may also contribute via its communication with the vagus nerve.

EXTERNAL SURGICAL APPROACHES TO THE MIDDLE EAR

Surgical access to the middle ear can be achieved by per-meatal, endaural and postauricular approaches.

Provided the external acoustic meatus is wide enough, the tympanic membrane can be elevated by incising the skin of the bony meatus circumferentially, leaving a vascular pedicle superiorly. The canal skin is elevated from the underlying bone until the fibrous anulus of the tympanic membrane is visualized, and this can then be elevated from the tympanic groove and the middle ear mucosa incised so that the tympanic membrane can be reflected forwards and upwards. This per-meatal approach is called a tympanotomy and is used for stapedectomy, ossuloplasty, myringoplasty and the removal of small middle ear tumours.

If the external acoustic meatus is too narrow to allow adequate visualization of the middle ear, or if access is required to the mastoid aditus and antrum, superficial soft tissues must be displaced. The two main external approaches to the middle ear are the endaural and postauricular approaches.

The endaural approach involves making an incision in the notch between the tragus and the helix. This is carried down to expose the lower margin of temporalis (which can be used to harvest a robust fascial graft for reconstruction) and the bone of the bony external acoustic meatus. The cartilaginous meatus is separated from the bony meatus and reflected laterally as a conchomeatal flap. The bony meatus can then be widened by drilling away bone (canaloplasty), which gives more space to manipulate the delicate structures of the middle ear as well as improving subsequent visualization of the tympanic membrane when the incision has healed.

The postauricular approach involves making an incision approximately 1 cm behind the postauricular skin crease and deepening the incision to the periosteum of the mastoid process, dividing the posterior auricular muscles on the way. Grafts can be harvested from the temporalis fascia. The periosteum is incised and elevated to expose the bony external acoustic meatus from behind. The skin over the junction of the bony and cartilaginous meatus is incised to allow the cartilage of the auricle and meatus to be swung forward on its blood supply and so expose the bony meatus and mastoid process. Access can then be gained by drilling and elevating a tympanomeatal skin flap as described for the endaural approach.

Temporalis fascia is the most popular tissue used as a free graft for repair of the tympanic membrane because it is easily obtainable. In recent years, tragal perichondrium has become a popular alternative: it has the additional advantage that the cartilage can also be harvested and used to reinforce the repair.

More extensive resections of the temporal bone are undertaken using extended pre- or postauricular incisions into the temporal region and neck. The blood supply of the pinna is sufficient to maintain viability despite significant elevation and undermining.

MIDDLE EAR

The middle ear is an irregular, laterally compressed space in the petrous part of the temporal bone. It is lined with mucous membrane and filled with air, which reaches it from the nasopharynx via the pharyngotympanic tube (Figs 36.6, 36.7, 36.9). The middle ear contains three small bones, the malleus, incus and stapes, collectively called the auditory ossicles, which form an articulated chain connecting the lateral and medial walls of the cavity, and which transmit the vibrations of the tympanic membrane across the cavity to the cochlea.

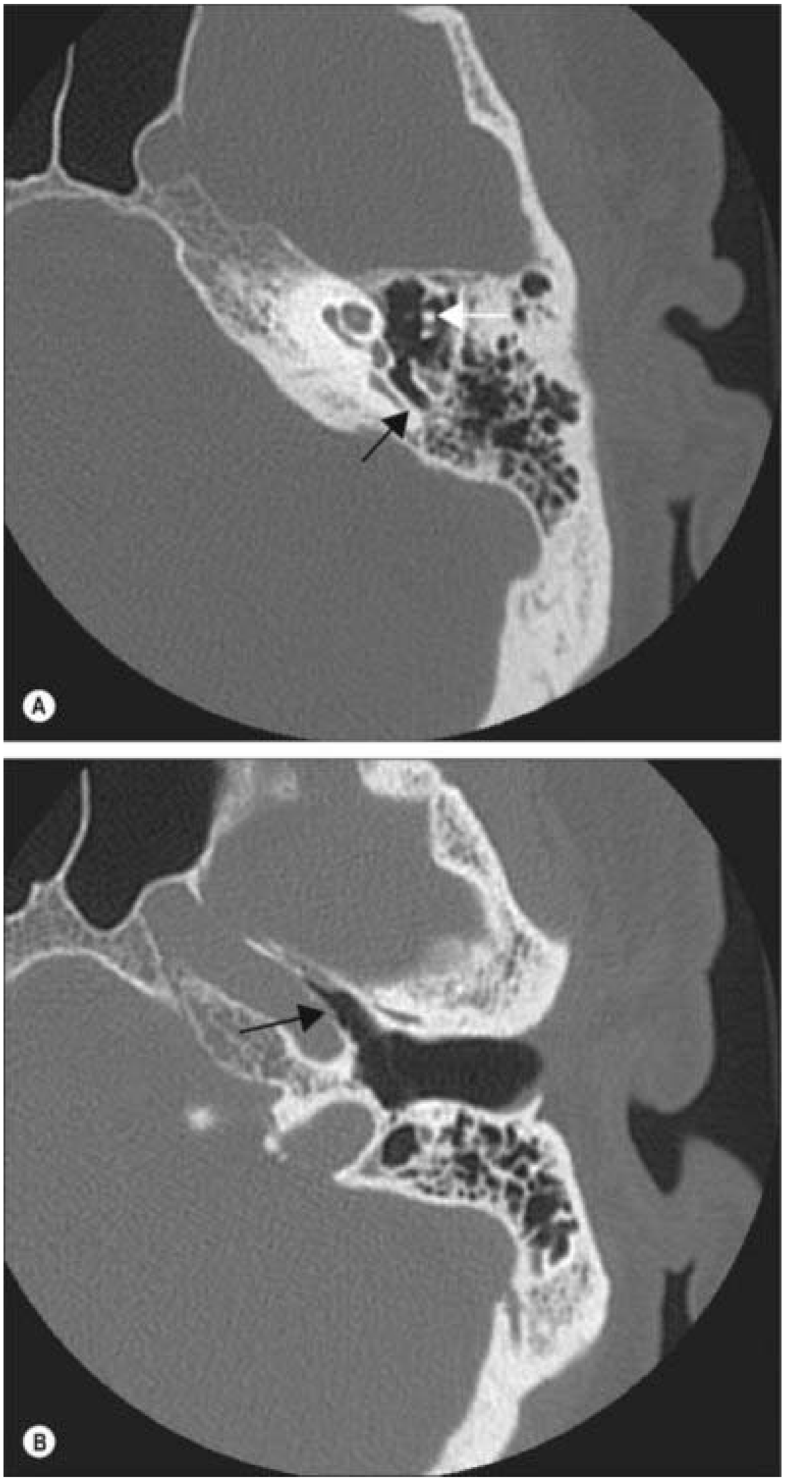

Fig. 36.9 **A**, Axial CT scan at level of the ossicular mass (white arrow) in the epitympanum, showing the mastoid antrum and its relationship to the lateral (horizontal) semicircular canal (black arrow). **B**, Axial CT scan at the

level of the entrance of the pharyngotympanic tube, showing its relationship to the internal carotid artery (black arrow).

(By courtesy of Dr Steven Connor.)

The essential function of the middle ear is to transfer energy efficiently from relatively weak vibrations in the elastic, compressible air in the external acoustic meatus to the incompressible fluid around the delicate receptors in the cochlea. Mechanical coupling between the two systems must match their resistance to deformation or ‘flow’, i.e. their impedance, as closely as possible. Aerial waves of low amplitude and low force per unit area arrive at the tympanic membrane, which has 15–20 times the area of the stapedial footplate that contacts the perilymph in the inner ear: the force per unit area generated by the footplate is increased by a similar amount, while the amplitude of vibration is almost unchanged.

Protective mechanisms incorporated into the design of the middle ear include the presence of the pharyngotympanic tube (to equalize pressure on both sides of the delicate tympanic membrane); the shape of the articulations between the ossicles; and the reflex contractions of stapedius and tensor tympani in response to sounds of fairly high intensity (preventing damage caused by sudden or excessive excursions of the ossicles).

The space within the middle ear can be subdivided into three parts. These are the mesotympanum or tympanic cavity proper, which is opposite the tympanic membrane; the epitympanum or attic, which is above the level of the membrane, and contains the head of the malleus and the body and short process of the incus; and the hypotympanum, which is in the floor of the cavity between the jugular bulb and the lower margin of the tympanic membrane. The vertical and anteroposterior diameters of the mesotympanum and hypotympanum are each approximately 15 mm; the transverse diameter is 6 mm superiorly and 4 mm inferiorly, narrowing to 2 mm opposite the umbo. The cavity is bounded laterally by the tympanic membrane and medially by the lateral wall of the internal ear, the promontory. It communicates posteriorly with the mastoid antrum and the mastoid air cells, and anteriorly with the nasopharynx via the pharyngotympanic tube (Figs 36.6, 36.7).

The tympanic cavity and mastoid antrum, auditory ossicles and structures of the internal ear are all almost fully developed at birth and subsequently alter little. In the fetus the cavity contains a gelatinous tissue which has practically disappeared by birth, when it is filled by a fluid which is absorbed when air enters via the pharyngotympanic tube. The tympanic cavity is a common site of infection in childhood.

BOUNDARIES OF THE TYMPANIC CAVITY

The tympanic cavity has a roof and a floor, and lateral, medial, posterior and anterior walls.

Roof

A thin plate of compact bone, the tegmen tympani, separates the cranial and tympanic cavities, and forms much of the anterior surface of the petrous temporal bone. It is prolonged posteriorly as the roof of the mastoid antrum and anteriorly it covers the canal for tensor tympani. In youth, the unossified petrosquamosal suture may allow the spread of infection from the tympanic cavity to the meninges. In adults, veins from the tympanic cavity traverse this suture to reach the superior petrosal or petrosquamous sinus and thus may also transmit infection to these structures through a process of thrombophlebitis.

Longitudinal fractures of the middle cranial fossa almost always involve the tympanic roof, accompanied by dislocation of the ossicular chain, rupture of the tympanic membrane, or a fractured roof of the osseous external acoustic meatus, which can be seen as a notch. Such injuries usually cause bleeding from the ear, with escape of cerebrospinal fluid if the dura mater has been torn (CSF otorrhea).

Floor

The floor of the tympanic cavity is a narrow, thin, convex plate of bone which separates the cavity from the superior bulb of the internal jugular vein. The bone may be patchily deficient, in which case the tympanic cavity and the vein are separated only by mucous membrane and fibrous tissue. Alternatively, the floor is sometimes thick and may contain some accessory mastoid air cells. A small aperture for the tympanic branch of the glossopharyngeal nerve lies near the medial wall.

Lateral wall

The lateral wall consists mainly of the tympanic membrane, but also contains the ring of bone to which the membrane is attached (see Figs 36.6B, 36.14A),. The lateral epitympanic bony wall is wedge-shaped in section and its sharp inferior portion is known as the outer attic wall or scutum. This part is easily eroded or blunted by cholesteatoma, a feature easily detected on CT scans (see Fig. 36.8). There is a deficiency or notch in the upper part of this ring, close to which are the small openings of the anterior and posterior canaliculi for the chorda tympani and the petrotympanic fissure. The posterior canaliculus for the chorda tympani is situated in the angle between the posterior and lateral walls of the tympanic cavity just behind the tympanic membrane, at a variable position approximately level with the upper end of the handle of the malleus. It leads into a minute canal that descends in front of the facial canal and ends in it about 6 mm above the stylomastoid foramen. The canaliculus transmits the chorda tympani and a branch of the stylomastoid artery to the tympanic cavity. The chorda tympani leaves the tympanic cavity through the anterior canaliculus, which opens at the medial end of the petrotympanic fissure.

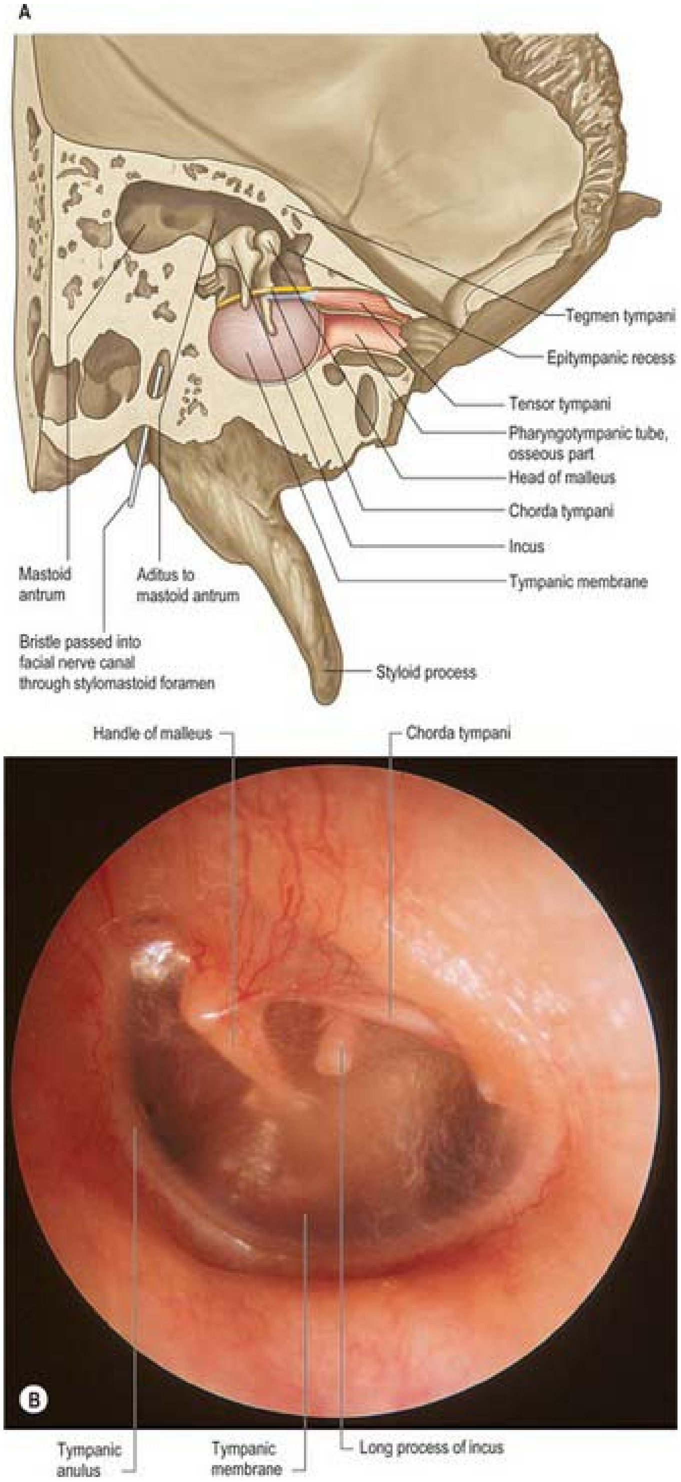
A
Tegmen tympani
Epitympanic recess
Tensor tympani
Pharyngotympanic tube, osseous part
Head of malleus
Chorda tympani
Incus
Tympanic membrane
Mastoid antrum
Aditus to mastoid antrum
Bristle passed into facial nerve canal through stylomastoid foramen
Styloid process
Handle of malleus
Chorda tympani
B
Tympanic anulus
Tympanic membrane
Long process of incus

Fig. 36.14 The chorda tympani nerve. **A**, Oblique vertical section through the left temporal bone, to show roof and lateral wall of the middle ear, the chorda tympani and the mastoid antrum. **B**, Chorda tympani crossing the tympanic membrane, auroscopic view.

*(**B**, By courtesy of Mr Simon A Hickey).*

The petrotympanic fissure is a mere slit approximately 2 mm in length which opens just above and in front of the ring of bone to which the tympanic membrane is attached. It contains the anterior process and anterior ligament of the malleus and transmits the anterior tympanic branch of the maxillary artery to the tympanic cavity.

Tympanic membrane

The tympanic membrane separates the tympanic cavity from the external acoustic meatus (Fig. 36.10; see also Figs 38.6, 36.14). It is thin, semi-transparent, and almost oval, though somewhat broader above than below. It lies obliquely, at an angle of approximately 55° with the meatal floor. Its longest, anteroinferior diameter is 9 to 10 mm, and its shortest is 8 to 9 mm. Most of its circumference is a thickened fibrocartilaginous ring or anulus which is attached to the tympanic sulcus at the medial end of the meatus. The anulus contains radially orientated smooth muscle cells in several locations that possibly play a role in controlling blood flow or maintaining tension (Henson et al 2005). The sulcus is deficient superiorly, i.e. it is notched. Two bands, the anterior and posterior malleolar folds, pass from the ends of this notch to the lateral process of the malleus. The small triangular part of the membrane, the pars flaccida, lies above these folds and is lax and thin. The major part of the tympanic membrane, the pars tensa, is taut. The handle of the malleus is firmly attached to the internal surface of the tympanic membrane as far as its centre, which projects towards the tympanic cavity. The inner surface of the membrane is thus convex and the point of greatest convexity is termed the umbo. Although the membrane as a whole is convex on its inner surface, its radiating fibres are curved with their concavities directed inwards.

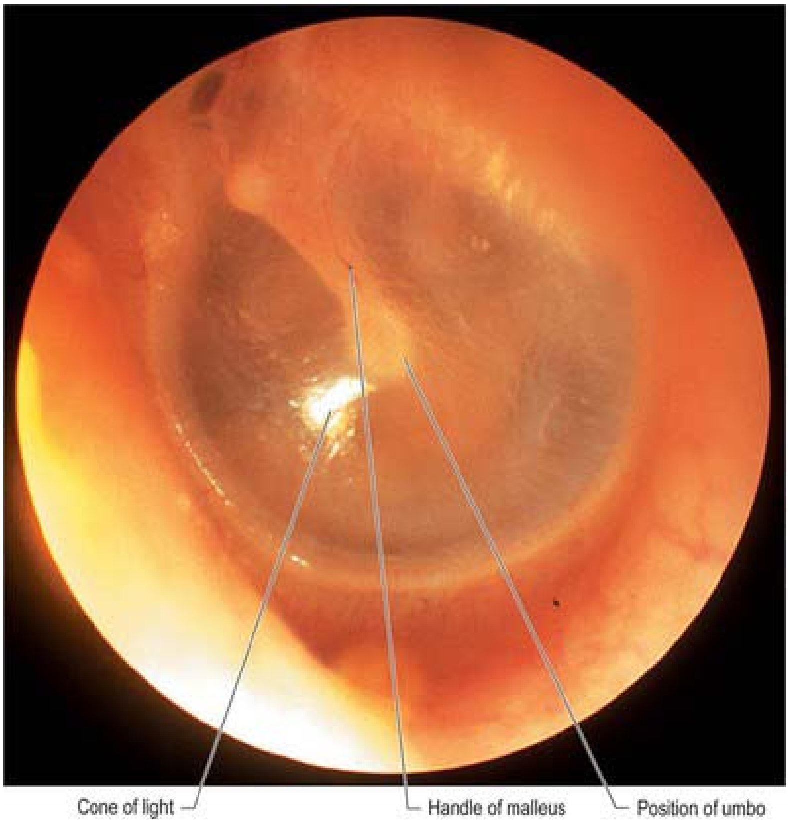

Fig. 36.10 Auroscopic view of left tympanic membrane. Note that a bright cone of light is seen in the anteroinferior quadrant of the membrane when it is illuminated.

(By courtesy of Mr Simon A Hickey.)

Microstructure

Histologically, the tympanic membrane is composed of an outer cuticular layer, an intermediate fibrous layer and an inner mucous layer.

The cuticular stratum is continuous with the thin skin of the meatus. It is keratinized, stratified squamous in type, devoid of dermal papillae and hairless. Its subepithelial tissue is vascularized and may develop a few peripheral papillae. Ultrastructurally, it is typically 10 cells thick and has two zones, a superficial layer of non-nucleated squames, and a deep zone which resembles the epidermal prickle cell layer (stratum spinosum). There are numerous desmosomes between cells, the deepest of which lie on a continuous basal lamina, but lack epithelial pegs and hemidesmosomes. The cells of this stratum have a propensity for lateral migration and differentiation not shared with any other stratified squamous epithelia in the body.

The fibrous stratum consists of an external layer of radiating fibres which diverge from the handle of the malleus, and a deep layer of circular fibres, which are plentiful peripherally, but sparse and scattered centrally. Ultrastructurally, the filaments are 10 nm in diameter, and are linked at 25 nm intervals. They have a distinctive amino acid composition, and may consist of a protein peculiar to the tympanic membrane. Small groups of collagen fibrils appear at 11 weeks *in utero*, interspersed with small bundles of elastin microfibrils. Older specimens contain more typically cross-banded collagen fibrils and an amorphous elastin component. The fibrous stratum is replaced by loose connective tissue in the pars flaccida.

The mucous stratum is a part of the mucosa of the tympanic cavity, and is thickest near the upper part of the membrane. It consists of a single layer of very flat cells, with overlapping interdigitating boundaries and desmosomes and tight junctions between adjacent cells. The cytoplasm contains only a few organelles: the luminal surfaces of these apparently metabolically inert cells have a few irregular microvilli and are covered by an amorphous electron-dense material. There are no ciliated columnar cells.

Innervation

The tympanic membrane is mainly innervated by the auriculotemporal nerve, and appears to perceive only pain. There is a minor, inconstant and overlapping sensory supply from cranial nerves VII, IX and X.

The auricular branch of the vagus arises from the superior vagal ganglion and is joined soon after by a ramus from the inferior ganglion of the glossopharyngeal nerve. It passes behind the internal jugular vein and enters the mastoid canaliculus on the lateral wall of the jugular fossa. It traverses the temporal bone and crosses the facial canal about 4 mm above the stylomastoid foramen. At this point it supplies an ascending branch to the facial nerve. Fibres of the nervus intermedius may pass to the auricular branch of the vagus here, which may explain the cutaneous vesiculation that sometimes accompanies geniculate herpes. The auricular branch then traverses the tympanomastoid fissure, and divides into two rami. One ramus joins the posterior auricular nerve and the other is distributed to the skin of part of the cranial surface of the auricle, the posterior wall and floor of the external acoustic meatus, and to the adjoining part of the outer surface of the tympanic membrane. The auricular branch therefore contains somatic afferent nerve fibres, which probably terminate in the spinal trigeminal nucleus. Stimulation of the vagus nerve, e.g. in syringing the ear, can have a reflex reaction on heart rate.

Myringoplasty

Persistent perforation of the tympanic membrane caused by infection or trauma causes hearing impairment and predisposes to continuing infection as a result of contamination with organisms from the external acoustic meatus. This condition is known as chronic suppurative otitis media of the tubo-tympanic type. Myringoplasty is a surgical procedure that uses a connective tissue scaffold or graft to support healing of the perforation. The commonest technique involves the elevation of the tympanic anulus and the placement of a piece of fibrous connective tissue, e.g. part of the fibrous deep fascia which invests the lateral surface of temporalis or the perichondrium of the tragal cartilage, onto the undersurface of the tympanic membrane to close the perforation. The healed edges of the perforation are stripped of epithelium to encourage healing and scar formation. The fibrous tissue supports the healing tympanic membrane and may in part be incorporated into the repair. Once the perforation is healed, the vibratory function of the tympanic membrane is usually restored to normal.

Medial wall

The medial wall of the tympanic cavity is also the lateral boundary of the internal ear. Its features are the promontory, fenestra vestibuli (fenestra ovalis, oval window), fenestra cochleae (fenestra rotunda, round window) and the facial prominence (Fig. 36.11).

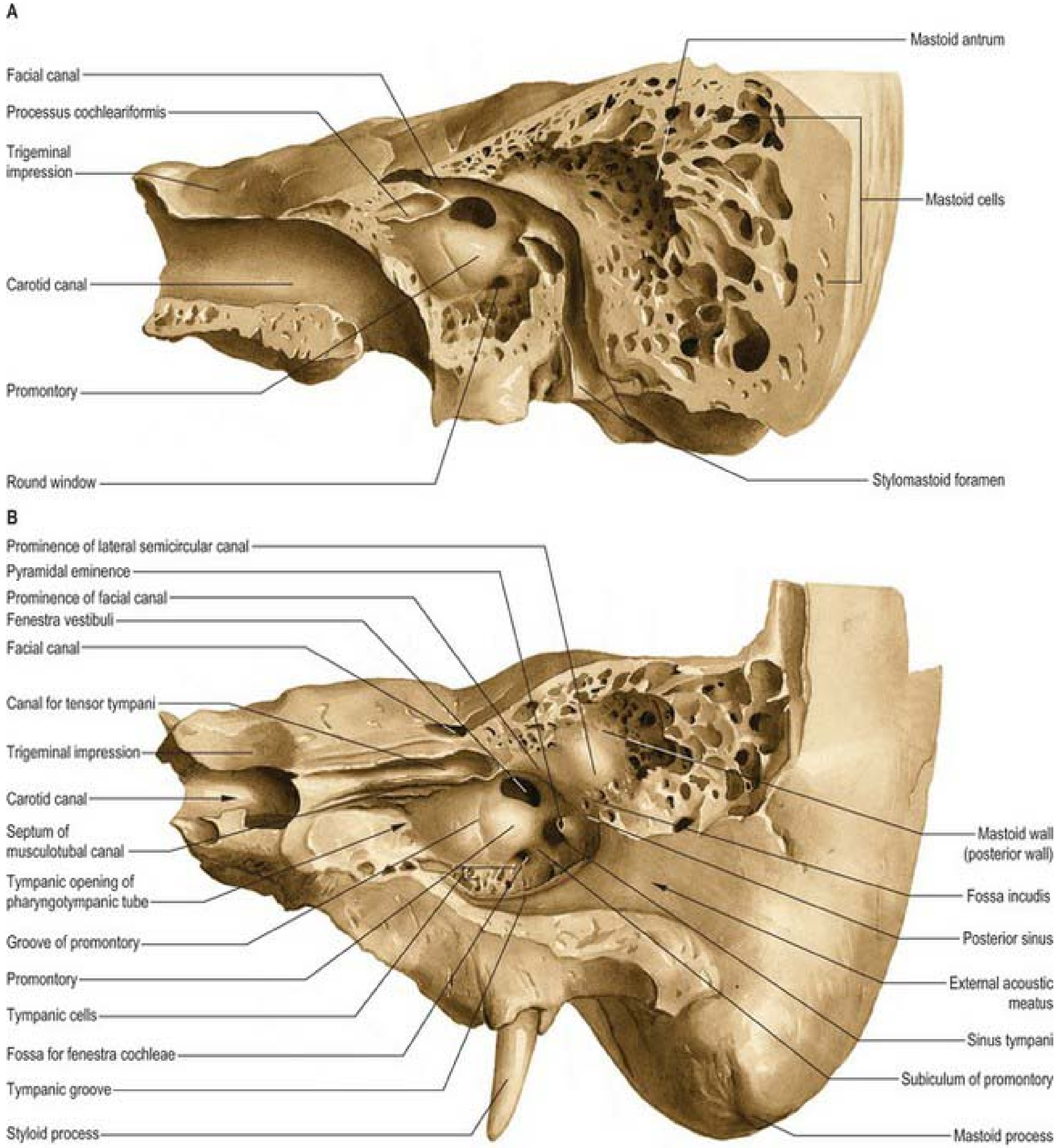
A
Facial canal
Processus cochleariformis
Trigeminal impression
Carotid canal
Promontory
Round window
Mastoid antrum
Mastoid cells
Stylomastoid foramen
B
Prominence of lateral semicircular canal
Pyramidal eminence
Prominence of facial canal
Fenestra vestibuli
Facial canal
Canal for tensor tympani
Trigeminal impression
Carotid canal
Septum of musculotubal canal
Tympanic opening of pharyngotympanic tube
Groove of promontory
Promontory
Tympanic cells
Fossa for fenestra cochleae
Tympanic groove
Styloid process
Mastoid wall (posterior wall)
Fossa incudis
Posterior sinus
External acoustic meatus
Sinus tympani
Subiculum of promontory
Mastoid process

Fig. 36.11 Medial wall of the left tympanic cavity, anterolateral aspect. **A**, Lateral wall and adjacent parts of anterior and superior walls removed; facial canal and carotid canal opened. **B**, Section along the axis of the petrous part of the temporal bone.

(From Sobotta 2006.)

The promontory is a rounded prominence furrowed by small grooves which lodge the nerves of the tympanic plexus. It lies over the lateral projection of the basal turn of the cochlea. A minute spicule of bone frequently connects the promontory to the pyramidal eminence of the posterior wall. The apex of the cochlea lies near the medial wall of the tympanic cavity, anterior to the promontory. A depression behind the promontory is known as the sinus tympani.

The fenestra vestibuli is a kidney-shaped opening situated above and behind the promontory, and leading from the tympanic cavity to the vestibule of the inner ear. Its long diameter is horizontal and its convex border is directed upwards. It is occupied by the base of the stapes, the footplate: the circumference of the footplate is attached to the margin of the fenestra by an anular ligament.

The fenestra cochleae is situated below and a little behind the fenestra vestibuli, from which it is separated by a posterior extension of the promontory, called the subiculum. Occasionally, another ridge of bone, the ponticulus, leaves the promontory above the subiculum and runs to the pyramid on the posterior wall of the cavity. The fenestra cochleae lies completely under the overhanging edge of the promontory in a deep hollow or niche, and is placed very obliquely. In dried specimens it opens anterosuperiorly from the tympanic cavity into the scala tympani of the cochlea, but in life it is closed by the secondary tympanic membrane. This is somewhat concave towards the tympanic cavity and convex towards the cochlea, and is bent so that its posterosuperior one-third forms an angle with its anteroinferior two-thirds. The membrane is composed of an external layer derived from the tympanic mucosa; an internal layer, derived from the cochlear lining membrane; and an intermediate, fibrous layer.

The prominence of the facial nerve canal indicates the position of the upper part of the bony facial canal (Fallopian canal) which contains the facial nerve. The canal crosses the medial tympanic wall from the cochleariform process anteriorly, runs just above the fenestra vestibuli, and then curves down into the posterior wall of the cavity. Its lateral wall may be partly deficient.

Posterior wall

The posterior wall of the tympanic cavity is wider above than below. Its main features are the aditus to the mastoid antrum, the pyramid, and the fossa incudis (Fig. 36.11).

The aditus to the mastoid antrum is a large irregular aperture which leads back from the epitympanic recess into the upper part of the mastoid antrum. A rounded eminence on the medial wall of the aditus, above and behind the prominence of the facial nerve canal, corresponds to the position of the lateral semicircular canal.

The pyramidal eminence is situated just behind the fenestra vestibuli and in front of the vertical part of the facial nerve canal. It is hollow and contains the stapedius muscle. Its summit projects towards the fenestra vestibuli and is pierced by a small aperture which transits the tendon of stapedius. The cavity in the pyramidal eminence is prolonged down and back in front of the facial nerve canal; it communicates with the canal by an aperture through which a small branch of the facial nerve passes to stapedius.

The fossa incudis is a small depression in the lower and posterior part of the epitympanic recess. It contains the short process of the incus, which is fixed to the fossa by ligamentous fibres.

Mastoid antrum

The mastoid antrum is an air sinus in the petrous part of the temporal bone. Its topographical relations are of considerable surgical importance. The aditus to the mastoid antrum, which leads back from the epitympanic recess, opens in the upper part of its anterior wall. The lateral semicircular canal lies medial to the aditus. The descending part of the facial nerve canal is anteroinferior. The medial wall is related to the posterior semicircular canal (see Ch. 37). The sigmoid sinus lies some distance posteriorly: the distance can be extremely variable and is dependent on the degree of pneumatization of the mastoid. The roof is formed by the tegmen tympani, and so the antrum lies below the middle cranial fossa and the temporal lobe of the brain. The floor has several openings which communicate with the mastoid air cells.

The lateral wall, which offers the usual surgical approach to the cavity, is formed by the postmeatal process of the squamous part of the temporal bone. This is only 2 mm thick at birth but increases at an average rate of 1 mm a year, attaining a final thickness of 12–15 mm. In adults, the lateral wall of the antrum corresponds to the suprameatal triangle (Macewen's triangle) on the outer surface of the skull. This is palpable through the cymba conchae: the superior side of the triangle, the supramastoid crest, is level with the floor of the middle cranial fossa; the anteroinferior side, which forms the posterosuperior margin of the external acoustic meatus, indicates approximately the position of the descending part of the facial nerve canal; the posterior side, formed by a posterior vertical tangent to the posterior margin of the external acoustic meatus, is anterior to the sigmoid sinus.

The adult capacity of the mastoid antrum is variable, but on average is 1 mL, with a general diameter of 10 mm. Unlike the other air sinuses in the skull, it is present at birth, and is indeed then almost adult in size, although it is at a higher level relative to the external acoustic meatus than it is in adults. In the very young, the thinness of the lateral antral wall and the absence or under-development of the mastoid process means that the stylomastoid foramen and emerging facial nerve are very superficially situated.

Mastoid air cells

Though the mastoid process antrum is well developed at birth, the mastoid air cells are merely minute antral diverticula at this stage. As the mastoid develops in the second year, the air cells gradually extend into it and by the fourth year they are well formed, although their greatest growth occurs at puberty. They vary considerably in number, form and size. Usually, they interconnect and are lined by a mucosa with squamous non-ciliated epithelium, continuous with that in the mastoid antrum and tympanic cavity. They may fill the mastoid process, even to its tip, and some may be separated from the sigmoid sinus and posterior cranial fossa only by extremely thin bone, which is occasionally deficient (Fig. 36.11). Some may lie superficial to, or even behind, the sigmoid sinus, and others may be present in the posterior wall of the descending part of the facial nerve canal. Those in the squamous part of the temporal bone may be separated from deeper cells in the petrous part by a plate of bone in the line of the squamomastoid suture (Körner’s septum). Sometimes they extend only minimally into the mastoid process, in which case the process consists largely of dense bone or trabecular bone containing bone marrow. Varieties of the mastoid process are recognized. The three types most commonly described are pneumatized (with many air cells); sclerotic or diploic (with few or no air cells); and mixed (contain both air cells and bone marrow).

The mastoid process may have no air cells at all in 20% of skulls. Alternatively, air cells may extend beyond the mastoid process into the squamous part of the temporal bone above the supramastoid crest; into the posterior root of the zygomatic process of the temporal bone; into the osseous roof of the external acoustic meatus just below the middle cranial fossa; or into the floor of the tympanic cavity very close to the superior jugular bulb. Rarely, a few may excavate the jugular process of the occipital bone. An important group may extend medially into the petrous part of the temporal bone, even to its apex, and are related to the pharyngotympanic tube, carotid canal, labyrinth and abducens nerve. Some investigators maintain that these are not continuous with the mastoid cells, but grow independently from the tympanic cavity. All of these extensions of the mastoid air cells are pathologically important since infection may spread to the structures around them.

Innervation

The mastoid air cells are innervated by a meningeal branch of the mandibular division of the trigeminal nerve.

Mastoiditis

Mastoiditis is a potentially dangerous, life-threatening condition that develops as a result of the spread of bacterial infection from the tympanic cavity via the aditus to the mastoid antrum and associated mastoid air cells. In particular, the infection may spread through the tegmen tympani to the dura mater of the middle cranial fossae, to cause an extradural collection.

This in turn may cause necrosis of the adjacent dura mater and infection may spread to form a subdural empyema in the subarachnoid space, or an abscess in the substance of the adjacent temporal lobe. Bacterial meningitis may also develop. Similar spread may be seen into the posterior cranial fossa. In both sites the infection may prove fatal.

Infection may spread laterally through the cortical bone of the lateral aspect of the mastoid process to form a subperiosteal postauricular abscess (Bezold's abscess), or through the cortical bone of the tip of the mastoid process to the attachment of the posterior belly of digastric and sternocleidomastoid, which stimulates painful muscular contraction and torticollis.

Anterior wall

The inferior, larger area of the anterior wall of the tympanic cavity is narrowed by the approximation of the medial and lateral walls of the cavity (Fig. 36.6). It is a thin lamina and forms the posterior wall of the carotid canal. It is perforated by the superior and inferior caroticotympanic nerves and the tympanic branch or branches of the internal carotid. The canals for tensor tympani and the osseous part of the pharyngotympanic tube open above it, the canal for tensor tympani being superior to that for the pharyngotympanic tube. Both canals incline downwards and anteromedially, to open in the angle between the squamous and petrous parts of the temporal bone, and are separated by a thin, osseous septum. The canal for tensor tympani and the bony septum runs posterolaterally on the medial tympanic wall, and ends immediately above the fenestra vestibuli. Here, the posterior end of the septum is curved laterally to form a pulley, the processus trochleariformis (cochleariform process), which is a surgical landmark for the identification of the geniculate ganglion of the facial nerve. The tendon of tensor tympani turns laterally over the pulley before attaching to the upper part of the handle of the malleus.

Pharyngotympanic tube blockage in children

The pharyngotympanic tube serves to ventilate the middle ear, exchanging nasopharyngeal air with the air in the middle ear, which has been altered in its composition via transmucosal gas exchange with the haemoglobin in the blood vessels of the mucosa. The tube also carries mucus from the middle ear cleft to the nasopharynx as a result of ciliary transport.

In children, the pharyngotympanic tube is relatively narrow. It is prone to obstruction when the mucosa swells in response to infection or allergic challenge: obstruction results in a relative vacuum being created in the middle ear secondary to transmucosal gas exchange, and this in turn promotes mucosal secretion and the formation of a middle ear effusion. Because of the collapsibility of the pharyngotympanic tube, the vacuum thus created can overcome the distending effect of the muscles of the tube and ‘lock’ the tube shut. The resultant persistent middle ear effusion, otitis media with effusion (glue ear), can cause hearing loss by splinting the tympanic membrane and impeding its vibration. It can also provide an ideal environment for the proliferation of bacteria, with the result that an acute otitis media may develop. It is possible to relieve the vacuum and unlock the tube, and then remove the effusion by myringotomy, i.e. by surgically creating a hole in the tympanic membrane. This hole will generally heal rapidly and it is common practice to insert a flanged ventilation tube (a grommet or tympanostomy tube) to keep the hole open. Migration of the outer squamous layer of the tympanic membrane eventually displaces the tube and the myringotomy heals.

Otitis media

It is assumed that acute otitis media usually arises as a result of ascending infection from the nasopharynx via the pharyngotympanic tube to the middle ear cleft. From there it may extend to the mastoid aditus and antrum. Swelling secondary to the infection may result in the closure of both exits from the middle ear, i.e. the pharyngotympanic tube and the aditus, with subsequent accumulation of pus under pressure, which causes lateral bulging and inflammation of the tympanic membrane. The latter may burst, releasing mucopurulent discharge into the external acoustic meatus, which results in a release of the pressure in the middle ear and a diminution in the levels of pain. After a brief period the discharge dries up, and for the most part the resultant perforation of the tympanic membrane heals. Normal ventilation and drainage of mucus from the middle ear is restored once the swelling in the pharyngotympanic tube resolves. On occasion the process will fail to produce a perforation of the tympanic membrane and the inflammatory exudates will not drain. The immune defence system sterilizes the exudates of organisms, resulting in a sterile mucoid effusion, otitis media with effusion (see above).

AUDITORY OSSICLES

A chain of three mobile ossicles, the malleus, incus and stapes, transfers sound waves across the tympanic cavity from the tympanic membrane to the fenestra vestibuli. The malleus is attached to the tympanic membrane and the base (footplate) of the stapes is attached to the rim of the fenestra vestibuli. The incus is suspended between them, and articulates with both bones.

Malleus

The malleus is the largest of the ossicles, and is shaped somewhat like a mallet (Fig. 36.12). It is 8–9 mm long and has a head, neck, handle (manubrium) and anterior and lateral processes. The head is the large upper end of the bone and is situated in the epitympanic recess. It is ovoid in shape, articulates posteriorly with the incus, and is covered elsewhere by mucosa. The cartilaginous articular facet for the incus is narrowed near its middle and consists of a larger upper part and a smaller lower part, orientated almost at right angles to each other. Opposite the constriction, the lower margin of the facet projects in the form of a process, the spur of the malleus. The neck is the narrowed part below the head, and inferior to this is an enlargement from which the anterior and lateral processes project.

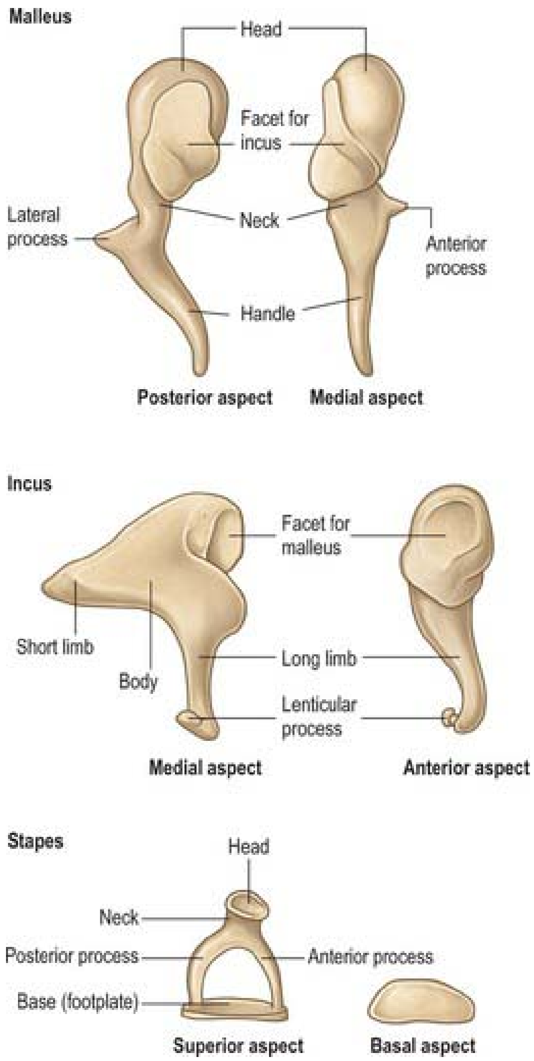
Malleus
Head
Facet for incus
Lateral process
Neck
Anterior process
Handle
Posterior aspect
Medial aspect
Incus
Facet for malleus
Short limb
Body
Long limb
Lenticular process
Medial aspect
Anterior aspect
Stapes
Head
Neck
Posterior process
Anterior process
Base (footplate)
Superior aspect
Basal aspect

Fig. 36.12 The left auditory ossicles.

The handle of the malleus is connected by its lateral margin to the tympanic membrane (Figs 36.6, 36.10; see also Fig. 36.14A). It is directed downwards, medially and backwards. It decreases in size towards its free end, which is curved slightly forwards and is flattened transversely. Near the upper end of its medial surface there is a slight projection to which the tendon of tensor tympani is attached. The anterior process is a delicate bony spicule, directed forwards from the enlargement below the neck, and connected to the petrotympanic fissure by ligamentous fibres. In fetal life it is the longest process of the malleus and is continuous in front with Meckel’s cartilage. The lateral process is a conical projection from the root of the handle of the malleus. It is directed laterally and is attached to the upper part of the tympanic membrane and, via the anterior and posterior malleolar folds, to the sides of the notch in the upper part of the tympanic sulcus.

Ossification

The cartilaginous precursor of the malleus originates as part of the dorsal end of Meckel's cartilage. With the exception of its anterior process, the malleus ossifies from a single endochondral centre which appears near the future neck of the bone in the fourth month *in utero*. The anterior process ossifies separately in dense connective tissue and joins the rest of the bone at about the sixth month of fetal life.

Incus

The incus is shaped less like an anvil, from which it is named, than a premolar tooth with its two diverging roots. It has a body and two processes (Fig. 36.12). The body is somewhat cubical but laterally compressed. On its anterior surface it has a saddle-shaped facet for articulation with the head of the malleus. The long process, rather more than half the length of the handle of the malleus, descends almost vertically, behind and parallel to the handle. Its lower end bends medially and ends in a rounded lenticular process, the medial surface of which is covered with cartilage and articulates with the head of the stapes. The short process, somewhat conical, projects backwards and is attached by ligamentous fibres to the fossa incudis in the lower and posterior part of the epitympanic recess.

Ossification

The incus has a cartilaginous precursor continuous with the dorsal extremity of Meckel's cartilage. Ossification often spreads from a single centre in the upper part of its long process in the fourth fetal month; the lenticular process may have a separate centre.

Stapes

The stapes is also known as the stirrup. It has a head, neck, two limbs (processes or crura) and a base (footplate) (Fig. 36.12). The head (caput) is directed laterally and has a small cartilaginous facet for articulation with the lenticular process of the incus. The neck is the constricted part supporting the head, and the tendon of stapedius is attached to its posterior surface. The processes diverge from the neck and are connected at their ends by a flattened oval plate, the base, which forms the footplate of the stapes. The footplate is attached to the margin of the fenestra vestibuli by a ring of fibres (the anular ligament). The anterior process is shorter, thinner and less curved than the posterior.

Ossification

The stapes is preformed in the perforated dorsal moiety of the hyoid arch cartilage of the fetus. Ossification starts from a single endochondral centre, which appears in the base in the fourth fetal month and then gradually spreads through the limbs of the stapes to reach the head.

At birth the auditory ossicles have reached an advanced state of maturity.

Ossicular ligaments

The ossicles are connected to the tympanic walls by ligaments (Fig. 36.6B): three for the malleus and one each for the incus and stapes. Some are mere mucosal folds which carry blood vessels and nerves to and from the ossicles and their articulations, and others contain a central, strong band of collagen fibres.

The anterior ligament of the malleus stretches from the neck of the malleus, just above the anterior process, to the anterior wall of the tympanic cavity near the petrotympanic fissure. Some of its collagen fibres traverse this fissure to reach the spine of the sphenoid, and others continue into the sphenomandibular ligament. The latter, like the anterior malleolar ligament, is derived from the perichondrial sheath of Meckel’s cartilage. The anterior malleolar ligament may contain muscle fibres, called laxator tympani or musculus externus mallei. The lateral ligament of the malleus is a triangular band which stretches from the posterior part of the border of the tympanic incisure to the head of the malleus. The superior ligament of the malleus connects the head of the malleus to the roof of the epitympanic recess.

The posterior ligament of the incus connects the end of its short process to the fossa incudis. The superior ligament of the incus is little more than a mucosal fold passing from the body of the incus to the roof of the epitympanic recess.

The vestibular surface and rim of the stapedial base are covered with hyaline cartilage. The cartilage encircling the base is attached to the margin of the fenestra vestibuli by a ring of elastic fibres, the anular ligament of the base of the stapes. The posterior part of this ligament is much narrower than the anterior part: it acts as a kind of hinge on which the stapedial base moves when stapedius contracts and during acoustic oscillation.

Ossicular articulations

The ossicular articulations are typical synovial joints. The incudomalleolar joint is saddle-shaped and the incudostapedial joint is a ball and socket articulation. The articular surfaces are covered with articular cartilage, and each joint is enveloped by a capsule rich in elastic tissue and lined by synovial membrane.

Movements of the auditory ossicles

The handle of the malleus faithfully follows all movements of the tympanic membrane. The malleus and incus rotate together around an axis which runs from the short process and posterior ligament of the incus to the anterior ligament of the malleus. When the tympanic membrane and handle of the malleus move inwards (medially), the long process of the incus moves in the same direction and pushes the stapedial footplate towards the labyrinth and the perilymph contained within the labyrinth. The movement of the perilymph causes a compensatory outward bulging of the secondary tympanic membrane. These events are reversed when the tympanic membrane moves outwards. However, if the movement of the tympanic membrane is considerable, the incus does not follow the full outward excursion of the malleus, and merely glides on it at the incudomalleolar joint, so preventing a dislocation of the footplate of the stapes from the fenestra vestibuli. When the handle of the malleus is carried medially, the spur at the lower margin of the head of the malleus locks the incudomalleolar joint, and this necessitates an inward movement of the long process of the incus. The joint is unlocked again when the handle of the malleus is carried outwards. The three bones together act as a bent lever so that the stapedial footplate does not move in the fenestra vestibuli like a piston, but rocks on a fulcrum at its anteroinferior border, where the anular ligament is thick. The rocking movement around a vertical axis, which is like a swinging door, is said to happen only at moderate intensities of sound. With loud, low-pitched sounds, the axis becomes horizontal, and the upper and lower margins of the stapedial footplate oscillate in opposite directions around this central axis, thus preventing excessive displacement of the perilymph.

Otosclerosis, stapedectomy and stapedotomy

Otosclerosis is a hereditary localized disease of the bone derived from the embryonic otic capsule in which lamellar bone is replaced by woven bone of greater thickness and vascularity. The position of the focus of new bone formation determines its effect on the function of the ear. When new bone develops around the footplate of the stapes it may fix the footplate to the margin of the fenestra vestibuli and prevent it from moving. This impedes the passage of vibrations of the tympanic membrane passing through the ossicular chain to the inner ear, producing a conductive hearing loss. Complete deafness does not result, because vibrations can still pass directly to the cochlea via the bones of the skull, albeit in a markedly less efficient manner.

Stapedectomy is a surgical procedure designed to bypass the fixation of the stapes footplate caused by otosclerosis. The tympanic membrane is temporarily elevated for access to the middle ear and, under microscopic control, the incudostapedial joint is disarticulated using microinstruments. The limbs of the stapes and stapedius are then both divided, usually with microscissors or a laser, and the superstructure of the stapes removed. A small hole (stapedotomy) is then made in the fixed footplate of the stapes using a microdrill, reamer or laser to expose the fluids of the inner ear. In some, the whole footplate becomes detached (stapedectomy). A small graft of connective tissue derived from local fascia or perichondrium is used to seal the hole with a flexible membrane. A small piston, usually made of Teflon or titanium incorporating a wire made of stainless steel, platinum or titanium, is crimped onto the long process of the incus and placed in the perforation in the stapes footplate. The tympanic membrane is then returned. The connection between the tympanic membrane and the inner ear is thus reconstituted and hearing restored.

MUSCLES

There are two intratympanic muscles, tensor tympani and stapedius.

Tensor tympani

Tensor tympani is a long slender muscle which occupies the bony canal above the osseous part of the pharyngotympanic tube, from which it is separated by a thin bony septum (Fig. 36.6). It arises from the cartilaginous part of the pharyngotympanic tube and the adjoining region of the greater wing of the sphenoid, as well as from its own canal. It passes back within its canal, and ends in a slim tendon which bends laterally round the pulley-like processus cochleariformis and attaches to the handle of the malleus, near its root.

Vascular supply

Tensor tympani receives its arterial blood supply from the superior tympanic branch of the middle meningeal artery.

Innervation

Tensor tympani is innervated by a branch of the nerve to medial pterygoid (a ramus of the mandibular division of the trigeminal nerve) which traverses the otic ganglion without interruption to reach the muscle.

Actions

Tensor tympani draws the handle of the malleus medially, and so tenses the tympanic membrane and helps to damp sound vibrations: its action also pushes the base of the stapes more tightly into the fenestra vestibuli.

Stapedius

Stapedius arises from the wall of a conical cavity in the pyramidal eminence on the posterior wall of the tympanic cavity, and from its continuation anterior to the descending part of the facial nerve canal. Its minute tendon emerges from the orifice at the apex of the pyramid and passes forwards to attach to the posterior surface of the neck of the stapes. The muscle is of an asymmetric bipennate form. It contains numerous small motor units, each of only six to nine muscle fibres; a few neuromuscular spindles exist near the myotendinous junction.

Vascular supply

Stapedius receives its arterial blood supply from branches of the posterior auricular, anterior tympanic and middle meningeal arteries.

Innervation

Stapedius is supplied by a branch of the facial nerve which is given off in the facial canal.

Actions

Stapedius helps to damp down excessive sound vibrations. It opposes the action of tensor tympani (which pushes the stapes more tightly into the fenestra vestibuli). Paralysis of stapedius results in hyperacusis.

Stapedial and tensor tympani reflex

When noises are loud, and immediately before speaking, a reflex contraction of stapedius and tensor tympani takes place that helps damp down the movement of the ossicular chain before vibrations reach the internal ear. The afferent pathways involve the auditory component of cranial nerve VIII, and higher centres prior to speech. The efferent pathway involves the facial nerve (stapedius) and the mandibular nerve (tensor tympani).

VASCULAR SUPPLY AND LYMPHATIC DRAINAGE

A number of arteries supply the walls and contents of the tympanic cavity. The deep auricular, anterior tympanic and stylomastoid arteries are larger than the others.

The deep auricular branch of the first part of the maxillary artery often arises with the anterior tympanic artery. It ascends in the parotid gland behind the temporomandibular joint, pierces the cartilaginous or bony wall of the external acoustic meatus and supplies its cuticular lining, the exterior of the tympanic membrane and the temporomandibular joint.

The anterior tympanic branch of the first part of the maxillary artery ascends behind the temporomandibular joint and enters the tympanic cavity through the petrotympanic fissure. It ramifies on the interior of the tympanic membrane, and forms a vascular circle around it with the posterior tympanic branch of the stylomastoid artery. It also anastomoses with twigs of the artery of the pterygoid canal and caroticotympanic branches of the internal carotid artery in the mucosa of the tympanic cavity.

The stylomastoid branch of the occipital or posterior auricular arteries supplies the posterior part of the tympanic cavity and mastoid air cells. It also enters the stylomastoid foramen to supply the facial nerve and semicircular canals. In the young, its posterior tympanic branch forms a circular anastomosis with the anterior tympanic artery.

The smaller arteries supplying the tympanic cavity include the petrosal branch of the middle meningeal artery, which enters through the hiatus for the greater petrosal nerve; the superior tympanic branch of the middle meningeal artery, which traverses the canal for tensor tympani; an inferior tympanic branch from the ascending pharyngeal artery, which traverses the tympanic canaliculus together with the tympanic branch of the glossopharyngeal nerve, to supply the medial wall of the tympanic cavity; a branch from the artery of the pterygoid canal, which accompanies the pharyngotympanic tube; and a tympanic branch or branches from the internal carotid artery, which is given off in the carotid canal and perforates the thin anterior wall of the tympanic cavity.

The mastoid air cells and dura mater are also supplied by a mastoid branch from the occipital artery. It is small in size and sometimes absent. When present, it enters the cranial cavity via the mastoid foramen near the occipitomastoid suture.

In early fetal life, a stapedial artery traverses the stapes.

The veins from the tympanic cavity terminate in the pterygoid venous plexus and the superior petrosal sinus. A small group of veins runs medially from the mucosa of the mastoid antrum through the arch formed by the superior (anterior) semicircular canal, and emerges onto the posterior surface of the petrous temporal bone at the subarcuate fossa. These veins drain into the superior petrosal sinus and are the remains of the large subarcuate veins of childhood. They represent a potential route for the spread of infection from the mastoid antrum to the meninges.

Lymphatic vessels of the tympanic and antral mucosae drain to the parotid or upper deep cervical lymph nodes. Vessels draining the tympanic end of the pharyngotympanic tube probably end in the deep cervical nodes.

INNERVATION

The tympanic cavity contains the tympanic plexus and the facial nerve. Branches from the plexus and the facial nerve supply structures within the tympanic cavity but also leave the cavity to supply structures on the face.

Tympanic plexus

The nerves that constitute the tympanic plexus ramify on the surface of the promontory on the medial wall of the tympanic cavity. They are derived from the tympanic branch of the glossopharyngeal nerve and the caroticotympanic nerves (Fig. 36.13). The former arises from the inferior ganglion of the glossopharyngeal nerve, and reaches the tympanic cavity via the tympanic canaliculus for the tympanic nerve. The superior and inferior caroticotympanic nerves are postganglionic sympathetic fibres which are derived from the carotid sympathetic plexus and traverse the wall of the carotid canal to join the plexus.

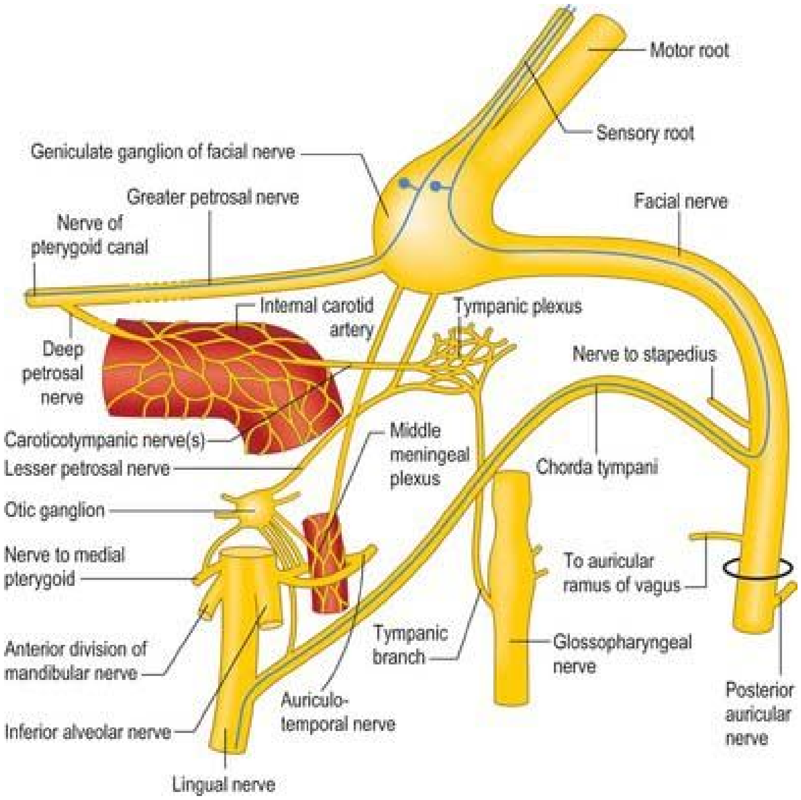

Motor root
Sensory root
Geniculate ganglion of facial nerve
Greater petrosal nerve
Facial nerve
Nerve of pterygoid canal
Internal carotid artery
Tympanic plexus
Deep petrosal nerve
Nerve to stapedius
Caroticotympanic nerve(s)
Lesser petrosal nerve
Middle meningeal plexus
Chorda tympani
Otic ganglion
Nerve to medial pterygoid
To auricular ramus of vagus
Tympanic branch
Glossopharyngeal nerve
Anterior division of mandibular nerve
Auriculo-temporal nerve
Posterior auricular nerve
Inferior alveolar nerve
Lingual nerve

Fig. 36.13 The intracranial branches of the facial and glossopharyngeal nerves and the connections of the tympanic plexus and the otic ganglion. The course of the taste fibres from the mucous membrane of the palate and from the anterior presulcal part of the tongue is represented by the blue lines.

The tympanic plexus supplies branches to the mucosa of the tympanic cavity, pharyngotympanic tube and mastoid air cells. It sends a branch to the greater petrosal nerve via an opening anterior to the fenestra vestibuli. The lesser petrosal nerve, which may be regarded as the continuation of the tympanic branch of the glossopharyngeal nerve, traverses the tympanic plexus. It occupies a small canal below that for the tensor tympani. It runs past, and receives a connecting branch from, the geniculate ganglion of the facial nerve. The lesser petrosal nerve emerges from the anterior surface of the temporal bone via a small opening lateral to the hiatus for the greater petrosal nerve and then traverses the foramen ovale or the small canaliculus innominatus to join the otic ganglion. Postganglionic secretomotor fibres leave this ganglion in the auriculotemporal nerve to supply the parotid gland. In former times, the operation of tympanic neurectomy was undertaken to reduce salivation in patients who drooled and to diminish facial sweating in those with Frey’s syndrome following parotidectomy: less invasive and more effective procedures are employed nowadays.

Facial nerve

The facial nerve enters the temporal bone through the internal acoustic meatus accompanied by the vestibulocochlear nerve (Fig. 36.7). At this point, the motor root, which supplies the muscles of the face, and the nervus intermedius, which contains sensory fibres concerned with the perception of taste and parasympathetic (secretomotor) fibres to various glands, are separate components. They merge within the meatus. At the end of the meatus, the facial nerve enters its own canal, the facial canal, which runs across the medial wall and down the posterior wall of the tympanic cavity to the stylomastoid foramen. As the nerve enters the facial canal, there is a bend (genu) which houses the geniculate ganglion (Figs 36.7, 36.13).

The branches which arise from the facial nerve within the temporal bone can be divided into those which come from the geniculate ganglion and those which arise within the facial canal.

The main branch from the geniculate ganglion is the greater (superficial) petrosal nerve, a branch of the nervus intermedius. The greater petrosal nerve passes anteriorly, receives a branch from the tympanic plexus and traverses a hiatus on the anterior surface of the petrous part of the temporal bone. It enters the middle cranial fossa, runs forwards in a groove on the bone above the lesser petrosal nerve and then passes beneath the trigeminal ganglion to reach the foramen lacerum. Here it is joined by the deep petrosal nerve from the internal carotid sympathetic plexus, to become the nerve of the pterygoid canal (Vidian nerve). The greater petrosal nerve contains parasympathetic fibres destined for the pterygopalatine ganglion, and taste fibres from the palate.

The nerve to stapedius arises from the facial nerve in the facial nerve canal behind the pyramidal eminence of the posterior wall of the tympanic cavity. It passes forwards through a small canal to reach the muscle.

The chorda tympani (Figs 36.13, 36.14) leaves the facial nerve some 6 mm above the stylomastoid foramen and runs anterosuperiorly in a canal to enter the tympanic cavity via the posterior canaliculus. It then curves anteriorly in the substance of the tympanic membrane between its mucous and fibrous layers (Fig. 36.14A), and crosses medial to the upper part of the handle of the malleus to the anterior wall of the tympanic cavity, where it enters the anterior canaliculus. It exits the skull at the petrotympanic fissure, and its further course is described on page 543. The chorda tympani contains parasympathetic fibres which supply the submandibular and sublingual salivary glands via the submandibular ganglion and taste fibres from the anterior two-thirds of the tongue.

The geniculate ganglion also communicates with the lesser petrosal nerve.

Dehiscences of the facial nerve canal

The facial nerve may be somewhat variable in its anatomical course through the temporal bone (Proctor & Nager 1982). It may split into two or three strands, starting at the geniculate ganglion and then make its way across the promontory to the stylomastoid foramen, or pass a few millimetres posteriorly to its second genu, before it turns inferiorly posterior to the fossa incudis, a position where it is particularly vulnerable during surgical exploration of the mastoid antrum. The more proximal the division into strands, the more bizarre is the subsequent course. More distal bifurcations pass either side of the fenestra vestibuli. It may be dehiscent, particularly in its second part, when it occasionally overhangs the stapes, or run inferior to the stapedial superstructure, a position which renders it vulnerable during surgery to the stapes (Barnes et al 2001). The motor fibres to the face may be carried through the chorda tympani, which is then enlarged. When this is the case, the distal facial nerve dwindles to a fibrous strand in a narrowed stylomastoid foramen. In chronic bone disease in the tympanic cavity, the facial nerve may be exposed in its canal. Inflammation may lead to facial paralysis of the infranuclear or lower motor neurone type.

Bell’s palsy

Bell’s palsy is the name given to a lower motor neurone palsy of the facial nerve which happens spontaneously and without obvious cause. It is characterized by a flaccid paralysis of the ipsilateral muscles of facial expression; decreased lacrimation in the ipsilateral eye (which is controlled by neurones in the greater petrosal nerve); and hyperacusis or decreased tolerance of loud noises in the ipsilateral ear as a result of paralysis of stapedius. Its cause remains the subject of speculation, but recent MRI studies suggest that it may be caused by viral neuronitis either in the bony first part of the facial canal (labyrinthine segment) at the apex of the internal auditory canal, or in the adjacent brainstem. In the vast majority of cases, spontaneous full recovery takes place after a few weeks.

TYMPANIC MUCOSA

The mucosa of the tympanic cavity is pale, thin and slightly vascular. It is continuous with that of the pharynx, via the pharyngotympanic tube, and covers the ossicles, muscles and nerves in the cavity to form the inner layer of the tympanic membrane and the outer layer of the secondary tympanic membrane. It also spreads into the mastoid antrum and air cells. The middle ear mucosa is a mucus-secreting respiratory mucosa bearing cilia on its surface. The precise distribution of the mucociliary epithelium varies in normal middle ears, being more widespread in the young. Three distinct mucociliary pathways have been identified, epitympanic, promontorial and hypotympanic, the latter being the largest. Each of these pathways coalesces at the tympanic orifice of the pharyngotympanic tube (Gleeson et al 1991).

The mucosa forms several vascular folds which extend from the tympanic walls to the ossicles: one descends from the roof of the cavity to the head of the malleus and the upper margin of the body of the incus, and a second surrounds stapedius. Other folds invest the chorda tympani nerve and tensor tympani. The folds separate off saccular recesses which give the interior of the tympanic cavity a somewhat honeycombed appearance: these mucosal folds have described in greater detail by Proctor (1964). Of note, the superior recess of the tympanic membrane, Prussak’s space, lies between the neck of the malleus and the pars flaccida, bounded by the lateral malleolar fold. This space can play an important role in the retention of keratin and subsequent development of cholesteatoma.

Cholesteatoma

Cholesteatoma is the name given to keratinizing squamous epithelium within the middle ear. There is debate as to how such epithelium comes to be in the middle ear. Theories include development from embryological cell rests, metaplasia from inflamed mucoperiosteum, and aberrant migration of squamous epithelium either through a perforation in the tympanic membrane (usually in the pars flaccida or posterosuperior pars tensa) or within an area of tympanic membrane atelectasis where the tympanic membrane becomes adherent to the medial wall of the tympanic cavity. It is likely that all of these processes may be implicated at some time. A feature of cholesteatoma that is poorly understood is its ability to erode bone, by activating osteoclasts, thus allowing the epithelium to proliferate and invade, destroying the temporal bone and carrying infection to the soft tissues. Cholesteatoma can therefore cause deafness through damage to the ossicles and inner ear; problems with balance through damage to the vestibule and semicircular canals; facial palsy through ischaemia and necrosis of the facial nerve; and intracranial sepsis. Treatment involves microsurgical dissection of the invading sac of epithelium with, wherever possible, preservation of the delicate structures just listed.

REFERENCES

nderson SD. The intratympanic muscles. In: Hinchcliffe R, editor. *Scientific Foundations of Otolaryngology*. London: Heinemann; 1976:257-280.

nson BJ, Donaldson JA. The Surgical Anatomy of the Temporal Bone and Ear. Philadelphia: Saunders, 1976.

arnes G, Liang J, Hall S, Michaels L, Wright A, Gleeson MJ. Development of the Fallopian canal in humans – a morphologic and radiologic study. *Otol Neurotol*. 2001;22:931-937.

uestone C, Klein J. Otitis media, atelectasis and Eustachian tube dysfunction. Bluestone CD, Stool SE, editors. Pediatric Otolaryngology, 4th edn., vol 1. Philadelphia: Saunders, 2002;474-486.

ampos A, Betancor L, Arias A, et al. Influence of human wet cerumen on the growth of common and pathogenic bacteria of the ear. *J Laryngol Otol*. 2000;114:925-929.

outer RT. A Colour Atlas of Temporal Bone Surgical Anatomy. London: Wolfe Medical, 1980.

assock MEIII, Shambaugh GE. Surgery of the Ear, 4th edn. Philadelphia: Saunders, 1990.

eeson M, Felix H, Neivergelt J. Quantitative and qualitative analysis of the human middle ear mucosa. In: Sade J, editor. *The Eustachian Tube, Basic Aspects*. Amsterdam: Kugler & Ghedini; 1991:125-131.

ey P. The clinical significance of the communicating branches of the somatic sensory supply of the middle and external ear. *J Laryngol Otol*. 1995;109:1141-1145.

enson MM, Madden VJ, Rask-Andersen H, Henson OW. Smooth muscle in the annulus fibrosus of the tympanic membrane in bats, rodents, insectivores and humans. *Hear Res*. 2005;200:29-37.

onjo I. Eustachian Tube and Middle Ear Diseases. Berlin: Springer-Verlag, 1988.

anishi N, Nakajima H, Aiso S. Arterial anatomy of the ear. *Okajimas Folia Anat Jpn*. 1997;73:313-323.

oschella F, Cordova A, Pirrello R, De Leo A. The supra-auricular arterial network: anatomical bases for the use of superior pedicle retro-auricular skin flaps. *Surg Radiol Anat*. 2003;25:3-4.

Flynn P, Bailey M. Anatomy of the skull base and infratemporal fossa. Gleeson MJ, editor. Scott-Brown’s Otolaryngology, Head and Neck Surgery, 7th edn., vol 3. London: Hodder Arnold, 2008;3897-3910.

ta YS, Ozturk C, Akbas Y, Gorur K, Unal M, Ozcan C. Has cerumen a protective role in recurrent external otitis? *Am J Otolaryngol*. 2003;24:209-212.

elps PD, Lloyd GAS. Diagnostic Imaging of the Ear, 2nd edn. Berlin: Springer-Verlag, 1990.

rter CJW, Tan ST. Congenital auricular anomalies: topographic anatomy, embryology, classification and treatment strategies. *Plast Reconstr Surg*. 2005;115:1701-1712.

octor B. The development of the middle ear spaces and their surgical significance. *J Otolaryngol*. 1964;78:631-649.

octor B, Nager GT. The facial canal: normal anatomy, variations and anomalies. *Ann Otol Rhinol Laryngol*. 1982;91(suppl 93):33-61.

right A. Anatomy and ultrastructure of the human ear. Kerr GA, editor. 6th edn. *Scott Brown's Otolaryngology*. vol 1. London: Butterworth Heinemann; 1997:1-50.

oshiura K, Kinoshita A, Ishida T, et al. A SNP in the *ABCC11* gene is the determinant of human earwax type. *Nat Genet*. 2006;38:324-330.

CHAPTER 37

Inner ear

The inner ear contains the organ of hearing, the cochlea, and the organs of balance, the utricle, saccule and semicircular canals. It consists of the bony (osseous) labyrinth, a series of interlinked cavities in the petrous temporal bone, and the membranous labyrinth of interconnected membranous sacs and ducts that lie within the bony labyrinth. The gap between the internal wall of the bony labyrinth and the external surface of the membranous labyrinth is filled with perilymph, a clear fluid with an ionic composition similar to that of other extracellular fluids, i.e. low in potassium ions and high in sodium and calcium. The membranous labyrinth contains endolymph, a fluid with an ionic composition more like that of cytosol, i.e. high in potassium ions and low in sodium and calcium. Moreover, the endolymphatic compartment is approximately 80 mV more positive than the perilymphatic compartment. These differences in ionic composition and potential are essential to the primary function of the inner ear because they provide the driving force for mechanotransduction, the process by which sensory hair cells convert the vibrations set up in the inner ear fluids by head or sound movements into electrical signals that are transmitted via the vestibulocochlear nerve to the vestibular and cochlear nuclei respectively in the brain stem.

The disarticulated temporal bone is described in detail in Chapter 36. The internal acoustic meatus and bony labyrinth are described here.

OSSEOUS (BONY) LABYRINTH

The bony labyrinth lies within the petrous part of the temporal bone. It consists of the vestibule, semicircular canals and cochlea, which are all cavities lined by periosteum and which contain the membranous labyrinth (Fig. 37.1; see Fig. 37.3A). The bone is denser and harder than that of the other parts of the petrous bone, and it is therefore possible, particularly in young skulls, to dissect the bony labyrinth out from the petrous temporal bone.

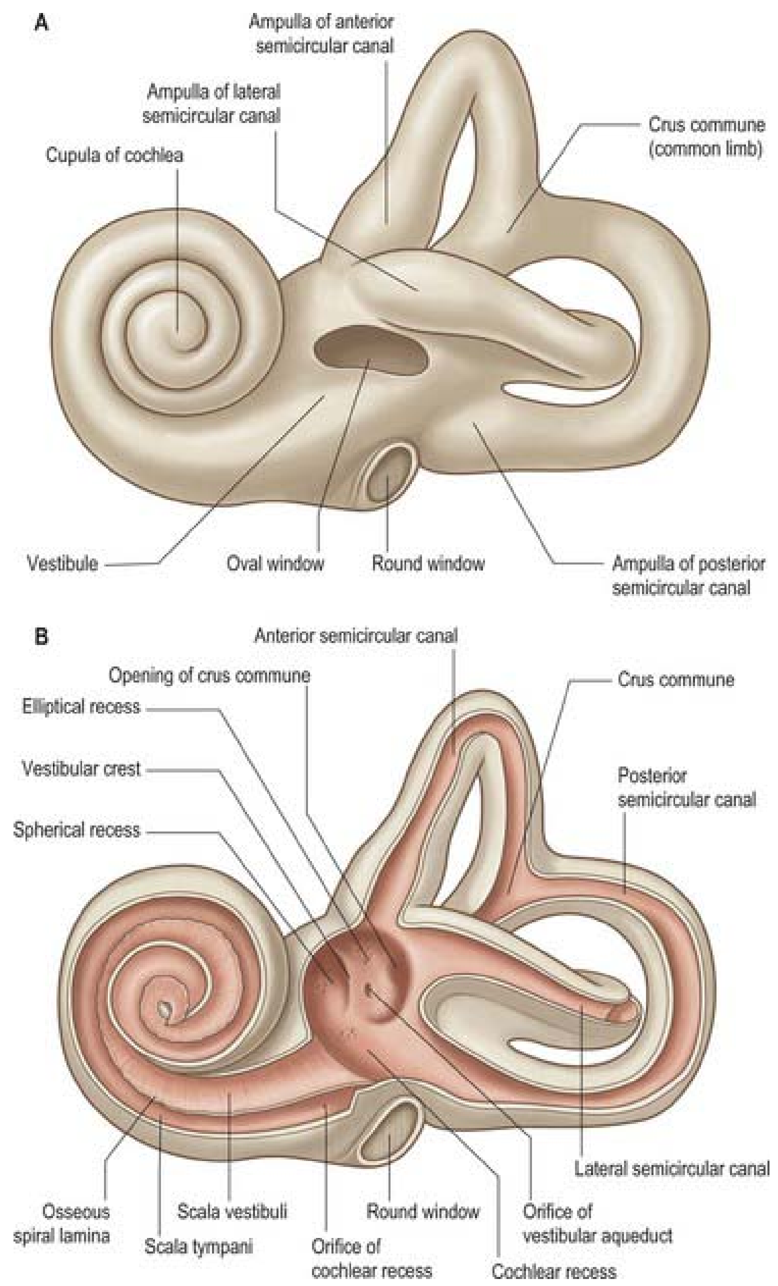
A
Ampulla of anterior semicircular canal
Ampulla of lateral semicircular canal
Cupula of cochlea
Crus commune (common limb)
Vestibule
Oval window
Round window
Ampulla of posterior semicircular canal
B
Anterior semicircular canal
Opening of crus commune
Elliptical recess
Vestibular crest
Spherical recess
Crus commune
Posterior semicircular canal
Lateral semicircular canal
Osseous spiral lamina
Scala tympani
Scala vestibuli
Orifice of cochlear recess
Round window
Cochlear recess
Orifice of vestibular aqueduct

Fig. 37.1 The left bony labyrinth. **A**, lateral aspect. **B**, interior.

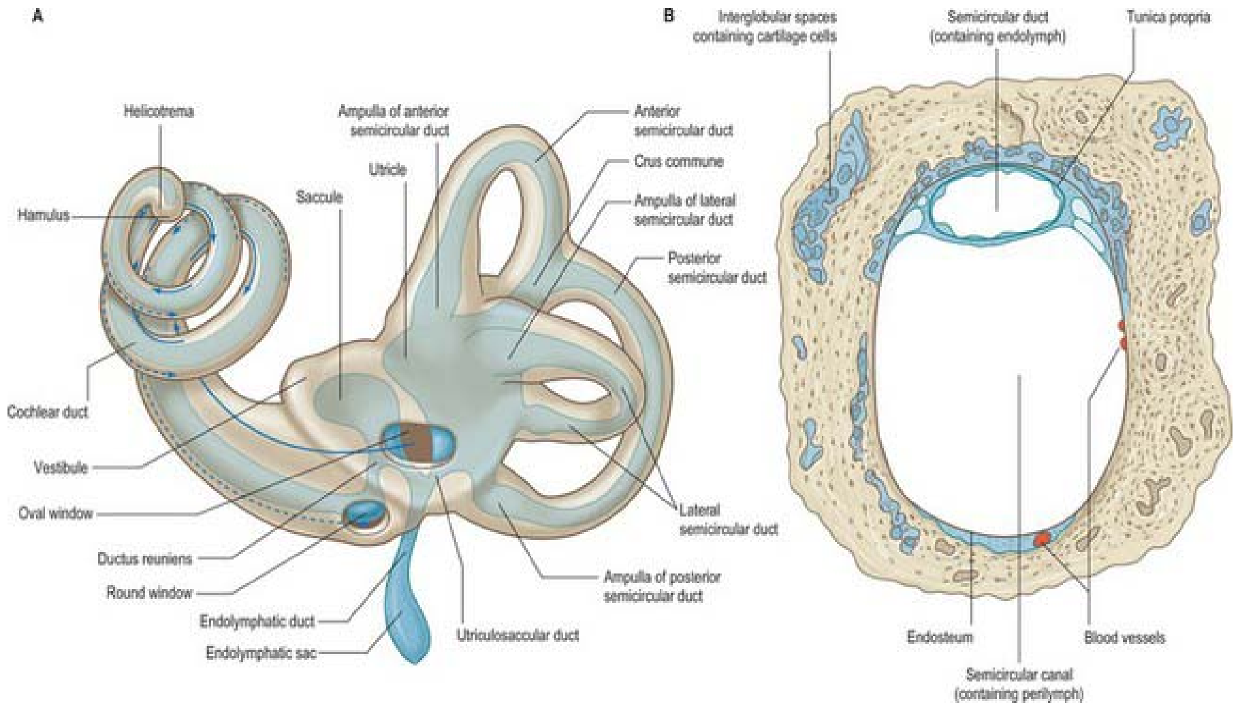
A
Helicotrema
Hamulus
Cochlear duct
Vestibule
Oval window
Ductus reuniens
Round window
Endolymphatic duct
Endolymphatic sac
Saccule
Utricle
Ampulla of anterior semicircular duct
Anterior semicircular duct
Crus commune
Ampulla of lateral semicircular duct
Posterior semicircular duct
Lateral semicircular duct
Ampulla of posterior semicircular duct
Utriculosaccular duct
B
Interglobular spaces containing cartilage cells
Semicircular duct (containing endolymph)
Tunica propria
Endosteum
Blood vessels
Semicircular canal (containing perilymph)

Fig. 37.3 **A**, The membranous labyrinth (blue) projected onto the bony labyrinth. The arrows indicate the direction of pressure waves in the cochlea. **B**, Transverse section through the left posterior semicircular canal and duct.

VESTIBULE

The vestibule is the central part of the bony labyrinth and lies medial to the tympanic cavity, posterior to the cochlea and anterior to the semicircular canals (Figs 37.1 and 37.2). It is somewhat ovoid in shape but flattened transversely, and (on average) measures 5 mm from front to back and vertically, and 3 mm across. In its lateral wall is the opening of the oval window (fenestra vestibuli) into which the base of the stapes inserts, and to which the base of the stapes is attached by an anular ligament. Anteriorly, on the medial wall, is a small spherical recess that contains the saccule; it is perforated by several minute holes, the macula cribrosa media, which transmit fine branches of the vestibular nerve to the saccule. Behind the recess is an oblique vestibular crest, the anterior end of which forms the vestibular pyramid. This crest divides below to enclose a small depression, the cochlear recess, which is perforated by vestibulocochlear fascicles as they pass to the vestibular end of the cochlear duct. Posterosuperior to the vestibular crest, in the roof and medial wall of the vestibule, is the elliptical recess (Fig. 37.1B), which contains the utricle. The pyramid and adjoining part of the elliptical recess are perforated by a number of holes, the macula cribrosa superior. The holes in the pyramid transmit the nerves to the utricle and those in the recess transmit the nerves to the ampullae of the superior and lateral semicircular canals (Fig. 37.1B). The region of the pyramid and elliptical recess corresponds to the superior vestibular area in the internal acoustic meatus (see Fig. 37.4). The vestibular aqueduct opens below the elliptical recess. It reaches the posterior surface of the petrous bone and contains one or more small veins and part of the membranous labyrinth, the endolymphatic duct (see Fig. 37.3A). In the posterior part of the vestibule are the five openings of the semicircular canals; in its anterior wall is an elliptical opening that leads into the scala vestibuli of the cochlea.

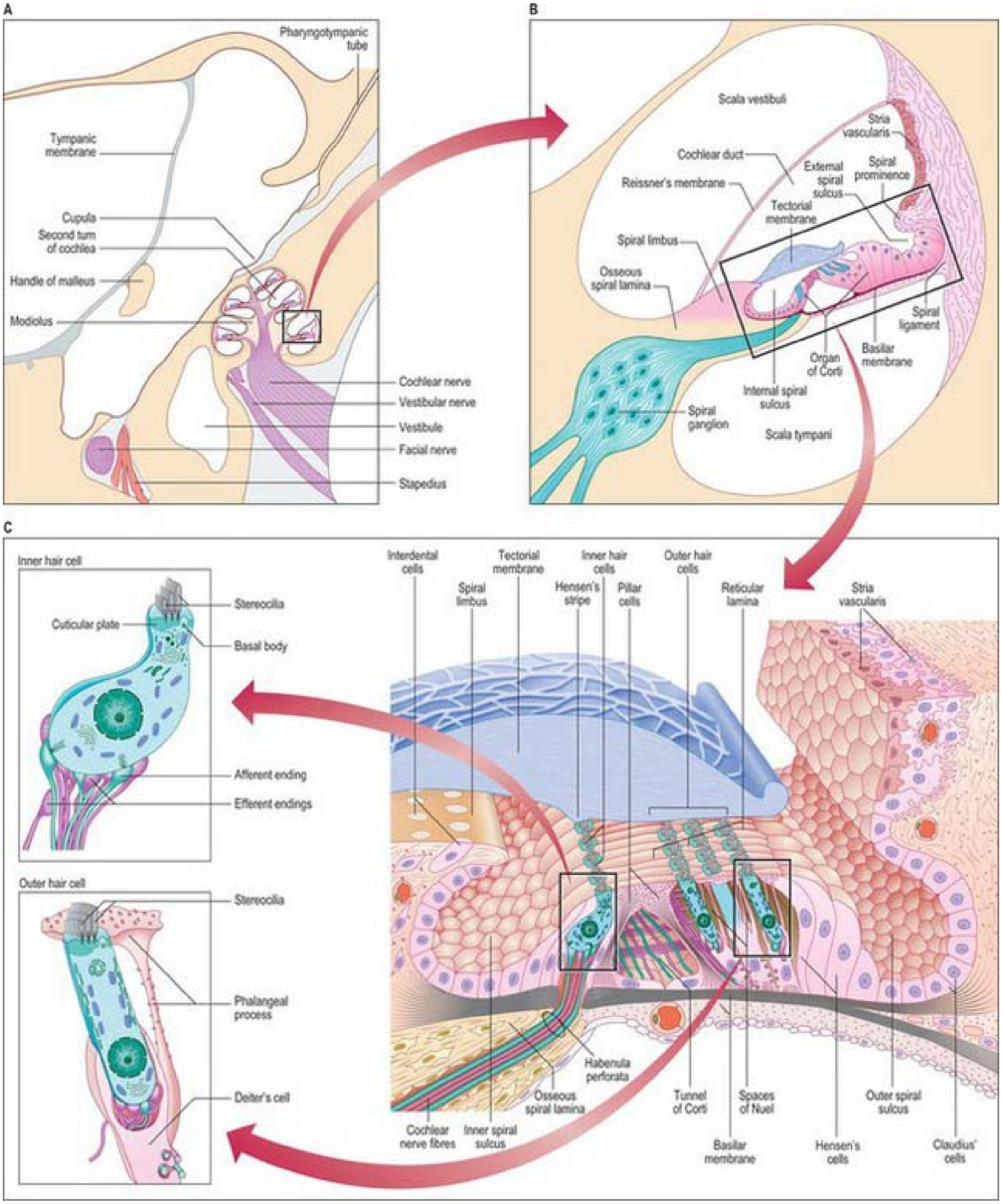
A
Pharyngotympanic tube
Tympanic membrane
Cupula
Second turn of cochlea
Handle of malleus
Modiolus
Cochlear nerve
Vestibular nerve
Vestibule
Facial nerve
Stapedius
B
Scala vestibuli
Stria vascularis
Cochlear duct
External spiral sulcus
Spiral prominence
Reissner's membrane
Tectorial membrane
Spiral limbus
Osseous spiral lamina
Spiral ligament
Basilar membrane
Organ of Corti
Internal spiral sulcus
Spiral ganglion
Scala tympani
C
Inner hair cell
Stereocilia
Cuticular plate
Basal body
Afferent ending
Efferent endings
Outer hair cell
Stereocilia
Phalangeal process
Deiter's cell
Interdental cells
Spiral limbus
Tectorial membrane
Hensen's stripe
Inner hair cells
Pillar cells
Outer hair cells
Reticular lamina
Stria vascularis
Habenula perforata
Osseous spiral lamina
Cochlear nerve fibres
Inner spiral sulcus
Tunnel of Corti
Spaces of Nuel
Basilar membrane
Hensen's cells
Outer spiral sulcus
Claudius' cells

Fig. 37.2 The cochlea. **A**, Horizontal section through the left temporal bone showing the position of the cochlea with respect to the tympanic cavity. **B**, Section through the second turn of the cochlea seen in **A**. The modiolus is to the left. **C**, Structure of the cochlear organ of Corti and stria

vascularis, showing the arrangement of the various types of cell and their overall innervation. The organization of the inner and outer hair cells and their synaptic connections are also depicted. A and B are drawn from histological sections.

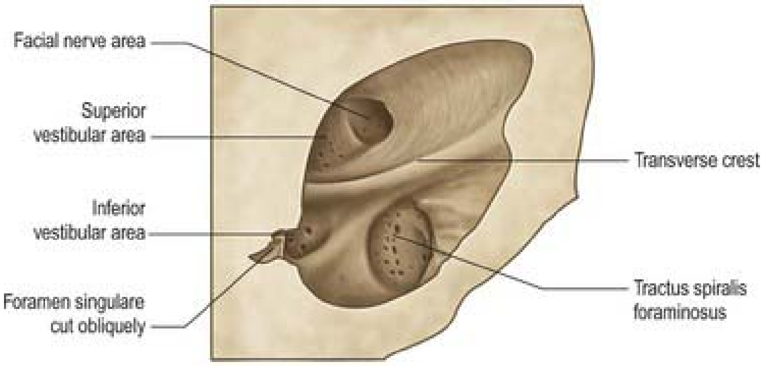
Facial nerve area
Superior vestibular area
Inferior vestibular area
Foramen singulare cut obliquely
Transverse crest
Tractus spiralis foraminosus

Fig. 37.4 The fundus of the left internal acoustic meatus, exposed by a section through the petrous part of the left temporal bone nearly parallel to the line of its superior border.

SEMICIRCULAR CANALS

The three semicircular canals, anterior (superior), posterior and lateral (horizontal), are located posterosuperior to the vestibule (Fig. 37.1; see Fig. 37.3). They are compressed from side to side and each forms approximately two-thirds of a circle. They are unequal in length, but similar in diameter along their lengths, except where they bear a terminal swelling, an ampulla, which is almost twice the diameter of the canal.

The anterior semicircular canal is 15–20 mm long. It is vertical in orientation and lies transverse to the long axis of the petrous temporal bone under the anterior surface of its arcuate eminence. The eminence may not accurately coincide with this semicircular canal, but may instead be adapted to the occipitotemporal sulcus on the inferior surface of the temporal lobe of the brain. The ampulla at the anterior end of the canal opens into the upper and lateral part of the vestibule. Its other end unites with the upper end of the posterior canal to form the crus commune (common limb), which is 4 mm long, and opens into the medial part of the vestibule.

The posterior semicircular canal is also vertical but curves backwards almost parallel with the posterior surface of the petrous bone. It is 18–22 mm long and its ampulla opens low in the vestibule, below the cochlear recess where the macula cribrosa inferior transmits nerves to it. Its upper end joins the crus commune.

The lateral (horizontal) canal is 12–15 mm long and its arch runs horizontally backwards and laterally. Its anterior ampulla opens into the upper and lateral angle of the vestibule, above the oval window and just below the ampulla of the superior canal; its posterior end opens below the opening of the crus commune.

The two lateral semicircular canals of the two ears are often described as being in the same plane and the anterior canal of one side as being almost parallel with the opposite posterior canal. However, measurements of the angular relations of the planes of the semicircular osseous canals in 10 human skulls led Blanks et al (1975) to suggest that the planes of the three ipsilateral canals are not completely perpendicular to each other. The angles were measured as: horizontal/anterior 111.76 ± 7.55°, anterior/posterior 86.16 ± 4.72°, posterior/horizontal 95.75 ± 4.66°. The planes of similarly orientated canals of the two sides also showed some departure from being parallel: left anterior/right posterior 24.50 ± 7.19°, left posterior/right anterior 23.73 ± 6.71°, left horizontal/right horizontal 19.82 ± 14.93°. The same observers (Curthoys et al 1977) also measured the dimensions and radii of the canals. The means for the radii of the osseous canals were found to be as follows: horizontal 3.25 mm, anterior 3.74 mm, posterior 3.79 mm. The diameters of the osseous canals are 1 mm (minor axis) and 1.4 mm (major axis). The membranous ducts within them are much smaller, but are also elliptical in transverse section, and have major and minor axes of 0.23 and 0.46 mm (see Fig. 37.3B). Representative means for ampullary dimensions are as follows: length 1.94 mm, height 1.55 mm. Phylogenetic studies suggest that the arc sizes of the semicircular canals in humans and other primates may be functionally linked to sensory control of body movements. The angulation and dimensions of the canals may be related to locomotor behaviour and possibly to agility, or more specifically to the frequency spectra of natural head movements (see review by Spoor & Zonneveld 1998).

COCHLEA

The cochlea (from the Greek *cochlos* for snail) is the most anterior part of the labyrinth, lying in front of the vestibule (Figs 37.1 and 37.2A; see Fig. 37.3A). It is 5 mm from base to apex, and 9 mm across its base. Its apex, or cupula, points towards the anterosuperior area of the medial wall of the tympanic cavity (Fig. 37.2A). Its base faces the bottom of the internal acoustic meatus and is perforated by numerous apertures for the cochlear nerve. The cochlea has a conical central bony core, the modiolus, and a spiral canal runs around it. A delicate osseous spiral lamina (or ledge) projects from the modiolus, partially dividing the canal (Fig. 37.2B). Within this bony spiral lies the membranous cochlear duct, attached to the modiolus at one edge and to the outer cochlear wall by its other edge. There are therefore three longitudinal channels within the cochlea. The middle canal (the cochlear duct or scala media) is blind, and ends at the apex of the cochlea; its flanking channels communicate with each other at the modiolar apex at a narrow slit, the helicotrema (Fig. 37.3A). Two elastic membranes form the upper and lower bounds of the scala media. One is Reissner’s membrane, the thin vestibular membrane that separates the scala media from the scala vestibuli. The other is the basilar membrane, which forms the partition between the scala media and the scala tympani. The organ of Corti, the sensory epithelium underlying hearing, sits on the inner surface of the basilar membrane. At the base of the scala vestibuli is the oval window (fenestra vestibuli), which leads onto the vestibular cavity but is sealed by the footplate of the stapes. The scala tympani is separated from the tympanic cavity by the secondary tympanic membrane at the round window (fenestra cochleae). The central cochlear core, the modiolus, has a broad base near the lateral end of the internal acoustic meatus, where it corresponds to the spiral tract (tractus spiralis foraminosus). There are several openings in this area for the fascicles of the cochlear nerve: those for the first 1½ turns run through the small holes of the spiral tract, and those for the apical turn run through the hole that forms the centre of the tract. Canals from the spiral tract go through the modiolus and open in a spiral sequence into the base of the osseous spiral lamina. Here the small canals enlarge and fuse to form Rosenthal’s canal, a spiral canal in the modiolus which follows the course of the osseous spiral lamina and contains the spiral ganglion (Fig. 37.2B). The main tract continues through the centre of the modiolus to the cochlear apex.

The osseous cochlear canal spirals for about 2¾ turns around the modiolus and is 35 mm long. At its first turn, the canal bulges towards the tympanic cavity where it underlies the promontory. At the base of the cochlea, the canal is 3 mm in diameter but it becomes progressively reduced in diameter as it spirals apically to end at the cupula. In addition to the round and oval windows, which are the two main openings at it base, the canal has a third smaller opening for the cochlear aqueduct or canaliculus. The latter is a minute funnel-shaped canal that runs to the inferior surface of the petrous temporal bone; it transmits a small vein to the inferior petrosal sinus and connects the subarachnoid space to the scala tympani.

The osseous or primary spiral lamina is a ledge that projects from the modiolus into the osseous canal like the thread of a screw (Fig. 37.2B). It is attached to the inner edge of the basilar membrane and ends in a hook-shaped hamulus at the cochlear apex, partly bounding the helicotrema (Fig. 37.3A), which is an opening connecting the scala tympani and scala vestibuli. From Rosenthal’s canal, many tiny canals, the habenula perforata, radiate through the osseous lamina to its rim; they carry fascicles of the cochlear nerve to the organ of Corti. A secondary spiral lamina projects inwards from the outer cochlear wall towards the osseous spiral lamina and is attached to the outer edge of the basilar membrane. It is most prominent in the lower part of the first turn: the gap between the two laminae increases progressively towards the cochlear apex, which means that the basilar membrane is wider at the apex of the cochlea than at the base.

MICROSTRUCTURE OF THE BONY LABYRINTH

The wall of the bony labyrinth is lined by fibroblast-like perilymphatic cells and extracellular fibres (Fig. 37.3B). The morphology of the cells varies in different parts of the labyrinth. Where the perilymphatic space is narrow, as in the cochlear aqueduct, the cells are reticular or stellate in form, and give off sheet-like cytoplasmic extensions that cross the space. Where the space is wider, as in the scalae vestibuli and tympani of the cochlea and much of the vestibule, the perilymphatic cells on the periosteum and the external surface of the membranous labyrinth are extremely flat, and resemble a squamous epithelium. Elsewhere, on parts of the perilymphatic surface of the basilar membrane, the cells are cuboidal. Bundles of collagen fibres are closely related to the periosteal and labyrinthine aspects of these cells.

Recent evidence suggests that micropores or canaliculi (canaliculi perforantes) (0.2–23.0 μm diameter) are more widely distributed within the bony surfaces lining the perilymphatic space than was previously suspected: they are numerous in the peripheral and modiolar portions of the osseous spiral lamina and the floor of the scala tympani, but sparse in the osseous wall of the scala vestibuli. The proposal that these canaliculi normally provide an extensive fluid communication channel between the scala tympani and the spiral canal of the cochlea could have implications not only for novel drug-based cochlear therapies delivered via the scala tympani and the delivery of stem cells or appropriate cell lines into the deafened cochlea, but also for the design of implanted perimodiolar electrode arrays (Shepherd & Colreavy 2004). (For further reading about the changes in the inner ear that are induced by implanted cochlear electrodes, both acute and long term, see Kiefer et al 2006.)

Composition of inner ear fluids

The space between the bony and membranous labyrinths is filled with perilymph (Fig. 37.3B). The membranous labyrinth is filled with endolymph, a fluid produced by the marginal cells of the stria vascularis and the dark cells of the vestibule (see review by Wangemann & Schacht 1996) (Fig. 37.2B). Whatever their relative contributions, endolymph probably circulates in the labyrinth; it enters the endolymphatic sac, where it is transferred into the adjacent vascular plexus via the specialized epithelium of the sac. Pinocytotic removal of fluid may also occur in other labyrinthine regions.

Perilymph was initially considered to be an ultrafiltrate of plasma because of its low protein content. However, it more closely resembles cerebrospinal fluid in ionic composition, particularly in the scala tympani. Its composition is not precisely the same in both cochlear scalae: concentrations of potassium, glucose, amino acids and proteins are greater in the scala vestibuli. This has led to the suggestion that perilymph in the scala vestibuli is derived from plasma via the endothelial boundary of the cochlear blood vessels, whereas the perilymph in the scala tympani contains some cerebrospinal fluid derived from the subarachnoid spaces via the cochlear canaliculus. However, the lack of significant bulk flow suggests that perilymph homeostasis is predominantly locally regulated. Perilymph contains approximately 5 mM K^+, 150 mM Na^+, 120 mM Cl^- and 1.5 mM Ca^{2+}. Endolymph contains greater K^+ (150 mM) and Cl^- (130 mM) concentrations and lower Na^+ (2 mM) and Ca^{2+} (20 μM) concentrations than perilymph. The major differences in ionic composition between the two fluids are important for the function of the inner ear. Displacements of the stereociliary bundles of the sensory cells activate relatively non-specific cationic channels in the stereociliary tips which allow an influx of cations, particularly K^+ and Ca^{2+}, from the endolymph. Hair cells also possess K^+ channels activated by membrane voltage or intracellular Ca^{2+} concentrations, and these allow efflux of K^+ into the perilymph which bathes their basal and lateral membranes. In addition, synaptic transmission at the base and sides of hair cells depends on the influx of Ca^{2+} from the perilymph through voltage-dependent calcium channels in order to release neurotransmitter.

INTERNAL ACOUSTIC MEATUS

The internal acoustic meatus is separated from the internal ear at its lateral fundus by a vertical plate divided unequally by a transverse crest (Fig. 37.4). The canal for the facial nerve passes above and anterior to the crest. Posterior to the crest, the superior vestibular area contains openings for nerves to the utricle and anterior and lateral semicircular ducts. Below the crest, an anterior cochlear area contains a spiral of small holes, the tractus spiralis foraminosus, which encircles the central cochlear canal. Behind this, the inferior vestibular area contains openings for saccular nerves, and most posteroinferior, a single hole (foramen singulare) admits the nerve to the posterior semicircular duct.

It has been suggested that vascular loops in the internal auditory canal (from the anterior inferior cerebellar artery) might generate pulsatile tinnitus.

MEMBRANOUS LABYRINTH

The membranous labyrinth is separated from the periosteum by a space that contains perilymph and a web-like network of fine blood vessels (Fig. 37.3). It can be divided into two major regions, the vestibular apparatus and the cochlear duct.

VESTIBULAR APPARATUS

The vestibular apparatus consists of three membranous semicircular canals which communicate with the utricle, a membranous sac leading into a smaller chamber, the saccule, via the utriculosaccular duct. This Y-shaped duct has a side branch to the endolymphatic duct, which passes to the endolymphatic sac, a small but functionally important expansion situated under the dura of the petrous temporal bone. From the saccule, a narrow canal, the ductus reuniens, leads to the base of the cochlear duct. These various ducts and sacs form a closed system of inter-communicating channels. Endolymph is resorbed into the cerebrospinal fluid from the endolymphatic sac, which therefore provides the site for the drainage of endolymph for the entire membranous labyrinth.

The terminal fibres of the vestibular nerve are connected to five distinct areas of specialized sensory epithelium (two maculae and three crests) in the walls of the membranous labyrinth. Maculae are flat plaques of sensory hair cells surrounded by supporting cells, and are found in the utricle and saccule. The crests are ridges bearing sensory hair cells and supporting cells. They are found in the walls of the ampullae near the utricular openings of the three semicircular canals, one for each canal.

Utricle

The utricle is the larger of the two major vestibular sacs. It is an irregular, oblong, dilated sac that occupies the posterosuperior region of the vestibule (Fig. 37.3A), and contacts the elliptical recess (where it is a blind-ended pouch) and the area inferior to it.

The macula of the utricle (or utriculus) is a specialized area of neurosensory epithelium lining the membranous wall, and is the largest of the vestibular sensory areas (Fig. 37.5). It is triangular or heart-shaped in surface view and lies horizontally with its long axis orientated anteroposteriorly and its sharp angle pointing posteriorly (Fig. 37.6). It is flat except at the anterior edge, where it is gently folded in on itself, and it measures 2.8 mm long by 2.2 mm wide. The mature form of the macula is reached early in development, but in the adult a bulge is often present on the anterolateral border; there is sometimes an indentation at the anteromedial border. The epithelial surface is covered by the otolithic membrane (statoconial membrane), a gelatinous structure in which many small crystals, the otoconia (otoliths, statoliths), are embedded. A curved ridge, the ‘snowdrift line’, runs along the length of the otolithic membrane. It corresponds to a narrow crescent of underlying sensory epithelium termed the striola, 0.13 μm wide. The density of sensory hair cells in this strip of epithelium is 20% less than in the rest of the macula. The striola is convex laterally and runs from the medial aspect of the anterior margin in a posterior direction towards, but not reaching, the posterior pole. The part of the macula medial to the striola is called the pars interna and is slightly larger than the pars externa, which is lateral to it. The significance of this area is that the sensory cells are functionally and anatomically polarized towards it (Fig. 37.6). The macula in each utricle is approximately horizontal when the head is in its normal position. Linear acceleration of the head in any horizontal plane will result in the otolithic membrane lagging behind the movement of the membranous labyrinth as a result of the inertia produced by its mass. The membrane thus maximally stimulates one group of hair cells by deflecting their bundles towards the striola whilst inhibiting others by deflecting their bundles away from it. Hence each horizontal movement of the head will produce a specific pattern of firing in the utricular efferents.

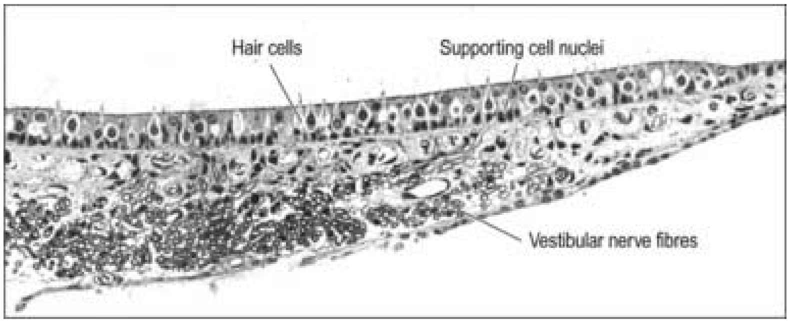

Fig. 37.5 Section of the utricular macula from a guinea pig, showing the relative positions of the hair cells and supporting cell nuclei. Semi-thin resin section, toluidine blue stain. (The inner ear is extremely vulnerable to hypoxia and situated in one of the hardest bones in the body, which means

that well-fixed human tissue is rarely obtained for histology. Guinea pigs are one of the most frequently used animal models of human hearing and their inner ear ultrastructure is very similar.)

(By courtesy of RM Walsh, DN Furness and CM Hackney, The Institute of Science and Technology in Medicine, School of Life Sciences, Keele University.)

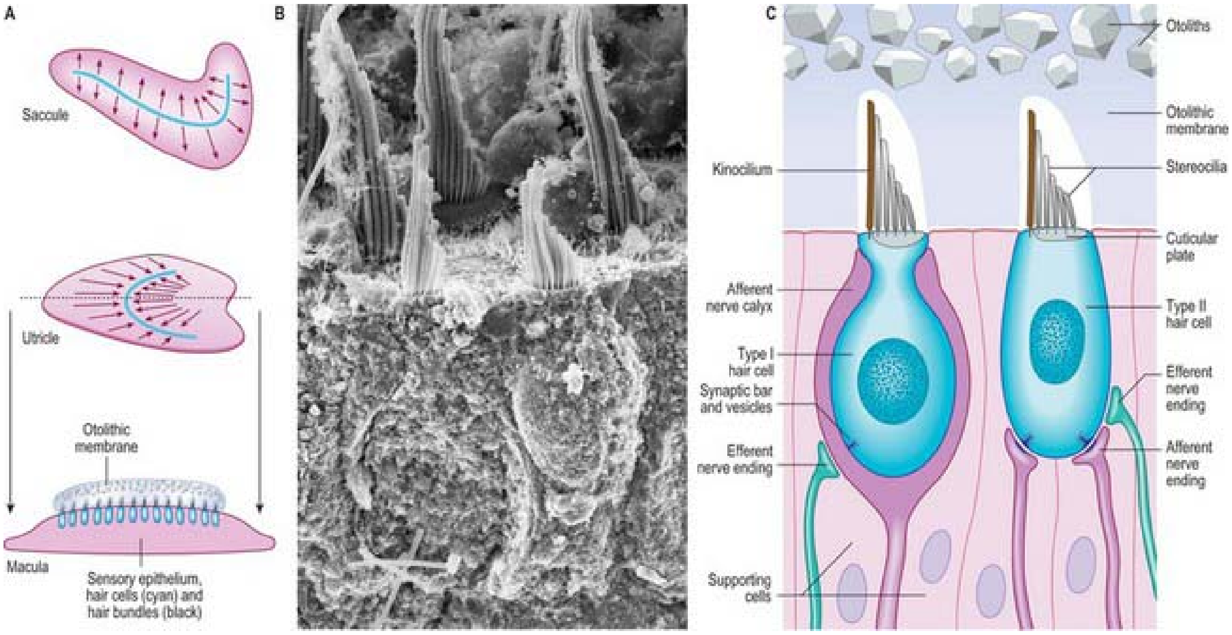
A
Saccule
Utricle
Otolithic membrane
Macula
Sensory epithelium, hair cells (cyan) and hair bundles (black)
B
C
Otoliths
Otolithic membrane
Kinocilium
Stereocilia
Cuticular plate
Afferent nerve calyx
Type II hair cell
Type I hair cell
Synaptic bar and vesicles
Efferent nerve ending
Efferent nerve ending
Afferent nerve ending
Supporting cells

Fig. 37.6 **A**, Morphological organization of the saccular and utricular maculae and the relationship of their hair cells to the otolithic membrane. The utricular macula has been tilted in the plane of the page to emphasize that it lies horizontally, whereas the saccular macula lies vertically when the head is in an upright position. Note the different shapes of the maculae, the position of the striola as indicated by a curved line in each case, and the different orientations of their stereociliary bundles. The arrows indicate the excitatory direction of deflection. **B**, Scanning electron micrograph of a fracture of a utricular macula (guinea pig) showing a type I hair cell (left) and a type II hair cell (right). **C**, The differing innervation patterns of the two types of hair cell.

*(Part **B** by courtesy of DN Furness, The Institute of Science and Technology in Medicine, School of Life Sciences, Keele University.)*

Saccule

The saccule (or sacculus) is a slightly elongated, globular sac lying in the spherical recess near the opening of the scala vestibuli of the cochlea (Fig. 37.6). As already noted, it is connected to the utricle and endolymphatic duct by the utriculosaccular duct, and to the cochlea by the ductus reuniens, which leaves inferiorly to open into the base of the cochlear duct (Fig. 37.3A).

The saccular macula is an almost elliptical structure, 2.6 mm long and 1.2 mm at its widest point. Its long axis is orientated anteroposteriorly but, in contrast to the utricular macula, the saccular macula lies in a vertical plane on the wall of the saccule. Its elliptical shape is very slightly distorted by a small anterosuperior bulge. Like the utricular macula, it is covered by an otolithic (statoconial) membrane and possesses a striola, 0.13 mm wide, which extends along its long axis as an S-shaped strip about which the sensory cells are functionally and anatomically polarized (Fig. 37.6). The part of the macula above the striola is termed the pars interna, and that below it, the pars externa. The operation of the saccule is similar to that of the utricle. However, because of its vertical orientation, the saccule is particularly sensitive to linear acceleration of the head in the vertical plane, and is, therefore, a major gravitational sensor when the head is in an upright position. It is also particularly sensitive to movement along the anteroposterior axis.

Semicircular canals

The lateral, anterior and posterior semicircular ducts follow the course of their osseous canals. Throughout most of their length they are securely attached, by much of their circumference, to the osseous walls. They are approximately one-quarter of the diameter of their osseous canals (Fig. 37.3B). The medial ends of the anterior and posterior canals fuse to form a single common duct, the crus commune, before entering the utricle. The lateral end of each canal is dilated to form an ampulla, which lies within the ampulla of the osseous canal. The short segment of duct between the ampullae and utricle is the crus ampullaris.

The membranous wall of each ampulla contains a transverse elevation (septum transversum) on the central region of which is a sensory area, the ampullary crest (crista). This is a saddle-shaped ridge that lies transversely across the duct. It is broadly concave on its free edge along most of its length and has a concave gutter (planum semilunatum) at either end between the ridge and the duct wall. Sectioned across the ridge, the crests of the lateral and anterior semicircular canals have smoothly rounded corners; the posterior crest is more angular. A vertical plate of gelatinous extracellular material, the cupula, is attached along the free edge of the crest (Fig. 37.7). It projects far into the lumen of the ampulla so that movements of endolymph within the duct readily deflect the cupula and therefore also the stereocilia of the sensory cells that are inserted into its base. The three semicircular canals thus detect angular accelerations during tilting or turning movements of the head in any direction.

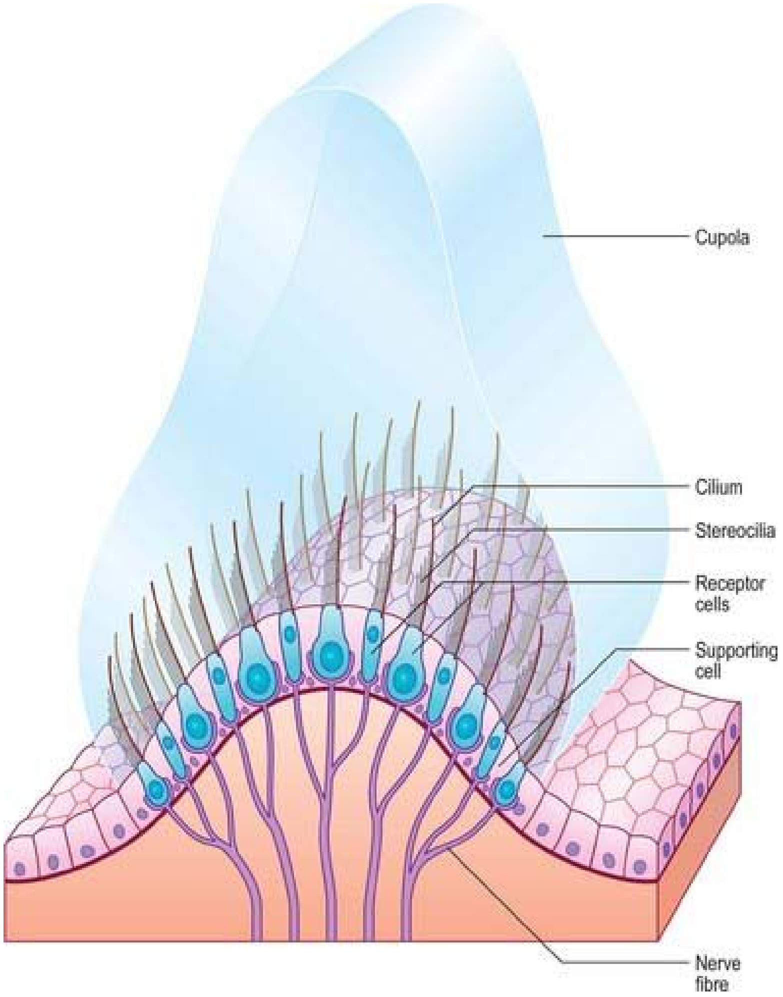

Fig. 37.7 Section of an ampullary crest.

Microstructure of the vestibular system

The maculae and crests detect the orientation of the head with respect to gravity and changes in head movement by means of the mechanosensitive hair cells that are interspersed among the non-sensory supporting cells in their sensory epithelia. These hair cells are in contact with afferent and efferent endings of vestibular nerve fibres by synapses at their base. The entire epithelium lies on a bed of thick, fibrous connective tissue containing myelinated vestibular nerve fibres and blood vessels. The axons lose their myelin sheaths as they perforate the basal lamina of the sensory epithelium. There are two types of sensory hair cell in the vestibular system, type I and type II.

Type I vestibular sensory cells measure 25 μm in length, with a free surface of 6–7 μm in diameter. The basal part of the cell does not reach the basal lamina of the epithelium. Each cell is typically bottle-shaped, with a narrow neck and a rather broad, rounded basal portion containing the nucleus (Fig. 37.6). The apical surface is characterized by 30–50 stereocilia (large, regularly-arranged, modified microvilli about 0.25 μm across) and a single kinocilium (with the typical ‘9 + 2′ arrangement of microtubules characteristic of true cilia). The kinocilium is considerably longer than the stereocilia, and may attain 40 μm, whereas the stereocilia are of graded lengths. They are characteristically arranged in regular rows behind the kinocilium in descending order of height, the longest being next to the kinocilium (Fig. 37.8). The kinocilium emerges basally from a typical basal body, with a centriole immediately beneath it. Close to the inner surface of their basal two-thirds, every cell contains numerous synaptic ribbons with associated synaptic vesicles (see p. 45). The postsynaptic surface of an afferent nerve ending encloses the greater part of the sensory cell body in the form of a cup (chalice or calyx). Efferent nerve fibres make synapses with the external surface of the calyx, rather than directly with the sensory cell.

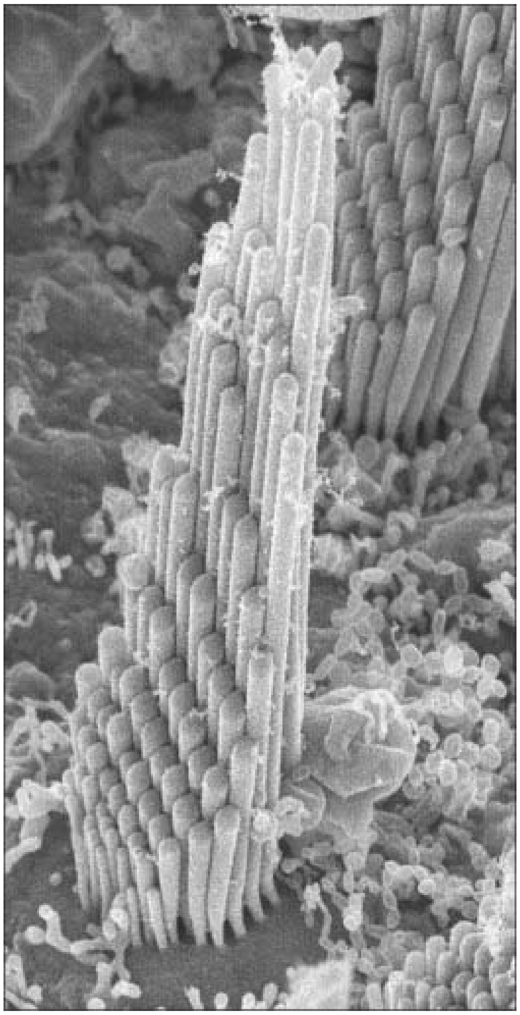

Fig. 37.8 Scanning electron micrograph of a stereociliary bundle from the utricle (guinea pig). The stereocilia are arranged in rows of increasing height towards the tallest element, the kinocilium. Deflection in the direction of the kinocilium results in depolarization of the hair cell.

(By courtesy of DN Furness, The Institute of Science and Technology in Medicine, School of Life Sciences, Keele University.)

There is much greater variation in the sizes of type II sensory cells (Fig. 37.9). Some are up to 45 μm long, and almost span the entire thickness of the sensory epithelium, whereas others are shorter than type I cells. They are mostly cylindrical, but otherwise resemble type I cells in their contents and the presence of an apical kinocilium and stereocilia. However, their kinocilia and stereocilia tend to be shorter and less variable in length. The most striking difference between type I and II cells is their efferent nerve terminals: type II cells receive several efferent nerve boutons containing a mixture of small clear and dense-core vesicles around their bases. Afferent endings are small expansions rather than chalices.

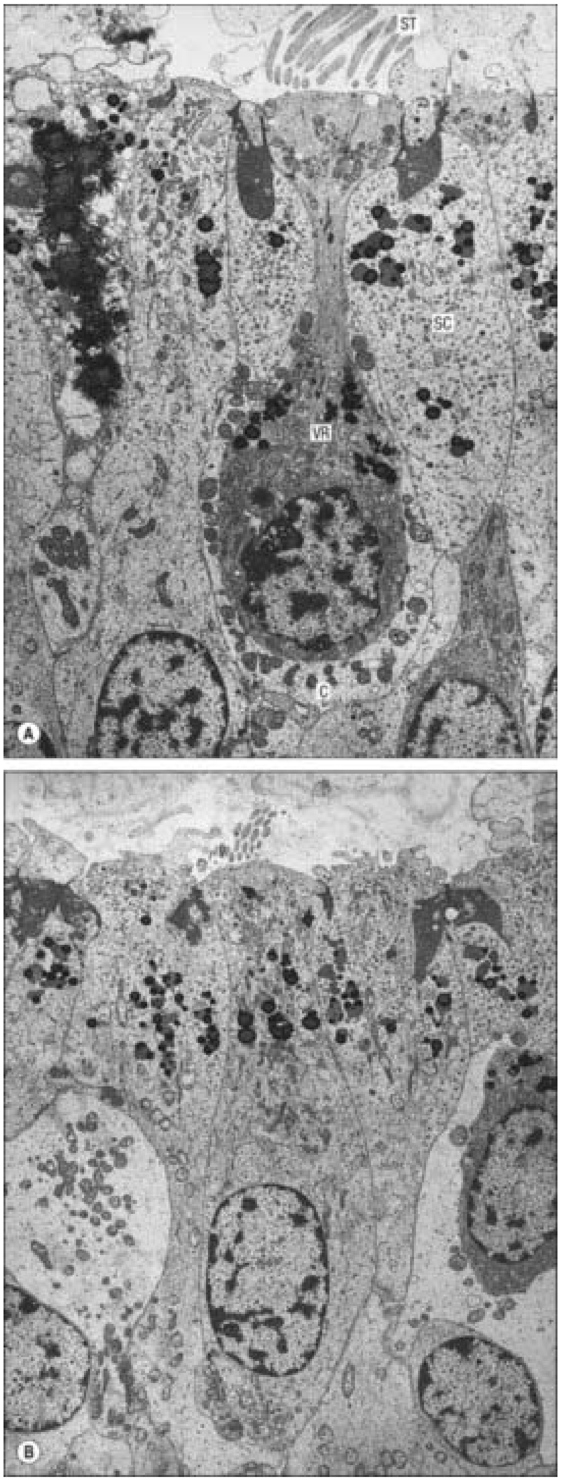

Fig. 37.9 Human vestibular hair cells (transmission electron micrograph). **A**, Type I cell (VR) bearing an apical group of stereocilia (ST) seen in a vertical section through the macula. Note that the hair cell is bottle-shaped, and that much of it is enclosed in the calyceal ending (C) of an afferent

nerve terminal. SC, supporting cells. **B**, Human type II vestibular hair cell: a bouton-type afferent nerve terminal is in contact with the basal part.

(By courtesy of H Felix, M Gleeson and L-G Johnsson, ENT Department, University of Zurich and GKT School of Medicine, London.)

Each sensory cell is structurally and functionally polarized (Fig. 37.6). Deflection of the hair bundle towards the kinocilium results in depolarization of the hair cell, and increases the rate of neurotransmitter release from its base. Deflection away from the kinocilium hyperpolarizes the hair cell and reduces the release of neurotransmitter. The hair cells have specific orientations within each sensory organ. In the maculae, they are arranged symmetrically on either side of the striola. In the utricle, the kinocilia are positioned on the side of the sensory cell nearest to the striola. In the saccule, they are furthest from it. In the ampullary crests, the cells are orientated with their rows of stereocilia at right angles to the long axis of the semicircular duct. In the lateral crest the kinocilia are on the side towards the utricle, whereas in the anterior and posterior crests they are away from it. These different arrangements are important functionally, because any given acceleration of the head maximally depolarizes one group of hair cells and maximally inhibits a complementary set, thus providing a unique representation of the magnitude and orientation of any movement (for further details, see Furness 2002).

The type I and II sensory cells are set within a matrix of supporting cells that reach from the base of the epithelium to its surface, and form rosettes round the sensory cells, as seen in surface view. Although their form is irregular, they can easily be recognized by the position of their nuclei, which tend to lie below the level of sensory cell nuclei and just above the basal lamina (Fig. 37.5). The apices of the supporting cells are attached by tight junctions to neighbouring cells to produce the reticular lamina, a composite layer which forms a plate that is relatively impermeable to cations other than via the mechanosensitive transduction channels of the hair cells.

The otolithic membrane is a layer of extracellular material with a complex structure. It can be divided into two strata. The external layer is composed of otoliths or otoconia, which are barrel-shaped crystals of calcium carbonate with angular ends, up to 30 μm long, and heterogeneous in distribution (Fig. 37.6). They are attached to a more basal gelatinous layer into which the stereocilia and kinocilia of the sensory cells are inserted (Fig. 37.8). The gelatinous material consists largely of glycosaminoglycans associated with fibrous protein.

Epley’s manoeuvre

Benign paroxysmal positional vertigo is a condition in which a sensation of rotation with associated nystagmus is induced by adopting a particular position (with the abnormal ear dependent). It is believed that calcium carbonate crystals from the otoliths become freed from their hair cells and, in certain positions, drop into the ampulla of the posterior semicircular canal, possibly becoming adherent to the cupula and rendering it gravity-sensitive. In certain positions, the alignment of the axis of the posterior semicircular canal with gravity results in the displacement of the cupula and the activation of the vestibulo-ocular reflex resulting in compensatory nystagmoid eye movements in response to apparent head movements.

Epley’s canalith repositioning procedure relies on the adoption of a series of body postures designed to allow the aberrant crystals (or canaliths) to float out of the posterior semicircular canal and to stick to the wall of the vestibule. Cure rates in excess of 80% have been recorded and the procedures have largely superseded surgical procedures designed to denervate the ampulla of the posterior semicircular canal (cingular neurectomy) or obliterate the canal completely.

Endolymphatic duct and sac

The endolymphatic duct runs in the osseous vestibular aqueduct and becomes dilated distally to form the endolymphatic sac. This is a structure of variable size, which may extend through an aperture on the posterior surface of the petrous bone to end between the two layers of the dura on the posterior surface of the petrous temporal bone near the sigmoid sinus (Fig. 37.3A). The surface cells throughout the entire endolymphatic duct resemble those lining the non-specialized parts of the membranous labyrinth and consist of squamous or low cuboidal epithelium. The epithelial lining and subepithelial connective tissue become more complex where the duct dilates to form the endolymphatic sac. An intermediate or rugose segment and a distal sac can be distinguished. In the intermediate segment, the epithelium consists of light and dark cylindrical cells. Light cells are regular in form and have numerous long surface microvilli with endocytic invaginations between them and large clear vesicles in their apical region. In contrast, dark cells are wedge-shaped and have a narrow base, few apical microvilli and dense, fibrillar cytoplasm.

The endolymphatic sac has important roles in the maintenance of vestibular function. Endolymph produced elsewhere in the labyrinth is absorbed in this region, probably mainly by the light cells. Damage to the sac, or blockage of its connection to the rest of the labyrinth, causes endolymph to accumulate; this produces hydrops, which affects both vestibular and cochlear function. The epithelium is also permeable to leukocytes, including macrophages which can remove cellular debris from the endolymph, and to various cells of the immune system that contribute antibodies to this fluid.

A unique positive electrical potential exists in the endolymphatic spaces, varying from +77 mV in the cochlear duct near the stria vascularis to +44 mV in the utricle. This is additional to the normal resting potentials of the receptor cells so that there is a very considerable potential difference across their membranes. This undoubtedly contributes to the extreme sensitivity to mechanical deformation of the labyrinthine sensory receptors.

COCHLEAR DUCT

The cochlear duct is a spiral tube that runs within the bony cochlea (Figs 37.2A and B, 37.3). The osseous spiral lamina projects for part of the distance between the modiolus and the outer wall of the cochlea and is attached to the inner edge of the basilar membrane. The endosteum of the outer wall is thickened to form a spiral cochlear ligament which projects inwards as a triangular basal crest attached to the outer rim of the basilar membrane. Immediately above this is a concavity, the external spiral sulcus (sulcus spiralis externus), above which the thick, highly vascular periosteum projects as a spiral prominence. Above the prominence is a specialized, thick epithelial layer, the stria vascularis. A second, thinner vestibular membrane, Reissner's membrane, extends from the thickened endosteum on the osseous spiral lamina to the outer wall of the cochlea, where it is attached above the stria. Reissner's membrane consists of two layers of squamous epithelial cells separated by a basal lamina. The side facing the scala vestibuli bears flattened perilymphatic cells, with tight junctions between them, creating a diffusion barrier. The endolymphatic side is lined by squamous epithelial cells; these are also joined by tight junctions and are involved in ion transport. The canal thus enclosed between the scala tympani and the scala vestibuli is the cochlear duct (Fig. 37.2B). It is triangular in cross-section throughout the length of the cochlea. Its closed upper end, the lagena, is attached to the cupula. The lower end of the duct turns medially, narrowing into the ductus reuniens, and connects with the saccule (Fig. 37.3A).

The organ of Corti, the sensory epithelium of the cochlea, sits upon the basilar membrane. The apices of the sensory hair cells and the supporting cells it contains are joined by tight junctions to form the reticular lamina. The diffusion barriers which line the cochlear duct ensure that the apices of the sensory hair cells are bathed by endolymph whereas their lateral and basal regions are bathed in perilymph.

The stria vascularis lies on the outer wall of the cochlear duct, above the spiral eminence (Fig. 37.2B and C). It has a special stratified epithelium containing a dense intraepithelial capillary plexus and three cell types:

superficial marginal, dark or chromophil cells; intermediate light, or chromophobe cells, and basal cells. The endolymphatic surface consists only of the apices of marginal cells. The intermediate and basal cells lie deeper within the stria and send cytoplasmic processes towards the surface, between the deeper parts of the marginal cells. The long descending cytoplasmic processes of the marginal dark cells and the ascending processes of the intermediate and basal cells envelop the intraepithelial capillaries. The stria vascularis is involved in ion transport, and it helps to produce the unusual ionic composition of endolymph. It is the source of the large positive endocochlear electrical potential, maintenance of which is directly dependent upon adequate oxygenation of the epithelial cells which is provided by the intraepithelial capillary plexus.

The osseous spiral lamina consists of two plates of bone between which are canals for the cochlear nerve filaments. On the upper plate, the periosteum is thickened to form the spiral limbus (limbus laminae spiralis) (Fig. 37.2B). It ends externally in the internal spiral sulcus, which in section is shaped like a C. Its upper part, the overhanging limbic edge, is the vestibular labium and the lower tapering part is the tympanic labium which is perforated by small holes (the habenula perforata) for branches of the cochlear nerve. The upper surface of the vestibular labium is crossed at right angles by furrows, separated by numerous elevations, the auditory teeth (dentes acustici). The limbus is covered by a layer that appears superficially to be squamous epithelium, however, only the cells over the 'teeth' are flat, and those in the furrows are flask-shaped interdental cells. The epithelium is continuous with the epithelium in the internal spiral sulcus and on the inferior surface of Reissner's membrane. During development the interdental cells secrete some of the material that forms the tectorial membrane.

Basilar membrane

The basilar membrane stretches from the tympanic lip of the osseous spiral lamina to the basal crest of the spiral ligament (Fig. 37.2B and C). It consists of two zones. The thin zona arcuata stretches from the spiral limbus to the bases of the outer pillar cells and supports the organ of Corti. It is composed of compact bundles of small (8–10 nm diameter) collagenous filaments, mainly radial in orientation. The outer thicker zona pectinata starts beneath the bases of the outer pillar cells and is attached to the crista basilaris. The basilar membrane is trilaminar in the zona pectinata, but the upper and lower layers fuse at its attachment to the crista basilaris. The length of the basilar membrane is 35 mm; its width increases from 0.21 mm basally to 0.36 mm at its apex, accompanied by corresponding narrowing of the osseous spiral lamina and a decrease in the thickness of the basal crest. The lower or tympanic surface of the basilar membrane is covered by a layer of vascular connective tissue and elongated perilymphatic cells. One vessel, the spiral vessel (vas spirale), is larger; it lies immediately below the tunnel of Corti.

Organ of Corti

The organ of Corti consists of a series of epithelial structures that lie on the zona arcuata of the basilar membrane (Fig. 37.2B and C). The more central of these structures are two rows of cells, the internal and external pillar cells. The bases of the pillar cells are expanded, and rest contiguously on the basilar membrane, but their rod-like cell bodies are widely separated. The two rows incline towards each other and come into contact again at the heads of the pillars, enclosing between them and the basilar membrane the tunnel of Corti, which has a triangular cross-section (Fig. 37.2C). Internal to the inner pillar cells is a single row of inner hair cells. External to the outer pillar cells are three or four rows of outer hair cells. The bases of the outer hair cells are cupped by supporting cells called outer phalangeal (Deiters') cells, except for a gap where cochlear axons synapse with them. The apical ends of the hair cells and apical processes of the supporting cells form a regular mosaic called the reticular lamina, which is covered by the tectorial membrane, a gel-like structure projecting from the spiral limbus. The reticular lamina is impervious to ions and thus maintains the electrochemical gradient between the fluids surrounding the apices and the basolateral membranes of the sensory hair cells. A narrow gap separates the tectorial membrane from the reticular lamina except where the apical stereocilia of the outer hair cells project to make contact with it.

In addition to the tunnel of Corti, other intercommunicating spaces, the spaces of Nuel, surround the outer hair cells. This entire intercommunicating complex of spaces of Nuel and tunnel of Corti is filled with perilymph, which diffuses through the matrix of the basilar membrane. The fluid in these spaces is also sometimes called the cortilymph; it is possible that minor alterations in perilymphatic composition occur within it, because it is exposed to the activities of synaptic endings and specialized excitable cells.

Each pillar cell has a base or crus, an elongated scapus (rod) and an upper end or caput (head) (Fig. 37.2C); each crus and caput are in contact, but the scapi are separated by the tunnel of Corti. Electron microscopy shows many microtubules, 30 nm in diameter, arranged in linked parallel bundles of 2000 or more in the scapus, originating in the crus and diverging above the scapus to terminate in the head region. The nucleus is situated in the foot-like expansion resting on the basal lamina.

There are almost 6000 internal pillar cells. Their bases rest on the basilar membrane near the tympanic lip of the internal spiral sulcus, and their bodies form an angle of approximately 60° with the basilar membrane. Their heads resemble the proximal end of the ulna, with deep concavities for the heads of the outer pillar cells, which they overhang. There are almost 4000 external pillar cells. They are longer and more oblique than the internal pillar cells, and form an angle of approximately 40° with the basilar membrane. Their heads fit into the concavities on the heads of the inner pillar cells and project externally as thin processes that contact the processes of the Deiters’ cells. The distances between the bases of the internal and external pillar cells increase from the cochlear base to its apex, whereas the angles they make with the basilar membrane diminish.

Cochlear hair cells are the sensory transducers of the cochlea: collectively, they detect the amplitude and frequency of the sound waves that enter the cochlea. All cochlear hair cells have a common pattern of organization. They are elongated cells with a group of modified apical microvilli or stereocilia (which contain parallel arrays of actin filaments) and a group of synaptic contacts with cochlear axons at their rounded bases (Fig. 37.10B). The inner hair cells form a single row along the inner edge of inner pillar cells (and the spiral tunnel), whereas the outer hair cells are arranged in three or, in some regions of the human cochlea, in four or even five rows, interspersed with supporting cells (Fig. 37.10A). These two groups have distinctive roles in sound reception; the differences in their detailed structure reflect this functional divergence. There are 3500 inner hair cells and 12,000 outer hair cells. The two sets of hair cells lean towards each other apically at about the same angles as the neighbouring inner and outer pillar cells. The geometric arrangement of these cells is very precise, and this pattern is closely related to the sensory performance of the cochlea.

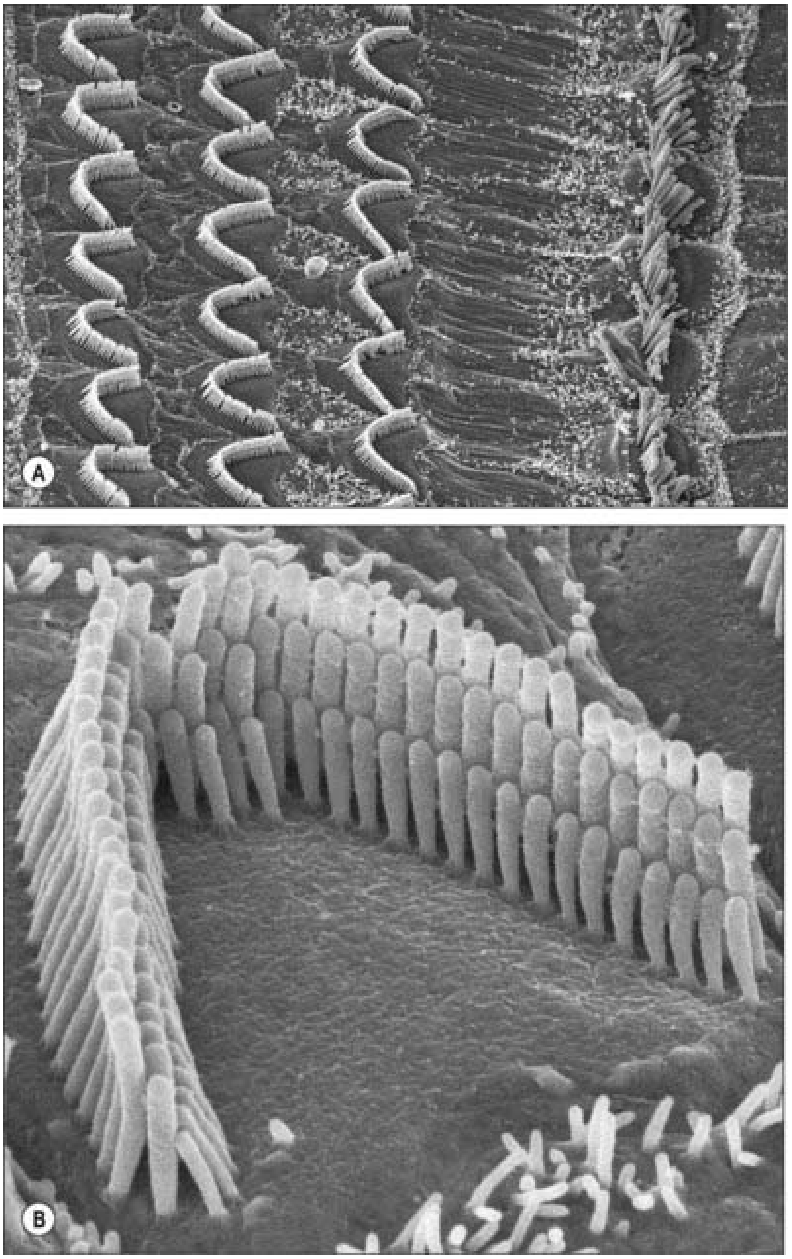

Fig. 37.10 Scanning electron micrographs of the surface of the organ of Corti (guinea pig). **A**, The reticular lamina: three rows of V-shaped stereociliary bundles can be seen protruding from the apices of the outer hair cells. They are separated from the single row of inner hair cells (which have relatively linear stereociliary bundles) by the apices of the inner pillar cells. **B**, The stereociliary bundle of one outer hair cell, showing three rows of stereocilia increasing in height: deflection of the stereocilia in the

direction of the tallest row results in depolarization of the hair cell. Microvilli can be seen on the surface of Deiters' cells (front right).

*(**A** and **B** by courtesy of DN Furness, The Institute of Science and Technology in Medicine, School of Life Sciences, Keele University.)*

The inner hair cells are pear-shaped and slightly curved; the narrower end is directed towards the surface of the organ of Corti and the wider basal end is positioned some distance above the inner end of the basilar membrane (Fig. 37.2C). The inner hair cells are surrounded by inner border cells and by inner phalangeal cells which are attached externally to the heads of the inner pillar cells. The flat apical surface of each inner hair cell is elliptical when viewed from above, its long axis directed in the direction of the row of hair cells (Fig. 37.10A). The breadth of the apex exceeds that of the inner pillar cells so that each inner hair cell is related to more than one inner pillar cell. The apex bears 50–60 stereocilia, arranged in several ranks of progressively ascending height, the tallest on the strial side. The tips of the shorter rows are connected diagonally to the sides of the adjacent taller stereocilia by thin filaments called tip links; each stereocilium is also connected to all its neighbours by lateral links. The length of a stereociliary row varies along the length of the cochlea, being longest at the apex and shortest at its base. The stereociliary bases insert into a transverse lamina of dense fibrillar material, the cuticular plate, which lies immediately beneath the apical surface of each inner hair cell. The cuticular plate includes a small aperture containing a basal body. During development, a kinocilium containing microtubules is anchored here, a condition which persists in vestibular hair cells.

At its base, each inner hair cell forms ten or more synaptic contacts with afferent endings, each being marked by a presynaptic structure similar to the ribbon synapses of the retina. Occasionally, an efferent synapse makes direct contact with a hair cell base but these are usually presynaptic to the terminal expansions of afferent endings, rather than to the hair cell itself.

Outer hair cells are long cylindrical cells which are nearly twice as tall as the inner hair cells (Figs 37.2C, 37.6, 37.10A). There is a gradation of length: the outermost row is longest in any one cochlear region, and those of the cochlear apex are taller than those of the base. They are surrounded by the apical or phalangeal processes of the Deiters' cells or, on the internal side of the inner row, by the heads of the outer pillar cells. The stereocilia, which may number up to 100 per cell, are arranged in three rows of graded heights; the longest is on the outer side. The rows are arranged in the form of a V or W depending on cochlear region, the points of the angles directed externally. The stereocilia are also graded in length according to cochlear region: those of the cochlear base are shortest. Like those of inner hair cells, the stereocilia possess tip links and other filamentous connections with their neighbours, and are inserted at their narrow bases into a cuticular plate. The tallest stereocilia are embedded in shallow impressions on the underside of the tectorial membrane.

The rounded nucleus is positioned near the base of the cell. Below the nucleus are a few ribbon-like synapses associated with afferent endings of the cochlear nerve. The latter are fewer in number and smaller than the cluster of efferent boutons that contact the base of the cell. The neurotransmitter at the afferent synapse in both inner and outer hair cells is glutamate whereas that of the efferent endings is acetylcholine, although other neurotransmitters or neuromodulators have been demonstrated.

Cochlear hair cells respond with phenomenal speed and sensitivity to sound vibrations that cause submicron deflections of their stereociliary hair bundles. Outer hair cells not only detect these vibrations but also generate force to increase auditory sensitivity and frequency discrimination. (See Fettiplace & Hackney 2006, for further details about the sensory and motor functions of auditory hair cells.)

Deiters' or phalangeal cells lie between the rows of outer hair cells. Their expanded bases lie on the basilar membrane and their apical ends partially envelop the bases of the outer hair cells (Figs 37.2C and 37.11). Each has a finger-like (phalangeal) process that extends diagonally upwards between the hair cells to the reticular membrane, where it forms a plate-like expansion that fills the gaps between hair cell apices.

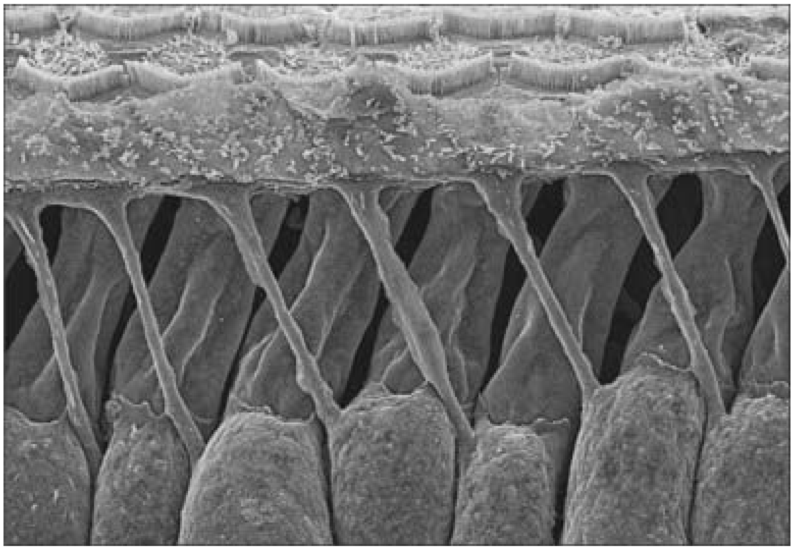

Fig. 37.11 Scanning electron micrograph of a portion of the organ of Corti (guinea pig) dissected to expose the outer row of outer hair cells and their attendant Deiters' cells with narrow phalangeal processes. The stereociliary bundles of two rows of outer hair cells are visible above the reticular lamina.

(By courtesy of DN Furness, The Institute of Science and Technology in Medicine, School of Life Sciences, Keele University.)

Five or six rows of columnar supporting cells or external limiting cells, such as Hensen's cells and Claudius' cells lie external to the Deiters' cells (Fig. 37.2C).

The apices of the hair cells and supporting cells that form the reticular lamina are linked by tight junctions, desmosomes and extensive gap junctions which couple them electrically. This arrangement is significant for two reasons. The reticular lamina creates a highly impermeable barrier to the passage of ions other than via the mechanotransducer channels in the stereociliary membranes. It also forms a rigid support between the apices of the hair cells, coupling them mechanically to the movements of the underlying basilar membrane, which causes lateral shearing movements between the stereocilia and the overlying tectorial membrane. If there is hair cell loss as a result of trauma such as excessive noise or ototoxic drugs, the supporting cells expand rapidly to fill the gap, disturbing the regular pattern of the reticular lamina (phalangeal scars), but restoring its function.

Tectorial membrane

The tectorial membrane overlies the sulcus spiralis internus and organ of Corti and is a stiff, gelatinous plate (Fig. 37.2B and C). It contains collagen types II, V and IX, interspersed with glycoproteins (tectorins), which contribute approximately half of the total protein.

In transverse section, the tectorial membrane has a characteristic shape. The underside is nearly flat and the upper surface is convex, and it is thin on the modiolar side where it is attached to the vestibular labium of the spiral limbus. Its outer part forms a thickened ridge, overhanging the edge of the reticular lamina. The lower surface is relatively smooth, except where the stereocilia of the outer hair cells are embedded in the membrane, leaving a pattern of W- or V-shaped impressions, an S-shaped ridge called Hensen’s stripe which projects towards the stereocilia of the inner hair cells. The interdental cells of the spiral limbus are believed to secrete the membrane.

VASCULAR SUPPLY

ARTERIES

The inner ear is principally supplied by the labyrinthine artery. The stylomastoid branch of either the occipital artery or the posterior auricular artery also supplies the semicircular canals.

Labyrinthine artery

The labyrinthine artery arises from the basilar artery, or sometimes from the anterior inferior cerebellar artery. It divides at the bottom of the internal auditory meatus into cochlear and vestibular branches. The cochlear branch divides into 12–14 twigs, which traverse the canals in the modiolus and are distributed as a capillary plexus to the spiral lamina, basilar membrane, stria vascularis and other cochlear structures. Vestibular arterial branches supply the utricle, saccule and semicircular ducts.

VEINS

The veins draining the vestibule and semicircular canals accompany the arteries. They receive the cochlear veins at the base of the modiolus, and form the labyrinthine vein, which ends in the posterior part of the superior petrosal sinus or in the transverse sinus. A small vessel from the basal cochlear turn traverses the cochlear canaliculus to join the internal jugular vein.

For details of the microvasculature of the cochlea of man and other mammals, see Axelsson (1988).

INNERVATION

VESTIBULOCOCHLEAR NERVE

The vestibulocochlear nerve emerges from the cerebellopontine angle (see Fig. 19.3). It courses through the posterior cranial fossa to enter the petrous temporal bone via the internal acoustic meatus, where it divides into an anterior trunk, the cochlear nerve, and a posterior trunk, the vestibular nerve (Fig. 37.12A; see Fig. 27.8). Both contain the centrally directed axons of bipolar neurones, together with a smaller number of efferent fibres that arise from brain stem neurones and terminate on cochlear and vestibular sensory cells. In humans, the intratemporal portion of the vestibulocochlear nerve consists of two histologically distinct portions: a central glial zone adjacent to the brain stem, and a peripheral or non-glial zone (Bridger & Farkashidy 1980). In the glial zone the axons are supported by central neuroglia, whereas in the non-glial zone they are ensheathed by Schwann cells. The non-glial zone extends into the cerebellopontine angle medial to the internal acoustic meatus in more than 50% of human vestibulocochlear nerves. During development, a gap of several weeks has been reported between the onset of Schwann cell myelination distally and glial myelination proximally: it has been suggested that the gap may coincide with the time of the final maturation of the organ of Corti. (For further details about the development of the human cochlear nerve see Ray et al 2005.)

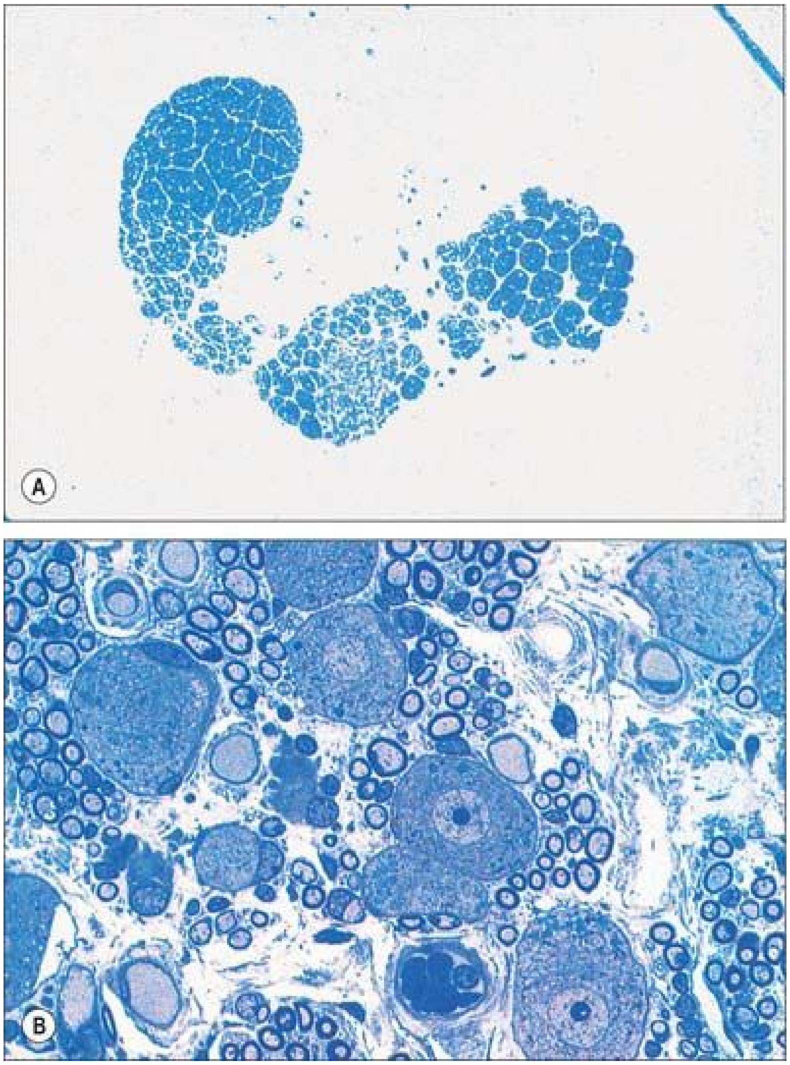

Fig. 37.12 The vestibulocochlear nerve (human). **A**, Transverse section. The cochlear nerve (comma-shaped profile on the left) abuts the inferior division of the vestibular nerve (right). The singular nerve is a separate fascicle between the superior and inferior divisions of the vestibular nerve. **B**, A portion of a vestibular ganglion, showing neuronal perikarya, myelinated axons and small blood vessels.

(Toluidine blue stained resin sections by courtesy of H Felix, M Gleeson and L-G Johnsson, ENT Department, University of Zurich and School of Medicine, King's College London.)

In audiological practice, it is important to distinguish between intratemporal and intracranial lesions. However, this surgical distinction does not correlate with the precise anatomical description of peripheral and central portions of the auditory and vestibular systems. Clinically, the term ‘peripheral auditory lesion’ is used to describe lesions peripheral to the spiral ganglion, and the term ‘peripheral vestibular disturbance’ includes lesions of the vestibular ganglion and the entire vestibular nerve.

Vestibular nerve

The cell bodies of the bipolar neurones that contribute to the vestibular nerve lie in the vestibular ganglion, which is situated in the trunk of the nerve within the lateral end of the internal auditory meatus (Fig. 37.12B). Their peripheral processes innervate the maculae of the utricle and saccule and the ampullary crests of the semicircular canals (see below). Their axons travel to the CNS in the vestibular nerve, which enters the brain stem at the cerebellopontine angle, and terminates in the vestibular nuclear complex. Neurones in this complex project to motor nuclei in the brain stem and upper spinal cord, and to the cerebellum and thalamus. Thalamic efferent projections pass to a cortical vestibular area which is probably located near the intraparietal sulcus in area 2 of the primary somatosensory cortex.

Vestibular (Scarpa’s) ganglion

The cell bodies of the neurones in the vestibular ganglion vary considerably in size: their circumferences range from 45 to 160 μm (Felix et al 1987). No topographically ordered distribution relating to size has been found. The cell bodies are notable for their abundant granular endoplasmic reticulum, which in places forms Nissl bodies, and prominent Golgi complexes. They are covered by a thin layer of satellite cells and are often arranged in pairs, closely abutting each other so that only a thin layer of endoneurium separates the adjacent coverings of satellite cells. This arrangement has led to speculation that ganglion cells may affect each other directly by electrotonic spread (ephaptic transmission: see Felix et al 1987).

Two distinct sympathetic components have been identified in the vestibular ganglion: a perivascular adrenergic system derived from the stellate ganglion, and a blood vessel-independent system derived from the superior cervical ganglion.

Intratemporal vestibular nerve

The peripheral processes of the vestibular ganglion cells are aggregated into definable nerves, each with a specific distribution. The main nerve divides at and within the ganglion into superior and inferior divisions, which are connected by an isthmus. The superior division, the larger of the two, passes through the small holes in the superior vestibular area at the fundus of the internal acoustic meatus (Fig. 37.4) and supplies the ampullary crests of the lateral and anterior semicircular canals via the lateral and anterior ampullary nerves, respectively. A secondary branch of the lateral ampullary nerve supplies the macula of the utricle; however, the greater part of the utricular macula is innervated by the utricular nerve, which is a separate branch of the superior division. Another branch of the superior division, Voit's nerve, supplies part of the saccule.

The inferior division of the vestibular nerve passes through small holes in the inferior vestibular area (Fig. 37.4) to supply the remainder of the saccule and the posterior ampullary crest via saccular and singular branches, respectively; the latter passes through the foramen singulare. Occasionally, a very small supplementary or accessory branch innervates the posterior crest; it is probably a vestigial remnant of the crista neglecta, an additional area of sensory epithelium found in some other mammals but seldom in man.

Afferent and efferent cochlear fibres are also present in the inferior division of the vestibular nerve, but leave at the anastomosis of Oort to join the main cochlear nerve (see review by Warr 1992). Another anastomosis, the vestibulofacial anastomosis, is situated more centrally between the facial and vestibular nerves, and is the point at which fibres originating in the intermediate nerve pass from the vestibular nerve to the main trunk of the facial nerve.

There are approximately 20,000 fibres in the vestibular nerve of which 12,000 travel in the superior division and 8000 travel in the inferior division.

The distribution of fibre diameters is bimodal, with peaks at 4 μm and 6.5 μm. The smaller fibres go mainly to the type II hair cells and the larger fibres tend to supply the type I hair cells. In addition to the afferents, efferent and autonomic fibres have been identified. Efferent fibres synapse exclusively with the afferent calyceal terminals around type I cells and usually with the afferent boutons on type II cells, although a few are in direct contact with the cell bodies of type II cells. The autonomic fibres do not contact vestibular sensory cells, but terminate beneath the sensory epithelia.

Anatomy of balance and posture

The vestibular labyrinths on each side of the head are arranged symmetrically with respect to each other. Vestibular sensory pathways are concerned with perception of the position of the head in space and movement of the head; they also establish important connections for reflex movements that govern the equilibrium of the body and the fixity of gaze.

The vestibular system consists of two otolithic organs, the utricle and the saccule, and three semicircular canals. The otolithic organs detect linear acceleration due to gravitational pull (gravitoinertial acceleration) and the direction of other linear accelerations such as the up and down movements of the head that occur in running. They also respond when the head is tilted relative to gravity, so called pitch (forward and backward tilting) and roll (side-to-side tilting) movements. The semicircular canals detect angular accelerations resulting from rotations of the head or body.

The stereocilia in the apical hair bundles of the mechanosensitive hair cells in each of these organs are embedded in an overlying accessory gel-like structure, the otolithic membrane (in the utricle and the saccule) and the cupula (in the semicircular canals). Their apical surfaces are bathed in endolymph: tight junctional complexes between the apices of the hair cells and their adjacent supporting cells separate the endolymph from the perilymph that bathes their basolateral surfaces. Deflection of the stereocilia (caused by displacements of their overlying accessory membranes by fluid movements in the membranous labyrinth) produces either an increased or decreased rate of opening of the mechanotransduction channels at their tips, depending on whether they are deflected towards or away from the tallest row respectively. The change in the membrane potential of the receptor cell is signalled to the brain as a change in the firing frequency of the vestibular nerve afferents (either an increase or a decrease of the basal resting discharge, depending on the direction of stimulation). The signals are compared centrally with visual and somatosensory signals, which also signal the position of the head in space (for a more detailed account, see Furness 2002).

Semicircular canals

Angular acceleration and deceleration of the head cause a counterflow of endolymph in the semicircular canals, which deflects the cupola of each crista and bends the stereociliary/kinociliary bundles. When a steady velocity of head movement is reached, the endolymph rapidly adopts the same velocity as the surrounding structures because of friction with the canal walls, so that the cupula and receptor cells return to their resting state. The three semicircular canals are orientated at right angles to each other, which means that all possible directions of acceleration can be detected. Directional sensitivity to head movement is coded by opposing receptor signals: the left and right semicircular canals of each functional pair (e.g. the left and right superior canals), respond oppositely to any movement of the head that affects them (Fig. 37.13). Some vestibular neurones receive a bilateral input from vestibular receptors, which means that they can compare the discharge rates of right and left canal afferents, a mechanism that increases the sensitivity of the system.

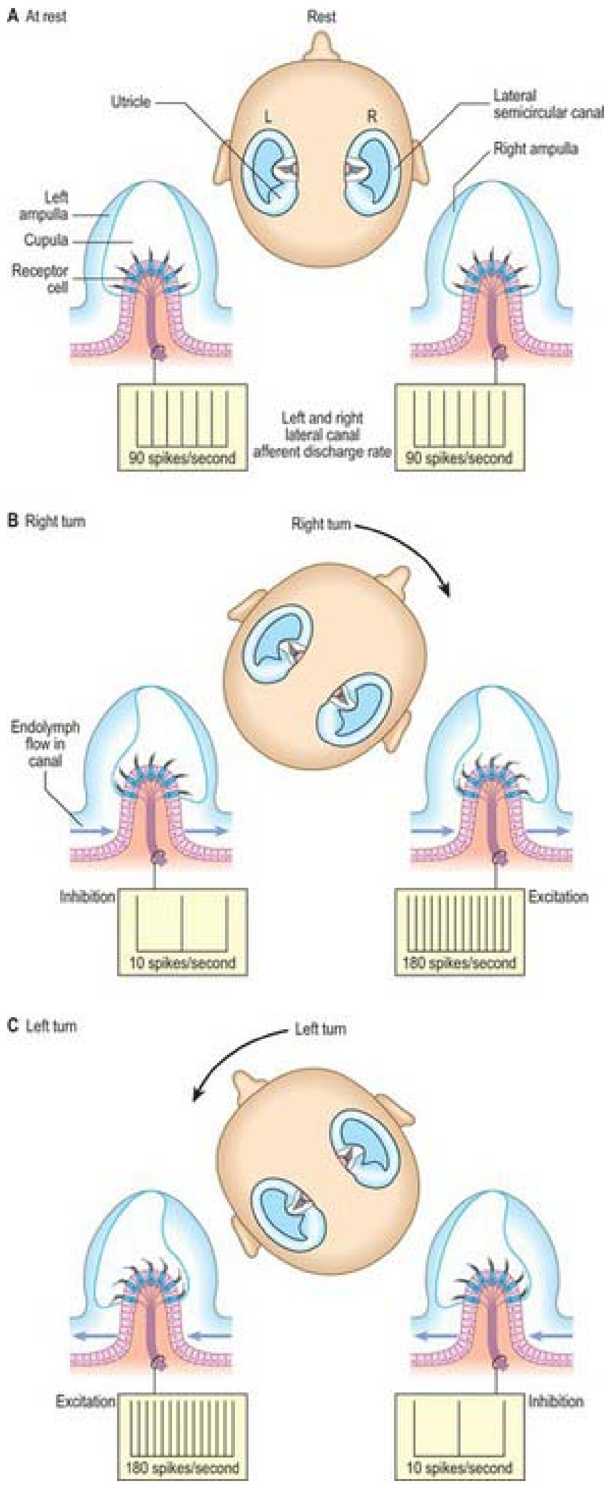
A At rest
Rest
Utricle
L
R
Lateral semicircular canal
Right ampulla
Left ampulla
Cupula
Receptor cell
90 spikes/second
Left and right lateral canal afferent discharge rate
90 spikes/second
B Right turn
Right turn
Endolymph flow in canal
Inhibition
10 spikes/second
Excitation
180 spikes/second
C Left turn
Left turn
Excitation
180 spikes/second
Inhibition
10 spikes/second

Fig. 37.13 Response of the horizontal semicircular canals to head rotation in the horizontal plane. The firing rates of afferents from the left and right horizontal canals are equivalent at rest (**A**). However, when the head is turned to the right (**B**) or to the left (**C**), receptor depolarization and afferent

fibre excitation occurs on the side to which the head turns; there is inhibition on the contralateral side.

Maculae

In the maculae, the weight of the otoconial crystals creates a gravitational pull on the otoconial membrane and thus on the stereociliary bundles of the sensory cells which are inserted into its base. Because of this, they are able to detect the static orientation of the head with respect to gravity. They also detect shifts in position according to the extent to which the stereocilia are deflected from the perpendicular. The two maculae are set at right angles to each other, and the cells of both maculae are orientated functionally in opposite directions across their striolar boundaries. Movement causes depolarization of the hair cells on one side of the striola and hyperpolarization of cells on the other side; because the striola is curved, small groups of hair cells on the macular epithelium each respond to a specific direction of head tilt or linear acceleration (Fig. 37.14). Moreover, because the otoconia have a collective inertia/momentum, linear acceleration and deceleration along the anteroposterior axis can be detected by the lag or overshoot of the otoconial membrane with respect to the epithelial surface, and so the saccular macula is able to signal these changes of velocity.

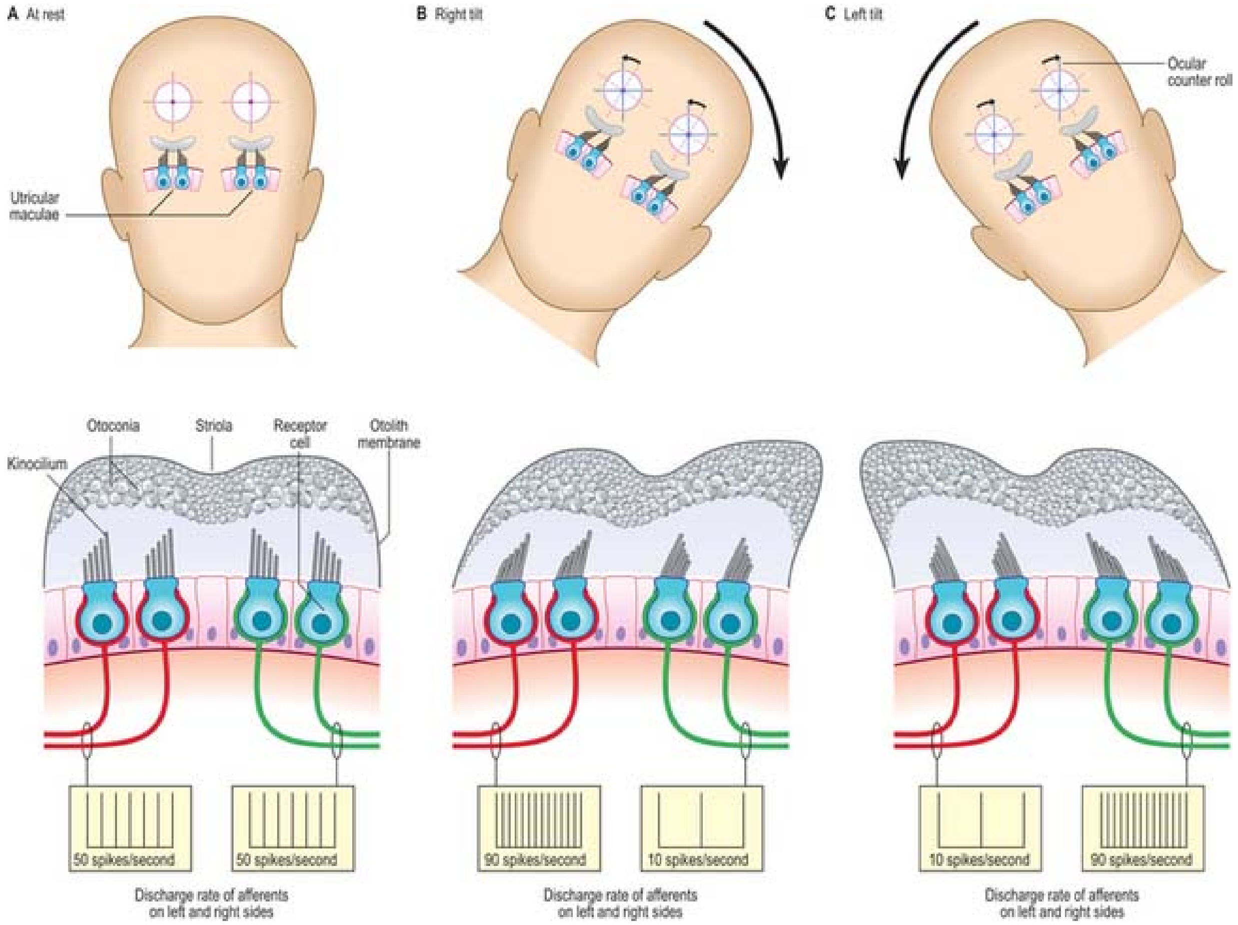
A At rest
B Right tilt
C Left tilt
Ocular counter roll
Utricular maculae
Otoconia
Striola
Receptor cell
Otolith membrane
Kinocilium
50 spikes/second
50 spikes/second
Discharge rate of afferents on left and right sides
90 spikes/second
10 spikes/second
Discharge rate of afferents on left and right sides
10 spikes/second
90 spikes/second
Discharge rate of afferents on left and right sides

Fig. 37.14 Head tilt is encoded by a macular map of directional space. These diagrams depict the responses of the utricular maculae to head tilt. Firing rates in the vestibular afferents that innervate receptors on either side of the striola (red and blue lines) are equivalent when the head is upright (**A**). When the head is tilted to the right (**B**) or to the left (**C**), the stereocilia are deflected by displaced otoconia: hair cells on the upward slope side of the striola increase their firing rate, while those on the downward slope decrease their firing rate.

The macular receptors can also be stimulated by low frequency sound which sets up vibratory movements in the otoconial membrane, although this appears to require relatively high sound levels. Efferent synapses on the afferent endings of the type I sensory cells and on the bases of type II cells receive inputs from the brain stem which appear to be inhibitory. They serve to reduce the activity of the afferent fibres either indirectly, in the case of the type I cells, or directly, for the type II cells.

Visual reflexes

The vestibular system plays a major role in the control of visual reflexes, which allow the fixation of gaze on an object in spite of movements of the head, and require the coordinated movements of the eye, neck and upper trunk. Constant adjustments of the visual axes are achieved chiefly through the medial longitudinal fasciculus, which connects the vestibular nuclear complex with neurones in the oculomotor, trochlear and abducens nuclei and with upper spinal motor neurones (Fig. 37.15; see Fig. 39.12), and also by the vestibulospinal tracts.

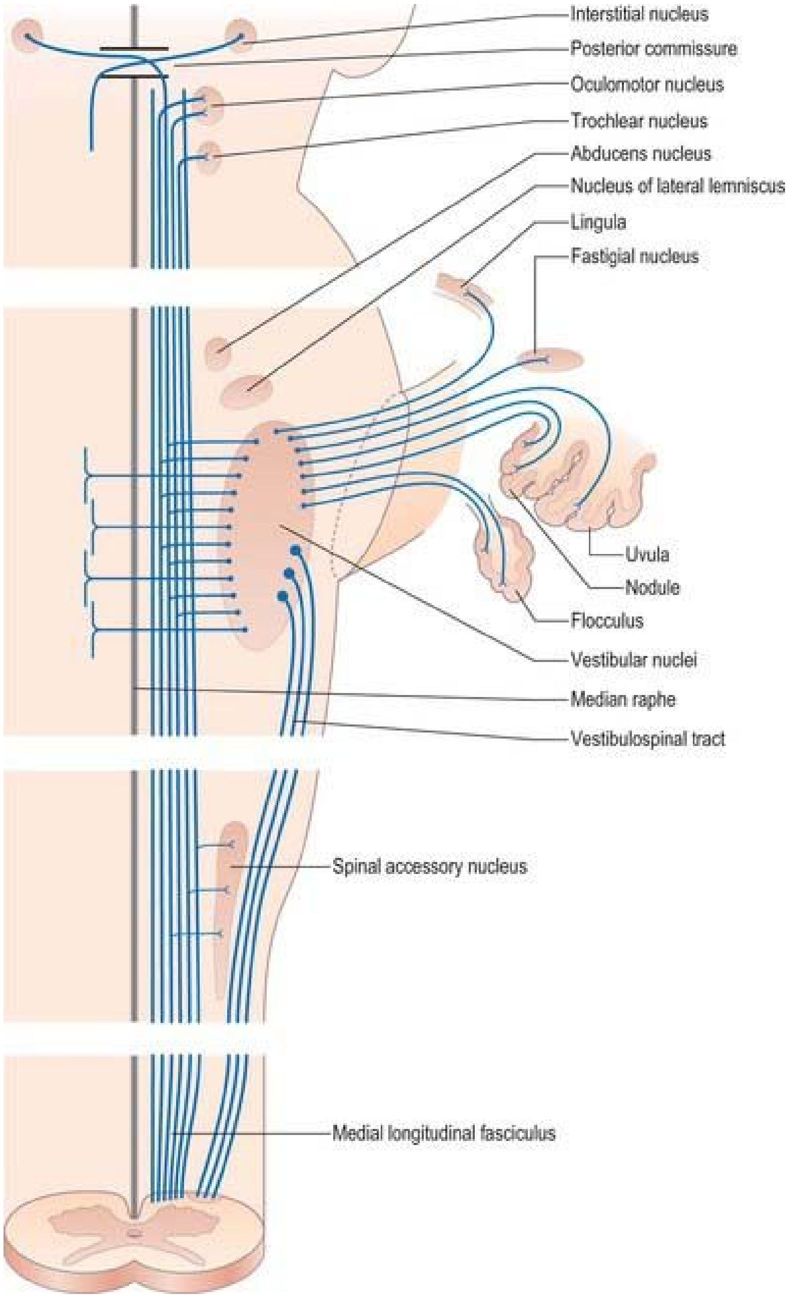
Interstitial nucleus
Posterior commissure
Oculomotor nucleus
Trochlear nucleus
Abducens nucleus
Nucleus of lateral lemniscus
Lingula
Fastigial nucleus
Uvula
Nodule
Flocculus
Vestibular nuclei
Median raphe
Vestibulospinal tract
Spinal accessory nucleus
Medial longitudinal fasciculus

Fig. 37.15 Some of the fibre components of the medial longitudinal fasciculus.

Abnormal activity of the vestibular input or central connections has various effects on these reflexes, e.g. the production of nystagmus. This can be elicited by the caloric test, a clinical test of vestibular function, by syringing the external auditory meatus with water above or below body temperature, a procedure which appears to stimulate the cristae of the lateral semi-circular canal directly. Spontaneous high activity in the afferent fibres of the vestibular nerve is seen in Ménière’s disease, in which those affected experience a range of disturbances including the sensation of dizziness and nausea, the latter reflecting the vestibular input to the vagal reflex pathway.

Cochlear nerve

Intratemporal cochlear nerve

The cochlear nerve connects the organ of Corti to the cochlear and related nuclei of the brain stem. The cochlear nerve lies inferior to the facial nerve throughout the internal acoustic meatus (see above). It becomes intimately associated with the superior and inferior divisions of the vestibular nerve, which are situated in the posterior compartment of the canal, and leaves the internal acoustic meatus in a common fascicle (Fig. 37.12A).

There are approximately 30–40,000 nerve fibres in the human cochlear nerve (for review, see Nadol 1988). Their fibre diameter distribution is unimodal, and ranges from 1 to 11 μm, with a peak at 4–5 μm. Functionally, the nerve contains both afferent and efferent somatic fibres, together with adrenergic postganglionic sympathetic fibres from the cervical sympathetic system.

Afferent cochlear innervation

The afferent fibres are myelinated axons with bipolar cell bodies that lie in the spiral ganglion in the modiolus (Fig. 37.2B; Fig. 37.16). There are two types of ganglion cell: most (90–95%) are large type I cells, the remainder are smaller type II cells (see reviews by Nadol 1988, Eybalin 1993). Type I cells contain a prominent spherical nucleus, abundant ribosomes and many mitochondria; in many mammals (although possibly not in humans) they are surrounded by myelin sheaths. In contrast, type II cells are smaller, always unmyelinated, and have a lobulated nucleus. The cytoplasm of type II cells is enriched with neurofilaments, but has fewer mitochondria and ribosomes than type I cells.

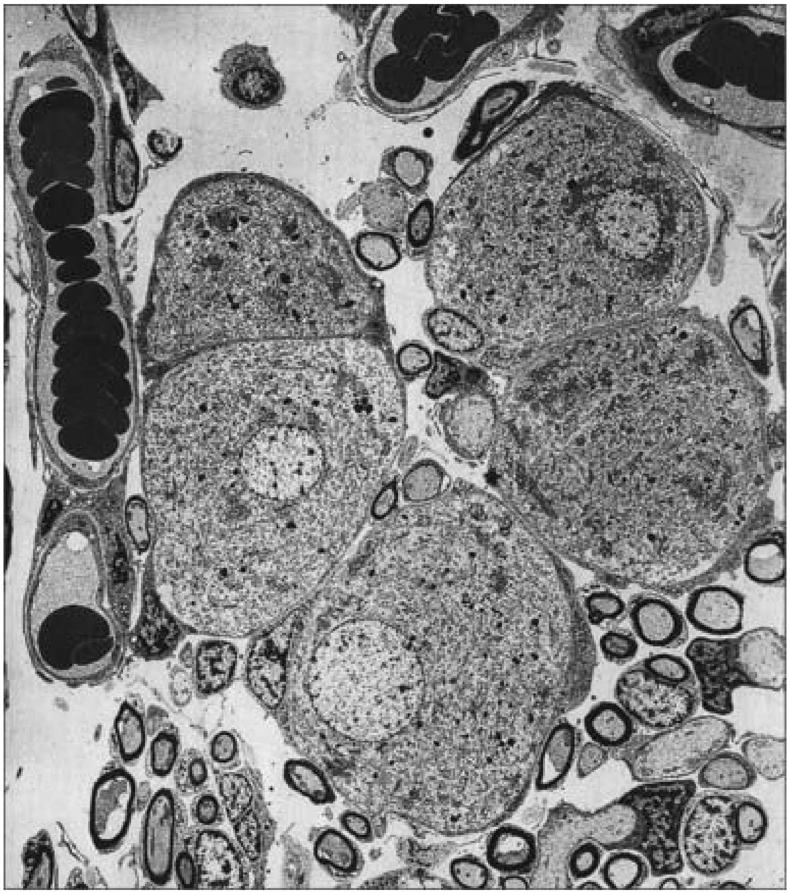

Fig. 37.16 Transmission electron micrograph showing several type II ganglion cells and nerve fibres in a human spiral ganglion. Note the absence of myelin from the surrounding sheaths of the ganglion cells.

(By courtesy of H Felix, M Gleeson and L-G Johnsson, ENT Department, University of Zurich and GKT School of Medicine, London.)

Each inner hair cell is in synaptic contact with the unbranched peripheral processes of approximately 10 type I ganglion cells. The processes of type II ganglion cells diverge within the organ of Corti and innervate more than 10 outer hair cells. The peripheral and central processes of type I ganglion cells are relatively large in diameter and are myelinated, whereas those of type II are smaller and unmyelinated. The peripheral processes of both types of cell radiate from the modiolus into the osseous spiral lamina, where the type I axons lose their myelin sheaths before entering the organ of Corti through the habenula perforata.

Three distinct groupings of afferent fibres have been identified: inner radial, basilar and outer spiral fibres (Fig. 37.17).

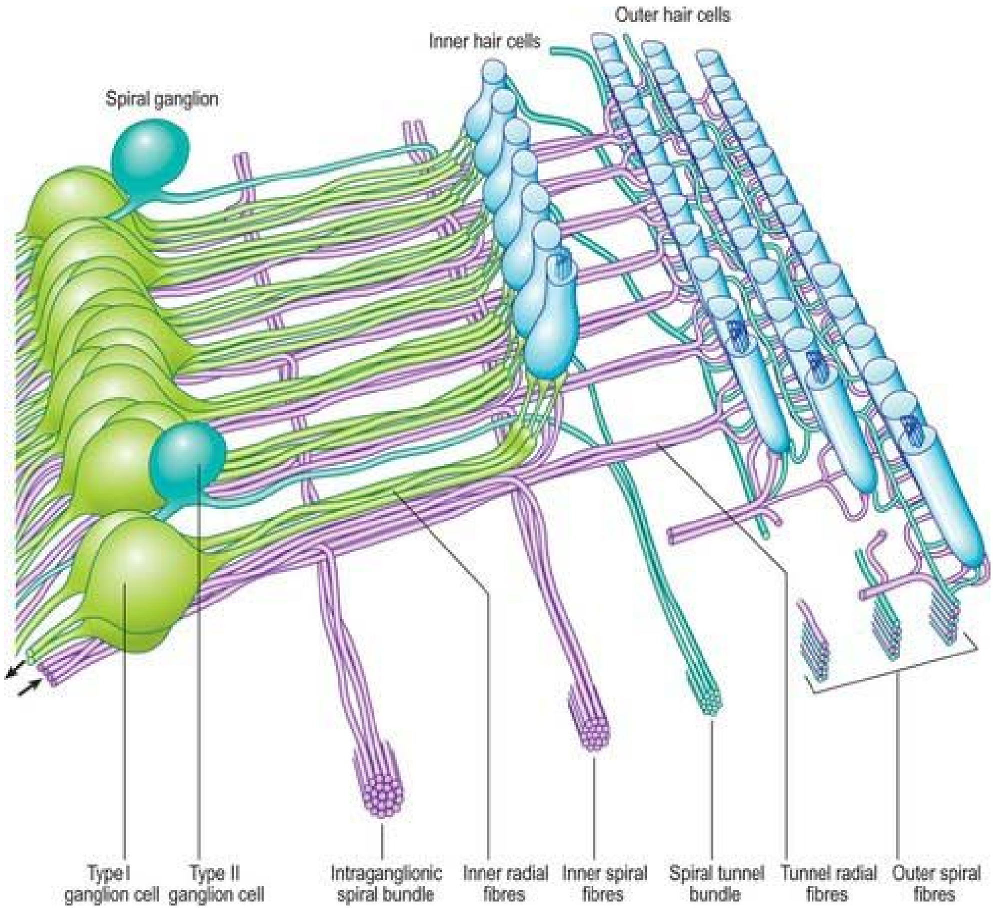
Outer hair cells
Inner hair cells
Spiral ganglion
Type I ganglion cell
Type II ganglion cell
Intraganglionic spiral bundle
Inner radial fibres
Inner spiral fibres
Spiral tunnel bundle
Tunnel radial fibres
Outer spiral fibres

Fig. 37.17 A simplified view of the innervation of the organ of Corti (see text for further details). There is a great contrast between the convergent afferent innervation of the inner hair cells (approximately 10 fibres to each cell) and the divergent supply of the outer hair cells (one afferent fibre to 10 cells).

Inner radial fibres

The inner radial fibre group consists of the majority of afferent fibres. They run directly in a radial direction to the inner hair cells, each of which receives endings from several of these fibres.

Basilar fibres

Basilar fibres are afferent to the outer hair cells and take an independent spiral course, turning towards the cochlear apex near the bases of the inner hair cells. They run for a distance of about five pillar cells before turning radially again and crossing the floor of the tunnel of Corti, often diagonally, to form part of the outer spiral bundle.

Outer spiral bundles

The afferent fibres of the bundles of the outer spiral group course towards the basal part of the cochlea, continually branching off en route to supply several outer hair cells. The outer spiral bundles also contain efferent fibres (see below).

Efferent cochlear fibres

The efferent nerve fibres in the cochlear nerve are derived from the olivocochlear system (see reviews by Warr 1992, Guinan 1996). Within the modiolus, the efferent fibres form the intraganglionic spiral bundle, which may be one or more discrete groups of fibres situated at the periphery of the spiral ganglion (Fig. 37.17). There are two main groups of olivocochlear efferents: lateral and medial. The lateral efferents come from small neurones in and near the lateral superior olivary nucleus and arise mainly, but not exclusively, ipsilaterally. They are organized into inner spiral fibres that run in the inner spiral bundle before terminating on the afferent axons that supply the inner hair cells. The medial efferents originate from larger neurones in the vicinity of the medial superior olivary nucleus, and the majority arise contralaterally. They are myelinated and cross the tunnel of Corti to synapse with the outer hair cells mainly by direct contact with their bases, although a few synapse with the afferent terminals. The efferent innervation of the outer hair cells decreases along the organ of Corti from cochlear base to apex, and from the first (inner) row to the third. The efferents use acetylcholine, γ-aminobutyric acid (GABA), or both as their neurotransmitter. They may also contain other neurotransmitters and neuromodulators.

Activity of the medial efferents inhibits cochlear responses to sound: the strength of the activity grows slowly with increasing sound level. They are believed to modulate the micromechanics of the cochlea by altering the mechanical responses of the outer hair cells thus changing their contribution to frequency selectivity and sensitivity. The lateral efferents related to the inner hair cells also respond to sound. They appear to modify transmission through their postsynaptic action on inner hair cell afferents. The cholinergic fibres may excite the radial fibres, while those containing GABA may inhibit them, although their role is less well understood than that of the medial efferents (see review by Guinan 1996).

Autonomic cochlear innervation

Autonomic nerve endings appear to be entirely sympathetic. Two adrenergic systems have been described within the cochlea: a perivascular plexus derived from the stellate ganglion and a blood vessel-independent system derived from the superior cervical ganglion. Both systems travel with the afferent and efferent cochlear fibres and seem to be restricted to regions away from the organ of Corti. The sympathetic nervous system may cause primary and secondary effects in the cochlea by remotely altering the metabolism of various cell types and by influencing the blood vessels and nerve fibres with which it makes contact.

Anatomy of hearing

Sounds waves entering the external ear are converted into electrical signals in the cochlear nerve by the peripheral auditory system (Fig. 37.18). The axons in the cochlear nerve constitute the auditory component of the vestibulocochlear nerve and terminate in the dorsal and ventral cochlear nuclei: onward connections make up the ascending (central) auditory pathway.

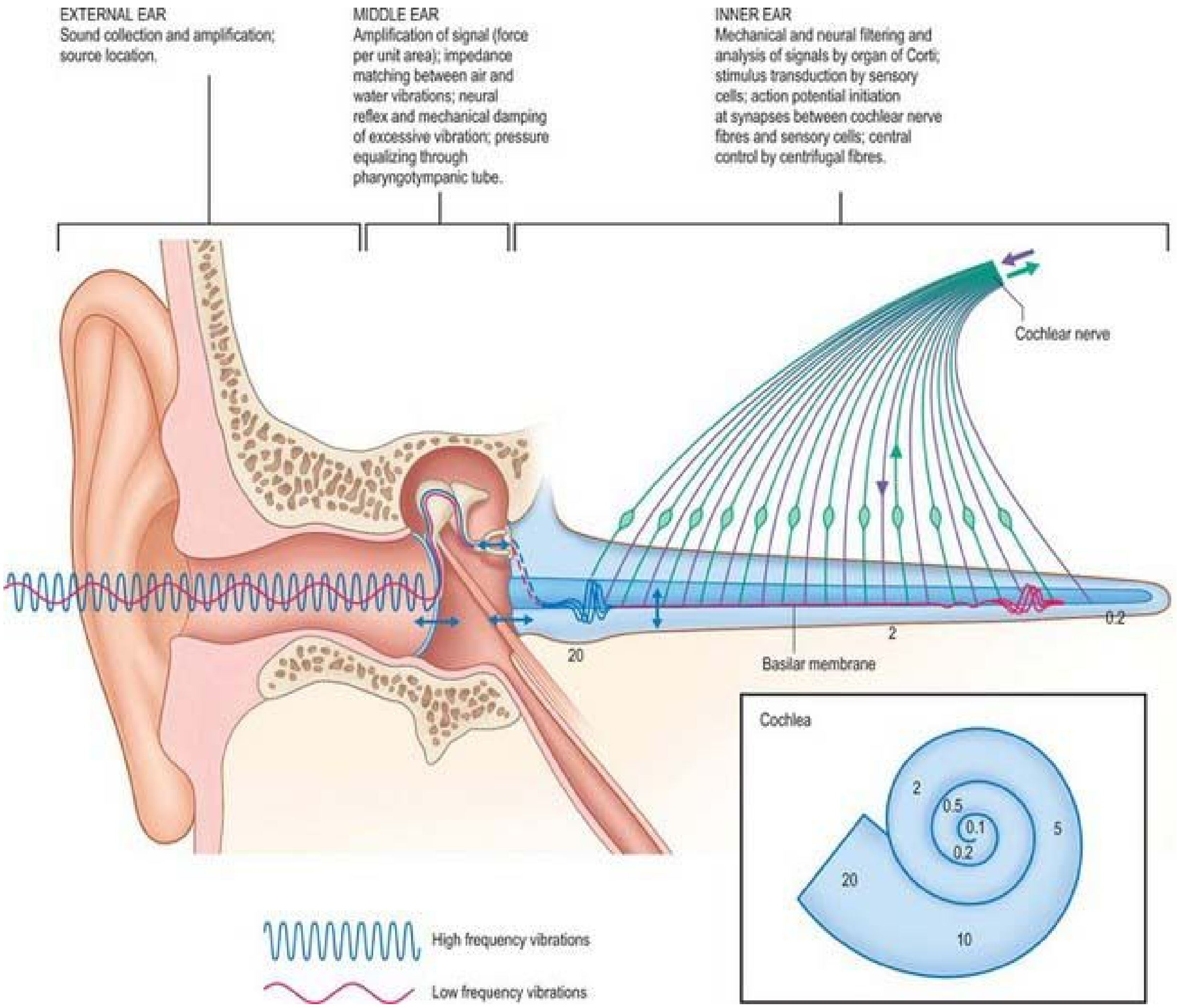
EXTERNAL EAR
Sound collection and amplification; source location.
MIDDLE EAR
Amplification of signal (force per unit area); impedance matching between air and water vibrations; neural reflex and mechanical damping of excessive vibration; pressure equalizing through pharyngotympanic tube.
INNER EAR
Mechanical and neural filtering and analysis of signals by organ of Corti; stimulus transduction by sensory cells; action potential initiation at synapses between cochlear nerve fibres and sensory cells; central control by centrifugal fibres.
Cochlear nerve
20
2
0.2
Basilar membrane
Cochlea
2
0.5
0.1
0.2
5
20
10
High frequency vibrations
Low frequency vibrations

Fig. 37.18 The principal activities of the peripheral auditory apparatus. For clarity, the cochlea is depicted as though it had been uncoiled, but it is normally coiled as in the inset. Different sound frequencies differentially excite different regions of the cochlea, the specific locations being given in kHz from 0.1 to 20 kHz in humans. Note that the frequency map is logarithmic, so that each decade occupies an equivalent distance on the basilar membrane. The components are drawn roughly to scale for the human ear, in which the cochlea is 35 mm in length. The points of maximal stimulation of the basilar membrane by high frequency and low frequency vibrations, together with their transmission pathways through the external and middle ear, are also indicated.

Peripheral auditory system

Vibrations in the air column in the external acoustic meatus cause a comparable set of vibrations in the tympanic membrane and auditory ossicles. The chain of ossicles acts as a lever which increases the force per unit area at the round window by 1.2 times while the reduction in size of the round window compared with the tympanic membrane increases the force per unit area of the oscillating surface a further 17 times. This overcomes the inertia of the cochlear fluids and produces in them pressure waves that are conducted almost instantaneously to all parts of the basilar membrane. The latter varies continuously in width, mass and stiffness from the basal to the apical end of the cochlea. Each part of the basilar membrane vibrates, but only the region tuned to a specific frequency will respond maximally to a pure tone entering the ear. A wave of mechanical motion, the travelling wave, is propagated along the basilar membrane to the position where it responds maximally and then dies away again. With increasing frequency, the locus of maximum amplitude moves progressively from the apical to the basal end of the cochlea. The pattern of vibrations in the basilar membrane thus varies with the intensity and frequency of the acoustic waves reaching the perilymph. Because of the arrangement of the hair cells on the basilar membrane, these oscillations generate a largely transverse shearing force between the outer hair cells and the overlying tectorial membrane (in which the apices of the hair cell stereocilia are embedded). This movement depends on the mechanical properties of the entire organ of Corti, including its cytoskeleton, which stiffens this structure. The inner hair cell stereocilia, which probably do not touch the tectorial membrane although they come very close to it, are likely to be stimulated by local movements of the endolymph. Displacement of the stereociliary bundle of a hair cell activates mechanoelectrical transduction (MET) ion channels near the tips of its stereocilia, and this allows potassium and calcium ions from the endolymph to enter the hair cell (see overviews by Fettiplace 2002, Fettiplace & Hackney 2006). This induces a depolarizing receptor potential and the release of neurotransmitter onto the cochlear afferents at the base of the cell. In this way a specific group of auditory axons is activated at the position of maximal basilar membrane vibration.

The mechanical behaviour of the basilar membrane is responsible for a rather broad discrimination between different frequencies (passive tuning, see overview by Ashmore 2002), but fine frequency discrimination in the cochlea appears to be related to physiological differences between the hair cells. Individual tuning of hair cells may result from differences in shape, stereociliary length, or possibly variations in the molecular composition of sensory membranes, and may have a role in cochlear amplification (active tuning).

The activity of the outer hair cells appears to play an important part in regulating inner hair cell sensitivity at specific frequencies. Outer hair cells can change length when stimulated electrically at frequencies of many thousands of cycles per second. The rapidity of these changes in length indicates a novel type of motile mechanism, which is believed to depend on conformational changes in proteins located in the plasma membrane of the cells (see Fettiplace & Hackney 2006) (Fig. 37.19). When the membrane potential of the outer hair cells changes, they generate forces along their axes. When the mechanoelectrical transduction channels open, they are thought to oppose the viscous forces which tend to damp down the vibration of the cochlear partition, and adjust the mechanics of the organ of Corti on a cycle-by-cycle basis. Alternatively they may alter the mechanics of the partition more slowly under the influence of the efferent pathway.

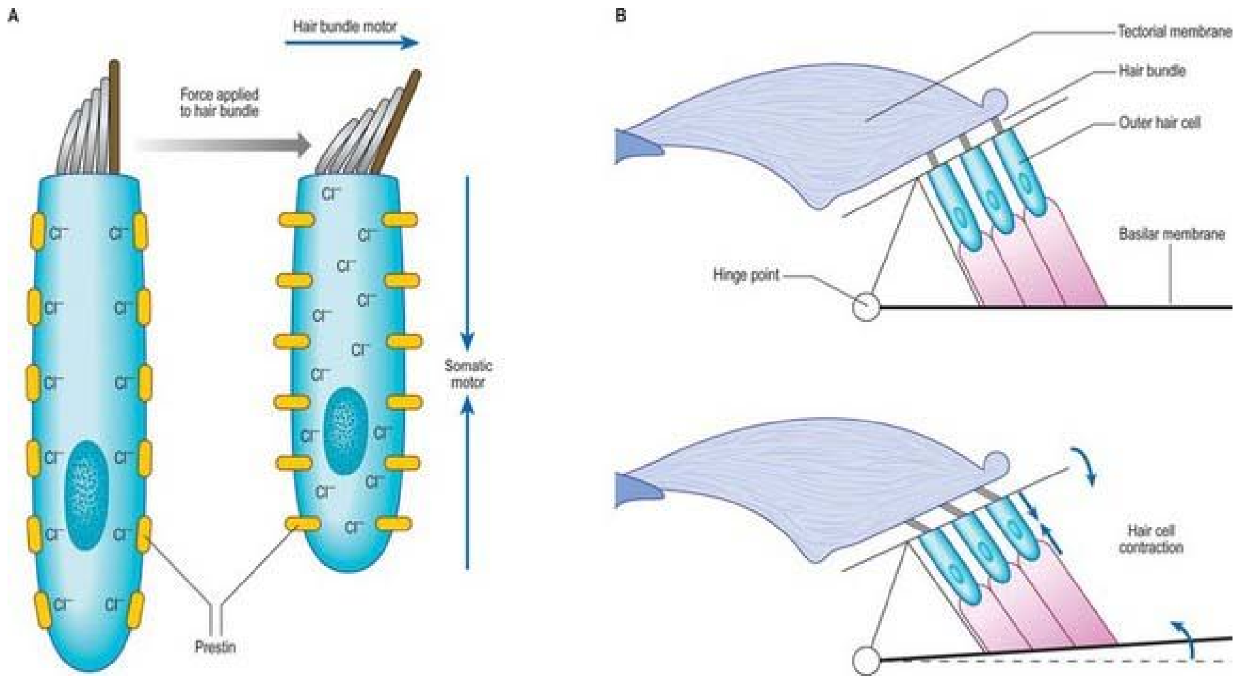
A
Hair bundle motor
Force applied to hair bundle
Cl^-
Somatic motor
Prestin
B
Tectorial membrane
Hair bundle
Outer hair cell
Basilar membrane
Hinge point
Hair cell contraction

Fig. 37.19 The putative motors of outer hair cells. Outer hair cells can generate force, mechanically boosting sound-induced vibrations of the hair bundle and augmenting frequency tuning. Two mechanisms have been advanced to explain this cochlear amplifier: the somatic motor and the hair bundle motor. **A**, In the resting state, Cl^- ions are bound to prestin molecules in the lateral membrane of the hair cell. When force is applied to the hair bundle, the cell is depolarized, the Cl^- ions dissociate and the prestin changes conformation, reducing its area in the plane of the membrane and shortening the hair cell body (the somatic motor). Adaptation of mechanoelectrical transduction (MET) channels, which are activated by bending of the stereocilia at their tapered base, also causes the hair bundle to produce extra force in the direction of the stimulus (the hair bundle motor). The amplitudes of the hair bundle movements have been exaggerated to illustrate the concept. **B**, The effects of the somatic motor (blue arrows) on the organ of Corti mechanics, which leads to downward motion of the reticular lamina (the upper surface of the organ of Corti) and a negative deflection of the hair bundle. This is a negative feedback pathway, as a positive deflection of the hair bundle causes outer hair cell depolarization, cell contraction and opposing motion of the bundle. (See Fettiplace & Hackney 2006.)

At a particular frequency, an increase in the intensity of stimulus is signalled by an increase in the rate of discharge in individual cochlear axons. At greater intensities it is signalled by the number of activated cochlear axons (recruitment).

The respective roles of the two groups of hair cells have been much debated, particularly since differences in their innervation and physiological behaviour have become apparent. Because of their rich afferent supply, inner hair cells are believed to be the major source of auditory signals in the cochlear nerve. Some evidence for this view is based on the finding that animals treated with antibiotics that are specifically toxic to outer hair cells are still able to hear, but their sensitivity and frequency discrimination is impaired.

Some electrical responses of the cochlea can be recorded with extracellular electrodes. The most significant is the endolymphatic potential, a steady potential recordable between the cochlear duct and the scala tympani, which is caused by the different ionic compositions of their fluids. As the resting potential of hair cells is approximately 70 mV (negative inside) and the endolymphatic potential is positive in the cochlear duct, the total transmembrane potential across the apices of hair cells is 150 mV. This is a greater resting potential than is found anywhere else in the body, and provides the driving force for mechanotransduction and for the cochlear amplifier.

Under stimulation by sound, a rapid oscillatory cochlear microphonic potential can be recorded. It matches the frequency of the stimulus and movements of the basilar membrane precisely, and appears to depend on fluctuations in the conductance of hair cell membranes, probably of the outer hair cells. At the same time, an extracellular summating potential develops, a steady direct current shift related to the (intracellular) receptor potentials of the hair cells. Cochlear nerve fibres then begin to respond with action potentials which are also recordable from the cochlea. Intracellular recording of auditory responses from inner hair cells has confirmed that these cells resemble other receptors: their steady receptor potentials are related in size to the amplitude of the acoustic stimulus. At the same time, afferent axons are stimulated by synaptic action at the bases of the inner hair cells. They fire more rapidly as the vibration of the basilar membrane increases in amplitude, up to a threshold that depends on the sensitivity of the specific nerve fibre involved. Each inner hair cell is contacted by axons with response thresholds that range from 0 decibels sound pressure level (dBSPL), the approximate threshold of human hearing, to those which respond to intensities in excess of 100 dBSPL; the loudest sound tolerable is around 120 dBSPL. Each axon responds most sensitively to the frequency represented by its particular cochlear location, its characteristic frequency (Fig. 37.18).

Central auditory pathway

The primary afferents of the auditory pathway arise from cell bodies in the spiral ganglion of the cochlea. The axons travel in the vestibulocochlear nerve, which enters the brain stem at the cerebellopontine angle. Afferent fibres bifurcate, and terminate in the dorsal and ventral cochlear nuclei (Fig. 37.20). The dorsal cochlear nucleus projects via the dorsal acoustic stria to the contralateral inferior colliculus. The ventral cochlear nucleus projects via the trapezoid body or the intermediate acoustic stria to relay centres in either the superior olivary complex, the nuclei of the lateral lemniscus, or the inferior colliculus. The superior olivary complex is dominated by the medial superior olivary nucleus which receives direct input from the ventral cochlear nucleus on both sides, and is involved in localization of sound by measuring the time difference between afferent impulses arriving from the two ears.

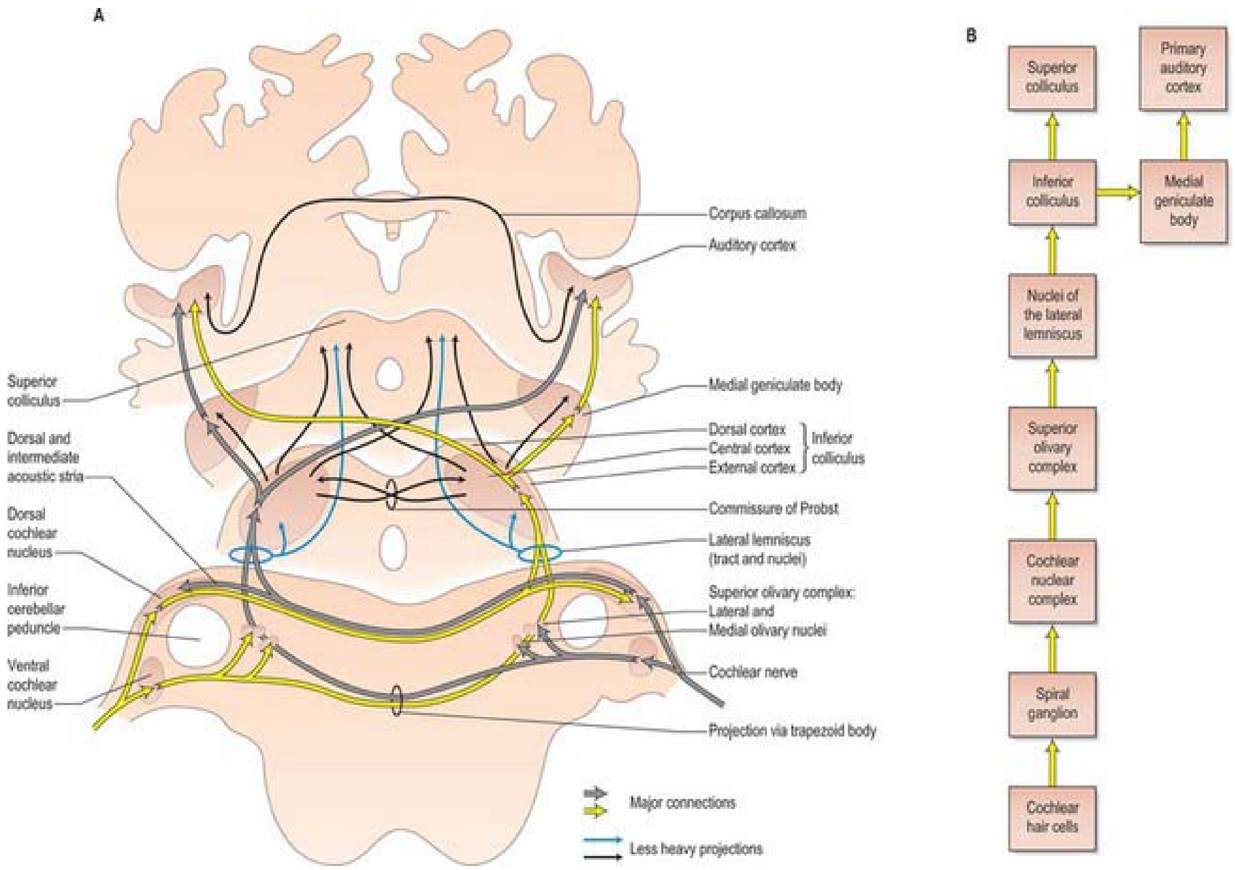
A
Corpus callosum
Auditory cortex
Superior colliculus
Medial geniculate body
Dorsal and intermediate acoustic stria
Dorsal cortex
Central cortex
External cortex
Inferior colliculus
Commissure of Probst
Dorsal cochlear nucleus
Lateral lemniscus (tract and nuclei)
Inferior cerebellar peduncle
Superior olivary complex:
Lateral and
Medial olivary nuclei
Ventral cochlear nucleus
Cochlear nerve
Projection via trapezoid body
Major connections
Less heavy projections
B
Superior colliculus
Primary auditory cortex
Inferior colliculus
Medial geniculate body
Nuclei of the lateral lemniscus
Superior olivary complex
Cochlear nuclear complex
Spiral ganglion
Cochlear hair cells

Fig. 37.20 The main features of the human ascending auditory pathway. **A**, A series of sections showing that ipsilateral and commissural connections occur at most levels in this system. The major connections are shown by the thicker arrows; thinner arrows denote less heavy projections. **B**, The main stations of the auditory pathway.

The inferior colliculus consists of a central nucleus and two cortical areas. The dorsal cortex lies dorsomedially, and the external cortex lies ventromedially. Secondary and tertiary fibres ascend in the lateral lemniscus. They converge in the central nucleus, which projects to the ventral division of the medial geniculate body of the thalamus. The external cortex receives both auditory and somatosensory input. It projects to the medial division of the medial geniculate body, and, together with the central nucleus, also projects to olivocochlear cells in the superior olivary complex and to cells in the cochlear nuclei. The dorsal cortex receives an input from the auditory cortex and projects to the dorsal division of the medial geniculate body (see

Ch. 21). Connections also run from the nucleus of the lateral lemniscus to the deep part of the superior colliculus, to coordinate auditory and visual responses.

The ascending auditory pathway crosses the midline at several points both below and at the level of the inferior colliculus. However, the input to the central nucleus of the inferior colliculus and higher centres has a clear contralateral dominance: during the initial stages of cortical auditory processing, both hemispheres respond most strongly to the contralateral ear. The medial geniculate body is connected reciprocally to the primary auditory cortex, which lies in the posterior half of the superior temporal gyrus and also dives into the lateral sulcus as the transverse temporal gyri (Heschl’s gyri) (see Ch. 23). Secondary areas of the auditory cortex are located in an adjacent belt region, and other regions of auditory association cortex have been described in a parabelt region beyond the secondary cortex.

The corpus callosum, particularly the posterior third of the body, contains auditory interhemispheric fibres that originate from the primary and second auditory cortices. Asymmetries of minicolumn number in primary and association auditory regions have been correlated with axonal fibre numbers in the subregions of the corpus callosum through which they project (Chance et al 2006).

The presence of tonotopic gradients in the primary auditory cortex is well established in animals and in humans. Hemispheric differences for frequency selectivity (i.e. the ability of the cochlea to separate the acoustic frequencies along its length like an acoustic prism) and tonotopic organization have been reported, for example, the right hemisphere appears to be most responsive to acoustic sound features such as pitch, whereas the left hemisphere seems to be more involved in processing temporal dynamics such as the phonological aspects of speech. Morphological asymmetries favouring the left hemisphere in the planum temporale and Heschl’s gyri have been correlated with left hemispheric dominance for language functions, but a direct link between structure and function has not been clearly established: studies often show relative rather than absolute differences in hemispheric specialization for particular attributes.

The transformation of the physical characteristics of sound into ‘auditory objects’ is thought to occur in the transition from primary to secondary auditory cortex. (For a critical perspective on auditory objects, see Griffiths & Warren 2004.)

Deafness

Hearing impairment is the most common disabling sensory defect in humans. Two causes of deafness are usually distinguished: conductive hearing loss and sensorineural hearing loss.

Conductive hearing loss may result from trauma to the external or middle ears, blockage of the external auditory meatus, or disruption of the tympanic membrane (e.g. by intense sounds or extreme pressure changes) (Ch. 36). It may also result from chronic inflammation of the tympanic membrane (e.g. by a cholesteatoma, which may also damage the ossicles); from an infection of the middle ear (otitis media with effusion), which produces a fluid build-up in the normally air-filled middle ear and so impedes the movements of the ossicles; or from otosclerosis, an inappropriate thickening of bone around the footplate of the stapes.

Sensorineural hearing loss is the most prevalent form of hearing impairment. It refers to loss or damage of the sensory hair cells or their innervation. The sensory cells of the inner ear are particularly vulnerable to mechanical trauma produced by high intensity noise and to changes in their physiological environment caused by infection or hypoxia. Changes in their ionic environment rapidly lead to degenerative processes that result in hair cell loss, often by apoptosis, and produce either hearing loss or vestibular dysfunction. These changes can be induced by drugs such as the aminoglycoside antibiotics, some diuretics, and certain anticancer drugs. A decrease in cochlear sensitivity, presbyacusis, almost invariably occurs with age: hair cells at the high frequency end of the cochlea tend to be lost first. At least 60% of hearing loss may have a genetic basis, a significant proportion may be non-syndromic, and most of these genes are inherited in an autosomal recessive mode.

Ménière’s disease is a distressing disorder of the inner ear characterized by episodes of hearing loss, tinnitus and vertigo. Histological examination of an affected ear reveals endolymphatic hydrops (swelling of the endolymphatic spaces), suggesting poor drainage of the endolymph via the endolymphatic sac.

Surgical approaches to the inner ear

The inner ear may be approached surgically from various directions. The promontory that overlies the basal turn of the cochlea and the oval window may be opened via the middle ear (after elevating the tympanic membrane). The lateral semicircular canal may be opened via the aditus (after widening the bony external acoustic meatus and removing the incus). The arcuate eminence may be opened to give access to the anterior semicircular canal via the floor of the middle cranial fossa. The posterior semicircular canal may be opened deep to the mastoid segment of the facial (Fallopian) canal via the mastoid process (after drilling away the overlying air cells). All of these approaches are usually reserved for destructive operations on the labyrinth to treat intractable vertigo.

The round window niche and its membrane may be approached via a posterior tympanotomy. In this procedure, the mastoid air cells are removed to allow access to the bony triangle bounded above by the fossa of incus, superficially by the chorda tympani, and deeply by the descending portion of the facial nerve. This bone is drilled away carefully to expose the facial recess of the tympanic cavity and the round window niche. Using this access, the stimulating electrode of a multichannel intracochlear implant can be passed into the scala tympani of the cochlea so that it lies against the spiral lamina and can stimulate the adjacent fibres of the cochlear nerve.

The endolymphatic sac may be approached after exenteration of the mastoid air cells by elevating the cortical bone of the anterolateral wall of the posterior cranial fossa, anterior to the sigmoid venous sinus and posterior to the posterior semicircular canal (below a line extended from the axis of the lateral semicircular canal). Access to the sac is required in some operations that aim to control vertigo secondary to Ménière’s disease.

The internal acoustic meatus may be approached, at a cost to hearing, by drilling away the entire bony labyrinth via the posterior cranial fossa (after craniectomy in the occipital region and retraction of the cerebellum), or via the middle cranial fossa (after a temporal craniotomy and retraction of the dura of the middle fossa and the temporal lobe). These approaches are usually used to access tumours of the cerebellopontine angle and internal acoustic meatus.

REFERENCES

shmore J. The mechanics of hearing. In: Roberts D, editor. *Signals and Perception: The Fundamentals of Human Sensation*. Basingstoke and New York: Palgrave Macmillan; 2002:3-16.

kelsson A. Comparative anatomy of cochlear blood vessels. *Am J Otolaryngol*. 1988;9:278-290.

anks RH, Curthoys IS, Markham CH. Planar relationships of the semicircular canals in man. *Acta Otolaryngol*. 1975;80:185-196.

ridger MW, Farkashidy J. The distribution of neuroglia and Schwann cells in the 8th nerve of man. *J Laryngol Otol*. 1980;94:1353-1362.

hance SA, Casanova MF, Switala AE, Crow TJ. Minicolumnar structure in Heschl’s gyrus and planum temporale: asymmetries in relation to sex and callosal fiber number. *Neuroscience*. 2006;143:1041-1050.

urthoys IS, Blanks RH, Markham CH. Semicircular canal radii of curvature (R) in cat, guinea pig and man. *J Morphol*. 1977;115:1-15.

ybalin M. Neurotransmitters and neuromodulators of the mammalian cochlea. *Physiol Rev*. 1993;73:309-373.

elix H, Hoffman V, Wright A, Gleeson MJ. Ultrastructural findings on human Scarpa’s ganglion. *Acta Otolaryngol Suppl*. 1987;436:85-92.

ettiplace R. The transformation of sound stimuli into electrical signals. In: Roberts D, editor. *Signals and Perception: The Fundamentals of Human Sensation*. Basingstoke and New York: Palgrave Macmillan; 2002:17-28.

ttiplace R, Hackney CM. The sensory and motor roles of auditory hair cells. *Nat Rev Neurosci*. 2006;7:19-29.

Describes recently identified proteins involved in the sensory and motor functions of auditory hair cells and presents evidence for each force generator..

rness DN. The vestibular system. In: Roberts D, editor. *Signals and Perception: The Fundamentals of Human Sensation*. Basingstoke and New York: Palgrave Macmillan; 2002:77-90.

iffiths TD, Warren JD. What is an auditory object? *Nat Rev Neurosci*. 2004;5:887-892.

inan JJr. Physiology of olivocochlear efferents. In: Dallos P, Popper AN, Fay RR. *The Cochlea*. New York: Springer Verlag; 1996:435-502.

Comprehensive description of the efferent innervation of the cochlea and its function..

ifer J, Böhnke F, Adunka O, Arnold W. Representation of acoustic signals in the human cochlea in presence of a cochlear implant electrode. *Hearing Res*. 2006;221:36-43.

dol JB. Comparative anatomy of the cochlea and auditory nerve in mammals. *Hear Res*. 1988;34:253-266.

rtel D, Fay RR, Popper AN, editors. Integrative Functions in the Mammalian Auditory Pathway. Springer Handbook of Auditory Research, vol. 15. New York: Springer, 2002.

y B, Roy TS, Wadhwa S, Roy KK. Development of the human fetal cochlear nerve. *Hearing Res*. 2005;202:74-86.

epherd RK, Colreavy MP. Surface microstructure of the perilymphatic space. Implications for cochlear implants and cell- or drug-based therapies. *Arch Otolaryngol Head Neck Surg*. 2004;130:518-523.

oor F, Zonneveld F. Comparative review of the human bony labyrinth. *Am J Phys Anthropol Suppl*. 1998;27:211-251.

angemann P, Schacht J. Homeostatic mechanisms in the cochlea. In: Dallos P, Popper AN, Fay RR. *The Cochlea*. New York: Springer Verlag; 1996:130-

135.

Reviews what is known about inner ear fluids (perilymph and endolymph), how they are produced and their possible functional significance..

arr WB. Organization of olivocochlear efferent systems in mammals. In: Webster DB, Popper AN, Fay RR. *Mammalian Auditory Pathway: Neuroanatomy*. New York: Springer Verlag; 1992:410-448.

CHAPTER 38

Development of the ear

INNER EAR

The production of a precisely positioned and functionally well tuned inner ear depends on genetic patterning and a cascade of transcription signals expressed by numerous tissues, including the developing inner ear and its surrounding periotic mesenchyme, the adjacent hindbrain, neural crest and notochord (e.g. Liu et al 2003).

The first signs of inner ear development are visible shortly after those associated with the developing eyes. Two patches of ectodermal thickening, the otic placodes, appear lateral to the hindbrain at stage 9. Each otic placode invaginates as an otic pit, adjacent to rhombomeres 5 and 6 of the hindbrain and dorsal to the second pharyngeal cleft. The pit becomes pinched off from the surface ectoderm to form a simple epithelial sac, the otocyst (auditory or otic vesicle), during stage 12 (Fig. 38.1).

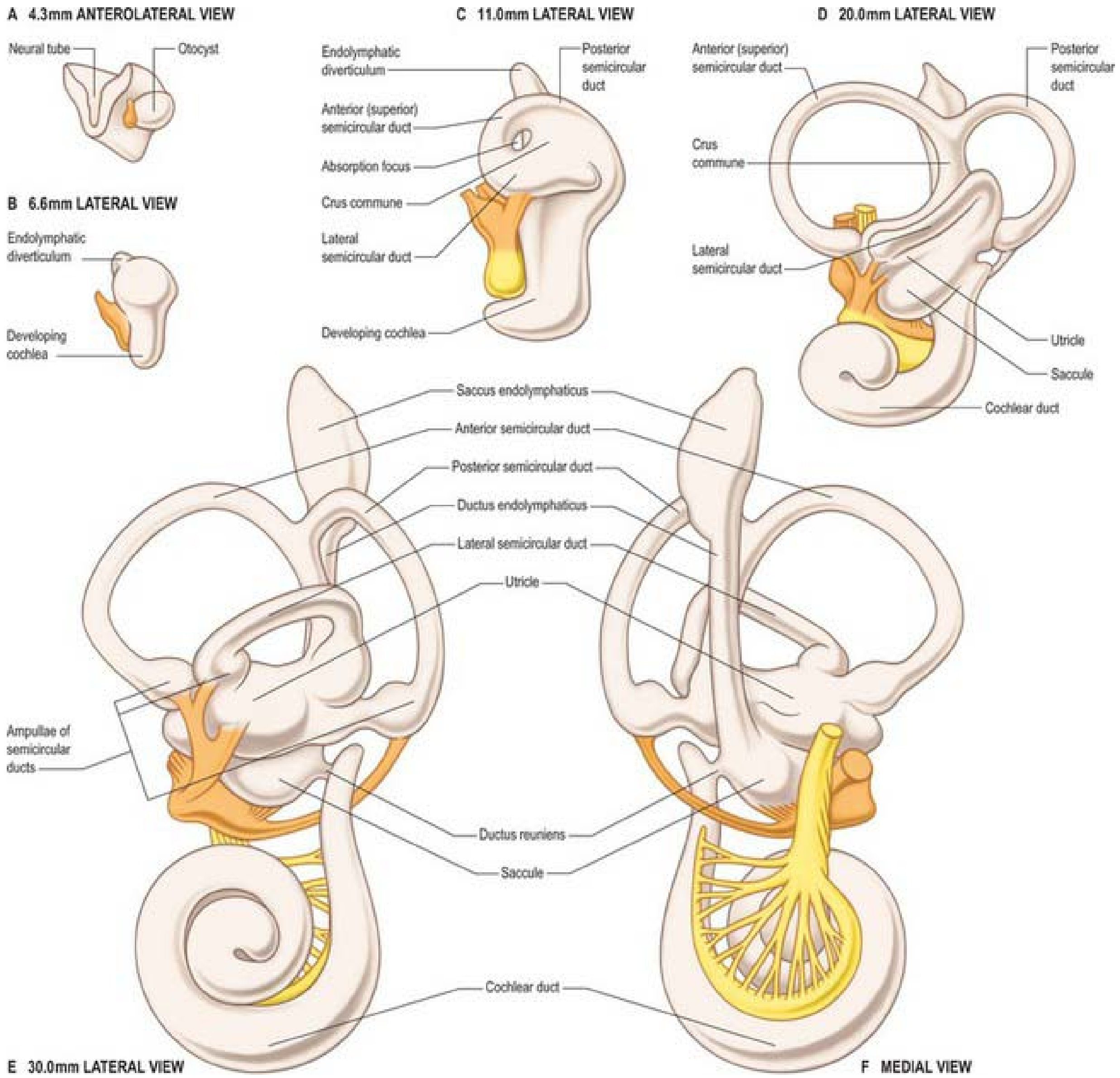
A 4.3mm ANTEROLATERAL VIEW
Neural tube
Otocyst
B 6.6mm LATERAL VIEW
Endolymphatic diverticulum
Developing cochlea
C 11.0mm LATERAL VIEW
Endolymphatic diverticulum
Posterior semicircular duct
Anterior (superior) semicircular duct
Absorption focus
Crus commune
Lateral semicircular duct
Developing cochlea
D 20.0mm LATERAL VIEW
Anterior (superior) semicircular duct
Posterior semicircular duct
Crus commune
Lateral semicircular duct
Utricle
Saccule
Cochlear duct
Saccus endolymphaticus
Anterior semicircular duct
Posterior semicircular duct
Ductus endolymphaticus
Lateral semicircular duct
Utricle
Ampullae of semicircular ducts
Ductus reuniens
Saccule
Cochlear duct
E 30.0mm LATERAL VIEW
F MEDIAL VIEW

Fig. 38.1 **A–F**, The stages in the development of the membranous labyrinth from the otocyst, at the embryonic stages and aspects indicated. Note the relationship of the vestibular (orange) and cochlear (yellow) parts of the vestibulocochlear nerve.

The first morphological differentiation of the otic vesicle is visible during stage 14 (approximately 33 days) and presages the three major subdivisions of the inner ear, i.e. the endolymphatic sac and duct, the dorsal utricular portion that later gives rise to the semicircular canals, and the ventral saccular portion that later gives rise to the cochlea. At this time the otocyst is piriform in shape. A tubular diverticulum develops from its medial rim and differentiates into the endolymphatic duct and sac. The sac communicates via the endolymphatic duct with the remainder of the otocyst which is placed laterally and can be regarded as the utriculosaccular chamber. At the same time, two plate-like diverticulae, one vertical and one horizontal, emerge from the dorsal part of the utriculosaccular chamber. The opposing epithelia in the central region of each outgrowth coalesce to form a fusion plate, and the central part of this plate is eventually resorbed, producing a tubular canal. The vertical plate gives rise to the anterior and posterior semicircular canals that share a common crural attachment to the utriculosaccular chamber, and the horizontal plate gives rise to the horizontal or lateral semicircular canal. A medially directed evagination, the cochlear anlagen, is evident in the ventral part of the utriculosaccular chamber in a 7–9 mm (approximately 35 days) embryo. The proximal region of the cochlear duct continues to increase in length and its distal region becomes progressively more coiled. When the duct has achieved its final length and spiral configuration, its proximal part becomes constricted, forming the ductus reuniens.

The central part of the utriculosaccular chamber now represents the membranous vestibule, which becomes divided into a small ventral saccule and a larger dorsal utricle. This is achieved mainly by horizontal infolding that extends from the lateral wall of the chamber towards the opening of the endolymphatic duct until only a narrow utriculosaccular duct remains between the saccule and utricle. The duct becomes acutely bent on itself: its apex is continuous with the ductus endolymphaticus. During this period the membranous labyrinth rotates so that its long axis, which was originally vertical, becomes more or less horizontal.

Cells derived from the otocyst differentiate into the bipolar neurones that populate the vestibular and cochlear ganglia; sustentacular cells; the unique endolymph-producing epithelia of the stria vascularis; the absorbing epithelia of the endolymphatic sac; the general epithelial lining of the membranous labyrinth; specialized cells in the six sensory patches of the inner ear (crista ampullaris of the three semicircular canals, maculae of the utricle and saccule, organ of Corti in the cochlea). Each of the sensory patches consists of mechanosensory hair cells and non-sensory supporting cells arranged into a mosaic pattern. The only cells in the mature inner ear that are not of otocyst origin are melanocytes in the stria vascularis, which are derived from the neural crest. The very different morphologies of the mature cristae, maculae and organ of Corti reflect the differential expression of multiple genes during their development.

At the same time that these changes are taking place within the membranous labyrinth, the developing inner ear also recruits surrounding mesenchymal cells to coalesce around it to form an encasing cartilaginous otic capsule. This later ossifies to form all of the bony labyrinth of the internal ear except the modiolus and osseous spiral lamina, which ossify directly from connective tissue. The cartilaginous capsule is initially incomplete and the cochlear, vestibular and facial ganglia are temporarily exposed in the gap between its canalicular and cochlear parts. They subsequently become covered by an outgrowth of cartilage, in which the facial nerve becomes enclosed.

Perilymphatic spaces develop in the embryonic connective tissue between the cartilaginous capsule and the epithelial wall of the membranous labyrinth. The rudiment of the periotic cistern or vestibular perilymphatic space can be seen in the reticulum between the saccule and fenestra vestibuli in an 11–14 mm (approximately 42 days) embryo. The scala tympani develops opposite the fenestra cochleae and is followed later by the scala vestibuli. The two scalae gradually extend along each side of the ductus cochlearis; when they reach the tip of the coiled ductus, a communication, the helicotrema, opens between them.

The rudiment of the eighth cranial nerve appears in the 4–6 mm (approximately 28 days) embryo as the vestibulocochlear (statoacoustic) ganglion. It lies between the otocyst and the hindbrain and is initially temporarily fused with the ganglion of the facial nerve. The cells of the vestibulocochlear ganglion are neuroblasts whose fate is already specified in the otic placode ectoderm. They delaminate from the anteroventral region of the otocyst and proliferate and migrate to the site of the presumptive ganglion where they coalesce. They differentiate into mature bipolar sensory neurones and segregate into vestibular and spiral ganglia, each associated with the corresponding division of the eighth cranial nerve. Ganglionic neurones are unusual in that they are exclusively placodal in origin (unlike neurones in most cranial ganglia which have a dual placodal and neural crest origin), and many of their somata become enveloped in thin myelin sheaths. Their peripheral processes collectively provide the afferent innervation of the labyrinthine hair cells, relaying balance and auditory information. The olivocochlear bundle, an outgrowth of axons from neurones in the superior olivary complexes in the pons, accompanies the axons of the developing eighth cranial nerve: these axons provide the inner ear with an efferent innervation, mainly to the outer hair cells in the organ of Corti, where they are associated with modulation of hearing.

MIDDLE EAR (TYMPANIC CAVITY) AND PHARYNGOTYMPANIC (AUDITORY) TUBE

All the components of the outer and middle ears develop from the first and second pharyngeal arches. The pharyngotympanic tube and tympanic cavity are lateral extensions of the early pharynx (see Fig. 35.4). They become visible in a 4–6 mm (approximately 28 days) embryo as a hollow, the tubotympanic recess, lying between the first and second pharyngeal arches, with a floor which consists of the second arch and its limiting pouches. The forward growth of the third pharyngeal arch causes the proximal part of the recess to remain narrow, forming the pharyngotympanic tube region, and also excludes the inner part of the second arch from this portion of the floor. The more lateral part of the recess eventually comes in contact with the first pharyngeal cleft and widens and develops into the tympanic cavity; its floor later forms the lateral wall of the tympanic cavity up to approximately the level at which the chorda tympani branches off from the facial nerve. The lateral wall of the tympanic cavity contains first and second arch elements. The first arch territory is limited to that part in front of the anterior process of the malleus, and the second arch forms the outer wall behind this and also turns on to the posterior wall to include the tympanohyal region.

The tubotympanic recess at first lies inferolateral to the cartilaginous otic capsule; this spatial relationship alters as the capsule enlarges and the tympanic cavity becomes anterolateral. A cartilaginous process grows from the lateral part of the capsule to form the tegmen tympani. It curves caudally to form the lateral wall of the pharyngotympanic tube, incorporating the tympanic cavity and the proximal part of the pharyngotympanic tube into the petrous region of the temporal bone. The mastoid antrum appears as a dorsal expansion of the tympanic cavity during the sixth to seventh month.

The middle ear ossicles are of neural crest origin, i.e. crest cells that have migrated from rhombomeres 1–4 into the mesenchyme of the first and second pharyngeal arches. The malleus develops from the dorsal end of the ventral mandibular (Meckel’s) cartilage of the first arch. The incus develops from the dorsal cartilage of the first arch which is probably homologous to the quadrate bone of birds and reptiles. The origin of the stapes in humans remains controversial. It is thought to be derived mainly from an anlage situated in the cranial end of the cartilage of the second pharyngeal arch, initially as a ring (anulus stapes) that encircles the small stapedial artery (for a recent analysis of the development of the stapes, consult Rodriguez-Vazquez 2005). The primordium of the stapedius muscle appears close to the artery and facial nerve in a 13–17 mm (approximately 48 days) embryo, and tensor tympani starts to appear near the extremity of the tubotympanic recess at almost the same time. At first the ossicles are embedded in the mesenchymal roof of the tympanic cavity, later they become covered by the mucosa of the middle ear as the tympanic cavity fills with air after birth. Further postnatal developmental changes contribute to the functional maturation of the middle ear.

EXTERNAL EAR

The external acoustic meatus develops from the dorsal end of the first pharyngeal (hyomandibular) cleft (see Fig. 35.4). Close to its dorsal extremity this groove extends inwards as a funnel-shaped primary meatus from which the entire cartilaginous part of the meatus, and a small area of its roof, are developed. A solid epidermal plug extends inwards from the tube along the floor of the tubotympanic recess. The cells in the centre of the plug subsequently degenerate to produce the inner part of the meatus (secondary meatus). The epidermal stratum of the tympanic membrane is formed from the deepest ectodermal cells of the epidermal plug, and the fibrous stratum is formed from the mesenchyme between the meatal plate and the endodermal floor of the tubotympanic recess.

The development of the auricle is initiated by the appearance of six tissue elevations, the auricular hillocks, which form round the margins of the dorsal portion of the first pharyngeal cleft. Of the six, three are on the caudal edge of the first pharyngeal (mandibular) arch and three on the cranial edge of the second pharyngeal (hyoid) arch. The hillocks appear from stage 15; before then, only the most ventral hillock on the mandibular arch, which subsequently forms the tragus, can be identified. The rest of the auricle is formed in the mesenchyme of the hyoid arch which extends forwards round the dorsal end of the remains of the first pharyngeal cleft, forming a keel-like elevation which is the forerunner of the helix. The contribution made by the mandibular arch to the auricle is greatest at the end of the second month, thereafter this contribution becomes relatively reduced as growth continues, until eventually the area of skin supplied by the mandibular nerve extends little above the tragus. The lobule is the last part of the auricle to develop.

Common congenital deformities of the auricle are described in Chapter 36.

REFERENCES

u W, Oh SH, Kang Yk Y, Li G, Doan TM, Little M, Li L, Ahn K, Crenshaw EB, Frenz DA. Bone morphogenetic protein 4 (BMP4): a regulator of capsule chondrogenesis in the developing mouse inner ear. *Develop Dynamics*. 2003;226:427-438.

odriguez-Vazquez JF. Development of the stapes and associated structures in human embryos. *J Anat*. 2005;207:165-173.

CHAPTER 39

The orbit and accessory visual apparatus

BONY ORBIT

The bony orbits are skeletal cavities located on either side of the root of the nose. They house the eyes, the paired peripheral organs of vision. The walls of each orbit protect the eye from injury, provide points of attachment for six extraocular muscles which allow the accurate positioning of the visual axis, and determine the spatial relationship between the two eyes, which is essential for both binocular vision and conjugate eye movements.

Each cavity approximates to a quadrilateral pyramid with its base at the orbital opening, narrowing to its apex along a posteromedially directed axis. Each orbit has a roof, floor, medial and lateral walls. The medial walls lie approximately 25 mm apart in adults and are nearly parallel. The angle between the medial and lateral walls is about 45°. The compromise between protection and ensuring a good field of view dictates that each eyeball is located anteriorly within the orbit. The eyeball thus occupies only one fifth of the volume of the orbit (Fig. 39.1): the remainder of the cavity is filled with vessels and nerves that are contained within and supported by orbital fat and connective tissue. In brief, the orbit also contains the extraocular muscles; the optic, oculomotor, trochlear and abducent nerves, and branches of the ophthalmic and maxillary divisions of the trigeminal nerve; the ciliary parasympathetic ganglion; the ophthalmic vessels; the nasolacrimal apparatus.

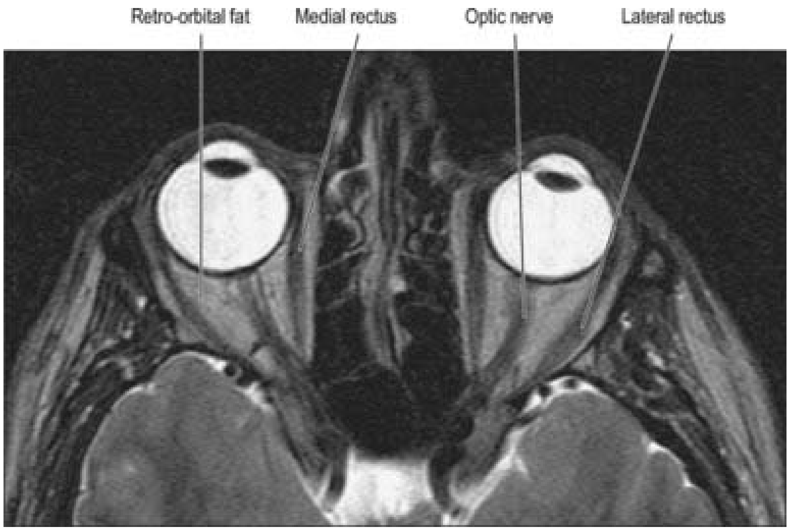

Fig. 39.1 T2-weighted axial MRI scan though the mid-orbit.

(By courtesy of Dr Timothy Beale FRCR, Royal National Throat Nose and Ear Hospital, London.)

Roof

The roof of the orbit is formed principally by the thin orbital plate of the frontal bone (Fig. 39.2). It is gently concave on its orbital aspect, which separates the orbital contents and the brain in the anterior cranial fossa. Anteromedially it contains the frontal sinus and displays a small trochlear fovea, sometimes surmounted by a small spine, where the cartilaginous trochlea (pulley) for superior oblique is attached. Anterolaterally there is a shallow lacrimal fossa which houses the orbital part of the lacrimal gland. The roof slopes significantly towards the apex, joining the lesser wing of the sphenoid, which completes the roof. The optic canal lies between the roots of the lesser wing, and is bounded medially by the body of the sphenoid.

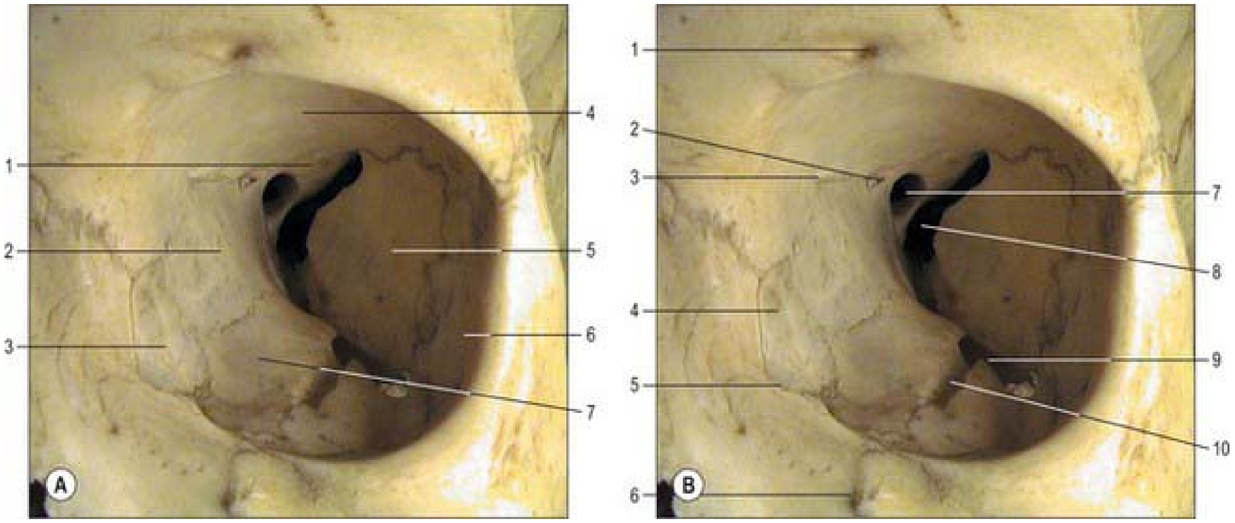

Fig. 39.2 Anterior view of the left orbit indicating the bones forming the walls (**A**) and the principal apertures (**B**). **A**, **1**. Lesser wing of sphenoid. **2**. Orbital plate of ethmoid. **3**. Lacrimal bone. **4**. Orbital plate of frontal bone. **5**. Greater wing of sphenoid. **6**. Zygomatic. **7**. Orbital plate of maxilla. **B**, **1**. Supraorbital foramen. **2**. Posterior ethmoidal foramen. **3**. Anterior ethmoidal foramen. **4**. Lacrimal fossa. **5**. (Canal for) Nasolacrimal duct. **6**. Infraorbital foramen. **7**. Optic canal. **8**. Superior orbital fissure. **9**. Inferior orbital fissure. **10**. Infraorbital groove.

Medial wall

The medial wall of the orbit is formed principally by the orbital plate (lamina papyracea) of the ethmoid bone (Fig. 39.2). This paper thin, rectangular plate covers the middle and posterior ethmoidal air cells, providing a route by which infection can spread into the orbit (see Ch. 32). The ethmoid articulates with the medial edge of the orbital plate of the frontal bone at a suture which is interrupted by anterior and posterior ethmoidal foramina. Posteriorly, it articulates with the body of the sphenoid, which forms the medial wall of the orbit to its apex. The lacrimal bone lies anterior to the ethmoid: it contains a fossa for the nasolacrimal sac that is limited in front by the anterior lacrimal crest on the frontal process of the maxilla and behind by the posterior lacrimal crest of the lacrimal bone (to which the lacrimal part of orbicularis oculi and lacrimal fascia are attached). A descending process of the lacrimal bone at the lower end of the posterior lacrimal crest contributes to the formation of the upper part of the nasolacrimal canal, which is completed by the maxilla (Fig. 39.3).

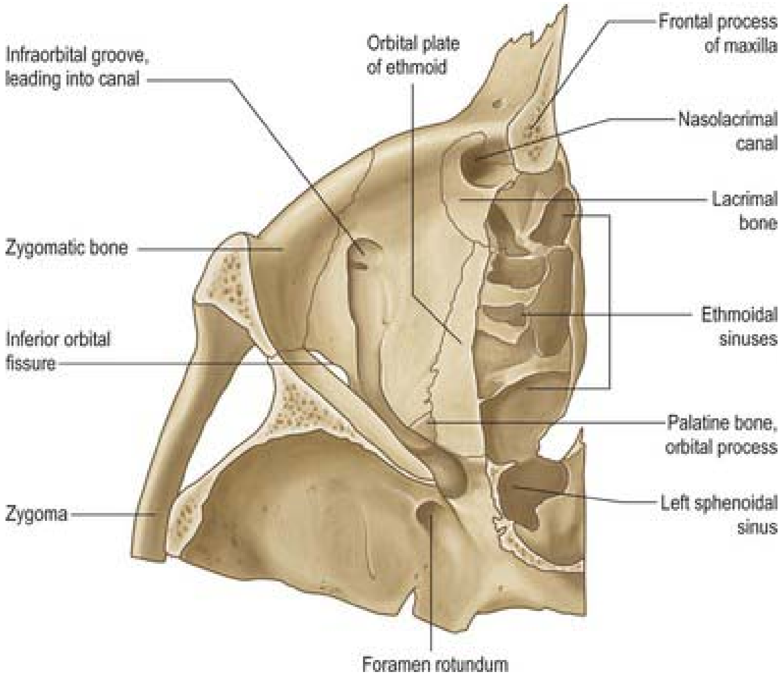
Infraorbital groove, leading into canal
Orbital plate of ethmoid
Frontal process of maxilla
Nasolacrimal canal
Lacrimal bone
Zygomatic bone
Ethmoidal sinuses
Inferior orbital fissure
Palatine bone, orbital process
Zygoma
Left sphenoidal sinus
Foramen rotundum

Fig. 39.3 Horizontal section through the left orbit and nasal cavity viewed from above.

Floor

The floor of the orbit is mostly formed by the orbital plate of the maxilla which articulates with the zygomatic bone anterolaterally and the small triangular orbital process of the palatine bone posteromedially (Fig. 39.3). The floor is thin and largely roofs the maxillary sinus. Not quite horizontal, it ascends a little laterally. Anteriorly it curves into the lateral wall, and posteriorly it is separated from the lateral wall by the inferior orbital fissure, which connects the orbit posteriorly to the pterygopalatine fossa, and more anteriorly to the infratemporal fossa. The medial lip is notched by the infraorbital groove. The latter passes forwards and sinks into the floor to become the infraorbital canal, which opens on the face at the infraorbital foramen: the infraorbital groove, canal and foramen contain the infraorbital nerve and vessels. Proportionally more orbital fractures involve the floor, particularly in the region of the infraorbital groove. The classic ‘blowout fracture’ leaves the orbital rim intact and typically entraps soft tissue structures, leading to diplopia, impaired ocular motility and enophthalmos; infra-orbital nerve involvement leads to ipsilateral sensory disturbance of the skin of the mid face.

Lateral wall

The lateral wall of the orbit is formed by the orbital surface of the greater wing of the sphenoid posteriorly and the frontal process of the zygomatic bone anteriorly: the bones meet at the sphenozygomatic suture (Fig. 39.2). The zygomatic surface contains the openings of minute canals for the zygomaticofacial and zygomaticotemporal nerves, the former near the junction of the floor and lateral wall, the latter at a slightly higher level, sometimes near the suture. The orbital tubercle, to which the lateral palpebral ligament, the check ligament of lateral rectus and the aponeurosis of levator palpebrae are all attached, lies just inside the midpoint of the lateral orbital margin. The lateral wall is the thickest wall of the orbit, especially posteriorly where it separates the orbit from the middle cranial fossa. Anteriorly the lateral wall separates the orbit and the infratemporal fossa. The lateral wall and roof are continuous anteriorly but are separated posteriorly by the superior orbital fissure, which lies between the greater wing (below) and lesser wing (above) of the sphenoid, and communicates with the middle cranial fossa. The fissure tapers laterally but widens at its medial end, its long axis descending posteromedially. Where the fissure begins to widen, its inferolateral edge shows a projection, often a spine, for the lateral attachment of the common tendinous ring. An infraorbital sulcus which runs from the superolateral end of the superior orbital fissure towards the orbital floor is sometimes associated with an anastomosis between the middle meningeal and infraorbital arteries.

ORBITAL FISSURES AND FORAMINA

Optic canal

The lesser wing of the sphenoid is connected to the body of the sphenoid by a thin, flat anterior root and a thick, triangular posterior root. The optic canal lies between these roots (Fig. 39.2) and connects the orbit to the middle cranial fossa, transmitting the optic nerve and its meningeal sheaths, and the ophthalmic artery. The common tendinous ring, which gives origin to the four recti, is attached to the bone near the superior, medial and lower margins of the orbital opening of the canal.

Superior orbital fissure

The superior orbital fissure is the gap between the greater and lesser wings of the sphenoid, bounded medially by the body of the sphenoid, and closed at its anterior extremity by the frontal bone (Fig. 39.2). It connects the cranial cavity with the orbit and transmits the oculomotor, trochlear and abducens nerves, branches of the ophthalmic nerve and the ophthalmic veins.

Inferior orbital fissure

The inferior orbital fissure is bounded above by the greater wing of the sphenoid, below by the maxilla and the orbital process of the palatine bone, and laterally by the zygomatic bone (Fig. 39.2). The maxilla and sphenoid often meet at the anterior end of the fissure, excluding the zygomatic bone. The inferior orbital fissure connects the orbit with the pterygopalatine and infratemporal fossae and transmits the infraorbital and zygomatic branches of the maxillary nerve and accompanying vessels, orbital rami from the pterygopalatine ganglion and a connection between the inferior ophthalmic vein and pterygoid venous plexus. A small maxillary depression may mark the attachment of inferior oblique anteromedially, lateral to the lacrimal hamulus.

Ethmoidal foramina

The anterior and posterior ethmoidal foramina usually lie in the frontoethmoidal suture (Fig. 39.2). The posterior foramen may be absent, and occasionally there is a middle ethmoidal foramen. The foramina open into canals which transmit their vessels and nerves into the ethmoidal sinuses, anterior cranial fossa and nasal cavity.

COMMON TENDINOUS RING

The common tendinous ring is a fibrous ring which surrounds the optic canal and part of the superior orbital fissure at the apex of the orbit, and gives origin to the four recti (Fig. 39.4). The optic nerve and ophthalmic artery enter the orbit via the optic canal, and so lie within the common tendinous ring. The superior and inferior divisions of the oculomotor nerve, the nasociliary branch of the ophthalmic nerve, and the abducens nerve, also enter the orbit within the common tendinous ring, but they do so via the superior orbital fissure (see Fig. 39.15). The trochlear nerve and the frontal and lacrimal branches of the ophthalmic nerve all enter the orbit through the superior orbital fissure but lie outside the common tendinous ring. Structures which enter the orbit through the inferior orbital fissure lie outside the common tendinous ring. The close anatomical relationship of the optic nerve and other cranial nerves at the orbital apex means that lesions in this region may lead to a combination of visual loss from optic neuropathy and ophthalmoplegia from multiple cranial nerve involvement.

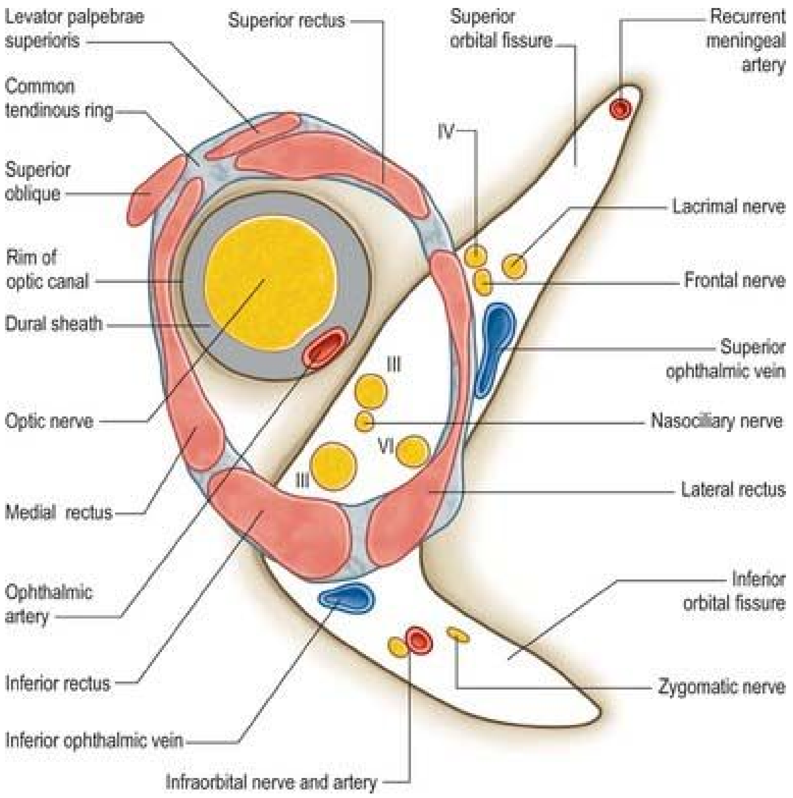
Levator palpebrae superioris
Superior rectus
Superior orbital fissure
Recurrent meningeal artery
Common tendinous ring
IV
Superior oblique
Lacrimal nerve
Rim of optic canal
Frontal nerve
Dural sheath
Superior ophthalmic vein
III
Optic nerve
Nasociliary nerve
VI
III
Lateral rectus
Medial rectus
Ophthalmic artery
Inferior orbital fissure
Inferior rectus
Zygomatic nerve
Inferior ophthalmic vein
Infraorbital nerve and artery

Fig. 39.4 The common tendinous ring with its muscle origins superimposed. The relative positions of the nerves and vessels which enter the orbital cavity by passing through the superior orbital fissure or optic canal are shown. Note that the attachments of levator palpebrae superioris and superior oblique lie external to the common tendinous ring but are attached to it. The ophthalmic veins frequently pass through the ring. The recurrent meningeal artery (a branch of the ophthalmic artery), is often conducted from the orbit to the cranial cavity through its own foramen.

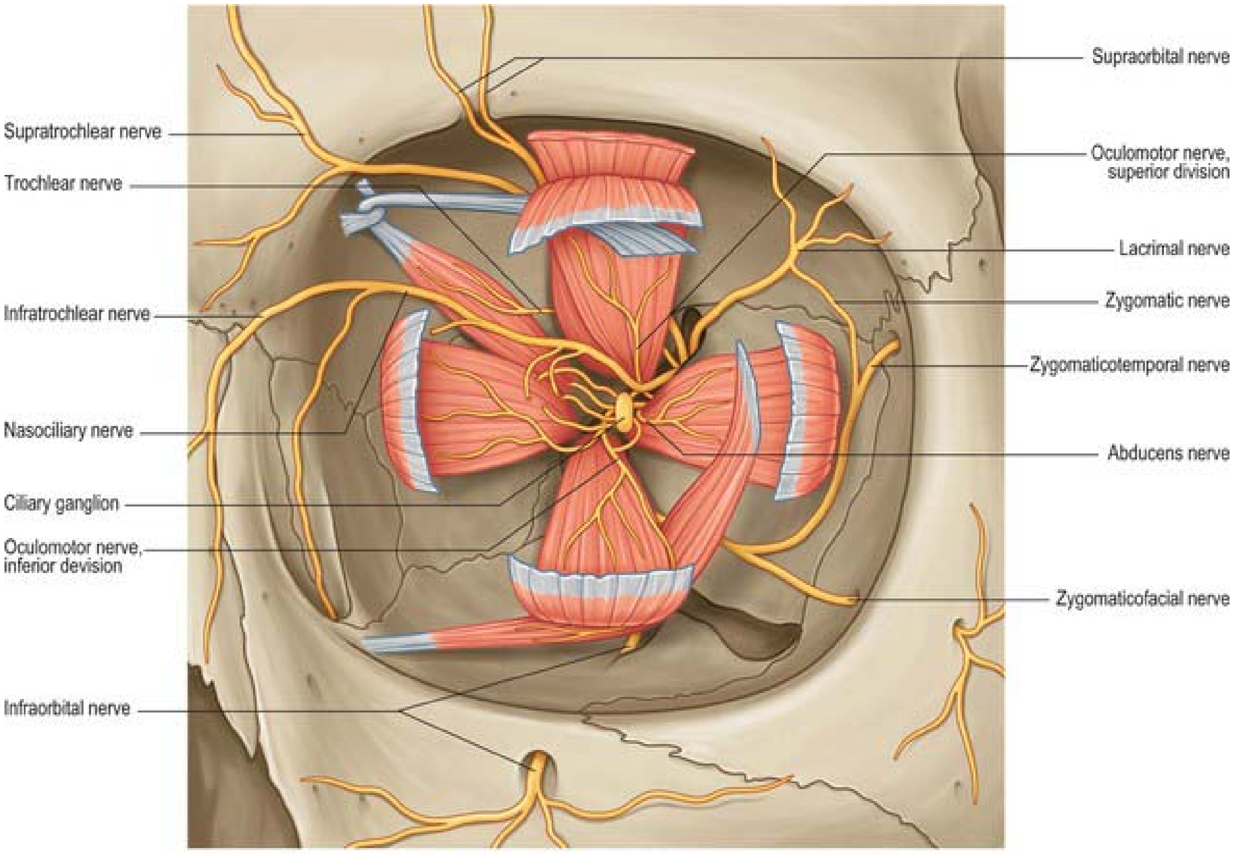
Supraorbital nerve
Supratrochlear nerve
Oculomotor nerve, superior division
Trochlear nerve
Lacrimal nerve
Zygomatic nerve
Infratrochlear nerve
Zygomaticotemporal nerve
Nasociliary nerve
Abducens nerve
Ciliary ganglion
Oculomotor nerve, inferior devision
Zygomaticofacial nerve
Infraorbital nerve

Fig. 39.15 Left orbit viewed from in front showing motor and sensory nerves and the origins of the extraocular muscles. Note that in this figure the trochlear nerve is shown inserting on the superior aspect of the superior oblique, whereas it more commonly inserts on the inferior surface of the muscle.

(By permission from Dutton 1994 Atlas of Clinical and Surgical Orbital Anatomy. Philadelphia: Saunders.)

ORBITAL CONNECTIVE TISSUE AND FAT

The orbit contains a complex arrangement of connective tissue which forms a supporting framework for the eyeball and also acts to limit ocular rotations and compartmentalize orbital fat (Fig. 39.5). Certain regions have anatomical and clinical significance, including the orbital septum, fascial sheath of the eye, ‘check’ ligaments, suspensory ligament and periosteum.

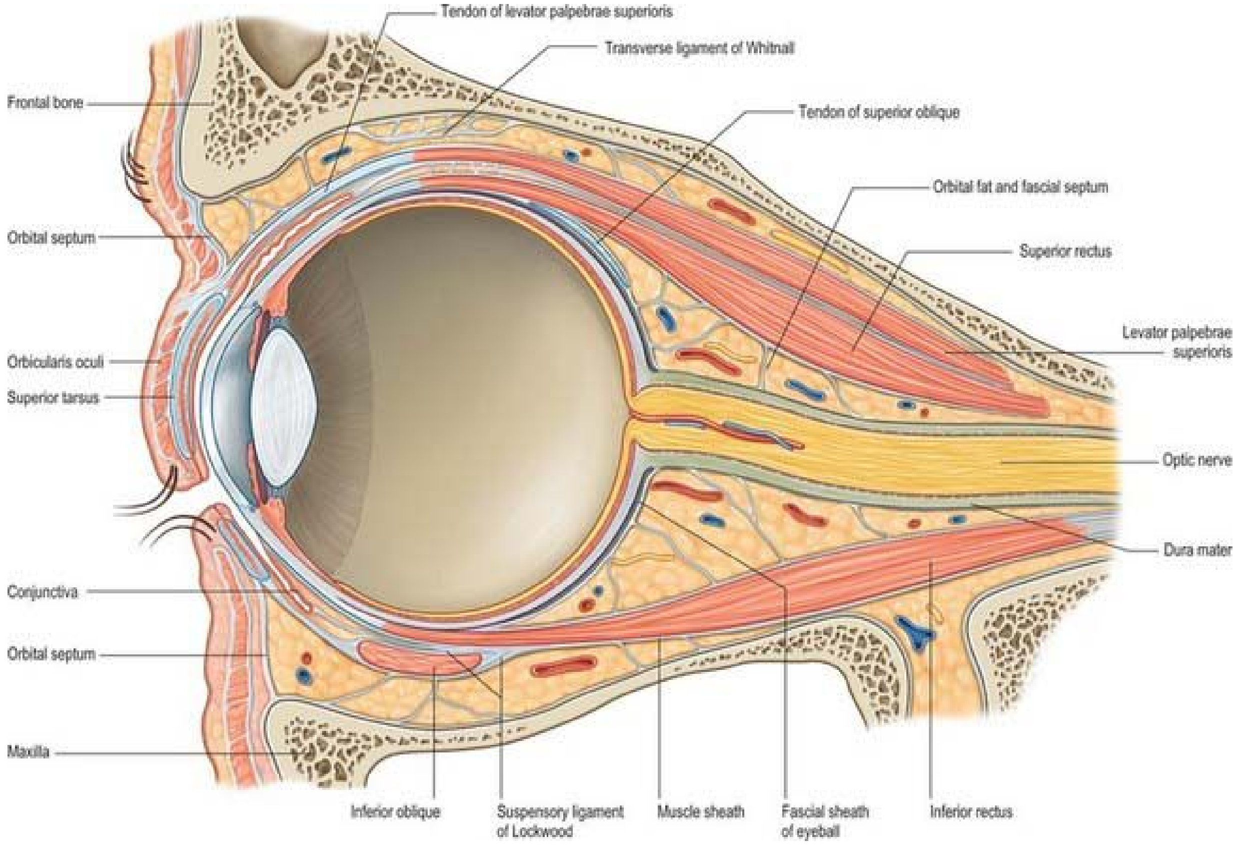
Tendon of levator palpebrae superioris
Transverse ligament of Whitnall
Frontal bone
Tendon of superior oblique
Orbital fat and fascial septum
Orbital septum
Superior rectus
Levator palpebrae superioris
Orbicularis oculi
Superior tarsus
Optic nerve
Dura mater
Conjunctiva
Orbital septum
Maxilla
Inferior oblique
Suspensory ligament of Lockwood
Muscle sheath
Fascial sheath of eyeball
Inferior rectus

Fig. 39.5 The contents of the orbit, sagittal section.

ORBITAL SEPTUM

The orbital septum is a weak membranous sheet, attached to the orbital rim where it becomes continuous with the periosteum (Fig. 39.5). It passes inwards into each eyelid and blends with the tarsal plates, and, in the upper eyelid, with the superficial lamella of levator palpebrae superioris. The orbital septum is thickest laterally, where it lies in front of the lateral palpebral ligament. It passes behind the medial palpebral ligament and nasolacrimal sac, but in front of the pulley of superior oblique. The septum is pierced above by levator palpebrae superioris and below by a fibrous extension from the sheaths of inferior rectus and inferior oblique. The lacrimal, supratrochlear, infratrochlear and supraorbital nerves and vessels pass through the septum from the orbit en route to the face and scalp.

FASCIAL SHEATH OF THE EYEBALL

A thin fascial sheath, the fascia bulbi (Tenon’s capsule), envelops the eyeball from the optic nerve to the corneoscleral junction, separating it from the orbital fat, and forming a socket for the eyeball (Figs 39.5, 39.6). The ocular aspect of the sheath is loosely attached to the sclera by delicate bands of episcleral connective tissue. Posteriorly, it is traversed by ciliary vessels and nerves. It fuses with the sclera and with the sheath of the optic nerve where the latter enters the eyeball: attachment to the sclera is strongest in this position and again anteriorly, just behind the corneoscleral junction at the limbus. The fascia bulbi is perforated by the tendons of the extraocular muscles and is reflected on to each as a tubular sheath called the muscular fascia. The sheath of superior oblique reaches the fibrous pulley (trochlea) associated with the muscle. The sheaths of the four recti are very thick anteriorly but are reduced posteriorly to a delicate perimysium. Just before they blend with the fascia bulbi, the thick sheaths of adjacent recti become confluent and form a fascial ring.

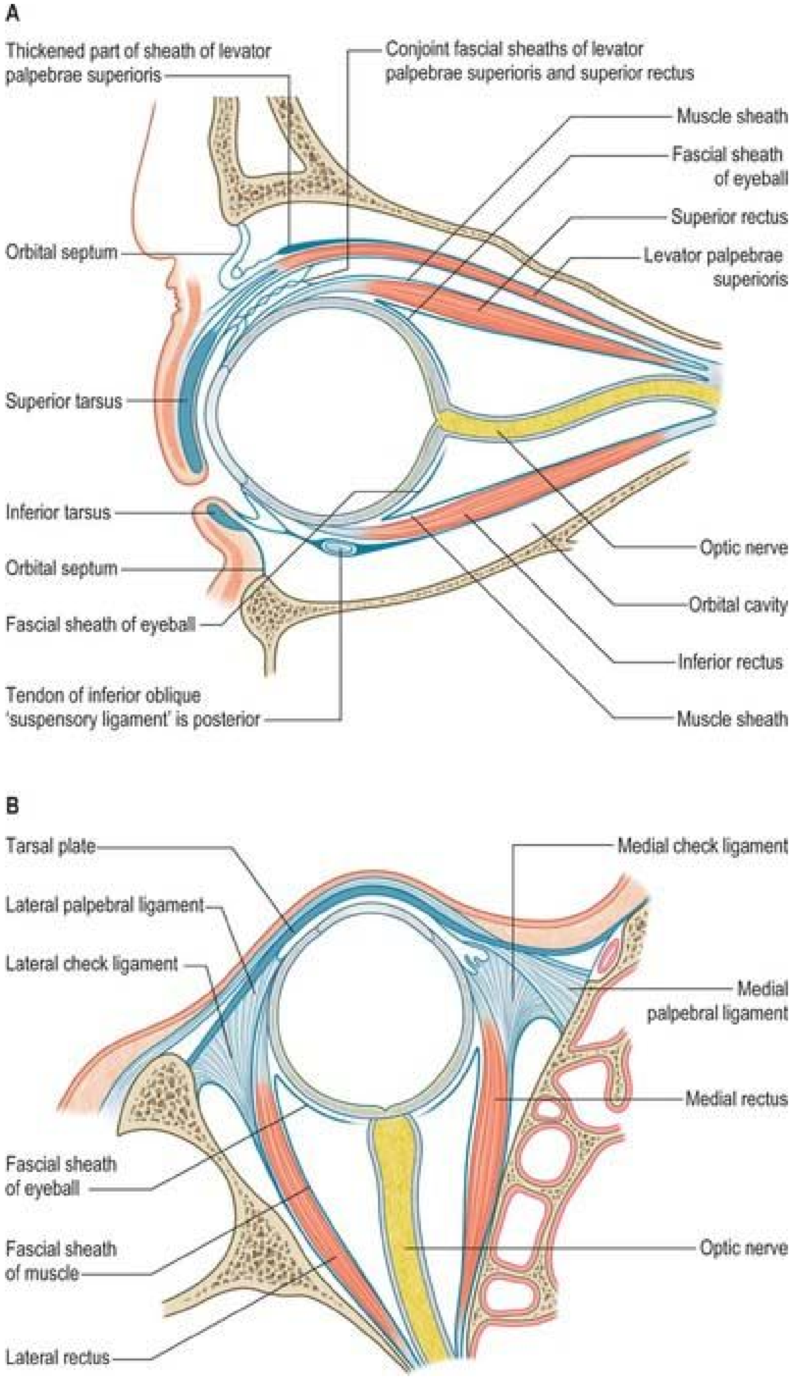
A
Thickened part of sheath of levator palpebrae superioris
Conjoint fascial sheaths of levator palpebrae superioris and superior rectus
Muscle sheath
Fascial sheath of eyeball
Superior rectus
Levator palpebrae superioris
Orbital septum
Superior tarsus
Inferior tarsus
Orbital septum
Fascial sheath of eyeball
Tendon of inferior oblique 'suspensory ligament' is posterior
Optic nerve
Orbital cavity
Inferior rectus
Muscle sheath
B
Tarsal plate
Lateral palpebral ligament
Lateral check ligament
Medial check ligament
Medial palpebral ligament
Medial rectus
Fascial sheath of eyeball
Fascial sheath of muscle
Optic nerve
Lateral rectus

Fig. 39.6 **A**, The orbital fascia, sagittal section. **B**, The orbital fascia, horizontal section.

Expansions from the muscular fascia are important for the attachments they make. Those from the medial and lateral recti are triangular and strong, and are attached to the lacrimal and zygomatic bones respectively: since they may limit the actions of the two recti, they are termed the medial and lateral check ligaments (Fig. 39.6). Other extraocular muscles have less substantial check ligaments, and the capacity of any of them to actually limit movement has been questioned.

The sheath of inferior rectus is thickened on its underside and blends with the sheath of inferior oblique. These two, in turn, are continuous with the fascial ring noted earlier and therefore with the sheaths of the medial and lateral recti. Since the latter are attached to the orbital walls by check ligaments, a continuous fascial band, the suspensory ligament of the eye, is slung like a hammock below the eye, providing sufficient support such that, even when the maxilla (forming the floor of the orbit) is removed, the eye will retain its position.

The thickened fused sheath of inferior rectus and inferior oblique also has an anterior expansion into the lower eyelid, where, augmented by some fibres of orbicularis oculi, it attaches to the inferior tarsus as the inferior tarsal muscle: contraction of inferior rectus in downward gaze therefore also draws the lid downward. The sheath of levator palpebrae superioris is also thickened anteriorly, and just behind the aponeurosis it fuses inferiorly with the sheath of superior rectus. It extends forward between the two muscles and attaches to the upper fornix of the conjunctiva.

Other extensions of the fascia bulbi pass medially and laterally and attach to the orbital walls, forming the transverse ligament of the eye. This structure is of uncertain significance, but presumably plays a part in drawing the fornix upwards in gaze elevation and may act as a fulcrum for levator movements. Other numerous finer fasciae form radial septa which extend from the fascia bulbi and the muscle sheaths to the periosteum of the orbit, and so provide compartments for orbital fat. Many of the fasciae contain smooth muscle cells. The ocular and orbital fasciae are arranged to assist in the location of the eye within the orbit without obstructing the activities of the extraocular muscles, except possibly in the extremes of rotation. They also prevent the gross displacement of orbital fat, which could interfere with the accurate positioning of the two eyes that is essential for binocular vision.

The periosteum of the orbit is only loosely attached to bone. Behind, it is united with the dura mater surrounding the optic nerve and in front it is continuous with the periosteum of the orbital margin, where it gives off a stratum which contributes to the orbital septum. It also attaches to the trochlea, and, as the lacrimal fascia, forms the roof and lateral wall of the fossa for the nasolacrimal sac.

ORBITAL FAT

The spaces between the main structures of the orbit are occupied by fat, particularly in the region between the optic nerve and the surrounding cone of muscles (Figs 39.5, 39.7). Fat also lies between the muscles and periosteum and is limited anteriorly by the orbital septum. Collectively, the fat helps to stabilize the position of the eyeball and also acts as a socket within which the eye can rotate. Conditions resulting in an increased overall volume of orbital fat, e.g. hyperthyroidism (Graves' disease), may lead to forward protrusion of the eyeball (exophthalmos).

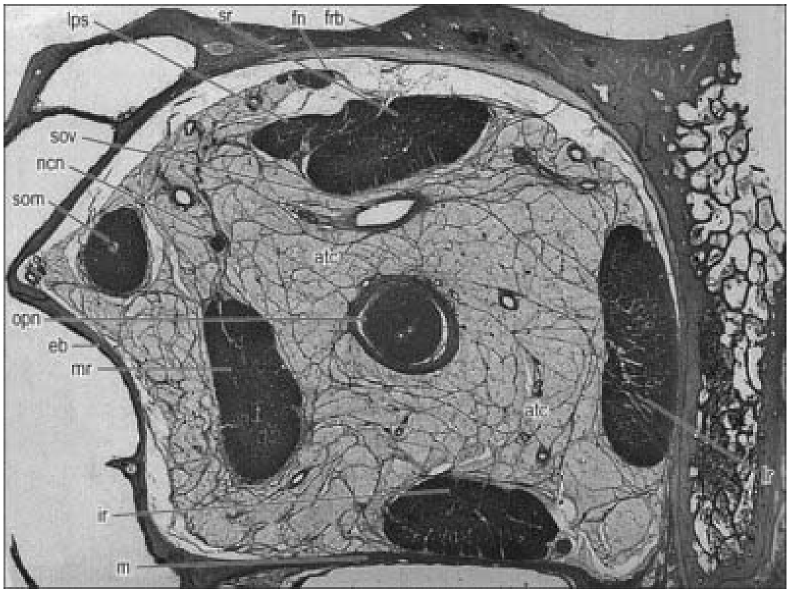

Fig. 39.7 Coronal section through the left orbit (viewed from in front) cut through a plane passing 5 mm behind the posterior pole of the globe. atc, adipose tissue compartments; eb, ethmoid bone; fn, frontal nerve; frb, frontal bone; ir, inferior rectus; lr, lateral rectus; m, maxilla (bone); mr, medial rectus; ncn, nasociliary nerve; opn, optic nerve; lps, levator palpebrae superioris; som, superior oblique; sov, superior ophthalmic vein; sr, superior rectus.

(By permission from Kornneef 1977.)

EXTRAOCULAR MUSCLES

There are seven skeletal extraocular (extrinsic) muscles associated with the eye. Levator palpebrae superioris is an elevator of the upper eyelid, and the other six, i.e. four recti (superior, inferior, medial and lateral), and two obliques (superior and inferior), are capable of moving the eye in almost any direction.

LEVATOR PALPEBRAE SUPERIORIS

Levator palpebrae superioris is a thin, triangular muscle which arises from the inferior aspect of the lesser wing of the sphenoid, above and in front of the optic canal, and separated from it by the attachment of superior rectus (Fig. 39.5). It has a short narrow tendon at its posterior attachment, and broadens gradually, then more sharply as it passes anteriorly above the eyeball. The muscle ends in front in a wide aponeurosis. Some of its tendinous fibres pass straight into the upper eyelid to attach to the anterior surface of the tarsus, while the rest radiate and pierce orbicularis oculi to pass to the skin of the upper eyelid. A thin lamina of smooth muscle, the superior tarsal muscle, passes from the underside of levator palpebrae superioris to the upper margin of the superior tarsus.

The connective tissue sheaths of the adjoining surfaces of levator palpebrae superioris and superior rectus are fused (Fig. 39.5). Where the two muscles separate to reach their anterior attachments, the fascia between them forms a thick mass to which the superior conjunctival fornix is attached: this is usually described as an additional attachment of levator palpebrae superioris. Traced laterally, the aponeurosis of the levator passes between the orbital and palpebral parts of the lacrimal gland to attach to the orbital tubercle of the zygomatic bone. Traced medially, it loses its tendinous nature as it passes closely over the reflected tendon of superior oblique, and continues on to the medial palpebral ligament as loose strands of connective tissue.

Vascular supply

Levator palpebrae superioris receives its arterial supply both directly from the ophthalmic artery and indirectly from its supraorbital branch.

Innervation

Levator palpebrae superioris is innervated by a branch of the superior division of the oculomotor nerve which enters the inferior surface of the muscle. Sympathetic fibres to the smooth muscle component of levator palpebrae superioris (superior tarsal muscle) are derived from the plexus surrounding the internal carotid artery; these nerve fibres may join the oculomotor nerve in the cavernous sinus and pass forward in its superior branch.

Actions

Levator palpebrae superioris elevates the upper eyelid. During this process the lateral and medial parts of its aponeurosis are stretched and thus limit its action: the elevation is also checked by the orbital septum. Elevation of the eyelid is opposed by the palpebral part of orbicularis oculi. Levator palpebrae superioris is linked to superior rectus by a check ligament, thus the upper eyelid elevates when the gaze of the eye is directed upwards.

The position of the eyelids depends on reciprocal tone in orbicularis oculi and levator palpebrae superioris, and on the degree of ocular protrusion. In the opened position the upper eyelid covers the upper part of the cornea, while the lower lid lies just below its lower margin. The eyes are closed by movements of both lids, produced by the contraction of the palpebral part of orbicularis oculi and relaxation of levator palpebrae superioris. In looking upwards, the levator contracts and the upper lid follows the ocular movement. At the same time, the eyebrows are also usually raised by the frontal parts of occipitofrontalis to diminish their overhang. The lower lid lags behind ocular movement, so that more sclera is exposed below the cornea and the lid is bulged a little by the lower part of the elevated eye. When the eye is depressed both lids move: the upper retains its normal relation to the eyeball and still covers about a quarter of the cornea, whereas the lower lid is depressed because the extension of the thickened fascia of inferior rectus and inferior oblique pull on its tarsus as the former contracts.

The palpebral apertures are widened in states of fear or excitement by contraction of the smooth muscle of the superior and inferior tarsal muscles as a result of increased sympathetic activity. Lesions of the sympathetic supply result in drooping of the upper eyelid (ptosis), as seen in Horner’s syndrome.

THE FOUR RECTI

The four recti are approximately strap-shaped; each has a thickened middle part which thins gradually to a tendon (Figs 39.8, 39.9). They are attached posteriorly to a common tendinous ring that encircles the superior, medial and inferior margins of the optic canal, continues laterally across the inferior and medial parts of the superior orbital fissure, and is attached to a tubercle or spine on the margin of the greater wing of the sphenoid (Fig. 39.4). The tendinous ring is closely adherent to the dural sheath of the optic nerve medially and to the surrounding periosteum. Inferior rectus, part of medial rectus and the lower fibres of lateral rectus, are all attached to the lower part of the ring, whereas superior rectus, part of medial rectus and the upper fibres of lateral rectus are all attached to the upper part. A second small tendinous slip of lateral rectus is attached to the orbital surface of the greater wing of the sphenoid, lateral to the common tendinous ring.

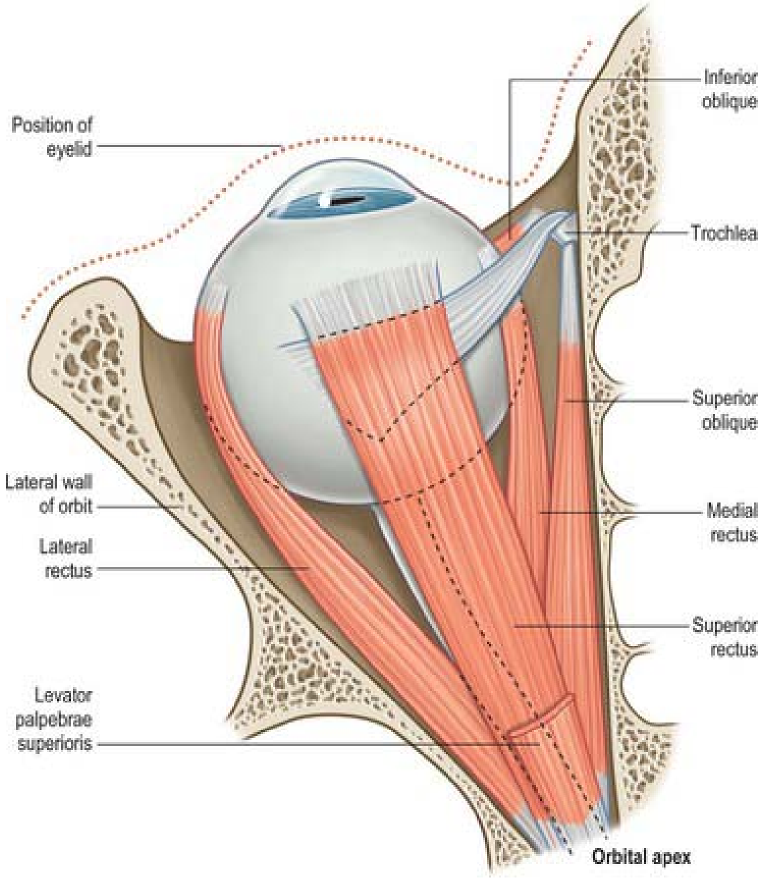
Position of eyelid
Inferior oblique
Trochlea
Superior oblique
Lateral wall of orbit
Medial rectus
Lateral rectus
Superior rectus
Levator palpebrae superioris
Orbital apex

Fig. 39.8 Extraocular muscles viewed from above.

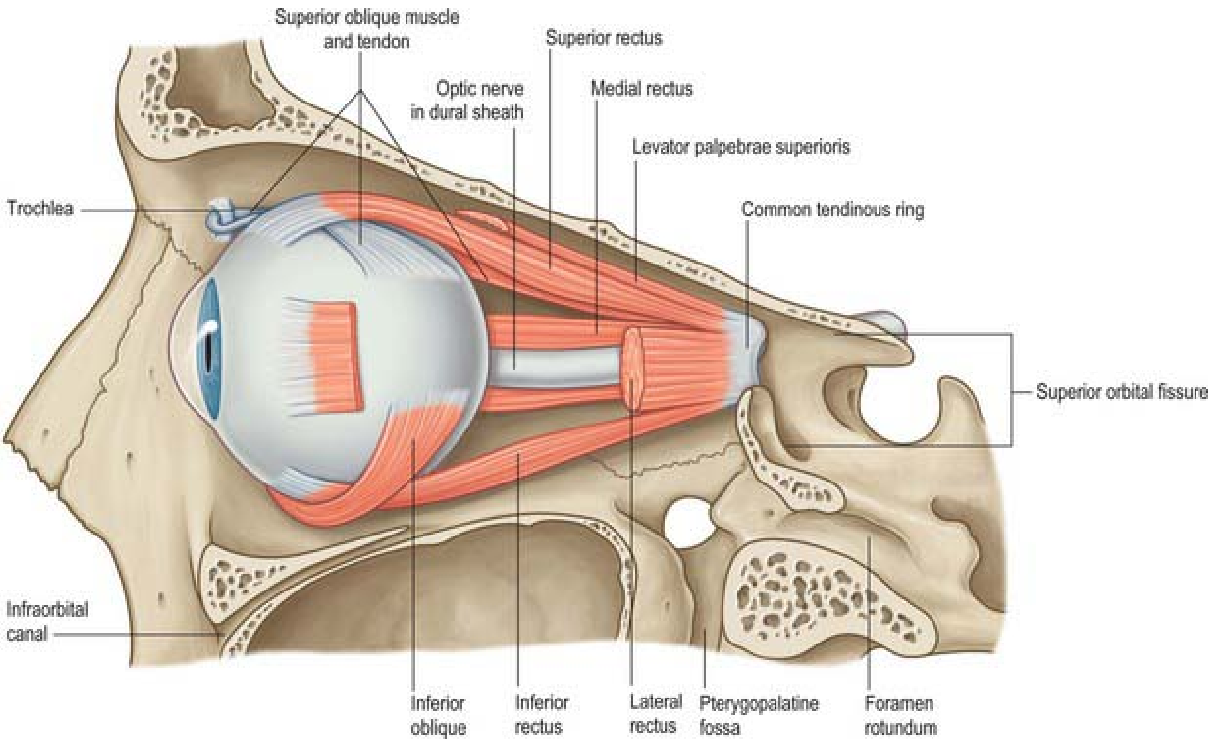
Superior oblique muscle and tendon
Superior rectus
Optic nerve in dural sheath
Medial rectus
Levator palpebrae superioris
Common tendinous ring
Trochlea
Superior orbital fissure
Infraorbital canal
Inferior oblique
Inferior rectus
Lateral rectus
Pterygopalatine fossa
Foramen rotundum

Fig. 39.9 The muscles of the left orbit, lateral view.

Each rectus muscle passes forwards, in the position implied by its name, to be attached anteriorly by a tendinous expansion into the sclera, posterior to the margin of the cornea.

Superior rectus

Superior rectus is slightly larger than the other rectus muscles. It arises from the upper part of the common tendinous ring, above and lateral to the optic canal. Some fibres also arise from the dural sheath of the optic nerve. The fibres pass forwards and laterally (at an angle of approximately 25° to the median plane of the eye in the primary position) to insert into the upper part of the sclera, approximately 8 mm from the limbus (Fig. 39.8). The insertion is slightly oblique, the medial margin more anterior than the lateral margin.

Vascular supply

Superior rectus receives its arterial supply both directly from the ophthalmic artery and indirectly from its supraorbital branch.

Innervation

Superior rectus is innervated by the superior division of the oculomotor nerve which enters the inferior surface of the muscle.

Actions

Superior rectus moves the eye so that the cornea is directed upwards (elevation) and medially (adduction). To obtain upward movement alone, the muscle must function with inferior oblique. Superior rectus also causes intorsion of the eye (i.e. medial rotation). Because a check ligament extends from the muscle to levator palpebrae superioris, elevation of the eye also results in elevation of the upper eyelid. For more detailed discussion of its actions, see p. 661.

Inferior rectus

Inferior rectus arises from the common tendinous ring, below the optic canal. It runs along the orbital floor in a similar direction to superior rectus (i.e. forwards and laterally) and inserts obliquely into the sclera below the cornea, approximately 6.5 mm from the limbus (Fig. 39.9).

Vascular supply

Inferior rectus receives its arterial supply from the ophthalmic artery and from the infraorbital branch of the maxillary artery.

Innervation

Inferior rectus is innervated by a branch of the inferior division of the oculomotor nerve which enters the superior surface of the muscle.

Actions

The principal activity of inferior rectus is to move the eye so that it is directed downwards (depression). It also causes the eye to deviate medially, and extorts the eye (i.e. produces lateral rotation). To obtain downward movement alone, inferior rectus must function with superior oblique. A fibrous extension from inferior rectus to the inferior tarsal plate of the eyelid causes the lower eyelid to be depressed when the muscle contracts. For more detailed discussion of its actions, see p. 661.

Medial rectus

Medial rectus is slightly shorter than the other recti, but is the strongest of the group. It arises from the medial part of the common tendinous ring, and also from the dural sheath of the optic nerve, passing horizontally forwards along the medial wall of the orbit, below superior oblique (Fig. 39.8). It inserts into the medial surface of the sclera, approximately 5.5 mm from the limbus and slightly anterior to the other recti.

Vascular supply

Medial rectus receives its arterial supply from the ophthalmic artery.

Innervation

Medial rectus is innervated by a branch from the inferior division of the oculomotor nerve which enters the lateral surface of the muscle.

Actions

Medial rectus moves the eye so that it is directed medially (adducted). The two medial recti acting together are responsible for convergence. For more detailed discussion of its actions, see p. 661.

Lateral rectus

Lateral rectus arises principally from the lateral part of the common tendinous ring and bridges the superior orbital fissure; some fibres also arise from a spine on the greater wing of the sphenoid. The muscle passes horizontally forward along the lateral wall of the orbit to insert into the lateral surface of the sclera, approximately 7 mm from the limbus (Fig. 39.8).

Vascular supply

Lateral rectus receives its arterial supply from the ophthalmic artery directly and/or from its lacrimal branch.

Innervation

Lateral rectus is innervated by the abducens nerve by branches which enter the medial surface of the muscle.

Actions

Lateral rectus moves the eye so that it is directed laterally (abducted). For more detailed discussion of its actions, see p. 661.

THE OBLIQUES

Superior oblique

Superior oblique is a fusiform muscle which arises from the body of the sphenoid superomedial to the optic canal and the tendinous attachment of the superior rectus. It passes forwards to end in a round tendon which plays through a fibrocartilaginous loop, the trochlea, attached to the trochlear fossa of the frontal bone (Fig. 39.8). Tendon and trochlea are separated by a delicate synovial sheath. The tendon subsequently descends posterolaterally and inferior to superior rectus, and is attached to the sclera in the superolateral part of the posterior quadrant behind the equator, between the superior and lateral recti.

Vascular supply

Superior oblique receives its arterial supply directly from the ophthalmic artery and indirectly from its supraorbital branch.

Innervation

Superior oblique is innervated by the trochlear nerve which enters the superior surface of the muscle.

Actions

Superior oblique is inserted into the posterior part of the eyeball; when it contracts, the back of the eyeball is elevated, and the front of the eyeball is depressed (particularly in the adducted position). Superior oblique also moves the eye laterally (abducted) and intorts the eyeball. For more detailed discussion of its actions, see p. 695.

Inferior oblique

Inferior oblique is a thin, narrow muscle that lies near the anterior margin of the floor of the orbit. It arises from the orbital surface of the maxilla lateral to the nasolacrimal dossa and ascends posterolaterally, at first between inferior rectus and the orbital floor, and then between the eyeball and lateral rectus. It is inserted into the lateral part of the sclera behind the equator of the eyeball, in the inferolateral part of the posterior quadrant between the inferior and lateral recti, near, but slightly posterior to, the attachment of superior oblique (Fig. 39.9). The muscle broadens and thins, and, in contrast to the other extraocular muscles, its tendon is barely discernible at its scleral attachment.

Vascular supply

Inferior oblique receives its arterial supply from the ophthalmic artery and from the infraorbital branch of the maxillary artery.

Innervation

Inferior oblique is innervated by a branch of the inferior division of the oculomotor nerve which enters the orbital surface of the muscle.

Actions

Inferior oblique is inserted into the posterior part of the eyeball; when it contracts, the back of the eyeball is depressed, and the front of the eyeball is elevated (particularly in the adducted position). The muscle moves the eye laterally (abduction) and also causes extorsion. For more detailed discussion of its actions, see p. 661.

MINOR MUSCLES OF THE EYELIDS

Several smooth muscles are associated with the orbit, although they are not directly attached to the eyeball. Orbitalis, the orbital muscle of Müller, lies at the back of the orbit and spans the infraorbital fissure. Its functions are uncertain, but its contraction may possibly produce a slight forward protrusion of the eyeball. The superior and inferior tarsal muscles are small muscle laminae inserted into the upper and lower eyelids and are described in more detail with the tarsal plates (p. 670). All three minor muscles receive a sympathetic innervation from the superior cervical ganglion via the internal carotid plexus.

MOVEMENTS OF THE EYES

Movements of the eyes involve rotations around a centre of rotation within the globe. For practical purposes this can be considered to lie 13.5 mm behind the corneal apex. Normal eye movements are binocular. Movements of the eyes in the same direction are termed versions, whilst those in opposite directions are termed vergences. Eye movements are often accompanied by corresponding movements of the eyelids, particularly in upgaze where the activity of levator palpebrae superioris is closely coupled to that of superior rectus. The following section describes the ocular motor system in terms of the actions of individual extraocular muscles, the diversity of eye movements and their neural control.

Actions of the extraocular muscles

Levator palpebrae superioris elevates the upper lid, and its antagonist is the palpebral part of orbicularis oculi. The degree of elevation, which, apart from blinking, is maintained for long periods during waking hours, is a compromise between ensuring an adequate exposure of the cornea and controlling the amount of incident light. In bright sunshine, the latter can be reduced by lowering the upper lid, so limiting glare. Electrically, the levator discharges steadily for a given fixation, but with increasing rates with upward lid position, and relaxes during closure of the palpebral fissure. The role of the superior tarsal muscle is less clear. Its tonus is related to sympathetic activity, and since ptosis is a consequence of impairment of its sympathetic nerve supply, it may function as an accessory elevator of the upper eyelid.

The six extraocular muscles all rotate the eyeball in directions dependent on the geometrical relation between their bony and global attachments (Fig. 39.10), which are altered by the ocular movements themselves. For convenience, each muscle will be considered in isolation, but it must be appreciated that any movement of the eyeball alters the tension and/or length in all six muscles. It is useful to consider the four recti and two obliques as separate groups, (remembering always that they act in concert), because they form more obvious groupings as antagonists or synergists. The extrinsic ocular muscles collectively position the eyeball in the orbital cavity and prevent its anteroposterior movements, other than a slight retraction during blinks, because the recti exert a posterior traction while the obliques pull the eyeball to some degree anteriorly. They may be assisted by various ‘check ligaments’ (see above). A simplified description of the actions of the extraocular muscles is summarized in Figure 39.11.

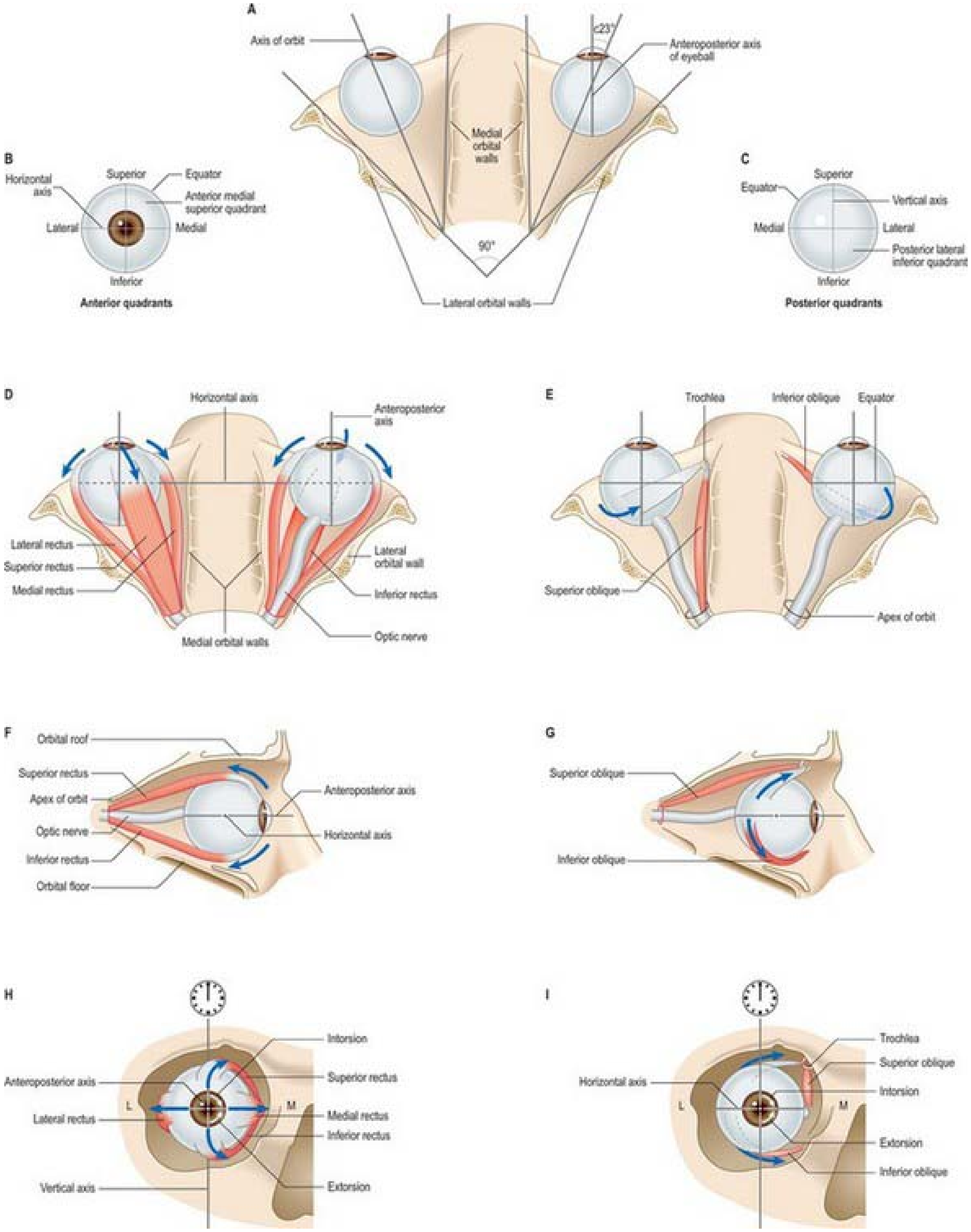
A
Axis of orbit
c23°
Anteroposterior axis of eyeball
Medial orbital walls
90°
Lateral orbital walls
B
Horizontal axis
Superior
Equator
Anterior medial superior quadrant
Lateral
Medial
Inferior
Anterior quadrants
C
Superior
Equator
Vertical axis
Medial
Lateral
Posterior lateral inferior quadrant
Inferior
Posterior quadrants
D
Horizontal axis
Anteroposterior axis
Lateral rectus
Superior rectus
Medial rectus
Lateral orbital wall
Inferior rectus
Optic nerve
Medial orbital walls
E
Trochlea
Inferior oblique
Equator
Superior oblique
Apex of orbit
F
Orbital roof
Superior rectus
Apex of orbit
Optic nerve
Inferior rectus
Orbital floor
Anteroposterior axis
Horizontal axis
G
Superior oblique
Inferior oblique
H
Intorsion
Superior rectus
Anteroposterior axis
Lateral rectus
L
M
Medial rectus
Inferior rectus
Vertical axis
Extorsion
I
Trochlea
Superior oblique
Horizontal axis
Intorsion
L
M
Extorsion
Inferior oblique

Fig. 39.10 The geometrical basis of ocular movements. **A**, The relationship between the orbital and ocular axes, with the eyes in the primary position, where the visual axes are parallel. **B** and **C**, The ocular globe in anterior and posterior views to show conventional geometry. **D**,

The orbits from above showing the medial and lateral recti and the superior rectus (left) and the inferior rectus (right), indicating turning moments primarily around the vertical axis. **E**, Superior (left) and inferior (right) oblique muscles showing turning moments primarily around the vertical and also anteroposterior axes. **F**, Lateral view to show the actions of the superior and inferior recti around the horizontal axis. **G**, Lateral view to show the action of the superior and inferior oblique muscles around the anteroposterior axis. **H**, Anterior view to show the medial rotational movement of the superior and inferior recti around the vertical axis. Conventionally the 12 o’clock position indicated is said to be intorted (superior rectus) or extorted (inferior rectus) as indicated by the small arrows on the cornea. **I**, Anterior view to show the torsional effects of the superior oblique (intorsion) and inferior oblique (extorsion) around the anteroposterior axis, as indicated by the small arrows on the cornea.

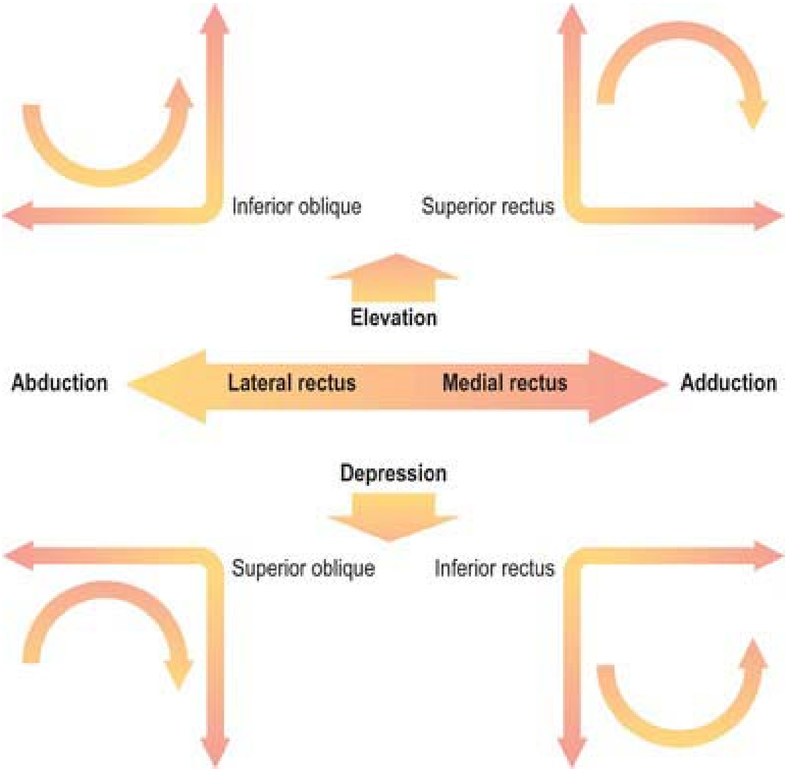
Inferior oblique
Superior rectus
Elevation
Abduction
Lateral rectus
Medial rectus
Adduction
Depression
Superior oblique
Inferior rectus

Fig. 39.11 Simplified summary of the actions of the extraocular muscles.

Of the four recti, the medial and lateral exert comparatively straightforward forces on the eyeball. Being approximately horizontal, when the visual axis is in its primary position, i.e. directed to the horizon, they rotate the eye medially (adduction) or laterally (abduction) about an imaginary vertical axis. They are antagonists. The visual axis can be swept through a horizontal arc by reciprocal adjustment of their lengths. When, as is usual, both eyes are involved, four medial and lateral recti of each eye can either adjust both visual axes in a conjugate movement from point to point at infinity (their axes remaining parallel), or they can converge or diverge the axes to or from nearer or more distant objects of attention in the visual field.

The medial and lateral recti do not rotate the eye around its horizontal axis and so cannot elevate or depress the visual axes as gaze is transferred from nearer to more distant objects or the reverse. This movement requires the superior and inferior recti (aided by the two oblique muscles). It must be remembered that the orbital axis does not correspond with the visual axis in its primary position but diverges from it at an angle of approximately 23° (the value varies between individuals, and depends on the angle between the orbital axes and the median plane). Thus, the simple rotation caused by an isolated superior rectus, analysed with reference to the three hypothetical ocular axes, appears more complex, being primarily elevation (horizontal axis), and secondarily a less powerful medial rotation (vertical axis) and slight intorsion (anteroposterior axis) in which the midpoint of the upper rim of the cornea (often referred to as ‘12 o’clock’) is rotated medially towards the nose. These actions, compounded as a single, simple rotation, are easily appreciated when it is seen that the direction of traction of superior rectus runs in a posteromedial direction from its attachment in front, which is anterior to the equator and superior to the cornea, to its bony attachment near the orbital apex (Fig. 39.10). Inferior rectus pulls in a similar direction to superior rectus, but rotates the visual axis downwards about the horizontal axis. It rotates the eye medially on a vertical axis but its action around the anteroposterior axis extorts the eye, i.e. rotates it so that the corneal ‘12 o’clock’ point turns laterally. The combined, equal contractions of the superior and inferior recti therefore rotate the eyeball medially, since their effects around the horizontal and anteroposterior axes are opposed. In binocular movements they assist the medial recti in converging the visual axes, and by reciprocal adjustment can elevate or depress the visual axes. As the eyeball is rotated laterally, the lines of traction of the superior and inferior recti approach the plane of the anteroposterior ocular axis (Fig. 39.10), and so their rotational effects about this and the vertical ocular axis diminish. In abduction to approximately 23°, they become almost purely an elevator and depressor respectively of the visual axis.

Superior oblique acts on the eye from the trochlea, and, since the attachment of inferior oblique is for practical purposes vertically below this, both muscles approach the eyeball at the same angle, being attached in approximately similar positions in the superior and inferior posterolateral ocular quadrants (Fig. 39.10). Superior oblique elevates the posterior aspect of the eyeball, and inferior oblique depresses it, which means that the former rotates the visual axis downwards and the latter rotates it upwards, and both movements occur around the horizontal axis. When the eye is in the primary position, the obliquity of both muscles means that they pull in a direction posterior to the vertical axis and both therefore rotate the eye laterally around this axis. With regard to the anteroposterior axis, in isolation, superior oblique intorts the eye and inferior oblique extorts it. Like the superior and inferior recti, therefore, the two obliques have a common turning movement around the vertical axis but are opposed forces in respect of the other two. Acting in concert they could therefore assist the lateral rectus in abducting the visual axis, as in divergence of the eyes in transferring attention from near to far. Again, like the superior and inferior recti, the directions of traction of the oblique muscles also vary with ocular position, such that they become more nearly a pure elevator and a depressor as the eye is adducted.

Ocular rotations are for the most part under voluntary control, whereas torsional movements cannot be voluntarily initiated. When the head is tilted in a frontal plane, reflex torsions occur. Any small lapse in the concerted adjustment of both eyes produces diplopia.

Movements that shift or stabilize gaze

The role of eye movements is to bring the image of objects of visual interest onto the fovea of the retina and to hold the image steady in order to achieve the highest level of visual acuity. Several types of eye movement are required to ensure that these conditions are met. Moreover, the movements of both eyes must be near perfectly matched to achieve the benefits of binocularity. Both voluntary and reflex movements are involved and may be so classified. Alternatively, they may be grouped into those movements that shift gaze as visual interest changes, and those that stabilize gaze by maintaining a steady image on the retina. They have distinct characteristics, and are generated by different neural mechanisms in response to different stimuli, but share a common final motor pathway. Movements that shift or stabilize gaze are of three types; saccades, vergence, and vestibular-generated changes in fixation.

In so-called ‘fixation’ of a focus of attention, whether uniocular or binocular, the visual axis is not ‘fixed’ in a perfectly steady manner but undergoes minute, but measurable, flicking (of a few minutes or even seconds of arc) across the true line of fixation. These microsaccades are rapid and surprisingly complex. When interest changes to another feature of the visual scene, the eyes execute a fast or saccadic movement to take up fixation. If the required rotation is small the saccade is accurate, whereas small supplementary corrective saccades are needed if the shift is substantial. Saccades may also occur in response to other, i.e. non-visual, exteroceptive stimuli (e.g. auditory, tactile, or centrally evoked). They may be volitional or reflex. As an example of the latter, in reading a line of print the eyes make three or four jerky saccades rather than following the line smoothly: the line is usefully imaged only when the eye is stationary, which means that little of the line is seen by the centre of the fovea. In general, reaction times and movements are measured in microseconds, amplitude varies from seconds of arc to many degrees, with an accuracy of 0.2° or better, and the velocity of a large saccade may reach 500° sec^{-1}. The speed of saccades is assured by an initial, slightly excessive, contraction of the appropriate muscles. The necessary deceleration when the target is fixated is largely dependent on the viscoelasticity of the extraocular muscles and orbital soft tissues, and not on antagonistic muscular activity.

Vergence is a relatively slow movement permitting maintenance of single binocular vision of close objects. The eyes converge towards the midline between the two eyes to achieve imagery of the object on both foveas. The view of the object at the two eyes is not quite the same and the disparity is used to assess depth. In addition, the pupils constrict and the eyes accommodate to achieve sharp focused images. These three activities constitute the near reflex.

The vestibular apparatus induces a variety of reflex eye movements to compensate for the potentially disruptive effects on vision caused by head and body movement (see Ch. 37). Receptors in the semicircular canals respond to active or passive rotational (angular) accelerations of the head. When the body makes substantial rotational movements a vestibulo-ocular reflex generates a cycle of responses involving both the shifting and stabilizing of gaze. Body rotation is matched by counter-rotation of the eyes so that gaze direction is unaltered and clear vision is maintained. Physical constraint limits the rotation to 30° or less and is followed by a rapid saccadic movement of the eyes to another object in the visual scene and the cycle is repeated. Vision is therefore clear throughout most of the cycle while the image is stationary, but at the cost of no useful vision during the brief periods of the saccades. The reflex is efficient and rapid: this speed could not be generated by the visual system, which is slow relative to the short latency of vestibular receptors.

Other reflexes generated by the vestibular system, which induce compensatory eye movements to stabilize gaze, are activated during brief head movements. When the head is sharply rotated in any direction, the eyeball rotates by an equal amount in the opposite direction in response to the stimulation of semicircular canal cristae (angular acceleration), and gaze is undisturbed. Brief rotational movements are commonly combined with translational movements (linear acceleration) that are monitored by otolith organs. For example, a linear displacement occurs in walking as the head bobs vertically with each stride, and a rotational displacement occurs as the head rolls, invoking otolith and canal responses respectively to stabilize the retinal image. Vestibular disease incurring the loss of the rapid, fine compensatory eye movements in locomotion destabilizes the retinal image, blurs vision and may render locomotion intolerable.

The otoliths also respond to the pull of gravity, generating static vestibulo-ocular reflexes associated with head tilt. When static otolith orientation is changed, e.g. when the head is tilted upwards or downwards, the eyes counter-rotate to maintain fixation of the horizontal meridian. Lateral tilt towards a shoulder generates a torsional counter-rotation of the eyes, a movement which cannot be made voluntarily. The torsional tilt reflex, equal and opposite in direction by the two eyes, is fully compensatory over 40° or so in afoveate animals, but in man it is vestigial: it is fractionally compensatory and varies in extent between individuals. Because the foveal image is unaffected by torsional movements, the subject is unaware of any visual penalty.

Pursuit eye movements are used to track a moving object of visual interest, maintaining the image approximately on the fovea. They are usually preceded by a saccade to capture the image but, unlike saccades, they are slow and motivated by vision. If the angular shift required to track the moving object is large or is moving swiftly, the initial saccade is frequently inaccurate and one or more small corrective saccades are made before tracking begins. Because the stimulus is visual, the pursuit system response is subject to a relatively long latency (approximately 100 msec): the limitation in performance this imposes may be offset by a predictive capacity when object movement follows a regular pattern, and the eye movements adjust in anticipation to speed and direction.

The optokinetic response is another visually mediated reflex which stabilizes retinal imagery when a visual scene is rotated about a stationary subject. As the visual scene changes, the eyes follow and hold the retinal image steady until the eyes shift rapidly in the opposite direction to another area of the visual scene. The full field of vision, rather than small objects within it, is the stimulus, and the alternating slow and fast phases of movement that are generated describes optokinetic nystagmus. This reflex functions in collaboration with the rotational vestibulo-ocular reflex. In sustained rotations of the body, the vestibulo-ocular reflex fades because of the mechanical arrangements of the semicircular canals. In darkness the reflex, which is initially compensatory, loses velocity, and after approximately 45 seconds the eyeballs become stationary. With a visual input, the reflex is sustained by the optokinetic response. Because the reflex is already initiated, the relative delay of visual input is overcome. The integration of the two systems is served by an accessory visual system projection to the vestibular nuclei via the inferior olive and cerebellum. The usual method of evoking optokinetic nystagmus in the laboratory or clinic is to present a horizontally moving pattern of vertical black-on-white stripes while the head of the subject is held stationary.

Saccadic activity is almost omnipresent in human vision. Thus, both visual axes are endlessly and rapidly transferred to new points of interest in any part of the visual field. Binocular gaze is frequently made to travel routes of the most variable complexity in examining objects of interest in the field, and both visual axes must be maintained with sufficient accuracy to avoid diplopia. Binocular movements involving convergence are markedly slower than conjugate movements, presumably reflecting the greater complexity of neural control that these movements require. Most human visual activity concerns targets near enough to demand convergence and hence a neuronal intermediation of greater flexibility. Since the prime purpose is the clear perception of a ‘target’, it is not surprising that the visual input is itself utilized in continuous feedback to achieve the correct aiming of visual axes.

Continual movements of the eyeball are essential for vision. Retinal and more central neural networks appear to be designed primarily to detect transient events such as movements, rather than static, maintained stimuli. Indeed, images which are essentially static, such as those due to retinal blood vessels, are not detectable unless the shadows they cast on photoreceptors are made to move, e.g. by shifting narrow-angle illumination with an ophthalmoscope.

Neural control of gaze

Although the detailed anatomical substrates for the different types of eye movement differ, they share common neural circuitry which lies mainly in the pons and midbrain, for horizontal and vertical gaze movements respectively (Fig. 39.12). The common element for all types of horizontal gaze movements is the abducens nucleus. It contains motor neurones which innervate the ipsilateral lateral rectus and interneurones which project via the medial longitudinal fasciculus (MLF) to the contralateral oculomotor nucleus which controls medial rectus. A lesion of the abducens nucleus leads to a total loss of ipsilateral horizontal conjugate gaze. A lesion of the MLF produces slowed or absent adduction of the ipsilateral eye, usually associated with jerky movements (nystagmus) of the abducting eye, a syndrome called internuclear ophthalmoplegia. The gaze motor command involves specialized areas of the reticular formation of the brain stem which receive a variety of supranuclear inputs. The main region for horizontal gaze is the paramedian pontine reticular formation (PPRF), located on each side of the midline in the central paramedian part of the tegmentum, and extending from the pontomedullary junction to the pontopeduncular junction. Each PPRF contains excitatory neurones (referred to as ‘burst’ cells) which discharge at high frequencies just prior to and during ipsilateral saccades. Pause neurones, located in a midline caudal pontine nucleus called the nucleus raphe interpositus, discharge tonically except just before and during saccades. They appear to exert an inhibitory influence on the burst neurones and so prevent extraneous saccades occurring during fixation.

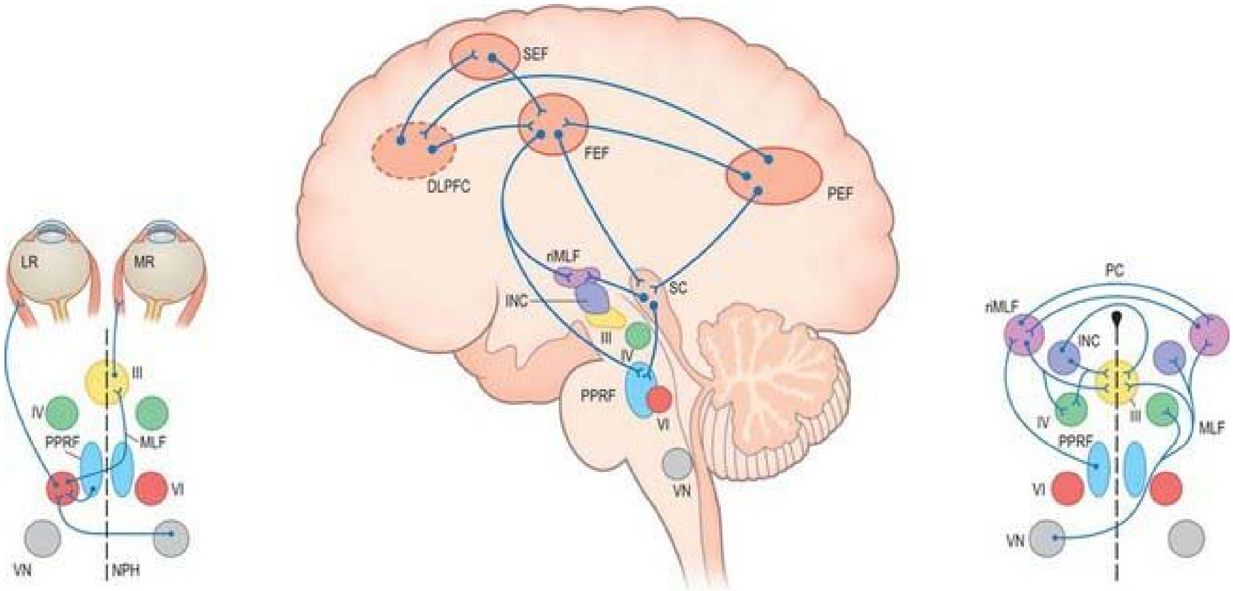

Fig. 39.12 Summary of the control of eye movements. The central drawing shows the supranuclear connections from the frontal eye field (FEF) and the posterior eye field (PEF) to the superior colliculus (SC), rostral interstitial nucleus of the medial longitudinal fasciculus (riMLF), and the paramedian pontine reticular formation (PPRF). The FEF and SC are involved in the production of saccades, while the PEF is thought to be important in the production of pursuit movements. The diagram on the left shows the brain stem pathways for horizontal gaze. Axons from the PPRF travel to the ipsilateral abducens nucleus innervating lateral rectus (LR). Abducens internuclear axons cross the midline and travel in the medial longitudinal fasciculus (MLF) to the neuronal pool in the oculomotor nucleus (III) that innervates medial rectus (MR) of the contralateral eye. The diagram on the right shows the brain stem pathways for vertical gaze. Important structures include the riMLF, PPRF, the interstitial nucleus of Cajal (INC), and the posterior commissure (PC). Other abbreviations are: DLPFC, dorsolateral prefrontal cortex; IV, trochlear nucleus; NPH, nucleus propositus hypoglossi; SEF, supplementary eye field; VI, abducens nucleus; VN, vestibular nucleus.

The vestibular nuclei and the perihypoglossal complex (especially the nucleus prepositus hypoglossi) project directly to the abducens nuclei. These projections probably carry both smooth pursuit signals, via the cerebellum, and vestibular signals. In addition, these nuclei, via reciprocal innervation with the PPRF, contain integrator neurones which control the step change in innervation required to maintain the eccentric position of the eye against the viscoelastic forces in the orbit. These forces tend to move the eyeball back to the position of looking straight ahead, i.e. the primary position, after a saccade.

The final common pathway of vertical gaze movements is formed by the oculomotor and trochlear nuclei. The rostral interstitial nucleus of the medial longitudinal fasciculus (riMLF) contains neurones which discharge in relation to up-and-down vertical saccadic movements. The riMLF projects through the posterior commissure to its equivalent on the other side of the mesencephalon, as well as directly to the oculomotor nucleus. Lesions within the posterior commissure therefore give rise to disturbance in vertical gaze, especially upgaze. Lesions placed more ventrally in the region of the riMLF cause vertical gaze disorders which may be mixed up-and-down, or mainly downgaze. The interstitial nucleus of Cajal lies slightly caudal to the riMLF, and is directly connected to it: it contains neurones which appear to be involved in vertical gaze holding.

The cerebellum plays an important role in the control of eye movements (see Ch. 20). The vestibulo-cerebellum (floculus and nodule) is involved in gaze holding, smooth pursuit and the vestibulo-ocular reflex. The dorsal vermis and fastigial nucleus play a major role in programming accurate saccades and smooth pursuit.

The cerebral hemispheres are extremely important for the programming and coordination of both saccadic and pursuit conjugate eye movements (see Ch. 23). There appear to be four main cortical areas in the cerebral hemispheres involved in the generation of saccades. These are the frontal eye field (FEF), which lies laterally at the caudal end of the second frontal gyrus in the premotor cortex (Brodmann area 8); the supplementary eye field (SEF), which lies at the anterior region of the supplementary motor area in the first frontal gyrus (Brodmann area 6); the dorsolateral prefrontal cortex (DLPFC), which lies anterior to the FEF in the second frontal gyrus

(Brodmann area 46); and a posterior eye field (PEF), which lies in the parietal lobe, possibly in the superior part of the angular gyrus (Brodmann area 39), and the adjacent lateral intraparietal sulcus. These areas all appear to be interconnected with each other and to send projections to the superior colliculus and the brain stem areas controlling saccades.

There are two parallel pathways involved in the cortical generation of saccades. An anterior system originates in the FEF and projects both directly, and via the superior colliculus, to the brain stem saccadic generators. This pathway also passes indirectly via the basal ganglia to the superior colliculus. Projections from the frontal cortex influence cells in the pars reticulata of the substantia nigra, via a relay in the caudate nucleus. An inhibitory pathway from the pars reticulata projects directly to the superior colliculus. This may be a gating circuit related to voluntary saccades, especially of the memory-guided type. A posterior pathway originates in the PEF and passes to the brain stem saccadic generators via the superior colliculus.

The smooth pursuit system has developed relatively independently of the saccadic oculomotor system to maintain foveation of a moving target, although there are inevitable interconnections between the two. The first task is to identify and code the velocity and direction of a moving target. This is carried out in the extrastriate visual area known as the middle temporal visual area (MT; also called visual area V5), which contains neurones sensitive to visual target motion. In man, this lies immediately posterior to the ascending limb of the inferior temporal sulcus at the occipitotemporal border. Area MT sends this motion signal to the medial superior temporal visual area (MST), thought to lie superior and a little anterior to area MT within the inferior parietal lobe: damage to this area results in an impairment of smooth pursuit of targets moving towards the damaged hemisphere.

Both area MST and FEF send direct projections to a group of nuclei which lie in the basal part of the pons. In the monkey, the dorsolateral and lateral groups of pontine nuclei receive direct cortical inputs related to smooth pursuit. Lesions of similarly located nuclei in man result in abnormal pursuit. These nuclei transfer the pursuit signal bilaterally to the posterior vermis, contralateral flocculus and fastigial nuclei of the cerebellum (see Ch.

20). The pursuit signal ultimately passes from the cerebellum to the brain stem, specifically to the medial vestibular nucleus and nucleus propositus hypoglossi, thence to the PPRF and possibly directly to the ocular motor nuclei. This circuitry therefore involves a double decussation, firstly at the level of the midpons (ponto-cerebellar neurones), and secondly in the lower pons (vestibuloabducens neurones).

The vestibulo-ocular reflex maintains coordination of vision during movement of the head and results in a compensatory conjugate eye movement which is equal but opposite to the movement of the head. This essentially three-neurone arc consists of primary vestibular neurones which project to the vestibular nuclei, secondary neurones which project from these nuclei directly to the abducens and oculomotor nuclei, and tertiary neurones which innervate the extraocular muscles. Vestibular neurones responding to head rotation also respond to optokinetic stimuli, which means that the neural substrate is likely to include both the visual and vestibular systems.

VASCULAR SUPPLY AND LYMPHATIC DRAINAGE

ARTERIES

The main vessel supplying orbital structures is the ophthalmic artery (Fig. 39.13). Its terminal branches anastomose on the face and scalp with those of the facial, maxillary and superficial temporal arteries, thereby establishing connections between the external and internal carotid arteries. The infraorbital branch of the maxillary artery, and possibly the recurrent meningeal artery, also supply orbital structures.

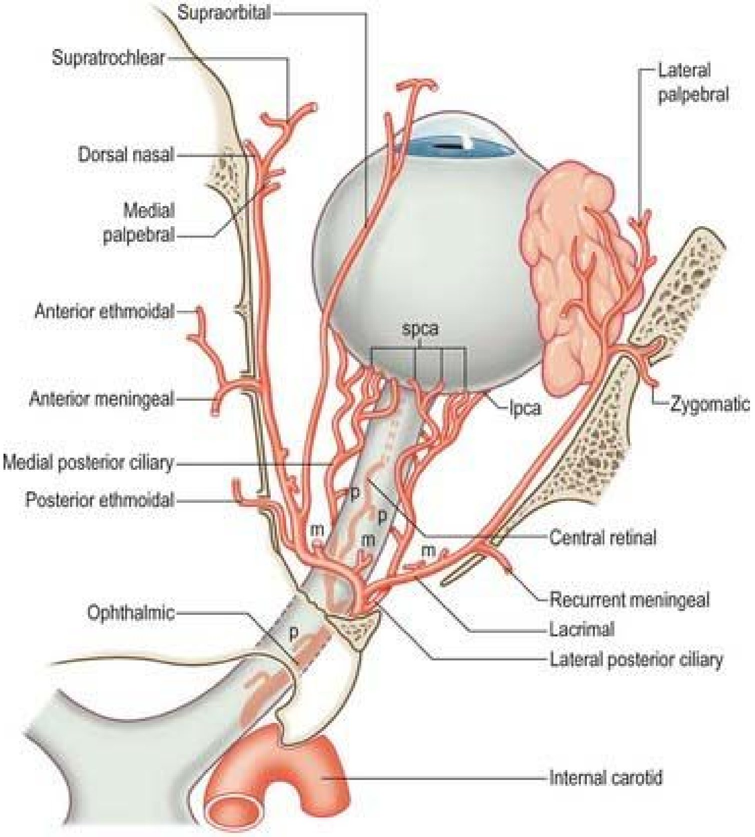
Supraorbital
Supratrochlear
Lateral palpebral
Dorsal nasal
Medial palpebral
Anterior ethmoidal
spca
Anterior meningeal
lpca
Zygomatic
Medial posterior ciliary
Posterior ethmoidal
p
m
p
m
m
Central retinal
Ophthalmic
p
Recurrent meningeal
Lacrimal
Lateral posterior ciliary
Internal carotid

Fig. 39.13 The orbital distribution of the ophthalmic artery. lpca, long posterior ciliary artery; m, muscular arteries; p, pial arteries; spca, short posterior ciliary arteries.

Ophthalmic artery

The ophthalmic artery leaves the internal carotid artery as it exits the cavernous sinus medial to the anterior clinoid process. It enters the orbit by the optic canal, inferolateral to the optic nerve and continues forward for a short distance before turning medially by crossing over (80%) or under (20%) the optic nerve. The main trunk of the artery continues along the medial wall of the orbit between the superior oblique and lateral rectus, and divides into supratrochlear (frontal) and dorsal nasal branches at the medial end of the upper eyelid. Although the order of branches from the ophthalmic artery is quite variable, a number may be identified consistently, including the central retinal artery, lacrimal artery, muscular branches, ciliary arteries, supraorbital artery, anterior and posterior ethmoidal arteries, meningeal branch, medial palpebral arteries, supratrochlear artery and dorsal nasal artery. Many of the branches of the ophthalmic artery accompany sensory nerves of the same name and have a similar distribution.

Central retinal artery

The small central artery of the retina is the first branch of the ophthalmic artery. It begins below the optic nerve and for a short distance lies in the dural sheath of the nerve. It enters the inferomedial surface of the nerve approximately 1.2 cm behind the eye, and runs to the retina (accompanying the central retinal vein) along its axis. The further distribution of the central retinal artery is described on p. 693.

Muscular branches

Muscular branches frequently spring from a common trunk to form superior and inferior groups, most of which accompany branches of the oculomotor nerve. The inferior branch contains most of the anterior ciliary arteries. Other muscular vessels branch from the lacrimal and supraorbital arteries or from the trunk of the ophthalmic artery.

Ciliary arteries

The ciliary arteries are distributed in long and short posterior, and anterior groups. Long posterior ciliary arteries, usually two, pierce the sclera near the optic nerve, pass anteriorly along the horizontal meridian and join the major arterial circle of the iris (see Fig. 40.10). About seven short posterior ciliary arteries pass close to the optic nerve to reach the eyeball where they divide into 15–20 branches. They pierce the sclera around the optic nerve to supply the choroid, and anastomose with twigs of the central retinal artery at the optic disc (see Fig. 40.31). Anterior ciliary arteries arise from muscular branches of the ophthalmic artery. They reach the eyeball on the tendons of the recti, form a circumcorneal subconjunctival vascular zone, and pierce the sclera near the sclerocorneal junction to end in the major arterial circle of the iris (see p. 685).

Lacrimal artery

The lacrimal artery is a large branch which usually leaves the ophthalmic artery near its exit from the optic canal, although it occasionally arises before the ophthalmic artery enters the orbit. It accompanies the lacrimal nerve along the upper border of lateral rectus, supplies and traverses the lacrimal gland, and ends in the eyelids and conjunctiva as the lateral palpebral arteries. The latter run medially in the upper and lower lids and anastomose with the medial palpebral arteries. The lacrimal artery gives off one or two zygomatic branches. One reaches the temporal fossa via the zygomaticotemporal foramen, and anastomoses with the deep temporal arteries. The other reaches the cheek by the zygomatico-facial foramen, and anastomoses with transverse facial and zygomatico-orbital arteries. A recurrent meningeal branch, usually small, passes back via the lateral part of the superior orbital fissure to anastomose with a middle meningeal branch. This branch is sometimes large and replaces the lacrimal artery, in which case it becomes a more significant contributor to the orbital blood supply.

Supraorbital artery

The supraorbital artery leaves the ophthalmic artery where it crosses the optic nerve, and ascends medial to superior rectus and levator palpebrae superioris. It accompanies the supraorbital nerve between the periosteum and levator palpebrae superioris, passes through the supraorbital foramen or notch, and divides into superficial and deep branches. These supply the skin, muscles and frontal periosteum, and anastomose with the supratrochlear artery, and the frontal branch of the superficial temporal artery and its contralateral fellow. The supraorbital artery supplies superior rectus and levator palpebrae superioris, and sends a branch across the trochlea to the medial canthus. It often sends a branch to the diploë of the frontal bone at the supraorbital margin, and may also supply the mucoperiosteum in the frontal sinus.

Posterior ethmoidal artery

The posterior ethmoidal artery runs through the posterior ethmoidal canal and supplies the posterior ethmoidal air sinuses. Entering the cranium, it gives off a meningeal branch to the dura mater, and nasal branches which descend into the nasal cavity via the cribriform plate and anastomose with branches of the sphenopalatine artery.

Anterior ethmoidal artery

The anterior ethmoidal artery passes with its accompanying nerve through the anterior ethmoidal canal to supply the ethmoidal and frontal air sinuses. Entering the cranium, it gives off a meningeal branch to the dura mater and nasal branches which descend into the nasal cavity with the anterior ethmoidal nerve. It runs in a groove on the deep surface of the nasal bone to supply the lateral nasal wall and septum. A terminal branch appears on the nose between the nasal bone and the upper nasal cartilage (see Ch. 32).

Meningeal branch

A meningeal branch, usually small, passes back through the superior orbital fissure to the middle cranial fossa, where it anastomoses with the middle and accessory meningeal arteries. It is sometimes large, in which case when it becomes a major contributor to the orbital blood supply.

Medial palpebral arteries

Above the trochlea, two medial palpebral arteries branch separately from the ophthalmic artery and join the lateral palpebral arteries to complete the arcades of the upper and lower eyelids.

Supratrochlear artery

The supratrochlear artery is a terminal branch of the ophthalmic artery. It leaves the orbit superomedially with the supratrochlear nerve, ascends on the forehead to supply the skin, muscles and pericranium, and anastomoses with the supraorbital artery and with its contralateral fellow.

Dorsal nasal artery

The dorsal nasal artery is the other terminal branch of the ophthalmic artery, and emerges from the orbit between the trochlea and medial palpebral ligament. It gives a branch to the upper part of the nasolacrimal sac and then divides into two branches. One branch joins the terminal part of the facial artery, and the other runs along the dorsum of the nose, supplies its outer surface and anastomoses with its contralateral fellow and the lateral nasal branch of the facial artery.

Infraorbital branch of the maxillary artery

The infraorbital branch of the maxillary artery enters the orbit through the posterior part of the inferior orbital fissure. It passes along the infraorbital groove of the maxilla in the floor of the orbit before entering the infraorbital canal, and comes out onto the face through the infraorbital foramen. Whilst in the infraorbital groove, it gives off branches which supply inferior rectus and inferior oblique, the nasolacrimal sac and, occasionally, the lacrimal gland.

VEINS

The orbit is drained by the superior and inferior ophthalmic veins and the infraorbital vein (Fig. 39.14). The veins of the eyeball mainly drain into the vortex veins; the retinal veins drain into the central retinal vein (see p. 693).

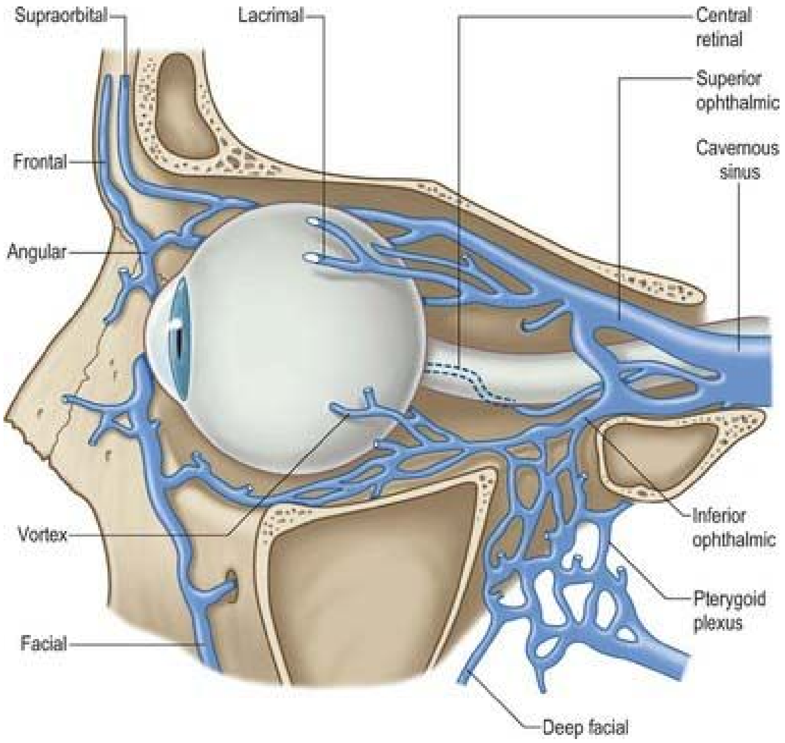
Supraorbital
Lacrimal
Central retinal
Superior ophthalmic
Cavernous sinus
Frontal
Angular
Vortex
Inferior ophthalmic
Pterygoid plexus
Facial
Deep facial

Fig. 39.14 The principal veins of the orbit.

Superior and inferior ophthalmic veins

The superior and inferior ophthalmic veins link the facial and intracranial veins and are devoid of valves. The superior ophthalmic vein forms posteromedial to the upper eyelid from two tributaries which connect anteriorly with the facial and supraorbital veins. It runs with the ophthalmic artery, lying between the optic nerve and superior rectus, and receives the corresponding tributaries, the two superior vortex veins of the eyeball, and the central vein of the retina. The central vein of the retina sometimes drains directly into the cavernous sinus, although it still gives a communicating branch to the superior ophthalmic vein. The superior ophthalmic vein may also receive the inferior ophthalmic vein. It traverses the superior orbital fissure, usually above the common tendinous ring of the recti, and ends in the cavernous sinus.

The inferior ophthalmic vein begins in a network near the anterior region of the orbital floor and medial wall. It runs backwards on inferior rectus and across the inferior orbital fissure, and then either joins the superior ophthalmic vein or passes through the superior orbital fissure, within or below the common tendinous ring, to drain directly into the cavernous sinus. The inferior ophthalmic vein receives tributaries from inferior rectus and inferior oblique, the nasolacrimal sac and the eyelids and receives the two inferior vortex veins of the eyeball. It communicates with the pterygoid venous plexus by a branch which passes through the inferior orbital fissure, and may also communicate with the facial vein across the inferior margin of the orbit.

Infraorbital vein

The infraorbital vein runs with the infraorbital nerve and artery in the floor of the orbit, and passes backwards through the inferior orbital fissure into the pterygoid venous plexus. It drains structures in the floor of the orbit and communicates with the inferior ophthalmic vein; it may also communicate with the facial vein on the face.

LYMPHATIC DRAINAGE

Lymphatic vessels other than those draining the conjunctiva have not been identified.

INNERVATION

Somatic and autonomic motor and somatic sensory nerves are found in the orbit (Figs 39.15, 39.16, 39.17). The oculomotor, trochlear and abducens nerves supply the extraocular muscles. Parasympathetic fibres from the oculomotor nerve supply sphincter pupillae and the ciliary muscle (ciliaris) via the ciliary ganglion, and from the facial nerve innervate the lacrimal gland and choroid via the pterygopalatine ganglion (see Ch. 31). Sympathetic fibres supply dilator pupillae. Both sympathetic and parasympathetic nerves supply the arteries. The sensory nerves within the orbit are the optic, ophthalmic and maxillary nerves (the maxillary nerve and most of the ophthalmic branches only pass through the orbit en route to supply the face and jaws).

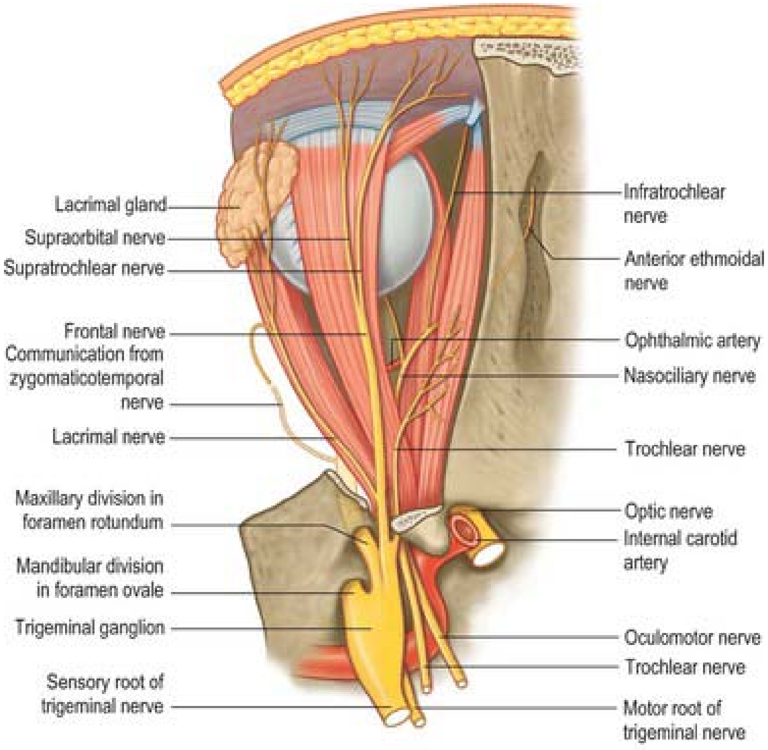
Lacrimal gland
Supraorbital nerve
Supratrochlear nerve
Frontal nerve
Communication from zygomaticotemporal nerve
Lacrimal nerve
Maxillary division in foramen rotundum
Mandibular division in foramen ovale
Trigeminal ganglion
Sensory root of trigeminal nerve
Infratrochlear nerve
Anterior ethmoidal nerve
Ophthalmic artery
Nasociliary nerve
Trochlear nerve
Optic nerve
Internal carotid artery
Oculomotor nerve
Trochlear nerve
Motor root of trigeminal nerve

Fig. 39.16 The nerves of the left orbit: superior aspect.

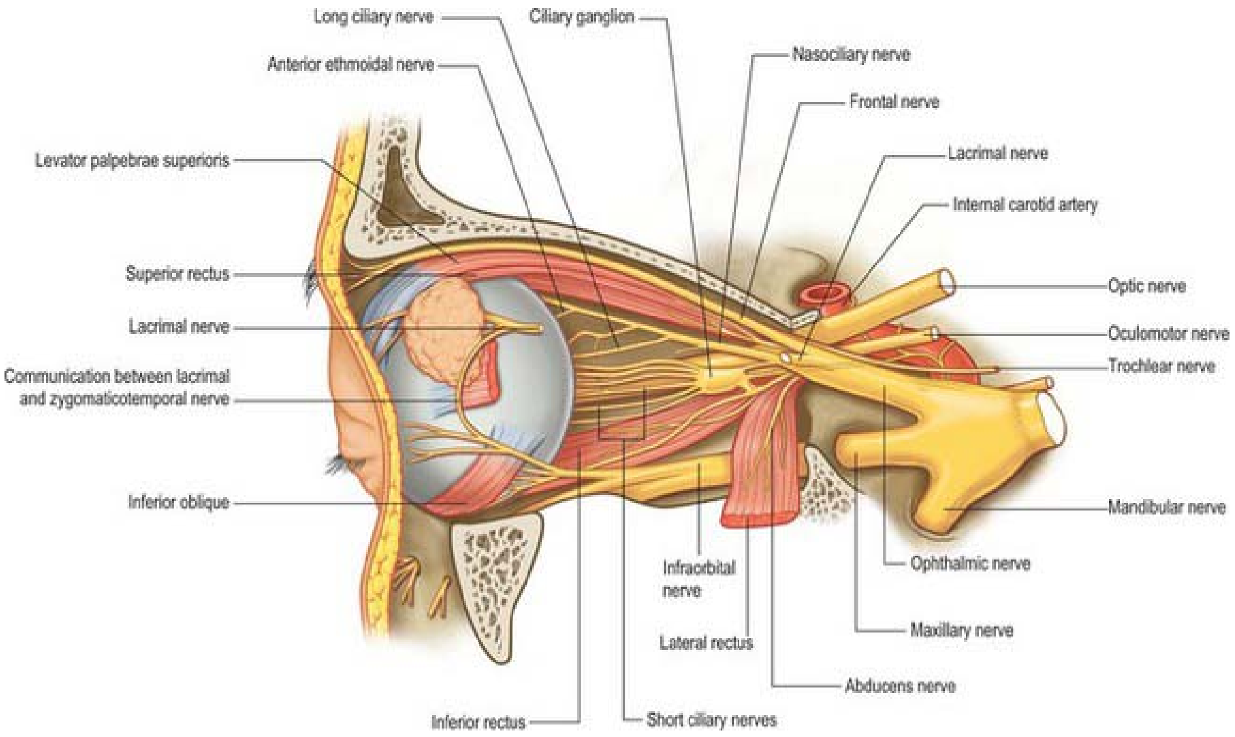
Long ciliary nerve
Ciliary ganglion
Anterior ethmoidal nerve
Nasociliary nerve
Frontal nerve
Levator palpebrae superioris
Lacrimal nerve
Internal carotid artery
Superior rectus
Optic nerve
Lacrimal nerve
Oculomotor nerve
Trochlear nerve
Communication between lacrimal and zygomaticotemporal nerve
Mandibular nerve
Inferior oblique
Ophthalmic nerve
Infraorbital nerve
Maxillary nerve
Lateral rectus
Abducens nerve
Short ciliary nerves
Inferior rectus

Fig. 39.17 The nerves of the left orbit and the ciliary ganglion: lateral aspect.

Oculomotor nerve

The oculomotor nerve is the third cranial nerve (Fig. 39.15). It innervates four of the extraocular muscles (superior, inferior and medial rectus and inferior oblique), and also conveys parasympathetic fibres which relay in the ciliary ganglion. The nerve emerges at the midbrain, on the medial side of the crus of the cerebral peduncle and passes along the lateral dural wall of the cavernous sinus, dividing into superior and inferior divisions which run beneath the trochlear and ophthalmic nerves. The two divisions enter the orbit through the superior orbital fissure, within the common tendinous ring of the recti, separated by the nasociliary branch of the ophthalmic nerve.

The superior division of the oculomotor nerve passes above the optic nerve to enter the inferior (ocular) surface of superior rectus. It supplies this muscle and gives off a branch which runs to innervate levator palpebrae superioris. The inferior division of the oculomotor nerve divides into medial, central and lateral branches. The medial branch passes beneath the optic nerve to enter the lateral (ocular) surface of medial rectus; the central branch runs downwards and forwards to enter the superior (ocular) surface of inferior rectus; the lateral branch travels forwards on the lateral side of inferior rectus to enter the orbital surface of inferior oblique and also communicates with the ciliary ganglion to distribute parasympathetic fibres to sphincter pupillae and the ciliary muscle.

Trochlear nerve

The trochlear nerve is the fourth cranial nerve and innervates superior oblique exclusively. It is the only cranial nerve to emerge from the dorsal surface of the brain stem, passing from the midbrain onto the lateral surface of the crus of the cerebral peduncle. It runs through the lateral dural wall of the cavernous sinus and then crosses the oculomotor nerve to enter the orbit through the superior orbital fissure, above the common tendinous ring and levator palpebrae superioris, and medial to the frontal and lacrimal nerves (Fig. 39.15). The trochlear nerve travels but a short distance to enter the superior (orbital) surface of superior oblique.

Abducens nerve

The abducens nerve is the sixth cranial nerve and innervates lateral rectus exclusively. It emerges from the brain stem between the pons and the medulla oblongata and usually runs through the inferior venous compartment of the petroclival venous confluence in a bow-shaped canal, Dorello’s canal (see Ch. 27). It then bends sharply across the upper border of the petrous part of the temporal bone to enter the cavernous sinus, where it lies lateral to the internal carotid artery (unlike the oculomotor, trochlear, ophthalmic and maxillary nerves, which merely invaginate the lateral dural wall of the sinus). The abducens nerve enters the orbit through the superior orbital fissure, within the common tendinous ring, at first below, and then between, the two divisions of the oculomotor nerve and lateral to the nasociliary nerve (Fig. 39.15). It passes forwards to enter the medial (ocular) surface of lateral rectus.

Optic nerve

The optic nerve is the second cranial nerve. It arises from the optic chiasma on the floor of the diencephalon and enters the orbit through the optic canal, accompanied by the ophthalmic artery. It changes its shape from being flattened at the chiasma to rounded as it passes through the optic canal. In the orbit the optic nerve passes forwards, laterally and downwards, and pierces the sclera at the lamina cribrosa (see p. 695), slightly medial to the posterior pole. It has a somewhat tortuous course within the orbit to allow for movements of the eyeball, and is surrounded by extensions of the three layers of the meninges.

The optic nerve has important relationships with other orbital structures. As it leaves the optic canal, it lies superomedial to the ophthalmic artery, and is separated from lateral rectus by the oculomotor, nasociliary and abducens nerves, and sometimes by the ophthalmic veins. It is closely related to the origins of the four recti, whereas more anteriorly, where the muscles diverge, it is separated from them by a substantial amount of orbital fat. Just beyond the optic canal, the ophthalmic artery and the nasociliary nerve cross the optic nerve to reach the medial wall of the orbit. The central artery of the retina enters the substance of the optic nerve about halfway along its length. Near the back of the eyeball, the optic nerve becomes surrounded by the long and short ciliary nerves and vessels.

Ophthalmic nerve

The ophthalmic division of the trigeminal nerve arises from the trigeminal ganglion in the middle cranial fossa. It passes forwards along the lateral dural wall of the cavernous sinus, giving off three main branches, the lacrimal, frontal and nasociliary nerves, just before it reaches the superior orbital fissure (Figs 39.16, 39.17). These branches subsequently travel through the orbit to supply targets that are primarily in the upper part of the face (see Ch. 29 for further details of this distribution).

Lacrimal nerve

The lacrimal nerve enters the orbit through the superior orbital fissure above the common tendinous ring and lateral to the frontal and trochlear nerves. It passes forwards along the lateral wall of the orbit on the superior border of lateral rectus, and travels through the lacrimal gland and the orbital septum to supply the conjunctiva and skin covering the lateral part of the upper eyelid. The nerve also communicates with the zygomatic branch of the maxillary nerve, which carries postganglionic parasympathetic fibres from the pterygopalatine ganglion to the lacrimal gland.

Frontal nerve

The frontal nerve is the largest branch of the ophthalmic nerve. It enters the orbit through the superior orbital fissure above the common tendinous ring, and lies between the lacrimal nerve laterally and the trochlear nerve medially. It passes forwards towards the rim of the orbit on levator palpebrae superioris; about halfway along this course it divides into the supraorbital and supratrochlear nerves.

Supraorbital nerve

The supraorbital nerve, the larger of the two terminal branches of the frontal nerve, continues forwards along levator palpebrae superioris until it leaves the orbit through the supraorbital notch or foramen. It emerges onto the forehead and supplies the mucous membrane which lines the frontal sinus, the skin and conjunctiva covering the upper eyelid, and the skin over the forehead and scalp (see Ch. 29). The postganglionic sympathetic fibres which innervate the sweat glands of the supraorbital area probably travel in the supraorbital nerve, having entered the ophthalmic nerve via its communication with the abducens nerve within the cavernous sinus.

Supratrochlear nerve

The supratrochlear nerve runs medially above the trochlea for the tendon of superior oblique. It gives a descending branch to the infratrochlear nerve and ascends onto the forehead through the frontal notch to supply the skin and conjunctiva covering the upper eyelid, and the skin over the forehead.

Nasociliary nerve

The nasociliary nerve is intermediate in size between the frontal and lacrimal nerves, and is more deeply placed in the orbit, which it enters through the common tendinous ring, lying between the two rami of the oculomotor nerve. It crosses the optic nerve with the ophthalmic artery and runs obliquely below superior rectus and superior oblique to reach the medial orbital wall, where it gives off the anterior and posterior ethmoidal nerves. The nasociliary nerve also has long ciliary and infratrochlear branches and a connection with the ciliary ganglion.

Anterior ethmoidal nerve

The anterior ethmoidal nerve passes through the anterior ethmoidal foramen and canal and enters the cranial cavity. It runs forwards in a groove on the upper surface of the cribriform plate beneath the dura mater, and descends through a slit lateral to the crista galli into the nasal cavity, where it occupies a groove on the internal surface of the nasal bone and gives off the medial and lateral internal nasal branches. For a description of the subsequent distribution of the anterior ethmoidal nerve, see Chapter 32.

Posterior ethmoidal nerve

The posterior ethmoidal nerve leaves the orbit by the posterior ethmoidal foramen and supplies the ethmoidal and sphenoidal sinuses.

Infratrochlear nerve

The infratrochlear nerve leaves the orbit below the trochlea and supplies the skin of the eyelids, the conjunctiva, lacrimal sac, lacrimal caruncle and the side of the nose above the medial canthus.

Long ciliary nerves

Two or three long ciliary nerves branch from the nasociliary nerve as it crosses the optic nerve. They accompany the short ciliary nerves, pierce the sclera near the attachment of the optic nerve, and run forwards between the sclera and choroid. They supply the ciliary body, iris and cornea, and contain postganglionic sympathetic fibres for the dilator pupillae from neurones in the superior cervical ganglion. An alternative pathway for the supply of the dilator pupillae is via the sympathetic root associated with the ciliary ganglion.

Ramus communicans to the ciliary ganglion

The ramus communicans to the ciliary ganglion usually branches from the nasociliary nerve as the latter enters the orbit lateral to the optic nerve. It is sometimes joined by a filament from the internal carotid sympathetic plexus or from the superior ramus of the oculomotor nerve as it enters the posterosuperior angle of the ganglion.

Maxillary nerve

Most of the branches of the maxillary division of the trigeminal nerve arise in the pterygopalatine fossa (see Ch. 31). They include the zygomatic and infraorbital nerves, which pass into the orbit through the inferior orbital fissure (Fig. 39.17).

Zygomatic nerve

The zygomatic nerve lies close to the base of the lateral wall of the orbit. It divides soon after entering the orbit into two branches, the zygomaticotemporal and the zygomaticofacial nerves, which run within the orbit for only a short distance before passing onto the face through the lateral wall of the orbit. They may either enter separate canals within the zygomatic bone or the zygomatic nerve itself may enter the bone before dividing. For a description of the distribution of the zygomaticotemporal and zygomaticofacial nerves on the face, see Chapter 29.

Infraorbital nerve

The infraorbital nerve initially lies in the infraorbital groove on the floor of the orbit. As it approaches the rim of the orbit it runs into the infraorbital canal through which it passes to emerge onto the face at the infraorbital foramen. It supplies the skin of the lower eyelid and possibly the conjunctiva. For a description of the subsequent distribution of the infraorbital nerve on the face, see Chapter 29.

Ciliary ganglion

The ciliary ganglion is a parasympathetic ganglion concerned with the innervation of certain intraocular muscles. It is a small, flat, reddish-grey swelling, 1–2 mm in diameter, connected to the nasociliary nerve, and located near the apex of the orbit in loose fat approximately 1 cm in front of the medial end of the superior orbital fissure. It lies between the optic nerve and lateral rectus, usually lateral to the ophthalmic artery. Its neurones, which are multipolar, are larger than those found in typical autonomic ganglia; a very small number of more typical neurones are also present.

Its connections or roots (motor, sensory and sympathetic) enter or leave the ganglion posteriorly (Fig. 39.18). Eight to ten delicate filaments, termed the short ciliary nerves, emerge anteriorly from the ganglion, arranged in two or three bundles, the lower being larger. They run forwards sinuously with the ciliary arteries, above and below the optic nerve, and divide into 15–20 branches that pierce the sclera around the optic nerve and run in small grooves on the internal scleral surface. They convey parasympathetic, sympathetic and sensory fibres between the eyeball and the ciliary ganglion: only the parasympathetic fibres synapse in the ganglion.

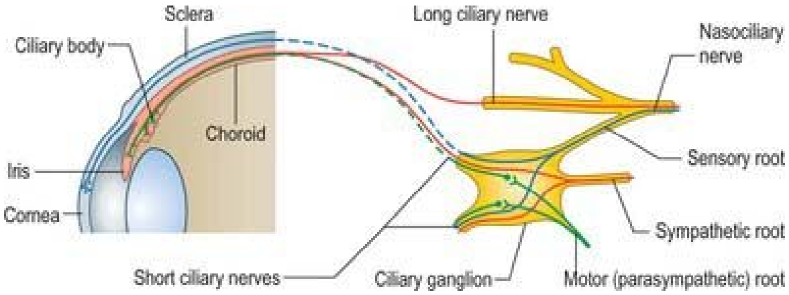

Fig. 39.18 The ciliary ganglion, with its roots and branches of distribution. Red, sympathetic fibres; green, parasympathetic fibres; blue, sensory fibres. Alternative pathways are given for the sympathetic fibres.

The parasympathetic root, derived from the branch of the oculomotor nerve to the inferior oblique, consists of preganglionic fibres from the Edinger–Westphal nucleus, which relay in the ganglion. Postganglionic fibres travel in the short ciliary nerves to the sphincter pupillae and ciliary muscle. More than 95% of these fibres supply the ciliary muscle, which is much the larger muscle in volume.

The sympathetic root contains fibres from the plexus around the internal carotid artery within the cavernous sinus. These postganglionic fibres, derived from the superior cervical ganglion, form a fine branch which enters the orbit through the superior orbital fissure inside the common tendinous ring. The fibres may pass directly to the ganglion, or may join the nasociliary nerve and travel to the ganglion in its sensory root: either way, they traverse the ganglion without synapsing to emerge into the short ciliary nerves. They are distributed to the blood vessels of the eyeball. Sympathetic fibres innervating dilator pupillae may sometimes travel via the short ciliary nerves (rather than the more usual route via the ophthalmic, nasociliary and long ciliary nerves).

The sensory fibres which pass through the ciliary ganglion are derived from the nasociliary nerve. They enter the short ciliary nerves and carry sensation from the cornea, the ciliary body and the iris.

Orbital branches of the pterygopalatine ganglion

Several rami orbitales arise dorsally from the pterygopalatine ganglion and enter the orbit through the inferior orbital fissure. Branches leave the orbit through the posterior ethmoidal air sinus. There is strong experimental evidence from studies of animals, including monkeys, that postganglionic parasympathetic branches pass directly to the lacrimal gland, ophthalmic artery and choroid.

EYELIDS, CONJUNCTIVA AND LACRIMAL SYSTEM

The exposed ocular surface is protected by retractable eyelids and by a tear film produced mainly by the lacrimal gland, with contributions from glands within the eyelid and conjunctiva (a transparent mucous membrane that covers the inner surface of the eyelid and the exposed surface of the sclera) (see Fig. 40.1).

EYELIDS

The eyelids (palpebrae) are two folds of modified skin which cover the anterior surface of the eye (Fig. 39.19). By their reflex closure, achieved by contraction of orbicularis oculi, they protect the eye from injury and shield the eyes from excessive light. Periodic blinking maintains a thin film of tears over the cornea which prevents desiccation: movement of the eyelid during blinking helps ensure the even distribution of the tear film.

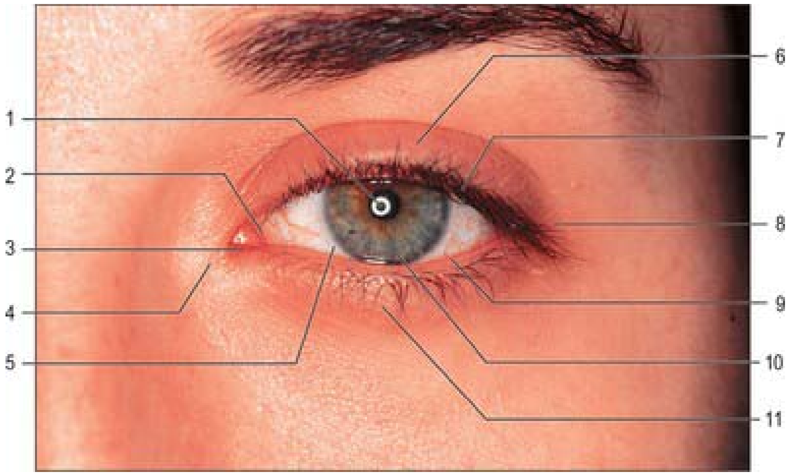

Fig. 39.19 The eyelids and anterior aspect of the eyeball. **1**. Pupil. **2**. Plica semilunaris. **3**. Lacrimal caruncle. **4**. Medial canthus. **5**. Conjunctiva. **6**. Upper eyelid. **7**. Eyelashes. **8**. Lateral canthus. **9**. Lid margin. **10**. Iris. **11**. Lower eyelid.

(By permission from Berkovitz BKB, Moxham BJ 2002 Head and Neck Anatomy. London: Martin Dunitz.)

The upper eyelid is larger and more mobile than the lower eyelid, and contains an elevator muscle, levator palpebrae superioris (see above). A transverse opening, the palpebral fissure, lies between the free margins of the lids, which join at their extremities (termed the medial and lateral canthus). The lateral canthi is relatively featureless. The medial canthus is approximately 2 mm lower than the lateral canthus: this distance is increased in some Asiatic groups. It is separated from the eyeball by a small triangular space, the lacrimal lake (lacus lacrimalis), in which a small, reddish body called the lacrimal caruncle is situated. The caruncle represents an area of modified skin containing some fine hairs, and is mounted on the plica semilunaris, a fold of conjunctiva which is believed by some to be a vestige of the nictitating membrane of other animals.

A small elevation, the lacrimal papilla, is located on each palpebral margin approximately one-sixth of the way along from the medial canthus of the eye. There is a small aperture, the punctum lacrimale, in the centre of the papilla that forms the opening to the lacrimal drainage system. The margin of the eyelid lateral to the lacrimal papilla bears the eyelashes and is termed the ciliary part of the eyelid. The margin medial to the papilla lacks eyelashes and forms the lacrimal part of the eyelid.

When looking straight ahead, the upper eyelid overlaps the upper part of the cornea by 2–3 mm, whereas the lower lid lies just below the corneo-scleral junction (limbus). When the eyelids are closed, the upper lid moves down to cover the whole of the cornea. Malposition of the lower eyelid is common, particularly in the elderly. Ectropion describes the rolling out of the lower eyelid so that it is no longer in contact with the cornea leading to epiphora (watering). Entropion describes the inversion of the eyelid with corresponding inturning of the eyelashes (trichiasis) which contact the cornea and cause irritation.

Each eyelid margin is 2–3 mm thick from front to back. The anterior two thirds is skin and the posterior third is conjunctival mucosa. A narrow ‘grey line’ lies anterior to the mucocutaneous junction. This corresponds to the location of the ciliary (marginal) part of orbicularis oculi and is an important surgical landmark, since an incision at this point allows the eyelid to be split into anterior and posterior lamellae along a relatively bloodless plane. The eyelashes lie in front of the grey line, and the circular openings of the tarsal glands (meibomian glands) lie behind it. The tarsal glands are visible through the palpebral conjunctiva, when the eyelids are everted, as a series of parallel, faint yellow lines arranged perpendicular to the lid margins.

Eyelashes are short, thick, curved hairs, arranged in double or triple rows. The upper, which are longer and more numerous, curve upwards, while those in the lower lid curve down, so that upper and lower lashes do not interlace when the lids are closed.

The eyelids pass to adjacent facial skin without obvious demarcation, although their limits are clearly defined in pathological conditions such as oedema. Various skin folds or furrows are of topographical interest. A prominent superior palpebral furrow or fold lies approximately opposite the upper margin of the tarsal plate and is deeply recessed when the lids are open. Oriental Asians have a skin flap, the epicanthus, which begins laterally in the superior palpebral fold and progresses medially to cover the medial canthus. Infant Caucasians frequently have a transient epicanthus which sometimes persists in the adult. A less prominent inferior palpebral furrow occupies a similar position in the skin of the lower lid and deepens on downward gaze. A naso-jugal furrow extends obliquely from the medial lower margin of the bony orbit to the cheek, and a malar furrow may be seen laterally along the inferior orbital rim in middle age, but only infrequently and faintly in the young.

Structure

From its anterior surface inwards each eyelid consists of skin, subcutaneous connective tissue, fibres of the palpebral part of orbicularis oculi (see Fig. 29.11A), submuscular connective tissue, the tarsal plate (tarsus) with its tarsal glands and orbital septum, and palpebral conjunctiva (Fig. 39.20). The upper lid also contains the aponeurosis of levator palpebrae superioris.

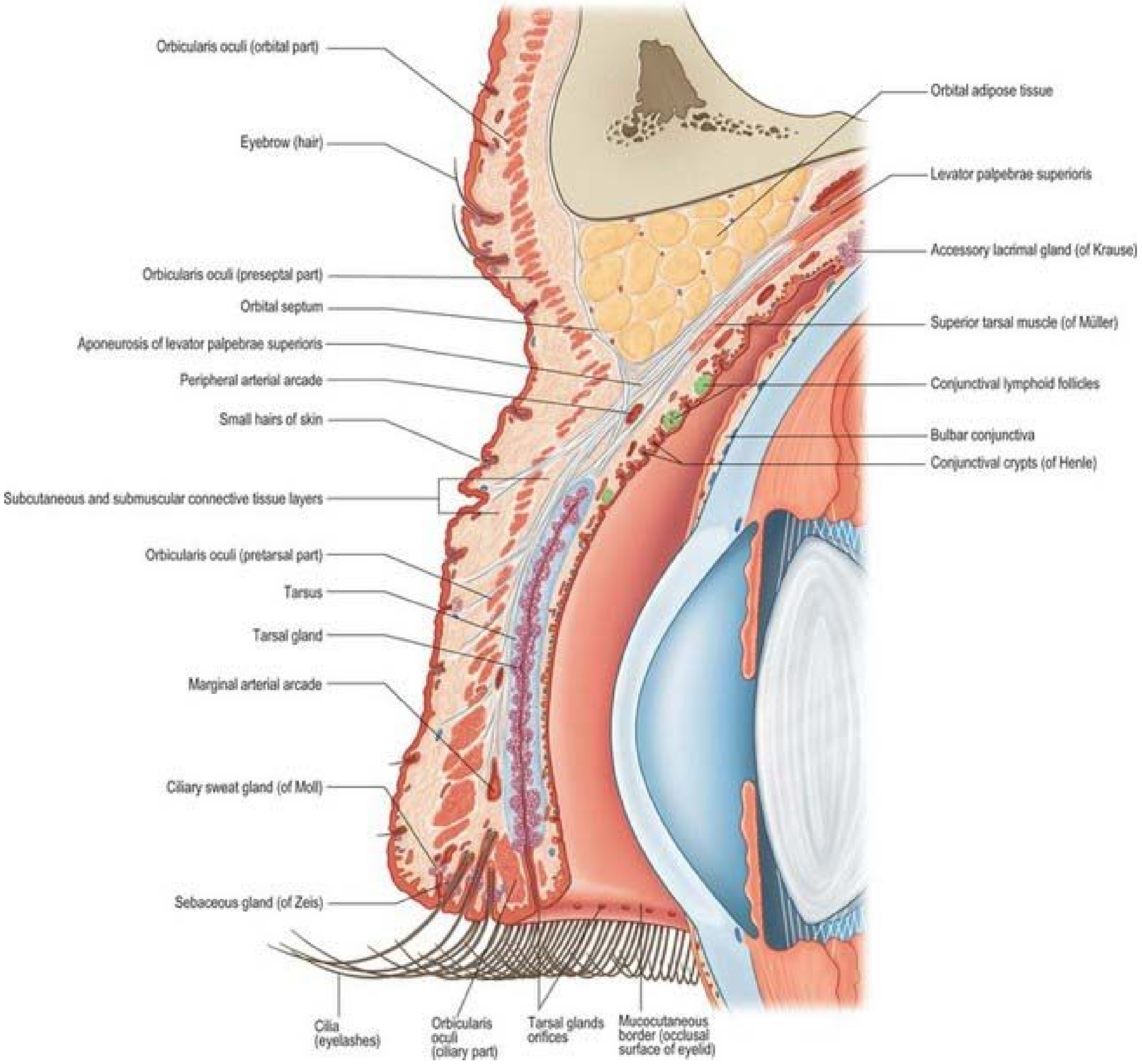
Orbicularis oculi (orbital part)
Eyebrow (hair)
Orbicularis oculi (preseptal part)
Orbital septum
Aponeurosis of levator palpebrae superioris
Peripheral arterial arcade
Small hairs of skin
Subcutaneous and submuscular connective tissue layers
Orbicularis oculi (pretarsal part)
Tarsus
Tarsal gland
Marginal arterial arcade
Ciliary sweat gland (of Moll)
Sebaceous gland (of Zeis)
Orbital adipose tissue
Levator palpebrae superioris
Accessory lacrimal gland (of Krause)
Superior tarsal muscle (of Müller)
Conjunctival lymphoid follicles
Bulbar conjunctiva
Conjunctival crypts (of Henle)
Cilia (eyelashes)
Orbicularis oculi (ciliary part)
Tarsal glands orifices
Mucocutaneous border (occlusal surface of eyelid)

Fig. 39.20 The upper eyelid and anterior segment of the eye: sagittal section.

The skin is extremely thin and is continuous at the palpebral margins with the conjunctiva. The subcutaneous connective tissue is very delicate, seldom contains any adipose tissue, and lacks elastic fibres.

The palpebral part of orbicularis oculi is subdivided anatomically into ciliary, pretarsal and preseptal parts. The palpebral fibre bundles are thin and pale and lie parallel with the palpebral margins. Deep to them is the submuscular connective tissue, a loose fibrous layer that is continuous in the upper lid with the subaponeurotic layer of the scalp: effusions of blood or pus at this level can therefore pass down from the scalp into the upper eyelid. The main nerves lie in the submuscular layer, which means that local anaesthetics should be injected deep to orbicularis oculi.

Tarsal plates

The two tarsal plates (Fig. 39.21) are thin, elongated, crescent-shaped plates of firm, dense fibrous tissue approximately 2.5 cm long. There is one in each eyelid to provide support and determine eyelid form. Each is convex and conforms to the configuration of the anterior surface of the eye. The free ciliary border is straight and adjacent to the eyelash follicles. The orbital border is convex and attached to the orbital septum. The superior tarsus, the larger of the two, is semi-oval, approximately 10 mm in height centrally. Its inferior edge is parallel to, and approximately 2 mm from, the lid margin. The smaller inferior tarsus is narrower and approximately 4 mm in vertical height.

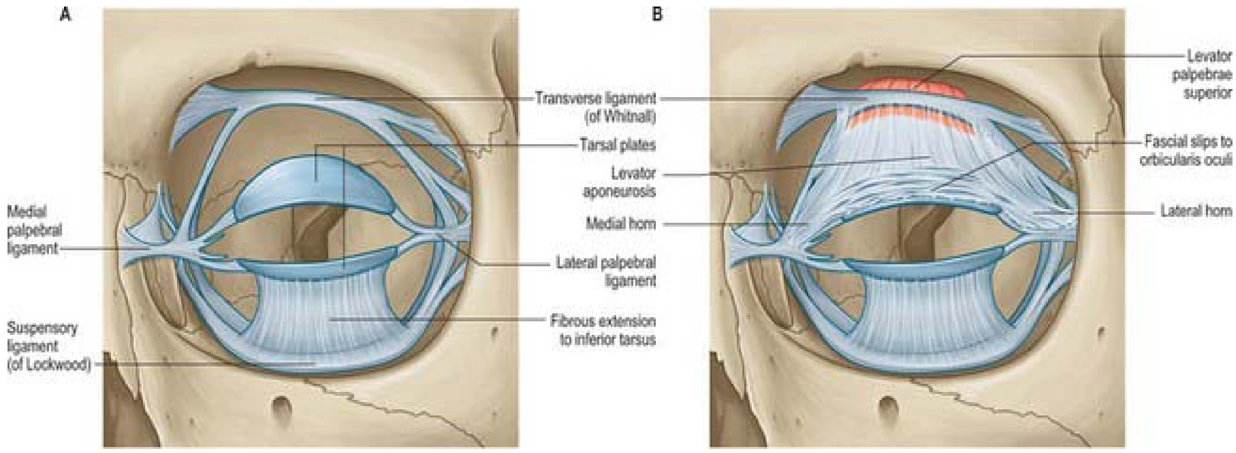
A
B
Transverse ligament (of Whitnall)
Tarsal plates
Levator aponeurosis
Medial horn
Lateral palpebral ligament
Fibrous extension to inferior tarsus
Medial palpebral ligament
Suspensory ligament (of Lockwood)
Levator palpebrae superior
Fascial slips to orbicularis oculi
Lateral horn

Fig. 39.21 **A**, Tarsal plates and their attachments. **B**, Anterior insertion of levator palpebrae superioris.

The tarsal plates are connected to the margins of the orbit by the orbital septum and by the medial and lateral palpebral (canthal) ligaments (Fig. 39.21). The medial palpebral ligament passes from the medial ends of the two tarsal plates to the anterior lacrimal crest and the frontal process of the maxilla. It splits at its insertion into the tarsal plates to surround the lacrimal canaliculi, and lies in front of the nasolacrimal sac and the orbital septum. The lateral palpebral ligament is relatively poorly developed. It passes from the lateral ends of the tarsal plates to a small tubercle on the zygomatic bone within the orbital margin and is more deeply situated than the medial palpebral ligament. It lies beneath the orbital septum and the lateral palpebral raphe of orbicularis oculi.

The deepest fibres of the aponeurosis of levator palpebrae superioris are attached to the anterior surface of the superior tarsus. The superior and inferior tarsal plates are also associated with a thin lamina of smooth muscle forming the superior and inferior tarsal muscles respectively. Opposite the equator of the eye the superior tarsal muscle passes from the inferior face of levator palpebrae superioris to a fibrous extension which projects to the upper margin of the superior tarsus (Fig. 39.20). The muscle is innervated by the sympathetic nervous system and on contraction, elevates the eyelid. Although it may be regarded as supplementing the action of the levator muscle, its full role is not clear. (The mild ptosis that is a characteristic feature of Horner's syndrome is the result of an interruption to the sympathetic supply to the superior tarsal muscle.) A corresponding but less prominent inferior tarsal muscle in the lower eyelid unites the inferior border, and possibly also the anterior surface, of the inferior tarsus to the capsulopalpebral fascia, which is the anterior expansion of the fused fascial sheath of inferior rectus and inferior oblique. Contraction of inferior rectus during downward gaze therefore also pulls the lower lid downwards. The lower lid is capable of depressing by 4–5 mm, although it is not equipped with a striated muscle counterpart to the levator of the upper lid.

Palpebral glands

Tarsal (Meibomian) glands are modified sebaceous glands embedded in the tarsi. They are yellow and arranged in approximately 25 parallel rows perpendicular to the eyelid margin in the upper lid, and slightly fewer in the lower lid. They occupy the full tarsal height, and are therefore longer centrally where the tarsi are higher. Each gland consists of a straight tube with many lateral diverticula, and opens by a minute orifice on the free palpebral margin. It is enclosed by a basement membrane, and is lined at its orifice by stratified epithelium and elsewhere by a single layer of polyhedral cells. The oily secretion of the tarsal glands spreads over the margins of the eyelids, and so an oily layer is drawn over the tear film as the palpebral fissure opens after a blink, reducing evaporation and contributing to tear film stability. The presence of the oily, hydrophobic secretions of tarsal glands along the margins of the eyelids also inhibits the spillage of tears onto the face. Obstruction of the tarsal gland ducts by lipid and cellular debris may result in lipogranulomatous inflammation and the clinical manifestations of chalazion (internal hordeolum).

Small sebaceous glands (of Zeis) and sweat glands (of Moll) are associated with the eyelashes, and are prone to infection, producing an external hordeolum (stye).

Vascular supply and lymphatic drainage

The arterial supply to the eyelids is derived principally from the medial and lateral palpebral branches of the ophthalmic artery. Their branches course laterally along the tarsal edges to form superior and inferior arcades (two in the upper eyelid and one in the lower). The eyelids are also supplied by branches of the infraorbital, facial, transverse facial and superficial temporal arteries.

The veins which drain the eyelids are larger and more numerous than the arteries; they pass either superficially to veins on the face and forehead, or deeply to the ophthalmic veins within the orbit.

The lymph vessels which drain the eyelids and conjunctiva commence in a superficial plexus beneath the skin, and in a deep plexus in front of and behind the tarsi. These plexuses communicate with one another, and medial and lateral sets of vessels arise from them. The lymph vessels of the lateral set drain the whole thickness of the lateral part of the upper and lower lids and pass laterally from the lateral canthus to end in the superficial and deep parotid lymph nodes. The lymph vessels of the medial set drain the skin over the medial part of the upper eyelid, the whole thickness of the medial half of the lower lid, and the caruncle; they follow the course of the facial vein to end in the submandibular group of lymph nodes.

Innervation

The cutaneous innervation of the eyelids comes from both the ophthalmic and maxillary divisions of the trigeminal nerve. The upper eyelid is supplied mainly by the supraorbital branch of the frontal nerve. Additional contributions come from the lacrimal nerve, the supratrochlear branch of the frontal nerve, and the infratrochlear branch of the nasociliary nerve. The nerve supply to the lower eyelid is derived principally from the infraorbital branch of the maxillary nerve, with small contributions from the lacrimal and infratrochlear nerves.

CONJUNCTIVA

The conjunctiva is a thin, transparent mucous membrane that extends from the eyelid margins anteriorly, providing a lining to the lids, before turning sharply upon itself to form the fornices whence it is reflected onto the globe to cover the sclera up to its junction with the cornea. The conjunctiva thus forms a sac that opens anteriorly through the palpebral fissure (Fig. 39.22). At the free palpebral margins the conjunctiva is continuous with the skin, the lining epithelium of the ducts of the tarsal glands, and with the lacrimal canaliculi and lacrimal sac (see below). The continuity between the conjunctiva and the nasolacrimal duct and nasal mucosa is important in the spread of infection (see Ch. 32).

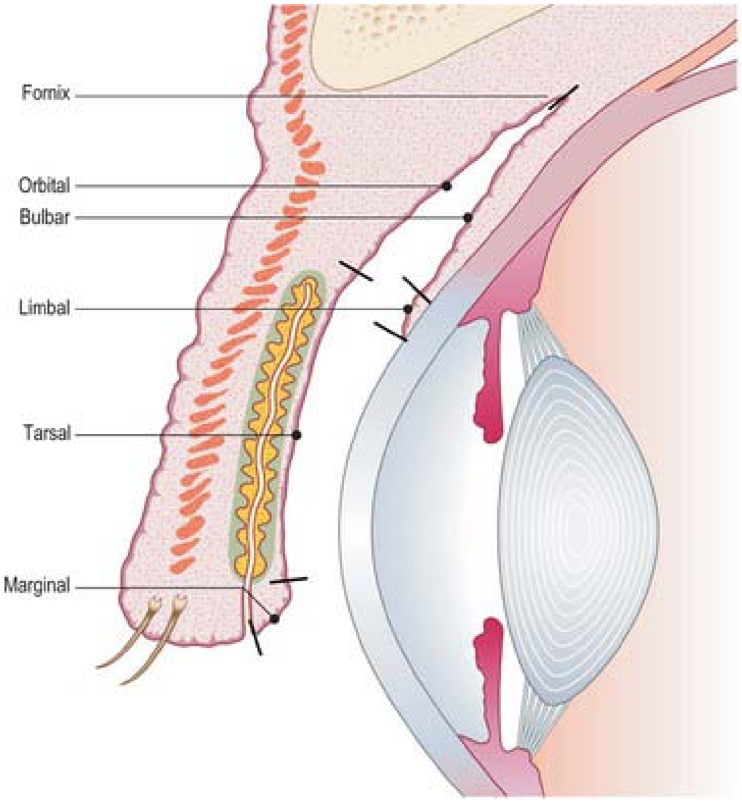

Fig. 39.22 The regions of the conjunctiva: sagittal section.

The conjunctiva contributes the mucin component of the pre-ocular tear film and plays a central role in the defence of the ocular surface against microbial infection. It is conventionally divided into five regions: marginal, tarsal, orbital, bulbar and limbal (Fig. 39.22). The marginal, tarsal and orbital regions are collectively referred to as the palpebral conjunctiva.

The marginal zone extends from a line immediately posterior to the openings of the tarsal glands and passes around the eyelid margin to continue on the inner surface of the lid as far as the sub-tarsal groove (a shallow sulcus which marks the inferior edge of the tarsus). The tarsal conjunctiva is highly vascular and is firmly attached to the underlying tarsal plate. The orbital zone extends as far as the fornices, which mark the line of reflection of the conjunctiva from the lids onto the eyeball. The conjunctiva is more loosely attached to underlying tissues over the orbital zone and so folds readily. Elevations of the conjunctival surface in the form of papillae and lymphoid follicles (part of the mucosa associated lymphoid tissue, MALT) are commonly observed in this region (Knop & Knop 2002).

Ducts of the lacrimal gland open into the lateral part of the superior fornix. The bulbar conjunctiva is loosely connected to the eyeball over the exposed sclera, is thin and transparent, and readily permits the visualization of conjunctival and episcleral blood vessels. The loose attachment of the conjunctiva to the fascial sheath of the globe (Tenon’s capsule) in this region means that the conjunctiva is freely movable here: as the bulbar conjunctiva approaches the cornea its surface becomes smoother and its attachment to the sclera increases. The limbal conjunctiva extends approximately 1–1.5 mm around the cornea and contains a dense network of capillaries.

Structure

The conjunctiva is composed of an epithelial layer and an underlying fibrous layer or substantia propria. The form of the epithelium and thickness of the substantia propria varies with location. At the margin of the lids the epithelium is non-keratinized stratified squamous and 10–12 cells thick. The epithelium of the tarsal conjunctiva thins to two or three layers and consists of columnar and flat surface cells. Near the fornices the cells are taller, and a trilaminar conjunctival epithelium covers much of the bulbar conjunctiva. It thickens closer to the corneoscleral junction and then changes to stratified squamous epithelium typical of the cornea (see p. 678). A proportion of limbal conjunctival epithelial cells serve as stem cells for the corneal epithelium: this region of the conjunctiva is therefore essential for maintaining corneal integrity.

Mucous-secreting goblet cells are scattered within the conjunctival epithelium. They show a marked regional variation in density, being most frequent on either side of the fornix, but absent from the exposed surfaces of the bulbar conjunctiva and the corneoscleral junction.

The substantia propria, fibrous layer, or stroma, is thickest at the fornix and thinnest over the tarsi where conjunctival attachment is firmest. With the exception of the tarsal conjunctiva, the substantia propria adjacent to the epithelium is mainly loose. It merges with the fibrous fascia bulbi and episclera in the limbal and bulbar regions, and is loosely attached to the sheaths of the recti. At the fornix it is continuous with orbital fascial tissues and has loose attachments to the overlying tendon of levator palpebrae superioris and the superior tarsal muscle fascia superiorly, an arrangement which provides support for the fornix during eyeball rotation.

Vascular supply and lymphatic drainage

The arteries of the palpebral conjunctiva are derived from the vascular arcades of the eyelids. Many of the small vessels of the eyelid drain to the conjunctival veins which in turn pass back to the orbital and facial veins. The substantia propria of the tarsal and orbital conjunctiva is richly vascular. A dense capillary network is arranged in a single subepithelial lamina, a distribution which meets the requirement of the cornea during sleep, when oxygen is available to the cornea only through this vascular system. The bulbar conjunctiva receives blood from the palpebral arcades and from the anterior ciliary arteries which reach the conjunctiva on the orbital surface of the recti. The veins drain by the same route and join the ophthalmic veins.

Lymphatics drain into pre-auricular and sub-mandibular lymph nodes.

Innervation

The conjunctiva is innervated by sensory nerves from the same ophthalmic and maxillary branches of the trigeminal nerve that serve the eyelid. Autonomic nerve fibres are abundant in the conjunctiva, particularly in bulbar and limbal regions and are probably vasomotor in function.

LACRIMAL SYSTEM

The lacrimal system consists of structures responsible for the production of tears (principally the main lacrimal gland with a contribution from accessory lacrimal glands) and the lacrimal drainage pathway which collects the tear fluid and conveys it into the nasal cavity (paired lacrimal canaliculi, lacrimal sac and nasolacrimal duct) (Fig. 39.23).

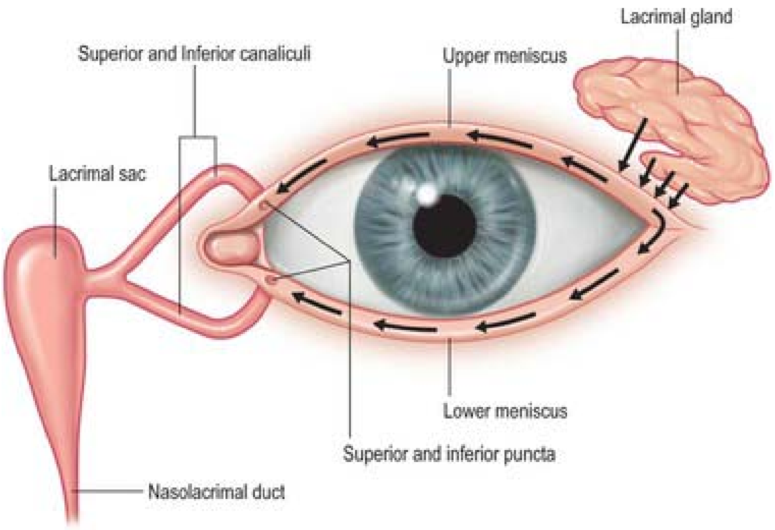
Lacrimal gland
Superior and Inferior canaliculi
Upper meniscus
Lacrimal sac
Lower meniscus
Superior and inferior puncta
Nasolacrimal duct

Fig. 39.23 Representation of tear dynamics on the ocular surface. Tears are produced by the lacrimal gland and flow within the upper and lower meniscus. Tears drain sequentially through the puncta, canaliculi, lacrimal sac and nasolacrimal duct.

The total tear volume is approximately 7 µl. It is distributed within the precorneal tear film (1–2 µl), and along the upper and lower marginal tear strips (5–6 µl), which are wedge-shaped menisci that run along the posterior border of the lid margins and join together at the canthi.

Lacrimal gland

The lacrimal gland is the primary producer of the aqueous component of the tear layer. Its secretion is a watery fluid with an electrolyte content similar to that of plasma and containing several proteins including the bacteriocidal enzymes lysozyme and lactoferrin, IgA, and tear lipocalin (previously called tear-specific pre-albumen).

The lacrimal gland consists of orbital and palpebral parts which are continuous posterolaterally around the concave lateral edge of the aponeurosis of levator palpebrae superioris. The orbital part, about the size and shape of an almond, lodges in the lacrimal fossa on the medial aspect of the zygomatic process of the frontal bone, just within the orbital margin. It lies above levator palpebrae superioris and, laterally, above lateral rectus. Its lower surface is connected to the sheath of levator palpebrae superioris and its upper surface is connected to the orbital periosteum. Its anterior border is in contact with the orbital septum and its posterior border attached to the orbital fat. The palpebral part, about one-third the size of the orbital part, is subdivided into two or three lobules and extends below the aponeurosis of levator palpebrae superioris into the lateral part of the upper lid, where it is attached to the superior conjunctival fornix. It is visible through the conjunctiva when the lid is everted.

The main ducts of the lacrimal gland, about six in number, discharge into the conjunctival sac at the superior lateral fornix. Those from the orbital part (four or five) penetrate the aponeurosis of levator palpebrae superioris to join those from the palpebral part. Excision of the palpebral part is therefore functionally equivalent to the total removal of the gland.

Many small accessory lacrimal glands (glands of Krause and Wolfring) occur in or near the fornix. They are more numerous in the upper eyelid and their presence may explain why the conjunctiva does not dry up after extirpation of the main lacrimal gland.

Microstructure

The lacrimal gland is lobulated and tubuloacinar in form. Its secretory units are acini similar to those found in the salivary glands (Fig. 39.24; see also Ch. 30) (Ruskell 1975). Acini consist of secretory cells which discharge their product into a central lumen continuous with an intercalated duct formed from a single layer of epithelial cells that lack secretory granules.

Myoepithelial cells extend processes around the perimeter of acini and ducts; their contraction imparts a mechanical force on the acini and ducts which promotes the expulsion of tears from the gland. The interstices of the gland are composed of loose connective tissue which contains numerous immune cells, mainly B-lymphocytes and plasma cells (particularly IgA-secreting cells).

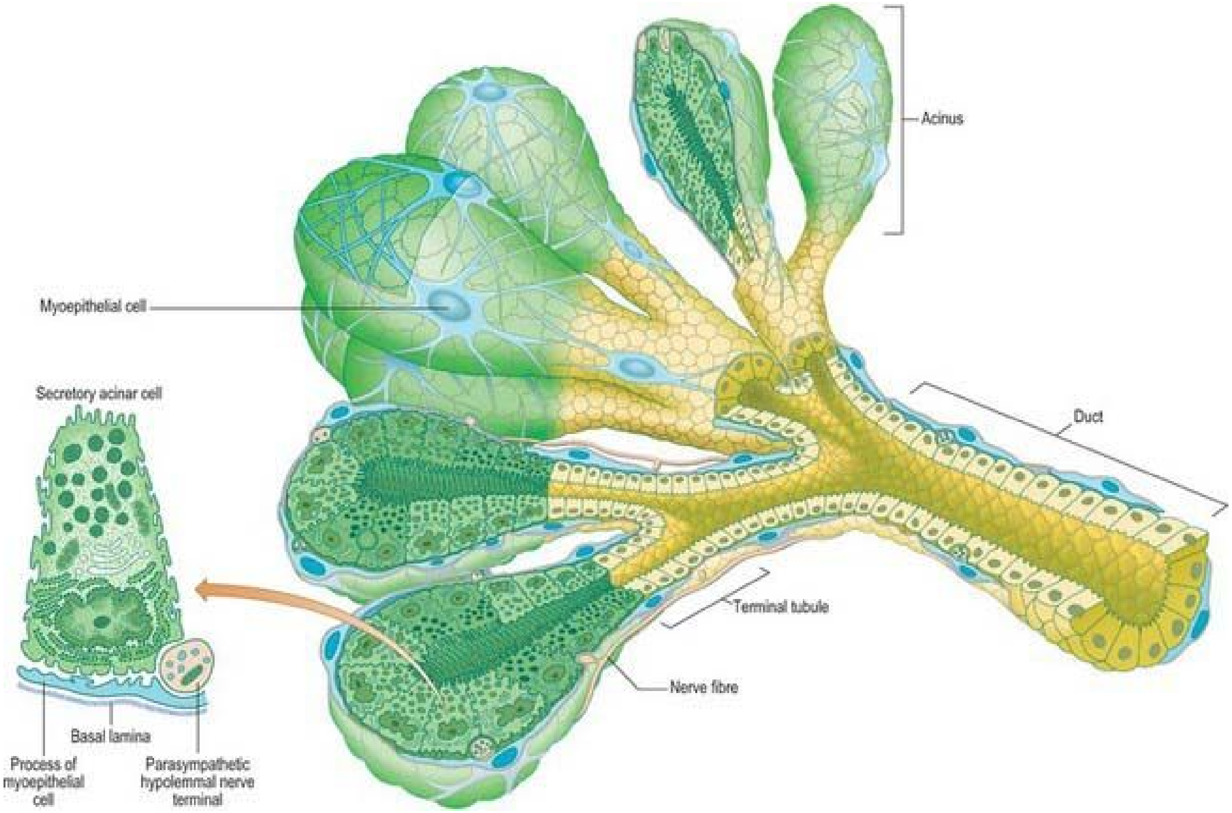
Acinus
Myoepithelial cell
Secretory acinar cell
Duct
Terminal tubule
Nerve fibre
Basal lamina
Process of myoepithelial cell
Parasympathetic hypolemmal nerve terminal

Fig. 39.24 Organization of the secretory units in the lacrimal gland.

Vascular supply

The lacrimal gland receives its arterial blood supply from the lacrimal branch of the ophthalmic artery. It may also receive blood from the infraorbital artery. Venous drainage is into the superior ophthalmic vein.

Innervation

The lacrimal gland is innervated by secretomotor postganglionic parasympathetic fibres from the pterygopalatine ganglion. They reach the gland either via zygomatic and lacrimal branches of the maxillary nerve or pass directly from the ganglion. Sympathetic fibres which issue from the superior cervical ganglion also supply the lacrimal gland. These fibres may be involved in the regulation of blood flow and the modulation of gland secretion.

Lacrimation reflex

The lacrimation reflex (Fig. 39.25) is stimulated by irritation of the conjunctiva and cornea, which elicits a large increase in tear volume. The afferent limb of the reflex involves branches of the ophthalmic nerve, with an additional contribution from the infraorbital nerve if the conjunctiva of the lower eyelid is involved. Impulses enter the brain and spread by interneurones to activate parasympathetic neurones in the superior salivatory nucleus (associated with the facial nerve) and sympathetic neurones in the upper thoracic spinal cord. The efferent pathway to the lacrimal gland involves the greater petrosal nerve, which carries preganglionic parasympathetic secretomotor fibres, and the deep petrosal nerve, which conveys postganglionic sympathetic fibres: the parasympathetic fibres relay in the pterygopalatine ganglion, and the sympathetic fibres pass through the ganglion without synapsing.

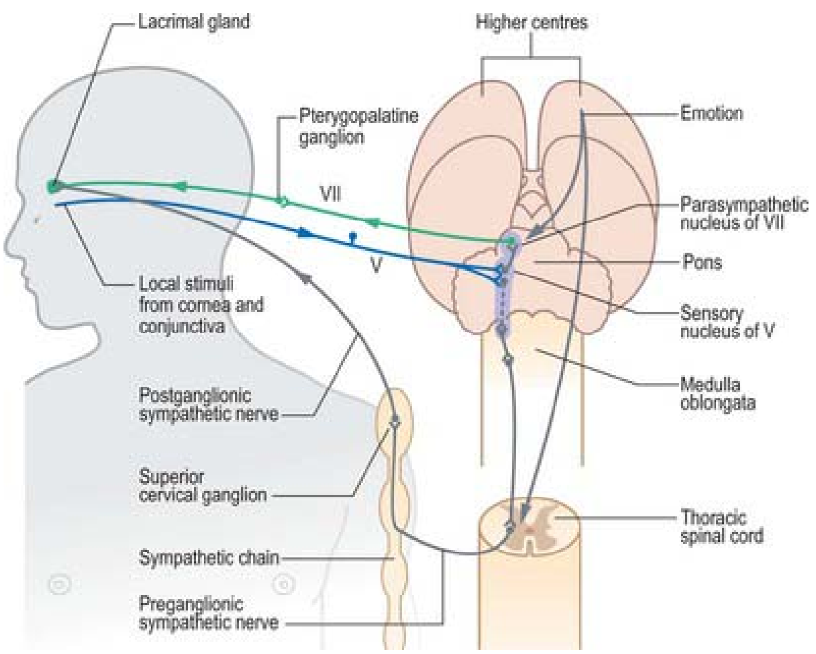
Lacrimal gland
Higher centres
Pterygopalatine ganglion
Emotion
VII
Parasympathetic nucleus of VII
Pons
V
Local stimuli from cornea and conjunctiva
Sensory nucleus of V
Medulla oblongata
Postganglionic sympathetic nerve
Superior cervical ganglion
Thoracic spinal cord
Sympathetic chain
Preganglionic sympathetic nerve

Fig. 39.25 Lacrimation reflex.

(Redrawn from MacKinnon P, Morris J 2005 Oxford Textbook of Functional Anatomy, Vol 3, 2nd edn. Head and Neck. Oxford: Oxford University Press. By permission of Oxford University Press.)

Lacrimation may also occur in response to emotional triggers.

Pre-ocular tear film

The tear film is a complex fluid that covers the exposed parts of the ocular surface framed by the eyelid margins. Classically the tear film has been regarded as a trilaminar structure, with a superficial lipid layer (secreted by the meibomian glands) that overlies an aqueous phase (derived from the main and accessory lacrimal glands) and an inner mucinous layer (produced mainly by conjunctival goblet cells) (Fig. 39.26). The tear film performs a number of important functions. By smoothing out irregularities of the corneal epithelium, it creates an even surface of good optical quality that is reformed with each blink. The air-tear interface forms the principal refractive surface of the optical system of the eye. Since the cornea is avascular, it is dependent on the tear film for its oxygen provision. When the eye is open, the tear film is in a state of equilibrium with the oxygen in the atmosphere, and gaseous exchange takes place across the tear-epithelial interface. The constant turnover of the tear film also provides a mechanism for the removal of metabolic waste products. Tears play a major role in the defence of the eye against microbial colonization: the washing action of the tear fluid reduces the likelihood of microbial adhesion to the ocular surface, and the tears contain a host of protective antimicrobial proteins.

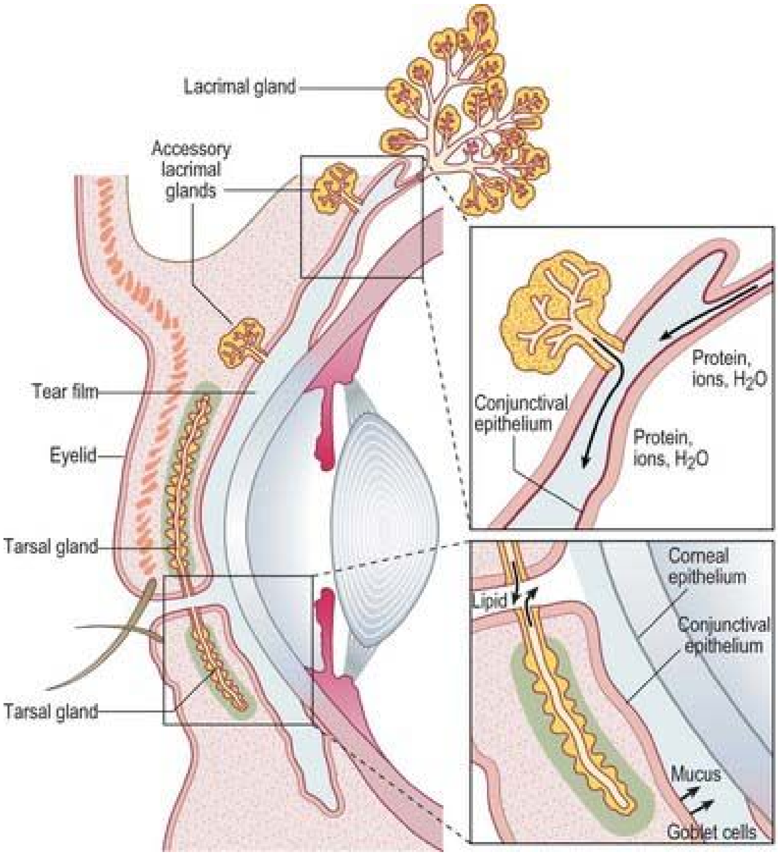
Lacrimal gland
Accessory lacrimal glands
Tear film
Eyelid
Tarsal gland
Tarsal gland
Conjunctival epithelium
Protein, ions, H_2O
Protein, ions, H_2O
Corneal epithelium
Lipid
Conjunctival epithelium
Mucus
Goblet cells

Fig. 39.26 Orbital glands which contribute the various components of the preocular tear film. The aqueous component (consisting primarily of proteins, ions and water) is produced by the main and accessory lacrimal glands. Tarsal glands in the eyelids produce the lipid layer of the tear film and the mucous component is derived from conjunctival goblet cells.

Lacrimal drainage pathway

There is a constant turnover of tears: production is matched by elimination. Some tears are lost by evaporation or absorption across the conjunctiva, but the majority are eliminated via the nasolacrimal drainage system (Fig. 39.23). Tears collect at the medial canthal angle where they drain into the puncta of the upper and lower lids, which are directed towards the surface of the eye to receive tear fluid. From each punctum tears drain into lacrimal canaliculi. There is one canaliculus, approximately 10 mm long, in each lid. Each canaliculus first passes vertically from its punctum for about 2 mm and widens to form an ampulla before passing medially towards the lacrimal sac. The superior canaliculus is smaller and shorter than the inferior. In approximately 80% of adults the canaliculi unite to form a common canaliculus before reaching the lacrimal sac.

The mucosa lining the canaliculi has a non-keratinized stratified squamous epithelium lying on a basement membrane, outside which is a lamina propria rich in elastic fibres (the canaliculi are therefore easily dilated when probed). Striated muscle fibres of orbicularis oculi interweave on each side of the canaliculus in a manner suggesting a sphincter-like spiraling, and supporting the claim that lumen size is regulated on blinking, possibly facilitating tear drainage.

The lacrimal sac is the closed upper end of the nasolacrimal duct. It is approximately 12 mm long and lies in a fossa in the lacrimal bone in the anterior part of the medial wall of the orbit (Fig. 39.2). The sac is bounded in front by the anterior lacrimal crest of the maxilla and behind by the posterior lacrimal crest of the lacrimal bone. Its closed upper end is laterally flattened, its lower part is rounded and merges into the duct, and the lacrimal canaliculi open into its lateral wall near its upper end.

A layer of lacrimal fascia, continuous with the orbital periosteum, passes between the lacrimal crest of the maxilla and the lacrimal bone. It forms a roof and lateral wall to the lacrimal fossa and separates the lacrimal sac from the medial palpebral ligament in front and the lacrimal part of orbicularis oculi behind. A plexus of minute veins lies between the fascia and the sac. The upper half of the lacrimal fossa is related medially to the anterior ethmoidal sinuses, and the lower half to the anterior part of the middle meatus. The lacrimal sac has a fibroelastic wall and is lined internally by mucosa which is continuous with the conjunctiva through the lacrimal canaliculi, and with the nasal mucosa through the nasolacrimal duct.

The nasolacrimal duct is approximately 18 mm long, and descends from the lacrimal sac to open anteriorly in the inferior meatus of the nose at an expanded orifice. A fold of mucosa (plica lacrimalis) forms an imperfect valve just above its opening (ostium lacrimalis). The duct runs down an osseous canal formed by the maxilla, lacrimal bone and inferior nasal concha. It is narrowest in the middle and is directed downwards, backwards and a little laterally. The mucosa of the lacrimal sac and the nasolacrimal duct has a bilaminar columnar epithelium, which is ciliated in places. A rich plexus of veins forms erectile tissue around the duct: engorgement of these veins may obstruct the duct.

REFERENCES

nop E, Knop N. A functional unit for ocular surface immune defence formed by the lacrimal gland, conjunctiva and lacrimal drainage system. *Adv Exp Med Biol*. 2002;506B:635-644.

oornneef L. The architecture of the musculo-fibrous apparatus in the human orbit. *Acta Morphol Neerl Scand*. 1977;15:35-64.

eigh RJ, Zee DS. The Neurology of Eye Movement, 4th edn. Oxford: Oxford University Press, 2006.

uskell GL. Nerve terminals and epithelial cell variety in the human lacrimal gland. *Cell Tiss Res*. 1975;138:121-136.

CHAPTER 40

The eye

The outer surface of the eye is composed of parts of two spheres with different radii. The anterior segment, part of the smaller sphere, is formed by the transparent cornea and accounts for approximately 7% of the ocular surface. The posterior segment of the eyeball is part of the larger sphere formed by the opaque sclera (Fig. 40.1).

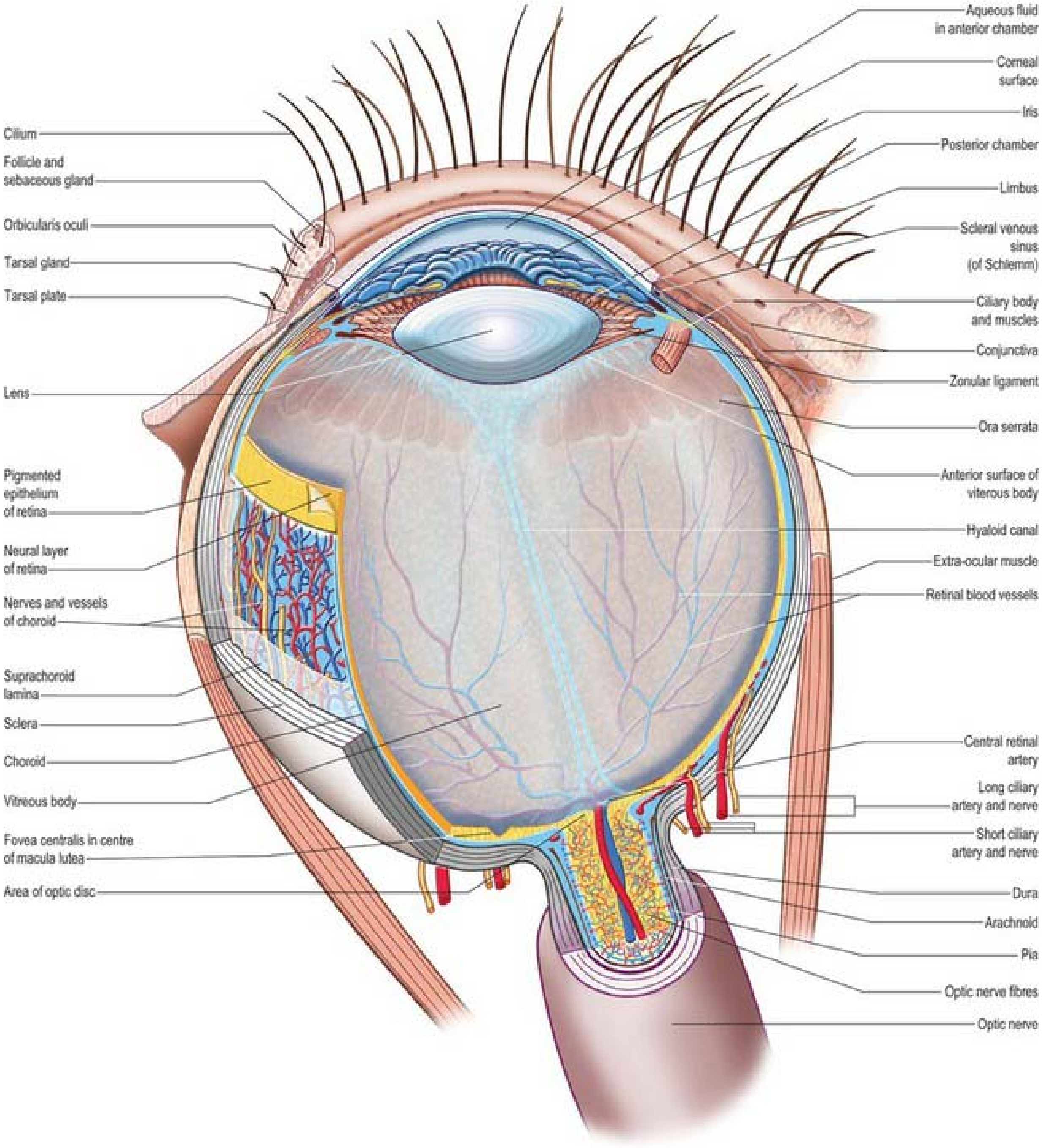
Cilium
Follicle and sebaceous gland
Orbicularis oculi
Tarsal gland
Tarsal plate
Lens
Pigmented epithelium of retina
Neural layer of retina
Nerves and vessels of choroid
Suprachoroid lamina
Sclera
Choroid
Vitreous body
Fovea centralis in centre of macula lutea
Area of optic disc
Aqueous fluid in anterior chamber
Corneal surface
Iris
Posterior chamber
Limbus
Scleral venous sinus (of Schlemm)
Ciliary body and muscles
Conjunctiva
Zonular ligament
Ora serrata
Anterior surface of viterous body
Hyaloid canal
Extra-ocular muscle
Retinal blood vessels
Central retinal artery
Long ciliary artery and nerve
Short ciliary artery and nerve
Dura
Arachnoid
Pia
Optic nerve fibres
Optic nerve

Fig. 40.1 Left eye and part of the lower eyelid in horizontal section viewed from above: parts have been cut away to show internal structures.

Internal to the sclera is a vascular, pigmented layer consisting of three continuous parts that collectively make up the uveal tract: a thin choroid lying posteriorly, a thicker ciliary body and an anterior iris which is displaced from the outer coat and terminates at the pupillary aperture (Fig. 40.1). The internal surface of the choroid is covered by the photosensory retina, which terminates anteriorly at the ora serrata, which also marks the junction between the ciliary body and choroid. The vasculature of the choroid supplies nutrients to the avascular outer retina.

The ocular lens is located immediately behind the iris and is suspended from the ciliary body via zonular fibres (Fig. 40.1). Smooth muscles within the ciliary body regulate the tension exerted on the elastic lens and hence determine its shape, thereby adjusting the focus of the eye in the process of accommodation. The iris, which does not allow the transmission of light due to a heavily pigmented posterior surface, also contains smooth muscle, allowing it to regulate the size of the pupillary aperture.

The iris and lens separate the eye into three chambers. The largest, the vitreous chamber, is filled with the gel-like vitreous humour, and lies posterior to the lens, comprising about two-thirds of the volume of the eye (Fig. 40.1). The spaces between the lens and iris, and the iris and cornea, are the posterior and anterior chambers respectively of the eye. Both are filled with aqueous humour, which is produced by the epithelium of the ciliary body, travels through the pupil, circulates in the anterior chamber and is drained principally through the canal of Schlemm at the iridocorneal filtration angle. Aqueous humour provides metabolic support to the avascular lens and cornea.

The sole purpose of the eyes and their associated structures within the bony orbit is to form a good image on a healthy retina. The photoreceptors of the retina transduce the optical radiation into neurobiological activity and other cells within the retina then begin to process the image. The retinal signal is transferred via the optic nerve, along the visual pathway (see Fig. 40.33) to various regions within the brain, where further processing results in visual perception.

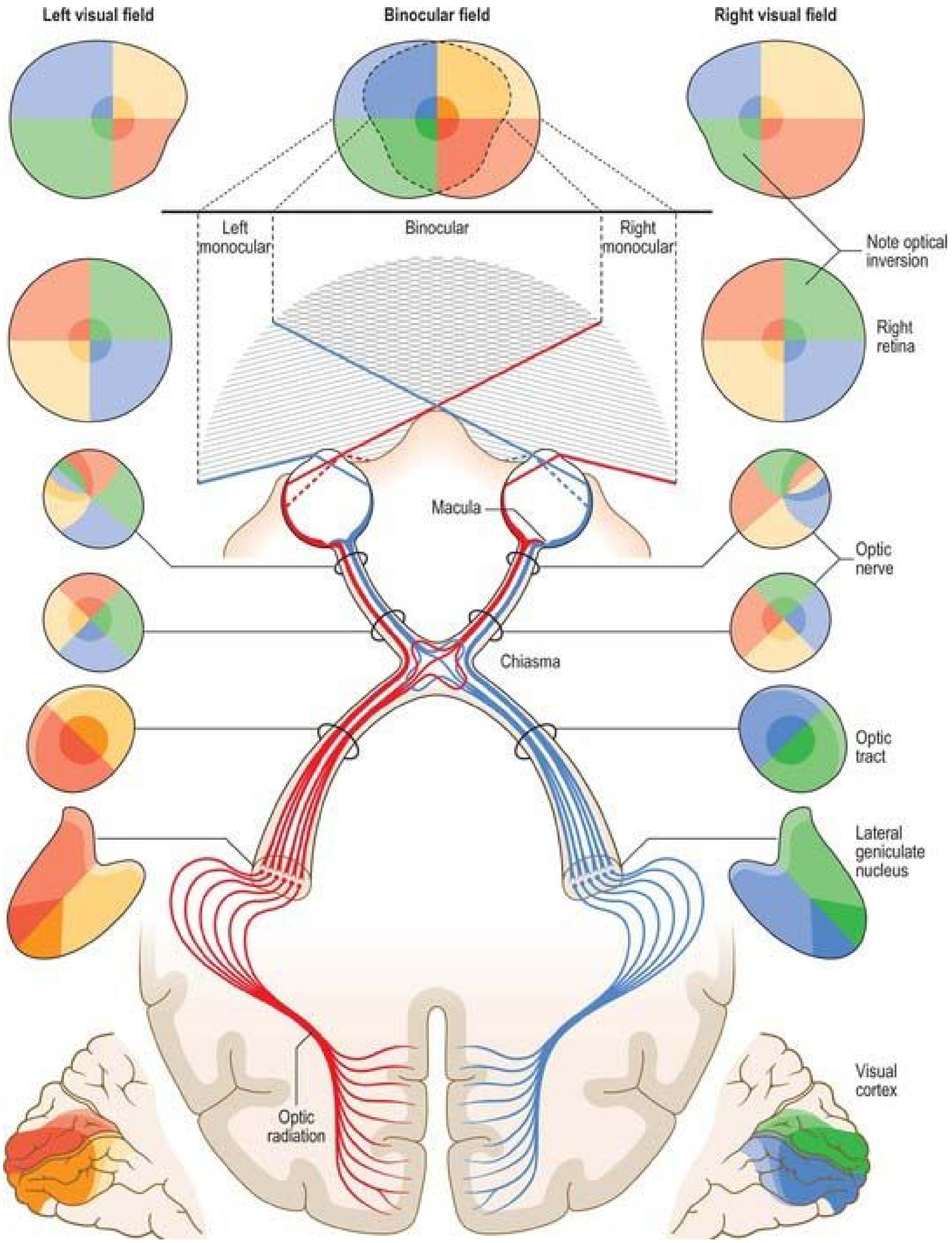
Left visual field
Binocular field
Right visual field
Left monocular
Binocular
Right monocular
Note optical inversion
Right retina
Macula
Optic nerve
Chiasma
Optic tract
Lateral geniculate nucleus
Visual cortex
Optic radiation

Fig. 40.33 The visual pathway, showing the spatial arrangement of neurones and their fibres in relation to the quadrants of the retinae and visual fields. The proportions at various levels are not exactly to scale. In particular the macula is exaggerated in size in the visual fields and retinae. In each quadrant of the visual field, and in the parts of the visual pathway subserving it, two shades of each respective colour are used; the paler shade

denotes the peripheral field and the darker shade denotes the macular part of the quadrant. From the optic tract onwards these two shades are both made more saturated to denote intermixture of neurones from both retinae, the palest shade being reserved for parts of the visual pathway concerned with monocular vision.

OUTER COAT

The fibrous outer coat of the eye consists of the opaque posterior sclera and the transparent anterior cornea. Together they form a semi-elastic protective capsule enclosing the eye, which when made turgid by intraocular pressure, determines the optical geometry of the eye and ensures its shape is not distorted when it moves. The sclera also provides attachments for the extraocular muscles, and its smooth external surface rotates easily on the adjacent tissues of the orbit when these muscles contract (see Ch. 39). The opacity of the sclera helps ensure that only light that enters the eye through the pupil reaches the retina. The cornea, on the other hand, not only admits light but its covering tear film (see p. 673) is also the major refractive surface of the eye.

SCLERA

The sclera accounts for approximately 93% of the outer coat of the eye. Anteriorly, it is continuous with the cornea at the corneoscleral junction (limbus) (Fig. 40.1). It is punctured by a number of foramina containing nerves and blood vessels, most notably the optic foramen, which lies 3 mm medial to the midline and 1 mm below the horizontal and houses the optic nerve. Smaller openings contain anterior ciliary arteries which penetrate anteriorly, vortex veins which cross the sclera equatorially, and the long and short ciliary nerves and arteries which enter posteriorly. The sclera is thickest posteriorly (1–1.35 mm), decreasing gradually towards the equator to reach a minimum of 300 μm under the tendons of the recti. Going forwards from the insertions of the recti, it gradually increases in thickness once more to 800 μm at the limbus.

The external surface of the sclera is covered by a delicate episcleral lamina of loose fibro-vascular tissue, which contains sparse blood vessels and is in contact with the inner surface of the fascial sheath of the eyeball (see p. 657). Anteriorly the external scleral surface is covered by conjunctiva which is reflected onto it from the deep surfaces of the eyelids. The scleral internal surface adjacent to the choroid is attached to it by a delicate fibrous layer, the suprachoroid lamina, which contains numerous fibroblasts and melanocytes. Anteriorly, the inner sclera is attached to the ciliary body by the lamina supraciliaris. Posteriorly, the sclera is pierced by the optic nerve. Here the outer half of the sclera turns back to become continuous with the dura mater, while the inner half is modified to form a perforated plate, the lamina cribrosa sclerae. The optic nerve fascicles pass through these minute orifices, while the central retinal artery and vein pass through a larger, central aperture. The lamina cribrosa sclerae is the weakest part of the sclera and bulges outwards (a cupped disc) when intraocular pressure is raised chronically as in glaucoma (see p. 686).

Like the cornea, the scleral stroma is composed mainly of densely packed collagen embedded in a matrix of proteoglycans, which are mixed with occasional elastic fibres and fibroblasts. However, in contrast to the cornea, scleral collagen fibrils show a large variation in diameter and spacing, and the lamellae branch and interlace extensively. This arrangement of fibres results in increased light scatter, which is responsible for the opaque dull white appearance of the sclera, and also imparts a high tensile strength to the sclera to resist the pull of the extraocular muscles and contain the intraocular pressure. Collagen fibre bundles are arranged circumferentially around the optic disc and the orifices of the lamina cribrosa. The fibres of the tendons of the recti intersect scleral fibres at right angles at their attachments, and then interlace deeper in the sclera. Collagen fibres of the scleral spur are orientated circularly, and there is an increased incidence of elastic fibres here. Although the sclera acts as a conduit for blood vessels, scleral vessels are few and mainly disposed in the episcleral lamina, especially close to the limbus. Its nerve supply is surprisingly rich, accounting for the intense pain associated with scleral inflammation (Watson & Young 2004).

Filtration angle and aqueous drainage

Aqueous humour is produced by the ciliary epithelium, passes through the pupil and circulates within the anterior chamber supplying the avascular cornea and lens with nutrients. It drains from the eye mainly through the trabecular meshwork into the canal of Schlemm at the iridocorneal (filtration) angle (Figs 40.2, 40.3), formed between the posterior aspect of the corneoscleral limbus and the periphery of the iris.

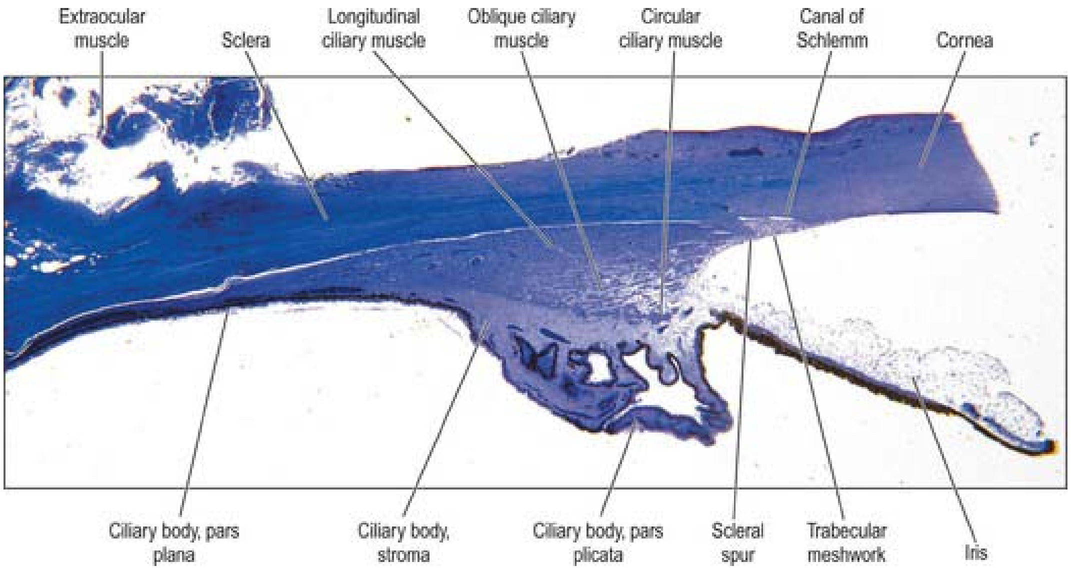
Extraocular muscle
Sclera
Longitudinal ciliary muscle
Oblique ciliary muscle
Circular ciliary muscle
Canal of Schlemm
Cornea
Ciliary body, pars plana
Ciliary body, stroma
Ciliary body, pars plicata
Scleral spur
Trabecular meshwork
Iris

Fig. 40.2 Meridional section through the anterior eye highlighting the ciliary body and drainage apparatus.

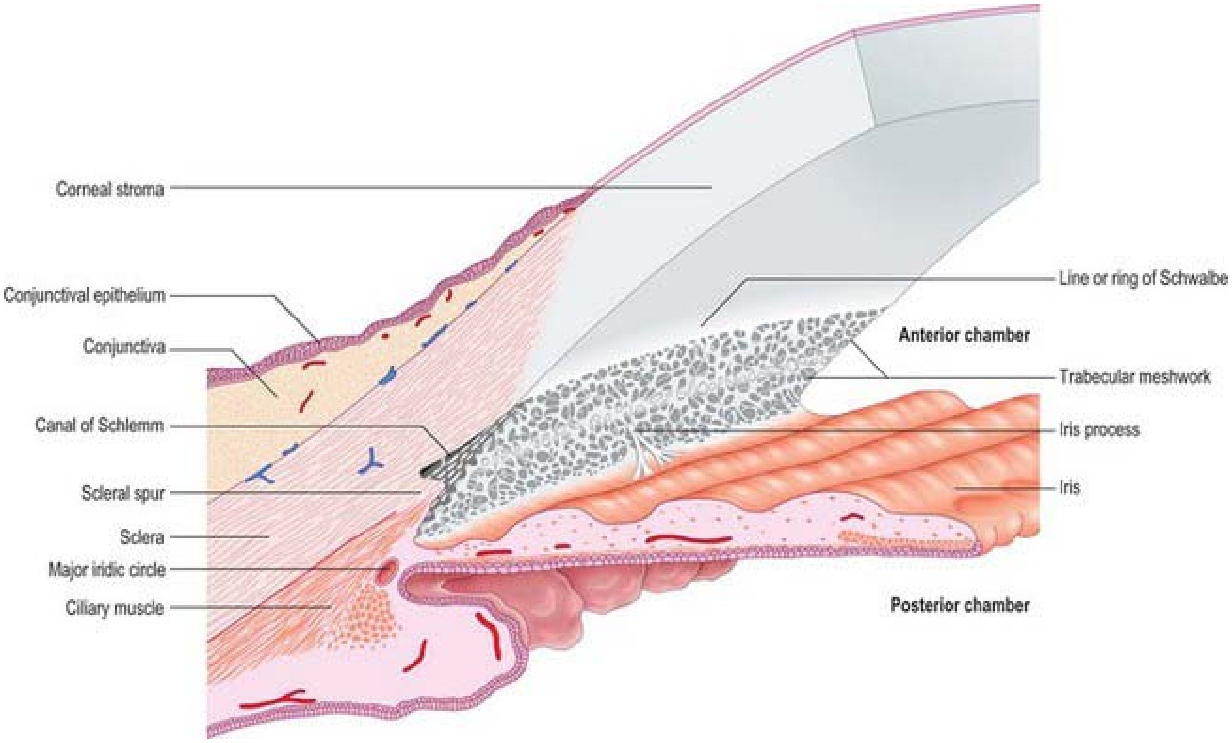
Corneal stroma
Conjunctival epithelium
Conjunctiva
Canal of Schlemm
Scleral spur
Sclera
Major iridic circle
Ciliary muscle
Line or ring of Schwalbe
Anterior chamber
Trabecular meshwork
Iris process
Iris
Posterior chamber

Fig. 40.3 Tissues bordering the anterior chamber angle. The trabecular meshwork is an anulus of tissue spanning the angle: its meshes are shown in transverse section opposite the canal of Schlemm and partly attached to the

scleral spur. A single iris process bridges the angle, connecting the trabecular meshwork to the anterior tissues of the iris.

The trabecular meshwork consists of loose trabecular tissue which is continuous anteriorly with Descemet’s membrane and the endothelium of the cornea. Aqueous humour filters from the anterior chamber through interconnected spaces among trabecular fibres. Most of these fibres are attached to the anterior, external aspect of the scleral spur. Of the remainder, most are continuous with longitudinal fibres of the ciliary muscle, some of which attach to the posterior internal aspect of the scleral spur. The trabecular meshwork provides sufficient resistance to aqueous humour outflow to generate an intraocular pressure of approximately 15 mmHg. It also acts as a filter and has the capacity to phagocytose particulate matter, although overloading may contribute to the pathogenesis of various forms of obstructive secondary glaucomas.

The canal of Schlemm (sinus venosus sclerae) is an anular endothelial canal located near the internal surface of the sclera close to the limbus. In section, the canal appears as an oval cleft, with an outer wall that grooves the sclera. Posteriorly, the cleft extends as far as a rim of scleral tissue, the scleral spur, which in section forms a triangle with its apex directed forwards (Figs 40.2, 40.3). The canal of Schlemm may be double or multiple in part of its course, and its walls are constructed of a continuous single thin endothelial layer. Passage of aqueous humour to the canal probably occurs via giant pinocytotic vacuoles, which form on the inner face of the endothelium and discharge into the canal at the outer face, and through intercellular clefts. Aqueous humour passes through a plexus of fine intrascleral vessels which connect the canal of Schlemm with anterior ciliary veins (Fig. 40.4). Normally the canal does not contain blood: pressure gradients prevent the reflux of blood even though the channels between the canal and veins have no valves. However, in venous congestion, blood may enter the canal: the continuous endothelial outer wall of the canal prevents further reflux.

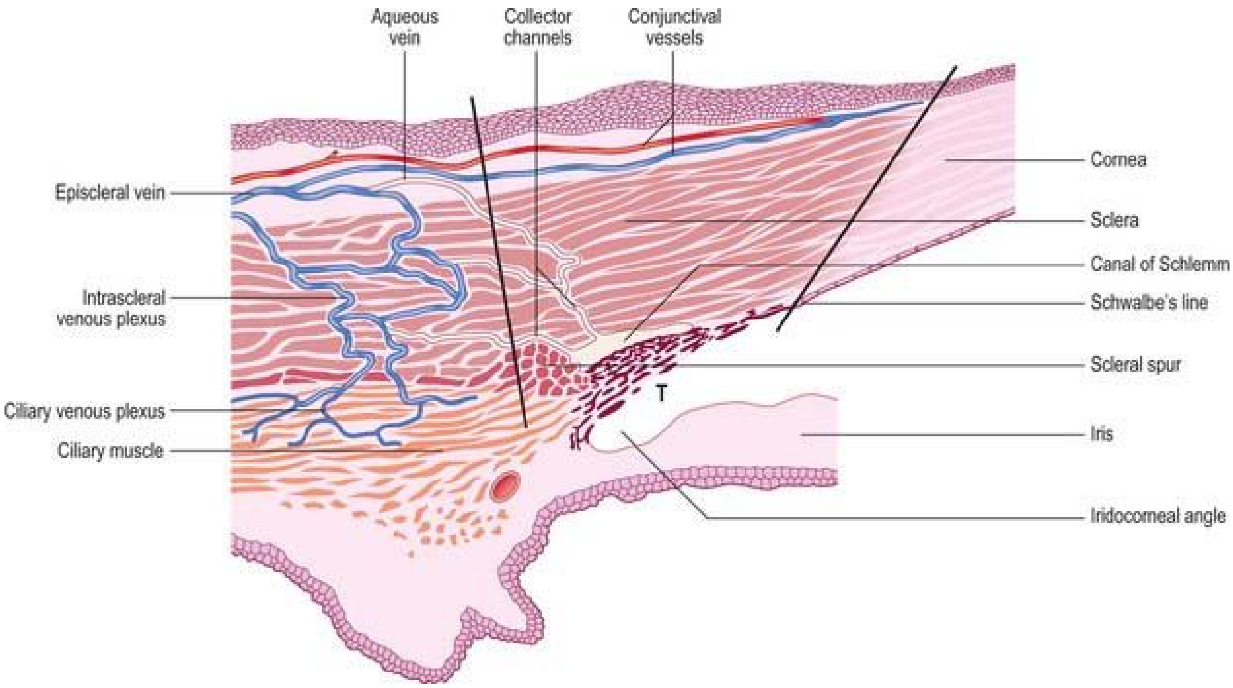
Aqueous vein
Collector channels
Conjunctival vessels
Episcleral vein
Intrascleral venous plexus
Ciliary venous plexus
Ciliary muscle
Cornea
Sclera
Canal of Schlemm
Schwalbe's line
Scleral spur
T
Iris
Iridocorneal angle

Fig. 40.4 Tissues of the filtration angle in section. The approximate borders of the limbal region are indicated by the solid lines. Aqueous humour drains from the anterior chamber at T through the trabecular meshwork into the canal of Schlemm from where it flows through collector channels either to the intrascleral venous plexus, where it mixes with blood from the ciliary venous plexus, or directly to the surface tissues of the eye as an aqueous vein. The aqueous vein is shown joining an episcleral vein at the surface to form a laminated vessel. Aqueous and blood drain posteriorly in episcleral veins which in turn join anterior ciliary veins.

An alternative route for aqueous outflow, the uveo-scleral pathway, has been described. Since there is no epithelial barrier between the anterior chamber and the ciliary body, aqueous humour is able to enter the loose connective tissue in front of the ciliary muscle and pass between the muscle fibres into the supraciliary and suprachoroidal spaces, where potentially it can be absorbed by vessels that drain the uvea.

CORNEA

The avascular cornea is the anterior transparent part of outer coat. Convex anteriorly, it projects from the sclera as a dome-shaped elevation with an area of 1.1 cm^2, forming approximately 7% of the external tunic area. Since it is more curved (average radius, $r = 7.8$ mm) than the sclera ($r = 11.5$ mm), a slight sulcus sclerae marks the corneoscleral junction (limbus). The cornea is approximately 670 μm thick close to the corneoscleral junction, and 520 μm at its centre. At the nasal and temporal limbus the transition from cornea to sclera occurs in a line that is approximately perpendicular to the cornea: this transition occurs more obliquely superiorly and inferiorly, with the sclera overlapping the cornea to a greater extent anteriorly. Consequently, when viewed from in front, the corneal perimeter is slightly elliptical, as its horizontal diameter (11.7 mm) is a little greater than its vertical (10.6 mm). Its posterior perimeter is circular (diameter 11.7 mm).

Microscopically, the cornea consists of five layers, namely, corneal epithelium, anterior limiting lamina (Bowman’s layer), substantia propria (stroma), posterior limiting lamina (Descemet’s membrane) and endothelium, arranged anteroposteriorly (Fig. 40.5A).

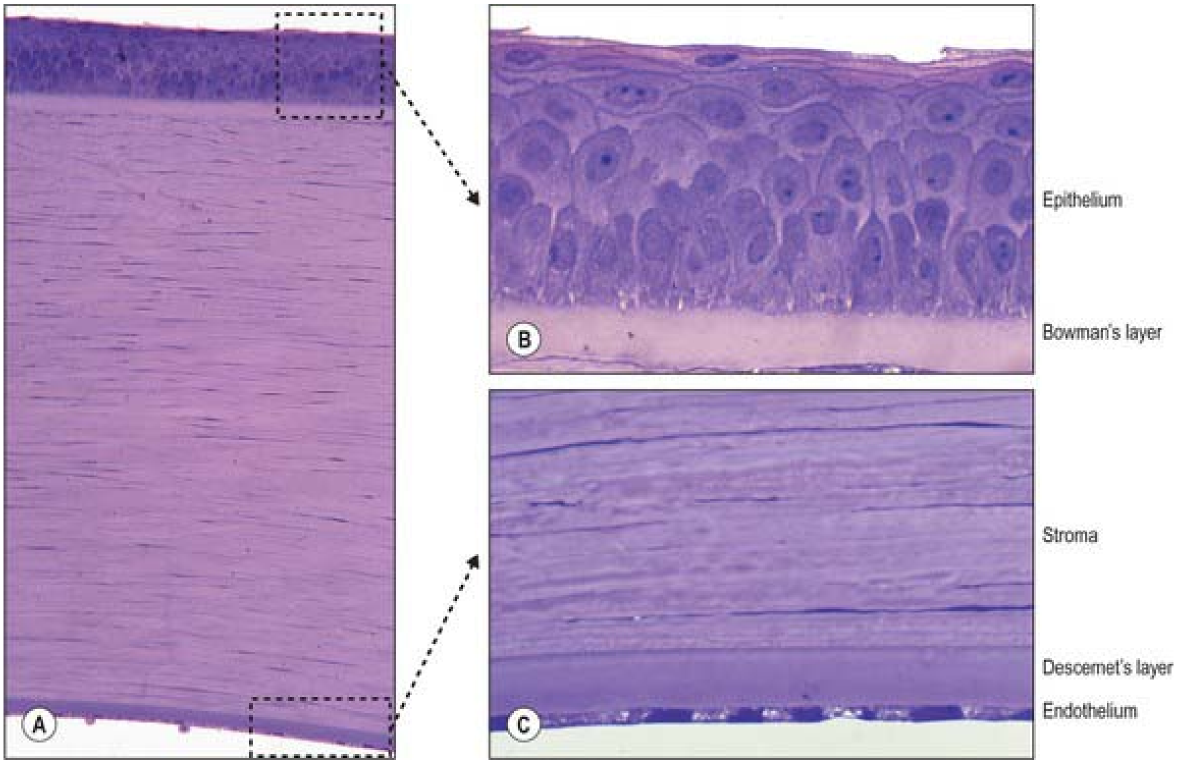

Fig. 40.5 **A**, Low power light micrograph of the five layers of the cornea. **B**, High power light micrograph of the corneal epithelium and Bowman's layer. **C**, High power light micrograph of the corneal endothelium, Descemet's layer and part of the stroma. The darkly staining cells in the stroma are keratocytes.

Corneal epithelium

The corneal epithelium accounts for approximately 10% of the corneal thickness (50 µm). It usually consists of 5–6 layers of cells (Fig. 40.5B) that protect the ocular surface from mechanical abrasion, form a permeability barrier (to small molecules, water and ions) and prevent the entry of pathogens. The deepest cells are columnar with flat bases, rounded apices, and large round or oval nuclei. Outside these are 2–3 layers of polyhedral (often wing-shaped) cells. In the more superficial layers the cells become progressively flatter, and present a smooth, optically perfect surface. Scanning electron microscopy of surface cells reveals extensive finger-like and ridge-like projections (microvilli and microplicae). A complex network of tight junctions links the superficial cells, consistent with their barrier function.

Anterior limiting lamina (Bowman’s layer)

The anterior limiting lamina lies behind the corneal epithelium. It contains a dense mass of collagen fibrils set in a matrix similar to that of the substantia propria. The lamina is 12 μm thick, is readily distinguishable from the substantia propria because it does not contain fibroblasts, and appears amorphous by light microscopy (Fig. 40.5B).

Substantia propria (stroma)

The substantia propria is approximately 500 μm thick and forms the bulk of the cornea. It is a compact and transparent layer, composed of 200–250 sequential lamellae, each made up of fine parallel collagen fibrils mainly of type I collagen. Flat dendritic interconnecting fibroblasts (keratocytes) form a coarse mesh between the lamellae. Alternate lamellae are typically orientated at large angles to each other (Fig. 40.6). X-ray diffraction studies indicate that they run along two preferred directions, superior-inferior and nasal-temporal, to account for the additional tensile stress exerted by the recti along these meridians (Boote et al 2005). Each lamella is approximately 2 μm thick and of variable width (10–250 μm, or, rarely, more). In the central cornea fibrils within the lamellae have a similar diameter of approximately 31 nm. This increases slightly with age and approaching the limbus. The small size of the fibrils (much smaller than the wavelength of light), along with the regularity of their spacing (maintained by collagen: proteoglycan interactions), and the careful control of corneal hydration, are the principal factors which determine stromal transparency. Light scattered by the collagen fibrils is eliminated by destructive interference in all directions other than forwards.

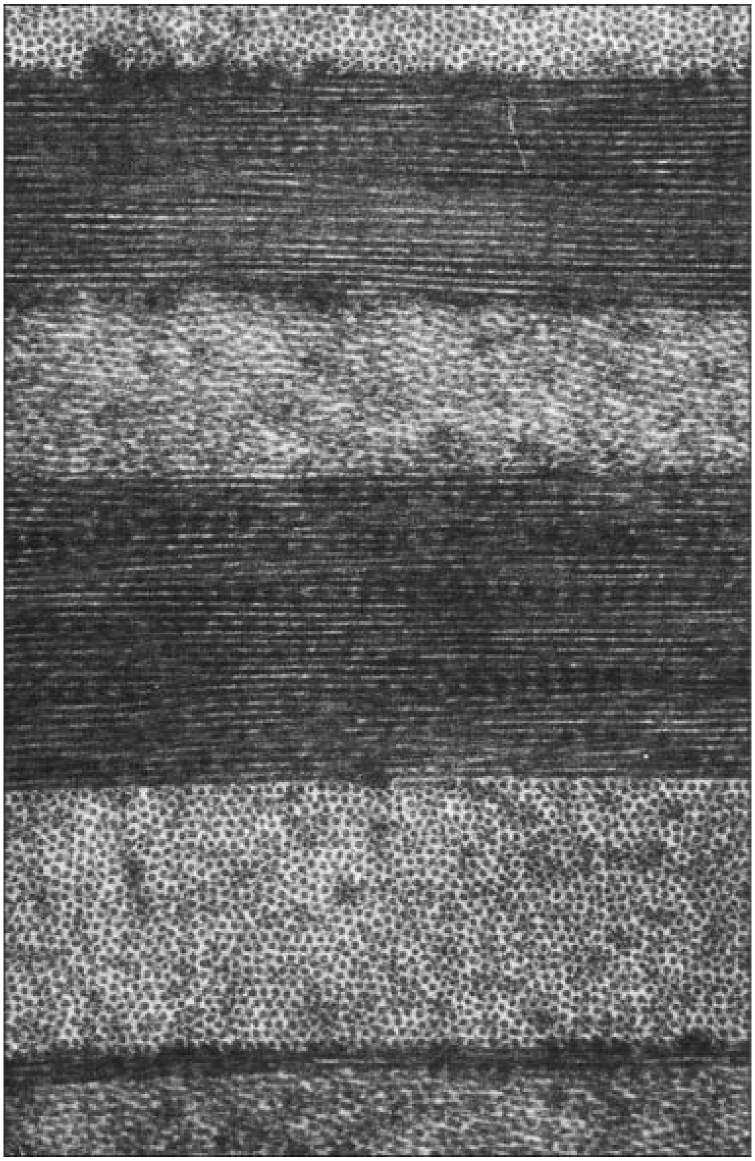

Fig. 40.6 Stroma of the human cornea showing the geometric precision of the alternation in direction of adjacent layers of fibres.

(By courtesy of John Marshall, St Thomas' Hospital, London).

Posterior limiting lamina (Descemet's layer)

The posterior limiting lamina covers the substantia propria posteriorly. It is thin and apparently homogeneous, and is regarded as the basement membrane of the endothelium. It is 4 μm thick at birth, and may increase to 12 μm by the eighth decade.

Endothelium

The endothelium covers the posterior surface of the cornea and consists of a single layer of squamous cells (Fig. 40.5C) with prominent interdigitations between adjacent cells, which are also connected by tight and gap junctions. When viewed en face, the endothelium appears as a mosaic of polygonal (typically hexagonal) cells. As these cells have a limited capacity for mitosis, in response to pathology, trauma, age and prolonged contact lens wear, the endothelial mosaic becomes less regular, and shows a greater variation in cell size and shape, as cells spread to fill gaps caused by cell loss. The numerous mitochondria and prominent rough ER within these cells reflects their high metabolic activity. Thus, for example, active pumping mechanisms largely control the degree of corneal hydration.

Corneal innervation

The cornea is innervated by numerous branches of the ophthalmic nerve (see p. 667) which either form an anular plexus around the periphery of the cornea, or pass directly from the sclera and enter the corneal stroma radially as 70–80 small groups of fibres. Upon entering the cornea, the few myelinated nerves lose their myelin sheaths and ramify throughout the corneal matrix in a delicate reticulum, their terminal filaments forming an intricate subepithelial plexus. Axon bundles from this plexus cross the anterior limiting membrane and form a subbasal plexus from which individual beaded axons pass to more superficial epithelial layers, eventually terminating as free nerve endings. Corneal nerves provide the afferent arm of the blink and lacrimal (see p. 673) reflexes and may also have a neurotrophic function.

CORNEOSCLERAL JUNCTION (LIMBUS)

The limbus marks the transitional zone between the cornea and sclera. Here the corneal epithelium merges with the epithelium of the conjunctiva, which thickens (up to 12 cells). Bowman’s layer terminates and the corneal stromal collagen loses its regularity. As the cornea contains neither blood nor lymphatic vessels, the capillaries of the conjunctiva and episclera end in loops near the limbus. Internally, Descemet’s membrane disperses into the fibres of trabecular meshwork and the corneal endothelium is continuous with that covering the trabeculae.

The cornea does not possess epithelial stem cells and cell replacement depends on the centripetal migration of cells from the edges of the cornea which are the progeny of mitotic limbal stem cells.

UVEA

The vascular tunic of the eye consists of the choroid, ciliary body and iris, which collectively form a continuous structure, the uvea (Fig. 40.1). The choroid covers the internal scleral surface, and extends forwards to the ora serrata. The ciliary body continues forward from the choroid to the circumference of the iris, which is a circular diaphragm behind the cornea and in front of the lens, presenting an almost central aperture, the pupil.

CHOROID

The choroid is a thin (60–160 μm, thickest behind macula) highly vascular, pigmented layer which lines almost five-sixths of the eye posteriorly. It is pierced by the optic nerve where it is firmly adherent to the sclera. Elsewhere its external surface is only loosely connected to the sclera by the suprachoroid layer (lamina fusca). Internally it is attached to the retinal pigment epithelium, and at the optic disc is continuous with the pia-arachnoid tissues around the optic nerve.

Four layers can be identified in transverse section (Fig. 40.7, see also Fig. 40.23): suprachoroid, vascular stroma, choriocapillaris and lamina vitrea (Bruch’s membrane).

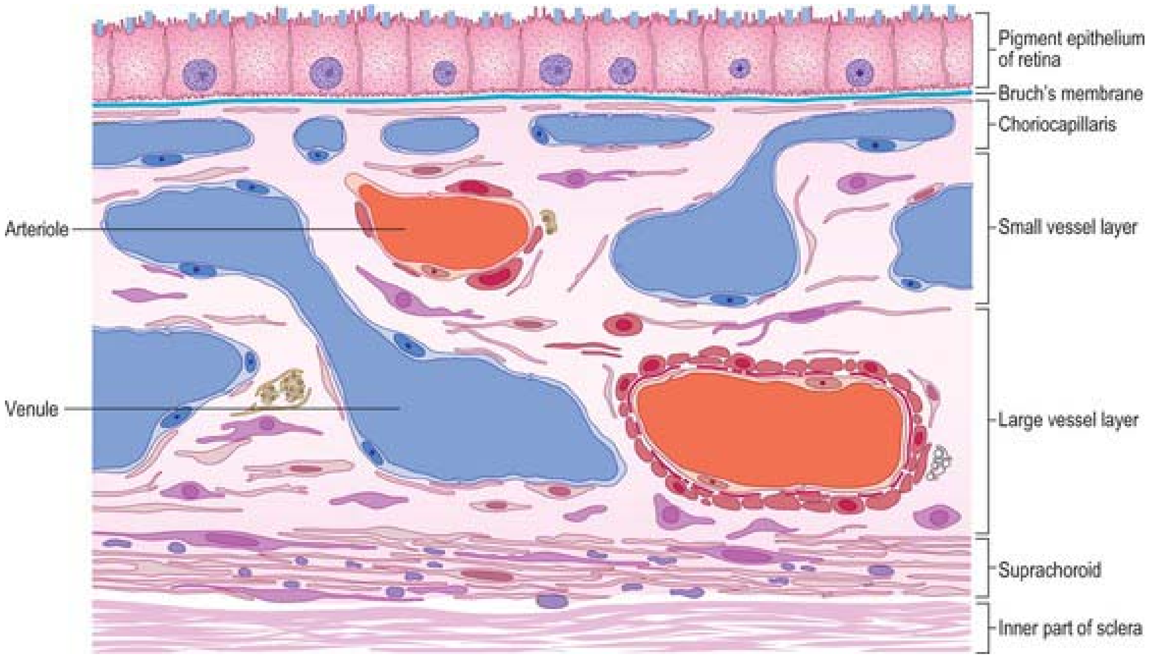
Pigment epithelium of retina
Bruch's membrane
Choriocapillaris
Arteriole
Small vessel layer
Venule
Large vessel layer
Suprachoroid
Inner part of sclera

Fig. 40.7 Drawing of a histological section through the choroid close to the posterior pole.

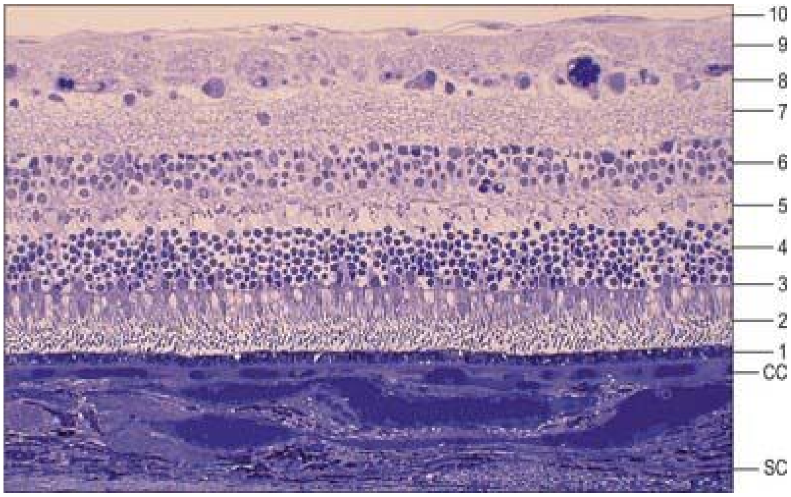

Fig. 40.23 Transverse section of the retina and choroid. The ten layers of the retina are: **1**. Pigment epithelial layer. **2**. Rod and cone layer. **3**. External limiting membrane. **4**. Outer nuclear layer. **5**. Outer plexiform layer. **6**. Inner nuclear layer. **7**. Inner plexiform layer. **8**. Ganglion cell layer. **9**. Nerve fibre layer. **10**. Internal limiting membrane. CC, choriocapillaris; SC, suprachoroid.

Suprachoroid

The suprachoroid covers the external surface of the choroid, is approximately 30 µm thick and composed of delicate non-vascular lamellae, each one a network of fine collagen and elastic fibres, fibroblasts and melanocytes. Ciliary nerves and long posterior ciliary arteries pass forward to the anterior uvea in this layer.

Vessel layer (stroma)

Internal to the suprachoroid lies a layer composed mainly of arteries and veins, but also some loose connective tissue containing scattered pigment cells. These melanocytes limit the passage of light through the sclera to the retina. More importantly, like the retinal pigment epithelium (see p. 689), they also absorb light traversing the retina that is not absorbed by the photoreceptors, so preventing internal reflection.

The blood supply of the choroid, as well as the rest of the uvea, is summarized in Figure 40.10. Short posterior ciliary arteries enter the eye through the sclera near the optic disc and supply the posterior choroid. These vessels branch and gradually decrease in size as they approach the retinal border. The choroidal stroma can be divided into layers based on the change in the calibre of these vessels; an outer layer of larger vessels (Haller’s layer), an inner layer of smaller vessels (Sattler’s layer) which eventually give rise to the choriocapillaris (Fig. 40.7). Long posterior ciliary arteries and recurrent branches of anterior ciliary arteries supply the anterior part of the choriocapillaris.

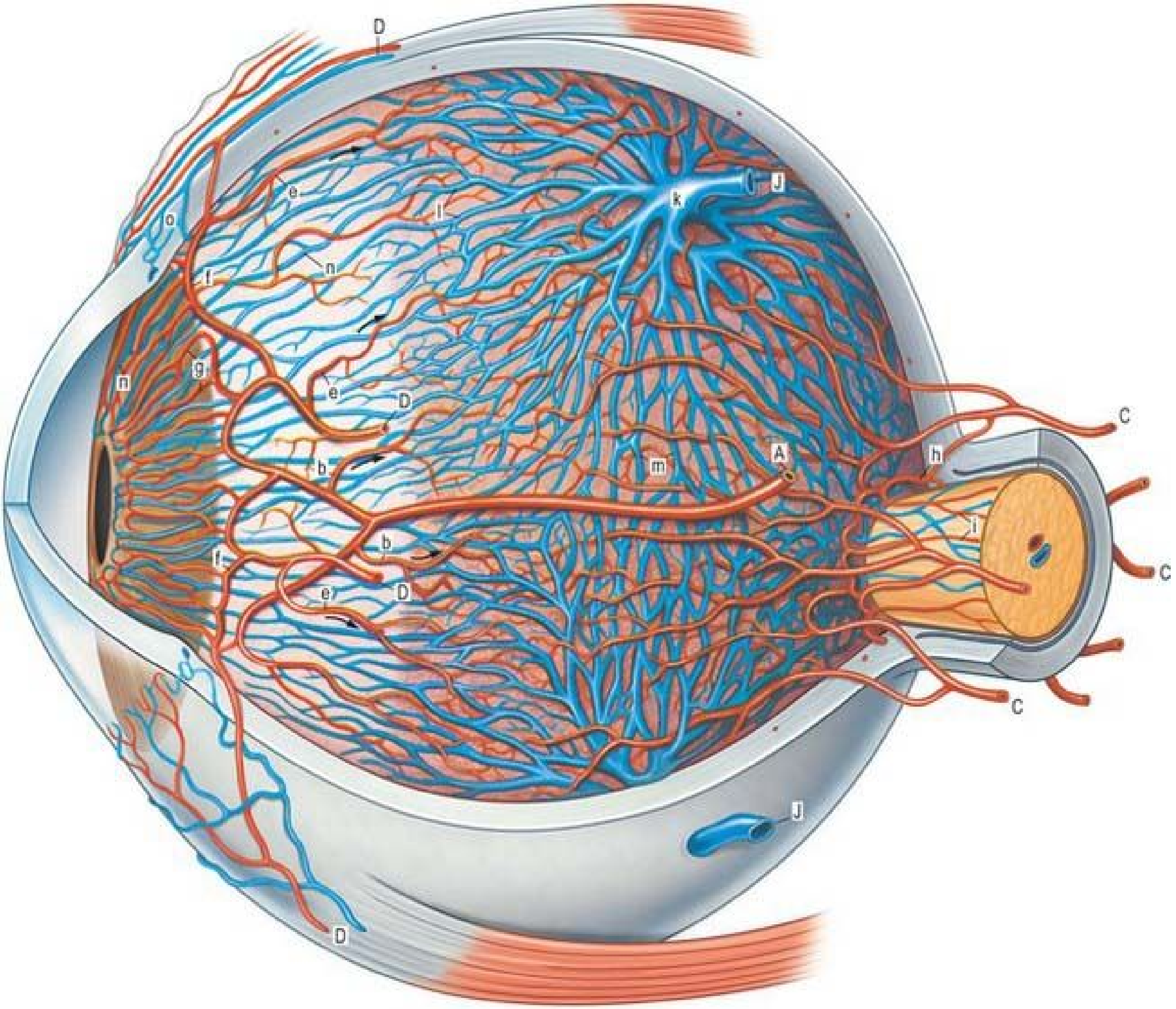

Fig. 40.10 The vasculature of the uveal tract. The long posterior ciliary arteries, one of which is visible (A), branch at the ora serrata (b) and feed the capillaries of the anterior part of the choroid. Short posterior ciliary arteries (C) divide rapidly to form the posterior part of the choriocapillaris. Anterior ciliary arteries (D) send recurrent branches to the choriocapillaris (e) and anterior rami to the major arterial circle (f). Branches from the circle extend into the iris (g) and to the limbus. Branches of the short posterior ciliary arteries (C) form an anastomotic circle (of Zinn) (h) round the optic disc, and twigs from this (i) join an arterial network on the optic nerve. The vortex veins (J) are formed by the junctions (k) of suprachoroidal tributaries (l). Smaller tributaries are also shown (m, n). The veins draining the scleral venous sinus (o) join anterior ciliary veins and vorticose tributaries.

(By permission from Hogan MJ, Alvarado JA, Weddell JE 1971 Histology of the Human Eye. Philadelphia: WB Saunders.)

Veins within the choroid converge spirally onto four, or very occasionally more, principal vortex veins. These pierce the sclera behind the equator to reach tributaries of the ophthalmic veins.

The vessels of the choroid have a rich autonomic vasomotor supply.

The blood flow through the choroid is high, a feature probably associated with an intraocular pressure of 15–20 mm Hg, which means that a venous pressure above 20 mm Hg is required to maintain circulation. The choroidal perfusion rate exceeds that required to supply nutrients and may serve to cool the retina during exposure to bright light.

Choriocapillaris

The choriocapillaris provides nutrients to the outer five layers of the retina and is composed of large (up to 20 μm thick) densely packed, freely anastomosing, fenestrated capillaries. While pericytes occur mainly on the scleral surface, most fenestrations face the retina. The permeability of choriocapillaris is exceptionally high even compared to other structures invested with fenestrated capillaries.

Lamina vitrea (Bruch’s membrane)

The lamina vitrea lies between the choriocapillaris and the retinal pigment epithelium from both of which it is derived. It appears as a glassy, homogeneous layer, only 2–4 μm in diameter, under the light microscope. It consists largely of an elastic fibre mesh, although some authors include internal and external layers of collagen and the basal laminae of the choriocapillaris and retinal pigment epithelium in this structure. Its function is thought to be related to the passage of fluid and solutes from the choroidal capillaries to the retina. In advancing years, extracellular deposits may accumulate in this membrane (drüsen), which impairs the exchange of gases, nutrients and metabolites between the choroidal blood and the outer layers of the retina, potentially contributing to degenerative disease in the photoreceptor layer of the neural retina.

CILIARY BODY

The ciliary body serves to anchor the lens via suspensory ligaments and by the contraction of its smooth muscle changes the refractive power of the lens (accommodation). Its anterior internal surface is also the source of aqueous humour, while posteriorly its inner surface is contiguous with the vitreous humour, and secretes several of its components. The anterior and the long ciliary arteries meet in the ciliary body and the major nerves to all the anterior tissues of the eyeball pass through it.

Externally, the ciliary body may be represented by a line which extends from approximately 1.5 mm posterior to the limbus of the cornea (corresponding also to the scleral spur) to a line approximately 7.5–8 mm posterior to this on the temporal side, and 6.5–7 mm on the nasal side. The ciliary body is thus slightly eccentric. It projects posteriorly from the scleral spur, which is its attachment, with a meridional width varying from 5.5 to 6.5 mm. Internally, it exhibits a posteriorly crenated or scalloped periphery, the ora serrata, where it is continuous with the choroid and retina (Figs 40.8, 40.9). Anteriorly, it is confluent with the periphery of the iris, and externally bounds the iridocorneal angle of the anterior chamber.

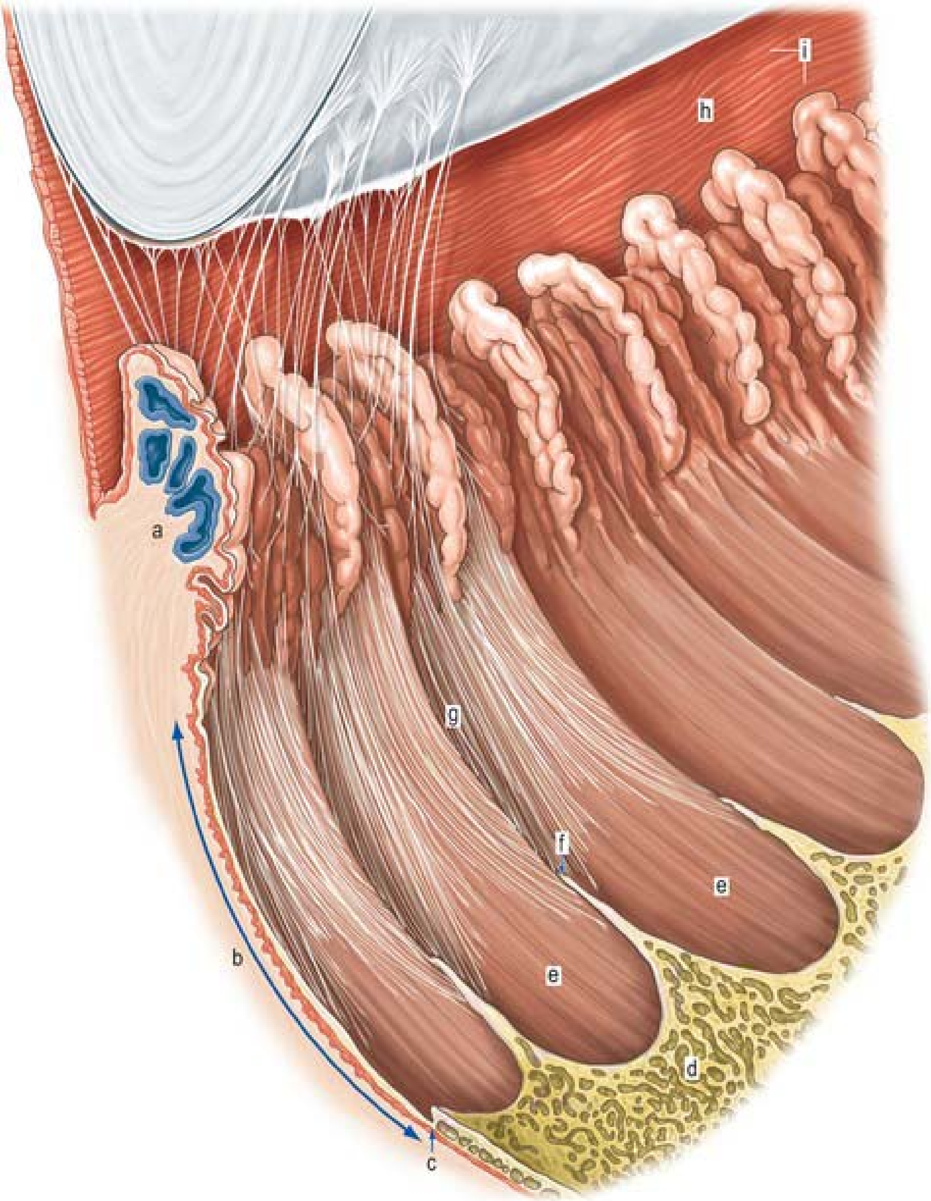

Fig. 40.8 The ciliary region seen from the ocular interior. Above is the periphery of the lens, attached by the fibres of the zonule (suspensory ligament) to the processes of the corona ciliaris (pars plicata) of the ciliary body (a). The orbiculus ciliaris or pars plana ciliaris (b) has a scalloped boundary, the ora serrata (c), which separates it from the retina (d). Flanking the ‘bays’ (e) of this are the dentate processes (f), with which linear ridges or striae (g) are continuous: the striae extend forwards between the main ciliary processes, providing an attachment for the longer zonular fibres. The posterior aspect of the iris shows radial (h) and circumferential (i) sulci.

(By permission from Hogan MJ, Alvarado JA, Weddell JE 1971 Histology of the Human Eye. Philadelphia: WB Saunders.)

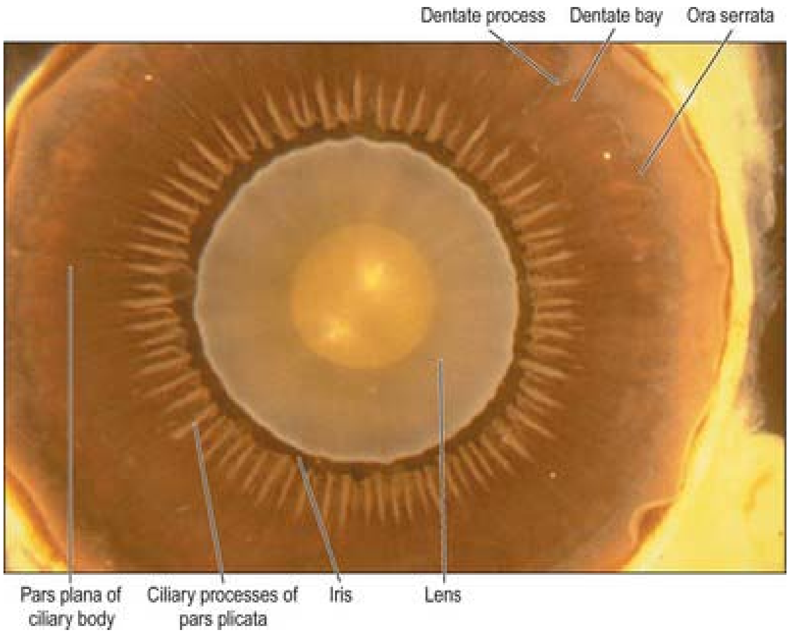

Fig. 40.9 The posterior aspect of the anterior half of the eye showing the termination of the neural retina at the ora serrata and the ciliary body. The lens has retained sufficient transparency to reveal the iris border: the crenated perimeter of the lens is due to tension imposed by the attached suspensory ligaments (unseen).

In cross section the ciliary body is composed of four layers (from internal to external), namely a double layer of epithelial cells, the stroma, ciliary muscle, and a supraciliary layer (Fig. 40.2).

Meridionally, the ciliary body can be divided into two parts (Figs 40.2, 40.9). Anteriorly, the ridged anterior pars plicata (corona ciliaris) surrounds the base of the iris and accounts for about ⅓ rd of the ciliary body. Posteriorly, the relatively smooth and thin pars plana (orbicularis ciliaris) lies adjacent to the ora serrata, and forms a convenient access point for instruments during vitreo-retinal surgery and for intraocular injection. The whole ciliary body is covered by a double epithelium, in which the inner layer is unpigmented, while the outer layer contains melanin. At the ora serrata the retinal pigment epithelium is continuous with the outer pigmented epithelium of the pars plana, while the neural retina is replaced by inner unpigmented ciliary epithelium. Anteriorly, this double epithelium continues over the pars plicata until it merges with the double epithelium on the posterior surface of the iris (where the inner layer of cells also accumulates melanin) (see p. 682). The anterior pars plicata is ridged meridionally by 70–80 ciliary processes radiating from the base of the iris (Figs 40.2, 40.9). In the young eye these process are approximately parallel-sided structures, but in the adult their flanks become less regular and appear thicker. A minor ridge, or ciliary plica, lies in the valley between most of the processes. The crests of the processes are less pigmented, giving them the appearance of white (or light) striae, from which the name ciliary is derived. Fibres of the zonule (the suspensory ligaments of the lens) extend into the valleys. They pass beyond the ciliary processes to fuse with the basal lamina of the superficial epithelial layer of pars plana. Their sites of attachment are marked by striae which pass back from the valleys of the pars plicata, across the pars plana, almost as far as the apices of the dentate processes of the ora serrata (Fig. 40.8).

Ciliary epithelium

The ciliary epithelium is bilaminar, consisting of two layers of simple epithelium which are derived embryonically from the two layers of the optic cup. The superficial layer consists of columnar cells over the pars plana, and cuboidal cells over the ciliary processes of the pars plicata: it becomes irregular and more flattened between the processes. These cells contain little or no pigment. The outer layer of the ciliary epithelium, in contrast contains cuboidal cells which are loaded with melanin. The two layers are normally firmly united, but fluid may separate them pathologically. The pigment layer is attached to the stroma of the ciliary body by its basal lamina, which continues back into the basal lamina of the choroid. As a consequence of the invagination of the optic cup during development, a basal lamina covers the free surface of the bilayer which is continuous with the internal limiting membrane of the retina (see p. 692).

The ciliary epithelium is responsible for the secretion of aqueous humour (see p. 685), while the outer pigmented epithelium additionally contributes to the eye's 'black box effect', like the retinal pigment epithelium, choroidal pigment and posterior iris epithelium, absorbing stray light to enhance image quality.

Ciliary stroma

The ciliary stroma is composed largely of loose bundles of collagen, which form a considerable mass between the ciliary muscle and overlying processes, and extend into both of them. This inner layer of connective tissue contains numerous larger branches of the ciliary vessels. A dense reticulum of large (up to 35 μm diameter) fenestrated capillaries is concentrated in the ciliary processes. This facilitates the passage of substances from the blood plasma during aqueous production (see p. 685). Anteriorly, near the periphery of the iris, the major arterial circle (Fig. 40.10; see also Fig. 40.14) is formed chiefly by long posterior ciliary branches of the ophthalmic artery. These enter the eye some distance behind the ocular equator and pass between the choroid and sclera to the ciliary body. Ciliary veins, also draining the iris, pass posteriorly to join the vortex veins of the choroid.

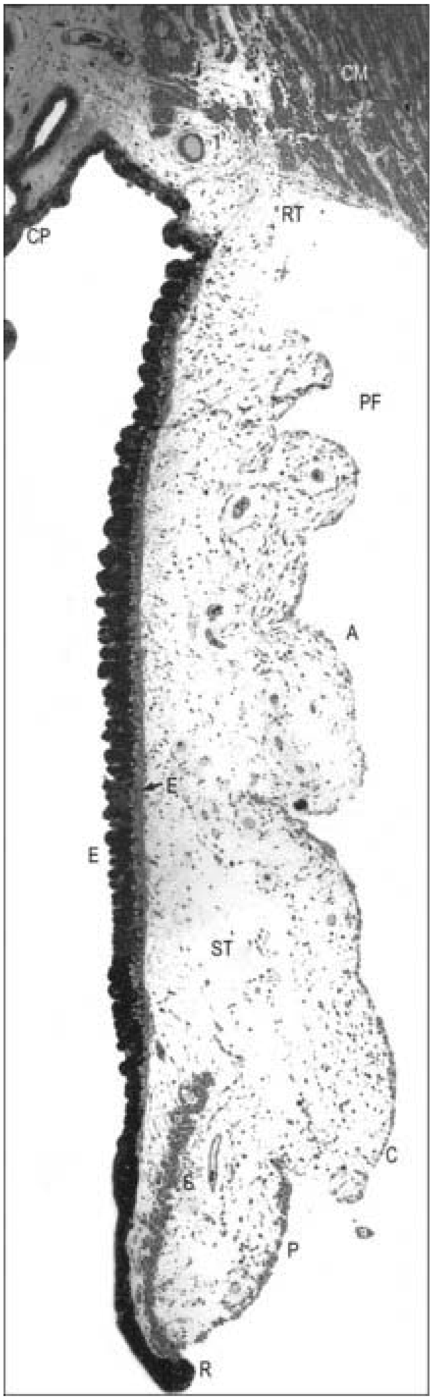

Fig. 40.14 Meridional section of an iris. The posterior surface is lined with a double epithelium (E, E’): the arrow points to the processes of the anterior layer of the epithelium forming the dilator pupillae muscle. ST, Stroma. C, Collarette. RT, Root. A, Anterior border layer. PF, Folds in anterior surface towards the root. R, Pupillary ruff. S, Sphincter pupillae muscle. P, Pupillary region of the iris. The iris is in a contracted state, as

shown by the thickened epithelium opposite the dilator muscle and thinning opposite the sphincter, and by the shortness of the pupillary zone. CM, Ciliary muscle. CP, Ciliary processes. I, Major iridic circle.

Ciliary muscle

Ciliary muscle is composed of smooth muscle cells, most of which are attached to the scleral spur and arranged in three different orientations. The outermost fibres are meridional or longitudinal, and pass posteriorly into the stroma of the choroid. The innermost fibres swerve acutely from the spur to run circumferentially as a sphincter near the periphery of the lens. Obliquely interconnecting radial fibres run between these two muscular strata, frequently forming an interweaving lattice (Figs 40.2, 40.11).

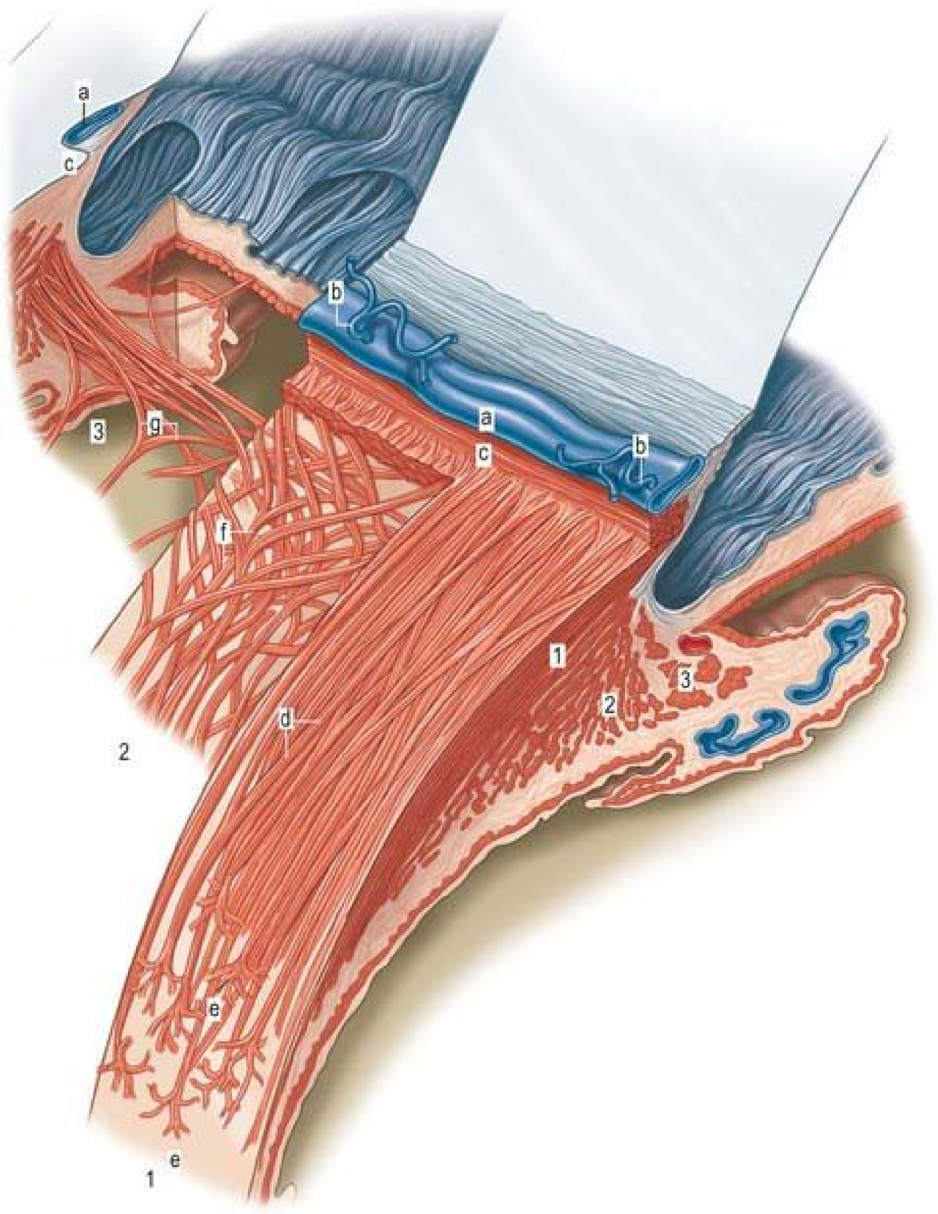

Fig. 40.11 The ciliary muscle and its components. The meridional or longitudinal (1), radial or oblique (2), and circular or sphincteric (3) layers of muscle fibres are displayed by successive removal towards the ocular interior. The cornea and sclera have been removed, leaving the canal of Schlemm (a), collecting venules (b) and scleral spur (c). The meridional fibres (1) often display acutely angled junctions (d) and terminate in epichoroidal stars (e). The radial fibres meet at obtuse angles (f) and similar junctions, at even wider angles (g), occur in the circular ciliary muscle.

(By permission from Hogan MJ, Alvarado JA, Weddell JE 1971 Histology of the Human Eye. Philadelphia: WB Saunders.)

Accommodation reflex

At rest distant objects are focused on the retina in an emmetropic eye (see p. 687). In order to focus closer objects the dioptric power of the eye has to be increased, which is achieved by increasing the curvature of the lens. At rest the lens is under tension from the zonular ligaments and hence flattened. On accommodation, the ciliary muscle contracts, moving the ciliary body forwards and inwards towards the optic axis. All parts of the muscle act in concert, and tension on the zonular ligaments is relaxed. As the lens is covered by an elastic capsule (see p. 686), once tension on it is released it assumes a more convex shape suitable for focusing closer objects. The radius of curvature of the anterior lens surface changes most during accommodation.

Information from the retina passing to the visual cortex does not constitute the afferent limb of a simple reflex in the usual sense of the term, but permits the visual areas to assess the clarity of objects in the visual field. Cortical efferent information passes to the pretectal area and thence to the Edinger–Westphal nucleus, which contains preganglionic parasympathetic neurones whose axons travel in the oculomotor nerve (Fig. 40.12). Efferent impulses pass in the oculomotor nerve to the orbit where they synapse in the ciliary ganglion. Postganglionic fibres (short ciliary nerves) innervate the ciliary muscle causing it to contract. There is also a sparse sympathetic innervation of ciliary muscle, which has a very limited capacity to relax the muscle.

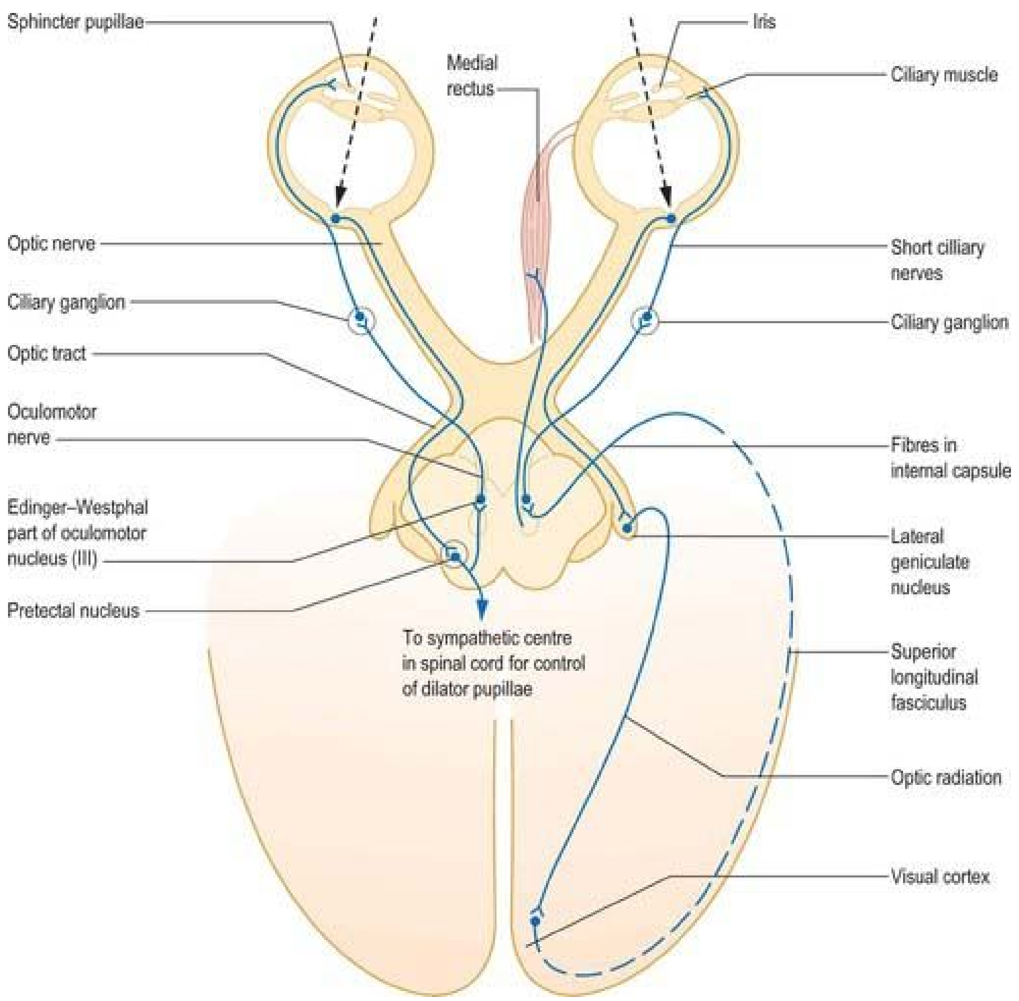
Sphincter pupillae
Medial rectus
Iris
Ciliary muscle
Optic nerve
Short cilliary nerves
Ciliary ganglion
Ciliary ganglion
Optic tract
Oculomotor nerve
Fibres in internal capsule
Edinger–Westphal part of oculomotor nucleus (III)
Lateral geniculate nucleus
Pretectal nucleus
To sympathetic centre in spinal cord for control of dilator pupillae
Superior longitudinal fasciculus
Optic radiation
Visual cortex

Fig. 40.12 The neural pathways of the pupillary light reflex (left) and the accommodation reflex (right).

(From Oxford Textbook of Functional Anatomy, Vol 3 Head and Neck, MacKinnon P, Morris J (eds) 1990. By permission of Oxford University Press.)

Accommodation is usually accompanied by constriction of the pupil brought about by contraction of the sphincter pupillae (see p. 682) and convergent eye movements caused by contraction of the medial, superior, and inferior recti (all innervated by the oculomotor nerve). This is the ‘near triad’ which may become disrupted in various diseases.

Supraciliary layer

The thin supraciliary layer separates the sclera from the ciliary muscle and is largely composed of collagen fibres derived from the two layers it divides. It also forms an alternative ‘unconventional’ route (other than the canal of Schlemm) for the drainage of aqueous humour (see p. 686).

IRIS

The iris is an adjustable diaphragm around a central aperture (slightly medial to true centre), the pupil. It lies between the cornea and lens and is immersed in aqueous fluid (Fig. 40.1), partially dividing the anterior segment into an anterior chamber, enclosed by the cornea and iris and a posterior chamber, which lies between the iris and the lens anterior to the vitreous. The efficacy of the iris as a light stop is mainly due to a densely pigmented posterior double epithelium. The pupillary aperture is adjusted by the action of two muscles, dilator and sphincter pupillae.

Seen from the front the iris is divided into a large ciliary zone adjacent to the ciliary body and a smaller, inner, pupillary zone (Fig. 40.13). The two regions join at the collarette. The anterior surface of the iris often contains large depressions and at the pupillary margin the posterior pigmented epithelium is visible as the pupillary ruff (Fig. 40.13).

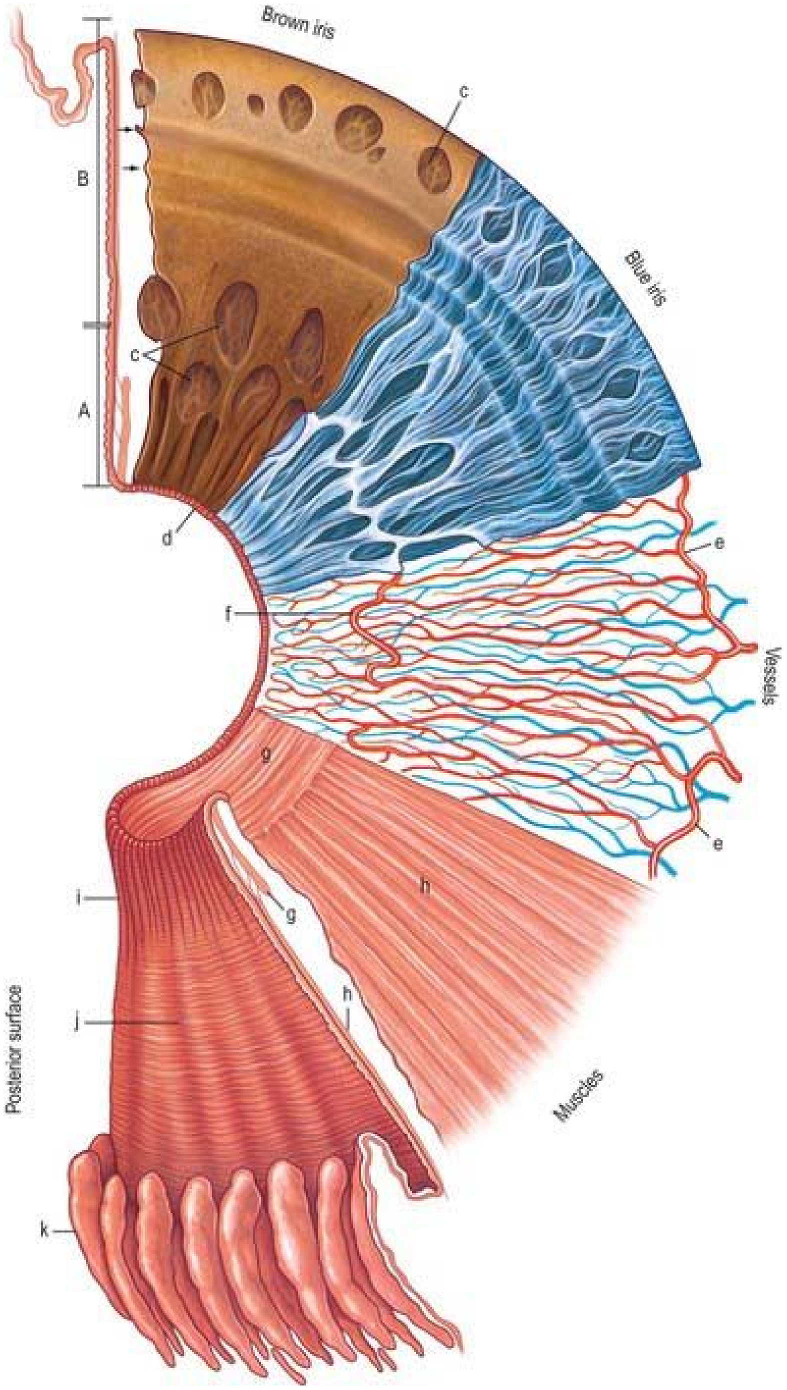
Brown iris
c
B
A
c
d
Blue iris
e
f
Vessels
e
g
h
i
g
h
j
Posterior surface
Muscles
k

Fig. 40.13 Composite view of the surfaces and internal strata of the iris. In a clockwise direction from above, the pupillary (A) and ciliary (B) zones are shown in successive segments. The first (brown iris) shows the anterior border layer and the openings of crypts (c). In the second segment (blue iris), the layer is much less prominent and the trabeculae of the stroma are more visible. The third segment shows the iridial vessels, including the

major arterial circle (e) and the incomplete minor arterial circle (f). The fourth segment shows the muscle stratum, including the sphincter (g) and dilator (h) of the pupil. The everted ‘pupillary ruff’ of the epithelium on the posterior aspect of the iris (d) appears in all segments. The final segment, folded over for pictorial purposes, depicts this aspect of the iris, showing radial folds (i and j) and the adjoining ciliary processes (k).

(By permission from Hogan MJ, Alvarado JA, Weddell JE 1971 Histology of the Human Eye. Philadelphia: WB Saunders.)

In transverse section several subdivisions of the iris are evident (Fig. 40.14). From anterior to posterior they are an anterior border layer, the stroma (which contains the sphincter pupillae), and two pigmented epithelial layers, the most anterior of which contains the dilator pupillae. It is thinnest at its root (approximately 200 µm), where the ciliary body is attached, and thickest at the collarette.

Anterior border layer

The anterior surface of the iris is not a distinct epithelium, but a modified layer of the iris stroma, formed mainly by an increased number of fibroblasts forming a network on the anterior surface with a layer of underlying melanocytes. At the periphery of the iris the anterior border layer blends with the trabecular connective tissue of the iridocorneal angle, and at the pupillary rim it meets the epithelium of the posterior surface of the iris.

The colour of the iris is a product of the combined effect of reflection/absorption by the iridial connective tissue and the concentration of pigment in the anterior border layer and to a lesser extent in the iris stroma. The distribution of pigment is often irregular, which produces a flecked appearance. When pigment is largely absent, other than in the posterior epithelial layers (the condition at birth), the colour is light blue.

Stroma

The stroma of the iris is formed of fibroblasts, melanocytes and a loose collagenous matrix. The intercellular spaces appear to communicate freely with the anterior chamber, and interchange of fluid between the two may assist the considerable changes in thickness which occur during contraction and relaxation of the iris. There is no elastic tissue. A few large heavily pigmented ‘clump cells’ may be present; these are phagocytes and contain lysosomes and ingested melanosomes. The stroma contains regional vessels and nerves. An aggregation of smooth muscle cells near the pupillary rim forms an anular contractile sphincter pupillae (see below).

Epithelial layers

The epithelial surface covering the iris posteriorly is a continuation of the bilaminar epithelium of the ciliary body and is formed from the two layers of the optic cup. The pupil, through which this epithelium curves for a short distance on to the anterior surface as the pigment ruff or ‘border’, corresponds to the opening of the optic cup.

The layer of epithelial cells nearest the stroma is, somewhat confusingly, termed the anterior epithelium, although it lies posterior to the stroma. Its cells are pigmented, as are those of the same layer in the ciliary epithelium. They give rise to the dilator pupillae (see below). Vitreal to this stratum is a layer of heavily pigmented cells, the posterior epithelium, which is continuous with the inner non-pigmented layer of the ciliary epithelium. Its free surface bears numerous radial ridges which facilitate the movement of aqueous humour from the posterior to the anterior chamber (because the front surface of the lens rests on the iris). Adjacent epithelial cells are extensively joined by various junctions which ensure that the layer can withstand the excursions of the iris during changes in pupillary size (Fig. 40.15).

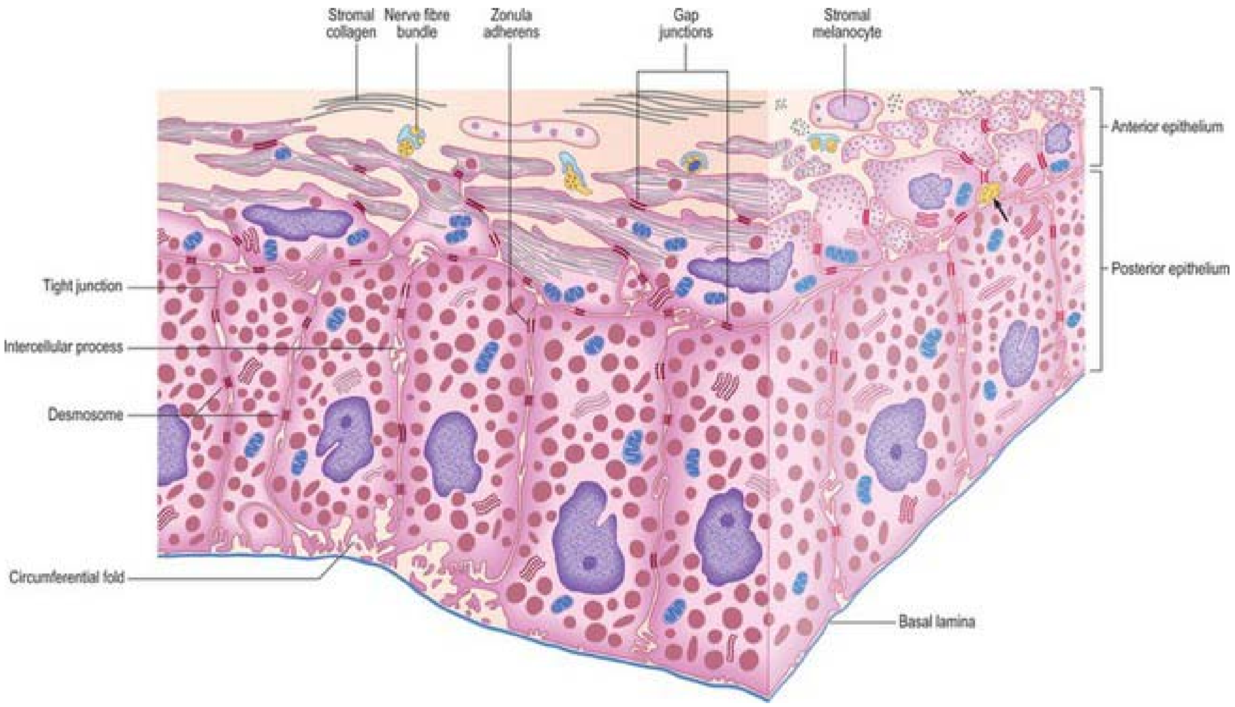
Stromal collagen
Nerve fibre bundle
Zonula adherens
Gap junctions
Stromal melanocyte
Anterior epithelium
Posterior epithelium
Tight junction
Intercellular process
Desmosome
Circumferential fold
Basal lamina

Fig. 40.15 Posterior structures of the iris. The dilator pupillae is shown in transverse section on the right and in longitudinal section on the left (arrow shows a rarer deeper nerve terminal).

Iris muscles

Sphincter pupillae

The sphincter pupillae is a flat anulus of smooth muscle approximately 750 µm wide and 150 µm thick. Its densely packed fusiform muscle cells are often arranged in small bundles, as in the ciliary muscle, and pass circumferentially around the pupil (Fig. 40.13). Collagenous connective tissue lies in front of and behind the muscle fibres. It is very dense posteriorly, where it binds the sphincter to the pupillary end of the dilator muscle, and is attached to the epithelial layer at the pupil margin. Small axons, mostly non-myelinated, ramify in the connective tissue between bundles.

Dilator pupillae

The dilator (dilatator) pupillae is a thin layer which lies immediately anterior to the epithelium of the posterior surface of the iris. Its ‘fibres’ are the muscular processes of the anterior layer of this epithelium, whose cells are therefore myoepithelial. Myofilaments are present throughout these cells, but are more abundant in their fusiform basal muscular processes, which are approximately 4 μm thick, 7 μm wide and 60 μm in length. They form a layer 3–5 elements thick through most of the iris, from its periphery to the outer perimeter of the sphincter, which it slightly overlaps. Here the dilator thins out, and sends spurs to blend with the sphincter. Unlike the apical parts of the myoepithelial cells, these have a basal lamina and are joined by gap junctions like those between the sphincteric muscle cells. Small non-myelinated axons pass between, and terminate on, their muscular processes (Fig. 40.15).

Innervation of muscles of the iris

The iris is innervated mainly by the long and short ciliary nerves. Short ciliary nerves, which contain parasympathetic postganglionic myelinated axons derived from the ciliary ganglion (see Fig. 39.17) innervate the sphincter pupillae, losing their myelin well before entering the muscle. The dilator is supplied with non-myelinated postganglionic fibres from the superior cervical ganglion; their routes are less well established. Some go via the ciliary ganglion and reach the eye in the short ciliary nerves, whereas other fibres may travel in the long ciliary nerves, which are branches of the nasociliary nerve. Both the sphincter and the dilator may have a double autonomic supply. An additional small fraction of nerve endings in the dilator and sphincter muscles have been identified as parasympathetic and sympathetic respectively in experimental animal studies, including those on primates. Although ganglion cells have been noted in the iris, the majority of axons are probably postganglionic. They form a plexus around the periphery of the iris, from which fibres extend to innervate the two muscles, the vessels, and the anterior border layer: some fibres may be afferent and others are vasomotor.

Pupillary light reflex

Pupillary diameter varies from around 2 mm when fully constricted (miosis) in bright light to at least 8 mm when dilated in darkness (mydriasis), and has an even wider range under the influence of drugs. The resulting variation in pupil area (maximally a factor of 16) will obviously affect the amount of light impinging on the retina. However, compared to the total range of illumination where humans can maintain some degree of vision (approximately 10 log units), this effect, though important, is small. Most mechanisms for dark/light adaptation are neural or biochemical. Enhancing visual acuity by restricting light to the centre of the lens, and thereby decreasing the amount of spherical aberration, is at least as important a function of pupillary constriction.

If only one eye is illuminated, the pupil of that eye constricts (direct response), as does the pupil of the contralateral, unilluminated, eye (consensual response). While change in pupillary diameter is usually considered a reflex response to changes in light level, the pupil also constricts on viewing near objects (as part of the accommodation reflex) and in response to painful stimuli; it can also be influenced to some degree by more complex cortical factors.

In pupillary constriction, light acting on both traditional retinal photoreceptors (rods and cones) and on intrinsically photosensitive retinal ganglion cells, gives rise to activity in retinal ganglion cells. This activity is conducted along the optic nerve, through the optic chiasma and along the optic tract. Although the majority of tract fibres end in the lateral geniculate nucleus of the thalamus, a small number leave the optic tract before it reaches the thalamus, at the superior brachium, and synapse in the olivary pretectal nucleus. The information is relayed from the pretectal nucleus by short neurones which synapse bilaterally on preganglionic parasympathetic neurones in the Edinger–Westphal nucleus (in the oculomotor nerve complex in the rostral midbrain). Efferent impulses pass along parasympathetic fibres carried by the oculomotor nerve to the orbit, where they synapse in the ciliary ganglion. Postganglionic fibres travel in the short ciliary nerves to the sphincter pupillae, which reduces the size of the pupil when it contracts (Fig. 40.12).

Pupillary dilation is brought about by lessening the parasympathetic drive to the sphincter (see above) and by sympathetic activation of the dilator. Sympathetic preganglionic fibres arise from neurones in the lateral column of the first and second thoracic segments, and pass via the sympathetic trunk to the superior cervical ganglion. Postganglionic neurones travel up the neck next to the internal carotid artery as the internal carotid nerve; at the level of the cavernous sinus the nerve breaks up to form an interweaving network of fibres, the carotid plexus, around the carotid artery. Some of the axons from the plexus form the sympathetic root of the ciliary ganglion, passing through the ciliary ganglion without synapsing, and, mostly travelling in the short ciliary nerves, innervate the dilator.

Vascular supply of the iris

The iris receives its blood supply from the long posterior and anterior ciliary arteries (Fig. 40.10). On reaching the attached margin of the iris, both long ciliary arteries divide into an upper and a lower branch. The branches anastomose with the corresponding contralateral arteries, and with the anterior ciliary arteries, to form the major arterial (iridic) circle (circulus arteriosus major) at the base of the iris (Figs 40.10, 40.13, 40.14). Vessels converge from this circle to the free margin of the iris, where they anastomose to form an incomplete circulus arteriosus minor: there is a view that these vessels are venous. The smaller arteries and veins are very similar in their structure and are often slightly helical, which allows them to adapt to changes in iridial shape as the pupil varies in size. All of the vessels, including the capillaries, have a non-fenestrated endothelium and a prominent, often thick, basal lamina. There is no elastic lamina in the arteries or veins, and there are few smooth muscle cells, especially in the veins. Connective tissue in the tunica media is loose, whereas the adventitia is remarkably dense and collagenous, so that it appears to form almost a separate tube.

LENS AND HUMOURS

The cornea, aqueous humour, lens and vitreous body, often collectively termed the ocular media, serve to form an image on the retina by transmitting and refracting light. Additionally, the aqueous provides nutrients to the avascular cornea and lens and removes their metabolic waste, as well as generating the intraocular pressure which maintains the shape of the eye.

AQUEOUS HUMOUR

Aqueous humour is derived from the plasma within the fenestrated capillaries of the ciliary processes. The major component of aqueous, like plasma, is water and the composition of the two fluids is broadly similar, although they do differ in the concentration of some electrolytes and organic solutes. In the interests of optical clarity, the blood–aqueous barrier also ensures a very low concentration of protein in the aqueous (generally <1 per cent of the level in plasma). Inflammation of the anterior uvea can lead to a breakdown of this barrier and the presence of protein in the aqueous, resulting in light scatter that is manifest clinically as ‘flare’.

The aqueous is actively secreted into the posterior chamber by the epithelium overlying the ciliary processes. It passes around the equator of the lens and flows through the pupil into the anterior chamber, where it circulates as a result of convection currents derived from temperature differences between the cornea and iris. Most aqueous is drained from the eye through the trabecular meshwork into the canal of Schlemm from where it drains into episcleral veins. However, some exits through the ciliary muscle into the supraciliary and suprachoroidal spaces (uveo-scleral pathway).

Any interference with the drainage of aqueous into the canal of Schlemm increases intraocular pressure and leads to glaucoma. Glaucoma is either ‘primary’ or secondary to a specific anomaly or disease of the eye. Primary glaucoma can be either ‘closed angle’, where the filtration angle is narrowed by the proximity of the root of the iris to the cornea, or more commonly ‘open angle’, where aqueous access to angle tissues is unimpeded. In the most common form of primary open angle glaucoma, pathological changes within the trabecular meshwork reduce the facility of aqueous drainage, thus raising intraocular pressure. Sustained raised pressure leads to progressive defects in the visual field, either because of direct mechanical damage to retinal ganglion cell axons (particularly at the optic nerve head), or impairment of the optic nerve head blood supply, or both.

LENS

The lens is a transparent, encapsulated, biconvex body bathed in aqueous humour, which serves to adjust the focus of the eye. Posteriorly, it contacts the hyaloid fossa of the vitreous body. Anteriorly, it forms a ring of contact with the posterior border of the iris, but further away from the axis of the lens the gap between the two increases to form the posterior chamber of the eye (Figs 40.1, 40.16). The lens is encircled by the ciliary processes, and is attached to them by the zonular fibres which issue mainly from the pars plana of the ciliary body. Collectively, the fibres form the zonule which holds the lens in place and transmits the forces which stretch the lens.

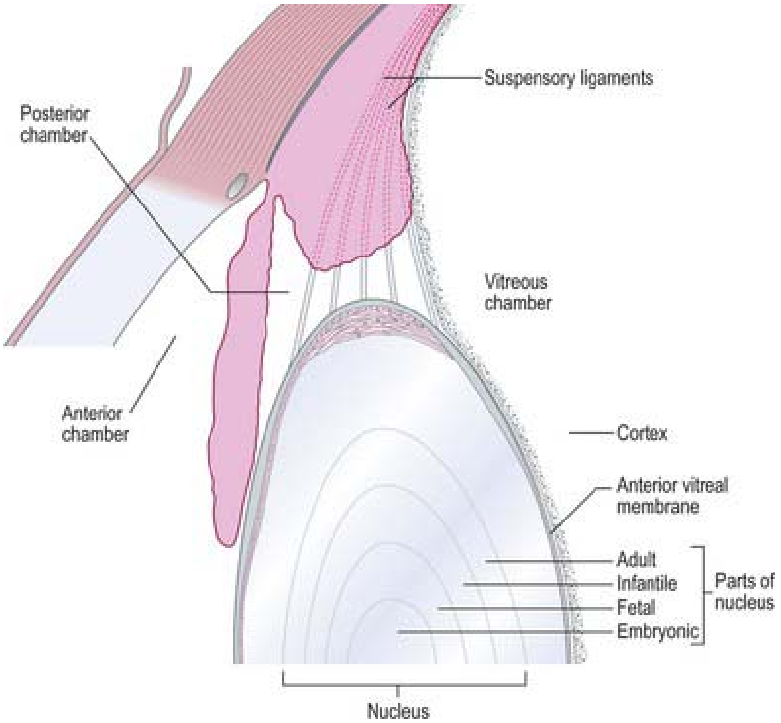
Suspensory ligaments
Posterior chamber
Vitreous chamber
Anterior chamber
Cortex
Anterior vitreal membrane
Adult
Infantile
Fetal
Embryonic
Parts of nucleus
Nucleus

Fig. 40.16 Sagittal section through part of the lens and related structures. The cortex is distinguished from the nucleus, which is composed of embryonic, fetal, infantile and adult parts. The capsule is drawn in blue, exaggerated in thickness 100 times and is based on observations from a 35-year-old.

The anterior convexity of the lens is less steep than that of the posterior surface. The central points of these surfaces are the anterior and posterior poles of the lens and a line connecting them is its axis. The marginal circumference of the lens is its equator.

At birth the lens is colourless and transmits all wavelengths from the infrared to the near UV well. However, throughout life, the amount of short-wave radiation transmitted diminishes until in old age the lens takes on an amber tinge as it absorbs visible short-wave radiation, decreasing blue sensitivity in older people. In cataract, the lens gradually becomes opaque.

The dimensions of the lens are optically and clinically important, but change with age as a consequence of continuous growth. Its equatorial diameter at birth is 6.5 mm, increasing rapidly at first, then more slowly to 9.0 mm at 15 years of age, and even more gradually to reach 9.5 mm in the ninth decade. Its axial dimension increases from 3.5–4.0 mm at birth to 4.75–5.0 mm at age 95. Average adult radii of the anterior and posterior surfaces are 10 mm and 6 mm respectively. These radii reduce throughout life, the anterior surface increasing most in curvature as the lens thickens, so that in old age the lens pushes the iris forward slightly.

The lens consists of three layers (Fig. 40.17). Most of the lens is composed of elongated cells known as lens fibres. The anterior surface, as far as the equator, is covered by a layer of epithelial cells and the whole is surrounded by the lens capsule. The lens is avascular and devoid of nerve fibres or other structures which might affect its transparency. Its surface forms a very effective barrier against invasion by cells or elements of the immune system, and so creates an immunologically sequestered environment. It is unique because it retains all the cells formed throughout its life.

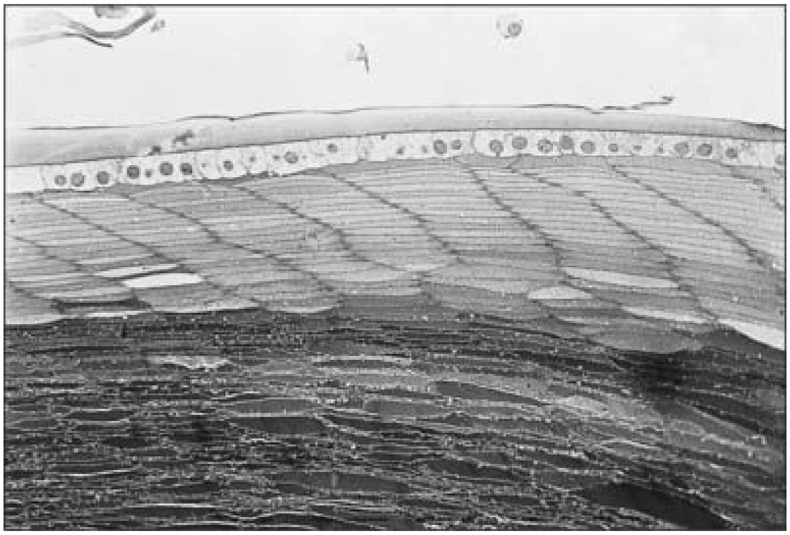

Fig. 40.17 Section through the anterior layers of the lens. The thin capsule covers the single row of epithelial cells and the lens substance is composed of regularly stacked younger fibres and more densely stained and complex deeper fibres.

Lens capsule

The lens capsule is a basement membrane that covers the surface of the lens. It consists of various classes of collagen fibre (I, III and IV), as well as a range of glycosaminoglycans and glycoproteins. It is derived from the anterior lens epithelial cells and their fetal precursors and is firmly attached to the epithelium anteriorly and to lens fibres posteriorly. The capsule is elastic, a property it owes to the arrangement of its collagen, and which is central to the process of accommodation. Capsule thickness varies with position and age. One view is that it is thicker at the anterior pole and equator than at the posterior pole, with a band of increased thickness between the pole and equator (Fig. 40.16). Zonular fibres insert into the capsule at the equator. They are composed of thin (4–7 nm) fibrils with hollow centres, and resemble fibrils associated with elastic connective tissue.

Lens epithelium

The anterior surface of the lens between the outer capsule and the underlying lens fibres is covered by a layer of simple, roughly cuboidal (10 μm high and 13 μm wide), epithelial cells which, in surface view, are polygonal (Fig. 40.17). These cells differentiate into lens fibres: they undergo mitosis at a germinative zone just anterior to the equator and are displaced towards the equator, where they synthesize characteristic lens fibre proteins and undergo extreme elongation. As other cells follow suit, the earlier cells come to occupy a deeper position within the lens.

Lens fibres

The inwardly displaced epithelial cells elongate further in both an anterior and posterior direction, becoming up to 12 mm long, depending on age and position in the lens. Fibres near the surface at the equator are nucleated; the nuclei form a short S-shaped bow which extends inwards from the surface. The deeper fibres lose their nuclei and most other organelles.

Variations in lens fibre structure and composition make it possible to distinguish a softer cortical zone, representing younger fibres and a firmer central part, representing the older nucleus (Fig. 40.16). The nucleus can be further subdivided into layers representing the age at which the fibres within them were formed.

In cross-section, individual fibres are flattened hexagons measuring approximately 10 μm by 2 μm (Fig. 40.17). They are tightly packed, and fibres are firmly attached to their neighbours by a variety of mechanical junctions (Fig. 40.18). Lens fibres are also in contact through desmosomes and numerous gap junctions.

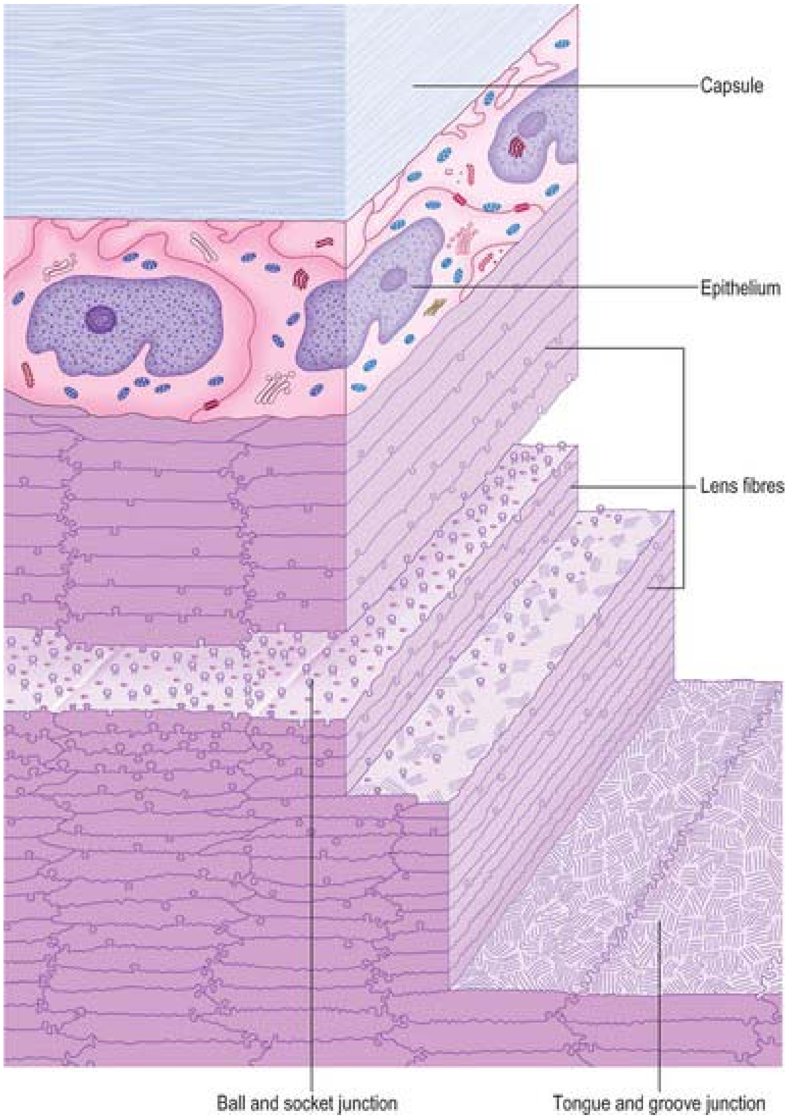
Capsule
Epithelium
Lens fibres
Ball and socket junction
Tongue and groove junction

Fig. 40.18 The mechanical junctions between lens fibres. There are no junctions immediately below the epithelium. Ball and socket junctions develop in deeper layers: these are subsequently eliminated towards the nucleus, where tongue and groove junctions gradually deepen. Angle joints are present at most levels.

All lens fibres cross the equator (or the plane passing through it) and terminate on both the anterior and posterior lens surfaces at lens ‘sutures’. These radiate out from the poles towards the equator and represent lines of linearly registered interlocking junctions between terminating lens fibres. In fetuses, the sutures on the anterior surface of the lens form a triradiate pattern centred on the anterior pole resembling the limbs of an upright letter Y (Fig. 40.19A). Posteriorly, the sutural configuration is similar but inverted. The sutures increase in number and complexity as a consequence of lens growth and other changes in the arrangement of lens fibres (Fig. 40.19B). Fibres which start near the central axis of the lens anteriorly, terminate posteriorly on a suture near the periphery, and *vice versa*.

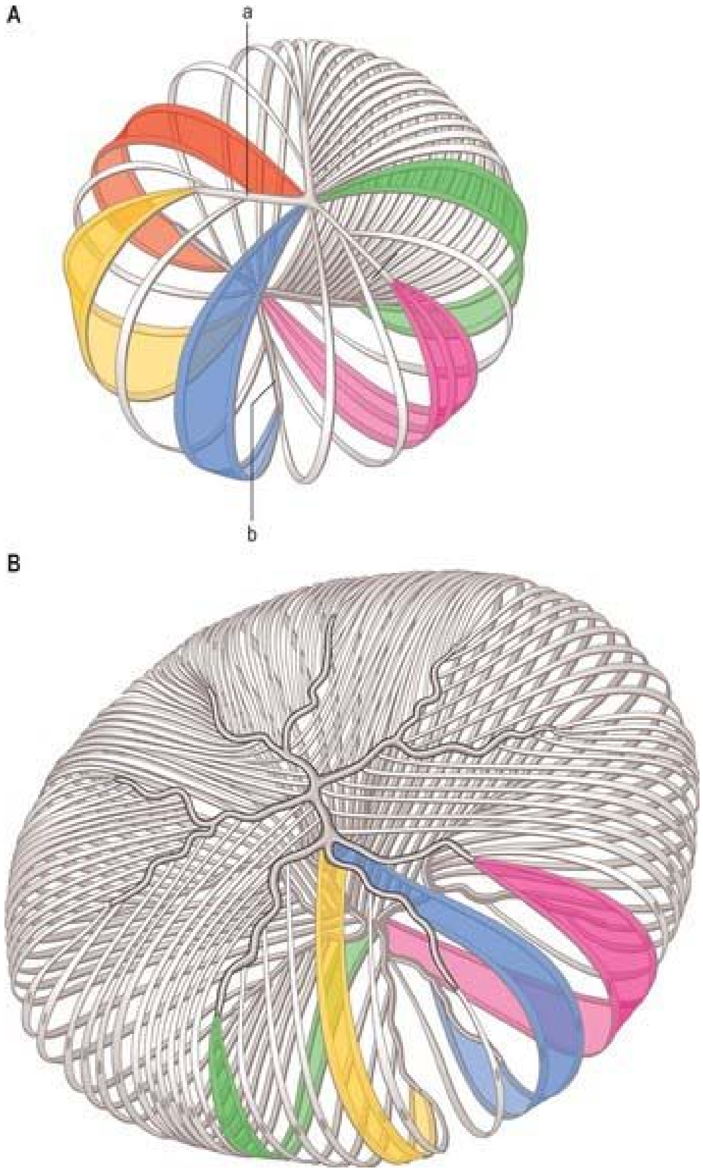

Fig. 40.19 The structure of the fetal (**A**) and adult (**B**) human lens, showing the major details of arrangement of the lens fibres. The anterior (a) and posterior (b) triradiate sutures are shown in the fetal lens. Fibres pass

from the apex of an arm of one suture to the angle between two arms at the opposite pole, as shown in the coloured segments. Intermediate fibres show the same reciprocal behaviour. The suture pattern becomes much more complex as successive strata are added to the exterior of the growing lens, and the original arms of each triradiate suture show secondary and tertiary dichotomous branchings.

(By permission from Hogan MJ, Alvarado JA, Weddell JE 1971 Histology of the Human Eye. Philadelphia: WB Saunders.)

Lens fibres contain crystallins, proteins which are responsible for the transparency and refractile properties, and for much of the elasticity, of the lens. At least three varieties coexist, α, β and γ, their relative proportions changing throughout life. They occur in very high concentrations, and form up to 60% of the lens fibre mass. Variations in their concentration in different parts of the lens give rise to regional differences in refractive index, correcting for the spherical and chromatic aberrations which might otherwise occur in a homogeneous lens.

Ocular refraction

The cornea and humours have a refractive index close to that of water, but the tear film covering the curved corneal surface is in contact with air and therefore approximately ⅔ rds (approximately 40 dioptres) of the refractive power of the eye is effected here. The lens has a greater refractive index than the adjacent media, varying from 1.386 at its periphery to 1.406 at its core, and contributes the remaining approximately 20 dioptres of the power of the relaxed eye. The main value of the lens is its ability to vary its dioptric power during the process of accommodation. Accommodation allows an increase in refraction of 12 dioptres in youth, but this decreases with age, being halved at 40 years and reduced to 1 dioptre or less at 60 years (presbyopia).

Disorders of refraction

A relaxed eye is said to be emmetropic when the refracting structures are so related to its length that the retina receives a focused image of a distant object. Although the majority of eyes are emmetropic, a large minority have errors of refraction or ametropia that can take three different forms. In myopia, the eye is too long for its refractive power and distant objects are focused in front of the retina when relaxed: closer objects will be in focus and consequently the eye is said to be ‘short-sighted’. Conversely, in hyperopia (long sight), the eye is too short for its refractive power and, when relaxed, distant objects are focused behind the retina. In astigmatism, the refractive power of the eye is not the same in different meridians, which are approximately 90 degrees apart in regular astigmatism. There is a hereditable factor in ametropia, and a relationship between myopia and the demands of close work in the young is widely accepted. These errors of refraction are amenable to correction using spectacle or contact lenses and by various forms of refractive surgery.

As noted above, the ability to change the power of the lens through accommodation diminishes during the fifth decade to an extent that neither the corrected ametrope nor the emmetrope is able to focus near objects clearly, and reading spectacles become necessary. This is offset to a very limited extent by the reduction of the pupil aperture with age, which increases the depth of focus, but at the cost of creating the further problem of requiring greater illumination.

Other errors of refraction are the concomitants of eye disease, especially those which affect the cornea. Corneal curvature, for example, may be sufficiently altered as a residual defect of past disease to cause irregular astigmatism. In keratoconus, the cornea is thinned and steepened centrally, distorting the refracting surface, and a dislocated lens, caused for example by Marfan’s syndrome, also disrupts the refractive status of the eye.

VITREOUS HUMOUR

The vitreous body occupies about four-fifths of the eyeball. Posteriorly it is in contact with the retina, while further forward it abuts the ciliary body, zonule and lens. Its anterior surface is hollowed into a deep concavity, the hyaloid fossa, fitting the shape of lens (Fig. 40.1). It is colourless, consisting of approximately 99% water, but is not entirely structureless. At its perimeter it has a gel-like consistency (100–300 μm thick); nearer the centre it contains a more liquid zone. Hyaluronan, in the form of long glycosaminoglycan chains, fills the whole vitreous. In addition, the peripheral gel or cortex contains a random loose network of type II collagen fibrils which are occasionally grouped into fibres. The cortex also contains scattered cells, the hyalocytes, which possess the characteristics of mononuclear phagocytes and may contribute to the production of hyaluronan. While they are normally in a resting state, they have the capacity to be actively phagocytic in inflammatory conditions. Hyalocytes are not present in the cortex bordering the lens.

The liquid vitreous is absent at birth, appears first at 4 or 5 years, and increases to occupy half the vitreous space by the seventh decade. The cortex is most dense at the pars plana of the ciliary body adjacent to the ora serrata, where attachment is strongest, and this is often referred to as the base of the vitreous. Here the vitreous is thickened into a mass of radial (zonular) fibres which form the suspensory ligament of the lens. Apart from the vitreous base, the vitreous also has a firm (peripapillary) attachment at the edge of the optic disc. This adherence of the vitreous to the retina can result in traction on the retina if the vitreous shrinks, such as occurs in old age, resulting in macular holes or peripheral breaks, possibly leading to retinal detachment.

A narrow hyaloid canal runs from the optic nerve head to the central posterior surface of the lens (Fig. 40.1). In the fetus this contains the hyaloid artery which normally disappears about 6 weeks before birth. The canal persists in adult life as a very delicate fibrous structure and is of no functional importance.

RETINA

The retina is a thin sheet of cells, ranging from less than 100 µm at its edge, to a maximum around 300 µm at the foveal rim. It lines the inner posterior surface of the eyeball, sandwiched between the choroid externally and the vitreous body internally, and terminates anteriorly at the ora serrata (Fig. 40.1).

When viewed with an ophthalmoscope to show the fundus oculi, the most prominent feature is the blood vessels emanating from and entering the optic disc (Fig. 40.20). Centred temporal and inferior to the disc lies the 'central retina' or macula (approximate diameter 5–6 mm), the middle of which is composed of the fovea and foveola, and easily identified with an ophthalmoscope as an avascular area with a yellow tinge (Fig. 40.20). The lack of blood vessels at the foveola is even more apparent in a fluorescein angiogram (Fig. 40.21). The peripheral retina lies outside the central retina.

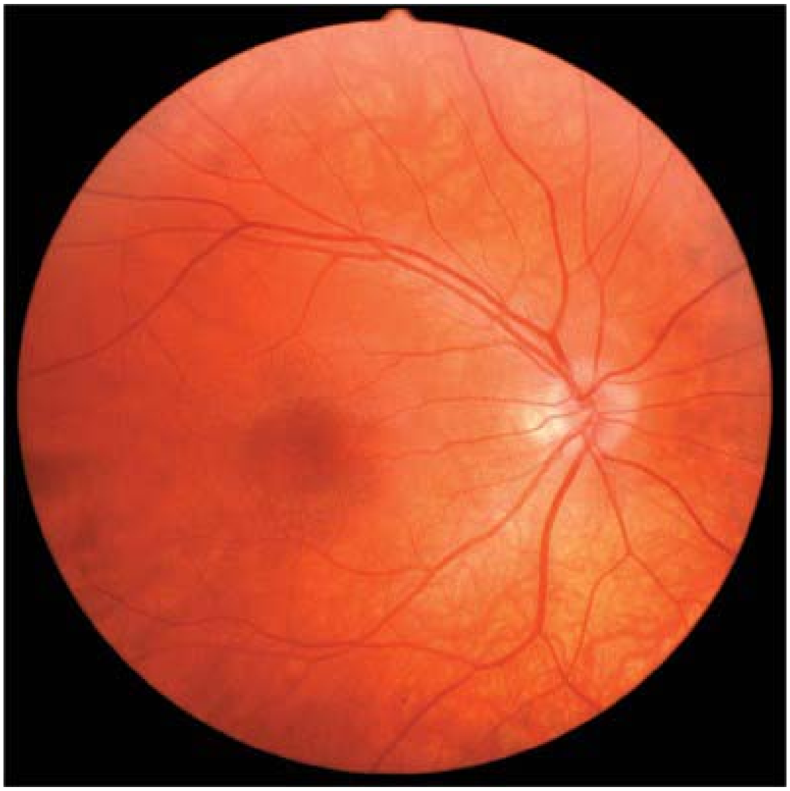

Fig. 40.20 Fundus photograph of the right eye of a 26-year-old Caucasian male. The central retinal vessels are seen emanating from the optic disc. Retinal arteries are lighter in colour and narrower than the veins. The avascular centre of the macular region can be seen temporal to the disc. The 6.25D of myopia of the subject is consistent with the peripapillary atrophy temporal to the optic nerve head and the visibility of the choroidal vessels.

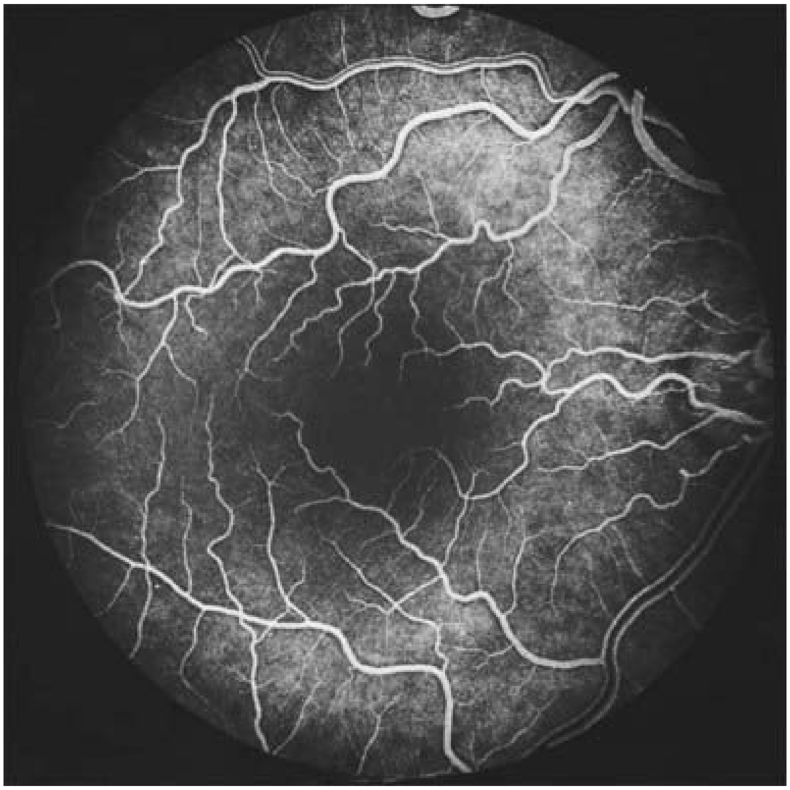

Fig. 40.21 Fluorescein angiogram showing the macular region of a right eye. The main macular vessels are approaching from the right. The subject was an elderly person with considerable macular pigmentation, which masks fluorescence from the choroidal circulation.

MICROSTRUCTURE

The retina is composed of a variety of epithelial, neural and glial cell types whose distribution conventionally divides it into 10 layers (Fig. 40.22). These are usually apparent in conventional histological sections (Fig. 40.23), but can also be seen *in vivo* using techniques such as optical coherence tomography, which uses backscattered light to visualize layers by differences in their optical scattering properties (Fig. 40.24). Embryologically, the retina is derived from the two layers of the invaginated optic vesicle. The outer layer becomes a layer of cuboidal pigment cells which separates the choroidal lamina vitrea from the neural retina, and therefore forms the outermost layer of the retina, the retinal pigment epithelium (RPE – layer 1). The other nine strata of the retina develop from the inner layer of the optic vesicle and form the neural retina.

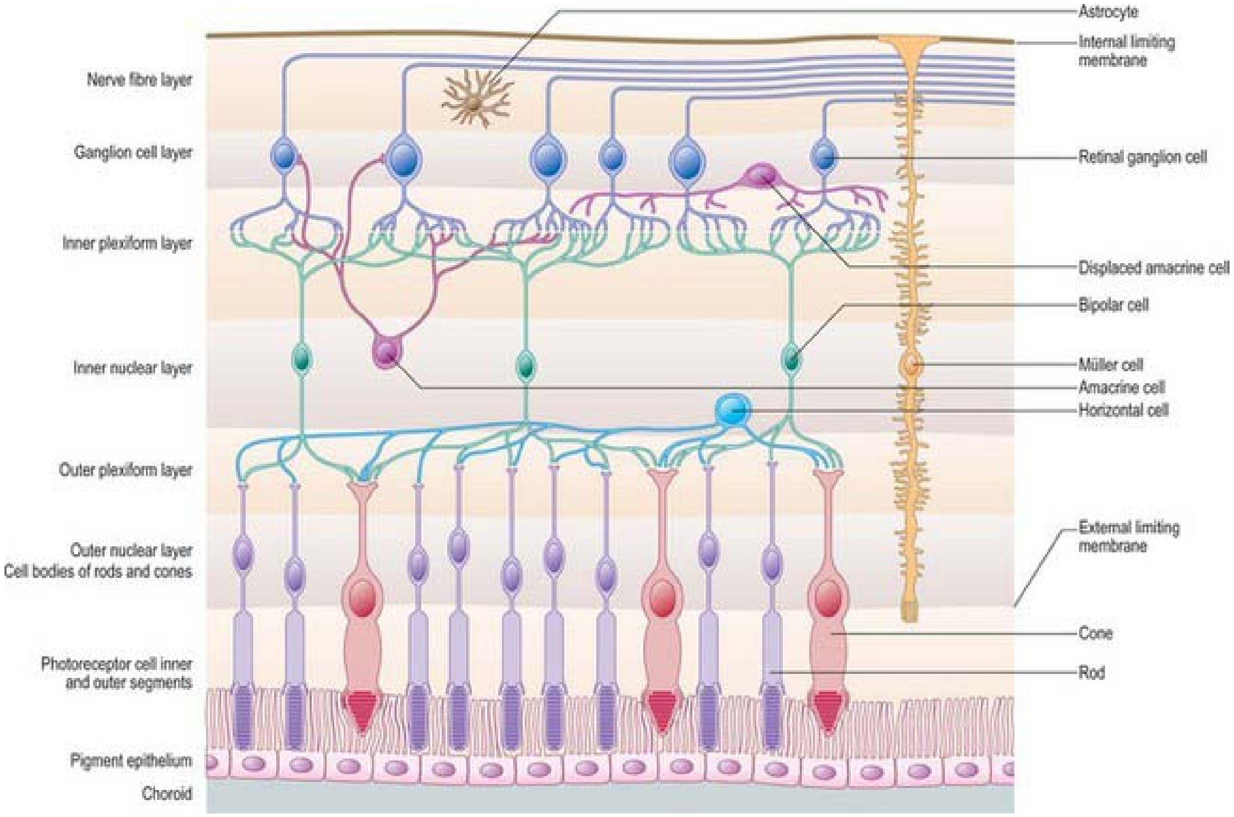
Nerve fibre layer
Ganglion cell layer
Inner plexiform layer
Inner nuclear layer
Outer plexiform layer
Outer nuclear layer
Cell bodies of rods and cones
Photoreceptor cell inner and outer segments
Pigment epithelium
Choroid
Astrocyte
Internal limiting membrane
Retinal ganglion cell
Displaced amacrine cell
Bipolar cell
Müller cell
Amacrine cell
Horizontal cell
External limiting membrane
Cone
Rod

Fig. 40.22 Neural cells whose cell bodies and interconnections account for the layered appearance of the retina in histological section (compare

with Fig. 40.23). Also shown are the two principal types of neuroglial cell in the retina (although microglia are also present they are not shown).

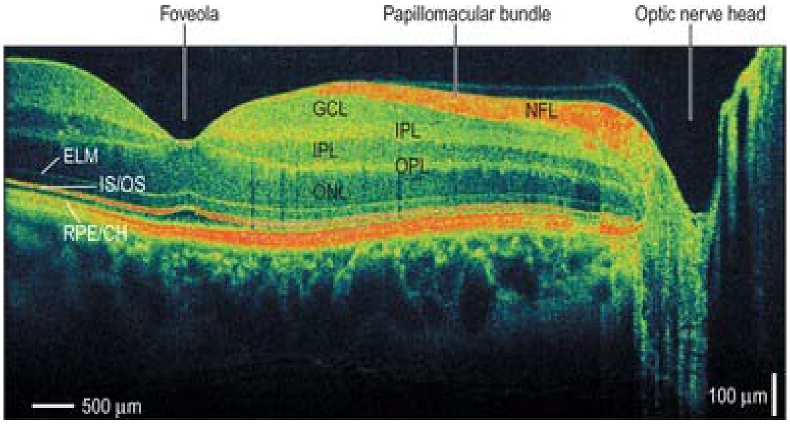

Fig. 40.24 High definition optical coherence tomography (OCT) *in vivo* image of the human retina. The image has approximately 2 µm axial resolution, is 8 mm long and consists of 10,000 axial scans. NFL, Nerve fibre layer. GCL, Ganglion cell layer. IPL, Inner plexiform layer. INL, Inner nuclear layer. OPL, Outer plexiform layer. ONL, Outer nuclear layer. ELM, External limiting membrane. IS/OS, Boundary between the photoreceptor inner and outer segments. RPE/CH, Retinal pigment epithelium and choriocapillaris. The image is expanded in the vertical direction to permit better visualization of retinal layers.

(By courtesy of Professor James Fujimoto, Department of Electrical Engineering and Computer Science, MIT, Boston, USA.)

The outermost layer of the neural retina contains the light sensitive parts of the photoreceptors, which convert the optical image into neural activity. From the photoreceptors, neural activity flows radially to bipolar and ganglion cells, and laterally via horizontal cells in the outer retina and amacrine cells in the inner retina. Photoreceptors synaptically contact each other and bipolar and horizontal cells in the outer plexiform layer (OPL – layer 5), while bipolar, amacrine and ganglion cells synapse in the inner plexiform layer (IPL – layer 7). The axons of ganglion cells run towards the optic disc in the nerve fibre layer (NFL – layer 9), where they leave the retina as the optic nerve, which transmits the retinal output to the visual areas of the brain where visual processing is completed. Although most neural activity flows from the photoreceptors towards the brain, some information flow occurs in the opposite direction via centripetal fibres in the optic nerve and interplexiform cells in the retina which connect the inner and outer plexiform layers.

The classic ten layered appearance of the retina is absent in the optic nerve head, the fovea and foveola, and the ora serrata. At the optic nerve head, the axons of the retinal ganglion cells leave the retina to form the optic nerve and all the other neural cell types of the retina are missing. At the fovea and foveola, the inner five layers of the retina are ‘pushed aside’. At the ora serrata, where the retina borders the ciliary body (Fig. 40.9), the retinal pigment epithelium merges with the outer pigmented epithelium of the ciliary body, while the neural retina borders the inner unpigmented ciliary epithelium: the retina is thinnest at this point. The normal layered arrangement of the neural retina approaching the ora serrata is frequently disrupted by cysts in older individuals (Fig. 40.25).

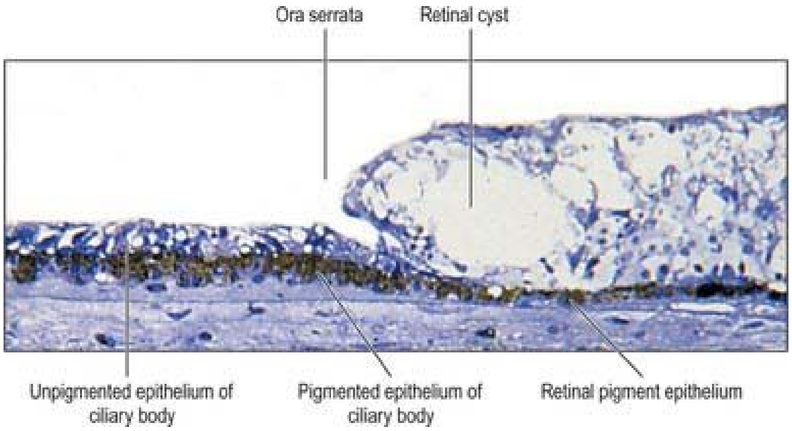
Ora serrata
Retinal cyst
Unpigmented epithelium of ciliary body
Pigmented epithelium of ciliary body
Retinal pigment epithelium

Fig. 40.25 Junction between the retina and ciliary body (ora serrata). The retinal pigment epithelium is continuous with the outer pigmented epithelium of the ciliary body, while the neural retina abuts the inner unpigmented epithelium of the ciliary body. The layered appearance that is apparent elsewhere in the neural retina is disrupted adjacent to the ora serrata by cystic degeneration.

Cells of the retina

Retinal pigment epithelium

The retinal pigment epithelium, RPE, is composed of approximately cuboidal cells that form a single continuous layer extending from the periphery of the optic disc to the ora serrata, where it continues as the outer ciliary epithelium. The cells are flat in radial section and hexagonal or pentagonal in surface view, and number 4–6 million in the human retina. Their cytoplasm contains numerous melanosomes. Apically (towards the rods and cones), the cells bear long (5–7 μm) microvilli which contact, or project between, the outer segments of rods and cones. The tips of rod outer segments are deeply inserted into invaginations in the apical membrane of the RPE. The different embryological origins of the RPE and neural retina mean that the attachments between these two layers are unsupported by junctional complexes; the neural retina and RPE are therefore easily parted in the clinical condition of retinal detachment arising from trauma or disease.

RPE cells play a major role in the turnover of rod and cone photoreceptive components. Their cytoplasm contains the phagocytosed tips of rods and cones undergoing lysosomal destruction. The final products of this process are lipofuscin granules, which accumulate in these cells with age.

Light reaching the outer retina but missing the photoreceptors is absorbed by the RPE, which, like melanin elsewhere in the eye, prevents such stray light degrading image quality. The zone of tight junctions between adjacent cells also allows the epithelium to function as an important blood-retinal barrier between the retina and the vascular system of the choroid. The RPE is required for the regeneration of bleached visual pigment and may have antioxidant properties. It also secretes a variety of growth factors necessary for the integrity of the choriocapillaris endothelium and the photoreceptors, and produces a number of immunosuppressive factors. A failure of any of the diverse functions of the RPE could result in compromised retinal function and eventual blindness (Strauss 2005).

Rods and cones

Rods and cones are the ‘image forming’ photoreceptors of the outer retina and function at low (scotopic) and higher (photopic) light levels respectively. Both are long, radially orientated structures with a similar organization, although details differ (Fig. 40.26). From the choroidal end inwards, the cells consist of outer and inner segments connected by a thin connecting cilium (together making up layer 2 of the retina), a cell body containing the nucleus, and a synaptic terminal (either a more complex pedicle for cones or a simpler rod spherule) where they make synaptic connections with adjacent bipolar and horizontal cells and with other cone or rod cells within the OPL.

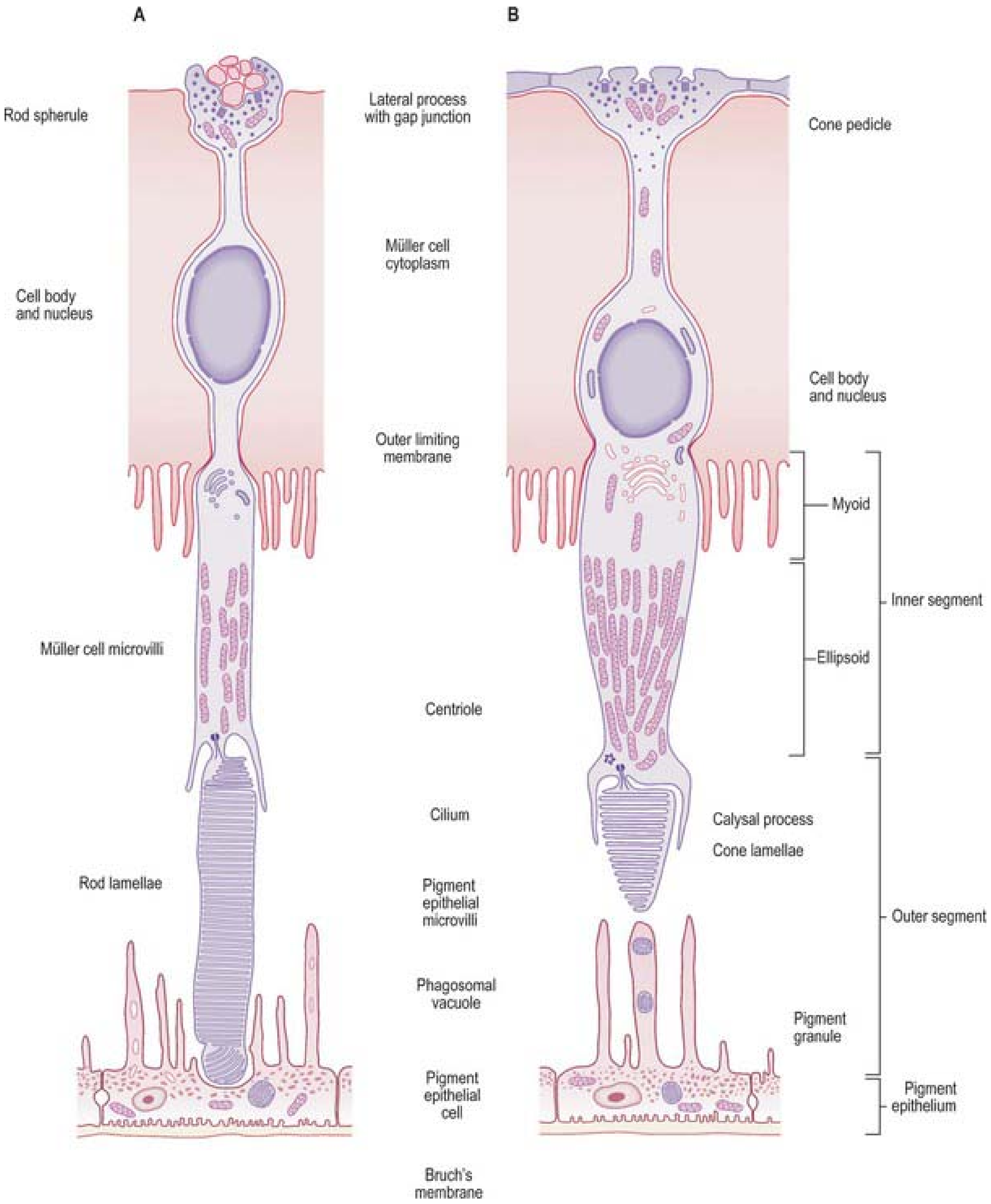
A
B
Rod spherule
Lateral process with gap junction
Cone pedicle
Müller cell cytoplasm
Cell body and nucleus
Cell body and nucleus
Outer limiting membrane
Myoid
Inner segment
Müller cell microvilli
Ellipsoid
Centriole
Cilium
Calysal process
Cone lamellae
Rod lamellae
Pigment epithelial microvilli
Outer segment
Phagosomal vacuole
Pigment granule
Pigment epithelial cell
Pigment epithelium
Bruch's membrane

Fig. 40.26 The major features of a retinal rod cell (**A**) and a retinal cone cell (**B**). The relative size of the pigment epithelial cells has been exaggerated for illustrative purposes.

The nuclei of the rods and cones form the outer nuclear layer (ONL – layer 4). The cone nuclei are relatively large, oval and generally form a single layer that often penetrates the external limiting membrane (ELM – layer 3). They also contain less heterochromatin and thus usually stain more lightly. Rod nuclei are round and smaller, stain more darkly and form several layers vitreal to the cone nuclei.

The ELM is in fact not a membrane at all, although it appears as such in the light microscope, but a series of zonula adherentes between photoreceptors and the glial (Müller) cells that separate them. These junctions most likely serve to anchor the photoreceptors and prevent leakage of the interphotoreceptor matrix that surrounds the photoreceptor outer and inner segments.

Rod outer segments are cylindrical and consist of around 1000 flattened lobulated membranous discs. These form as deep infoldings of the plasma membrane at the base of the outer segment; they 'bud off' after formation so that the discs are not attached to the plasma membrane and are free floating within the outer segment. Cone outer segments are generally shorter and, as their name implies, often conical (especially in the peripheral retina). Cone discs do not bud off after formation and remain as infoldings of the plasma membrane.

The inner segment of both rods and cones is divided into an outer, mitochondria-rich, ellipsoid and an inner myoid which contains endoplasmic reticulum (Fig. 40.26). In most of the retina these inner segments are much wider in cones (5–6 μm at their widest point) than rods (1.5 μm) (Fig. 40.27). In both rods and cones proteins are manufactured within the myoid and incorporated into the newly formed discs at the base of the outer segment. In rods, as new discs are added, old discs are pushed up the outer segment and eventually phagocytosed by the RPE. Cone discs are also phagocytosed but the incorporation of new proteins within the discs is more diffuse. While all rods within the retina have a similar structure, the cones at the foveola are highly modified compared to those situated more peripherally, and in many ways resemble rods with a longer outer segment and a thinner inner segment.

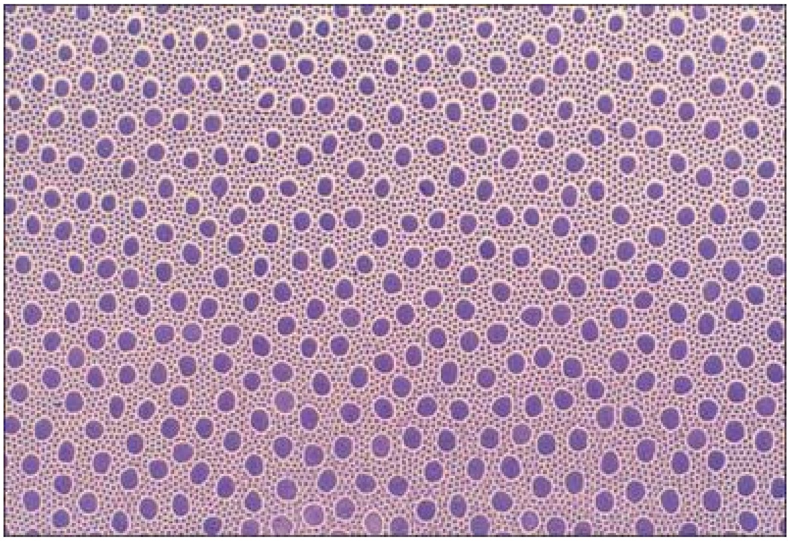

Fig. 40.27 Tangential section of a human retina in the parafovea cut at the level of the inner/outer segments, showing the ‘mosaic’ of both the larger cones and the more numerous, but smaller, rods. Photoreceptors at the top of the image are sectioned at a level closer to the retinal pigment epithelium than receptors lower in the figure. The reduction in size of the cones at the top of the figure is explained by the conical shape of their outer segment. If the figure were continued upwards, representing sections closer to the RPE, the size of the cones would continue to decrease and the amount of surrounding white space increase. Rod outer segment diameter, however, would change little.

Light is absorbed by rhodopsins, visual pigments consisting of a protein, opsin, that spans the membrane of the outer segment discs, bound to a light absorbing chromophore, retinal, which is an aldehyde of vitamin A_1. Such rhodopsins have a smooth bell-shaped absorption profile with a point of maximum absorbance (λ_{max}), indicating the wavelength at which they are most sensitive. Humans possess four different opsins resulting in four spectrally distinct visual pigments, one located within the rods (λ_{max} 498 nm) and three within different populations of cones absorbing maximally at the short (λ_{max} 420 nm); middle (λ_{max} 534 nm) and longer wave (λ_{max} 563 nm) end of the visible spectrum. The three cone classes are sometimes referred to as the blue, green and red cones, but are better classed as S, M and L cones.

The action of light is to isomerize the retinal separating it from the opsin, a process which, via a G-protein coupled enzyme cascade and a second messenger system, results in the closure of cation channels in the receptor outer segment membrane, a hyperpolarization of the photoreceptor, and a consequent decrease in the release of the neurotransmitter glutamate from its synapses.

The human retina contains on average 4.6 million cones and 92 million rods, although there is significant inter-individual variation (Curcio et al 1990). Although cones populate the whole retina, their density is highest in the foveola, where approximately 7000 cones reach an average density of 199,000 cones/mm^2: this area is entirely rod free. Going outwards from the foveola, rod numbers rise, reaching a peak density in a horizontal elliptical ring at the eccentricity of the optic disc, before declining once more toward the periphery. Cone density is 40–45% higher in the nasal compared to the temporal retina, and slightly higher inferiorly than superiorly.

The number of S cones in all human retinae is similar, making up less than 10% of all cones (Curcio et al 1991; Hofer et al 2005). The distribution of S cones is relatively even throughout the retina, although they are absent from the central fovea. The relative proportions of L and M cones shows a much greater degree of variation between individuals, the L : M cone ratio varying from close to unity to over 10. The distribution of L and M cones is more irregular than that of S cones, and appears random with some indication of clumping (Bowmaker et al 2003; Hofer et al 2005).

The high packing density of cones at the foveola, achieved by decreasing inner segment size, ensures maximal resolution, while the presence of more than one spectral cone type allows colour vision. S cones probably contribute little to spatial resolution because they are absent from the foveola. Rod-based vision provides high sensitivity, but with relatively low spatial discrimination and no ability to distinguish wavelengths. Although many of the functional differences between rods and cones rely on the different properties of the photoreceptors themselves, their connectivity to other retinal neurones is equally important.

Horizontal cells

Horizontal cells are inhibitory interneurones. Their dendrites and axons extend laterally within the OPL, making synaptic contacts with cone pedicles and rod spherules, and, via gap junctions at the tips of their dendrites, with each other. Their cell bodies lie in the outer part of the inner nuclear layer (INL – layer 6). Three morphological types of horizontal cell can be distinguished in the human retina (Kolb et al 1992). The dendrites of HI and HIII cells contact cones, and their axons terminate on rods. Both the axons and dendrites of HII cells synapse only with cones.

Bipolar cells

Bipolar cells are radially orientated neurones. Their dendrites synapse on photoreceptors, horizontal cells and interplexiform cells in the OPL. Their somata are located in the INL, and axonal branches in the IPL synapse with dendrites of ganglion cells or amacrine cells. Golgi staining has identified nine distinct types of bipolar cell in the human retina (Kolb et al 1992), eight of which contact cones exclusively, and the remaining type synapses only on rods.

Cone bipolars are of three major types, midget, S (blue) cone and diffuse, according to their connectivity and size. Midget cone bipolar cells either invaginate the cone pedicle or synapse on its base (flat subtype). In the central retina, each midget bipolar cell contacts only a single cone (2–3 in the periphery) forming part of a one-to-one channel from cone to ganglion cell that mediates high spatial resolution. S cones form part of a short wavelength mediating channel, while the larger diffuse cone bipolars are connected to up to ten cones and are thought to signal luminosity rather than colour.

Cone bipolar cells can be of two types, according to their response to the light-induced decrease in glutamate release from the photoreceptors to which they are synaptically connected. If illumination of the photoreceptors with a point of light causes a depolarization of the connected bipolar cell, it is said to be an ‘ON’ bipolar, connected to the cone by ‘sign-inverting’ synapses with metabotropic receptors. However, if cones are connected to an ‘OFF’ bipolar cell via ‘sign-conserving’ synapses with ionotropic receptors, illumination of the photoreceptor will result in hyperpolarization of the bipolar cell. Illumination of a concentric area of surrounding photoreceptors causes the opposite response in the bipolar cell. This inhibition is mediated via horizontal cells and gives rise to the antagonistic centre-surround type receptive field that is characteristic of all levels of the visual system up to and including the occipital cortex.

The single morphological type of rod bipolar cell contacts 30–35 rods in the central retina, increasing to 40–45 rods in the periphery. Such convergence serves to increase the absolute sensitivity of the rod system. All rod bipolar cells are ‘ON-centre’ and do not contact ganglion cells directly, but synapse with a class of amacrine cell (AII) which then contacts cone bipolar cells.

The IPL can be divided into two main layers, an outer layer containing the synaptic endings of ‘OFF’ cone bipolar cells, and an inner layer of ‘ON’ cone and rod bipolar cell synapses.

Amacrine cells

Most amacrine cells lack typical axons and consequently their dendrites make both incoming and outgoing synapses. Each neurone has a cell body either in the INL near its boundary with the IPL, or on the outer aspect of the ganglion cell layer, when it is known as a displaced amacrine cell. The processes of amacrine cells make a variety of synaptic contacts in the IPL with bipolar and ganglion cells as well as with other amacrine cells.

The various classes of amacrine cell serve a number of important functions in vision. AII cells play an essential role in the rod pathway (see above). Other cells appear to be important modulators of photoreceptive signals, and serve to adjust or maintain relative colour and luminosity inputs under changing light conditions. They are probably also responsible for some of the complex forms of image analysis known to occur within the retina, such as directional movement detection. Up to 24 different morphological types are recognized in humans (Kolb et al 1992): coupled to their neurochemical complexity, this makes them perhaps the most diverse neural cell type in the body.

Interplexiform cells

Interplexiform cells, often regarded as a subclass of amacrine cells, generally have cell bodies in the INL. They are postsynaptic to cells in the inner retina, and send signals against the general direction of information flow in the retina, synapsing with bipolar, horizontal and photoreceptor cells in the OPL. Although their function is uncertain, it is likely that they adjust some aspect of retinal function such as sensitivity.

Ganglion cells

The human retina contains 0.7–1.5 million ganglion cells, the output neurones of the retina (Curcio & Allen 1990). Their dendrites synapse with processes of bipolar and amacrine cells in the IPL. Ganglion cell bodies, together with displaced amacrine cells, form the ganglion cell layer of the retina (GCL – layer 8). Throughout most of the retina they form a single layer; they become progressively more numerous near the macula, where they are ranked in up to 10 rows, reaching a peak density of up to 38,000/mm^2 in a horizontally orientated elliptical ring 0.4–2.0 mm from the foveal centre. Their number diminishes again towards the fovea, from which they are almost totally excluded.

Up to 15 ganglion cell types have been identified in the mammalian retina based on morphology, physiology, and target area in the brain, each of them presumably functionally distinct. For example, some project to different regions of the LGN and form three parallel visual pathways involved in conscious visual perception, namely the magnocellular and parvocellular systems and a pathway carrying the S cone signal (Wässle 2004). Midget ganglion cells (P cells) contact only single midget bipolar cells in the central retina, which in turn connect to single cones, giving each cone a ‘private line’ out of the retina and ensuring optimal acuity. The large dendritic field of parasol (M cells) is consistent with a role in motion detection. Parasol and midget ganglion cells together make up around 80% of human retinal ganglion cells. The remaining cells (approximately 200,000) project to the superior colliculus of the midbrain, the thalamic pulvinar, the pretectum and the accessory optic system, and contribute to various subconscious visual reflexes such as the pupillary and accommodation responses. In addition, a population of around 3000 large, intrinsically light-sensitive ganglion cells form a network composed of extensive overlapping dendrites (Dacey et al 2005). Such ‘inner retinal photoreceptors’ contain a retinal-based visual pigment (melanopsin; λ_{max} approximately 479 nm) which resembles an invertebrate-type visual pigment in many of its characteristics. These light-sensitive ganglion cells are part of a pathway parallel to the rod and cone-mediated ‘image-forming’ system that monitors overall levels of illumination. This ‘non-imaging’ pathway is the major route by which the eye influences circadian rhythms via the suprachiasmatic nucleus; it also contributes to light-evoked pupillary constriction via projections to the olivary pretectal nucleus.

Ganglion cell axons, which form the NFL on the inner surface of the retina, run parallel to the surface of the retina, and converge on the optic nerve head where they leave the eye as the optic nerve. Fibres from the medial (nasal) retina approach the disc in a simple radial pattern (Fig. 40.28), whereas axons from the lateral (temporal) retina take an arcuate route as they avoid the fovea. Axons from the macula form a papillomacular fasciculus which passes almost straight to the disc. The thickness of the NFL increases dramatically near the optic disc as fibres from the peripheral retina traverse more central areas. Towards the edge of the disc the other retinal layers thin, and at the disc all neural elements of the retina other than ganglion cell axons are excluded.

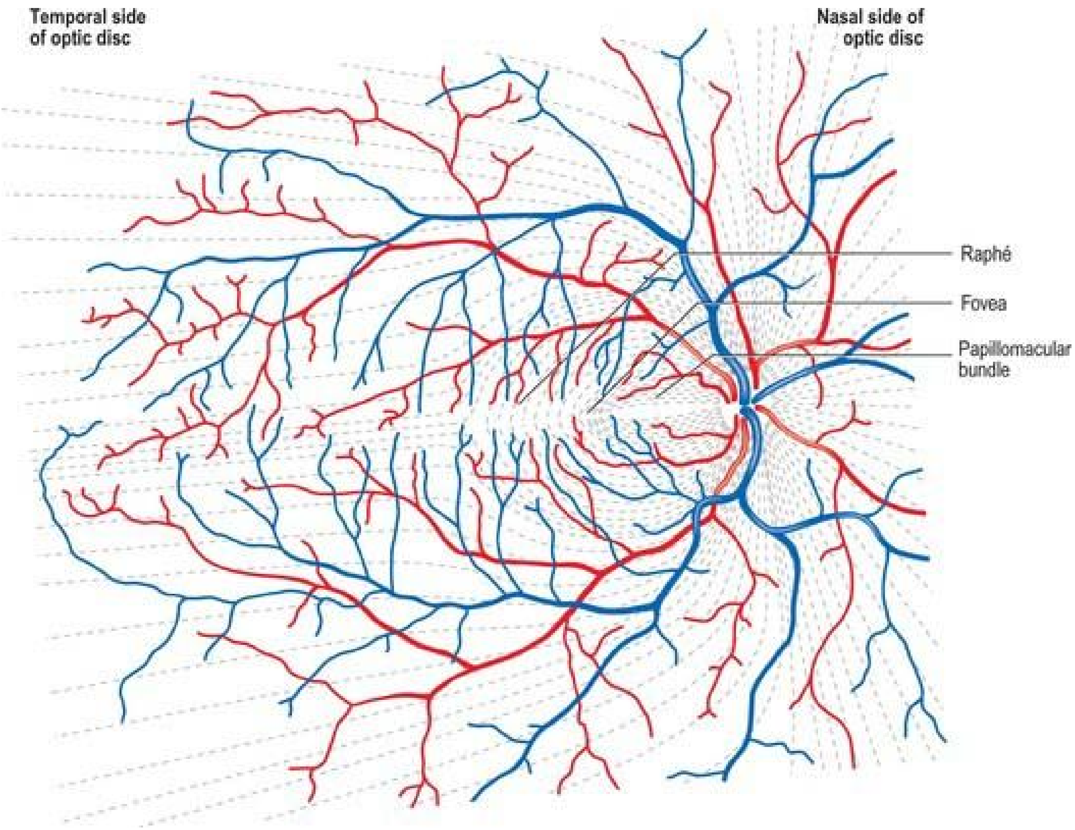

Fig. 40.28 Directions of axons (dashed lines) and blood vessels of the nerve fibre layer of the retina. Axons pass radially on the nasal side of the optic disc, whereas fibres on the temporal side avoid crossing the fovea by arching around it. Some of the fibres from the fovea and central region pass straight to the optic disc and others arch above and below the horizontal; together these form the papillomacular bundle. A raphé is formed by the central fibres temporal to the fovea. Venules are shown crossing in front of arteries: the reverse relationship is probably the more common pattern. All vessels issue from the disc on the right of the figure; the larger temporal branches tend to arch around the central region of the retina and do not approach the fovea. The peripheral retina and most of the nasal retina are not shown.

Axons of ganglion cells are surrounded by the processes of radial glial cells and retinal astrocytes and are almost always non-myelinated within the retina, which is an optical advantage because myelin is refractile. Although a few small myelinated axons may occur, myelination does not generally start until axons enter the optic disc to become the optic nerve.

Retinal glial cells

There are three types of retinal glial cells, namely, radial Müller cells, astrocytes and microglia. Müller cells form the predominant glial element of the retina; retinal astrocytes are largely confined to the ganglion cell and nerve fibre layers; microglial cells are scattered throughout the neural part of the retina in small numbers.

Müller cells span almost the entire thickness of the neural retina, ensheathing and separating the various neural cells except at synaptic sites. They constitute much of the total retinal volume, and almost totally fill the extracellular space between neural elements. Their nuclei lie within the INL, and from this region each cell body extends a single thick fibre that runs radially outwards, giving off complex lateral lamellae which branch among the processes of the OPL. Apically, each central process terminates at the ELM from which microvilli project for a short distance into the space between the rod and cone inner segments (fibre baskets) (Fig. 40.22). On the inner surface of the retina, the main Müller cell process expands into a terminal foot plate which contacts those of neighbouring glial cells and forms part of the internal limiting membrane (ILM; see below).

Like astrocytes, Müller cells also contact blood vessels, especially capillaries of the INL, and their basal laminae fuse with those of perivascular cells or vascular endothelia, contributing to the formation of the blood–retinal barrier. They also maintain the stability of the retinal extracellular environment by, for example; regulation of K^+ levels, uptake of neurotransmitter, removal of debris, storage of glycogen, electrical insulation of receptors and other neurones, and mechanical support of the neural retina.

The cell bodies of retinal astrocytes lie within the NFL and their processes branch to form sheaths around ganglion cell axons. The close association between astrocytes and blood vessels in the inner retina suggests that they contribute to the blood–retinal barrier. Retinal microglia are scattered mainly within the IPL. Their radiating branched processes spread mainly parallel to the retinal plane, giving them a star-like appearance when viewed microscopically from the surface of the retina. They can act as phagocytes, and their number increases in the injured retina.

The inner border of the retina is formed by the internal limiting membrane (ILM – layer 10) which consists of collagen fibres and proteoglycans from the vitreous, a basement membrane (which is continuous with the basal lamina of the ciliary epithelium), and the plasma membrane of expanded Müller cell terminal foot plates. It is 0.5–2 µm thick in the posterior retina and thickens with age. The ILM is involved in fluid exchange between the vitreous and the retina and, perhaps through the latter, with the choroid. It also has various other functions including anchorage of retinal glial cells, and inhibition of cell migration into the vitreous body.

Modifications of the central retina

The central retina, clinically referred to as the macula, is composed of four concentric areas, which, starting with the innermost, are: the foveola (0.35 mm diameter, equivalent of an angular subtense at the nodal point of around 1.25°), the fovea (1.5 mm, 5.2°), the parafovea (2.5 mm, 8.6°), and the vaguely defined perifovea (approximately 5–6 mm, 20°). The foveola, which contains no rods or S cones, is centred about 3 mm temporal and 1 mm inferior to the optic disc (Fig. 40.20). In the foveola and surrounding fovea all the inner layers of the neural retina beyond the ONL have been displaced peripherally resulting in a retinal thickness around half of that elsewhere in the retina (Figs 40.24, 40.29). This foveal pit is created by the cone ‘axons’, known here as Henle fibres, running almost parallel to the retinal surface before connecting to post-receptoral retinal neurones outside the fovea. The Henle fibres contain two xanthophyll carotenoid pigments (lutein and zeaxanthin) which create an elliptical yellowish area (approximately 2 mm horizontally and 1 mm vertically), the macula lutea. Macular pigment density varies by more than an order of magnitude between individuals, is influenced by several environmental factors including diet, and is negligible in the central foveola.

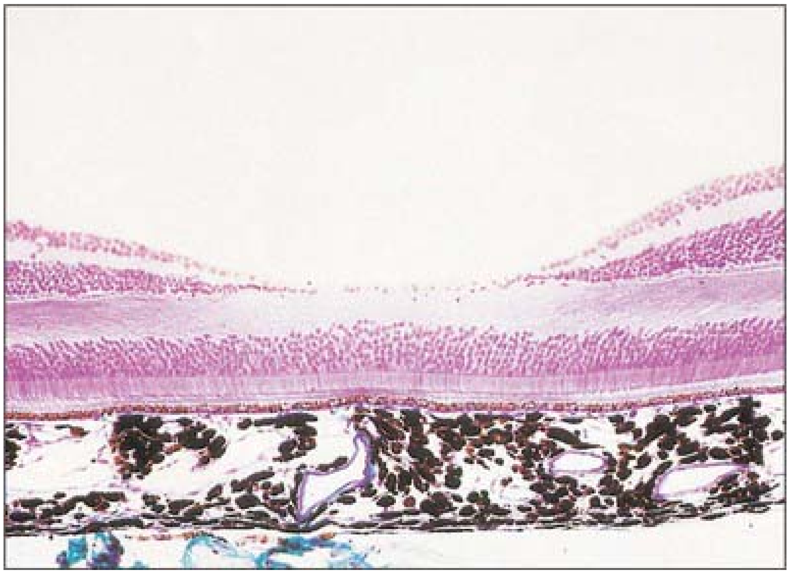

Fig. 40.29 Section through the fovea centralis

(By permission from Young B, Heath JW 2000 Wheater's Functional Histology. Edinburgh; Churchill Livingstone.)

The absence of the inner retinal layers, including blood vessels (Figs 40.20, 40.21), reduces light scatter, which, along with the increased packing density of cones in the foveola and their lack of convergence with ganglion cells, ensures visual resolution is highest in this part of the retina. Acuity may be further enhanced by the macular pigment, which apart from having antioxidant properties and removing potentially harmful short-wave radiation, will absorb those wavelengths most prone to chromatic aberration and Rayleigh scatter.

VASCULAR SUPPLY

The retina has a dual arterial supply and both parts are necessary to maintain retinal function. The outer five layers of the retina are avascular and rely on an indirect supply from the choriocapillaris in the choroid. The inner retina receives a direct blood supply through capillaries connected to branches of the central retinal artery and vein. Only the inner retinal circulation is described here. The choroidal blood supply is discussed on p. 680.

The central retinal artery enters the optic nerve as a branch of the ophthalmic artery approximately 1.2 cm behind the eyeball, and travels within the optic nerve to its head, where it passes through the lamina cribrosa. At this level the central artery divides into equal superior and inferior branches, which, after a few millimetres, divide into superior and inferior nasal, and superior and inferior temporal, branches, each supplying a ‘quadrant’ of the retina (Fig. 40.28). Although similar retinal veins unite to form the central retinal vein, the courses of the arteries and veins do not correspond exactly. These vessels mainly run within the nerve fibre and ganglion cell layers of the retina, accounting for their clarity when seen through an ophthalmoscope (Fig. 40.20). Arteries often cross veins, usually lying superficial to them: in severe hypertension the arteries may press on the veins and cause visible dilations distal to these crossings. The vitreal location of arteries, and their lighter, bright red colouration and smaller diameter in comparison to veins, allows the two vessel types to be distinguished ophthalmoscopically.

From the four major arteries subsequent dichotomous branches run from the posterior pole to the periphery, supplying the whole retina (Zhang 1994). Arteries and veins ramify in the nerve fibre layer, near the ILM, and arterioles pass deeper into the retina to supply capillary beds. Venules return from these beds to larger superficial veins which converge towards the disc to form the central retinal vein.

Retinal capillary networks can occur in three different layers, the number of layers depending on location (Zhang 1994). Radial peripapillary capillaries are the most superficial of the capillary networks and lie within the inner nerve fibre layer. A layer of inner capillaries runs within the nerve fibre and ganglion cell layers, while an outer capillary layer is located in the inner plexiform and inner nuclear layers (Fig. 40.30). Approaching the fovea, capillaries are restricted to two layers, and terminal capillaries eventually join to form a single-layered macular capillary ring, producing a capillary-free zone 450–500 μm in diameter at the fovea. This avascular region is clearly visible in a fluorescein angiogram (Fig. 40.21). Capillaries become less numerous in the peripheral retina and are absent from a zone approximately 1.5 mm wide adjoining the ora serrata.

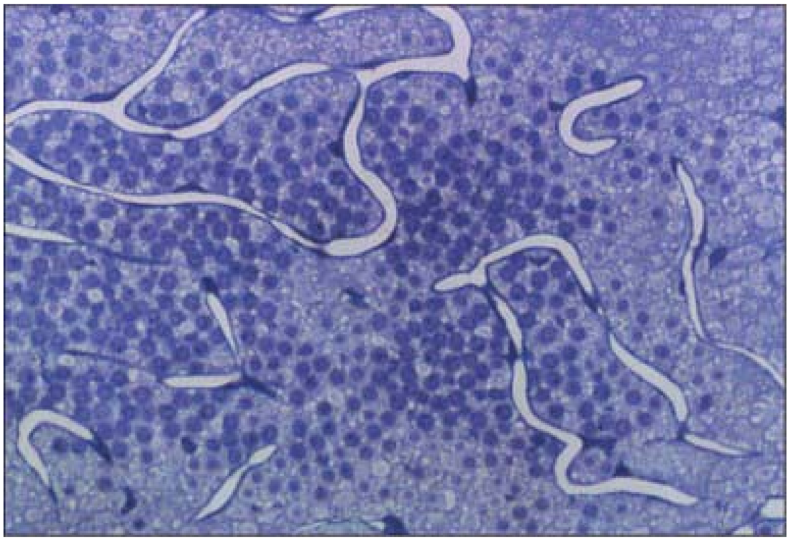

Fig. 40.30 Tangential section of the retina at the level of the inner nuclear layer, highlighting the dense network of capillaries.

The territories of the arteries which supply a particular quadrant do not overlap, nor do the branches within a quadrant anastomose with each other, and consequently a blockage in a retinal artery causes loss of vision in the corresponding part of the visual field. The only exception to this end-arterial pattern is in the vicinity of the optic disc. Here, the posterior ciliary arteries enter the eye near the disc (Figs 40.10, 40.31), and their rami not only supply the adjacent choroid, but also form an anastomotic circle in the sclera around the head of the optic nerve (Fig. 40.31). Branches from this ring join the pial arteries of the nerve, and small cilioretinal arteries from any arteries in this region may enter the eye and contribute to the retinal vasculature, possibly resulting in the preservation of visual function following central retinal artery occlusion. Similarly, small retinociliary veins may sometimes also be present.

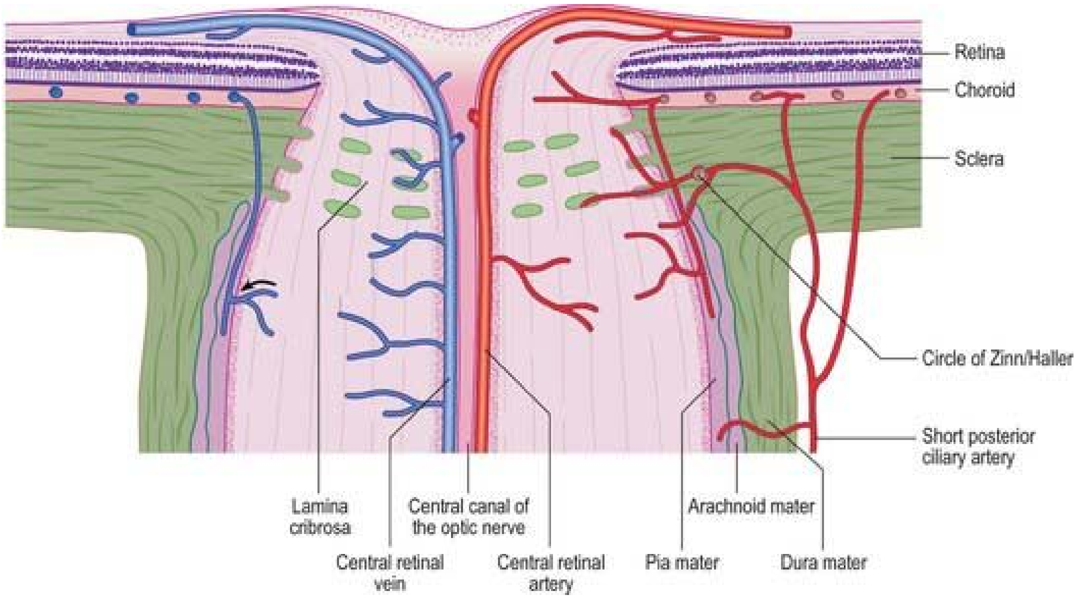
Retina
Choroid
Sclera
Circle of Zinn/Haller
Short posterior ciliary artery
Lamina cribrosa
Central canal of the optic nerve
Arachnoid mater
Central retinal vein
Central retinal artery
Pia mater
Dura mater

Fig. 40.31 Vessels of the optic nerve head. The dotted areas represent the principal glial membranes.

The structure of retinal blood vessels resembles that of vessels elsewhere, except that the internal elastic lamina is absent from the arteries, and muscle cells may appear in their adventitia. Capillaries are non-fenestrated and endothelial cells are joined by complex tight junctions, fulfilling the requirements of a functional blood–retinal barrier. Within the optic nerve, the central artery is innervated by sympathetic and parasympathetic fibres: this innervation does not extend to the vessels in the retina. The parasympathetic supply is derived from the pterygopalatine ganglion, and the fibres are predominantly VIP-ergic (and probably NO-ergic) and vasodilatory. The sympathetic supply is derived from the plexus around the internal carotid and ophthalmic arteries.

RETINOPETAL INNERVATION OF THE RETINA

The human retina receives modulating input from the brain via fibres within the optic nerve which emerge at the optic disk as large axons, and then course through the NFL, gradually diminishing in size. Although there are only a small number of these retinopetal axons (usually less than 10), they branch extensively before terminating in the IPL (Reperant et al 2006). One set of such axons arises from perikarya in the posterior hypothalamus and uses histamine as a neurotransmitter, while other, serotoninergic, fibres arise from cell bodies in the dorsal raphé. These neurones project to many targets in the central nervous system including the retina, forming components of an ascending arousal system. Such fibres allow higher central areas to modulate aspects of retinal activity; in man they may, among other things, affect sensitivity and modulate retinal blood flow (Gastinger et al 2006).

OPTIC NERVE HEAD

The axons of more than a million retinal ganglion cells converge at the optic nerve head (ONH) and leave the eye by penetrating the sclera to form the optic nerve (ON). The ONH represents that part of the optic nerve lying within the bulb of the eye. Since all retinal neural elements, apart from ganglion cell axons, are absent from this region it is insensitive to light and forms the ‘blind spot’.

Histologically the ONH can be divided into three zones (Fig. 40.32). These are prelaminar (the anterior part terminating at the vitreous); laminar (formed by the lamina cribrosa); postlaminar (continuous with the retrobulbar optic nerve). The surface view of the ONH, usually seen with an ophthalmoscope, is referred to as the optic disc.

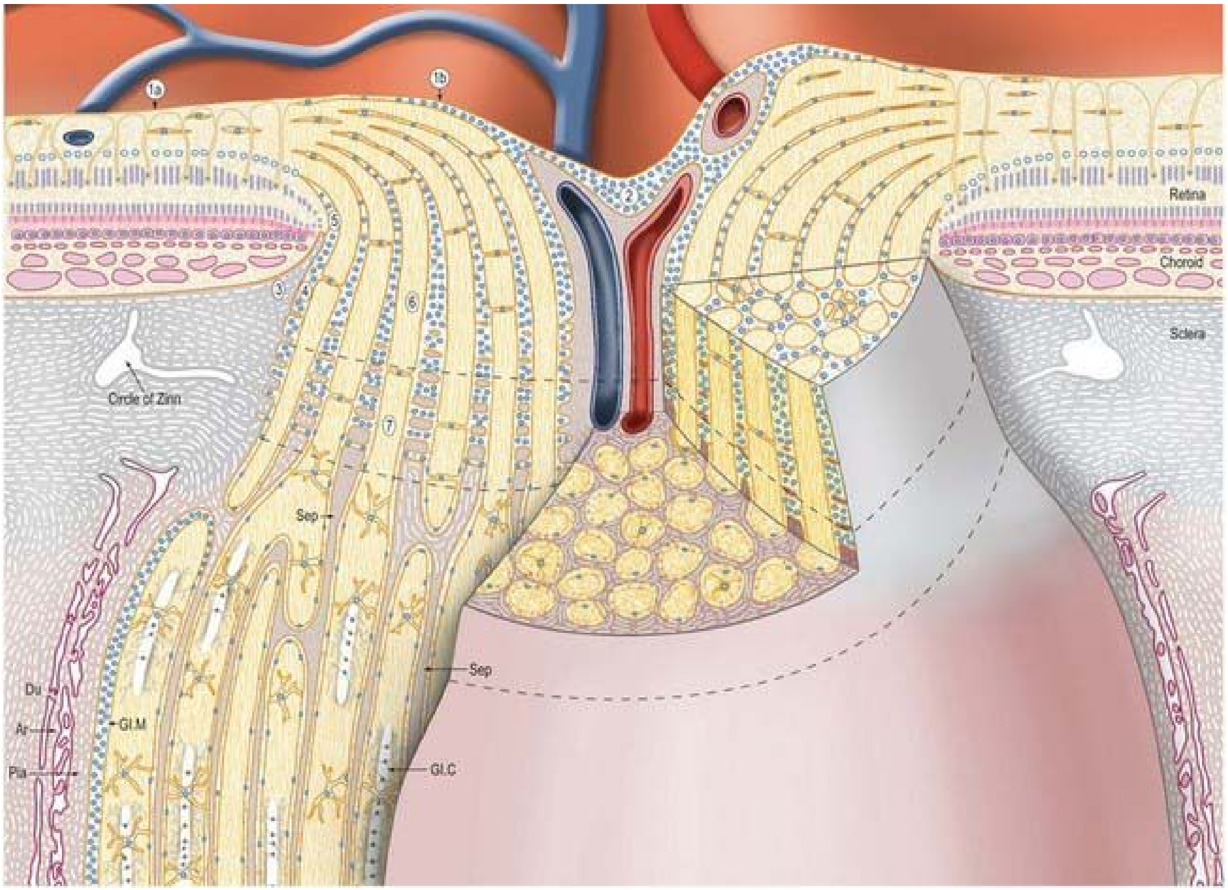

Fig. 40.32 The optic nerve head, showing the distribution of collagenous tissue (grey) and neuroglial nuclei (solid blue circles). **1a**, retinal internal limiting membrane; **1b**, inner limiting membrane of Elschnig; **2**, central meniscus of Kuhnt; **3**, spur of collagenous tissue separating the anterior lamina cribrosa (**6**) from the choroid; **4**, border tissue of Jacoby; **5**, intermediary tissue of Kuhnt; **7**, posterior lamina cribrosa; Sep, connective tissue septa from pia mater; Gl. M, astroglial membrane; Gl. C, astrocytes and oligodendrocytes among the fibres in their fascicles; Du, Ar, Pia: dura, arachnoid and pia mater, respectively. The dotted lines represent the borders of the lamina cribrosa.

(By permission from Anderson DR, Hoyt W 1969 Ultrastructure of intraorbital portion of human and monkey optic nerve. Arch Ophthalmol 82: 506–30.

Prelaminar zone

The inner surface of the ONH is covered by an astroglial membrane (of Elschnig) that is continuous with the ILM of the retina. At the centre of the disc, the layer of astrocytes thickens into a central meniscus (of Kuhnt). Retinal ganglion cells turn into the ONH accompanied by astrocytes, which gradually increase in number posteriorly, eventually forming a sieve-like structure, the glial lamina cribrosa, through which the nerve fibres pass as separate fasciculi. At the perimeter of the ONH, a collar of astrocytes several cells thick (the intermediary tissue of Kuhnt) separates the ON from the terminating outer layers of the retina. This layer continues posteriorly and forms a barrier between the ONH and the choroid (the border tissue of Jacoby) (Fig. 40.32).

Laminar zone

The lamina cribrosa is composed of discrete trabeculae of collagenous and elastic connective tissue which extend from the sclera to form a meshwork through which the optic nerve fascicles and central retinal vessels pass. Each trabecula has a lining of astrocytes which are continuous with those of the glial lamina cribrosa.

Postlaminar zone

The ON thickens in the postlaminar zone as its axons become myelinated. The reflected sclera, and the dura mater with which it is continuous, invests the nerve together with the other two meningeal sheaths, the arachnoid and pia mater. Fine fibrous septa penetrate the optic nerve from the pia mater dividing it into 300–400 fascicles, giving pial blood vessels access to the nerve.

Optic disc

As it is visible by ophthalmoscopy (Fig. 40.20), the disc is a region of much clinical importance. Oedema of the disc (papilloedema) may be the first sign of raised intracranial pressure, which is transmitted into the subarachnoid space around the ON. The disc is also sensitive to the raised intra-ocular pressure which occurs in glaucoma and shows characteristic structural changes due to retinal ganglion cell loss.

The optic disc is superomedial to the posterior pole of the eye, and so lies away from the visual axis. It is round or oval, usually approximately 1.6 mm in transverse diameter and 1.8 mm in vertical diameter, and its appearance is very variable. In light-skinned subjects, the general retinal hue is a bright terracotta-red, with which the pale pink of the disc contrasts sharply; its central part is usually even paler and may be light grey. These differences are due in part to the degree of vascularization of the two regions, which is much less at the optic disc, and also to the total absence of choroidal or retinal pigment cells. In subjects with strongly melanized skins, both retina and disc are darker. The optic disc rarely projects sufficiently to justify the term papilla, although it is usually a little elevated on its lateral side, where the papillomacular nerve fibres turn into the optic nerve (Fig. 40.28). There is usually a slight depression where the retinal vessels traverse its centre.

Vascular supply

The blood supply to the three regions of the ONH differs. The prelaminar region is supplied mainly by branches of the central retinal artery (Fig.

40.31). Branches from the short posterior ciliary arteries form an often incomplete circle within the sclera around the ONH (circle of Zinn/Haller); centripetal branches from this structure supply the laminar region of the ONH. The short posterior ciliary arteries may also give off centripetal branches directly to supply the lamina, and branches that pass anteriorly to augment the prelaminar blood supply (Fig. 40.31). In the postlaminar region, arteries from the prepapillary choroid and circle of Zinn pass retrogradely as pial vessels, providing centripetal branches that supply the optic nerve. More posteriorly, the optic nerve receives pial arterioles directly from the posterior ciliary arteries. The central retinal artery may also contribute some centrifugal branches in this region.

The central retinal vein drains the ONH at all levels; other drainage pathways are minor.

VISUAL PATHWAY

The visual pathway includes the interneurones of the retina, retinal ganglion cells whose axons project via the optic nerve, chiasma, and optic tract to the lateral geniculate nucleus (LGN) and neurones within the LGN which project via the optic radiation to the primary visual cortex (Fig. 40.33).

The retina can be divided by a horizontal line bisecting the fovea. Axons arising from the nasal half of this line within each retina cross in the chiasma to enter the contralateral optic tract. Fibres from the temporal hemiretinas do not cross in the chiasma. Upper and lower temporal fibres pass laterally in the chiasma and shift respectively to medial and inferolateral positions in the ipsilateral optic tract. They are joined by the crossed fibres, the upper and lower nasal quadrants sharing the same positions as their uncrossed counterparts. Thus, each tract carries a binocular representation of the contralateral half fields as shown in Figure 40.33. It is important to remember that visual space is optically inverted by the crystalline lens when relating the spatial location of neurones within the visual pathway to corresponding visual field locations.

The LGN contains cells arranged in six laminae. Each layer receives input from either crossed or uncrossed projections from the retina. The contralateral nasal retina projects to laminae 1, 4, and 6, whereas the ipsilateral temporal retina projects to layers 2, 3 and 5. Layers 1 and 2 contain magnocellular cells, the remaining layers are parvocellular. There is a point-to-point retinotopic arrangement between corresponding points in each hemiretina so that the contralateral visual field is mapped within each lateral geniculate nucleus.

Axons from the LGN run in the retrolenticular part of the internal capsule and form the optic radiation. This curves dorsomedially to the primary visual cortex, located around and within the depths of the calcarine sulcus in the occipital lobe (also known as the striate cortex, Brodmann area 17, or V1; see Ch. 23). The visual cortex also has a strict retinotopic organization. Fibres representing the lower half of the visual field sweep superiorly to reach the visual cortex above the calcarine sulcus, while those representing the upper half of the visual field curve inferiorly into the temporal lobe (Meyer’s loop) before reaching the visual cortex below the calcarine sulcus. The periphery of the retina is represented anteriorly within the visual cortex, and the macula is represented towards the posterior pole, occupying a disproportionately large area that reflects the high number of foveal retinal ganglion cells that subserve the enhanced acuity of this region.

The primary visual cortex is connected to pre-striate and other cortical regions where further processing of visual stimuli occurs (see Ch. 23).

Almost all of the RGC axons (90%) terminate on neurones in the LGN. Extra-geniculate axons (10%) leave the optic tract before the LGN: they may leave the optic chiasma dorsally and project to the suprachiasmatic nucleus of the hypothalamus, others branch off the optic tract at the superior brachium and project to the superior colliculus, pretectal areas, and inferior pulvinar.

VISUAL FIELD DEFECTS

The basis for clinical assessment of damage to the visual pathway is an understanding of the retinotopic projections within the pathway. Moreover, plotting visual field loss frequently reveals the approximate location of the causative lesion and sometimes its nature (Fig. 40.33). Since retinal lesions can be visualized with an ophthalmoscope, field testing might appear to be redundant for such defects, but visual field measurement is still helpful in assessing the extent of the damage and may be the key factor in confirming a diagnosis. Glaucoma serves as an example. Field defects in glaucoma, occurring as a consequence of damage to the nerve fibre bundles at the optic nerve head, may be detectable ophthalmoscopically, but confirmation of the diagnosis frequently depends on field assessment. Early defects consist of one or more areas of paracentral focal field loss, progressing to arcuate scotomas. The shape of the defect corresponds to the anatomical arrangement of ganglion cell axons (Fig. 40.28).

So far as the location of lesions central to the retina is concerned, deficits in the vision of one eye are usually attributable to optic nerve lesions. Lesions of the optic chiasma, involving crossing nerve fibres, produce a bilateral field loss as exemplified by a pituitary adenoma (Fig. 40.33). The tumour expands upwards from the pituitary fossa, compressing the inferior midline of the chiasma, and eventually produces bitemporal hemianopia, starting with an early loss in the upper temporal quadrants. Field defects in the rare instances of optic tract lesions are distinctive. The tract contains contralateral nasal and ipsilateral temporal retinal projections and damage will cause a homonymous contralateral loss of field with substantial incongruity (dissimilar defects in the two fields). Incongruity probably results from a delay in achieving coincidence between retinal topographical projections of the two inputs of the visual pathway, as contiguous projections adjust their location, gradually achieving coincidence. It also probably reflects the reorganization of fibres which occurs normally in the optic tracts, as some fibres leave the tract in the superior brachium and others progress to the lateral geniculate nucleus. Incongruity is most marked in defects of the optic tract, less obvious in optic radiation defects, and is usually absent in cortically induced field defects, thus providing an additional clue in assessing location of the cause.

Lesions of the optic radiations are usually unilateral, and commonly vascular in origin. Field defects therefore develop abruptly, in contrast to the slow progression of defects associated with tumours, and the resulting hemifield loss follows the general rule that visual field defects central to the chiasma are on the opposite side to the lesion. Little or no incongruity is seen in visual cortical lesions, but they commonly display the phenomenon of macular sparing, the central 5–10° field being retained in an otherwise hemianopic defect.

REFERENCES

ote C, Dennis S, Huang YF, Quantock AJ, Meek KM. Lamellar orientation in human cornea in relation to mechanical properties. *J Struct Biol*. 2005;149:1-6.

wmaker JK, Parry JWL, Mollon JD. The arrangement of L and M cones in human and a primate retina. In: Mollon JD, Pokorny J, Knoblauch K. *Normal and Defective Colour Vision*. Oxford: Oxford University Press, 2003.

rcio CA, Allen KA. Topography of ganglion cells in human retina. *J Comp Neurol*. 1990;300:5-25.

rcio CA, Sloan KR, Kalina RE, Henrickson AE. Human photoreceptor topography. *J Comp Neurol*. 1990;292:497-523.

rcio CA, Allen KA, Sloan KR, Lerea CL, Hurley JB, Klock IB, Milam AH. Distribution and morphology of human cone photoreceptors stained with anti-blue opsin. *J Comp Neurol*. 1991;312:610-624.

acey DM, Liao H-S, Peterson BB, Robinson FR, Smith WC, Pokorny J, Yau K-W, Gamlin PD. Melanopsin-expressing ganglion cells in primate retina signal colour and irradiance and project to the LGN. *Nature*. 2005;433:749-754.

astinger MJ, Tian N, Horvath T, Marshak D. Retinopetal axons in mammals: emphasis on histamine and serotonin. *Curr Eye Res*. 2006;31:655-667.

ofer H, Carroll J, Neitz J, Neitz M, Williams DR. Organization of the human trichromatic cone mosaic. *J Neurosci*. 2005;25:9669-9679.

olb H, Linberg KA, Fisher SK. Neurons of the human retina – a Golgi study. *J Comp Neurol*. 1992;318:147-187.

epérant J, Ward R, Miceli D, Rio JP, Médina M, Kenigfest NB, Vesselkin NP. The centrifugal visual system of vertebrates: a comparative analysis of its functional anatomical organization. *Brain Res Rev*. 2006;52:1-57.

rauus O. The retinal pigment epithelium in visual function. *Phys Rev*. 2005;85:845-881.

ässle H. Parallel processing in the mammalian retina. *Nature Rev Neurosci*. 2004;5:1-11.

atson PG, Young RD. Scleral structure; organisation and disease. A review. *Exp Eye Res*. 2004;278:609-623.

ang HR. Scanning electron-microscopic study of corrosion casts on retinal and choroidal angioarchitecture in man and animals. *Prog Retinal Eye Res*. 1994;13:243-270.

CHAPTER 41

Development of the eye

The development of the eye involves a series of inductive interactions between neighbouring tissues in the embryonic head. These are the neurectoderm of the forebrain (which forms the sensory retina and accessory pigmented structures), the surface ectoderm (which forms the lens and the corneal epithelium) and the intervening neural crest mesenchyme (which contributes to the fibrous coats of the eye and to tissues of the anterior segment of the eye). A broad anterior domain of neurectoderm characterized by the activation of several homeobox-containing transcriptional regulators, including *PAX6*, *RX*, *SIX3* and *OTX2*, develops the potential to form optic vesicles. Subsequent interactions between mesenchyme and neurectoderm involving expression of the secreted protein SHH at the midline subdivides this eye field region into bilateral domains at the future sites of the eyes (Chow & Lang 2001). Loss of SHH function causes holoprosencephaly and a range of malformations that can include cyclopia. The parallel process of lens determination appears to depend on a brief period of inductive influence that spreads through the surface ectoderm from the rostral neural plate and elicits a lens-forming area of the head. Reciprocal interactions that are necessary for the complete development of both tissues take place as the optic vesicle forms and contacts the potential lens ectoderm (Saha et al 1992). Vascular tissue of the developing eye may form by local angiogenesis or vasculogenesis of angiogenetic mesenchyme. (Accounts of the development of the eye are given in O’Rahilly 1966 and 1983.)

EMBRYONIC COMPONENTS OF THE EYE

The first morphological sign of eye development is a thickening of the diencephalic neural folds at 29 days postovulation, when the embryo has seven to eight somites. This optic primordium (eye field) extends on both sides of the neural plate and crosses the midline at the primordium chiasmatis. A slight transverse indentation, the optic sulcus, appears in the inner surface of the optic primordium on each side of the brain. During the period when the rostral neuropore closes, at about 30 days (stage 11), the walls of diencephalon 1 (see Fig. 24.2) begin to evaginate at the optic sulcus, projecting laterally towards the surface ectoderm, so that, by 32 days, the optic vesicles are formed. Failure of the specification and development of the optic vesicle is associated with mutation of several transcriptional regulator genes expressed in the eye field and leads to anophthalmia (absence of the eye) (Graw 2003). The lumen of each optic vesicle is continuous with that of the neuromere diencephalon 1; the vesicle is surrounded by a sheath of mesenchymal cells derived from the head mesenchyme and neural crest. By 31 days, regional differentiation is apparent in each of the source tissues of the eye. The optic vesicle is visibly differentiated into its three primary parts: at the junction with the diencephalon, a thick-walled region marks the future optic stalk; laterally, the tissue which will become the sensory (neural) retina forms a flat disc of thickened epithelium in close contact with the surface ectoderm; the thin-walled part that lies between these regions will later form the pigmented layer of the retina (retinal pigmented epithelium). The area of surface ectoderm that is closely apposed to the distal optic vesicle thickens to form the lens placode, and the mesenchymal sheath of the vesicle begins to show signs of angiogenesis. Between 33 and 35 days postovulation, the lens placode and optic vesicle, responding to inductive signalling interactions involving fibroblast growth factors (FGFs) between these two tissues (Chow & Lang 2001), undergo coordinated morphogenesis. The lens placode invaginates, forming a pit which pinches off from the surface ectoderm to form the lens vesicle (Fig. 41.1). The surface ectoderm reforms a continuous layer which will become the corneal epithelium. The lateral part of the optic vesicle invaginates to form a cup: the inner layer (facing the lens vesicle) will become the sensory (neural) retina, and the outer layer, influenced by signals from the surrounding extra ocular mesenchyme, becomes the retinal pigmented epithelium. As a result of these folding movements, what were the apical (luminal) surfaces of the two layers of the cup now face one another across a much reduced lumen, the intraretinal space. The pigmented layer becomes attached to the mesenchymal sheath, but the junction between the pigmented and sensory layers is less firm and is the site of pathological detachment of the retina. The two layers are continuous at the lip of the cup (Fig. 41.2). The narrow part of the optic vesicle between the base of the cup and the brain forms the optic stalk. As well as the invagination of the lateral part of the optic vesicle, the ventral surface of the vesicle and distal part of the stalk similarly invaginate, forming a wide groove, the choroid (optic) fissure, through which mesenchyme and the hyaloid artery extend. These infoldings involve differential growth and cell movement, high and levels of proliferation in the inner neuroepithelial layer. As growth proceeds, the fissure closes and the artery is included in the distal part of the stalk. The fusion process is characterized by apoptosis at the margins of the fissure. Failure of the optic fissure to close is a rare anomaly that is accompanied by a corresponding deficiency in the choroid and iris (congenital coloboma) and is often associated with microphthalmia (small eyes). Reduced growth of the optic cup caused by mutation of the homeobox gene *CHX10*, which is important for specification and growth of the neural retina, is one known cause of microphthalmia (Graw 2003).

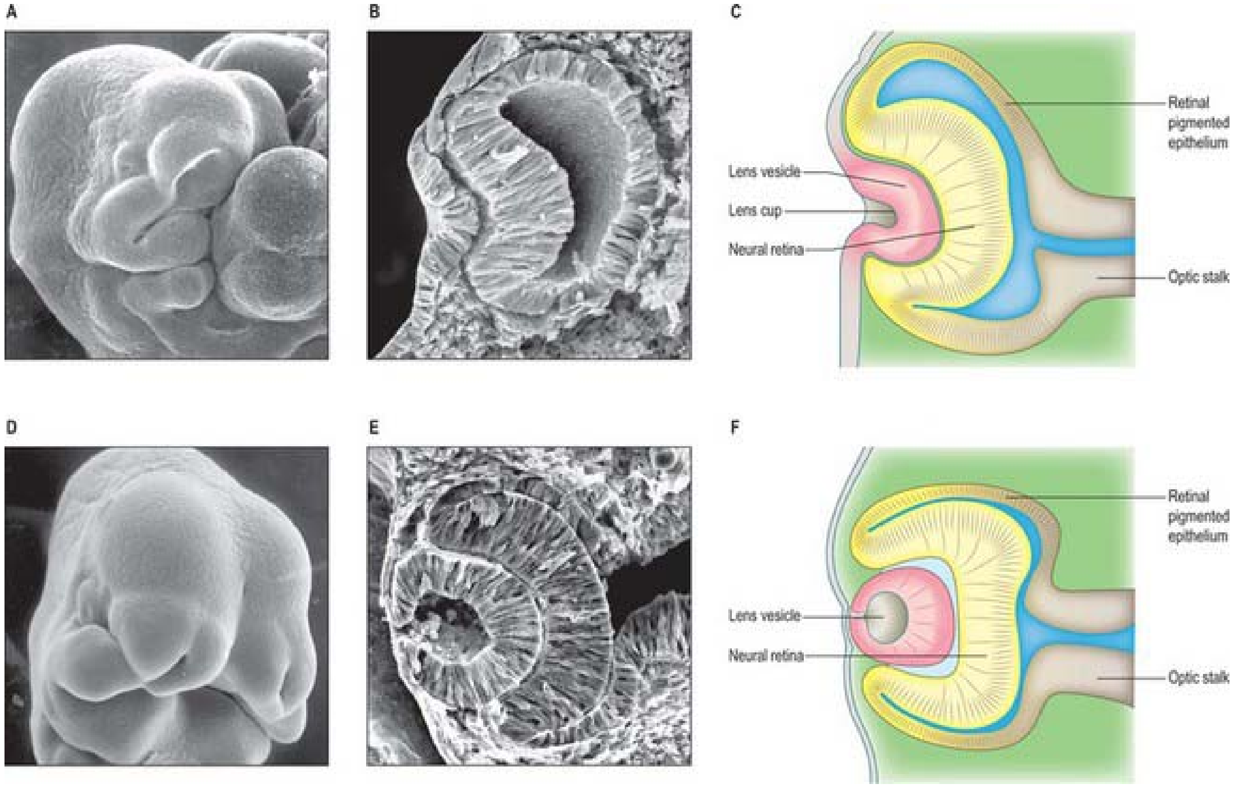
A
B
C
Retinal pigmented epithelium
Lens vesicle
Lens cup
Neural retina
Optic stalk
D
E
F
Retinal pigmented epithelium
Lens vesicle
Neural retina
Optic stalk

Fig. 41.1 Development and morphogenesis of the optic vesicle.

(A, B, D, E By courtesy of Kathleen Sulik PhD, Professor, University of North Carolina.)

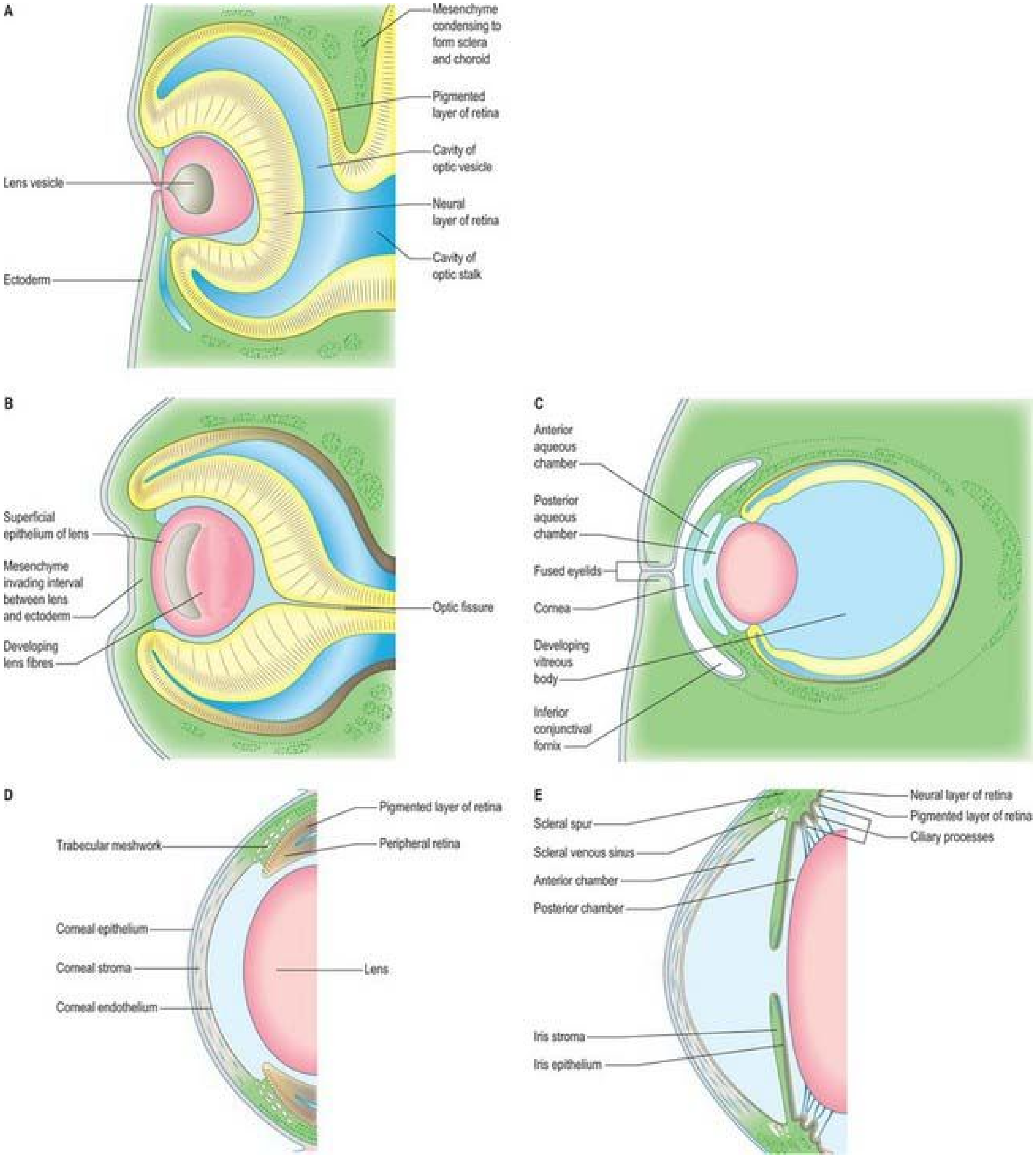
A
Mesenchyme condensing to form sclera and choroid
Pigmented layer of retina
Cavity of optic vesicle
Lens vesicle
Neural layer of retina
Cavity of optic stalk
Ectoderm
B
Superficial epithelium of lens
Mesenchyme invading interval between lens and ectoderm
Developing lens fibres
Optic fissure
C
Anterior aqueous chamber
Posterior aqueous chamber
Fused eyelids
Cornea
Developing vitreous body
Inferior conjunctival fornix
D
Pigmented layer of retina
Trabecular meshwork
Peripheral retina
Corneal epithelium
Corneal stroma
Lens
Corneal endothelium
E
Neural layer of retina
Pigmented layer of retina
Ciliary processes
Scleral spur
Scleral venous sinus
Anterior chamber
Posterior chamber
Iris stroma
Iris epithelium

Fig. 41.2 Sections through the developing eyes of human embryos. **A**, Equivalent to 8 mm crown–rump length (CRL); stage 16. The thick nervous and the thinner pigmented layers of the retina and the developing lens are shown. **B**, Equivalent to 13.2 mm CRL; stage 17. **C**, Mesenchymal proliferation at the anterior part of the retina gives rise to the choroidal extensions which form the ciliary body and iris. The surface ectoderm

anterior to the lens forms the cornea. **D**, Equivalent to 40 mm CRL. The development of the anterior and posterior aqueous chambers is apparent. The eyelids have developed and are fused and the extent of the conjunctival fornices can be seen. **E**, Details of the developing uveal tract

DIFFERENTIATION OF THE FUNCTIONAL COMPONENTS OF THE EYE

The developments just described bring the embryonic components of the eye into the spatial relationships necessary for the passage, focusing and sensing of light. The next phase of development involves further patterning and phenotypic differentiation in order to develop the specialized structures of the adult organ.

The optic cup becomes patterned, from the base to the rim, into regions with distinct functions. Several secreted factors, including bone morphogenetic proteins (BMP), retinoic acid and SHH, and transcriptional regulators, including *PAX6* and *PAX2*, are important for specifying each region (Chow & Lang 2001). The outer layer of the optic cup remains as a thin layer of cells which begin to acquire pigmented melanosomes and form the pigmented epithelium of the retina around 36 days. In a parallel process, which begins before invagination, the cells of the inner layer of the cup proliferate to form a thick pseudostratified neuroepithelium, the future neural retina, over the base and sides of the cup. The peripheral region around the lip of the cup is further differentiated into the components of the prospective iris at the rim, and the ciliary body a little further back adjacent to the neural retina (Fig. 41.2). The development of this pattern is reflected in regional differences in the expression of various genes which encode transcriptional regulators and which are therefore likely to play key roles in controlling and coordinating development. Distinct sets of genes are expressed prior to and during overt cell-type differentiation. For example, *PAX6* is expressed in the prospective ciliary and iris regions of the optic cup: individuals heterozygous for mutations in *PAX6* lack an iris (aniridia), which suggests a causal role for this gene in the development of the iris. The genes expressed in the eye are also often active at a variety of other specific sites in the embryo, which may, in part, account for the co-involvement of the eye and other organs in syndromes which result from single genetic lesions, e.g. *PAX2* mutation causes coloboma and kidney defects, reflecting the sites of expression of the gene (Graw 2003).

Developing neural retina

The developing neural retina consists of an outer nuclear zone, which contains dividing neuroepithelial retinal progenitor cells, and an inner marginal zone, which is initially devoid of nuclei. At around 37 days, the cells of the nuclear zone invade the marginal zone, and by stage 18 (44 days) the nervous stratum of the retina consists of inner and outer neuroblastic layers. Cell lineage analyses have shown that seven retinal cell types are all derived from a common multipotential retinal progenitor cell. Different types of retinal cells are born (cease dividing) in a conserved sequence during development: ganglion cells, amacrine cells, cone photoreceptors and horizontal cells develop early, whereas bipolar cells, rod photoreceptors and Müller glial cells develop later (Cepko et al 1996). Newly born cells migrate from the apical (ventricular) surface to the appropriate cell layer in the developing retina, establishing its characteristic laminar structure. The developing ganglion cell layer first separates from the neuroblastic layers by formation of the inner plexiform layer. The inner nuclear layer containing developing amacrine, horizontal, bipolar and Müller glial cells then separates from the outer nuclear layer containing the developing rod and cone photoreceptors by formation of the outer plexiform layer. Mature retinal neurones first appear in the central part of the retina. By the eighth month all the named layers of the retina can be identified. However, the photoreceptor cells continue to differentiate after birth, generating an array of increasing resolution and sensitivity; the macula does not reach maturity until 15–45 months after birth (Hendrickson & Yuodelis 1984).

The divergent differentiation of the pigmented and sensory layers of the retina from the initially bipotential optic vesicle neuroepithelium depends on interactions mediated by diffusible molecules derived from surrounding tissues. Activation of region-specific regulatory genes, for example *CHX10* in the presumptive neural retina and *MITF* in the presumptive pigmented epithelium, is an important aspect of establishing regional identity of the optic cup and the subsequent maturation of these respective tissues. Soluble factors from the retina elicit the polarized distribution of plasma membrane proteins and the formation of tight junctions in the pigmented epithelium. Neural retinal differentiation is mediated by several growth factors, including fibroblast growth factors, SHH and retinoic acid. Basic helix-loop-helix proneural transcriptional regulatory genes also play a central role in regulating retinal cell fate. However, the pigmented epithelium initially retains the potential to become neural retina and will do so if the embryonic retina is wounded, demonstrating the plasticity of the early commitment to pigment epithelium or neural retinal fate.

Optic nerve

The optic nerve develops from the optic stalk. The centre of the optic cup, where the optic fissure is deepest, will later form the optic disc, where the neural retina is continuous with the corresponding invaginated cell layer of the optic stalk: the developing axons of the ganglion cells therefore pass directly into the wall of the stalk and convert it into the optic nerve. Myelination of the axons within the optic nerve begins shortly before birth, but the process is not completed until some time later. The optic chiasma is formed by the meeting and partial decussation of the axons within the two optic nerves in the ventral part of the lamina terminalis (at the junction of the telencephalon with the diencephalon in the floor of the third ventricle). Beyond the chiasma, the axons continue as the optic tracts, and pass principally to the lateral geniculate bodies and to the superior tectum of the midbrain.

Ciliary body

The ciliary body is a compound structure. Its epithelial components are the region of the inner layer of the retina between the iris and the neural retina and the adjacent outer layer of pigmented epithelium. The cells here differentiate in close association with the surrounding mesenchyme to form highly vascularized folds that secrete aqueous fluid into the globe of the eye. The ciliary epithelium also retains a population of cells with properties of embryonic retinal progenitor cells (retinal stem cells) that even in adulthood can be induced to form new neurones.

The inner surface of the ciliary body forms the site of attachment of the lens. The outer layer is associated with smooth muscle derived from mesenchymal cells in the choroid that lie between the anterior scleral condensation and the pigmented ciliary epithelium.

Iris

The iris develops from the tip of the optic cup where the two neuroepithelial layers remain thin and are associated with vascularized, muscular connective tissue. The muscles of the sphincter and dilator pupillae are unusual in that they are of neurectodermal origin, and develop as a result of further growth and differentiation of the two layers of the optic cup. Mesenchymal cells, largely composed of neural crest cells that have migrated anterior to the lens, form the collagen-rich iris stroma; they overlay the pigmented epithelium of the iris, which is continuous with the ciliary body and neural retina and is of neuroecto-dermal origin. The mature colour of the iris develops after birth and is dependent on the relative contributions made by the pigmented epithelium on the posterior surface of the iris and by the neural crest-derived melanocytes in the mesenchymal stroma of the iris. If only epithelial pigment is present, the eye appears blue, whereas if there is an additional contribution from the melanocytes, the eye appears brown.

Lens

The lens develops from the lens vesicle (Figs 41.1F, 41.2A),. Initially this is a ball of actively proliferating epithelium, but by stage 16 there is a discernible difference between the thin anterior (i.e. outward-facing) epithelium and the thickened posterior epithelium. Cells of the posterior wall lengthen and fill the vesicle (Fig. 41.2B,C), reducing the original cavity to a slit by about 44 days. The posterior cells become filled with a very high concentration of proteins (crystallins) which render them transparent; they also become densely packed within the lens as primary lens fibres. Cells at the equatorial region of the lens elongate and contribute secondary lens fibres to the body of the lens in a process which continues into adult life, sustained by continued proliferation of cells in the anterior epithelium. The polarity and growth of the lens appear to depend on the differential distribution of soluble factors which promote either cell division or lens fibre differentiation and are present in the anterior chamber and vitreous humour respectively. Congenital cataracts can be associated with mutations in genes that encode structural lens proteins, particularly crystallin proteins, as well as genes that encode transcriptional regulatory factors expressed specifically in the lens, such as *MAF* and *PITX3*, that are needed for normal lens development and which also influence normal growth of the globe of the eye (Graw 2003).

The developing lens is surrounded by a vascular mesenchymal condensation, the vascular capsule, the anterior part of which is named the pupillary membrane. The posterior part of the capsule is supplied by branches from the hyaloid artery, and the anterior part is supplied by branches from the anterior ciliary arteries. During the fourth month, the hyaloid artery gives off retinal branches. By the sixth month, all of the vessels have atrophied except the hyaloid artery, which becomes occluded during the eighth month of intrauterine life, although its proximal part persists in the adult as the central artery of the retina. Atrophy of the hyaloid vasculature and of the pupillary membrane appears to be an active process of programmed tissue remodelling which is macrophage-dependent: visual impairment occurs in persistent hyperplastic primary vitreous, a condition when normal regression of the hyaloid vasculature fails to occur. The hyaloid canal, which carries the vessels through the vitreous, persists after the vessels have become occluded. In the newly born child it extends more or less horizontally from the optic disc to the posterior aspect of the lens, but when the adult eye is examined with a slit-lamp it can be seen to follow an undulating course, sagging downwards as it passes forwards to the lens. With the loss of its blood vessels, the vascular capsule disappears and the lens becomes dependent for its nutrition on diffusion via the aqueous and vitreous humours. The lens remains enclosed in the lens capsule, a thickened basal lamina derived from the lens epithelium. Sometimes the pupillary membrane persists at birth, which gives rise to congenital atresia of the pupil.

Vitreous body

The vitreous body develops between the lens and the optic cup as a transparent, avascular gel of extracellular substance. The precise derivation of the vitreous remains controversial. The lens rudiment and the optic vesicle are at first in contact, but they draw apart after closure of the lens vesicle and formation of the optic cup, and remain connected by a network of delicate cytoplasmic processes. This network, derived partly from cells of the lens and partly from those of the retina, is the primitive vitreous body. At first these cytoplasmic processes are connected to the whole of the neuroretinal area of the cup, but later they become limited to the ciliary region, where, by a process of condensation, they form the basis of the suspensory ligaments of the ciliary zonule. The vascular mesenchyme which enters the cup through the choroidal fissure and around the equator of the lens associates locally with this reticular tissue and thus contributes to the formation of the vitreous body.

Anterior segment

Mesenchymal cells of neural crest origin migrate anteriorly around the optic cup and between the surface ectoderm and the lens to contribute to the development of anterior segment structures, including the ciliary body, the iris, the cornea and the iridocorneal angle tissues (Fig. 41.2C–E) (Gould et al 2004). The anterior chamber initially appears as a cleft in this mesenchymal tissue. The mesenchyme superficial to the cleft forms the stroma (substantia propria) and endothelium of the cornea, and that deep to the cleft forms the stroma of the iris and the pupillary membrane. Tangentially, this early cleft extends as far as the iridocorneal angle, where communications are established with the scleral venous sinus (canal of Schlemm). Mesenchymal cells of neural crest origin lying at the angle of the anterior chamber differentiate to form a specialized meshwork of trabecular beams (collagen fibrils covered by cells): the open spaces of the meshwork become open to the anterior chamber as the beams develop. The canal of Schlemm develops deep to the trabecular meshwork and is derived from mesodermal mesenchyme. Initially a vascular structure lined by endothelial cells, the canal acts as an aqueous sinus from the fifth month of gestation. The forward-growing optic cup rim differentiates into the ciliary epithelium and the iris; the posterior chamber is formed between the iris, the lens capsule and the zonular suspensory fibres and the ciliary processes. The ciliary processes produce the aqueous humour that flows through the pupil and is drained in the iridocorneal angle mainly by the trabecular meshwork and the canal of Schlemm. In this way the walls of the anterior and posterior segment chambers furnish both the sites of production of, and the channels for circulation and reabsorption of, the aqueous humour. The *FOXC1* and *PITX2* transcriptional regulatory genes are expressed in the neural crest cells migrating into the presumptive anterior segment, and regulate differentiation of the anterior segment tissues. Anterior segment dysgenesis involving malformation of the iris, cornea and angle occurs when these genes are mutated (e.g. Axenfeld–Rieger syndrome) and is often associated with raised intraocular pressure and glaucoma (Gould et al 2004).

Cornea

The cornea is induced in front of the anterior chamber by the lens and optic cup. The corneal epithelium is formed from surface ectoderm, and the primordial corneal endothelium lining the front of the anterior chamber is formed from mesenchymal cells derived from the neural crest (Fig. 41.2D,E). Mesenchymal cells migrate between these layers and differentiate to form fibroblasts and keratocytes which secrete the extracellular matrix of the corneal stroma. A regular array of collagen fibres (lamellae) is established between these two layers and serves to reduce scattering of light entering the eye. The most anterior region of the stroma (Bowman’s layer) develops as an acellular zone packed with collagen fibrils which confer strength on the layer. From the third month, the endothelium is organized as a monolayer of cells and develops a strong laminated basal lamina (Descemet’s membrane) adjacent to the stroma. The endothelium maintains corneal trans-parency by regulating the water content of the stroma.

Choroid and sclera

The choroid and sclera differentiate as inner, vascular, and outer, fibrous, layers from the mesenchyme that surrounds the optic cup: the choroid is continuous with the leptomeningeal internal sheath of the optic nerve and the sclera is continuous with the outer dural sheath of the optic nerve. The blood vessels of the choroid develop from the 15th week and include the vasculature of the ciliary body.

DIFFERENTIATION OF STRUCTURES AROUND THE EYE

Extraocular muscles

The extrinsic ocular muscles are derived from prechordal mesenchyme which ingresses at the primitive node very early in development. The prechordal cells lie at the rostral tip of the notochordal process (see Fig. 12.4); they remain mesenchymal after the notochordal process becomes epithelial and gains a basal lamina. The prechordal mesenchyme migrates laterally towards the paraxial mesenchyme. Although this is a singular origin for muscle, the early myogenic properties of these cells have been demonstrated experimentally; if transplanted into limb buds, the cells are able to develop into muscle tissue (Wachtler & Jacob 1986).

Early embryos develop bilateral premandibular, intermediate and caudal cavities in the head (previously described as preotic somites). The walls of the premandibular head cavities are lined by flat or cylindrical cells that do not exhibit the characteristics of a germinal epithelium. As the oculomotor nerve grows down to the level of the head cavity, a condensation of premuscle cells appears at its ventrolateral side and later subdivides into the blastemata of the muscles that the nerve will supply. Similar events occur in the intermediate head cavity (trochlear nerve and superior oblique) and the caudal head cavity (abducens nerve and lateral rectus) (see Figs 12.4 and 35.7).

Eyelids

The eyelids are formed as small cutaneous folds of surface ectoderm with a core of neural crest mesenchyme (Fig. 41.2C). During the middle of the third month, their edges come together and unite over the cornea to enclose the conjunctival sac; they usually remain united until about the end of the sixth month. When the eyelids open, the conjunctiva lining their inner surfaces and covering the white (scleral) region of the eye fuses with the corneal epithelium. Transforming growth factor alpha (TGF-α) and several other growth factors regulate the mesenchyme–epithelium interactions and cell migration that are required for eyelid formation; keratinization is thought to play an important role in lid separation. The eyelashes and lid glands, i.e. sebaceous glands associated with the eyelashes, and tarsal (Meibomian) glands develop from ectoderm, as do the lacrimal and accessory lacrimal glands. Orbicularis oculi, which closes the eyelids, develops on each side from skeletal myoblasts which invade the eyelids from the second pharyngeal arch. The muscles that widen the palpebral fissure develop within the orbit from mesenchymal cells: the superior and inferior tarsal muscles are smooth muscle, whereas levator palpebrae superioris is striated muscle that is attached to each upper eyelid by a tendon derived from the neural crest.

Lacrimal apparatus

The ectodermal epithelium of the superior conjunctival fornix proliferates and gives rise to a series of tubular buds which form the alveoli and ducts of the lacrimal gland. These buds are arranged in two groups: one forms the gland proper and the other forms its palpebral process (de la Cuadra-Blanco et al 2003). The lacrimal sac and nasolacrimal duct are derived from ectoderm in the nasomaxillary groove (between the lateral nasal process and the maxillary process of the developing face). The ectoderm thickens to form a solid cord of cells, the nasolacrimal ridge, which subsequently sinks into the mesenchyme and becomes canalized during the third month to form the nasolacrimal duct. The lacrimal canaliculi arise from the cranial extremity of the cord as buds which establish openings (puncta lacrimalia) on the margins of the lids. The inferior canaliculus isolates a small part of the lower eyelid to form the lacrimal caruncle and plica semilunaris.

REFERENCES

arti K, Nguyen MT, Skuntz S, Bertuzzi S, Arnheiter H. The other pigment cell: specification and development of the pigmented epithelium of the vertebrate eye. *Pigment Cell Res*. 2006;19:390-394.

epko CL, Austin CP, Yang X, Alexiades M, Ezzeddine D. Cell fate determination in the vertebrate retina. *Proc Natl Acad Sci USA*. 1996;93:589-595.

now RL, Lang RA. Early eye development in vertebrates. *Annu Rev Cell Dev Biol*. 2001;17:255-296.

la Cuadra-Blanco C, Peces-Peña MD, Mérida-Velasco JR. Morphogenesis of the human lacrimal gland. *J Anat*. 2003;203:531-536.

ould DB, Smith RS, John SW. Anterior segment development relevant to glaucoma. *Int J Dev Biol*. 2004;48:1015-1029.

raw J. The genetic and molecular basis of congenital eye defects. *Nat Rev Genet*. 2003;4:876-888.

endrickson AE, Yuodelis C. The morphological development of the human fovea. *Ophthalmology*. 1984;91:603-612.

'Rahilly R. The early development of the eye in staged human embryos. *Contrib Embryol Carnegie Inst*. 1966;38:1.

'Rahilly R. The timing and sequence of events in the development of the human eye and ear during the embryonic period proper. *Anat Embryol*. 1983;168:87-99.

ha MS, Servetnick M, Grainger RM. Vertebrate eye development. *Curr Opin Genet Dev*. 1992;2:582-588.

Reviews the interactions involved in eye development and discusses genes responsible for development of the eye..

achtler F, Jacob M. Origin and development of the cranial skeletal muscles. *Bibl Anat*. 1986;29:24-46.

Section 5
THE BACK

CHAPTER 42

The back

Most clinical disorders of the back present as low back pain with or without associated lower limb pain, so historically most attention has been paid to the anatomy of the lower (lumbosacral) back. In this Section, the term ‘the back’ will include the whole of the posterior aspect of the trunk and of the neck. The whole of this region has great clinical importance but its anatomy has often been neglected. Recent understanding of the detailed topography of the bony and soft-tissue elements of the lower back owes much to the work of Bogduk (2005).

The soft tissues of the back of the trunk and neck include the skin and subcutaneous fat, the underlying fascial layers and the musculature. The deep, ‘true’ or epaxial muscles lie within compartments in their own fascial ‘skeleton’. The bony framework to which the muscles and fasciae attach includes not only elements of the axial skeleton, i.e. the vertebral column and occiput, but also elements of the pectoral and pelvic girdles as well as the ribs. The occiput is described below, the scapula on page 793, the ribs on page 918 and the pelvis on page 1352.

SKIN

The skin of the back of the trunk is thick and highly protective, but has low discriminatory sensation. The superficial fascia is thick and fatty in most areas of the back. Its attachment to the deeper fascial layers is strong in the midline, especially in the neck, but becomes weaker more laterally. The skin of the back of the neck is thicker than that of the front of the neck, but thinner than that of the back of the trunk. The quantity, texture and distribution of hair vary with sex, race and the individual, though well-defined hair tracts have been delineated (Fig. 42.1).

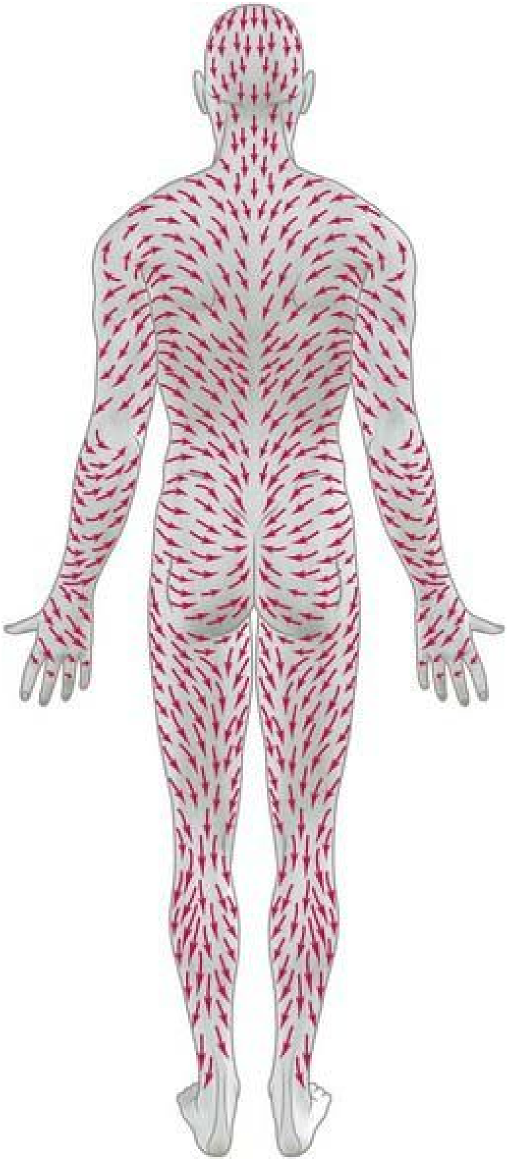

Fig. 42.1 Hair tracts on the dorsal surface of the body.

(Redrawn by permission from Wood Jones F (ed) 1949 Buchanan's Manual of Anatomy, 8th edn. London: Baillière Tindall and Cox.)

Lines of skin tension run horizontally in the cervical and lumbosacral regions but form segments of two adjacent circles in the thoracic region (Fig. 42.2).

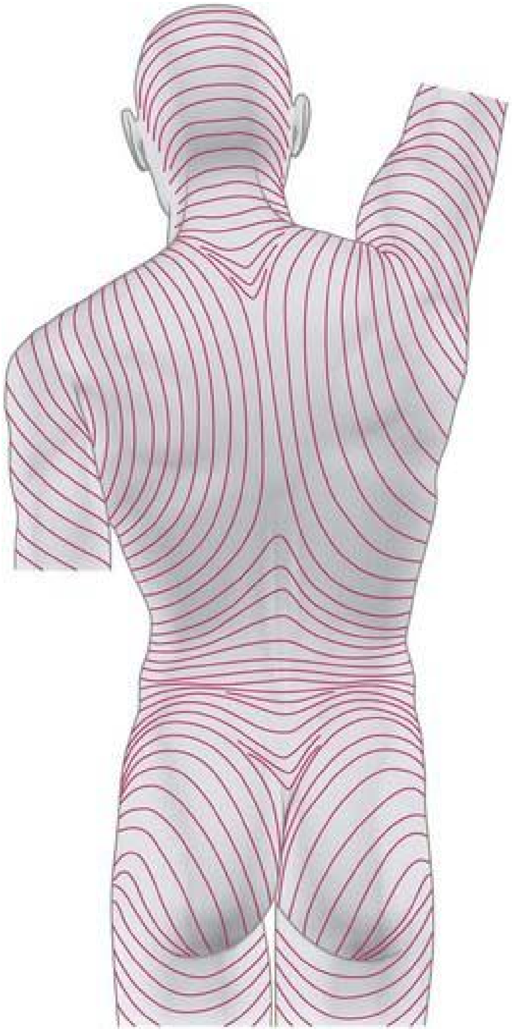

Fig. 42.2 Lines of skin tension on the dorsum of the trunk and head.

(From Kraissl CL, Plast Reconstruct Surg 8: 1–28, 1951. By permission from Lippincott Williams and Wilkins.)

CUTANEOUS INNERVATION AND DERMATOMES

The skin of the back of the neck and trunk is innervated by the dorsal (posterior primary) rami of the spinal nerves (see Fig. 43.6 and pp. 755–756 where dorsal rami are covered in detail). In the cervical and upper thoracic regions (down to T6) skin is supplied by the medial branches of these rami, while in the lower thoracic, lumbar and sacral regions it is supplied by the lateral branches. The total area supplied by these dorsal rami is shown in Fig. 43.6. The spinal nerves involved include C2 to C5, T2 to L3, S2 to S4, and Co1. The pattern of their dermatomes is shown in Fig. 42.3. There is about half a segment of overlap between these cutaneous 'strips': the strips supplied by the dorsal rami do not correspond exactly to those served by ventral rami, and differ slightly in both width and position.

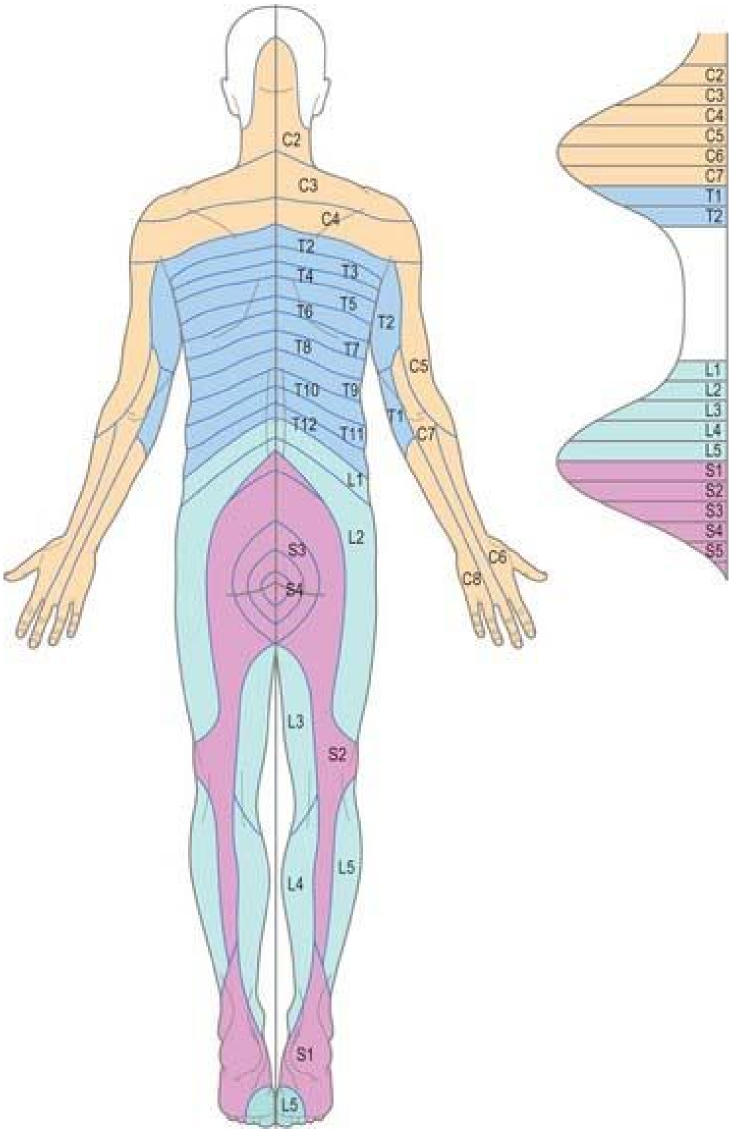
C2
C3
C4
T2
T4
T3
T6
T5
T2
T8
T7
C5
T10
T9
T12
T11
T1
C7
L1
L2
S3
S4
C6
C8
L3
S2
L5
L4
S1
L5
C2
C3
C4
C5
C6
C7
T1
T2
L1
L2
L3
L4
L5
S1
S2
S3
S4
S5

Fig. 42.3 Dermatomes on the dorsal surface of the body. The small diagram shows the regular arrangement of dermatomes in the upper and lower limbs of the embryo.

(Adapted with permission from Moffat DB 1993 Lecture Notes on Anatomy, 2nd edn. Oxford: Blackwell Scientific.)

CUTANEOUS VASCULAR SUPPLY AND LYMPHATIC DRAINAGE

The skin of the back of the trunk receives its arterial blood supply mainly from musculocutaneous branches of posterior intercostal, lumbar and lateral sacral arteries (Fig. 42.4), which all accompany the cutaneous branches of their respective dorsal rami. In addition, there is a supply from the dominant vascular pedicles of the superficial (extrinsic) back muscles. The skin over the scapula is supplied by branches of the suprascapular, dorsal scapular and subscapular arteries. The skin of the back of the neck is supplied mainly from the occipital and deep cervical arteries. The superficial cervical or transverse cervical artery supplies the skin of the lower part of the back of the neck (see Cormack & Lamberty 1994 in the Bibliography).

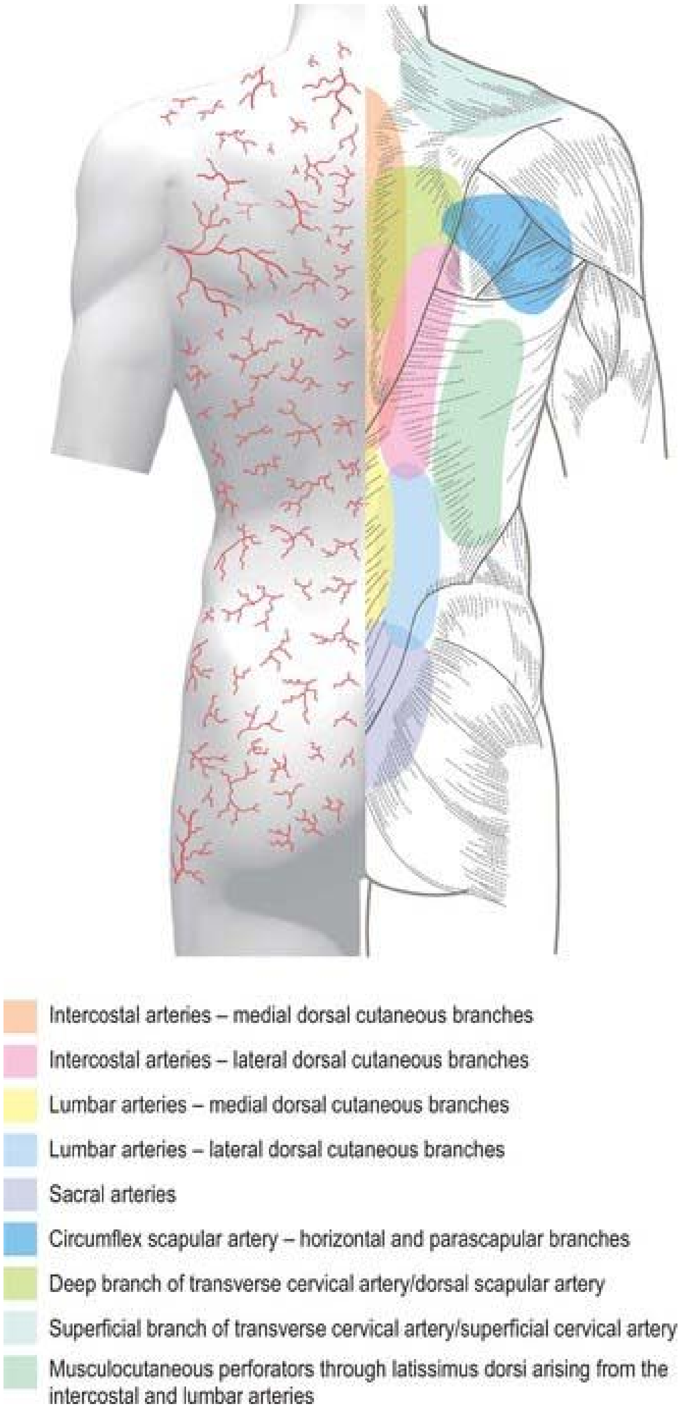
Intercostal arteries – medial dorsal cutaneous branches
Intercostal arteries – lateral dorsal cutaneous branches
Lumbar arteries – medial dorsal cutaneous branches
Lumbar arteries – lateral dorsal cutaneous branches
Sacral arteries
Circumflex scapular artery – horizontal and parascapular branches
Deep branch of transverse cervical artery/dorsal scapular artery
Superficial branch of transverse cervical artery/superficial cervical artery
Musculocutaneous perforators through latissimus dorsi arising from the intercostal and lumbar arteries

Fig. 42.4 Areas of cutaneous arterial supply on the dorsum of the trunk.

(Redrawn with permission from Cormack GC, Lamberty BGH 1994 The Arterial Anatomy of Skin Flaps. Edinburgh: Churchill Livingstone.)

Veins drain the skin of the back of the neck into tributaries of the occipital and deep cervical veins. The skin of the back of the trunk drains into the azygos system, via tributaries of the posterior intercostal and lumbar veins.

Lymph from the skin of the back of the neck drains into occipital, lateral deep cervical and axillary nodes (Fig. 42.5). From the back of the trunk, drainage is to the posterior (subscapular) axillary nodes and to the lateral superficial inguinal nodes.

Rights were not granted to include this figure in electronic media. Please refer to the printed book.

Fig. 42.5 Cutaneous lymphatics on the dorsum of the trunk.

(By permission from Romanes GJ (ed) 1964 Cunningham's Textbook of Anatomy, 10th edn. London: Oxford University Press.)

FASCIAL LAYERS

The main fascial layers in the axial and paraxial regions of the trunk and neck are the thoracolumbar fascia, the deep cervical fascia and the prevertebral, endothoracic, retroperitoneal and posterior part of the pelvic fasciae (the latter four layers collectively form the continuous prevertebral plane). Other important structures with fascial components are the ligamentum nuchae and the aponeurosis of erector spinae (see below).

THORACOLUMBAR FASCIA

The thoracolumbar (lumbodorsal) fascia covers the deep muscles of the back and the trunk. Above, it passes anterior to serratus posterior superior and is continuous with the superficial lamina of the deep cervical fascia on the back of the neck. In the thoracic region the thoracolumbar fascia provides a thin fibrous covering for the extensor muscles of the vertebral column and separates them from the muscles connecting the vertebral column to the upper extremity. Medially it is attached to the spines of the thoracic vertebrae, and laterally to the angles of the ribs. In the lumbar region the thoracolumbar fascia is in three layers (Fig. 42.6, Fig. 42.7, Fig. 62.1). The posterior layer is attached to the spines of the lumbar and sacral vertebrae and to the supraspinous ligaments. The middle layer is attached medially to the tips of the lumbar transverse processes and the intertransverse ligaments, below to the iliac crest, and above to the lower border of the 12th rib and the lumbocostal ligament. The anterior layer covers quadratus lumborum and is attached medially to the anterior surfaces of the lumbar transverse processes behind the lateral part of psoas major; below, it is attached to the iliolumbar ligament and the adjoining part of the iliac crest; above, it forms the lateral arcuate ligament. The posterior and middle layers unite to form a tough raphe at the lateral margin of erector spinae, and at the lateral border of quadratus lumborum they are joined by the anterior layer to form the aponeurotic origin of transversus abdominis. At sacral levels, the posterior layer is attached to the posterior superior iliac spine and posterior iliac crest, and fuses with the underlying erector spinae aponeurosis. Bogduk (2005) describes two laminae in the posterior layer at lumbar levels, with varying orientation of the constituent collagen fibres relating to the biomechanical function of the fascia. The posterior and middle layers of the thoracolumbar fascia and the vertebral column together form an osteofascial compartment which encloses the erector spinae muscle group. The attachments of the fascia, especially those which give it continuity with the abdominal wall musculature, putatively give it an important role in lifting, though the exact details of this role remain controversial. The fascia may also play an important role in load transfer between the trunk and the limbs: its tension is affected by the actions of latissimus dorsi, gluteus maximus, and the hamstrings. An erector spinae compartment syndrome may be one cause of low back pain.

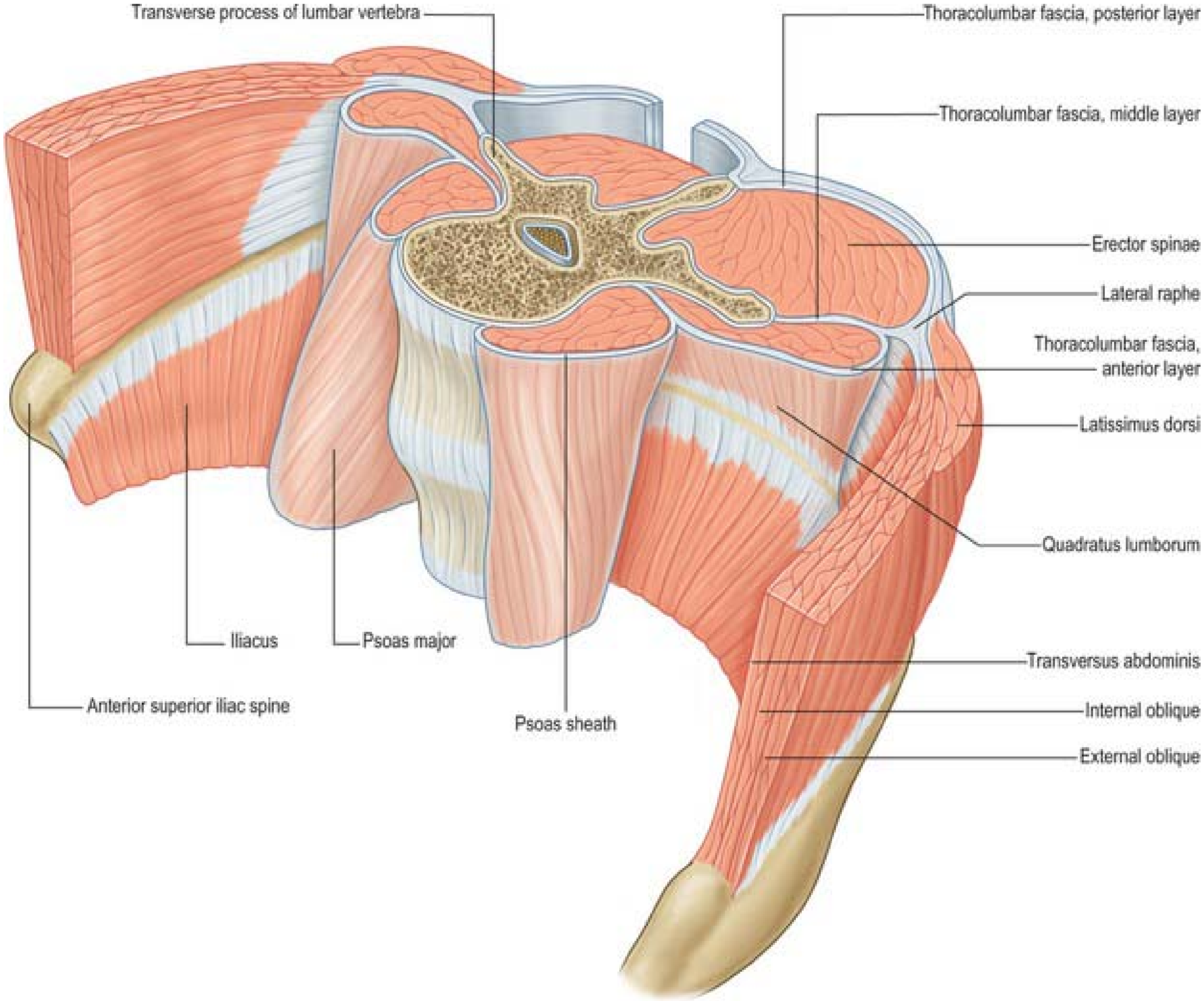
Transverse process of lumbar vertebra
Thoracolumbar fascia, posterior layer
Thoracolumbar fascia, middle layer
Erector spinae
Lateral raphe
Thoracolumbar fascia, anterior layer
Latissimus dorsi
Quadratus lumborum
Transversus abdominis
Internal oblique
External oblique
Iliacus
Psoas major
Anterior superior iliac spine
Psoas sheath

Fig. 42.6 Muscles and fasciae of the posterior abdominal wall.

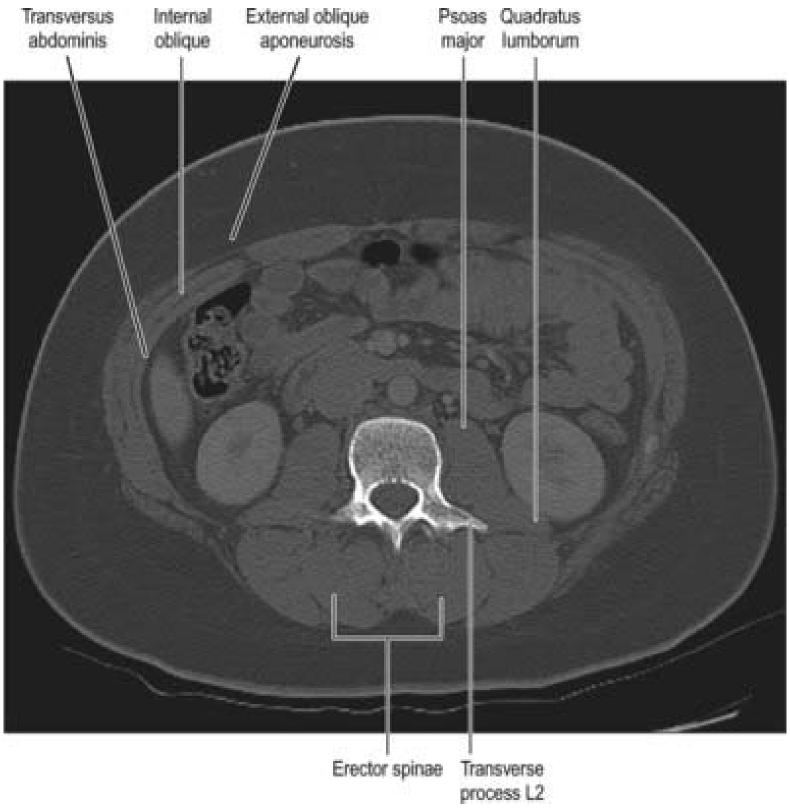
Transversus abdominis
Internal oblique
External oblique aponeurosis
Psoas major
Quadratus lumborum
Erector spinae
Transverse process L2

Fig. 42.7 Axial CT scan of the abdomen in a 32-year-old female.

DEEP CERVICAL FASCIA

The investing layer of the deep cervical fascia forms the deep fascia of the posterior aspect of the neck (Fig. 28.4). It attaches in the midline to the external occipital protuberance, the ligamentum nuchae and the spine of the seventh cervical vertebra, and splits to enclose trapezius on each side. Inferiorly the posterior part of the investing layer attaches with trapezius to the spine and acromion of the scapula.

BONE

OCCIPITAL BONE

The occipital bone forms much of the back and base of the cranium (Fig. 42.8). It is trapezoid, internally concave and encloses the foramen magnum. It has four parts: basilar (basioccipital), which is the quadrilateral part in front of the foramen magnum; squamous, which is the expanded plate posterosuperior to the foramen; and two lateral (condylar or exoccipital), one on each side of the foramen magnum. The latter is anteromedian and wider behind, with an anteroposterior diameter greater than its transverse diameter.

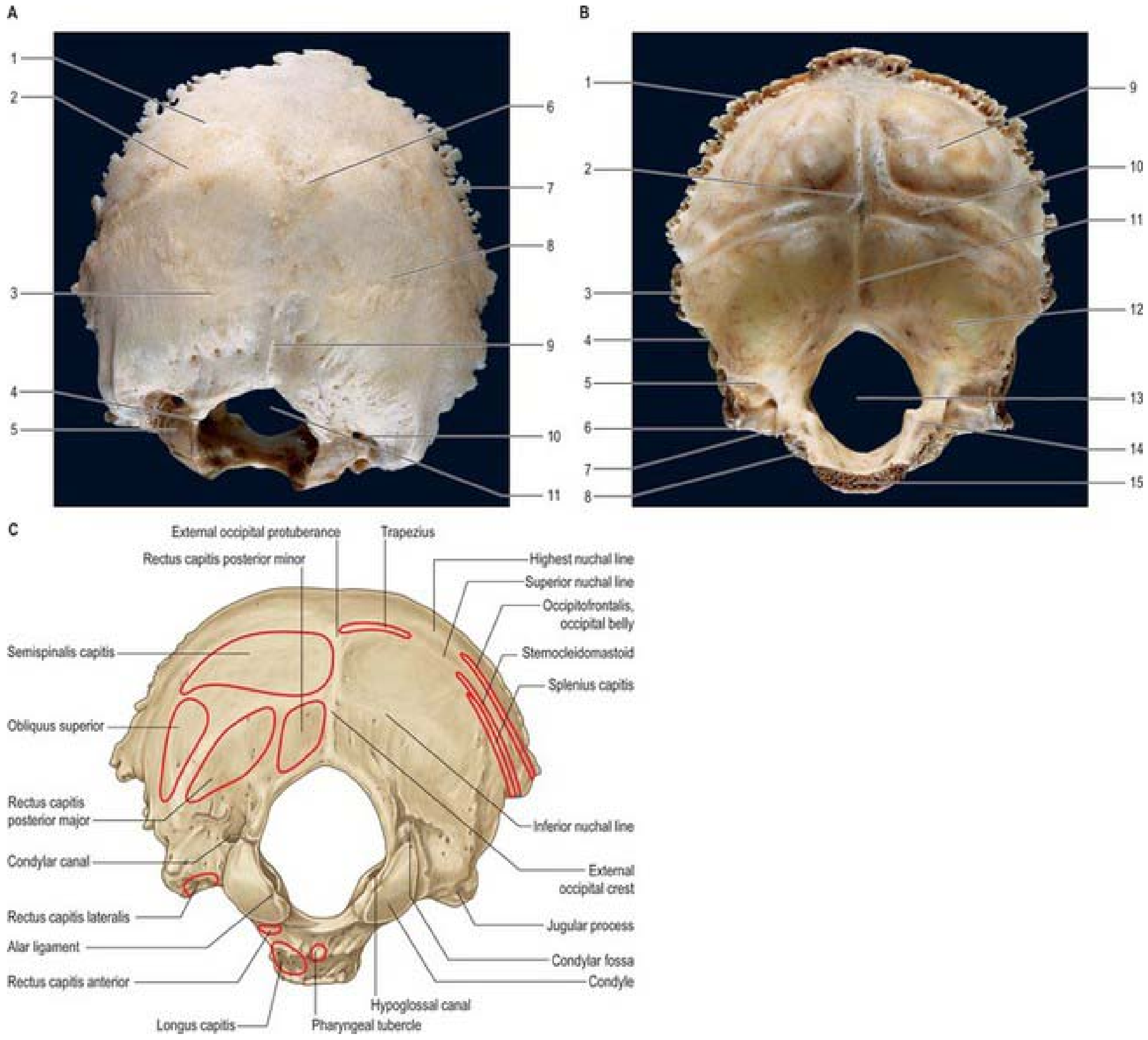
A
1
2
3
4
5
6
7
8
9
10
11
B
1
2
3
4
5
6
7
8
9
10
11
12
13
14
15
C
External occipital protuberance
Trapezius
Rectus capitis posterior minor
Highest nuchal line
Superior nuchal line
Occipitofrontalis, occipital belly
Semispinalis capitis
Sternocleidomastoid
Splenius capitis
Obliquus superior
Rectus capitis posterior major
Inferior nuchal line
Condylar canal
External occipital crest
Rectus capitis lateralis
Jugular process
Alar ligament
Condylar fossa
Rectus capitis anterior
Condyle
Hypoglossal canal
Longus capitis
Pharyngeal tubercle

Fig. 42.8 Occipital bone. **A**, External surface; **B**, internal surface; **C**, muscle attachments. (A and B by permission from Berkovitz BKB, Moxham BJ 1994 Colour Atlas of the Skull. London: Mosby.) **A: 1**. Highest nuchal line. **2**. Superior nuchal line. **3**. Inferior nuchal line. **4**. Hypoglossal canal. **5**. Occipital condyle. **6**. External occipital protuberance. **7**. Lambdoid margin. **8**. Squamous part. **9**. External occipital crest. **10**. Condylar canal. **11**. Foramen magnum. **B: 1**. Lambdoid margin. **2**. Internal occipital protuberance at 'confluence of sinuses'. **3**. Lateral angle. **4**. Mastoid margin. **5**. Groove for sigmoid sinus. **6**. Jugular process. **7**. Jugular notch. **8**. Groove for inferior petrosal sinus. **9**. Cerebral fossa. **10**. Groove for transverse sinus. **11**. Internal occipital crest. **12**. Cerebellar fossa. **13**. Foramen magnum. **14**. Jugular tubercle. **15**. Margin of basilar part for articulation with body of sphenoid.

The occipital bone provides attachment for a number of the muscles of the neck and upper part of the back (longus capitis; recti capitis anterior, lateralis, posterior major and minor; superior oblique; semispinalis capitis; splenius capitis; occipitofrontalis; trapezius; sternocleidomastoid), and articulates with the first cervical vertebra at the atlanto-occipital joints.

Squamous part

The squamous part is an expanded plate posterosuperior to the foramen magnum, convex externally and concave internally. On its external surface the external occipital protuberance lies midway between its summit and the foramen magnum. On each side, two curved lines extend laterally from this protuberance. The upper, faintly marked and often almost imperceptible, is the highest nuchal line, and the lower is the superior nuchal line. The epicranial aponeurosis is attached to the medial part of the highest nuchal line. The median external occipital crest is often faint; it descends from the external occipital protuberance to the foramen magnum. On each side an inferior nuchal line spreads laterally from the midpoint of the crest.

The internal surface of the squamous part is divided into four deep fossae by an irregular internal occipital protuberance and by ridged sagittal and horizontal extensions from the protuberance. The two superior fossae are triangular and adapted to the occipital poles of the cerebral hemispheres; the inferior fossae are quadrilateral and shaped to accommodate the cerebellar hemispheres. A wide groove with raised banks, the superior sagittal sulcus, ascends from the protuberance to the superior angle of the squamous part. The posterior part of the falx cerebri is attached to the margins of the sulcus. A prominent internal occipital crest descends from the protuberance and bifurcates near the foramen magnum, and provides an attachment for the falx cerebelli. The occipital sinus, sometimes double, lies in this attachment. A small vermian fossa may exist at the lower end of the internal occipital crest; when present, it is occupied by part of the inferior cerebellar vermis. On each side a wide sulcus for the transverse sinus extends laterally from the internal occipital protuberance; the tentorium cerebelli is attached to the margins of these sulci. The right sulcus is usually larger than the left, and passes into the sulcus for the superior sagittal sinus, whereas the left usually receives the straight sinus. The position of the confluence of the sinuses is indicated by a depression on one side of the protuberance.

The position of the fetal posterior fontanelle coincides with the junction between the superior angle of the squamous part of the occipital bone and the occipital angle of the parietal bone on either side. The lateral angles of the squamous part are marked internally by the ends of the transverse sulci and project between the parietal and temporal bones. The lambdoid borders extend from superior to lateral angles and are serrated for articulation with the occipital borders of the parietal bones at the lambdoid suture. The mastoid borders extend from the lateral angles to the jugular processes, articulating with the mastoid parts of the temporal bones. A variety of sutural bones (ossicles) may occur at or near the lambda, e.g. the ‘interparietal’ (Inca bone or ossicle of Goethe).

Muscle attachments

The occipital part of occipitofrontalis is attached to the lateral part of the highest nuchal line (Fig. 42.8C). Trapezius attaches to the medial third of the superior nuchal line and to the external occipital protuberance. Sternocleidomastoid attaches to the lateral half of the superior nuchal line, with splenius capitis just below the lateral third of that line. Semispinalis capitis is attached to the medial part of the area between the superior and inferior nuchal lines; obliquus capitis superior attaches to the lateral part of this area. Rectus capitis posterior major attaches to the lateral part of the inferior nuchal line and to the bone immediately below, and rectus capitis posterior minor attaches to the medial part of the inferior nuchal line and to the bone between that line and the foramen magnum.

Basilar part

The basilar part extends anterosuperiorly from the foramen magnum. In young skulls it presents a rough and uneven surface where it is joined to the body of the sphenoid by a growth cartilage (spheno-occipital synchondrosis). This plate has fully ossified by the 25th year, at which time the occipital and sphenoid bones are fused.

The inferior surface bears a small pharyngeal tubercle, about 1 cm in front of the foramen magnum, which gives attachment to the fibrous pharyngeal raphe. A small depression immediately anterior to the occipital condyle may occasionally be replaced by a small precondylar tubercle. The anterior atlanto-occipital membrane is attached to the anterior margin of the foramen magnum.

The superior surface has the form of a broad groove which slopes upwards and forwards from the foramen magnum, directly into the basilar part of the sphenoid: together these bones form the clivus. The lateral margins articulate below with the petrous part of the temporal bones.

Muscle attachments

Longus capitis is attached anterolateral to the pharyngeal tubercle, and rectus capitis anterior is attached to the small depression anterior to the occipital condyle (Fig. 42.8C).

Lateral (condylar) parts

The lateral (condylar) parts of the occipital bone flank the foramen magnum. On their inferior surfaces are occipital condyles for articulation with the superior articular facets of the atlas vertebra. The condyles are oval or reniform, their long axes converging anteromedially. The articular surfaces, wholly convex, face inferolaterally. They are occasionally constricted and a condyle may be in two parts (as may be the reciprocal surfaces of the atlas vertebra). A tubercle gives attachment to an alar ligament medial to each articular facet. The hypoglossal (anterior condylar) canal, which is situated anteriorly above each condyle, starts internally a little above the anterolateral part of the foramen magnum and continues anterolaterally. It may be partly or wholly divided by a spicule of bone and transmits the hypoglossal nerve and a meningeal branch of the ascending pharyngeal artery. A condylar fossa, behind each condyle, fits the posterior margin of the superior facet of the atlas vertebra in full extension of the skull. Its floor is sometimes perforated by a posterior condylar canal for a sigmoid emissary vein. A quadrilateral plate, the jugular process, projects laterally from the posterior half of each condyle, and contributes the posterior part of the jugular foramen. The jugular process is indented in front by a jugular notch, which may be partly divided by a small intrajugular process projecting anterolaterally. A paramastoid process sometimes projects downwards and may even articulate with the transverse process of the atlas vertebra. Laterally, the jugular process has a rough quadrilateral or triangular area that is joined to the jugular surface of the temporal bone by cartilage: it begins to ossify at around 25 years.

An oval jugular tubercle overlies the hypoglossal canal on the superior surface of the occipital condyle. Its posterior part often bears a shallow furrow for the glossopharyngeal, vagus and accessory nerves. A deep groove containing the end of the sigmoid sinus curves anteromedially around a hook-shaped process to end at the jugular notch. The posterior condylar canal opens into the posterior cranial fossa near the medial end of the groove.

Muscle attachments

Rectus capitis lateralis attaches to a roughened area on the inferior surface of the jugular process (Fig. 42.8C).

Ossification

Above the highest nuchal lines the squamous part of the occipital bone is developed in a fibrous membrane and is ossified from two centres (one on each side) from about the second fetal month. This part of the occipital bone may remain separate as the interparietal bone. The remainder of the occipital bone is preformed in cartilage. Below the highest nuchal lines, the squamous part ossifies from two centres that appear in about the seventh week and soon unite. The two components of the squamous part unite in the third postnatal month, but the line of their union is recognizable at birth. The remainder of the cartilage of the occipital bone is ossified from five centres; two each for the lateral parts appear during the eighth week, and one for the basilar part appears around the sixth week.

At birth the occipital bone consists of four separate parts (Fig. 42.9), a basilar part, two lateral parts and a squamous part, all joined by cartilage and forming a ring around the foramen magnum. The squamous and lateral parts fuse together from the second year. The lateral parts fuse with the basilar part during years 3 and 4, but fusion may be delayed until the 7th year.

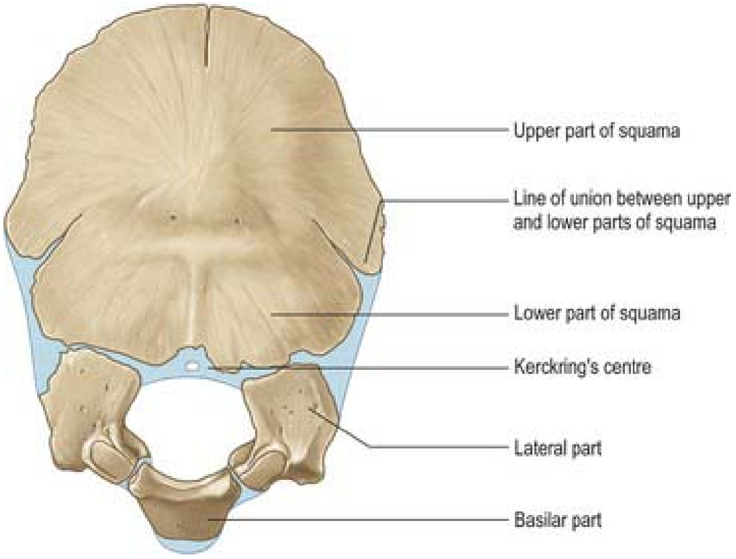

Fig. 42.9 The occipital bone of a newborn child: external surface. Parts of the chondrocranium which are still unossified are shown in blue.

VERTEBRAL COLUMN

The vertebral column is a curved linkage of individual bones or vertebrae (Fig. 42.10). A continuous series of vertebral foramina runs through the articulated vertebrae posterior to their bodies, and collectively constitutes the vertebral canal, which transmits and protects the spinal cord and nerve roots, their coverings and vasculature (Fig. 42.11, 42.16). A series of paired lateral intervertebral foramina transmits the spinal nerves and their associated vessels between adjacent vertebrae. The linkages between the vertebrae include cartilaginous interbody joints and paired synovial facet (zygapophysial) joints, together with a complex of ligaments and overlying muscles and fasciae. The muscles directly concerned with vertebral movements and attached to the column lie mainly posteriorly. Several large muscles producing major spinal movements lie distant from the column and without direct attachment to it, e.g. the anterolateral abdominal wall musculature. Movements of the column and the muscles concerned are described on page 743. The column as a whole receives its vascular supply and innervation according to general anatomical principles which are considered below.

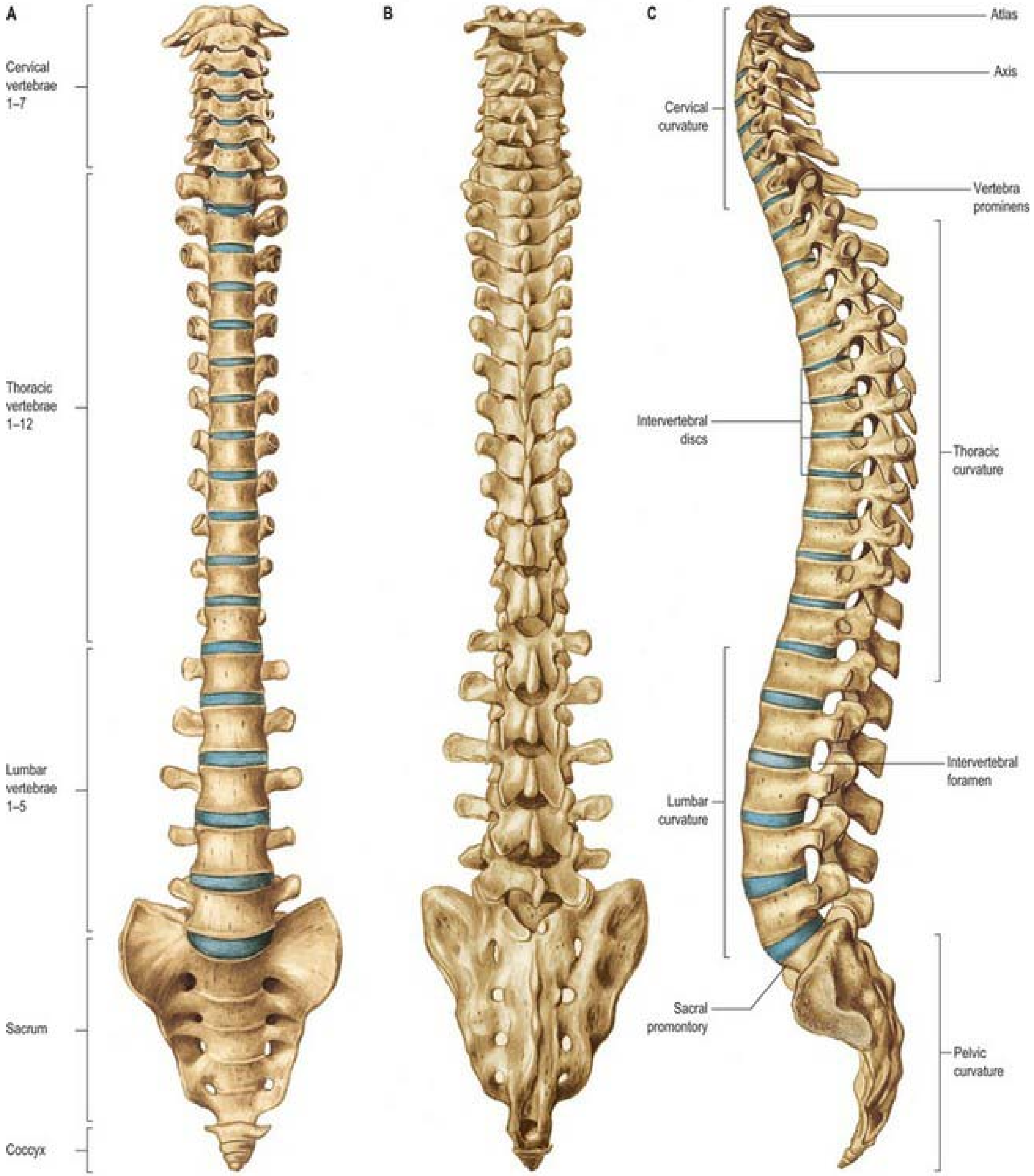
A
B
C
Cervical vertebrae 1–7
Thoracic vertebrae 1–12
Lumbar vertebrae 1–5
Sacrum
Coccyx
Atlas
Axis
Cervical curvature
Vertebra prominens
Intervertebral discs
Thoracic curvature
Intervertebral foramen
Lumbar curvature
Sacral promontory
Pelvic curvature

Fig. 42.10 The vertebral column: **A**, anterior aspect; **B**, posterior aspect; **C**, lateral aspect.

(From Sobotta 2006.)

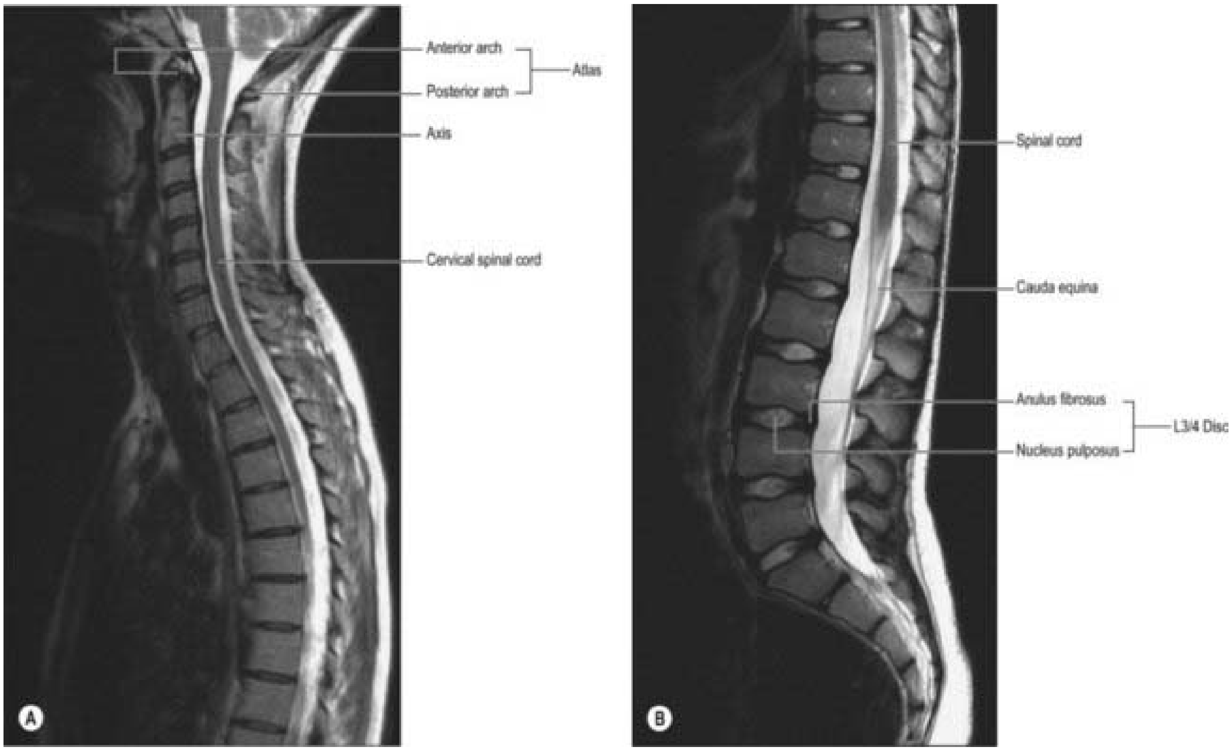
Anterior arch
Posterior arch
Atlas
Axis
Cervical spinal cord
A
Spinal cord
Cauda equina
Anulus fibrosus
Nucleus pulposus
L3/4 Disc
B

Fig. 42.11 Sagittal MRI of the cervical (**A**) and lumbar (**B**) spine.

Vertebral column morphology is influenced externally by mechanical and environmental factors and internally by genetic, metabolic and hormonal factors. These all affect its ability to react to the dynamic forces of everyday life, such as compression, traction and shear. These dynamic forces can vary in magnitude and are much influenced by occupation, locomotion and posture.

The adult vertebral column usually consists of 33 vertebral segments. Each presacral segment (except the first two cervical) is separated from its neighbour by a fibrocartilaginous intervertebral disc. The functions of the column are to support the trunk, to protect the spinal cord and nerves, and to provide attachments for muscles. It is also an important site of haemopoiesis throughout life. Its total length in males is about 70 cm and in females about 60 cm. The intervertebral discs contribute about a quarter of this length in young adults, though there is some diurnal variation in this contribution (p. 744). Approximately 8% of overall body length is accounted for by the cervical spine, 20% by the thoracic, 12% by the lumbar and 8% by the sacrococcygeal regions. Although the usual number of vertebrae is 7 cervical, 12 thoracic, 5 lumbar, 5 sacral and 4 coccygeal, this total is subject to frequent variability, and there have been reports of variation between 32 and 35 bones. The demarcation of groups by their morphological characteristics may be blurred: thus there may be thoracic costal facets on the seventh cervical vertebra, giving it the appearance of an extra thoracic vertebra; lumbar-like articular processes may be found on the lowest thoracic vertebra; the fifth lumbar vertebra may be wholly or partially incorporated into the sacrum. As a result of these changes in transition between vertebral types, there may be 23–25 mobile presacral vertebrae.

Anterior aspect

The anterior aspect of the column is formed by the anterior surfaces of the vertebral bodies and of the intervertebral discs (Fig. 42.10A). It has important anatomical relations at all levels, and should be considered in continuity. It forms part of several clinically significant junctional or transitional zones, including the prevertebral/retropharyngeal zone of the neck, the thoracic inlet, the diaphragm and the pelvic inlet. The anterior aspect of the column is covered centrally by the anterior longitudinal ligament, which forms a fascial plane with the prevertebral and endothoracic fascia and with the subperitoneal areolar tissue of the posterior abdominal wall. Infection and other pathological processes may spread along this fascial plane.

Lateral aspect

The lateral aspect of the vertebral column is arbitrarily separated from the posterior by articular processes in the cervical and lumbar regions and by transverse processes in the thoracic region (Fig. 42.10C). Anteriorly it is formed by the sides of vertebral bodies and intervertebral discs. The oval intervertebral foramina, behind the bodies and between the pedicles, are smallest at the cervical and upper thoracic levels, and increase progressively in size in the thoracic and upper lumbar regions. The lumbosacral (L5/S1) intervertebral foramen is the smallest of the lumbar foramina. The foramina permit communication between the lumen of the vertebral canal and the paravertebral soft tissues (a ‘paravertebral space’ is sometimes described), which may be important in the spread of tumours and other pathological processes. The lateral aspects of the column have important anatomical relations, some of which vary considerably between the two sides.

Posterior aspect

The posterior aspect of the column is formed by the posterior surfaces of the laminae and spinous processes, their associated ligaments, and the facet joints (Fig. 42.10B). It is covered by the deep muscles of the back.

Structural defects of the posterior bony elements

Deformity and bony deficiency may occur at several sites within the posterior elements. The laminae may be wholly or partially absent, or the spinous process alone may be affected, with no abnormalities in the overlying soft tissues (spina bifida occulta). A defect may occur in the part of the lamina between the superior and inferior articular processes (pars interarticularis): this condition is spondylolysis, and may be developmental or result from acute or fatigue fracture. If such defects are bilateral, the column becomes unstable at that level, and forward displacement of that part of the column above (cranial to) the defects may occur: this is spondylolisthesis. Abnormality of the laminar bone, or degenerative changes in the facet joints, may also lead to similar displacement in the absence of pars defects. The deformity of the vertebral canal resulting from severe spondylolisthesis may lead to neural damage. Much more rarely, bony defects may occur elsewhere in the posterior elements, e.g. in the pedicles.

Detailed anatomical relations of all aspects of the vertebral column at the various levels are best appreciated by the study of horizontal (axial) sections and images (see Fig. 42.33B and Fig. 42.55).

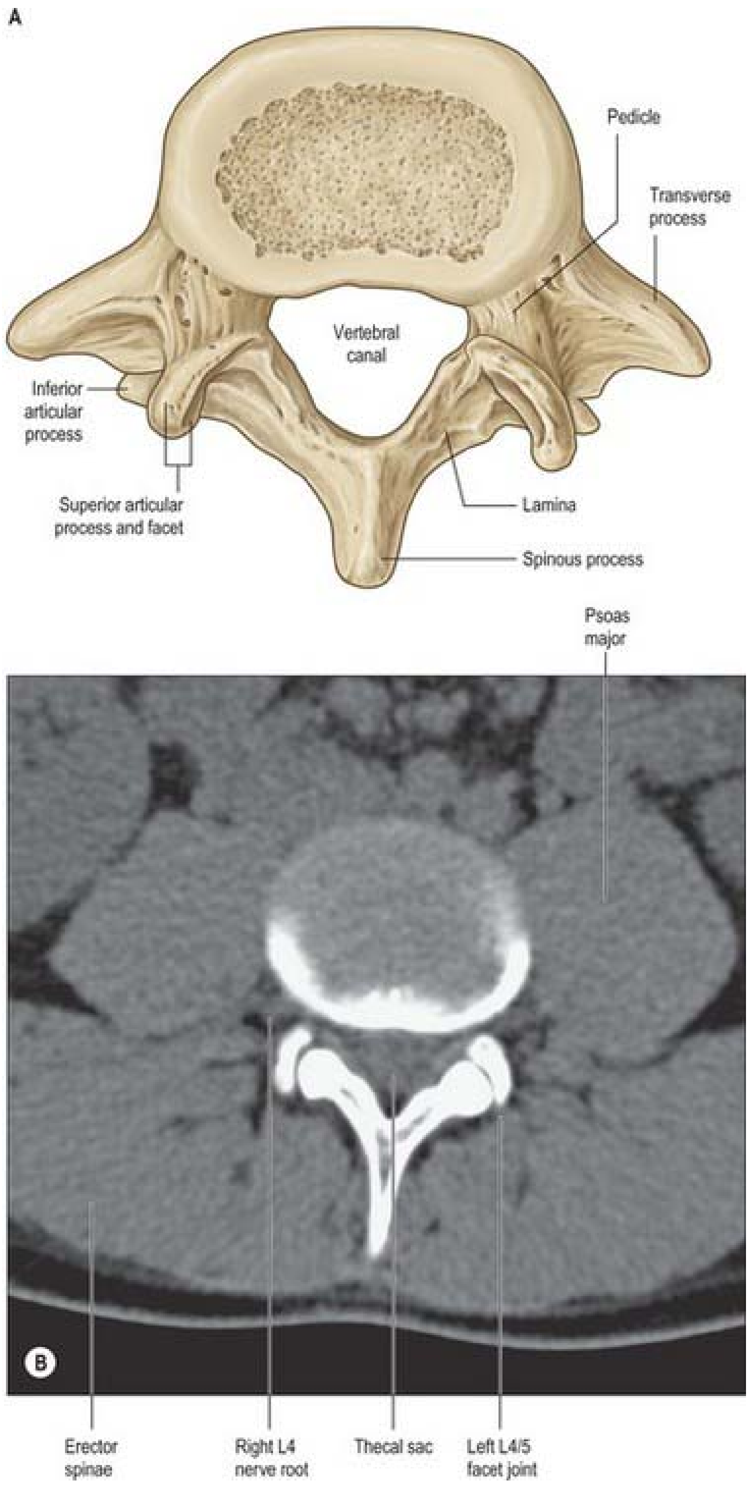
A
Pedicle
Transverse process
Vertebral canal
Inferior articular process
Superior articular process and facet
Lamina
Spinous process
Psoas major
B
Erector spinae
Right L4 nerve root
Thecal sac
Left L4/5 facet joint

Fig. 42.33 Lumbar vertebrae. **A**, Fifth lumbar vertebra, superior aspect. **B**, High resolution axial CT scan through the lumbar spine at the level of the fourth lumbar vertebra.

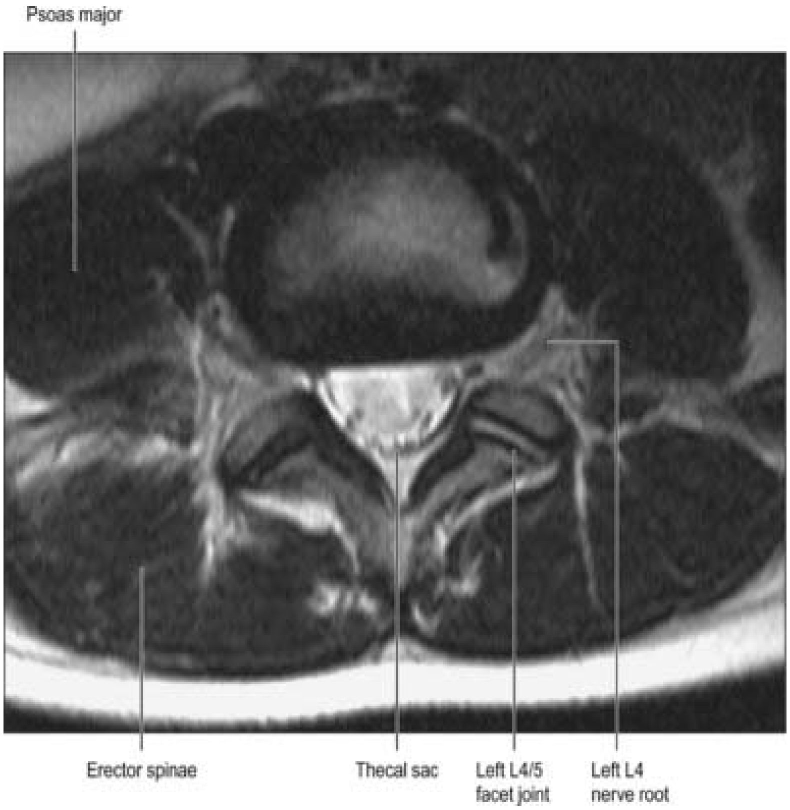

Fig. 42.55 Axial MRI of lumbar spine at the level of the L4/5 intervertebral disc.

Curvatures

Embryonic and fetal curvatures

The embryonic body appears flexed. It has primary thoracic and pelvic curves which are convex dorsally. Functional muscle development leads to the early appearance of secondary cervical and lumbar spinal curvatures in the sagittal plane. The cervical curvature appears at the end of the embryonic period, and reflects the development of function in the muscles responsible for head extension, an important component of the ‘grasp reflex’. Radiographic examination of human fetuses aged from 8 to 23 weeks shows that the secondary cervical curvature is almost always present. Lumbar flattening has also been identified as early as the eighth week. Ultrasound investigations support the role of movement in the development of these curvatures. The early appearance of the secondary curves is probably accentuated by postnatal muscular and nervous system development at a time when the vertebral column is highly flexible and is capable of assuming almost any curvature.

Neonatal curvatures

In the neonate the vertebral column has no fixed curvatures. It is particularly flexible and if dissected free from the body it can easily be bent (flexed or extended) into a perfect half circle. A slight sacral curvature can be seen which develops as the sacral vertebrae ossify and fuse. The thoracic part of the column is the first to develop a relatively fixed curvature, which is concave anteriorly. An infant can usually support its head at 3 or 4 months, sit upright at around 9 months, and will commence walking between 12 and 15 months. These functional changes exert a major influence on the development of the secondary curvatures in the vertebral column and changes in the proportional size of the vertebrae, in particular in the lumbar region. The secondary lumbar curvature becomes important in maintaining the centre of gravity of the trunk over the legs when walking starts, and thus changes in body proportions exert a major influence on the subsequent shape of curvatures in the vertebral column.

Adult curvatures

In adults, the cervical curve is a lordosis (convex forwards), and the least marked. It extends from the atlas to the second thoracic vertebra, with its apex between the fourth and fifth cervical vertebrae. Sexual dimorphism has been described in the cervical curvatures. The thoracic curve is a kyphosis (convex dorsally). It extends between the second and the 11th and 12th thoracic vertebrae, and its apex lies between the sixth and ninth thoracic vertebrae. This curvature is caused by the increased posterior height of the thoracic vertebral bodies. The lumbar curve is also a lordosis. It has a greater magnitude in females and extends from the 12th thoracic vertebra to the lumbosacral angle: there is an increased convexity of the last three segments as a result of the greater anterior height of the intervertebral discs and some posterior wedging of the vertebral bodies. Its apex is at the level of the third lumbar vertebra. The pelvic curve is concave anteroinferiorly and involves the sacrum and coccygeal vertebrae. It extends from the lumbosacral junction to the apex of the coccyx.

The presence of these curvatures means that the cross-sectional profile of the trunk changes with spinal level. The anteroposterior diameter of the thorax is much greater than that of the lower abdomen. In the normal vertebral column there are well-marked curvatures in the sagittal plane and no lateral curvatures other than in the upper thoracic region, where there is often a slight lateral curvature, convex to the right in right-handed persons, and to the left in the left-handed. Compensatory lateral curvature may also develop to cope with pelvic obliquity such as that imposed by inequality of leg length. The sagittal curvatures are present in the cervical, thoracic, lumbar and pelvic regions (Fig. 42.10). These curvatures have developed with rounding of the thorax and pelvis as an adaptation to bipedal gait.

Vertebral column in the elderly

In older people, age-related changes in the structure of bone lead to broadening and loss of height of the vertebral bodies. These changes are more severe in females. The bony changes in the vertebral column are accompanied by changes in the collagen content of the discs and by decline in the activity of the spinal muscles. This leads to progressive decline in vertebral column mobility, particularly in the lumbar spine. The development of a ‘dowager’s hump’ in the midthoracic region in females, caused by age-related osteoporosis, increases the thoracic kyphosis and cervical lordosis. Overall, these changes in the vertebral column lead directly to loss of total height in the individual.

In mid-lumbar vertebrae the width of the body increases with age. In men there is a relative decrease of posterior to anterior body height, while in both sexes anterior height decreases relative to width. Twomey et al (1983) observed a reduction in bone density of lumbar vertebral bodies with age, principally as a result of a reduction in transverse trabeculae (more marked in females as a result of postmenopausal osteoporosis), which was associated with increased diameter and increasing concavity in their juxtadiscal surfaces (end-plates).

Other changes affect the vertebral bodies. Osteophytes (bony spurs) may form from the compact cortical bone on the anterior and lateral surfaces of the bodies. Although individual variations occur, these changes appear in most individuals from 20 years onwards. They are most common on the anterior aspect of the body, and never involve the ring epiphysis. Osteophytic spurs are frequently asymptomatic, but may result in diminished movements within the spine.

Vascular supply and lymphatic drainage

Arteries

(See Crock 1996.)

The vertebral column, its contents and its associated soft tissues, all receive their arterial supply from derivatives of dorsal branches of the embryonic intersegmental somatic arteries (see Ch. 59). The named artery concerned depends on the level of the column. These intersegmental vessels persist in the thoracic and lumbar regions as the posterior intercostal and lumbar arteries. In the cervical and sacral regions, longitudinal anastomoses between the intersegmental vessels persist as longitudinal vessels which themselves give spinal branches to the vertebral column. In the neck the postcostal anastomosis becomes most of the vertebral artery, while the post-transverse anastomosis forms most of the deep cervical artery. The ascending cervical artery and the lateral sacral artery are persistent parts of the precostal anastomosis.

In the thorax and abdomen the primitive arterial pattern is retained by the paired branches of the descending aorta which supply the vertebral column (Fig. 42.12A). On each side, the main trunk of the artery (posterior intercostal or lumbar) passes around the vertebral body, giving off primary periosteal and equatorial branches to the body, and then a major dorsal branch. The latter gives off a spinal branch which enters the intervertebral foramen, before itself supplying the facet joints, the posterior surfaces of the laminae and the overlying muscles and skin. There is free anastomosis between these dorsal articular and soft-tissue branches, extending over several segments (Crock & Yoshizawa 1976; Boelderl et al 2002). At cervical and sacral levels the longitudinally running arteries described above have direct spinal branches. The spinal branches are the main arteries of supply to all bony elements of the vertebrae and to the dura and epidural tissues, and also contribute to the supply of the spinal cord and nerve roots via radicular branches. As they enter the vertebral canal the spinal arteries divide into postcentral, prelaminar and radicular branches. The postcentral branches, which are the main nutrient arteries to the vertebral bodies and to the periphery of the intervertebral discs, anastomose beneath the posterior longitudinal ligament with their fellows above and below as well as across the midline (Fig. 42.12A,B). This anastomosis also supplies the anterior epidural tissues and dura. The majority of the vertebral arch, the posterior epidural tissues and dura and the ligamentum flavum are supplied by the prelaminar branches and their anastomotic plexus on the posterior wall of the vertebral canal.

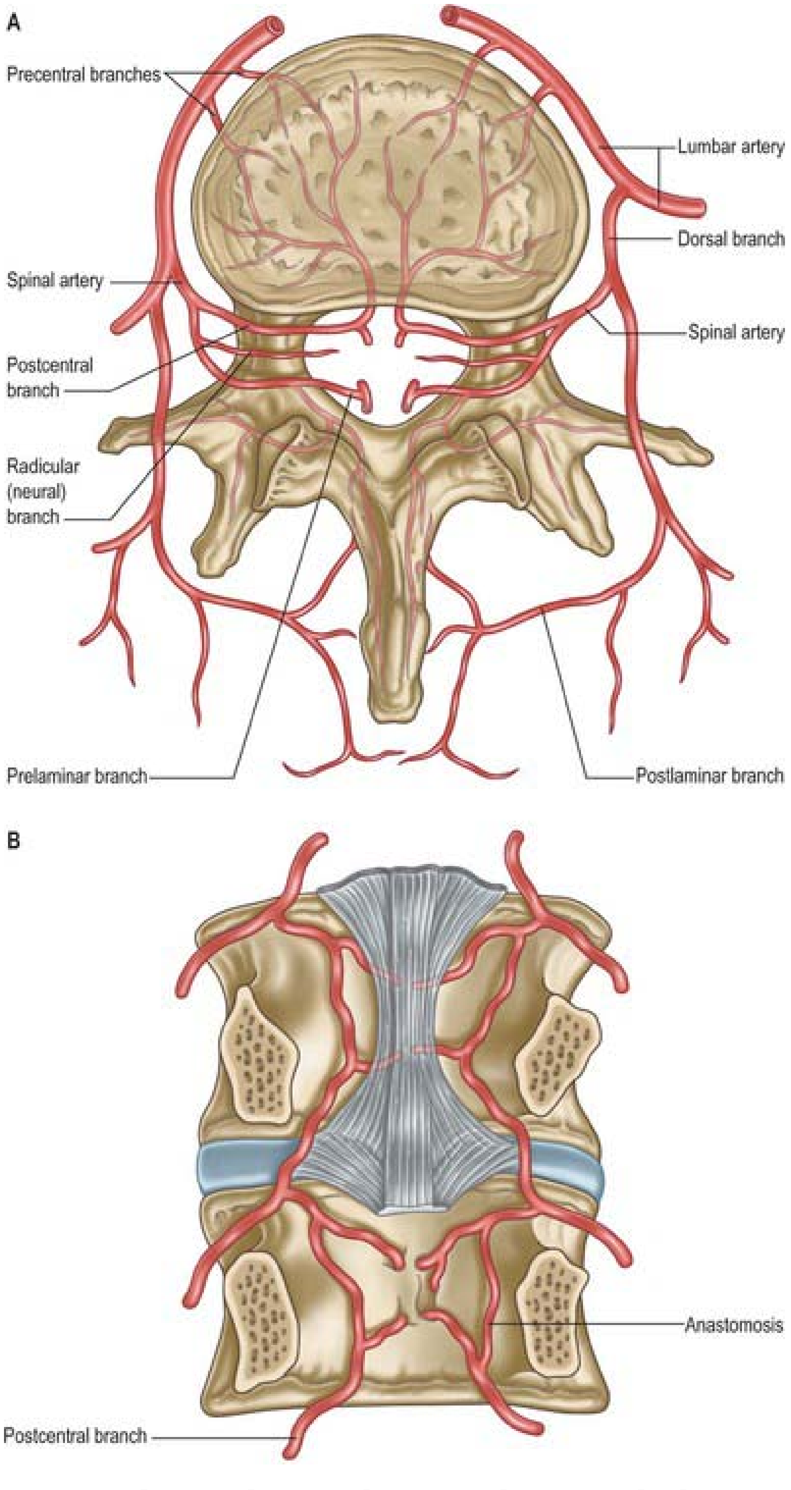
A
Precentral branches
Lumbar artery
Dorsal branch
Spinal artery
Spinal artery
Postcentral branch
Radicular (neural) branch
Prelaminar branch
Postlaminar branch
B
Anastomosis
Postcentral branch

Fig. 42.12 Arterial supply to the vertebrae and the contents of the vertebral canal. **A**, Branching pattern of lumbar segmental arteries. **B**, Arterial anastomoses between postcentral branches of spinal arteries within the vertebral canal.

Veins

Veins of the vertebral column form intricate plexuses along the entire column, external and internal to the vertebral canal (Fig. 42.13). Both groups are devoid of valves, anastomose freely with each other, and join the intervertebral veins. Interconnections are widely established between these plexuses and longitudinal veins early in fetal life. When development is complete, the plexuses drain into the caval and azygos/ascending lumbar systems via named veins which accompany the arteries described above.

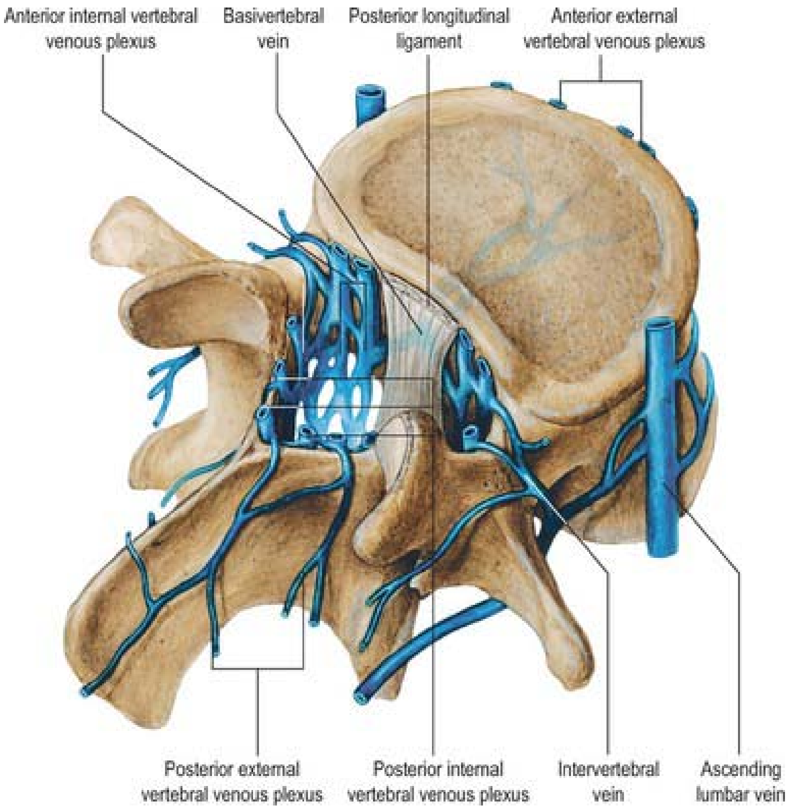
Anterior internal vertebral venous plexus
Basivertebral vein
Posterior longitudinal ligament
Anterior external vertebral venous plexus
Posterior external vertebral venous plexus
Posterior internal vertebral venous plexus
Intervertebral vein
Ascending lumbar vein

Fig. 42.13 Venous drainage of the vertebral column.

(From Sobotta 2006.)

The veins also communicate with cranial dural venous sinuses and with the deep veins of the neck and pelvis. The venous complexes associated with the vertebral column can dilate considerably, and can form alternative routes of venous return in patients with major venous obstruction in the neck, chest or abdomen. The absence of valves allows pathways for the wide and sometimes paradoxical spread of malignant disease and sepsis. Pressure changes in the body cavities are transmitted to these venous plexuses and thus to the CSF, though the cord itself may be protected from such congestion by valves in the small veins which drain from the cord into the internal vertebral plexus.

External vertebral venous plexuses

The external vertebral venous plexuses are anterior and posterior. They anastomose freely, and are most developed in the cervical region. Anterior external plexuses are anterior to the vertebral bodies, communicate with basivertebral and intervertebral veins, and receive tributaries from vertebral bodies. Posterior external plexuses lie posterior to the vertebral laminae and around spines, transverse and articular processes. They anastomose with the internal plexuses and join the vertebral, posterior intercostal and lumbar veins.

Internal vertebral venous plexuses

The internal vertebral venous plexuses occur between the dura mater and vertebrae, and receive tributaries from the bones, red bone marrow and spinal cord. (For the venous drainage of the spinal cord see p. 757 and Fig. 43.11.)

They form a denser network than the external plexuses and are arranged vertically as four interconnecting longitudinal vessels, two anterior and two posterior.

The anterior internal plexuses are large plexiform veins on the posterior surfaces of the vertebral bodies and intervertebral discs. They flank the posterior longitudinal ligament, beneath which they are connected by transverse vessels into which the large basivertebral veins open. The posterior internal plexuses, on each side in front of the vertebral arches and ligamenta flava, anastomose with the posterior external plexuses via veins which pass through and between the ligaments. The internal plexuses interconnect by venous rings near each vertebra. Around the foramen magnum they form a dense network connecting with vertebral veins, occipital and sigmoid sinuses, the basilar plexus, the venous plexus of the hypoglossal canal, and the condylar emissary veins.

Basivertebral veins

The basivertebral veins are large and tortuous channels in bone, like those in the cranial diploë. They emerge from the posterior foramina of the vertebral bodies and drain into the anterior external vertebral plexuses through small openings in the vertebral bodies. Posteriorly they form one or two short trunks that open into the transverse vessels which unite the anterior internal vertebral plexuses. The basivertebral veins enlarge in advanced age.

Intervertebral veins

The intervertebral veins accompany the spinal nerves through intervertebral foramina, draining the spinal cord and internal and external vertebral plexuses, and ending in the vertebral, posterior intercostal, lumbar and lateral sacral veins. Upper posterior intercostal veins may drain into the caval system via brachiocephalic veins, whereas the lower intercostals drain into the azygos system. Lumbar veins are joined longitudinally in front of the transverse processes by the ascending lumbar veins, in which they may terminate. Alternatively, they may proceed around the vertebral bodies to drain into the inferior vena cava. Whether the basivertebral or intervertebral veins contain effective valves is uncertain but experimental evidence strongly suggests that their blood flow can be reversed (Batson 1957). This may explain how pelvic neoplasms, e.g. carcinoma of the prostate, may metastasize in vertebral bodies: the cells spread into the internal vertebral plexuses via their connections with the pelvic veins when blood flow is temporarily reversed by raised intra-abdominal pressure or postural alterations.

Lymphatic drainage

Little is known in detail about the lymphatic drainage of the vertebral column and its associated soft tissues. In general, deep lymphatic vessels tend to follow the arteries. The cervical vertebral column drains to deep cervical nodes, the thoracic to (posterior) intercostal nodes, and the lumbar column to lateral aortic and retro-aortic nodes. The pelvic part of the column drains to lateral sacral and internal iliac nodes.

Innervation

The innervation of the vertebral column and its associated soft tissues has been studied in greatest detail in the lumbar region (see below Fig. 42.44). The account given here relies particularly on the work of Bogduk, to whose textbook on the lumbosacral spine (Bogduk 2005) the interested reader is referred. See also the work of Groen et al (1990).

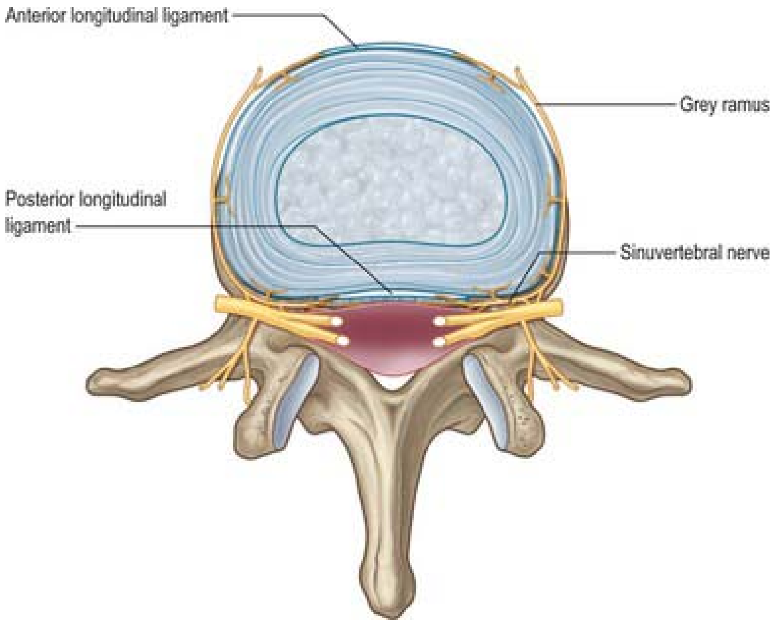
Anterior longitudinal ligament
Grey ramus
Posterior longitudinal ligament
Sinuvertebral nerve

Fig. 42.44 The nerve supply of a lumbar intervertebral disc. Branches of the grey rami communicantes and the sinuvertebral nerves are shown entering the disc and the anterior and posterior longitudinal ligaments. Branches from the sinuvertebral nerves also supply the ventral aspect of the dural sac and the dural nerve-root sleeve.

Innervation is derived from the spinal nerves where they branch, in and just beyond the intervertebral foramina. There is an input from the sympathetic system via either grey rami communicantes or directly from thoracic sympathetic ganglia. The branches of the spinal nerve concerned are the dorsal ramus and the recurrent meningeal or sinuvertebral nerves (usually more than one at each level) (p. 753 and also Fig. 43.5). The dorsal ramus branches to supply the facet joints, periosteum of the posterior bony elements, overlying muscles and skin. The exact origin and branching pattern of the sinuvertebral nerves is controversial, but they may be best considered to be recurrent branches of the ventral rami. They receive the sympathetic input described above, then re-enter the intervertebral foramina to supply the structures that form the walls of the vertebral canal, the dura and epidural soft tissues. Their subsequent course is described on page 754.

VERTEBRAE: GENERAL FEATURES

A typical vertebra has a ventral body, a dorsal vertebral (neural) arch, extended by lever-like processes, and a vertebral foramen, which is occupied in life by the spinal cord, meninges and their vessels (Fig. 42.14).

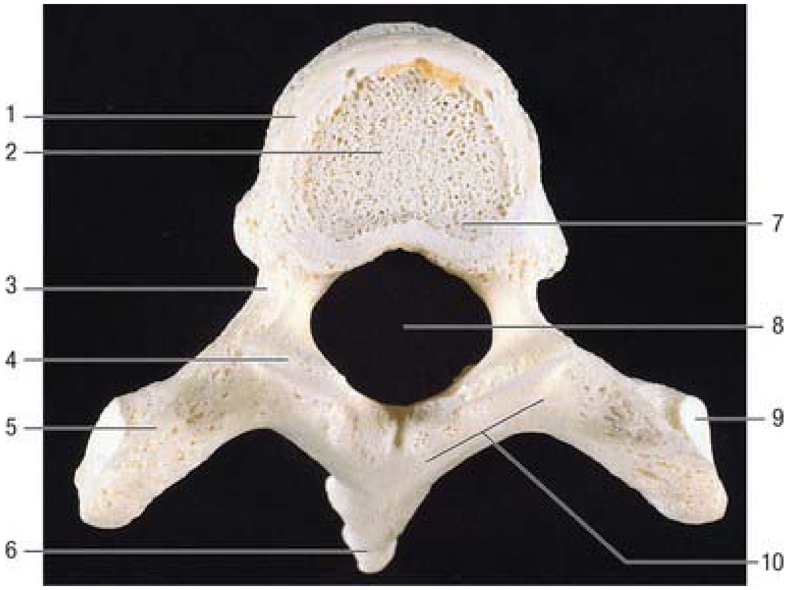

Fig. 42.14 Fourth thoracic vertebra, superior aspect. **1**. Bone derived from anular epiphysis. **2**. Vertebral body – bone derived from centrum. **3**. Pedicle. **4**. Superior articular facet. **5**. Transverse process. **6**. Spinous process. **7**. Vertebral body – bone derived from neural arch. **8**. Vertebral foramen. **9**. Costal facet. **10**. Lamina.

Opposed surfaces of adjacent bodies are bound together by intervertebral discs of fibrocartilage. The complete column of bodies and discs forms the strong but flexible central axis of the body and supports the full weight of the head and trunk. It also transmits even greater forces generated by muscles attached to it directly or indirectly. The foraminae form a vertebral canal for the spinal cord, and between adjoining neural arches, near their junctions with vertebral bodies, intervertebral foraminae transmit mixed spinal nerves, smaller recurrent nerves and blood and lymphatic vessels.

The cylindroid vertebral body varies in size, shape and proportions in different regions of the vertebral column. Its superior and inferior (discal) surfaces vary in shape from approximately flat (but not parallel) to sellar, with a raised peripheral smooth zone, formed from an ‘anular’ epiphysial disc, within which the surface is rough. These differences in texture reflect variations in the early structure of intervertebral discs. In the horizontal plane the profiles of most bodies are convex anteriorly, but concave posteriorly where they complete the vertebral foramen. Most sagittal profiles are concave anteriorly but flat posteriorly. Small vascular foramina appear on the front and sides, and posteriorly there are small arterial foramina and a large irregular orifice (sometimes double) for the exit of basivertebral veins (Fig. 42.15). The adult vertebral body is not coextensive with the developmental centrum but includes parts of the neural arch posterolaterally.

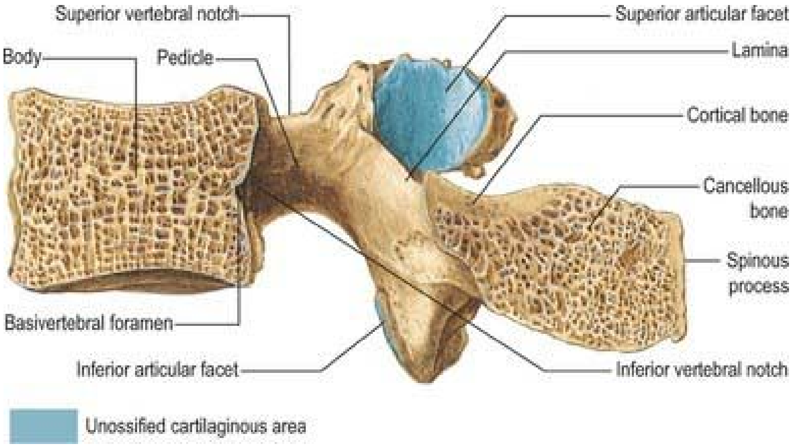
Superior vertebral notch
Body
Pedicle
Superior articular facet
Lamina
Cortical bone
Cancellous bone
Spinous process
Basivertebral foramen
Inferior articular facet
Inferior vertebral notch
Unossified cartilaginous area

Fig. 42.15 Median sagittal section through a lumbar vertebra.

(From Sobotta 2006.)

Viewed anteriorly there is a cephalocaudal increase in vertebral body width from the second cervical to the third lumbar vertebra, which is associated with an increased load-bearing function. The increase is linear in the neck but not in the thoracic and lumbar regions. There is some variation in size of the last two lumbar bodies, but thereafter width diminishes rapidly to the coccygeal apex. In the two lowest lumbar vertebrae there is an inverse relation between the areas of the upper and lower surfaces of the bodies and the size of the pedicles and transverse processes.

On each side the vertebral arch has a vertically narrower ventral part, the pedicle, and a broader lamina dorsally. Paired transverse, superior and inferior articular processes project from their junctions. There is a median dorsal spinous process.

Pedicles are short, thick, rounded dorsal projections from the superior part of the body at the junction of its lateral and dorsal surfaces: the concavity formed by the curved superior border of the pedicle is shallower than the inferior one (Fig. 42.15). When vertebrae articulate by the intervertebral disc and facet joints, these adjacent vertebral notches contribute to an intervertebral foramen. The complete perimeter of an intervertebral foramen consists of the notches, the dorsolateral aspects of parts of adjacent vertebral bodies and the intervening disc, and the capsule of the synovial facet joint.

The laminae are directly continuous with the pedicles. They are vertically flattened and curve dorsomedially.

Lateral to the spinous processes, vertebral grooves contain the deep dorsal muscles. At cervical and lumbar levels these grooves are shallow and mainly formed by laminae. In the thoracic region they are deeper, broader and formed by the laminae and transverse processes. The laminae are broad for the first thoracic vertebra, narrow for the second to seventh, broaden again from the eighth to 11th, but become narrow thereafter down to the third lumbar vertebra.

The spinous process (vertebral spine) projects dorsally and often caudally from the junction of the laminae. Spines vary considerably in size, shape and direction. They lie approximately in the median plane and project posteriorly, although in some individuals a minor deflection of the processes to one side may be seen. The spines act as levers for muscles which control posture and active movements (flexion/extension, lateral flexion and rotation) of the vertebral column.

The paired superior and inferior articular processes (zygapophyses) arise from the vertebral arch at the pediculolaminar junctions. The superior processes project cranially, bearing dorsal facets which may also have a lateral or medial inclination, depending on level. Inferior processes run caudally with articular facets directed ventrally, again with a medial or lateral inclination which depends on vertebral level. Articular processes of adjoining vertebrae thus contribute to the synovial zygapophysial or facet joints, and form part of the posterior boundaries of the intervertebral foramina. These joints permit limited movement between vertebrae: mobility varies considerably with vertebral level.

Transverse processes project laterally from the pediculolaminar junctions as levers for muscles and ligaments, particularly those concerned in rotation and lateral flexion. In the cervical region, the transverse processes are anterior to the articular processes, lateral to the pedicles and between the intervertebral foramina. In the thoracic region, they are posterior to the pedicles, considerably behind those of the cervical and lumbar processes. In the lumbar region, the transverse processes are anterior to the articular processes, but posterior to the intervertebral foramina. There is considerable regional variation in the structure and length of the transverse processes. In the cervical region, the transverse process of the atlas is long and broad, which allows the rotator muscles maximum mechanical advantage. Breadth varies little from the second to the sixth cervical vertebra, but increases in the seventh. In thoracic vertebrae, the first is widest, and breadth decreases to the 12th, where the transverse elements are usually vestigial. The transverse processes become broader in the upper three lumbar vertebrae, and diminish in the fourth and fifth. The transverse process of the fifth lumbar vertebra is the most robust. It arises directly from the body and pedicle to allow for force transmission to the pelvis through the iliolumbar ligament.

The thoracic transverse processes articulate with ribs, but at other levels the mature transverse process is a composite of ‘true’ transverse process and an incorporated costal element. Costal elements develop as basic parts of neural arches in mammalian embryos, but become independent only as thoracic ribs. Elsewhere they remain less developed and fuse with the ‘transverse process’ of descriptive anatomy (Fig. 44.11).

Vertebrae are internally trabecular, and have an external shell of compact bone perforated by vascular foramina (Fig. 42.15). The shell is thin on the superior and inferior body surfaces but thicker in the arch and its processes. The trabecular interior contains red bone marrow and one or two large ventrodorsal canals which contain the basivertebral veins.

Sexual dimorphism in vertebrae has received little attention, but Taylor & Twomey (1984) have described radiological differences in adolescent humans and have reported that female vertebral bodies have a lower ratio of width to depth. Vertebral body diameter has also been used as a basis for sex prediction in the analysis of skeletal material (MacLaughlin & Oldale 1992).

Vertebral canal

The vertebral canal (Fig. 42.16) extends from the foramen magnum to the sacral hiatus, and follows the vertebral curves. In the cervical and lumbar regions, which exhibit free mobility, it is large and triangular, but in the thoracic region, where movement is less, it is small and circular. These differences are matched by variations in the diameter of the spinal cord and its enlargements. In the lumbar region, the vertebral canal decreases gradually in size between L1 and L5, with a greater relative width in the female.

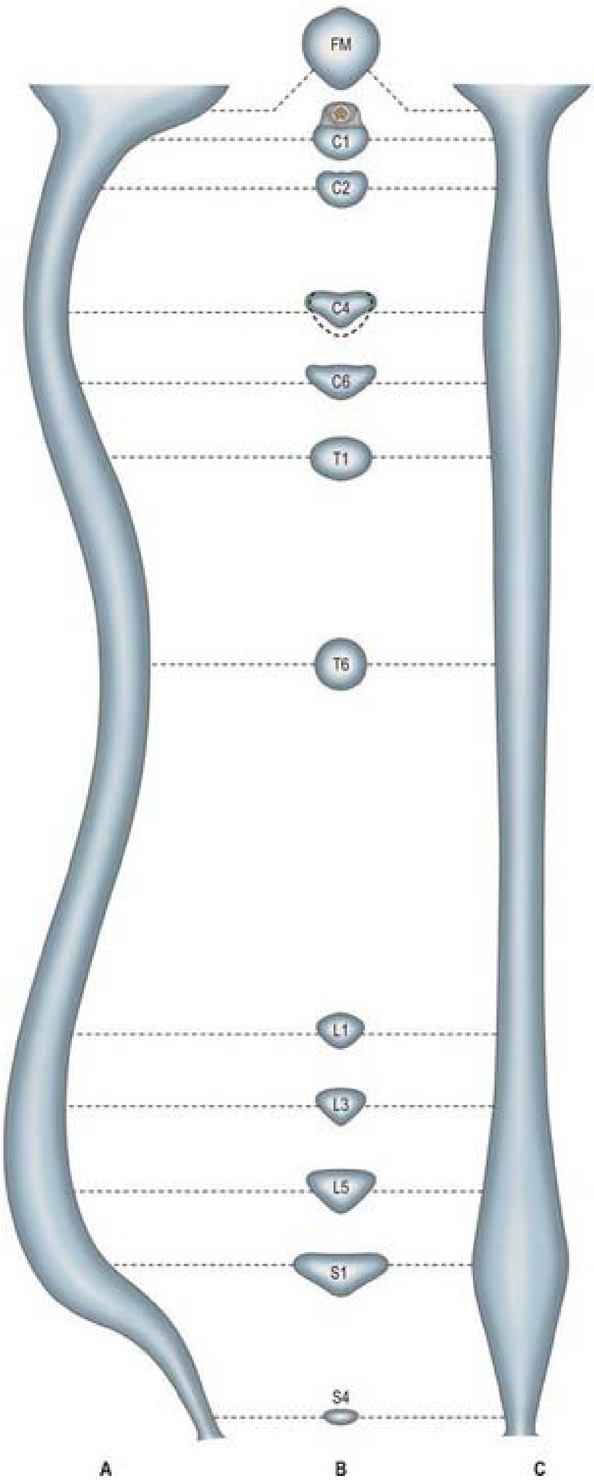
FM
C1
C2
C4
C6
T1
T6
L1
L3
L5
S1
S4
A
B
C

Fig. 42.16 The vertebral canal in section: **A**, sagittal; **B**, transverse (axial); **C**, coronal. FM: foramen magnum.

For clinical purposes it is useful to consider the vertebral canal as having three zones. These are a central zone, between the medial margins of the facet joints, and two lateral zones, beneath the facet joints and entering the intervertebral foramina. Each lateral zone, which passes into and just beyond the intervertebral foramen, can be further subdivided into subarticular (lateral recess), foraminal and extraforaminal regions (Macnab & McCulloch 1990). The lateral zone thus described forms the canal of the spinal nerve (the radicular or 'root' canal). The central zone of the canal is a little narrower than the radiological interpedicular distance if the lateral recess is considered to be part of the radicular canal rather than part of the central zone.

Spinal stenosis

Narrowing (stenosis) of the vertebral canal may occur at single or multiple spinal levels, and mainly affects the lumbar and cervical regions. Stenosis may affect the central canal and the 'root canals' either together or separately. There is a developmental form of the condition which mainly affects the central canal, but more commonly the stenosis is degenerative, and results from intervertebral disc narrowing and osteoarthritic changes in the facet joints. This latter combination is more likely to narrow the intervertebral foramen and the 'root canal', even though the sectional profile of the vertebral canal in affected lumbar vertebrae typically changes from the shape of a bell to that of a trefoil. The lumbosacral intervertebral foramen, which is normally the smallest in the region, is particularly liable to such stenosis. Severe spinal stenosis may compress the spinal cord and compromise its arterial supply. More localized 'root canal' stenosis will present with the clinical features of spinal nerve compression, but without the tension signs that characterize the stretching of nerve roots over a prolapsed disc. Ischaemia of the nerves and roots may provoke more damage than the actual physical compression of the neural tissue.

Intervertebral foramina

Intervertebral foramina (see also p. 712) are the principal routes of entry and exit to and from the vertebral canal, and are closely related to the main intervertebral articulations. (Minor routes occur between the median, often partly fused, margins of the ligamenta flava.) The same general arrangement applies throughout the vertebral column, between the axis and sacrum, although there are some quantitative and structural regional variations. Because of their construction, contents and susceptibilities to multiple disorders, the intervertebral foramina are loci of great biomechanical, functional and clinical significance. The specializations cranial to the axis and at sacral levels are described with the individual bones and articulations.

The boundaries of a generalized intervertebral foramen (Fig. 42.17) are anteriorly, from above downwards, the posterolateral aspect of the superior vertebral body, the posterolateral aspect of the intervertebral symphysis (including the disc), and a small (variable) posterolateral part of the body of the inferior vertebra; superiorly, the compact bone of the deep arched inferior vertebral notch of the vertebra above; inferiorly, the compact bone of the shallow superior vertebral notch of the vertebra below; and posteriorly a part of the ventral aspect of the fibrous capsule of the facet synovial joint. Cervical intervertebral foramina are distinct in having superior and inferior vertebral notches of almost equal depth which, in accord with the direction of the pedicles, face anterolaterally. External to them, and oriented in the same direction, is a transverse process. The thoracic and lumbar intervertebral foramina face laterally and their transverse processes are posterior. In addition, the anteroinferior boundaries of the first to tenth thoracic foramina are formed by the articulations of the head of a rib and the capsules of double synovial joints (with the demifacets on adjacent vertebrae and the intra-articular ligament between the costocapitular ridge and the intervertebral symphysis). Lumbar foramina lie between the two principal lines of vertebral attachment of psoas major. The walls of each foramen are covered throughout by fibrous tissue which is in turn periosteal (though the presence of a true periosteum lining the vertebral canal is controversial [Newell 1999]), perichondrial, anular and capsular. The more lateral parts of the foramina may be crossed at a variable level by narrow fibrous bands, the transforaminal ligaments (for detail of these ligaments see Bogduk 2005). The true foramen is the foraminal region of the canal of the spinal nerve (the radicular or 'root' canal). A foramen contains a segmental mixed spinal nerve and its sheaths, from two to four recurrent meningeal (sinuvertebral) nerves, variable numbers of spinal arteries, and plexiform venous connections between the internal and external vertebral venous plexuses. These structures, particularly the nerves, may be affected by trauma or one of the many disorders which may affect tissues bordering the foramen. In particular, nerve compression and irritation may be caused by intervertebral disc prolapse, or by bony entrapment as the size of the foramen decreases. This decrease may result from facet joint osteoarthritis, osteophyte formation, disc degeneration and degenerative spondylolisthesis, all of which may lead to lateral or foraminal spinal stenosis.

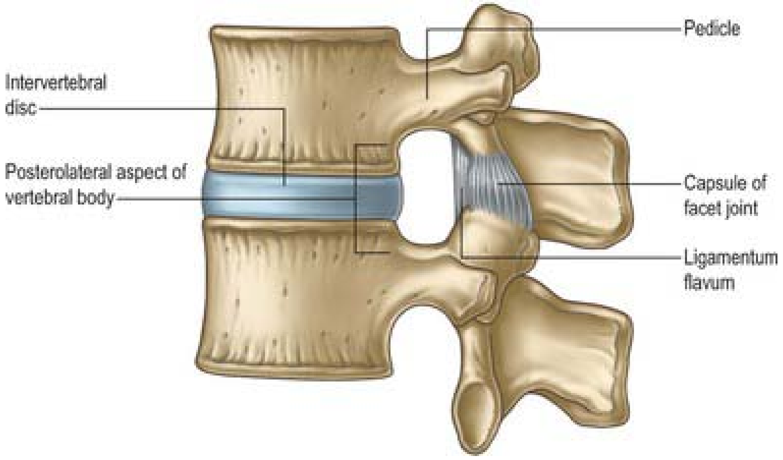
Pedicle
Intervertebral disc
Posterolateral aspect of vertebral body
Capsule of facet joint
Ligamentum flavum

Fig. 42.17 The boundaries of an intervertebral foramen.

CERVICAL VERTEBRAE

The cervical vertebrae (Fig. 42.18, Fig. 42.19) are the smallest of the moveable vertebrae, and are characterized by a foramen in each transverse process. The first, second and seventh have special features and will be considered separately. The third, fourth and fifth cervical are almost identical, and the sixth, while typical in its general features, has minor distinguishing differences.

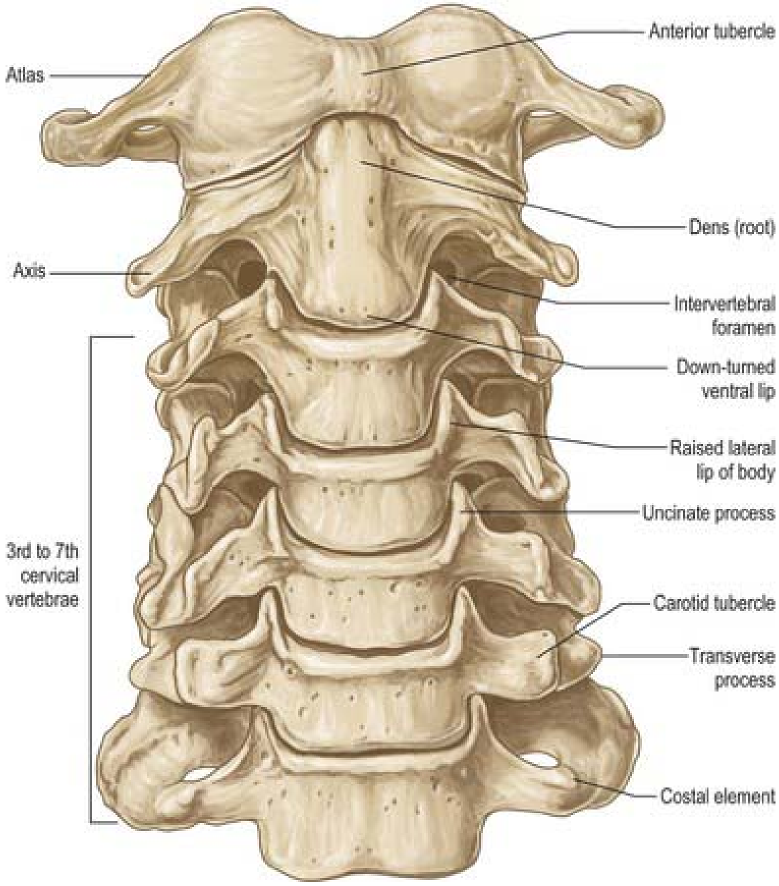
Atlas
Anterior tubercle
Dens (root)
Axis
Intervertebral foramen
Down-turned ventral lip
Raised lateral lip of body
Uncinate process
3rd to 7th cervical vertebrae
Carotid tubercle
Transverse process
Costal element

Fig. 42.18 The cervical vertebrae (anterior aspect).

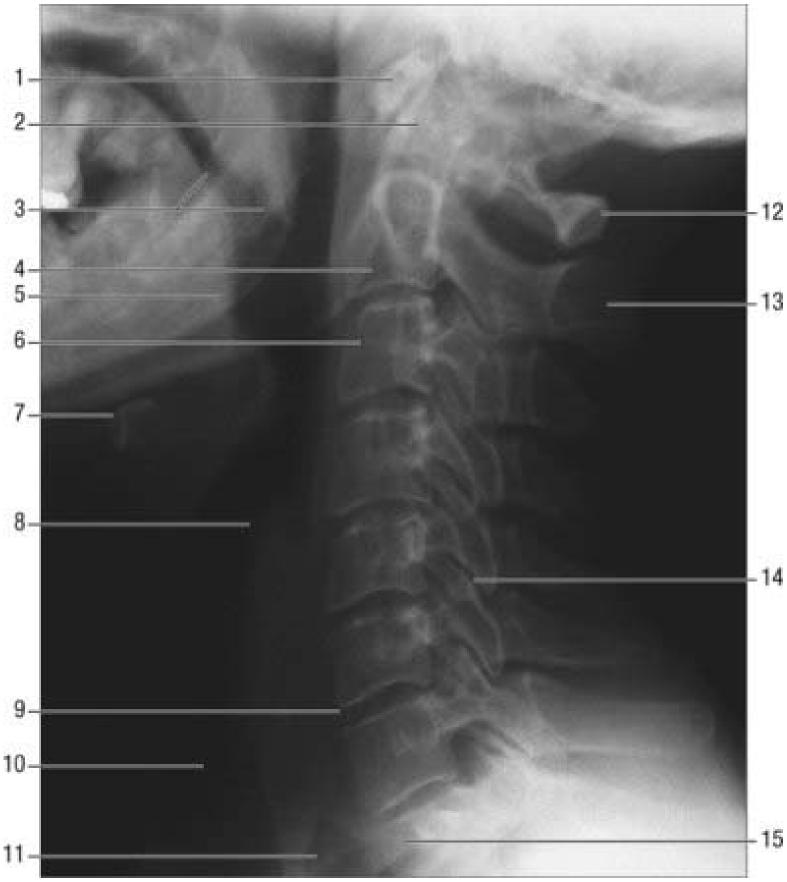

Fig. 42.19 Lateral radiograph of the cervical spine. **1**. Anterior tubercle of atlas. **2**. Dens of C2. **3**. Soft palate. **4**. Body of C2. **5**. Pharyngeal part of tongue. **6**. C3 characteristic cervical body. **7**. Body of hyoid. **8**. Epiglottis. **9**. C6/7 intervertebral disc. **10**. Air in trachea. **11**. Air in oesophagus. **12**. Posterior arch of atlas. **13**. Spinous process of axis. **14**. C5/6 facet joint. **15**. Body of T1.

Typical cervical vertebra

A typical cervical vertebra (Fig. 42.20, Fig. 42.21) has a small, relatively broad vertebral body. The pedicles project posterolaterally and the longer laminae posteromedially, enclosing a large, roughly triangular vertebral foramen; the vertebral canal here accommodates the cervical enlargement of the spinal cord. The pedicles attach midway between the discal surfaces of the vertebral body, so the superior and inferior vertebral notches are of similar depth. The laminae are thin and slightly curved, with a thin superior and slightly thicker inferior border. The spinous process (‘spine’) is short and bifid, with two tubercles which are often unequal in size. The junction between lamina and pedicle bulges laterally between the superior and inferior articular processes to form an articular pillar (‘lateral mass’) on each side. The transverse process is morphologically composite around the foramen transversarium. Its dorsal and ventral bars terminate laterally as corresponding tubercles. The tubercles are connected, lateral to the foramen, by the costal (or intertubercular) lamella: these three elements represent morphologically the capitellum, tubercle and neck of a cervical costal element (p. 770, Fig. 44.11). The attachment of the dorsal bar to the pediculolaminar junction represents the morphological transverse process and the attachment of the ventral bar to the ventral body represents the capitellar process. In all but the seventh cervical vertebra, the foramen transversarium normally transmits the vertebral artery and vein and a branch from the cervicothoracic ganglion (vertebral nerve).

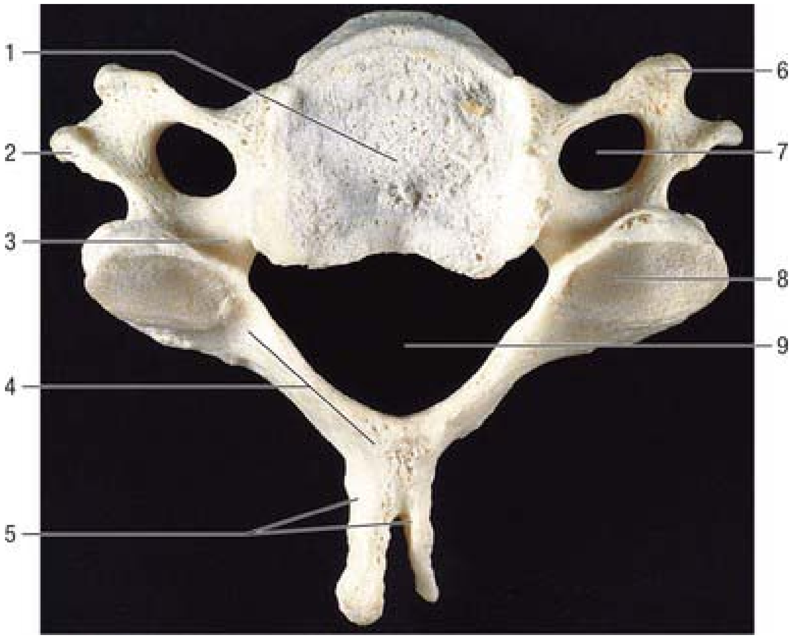

Fig. 42.20 Fourth cervical vertebra, superior aspect. **1**. Body. **2**. Posterior tubercle of transverse process. **3**. Pedicle. **4**. Lamina. **5**. Bifid spinous process. **6**. Anterior tubercle of transverse process. **7**. Foramen transversarium. **8**. Superior articular facet. **9**. Vertebral foramen.

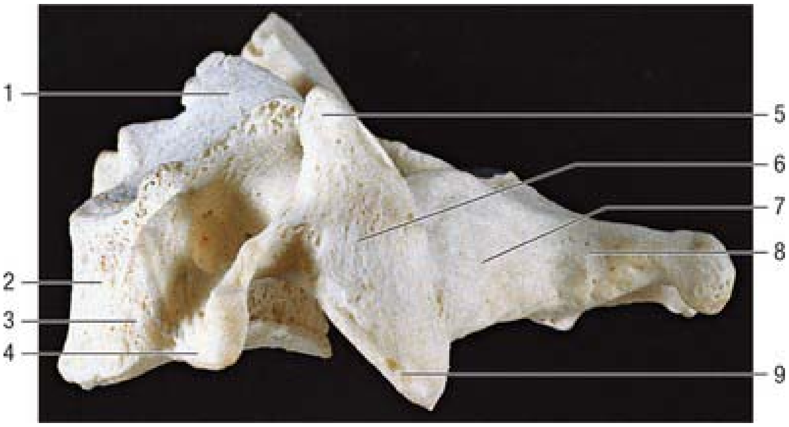

Fig. 42.21 Fourth cervical vertebra, lateral aspect. **1**. Uncinate process. **2**. Body. **3**. Anterior tubercle of transverse process. **4**. Posterior tubercle of transverse process. **5**. Superior articular process. **6**. Lateral mass. **7**. Lamina. **8**. Spinous process. **9**. Inferior articular process.

The vertebral body has a convex anterior surface. The discal margin gives attachment to the anterior longitudinal ligament. The posterior surface is flat or minimally concave, and its discal margins give attachment to the posterior longitudinal ligament. The central area displays several vascular foramina, of which two are commonly relatively larger. These are the basivertebral foramina which transmit basivertebral veins to the anterior internal vertebral veins. The superior discal surface is saddle-shaped, formed by flange-like lips which arise from most of the lateral circumference of the upper margin of the vertebral body; these are sometimes referred to as uncinate or neurocentral lips or processes. The inferior discal surface is also concave: the concavity is produced mainly by a broad projection from the anterior margin which partly overlaps the anterior surface of the intervertebral disc. The discal surfaces of cervical vertebrae are so shaped in order to restrict both lateral and anteroposterior gliding movements during articulation. The paired ligamenta flava extend from the superior border of each lamina below to the roughened inferior half of the anterior surfaces of the lamina above. The superior part of the anterior surface of each lamina is smooth, like the immediately adjacent surfaces of the pedicles, which are usually in direct contact with the dura mater and cervical root sheaths to which they may become loosely attached. The spinous process of the sixth cervical vertebra is larger, and is often not bifid.

The superior articular facets, flat and ovoid, are directed superoposteriorly, whereas the corresponding inferior facets are directed mainly anteriorly, and lie nearer the coronal plane than the superior facets. The dorsal rami of the cervical spinal nerves curve posteriorly, close to the anterolateral aspects of the lateral masses, and may actually lie in shallow grooves, especially on the third and fourth pair. The dorsal root ganglion of each cervical spinal nerve lies between the superior and inferior vertebral notches of adjacent vertebrae. The large anterior ramus passes posterior to the vertebral artery, which lies on the concave upper surface of the costal lamella: the concavity of the lamellae increases from the fourth to the sixth vertebra. The fourth to sixth anterior tubercles are elongated and rough for muscle attachment. The sixth is the longest, the carotid tubercle of Chassaignac. The carotid artery can be forcibly compressed in the groove formed by the vertebral bodies and the larger anterior tubercles, especially the sixth. The posterior tubercles are rounded and more laterally placed than the anterior, and all but the sixth are also more caudal; the sixth is at about the same level as the anterior.

Muscle attachments

The ligamentum nuchae and numerous deep extensors, including semispinalis thoracis and cervicis, multifidus, spinales and interspinales, are all attached to the spinous processes. Tendinous slips of scalenus anterior, longus capitis and longus colli are attached to the fourth to sixth anterior tubercles. Splenius, longissimus and iliocostalis cervicis, levator scapulae and scalenus posterior and medius are all attached to the posterior tubercles. Shallow anterolateral depressions on the anterior surface of the body lodge the vertical parts of the longus colli.

Ossification

Cervical vertebrae ossify according to the standard vertebral pattern described on page 768. Incomplete segmentation (‘block vertebra’) is common in the cervical spine and most commonly involves the axis and third cervical vertebra.

C1, atlas

The atlas, the first cervical vertebra (Fig. 42.22), supports the head. It is unique in that it fails to incorporate a centrum, whose expected position is occupied by the dens, a cranial protuberance from the axis. The atlas consists of two lateral masses connected by a short anterior and a longer posterior arch. The transverse ligament retains the dens against the anterior arch.

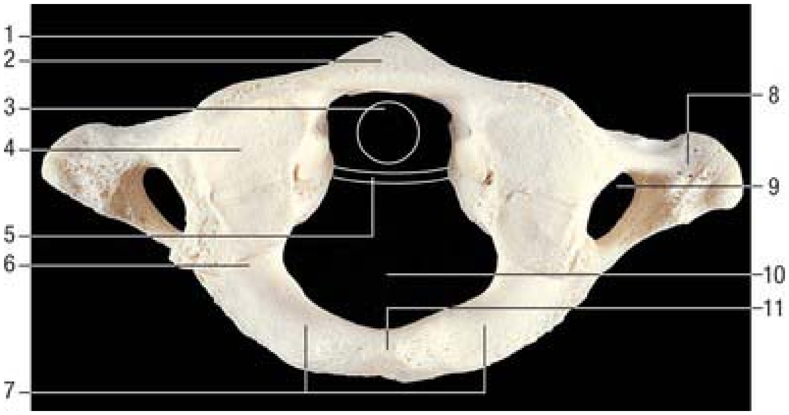

Fig. 42.22 First cervical vertebra (atlas), superior aspect. **1**. Anterior tubercle. **2**. Anterior arch. **3**. Outline of dens. **4**. Superior articular facet, on lateral mass (bipartite facet in this specimen). **5**. Outline of transverse ligament. **6**. Groove for vertebral artery and C1 (beneath bony overhang from lateral mass here). **7**. Posterior arch. **8**. Transverse process. **9**. Foramen transversarium. **10**. Vertebral foramen. **11**. Posterior tubercle.

The transverse ligament divides the vertebral canal into two compartments. The anterior third (approximately) of the canal is occupied by the dens. The posterior compartment is occupied by the spinal cord and its coverings, and the cord itself takes up about half of this space (i.e. the cord, like the dens, occupies one third of the canal).

The anterior arch is slightly convex anteriorly, and carries a roughened anterior tubercle to which is attached the anterior longitudinal ligament (which is cylindrical at this level). Its upper and lower borders provide attachment for the anterior atlanto-occipital membrane and diverging lateral parts of the anterior longitudinal ligament. The posterior surface of the anterior arch carries a concave, almost circular, facet for the dens.

The lateral masses are ovoid, their long axes converging anteriorly. Each bears a kidney-shaped superior articular facet for the respective occipital condyle, which is sometimes completely divided into a larger anterior and a smaller posterior part (Lang 1986). The inferior articular facet of the lateral mass is almost circular and is flat or slightly concave. It is orientated more obliquely to the transverse plane than the superior facet, and faces more medially and very slightly backwards. On the medial surface of each lateral mass is a roughened area which bears vascular foramina and a tubercle for attachment of the transverse ligament. In adults the distance between these tubercles is shorter than the transverse ligament itself, with a mean value of approximately 16 mm.

The posterior arch forms three-fifths of the circumference of the atlantal ring. The superior surface bears a wide groove for the vertebral artery and venous plexus immediately behind, and is variably overhung by the lateral mass; the first cervical nerve intervenes. The flange-like superior border gives attachment to the posterior atlanto-occipital membrane, and the flatter inferior border to the highest pair of ligamenta flava. The posterior tubercle is a rudimentary spinous process, roughened for attachment of the ligamentum nuchae.

The transverse processes are longer than those of all cervical vertebrae except the seventh (Fig. 42.18). They act as strong levers for the muscles which make fine adjustments to keep the head balanced. Maximum atlantal width varies from 74–95 mm in males and 65–76 mm in females, and this affords a useful criterion for assessing sex in human remains. The apex of the transverse process, which is usually broad, flat and palpable between the mastoid process and ramus of the mandible, is homologous with the posterior tubercle of typical cervical vertebrae: the remaining part of the transverse process consists of the costal lamella. A small anterior tubercle is sometimes visible on the anterior aspect of the lateral mass. The costal lamella is sometimes deficient, which leaves the foramen transversarium open anteriorly.

Muscle attachments

The superior oblique parts of longus colli are attached on each side of the anterior tubercle. The anterior surface of the lateral mass gives attachment to rectus capitis anterior. Rectus capitis posterior minor is attached just lateral to the posterior tubercle. Rectus capitis lateralis is attached to the transverse process superiorly, and obliquus capitis superior is located more posteriorly. Obliquus capitis inferior is attached laterally on the apex, below which are slips of levator scapulae, splenius cervicis and scalenus medius.

Ossification

The atlas is commonly ossified from three centres (Fig. 42.23). One appears in each lateral mass at about the seventh week, gradually extending into the posterior arch where they unite between the third and fourth years, usually directly but occasionally through a separate centre. At birth, the anterior arch is fibrocartilaginous, and a separate centre appears about the end of the first year. This unites with the lateral masses between the sixth and eighth year, the lines of union extending across anterior parts of the superior articular facets. Occasionally the anterior arch is formed by the extension and ultimate union of centres in the lateral masses and sometimes from two lateral centres in the arch itself.

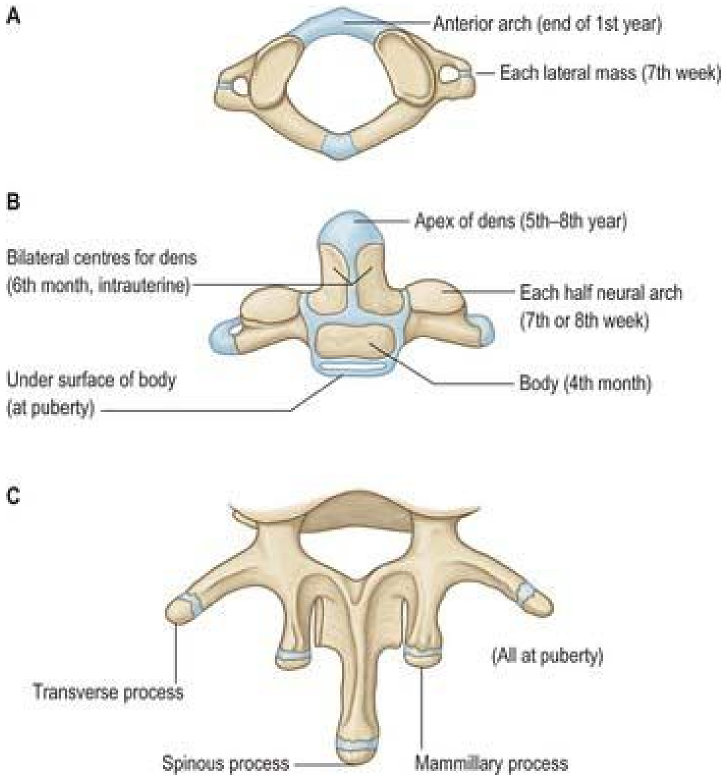
A
Anterior arch (end of 1st year)
Each lateral mass (7th week)
B
Apex of dens (5th–8th year)
Bilateral centres for dens (6th month, intrauterine)
Each half neural arch (7th or 8th week)
Under surface of body (at puberty)
Body (4th month)
C
(All at puberty)
Transverse process
Spinous process
Mammillary process

Fig. 42.23 Ossification in the vertebral column. **A**, The atlas. **B**, The axis. **C**, Lumbar vertebra.

The central part of the posterior arch may be absent and replaced by fibrous tissue. Frequently bony spurs arise from the anterior and posterior margins of the groove for the vertebral artery. These are sometimes referred to as ponticles, and they occasionally convert the groove into a foramen. More often the foramen is incomplete superiorly. Rarely the atlas may be wholly or partially assimilated into (fused with) the occiput.

C2, axis

The axis, the second cervical vertebra (Fig. 42.24, Fig. 42.25), acts as an axle for rotation of the atlas and head around the strong dens (odontoid process), which projects cranially from the superior surface of the body.

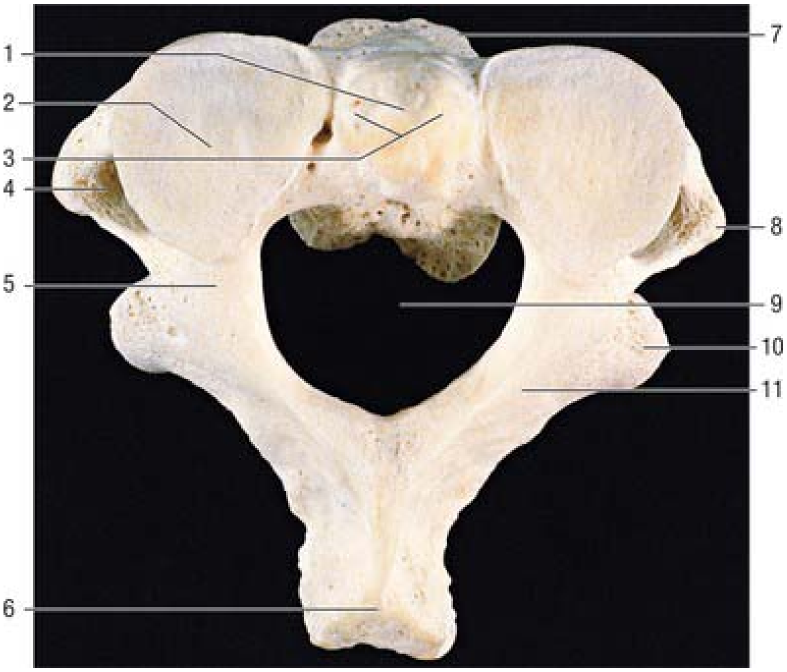

Fig. 42.24 Second cervical vertebra (axis), superior aspect. **1**. Dens – attachment of apical ligament. **2**. Superior articular facet on lateral mass. **3**. Dens – attachments of alar ligaments. **4**. Foramen transversarium. **5**. Pedicle. **6**. Spinous process. **7**. Body. **8**. Transverse process. **9**. Vertebral foramen. **10**. Inferior articular process. **11**. Lamina.

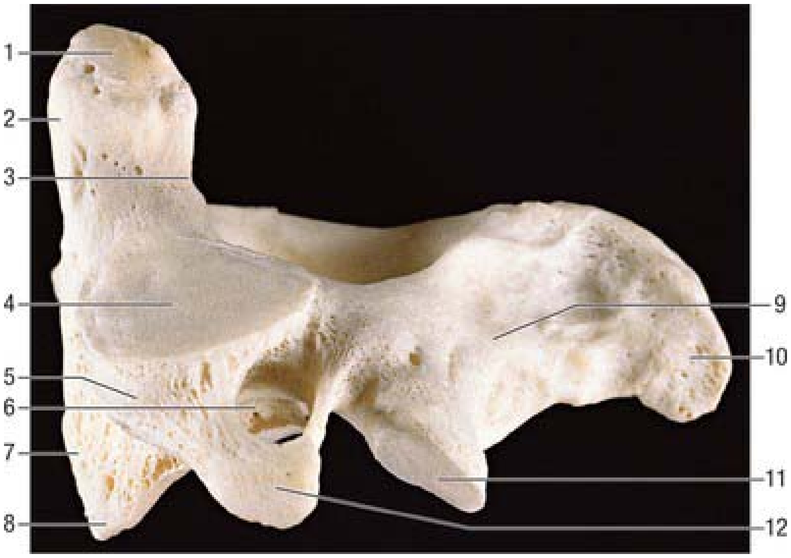

Fig. 42.25 Second cervical vertebra (axis), lateral aspect. **1**. Dens – attachment of alar ligament. **2**. Facet for anterior arch of atlas. **3**. Groove for

transverse ligament of atlas. **4**. Superior articular facet. **5**. Lateral mass. **6**. Divergent foramen transversum. **7**. Body. **8**. Ventral lip of body. **9**. Lamina. **10**. Spinous process. **11**. Inferior articular facet. **12**. Transverse process.

The dens is conical in shape with a mean length of 15 mm in adults. It may be tilted a little, up to 14°, posteriorly, or, less often, anteriorly on the body of the axis: it may also tilt laterally up to 10°. The posterior surface bears a broad groove for the transverse ligament which is covered in cartilage. The apex is pointed, and from this point arises the apical ligament. The alar ligaments are attached to the somewhat flattened posterolateral surfaces above the groove for the transverse ligament. The anterior surface bears an ovoid articular facet for the anterior arch of the atlas, and the surface is pitted by many vascular foramina, which are most numerous near the apex.

The body consists of less compact bone than the dens. It is composite, and consists of the partly fused centra of the atlas and axis, and a rudimentary disc (synchondrosis) between them which usually remains detectable deep within the body of the axis throughout life. Large ovoid articular facets are present on either side of the dens at the junction of the body and neural arch: they are flat or slightly convex for articulation with the masses of the atlas. The facets lie in a plane anterior to the plane of the intercentral (Luschka) articulations, with which they are, in part, homologous. The somewhat triangular downward projecting anterior border gives attachment to the anterior longitudinal ligament. Posteriorly, the lower border receives the posterior longitudinal ligament and the membrana tectoria.

The pedicles are stout, and the superior surface carries part of the superior articular facet, which also projects laterally and downwards onto the transverse process. The anterolateral surface is deeply grooved by the vertebral artery, running beneath the thin lateral part of the inferior surface of the superior articular facet, which can become quite thin. The inferior surface of each pedicle bears a deep, smooth inferior intervertebral notch, in which the large root sheath of the third cervical nerve lies. The interarticular part of the pedicle is short and lies between the relatively small inferior posterior articular process (which is located at the pediculolaminar junction and bearing a small anteriorly facing facet) and the superior articular surface.

The transverse process is pointed, projects inferiorly and laterally, and arises from the pediculolaminar junction and the lateral aspect of the interarticular area of the pedicle. The rounded tip is homologous with the posterior tubercle of a typical cervical vertebrae. The foramen transversarium is directed laterally as the vertebral artery turns abruptly laterally under the superior articular facet. Small anterior tubercles may be present near the junction of the costal lamella with the body.

The laminae are thick, and give attachment to the ligamenta flava.

The spinous process is large, with a bifid tip and a broad base, which is concave inferiorly. The ligamentum nuchae is attached to the apical notch.

Muscle attachments

The anterior surface of the body carries a deep depression on each side for the attachment of the vertical part of longus colli. Levator scapulae, scalenus medius and splenius cervicis are all attached to the tips of the transverse processes and the intertransverse muscles are attached to their upper and lower surfaces. The lateral surfaces of the spinous process give origin to obliquus capitis inferior, and rectus posterior major is attached a little more posteriorly. The inferior concavity of the process receives semispinalis and spinalis cervicis, multifidus more deeply, and the interspinales near the apex.

Arterial supply

Small branches arise mainly from the vertebral artery at the level of the intervertebral foramen for the third cervical nerve and form paired anterior and posterior longitudinal channels, branches of which enter the dens near the base and near the apex. The anterior channel also receives numerous twigs from nearby branches of the external carotid artery via branches to longus colli and the ligaments of the apex, hence avascular necrosis does not occur after fracture of the base of the dens.

Ossification

The axis is ossified from five primary and two secondary centres (Fig. 42.23). The vertebral arch has two primary centres and the centrum one, as in a typical vertebra. The former appear about the seventh or eighth week, and that for the centrum about the fourth or fifth month. The dens is largely ossified from bilateral centres, appearing about the sixth month and joining before birth to form a conical mass, deeply cleft above by cartilage. This cuneiform cartilage forms the apex of the odontoid process. A centre appears in it which shows considerable individual variation in both time of appearance and time of fusion to the rest of the dens: it most often appears between five and eight years, but sometimes even later, fusing with the main mass about the 12th year. The cartilage was thought to be part of the cranial sclerotomal half of the first cervical segment or pro-atlas. It has also been suggested that the apical centre for the dens is itself derived from the pro-atlas, which may also contribute to lateral atlantal masses. The dens is separated from the body by a cartilaginous disc, the circumference of which ossifies while its centre remains cartilaginous until old age; possible rudiments of adjacent epiphyses of atlas and axis may occur in the disc. A thin epiphysial plate is formed inferior to the body around puberty.

Ossification may sometimes be incomplete. Thus the apical cuneiform centre may fail to fuse with the dens, or the dens itself may fail to fuse with the body, instead forming an os odontoideum. Some believe that this results from old unrecognized trauma rather than ossification failure. Interposition of the transverse ligament may prevent union of fractures through the base of the dens. Hypoplasia of the dens is usually accompanied by atlanto-occipital assimilation and basilar invagination. Abnormalities of the dens are common, and can result in atlanto-axial subluxation. In some skeletal dysplasias there is abnormal ossification in which the dens ossifies separately and much later than the atlantal centrum. This is probably a result of abnormal mobility in the cartilaginous anlage, and normal ossification may be restored if motion is prevented by surgical fusion.

C7, seventh cervical vertebra

The seventh cervical vertebra, the vertebra prominens (Fig. 42.26), has a long spinous process which is visible at the lower end of the nuchal furrow. It ends in a prominent tubercle for the attachment of the ligamentum nuchae, and the muscles detailed below. The thick and prominent transverse processes lie behind and lateral to the foramina transversaria. The latter transmit vertebral veins, but not the vertebral artery, and each is often divided by a bony spicule. The costal lamella is relatively thin and may be partly deficient. It is grooved superiorly for the anterior ramus of the seventh cervical nerve, and usually carries a small and inconspicuous anterior tubercle. The posterior tubercle is prominent. The suprapleural membrane is attached to the anterior border of the transverse process.

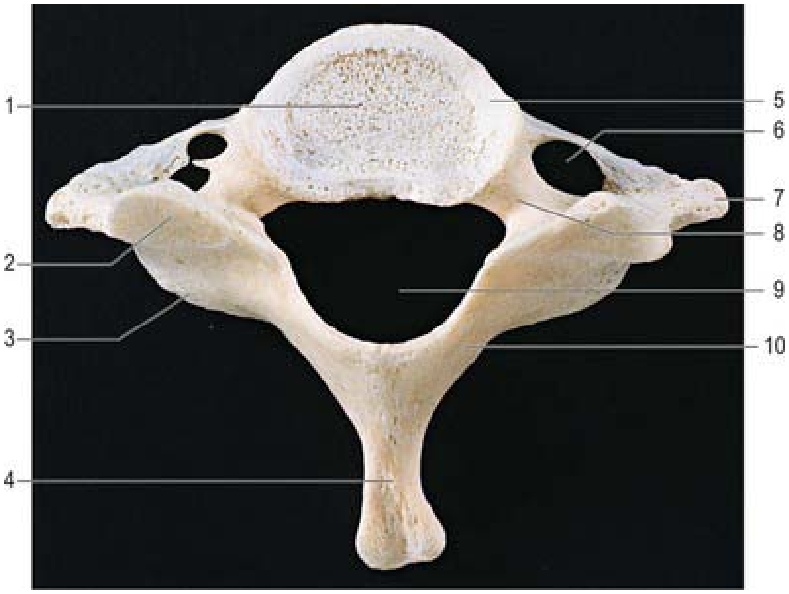

Fig. 42.26 Seventh cervical vertebra, superior aspect. **1**. Body. **2**. Superior articular facet. **3**. Inferior articular process. **4**. Spinous process. **5**. Uncinate process. **6**. Foramen transversarium (foramina are asymmetrical in this specimen). **7**. Transverse process. **8**. Pedicle. **9**. Vertebral foramen. **10**. Lamina.

The costal lamella of the transverse process may be separate as a cervical rib. The foramina transversaria may be asymmetrical: sometimes one is absent if the costal lamella is undeveloped.

Muscle attachments

Trapezius, spinalis capitis, semispinalis thoracis, multifidus and interspinales all attach to the tubercle of the spinous process. The anterior border of the transverse process receives the attachment of scalenus minimus (pleuralis), when present. The first pair of levatores costarum is attached to the transverse processes.

Ossification

Ossific centres for the costal processes appear about the sixth month and join the body and transverse processes between the fifth and sixth years; they may remain separate and grow anterolaterally as cervical ribs. Separate ossific centres may, on occasion, also occur in the costal processes of the fourth to sixth cervical vertebrae.

THORACIC VERTEBRAE

Thoracic vertebrae in general and changes with descending level

All thoracic vertebral bodies display lateral costal facets and all but the lowest two or three transverse processes also have facets (Fig. 42.27). The facets articulate with the head of the rib (costocapitular facet) and its tubercle (costotubercular facet) respectively. The first and ninth to 12th vertebrae also have atypical features, but the remainder are very similar, except for relatively minor details.

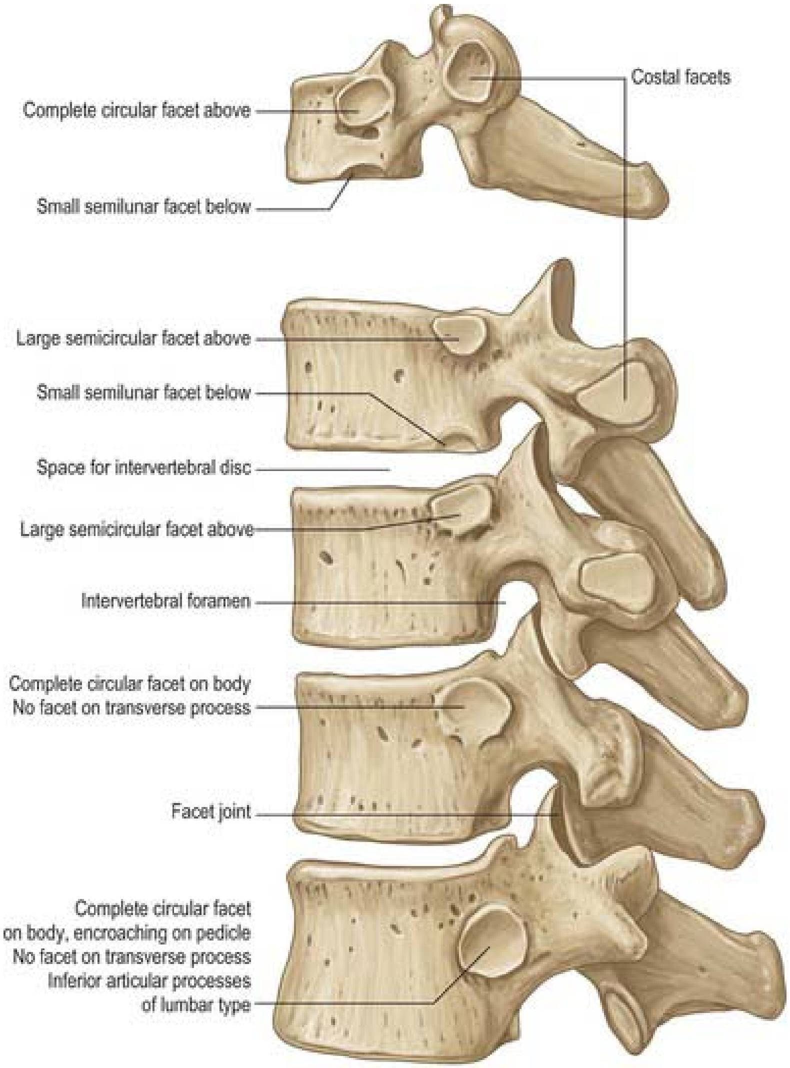
Costal facets
Complete circular facet above
Small semilunar facet below
Large semicircular facet above
Small semilunar facet below
Space for intervertebral disc
Large semicircular facet above
Intervertebral foramen
Complete circular facet on body
No facet on transverse process
Facet joint
Complete circular facet
on body, encroaching on pedicle
No facet on transverse process
Inferior articular processes
of lumbar type

Fig. 42.27 The first, ninth, tenth, eleventh and twelfth thoracic vertebrae, lateral aspect.

The body is typically a waisted cylinder (Fig. 42.28) except where the vertebral foramen encroaches, and transverse and anteroposterior dimensions are almost equal. On each side there are two costal facets (which are really demifacets): the superior and usually larger pair at the upper border are anterior to the pedicles, while the inferior pair at the lower border are anterior to the vertebral notches. The vertebral foramen (Fig. 42.14) is small and circular, so the pedicles do not diverge as they do in cervical vertebrae: the thoracic spinal cord is smaller and more circular than the cervical cord. The laminae are short, thick and broad, and overlap from above downwards. The spinous process slants downward. The thin and almost flat superior articular processes project from the pediculolaminar junctions and face posteriorly and a little superolaterally. The inferior processes project down from the laminae and their facets are directed forwards and a little superomedially. The large, club-like transverse processes also project from the pediculolaminar junctions. Each passes posterolaterally and bears, near its tip, anterior oval facets for articulation with the tubercle of the corresponding rib.

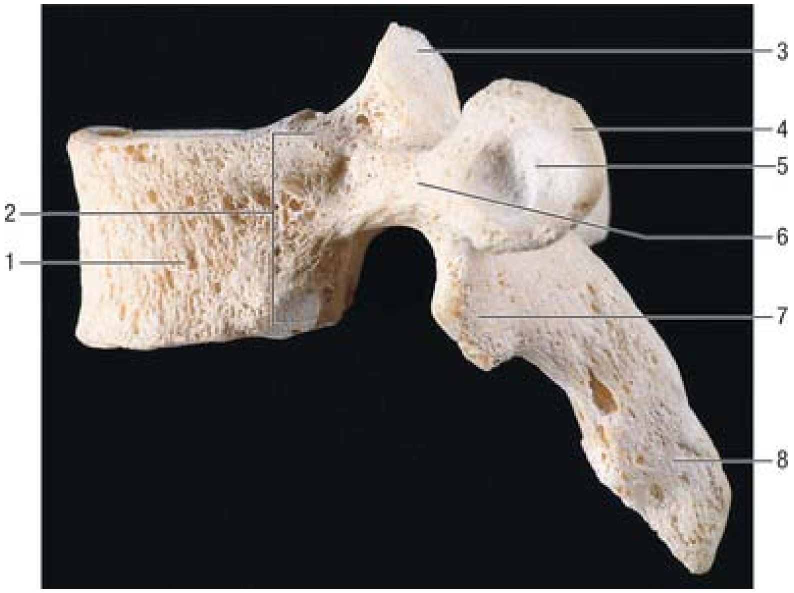

Fig. 42.28 Fourth thoracic vertebra, lateral aspect. **1**. Body. **2**. Costocapitular demifacets. **3**. Superior articular facet. **4**. Transverse process. **5**. Costotubercular facet. **6**. Pedicle. **7**. Inferior articular process. **8**. Spinous process.

The bodies of upper thoracic vertebrae gradually change from cervical to thoracic in type, and the lower change from thoracic to lumbar. The body of the first is typically cervical, its transverse diameter being almost twice the anteroposterior; the second retains a cervical shape, but its two diameters differ less. The third body is the smallest, and has a convex anterior aspect unlike the flattened first and second thoracic vertebrae. The remaining bodies increase in size and, because of its increased anteroposterior diameter, the fourth is typically ‘heart-shaped’. The fifth to eighth increase their anteroposterior dimension but change little transversely. These four, in transverse section, are asymmetrical, their left sides being flattened by pressure of the thoracic aorta. The rest increase more rapidly in all measurements, so that the 12th body resembles that of a typical lumbar vertebra. These modifications may contribute to the greater range of flexion-extension seen at the cervical and lumbar ends of the thoracic vertebral column.

The anterior and posterior longitudinal ligaments are attached to the borders of the bodies, and around the margins of the costal facets there are the capsular and radiate ligaments of the costovertebral joints. Thoracic pedicles show a successive caudal increase in thickness. The superior vertebral notch is recognizable only in the first thoracic vertebra, whereas the inferior notch is deep in all. Ligamenta flava are attached at the upper borders and lower anterior surfaces of the laminae.

Thoracic transverse processes shorten in caudal succession. In the upper five or six vertebrae the costal facets are concave and face anterolaterally, and at lower levels the facets are flatter and face superolaterally and slightly forwards. The costotransverse ligament is attached to the anterior surface medial to the facet; the lateral costotransverse ligament is attached to its tuberculated apex and the superior costotransverse ligament is attached to its lower border.

Thoracic spines overlap from the fifth to the eighth vertebra, whose spine is the longest and most oblique. Supraspinous and interspinous ligaments are attached to the spines.

A change in orientation of articular processes from thoracic to lumbar type usually occurs at the 11th thoracic vertebra, but sometimes at the 12th or 10th. In the transitional vertebra the superior articular processes are thoracic, and face posterolaterally, while the inferior are transversely convex and face anterolaterally. The transitional vertebra marks the site of a sudden change of mobility from predominantly rotational to predominantly flexion–extension.

Muscle attachments

Longus colli arises from the upper three thoracic vertebral bodies, lateral to the anterior longitudinal ligament, and psoas major and minor arise from the sides of the 12th near its lower border. Upper and lower borders of the transverse processes provide attachment for the intertransverse muscles or their fibrous vestiges. The posterior surfaces of the transverse processes provide attachment for the deep dorsal muscles, and levator costae is attached posteriorly on the apex. Trapezius, rhomboid major and minor, latissimus dorsi, serratus posterior superior and inferior and many deep dorsal muscles are attached to the spines. Rotatores attach to the posterior aspects of the laminae.

Ossification

Thoracic vertebrae all ossify according to the standard vertebral pattern described on page 768.

T1

The first thoracic vertebra (Fig. 42.27) resembles a cervical vertebra in its body, both in shape and in the distinctive posterolateral ‘lipping’ which forms the anterior border of the superior vertebral notch. There are circular superior costal facets for articulation with the whole facet on the head of the first rib.

The smaller, semilunar inferior facets articulate with a demifacet on the head of the second rib. The upper costal facet is often incomplete, in which case the first rib articulates with the seventh cervical vertebra and the intervening disc. A small, deep depression often occurs below the facet. The long, thick spine is horizontal and commonly as prominent as that of the seventh cervical vertebra.

T9

The ninth thoracic vertebra (Fig. 42.27) is otherwise typical, but it often fails to articulate with the tenth ribs, in which case the inferior demifacets are absent.

T10

The 10th thoracic vertebra (Fig. 42.27) only articulates with the 10th pair of ribs, so that superior facets only appear on the body. These are usually large and semilunar, but are oval when the tenth ribs fail to articulate with the ninth vertebra and intervening disc. The transverse process may or may not bear a facet for the tubercle of the 10th rib.

T11

The 11th thoracic vertebra (Fig. 42.27) articulates only with the heads of the 11th ribs. The circular costal facets are close to the upper border of the body and extend onto the pedicles. The small transverse processes lack articular facets. The 11th and 12th thoracic spinous processes are triangular, with blunt apices, a horizontal lower and an oblique upper border.

T12

The 12th thoracic vertebra (Fig. 42.27) articulates with the heads of the 12th ribs by circular facets somewhat below the upper border, spreading on to the pedicles. The body is large and the vertebra has some lumbar features. The transverse process is replaced by three small tubercles: the superior is largest, projects upwards and corresponds to a lumbar mammillary process, though it does not lie as close to the superior articular process; the lateral tubercle is the homologue of a transverse process; the inferior is the homologue of a lumbar accessory process. The superior and inferior processes are surprisingly long in some specimens.

LUMBAR VERTEBRAE

Lumbar vertebrae in general

The five lumbar vertebrae are distinguished by their large size and absence of costal facets and transverse foramina. The body is wider transversely (Fig. 42.29, see Fig. 42.33B). The vertebral foramen is triangular, larger than at thoracic levels but smaller than at cervical levels. The pedicles are short. The spinous process is almost horizontal, quadrangular and thickened along its posterior and inferior borders. The superior articular processes bear vertical concave articular facets facing posteromedially, with a rough mammillary process on their posterior borders (Fig. 42.30A). The inferior articular processes have vertical convex articular facets which face anterolaterally. The transverse processes are thin and long, except on the more substantial fifth pair. A small accessory process marks the posteroinferior aspect of the root of each transverse process. The accessory and mammillary processes are linked by a fine ligament, the mammillo-accessory ligament, which is sometimes ossified, and beneath which runs the medial branch of the dorsal primary ramus of the spinal nerve (Bogduk 2005).

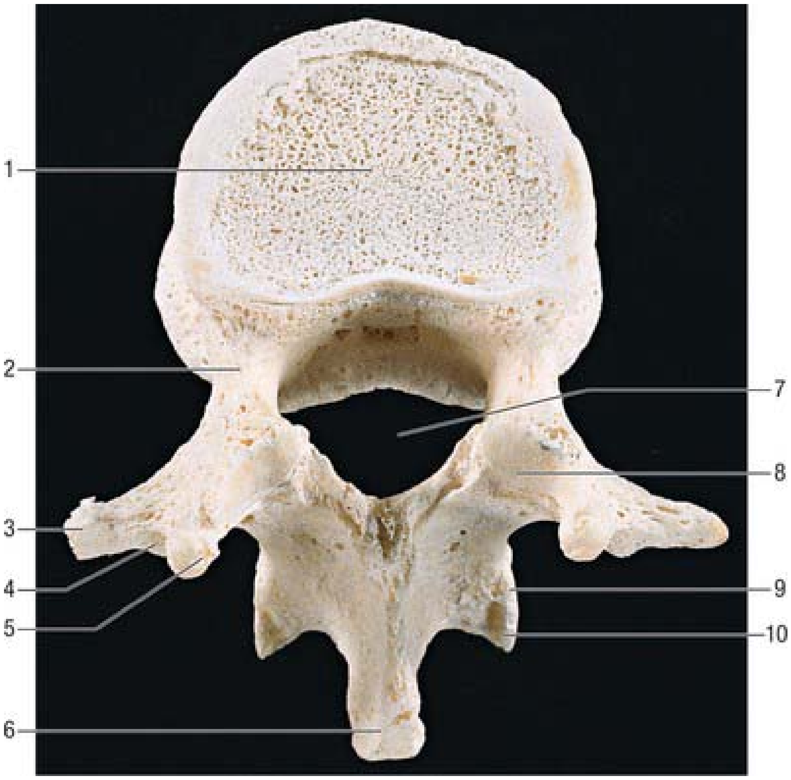

Fig. 42.29 First lumbar vertebra, superior aspect. **1**. Body. **2**. Pedicle. **3**. Transverse process. **4**. Accessory process. **5**. Mammillary process. **6**. Spinous process. **7**. Vertebral foramen. **8**. Superior articular facet. **9**. Lamina. **10**. Inferior articular facet.

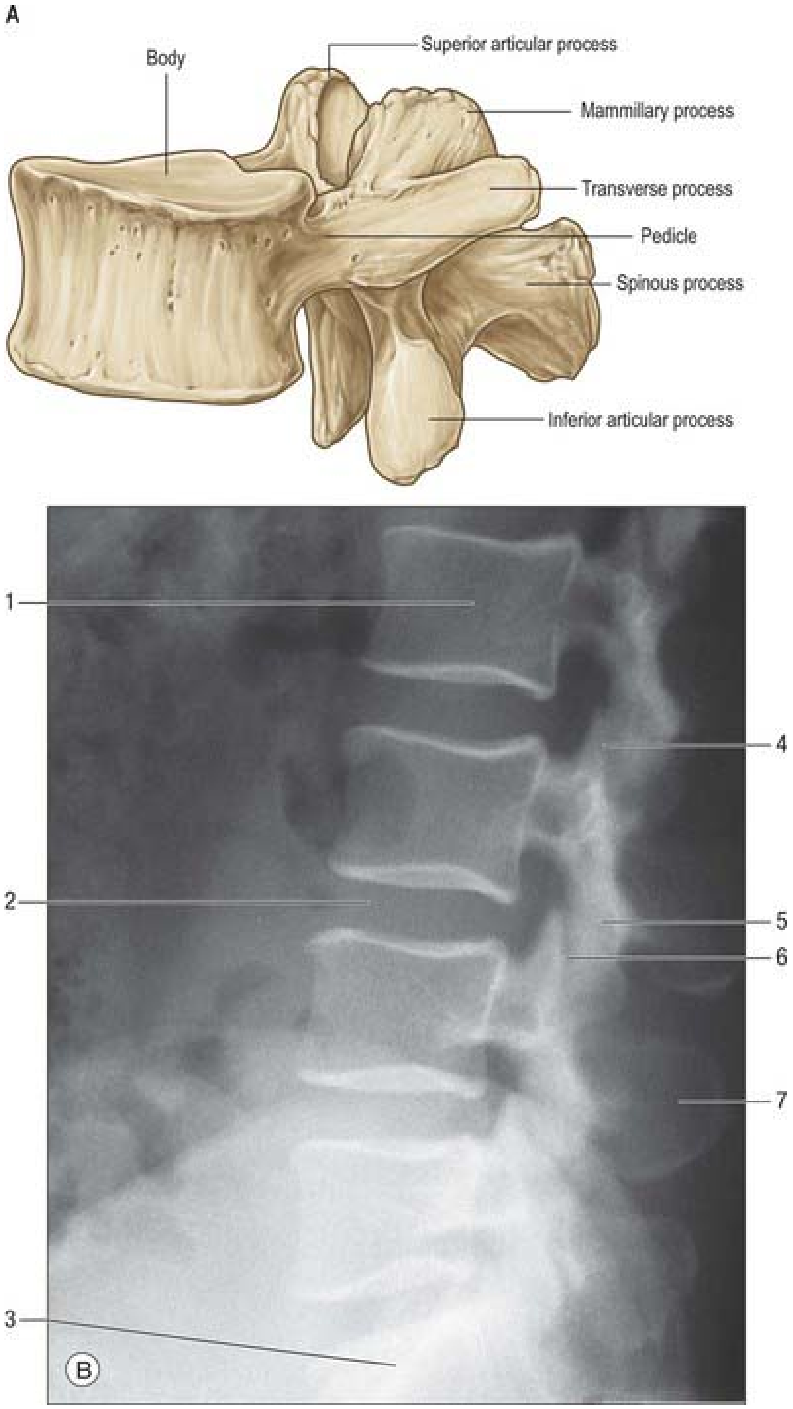
A
Body
Superior articular process
Mammillary process
Transverse process
Pedicle
Spinous process
Inferior articular process
1
2
3
4
5
6
7
B

Fig. 42.30 Lumbar spine. **A**, Lumbar vertebra, lateral aspect. **B**, Lateral radiograph, 24-year-old male. **1**. L2 vertebral body. **2**. Site of L3–4 intervertebral disc. **3**. S1 vertebral body. **4**. Superior facet. **5**. Inferior facet. **6**. L3–4 facet joint. **7**. L4 spinous process.

Strong paired pedicles arise posterolaterally from each body near its upper border. Superior vertebral notches are shallow and the inferior ones are deep. The laminae are broad and short, but do not overlap as much as those of the thoracic vertebrae. The fifth spine is the smallest, and its apex is often rounded and down-turned. Upper lumbar superior articular processes are further apart than inferior ones, but the difference is slight in the fourth and negligible in the fifth. The articular facets are reciprocally concave (superior) and convex (inferior), which allows flexion, extension, lateral bending and some degree of rotation. There are sex differences in the angle of inclination and depth of curvature of the articular facets. The facets are sometimes asymmetrical. Transverse processes, except the fifth, are anteroposteriorly compressed and project posterolaterally. The lower border of the fifth transverse process is angulated, passes laterally and then superolaterally to a blunt tip, and the whole process presents a greater upward inclination than the fourth. The angle on the inferior border may represent the tip of the costal element and the lateral end the tip of the true transverse process. The lumbar transverse processes increase in length from first to third and then shorten (Fig. 42.31). The fifth pair incline both upwards and posterolaterally. The costal element is incorporated in the mature transverse process.

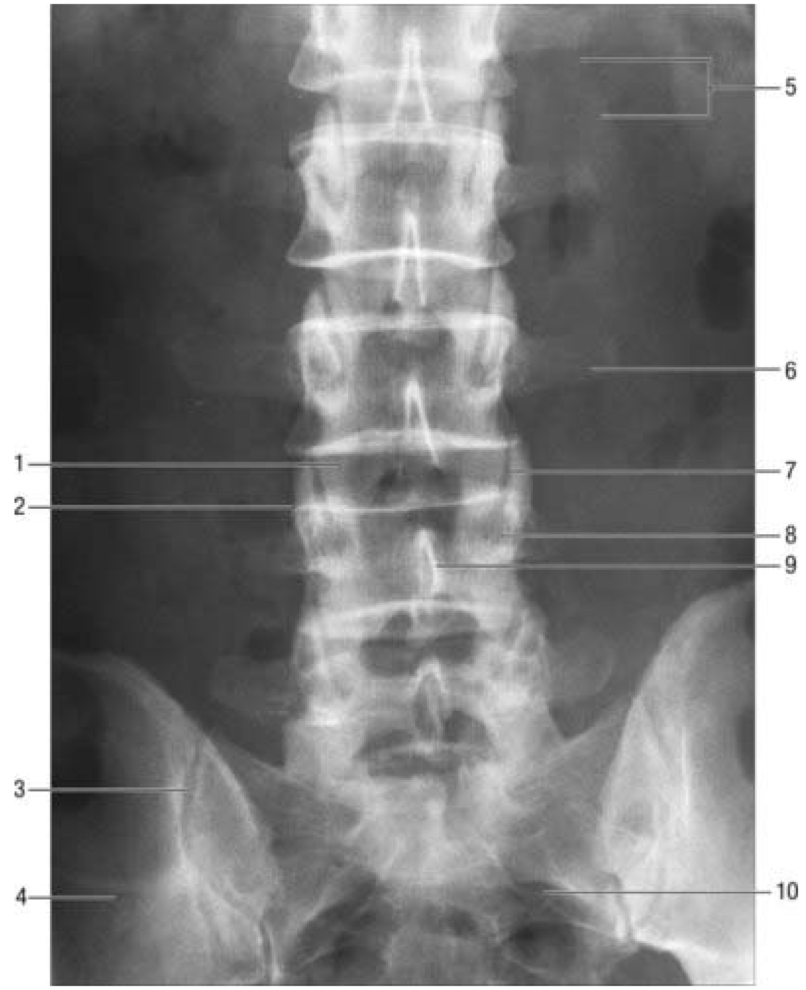

Fig. 42.31 Anteroposterior radiograph of lumbosacral spine in a 22-year-old male. **1**. L3 inferior articular process. **2**. L4 superior articular process. **3**. Right sacroiliac joint. **4**. Ilium. **5**. Psoas lateral border. **6**. L3 transverse process. **7**. Facet joint. **8**. L4 pedicle. **9**. L4 spinous process. **10**. Anterior sacral foramen.

The first lumbar vertebral foramen contains the conus medullaris of the spinal cord, while lower foramina contain the cauda equina and spinal meninges (Fig. 42.11B, Fig. 42.32A). Variation occurs in the sagittal and coronal dimensions of the lumbar vertebral canal, both within and between normal populations.

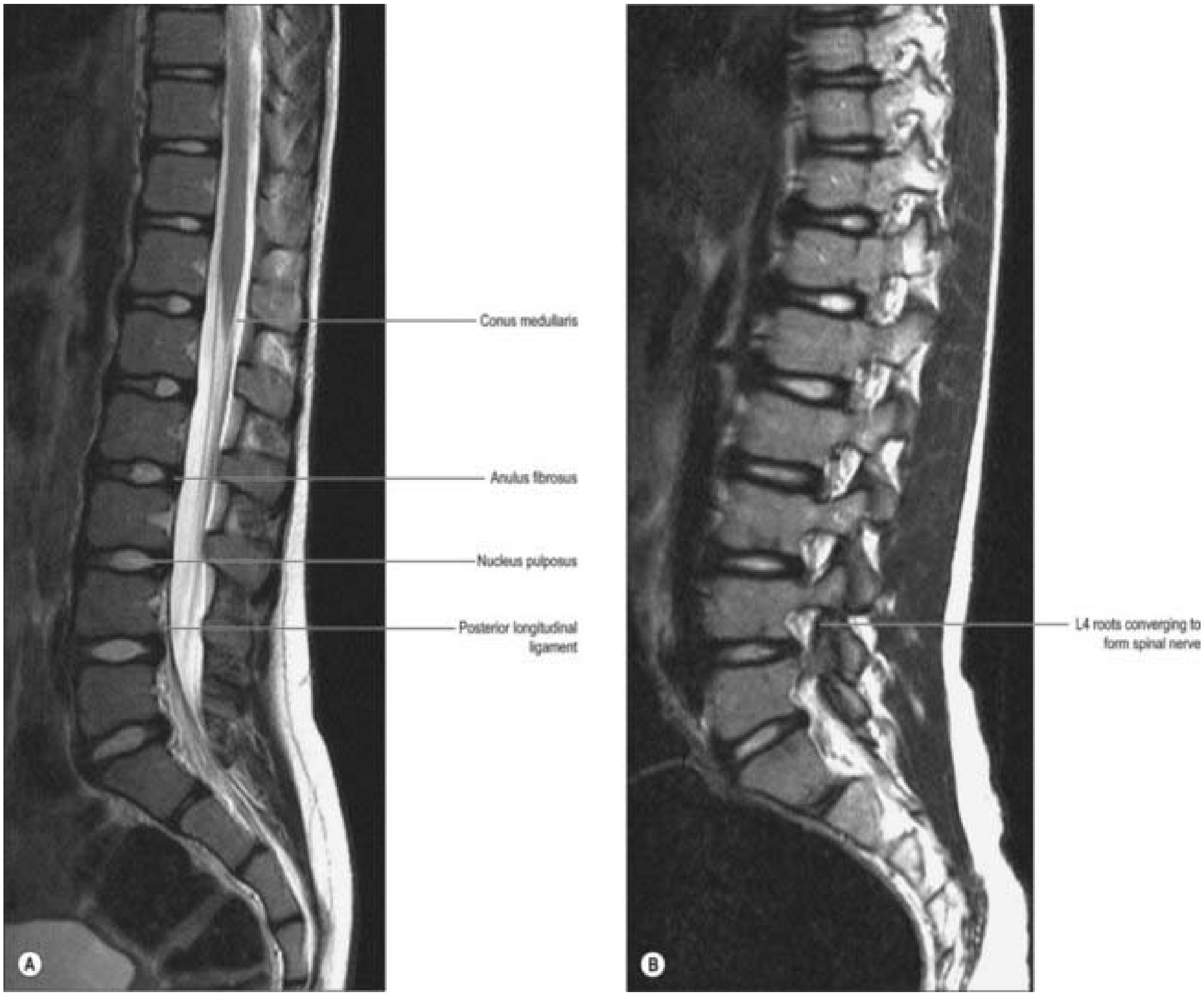
Conus medullaris
Anulus fibrosus
Nucleus pulposus
Posterior longitudinal ligament
L4 roots converging to form spinal nerve
A
B

Fig. 42.32 Lumbar spine. **A**, Median sagittal MRI. **B**, Paramedian sagittal MRI lumbar spine.

Muscle and fascial attachments (see also p. 708)

Upper and lower borders of lumbar bodies give attachment to the anterior and posterior longitudinal ligaments. The upper bodies (three on the right, two on the left) give attachments to the crura of the diaphragm lateral to the anterior longitudinal ligament. Posterolaterally, psoas major is attached to the upper and lower margins of all the lumbar bodies, and between them, tendinous arches carry its attachments across their concave sides (see Fig. 62.5). The posterior lamella of the thoracolumbar fascia, erectores spinae, spinales thoracis, multifidi, interspinal muscles and ligaments, and supraspinous ligaments are all attached to spinous processes. All lumbar transverse processes present a vertical ridge on the anterior surface, nearer the tip, which marks the attachment of the anterior layer of the thoracolumbar fascia, and separates the surface into medial and lateral areas for psoas major and quadratus lumborum respectively. The middle layer of the fascia is attached to the apices of the transverse processes; the medial and lateral arcuate ligaments attach to the vertical ridge on the anterior aspect of the first pair, and the iliolumbar ligament attaches to the apices of the fifth pair. Posteriorly the transverse processes are covered by deep dorsal muscles, and fibres of longissimus thoracis are attached to them and to their accessory processes. The ventral lateral intertransverse muscles are attached to their upper and lower borders, while the dorsal attach cranially to the accessory process and caudally to the upper border of the transverse process. The mammillary process, homologous with the superior tubercle of the 12th thoracic vertebra, gives attachment to multifidus and the medial intertransverse muscle. The latter also attaches to the accessory process, which is sometimes difficult to identify.

Ossification

Lumbar vertebrae ossify according to the standard vertebral pattern described on page 768, but also have two additional centres for the mammillary processes. A pair of scale-like epiphyses usually appear on the tips of the costal elements of the fifth lumbar vertebra (Fig. 42.23).

L5

The fifth lumbar vertebra (Fig. 42.33) has a massive transverse process which is continuous with the whole of the pedicle and encroaching on the body. The body is usually the largest and markedly deeper anteriorly, so contributing to the lumbosacral angle.

Segmentation anomalies (sacralization) are considered below with the sacrum. The costal element of the first lumbar vertebra may form a short lumbar rib, which articulates with the transverse process, but not usually with the body, of the vertebra.

SACRUM

The sacrum is a large, triangular fusion of five vertebrae and forms the posterosuperior wall of the pelvic cavity, wedged between the two hip (innominate) bones. Its blunted, caudal apex articulates with the coccyx and its superior, wide base with the fifth lumbar vertebra at the lumbosacral angle. It is set obliquely and curved longitudinally, the dorsal surface is convex, and the pelvic surface is concave: this ventral curvature increases pelvic capacity. Between base and apex are dorsal, pelvic and lateral surfaces and a sacral canal. In childhood, individual sacral vertebrae are connected by cartilage, and the adult bone retains many vertebral features. The sacrum consists of trabecular bone enveloped by a shell of compact bone of varying thickness.

Base

The base (Fig. 42.34) is the upper surface of the first sacral vertebra, the least modified from the typical vertebral plan. The body is large and wider transversely, and its anterior projecting edge is the sacral promontory. The vertebral foramen is triangular, its pedicles are short and diverge posterolaterally. The laminae are oblique, inclining down posteromedially to meet at a spinous tubercle. The superior articular processes project cranially, with concave articular facets directed posteromedially to articulate with the inferior articular processes of the fifth lumbar vertebra. The posterior part of each process projects backwards and its lateral aspect bears a rough area homologous with a lumbar mammillary process.

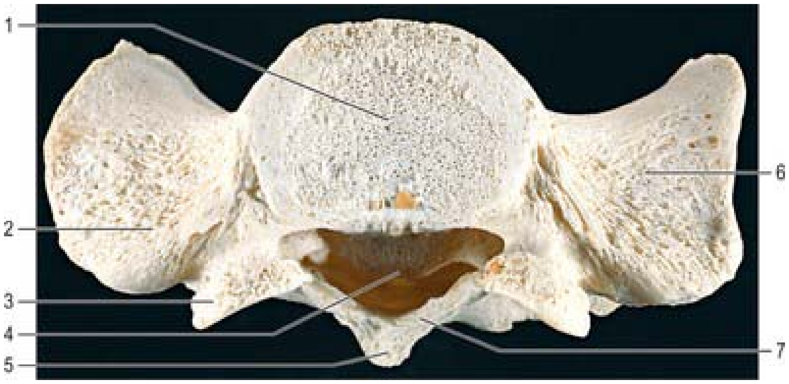

Fig. 42.34 Sacrum, superior aspect (base). **1**. Body of S1. **2**. Posterosuperior ala (transverse process element). **3**. Superior articular process. **4**. Sacral canal. **5**. Spinous process of S1. **6**. Anterosuperior ala (costal element). **7**. Lamina.

The transverse process is much modified as a broad, sloping mass which projects laterally from the body, pedicle and superior articular process. It is formed by the fusion of the transverse process and the costal element to each other and to the rest of the vertebra, and forms the upper surface of the sacral lateral mass or ala.

Terminal fibres of the anterior and posterior longitudinal ligaments are attached to the ventral and dorsal surfaces of the first sacral body. Its upper laminar borders receive the lowest pair of ligamenta flava. The ala is smooth superiorly, concave medially and rough laterally, and covered almost entirely by psoas major. The smooth area is grooved obliquely by the lumbosacral trunk. The rough area is for the lower band of the iliolumbar ligament, which lies lateral to the fifth lumbar spinal nerve and to the anterior sacroiliac ligament.

Pelvic surface

The anteroinferior pelvic surface (Fig. 42.35) is vertically and transversely concave, but the second sacral body may produce a convexity. Four pairs of pelvic sacral foramina communicate with the sacral canal through intervertebral foramina, and transmit ventral rami of the upper four sacral spinal nerves. The large area between the right and left foramina, which is formed by the flat pelvic aspects of the sacral bodies, bears evidence of their fusion at four transverse ridges. The longitudinal bars between the foramina are costal elements, which fuse to the vertebrae. Lateral to the foramina the costal elements unite. Posteriorly they unite with the transverse processes to form the lateral part of the sacrum, which expands basally as the ala.

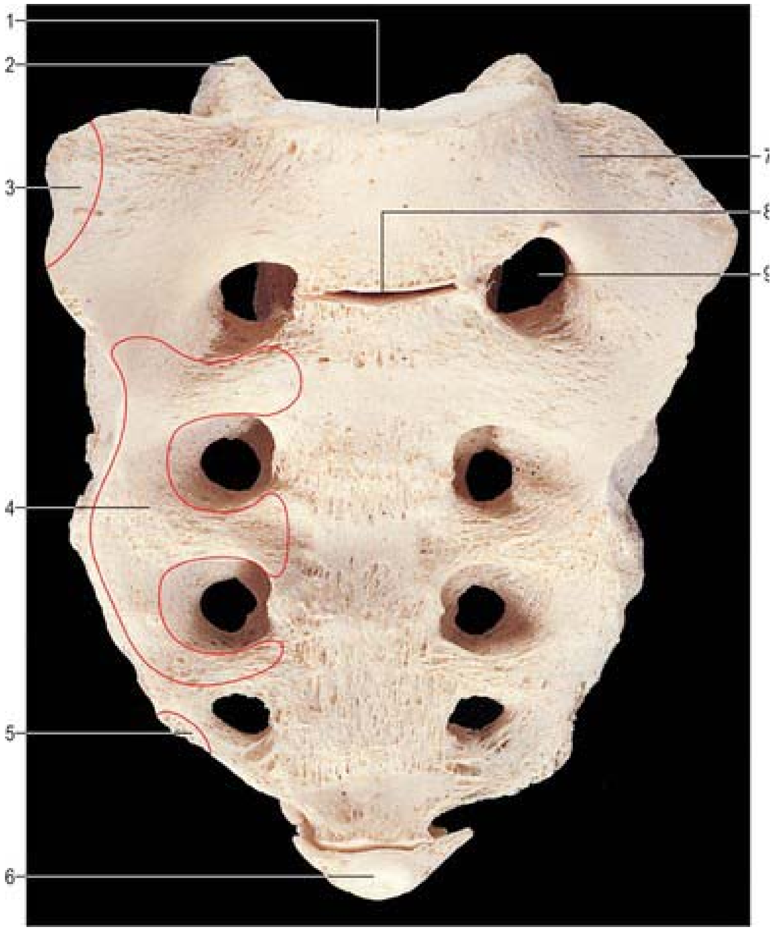

Fig. 42.35 Sacrum, anterior (pelvic) surface. **1**. Upper border of body of S1 (sacral promontory). **2**. Superior articular process of S1. **3**. Attachment of iliacus. **4**. Attachment of piriformis. **5**. Attachment of coccygeus. **6**. Coccyx. **7**. Ala. **8**. Incompletely fused S1–2 intervertebral joint. **9**. First pelvic sacral foramen.

The first three sacral ventral rami emerge from the pelvic sacral foramina and pass anterior to piriformis. The sympathetic trunks descend in contact with bone, medial to the foramina, as do the median sacral vessels in the midline. Lateral to the foramina, lateral sacral vessels are related to bone. Ventral surfaces of the first, second, and part of the third sacral bodies are covered by parietal peritoneum and crossed obliquely, left of the midline, by the attachment of the sigmoid mesocolon. The rectum is in contact with the pelvic surfaces of the third to fifth sacral vertebrae and with the bifurcation of the superior rectal artery between the rectum and third sacral vertebra.

Dorsal surface

The posterosuperior aspect of the dorsal surface bears a raised, interrupted, median sacral crest with four (sometimes three) spinous tubercles which represent fused sacral spines (Fig. 42.36). Below the fourth (or third) tubercle there is an arched sacral hiatus in the posterior wall of the sacral canal. This hiatus is produced by the failure of the laminae of the fifth sacral vertebra to meet in the median plane, and as a result the posterior surface of the body of that vertebra is exposed on the dorsal surface of the sacrum. Flanking the median crest, the posterior surface is formed by fused laminae, and lateral to this are four pairs of dorsal sacral foramina. Like the pelvic foramina, they lead into the sacral canal through intervertebral foramina, and each transmits the dorsal ramus of a sacral spinal nerve. Medial to the foramina, and vertically below each articular process of the first sacral vertebra, is a row of four small tubercles, which collectively constitute the intermediate sacral crest. These are sometimes termed articular tubercles, and represent fused contiguous articular processes. The inferior articular processes of the fifth sacral vertebra are free and project downwards at the sides of the sacral hiatus as sacral cornua, connected to coccygeal cornua by intercornual ligaments. The interrupted roughened crest to the lateral side of the dorsal sacral foramina is the lateral sacral crest which is formed by fused transverse processes, whose apices appear as a row of transverse tubercles.

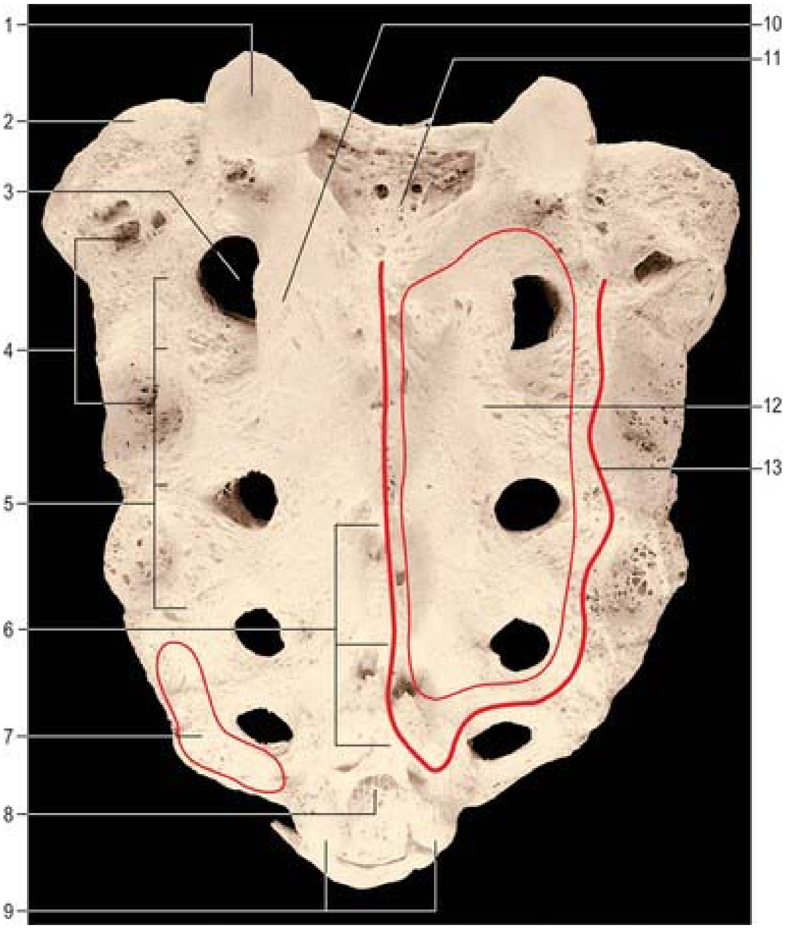

Fig. 42.36 Sacrum, posterior (dorsal) surface. **1**. Superior articular facet of S1. **2**. Ala. **3**. First dorsal sacral foramen. **4**. Attachments of interosseous sacroiliac ligaments. **5**. Lateral crest and transverse tubercles. **6**. Median crest and spinous processes. **7**. Attachment of gluteus maximus. **8**. Sacral hiatus. **9**. Cornua. **10**. Intermediate crest and articular tubercle (inferior articular process). **11**. Posterior surface of body of S1 forming anterior wall of sacral canal. **12**. Area of attachment of multifidus (bounded by thin line). **13**. Attachment of erector spinae aponeurosis (thick line).

The upper three sacral spinal dorsal rami pierce multifidus as they emerge via dorsal foramina.

Lateral surface

The lateral surface (Fig. 42.37A) is a fusion of transverse processes and costal elements. It is wide above, and rapidly narrows in its lower part. The broad upper part bears an auricular surface for articulation with the ilium, and the area posterior to this is rough and deeply pitted by the attachment of ligaments. The auricular surface, borne by costal elements, is like an inverted letter L. The shorter, cranial limb is restricted to the first sacral vertebra; the caudal limb descends to the middle of the third. Beyond this the lateral surface is non-articular and reduced in breadth. Caudally it curves medially to the body of the fifth sacral vertebra at the inferior lateral angle, beyond which the surface becomes a thin lateral border. A variable accessory sacral articular facet sometimes occurs, posterior to the auricular surface.

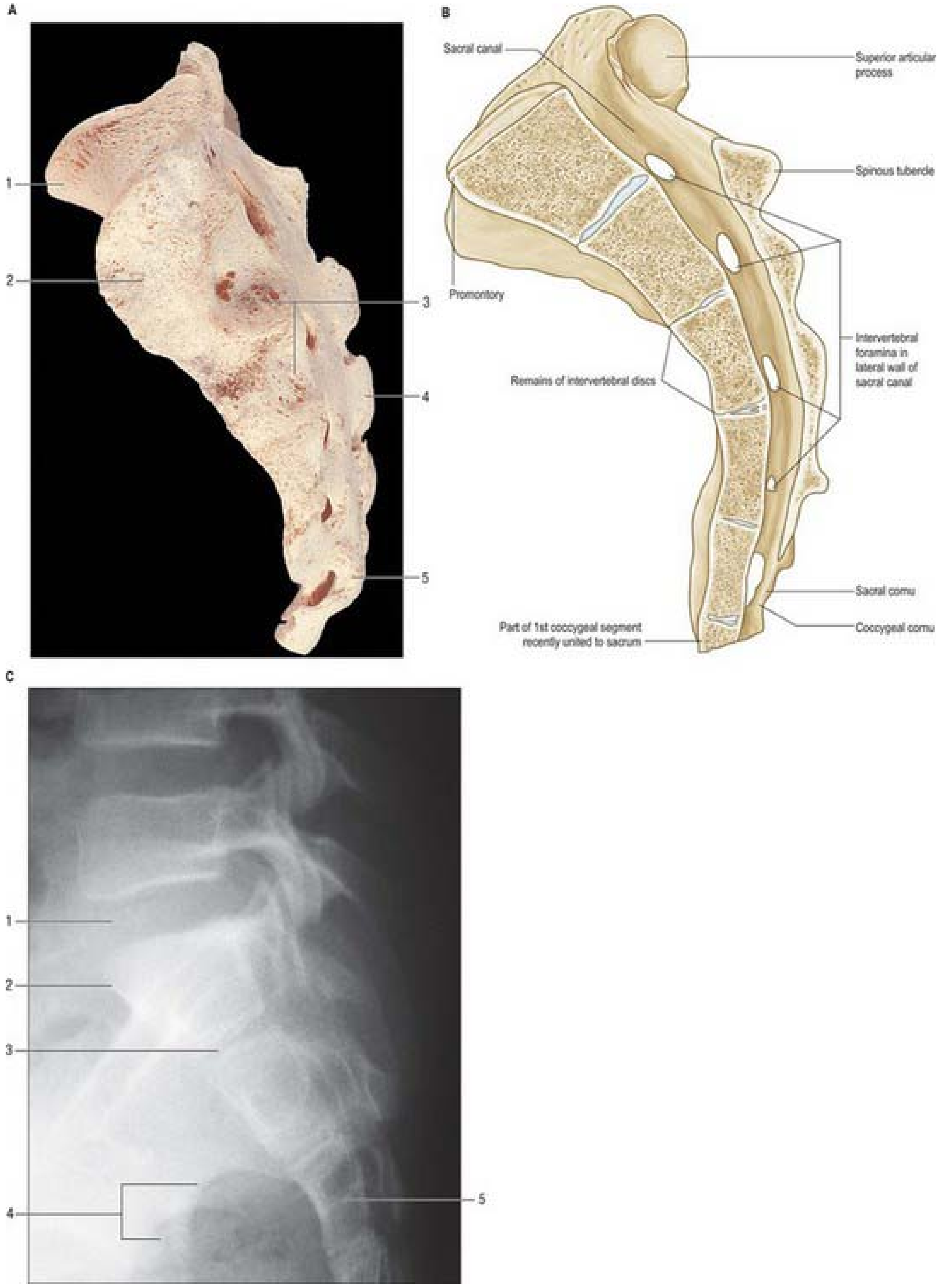
A
1
2
3
4
5
B
Sacral canal
Superior articular process
Spinous tubercle
Promontory
Intervertebral foramina in lateral wall of sacral canal
Remains of intervertebral discs
Sacral cornu
Coccygeal cornu
Part of 1st coccygeal segment recently united to sacrum
C
1
2
3
4
5

Fig. 42.37 **A**, Sacrum, lateral aspect: **1**. Promontory. **2**. Auricular (articular) surface. **3**. Attachments of interosseous sacroiliac ligaments. **4**. Spinous process. **5**. Sacral cornu (left). **B**, Median sagittal section through the sacrum. **C**. Lateral radiograph of lumbosacral junction in a 14-year-old

male **1**. L5–S1 disc. **2**. Sacral promontory. **3**. S1–2 disc. **4**. Greater sciatic notches. **5**. S3.

The auricular surface is covered by hyaline cartilage, and formed entirely by costal elements. It shows cranial and caudal elevations and an intermediate depression, behind which a third elevation is visible in the elderly. The surface becomes more corrugated with age. The rough area behind the auricular surface shows two or three marked depressions for the attachment of strong interosseous sacroiliac ligaments. Below the auricular surface the sacrotuberous and sacrospinous ligaments are attached between gluteus maximus dorsally and coccygeus ventrally.

Apex

The apex is the inferior aspect of the fifth sacral vertebral body, and bears an oval facet for articulation with the coccyx.

Sacral canal

The sacral canal (Fig. 42.37B) is formed by sacral vertebral foramina, and is triangular in section (Fig. 42.34). Its upper opening, seen on the basal surface, appears to be set obliquely. The inclination of the sacrum means that it is directed cranially in the standing position. Each lateral wall presents four intervertebral foramina, through which the canal is continuous with pelvic and dorsal sacral foramina. Its caudal opening is the sacral hiatus. The canal contains the cauda equina and the filum terminale, and the spinal meninges. Opposite the middle of the sacrum, the subarachnoid and subdural spaces close: the lower sacral spinal roots and filum terminale pierce the arachnoid and dura mater at that level. The filum terminale with its meningeal coverings emerges below the sacral hiatus and passes downwards across the dorsal surface of the fifth sacral vertebra and sacrococcygeal joint to reach the coccyx. The fifth sacral spinal nerves also emerge through the hiatus medial to the sacral cornua, and groove the lateral aspects of the fifth sacral vertebra.

Muscle attachments

The pelvic surface gives attachment to piriformis in its second to fourth segments, to iliacus superolaterally, and to coccygeus inferolaterally. The dorsal surface gives attachment to the aponeurosis of erector spinae along a U-shaped area of spinous and transverse tubercles, covering multifidus which occupies the enclosed area (Fig. 42.34). On the lateral border below the auricular surface, gluteus maximus is attached dorsal and coccygeus is attached ventral to the sacrotuberous and sacrospinous ligaments.

Ossification

The sacrum resembles typical vertebrae in the ossification of its segments (Fig. 42.38). Primary centres for the centrum and each half vertebral arch appear between the 10th and 20th weeks. Primary centres for the costal elements of the upper three or more segments appear superolateral to the pelvic sacral foramina, between the sixth and eighth prenatal months. Each costal element unites with its half vertebral arch between the second and fifth years, and the conjoined element so formed unites anteriorly with the centrum and posteriorly with its opposite fellow at about the eighth year. Thereafter the upper and lower surfaces of each sacral body are covered by an epiphysial plate of hyaline cartilage which is separated from its neighbour by the fibrocartilaginous precursor of an intervertebral disc. Laterally, successive conjoined vertebral arches and costal elements are separated by hyaline cartilage; a cartilaginous epiphysis, sometimes divided into upper and lower parts, develops on each auricular and adjacent lateral surface. Soon after puberty the fused vertebral arches and costal elements of adjacent vertebrae begin to coalesce from below upwards. At the same time individual epiphysial centres develop for the upper and lower surfaces of bodies, spinous tubercles, transverse tubercles and costal elements.

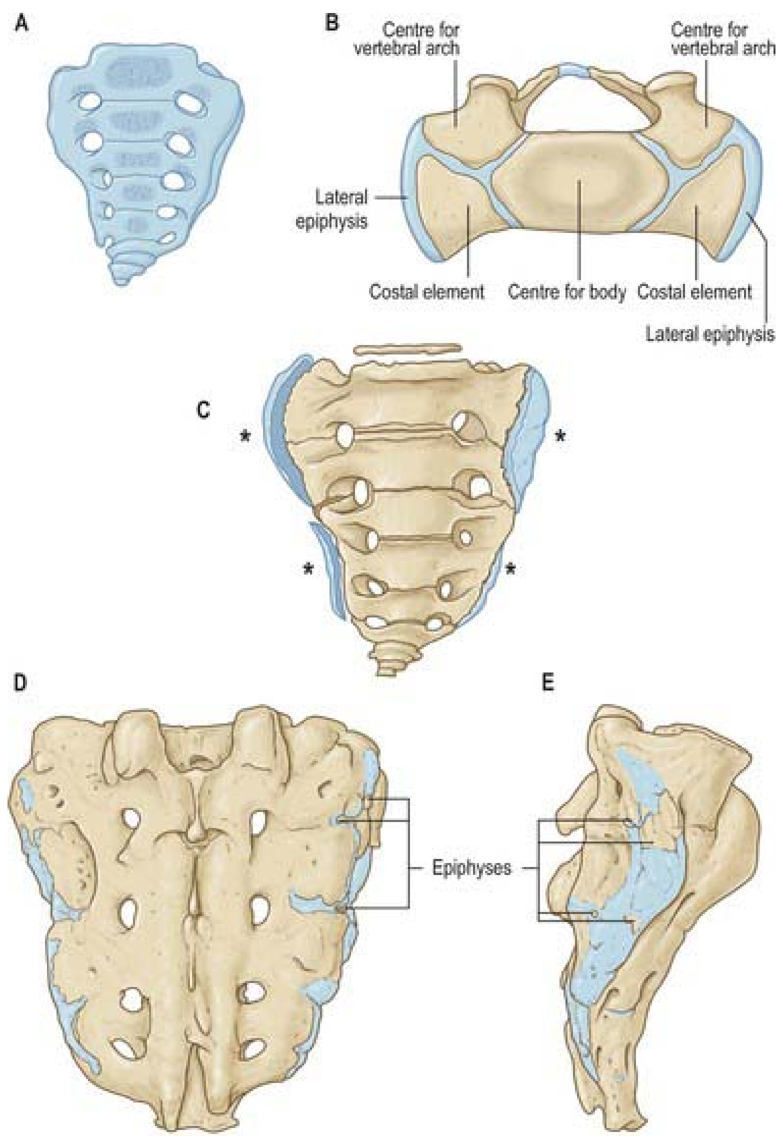
A
B
Centre for vertebral arch
Centre for vertebral arch
Lateral epiphysis
Costal element
Centre for body
Costal element
Lateral epiphysis
C
*
*
*
*
D
E
Epiphyses

Fig. 42.38 Ossification of the sacrum and coccyx. **A**, At birth. **B**, The base of the sacrum of a child about four years old. **C**, At the 25th year: epiphysial plates for each lateral surface are marked by asterisks. **D**, **E**, The epiphyses of the costal and transverse process of the sacrum at the 18th year.

The costal epiphysial centres appear at the lateral extremities of the hyaline cartilages between adjacent costal elements; two anterior and two posterior centres appear in each of the intervals between the first, second and third sacral vertebrae. Ossification spreads from these into the auricular epiphysial plates. One costal epiphysial centre, placed anteriorly, occurs in each remaining interval and from them ossification spreads to the epiphysial plate covering the lower part of the lateral surface of the sacrum. Sacral bodies unite at their adjacent margins after the twentieth year, but the central and greater part of each intervertebral disc remains unossified up to or beyond middle life.

Variants

The sacrum may contain six vertebrae, by development of an additional sacral element or by incorporation of the fifth lumbar or first coccygeal vertebrae. Inclusion of the fifth lumbar vertebra (sacralization) is usually incomplete and limited to one side. In the most minor degree of the abnormality a fifth lumbar transverse process is large and articulates, sometimes by a synovial joint, with the sacrum at the posterolateral angle of its base. Reduction of sacral constituents is less common but lumbarization of the first sacral vertebra does occur: it remains partially or completely separate. The bodies of the first two sacral vertebrae may remain unfused when the lateral masses are fused. The dorsal wall of the sacral canal may be variably deficient, due to imperfect development of laminae and spines. Orientation of the superior sacral articular facets displays wide variation, as does the sagittal curvature of the sacrum. Asymmetry (facet tropism) of the superior facets alters the relation between the planes of the two lumbosacral facet joints.

Sex differences in sacra

Sex differences in sacra are described on page 1359.

COCCYX

The coccyx (Fig. 42.39) is a small triangular bone and is often asymmetrical in shape. It usually consists of four fused rudimentary vertebrae, although the number varies from three to five, and the first is sometimes separate. The bone is directed downwards and ventrally from the sacral apex: its pelvic surface is tilted upwards and forwards, its dorsum downwards and backwards. Orientation varies with mobility and between individuals.

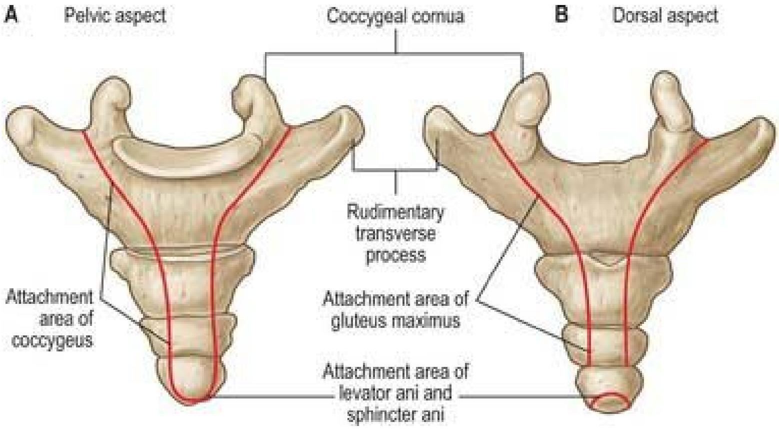
A
Pelvic aspect
Coccygeal cornua
B
Dorsal aspect
Rudimentary transverse process
Attachment area of coccygeus
Attachment area of gluteus maximus
Attachment area of levator ani and sphincter ani

Fig. 42.39 The coccyx. **A**, Anterior (pelvic) aspect. **B**, Posterior (dorsal) aspect.

The base or upper surface of the first coccygeal vertebral body has an oval, articular facet for the sacral apex. Posterolateral to this, two coccygeal cornua project upwards to articulate with sacral cornua: they are homologues of the pedicles and superior articular processes of other vertebrae. A rudimentary transverse process projects superolaterally from each side of the first coccygeal body and may articulate or fuse with the inferolateral sacral angle, completing the fifth sacral foramina.

The second to fourth coccygeal vertebrae diminish in size and are usually mere fused nodules. They represent rudimentary vertebral bodies, though the second may show traces of transverse processes and pedicles.

The gap between the fifth sacral body and the articulating cornua represents, on each side, an intervertebral foramen which transmits the fifth sacral spinal nerve. The dorsal ramus descends behind the rudimentary transverse process, and the ventral ramus passes anterolaterally between the transverse process and sacrum.

Muscle and ligament attachments

The lateral parts of the pelvic surface, including the rudimentary transverse processes, give attachment to the levatores ani and coccygei. The anterior sacrococcygeal ligament is attached to the front of the first and sometimes second coccygeal vertebral bodies (Fig. 80.8). The cornua give attachment to the intercornual ligaments. The lateral sacrococcygeal ligament connects the transverse process to the inferolateral sacral angle. Gluteus maximus is attached to the dorsal surface, and both levator ani and sphincter ani externus are attached to the tip of the bone. The median area gives attachment to the deep and superficial posterior sacrococcygeal ligaments, the superficial descending from the margins of the sacral hiatus and sometimes closing the sacral canal. The filum terminale, which is situated between the two ligaments, blends with them on the dorsum of the first coccygeal vertebra.

Ossification

Each coccygeal segment is ossified from one primary centre. A centre in the first segment appears about birth and its cornua may soon ossify from separate centres. Remaining segments ossify at wide intervals up to the 20th year or later. Segments slowly unite: union between the first and second is frequently delayed until 30 years. The coccyx often fuses with the sacrum in later decades, especially in females.

LIGAMENTS OF THE VERTEBRAL COLUMN

ANTERIOR LONGITUDINAL LIGAMENT

The anterior longitudinal ligament (Fig. 42.40B) is a strong band extending along the anterior surfaces of the vertebral bodies. It is broader caudally, thicker and narrower in thoracic than in cervical and lumbar regions, and is also relatively thicker and narrower opposite vertebral bodies than at the levels of intervertebral symphyses. It extends from the basilar part of the occipital bone to the anterior tubercle of C1 and the front of the body of C2, then continues caudally to the front of the upper sacrum. Its longitudinal fibres are strongly adherent to the intervertebral discs, hyaline cartilage end-plates and margins of adjacent vertebral bodies, and are loosely attached at intermediate levels of the bodies, where the ligament fills their anterior concavities, flattening the vertebral profile. At these various levels ligamentous fibres blend with the subjacent periosteum, perichondrium and periphery of the anulus fibrosus. The anterior longitudinal ligament has several layers. The most superficial fibres are the longest and extend over three or four vertebrae, the intermediate extend between two or three, and the deepest from one body to the next. Laterally, short fibres connect adjacent vertebrae.

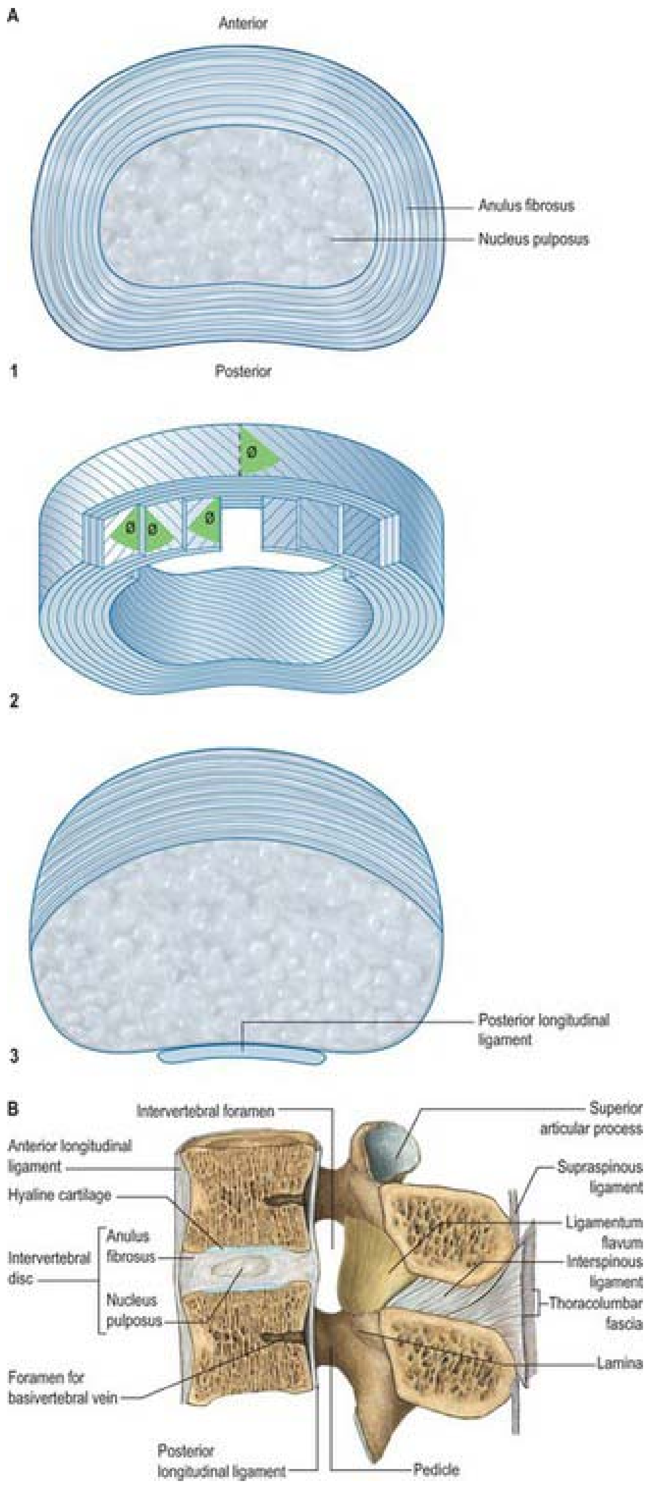
A
Anterior
Anulus fibrosus
Nucleus pulposus
1
Posterior
ø
ø
ø
ø
2
3
Posterior longitudinal ligament
B
Intervertebral foramen
Superior articular process
Anterior longitudinal ligament
Supraspinous ligament
Hyaline cartilage
Ligamentum flavum
Intervertebral disc
Anulus fibrosus
Interspinous ligament
Nucleus pulposus
Thoracolumbar fascia
Lamina
Foramen for basivertebral vein
Posterior longitudinal ligament
Pedicle

Fig. 42.40 **A**, The main structural features of an intervertebral disc. For clarity the number of fibrocartilaginous laminae has been greatly reduced. Note alternating obliquity of collagen fascicles in adjacent laminae. **1**. Lumbar disc. **2**. Detailed structure of anulus fibrosus. ø = approximately

65°. **3**. Cervical disc. (After Bogduk.) **B**, Median sagittal section through upper lumbar vertebral column showing discs and ligaments.

(From Sobotta 2006.)

POSTERIOR LONGITUDINAL LIGAMENT

The posterior longitudinal ligament (Fig. 42.41) lies on the posterior surfaces of the vertebral bodies in the vertebral canal, attached between the body of C2 and the sacrum, and continuous with the membrana tectoria above. Its smooth glistening fibres, attached to intervertebral discs, hyaline cartilage end-plates and adjacent margins of vertebral bodies, are separated between attachments by basivertebral veins and the venous channels which drain them into anterior internal vertebral plexuses. At cervical and upper thoracic levels the ligament is broad and of uniform width, but in lower thoracic and lumbar regions it is denticulated, narrow over vertebral bodies and broad over discs. Its superficial fibres bridge three or four vertebrae, while deeper fibres extend between adjacent vertebrae as perivertebral ligaments, which are close to and, in adults, fused with, the anulus fibrosus of the intervertebral disc. The layers of the posterior longitudinal ligament and the relationship of the ligament to associated membranes in the epidural space are fully discussed by Loughenbury et al (2006).

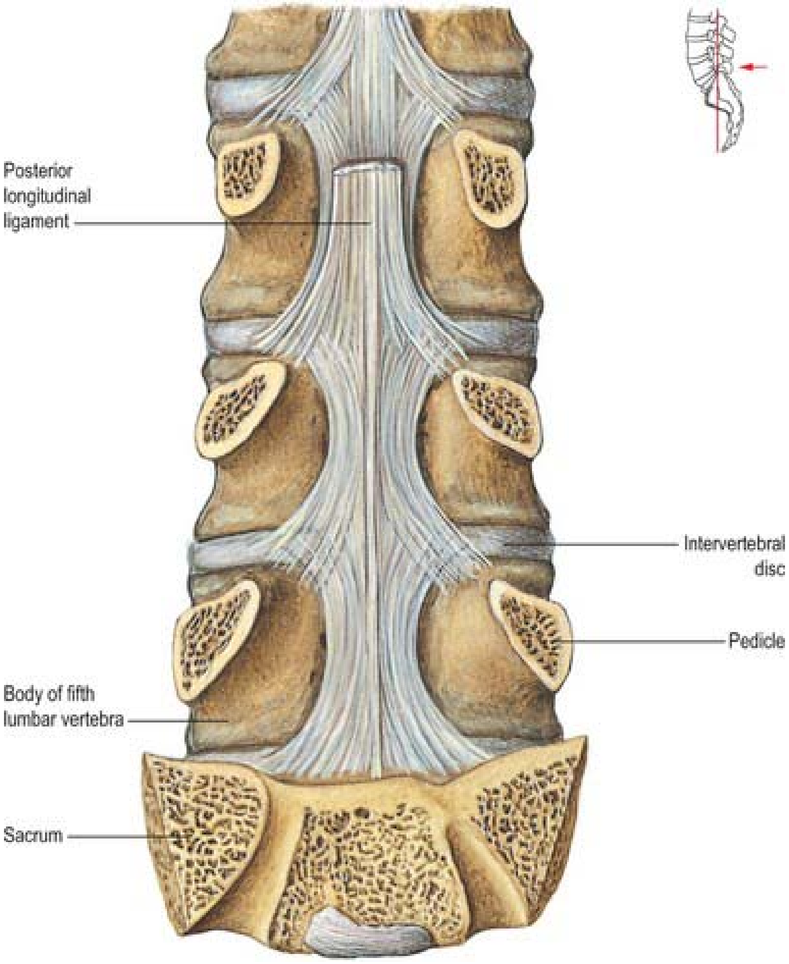
Posterior longitudinal ligament
Intervertebral disc
Pedicle
Body of fifth lumbar vertebra
Sacrum

Fig. 42.41 The posterior longitudinal ligament in the lumbar region.

(From Sobotta 2006.)

LIGAMENTA FLAVA

The ligamenta flava (Fig. 42.40B, Fig. 42.42) connect laminae of adjacent vertebrae in the vertebral canal. Their attachments extend from facet joint capsules to the point where laminae fuse to form spines. Here their posterior margins meet and are partially united; the intervals between them admit veins which connect the internal and posterior external vertebral venous plexuses. Their predominant tissue is yellow elastic tissue, whose almost perpendicular fibres descend from the lower anterior surface of one lamina to the posterior surface and upper margin of the lamina below. The anterior surface of the ligaments is covered by a fine, continuous smooth lining membrane (Newell 1999). The ligaments are thin, broad and long in the cervical region, thicker in the thoracic and thickest at lumbar levels. They arrest separation of the laminae in spinal flexion, preventing abrupt limitation, and also assist restoration to an erect posture after flexion, perhaps protecting discs from injury.

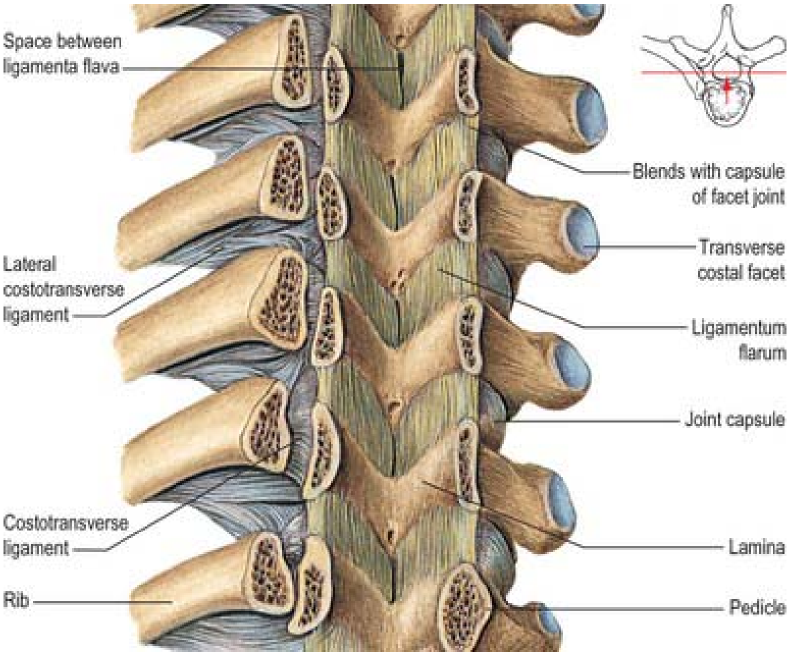
Space between ligamenta flava
Lateral costotransverse ligament
Costotransverse ligament
Rib
Blends with capsule of facet joint
Transverse costal facet
Ligamentum flarum
Joint capsule
Lamina
Pedicle

Fig. 42.42 Ligamenta flava and costotransverse ligaments (ventral aspect).

(From Sobotta 2006.)

INTERSPINOUS LIGAMENTS

Interspinous ligaments (Fig. 42.40B) connect the facing edges of consecutive spinous processes, and extend ventrally as far as the ligamentum flavum and dorsally to the supraspinous ligament, when this ligament is present (see below). They differ structurally in thoracic, lumbar and cervical levels. The thoracic interspinous ligaments are narrow and elongated, whereas those at lumbar levels are thick and quadrilateral, and occur as closely applied pairs, the left and right ligaments being separated by a narrow or potential cleft. In the lumbar ligaments, collagen fibres run obliquely inferiorly and ventrally and only the deepest fibres are truly ligamentous. The more dorsal fibres are derived from tendons of longissimus thoracis that dip into the interspinous space to gain attachment to the superior edge of the spinous process rather than to its tip. Distinctive interspinous ligaments are not evident at cervical levels, where they are represented by the median septum of the ligamentum nuchae as it passes between the cervical spinous processes.

SUPRASPINOUS LIGAMENT

The supraspinous ligament (Fig. 42.40B) is a strong fibrous cord which connects the tips of spinous process from C7 to L3 or L4. It is regularly deficient. The most superficial fibres extend over three or four vertebrae, the deeper span two or three, and the deepest connect adjacent spines and are continuous with the interspinous ligament. Most of the ligament is formed by the tendons of muscles with posterior midline attachments, i.e. semispinalis, longissimus, trapezius and latissimus dorsi. Only the most superficial fibres lack any connection with muscle. Below L4 the ligament is replaced by the decussating fibres of latissimus dorsi.

INTERTRANSVERSE LIGAMENTS

Intertransverse ligaments run between adjacent transverse processes. At cervical levels they consist of a few, irregular fibres which are largely replaced by intertransverse muscles; in the thoracic region they are cords intimately blended with adjacent muscles; in the lumbar region they are thin and membranous. For the detailed anatomy of the lumbar intertransverse ligaments, see Bogduk (2005).

LIGAMENTOUS INSTABILITY

Damage to the ligaments controlling stability of the column may occur in the absence of evident bony pathology. This is particularly prevalent in inflammatory disease of the upper cervical spine, where rheumatoid arthritis may weaken or destroy the ligaments on which atlanto-axial stability depends. The transverse ligament is stronger than the dens, which therefore usually fractures before the ligament ruptures. The alar ligaments are weaker, and combined head flexion and rotation may avulse one or both alar ligaments: rupture of one side results in an increase of about a third in the range of rotation to the opposite side. Pathological softening of the transverse and adjacent ligaments or of the lateral atlanto-axial joints results in atlanto-axial subluxation, which may cause spinal cord injury. Ligamentous damage may also occur in spinal injuries, particularly at cervical levels.

Developmental laxity of ligaments may also lead to problems with instability, especially if there is an episode of trauma: this combination is probably responsible for atlanto-axial rotational instability. Laxity of cervical spinal ligaments may be a normal variant in children, and lead to diagnostic difficulties. In radiographs of the upper cervical spine in children aged less than 8, a deceptive appearance of subluxation (‘pseudosubluxation’) may result from a combination of ligamentous laxity and facet orientation. This usually occurs between C2 and C3, but may occasionally be seen at C3/4. Clinical and other radiological features should facilitate the correct diagnosis.

JOINTS

All vertebrae from C2 to S1 articulate by secondary cartilaginous joints (symphyses) between their bodies, synovial joints between their articular processes, and fibrous joints between their laminae, transverse and spinous processes. In the cervical region, from C3 to C7, joints have been described between the uncinate or neurocentral processes of the inferior vertebral body and the bevelled lateral border of the superior body at each level. These small unco-vertebral or neurocentral ‘joints’ are absent at birth, do not contain synovium, and are probably clefts in the intervertebral discs.

INTERVERTEBRAL JOINTS

Joints between the vertebral bodies

Joints between vertebral bodies are symphyses. Typical vertebral bodies are united by anterior and posterior longitudinal ligaments and by fibrocartilaginous intervertebral discs between sheets of hyaline cartilage (vertebral end-plates).

Articulating surfaces: intervertebral discs

The intervertebral discs are the chief bonds between the adjacent surfaces of vertebral bodies from C2 to the sacrum. Except at the sites of the uncovertebral (neurocentral) joints of Luschka, disc outlines correspond with the adjacent bodies. Their thickness varies in different regions and within individual discs. Each disc consists of an outer lamellated anulus fibrosus and an inner nucleus pulposus. (Fig. 42.40A1).

In cervical and lumbar regions the discs are thicker anteriorly, contributing to the anterior convexity of the vertebral column. In the thoracic region they are nearly uniform, and the anterior concavity is largely due to the vertebral bodies. Discs are thinnest in the upper thoracic region and thickest in the lumbar region. They adhere to thin layers of cartilage on the superior and inferior vertebral surfaces, the vertebral end-plates. The latter do not reach the periphery of the vertebral bodies but are encircled by ring apophyses. The end-plates contain both hyaline cartilage and fibrocartilage. The fibrocartilaginous component lies nearer to the disc, and is sometimes considered not to be part of the end-plate itself. The fibrocartilaginous components of the end-plates above and below the nucleus pulposus, together with the innermost lamellae of the anulus fibrosus, form a flattened sphere of collagen which surrounds and encloses the nucleus (Fig. 42.43). The overall proportion of fibrocartilage in the end-plate increases with age. While all discs are attached to the anterior and posterior longitudinal ligaments, discs in the thoracic region are additionally tied laterally, by intra-articular ligaments, to the heads of ribs articulating with adjacent vertebrae. Intervertebral discs form about a quarter of the length of the postaxial vertebral column: cervical and lumbar regions make a greater contribution than the thoracic and are thus more pliant.

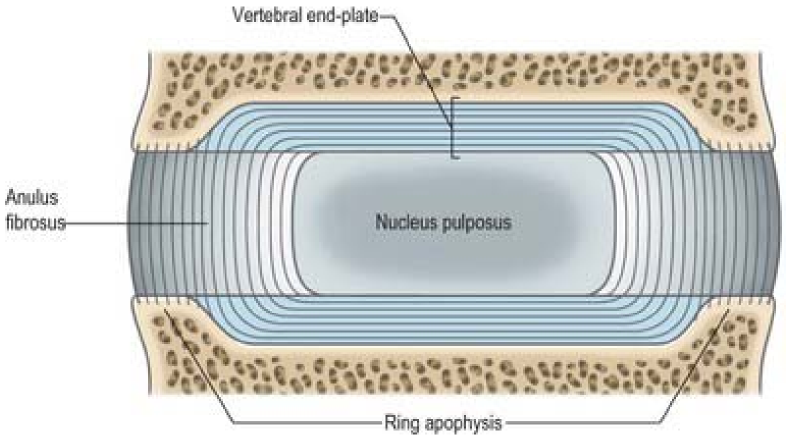

Fig. 42.43 Structure of the vertebral end-plate: the collagen fibres of the inner two-thirds of the anulus fibrosus sweep around into the vertebral end-plate and form its fibrocartilaginous component. The peripheral fibres of the anulus are anchored into the bone of the ring apophysis.

(By permission from Bogduk N 1997 Clinical Anatomy of the Lumbar Spine and Sacrum, 3rd edn. Edinburgh: Churchill Livingstone.)

Anulus fibrosus

The anulus fibrosus has a narrow outer collagenous zone and a wider inner fibrocartilaginous zone. Its lamellae, which are convex peripherally when seen in vertical section, are incomplete collars. The internal vertical concavity of the lamellae conforms to the surface profile of the nucleus pulposus. In all quadrants of the anulus, about half the lamellae are incomplete; the proportion increases in the posterolateral region. The exact nature of the interlamellar substance remains in some doubt. Posteriorly, lamellae join in a complex manner. Fibres in the rest of each lamella are parallel and run obliquely between vertebrae at about 65° to the vertical (Fig. 42.40A2). Fibres in successive lamellae cross each other obliquely in opposite directions, thus limiting rotation. The obliquity of fibres in deeper zones varies in different lamellae. Posterior fibres may sometimes be predominantly vertical, which possibly predisposes them to herniation.

This standard description of the anulus may not apply at all spinal levels: a recent cadaveric study indicates that the anulus is usually incomplete posteriorly in adult cervical discs (Mercer & Bogduk 1999) (Fig. 42.40A3).

Nucleus pulposus

The nucleus pulposus is better developed in cervical and lumbar regions and lies between the centre of the disc and its posterior surface. At birth it is large, soft, gelatinous and composed of mucoid material. It contains a few multinucleated notochordal cells and is invaded by cells and collagen fibres from the inner zone of the adjacent anulus fibrosus. Notochordal cells disappear in the first decade, and the mucoid material is gradually replaced by fibrocartilage, derived mainly from the anulus fibrosus and the plates of hyaline cartilage adjoining the vertebral bodies. The nucleus pulposus becomes less differentiated from the remainder of the disc as age progresses, and gradually becomes less hydrated and increasingly fibrous. The type II collagen of the nucleus becomes more like the type I of the anulus as its fibril diameter increases. The quantity of aggregated proteoglycans in the nucleus decreases, while the keratan sulphate/chondroitin sulphate ratio increases. As increased cross-linking occurs between collagen and the proteoglycans the discs lose their water-binding capacity, become stiffer and more liable to injury. Contrary to what was previously thought, it has now been shown that lumbar discs do not decrease in overall height as a part of normal ageing. The anulus gradually loses height as its radial bulge increases, but the nucleus retains height and may increase in convexity as it increasingly indents the end-plate. Loss of trunk height with age results from a decrease in vertebral body height (Bogduk 2005). When the disc is not loaded, pressure in the nucleus pulposus is low at all ages.

For a review of the structure and function of the human intervertebral disc see Adams et al (2006).

Ligaments

The ligaments associated with the joints between the vertebral bodies are described on page 728.

Vascular supply

Small offshoots of spinal branches of arteries supplying the vertebral column (see p. 714) form an anastomosis on the outer surface of the anulus fibrosus and supply its most peripheral fibres. Normal discs are otherwise avascular and are dependent for their nutrition on diffusion from vertebral bone beneath adjacent end-plates and from the peripheral anulus. Vascular and avascular parts differ in their reaction to injury. Venous drainage is via the external and internal vertebral venous plexuses to the intervertebral veins and thence to the larger named veins which drain the vertebral column. Lymphatic drainage of the vertebral column is briefly considered above (see p. 715). Nothing specific is known about the lymphatic drainage of the disc.

Innervation

The nerve supply of intervertebral discs has been studied in detail in the lumbar region (Fig. 42.44). The outer third of the anulus is innervated by the sinuvertebral nerves (see p. 754): each sinuvertebral nerve supplies both the disc at the level of its spinal nerve of origin and the disc one level above. The anterior part of the anulus is supplied by the sympathetic (grey ramus communicans) rather than by the mixed nerve. In damaged and degenerate discs the nerves may penetrate more centrally into the disc substance. The sinuvertebral nerves are condensations within extensive nerve plexuses which lie on the posterior longitudinal ligament. Similar plexuses have been demonstrated anteriorly, covering the anterior longitudinal ligament, and laterally in the fetus.

Relations and ‘at risk’ structures

Posterior, lateral and anterior relations of the intervertebral disc are important in the planning of interventional investigative and therapeutic procedures ranging from discography to open disc surgery. The posterolateral surface of the disc forms the anterior boundary of the intervertebral foramen on each side, and so is closely related to the spinal nerve and its accompanying vessels. More centrally the disc is related posteriorly to the dura mater covering the spinal cord and the cauda equina. Anterior relations of the discs vary considerably with vertebral level, but important ‘at risk’ structures include the pharynx and oesophagus, the descending aorta and the inferior vena cava. Laterally, relations change with level, but the parietal pleura in the thorax, and the sympathetic trunk and psoas muscles in the lumbar region, are important examples.

Prolapsed intervertebral disc

A prolapsed intervertebral disc most commonly affects the 20–55 year age group, and is most often seen at the L4/5 and lumbosacral levels. It may also affect the cervical discs, particularly at C5/6 and C6/7. The thoracic discs are rarely affected. Acute tearing or chronic degeneration of the posterior lamellae of the anulus fibrosus allows deformation and herniation of the disc contents. The disc most often prolapses just lateral to the posterior longitudinal ligament and can compress one or two spinal nerves unilaterally (Fig. 42.45). Much less commonly, the prolapse is central, in the midline posteriorly. The compression of neural structures may then be bilateral, affecting the cord itself or the whole cauda equina. If the damaged anulus ruptures completely, some of the nuclear tissue may escape into the vertebral and ‘root’ canals. This sequestrated material may migrate within the canals and cause nerve compression at spinal levels distant from that of the disc rupture. The disc material itself may have an irritative effect on the spinal nerve.

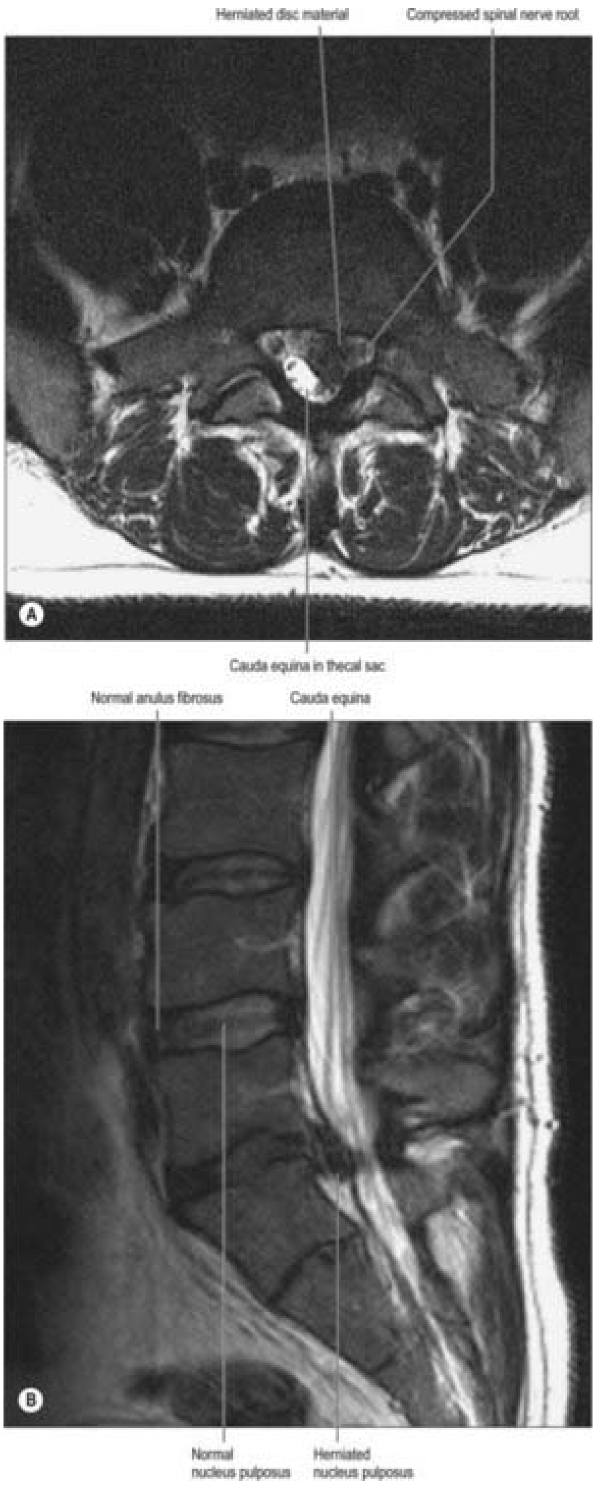
Herniated disc material
Compressed spinal nerve root
A
Cauda equina in thecal sac
Normal anulus fibrosus
Cauda equina
B
Normal nucleus pulposus
Herniated nucleus pulposus

Fig. 42.45 Posterolateral disc prolapse. **A**, Axial view. **B**, Sagittal view.

Regarding the anatomy of the vertebral canal and intervertebral foramen in relation to disc prolapse, it is important to understand that one or both of two spinal nerves and their roots may be affected by a single prolapse, depending upon the exact site of the prolapse in the horizontal plane. At the level of each disc and foramen, there are two spinal nerves (and their roots) to consider: these are the exiting nerve and the traversing nerve (Macnab & McCulloch 1990) (Fig. 42.46). The nerve usually affected at lumbar levels is the traversing nerve, which crosses the back of the disc on its way to become the exiting nerve at the level below. Thus a lumbosacral (i.e. L5/S1) disc prolapse usually compresses the S1 nerve. However, a prolapse may affect the exiting nerve at its own level. This is especially likely if the prolapse is in the extraforaminal zone of the ‘root’ canal, the so-called ‘far lateral’ prolapse. At cervical levels, because the roots and nerve leave the vertebral canal almost horizontally, the prolapse usually affects the exiting nerve. This nerve will still bear the number of the vertebra below the affected disc, because cervical nerves exit the canal above the pedicle of their numerically corresponding vertebra. Neurological presentation will include signs and symptoms of spinal nerve damage at the affected level. Thus pain and sensory loss will be dermatomal in distribution. Sensory changes usually precede motor loss.

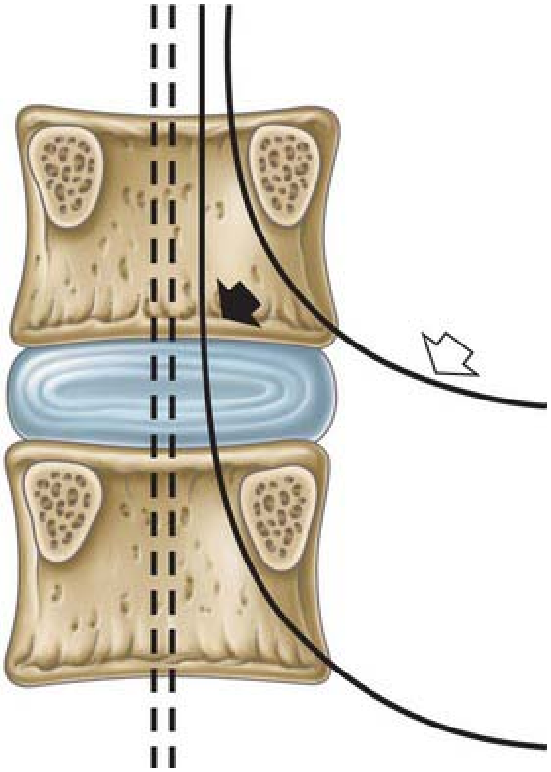

Fig. 42.46 Exiting and traversing nerve roots. The upper root (open arrow) is the exiting root at this level: the lower (closed arrow) is the traversing root here, which becomes the exiting root at the level below. The dotted roots are traversing roots of the lower segment.

Internal disruption of a lumbar intervertebral disc is more common than disc prolapse, and is now an increasingly recognized cause of back pain. Typically, the nucleus is decompressed and the inner lamellae of the anulus appear to collapse into it.

For more detail on disc pathology and its consequences, see Adams et al (2006).

Facet (zygapophysial) joints

Joints between the vertebral articular processes (zygapophyses) are synovial and have long been called zygapophysial joints by anatomists. However, in current clinical practice they are commonly called ‘facet joints’.

Detailed description of the anatomy of these joints is to be found in Bogduk (2005), where Bogduk explains why the term ‘facet joint’ is both incorrect and essentially ambiguous, on the grounds that facets are not restricted to zygapophysial articular processes and occur, for example, in both costovertebral and costotransverse joints.

Articulating surfaces

Facet joints are of the simple (cervical and thoracic) or complex (lumbar) synovial variety: the articulating surfaces are covered in hyaline cartilage and are carried on mutually adapted articular processes. The size and shape of these processes vary with spinal level and are described with the individual vertebrae.

Fibrous capsule

The fibrous capsule is thin and loose and attached peripherally to the articular facets of adjacent articular processes. The capsules are longer and looser in the cervical region. According to Bogduk, the anterior fibrous capsule is replaced entirely by the ligamentum flavum in the lumbar spine.

Intracapsular structures

Bogduk describes two types of intra-articular structure in lumbar facet joints, namely subcapsular fat and ‘meniscoid’ structures. The latter structures may be collagenous, fibroadipose or purely adipose, and project into the crevices between non-congruent articular surfaces. They resemble inclusions seen in the small joints of the hand; their function is conjectural.

Ligaments

Ligaments which work in conjunction with, and modify the function of, the facet joints throughout the vertebral column are described on page 728.

Synovial membrane

The synovium is attached around the periphery of the articular cartilages and lines the fibrous capsule. In the lumbar region it is reflected over the intracapsular structures described above.

Vascular supply

The posterior spinal branches of the arteries that supply the vertebral column form arterial anastomoses around the facet joints. Venous drainage is via the external and internal posterior vertebral venous plexuses to the intervertebral veins and thence to the larger named veins that drain the vertebral column. Lymphatic drainage follows the principles described for the vertebral column (p. 715).

Innervation

The facet joints are profusely innervated by medial branches of the dorsal primary rami of the spinal nerves, which give articular branches to the joints above and below them.

Relations and ‘at risk’ structures

Anteriorly the capsules of the facet joints form the posterior boundaries of the intervertebral foramina. Posteriorly and laterally the joints are related to the deep muscles of the back, some of whose fibres attach to the capsules. The joints also lie in close relation to the medial branches of the dorsal rami of the spinal nerves and to their accompanying arteries and veins. Damage to the medial branches of the dorsal rami may denervate the deep back muscles. Access to the facet joints and their related nerves may be required in the diagnosis and treatment of spinal pain.

Lumbar articular tropism

In the lumbar region, asymmetrical orientation of the facet joints occurs in about one fifth of the population. Such facet tropism does not appear to predispose to degenerative disc disease.

CRANIOVERTEBRAL JOINTS

The articulation between the cranium and vertebral column is specialized to provide a wider range of movement than those which occur in the rest of the axial skeleton. It consists of the occipital condyles, the atlas and the axis, and functions like a universal joint that permits horizontal and vertical scanning movements of the head, and is adapted for eye–head co-ordination.

Atlanto-occipital joints

The atlas articulates with the occipital bone of the skull by a pair of synovial joints. The bones are connected by articular capsules and by the anterior and posterior atlanto-occipital membranes (Fig. 42.47, Fig. 42.48).

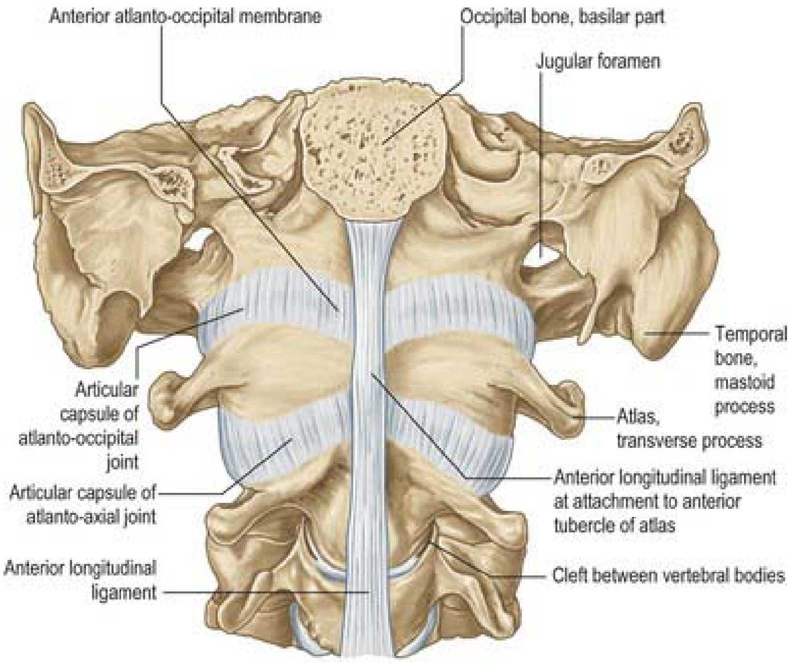
Anterior atlanto-occipital membrane
Occipital bone, basilar part
Jugular foramen
Temporal bone, mastoid process
Articular capsule of atlanto-occipital joint
Atlas, transverse process
Articular capsule of atlanto-axial joint
Anterior longitudinal ligament at attachment to anterior tubercle of atlas
Anterior longitudinal ligament
Cleft between vertebral bodies

Fig. 42.47 Atlanto-occipital and atlanto-axial joints: anterior aspect. On each side a small cleft has been opened between the lateral part of the upper surface of the body of the third cervical vertebra and the bevelled, inferior surface of the body of the axis.

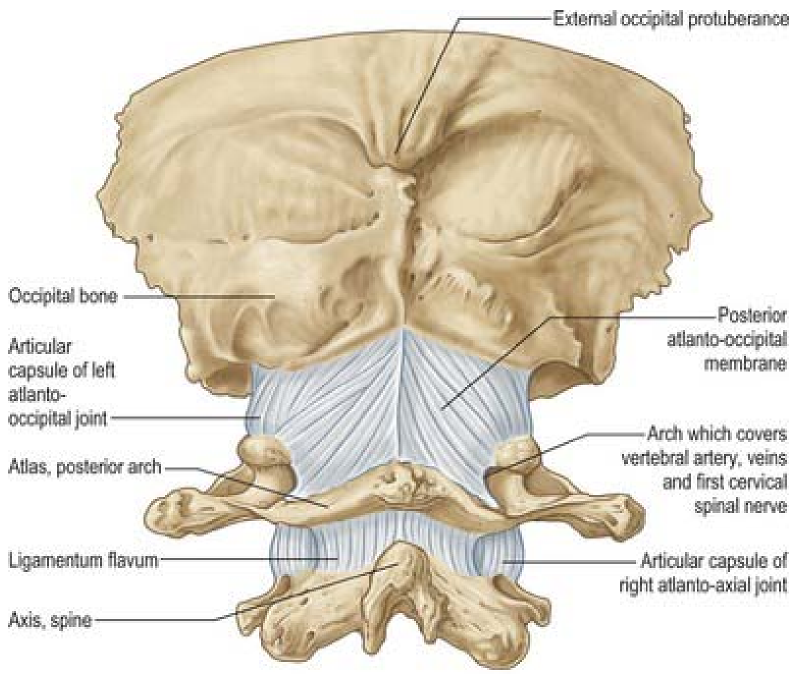
External occipital protuberance
Occipital bone
Articular capsule of left atlanto-occipital joint
Posterior atlanto-occipital membrane
Atlas, posterior arch
Arch which covers vertebral artery, veins and first cervical spinal nerve
Ligamentum flavum
Articular capsule of right atlanto-axial joint
Axis, spine

Fig. 42.48 Atlanto-occipital and atlanto-axial joints: posterior aspect.

Articulating surfaces

Each joint consists of two reciprocally curved articular surfaces, one on the occipital condyle and the other on the lateral mass of the atlas. The atlantal facets are concave and tilted medially.

Fibrous capsules

The fibrous capsules surround the occipital condyles and superior atlantal articular facets. They are thicker posteriorly and laterally, where the capsule is sometimes deficient, and may communicate with the joint cavity between the dens and the transverse ligament of the atlas.

Ligaments

The ligaments are the anterior and posterior atlanto-occipital membranes.

Anterior atlanto-ocipital membrane

The anterior atlanto-occipital membrane (Fig. 42.47, Fig. 42.49) is a broad, dense fibrous structure which connects the anterior margin of the foramen magnum to the upper border of the anterior arch of the atlas. Laterally, it blends with the joint capsule, and medially it is strengthened by a median cord, which is the anterior longitudinal ligament stretching between the basilar occipital bone and anterior atlantal tubercle.

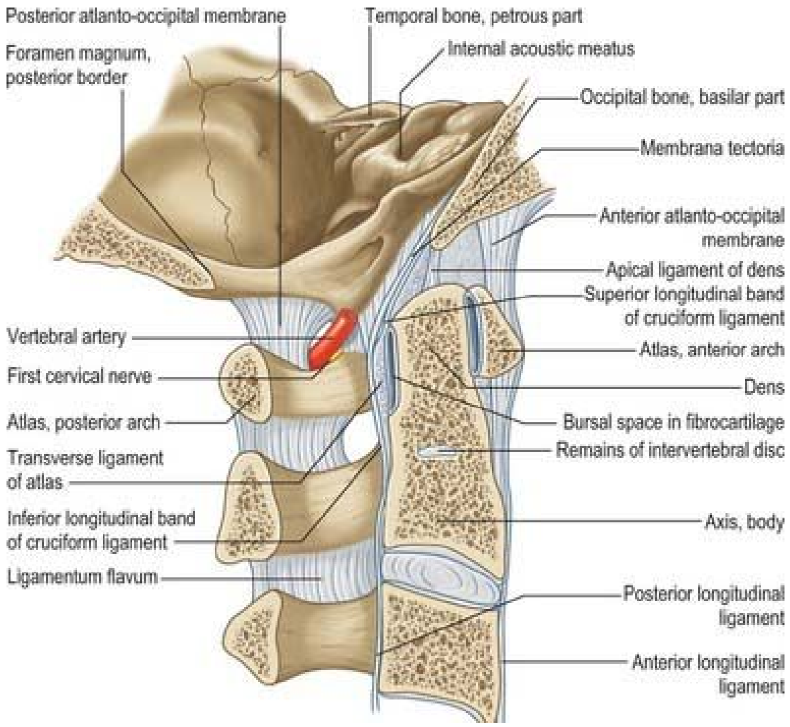
Posterior atlanto-occipital membrane
Foramen magnum, posterior border
Vertebral artery
First cervical nerve
Atlas, posterior arch
Transverse ligament of atlas
Inferior longitudinal band of cruciform ligament
Ligamentum flavum
Temporal bone, petrous part
Internal acoustic meatus
Occipital bone, basilar part
Membrana tectoria
Anterior atlanto-occipital membrane
Apical ligament of dens
Superior longitudinal band of cruciform ligament
Atlas, anterior arch
Dens
Bursal space in fibrocartilage
Remains of intervertebral disc
Axis, body
Posterior longitudinal ligament
Anterior longitudinal ligament

Fig. 42.49 Median sagittal section through the occipital bone and first to third cervical vertebrae.

Posterior atlanto-occipital membrane

The posterior atlanto-occipital membrane (Fig. 42.48, Fig. 42.49) is broad, but relatively thin, and connects the posterior margin of the foramen magnum to the upper border of the posterior atlantal arch, blending laterally with the joint capsules. It arches over the grooves for the vertebral arteries, venous plexuses and first cervical nerve, and forms the ‘floor’ of the suboccipital triangle. The ligamentous border of this arch is sometimes ossified. The membrane is usually attached by a soft-tissue ‘bridge’, which may contain muscle or tendon fibres, to rectus capitis posterior minor, and is firmly attached anteriorly to the spinal dura in the same area (Zumpano et al 2006).

The ligaments connecting the axis and the occipital bone are functionally involved with the posterior atlanto-occipital membrane.

Synovial membrane

The synovial cavities of one or both joints may communicate with that of the posterior component of the median atlanto-axial joint.

Vascular supply

The arterial supply of this region is derived from an anastomosis between branches of the deep cervical, occipital and vertebral arteries.

Innervation

The joints are innervated by branches of the ventral primary ramus of the first cervical spinal nerves.

Factors maintaining stability

Factors maintaining stability include the fibrous capsules, the atlanto-occipital membranes, the shape of the articular surfaces, the ligaments connecting the axis and the occipital bone, the ligamentum nuchae and the posterior neck muscles. The suboccipital muscles play an important proprioceptive and postural role.

Movements and muscles

The orientation and shape of the atlanto-occipital joints allow mainly for flexion-extension, which has a total range of about 15°. Axial rotation and lateral flexion have not been measured in living subjects, but a few degrees of motion in these directions can be produced by forceful movement in cadavers.

The following muscles produce these movements. For flexion: longus capitis and rectus capitis anterior; for extension: recti capitis posteriores major and minor, obliquus capitis superior, semispinalis capitis, splenius capitis and trapezius (cervical part); for lateral flexion: rectus capitis lateralis, semispinalis capitis, splenius capitis, sternocleidomastoid and trapezius (cervical part); and for rotation: obliquus capitis superior, rectus capitis posterior minor, splenius capitis and sternocleidomastoid.

Relations and ‘at risk’ structures

Posteriorly the joints are closely related to the vertebral arteries as they pass from the foramina transversaria into the foramen magnum. The dorsal primary ramus of the first cervical nerve and rectus capitis posterior major lie posteromedially and rectus capitis anterior lies anteriorly.

Atlanto-axial joints

The atlas articulates with the axis at three synovial joints. These are a pair between the lateral masses and a median complex between the dens of the axis and the anterior arch and transverse ligament of the atlas.

Articulating surfaces

The articular surfaces of the joints between the lateral masses are often classified as planar. The bony articular surfaces are more complex in shape and are usually reciprocally concave in the coronal plane; the medial parts are somewhat convex in the sagittal plane (especially that of the axis). The cartilaginous articular surfaces are usually less concave. The median joint is a pivot between the dens and a ring formed by the anterior arch and transverse ligament of the atlas. A vertically ovoid facet on the anterior dens articulates with a facet on the posterior aspect of the anterior atlantal arch.

Fibrous capsules

The fibrous capsules for the lateral joints are attached to the articular margins and are thin and loose. Each has a posteromedial accessory ligament attached below to the axial body near the base of its dens, and above to the lateral atlantal mass near the transverse ligament. The fibrous capsule for the median joint is also relatively weak and loose, especially superiorly.

Ligaments

Anteriorly, the vertebral bodies are connected by the anterior longitudinal ligament (Fig. 42.47, Fig. 42.49): here a strong, thickened band attaches above to the lower border of the anterior tubercle of the anterior arch of the atlas and below to the front of the axial body. Posteriorly the vertebral arches are joined by the ligamenta flava (Fig. 42.48, Fig. 42.49) which are attached to the lower border of the atlantal arch above, and to the upper borders of the axial laminae. At this level these ligaments form a thin membrane, pierced laterally by the second cervical nerves.

Transverse atlantal and cruciform ligaments

The transverse atlantal ligament (Fig. 42.50) is a broad, strong band which arches across the atlantal ring behind the dens: its length varies about a mean of 20 mm. It is attached laterally to a small but prominent tubercle on the medial side of each atlantal lateral mass, and broadens medially where it is covered anteriorly by a thin layer of articular cartilage. It consists almost entirely of collagen fibres, which, in the central part of the ligament, cross one another at an angle to form an interlacing mesh. From its upper margin a strong median longitudinal band arises which inserts into the basilar part of the occipital bone between the apical ligament of the dens and membrana tectoria, and from its inferior surface a weaker and less consistent longitudinal band passes to the posterior surface of the axis. These transverse and longitudinal components together constitute the cruciform ligament. The transverse ligament divides the ring of the atlas into unequal parts (Fig. 42.22). The posterior two-thirds surrounds the spinal cord and meninges, the anterior third contains the dens, which the transverse ligament retains in position even when all other ligaments are divided.

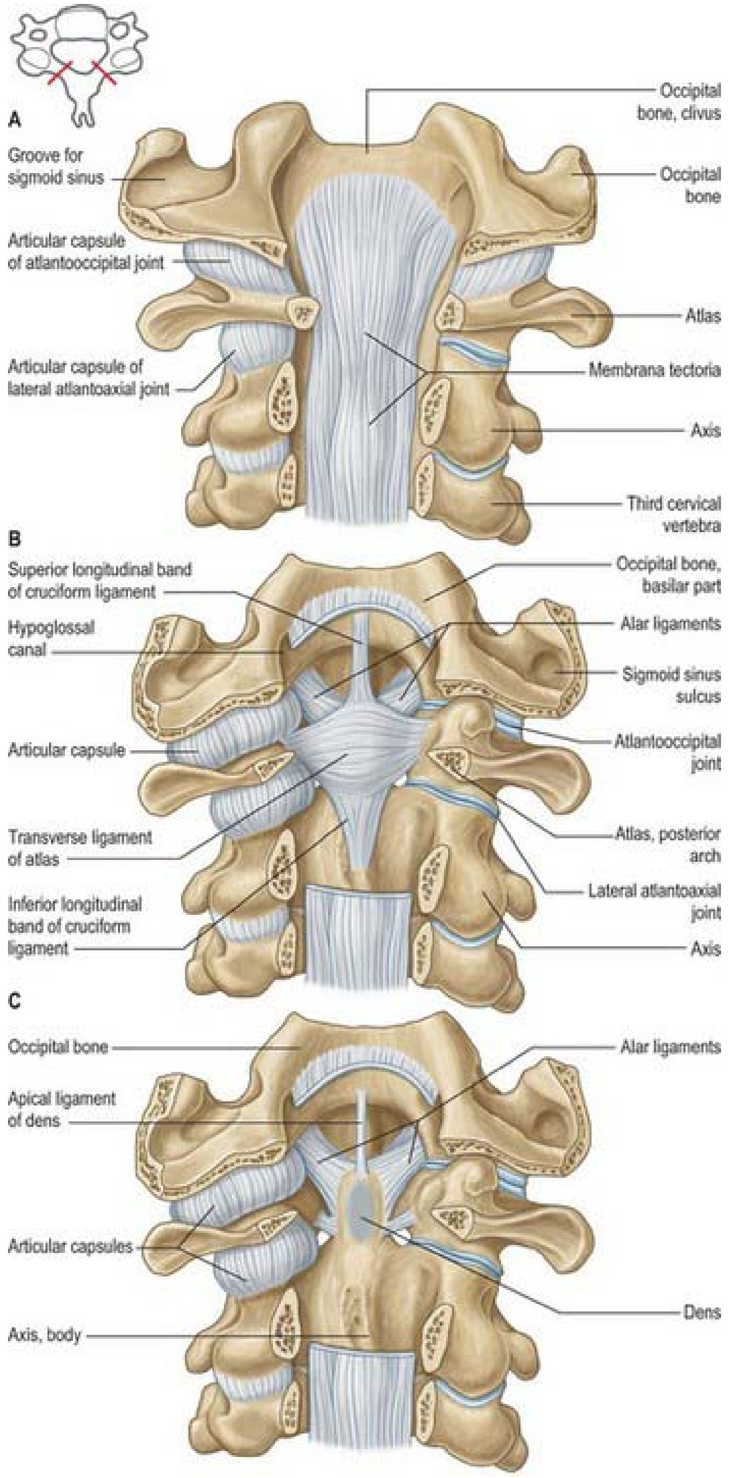
A
Groove for sigmoid sinus
Articular capsule of atlantooccipital joint
Articular capsule of lateral atlantoaxial joint
Occipital bone, clivus
Occipital bone
Atlas
Membrana tectoria
Axis
Third cervical vertebra
B
Superior longitudinal band of cruciform ligament
Hypoglossal canal
Articular capsule
Transverse ligament of atlas
Inferior longitudinal band of cruciform ligament
Occipital bone, basilar part
Alar ligaments
Sigmoid sinus sulcus
Atlantooccipital joint
Atlas, posterior arch
Lateral atlantoaxial joint
Axis
C
Occipital bone
Apical ligament of dens
Articular capsules
Axis, body
Alar ligaments
Dens

Fig. 42.50 Posterior aspect of the atlanto-occipital and atlanto-axial joints. The posterior part of the occipital bone and the laminae of the cervical vertebrae have been removed and the atlanto-occipital joint cavities opened.

(Adapted from Sobotta 2006.)

Ligaments connecting axis and occipital bone

Ligaments connecting the axis and the occipital bone consist of the membrana tectoria, the paired alar ligaments, the median apical ligament, and the longitudinal components of the cruciform ligament (Fig. 42.49, Fig. 42.50).

Membrana tectoria.

Inside the vertebral canal, the membrana tectoria is a broad strong band representing the upward continuation of the posterior longitudinal ligament. Its superficial and deep laminae are both attached to the posterior surface of the axial body. The superficial lamina expands as it ascends to the upper surface of the basilar occipital bone, and attaches above the foramen magnum, where it blends with the cranial dura mater. The deep lamina consists of a strong median band which ascends to the foramen magnum, and two lateral bands which pass to, and blend with, the capsules of the atlanto-occipital joints as they reach the foramen magnum. The membrane is separated from the cruciform ligament of the atlas by a thin layer of loose areolar tissue, and sometimes by a bursa.

Alar ligaments.

The alar ligaments are thick cords, about 11 mm long, which pass horizontally and laterally from the longitudinally ovoid flattenings on the posterolateral aspect of the apex of the dens to the roughened areas on the medial side of the occipital condyles. In most individuals there is also an anteroinferior band, approximately 3 mm long, which inserts into the lateral mass of the atlas in front of the transverse ligament. Fibres occasionally pass from the dens to the anterior arch of the atlas. In addition, in some 10% of cases a continuous transverse band of fibres, the transverse occipital ligament, passes between the occipital condyles immediately above the transverse ligament. The ligaments consist mainly of collagen fibres arranged in parallel. The main function of the alar ligaments is now considered to be limitation of atlanto-axial rotation, the left becoming taut on rotation to the right and vice versa. The slightly downward movement of the atlas during rotation helps permit a wider range of movement by reducing tension in the alar ligaments, and in the capsules and accessory ligaments of the lateral atlanto-occipital joint.

Apical ligament of the dens.

The apical ligament of the dens fans out from the apex of the dens into the anterior margin of the foramen magnum between the alar ligaments, and represents the cranial continuation of the notochord and its sheath. It is separated for most of its extent from the anterior atlanto-occipital membrane and cruciform ligament by pads of fatty tissue, though it blends with their attachments at the foramen magnum, and with the alar ligaments at the apex of the dens.

The ligamentum nuchae and the anterior longitudinal ligament also connect cervical vertebrae with the cranium.

Synovial membrane

The synovial membranes of the lateral joints have no special features. The median joint has two synovial cavities which sometimes communicate. The synovial cavity of the posterior component of the median joint complex is larger, lying between the horizontally orientated ovoid facet, on the posterior surface of the dens and the cartilaginous anterior surface of the transverse ligament: communication often exists with one or both of the atlanto-occipital joint cavities.

Vascular supply

The arterial supply of this region is derived from an anastomosis between branches of the deep cervical, occipital and vertebral arteries.

Innervation

The joints are innervated by branches of the ventral primary ramus of the second cervical spinal nerve.

Factors maintaining stability

The most important factors maintaining stability are the ligaments, of which the transverse atlantal ligament is the strongest. The alar ligaments are weaker. Other ligaments connecting the axis and the occipital bone, the fibrous capsules, the ligamentum nuchae and the posterior neck muscles also contribute to stability: the suboccipital muscles play an important proprioceptive and postural role.

Movements and muscles

Movement is simultaneous at all three joints, and consists almost exclusively of rotation around the axis. The shape of the articular surfaces is such that, when rotation occurs, the axis ascends slightly into the atlantal ring, limiting stretch on the lateral atlanto-axial joint capsules. Rotation is limited mainly by the alar ligaments, with a minor contribution from the accessory atlanto-axial ligament. The normal range of atlanto-axial rotation is about 40°.

The muscles that produce atlanto-axial rotation act on the cranium, transverse processes of the atlas and spinous process of the axis. They are mainly obliquus capitis inferior, rectus capitis posterior major and splenius capitis of one side, and the contralateral sternocleidomastoid.

Relations and ‘at risk’ structures

The most important ‘at risk’ relation is the spinal cord, lying posterior to the median atlanto-axial joint. Anteriorly the atlanto-axial articulations, capsules and ligaments are separated from the buccopharyngeal fascia and superior constrictor by longus capitis and longus colli, the prevertebral fascia and the retropharyngeal (potential) space.

Variants of craniovertebral joints

Anomalies of the craniovertebral joints are sometimes seen. Many are minor segmentation anomalies, and may be incidental radiological or osteological findings. More severe anomalies may lead to craniocervical instability (Piper & Traynelis 1998).

LUMBOSACRAL JUNCTION

Articulations between the fifth lumbar and first sacral vertebrae resemble those between other vertebrae. The bodies are united by a symphysis which includes a large intervertebral disc. The latter is deeper anteriorly at the lumbosacral angle. The synovial facet joints are separated by a wider interval than those above.

Articulating surfaces

The reciprocally curved surfaces of the facet joints show considerable individual variation in alignment and shape. Asymmetry (facet tropism) is not unusual.

Ligaments

The major ligament associated with the lumbosacral junction is the iliolumbar ligament (Fig. 80.8, Fig. 42.51).

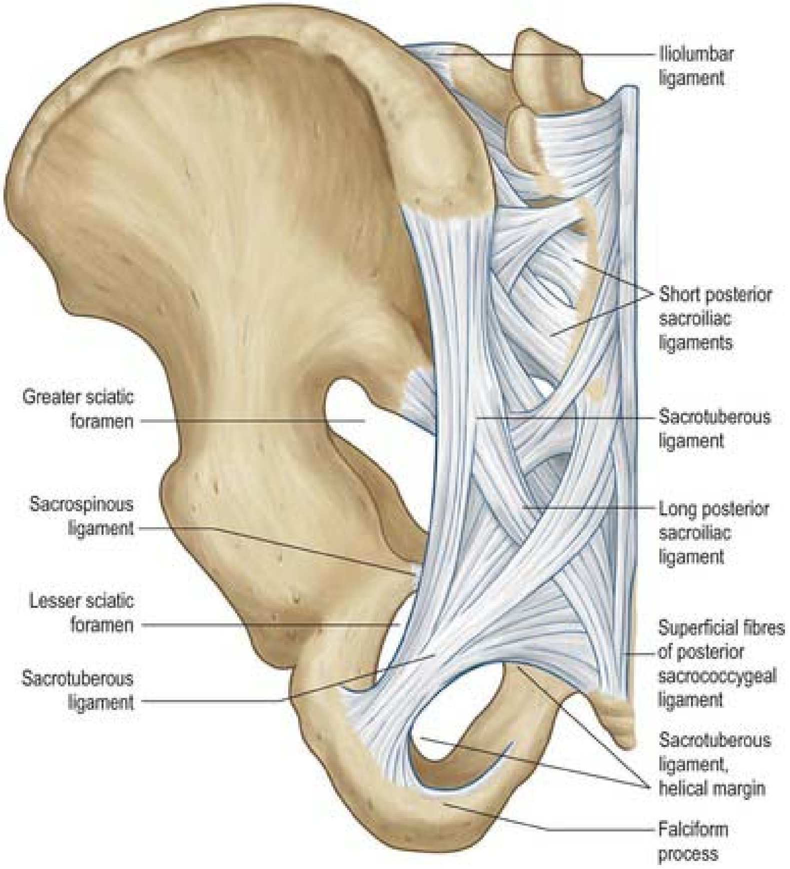
Iliolumbar ligament
Short posterior sacroiliac ligaments
Greater sciatic foramen
Sacrotuberous ligament
Sacrospinous ligament
Long posterior sacroiliac ligament
Lesser sciatic foramen
Superficial fibres of posterior sacrococcygeal ligament
Sacrotuberous ligament
Sacrotuberous ligament, helical margin
Falciform process

Fig. 42.51 Joints and ligaments on the posterior aspect of the left half of the pelvis and the fifth lumbar vertebra.

Iliolumbar ligament

The iliolumbar ligament is attached to the tip and anteroinferior aspect of the fifth lumbar transverse process, and sometimes has a weak attachment to the fourth transverse process. It radiates laterally and is attached to the pelvis by two main bands. A lower band passes from the inferior aspect of the fifth lumbar transverse process and the body of the fifth lumbar vertebra across the anterior sacroiliac ligament to reach the posterior margin of the iliac fossa. An upper band, part of the attachment of quadratus lumborum, passes to the iliac crest anterior to the sacroiliac joint, and is continuous above with the anterior layer of the thoracolumbar fascia. The lower ligament has a more vertical component that reaches the posterior iliopectineal line: this component is a lateral relation of the L5 ventral ramus. A posterior component of the iliolumbar ligament passes behind quadratus lumborum to attach to the ilium.

In neonates and children the iliolumbar ‘ligament’ is muscular: the muscle is gradually replaced by ligament up to the fifth decade of life.

Vascular supply

The vascular supply of the lumbosacral junction is derived mainly from the iliolumbar and superior lateral sacral arteries.

Innervation

The lumbosacral junction is innervated by branches derived from the fourth and fifth lumbar spinal nerves: the pattern of distribution is as described on page 707.

Relations and ‘at risk’ structures

The lumbosacral disc is related anteriorly to the common iliac veins, the median sacral vessels, and the superior hypogastric plexus of nerves. The sympathetic trunks cross it anterolaterally, while the obturator nerves and lumbosacral trunks pass close laterally. The relations of the lumbosacral facet joints are similar to those of the lumbar facet joints (see above).

SACROCOCCYGEAL JUNCTION

The sacrococcygeal joint is usually a symphysis between the sacral apex and coccygeal base, united by a thin fibrocartilaginous disc which is somewhat thicker in front and behind than laterally. Its surfaces carry hyaline cartilage which varies from thin veils to small islands. Occasionally the coccyx is more mobile and the joint is synovial.

Ligaments

The anterior sacrococcygeal ligament consists of irregular fibres that descend on the pelvic surfaces of both sacrum and coccyx, and is attached in the same way as the anterior longitudinal ligament. The flat superior posterior sacrococcygeal ligament passes from the margin of the sacral hiatus to the dorsal coccygeal surface, roofing the lower sacral canal (Fig. 42.51). The deep posterior sacrococcygeal ligament passes from the back of the fifth sacral vertebral body to the dorsum of the coccyx and corresponds to the posterior longitudinal ligament. On each side, the lateral sacrococcygeal ligaments connect the coccygeal transverse processes to the inferolateral sacral angles, completing foramina for the fifth sacral spinal nerves. Similarly, the intercornual ligaments connect the sacral and coccygeal cornua, and a fasciculus connects the sacral cornua to the coccygeal transverse processes.

Vascular supply

The arterial supply of the sacrococcygeal junction is derived from the inferior lateral sacral and median sacral arteries.

Innervation

The innervation of the sacrococcygeal junction is derived from the lower two sacral and the coccygeal nerves.

INTERCOCCYGEAL JOINTS

In the young the intercoccygeal joints are symphyses, with thin discs of fibrocartilage between coccygeal segments. Segments are also connected by extensions of the anterior and posterior sacrococcygeal ligaments. In adult males all segments unite comparatively early, but in females union is later. In advanced age the sacrococcygeal joint becomes obliterated. Occasionally the joint between the first and second segments is synovial. The apex of the terminal segment is connected to overlying skin by white fibrous tissue.

MUSCLES

The musculature of the back is arranged in a series of layers, of which only the deeper are true, intrinsic, back muscles (Fig. 42.52). The true back muscles are characterized by their position and by their innervation by branches of the posterior (dorsal) rami of the spinal nerves. The true back muscles below the neck lie deep to the posterior layer of the thoracolumbar fascia. In the lumbar region, where the layers of the thoracolumbar fascia are well-defined, they occupy the compartment between its posterior and middle layers.

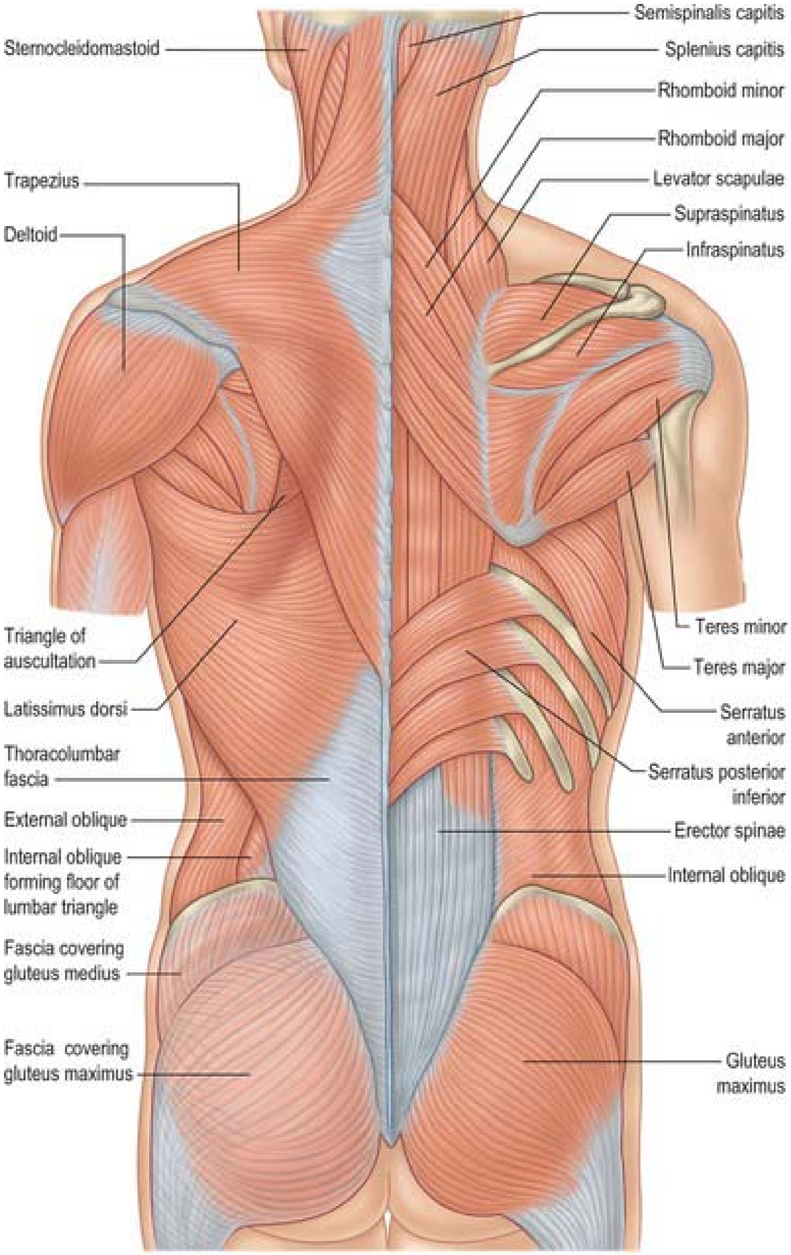
Sternocleidomastoid
Trapezius
Deltoid
Triangle of auscultation
Latissimus dorsi
Thoracolumbar fascia
External oblique
Internal oblique forming floor of lumbar triangle
Fascia covering gluteus medius
Fascia covering gluteus maximus
Semispinalis capitis
Splenius capitis
Rhomboid minor
Rhomboid major
Levator scapulae
Supraspinatus
Infraspinatus
Teres minor
Teres major
Serratus anterior
Serratus posterior inferior
Erector spinae
Internal oblique
Gluteus maximus

Fig. 42.52 Superficial muscles of the back of the neck and trunk. On the left only the skin, superficial and deep fasciae (other than gluteofemoral) have been removed; on the right, sternocleidomastoid, trapezius, latissimus dorsi, deltoid and external oblique have been dissected away.

Lying superficial to the true, intrinsic muscles are the extrinsic, 'immigrant' muscles (Fig. 42.52). The most superficial of these run between the upper limb and the axial skeleton, and consist of trapezius, latissimus dorsi, levator scapulae and the rhomboid muscles. Beneath this layer lie the serratus posterior group, superior and inferior, which are variably developed but usually thin muscles whose function may be respiratory or possibly proprioceptive. All the extrinsic muscles are innervated by ventral rami.

Trapezius, latissimus dorsi, levator scapulae, rhomboid major and rhomboid minor are described on pages 809–811; serratus posterior superior and inferior are described on pages 925–926. The muscles of the posterior abdominal wall are described on page 1070.

The intrinsic muscles are also arranged in layers. The more superficial layers contain the splenius muscles in the neck and upper thorax, and the erector spinae group in the trunk as a whole. The deeper layers include the spinotransverse group, which is itself layered into semi-spinalis, multifidus and the rotatores, and the suboccipital muscles. Deepest of all lie the interspinal and intertransverse muscles. The latter group constitute a mixture of dorsal and ventral spinal muscles. The lumbar intertransversarii mediales, thoracic intertransversarii and medial parts of cervical posterior intertransversarii are innervated by dorsal rami, but the others are supplied by ventral rami.

Muscle attachments and fibre direction

Although developmentally the muscles of the back extend caudally as the vertebral column elongates, drawing their nerve supply with them, they have traditionally been described as if their fibres ran caudocranially, so that the 'origins' of the muscles lay distal to their 'insertions'.

It has been shown (Bogduk 2005) that in the lumbar spine it is more appropriate morphologically and biomechanically to view the muscles in the reverse direction – from above downwards. It is reasonable to argue that this view may also be applied to the cervical and thoracic muscles, and so for uniformity in this section, all muscles have been described in this way.

Ligamentum nuchae

The ligamentum nuchae is not a ligament of the neck, for it does not connect adjacent bones and lacks the internal structure typical of a ligament. It is a unique arrangement of tendons and fascia between the posterior muscles of the neck. It consists of a dorsal raphe and a median septal portion. The dorsal raphe lies superficially along the posterior midline of the neck. It is attached to the external occipital protruberance superiorly, and the tip of the C7 spinous process inferiorly. In its superior half it consists of the aggregated tendons of the most medial fibres of the cervical trapezius. Because of their longitudinal arrangement, these tendons have been described as forming the funicular portion of the ligamentum nuchae (Mercer & Bogduk 2003). In its inferior half the funicular portion is joined by the obliquely orientated tendons of splenius capitis and rhomboid minor. Across the midline the tendons of splenius capitis are continuous with those of rhomboid minor on the other side, and they interweave with the tendons of the reciprocal sets of muscles to produce the raphenous structure of the ligamentum nuchae. From the ventral surface of the dorsal raphe, a median fascial septum extends deeply towards the vertebral column and separates semispinalis capitis from its opposite partner. A lateral expansion of the septum extends laterally ventral to semispinalis capitis, separating it from multifidus and semispinalis cervicis. The median continuation of the septum reaches the tips of the cervical spinous processes, and extends into the cervical interspinous spaces as far as the ligamentum flavum. At upper cervical levels the septum is attached to the external occipital crest and the posterior tubercle of the atlas, and it blends with the posterior atlanto-occipital and posterior atlanto-axial membranes. Passing through these membranes it is attached to the posterior surface of the dura mater (Dean & Mitchell 2002). Only the dorsal raphe affords attachment to muscles: no muscles arise from the median septum.

Splenius capitis

Attachments

Splenius capitis arises from the mastoid process and the rough surface on the occipital bone just below the lateral third of the superior nuchal line. Its fibres pass downwards and medially to reach the midline. The lower fibres insert into the tips of the spinous processes of the seventh cervical and upper three or four thoracic vertebrae and the intervening supraspinous ligaments. The tendons of the upper fibres interlace in the midline with those of the opposite side in the dorsal raphe of the ligamentum nuchae in the lower half of the cervical region (Fig. 42.53).

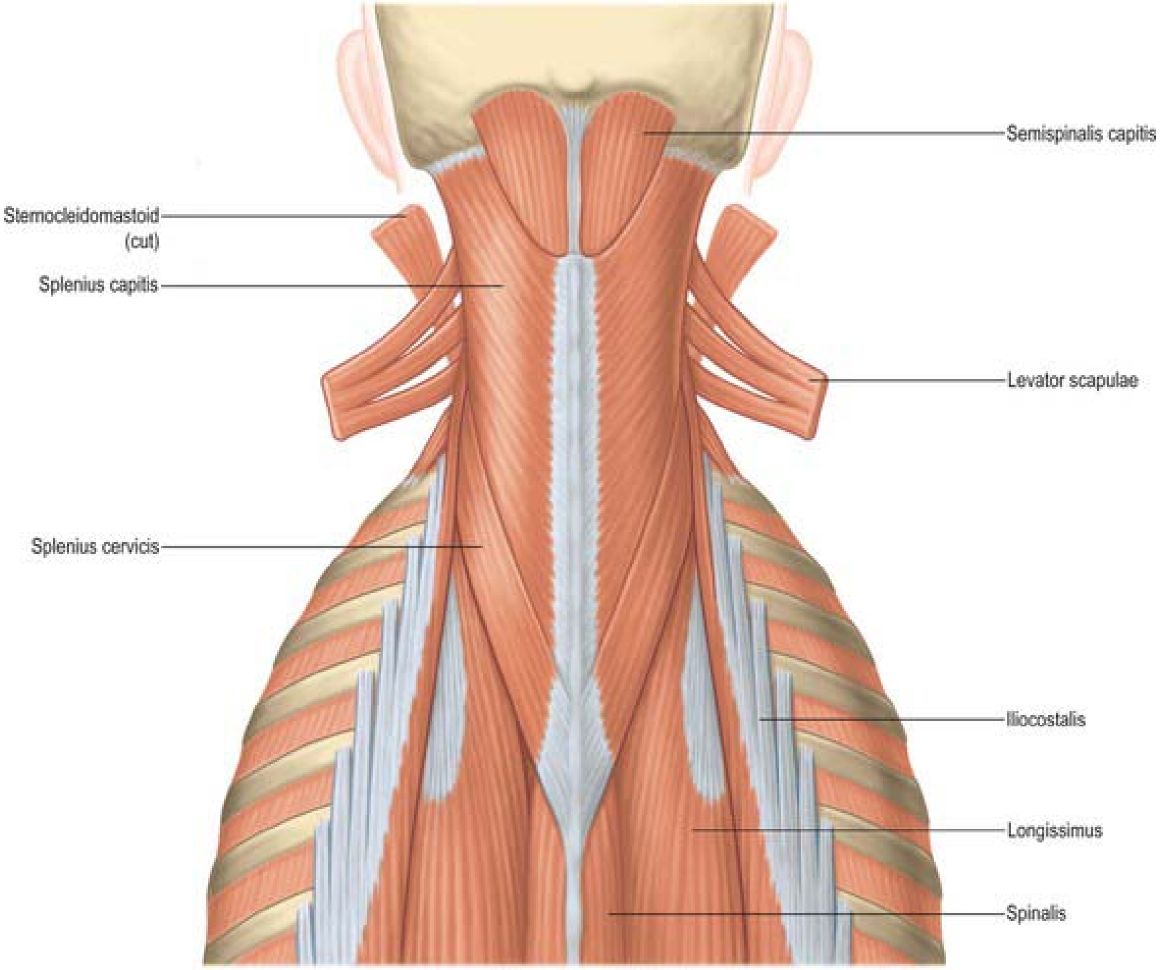
Semispinalis capitis
Sternocleidomastoid (cut)
Splenius capitis
Levator scapulae
Splenius cervicis
Iliocostalis
Longissimus
Spinalis

Fig. 42.53 Splenius cervicis and splenius capitis.

Relations

Splenius capitis lies deep to trapezius and covers semispinalis capitis and longissimus capitis. The upper part of the muscle lies beneath sternocleidomastoid. Between sternocleidomastoid and trapezius it forms part of the floor of the posterior triangle of the neck, above and behind levator scapulae.

Vascular supply

See below.

Innervation

Splenius capitis is innervated by lateral branches of the second and third cervical dorsal rami.

Actions

Acting unilaterally, and synergistically with the contralateral sternocleidomastoid, splenius capitis rotates the head to the same side. Acting bilaterally, splenius capitis extends the head.

Splenius cervicis

Attachments

Splenius cervicis is confluent with splenius capitis, but covers more caudal regions of the neck and thoracic region (Fig. 42.53). It arises from the transverse process of the atlas, the tip of the transverse process of the axis and the posterior tubercle of the third cervical vertebra. Its fibres pass downwards and medially, wrapping around the other posterior intrinsic neck muscles, to insert into the third to sixth thoracic spinous processes.

Relations

Splenius cervicis lies deep to serratus posterior superior, the rhomboids and trapezius. It covers the upper parts of the erector spinae and the lower semispinalis muscles.

Vascular supply

See below.

Innervation

Splenius cervicis is innervated by lateral branches of the lower cervical dorsal rami.

Actions

Acting unilaterally, splenius cervicis rotates the upper cervical vertebra, in the same way that the splenius capitis rotates the head. Acting bilaterally, splenius cervicis extends the upper cervical spine.

Variations

The splenii may be absent or vary in their vertebral attachments. Accessory slips also occur.

Erector spinae

Erector spinae (Fig. 42.6, Fig. 42.7, Fig. 42.54, Fig. 42.55) is a large musculotendinous mass which differs in size and composition at different vertebral levels. It consists of fascicles that assume systematic attachments to homologous parts of the skull, the cervical, thoracic, and lumbar vertebrae, the sacrum, and the ilium. Individual muscles are defined by the attachments of their fascicles and the regions that they span. There are three muscles each with three regional parts:

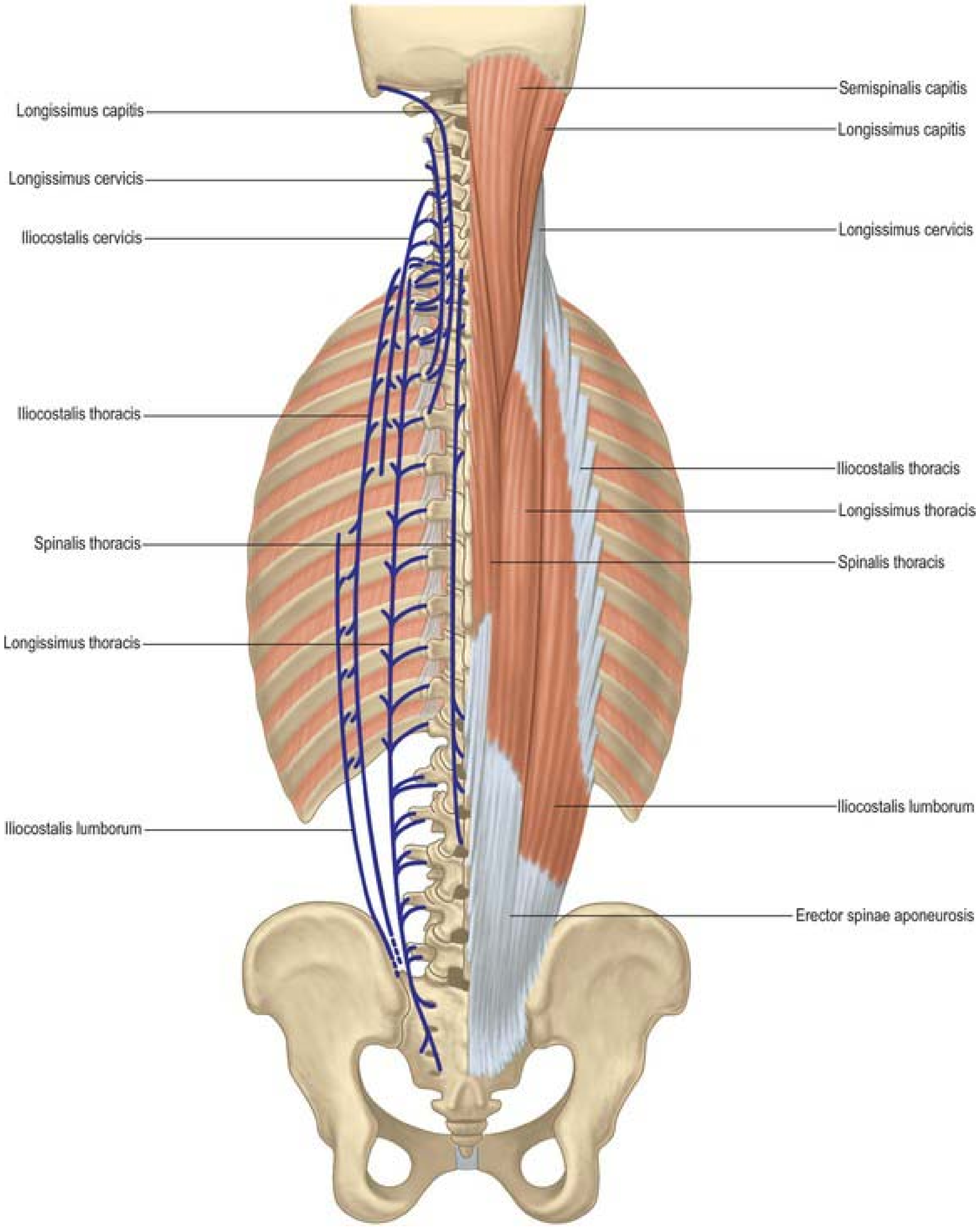
Longissimus capitis
Longissimus cervicis
Iliocostalis cervicis
Iliocostalis thoracis
Spinalis thoracis
Longissimus thoracis
Iliocostalis lumborum
Semispinalis capitis
Longissimus capitis
Longissimus cervicis
Iliocostalis thoracis
Longissimus thoracis
Spinalis thoracis
Iliocostalis lumborum
Erector spinae aponeurosis

Fig. 42.54 Erector spinae muscle group.

Spinalis	**Longissimus**	**Iliocostalis**
Spinalis thoracis	Longissimus capitis	Iliocostalis cervicis

Spinalis cervicis	Longissimus cervicis	Iliocostalis thoracis
Spinalis capitis	Longissimus thoracis	Iliocostalis lumborum

Spinalis

Spinalis thoracis is the most medial portion of erector spinae in the thoracic region. It consists of fascicles that arise from the spinous processes of the upper thoracic vertebra and insert into the spinous processes of the 11th and 12th thoracic and first two lumbar vertebrae. The number of fascicles and their segmental attachments vary. The fascicles are arranged in an overlapping series of increasingly longer, flat arcs. The shortest fascicles have the lowest origin and highest insertion, and the longest fascicles have the highest origin and lowest insertion. Laterally the muscle blends intimately with longissimus thoracis, and is considered by some to be a component of that muscle.

Spinalis is irregularly and poorly developed in other regions. When present, spinalis cervicis consists of paramedian fibres that arise variously from the spinous processes of the axis and the third and fourth cervical vertebrae, and insert into the lower part of the ligamentum nuchae and the spine of the seventh cervical vertebra (sometimes also to the first and second thoracic vertebrae). Spinalis capitis is represented by occasional fibres of semispinalis capitis that insert into the spines of the seventh cervical and first thoracic vertebrae instead of reaching thoracic transverse processes.

Longissimus

Longissimus is the central component of erector spinae. It assumes a series of attachments at sites that are homologous to the junction of the transverse and costal elements of the segment. These sites are represented at thoracic levels by the tip of a transverse process and the immediately adjacent posterior surface of the rib; at cervical levels by the transverse process and posterior tubercle; and at lumbar levels by the accessory process (the transverse element) and medial half of the transverse process (the costal element).

Longissimus capitis is a narrow flat band of muscle that arises from the posterior edge of the mastoid process, under cover of splenius capitis and sternocleidomastoid. It descends across the lateral surface of semispinalis capitis and inserts by a series of tendons into the transverse processes of the lower three or four cervical and upper four or so thoracic vertebrae.

Longissimus cervicis is a long thin muscle that arises by tendons from the posterior tubercles of the transverse processes of the second to sixth cervical vertebra. It descends into the thoracic region, between the tendons of longissimus capitis and longissimus thoracis, to insert by tendons into the transverse processes of the upper four or five thoracic vertebrae.

Longissimus thoracis is the largest component of erector spinae. It consists of many small fascicles that are aggregated in a particular manner to produce a very long, and in some places thick, muscle. It has lumbar and thoracic parts.

The lumbar part is formed by fleshy bundles that arise from the accessory process and the medial half or so of the posterior surface of the transverse process of each of the five lumbar vertebrae. The fascicles pass inferiorly and slightly laterally. Those from the first four lumbar vertebrae converge onto a common flat tendon that covers the lateral surface of the muscle, and separates it from the lumbar fibres of iliocostalis, for which reason it is called the lumbar intermuscular aponeurosis. The aponeurosis commences in the mid lumbar region, with a broad irregular base, and inferiorly it tapers to a truncated point that inserts into the medial surface of the ilium just dorsal to the ala of the sacrum. The fascicle from the first lumbar vertebra attaches rostrally and dorsally to the aponeurosis. Successive fascicles attach to it more ventrally and caudally. The fascicle from the fifth lumbar vertebra inserts separately, deep to the intermuscular aponeurosis, into the ventromedial aspect of the ilium and the upper fibres of the dorsal sacroiliac ligament. Medially the lumbar fibres of longissimus are separated from the multifidus by a wide cleavage plane filled with fat and veins.

The thoracic part consists of fascicles with small, fusiform muscle bellies that have short rostral tendons and long caudal tendons. The muscle bellies are arranged in a tiered fashion across the length of the posterior thoracic wall, with the highest lying medially and the lowest lying laterally. The upper four fascicles arise from the tips of the first four thoracic transverse processes. The succeeding fascicles have bifid tendons that arise from the transverse process and the adjacent rib at each of the lower eight thoracic segments. The long caudal tendons of the thoracic fascicles of longissimus are aggregated in parallel to form a wide aponeurosis, that allows them to assume a variety of caudal insertions. The tendons of the uppermost fascicles insert into the lumbar spinous processes and their supraspinous ligament. Those from the first thoracic segment reach the L1–2 level, and those from the sixth thoracic segment reach the L5 level. The fascicles from the seventh to ninth thoracic segments reach the median sacral crest, and those from the tenth and 11th thoracic segments attach transversely across the posterior surface of the third segment of the sacrum. The fascicle from the 12th thoracic segment reaches the sacrum and dorsal segment of the iliac crest just below where the intermuscular aponeurosis of the lumbar fibres of longissimus inserts into the ilium. The aponeurosis covers the multifidus and the lumbar fibres of longissimus; it extends from the midline as far laterally as the dorsal edge of the lumbar intermuscular aponeurosis, with which it fuses. Within the lumbar intermuscular aponeurosis the lumbar fibres of longissimus, from L1 to L5, complete the systematic progression of attachments exhibited by the thoracic fibres.

Iliocostalis

Iliocostalis is the most lateral component of the erector spinae. Its fascicles are attached to sites that are homologous with the ribs.

Iliocostalis cervicis consists of slender fascicles that arise by long tendons from the posterior tubercles of the fourth, fifth, and sixth cervical vertebra. They descend over the posterior thorax to insert into the third to sixth ribs at their angles.

Iliocostalis thoracis is a narrow, fusiform muscle. The fibres arise from the back of the transverse process of the seventh cervical vertebra and the superior borders of the angles of the upper six ribs: they lie lateral to iliocostalis cervicis, and insert into the upper borders of the angles of the lower six ribs.

Iliocostalis lumborum consists of lumbar and thoracic parts. The lumbar part is formed by fleshy fascicles that arise from the tips of the first four lumbar transverse processes and the posterior surface of the middle layer of thoracolumbar fascia lateral to these tips. These fascicles descend to the ilium in a laminated fashion, such that those from higher levels cover those from lower levels. They insert into the medial end of the iliac crest and the dorsal segment of the iliac crest, with the fascicle from L4 assuming the most ventral and lateral attachment, and the fascicle from L1 assuming the most dorsal and medial attachment. The attachment to the ilium is largely by fleshy fibres but the more superficial fibres are aponeurotic. The thoracic part consists of eight or nine small fascicles that respectively arise from the lower eight or nine ribs at their angles, lateral to the iliocostalis thoracis. Each fascicle arises from its rib by a ribbon-like tendon. The tendons are longer at high levels but become progressively shorter at lower levels. The muscle bellies of the fascicles are uniform in length, and each gives rise to a caudal tendon. These tendons are aggregated to form a dorsal aponeurosis that covers the lumbar part of iliocostalis lumborum and inserts in a linear fashion into the medial end of the iliac crest and its dorsal segment. Along this line the fascicles are represented serially, such that the fascicle from the 12th rib attaches most laterally and that from the four or fifth rib attaches most medial and inferiorly.

Erector spinae aponeurosis

Together, the dorsal aponeuroses of the thoracic fibres of longissimus and the thoracic fibres of iliocostalis lumborum form a wide sheet of parallel tendons known as the erector spinae aponeurosis. It is attached to the lumbar spinous processes and supraspinous ligaments, the median sacral crest, the third sacral segment, the dorsal segment of the iliac crest, and the medial end of the iliac crest, and covers multifidus, and the lumbar fibres of both longissimus and iliocostalis. Significantly, the erector spinae aponeurosis is formed exclusively by the tendons of the thoracic fibres of longissimus thoracis and iliocostalis lumborum; it does not give rise to the lumbar fibres of these muscles, which are attached independently to the ilium. Some of the more superficial fibres of multifidus may insert into the deep surface of the erector aponeurosis over the sacrum, but otherwise the substantive insertion of multifidus is into the sacrum. A portion of the uppermost fibres of gluteus maximus arise from the dorsal surface of the inferolateral corner of the erector spinae aponeurosis. The lumbar intermuscular aponeurosis is a ventral extension of the erector spinae aponeurosis, separating the lumbar fibres of longissimus from those of iliocostalis.

Relations

Erector spinae is covered in the lumbar and thoracic regions by the thoracolumbar fascia, and by serratus posterior inferior below and the rhomboids and splenii above. In the lumbar region it lies in the compartment between the posterior and middle layers of the thoracolumbar fascia.

Vascular supply

See below.

Innervation

Erector spinae is innervated by the lateral branches of the dorsal rami of the cervical, thoracic, and lumbar spinal nerves. At lumbar levels, lateral branches innervate iliocostalis and intermediate branches innervate longissimus.

Actions

The thoracic and lumbar components of erector spinae are powerful extensors of the vertebral column. Acting concentrically and bilaterally they can extend the thoracic and lumbar spines whereas acting unilaterally they can laterally flex the trunk. However, more commonly, erectores spinae act eccentrically.

From the upright posture, the trunk can flex forwards under the influence of gravity. This movement is initiated by flexor muscles, such as rectus abdominis, in order to bring the centre of gravity of the trunk forwards. Thereafter, erectores spinae control the descent of the thorax under gravity. When the trunk is fully flexed, many parts of erector spinae cease to contract and become electromyographically silent. In this position, flexion is limited by passive tension in the back muscles, and tension in the thoracolumbar fascia, the posterior spinal ligaments, and the intervertebral discs. Similarly, lateral flexion under gravity is controlled by the contralateral erector spinae, with input from the abdominal oblique muscles.

The function of the cervical and capital components of erector spinae has not been determined. These are small muscles with very little force capacity, and are poorly orientated to exercise extension or to control flexion of the head or cervical spine. As putative extensors they are dwarfed by semispinalis and splenius. Axial rotation of the head draws longissimus capitis around the perimeter of the cervical spine, orientating it perhaps so that it is able to restore the head to neutral from the rotated position.

Spinotransverse group

The spinotransverse muscle group consists of muscles where the fascicles span between a spinous process and the transverse elements of vertebrae at various levels below. The muscles are grouped according to the length of their fascicles and the region that they cover.

Rotatores	**Multifidus**	**Semispinalis**
Rotatores thoracis	Multifidus	Semispinalis cervicis
Rotatores cervicis		Semispinalis thoracis
Rotatores capitis		Semispinalis capitis

Rotatores have the deepest and shortest fascicles, and span one and two segments, whereas the fascicles of multifidus span two, three, four or five segments, and those of semispinalis span about six segments.

Rotatores

Rotatores thoracis (Fig. 42.56) consist of eleven pairs of small quadrilateral muscles. The first pair lies between the first and second thoracic vertebrae, and the last between the 11th and 12th thoracic vertebrae. One or more may be absent from the upper or lower ends of the series. In each segment, a rotator brevis connects the lower border and lateral surface of the lamina above to the upper, posterior part of the transverse process of the vertebra immediately below; a rotator longus connects the base of the spinous process above to the transverse process two levels below. Rotatores are not obviously present at lumbar and cervical levels, where they may be represented by some of the deeper fascicles of multifidus.

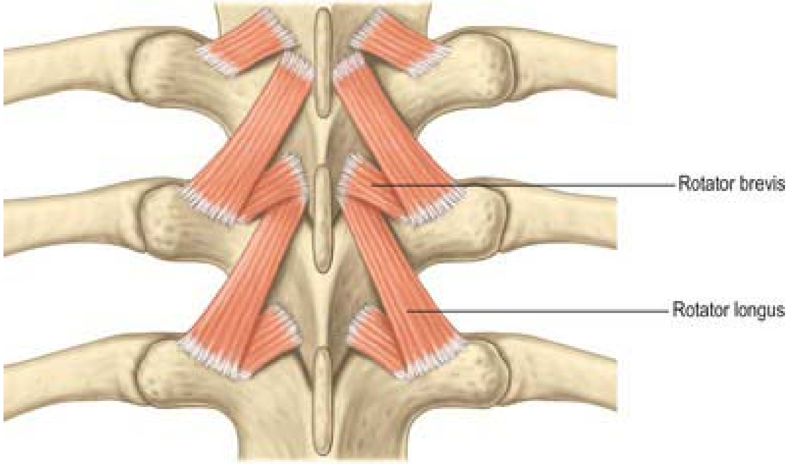

Fig. 42.56 Rotatores (thoracic region).

(By permission from Benninghoff, Anatomie, 15th edition © Urban and Schwarzenberg, 1994.)

Multifidus

At cervical, thoracic, and upper lumbar levels, multifidus lies lateral to the spinous processes and covers the laminae of the underlying vertebrae, but at lumbosacral levels it expands to cover the posterior surface of the sacrum (Fig. 42.57). At each segmental level, multifidus is formed by several fascicles that arise from the caudal edge of the lateral surface of the spinous process and from the caudal end of its tip. They radiate caudally to insert into the transverse elements of vertebrae two, three, four and five levels below (Macintosh et al 1986). These sites are represented at cervical levels by the superior articular processes, at thoracic levels by the posterior surface of each transverse process near its base, and at lumbar levels by the mammillary processes. Fascicles that extend beyond the fifth lumbar vertebra insert into the dorsal surface of the sacrum. The longest fascicles from the first and second lumbar vertebrae insert into the dorsal segment of the iliac crest. From each spinous process the shortest fascicles pass inferiorly and laterally to their insertion; the longer fascicles assume a progressively steeper course and are arranged progressively more medially. The fascicles from a given segment are flanked and overlapped dorsolaterally by fascicles from successively higher segments, an arrangement that endows the intact muscle with a laminated structure.

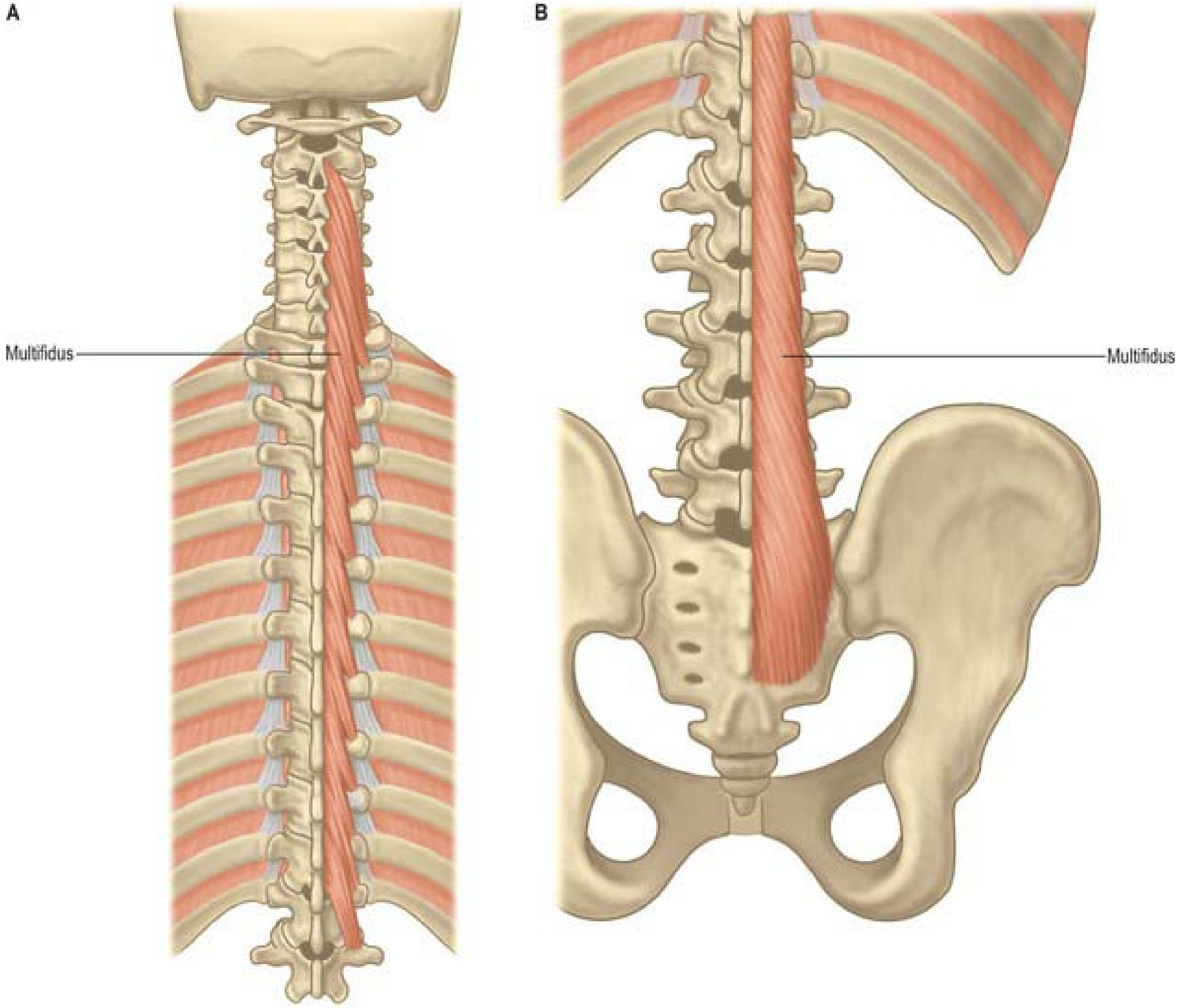

Fig. 42.57 Multifidus. **A**, cervicothoracic. **B**, lumbosacral parts.

Semispinalis

The semispinalis muscles are formed by the longest fascicles of the spinotransverse group. Three divisions are defined essentially by their origins (Fig. 42.58).

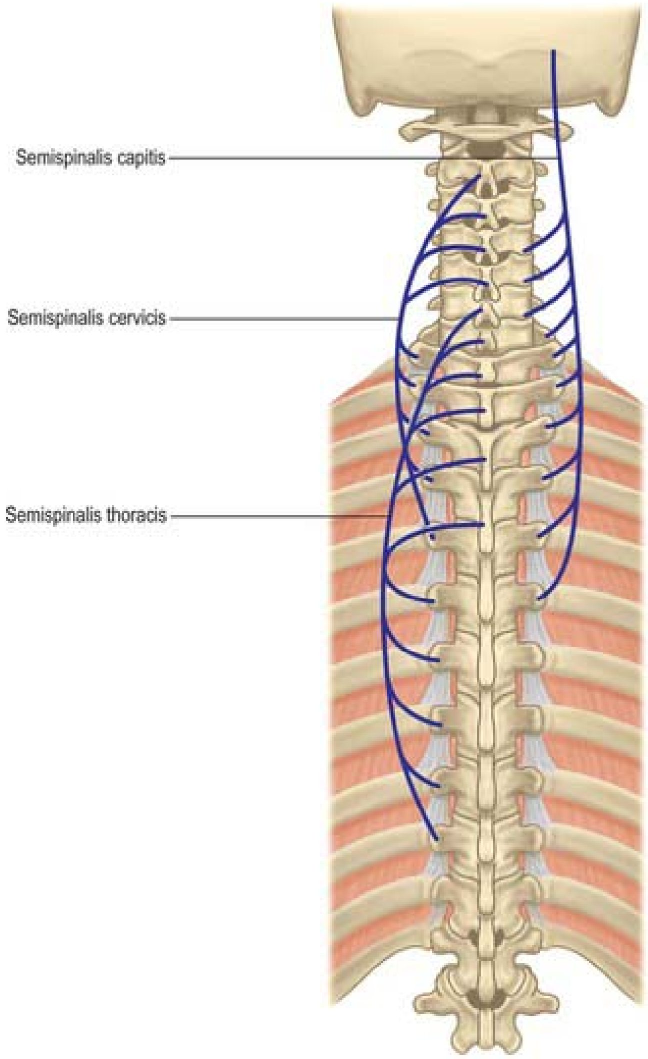
Semispinalis capitis
Semispinalis cervicis
Semispinalis thoracis

Fig. 42.58 Attachments of semispinalis.

Semispinalis cervicis arises from the spinous processes of the second to fifth cervical vertebrae. Its fascicles span about six segments and cover the cervical and thoracic multifidus. They insert by fleshy or tendinous fibres into the posterior surfaces of the upper five or six thoracic transverse processes. The fascicle from the axis is the largest, and is composed chiefly of muscle.

Semispinalis thoracis consists of thin, fleshy fascicles that have long tendons at both ends. They arise from the lower two cervical and the upper four thoracic spinous processes, and insert into the transverse processes of the sixth to tenth thoracic vertebrae. They cover the thoracic multifidus.

Semispinalis capitis covers semispinalis cervicis. It arises from the medial part of the area between the superior and inferior nuchal lines of the occipital bone and forms a thick muscle bundle in the suboccipital region. Individual fascicles pass inferiorly, laterally and ventrally from the muscle, ending as flat tendons that insert successively into the superior articular processes of the lower four cervical vertebrae and the tips of the transverse processes of the upper six or seven thoracic vertebrae. The medial part of the muscle in the cervical region is formed by the thoracic fascicles, which are more or less distinct from the rest, and has been called biventer cervicis because it is traversed by an incomplete tendinous intersection.

Semispinalis is not formed in the lumbar region, but vestiges of its caudal tendons are represented as the mammillo-accessory ligaments of the lumbar vertebrae.

Relations

At cervical, thoracic, and lumbar levels components of erector spinae lie lateral to the spinotransverse group of muscles. They are covered at cervical levels by splenius, at thoracic levels by spinalis thoracis, and at lumbar levels by the erector spinae aponeurosis. In the neck, semispinalis capitis lies mainly deep to splenius and trapezius, but a small portion may be exposed to form the uppermost part of the floor of the posterior triangle of the neck.

Vascular supply

See below.

Innervation

Rotatores, multifidus, semispinalis thoracis, and semispinalis cervicis are all innervated by the medial branches of the dorsal rami of the appropriate spinal nerves. Semispinalis capitis is innervated by descending branches of the greater occipital nerve (C2) and the third cervical nerve (C3).

Actions

All the spinotransverse muscles are extensors. They extend the vertebrae from which they arise, or the head in the case of semi-spinalis capitis. The predominantly longitudinal orientation of their fascicles precludes any substantive action as rotators. Although rotatores have been presumed to rotate the thoracic vertebrae, this action has not been validated. Axial rotation has been expressly refuted as an action of the lumbar multifidus.

Interspinales

Interspinales are short paired muscular fasciculi attached above and below to the apices of the spines of contiguous vertebrae, one on either side of the interspinous ligament. They are most distinct in the cervical region, where they consist of six pairs, the first between the axis and third vertebra, and the last between the seventh cervical and first thoracic vertebrae. In the thoracic region they occur between the first and second vertebrae (sometimes between the second and third), and the 11th and 12th vertebrae. In the lumbar region there are four pairs between the five lumbar vertebrae. A pair is occasionally found between the last thoracic and first lumbar vertebrae, and another between the fifth lumbar vertebra and the sacrum. Sometimes cervical interspinales span more than two vertebrae.

Intertransversarii

Intertransversarii are small muscles between the transverse processes of the vertebrae. They are best developed in the cervical region, where they consist of posterior and anterior sets of muscles separated by the ventral rami of spinal nerves. Posterior intertransverse muscles are divisible into medial and lateral slips. Each medial slip, the intertransverse muscle ‘proper’, is often further subdivided into medial and lateral parts by the passage through it of the dorsal ramus of a spinal nerve. There are seven pairs of these muscles, the highest between the atlas and axis, and the lowest between the seventh cervical vertebra and the first thoracic vertebra; the anterior muscles between atlas and axis are often absent. In the thoracic region, intertransversarii consist of single muscles that span between the transverse processes of the last three thoracic and the first lumbar vertebrae. In the lumbar region they again consist of two sets of muscles. One set, intertransversarii mediales, connects the accessory process of one vertebra with the mammillary process of the next. The other set, intertransversarii laterales, can be divided into ventral and dorsal parts: the ventral parts connect the transverse processes of the lumbar vertebrae, and the dorsal parts connect the accessory processes to the transverse processes of succeeding vertebrae.

Different parts of the intertransversarii in the cervical and lumbar regions are homologous with certain muscles found in the thoracic region. The homologies are determined according to whether the muscle attaches between consecutive transverse elements of the vertebrae, or between transverse and costal elements, or between consecutive costal elements. They are reinforced by the nerve supply of the muscle, and by the relationship between the muscles and certain nerves.

The medial slips of the ‘proper’ posterior intertransverse muscles of the neck connect consecutive transverse elements, as do the intertransversarii mediales of the lumbar region. These muscles are homologous with the thoracic intertransverse muscles and ligaments. All are supplied by dorsal rami. The lateral slips of the ‘proper’ posterior intertransverse muscles connect a transverse element to a costal element, as do the intertransversarii laterales dorsales. They are homologous with levatores costarum, and are supplied by the ventral rami of spinal nerves. At each level the medial branch of a dorsal ramus separates the true intertransverse muscle from levator costae or its equivalent. The anterior intertransverse muscles of the neck and lateral parts of the posterior intertransversarii connect the costal processes of consecutive vertebrae, as do the intertransversarii laterales ventrales of the lumbar region: they are homologous with the intercostal muscles, and are supplied by ventral rami.

Actions of the short muscles of the back

The functions of interspinales and intertransversarii have not been established. They are very small muscles, and are unlikely to be able to generate enough force to be prime movers of the vertebrae. However, they are richly endowed with muscle spindles: the density approaches that found in the lumbricals of the hand and in the extraocular muscles. It therefore seems reasonable to assume that the short muscles of the back may serve a proprioceptive function in controlling the position of the vertebral column and its movements.

Vascular supply of the true back muscles

The true (intrinsic) muscles of the back receive their blood supply from: the vertebral artery; deep cervical artery; superficial and deep descending branches of the occipital artery; deep branch of the transverse cervical artery (when present); superior intercostal artery, via dorsal branches of the upper two posterior intercostal arteries; posterior intercostal arteries of the lower nine spaces via dorsal branches; dorsal branches of the subcostal arteries; dorsal branches of the lumbar arteries; dorsal branch of arteria lumbalis ima; dorsal branches of the lateral sacral arteries.

The detailed pattern of the arterial supply of the deep muscles of the back has been described by Michel Salmon (Taylor & Razaboni 1994). These muscles are supplied by dorsal branches of the posterior intercostal and lumbar arteries. In the thoracic and upper lumbar regions, where the components of erector spinae run in well-defined longitudinal columns, arterial trunks from these dorsal branches run in the sulci between the columns and between erector spinae and multifidus, giving off branches to supply the muscles. This vascular pattern is less regular in the lumbar region.

Suboccipital muscles

The suboccipital muscles (Fig. 42.59) are four small muscles that connect the occipital bone, atlas and axis posteriorly. They lie inferior to the anterior part of the occipital bone, where three of the muscles form the boundaries of the suboccipital triangle: rectus capitis posterior major lies above and medially;

obliquus capitis superior lies above and laterally, and obliquus capitis inferior lies below and laterally. With the head in the anatomical position the suboccipital triangle lies almost in the horizontal plane.

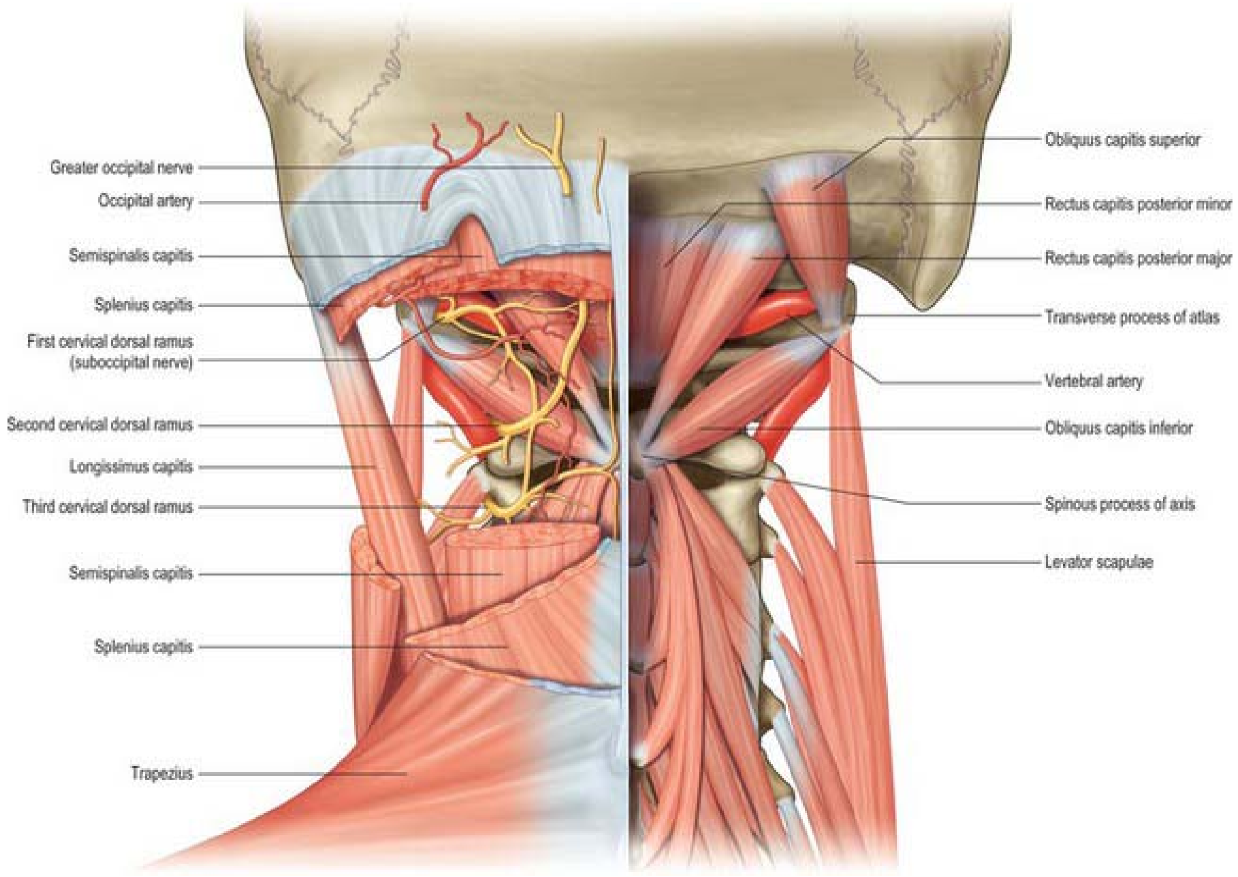
Greater occipital nerve
Occipital artery
Semispinalis capitis
Splenius capitis
First cervical dorsal ramus (suboccipital nerve)
Second cervical dorsal ramus
Longissimus capitis
Third cervical dorsal ramus
Semispinalis capitis
Splenius capitis
Trapezius
Obliquus capitis superior
Rectus capitis posterior minor
Rectus capitis posterior major
Transverse process of atlas
Vertebral artery
Obliquus capitis inferior
Spinous process of axis
Levator scapulae

Fig. 42.59 Posterior view of the suboccipital triangles.

(From Drake, Vogl, Mitchell, Tibbitts and Richardson 2008.)

Rectus capitis posterior major

Rectus capitis posterior major is attached by a pointed tendon to the spine of the axis, becomes broader as it ascends, and is attached to the lateral part of the inferior nuchal line and the occipital bone immediately below it. As the muscles of the two sides pass upwards and laterally, they leave between them a triangular space in which parts of recti capitis posteriores minores are visible.

Rectus capitis posterior minor

Rectus capitis posterior minor is attached by a narrow pointed tendon to the tubercle on the posterior arch of the atlas. As it ascends it broadens before attaching to the medial part of the inferior nuchal line and to the occipital bone between the inferior nuchal line and the foramen magnum. Either muscle may be doubled longitudinally. There is usually a soft-tissue attachment to the posterior atlanto-occipital membrane, which itself is firmly attached anteriorly to the spinal dura in the same area (Zumpano et al 2006).

Obliquus capitis inferior

Obliquus capitis inferior, the larger of the two oblique muscles, passes laterally and slightly upwards from the lateral surface of the spine and the adjacent upper part of the lamina of the axis to the inferoposterior aspect of the transverse process of the atlas.

Obliquus capitis superior

Obliquus capitis superior is attached by tendinous fibres to the upper surface of the transverse process of the atlas. It expands in width as it ascends dorsally, and is attached to the occipital bone between the superior and inferior nuchal lines, lateral to semispinalis capitis and overlapping the insertion of rectus capitis posterior major.

Relations of the suboccipital triangle

Medially the suboccipital triangle is covered by a layer of dense adipose tissue, deep to semispinalis capitis. Laterally it lies under longissimus capitis and sometimes splenius capitis, both of which overlap obliquus capitis superior. The ‘floor’ of the triangle is formed by the posterior atlanto-occipital membrane and the posterior arch of the atlas. The vertebral artery and the dorsal ramus of the first cervical nerve lie in a groove on the upper surface of the posterior arch of the atlas.

Vascular supply

The suboccipital muscles receive their blood supply from the vertebral artery and deep descending branches of the occipital artery.

Innervation

All the suboccipital muscles are supplied by the dorsal ramus of the first cervical spinal nerve.

Actions of the suboccipital muscles

The suboccipital muscles are involved in extension of the head at the atlanto-occipital joints and rotation of the head and atlas on the axis. Obliquus capitis superior and the two recti are probably more important as postural muscles than as prime movers, but this is difficult to confirm by direct observation. Rectus capitis posterior major extends the head and, acting with obliquus capitis inferior, rotates the face towards the ipsilateral side. Rectus capitis posterior minor extends the head. Obliquus capitis superior extends the head and laterally flexes it to the ipsilateral side.

MOVEMENTS OF THE VERTEBRAL COLUMN

Spinal movements between individual vertebrae cannot be measured accurately by skin-surface techniques: only biplanar radiography is sufficient for this purpose. The best values for the normal adult lumbar spine are from Pearcy (1984a,b). Movements of the entire lumbar spine can be measured using skin-surface techniques, but the results are of limited clinical use because there is high inter- and intra-observer variation.

The intervertebral discs are the principal sites of vertebral column movement. Conversely, at most levels, the extent to which the discs may be deformed is also the limiting factor for motion. Bony deformation in the subchondral bone and articular cartilage may contribute to movement. Regional variations in mobility of the spine depend on the geometry, orientation and properties of the facet joints and related ligamentous complexes. Physiological intervertebral movements usually combine tilting (bending) and gliding (shear), so the instantaneous centre of rotation moves continually during the movement. During flexion and extension of the lumbar vertebrae, the centre of rotation usually lies near the centre of the intervertebral disc when viewed in the transverse plane, close to the superior end-plate of the vertebra below.

The oblique and ovoid articular surfaces of the facet joints ensure that spinal movements in different planes are usually ‘coupled’ to a certain extent. For example, lateral flexion would cause impingement of the articular surfaces on that side, leading to a posteriorly directed force on the upper vertebra that would act to rotate it about its long axis. Physiologically, coupled movements are variable. Although movements between individual vertebrae are small, their summation gives a large total range to the vertebral column in flexion, extension, lateral flexion, and axial rotation. Each pair of vertebrae with its interposed disc and ligaments is termed a motion segment or functional spinal unit.

In flexion, the anterior longitudinal ligament becomes relaxed as the anterior parts of the intervertebral discs are compressed. At its limit, the posterior longitudinal ligament, ligamenta flava, interspinous and supraspinous ligaments and the posterior fibres of the intervertebral discs are all tensed, the interlaminar intervals widen, the inferior articular processes glide on the superior processes of subjacent vertebrae, and their capsules become taut. Tension of extensor muscles is also important in limiting flexion, e.g. when carrying a load on the shoulders. Flexion is effectively absent in the thoracic region. In forward flexion of the lumbar spine, the muscles normally protect the osteoligamentous spine from injury. However, the margin of safety can be compromised during repetitive or sustained bending by a failure of the spinal reflexes. Once the muscle protection is lost, flexion injury affects first the interspinous ligaments and then the capsules of the facet joints. The ligamentum flavum has such a high content of elastin that it is always under tension, and can be stretched by 80% without damage. This ligament probably functions to provide a constant smooth lining to the vertebral canal which is never overstretched in flexion, and which never goes slack in extension.

In extension, the opposite events occur, and there is compression of posterior discal fibres. Extension is limited by tension of the anterior longitudinal ligament, anterior discal fibres and impaction of spines or articular processes. It is marked in cervical and lumbar regions, and much less at thoracic levels, partly because the discs are thinner, but also because of the presence of the ribs and chest musculature. In full extension, the axis of movement passes posterior to the disc, moves forwards as the column straightens and passes into flexion, and reaches the centre of the intervertebral disc in full flexion.

In lateral flexion, which is always combined with ‘coupled’ axial rotation, intervertebral discs are laterally compressed and contralaterally tensed and lengthened, and motion is limited by tension of antagonist muscles and ligaments. Lateral movements occur in all parts of the column but are greatest in cervical and lumbar regions.

Axial rotation involves twisting of vertebrae relative to each other with accompanying torsional deformation of intervening discs. About 50% of cervical rotation occurs at the atlanto-axial joint. Elsewhere in the column, although movement is slight between individual vertebrae, the range summates to become considerable for the column as a whole. In the post-cervical column, the effective range of rotation is greatest at the thoracolumbar junction. There is very little rotation in the remainder of the lumbar region.

In the cervical region the upward inclination of the superior articular facets allows free flexion and extension. The latter is usually greater, and is checked above by locking of the posterior edges of the superior facets of C1 in the occipital condylar fossae, and below by slipping of the inferior processes of C7 into grooves inferoposterior to the first thoracic superior articular processes. Flexion stops where the cervical convexity is straightened, checked by apposition of the projecting lower lips of vertebral bodies on subjacent bodies. Cervical lateral flexion and rotation are always coupled, and the superomedial inclination of the superior articular facets imparts rotation during lateral flexion.

Cervical motion can be considered to involve the upper (i.e. the atlanto-occipital and atlanto-axial complexes) and the lower cervical spine (C3–7). Two physiological movements take place at the atlanto-occipital joints, those of flexion-extension and lateral flexion. The atlanto-axial joints allow flexion-extension and rotation. Some studies have suggested that maximum flexion-extension occurs between the occiput and C1; however, Frobin et al (2002) noted between 12.6° and 14.5° at this level, which is less than at some of the other cervical levels. Global cervical flexion ranges from 45° to 58° depending on the method of assessment, age and sex: older subjects and females exhibit less motion (Ordway et al 1997; Trott et al 1996). At an intersegmental level, motion increases from the second cervical level, peaks at the mid cervical level (14–17° recorded at C4/5), before reducing at the junction of the cervical and thoracic spine (9.8–11.5° noted at C6/7) (Frobin et al 2002). Global ranges of lateral flexion range from 32° to 47°, with a gradual reduction in range with age and sex, while rotational movements range from 63° to 78°. Intersegmental ranges of motion vary from 4.7° to 6° for lateral flexion between C2 and C7, and 2–12° for rotation (White & Panjabi 1990).

In the thoracic region, especially superiorly, all movements are limited, reducing interference with respiration. Lack of upward inclination of the superior articular facets prohibits much flexion, and extension is checked by contact of the inferior articular margins with the laminae and of adjacent spines. Thoracic rotation is freer, though limited by the ribs at upper levels. Its axis is in the vertebral bodies in the midthoracic region, and in front of them elsewhere, so that rotation involves some lateral displacement. The direction of articular facets would allow free lateral flexion, but this is limited in the upper thoracic region by the resistance of the ribs and sternum. Rotation is usually combined with slight lateral flexion to the same side.

Movement in the thoracic spine is frequently regionalized to upper, mid- and lower thoracic. In the upper thoracic, flexion ranges from 7.8° to 9.5°, increasing to 10–11.4° in the mid-thoracic and 12.5° to 12.8° in the lower thoracic (Willems et al 1996). Extension is more consistent, ranging from 7.1° to 9.7° throughout the thoracic spine. Lateral flexion is greater in the lower thoracic spine, ranging from 5.6° to 6.2° in the upper thoracic, 7.9° to 8.1° in the mid-thoracic and 11.9° to 13.2° in the lower thoracic. However, rotation is greatest in the mid-thoracic region, being 11.8° to 15.9° in the upper thoracic, 21.5° to 25.3° in the mid-thoracic, and 8.3° to 11.8° in the lower thoracic.

Flexion movements are generally greater than extension or lateral flexion in the lumbar region. Axial rotation occurs about a centre of rotation in the posterior anulus, and is limited by bony contact in the facet joints after only 1–2° of movement. Functional transition between thoracic and lumbar regions is usually between the 11th and 12th thoracic vertebrae, where the facet joints usually fit so tightly that slight compression locks them, and prevents all movements but flexion.

During flexion of the lumbar spine there is an unfolding or straightening of the lumbar lordosis. Thus in full flexion the lumbar spine assumes a straight alignment or is curved slightly forwards. Normal ranges of global lumbar flexion range from 58° to 72° in under 40-year-olds and 40° to 60° in the over forties: females exhibit a reduced range compared with males (McGregor et al 1995; Dvorák et al 1995). At an intersegmental level, the L3/4 junction and L4/5 junction exhibit the greatest mobility, approximately 12° and 13° respectively, while at the lowest level (L5/S1) there is only 9°, and at the upper lumbar levels only 8° and 10° respectively (Pearcy et al 1984). Movements into extension are the converse of those seen in flexion. Normal ranges of global extension range from 25° to 30° in under 40-year-olds and 15° to 20° in those over forty. At an intersegmental level, L5/S1 and L1/2 exhibit the greatest mobility at approximately 5°, while the remaining levels exhibit less than 5° of extension. Ranges of lateral flexion and rotation in the lumbar spine are reduced compared to other regions of the spine. Global lateral flexion ranges from 20° to 35°, and rotation ranges from 25° to 40°: the ranges of both movements are reduced with age. Assessment of intersegmental rotation and lateral flexion has proven difficult because of the limitations of measurement techniques.

ROLE OF MUSCULATURE

Although muscles will move the spinal column, the majority of muscular activity is involved in providing stability to maintain posture and to provide a firm platform for limb function. Hence the concept of ‘core stability’ in modern rehabilitation programmes, especially in sports-related problems.

It is important to recognize the way in which the muscles of the back work in conjunction with those of the abdominal wall, particularly the oblique and transversus muscles, and with those of the lower limbs. The erector spinae group and internal oblique and transversus abdominis are anatomically and functionally connected by the thoracolumbar fascia (which encloses the former, and into which the latter are inserted). This fascia, together with collagenous tissue within the back muscles, plays an important role in resisting forward bending of the trunk, and during manual handling. The fascia is tensioned primarily by flexing the trunk, although this tension may be enhanced slightly by the lateral pull of the abdominal muscles. It is functionally advantageous to generate tension in the fascia and muscle sheaths, because the elastic strain energy stored in these stretched tissues can be used to help bring the trunk to an upright position and so reduce the metabolic cost of the movement (Adams et al 2002). The thoracolumbar fascia may also have an important function in transferring load between the trunk and the lower limbs: tension in the fascia can be increased by the actions of gluteus maximus and the hamstrings as well as by trunk flexion.

Muscles producing vertebral movements

The spinal column is moved both directly by muscles attached to it, and indirectly by muscles attached to other bones. Gravity always plays a part: movements with gravity usually involve the eccentric contraction of antagonists. Flexion is effected by longus capitis and longus colli, scaleni, sternocleidomastoid and rectus abdominis of both sides, aided in the lumbar region by the abdominal obliques; extension by the erector spinae complex and the transversospinalis group, splenius, semispinalis capitis and trapezius of both sides, together with the sub-occipital muscles; lateral flexion by ipsilateral longissimus, iliocostalis, abdominal obliques and flexors, and quadratus lumborum; rotation by sternocleidomastoid, splenius cervicis, abdominal obliques, rotatores and multifidus.

FACTORS INVOLVED IN STABILITY

The vertebral column is remarkable in that it combines mobility, stability and load-bearing capacity and also protects its contained neural structures, irrespective of its position. Much of the stability of the vertebral column depends on dynamic muscular control, but there are also bony and ligamentous ‘static’ stabilizers. There is considerable variation between segments of the column in terms of stability and mobility: the most mobile levels are the least stable. The latter are those in which the ratio of intervertebral disc height to vertebral body height is highest. Stability may be compromised by damage to any of these structures.

Trauma may affect any vertebral region. Levels of specialized mobility (e.g. atlanto-axial joint) and the junctions of mobile and relatively fixed regions (e.g. cervicothoracic, thoracolumbar) are particularly vulnerable to severe structural damage, often accompanied by spinal cord and nerve injury. Injuries of the vertebral column may be purely soft-tissue (ligaments, joint capsules and muscles) or may affect bony structures. Pure ligamentous/capsular injuries leading to instability may be particularly difficult to diagnose in the absence of gross radiological signs. In the cervical spine, subluxation and dislocation of the facet joints commonly occur without bony injury because of the orientation of the articular facets.

Chronic infections of many types (e.g. tuberculosis) may involve the vertebrae and lead to their deformity and collapse, affect their mechanical properties and compromise their neuroprotective function. Acute infections, spreading locally or via the bloodstream, may lead to the collection of pus within the vertebral canal causing spinal cord compression (epidural abscess).

The integrity of the vertebrae may also be affected by malignant disease, most commonly metastatic. Vertebrae have a copious blood supply throughout life, and many of the common cancers (e.g. breast, bronchus) spread via the arterial system. Cancers of the haemopoietic system (e.g. multiple myeloma) also commonly affect the vertebrae. Prostatic carcinoma has a predilection to metastasize to the vertebral column, often using the venous (Batson’s plexus) rather than the arterial route. Metastatic deposits may occur within the epidural space, compressing the contents of the dural sac at multiple levels.

Systemic inflammatory diseases may cause both deformity and instability of the vertebral column. Rheumatoid arthritis inflames facet joints and weakens ligaments, leading to instability, especially in the cervical spine. Ankylosing spondylitis and other seronegative arthritides affect joints and ligamentous attachments (entheses), leading to ectopic ossification of collagenous structures, fusion (ankylosis) of interbody and facet joints, and loss of the normal spinal curvatures. Widespread new bone formation at and around the joints of the column occurs in DISH (diffuse idiopathic skeletal hyperostosis). Such conditions would seem to increase stability of the column, at the expense of its mobility and function, but an ankylosed spine is very liable to fracture, with an associated risk of neural damage.

Full stability and load-bearing capacity both require intact vertebral bodies and intervertebral discs. Earlier views regarding the relative importance of the disc-body complex and the posterior elements have proved somewhat simplistic. Clinical observation led to the ‘three-column concept’ of spinal stability (Denis 1983), in which the column is divided into three longitudinal parts rather than two. The anterior column is formed by the anterior longitudinal ligament, the anterior half of the vertebral body and the anterior anulus fibrosus. The middle column is made up of the posterior longitudinal ligament, the posterior half of the vertebral body and pedicles and the posterior anulus fibrosus. The posterior column consists of the neural arch and facet joints and the posterior ligamentous complex. Failure of any column can lead to some instability, the status of the middle column being the most important. The more columns that are affected, the worse is the instability: an injury to two columns is usually unstable.

The elastic deformability of intervertebral discs permits tilting and axial rotation between vertebral bodies, and also helps to reduce vertical accelerations of the head. The main shock-absorbing mechanism of the column stems from the spinal curves, which increase and decrease slightly during locomotion against the restraining tension of the trunk muscles. The elastic strain energy in the stretched tendons of the muscle is responsible for shock absorption.

Both body height and spinal stability are subject to a marked diurnal variation. Body height is affected by changes from recumbency to the upright posture. These diurnal variations appear to be due to changes that occur within the cervical, thoracic and lumbar regions of the spine. Investigations using stereophotogrammetry have demonstrated that 40% of diurnal changes occur in the thoracic spine and affect the degree of kyphosis, and a further 40% in the lumbar spine, but do not affect the lordosis (Wing et al 1992). The greatest change in vertebral column length is found in adolescents and young adults. The height loss occurs within 3 hours of rising in the morning, with an overall loss of about 15 mm.

Although the curvatures within the vertebral column contribute to the changes in height, changes within the intervertebral disc contribute both to observed height loss and to variation in stability. Magnetic resonance imaging investigations reveal a dynamic movement of fluid into and out of an intervertebral disc and adjacent vertebral body over a 24-hour period. Body position affects the movement of fluid. In the early morning, the discs are swollen with water, the intervertebral ligaments and the anulus fibrosus are taut, and the intrinsic bending stiffness and stability of the osteoligamentous spine are relatively high. After several hours of normal activity, the discs lose approximately 20% of their water and height. This change makes the ligaments slack and greatly reduces the bending stiffness of the spine, so that relatively more of the stability of the spine must then be provided by the musculature. The diurnal expulsion of water from intervertebral discs also affects the distribution of compressive loading in the spine. As the day progresses, the hydrostatic pressure in the nucleus pulposus falls, and stress concentrations arise in the anulus fibrosus and facet joints.

All ligaments of the column, as well as the facet joint capsules, are important in the maintenance of stability. The anterior longitudinal ligament is very strong, and resists translational displacement (shear) of the vertebrae as well as extension. All the ligaments of the posterior complex resist flexion and rotation, and their integrity determines the range of movements allowed.

These ligaments can support the whole column when the muscles are inactive, e.g. in quiet standing. At the limit of lumbar flexion the column is supported mainly by the thoracolumbar fascia and by collagenous tissue within the electrically silent muscles of the back.

Movements are both determined and constrained by the shape and orientation of the facet joints, whose articular surfaces stabilize the column primarily by resisting horizontal gliding (shear) movements and axial rotation. In the most mobile regions the joint surfaces are flatter and more horizontally placed, as will become apparent if a typical cervical facet joint is compared with a typical lumbar joint.

Certain regions of the vertebral column are further stabilized by additional extraspinal factors. The thoracic spine is stabilized by its position as an integral part of the thoracic cage and by its strong ligamentous linkages with the ribs. The sacrum is effectively a virtually fixed integral element of the bony pelvis.

The contribution to stability conferred by the musculature has been grossly underrated. The whole vertebral column is stabilized by the ‘guy-rope’ or staying effect of the long muscles which attach it to the girdles, the head and the appendicular skeleton. This effect is particularly marked for erector spinae, which controls global posture and movement. The small and deep muscles of the back are best able to resist shear movements between vertebrae because only they have sufficient angulation to the long axis of the vertebral column to do this effectively. The deep muscles can also fine-tune intervertebral movements.

For most back problems in clinical practice, especially chronic low back pain, enhancing muscle strength, stamina, and coordination with the many other muscle groups that contribute to stability, e.g. pelvic girdle muscles, is the most appropriate and effective therapeutic avenue. Only a minority of cases benefit from surgery. Furthermore, neglecting the musculature may explain the relatively high failure rates from surgery.

Mechanical injury to the vertebral column may be produced by flexion, extension, distraction, rotation, shear or compression: movements that cause damage are commonly combined, e.g. flexion, axial rotation and compression.

POSTURE AND ERGONOMICS

Posture is a descriptive term for the relative position of the body segments during rest or activity. The maintenance of good posture is a compromise between minimizing the load on the spine and minimizing the muscle work required.

The well-balanced erect body has a line of gravity which extends from the level of the external auditory meatus, through the dens of the axis just anterior to the body of the second thoracic vertebra, through the centre of the body of the 12th thoracic vertebra, and through the rear of the body of the fifth lumbar vertebra to lie anterior to the sacrum. The position of the line of gravity may move anteriorly with locomotion, and may vary between individuals.

The normal curvature of the cervical spine is a lordosis. However, as a result of pain, injury or poor ergonomics, this curve can become exaggerated to give a ‘protruding chin’ stance, i.e. hyperlordosis in the lower cervical spine.

The thoracic spine is held convex posteriorly, and this posture primarily results from the structure of the underlying vertebrae. However, this curve or kyphosis can become exaggerated to give the impression of a rounded back. Poor posture and ergonomics can lead to this exaggerated curvature but other important causes include tuberculosis, a wedge or compression fracture of a vertebral body, Scheuermann’s osteochondritis, ankylosing spondylitis, osteoporosis, and metastatic carcinoma.

The lumbar spine is held in a lordosis. The degree of this lordosis is determined by the lumbosacral angle and is normally 30–45°. The muscles responsible for this posture include erector spinae, rectus abdominus, the internal and external obliques, psoas major, iliacus, the gluteal and hamstring muscles. The lordosis can be increased (as a result of weak abdominal muscles and tight hamstring muscles), decreased, flattened (common in people either with acute or chronic low back pain), or reversed.

A common postural deviation seen throughout the spine is scoliosis or lateral curvature of the spine. It can be structural, compensatory or protective. In structural scoliosis, the lateral curvature is associated with vertebral rotation, and both the curve and the rotation become more accentuated on forward flexion. Such a scoliosis is common in adolescent girls and its cause is unknown. It may also be secondary to an underlying disorder, e.g. muscular dystrophy, spinal muscular atrophy or spina bifida. A compensatory scoliosis occurs when the pelvis is tilted laterally, e.g. as a result of unequal leg length or of a fixed abduction or adduction deformity at the hip joint. Usually there is no intrinsic abnormality of the spine itself and the scoliosis disappears when the pelvic tilt is corrected. A sciatic or antalgic scoliosis is a temporary deformity produced by the protective action of muscles in certain painful conditions of the spine.

Ergonomics has been defined as ‘the way humans work’, and it permits an appreciation of the effects of tasks and the work environment on underlying postural biomechanics. Nachemson (1975) showed that discs were loaded maximally in sitting and in lifting in a forward leaning position, so sitting posture and lifting have received considerable ergonomic attention.

In sitting the goal has been to determine the seat type and reclining angle associated with lowest disc pressure and the least paraspinal muscle activity. When sitting with the hips and knees flexed to 90° the pelvis rotates posteriorly, flattening the lumbar lordosis and consequently increasing the load on the intervertebral discs. Thus it is now advised that in sitting the angle between trunk and thigh should be between 105 and 135°, with the sacrum tilted at 16° and the fourth and fifth lumbar vertebrae supported.

In lifting heavy weights there is considerable initial compression of lumbar intervertebral discs, and large increases in thoracic and intra-abdominal pressure. The compressive force acting on the spine is shared between the vertebral bodies and the neural arch. In the lumbar spine, the neural arch typically resists 20% of this force once the disc height has been reduced by diurnal fluid expulsion, and when the spine is positioned upright. However, age-related narrowing of the disc can cause more than 50% of the compressive force to be resisted by the neural arch, which may explain why osteoarthritis of the facet joints commonly follows disc degeneration.

When lifting, manual handling advisors emphasize the importance of leg lifting as opposed to back lifting. Loads should also be kept close to the body to reduce the lever arm of the load. The use of deep inspiration to raise intra-abdominal pressure while lifting has also been advised, as this is believed to offer further support to the lumbar spine. The spine is at risk when lifting is combined with twisting, lateral bending, and asymmetric postures. However, heavy lifting remains one of the key work related risk factors for the spine together with whole body vibration, prolonged sitting, twisting and bending.

SURFACE ANATOMY

SKELETAL LANDMARKS

Vertebral spines

In the midline a median furrow runs from the external occipital protuberance above to the natal cleft below (Fig. 42.60, Fig. 42.61, Fig. 42.62). The furrow is most shallow in the lower cervical region and is deepest in the midlumbar zone. Inferiorly, it widens out into a flattened, triangular area, the apex of which lies at the start of the natal cleft and corresponds to the third sacral spine. Palpation of the median furrow reveals the sagittal curves of the spine: the cervical curve is convex forwards (lordosis) and extends from the first cervical to the second thoracic vertebra; the thoracic curvature is concave forwards (kyphosis) and extends from the second to the 12th thoracic vertebra; the lumbar curvature is convex forwards and extends from the 12th thoracic vertebra to the lumbosacral prominence. The external occipital protuberance is subcutaneous and can be felt and often seen (Fig. 42.61), and it can be palpated without difficulty when it is approached from below. The inion is the point situated on this protuberance in the median plane. The tips of the spines of the cervical vertebrae are obscured by the overlying ligamentum nuchae. The tubercle on the posterior arch of the atlas is impalpable; the first bony prominence which is encountered when the finger is drawn downwards in the midline from the external occipital protuberance is the spine of the second cervical vertebra. The ligamentum nuchae terminates inferiorly at the spine of the seventh cervical vertebra, which is the highest, and sometimes the only, visible projection in this region (vertebra prominens). Immediately below this the spine of the first thoracic vertebra is palpable; it is usually more prominent than the seventh cervical vertebra. The spine of the second thoracic vertebra can also often be felt. The third thoracic spinous process is level with the spine of the scapula (Fig. 42.60), and the seventh with the inferior scapular angle when the arm is by the side. The identification of the remaining thoracic spines is not easy, even in a thin subject when the trunk is fully flexed, because of the manner in which they overlap one another in the midthoracic region. In the upper and lower thoracic regions, the tips of the thoracic spines lie opposite the upper part of the body of the immediately subjacent vertebra. In the midthoracic region, they lie opposite the lower part of the vertebra below. The tip of the spine of each lumbar vertebra can usually be palpated without difficulty, especially if the trunk is flexed. Each lies opposite the inferior part of its own body. The body of the fourth lumbar vertebra is level with the summits of the iliac crests, so the fourth lumbar spine overlies the L4/5 interspace (a point useful in lumbar puncture). The second sacral spine is level with the posterior superior iliac spines. Sacral and coccygeal landmarks are described below.

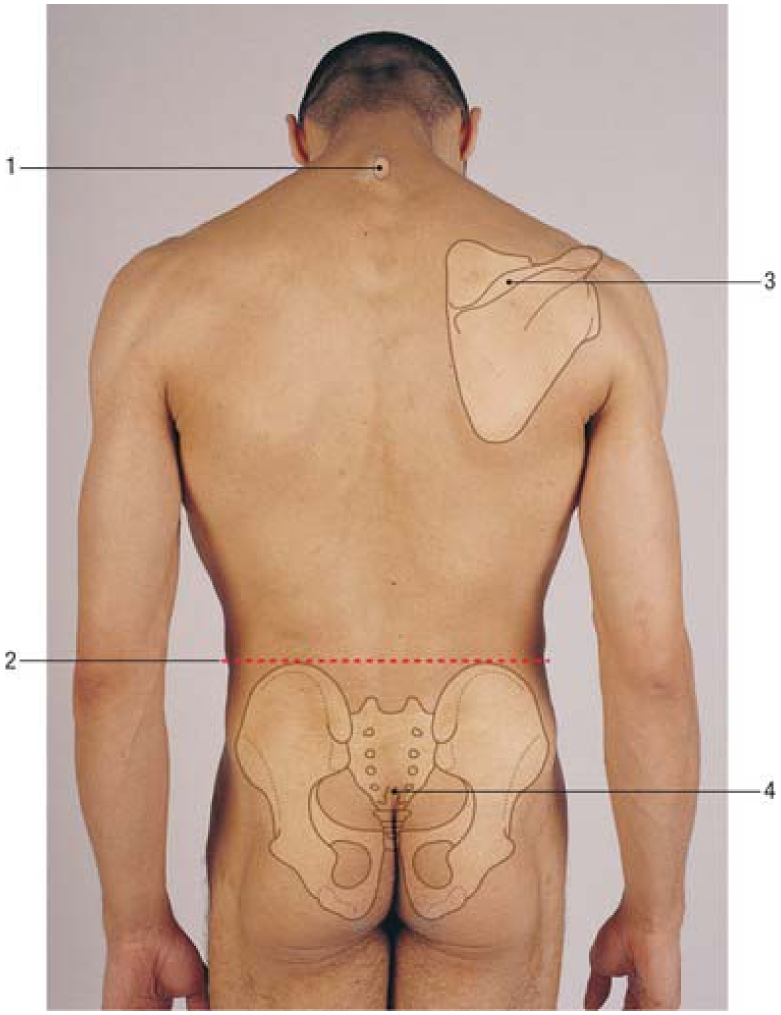

Fig. 42.60 Back view of trunk. **1**. Vertebra prominens (spine of C7) **2**. Supracristal plane. **3**. Spine of scapula. **4**. Position of sacral hiatus.

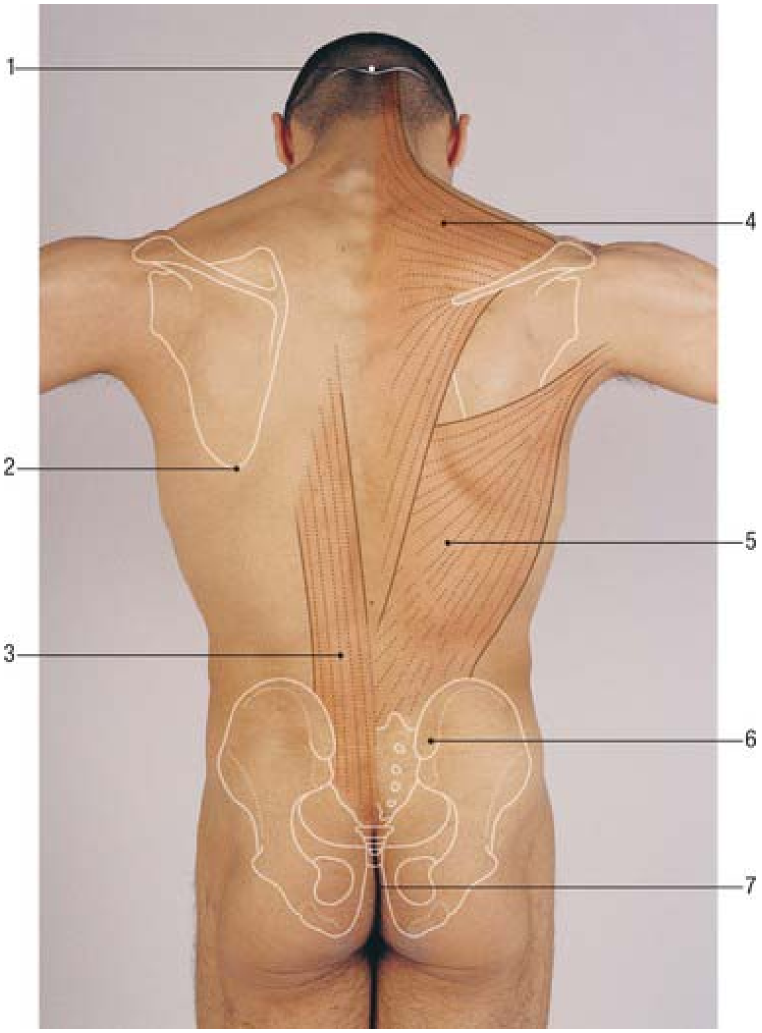

Fig. 42.61 Back view of trunk, arms abducted. **1**. External occipital protuberance. **2**. Inferior angle of scapula. **3**. Erector spinae. **4**. Trapezius. **5**. Latissimus dorsi. **6**. Posterior superior iliac spine underlying sacral dimple. **7**. Natal cleft.

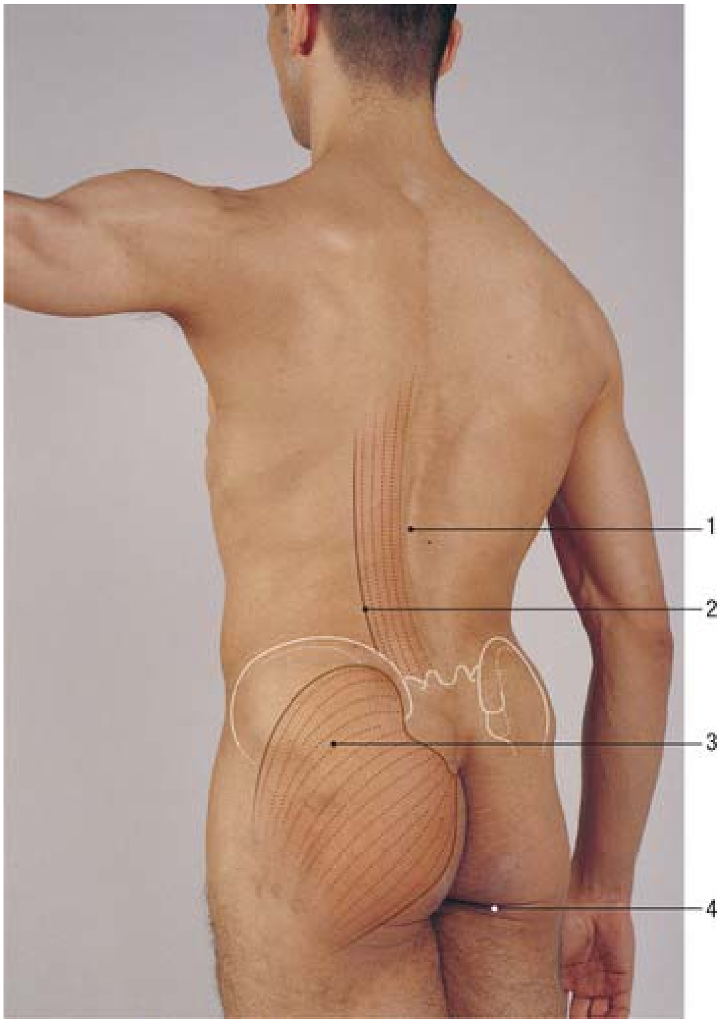

Fig. 42.62 Back of trunk, oblique view. **1**. Median furrow. **2**. Lateral border of erector spinae. **3**. Gluteus maximus. **4**. Gluteal fold.

Note that when the subject lies in the lateral position (on the side), the median soft-tissue furrow may not coincide with the median plane, especially in the lumbar region in the obese. Careful palpation may be necessary to identify the spines, a point which is of particular importance during lumbar or epidural puncture in this position.

Spinal levels of viscera

The palpable vertebral spines can be used as landmarks for the levels of the viscera. Some of the more important are shown in Table 42.1 (minor differences between the two sides are ignored).

Table 42.1 Vertebral spines as landmarks for the viscera.

Spine	Viscera
C5	Cricoid cartilage, start of oesophagus
C7	Apex of lung
T3	Aorta reaches spine. Tracheal bifurcation
T4	Aortic arch ends. Upper border of heart
T8	Lower border of heart. Central tendon of diaphragm
T10	Lower border of lung. Cardia of stomach. Upper border of kidney
T12	Lowest level of pleura. Pylorus
L1	Hilum of kidney. Renal arteries. Superior mesenteric artery
L2	Spinal cord terminates. Pancreas. Duodenojejunal flexure
L3	Lower border of kidney
L4	Bifurcation of aorta
L5	Inferior vena cava begins

Scapular landmarks

The shape of the back in the upper thoracic region is determined largely by the scapula and the muscles which attach to it, especially trapezius. The relative prominence of the scapula and its muscles depends upon the state of contraction of the latter. Bony scapular landmarks are most evident when the arms hang by the sides.

The scapula overlies the second to seventh ribs. Its superior angle is palpable beneath trapezius, and its inferior angle is just covered by latissimus dorsi: these angles are joined by the medial border of the scapula which runs vertically (Fig. 42.60, Fig. 42.61). The scapular spine runs subcutaneously and is easily palpable from its root medially to the acromion process laterally.

The root of the spine of the scapula lies opposite the third thoracic spine and the inferior angle lies opposite the seventh thoracic spine when the arm is by the side.

Posterior pelvic and sacrococcygeal bony landmarks

At the lower part of the back the iliac crest can be palpated throughout its whole length, and can be traced backwards and upwards from the anterior superior iliac spine to its highest point, and then downwards and medially to the posterior superior iliac spine, which is overlain by a dimple in the skin (Fig. 42.61). A line joining these sacral dimples passes through the second sacral spine and the body of the second sacral vertebra, and is a useful landmark for the lower end of the adult dural sac. There may also be a less prominent pair of dimples at the level of the L4/5 intervertebral disc. The posterior superior iliac spine lies over the centre of the sacroiliac joint. The supracristal plane joins the highest points of the iliac crest on each side. It passes through the body of the fourth lumbar vertebra and has been used as a clinical landmark when performing a lumbar puncture (p. 760) though difficulty in its definition reduces its reliability in this procedure. The tip of the coccyx can be felt deeply near the centre of the natal cleft. As the examining finger passes cranially, the sacral cornua can be felt on either side: these demarcate the sacral hiatus, and form the landmark for performing a caudal anaesthetic block.

MUSCULOTENDINOUS LANDMARKS

In the upper and middle cervical region the median furrow lies between the cylindrical prominences formed mainly by the semispinalis muscles, which are accentuated by neck extension against resistance. In the thoracic and lumbar regions, a broad elevation produced by the erector spinae muscle group extends for about one hand's breadth on either side of the median furrow and is present between the iliac crest and the 12th rib (Fig. 42.62). The lateral border of this elevation then crosses the ribs at their angles, passing medially as it ascends. The muscle group can be demonstrated by extending the back against resistance.

Trapezius is a flat, triangular muscle that covers the back of the neck and shoulder (Fig. 42.61). Together, the two trapezius muscles resemble a trapezium or quadrilateral in which two of the angles correspond to the shoulders, a third to the occipital protuberance and the fourth to the spine of the 12th thoracic vertebra. The two muscles cover the back of the neck and shoulders like a monk's cowl, hence the ancient name of the trapezius was musculus cucullaris. The upper part of trapezius is demonstrated by elevation of the shoulders, or by extension and lateral flexion of the neck, against resistance. The lower fibres are best seen when the subject pushes both hands hard against a wall with the elbows extended. The anterosuperior border of the muscle forms the posterior boundary of the posterior triangle of the neck and can be seen in muscular subjects, especially during elevation of the shoulder against resistance.

In a well-muscled subject the outline of latissimus dorsi can easily be traced, particularly if the arm is adducted against resistance. The triangle of auscultation (Fig. 42.52) lies between the upper border of latissimus dorsi, the lower lateral border of trapezius and the medial border of the scapula.

The lumbar triangle (Fig. 42.52), one of the sites of the rare primary lumbar hernia, lies inferiorly, between the lowermost outer border of latissimus dorsi, the posterior free border of external oblique, and the iliac crest.

CLINICAL EXAMINATION

Clinical examination of the back of the trunk and neck best follows the order of inspection, palpation and movement. The examination will be determined by the circumstances of presentation and by the history, and may include musculoskeletal, neurological and vascular observations. Information relevant to the neurological and vascular examination of the skin and material relating to spinal movements and deeper innervation are found above. Palpation of the region involves careful assessment of the bony and musculotendinous landmarks described above, looking in particular for asymmetry, deformity and tenderness. Note that, apart from the spines, most of the bony elements of the vertebrae and almost all of the intervertebral joints are not palpable from behind. In regions of lordosis (sagittal plane curves of the spine with anterior convexity, i.e. midcervical and mid- and lower lumbar), parts of the vertebral column can often be palpated anteriorly with care in well-relaxed, thin subjects.

REFERENCES

lams MA, Bogduk N, Burton K, Dolan P. The Biomechanics of Back Pain, 2nd edn. Edinburgh: Churchill Livingstone, 2006.

A comprehensive and detailed source of information on the functional anatomy, tissue biology and biomechanics of the lumbar spine..

tson OV. The vertebral vein system. *Am J Roentgenol*. 1957;78:195-212.

A pioneering study of the venous plexuses of the vertebral column which has become the standard of reference in its field..

elderl A, Daniaux H, Kathrein A, Maurer H. Danger of damaging the medial branches of the posterior rami of spinal nerves during a dorsomedian approach to the spine. *Clin Anat*. 2002;15:77-81.

Detailed descriptions of the vascular supply and innervation of the posterior elements of the thoracolumbar spine and the overlying muscles..

ogduk N. Clinical Anatomy of the Lumbar Spine and Sacrum, 4th edn. Edinburgh: Elsevier Churchill Livingstone, 2005.

The most thorough text currently available on the topographical and functional anatomy of the lumbosacral spine, with over 1000 references. The book incorporates biomechanical and physiological information which is related to the clinical problem of low back pain..

rock HV. Atlas of Vascular Anatomy of the Skeleton and Spinal Cord. London: Martin Dunitz, 1996.

rock HV, Yoshizawa H. The blood supply of the lumbar vertebral column. *Clin Orthop*. 1976;115:6-21.

ean NA, Mitchell BS. Anatomic relation between the nuchal ligament (ligamentum nuchae) and the spinal dura mater in the craniocervical region. *Clin Anat*. 2002;15:182-185.

Describes continuity in the midline between the spinal dura and the ligamentum nuchae in human cadavers..

enis F. The three column spine and its significance in the classification of acute thoracolumbar spinal injuries. *Spine*. 1983;8:817-831.

Seminal paper for the understanding and classification of spinal instability..

vorák J, Vajda EG, Grob D, Panjabi MM. Normal motion of the lumbar spine related to age and gender. *Eur Spine J*. 1995;4:18-23.

obin W, Leivseth G, Biggeman M, Brinckmann P. Sagittal plane segmental motion of the cervical spine. A new precision measurement protocol and normal motion data of healthy adults. *Clin Biomech*. 2002;17:21-31.

roen G, Baljet B, Drukker J. The nerves and nerve plexuses of the human vertebral column. *Amer J Anat*. 1990;188:282-296.

An acetylcholinesterase whole-mount study of human fetal material giving detail of the perivertebral nerve plexuses and of the sinuvertebral nerves..

ng J. Craniocervical region, osteology and articulations. *Neuro Orthop*. 1986;1:67-92.

ughenbury PR, Wadhwani S, Soames RW. The posterior longitudinal ligament and peridural (epidural) membrane. *Clin Anat*. 2006;19:487-492.

acintosh JE, Valencia F, Bogduk N, Munro RR. The morphology of the lumbar multifidus muscles. *Clin Biomech*. 1986;1:196-204.

acLaughlin SM, Oldale KNM. Vertebral body diameters and sex prediction. *Ann Hum Biol*. 1992;19:285-293.

Describes the archaeological and forensic examination of skeletal material..

acnab I, McCulloch J. Backache, 2nd edn. Baltimore: Williams and Wilkins, 1990. Chapter 1.

The functional anatomy of the lumbar spine, described as a basis for the clinical management of low back pain..

cGregor AH, McCarthy ID, Hughes SPF. Motion characteristics of the lumbar spine in the normal population. *Spine*. 1995;20(22):2421-2428.

ercer S, Bogduk N. The ligaments and anulus fibrosus of human adult cervical intervertebral discs. *Spine*. 1999;24:619-628.

A human cadaveric microdissection study showing that the cervical anulus fibrosus is an anterior crescent rather than a uniformly circumferential structure..

ercer SR, Bogduk N. Clinical anatomy of ligamentum nuchae. *Clin Anat*. 2003;16:484-493.

chemson A. Towards a better understanding of low-back pain: a review of the mechanics of the lumbar disc. *Rheumatol Rehab*. 1975;14:129-143.

well RLM. The spinal epidural space. *Clin Anat*. 1999;12:375-379.

Review of the morphological, developmental and topographical aspects of the spinal epidural space..

dway NR, Seymour R, Donelson RG, Hojnowski L, Lee E, Edwards T. Cervical sagittal range of motion using three methods. *Spine*. 1997;22:501-508.

arcy M, Protek I, Shepherd J. Three-dimensional X-ray analysis of normal movement in the lumbar spine. *Spine*. 1984;9:294-297.

arcy M, Tibrewal SB. Axial rotation and lateral bending in the normal lumbar spine. *Spine*. 1984;9:582-587.

per JG, Traynelis VC. Congenital malformations of the craniovertebral junction. In: Dickman CA, Spetzler RF, Sonntag VKH. *Surgery of the Craniovertebral Junction*. New York: Thieme, 1998.

ylor GI, Razaboni RM. Michel Salmon: Anatomic Studies, Book 1. Arteries of the Muscles of the Extremities and Trunk. St Louis: Quality Medical Publishing, 1994.

A translated, updated and edited version of a classic French text first published in 1933. Now a major source-book in plastic surgery..

ylor JR, Twomey LT. Sexual dimorphism in human vertebral shape. *J Anat*. 1984;138:281-286.

ott PH, Pearcy MJ, Ruston SA, Fulton I, Brien C. Three-dimensional analysis of active cervical motion: the effect of age and gender. *Clin Biomech*. 1996;11:201-206.

vomey L, Taylor J, Furniss B. Age changes in the bone density and structure of the lumbar vertebral column. *J Anat*. 1983;136:15-25.

hite AA, Panjabi MM. Clinical Biomechanics of the Spine, 2nd edn. Philadelphia: JB Lippincott, 1990.

illems JM, Jull GA, Ng JK-F. An in vivo study of the primary and coupled rotations of the thoracic spine. *Clin Biomech*. 1996;11:311-316.

ing P, Tsang I, Gagnon F, Susak L, Gagnon R. Diurnal changes in the profile shape and range of motion of the back. *Spine*. 1992;17:761-765.

impano MP, Hartwell S, Jagos CS. Soft tissue connection between rectus capitis posterior minor and the posterior atlanto-occipital membrane. *Clin Anat*. 2006;19:522-527.

CHAPTER 43

Spinal cord and spinal nerves: gross anatomy

This chapter deals with the gross anatomy of the structures which lie within the vertebral canal and its extensions through the intervertebral foramina, the spinal nerve or radicular (‘root’) canals. The spinal cord, its blood vessels and nerve roots lie within a meningeal sheath, the theca, which occupies the central zone of the vertebral canal and extends from the foramen magnum, where it is in continuity with the meningeal coverings of the brain, to the level of the second sacral vertebra in the adult. Distal to this level the dura extends as a fine cord, the filum terminale externum, which fuses with the posterior periosteum of the first coccygeal segment. Tubular prolongations of the dural sheath extend around the spinal roots and nerves into the lateral zones of the vertebral canal and out into the root canals, eventually fusing with the epineurium of the spinal nerves. Between the theca and the walls of the vertebral canal is the epidural (spinal extradural) space, which is loosely filled with fat, connective tissue containing small arteries and lymphatics, and an important venous plexus. Three-dimensional appreciation of the anatomy of the spinal theca and its surroundings is essential for the efficient management of spinal pain and of spinal injuries, tumours and infections. Equally significant clinically is the anatomy of the often precarious blood supply of the spinal cord and its associated structures. The increasing application and refinement of diagnostic imaging and endoscopic procedures lend a new importance to topographical detail here.

SPINAL CORD (MEDULLA)

The spinal cord occupies the superior two-thirds of the vertebral canal (Fig. 18.1, Fig. 43.1). It is continuous cranially with the medulla oblongata, and narrows caudally to the conus medullaris, from whose apex a connective tissue filament, the filum terminale, descends to the dorsum of the first coccygeal vertebral segment. The cord extends from the upper border of the atlas to the junction between the first and second lumbar vertebrae: its average length in European males is 45 cm, its weight approximately 30 g. (For dimensional data consult Barson & Sands 1977.)

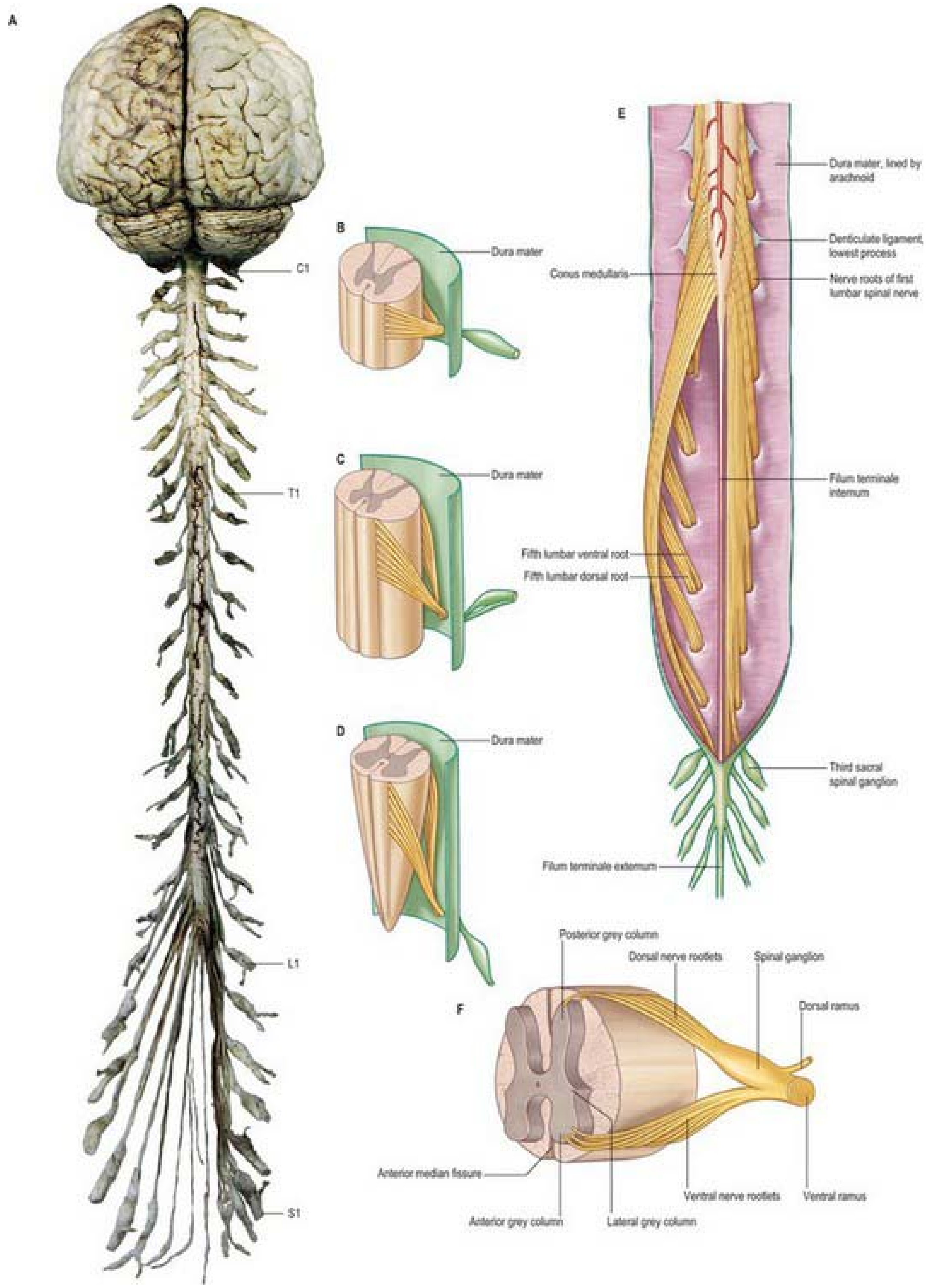
A
C1
T1
L1
S1
B
Dura mater
C
Dura mater
D
Dura mater
E
Dura mater, lined by arachnoid
Denticulate ligament, lowest process
Conus medullaris
Nerve roots of first lumbar spinal nerve
Filum terminale internum
Fifth lumbar ventral root
Fifth lumbar dorsal root
Third sacral spinal ganglion
Filum terminale externum
F
Posterior grey column
Dorsal nerve rootlets
Spinal ganglion
Dorsal ramus
Anterior median fissure
Ventral nerve rootlets
Ventral ramus
Anterior grey column
Lateral grey column

Fig. 43.1 **A**, Brain and spinal cord with attached spinal nerve roots and dorsal root ganglia, photographed from the dorsal aspect. Note the fusiform cervical and lumbar enlargements of the cord, and the changing

obliquity of the spinal nerve roots as the cord is descended. The cauda equina is undisturbed on the right but has been spread out on the left to show its individual components. **B–D**, Formation of typical spinal nerve, ventral aspect. **B**, Cervical level; **C**, Thoracic level; **D**, Lumbar level. **E**, Lower end of spinal cord, filum terminale and cauda equina exposed from behind. The dura mater and the arachnoid have been opened and spread out. **F**, Spinal cord segment showing mode of formation of a typical spinal nerve and the gross relationships of the grey and white matter. (B–D, From Sobotta 2006.)

(Dissection by MCE Hutchinson, GKT School of Medicine; photograph by Kevin Fitzpatrick on behalf of GKT School of Medicine, London.)

During development, the vertebral column elongates more rapidly than the spinal cord, so that there is an increasing discrepancy between the anatomical level of spinal cord segments and their corresponding vertebrae. At stage 23, the vertebral column and spinal cord are the same length, and the cord ends at the last coccygeal vertebra: this arrangement continues until the third fetal month. At birth, the spinal cord terminates at the lower border of the second lumbar vertebra, and may sometimes reach the third lumbar vertebra. In the adult, the spinal cord is said to terminate at the level of the disc between the first and second lumbar vertebral bodies, which lies a little above the level of the elbow joint when the arm is by the side, and also lies approximately in the transpyloric plane (p. 1054). However, there is considerable variation in the level at which the spinal cord ends. It may end below this level in as many as 40% of subjects, or opposite the body of either the first or second lumbar vertebra: very occasionally it ends as high as the caudal third of twelfth thoracic or as low as the disc between the second and third lumbar vertebrae. Its position rises slightly in vertebral flexion, and there is some correlation with the length of the trunk, especially in females. The spinal cord varies in transverse width, gradually tapering craniocaudally, except at the levels of the enlargements. It is not cylindrical, being wider transversely at all levels, especially in the cervical segments.

The cervical enlargement is the source of the large spinal nerves that supply the upper limbs. It extends from the third cervical to the second thoracic segments, its maximum circumference (approximately 38 mm) is in the sixth cervical segment. (A spinal cord segment provides the attachment of the rootlets of a pair of spinal nerves.) The lumbar enlargement is the source of the large spinal nerves that supply the lower limbs, and extends from the first lumbar to the third sacral segments, the equivalent vertebral levels being the ninth to twelfth thoracic vertebrae. Its greatest circumference (approximately 35 mm) is near the lower part of the body of the twelfth thoracic vertebra, below which it rapidly dwindles into the conus medullaris.

Fissures and sulci extend along most of the external surface. An anterior median fissure and a posterior median sulcus and septum almost completely separate the cord into right and left halves, but they are joined by a commissural band of nervous tissue which contains a central canal.

The anterior median fissure extends along the whole ventral surface with an average depth of 3 mm, although it is deeper at caudal levels. It contains a reticulum of pia mater. Dorsal to it is the anterior white commissure. Perforating branches of the spinal vessels pass from the fissure to the commissure to supply the central spinal region. The posterior median sulcus is shallower, and from it a posterior median septum penetrates more than halfway into the cord, almost to the central canal. The septum varies in anteroposterior extent from 4 to 6 mm, and diminishes caudally as the canal becomes more dorsally placed and the cord contracts.

A posterolateral sulcus exists from 1.5 to 2.5 mm lateral to each side of the posterior median sulcus. Dorsal roots (strictly rootlets) of spinal nerves enter the cord along the sulcus. The white substance between the posterior median and posterolateral sulcus on each side is the posterior funiculus. In cervical and upper thoracic segments a longitudinal posterointermediate sulcus marks a septum dividing each posterior funiculus into two large tracts: the fasciculus gracilis (medial) and fasciculus cuneatus (lateral). Between the posterolateral sulcus and anterior median fissure is the anterolateral funiculus. This is subdivided into anterior and lateral funiculi by ventral spinal rootlets which pass through its substance to issue from the surface of the cord. The anterior funiculus is medial to, and includes, the emerging ventral rootlets, whilst the lateral funiculus lies between the roots and the posterolateral sulcus. In upper cervical segments, nerve rootlets emerge through each lateral funiculus to form the spinal accessory nerve which ascends in the vertebral canal lateral to the spinal cord and enters the posterior cranial fossa via the foramen magnum (Fig. 28.11).

The filum terminale, a filament of connective tissue approximately 20 cm long, descends from the apex of the conus medullaris. Its upper 15 cm, the filum terminale internum, is continued within extensions of the dural and arachnoid meninges and reaches the caudal border of the second sacral vertebra. Its final 5 cm, the filum terminale externum, fuses with the investing dura mater, and then descends to the dorsum of the first coccygeal vertebral segment. The filum is continuous above with the spinal pia mater. A few strands of nerve fibres which probably represent roots of rudimentary second and third coccygeal spinal nerves adhere to its upper part. The central canal is continued into the filum for 5–6 mm. A capacious part of the subarachnoid space surrounds the filum terminale internum, and is the site of election for access to the CSF (lumbar puncture).

DORSAL AND VENTRAL ROOTS

The paired dorsal and ventral roots of the spinal nerves are continuous with the spinal cord (Fig. 43.1F; see also p. 754). They cross the subarachnoid space and traverse the dura mater separately, uniting in or close to their intervertebral foramina to form the (mixed) spinal nerves. Since the spinal cord is shorter than the vertebral column, the more caudal spinal roots descend for varying distances around and beyond the cord to reach their corresponding foramina. In so doing they form a divergent sheaf of spinal nerve roots, the cauda equina, which is gathered round the filum terminale in the spinal theca, mostly distal to the apex of the cord.

Ventral spinal roots contain efferent somatic and, at some levels, preganglionic sympathetic, axons which extend from neuronal cell bodies in the ventral horns and intermediolateral columns respectively. There are also afferent nerve fibres in these roots. The rootlets comprising each ventral root emerge from the anterolateral sulcus in groups over an elongated vertical elliptical area (Fig. 43.1F). Dorsal spinal roots bear ovoid swellings, the spinal ganglia, one on each root proximal to its junction with a corresponding ventral root in an intervertebral foramen. Each root fans out into six to eight rootlets before entering the cord in a vertical row in the posterolateral sulcus. Dorsal roots are usually said to contain only afferent axons (both somatic and visceral) which are the central processes of unipolar neurones in the spinal root ganglia, but they may also contain a small number (3%) of efferent fibres and autonomic vasodilator fibres.

Each ganglionic neurone has a single short stem which divides into a medial (central) branch which enters the spinal cord via a dorsal root, and a lateral (peripheral) branch which passes peripherally to a sensory end organ. The central branch is an axon while the peripheral one is an elongated dendrite (but when traversing a peripheral nerve is, in general structural terms, indistinguishable from an axon). The region of spinal cord associated with the emergence of a pair of nerves is a spinal segment, but there is no actual surface indication of segmentation. Moreover, the deep neural sources or destinations of radicular fibres may lie far beyond the confines of the ‘segment’ so defined.

MENINGES

DURA MATER

In some areas within the skull the dura mater can be distinguished from the endosteum, but at the base of the skull around the foramen magnum the two layers are fused and adherent to the bone. Distal to the foramen magnum, within the vertebral column, the dura is distinct from the tissues which line the vertebral canal, and separated from them by the epidural space (see below). The spinal dura mater forms a tube whose upper end is attached to the edge of the foramen magnum and to the posterior surfaces of the second and third cervical vertebral bodies, and also by fibrous bands to the posterior longitudinal ligament, especially towards the caudal end of the vertebral canal. The dural tube narrows at the lower border of the second sacral vertebra. It invests the thin spinal filum terminale, descends to the back of the coccyx, and blends with the periosteum.

Epidural space

The epidural space lies between the spinal dura mater and the tissues which line the vertebral canal (Fig. 43.2). It is closed above by fusion of the spinal dura with the edge of the foramen magnum, and below by the posterior sacrococcygeal ligament which closes the sacral hiatus. It contains loosely packed connective tissue, fat, a venous plexus, small arterial branches, lymphatics and fine fibrous bands which connect the theca with the lining tissue of the vertebral canal. These bands, the meningovertebral ligaments, are best developed anteriorly and laterally. Similar bands tether the nerve root sheaths or ‘sleeves’ within their canals. There is also a midline attachment from the posterior spinal dura to the ligamentum nuchae at atlanto-occipital and atlanto-axial levels (Dean & Mitchell 2002). The venous plexus consists of longitudinally arranged chains of vessels, connected by circumdural venous ‘rings’. The anteriorly placed vessels receive the basivertebral veins.

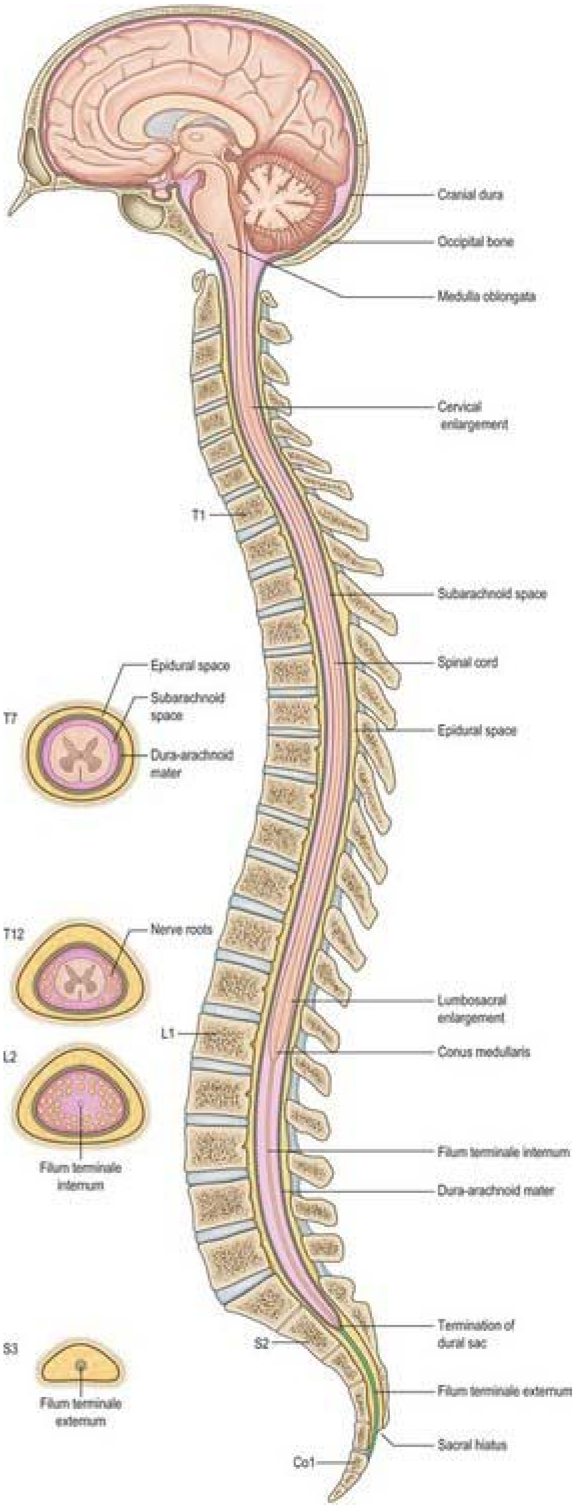
Cranial dura
Occipital bone
Medulla oblongata
Cervical enlargement
T1
Subarachnoid space
Spinal cord
Epidural space
Epidural space
Subarachnoid space
T7
Dura-arachnoid mater
T12
Nerve roots
Lumbosacral enlargement
L1
Conus medullaris
L2
Filum terminale internum
Dura-arachnoid mater
Filum terminale internum
Termination of dural sac
S2
S3
Filum terminale externum
Filum terminale externum
Sacral hiatus
Co1

Fig. 43.2 The epidural and subarachnoid spaces.

The shape of the space within each spinal segment is not uniform, though the segmental pattern is metamerically repeated. It is difficult to define the true shape of the 'space', because it changes with the introduction of fluid or as a result of preservation techniques. In the lumbar region, the dura mater is apposed to the walls of the vertebral canal anteriorly and attached by connective tissue in a manner that permits displacement of the dural sac during movement and venous engorgement. Adipose tissue is present posteriorly in recesses between the ligamentum flavum and the dura. The connective tissue extends for a short distance through the intervertebral foramina along the sheaths of the spinal nerves. Like the main thecal sac, the root sheaths are partially tethered to the walls of the foramina by fine meningovertebral ligaments.

Epidural injections

Contrast media and other fluids injected into the epidural space at the sacral level can spread up to the cranial base (p. 760). Local anaesthetics injected near the spinal nerves, just outside the intervertebral foramina, may spread up or down the epidural space to affect the adjacent spinal nerves or may pass to the opposite side. The paravertebral spaces of each side communicate via the epidural space, particularly at lumbar levels.

For a review of the morphology of the epidural space and a discussion of the nature of the lining layer of the vertebral canal, see Newell (1999).

Subdural space

The subdural space is a potential space in the normal spine because the arachnoid and dura are closely apposed (Haines et al 1993). It does not connect with the subarachnoid space, but continues for a short distance along the cranial and spinal nerves. Accidental subdural catheterization may occur during epidural injections. Injection of fluid into the subdural space may either damage the cord by direct toxic effects or by compression of the vasculature.

ARACHNOID MATER

The spinal arachnoid mater, which surrounds the spinal cord, is continuous with the cranial arachnoid mater (Fig. 43.3). It is closely applied to the deep aspect of the dura mater. At sites where vessels and nerves enter or leave the subarachnoid space, the arachnoid mater is reflected on to the surface of these structures and forms a thin coating of leptomeningeal cells over the surface of both vessels and nerves. Thus a subarachnoid angle is formed as nerves pass through the dura into the intervertebral foramina. At this point, the layers of leptomeninges (arachnoid and pia) fuse and become continuous with the perineurium. The epineurium is in continuity with the dura. Such an arrangement seals the subarachnoid space so that particulate matter does not pass directly from the subarachnoid space into nerves. The existence of a pathway of lymphatic drainage from the CSF is controversial.

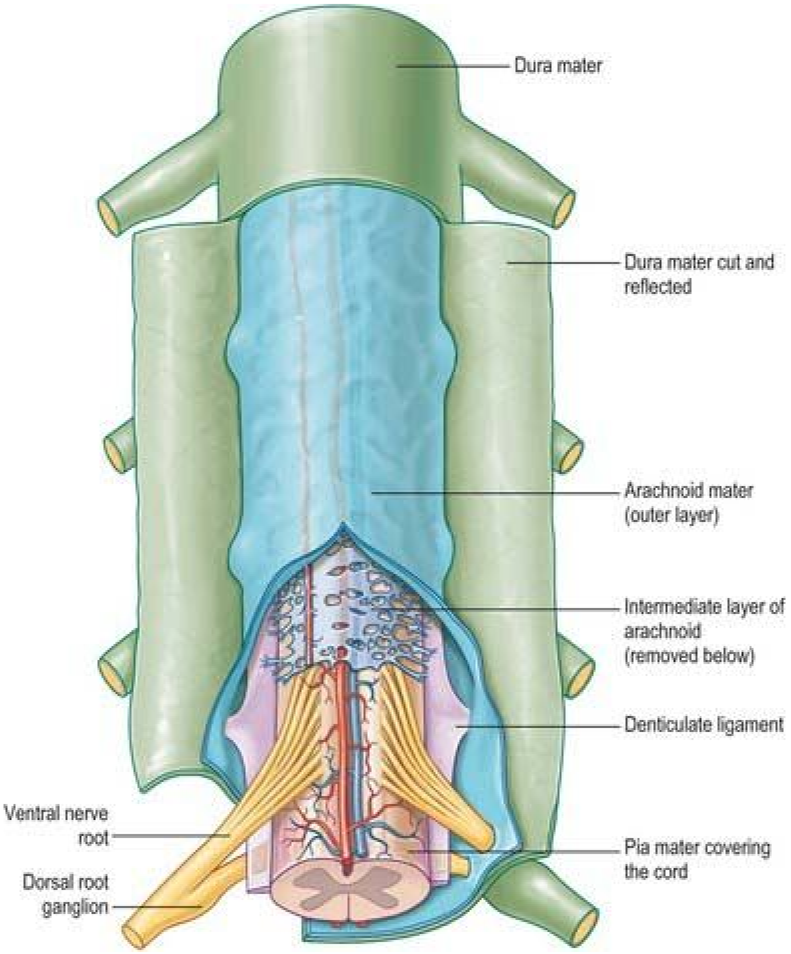
Dura mater
Dura mater cut and reflected
Arachnoid mater (outer layer)
Intermediate layer of arachnoid (removed below)
Denticulate ligament
Ventral nerve root
Pia mater covering the cord
Dorsal root ganglion

Fig. 43.3 Part of the spinal cord exposed from the anterior aspect to show meningeal coverings.

PIA MATER

The spinal pia mater (Fig. 43.3) closely invests the surface of the spinal cord and passes into the anterior median fissure. As in the cranial region, there is a subpial ‘space’, however over the surface of the spinal cord the subpial collagenous layer is thicker than in the cerebral region, and it is continuous with the collagenous core of the ligamentum denticulatum.

The ligamentum denticulatum is a flat, fibrous sheet which lies on each side of the spinal cord between the ventral and dorsal spinal roots. Its medial border is continuous with the subpial connective tissue of the cord and its lateral border forms a series of triangular processes, the apices of which are fixed at intervals to the dura mater. There are usually 21 processes on each side. The first crosses behind the vertebral artery where it is attached to the dura mater, and is separated by the artery from the first cervical ventral root. Its site of attachment to the dura mater is above the rim of the foramen magnum, just behind the hypoglossal nerve: the spinal accessory nerve ascends on its posterior aspect (Fig. 28.11). The last of the dentate ligaments lies between the exiting twelfth thoracic and first lumbar spinal nerves and is a narrow, oblique band which descends laterally from the conus medullaris. Changes in the form and position of the dentate ligaments during spinal movements have been demonstrated by cine-radiography.

Beyond the conus medullaris, the pia mater continues as a coating of the filum terminale.

INTERMEDIATE LAYER

In addition to the well-defined coats of arachnoid and pia mater, the cord is also surrounded by an extensive intermediate layer of leptomeninges. This layer is concentrated in the dorsal and ventral regions and forms a highly perforated, almost lace-like structure which is focally compacted to form the dorsal, dorsolateral and ventral ligaments of the spinal cord. Dorsally, the intermediate layer is adherent to the deep aspect of the arachnoid mater and forms a discontinuous series of dorsal ligaments which attach the spinal cord to the arachnoid. The dorsolateral ligaments are more delicate and fenestrated, and they extend from the dorsal roots to the parietal arachnoid. As the intermediate layer spreads laterally over the dorsal surface of the dorsal roots, it becomes increasingly perforated and eventually disappears. A similar arrangement is seen over the ventral aspect of the spinal cord, but the intermediate layer is less substantial.

The intermediate layer is structurally similar to the trabeculae which cross the cranial subarachnoid space, in that a collagenous core is coated by leptomeningeal cells. The intermediate layers of leptomeninges around the spinal cord may act as a baffle within the subarachnoid space to dampen waves of CSF in the spinal column. Inflammation within the spinal subarachnoid space may result in extensive fibrosis within the intermediate layer and the complications of chronic arachnoiditis.

COVERINGS AND RELATIONS OF THE SPINAL ROOTS AND NERVES IN THE RADICULAR CANAL

Tubular prolongations of the spinal dura mater, closely lined by the arachnoid, extend around the spinal roots and nerves as they pass through the lateral zone of the vertebral canal and through the intervertebral foramina (Fig. 43.3, Fig. 43.4A). These prolongations, the spinal nerve sheaths or root sheaths, gradually lengthen as the spinal roots become increasingly oblique. Each individual dorsal and ventral root runs in the subarachnoid space with its own covering of pia mater. Each root pierces the dura separately, taking a sleeve of arachnoid with it, before joining within the dural prolongation just distal to the spinal ganglion. The dural sheaths of the spinal nerves fuse with the epineurium, within or slightly beyond the intervertebral foramina. The arachnoid prolongations within the sheaths do not extend as far distally as their dural coverings, but the subarachnoid space and its contained CSF extend sufficiently distally to form a radiologically demonstrable root sleeve for each nerve. Shortening or obstruction of this sleeve seen on MRI indicates compression of the spinal nerve. At the cervical level, where the nerves are short and the vertebral movement is greatest, the dural sheaths are tethered to the periosteum of the adjacent transverse processes. In the lumbosacral region there is less tethering of the dura to the periosteum, though there may be an attachment posteriorly to the facet joint capsule.

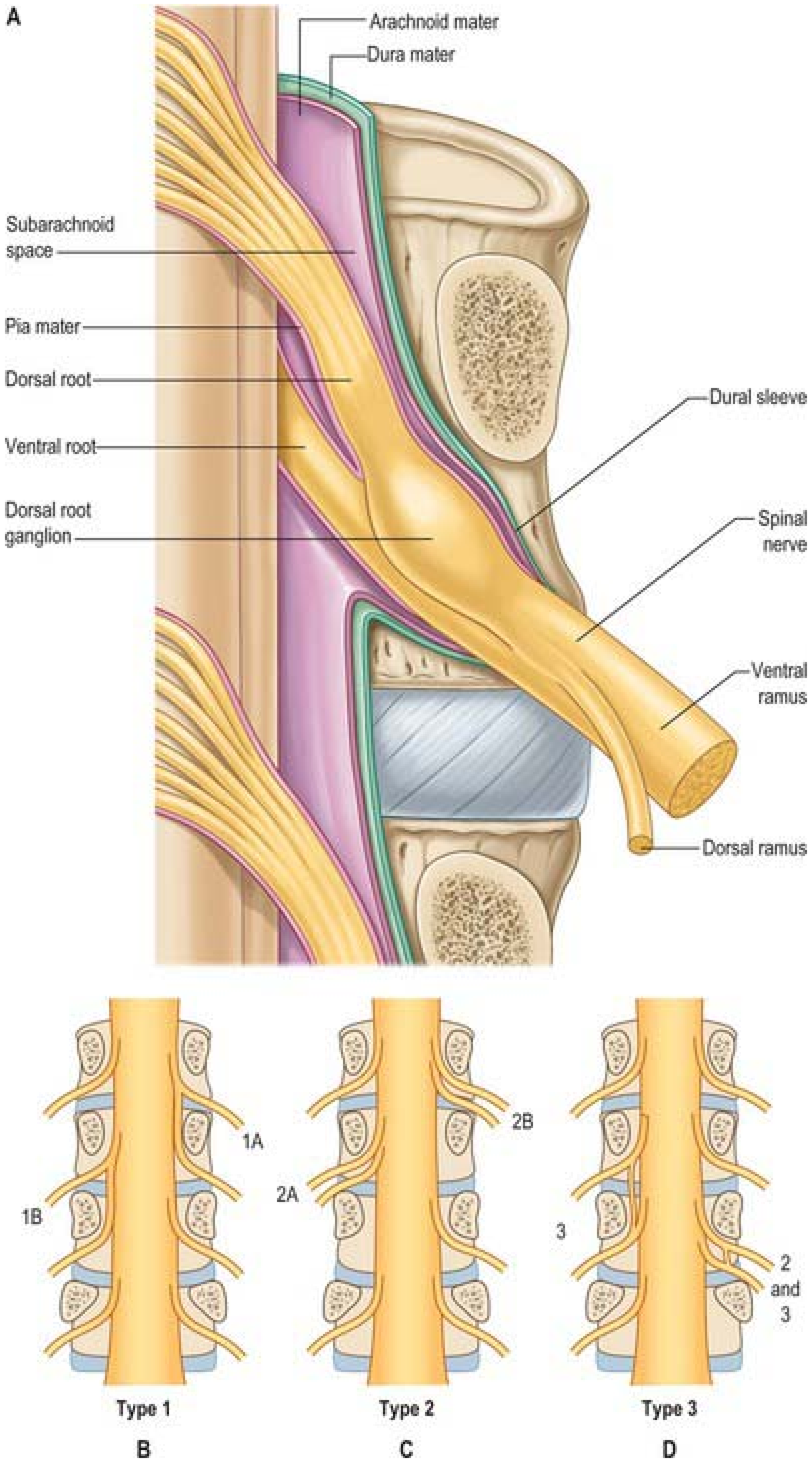
A
Arachnoid mater
Dura mater
Subarachnoid space
Pia mater
Dorsal root
Ventral root
Dorsal root ganglion
Dural sleeve
Spinal nerve
Ventral ramus
Dorsal ramus
1A
1B
2B
2A
3
2 and 3
Type 1
Type 2
Type 3
B
C
D

Fig. 43.4 **A**, A lumbar spinal nerve and its roots and meningeal coverings. **B–D**, Extradural anomalies of the lumbar nerve roots.

CEREBROSPINAL FLUID (CSF)

The cerebrospinal fluid is described in detail on page 242. Although there is free communication between the spinal and cerebral subarachnoid spaces, the mode of circulation of the spinal CSF and the contribution that it makes to the overall circulation of CSF remains uncertain in man: CSF may be absorbed from the spinal subarachnoid space, and spinal arachnoid granulations and villi have been described (Kiddo et al 1976).

SPINAL NERVES

In those body segments which largely retain a metameric (segmental) structure, e.g. the thoracic region, spinal nerves show a common plan (Fig. 43.5). The dorsal, epaxial, ramus passes back lateral to the articular processes of the vertebrae and divides into medial and lateral branches which penetrate the deeper muscles of the back: both branches innervate the adjacent muscles and supply a band of skin from the posterior median line to the lateral border of the scapula (Fig. 43.6). The ventral, hypaxial, ramus is connected to a corresponding sympathetic ganglion by white and grey rami communicantes. It innervates the prevertebral muscles and curves round in the body wall to supply the lateral muscles of the trunk. Near the midaxillary line it gives off a lateral branch which pierces the muscles and divides into anterior and posterior cutaneous branches. The main nerve advances in the body wall, where it supplies the ventral muscles and terminates in branches to the skin.

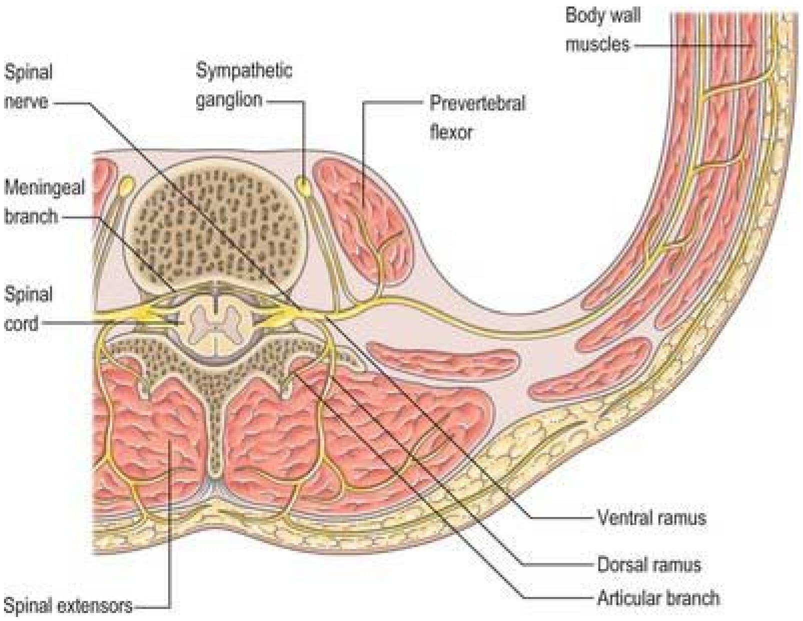
Body wall muscles
Spinal nerve
Sympathetic ganglion
Prevertebral flexor
Meningeal branch
Spinal cord
Ventral ramus
Dorsal ramus
Articular branch
Spinal extensors

Fig. 43.5 Formation and branching pattern of a typical spinal nerve.

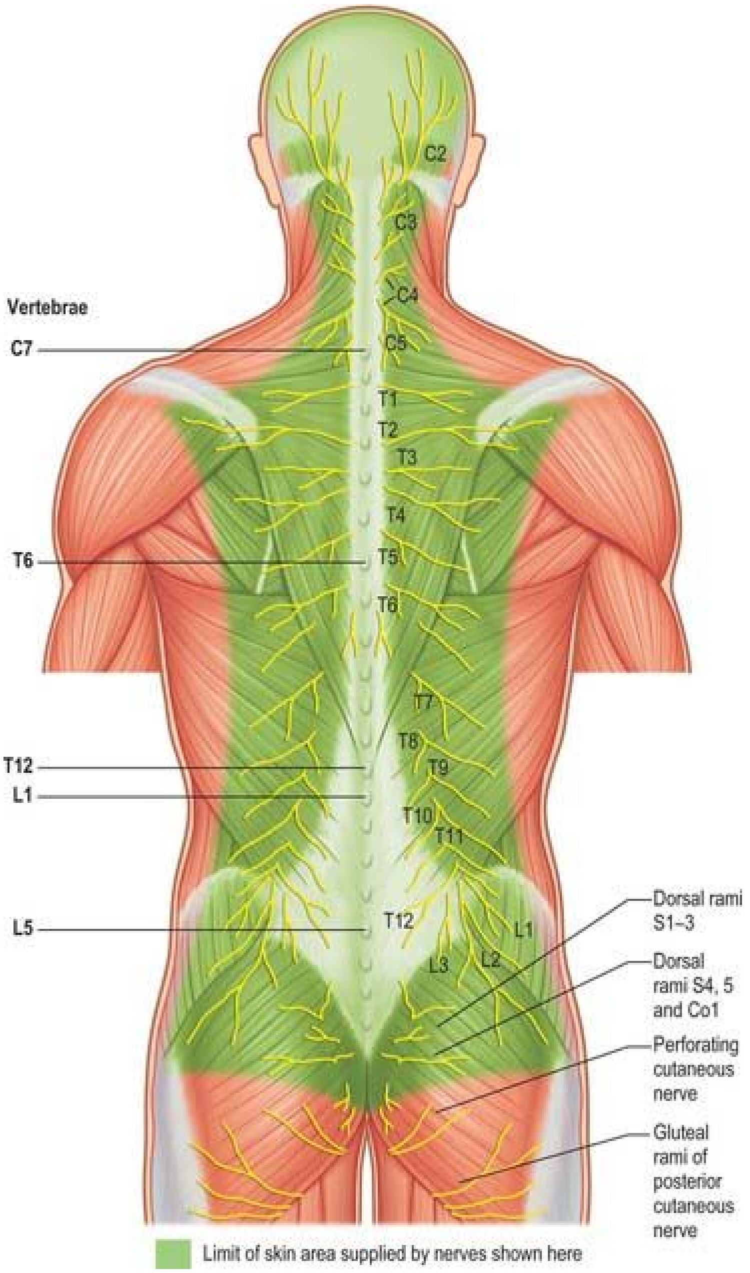
C2
C3
C4
C5
Vertebrae
C7
T1
T2
T3
T4
T6
T5
T6
T7
T8
T9
T12
L1
T10
T11
L5
T12
L1
L3
L2
Dorsal rami S1–3
Dorsal rami S4, 5 and Co1
Perforating cutaneous nerve
Gluteal rami of posterior cutaneous nerve
🟩 Limit of skin area supplied by nerves shown here

Fig. 43.6 Cutaneous distribution of the dorsal rami of the spinal nerves. The nerves are shown lying on the superficial muscles. The nerves are numbered on the right side; the spines of the seventh cervical, sixth and twelfth thoracic, and first and fifth lumbar vertebrae are labelled in on the left side.

Spinal nerves are united ventral and dorsal spinal roots, attached in series to the sides of the spinal cord. The term spinal nerve strictly applies only to the short segment after union of the roots and before branching occurs. This segment, the spinal nerve proper, lies in the intervertebral foramen: it is sometimes mistakenly called the ‘nerve root’. There are 31 pairs of spinal nerves: 8 cervical, 12 thoracic, 5 lumbar, 5 sacral, 1 coccygeal. The abbreviations C, T, L, S and Co, with appropriate numerals, are commonly applied to individual nerves. The peripheral nerves emerge through the intervertebral foramina. At thoracic, lumbar, sacral and coccygeal levels the numbered nerve exits the vertebral canal by passing below the pedicle of the corresponding vertebra, e.g. L4 nerve exits the intervertebral foramen between L4 and L5. However, in the cervical region, nerves C1–7 pass above their corresponding vertebrae. C1 leaves the vertebral canal between the occipital bone and atlas and hence is often termed the suboccipital nerve. The last pair of cervical nerves does not have a correspondingly numbered vertebra and C8 passes between the seventh cervical and first thoracic vertebrae. Each nerve is continuous with the spinal cord by ventral and dorsal roots; the latter each bears a spinal ganglion (‘dorsal root ganglion’).

SPINAL ROOTS AND GANGLIA

Ventral (anterior) roots

Ventral roots contain axons of neurones in the anterior and lateral spinal grey columns. Each emerges as a series of rootlets in two or three irregular rows in an area approximately 3 mm in horizontal width.

Dorsal (posterior) roots

Dorsal roots contain centripetal processes of neurones sited in the spinal ganglia. Each consists of medial and lateral fascicles which both diverge into rootlets which enter the spinal cord along the posterolateral sulcus. The rootlets of adjacent dorsal roots are often connected by oblique filaments, especially in the lower cervical and lumbosacral regions.

Little is known of the detail of the regions of entry and emergence of afferent and efferent rootlets in humans, but these zones of transition between the central and peripheral nervous systems have been extensively described in rodents (Fraher 2000) (see also p. 63).

Appearance and orientation of roots at each spinal level

The size and direction of spinal nerve roots vary. The upper four cervical roots are small, the lower four are large. Cervical dorsal roots have a thickness ratio to the ventral roots of 3 : 1, which is greater than in other regions. The first dorsal root is an exception, being smaller than the ventral and it is occasionally absent. The conventional view is that the first and second cervical spinal roots are short, running almost horizontally to their exits from the vertebral canal, and that from the third to the eighth cervical levels the roots slope obliquely down. Obliquity and length increase successively, although the distance between spinal attachment and vertebral exit never exceeds the height of one vertebra. An alternative view (Kubik & Müntener 1969) states that upper cervical roots descend, the fifth is horizontal, the sixth to eighth ascend, the first two thoracic roots are horizontal, the next three ascend, the sixth is horizontal and the rest descend. This view is based on the observation that the cervicothoracic part of the spinal cord grows more in length than other parts.

Thoracic roots, except the first, are small, and the dorsal root only slightly exceeds the ventral in thickness. They increase successively in length. In the lower thoracic region, the roots descend in contact with the spinal cord for at least two vertebrae before emerging from the vertebral canal.

Lower lumbar and upper sacral roots are the largest, and their rootlets are the most numerous. Coccygeal roots are the smallest. Kubik & Müntener (1969) confirm that lumbar, sacral and coccygeal roots descend with increasing obliquity to their exits. The spinal cord ends near the lower border of the first lumbar vertebra, and so the lengths of successive roots rapidly increase: the consequent collection of roots is the cauda equina (Fig. 43.1A). The largest roots, and hence the largest spinal nerves, are continuous with the spinal cervical and lumbar enlargements and innervate the upper and lower limbs.

Spinal ganglia (dorsal root ganglia)

Spinal ganglia are large groups of neurones on the dorsal spinal roots. Each is oval and reddish; its size is related to that of its root. A ganglion is bifid medially where the two fascicles of the dorsal root emerge to enter the cord. Ganglia are usually sited in the intervertebral foramina, immediately lateral to the perforation of the dura mater by the roots (Fig. 43.1B). However, the first cervical ganglion lies on the vertebral arch of the atlas, the second lies behind the lateral atlantoaxial joint, the sacral lie inside the vertebral canal, and the coccygeal ganglion usually lies within the dura mater. The first cervical ganglia may be absent. Small aberrant ganglia sometimes occur on the upper cervical dorsal roots between the spinal ganglia and the cord.

SPINAL NERVES PROPER

Immediately distal to the spinal ganglia, ventral and dorsal roots unite to form spinal nerves (see Fig. 43.5, Fig. 15.15). These very soon divide into dorsal and ventral rami, both of which receive fibres from both roots. At all levels above the sacral, this division occurs within the intervertebral foramen. Division of the sacral spinal nerves occurs within the sacral vertebral canal, and the dorsal and ventral rami exit separately through posterior and anterior sacral foramina at each level. Spinal nerves trifurcate at some cervical and thoracic levels, in which case the third branch is called a ramus intermedius. At or distal to its origin each ventral ramus gives off recurrent meningeal (sinuvertebral) branches and receives a grey ramus communicans from the corresponding sympathetic ganglion. The thoracic and first and second lumbar ventral rami each contributes a white ramus communicans to the corresponding sympathetic ganglia. The second, third and fourth sacral nerves also supply visceral branches, unconnected with sympathetic ganglia, which carry a parasympathetic outflow direct to the pelvic plexuses.

Cervical spinal nerves enlarge from the first to the sixth nerve. The seventh and eighth cervical and the first thoracic nerve are similar in size to the sixth cervical nerve. The remaining thoracic nerves are relatively small. Lumbar nerves are large, increasing in size from the first to the fifth. The first sacral is the largest spinal nerve, thereafter the sacral nerves decrease in size. The coccygeal nerves are the smallest spinal nerves. The size of the spinal nerve and its associated structures within the intervertebral foramen is not in direct relation to the size of the foramen. At lumbar levels, though L5 is the largest nerve, its foramen is smaller than those of L1–4, which renders this nerve particularly liable to compression.

In the radicular (‘root’) canal and intervertebral foramen, the spinal nerve is related to the spinal artery of that level and its radicular branch, and to a small plexus of veins. At the outer end of the foramen the nerve may lie above or below transforaminal ligaments.

Meningeal nerves

Recurrent meningeal (or sinuvertebral) nerves (Fig. 43.7) occur at all vertebral levels. They are mixed sensory and sympathetic nerves, represented by numerous fine filaments amongst which one, or two to four, larger trunks may be evident. At cervical levels the autonomic roots arise from the grey rami that form the vertebral nerve (p. 461). At thoracic and lumbar levels, each nerve is formed by a somatic root from the ventral ramus and by an autonomic root from the grey ramus communicans of that segment. Each nerve pursues a recurrent course through the intervertebral foramen, passing ventral to the spinal nerve, to enter the vertebral canal, where it divides into ascending, descending, and transverse branches. These branches communicate with corresponding branches from the segments above and below, and from the opposite side, forming arcades along the floor of the vertebral canal. Meningeal branches of the arcades form a plexus on the ventral surface of the dural sac and nerve root sleeves which attenuates laterally; the posterior paramedian dura is devoid of nerve endings. Skeletal branches are distributed to the posterior longitudinal ligament, the periosteum of the vertebral bodies, and to the posterior and posterolateral aspects of the intervertebral discs. Vascular branches accompany the veins and arteries of the vertebral canal and those of the vertebral bodies. The upper three cervical meningeal nerves ascend through the foramen magnum into the posterior cranial fossa, where they innervate the dura mater that covers the clivus. En route, they innervate the median atlanto-axial joint and its ligaments.

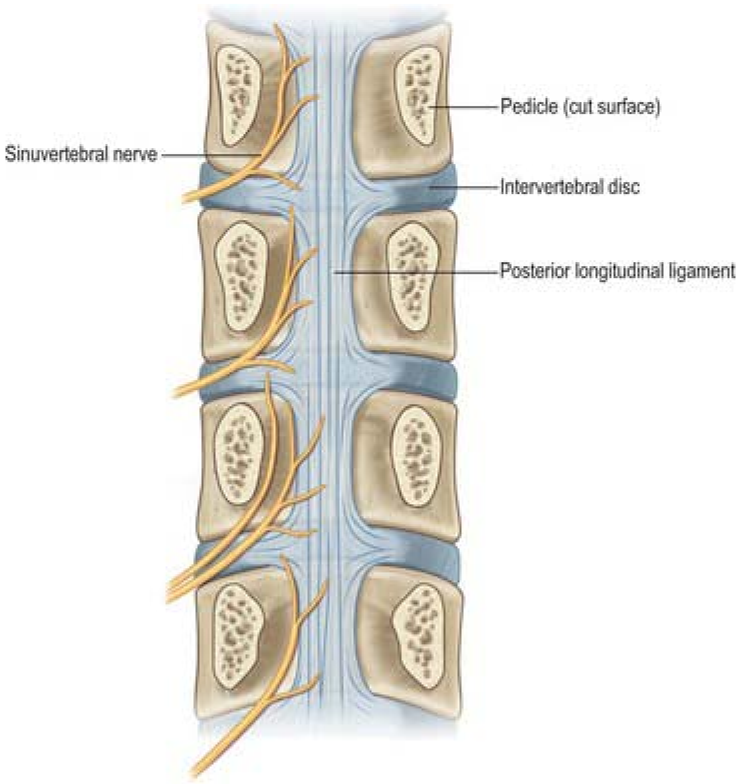
Pedicle (cut surface)
Sinuvertebral nerve
Intervertebral disc
Posterior longitudinal ligament

Fig. 43.7 The course and skeletal distribution of the lumbar sinuvertebral nerves. Each nerve supplies the intervertebral disc at its level of entry into the vertebral canal, the disc above, and the intervening posterior longitudinal ligament. In about one-third of cases, the nerve at a particular level may be represented by more than one filament.

Functional components of spinal nerves

A typical spinal nerve contains somatic efferent fibres and somatic and visceral afferent fibres. Some, but not all, spinal nerves also contain preganglionic autonomic fibres.

Somatic components

Somatic efferent fibres innervate skeletal muscles and are axons of α, β and γ neurones in the spinal ventral grey column. Somatic afferent fibres convey impulses into the CNS from receptors in the skin, subcutaneous tissue, muscles, tendons, fasciae and joints: they are peripheral processes of unipolar neurones in the spinal ganglia.

Visceral components

Preganglionic visceral efferent sympathetic fibres are axons of neurones in the spinal intermediolateral grey column throughout the thoracic and upper two or three lumbar segments: they join the sympathetic trunk via corresponding white rami communicantes and synapse with postganglionic neurones which are distributed to smooth muscle, myocardium or exocrine glands. The preganglionic visceral efferent parasympathetic fibres are axons of neurones in the spinal lateral grey column of the second to fourth sacral segments: they leave the ventral rami of corresponding sacral nerves and synapse in pelvic ganglia. The postganglionic axons are distributed mainly to smooth muscle or glands in the walls of the pelvic viscera. Visceral afferent fibres have cell bodies in the spinal ganglia. Their peripheral processes pass through white rami communicantes and, without synapsing, through one or more sympathetic ganglia to end in the walls of the viscera. Some visceral afferent fibres may enter the spinal cord in the ventral roots.

Central processes of ganglionic unipolar neurones enter the spinal cord by dorsal roots and synapse on somatic or sympathetic efferent neurones, usually through interneurones, completing reflex paths. Alternatively, they may synapse with other neurones in the spinal or brain stem grey matter which give origin to a variety of ascending tracts.

VARIATIONS OF SPINAL ROOTS AND NERVES

The courses of spinal roots and nerves in relation to the thecal sac and vertebral and radicular canals may be aberrant. An individual intervertebral foramen may contain a duplicated sheath, nerve and roots, which will then be absent at an adjacent level. Abnormal communications between roots may occur within the vertebral canal. These anomalies have been described and classified for the lumbosacral spine by Neidre & Macnab (1983) (Fig. 43.4).

RAMI OF THE SPINAL NERVES

Ventral (anterior primary) rami supply the limbs and the anterolateral aspects of the trunk, and in general are larger than the dorsal rami. Thoracic ventral rami run independently and retain a largely segmental distribution. Cervical, lumbar and sacral ventral rami connect near their origins to form plexuses. Dorsal rami do not join these plexuses. The ventral rami are described in the appropriate regional Sections.

Dorsal (posterior primary) rami of spinal nerves are usually smaller than the ventral rami and are directed posteriorly. Retaining a segmental distribution, all, except for the first cervical, fourth and fifth sacral and the coccygeal, divide into medial and lateral branches which supply the muscles and skin of the posterior regions of the neck and trunk (Fig. 43.6).

Cervical dorsal spinal rami

Each cervical spinal dorsal ramus, except the first, divides into medial and lateral branches which all innervate muscles. In general only medial branches of the second to fourth, and usually the fifth, supply the skin. Except for the first and second, each dorsal ramus passes posteriorly around an articular pillar as far as the root of the transverse process medial to a posterior intertransverse muscle, which it supplies.

First cervical dorsal ramus (suboccipital nerve)

The first cervical dorsal ramus, the suboccipital nerve, is larger than the ventral (Fig. 42.59). It emerges superior to the posterior arch of the atlas and inferior to the vertebral artery and enters the suboccipital triangle to supply rectus capitis posterior major and minor, obliquus capitis superior and inferior, and semispinalis capitis. A filament from the branch to the inferior oblique joins the second dorsal ramus. The suboccipital nerve occasionally has a cutaneous branch which accompanies the occipital artery to the scalp, and connects with the greater and lesser occipital nerves. It may also communicate with the accessory nerve.

Second cervical dorsal ramus

The second cervical dorsal ramus is slightly larger than the ventral and all the other cervical dorsal rami (Fig. 42.59, Fig. 29.15). It runs between the lamina of the axis and the inferior oblique, below which it divides into a large medial and smaller lateral branch. The dorsal ramus or its medial branch receives communicating branches from the first cervical dorsal ramus which pass both through and around inferior oblique. A descending communicating branch crosses the C2–3 facet joint to reach the third cervical dorsal ramus.

Greater occipital nerve

The medial branch, termed the greater occipital nerve, passes transversely across inferior oblique deep to semispinalis capitis, which it innervates. Near the origin of inferior oblique, it turns rostrally along rectus capitis posterior major, where it receives a communicating branch from the third occipital nerve before turning dorsally to pierce semispinalis capitis. It emerges onto the scalp by passing above an aponeurotic sling between trapezius and sternocleidomastoid near their occipital attachments It ascends with the occipital artery, divides into branches which connect with the third occipital and lesser occipital nerves, and which supply the back of the auricle and the skin of the scalp as far forward as the coronal suture. The lateral branch of the second cervical dorsal ramus supplies longissimus capitis, semispinalis capitis and splenius capitis, and sends a communicating branch to the lateral branch of the third cervical dorsal ramus.

Greater occipital neuralgia

Greater occipital neuralgia is a syndrome of pain and paraesthesiae felt in the distribution of the greater occipital nerve. The pathology lies at the dorsal root ganglion. A similar syndrome may be caused by upper facet joint arthritis involving the second cervical root.

Third cervical dorsal ramus

The third cervical dorsal ramus is intermediate in size between the second and fourth. It courses back round the articular pillar of the third cervical vertebra, medial to the posterior intertransverse muscle, and divides into medial and lateral branches. The lateral branch passes dorsally across the surface of semispinalis capitis to supply it and the overlying longissimus capitis and splenius capitis. It receives a communicating branch from the lateral branch of the second cervical dorsal ramus, and sends a similar branch to the lateral branch of the fourth cervical dorsal ramus. The deep medial branch curves dorsally and medially around the waist of the articular pillar before ending in multifidus. It sends an articular branch to the C3–4 facet joint, and may also send a branch into semispinalis capitis. The superficial medial branch, the third occipital nerve, curves around the lateral and dorsal surfaces of the C2–3 facet joint, which it supplies. It continues transversely, deep to semispinalis, which it supplies, and sends a communicating branch to the greater occipital nerve. Just above the second cervical spinal process, the third occipital nerve turns dorsally to pierce semispinalis capitis, splenius capitis and trapezius, and becomes cutaneous over a small area immediately below the superior nuchal line. Communicating branches join the cutaneous branches of the greater and lesser occipital nerves.

Dorsal rami of the lower five cervical nerves

The dorsal rami of the lower five cervical nerves curve back round the vertebral articular pillars and divide into lateral and medial branches. The lateral branches supply longissimus cervicis, splenius cervicis and iliocostalis cervicis. The medial branches curve around the lateral and dorsal surfaces of the articular pillar of their segment, deep to semispinalis capitis. They send articular branches to the facet joints above and below their course before entering and supplying multifidus. Terminal branches reach interspinalis at each segment. Cutaneous branches arise consistently from the fourth, commonly from the fifth, sixth and eighth, but not usually from the seventh medial branches. These branches pass across multifidus or through semispinalis cervicis and turn dorsally around the medial border of semispinalis capitis, to pierce splenius cervicis and trapezius and reach the skin.

Thoracic dorsal spinal rami

At each segmental level, the thoracic dorsal rami pass dorsally through an aperture bounded by the transverse processes superiorly and inferiorly, the facet joint medially, and the superior costotransverse ligament laterally. Thereafter, each dorsal ramus follows a prolonged course laterally, between the anterior lamella of the superior costotransverse ligament anteriorly, and the costolamellar ligament and the posterior lamella of the superior costotransverse ligament posteriorly. In this narrow space, the dorsal ramus divides into lateral and medial branches. The lateral branches continue laterally as far as the costotransverse joint, above which they turn dorsally and inferiorly to supply the levatores costarum, and enter the longissimus thoracis and iliocostalis muscles. Lateral branches from the upper six thoracic dorsal rami remain intramuscular. Those from the lower six levels emerge from iliocostalis lumborum to pierce serratus posterior inferior and latissimus dorsi in line with the costal angles. They descend across as many as four ribs before becoming superficial. The twelfth thoracic lateral branch sends a filament medially along the iliac crest, then passes down to the anterior gluteal skin. Some upper thoracic lateral branches may become cutaneous.

Each medial branch hooks dorsally around the lateral margin of the posterior lamella of the superior costotransverse ligament, lying a variable distance above the tip of the transverse process. At the first to fourth, and at the ninth and tenth thoracic levels, the medial branch cross the superior tip of the transverse process to turn inferiorly and medially across the posterior surface of the transverse process, lying between the attachment sites of multifidus medially and semispinalis laterally. Each nerve continues this oblique course to supply the multifidus and semispinalis. At the fifth to eighth thoracic levels, the medial branches assume a course parallel to that of other levels, but do not reach the transverse process, instead passing superior and dorsal to the plane of the transverse processes. At the eleventh and twelfth levels, in keeping with the relatively short transverse processes at these levels, the medial branches run close to the superior articular processes. Each medial branch supplies articular branches to the facet joints above and below its course. Medial branches of the upper six thoracic dorsal rami furnish cutaneous branches that pierce trapezius and the rhomboids to reach the skin near the spinous processes. Cutaneous branches may occasionally arise from the medial branches of the lower six thoracic dorsal rami.

Lumbar dorsal spinal rami

After leaving its spinal nerve, each of the first to fourth lumbar dorsal rami passes through an aperture in the dorsal leaf of the intertransverse ligament just above a transverse process (Fig. 43.8). Each dorsal ramus supplies the overlying medial intertransverse muscle before dividing into lateral and medial branches. The lateral branches supply the longissimus and iliocostalis components of the lumbar erector spine. The upper three lumbar lateral branches emerge from the lateral border of iliocostalis lumborum and pierce the aponeurosis of latissimus dorsi to become cutaneous, They cross the iliac crest to reach the gluteal skin, some reach as far as the level of the greater trochanter. Medial branches cross the junction of the superior articular process and transverse process and hook medially between the mammillary and accessory processes, deep to the mammillo-accessory ligament. Medial to the ligament, each medial branch sends articular branches to the facet joints above and below its course, before entering multifidus, which it supplies. Terminal branches reach interspinalis at each segment.

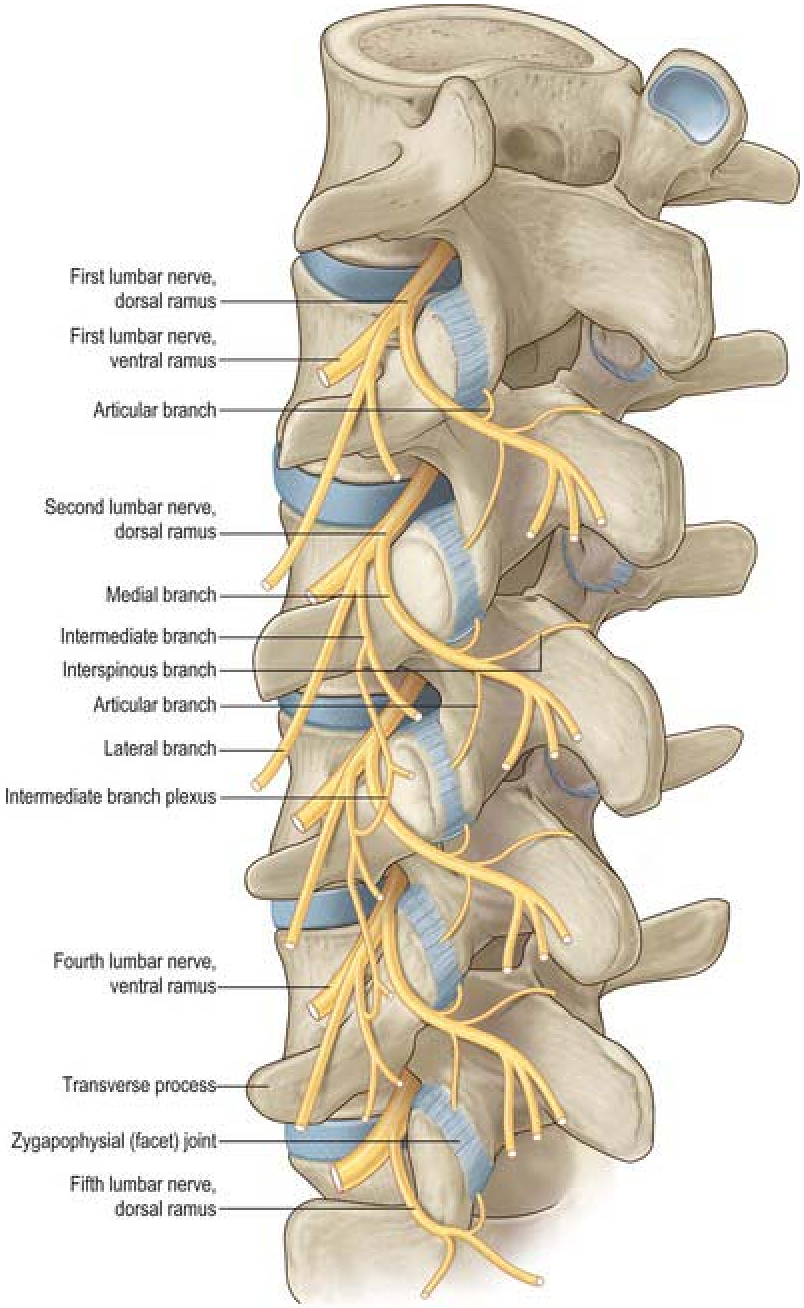
First lumbar nerve, dorsal ramus
First lumbar nerve, ventral ramus
Articular branch
Second lumbar nerve, dorsal ramus
Medial branch
Intermediate branch
Interspinous branch
Articular branch
Lateral branch
Intermediate branch plexus
Fourth lumbar nerve, ventral ramus
Transverse process
Zygapophysial (facet) joint
Fifth lumbar nerve, dorsal ramus

Fig. 43.8 A left posterolateral view of the lumbar spine showing the branches of the lumbar dorsal rami.

The fifth dorsal ramus has a longer course than other dorsal rami. It arches over the ala of the sacrum, lying against the root of the first sacral superior articular process. Opposite the base of the lumbosacral joint it sends a branch into the lowest fibres of longissimus thoracis, and a communicating branch to the first sacral dorsal ramus, before terminating as a medial branch that hooks around the lumbosacral joint to end in multifidus.

Sacral dorsal spinal rami

Sacral dorsal rami are small, diminishing in size inferiorly, and other than the fifth, all emerge though the dorsal sacral foramina. The upper three are covered at their exit by multifidus, and divide into medial and lateral branches. Medial branches are small and end in multifidus. Lateral branches join together and with branches of the last lumbar and fourth sacral dorsal rami to form loops dorsal to the sacrum. Branches from these loops run dorsal to the sacrotuberous ligament and form a second series of loops under gluteus maximus. From these, two or three gluteal branches pierce gluteus maximus (along a line from the posterior superior iliac spine to the coccygeal apex) to supply the posterior gluteal skin.

The dorsal rami of the fourth and fifth sacral nerves are small and lie caudal to multifidus. They unite with each other and with the coccygeal dorsal ramus to form loops dorsal to the sacrum: filaments from these supply the skin over the coccyx.

Coccygeal dorsal spinal ramus

The coccygeal dorsal spinal ramus does not divide into medial and lateral branches. It communicates with the fourth and fifth sacral dorsal rami to supply the skin over the coccyx.

VASCULAR SUPPLY OF SPINAL CORD, ROOTS AND NERVES

ARTERIES

The spinal cord, its roots and nerves are supplied with blood by both longitudinal and segmental vessels (Fig. 43.9). Three major longitudinal vessels, a single anterior and two posterior spinal arteries (each of which is sometimes doubled to pass on either side of the dorsal rootlets), originate intracranially from the vertebral artery and terminate in a plexus around the conus medullaris. The anterior spinal artery forms from the fused anterior spinal branches of the vertebral artery, and descends in the anterior median fissure of the cord. Each posterior spinal artery originates either directly from the ipsilateral vertebral artery or from its posterior inferior cerebellar branch, and descends in a posterolateral sulcus of the cord. The segmental arteries are derived in craniocaudal sequence from spinal branches of the vertebral, deep cervical, intercostal and lumbar arteries. These vessels enter the vertebral canal through the intervertebral foramina and anastomose with branches of the longitudinal vessels to form a pial plexus on the surface of the cord. The segmental spinal arteries send anterior and posterior radicular branches to the spinal cord along the ventral and dorsal roots. Most anterior radicular arteries are small, and end in the ventral nerve roots or in the pial plexus of the cord. The small posterior radicular arteries also supply the dorsal root ganglia: branches enter at both ganglionic poles to be distributed around ganglion cells and nerve fibres. (See also Crock 1996.)

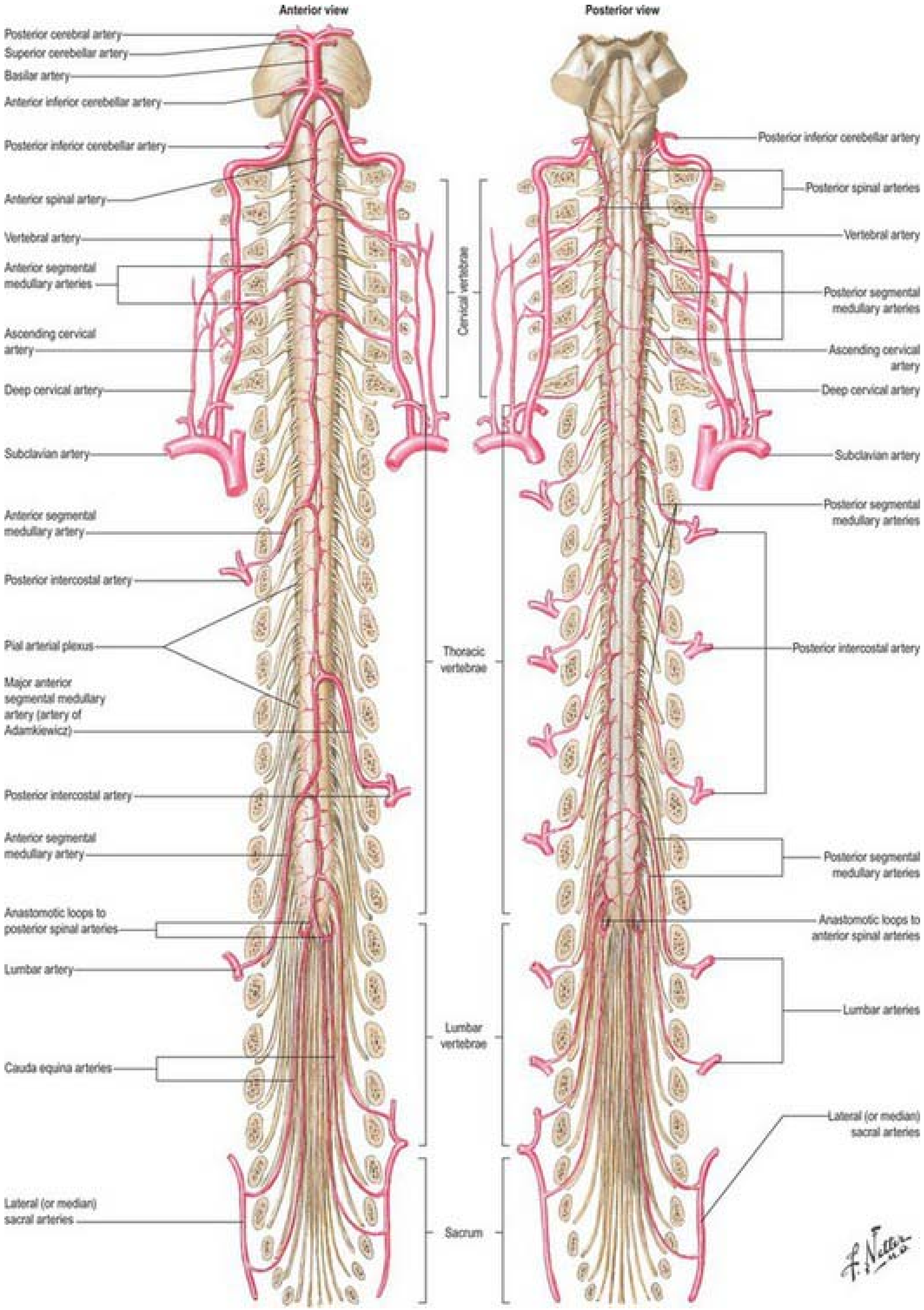
Anterior view
Posterior view
Posterior cerebral artery
Superior cerebellar artery
Basilar artery
Anterior inferior cerebellar artery
Posterior inferior cerebellar artery
Anterior spinal artery
Vertebral artery
Anterior segmental medullary arteries
Ascending cervical artery
Deep cervical artery
Subclavian artery
Anterior segmental medullary artery
Posterior intercostal artery
Pial arterial plexus
Major anterior segmental medullary artery (artery of Adamkiewicz)
Posterior intercostal artery
Anterior segmental medullary artery
Anastomotic loops to posterior spinal arteries
Lumbar artery
Cauda equina arteries
Lateral (or median) sacral arteries
Cervical vertebrae
Thoracic vertebrae
Lumbar vertebrae
Sacrum
Posterior inferior cerebellar artery
Posterior spinal arteries
Vertebral artery
Posterior segmental medullary arteries
Ascending cervical artery
Deep cervical artery
Subclavian artery
Posterior segmental medullary arteries
Posterior intercostal artery
Posterior segmental medullary arteries
Anastomotic loops to anterior spinal arteries
Lumbar arteries
Lateral (or median) sacral arteries

Fig. 43.9 Arteries of the spinal cord.

(Reprinted from Netter Anatomy Illustration Collection, © Elsevier Inc. All Rights Reserved.)

Segmental medullary feeder arteries

Some radicular arteries, mainly situated in the lower cervical, lower thoracic and upper lumbar regions, are large enough to reach the anterior median sulcus where they divide into slender ascending and large descending branches. These are the anterior medullary feeder arteries (Dommisse 1975). They anastomose with the anterior spinal arteries to form a single or partly double longitudinal vessel of uneven calibre along the anterior median sulcus. The largest anterior medullary feeder, the great anterior segmental medullary artery of Adamkiewicz, varies in level, arising from a spinal branch of either one of the lower posterior intercostal arteries (T9–11), or of the subcostal artery (T12), or less frequently of the upper lumbar arteries (L1 and L2). It most often arises on the left side (Carmichael & Gloviczki 1999). Reaching the spinal cord, it sends a branch to the anterior spinal artery below and another to anastomose with the ramus of the posterior spinal artery which lies anterior to the dorsal roots. It may be the main supply to the lower two-thirds of the cord. Central branches of the anterior spinal artery enter the anterior median fissure, and then turn right or left to supply the ventral grey column, the base of the dorsal grey column, including the dorsal nucleus, and the adjacent white matter (Fig. 43.9).

Each posterior spinal artery contributes to a pair of longitudinal anastomotic channels, anterior and posterior to the dorsal spinal roots. These are reinforced by posterior medullary feeders from the posterior radicular arteries. The latter are variable in number and size, but smaller, more numerous and more evenly distributed than the anterior medullary feeders. The anterior channel is joined by a ramus from the descending branch of the great anterior segmental medullary artery of Adamkiewicz. In all longitudinal spinal arteries the width of the lumen is uneven, and complete interruptions may occur. At the conus medullaris they communicate by anastomotic loops. Anastomoses other than those between the pial or peripheral spinal arterial branches may be important, e.g. a posterior spinal series of anastomoses between rami of the dorsal divisions of segmental arteries near the spinous processes.

Intramedullary arteries

The central branches of the anterior spinal artery supply about two-thirds of the cross-sectional area of the cord. The rest of the dorsal grey and white columns and peripheral parts of the lateral and ventral white columns are supplied by numerous small radial vessels which branch from posterior spinal arteries and the pial plexus. In a microangiographic study of the human cervical spinal cord, up to six anterior, and eight posterior, radicular spinal arteries were described, and up to eight central branches arose from each centimetre of the anterior spinal artery (Turnbull et al 1966).

Spinal cord ischaemia

The spinal cord can rely neither for its transverse nor for its longitudinal blood supply entirely on the longitudinal arteries. The anterior longitudinal artery and the intramedullary arteries are functional endarteries, although overlap of territories of supply has been described. Damage to the anterior longitudinal artery can result in loss of function of the anterior two-thirds of the cord. The longitudinal arteries cannot supply the whole length of the cord, and the input of the segmental medullary feeder vessels is essential. This is especially true of the artery of Adamkiewicz (great anterior segmental medullary artery), which may effectively carry the major supply for the lower cord. The midthoracic cord, distant from the main anterior medullary feeders, is particularly liable to become ischaemic after periods of hypotension.

VEINS

The venous drainage of the spinal cord (Fig. 43.11) follows a similar pattern to that of its arterial supply (Gillilan 1970). Intramedullary veins within the substance of the cord drain into a plexus of surface veins, the coronal plexus. There are six tortuous longitudinal channels within this plexus, one in each of the anterior and posterior median fissures, and four others which run on either side of the ventral and dorsal nerve roots. Only the anterior median vein, which drains the central grey matter, is consistently complete. These vessels connect freely and drain superiorly into the cerebellar veins and cranial sinuses, and segmentally mainly into medullary veins. The segmental veins drain into the intervertebral veins and thence into the external vertebral venous plexuses, the caval and azygos systems.

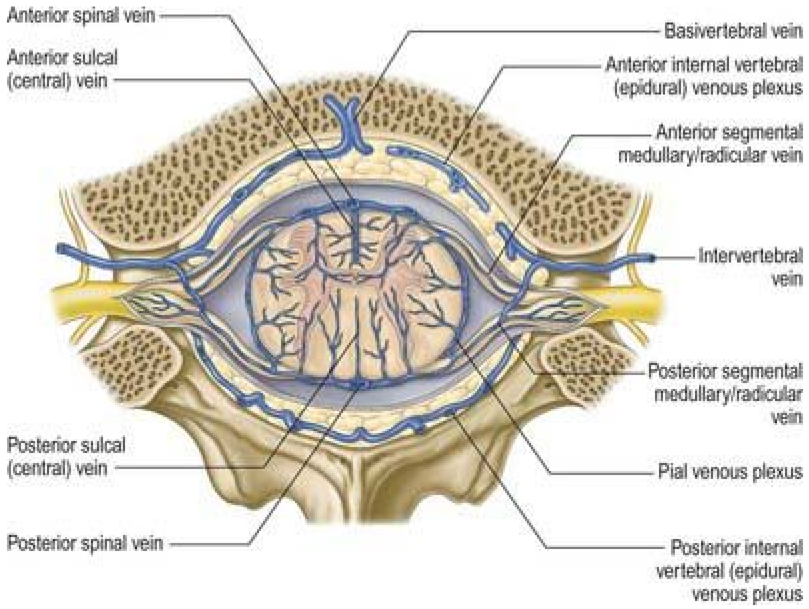
Anterior spinal vein
Anterior sulcal (central) vein
Basivertebral vein
Anterior internal vertebral (epidural) venous plexus
Anterior segmental medullary/radicular vein
Intervertebral vein
Posterior segmental medullary/radicular vein
Pial venous plexus
Posterior sulcal (central) vein
Posterior spinal vein
Posterior internal vertebral (epidural) venous plexus

Fig. 43.11 Venous disposition within the spinal cord.

Segmental veins

Anterior and posterior medullary veins run along some of the ventral and dorsal roots. They are larger than radicular veins, and drain the cord but not the roots themselves. Like the medullary feeder arteries, they are largest in the cervical and lumbar regions of the cord, but do not necessarily occur in the same segments as the medullary feeders. Anterior and posterior great medullary veins may arise in the lower thoracic or upper lumbar cord segments. There are 8–14 anterior medullary veins; posterior medullary veins are more numerous.

Very small anterior and posterior radicular veins occur in most spinal segments, accompanying and draining the ventral and dorsal roots and some of the cord at the points of entry and exit of the rootlets: they usually drain into the intervertebral veins.

THE EFFECTS OF INJURY

SPINAL CORD INJURY AND VERTEBRAL COLUMN INJURY

In the assessment of a patient with spinal injury and neurological damage, it is important to remember that the level of cord and root injury will not coincide with that of the skeletal damage to the vertebral column.

In estimating the vertebral levels of cord segments in the adult, a useful approximation is that in the cervical region the tip of a vertebral spinous process corresponds to the succeeding cord segment (i.e. the sixth cervical spine is opposite the seventh spinal segment); at upper thoracic levels the tip of a vertebral spine corresponds to the cord two segments lower (i.e. the fourth spine is level with the sixth segment), and in the lower thoracic region there is a difference of three segments (i.e. the tenth thoracic spine is level with the first lumbar segment). The eleventh thoracic spine overlies the third lumbar segment and the twelfth is opposite the first sacral segment. In making this estimate by palpation of the vertebral spines, the relationship of the individual spines to their vertebral bodies should be remembered (p. 745).

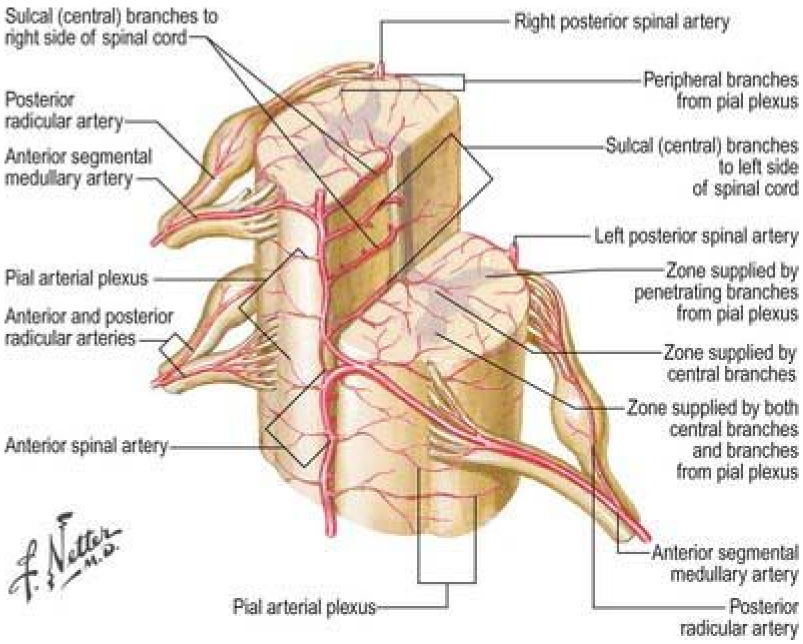
Sulcal (central) branches to right side of spinal cord
Right posterior spinal artery
Peripheral branches from pial plexus
Posterior radicular artery
Anterior segmental medullary artery
Sulcal (central) branches to left side of spinal cord
Left posterior spinal artery
Pial arterial plexus
Zone supplied by penetrating branches from pial plexus
Anterior and posterior radicular arteries
Zone supplied by central branches
Zone supplied by both central branches and branches from pial plexus
Anterior spinal artery
Anterior segmental medullary artery
Pial arterial plexus
Posterior radicular artery
F. Netter M.D.

Fig. 43.10 Arterial disposition within the spinal cord.

(Reprinted from Netter Anatomy Illustration Collection, © Elsevier Inc. All Rights Reserved.)

Complete division above the fourth cervical segment causes respiratory failure because of the loss of activity in the phrenic and intercostal nerves. Lesions between C5 and T1 paralyse all four limbs (quadriplegia), the effects in the upper limbs varying with the site of injury: at the fifth cervical segment paralysis is complete; at the sixth, each arm is positioned in abduction and lateral rotation, with the elbow flexed and the forearm supinated, due to unopposed activity in the deltoid, supraspinatus, rhomboid and brachial flexors (all supplied by the fifth cervical spinal nerves). In lower cervical lesions upper limb paralysis is less marked. Lesions of the first thoracic segment paralyse small muscles in the hand and damage the sympathetic outflow to the head and neck, resulting in contraction of the pupil, recession of the eyeball, narrowing of the palpebral fissure and loss of sweating in the face and neck (Horner's syndrome). However, sensation is retained in areas innervated by segments above the lesion, thus cutaneous sensation is retained in the neck and chest down to the second intercostal space, because this area is innervated by the supraclavicular nerves (C3 and C4). At thoracic levels, division of the cord paralyses the trunk below the segmental level of the lesion, and both lower limbs (paraplegia). The first sacral neural segment is approximately level with the thoracolumbar vertebral junction: injury, which commonly occurs here, paralyses the urinary bladder, the rectum and muscles supplied by the sacral segments, and cutaneous sensibility is lost in the perineum, buttocks, the back of the thighs and the legs and soles of the feet. The roots of lumbar nerves descending to join the cauda equina may be damaged at this level, causing complete paralysis of both lower limbs. Lesions below the first lumbar vertebra may divide or damage the cauda equina, but severe nerve damage is uncommon and is usually confined to the spinal roots at the level of the trauma. Neurological symptoms may also occur as a result of interference with the spinal blood supply, particularly in the lower thoracic and upper lumbar segments.

Spinal cord injury without radiological abnormality: ‘SCIWORA’

The spinal cord may be damaged without radiological evidence of skeletal injury in some injuries to the vertebral column. This is particularly liable to occur if the vertebral canal is abnormally narrowed, usually by osteoarthritic changes. In the elderly patient there may in addition be occlusive arterial disease, directly compromising an already precarious blood supply to the cord. This type of injury not uncommonly occurs in hyperextension injuries of the cervical spine in this age group. The cause of the damage may be direct injury to neural tissue by osteophytes or by an infolded ligamentum flavum, or direct or indirect injury to the vasculature of the cord. For cervical spinal injury, several cord syndromes have been described, relating the clinical picture to the anatomy of the neurological lesion within the cord. The commonest of these is central cord syndrome, which usually results from hyperextension injury to an osteoarthritic neck, in which the major injury is to the central grey matter. This gives a greater motor loss in the upper than in the lower limbs, with variable sensory loss. In anterior cord syndrome, which may occur in flexion–compression injuries of the neck, the damage occurs in the area of supply of the anterior spinal artery, sparing the posterior columns: the motor loss is usually proportionately greater in the lower than in the upper limbs, while sensory loss is less of a problem.

LESIONS OF THE SPINAL ROOTS, NERVES AND GANGLIA

Spinal roots, nerves and ganglia may be damaged in the vertebral and root canals and at the intervertebral foramina. Neurofibromas may occur on the roots and nerves in the root canals. As they enlarge these tumours become dumb-bell shaped, with both an intra- and an extra-spinal component in continuity: the clinical picture may thus include paradoxical features as the asymmetrical space-occupying lesion grows. Root compression usually presents acutely with pain which may be severe. The pain, paraesthesiae and numbness occur in a dermatomal distribution, and it may be difficult to demonstrate sensory loss on the trunk, because of dermatomal overlap. Severe traction injuries of the upper limbs may cause avulsion of spinal roots from the cord in the cervical region.

The anatomical basis for pain of spinal origin

In the diagnosis and description of pain of spinal origin it is particularly important to distinguish between radicular pain and somatic referred pain.

Radicular pain is caused by disorders that affect a spinal nerve or its dorsal root ganglion. This type of pain characteristically radiates, along a narrow band, into the area of the limb (or trunk wall) that the spinal nerve supplies, and is typically (although not always) lancinating in quality, not unlike an electric shock.

Referred pain is pain felt in the distribution of a nerve that is not the nerve that innervates the source of pain. Typically these nerves are derived from the same spinal cord segment. Referred pain is felt deeply, is typically aching in quality, and is felt across a broad area; although it may radiate into a limb (or around the trunk wall), it is typically constant in location. Patients may find it hard to define the outer boundaries of this pain, but they can clearly identify the centre of its distribution. Referred pain can be subdivided into somatic referred pain and visceral referred pain, according to its origin. Visceral referred pain is caused by disorders in viscera. In some instances, the referral can be quite remote from the viscus, as in cardiac pain that radiates into the neck. Somatic referred pain is caused by disorder of muscle and skeletal structures. Examples include lumbar spinal pain referred to the gluteal region, thigh, or leg; cervical spinal pain referred to the upper limb girdle; and cervical or thoracic spinal pain referred to the chest wall, where it can mimic cardiac pain. Often the source of somatic referred pain cannot be determined by clinical examination, and requires invasive tests to pinpoint its location.

LESIONS OF THE CONUS AND CAUDA EQUINA

Lesions of the conus and cauda equina, e.g. tumours, cause bilateral deficit, often with pain in the back extending into the sacral segments and to the legs. Loss of bladder and erectile function can be early features. There are lower motor neurone signs in the legs with fasciculation and muscle atrophy. Sensory loss usually involves the perineal or ‘saddle area’ as well as involving other lumbar and sacral dermatomes. There may be congenital abnormalities, e.g. spina bifida, lipomata or dystematomyelia, and the conus may extend below the lower border of L1, often with a tethered filum terminale. Extramedullary lesions include prolapsed intervertebral discs. A midline (central) disc protrusion in the lumbar region may present with involvement of only the sacral segments.

CLINICAL PROCEDURES

ACCESS TO CEREBROSPINAL FLUID

The safest approach to the cerebrospinal fluid (CSF) is to enter the lumbar cistern of the subarachnoid space in the midline, well below the level at which the spinal cord normally terminates (see above). The fine needle employed is unlikely to damage the mobile nerve roots of the cauda equina. This procedure is called lumbar puncture. It is also possible to access the CSF by midline puncture of the cerebello-medullary cistern (cisterna magna) (Ch. 16): this is cisternal puncture.

Lumbar puncture: adult

Lumbar puncture in the adult may be performed with the patient either sitting or lying on the side on a firm flat surface. In each position, the lumbar spine must be flexed as far as possible, in order to separate the vertebral spines maximally and expose the ligamentum flavum in the interlaminar window (Fig. 43.12). A line is then taken between the highest points of the iliac crests: this line intersects the vertebral column just above the palpable spine of L4. With the spines now identified, the skin is anaesthetized and a needle is inserted between the spines of L3 and L4 (or L4 and L5). Exact identification of the level by palpation is difficult (Broadbent et al 2000). The soft tissues which the needle will ultimately traverse should also be anaesthetized, though care should be taken lest the injection of an excessive amount of local anaesthetic compromises appreciation of the structures being traversed. These include the subcutaneous fat, and supraspinous and interspinous ligaments down to the ligamentum flavum itself. The lumbar puncture needle may then be inserted in the midline or just to one side, and angled in the horizontal and sagittal planes sufficiently to pierce the ligamentum flavum in or very near the midline. There is then a slight loss of resistance as the needle enters the epidural space, and careful advancement will next pierce the dura and arachnoid to release CSF.

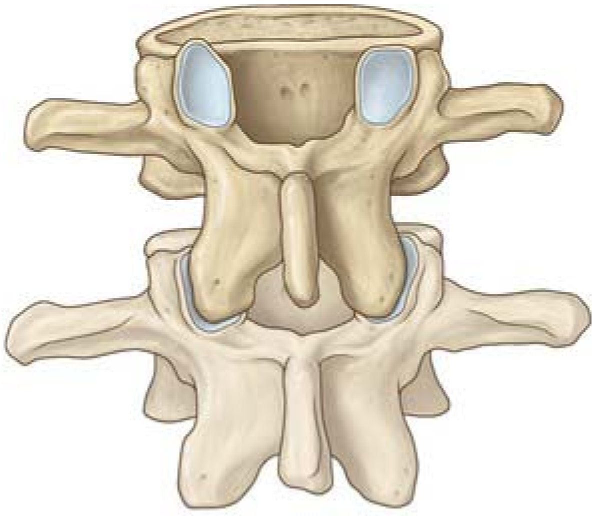

Extension

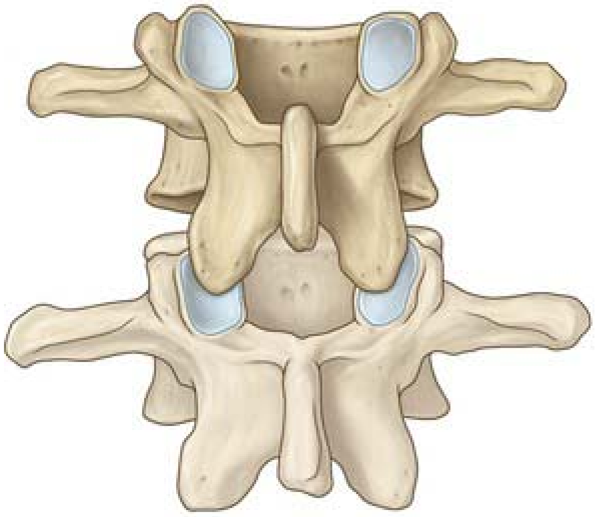

Flexion

Fig. 43.12 The lumbar interlaminar window in extension and flexion.

Lumbar puncture: neonate and infant

At full term (40 weeks) the spinal cord usually terminates somewhat lower than the adult level, sometimes reaching the body of L3. The supracristal plane intersects the vertebral column slightly higher (L3–4). By the second postnatal month the level of cord termination has usually reached its permanent position level with the body of the first lumbar vertebra. The lower end of the subarachnoid spine is found at sacral levels 1 or 2. These differences must be borne in mind when identifying the landmarks before undertaking lumbar puncture in the neonate and infant.

A lumbar puncture is performed by placing the baby in a position, either lying or ‘sitting’, which gives maximum convex curvature to the lumbar spine. A needle with trocar is inserted into the back between the spines of the third and fourth lumbar vertebrae and into the subarachnoid space below the level of the conus medullaris. The space between L3 and L4 is approximately level with the iliac crests and it is usual to insert the needle and trocar into the intervertebral space immediately above or below the iliac crests.

Cisternal puncture

In cisternal puncture, the cisterna magna (Ch. 16) is entered by midline puncture through the posterior atlanto-occipital membrane. Further details of this difficult specialist technique are beyond the scope of this book.

ACCESS TO THE EPIDURAL SPACE

The epidural space lies between the spinal dura and the wall of the vertebral canal. It contains epidural fat and a venous plexus. Access to this space, usually in the lumbar region, is required for the administration of anaesthetic and analgesic drugs, and for endoscopy. The caudal route is used mainly for analgesic injections.

Thoracic and cervical epidurals

It is possible to access the epidural space at thoracic and cervical levels, but the specialist techniques required are outside the scope of this book. The principles are the same as those for lumbar epidurals, but the special anatomy of the vertebral spines at the other levels requires the angle of approach to be modified.

Lumbar epidural

For access to the lumbar epidural space, the approach is as for lumbar puncture. The intention in epidural injection is to avoid dural puncture, so it is best to enter the epidural space in the midline posteriorly, where the depth of the space is greatest. Techniques for entering the epidural space rely on the appreciation of loss of resistance to injection of the chosen medium (usually air or saline) as the space is entered. This loss of resistance results from the fact that the pressure in the epidural space is subatmospheric. There is very little distance between the ligamentum flavum and the underlying dura on either side of the median plane.

Caudal epidural

The route of access to the caudal epidural space is via the sacral hiatus. The space is therefore entered below the level of termination of the dural sac, i.e. the subarachnoid space and its contained CSF, which usually extends to the level of the second sacral segment. Occasionally the dural sac ends as high as the fifth lumbar vertebra, and very rarely it may extend to the third part of the sacrum, in which case it is occasionally possible to enter the subarachnoid space inadvertently during the course of a sacral nerve block.

With the patient in the lateral position or lying prone over a pelvic pillow, the sacral hiatus is identified by palpation of the sacral cornua (Fig. 43.13). These are felt at the upper end of the natal cleft approximately 5 cm above the tip of the coccyx. Alternatively, the sacral hiatus may be identified by constructing an equilateral triangle based on a line joining the posterior superior iliac spines: the inferior apex of this triangle overlies the hiatus. After local anaesthetic infiltration, a needle is introduced at 45° to the skin, to penetrate the posterior sacrococcygeal ligament and enter the sacral canal. Once the canal is entered, the hub of the needle is lowered so that the needle may pass along the canal (Fig. 43.2, Fig. 43.14). If the needle is angled too obliquely it will strike bone; if it is placed too superficially it will lie outside the canal. The latter malposition can be confirmed by careful injection of air while palpating the skin over the lower sacrum.

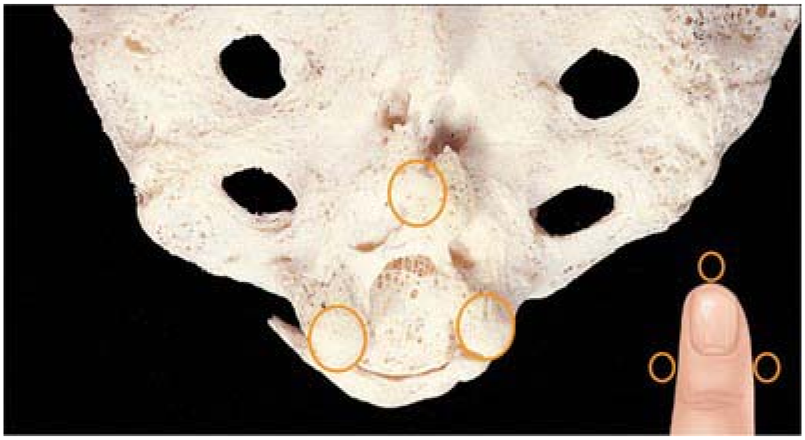

Fig. 43.13 Palpation of the sacral cornua for caudal epidural injection.

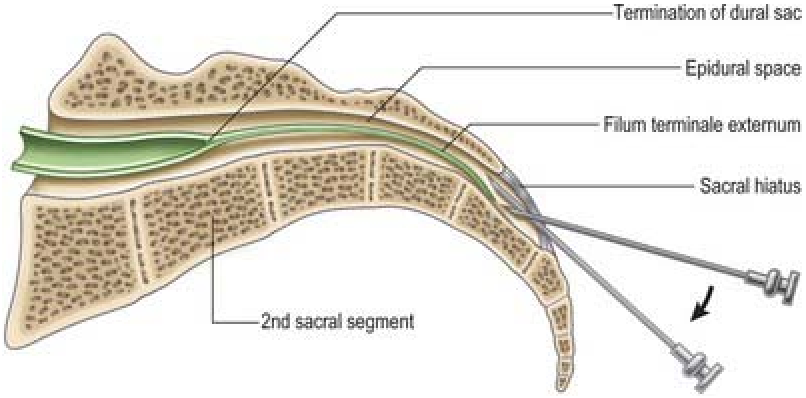

Fig. 43.14 Position of the needle in caudal epidural injection.

REFERENCES

rson AJ, Sands J. Regional and segmental characteristics of the human adult spinal cord. *J Anat*. 1977;123:797-803.

gduk N. Clinical Anatomy of the L Spine and Sacrum, 4th edn. Edinburgh: Elsevier Churchill Livingstone, 2005.

oadbent CR, Maxwell WE, Ferrie R, Wilson DJ, Gawne-Cain M, Russell R. Ability of anaesthetists to identify a marked lumbar interspace. *Anaesthesia*. 2000;55:1122-1126.

rmichael SW, Gloviczki P. Anatomy of the blood supply to the spinal cord: the artery of Adamkiewicz revisited. *Perspect Vasc Surg*. 1999;12:113-122.

ock HV. An Atlas of Vascular Anatomy of the Skeleton and Spinal Cord. London: Martin Dunitz, 1996.

an NA, Mitchell BS. Anatomic relation between the nuchal ligament (ligamentum nuchae) and the spinal dura mater in the craniocervical region. *Clin Anat*. 2002;15:182-185.

mmisse GF. The Arteries and Veins of the Human Spinal Cord From Birth. Edinburgh: Churchill Livingstone, 1975.

aher JP. The transitional zone and CNS regeneration. *J Anat*. 2000;196:137-158.

llilan LA. Veins of the spinal cord. Anatomic details; suggested clinical applications. *Neurology*. 1970;20:860-868.

ines DE, Harkey HL, Al-Mefty O. The ‘subdural’ space: a new look at an outdated concept. *Neurosurgery*. 1993;32:111-120.

Proposes the view that the subdural ‘space’ is a pathological cleavage plane rather than a normal anatomical element..

ddo DK, Gomez DG, Pavese AM, Potts DG. Human spinal arachnoid granulations. *Neuroradiol*. 1976;11:221-228.

bik S, Müntener M. Zur Topographie der spinalen Nervenwurzeln. II Der Einfuss des Wachstums des Duralsackes, sowie der Krümmagen und der Bewegungen der spinalen Nervenwurzeln. *Acta Anat*. 1969;74:149-168.

An alternative view of the obliquity of the cervicothoracic spinal nerve roots based on observations of differential cord growth..

idre A, Macnab I. Anomalies of the lumbosacral nerve roots. *Spine*. 1983;8:294-299.

well RLM. The spinal epidural space. *Clin Anat*. 1999;12:375-379.

rnbull IM, Brieg A, Hassler O. Blood supply of cervical spinal cord in man. A microangiographic cadaver study. *J Neurosurg*. 1966;24:951-965.

CHAPTER 44

Development of the back

Vertebrae and their alternating intervertebral discs are one of the main manifestations of body segmentation or metamerism. A chain of segments arranged in sequence allows the overall structure to bend when it is moved by the associated muscles. The original body segments, the somites, are formed by the paraxial mesenchyme which is found lateral to the neural tube and notochord in the early embryo. The somites provide the embryonic cell populations for bone and muscle. The vertebrae form between the early body segments by the recombination of portions of the somites on the craniocaudal axis, and the muscles attach to adjacent vertebrae. Each vertebra develops from bilateral origins to form a midline centrum, two lateral arches bearing transverse processes which develop lateral and dorsal to the spinal cord, and a midline fused dorsal portion with a spinous process. Individual vertebrae may be distinguished by modifications of these component parts. The intervertebral discs develop from the same origins as the centra, and are composed of outer dense fibrous tissue surrounding a softer central zone.

SEGMENTATION OF PARAXIAL MESENCHYME

Epiblast cells which ingress through the lateral aspect of the primitive node and the rostral primitive streak (see Fig. 10.3) become committed to a somitic lineage (see p. 184). After passing through the streak the cells retain contact with both the epiblast and hypoblast basal laminae as they migrate and for some time after reaching their destination. The cells form populations of paraxial mesenchyme on each side of the notochord, termed presomitic or unsegmented mesenchyme. Somites will form from cultured presomitic mesenchyme with or without the presence of neural tube tissue or primitive node tissue. As well as specifying somitic lineage, the position of ingression of the epiblast informs the specific destination of the cells. Thus those cells which ingress through the lateral portion of Hensen's node form the medial halves of the somites, whereas those ingressing through the primitive streak approximately 200 μm caudal to the node produce the lateral halves of the somites. The two somite halves do not appear to intermingle.

The segmentation of the paraxial presomitic mesenchyme occurs as a sequential process along the craniocaudal axis. In some amniote embryos a pair of somites is formed every 90 minutes until the full number is obtained. The molecular pathway for this synchronous segmentation has been termed the segmentation clock. It has been identified as a conserved process in vertebrates from fish to mammals, and is based on the rhythmic production of mRNAs for the transcription of genes related to Notch, a large transmembrane receptor, and a number of transmembrane ligands.

Intrinsically coordinated pulses of mRNA expression appear as a wave within the presomitic mesenchyme as each somite forms. As new cells enter the paraxial mesenchyme caudally they begin phases of up-regulation of the cycling genes followed by downregulation of these genes. During each cycle the most cranial presomitic mesenchyme will segment to form the next somite.

Experimental evidence (from chick embryos) shows that newly formed paraxial mesenchyme cells undergo 12 such cycles before they finally form a somite (Pourquie & Kusumi 2001). Thus from ingression through the primitive streak to segmentation into a somite takes approximately 18 hours. As the somite number varies between vertebrate species, it is likely that the rate of somite formation also varies and may be longer in human embryos. Indeed those vertebrates with elongated bodies and many somites appear to form somites more rapidly than those with shorter bodies, a finding which supports the concept that somite number is controlled in part by species-specific cyclical properties of the presomitic mesenchyme (Richardson et al 1998).

The final determination of somitic boundary formation has not yet been fully elucidated, but seems to require a periodic repression of the Notch pathway genes. The caudal presomitic mesenchyme cells are thought to be maintained in an immature state by their production of FGF8. The cells become competent for segmentation when FGF8 levels drop below a certain threshold. They would then be in close apposition to cells that have segmented (i.e. the next cranial somite).

This area of research is moving rapidly. A detailed critique of the conceptual models of segmentation is given by Stern & Vasiliauskas (2000). An overview of the processes involved in the development of the paraxial mesenchyme, based on the work of Christ et al (2000), is shown in Figure 44.1.

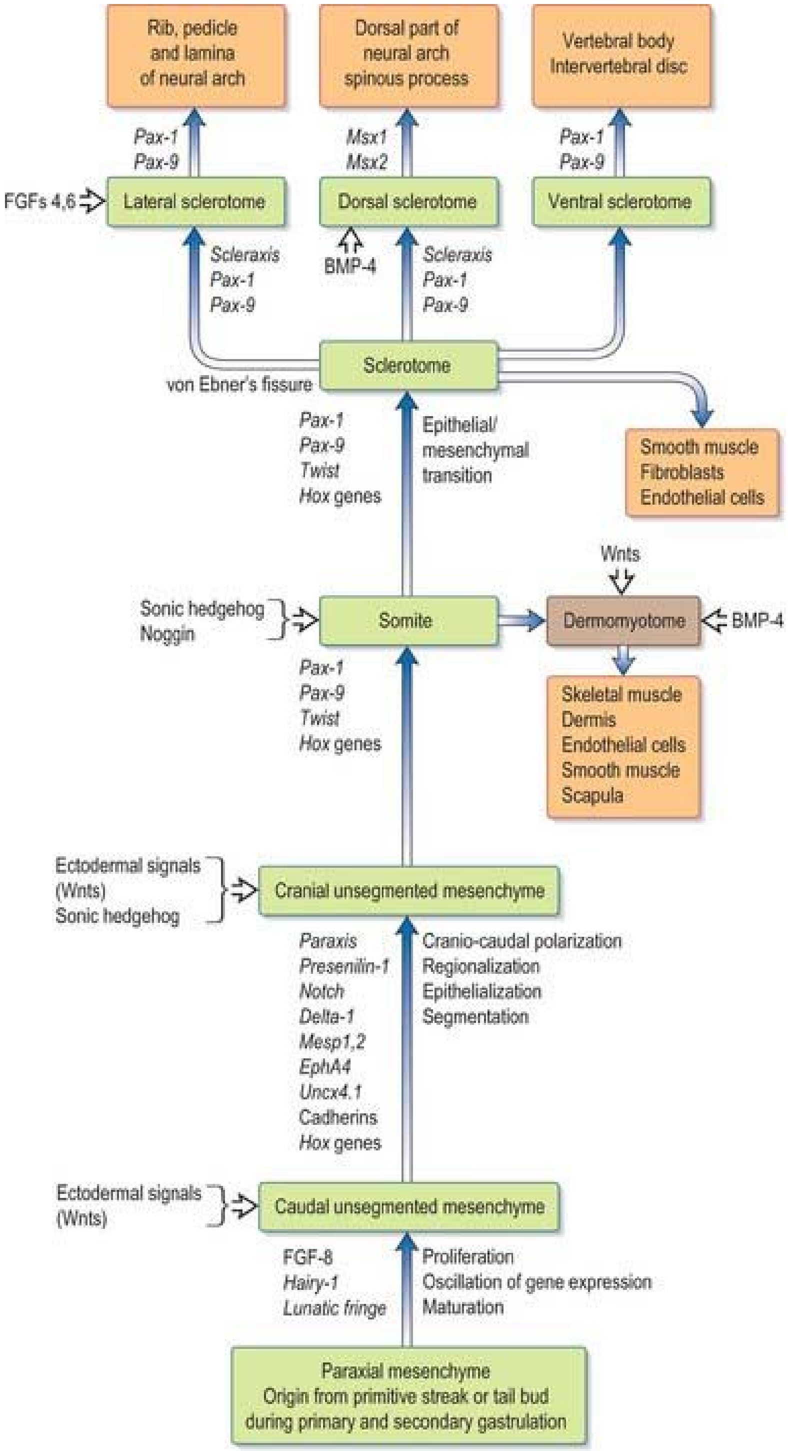
Rib, pedicle and lamina of neural arch
Dorsal part of neural arch spinous process
Vertebral body Intervertebral disc
Pax-1
Pax-9
Msx1
Msx2
Pax-1
Pax-9
FGFs 4,6
Lateral sclerotome
Dorsal sclerotome
Ventral sclerotome
Scleraxis
Pax-1
Pax-9
BMP-4
Scleraxis
Pax-1
Pax-9
Sclerotome
von Ebner's fissure
Pax-1
Pax-9
Twist
Hox genes
Epithelial/ mesenchymal transition
Smooth muscle
Fibroblasts
Endothelial cells
Wnts
Sonic hedgehog
Noggin
Somite
Dermomyotome
BMP-4
Pax-1
Pax-9
Twist
Hox genes
Skeletal muscle
Dermis
Endothelial cells
Smooth muscle
Scapula
Ectodermal signals (Wnts)
Sonic hedgehog
Cranial unsegmented mesenchyme
Paraxis
Presenilin-1
Notch
Delta-1
Mesp1,2
EphA4
Uncx4.1
Cadherins
Hox genes
Cranio-caudal polarization
Regionalization
Epithelialization
Segmentation
Ectodermal signals (Wnts)
Caudal unsegmented mesenchyme
FGF-8
Hairy-1
Lunatic fringe
Proliferation
Oscillation of gene expression
Maturation
Paraxial mesenchyme
Origin from primitive streak or tail bud during primary and secondary gastrulation

Fig. 44.1 Processes in the development of the paraxial mesenchyme in the avian embryo. Signals are indicated by open arrows; genes are italicized.

(Redrawn with permission from Christ B, Huang R, Wilting J 2000 The development of the avian vertebral column. Anat Embryol 202: 179–94, Springer.)

SOMITOGENESIS

Somitogenesis is a process in which five main stages can be identified (Figs 44.2, 44.3). Compaction and formation of the spherical epithelial somite surrounding free somitocele cells occur prior to segmentation of the paraxial mesenchyme. Once the somite boundaries have been defined there is an epithelial/mesenchymal transition of the ventral and ventromedial walls of the somite to form the sclerotome. This is followed by bilateral movement of these ventral and medial mesenchyme populations around the notochord and the neural tube. The final stage is formation of the epithelial plate of the somite, also termed the dermomyotome, from the remaining somitic epithelium. Segmentation of the paraxial mesenchyme, formation of somites and resultant somitogenetic processes occur in a craniocaudal progression caudal to the otic vesicle from stage 9.

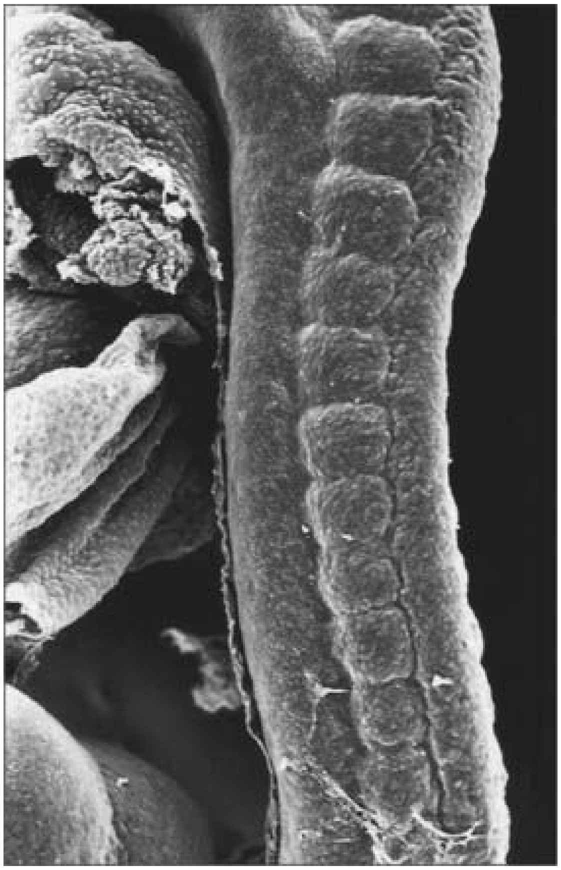

Fig. 44.2 Scanning electron micrograph of a lateral view of an embryo showing the somites. The cranial somites are at the upper border and the more caudal somites are at the lower border. A change in size of the cranially more advanced somites is apparent.

(Photograph by P Collins; printed by S Cox, Electron Microscopy Unit, Southampton General Hospital.)

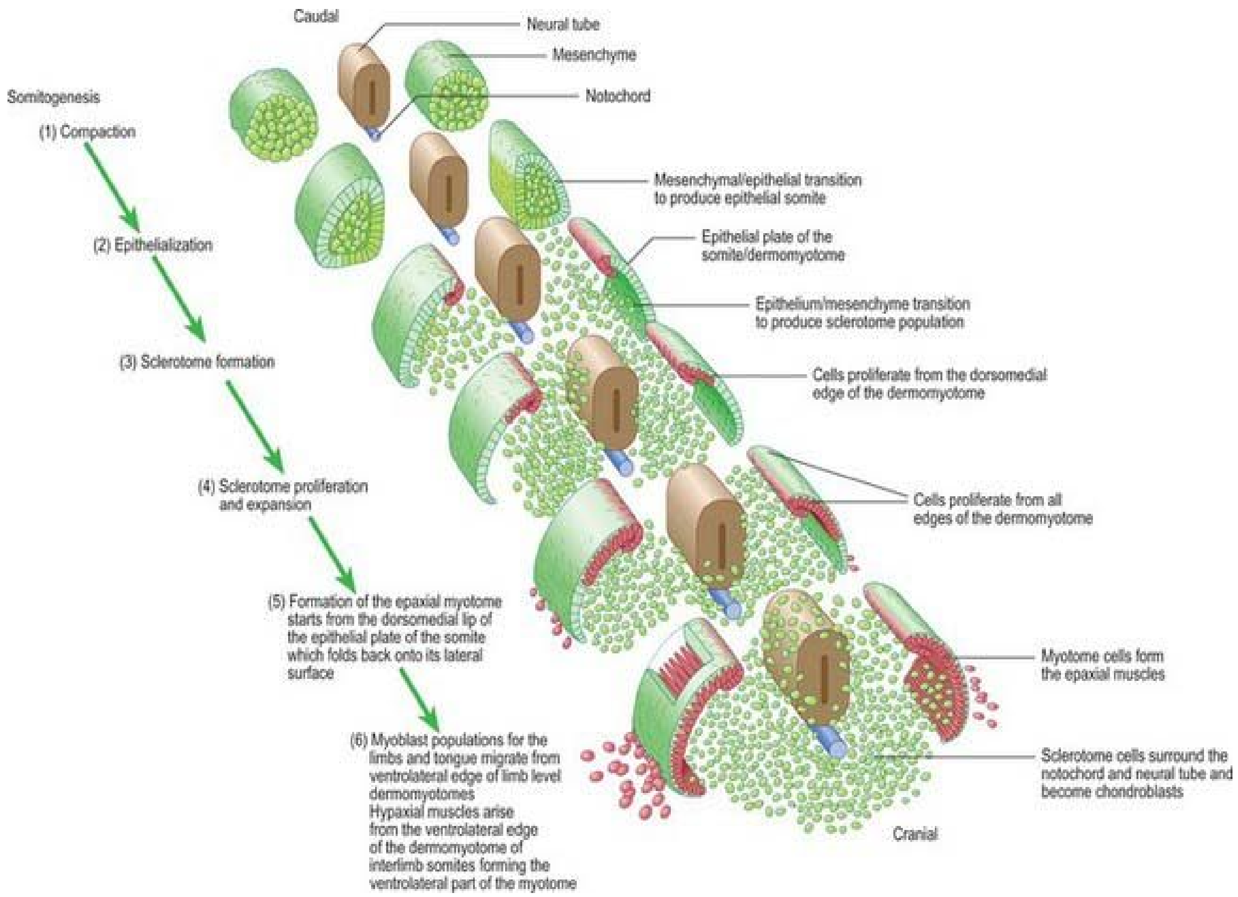
Caudal
Neural tube
Mesenchyme
Notochord
Somitogenesis
(1) Compaction
(2) Epithelialization
(3) Sclerotome formation
(4) Sclerotome proliferation and expansion
(5) Formation of the epaxial myotome starts from the dorsomedial lip of the epithelial plate of the somite which folds back onto its lateral surface
(6) Myoblast populations for the limbs and tongue migrate from ventrolateral edge of limb level dermomyotomes
Hypaxial muscles arise from the ventrolateral edge of the dermomyotome of interlimb somites forming the ventrolateral part of the myotome
Mesenchymal/epithelial transition to produce epithelial somite
Epithelial plate of the somite/dermomyotome
Epithelium/mesenchyme transition to produce sclerotome population
Cells proliferate from the dorsomedial edge of the dermomyotome
Cells proliferate from all edges of the dermomyotome
Myotome cells form the epaxial muscles
Sclerotome cells surround the notochord and neural tube and become chondroblasts
Cranial

Fig. 44.3 The stages of somitogenesis. Development occurs in a craniocaudal progression. The more cranially placed somites (at the lower right of the figure) are further developed than those caudally placed (at the upper left of the figure). The stages in somitogenesis are given on the left of the figure; more detailed information is given on the right.

The Golgi apparatus, and actin and α-actinin are all located in the apical region of the epithelial somite cells. Cilia develop on the free surface. The cells are joined by tight junctions (a variety of cell adhesion molecules has been demonstrated in epithelial somites). The basal surface rests on a basal lamina which contains collagen, laminin, fibronectin and cytotactin. Processes from the somite cells pass through this basal lamina to contact the basal laminae of the neural tube and notochord. Dorsoventral patterning of the putative vertebral column is dependent on the interaction of SHH from the notochord/floor plate with Wnt1 and Wnt3a from the roof plate and Wnt6 from the overlying ectoderm.

The epithelial somite undergoes rapid development (Fig. 44.3). The cells of the ventromedial wall which were abutting the neural tube undergo an epithelial/mesenchyme transformation and break apart. The newly formed mesenchymal cells, which are collectively termed the sclerotome, proliferate. The remaining cells of the somite are now termed the epithelial plate of the somite (or dermomyotome). This epithelium is proliferative; it produces the cell lines which will give rise to (nearly) all the striated muscles of the body.

The sclerotomal population has been subdivided in the chick and the fates of the cells followed (Christ, Huang & Scaal 2004) (Fig. 44.4-44.6). The main mass of the sclerotome is termed the central sclerotome, that portion close to the notochord is termed the ventral sclerotome, and the portions adjacent to the dermomyotome are termed dorsal sclerotome and lateral sclerotome. The central sclerotome remains close to the dermomyotome; it will give rise to the pedicles and ventral parts of the neural arches, and the proximal ribs. The ventral sclerotomal cells, which were always lateral to the notochord, proliferate to form an axial cell population within the extracellular matrix of the perinotochordal space, now termed the perinotochordal sheath. The dorsal sclerotomal cells develop relatively late and invade the space between the surface ectoderm and growing neural tube and form the dorsal part of the neural arches. The lateral sclerotomal cells give rise to distal ribs and endothelial cells of blood vessels. Generally there is a dorsolateral expansion of the whole sclerotome rather than the medial migration of a population of sclerotomal cells (Gasser 2006). This can be seen in Figures 44.4-44.6. Sclerotomal cells also give rise to the meninges surrounding the spinal cord, local tendons and ligaments. The somitocele cells which remain mesenchymal throughout somite formation give rise to the vertebral joints, intervertebral discs and the proximal ribs (Christ, Huang & Scaal 2004).

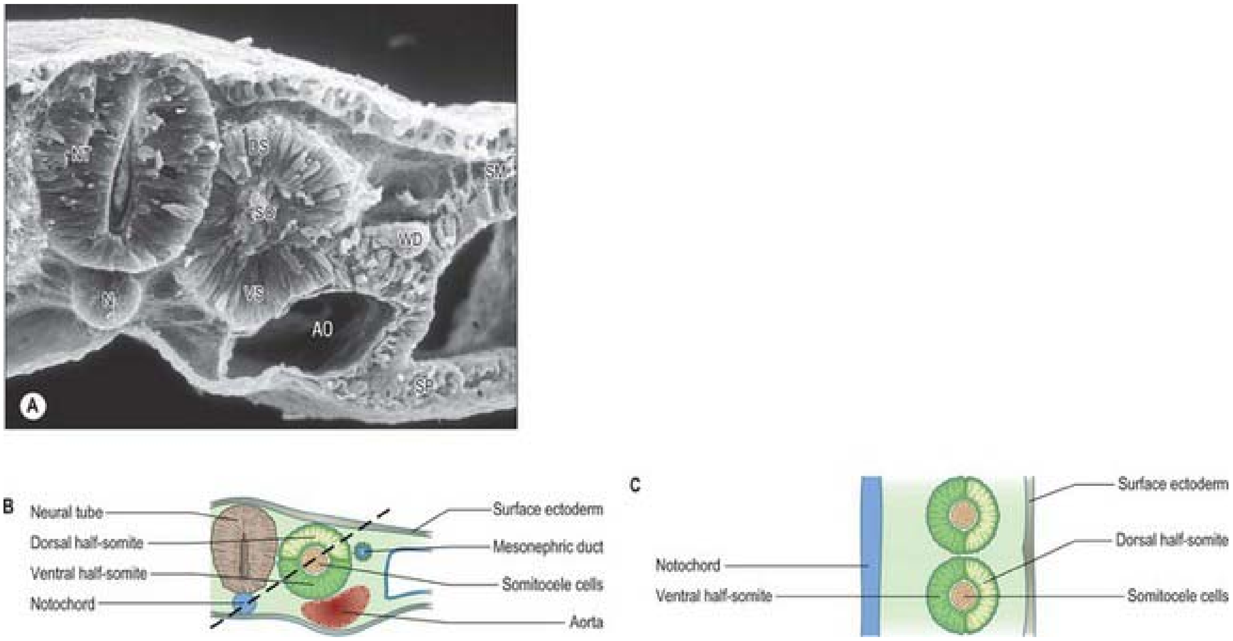
A
NT
DS
SM
SO
WD
N
VS
AO
SP
B
Neural tube
Dorsal half-somite
Ventral half-somite
Notochord
Surface ectoderm
Mesonephric duct
Somitocele cells
Aorta
C
Surface ectoderm
Dorsal half-somite
Notochord
Ventral half-somite
Somitocele cells

Fig. 44.4 Development of the sclerotome. Scanning electron micrograph of a transverse fracture of a 2 day chick embryo (**A**) and transverse (**B**) and longitudinal (**C**) section through the somites, indicated by dotted line in **B**. The somites here are in the epithelialization phase of somitogenesis. AO, aorta; DS, dorsal somite; N, notochord; NT, neural tube; SM, somatopleure; SO, somitocele; SP, splanchnopleure; VS, ventral somite; WD, Wolffian duct (mesonephric duct).

*(**A** By courtesy of Dr Heinz Jürgen Jacob, Bochum, Germany)*

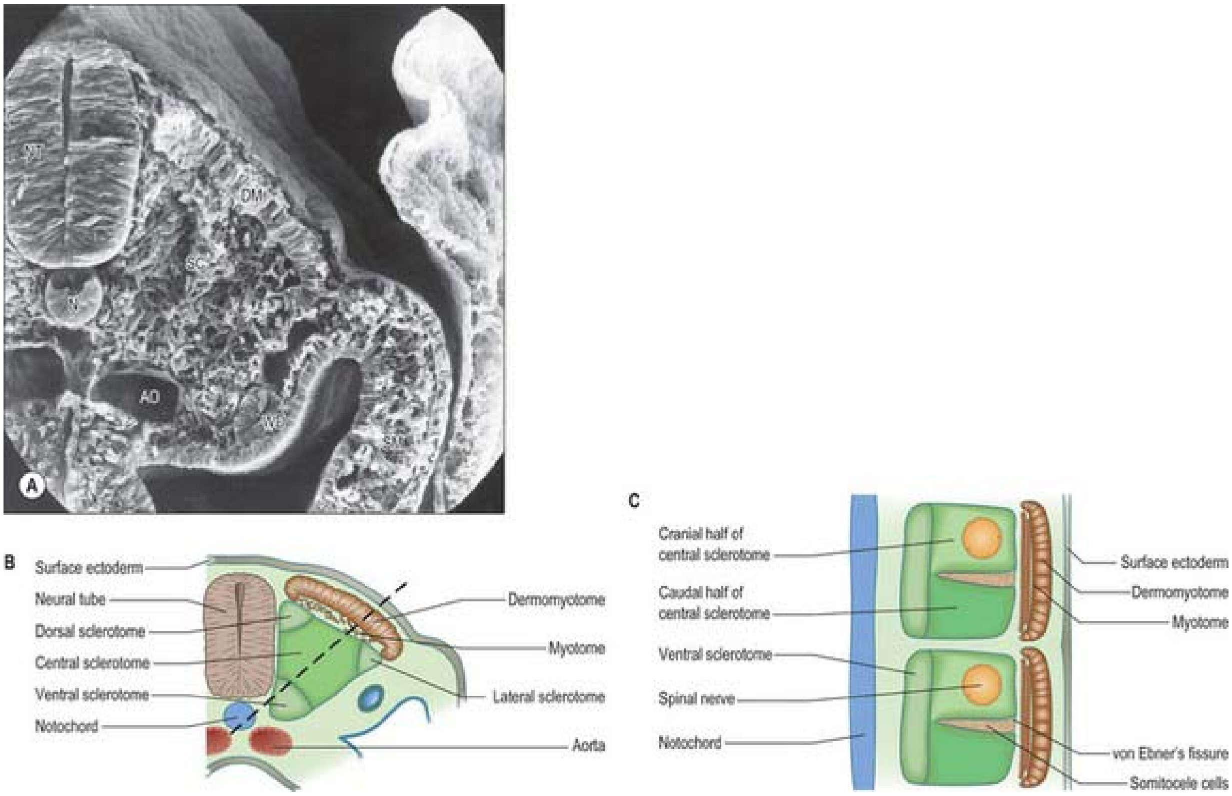
A
NT
DM
SC
N
AO
WD
SM
B
Surface ectoderm
Neural tube
Dorsal sclerotome
Central sclerotome
Ventral sclerotome
Notochord
Dermomyotome
Myotome
Lateral sclerotome
Aorta
C
Cranial half of central sclerotome
Caudal half of central sclerotome
Ventral sclerotome
Spinal nerve
Notochord
Surface ectoderm
Dermomyotome
Myotome
von Ebner's fissure
Somitocele cells

Fig. 44.5 Development of the sclerotome. Scanning electron micrograph of a transverse fracture of a 3 day chick embryo (**A**) and transverse (**B**) and longitudinal (**C**) section through the developing sclerotome, indicated by dotted line in **B**. AO, aorta; DM, dermomyotome; N, notochord; NT, neural tube; SC, sclerotome; SM, somatopleure; WD, Wolffian duct (mesonephric duct).

*(**A** By courtesy of Dr Heinz Jürgen Jacob, Bochum, Germany)*

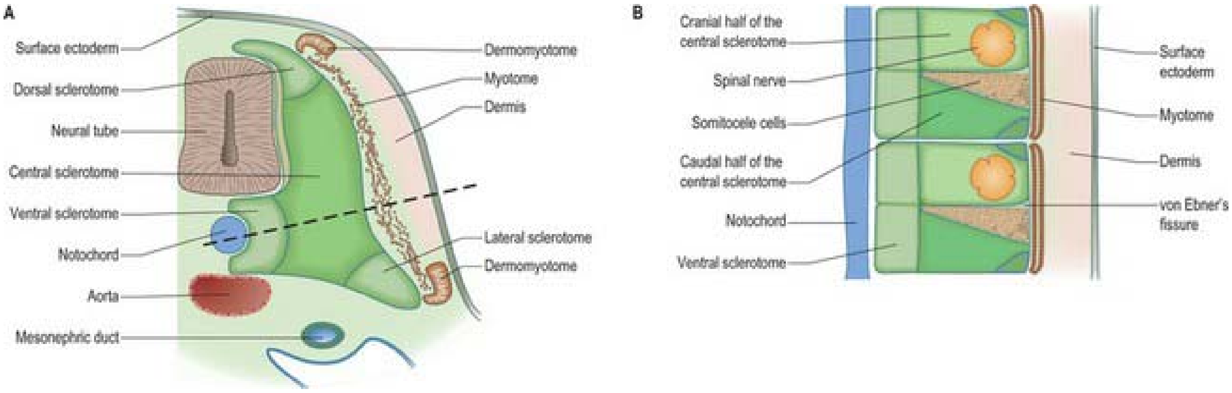
A
Surface ectoderm
Dorsal sclerotome
Neural tube
Central sclerotome
Ventral sclerotome
Notochord
Aorta
Mesonephric duct
Dermomyotome
Myotome
Dermis
Lateral sclerotome
Dermomyotome
B
Cranial half of the central sclerotome
Spinal nerve
Somitocele cells
Caudal half of the central sclerotome
Notochord
Ventral sclerotome
Surface ectoderm
Myotome
Dermis
von Ebner's fissure

Fig. 44.6 Later development of the sclerotome. Transverse (**A**) and longitudinal (**B**) section through dotted line indicated in A showing the sclerotomal subdivisions.

The dermomyotome is a proliferative epithelium which produces cells from four borders (Fig. 44.7). Proliferation at the dorsomedial edge produces cells from the cranial to the caudal edge of the dermomyotome; they elongate beneath its basal lamina as they move laterally. Cells similarly proliferate from the cranial and caudal edges of the dermomyotome and these cells also elongate across it. The cells that are produced from these three edges are collectively termed the myotome, and will give rise to skeletal muscle dorsal to the vertebrae, i.e. the epaxial musculature. At limb levels cells de-epithelialize and migrate from the ventrolateral edges of the dermomyotome into the limb bud. Cells produced from this portion of the occipital somites migrate anteriorly to give rise to the intrinsic muscles of the tongue. At interlimb levels a hypaxial proliferation of myogenic cells that will give rise to intercostal and abdominal muscles extends from the ventrolateral edge of the epithelial dermomyotome into the body wall as development proceeds (Scaal & Christ 2004).

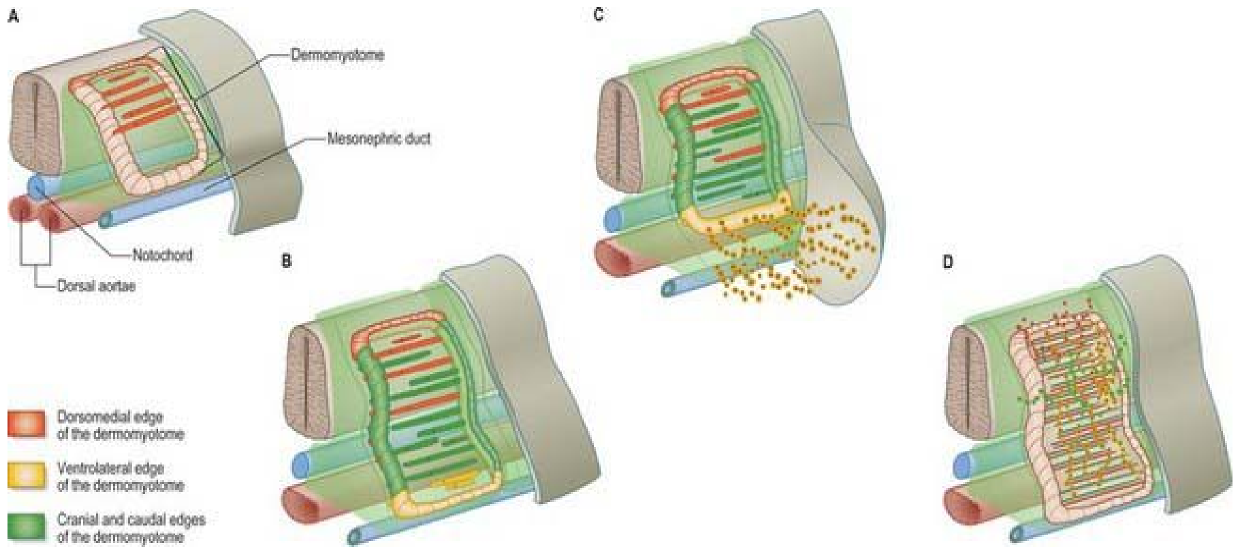
A
Dermomyotome
Mesonephric duct
Notochord
Dorsal aortae
B
C
D
Dorsomedial edge of the dermomyotome
Ventrolateral edge of the dermomyotome
Cranial and caudal edges of the dermomyotome

Fig. 44.7 **A–D**, Epaxial and hypaxial muscle origin from the dermomyotome. **A**, Early dermomyotome proliferation. **B**, Dermomyotome

at interlimb level producing expaxial myoblasts. **C**, Dermomyotome at limb level. Hypaxial dermomyotome cells de-epithelialize from the ventrolateral edge and migrate into the limb bud. **D**, Local dermis is formed later by superficial de-epithelialization of dermomyotome cells.

It was thought that the somite gave rise to segmental portions of the dermis of the skin as well as bone and muscle. However, it is now clear that the somitic contribution to the skin from the epithelial plate is limited to de-epithelialization of dermomyotome cells over the epaxial muscles alone, which is a much smaller distribution than the segmental portion of skin usually implied by the term dermatome. The concept that an embryological dermatome, derived from the somite, produces all of the dermis of the skin is therefore outdated.

The regularity of somite formation provides criteria for staging embryos. The staging scheme proposed by Ordahl (1993) will be used in the following account of relative somite development. Ordahl noted that morphogenetic events occur in successive somites at approximately the same rate. The somite most recently formed from the unsegmented mesenchyme is designated as stage I, the next most recent as stage II, etc. After the embryo forms an additional somite, the ages of the previously formed somites increase by one Roman numeral. According to this scheme, compaction occurs at stage I; epithelialization at stages II to III; formation of mesenchymal sclerotome cells from stage V; myotome formation at stage VI; early migration of the ventrolateral lip of the epithelial plate and production of myotome cells are still occurring at stage X.

DEVELOPMENT OF SCLEROTOMES

Sclerotomal populations form from the ventral half of the epithelial somite. An intrasegmental boundary (fissure or cleft, sometimes termed von Ebner's fissure) that is initially filled with extracellular matrix and a few cells, appears within the sclerotome and divides it into loosely packed cranial and densely packed caudal halves. The epithelial plate, and later the dermomyotome, spans the two half-sclerotomes. The bilateral sclerotomal cell populations migrate towards the notochord and surround it to form the perinotochordal sheath. They undergo a matrix-mediated interaction with the notochord, differentiating chondrogenetically to form the cartilaginous precursor of the vertebral centrum. The perinotochordal sheath transiently expresses type II collagen, and this is believed to initiate type II collagen expression, and thereafter a chondrogenic fate, in those mesenchyme cells which contact it. Each vertebra is formed by the combination of much of the caudal half of one bilateral pair of sclerotomes with much of the cranial half of the next caudal pair of sclerotomes. Their fusion around the notochord produces the blastemal centrum of the vertebra (Figs 44.8 and 44.9). The mesenchyme adjoining the intrasegmental sclerotomic fissure now increases greatly in density to form a well-defined perichordal disc which intervenes between the centra of two adjacent vertebrae and is the future anulus fibrosus of the intervertebral symphysis ('disc') (see below).

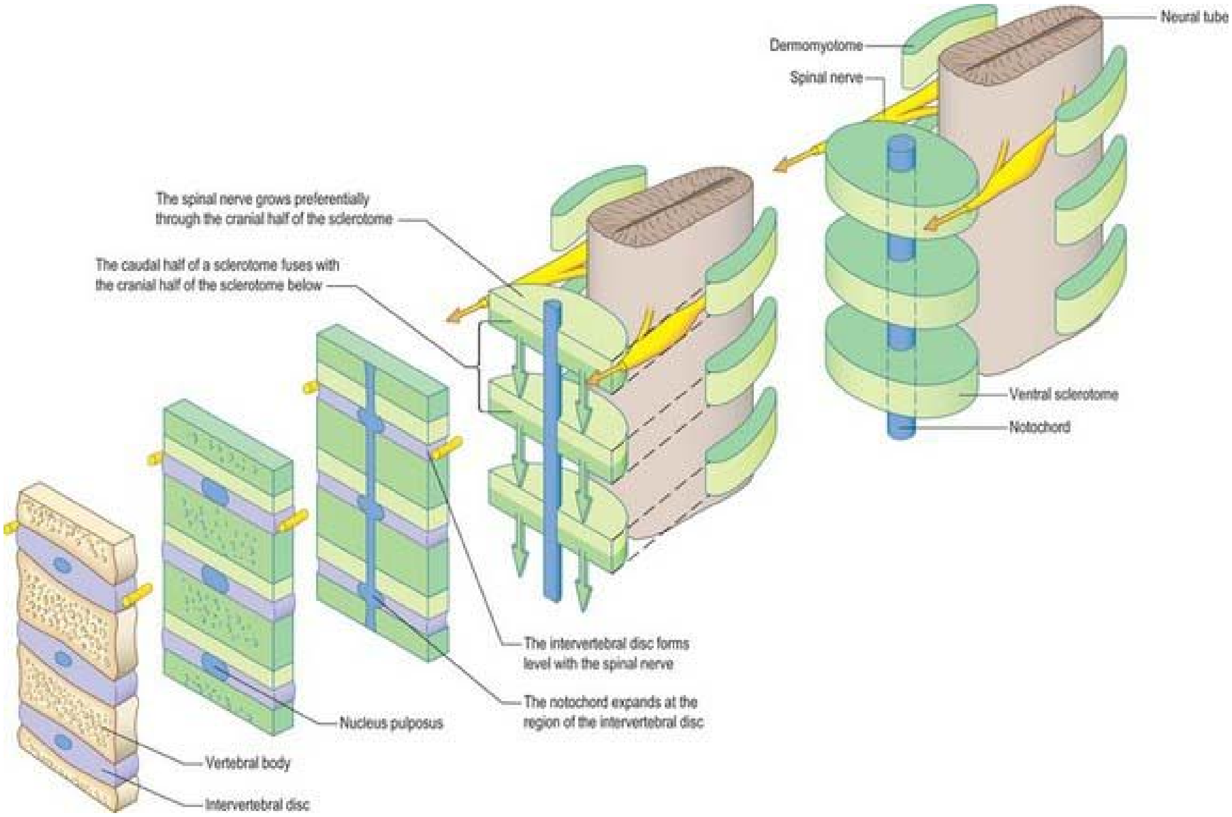
Neural tube
Dermomyotome
Spinal nerve
The spinal nerve grows preferentially through the cranial half of the sclerotome
The caudal half of a sclerotome fuses with the cranial half of the sclerotome below
Ventral sclerotome
Notochord
The intervertebral disc forms level with the spinal nerve
The notochord expands at the region of the intervertebral disc
Nucleus pulposus
Vertebral body
Intervertebral disc

Fig. 44.8 Formation of vertebrae and intervertebral discs from the mesenchymal sclerotomes. Each vertebra is formed from the cranial half of one bilateral pair of sclerotomes and the caudal half of the next pair of sclerotomes.

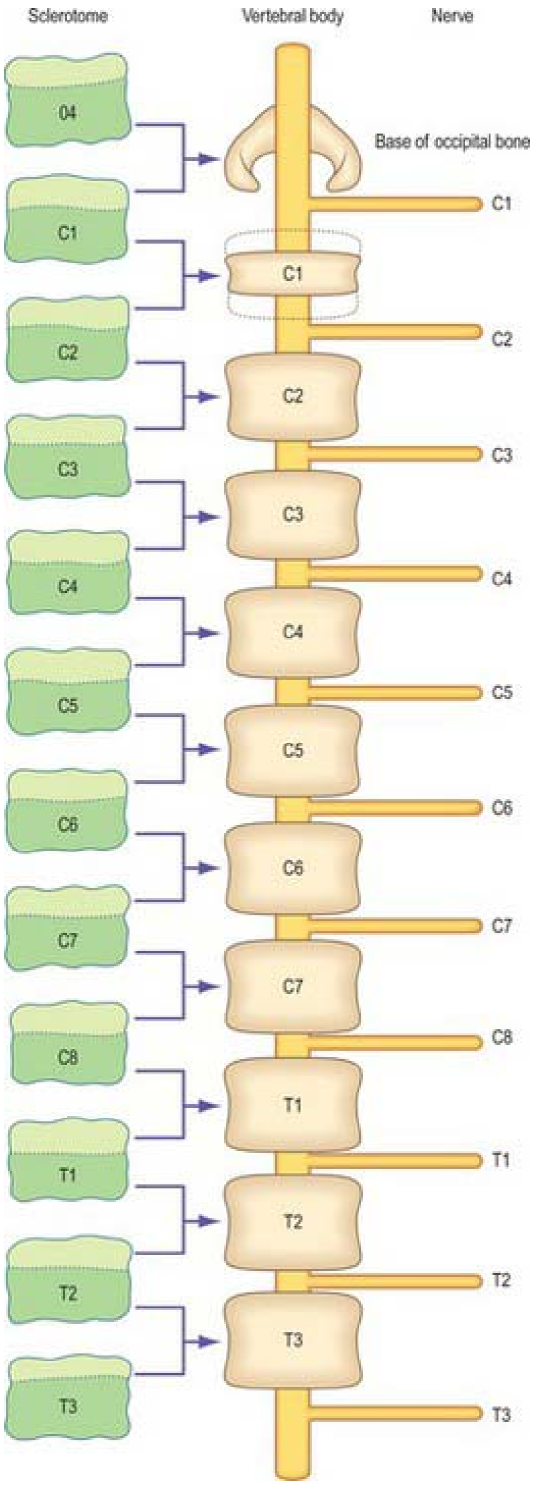
Sclerotome
Vertebral body
Nerve
04
C1
C2
C3
C4
C5
C6
C7
C8
T1
T2
T3
Base of occipital bone
C1
C2
C3
C4
C5
C6
C7
T1
T2
T3
C1
C2
C3
C4
C5
C6
C7
C8
T1
T2
T3

Fig. 44.9 Contribution of the somites to the vertebrae. Each somite induces a ventral root to grow out from the spinal cord. When the sclerotomes recombine, the cranial half of the first cervical sclerotome fuses with the occipital sclerotome above contributing to the occipital bone of the

skull. The cervical nerves beginning with C1 exit above the corresponding vertebra. Nerve C8 exits below the seventh cervical vertebra (C7), and thereafter nerves arise below their numbered vertebrae.

(By permission from Larsen WJ 1997 Human Embryology, 2nd edn. Edinburgh: Churchill Livingstone.)

The basic pattern of a typical vertebra is initiated by this recombination of caudal and cranial sclerotome halves (Fig. 44.10), followed by differential growth and sculpturing of the sclerotomal mesenchyme which encases the notochord and neural tube. The centrum encloses the notochord and lies ventral to the neural tube. Condensation of the sclerotomal mesenchyme around the notochord and right and left neural processes can be seen in stage 15 human embryos. The neural processes curve to enclose the neural tube and extend to the dorsolateral angles of the centrum. The neural arch consists of paired bilateral pedicles (ventrolaterally) and laminae (dorsolaterally) which coalesce in the midline dorsal to the neural tube to form the spinous process. On each side three further processes project cranially, caudally and laterally from the junction of the pedicle and laminae. The cranial and caudal projections are the blastemal articular processes (zygapophyses) which become contiguous with reciprocal processes of adjacent vertebrae; their junctional zones mark the future zygapophysial or facet joints. The lateral projections are the true vertebral transverse processes. Bilateral costal processes (ribs) grow anterolaterally from the ventral part of the pedicles (i.e. near the centrum), from the neighbouring perichordal disc, and, at most thoracic levels, with accessions from the next adjacent caudal pedicles. The costal processes expand to meet the tips of the transverse processes. The definitive vertebral body is compound, and is formed from a median centrum (derived from the cells of the peri-notochordal sheath), and bilaterally from the expanded pedicle ends (derived from the migrating sclerotomal populations). These portions of the vertebral body fuse at the neurocentral synchondroses.

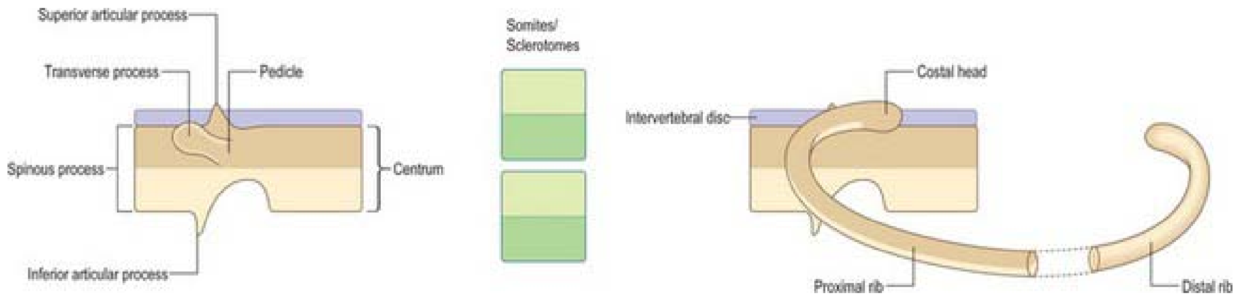
Superior articular process
Transverse process
Pedicle
Spinous process
Centrum
Inferior articular process
Somites/
Sclerotomes
Costal head
Intervertebral disc
Proximal rib
Distal rib

Fig. 44.10 Contribution of two adjacent somites to one vertebra and rib. The intervertebral disc and the costal head are derived from somitocele cells from one somite which migrate with the caudal half of the sclerotome. The proximal rib is formed from caudal and cranial somite halves with no mixing of cells; in the distal rib there is more mixing of cranial and caudal cells as segmentation diminishes in the ventral body wall.

(Redrawn with permission from Christ B, Huang R, Wilting J 2000 The development of the avian vertebral column. Anat Embryol 202: 179–94, Springer.)

The segmental nature of the vertebrae is promoted by the notochord, which induces the ventral elements of the vertebrae and represses dorsal structures, e.g. the spinous processes. Excision of the notochord in early embryos results in fusion of the centra and formation of a cartilaginous plate ventral to the neural tube. Dorsal segmentation is influenced by the spinal ganglia: experimental removal of the ganglia results in fusion of the neural arches and the formation of a uniform cartilaginous plate dorsal to the neural tube.

INTERVERTEBRAL DISCS

Vertebral centra are derived from caudal and cranial sclerotomal halves. An intervertebral disc is formed from the free somitocele cells within the epithelial somite which migrate with the caudal sclerotomal cells. The sclerotomal mesenchyme which forms the centra of the vertebrae replaces the notochordal tissue which it surrounds. In contrast, the notochord expands between the developing vertebrae as localized aggregates of cells and matrix which form the nucleus pulposus of the intervertebral disc (Figs 44.8 and 44.11). The intermediate part of each perichordal disc, which forms the anulus fibrosus, surrounds the nucleus pulposus and differentiates into an external laminated fibrous zone and an internal cuff (which lies next to the nucleus pulposus). The inner zone contributes to the growth of the outer. Near the end of the second month of embryonic life it begins to merge with the notochordal tissue, and is ultimately converted into fibrocartilage. After the sixth month of fetal life, notochordal cells in the nucleus pulposus degenerate, and are replaced by cells from the internal zone of the anulus fibrosus. This degeneration continues until the second decade of life, by which time all the notochordal cells have disappeared. In the adult, notochordal vestiges are limited, at the most, to non-cellular matrix.

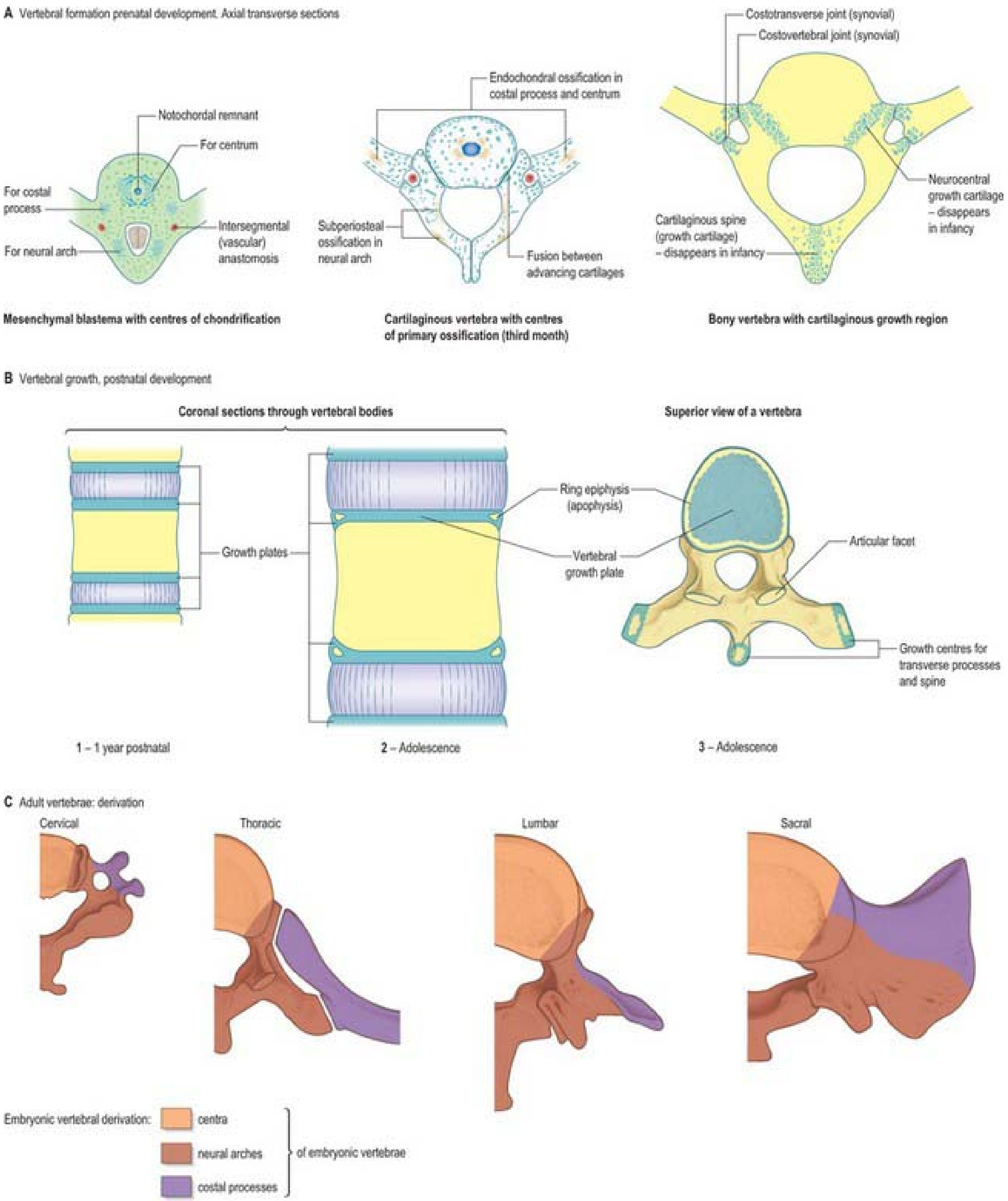
A Vertebral formation prenatal development. Axial transverse sections
Notochordal remnant
For centrum
For costal process
Intersegmental (vascular) anastomosis
For neural arch
Mesenchymal blastema with centres of chondrification
Endochondral ossification in costal process and centrum
Subperiosteal ossification in neural arch
Fusion between advancing cartilages
Cartilaginous vertebra with centres of primary ossification (third month)
Costotransverse joint (synovial)
Costovertebral joint (synovial)
Neurocentral growth cartilage – disappears in infancy
Cartilaginous spine (growth cartilage) – disappears in infancy
Bony vertebra with cartilaginous growth region
B Vertebral growth, postnatal development
Coronal sections through vertebral bodies
Growth plates
Ring epiphysis (apophysis)
Vertebral growth plate
1 – 1 year postnatal
2 – Adolescence
Superior view of a vertebra
Articular facet
Growth centres for transverse processes and spine
3 – Adolescence
C Adult vertebrae: derivation
Cervical
Thoracic
Lumbar
Sacral
Embryonic vertebral derivation:
centra
neural arches
costal processes
of embryonic vertebrae

Fig. 44.11 **A**,**B**, Vertebral development through blastemal, cartilaginous and pre- and postnatal ossificatory stages. **C**, Derivation of principal morphological parts of adult vertebrae.

The original sclerotomes are coextensive with the individual metameric body segments: each sclerotomic fissure, perichordal disc, and maturing intervertebral disc lie opposite the centre of each fundamental body segment. It therefore follows that the discs correspond in level to (i.e. form the anterior boundary of) the intervertebral foramina and their associated mixed spinal nerves, ganglia, vessels and sheaths. Posteriorly, the foramina are bounded by the capsules of the synovial facet joints; the rims of the vertebral notches of adjacent vertebrae lie cranially and caudally. Thus all the structures listed (and other associated ones) are often designated segmental, whereas vertebral bodies are designated intersegmental because of their mode of development.

(For further discussion of resegmentation theories, the reader is directed to Müller & O’Rahilly 1986; Huang et al 2000; Stern & Vasiliauskas 2000.)

DEVELOPMENT OF VERTEBRAE

The initial movements of sclerotomal cells round the neural tube and the expression of type II collagen signals the blastemal stage of vertebral development (Fig. 44.11). Chondrification begins at stage 17, initiating the cartilaginous stage. Each centrum chondrifies from one cartilage anlage. Each half of a neural arch is chondrified from a centre, starting in its base and extending dorsally into the laminae and ventrally into the pedicles, to meet, expand and blend with the centrum. By stage 23 there are 33 or 34 cartilaginous vertebrae, but the spinous processes have not yet developed, so the overall appearance is of total spina bifida occulta. Fusion of the spines does not occur until the fourth month. The transverse and articular processes are chondrified in continuity with the neural arches. Intervening zones of mesenchyme which do not become cartilage mark the sites of the facet joints and the complex of costovertebral joints, within which synovial cavities later appear.

A typical vertebra is ossified from three primary centres, one in each half vertebral arch and one in the centrum (see Fig. 42.24). Centres in arches appear at the roots of the transverse processes, and ossification spreads backwards into laminae and spines, forwards into pedicles and posterolateral parts of the body, laterally into transverse processes and upwards and downwards into articular processes. Classically centres in vertebral arches are said to appear first in upper cervical vertebrae in the ninth to 10th week, and then in successively lower vertebrae, reaching lower lumbar levels in the 12th week. However, in a radiographic study of unsexed human fetuses (Bagnall et al 1977), a pattern was noted which differed from such a simple craniocaudal sequence. A regular cervical progression was not observed. Centres first appeared in the lower cervical/upper thoracic region, quickly followed by others in the upper cervical region. After a short interval a third group appeared in the lower thoracolumbar region and remaining centres then appeared, spreading regularly and rapidly in craniocaudal directions.

The major part of the body, the centrum, ossifies from a primary centre dorsal to the notochord. Centra are occasionally ossified from bilateral centres which may fail to unite. Suppression of one of these produces a cuneiform vertebra (hemivertebra), which is one cause of lateral spinal curvature (scoliosis). At birth and during early postnatal years the centrum is connected to each half neural arch by a synchondrosis or neurocentral joint. In thoracic vertebrae costal facets on the bodies are posterior to neurocentral joints.

During the first year the arches unite behind, first in the lumbar region and then throughout the thoracic and cervical regions. In upper typical cervical vertebrae, centra unite with arches about the third year, but in lower lumbar vertebrae, union is not complete until the sixth. The upper and lower surfaces of bodies and apices of transverse and spinous processes are cartilaginous until puberty, at which time five secondary centres appear, one in the apex of each transverse and spinous process and two annular epiphyses (‘ring apophyses’) for the circumferential parts of the upper and lower surfaces of the body. Costal articular facets are extensions of these anular epiphyses. They fuse with the rest of the bone at about 25 years. There are two secondary centres in bifid cervical spinous processes. Exceptions to this pattern of ossification are described in the appropriate subsections in Chapter 42.

Vertebrae are specified as to region very early in development. If a group of thoracic somites is transplanted to the cervical region, ribs will still develop. It is the sclerotome which is restricted: the myotome will produce muscle characteristic of the new location.

Occipitocervical junction

In humans, the junction between the head and neck (termed occipitocervical, craniovertebral or spinomedullary) is placed at the boundary between the fourth and fifth somites (Müller & O’Rahilly 1994). In avian embryos, where all embryonic stages may be obtained experimentally, the occipitocervical boundary has been determined as the fifth to sixth somite boundary (Wilting et al 1995). The boundary can first be determined in the human at stage 12 by the observation of hypoglossal nerve rootlets (Fig. 44.12). At stages 14 and

15 the junction is seen between the hypoglossal rootlets and the 1st spinal ganglion.

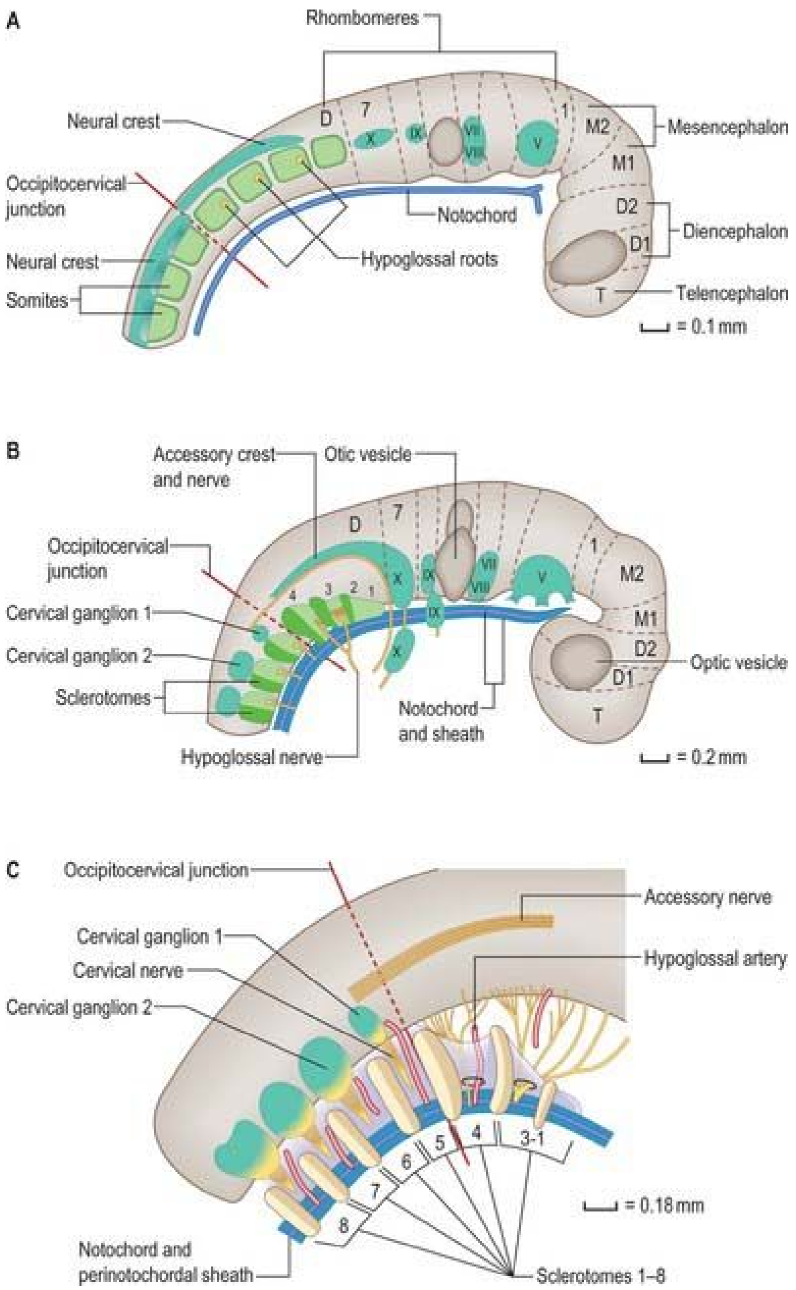
A
Rhombomeres
D
7
X
IX
VII
VIII
V
1
M2
M1
D2
D1
T
Mesencephalon
Diencephalon
Telencephalon
Neural crest
Occipitocervical junction
Neural crest
Somites
Notochord
Hypoglossal roots
= 0.1 mm
B
Accessory crest and nerve
Otic vesicle
Occipitocervical junction
Cervical ganglion 1
Cervical ganglion 2
Sclerotomes
Hypoglossal nerve
Notochord and sheath
Optic vesicle
4
3
2
1
D
7
X
IX
VII
VIII
V
1
M2
M1
D2
D1
T
= 0.2 mm
C
Occipitocervical junction
Cervical ganglion 1
Cervical nerve
Cervical ganglion 2
Accessory nerve
Hypoglossal artery
3-1
4
5
6
7
8
= 0.18 mm
Notochord and perinotochordal sheath
Sclerotomes 1–8

Fig. 44.12 Reconstructions of the occipitocervical region of human embryos. **A**, Stage 12: occipital somites innervated by hypoglossal fibres (small yellow circles). Three cervical somites are shown. The crest-derived ganglia of cranial nerves V, VII, VIII, IX, and X are shown in green. Neural crest associated with the occipital somites is hypoglossal and perhaps

accessory (also shown in green). **B**, Stage 14: the somites have transformed into sclerotomes and moved ventrally. The less dense cranial and dense caudal parts of the sclerotomes and occipital sclerotomes 1–4 are indicated. Hypoglossal fibres and cervical ventral rami migrate through the less dense parts of the sclerotomes. The occipital neural crest is now seen to be mostly accessory. The cervical crest is subdivided into spinal ganglia. A perinotochordal sheath can be seen extending rostrally to the termination of the notochord. **C**, Stage 15: the dense parts of sclerotomes 1–8 are shown. Intersegmental arteries are visible in the less dense areas of the sclerotomes, as are the spinal nerve fibres. In all diagrams the occipitocervical junction is indicated by the asterisks and line.

(After Müller F, O'Rahilly R 1994 Occipitocervical segmentation in staged human embryos. J Anat 185: 251–8. Permission by Blackwell Publishing.)

The first occipital somite disappears early and the caudal three fuse to form the basiocciput. Occipital sclerotomes 3 and 4 are the most distinct at stage 14, by which time the first three sclerotomes have fused. Vertebrae are formed from the fifth somite caudally: the first cervical vertebra is formed by the caudal half of occipital somite 4 and the cranial half of cervical somite 1 (Fig. 44.9). This shift of somite number and vertebral number accounts for the production of seven cervical vertebrae from eight cervical somites.

The segmental pattern present in the cervical somites can be seen rostrally in the developing skull base, where mesenchymal condensations equivalent to the centra of occipital somites 2, 3 and 4 are apparent. The hypoglossal rootlets pass through the less dense portion of occipital sclerotome 4, accompanied by the hypoglossal artery. Occipital sclerotome 4 forms an incomplete centrum axially and exoccipital elements laterally, which are regarded as corresponding to neural arches. They form the rim of the foramen magnum. The occipital condyles develop from the first cervical somite (as also happens in the chick).

In the occipitocervical junctional region the centra formed from sclerotomes 5, 6 and 7 have a different fate from those more caudally placed.

The lateral portions of these sclerotomes generally develop similarly to those of lower ones. In a study of occipitocervical segmentation in human embryos, Müller & O’Rahilly designated the three complete rostral centra which develop in the atlanto-axial region X, Y and Z (Fig. 44.13; Müller & O’Rahilly 1986). They noted that the height of the XYZ complex is equal to that of three centra elsewhere. X is on the level of sclerotome 5, and Y and Z are in line with sclerotome 6 and with the less dense portion of sclerotome 7. During stage 17 a temporary intervertebral disc appears peripherally between Y and Z. It begins to disappear in stage 21, although remains may be found in the adult. No disc develops between X and Y.

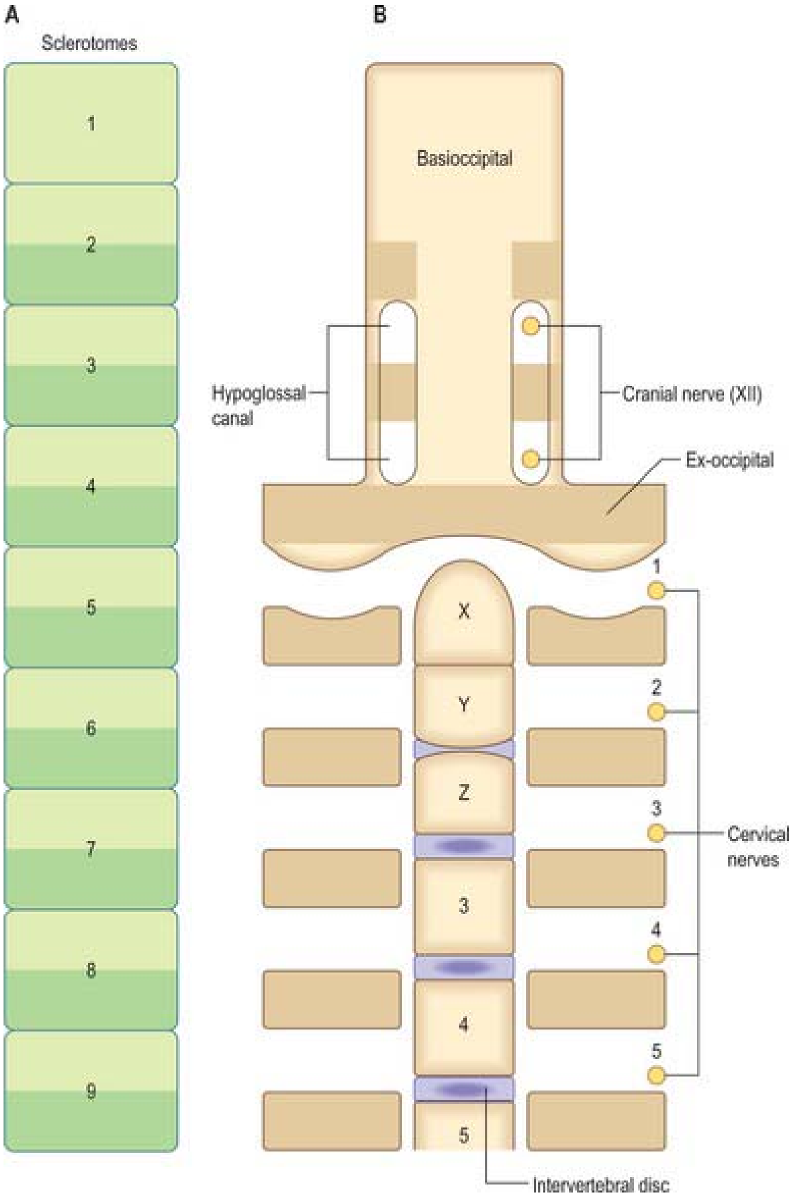
A
Sclerotomes
1
2
3
4
5
6
7
8
9
B
Basioccipital
Hypoglossal canal
Cranial nerve (XII)
Ex-occipital
X
Y
Z
3
4
5
1
2
3
4
5
Cervical nerves
Intervertebral disc

Fig. 44.13 The relationship between the centra and neural arches of the vertebrae and the related spinal ganglia and nerves. Scheme of the details of the early development of the occipitocervical region. **A**, The column of sclerotomes from occipital somite 1. **B**, Dorsal view of the developing vertebrae with the centra in the middle and the bilateral components of the neural processes laterally. X, Y and Z are three centra which will produce the tip of the dens of the axis (X), the base of the dens of the axis (Y) and the centrum of the axis (Z). An intervertebral disc appears temporarily between Y and Z during stage 17. No disc develops between X and Y. The occipital condyles are derived from the first cervical sclerotome.

(After Müller F, O’Rahilly R 1994 Occipitocervical segmentation in staged human embryos. J Anat 185: 251–8. Permission by Blackwell Publishing.)

The origin of the anterior arch of the atlas is unclear. It is evident at stages 21–23 at the level of X or sometimes between X and Y. The posterior arch of the atlas arises from the dense area of sclerotome 5 at the level of X. The XYZ complex belongs to the axis, which means that the atlas does not incorporate a part of the central column (Müller & O’Rahilly 1994).

The posterior arch of the axis arises from the dense area of sclerotome 6 and is at the level of Y and Z, particularly Z. XYZ correspond to the three parts of the median column of the axis, where X represents the tip of the dens, Y represents the base of the dens and Z represents the centrum of the axis. The latter differs from other cervical vertebrae in that it is thicker and square-shaped.

The development of the cervical spine, particularly the upper cervical vertebrae, is closely related to the development of the basiocciput and exocciput: anomalous development will affect both regions. Anomalies of the occiput are associated with decreased skull base height; the dens lies at or above the level of the foramen magnum; a distinctive margin of the foramen magnum lies above the bottom of the posterior fossa; and the posterior arch of the atlas is at the same level as the foramen magnum. The last three structural defects are collectively termed basilar invagination. Malfusions of the caudal portion of occipital sclerotome 4 and the cranial portion of cervical sclerotome 1 may produce defects of the occipital condyles. Disassociated occipital condyles are called a proatlas, because in lower vertebrates the cranial half of the first cervical sclerotome forms a separate bone between the occipital bone and the atlas.

Decreased skull base height and diminished volume in the posterior fossa are structural anomalies associated with the Arnold–Chiari malformation. Although this is considered clinically to be a neurological defect, in that the medulla oblongata, and sometimes the cerebellar tonsils, project through the foramen magnum, there is good evidence that the underlying cause is a series of abnormalities of the occipitocervical junction.

When the volume of the brain in the posterior cranial fossa and the volume of the fossa (delineated by bone and the tentorium cerebelli) were compared in controls and Arnold–Chiari cases, no significant difference was found between brain volume in the two groups, though the basiocciput, exocciput and supraocciput were significantly smaller in affected individuals (Nishikawa et al 1997). In patients with the Arnold–Chiari malformation, proatlas remnants and atlas assimilation are found. The sagittal canal diameter of the foramen magnum is critical: patients become symptomatic when this is less than 19 mm (Menezes 1995). Secondary skull base and cervical spine deformations, e.g. foramen magnum and cervical canal enlargement, may develop in association with the Arnold–Chiari malformation.

Most defects of the atlas do not contribute to abnormal occipito-cervical anomalies and are not associated with basilar invagination.

Abnormalities of the axis are usually concerned with fusion of the dens with the centrum of the second cervical sclerotomes. Using the classification of the three complete centra which develop in the atlanto-axial region as X, Y and Z (Müller & O’Rahilly 1986), failure of fusion of X with the YZ complex produces an ossiculum terminale, a dissociated apical odontoid epiphysis. Failure of fusion of the XY complex with Z at the dentocentral synchondrosis, or maintenance of the transitory intervertebral disc at this point, produces an os odontoideum, thought to be induced by excessive movement at the time of ossification of the dens (Crockard & Stevens 1995). Hypoplasia and aplasia of the X and Y centra, and aplasia of the Z centrum, will all lead to reduced size of the dens. There are widely differing views about whether this will lead to atlanto-axial instability.

C3–7, third to seventh cervical vertebrae

In cervical vertebrae 3–7 (Fig. 44.11) the transverse process is dorsomedial to the foramen transversarium. The costal process, corresponding to the head, neck and tubercle of a rib, limits the foramen ventrolaterally and dorsolaterally. The distal parts of these cervical costal processes do not normally develop; they do so occasionally in the case of the seventh cervical vertebra, and may even develop costovertebral joints. These cervical ribs may reach the sternum.

The seventh cervical vertebra is transitional in shape between cervical and thoracic vertebrae. The laminae are longer than other cervical vertebrae in the neonate and lie almost perpendicular to the basal plane; the inferior articular facets are more upright, and resemble those of thoracic vertebrae; and, in the lateral view, the superior articular facets extend transversely to the top of the transverse processes.

Anomalies of the lower cervical vertebrae are generally caused by inappropriate cervical vertebral fusion: collectively this is termed Klippel–Feil syndrome. This term includes all congenital fusions of the cervical spine, from two segments to the entire cervical spine. Affected individuals have a low posterior hairline, short neck and limitations of head and neck movement. Scoliosis and/or kyphosis is common.

Thoracic vertebrae

At stage 23 the neural processes of thoracic vertebrae are short, slightly bifurcated and joined by collagenous fibres. The transverse process is prominent. The three facets for articulation with the ribs at the costovertebral and costotransverse joints are present. The thoracic neurocentral and posterior synchondroses are not fused in the neonate: the posterior synchondroses close within 2 to 3 months of postnatal development and the neurocentral synchondroses are open until 5 to 6 years of age.

In general, the thoracic spine develops ahead of the cervical and lumbar spine. However, towards the end of the second month, ossification begins in the cartilaginous vertebrae in a craniocaudal progression.

Ribs

Ribs usually develop in association with the thoracic vertebrae. Occasionally they can arise from the seventh cervical and first lumbar vertebrae.

The costal processes attain their maximum length as the ribs in the thoracic region. Each rib originates from lateral sclerotomal populations, and forms from the caudal half of one sclerotome and the cranial half of the next subjacent sclerotome (Fig. 44.10). The head of the rib develops from somitocele cells from one somite, which migrate with the caudal half of the sclerotome. The proximal portion of the rib forms from both caudal and cranial sclerotomal halves; there is no mixing of cells from these origins. The distal portion of the rib forms from caudal and cranial sclerotomal halves; these cells mix as the rib extends into the ventral body wall and segmentation diminishes.

The ribs arise anterolaterally from the ventral part of the pedicles, and form bilateral costal processes which expand to meet the tips of the transverse processes. As they elongate laterally and ventrally they come to lie between the myotomic muscle plates. In the thorax (Fig. 44.11) the costal processes grow laterally to form a series of precartilaginous ribs. The transverse processes grow laterally behind the vertebral ends of the costal processes, at first connected by mesenchyme which later becomes differentiated into the ligaments and other tissues of the costotransverse joints. The capitular costovertebral joints are similarly formed from mesenchyme between the proximal end of the costal processes and the perichordal disc, and the adjacent parts of two (sometimes one) vertebral bodies, which are derived from the neural arch. Ribs 1–7 (vertebrosternal) curve round the body wall to reach the developing sternal plates. Ribs 8–10 (vertebrochondral) are progressively more oblique and shorter, only reaching the costal cartilage of the rib above, and contributing to the costal margin. Ribs 11 and 12 are free (floating), and have cone-shaped terminal cartilages to which muscles become attached (p. 921).

Lumbar vertebrae

The costal processes do not develop distally in lumbar vertebrae (Fig. 44.11). Their proximal parts become the ‘transverse processes’, while the morphologically true transverse processes may be represented by the accessory processes of the vertebrae. Occasionally, movable ribs may develop in association with the first lumbar vertebra.

Lumbar intervertebral discs are thicker than thoracic discs. By stage 23 the anulus fibrosus can be seen in the peripheral part, and internally the notochordal cells are expanding to form the nucleus pulposus.

Sacrum

Sacral vertebrae have lower centra and are narrower overall from side to side than their thoracic and lumbar counterparts. Each sacral vertebra is composed of a centrum and bilateral neural processes. The contribution of the costal processes to sacral development was examined by O'Rahilly et al (1990). These authors divided the neurocentral junctional area into two parts, anterolateral or alar, and posterolateral. They found the alar element in sacral vertebra 1 to be novel, since it was absent in lumbar vertebra 5. There is support for this view if the course of the dorsal rami of the spinal nerves is used to distinguish the costal elements ventrally from the transverse elements dorsally. The alar elements of the sacral vertebrae are ventral to the sacral dorsal rami, and both costal and transverse portions are posterolateral. The alar element of S1 and S2 forms the auricular surface of the sacrum. At stage 23 the cartilaginous sacral vertebrae have joined and the outline of the future bone can be recognized. Individual pedicles and laminae are very small and can be detected in S3–5.

Ossification of the vertebral column proceeds in a craniocaudal direction. After 16 weeks it has progressed to L5. Ossification of each additional vertebra occurs over a period of 2–3 weeks; S2 is ossified by 22 weeks.

Very rarely significant malformation of the sacral or lumbosacral vertebrae may develop, often in association with a maternal history of diabetes. When there is sacral agenesis, motor paralysis is profound below the affected vertebral level, whereas the sensory disturbance does not relate to the vertebral level so clearly and sensation may be present down to the knees. Bladder involvement is a consistent feature.

SPINA BIFIDA

Spina bifida is the generic term for a range of discrete defects of neurulation and subsequent vertebral formation. The spectrum of neural tube and vertebral defects includes a range of open neural tube defects: craniorachischisis (non-fusion of the entire neural tube and no vertebral arch development); anencephaly (non-fusion of the rostal portion of the neural tube with no calvarial or occipital development); and myelocele (non-fusion of caudal portions of the neural tube and local failure of vertebral arch development) (see Fig. 24.8).

Spina bifida cystica occurs where the meninges have developed adjacent to or over the defective neural tissue. Local accumulation of CSF may push a defective neural plaque or spinal cord superficial to the level of the vertebrae forming a meningomyelocele. Alternatively, a meningeal sac may protrude in the midline if one or two spinous processes are absent; this condition is a meningocele. In both cases the meningeal sac may be covered with skin or skin may be contiguous with the edges of a neural plaque.

Prior to antenatal diagnosis of spina bifida by ultrasonography, most live births with spina bifida cystica had meningomyelocele. Meningomyelocele occurs in thoracolumbar, lumbar or lumbosacral regions. Sacral lesions are less common. The vertebral lesion usually extends cranially further than the neural lesion, showing deformities of the vertebral bodies and laminae. Vertebrae may be wedge-shaped or hemivertebrae and ribs may be fused or absent. Concomitant kyphosis at birth is associated with a worse prognosis. Prenatal diagnosis of meningomyelocele and termination of affected fetuses has led to a significant decrease in the incidence of live births with this condition.

Up to 10% of spina bifida cystica cases are meningocele. This lesion may occur in cervical and upper thoracic levels or in lower lumbar and sacral levels: the latter are most common. In its mildest form no neurological abnormality occurs with this condition.

Spina bifida occulta affects about 5% of the population. Affected individuals have bifid spinous processes often at the lumbosacral junction. A very small proportion of those with this condition have a naevus, dimple or tuft of hair over the lesion.

Tethering of the cord and diastematomyelia

The greatest change of vertebral length occurs within the last 6 months of intrauterine life. When there is any degree of spina bifida, the upward migration of the spinal cord which normally occurs within the vertebral canal during growth is limited, and the cord is said to be tethered. Neurological deficits caused by this condition in neonates become apparent soon after birth, although some individuals show symptoms later in life, especially degrees of urinary dysfunction.

Very rarely, tethering symptoms may be associated with abnormal development of the vertebral centra, e.g. when a midline cartilaginous or osseous spicule or a fibrous septum projects into the vertebral canal. These obstacles may split the spinal cord or intraspinal nerve roots into two columns, a condition termed diastematomyelia. Usually patients with this condition have a cutaneous abnormality, such as a dimple, pigmented naevi or patch of hair, along their back at the level of the tethering.

DEVELOPMENT OF DERMOMYOTOMES

The dermomyotome, which forms from the dorsal half of the early somite, gives rise to all the skeletal muscle in the trunk and limbs and the intrinsic muscles of the tongue. Muscles in the head arise from the unsegmented paraxial mesenchyme rostral to the occipital somites. The dorsomedial lip (border) of the dermomyotome is an infolding of the epithelial plate of the somite and becomes a proliferative epithelial site from which mediolateral growth of the dermomyotome itself occurs. Three structures are required for myogenesis, the neural tube, the notochord/neural floor plate complex and the (early) dorsally placed ectoderm. There is a balance between levels of Shh from the notochord and Wnts from the dorsal neural tube and ectoderm which promotes myogenesis; high levels of either alone lead to sclerotomal or nonmyogenic dermomyotomal development (Scaal & Christ 2004). Myogenic determination factors, MyoD, myogenin, Myf 5 and herculin/MRF 4 can first be detected in the medial half of the somite as early as stage II, several hours prior to the onset of myotome formation.

The mode of formation of mononucleated, postmitotic, primitive myotubes from the dermomyotome has been elucidated in the chick but not yet confirmed in mammals (Gros, Scaal & Marcelle 2004). In this model all four borders of the dermomyotome give rise to myotomal cells which are produced in two phases: initially from the dorsomedial dermomyotomal lip by direct ingression and bidirectional extension; later, in a second phase, the caudal dermomyotomal border, followed in turn by the cranial dermomyotomal border and lastly the ventrolateral dermomyotomal lip, start to release myotomal precursor cells. Those myotomal cells arising from the dorsomedial dermomyotomal border contribute cells exclusively to the epaxial domain, those from the ventrolateral border contribute cells exclusively to the hypaxial domain, and the cells arising from the cranial and caudal borders move into both epaxial and hypaxial domains (Scaal & Christ 2004) (Fig. 44.7).

EPAXIAL MUSCLE: DORSAL TRUNK MUSCLES

Epaxial muscles arise from the dorsomedial lip of the dermomyotome. Myotome cells are all postmitotic embryonic myoblasts: later in development they fuse to form syncytia which produce the intrinsic muscles of the back. They bridge the early segmental borders, joining vertebrae together. The epaxial muscles are innervated by the dorsal ramus of each spinal nerve. At later stages satellite cells enter the myotome. The mechanism of development of endo-, peri- and epimysium in relation to the epaxial muscles has not been determined.

HYPAXIAL MUSCLE: VENTROLATERAL TRUNK MUSCLES

Two modes of production of hypaxial musculature are seen, related to axial level (Fig. 44.7). At cervical and trunk levels, myotubes are produced by the ventrolateral edge of the dermomyotome in a manner similar to the production of epaxial muscles. As development proceeds there is lateral growth of the dermomyotome so that the ventrolateral border extends ventrolaterally into the developing lateral and ventral body wall. The somite structures that invade the somatopleure of the abdominal and thoracic wall thus consist of two layers, dermomyotome and myotome, that give rise to the muscle blastemata for the intercostal and oblique muscles, transversus abdominis and rectus abdominis. At this time the number of somatopleural fibroblasts situated within the muscle-forming zone increases, and myotubes can be first seen. There is a subsequent ventral shift of the already separated muscle blastemata within the growing abdominal wall as they attain their definitive positions. Muscle differentiation continues and muscular connective tissue, tendons and aponeuroses develop.

At occipital and limb levels a ventrolateral dermomyotomal lip is not formed in the same way; cells undergo epithelial/mesenchymal transformation and migrate to their destination. Myoblasts move from the occipital dermomyotomes into the developing mandibular processes to form the intrinsic muscles of the tongue, whereas those opposite the early limb buds migrate into the limbs as dorsal and ventral muscle masses which give rise to the shoulder, hip and appendicular muscles. (For a review of dermomyotomal development see Scaal & Christ 2004.)

OTHER STRUCTURES DERIVED FROM THE SOMITES

Dermal precursors arise from the central portion of the dermomyotome and possibly also from the dorsomedial dermomyotome lip (Fig. 44.7). The cells undergo an epithelial/mesenchyme transformation from the dermomyotome and migrate to the dorsomedial subectodermal space overlying the dorsal neural tube. Their transformation seems to be controlled by factors from the neural tube. There is a sharp boundary between dermis which is somite-derived and that which is derived from the splachnopleuric mesenchyme of the lateral plate (and which covers the limbs, part of the lateral and all of the ventral body wall).

Smooth muscle cells within and around the developing somites and endothelial cell precursors are now considered to arise from somitic cells. All compartments of the epithelial somite, including the somitocele cells, give rise to angioblasts. The early ventral half of the somite gives rise to the endothelium of ventrolateral blood vessels. Angioblastic cells arising from the dorsomedial dermomyotome migrate mainly into the dorsal dermis, whereas those arising from the dorsolateral part move to the ventrolateral body wall and limbs (Scaal & Christ 2004).

REFERENCES

agnall KM, Harris PF, Jones PRM. A radiographic study of the human spine II. The sequence of development of ossification centres in the vertebral column. *J Anat*. 1977;124:791-802.

hrist B, Huang R, Wilting J. The development of the avian vertebral column. *Anat Embryol*. 2000;202:179-194.

hrist B, Huang R, Scaal M. Formation and differentiation of the avian sclerotome. *Anat Embryol*. 2004;208:333-350.

rockard HA, Stevens JM. Craniovertebral junction anomalies in inherited disorders: part of the syndrome or caused by the disorder? *Eur J Pediatr*.

1995;154:504-512.

sser RF. Evidence that some events of mammalian embryogenesis can result from differential growth, making migration unnecessary. *Anat Rec*. 2006;289B:53-63.

mpel-Pinot M. Muscle and skeleton of limbs and body wall. In: Le Douarin N, McLaren A. *Chimeras in Developmental Biology*. London: Academic Press; 1984:281-310.

ang R, Zhi Q, Brand-Saberi B, Christ B. New experimental evidence for somite resegmentation. *Anat Embryol*. 2000;202:195-200.

enezes AH. Primary craniovertebral anomalies and the hindbrain herniation syndrome (Chiari 1); database analysis. *Pediatr Neurosurg*. 1995;23:260-269.

üller F, O'Rahilly R. Somitic-vertebral correlation and vertebral levels in the human embryo. *Am J Anat*. 1986;177:3-19.

üller F, O'Rahilly R. Occipitocervical segmentation in staged human embryos. *J Anat*. 1994;185:251-258.

shikawa M, Sakamoto H, Hakuba A, Nakanishi N, Inoue Y. Pathogenesis of Chiari malformations: a morphometric study of the posterior cranial fossa. *J Neurosurg*. 1997;86:40-47.

'Rahilly R, Müller F, Meyer DB. The human vertebral column at the end of the embryonic period proper. 4. The sacrococcygeal region. *J Anat*. 1990;168:95-111.

dahl CP. Myogenic lineages within the developing somite. In: Bernfield M, editor. *Molecular Basis of Morphogenesis*. New York: Wiley Liss; 1993:165-176.

urquie O, Kusumi K. When body segmentation goes wrong. *Clin Genet*. 2001;60:409-416.

chardson MK, Allen SP, Wright GM, Raynaud A, Hanken J. Somite number and vertebrate evolution. *Development*. 1998;125:151-160.

aal M, Christ B. Formation and differentiation of the avian dermomyotome. *Anat Embryol*. 2004;208:411-424.

ern CD, Vasiliauskas D. Segmentation: a view from the border. Current Topics in Developmental Biology. vol 47. New York: Academic Press; 2000.

Presents three different models of somite formation in the context of molecular data..

ilting J, Ebensperger C, Müller TS, Kosecki H, Wallin J, Christ B. *Pax-1* in the development of the cervico-occipital transitional zone. *Anat Embryol*. 1995;192:221-227.

Section 6

PECTORAL GIRDLE AND UPPER LIMB

CHAPTER 45

Pectoral girdle and upper limb: overview and surface anatomy

This chapter is divided into two sections. The first is an overview of the general organization of the upper limb, with particular emphasis on the distribution of the major blood vessels and lymphatic channels, and of the branches of the brachial plexus: it is intended to complement the detailed regional anatomy described in Chapters 46 to 50 Chapter 47 Chapter 48 Chapter 49 Chapter 50. The second section describes the surface anatomy of the upper limb.

BONES AND JOINTS

The bones of the upper limb are the clavicle, scapula, humerus, radius and ulna (connected for a large portion of their length by an interosseous membrane) and the bones of the hand, i.e. the carpals, metacarpals and phalanges (Figs 45.1, 45.2).

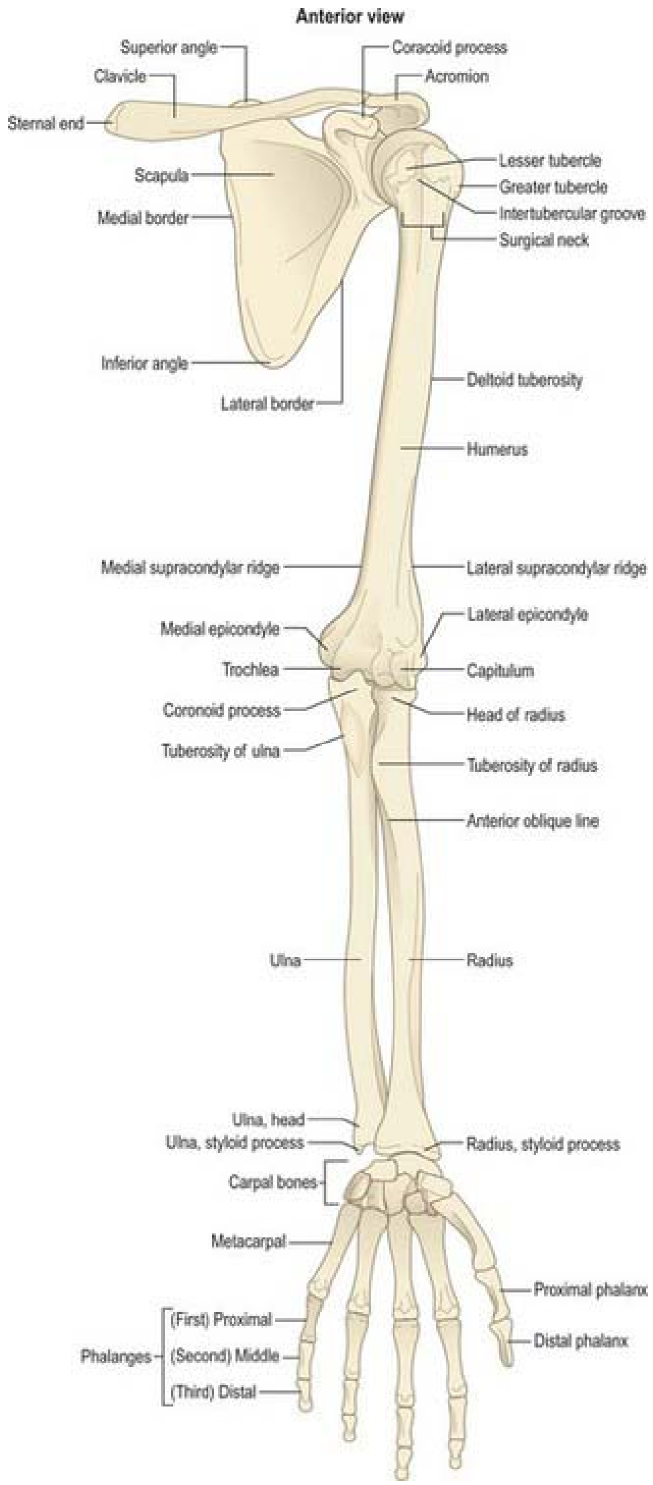
Anterior view
Superior angle
Coracoid process
Clavicle
Acromion
Sternal end
Scapula
Lesser tubercle
Greater tubercle
Medial border
Intertubercular groove
Surgical neck
Inferior angle
Deltoid tuberosity
Lateral border
Humerus
Medial supracondylar ridge
Lateral supracondylar ridge
Lateral epicondyle
Medial epicondyle
Trochlea
Capitulum
Coronoid process
Head of radius
Tuberosity of ulna
Tuberosity of radius
Anterior oblique line
Ulna
Radius
Ulna, head
Ulna, styloid process
Radius, styloid process
Carpal bones
Metacarpal
Proximal phalanx
(First) Proximal
Distal phalanx
Phalanges
(Second) Middle
(Third) Distal

Fig. 45.1 Overview of the bones of the left pectoral girdle and upper limb: anterior view.

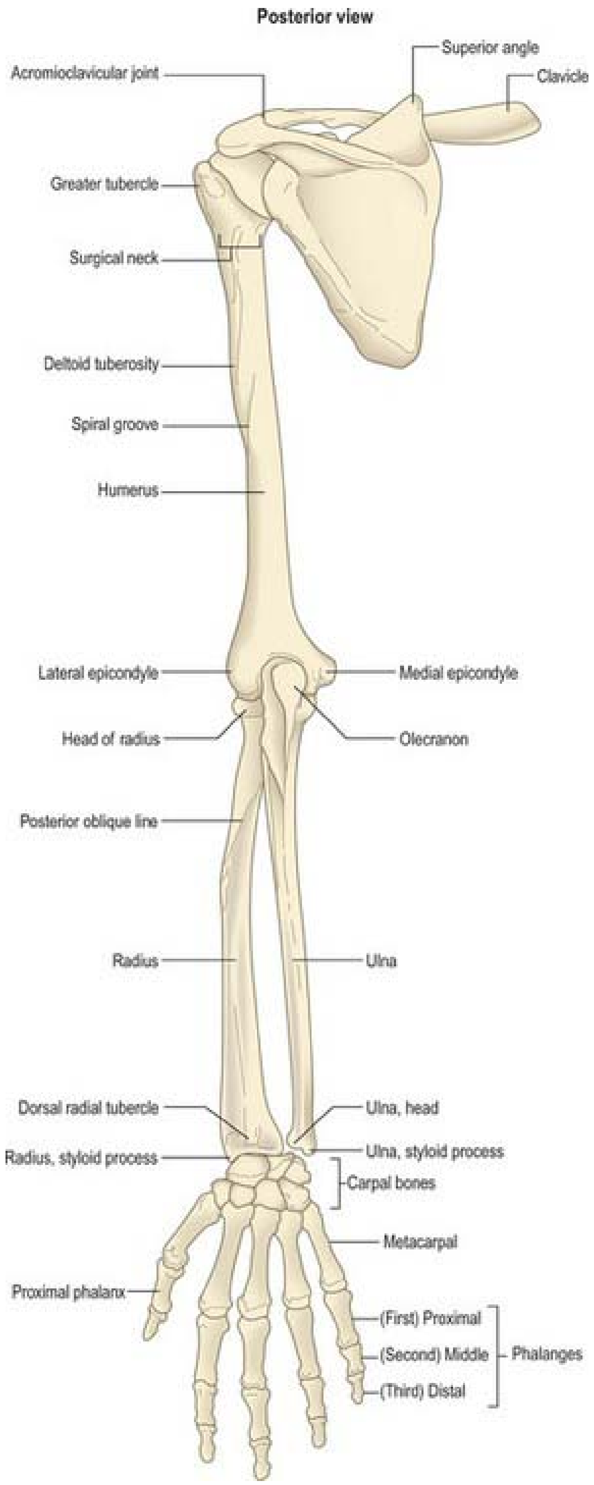
Posterior view
Superior angle
Acromioclavicular joint
Clavicle
Greater tubercle
Surgical neck
Deltoid tuberosity
Spiral groove
Humerus
Lateral epicondyle
Medial epicondyle
Head of radius
Olecranon
Posterior oblique line
Radius
Ulna
Dorsal radial tubercle
Ulna, head
Radius, styloid process
Ulna, styloid process
Carpal bones
Metacarpal
Proximal phalanx
(First) Proximal
(Second) Middle
(Third) Distal
Phalanges

Fig. 45.2 Overview of the bones of the left pectoral girdle and upper limb: posterior view.

The shoulder girdle is extremely mobile because reciprocal movements at the sternoclavicular and glenohumeral joints enable 180° abduction of the upper limb. Movement occurs in all three planes at the glenohumeral joint.

The elbow joint is a hinge joint. It incorporates the superior (proximal) radio-ulnar joint within its capsule. The proximal and distal radio-ulnar joints permit pronation and supination of the forearm – a unique feature of the primate upper limb.

The range of movement at the condyloid wrist joint, between the distal ends of the radius and ulna and the proximal carpal bones, is supplemented by gliding movements between the carpal bones. The saddle-shaped first carpometacarpal joint, between the trapezium and the base of the first metacarpal, is unique to the primate forelimb and permits opposition of the thumb. The hand is clenched by flexion at the metacarpophalangeal joints, supplemented by gliding movements of the fourth and fifth carpometacarpal joints. In grasping, the thumb is of equal value to the remaining four digits: loss of the thumb is almost as disabling as loss of all of the other digits.

SKIN, FASCIA AND SOFT TISSUES

The skin of the anterior aspect of the upper arm and forearm differs from that of the posterior aspect in that it is thinner and hairless. The palmar skin is thick and hairless: firm attachments to the underlying palmar fascia reflect its role in gripping and shock absorption. The dorsal skin of the hand is much thinner, lax and mobile, and this allows the extensor tendons to glide underneath the subcutaneous tissue.

The direction in which skin tension is greatest varies regionally in the upper limb as in other areas of the body. Skin tension lines that follow the furrows formed when the skin is relaxed are known as ‘relaxed skin tension lines’ and can act as a guide in planning elective incisions.

The superficial fascia is a layer of subcutaneous fatty tissue. Its thickness depends on the degree of obesity of the subject: measurement of the thickness of the subcutaneous tissue of the posterior upper arm is used as an indicator of obesity. With the exception of the digital pads, there is less subcutaneous tissue in the palm of the hand than on the dorsum of the hand.

The depth of deep fascia varies according to the stresses to which it is subjected in the different areas of the limb. In the upper arm it is a thin but quite obvious layer. Intermuscular septa pass to the medial and lateral sides of the humerus, separating the upper arm muscles into anterior and posterior groups within their respective compartments. Each muscle also lies within its own delicate fascial shea than arrangement that allows individual muscles to glide upon each other.

The deep fascia condenses anteriorly at the elbow as the tough bicipital aponeurosis; it is otherwise relatively thin in the forearm where it is attached along the subcutaneous border of the ulna. Intermuscular septa divide the forearm into three compartments, namely, anterior (contains the flexor group of muscles), posterior (extensors) and the mobile wad compartment for brachioradialis and extensor carpi radialis longus and brevis.

At the wrist the deep fascia becomes condensed anteriorly and posteriorly as the flexor and extensor retinacula respectively. Further condensation occurs in the palm of the hand, where the palmar aponeurosis is reinforced by the insertion of the tendon of palmaris longus, and in the flexor tendon sheaths and fascial system associated with the digits.

MUSCLES

Posterior and anterior muscle groups connect the pectoral girdle to the axial skeleton; the only bony connection is at the sternoclavicular joint. The posterior muscles are trapezius, levator scapulae and the rhomboid muscles: their actions include raising the shoulder and drawing the scapula medially. The anterior muscles are pectoralis minor, serratus anterior, and subclavius. Serratus anterior and trapezius together rotate the scapula in abduction of the arm.

Latissimus dorsi (posteriorly) and pectoralis major (anteriorly) run from the axial skeleton to the humerus. They are both powerful adductors and medial rotators of the shoulder; latissimus dorsi is also a powerful extensor.

A large group of muscles arise from the shoulder girdle and pass to the humerus. They are the four muscles of the rotator cuff (subscapularis, supraspinatus, infraspinatus and teres minor), teres major, deltoid, the clavicular origin of pectoralis major, biceps brachii, coracobrachialis and the long head of triceps.

The muscles of the upper arm can be divided into an anterior group of elbow flexors (biceps brachii, brachialis and coracobrachialis) and a posterior group of elbow extensors (triceps and anconeus). Biceps brachii is also a powerful supinator of the radio-ulnar joints.

The extensor muscles of the wrist and fingers, together with brachioradialis and a slip of origin of supinator, arise from the lateral epicondyle of the humerus. The principal head of pronator teres, the carpal flexor muscles, palmaris longus and, at a deeper level, the main origin of flexor digitorum superficialis, all arise from the medial epicondyle of the humerus. More deeply, flexor pollicis longus, flexor digitorum profundus and pronator quadratus arise from the anterior aspects of the shafts of the radius and ulna and the intervening interosseous membrane. Abductor pollicis longus, extensors pollicis longus and brevis and extensor indicis all arise from the posterior aspects of these bones and the intervening interosseous membrane.

The small, intrinsic, muscles of the hand consist of a thenar and a hypothenar group, and the muscles of the palm (the anterior and posterior interossei and the lumbricals). They are all concerned with the intricate movements of the digits.

VASCULAR SUPPLY AND LYMPHATIC DRAINAGE

ARTERIAL SUPPLY

The blood supply to the skin of the upper limb comes from a combination of direct cutaneous, fasciocutaneous and musculocutaneous vessels (Figs 45.3, 45.4; see Fig. 7.19).

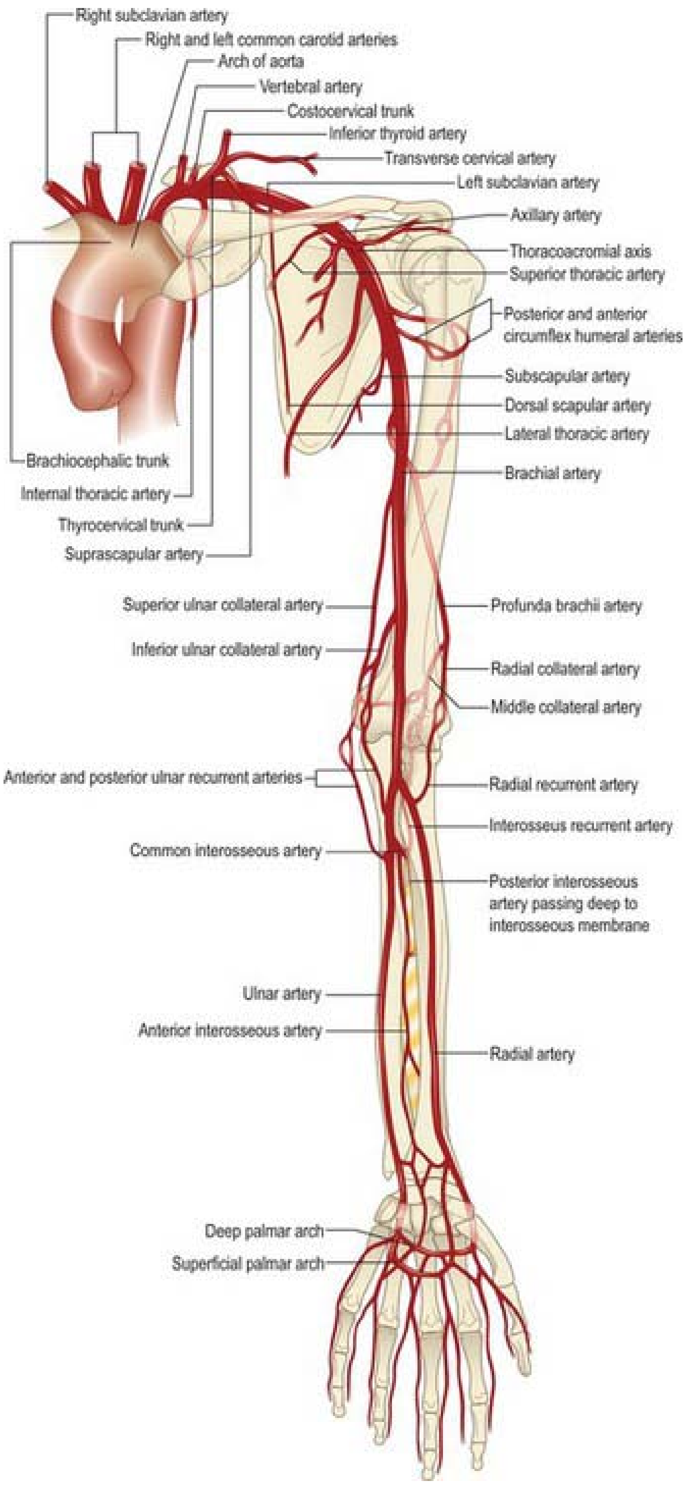
Right subclavian artery
Right and left common carotid arteries
Arch of aorta
Vertebral artery
Costocervical trunk
Inferior thyroid artery
Transverse cervical artery
Left subclavian artery
Axillary artery
Thoracoacromial axis
Superior thoracic artery
Posterior and anterior circumflex humeral arteries
Subscapular artery
Dorsal scapular artery
Lateral thoracic artery
Brachial artery
Brachiocephalic trunk
Internal thoracic artery
Thyrocervical trunk
Suprascapular artery
Superior ulnar collateral artery
Profunda brachii artery
Inferior ulnar collateral artery
Radial collateral artery
Middle collateral artery
Anterior and posterior ulnar recurrent arteries
Radial recurrent artery
Interosseus recurrent artery
Common interosseous artery
Posterior interosseous artery passing deep to interosseous membrane
Ulnar artery
Anterior interosseous artery
Radial artery
Deep palmar arch
Superficial palmar arch

Fig. 45.3 Overview of arteries of the left upper limb.

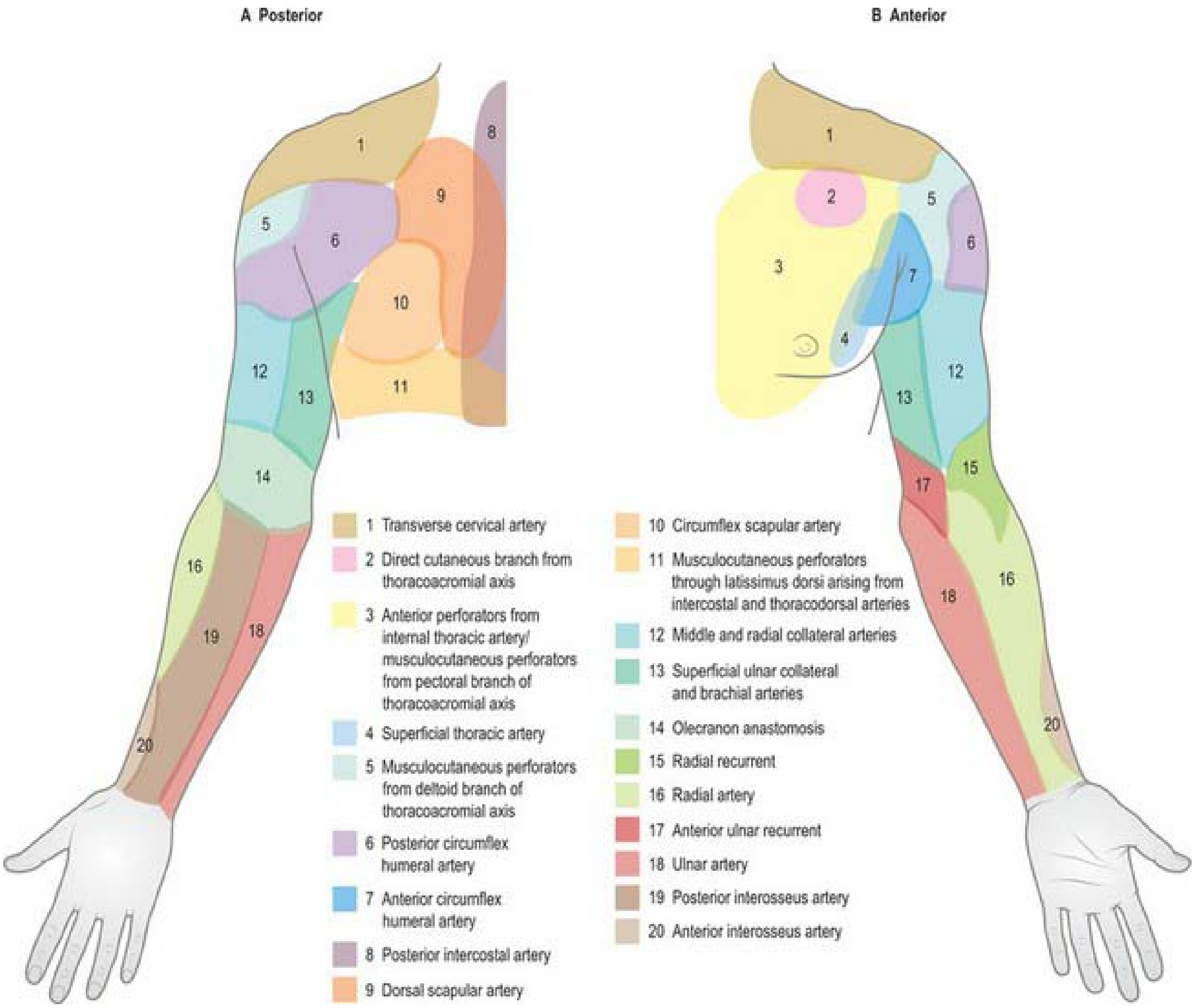
A Posterior
B Anterior
1
2
3
4
5
6
7
8
9
10
11
12
13
14
15
16
17
18
19
20
1 Transverse cervical artery
2 Direct cutaneous branch from thoracoacromial axis
3 Anterior perforators from internal thoracic artery/ musculocutaneous perforators from pectoral branch of thoracoacromial axis
4 Superficial thoracic artery
5 Musculocutaneous perforators from deltoid branch of thoracoacromial axis
6 Posterior circumflex humeral artery
7 Anterior circumflex humeral artery
8 Posterior intercostal artery
9 Dorsal scapular artery
10 Circumflex scapular artery
11 Musculocutaneous perforators through latissimus dorsi arising from intercostal and thoracodorsal arteries
12 Middle and radial collateral arteries
13 Superficial ulnar collateral and brachial arteries
14 Olecranon anastomosis
15 Radial recurrent
16 Radial artery
17 Anterior ulnar recurrent
18 Ulnar artery
19 Posterior interosseus artery
20 Anterior interosseus artery

Fig. 45.4 The anatomical territories served by the cutaneous blood supply to the upper limb.

(From Cormack GC, Lamberty BGH 1994 The Arterial Anatomy of Skin Flaps, 2nd edn. Edinburgh: Churchill Livingstone, with permission.)

The axial artery to the upper limb is the subclavian artery, which becomes the axillary artery after crossing the lateral edge of the first rib. The axillary artery becomes the brachial artery as it crosses the distal edge of the posterior axillary fold, i.e. at the lower border of teres major. At first, the brachial artery lies in the flexor compartment on the medial side of the upper arm, but later it inclines laterally until it lies anterior to the elbow joint. Just distal to the elbow, it divides into the radial and ulnar arteries, both of which remain in, and supply, the flexor compartment. The ulnar artery almost immediately gives rise to the common interosseous artery, and this divides into anterior and posterior interosseous arteries which travel towards the wrist on either side of the interosseous membrane (the anterior interosseous artery lies directly on the membrane and the posterior interosseous artery is separated from it by the deep extensor muscles).

The muscles and other components of the extensor aspect are supplied by the profunda brachii artery in the upper arm, and by the posterior interosseous artery in the forearm. The hand is supplied by rich, and somewhat variable, anastomoses between branches of the radial and ulnar arteries, principally on its palmar aspect.

Each upper limb joint is supplied by an extensive anastomosis of arteries fed by descending vessels that arise proximal to the joint and ascending recurrent branches that arise distal to the joint.

VENOUS DRAINAGE

The venous drainage of the upper limb is composed of superficial and deep groups of vessels.

The superficial group starts as an irregular dorsal arch on the back of the hand. The cephalic vein begins at the radial extremity of the arch, ascends along the lateral aspect of the arm within the superficial fascia and then pierces the deep fascia to enter the axillary vein just distal to the clavicle (Fig. 45.5). The basilic vein drains the ulnar end of the arch, passes along the medial aspect of the forearm, pierces the deep fascia at the elbow and joins the venae comitantes of the brachial artery to form the axillary vein. In front of the elbow, the prominent median cubital vein links the cephalic and basilic veins. It receives a number of tributaries from the front of the forearm and gives off the deep median vein which pierces the fascial roof of the antecubital fossa to join the venae comitantes of the brachial artery.

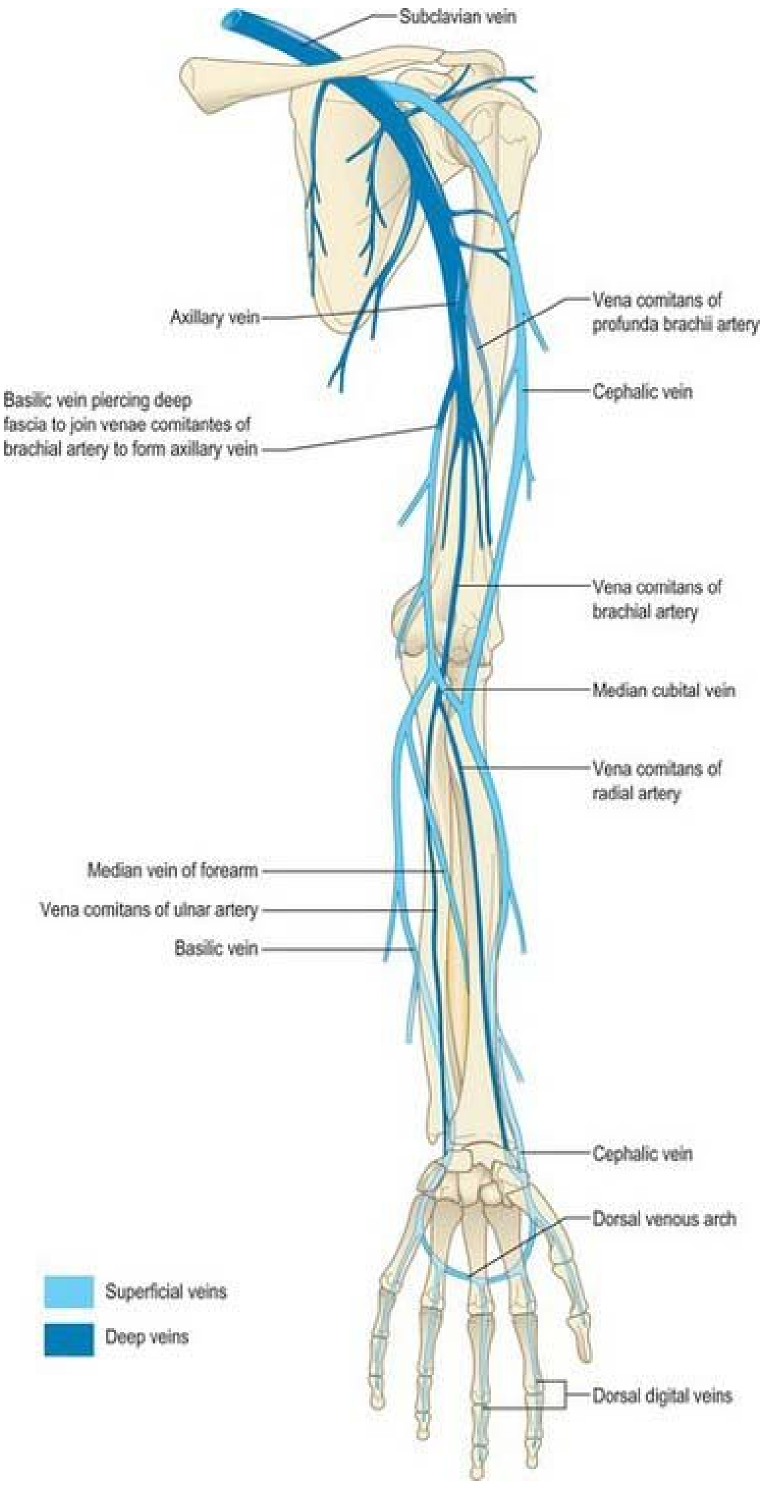
Subclavian vein
Axillary vein
Vena comitans of profunda brachii artery
Cephalic vein
Basilic vein piercing deep fascia to join venae comitantes of brachial artery to form axillary vein
Vena comitans of brachial artery
Median cubital vein
Vena comitans of radial artery
Median vein of forearm
Vena comitans of ulnar artery
Basilic vein
Cephalic vein
Dorsal venous arch
Superficial veins
Deep veins
Dorsal digital veins

Fig. 45.5 Overview of veins of the left upper limb.

The deep group of veins accompany the arteries, usually as venae comitantes, and ultimately become the axillary and then the subclavian vein.

They drain the tissues beneath the deep fascia of the upper limb and are connected to the superficial system by perforating veins.

LYMPH NODES AND DRAINAGE

Superficial tissues

Superficial lymphatic vessels begin in cutaneous plexuses. In the hand, the palmar plexus is denser than the dorsal plexus. Digital plexuses drain along the digital borders to their webs, where they join the distal palmar vessels, which pass back to the dorsal aspect of the hand. The proximal palm drains towards the carpus, medially by vessels that run along its ulnar border, and laterally to join vessels draining the thumb. Several vessels from the central palmar plexus form a trunk that winds round the second metacarpal bone to join the dorsal vessels that drain the index finger and thumb.

In the forearm and arm, superficial vessels run with the superficial veins. Collecting vessels from the hand pass into the forearm on all carpal aspects. Dorsal vessels, after running proximally in parallel, curve successively round the borders of the limb to join the ventral vessels. Anterior carpal vessels run through the forearm parallel with the median vein of the forearm to the cubital region, then follow the medial border of biceps brachii before piercing the deep fascia at the anterior axillary fold to end in the lateral axillary lymph nodes (Fig. 45.6).

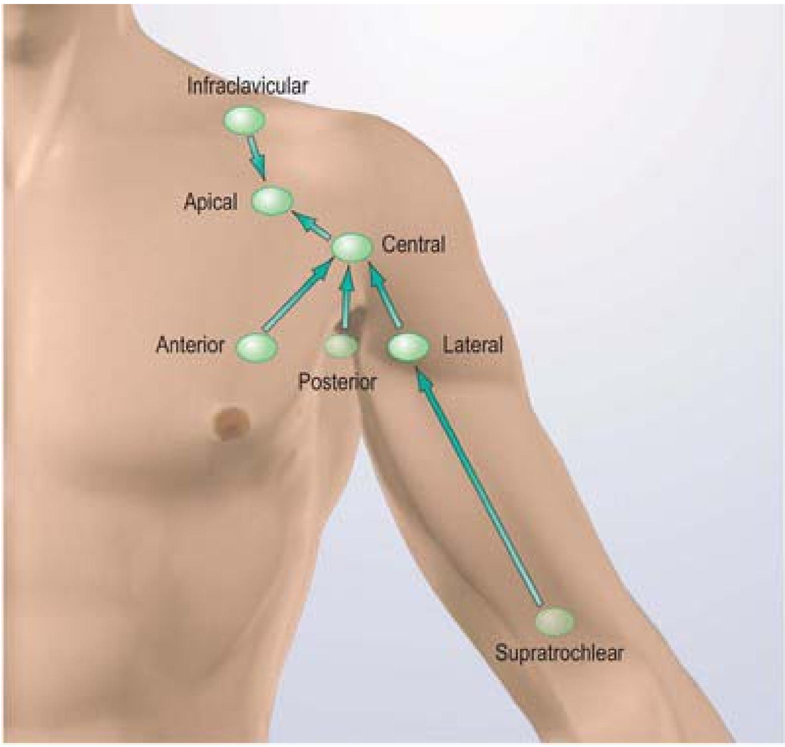

Fig. 45.6 Lymph nodes of the left upper limb.

Lymph vessels that lie laterally in the forearm receive vessels that curve round the lateral border from the dorsal aspect of the limb. They follow the cephalic vein to the level of the deltoid tendon, where most incline medially to reach the lateral axillary nodes; a few continue with the vein and drain into the infraclavicular nodes. Vessels lying medially in the forearm are joined by vessels that curve round the medial border of the limb. They follow the basilic vein. Proximal to the elbow some end in supratrochlear lymph nodes whose efferents, together with the medial vessels that have bypassed them, pierce the deep fascia with the basilic vein and end in the lateral axillary nodes or deep lymphatic vessels.

Collecting vessels from the deltoid region pass round the anterior and posterior axillary folds to end in the axillary nodes. The scapular skin drains either to subscapular axillary nodes or by channels that follow the transverse cervical vessels to the inferior deep cervical nodes.

Lymphatic drainage of deep tissues

Deep lymph vessels follow the main neurovascular bundles (radial, ulnar, interosseous and brachial) to the lateral axillary nodes. They are less numerous than the superficial vessels and communicate with them at intervals. A few lymph nodes occur along the vessels. Scapular muscles drain mainly to the subscapular axillary nodes, and pectoral muscles drain mainly to the pectoral, central and apical nodes (Fig. 45.6).

INNERVATION

OVERVIEW OF THE BRACHIAL PLEXUS

The brachial plexus is formed by the union of the ventral rami of the lower four cervical nerves and the greater part of the first thoracic ventral ramus (Fig. 45.7; see Fig. 46.29).

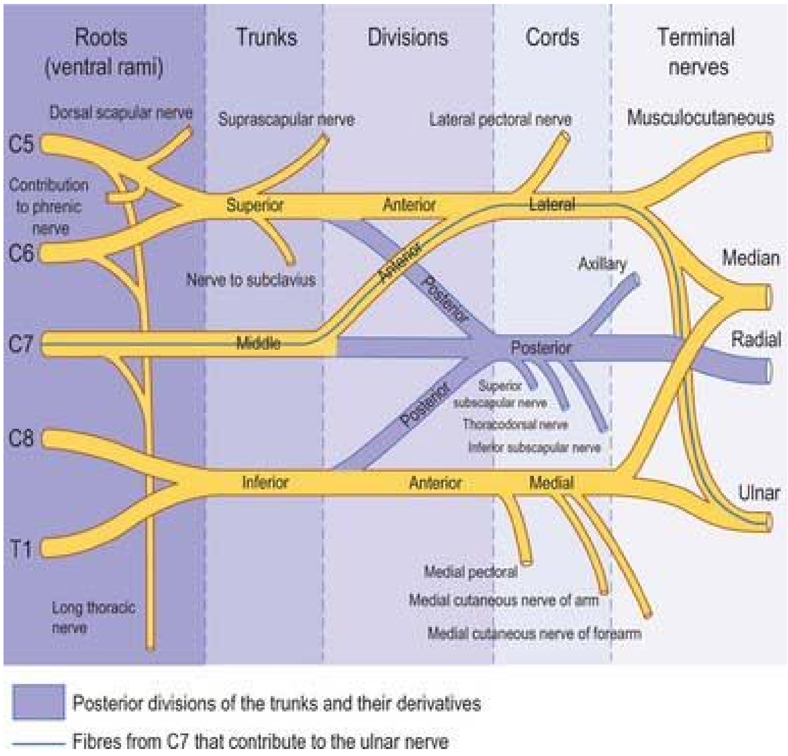
Roots (ventral rami)
Trunks
Divisions
Cords
Terminal nerves
Dorsal scapular nerve
Suprascapular nerve
Lateral pectoral nerve
Musculocutaneous
C5
Contribution to phrenic nerve
Superior
Anterior
Lateral
C6
Axillary
Median
Nerve to subclavius
Anterior
Posterior
C7
Middle
Posterior
Radial
Superior subscapular nerve
Thoracodorsal nerve
Inferior subscapular nerve
Posterior
C8
Inferior
Anterior
Medial
Ulnar
T1
Medial pectoral
Medial cutaneous nerve of arm
Medial cutaneous nerve of forearm
Long thoracic nerve
▨ Posterior divisions of the trunks and their derivatives
— Fibres from C7 that contribute to the ulnar nerve

Fig. 45.7 A schematic plan of the left brachial plexus.

(Adapted from Drake, Vogl and Mitchell 2005.)

The fourth ramus usually gives a branch to the fifth, and the first thoracic ramus frequently receives a branch from the second. These ventral rami are the roots of the plexus: they are almost equal in size but variable in their mode of junction. Contributions to the plexus by C4 and T2 vary. When the branch from C4 is large, that from T2 is frequently absent and the branch from T1 is reduced, forming a ‘prefixed’ type of plexus. If the branch from C4 is small or absent, the contribution from C5 is reduced but that from T1 is larger and there is always a contribution from T2: this arrangement constitutes a ‘postfixed’ type of plexus.

Close to their exit from the intervertebral foramina, the fifth and sixth cervical ventral rami receive grey rami communicantes from the middle cervical sympathetic ganglion, and the seventh and eighth rami receive grey rami from the cervicothoracic ganglion. The first thoracic ventral ramus receives a grey ramus from, and contributes a white ramus to, the cervicothoracic ganglion.

The most common arrangement of the brachial plexus is as follows: the fifth and sixth rami unite at the lateral border of scalenus medius as the upper trunk; the eighth cervical and first thoracic rami join behind scalenus anterior as the lower trunk; the seventh cervical ramus becomes the middle trunk. The three trunks incline laterally, and either just above or behind the clavicle each bifurcates into anterior and posterior divisions. The anterior divisions of the upper and middle trunks form a lateral cord that lies lateral to the axillary artery. The anterior division of the lower trunk descends at first behind and then medial to the axillary artery and forms the medial cord; it often receives a branch from the seventh cervical ramus. Posterior divisions of all three trunks form the posterior cord, which is at first above, and then behind, the axillary artery. The posterior division of the lower trunk is much smaller than the others and is frequently derived from the eighth cervical ramus before the trunk is formed; it contains few, if any, fibres from the first thoracic ramus.

Axillary nerve (C5, 6)

The axillary nerve is a branch of the posterior cord of the brachial plexus. It winds posteriorly around the neck of the humerus together with the circumflex humeral vessels, and supplies deltoid and teres minor and an area of skin over the deltoid region (Fig. 45.8).

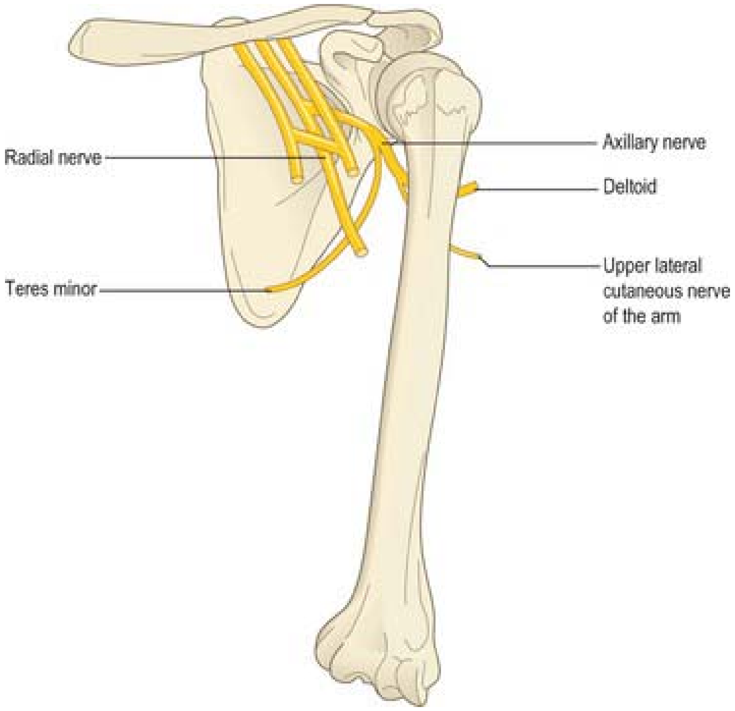

Fig. 45.8 Motor and sensory branches of the axillary nerve.

Radial nerve (C5–8, T1)

The radial nerve is the continuation of the posterior cord of the brachial plexus (Fig. 45.9). In the upper arm it lies in the spiral groove of the humerus where it is accompanied by the profunda brachii artery and its venal comitantes. It enters the posterior (extensor) compartment and supplies triceps, then re-enters the anterior compartment of the arm by piercing the lateral intermuscular septum. At the level of the lateral epicondyle it gives off the posterior interosseous nerve, which passes between the two heads of supinator and enters the extensor compartment of the forearm. The posterior interosseous nerve supplies these muscles, while the radial nerve proper continues into the forearm in the anterior compartment deep to brachioradialis and terminates by supplying the skin over the posterior aspect of the thumb, index, middle and radial half of the ring finger.

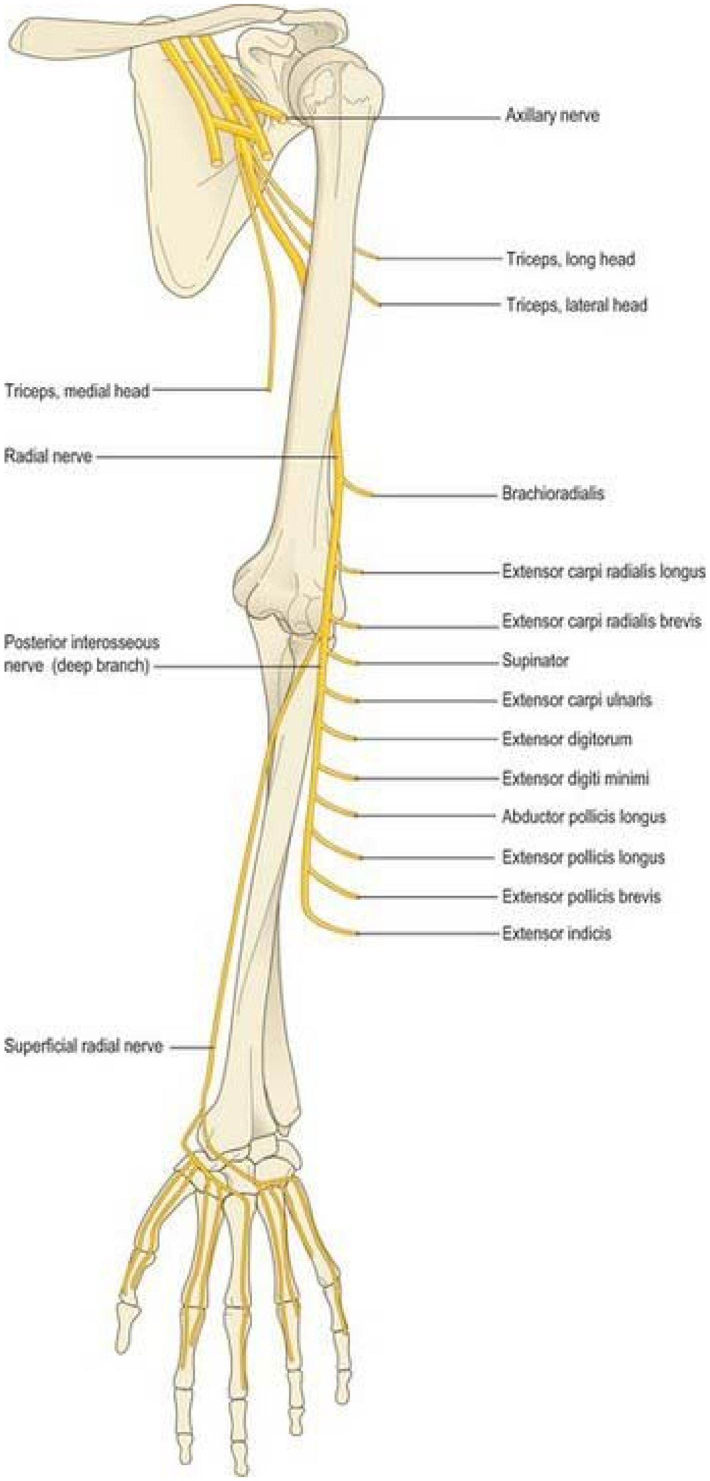
Axillary nerve
Triceps, long head
Triceps, lateral head
Triceps, medial head
Radial nerve
Brachioradialis
Extensor carpi radialis longus
Extensor carpi radialis brevis
Posterior interosseous nerve (deep branch)
Supinator
Extensor carpi ulnaris
Extensor digitorum
Extensor digiti minimi
Abductor pollicis longus
Extensor pollicis longus
Extensor pollicis brevis
Extensor indicis
Superficial radial nerve

Fig. 45.9 Motor and sensory branches of the radial nerve. Variation exists in the cutaneous innervation of the dorsal aspects of the digits. Here the radial nerve is shown to supply all five digits. The dorsum of the ring and little fingers is frequently innervated by the dorsal branch of the ulnar nerve.

Musculocutaneous nerve (C5–7)

The musculocutaneous nerve is formed from the continuation of the lateral cord of the brachial plexus. It pierces and supplies coracobrachialis, biceps and brachialis, and then continues into the forearm as the lateral cutaneous nerve of the forearm (Fig. 45.10).

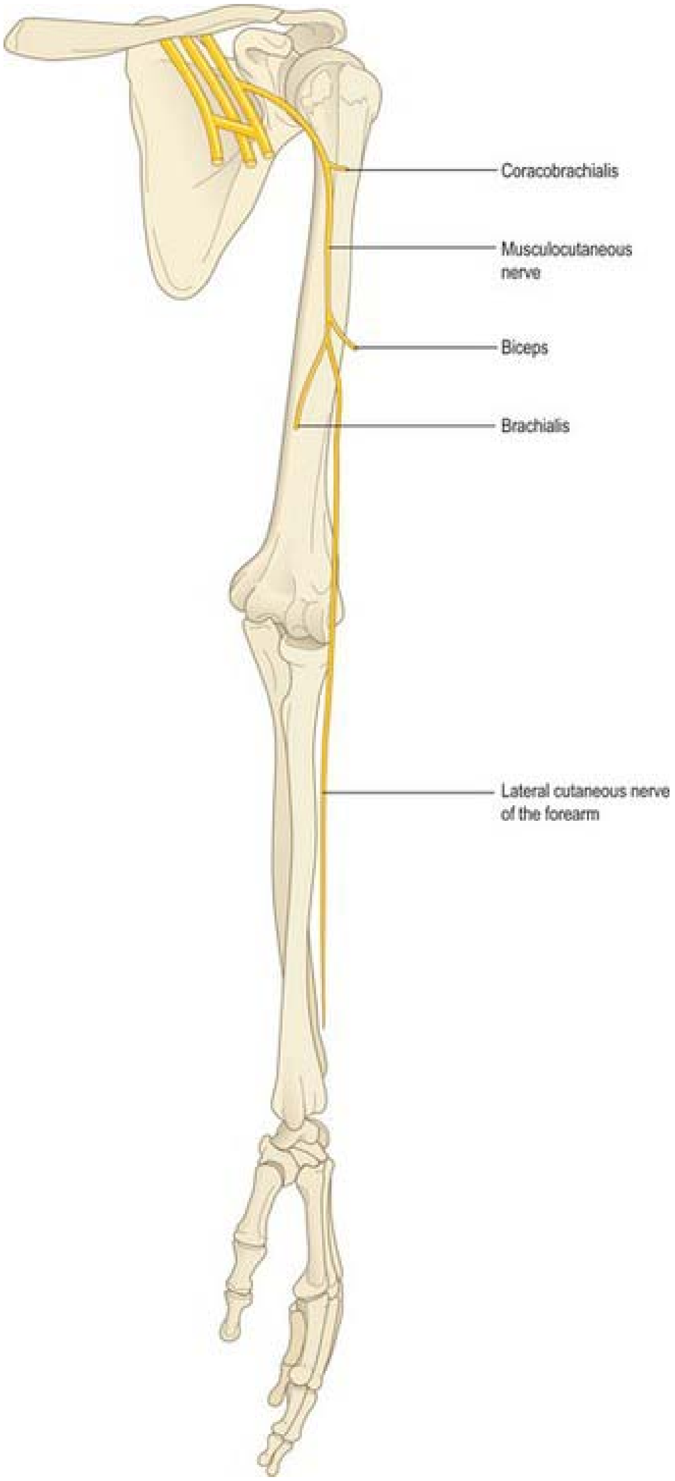
Coracobrachialis
Musculocutaneous nerve
Biceps
Brachialis
Lateral cutaneous nerve of the forearm

Fig. 45.10 Motor and sensory branches of the musculocutaneous nerve.

Median nerve (C6–8, T1)

The median nerve is formed by the union of the terminal branch of the lateral and medial cords of the brachial plexus (Fig. 45.11). It has no branches in the upper arm. It enters the forearm between the two heads of pronator teres and gives off the anterior interosseous nerve, which supplies all the flexor muscles of the forearm apart from flexor carpi ulnaris and the ulnar half of flexor digitorum profundus. The median nerve itself passes deep to the flexor retinaculum at the wrist. On entering the palm, it gives off motor branches to the thenar muscles and the radial two lumbricals, and cutaneous branches to the palmar aspect of the thumb, index and middle fingers and the radial half of the ring finger.

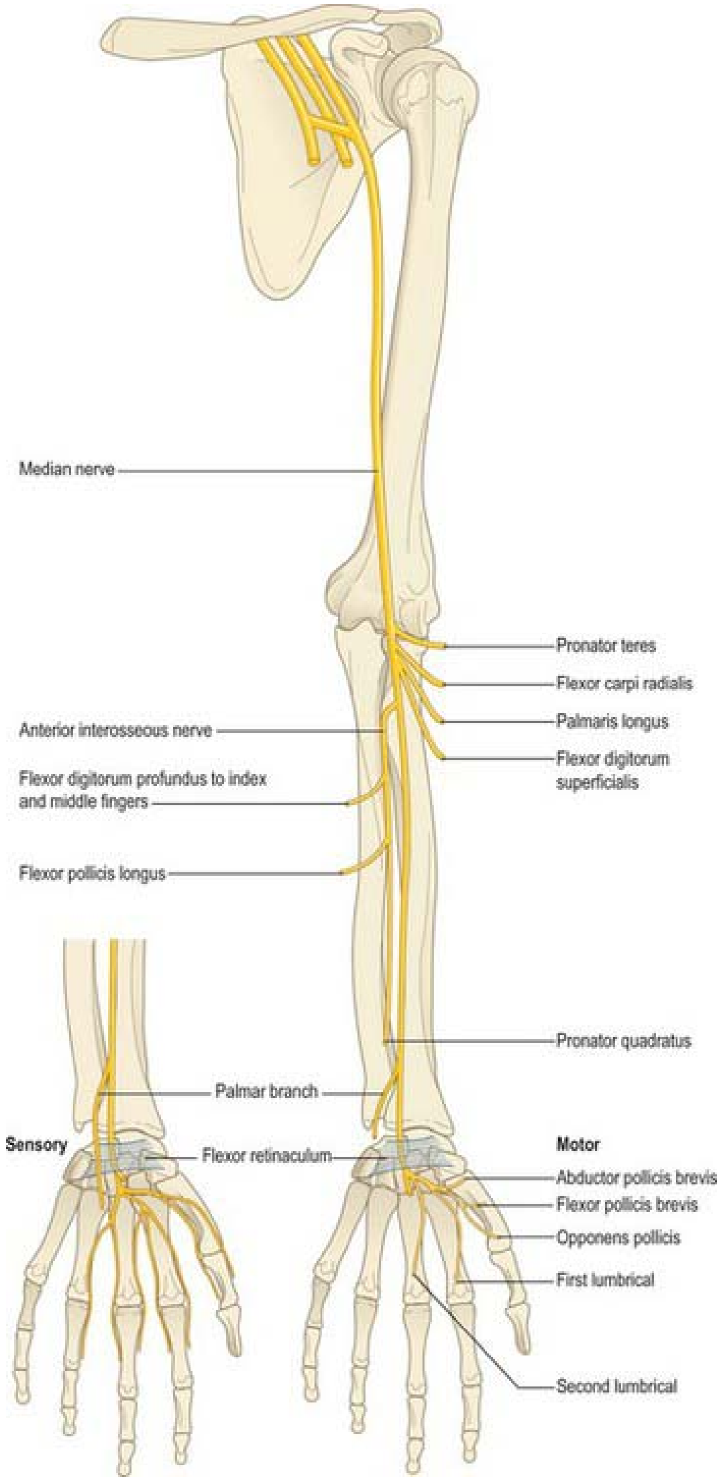
Median nerve
Pronator teres
Flexor carpi radialis
Palmaris longus
Anterior interosseous nerve
Flexor digitorum superficialis
Flexor digitorum profundus to index and middle fingers
Flexor pollicis longus
Pronator quadratus
Palmar branch
Sensory
Flexor retinaculum
Motor
Abductor pollicis brevis
Flexor pollicis brevis
Opponens pollicis
First lumbrical
Second lumbrical

Fig. 45.11 Motor and sensory branches of the median nerve. Flexor pollicis brevis may be supplied by both median nerve and ulnar nerve.

Ulnar nerve (C7, C8, T1)

The ulnar nerve is the continuation of the medial cord of the brachial plexus (Fig. 45.12). Like the median nerve, it has no branches in the upper arm. It enters the posterior compartment of the upper arm midway down its length by piercing the medial intermuscular septum, passes behind the medial epicondyle of the humerus to enter the forearm and descends to the wrist deep to flexor carpi ulnaris. The ulnar nerve supplies flexor carpi ulnaris and the ulnar half of flexor digitorum profundus. Just proximal to the wrist it gives off a dorsal cutaneous branch that supplies the skin over the dorsal aspect of the little finger and the ulnar half of the ring finger, and then crosses into the palm superficial to the flexor retinaculum in Guyon’s canal. It divides into a motor branch, which supplies the hypothenar muscles, the intrinsic muscles of the hand (apart from the radial two lumbricals) and adductor pollicis, and cutaneous branches, which supply the skin of the palmar aspect of the little finger and the ulnar half of the ring finger.

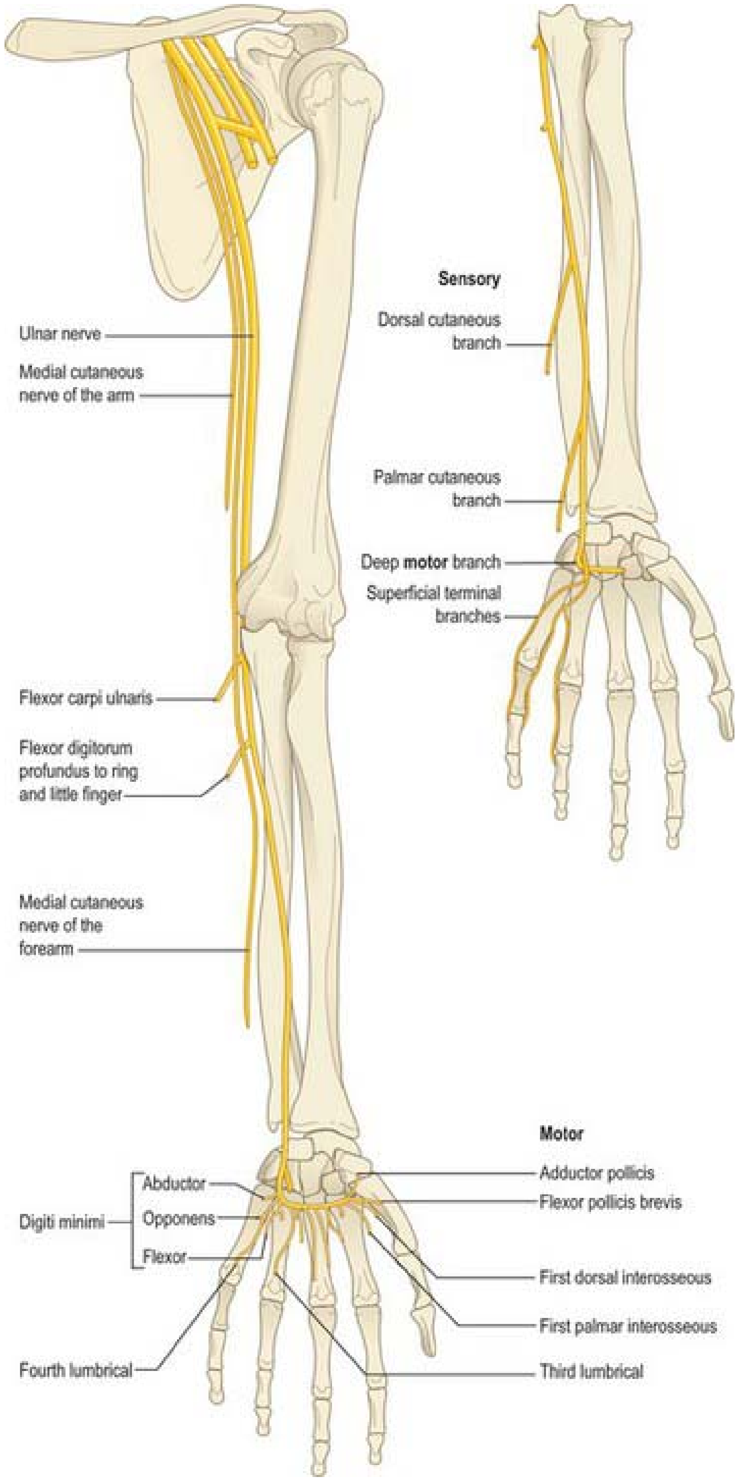
Sensory
Dorsal cutaneous branch
Palmar cutaneous branch
Deep motor branch
Superficial terminal branches
Ulnar nerve
Medial cutaneous nerve of the arm
Flexor carpi ulnaris
Flexor digitorum profundus to ring and little finger
Medial cutaneous nerve of the forearm
Motor
Adductor pollicis
Flexor pollicis brevis
Digiti minimi
Abductor
Opponens
Flexor
First dorsal interosseous
First palmar interosseous
Fourth lumbrical
Third lumbrical

Fig. 45.12 Motor and sensory branches of the ulnar nerve together with the medial cutaneous nerve of the arm and the forearm. Flexor pollicis brevis may be supplied by both median nerve and ulnar nerve.

AUTONOMIC INNERVATION

The autonomic supply to the limbs is exclusively sympathetic. The preganglionic sympathetic inflow to the upper limb is derived from neurones in the lateral horn of the upper thoracic spinal segments T2–6(7). Fibres pass in white rami communicantes to the thoracic sympathetic chain and synapse in the stellate and second thoracic ganglia. Postganglionic fibres to the skin are distributed via cutaneous branches of the brachial plexus. The blood vessels to the upper limb receive their sympathetic supply via adjacent peripheral nerves, thus the median nerve supplies postganglionic sympathetic fibres to the brachial artery and the palmar arches, and the ulnar nerve supplies the ulnar artery.

MOVEMENTS, MUSCLES AND SEGMENTAL INNERVATION

Most limb muscles are innervated by neurones derived from more than one segment of the spinal cord. The predominant segmental origin of the nerve supply for each of the muscles of the upper limb and for the movements which take place at the joints of the upper limb is summarized in Tables 45.1-45.4. Red has been used in Table 45.1 to highlight those muscles or movements which have diagnostic value (see below). The following caveats should be borne in mind when consulting these tables.

Table 45.1 Movements, muscles and segmental innervation in the upper limb. Muscles and movements that have diagnostic value are marked in red

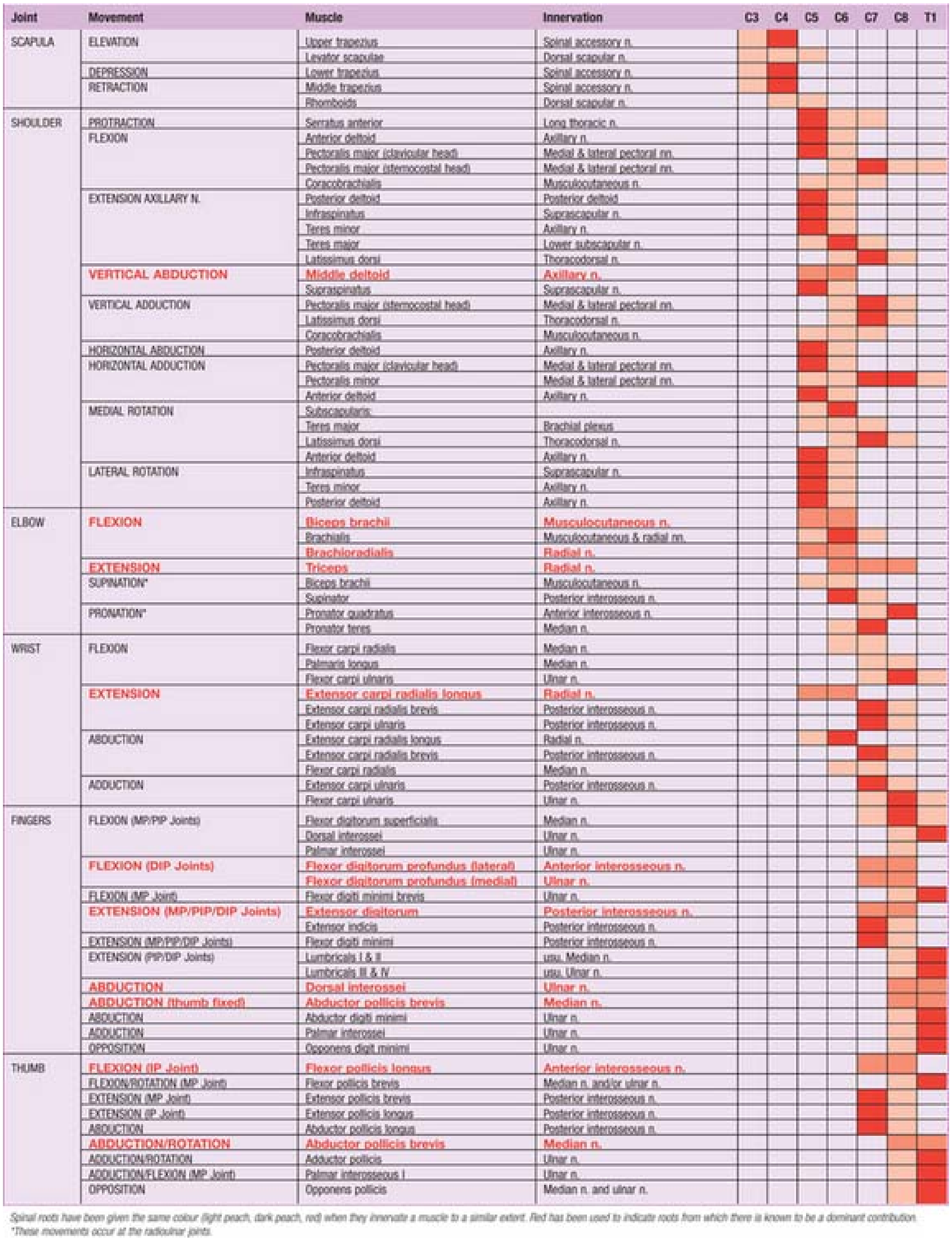

Joint	Movement	Muscle	Innervation	C3	C4	C5	C6	C7	C8	T1
SCAPULA	ELEVATION	Upper trapezius	Spinal accessory n.	░	█					
		Levator scapulae	Dorsal scapular n.	░	░	░				
	DEPRESSION	Lower trapezius	Spinal accessory n.	░	█					
	RETRACTION	Middle trapezius	Spinal accessory n.	░	█					
		Rhomboids	Dorsal scapular n.		░	░				
SHOULDER	PROTRACTION	Serratus anterior	Long thoracic n.			█	░	░		
	FLEXION	Anterior deltoid	Axillary n.			█	░			
		Pectoralis major (clavicular head)	Medial & lateral pectoral nn.			█	░			
		Pectoralis major (sternocostal head)	Medial & lateral pectoral nn.				░	█	░	░
		Coracobrachialis	Musculocutaneous n.			░	░	░		
	EXTENSION AXILLARY N.	Posterior deltoid	Posterior deltoid			█	░			
		Infraspinatus	Suprascapular n.			█	░			
		Teres minor	Axillary n.			█	░			
		Teres major	Lower subscapular n.			░	█	░		
		Latissimus dorsi	Thoracodorsal n.				░	█	░	
	VERTICAL ABDUCTION	**Middle deltoid**	**Axillary n.**			▒	▒			
		Supraspinatus	Suprascapular n.			█	░			
	VERTICAL ADDUCTION	Pectoralis major (sternocostal head)	Medial & lateral pectoral nn.				░	█	░	
		Latissimus dorsi	Thoracodorsal n.				░	█	░	
		Coracobrachialis	Musculocutaneous n.			░	░	░		
	HORIZONTAL ABDUCTION	Posterior deltoid	Axillary n.			█	░			
	HORIZONTAL ADDUCTION	Pectoralis major (clavicular head)	Medial & lateral pectoral nn.			█	░			
		Pectoralis minor	Medial & lateral pectoral nn.			░	░	█	█	░
		Anterior deltoid	Axillary n.			█	░			
	MEDIAL ROTATION	Subscapularis				░	█			
		Teres major	Brachial plexus			░	░	░		
		Latissimus dorsi	Thoracodorsal n.				░	█	░	
		Anterior deltoid	Axillary n.			█	░			
	LATERAL ROTATION	Infraspinatus	Suprascapular n.			█	░			
		Teres minor	Axillary n.			█	░			
		Posterior deltoid	Axillary n.			█	░			
ELBOW	**FLEXION**	**Biceps brachii**	**Musculocutaneous n.**			▒	▒			
		Brachialis	Musculocutaneous & radial nn.			░	█	░		
		Brachioradialis	**Radial n.**			▒	▒			
	EXTENSION	**Triceps**	**Radial n.**				▒	▒	▒	
	SUPINATION*	Biceps brachii	Musculocutaneous n.			░	░			
		Supinator	Posterior interosseous n.				█	░		
	PRONATION*	Pronator quadratus	Anterior interosseous n.					░	█	
		Pronator teres	Median n.				░	█		
WRIST	FLEXION	Flexor carpi radialis	Median n.				░	░		
		Palmaris longus	Median n.					░	░	
		Flexor carpi ulnaris	Ulnar n.					░	█	░
	EXTENSION	**Extensor carpi radialis longus**	**Radial n.**			▒	▒			
		Extensor carpi radialis brevis	Posterior interosseous n.					█	░	
		Extensor carpi ulnaris	Posterior interosseous n.					█	░	
	ABDUCTION	Extensor carpi radialis longus	Radial n.			░	█			
		Extensor carpi radialis brevis	Posterior interosseous n.					█	░	
		Flexor carpi radialis	Median n.				░	░		
	ADDUCTION	Extensor carpi ulnaris	Posterior interosseous n.					█	░	
		Flexor carpi ulnaris	Ulnar n.					░	█	░
FINGERS	FLEXION (MP/PIP Joints)	Flexor digitorum superficialis	Median n.					░	█	░
		Dorsal interossei	Ulnar n.						░	█
		Palmar interossei	Ulnar n.						░	
	FLEXION (DIP Joints)	**Flexor digitorum profundus (lateral)**	**Anterior interosseous n.**					▒	▒	
		Flexor digitorum profundus (medial)	**Ulnar n.**					▒	▒	
	FLEXION (MP Joint)	Flexor digiti minimi brevis	Ulnar n.						░	█
	EXTENSION (MP/PIP/DIP Joints)	**Extensor digitorum**	**Posterior interosseous n.**					▒	▒	
		Extensor indicis	Posterior interosseous n.					█	░	
	EXTENSION (MP/PIP/DIP Joints)	Flexor digiti minimi	Posterior interosseous n.					█	░	
	EXTENSION (PIP/DIP Joints)	Lumbricals I & II	usu. Median n.						░	█
		Lumbricals III & IV	usu. Ulnar n.						░	█
	ABDUCTION	**Dorsal interossei**	**Ulnar n.**						▒	▒
	ABDUCTION (thumb fixed)	**Abductor pollicis brevis**	**Median n.**						▒	▒
	ABDUCTION	Abductor digiti minimi	Ulnar n.						░	█
	ADDUCTION	Palmar interossei	Ulnar n.						░	█
	OPPOSITION	Opponens digiti minimi	Ulnar n.						░	█
THUMB	**FLEXION (IP Joint)**	**Flexor pollicis longus**	**Anterior interosseous n.**					▒	▒	
	FLEXION/ROTATION (MP Joint)	Flexor pollicis brevis	Median n. and/or ulnar n.						░	█
	EXTENSION (MP Joint)	Extensor pollicis brevis	Posterior interosseous n.					█	░	
	EXTENSION (IP Joint)	Extensor pollicis longus	Posterior interosseous n.					█	░	
	ABDUCTION	Abductor pollicis longus	Posterior interosseous n.					█	░	
	ABDUCTION/ROTATION	**Abductor pollicis brevis**	**Median n.**						▒	▒
	ADDUCTION/ROTATION	Adductor pollicis	Ulnar n.						░	█
	ADDUCTION/FLEXION (MP Joint)	Palmar interosseous I	Ulnar n.						░	█
	OPPOSITION	Opponens pollicis	Median n. and ulnar n.						░	█

Spinal roots have been given the same colour (light peach, dark peach, red) when they innervate a muscle to a similar extent. Red has been used to indicate roots from which there is known to be a dominant contribution.
**These movements occur at the radioulnar joints.*

Table 45.2 Segmental innervation of the muscles of the upper limb

C3,	Trapezius, levator scapulae

4	
C5	Rhomboids, deltoids, supraspinatus, infraspinatus, teres minor, biceps
C6	Serratus anterior, latissimus dorsi, subscapularis, teres major, pectoralis major (clavicular head), biceps, coracobrachialis, brachialis, brachioradialis, supinator, extensor carpi radialis longus
C7	Serratus anterior, latissimus dorsi, pectoralis major (sternal head), pectoralis minor, triceps, pronator teres, flexor carpi radialis, flexor digitorum superficialis, extensor carpi radialis longus, extensor carpi radialis brevis, extensor digitorum, extensor digiti minimi
C8	Pectoralis major (sternal head), pectoralis minor, triceps, flexor digitorum superficialis, flexor digitorum profundus, flexor pollicis longus, pronator quadratus, flexor carpi ulnaris, extensor carpi ulnaris, abductor pollicis longus, extensor pollicis longus, extensor pollicis brevis, extensor indicis, abductor pollicis brevis, flexor pollicis brevis, opponens pollicis
T1	Flexor digitorum profundus, intrinsic muscles of the hand (except abductor pollicis brevis, flexor pollicis brevis, opponens pollicis)

Table 45.3 Segmental innervation of joint movements of the upper limb

Shoulder	Abductors and lateral rotators	C5
	Adductors and medial rotators	C6–8
Elbow	Flexors	C5, 6
	Extensors	C7, 8
Forearm	Supinators	C6
	Pronators	C7, 8
Wrist	Flexors and extensors	C6, 7
Digits	Long flexors and extensors	C7, 8
Hand	Intrinsic muscles	C8, T1

Table 45.4 Movements and muscles tested to determine the location of a lesion in the upper limb

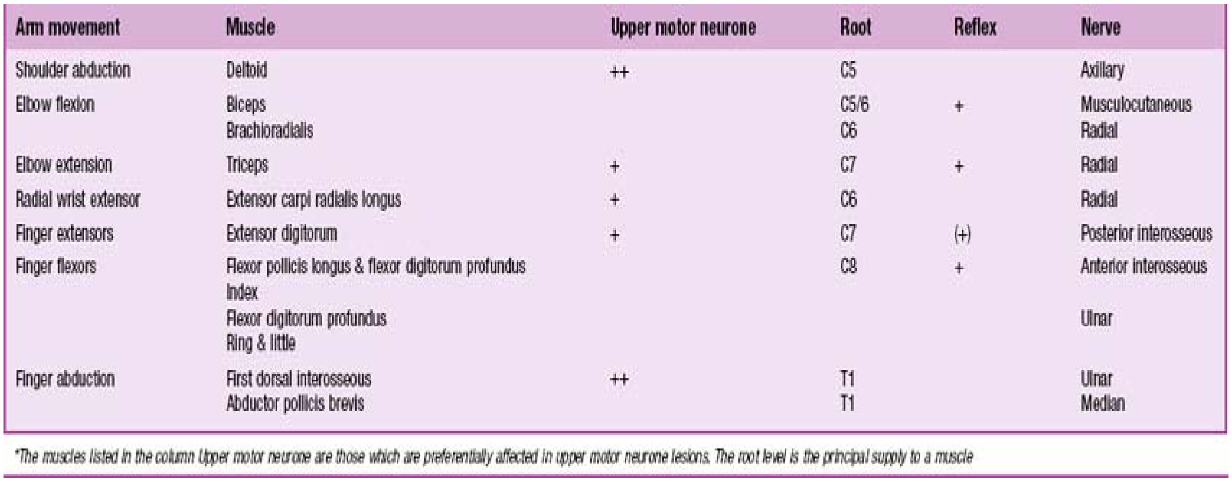

Arm movement	Muscle	Upper motor neurone	Root	Reflex	Nerve
Shoulder abduction	Deltoid	++	C5		Axillary
Elbow flexion	Biceps Brachioradialis		C5/6 C6	+	Musculocutaneous Radial
Elbow extension	Triceps	+	C7	+	Radial
Radial wrist extensor	Extensor carpi radialis longus	+	C6		Radial
Finger extensors	Extensor digitorum	+	C7	(+)	Posterior interosseous
Finger flexors	Flexor pollicis longus & flexor digitorum profundus Index		C8	+	Anterior interosseous
	Flexor digitorum profundus Ring & little				Ulnar
Finger abduction	First dorsal interosseous Abductor pollicis brevis	++	T1 T1		Ulnar Median

*The muscles listed in the column Upper motor neurone are those which are preferentially affected in upper motor neurone lesions. The root level is the principal supply to a muscle

Movements

At the central nervous level of control, muscles are not recognized as individual actuators but as components of movement, and may therefore contribute to several types of movement, acting variously as prime movers, antagonists, fixators or synergists. For example, serratus anterior acts as an antagonist of trapezius as the scapula moves around the thorax, whereas both muscles act together as prime movers during the forward rotation of the scapula. Some muscles have been included in more than one place in Table 45.1, on the basis that a muscle which acts across one joint can produce a combination of movements (e.g. flexion with medial rotation, or extension with adduction) and a muscle which crosses two joints can produce more than one movement. It must also be remembered that these listings are not exhaustive.

Nerve roots

There is no universal consensus concerning the contribution that individual spinal roots make to the innervation of individual muscles: the most positive identifications, which are limited, have been obtained by electrically stimulating spinal roots and recording the evoked electromyographic activity in the muscles. Much of the information in Tables 45.1-45.4 is therefore based on neurological experience gained in examining the effects of lesions, and some of it is far from new. In Table 45.1, spinal roots have been given the same colour (light peach, dark peach, red) when they innervate a muscle to a similar extent, or when differences in their contribution have not been described. Red has been used to indicate roots from which there is known to be a dominant contribution. From a clinical viewpoint, some of these roots may be regarded as innervating the muscle almost exclusively, e.g. deltoid by C5, brachioradialis by C6, and triceps by C7. Minor contributions have been retained in the table in order to increase its utility in other contexts, such as electromyography and comparative anatomy.

Neurological location of a lesion

In clinical practice it is only necessary to test a relatively small number of muscles in order to determine the location of a lesion. Any muscle to be tested must satisfy a number of criteria. It should be visible, so that wasting or fasciculation can be observed, and the muscle consistency with contraction can be felt. It should have an isolated action, so that its function can be tested separately. It should help to differentiate between lesions at different levels in the neuraxis and in the peripheral nerve, or between peripheral nerves. It should be tested in such a way that normal can be differentiated from abnormal, so that slight weakness can be detected early with reliability. Some preference should be given to muscles with an easily elicited reflex.

Table 45.4 gives a list of movements and muscles chosen according to these criteria. For example, with an upper motor neurone lesion, shoulder abduction, elbow extension, wrist and finger extension and finger abduction are weaker than their opposing movements. Since this weakness may be more distal than proximal or *vice versa*, normal shoulder abduction and finger abduction excludes an upper motor neurone weakness of the arm. Some muscles are difficult to test but are included for special reasons, e.g. the strength of brachioradialis is difficult to assess but it can be seen and felt, it is mostly innervated by the C6 root, and it has an easily elicited reflex.

Knowledge of the sequence in which motor branches leave a peripheral nerve to innervate specific muscles is very helpful in locating the level of a lesion. For example, with radial nerve lesions, if triceps is involved, then the lesion must be high in the axilla; if (as is usual), triceps is spared but brachioradialis, wrist extensors, finger extensors and the superficial radial nerve are all involved, then the lesion is in the arm, where the radial nerve is vulnerable to pressure against the humerus; if wrist extension is normal and the superficial radial nerve is not involved but finger extension is weak, then the lesion involves the posterior interosseous branch of the radial nerve.

SURFACE ANATOMY

SKIN

Palmar skin is marked by a number of creases, but they are of little value as points of reference. Transverse skin creases cross the palmar aspects of the fingers in three situations. The most proximal crease is placed at the junction of the digit with the palm and lies nearly 2 cm distal to the metacarpophalangeal joint, the intermediate crease lies opposite the proximal interphalangeal joint, and the distal crease is placed just proximal to the distal interphalangeal joint.

The flexor retinaculum may be outlined by defining its bony attachments. Its distal border, concave downwards, may be indicated on the surface by a curved line that joins the crest of the trapezium to the hook of the hamate. Its proximal border may be indicated by a curved line, concave upwards, that joins the tubercle of the scaphoid to the pisiform. Flexion of the wrist produces a number of transverse skin creases (usually two or three) at the wrist. The dominant crease, which is distal, overlies the proximal edge of the flexor retinaculum; the carpal tunnel lies distal to this crease, under the palmar skin.

SKELETAL LANDMARKS

The clavicle is both visible and palpable throughout its course. Its outline can be traced from the expanded sternal end, which forms the lateral boundary of the suprasternal notch, to the flattened acromial extremity. The line of the acromioclavicular joint is palpable as a distinct ‘step’ in an anteroposterior plane. The acromion can be traced from the acromioclavicular joint to its tip, and then backwards across the top of the shoulder until it meets the crest of the spine of the scapula at the prominent acromial angle. From this point, the spine of the scapula can be palpated as it passes medially from the acromial angle to the medial (vertebral) border of the scapula, where it lies opposite the spine of the third thoracic vertebra. The spine is subcutaneous and is easily visible in a thin subject.

The medial border of the scapula is hidden in its upper part by trapezius, but below the spine it can be palpated as it passes downwards to the inferior angle. Although covered by teres major and latissimus dorsi, the inferior angle can easily be felt when it is approached from below, and it can be seen to move laterally and forwards around the chest wall when the arm is raised above the head. The inferior angle of the scapula is at the level of the spine of the seventh thoracic vertebra and overlies the seventh rib. When a thoracotomy is being performed, it is a convenient landmark from which the ribs can be counted along the lateral chest wall.

A small depression can be seen inferior to the clavicle at the junction of its convex medial and concave lateral portions. This is the infraclavicular fossa (or deltopectoral triangle) and it intervenes between the surface elevations produced by the clavicular origins of pectoralis major and deltoid. The apex of the coracoid process lies 2.5 cm below the clavicle immediately to the lateral side of this fossa, under cover of the anterior fibres of deltoid. If the examining finger is passed laterally from the coracoid process, the lesser tubercle of the humerus will be felt below the tip of the acromion on deep pressure through deltoid. This bony prominence slips away from the examining finger when the humerus is rotated laterally or medially. The greater tubercle of the humerus is the most lateral bony point in the shoulder region and projects laterally below and in front of the acromial angle. It can also be felt to move on rotation of the humerus. When the arm is abducted, the head of the humerus can be palpated on deep pressure in the apex of the axilla.

The shaft of the humerus can only be felt indistinctly through its course because its outline is obscured by overlying muscles. Distally, the medial epicondyle of the humerus is a conspicuous landmark and is easily felt, particularly when the elbow is flexed; proximally it can be traced upwards into the medial supracondylar ridge. The ulnar nerve can be rolled from side to side posterior to the base of the medial epicondyle. The lateral epicondyle is not so prominent, but its posterior surface is easily palpated and its lateral margin can be traced upwards into the lateral supracondylar ridge on deep pressure. Inspection of the posterior aspect of the extended elbow reveals a well-marked depression to the lateral side of the midline. This is bounded laterally by the fleshy elevation formed by the superficial group of forearm extensor muscles and medially by the lateral side of the olecranon. The floor of this depression contains, in its upper part, the posterior surface of the lateral epicondyle and, in its lower part, the head of the radius. Although the latter is covered by the anular ligament, it can be felt to rotate when the forearm is pronated and supinated. Between the lateral epicondyle and the radial head, the humero-radial part of the elbow joint can be felt as a distinct transverse depression.

When the elbow is extended, the apex of the olecranon can be felt and seen to lie in a line level with the two epicondyles. When the elbow is flexed, the apex of the olecranon descends and the three bony points then form the angles of a triangle. This relationship is lost in dislocation of the elbow. The posterior surface of the olecranon is subcutaneous and tapers from above downwards. It can be felt with ease immediately below the apex.

The level of the elbow joint is situated 2 cm below a line joining the two epicondyles. It slopes downwards and medially from its lateral extremity, and this obliquity produces the ‘carrying angle’. When the elbow is fully extended and the forearm and hand are in supination (‘the anatomical position’), the carrying angle is normally 165° in the female and 175° in the male. It disappears on full flexion of the elbow, when the shafts of the ulna and humerus come to lie in the same plane, and is also obscured in full pronation of the forearm.

The posterior border of the ulna is subcutaneous throughout its whole extent, from the subcutaneous surface of the olecranon superiorly to the styloid process below. Its position corresponds to the longitudinal furrow that can be seen on the posterior aspect of the forearm when the elbow is fully flexed, and which separates the flexor group of muscles from the extensors. In contrast, the shaft of the radius can only be felt indistinctly because it is covered by muscles. The rounded head of the ulna forms a surface elevation on the medial part of the posterior aspect of the wrist when the hand is pronated. The styloid process of the ulna projects distally from the posteromedial aspect of the head.

The expanded lower end of the radius forms a slight surface elevation on the lateral side of the wrist and can be traced downwards into the styloid process of the radius. The posterior aspect of the lower end of the radius is partly obscured by the extensor tendons but can be palpated without difficulty. It presents a tubercle (of Lister), which is grooved on its ulnar aspect by the tendon of extensor pollicis longus. The tubercle lies in line with the cleft between the index and the middle fingers.

The wrist joint is easily identified between the carpus and the distal ends of the radius and ulna on flexion and extension of the wrist, even though it is covered by tendons. The line of the wrist joint corresponds to a line, convex upwards, that joins the styloid process of the radius to that of the ulna. It is delineated by the proximal of the two transverse anterior wrist skin creases.

Four of the bones of the carpus can be palpated and identified. The pisiform forms an elevation that can be both seen and felt on the palmar aspect of the wrist at the base of the hypothenar eminence. It can be moved over the articular surface of the triquetrum when the wrist is passively flexed. The hook of the hamate lies 2.5 cm distal to the pisiform and is in line with the ulnar border of the ring finger. It can be felt by deep pressure in this situation, and here the superficial division of the ulnar nerve can be rolled from side to side over the tip of the hook. The tubercle of the scaphoid is situated at the base of the thenar eminence, and in many subjects forms a small visible elevation. Immediately distal to it, but covered by the muscles of the thenar eminence, the crest of the trapezium can be identified on deep pressure. The scaphoid and trapezium can also be palpated in the ‘anatomical snuffbox’.

The heads of the metacarpal bones form the prominence of the knuckles, that of the middle finger being the most prominent. Their convex palmar aspects can be felt on deep pressure over the front of the metacarpophalangeal joints and can be gripped between the finger and the thumb. Deep pressure over the distal aspect of the head of the metacarpal bone reveals the base of the corresponding proximal phalanx; the line of the metacarpophalangeal joint can be detected on the dorsum of the hand as the fingers are flexed and extended. The dorsal aspects of the shafts of the metacarpal bones of the fingers and thumb and of the trapezium can be felt rather indistinctly, since they are obscured by the extensor tendons. The interphalangeal joints can be felt on the dorsal aspect of the flexed finger, just distal to the prominences caused by the heads of the proximal and middle phalanges.

MUSCULOTENDINOUS LANDMARKS

Deltoid may be delineated when the arm is abducted against resistance, and its tendon can be identified about half-way down the lateral aspect of the humerus. Its anterior border can be traced upwards and medially from the anterior aspect of the humerus, across the tendon of pectoralis major, to form the lateral boundary of the infraclavicular fossa. The posterior border runs upwards and medially from the posterior aspect of the deltoid tendon and reaches the crest of the spine of the scapula near its medial end. The normal rounded contour of the shoulder is produced by deltoid, which spreads out over the lateral aspect of the greater tubercle of the humerus. In dislocation of the shoulder, the greater tubercle is displaced medially, deltoid descends vertically to its humeral attachment, and the normal rounded contour of the shoulder is lost.

The rounded lower border of pectoralis major forms the anterior axillary fold. It is rendered more conspicuous when the abducted arm is adducted against resistance, e.g. when the hand is placed on the hip and pressed firmly against the trunk. When the arm is flexed to a right angle against resistance, the clavicular head of the muscle can be felt and seen to contract. When the flexed arm is extended against resistance, the clavicular head becomes relaxed but the sternocostal head stands out in relief.

The posterior fold of the axilla, produced by latissimus dorsi and the underlying teres major, reaches a lower level on the humerus than the anterior fold. Both latissimus dorsi and teres major participate in adduction of the arm: when the abducted arm is adducted against resistance, the posterior fold of the axilla is accentuated and the lateral border of latissimus dorsi can be traced downwards to its attachment to the iliac crest. When the arm is raised above the head, the lower five or six serrations of serratus anterior can be seen on the lateral aspect of the chest; they pass downwards and forwards to interdigitate with the serrations of external oblique. When serratus anterior is paralysed following injury to its nerve, the medial border, and especially the lower angle of the scapula, stand out prominently to produce a characteristic ‘winged’ appearance that can be accentuated by asking the patient to press both hands against a wall.

The belly of biceps brachii produces a conspicuous elevation on the anterior aspect of the arm. It diminishes above, where it is covered by pectoralis major, and below, where it is replaced by its tendon just above the elbow joint. Shallow furrows indicate its medial and lateral borders. When the elbow is flexed against resistance, biceps becomes still more obvious, and the bicipital tendon can be held between finger and thumb and traced down into the cubital fossa. With the arm held in this position, the sharp upper margin of the bicipital aponeurosis can be traced downwards and medially over the elevation produced by the superficial group of forearm flexor muscles. Coracobrachialis emerges from the lateral wall of the axilla and forms a rounded ridge on the upper part of the medial side of biceps.

Posteriorly, the lateral head of triceps forms an elevation medial and parallel to the posterior border of deltoid and is thrown into prominence when the elbow is extended against resistance. On its medial side, the fleshy mass produced by the long head of triceps disappears above under cover of deltoid.

Brachioradialis is the most superficial of the muscles on the lateral side of the forearm. When the elbow is flexed in the semi-prone position against resistance, brachioradialis stands out as a prominent ridge extending upwards beyond the level of the elbow joint on the lateral side of the arm.

Proximal to the wrist crease, the prominent tendon of flexor carpi radialis can be seen and palpated when the wrist is flexed; the radial artery lies on its lateral side. By palpating lateral to flexor carpi radialis, 3 or 4 cm proximal to the wrist crease, it is possible to feel flexor pollicis longus (bending and straightening the thumb will confirm that the examining finger is in the correct place). The area on the ulnar side of flexor carpi radialis is packed most densely with functionally important structures. The median nerve lies very close to the skin surface and is therefore often injured in lacerations. It is covered by palmaris longus, when that muscle is present (best confirmed by pinching thumb and ring finger together, when the muscle will be seen to stand out). When palmaris longus is absent, only a thin covering of subcutaneous fat and deep fascia separates skin and nerve. The four tendons of flexor digitorum superficialis lie deep to the median nerve: the tendons for the middle and ring fingers lie in front of those for the index and little fingers as they pass deep to the flexor retinaculum and can be felt, and usually seen, to move on flexion of the fingers. Deeper still are the tendons of flexor digitorum profundus. The large and robust tendon of flexor carpi ulnaris is easily palpated on the ulnar side of the front of the wrist; the ulnar nerve, artery and venae comitantes lie in the shelter of its radial edge. Any sharp injury powerful enough to cut through this strong tendon usually has enough energy left to cut the nerve and vessel.

When the thumb is fully extended, a depression known as the anatomical snuffbox is seen on the lateral aspect of the wrist, immediately distal to the radial styloid process (Fig. 45.13). Palpating distally from the styloid process, three structures are usually encountered: the convex ovoid proximal articular surface of the scaphoid (best felt during alternate ulnar and radial deviation at the wrist); less distinctly, the radial aspect of the trapezium; and the expanded base of the first metacarpal (best felt during circumduction of the thumb). When clinically assessing wrist stability throughout the range of wrist movements, the scaphoid may be effectively compressed bidigitally, between index finger and thumb, along its oblique long axis between tubercle and articular surface. The trapezium may be similarly compressed between its crest and radial aspect.

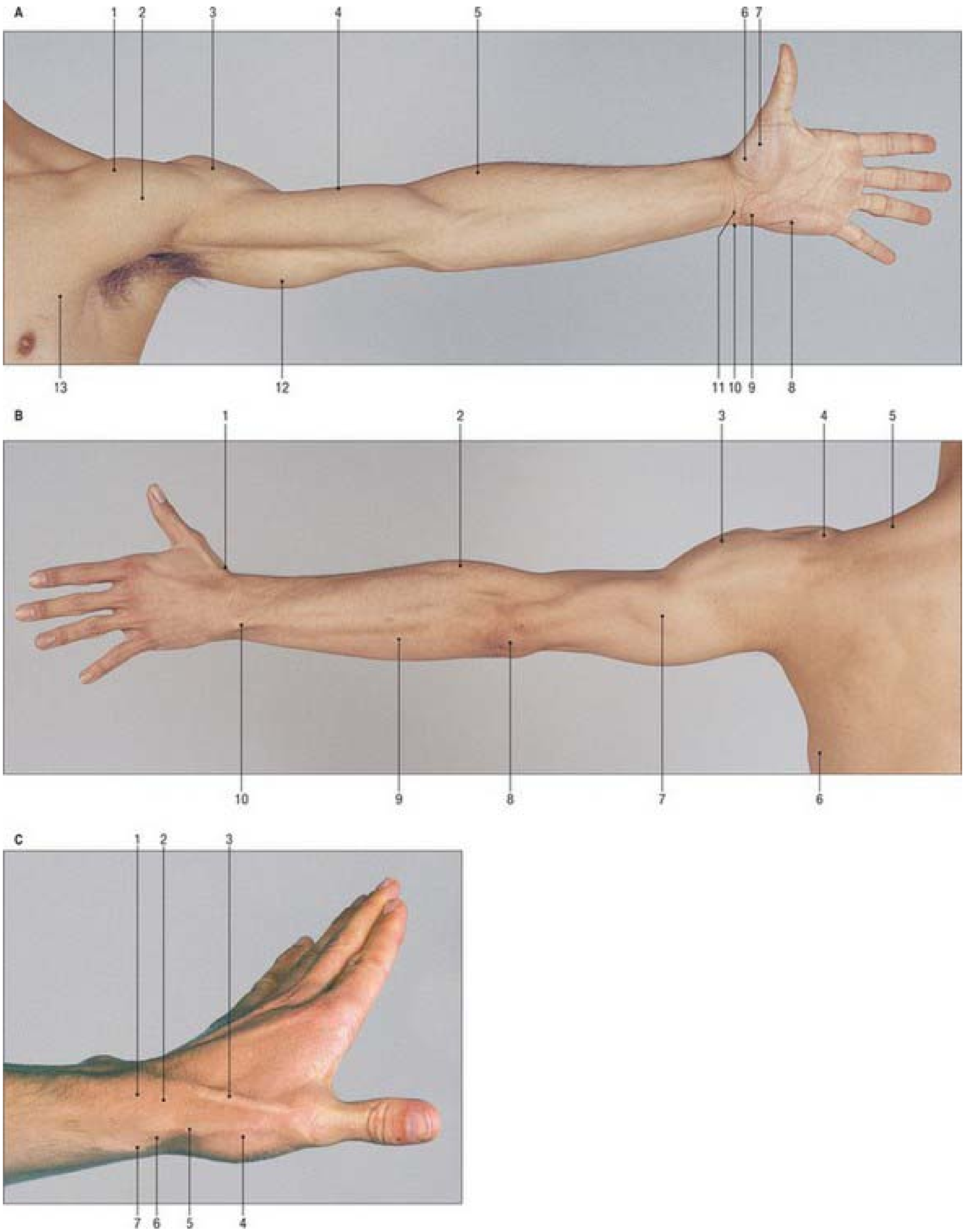
A
1
2
3
4
5
6
7
13
12
11
10
9
8
B
1
2
3
4
5
10
9
8
7
6
C
1
2
3
7
6
5
4

Fig. 45.13 Surface anatomy of left upper limb. **A**, Anterior view of the arm abducted at the shoulder. **1**. Acromion. **2**. Greater tubercle (tuberosity). **3**. Deltoid. **4**. Biceps brachii. **5**. Brachioradialis. **6**. Scaphoid. **7**. Thenar eminence. **8**. Hypothenar eminence. **9**. Triquetrum. **10**. Styloid process of

ulna. **11**. Proximal wrist crease. **12**. Triceps. **13**. Pectoralis major. **B**, Posterior view of the arm abducted at the shoulder. **B**, **1**. Anatomical snuffbox. **2**. Brachioradialis. **3**. Deltoid. **4**. Acromion. **5**. Trapezius. **6**. Latissimus dorsi. **7**. Triceps. **8**. Olecranon process. **9**. Common extensor muscle group. **10**. Extensor carpi ulnaris. **C**, Radial aspect of the distal forearm and wrist to show the anatomical snuffbox. **1**. Tendon of extensor carpi radialis brevis. **2**. Tendon of extensor carpi radialis longus. **3**. Tendon of extensor pollicis longus. **4**. First metacarpal. **5**. Tendon of extensor pollicis brevis. **6**. Tendon of abductor pollicis longus. **7**. Radial styloid.

*(**C** By permission from Lumley JSP 2002 Surface Anatomy, 3rd edn. Edinburgh: Churchill Livingstone.)*

The cephalic vein can be seen in the proximal roof of the snuffbox, and the pulsation of the radial artery can be felt in its depth. The snuffbox is bounded on the radial side by the tendons of abductor pollicis longus laterally and extensor pollicis brevis medially; these tendons lie close to each other. The tendon of extensor pollicis longus lies on the ulnar side of the snuffbox. It stands out conspicuously in full extension of the thumb, and can be seen to extend to the base of the distal phalanx of the thumb. If a finger is run along this tendon proximally, the superficial radial nerve can be rolled from side to side as it crosses the tendon.

The tendons of the radial extensors of the wrist can be identified on the back of the carpus when the fist is alternately clenched and relaxed. The tendons of extensor digitorum can readily be seen on the back of the hand when the fingers are fully extended. When the wrist is extended and deviated to the ulnar side, the tendon of extensor carpi ulnaris may be felt distal to the ulnar styloid as it crosses the wrist. The lateral part of the dorsal aspect of the hand between the index finger and thumb shows a fleshy elevation caused by the first dorsal interosseous: it becomes more conspicuous when the index finger is abducted against resistance. The corresponding anterior aspect of the first web space is formed by adductor pollicis.

The thenar eminence is a fleshy elevation produced by abductor and flexor pollicis brevis, which overlie opponens pollicis. On the medial side of the palm the hypothenar eminence is formed by the corresponding muscles of the little finger but is not so prominent. The medial border of the hand is formed by the medial aspect of the hypothenar eminence. The lateral border of the hand is formed by the dorsal aspect of the metacarpal bone of the thumb, which can be palpated throughout its extent.

VESSELS, PULSES AND NERVES

Arteries

By applying pressure laterally against the shaft of the humerus, the pulsation of the brachial artery can be felt in the furrow along the medial side of biceps and, more superiorly, in the depression posterior to coracobrachialis. In its lower part, the artery can be felt adjacent and posteromedial to the tendon of biceps before it disappears deep to the bicipital aponeurosis. Note that the brachial artery lies medial to the humerus in its upper part, but then lies directly in front of the distal end of the shaft of the bone. The proximity of the artery to a bone against which it can be compressed makes this the favoured site for non-invasive measurement of blood pressure. The median nerve is intimately related to the brachial artery throughout its course in the arm. It is at first lateral to the artery, then half-way along the arm the nerve crosses the artery, usually by passing in front of it, and descends on its medial side into the cubital fossa.

The ulnar artery begins in the midline of the forearm opposite the neck of the radius. In the upper, and deepest, part of its course through the forearm it can be represented by a line which passes downwards and medially across the elevation produced by the superficial flexor muscles of the forearm to reach the radial side of the ulnar nerve at the junction of the upper one-third with the lower two-thirds of the forearm. In the rest of its course, the ulnar artery lies along the radial side of the ulnar nerve.

The radial artery begins opposite the neck of the radius on the medial side of the tendon of biceps. It runs downwards and radially through the forearm to the wrist, where it crosses the anterior margin of the expanded lower end of the radius, passes posteriorly, deep to the tendons of abductor pollicis longus and extensor pollicis brevis, and enters the anatomical snuffbox where its pulsation can be felt. The upper part of its course can be represented by a line that passes deep to the medial part of the elevation produced by brachioradialis on the anterior aspect of the forearm.

The superficial palmar arch is indicated by a horizontal line that is usually 4 cm long at the level of the fully extended and partially abducted thumb. The deep palmar arch is indicated by a horizontal line 4 cm long from a point just distal to the hook of the hamate, and is about 1 cm proximal to the superficial arch.

Pulses, palpation and arterial gases

Brachial artery

The pulsation of the brachial artery can be felt in the furrow along the medial side of biceps and, more superiorly, in the depression posterior to coracobrachialis, by applying pressure laterally against the shaft of the humerus. In its lower part, the artery can be felt adjacent and posteromedial to the tendon of biceps before it disappears deep to the bicipital aponeurosis. This is a useful site at which to pass an arterial catheter for coronary angiography or cardiac catheterization.

Radial artery

The radial pulse is most easily felt on the ventral aspect of the wrist in the interval between the tendon of flexor carpi radialis medially and the lower lateral aspect of the radius. This is the most accessible pulse for palpation under normal clinical circumstances.

Ulnar artery

The pulse of the ulnar artery is usually palpable on deep pressure radial to the tendon of flexor carpi ulnaris at the wrist.

Sites for arterial cannulation

The most useful and commonly used site for cannulation of an artery (for blood pressure monitoring and arterial blood sampling) in the upper limb is the radial artery at the wrist. The presence of the palmar arches, which supply a collateral circulation to the hand, means that thrombosis at this site will not normally jeopardize the circulation of the hand.

The deep branch of the ulnar artery supplies the intrinsic muscles of the thumb via the deep palmar anastomosis. Cannulation should therefore be avoided if the ulnar artery has previously been damaged. An adequate collateral circulation is demonstrated by Allen’s test.

Allen’s test

Allen’s test examines the patency of the radial and ulnar arteries at the wrist and so determines whether each individual artery is sufficient to maintain the arterial supply to the hand in isolation. Both the radial and ulnar arteries are compressed by the examiner’s index and middle fingers of both hands. The forearm is then elevated and the hand exsanguinated by clenching the fist. The hand is then opened while continuing the arterial compression. The palm of the hand appears pale unless there is an anomalous arterial supply, e.g. from a persistent median artery. The brisk return of a normal pink colour to the palmar skin following removal of digital pressure from one of the arteries suggests that that artery is patent and capable of perfusing the hand adequately in isolation. If the palmar skin remains pale, it must be assumed that there is either a distal obstruction to the artery or that this artery cannot adequately perfuse the hand in isolation. The test is then repeated with release of digital pressure on the other artery.

Veins

At the wrist the cephalic vein is situated over the dorsolateral aspect of the lower end of the radius just proximal to the anatomical snuffbox. This is one of the few constantly sited peripheral veins. In the upper arm, the cephalic vein lies in the deltopectoral groove between deltoid and pectoralis major, and then ascends to the infraclavicular fossa, where it pierces the clavipectoral fascia to enter the axillary vein.

The median cubital and basilic veins may be identified in the cubital fossa. They are frequently covered by fat, especially in the female, which makes them difficult to see; however, they are usually palpable, especially if the venous return is occluded proximally by a tourniquet. The median cubital vein usually arises from the cephalic vein 2.5 cm distal to the lateral epicondyle of the humerus and runs upwards and medially to join the basilic vein 2.5 cm above the transverse crease of the elbow. The median vein of the forearm drains the venous plexuses on the palmar surface of the hand. It ascends on the front of the forearm and usually ends in either the basilic vein or the median cubital vein: sometimes it divides just distal to the elbow into two branches, one of which joins the basilic vein and the other the cephalic vein.

The bicipital aponeurosis is crossed by the median cubital vein, which runs medially and proximally from the cephalic vein to join the basilic vein. It may be distended into prominence by applying gentle constriction to the upper arm.

Venepuncture at the elbow

Blood sampling, blood transfusion and intravenous injection are commonly carried out near the elbow or more distally in the forearm: the largest vein is usually the median cubital. The cubital veins are also used for cardiac catheterization.

A high bifurcation of the brachial artery is seen occasionally and may produce an anomalous superficial ulnar artery that descends superficial to the common origin of the forearm flexor muscles. When this occurs, the ulnar artery, although deep to the deep fascia, may lie subcutaneously, either at the elbow or in the upper forearm. It is this anomalous ulnar artery, superficial to the bicipital aponeurosis and immediately deep to the median cubital vein, that is at greatest risk of intra-arterial puncture when the median cubital vein is selected for intravenous injection.

The cephalic vein may be accessed where it lies superficial to the distal end of the radius in the anatomical snuffbox. This site has many advantages for placing an indwelling cannula when a lengthy period is contemplated: the position of the arm, forearm and hand are all optimal for this purpose.

Lymph nodes

Outlying supratrochlear nodes (in reality supra-epicondylar nodes) lie next to the basilic vein. If enlarged, they may be palpated along the line of the vein a few centimetres above the elbow joint.

Nerves

The trunks of the brachial plexus lie in the posterior triangle of the neck in the angle between the clavicle and lower posterior border of sternocleidomastoid, where they are palpable through the skin, platysma and deep fascia.

The initial course of the radial nerve may be indicated on the posterior aspect of the arm. It passes laterally from the start of the brachial artery to the junction of the upper and middle thirds of a line between the lateral epicondyle and deltoid tuberosity, and then continues anteriorly as far as the lateral epicondyle, a finger's breadth to the lateral side of the tendon of biceps. From here its course in the forearm can be mapped out along a line descending vertically to a point on the dorsum of the wrist midway between the head of the ulna and the dorsal tubercle of the radius. The point at which the posterior interosseous nerve winds round the upper end of the radius may be indicated by placing the index finger of the contralateral hand on the dorsal aspect of the head of the radius, and aligning the middle and ring fingers below the index finger. The ring finger then lies over the posterior interosseous nerve. This is an important surgical landmark in making an incision for exposure and removal of a fractured head of radius: the incision should not extend more than a finger's breadth below the head of the radius. The terminal branches of the superficial radial nerve can be palpated in the region of the anatomical snuffbox as they pass over the tendon of extensor pollicis longus.

The median nerve is intimately related to the brachial artery throughout its course in the upper arm. Its course can be marked on the surface by a line from the medial side of the brachial artery in the cubital fossa along the midline of the forearm to the wrist.

The ulnar nerve can be palpated and rolled by the examining fingers as it passes posterior to the medial epicondyle of the humerus. In the forearm its course corresponds to a line drawn from the base of the posterior aspect of the medial epicondyle of the humerus to the radial side of the pisiform and across the hook of the hamate. Deep pressure at these bony landmarks will produce paraesthesia. In the lower part of the forearm the line of the nerve lies along the radial side of the tendon of flexor carpi ulnaris medial to the ulnar artery and its venae comitantes.

Dermatomes

Our knowledge of the extent of individual dermatomes, especially in the limbs, is largely based on clinical evidence. The dermatomes of the upper limb arise from spinal nerves C5–8 and T1: C7 supplies the central part of the hand (Figs 45.14, 45.15). Considerable overlap exists between adjacent dermatomes innervated by nerves derived from consecutive spinal cord segments.

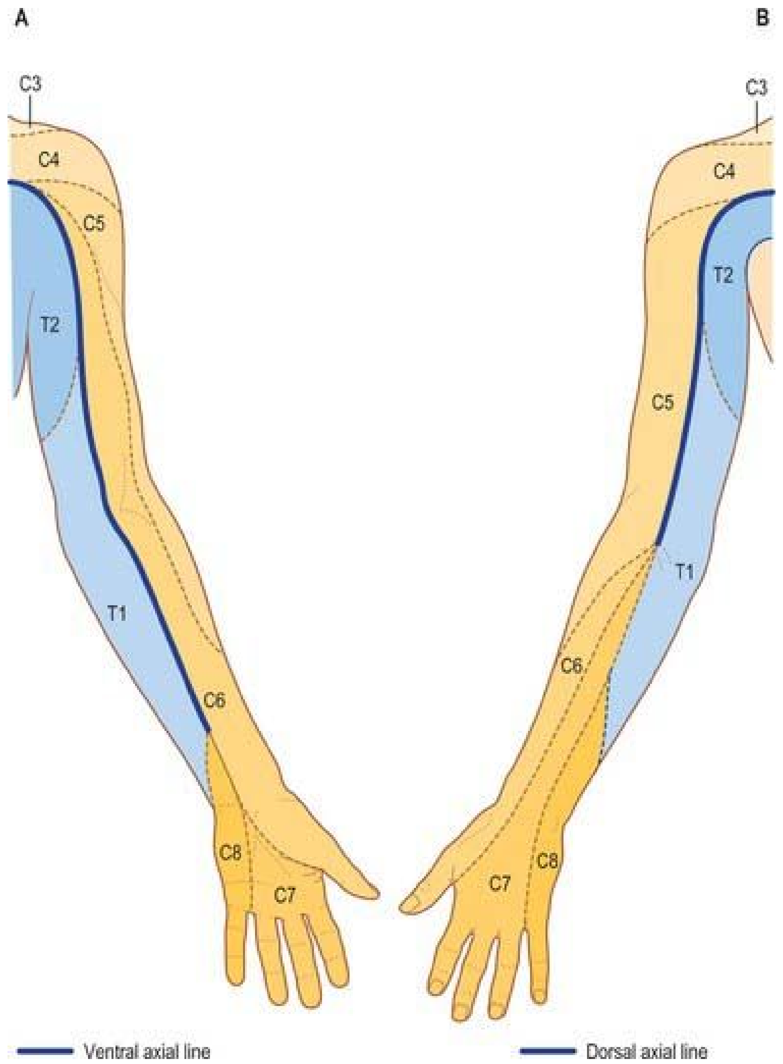
A
B
C3
C4
C5
T2
T1
C6
C8
C7
C3
C4
T2
C5
T1
C6
C8
C7
Ventral axial line
Dorsal axial line

Fig. 45.14 The dermatomes of the left upper limb. Overlap across the axial lines is minimal, whereas overlap is considerable across the interrupted lines. **A**, Viewed from the anterior aspect. **B**, Viewed from the posterior aspect.

(Adapted from Drake, Vogl and Mitchell 2005.)

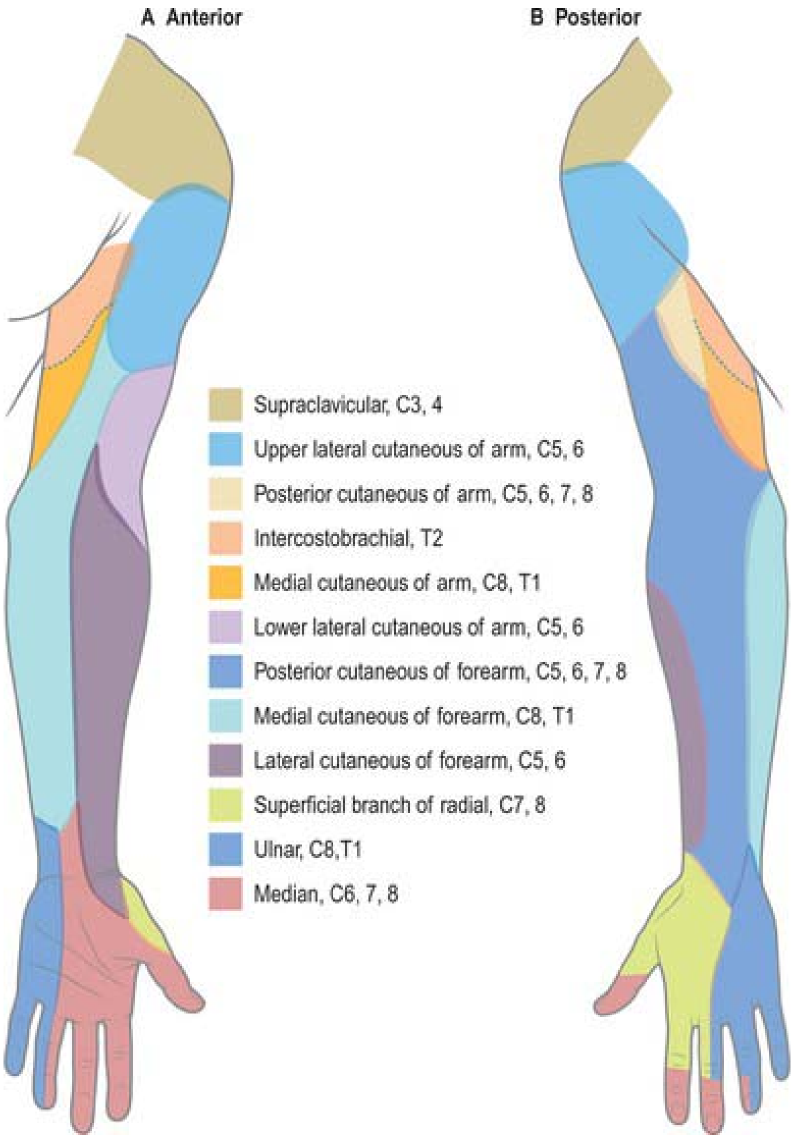

A Anterior
B Posterior
Supraclavicular, C3, 4
Upper lateral cutaneous of arm, C5, 6
Posterior cutaneous of arm, C5, 6, 7, 8
Intercostobrachial, T2
Medial cutaneous of arm, C8, T1
Lower lateral cutaneous of arm, C5, 6
Posterior cutaneous of forearm, C5, 6, 7, 8
Medial cutaneous of forearm, C8, T1
Lateral cutaneous of forearm, C5, 6
Superficial branch of radial, C7, 8
Ulnar, C8,T1
Median, C6, 7, 8

Fig. 45.15 The distribution of skin territories supplied by the cutaneous nerves of the left upper limb. **A**, Viewed from the anterior aspect. **B**, Viewed from the posterior aspect.

Myotomes

The predominant segmental origin of the nerve supply for each of the muscles of the upper limb and for the movements which take place at the joints of the upper limb are summarized in Tables 48.1–48.4.

Reflexes

Biceps jerk (C5, 6)

The elbow is flexed to a right angle and slightly pronated. A finger is placed on the biceps tendon and struck with a percussion hammer: this should elicit flexion and slight supination of the forearm.

Triceps jerk (C6–8)

The arm is supported at the wrist and flexed to a right angle. Triceps is struck with a percussion hammer just proximal to the olecranon: this should elicit extension of the elbow.

Radial jerk (C7, 8)

The radial jerk is a periosteal, not a tendon, reflex. The elbow is flexed to a right angle and the forearm placed in the mid position. The radial styloid is struck with the percussion hammer. This elicits contraction of brachioradialis, which causes flexion of the elbow.

Nerve blocks

Brachial plexus

There are three common approaches to achieve anaesthetic blockade of the brachial plexus: the interscalene, supraclavicular and axillary routes.

The interscalene route requires identification of the interscalene groove. The patient is asked to sniff, an action that involves the scalene muscles as accessory muscles of respiration. A needle is inserted perpendicular to the skin and enters the interscalene groove. Paraesthesia may be elicited, and local anaesthetic solution is injected. There is a risk that some local anaesthetic may move in a retrograde direction and reach the cervical epidural space. The proximal nature of the block means that there is almost always some involvement of the phrenic nerve, and sympathetic block (as evidenced by a Horner’s syndrome) is universal.

The supraclavicular route places local anaesthetic solution in the plane occupied by the trunks of the brachial plexus as they emerge between scalenus anterior and medius on the first rib, immediately posterior to the third part of the subclavian artery. The site of injection is 2 cm above the midpoint of the clavicle. The needle is directed backwards, inwards and downwards to make contact with the upper surface of the first rib. During this procedure the patient will usually complain of paraesthesia down the arm, which indicates that the needle is correctly placed. Preliminary aspiration ensures that a major vessel has not been punctured. If the first rib is missed, there is the risk of producing a pneumothorax. There is often a transient Horner’s syndrome, caused by diffusion of the local anaesthetic towards the stellate ganglion.

The axillary approach blocks the nerves as they group around the axillary artery.

Wrist

Useful anaesthesia of the palm of the hand (except for the lateral surface of the thumb base) can be achieved by blockade of the ulnar and median nerves at the wrist. The ulnar nerve may be blocked via a needle inserted lateral to the tendon of flexor carpi ulnaris at the wrist. The median nerve may be blocked via a needle inserted at the midline between the tendons of palmaris longus and flexor carpi radialis at the level of the proximal wrist crease.

The radial nerve, which supplies the dorsal skin of the hand, may be blocked by injecting local anaesthetic around the subcutaneous dorsoradial border of the wrist, where branches of the nerve can be rolled over the tendon of extensor pollicis longus.

Digital nerve

The digital nerves lie on either side of the flexor sheath in a plane immediately anterior to the phalanx. Therefore the needle should be inserted on either side of the base of the digit, just anterior to the anterolateral margin of the phalanx. A common alternative approach to blocking the digital nerves is via a dorsal skin approach: the needle is inserted through the dorsal skin on either side of the base of the proximal phalanx and advanced towards the volar location of the digital nerves while continually infusing the local anaesthetic agent. This is thought to be less painful than the volar approach because the dorsal skin is less sensitive than the volar skin.

CHAPTER 46

Pectoral girdle, shoulder region and axilla

SKIN AND SOFT TISSUE

SKIN

Cutaneous vascular supply

The area over the lateral end of the clavicle is supplied by the supraclavicular artery which pierces the deep fascia superior to the clavicle and anterior to trapezius (Fig. 45.4). In the majority of cases this artery arises from the superficial cervical/transverse cervical artery, but it occasionally arises from the suprascapular artery. The area over the deltoid is supplied by the anterior and posterior circumflex humeral arteries. The deltoid branch of the thoraco-acromial axis contributes to the blood supply of the anterior aspect of the shoulder via musculocutaneous perforators through deltoid. For details of the cutaneous supply to the anterior, lateral and posterior chest wall see page 915.

Cutaneous innervation

The segmental supply is described in Chapter 45, page 789. The cutaneous supply to the shoulder region comes from the supraclavicular nerves (p. 436, Fig. 45.15). The floor of the axilla together with part of the upper medial aspect of the arm is supplied by the intercostobrachial nerve (lateral branch of the second intercostal nerve). Occasionally the lateral branch of the third intercostal nerve contributes to the supply of skin in the floor of the axilla. The upper lateral cutaneous nerve of the arm supplies the skin over the inferolateral part of the shoulder.

SOFT TISSUE

Deep fascia

Fascia over deltoid

The deep fascia over deltoid sends numerous septa between its fasciculi and is continuous with the pectoral fascia in front and the thick and strong infraspinous fascia behind. Above it is attached to the clavicle, acromion and crest of the scapular spine; below it is continuous with the brachial fascia.

Subscapular fascia

The subscapular fascia is a thin aponeurosis attached to the entire circumference of the subscapular fossa; subscapularis itself is partly attached to its deep surface.

Supraspinous fascia

The supraspinous fascia completes the osseofibrous compartment in which supraspinatus is attached. It is thick medially, but thinner laterally under the coraco-acromial ligament. It is attached to the scapula around the boundaries of the attachment of supraspinatus.

Infraspinous fascia

The infraspinous fascia covers infraspinatus and is attached to the margins of the infraspinous fossa. The fascia is continuous with the deltoid fascia along the overlapping posterior border of deltoid.

Pectoral and axillary fascia

The pectoral fascia is a thin lamina which covers pectoralis major and extends between its fasciculi. It is attached medially to the sternum, above to the clavicle and is continuous inferolaterally with the fascia of the shoulder, axilla and thorax. Although thin over pectoralis major, it is thicker between this muscle and latissimus dorsi, and forms the floor of the axilla as the axillary fascia. The latter divides at the lateral margin of latissimus dorsi into two layers, which ensheathe the muscle and are attached behind to the spines of the thoracic vertebrae. As the fascia leaves the lower edge of pectoralis major to cross the axilla, a layer ascends under cover of the muscle and splits to envelop pectoralis minor: it becomes the clavipectoral fascia at the upper edge of pectoralis minor. The hollow of the armpit is produced mainly by the action of this fascia in tethering the skin to the floor of the axilla, and it is sometimes referred to as the suspensory ligament of the axilla. The axillary fascia is pierced by the tail of the breast (Ch. 54).

Clavipectoral fascia

The clavipectoral fascia is a strong fibrous sheet behind the clavicular part of pectoralis major. It fills the gap between pectoralis minor and subclavius, and covers the axillary vessels and nerves. It splits around subclavius and is attached to the clavicle both anterior and posterior to the groove for subclavius. The posterior layer fuses with the deep cervical fascia which connects omohyoid to the clavicle and with the sheath of the axillary vessels. Medially it blends with the fascia over the first two intercostal spaces and is attached to the first rib, medial to subclavius. Laterally, it is thick and dense, and is attached to the coracoid process, blending with the coracoclavicular ligament. Between the first rib and coracoid process the fascia often thickens to form a band, the costocoracoid ligament. Below this the fascia becomes thin, splits around pectoralis minor and descends to blend with the axillary fascia and laterally with the fascia over the short head of biceps. The cephalic vein, thoraco-acromial artery and vein, and lateral pectoral nerve pass through the fascia.

Spread of infection

When axillary suppuration occurs the local fascial arrangement affects the spread of pus. Suppuration may be superficial or deep to the clavipectoral fascia, either between the pectoral muscles or behind pectoralis minor. In the former, an abscess would appear at the edge of the anterior axillary fold or the groove between deltoid and pectoralis major; in the latter, pus would tend to surround vessels and nerves and ascend into the neck, the direction of least resistance. Pus may also track along vessels into the arm. When an axillary abscess is incised, the knife should enter the axillary ‘base’, midway between the anterior and posterior margins and near the thoracic side to avoid the lateral thoracic, subscapular and axillary vessels on the anterior, posterior and lateral walls respectively.

BONE

CLAVICLE

The clavicle lies almost horizontally at the root of the neck and is subcutaneous throughout its whole extent (Fig. 46.1). It acts as a prop which braces back the shoulder and enables the limb to swing clear of the trunk and transmits part of the weight of the limb to the axial skeleton. The lateral or acromial end of the bone is flattened and articulates with the medial side of the acromion, whereas the medial or sternal end is enlarged and articulates with the clavicular notch of the manubrium sterni and first costal cartilage. The shaft is gently curved and in shape resembles the italic letter *f*, being convex forwards in its medial two-thirds and concave forwards in its lateral third. The inferior aspect of the intermediate third is grooved in its long axis. The clavicle is trabecular internally, with a shell of much thicker compact bone in its shaft. Although elongated, the clavicle is unlike typical long bones in that it usually has no medullary cavity.

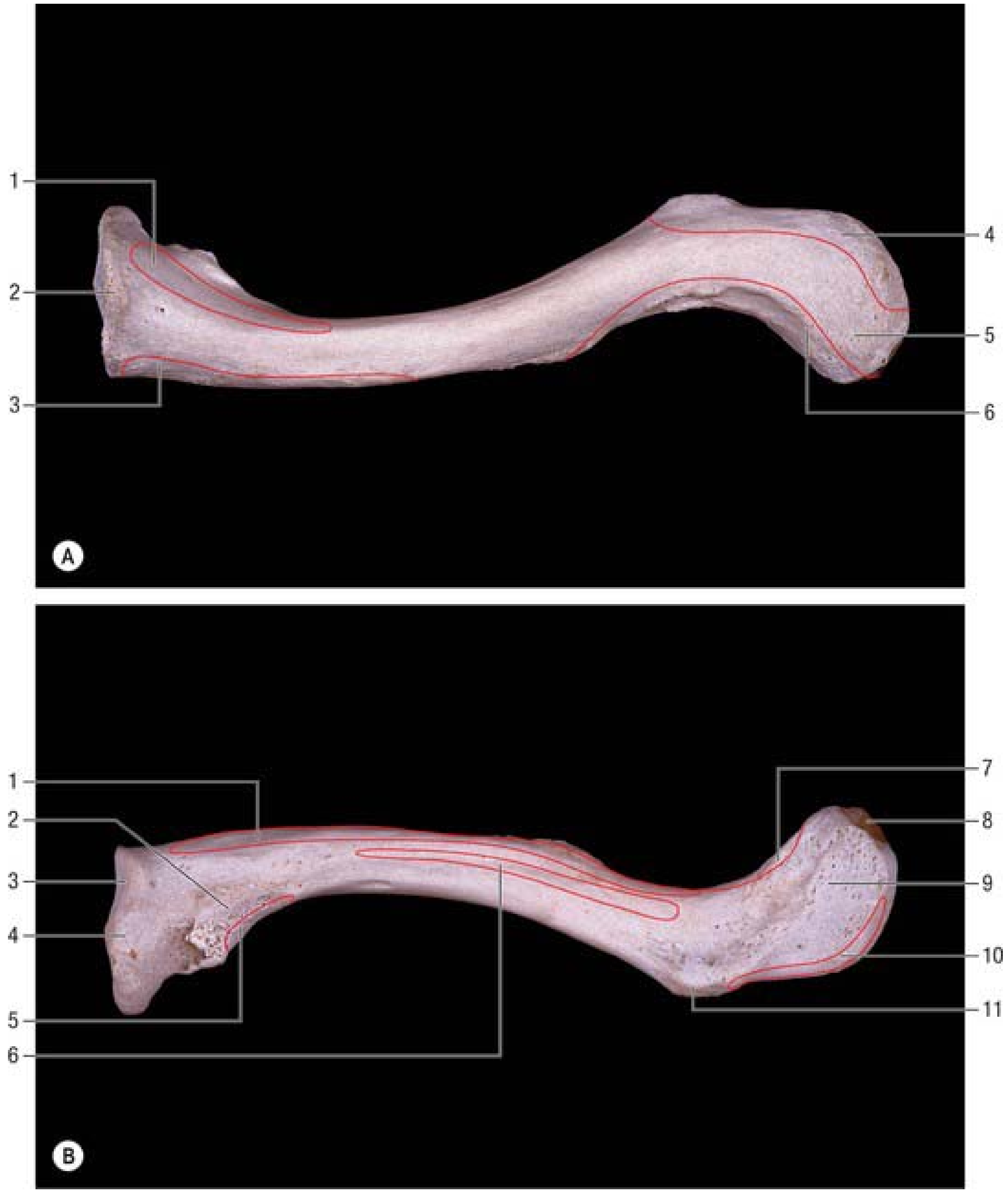

Fig. 46.1 **A**, Superior view of left clavicle. **B**, Inferior view of left clavicle. **A:** **1**. Sternocleidomastoid (clavicular head). **2**. Sternal end. **3**. Pectoralis major. **4**. Trapezius. **5**. Acromial end. **6**. Deltoid. **B:** **1**. Pectoralis major. **2**. For costoclavicular ligament. **3**. For first costal cartilage. **4**. For sternum. **5**. Sternohyoid. **6**. Subclavius. **7**. Deltoid. **8**. For acromion. **9**. Trapezoid line. **10**. Trapezius. **11**. Conoid tubercle.

The female clavicle is shorter, thinner, less curved and smoother, and its acromial end is carried lower than the sternal in comparison with the male. In males the acromial end is on a level with, or slightly higher than, the sternal end when the arm is pendent. Midshaft circumference is the most reliable single indicator of sex: a combination of this measurement with weight and length yields better results. The clavicle is thicker and more curved in manual workers, and its ridges for muscular attachment are better marked.

Lateral third

The lateral third of the clavicle is flattened and has a superior and an inferior surface, limited by an anterior and a posterior border. The anterior border is concave, thin and roughened and may be marked by a small deltoid tubercle.

The posterior border, also roughened by muscular attachments, is convex backwards. The superior surface is roughened near its margins but is smooth centrally, where it can be felt through the skin. The inferior surface presents two obvious markings. Close to the posterior border, at the junction of the lateral fourth with the rest of the bone, there is a prominent conoid tubercle which gives attachment to the conoid part of the coracoclavicular ligament. A narrow, roughened strip, the trapezoid line, runs forwards and laterally from the lateral side of this tubercle, almost as far as the acromial end (Fig. 46.1B). The trapezoid part of the coracoclavicular ligament is attached to it. A small oval articular facet, for articulation with the medial aspect of the acromion, faces laterally and slightly downwards at the lateral end of the shaft.

Subclavius lies in a groove on the inferior surface (Fig. 46.1B). The clavipectoral fascia is attached to the edges of the groove; the posterior edge of the groove runs to the conoid tubercle, where fascia and conoid ligament merge. Lateral to the groove there is a laterally inclined nutrient foramen. Deltoid (anterior) and trapezius (posterior) are attached to the lateral third of the shaft: both muscles reach the superior surface. The coracoclavicular ligament, which is attached to the conoid tubercle and trapezoid line (Fig. 46.1B), transmits the weight of the upper limb to the clavicle, counteracted by trapezius which supports its lateral part. From the conoid tubercle this weight is transmitted through the medial two-thirds of the shaft to the axial skeleton.

The clavicle is often fractured, commonly by indirect forces, as a result of a violent impact to the hand or shoulder. The break is usually at the junction of the lateral and intermediate thirds, where the curvature changes, for this is the weakest part of the bone. A fracture medial to the conoid tubercle interrupts weight transmission from the arm to the axial skeleton. The resulting deformity is caused by the weight of the arm, which acts on the lateral fragment through the coracoclavicular ligament and draws it downwards. The medial fragment, as a rule, is a little displaced.

Medial two-thirds

The medial two-thirds of the shaft of the clavicle is cylindrical or prismoid in form and possesses four surfaces, but the inferior surface is often reduced to a mere ridge. The anterior surface is roughened over most of its extent but it is smooth and rounded at its lateral end, where it forms the upper boundary of the infraclavicular fossa. The upper surface is roughened in its medial part and smooth at its lateral end. The posterior surface is smooth and featureless. The inferior surface is marked, near the sternal end, by a roughened oval impression, which is often depressed below the surface. Its margins give attachment to the costoclavicular ligament, which connects the clavicle to the upper surface of the first rib and its cartilage. Rarely, this area is smooth or raised to form an eminence which may articulate with the upper surface of the first rib by means of a synovial joint. There is a groove in the long axis of the bone in the lateral half of the posterior surface.

The medial two-thirds provide attachment, anteriorly, for the clavicular head of pectoralis major: the area is usually clearly indicated on the bone. The clavicular head of sternocleidomastoid is attached to the medial half of the superior surface, but the marking on the bone is not very conspicuous. The smooth, posterior surface is devoid of muscular attachments except at its lower part immediately adjoining the sternal end, where the lateral fibres of sternohyoid are attached. Medially, this surface is related to the lower end of the internal jugular vein (from which it is separated by sternohyoid), the termination of the subclavian vein, and the start of the brachiocephalic vein. More laterally, it arches in front of the trunks of the brachial plexus and the third part of the subclavian artery. The suprascapular vessels are related to the upper part of this surface. The inferior surface gives insertion to subclavius in the subclavian groove: the clavipectoral fascia, which encloses subclavius, is attached to the edges of the groove. The posterior lip of the groove runs into the conoid tubercle and carries the fascia into continuity with the conoid ligament. A nutrient foramen is found in the lateral end of the groove, running in a lateral direction: the nutrient artery is derived from the suprascapular artery. The impression for the costoclavicular ligament is very variable in its character.

Sternal end

The sternal end of the clavicle is directed medially, and a little downwards and forwards, to articulate with the clavicular notch of the manubrium sterni. The sternal surface, usually irregular and pitted, is quadrangular (sometimes triangular). Its uppermost part is slightly roughened for attachment of the interclavicular ligament, sternoclavicular capsule and articular disc. Elsewhere the surface is smooth and articular and it extends onto the inferior surface for a short distance, where it articulates with the first costal cartilage. The sternal end of the clavicle projects upwards beyond the manubrium sterni and can be felt without difficulty and usually seen (a prominent clinical landmark), in the lateral wall of the jugular fossa.

Ossification

The clavicle begins to ossify before any other bone in the body, and is ossified from three centres. The shaft of the bone is ossified in condensed mesenchyme from two primary centres, medial and lateral, which appear between the fifth and sixth weeks of intrauterine life, and fuse about the 45th day. Cartilage then develops at both ends of the clavicle. The medial cartilaginous mass contributes more to growth in length than does the lateral mass: the two centres of ossification meet between the middle and lateral thirds of the clavicle. A secondary centre for the sternal end appears in late teens, or even early twenties, usually 2 years earlier in females (Fig. 46.2). Fusion is probably rapid but reliable data are lacking. An acromial secondary centre sometimes develops at around 18 to 20 years, but this epiphysis is always small and rudimentary and rapidly joins the shaft.

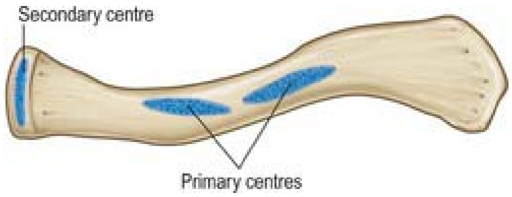

Fig. 46.2 The three constant centres of ossification of the clavicle.

The clavicle does not ossify exclusively by intramembranous ossification. In 14 mm embryos the clavicle is a band of condensed mesenchyme between the acromion and apex of the first rib, which is continuous with the sternal rudiment. Medial and lateral zones of early cartilage transformation (‘precartilage’) occur within this band, and intramembranous centres of ossification appear, and soon fuse, in the mesenchyme between them. Sternal and acromial zones soon become true cartilage into which ossification extends from the shaft. Length increases by interstitial growth of these terminal cartilages; the latter develop zones of hypertrophy, calcification and advancing endochondral ossification like other growth cartilages. Diameter increases by subperichondral deposition in the extremities and subperiosteal deposition in the shaft. Epiphyses are endochondral and probably fuse in the same way as they do in long bones. Defects of ossification in the clavicle and those cranial bones which ossify by intramembranous ossification occasionally coincide, e.g. in cleidocranial dysostosis.

SCAPULA

The scapula is a large, flat, triangular bone which lies on the posterolateral aspect of the chest wall, covering parts of the second to seventh ribs (Fig. 46.3, Fig. 46.4). It has costal and dorsal surfaces, superior, lateral and medial borders, inferior, superior and lateral angles, and three processes, the spine, its continuation the acromion and the coracoid process. The lateral angle is truncated and bears the glenoid cavity for articulation with the head of the humerus. This part of the bone may be regarded as the head, and it is connected to the plate-like body by an inconspicuous neck. The long axis of the scapula is nearly vertical and the relatively featureless costal surface can easily be distinguished from the dorsal surface, which is interrupted by the shelf-like projection of the spine (Fig. 46.3A). The bone is very much thickened in the immediate neighbourhood of the lateral border, which runs from the inferior angle below, to the glenoid cavity above. The main processes, and thicker parts of the scapula, contain trabecular bone; the rest consists of a thin layer of compact bone. The central supraspinous fossa and the greater part of the infraspinous fossa are thin and even translucent; occasionally the bone in them is deficient, and the gaps are filled by fibrous tissue.

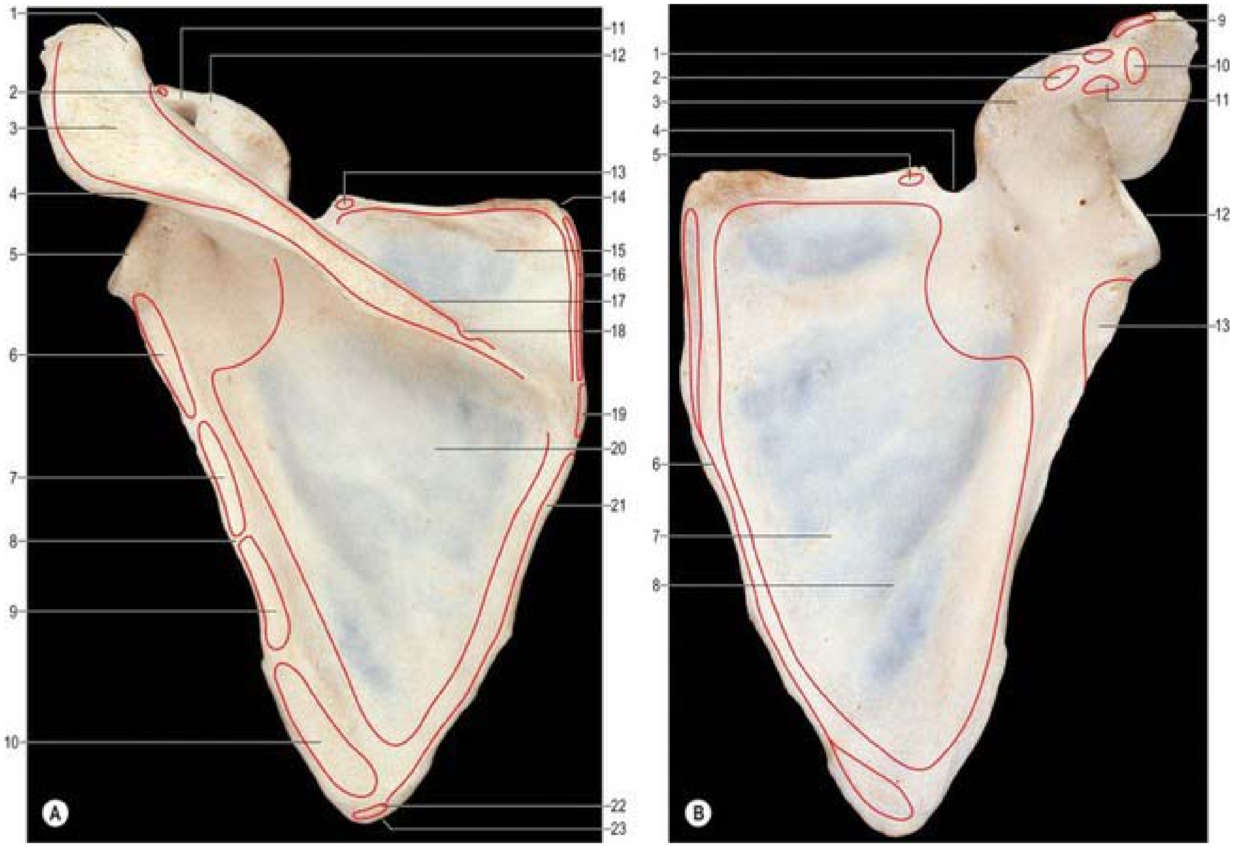

Fig. 46.3 **A**, Posterior aspect of left scapula. **1**. Clavicular facet. **2**. Biceps (short head). **3**. Acromion. **4**. Deltoid. **5**. Glenoid fossa. **6**. Triceps brachii (long head). **7 and 9**. Teres minor. **8**. Groove for circumflex scapular artery. **10**. Teres major. **11**. Conoid tubercle. **12**. Coracoid process. **13**. Omohyoid (inferior belly). **14**. Superior angle. **15**. Supraspinatus. **16**. Levator scapulae. **17**. Spine. **18**. Trapezius. **19**. Rhomboid minor. **20**. Infraspinatus. **21**. Rhomboid major. **22**. Latissimus dorsi. **23**. Inferior angle. **B**, Anterior aspect of left scapula. **1**. Trapezoid ligament attachment. **2**. Conoid ligament attachment. **3**. Acromion process. **4**. Suprascapular notch. **5**. Omohyoid (inferior belly). **6**. Serratus anterior. **7**. Subscapularis. **8**. Ridge for intermuscular tendon of subscapularis. **9**. Deltoid. **10**. Biceps (short head) and coracobrachialis. **11**. Pectoralis minor. **12**. Glenoid fossa. **13**. Triceps (long head).

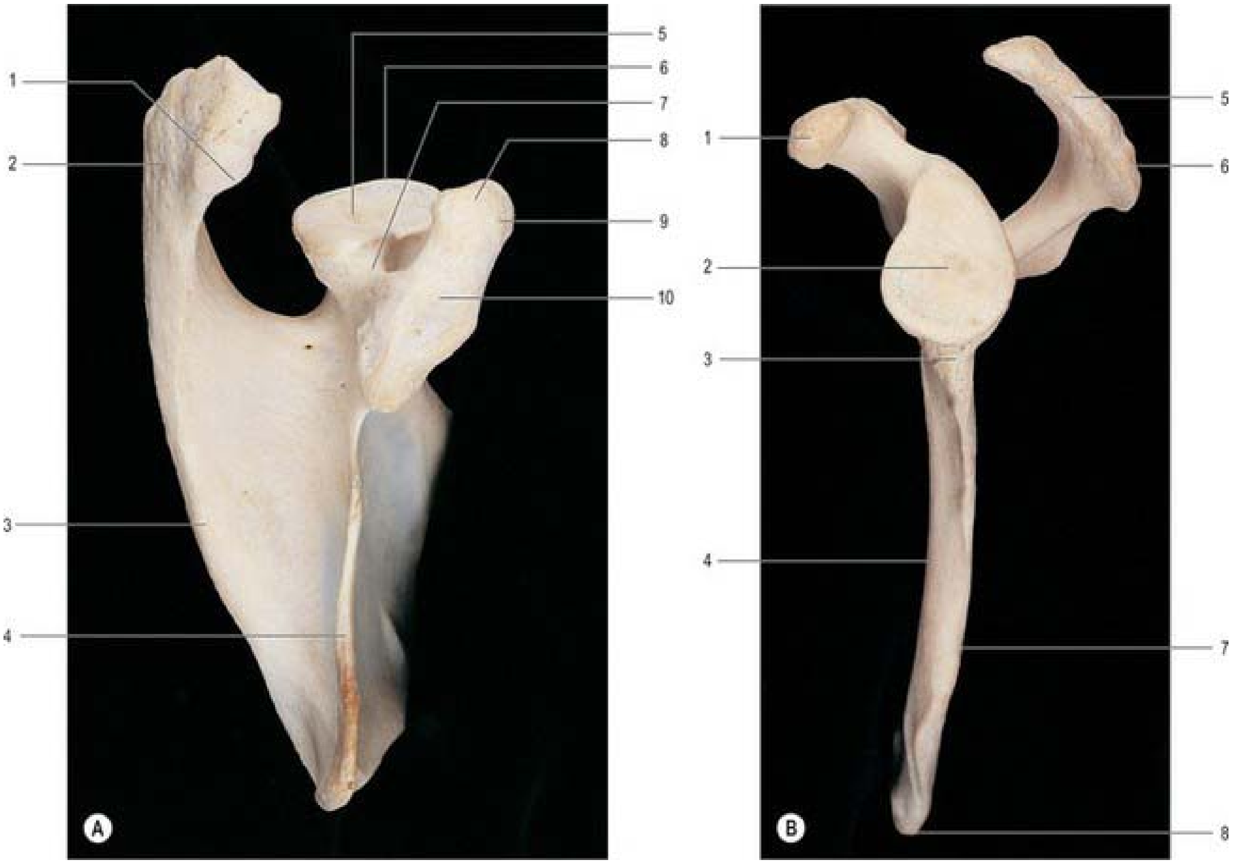

Fig. 46.4 **A**, Superior aspect of left scapula. **1**. Facet for clavicle. **2**. Acromial process. **3**. Spine. **4**. Superior border. **5**. Head. **6**. Glenoid fossa. **7**. Neck. **8**. Conoid tubercle (for conoid ligament). **9**. Coracoid process. **10**. Trapezoid ligament attachment. **B**, Lateral aspect of left scapula. **1**. Coracoid process. **2**. Glenoid fossa. **3**. Infraglenoid tubercle for long head of triceps. **4**. Ventral surface. **5**. Acromion. **6**. Acromial angle. **7**. Lateral border. **8**. Inferior angle.

The inferior angle lies over the seventh rib, or over the seventh intercostal space. It can be felt through the skin and the muscles which cover it and, when the arm is raised above the head, it can be seen to pass forwards round the chest wall. The superior angle is placed at the junction of the superior and medial borders, and is obscured by the muscles which cover it. The lateral angle is truncated and broadened. It constitutes the head of the bone. On its free surface it bears the glenoid cavity for articulation with the head of the humerus in the shoulder joint. Very gently hollowed out, the glenoid forms a poor socket for the humeral head. It is narrow above and wider below, and is pear-shaped in outline. Immediately above the glenoid cavity a small, roughened area encroaches on the root of the coracoid process and is termed the supraglenoid tubercle. The neck of the scapula is the constriction immediately adjoining the head. It can be identified most easily on its inferior and dorsal aspects. Ventrally, it can be regarded as extending between the infraglenoid tubercle and the anterior margin of the suprascapular notch.

Costal surface

The costal surface, which is directed medially and forwards when the arm is by the side, is slightly hollowed out, especially in its upper part (Fig. 46.3B).

Near the lateral border there is a longitudinal rounded ridge, prominent near the neck, but less so below, which is separated from the lateral border by a narrow grooved area.

Subscapularis arises from nearly the whole of the costal surface, including the grooved area immediately adjoining the lateral border, but excluding the area next to the neck of the bone. Small intramuscular tendons are attached to the roughened ridges which subdivide this surface incompletely into a number of smooth areas. The anterior aspect of the neck is separated from subscapularis by a bursal protrusion of the synovial membrane of the shoulder joint (subscapular ‘bursa’). The lower five or six digitations of serratus anterior are attached to an oval area near the inferior angle. The remainder of the muscle is inserted into a narrow strip along the ventral aspect of the medial border, which is wider above, where it receives the large first digitation. The longitudinal thickening of the bone near the lateral border provides a lever of the necessary strength to withstand the pull of serratus anterior on the inferior angle during lateral scapular rotation, when the glenoid cavity is turned to face more directly upwards as the arm is raised from the side and carried above the head against gravity.

Dorsal surface

The dorsal surface is divided by the shelf-like spine of the scapula into a small upper and a large lower area, which are confluent at the spinoglenoid notch between the lateral border of the spine and the dorsal aspect of the neck (Fig. 46.3A).

Supraspinatus is attached to the medial two-thirds of the supraspinous fossa on the dorsal surface: the fascia which covers the muscle is attached to the margins of the fossa. Teres minor is attached to the upper two-thirds of a flattened strip which adjoins the lateral border. The strip is grooved near its upper end by the circumflex scapular vessels, which pass between teres minor and the bone as they enter the infraspinous fossa. The lower limit of the attachment of teres minor is indicated by an oblique ridge, which runs from the lateral border to the neighbourhood of the inferior angle and cuts off a somewhat oval area where teres major is attached. The dorsal aspect of the inferior angle may give origin to a small slip which joins the deep surface of latissimus dorsi. The infraspinous fossa is hollowed out laterally but is convex medially. Infraspinatus is attached to the infraspinous fossa, with the exception of an area near the neck of the bone. The strong infraspinatus fascia passes onto teres minor and teres major, and sends fascial partitions between them which reach the bone along the ridges which mark the limits of their attachments.

Superior border

The superior border, thin and sharp, is the shortest. At its anterolateral end it is separated from the root of the coracoid process by the suprascapular notch (Fig. 46.3B). Near the suprascapular notch it gives origin to the inferior belly of omohyoid. The notch is bridged by the superior transverse ligament which is attached laterally to the root of the coracoid process and medially to the limit of the notch. The ligament is sometimes ossified. The foramen, thus completed, transmits the suprascapular nerve to the supraspinous fossa, whereas the suprascapular vessels pass backwards above the ligament.

Lateral border

The lateral border of the scapula forms a clearly defined, sharp, roughened ridge, which runs sinuously from the inferior angle to the glenoid cavity. At its upper end it widens into a rough, somewhat triangular area, which is termed the infraglenoid tubercle (Fig. 46.4B). The lateral border separates the attachments of subscapularis and teres minor and major. These muscles project beyond the bone and, with latissimus dorsi, cover it so completely that it cannot be felt through the skin. The long head of triceps is attached to the infraglenoid tubercle.

The grooved part of the costal surface, the narrow flat lateral strip of the dorsal surface and the adjacent thickened ridge (Fig. 46.4B), are often included in the 'lateral border' during clinical examination.

Medial border

The medial border of the scapula extends from the inferior to the superior angle. In its lower two-thirds this border can easily be felt through the skin, but its upper third is more deeply placed and cannot be palpated. It is thin and often angled opposite the root of the spine. Levator scapulae is attached to a narrow strip, extending from the superior angle to the root of the spine, and rhomboid minor is attached below this, opposite the root of the spine. Rhomboid major is attached to the remainder of the border.

Scapular angles

The inferior angle overlies the seventh rib or intercostal space. Palpable through the skin and covering muscles, it is also visible as it advances round the thoracic wall when the arm is raised. It is covered on its dorsal aspect by the upper border of latissimus dorsi, a small slip from which is frequently attached to the inferior angle. The superior angle, at the junction of the superior and medial borders, is obscured by the upper part of trapezius. The lateral angle, truncated and broad, bears the glenoid cavity which articulates with the head of the humerus at the glenohumeral joint. It provides a shallow, and limited, socket for the humeral head. Its outline is piriform, narrower above (Fig. 46.4B). The glenohumeral ligaments are attached to its anterior margin. When the arm is by the side, the cavity is directed forwards, laterally and slightly upwards. When the arm is raised above the head it is directed almost straight upwards. Just above it a small rough supraglenoid tubercle encroaches on the root of the coracoid process. The anatomical neck, the constriction adjoining the rim of the glenoid cavity, is most distinct at its inferior and dorsal aspects. Anteriorly and posteriorly it extends between the infraglenoid and supraglenoid tubercles, passing lateral to the root of the coracoid process. The long head of biceps brachii is attached to the supraglenoid tubercle, and the long head of triceps brachii is attached to the infraglenoid tubercle.

Spine of the scapula

The spine of the scapula forms a shelf-like projection on the upper part of the dorsal surface of the bone, and is triangular in shape (Fig. 46.3A). Its lateral border is free, thick and rounded and helps to bound the spinoglenoid notch, which lies between it and the dorsal surface of the neck of the bone. Its anterior border joins the dorsal surface of the scapula along a line which runs laterally and slightly upwards from the junction of the upper and middle thirds of the medial border. The plate-like body of the bone is bent along this line, which accounts for the concavity of the upper part of the costal surface. The dorsal border is the crest of the spine, and is subcutaneous throughout nearly its whole extent. At its medial end the crest expands into a smooth, triangular area. Elsewhere the upper and lower edges and the surface of the crest are roughened for muscular attachments. The upper surface of the spine widens as it is traced laterally, and is slightly hollowed out. Together with the upper area of the dorsal surface of the bone, the upper surface of the spine forms the supraspinous fossa. The lower surface is overhung by the crest at its medial, narrow end, but is gently convex in its wider, lateral portion. Together with the lower area of the dorsal surface of the bone, the lower surface of the spine forms the infraspinous fossa, which communicates with the supraspinous fossa through the spinoglenoid notch.

Supra- and infraspinatus are attached to the upper and lower surfaces of the spine of the scapula, respectively. The flattened triangular area at its root lies opposite the spine of the third thoracic vertebra and is covered by the tendon of trapezius; a bursa intervenes to enable the tendon to play over this part of the bone. The posterior fibres of deltoid are attached to the lower border of the crest. The middle fibres of trapezius are attached to the upper border of the crest, and the lowest fibres of trapezius terminate in a flat triangular tendon which glides over the smooth area at the base of the spine and inserts into a rough prominence, erroneously called the deltoid tubercle, on the dorsal or subcutaneous aspect of the spine near its medial end.

Acromion

The acromion projects forwards, almost at right angles, from the lateral end of the spine, with which it is continuous. The lower border of the crest of the spine becomes continuous with the lateral border of the acromion at the acromial angle, which forms a subcutaneous, bony landmark. The medial border of the acromion is short and is marked anteriorly by a small, oval facet, directed upwards and medially, for articulation with the lateral end of the clavicle. The lateral border, tip and upper surface of the acromion can all be felt through the skin without difficulty. There may be an accessory articular facet on the inferior surface of the acromion.

The acromion is subcutaneous over its dorsal surface, being covered only by the skin and superficial fascia. The lateral border, which is thick and irregular, and the tip of the process, as far round as the clavicular facet, give origin to the middle fibres of deltoid. The medial aspect of the tip gives attachment, below deltoid, to the lateral end of the coraco-acromial ligament. The articular capsule of the acromioclavicular joint is attached around the margins of the clavicular facet. Behind the facet, the medial border of the acromion gives insertion to the horizontal fibres of trapezius. The inferior aspect of the acromion is relatively smooth, and together with the coraco-acromial ligament and the coracoid process forms a protective arch over the shoulder joint. The tendon of supraspinatus passes below the overhanging acromion and is separated from it and from deltoid by the subacromial bursa.

Coracoid process

The coracoid process arises from the upper border of the head of the scapula and is bent sharply so as to project forwards and slightly laterally (Fig. 46.3B, Fig. 46.4A). When the arm is by the side, the coracoid process points almost straight forwards and its slightly enlarged tip can be felt through the skin, although it is covered by the anterior fibres of deltoid. The supraglenoid tubercle marks the root of the coracoid process where it adjoins the upper part of the glenoid cavity. There is another impression on the dorsal aspect of the coracoid process at the point where it changes direction: it gives attachment to the conoid part of the coracoclavicular ligament.

The coracoid process lies about 2.5 cm below the clavicle at the junction of the lateral fourth with the rest of the bone and is connected to its under surface by the coracoclavicular ligament. It is covered by the anterior fibres of deltoid and can be identified only on deep pressure through the lateral border of the infraclavicular fossa. The attachment of the conoid part of the ligament has already been considered: the trapezoid part is attached to the upper aspect of the horizontal part of the process. Pectoralis minor is attached to the superior aspect of the coracoid process. The wider, medial end of the coraco-acromial ligament and, below that, the coracohumeral ligament, are attached to the lateral border. Coracobrachialis is attached to the medial side of the tip of the process, and the short head of biceps is attached to the lateral side of the tip. The inferior aspect of the process is smooth and helps to complete the coraco-acromial arch.

Ligaments

The main scapular ligaments are the coracoacromial and superior transverse scapular; there may also be a weaker, variable inferior transverse scapular (spinoglenoid) ligament (see below Fig. 46.13, see below Fig. 46.14).

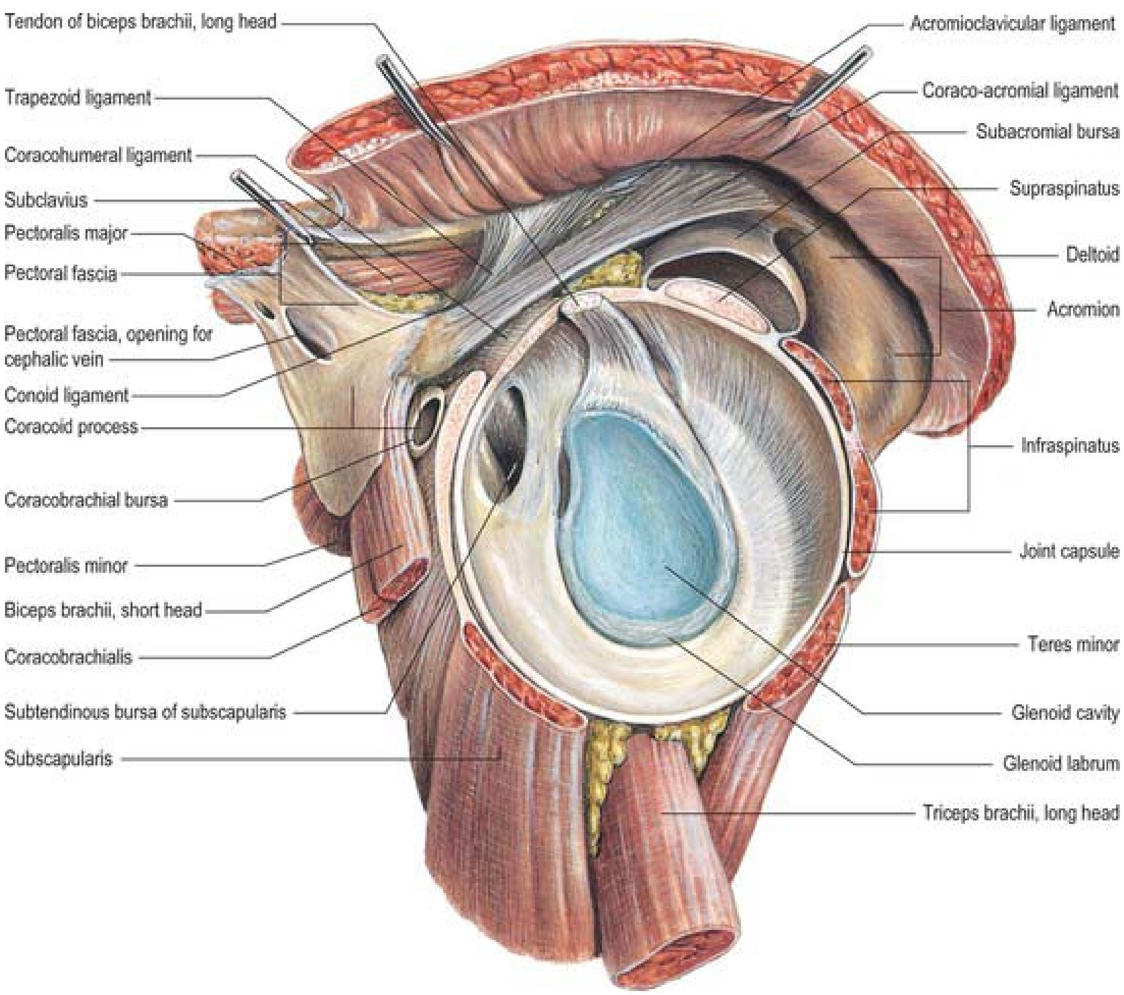
Tendon of biceps brachii, long head
Trapezoid ligament
Coracohumeral ligament
Subclavius
Pectoralis major
Pectoral fascia
Pectoral fascia, opening for cephalic vein
Conoid ligament
Coracoid process
Coracobrachial bursa
Pectoralis minor
Biceps brachii, short head
Coracobrachialis
Subtendinous bursa of subscapularis
Subscapularis
Acromioclavicular ligament
Coraco-acromial ligament
Subacromial bursa
Supraspinatus
Deltoid
Acromion
Infraspinatus
Joint capsule
Teres minor
Glenoid cavity
Glenoid labrum
Triceps brachii, long head

Fig. 46.13 Interior of the left shoulder joint: anterolateral aspect.

(From Sobotta 2006.)

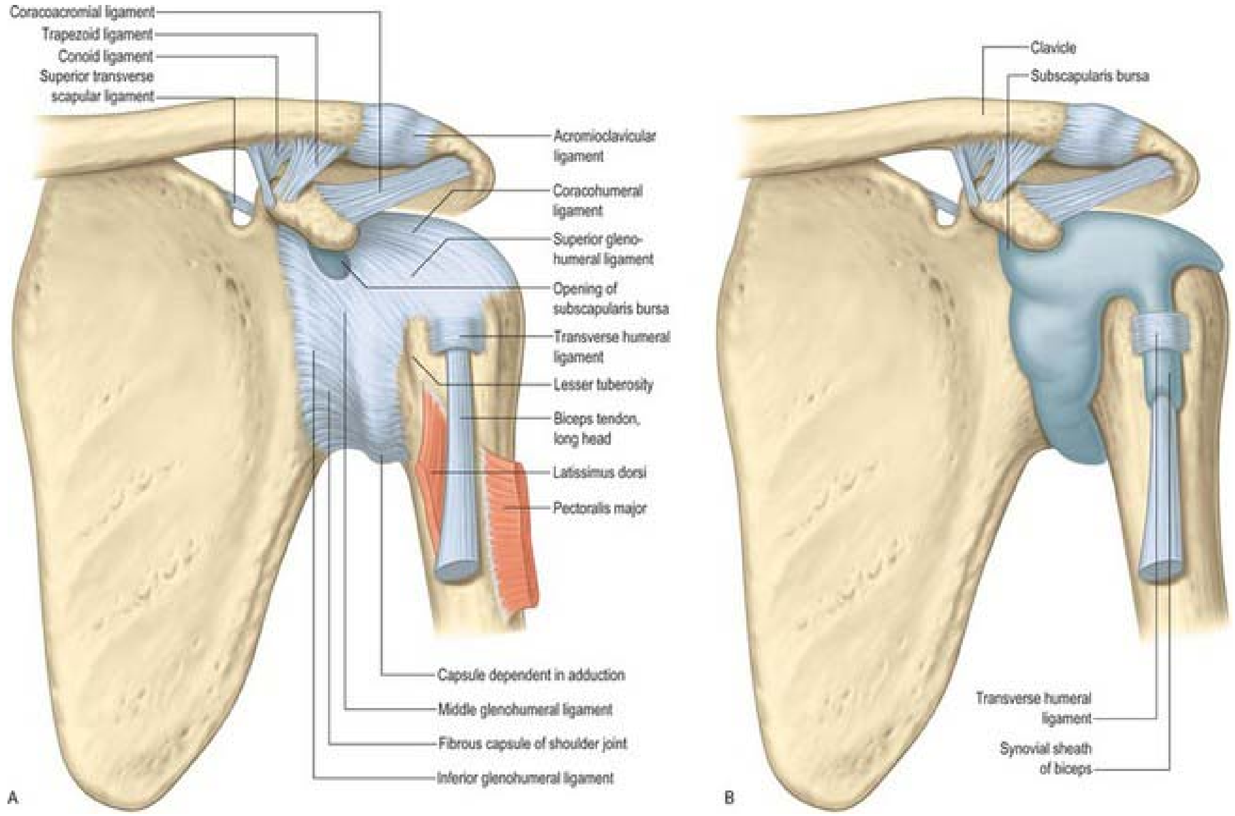
Coracoacromial ligament
Trapezoid ligament
Conoid ligament
Superior transverse scapular ligament
Acromioclavicular ligament
Coracohumeral ligament
Superior gleno-humeral ligament
Opening of subscapularis bursa
Transverse humeral ligament
Lesser tuberosity
Biceps tendon, long head
Latissimus dorsi
Pectoralis major
Capsule dependent in adduction
Middle glenohumeral ligament
Fibrous capsule of shoulder joint
Inferior glenohumeral ligament
A
Clavicle
Subscapularis bursa
Transverse humeral ligament
Synovial sheath of biceps
B

Fig. 46.14 **A**, The anterior aspect of the left shoulder. **B**, A deeper view of the anterior aspect than in (**A**), showing the subscapularis bursa.

Coracoacromial ligament

The coracoacromial ligament is a strong triangular band between the coracoid process and acromion. It is attached apically to the acromion anterior to its clavicular articular surface and by its base along the whole lateral border of the coracoid. Together with the coracoid process and acromion it completes an arch above the humeral head. It may be composed of two strong marginal bands with a thinner centre; when pectoralis minor is inserted into the humeral capsule instead of the coracoid process, which happens occasionally, its tendon passes between the bands. The subacromial bursa facilitates movement between the coracoacromial arch and the subjacent supraspinatus and shoulder joint, functioning as a secondary synovial articulation.

Superior transverse scapular (suprascapular) ligament

The superior transverse scapular (suprascapular) ligament converts the scapular notch into a foramen: it is sometimes ossified. A flat fasciculus, it narrows towards its attachments to the base of the coracoid process and medial side of the scapular notch. The suprascapular nerve traverses the foramen and the suprascapular vessels cross above the ligament.

Inferior transverse scapular (spinoglenoid) ligament

When present, the inferior transverse scapular ligament is a membranous ligament which may stretch from the lateral border of the spine of the scapula to the glenoid margin. It forms an arch over the suprascapular nerve and vessels entering the infraspinous fossa.

Ossification

The cartilaginous scapula is ossified from eight or more centres: one in the body, two each in the coracoid process and the acromion, one each in the medial border, inferior angle and lower part of the rim of the glenoid cavity (Fig. 46.5). The centre for the body appears in the eighth intrauterine week. Ossification begins in the middle of the coracoid process in the first year or in a small proportion of individuals before birth and the process joins the rest of the bone about the 15th year. At or soon after puberty centres of ossification occur in the rest of the coracoid process (subcoracoid centre), in the rim of the lower part of the glenoid cavity, frequently at the tip of the coracoid process, in the acromion, in the inferior angle and contiguous part of the medial border and in the medial border. A variable area of the upper part of the glenoid cavity, usually the upper third, is ossified from the subcoracoid centre; it unites with the rest of the bone in the 14th year in the female and the 17th year in the male. A horse-shoe shaped epiphysis appears for the rim of the lower part of the glenoid cavity; thicker at its peripheral than at its central margin, it converts the flat glenoid cavity of the child into the gently concave fossa of the adult. The base of the acromion is formed by an extension from the spine; the rest of the acromion is ossified from two centres which unite and then join the extension from the spine. The various epiphyses of the scapula have all joined the bone by about the 20th year.

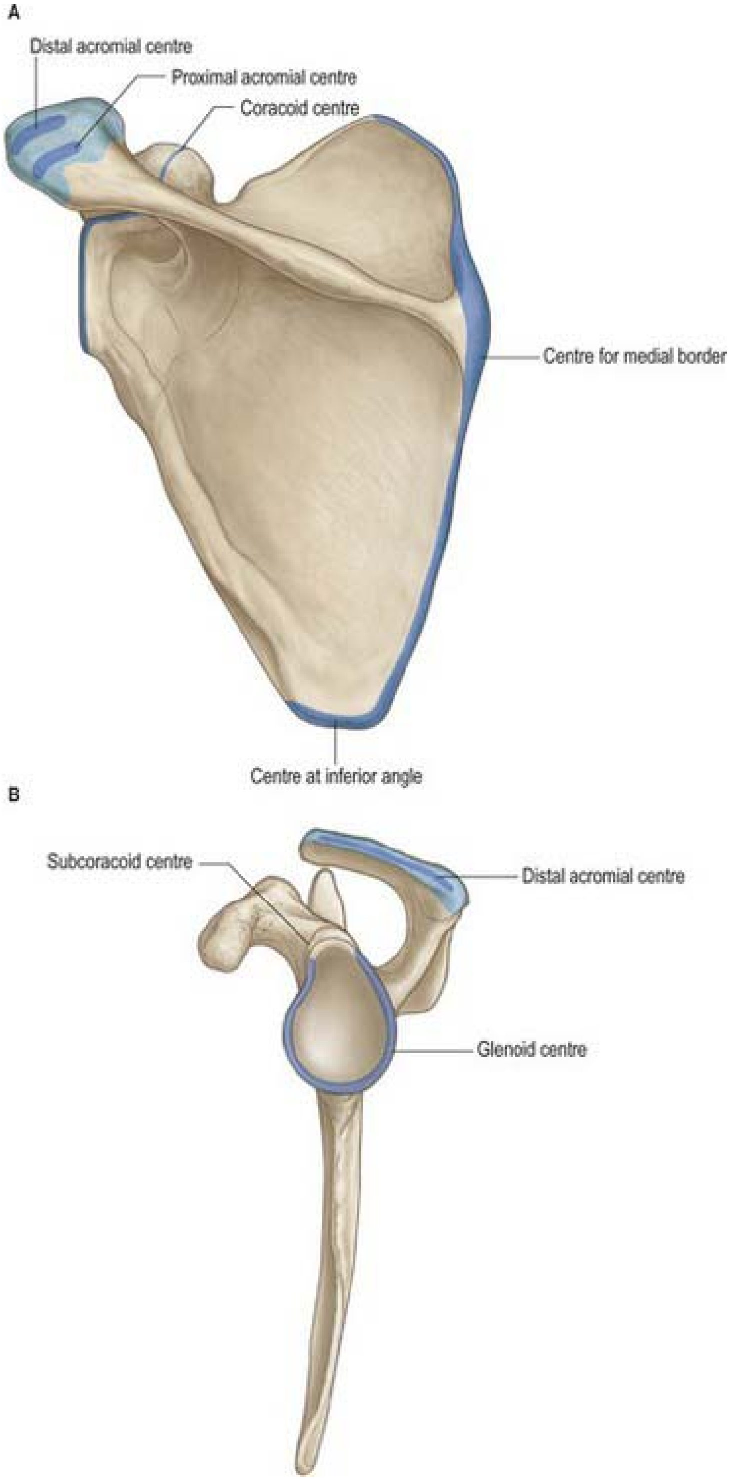
A
Distal acromial centre
Proximal acromial centre
Coracoid centre
Centre for medial border
Centre at inferior angle
B
Subcoracoid centre
Distal acromial centre
Glenoid centre

Fig. 46.5 Ossification of the scapula. **A**, Dorsal aspect; **B**, Lateral aspect.

(Adapted from Drake, Vogl and Mitchell 2005.)

HUMERUS

The humerus, the longest and largest bone in the upper limb, has expanded ends and a shaft (Fig. 46.6, Fig. 46.7, Fig. 46.8). The rounded head occupies the proximal and medial part of the upper end of the bone and forms an enarthrodial articulation with the glenoid cavity of the scapula. The lesser tubercle projects from the front of the shaft, close to the head, and is limited on its lateral side by a well-marked groove. The distal end, loosely termed ‘condylar’, is adapted to the forearm bones at the elbow joint.

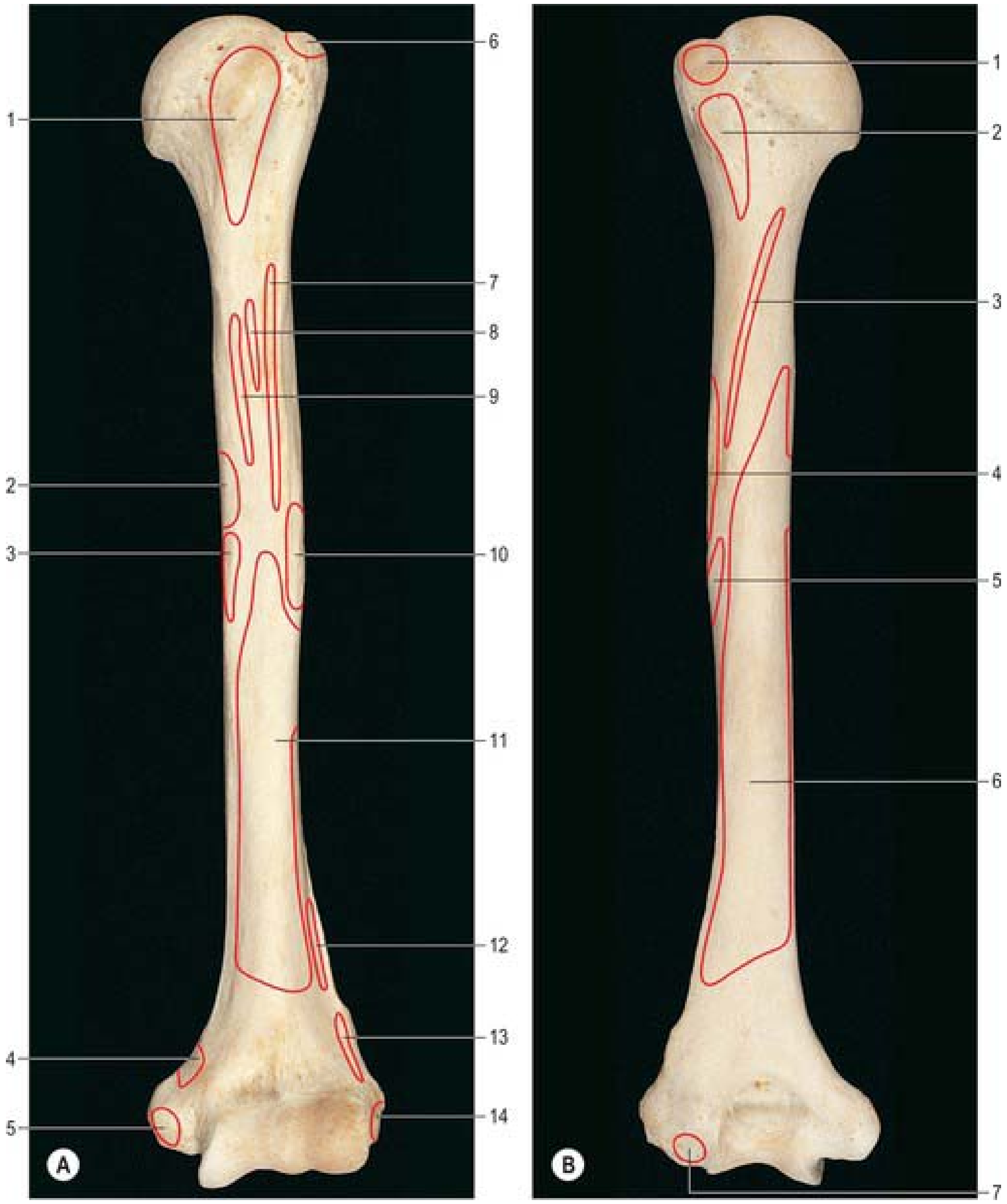

Fig. 46.6 Left humerus showing muscular attachments. **A**, Anterior aspect. **B**, Posterior aspect. **A: 1**. Subscapularis. **2**. Triceps (medial head). **3**. Coracobrachialis. **4**. Pronator teres (humeral head). **5**. Common flexor origin. **6**. Supraspinatus. **7**. Pectoralis major. **8**. Latissimus dorsi. **9**. Teres major. **10**. Deltoid. **11**. Brachialis. **12**. Brachioradialis. **13**. Extensor carpi radialis longus. **14**. Common extensor origin. **B: 1**. Infraspinatus. **2**. Teres minor. **3**. Triceps (lateral head). **4**. Deltoid. **5**. Brachialis. **6**. Triceps (medial head). **7**. Anconeus.

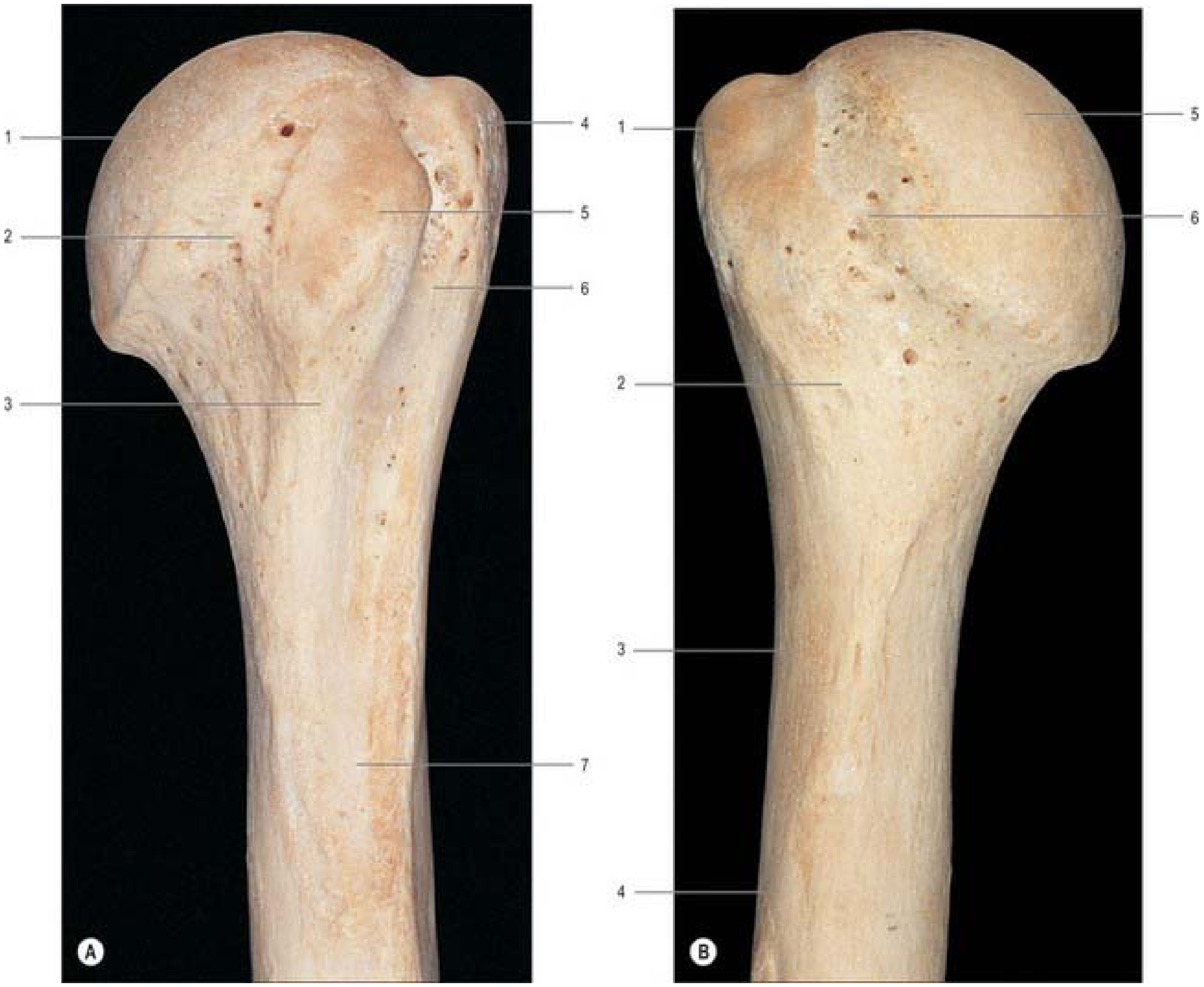

Fig. 46.7 **A**, Anterior aspect of proximal end of left humerus. **B**, Posterior aspect of proximal end of left humerus. **A: 1**. Head. **2**. Anatomical neck. **3**. Surgical neck. **4**. Greater tubercle. **5**. Lesser tubercle. **6**. Intertubercular sulcus. **7**. Shaft. **B: 1**. Greater tubercle. **2**. Surgical neck. **3**. Shaft. **4**. Radial groove. **5**. Head. **6**. Anatomical neck.

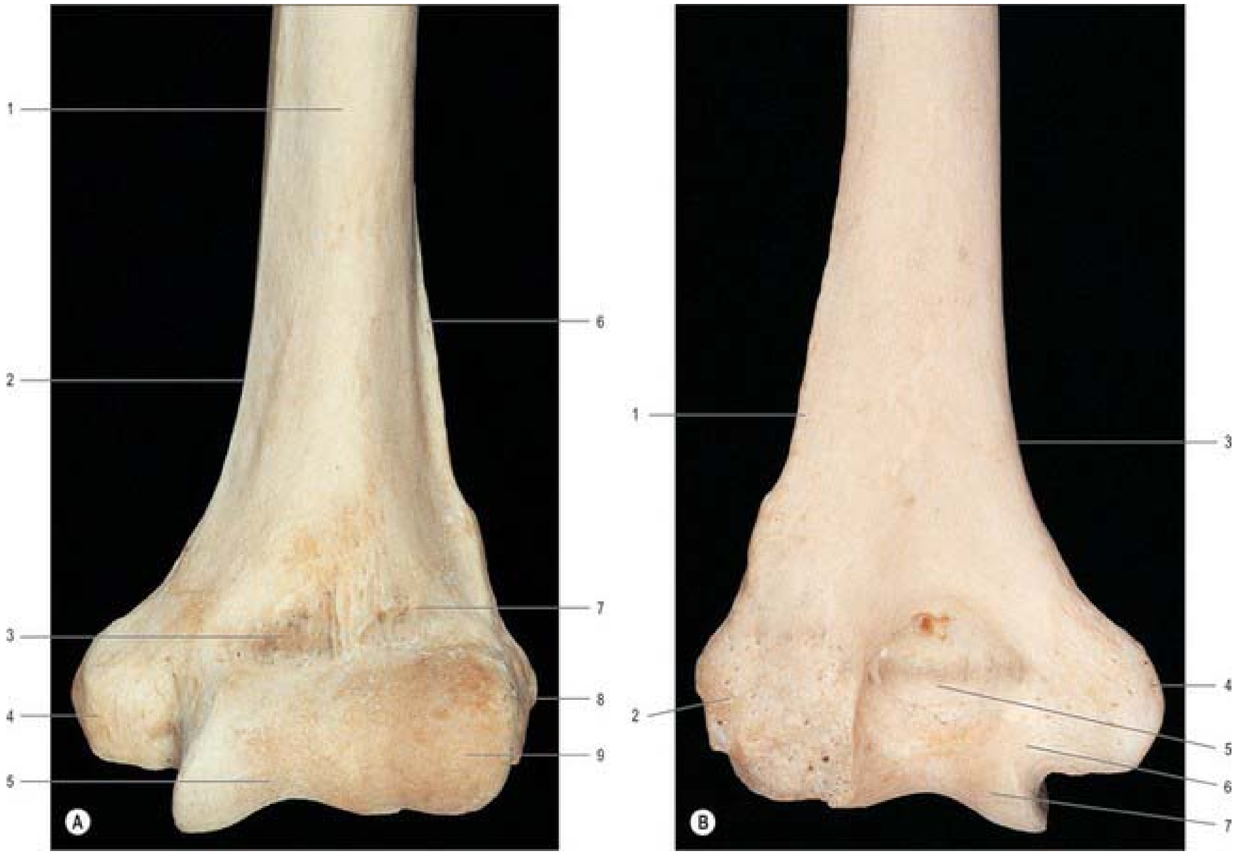

Fig. 46.8 **A**, Anterior aspect of distal end of left humerus. **B**, Posterior aspect of distal end of left humerus. **A:** **1**. Shaft. **2**. Medial supracondylar ridge. **3**. Coronoid fossa. **4**. Medial epicondyle. **5**. Trochlea. **6**. Lateral supracondylar ridge. **7**. Radial fossa. **8**. Lateral epicondyle. **9**. Capitulum. **B:** **1**. Lateral supracondylar ridge. **2**. Lateral epicondyle. **3**. Medial supracondylar ridge. **4**. Medial epicondyle. **5**. Olecranon fossa. **6**. Sulcus for ulnar nerve. **7**. Trochlea.

The capsular ligament of the elbow joint is attached anteriorly to the upper limits of the radial and coronoid fossae, so that both these bony depressions are intracapsular and therefore lined with synovial membrane. Medially it is attached to the medial non-articular aspect of the projecting lip of the trochlea and to the root of the medial epicondyle. Posteriorly it ascends to, or almost to, the upper margin of the olecranon fossa, which is therefore intracapsular and covered with synovial membrane. Laterally it skirts the lateral borders of the trochlea and capitulum, lying medial to the lateral epicondyle.

With the arm by the side, the medial epicondyle lies on a plane which is posterior to that of the lateral epicondyle, so that the humerus *appears* to be rotated medially. In this position the head of the humerus is directed almost equally backwards and medially, and the posterior surface of the shaft faces posterolaterally. Since the glenoid fossa of the scapula faces anterolaterally, the humerus is not rotated medially relative to the scapula in this position of rest, but it is so rotated relative to the conventional anatomical position. This position of the bone must be remembered when movements of the arm and forearm are considered.

Proximal end

The proximal end of the humerus consists of the head, anatomical neck and the greater and lesser tubercles. It joins the shaft at an ill-defined ‘surgical neck’, which is closely related on its medial side to the axillary nerve and posterior humeral circumflex artery (Fig. 46.7).

Head

The head of the humerus forms rather less than half a spheroid; in sectional profile it is spheroidal (strictly ovoidal) (Fig. 46.7). Its smooth articular surface is covered with hyaline cartilage, which is thicker centrally. When the arm is at rest by the side, it is directed medially, backwards and upwards to articulate with the glenoid cavity of the scapula. The humeral articular surface is much more extensive than the glenoid cavity, and only a portion of it is in contact with the cavity in any one position of the arm.

Anatomical neck

The anatomical neck of the humerus immediately adjoins the margin of the head and forms a slight constriction, which is least apparent in the neighbourhood of the greater tubercle, and superiorly, and for some distance anteriorly and posteriorly: it indicates the line of capsular attachment of the shoulder joint (Fig. 46.7), other than at the intertubercular sulcus, where the long tendon of biceps emerges. Medially, the capsular attachment diverges from the anatomical neck and descends 1 cm or more onto the shaft.

Lesser tubercle

The lesser tubercle is anterior to and just beyond the anatomical neck. It has a smooth, muscular impression on its upper part palpable through the thickness of deltoid 3 cm below the acromial apex. The bony prominence slips away from the examining finger when the humerus is rotated. The lateral edge of the lesser tubercle is sharp and forms the medial border of the intertubercular sulcus. Subscapularis is attached to the lesser tubercle (Fig. 46.6A), and the transverse ligament of the shoulder joint is attached to the lateral margin.

Greater tubercle

The greater tubercle is the most lateral part of the proximal end of the humerus. It projects beyond the lateral border of the acromion. Its posterosuperior aspect, near the anatomical neck, bears three smooth flattened impressions for the attachment of supraspinatus (uppermost), infraspinatus (middle) and teres minor (lowest and placed on the posterior surface of the tubercle) (Fig. 46.6). The attachments of subscapularis and teres minor are not confined to their respective tubercles, but extend for varying distances on to the adjacent metaphysis. The projecting lateral surface of the tubercle presents numerous vascular foramina and is covered by the thick, fleshy deltoid, which produces the normal rounded contour of the shoulder. A part of the subacromial bursa may cover the upper part of this area and separate it from deltoid.

The intertubercular sulcus (bicipital groove) lies between the tubercles. It contains the long tendon of biceps, its synovial sheath, and an ascending branch from the anterior circumflex humeral artery. The rough lateral lip of the groove is marked by the bilaminar tendon of pectoralis major, its floor by the tendon of latissimus dorsi and its medial lip by the tendon of teres major;

the attachment of pectoralis major extends beyond that of teres major, that of latissimus dorsi is least extensive.

Shaft

The shaft of the humerus is almost cylindrical in its proximal half but is triangular on section in its distal half, which is compressed in an anteroposterior direction. It can be identified when the arm is grasped firmly, but its outline is obscured by the strong muscles which surround it. It has three surfaces and three borders – which are not everywhere equally obvious.

Anterior border

The anterior border starts on the front of the greater tubercle and runs downwards almost to the lower end of the bone. Its proximal third forms the lateral lip of the intertuberculous sulcus and is roughened for muscular attachments. The succeeding portion is also roughened and forms the anterior limit of the deltoid tubercle; the lower half of the border is smooth and rounded.

Lateral border

The lateral border is conspicuous at the lower end of the bone, where it is thickened to form the lateral supracondylar ridge and its sharp edge is roughened along its anterior aspect. In its middle and upper thirds the border is barely discernible, but in a well-marked bone it can be traced upwards to the posterior surface of the greater tubercle. A little above its middle it is marked by a V-shaped roughened area, the deltoid tubercle. The limbs of the V are broad: the groove for the radial nerve runs downwards behind the posterior limb and fades away on the lower part of the surface.

Medial border

The medial border, although rounded, can be identified without difficulty in the lower half of the shaft, where it becomes the medial supracondylar ridge. In the proximal third the medial border is indistinct until it reappears as the medial lip of the intertubercular sulcus, where it is again rough and reaches the lesser tubercle. In its middle third, the border is interrupted by a wide, shallow groove, the radial or spiral groove, which crosses the bone obliquely, passing downwards and forwards from its posterior to its anterior surface.

Surfaces

The anterolateral surface is bounded by the anterior and lateral borders and is smooth and featureless in its upper part, which is covered by deltoid. About, or a little above, the middle of this surface, deltoid is inserted into the deltoid tubercle; further distally the surface gives origin to the lateral fibres of brachialis, which extend upwards into the floor of the lower end of the groove for the radial nerve (Fig. 46.6). Brachioradialis is attached to the proximal two-thirds of the roughened anterior aspect of the lateral supracondylar ridge, and extensor carpi radialis longus is attached to its distal third. Behind these muscles, the ridge gives attachment to the lateral intermuscular septum of the arm.

The anteromedial surface is bounded by the anterior and medial borders. Rather less than its upper third forms the rough floor of the intertubercular sulcus; the rest of the surface is smooth. Distal to the intertubercular sulcus a small area of the anteromedial surface is devoid of muscular attachment, but its lower half is occupied by the medial part of brachialis (Fig. 46.6A). Coracobrachialis is attached to a roughened strip on the middle of the medial border. The humeral head of pronator teres is attached to a narrow area close to the lowest part of the medial supracondylar ridge, and the ridge itself gives attachment to the medial intermuscular septum of the arm.

A little below its midpoint, the nutrient foramen, which is directed downwards, opens close to the medial border. A hook-shaped process of bone, the supracondylar process, from 2 to 20 mm in length, occasionally projects from the anteromedial surface of the shaft, approximately 5 cm proximal to the medial epicondyle. It is curved downwards and forwards, and its pointed apex is connected to the medial border, just above the epicondyle, by a fibrous band to which part of pronator teres is attached. The foramen completed by this fibrous band usually transmits the median nerve and brachial artery, but sometimes encloses only the nerve, or the nerve plus the ulnar artery (in cases of high division of the brachial artery). A groove which lodges the artery and nerve usually exists behind the process, and may protect the nerve and artery from compression by muscles.

The posterior surface, between the medial and lateral borders, is the most extensive surface and is occupied mostly by the medial head of triceps. A ridge, sometimes rough, descends obliquely and laterally across its proximal third, and gives attachment to the lateral head of triceps. Above triceps, the axillary nerve and the posterior circumflex humeral vessels wind round this aspect of the bone under cover of deltoid. Below and medial to the attachment of the lateral head of triceps, a shallow groove which contains the radial nerve and the profunda brachii vessels, runs downwards and laterally to gain the anterolateral surface of the shaft. The area for the origin of the fleshy medial head of triceps includes a very large part of the posterior surface of the bone. It covers an elongated triangular area, the apex of which is placed on the medial part of the posterior surface above the level of the lower limit of the insertion of teres major. The area widens below and covers the whole surface almost down to the lower end of the bone.

Fractures of the humeral shaft

Fractures of the humerus are comparatively common and may occur at almost any level. The humerus is fractured by muscular action probably more frequently than any other long bone: usually the shaft is broken below the attachment of deltoid. The radial nerve may be injured in its groove or may very rarely become involved later in the growth of callus. Fractures at the proximal end of the humerus may rarely damage the axillary nerve, and similarly fractures of the medial epicondyle may be complicated by damage to the ulnar nerve. Supracondylar fractures are relatively common in children: the end of the proximal fragment can sometimes injure the brachial artery or median nerve. In adults, non-union is more common in the humerus than in any other long bone, although contemporary management of humeral fractures has rendered non-union rare: the incidence of scaphoid non-union is similar, if not greater.

Distal end

The distal end of the humerus is a modified condyle: it is wider transversely and has articular and non-articular parts (Fig. 46.8, Fig. 46.9). The articular part is curved forwards, so that its anterior and posterior surfaces lie in front of the corresponding surfaces of the shaft. It articulates with the radius and the ulna at the elbow joint, and is divided by a faint groove into a lateral capitulum, and a medial trochlea.

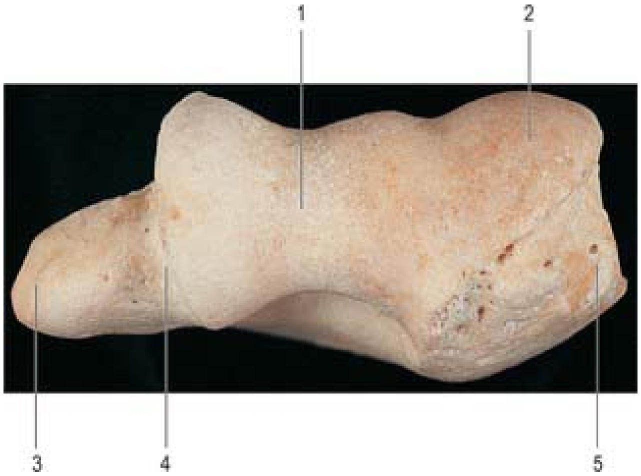

Fig. 46.9 Inferior aspect of distal end of left humerus. **1**. Trochlea. **2**. Capitulum. **3**. Medial epicondyle. **4**. Sulcus for ulnar nerve. **5**. Lateral epicondyle.

The capitulum is a rounded, convex projection, considerably less than half a sphere, which covers the anterior and inferior surfaces of the lateral part of the condyle of the humerus but does not extend onto its posterior surface. It articulates with the discoid head of the radius, which lies in contact with its inferior surface in full extension of the elbow but slides onto its anterior surface during flexion. The groove of the trochlea winds backwards and laterally as it is traced from the anterior to the posterior surface of the bone, and it is wider, deeper and more symmetrical posteriorly. Anteriorly, the medial flange of the pulley is much longer than the lateral, and the surface adjoining its projecting medial margin is convex to accommodate itself to the medial part of the upper surface of the coronoid process of the ulna. These asymmetries entail varying angulation between the humeral and ulnar axes, together with some conjunct rotation. The non-articular part of the condyle includes the medial and lateral epicondyles, olecranon and coronoid and radial fossae.

Trochlea

The trochlea is a pulley-shaped surface that covers the anterior, inferior and posterior surfaces of the condyle of the humerus medially. It articulates with the trochlear notch of the ulna. On its lateral side it is separated from the capitulum by a faint groove; its medial margin projects distally beyond the rest of the bone. When the elbow is extended the inferior and posterior aspects of the trochlea are in contact with the ulna, but, as the joint is flexed, the trochlear notch slides on to the anterior aspect and the posterior aspect is then left uncovered. The downward projection of the medial edge of the trochlea is the principal factor in determining the angulation between the long axis of the humerus and the long axis of the supinated forearm when the elbow is extended.

Medial epicondyle

The medial border of the humerus ends by turning slightly backwards as the medial epicondyle, which forms a conspicuous, blunt projection on the medial side of the condyle. It is subcutaneous and usually visible, especially in passive flexion of the elbow. Its posterior surface is smooth and is crossed by the ulnar nerve, which lies in a shallow sulcus as it enters the forearm. In this situation the nerve can be felt and rolled against the bone, and if it is jarred against the epicondyle, characteristic tingling sensations result. The lower part of the anterior surface of the medial epicondyle is marked by the attachment of the superficial group of forearm flexors. They arise from the epiphysis for the epicondyle, but are entirely extracapsular.

Lateral epicondyle

The lateral border of the humerus terminates at the lateral epicondyle, and its lower portion constitutes the lateral supracondylar ridge. The lateral epicondyle occupies the lateral part of the non-articular portion of the condyle, but does not project beyond the lateral supracondylar ridge. It turns slightly forwards, unlike the medial epicondyle, which turns slightly backwards. Its lateral and anterior surfaces show a well-marked impression for the superficial group of the extensor muscles of the forearm (Fig. 46.6B), which arise from the lateral side of the lower humeral epiphysis, and, like the flexors, are situated outside the articular capsule. The posterior surface, which is very slightly convex, is easily felt in a depression visible behind the extended elbow. A small area on the posterior surface gives origin to anconeus.

Olecranon, coronoid and radial fossae

The olecranon fossa is a deep hollow on the posterior surface of the condyle, immediately above the trochlea, that lodges the tip of the olecranon of the ulna when the elbow is extended. The floor of the fossa is always thin and may be partially deficient. A similar but smaller hollow lies immediately above the trochlea on the anterior surface of the condyle and is termed the coronoid fossa. It accommodates the anterior margin of the coronoid process of the ulna during flexion of the elbow. A very slight depression lies above the capitulum on the lateral side of the coronoid fossa. It is termed the radial fossa, since it is related to the margin of the head of the radius in full flexion of the elbow.

Ossification

The humerus is ossified from eight centres, in the shaft, head, greater and lesser tubercles, capitulum with the lateral part of the trochlea, the medial part of the trochlea, and one for each epicondyle (Fig. 46.10). The centre for the shaft appears near its middle in the eighth week of intrauterine life, and gradually extends towards the ends. Before birth (20%), or in the first six months afterwards, ossification begins in the head, during the first year in females and second year in males in the greater tubercle, and about the fifth in the lesser tubercle. The existence of a centre in the lesser tubercle is often questioned, perhaps because it is often obscured in the usual anteroposterior radiological views (Fig. 46.11).

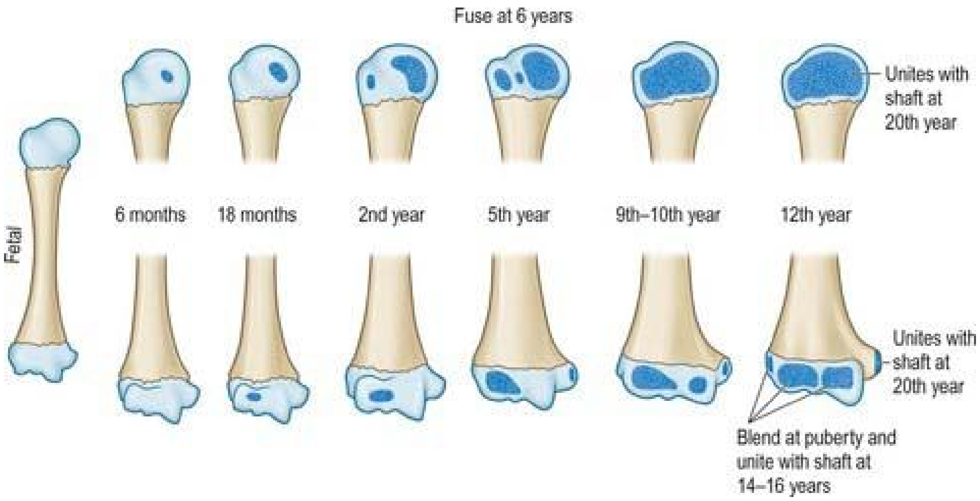
Fuse at 6 years
Unites with shaft at 20th year
Fetal
6 months
18 months
2nd year
5th year
9th–10th year
12th year
Unites with shaft at 20th year
Blend at puberty and unite with shaft at 14–16 years

Fig. 46.10 The stages in ossification of the humerus (not to scale).

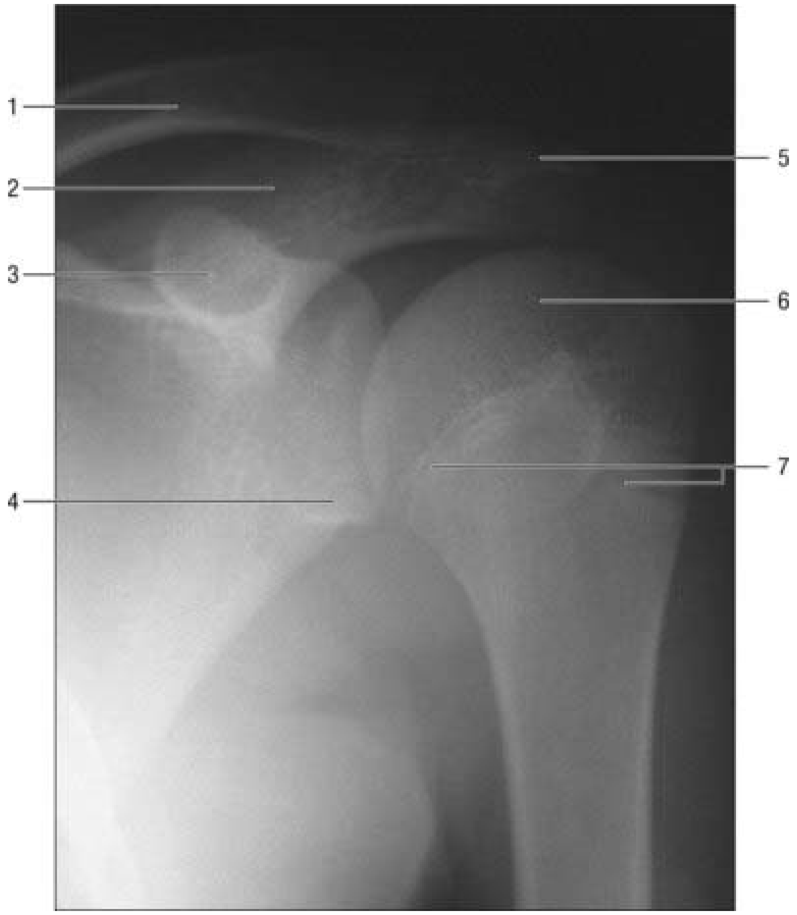

Fig. 46.11 Anteroposterior radiograph of the left shoulder in a boy aged 11. Note the conical junction of the humeral epiphysis with the diaphysis. **1**. Clavicle. **2**. Spine of scapula. **3**. Coracoid process. **4**. Glenoid cavity. **5**. Acromion. **6**. Proximal humeral epiphysis. **7**. Proximal humeral growth plate.

By the sixth year the centres for the head and tubercles have joined to form a single large epiphysis, which is hollowed out on its inferior surface to adapt it to the somewhat conical upper end of the metaphysis. It fuses with the shaft of the humerus about the twentieth year in males, two years earlier in females. The lower end is ossified as follows. During the first year ossification begins in the capitulum and extends medially to form the chief part of the articular surface; the centre for the medial part of the trochlea appears in the ninth year in females and tenth year in males.

Ossification begins in the medial epicondyle in the fourth year in females, sixth in males, and in the lateral epicondyle about the 12th year. The centres for the lateral epicondyle, capitulum and trochlea fuse around puberty and the composite epiphysis unites with the shaft in the fourteenth year in females, sixteenth in males. The centre for the medial epicondyle forms a separate epiphysis, which is entirely extracapsular and is placed on the posteromedial aspect of the epicondyle. It is separated from the rest of the lower epiphysis by a downgrowth from the shaft, with which it unites about the 20th year.

Amputation of the humerus in youth

The proximal epiphysis joins the humeral shaft later than the distal, which means that growth in length is mainly attributable to growth from the proximal epiphysial plate. After amputation through the arm in youth, the humerus continues to grow and its lower end progressively moulds the surrounding soft tissues so that the stump becomes conical.

JOINTS

STERNOCLAVICULAR JOINT

The sternoclavicular joint is a synovial sellar joint and represents the only skeletal articulation between the upper limb and the axial skeleton.

Articulating surfaces

The articulating surfaces are the sternal end of the clavicle and the clavicular notch of the sternum, together with the adjacent superior surface of the first costal cartilage (Fig. 46.12). The larger clavicular articular surface is covered by fibrocartilage, which is thicker than the fibrocartilaginous lamina on the sternum. The joint is convex vertically but slightly concave anteroposteriorly, and is therefore sellar; the clavicular notch of the sternum is reciprocally curved, but the two surfaces are not fully congruent. An articular disc completely divides the joint.

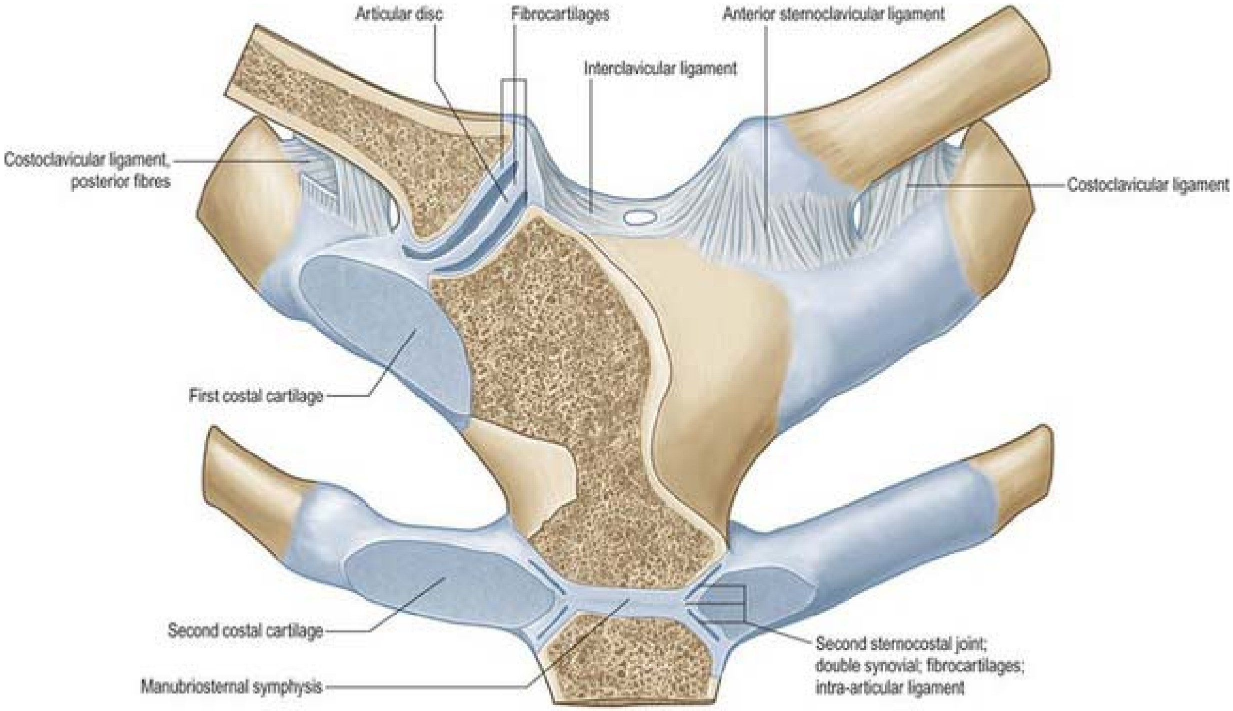
Articular disc
Fibrocartilages
Anterior sternoclavicular ligament
Interclavicular ligament
Costoclavicular ligament, posterior fibres
Costoclavicular ligament
First costal cartilage
Second costal cartilage
Manubriosternal symphysis
Second sternocostal joint; double synovial; fibrocartilages; intra-articular ligament

Fig. 46.12 Sternoclavicular joints: anterior aspect; left joint intact and right in coronal section.

Fibrous capsule

The capsule is thickened in front and behind, but above, and especially below, it is little more than loose areolar tissue.

Ligaments

The ligaments are the anterior and posterior sternoclavicular and the costoclavicular on each side, and the midline interclavicular.

Anterior sternoclavicular ligament

The anterior sternoclavicular ligament is broad and attached above to the anterosuperior aspect of the sternal end of the clavicle. It passes inferomedially to the upper anterior aspect of the manubrium, spreading onto the first costal cartilage.

Posterior sternoclavicular ligament

The posterior sternoclavicular ligament is a weaker band posterior to the joint. It descends inferomedially from the back of the sternal end of the clavicle to the back of the upper manubrium.

Interclavicular ligament

The interclavicular ligament is continuous above with deep cervical fascia, and unites the superior aspect of the sternal ends of both clavicles; some fibres are attached to the superior manubrial margin.

Costoclavicular ligament

The costoclavicular ligament is like an inverted cone, but short and flattened. It has anterior and posterior laminae which are attached to the upper surface of the first rib and costal cartilage, and ascends to the margins of an impression on the inferior clavicular surface at its medial end. Fibres of the anterior lamina ascend laterally and those of the posterior lamina (which are shorter) ascend medially (Fig. 46.12); they fuse laterally and merge medially with the capsule.

Articular disc

The articular disc is flat and almost circular, between the sternal and clavicular surfaces. It is attached above to the posterosuperior border of the articular surface of the clavicle, below to the first costal cartilage near its sternal junction, and by the rest of its circumference to the capsule. It is thicker peripherally, especially in its superoposterior part and a smaller inferomedial one. The capsule around the former is more lax: movements between the clavicle and the disc are more extensive than those between the disc and sternum. The sellar shape of the articular surfaces permits movement in approximately anteroposterior and vertical planes, and some rotation about the long axis of the clavicle. Close-packing probably coincides with maximum posterior rotation associated with full scapular rotation. Some anteroposterior translation also occurs.

Vascular supply

The sternoclavicular joint is supplied by branches from the internal thoracic and suprascapular arteries.

Innervation

The sternoclavicular joint is innervated by branches from the medial supraclavicular nerve and the nerve to subclavius.

Factors maintaining stability

There is relatively little bony articular congruence at the sternoclavicular joint. However, the strength of its associated ligaments, and especially its articular disc, actually make it very stable. These factors, and the usual transmission of forces along the clavicle, make dislocation rare: fracture along the clavicular shaft is far more common.

ACROMIOCLAVICULAR JOINT

The acromioclavicular joint is a synovial plane joint.

Articulating surfaces

The articulating surfaces are between the acromial end of the clavicle and the medial acromial margin (Fig. 46.13). The joint is approximately plane, but either surface may be slightly convex, the other being reciprocally concave, and both are covered by fibrocartilage. The clavicular surface is a narrow, oval area which faces inferolaterally and overlaps a corresponding facet on the medial acromial border. The long axis is anteroposterior.

Fibrous capsule

The capsule completely surrounds the articular margins and is strengthened above by the acromioclavicular ligament. The capsule is lined by synovial membrane.

Ligaments

The acromio- and coraco-clavicular ligaments run between the clavicle and the acromion and coracoid processes respectively.

Acromioclavicular ligament

The acromioclavicular ligament is quadrilateral. It extends between the upper aspects of the lateral end of the clavicle and the adjoining acromion. Its parallel fibres interlace with the aponeuroses of trapezius and deltoid.

Coracoclavicular ligament

The coracoclavicular ligament connects the clavicle and the coracoid process of the scapula (Fig. 46.14). Though separate from the acromioclavicular joint, it is a most efficient accessory ligament, and maintains the apposition of the clavicle to the acromion. The trapezoid and conoid parts of the ligament, usually separated by fat or, frequently, by a bursa, connect the medial horizontal part of the coracoid process and lateral end of the subclavian groove of the clavicle; these adjacent areas may even be covered by cartilage to form a coracoclavicular joint.

The trapezoid part is anterolateral and is broad, thin and quadrilateral, ascending slightly from the upper coracoid surface to the trapezoid line on the inferior clavicular surface. It is almost horizontal, its anterior border is free, and its posterior border is joined to the conoid part, forming an angle which projects backwards.

The conoid part is posteromedial and is a dense, almost vertical triangular band. Its base is attached to the conoid tubercle of the clavicle and its inferior apex is attached posteromedially to the root of the coracoid process in front of the scapular notch.

Articular disc

The articular disc often occurs in the upper part of the joint, partially separating the articular surfaces: occasionally it completely divides the joint.

Vascular supply

The acromioclavicular joint receives its arterial supply from branches from the suprascapular and thoracoacromial arteries.

Innervation

The acromioclavicular joint is innervated by branches from the suprascapular and lateral pectoral nerves.

Factors maintaining stability

The coracoclavicular ligament stabilizes the acromioclavicular joint. In acromioclavicular dislocation, the ligament is torn and the scapula falls away from the clavicle, which may be slightly elevated by the unopposed pull of trapezius. Dislocation can occur because of the flatness and orientation of the joint surfaces; once the acromioclavicular joint dislocates it never reduces.

Movements

Movements at the joint are like those of the sternoclavicular joint. These are passive, i.e. no muscle directly moves the joint, but muscles which move the scapula indirectly move the clavicle. Axial rotation of the clavicle is about 30°, the two joints together therefore, permit about 60° of scapular rotation. Angulation with the scapula occurs in any direction.

MOVEMENTS OF THE PECTORAL (SHOULDER) GIRDLE

Clavicular movements at the sternoclavicular and acromioclavicular joints are inevitably associated with movements of the scapula, and these are usually accompanied by movements of the humerus. The acromioclavicular joint allows anteroposterior gliding and rotation of the acromion, and hence the scapula, on the clavicle: scapular range is increased by movements at the sternoclavicular joint. The sternoclavicular and the acromioclavicular joints, in combination with the fascial space between the scapula and underlying chest wall, are collectively known as the scapulothoracic articulation.

In all scapular movements, it is assumed that subclavius probably steadies the clavicle by drawing it medially and downwards, although its inaccessibility for electromyographic analysis makes its role uncertain. Scapular movements on the thoracic wall are facilitated by areolar tissue between subscapularis, serratus anterior and the chest wall. With the arm by the side, the normal posture of the shoulder girdle relative to the trunk involves moderate activity in trapezius and serratus anterior, and this increases when the limb is loaded.

The following account should be read together with the description of movements of the glenohumeral joint.

Elevation and depression

Scapular elevation and depression, as in ‘shrugging the shoulders’, do not necessarily imply movement at the shoulder joint. In elevation, slight angulation or swing occurs at the acromioclavicular joint. The sternal end of the clavicle, rotating about an anteroposterior axis through the bone above the medial attachment of the costoclavicular ligament, slides down over the articular disc (translation). This is checked by antagonist muscles and tension in the costoclavicular ligament and lower capsule. It is produced by the upper part of trapezius and levator scapulae, and since these tend to rotate the scapula in opposite directions, pure elevation can occur. In depression, slight angulation occurs at the acromioclavicular joint, and the clavicle slides up on the disc at the sternoclavicular joint. The movements are checked by antagonist muscles, the interclavicular and sternoclavicular ligaments and the articular disc. Usually gravity alone is sufficient: when necessary, the lowest part of serratus anterior and pectoralis minor are active depressors.

Protraction and retraction

Protraction (forward movement) round the thoracic wall occurs in pushing, thrusting and reaching movements, usually with some lateral rotation. The acromion advances over the clavicular facet to the limit, and the shoulder is simultaneously advanced by forward movement of the lateral end of the clavicle and posterior translation of its sternal end over the sternal facet, carrying the disc with it. Antagonist muscles, together with the anterior sternoclavicular ligament and posterior lamina of the costoclavicular ligament, check backward slide of the sternal end. Serratus anterior and pectoralis minor are prime movers and maintain continuous apposition of the scapula, especially its medial border, in smooth gliding on the thoracic wall. The upper part of latissimus dorsi also acts like a strap across the inferior scapular angle in protraction and lateral rotation.

In scapular retraction, i.e. bracing back the shoulders, these movements are reversed and checked at the sternoclavicular joint by the posterior sternoclavicular ligament and anterior lamina of the costoclavicular ligament. Trapezius and the rhomboids are prime movers, but gravity may also produce retraction when the weight of the trunk is taken by the arms in leaning forwards, which is to a degree controlled by protractive musculature.

When force is applied at the end of an outstretched arm, e.g. in a fall on the hand, pressure transmitted to the glenoid fossa tends to drive the sloping acromial facet below the acromial end of the clavicle. It also tenses the trapezoid ligament, which resists the displacement.

Lateral and medial rotation

Lateral (upward) rotation of the scapula increases the range of humeral elevation by turning the glenoid cavity to face almost directly up, e.g. raising an arm above the head. This movement is always associated with some humeral elevation and with protraction of the scapula. Scapular rotation requires movement at both sternoclavicular and acromioclavicular joints: the sternoclavicular joint permits elevation of the lateral end of the clavicle, a movement which is almost complete when the arm is abducted to 90°. The acromioclavicular joint moves in the first 30° of abduction, when the conoid ligament becomes taut, and is subsequently accompanied by clavicular rotation at the sternoclavicular joint around the longitudinal axis of the bone. The medial end is depressed further as the lateral end continues to rise. Some acromioclavicular movement also occurs in the final stages of humeral abduction. Trapezius (upper part) and serratus anterior (lower part) are prime movers.

Medial (downward) rotation is usually effected by gravity: gradual active lengthening of trapezius and serratus anterior is sufficient to control it. When more force is needed, levator scapulae, the rhomboids and, in the initial stages, pectoralis minor, are prime movers in returning the scapula to a position of rest.

Muscles which are antagonists in one movement may combine as prime movers in another. Movements, not muscles, are represented in cerebral motor areas. Muscles are not grouped unalterably in nervous control but can be variably combined as demands dictate. Thus serratus anterior and trapezius are opposed in scapular movement round the thorax, but combine as prime movers in lateral rotation of the scapula.

GLENOHUMERAL (SHOULDER) JOINT

The glenohumeral joint is a synovial multiaxial spheroidal joint between the roughly hemispherical head of the humerus and the shallow glenoid fossa of the scapula (Fig. 46.15). Notable for its relative lack of bony constraint, the joint possesses three degrees of freedom. Its static and dynamic stability depends on the surrounding muscular and soft tissue envelope more than on its shape and ligaments: effective function is achieved by a complex interaction between the articular and soft tissue restraints. It is the most mobile joint in the body and the most frequently dislocated.

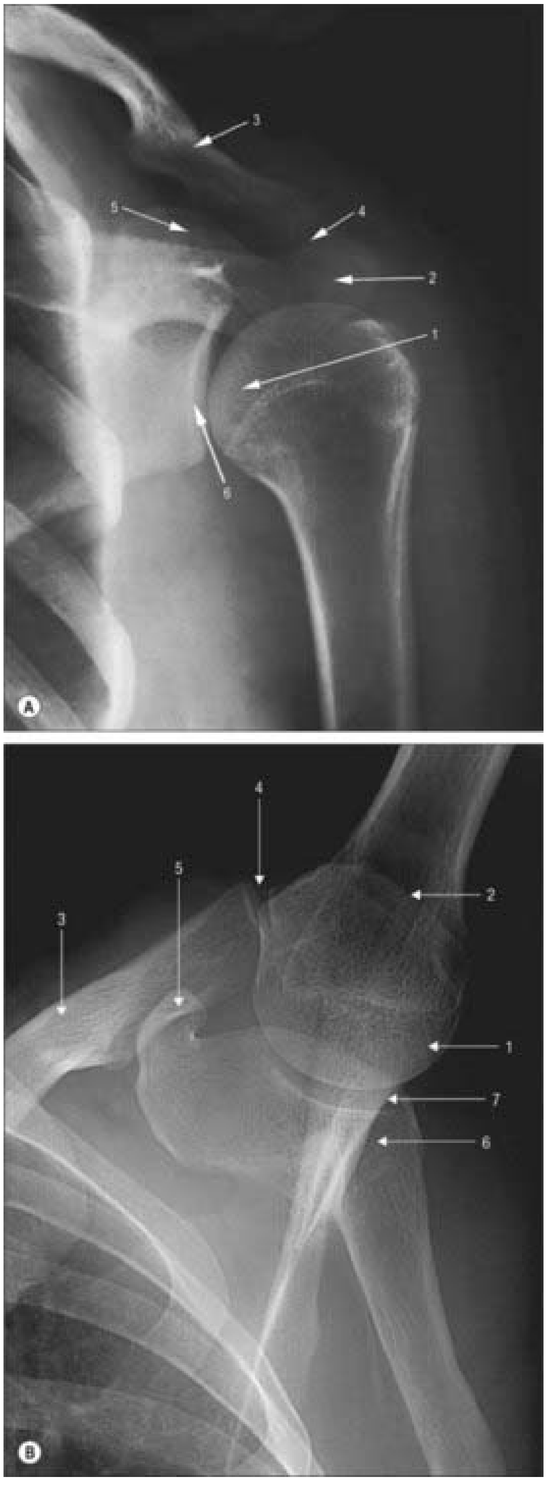

Fig. 46.15 Radiographs of the left shoulder of an 18 year old female in anteroposterior view (**A**) and axillary view with the arm abducted (**B**). **1**. Head of humerus. **2**. Acromion. **3**. Clavicle. **4**. Acromioclavicular joint. **5**. Coracoid. **6**. Glenoid. **7**. Glenohumeral articulation.

Articulating surfaces

The articular surfaces are reciprocally curved and are really ovoids. (Here, as in the hip, where ovoid surfaces are almost spherical they are often termed spheroidal.) The area of the humeral convexity exceeds that of the glenoid concavity such that only a small portion opposes the glenoid in any position (Fig. 46.16). The remaining capitular articular surface is in contact with the capsule, so that contact on the glenoid fossa is much more uniformly distributed over its entire articular surface. The radius of curvature of the glenoid fossa in the coronal plane is greater than that of the humeral head, and is deepened by a fibrocartilaginous rim, the glenoid labrum (Fig. 46.13, Fig. 46.17). Both articular surfaces are covered by hyaline cartilage, which is thickest centrally and thinner peripherally over the humerus, and the reverse in the glenoid cavity. In most positions, their curvatures are not fully congruent, and the joint is loose-packed. Close packing (full congruence) is reached with the humerus abducted and laterally rotated (Fig. 5.61).

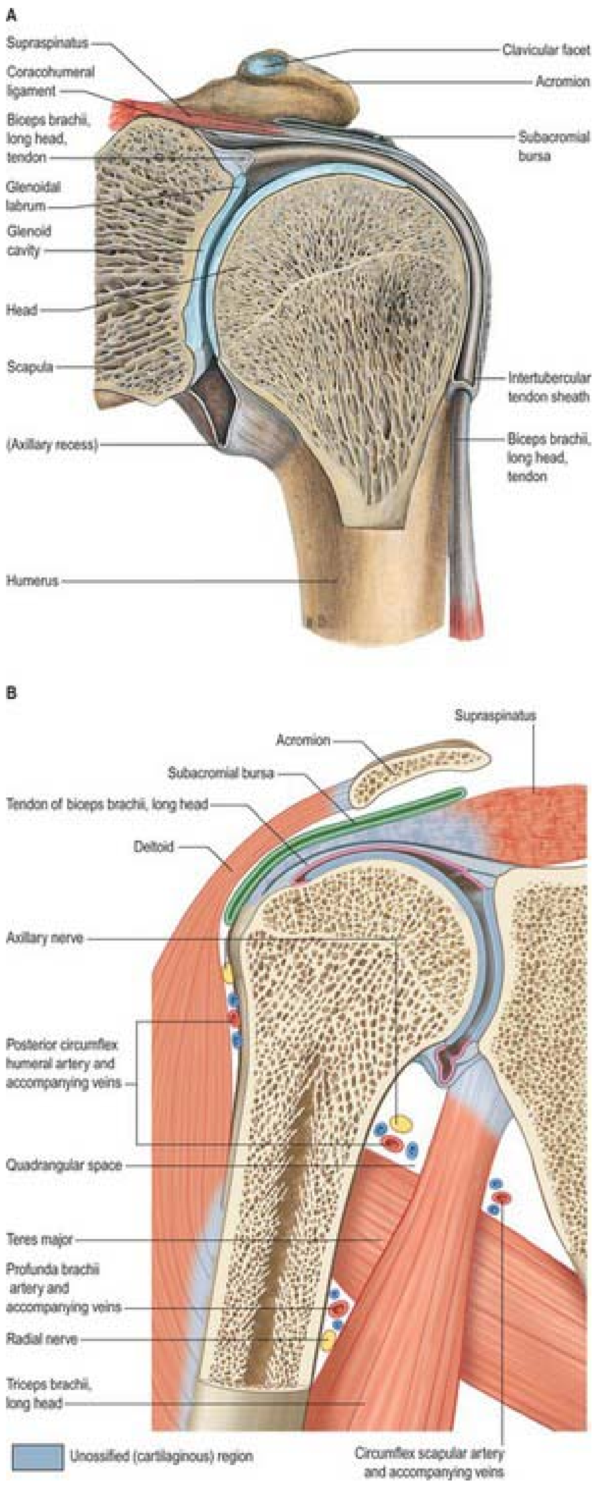
A
Supraspinatus
Coracohumeral ligament
Biceps brachii, long head, tendon
Glenoidal labrum
Glenoid cavity
Head
Scapula
(Axillary recess)
Humerus
Clavicular facet
Acromion
Subacromial bursa
Intertubercular tendon sheath
Biceps brachii, long head, tendon
B
Supraspinatus
Acromion
Subacromial bursa
Tendon of biceps brachii, long head
Deltoid
Axillary nerve
Posterior circumflex humeral artery and accompanying veins
Quadrangular space
Teres major
Profunda brachii artery and accompanying veins
Radial nerve
Triceps brachii, long head
Unossified (cartilaginous) region
Circumflex scapular artery and accompanying veins

Fig. 46.16 Coronal sections through the left shoulder joint viewed from the posterior aspect. **A**, Anteriorly placed coronal section to show tendon of biceps, long head. **B**, Posteriorly placed coronal section to show subacromial bursa and contents of quadrangular space.

(From Sobotta 2006.)

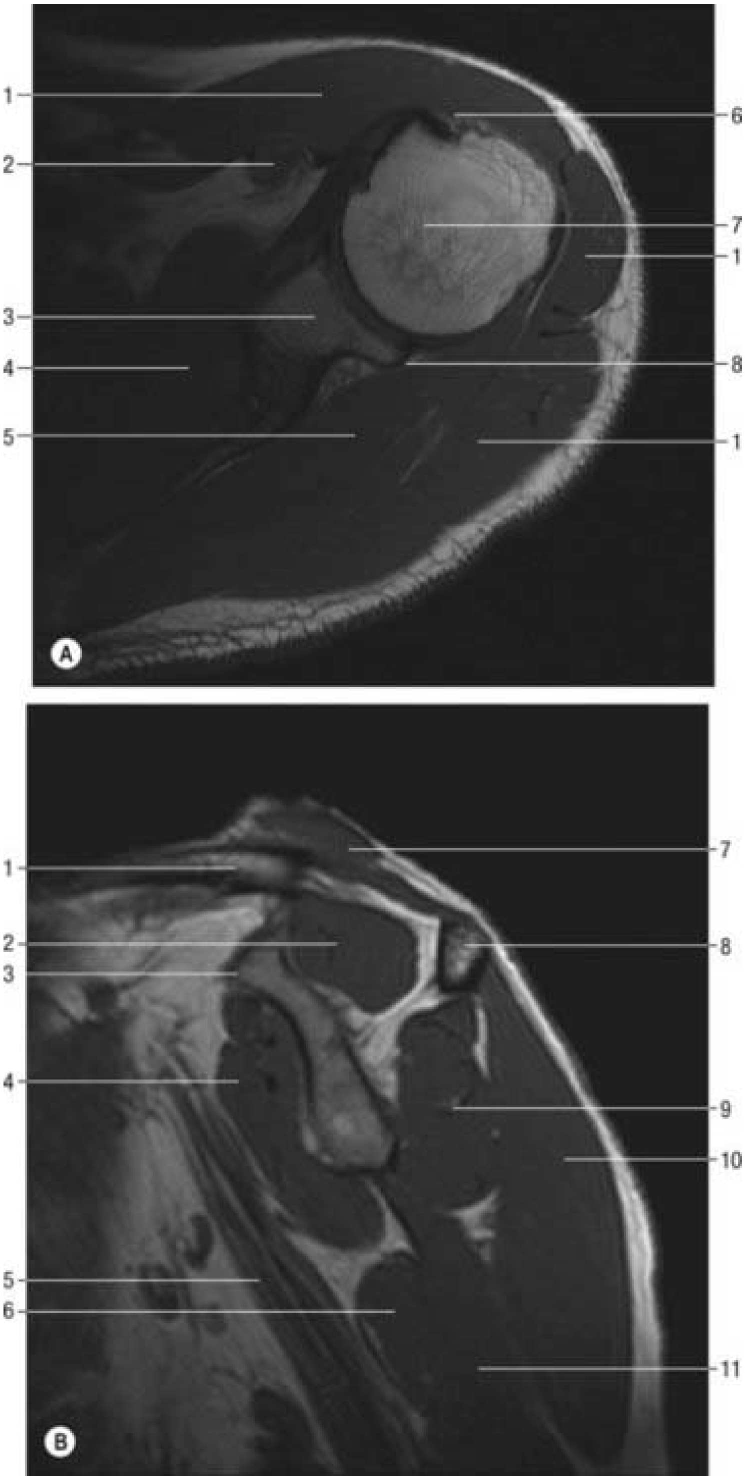
1
2
3
4
5
6
7
1
8
1
A
1
2
3
4
5
6
7
8
9
10
11
B

Fig. 46.17 MRI of shoulder. **A**, Axial image. **B**, Median sagittal oblique image at base of coracoid. **A: 1**. Deltoid. **2**. Coracobrachialis. **3**. Glenoid. **4**.

Subscapularis. **5**. Infraspinatus. **6**. Tendon of the long head of biceps. **7**. Head of humerus. **8**. Posterior labrum. **B: 1**. Clavicle. **2**. Supraspinatus. **3**. Coracoid. **4**. Subscapularis. **5**. Axillary nerve. **6**. Latissimus dorsi. **7**. Trapezius. **8**. Scapular spine. **9**. Infraspinatus. **10**. Deltoid. **11**. Triceps. Compare **A** with Fig. 46.23.

Glenoid labrum

The glenoid labrum is a fibrocartilaginous rim around the glenoid fossa. It is triangular in section and varies in size and thickness; its base is attached to the margin of the fossa and its free inner edge projects as a continuation of the curve of the glenoid. It blends above with two fasciculi from the long tendon of biceps. The labrum deepens the cavity, may protect the bone, and probably assists lubrication. Its attachment is sometimes partly deficient anterosuperiorly, in which case synovial membrane may protrude through the gaps.

Fibrous capsule

A fibrous capsule envelops the joint (Fig. 46.14, Fig. 46.16). It is attached medially to the glenoid neck outside the glenoid labrum, and encroaches on the coracoid process to include the attachment of the long head of biceps. The capsule often extends and attaches to the base of the coracoid and to the body of the scapula, forming anterior and posterior recesses. Laterally, it is attached to the anatomical neck of the humerus, i.e. near the articular margin, except inferomedially, where it descends more than 1 cm on the humeral shaft. It is so lax that the bones can be distracted for 2 or 3 cm, which accords with the very wide range of movement possible at the glenohumeral joint. However, such unnatural separation requires relaxation of the upper capsule by abduction.

The fibrous capsule is supported by the tendons of supraspinatus (above), infraspinatus and teres minor (behind), subscapularis (in front) and by the long head of triceps (below). The rotator interval is a medially based triangular area of uncovered capsule between the superior edge of subscapularis and the anterior edge of supraspinatus as these tendons pass on either side of the base of the coracoid: it may represent an area of weakness that increases instability in some shoulders. Triceps is separated from the capsule by the axillary nerve and posterior circumflex humeral vessels as they pass back from the axilla (Fig. 46.14). The capsule is least supported inferiorly, and subjected to the greatest strain in full abduction, when it is stretched tightly across the humeral head. It is strengthened anteriorly by extensions from the tendons of pectoralis major and teres major.

There are usually two or three openings in the capsule: below the coracoid process, connecting the joint to a bursa behind the tendon of subscapularis (anterior); between the humeral tubercles, transmitting the long tendon of biceps and its synovial sheath; connecting the joint to a bursa under the tendon of infraspinatus (posterior and inconstant).

Ligaments

The ligaments associated with the glenohumeral joint are the glenohumeral (superior, middle and inferior), coracohumeral and transverse humeral.

Glenohumeral ligaments

Three glenohumeral ligaments, only visible from within the joint, reinforce the capsule anteriorly and inferiorly (Fig. 46.18). They do not act as traditional ligaments (which carry a pure tensile force along their length), but become taut at varying positions of abduction and humeral rotation, acting as ‘check-reins’. Moreover, they do not have the strength characteristics of the ligaments at the knee. The superior glenohumeral ligament passes from the supraglenoid tubercle, just anterior to the origin of the long head of biceps, to the humerus near the proximal tip of the lesser tubercle on the medial ridge of the intertuberculous groove, the fovea capitis. It forms an anterior cover around the long head of biceps, and is part of the rotator interval. Together with the coracohumeral ligament it is an important stabilizer in the inferior direction, helping to keep the humeral head suspended (the coracohumeral ligament is more robust than the superior glenohumeral ligament). The middle glenohumeral ligament arises from a wide attachment below the superior glenohumeral ligament, along the anterior glenoid margin as far as the inferior third of the rim, and passes obliquely inferolaterally, enlarging as it does, to attach to the lesser tubercle deep to the tendon of subscapularis, with which it blends. The width and thickness of this ligament may be as much as 2 cm and 4 mm respectively. It provides anterior stability at 45° and 60° abduction. The thicker and longer inferior glenohumeral ligament complex is a hammock-like structure with anchor points on the anterior and posterior sides of the glenoid. It arises from the anterior, middle and posterior margins of the glenoid labrum, below the epiphysial line, and passes anteroinferiorly to the inferior and medial aspects of the neck of the humerus. The anterior, superior edge of the inferior ligament is thickened as the superior band, and the diffuse thickening of the anterior part of the capsule to which it is attached is known as the axillary pouch. The anterior band of the inferior glenohumeral ligament is thought to be the primary static anterior stabilizer of the abducted and externally rotated glenohumeral joint. (For further details consult Burkart & Debski 2002.)

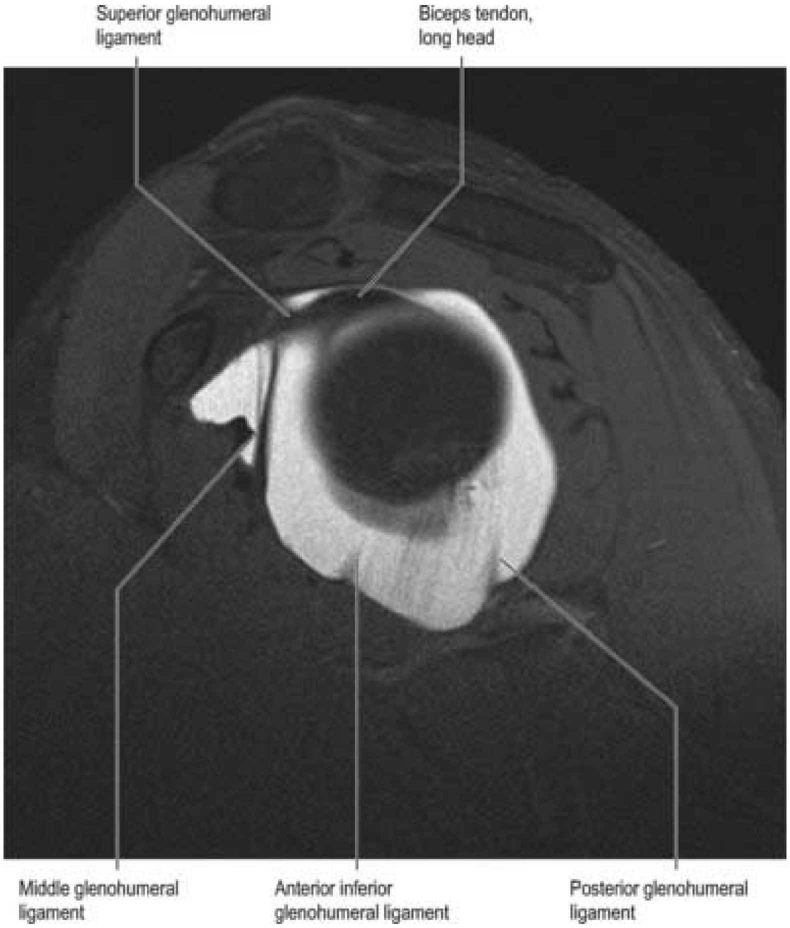
Superior glenohumeral ligament
Biceps tendon, long head
Middle glenohumeral ligament
Anterior inferior glenohumeral ligament
Posterior glenohumeral ligament

Fig. 46.18 Sagittal magnetic resonance arthrogram image following distension of the glenohumeral joint by intra-articular contrast injection in a 28-year-old male. Note the clearly outlined glenohumeral ligaments.

Coracohumeral ligament

The coracohumeral ligament is attached to the dorsolateral base of the coracoid process and extends as two bands, which blend with the capsule, to the greater and lesser tubercles (Fig. 46.14). Portions of the coracohumeral ligament form a tunnel for the biceps tendon on the anterior side of the joint. The rotator interval is reinforced by the coracohumeral ligament. It also blends inferiorly with the superior glenohumeral ligament.

Transverse humeral ligament

The transverse humeral ligament is a broad band which passes between the humeral tubercles, and is attached superior to the epiphysial line (Fig. 46.14). It converts the intertubercular sulcus into a canal, and acts as a retinaculum for the long tendon of biceps.

Synovial membrane

The synovial membrane lines the capsule and covers parts of the anatomical neck. The long tendon of biceps traverses the joint in a synovial sheath which continues into the intertubercular sulcus as far as the surgical neck of the humerus (Fig. 46.14, Fig. 46.16).

Bursae Many bursae adjoin the shoulder joint.

They are usually found between the tendon of subscapularis and the capsule, communicating with the joint between the superior and middle glenohumeral ligaments; on the superior acromial aspect; between the coracoid process and capsule; between teres major and the long head of triceps: anterior and posterior to the tendon of latissimus dorsi. The subacromial bursa, between deltoid and the capsule, does not communicate with the joint cavity but is prolonged under the acromion and coracoacromial ligament, and between them and supraspinatus: it appears to be attached, together with the subdeltoid fascia, to the acromion. Bursae sometimes occur behind coracobrachialis and between the tendon of infraspinatus and the capsule, occasionally opening into the joint.

Vascular supply

The glenohumeral joint is supplied by branches from the anterior and posterior circumflex humeral, suprascapular and circumflex scapular vessels.

Innervation

The glenohumeral joint is innervated mainly from the posterior cord of the brachial plexus. The capsule is supplied by the suprascapular nerve (posterior and superior parts), axillary nerve (anteroinferior) and the lateral pectoral nerve (anterosuperior).

Factors maintaining stability

The articulation between the relatively large humeral head and the shallow glenoid fossa allow a wide range of movement at the expense of providing an unstable bony complex. The anterior joint capsule is strong but lax. A variety of additional factors help to increase the stability of the joint: the glenoid labrum deepens the concavity of the articulating glenoid, the glenohumeral ligaments act as static stabilizers in certain positions, and there is a negative pressure within the joint. The coracoacromial arch (coracoid, acromion and coracoacromial ligament) prevents upward dislocation of the humerus. The tendons of subscapularis, supraspinatus, infraspinatus and teres minor fuse with the lateral part of the joint capsule to form the 'rotator cuff'. These short muscles collectively produce a compressive force during active glenohumeral movements which maintains congruent contact between the head of the humerus and the glenoid fossa, helps to resist skid, and checks excessive translation. The rotator cuff also provides strong lateral stability and prevents this part of the lax capsule from being nipped during joint movements. The long head of biceps offers additional superior support. The long head of triceps offers inferior support which is particularly important when the shoulder is abducted. However, the glenohumeral joint is least stabile inferiorly when the shoulder is fully abducted.

Movements at the shoulder (glenohumeral) joint

The shoulder is capable of any combination of swing and spin over a very wide range. Laxity of the capsule, and a humeral head which is large relative to a shallow glenoid fossa, afford a wider range of movement than at any other joint. Flexion–extension, abduction–adduction, circumduction and medial and lateral rotation all occur at the shoulder. Although the majority of the movement of the shoulder occurs at the glenohumeral joint, there is a varying contribution from the scapulothoracic articulation in most directions, most significantly in abduction, and excluding lateral rotation.

In analysis of shoulder movements it is preferable to refer humeral movement to the scapula, rather than to conventional anatomical planes (Fig. 46.19). When the arm hangs at rest the glenoid fossa faces almost equally forwards and laterally, and the humeral capitular and scapular (topographical) axes correspond, although the humerus, relative to the anatomical position, is medially rotated. Flexion carries the arm anteromedially on an axis through the humeral head orthogonal to the glenoid fossa at its centre. Abduction and adduction occur in a vertical plane orthogonal to that of flexion–extension; the axis is horizontal, through the humeral head, parallel with the glenoid plane. Pure abduction raises the arm anterolaterally in the plane of the scapula. However, when referred to the trunk, flexion and extension occur in the paramedian plane, and abduction and adduction in the coronal plane. In this sense, raising the arm vertically from flexion or raising it from abduction are both accompanied by humeral rotation in opposite directions. Whether ‘scapular’ or any other plane of abduction is described, these are selections from an infinite series. In scapular abduction points on the humeral surface pursue vertical cords but in rotation they are horizontal. In ‘pure’ flexion–extension, in a plane orthogonal to the scapula the axis of movement, and the notional ‘mechanical axis’, are regarded as projected from the centre of the glenoid cavity.

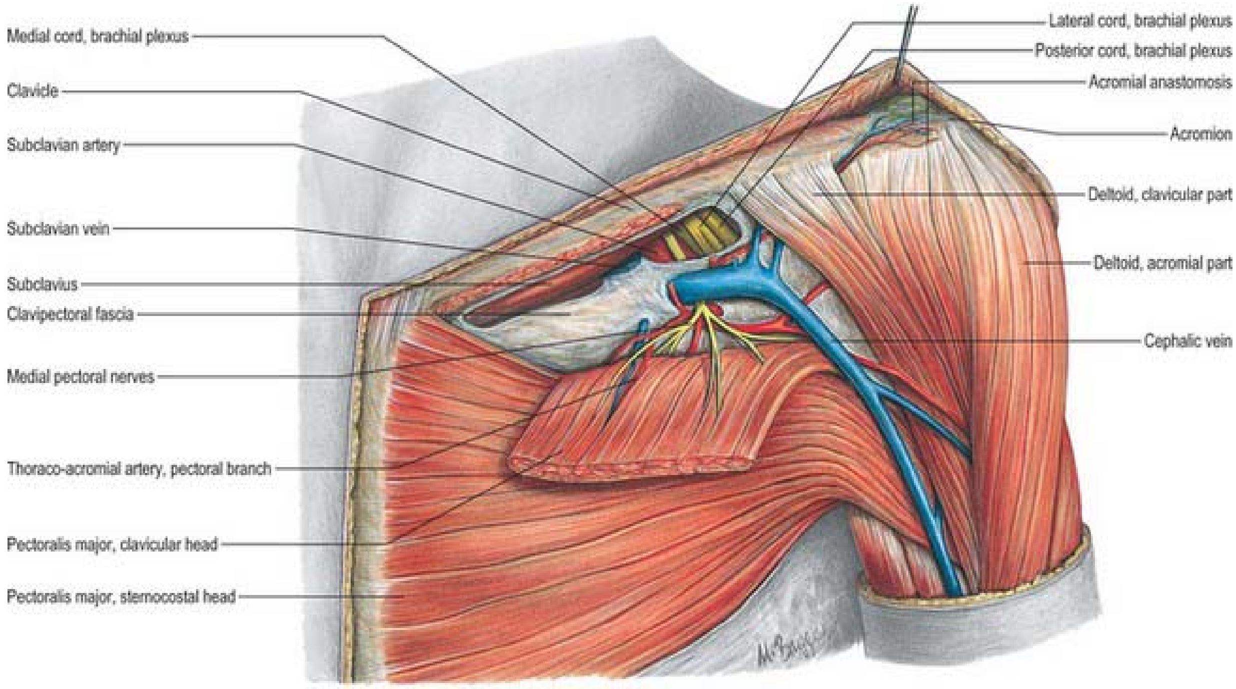
Medial cord, brachial plexus
Clavicle
Subclavian artery
Subclavian vein
Subclavius
Clavipectoral fascia
Medial pectoral nerves
Thoraco-acromial artery, pectoral branch
Pectoralis major, clavicular head
Pectoralis major, sternocostal head
Lateral cord, brachial plexus
Posterior cord, brachial plexus
Acromial anastomosis
Acromion
Deltoid, clavicular part
Deltoid, acromial part
Cephalic vein

Fig. 46.19 Left deltopectoral groove showing clavipectoral fascia and thoracoacromial axis.

(From Sobotta 2006.)

Glenohumeral abduction is approximately 90°, but angles up to 120° have been reported. Some 60° further abduction occurs at the sterno- and acromioclavicular articulations. Contralateral vertebral flexion also aids in bringing the arm to the vertical. During active elevation, movements at the glenohumeral and acromioclavicular joints are simultaneous, except in the initial few degrees, when most, often all, movement is glenohumeral. For every 15° of elevation, glenohumeral movement is said to be 10° and scapular movement 5°. During the initial stages of abduction, subscapularis, infraspinatus and teres minor counteract the strong upward component of pull of deltoid, which would otherwise cause the humeral head to slide up; the additive turning moments exerted by deltoid and supraspinatus about the shoulder joint can then abduct the arm.

In flexion, the humerus swings at right angles to the scapular plane and scapular rotation cannot increase the elevation (120°) obtainable in full flexion. If the fully flexed humerus is also abducted, elevation increases pro rata until, when the humerus reaches the scapular plane, i.e. when true abduction is reached, 180° of elevation becomes possible. In medial or lateral rotation, the humerus revolves about one-quarter of a circle around a vertical axis; the range is greatest when the arm is pendent, and least when it is vertical. When assessing the rotational range at the glenohumeral joint, the forearm should be flexed to a right angle at the elbow: this will prevent the effects of superadded pronation or supination in the pendent limb. In circumduction, which is a succession of the foregoing movements, the distal end of the humerus describes the base of a cone, its apex at the humeral head. This glenohumeral movement can be much increased by scapular movements, e.g. in acts of slinging objects with force.

The peculiar relation of the long head of biceps to the shoulder joint may serve several purposes. By its connection with both the shoulder and elbow, the muscle harmonizes their actions as an elastic ligament during all their movements. It helps to prevent the humeral head impinging on the acromion when deltoid contracts and to steady it in movements of the arm. In paralysis of supraspinatus it may also help initiate abduction of the arm, particularly when the humerus is laterally rotated.

Muscles producing movements

The muscles which produce movements at the glenohumeral joint are principally deltoid, pectoralis major, latissimus dorsi and teres major. These long muscles all converge on the humerus, acting at mechanical advantage on a joint which, as a result of glenoid shallowness and capsular laxity, is relatively unstable. The long muscles are counteracted by the rotator cuff, a group of short muscles (subscapularis, supraspinatus, infraspinatus and teres minor) which are attached nearer to the joint, and which centre the head of the humerus in the glenoid fossa through the midrange of motion, when the capsuloligamentous structures are lax.

Flexion

Pectoralis major (clavicular part), deltoid (anterior fibres) and coracobrachialis assisted by biceps. The sternocostal part of pectoralis major is a major force in flexion forwards to the coronal plane from full extension.

Extension

Deltoid (posterior fibres) and teres major, from the dependent position. When the fully flexed arm is extended against resistance, latissimus dorsi and the sternocostal part of pectoralis major act powerfully until the arm reaches the coronal plane.

Abduction

Deltoid. Initially its effect is mainly upward and, unless opposed, this would displace the humerus upwards. Subscapularis, infraspinatus and teres minor exert downward traction and so apply an opposing force: together with deltoid they constitute a ‘couple’ to produce abduction in the scapular plane.

Supraspinatus assists in effecting and maintaining this movement, but its precise role is controversial.

Medial rotation

Pectoralis major, deltoid (anterior fibres), latissimus dorsi, teres major and, with the arm pendent, subscapularis.

Lateral rotation

Infraspinatus, deltoid (posterior fibres) and teres minor. Lateral rotation is important for clearance of the greater tubercle and its associated tissues as it passes under the coracoacromial arch, as well as for relaxation of the capsular ligamentous constraints.

Rotator cuff disease

The subacromial space is defined inferiorly by the humeral head, and superiorly by the anterior edge and inferior surface of the anterior third of the acromion, coracoacromial ligament and acromioclavicular joint, forming the coracoacromial arch. It is occupied by the supraspinatus tendon, subacromial bursa, tendon of the long head of biceps brachii, and the capsule of the shoulder joint. Rotator cuff disease is a painful condition with a multifactorial aetiology in which severe or chronic impingement of the rotator cuff tendons on the undersurface of the coracacromial arch is often a significant factor. The cuff normally impinges against the coracoacromial arch when the humerus is abducted, flexed and internally rotated. This is known as the impingement position. The supraspinatus tendon is anatomically affected most by the impingement, which interestingly also coincides with an area of reduced vascularity in this tendon. Severe impingement can be caused by thickening of the coracoacromial arch, by inflammation of the cuff from disorders such as rheumatoid arthritis, or as a result of prolonged overuse in the impingement position, e.g. in cleaning windows. When associated with a tendinopathy from age-related degenerative changes within the tendon, impingement may be associated with partial or complete tears of the cuff. Clinically, this condition causes tenderness over the anterior portion of the acromion, and pain which typically occurs on abducting the shoulder between 60° and 120° (the painful arc).

Glenohumeral joint dislocations

The glenohumeral joint is the most frequently dislocated joint in the body. It is most unstable anteroinferiorly, which explains why the vast majority of dislocations are anterior, and occur when the arm is forced backwards when it is in abduction, external rotation and extension. Clinically, a dislocated shoulder loses its normal contour, and the acromion process, rather than the greater tubercle, becomes the most lateral bony structure. The axillary nerve and artery may be injured during dislocation, and this can lead to inability to abduct the shoulder as a result of paralysis of deltoid together with an area of anaesthesia over the distal part of the muscle (sometimes referred to as the ‘badge area’ of skin), as well as ischaemic changes in the limb. Posterior dislocation is rare and typically occurs when violent movements produce marked internal rotation and adduction, e.g. in epileptic seizures or electric shock.

MUSCLES

Pectoralis major

Attachments

Pectoralis major (Fig. 46.19) is a thick, fan-shaped muscle. It arises from the anterior surface of the sternal half of the clavicle; half the breadth of the anterior surface of the sternum down to the level of the sixth or seventh costal cartilage; the first to the seventh costal cartilages (first and seventh often omitted); the sternal end of the sixth rib; and the aponeurosis of external oblique. The clavicular fibres are usually separated from the sternal fibres by a slight cleft. The muscle converges to a flat tendon, approximately 5 cm across, which is attached to the lateral lip of the intertubercular sulcus of the humerus. The tendon is bilaminar. The thicker anterior lamina is formed by fibres from the manubrium, which are joined superficially by clavicular fibres and deeply by fibres from the sternal margin and the second to fifth costal cartilages. Clavicular fibres may be prolonged into the deltoid tendon. The posterior lamina receives fibres from the sixth (and often seventh) costal cartilages, sixth rib, sternum, and aponeurosis of the external oblique. Costal fibres join the lamina without twisting. Fibres from the sternum and aponeurosis curve around the lower border, turning successively behind those above them, which means that this part of the muscle is twisted so that the fibres that are lowest at their medial origin are highest at their insertion on the humerus. The posterior lamina reaches higher on the humerus than the anterior, and gives off an expansion which covers the intertubercular sulcus and blends with the capsular ligament of the shoulder joint. An expansion from the deepest part of the lamina lines the intertubercular sulcus at its linear insertion; from its lower border another expansion descends into the deep fascia of the upper arm.

The rounded lower border of the muscle forms the anterior axillary fold, and becomes conspicuous in abduction against resistance.

Variants

The abdominal slip from the aponeurosis of the external oblique is sometimes absent. The number of costal attachments and the extent to which the clavicular and costal parts are separated vary. Right and left muscles may decussate across the sternum. A superficial vertical slip, or slips, may ascend from the lower costal cartilages and rectus sheath to blend with sternocleidomastoid or to attach to the upper sternum or costal cartilages. This is sternalis (rectus sternalis). The muscle may be partially or completely absent.

Relations

Skin, superficial fascia, platysma, medial and intermediate supraclavicular nerves, breast, and deep fascia are all anterior. The sternum, ribs and costal cartilages, clavipectoral fascia, subclavius, pectoralis minor, serratus anterior, external intercostal muscles and membranes are all posterior. Pectoralis major forms the superficial layer of the anterior axillary wall, and hence lies anterior to the axillary vessels and nerves and the upper parts of biceps and coracobrachialis. Its upper border is separated from deltoid by the infraclavicular fossa, which contains the cephalic vein and deltoid branch of the thoraco-acromial artery. Its lower border forms the anterior axillary fold. Pectoralis major is separated from latissimus dorsi on the medial axillary wall, but the two muscles converge as they approach the lateral axillary wall: the floor of the intertuberculous sulcus lies between their attachments.

Vascular supply

Pectoralis major is supplied by one dominant vascular pedicle from the pectoral branch of the thoraco-acromial axis, supplemented by several smaller secondary segmental vessels from the deltoid and clavicular branches of the thoraco-acromial axis, and perforating branches of the internal thoracic arteries and superior and lateral thoracic arteries.

The presence of a dominant vascular pedicle (together with its musculocutaneous perforators) means that a musculocutaneous flap in this region can be surgically raised solely on the pectoral branch (the pectoralis major musculocutaneous flap). This flap can be used to reconstruct areas of missing tissue following head and neck cancer resections.

Innervation

Pectoralis major is supplied through the medial and lateral pectoral nerves. Fibres for the clavicular part are from C5 and 6; those for the sternocostal part are from C6, 7, 8, and T1.

Action

The two parts of the muscle can act separately or together. The whole muscle assists adduction and medial rotation of the humerus against resistance. It swings the extended arm forwards and medially, its clavicular part acting with the anterior fibres of deltoid and coracobrachialis: the sternocostal part is relaxed. The opposite movement is usually aided by gravity. When it is resisted, the sternocostal part acts together with latissimus dorsi, teres major and the posterior fibres of deltoid: the clavicular part is relaxed. With the raised arms fixed, e.g. gripping a branch, the same combination of muscles draws the trunk up and forwards. Pectoralis major is active in deep inspiration. Electromyography suggests that the clavicular part acts alone in medial rotation.

Clinical anatomy: testing

To test the clavicular head, the abducted arm is flexed against resistance. To test the sternocostal head, the arm is adducted against resistance.

Poland syndrome

Poland syndrome is a rare congenital anomaly where there is hypoplasia of the thoracic chest wall muscles and ipsilateral hypoplasia of the arm and hand. It occurs in approximately 1 : 50,000 live births. The major clinical features are that the sternocostal head of pectoralis major and all of pectoralis minor are absent. In addition, there may be hypoplasia of latissimus dorsi, serratus anterior, external oblique, supraspinatus, infraspinatus, deltoid and the intercostal muscles, and hypoplasia of the hemithorax and ribs. There may be ipsilateral breast hypoplasia and absent nipple-areolar-complex (Ch. 55).

Hypoplasia affecting the arm ranges from syndactyly to symbrachydactyly and ectrodactyly. The second, third and fourth fingers are the most affected; the wrist, forearm, upper arm and scapula are variably involved.

The aetiology is unclear. It has been suggested that the condition is caused by disruption of the arterial blood supply to the subclavian vessels during the sixth and seventh week of embryonic life, or by disruption of lateral plate mesoderm 2–4 weeks after fertilization.

Pectoralis minor

Attachments

Pectoralis minor is a thin, triangular muscle lying posterior (deep) to pectoralis major (Fig. 46.20). It arises from the upper margins and outer surfaces of the third to fifth ribs (frequently second to fourth), near their cartilages, and from the fascia over the adjoining external intercostal muscles. Its fibres ascend laterally under cover of pectoralis major, converging in a flat tendon which is attached to the medial border and upper surface of the coracoid process of the scapula. Part or all of the tendon may cross the coracoid process into the coraco-acromial ligament, or even beyond to the coracohumeral ligament, thereby gaining attachment to the humerus.

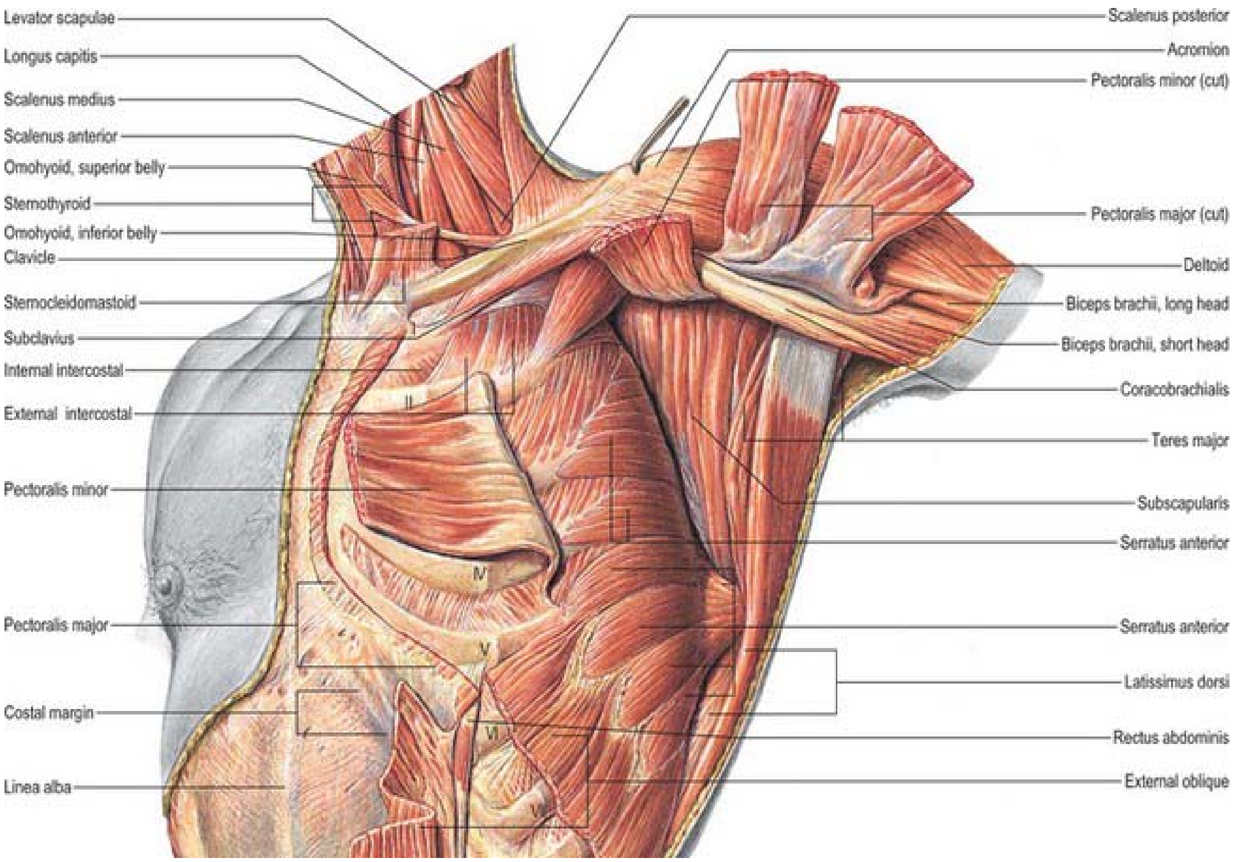
Levator scapulae
Longus capitis
Scalenus medius
Scalenus anterior
Omohyoid, superior belly
Sternothyroid
Omohyoid, inferior belly
Clavicle
Sternocleidomastoid
Subclavius
Internal intercostal
External intercostal
Pectoralis minor
Pectoralis major
Costal margin
Linea alba
Scalenus posterior
Acromion
Pectoralis minor (cut)
Pectoralis major (cut)
Deltoid
Biceps brachii, long head
Biceps brachii, short head
Coracobrachialis
Teres major
Subscapularis
Serratus anterior
Serratus anterior
Latissimus dorsi
Rectus abdominis
External oblique
II
III
IV
V
VI
VII

Fig. 46.20 Deep muscles of the front of the chest and left arm. Roman numerals refer to costal cartilages.

(From Sobotta 2006.)

Variants

Slips of the muscle are sometimes separated and vary in number and level. In rare cases, one passes from the first rib to the coracoid (pectoralis minimus). The costal attachments can be 2nd to 5th ribs; 3rd to 5th; 2nd to 4th; 3rd to 4th. The muscle can be present or absent when the pectoralis major is absent.

Relations

Pectoralis major, the lateral pectoral nerve and pectoral branches of the thoraco-acromial artery are anterior. The ribs, external intercostals, serratus anterior, the axilla, axillary vessels, lymphatics and brachial plexus are all posterior. The upper border of pectoralis minor is separated from the clavicle by a triangular gap which is filled by the clavipectoral fascia, behind which are the axillary vessels, lymphatics and nerves. The lateral thoracic artery follows the lower border of the muscle. The medial pectoral nerves pierce and partly supply the muscle.

Vascular supply

Pectoralis minor is supplied by pectoral and deltoid branches of the thoraco-acromial and superior and lateral thoracic arteries.

Innervation

Pectoralis minor is innervated by branches of the medial and lateral pectoral nerves, C5, 6, 7, 8 and T1.

Action

Pectoralis minor assists serratus anterior in drawing the scapula forwards around the chest wall. With levator scapulae and the rhomboids it rotates the scapula, depressing the point of the shoulder. Both pectoral muscles are electromyographically quiescent in normal inspiration, but are active in forced inspiration.

Subclavius

Attachments

Subclavius is a small, triangular muscle tucked between the clavicle and the first rib (Fig. 46.20). It arises from the junction of the first rib and its costal cartilage by a thick tendon, prolonged at its inferior margin and anterior to the costoclavicular ligament. It passes upwards and laterally to a groove on the under surface of the middle third of the clavicle, where it is attached by muscular fibres.

Subclavius may be attached to the coracoid process or the upper border of the scapula as well as, or instead of, the clavicle.

Relations

Posteriorly subclavius is separated from the first rib by the subclavian vessels and brachial plexus, and anteriorly it is separated from pectoralis major by the anterior lamina of the clavipectoral fascia.

Vascular supply

Subclavius is supplied by the clavicular branch of the thoraco-acromial artery and the suprascapular artery.

Innervation

Subclavius is supplied by the subclavian branch of the brachial plexus, which contains fibres from C5 and 6.

Action

Subclavius probably pulls the point of the shoulder down and forwards and braces the clavicle against the articular disc of the sternoclavicular joint: however it is inaccessible to palpation, and difficult to investigate by electromyography. It ‘protects’ the subclavian vessels in fractures of the clavicle, which rarely involve these vessels.

Trapezius

Attachments

Trapezius is a flat, triangular muscle which extends over the back of the neck and upper thorax (Fig. 54.15). The paired trapezius muscles form a diamond shape, from which the name is derived: the lateral angles occur at the shoulder tips, the superior angle at the occipital protuberance and superior nuchal lines, and the inferior angle at the spine of the twelfth thoracic vertebra. On either side, the muscle is attached to the medial third of the superior nuchal line, external occipital protuberance, ligamentum nuchae, and apices of the spinous processes and their supraspinous ligaments from C7 to T12. Superior fibres descend, inferior fibres ascend, and the fibres between them proceed horizontally: all converge laterally on the shoulder. The superior fibres are attached to the posterior border of the lateral third of the clavicle; the middle fibres to the medial acromial margin and superior lip of the crest of the scapular spine; and the inferior fibres pass into an aponeurosis which glides over a smooth triangular surface at the medial end of the scapular spine and is attached to a tubercle at its lateral apex. The occipital attachment is by a fibrous lamina, which is also adherent to the skin. The spinal attachment is by a broad triangular aponeurosis from the sixth cervical to the third thoracic vertebrae, and by short tendinous fibres below this.

Variants

The clavicular attachment of trapezius varies in extent, sometimes reaching mid-clavicle, and occasionally blending with sternocleidomastoid. The vertebral attachment sometimes stops at the eighth thoracic spine. The occipital attachment may be absent. Cervical and dorsal parts are occasionally separate.

Vascular supply

The upper third of trapezius is supplied by a transverse muscular branch which arises from the occipital artery at the level of the mastoid process. It enters the muscle on its deep surface and gives off several musculocutaneous perforators to the overlying skin.

The middle portion of trapezius, together with an area of overlying skin, is supplied by the superficial cervical artery or by a superficial branch of the transverse cervical artery, via musculocutaneous perforators.

The lower third of trapezius is supplied by a muscular branch from the dorsal scapular artery, passing medial to the medial border of the scapula. It reaches the deep surface of the muscle either by piercing the rhomboids or by passing between rhomboid major and minor at the level of the base of the spine of the scapula. It anastomoses with the medial and lateral perforating branches of the posterior intercostal arteries.

The presence of these three discrete vascular pedicles means that musculocutaneous flaps can be surgically raised based on these individual arteries and their accompanying venae comitantes. These flaps can be used for reconstructing areas in the posterior head and neck.

Innervation

Trapezius is innervated by the spinal part of the accessory nerve. Sensory (proprioceptive) branches are derived from the ventral rami of C3 and C4.

Action

Trapezius cooperates with other muscles in steadying the scapula, controlling it during movements of the arm, and maintaining the level and poise of the shoulder. Electromyographic activity is minimal in the unloaded arm, and heavy loads can be suspended with a small contribution from the upper part. Acting with levator scapulae, the upper fibres elevate the scapula and with it the point of the shoulder; acting with serratus anterior, trapezius rotates the scapula forward (upwards) so that the arm can be raised above the head; and acting with the rhomboids, it retracts the scapula, bracing back the shoulder. With the shoulder fixed, trapezius may bend the head and neck backwards and laterally. Trapezius, levator scapulae, rhomboids and serratus anterior combine in producing a variety of scapular rotations (p. 803).

Clinical anatomy: testing

Trapezius is palpated while the shoulder is shrugged against resistance.

Deltoid

Attachments

Deltoid is a thick, curved triangle of muscle. It arises from the anterior border and superior surface of the lateral third of the clavicle, the lateral margin and superior surface of the acromion, and the lower edge of the crest of the scapular spine (other than its smooth medial triangular surface) (Fig. 46.19). The fibres converge inferiorly to a short, substantial tendon which is attached to the deltoid tubercle on the lateral aspect of the midshaft of the humerus. Anterior and posterior fibres converge directly to this tendon. The intermediate part is multipennate: four intramuscular septa descend from the acromion to interdigitate with three septa ascending from the deltoid tubercle. The septa are connected by short muscle fibres, which provide powerful traction. The fasciculi are large, producing a coarse longitudinal striation. The muscle surrounds the glenohumeral articulation on all sides except inferomedially, lending the shoulder its rounded profile. In contraction its borders are easily seen and felt. The tendon gives off an expansion into the brachial deep fascia which may reach the forearm.

Variants

Deltoid may fuse with pectoralis major or may receive additional slips from trapezius, the infraspinous fascia or the lateral scapular border.

Relations

The skin, superficial and deep fasciae, platysma, lateral supraclavicular and upper lateral brachial cutaneous nerves are all superficial. The coracoid process, coraco-acromial ligament, subacromial bursa, tendons of pectoralis minor, coracobrachialis, both heads of biceps, pectoralis major, subscapularis, supraspinatus, infraspinatus, teres minor, long and lateral heads of triceps, the circumflex humeral vessels, axillary nerve, and the surgical neck and upper shaft of the humerus, including both tubercles, all lie deep to deltoid. The anterior border of the muscle is separated proximally from pectoralis major by the infraclavicular fossa, which contains the cephalic vein and deltoid branches of the thoraco-acromial artery. Distally, the muscles are in contact, and their tendons are usually united. The posterior border overlies infraspinatus and triceps.

Vascular supply

Deltoid is supplied by acromial and deltoid branches of the thoraco-acromial artery; the anterior and posterior circumflex humeral arteries; subscapular artery; and the deltoid branch of profunda brachii.

Innervation

Deltoid is innervated by the axillary nerve, C5 and 6.

Action

Different parts of the muscle can act independently as well as together. Anterior fibres assist pectoralis major in drawing the arm forwards and rotating it medially. Posterior fibres act with latissimus dorsi and teres major in drawing the arm backwards and rotating it laterally. The multipennate acromial part of deltoid is a strong abductor: aided by supraspinatus it abducts the arm until the joint capsule is tense below. Movement takes place in the plane of the body of the scapula, which is the only way that scapular rotation can be fully effective in raising the arm above the head. In true abduction (Fig. 46.19), acromial fibres contract strongly, while clavicular and posterior fibres prevent departure from the plane of motion. In the early stages of abduction, traction by the deltoid is upward, but the humeral head is prevented from translating upward by the synergistic downward pull of subscapularis, infraspinatus and teres minor. Electromyography suggests that deltoid contributes little to medial or lateral rotation but confirms that it takes part in most other shoulder movements. It may also aid supraspinatus in resisting the downward drag of a loaded arm. A common action of the deltoid is arm-swinging while walking.

Clinical anatomy: testing

Deltoid can be seen and felt to contract when the arm is abducted against resistance.

Levator scapulae

Attachments

Levator scapulae is a slender muscle attached by tendinous slips to the transverse processes of the atlas and axis, and to the posterior tubercles of the transverse processes of the third and fourth cervical vertebrae (Fig. 28.6, see below Fig. 46.21). It descends diagonally to approach the medial scapular border between its superior angle and the triangular smooth surface at the medial end of the scapular spine.

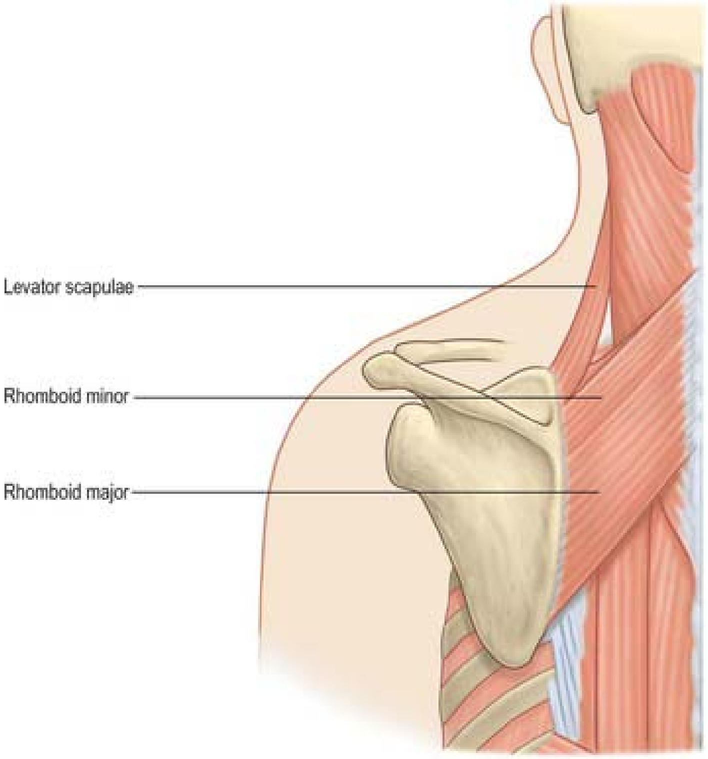

Fig. 46.21 Rhomboid muscles.

Variants

Levator scapulae varies considerably in its vertebral attachments and the extent to which it separates into slips. There may be accessory attachments to the mastoid process, occipital bone, first or second rib, scaleni, trapezius, and serratus muscles.

Vascular supply

Levator scapulae receives its arterial supply mainly from the transverse cervical and ascending cervical arteries. The vertebral extremity of the muscle is supplied by branches from the vertebral artery.

Innervation

Levator scapulae is innervated directly by branches of the third and fourth cervical spinal nerves, and from the fifth cervical nerve via the dorsal scapular nerve.

Action

The levator scapulae and the rhomboids assist other scapular muscles in controlling the position and movement of the scapula. Acting with trapezius, rhomboids retract the scapula, bracing back the shoulder; with levator scapulae and pectoralis minor they rotate the scapula, depressing the point of the shoulder. With the cervical vertebral column fixed, levator scapulae acts with trapezius to elevate the scapula or to sustain a weight carried on the shoulder; with the shoulder fixed, the muscle inclines the neck to the same side.

Rhomboid major

Attachments

Rhomboid major is a quadrilateral sheet of muscle which arises by tendinous fibres from the spines and supraspinous ligaments of the second to fifth thoracic vertebrae, and descends laterally to the medial border of the scapula between the root of the spine and the inferior angle (Fig. 46.21). Most of its fibres usually end in a tendinous band between these two points, joined to the medial border by a thin membrane. Occasionally this is incomplete, in which case some muscular fibres are attached directly into the scapula. The attachments of rhomboid major – and also those of rhomboid minor, levator scapulae and serratus anterior – can be more extensive, with ‘folds’ or extensions passing to both dorsal and costal aspects of the scapula adjacent to its medial margin.

Vascular supply, innervation, action and clinical anatomy: testing

All are described with rhomboid minor.

Rhomboid minor

Attachments

Rhomboid minor is a small, cylindrical muscle. It runs from the lower ligamentum nuchae and the spines of the seventh cervical and first thoracic vertebrae to the base of a smooth triangular surface at the medial end of the spine of the scapula, where dorsal and ventral layers enclose the inferior border of levator scapulae (Fig. 46.21). The dorsal layer of rhomboid minor is attached to the rim of the triangular surface, dorsolateral to and below levator scapulae. The ventral layer is strong and wide, extending 2–3 cm medial to and below levator scapulae; here the fasciae of rhomboid minor and serratus anterior are tightly fused. Rhomboid minor is usually separate from rhomboid major, but the muscles overlap and are occasionally united.

Variants

There is some variability in the vertebral and scapular attachments of rhomboids major and minor. A slip of muscle may extend from the upper border of rhomboid minor to reach the occipital bone (rhomboid occipitalis).

Vascular supply of the rhomboids

Rhomboids major and minor are supplied by the dorsal scapular artery or deep branch of the transverse cervical artery and by dorsal perforating branches from the upper five or six posterior intercostal arteries.

Innervation of the rhomboids

Rhomboids major and minor are innervated by a branch of the dorsal scapular nerve, C4, 5.

Action of the rhomboids

Both rhomboid major and minor retract the medial border of the scapula superiorly and medially. They are used in squaring the shoulders.

Clinical anatomy: testing of the rhomboids

Rhomboids major and minor can be palpated deep to trapezius on bracing the shoulder back against resistance.

Latissimus dorsi

Attachments

Latissimus dorsi is a large, flat, triangular muscle that sweeps over the lumbar region and lower thorax and converges to a narrow tendon (Fig. 46.22, Fig. 54.15). It arises by tendinous fibres from the spines of the lower six thoracic vertebrae anterior to trapezius; from the posterior layer of thoracolumbar fascia, by which it is attached to the spines and supraspinous ligaments of the lumbar and sacral vertebrae; and from the posterior part of the iliac crest. It also springs by muscular fibres from the posterior part (outer lip) of the iliac crest lateral to erector spinae, and by fleshy slips from the three or four lower ribs, interdigitating with external oblique (Fig. 61.9). From this extensive attachment, fibres pass laterally with different degrees of obliquity (the upper fibres are nearly horizontal, the middle oblique, and the lower almost vertical) to form a sheet approximately 12 or 13 mm thick that overlaps the inferior scapular angle. The muscle curves around the inferolateral border of teres major to gain its anterior surface. Here it ends as a flattened tendon, approximately 7 cm long, in front of the tendon of teres major. It is attached to the floor of the intertubercular sulcus of the humerus, with an expansion to the deep fascia. The attachment extends higher on the humerus than that of teres major. As the muscle curves round teres major, the fasciculi rotate around each other, so that fibres that originate lowest at the midline insert highest on the humerus, and fibres that originate highest at the midline insert lowest on the humerus. A bursa sometimes occurs between the muscle and the inferior scapular angle. The tendons of latissimus dorsi and teres major are united at their lower borders: they are separated by a bursa near their humeral attachments.

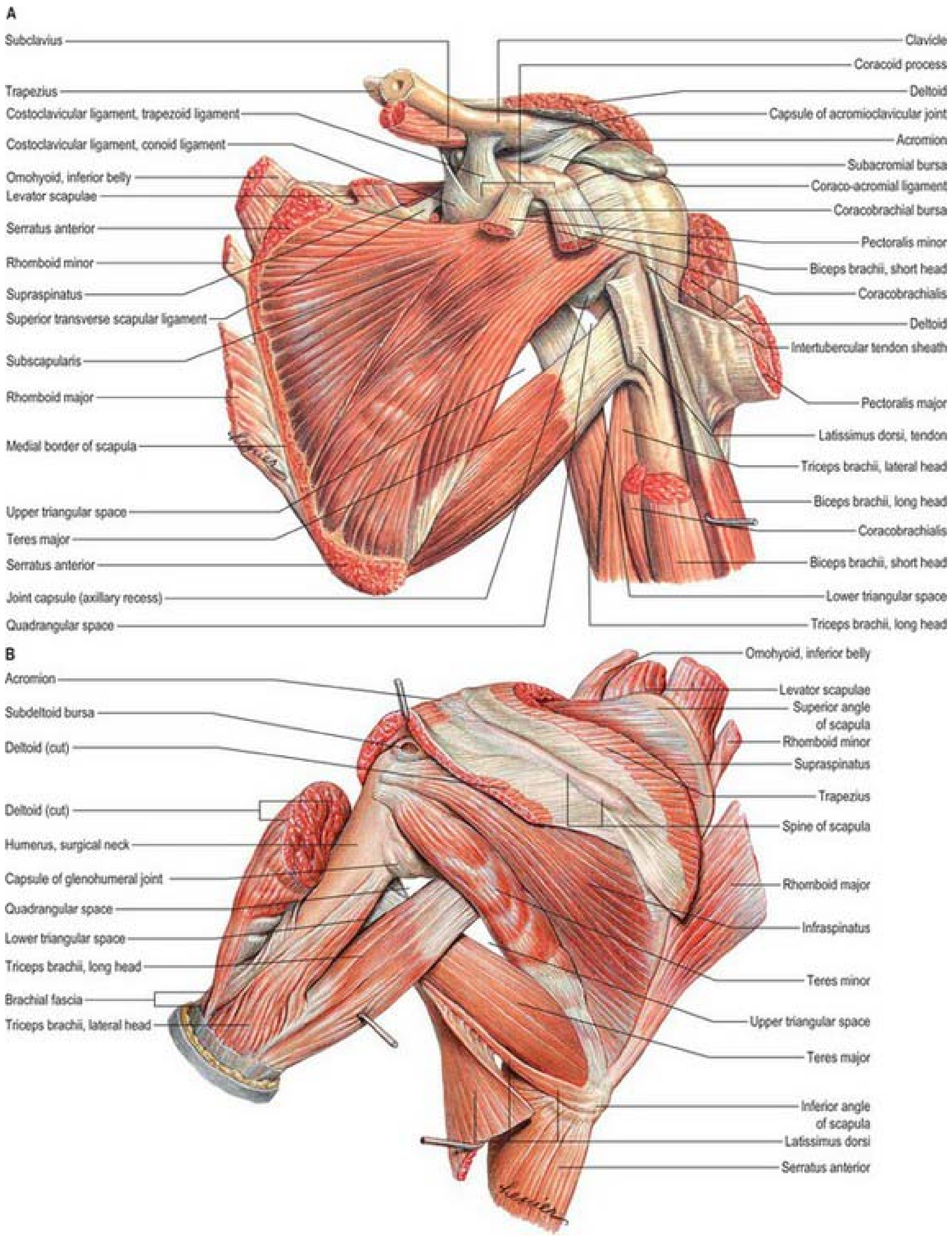
A
Subclavius
Trapezius
Costoclavicular ligament, trapezoid ligament
Costoclavicular ligament, conoid ligament
Omohyoid, inferior belly
Levator scapulae
Serratus anterior
Rhomboid minor
Supraspinatus
Superior transverse scapular ligament
Subscapularis
Rhomboid major
Medial border of scapula
Upper triangular space
Teres major
Serratus anterior
Joint capsule (axillary recess)
Quadrangular space
Clavicle
Coracoid process
Deltoid
Capsule of acromioclavicular joint
Acromion
Subacromial bursa
Coraco-acromial ligament
Coracobrachial bursa
Pectoralis minor
Biceps brachii, short head
Coracobrachialis
Deltoid
Intertubercular tendon sheath
Pectoralis major
Latissimus dorsi, tendon
Triceps brachii, lateral head
Biceps brachii, long head
Coracobrachialis
Biceps brachii, short head
Lower triangular space
Triceps brachii, long head
B
Acromion
Subdeltoid bursa
Deltoid (cut)
Deltoid (cut)
Humerus, surgical neck
Capsule of glenohumeral joint
Quadrangular space
Lower triangular space
Triceps brachii, long head
Brachial fascia
Triceps brachii, lateral head
Omohyoid, inferior belly
Levator scapulae
Superior angle of scapula
Rhomboid minor
Supraspinatus
Trapezius
Spine of scapula
Rhomboid major
Infraspinatus
Teres minor
Upper triangular space
Teres major
Inferior angle of scapula
Latissimus dorsi
Serratus anterior

Fig. 46.22 Deep muscles of the left shoulder girdle. **A**, Anterior aspect after removal of several superficial muscles. **B**, Posterior aspect.

(From Sobotta 2006.)

Latissimus dorsi and teres major together form the posterior axillary fold. When the arm is adducted against resistance, this fold is accentuated, and the whole inferolateral border of latissimus dorsi can then be traced to its attachment to the iliac crest.

The lower, lateral margin of the muscle is usually separated from the posterior border of external oblique by the lumbar triangle; the base of this small triangle is the iliac crest and its floor the internal oblique. It should not be confused with the triangle of auscultation, which is medial to the scapula, and is bounded above by the trapezius, below by latissimus dorsi and laterally by the medial border of the scapula; part of rhomboid major is exposed in the triangle. If the scapulae are drawn forwards, by folding the arms across the chest, and the trunk is bent forwards, parts of the sixth and seventh ribs and the interspace between them (overlying the apex of the lower pulmonary lobe) become subcutaneous.

Variants

Latissimus dorsi commonly receives some additional fibres from the scapula as it crosses the inferior scapular angle. A muscular axillary arch, 7–10 cm in length and 5–15 mm in breadth, may sometimes be present: it crosses from the edge of latissimus dorsi, midway in the posterior fold, over the front of the axillary vessels and nerves to join the tendons of pectoralis major, coracobrachialis or the fascia over the biceps. The vertebral and costal attachments of latissimus dorsi may be reduced or, in rare cases, increased. A fibrous slip usually passes from the tendon, near its humeral insertion, to the long head of triceps.

Vascular supply

Latissimus dorsi is supplied by a single dominant vascular pedicle, the thoracodorsal artery, itself a continuation of the subscapular artery (p. 817). The thoracodorsal artery (and its accompanying venae comitantes) enters the muscle at a single neurovascular hilum on its costal surface, 6–12 cm from the subscapular artery and 1–4 cm medial to the lateral border of the muscle. The artery gives off one to three large branches to serratus anterior before dividing at, or even before, the hilum to supply latissimus dorsi itself. The basic pattern of branching is a bifurcation into lateral and medial branches. The larger lateral branch follows a course parallel to, and 1–4 cm from, the upper border of the muscle; the smaller branch diverges at an angle of 45° and travels medially. In a small number of cases the artery trifurcates: this usually yields a small recurrent branch which returns to supply the proximal part of the muscle, but in some cases it provides a third major branch which supplies the distal part of the muscle. Occasionally the lateral branch gives off a further collateral to serratus anterior. The major branches give off 5–9 longitudinal branches which travel distally, parallel with the muscle fibres. Musculocutaneous perforators arising from these vessels supply the overlying skin.

In addition to the dominant vascular pedicle, latissimus dorsi is supplied inferiorly by several smaller secondary segmental vascular pedicles. These are dorsal perforating arteries derived from the 9th, 10th and 11th posterior intercostal and 1st, 2nd and 3rd lumbar arteries, and they all enter the muscle on its deep surface. They anastomose within the muscle with branches of the thoracodorsal artery.

The blood supply of latissimus dorsi is particularly important because of its applications in plastic and reconstructive surgery. The presence of the dominant vascular pedicle provides the anatomical basis for raising the muscle either alone, or together with an overlying paddle of skin in the form of a musculocutaneous flap based solely on the thoracodorsal artery and its accompanying venae comitantes. These flaps can be used in a pedicle fashion, e.g. in reconstructing a breast following a mastectomy, or used as free tissue transfer to cover large areas of tissue loss anywhere in the body.

Innervation

Latissimus dorsi is supplied by the thoracodorsal nerve, from the posterior cord of the brachial plexus, C6, 7 and 8. This nerve runs in the neurovascular pedicle and divides approximately 1.3 cm proximal to the point of bifurcation or trifurcation of the thoracodorsal artery. The pattern of branching follows that of the artery closely, and the neural and vascular branches travel together.

Action

Latissimus dorsi is active in adduction, extension and especially in medial rotation of the humerus. Humeral adduction and extension are most powerful when the initial position of the arm is one of partial abduction, flexion or a combination of the two. With the sternocostal part of pectoralis major and teres major it adducts the raised arm against resistance. It assists backward swinging of the arm, as in walking and many athletic pursuits. When the arms are raised above the head, as in climbing, it pulls the trunk upwards and forwards. It takes part in all violent expiratory efforts, such as coughing or sneezing: this is readily confirmed by palpation. Electromyography suggests that it aids deep inspiration, but it is also active towards the end of forcible expiration, e.g. when blowing a sustained note on a musical instrument. When the arm is elevated, the stretched fibres of latissimus dorsi press on the inferior scapular angle, keeping it in contact with the chest wall. Despite this range of actions, surgical transposition of the muscle does not produce any serious restriction of normal activity.

Clinical anatomy: testing

Latissimus dorsi is palpated when the abducted arm is adducted against resistance and can be felt to contract during coughing.

Serratus anterior

Attachments

Serratus anterior is a large muscular sheet which curves around the thorax. It arises from an extensive costal attachment and inserts on the scapula (Fig. 46.19, Fig. 46.20). Fleshy digitations spring anteriorly from the outer surfaces and superior borders of the upper eight, nine or even ten ribs, and from fasciae which cover the intervening intercostals. They lie on a long, slightly curved, line which passes inferolaterally across the thorax. The first digitations spring from the first and second ribs and intercostal fascia, the others from a single rib, and the lower four interdigitate with the upper five slips of external oblique. The muscle follows the contour of the chest wall closely. It passes ventral to the scapula and reaches the medial border of the scapula in the following way. The first digitation encloses, and is attached to, a triangular area of both the costal and dorsal surfaces of the superior scapular angle. The next two or three digitations form a triangular sheet which is attached to the costal surface along almost its entire medial border. The lower four or five digitations converge to be attached by musculotendinous fibres to a triangular impression on the costal surface of the inferior angle: they enclose the inferior angle and are also attached to a smaller triangular part of its dorsal surface near its tip.

Variants

Digitations may be absent, particularly the first and eighth, and sometimes also the intermediate part. Serratus anterior may be partly fused with levator scapulae, adjacent external intercostals or external oblique.

Vascular supply

Serratus anterior is supplied by superior and lateral thoracic arteries, and branches from the thoracodorsal artery before (occasionally after) it divides in latissimus dorsi.

Innervation

Serratus anterior is innervated by the long thoracic nerve, C5, 6 and 7, which descends on the external surface of the muscle.

Action

With pectoralis minor, serratus anterior protracts (draws forward) the scapula, as a prime mover in all reaching and pushing movements. The upper part, with levator scapulae and upper fibres of trapezius, suspends the scapula, but slight activity is sufficient to support the unloaded arm. The heavier insertion lower down pulls the inferior scapular angle forwards around the thorax, assisting trapezius in upward rotation of the bone, an action that is essential to raising the arm above the head. In the initial stages of abduction, serratus anterior helps other muscles to fix the scapula, so that deltoid acts effectively on the humerus, and not the scapula. While deltoid is raising the arm to a right angle with the scapula, serratus anterior and trapezius are simultaneously rotating the scapula: the combination allows the arm to be raised to the vertical. To effect this upward rotation of the scapula, forward pull on the inferior angle by the lower digitations of serratus anterior is coupled with an upward and medial pull on the lateral end of the clavicle and acromion by the upper fibres of trapezius, and a downward pull on the base of the scapular spine by the lower fibres of trapezius. Conversely, slow downward scapular rotation assisted by gravity is achieved by controlled lengthening of these muscles. More powerful downward rotation requires balanced contraction of the upper fibres of serratus anterior, levator scapulae, rhomboids, pectoralis minor and the middle part of trapezius. When weights are carried in front of the body, serratus anterior prevents backward rotation of the scapula. Electromyography shows that serratus anterior is not active in normal human respiration. This may not apply to laboured respiration, e.g. when asthmatics and athletes may be observed to fix the scapula by grasping a rail or other support.

Clinical anatomy: testing

The muscular digitations of serratus anterior can be seen and felt when the outstretched hand pushes against resistance.

When serratus anterior is paralysed, the medial border of the scapula, and especially its lower angle, stand out prominently. The arm cannot be raised fully. Pushing is ineffective, indeed attempts to do so produce further projection, known as ‘winging’ of the scapula.

Supraspinatus

Attachments

Supraspinatus arises from the medial two-thirds of the supraspinous fossa and from the supraspinous fascia (Fig. 46.22). The fibres converge, under the acromion, into a tendon which crosses above the shoulder joint and is attached to the highest facet of the greater tubercle of the humerus. The tendon blends into the articular capsule and may give a slip to the tendon of pectoralis major. Fibrocartilage has been described at the tendinous insertion, as in other tendons attached to epiphysial bone.

Vascular supply

Supraspinatus is supplied by the suprascapular and dorsal scapular arteries.

Innervation

Supraspinatus is innervated by the suprascapular nerve, C5 and 6.

Action

The conventional view is that supraspinatus initiates abduction of the shoulder and assists deltoid in abduction thereafter. However, there is evidence that both supraspinatus and deltoid are involved throughout the range of abduction, including initiation of the movement. As part of the rotator cuff, supraspinatus helps to stabilize the head of the humerus in the glenoid fossa during movements of the glenohumeral joint. With the arm dependent, even when moderately loaded, supraspinatus and tension in the upper capsule prevent downward displacement of the humerus.

Clinical anatomy: testing

Supraspinatus can be palpated deep to trapezius when the arm is abducted at the shoulder joint against resistance.

The tendon of supraspinatus is separated from the coraco-acromial ligament, acromion and deltoid by the large subacromial bursa; when this is inflamed, abduction of the shoulder joint is painful. The tendon is the most frequently torn element of the musculotendinous cuff around the shoulder joint.

Infraspinatus

Attachments

Infraspinatus is a thick triangular muscle which occupies most of the infraspinous fossa (Fig. 46.22). It arises by muscular fibres from the medial two-thirds of the fossa, by tendinous fibres from ridges on its surface and from the deep surface of the infraspinous fascia, which separates it from teres major and minor. Its fibres converge to a tendon which glides under the lateral border of the spine of the scapula, and then passes across the posterior aspect of the capsule of the shoulder joint to be attached to the middle facet on the greater tubercle of the humerus. The tendon is sometimes separated from the capsule by a bursa, which may communicate with the joint cavity. Infraspinatus is sometimes fused with teres minor.

Vascular supply

Infraspinatus is supplied by the suprascapular and circumflex scapular arteries.

Innervation

Infraspinatus is innervated by the suprascapular nerve, C5 and 6.

Action

Infraspinatus is a lateral rotator of the humerus. Together with supraspinatus, subscapularis and teres minor, it helps to stabilize the head of the humerus in the glenoid fossa during shoulder movements (p. 806).

Subscapularis

Attachments

Subscapularis is a bulky, triangular muscle which fills the subscapular fossa (Fig. 46.20). In its medial two-thirds, the fibres are attached to the periosteum of the costal surface of the scapula. Other fibres arise from tendinous intramuscular septa, which are attached to ridges on the bone, and from the aponeurosis which covers the muscle and separates it from teres major and the long head of triceps. The fibres converge laterally into a broad tendon which is attached to the lesser tubercle of the humerus and the front of the articular capsule. The tendon is separated from the neck of the scapula by the large subscapular bursa, which communicates with the shoulder joint.

Variation is unusual. A separate slip may pass from the medial border of the scapula to the glenohumeral capsule or to the periosteum medial to the intertuberculous sulcus of the humerus.

Relations

Subscapularis forms much of the posterior axillary wall. Its anterior surface is apposed inferomedially to serratus anterior, and superolaterally to coracobrachialis and biceps, the axillary vessels, brachial plexus and subscapular vessels and nerves. Its posterior surface is attached to the scapula and glenohumeral capsule. Its lower border contacts teres major and latissimus dorsi.

Vascular supply

Subscapularis is supplied by small branches from the suprascapular, axillary and subscapular arteries.

Innervation

Subscapularis is innervated by the upper and lower subscapular nerves, C5, 6.

Action

Subscapularis is a medial rotator of the humerus. Together with supraspinatus, infraspinatus and teres minor, it helps to stabilize the head of the humerus in the glenoid fossa during shoulder movements (p. 806).

Teres major

Attachments

Teres major is a thick, flat muscle which arises from the oval area on the dorsal surface of the inferior scapular angle, and from the fibrous septa interposed between the muscle and teres minor and infraspinatus (Fig. 46.22). Its fibres ascend laterally and end in a flat tendon, approximately 5 cm long, which is attached to the medial lip of the intertubercular sulcus of the humerus. The tendon lies behind that of latissimus dorsi, from which it is separated by a bursa; the tendons are united along their lower borders for a short distance.

Variants

Teres major may be fused with the scapular part of latissimus dorsi, and it may send a slip to join the long head of triceps or the brachial fascia.

Vascular supply

Teres major is supplied by the thoracodorsal branch of the subscapular artery on its way to latissimus dorsi and by the posterior circumflex humeral artery.

Innervation

Teres major is innervated by the lower subscapular nerve, C5, 6 and 7.

Action

Despite its name, teres major has a nerve supply and action that is distinct from teres minor. Teres major draws the humerus backwards and rotates it medially. Electromyographic studies are equivocal about its major role in movement, but its involvement as a contributor to static posture and arm-swinging is not contested.

Clinical anatomy: testing

Teres major can be palpated posterior to the posterior axillary fold during adduction of the humerus against resistance.

Teres minor

Attachments

Teres minor is a narrow elongated muscle which arises from the upper two-thirds of a flattened strip on the dorsal surface of the scapula adjoining its lateral border, and from two aponeurotic laminae which separate it from infraspinatus and teres major (Fig. 46.22). It runs upwards and laterally. The upper fibres end in a tendon attached to the lowest facet on the greater tubercle of the humerus. The lower fibres are attached directly into the humerus distal to this facet and above the origin of the lateral head of triceps. The tendon passes across, and blends with, the lower posterior surface of the capsule of the shoulder joint.

Teres minor may be fused with infraspinatus.

Vascular supply

Teres minor is supplied by the circumflex scapular artery, which pierces the origin of the muscle as it turns upward in the infraspinous fossa, and by the posterior circumflex humeral artery.

Innervation

Teres minor is innervated by the axillary nerve, C5 and 6.

Action

Teres minor acts as a lateral rotator and weak adductor of the humerus. Together with supraspinatus, infraspinatus and subscapularis, it helps stabilize the head of the humerus in the glenoid fossa during shoulder movements (p. 803).

The quadrangular and triangular spaces

Anteriorly, the quadrangular space is bounded by subscapularis, the capsule of the shoulder joint and teres minor above, teres major below, the long head of triceps medially, and the surgical neck of the humerus laterally. Posteriorly, the quadrangular space is bounded above by teres minor. The axillary nerve and the posterior circumflex artery and vein pass through the space (Fig. 46.22).

There are two triangular spaces (Fig. 46.22). The upper triangular space is bounded above by subscapularis anteriorly, teres minor posteriorly, teres major below, and the long head of triceps laterally. The circumflex scapular artery passes through this space. The lower triangular space (triangular interval) is bounded above by subscapularis anteriorly and teres major posteriorly; the long head of triceps medially and the humerus laterally. The radial nerve and the profunda brachii vessels pass through this space.

AXILLA

BOUNDARIES

The axilla is a pyramidal region between the upper thoracic wall and the arm (Fig. 46.23, Fig. 46.24). Its blunt apex continues into the root of the neck (cervico-axillary canal) between the external border of the first rib, superior border of the scapula, posterior surface of the clavicle and the medial aspect of the coracoid process. Its base, which is virtual, can be imagined as facing downwards: it is broad at the chest and narrow at the arm, and corresponds to the skin and a thick layer of axillary fascia between the inferior borders of pectoralis major anteriorly and latissimus dorsi posteriorly. It is convex upwards, conforming to the concavity of the armpit.

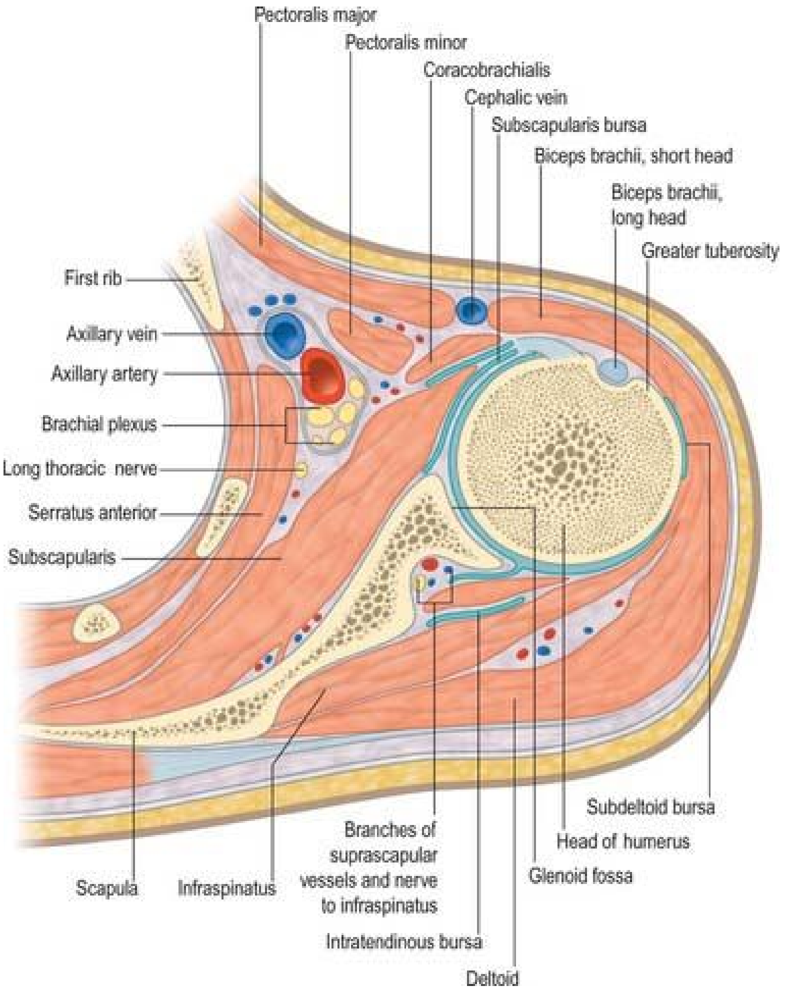
Pectoralis major
Pectoralis minor
Coracobrachialis
Cephalic vein
Subscapularis bursa
Biceps brachii, short head
Biceps brachii, long head
Greater tuberosity
First rib
Axillary vein
Axillary artery
Brachial plexus
Long thoracic nerve
Serratus anterior
Subscapularis
Subdeltoid bursa
Head of humerus
Glenoid fossa
Scapula
Infraspinatus
Branches of suprascapular vessels and nerve to infraspinatus
Intratendinous bursa
Deltoid

Fig. 46.23 Transverse section through left shoulder joint and axilla, viewed from below. Compare with Fig. 46.17A.

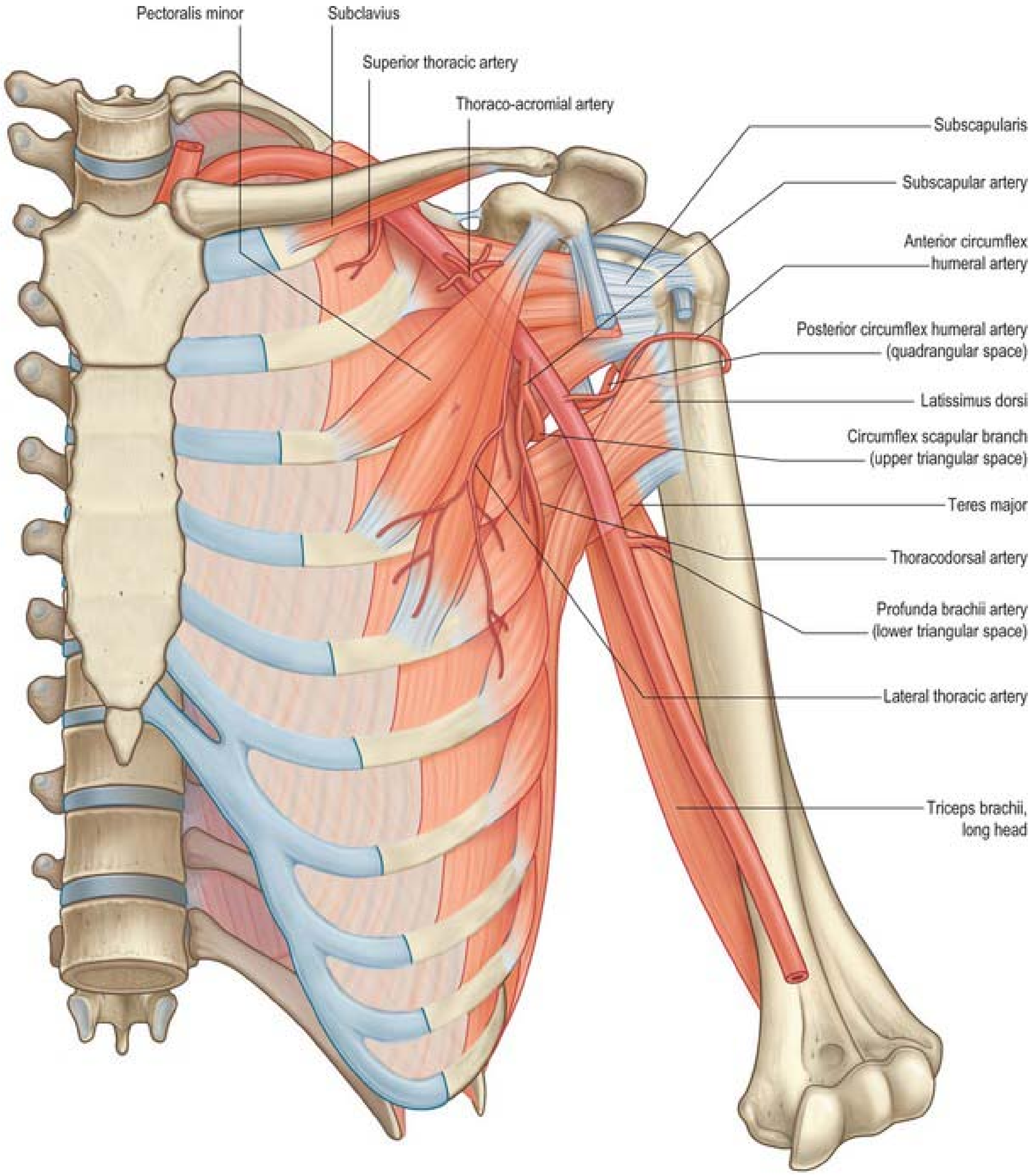
Pectoralis minor
Subclavius
Superior thoracic artery
Thoraco-acromial artery
Subscapularis
Subscapular artery
Anterior circumflex humeral artery
Posterior circumflex humeral artery (quadrangular space)
Latissimus dorsi
Circumflex scapular branch (upper triangular space)
Teres major
Thoracodorsal artery
Profunda brachii artery (lower triangular space)
Lateral thoracic artery
Triceps brachii, long head

Fig. 46.24 The left axillary artery and its branches.

(From Drake, Vogl and Mitchell 2005.)

The anterior wall is formed by pectorales major and minor, the former covering the whole wall, the latter its intermediate part. The interval between the upper border of pectoralis minor and clavicle is occupied by the clavipectoral fascia. The posterior wall is formed by subscapularis above, and teres major and latissimus dorsi below. The medial ‘wall’ is convex laterally and is composed of the first four ribs and their associated intercostal muscles, together with the upper part of serratus anterior. The anterior and posterior walls converge laterally: the ‘wall’ is narrow and consists of the humeral intertubercular sulcus. The lateral angle lodges coracobrachialis and biceps.

CONTENTS

The axilla contains the axillary vessels, the infraclavicular part of the brachial plexus and its branches, lateral branches of some intercostal nerves, many lymph nodes and vessels, loose adipose areolar tissue and, in many instances, the ‘axillary tail’ of the breast. The axillary vessels and brachial plexus run from the apex to the base along the lateral wall, nearer to the anterior wall: the axillary vein is anteromedial to the artery. The obliquity of the upper ribs means that the neurovascular bundle, after it emerges from behind the clavicle, crosses the first intercostal space: its relations are therefore different at upper and lower levels. Thoracic branches of the axillary artery are in contact with the pectoral muscles; the lateral thoracic artery reaches the thoracic wall along the lateral margin of pectoralis minor. Subscapular vessels descend on the posterior wall at the lower margin of subscapularis. The subscapular and thoracodorsal nerves cross the anterior surface of latissimus dorsi at different inclinations. Circumflex scapular vessels wind round the lateral border of the scapula; posterior circumflex humeral vessels and the axillary nerve curve back and laterally around the surgical neck of the humerus.

No large vessel lies on the medial ‘wall’, which is crossed proximally only by small branches of the superior thoracic artery. The long thoracic nerve descends on serratus anterior and the intercostobrachial nerve perforates the upper anterior part of this wall, crossing the axilla to its lateral ‘wall’.

VASCULAR SUPPLY AND LYMPHATIC DRAINAGE

ARTERIES

Suprascapular artery

The suprascapular artery usually arises from the thyrocervical trunk of the subclavian artery, although it may arise from the third part of the subclavian artery (Fig. 28.7). It first descends laterally across scalenus anterior and the phrenic nerve, posterior to the internal jugular vein and sternocleidomastoid, then crosses anterior to the subclavian artery and brachial plexus, posterior and parallel with the clavicle and subclavius and the inferior belly of omohyoid, to reach the superior border of the scapula. Here it passes above (sometimes under) the superior transverse ligament, separating it from the suprascapular nerve, and enters the supraspinous fossa (Fig. 46.25), where it lies on the bone, and supplies supraspinatus. It descends behind the scapular neck, and passes through the spinoglenoid notch deep to the inferior transverse ligament to gain the deep surface of infraspinatus, where it anastomoses with the circumflex scapular and deep branch of the transverse cervical artery. Its muscular branches supply sternocleidomastoid, subclavius and infraspinatus. It also gives off a suprasternal branch which crosses the sternal end of the clavicle to supply the skin of the upper thorax, and an acromial branch which pierces trapezius to supply the skin over the shoulder. This last branch anastomoses with the thoraco-acromial and posterior circumflex humeral arteries.

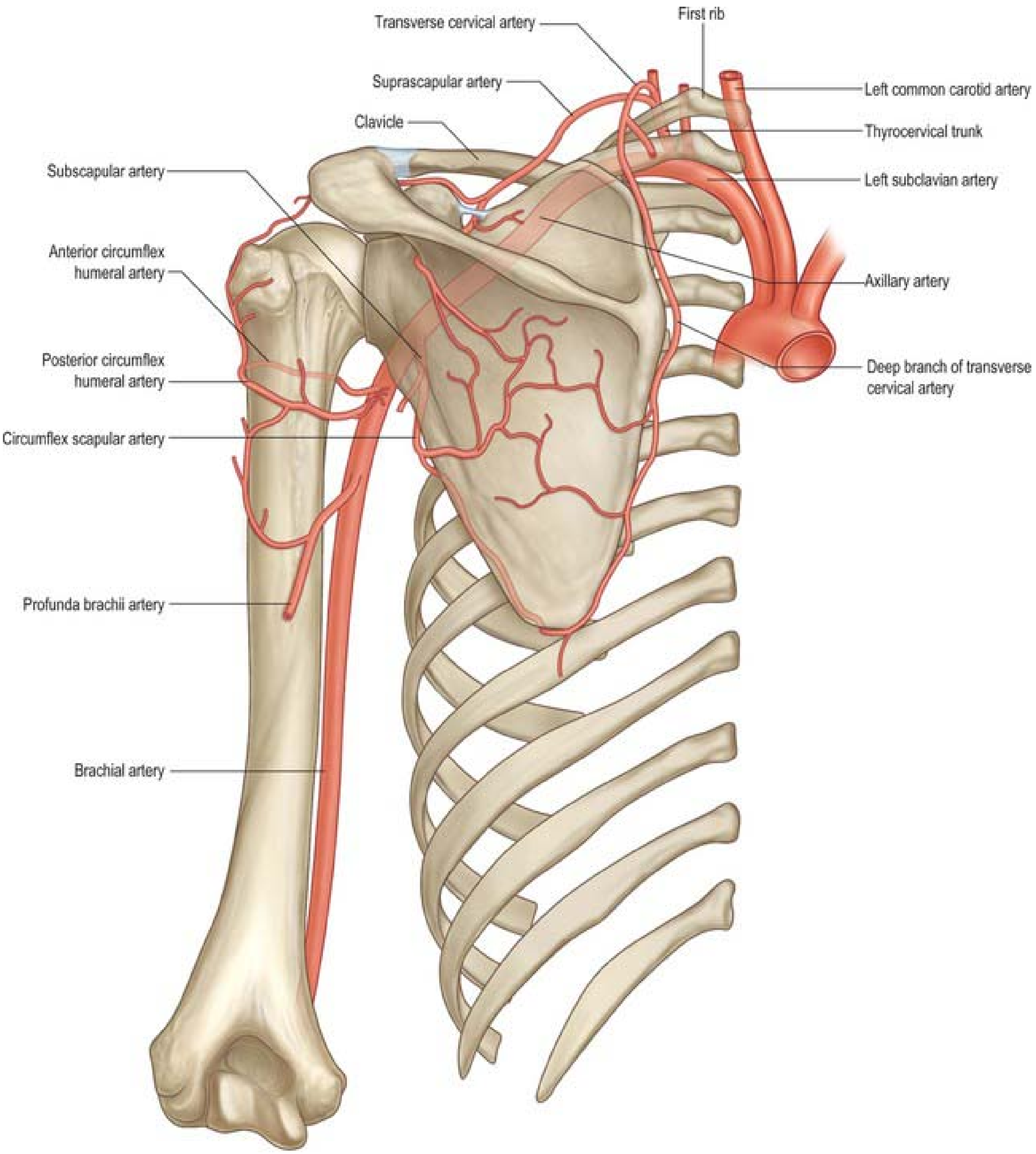
Transverse cervical artery
First rib
Suprascapular artery
Left common carotid artery
Clavicle
Thyrocervical trunk
Subscapular artery
Left subclavian artery
Anterior circumflex humeral artery
Axillary artery
Posterior circumflex humeral artery
Deep branch of transverse cervical artery
Circumflex scapular artery
Profunda brachii artery
Brachial artery

Fig. 46.25 The scapular anastomosis of the left side.

(From Drake, Vogl and Mitchell 2005.)

As the suprascapular artery passes over the superior transverse ligament, it gives off a branch which enters the subscapular fossa beneath subscapularis and anastomoses with the subscapular artery and the deep branch of the transverse cervical artery. It also supplies the acromioclavicular and glenohumeral joints, the clavicle and the scapula.

Dorsal scapular artery

In the majority of cases, the dorsal scapular artery arises from the third, or less often the second, part of the subclavian artery. It passes laterally through the trunks of the brachial plexus in front of scalenus medius and then deep to levator scapulae to reach the superior scapular angle. Here it descends with the dorsal scapular nerve under the rhomboids along the medial border of the scapula to the inferior angle (Fig. 46.25). It supplies the rhomboids, latissimus dorsi and the inferior portion of trapezius. It supplies the skin over the inferomedial aspect of trapezius via musculocutaneous perforators. It anastomoses with the suprascapular and subscapular and with posterior branches of some posterior intercostal arteries. It sends a small branch to scalenus anterior: sometimes this arises directly from the subclavian artery.

Variants

About a third of the superficial cervical and dorsal scapular arteries arise in common from the thyrocervical trunk as a transverse cervical artery, together with a superficial and a deep branch (superficial cervical and dorsal scapular arteries respectively). In this case the dorsal scapular artery arises near the superior border of the scapula: it passes laterally, anterior to the brachial plexus and then posterior to levator scapulae (Fig. 46.26).

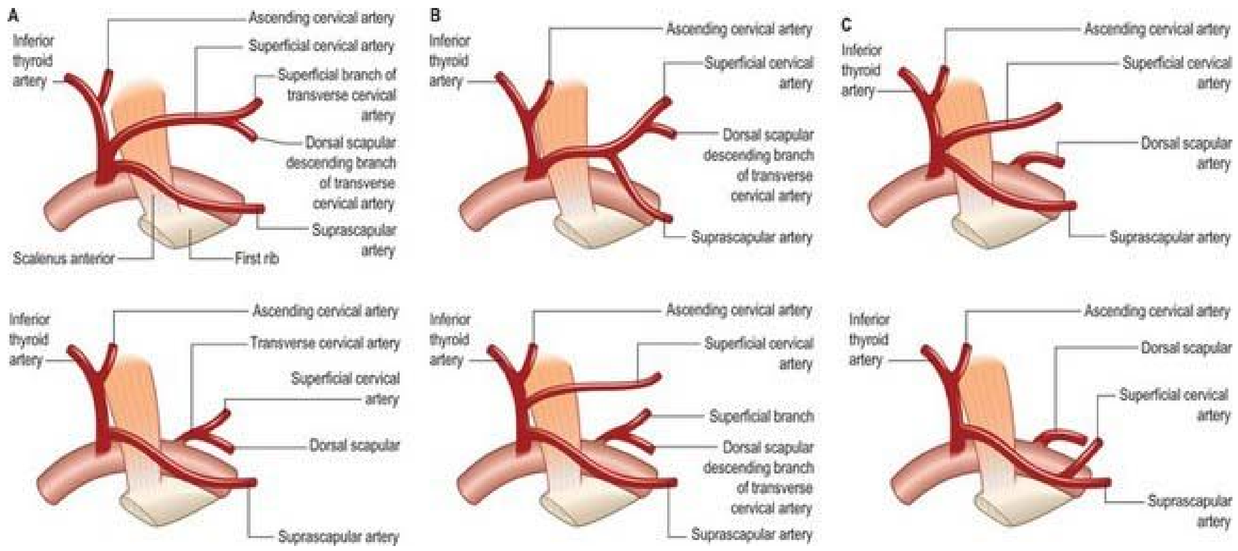
A
Inferior thyroid artery
Ascending cervical artery
Superficial cervical artery
Superficial branch of transverse cervical artery
Dorsal scapular descending branch of transverse cervical artery
Suprascapular artery
Scalenus anterior
First rib
B
Inferior thyroid artery
Ascending cervical artery
Superficial cervical artery
Dorsal scapular descending branch of transverse cervical artery
Suprascapular artery
C
Inferior thyroid artery
Ascending cervical artery
Superficial cervical artery
Dorsal scapular artery
Suprascapular artery
Inferior thyroid artery
Ascending cervical artery
Transverse cervical artery
Superficial cervical artery
Dorsal scapular
Suprascapular artery
Inferior thyroid artery
Ascending cervical artery
Superficial cervical artery
Superficial branch
Dorsal scapular descending branch of transverse cervical artery
Suprascapular artery
Inferior thyroid artery
Ascending cervical artery
Dorsal scapular
Superficial cervical artery
Suprascapular artery

Fig. 46.26 **A–F**, Variations in origin and branches of the thyrocervical trunk. The superficial cervical artery is the distinct vessel arising from the thyrocervical trunk (**C** and **E**) or from the suprascapular artery (**D**), which supplies the territory of the superficial branch of the (absent) transverse cervical artery.

(By permission from Cormack GC, Lamberty BGH 1994 The Arterial Anatomy of Skin Flaps, 2nd edn. Edinburgh: Churchill Livingstone.)

Supraclavicular artery

This small vessel arises from either the transverse cervical or superficial cervical artery. It pierces the deep fascia just superior to the clavicle and anterior to trapezius and supplies an area of skin over the lateral end of the clavicle.

Axillary artery

The axillary artery, a continuation of the subclavian artery, begins at the outer border of the first rib, and ends nominally at the inferior border of teres major where it becomes the brachial artery. Its direction varies with the position of the limb: it is almost straight when the arm is raised at right angles, concave upwards when the arm is elevated above this, and convex upwards and laterally when the arm is by the side. At first deep, it subsequently becomes superficial, when it is covered only by the skin and fasciae. Pectoralis minor crosses it and so divides it into three parts which are proximal, posterior and distal to the muscle.

Relations of the first part

The skin, superficial fascia, platysma, supraclavicular nerves, deep fascia, clavicular fibres of pectoralis major and the clavipectoral fascia, lateral pectoral nerve and the loop of communication between the lateral and medial pectoral nerves, and the thoraco-acromial and cephalic veins are all anterior. The first intercostal space and external intercostal, first and second digitations of serratus anterior, long thoracic and medial pectoral nerves and the medial cord of the brachial plexus are all posterior. The posterior cord of the brachial plexus is lateral and the axillary vein is anteromedial. The first part is enclosed with the axillary vein and brachial plexus in a fibrous axillary sheath, which is continuous with the prevertebral layer of the deep cervical fascia.

Relations of the second part

The skin, superficial and deep fascia, and pectorales major and minor are all anterior. The posterior cord of the brachial plexus and the areolar tissue between it and subscapularis are posterior. The axillary vein is medial, separated from the artery by the medial cord of the brachial plexus and the medial pectoral nerve. The lateral cord of the brachial plexus is lateral, separating the artery from coracobrachialis. The cords of the brachial plexus thus surround the second part on three sides, with the dispositions implied by their names, and separate it from the vein and adjacent muscles.

Relations of the third part

Pectoralis major, and, distal to the muscle, skin and fasciae, are anterior. The lower part of subscapularis and the tendons of latissimus dorsi and teres major are posterior. Coracobrachialis is lateral and the axillary vein is medial. Branches of the brachial plexus are arranged as follows: laterally, the lateral root and then trunk of the median nerve and, for a short distance, the musculocutaneous nerve; medially, the medial cutaneous nerve of the forearm between the axillary artery and vein anteriorly, and the ulnar nerve between these vessels posteriorly; anteriorly, the medial root of the median nerve; posteriorly, the radial and axillary nerves, the latter only to the distal border of subscapularis.

Branches

The branches of the axillary artery are superior thoracic, thoracoacromial, lateral thoracic, subscapular, anterior and posterior circumflex humeral.

Superior thoracic artery

The superior thoracic artery is a small vessel which arises from the first part of the axillary artery near the lower border of subclavius: it sometimes arises from the thoraco-acromial artery (Fig. 46.24). It runs anteromedially above the medial border of pectoralis minor, then passes between it and pectoralis major to gain the thoracic wall. It supplies these muscles and the thoracic wall, and anastomoses with the internal thoracic and upper intercostal arteries.

Thoraco-acromial (acromio-thoracic) artery

The thoraco-acromial artery is a short branch which arises from the second part of the axillary artery (Fig. 28.7, Fig. 46.19). It is at first overlapped by pectoralis minor; skirting its medial border, next pierces the clavipectoral fascia and divides into pectoral, acromial, clavicular and deltoid branches, which supply pectoralis major and minor, an area of skin over the clavipectoral fascia and the anterior portion of deltoid.

Pectoral branch

The pectoral branch is the largest branch. It descends between the pectoral muscles, gives a branch to pectoralis minor, and then continues on the deep surface of pectoralis major. It enters the muscle and anastomoses with the intercostal branches of the internal thoracic and lateral thoracic arteries. It gives off perforating branches to the breast, and musculocutaneous perforators to the skin over pectoralis major.

Acromial branch

The acromial branch crosses the coracoid process under deltoid, which it supplies, pierces the muscle and ends on the acromion. It anastomoses with branches of the suprascapular artery, the deltoid branch of the thoraco-acromial artery and the posterior circumflex humeral arteries.

Clavicular branch

The clavicular branch ascends medially between the clavicular part of pectoralis major and the clavipectoral fascia. It supplies the sternoclavicular joint and subclavius.

Deltoid branch

The deltoid branch often arises with the acromial branch. It crosses pectoralis minor to accompany the cephalic vein between pectoralis major and deltoid, and supplies both muscles.

Lateral thoracic artery

The lateral thoracic artery arises from the second part of the axillary artery. Following the lateral border of pectoralis minor, it passes to the deep surface of pectoralis major as far distally as the fifth intercostal space. It supplies serratus anterior and the pectoral muscles, the axillary lymph nodes and subscapularis. It anastomoses with the internal thoracic, subscapular, and intercostal arteries and with the pectoral branch of the thoraco-acromial artery. In females it is large and has lateral mammary branches, which curve round the lateral border of pectoralis major to the breast. In both males and females, it gives off cutaneous branches which pass around the lateral border of pectoralis major to supply the skin in this region.

Subscapular artery

The subscapular artery is the largest branch of the axillary artery (Fig. 46.24, Fig. 46.25). It usually arises from the third part of the axillary artery at the distal (inferior) border of subscapularis, which it follows to the inferior scapular angle, where it anastomoses with the lateral thoracic and intercostal arteries and the deep branch of the transverse cervical artery. It supplies adjacent muscles and the thoracic wall. It is accompanied distally by the nerve to latissimus dorsi. Approximately 4 cm from its origin the subscapular artery divides into the circumflex scapular and thoracodorsal arteries.

Circumflex scapular artery

The circumflex scapular artery, the larger of the two terminal branches of the subscapular artery, curves backwards around the lateral border of the scapula, traversing a triangular space between subscapularis above and teres major below and the long head of the triceps laterally. It enters the infraspinous fossa under teres minor and then divides. One branch (infrascapular) enters the subscapular fossa deep to subscapularis, and anastomoses with the suprascapular and dorsal scapular arteries (or deep branch of the transverse cervical artery). The other branch continues along the lateral border of the scapula between teres major and minor and, dorsal to the inferior angle, anastomoses with the dorsal scapular artery. Small branches supply the posterior part of deltoid and the long head of triceps, and anastomose with an ascending branch of the profunda brachii artery.

Two significant cutaneous branches arise from the circumflex scapular artery as it emerges through the upper triangular space. The superior, or horizontal, branch is a direct cutaneous artery which passes medially at the level of the deep fascia parallel with the spine of the scapula: it supplies a band of skin overlying the spine of the scapula. The lower branch (parascapular branch) is also a direct cutaneous vessel which passes in an inferomedial direction, again at the level of the deep fascia, and supplies an area of skin overlying the lateral border of the scapula. Both these cutaneous vessels provide the anatomical basis of skin flaps which can be surgically raised in this region (scapular flap based on the horizontal branch and parascapular flap based on the lower, parascapular branch) to reconstruct areas of missing tissue elsewhere in the body.

Thoracodorsal artery

The other terminal branch of the subscapular artery, the thoracodorsal artery, follows the lateral margin of the scapula, posterior to the lateral thoracic artery, between latissimus dorsi and serratus anterior. Before entering the deep surface of latissimus dorsi, it supplies teres major and the intercostals and sends one or two branches to serratus anterior. It enters latissimus dorsi muscle with the thoracodorsal nerve: this constitutes the principle neurovascular pedicle to the muscle. It provides numerous musculocutaneous perforators which supply the skin over the superior part of latissimus dorsi. The intramuscular portion of the artery anastomoses with intercostal arteries and lumbar perforating arteries.

Anterior circumflex humeral artery

The anterior circumflex humeral artery arises from the lateral side of the axillary artery at the distal border of subscapularis. It runs horizontally behind coracobrachialis and the short head of biceps, anterior to the surgical neck of the humerus. Reaching the intertubercular sulcus, it sends an ascending branch to supply the humeral head and shoulder joint. It continues laterally under the long head of biceps and deltoid, and anastomoses with the posterior circumflex humeral artery.

Posterior circumflex humeral artery

The posterior circumflex humeral artery is larger than the anterior (Fig. 46.25, Fig. 46.27). It branches from the third part of the axillary artery at the distal border of subscapularis and runs backwards with the axillary nerve through a quadrangular space which is bounded by subscapularis, the capsule of the shoulder joint and teres minor above, teres major below, the long head of triceps medially, and the surgical neck of the humerus laterally. It curves round the humeral neck and supplies the shoulder joint, deltoid, teres major and minor, and long and lateral heads of triceps. It gives off a descending branch which anastomoses with the deltoid branch of the profunda brachii artery and with the anterior circumflex humeral and acromial branches of the suprascapular and thoraco-acromial arteries.

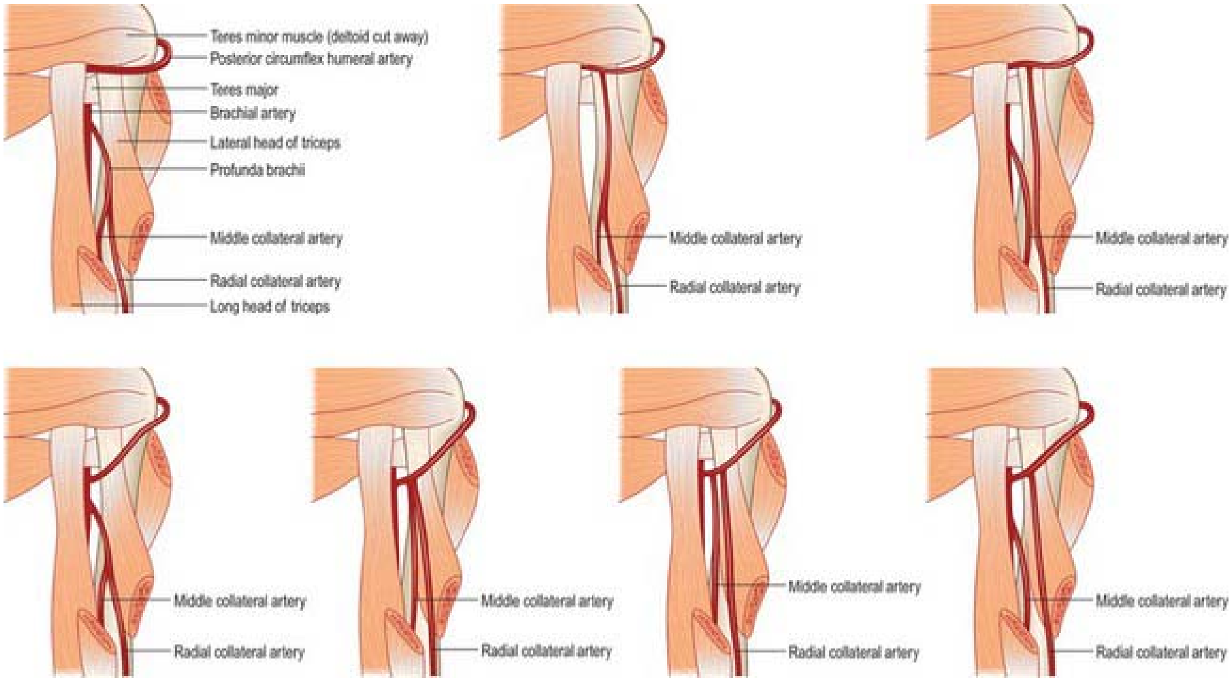
Teres minor muscle (deltoid cut away)
Posterior circumflex humeral artery
Teres major
Brachial artery
Lateral head of triceps
Profunda brachii
Middle collateral artery
Radial collateral artery
Long head of triceps
Middle collateral artery
Radial collateral artery
Middle collateral artery
Radial collateral artery
Middle collateral artery
Radial collateral artery
Middle collateral artery
Radial collateral artery
Middle collateral artery
Radial collateral artery
Middle collateral artery
Radial collateral artery

Fig. 46.27 Variation in origin and course of the posterior circumflex humeral artery. The axillary artery, shown in red outline, runs anterior to the radial nerve.

(By permission from Cormack GC, Lamberty BGH 1994 The Arterial Anatomy of Skin Flaps, 2nd edn. Edinburgh: Churchill Livingstone.)

Variants

Branches exhibit considerable variation. An alar thoracic artery, often from the second part, may supply fat and lymph nodes in the axilla. The lateral thoracic artery may be absent, in which case it is replaced by lateral perforating branches of the intercostal arteries, alternatively, it may become, or give off, a direct cutaneous vessel (named the superficial thoracic artery by some sources) which supplies the skin over the lateral border of pectoralis major. In up to 30% of cases, the subscapular artery can arise from a common trunk with the posterior circumflex humeral artery. Occasionally the subscapular, circumflex humeral and profunda brachii arteries arise in common, in which case, branches of the brachial plexus surround this common vessel instead of the axillary artery. The posterior circumflex humeral artery may arise from the profunda brachii artery, and pass back below teres major instead of passing through the quadrangular space. Sometimes the axillary divides into radial and ulnar arteries (anomalous ‘high division’), and is occasionally the source of the anterior interosseous artery.

VEINS

Axillary vein

The axillary vein is the continuation of the basilic vein. It begins at the lower border of teres major, and ascends to the outer border of the first rib, where it becomes the subclavian vein. It is joined by the brachial vein near subscapularis, and by the cephalic vein near its costal end; other tributaries follow the axillary arterial branches. It lies medial to the axillary artery, which it partly overlaps. The medial pectoral nerve, medial cord of the brachial plexus, ulnar nerve and medial cutaneous nerve of the forearm lie between the artery and the vein. The medial cutaneous nerve of the arm is medial to the vein; the lateral group of axillary lymph nodes is posteromedial. There are a pair of valves near its distal end, and valves also occur near the ends of the cephalic and subscapular veins.

Subclavian vein

The subclavian vein is a continuation of the axillary vein. It extends from the outer border of the first rib to the medial border of scalenus anterior, where it joins the internal jugular to form the brachiocephalic vein. The clavicle and subclavius are anterior, the subclavian artery is posterosuperior, separated by scalenus anterior and the phrenic nerve, and the first rib and pleura are inferior. The vein usually has a pair of valves about 2cm from its end. Its tributaries are the external jugular, dorsal scapular and (sometimes) anterior jugular veins, and occasionally a small branch from the cephalic vein which ascends anterior to the clavicle. At its junction with the internal jugular vein, the left subclavian receives the thoracic duct: the right subclavian vein receives the right lymphatic duct.

AXILLARY LYMPH NODES

There are between 20 to 30 axillary nodes, which may be divided into five not wholly distinct groups, namely, lateral, anterior (pectoral), posterior (subscapular), central and apical (Fig. 54.21, Fig. 45.6, Fig. 46.28). Four of the groups are intermediary, and only the apical group is terminal. Collectively they drain the entire upper limb, breast and trunk above the umbilicus.

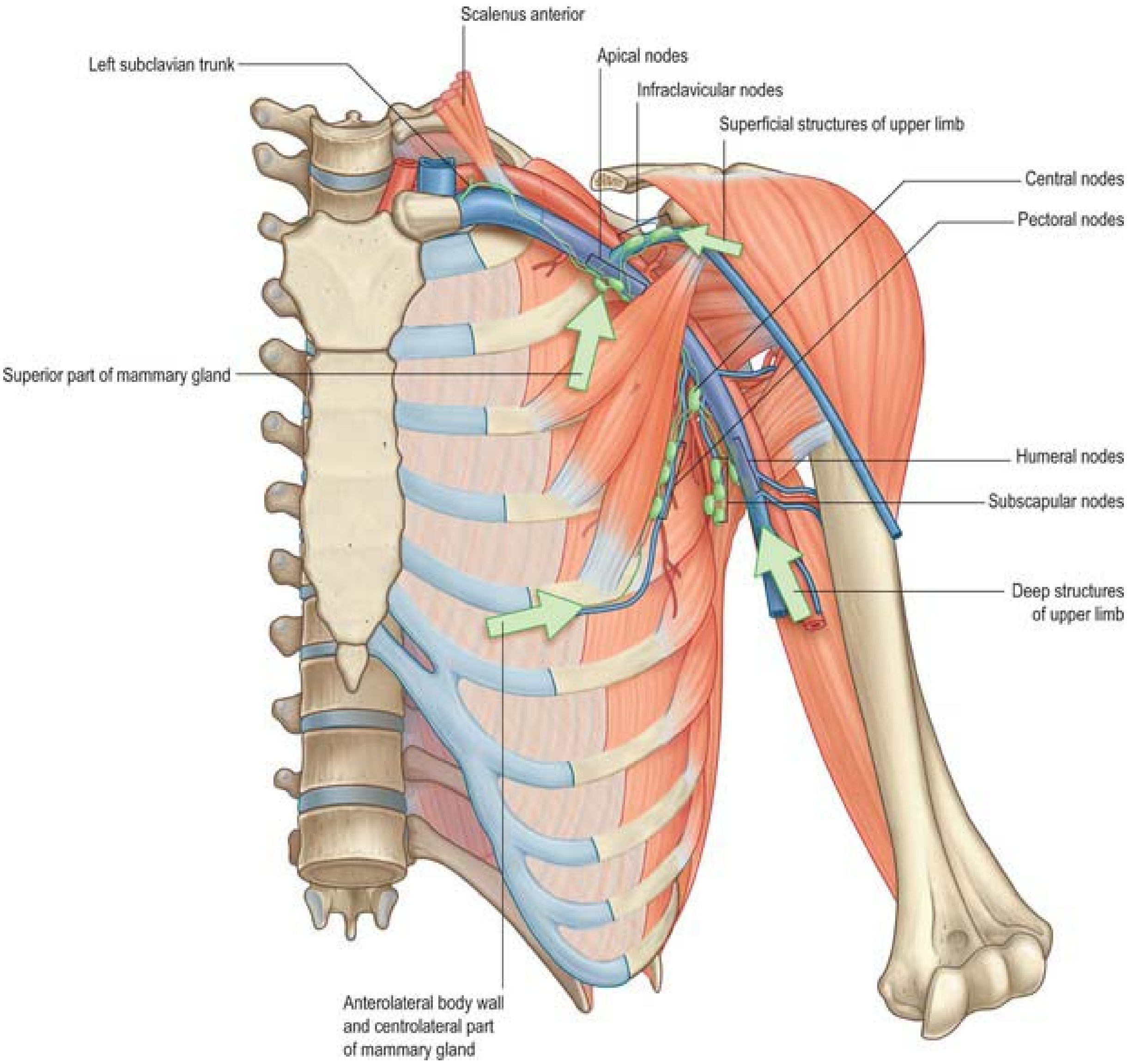
Scalenus anterior
Left subclavian trunk
Apical nodes
Infraclavicular nodes
Superficial structures of upper limb
Central nodes
Pectoral nodes
Superior part of mammary gland
Humeral nodes
Subscapular nodes
Deep structures of upper limb
Anterolateral body wall and centrolateral part of mammary gland

Fig. 46.28 Lymph nodes and vessels in the left axilla.

(From Drake, Vogl and Mitchell 2005.)

The lateral group of four to six nodes is posteromedial to the axillary vein, its afferents drain the whole limb except the vessels accompanying the cephalic vein (Fig. 54.21, Fig. 45.6, Fig. 46.28). Efferent vessels pass partly to the central and apical axillary groups, and partly to the inferior deep cervical nodes. The anterior group of four or five nodes spreads along the inferior border of pectoralis minor near the lateral thoracic vessels. Their afferents drain the skin and muscles of the supraumbilical anterolateral body wall and breast, and efferents pass partly to the central and partly to the apical axillary nodes. The posterior group of six or seven nodes lie on the inferior margin of the posterior axillary wall, along the subscapular vessels. Their afferents drain the skin and superficial muscles of the inferior posterior region of the neck and the dorsal aspect of the trunk down to the iliac crest, and efferents pass to the apical and central axillary nodes. A central group of three or four large nodes embedded in axillary fat receives afferents from all preceding groups, and their efferents drain to the apical nodes. An apical group of six to twelve nodes is partly posterior to the superior part of pectoralis minor and partly above its superior border, extending to the apex of the axilla medial to the axillary vein. The only direct territorial afferents are those which accompany the cephalic vein or some which drain the upper peripheral region of the breast: the group drains all the other axillary nodes. Their efferents unite as the subclavian trunk and drain directly to the jugulosubclavian venous junction, or the subclavian vein, or jugular lymphatic trunk or (occasionally) to a right lymphatic duct; the left trunk usually ends in the thoracic duct. A few efferents from apical nodes usually reach the inferior deep cervical nodes.

One or two infraclavicular nodes appear beside the cephalic vein, in the groove between pectoralis major and deltoid, just inferior to the clavicle. Their efferents pass through the clavipectoral fascia to the apical axillary nodes. Occasionally some pass anterior to the clavicle to the inferior deep cervical (supraclavicular) nodes.

INNERVATION

BRACHIAL PLEXUS

For an overview of the brachial plexus see page 779 and Fig. 45.7.

In the axilla, the lateral and posterior cords of the brachial plexus are lateral to the first part of the axillary artery, and the medial cord is behind the artery. The cords surround the second part of the artery, their names indicating their relationship. In the lower axilla the cords divide into nerves that supply the upper limb (Fig. 46.29). Other than the medial root of the median nerve, these nerves are related to the third part of the artery in the same way as their cords are related to the second part, i.e. branches of the lateral cord are lateral to the artery, branches of the medial cord are medial, and branches of the posterior cord are posterior.

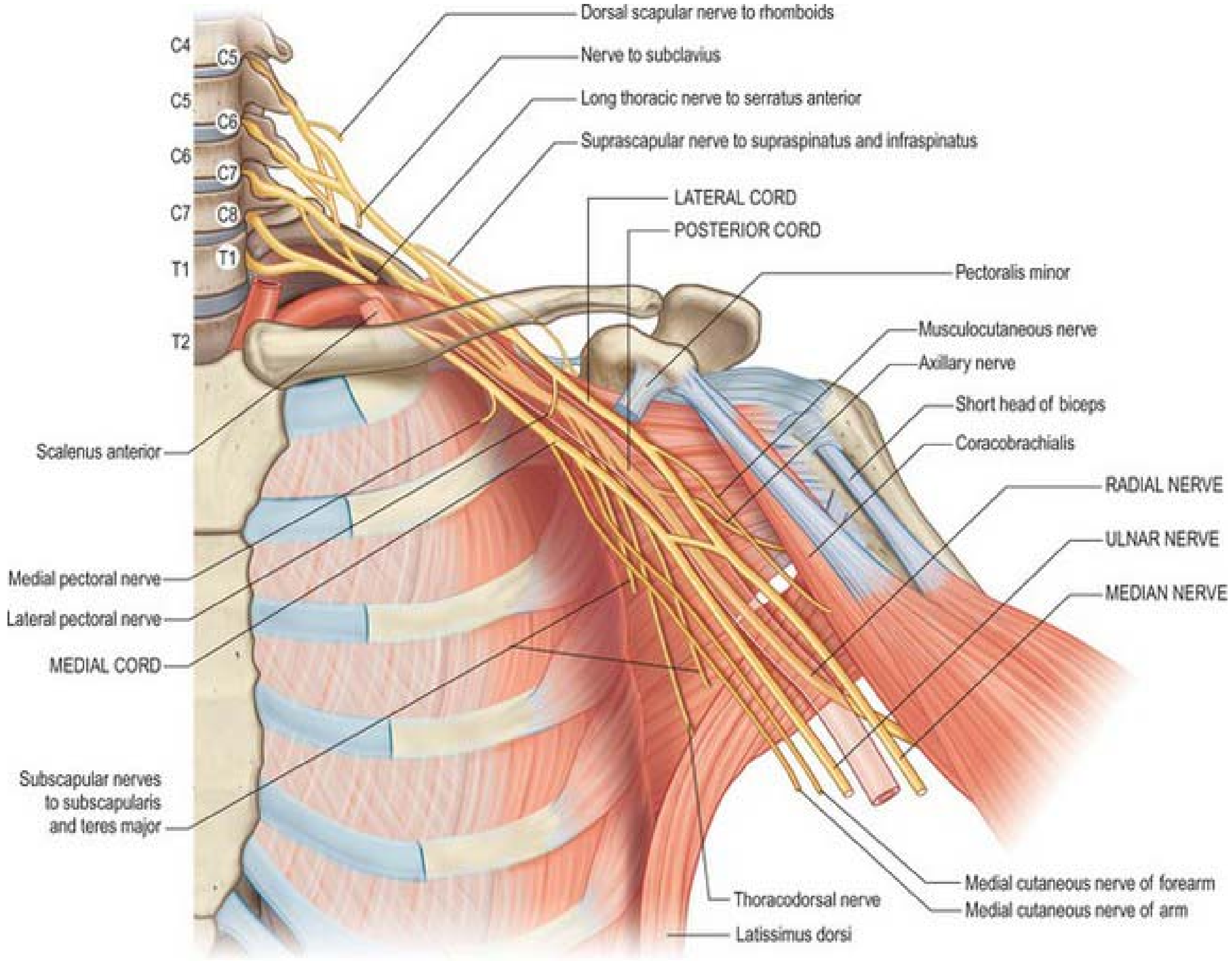
Dorsal scapular nerve to rhomboids
Nerve to subclavius
Long thoracic nerve to serratus anterior
Suprascapular nerve to supraspinatus and infraspinatus
C4
C5
C6
C7
T1
T2
C5
C6
C7
C8
T1
LATERAL CORD
POSTERIOR CORD
Pectoralis minor
Musculocutaneous nerve
Axillary nerve
Short head of biceps
Coracobrachialis
RADIAL NERVE
ULNAR NERVE
MEDIAN NERVE
Scalenus anterior
Medial pectoral nerve
Lateral pectoral nerve
MEDIAL CORD
Subscapular nerves to subscapularis and teres major
Thoracodorsal nerve
Latissimus dorsi
Medial cutaneous nerve of forearm
Medial cutaneous nerve of arm

Fig. 46.29 The brachial plexus, its branches and the muscles which they supply. The axillary artery, shown in red outline, runs anterior to the radial nerve. The vertebral levels are labelled C4–T2. The nerve roots are labelled C5–T1 (white circles).

Branches of the brachial plexus may be described as supraclavicular and infraclavicular.

Supraclavicular branches

Supraclavicular branches arise from roots or from trunks as follows:

From roots	1. Nerves to scaleni and longus colli	C5, 6, 7, 8
	2. Branch to phrenic nerve	C5
	3. Dorsal scapular nerve	C5
	4. Long thoracic nerve	C5, 6 (7)
From trunks	1. Nerve to subclavius	C5, 6
	2. Suprascapular nerve	C5, 6

Branches to the scaleni and longus colli arise from the lower cervical ventral rami near their exit from the intervertebral foramina. The phrenic nerve is joined by a branch from the fifth cervical ramus anterior to scalenus anterior.

Dorsal scapular nerve

The dorsal scapular nerve comes from the fifth cervical ventral ramus, pierces scalenus medius, passes behind levator scapulae, which it occasionally supplies, and runs with the deep branch of the dorsal scapular artery to the rhomboids, which it supplies.

Long thoracic nerve

The long thoracic nerve is usually formed by roots from the fifth to the seventh cervical rami, although the last ramus may be absent (Fig. 46.30). The upper two roots pierce scalenus medius obliquely, uniting in or lateral to it. The nerve descends dorsal to the brachial plexus and the first part of the axillary artery and crosses the superior border of serratus anterior to reach its lateral surface. It may be joined by the root from C7, which emerges between scalenus anterior and scalenus medius, and descends on the lateral surface of medius. The nerve continues downwards to the lower border of serratus anterior, and supplies branches to each of its digitations.

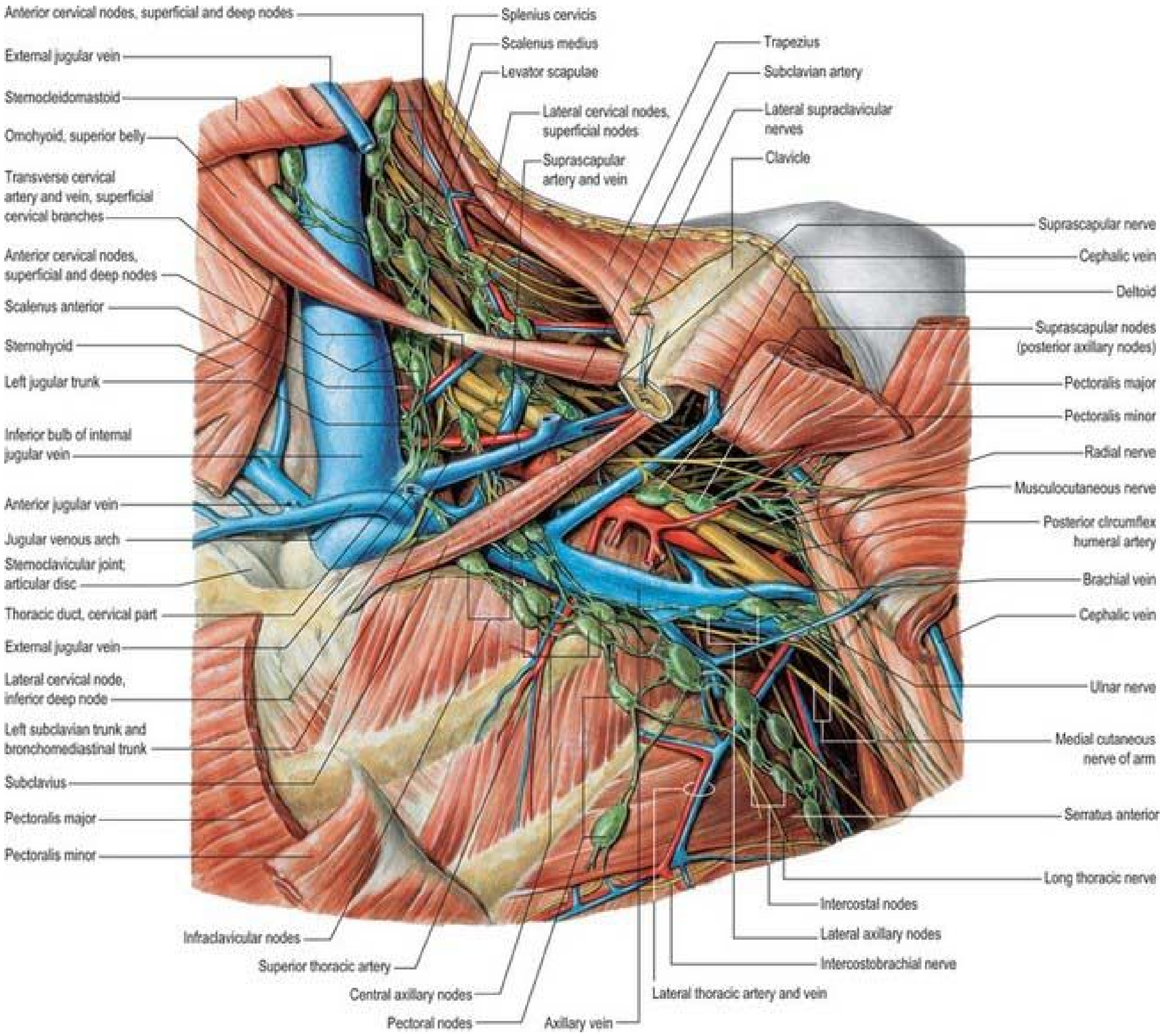
Anterior cervical nodes, superficial and deep nodes
External jugular vein
Sternocleidomastoid
Omohyoid, superior belly
Transverse cervical artery and vein, superficial cervical branches
Anterior cervical nodes, superficial and deep nodes
Scalenus anterior
Sternohyoid
Left jugular trunk
Inferior bulb of internal jugular vein
Anterior jugular vein
Jugular venous arch
Sternoclavicular joint; articular disc
Thoracic duct, cervical part
External jugular vein
Lateral cervical node, inferior deep node
Left subclavian trunk and bronchomediastinal trunk
Subclavius
Pectoralis major
Pectoralis minor
Splenius cervicis
Scalenus medius
Levator scapulae
Lateral cervical nodes, superficial nodes
Suprascapular artery and vein
Trapezius
Subclavian artery
Lateral supraclavicular nerves
Clavicle
Suprascapular nerve
Cephalic vein
Deltoid
Suprascapular nodes (posterior axillary nodes)
Pectoralis major
Pectoralis minor
Radial nerve
Musculocutaneous nerve
Posterior circumflex humeral artery
Brachial vein
Cephalic vein
Ulnar nerve
Medial cutaneous nerve of arm
Serratus anterior
Long thoracic nerve
Intercostal nodes
Lateral axillary nodes
Intercostobrachial nerve
Lateral thoracic artery and vein
Axillary vein
Pectoral nodes
Central axillary nodes
Superior thoracic artery
Infraclavicular nodes

Fig. 46.30 Anterior aspect of left axillary fossa and deep aspect of thoracic inlet. The clavicle has been partially removed and the pectoral muscles have been reflected.

(From Sobotta 2006.)

The long thoracic nerve is the most common nerve to be affected by neuralgic amyotrophy. Winging of the scapula may be the only clinical manifestation: it is best demonstrated by asking the patient to push against resistance with the arm extended at the elbow and flexed to 90° at the shoulder.

Nerve to subclavius

The nerve to subclavius is small and arises near the junction of the fifth and sixth cervical ventral rami. It descends anterior to the plexus and the third part of the subclavian artery and is usually connected to the phrenic nerve. It passes above the subclavian vein to supply subclavius.

Suprascapular nerve

The suprascapular nerve is a large branch of the superior trunk (Fig. 28.17). It runs laterally, deep to trapezius and omohyoid and enters the supraspinous fossa through the suprascapular notch inferior to the superior transverse scapular ligament. It runs deep to supraspinatus, supplies it, and curves round the lateral border of the spine of the scapula with the suprascapular artery to reach the infraspinous fossa, where it gives two branches to infraspinatus and articular rami to the shoulder and acromioclavicular joints. The suprascapular nerve rarely has a cutaneous branch. When present, it pierces deltoid close to the tip of the acromion and supplies the skin of the proximal third of the arm within the territory of the axillary nerve.

Lesions of the suprascapular nerve

The commonest cause involving the suprascapular nerve is neuralgic amyotrophy. An entrapment neuropathy may occur in the scapular notch, often related to a degenerate cyst originating from the posterior glenoid labrum, or the nerve may be damaged by trauma to the scapula and shoulder. There is pain in the shoulder and wasting and weakness of supraspinatus and infraspinatus.

Infraclavicular branches

Infraclavicular branches come from the cords, but their axons may be traced back to the spinal nerves detailed in the box below.

Lateral cord	Lateral pectoral	C5, 6, 7
	Musculocutaneous	C5, 6 7
	Lateral root of median	C(5), 6, 7
Medial cord	Medial pectoral	C8, T1
	Medial cutaneous of forearm	C8, T1
	Medial cutaneous of arm	C8, T1
	Ulnar	C(7), 8, T1
	Medial root of median	C8, T1
Posterior cord	Upper subscapular	C5, 6
	Thoracodorsal	C6, 7,8
	Lower subscapular	C5, 6
	Axillary	C5, 6
	Radial	C5, 6, 7, 8, (T1)

Lateral pectoral nerve

The lateral pectoral nerve is larger than the medial, and may arise from the anterior divisions of the upper and middle trunks, or by a single root from the lateral cord. Its axons are from the fifth to seventh cervical rami. It crosses anterior to the axillary artery and vein, pierces the clavipectoral fascia and supplies the deep surface of pectoralis major. It sends a branch to the medial pectoral nerve, forming a loop in front of the first part of the axillary artery (Fig. 46.30), to supply some fibres to pectoralis minor.

Medial pectoral nerve

The medial pectoral nerve is derived from the eighth cervical and first thoracic ventral rami and branches from the medial cord while the latter lies posterior to the axillary artery. It curves forwards between the axillary artery and vein. Anterior to the artery it joins a ramus of the lateral pectoral nerve, and enters the deep surface of pectoralis minor, which it supplies. Two or three branches pierce pectoralis minor and others may pass round its inferior border to end in pectoralis major.

Upper (superior) subscapular nerve

The superior subscapular nerve is smaller than the inferior. It arises from the posterior cord (C5 and 6), enters subscapularis at a high level, and is frequently double.

Lower (inferior) subscapular nerve

The inferior subscapular nerve arises from the posterior cord (C5 and 6). It supplies the lower part of subscapularis, and ends in teres major, which is sometimes supplied by a separate branch.

Thoracodorsal nerve

The thoracodorsal nerve arises from the posterior cord (C6 to 8) between the subscapular nerves. It accompanies the subscapular artery along the posterior axillary wall and supplies latissimus dorsi, reaching its distal border.

Axillary nerve

The axillary nerve arises from the posterior cord (C5, 6) (Fig. 46.22). It is at first lateral to the radial nerve, posterior to the axillary artery and anterior to subscapularis. At the lower border of subscapularis it curves back inferior to the humeroscapular articular capsule and, with the posterior circumflex humeral vessels, traverses a quadrangular space bounded above by subscapularis (anterior) and teres minor (posterior), below by teres major, medially by the long head of triceps, and laterally by the surgical neck of the humerus. It divides in the space into anterior and posterior branches. The anterior branch curves round the neck of the humerus with the posterior circumflex humeral vessels, deep to deltoid. It reaches the anterior border of the muscle and supplies it, and gives off a few small cutaneous branches which pierce deltoid and ramify in the skin over its lower part. The posterior branch courses medially and posteriorly along the attachment of the lateral head of triceps, inferior to the glenoid rim. It usually lies medial to the anterior branch in the quadrangular space. It gives off the nerve to teres minor and the upper lateral cutaneous nerve of the arm at the lateral edge of the origin of the long head of triceps. The nerve to teres minor enters the muscle on its inferior surface. The posterior branch frequently supplies the posterior aspect of deltoid, usually via a separate branch from the main stem, occasionally from the superior lateral cutaneous nerve of the arm. However, the posterior part of deltoid has a more consistent supply from the anterior branch of the axillary nerve, which should be remembered when performing a posterior deltoid-splitting approach to the shoulder. The upper lateral cutaneous nerve of the arm pierces the deep fascia at the medial border of the posterior aspect of deltoid and supplies the skin over the lower part of deltoid and the upper part of the long head of triceps. The posterior branch is intimately related to the inferior aspects of the glenoid and shoulder joint capsule, which may place it at particular risk during capsular plication or thermal shrinkage procedures (Ball et al 2003). There is often an enlargement or pseudoganglion on the branch to teres minor. The axillary trunk supplies a branch to the shoulder joint below subscapularis.

Lesions of the axillary nerve

The commonest causes of axillary nerve lesions are trauma (dislocation of the shoulder, fracture of the surgical neck of the humerus), and neuralgic amyotrophy. There is wasting and weakness of deltoid, which is usually clinically evident, and a patch of sensory loss on the outer aspect of the arm.

This can be differentiated from a C5 root lesion by finding normal function in the distribution of the suprascapular nerve.

Musculocutaneous nerve

The musculocutaneous nerve arises from the lateral cord (C5–7), opposite the lower border of pectoralis minor (Fig. 46.30). It pierces coracobrachialis and descends laterally between biceps and brachialis to the lateral side of the arm. Just below the elbow it pierces the deep fascia lateral to the tendon of biceps, and continues as the lateral cutaneous nerve of the forearm. A line drawn from the lateral side of the third part of the axillary artery across coracobrachialis and biceps to the lateral side of the biceps tendon is a surface projection for the nerve (but this varies according to its point of entry into coracobrachialis). It supplies coracobrachialis, both heads of biceps and most of brachialis. The branch to coracobrachialis is given off before the musculocutaneous nerve enters the muscle: its fibres are from the seventh cervical ramus and may branch directly from the lateral cord. Branches to biceps and brachialis leave after the musculocutaneous has pierced coracobrachialis: the branch to brachialis also supplies the elbow joint. The musculocutaneous nerve supplies a small branch to the humerus, which enters the shaft with the nutrient artery.

Lesions of the musculocutaneous nerve

An isolated lesion of the musculocutaneous nerve is rare, but may occur in injuries to the upper arm and shoulder, e.g. fracture of the humerus, and in patients with neuralgic amyotrophy. There is marked weakness of elbow flexion, because biceps brachii and much of brachialis are paralysed, and sensory impairment on the extensor aspect of the forearm in the distribution of the lateral cutaneous nerve of the forearm. Pain and paraesthesiae may be aggravated by elbow extension.

Medial cutaneous nerve of arm

The medial cutaneous nerve of the arm is the smallest and most medial branch of the brachial plexus, and arises from the medial cord (C8, T1). It crosses the axilla, either anterior or posterior to the axillary vein, then passes medial to the axillary vein, communicates with the intercostobrachial nerve, and descends medial to the brachial artery and basilic vein. It pierces the deep fascia at the midpoint of the upper arm to supply the skin over the medial aspect of the distal third of the upper arm.

Medial cutaneous nerve of forearm

The medial cutaneous nerve of the forearm arises from the medial cord (C8, T1). It is described further on pages 830 and 856.

Median nerve

The median nerve has two roots from the lateral (C5, 6, 7) and medial (C8, T1) cords, which embrace the third part of the axillary artery, and unite anterior or lateral to it (Fig. 46.30). Some fibres from C7 often leave the lateral root in the lower part of the axilla and pass distomedially posterior to the medial root, and usually anterior to the axillary artery, to join the ulnar nerve. They may branch from the seventh cervical ventral ramus. Clinically they are believed to be mainly motor and to supply flexor carpi ulnaris. If the lateral root is small, the musculocutaneous nerve (C5, 6, 7) connects with the median nerve in the arm.

Ulnar nerve

The ulnar nerve arises from the medial cord (C8, T1) but often receives fibres from the ventral ramus of C7 (Fig. 46.30). It runs distally through the axilla medial to the axillary artery, between it and the vein. It is described further on page 827.

Radial nerve

The radial nerve is the largest branch of the brachial plexus. It arises from the posterior cord (C5, 6, 7, 8, (T1)) (Fig. 46.22), and descends behind the third part of the axillary artery and the upper part of the brachial artery, anterior to subscapularis and the tendons of latissimus dorsi and teres major. With the profunda brachii artery it inclines dorsally, and passes through the triangular space below the lower border of teres major, between the long head of triceps and the humerus. It is described further on page 827.

Brachial plexus lesions

Lesions of the brachial plexus commonly affect either the upper part of the plexus, i.e. C5 and C6 roots and the upper trunk, or the lower part of the plexus, i.e. C8 and T1 roots and the lower trunk. Lesions affecting the upper part are usually traumatic, whereas those affecting the lower part may be caused by trauma but may also be produced by malignant infiltration or a thoracic outlet syndrome. Severe trauma may affect the whole plexus.

Upper plexus palsies

Downward traction of an infant’s arm during birth, or, in adults, a severe fall on the side of the head and the shoulder, forcing the two apart, as frequently occurs in motor cycle injuries, may tear the roots of C5 and C6. This will result in paralysis of deltoid, the short muscles of the shoulder, and of brachialis and biceps. The last two are both elbow flexors, and biceps is also a powerful supinator of the superior radio-ulnar joint. The arm therefore hangs by the side, with the forearm pronated and the palm facing backwards, like a waiter hinting for a tip (Erb–Duchenne paralysis). There is sensory loss over the lateral aspect of the upper arm.

Lower plexus palsies

Upward traction on the arm, e.g. in a forcible breech delivery, may tear the lowest root, T1, which provides the segmental supply to the intrinsic muscles of the hand. The hand assumes a clawed appearance reflecting the unopposed action of the long flexors and extensors of the fingers (Klumpke’s paralysis). There is sensory loss along the medial aspect of the forearm and there is often an associated Horner’s syndrome (ptosis and constriction of the pupil) which occurs as a result of traction on the cervical sympathetic chain.

Malignant infiltration of the brachial plexus may result from extension of an apical lung carcinoma (Pancoast tumour) or from metastatic spread, often from carcinoma of the breast. There is slowly progressive weakness which usually starts in the small muscles of the hand (T1) and spreads to involve the finger flexors (C8). This is usually a painful condition, and the pain may be severe. There is sensory loss on the medial aspect of the forearm (T1) extending into the medial side of the hand and to the little finger (C8). A Horner's syndrome may occur if there is involvement of the cervical sympathetic ganglia. A similar syndrome may occur following radiotherapy for breast carcinoma, but this is usually painless. Thoracic surgery involving a sternal split may cause traction on the brachial plexus and usually affects the lower part of the plexus.

The lower trunk of the brachial plexus (C8, T1), together with the subclavian artery, may be angulated over a cervical rib (thoracic outlet syndrome). Patients may present with vascular symptoms as a result of kinking of the subclavian artery (this is more likely to occur with large bony ribs), or they may present with neurological deficit (this is more likely in patients with small rudimentary ribs which extend into a fibrous band which joins the first rib anteriorly). Cervical ribs are quite common and are rarely associated with symptoms. There is a slow insidious onset of wasting of the small muscles of the hand, which often starts on the lateral side with involvement of the thenar eminence and first dorsal interosseous. There is pain and paraesthesiae in the medial aspect of the forearm extending to the little finger, and this is often aggravated by carrying shopping or suitcases. A bruit may be heard over the subclavian artery, and the radial pulse may be easily obliterated by movements of the arm, particularly with the arm extended and abducted at the shoulder.

REFERENCES

ll CM, Steger T, Galatz LM, Yamaguchi K. The posterior branch of the axillary nerve: an anatomic study. *J Bone Joint Surg*. 2003;85:1497-1501.

rkart AC, Debski RE. Anatomy and function of the glenohumeral ligaments in anterior shoulder instability. *Clin Orthopaed Related Res*. 2002;400:32-39.

ichael Salmon: Anatomic Studies. In: Taylor GI, Razaboni RM. *Book 1, Arteries of the Muscles of the Extremities and the Trunk, Book 2, Arterial anastomotic pathways of the extremities*. St Louis: Quality Medical Publishing, 1994.

Contains the translated work of Dr Michel Salmon and describes the blood supply to muscle as well as the anastomotic pathways in the limbs..

CHAPTER 47

Upper arm

SKIN AND SOFT TISSUE

SKIN

Cutaneous vascular supply

The blood supply to the skin of the upper arm can be divided into three regions with separate supply: the deltoid region, supplied by musculocutaneous perforators, and the medial and lateral regions, supplied by fasciocutaneous perforators (Cormack & Lamberty 1994; Salmon 1994) (Fig. 47.1, Fig. 47.2).

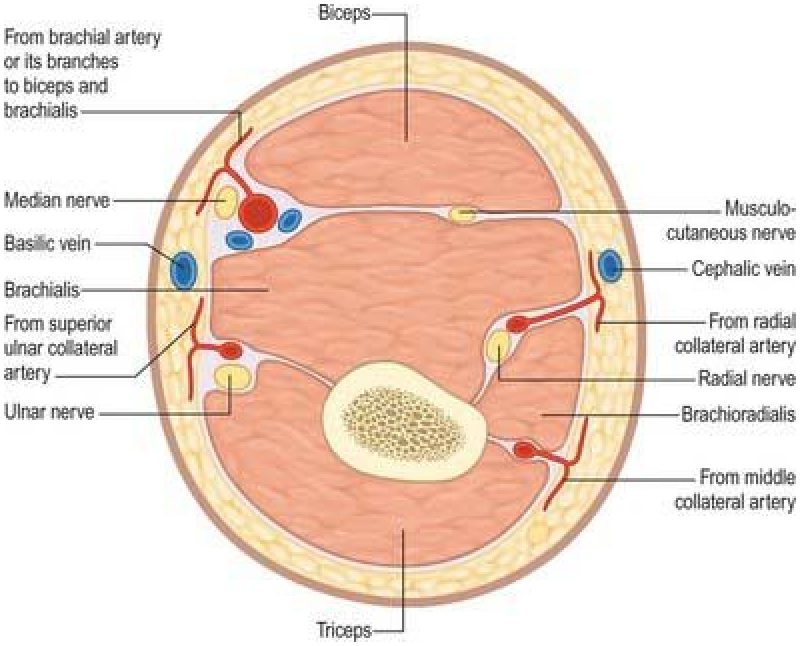
Biceps
From brachial artery or its branches to biceps and brachialis
Median nerve
Basilic vein
Brachialis
From superior ulnar collateral artery
Ulnar nerve
Musculo-cutaneous nerve
Cephalic vein
From radial collateral artery
Radial nerve
Brachioradialis
From middle collateral artery
Triceps

Fig. 47.1 Transverse section through the upper arm to show the location of fasciocutaneous perforators lying on the superficial aspect of the deep fascia.

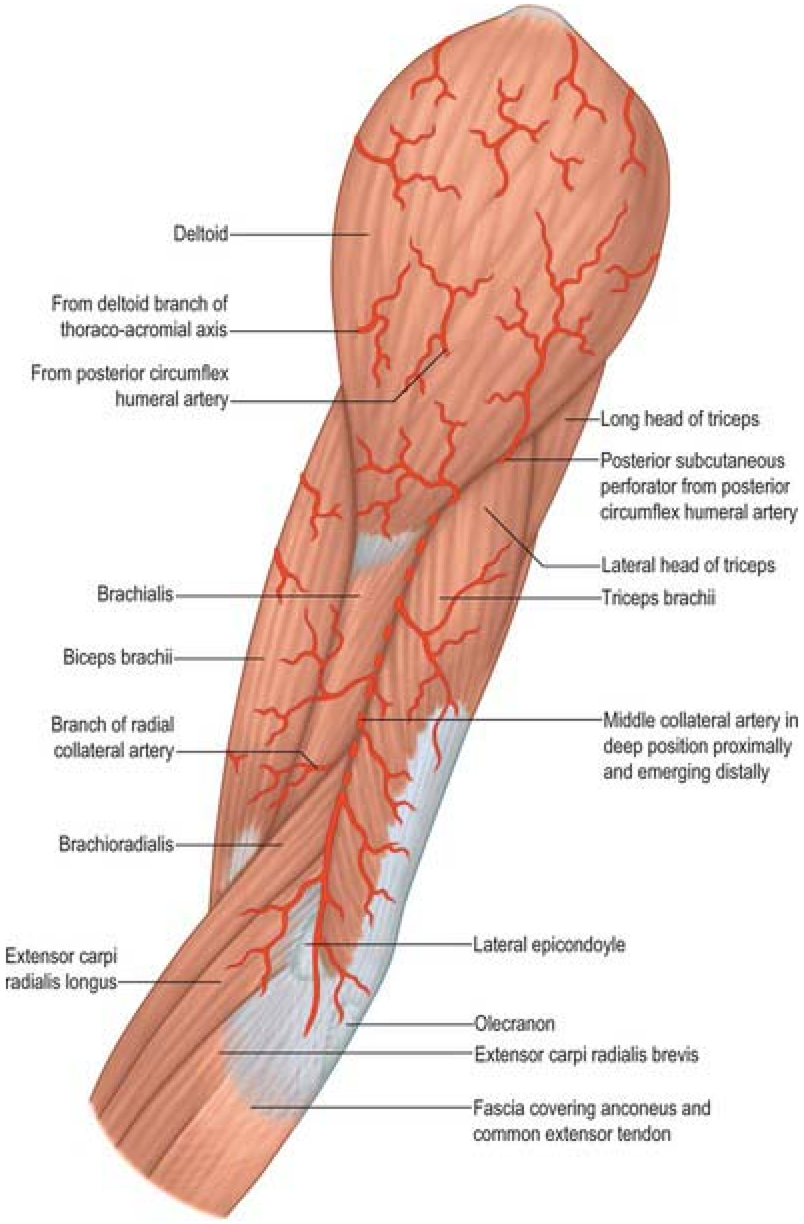
Deltoid
From deltoid branch of thoraco-acromial axis
From posterior circumflex humeral artery
Brachialis
Biceps brachii
Branch of radial collateral artery
Brachioradialis
Extensor carpi radialis longus
Long head of triceps
Posterior subcutaneous perforator from posterior circumflex humeral artery
Lateral head of triceps
Triceps brachii
Middle collateral artery in deep position proximally and emerging distally
Lateral epicondoyle
Olecranon
Extensor carpi radialis brevis
Fascia covering anconeus and common extensor tendon

Fig. 47.2 Muscles of the left upper arm, viewed from the lateral aspect showing fasciocutaneous and musculocutaneous perforating vessels.

The deltoid region is supplied by the posterior circumflex humeral artery (p. 817) via musculocutaneous perforators. After the posterior circumflex humeral artery passes through the quadrangular space (p. 814) it gives off a descending branch, which runs down to the deltoid insertion and the overlying skin, and an ascending branch which passes superiorly towards the acromion, pierces the edge of deltoid and the deep fascia to fan out and supply the overlying skin.

The medial side of the upper arm is supplied by five or six fasciocutaneous perforators which arise from the brachial artery, the superior ulnar collateral artery and, if present, the single artery to biceps. These perforators pass along the medial intermuscular septum to spread out in the deep fascia and anastomose with perforating vessels superiorly and inferiorly and from the lateral side. There are virtually no musculocutaneous perforators through biceps or triceps.

The lateral side of the upper arm below deltoid is supplied by perforating vessels from the middle collateral and radial collateral arteries (the terminating bifurcation of the profunda brachii). The middle collateral artery sends perforators to the skin via the lateral intermuscular septum between brachioradialis and triceps, while the radial collateral artery gives off cutaneous perforators via the intermuscular septum between brachialis and brachioradialis. These cutaneous vessels anastomose with those from the medial side.

Cutaneous innervation

The skin of the shoulder region is supplied by the supraclavicular nerves from the cervical plexus. The floor of the axilla and upper medial surface of the arm is supplied by the lateral branch of the second intercostal nerve (the intercostobrachial nerve). The lower aspect of the medial side of the upper arm is supplied by the medial cutaneous nerve of the arm. The lateral aspect of the upper arm is supplied by the upper lateral cutaneous nerve (a branch of the axillary nerve) and the lower lateral cutaneous nerve (a branch of the radial nerve). The posterior aspect is supplied by the posterior cutaneous nerve of the arm, a branch of the radial nerve (Fig. 45.15, Fig. 45.14).

SOFT TISSUE

Brachial fascia

Brachial fascia, the deep fascia of the upper arm, is continuous with the fascia covering deltoid and pectoralis major: it forms a thin, loose sheath for muscles of the upper arm, and sends septa between them. It is thin over biceps, but thicker over triceps and the humeral epicondyles, and is strengthened by fibrous aponeuroses from pectoralis major and latissimus dorsi medially and from deltoid laterally. Strong medial and lateral intermuscular septa extend from it on each side.

The lateral intermuscular septum extends distally from the lateral lip of the intertubercular sulcus of the humerus along the lateral supracondylar ridge to the lateral epicondyle, and blends with the tendon of deltoid. It gives attachment to triceps behind, and brachialis, brachioradialis and extensor carpi radialis longus in front. It is perforated in the middle third by the radial nerve and the radial collateral branch of the profunda brachii artery. The thicker medial intermuscular septum extends from the medial lip of the intertubercular sulcus, distal to teres major, along the medial supracondylar ridge to the medial epicondyle, and blends with the tendon of coracobrachialis. It gives attachment to triceps behind, and brachialis in front. It is perforated by the ulnar nerve, superior ulnar collateral artery, and the posterior branch of the inferior ulnar collateral artery. At the elbow, the brachial fascia is attached to the epicondyles of the humerus and the olecranon of the ulna, and is continuous with the antebrachial fascia. Medially, just below the middle of the upper arm, it is traversed by the basilic vein and lymphatic vessels and, at various levels, branches of the brachial cutaneous nerves.

Together, the lateral and medial intermuscular septa of the upper arm divide the upper arm into anterior and posterior compartments.

MUSCLES

The muscles of the upper arm are coracobrachialis, which acts only on the shoulder joint; biceps and triceps, which cross both shoulder and elbow joints; and brachialis, which acts only at the elbow joint (Fig. 47.2, Fig. 47.3).

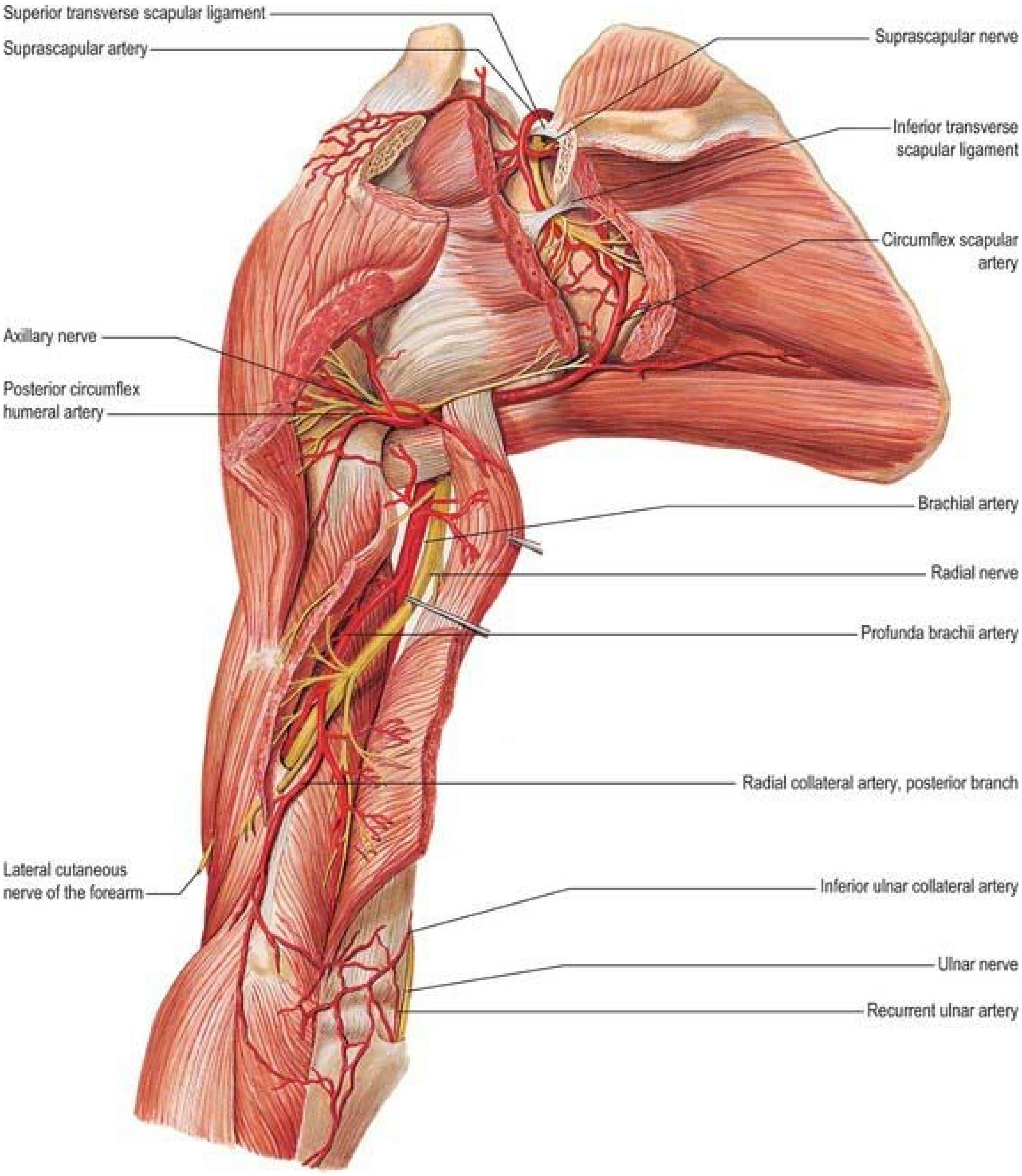
Superior transverse scapular ligament
Suprascapular artery
Suprascapular nerve
Inferior transverse scapular ligament
Circumflex scapular artery
Axillary nerve
Posterior circumflex humeral artery
Brachial artery
Radial nerve
Profunda brachii artery
Radial collateral artery, posterior branch
Lateral cutaneous nerve of the forearm
Inferior ulnar collateral artery
Ulnar nerve
Recurrent ulnar artery

Fig. 47.3 Muscles, vessels and nerves of the left upper arm, viewed from the posterior aspect.

(From Sobotta 2006.)

ANTERIOR COMPARTMENT

Coracobrachialis

Attachments

Coracobrachialis arises from the apex of the coracoid process, together with the tendon of the short head of biceps, and also by muscular fibres from the proximal 10 cm of this tendon; it ends on an impression, 3–5 cm in length, midway along the medial border of the humeral shaft between the attachments of triceps and brachialis (Fig. 46.20, Fig. 47.4). Accessory slips may be attached to the lesser tubercle, medial epicondyle or medial intermuscular septum.

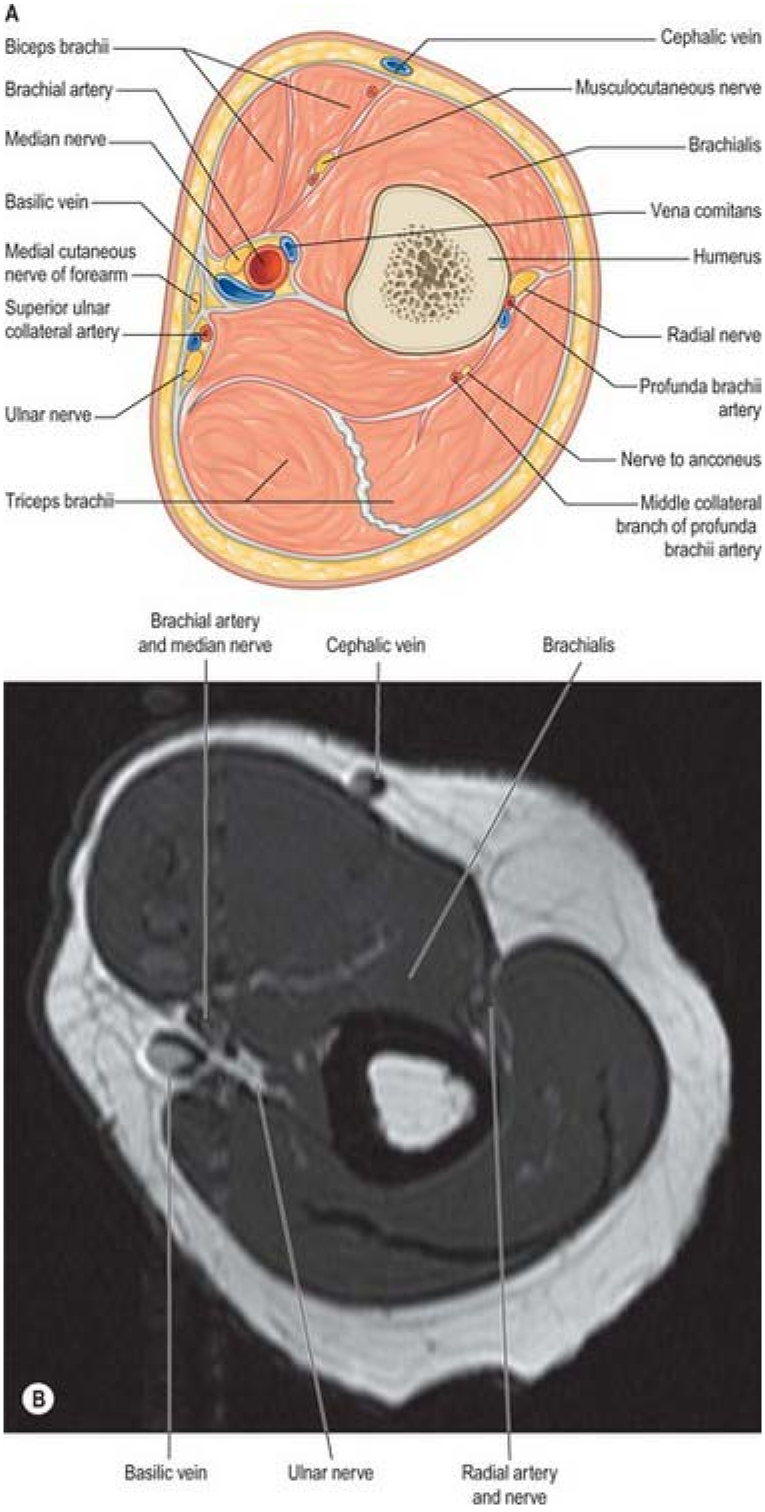
A
Biceps brachii
Brachial artery
Median nerve
Basilic vein
Medial cutaneous nerve of forearm
Superior ulnar collateral artery
Ulnar nerve
Triceps brachii
Cephalic vein
Musculocutaneous nerve
Brachialis
Vena comitans
Humerus
Radial nerve
Profunda brachii artery
Nerve to anconeus
Middle collateral branch of profunda brachii artery
Brachial artery and median nerve
Cephalic vein
Brachialis
B
Basilic vein
Ulnar nerve
Radial artery and nerve

Fig. 47.4 **A**, Transverse section through the left arm a little below the middle of the shaft of the humerus. **B**, MRI scan at similar level.

Relations

Coracobrachialis forms an inconspicuous rounded ridge on the upper medial side of the arm; pulsation of the brachial artery can be felt and often seen in the depression behind it. The muscle is perforated by the musculocutaneous nerve. Anteriorly it is related to pectoralis major above and, at its humeral insertion, to the brachial vessels and median nerve, which cross it. The tendons of subscapularis, latissimus dorsi, and teres major, the medial head of triceps, the humerus and the anterior circumflex humeral vessels all lie posterior. The axillary artery (third part) and proximal parts of the median and musculocutaneous nerves lie medial. Biceps and brachialis lie lateral.

Vascular supply

One or more branches from the axillary artery pass deep to the lateral root of the median nerve, and the musculocutaneous nerve, to reach the deep surface of the muscle. Branches from the anterior circumflex humeral artery also supply the deep surface of the muscle. The accompanying artery of the musculocutaneous nerve sends a recurrent branch to the coracoid attachment and gives off a series of branches to the muscle during its intramuscular course. Accessory branches from the thoracoacromial artery provide additional supply to the superficial part of coracobrachialis.

Innervation

Coracobrachialis is innervated by the musculocutaneous nerve, C5, 6 and 7.

Actions

Coracobrachialis flexes the arm forward and medially, especially from a position of brachial extension. In abduction it acts with anterior fibres of deltoid to resist departure from the plane of motion.

Clinical anatomy: testing

Coracobrachialis can be tested by palpating its fibres during shoulder flexion against resistance.

Biceps brachii

Attachments

Biceps brachii derives its name from its two proximally attached parts or ‘heads’ (Fig. 46.20). The short head arises by a thick flattened tendon from the coracoid apex, together with coracobrachialis. The long head starts within the capsule of the shoulder joint as a long narrow tendon, running from the supraglenoid tubercle of the scapula at the apex of the glenoidal cavity, where it is continuous with the glenoidal labrum (p. 805). The tendon of the long head, enclosed in a double tubular sheath (an extension of the synovial membrane of the joint capsule), arches over the humeral head, emerges from the joint behind the transverse humeral ligament, and descends in the intertubercular sulcus, where it is retained by the transverse humeral ligament and a fibrous expansion from the tendon of pectoralis major. The two tendons lead into elongated bellies that, although closely applied, can be separated to within 7 cm or so of the elbow joint. At this joint they end in a flattened tendon, which is attached to the rough posterior area of the radial tuberosity; a bursa separates the tendon from the smooth anterior area of the tuberosity. As it approaches the radius, the tendon spirals, its anterior surface becoming lateral before being applied to the tuberosity. The tendon has a broad medial expansion, the bicipital aponeurosis, which descends medially across the brachial artery to fuse with deep fascia over the origins of the flexor muscles of the forearm (Fig. 47.5). The tendon can be split without difficulty as far as the tuberosity, whence it can be confirmed that its anterior and posterior layers receive fibres from the short and long heads, respectively.

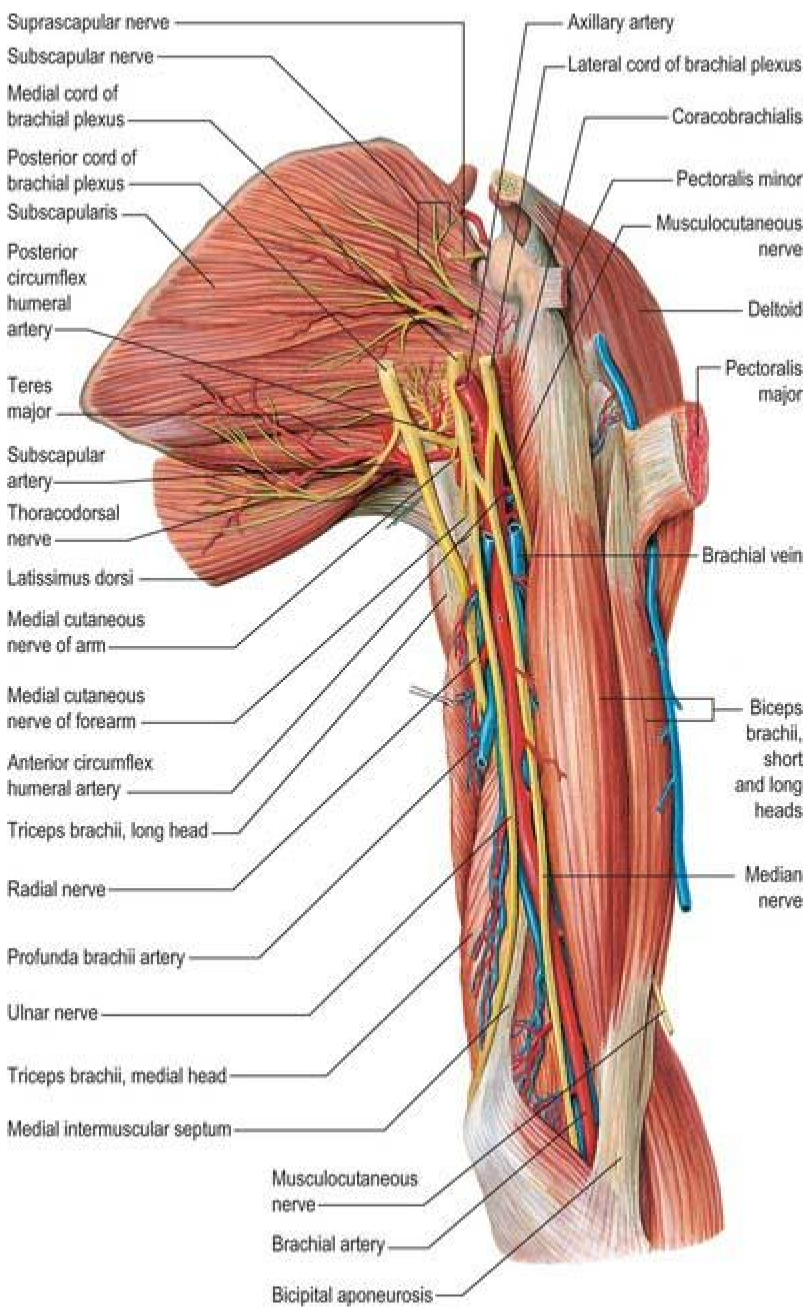
Suprascapular nerve
Subscapular nerve
Medial cord of brachial plexus
Posterior cord of brachial plexus
Subscapularis
Posterior circumflex humeral artery
Teres major
Subscapular artery
Thoracodorsal nerve
Latissimus dorsi
Medial cutaneous nerve of arm
Medial cutaneous nerve of forearm
Anterior circumflex humeral artery
Triceps brachii, long head
Radial nerve
Profunda brachii artery
Ulnar nerve
Triceps brachii, medial head
Medial intermuscular septum
Musculocutaneous nerve
Brachial artery
Bicipital aponeurosis
Axillary artery
Lateral cord of brachial plexus
Coracobrachialis
Pectoralis minor
Musculocutaneous nerve
Deltoid
Pectoralis major
Brachial vein
Biceps brachii, short and long heads
Median nerve

Fig. 47.5 Anterior aspect of left upper arm showing arteries and nerves.

(From Sobotta 2006.)

In 10% of cases, a third head arises from the superomedial part of brachialis and is attached to the bicipital aponeurosis and medial side of the tendon of insertion. It usually lies behind the brachial artery, but it may consist of two slips, which descend in front of and behind the artery. Less often, other slips may spring from the lateral aspect of the humerus or intertubercular sulcus.

Relations

Biceps is overlapped proximally by pectoralis major and deltoid; distally it is covered only by fasciae and skin, and it forms a conspicuous elevation on the front of the arm. Its long head passes through the shoulder joint; its short head is anterior to the joint. Distally it lies anterior to brachialis, the musculocutaneous nerve and supinator. Its medial border touches coracobrachialis, and overlaps the brachial vessels and median nerve; its lateral border is related to deltoid and brachioradialis.

Vascular supply

Biceps brachii is typically supplied by up to eight vessels originating from the brachial artery in the middle third of the arm. These vessels pass laterally, posterior to the median nerve and divide into ascending and descending branches just before reaching the deep surface of the muscle. Smaller branches arise from the anterior circumflex humeral artery and the deltoid branch of the acromial division of the thoracoacromial axis.

There is great variation in the arterial supply to the muscle. The main arterial supply may originate from the superior or inferior ulnar collateral artery, subscapular artery, axillary artery, ulnar or radial arteries in cases of proximal bifurcation of the brachial artery, or the profunda brachii artery.

Innervation

Biceps brachii is innervated by the musculocutaneous nerve, C5 and 6, with separate branches passing to each belly.

Actions

Biceps brachii is a powerful supinator, especially in rapid or resisted movements. It flexes the elbow, most effectively with the forearm supinated, and acts to a slight extent as a flexor of the shoulder joint. It is attached, via the bicipital aponeurosis, to the posterior border of the ulna, the distal end of which is drawn medially in supination. The long head helps to check upward translation of the humeral head during contraction of deltoid. When the elbow is flexed against resistance, the tendon of insertion and bicipital aponeurosis become conspicuous.

Lowering the hand under the influence of gravity by extension at the elbow calls for controlled lengthening of biceps. This is an example of a habitual movement in which muscle tension increases despite increasing length. As the hand descends and the elbow extends, the vertical through the centre of gravity of the forearm is carried further from the fulcrum of movement; the turning moment exerted by the load therefore increases and must be matched by an increase in the moment exerted by the muscle.

Clinical anatomy: testing

With the forearm supinated, biceps brachii can be tested by palpating its fibres during elbow flexion against resistance.

Brachialis

Attachments

Brachialis arises from the lower half of the front of the humerus, starting on either side of the insertion of deltoid, and extending distally to within 2.5 cm of the cubital articular surface (Fig. 46.20, Fig. 47.4). It also arises from the intermuscular septa, more from the medial than the lateral, since it is separated distally from the lateral intermuscular septum by brachioradialis and extensor carpi radialis longus. Its fibres converge to a thick, broad tendon which is attached to the ulnar tuberosity and to a rough impression on the anterior aspect of the coronoid process.

Brachialis may be divided into two or more parts. It may be fused with brachioradialis, pronator teres or biceps. In some cases it sends a tendinous slip to the radius or bicipital aponeurosis.

Relations

Anterior are biceps, the brachial vessels, musculocutaneous and median nerves. Posterior are the humerus and capsule of the elbow joint. Medial are pronator teres, and the medial intermuscular septum, which separates it from triceps and the ulnar nerve. Lateral are the radial nerve, radial recurrent and radial collateral arteries, brachioradialis and extensor carpi radialis longus.

Vascular supply

The blood supply to brachialis typically consists of two main arteries (superior and inferior) supplemented by a system of accessory arteries. The superior main artery originates from the brachial artery distal to the site of origin of the superior ulnar collateral artery and travels laterally to enter the anterior surface of the upper third of the muscle. The inferior main artery originates either from the superior ulnar collateral artery or directly from the brachial artery and enters the mid-portion of the muscle. The accessory arteries are small, variable in number, origin and course. They can arise from the brachial artery, the superior and inferior ulnar collateral arteries, or the profunda brachii artery.

Innervation

Brachialis is innervated by the musculocutaneous nerve (C5 and 6), and radial nerve (C7) to a small lateral part of the muscle.

Action

Brachialis is a flexor of the elbow joint with the forearm either prone or supine, whether or not the movement is resisted.

Clinical anatomy: testing

Brachialis can be tested by palpating its fibres during elbow flexion against resistance.

POSTERIOR COMPARTMENT

Triceps

Attachments

Triceps fills most of the extensor compartment of the upper arm (Fig. 46.22, Figs 47.2-47.4). It arises by three heads (long, lateral and medial), from which it takes its name.

The long head arises by a flattened tendon from the infraglenoid tubercle of the scapula, blending above with the glenohumeral capsule. Its muscular fibres descend medial to the lateral head and superficial to the medial head, and join them to form a common tendon.

The lateral head arises by a flattened tendon from a narrow, linear, oblique ridge on the posterior surface of the humeral shaft, and from the lateral intermuscular septum. The origin on the humerus ascends with varying obliquity from its lateral border above the radial groove and behind the deltoid tuberosity to the surgical neck medial to the insertion of teres minor. These fibres also converge to the common tendon.

The medial head, which is overlapped posteriorly by the lateral and long heads, has a particularly extensive origin, from the entire posterior surface of the humeral shaft, below the radial groove from the insertion of teres major to within 2.5 cm of the trochlea, from the medial border of the humerus; the medial intermuscular septum and the lower part of the lateral intermuscular septum. Some muscular fibres reach the olecranon directly, the rest converge to the common tendon.

The tendon of triceps begins near the middle of the muscle. It has two laminae, one superficial in the lower half of the muscle, the other in its substance. After receiving the muscle fibres, the two layers unite above the elbow and are attached, for the most part, to the upper surface of the olecranon. On the lateral side a band of fibres continues down over anconeus to blend with antebrachial fascia.

Relations

The long head descends between teres minor and major, dividing the wedge-shaped interval between them and the humerus into triangular and quadrangular parts (Fig. 46.22). The triangular space contains the circumflex scapular vessels; it is bounded above by teres minor, below by teres major, laterally by the long head of triceps. The quadrangular space transmits the posterior circumflex humeral vessels and the axillary nerve; it is bounded above by subscapularis, teres minor and the articular capsule, below by teres major, medially by the long head of triceps, and laterally by the humerus.

The lateral head of triceps forms an elevation, parallel and medial to the posterior border of the deltoid; it stands out prominently when the elbow is actively extended. The mass which lies medial to it, and disappears under the deltoid, is the long head.

Vascular supply

The blood supply to triceps is mainly from the profunda brachii artery and the superior ulnar collateral artery, with an accessory supply from the posterior circumflex humeral artery. The medial head of triceps is supplied on its anterior surface by two or three branches from the superior ulnar collateral artery. The posterior surface is supplied by a large proximal branch from the profunda which passes medially in front of the radial nerve. The long head of triceps is supplied on its anterior surface by two arteries, one arising from the axillary artery in front of the tendon of latissimus dorsi and the other arising from either the brachial artery or the superior ulnar collateral. The posterior surface receives a recurrent branch from the posterior circumflex humeral artery immediately after traversing the quadrangular space. The lateral surface receives a number of small branches from the profunda brachii in its distal portion. The lateral head of the triceps is primarily supplied by branches of the profunda brachii, with an additional supply from a branch of the posterior circumflex humeral artery.

Innervation

Triceps is innervated by the radial nerve, C6, 7 and 8, with separate branches for each head.

Action

Triceps is the major extensor of the forearm at the elbow joint. The medial head is active in all forms of extension. The lateral and long heads are minimally active except in extension against resistance, as in thrusting or pushing or supporting body weight on the hands with the elbows semiflexed. When the flexed arm is extended at the shoulder joint, the long head may assist in drawing back and adducting the humerus to the thorax. The long head supports the lower part of the capsule of the shoulder joint, especially when the arm is raised. Articularis cubiti probably draws up the posterior part of the capsule of the elbow joint during extension of the forearm. In forceful supination of the semiflexed forearm, involving contraction of both supinator and biceps brachii, the triceps contracts synergistically to maintain the semiflexed position.

Clinical anatomy: testing

The muscle can be tested by palpating its fibres during elbow extension against resistance.

Anconeus

Anconeus is described on page 850.

VASCULAR SUPPLY AND LYMPHATIC DRAINAGE

ARTERIES

Brachial artery

The brachial artery, a continuation of the axillary, begins at the distal (inferior) border of the tendon of teres major and ends about a centimetre distal to the elbow joint (at the level of the neck of the radius) by dividing into radial and ulnar arteries (Fig. 47.5, Fig. 47.6). At first it is medial to the humerus, but gradually spirals anterior to it until it lies midway between the humeral epicondyles. Its pulsation can be felt throughout.

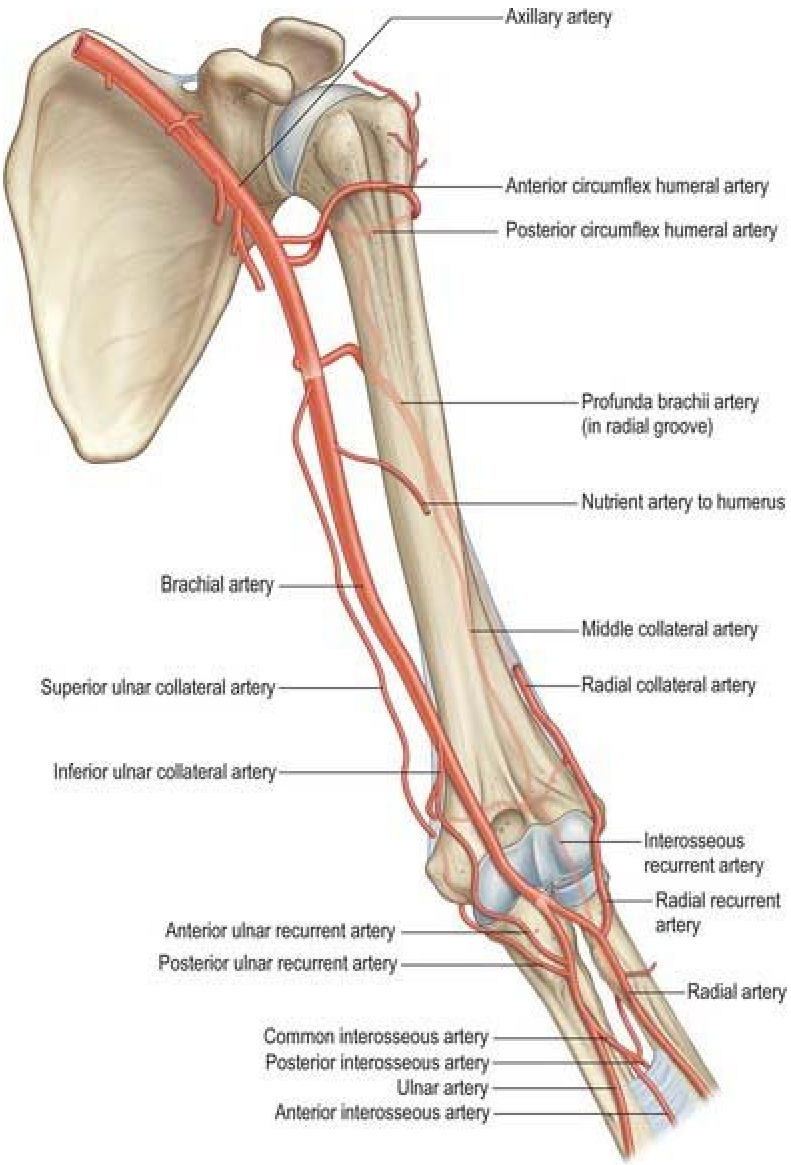
Axillary artery
Anterior circumflex humeral artery
Posterior circumflex humeral artery
Profunda brachii artery (in radial groove)
Nutrient artery to humerus
Brachial artery
Middle collateral artery
Superior ulnar collateral artery
Radial collateral artery
Inferior ulnar collateral artery
Interosseous recurrent artery
Radial recurrent artery
Anterior ulnar recurrent artery
Posterior ulnar recurrent artery
Radial artery
Common interosseous artery
Posterior interosseous artery
Ulnar artery
Anterior interosseous artery

Fig. 47.6 The arterial anastomoses around the left elbow joint viewed from the anterior aspect.

(From Drake, Vogl and Mitchell 2005.)

Relations

The brachial artery is wholly superficial, covered anteriorly only by skin and superficial and deep fasciae. The bicipital aponeurosis crosses it anteriorly at the elbow, separating it from the median cubital vein; the median nerve crosses it lateromedially near the distal attachment of coracobrachialis. Posterior are the long head of triceps, separated by the radial nerve and profunda brachii artery, and then successively by the medial head of triceps, the attachment of coracobrachialis and brachialis. Proximally the median nerve and coracobrachialis lie laterally while distally the biceps and the muscles overlap the artery. Proximally the medial cutaneous nerve of the forearm and ulnar nerve lie medially, while distally the median nerve and basilic vein lie medially. With the artery are two venae comitantes, connected by transverse and oblique branches.

At the elbow the brachial artery sinks deeply into the triangular intermuscular cubital fossa (p. 831).

Variants

The brachial artery, with the median nerve, may diverge from the medial border of the biceps, descending towards the medial humeral epicondyle, usually behind a supracondylar process from which a fibrous arch crosses the artery, and which then runs behind or through pronator teres to the elbow. Occasionally the artery divides proximally into two trunks which reunite. Frequently it divides more proximally than usual into radial, ulnar and common interosseous arteries. Most often the radial branches arise proximally, leaving a common trunk for the ulnar and common interosseous; sometimes the ulnar arises proximally, the radial and common interosseous forming the other division; the common interosseous may also arise proximally. Sometimes slender vasa aberrantia connect the brachial to the axillary artery or to one of the forearm arteries, usually the radial. The brachial artery may be crossed by muscular or tendinous slips from coracobrachialis, biceps, brachialis or pronator teres. Rarely the median nerve crosses behind, and not in front of, the brachial artery near the insertion of coracobrachialis.

Branches

These are profunda brachii, nutrient, superior, middle and inferior ulnar collateral, deltoid, muscular, radial and ulnar arteries.

Profunda brachii artery

The profunda brachii (Fig. 47.2, Fig. 47.3, Fig. 47.5, Fig. 47.6) is a large branch from the posteromedial aspect of the brachial artery, distal to teres major. It follows the radial nerve closely, at first posteriorly between the long and medial heads of triceps, then in the spiral groove covered by the lateral head of triceps. It supplies muscular branches, the nutrient artery of the humerus, and finally divides into terminal radial and middle collateral branches (Fig. 47.6). The radial collateral branch pierces the lateral intermuscular septum to reach the anterior aspect of the epicondyle of the humerus in the groove between brachioradialis and brachialis, and takes part in the anastomosis around the elbow. The middle collateral branch runs posterior to the septum and epicondyle.

The profunda brachii can originate from a common origin with the posterior circumflex humeral artery, from the axillary artery proximal to the tendon of latissimus dorsi or from the distal portion of the axillary artery.

Middle collateral (posterior descending) branch

The middle collateral artery is the larger terminal vessel. It arises posterior to the humerus and descends down the posterior surface of the lateral intermuscular septum to the elbow (Fig. 47.4, Fig. 47.6). Proximally, the artery lies between brachialis (anteriorly) and the lateral head of triceps (posteriorly) while distally it lies between brachioradialis (anteriorly) and the lateral head of triceps (posteriorly). It may pierce the deep fascia and become cutaneous or remain deep to the fascia until anastomosing with the interosseous recurrent artery behind the lateral epicondyle; it gives off about five small fasciocutaneous perforators and often has a small branch that accompanies the nerve to anconeus.

This artery and its fasciocutaneous perforators provide the anatomical basis to allow a skin flap (the lateral arm flap) to be surgically raised (either pedicled or by free tissue transfer) for reconstructing areas of tissue missing elsewhere in the body.

Radial collateral (anterior descending) branch

The radial collateral artery is the continuation of the profunda (Fig. 47.6). It accompanies the radial nerve through the lateral intermuscular septum, descending between brachialis and brachioradialis anterior to the lateral epicondyle, anastomosing with the radial recurrent artery. It supplies brachialis, brachioradialis, the radial nerve and a few fasciocutaneous perforators.

Nutrient artery of humerus

The nutrient artery of the humerus arises near the mid-level of the upper arm, and enters the nutrient canal near the attachment of coracobrachialis, posterior to the deltoid tuberosity; it is directed distally.

Superior ulnar collateral artery

The superior ulnar collateral artery arises a little distal to the mid-level of the upper arm, usually from the brachial artery, but often as a branch from the profunda brachii (Figs 47.4-47.6). It accompanies the ulnar nerve, piercing the medial intermuscular septum to descend in the posterior compartment and supply the medial head of triceps. It passes between the medial epicondyle and olecranon, ending deep to flexor carpi ulnaris by anastomosing with the posterior ulnar recurrent and inferior collateral arteries. A branch sometimes passes anterior to the medial epicondyle and anastomoses with the anterior ulnar recurrent artery.

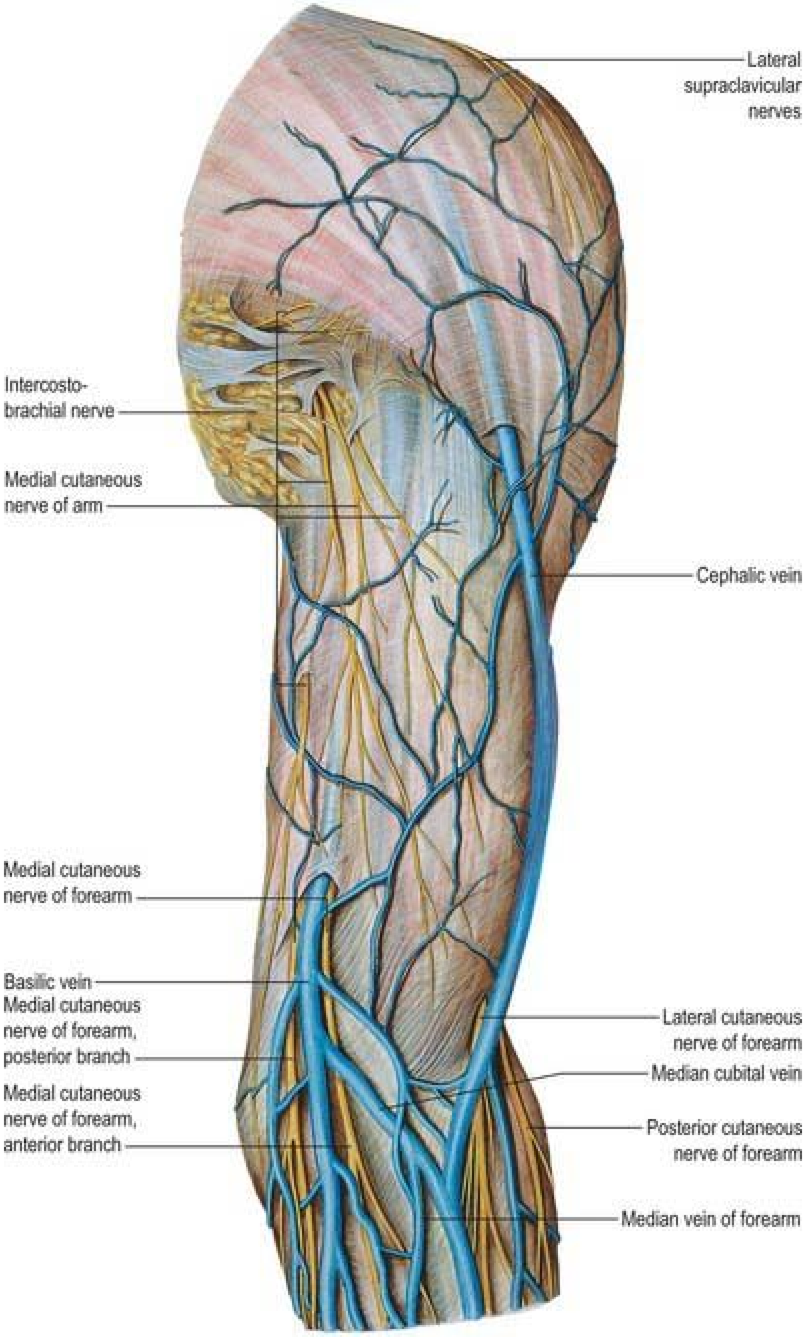
Lateral supraclavicular nerves
Intercosto-brachial nerve
Medial cutaneous nerve of arm
Cephalic vein
Medial cutaneous nerve of forearm
Basilic vein
Medial cutaneous nerve of forearm, posterior branch
Medial cutaneous nerve of forearm, anterior branch
Lateral cutaneous nerve of forearm
Median cubital vein
Posterior cutaneous nerve of forearm
Median vein of forearm

Fig. 47.7 Superficial veins and nerves of the left upper arm.

(From Sobotta 2006.)

Middle ulnar collateral artery

If present, the middle ulnar collateral artery arises from the brachial artery between the superior and inferior ulnar collaterals. It passes anterior to the medial epicondyle and anastomoses with the anterior ulnar recurrent artery. It supplies triceps and sends small fasciocutaneous perforators to the skin.

Inferior ulnar collateral (supratrochlear) artery

The inferior ulnar collateral artery begins approximately 5 cm proximal to the elbow, passes medially between the median nerve and brachialis and, piercing the medial intermuscular septum, curls round the humerus between the triceps and bone (Fig. 47.5, Fig. 47.6). It forms, by its junction with the middle collateral branch of the profunda brachii artery, an arch proximal to the olecranon fossa. As it lies on brachialis it gives off branches which descend anterior to the medial epicondyle to anastomose with the anterior ulnar recurrent artery. Behind the epicondyle a branch anastomoses with the superior ulnar collateral and posterior ulnar recurrent arteries.

Muscular branches

Muscular branches are distributed to the coracobrachialis, biceps and brachialis.

Deltoid (ascending) branch

The deltoid branch ascends between the lateral and long heads of triceps, and anastomoses with a descending branch of the posterior humeral circumflex artery.

Radial and ulnar arteries

The radial and ulnar arteries are described in detail on page 835.

VEINS

Brachial veins

The brachial veins flank the brachial artery, as venae comitantes with tributaries similar to the arterial branches; near the lower margin of subscapularis they join the axillary vein. The medial branch, however, often joins the basilic before it becomes the axillary.

These deep veins have numerous anastomoses with each other and with the superficial veins.

Superficial veins

The cephalic vein ascends in front of the elbow superficial to a groove between the brachioradialis and biceps, crosses superficial to the lateral cutaneous nerve of the forearm, ascends lateral to biceps and between pectoralis major and deltoid, where it adjoins the deltoid branch of the thoracoacromial artery (Fig. 45.5, Fig. 47.7). Entering the infraclavicular fossa to pass behind the clavicular head of pectoralis major, it pierces the clavipectoral fascia, crosses the axillary artery and joins the axillary vein just below clavicular level. It may connect with the external jugular by a branch anterior to the clavicle. Sometimes the median cubital vein is large, transferring most blood from the cephalic to the basilic vein; the proximal cephalic vein is then absent or much diminished.

LYMPHATIC DRAINAGE

Lymphatics follow the usual pattern in that superficial lymphatics follow the veins; deep lymphatics follow the arteries.

For details of supratrochlear nodes see page 836.

For details of infraclavicular nodes see page 818.

INNERVATION

Median nerve

The median nerve (Fig. 45.7, Fig. 47.5, Fig. 47.8) enters the arm lateral to the brachial artery. Near the insertion of coracobrachialis it crosses in front of (rarely behind) the artery, descending medial to it to the cubital fossa where it is posterior to the bicipital aponeurosis and anterior to brachialis, separated by the latter from the elbow joint.

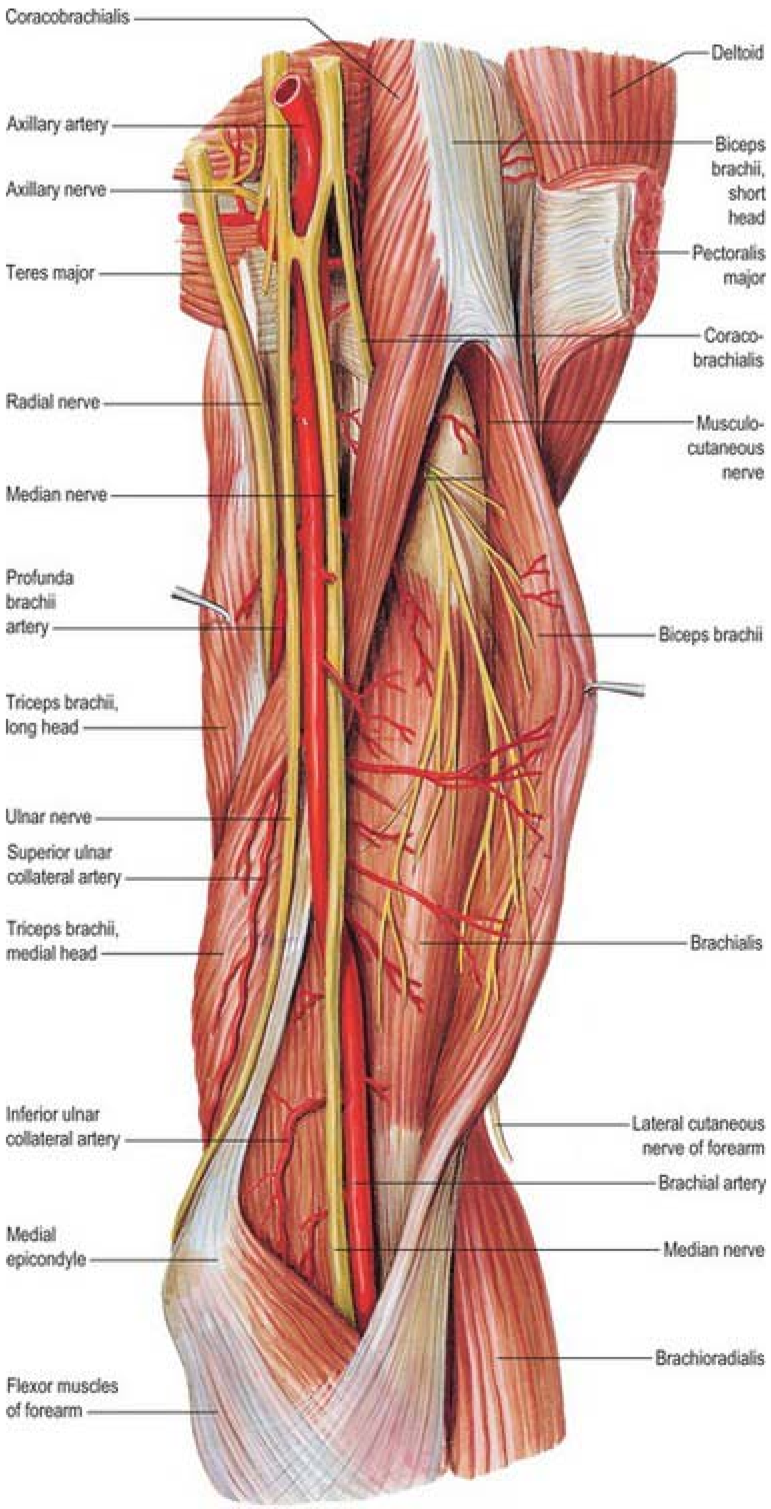
Coracobrachialis
Deltoid
Axillary artery
Biceps brachii, short head
Axillary nerve
Pectoralis major
Teres major
Coraco-brachialis
Radial nerve
Musculo-cutaneous nerve
Median nerve
Profunda brachii artery
Biceps brachii
Triceps brachii, long head
Ulnar nerve
Superior ulnar collateral artery
Triceps brachii, medial head
Brachialis
Inferior ulnar collateral artery
Lateral cutaneous nerve of forearm
Brachial artery
Medial epicondyle
Median nerve
Brachioradialis
Flexor muscles of forearm

Fig. 47.8 Anterior aspect of the left upper arm dissected to show the musculocutaneous nerve.

(From Sobotta 2006.)

It gives off vascular branches to the brachial artery and usually a branch to pronator teres, a variable distance proximal to the elbow joint.

Musculocutaneous nerve

The musculocutaneous nerve is the nerve of the anterior compartment of the arm (Fig. 47.5, Fig. 47.8). It gives a branch to the shoulder joint and then passes through coracobrachialis, which it supplies, emerging to pass between biceps and brachialis. It sends branches to both these muscles. In the cubital fossa it lies at the lateral margin of the biceps tendon where it continues as the lateral cutaneous nerve of the forearm.

The musculocutaneous nerve has frequent variations. It may run behind coracobrachialis or adhere for some distance to the median nerve and pass behind biceps. Some fibres of the median nerve may run in the musculocutaneous nerve, leaving it to join their proper trunk; less frequently the reverse occurs, and the median nerve sends a branch to the musculocutaneous. Occasionally it supplies pronator teres and may replace radial branches to the dorsal surface of the thumb.

Ulnar nerve

The ulnar nerve gives no branches in the arm (Fig. 47.5, Fig. 47.8). It runs distally through the axilla medial to the axillary artery and between it and the vein, continuing distally medial to the brachial artery as far as the midarm. Here it pierces the medial intermuscular septum, inclining medially as it descends anterior to the medial head of triceps to the interval between the medial epicondyle and the olecranon, with the superior ulnar collateral artery.

Radial nerve

The radial nerve descends behind the third part of the axillary artery and the upper part of the brachial artery, anterior to subscapularis and the tendons of latissimus dorsi and teres major (Figs 47.2-47.4, Fig. 47.8). With the profunda brachii artery it inclines dorsally, passing through the triangular space (see p. 814) below the lower border of teres major, between the long head of triceps and the humerus. Here it supplies the long head of triceps, and gives rise to the posterior cutaneous nerve of the arm which supplies the skin along the posterior surface of the upper arm. It then spirals obliquely across the back of the humerus, lying posterior to the uppermost fibres of the medial head of triceps which separate the nerve from the bone in the first part of the spiral groove. Here it gives off a muscular branch to the lateral head of triceps and a branch which passes through the medial head of triceps to anconeus. On reaching the lateral side of the humerus it pierces the lateral intermuscular septum to enter the anterior compartment; it then descends deep in a furrow between brachialis and proximally brachioradialis, then more distally extensor carpi radialis longus. Anterior to the lateral epicondyle it divides into superficial and deep terminal rami.

The branches of the radial nerve in the upper arm are: muscular, cutaneous, articular and superficial terminal and posterior interosseous.

Muscular branches

Muscular branches supply triceps, anconeus, brachioradialis, extensor carpi radialis longus and brachialis in medial, posterior and lateral groups. Medial muscular branches arise from the radial nerve on the medial side of the arm. They supply the medial and long heads of triceps; the branch to the medial head is a long, slender filament which, lying close to the ulnar nerve as far as the distal third of the arm, is often termed the ulnar collateral nerve. A large posterior muscular branch arises from the nerve as it lies in the humeral groove. It divides to supply the medial and lateral heads of triceps and anconeus, that for the latter being a long nerve which descends in the medial head of triceps and partially supplies it; it is accompanied by the middle collateral branch of the profunda brachii artery and passes behind the elbow joint to end in anconeus. Lateral muscular branches arise in front of the lateral intermuscular septum; they supply the lateral part of brachialis, brachioradialis and extensor carpi radialis longus.

Cutaneous branches

Cutaneous branches are the posterior and lower lateral cutaneous nerves of the arm and the posterior cutaneous nerve of the forearm.

Lower lateral cutaneous nerve of the arm

The lower lateral cutaneous nerve of the arm perforates the lateral head of triceps distal to the deltoid tuberosity, passes to the front of the elbow close to the cephalic vein and supplies the skin of the lateral part of the lower half of the arm.

Posterior cutaneous nerve of the arm

The small posterior cutaneous nerve of the arm arises in the axilla and passes medially to supply the skin on the dorsal surface of the arm nearly as far as the olecranon. It crosses posterior to and communicates with the intercostobrachial nerve.

Posterior cutaneous nerve of the forearm

The posterior cutaneous nerve of the forearm arises with the lower lateral cutaneous nerve of the arm. Perforating the lateral head of triceps, it descends first lateral in the arm, then along the dorsum of the forearm to the wrist, supplying the skin in its course and joining, near its end, with dorsal branches of the lateral cutaneous nerve of the forearm.

Articular branches to elbow joint

See page 836.

Lesions of the radial nerve in the upper arm

Lesions of the radial nerve at its origin from the posterior cord in the axilla may be caused by pressure from a long crutch (crutch palsy). Triceps is only involved when lesions occur at this level and is usually spared in the more common lesions of the radial nerve in the arm as it lies alongside the spiral groove, where the nerve is commonly affected by fractures of the humerus. Compression of the nerve against the humerus occurs if the arm is rested on a sharp edge such as the back of a chair (‘Saturday night palsy’). Both these injuries cause weakness of brachioradialis with wasting and loss of the reflex. There is both wrist and finger drop due to weakness of wrist and finger extensors, as well as weakness of extensor pollicis longus and abductor pollicis longus. There may be sensory impairment or paraesthesiae in the distribution of the superficial radial nerve. However, nerve overlap means that only a small area of anaesthesia usually occurs on the dorsum of the hand between the first and second metacarpal bones.

Medial cutaneous nerve of arm

The medial cutaneous nerve of arm supplies the skin of the medial aspect of the arm (Fig. 47.7). It is the smallest branch of the brachial plexus, and arises from the medial cord and contains fibres from the eighth cervical and first thoracic ventral rami. It traverses the axilla, crossing anterior or posterior to the axillary vein, to which it is then medial, and communicating with the intercostobrachial nerve; it descends medial to the brachial artery and basilic vein (Fig. 47.7) to a point midway in the upper arm, where it pierces the deep fascia to supply a medial area in the distal third of the arm, extending on to its anterior and posterior aspects. Rami reach the skin anterior to the medial epicondyle, and over the olecranon. It connects with the posterior branch of the medial cutaneous nerve of the forearm. Sometimes the medial cutaneous nerve of the arm and the intercostobrachial nerve are connected in a plexiform manner in the axilla. The intercostobrachial nerve may be large and reinforced by part of the lateral cutaneous branch of the third intercostal nerve. It then replaces the medial cutaneous nerve of the arm and receives a connection representing the latter from the brachial plexus (occasionally this connection is absent).

Medial cutaneous nerve of forearm

The medial cutaneous nerve of forearm comes from the medial cord (Fig. 47.7). It is derived from the eighth cervical and first thoracic ventral rami. At first it is between the axillary artery and vein and gives off a ramus which pierces the deep fascia to supply the skin over the biceps, almost to the elbow. The nerve descends medial to the brachial artery, pierces the deep fascia with the basilic vein midway in the arm and divides into anterior and posterior branches. The larger, anterior branch usually passes in front of, occasionally behind, the median cubital vein, descending anteromedial in the forearm to supply the skin as far as the wrist and connecting with the palmar cutaneous branch of the ulnar nerve. The posterior branch descends obliquely medial to the basilic vein, anterior to the medial epicondyle, and curves round to the back of the forearm, descending on its medial border to the wrist, supplying the skin. It connects with the medial cutaneous nerve of the arm, the posterior cutaneous nerve of the forearm, and the dorsal branch of the ulnar.

REFERENCES

ormack GC, Lamberty BGH. The Arterial Anatomy of Skin Flaps. Edinburgh: Churchill Livingstone, 1994.

lmon M. Anatomic studies. In: Taylor GI, Razaboni RM. *Book 1: Arteries of the Muscles of the Extremities and the Trunk. Book 2: Arterial Anastomotic Pathways of the Extremities*. New York: Quality Medical Publishing, 1994.

CHAPTER 48

Elbow

SKIN AND SOFT TISSUE

SKIN

Cutaneous vascular supply

The skin overlying the cubital fossa receives its blood supply on its anterolateral side by small perforating vessels from the radial collateral artery, together with some small musculocutaneous perforators from the radial recurrent artery which traverse brachioradialis (Fig. 45.4). On the anteromedial side, skin is supplied by small branches from the anastomosis between the inferior ulnar collateral artery and the anterior ulnar recurrent artery and by small branches from the brachial artery.

A plexus of anastomosing vessels covers the posterior aspect of the elbow region. On the medial side, the plexus is supplied by small branches from the superior and inferior ulnar collateral arteries and the posterior ulnar recurrent artery, and on the lateral side from the middle collateral artery and the posterior interosseous recurrent artery.

Cutaneous innervation

The skin of the cubital fossa and the epicondylar regions is innervated by the medial and lateral cutaneous nerves of the forearm (Fig. 45.15). A small proximal area on the lateral aspect is supplied by the distal part of the lower lateral cutaneous nerve of the arm. The skin over the olecranon region is innervated by the distal branches of the posterior cutaneous nerve of the arm, together with proximal branches of the posterior cutaneous nerve of the forearm.

SOFT TISSUE: CUBITAL FOSSA

The cubital fossa forms a triangular depression in the middle of the upper part of the anterior aspect of the forearm (Fig. 48.1). The superior border of the fossa is an imaginary line, which joins the two epicondyles of the humerus. The fleshy elevation which constitutes its medial border is formed by the lateral margin of pronator teres and the elevation which forms the lateral border is the medial edge of brachioradialis. The roof of the fossa is formed by the deep fascia of the forearm, reinforced by the bicipital aponeurosis on the medial aspect. The median cubital vein lies on this deep fascia crossed superficially (or sometimes deeply) by the medial cutaneous nerve of the forearm. Brachialis and supinator form the floor of the fossa.

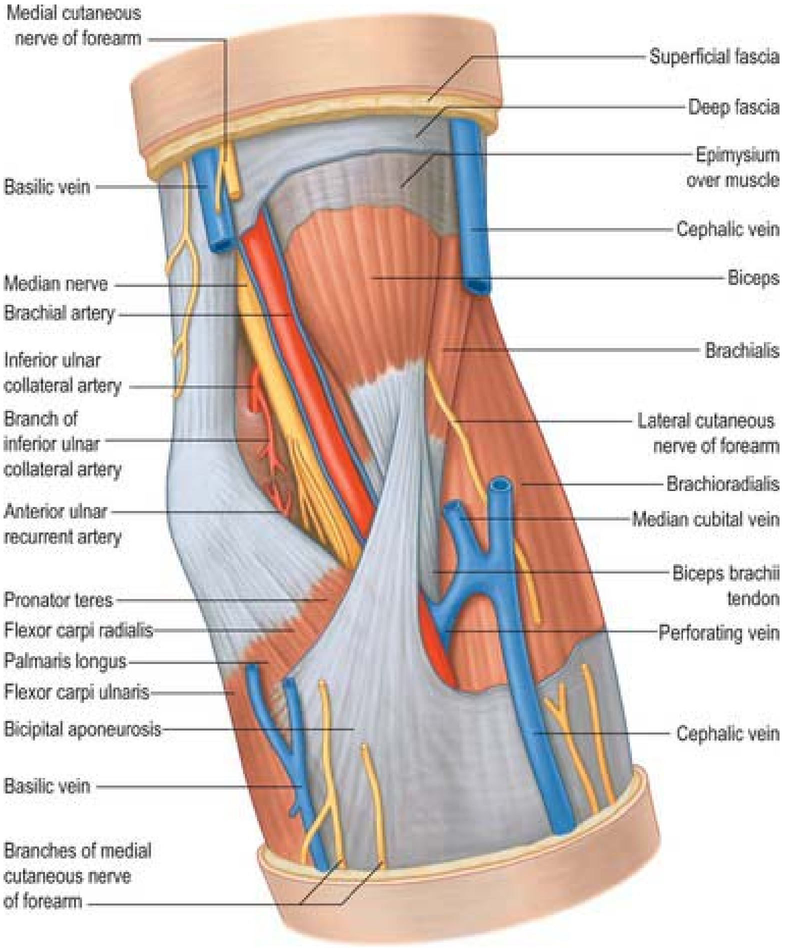
Medial cutaneous nerve of forearm
Basilic vein
Median nerve
Brachial artery
Inferior ulnar collateral artery
Branch of inferior ulnar collateral artery
Anterior ulnar recurrent artery
Pronator teres
Flexor carpi radialis
Palmaris longus
Flexor carpi ulnaris
Bicipital aponeurosis
Basilic vein
Branches of medial cutaneous nerve of forearm
Superficial fascia
Deep fascia
Epimysium over muscle
Cephalic vein
Biceps
Brachialis
Lateral cutaneous nerve of forearm
Brachioradialis
Median cubital vein
Biceps brachii tendon
Perforating vein
Cephalic vein

Fig. 48.1 Anterior aspect of the left elbow, superficial structures. The subcutaneous veins have been cut to reveal the subfascial structures. Compare with **Fig. 48.6**.

From medial to lateral, the fossa contains the median nerve, the terminal part of the brachial artery together with the start of the radial and ulnar arteries and accompanying veins, the tendon of biceps and the radial nerve just under cover of brachioradialis.

JOINTS

The humerus articulates with both the radius and the ulna at the elbow joint. The radius and ulna articulate by synovial superior (proximal) and inferior (distal) radio-ulnar joints and by an intermediate interosseous membrane and ligament, which constitute a fibrous middle radio-ulnar union.

ELBOW JOINT

The elbow joint is a synovial joint. Its complexity is increased by continuity with the superior radio-ulnar joint. It includes two articulations (Fig. 48.2). These are the humero-ulnar, between the trochlea of the humerus and the ulnar trochlear notch, and the humero-radial, between the capitulum of the humerus and the radial head.

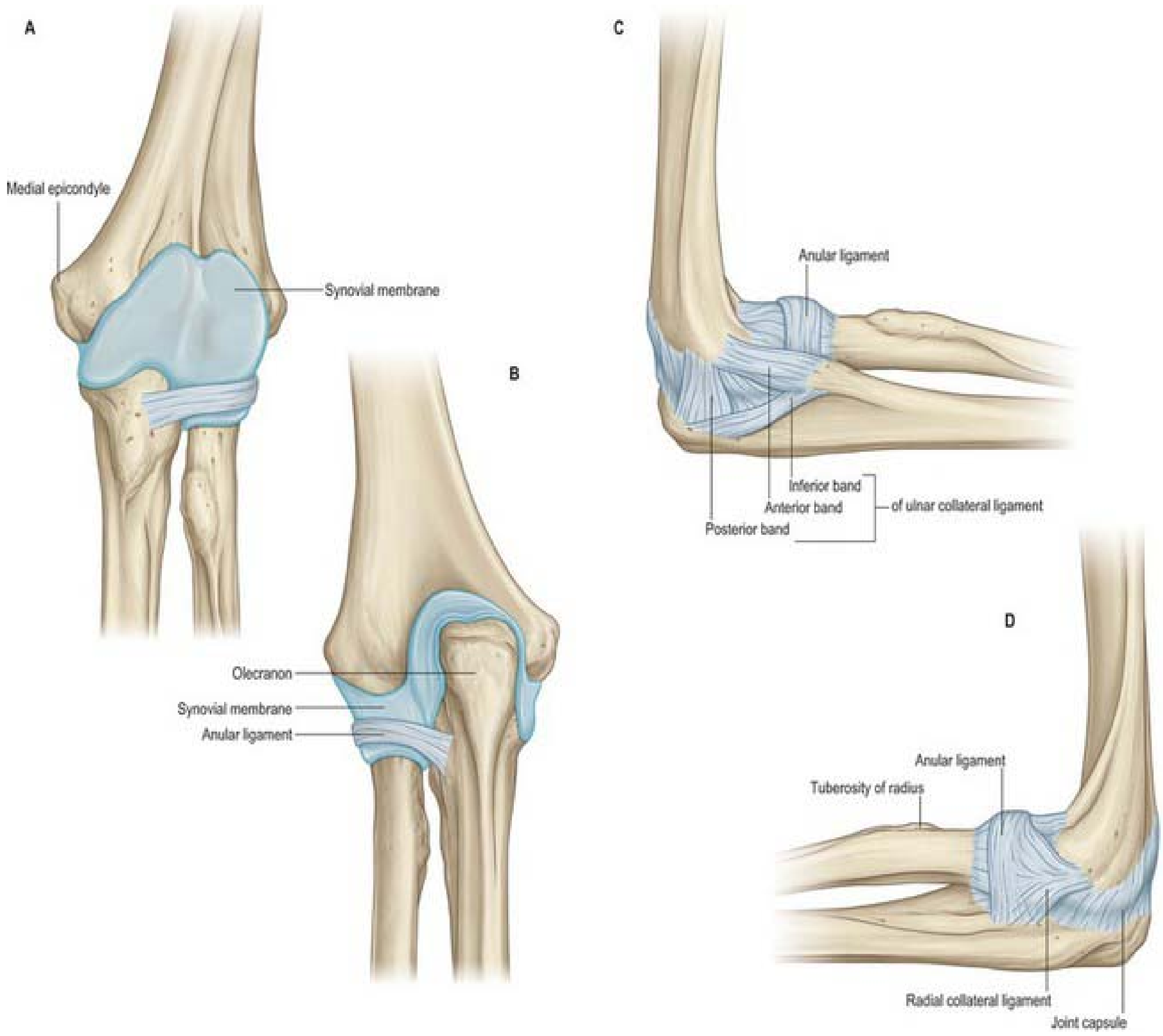
A
Medial epicondyle
Synovial membrane
C
Anular ligament
Inferior band
Anterior band
Posterior band
of ulnar collateral ligament
B
Olecranon
Synovial membrane
Anular ligament
D
Anular ligament
Tuberosity of radius
Radial collateral ligament
Joint capsule

Fig. 48.2 **A–D**, The left elbow joint. **A**, Synovial cavity partially distended: anterior aspect. The fibrous capsule of the elbow joint has been removed but the thick part of the anular ligament has been left *in situ*. Note that the synovial membrane (blue) descends below the lower border of the

anular ligament. **B**, Synovial cavity partially distended: posterior aspect of the specimen represented in A. In A and B a small part of the ulnar (medial) collateral ligament may be seen. **C**, Medial aspect. **D**, Lateral aspect.

Articulating surfaces

The articular surfaces are the humeral trochlea and capitulum, and the ulnar trochlear notch and radial head. The trochlea is not a simple pulley because its medial flange exceeds its lateral, thus projecting to a lower level. This means that the plane of the joint, approximately 2 cm distal to the inter-epicondylar line, is tilted inferomedially; the trochlea is also widest posteriorly where its lateral edge is sharp. The trochlear notch is not wholly congruent with it: in full extension the medial part of its upper half is not in contact with the trochlea and a corresponding lateral strip loses contact in flexion. The trochlea has an asymmetrical sellar surface, largely concave transversely, convex anteroposteriorly: sections show that these profiles are compounded spirals. Swing is therefore accompanied (as in all hinge joints) by screwing and conjunct rotation. The olecranon and coronoid parts of the trochlear notch are usually separated by a rough strip, devoid of articular cartilage and covered by fibroadipose tissue and synovial membrane. The capitulum and the radial head are reciprocally curved; closest contact occurs in midpronation with a semiflexed radius. The rim of the head, which is more prominent medially, fits the groove between humeral capitulum and trochlea.

The humero-ulnar and humero-radial articulations form a largely uniaxial joint which is one of the most congruent, and therefore most stable, joints in the body. The static soft tissue stability of the joint is derived from the anterior capsule and lunar and radial collateral ligaments.

Fibrous capsule

The fibrous capsule (Fig. 48.2, Fig. 48.3, 48.4) is broad and thin anteriorly. It is attached proximally to the front of the medial epicondyle and humerus above the coronoid and radial fossae, and distally to the edge of the ulnar coronoid process and anular ligament, and is continuous at its sides with the ulnar and radial collateral ligaments. Anteriorly it receives numerous fibres from brachialis. Posteriorly the capsule is thin and attached to the humerus behind its capitulum and near its lateral trochlear margin, to all but the lower part of the edge of the olecranon fossa, and to the back of the medial epicondyle. Inferomedially it reaches the superior and lateral margins of the olecranon and is laterally continuous with the superior radio-ulnar capsule deep to the anular ligament. It is related posteriorly to the tendon of triceps and to anconeus.

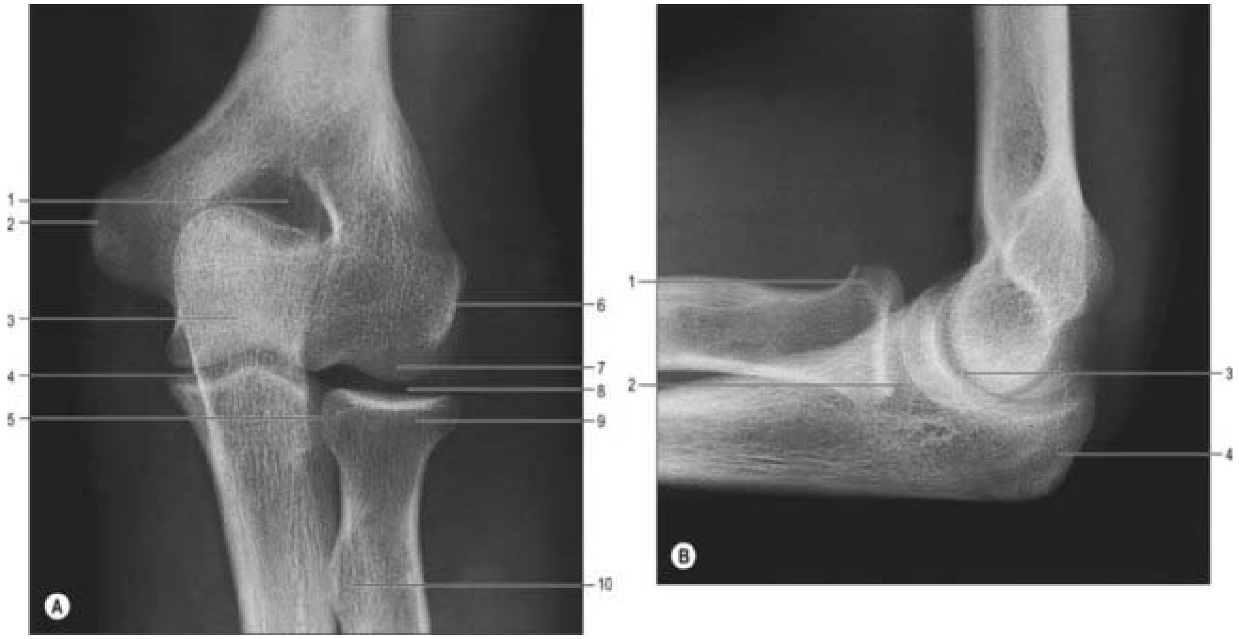

Fig. 48.3 Radiographs of the left elbow joint of an adult. **A**, Anteroposterior view: **1**. Olecranon fossa. **2**. Medial humeral epicondyle. **3**. Shadow of olecranon superimposed on trochlea. **4**. Humero-ulnar joint. **5**. Radial head articulating with radial notch of ulna. **6**. Lateral humeral epicondyle. **7**. Capitulum. **8**. Humero-radial joint. **9**. Head of radius. **10**. Radial tuberosity. **B**, Lateral view: **1**. Head of radius. **2**. Profile of capitulum. **3**. Profile of trochlea. **4**. Olecranon.

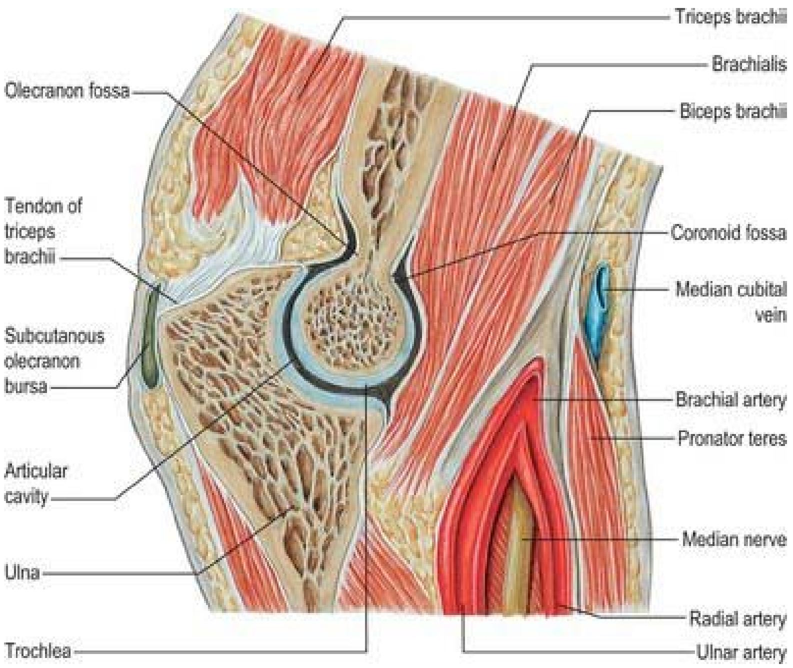
Triceps brachii
Brachialis
Biceps brachii
Olecranon fossa
Tendon of triceps brachii
Coronoid fossa
Median cubital vein
Subcutanous olecranon bursa
Brachial artery
Pronator teres
Articular cavity
Median nerve
Ulna
Radial artery
Trochlea
Ulnar artery

Fig. 48.4 Sagittal section through the left elbow joint: medial aspect. The synovial membrane is shown in blue.

(From Sobotta 2006.)

Ligaments

The humero-ulnar and humeroradial articulations have ulnar and radial collateral ligaments.

Ulnar collateral ligament

This is a triangular band, consisting of thick anterior, posterior and inferior parts united by a thin region (Fig. 48.2C). The strongest and stiffest anterior part is attached by its apex to the front of the medial epicondyle and by its broad distal base to a proximal tubercle on the medial coronoid margin. The posterior part, also triangular, is attached low on the back of the medial epicondyle and to the medial margin of the olecranon. Between these two bands intermediate fibres descend from the medial epicondyle to an inferior, oblique band, often weak, between the olecranon and coronoid processes. This converts a depression on the medial margin of the trochlear notch into a foramen, through which the intracapsular fat pad is continuous with extracapsular fat medial to the joint. The anterior band is taut throughout most of the range of flexion, while the posterior band becomes taut between half and full flexion.

The ulnar collateral ligament is related to triceps, flexor carpi ulnaris and the ulnar nerve. Along it, anteriorly, the attachment of flexor digitorum superficialis extends from the medial epicondyle to the medial coronoid border.

Radial collateral ligament

This is attached low on the lateral epicondyle and to the anular ligament (Fig. 48.2D). Some of its posterior fibres cross the ligament to the proximal end of the supinator crest of the ulna. It intimately blends with attachments of supinator and extensor carpi radialis brevis. It is taut throughout most of the range of flexion.

Synovial membrane

The synovial membrane (Figs 48.2-48.4) extends from the humeral articular margins, lines the coronoid, radial and olecranon fossae, the flat medial trochlear surface, the deep surface of the capsule and the lower part of the anular ligament. Projecting between the radius and ulna from behind is a crescentic synovial fold, which partly divides the joint into humero-radial and humero-ulnar parts. Irregularly triangular, it contains extrasynovial fat (Fig. 48.5). Between the capsule and synovial membrane are three other pads of fat: the largest, at the olecranon fossa, is pressed into the fossa by triceps during flexion; the other two, at the coronoid and radial fossae, are pressed in by brachialis during extension. They are all slightly displaced in contrary movements. Smaller synovial-covered tags of fat project into the joint near constrictions flanking the trochlear notch, and cover small non-articular areas of bone.

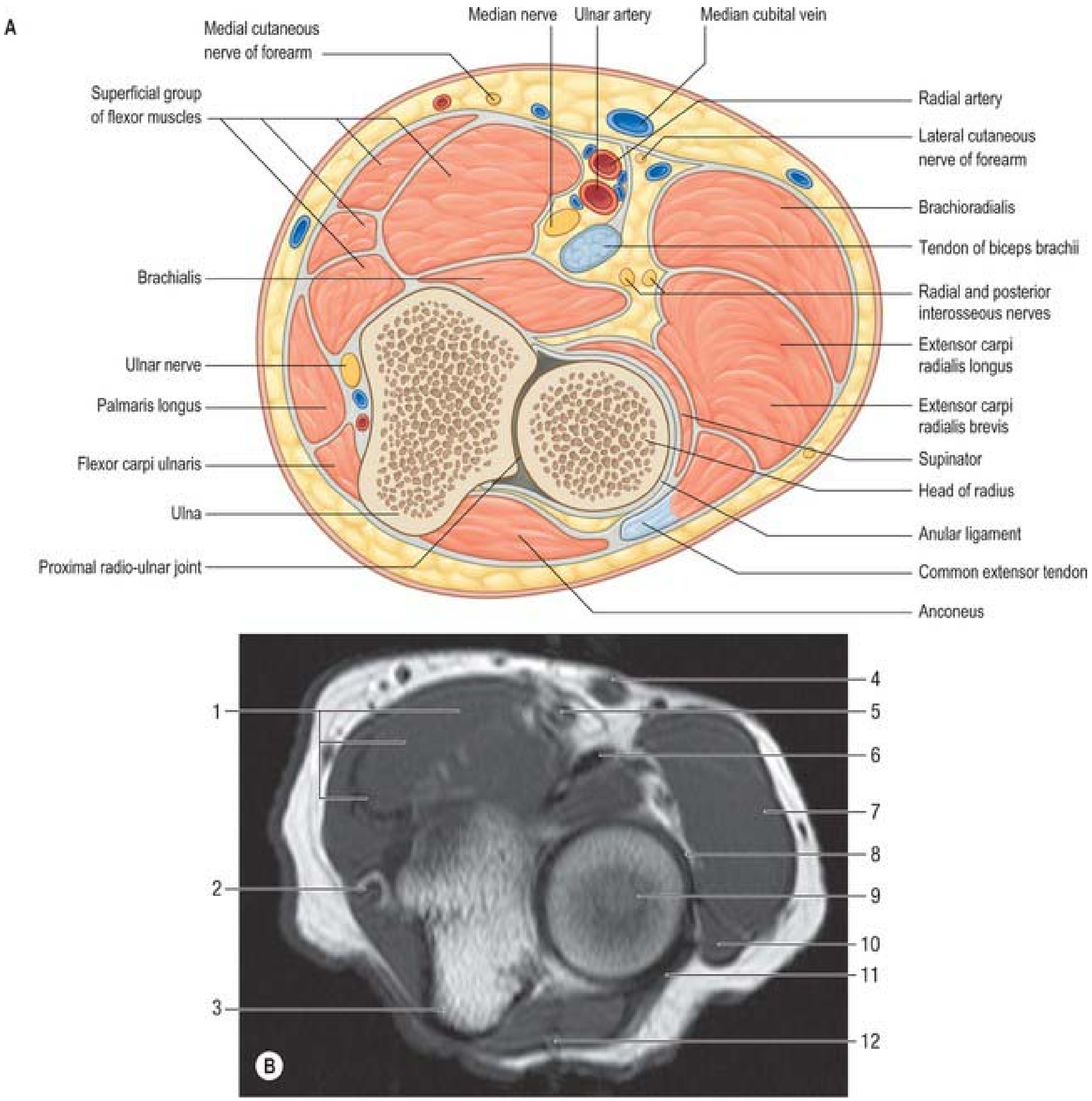
A
Median nerve
Ulnar artery
Median cubital vein
Medial cutaneous nerve of forearm
Superficial group of flexor muscles
Radial artery
Lateral cutaneous nerve of forearm
Brachioradialis
Tendon of biceps brachii
Brachialis
Radial and posterior interosseous nerves
Extensor carpi radialis longus
Ulnar nerve
Palmaris longus
Extensor carpi radialis brevis
Supinator
Flexor carpi ulnaris
Head of radius
Ulna
Anular ligament
Proximal radio-ulnar joint
Common extensor tendon
Anconeus
B
1
2
3
4
5
6
7
8
9
10
11
12

Fig. 48.5 The proximal left radio-ulnar joint. **A**, Transverse section. **B**, Axial MRI scan: **1**. Superficial group of flexor muscles. **2**. Ulnar nerve. **3**. Ulna. **4**. Median cubital vein. **5**. Brachial artery and median nerve. **6**. Biceps tendon. **7**. Brachioradialis. **8**. Anular ligament. **9**. Head of radius. **10**. Extensor carpi radialis brevis. **11**. Common extensor tendon. **12**. Anconeus.

A small bursa, the olecranon bursa, lies between the elbow joint capsule and the insertion of triceps tendon. Pressure and friction can lead to inflammation and enlargement of this bursa.

Vascular supply and lymphatic drainage

Articular arteries are derived from the numerous periarticular anastomoses (Fig. 47.6).

Innervation

Articular nerves are mainly from branches of the musculocutaneous and radial nerves, but the ulnar, median, and sometimes anterior interosseous nerves also contribute. The musculocutaneous branch is from the nerve to brachialis and innervates an anterior part of the capsule; branches of the radial supply posterior and anterolateral regions and come from the nerve to anconeus and the ulnar collateral branch to the medial head of triceps. The ulnar nerve supplies the ulnar collateral ligament behind the medial epicondyle. These articular nerves accompany blood vessels supplying the synovial membrane, fat pads and epiphyses; they presumably contain vasomotor fibres as well as afferent fibres serving pain and proprioception.

Movements

Being a uniaxial joint, the elbow allows flexion and extension, the ulna moving on the trochlea, and the radial head on the capitulum. However, ulnar flexion–extension is not a pure swing but is accompanied by slight conjunct rotation, the ulna being slightly pronated in extension, supinated in flexion. Since the capitulum is smaller than the radial facet, the head of the radius can be felt at the back of the joint in full extension, which is limited by tension in the capsule and muscles anterior to the joint (extension being the close-packed position) and the entry of the tip of the olecranon into the olecranon fossa. Flexion is limited chiefly by apposition of soft parts: in full flexion the rim of the radial head and the tip of the ulnar coronoid process enter the radial and coronoid fossae of the humerus respectively.

When the forearm is fully extended and supinated, it diverges laterally forming with the upper arm a ‘carrying angle’ of approximately 163°; its ulnar border cannot contact the lateral surface of the thigh. The ‘carrying angle’ is caused partly by projection of the medial trochlear edge about 6 mm beyond its lateral edge and partly by the obliquity of the superior articular surface of the coronoid, which is not orthogonal to the shaft of the ulna. Tilt of the humeral and ulnar articular surfaces is approximately equal, hence the carrying angle disappears in full flexion, the two bones reaching the same plane. When the adducted arm is flexed the little finger meets the clavicle, because of the position of the resting humerus; when the humerus is rotated laterally, the hand reaches the front of the shoulder. The carrying angle is also masked by pronation of the extended forearm, which brings the upper arm, semipronated forearm and hand into line, increasing manual precision in full extension of the elbow or during extension.

Accessory movements

These are limited to slight ulnar screwing, abduction and adduction, and anteroposterior translation of the radial head on the capitulum. In translation the radial head moves on the ulnar radial notch and the anular ligaments are slewed backwards and forwards, more so when the elbow is semiflexed.

Muscles producing movement

Flexion: brachialis, biceps brachii and brachioradialis. In slow flexion or its maintenance against gravity, brachialis and biceps are principally involved, even for light loads. With increasing speed, activity in brachioradialis is increasingly prominent; its attachments determine that it acts most effectively in midpronation. Against resistance, pronator teres and flexor carpi radialis may also act.

Extension: triceps, anconeus and gravity. In rapid extension, brachioradialis may be active.

Relations

Muscles related to the joint are: brachialis (anteriorly), triceps and anconeus (posteriorly), supinator and the common extensor tendon (laterally), and the common flexor tendon and flexor carpi ulnaris (medially).

PROXIMAL (SUPERIOR) RADIO-ULNAR JOINT

The proximal radio-ulnar joint is a uniaxial pivot joint.

Articulating surfaces

The articulating surfaces are between the circumference of the radial head and the fibro-osseous ring made by the ulnar radial notch and anular ligament.

Fibrous capsule

The capsule is continuous with that of the elbow joint and is attached to the anular ligament.

Ligaments

The proximal radio-ulnar joint has anular and quadrate ligaments.

Anular ligament

This is a strong band, which encircles the radial head, holding it against the radial notch of the ulna. Forming about four-fifths of the ring, it is attached to the anterior margin of the notch, broadens posteriorly and may divide into several bands. It is attached to a rough ridge at or behind the posterior margin of the notch; diverging bands may also reach the lateral margin of the trochlear notch above and proximal end of the supinator crest below. The proximal anular border blends with the elbow joint capsule, except posteriorly where the capsule passes deep to the ligament to reach the posterior and inferior margins of the radial notch. From the distal anular border a few fibres pass over reflected synovial membrane to attach loosely on the radial neck. The external surface of the anular ligament blends with the radial collateral ligament and provides an attachment for part of supinator. Posterior to it are anconeus and the interosseous recurrent artery. Internally the ligament is thinly covered by cartilage where it is in contact with the radial head; distally it is covered by synovial membrane, reflected up onto the radial neck.

Quadrate ligament

This thin, fibrous ligament stretches between the neck of the radius and the upper part of the supinator fossa of the ulna and covers the synovial membrane on the distal surface of the joint. It maintains constant tension throughout pronation and supination.

Synovial membrane

The synovial membrane is continuous with that of the elbow joint so that the proximal radio-ulnar joint and elbow joint form one continuous synovial cavity. It is attached to the articular margins and lines the capsule and anular ligament. It is prevented from herniation between the anterior and posterior free edges of the anular ligament by the quadrate ligament.

Vascular supply

Articular arteries are derived from the numerous periarticular anastomoses (Fig. 47.6).

Innervation

Innervation is by small branches from the musculocutaneous, median, radial and ulnar nerves.

Factors maintaining stability

The prime stabilizing factor (Fig. 48.2, Fig. 48.3) is the anular ligament which encircles the radial head and holds it against the radial notch of the ulna.

Movements and muscles producing movement

See the description of the distal radio-ulnar joint (p. 468).

Injuries around the elbow

Posterior dislocation of the elbow joint with ulnar abduction can be complicated by fracture of the coronoid process as it impinges against the trochlea of the humerus. The normal triangular relationship between the olecranon and the two humeral epicondyles is disrupted. The brachial artery and/or median and ulnar nerves can occasionally be damaged in these injuries. The strength of the collateral ligaments is such that the medial epicondyle is frequently torn off in lateral dislocations.

Subluxation of the radial head through the anular ligament arising from a sudden jerk on the arm is a relatively common injury in young children (known as ‘pulled elbow’). This is because the anular ligament has vertical sides in children compared with more funnel-shaped sides in adults. Reduction involves forcefully supinating and flexing the elbow which snaps the ligament back into place.

Supracondylar distal humeral fractures are usually seen in children following a fall on the outstretched hand. The distal fragment in usually displaced posteriorly. The jagged end of the proximal fragment can sometimes injure the brachial artery or the median nerve.

DISTAL (INFERIOR) RADIO-ULNAR JOINT

Movements at the radio-ulnar joint complex pronate and supinate the hand. The distal radio-ulnar joint and the movements which occur during supination and pronation are described on page 468.

VASCULAR SUPPLY AND LYMPHATIC DRAINAGE

ARTERIES

Brachial artery

The brachial artery is central and divides near the neck of the radius into its terminal branches, namely the radial and ulnar arteries (Fig. 48.1, Fig. 48.6). The skin, superficial fascia and median cubital vein are anterior, separated by the bicipital aponeurosis. Posteriorly, brachialis separates it from the elbow joint. The median nerve is medial proximally but is separated from the ulnar artery by the ulnar head of pronator teres. Lateral are the tendon of biceps and the radial nerve, the latter concealed between supinator and brachioradialis.

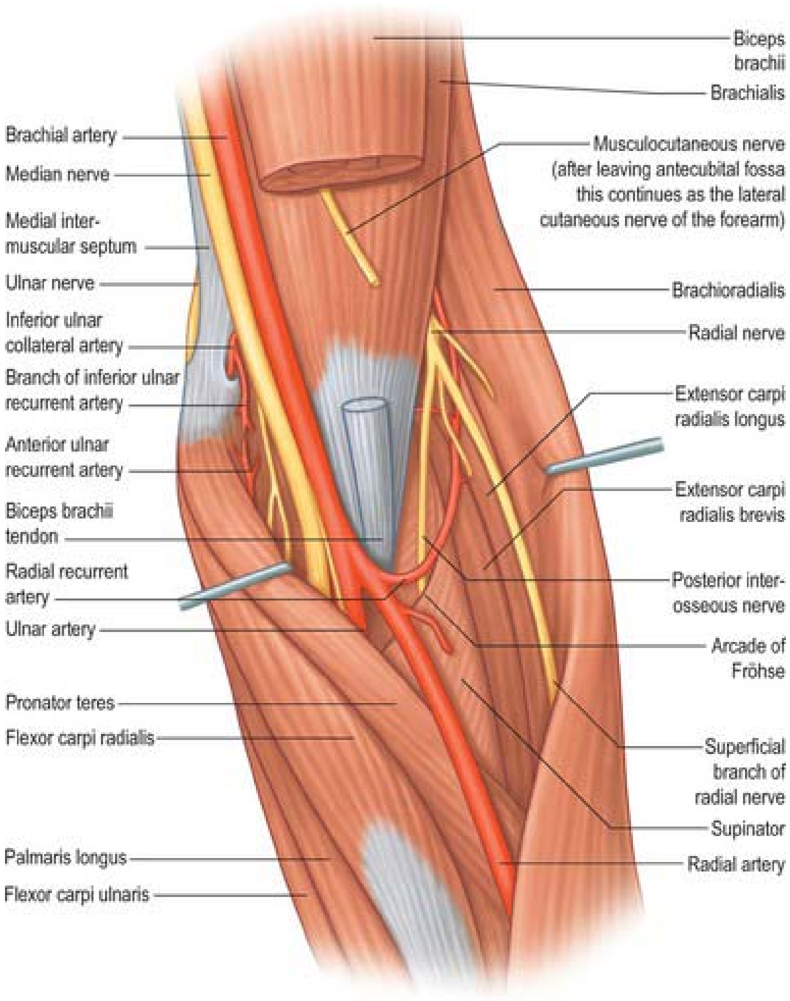
Brachial artery
Median nerve
Medial inter-muscular septum
Ulnar nerve
Inferior ulnar collateral artery
Branch of inferior ulnar recurrent artery
Anterior ulnar recurrent artery
Biceps brachii tendon
Radial recurrent artery
Ulnar artery
Pronator teres
Flexor carpi radialis
Palmaris longus
Flexor carpi ulnaris
Biceps brachii
Brachialis
Musculocutaneous nerve (after leaving antecubital fossa this continues as the lateral cutaneous nerve of the forearm)
Brachioradialis
Radial nerve
Extensor carpi radialis longus
Extensor carpi radialis brevis
Posterior inter-osseous nerve
Arcade of Fröhse
Superficial branch of radial nerve
Supinator
Radial artery

Fig. 48.6 Anterior aspect of the left elbow, deep structures. Compare with **Fig. 48.1**.

Radial artery

The radial artery passes deep to brachioradialis and gives off the radial recurrent artery before continuing into the forearm (Fig. 48.1, Fig. 48.6).

Radial recurrent artery

The radial recurrent artery (Fig. 47.6, Fig. 48.6) arises just distal to the elbow, passing between superficial and deep branches of the radial nerve to ascend behind brachioradialis, anterior to supinator and brachialis. It supplies these muscles and the elbow joint, anastomosing with the radial collateral branch of the profunda brachii.

Ulnar artery

The ulnar artery gives off the anterior and then the posterior ulnar recurrent arteries before passing deep to pronator teres to continue its course in the forearm (Fig. 48.1, Fig. 48.6). In the forearm, the posterior interosseous artery (a branch of the ulnar artery via the common interosseous artery), gives rise to the posterior interosseous recurrent artery which passes proximally to supply the elbow region.

The common interosseous, anterior interosseous and posterior interosseous arteries, and muscular branches of the ulnar artery, are described on p. 852.

Anterior ulnar recurrent artery

The anterior ulnar recurrent artery (Fig. 47.6) arises just distal to the elbow, ascends between brachialis and pronator teres, supplies them and anastomoses with the inferior ulnar collateral artery anterior to the medial epicondyle.

Posterior ulnar recurrent artery

The posterior ulnar recurrent artery (Fig. 47.6) arises distal to the anterior ulnar recurrent, and passes dorsomedially between flexors digitorum profundus and superficialis, ascending behind the medial epicondyle; between this and the olecranon, it is deep to flexor carpi ulnaris, ascending between its heads with the ulnar nerve. It supplies adjacent muscles, nerve, bone and elbow joint, and anastomoses with the ulnar collateral and interosseous recurrent arteries (Fig. 47.6).

Posterior interosseous recurrent artery

The posterior interosseous recurrent artery is a branch of the posterior interosseous artery. It passes proximally through supinator to lie deep to anconeous posterior to the lateral epicondyle. It gives off branches which take part in the anastomotic cutaneous plexus around the olecranon.

VEINS

The deep and superficial veins supplying the elbow and related structures are described on page 853. Fig. 48.7 shows the common variants of the superficial veins of the cubital fossa: their easy access means that the cubital veins are common sites for venous blood puncture and intravenous fluid and drug administration.

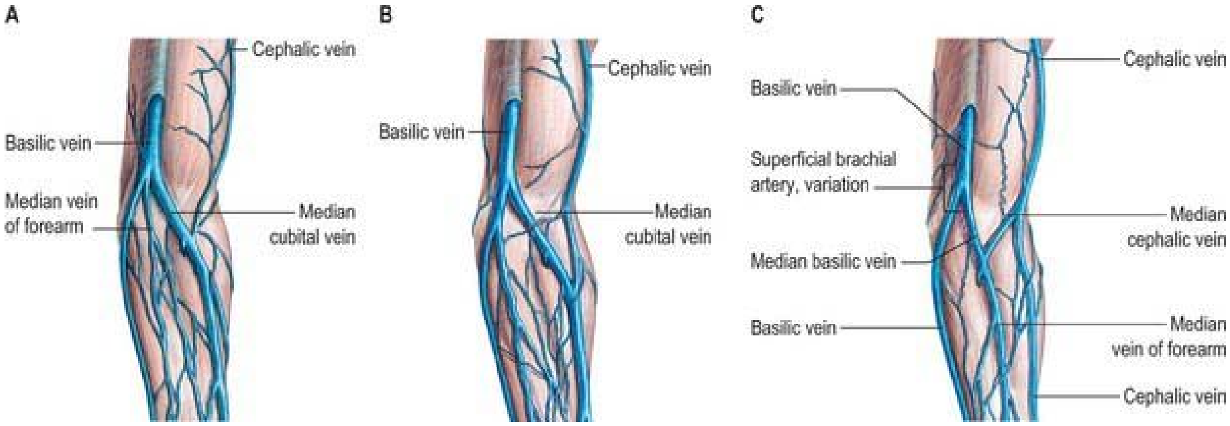
A
Cephalic vein
Basilic vein
Median vein of forearm
Median cubital vein
B
Cephalic vein
Basilic vein
Median cubital vein
C
Basilic vein
Cephalic vein
Superficial brachial artery, variation
Median cephalic vein
Median basilic vein
Basilic vein
Median vein of forearm
Cephalic vein

Fig. 48.7 **A–C**, Variations of superficial veins of the left cubital fossa.

(From Sobotta 2006.)

LYMPHATIC DRAINAGE: SUPRATROCHLEAR NODES

One or two supratrochlear nodes (Fig. 45.6) are superficial to the deep fascia proximal to the medial epicondyle and medial to the basilic vein; their efferents accompany the vein to join the deep lymph vessels.

Small isolated nodes sometimes occur along the radial, ulnar and interosseous vessels, in the cubital fossa near the bifurcation of the brachial artery, or in the arm medial to the brachial vessels.

INNERVATION

Median nerve

In the cubital fossa the median nerve lies medial to the brachial artery, deep to the bicipital aponeurosis and anterior to brachialis (Fig. 48.1, Fig. 48.6).

Pronator syndrome

This is an uncommon entrapment neuropathy of the median nerve occurring in the elbow region. Entrapment can occur typically at four sites. The first occurs at the site of the ligament of Struthers. This ligament represents an anatomical variant and when present connects a small supracondylar spur of bone to an accessory origin of pronator teres. The median nerve can be compressed as it passes under this ligament. The nerve may also be trapped as it passes deep to the bicipital aponeurosis; the aponeurotic edge of the deep head of pronator teres muscle; or the tendinous aponeurotic arch forming the proximal free edge of the radial attachment of flexor digitorum superficialis.

The syndrome presents with pain on the volar aspect of the distal arm and proximal forearm. The symptoms may be aggravated by flexing the elbow against resistance, pronating the forearm against resistance, or flexion of superficialis to the middle finger against resistance, depending on the precise cause of the entrapment. If the anterior interosseous nerve is also compressed there is weakness of all the muscles innervated by the median nerve, including abductor pollicis brevis and the long finger flexors, and sensory impairment on the palm of the hand. Treatment involves exploration of the nerve and surgical decompression.

Musculocutaneous nerve

In the cubital fossa the musculocutaneous nerve lies at the lateral margin of the biceps tendon where it continues on as the lateral cutaneous nerve of the forearm.

Ulnar nerve

At the elbow the ulnar nerve is in a groove on the dorsum of the medial epicondyle. It enters the forearm between the two heads of flexor carpi ulnaris superficial to the posterior and oblique parts of the ulnar collateral ligament (Fig. 48.6, Fig. 48.8, Fig. 48.9).

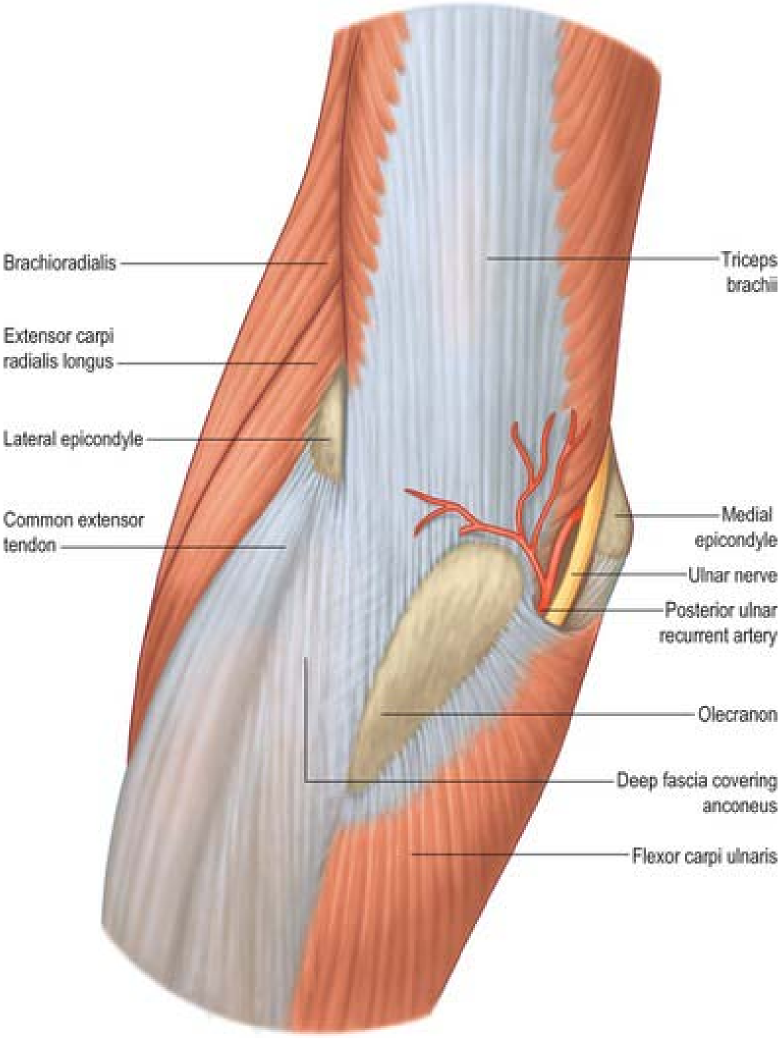
Brachioradialis
Extensor carpi radialis longus
Lateral epicondyle
Common extensor tendon
Triceps brachii
Medial epicondyle
Ulnar nerve
Posterior ulnar recurrent artery
Olecranon
Deep fascia covering anconeus
Flexor carpi ulnaris

Fig. 48.8 Posterior aspect of the left elbow, superficial structures.

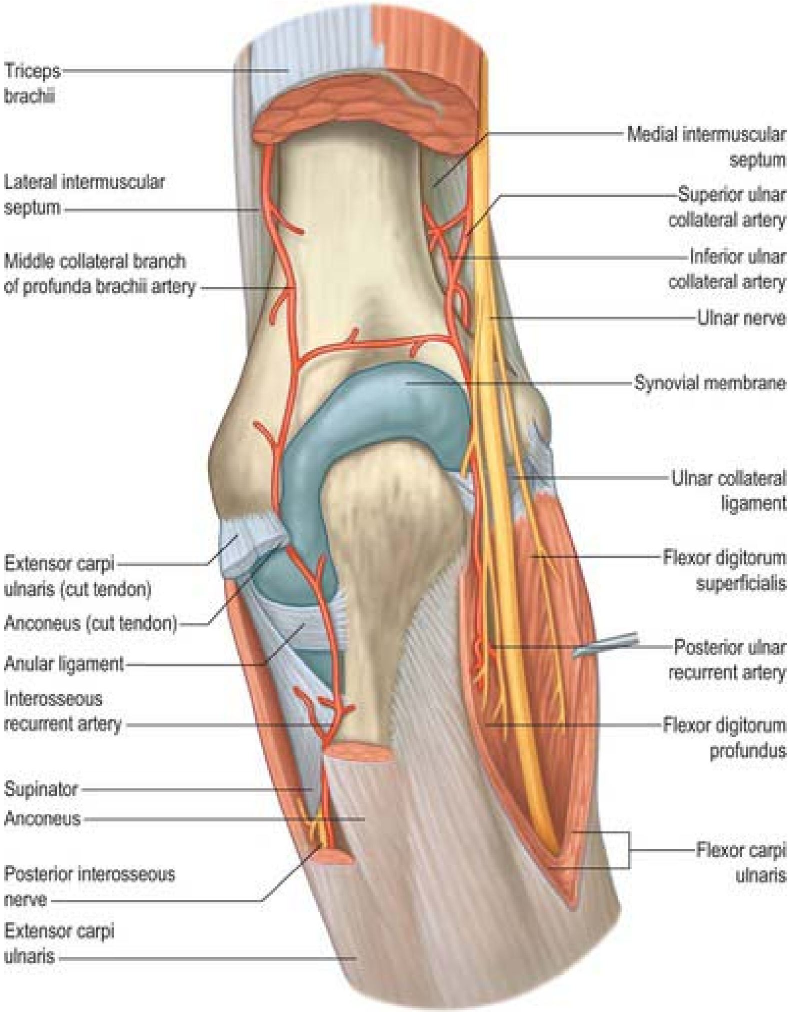
Triceps brachii
Lateral intermuscular septum
Middle collateral branch of profunda brachii artery
Extensor carpi ulnaris (cut tendon)
Anconeus (cut tendon)
Anular ligament
Interosseous recurrent artery
Supinator
Anconeus
Posterior interosseous nerve
Extensor carpi ulnaris
Medial intermuscular septum
Superior ulnar collateral artery
Inferior ulnar collateral artery
Ulnar nerve
Synovial membrane
Ulnar collateral ligament
Flexor digitorum superficialis
Posterior ulnar recurrent artery
Flexor digitorum profundus
Flexor carpi ulnaris

Fig. 48.9 Posterior aspect of the left elbow region, deep structures.

Articular branches

Articular branches to the elbow joint arise from the ulnar nerve between the medial epicondyle and olecranon.

Cubital tunnel syndrome

Typically the ulnar nerve can be compressed in the tunnel formed by the tendinous arch connecting the two heads of flexor carpi ulnaris at their humeral and ulnar attachments. Other local causes of compression and neuritis at this site include trauma, inflammatory arthritis, compression by the medial head of the triceps, osteophytes, recurrent subluxation of the nerve across the medial epicondyle of the humerus and abnormal muscular variants such as the anconeus epitrochlearis.

The symptoms are pain at the medial aspect of the proximal forearm together with paraesthesia and numbness of the little finger and ulnar half of the ring finger and the ulnar side of the dorsum of the hand. These symptoms are typically worse on forced elbow flexion. There may also be associated weakness of the muscles of the forearm and the intrinsic muscles of the hand innervated by the ulnar nerve. Interestingly, flexor carpi ulnaris and profundus to the ring and little fingers are frequently spared, presumably because the fascicles supplying these muscles are located on the deep aspect of the nerve. Clawing of the hand is therefore unusual in this syndrome.

Surgical treatment involves decompression of the tunnel by division of the aponeurosis of flexor carpi ulnaris with or without subsequent anterior transposition of the ulnar nerve.

Ulnar nerve division at the elbow

– The ulnar nerve is in a vulnerable position as it lies between the medial epicondyle and the olecranon: it lies on bone covered only by a thin layer of skin. It is easily damaged if the ulnar groove is shallow and the nerve may become more prominent than the medial epicondyle or the olecranon when the elbow is fully flexed.

Division of the nerve at the elbow paralyses flexor carpi ulnaris, flexor digitorum profundus to the ring and little fingers and all the intrinsic muscles of the hand (apart from the radial two lumbricals). The clawing of the hand is less intense than occurs after division of the ulnar nerve at the wrist, reflecting the imbalance in action between the long flexors and extensors to the ring and little fingers when finger flexion is produced only by superficialis. In addition there is sensory loss over the little finger and the ulnar half of the ring finger.

Radial nerve

The radial nerve at the elbow lies deep in a groove between brachialis and brachioradialis proximally and extensor carpi radialis distally. It divides into the superficial terminal branch and the posterior interosseous nerve just anterior to the lateral epicondyle (Fig. 48.6).

Articular branches are distributed to the elbow joint.

Medial and posterior cutaneous nerves of the forearm

The medial cutaneous nerve is described on pages 830 and 856, and the posterior cutaneous nerve is described on pages 829 and 856.

REFERENCES

reen DP, editor. Operative Hand Surgery. New York/London: Churchill Livingstone, 1982.

CHAPTER 49

Forearm

SKIN AND SOFT TISSUE

SKIN

Cutaneous vascular supply

Fasciocutaneous perforators from the radial artery supply the lateral two-thirds of the anterior surface of the forearm, the lateral (radial) border and the posterior one-quarter of the forearm (except in the distal third) (see Fig. 45.4). These perforators pass in the intermuscular fascia between brachioradialis and flexor carpi radialis and between flexor carpi radialis and flexor digitorum superficialis (see Fig. 49.17). Within the territory of the radial artery is the area of the largest fasciocutaneous perforator, which has recently been named the inferior cubital artery. It extends from the distal apex of the antecubital fossa to midway down the forearm. Fasciocutaneous perforators from the ulnar artery supply an anatomical area which extends from the cubital fossa to the wrist, and from the medial (ulnar) third of the anterior aspect of the forearm around the medial border to the medial one-quarter of the posterior surface of the forearm (see Fig. 49.17, Fig. 45.4).

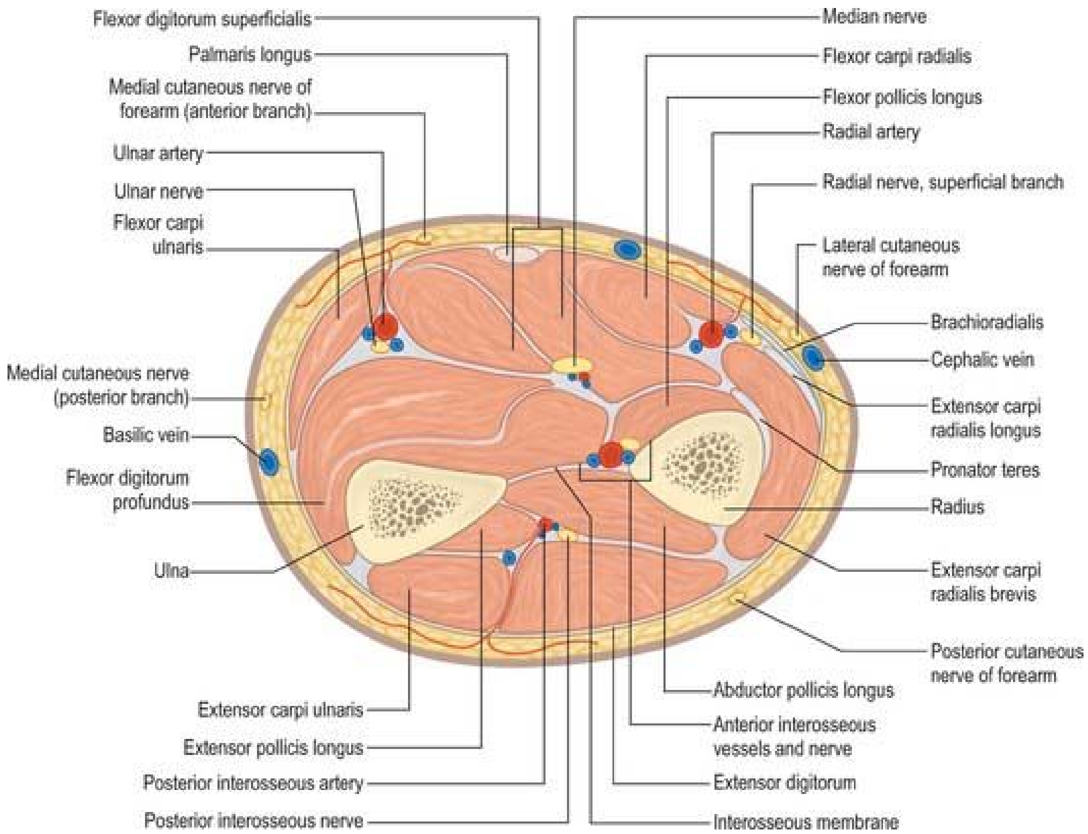
Flexor digitorum superficialis
Palmaris longus
Medial cutaneous nerve of forearm (anterior branch)
Ulnar artery
Ulnar nerve
Flexor carpi ulnaris
Medial cutaneous nerve (posterior branch)
Basilic vein
Flexor digitorum profundus
Ulna
Extensor carpi ulnaris
Extensor pollicis longus
Posterior interosseous artery
Posterior interosseous nerve
Median nerve
Flexor carpi radialis
Flexor pollicis longus
Radial artery
Radial nerve, superficial branch
Lateral cutaneous nerve of forearm
Brachioradialis
Cephalic vein
Extensor carpi radialis longus
Pronator teres
Radius
Extensor carpi radialis brevis
Posterior cutaneous nerve of forearm
Abductor pollicis longus
Anterior interosseous vessels and nerve
Extensor digitorum
Interosseous membrane

Fig. 49.17 Transverse section through the middle of the left forearm showing the fasciocutaneous perforating vessels.

Very small musculocutaneous perforators pass through brachioradialis and flexor carpi ulnaris. The contribution from these is far less than that of the fasciocutaneous perforators.

The distal third of the lateral (radial) aspect of the forearm is supplied by the terminal perforating branches of the anterior interosseous artery (see Fig. 45.4).

The central half of the posterior surface of the forearm, from the lateral edge of extensor digitorum, just below the lateral epicondyle of the humerus, to the wrist, is supplied by fasciocutaneous perforators which arise from the posterior interosseous artery. They reach the skin by passing along the intermuscular fascia between extensor carpi ulnaris and extensor digit minimi (see Fig. 49.17, Fig. 45.4).

For a detailed account of the cutaneous blood supply to the forearm, see Cormack & Lamberty (1994) and the translated works of Salmon (1994).

Cutaneous innervation

The anterior aspect of the forearm is supplied by the anterior branches of the medial and lateral cutaneous nerves of the forearm (see Fig. 45.15). The medial and lateral regions of the posterior aspect of the forearm are supplied by the posterior branches of the medial and lateral cutaneous nerves of the forearm respectively. The central part of the posterior aspect of the forearm is supplied by the posterior cutaneous nerve of the forearm.

SOFT TISSUE

Interosseous membrane

The radial and ulnar shafts are connected by syndesmoses – an oblique cord and an interosseous membrane.

Oblique cord

The oblique cord is a small inconstant flat fascial band on the deep head of supinator (Fig. 49.1). It extends from the lateral side of the ulnar tuberosity to the radius a little distal to its tuberosity. Its fibres are at right angles to those in the interosseous membrane. Its functional significance is dubious.

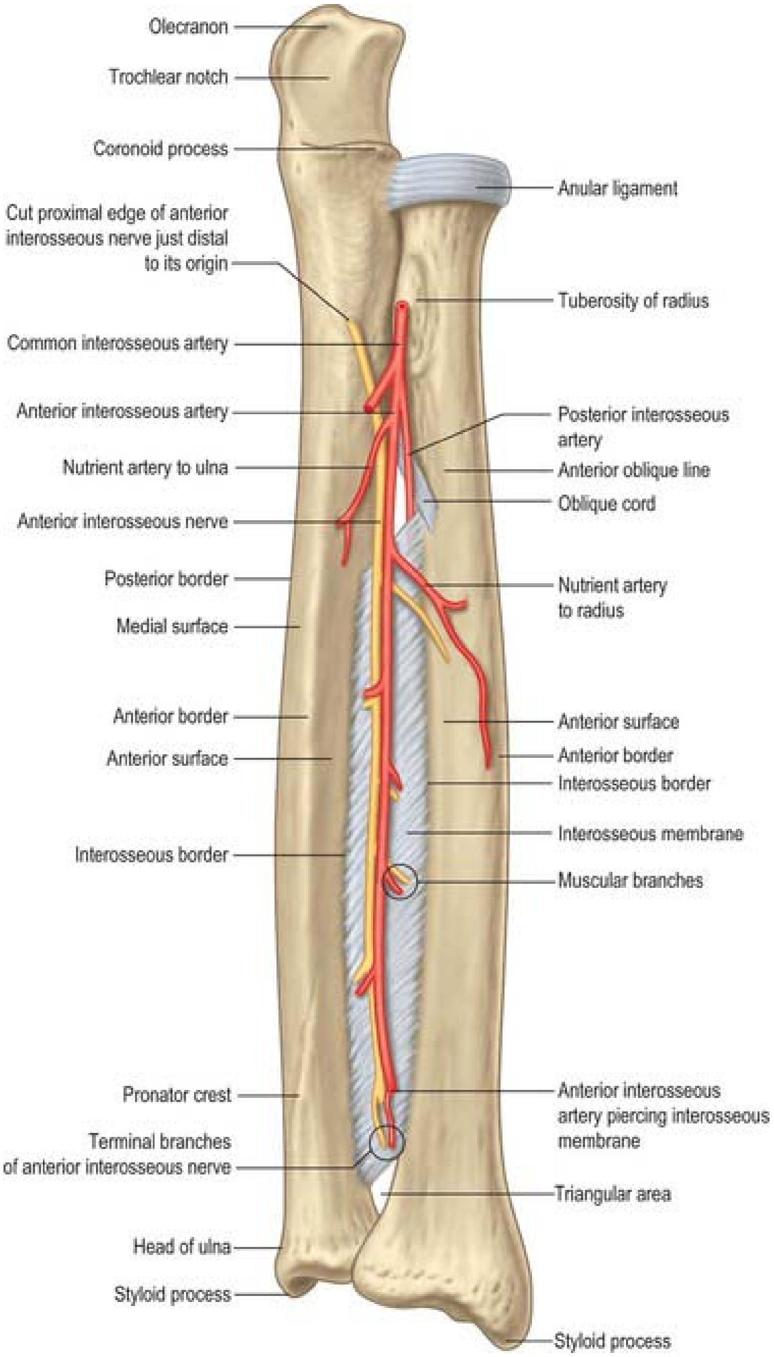
Olecranon
Trochlear notch
Coronoid process
Cut proximal edge of anterior interosseous nerve just distal to its origin
Common interosseous artery
Anterior interosseous artery
Nutrient artery to ulna
Anterior interosseous nerve
Posterior border
Medial surface
Anterior border
Anterior surface
Interosseous border
Pronator crest
Terminal branches of anterior interosseous nerve
Head of ulna
Styloid process
Anular ligament
Tuberosity of radius
Posterior interosseous artery
Anterior oblique line
Oblique cord
Nutrient artery to radius
Anterior surface
Anterior border
Interosseous border
Interosseous membrane
Muscular branches
Anterior interosseous artery piercing interosseous membrane
Triangular area
Styloid process

Fig. 49.1 Interosseous membrane and oblique cord of the forearm: anterior aspect. Membrane and cord are syndesmoses.

Interosseous membrane

The interosseous membrane is a broad, thin, collagenous sheet (Fig. 49.1). Its fibres slant distomedially between the radial and ulnar interosseous borders, and its distal part is attached to the posterior division of the radial border. Two or three posterior bands occasionally descend distolaterally across the other fibres. The membrane is deficient proximally, starting 2 or 3 cm distal to the radial tuberosity, and broader at midlevel. An oval aperture near its distal margin conducts the anterior interosseous vessels to the back of the forearm, and the posterior interosseous vessels pass through a gap between its proximal border and the oblique cord.

The membrane provides attachments for the deep forearm muscles and connects the radius and ulna. Its fibres appear to transmit forces which act proximally from the hand to the radius, thence to the ulna and humerus. However the hand is usually pronated when subject to these forces, and the membrane is relaxed in complete pronation and supination: the interosseous membrane is only tense when the hand is midway between prone and supine positions. Moreover, the radius can transmit substantial forces directly to the humerus. Anteriorly, in its proximal three-quarters, the membrane is related laterally to flexor pollicis longus and medially to flexor digitorum profundus, and between them to the anterior interosseous vessels and nerve. In its distal quarter it is related to pronator quadratus. Its posterior relations are supinator, abductor pollicis longus, extensors pollicis brevis, longus and indicis and, near the carpus, the anterior interosseous artery and posterior interosseous nerve.

Compartments of the forearm

The antebrachial fascia (deep fascia of the forearm), which is continuous above with the brachial fascia, is a dense general sheath for muscles, collectively and individually, in this region. It is attached to the olecranon and posterior border of the ulna. From its deep surface septa pass between muscles, providing partial attachment for them, and some of these septa reach bone. Muscles also arise from its internal aspect, especially in the upper forearm. This deep fascia, together with the interosseous membrane and fibrous intermuscular septa, divide the forearm into a number of compartments. These are the superficial and deep flexor (anterior) compartments, the extensor (posterior compartment) and a proximolateral compartment known as the mobile wad (encompassing brachioradialis and extensors carpi radialis longus and brevis) (Fig. 49.2). The fascia is much thicker posteriorly and in the lower forearm. It is strengthened above by tendinous fibres from biceps and triceps. Near the wrist, two localized thickenings, the flexor and extensor retinacula, retain the digital tendons in position (p. 879). Vessels and nerves pass through apertures in the fascia. One large aperture anterior to the elbow transmits a venous communication between superficial and deep veins.

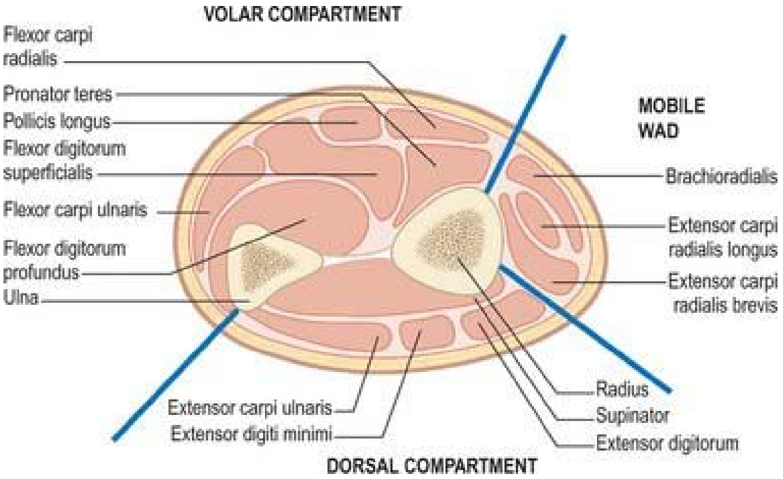
VOLAR COMPARTMENT
Flexor carpi radialis
Pronator teres
Pollicis longus
Flexor digitorum superficialis
Flexor carpi ulnaris
Flexor digitorum profundus
Ulna
MOBILE WAD
Brachioradialis
Extensor carpi radialis longus
Extensor carpi radialis brevis
Radius
Supinator
Extensor digitorum
Extensor carpi ulnaris
Extensor digiti minimi
DORSAL COMPARTMENT

Fig. 49.2 Compartments of the forearm. Cross-section through the upper third of the left forearm.

Compartment syndrome

The deep fascia in the forearm has limited elasticity and consequently any accumulation of fluid within this space (e.g. from haemorrhage, swelling from trauma, burns) can lead to increased tension in the compartment. If this pressure is high enough (35 mmHg), tissue perfusion pressure will be compromised and this will lead to a compartment syndrome where ischaemia and necrosis of the tissues ensues. Once muscle becomes infarcted the damage is irreversible: muscle fibres become contracted and replaced by inelastic fibrous tissue (termed Volkmann’s ischaemic contracture). The symptoms and signs associated with compartment syndrome are pain (particularly on passive stretching of the compartmental muscles), weakness of the compartment muscles, tenseness of the compartment, paraesthesia and hyperaesthesia. The pulse can still be normal in compartment syndrome, because systolic blood pressure is well above the critical closing pressure of vessels which supply the tissues within the compartment.

Compartment syndromes can occur at various sites in the body, but more commonly affect the anterior compartment of the forearm, the intrinsic muscles of the hand, and the lower leg. The identification of a compartment syndrome requires urgent surgical decompression. Here, both the skin and deep fascia are incised throughout the whole length of the compartment to relieve the pressure.

BONE

RADIUS

The radius is the lateral bone of the forearm (Fig. 49.3, Fig. 49.4, Fig. 49.5). It has expanded proximal and distal ends; the distal is much the broader. The shaft widens rapidly towards its distal end, is convex laterally and concave anteriorly in its distal part.

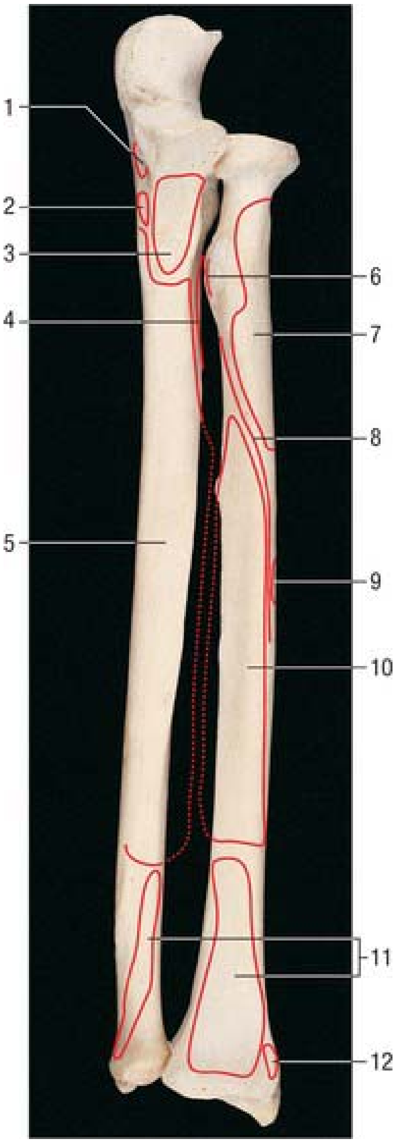

Fig. 49.3 Articulated radius and ulna: anterior view showing muscle attachments. Note that the hatched lines denote extension of muscular attachments onto the interosseous membrane. **1**. Flexor digitorum superficialis. **2**. Pronator teres (ulnar head). **3**. Brachialis. **4**. Supinator. **5**.

Flexor digitorum profundus. **6**. Biceps. **7**. Supinator. **8**. Flexor digitorum superficialis (oblique line). **9**. Pronator teres. **10**. Flexor pollicis longus. **11**. Pronator quadratus. **12**. Brachioradialis.

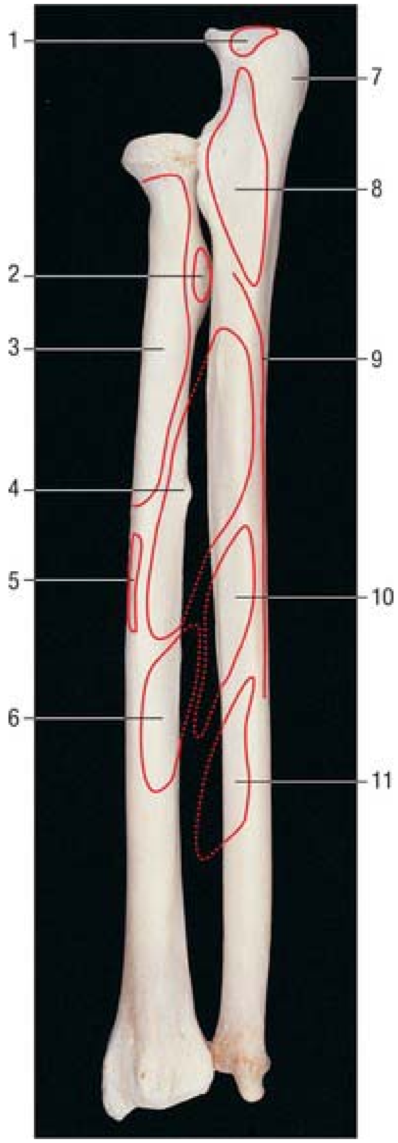

Fig. 49.4 Articulated radius and ulna: posterior view showing muscle attachments. **1**. Triceps. **2**. Biceps. **3**. Supinator. **4**. Abductor pollicis longus. **5**. Pronator teres. **6**. Extensor pollicis brevis. **7**. Subcutaneous area. **8**. Anconeus. **9**. Posterior border: attachment for common aponeurosis of extensor carpi ulnaris, flexor carpi ulnaris, flexor digitorum profundus. **10**. Extensor pollicis longus. **11**. Extensor indicis.

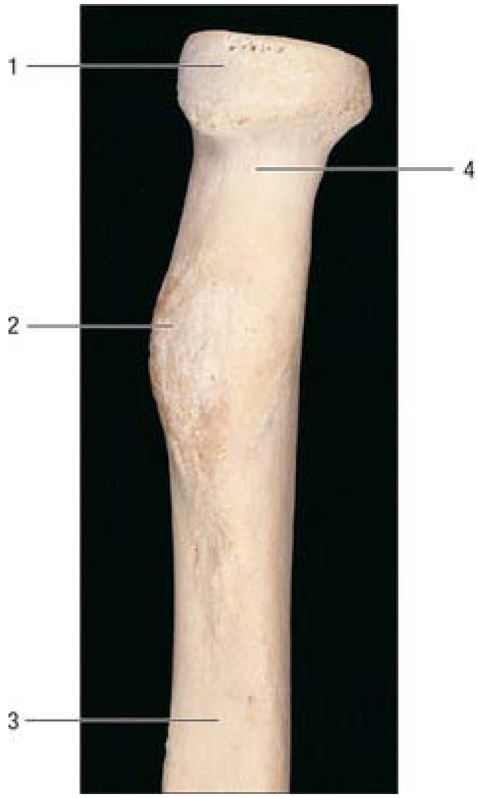

Fig. 49.5 Proximal end of left radius: anterior view. **1**. Head. **2**. Radial tuberosity. **3**. Shaft. **4**. Neck.

Proximal end

The proximal end includes a head, neck and tuberosity. The head is discoid, its proximal surface a shallow cup for the humeral capitulum. Its smooth articular periphery is vertically deepest medially, where it contacts the ulnar radial notch. Its posterior surface is palpable in a small depression on the lateral side of the back of the extended elbow. The neck is the constriction distal to the head, which overhangs it, especially on the lateral side. The tuberosity is distal to the medial part of the neck; posteriorly it is rough, but anteriorly it is usually smooth.

Shaft

The shaft has a lateral convexity, and is triangular in section (Fig. 49.1). The interosseous border is sharp, except for two areas: proximally, near the tuberosity; and distally, where the interosseous border is the posterior margin of a small, elongated, triangular area, proximal to the ulnar notch. These two areas form the so-called medial surface. The interosseous membrane is attached to its distal three-fourths, and connects the radius to the ulna. The anterior border is obvious at both ends, but rounded and indefinite between them. It descends laterally from the anterolateral part of the tuberosity as the anterior oblique line, which distally becomes a sharp, palpable crest along the lateral margin of the anterior surface. The posterior border is well defined only in its middle third: proximally it ascends medially towards the posteroinferior part of the tuberosity, and distally it is merely a rounded ridge. The anterior surface, between anterior and interosseous borders, is concave transversely and shows a distal forward curvature. Near its midpoint there is a proximally directed nutrient foramen and canal. The posterior surface, between interosseous and posterior borders, is largely flat but may be slightly hollow in the proximal area. The lateral surface is gently convex. Proximally, due to the obliquity of the anterior and posterior borders, it encroaches on the anterior and posterior aspects and is here slightly rough. A finely irregular oval area occurs near the midshaft, and beyond it the surface is smooth.

Distal end

The distal end of the radius (Fig. 49.6) is the widest part. It is four-sided in section. The lateral surface is slightly rough, projecting distally as a styloid process which is palpable when tendons around it are slack. The smooth carpal articular surface is divided by a ridge into medial and lateral areas. The medial is quadrangular, whereas the lateral is triangular and curves on to the styloid process. The anterior surface is a thick, prominent ridge, palpable even through overlying tendons, 2 cm proximal to the thenar eminence. The medial surface is the ulnar notch, which is smooth and anteroposteriorly concave for articulation with the head of the ulna. The posterior surface displays a palpable dorsal tubercle (Lister’s tubercle), which is limited medially by an oblique groove and is in line with the cleft between the index and middle fingers. Lateral to the tubercle there is a wide, shallow groove, divided by a faint vertical ridge.

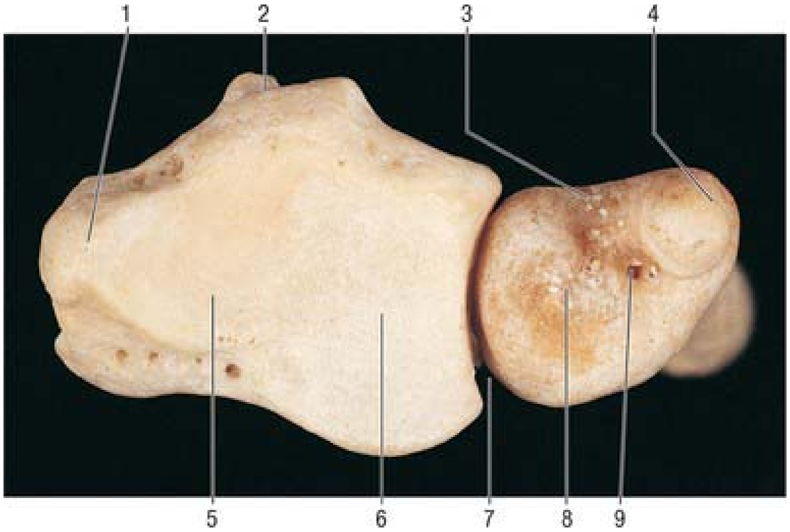

Fig. 49.6 Distal end of left radius and ulna. **1**. Styloid process of radius. **2**. Dorsal tubercle. **3**. Groove for tendon of extensor carpi ulnaris. **4**. Styloid process of ulna. **5**. Facet for scaphoid. **6**. Facet for lunate. **7**. Inferior radio-ulnar articulation. **8**. Area of contact with articular disc. **9**. Area for attachment of articular disc.

Muscle, ligament and articular attachments

The proximal articular surface of the radial head and its circumference are covered by hyaline cartilage. The upper rim (margin) fits the groove between the capitulum and trochlea and enters the radial fossa in flexion. The articular circumference articulates with the ulnar radial notch and annular ligament, within which it rotates in pronation and supination. The radial neck is enclosed by the narrower distal part of the ligament, from which it is separated by a synovial protrusion from the superior radio-ulnar joint. The posterior area of the tuberosity is marked by the biceps tendon, which is separated from a smooth anterior area by a bursa. The oblique cord is attached just distal to the bursa.

The thin, wide radial head of flexor digitorum superficialis is attached proximally on the anterior border. The lateral edge of the extensor retinaculum is attached to its conspicuous distal part. A small, triangular area proximal to the ulnar notch gives attachment to the deepest part of pronator quadratus.

The proximal two-thirds of the anterior surface provides an extensive area for attachment of flexor pollicis longus, which conceals the nutrient foramen. Pronator quadratus is attached to the distal quarter, and pronator teres is attached to a rough area near the midpoint of its lateral surface, at its maximal curvature. Proximally, the lateral surface widens into a long V-shaped area for supinator (Fig. 49.3, Fig. 49.4). Distal to pronator teres, the lateral surface is covered by tendons of the radial extensors. On the posterior surface, abductor pollicis longus is attached proximally and, more distally, extensor pollicis brevis. The remaining surface is devoid of attachments and covered by the long and short extensors of the thumb.

The radial styloid process projects beyond that of the ulna, its apex concealed by the tendons of abductor pollicis longus and extensor pollicis brevis. The lateral radiocarpal ligament is attached to its tip. The lateral surface, near the styloid process, receives the attachment of brachioradialis and is crossed obliquely, downwards and forwards, by the tendons of abductor pollicis longus and extensor pollicis brevis. The terminal ridge on the anterior surface of the lower end is an attachment for the palmar radiocarpal ligament. The base of the triangular articular disc of the inferior radio-ulnar joint is attached to a smooth ridge distal to the ulnar notch. From the latter, a narrow protrusion of synovial membrane extends proximally anterior to the lower end of the interosseous membrane (p. 839). The lateral part of the carpal articular surface articulates with the scaphoid, and the medial part with the lateral part of the lunate. In full adduction, the proximal surface of the lunate is wholly in contact with the radius.

The radial dorsal tubercle receives a slip from the extensor retinaculum and is grooved medially by the tendon of extensor pollicis longus. The wide groove lateral to the tubercle contains the tendons of extensor carpi radialis longus laterally, and extensor carpi radialis brevis medially, together with their synovial sheaths. Medially the dorsal surface is grooved by the tendons of extensor digitorum, which are separated from the bone by the tendons of extensor indicis and the posterior interosseous nerve. The dorsal radiocarpal ligament is attached to the distal margin of this surface.

Vascular supply

There are multiple metaphysial nutrient foramina that transmit branches of the radial, ulnar, anterior and posterior interosseous arteries. Typically, there is one nutrient diaphysial foramina located on the anterior surface of the bone and directed proximally toward the elbow. There is also a network of small fascioperiosteal and musculoperiosteal vessels which arise from the compartmental vessels and reach the bone via septal and muscular attachments.

The dorsal metaphysial supply of the distal radius is of particular importance to reconstructive hand surgeons because of its potential use in raising vascularized pedicled bone grafts (Fig. 49.7). Consistent branches connecting the anterior interosseous artery proximally to the dorsal carpal arch distally pass through the fourth and fifth extensor compartments of the wrist and provide metaphysial nutrient arteries. Intercompartmental vessels send nutrient arteries to the radius through the retinaculum between the first and second dorsal compartments, and the second and third dorsal compartments. These vessels originate from the radial artery and anterior interosseous arteries respectively, and anastomose with the dorsal carpal arch. For an anatomical description detailing the practical application of such pedicled bone grafts see Sheetz et al (1995).

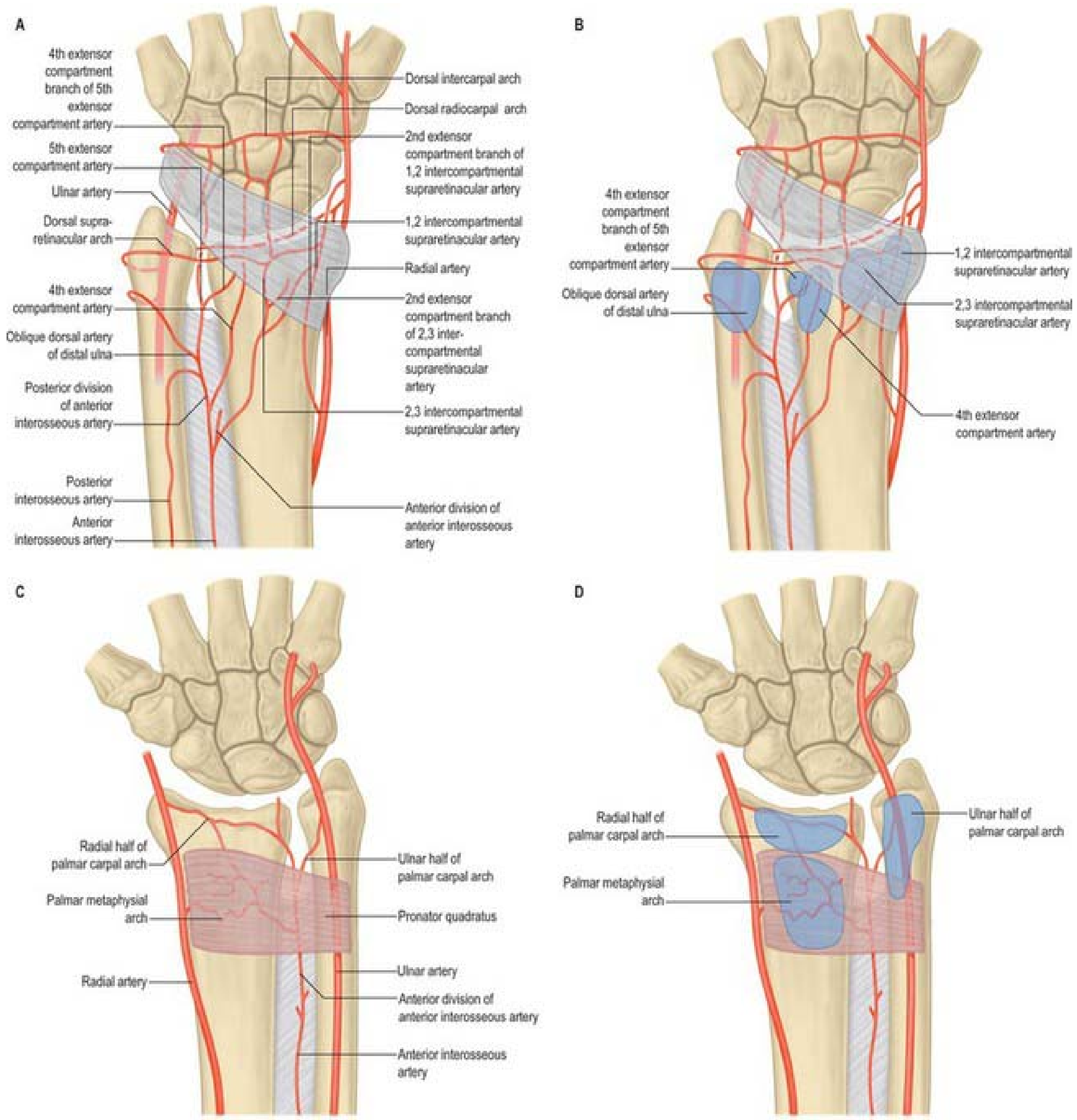
A
4th extensor compartment branch of 5th extensor compartment artery
5th extensor compartment artery
Ulnar artery
Dorsal supra-retinacular arch
4th extensor compartment artery
Oblique dorsal artery of distal ulna
Posterior division of anterior interosseous artery
Posterior interosseous artery
Anterior interosseous artery
Dorsal intercarpal arch
Dorsal radiocarpal arch
2nd extensor compartment branch of 1,2 intercompartmental supraretinacular artery
1,2 intercompartmental supraretinacular artery
Radial artery
2nd extensor compartment branch of 2,3 inter-compartmental supraretinacular artery
2,3 intercompartmental supraretinacular artery
Anterior division of anterior interosseous artery
B
4th extensor compartment branch of 5th extensor compartment artery
Oblique dorsal artery of distal ulna
1,2 intercompartmental supraretinacular artery
2,3 intercompartmental supraretinacular artery
4th extensor compartment artery
C
Radial half of palmar carpal arch
Palmar metaphysial arch
Radial artery
Ulnar half of palmar carpal arch
Pronator quadratus
Ulnar artery
Anterior division of anterior interosseous artery
Anterior interosseous artery
D
Radial half of palmar carpal arch
Palmar metaphysial arch
Ulnar half of palmar carpal arch

Fig. 49.7 **A**, **B**, Extraosseous arterial supply to the dorsal distal radius and ulna. **C**, **D**, Extraosseous arterial supply to the palmar distal radius and ulna. The shaded regions demonstrate where the nutrient vessels from the labelled arteries penetrate bone.

Ossification

The radius ossifies from three centres. One appears centrally in the shaft in the eighth week of fetal life, and the others appear in each end (Fig. 49.8, Fig. 49.9). Ossification begins in the distal epiphysis towards the end of the first postnatal year, and in the proximal epiphysis during the fourth year in females, and fifth in males. The proximal epiphysis fuses in the 14th year in females, 17th in males, and the distal in the 17th and 19th years respectively. A fourth centre sometimes appears in the tuberosity at about the 14th or 15th year.

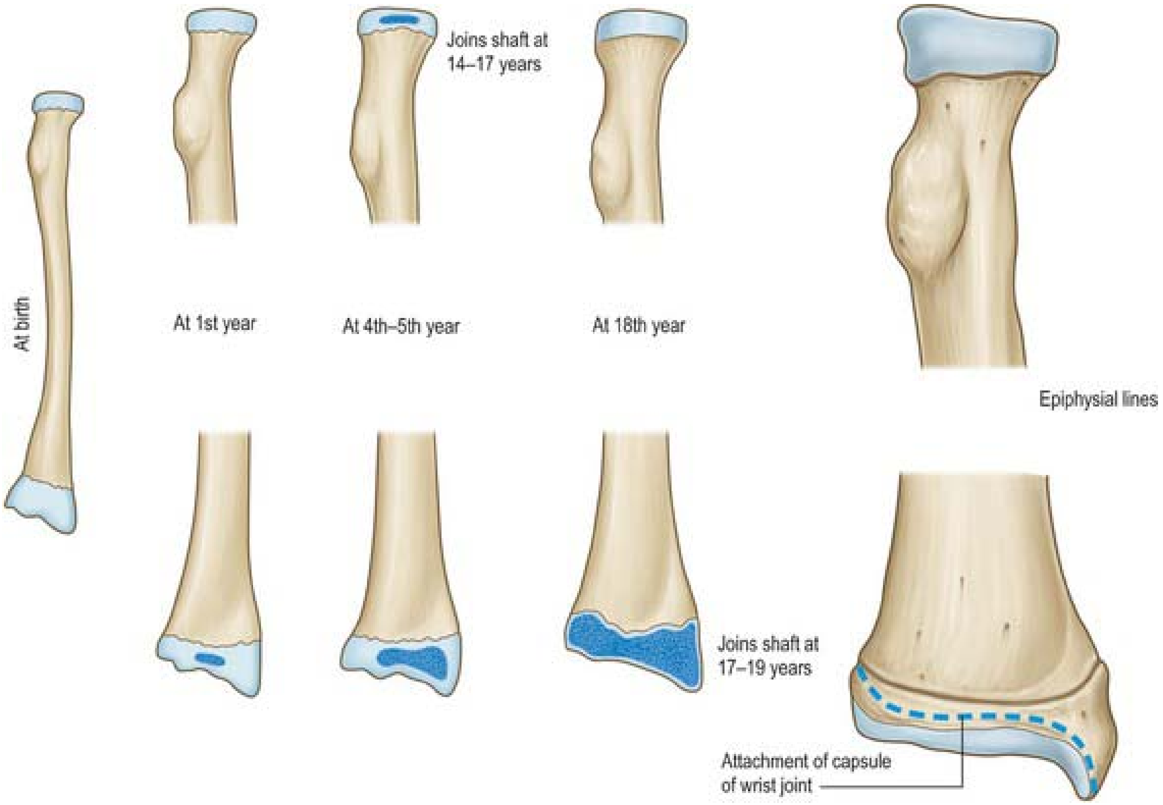
At birth
At 1st year
Joins shaft at 14–17 years
At 4th–5th year
At 18th year
Epiphysial lines
Joins shaft at 17–19 years
Attachment of capsule of wrist joint

Fig. 49.8 **A**, Stages in the ossification of the radius (not to scale). **B**, The epiphysial lines of the adolescent left radius, anterior aspect. The attachment of the wrist joint capsule is in blue.

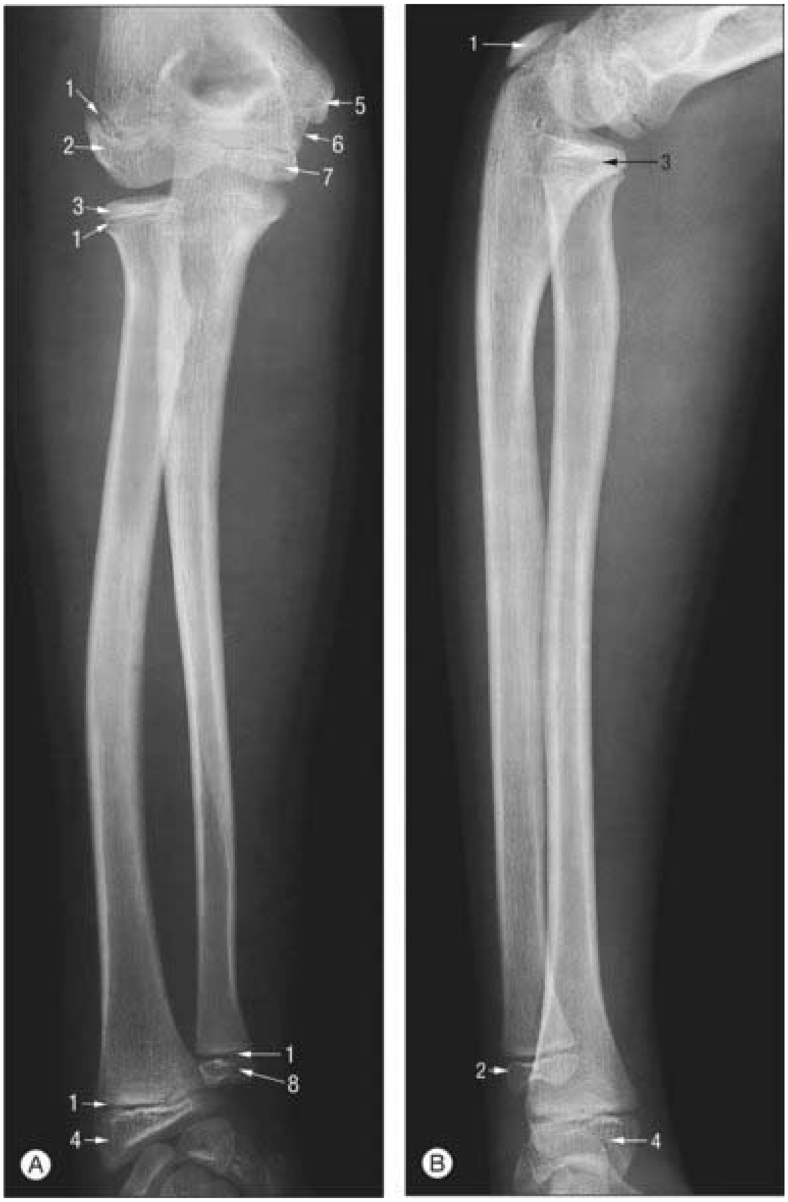

Fig. 49.9 Radiographs of the forearm of a girl aged 11. **A**, Anteroposterior view. **B**, Lateral view, semiflexed at the elbow. Note the epiphyses and adjacent radiotranslucent growth cartilages. **A: 1**. Cartilaginous growth plates. **2**. Conjoined epiphyses of capitulum and lateral epicondyle. **3**. Proximal radial epiphysis. **4**. Distal radial epiphysis. **5**. Epiphysis of medial epicondyle. **6**. Diaphysial bone. **7**. Trochlear epiphysis. **8**. Distal ulnar epiphysis. **B: 1**. Olecranon. **2**. Distal ulna. **3**. Proximal radial. **4**. Distal radial.

ULNA

The ulna is medial to the radius in the supinated forearm (Fig. 49.3, Fig. 49.4). Its proximal end is a massive hook which is concave forwards (Fig. 49.10). The lateral border of the shaft is a sharp interosseous crest. The bone diminishes progressively from its proximal mass throughout almost its whole length, but at its distal end expands into a small rounded head and styloid process. The shaft is triangular in section but has no appreciable double curve. In its whole length it is slightly convex posteriorly. Mediolaterally, its profile is sinuous. The proximal half has a slight laterally concave curvature, and the distal half a medially concave curvature.

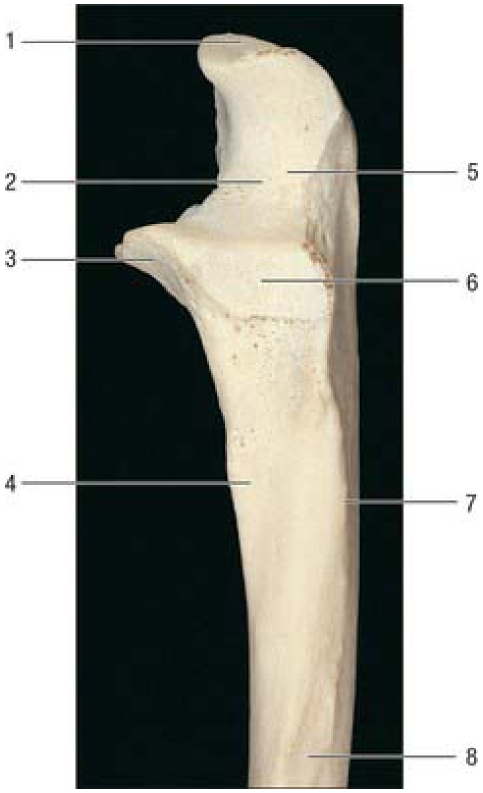

Fig. 49.10 Proximal end of left ulna: lateral view. **1**. Olecranon. **2**. Non-articular strip in trochlear notch. **3**. Coronoid process. **4**. Tuberosity. **5**. Trochlear notch. **6**. Radial notch. **7**. Supinator crest. **8**. Shaft.

Proximal end

The proximal end has large olecranon and coronoid processes and trochlear and radial notches which articulate with the humerus and radius (Fig. 49.10). The olecranon is more proximal and is bent forwards at its summit like a beak, which enters the humeral olecranon fossa in extension. Its posterior surface is smooth, triangular and subcutaneous, and its proximal border underlies the ‘point’ of the elbow. In extension it can be felt near a line joining the humeral epicondyles, but in flexion it descends, so that the three osseous points form an isosceles triangle. Its anterior, articular surface forms the proximal area of the trochlear notch. Its base is slightly constricted where it joins the shaft and is the narrowest part of the proximal ulna. The coronoid process projects anteriorly distal to the olecranon. Its proximal aspect forms the distal part of the trochlear notch. On the lateral surface, distal to the trochlear notch, there is a shallow, smooth, oval radial notch which articulates with the radial head. Distal to the radial notch the surface is hollow to accommodate the radial tuberosity during pronation and supination. The anterior surface of the coronoid is triangular. Its distal part is the tuberosity of the ulna. Its medial border is sharp and bears a small tubercle proximally.

The trochlear notch articulates with the trochlea of the humerus. It is constricted at the junction of the olecranon and coronoid processes, where their articular surfaces may be separated by a narrow rough non-articular strip. A smooth ridge, adapted to the groove on the humeral trochlea, divides the notch into medial and lateral parts. The medial fits into the trochlear flange. The radial notch, an oval or oblong proximal depression on the lateral aspect of the coronoid process, articulates with the periphery of the radial head, and is separated from the trochlear notch by a smooth ridge (Fig. 49.10).

Shaft

The shaft is triangular in section in its proximal three-fourths, but distally is almost cylindrical (Fig. 49.3, Fig. 49.4). It has anterior, posterior and medial surfaces and interosseous, posterior and anterior borders. The interosseous border is a conspicuous lateral crest in its middle two-fourths. Proximally it becomes the supinator crest, which is continuous with the posterior border of a depression distal to the radial notch. Distally, it disappears. The rounded anterior border starts medial to the ulnar tuberosity, descends backwards, and is usually traceable to the base of the styloid process. The posterior border, also rounded, descends from the apex of the posterior aspect of the olecranon, and curves laterally to reach the styloid process. It is palpable throughout its length in a longitudinal furrow which is most obvious when the elbow is fully flexed.

The anterior surface, between the interosseous and anterior borders, is longitudinally grooved, sometimes deeply (Fig. 49.3). Proximal to its midpoint there is a nutrient foramen, which is directed proximally and contains a branch of the anterior interosseous artery. Distally, it is crossed obliquely by a rough, variable prominence, descending from the interosseous to the anterior border. The medial surface, between the anterior and posterior borders, is transversely convex and smooth. The posterior surface, between the posterior and interosseous borders, is divided into three areas (Fig. 49.4). The most proximal is limited by a sometimes faint oblique line ascending laterally from the junction of the middle and upper thirds of the posterior border to the posterior end of the radial notch. The region distal to this line is divided into a larger medial and narrower lateral strip by a vertical ridge, usually distinct only in its proximal three-fourths.

Distal end

The distal end is slightly expanded and has a head and styloid process. The head is visible in pronation on the posteromedial carpal aspect, and can be gripped when the supinated hand is flexed. Its lateral convex articular surface fits the radial ulnar notch. Its smooth distal surface (Fig. 49.6) is separated from the carpus by an articular disc, the apex of which is attached to a rough area between the articular surface and styloid process. The latter, a short, round, posterolateral projection of the distal end of the ulna, is palpable (most readily in supination) about 1 cm proximal to the plane of the radial styloid. A posterior vertical groove is present between the head and styloid process.

Muscle, ligament and articular attachments

Anteriorly, the capsule of the elbow joint is attached to the proximal olecranon surface. The tendon of triceps is attached to its rough posterior two-thirds: the capsule and tendon can be separated by a bursa. The medial surface of the olecranon is marked proximally by the attachment of the posterior and oblique bands of the ulnar collateral ligament and the ulnar part of flexor carpi ulnaris. The smooth area distal to this is the most proximal attachment of flexor digitorum profundus. Anconeus is attached to the lateral olecranon surface and the adjoining posterior surface of the ulnar shaft as far as its oblique line. The posterior surface of the ulna is separated from the skin by a subcutaneous bursa.

Brachialis is attached to the anterior surface of the coronoid process, including the ulnar tuberosity. The oblique and anterior bands of the ulnar collateral ligament and the distal part of the humero-ulnar slip of flexor digitorum superficialis are attached to a small tubercle at the proximal end of the medial border. Distal to this the margin provides attachment for the ulnar part of pronator teres. An ulnar part of flexor pollicis longus may be attached to the lateral or, more rarely, the medial border of the coronoid process. Fibres of flexor digitorum profundus are attached to its medial surface. The annular ligament is attached to the anterior rim of the radial notch and posteriorly to a ridge at or just behind the posterior margin of the notch. The depressed area distal to the notch is limited behind by the supinator crest, and both provide attachment for supinator.

The olecranon area of the trochlear notch is usually divided into three areas. The most medial faces anteromedially, and is grooved to fit the medial flange of the humeral trochlea, with which it makes increasing contact during flexion. A flat intermediate area fits the lateral flange, and the most lateral area, a narrow strip, abuts the trochlea in extension. The articular surface is narrower than the base of the olecranon: non-articular parts are related to the synovial processes. The coronoid area of the trochlear notch is also divided, and its medial and lateral areas correspond to medial and intermediate areas of the olecranon. The medial is more hollow, and conforms to the convex medial trochlear flange. The medial and anterior parts of the capsular ligament are attached to its medial and anterior borders.

The deep fascia of the forearm is attached to the subcutaneous posterior border. This border also provides an attachment for the aponeurosis of flexor digitorum profundus in its proximal threequarters, for flexor carpi ulnaris in its proximal half, and for extensor carpi ulnaris in its middle third. These three muscles connect with the posterior border through a common blended aponeurosis. The interosseous membrane is attached to the interosseous border, except proximally.

Flexor digitorum profundus is attached to the proximal three-fourths of the anterior border and medial surface, attaching medial to the coronoid process and olecranon. The rough strip across the distal fourth of the anterior surface provides part of the bony attachment for pronator quadratus. Anconeus is attached to the posterior surface proximal to the oblique line and lateral to the olecranon. The narrow strip between the interosseous border and vertical ridge gives rise to the attachment of three deep muscles: abductor pollicis longus arises from the proximal fourth, extensor pollicis longus arises from the succeeding fourth (sometimes a ridge is interposed between them), and extensor indicis is attached to the third quarter. The broad strip medial to the vertical ridge is covered by extensor carpi ulnaris, whose tendon grooves the posterior aspect of the distal end of the ulna. The ulnar collateral ligament is attached to the apex of the styloid process.

Vascular supply

Multiple metaphysial nutrient foramina transmit branches of the radial, ulnar, anterior and posterior interosseous arteries (Fig. 49.7). These vessels give off a number of smaller segmental branches. Usually one, but occasionally two, major nutrient diaphysial foramina are located on the anterior surface of the bone, directed proximally toward the elbow. A network of small fascioperiosteal and musculoperiosteal branches given off from the compartmental vessels reaches the bone via septal and muscular attachments.

Ossification

The ulna ossifies from four main centres, one each in the shaft and distal end and two in the olecranon (Fig. 49.11). Ossification begins in the midshaft about the eighth fetal week, and extends rapidly. In the fifth (females) and sixth (males) years, a centre appears in the distal end, and extends into the styloid process. The distal olecranon is ossified as an extension from the shaft, the remainder from two centres, one for the proximal trochlear surface, and the other for a thin scale-like proximal epiphysis on its summit. The latter appears in the ninth year in females, 11th in males. The whole proximal epiphysis has joined the shaft by the 14th year in females, sixteenth in males. The distal epiphysis unites with the shaft in the 17th year in females, 18th in males.

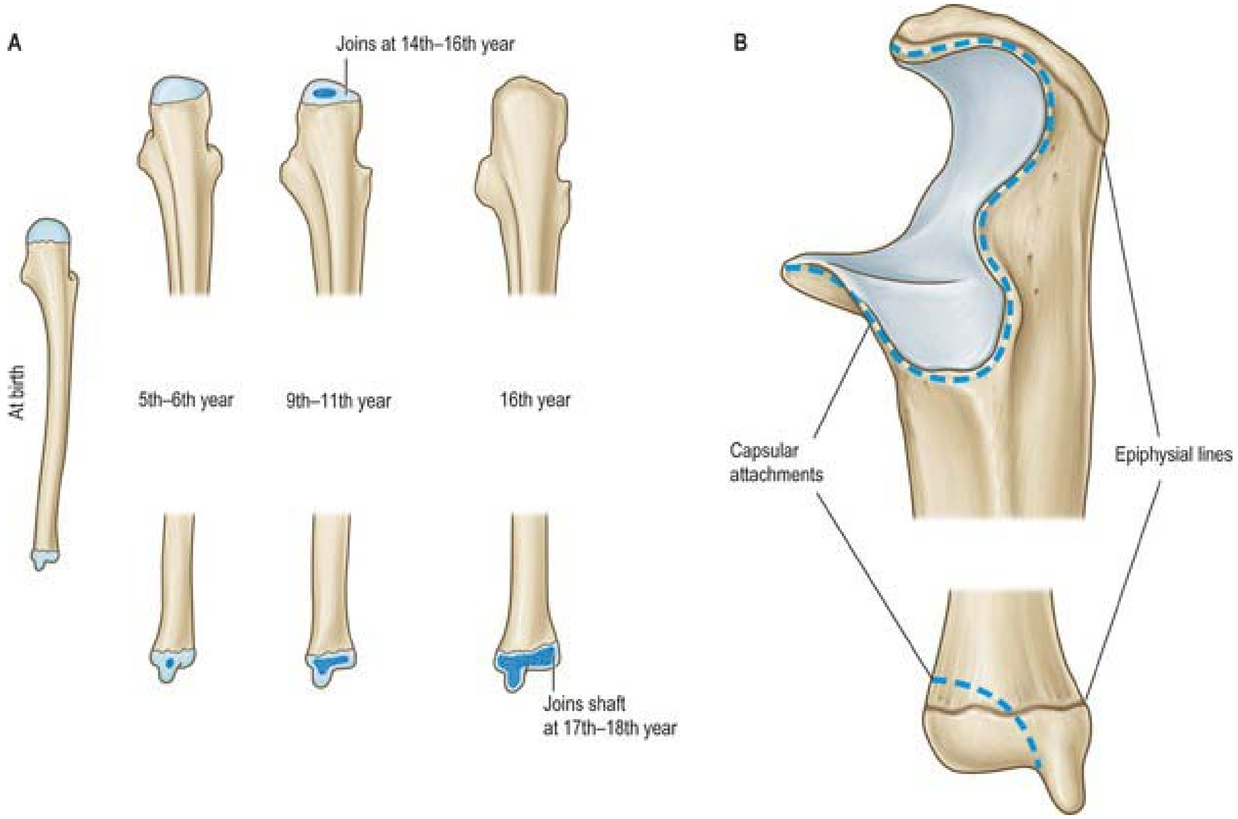
A
Joins at 14th–16th year
At birth
5th–6th year
9th–11th year
16th year
Joins shaft at 17th–18th year
B
Capsular attachments
Epiphysial lines

Fig. 49.11 **A**, Stages in the ossification of the ulna. The diagram is simplified in relation to the ossification of the olecranon epiphysis, which is said to have two centres. **B**, The epiphysial lines of the adolescent left ulna, lateral aspect. The attachment of the joint capsules is in blue.

MUSCLES

ANTERIOR COMPARTMENT

The anterior compartment contains the flexor muscles of the forearm which are arranged in superficial and deep groups. Chronic tendonitis of the common flexor tendon origin produces medial epicondylitis of the elbow, leading to pain and tenderness. It is a frequent complaint among golfers. A detailed account of the architectural properties of the muscles of the arm and forearm is given by Leiber et al (1992).

Superficial flexor compartment

Muscles of the superficial flexor compartment arise from the medial epicondyle of the humerus by a common tendon. They are pronator teres, flexor carpi radialis, palmaris longus, flexor digitorum superficialis, and flexor carpi ulnaris (Fig. 49.12). They have additional attachments to the antebrachial fascia near the elbow and to the septa that pass from this fascia between individual muscles.

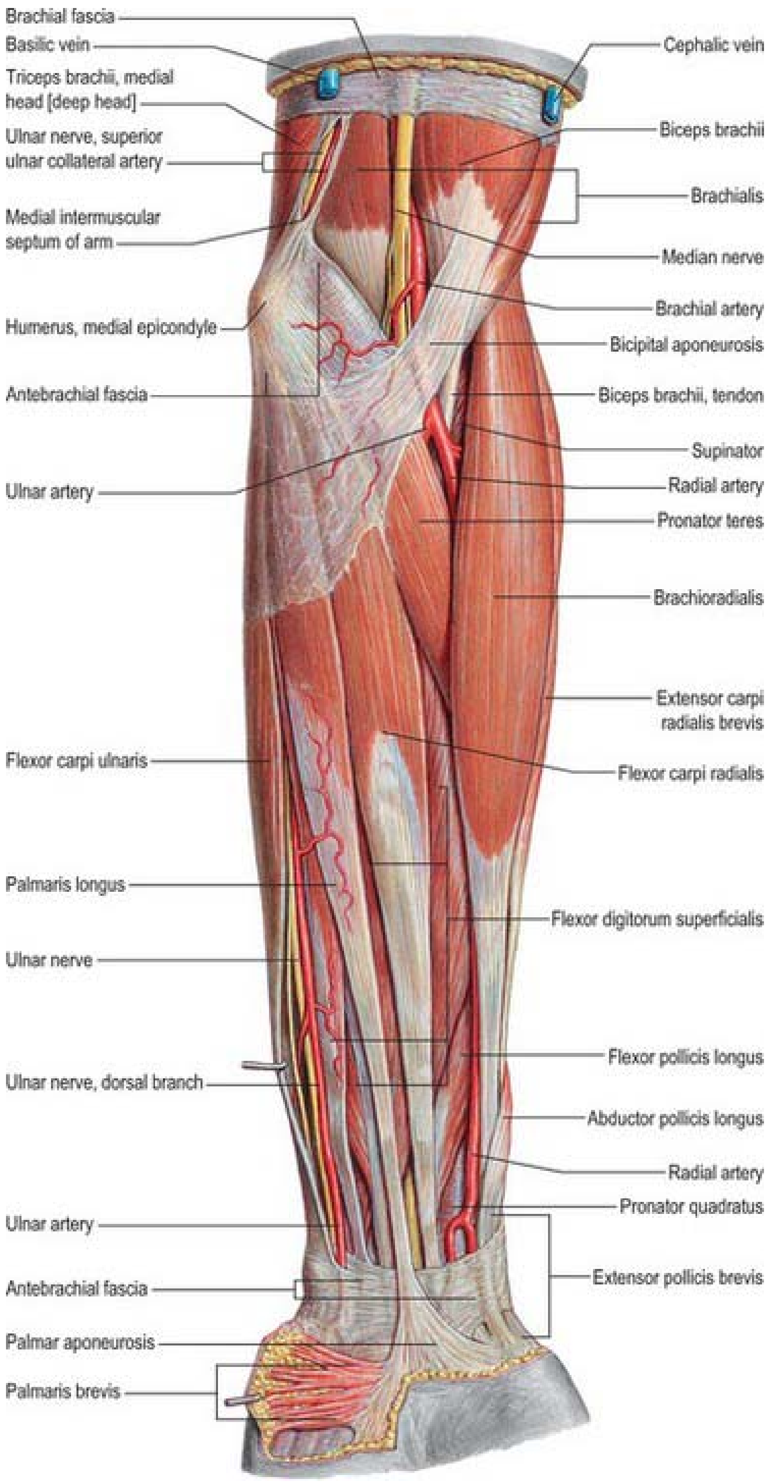
Brachial fascia
Basilic vein
Cephalic vein
Triceps brachii, medial head [deep head]
Biceps brachii
Ulnar nerve, superior ulnar collateral artery
Brachialis
Medial intermuscular septum of arm
Median nerve
Brachial artery
Humerus, medial epicondyle
Bicipital aponeurosis
Antebrachial fascia
Biceps brachii, tendon
Supinator
Ulnar artery
Radial artery
Pronator teres
Brachioradialis
Extensor carpi radialis brevis
Flexor carpi ulnaris
Flexor carpi radialis
Palmaris longus
Flexor digitorum superficialis
Ulnar nerve
Flexor pollicis longus
Ulnar nerve, dorsal branch
Abductor pollicis longus
Radial artery
Pronator quadratus
Ulnar artery
Extensor pollicis brevis
Antebrachial fascia
Palmar aponeurosis
Palmaris brevis

Fig. 49.12 The superficial flexor muscles of the left forearm.

(From Sobotta 2006.)

Pronator teres

Attachments

Pronator teres has humeral and ulna attachments (Fig. 49.3, Fig. 49.12, Fig. 49.13). The humeral head, the larger and more superficial of the two, arises just proximal to the medial epicondyle, from the common tendon of origin of the flexor muscles, from the intermuscular septum between it and flexor carpi radialis, and from antebrachial fascia. The smaller ulnar head springs from the medial side of the coronoid process of the ulna, distal to the attachment of flexor digitorum superficialis, and joins the humeral head at an acute angle. The muscle passes obliquely across the forearm to end in a flat tendon that is attached to a rough area midway along the lateral surface of the radial shaft at the ‘summit’ of its lateral curve. The coronoid attachment may be absent. Accessory slips may arise from a supracondylar process of the humerus, if it is present, or from biceps, brachialis or the medial intermuscular septum.

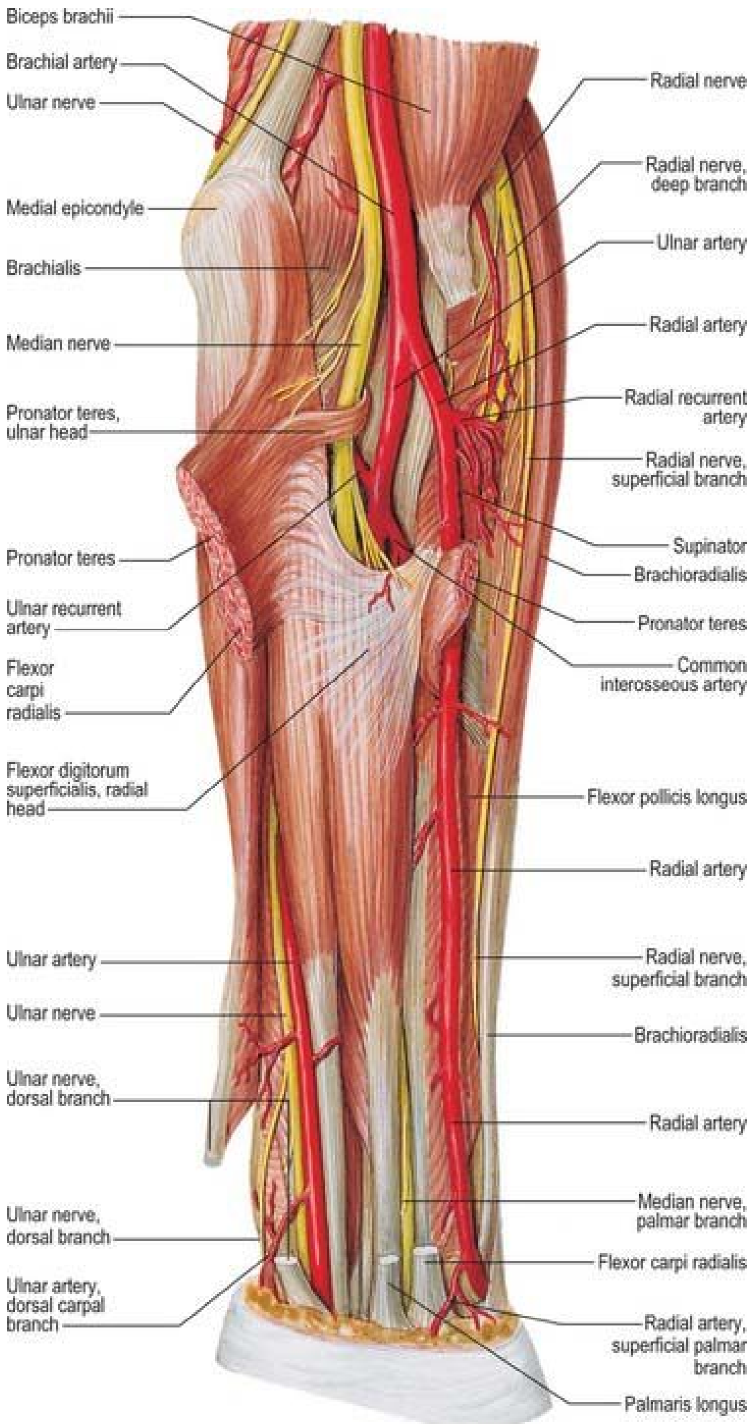
Biceps brachii
Brachial artery
Ulnar nerve
Medial epicondyle
Brachialis
Median nerve
Pronator teres, ulnar head
Pronator teres
Ulnar recurrent artery
Flexor carpi radialis
Flexor digitorum superficialis, radial head
Ulnar artery
Ulnar nerve
Ulnar nerve, dorsal branch
Ulnar nerve, dorsal branch
Ulnar artery, dorsal carpal branch
Radial nerve
Radial nerve, deep branch
Ulnar artery
Radial artery
Radial recurrent artery
Radial nerve, superficial branch
Supinator
Brachioradialis
Pronator teres
Common interosseous artery
Flexor pollicis longus
Radial artery
Radial nerve, superficial branch
Brachioradialis
Radial artery
Median nerve, palmar branch
Flexor carpi radialis
Radial artery, superficial palmar branch
Palmaris longus

Fig. 49.13 The deep flexor muscles of the left forearm.

(From Sobotta 2006.)

Relations

The median nerve usually enters the forearm between the two heads of pronator teres, and is separated from the ulnar artery by the ulnar head. The lateral border of pronator teres is the medial limit of the cubital fossa, the triangular hollow anterior to the elbow joint.

Vascular supply

The humeral head of pronator teres is supplied by the inferior ulnar collateral artery and the anterior ulnar recurrent artery. The ulnar head is supplied by the common interosseous artery. The mid portion of the muscle belly is supplied by direct branches from the ulnar artery, while the attachment to the radius is supplied by the radial artery.

Innervation

Pronator teres is innervated by the median nerve, C6 and 7.

Action

Pronator teres rotates the radius on the ulna (pronation of the forearm), turning the palm medially so that it faces backwards. It acts with pronator quadratus (which is always active in pronation) only in rapid or forcible pronation. Like all of the muscles which arise from the medial epicondyle, pronator teres acts as a weak flexor of the elbow joint.

Clinical anatomy: testing

Pronator teres is tested by palpating its contracting fibres during pronation against resistance.

Flexor carpi radialis

Attachments

Flexor carpi radialis lies medial to pronator teres, and arises from the medial epicondyle via the common flexor tendon, from the antebrachial fascia and from adjacent intermuscular septa (Fig. 49.12). Its fusiform belly ends, rather more than halfway to the wrist, in a long tendon which passes within a synovial sheath through a lateral canal, formed by the flexor retinaculum above and a groove on the trapezium beneath. It inserts on the palmar surface of the base of the second metacarpal, sending a slip to the third metacarpal. These distal attachments are hidden by the oblique head of adductor pollicis. The muscle rarely may be absent. It may have accessory slips from the biceps tendon, bicipital aponeurosis, coronoid process or radius. Distally it may also be attached to the flexor retinaculum, trapezium or fourth metacarpal.

Relations

In the lower part of the forearm the radial artery lies between the tendon of flexor carpi radialis and that of brachioradialis. The surface groove for the radial pulse is well known to all physicians.

Vascular supply

Flexor carpi radialis is supplied by a single dominant proximal pedicle and several distal minor pedicles. The dominant pedicle is formed by a branch which arises from either the anterior or posterior ulnar recurrent artery. The latter passes deep to pronator teres to enter the deep surface of flexor carpi radialis, whereupon it divides into a small ascending branch and a larger descending branch. The distal minor pedicles amount to six to eight branches from the radial artery which enter the muscle on the anterolateral side.

Innervation

Flexor carpi radialis is innervated by the median nerve, C6 and 7.

Action

Acting with flexor carpi ulnaris, and sometimes flexor digitorum superficialis, flexor carpi radialis flexes the wrist, and helps radial extensors of the wrist in abducting the hand.

Clinical anatomy: testing

Flexor carpi radialis is tested by palpating its contracting fibres during flexion of the wrist against resistance.

Flexor digitorum superficialis

Attachments

Flexor digitorum superficialis (sublimis) lies deep to the preceding muscles (Fig. 49.12). It is the largest of the superficial flexors, and arises by two heads. The humero-ulnar head arises from the medial epicondyle of the humerus via the common tendon; the anterior band of the ulnar collateral ligament; adjacent intermuscular septa, and from the medial side of the coronoid process proximal to the ulnar origin of pronator teres. The radial head, a thin sheet of muscle, arises from the anterior radial border extending from the radial tuberosity to the insertion of pronator teres. The median nerve and ulnar artery descend between the heads. The muscle usually separates into two strata, directed to digits 2–5. The superficial stratum, joined laterally by the radial head, divides into two tendons for the middle and ring finger. The deep stratum gives off a muscular slip to join the superficial fibres directed to the ring finger, and then ends in two tendons for the index and little finger. As the tendons pass behind the flexor retinaculum they are arranged in pairs: the superficial pair pass to the middle and ring fingers, the deep to the index and little finger. Distal to the carpal tunnel the four tendons diverge. Each passes towards a finger superficial to the corresponding flexor digitorum profundus tendon. The two tendons for each finger enter the digital flexor sheath (which starts over the metacarpophalangeal joint) in this relationship. The superficialis tendon then splits into two bundles which pass around the profundus to lie posteriorly. They subsequently reunite and insert into the anterior surface of the middle phalanx. Some fibres interchange from one bundle to another.

An intermediate tendon is always found in the central branching area of the muscle belly and is an important landmark in deep dissection: it can initially be confused with the median nerve. The radial head of flexor digitorum superficialis may be absent and the muscular slip from the deep stratum may provide most or all of the fibres acting on the index finger. The fibres associated with the little finger may be absent, when they are replaced by a separate slip from the ulna, flexor retinaculum or palmar fascia. Variations occur in the arrangement of the tendons.

Relations

The median nerve and ulnar artery descend between the heads of flexor digitorum superficialis.

Vascular supply

The humeral head of flexor digitorum superficialis is supplied by the anterior ulnar recurrent artery. The main part of the muscle is supplied on its anterior surface by three or four branches from both the ulnar and radial arteries. The posterior surface is supplied by the ulnar artery and median artery, and the lateral surface by additional branches from the radial artery.

Innervation

Flexor digitorum superficialis is innervated by the median nerve, C8 and T1.

Action

Flexor digitorum superficialis is potentially a flexor of all the joints over which it passes, i.e. proximal interphalangeal, metacarpophalangeal and wrist joints. Its precise action depends on which other muscles are acting. It has independent muscle slips to all four fingers, unlike flexor digitorum profundus, which has a muscle group common to the middle, ring and little fingers. It is therefore able to flex the proximal interphalangeal joints individually.

Clinical anatomy: testing

The independent action of flexor digitorum superficialis for a particular finger is tested by flexing that digit while holding the three other fingers in full extension. This eliminates any simultaneous contraction of the flexor digitorum profundus which might flex the digit.

Palmaris longus

Attachments

Palmaris longus is a slender, fusiform muscle medial to flexor carpi radialis (Fig. 49.12). It springs from the medial epicondyle by the common tendon, and from adjacent intermuscular septa and deep fascia. It converges on a long tendon, which passes anterior (superficial) to the flexor retinaculum. A few fibres leave the tendon and interweave with the transverse fibres of the retinaculum, but most of the tendon passes distally. As the tendon crosses the retinaculum it broadens out to become a flat sheet which becomes incorporated into the palmar aponeurosis. Palmaris longus is often absent on one or both sides.

Relations

The median nerve at the wrist lies partly under the cover of the tendon of palmaris longus, and partly between the tendons of palmaris longus and flexor carpi radialis.

Vascular supply

The muscle belly of palmaris longus is supplied by a small branch from the anterior ulnar recurrent artery. A small contribution is sometimes made by the median artery, if this is well developed.

Innervation

Palmaris longus is innervated by the median nerve, C7 and 8.

Action

It has been suggested that palmaris longus is a phylogenetically degenerate metacarpophalangeal joint flexor. Although consideration of the line of action would suggest that it plays a role in carpal flexion, its main function appears to be as an anchor for the skin and fascia of the hand, in resisting horizontal shearing forces in a distal direction (e.g. as in holding a golf club), which would tend to deglove the skin of the palm.

Clinical anatomy: testing

If the wrist is flexed against resistance, the taut tendon of palmaris longus will be seen in the midline of the flexor wrist crease as the tendon passes superficial to the flexor retinaculum. When testing palmaris longus it helps to oppose the thumb to the middle fingertip at the same time as the wrist is flexed in order to make palmaris stand out.

Flexor carpi ulnaris

Attachments

Flexor carpi ulnaris is the most medial of the superficial forearm flexors (Fig. 49.12). It arises by two heads, humeral and ulnar, connected by a tendinous arch. The small humeral head arises from the medial epicondyle via the common tendon. The ulnar head has an extensive origin from the medial margin of the olecranon and proximal two-thirds of the posterior border of the ulna, an aponeurosis (which it shares with extensor carpi ulnaris and flexor digitorum profundus), and from the intermuscular septum between it and flexor digitorum superficialis. Occasionally there is a slip from the coronoid process. A thick tendon forms along its anterolateral border in its distal half. The tendon is attached to the pisiform, and thence prolonged to the hamate and fifth metacarpal by pisohamate and pisometacarpal ligaments. The attachment to the flexor retinaculum and the fourth or fifth metacarpal bones is sometimes substantial.

Relations

The ulnar nerve and posterior ulnar recurrent artery pass under the tendinous arch between the humeral and ulnar heads of flexor carpi ulnaris. Ulnar vessels and nerve lie lateral to the tendon of insertion.

Vascular supply

The main arterial supply of flexor carpi ulnaris is derived from three pedicles. The proximal pedicle arises from a branch of the posterior ulnar recurrent artery as it passes between the humeral and ulnar heads. The middle and distal pedicles arise from the ulnar artery and enter the muscle at the junction of the upper and middle thirds, and the musculotendinous junctions, respectively. Flexor carpi ulnaris also receives a small supply near its origin which arises from the inferior ulnar collateral artery.

Innervation

Flexor carpi ulnaris is innervated by the ulnar nerve, C7 and 8 and T1.

Action

Acting with flexor carpi radialis, flexor carpi ulnaris flexes the wrist. Acting with extensor carpi ulnaris, it adducts (ulnar deviates) the hand.

Clinical anatomy: testing

Flexor carpi ulnaris is tested by palpating its fibres while the wrist is flexed against resistance. A more positive test is to palpate the tendon while the patient abducts the little finger against resistance. FCU synergistically contracts to stabilize the pisiform, giving abducted digiti minimi a stable origin.

Deep flexor compartment

The muscles of the deep flexor compartment are flexor digitorum profundus, flexor pollicis longus and pronator quadratus.

Flexor digitorum profundus

Attachments

Flexor digitorum profundus arises deep to the superficial flexors from about the upper three-quarters of the anterior and medial surfaces of the ulna (Fig. 49.13, see Fig. 49.19). It embraces the attachment of brachialis above and extends distally almost to pronator quadratus. It also arises from a depression on the medial side of the coronoid process, the upper three-quarters of the posterior ulnar border (by an aponeurosis which it shares with flexor and extensor carpi ulnaris), and the anterior surface of the ulnar half of the interosseous membrane. The muscle ends in four tendons, which run initially posterior (deep) to the tendons of flexor digitorum superficialis and the flexor retinaculum. The part of the flexor digitorum profundus muscle which acts on the index finger is usually distinct throughout. The tendons for the other fingers are interconnected by areolar tissue and tendinous slips as far as the palm. Anterior to their proximal phalanges, the tendons pass through the tendons of flexor digitorum superficialis to insert on the palmar surfaces of the bases of the distal phalanges. The tendons of the profundus undergo fascicular rearrangement as they pass through those of superficialis.

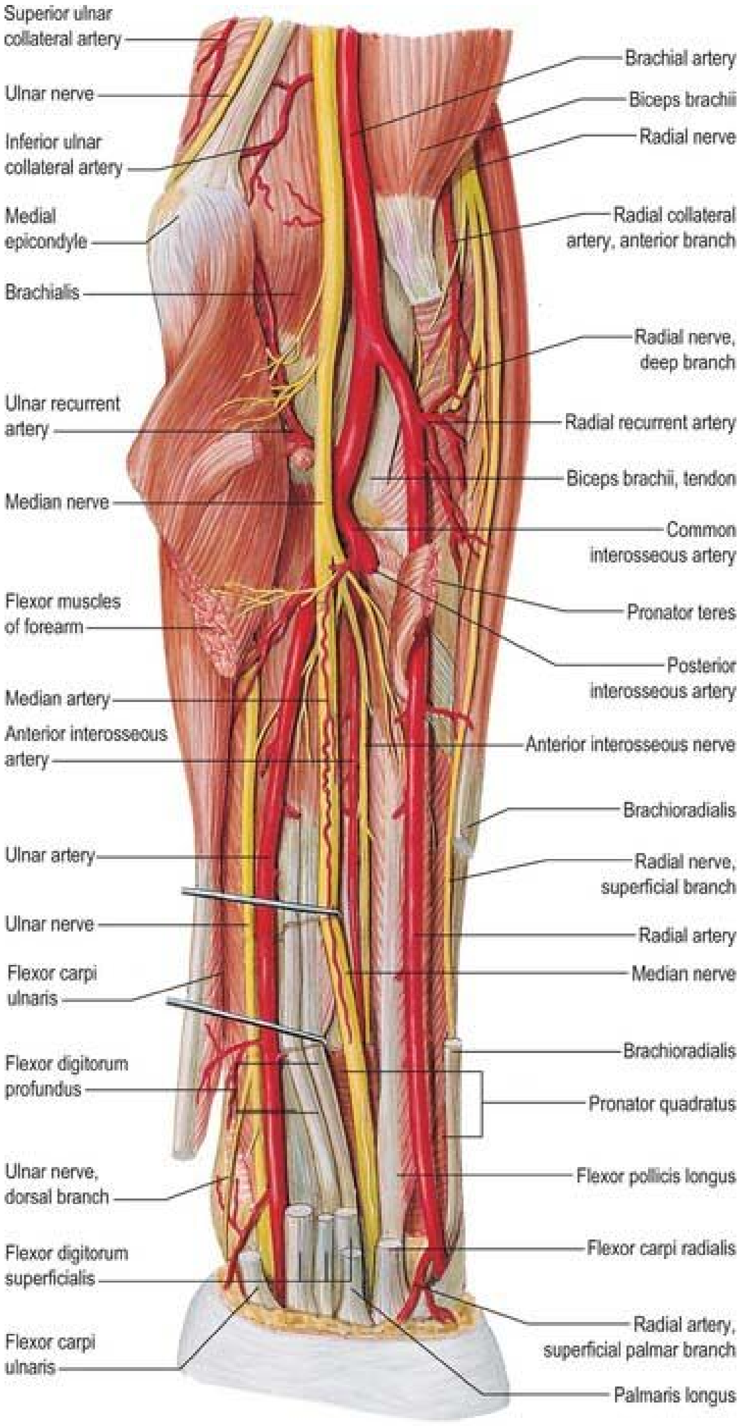
Superior ulnar collateral artery
Ulnar nerve
Inferior ulnar collateral artery
Medial epicondyle
Brachialis
Ulnar recurrent artery
Median nerve
Flexor muscles of forearm
Median artery
Anterior interosseous artery
Ulnar artery
Ulnar nerve
Flexor carpi ulnaris
Flexor digitorum profundus
Ulnar nerve, dorsal branch
Flexor digitorum superficialis
Flexor carpi ulnaris
Brachial artery
Biceps brachii
Radial nerve
Radial collateral artery, anterior branch
Radial nerve, deep branch
Radial recurrent artery
Biceps brachii, tendon
Common interosseous artery
Pronator teres
Posterior interosseous artery
Anterior interosseous nerve
Brachioradialis
Radial nerve, superficial branch
Radial artery
Median nerve
Brachioradialis
Pronator quadratus
Flexor pollicis longus
Flexor carpi radialis
Radial artery, superficial palmar branch
Palmaris longus

Fig. 49.19 The deep flexor aspect of the left forearm.

(From Sobotta 2006.)

Flexor digitorum profundus may be joined by accessory slips from the radius (which act on the index finger), flexor superficialis, flexor pollicis longus, the medial epicondyle or the coronoid process.

Relations

Flexor digitorum profundus forms most of the surface elevation medial to the palpable posterior ulnar border. In the palm, the lumbrical muscles are attached to its tendons.

Vascular supply

The origin of flexor digitorum profundus is supplied by the inferior ulnar collateral and ulnar recurrent arteries. The proximal part is supplied by one or two branches from either the ulnar or common interosseous arteries. The distal part is supplied by a series of branches from the ulnar artery, the anterior interosseous artery and the median artery.

Innervation

The medial part of flexor digitorum profundus, i.e. the muscle bellies to the little and ring fingers, is innervated by the ulnar nerve. The lateral part, i.e. the muscle bellies to the middle and index fingers, is innervated by the anterior interosseous branch of the median nerve, C8 and T1.

Action

Flexor digitorum profundus is capable of flexing any or all of the joints over which it passes. It therefore has a role in coordinated finger flexion, but it is the only muscle capable of flexing the distal interphalangeal joints. The index finger tendon is usually capable of independent function, whereas the other three work together. Electromyographically flexor digitorum profundus acts alone in gentle digital flexion and is reinforced by superficialis for greater force and/or velocity.

Clinical anatomy: testing

Flexor digitorum profundus is tested by flexing the distal interphalangeal joint while holding the proximal interphalangeal joint in extension.

Flexor pollicis longus

Attachments

Flexor pollicis longus is lateral to flexor digitorum profundus (Fig. 49.13). It arises from the grooved anterior surface of the radius, and extends from below its tuberosity to the upper attachment of pronator quadratus. It also arises from the adjacent interosseous membrane, and frequently by a variable slip from the lateral, or more rarely medial, border of the coronoid process, or from the medial epicondyle of the humerus. The muscle ends in a flattened tendon, which passes behind the flexor retinaculum, between opponens pollicis and the oblique head of adductor pollicis, to enter a synovial sheath. It inserts on the palmar surface of the base of the distal phalanx of the thumb.

Flexor pollicis longus is sometimes connected to flexor digitorum superficialis, or profundus, or pronator teres. The interosseous attachment, and indeed the whole muscle, may be absent. Anomalous tendon slips from the flexor pollicis longus to the flexor digitorum profundus are common.

Relations

The anterior interosseous nerve and vessels descend on the interosseous membrane between flexor pollicis longus and flexor digitorum profundus.

Vascular supply

The medial half of flexor pollicis longus is supplied by the anterior interosseous artery, while the lateral half is supplied by branches of the radial artery. The median artery may contribute if it is well developed.

Innervation

Flexor pollicis longus is innervated by the anterior interosseous branch of the median nerve, C7 and 8.

Action

Flexor pollicis longus flexes the phalanges of the thumb and the carpometacarpal joint of the thumb, especially if the more distal joints are stiff or fused.

Clinical anatomy: testing

Flexor pollicis longus is tested by flexing the interphalangeal joint of the thumb against resistance.

Pronator quadratus

Attachments

Pronator quadratus is a flat, quadrilateral muscle which extends across the front of the distal parts of the radius and ulna (Fig. 49.13, see Fig. 49.19). It arises from the oblique ridge on the anterior surface of the shaft of the ulna, the medial part of this surface, and a strong aponeurosis which covers the medial third of the muscle. The fibres pass laterally and slightly downwards to the distal quarter of the anterior border and surface of the shaft of the radius. Deeper fibres insert into the triangular area above the ulnar notch of the radius.

Vascular supply

Pronator quadratus receives its main arterial supply from the anterior interosseous artery as it passes through the interosseous membrane.

Innervation

Pronator quadratus is innervated by the anterior interosseous branch of the median nerve, C7 and 8.

Action

Pronator quadratus is the principal pronator of the forearm, and is assisted by pronator teres only in rapid or forceful pronation. The deeper fibres oppose separation of the distal ends of the radius and ulna when upward thrusts are transmitted through the carpus.

Clinical anatomy: testing

Pronator quadratus is tested by pronation of the forearm against resistance while the wrist finger flexors are relaxed. The simultaneous contraction of pronator teres makes it difficult to test the independent action of pronator quadratus.

POSTERIOR COMPARTMENT

The posterior compartment contains the extensor muscles of the forearm and brachioradialis and supinator. Chronic tendonitis of the common extensor tendon origin produces lateral epicondylitis of the elbow leading to pain and tenderness. It is a frequent complaint among tennis players.

Superficial extensor compartment

Brachioradialis

Attachments

Brachioradialis is the most superficial muscle along the radial side of the forearm, and forms the lateral border of the cubital fossa (Fig. 49.14). It arises from the proximal two-thirds of the lateral supracondylar ridge of the humerus and the anterior surface of the lateral intermuscular septum. The muscle fibres end above mid-forearm level in a flat tendon which inserts on the lateral side of the distal end of the radius, usually just proximal to its styloid process. Occasionally this attachment may be much more proximal.

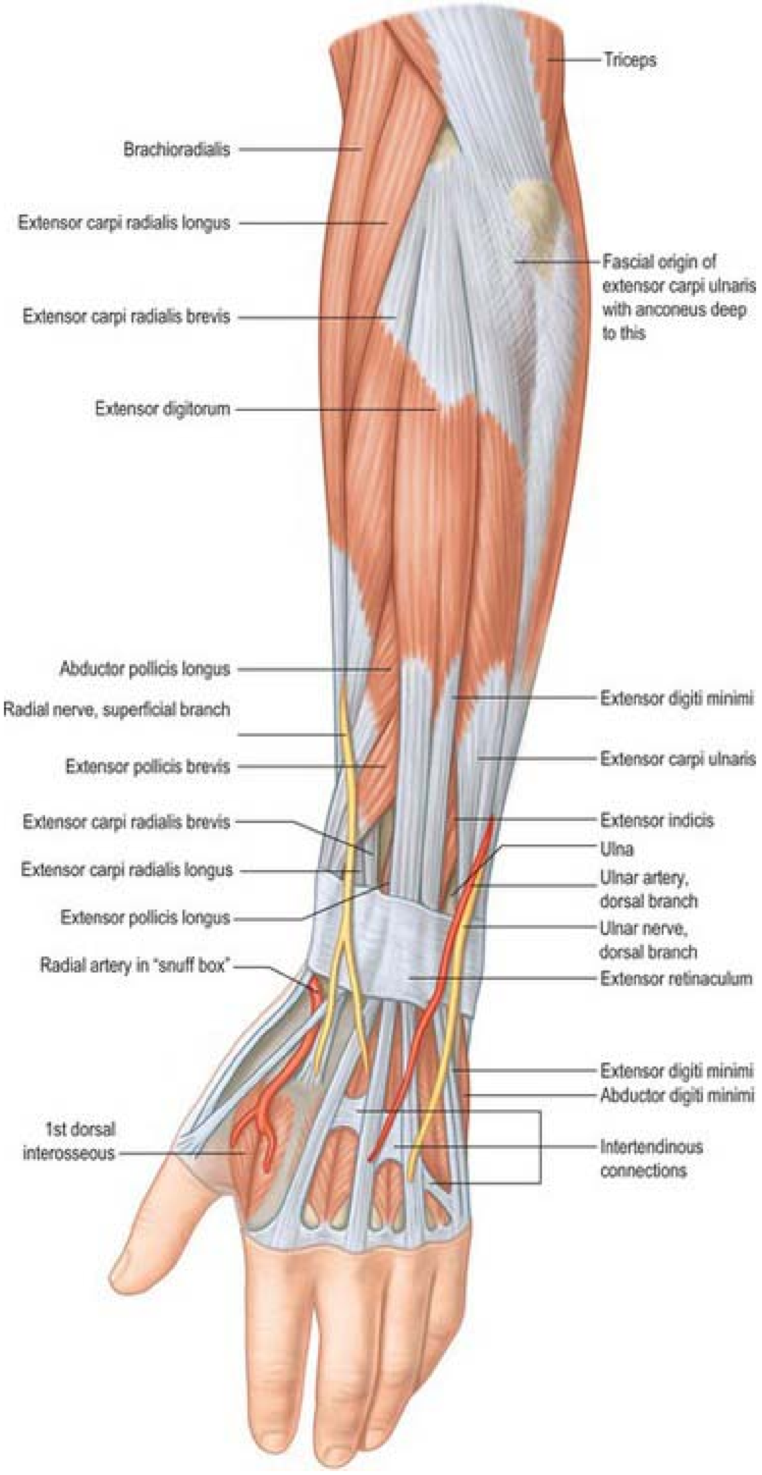
Triceps
Brachioradialis
Extensor carpi radialis longus
Extensor carpi radialis brevis
Fascial origin of extensor carpi ulnaris with anconeus deep to this
Extensor digitorum
Abductor pollicis longus
Radial nerve, superficial branch
Extensor pollicis brevis
Extensor carpi radialis brevis
Extensor carpi radialis longus
Extensor pollicis longus
Radial artery in "snuff box"
1st dorsal interosseous
Extensor digiti minimi
Extensor carpi ulnaris
Extensor indicis
Ulna
Ulnar artery, dorsal branch
Ulnar nerve, dorsal branch
Extensor retinaculum
Extensor digiti minimi
Abductor digiti minimi
Intertendinous connections

Fig. 49.14 The superficial extensor muscles of the left forearm.

The muscle is often fused proximally with brachialis. Its tendon may divide into two or three separately attached slips. In rare instances it is double or absent.

Relations

The radial nerve and the anastomosis between the profunda brachii artery and the radial recurrent artery lie between the lateral intermuscular septum and brachialis. The tendon is crossed near its distal termination by the tendons of abductor pollicis longus and extensor pollicis brevis. The radial artery is on its ulnar (medial) side.

Vascular supply

Brachioradialis is supplied by branches of the radial recurrent artery which pierce the posteromedial surface of the muscle. It also receives branches from the radial collateral branch of the profunda brachii and directly from the radial artery in the distal part of the muscle.

Innervation

Brachioradialis is innervated by the radial nerve, C5 and 6.

Action

Brachioradialis is a flexor of the elbow (despite being supplied by an ‘extensor’ nerve). It acts most effectively with the forearm in mid-pronation. It is minimally active in slow, easy flexions, or with the forearm supine, but generates a powerful burst of activity in both flexion and extension when movement is rapid. Under these conditions it develops a pronounced transarticular component of its force which helps to stabilize the elbow joint by balancing the centrifugal force of rapid swings in either direction.

Clinical anatomy: testing

Brachioradialis can be seen and felt when the semi-pronated forearm is flexed against resistance.

Extensor carpi radialis longus

Attachments

Extensor carpi radialis longus arises mainly from the distal third of the lateral supracondylar ridge of the humerus and the front of the lateral intermuscular septum. Some fibres come from the common tendon of origin of the forearm extensors. The belly ends at the junction of the proximal and middle thirds of the forearm in a flat tendon which runs along the lateral surface of the radius, deep to abductor pollicis longus and extensor pollicis brevis. The tendon then passes under the extensor retinaculum, where it lies in a groove on the back of the radius just behind the styloid process. It inserts on the radial side of the dorsal surface of the base of the second metacarpal, and may send slips to the first or third metacarpal bones. It contributes to the intermetacarpal ligaments.

Relations

Extensor carpi radialis longus is partly overlapped by brachioradialis (Fig. 49.14).

Vascular supply

Extensor carpi radialis longus receives its principal arterial supply from a single branch from the radial recurrent artery. Additional blood supply comes from branches from the radial collateral branch of the profunda brachii and directly from the radial artery in the distal part of the muscle.

Innervation

Extensor carpi radialis longus is innervated by the radial nerve, C6 and 7.

Action

Extensor carpi radialis longus acts as an extensor and abductor of the wrist and midcarpal joints. It acts in synergism with the finger flexors when making a fist.

Clinical anatomy: testing

The muscle belly and tendon of extensor carpi radialis longus can be palpated when the wrist is extended and abducted against resistance with the forearm pronated.

Extensor carpi radialis brevis

Attachments

Extensor carpi radialis brevis arises from the lateral epicondyle of the humerus by a tendon of origin which it shares with other forearm extensors, the radial collateral ligament of the elbow joint, a strong aponeurosis which covers its surface, and adjacent intermuscular septa. Its belly ends at about mid-forearm in a flat tendon which closely accompanies that of the longer carpal extensor to the wrist. The tendon passes under the extensor retinaculum and is attached to the dorsal surface of the base of the third metacarpal on its radial side, distal to its styloid process, and on adjoining parts of the second metacarpal base.

The tendons of both extensor carpi radialis longus and brevis may split into slips, which are variably attached to the second and third metacarpal bones. The muscles themselves may be united or may exchange muscular slips.

Relations

Extensor carpi radialis brevis is shorter than extensor carpi radialis longus and is covered by it (Fig. 49.14). The tendon passes deep to abductor pollicis longus and extensor pollicis brevis, then under the extensor retinaculum, where it lies in a shallow groove on the back of the radius, medial to the tendon of extensor carpi radialis longus, and separated from it by a low ridge. These two tendons share a common synovial sheath.

Vascular supply

Extensor carpi radialis brevis receives its arterial supply principally from two pedicles. One is a single branch from the radial recurrent artery, and the other is a branch of the radial artery which arises about one third of the way down the forearm. There is an additional blood supply proximally from branches from the radial collateral branch of the profunda brachii.

Innervation

Extensor carpi radialis brevis is innervated by the posterior interosseous nerve, C7 and 8.

Action

Extensor carpi radialis brevis acts with extensor carpi radialis longus as an extensor and abductor of the wrist and midcarpal joints. It acts in synergism with the finger flexors when making a fist.

Clinical anatomy: testing

The muscle belly and tendon of extensor carpi radialis brevis can be palpated when the wrist is extended and abducted against resistance with the forearm pronated.

Extensor digitorum

Attachments

Extensor digitorum arises from the lateral epicondyle of the humerus via the common extensor tendon, the adjacent intermuscular septa and the antebrachial fascia (Fig. 49.14). It divides distally into four tendons, which pass, in a common synovial sheath with the tendon of extensor indicis, through a tunnel under the extensor retinaculum. The tendons diverge on the dorsum of the hand, one to each finger. The tendon to the index finger is accompanied by extensor indicis, which lies ulnar (medial) to it. On the dorsum of the hand, adjacent tendons are linked by three variable intertendinous connections (juncturae tendinae), which are inclined distally and radially. The digital attachments enter a fibrous expansion on the dorsum of the proximal phalanges to which lumbrical, interosseous and digital extensor tendons all contribute.

The tendons of extensor digitorum may be variably deficient. More commonly, they are doubled or even tripled in one or more digits, most often the index finger or the middle finger. Occasionally a slip of tendon passes to the thumb. The arrangement of the intertendinous connections on the dorsum of the hand is highly variable. The medial connection is strong and pulls the tendon of the little finger towards that of the ring finger, whereas the connection between the middle two tendons is weak and may be absent.

Relations

The extensor tendon to the index finger lies radial (lateral) to the tendon of extensor indicis. The extensor tendon to the little finger lies radial (lateral) to the tendon of extensor digiti minimi.

Vascular supply

The proximal third of extensor digitorum is supplied by branches from the radial recurrent artery, and the distal two-thirds are supplied by branches from the posterior interosseous artery. The very distal portion is supplied by a perforating branch from the anterior interosseous artery which passes through the interosseous membrane.

Innervation

Extensor digitorum is innervated by the posterior interosseous nerve, C7 and 8.

Action

Extensor digitorum can extend any or all of the joints over which it passes, i.e. wrist, metacarpophalangeal, proximal and distal interphalangeal joints (the latter two via the extensor expansion of the digits). When acting on the metacarpophalangeal joints, extensor digitorum tends to spread the digits apart, an action that is due principally to the different axes of the individual joints imposed by the transverse arch of the hand. This is a ‘trick’ movement used by patients with interosseous muscle paralysis. The function of the intertendinous bands is not clear, but they may affect the independent extension of digits. Alternatively a junctura can maintain some active extension even when a tendon has been divided in the metacarpal section of the hand, although the extent to which this occurs will depend on the junctura’s orientation. For example, some extension of the ring finger may be possible in the absence of its own tendon via the junctura of the middle finger, but the converse does not occur

Testing

The tendons of extensor digitorum can be readily felt, and usually seen, when the fingers are extended against resistance and the forearm is pronated.

Extensor digiti minimi

Attachments

Extensor digiti minimi is a slender muscle medial to, and usually connected with, extensor digitorum (Fig. 49.14). It arises from the common extensor tendon by a thin tendinous slip and adjacent intermuscular septa. It frequently has an additional origin from the antebrachial fascia. Its long tendon slides in a separate compartment of the extensor retinaculum just behind the inferior radio-ulnar joint. Distal to the retinaculum, the tendon typically splits into two, and the lateral slip is joined by a tendon from extensor digitorum. All three tendons are attached to the dorsal digital expansion of the fifth digit, and there may be a slip to the fourth digit.

Extensor digiti minimi is rarely absent, but sometimes it is fused with extensor digitorum.

Relations

The tendon of extensor digiti minimi lies ulnar (medial) to the common extensor tendon to the little finger.

Vascular supply

Extensor digiti minimi is supplied by branches from the radial recurrent and posterior interosseous arteries, and by terminal branches from the anterior interosseous artery after it has pierced the interosseous membrane.

Innervation

Extensor digiti minimi is innervated by the posterior interosseous nerve, C7 and 8.

Action

Extensor digiti minimi can extend any of the joints of the little finger, or contribute to wrist extension. It permits extension of the little finger independently of the other digits even in extremes of ulnar or radial wrist deviation.

Clinical anatomy: testing

Extensor digiti minimi is tested by extending the little finger while holding the remaining fingers flexed at the metacarpophalangeal joints. This eliminates any simultaneous contraction of extensor digitorum.

Extensor carpi ulnaris

Attachments

Extensor carpi ulnaris arises from the lateral epicondyle via the common extensor tendon, the posterior border of the ulna (by an aponeurosis shared with flexor carpi ulnaris and flexor digitorum profundus), and overlying fascia (Fig. 49.14). It ends in a tendon that slides in a groove between the head and the styloid process of the ulna, in a separate compartment of the extensor retinaculum, and is ultimately attached to a tubercle on the medial side of the fifth metacarpal base.

Vascular supply

Proximally extensor carpi ulnaris receives branches from the radial recurrent artery. Distally, it is supplied by several branches from the posterior interosseous artery.

Innervation

Extensor carpi ulnaris is innervated by the posterior interosseous nerve, C7 and 8.

Action

Together with extensors carpi radialis longus and brevis, extensor carpi ulnaris acts synergistically with the digital flexors to extend and to fix the wrist when objects are being gripped or when the fist is clenched.

Observation shows that it is impossible to grip strongly unless the wrist is extended. Acting with flexor carpi ulnaris, extensor carpi ulnaris adducts the hand.

Clinical anatomy: testing

If the wrist is extended and adducted against resistance, and the forearm is pronated and the fingers are extended, extensor carpi ulnaris can be felt lateral to the groove that overlies the posterior subcutaneous border of the ulna.

Anconeus

Attachments

Anconeus is a small, triangular muscle posterior to the elbow joint and is partially blended with triceps (Fig. 49.14). Anconeus arises by a separate tendon from the posterior surface of the lateral epicondyle of the humerus. Its fibres diverge medially towards the ulna, covering the posterior aspect of the annular ligament, and are attached to the lateral aspect of the olecranon and proximal quarter of the posterior surface of the shaft of the ulna.

The extent to which anconeus fuses with triceps or extensor carpi ulnaris is variable.

Vascular supply

Anconeus is supplied by branches from the posterior interosseous recurrent artery. A small number of musculocutaneous perforators reach the skin overlying the muscle.

Innervation

Anconeus is innervated by the radial nerve, C6, 7 and 8.

Action

Anconeus assists triceps in extending the elbow joint. Its major function is not clear, but it may be the control of ulnar abduction in pronation, which is necessary if the forearm is to turn over the hand without translating it medially. In this way a tool can be revolved ‘on the spot’ or it can be swept through an arc.

Deep extensor compartment

The five deep forearm extensor muscles are abductor pollicis longus, extensor pollicis longus and extensor pollicis brevis (which all act on the thumb), extensor indicis and supinator (Fig. 49.15). Apart from supinator, all are attached proximally only to the forearm bones.

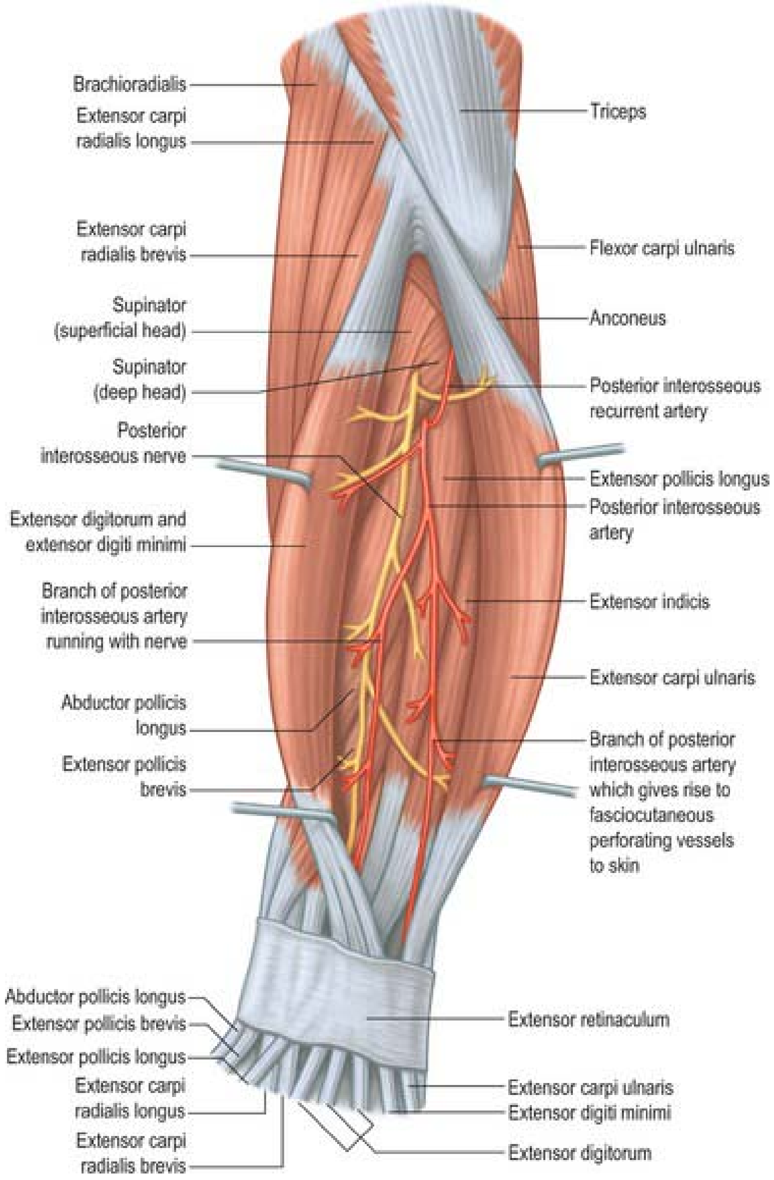
Brachioradialis
Extensor carpi radialis longus
Extensor carpi radialis brevis
Supinator (superficial head)
Supinator (deep head)
Posterior interosseous nerve
Extensor digitorum and extensor digiti minimi
Branch of posterior interosseous artery running with nerve
Abductor pollicis longus
Extensor pollicis brevis
Abductor pollicis longus
Extensor pollicis brevis
Extensor pollicis longus
Extensor carpi radialis longus
Extensor carpi radialis brevis
Triceps
Flexor carpi ulnaris
Anconeus
Posterior interosseous recurrent artery
Extensor pollicis longus
Posterior interosseous artery
Extensor indicis
Extensor carpi ulnaris
Branch of posterior interosseous artery which gives rise to fasciocutaneous perforating vessels to skin
Extensor retinaculum
Extensor carpi ulnaris
Extensor digiti minimi
Extensor digitorum

Fig. 49.15 The deep extensor muscles of the left forearm. Note the posterior interosseous artery divides into two main branches shortly after emerging from beneath supinator. One branch follows the posterior interosseous nerve, while the other travels more laterally and gives off fasciocutaneous perforator vessels which supply the posterior interosseous artery flap.

Abductor pollicis longus

Attachments

Abductor pollicis longus arises from the posterior surface of the shaft of the ulna distal to anconeus, the adjoining interosseous membrane, and the middle third of the posterior surface of the radius distal to the attachment of supinator (Fig. 49.15). It descends laterally, becoming superficial in the distal forearm, where it is visible as an oblique elevation (Fig. 49.14). The muscle fibres end in a tendon just proximal to the wrist. The tendon runs in a groove on the lateral side of the distal end of the radius accompanied by the tendon of extensor pollicis brevis. It usually splits into two slips, one of which is attached to the radial side of the first metacarpal base, and the other is attached to the trapezium. Slips from the tendon may continue into opponens pollicis or abductor pollicis brevis. Occasionally the muscle itself may be wholly or partially divided.

Vascular supply

Abductor pollicis longus is supplied proximally by a lateral branch from the posterior interosseous artery. Distally it is supplied on the medial side by a perforating branch from the anterior interosseous artery.

Innervation

Abductor pollicis longus is innervated by the posterior interosseous nerve, C7 and 8.

Action

Abductor pollicis longus abducts the wrist joint. Acting with abductor pollicis brevis it aids abduction of the thumb radially (i.e. in the plane of the palm). Acting with the pollicial extensors it extends the thumb at its carpometacarpal joint. The tendon may also stabilize the trapezium upon which the first metacarpal can move.

Clinical anatomy: testing

The tendon of abductor pollicis longus can be seen and felt at the radial aspect of the anatomical snuff box when the thumb and wrist are abducted against resistance at the carpometacarpal joint.

Extensor pollicis longus

Attachments

Extensor pollicis longus is larger than extensor pollicis brevis, whose proximal attachment it partly covers (Fig. 49.14, Fig. 49.15). It arises from the lateral part of the middle third of the posterior surface of the shaft of the ulna below abductor pollicis longus, and the adjacent interosseous membrane. The tendon passes through a separate compartment of the extensor retinaculum in a narrow, oblique groove on the back of the distal end of the radius. It turns around a bony fulcrum, Lister’s tubercle, which changes its line of pull from that of the forearm to that of the thumb, and is attached to the base of the distal phalanx of the thumb. The sides of the tendon are joined on the dorsum of the proximal phalanx by expansions from the tendon of abductor pollicis brevis laterally, and from the first palmar interosseous and adductor pollicis medially.

Relations

After passing around Lister’s tubercle, the tendon of extensor pollicis longus crosses the tendons of extensor carpi radialis brevis and longus obliquely (Fig. 49.14). When the thumb is fully extended the tendon is separated from extensor pollicis brevis by a triangular depression or fossa, the so-called ‘anatomical snuff-box’. Bony structures can be felt in the floor of this fossa by deep palpation. In proximal to distal order they are the radial styloid, the smooth convex articular surface of the scaphoid, the trapezium, and the base of the first metacarpal. The latter are more easily felt during metacarpal movement, while the scaphoid is more easily felt during adduction and abduction of the hand.

Vascular supply

Extensor pollicis longus is supplied on its superficial surface by branches from the posterior interosseous artery, and on its deep surface by perforating branches from the anterior interosseous artery.

Innervation

Extensor pollicis longus is innervated by the posterior interosseous nerve, C7 and 8.

Action

Extensor pollicis longus extends the distal phalanx of the thumb. Acting in association with extensor pollicis brevis and abductor pollicis longus, it extends the proximal phalanx and the metacarpal. In continued action, as a consequence of the obliquity of its tendon, extensor pollicis longus adducts the extended thumb and rotates it laterally.

Clinical anatomy: testing

The tendon of extensor pollicis longus can be palpated at the ulnar border of the anatomical snuff-box when the thumb is extended at the interphalangeal joint against resistance. When the thumb is opposed and adducted, abductor pollicis brevis can extend the interphalangeal joint of the thumb, mimicking the action of extensor pollicis longus.

Extensor pollicis brevis

Attachments

Extensor pollicis brevis arises from the posterior surface of the radius distal to abductor pollicis longus, and from the adjacent interosseous membrane (Fig. 49.14, Fig. 49.15). The tendon is inserted into the base of the proximal phalanx of the thumb, and commonly has an additional attachment to the base of the distal phalanx, usually through a fasciculus which joins the tendon of extensor pollicis longus. Extensor pollicis brevis may be absent or fused completely with abductor pollicis longus.

Relations

Extensor pollicis brevis is ulnar (medial) to, and closely connected with, abductor pollicis longus (Fig. 49.14, Fig. 49.15). In the distal forearm, the two muscles emerge between extensor carpi radialis brevis and extensor digitorum, and pass obliquely across the tendons of the radial extensors of the wrist. They cover the distal part of brachioradialis, and pass through the most lateral compartment of the extensor retinaculum in a single synovial sheath, sharing a groove in the distal radius. Ultimately they cross, superficial to the radial styloid process and radial artery, to reach the dorsolateral base of the proximal phalanx of the thumb.

Vascular supply

Extensor pollicis brevis is supplied from branches from the posterior interosseous artery together with perforating branches from the anterior interosseous artery.

Innervation

Extensor pollicis brevis is innervated by the posterior interosseous nerve, C7 and 8.

Action

Extensor pollicis brevis extends the proximal phalanx and metacarpal of the thumb.

Clinical anatomy: testing

The tendon of extensor pollicis brevis can be felt at the radial border of the anatomical snuff-box, lying medial to the tendon of abductor pollicis longus, when the metacarpophalangeal joint of the thumb is extended against resistance.

Extensor indicis

Attachments

Extensor indicis is a narrow, elongated muscle which lies medial and parallel to extensor pollicis longus (Fig. 49.15). It arises from the posterior surface of the ulna distal to extensor pollicis longus, and the adjacent interosseous membrane. Its tendon passes under the extensor retinaculum in a common compartment with the tendons of extensor digitorum. Opposite the head of the second metacarpal it joins the ulnar side of the tendon of extensor digitorum which serves the index finger.

Extensor indicis occasionally sends accessory slips to the extensor tendons of other digits. Rarely its tendon may be interrupted on the dorsum of the hand by an additional muscle belly (extensor indicis brevis manus).

Relations

The tendon of extensor indicis lies on the ulnar aspect of the extensor digitorum tendon to the index finger on the dorsum of the hand.

Vascular supply

Extensor indicis is supplied on its superficial surface by branches from the posterior interosseous artery, and on its deep surface by perforating branches from the anterior interosseous artery.

Innervation

Extensor indicis is innervated by the posterior interosseous nerve, C7 and 8.

Action

Extensor indicis helps to extend the index finger and the wrist. It permits extension of the index finger independently of the other digits, even in extremes of ulnar or radial wrist deviation.

Clinical anatomy: testing

Extensor indicis is tested by extending the index finger while holding the remaining fingers flexed at the metacarpophalangeal joints. This eliminates the effects of any simultaneous contraction of extensor digitorum.

Supinator

Attachments

Supinator surrounds the proximal third of the radius and has superficial and deep layers (Fig. 49.15). The two parts arise together, the superficial by tendinous, and the deep by muscular fibres, from the lateral epicondyle of the humerus; the radial collateral ligament of the elbow joint and the anular ligament of the superior radio-ulnar joint; the supinator crest of the ulna and the posterior part of the triangular depression in front of it; and an aponeurosis which covers the muscle. Supinator is attached distally to the lateral surface of the proximal third of the radius, down to the insertion of pronator teres. The radial attachment extends on to the anterior and posterior surfaces between the anterior oblique line and the fainter posterior oblique ‘ridge’ (Fig. 49.4).

Supinator is subject to frequent variation, and small parts of the muscle have acquired individual names, e.g. lateral and medial tensors of the annular ligament.

Relations

The posterior interosseous nerve enters the forearm by passing between the superficial and deep heads of supinator.

Vascular supply

The superficial part of supinator is supplied by branches from the radial recurrent artery. The deep part of supinator is supplied by branches from the posterior interosseous artery and the posterior interosseous recurrent artery.

Innervation

Supinator is innervated by the posterior interosseous nerve, C6 and 7 as it traverses the muscle.

Action

Supinator rotates the radius so as to bring the palm to face anteriorly. It acts alone in slow, unopposed supination, and together with biceps brachii in fast or forceful supination. An object which may potentially be heavy is often picked up with the forearm initially pronated. The more powerful supinators lift the object against gravity, and rotation is often combined with increasing elbow flexion to bring the object towards the eyes.

Clinical anatomy: testing

Supinator is too deep to be palpated and independent testing is difficult. Biceps is inactive on supination with the elbow fully extended, therefore this must be produced by supination alone and can be used to test its function.

VASCULAR SUPPLY AND LYMPHATIC DRAINAGE

ARTERIES

Radial artery

The radial artery is smaller than the ulnar artery, yet appears a more direct continuation of the brachial artery (Fig. 49.12, Fig. 49.13, see Fig. 49.19). It normally starts 1 cm distal to the flexion crease of the elbow. It descends along the lateral side of the forearm, accompanied by paired venae comitantes, from the medial side of the neck of the radius to the wrist, where it is palpable between flexor carpi radialis medially and the salient anterior border of the radius. The artery is medial to the radial shaft proximally, and anterior to it distally. Proximally it is overlapped anteriorly by the belly of brachioradialis, but elsewhere in its course it is covered only by the skin, and superficial and deep fasciae. Its posterior relations in the forearm are successively the tendon of biceps, supinator, the distal attachment of pronator teres, the radial head of flexor digitorum superficialis, flexor pollicis longus, pronator quadratus and the lower end of the radius (where its pulsation is most accessible). Brachioradialis is lateral to the artery throughout its length. Pronator teres is medial to the proximal part of the artery and the tendon of flexor carpi radialis is medial to the distal portion. The superficial radial nerve lies lateral to the middle third of the radial artery: multiple branches from the artery supply the nerve throughout its length.

The radial artery may occasionally arise from the continuation of a superficial brachial artery, or as a high proximal division of an otherwise normal brachial artery. It can give rise to the common interosseous artery.

The course and distribution of the radial artery in the wrist and hand are described on page 890.

Branches in the forearm

Radial recurrent artery

The radial recurrent artery is discussed on page 835.

Cutaneous branches

Cutaneous branches emerge between brachioradialis and pronator teres in the proximal third of the forearm. The largest perforator, which is also the largest in the forearm, has been named the inferior cubital artery. It reaches the deep fascia by passing superficially between brachioradialis and pronator teres in the apex of the antecubital fossa. It lies lateral to the tendon of biceps, emerging between the median cubital vein and its communicating branch to the venae comitantes of the radial artery. In the distal two-thirds of the forearm, the cutaneous perforators emerge through the fascia between brachioradialis and flexor carpi radialis and between flexor carpi radialis and flexor digitorum superficialis and fan out at the level of the deep fascia. These vessels anastomose with their counterparts from the ulnar artery and the posterior interosseous artery.

The fasciocutaneous branches provide the anatomical basis for raising a skin flap containing the whole width of forearm skin, either pedicled or as a free flap, based on the radial artery and its venae comitantes. Known as the radial forearm fasciocutaneous flap, it is used for reconstructing areas of missing tissue elsewhere in the body. It is possible to incorporate the lateral aspect of the radius with the flap because a few fascioperiosteal branches supply this part of the bone.

Muscular branches

Muscular branches are distributed to the muscles on the radial side of the forearm.

Ulnar artery

The ulnar artery is the larger terminal branch of the brachial artery (Fig. 49.12, Fig. 49.13, see Fig. 49.19). It starts 1 cm distal to the flexion crease of the elbow and reaches the medial side of the forearm midway between elbow and wrist. In the forearm the artery initially lies on brachialis and deep to pronator teres, flexor carpi radialis, palmaris longus and flexor digitorum superficialis. It subsequently lies on flexor digitorum profundus, between flexor carpi ulnaris and flexor digitorum superficialis, and is covered by the skin, superficial and deep fasciae. The median nerve is a medial relation for approximately 2.5 cm distal to the elbow, and then crosses the artery, from which it is separated by the ulnar head of pronator teres. The ulnar nerve lies medial to the distal two-thirds of the artery, which supplies the nerve throughout its length. The palmar cutaneous branch of the ulnar nerve descends along the ulnar artery to reach the hand. The ulnar artery crosses the flexor retinaculum lateral to the ulnar nerve and pisiform bone to enter the hand.

The ulnar artery is accompanied throughout its length by venae comitantes.

The ulnar artery may arise proximal to the elbow, usually from the brachial artery, when it usually lies superficial to the forearm flexors under the deep fascia: only rarely is it subcutaneous. When this occurs, the brachial artery supplies the common interosseous and the ulnar recurrent arteries.

The course and distribution of the ulnar artery in the wrist and hand are described on page 893.

Branches in the forearm

Anterior and posterior ulnar recurrent arteries

The anterior and posterior ulnar recurrent arteries are described on page 835.

Common interosseous artery

The common interosseous artery is a short branch of the ulnar artery (Fig. 49.13, see Fig. 49.19). It arises just distal to the radial tuberosity and passes back to the proximal border of the interosseous membrane, where it divides into the anterior and posterior interosseous arteries. Occasionally, the common interosseous artery is a branch of the radial artery.

Anterior interosseous artery

The anterior interosseous artery descends on the anterior aspect of the interosseous membrane with the anterior interosseous branch of the median nerve (see Fig. 49.19). It is overlapped by contiguous sides of flexor digitorum profundus and flexor pollicis longus. Shortly after its origin, it usually gives off a slender median artery. This accompanies and supplies the median nerve as far as the palm, where it may join the superficial palmar arch or end as one or two palmar digital arteries. (The median artery can also arise from the ulnar or the common interosseous artery.)

Muscular and nutrient branches from the anterior interosseous artery pierce the interosseous membrane to supply deep extensor muscles and the radius and ulna respectively. A branch descends deep to pronator quadratus before piercing the interosseous membrane to join the anterior ‘carpal’ arch.

The anterior interosseous artery proper leaves the anterior compartment by piercing the interosseous membrane proximal to pronator quadratus. It anastomoses with the posterior interosseous artery in the posterior compartment of the forearm, and travels through a tunnel under the extensor retinaculum with the tendons of the digital extensors before joining the dorsal carpal arch. Three small cutaneous perforating branches supply the skin over the lower lateral border of the forearm.

Posterior interosseous artery

The posterior interosseous artery is usually smaller than the anterior (Fig. 49.15, Fig. 49.17, Fig. 49.18). It passes dorsally between the oblique cord and proximal border of the interosseous membrane and then between supinator and abductor pollicis longus. It descends deep in the groove between extensor carpi ulnaris and the extensor digiti minimi part of extensor digitorum. While in the groove it gives rise to multiple muscular branches which supply these muscles and fasciocutaneous perforators which travel in the intermuscular septum between extensor carpi ulnaris and extensor digiti minimi. These fasciocutaneous vessels provide the anatomical basis for raising a dorsal forearm skin flap, which is usually pedicled, based on the posterior interosseous artery and its venae comitantes. Known as the posterior interosseous artery flap, it is used for reconstructing areas of missing tissue in the forearm and proximal part of the hand.

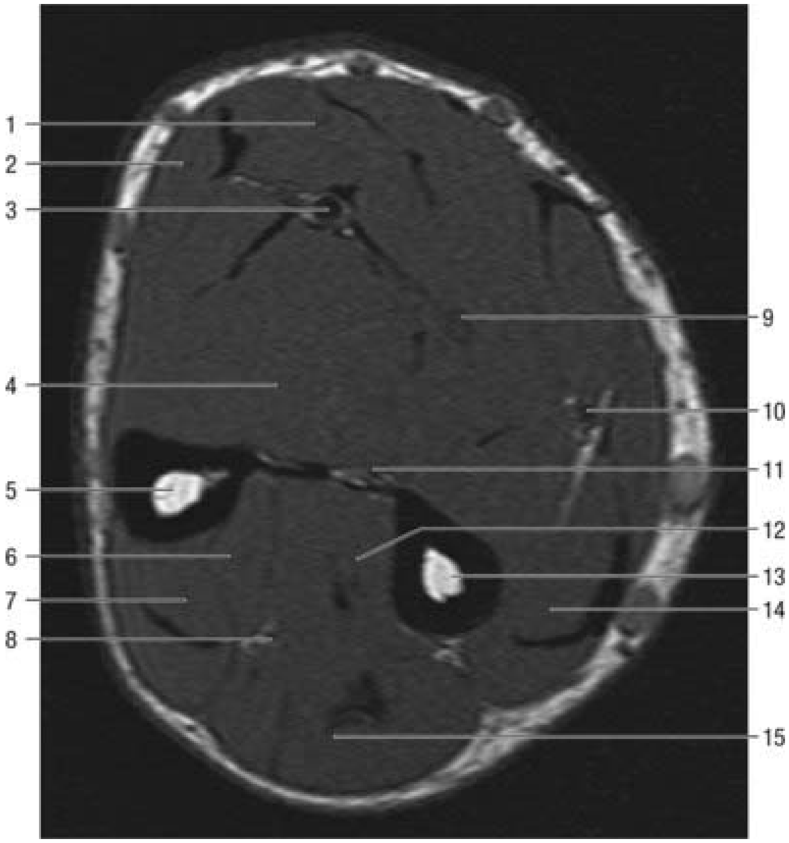

Fig. 49.18 Axial MRI through middle of left forearm. **1**. Flexor digitorum superficialis. **2**. Flexor carpi ulnaris. **3**. Ulnar artery. **4**. Flexor digitorum profundus. **5**. Ulna. **6**. Extensor pollicis longus. **7**. Extensor carpi ulnaris. **8**. Posterior interosseous neurovascular bundle. **9**. Median nerve. **10**. Radial artery. **11**. Anterior interosseous neurovascular bundle. **12**. Abductor pollicis longus. **13**. Radius. **14**. Extensor carpi radialis brevis. **15**. Extensor digitorum.

The posterior interosseous artery accompanies the deep branch of the radial nerve (posterior interosseous nerve) on abductor pollicis longus. Distally it anastomoses with the terminal part of the anterior interosseous artery and the dorsal carpal arch.

Sometimes the posterior interosseous artery disappears halfway down the forearm, in which case the anterior interosseous artery pierces the interosseous membrane more proximally to anastomose with it. Rarely no anastomosis occurs between the anterior and the posterior interosseous arteries.

Posterior interosseous recurrent artery

The posterior interosseous recurrent artery leaves the posterior interosseous artery near its origin and ascends between the lateral epicondyle and olecranon, either on or through supinator, and deep to anconeus. It anastomoses with the middle collateral branch of the profunda brachii artery, posterior ulnar recurrent and ulnar collateral arteries. Occasionally the artery is absent.

Cutaneous branches

The cutaneous perforators of the ulnar artery reach the skin by passing along the fascial septum between flexor carpi ulnaris and flexor digitorum superficialis throughout the length of the forearm. A constant dorso-ulnar perforator vessel is given off distally 2–5 cm proximal to the pisiform and it accompanies the dorsal cutaneous branch of the ulnar nerve. The vessel emerges between flexor carpi ulnaris and extensor carpi ulnaris. A few small musculocutaneous perforators reach the skin via flexor carpi ulnaris and anastomose with their counterparts derived from the radial and the posterior interosseous arteries.

Muscular branches

Muscular branches arise directly from the main vessel and are distributed to the muscles on the ulnar side of the forearm.

VEINS

Deep veins

The venae comitantes running with the radial and ulnar arteries drain the deep and superficial palmar venous arches respectively. They unite near the elbow as paired brachial veins. The radial veins are smaller, and receive the deep dorsal veins of the hand. The ulnar veins drain the deep palmar venous arch, and connect with superficial veins near the wrist. Near the elbow they receive the venae comitantes of the anterior and posterior interosseous arteries, and a large branch connects them to the median cubital vein.

Superficial veins

Cephalic vein

The cephalic vein (see Fig. 45.5) usually forms over the ‘anatomical snuff-box’ from the radial end of the dorsal venous plexus. It curves proximally around the radial side of the forearm to gain its ventral aspect, and receives veins from both aspects of the forearm. Distal to the elbow a branch, the median cubital vein, diverges proximomedially to reach the basilic vein. The median cubital vein is joined by a branch from the deep veins.

The further course of the cephalic vein is described in the arm on page 828.

Accessory cephalic vein

The accessory cephalic vein may arise either in a dorsal forearm plexus or from the ulnar side of the dorsal venous network in the hand. It joins the cephalic vein distal to the elbow. A large oblique vein often connects the basilic and cephalic veins dorsally in the forearm.

Basilic vein

The basilic vein starts medially in the dorsal venous network of the hand (Fig. 45.5). It ascends posteromedially in the forearm, inclining forwards to the anterior surface distal to the elbow, where it is joined by the median cubital vein. It then ascends superficial to and between biceps and pronator teres, and is crossed by filaments of the medial cutaneous nerve of the forearm which pass both superficial and deep to the vein.

The course of the basilic vein in the arm is described on page 828.

Median vein

The median vein (Fig. 45.5) of the forearm drains the superficial palmar venous plexus and ascends through the anterior part of the forearm to join either the basilic or median cubital vein. It may divide distal to the elbow to join both veins.

INNERVATION

Median nerve

The median nerve usually enters the forearm between the heads of pronator teres (Fig. 49.12, Fig. 49.13, Fig. 49.16, Fig. 49.17, Fig. 49.18). (Occasionally the nerve passes posterior to both heads of pronator teres, or it may pass through the humeral head). It crosses to the lateral side of the ulnar artery, from which it is separated by the deep head of pronator teres. It passes behind a tendinous bridge between the humero-ulnar and radial heads of the flexor digitorum superficialis, and descends through the forearm posterior and adherent to flexor digitorum superficialis and anterior to flexor digitorum profundus. About 5 cm proximal to the flexor retinaculum it emerges from behind the lateral edge of flexor digitorum superficialis, and becomes superficial just proximal to the wrist. Here it lies between the tendons of flexor digitorum superficialis and flexor carpi radialis, projecting laterally from beneath the tendon of palmaris longus (Fig. 49.13, Fig. 49.19). It then passes deep to the flexor retinaculum into the palm. In the forearm the median nerve is accompanied by the median branch of the anterior interosseous artery.

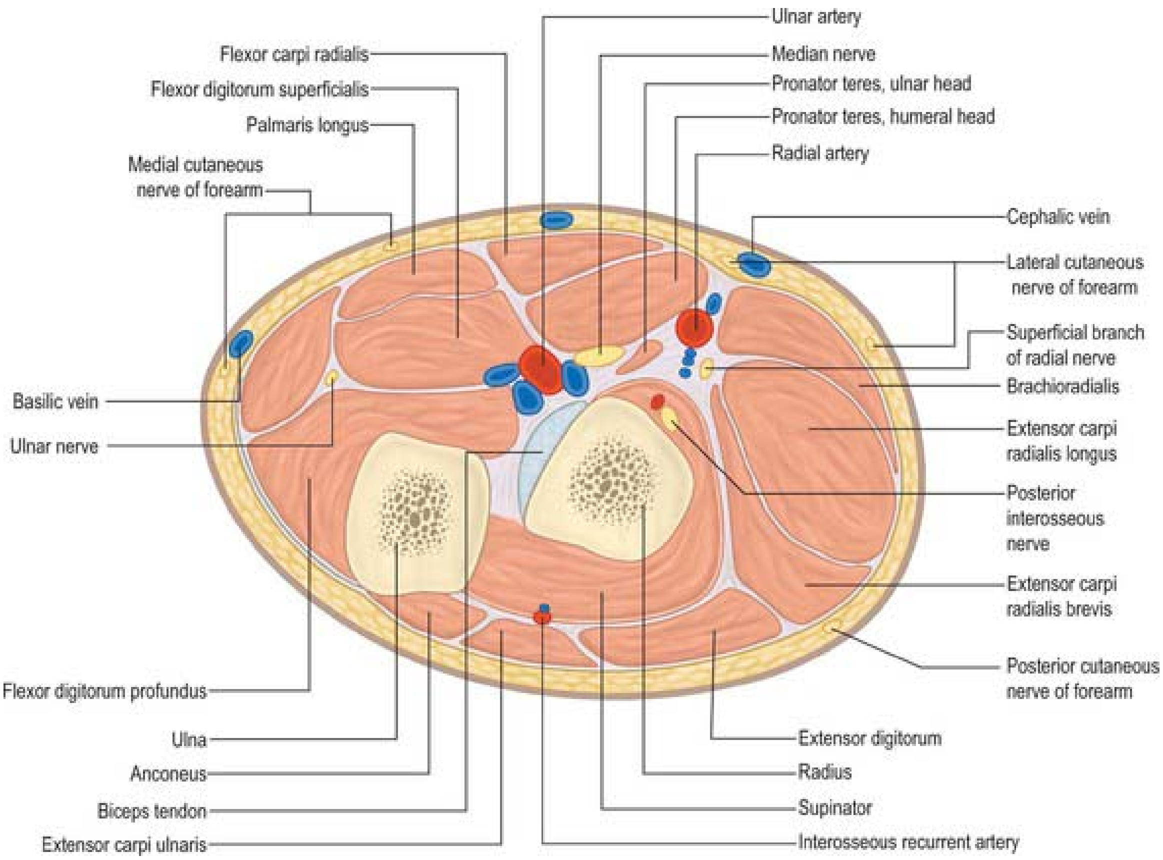
Ulnar artery
Median nerve
Pronator teres, ulnar head
Pronator teres, humeral head
Radial artery
Flexor carpi radialis
Flexor digitorum superficialis
Palmaris longus
Medial cutaneous nerve of forearm
Cephalic vein
Lateral cutaneous nerve of forearm
Superficial branch of radial nerve
Brachioradialis
Basilic vein
Ulnar nerve
Extensor carpi radialis longus
Posterior interosseous nerve
Extensor carpi radialis brevis
Posterior cutaneous nerve of forearm
Flexor digitorum profundus
Ulna
Anconeus
Biceps tendon
Extensor carpi ulnaris
Extensor digitorum
Radius
Supinator
Interosseous recurrent artery

Fig. 49.16 Transverse section through the left forearm at the level of the radial tuberosity: proximal aspect.

The course and distribution of the median nerve in the wrist and hand is described on page 895.

Martin–Gruber connection

Multiple communicating branches between the median nerve (and sometimes the anterior interosseous nerve) arise proximally and pass medially between flexors digitorum superficialis and profundus, deep to the ulnar artery, and join the ulnar nerve. This motor fibre communication (commonly referred to as the Martin–Gruber connection) is estimated to be present in 17% of individuals. It results in a median nerve innervation of a variable number of intrinsic muscles of the hand (Leibovic & Hastings 1992), and presumably explains why isolated ulnar and median nerve lesions can sometimes be unpredictable in terms of the pattern of intrinsic muscle paralysis.

Branches in the forearm

Anterior interosseous nerve

The anterior interosseous nerve branches posteriorly from the median nerve between the two heads of pronator teres, just distal to the origin of its branches to the superficial forearm flexors and proximal to the point at which the median nerve passes under the tendinous arch of flexor digitorum superficialis. With the anterior interosseous artery it descends anterior to the interosseous membrane, between and deep to flexor pollicis longus and flexor digitorum profundus. It supplies flexor pollicis longus and the lateral part of flexor digitorum profundus (which sends tendons to the index and middle finger). Terminally, the anterior interosseous nerve lies posterior to pronator quadratus, which it supplies via its deep surface. It also supplies articular branches to the distal radio-ulnar, radiocarpal and carpal joints.

Anterior interosseous nerve syndrome

The anterior interosseous nerve may be affected with the median nerve or by itself in any of the causes of pronator syndrome (p. 836). Median nerve compression is typically caused by pressure from fascial bands on the deep head of the pronator teres or the tendinous radial attachment of flexor digitorum superficialis. Anterior interosseous nerve palsy may be due to external pressure, a form of ‘Saturday night palsy’, and sometimes by tight grip in association with pronation without obvious cause. It may be a manifestation of neuralgic amyotrophy and tends to resolve spontaneously over several months. A variety of aberrant muscles, e.g. an accessory head of flexor pollicis longus, palmaris profundus, or flexor carpi radialis brevis, have all been described as causing entrapment neuropathy of the anterior interosseous nerve.

An anterior interosseous nerve palsy causes weakness of pinch grip due to involvement of flexor pollicis longus and flexor digitorum profundus to the index finger. Innervation of flexor digitorum profundus to the middle finger is rather variable, and therefore this muscle may or may not be weak. The branches to these three muscles may arise separately from the median nerve, so that isolated weakness of the terminal phalanx to the thumb or index finger may occur. Pronator quadratus is also involved but is not clinically significant. Anterior interosseous nerve palsy can be distinguished from pronator syndrome because there are no sensory symptoms. The treatment is exploration of the nerve and surgical decompression.

Muscular branches

Muscular branches are given off near the elbow to all the superficial flexor muscles except flexor carpi ulnaris, i.e. to pronator teres, flexor carpi radialis, palmaris longus and flexor digitorum superficialis. The branch to the part of flexor digitorum superficialis which serves the index finger is given off near mid-forearm and may be derived from the anterior interosseous nerve.

Other branches

Articular branches, arising at or just distal to the elbow joint, supply the joint and the proximal radio-ulnar joint. The palmar cutaneous branch is described on page 895.

Ulnar nerve

The ulnar nerve descends on the medial side of the forearm, lying on flexor digitorum profundus (Fig. 49.13, Figs 49.16-49.19). Proximally it is covered by flexor carpi ulnaris: its distal half lies lateral to the muscle and is covered only by skin and fasciae. In the upper third of the forearm, the nerve is distant from the ulnar artery, but more distally it comes to lie close to the medial side of the artery. About 5 cm proximal to the wrist it gives off a dorsal branch which continues distally into the hand, anterior to the flexor retinaculum on the lateral side of the pisiform and posteromedial to the ulnar artery. It passes deep to the superficial part of the retinaculum (in Guyon’s canal) with the artery and divides into superficial and deep terminal branches.

The course and distribution of the ulnar nerve in the hand is described on page 897.

Muscular branches

There are usually two muscular branches. They begin near the elbow and supply flexor carpi ulnaris and the medial half of flexor digitorum profundus.

Palmar cutaneous branch

The palmar cutaneous branch arises about mid-forearm. It descends on the ulnar artery, which it supplies, and then perforates the deep fascia to end in the palmar skin, after communicating with the palmar branch of the median nerve. It sometimes supplies palmaris brevis.

Dorsal branch

The dorsal branch of the ulnar nerve is described on page 897.

Radial nerve

There is some variation in the level at which branches of the radial nerve arise from the main trunk in different subjects (Fig. 49.12, Fig. 49.13, Fig. 49.17, Fig. 49.18). Branches to extensor carpi radialis brevis and supinator may arise from the main trunk of the radial nerve or from the proximal part of the posterior interosseous nerve, but almost invariably above the arcade of Frohse.

Radial tunnel syndrome

Radial tunnel syndrome is an entrapment neuropathy of the radial nerve near the elbow, where four structures can potentially cause compression of the nerve. These are fibrous bands (which can tether the radial nerve to the radiohumeral joint); the sharp tendinous medial border of extensor carpi radialis brevis; a leash of vessels from the radial recurrent artery as it passes to supply brachioradialis and extensor carpi radialis longus; the arcade of Frohse, which is the free aponeurotic proximal edge of the superficial part of supinator (see Fig. 48.6).

Usually the only presenting symptom is pain over the extensor mass just distal to the elbow. There is no sensory disturbance or motor loss, but there is frequently tenderness along the course of the radial nerve over the radial head. The pain is exacerbated when the elbow is extended and the wrist is passively flexed and pronated, or extended and supinated against resistance. Extension of the middle finger against resistance when the elbow is fully extended also may lead to increased pain. These manoeuvres tighten the anatomical structures which cause compression.

Superficial terminal branch

The superficial terminal branch descends from the lateral epicondyle anterolaterally in the proximal two-thirds of the forearm, initially lying on supinator, lateral to the radial artery and behind brachioradialis. In the middle third of the forearm it lies behind brachioradialis, close to the lateral side of the artery, and is successively anterior to pronator teres, the radial head of flexor digitorum superficialis and flexor pollicis longus. It usually leaves the artery 7 cm proximal to the wrist and passes deep to the tendon of brachioradialis. It curves round the lateral side of the radius as it descends, pierces the deep fascia and divides into five, sometimes four, dorsal digital nerves. On the dorsum of the hand it usually communicates with the posterior and lateral cutaneous nerves of the forearm.

As the nerve crosses the lateral aspect of the radius it is superficial and relatively unprotected: it is easily compressed here by tight bracelets, watch straps and handcuffs.

Radial sensory nerve entrapment (Wartenberg’s disease)

Entrapment of the superficial radial nerve can occur as the nerve emerges from beneath the edge of the brachioradialis tendon about 6 cm proximal to the radial styloid; it is probably pinched by the scissoring effect of brachioradialis and extensor carpi radialis brevis tendons. The condition is frequently associated with previous trauma in this region. The symptoms are pain and paraesthesia over the radial aspect of the dorsum of the wrist and hand.

Posterior interosseous nerve

The posterior interosseous nerve is the deep terminal branch of the radial nerve (Fig. 49.15, Fig. 49.16). It reaches the back of the forearm by passing round the lateral aspect of the radius between the two heads of supinator. It supplies extensor carpi radialis brevis and supinator before entering supinator: as it passes through the muscle it supplies it with additional branches. The branch to extensor carpi radialis brevis may arise from the beginning of the superficial branch of the radial nerve. As it emerges from supinator posteriorly, the posterior interosseous nerve gives off three short branches to extensor digitorum, extensor digiti minimi and extensor carpi ulnaris, and two longer branches, a medial to extensor pollicis longus and extensor indicis, and a lateral which supplies abductor pollicis longus and extensor pollicis brevis. The nerve at first lies between the superficial and deep extensor muscles, but at the distal border of extensor pollicis brevis it passes deep to extensor pollicis longus and, diminished to a fine thread, descends on the interosseous membrane to the dorsum of the carpus. Here it presents a flattened and somewhat expanded termination or 'pseudoganglion', from which filaments supply the carpal ligaments and articulations. Articular branches from the posterior interosseous nerve supply carpal, distal radio-ulnar and some intercarpal and intermetacarpal joints. Digital branches supply the metacarpophalangeal and proximal interphalangeal joints.

The distal portion of the nerve lies in a separate fascial sheath in the radial, deep aspect of the fourth dorsal compartment of the extensor retinaculum of the wrist, where it is located deep to extensor digitorum and extensor indicis. This portion of the nerve can be used as a donor nerve for grafting segmental digital nerve defects, as there is no clinically discernible donor site deficit.

Posterior interosseous nerve palsy

There are many causes of posterior interosseous nerve palsy. These include trauma and inflammatory swellings, as well as entrapment at the same anatomical sites that can cause radial tunnel syndrome. Pain is similar in nature to that of radial tunnel syndrome and is later accompanied by weakness and paralysis. When fully developed, there is inability to extend the fingers at the metacarpophalangeal joints, weakness of thumb extension and abduction. There is weakness and radial deviation of wrist extension because extensor carpi ulnaris is usually affected, while the radial wrist extensors and brachioradialis are normal (because their nerve supply is given off proximal to the origin of the posterior interosseous nerve). There are no sensory disturbances, because the superficial radial nerve arises above this level.

Medial cutaneous nerve of the forearm

The medial cutaneous nerve of the forearm has already divided into anterior and posterior branches before it enters the forearm (see Fig. 45.15). The larger anterior branch usually passes in front of, occasionally behind, the median cubital vein, and descends anteromedially in the forearm to supply the skin as far as the wrist. It curves round to the back of the forearm, descending on its medial border to the wrist, supplying the skin. It connects with the medial cutaneous nerve of the arm, the posterior cutaneous nerve of the forearm, and the dorsal branch of the ulnar nerve.

Lateral cutaneous nerve of the forearm

The lateral cutaneous nerve of the forearm is a direct continuation of the musculocutaneous nerve as it lies lateral to the biceps tendon in the antecubital fossa (see Figs 45.10 and 45.15). It passes deep to the cephalic vein, descending along the radial border of the forearm to the wrist. It supplies the skin of the anterolateral surface of the forearm and connects with the posterior cutaneous nerve of the forearm and the terminal branch of the radial nerve by branches which pass around its radial border. Its trunk gives rise to a slender recurrent branch which extends along the cephalic vein as far as the middle third of the upper arm, distributing filaments to the skin over the distal third of the anterolateral surface of the upper arm close to the vein. At the wrist joint the lateral cutaneous nerve of the forearm is anterior to the radial artery. Some filaments pierce the deep fascia and accompany the artery to the dorsum of the carpus. The nerve then passes to the base of the thenar eminence, where it ends in cutaneous rami. It has branches which connect with the terminal branch of the radial nerve and the palmar cutaneous branch of the median nerve.

Posterior cutaneous nerve of the forearm

The posterior cutaneous nerve of the forearm passes along the dorsum of the forearm to the wrist. It supplies the skin along its course and near its end joins the dorsal branches of the lateral cutaneous nerve of the forearm (see Fig. 45.15).

REFERENCES

rmack GC, Lamberty BGH. The Arterial Anatomy of Skin Flaps. Edinburgh: Churchill Livingstone, 1994.

iber RL, Jacobson MD, Fazeli BM, Abrams RA, Botte MJ. Architecture of selected muscles of the arm and forearm: anatomy and implications for tendon transfer. *J Hand Surg*. 1992;17A:787-798.

ibovic SJ, Hastings HII. Martin-Gruber revisited. *J Hand Surg*. 1992;17A:47-53.

Examines the literature on reported connections between the median and ulnar nerves in the forearm and classifies these connections..

lmon M. Anatomic studies. In: Taylor GI, Razaboni RM. *Book 1. Arteries of the Muscles of the Extremities and the Trunk. Book 2: Arterial Anastomotic Pathways of the Extremities*. St Louis, MO: Quality Medical Publishing, 1994.

Contains the translated work of Dr Michel Salmon concerning the blood supply to muscle as well as the anastomotic pathways in the limbs..

eetz KK, Bishop AT, Berger RA. The arterial blood supply of the distal radius and ulna and its potential use in vascularized pedicled bone grafts. *J Hand Surg*. 1995;20A:902-914.

n ST, Smith PJ. Anomalous extensor muscles of the hand: a review. *J Hand Surg*. 1999;24A:449-455.

CHAPTER 50

Wrist and hand

SKIN AND SOFT TISSUE

SKIN

Dorsal skin versus palmar skin

The skin over the dorsum of the hand is thin and mobile and this allows for flexion at the metacarpophalangeal and interphalangeal joints. The dorsal skin is frequently hirsute over the dorsal aspect of the proximal phalanges and the ulnar aspect of the dorsum of the hand. In comparison, the palm is adapted for padding and anchorage. The palmar skin and the skin over the volar surface of the digits is thick and hairless, and has a well-defined stratum lucidum, a higher density of nerve endings, and eccrine sweat glands, but no sebaceous glands.

Skin creases and fingerprints

Flexure lines commonly crease the skin across the flexor surfaces of the wrist and hand (Fig. 50.1). Though not all directly over their functionally related subjacent skeletal joints, they are produced by adhesion of the skin to subjacent deep fascia and are sites of folding of the skin during movement. These flexures are useful landmarks. Less regular, but quite prominent, crease-line complexes are centred over the dorsal (extensor) aspects of the radiocarpal, carpal, metacarpophalangeal and interphalangeal joints. They are mainly transverse but display varying curvatures. During flexion the dorsal skin is stretched and the lines become less prominent (but can still be identified). During extension the now redundant skin becomes increasingly puckered and the lines are finally maximally prominent. (For a general review of ‘skin lines’ see p. 160.)

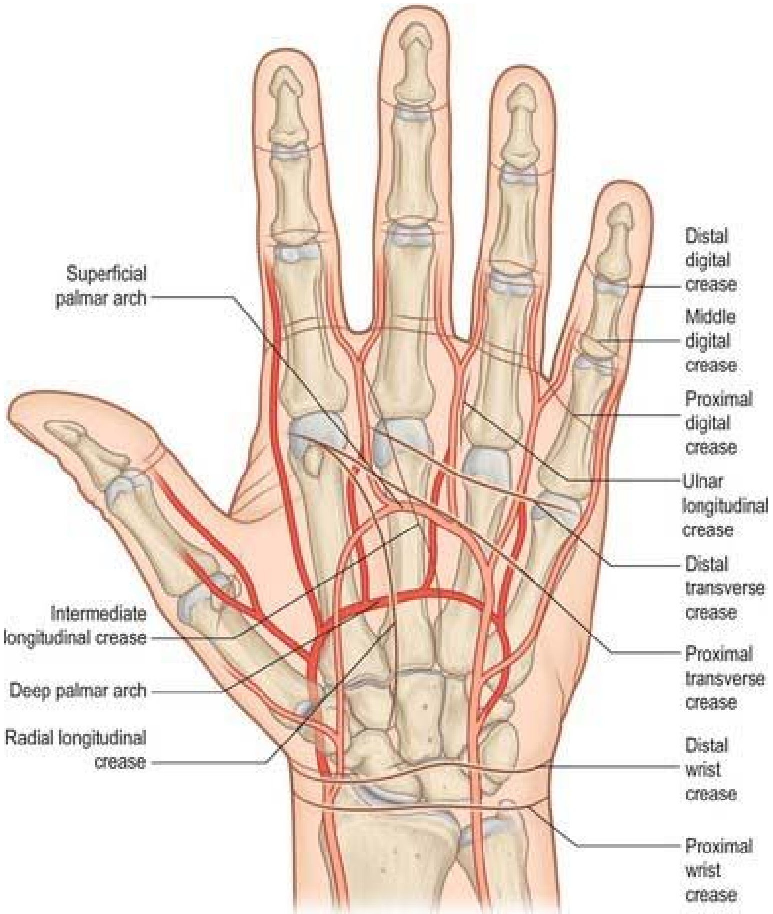
Superficial palmar arch
Intermediate longitudinal crease
Deep palmar arch
Radial longitudinal crease
Distal digital crease
Middle digital crease
Proximal digital crease
Ulnar longitudinal crease
Distal transverse crease
Proximal transverse crease
Distal wrist crease
Proximal wrist crease

Fig. 50.1 Relation of the skin flexure lines and palmar arterial arches to the bones of the left hand.

(Adapted from Drake, Vogl and Mitchell 2005.)

Near the junction of the carpus and forearm there are usually three anterior transverse lines. The proximal marks the proximal limit of the flexor synovial sheaths, an intermediate line overlies the wrist joint, and a distal line is at the proximal border of the flexor retinaculum.

In the palm a curved radial longitudinal line encircles the thenar eminence, ending at the radial (lateral) margin of the palm. Several less constant longitudinal lines lie medial and roughly parallel to it. Proximal and distal transverse lines ascend medially across the palm. The proximal line begins at the distal end of the radial longitudinal line and runs obliquely to the middle of the hypothenar eminence across the shafts of the metacarpals.

The distal line begins at or near the cleft between the index and middle finger and crosses the palm with a proximal convexity over the second to fourth metacarpal heads, near the proximal ends of the fibrous flexor sheaths.

The second to fifth digits show proximal, middle and distal sets of transverse lines. The proximal, often double, are at the digital roots, approximately 2 cm distal to the metacarpophalangeal joints. The middle lines are typically double, the proximal line lying directly over the proximal interphalangeal joint. The distal lines are usually single, and lie proximal to the distal interphalangeal joints: their levels are sometimes marked by a fainter, more distal line. The free pollicial base is partly encircled by a line which starts on the radial side and crosses distally over the metacarpophalangeal joint to end between the thumb and index finger level with the base of the proximal pollicial phalanx. There is a second, shorter crease usually 1 cm distal to this line. There are two lines comparable to the middle digital lines in other digits opposite the interphalangeal joint of the thumb (see also p. 160).

Cutaneous vascular supply

The skin of the volar aspect of the wrist is supplied directly by cutaneous branches from the superficial palmar branch of the radial artery, the ulnar artery and occasionally the median artery if it is large enough (Fig. 50.2). The skin over the thenar eminence is supplied by small perforating branches from the superficial palmar branch of the radial artery and the princeps pollicis. The skin over the hypothenar eminence is supplied by perforating branches from the ulnar artery, some of which pass through palmaris brevis. The remainder of the palm is supplied by small perforating branches from the common palmar digital arteries which pierce the palmar aponeurosis, and small branches from the radialis indicis artery. The blood supply to the volar aspect of the digital skin comes from small branches from each digital artery. At the level of the distal phalanx the two digital arteries typically form an H-shaped anastomosis from which cutaneous perforators fan out within the pulp. Deep digital veins accompanying the digital arteries are usually very small and frequently absent. More commonly, superficial palmar veins tend to pass dorsally and drain into the larger superficial dorsal venous system.

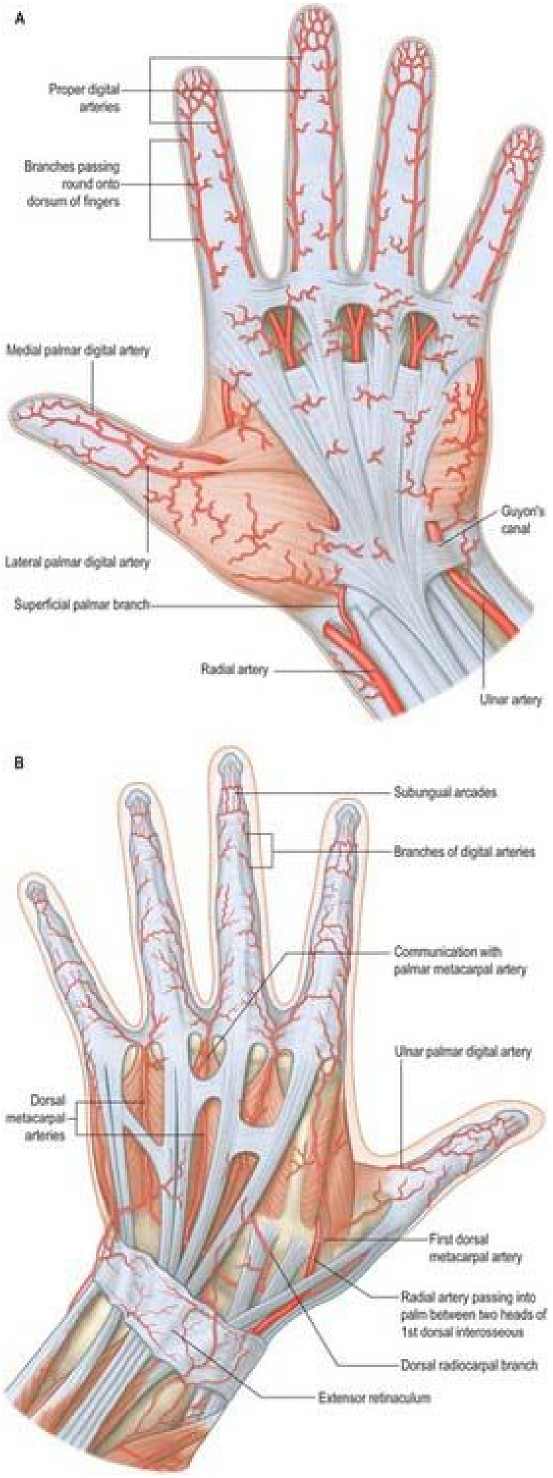
A
Proper digital arteries
Branches passing round onto dorsum of fingers
Medial palmar digital artery
Lateral palmar digital artery
Superficial palmar branch
Radial artery
Guyon's canal
Ulnar artery
B
Subungual arcades
Branches of digital arteries
Communication with palmar metacarpal artery
Ulnar palmar digital artery
Dorsal metacarpal arteries
First dorsal metacarpal artery
Radial artery passing into palm between two heads of 1st dorsal interosseous
Dorsal radiocarpal branch
Extensor retinaculum

Fig. 50.2 Cutaneous blood supply to the hand. **A**, Volar aspect. **B**, Dorsal aspect.

The skin of the dorsal aspect of the wrist is supplied by branches from a plexus overlying the extensor retinaculum. Branches from the radial artery, including its dorsal carpal branch, dorsal carpal branch of the ulnar artery, and anterior and posterior interosseous arteries all contribute to this plexus. The blood supply to the dorsum of the hand arises from longitudinal rows of four or five tiny branches from each of the dorsal metacarpal arteries, which usually arise either from the radial artery directly or the dorsal carpal arch. At the level of the neck of the metacarpals, where the second, third and fourth dorsal metacarpal arteries communicate with branches from the corresponding common palmar digital arteries, a large cutaneous perforating branch passes proximally to supply an area of skin as far as the dorsal aspect of the wrist.

The blood supply to the dorsum of the fingers comes proximally from the terminal branches of the dorsal metacarpal arteries – supplying a region as far distally as the proximal interphalangeal joint – as well as from dorsal branches of the palmar digital arteries which are given off at each phalangeal level. At the level of the distal phalanx the cutaneous supply comes from three dorsal arcades: a superficial arcade over the base of the distal phalanx, and two distal subungual arcades. The skin of the dorsum of the thumb is supplied by longitudinal axial branches of the princeps pollicis and dorsal branches from the palmar digital arteries.

Cutaneous innervation

The skin of the volar aspect of the wrist is innervated by the terminal branches of the lateral and medial cutaneous nerves of the forearm. The skin of the palm is innervated by the palmar branches of the ulnar nerve and the palmar branch of the median nerve (Fig. 50.3; see also Fig. 50.45. The skin of the volar aspect of the thumb, index, middle and radial aspect of the ring fingers is supplied by cutaneous branches of the median nerve, while that of the little finger and ulnar side of the ring finger is supplied by the ulnar nerve.

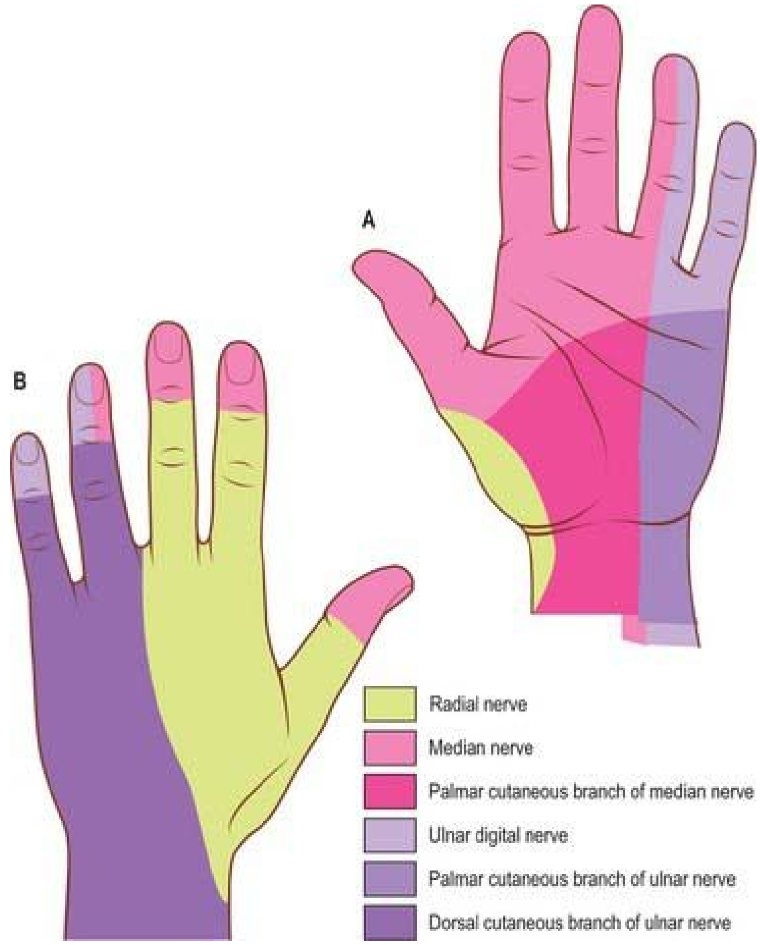
A
B
Radial nerve
Median nerve
Palmar cutaneous branch of median nerve
Ulnar digital nerve
Palmar cutaneous branch of ulnar nerve
Dorsal cutaneous branch of ulnar nerve

Fig. 50.3 Cutaneous nerve supply to the hand. **A**, Volar aspect. **B**, Dorsal aspect

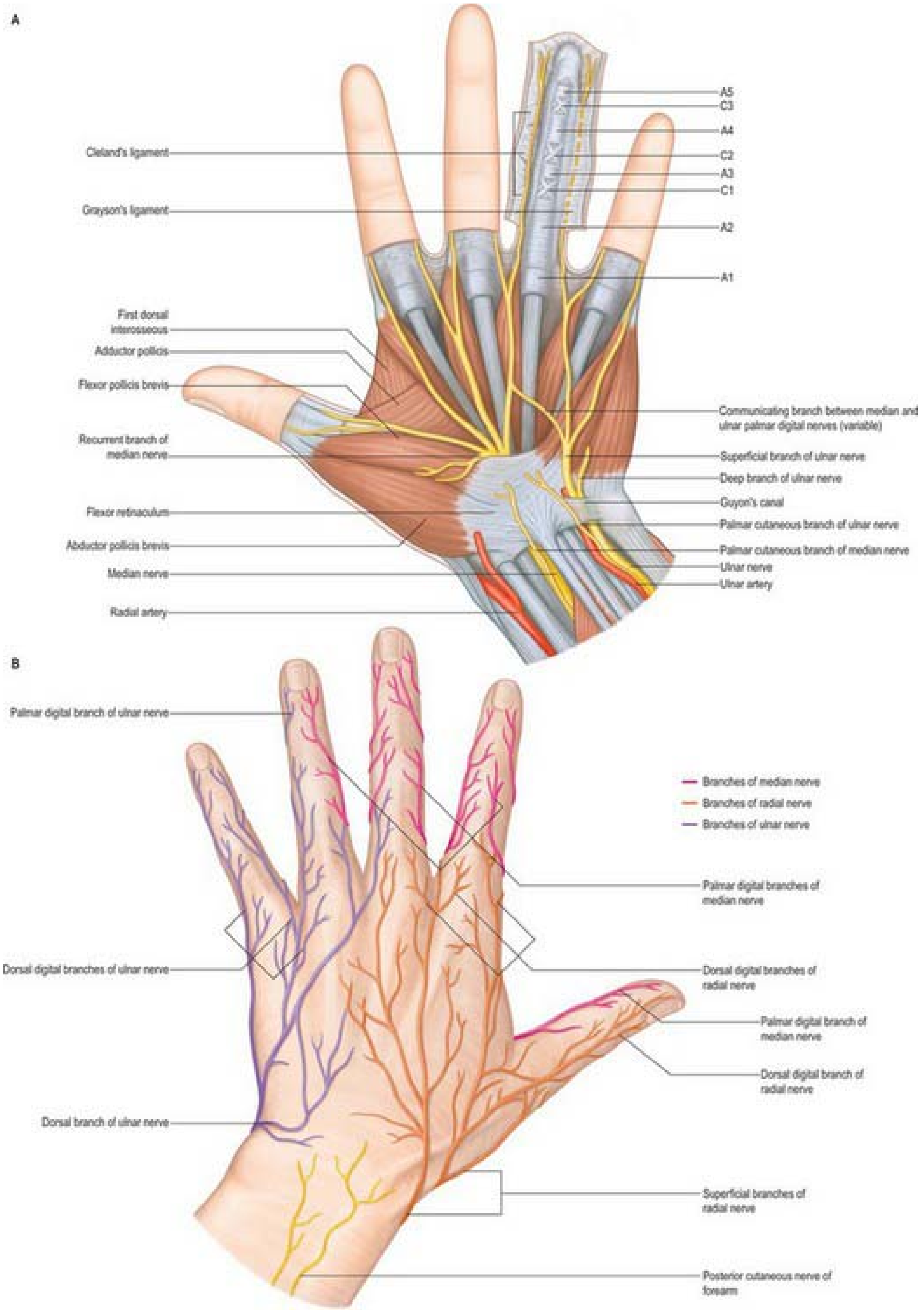
A
A5
C3
A4
Cleland's ligament
C2
A3
C1
Grayson's ligament
A2
A1
First dorsal interosseous
Adductor pollicis
Flexor pollicis brevis
Communicating branch between median and ulnar palmar digital nerves (variable)
Recurrent branch of median nerve
Superficial branch of ulnar nerve
Deep branch of ulnar nerve
Guyon's canal
Flexor retinaculum
Palmar cutaneous branch of ulnar nerve
Abductor pollicis brevis
Palmar cutaneous branch of median nerve
Median nerve
Ulnar nerve
Ulnar artery
Radial artery
B
Palmar digital branch of ulnar nerve
Branches of median nerve
Branches of radial nerve
Branches of ulnar nerve
Palmar digital branches of median nerve
Dorsal digital branches of ulnar nerve
Dorsal digital branches of radial nerve
Palmar digital branch of median nerve
Dorsal digital branch of radial nerve
Dorsal branch of ulnar nerve
Superficial branches of radial nerve
Posterior cutaneous nerve of forearm

Fig. 50.45 Cutaneous nerves of the hand. **A**, Palmar aspect. The anular and cruciate pulleys are shown schematically in the ring finger. **B**, Dorsal aspect.

The cutaneous innervation of the radial aspect of the dorsum of the wrist and hand, as well as the dorsal aspect of the radial three and a half digits as far distally as the nail bed, arises from the terminal branches of the radial nerve, the dorsal digital nerves. Between two and five dorsal digital nerves supply each digit. The cutaneous innervation of the ulnar aspect of the dorsum of the wrist and hand, and the dorsal aspect of the ulnar one and a half digits as far distally as the nail bed, arises from the dorsal branch of the ulnar nerve, again ending as dorsal digital nerves. The skin of the dorsum of the middle and distal phalanges is also supplied by dorsal branches of the palmar digital nerves.

NAIL APPARATUS

The nail apparatus consists of the nail plate, proximal and lateral nail folds, nail matrix, nail bed and hyponychium. It is described on page 154.

SOFT TISSUE

Palmar fascial complex

The palmar fascia is a three-dimensional ligamentous system composed of longitudinal, transverse and vertical fibres (Fig. 50.4).

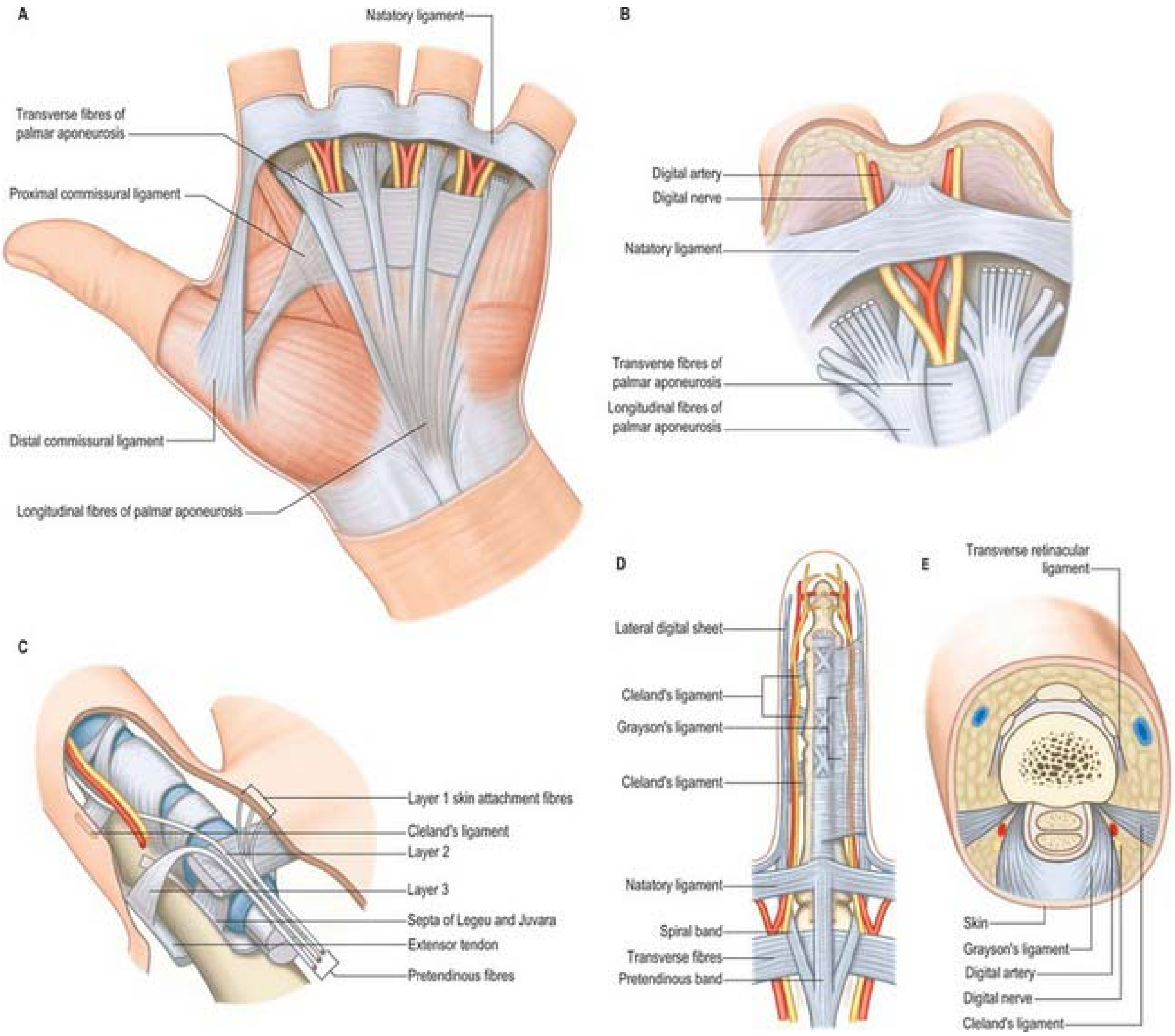
A
Natatory ligament
Transverse fibres of palmar aponeurosis
Proximal commissural ligament
Distal commissural ligament
Longitudinal fibres of palmar aponeurosis
B
Digital artery
Digital nerve
Natatory ligament
Transverse fibres of palmar aponeurosis
Longitudinal fibres of palmar aponeurosis
C
Layer 1 skin attachment fibres
Cleland's ligament
Layer 2
Layer 3
Septa of Legeu and Juvara
Extensor tendon
Pretendinous fibres
D
Lateral digital sheet
Cleland's ligament
Grayson's ligament
Cleland's ligament
Natatory ligament
Spiral band
Transverse fibres
Pretendinous band
E
Transverse retinacular ligament
Skin
Grayson's ligament
Digital artery
Digital nerve
Cleland's ligament

Fig. 50.4 Palmar aponeurosis and distal fascial complex. **A**, Schematic diagram of the palmar fascia. **B**, More detailed view of structures at the web space. **C**, Fate of the distal longitudinal fibres. **D**, **E**, Normal digital fascia.

Longitudinal fibre system

The longitudinal fibres represent the phylogenetically degenerated metacarpophalangeal joint flexor. They run distally from the palmaris longus tendon or the flexor retinaculum of the wrist across the whole width of the central third of the palm, producing four well-defined longitudinal bundles to the index, middle, ring and little fingers. A less well-defined bundle passes to the thumb. Distal to the transverse fibres of the palmar aponeurosis the longitudinal fibres pass in three layers (McGrouther 1982). The most superficial longitudinal fibres (layer 1) are inserted superficially into the skin of the distal palm between the distal palmar crease and the proximal digital crease. Some superficial fibres pass distally into the palmar midline of the digit. Deeper longitudinal fibres (layer 2) pass deep to the natatory ligament and neurovascular bundles into the apex of the web space skin and into the fingers themselves where they are continuous with Cleland's ligaments and the lateral digital sheet. These are known as the spiral bands of Gosset. Deeper still, the longitudinal fibres in layer 3 perforate the deep transverse metacarpal ligament to pass around the sides of the metacarpophalangeal joint and attach to the metacarpal bone and proximal phalanx, and extensor tendon.

Transverse fibre system

The transverse fibre system consists of the natatory ligament (also known as superficial transverse metacarpal ligament), the transverse fibres of the palmar aponeurosis (also known as fibres of Skoog), and the transverse metacarpal ligament (also known as the deep transverse metacarpal ligament).

Natatory ligament (superficial transverse metacarpal ligament)

The fibres of the natatory ligament (superficial transverse metacarpal ligament) cross the apex of the web skin and extend into the digit to blend with the lateral digital sheet, thus limiting the spreading of the skin of the distal palm and the separation of the adjacent fingers. The natatory ligament in the first web is called the distal commissural ligament.

Transverse fibres of the palmar aponeurosis

The transverse fibres of the palmar aponeurosis (fibres of Skoog) lie more proximally than the natatory fibres and represent the deepest layer of the palmar fascia. They lie proximal to the distal palmar crease in a band approximately 2 cm wide, and connect the anterior fibres of the flexor tendon sheaths with one another and to the fasciae over the thenar and hypothenar muscles groups. The extension to the first ray is called the proximal commissural ligament.

Transverse metacarpal ligament

The strong transverse fibres of the transverse metacarpal ligament are deep to the palmar aponeurosis and flexor sheaths. They connect the metacarpal heads of the index to little fingers by their attachment with the volar plates.

Vertical fibre system

The vertical fibres are more delicate, and pass from the dermis, between the longitudinal and transverse fibres, to the fibrous flexor sheaths and the metacarpal bones. They are concentrated on either side of the palmar skin creases as well as the thenar and hypothenar eminences.

A series of vertical septa lie deep to the transverse fibres of the palmar aponeurosis, and connect it to the underlying deep transverse ligament. They provide compartments which contain the flexor tendons and the lumbricals and neurovascular bundles.

Dupuytren’s disease

Dupuytren’s disease (contracture) is a progressive condition of uncertain aetiology resulting from fibrous contracture of the palmar aponeurosis: the little and ring fingers are especially affected. Longitudinal thickening in the palm produces cords and thickened nodules which can progress to flexion deformities of the metacarpophalangeal and proximal interphalangeal joints of the affected fingers. The palmar aponeurosis only extends as far as the sides of the middle phalanx, therefore the distal interphalangeal joint is uncommonly involved. Indeed, in advanced cases, the distal interphalangeal joint can be hyperextended as the distal phalanx is pushed backwards against the palm.

The pattern of fascial involvement in this condition can be complex. For example, the normal anatomical position of the digital nerves and arteries may be distorted because they are often displaced medially. Since surgical treatment involves excising the affected area of palmar fascia, the digital nerves and arteries may be at risk in this procedure.

A similar contracture may affect the plantar fascia in the sole of the foot.

Digital fascial complex

The superficial fascia within the finger is fibrofatty in the palmar and dorsal aspects, but more sheet-like laterally, where it is termed the lateral digital sheet. Within the core of the finger the fascia is thickened in areas, forming the flexor sheath, Cleland's, Grayson's and Landsmeer's ligaments (Fig. 50.4). The flexor sheath is discussed in detail on page 879. Cleland's ligaments extend from the sides of the phalanges, pass dorsal to the neurovascular bundles and insert into the lateral digital sheet. Grayson's ligaments are more delicate, may even be discontinuous and pass from the lateral sides of the phalanges volar to the neurovascular bundles to insert into the lateral digital sheet. Landsmeer's ligaments are inconsistent anatomical structures made up of transverse and oblique retinacular ligaments (see Fig. 50.30). The transverse retinacular ligament passes from the A3 pulley of the fibrous flexor sheath at the level of the proximal interphalangeal joint to the lateral border of the lateral extensor band. The oblique retinacular ligament lies deep to the transverse retinacular ligament. It originates from the lateral aspect of the proximal phalanx and flexor sheath (A2 pulley) and passes volar to the axis of rotation of the proximal interphalangeal joint in a dorsal and distal direction to insert into the terminal extensor tendon.

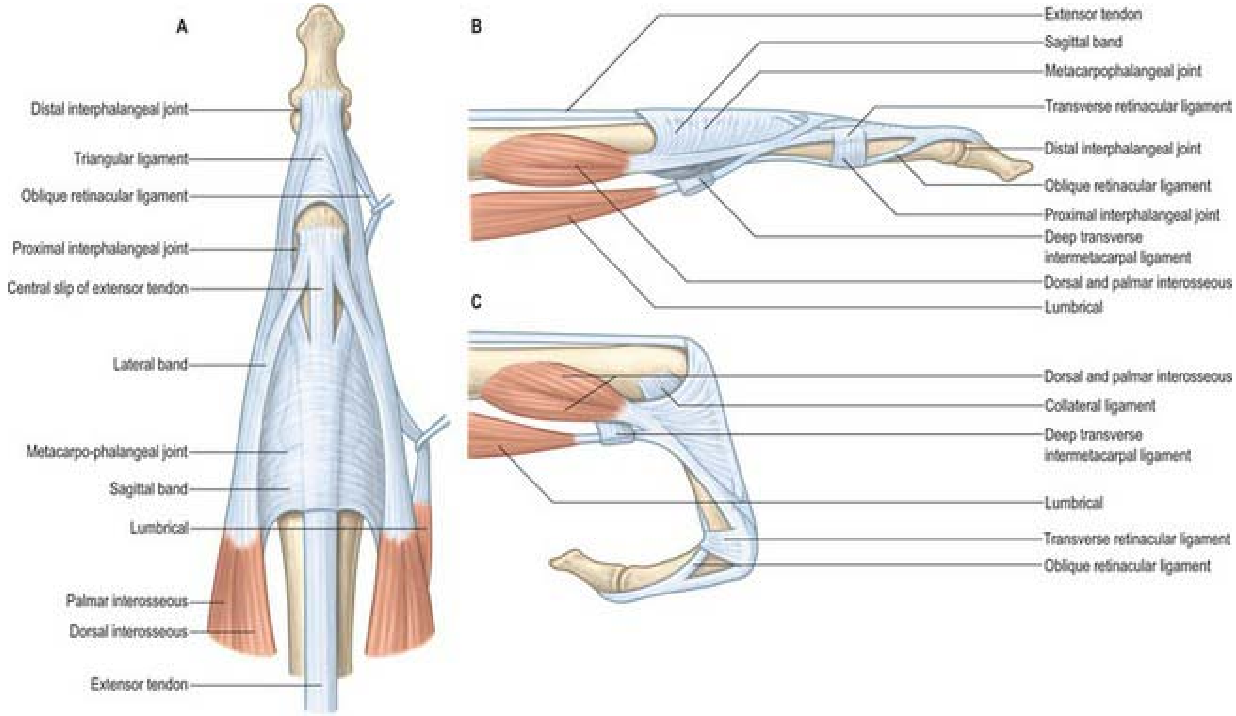
A
Distal interphalangeal joint
Triangular ligament
Oblique retinacular ligament
Proximal interphalangeal joint
Central slip of extensor tendon
Lateral band
Metacarpo-phalangeal joint
Sagittal band
Lumbrical
Palmar interosseous
Dorsal interosseous
Extensor tendon
B
Extensor tendon
Sagittal band
Metacarpophalangeal joint
Transverse retinacular ligament
Distal interphalangeal joint
Oblique retinacular ligament
Proximal interphalangeal joint
Deep transverse intermetacarpal ligament
Dorsal and palmar interosseous
Lumbrical
C
Dorsal and palmar interosseous
Collateral ligament
Deep transverse intermetacarpal ligament
Lumbrical
Transverse retinacular ligament
Oblique retinacular ligament

Fig. 50.30 Extensor mechanism of the finger. **A**, Dorsal view; **B**, lateral view; **C**, lateral view in flexion.

Functions of the fascia of the hand

The fascial continuum of the hand performs a number of different, but inter-related, functions. It channels and provides a gliding surface for structures in transit between the forearm and the digits; transmits loads; anchors the skin; protects underlying vessels; and provides a framework for muscle attachments.

Channelling of structures in transit between forearm and digits

The vertical septa act as spacers between the tendons and neurovascular bundles of the individual digital rays. Where tendons change direction around a concave surface the channels are thickened. They perform a retinacular role, forming sheaths with specialized pulleys to prevent the tendon springing away from the underlying skeleton (see flexor tendon sheaths, p. 879).

Transmission of loads

At points where compressive loading is applied to the hand, such as the finger pulp and palm, loculi of fat act as shock absorbers. The loculi are contained within defined fibrous boundaries, which means that the shape, but not the volume, of each loculus can change. The compliance or deformability of the boundaries determines the amount of shock absorption. Local ‘turgor’ (deformability) and blood volume are measures of this anatomical property.

The palm also contains much larger fibrous compartments between skin and skeleton which transmit muscles, tendons and other structures. The honeycomb pattern of these compartments constitutes the palmar shock absorption system. The soft padded parts of the hand are able to conform to the contours of objects which are grasped, and this permits better interpretation of sensation and better grip.

The hand must also resist tensile loading. Tendons and ligaments are particularly suitable for resisting such forces but many other parts of the fascial continuum, e.g. the anchorage system of the palm, also play a major role in resisting ‘pulling’ forces.

Anchorage

Skin is retained by fascial ligaments which allow the hand to flex while retaining the skin in position. Skin folds at palmar and digital creases possess few deep-anchoring fibres. However, the skin on either side of the crease lines contains deep anchorage ligaments, and these allow the unanchored skin between them to fold in a repetitive pattern. The palmar creases have been described as skin ‘joints’. Fascial anchors may be vertical (perpendicular to the palm), e.g. in the midpalm where scattered vertical fibres run from the dermis down into the depths of the hand; horizontal (in the plane of the palm); or oblique to the skin surface.

The insertion of the longitudinal (pretendinous) fibres of the palmar aponeurosis is an example of a well-developed horizontal anchorage system. The most superficial longitudinal fibres insert into the dermis of the distal palm. This arrangement resists horizontal shearing force in gripping tasks, e.g. holding a golf club, where it prevents distal skin slippage or degloving of the palm on striking the golf ball. The characteristic blisters on the palms of those unaccustomed to such sports map out the sites of the skin anchorage points. This anchorage system can be demonstrated by flexing the palm until the skin of the distal palm folds loosely. An attempt to pull the loose skin distally will reveal the anchoring longitudinal fibres of the palmar aponeurosis.

Oblique anchors occur in the fingers where Cleland’s ligaments tether the skin of the proximal and middle segments of the digits to the region of the proximal interphalangeal joints.

Binding

Transversely orientated fascial structures help to maintain the transverse arch of the hand by ‘binding’ the underlying skeletal structures or the tendon sheaths.

Limiting or tethering

Joint motion is limited not only by joint ligamentous action, but also in some cases by skin tightness. Skin in the interdigital webs is generally reinforced by fascial ligamentous fibres which run just beneath the dermis in a direction which resists stretch: they are well developed in the thumb web.

Lubrication

There are many other gliding planes, e.g. between periosteum and the extensor apparatus, and between the latter and the skin, on the dorsum of the digits. The flexor tendon sheaths possess low friction and are lubricated by synovial fluid.

Vascular protection and pumping action

The blood vessels of the palm are surrounded by a cuff of tough fascia or by a fatty pad. When the hand is compressed, as in gripping, these relatively incompressible fascial structures function as a venous pumping mechanism to assist return of blood from the limb. In contrast, large capacitance veins on the dorsum of the hand lie in gliding skin, surrounded by loose areolar tissue, which allows venous dilatation.

Framework for muscle attachments

Many of the small muscles of the hand are attached to the fascial skeleton, at least in part, e.g. abductor pollicis brevis, palmaris longus. The fascial framework can be visualized as a harness by which muscles can act on the underlying skeleton, e.g. the metacarpophalangeal joint is moved by a ring of fascial and ligamentous structures that surround the joint and to which tendons are attached.

Digital and palmar spaces

There are many potential spaces within the hand, often with ill-defined margins.

The nail fold is a ‘U-shaped’ space made up of the eponychium and the lateral nail fold. The apical spaces at the tip of the finger are formed by the fibrous attachments of the distal phalanx to the tip of the digital pulp skin. The digital pulp spaces are confined compartments bounded by the digital creases which overlie the joints, and are attached to the underlying pulleys. The synovial flexor tendon sheaths are described on page 879. The web space is bounded distally by the skin and natatory ligament, by the deep transverse metacarpal ligament posteriorly, and by the deep attachments of the palmar fascia, together with their lateral attachments to the tendon sheaths proximally. The deep palmar space is a complex three-dimensional space limited proximally by the carpal tunnel. It lies deep to the palmar aponeurosis, between the radial and ulnar condensations of vertical fibres which connect the palmar aponeurosis to the thenar and hypothenar eminences. Partitions that pass deeply from the longitudinal bands of the palmar aponeurosis form eight narrow compartments: four contain the digital flexor tendons and four contain the lumbricals and the neurovascular bundles.

Infections of the hand

The spaces of the hand limit the spread of infection. Infections in the digit can occur in the nail fold (paronychia), the apical spaces at the very tip of the finger, the distal pulps (a felon) and the flexor sheaths. Anatomically, because the flexor synovial sheath of the thumb and the little finger are continuous throughout the palm, they have the potential to spread infection to the palm and so communicate with other sheaths within the carpal tunnel. Pus can certainly spread proximally within flexor tendon sheaths, but from a clinical point of view it is as disastrous in those digits whose sheaths do not communicate with the carpal tunnel sheaths (index, middle, ring) as it is in those that do (thumb, little finger). It is preferable, therefore, to know the structures rather than the potential spaces between them. Deep infections in the palm are usually not confined to any particular space.

BONE

The skeleton of the hand consists of the carpus, metacarpus and the phalanges. In the following description, proximal and distal are used in preference to superior and inferior, and palmar and dorsal, rather than anterior and posterior.

CARPAL BONES

The carpus contains eight bones: four each in proximal and distal rows (Fig. 50.5 and Fig. 50.6). In radial (lateral) to ulnar (medial) order, the scaphoid, lunate, triquetrum and pisiform make up the proximal row, and the trapezium, trapezoid, capitate and hamate make up the distal row. The pisiform articulates with the palmar surface of the triquetrum, and is thus separated from the other carpal bones, all of which articulate with their neighbours. The other three proximal bones form an arch which is proximally convex, and which articulates with the radius and articular disc of the distal radio-ulnar joint. The concavity of the arch is a distal recess embracing, proximally, the projecting aspects of the capitate and hamate. The two rows of carpal bones are thus mutually and firmly adapted without any loss of movement.

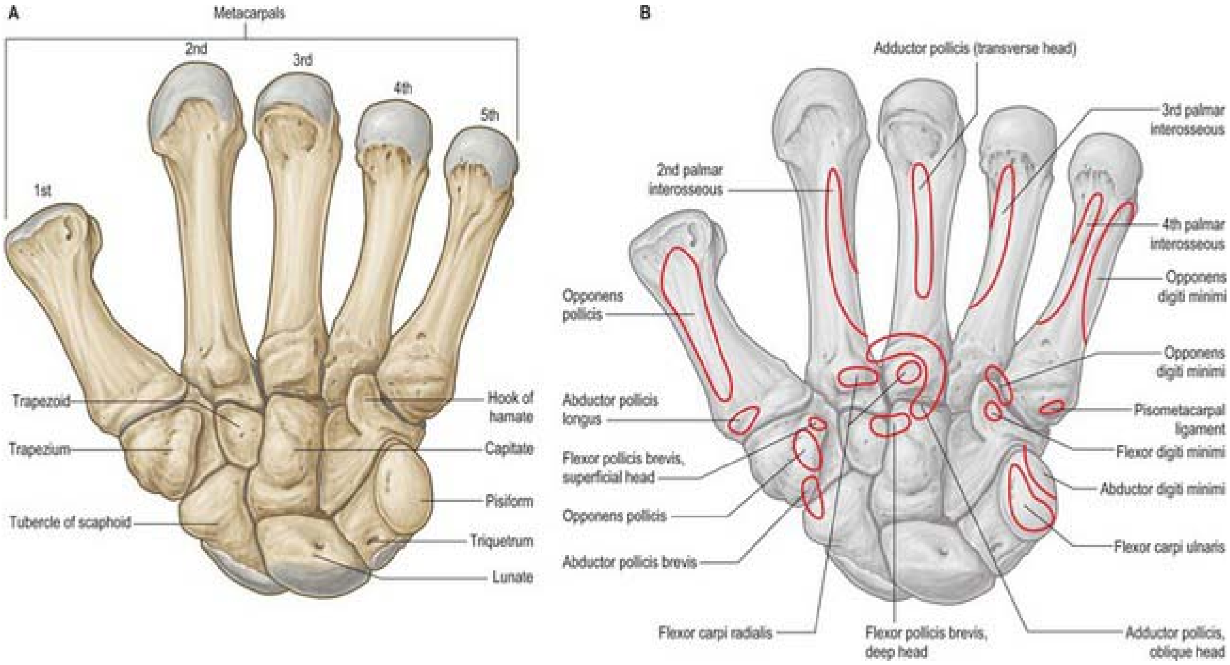
A
Metacarpals
2nd
3rd
4th
5th
1st
Trapezoid
Trapezium
Tubercle of scaphoid
Hook of hamate
Capitate
Pisiform
Triquetrum
Lunate
B
Adductor pollicis (transverse head)
3rd palmar interosseous
2nd palmar interosseous
4th palmar interosseous
Opponens digiti minimi
Opponens pollicis
Opponens digiti minimi
Abductor pollicis longus
Pisometacarpal ligament
Flexor digiti minimi
Flexor pollicis brevis, superficial head
Abductor digiti minimi
Opponens pollicis
Flexor carpi ulnaris
Abductor pollicis brevis
Flexor carpi radialis
Flexor pollicis brevis, deep head
Adductor pollicis, oblique head

Fig. 50.5 **A**, Palmar aspect of the carpal and metacarpal bones of the left hand. Muscle attachments, except for the dorsal interossei, are shown in **B**.

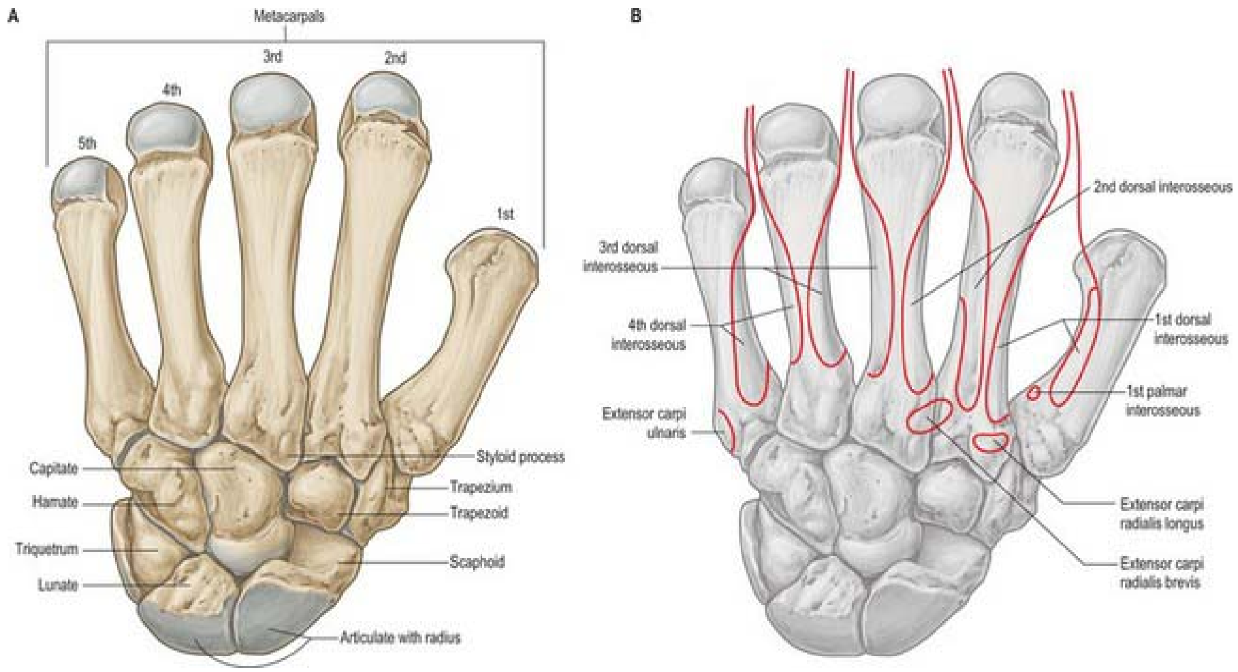
A
Metacarpals
3rd
2nd
4th
5th
1st
Capitate
Hamate
Triquetrum
Lunate
Styloid process
Trapezium
Trapezoid
Scaphoid
Articulate with radius
B
2nd dorsal interosseous
3rd dorsal interosseous
4th dorsal interosseous
1st dorsal interosseous
1st palmar interosseous
Extensor carpi ulnaris
Extensor carpi radialis longus
Extensor carpi radialis brevis

Fig. 50.6 **A**, Dorsal aspect of the carpal and metacarpal bones of the left hand. Muscle attachments are shown in **B**.

The dorsal carpal surface is convex. The palmar surface forms a deeply concave carpal groove, accentuated by the palmar projection of the radial (lateral) and ulnar (medial) borders. The ulnar projection is formed by the pisiform and the hamulus (hook), an unciform palmar process of the hamate. The pisiform is at the proximal border of the hypothenar eminence, on the ulnar side of the palm, and it is easily felt in front of the triquetrum. The hamulus is concave in a radial direction, its tip is palpable 2.5 cm distal to the pisiform, in line with the radial border of the ring finger. The superficial division of the ulnar nerve can be rolled on it. The radial border of the carpal groove is formed by the tubercles of the scaphoid and trapezium. The former is distal on the anterior scaphoid surface and palpable (sometimes also visible) as a small medial knob at the proximal border of the palmar thenar eminence, radial to the tendon of flexor carpi radialis. The tubercle of the trapezium is a vertically rounded ridge on the anterior surface of the bone, slightly hollow medially and just distal and radial to the scaphoid tubercle: it is difficult to palpate. (Both the scaphoid and trapezium may be grasped individually, and moved passively, by firm pressure between an opposed index finger and thumb applied to the palmar surface and ‘anatomical snuff-box’ simultaneously.) The carpal groove is made into an osseofibrous carpal tunnel by a fibrous retinaculum attached to its margins. The tunnel carries flexor tendons and the median nerve into the hand. The retinaculum strengthens the carpus and augments flexor efficiency. Radiocarpal, intercarpal and carpometacarpal ligaments are attached to the palmar and dorsal surfaces of all of the carpal bones, except the triquetrum and pisiform.

Individual carpal bones

Scaphoid

The scaphoid is the largest element in the proximal carpal row (Fig. 50.7A). It has a long axis which is distal, radial and slightly palmar in direction. A round tubercle on the distolateral part of its palmar surface is directed anterolaterally (Fig. 50.5), and provides an attachment for the flexor retinaculum and abductor pollicis brevis: it is crossed by the tendon of flexor carpi radialis. The rough dorsal surface is slightly grooved, narrower than the palmar, and pierced by small nutrient foramina, which are often restricted to the distal half (13%). The radial collateral ligament is attached to the lateral surface, which is also narrow and rough. The remaining surfaces are all articular. The radial (proximal) surface is convex, proximal and directed proximolaterally; the lunate surface is flat, semilunar, and faces medially; the capitate surface is large, concave and distal, and directed distomedially. The surface for the trapezium and trapezoid is continuous, convex and distal.

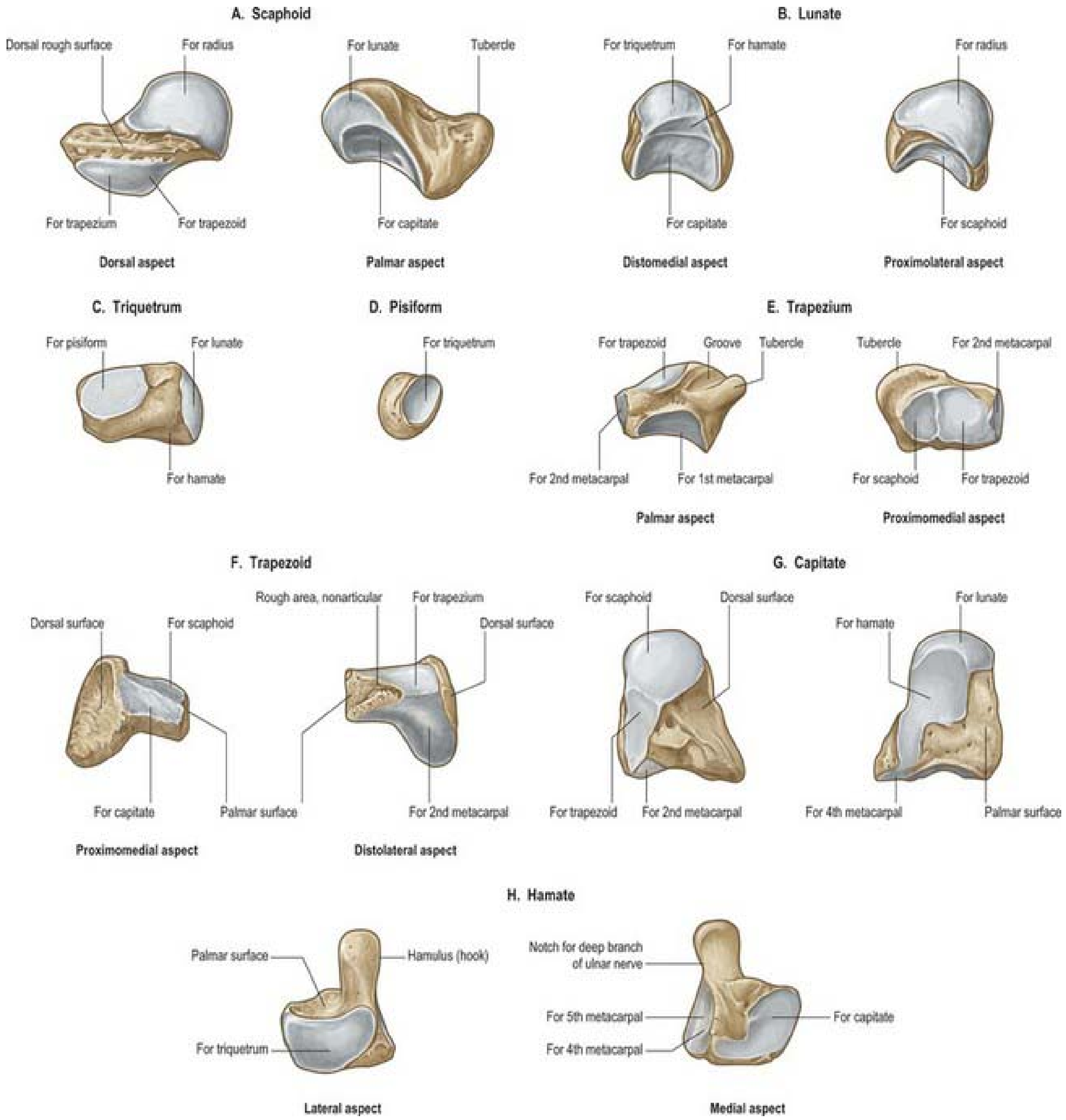
A. Scaphoid
Dorsal rough surface
For radius
For trapezium
For trapezoid
Dorsal aspect
For lunate
Tubercle
For capitate
Palmar aspect
B. Lunate
For triquetrum
For hamate
For capitate
Distomedial aspect
For radius
For scaphoid
Proximolateral aspect
C. Triquetrum
For pisiform
For lunate
For hamate
D. Pisiform
For triquetrum
E. Trapezium
For trapezoid
Groove
Tubercle
For 2nd metacarpal
For 1st metacarpal
Palmar aspect
Tubercle
For 2nd metacarpal
For scaphoid
For trapezoid
Proximomedial aspect
F. Trapezoid
Dorsal surface
For scaphoid
For capitate
Palmar surface
Proximomedial aspect
Rough area, nonarticular
For trapezium
Dorsal surface
For 2nd metacarpal
Distolateral aspect
G. Capitate
For scaphoid
Dorsal surface
For trapezoid
For 2nd metacarpal
For lunate
For hamate
For 4th metacarpal
Palmar surface
H. Hamate
Palmar surface
Hamulus (hook)
For triquetrum
Lateral aspect
Notch for deep branch of ulnar nerve
For 5th metacarpal
For 4th metacarpal
For capitate
Medial aspect

Fig. 50.7 Disarticulated carpal bones.

Scaphoid bone fractures

The scaphoid is the most frequently fractured carpal bone, typically as a result of a fall onto an outstretched hand. The fracture usually crosses the long axis of the bone. Fractures of its proximal part or its ‘waist’ may fail to unite because the proximal fragment has lost its blood supply: avascular necrosis of the proximal fragment is then inevitable.

Lunate

The lunate is approximately semilunar and articulates between the scaphoid and triquetrum in the proximal carpal row (Fig. 50.7B). Its rough palmar surface, almost triangular, is larger and wider than the rough dorsal surface. Its smooth convex proximal surface articulates with the radius and the articular disc of the distal radio-ulnar joint. Its narrow lateral surface bears a flat semilunar facet for the scaphoid. The medial surface, almost square, articulates with the triquetrum and is separated from the distal surface by a curved ridge, usually somewhat concave for articulation with the edge of the hamate in adduction (Fig. 50.7B, left). The distal surface is deeply concave to fit the medial part of the head of the capitate.

Triquetrum

The triquetrum is somewhat pyramidal and bears an oval isolated facet for articulation with the pisiform on its distal palmar surface (Fig. 50.7C). Its medial and dorsal surfaces are confluent, and marked distally by the attachment of the ulnar collateral ligament, but smooth proximally to receive the articular disc of the distal radio-ulnar joint in full adduction. The hamate surface, lateral and distal, is concavoconvex, broad proximally, narrow distally. The lunate surface, almost square, is proximal and lateral.

Pisiform

The pisiform is shaped like a pea, with a distolateral long axis (Fig. 50.7D). It bears a dorsal flat articular facet for the triquetrum. The tendon of flexor carpi ulnaris and the distal continuations of the tendon, the pisometacarpal and pisohamate ligaments, are all attached to the palmar non-articular area, which surrounds and projects distal to the articular surface: the pisiform therefore has attributes of a sesamoid bone.

Trapezium

The trapezium has a tubercle and groove on its rough palmar surface (Fig. 50.7E). The groove, which is medial, contains the tendon of flexor carpi radialis, and two layers of the flexor retinaculum are attached to its margins. The tubercle is obscured by the thenar muscles which are attached to it (opponens pollicis, flexor pollicis brevis and abductor pollicis brevis) (Fig. 50.5B). The elongated, rough dorsal surface is related to the radial artery. The large lateral surface is rough for attachment of the radial collateral ligament and capsular ligament of the thumb carpometacarpal joint. A large sellar surface faces distolaterally and articulates with the base of the first metacarpal. Most distally it projects between the bases of the first and second metacarpal bones and carries a small, quadrilateral, distomedially directed facet which articulates with the base of the second metacarpal. The large medial surface is gently concave for articulation with the trapezoid. The proximal surface is a small, slightly concave facet for articulation with the scaphoid. Its ridge, or ‘summit’, fits the concavity of the first metacarpal base, and extends in a palmar and lateral direction, at an angle of approximately 60° with the plane of the second and third metacarpals. Abduction and adduction occur in the plane of the ridge, which is shorter than the corresponding metacarpal groove. Their contours vary reciprocally: they are more curved near the second metacarpal base, whereas the radius of curvature is longer further away from this site. The two surfaces are not completely congruent, and the area of close contact probably moves towards the palm in adduction and dorsally in abduction. While the axis of flexion/extension passes through the trapezium, that for adduction/abduction is in the metacarpal base. Flexion is accompanied by medial rotation, and extension by lateral rotation (p. 875).

Trapezoid

The trapezoid is small and irregular. It has a rough palmar surface which is narrower and smaller than its rough dorsal surface: the former invades the lateral aspect (Fig. 50.7F). The distal surface, which articulates with the grooved base of the second metacarpal, is triangular, convex transversely and concave at right angles to this. The medial surface articulates by a concave facet with the distal part of the capitate, the lateral surface articulates with the trapezium, and the proximal surface articulates with the scaphoid.

Capitate

The capitate is the central and largest carpal bone. It articulates with the base of the third metacarpal via its triangular distal concavoconvex surface (Fig. 50.7G). Its lateral border is a concave strip for articulation with the medial side of the base of the second metacarpal. Its dorsomedial angle usually bears a facet for articulation with the base of the fourth metacarpal. The head projects into the concavity formed by the lunate and scaphoid: the proximal surface articulates with the lunate, and the lateral surface with the scaphoid. The facets for the scaphoid and trapezoid, though usually continuous on the distolateral surface, may be separated by a rough interval. The medial surface bears a large facet for articulation with the hamate, which is deeper proximally where it is partly non-articular. Palmar and dorsal surfaces are roughened for carpal ligaments, the dorsal being the larger.

Hamate

The hamate is cuneiform and bears an unciform hamulus (hook) which projects from the distal part of its rough palmar surface. The hamulus is curved with a lateral concavity and its tip inclines laterally, contributing to the medial wall of the carpal tunnel (Fig. 50.7H). The flexor retinaculum is attached to the apex of the hamulus. Distally, on the hamular base, a slight transverse groove may be in contact with the terminal deep branch of the ulnar nerve. The remaining palmar surface, like the dorsal, is roughened for attachment of ligaments. A faint ridge divides the distal surface into a smaller lateral facet which articulates with the base of the fourth metacarpal base, and a medial facet for articulation with the base of the fifth. The proximal surface, the thin margin of the wedge, usually bears a narrow facet which contacts the lunate in adduction. The medial surface is a broad strip, convex proximally, concave distally, which articulates with the triquetrum: distally a narrow medial strip is non-articular. The lateral surface articulates with the capitate by a facet covering all but its distal palmar angle.

Ossification

Carpal bones are cartilaginous at birth, although ossification may have started in the capitate and hamate. Each carpal bone is ossified from one centre, capitate first, and pisiform last: the order in the others varies (Fig. 50.8, Fig. 5.9, Fig. 5.10, Fig. 5.11, Fig. 50.12). The capitate begins to ossify in the second month, the hamate at the end of the third month, the triquetrum in the third year, the lunate, scaphoid, trapezium and trapezoid in the fourth year in females and fifth year in males. The pisiform begins to ossify in the ninth or tenth year in females, and the twelfth in males. The order varies according to sex, nutrition and, possibly, race. Occasionally an os centrale occurs between the scaphoid, trapezoid and capitate bones: during the second prenatal month it is a cartilaginous nodule which usually fuses with the scaphoid. Occasionally, lunate and triquetral elements may fuse. Other fusions and accessory ossicles have also been described.

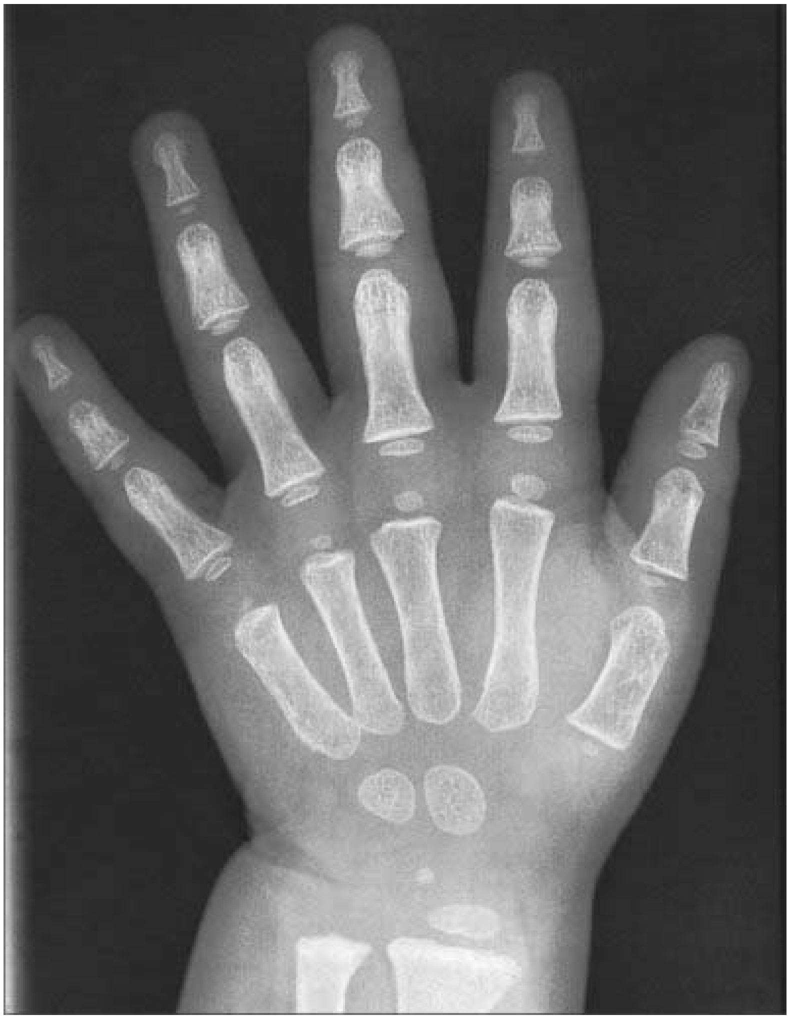

Fig. 50.8 Radiograph of a hand at 2½ years (male), dorsopalmar projection. Note early stages of ossification in the epiphyses at the proximal ends of the phalanges and first metacarpal; at the distal ends of the remaining metacarpals and radius; in the capitate, hamate and lunate. Typically, the centre for the lunate is preceded by the centre for the triquetrum. Compare with Figs **50.9** and **50.10**.

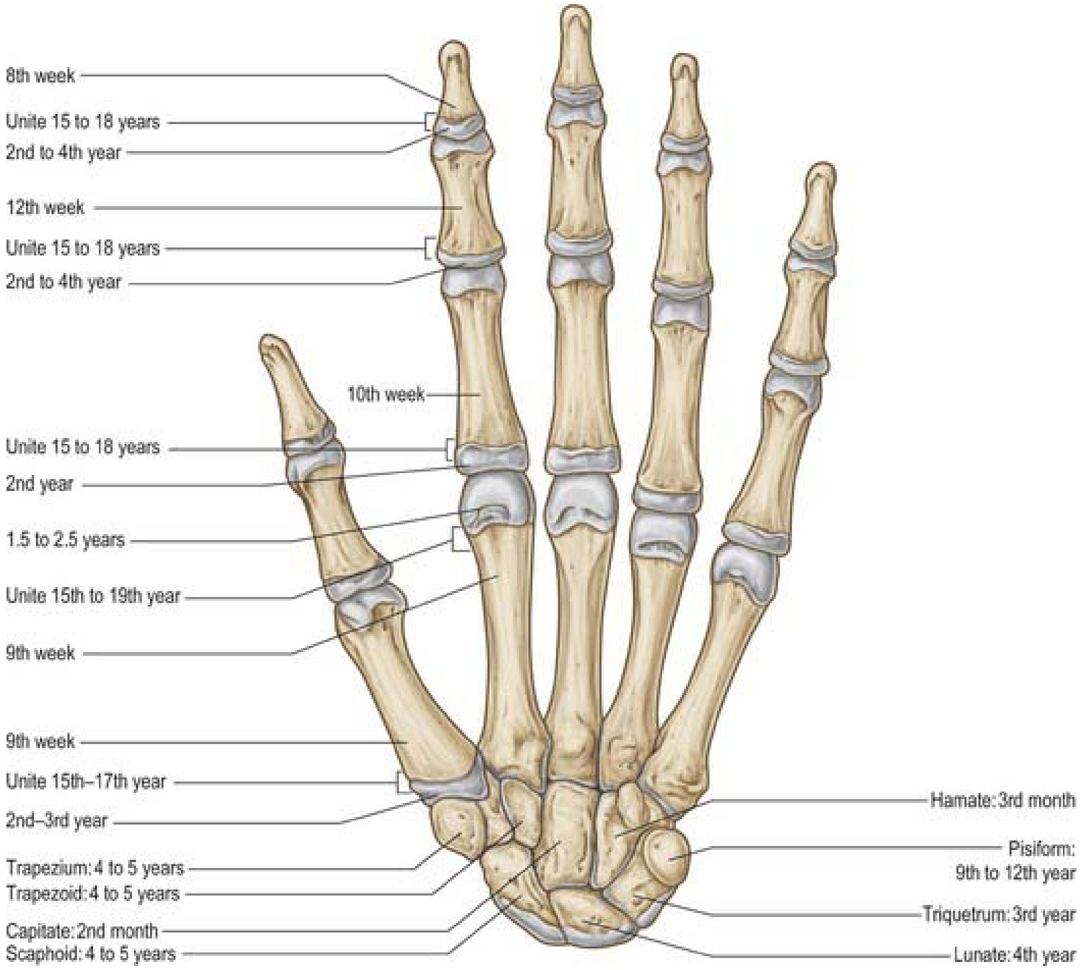
8th week
Unite 15 to 18 years
2nd to 4th year
12th week
Unite 15 to 18 years
2nd to 4th year
10th week
Unite 15 to 18 years
2nd year
1.5 to 2.5 years
Unite 15th to 19th year
9th week
9th week
Unite 15th–17th year
2nd–3rd year
Trapezium: 4 to 5 years
Trapezoid: 4 to 5 years
Capitate: 2nd month
Scaphoid: 4 to 5 years
Hamate: 3rd month
Pisiform:
9th to 12th year
Triquetrum: 3rd year
Lunate: 4th year

Fig. 50.12 The bones of the hand of a child, indicating the general plan of ossification.

METACARPALS

The metacarpus consists of five metacarpal bones, conventionally numbered in radio-ulnar order. These are miniature long bones, with a distal head, shaft and expanded base. The rounded heads articulate with the proximal phalanges. Their articular surfaces are convex, although less so transversely, and extend further on the palmar surfaces, especially at their margins. The knuckles are produced by the metacarpal heads. The metacarpal bases articulate with the distal carpal row and with each other, except the first and second. The shafts have longitudinally concave palmar surfaces, which form hollows for the palmar muscles. Their dorsal surfaces bear a distal triangular area, which is continued proximally as a round ridge. These flat areas are palpable proximal to the knuckles.

The medial four metacarpals are sometimes described as parallel; strictly speaking, they diverge somewhat, and radiate gently proximodistally. However, the first metacarpal, relative to the others, is more anterior and rotated medially on its axis through 90°, so that its morphologically dorsal surface is lateral, its radial border palmar, its palmar surface medial, and its ulnar border dorsal. Hence the thumb flexes medially across the palm and can be rotated into opposition with each finger. Opposition depends on medial rotation and is the prime factor in manual dexterity: when an object is grasped, fingers and thumb encircle it from opposite sides, greatly increasing the power and skill of the grip.

Individual metacarpal bones

First metacarpal

The first metacarpal is short and thick (Fig. 50.13A). Its dorsal (lateral) surface can be felt to face laterally; its long axis diverges distolaterally from its neighbour. The shaft is flattened, dorsally broad and transversely convex. The palmar (medial) surface is longitudinally concave and divided by a ridge into a larger lateral (anterior) and smaller medial (posterior) part. Opponens pollicis is attached to the radial border and adjoining palmar surface; the first dorsal interosseous muscle (radial head) is attached to its ulnar border and adjacent palmar surface. The base is concavoconvex and articulates with the trapezium. Abductor pollicis longus is attached on its lateral (palmar) side, the first palmar interosseous muscle to its ulnar side. The head is less convex than in other metacarpals and is transversely broad. Sesamoid bones glide on radial and ulnar articular eminences on its palmar aspect.

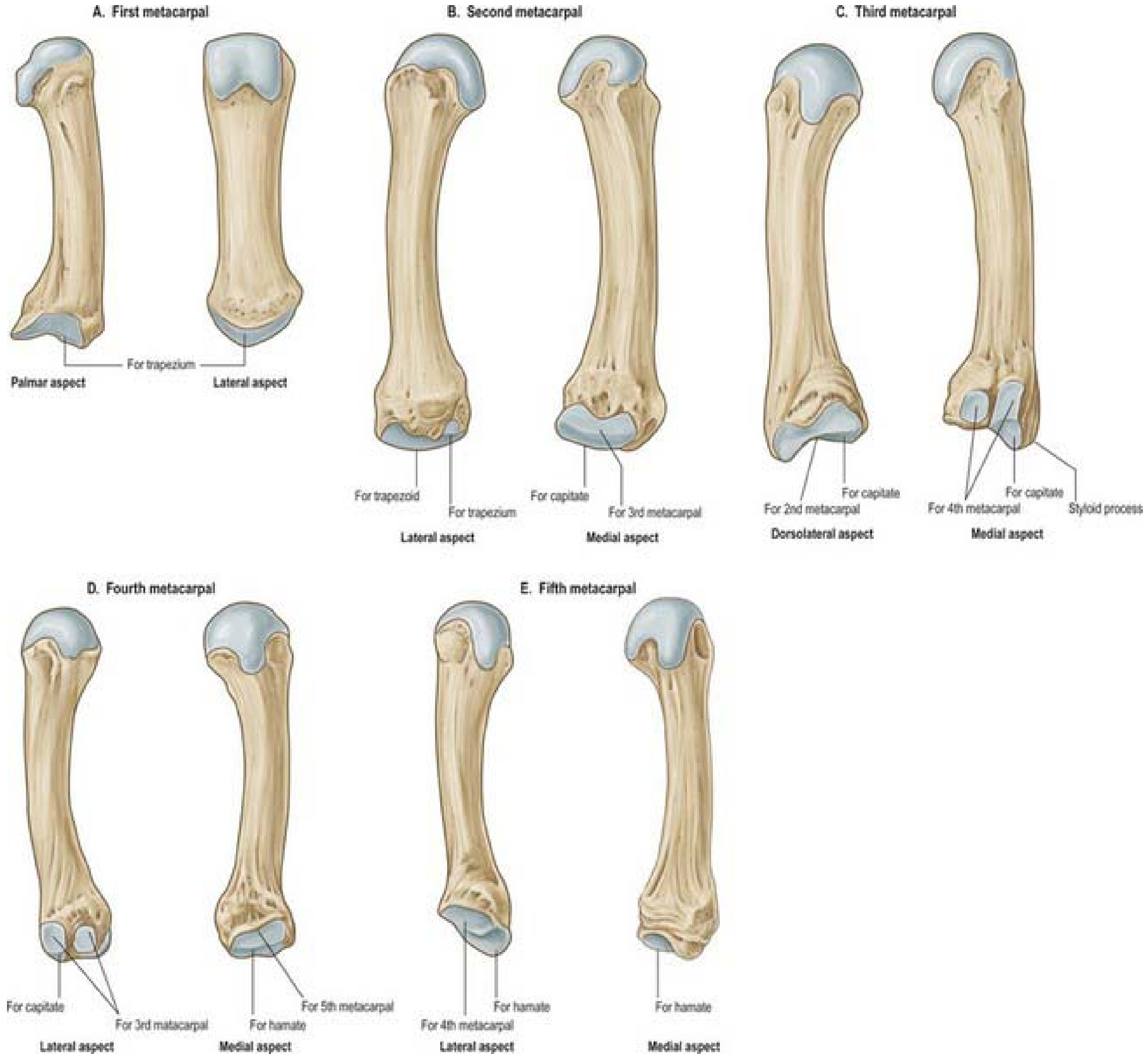
A. First metacarpal
For trapezium
Palmar aspect
Lateral aspect
B. Second metacarpal
For trapezoid
For trapezium
Lateral aspect
For capitate
For 3rd metacarpal
Medial aspect
C. Third metacarpal
For capitate
For 2nd metacarpal
Dorsolateral aspect
For capitate
For 4th metacarpal
Styloid process
Medial aspect
D. Fourth metacarpal
For capitate
For 3rd matacarpal
Lateral aspect
For 5th metacarpal
For hamate
Medial aspect
E. Fifth metacarpal
For hamate
For 4th metacarpal
Lateral aspect
For hamate
Medial aspect

Fig. 50.13 Metacarpal bones.

Second metacarpal

The second metacarpal has the longest shaft and largest base (Fig. 50.13B). The latter is grooved in a dorsopalmar direction for articulation with the trapezoid. Medial to the groove a deep ridge articulates with the capitate; laterally, nearer the dorsal surface of the base, there is a quadrilateral facet for articulation with the trapezium, and just dorsal to this facet a rough impression marks the attachment of extensor carpi radialis longus. On the palmar surface a small tubercle or ridge receives flexor carpi radialis. The medial side of the base articulates with that of the third metacarpal by a long facet, centrally narrowed. The shaft is prismatic in section and longitudinally curved, convex dorsally, concave towards the palm. Its dorsal surface is distally broad but proximally narrows to a ridge which is covered by extensor tendons of the index finger. Its converging borders begin at the tubercles, one on each side of its head for the attachment of collateral ligaments. Proximally the lateral surface inclines dorsally for the ulnar head of the first dorsal interosseous. The medial surface inclines similarly, and is divided by a faint ridge into a palmar strip for attachment of the second palmar interosseous, and a dorsal strip for attachment of the radial head of the second dorsal interosseous.

Third metacarpal

The third metacarpal has a short styloid process, projecting proximally from the radial side of the dorsal surface (Fig. 50.13C). Its base articulates with the capitate by a facet anteriorly convex but dorsally concave where it invades the styloid process on the lateral aspect of its base. A strip-like facet, constricted centrally, articulates with the bases of the second metacarpal (laterally) and the fourth metacarpal (medially), the latter by two oval facets. The palmar facet may be absent; less frequently the facets are connected proximally by a narrow bridge. The palmar surface of the base receives a slip from the tendon of flexor carpi radialis; extensor carpi radialis brevis is attached to its dorsal surface, beyond the styloid process. The shaft resembles that of the second metacarpal. The ulnar head of the second dorsal interosseous is attached to its lateral surface; the radial head of the third dorsal interosseous is attached to its medial surface, and the transverse head of adductor pollicis is attached to the intervening palmar ridge in its distal two-thirds. Its dorsal surface is covered by the extensor tendon.

Fourth metacarpal

The fourth metacarpal is shorter and thinner than the second and third (Fig. 50.13D). On its base it displays two lateral oval facets for articulation with the base of the third metacarpal; the dorsal is usually larger and proximally in contact with the capitate. A single medial elongated facet is for articulation with the base of the fifth metacarpal. The quadrangular proximal surface articulates with the hamate, and is anteriorly convex, dorsally concave. The shaft is like the second, but a faint ridge on its lateral surface separates the attachments of the third palmar interosseous and the ulnar head of the third dorsal interosseous. The radial head of the fourth dorsal interosseous is attached to the medial surface.

Fifth metacarpal

The fifth metacarpal (Fig. 50.13E) differs in its medial basal surface, which is non-articular and bears a tubercle for extensor carpi ulnaris. The lateral basal surface is a facet, transversely concave, convex from palm to dorsum, for articulation with the hamate. A lateral strip articulates with the base of the fourth metacarpal. The shaft bears a triangular dorsal area which almost reaches the base; the lateral surface inclines dorsally only at its proximal end. Opponens digiti minimi is attached to the medial surface. The lateral surface is divided by a ridge, which is sometimes sharp, into a palmar strip for the attachment of the fourth palmar interosseous and a dorsal strip for the ulnar part of the fourth dorsal interosseous.

Ossification

Each metacarpal ossifies from a primary centre for the shaft and a secondary centre which is in the base of the first metacarpal and in the heads of the other four (Figs 50.8-50.11). Ossification begins in the midshaft about the ninth week. Centres for the second to fifth metacarpal heads appear in that order in the second year in females, and between 1½ to 2½ years in males. They unite with the shafts about the 15th or 16th year in females, 18th or 19th in males. The first metacarpal base begins to ossify late in the second year in females, early in the third year in males, uniting before the 15th year in females and 17th in males. Sometimes the styloid process of the third metacarpal is a separate ossicle. The thumb metacarpal ossifies like a phalanx, and some authorities therefore consider that the thumb skeleton consists of three phalanges. Others believe that the distal phalanx represents fused middle and distal phalanges, a condition occasionally observed in the fifth toe. When the thumb has three phalanges, the metacarpal has a distal and a proximal epiphysis. It occasionally bifurcates distally. When it does, the medial branch has no distal epiphysis and bears two phalanges, while the lateral branch shows a distal epiphysis, and three phalanges. The existence of only a distal metacarpal epiphysis may be associated with a greater range of movement at the metacarpophalangeal joint. In the thumb, the carpometacarpal joint has the wider range, and the first metacarpal has a basal epiphysis. A distal epiphysis may appear in the first, and a proximal epiphysis in the second, metacarpal.

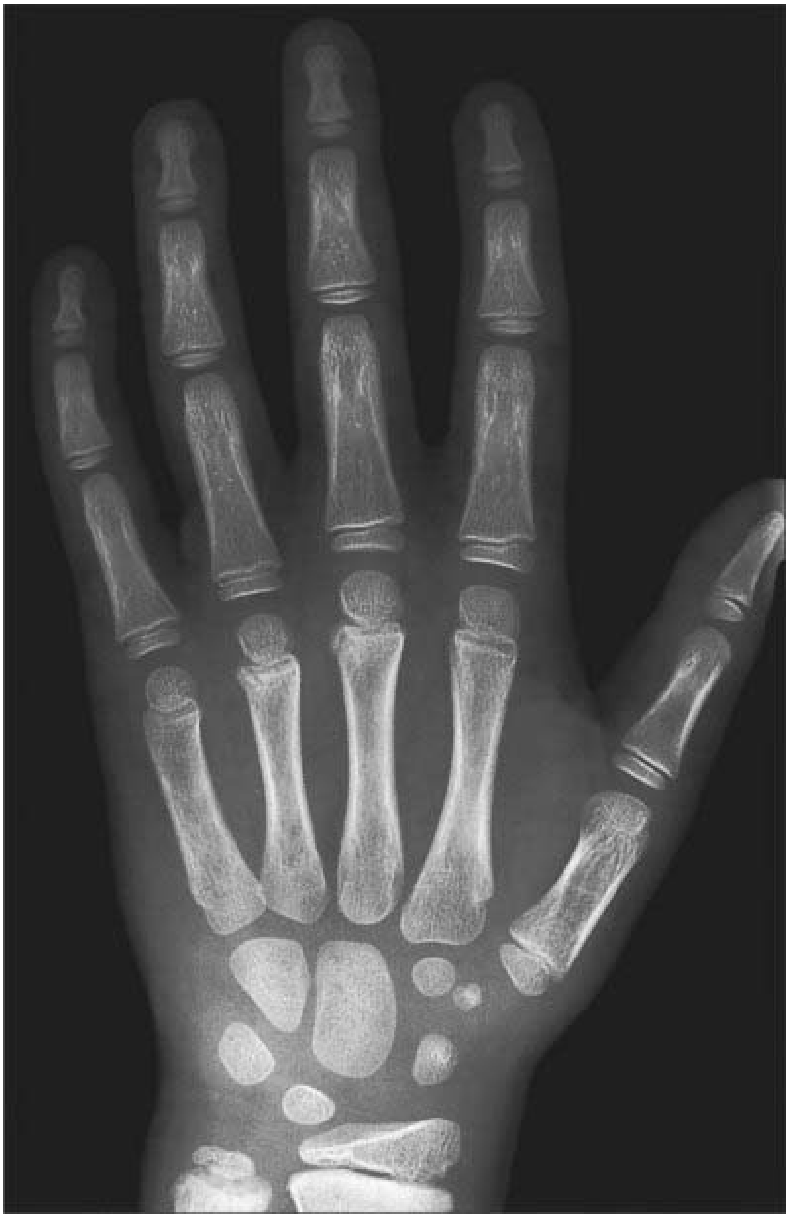

Fig. 50.9 Radiograph of a hand at 6½ years (male), dorsopalmar projection. Note the more advanced state of the centres of ossification which were already visible in **Fig. 50.8**, and the appearance of additional centres in the distal ulnar epiphysis and in the triquetrum, scaphoid, trapezium and trapezoid.

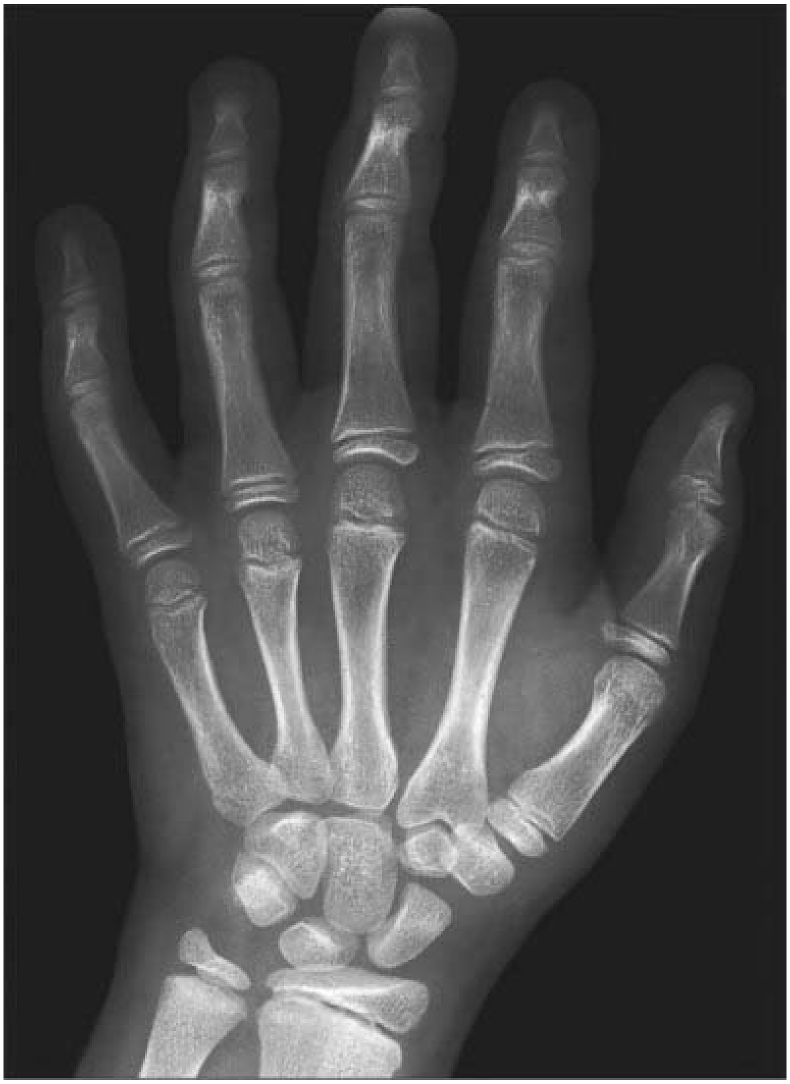

Fig. 50.10 Radiograph of a hand at 11 years (female), dorsopalmar projection. Note the maturing shapes of all the ossifications previously seen in **Figs 50.8** and **50.9**, with the addition of the pisiform.

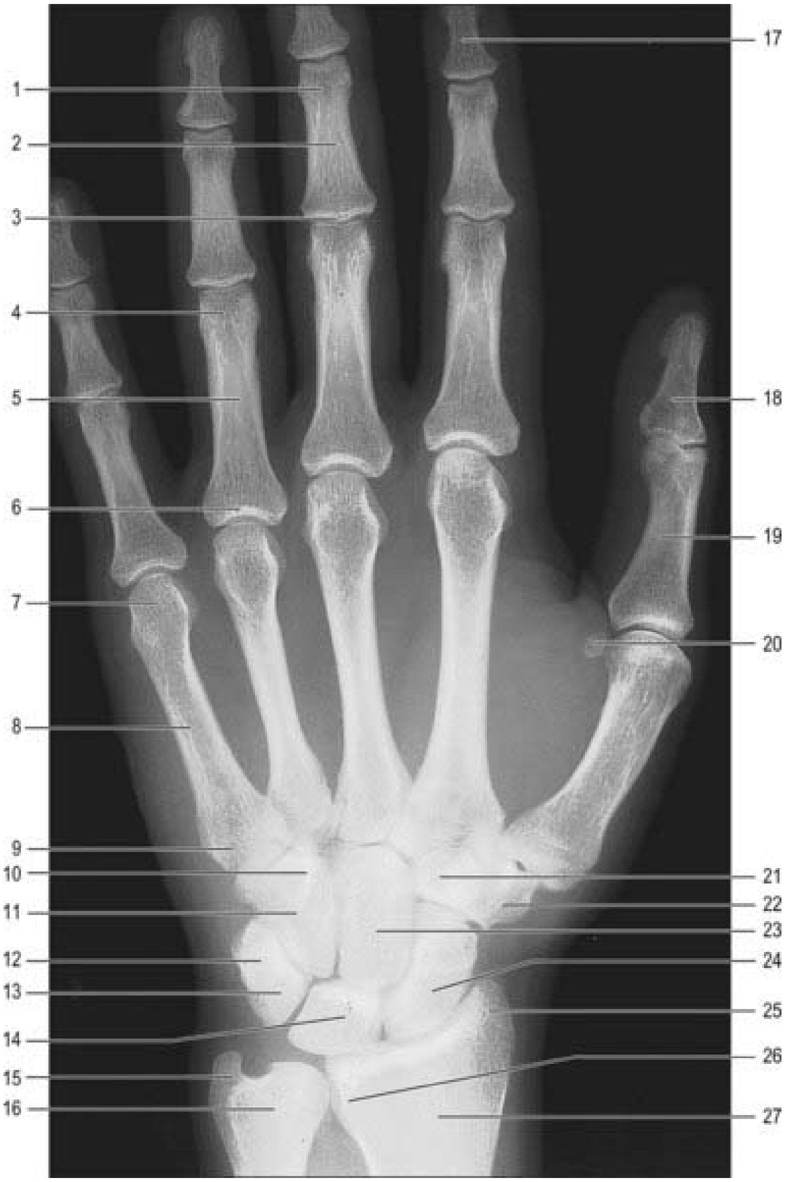

Fig. 50.11 Radiograph of adult hand for comparison (male of 19 years), dorsopalmar projection. Note additional ossification in the sesamoid bones of the thumb. **1**. Head of middle phalanx of middle finger. **2**. Shaft of middle phalanx of middle finger. **3**. Base of middle phalanx of middle finger. **4**. Head of proximal phalanx of ring finger. **5**. Shaft of proximal phalanx of ring finger. **6**. Base of proximal phalanx of ring finger. **7**. Head of fifth metacarpal. **8**. Shaft of fifth metacarpal. **9**. Base of fifth metacarpal. **10**. Hook of hamate. **11**. Hamate. **12**. Pisiform. **13**. Triquetrum. **14**. Lunate. **15**. Styloid process of ulna. **16**. Head of ulna. **17**. Distal phalanx of index finger. **18**. Distal phalanx of thumb. **19**. Proximal phalanx of thumb. **20**.

Sesamoid bone. **21**. Trapezoid. **22**. Trapezium. **23**. Capitate. **24**. Scaphoid. **25**. Styloid process of radius. **26**. Ulnar (sigmoid) notch of radius. **27**. Radius.

(By permission from Weir J, Abrahams PH 2003 Imaging Atlas of Human Anatomy, 3rd edn, London: Mosby, and contributions from Anna-Maria Belli, Margaret Hourihan, Niall Moore and Philip Owen.)

PHALANGES

There are 14 phalanges, three in each finger, two in the thumb. Each has a head, shaft and proximal base. The shaft tapers distally, its dorsal surface transversely convex. The palmar surface is transversely flat but gently concave anteriorly in its long axis. The bases of the proximal phalanges carry concave, oval facets adapted to the metacarpal heads. Their own heads are smoothly grooved like pulleys and encroach more on to the palmar surfaces. The bases of the middle phalanges carry two concave facets separated by a smooth ridge, conforming to the heads of the proximal phalanges. The bases of the distal phalanges are adapted to the pulley-like heads of the middle phalanges. The heads of the distal phalanges are non-articular and carry a rough, crescentic palmar tuberosity to which the pulps of the fingertips are attached.

Articular ligaments and numerous muscles are attached to the phalanges. A corresponding tendon of flexor digitorum profundus and, on its dorsal surface, extensor digitorum, are attached to the base of each distal phalanx on its palmar surface. A tendon of flexor digitorum superficialis and its fibrous sheath are attached to the sides of a middle phalanx, and a part of extensor digitorum is attached to the base dorsally. A fibrous flexor sheath is attached to the sides of a proximal phalanx, part of the corresponding dorsal interosseous is attached to its base laterally, and another dorsal interosseous is attached medially.

The phalanges of the little finger and the thumb differ. Abductor and flexor digiti minimi are attached to the medial side of the base of the proximal phalanx of the little finger. The tendon of extensor pollicis brevis and the oblique head of adductor pollicis (dorsally), and the oblique and transverse heads of adductor pollicis, sometimes conjoined with the first palmar interosseous (medially), are attached to the base of the proximal pollicial phalanx.

The margins of the proximal pollicial phalanx are not sharp, because the fibrous sheath is less strongly developed than it is in the other digits.

Ossification

Phalanges are ossified from a primary centre for the shaft and a proximal epiphysial centre (Figs 50.8-50.12). Ossification begins prenatally in shafts as follows: distal phalanges in the eighth or ninth week, proximal phalanges in the tenth, middle phalanges in the 11th week or later. Epiphysial centres appear in proximal phalanges early in the second year (females), and later in the same year (males), and in middle and distal phalanges in the second year (females), or third or fourth year (males). All epiphyses unite about the 15th to 16th year in females, and 17th to 18th year in males.

JOINTS

DISTAL RADIO-ULNAR JOINT

The distal radio-ulnar joint is a uniaxial pivot joint (Fig. 50.14).

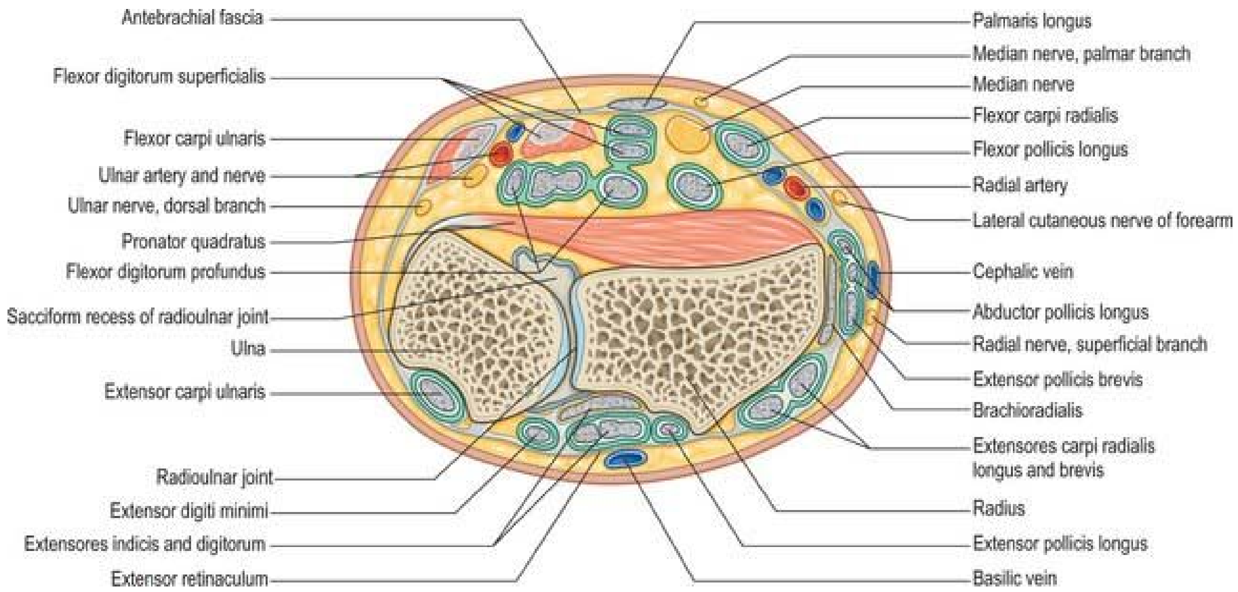
Antebrachial fascia
Flexor digitorum superficialis
Flexor carpi ulnaris
Ulnar artery and nerve
Ulnar nerve, dorsal branch
Pronator quadratus
Flexor digitorum profundus
Sacciform recess of radioulnar joint
Ulna
Extensor carpi ulnaris
Radioulnar joint
Extensor digiti minimi
Extensores indicis and digitorum
Extensor retinaculum
Palmaris longus
Median nerve, palmar branch
Median nerve
Flexor carpi radialis
Flexor pollicis longus
Radial artery
Lateral cutaneous nerve of forearm
Cephalic vein
Abductor pollicis longus
Radial nerve, superficial branch
Extensor pollicis brevis
Brachioradialis
Extensores carpi radialis longus and brevis
Radius
Extensor pollicis longus
Basilic vein

Fig. 50.14 Transverse section through the left wrist at the level of the distal radio-ulnar joint, showing the muscle tendons and their synovial sheaths.

(From Sobotta 2006.)

Articulating surfaces

The articulating surfaces are between the convex distal head of the ulna and the concave ulnar notch of the radius, and are connected by an articular disc.

Fibrous capsule

The fibrous capsule is thicker anteriorly and posteriorly, but the proximal part of the capsule is lax.

Articular disc

The articular disc is fibrocartilaginous (collagen with few elastic fibres in the young) and is triangular, binding the distal ends of the ulna and radius. Its periphery is thicker, its centre sometimes perforated. The disc is attached by a blunt, thick apex to a depression between the ulnar styloid process and distal articular surface, and by its wider thin base to the prominent edge between the ulnar notch and carpal articular surface of the radius. Its margins are united to adjacent carpal ligaments, its surfaces are smooth and concave: the proximal articulates with the ulnar head, the distal is part of the radiocarpal joint, and articulates with the lunate and, when the hand is adducted, the triquetrum. The disc shows age-related degeneration, becoming thinned and ultimately perforated in about half the subjects over the age of 60.

Synovial membrane

The capsule is lined by synovial membrane which projects proximally between the radius and ulna as a recessus sacciformis in front of the distal part of the interosseous membrane.

Vascular supply and lymphatic drainage

The arterial supply to the distal radio-ulnar joint and disc is mainly derived from the palmar and dorsal branches of the anterior interosseous artery, reinforced by the posterior interosseous and ulnar arteries.

Innervation

The distal radio-ulnar joint is innervated by branches of the anterior and posterior interosseous nerves.

Movements

Movements at the radio-ulnar joint complex pronate and supinate the hand. In pronation the radius, carrying the hand, turns anteromedially and obliquely across the ulna, its proximal end remains lateral, its distal becomes medial. During this action the interosseous membrane becomes spiralled. In supination the radius returns to a position lateral and parallel to the ulna and the interosseous membrane becomes unspiralled. The hand can be turned through 140–150°: with the elbow extended, this can be increased to nearly 360° by humeral rotation and scapular movements. Power is greater in supination, a fact which has affected the design of nuts, bolts and screws, which are tightened by supination in right-handed subjects. Moreover, supination is an antigravity movement with a pendent upper arm and semiflexed forearm; in seizing objects for examination or manipulation, pronation is merely a preliminary and is aided by gravity.

Forearm rotation occurs between the articulation of the head of the ulna and sigmoid notch distally, and the head of the radius and the radial notch of the ulna proximally. These distal and proximal radio-ulnar joints are pivot-type synovial joints: they act as a pair permitting stable rotary motion (pronation 61–66°, supination 70–77°). During rotation, the radius moves around the ulnar head. The axis for pronation and supination is often represented as a line through the centre of the radial head (proximal) and the ulnar attachment of the articular disc (distal). More correctly this is the axis of movement of the radius relative to the ulna and it does not remain stationary. The radial head rotates in the fibro-osseous ring: its distal lower end and articular disc swing round the ulnar head. During rotation of the radial head its proximal surface spins on the humeral capitulum. As the forearm moves from full pronation into supination the ulna translocates medially by 9–10 mm, such that the axis of rotation shifts but still passes through the ulnar head. In addition the sigmoid notch changes its contact position with the ulnar head, lying dorsal proximal in pronation and volar distal in supination. The distal end of the ulna is not stationary during these movements; it moves a variable amount along a curved course, posterolaterally in pronation, anteromedially in supination. The axis of movement, as defined above, is therefore displaced laterally in pronation, medially in supination. Hence the axis for supination and pronation of the whole forearm and hand passes between the bones at both the superior and distal radio-ulnar joints when ulnar movement is marked, but through the centres of the radial head and ulnar styloid when it is minimal. The axis may be prolonged through any digit, depending on the medial or lateral displacement of the distal end of the ulna. The hand will rotate further than the forearm because of the sliding–rotatory movement which occurs between the carpal bones and the bases of the metacarpals and, to a very minor degree, at the radiocarpal joint.

Accessory movements

Accessory movements include anterior and posterior translation of the radial head on the ulnar radial notch, and of the ulnar head likewise on the radial ulnar notch.

Muscles producing movement

The muscles producing movements at the distal radio-ulnar joint are as follows.

Pronation

Pronator quadratus, aided in rapid movement and against resistance by pronator teres. Gravity also assists.

Supination

Supinator, in slow unresisted movement and extension, assisted by biceps in fast movements in flexion, especially when resisted.

Electromyographic studies have not confirmed activity in brachioradialis during pronation and supination.

RADIOCARPAL (WRIST) JOINT

Articulating surfaces

The radiocarpal joint is a synovial biaxial and ellipsoid joint formed by articulation of the distal end of the radius and the triangular fibrocartilage with the scaphoid, lunate and triquetrum (Fig. 50.15 and Fig. 50.16). In the neutral position of the wrist, only the scaphoid and lunate are in contact with the radius and articular disc: the triquetrum comes into apposition with the disc only in full adduction of the wrist joint. The radial articular surface and distal discal surface form an almost elliptical, concave surface with a transverse long axis. The radial surface is bisected by a low ridge into two concavities. A similar ridge usually appears between the medial radial concavity and the concave distal discal surface. The proximal articular surfaces of the scaphoid, lunate and triquetrum, and their interosseous ligaments, form a smooth convex surface which is received into the proximal concavity.

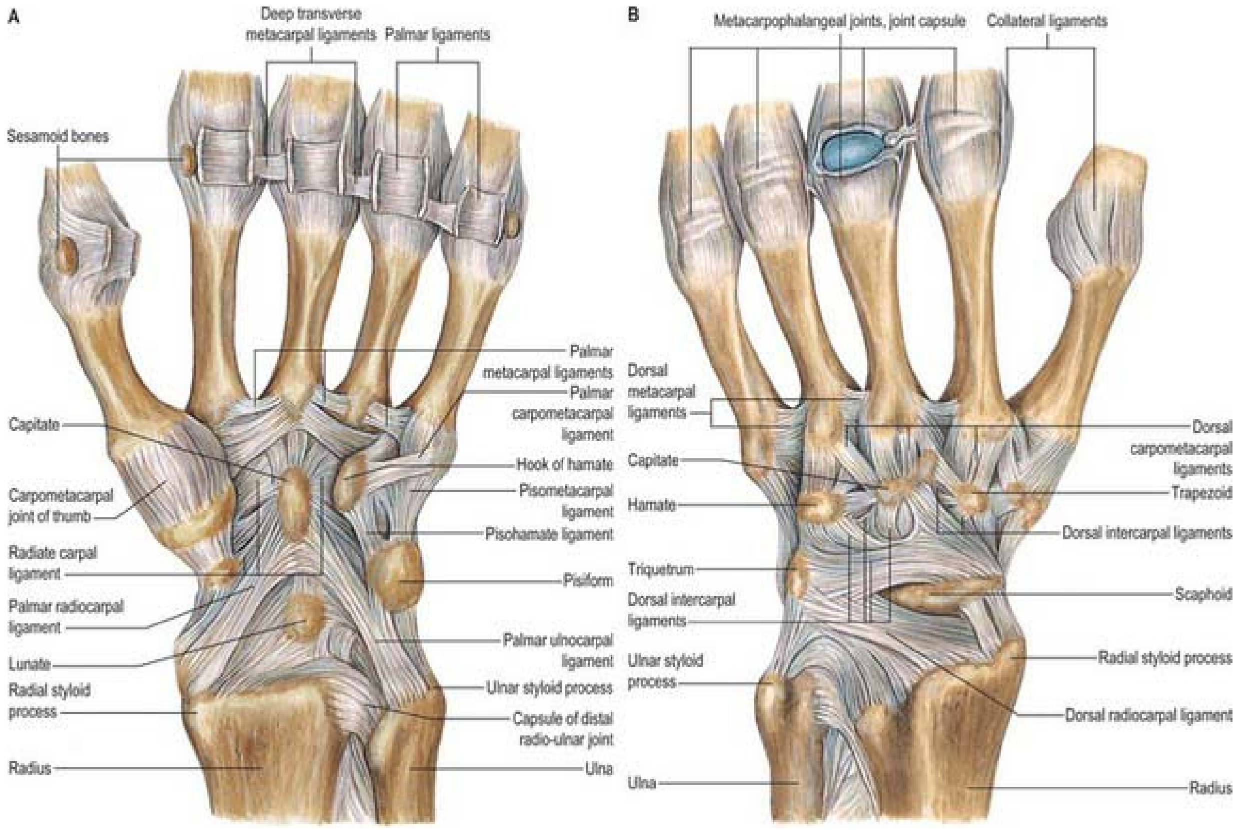
A
Deep transverse metacarpal ligaments
Palmar ligaments
Sesamoid bones
Capitate
Carpometacarpal joint of thumb
Radiate carpal ligament
Palmar radiocarpal ligament
Lunate
Radial styloid process
Radius
Palmar metacarpal ligaments
Palmar carpometacarpal ligament
Hook of hamate
Pisometacarpal ligament
Pisohamate ligament
Pisiform
Palmar ulnocarpal ligament
Ulnar styloid process
Capsule of distal radio-ulnar joint
Ulna
B
Metacarpophalangeal joints, joint capsule
Collateral ligaments
Dorsal metacarpal ligaments
Capitate
Hamate
Triquetrum
Dorsal intercarpal ligaments
Ulnar styloid process
Ulna
Dorsal carpometacarpal ligaments
Trapezoid
Dorsal intercarpal ligaments
Scaphoid
Radial styloid process
Dorsal radiocarpal ligament
Radius

Fig. 50.15 Joints and ligaments of the left hand. **A**, Palmar aspect. **B**, Dorsal aspect.

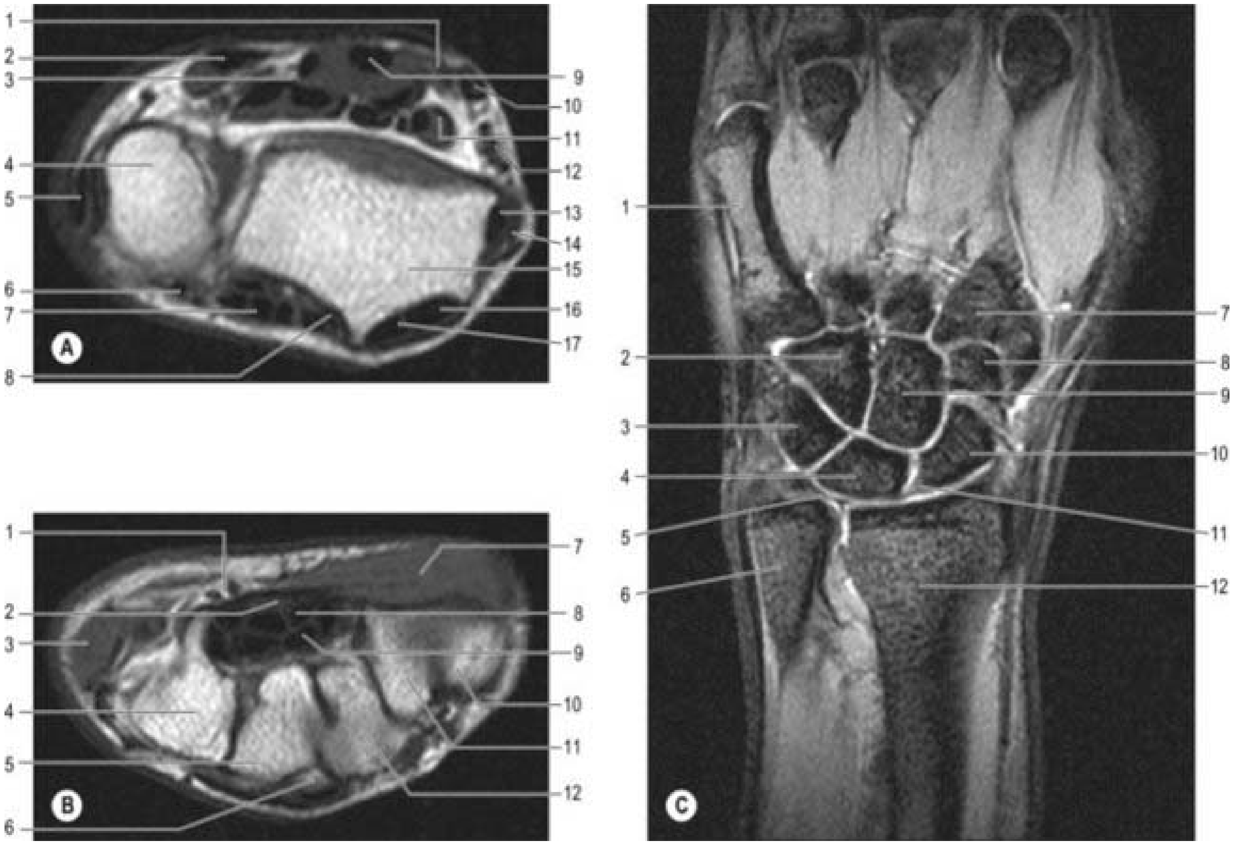

Fig. 50.16 MRI left wrist. **A**, Axial view at level of distal radio-ulnar joint. **B**, Axial view at level of carpal tunnel. **C**, Coronal MRI through the wrist demonstrating normal bony anatomy and the triangular fibrocartilage.

Part A: **1**. Median nerve. **2**. Flexor carpi ulnaris. **3**. Flexor digitorum profundus. **4**. Ulna. **5**. Extensor carpi ulnaris. **6**. Extensor digiti minimi. **7**. Extensor digitorum and extensor indicis. **8**. Extensor pollicis longus. **9**. Flexor digitorum superficiales. **10**. Flexor carpi radialis. **11**. Flexor pollicis longus. **12**. Radial artery. **13**. Abductor pollicis longus. **14**. Extensor pollicis brevis. **15**. Radius. **16**. Extensor carpi radialis longus. **17**. Extensor carpi radialis brevis.

Part B: **1**. Ulnar artery and nerve. **2**. Median nerve. **3**. Hypothenar muscles. **4**. Hamate. **5**. Capitate. **6**. Base of 3rd metacarpal. **7**. Thenar muscles. **8**.

Flexor digitorum superficialis. **9**. Flexor digitorum profundus. **10**. Base of 1st metacarpal. **11**. Trapezium. **12**. Trapezoid.
Part C: **1**. 5th metacarpal. **2**. Hamate. **3**. Triquetrum. **4**. Lunate. **5**. Triangular fibrocartilage. **6**. Distal ulna. **7**. Base of 2nd metacarpal. **8**. Trapezoid. **9**. Capitate. **10**. Scaphoid. **11**. Scapholunate ligament. **12**. Distal radius.

Fibrous capsule

The fibrous capsule is lined by synovial membrane which is usually separate from that of the distal radio-ulnar and intercarpal joints. A protruding prestyloid recess (recessus sacciformis), anterior to the articular disc, is present and ascends close to the styloid process. The recess is bounded distally by a fibrocartilaginous meniscus, which projects from the ulnar collateral ligament between the tip of the ulnar styloid process and the triquetrum; both are clothed with hyaline articular cartilage. The meniscus may ossify. The capsule is strengthened by palmar radiocarpal and ulnocarpal, dorsal radiocarpal and radial and ulnar collateral ligaments.

Synovial membrane

The synovial membrane lines the fibrous capsule.

Vascular supply

The radiocarpal joint is supplied by branches of the anterior interosseous artery, anterior and posterior carpal branches of the radial and ulnar arteries, palmar and dorsal metacarpal arteries and recurrent rami of the deep palmar arch.

Innervation

The radiocarpal joint is innervated by the anterior and posterior interosseous nerves with contributions from the median, ulnar and radial nerves.

Muscles producing movement

Movements accompany those of the intercarpal and midcarpal joints and are described on page 871.

CARPAL JOINTS

The intercarpal joints interconnect the carpal bones. They may be summarized as the joints between the proximal and distal rows of carpal bones, and the midcarpal joint, a complex joint between the rows.

Carpal bones are connected by an extensive array of ligaments, not all of which are specifically named. The flexor retinaculum is an accessory intercarpal ligament. Articular surfaces are either sellar, ellipsoid or spheroidal.

Joints of the proximal carpal row

Joints of the proximal carpal row are between the scaphoid, lunate and triquetrum. In addition, the pisiform articulates with the palmar surface of the triquetrum at a small, oval, almost flat, synovial pisotriquetral joint.

A thin capsule surrounds the joint. The synovial cavity is usually separate but may communicate with that of the radiocarpal joint.

Joints of the distal carpal row

Joints of the distal carpal row are between the trapezium, trapezoid, capitate and hamate. There is virtually no movement at these joints.

Midcarpal joint

The midcarpal joint, between the scaphoid, lunate and triquetrum (proximally) and trapezium, trapezoid, capitate and hamate (distally) is a compound articulation that may be divided descriptively into medial and lateral parts. Throughout most of the medial compartment the convexity formed by the head of the capitate and hamate articulates with a reciprocal concavity formed by the scaphoid, lunate and much of the triquetrum. However, most medially the curvatures are reversed, forming a compound sellar joint. In the lateral compartment the trapezium and trapezoid articulate with the scaphoid, forming a second compound articulation, often said to be plane, but which is also sellar.

Carpal synovial membrane

The carpal synovial membrane is most extensive, and lines an irregular articular cavity. Its proximal part is between the distal surfaces of the scaphoid, lunate and triquetrum and the proximal surfaces of the second carpal row. It has proximal prolongations between the scaphoid and lunate, and lunate and triquetrum, and three distal prolongations between the four bones of the second row. The absence of an interosseous ligament means that the prolongation between the trapezium and trapezoid and/or between the trapezoid and capitate is often continuous with corresponding carpometacarpal joints, variably from the second to the fifth, or often the second and third only. In the latter case, the joint between the hamate and fourth and fifth metacarpal bones has a separate synovial membrane and the carpometacarpal interosseous ligament is interposed. Synovial cavities of carpometacarpal joints are prolonged slightly between the metacarpal bases. The synovial joint between the pisiform and triquetrum is usually isolated.

Vascular supply

The carpal joints are supplied by the posterior carpal branches of the radial and ulnar arteries and by the anterior interosseous artery.

Innervation

Precise details about innervation of the carpal joints are lacking. They appear to be innervated by small branches from the deep terminal branch of the ulnar nerve, the median nerve and its anterior interosseous branch, the superficial radial nerve and the posterior interosseous branch of the radial nerve.

Wrist ligaments

Wrist ligaments situated between the fibrous and synovial layers of the wrist joint are termed intracapsular, while those lying superficial to the fibrous layer are extracapsular. Almost all ligaments of the wrist actually lie within the joint capsule and the only exceptions are the flexor and extensor retinaculae and the pisotriquetral ligament. The intracapsular ligaments appear to blend one into another and the edges of the ligaments may not be distinct or discrete.

The ligaments are further classified into extrinsic and intrinsic named ligaments. In addition there are superficial and deep parts to some of the extrinsic ligaments; the latter are identifiable at wrist arthroscopy, the former are not.

It is important to appreciate that the wrist ligaments are named from proximal to distal and from radial to ulnar. Thus a ligament passing between the capitate, scaphoid and radius is called the radioscaphocapitate ligament.

Extrinsic ligaments

Extrinsic ligaments connect the carpus with the forearm bones. The extrinsic ligaments as a group tend to be longer than the intrinsic ligaments. They are approximately one-third as strong but easier to repair following rupture.

Extrinsic palmar carpal ligaments

When the synovial lining of the carpal tunnel is dissected away, two V-shaped ligamentous bands are visible with their apices lying distally (Fig. 50.15A). The limbs of the 'V' take origin from the radius and ulna respectively: the apex of one 'V' attaches to the distal row and that of the second 'V' to the proximal row.

Radioscaphocapitate ligament

The radioscaphocapitate ligament originates from the radial styloid and the palmar lip of the radius. It courses distally and is then described by some authors as having three parts. The first is the most radial and inserts onto the lateral aspect of the waist of the scaphoid (radial collateral ligament). The second continues as part of the distal 'V' and inserts onto the distal pole of the scaphoid. The third passes over the proximal pole of the scaphoid towards the midcarpus and blends with the fibres originating from the ulnar side – part of the triangular fibrocartilage complex – to form the arcuate ligament over the palmar aspect of the capitate. A few of the fibres of the radioscaphocapitate ligament attach to the body of the capitate. There is a discrete interval between the inferior margin of this ligament and the palmar horn of the lunate which is known as the space of Poirier.

Long radiolunate ligament

The long radiolunate ligament takes origin adjacent to the radioscaphocapitate ligament on the palmar lip of the radius. It passes over and supports the proximal pole of the scaphoid before inserting into the palmar horn of the lunate. This ligament is discrete from the radioscaphocapitate ligament and the visible separation is known as the interligamentous sulcus (continuous with the space of Poirier).

Radioscapholunate (ligament of Testut)

Histological studies have shown the radioscapholunate ligament is not a true ligament because it contains neurovascular structures which supply the scapholunate interosseous membrane and is covered by a thick synovial lining. However it a visible landmark inside the wrist joint when undertaking wrist arthroscopy.

Short radiolunate ligament

The short radiolunate ligament is part of the proximal ‘V’. It arises from the palmar lip of the lunate fossa of the radius and passes directly to the palmar horn of the lunate. To the ulnar side its fibres blend with those of the palmar triangular fibrocartilage complex as these also pass to their insertion on the lunate. This ligament contributes to the stability of the lunate.

Ulnolunate ligament

The ulnolunate ligament originates from the palmar aspect of the ulna adjacent to the short radiolunate ligament and inserts onto the palmar horn of the lunate. Part of this fibre complex arches radially and blends with part of the radioscaphocapitate complex, forming the arcuate ligament.

Ulnotriquetral (ulnar collateral) ligament

The ulnotriquetral ligament arises from the palmar aspect of the ulna and inserts into the medial aspect of the triquetrum. It continues distally to a further attachment to the medial aspect of the hamate. It is generally thought that the ulnolunate and ulnotriquetral ligaments also take some origin from the marginal ligament of the triangular fibrocartilage complex.

Extrinsic dorsal carpal ligaments

The dorsal wrist ligaments are comparatively thin. They are reinforced by the floor and septa of the fibrous tunnels for the six dorsal compartments. The extrinsic dorsal carpal ligaments and the intrinsic dorsal intercarpal ligaments have a ‘Z-shaped’ configuration (Fig. 50.15B). The pattern and shape of these ligaments is utilized in one surgical approach to the dorsum of the wrist joint where incisions are oriented parallel with the ligaments: this reduces scarring and restriction of subsequent motion caused by the arthrotomy.

Dorsal radiolunotriquetral ligament

The dorsal radiolunotriquetral ligament is a true intracapsular ligament. It is the only extrinsic ligament on the dorsum of the carpus and has superficial and deep components. The superficial part connects the radius and triquetrum, and the deep part connects the radius, lunate and triquetrum. The two components are inseparable. The wide superficial component arises from the dorsal margin of the distal radius and courses ulnarly to insert on the dorsal edge of the triquetrum. The deep component takes a narrower origin from the ulnar aspect of the distal dorsal radius and passes in an ulnar direction to attach to part of the lunotriquetral articulation and the intrinsic lunotriquetral ligament.

Intrinsic ligaments

Intrinsic ligaments of the wrist are attached to carpal bones. They are stronger and shorter than extrinsic ligaments and are connected with the extrinsic ligament complexes by interdigitating fibres. Rupture of one or more intrinsic ligaments frequently leads to a clinical instability of the carpus. The intrinsic ligaments are subdivided into ligaments which connect the carpal bones of the proximal and distal rows respectively and ligaments which connect the rows by crossing over the midcarpal joint.

Proximal row interosseous ligaments

The scapholunate and lunotriquetral ligaments are clinically and biomechanically important structures. In the sagittal plane they have an approximately horseshoe-shape configuration with palmar, midcarpal and dorsal components. The scapholunate ligament contains short transverse fibres connecting the dorsal aspect of the respective bones and more obliquely oriented fibres connecting the palmar aspect. The functional significance of this arrangement is that the tighter dorsal component of the ligament acts as a hinge facilitating flexion and extension of the scaphoid: these movements are important to carpal mechanics. The ligament continues on its midcarpal section as an interosseous membrane. The lunotriquetral ligament has similar dorsal, midcarpal interosseous and palmar components, but the fibres of the dorsal and palmar components are similarly rather than differentially oriented, which precludes the same pattern of preferential movement as occurs between the lunate and scaphoid. The interosseous membranes of the scapholunate and lunotriquetral ligaments separate the midcarpal from the radiocarpal joint spaces. Dye injected into one of these joint spaces which leaks to the other denotes a tear of one of these ligaments.

Distal row interosseous ligaments

The distal row interosseous ligaments are powerful ligaments between the capitate, hamate, trapezium and trapezoid, with an important stabilizing function for the distal carpal row. They have superficial and deep components, and unlike the ligaments of the proximal row, are seldom torn.

Palmar midcarpal ligaments

Anterolaterally lies the fan-shaped palmar scaphocapitate – trapezoid ligament which originates from the scaphoid tuberosity and is thought to be an important stabilizer of the scaphoid. This ligament may be subdivided into two parts known as the scaphotrapeziotrapezoidal ligament (having the attachments as its name suggests) and a more ulnar component known as the scaphocapitate ligament. The triquetrohamate and triquetrocapitate ligaments lie towards the ulnar side of the carpus.

Dorsal midcarpal ligaments

The dorsal intercarpal ligament assists in stabilization of the proximal carpal row. It arises from the trapezoid and distal pole of scaphoid, and passes across the dorsal horn of the lunate to be attached to the triquetrum. The ligament forms the floor of the fourth and fifth extensor compartments. On the radial side is the lateral scaphotrapeziotrapezoidal ligament which acts as a stabilizer of the scaphoid and trapezium.

Triangular fibrocartilage complex (TFCC) and distal radio-ulnar ligaments

The triangular fibrocartilage complex (TFCC) is a ligamentous and cartilaginous structure which suspends the distal radius and ulnar carpus from the distal ulna. The TFCC stabilizes the ulnocarpal and radio-ulnar joints, transmits and distributes load from the carpus to the ulna, and facilitates complex movements at the wrist (Fig. 50.17). By definition, it is made up of the cartilaginous disc, the meniscus homologue (an embryological remnant of the ‘ulnar’ wrist that is only occasionally present), volar and dorsal distal radio-ulnar ligaments, ulnar collateral ligament, floor of extensor carpi ulnaris subsheath, ulnolunate and ulnotriquetral ligaments. The triangular fibrocartilage proper (TFC) is a biconcave body composed of chondroid fibrocartilage. It extends across the dome of the ulnar head and varies between 2 and 5 mm in thickness.

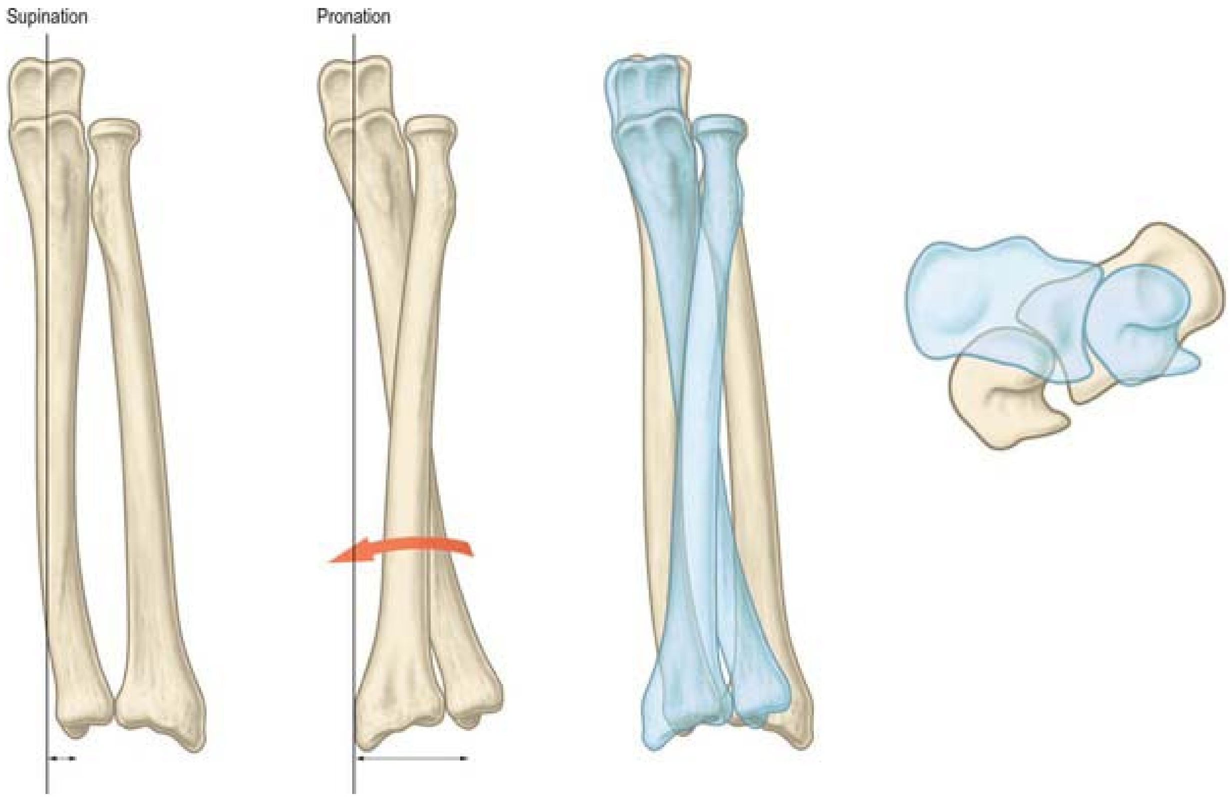

Fig. 50.17 Representation of the manner in which the radius moves around the ulna during forearm rotation. The curvature of the shaft of the radius is important in facilitating this movement. The axis of forearm rotation passes through the head of the ulna and varies slightly in position through the range of rotation. The degree of ulnar translocation of the ulna during pronation (shown by the difference in length between the two double arrowheads) can be seen with reference to the distance the ulnar styloid has moved from the plumb line (vertical black line shown)

From its distal aspect, the TFCC resembles a hammock supporting the ulnar carpus with the disc proper as the base of the hammock. From the proximal side, the TFCC appears in the shape of a fan extending from the fovea of the ulna along either side of the sigmoid notch. This fan-shaped structure is divided into dorsal, central and palmar portions where the central portion is the triangular fibrocartilage and the peripheral margins are thick lamellar collagen, structurally adapted to tensile loading and known as the distal (palmar and dorsal) radio-ulnar ligaments. In keeping with other extrinsic ligaments of the wrist joint proper there are thought to be superficial and deep components of the distal radio-ulnar ligaments which act as a functional couple stabilizing the rotation of the ulnar head on the sigmoid notch of the radius.

Stability of the distal radio-ulnar joint during forearm rotation is conferred by the TFCC complex, dorsal and volar distal radio-ulnar ligaments, interosseous membrane and subsheath of the extensor carpi ulnaris tendon (floor of sixth dorsal extensor compartment).

COORDINATED MOVEMENTS AND LOAD-BEARING AT THE WRIST JOINT

Wrist movements

The movements at the radiocarpal and intercarpal joints are considered together since they are both involved in all movements as well as being acted upon by the same muscles. Active movements are flexion (85°), extension (85°), adduction or ulnar deviation (45°), abduction or radial deviation (15°) and circumduction (all movements are approximate).

The range of flexion is greater at the radiocarpal joint, while in extension there is more movement at the midcarpal joint (Fig. 50.18). Hence the proximal surfaces extend further posteriorly on the lunate and scaphoid bones. These movements are limited chiefly by antagonistic muscles, and therefore the range of flexion is perceptibly diminished when the fingers are flexed, due to increased tension in the extensors. Only when the joints are forced to the limits of flexion or extension are the dorsal or palmar ligaments fully stretched (but see below).

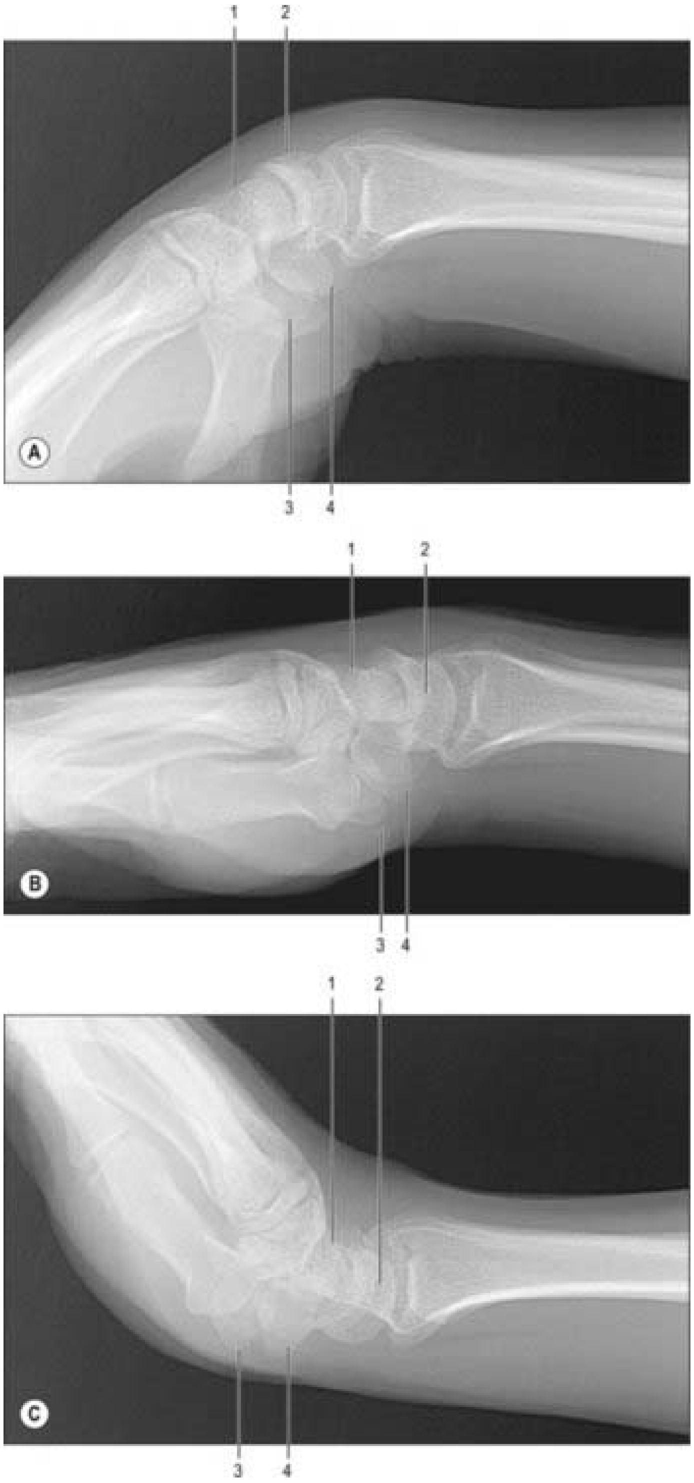

Fig. 50.18 **A**, Radiograph of the hand and wrist in full flexion: lateral aspect. Compare with **B**, and note the relative positions of the capitate and lunate, and the lunate and radius. **B**, Radiograph of the hand and wrist: lateral aspect. The long axes of the third metacarpal, capitate and lunate are,

approximately, in line with the long axis of the radius. Note the relative positions of the capitate and lunate, and the lunate and radius. **C**, Radiograph of the hand and wrist in full extension: lateral aspect. Compare with **B** and note the alterations in the relative positions of the capitate and lunate, and the lunate and the radius. **1**. Capitate. **2**. Lunate. **3**. Tubercle of the trapezium. **4**. Tubercle of the scaphoid.

Adduction of the hand is considerably greater than abduction, perhaps due to the more proximal site of the ulnar styloid process. Most adduction occurs at the radiocarpal joint. The lunate articulates with both the radius and articular disc when the hand is in the midposition, but in adduction it articulates solely with the radius, and the triquetrum now comes into contact with the articular disc (Fig. 50.19A). Much of the proximal articular surface of the scaphoid becomes subcapsular beneath the radial collateral ligament and forms a smooth, convex, palpable prominence in the floor of the ‘anatomical snuff-box’.

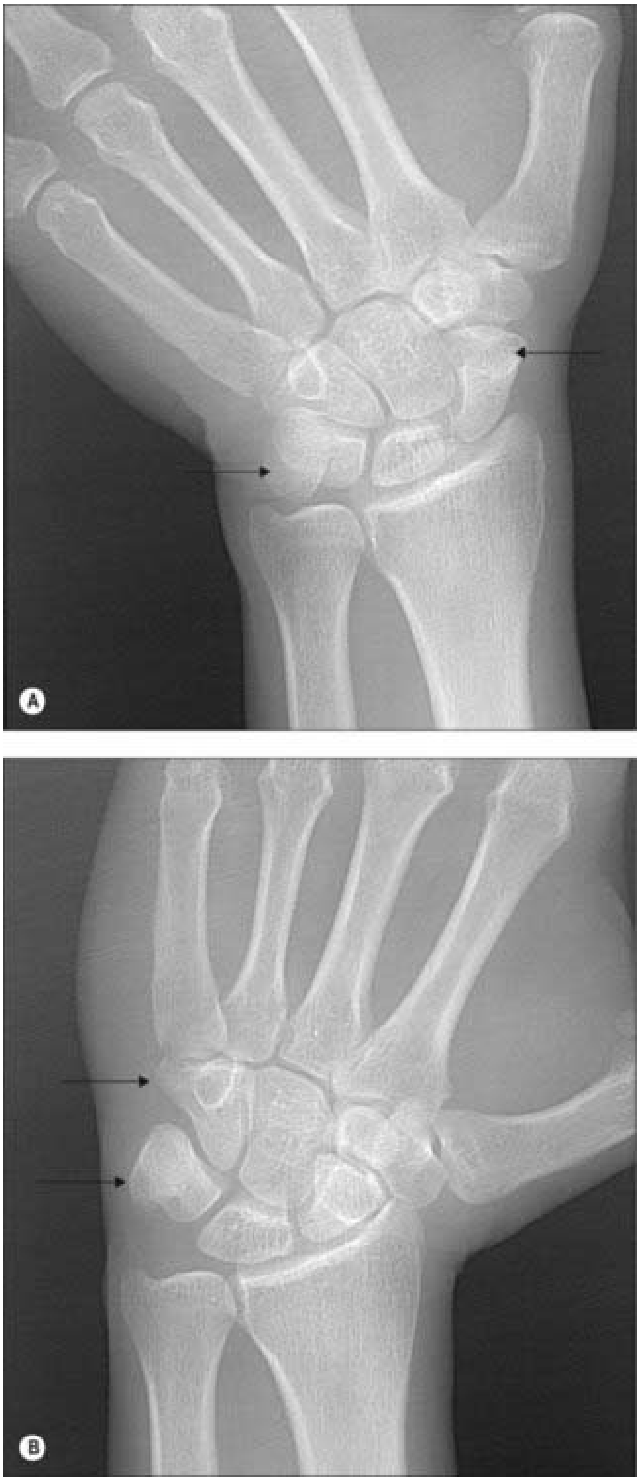

Fig. 50.19 **A**, Radiograph of the hand in full adduction (ulnar deviation), dorsopalmar projection. The arrows point to the scaphoid on the radial side and to the pisiform on the ulnar side. Note that the shadow of the pisiform bone overlaps the shadow of the tip of the styloid process of the ulna.

Compare with **B** and observe that the movements occur at both the radiocarpal and intercarpal joints. **B**, Radiograph of the same hand in full abduction (radial deviation). The arrows point to the hamate and pisiform. Compare with **A** and note that: (1) the scaphoid and lunate have passed medially (ulnarly) so that the latter articulates to a large extent with the articular disc of the distal radio-ulnar joint; (2) the pisiform is now widely separated from the styloid process of the ulna; (3) the scaphoid, having rotated round a transverse axis, is much foreshortened; (4) the apex of the hamate has been thrust away from the lunate by the rotation of the capitate around an anteroposterior axis; (5) a gap has opened up between the distal portions of the hamate and triquetrum; and (6) the long axes of the capitate and lunate are now almost in the same straight line.

Abduction from the neutral position occurs at the midcarpal joint, the proximal carpal row not moving. Radiographs of abducted hands show that the capitate rotates round an anteroposterior axis so that its head passes medially and the hamate conforms to this: the distance between the lunate and the apex of the hamate is increased (Fig. 50.19B). The scaphoid rotates around a transverse axis, and its proximal articular surface moves away from the capsule to articulate solely with the radius. Movements are limited by antagonistic muscles and, at extremes, by the carpal collateral ligaments.

Circumduction of the hand is not rotatory, but involves successive flexion, adduction, extension and abduction or vice versa.

Muscles producing movements

Flexion

Flexores carpi radialis and ulnaris and palmaris longus, assisted by flexores digitorum superficialis and profundus and flexor pollicis longus.

Extension

Extensores carpi radialis longus, brevis and ulnaris, assisted by extensores digitorum, digiti minimi, indicis and pollicis longus.

Adduction

Flexor and extensor carpi ulnaris.

Abduction

Flexor carpi radialis, extensores carpi radialis longus and brevis, with abductor pollicis longus and extensor pollicis brevis.

Integrated model of wrist movement (carpal kinematics)

The proximal row (scaphoid, lunate and triquetrum) is an intercalated segment: no tendons insert onto the bones of the row. It is inherently unstable and controlled by specific retaining and gliding ligaments. Its relative position is determined by the spatial configurations of the radius, triangular fibrocartilage complex (TFCC) and ulna on one side, and the rigid distal carpal row on the other. The proximal carpal row is subject to two opposing moments: the scaphoid straddles the proximal and distal rows and tends to rotate the proximal row into flexion under axial load and radial deviation. At the same time there is a force tending to extend the proximal row which is initiated by the distal row and transmitted via the midcarpal ligaments to the triquetrum (Fig. 50.20). Stability of the midcarpal joint is thus ensured during both movement and loading.

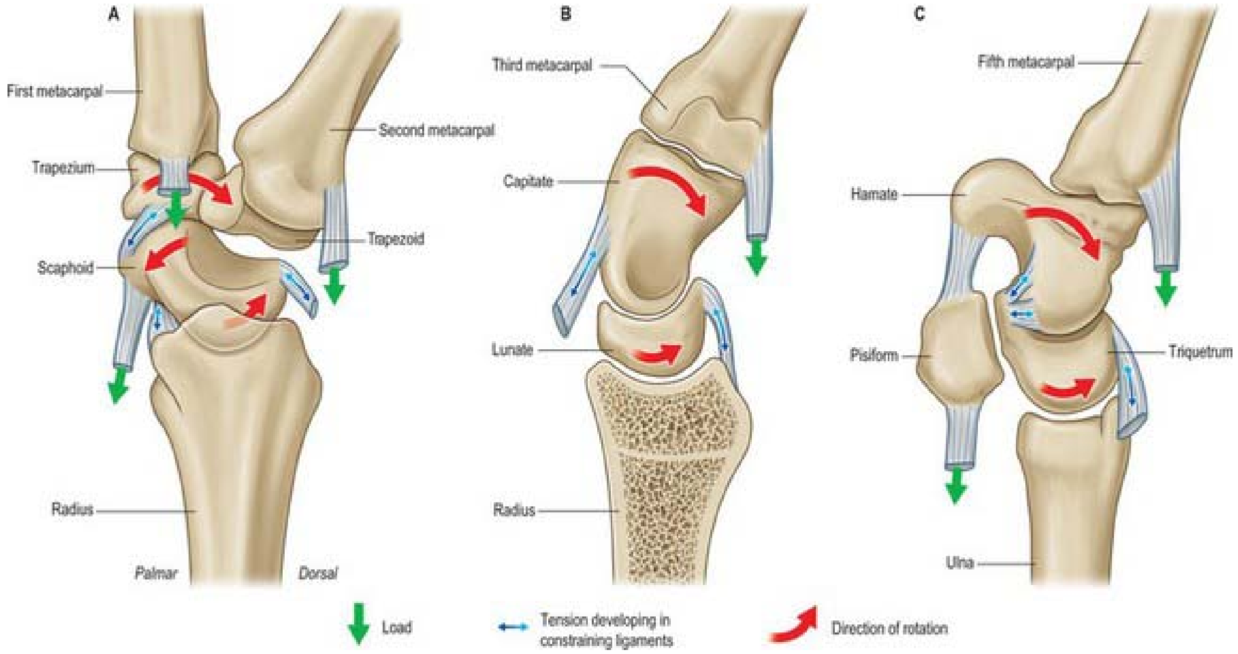
A
First metacarpal
Second metacarpal
Trapezium
Trapezoid
Scaphoid
Radius
Palmar
Dorsal
B
Third metacarpal
Capitate
Lunate
Radius
C
Fifth metacarpal
Hamate
Pisiform
Triquetrum
Ulna
Load
Tension developing in constraining ligaments
Direction of rotation

Fig. 50.20 The balance of rotatory moments occurring during axial loading are explained in this series of sagittal sections of the wrist. **A**, The scaphoid tends to move into flexion with axial loading and is simultaneously constrained palmarly by the scaphotrapeziotrapezoidal ligaments and dorsally by the scapholunate ligament. **B**, The lunate tends to follow the scaphoid restrained only by the dorsal radiolunate ligament. **C**, The triquetrum tends to flex along with the two other bones of the proximal carpal row and is constrained palmarly by the triquetrohamate and triquetrocapitate ligaments and dorsally by the radiotriquetral ligament.

The distal carpal row (trapezium, trapezoid, capitate and hamate) can be regarded as one rigid structure tightly bound together. The scaphoid bridges the proximal and distal carpal rows and provides a functional couple between the two.

The carpus was originally thought to move simply as proximal and distal rows (row or rigid body theory). According to this view, during the composite movement of wrist flexion and extension, approximately two-thirds of movement occurs at the radiocarpal joint and one-third at the midcarpal joint. The carpus was later judged to move in lateral central and medial columns more than it did in rows, and the radius–lunate–capitate was described as a three-bar linkage system (column theory). This theory was modified to incorporate the specific stabilizing role of the scaphoid as it bridges the proximal and distal rows. A further theory proposed that the bones were linked by their ligaments in a ring configuration, so that any breakage of the key links leads to instability (ring theory). Most recently the ‘four unit’ theory suggests that the distal carpal row moves as a single unit, and the scaphoid, lunate and triquetrum move in complex but characteristic relationships which are dependent on the given movement (Fig. 50.21). Clinical observation provides some support for each of these theories.

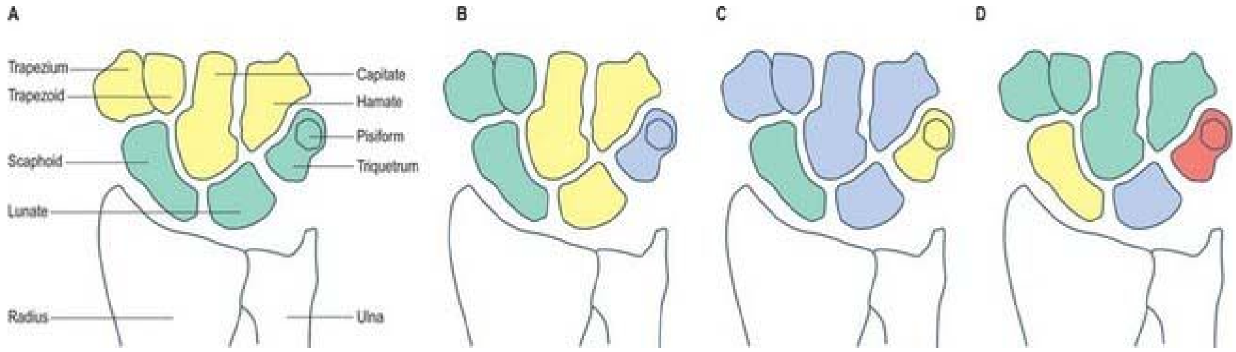

Fig. 50.21 Different theories of carpal mechanics. **A**, Row or rigid body theory; **B**, central column theory of Navarro; **C**, ring theory of Taleisnik; **D**, four-unit concept of Viegas.

Wrist loading

Axial loading refers to load or force applied along a line parallel to the long bones of the arm and therefore corresponds to power grip manoeuvres, e.g. clenching the fist. In the normal activities of daily living, loading is usually multiplanar with a combination of vectors of force, e.g. grasping an object and then lifting it against gravity with the elbow flexed would engender transverse and axial loading with respect to the long axis of the forearm.

Force transmission

Radiocarpal joint

The articulation of the carpus with the radius (radiocarpal) and ulna (ulnocarpal) can be described in terms of specific fossae, i.e. the scaphoid and lunate fossae of the radius and the facet formed by the distal aspect of the TFCC. The scaphoid fossa contributes 43%, the lunate fossa 46%, and the TFCC 11%, of the total area of this articulating surface. Under physiological conditions, the contact area between this surface and the proximal carpal row is of the order of 20% of the whole. It varies consistently with position: greater contact is seen in forearm supination, radial deviation and dorsiflexion of the wrist, and lesser contact in forearm pronation, ulnar deviation and palmar flexion of the wrist. Further increase in contact area is seen with axial loading. Maximum contact areas are recorded at 40%. Force across the joint also varies with the position of the forearm and the degree of wrist flexion. For a given load in wrist neutral position, 50% of force passes across the scaphoid fossa, 35% through the lunate fossa, and 15% across the TFCC. With a power grip there is slight ulnar deviation, and the proportion of force passing across the scaphoid and lunate fossae reverses.

Midcarpal joint

With the wrist in neutral position, 50–60% of a given load is transmitted from the distal row through the capitate to the scaphoid and lunate. Up to 30% of the load is transmitted via the scaphotrapeziotrapezoid joint, and up to 20% via the hamate-triquetral joint.

Distal radio-ulnar joint (DRUJ)

The DRUJ is part of a more complex articulation that includes the proximal radio-ulnar joint and the interosseous membrane. Static axial loading of the wrist increases the contact areas of the joint surfaces of the distal radio-ulnar joint, DRUJ. Force transmitted across the DRUJ also increases with axial loading and varies with position of forearm rotation. It is maximal at 60° supination, when the ulnar head lies most directly under the ulnar-sided carpus, and least in full pronation. It has been shown that with the wrist in neutral position, 70–80% of axial load passes down the radius and 20–30% down the ulna. The proportion of force passing down the ulna varies with increasing load, and changes with position of the hand and carpus relative to the forearm bones. The interosseous membrane between the radius and ulna plays a role in distributing load in the forearm. Distal radio-ulnar joint loading also depends on relative radial and ulnar lengths, i.e. ulnar negative, neutral or positive variance.

Specific actions

Power grip

There is a predictable pathway of force transmission during axial loading of the hand such as occurs in power grip. During this action the wrist is positioned in mid-dorsiflexion and the object is tightly gripped. Force is transmitted from the hand and wrist via the radiocarpal joint and TFCC to both bones of the forearm, through the elbow joint to the humerus, and thence via the glenohumeral joint to the pectoral girdle. Dynamic muscle action accounts for transmission of a large part of the force, and a smaller proportion is transmitted through the osseoligamentous structures. The distribution of force between the radius and ulna varies dynamically. It depends on the absolute value of load, degree of forearm rotation, and position of the carpus relative to the forearm.

Hammer action

The action exemplified by hammering, where the wrist alternates between the dorsoradial and the palmar-ulnar position, is an important movement. The reciprocal movement is more constrained and awkward to perform. The former movement is important in a wide variety of activities of daily living. In primates this movement is needed (along with forearm rotation at the distal radio-ulnar joint) for brachiation.

It is believed that load distributes dynamically as the position of the carpus moves relative to the forearm and there are consequent changes in the relative position of the carpal bones.

Wrist instability

During evolution the upper limb has developed to facilitate prehension, i.e. the placing of the hand in three-dimensional space. However, mobility of the hand on the forearm has evolved at the expense of stability. A wrist is said to be kinetically unstable when it cannot bear physiological loads without giving way or causing injury. A wrist is kinematically unstable when it exhibits sudden changes in carpal alignment, i.e. during a specific movement there is a ‘clunk’ as one or more of the carpal bones moves abnormally with respect to the others. Stability of the various joints such that the bones maintain normal anatomical relations with respect to each other throughout the normal range of motion is essential for physiological load-bearing.

Some degree of carpal instability may occur as part of inherent hypermobility in affected individuals, but usually it occurs only after rupture or attenuation of intrinsic and extrinsic carpal ligaments and may be detected either clinically or evidenced on radiographs as malalignment of the carpal bones (Fig. 50.22).

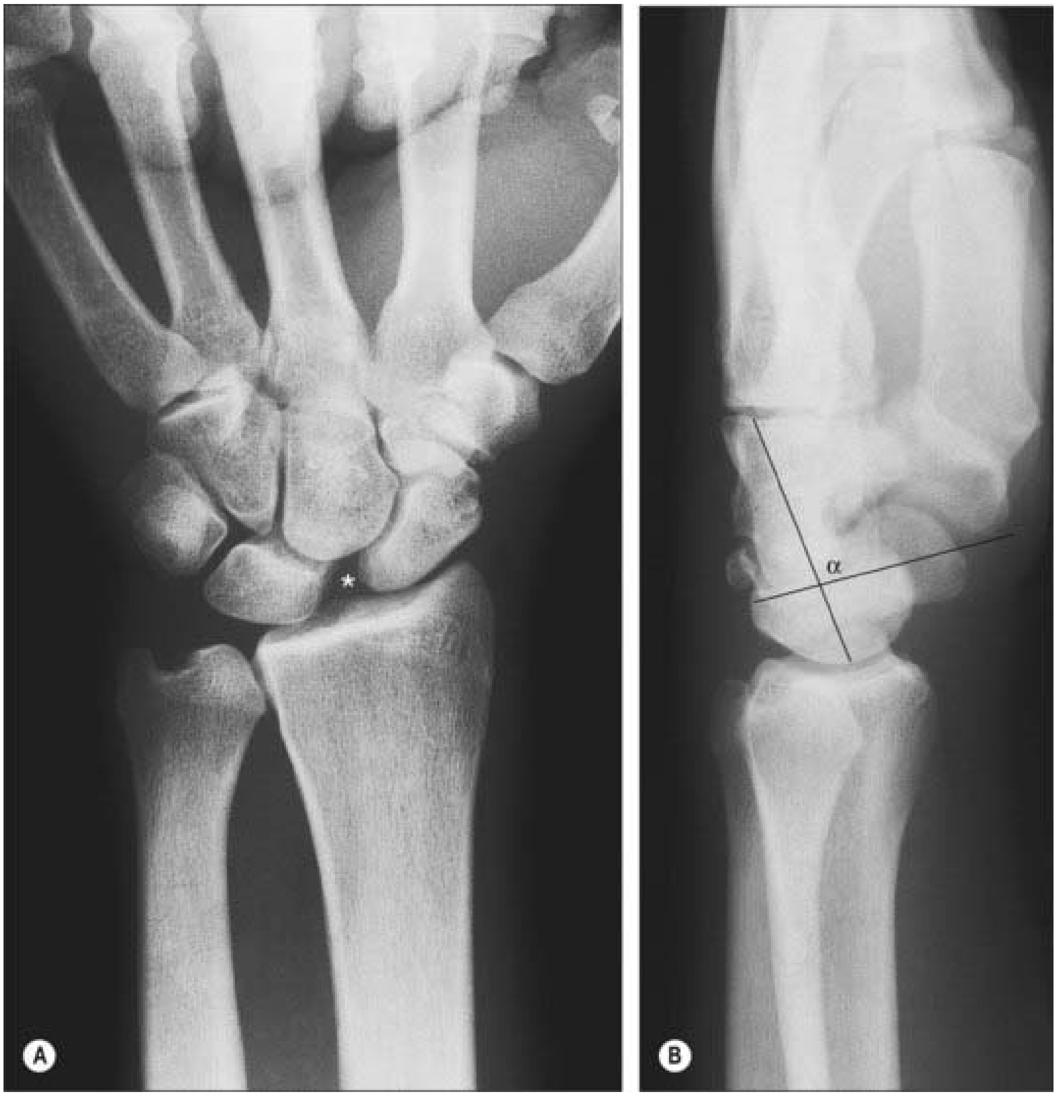

Fig. 50.22 Scapholunate dissociation shown in posteroanterior power grip view (**A**) and lateral view (**B**). Dissociation between the scaphoid and lunate as shown here leads to collapse of the scaphoid into flexion and the lunate into extension (dorsal intercalated segment instability, or DISI) thus removing the inbuilt tension across the proximal row. This causes the gap (so called Terry Thomas sign) between the scaphoid and lunate in the PA radiograph (marked with asterisk) and increased scapholunate angle above the upper limit of normal of 60 degrees, as shown in **B**.

CARPOMETACARPAL JOINTS

The first carpometacarpal joint, CMCJ, or basal joint of the thumb, is a modified saddle joint that permits opposition of the thumb and confers the ability to hold and manipulate objects: the actions of ‘pinch’ grip, ‘tripod’ pinch and ‘chuck’ grip are specifically facilitated. Significant forces pass across and compress this joint compared to the remaining CMCJs. The second to fifth CMCJs exhibit an increasing range of movement progressing from the radial to the ulnar side. Thus there is little mobility at the base of the index ray, but considerable mobility at the base of the small finger ray, which facilitates ‘cupping’ of the palm of the hand. Compressive forces between the metacarpals and the distal carpal row are estimated to be upwards of ten times the forces at the tips of the fingers during ‘pinch’ or ‘chuck’ grip.

Carpometacarpal joint of the thumb

Articulating surfaces

The carpometacarpal joint of the thumb is a sellar (saddle) joint between the first metacarpal base and trapezium. It enjoys wide mobility due to its extensive articular surfaces and their topology.

Ligaments

The first metacarpal and trapezium are connected by lateral, anterior and posterior ligaments and a fibrous capsule. The broad lateral ligament runs from the lateral surface of the trapezium to the radial side of the metacarpal base. The palmar and dorsal ligaments are oblique bands which converge to the ulnar side of the metacarpal base from the palmar and dorsal surfaces of the trapezium respectively.

Synovial membrane

The synovial membrane lines the joint capsule and is separate from it.

Vascular supply

The carpometacarpal joint of the thumb receives its blood supply from the radial artery and its first dorsal metacarpal branch.

Innervation

The carpometacarpal joint of the thumb is innervated by articular twigs from the posterior interosseous nerve and the superficial branch of the radial nerve.

Joint movements

Except at initiation, flexion is accompanied by medial rotation; conversely, medial rotation involves flexion. Linkage of movements is due largely to the shape of the articular surfaces (which impose some conjunct rotation), and to the obliquity of the dorsal ligament (which, when taut, anchors the ulnar side of the metacarpal base while its radial side continues to move). Contraction of flexor pollicis brevis, assisted by opponens pollicis, thus produces medial rotation with flexion; combined with abduction this brings the thumb pulp into contact with the pulps of the slightly flexed fingers, a movement termed opposition. (The flexed fingers have varying degrees of lateral metacarpophalangeal rotation, which is minimal in the index, and maximal in the minimus.) Conversely, full extension of the thumb metacarpal entails slight lateral rotation, attributable to the sellar form of the joint and to the action of the palmar ligament (which is similar to that of the dorsal ligament in flexion). (See also p. 888.)

Muscles producing movements

The muscles producing movements at the carpometacarpal joint of the thumb are as follows.

Flexion

Flexor pollicis brevis and opponens pollicis, aided by flexor pollicis longus when the other joints of the thumb are flexed. Flexion entails medial rotation.

Extension

Abductor pollicis longus and extensors pollicis brevis and longus. In full extension extensor pollicis longus, owing to its oblique pull and the disposition of the palmar ligament, rotates the thumb laterally and draws it dorsally, i.e. slightly adducts the thumb.

Abduction

Abductors pollicis brevis and longus. When abduction is maximal the digit and metacarpal are not in line, and the thumb is abducted at both metacarpophalangeal and carpometacarpal joints.

Adduction

Adductor pollicis alone.

Opposition

Opponens pollicis and flexor brevis pollicis simultaneously flex and medially rotate the abducted thumb. Interpulpal pressure, or that generated by digital grasping, is increased by adductor pollicis and flexor pollicis longus.

Circumduction

Extensors, abductors, flexors and adductors acting consecutively in this, or reverse, order.

Second to fifth carpometacarpal joints

The second to fifth carpometacarpal joints are synovial ellipsoid joints between the carpus and second to fifth metacarpals. Although widely classed as plane, they have curved articular surfaces which are often of complex sellar shape. The bones are united by articular capsules, and dorsal, palmar and interosseous ligaments.

Ligaments

The dorsal ligaments are the strongest, and connect the dorsal surfaces of the carpal and metacarpal bones. The second metacarpal has two ligaments, from the trapezium and trapezoid; the third has two, from the trapezoid and capitate; the fourth has two, from the capitate and hamate; the fifth has a single band from the hamate, which is continuous with a similar palmar ligament, forming an incomplete capsule.

The palmar ligaments are similar, except that the third metacarpal has three: a lateral from the trapezium, superficial to the tendon sheath of flexor carpi radialis, an intermediate from the capitate, and a medial from the hamate.

The interosseous ligaments consist of two short, thick, fibrous bands. They are limited to one part of the carpometacarpal articulation and connect contiguous distal margins of the capitate and hamate with adjacent surfaces of the third and fourth metacarpal bones: they may be united proximally.

Synovial membranes

The synovial membranes are often continuous with those of the intercarpal joints. Occasionally, the joint between the hamate and fourth and fifth metacarpal bones has a separate synovial cavity, bounded laterally by the medial interosseous ligament and its extensions to the palmar and dorsal parts of the capsule.

Vascular supply

The second to fifth carpometacarpal joints are supplied by the posterior carpal branches of the radial and ulnar arteries, by twigs from the anterior interosseous artery, and from the palmar digital arteries.

Innervation

The second to fifth carpometacarpal joints are innervated by the deep terminal branches of the ulnar nerve, the anterior interosseous branch of the median nerve, and the short branches of the superficial radial and dorsal ulnar nerves.

Muscles producing movements

Slight gliding movements are effected by the long flexor and extensor muscles of the digits.

INTERMETACARPAL JOINTS

Articulating surfaces

The second to fifth metacarpal bases articulate reciprocally by small cartilage-covered facets connected by dorsal, palmar and interosseous ligaments.

Fibrous capsule

The intermetacarpal joints have fibrous capsules.

Ligaments

The dorsal and palmar ligaments pass transversely from bone to bone. The interosseous ligaments connect contiguous surfaces just distal to their articular facets.

Synovial membranes

The synovial membranes are continuous with those of the carpometacarpal articulations.

Movements at the carpometacarpal and intermetacarpal joints

Movements at the carpometacarpal and intermetacarpal articulations are limited to slight gliding, sufficient to permit some flexion–extension and adjunct rotation: ranges vary in different joints. They are partly accessory movements occurring when the palm is ‘cupped’, as in grasping an object. Active movements also occur and are familiar, e.g. to the pianist or violinist. The fifth metacarpal is most movable and the second and third are the least mobile. These variations are easily demonstrated by opposing each digit to the thumb over the palmar centre. About two-thirds of the movements are pollicial, as described above, but during opposition to minimus, the latter is flexed, abducted and laterally rotated, accounting for the remaining third of the movement. These actions occur at both the carpometacarpal and metacarpophalangeal joints. The close-packed position probably coincides with carpal extension, as in gripping. Further accessory movements are spiral twisting of the whole metacarpus on the carpus.

Muscles producing movements

Movements at carpometacarpal and intermetacarpal joints are effected by the flexors and extensors of the second to fifth digits.

METACARPOPHALANGEAL JOINTS

The metacarpophalangeal joints are usually considered ellipsoid. However, the metacarpal heads are adapted to shallow concavities on the phalangeal bases: they are not regularly convex but partially divided on their palmar aspects and thus almost bicondylar (Fig. 50.23).

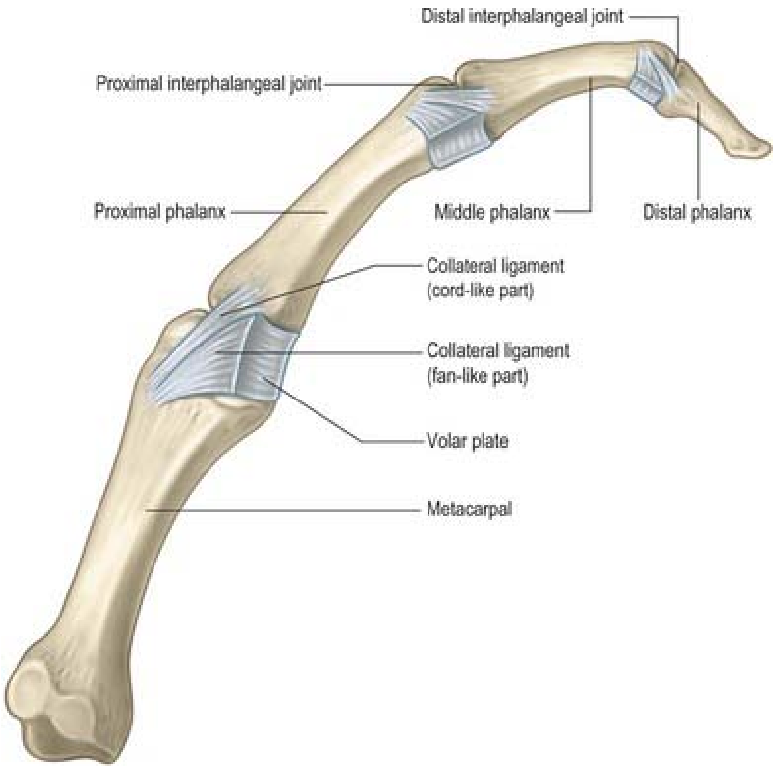
Distal interphalangeal joint
Proximal interphalangeal joint
Proximal phalanx
Middle phalanx
Distal phalanx
Collateral ligament (cord-like part)
Collateral ligament (fan-like part)
Volar plate
Metacarpal

Fig. 50.23 Metacarpophalangeal and digital joints of the left third finger: medial aspect.

Fibrous capsule

The metacarpophalangeal joints all have fibrous capsules.

Ligaments

Each metacarpophalangeal joint has a palmar and two collateral ligaments.

Palmar ligaments

The palmar (volar plates) ligaments are unusual. They are thick, dense and fibrocartilaginous, and sited between, and connected to, the collateral ligaments. They are attached loosely to the metacarpals but firmly to the phalangeal bases. Their palmar aspects are blended with the deep transverse palmar ligaments and are grooved for the flexor tendons, whose fibrous sheaths connect with the sides of the grooves. Their deep surfaces increase articular areas for the metacarpal heads.

Deep transverse metacarpal ligaments

The deep transverse metacarpal ligaments are three short, wide, flat bands which connect the palmar ligaments of the second to fifth metacarpophalangeal joints. They are related anteriorly to the lumbricals and digital vessels and nerves, and posteriorly to the interossei. Bands from the digital slips of the central palmar aponeurosis join their palmar surfaces. On both sides of the third and fourth metacarpophalangeal joints, but only the ulnar side of the second and radial side of the fifth, transverse bands of the dorsal digital expansions join the deep transverse metacarpal ligaments. The lumbricals and the phalangeal attachments of the dorsal interossei lie anterior to this band, and the remaining attachments of dorsal interossei and palmar interossei are posterior to it (see Fig. 50.30).

Collateral ligaments

The collateral ligaments are strong, round cords which flank the joints. Each is attached to the posterior tubercle and adjacent pit on the side of its metacarpal head, and each passes distoanteriorly to the side of the anterior aspect of its phalangeal base (Fig. 50.23).

Synovial membrane

The metacarpophalangeal joints are lined by a synovial membrane.

Vascular supply

The metacarpophalangeal joints receive their blood supply from the dorsal and palmar metacarpal arteries, the arteria princeps pollicis, and the arteria radialis indicis.

Innervation

The metacarpophalangeal joints are innervated by twigs from the palmar digital branches of the median nerve, the deep terminal branch of the ulnar nerve, and the posterior interosseous nerve.

Joint movements

Flexion, extension, adduction, abduction, circumduction and limited rotation all take place at the metacarpophalangeal joints. Rotation cannot occur in isolation, but may accompany flexion–extension. This may be initiated voluntarily in the free hand (e.g. each finger flexing and rotating to place its tip near the palmar centre); the range of rotation is frequently increased as a result of the resistance of a grasped object. Flexion is almost 90°, whereas extension is only a few degrees: both movements are limited mostly by antagonistic muscles. Flexion is often terminated by the resistance offered by a grasped object. The metacarpophalangeal joint of the thumb has a flexion–extension range of approximately 60°, which is almost entirely flexion. Slight lateral rotation accompanies digital flexion of digits 3–5. Flexion of the index finger may be accompanied by minimal lateral rotation or no rotation: a small degree of medial rotation is frequently observed. Other movements are adduction–abduction (maximal range 25°), which invariably accompanies the corresponding carpometacarpal movements and increases their combined range, and slight conjunct rotation, but greater adjunct rotation, which accompanies flexion–extension. Of the second to fifth metacarpophalangeal joints, the second is most mobile in adduction–abduction (approximately 30°), followed by the fifth, fourth, and third.

Accessory movements

Accessory movements are further rotation (most marked in the thumb), anteroposterior and lateral translation of a phalanx or metacarpal, and distraction.

Muscles producing movements

The muscles producing movements at the metacarpophalangeal joints are as follows.

Flexion

Flexores digitorum superficialis and profundus, assisted by the lumbricals and interossei and, in the minimus, flexor digiti minimi brevis. In the thumb, flexores pollicis longus and brevis and the first palmar interosseous.

Extension

Extensor digitorum, assisted in the second and fifth digits by extensor indicis and extensor digiti minimi respectively. In the thumb, extensors pollicis longus and brevis.

Adduction

In extended fingers, palmar interossei; the long flexors are predominant during flexion. In the thumb, limited metacarpophalangeal adduction is possible and may be attributable to adductor pollicis and the first palmar interosseous.

Abduction

In extended fingers, dorsal interossei assisted by the long extensors (except in the middle finger), and abductor digiti minimi in the little finger. In the thumb, abductor pollicis brevis (which also contributes to opposition). When the fingers are flexed at the IP joints, active abduction is impossible: if the long digital flexors are inactive, passive abduction is free. Inability to abduct actively in this position may be due to shortening of the dorsal interossei and abductor digiti minimi by flexion. However the altered line of pull of the interossei relative to the axis of movement is probably the determining factor: in digital extension the axis of lateral movements is anteroposterior, whereas in flexion it is proximodistal, and the line of pull of the interossei is then nearly parallel to the axis.

Gamekeeper’s thumb

The ulnar collateral ligament of the metacarpophalangeal joint of the thumb can be avulsed from its distal attachment to the base of the proximal phalanx by a combination of forced extension and radial deviation of the joint. The injury was reported to occur in gamekeepers while breaking the necks of game, but can occur following simple falls onto the outstretched hand, especially in skiers who have the straps of ski poles wrapped around their thumbs.

The ulnar collateral ligament is normally covered by the aponeurotic insertion of the adductor pollicis tendon. Following avulsion, the proximal end can become superficially displaced around the proximal free edge of the aponeurotic insertion of the adductor. This soft tissue interposition prevents the ends of the avulsed ligament from healing. If left untreated, a firm palpable inflammatory swelling occurs, known as the ‘Stener lesion’. Surgical repair requires division of the aponeurotic insertion of adductor pollicis, followed by bony reattachment of the avulsed ligament and repair of the aponeurosis.

INTERPHALANGEAL JOINTS

The interphalangeal joints are uniaxial hinge joints (Fig. 50.23).

Fibrous capsule

Each interphalangeal joint has a fibrous capsule.

Ligaments

Each interphalangeal joint has a palmar ligament (also known as the volar plate) and two collateral ligaments. The long extensor tendons take the place of the dorsal capsular ligaments. Extensions from the extensor expansion, each collateral ligament and the palmar ligament, all pass into the joint cavity and provide a significant increase to the articular surface area of the phalangeal base: their deformable nature improves joint congruence.

Palmar ligament (volar plate)

The volar plate constitutes the floor of the interphalangeal joint. In the proximal interphalangeal joint, the distal end of the volar plate is thickened laterally where it is firmly attached to the base of the middle phalanx at the position of the true collateral ligament attachment. Centrally, it is more delicate and blends with the volar periosteum of the middle phalanx. Proximally, the volar plate is also very delicate in its central portion, but it is thickened laterally to form the so-called check rein ligaments which attach to the periosteum of the proximal phalanx just within the walls of the A2 pulley component of the fibrous flexor sheath. Nutrient branches of the digital arteries pass underneath these check ligaments to reach the vinculae (Fig. 50.24). A detailed account of the anatomy of the volar plate can be found in Bowers et al (1980).

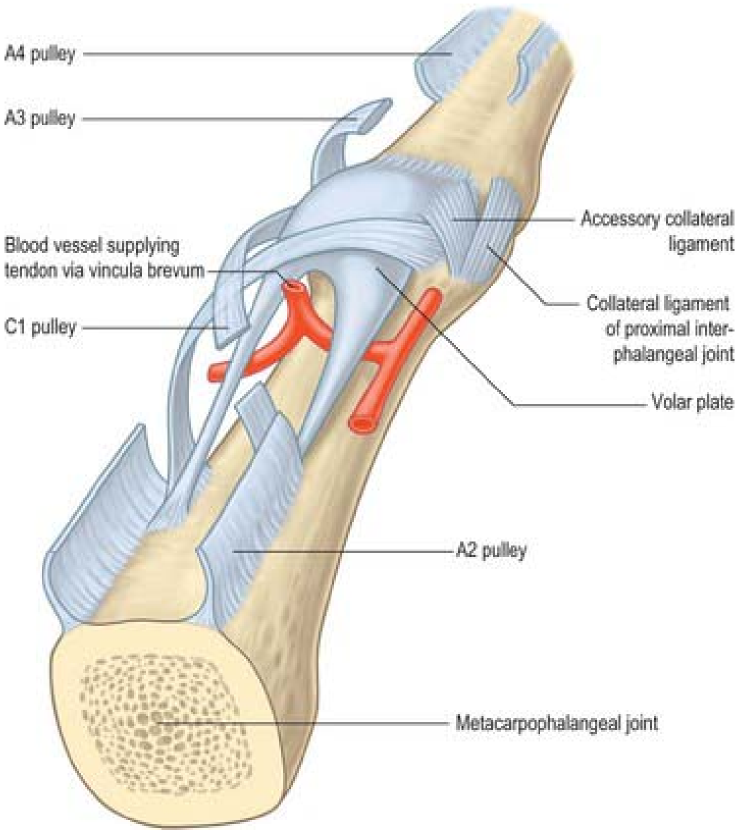
A4 pulley
A3 pulley
Blood vessel supplying tendon via vincula brevum
C1 pulley
Accessory collateral ligament
Collateral ligament of proximal inter-phalangeal joint
Volar plate
A2 pulley
Metacarpophalangeal joint

Fig. 50.24 Anatomy of the proximal interphalangeal joint volar plate. The blood vessel supplying the flexor tendons via the vincula brevum is shown, but the mesentery forming the vinculum has been omitted.

Collateral ligaments

The collateral ligaments pass from the lateral aspect of the head of one phalanx to the volar aspect of the base of the adjacent phalanx. An accessory component to the collateral ligament arises in continuity with the main ligament and passes in a volar direction to attach to the volar plate.

Synovial membrane

Each interphalangeal joint has a synovial lining.

Vascular supply

The interphalangeal joints are supplied by branches from the palmar digital arteries.

Innervation

The interphalangeal joints are innervated by the palmar digital branches of the median nerve (to the thumb, index, middle and ring fingers), and the ulnar nerve (to the ring and little fingers).

Factors maintaining stability

Stability is conferred by the articular contours of the joint surfaces and the collateral ligaments. The flexor and extensor tendons and retinacular ligaments provide secondary stabilization. Stability against hyperextension of the proximal interphalangeal joint is enhanced by the three-dimensional box arrangement that is produced by the collateral ligament–volar plate complex.

Joint movements

Movements (active) at the interphalangeal joints are flexion and extension, and are greater in range at the proximal joints. Flexion is considerable, whereas extension is limited by tension of the digital flexors and terminated by tension in the palmar ligaments and nonarticular compression. Full extension is the close-packed position, which is assumed whenever the fingers are used as props to transmit body weight or powerful thrust. In contrast, the fully clenched fist may also be used for this purpose. Flexion and extension are accompanied by slight conjunct rotation: during flexion this turns the digital pulps slightly laterally, i.e. to face the opposed thumb, and an opposite rotation occurs during extension.

Accessory movements

Accessory movements are limited rotation, abduction, adduction and anteroposterior translation. They permit the fingers to adapt to the shapes of gripped objects and help to protect against stresses and strains.

Muscles producing movements

The muscles producing movements at the interphalangeal joints are as follows.

Flexion

At proximal interphalangeal joints, flexores digitorum superficialis and profundus; at distal interphalangeal joints, flexor digitorum profundus; at the thumb interphalangeal joint, flexor pollicis longus.

Extension

Extensores digitorum, digiti minimi and pollicis longus, in association with abductor pollicis longus and extensor pollicis brevis. Extension occurs simultaneously in both joints in digits 2–5.

Simultaneous flexion at the metacarpophalangeal joints and extension at the interphalangeal joints of a digit are essential for the fine movements of writing, drawing, threading a needle, etc. The lumbricals and interossei have long been accepted as not only primary agents in flexing the metacarpophalangeal joints but also in extending the interphalangeal joints via their attachments to the dorsal digital expansions.

Mallet finger

Mallet finger is a traumatic rupture, avulsion fracture or laceration of the terminal slip of the extensor tendon to the terminal phalanx of the finger. It can result from forced flexion of the distal phalanx of the fully extended finger and is a well-known injury in cricketers. The patient is unable actively to extend the terminal phalanx although the distal interphalangeal joint can be extended passively.

Swan neck deformity

Swan neck deformity involves hyperextension of the proximal interphalangeal joint together with distal interphalangeal joint flexion. It is caused by a relative overactivity of the extensors acting at the proximal interphalangeal joint compared with the flexors. It arises as a result of intrinsic muscle spasm, long standing mallet finger or dysfunction of flexor digitorum superficialis and can only occur if there is also some laxity of the volar plate.

Boutonnière deformity

Boutonnière deformity is a flexion deformity of the proximal interphalangeal joint following either division or laxity in the central slip of the extensor tendon, which normally inserts into the base of the middle phalanx. An essential feaure is hyperextension at the distal interphalangeal joint. It usually occurs as a result of either trauma or rheumatoid arthritis which cause the lateral bands of the extensor tendon to migrate in a volar direction and the head of the proximal phalanx to migrate dorsally. Initially the deformity is passively correctable. With time, the soft tissues around the joint contract and a fixed deformity results.

MUSCLE

EXTRINSIC LONG FLEXORS AND EXTENSORS

The extrinsic long flexors and extensors are described on page 845.

Flexor retinaculum

The flexor retinaculum is a strong, fibrous band (Fig. 50.25). It crosses the front of the carpus and converts its anterior concavity into the carpal tunnel which transmits the flexor tendons of the digits and the median nerve. The retinaculum is short and broad, measuring 2.5–3 cm both transversely and proximodistally. It is attached medially to the pisiform and the hook of the hamate. Laterally, it splits into superficial and deep laminae. The superficial lamina is attached to the tubercles of the scaphoid and trapezium. The deep lamina is attached to the medial lip of the groove on the trapezium. Together with this groove, the two laminae form a tunnel, lined by a synovial sheath, which contains the tendon of flexor carpi radialis. The retinaculum is crossed superficially by the ulnar vessels and nerve – immediately radial to the pisiform – and by the palmar cutaneous branches of the median and ulnar nerves. A slender band of fascia, the superficial part of the flexor retinaculum, bridges over the ulnar neurovascular bundle and attaches to the radial side of the pisiform, forming a tunnel (Guyon’s canal) which is an occasional site of ulnar nerve entrapment. The tendons of palmaris longus and flexor carpi ulnaris are partly attached to the anterior surface of the retinaculum. Distally some of the intrinsic muscles of the thumb and little finger are attached to the retinaculum.

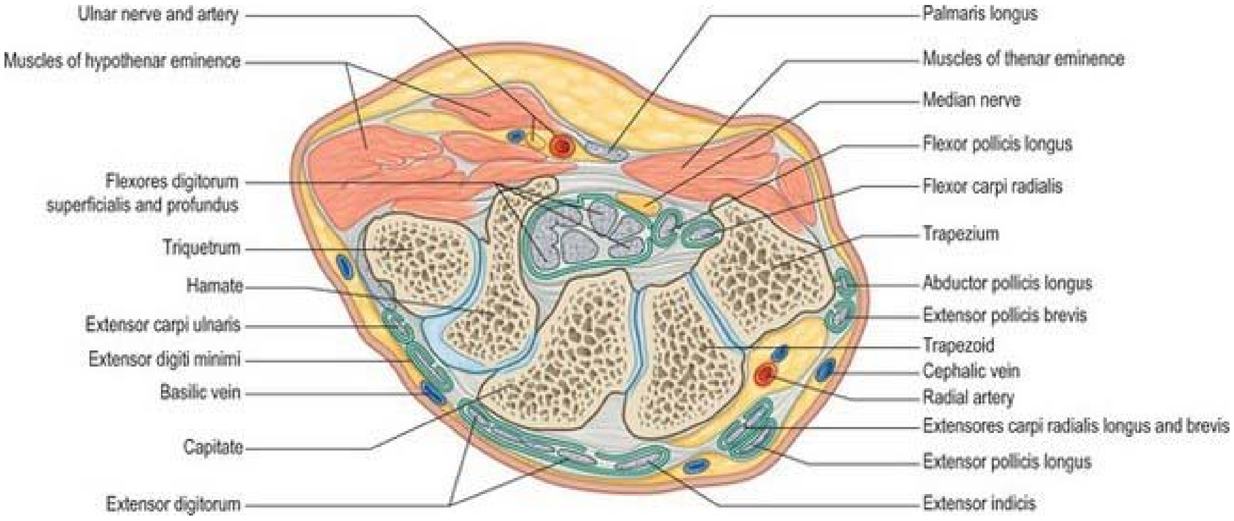
Ulnar nerve and artery
Muscles of hypothenar eminence
Flexores digitorum superficialis and profundus
Triquetrum
Hamate
Extensor carpi ulnaris
Extensor digiti minimi
Basilic vein
Capitate
Extensor digitorum
Palmaris longus
Muscles of thenar eminence
Median nerve
Flexor pollicis longus
Flexor carpi radialis
Trapezium
Abductor pollicis longus
Extensor pollicis brevis
Trapezoid
Cephalic vein
Radial artery
Extensores carpi radialis longus and brevis
Extensor pollicis longus
Extensor indicis

Fig. 50.25 Transverse section through the left wrist at the level of the carpus, showing the muscle tendons and their synovial sheaths.

Long flexor tendon apparatus

Flexor tendon sheaths

The fibrous sheaths of the flexor tendons are specialized parts of the palmar fascial continuum. Each finger has an osseoaponeurotic tunnel which extends from midpalm to the distal phalanx. The thumb has a tunnel for flexor pollicis longus which extends from the metacarpal to the distal phalanx. The proximal border is to some extent a matter of definition, because the transverse fibres of the palmar aponeurosis may be considered to be a part of the pulley system. The sheath consists of arcuate fibres which arch anteriorly over bone, tendons (where the sheath is required to be stiff), and the centres of joints (where a bucket-handle of arcuate fibres is a mechanically favourable arrangement). In contrast, where the sheath is required to fold to permit joint flexion, it consists of cruciate fibres. These fibrous sheaths are lined by a thin synovial membrane which provides a sealed lubrication system containing synovial fluid. The synovial membrane extends from the distal phalanx to midpalm in the case of the index, middle and ring fingers, and further proximally in the case of the little finger (Fig. 50.26). The sheaths around the thumb and little finger are continuous with the flexor sheaths in front of the wrist. The parietal synovial membrane is reflected onto the surface of the flexor tendon, forming a visceral synovium.

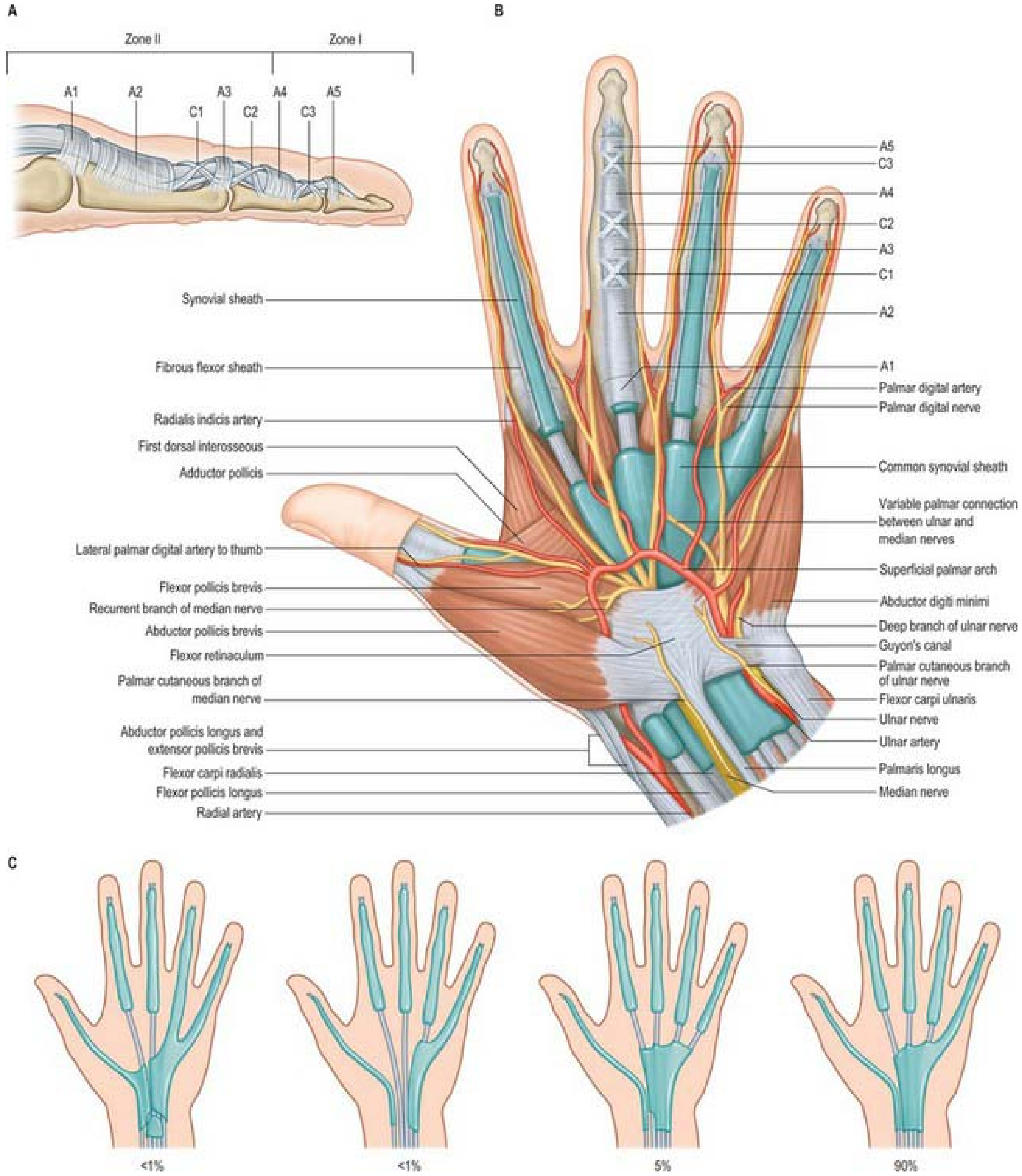
A
Zone II
Zone I
A1
A2
A3
A4
A5
C1
C2
C3
B
A5
C3
A4
C2
A3
C1
A2
A1
Synovial sheath
Fibrous flexor sheath
Radialis indicis artery
First dorsal interosseous
Adductor pollicis
Lateral palmar digital artery to thumb
Flexor pollicis brevis
Recurrent branch of median nerve
Abductor pollicis brevis
Flexor retinaculum
Palmar cutaneous branch of median nerve
Abductor pollicis longus and extensor pollicis brevis
Flexor carpi radialis
Flexor pollicis longus
Radial artery
Palmar digital artery
Palmar digital nerve
Common synovial sheath
Variable palmar connection between ulnar and median nerves
Superficial palmar arch
Abductor digiti minimi
Deep branch of ulnar nerve
Guyon's canal
Palmar cutaneous branch of ulnar nerve
Flexor carpi ulnaris
Ulnar nerve
Ulnar artery
Palmaris longus
Median nerve
C
<1%
<1%
5%
90%

Fig. 50.26 Synovial sheaths of the tendons and flexor tendon sheaths on the flexor aspect of the left wrist and hand. Where they are exposed, the

synovial sheaths are shown in blue. **A**, Lateral view of the anular and cruciate pulleys of the flexor tendon sheath. **B**, Palmar aspect showing the synovial sheaths and details of the anular and cruciate pulleys in the middle finger. Note the extension of the digital arteries and nerves to the end of the middle finger have been omitted to allow clarity in showing the pulley system. **C**, Variation in the arrangement to the synovial sheaths to the digits.

A standard nomenclature for the anular and cruciform pulleys that make up the sheath has been adopted by the American Society for Surgery of the Hand: the letters A and C respectively are used (Doyle & Blythe 1975).

The usual pattern is as follows (Fig. 50.26). The A1 pulley is situated anterior to the palmar cartilaginous plate of the metacarpophalangeal joint and may extend over the proximal part of the proximal phalanx. The A2 overlies the middle third of the proximal phalanx. It is the strongest pulley and arises from well-defined longitudinal ridges on the palmar aspect of the phalanx. Its distal edge is well developed. A pouch or recess of synovium extends superficial to the free edge of the pulley fibres so that the free edge forms a lip protruding into the synovial space. A3 is a narrow pulley lying palmar to the proximal interphalangeal joint. A4 overlies the middle third of the middle phalanx, and A5 overlies the distal interphalangeal joint. The cruciate fibres are numbered in a slightly different manner. C0 is palmar to the metacarpophalangeal joint. There are two cruciate zones, C1 and C2, at the proximal interphalangeal joint and they lie just proximal and distal respectively to A3. At the distal interphalangeal joint there is one pronounced cruciate system, C3, which lies between A4 and A5. Variations occur frequently. During flexion, the cruciate fibres become orientated more transversely in the digits and the edges of adjacent anular pulleys approximate so that they form, in full flexion, a continuous tunnel of transversely orientated fibres. Surgically the most important pulleys which prevent bowstringing of the flexor tendons are the A2 and A4 pulleys.

The pulley arrangement in the thumb is different from that in the other digits. There are three constant pulleys – two anular and one oblique (Fig. 50.27). The A1 pulley is located at the metacarpophalangeal joint. The oblique pulley is located over the mid-portion of the proximal phalanx, and its fibres pass from the ulnar aspect proximally to the radial aspect dorsally. The A2 pulley is thinner than the A1 pulley and is situated just proximal to the interphalangeal joint. The oblique pulley is the most important pulley in the thumb for maintaining the action of flexor pollicis longus.

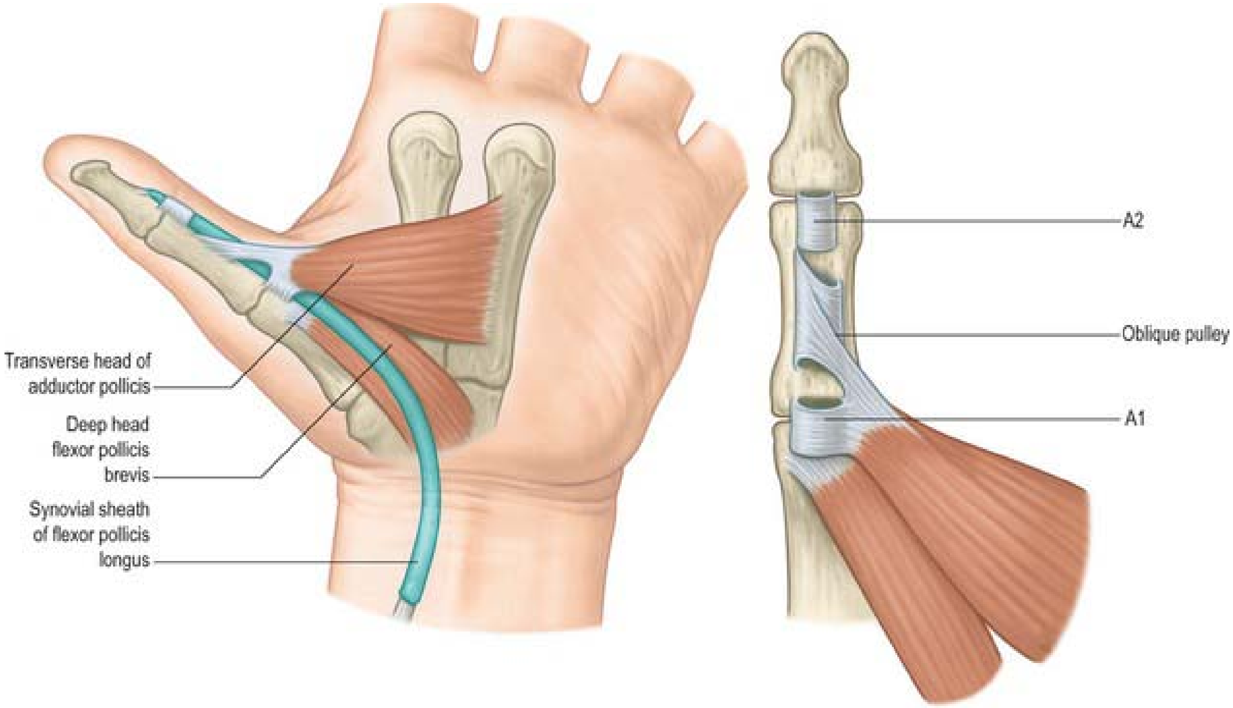
Transverse head of adductor pollicis
Deep head flexor pollicis brevis
Synovial sheath of flexor pollicis longus
A2
Oblique pulley
A1

Fig. 50.27 Flexor sheath of the left thumb showing the anular and oblique pulleys.

(From Doyle JR, Blythe WF 1977 Anatomy of the flexor tendon sheath and pulleys of the thumb. J Hand Surg 2: 149–51. With permission from the American Society for Surgery of the Hand.)

Synovial sheaths of the carpal flexor tendons

Two synovial sheaths envelop the flexor tendons as they traverse the carpal tunnel, one for the flexores digitorum superficialis and profundus, the other for flexor pollicis longus (Fig. 50.25). These sheaths typically extend into the forearm for 2.5 cm proximal to the flexor retinaculum, and occasionally communicate with each other deep to it. The sheath of the flexores digitorum tendons reaches about halfway along the metacarpal bones, where it ends in blind diverticula around the tendons to the index, middle and ring fingers (Fig. 50.26). The sheath is prolonged around the tendons to the little finger and is usually continuous with their digital synovial sheath. A transverse section through the carpus shows that the tendons are invaginated into the sheath from the lateral side (Fig. 50.25). The parietal layer lines the flexor retinaculum and the floor of the carpal tunnel. It is reflected laterally as the visceral layer over the tendons of flexor digitorum superficialis ventrally and flexor digitorum profundus dorsally. Medially a recess formed by the visceral layer of the sheath insinuates between the two groups of tendons and passes laterally for a variable distance. The sheath of flexor pollicis longus, which is usually separate, is continued along the thumb as far as the insertion of the tendon.

Vincula

The phenomenon of tendon gliding within a fibrous sheath requires a very specialized arrangement of the vascular supply. Folds of synovial membrane containing a loose plexus of fascial fibres carry blood vessels to the tendons at certain defined points (Fig. 50.28). These folds, vincula tendinum, are of two kinds. Vincula brevia, of which there are two in each finger, are attached to the deep surfaces of the tendons near to their insertions. There is thus one vinculum brevium attaching flexor digitorum profundus to the region of the distal interphalangeal joint, and a more proximal vinculum deep to flexor digitorum superficialis at the proximal interphalangeal joint. Vincula longa are filiform: usually two are attached to each superficial tendon, one to each deep tendon.

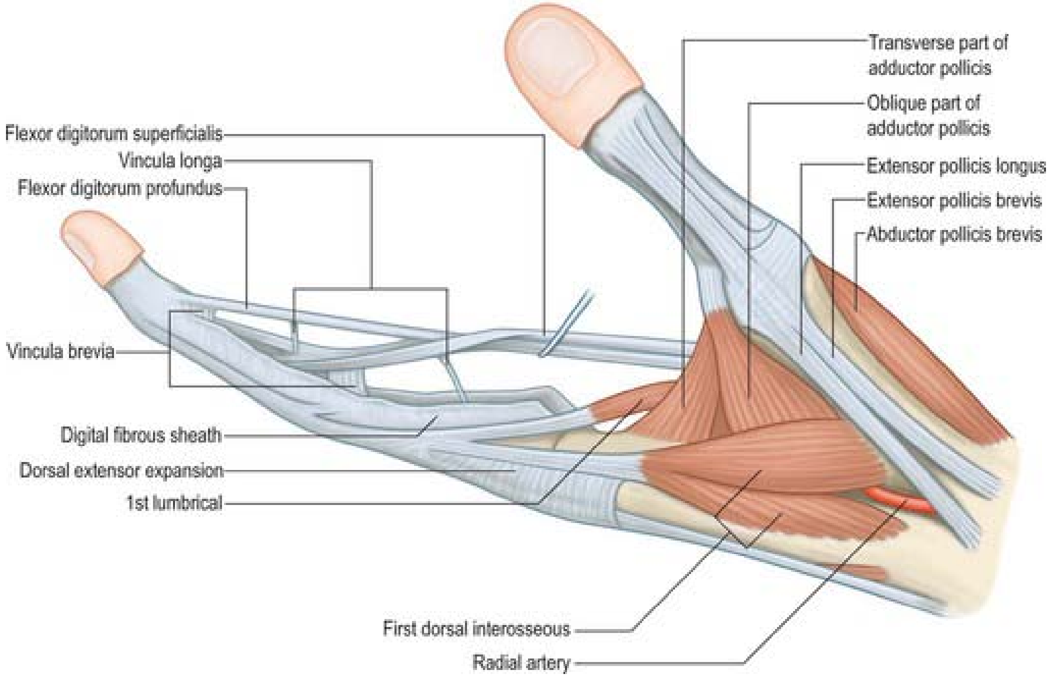
Transverse part of adductor pollicis
Oblique part of adductor pollicis
Flexor digitorum superficialis
Vincula longa
Flexor digitorum profundus
Extensor pollicis longus
Extensor pollicis brevis
Abductor pollicis brevis
Vincula brevia
Digital fibrous sheath
Dorsal extensor expansion
1st lumbrical
First dorsal interosseous
Radial artery

Fig. 50.28 Lateral part of the left hand showing the tendons and vincula tendinum of the index finger and the muscles in the first intermetacarpal space.

Trigger finger

Trigger finger is a stenosing tenovaginitis which affects the fibrous flexor sheaths of the fingers or thumb within the palm. The affected sheath thickens and entraps the contained tendons, which become constricted at the site of entrapment and bulge distal to it, to produce a distinct nodule in the palm of the hand. The finger now snaps as the tendon nodule passes through the constriction on flexing the finger. The corresponding extensor muscle is insufficiently powerful to extend the affected finger. The patient does this passively, accompanied by a painful snap. Treatment frequently requires surgical division of the A1 pulley of the flexor sheath to relieve the stricture.

Extensor retinaculum

The extensor retinaculum is a strong, fibrous band which extends obliquely across the back of the wrist (Fig. 50.29). It is attached laterally to the anterior border of the radius, medially to the triquetral and pisiform bones, and, in passing across the wrist, to the ridges on the dorsal aspect of the distal end of the radius. It prevents bowstringing of the tendons across the wrist joint.

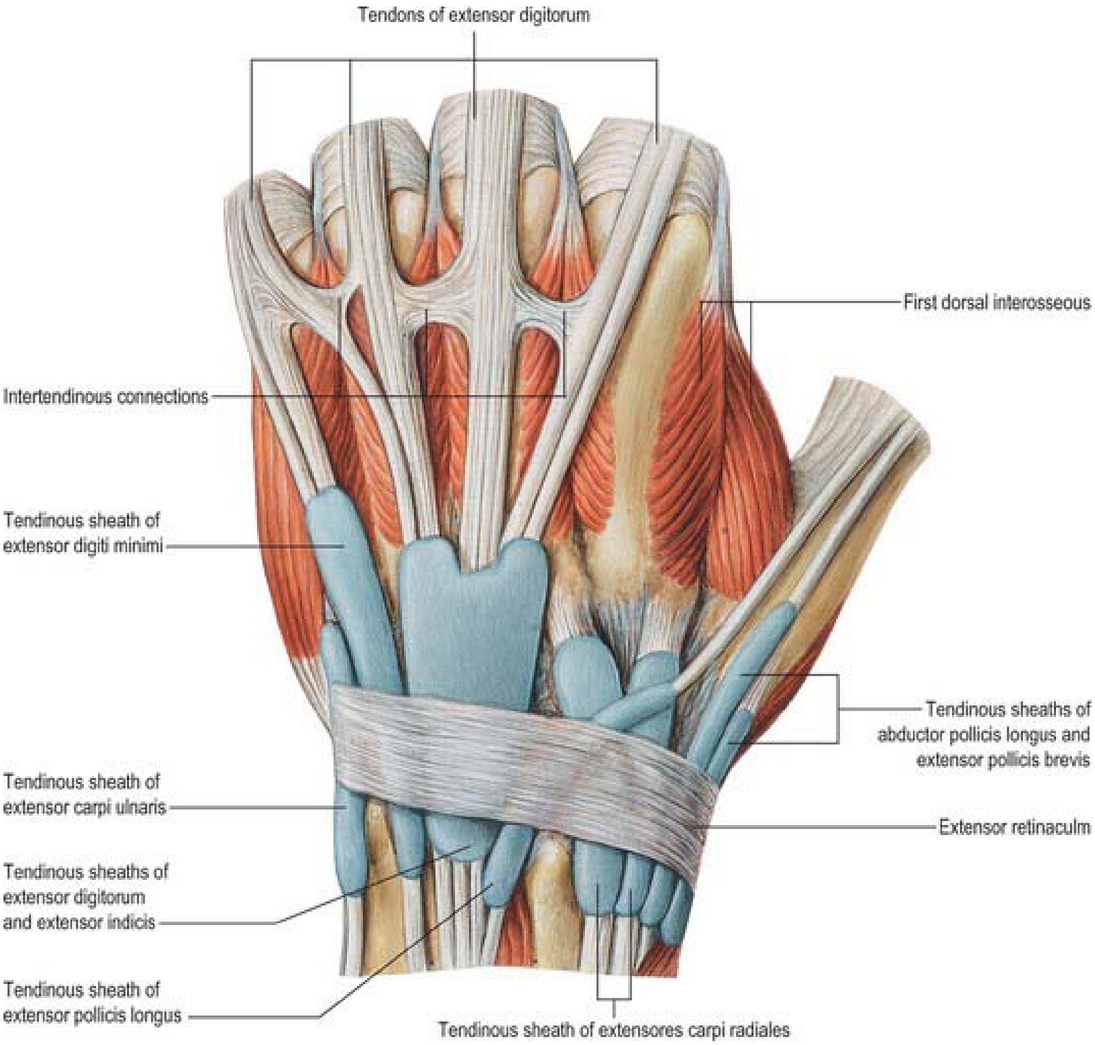
Tendons of extensor digitorum
First dorsal interosseous
Intertendinous connections
Tendinous sheath of extensor digiti minimi
Tendinous sheaths of abductor pollicis longus and extensor pollicis brevis
Tendinous sheath of extensor carpi ulnaris
Extensor retinaculm
Tendinous sheaths of extensor digitorum and extensor indicis
Tendinous sheath of extensor pollicis longus
Tendinous sheath of extensores carpi radiales

Fig. 50.29 The synovial sheaths of the tendons on the extensor aspect of the left wrist.

(From Sobotta 2006.)

Synovial sheaths of the carpal extensor tendons

Six tunnels deep to the extensor retinaculum transmit the extensor tendons, each contains a synovial sheath. The tendons of abductor pollicis longus and extensor pollicis brevis lie in a tunnel on the lateral side of the styloid process of the radius. Occasionally there may be a separate synovial sheath for each, or the tendon of the abductor may be double. The tendons of extensores carpi radiales longus and brevis lie behind the styloid process. The tendon of extensor pollicis longus lies on the medial side of the dorsal tubercle of the radius and the tendons of extensor digitorum and extensor indicis lie in a tunnel on the medial side of the tubercle. The tendon of extensor digiti minimi lies opposite the interval between the radius and ulna, and the tendon of extensor carpi ulnaris lies between the head and the styloid process of the ulna.

The tendon sheaths of abductor pollicis longus, extensores pollicis brevis and longus, extensores carpi radiales and extensor carpi ulnaris stop immediately proximal to the bases of the metacarpal bones; those of extensor digitorum, extensor indicis and extensor digiti minimi are sometimes prolonged a little more distally along the metacarpus.

De Quervain’s tenovaginitis

De Quervain’s tenovaginitis is a stenosing tenovaginitis of unknown aetiology which occurs in the first dorsal compartment at the level of the radial styloid. It involves the common extensor sheath containing the tendons of abductor pollicis longus and extensor pollicis brevis. There is palpable thickening of the tendon sheath with painful limitation of extension of the thumb. Treatment frequently requires division of the thickened sheath, care being taken to avoid the adjacent superficial radial nerve. Division of the sheath produces no functional impairment.

Extensor tendon apparatus

The extensor digitorum tendons emerge through the fourth dorsal compartment onto the dorsum of the hand, where they are joined together distally by a varying pattern of oblique interconnections, the juncturae tendinae. These typically pass in a distal direction from middle finger to index finger and from ring finger to middle and little fingers. Proximal lacerations to the middle finger extensor tendon may result in only partial loss of extension because of these tendinous interconnections.

At the level of the metacarpophalangeal joint, each extensor tendon is held in a central position over the dorsum of the joint by a flat fibrous extensor expansion (Fig. 50.30). The expansion extends onto the dorsum of the proximal phalanx of each digit. It forms a movable hood, which moves distally when the metacarpophalangeal joint is flexed, and proximally when it is extended (in which position it is most closely applied to the joint).

Each extensor tendon blends with the extensor expansion along its central axis, and is separated from the metacarpophalangeal joint by a small bursa. The expansion is triangular in shape, with its base proximal. It receives the conjoined tendons of the intrinsic muscles. The expansion is almost translucent between its margins and the extensor digitorum tendon. Transverse fibres (the sagittal bands) pass to the volar plate and transverse metacarpal ligaments. They separate the phalangeal attachment of the dorsal interosseus from the rest of the muscle, and the palmar interosseus from the lumbrical muscle. Injuries to the sagittal bands can lead to subluxation of the extensor tendon.

The margins of the extensor expansions are thickened on the radial side by the tendons of lumbrical and interosseous muscles and on the ulnar side by the tendon of an interosseous alone or, in the case of the fifth digit, by abductor digiti minimi.

The interossei tendons join the extensor expansion at the level of the proximal portion of the proximal phalanx, while the lumbrical tendons join the extensor mechanism further distally at the mid-portion of the proximal phalanx. Their line of pull is proximal to the axis of rotation at the metacarpophalangeal joint, but dorsal to the axis of rotation at the proximal interphalangeal joint. The extensor mechanism trifurcates into a central slip and two lateral bands just proximal to the proximal interphalangeal joint. The central slip receives a contribution from the lumbrical and interosseous tendons via the lateral bands. Similarly, some fibres from the central region pass to each lateral band, producing a criss-cross arrangement of fibres. The central slip attaches to the base of the middle phalanx, while the lateral bands continue distally and eventually fuse together and insert into the distal phalanx. The tension in the central slip and the lateral bands varies as the finger moves between flexion and extension and plays a crucial role in coordinating synchronous activity between the proximal and distal interphalangeal joints.

The transverse and oblique retinacular ligaments of Landsmeer connect the fibrous flexor sheath to the extensor apparatus. The transverse retinacular ligament passes from the A3 pulley of the fibrous flexor sheath at the level of the proximal interphalangeal joint to the lateral border of the lateral extensor band. The oblique retinacular ligament lies deep to the transverse retinacular ligament. It originates from the lateral aspect of the proximal phalanx and flexor sheath (A2 pulley) and passes volar to the axis of rotation of the proximal interphalangeal joint but in a dorsal and distal direction to insert into the terminal extensor tendon.

INTRINSIC MUSCLES OF THE HAND

The intrinsic muscles of the hand are organized into three groups plus a superficial muscle. Flexor pollicis brevis, abductor pollicis brevis, opponens pollicis and adductor pollicis all act on the thumb and are known collectively as the thenar muscles. Abductor digiti minimi, flexor digiti minimi brevis and opponens digiti minimi all act on the little finger and are known collectively as hypothenar muscles. Interossei and lumbricals act on the fingers. Palmaris brevis is a superficial muscle that lies beneath the ulnar palmar skin.

Flexor pollicis brevis

Attachments

Flexor pollicis brevis lies medial to abductor pollicis brevis (Fig. 50.31). It has superficial and deep parts. The superficial head arises from the distal border of the flexor retinaculum and the distal part of the tubercle of the trapezium, and passes along the radial side of the tendon of flexor pollicis longus. It is attached, by a tendon that contains a sesamoid bone, to the radial side of the base of the proximal phalanx of the thumb. The deep part arises from the trapezoid and capitate bones and from the palmar ligaments of the distal row of carpal bones, and passes deep to the tendon of flexor pollicis longus. It unites with the superficial head on the sesamoid bone and base of the first phalanx.

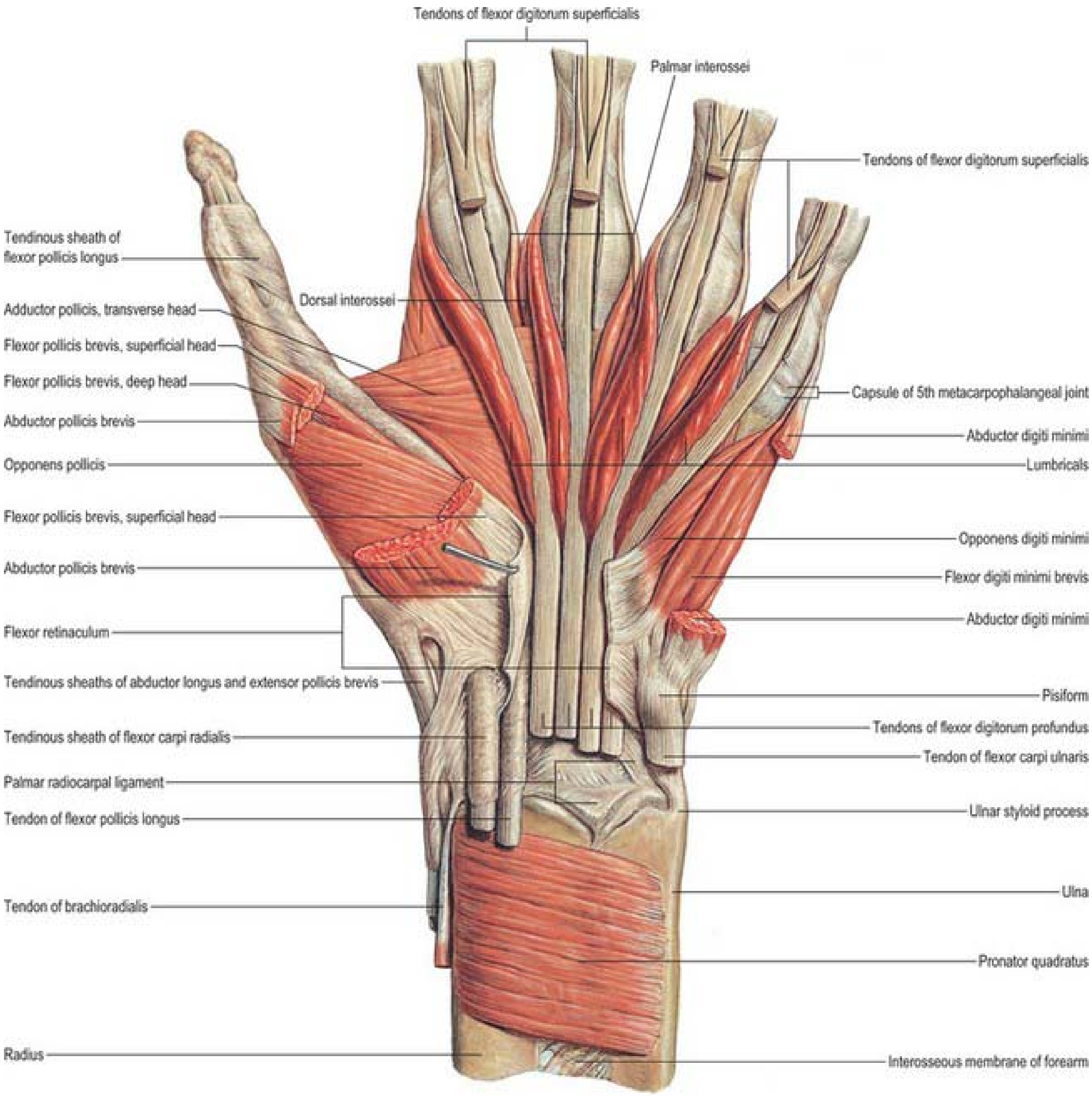
Tendons of flexor digitorum superficialis
Palmar interossei
Tendons of flexor digitorum superficialis
Tendinous sheath of flexor pollicis longus
Dorsal interossei
Adductor pollicis, transverse head
Flexor pollicis brevis, superficial head
Flexor pollicis brevis, deep head
Abductor pollicis brevis
Opponens pollicis
Flexor pollicis brevis, superficial head
Abductor pollicis brevis
Flexor retinaculum
Tendinous sheaths of abductor longus and extensor pollicis brevis
Tendinous sheath of flexor carpi radialis
Palmar radiocarpal ligament
Tendon of flexor pollicis longus
Tendon of brachioradialis
Radius
Capsule of 5th metacarpophalangeal joint
Abductor digiti minimi
Lumbricals
Opponens digiti minimi
Flexor digiti minimi brevis
Abductor digiti minimi
Pisiform
Tendons of flexor digitorum profundus
Tendon of flexor carpi ulnaris
Ulnar styloid process
Ulna
Pronator quadratus
Interosseous membrane of forearm

Fig. 50.31 Muscles of the left hand. Deep layer after cutting the flexor retinaculum and partial removal of several superficial muscles: palmar aspect.

(From Sobotta 2006.)

The superficial head is frequently blended with opponens pollicis. The deep head varies considerably in size and may even be absent.

Relations

Flexor pollicis brevis lies superficial in the thenar eminence and is distal to abductor pollicis brevis. It is crossed by the motor branch of the median nerve.

Vascular supply

Flexor pollicis brevis is supplied by the superficial palmar branch of the radial artery, and branches from the princeps pollicis artery and radialis indicis artery.

Innervation

The superficial head of flexor pollicis brevis is usually innervated by the lateral terminal branch (motor branch) of the median nerve. The deep head is usually innervated by the deep branch of the ulnar nerve, C8 and T1. Some variation is common.

Action

Flexor pollicis brevis flexes the metacarpophalangeal joint.

Testing

Flexor pollicis brevis is palpated in the thenar eminence while the subject flexes the metacarpophalangeal joint of the thumb, keeping the interphalangeal joint fully extended.

Abductor pollicis brevis

Attachments

Abductor pollicis brevis is a thin, subcutaneous muscle in the proximolateral part of the thenar eminence (Fig. 50.31). It arises mainly from the flexor retinaculum, but a few fibres spring from the tubercles of the scaphoid bone and trapezium, and from the tendon of abductor pollicis longus. Its medial fibres are attached by a thin, flat tendon to the radial side of the base of the proximal phalanx of the thumb, and its lateral fibres join the dorsal digital expansion of the thumb. The muscle may receive accessory slips from the long and short extensors of the thumb, opponens pollicis, or the styloid process of the radius.

Relations

Abductor pollicis brevis lies proximomedial to flexor pollicis brevis in the superficial part of the thenar eminence.

Vascular supply

Abductor pollicis brevis is supplied by the superficial palmar branch of the radial artery, and often by an independent branch directly from the radial artery lying on the radial aspect of thumb.

Innervation

Abductor pollicis brevis is innervated by the lateral terminal branch (motor branch) of the median nerve, C8 and T1. Note that this is the only muscle of the thenar eminence which is constantly supplied by the median nerve.

Action

Abductor pollicis brevis draws the thumb ventrally in a plane at right angles to the palm of the hand (abduction).

Testing

The hand is placed with its dorsum on the table. The subject's thumb is placed so that the nail is in a plane at right angles to the palm of the hand. The subject is instructed to touch with his thumb an object held vertically above the thumb. This is a highly specific test for a median nerve lesion.

Opponens pollicis

Attachments

Opponens pollicis lies deep to abductor pollicis brevis (Fig. 50.31). It arises from the tubercle of the trapezium and the flexor retinaculum, and is attached to the whole length of the lateral border, and the adjoining lateral half of the palmar surface of the metacarpal bone of the thumb.

Relations

Opponens pollicis lies deep between the other two muscles of the thenar eminence and is only revealed when they are retracted.

Vascular supply

Opponens pollicis is supplied by the superficial palmar branch of the radial artery, and by branches from the first palmar metacarpal artery (when present), princeps pollicis artery, radialis indicis artery and the deep palmar arch.

Innervation

Opponens pollicis is innervated by the lateral terminal branch of the median nerve, C8 and T1, and commonly by a branch of the deep terminal branch of the ulnar nerve.

Action

Opponens pollicis flexes the metacarpal bone of the thumb.

Testing

The subject tries, against resistance, to touch the tip of the little finger with the thumb. The key observation is whether or not the thumb can be strongly adducted without flexing the IP joint.

Adductor pollicis

Attachments

Adductor pollicis arises by oblique and transverse heads (Fig. 50.31). The oblique head is attached to the capitate bone, the bases of the second and third metacarpal bones, the palmar ligaments of the carpus and the sheath of the tendon of flexor carpi radialis. Most of the fibres converge into a tendon (which contains a sesamoid bone), which unites with the tendon of the transverse head, and is attached to the ulnar side of the base of the proximal phalanx of the thumb. The deepest fibres may pass into the medial side of the dorsal digital expansion of the thumb. On the lateral side of the oblique head a considerable fasciculus passes deep to the tendon of flexor pollicis longus to join flexor pollicis brevis; this has been described as the ‘deep head’ of flexor pollicis brevis. The transverse head is the deepest of the pollicial muscles, it is triangular, and arises from the distal two-thirds of the palmar surface of the third metacarpal. The fibres converge to be attached, with the oblique head and the first palmar interosseous, to the base of the proximal phalanx of the thumb. The two parts of the adductor vary in relative size and degree of connection.

Relations

The deep palmar arch and the deep branch of the ulnar nerve pass between the two heads of the muscle. Anteriorly adductor pollicis is crossed by the flexor tendons of the index finger and their sheath, and the first lumbrical, and is overlapped by flexor pollicis brevis. Posteriorly it abuts against the first dorsal interosseous muscle: together these muscles form the mass of the first web space of the hand.

Vascular supply

Adductor pollicis is supplied by the arteria princeps pollicis and the arteria radialis indicis (which are sometimes combined as the first palmar metacarpal artery) and by branches from the deep palmar arch.

Innervation

Adductor pollicis is innervated by the deep branch of the ulnar nerve, C8 and T1.

Action

Adductor pollicis approximates the thumb to the palm of the hand. It acts to greatest advantage when the abducted, rotated and flexed thumb is opposed to the fingers in gripping.

Testing

With the thumb lying along the palmar aspect of the index finger, and with its nail in a plane at right angles to the palm, the subject is asked to retain a strip of paper between the thumb and palm against resistance.

Abductor digiti minimi

Attachments

Abductor digiti minimi arises from the pisiform bone, the tendon of flexor carpi ulnaris and the pisohamate ligament (Fig. 50.31). It ends in a flat tendon which divides into two slips: one is attached to the ulnar side of the base of the proximal phalanx of the little finger, and the other to the ulnar border of the dorsal digital expansion of extensor digiti minimi.

The muscle may have two or three slips and may be fused with flexor digiti minimi brevis. An additional slip may arise from flexor retinaculum, antebrachial fascia, or tendons of palmaris longus or flexor carpi ulnaris. It may be partly attached to the fifth metacarpal by a slip from the pisiform.

Relations

Abductor digiti minimi lies along the ulnar border of flexor digiti minimi brevis and overlies opponens digiti minimi.

Vascular supply

Abductor digiti minimi is supplied by the deep palmar branch of the ulnar artery, branches from the ulnar end of the superficial palmar arch and the palmar digital artery for the medial border of the little finger.

Innervation

Abductor digiti minimi is innervated by the deep branch of the ulnar nerve, C8 and T1.

Action

Abductor digiti minimi abducts the little finger away from the fourth, e.g. in the habitual spreading of the digits when they are extended. Abduction is also possible when digits 2–4 are tightly adducted in flexion or extension.

Testing

Abductor digiti minimi is tested by abducting the little finger against resistance.

Flexor digiti minimi brevis

Attachments

Flexor digiti minimi brevis arises from the convex surface of the hook of the hamate and the palmar surface of the flexor retinaculum. It inserts into the ulnar side of the base of the proximal phalanx of the little finger with abductor digiti minimi.

It may be absent, or fused with the abductor, and it may attach to the distal end of the fifth metacarpal by a muscular slip.

Relations

Flexor digiti minimi brevis lies lateral to the abductor. Its origin is separated from that of the abductor by the deep branches of the ulnar artery and nerve.

Vascular supply

Flexor digiti minimi brevis is supplied by the deep palmar branch of the ulnar artery, branches from the ulnar end of the superficial palmar arch, and the palmar digital artery for the medial border of the little finger.

Innervation

Flexor digiti minimi brevis is innervated by the deep branch of the ulnar nerve, C8 and T1.

Action

Flexor digiti minimi brevis produces flexion of the little finger at its metacarpophalangeal joint, together with some lateral rotation.

Testing

The subject flexes the metacarpophalangeal joint of the little finger while the examiner maintains the interphalangeal joints in extension.

Opponens digiti minimi

Attachments

Opponens digiti minimi is a triangular muscle, lying under cover of the flexor and abductor. It arises from the convexity of the hook of the hamate, and the contiguous portion of the flexor retinaculum, and inserts along the whole length of the ulnar margin of the fifth metacarpal bone, and the adjacent palmar surface.

The muscle is often divided into two lamellae by the deep branches of the ulnar artery and nerve. It blends to a variable degree with its neighbours.

Relations

Opponens digiti minimi lies on the ulnar margin and adjacent palmar surface of the fifth metacarpal, overlapped by, and often partly fused with, the other two muscles of the hypothenar eminence.

Vascular supply

Opponens digiti minimi is supplied by the deep palmar branch of the ulnar artery, and branches from the medial end of the deep palmar arch.

Innervation

Opponens digiti minimi is innervated by the deep branch of the ulnar nerve, C8 and T1.

Action

Opponens digiti minimi flexes the fifth metacarpal bone, drawing it forwards and rotating it laterally at the carpometacarpal joint: this deepens the hollow of the palm. These actions, together with flexion and some lateral rotation at the metacarpophalangeal and interphalangeal joints, bring the digit into opposition with the thumb.

Testing

The subject is asked to place the tip of the little finger, against resistance, onto the tip of the opposed thumb while the examiner maintains the interphalangeal joints of the little finger in extension.

Palmaris brevis

Attachments

Palmaris brevis is a thin, quadrilateral muscle, lying beneath the skin of the ulnar side of the palm (see Fig. 50.4). It arises from the flexor retinaculum and the medial border of the central part of the palmar aponeurosis, and is attached to the dermis on the ulnar border of the hand.

Relations

Palmaris brevis is superficial to the ulnar artery and the superficial terminal branch of the ulnar nerve.

Vascular supply

Palmaris brevis is supplied by branches from the ulnar end of the superficial palmar arch.

Innervation

Palmaris brevis is innervated by the superficial branch of the ulnar nerve, C8 and T1.

Action

Palmaris brevis wrinkles the skin on the ulnar side of the palm of the hand and deepens the hollow of the palm by accentuating the hypothenar eminence. In this way it may contribute to the security of the palmar grip.

Testing

Against resistance, the subject touches the tip of the opposed thumb with the tip of the little finger; the skin on the ulnar side of the palm is seen to pucker.

Interossei

The interossei occupy the intervals between the metacarpal bones, and are divided into a palmar and a dorsal set.

Palmar interossei

Attachments

Palmar interossei are smaller than dorsal interossei and lie on the palmar surfaces of the metacarpal bones rather than between them (Fig. 50.32). With the exception of the first, each of the three arises from the entire length of the metacarpal bone of one finger, and passes to the appropriate (adductor) side of the dorsal digital expansion.

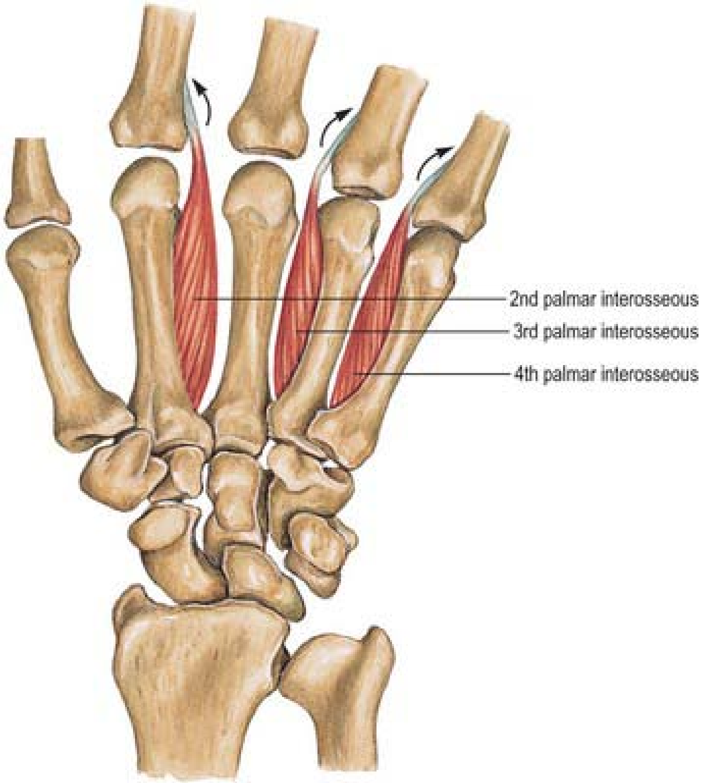

Fig. 50.32 Palmar interossei of the left hand: palmar aspect. Note that there is no first palmar interosseous in this specimen.

(From Sobotta 2006.)

The middle finger has no palmar interosseus. The remaining digits have palmar interossei on their aspects which face the middle finger. The first arises from the ulnar side of the palmar surface of the base of the first metacarpal bone, and is inserted into a sesamoid bone on the ulnar side of the proximal phalanx and from there passes to the phalanx and usually also into the dorsal digital expansion. It lies in front of the lateral head of the first dorsal interosseous, and is overlapped anteriorly by the oblique head of adductor pollicis (Fig. 50.31, Fig. 50.32). It is often very rudimentary because the thumb has its own powerful adductor. The second arises from the ulnar side of the second metacarpal bone, and is inserted into the same side of the digital expansion of the index finger. The third arises from the radial side of the fourth metacarpal bone, and is inserted together with the third lumbrical. The fourth arises from the radial side of the fifth metacarpal bone, and is attached with the fourth lumbrical and also to the base of the proximal phalanx. The attachment of these muscles to the dorsal digital expansions (Fig. 50.30) stabilizes the extensor tendons on the convex heads of the metacarpal bones during flexion and extension at the metacarpophalangeal joints.

The interossei show little variation in their arrangement. They are occasionally reduplicated.

Relations

The first palmar interosseous lies anterior to the lateral head of the first dorsal interosseous and is overlapped anteriorly by the oblique head of adductor pollicis, which also crosses anterior to the second palmar interosseous. The third and fourth are overlapped by the long flexor tendons of the ring and little finger respectively within their flexor sheaths.

Vascular supply

Palmar interossei are supplied by branches from the deep palmar arch, princeps pollicis artery, radialis indicis artery, palmar metacarpal arteries, proximal and distal perforating arteries and common and proper digital (palmar) arteries.

Innervation

All the interossei are innervated by the deep branch of the ulnar nerve, C8 and T1.

Action

Palmar interossei adduct the fingers to an imaginary longitudinal axis through the centre of the middle finger. Interossei have a considerable cross-sectional area and therefore contribute strongly to metacarpophalangeal joint flexion and interphalangeal extension. When paralysed, as in ulnar nerve paralysis, the grip strength of the hand is severely impaired and the arc of finger motion is abnormal, with a tendency for the fingers to claw. Each interosseous has a considerable ability to rotate the digit at the metacarpophalangeal joint. Generally this is not obvious, because interossei act in pairs, but it may occur where one interosseus is deficient as a result of injury or congenital deformity.

Testing

Adduction of the index, ring and little fingers against resistance. The subject grips a piece of paper between the index and middle fingers with the hand placed flat on the table. The examiner can assess the strength of adduction on trying to pull the paper away. This is a reliable test of ulnar nerve integrity.

Dorsal interossei

Attachments

Dorsal interossei consist of four bipennate muscles, each arising from the adjacent sides of two metacarpal bones, but more extensively from the metacarpal bone of the finger into which the muscle passes (Fig. 50.33). They insert on the bases of the proximal phalanges and separately into the dorsal digital expansions. Between the double origin of each of these muscles there is a narrow triangular interval. The radial artery passes through the first of these intervals, and a perforating branch from the deep palmar arch passes through each of the others. The first and largest muscle is sometimes named abductor indicis. It is attached to the radial side of the proximal phalanx of the index finger and to the capsule of the adjoining metacarpophalangeal joint. The second and third are attached to the radial and ulnar sides of the middle finger, respectively. Whereas the second generally reaches the digital expansion and the proximal phalanx, the third usually extends only to the digital expansion (Fig. 50.30). The fourth may be wholly attached to the digital expansion, but it often sends an additional slip to the proximal phalanx.

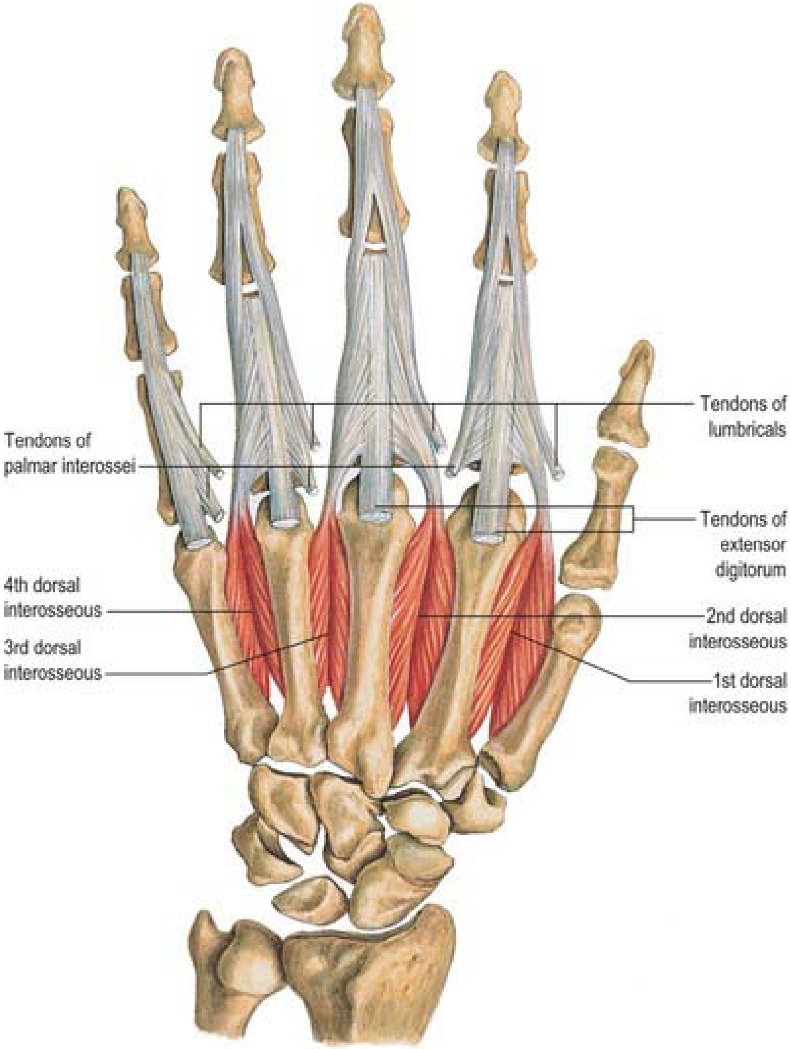
Tendons of palmar interossei
4th dorsal interosseous
3rd dorsal interosseous
Tendons of lumbricals
Tendons of extensor digitorum
2nd dorsal interosseous
1st dorsal interosseous

Fig. 50.33 Dorsal interossei of the left hand: palmar aspect.

(From Sobotta 2006.)

Relations

The first dorsal interosseous abuts anteriorly with adductor pollicis. The other dorsal interossei occupy the spaces between the second and the fifth metacarpal bones.

Vascular supply

Dorsal interossei are supplied by the dorsal metacarpal arteries (1st–4th), palmar metacarpal arteries (2nd–4th), radial artery (1st); princeps pollicis artery, radialis indicis artery, three perforating branches from the deep palmar arch (proximal perforating arteries), and three distal perforating branches. The tendons are supplied by branches from the common and proper palmar digital arteries and the dorsal digital arteries.

Innervation

All the interossei are innervated by the deep branch of the ulnar nerve, C8 and T1.

Action

Dorsal interossei abduct the fingers from an imaginary longitudinal axis through the centre of the middle finger. See also Action of palmar interossei.

Testing

Abduction of the index, middle and ring fingers against resistance. Most conveniently, the first dorsal interosseous is tested with the subject's fingers and palm flat upon the table. The subject tries to abduct the index finger against the examiner's resistance. The muscle belly can be felt and seen. This provides a reliable test for the integrity of the ulnar nerve.

Lumbricals

Attachments

The lumbricals are four small fasciculi which arise from the tendons of flexor digitorum profundus (Fig. 50.34). The first and second arise from the radial sides and palmar surfaces of the tendons of the index and middle fingers respectively. The third arises from the adjacent sides of the tendons of the middle and ring fingers, and the fourth from the adjoining sides of the tendons of the ring and little fingers. Each passes to the radial side of the corresponding finger, and is attached to the lateral margin of the dorsal digital expansion of extensor digitorum which covers the dorsal surface of the finger.

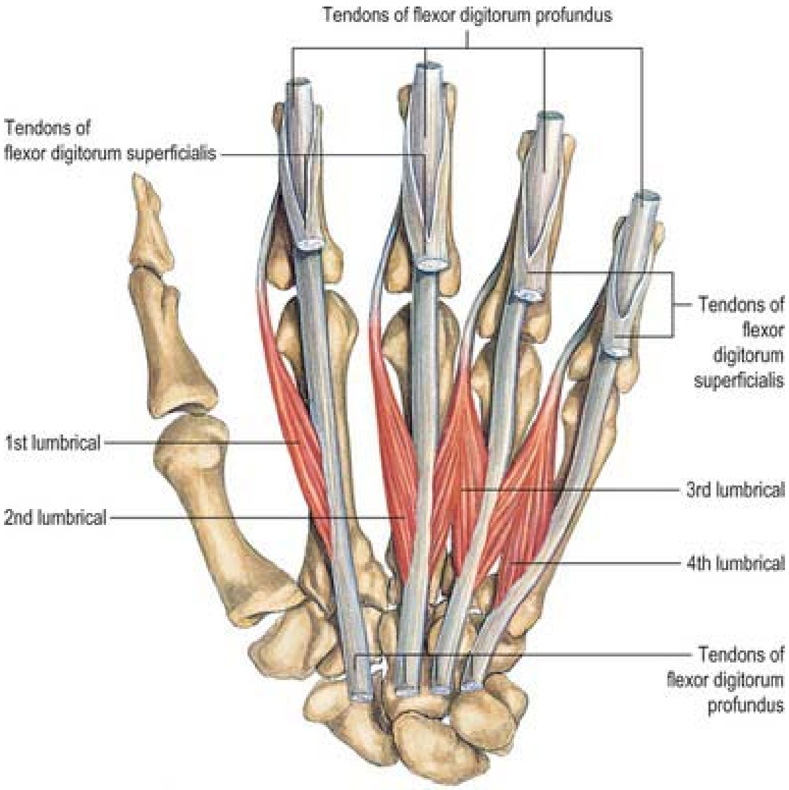
Tendons of flexor digitorum profundus
Tendons of flexor digitorum superficialis
Tendons of flexor digitorum superficialis
1st lumbrical
2nd lumbrical
3rd lumbrical
4th lumbrical
Tendons of flexor digitorum profundus

Fig. 50.34 The lumbricals of the left hand.

(From Sobotta 2006.)

Variations in the attachments of the lumbricals are common. Any of them may be unipennate or bipennate. When they are bipennate, the two heads arise from adjoining tendons of flexor digitorum profundus, and, in the case of the first lumbrical, from the tendon of flexor pollicis longus. Accessory lumbrical slips may be attached to an adjacent tendon of flexor digitorum superficialis.

Vascular supply

The first and second lumbricals are supplied by the first and second dorsal metacarpal and dorsal digital arteries. The third and fourth lumbricals are supplied by the second and third common palmar digital arteries, and the third and fourth dorsal digital arteries and their anastomoses with the palmar digital arteries.

Innervation

The first and second lumbricals are innervated by the median nerve, C8 and T1, and the third and fourth lumbricals by the deep terminal branch of the ulnar nerve, C8 and T1. The third lumbrical frequently receives a supply from the median nerve. The first and second lumbricals are occasionally innervated by the deep terminal branch of the ulnar nerve.

Action

Lumbricals arise from flexor tendons and insert into the extensor apparatus. Since both attachments are mobile, they have the potential for producing movement at either. The action on the extensor apparatus is easier to understand and consists of extension of both interphalangeal joints in a coordinated manner. The mode of action at the metacarpophalangeal joints is disputed, but if there is a flexor action it is very weak. The effect on the flexor digitorum profundus attachment is to pull the tendon distally. The combined action on both origin and insertion is therefore to alter the posture of the finger to allow more interphalangeal extension. Pinching the index finger against the thumb without a lumbrical would result in a nail-to-nail contact: the addition of the lumbrical increases the interphalangeal joint extension, and results in pulp-to-pulp pinch. Lumbricals contain many muscle spindles and have a long fibre length: it is therefore reasonable to assume that they play a role in proprioception.

Testing

Lumbricals cannot be tested in isolation, but the lumbrical–interosseous muscle complex can readily be examined together. The examiner holds the metacarpophalangeal joint of the index finger in hyperextension and the subject is the instructed to extend the two interphalangeal joints against resistance. This test is repeated seriatim on the middle, ring and little fingers.

COORDINATED MOVEMENTS OF THE HAND

The apparently simple human functions of closing the hand to grasp an object, or opening the palm to release it, are in reality tasks of considerable mechanical complexity, requiring the simultaneous contraction of many individual muscles. The isolated action of a single muscle may be inferred from the positions of its origin and insertion, and the estimated line of action (usually the centre line of the muscle) in relation to the axes of all the joints traversed by the muscle and its tendon. The limb can be regarded as a chain of joints crossed by muscles. If it is known which muscles are active, then the reason why one joint moves and others do not is a matter of simple mechanical relationships.

For example, flexor pollicis longus is considered to have a major role as a flexor of the interphalangeal joint of the thumb. However, the position of its tendon relative to more proximal joints in the limb gives it the potential for producing flexion at the metacarpophalangeal joint and also at the trapeziometacarpal and wrist joints. In the living subject the actual motion that takes place depends on which other muscle groups are acting, and so the potential for movement must be considered for each joint in the chain in turn. Motion at the wrist is generally balanced by wrist extensors. Motion at the trapeziometacarpal joint is balanced by abductor pollicis longus. Flexor pollicis longus will then have an action as a flexor of the metacarpophalangeal and interphalangeal joints only.

The factor that determines whether one or both of two joints will move is the turning moment at each. The greater the perpendicular distance from the line of muscle or tendon pull to the axis of the joint, the stronger is the turning effect of the muscle at the joint, but the smaller the range of joint motion that can be produced. In the case of flexor pollicis longus, the tendon is situated further from the axis of the metacarpophalangeal joint than from the axis of the interphalangeal joint: it will therefore tend to produce flexion preferentially at the metacarpophalangeal joint unless that joint is restrained by extensor pollicis brevis. In this way different postures of the thumb can be produced by the interplay of flexor and extensor forces. These simple guiding principles should provide an understanding of muscle action in the hand that is sufficient for most purposes.

In considering the role of a particular muscle, there is a tendency to concentrate on motion. Indeed, many muscles are named on the basis of the movements that they generate, although others – often those whose actions are the most difficult to interpret – are described according to their morphology or situation. A more important function may be the nature of the force generated. For example, although flexor pollicis longus flexes the thumb (see above), a large range of flexion is actually required in only a few activities, such as certain ripping tasks. In most pinch and manipulative tasks the role of the thumb is to apply isometric force, which it does with such precision that it is possible to pick up an egg and neither crush nor drop it. Thus for much of the time flexor pollicis longus behaves as an extremely sophisticated mechanism for the application of force, in which contraction and proprioception are equally important.

The anatomical position of the hand (palm flat and pointing anteriorly, forearm supinated) is a convenient standard for studying structural relationships. The hand in the relaxed (anaesthetized) position adopts a posture of partial flexion and mid-supination/pronation (the reader can verify this by relaxing completely and observing forearm and hand position).

SPECIAL FUNCTIONS OF THE HAND

Closing the hand

It is clear that the fingers and palm of the hand flex in gripping, grasping or making a fist, but there are subtle differences in hand posture in these various activities. The basic mechanisms of hand closure will be described before special grips are considered.

As the digits flex, the wrist usually extends (dorsiflexes) at the same time. The involvement of the long digital flexors in this movement will be considered first, followed by an analysis of the role of the wrist.

Role of the long digital flexors

Flexor digitorum superficialis acts principally to flex the proximal interphalangeal joints, through its insertions into the middle phalanges. However, in each digit it also has an action on the metacarpophalangeal joint, because the tendon passes anterior to that joint. The muscle has the potential to produce flexion at the wrist for the same reason. The fact that each tendon arises from an individual muscle slip allows the clinician to test one finger at a time. The reader can verify this by attempting to flex each digit individually while using the other hand to keep the distal interphalangeal joints of the remaining fingers in extension. This test is frequently used in clinical practice and is useful for the middle and ring fingers, where flexion of one finger alone must be attributed to flexor digitorum superficialis. The index finger, however, has its own profundus musculotendinous unit and may therefore move independently under the action of this tendon. Many individuals cannot flex the proximal interphalangeal joint of the little finger alone; usually this is because of linkage between the ring and little finger flexor digitorum superficialis tendons, but occasionally may be because superficialis is deficient. Most individuals can flex the metacarpophalangeal joint of the little finger using flexor digiti minimi.

Flexor digitorum profundus reaches further (to the distal phalanx), and is therefore the only muscle available for flexion of the distal interphalangeal joint. It also contributes, together with superficialis, to flexion at the proximal interphalangeal and metacarpophalangeal joints. These two long flexors (sometimes called extrinsic flexors, because the muscle bellies are outside the hand) can be considered to act together to flex the finger. However, their action alone would wind up the interphalangeal before the metacarpophalangeal joints and the finger would not move in a normal arc of flexion. This is precisely what happens in an ulnar nerve paralysis, in which the interossei and lumbricals are not functioning. These small (intrinsic) muscles have been described earlier in terms of their individual actions. For their role in coordinated activity it is sufficient to appreciate that their contribution changes the arc produced by the long flexors, increasing flexion at the metacarpophalangeal joint and reducing flexion at the proximal interphalangeal joint. All three joints are then angulated to the same degree and the fingers form a normal arc of flexion. As the finger flexes, the long extensor tendons (extensor digitorum, extensor indicis and extensor digiti minimi) aid the process by relaxing and allowing the extensor apparatus to glide distally on the dorsum of the phalanges. (See also p. 879.)

Role of the wrist

As the fingers wind up to make a fist, the wrist tends to extend, particularly when force is applied. This extension has a marked effect on the excursion of the long flexor tendons. On its own, digital flexion would require the long tendons to move proximally in their sheaths and the flexor muscles in the forearm would shorten. Extension of the wrist tends to produce a lengthening of the same muscles, which in normal use is almost enough to balance the shortening due to finger flexion; the net effect is a very slight shortening (approximately 1 cm) of the long flexors in the forearm. The wrist can therefore be seen as a mechanism for maximizing force, because it allows the fingers to flex while maintaining the resting length of the extrinsic muscles near to the peak of the force–length curve. It is, of course, possible to wind up the fingers with the wrist held in a neutral position, but the grip is somewhat weaker. With the wrist in full flexion it is not possible to flex the fingers fully.

Flexion of the fingers on gripping tends to result in a distal excursion of the long extensors. However, this tendency is counteracted by dorsiflexion of the wrist. The net effect is a very small proximal excursion of the long extensor tendons on gripping, mirroring the effect on the flexor surface. If the movement of the wrist is exaggerated so that the wrist is a little flexed on opening the hand, and fully dorsiflexed on closing it, the net excursion of long flexors and extensors is zero, i.e. this whole movement sequence can be completed with the forearm flexor and extensor muscles contracting isometrically.

The reader can observe the relationship between digits and wrist by performing the following manoeuvre. The wrist is held in a relaxed, mid-supinated position, with the elbow flexed at 90°. If the forearm is now rotated into pronation, the wrist will fall into flexion and the fingers will automatically extend. If the forearm is rotated into supination, the wrist will extend and the fingers flex. The finger movements compensate for the wrist movements and are entirely automatic; they are made without the need for any excursion of forearm flexor or extensor tendons. This test, the wrist tenodesis test, is a useful way of examining the limb for tendon injury. The pointing finger (which does not move with wrist motion) ‘points to’ a tendon injury.

Wrist motion is controlled principally by two wrist flexors (flexor carpi radialis and flexor carpi ulnaris) and three extensors (extensores carpi radialis longus and brevis, and extensor carpi ulnaris). Although the radiocarpal joint has some functional similarity to a ball and socket joint, it is possible to think of the wrist as a variable hinge joint, the axis of which may be set in a number of inclinations. For example, in using a hammer it is useful to rotate the wrist backwards and forwards about an axis that permits not only wrist flexion but also ulnar deviation. It would be very restricting to have a pure hinge joint with collateral ligaments of fixed length. In this context, the wrist flexors and extensors may be regarded as variable collateral ligaments which allow the joint to be set about a number of different axes.

For movement about major axes, the wrist tendons can be considered to act in pairs: flexores carpi radialis and carpi ulnaris produce wrist flexion;

extensores carpi radialis longus and brevis, and extensor carpi ulnaris produce wrist extension; extensor carpi ulnaris and flexor carpi ulnaris produce ulnar deviation; flexor carpi radialis, extensores carpi radialis longus and brevis, extensor policis and abductor policis longus produce radial deviations. (See also p. 871.)

Making a tight fist

It is possible to observe and to palpate the muscle groups that are active in making a tight fist. The flexor compartment of the forearm is contracted tightly and electromyogram evidence confirms that flexor digitorum profundus and flexor digitorum superficialis are active. Flexor carpi ulnaris may be seen and felt to contract strongly. The extensor compartment is tightly contracted and the wrist extensors would certainly be expected to be active. Palpation of the long digital extensors on the back of the wrist will show these to be contracting as well. It seems that when the fingers are held tightly closed, the long digital extensors are unable to move the extensor apparatus: they have acquired a new fixed point on which to act, namely the proximal limit of the extensor apparatus over the metacarpophalangeal joint. They therefore perform the only task available to them and act together as an additional wrist extensor.

In the thumb web, palpation confirms that the first dorsal interosseous is contracting, as are all the other interossei and the thenar and hypothenar muscles. As the firm fist is swung forward in anger the brachioradialis stands out, and at the moment of impact virtually every muscle in the limb is in a state of contraction, with the exception of the lumbricals.

Opening the hand

The hand is opened from its relaxed balanced posture, e.g. when stretching out to reach an object. This motion is made up of extension of the distal interphalangeal, proximal interphalangeal and metacarpophalangeal joints. The hand is provided with an ingenious mechanism that allows this to happen. The laws of mechanics would suggest that one motor would be required for every joint in a chain, together with some sort of controlling mechanism to ensure that the chain of joints moved together in a coordinated fashion. In the hand this is achieved through an extensor apparatus which minimizes the number of motors required for movement by allowing the muscles to act on more than one joint, and by linking different levels in the mechanism so that the arc of motion is controlled.

The tendons of extensor digitorum run distally over the metacarpal heads, forming the major component of the extensor apparatus. Extensor digitorum has no insertion into the proximal phalanx and therefore exerts its extensor action on the metacarpophalangeal joint indirectly through more distal insertions. The first point of insertion is at the base of the middle phalanx (in clinical practice the term central slip has been adopted). Acting at this insertion alone, extensor digitorum can extend both metacarpophalangeal and proximal interphalangeal joints together. The interossei are also active in hand opening, since they will tend to increase extension of the proximal interphalangeal joint. There is therefore a range of possibilities. At one extreme, with no interosseous contribution, the long extensor will exert all of its action at the metacarpophalangeal joint: this leads to full extension, and even hyperextension, while the proximal interphalangeal joint remains flexed (the typical claw hand of ulnar nerve paralysis, or ‘intrinsic minus’ hand). At the other extreme, when the intrinsics act strongly together with extensor digitorum, the proximal interphalangeal joint will extend completely while the metacarpophalangeal joint remains flexed (‘intrinsic plus’ hand). Thus the hand possesses in the proximal part of the extensor apparatus a variable mechanism that allows different amounts of relative metacarpophalangeal or proximal interphalangeal joint motion.

In contrast, the more distal part of the extensor apparatus acts as an automatic or fixed mechanism which determines that the two interphalangeal joints, proximal and distal, will move together. The lateral slips of the extensor apparatus arise from extensor digitorum and pass distally on either side of the central slip and thus over the proximal interphalangeal joint: being further lateral, they are nearer the joint axis, because the dorsal surface curves away on each side. A helpful analogy that has been suggested for this arrangement is to consider it as two pulleys of different size on one axle. The central slip can be regarded as a cord that passes over the larger wheel, and each lateral slip as a cord that passes over the smaller wheel. Since these latter pulleys are smaller there is less longitudinal excursion for a given rotation of the wheel, and this allows some of the excursion to be used for another function, namely extension at the distal joint. There is an additional mechanism by which the lateral slips move laterally during flexion of the proximal interphalangeal joint. The effect of this lateral movement is to reduce further the distance between the lateral slips and the joint axis, thereby reducing the amount of excursion at the proximal interphalangeal joint still more and allowing more excursion at the distal joint. When the hand flexes, this mechanical linkage system allows both interphalangeal joints to flex together in a coordinated way.

The extensor expansion also receives contributions from the interossei and lumbricals, which approach the digits from the webs and join the corresponding expansion in the proximal segment of the digit. These small muscles can therefore act on the extensor apparatus at two levels: they can extend the proximal interphalangeal joint through fibres that radiate towards the central slip, and they can act on the distal interphalangeal joint through fibres that join the lateral slip.

Apart from the components of the extensor expansion that are concerned with joint function, the whole structure requires additional anchorage. This must be arranged in such a way that it is not displaced from the underlying skeleton, yet it must not restrict longitudinal movement. These difficult requirements are met by transverse retinacular ligaments at the level of the joints, the transverse ligaments running to relatively fixed attachment points in the region of the joint axis. As the expansion glides backwards and forwards the transverse fibres move like bucket handles. Smooth gliding layers are required under the expansion and retinacular ligaments to allow motion to occur without friction.

One final component of the extensor apparatus provides an additional automatic function. This is a fibrous anchorage system, Landsmeer’s oblique retinacular ligament, which anchors the distal expansion to the middle phalanx. The role of the oblique retinacular ligament is controversial (reviewed by Bendz 1985). Some argue it may act in a dynamic tenodesis effect to synchronize the movements of the interphalangeal joints, i.e. it may initiate extension of the distal interphalangeal joint as the proximal interphalangeal joint is extended from a fully flexed position, and relax with proximal interphalangeal joint flexion to allow full distal interphalangeal joint flexion. Others argue that it only becomes taut when the proximal interphalangeal joint is fully extended and the distal interphalangeal joint is flexed, so that it functions as a restraining force to stabilize the fingertip when it is flexed against resistance, e.g. in the hook grip. A further suggestion is that the ligament is merely a secondary lateral stabilizer of the proximal interphalangeal joint and that it acts to centralize the extensor components over the dorsum of the middle phalanx.

Movements of the thumb

An opposable thumb requires a different system of control from the other digits. Since the metacarpal is much more mobile than in the digits, muscles are needed to control the extra freedom of movement.

The thumb does not easily assume the classical anatomical position. Therefore the normal descriptive anatomical terms – anterior, posterior, medial and lateral – do not readily apply. The terms ‘palmar, dorsal, ulnar and radial’ have been adopted in clinical practice.

The basic active movements are flexion–extension, abduction–adduction, rotation, and circumduction. In the resting position of the first metacarpal, flexion and extension are parallel with the palmar plane, and abduction and adduction occur at right angles to this.

Flexion and extension should be confined to motion at the interphalangeal or metacarpophalangeal joints (Fig. 50.35A–C). Palmar abduction (Fig. 50.35D,E), in which the first metacarpal moves away from the second at right angles to the plane of the palm, and radial abduction (Fig. 50.35D,F), in which the first metacarpal moves away from the second with the thumb in the plane of the palm, occur at the carpometacarpal joint. The opposite of radial abduction is ulnar adduction, or transpalmar adduction, in which the thumb crosses the palm towards its ulnar border. In clinical practice the term adduction is generally used without qualification. Circumduction describes the angular motion of the first metacarpal, solely at the carpometacarpal joint, from a position of maximal radial abduction in the plane of the palm towards the ulnar border of the hand, maintaining the widest possible angle between the first and second metacarpals (Fig. 50.35G). Lateral inclinations of the first phalanx maximize the extent of excursion of the circumduction arc. Opposition is a composite position of the thumb achieved by circumduction of the first metacarpal, internal rotation of the thumb ray and maximal extension of the metacarpophalangeal and interphalangeal joints (Fig. 50.35H). Retroposition is the opposite to opposition (Fig. 50.35I). Flexion and adduction is the position of maximal transpalmar adduction of the first metacarpal: the metacarpophalangeal and interphalangeal joints are flexed and the thumb is in contact with the palm (Fig. 50.35J).

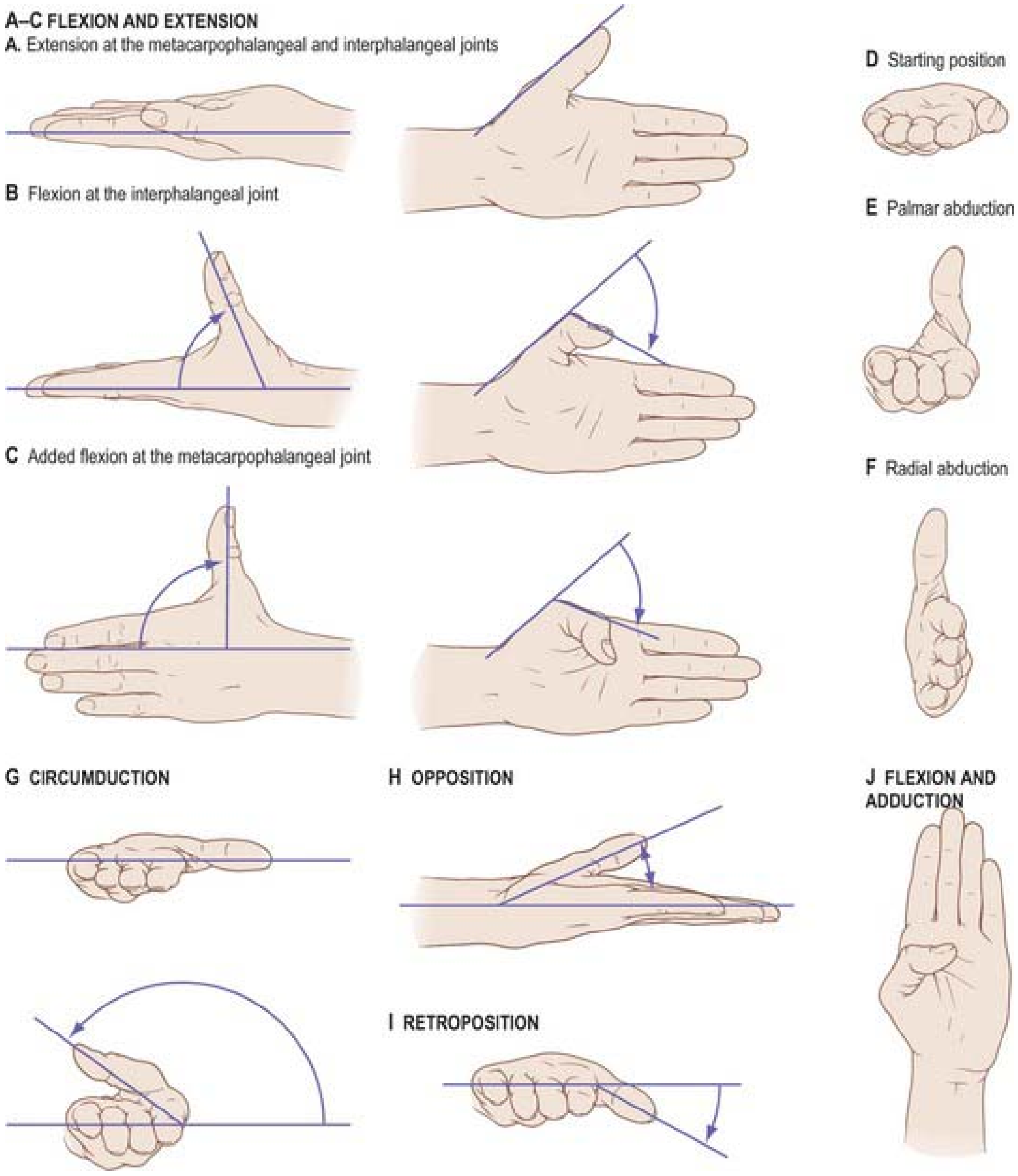
A–C FLEXION AND EXTENSION
A. Extension at the metacarpophalangeal and interphalangeal joints
B Flexion at the interphalangeal joint
C Added flexion at the metacarpophalangeal joint
D Starting position
E Palmar abduction
F Radial abduction
G CIRCUMDUCTION
H OPPOSITION
I RETROPOSITION
J FLEXION AND ADDUCTION

Fig. 50.35 Movements of the thumb.

Rotary movements occur during circumduction. The simple angular movements described above combine with rotation about the long axis of the metacarpal shaft. In opposition, the shaft must rotate medially into pronation. In retroposition, the thumb must rotate laterally into supination. Axial rotation of the thumb metacarpal is produced by muscle activity (which moves the thumb through its arc of circumduction); the geometry of the articular surfaces of the trapeziometacarpal joint; tensile forces in the ligaments (which combine with forces exerted by the muscles of opposition and retroposition to produce axial rotation). The stability of the first metacarpal is greatest after complete pronation in the position of full opposition, when ligamentary tension, muscular contraction and joint congruence combine to maximal effect. (See also p. 875.)

Position of rest

The hand has a well-recognized position of rest, with the wrist in extension and the digits in some degree of flexion. The precise position of the thumb in the position of rest appears to be rather variable. Typically it is considered as the midpoint between maximal palmar abduction and maximal retroposition. In this position the carpometacarpal joint lies within 20° of radial abduction and 30° of palmar abduction, and from clinical observations it seems that the metacarpophalangeal joint lies within approximately 40° of flexion and the interphalangeal joint between extension and 10° of flexion.

Grips

From the position of rest, the tip of the thumb can approach the radial aspect of the fingers without incurring axial rotation because the palmar and dorsal trapeziometacarpal ligaments remain relaxed (see below).

From different positions of the arc of circumduction, numerous different types of pinch grip are possible (Fig. 50.36). In clinical practice these have been classified into two main types: tip pinch and lateral (or key) pinch. Many forces contribute to these configurations.

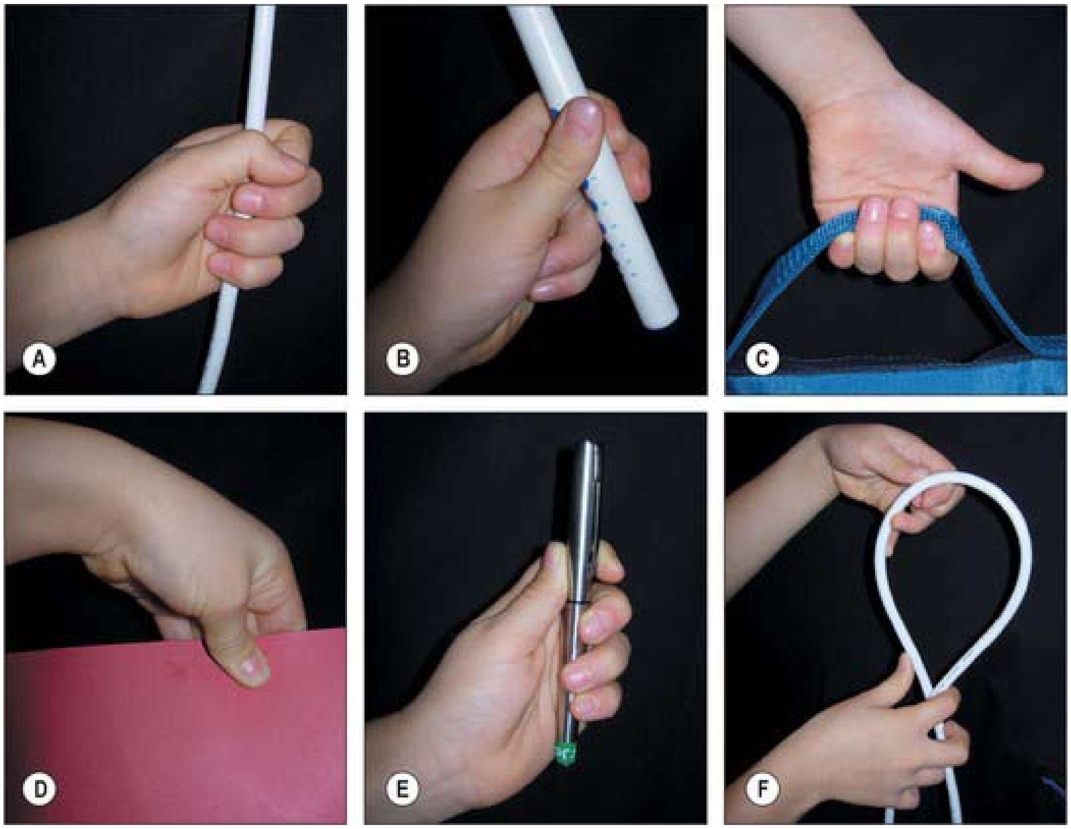

Fig. 50.36 Some of the many varieties of functional posture that may be adopted by the human hand. **A**, In the power grip, the fingers are flexed around an object, with counter pressure from the thumb. Any skill in wielding the object derives from the limb, including the wrist; relative movements of the thumb and fingers are not involved. **B**, The precision grip, which varies considerably with the task, stabilizes the object between the tips of one or more fingers and the thumb. The gross position of the object may be adjusted by movements at the wrist, elbow, or even shoulder, but the most skilled manipulations are carried out by the digits themselves, e.g. in advancing a thread through the eye of a needle. **C**, The hook grip is used to suspend or to pull open objects. The fingers are flexed around the object; the thumb may or may not be involved. It is a grip for the transmission of forces, not for skillful manipulation. **D**, Powerful opposition of the thumb to the radial side of the index finger produces a lateral pinch grip, e.g. to hold a door key; here the object is larger than a key, and all the fingers are involved. **E**, Many activities involve a combination of grips. Here a fountain pen is stabilized in a power grip by flexion of digits 4–5

against the palm, while the index finger and thumb, used in a precision grip, unscrew the cap. **F**, Complex manipulation.

(By courtesy of Olivia Pillai Johnson, Oxford.)

The thumb is a triarticular system, unlike the finger, which is a biarticular system. The thumb is activated by monoarticular muscles (abductor pollicis longus and opponens pollicis), biarticular muscles (extensor pollicis brevis, adductor pollicis, abductor pollicis brevis and flexor pollicis brevis), and triarticular muscles (extensor pollicis longus and flexor pollicis longus). It appears, however, that even a monoarticular muscle can change posture in all three joints by altering the overall balance of forces, and it is therefore very difficult to attribute function to the individual intrinsic muscles. However, the thumb muscles do seem to provide two broad functions. They control metacarpal positioning (the guy-rope function), an activity that is automatically accompanied by rotation. They also control the axial stability of the skeleton of the thumb.

The thumb muscles can be classified into those used for retroposition, opposition and pinch grip.

Retroposition muscles

The muscles that bring about retroposition are extensor pollicis longus, extensor pollicis brevis and abductor pollicis longus. As the thumb moves into retroposition, automatic axial rotation produces supination of the first metacarpal. This is produced by the off-axis action of two parallel, but oppositely directed, forces, one exerted by extensores pollicis longus and brevis and the other by abductor pollicis longus and the anterior oblique carpometacarpal ligament.

Opposition muscles

A succession of activity occurs in the thenar muscles during the movement of opposition. Three subgroups of radial (abductor pollicis longus and extensor pollicis brevis), central (abductor pollicis brevis and opponens pollicis) and ulnar (flexor pollicis brevis) muscles are involved. These forces act simultaneously but with different intensities, depending on the situation of the thumb. As the thumb moves into opposition there is automatic axial rotation of the first metacarpal shaft to produce pronation. This is produced by the paired action of oppositely directed forces: the opposition muscles provide one force, and the posterior oblique carpometacarpal ligament provides the other.

Pinch grip muscles

The muscles of pinch grip can be divided into lateral, medial and intermediate subgroups. The lateral subgroup (opposition muscles) moves the first metacarpal into palmar abduction. The metacarpal shaft rotates medially into pronation. Radial angulation at the metacarpophalangeal joint increases the span of the hand. The metacarpophalangeal joint is stabilized principally by extensor pollicis brevis and flexor pollicis brevis. Flexion of the proximal and distal phalanges is controlled. Muscles of the medial subgroup (abductor pollicis brevis and first dorsal interosseous) produce an approach of the first metacarpal towards the palm. Since they act with the lateral group they have a strong controlling effect on the position and rotation of the first metacarpal. The intermediate subgroup consists simply of flexor pollicis longus, which flexes the interphalangeal or metacarpophalangeal joint, as described earlier. Palpating the thenar eminence during tip and lateral pinch provides some appreciation of the action of the pinch grip muscles.

VASCULAR SUPPLY AND LYMPHATIC DRAINAGE

ARTERIES

Anastomoses occur between the radial and ulnar arteries at the wrist (via the palmar and dorsal carpal arches) and in the hand (via the superficial and deep palmar arches), and between their digital and metacarpal branches.

Radial artery

At the wrist the radial artery passes on to the dorsal aspect of the carpus between the lateral carpal ligament and the tendons of abductor pollicis longus and extensor pollicis brevis (Fig. 50.37). It crosses the scaphoid bone and trapezium (in the ‘anatomical snuff-box’), where again its pulsation is obvious, and as it passes between the heads of the first dorsal interosseous it is crossed by the tendon of extensor pollicis longus. Between the thumb extensors it is crossed by the start of the cephalic vein and the digital branches of the radial nerve which supply the thumb and index finger (Fig. 50.38). Occasionally it gives off a distal superficial dorsal branch which crosses the radial extensor tendons at the wrist together with the superficial radial nerve. Filaments of the lateral cutaneous nerve of the forearm run along its distal part as it curves round the carpus.

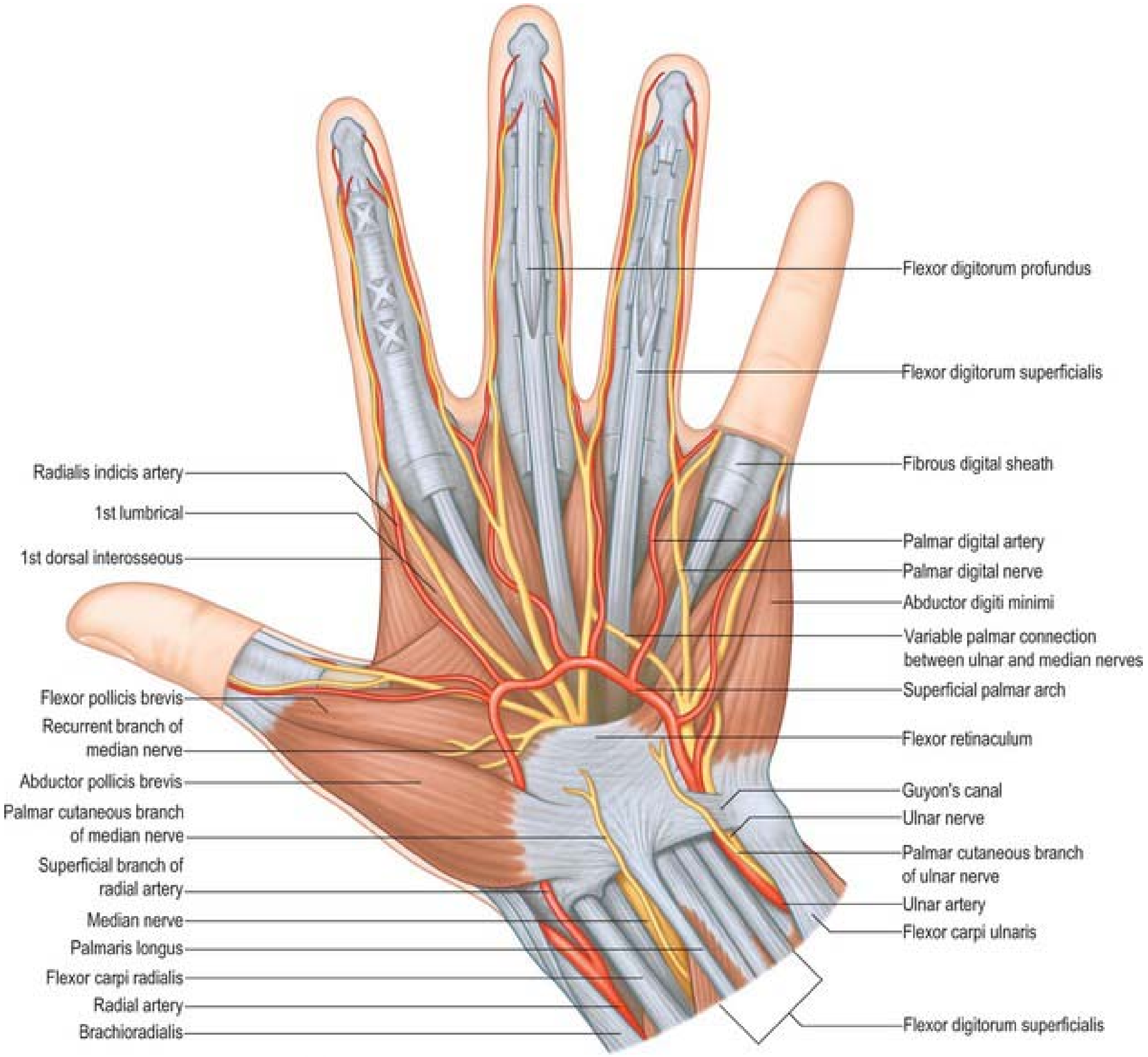
Flexor digitorum profundus
Flexor digitorum superficialis
Fibrous digital sheath
Radialis indicis artery
1st lumbrical
1st dorsal interosseous
Palmar digital artery
Palmar digital nerve
Abductor digiti minimi
Variable palmar connection between ulnar and median nerves
Superficial palmar arch
Flexor pollicis brevis
Recurrent branch of median nerve
Flexor retinaculum
Abductor pollicis brevis
Guyon's canal
Ulnar nerve
Palmar cutaneous branch of median nerve
Palmar cutaneous branch of ulnar nerve
Superficial branch of radial artery
Ulnar artery
Median nerve
Flexor carpi ulnaris
Palmaris longus
Flexor carpi radialis
Radial artery
Flexor digitorum superficialis
Brachioradialis

Fig. 50.37 Superficial structures of the left palm and wrist. See also **Fig. 50.26**.

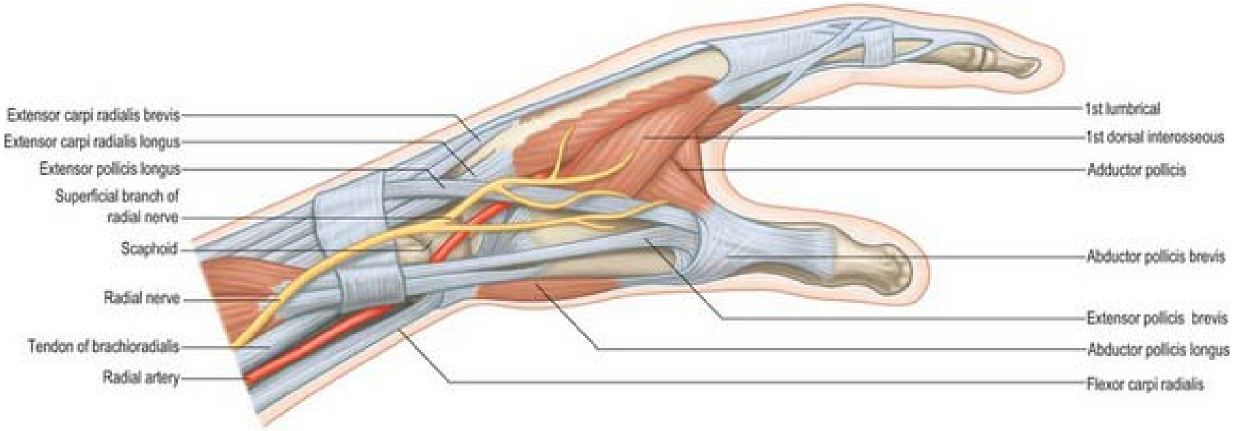
Extensor carpi radialis brevis
Extensor carpi radialis longus
Extensor pollicis longus
Superficial branch of radial nerve
Scaphoid
Radial nerve
Tendon of brachioradialis
Radial artery
1st lumbrical
1st dorsal interosseous
Adductor pollicis
Abductor pollicis brevis
Extensor pollicis brevis
Abductor pollicis longus
Flexor carpi radialis

Fig. 50.38 Radial aspect of the left wrist.

In the hand the radial artery passes through the first interosseous space between the heads of the first dorsal interosseous and crosses the palm. At first it lies deep to the oblique head of adductor pollicis and then passes between its oblique and transverse heads or through the transverse head. At the fifth metacarpal base it anastomoses with the deep branch of the ulnar artery, completing the deep palmar arch (Fig. 50.39).

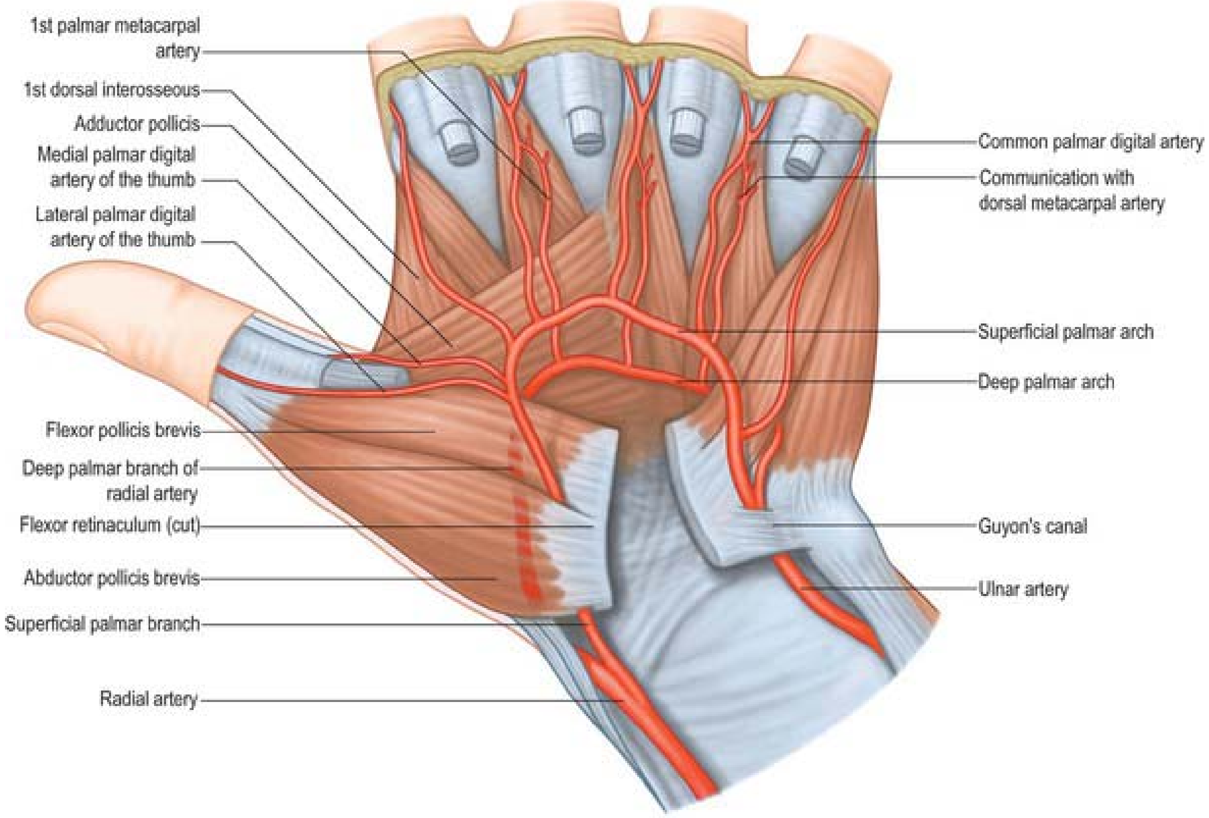
1st palmar metacarpal artery
1st dorsal interosseous
Adductor pollicis
Medial palmar digital artery of the thumb
Lateral palmar digital artery of the thumb
Flexor pollicis brevis
Deep palmar branch of radial artery
Flexor retinaculum (cut)
Abductor pollicis brevis
Superficial palmar branch
Radial artery
Common palmar digital artery
Communication with dorsal metacarpal artery
Superficial palmar arch
Deep palmar arch
Guyon's canal
Ulnar artery

Fig. 50.39 The deep palmar arch and its branches. Note the palmar digital arteries to the thumb have a separate origin from the superficial palmar arch in this specimen; this variation occurs in 20% of cases. The princeps pollicis artery is absent in this specimen.

Palmar carpal branch

The palmar carpal branch is a small vessel which arises from the radial artery near the distal border of pronator quadratus (Fig. 50.40). It crosses the anterior surface of the distal end of the radius, near the palmar carpal surface, and passes medially to anastomose behind the long flexor tendons with the palmar carpal branch of the ulnar artery. This transverse anastomosis is joined by longitudinal branches from the anterior interosseous artery and recurrent branches from the deep palmar arch, to form a cruciate palmar carpal arch which supplies the carpal articulations and bones by descending branches. (Although so named, this anastomosis is usually sited near the wrist joint on the distal forearm bones.)

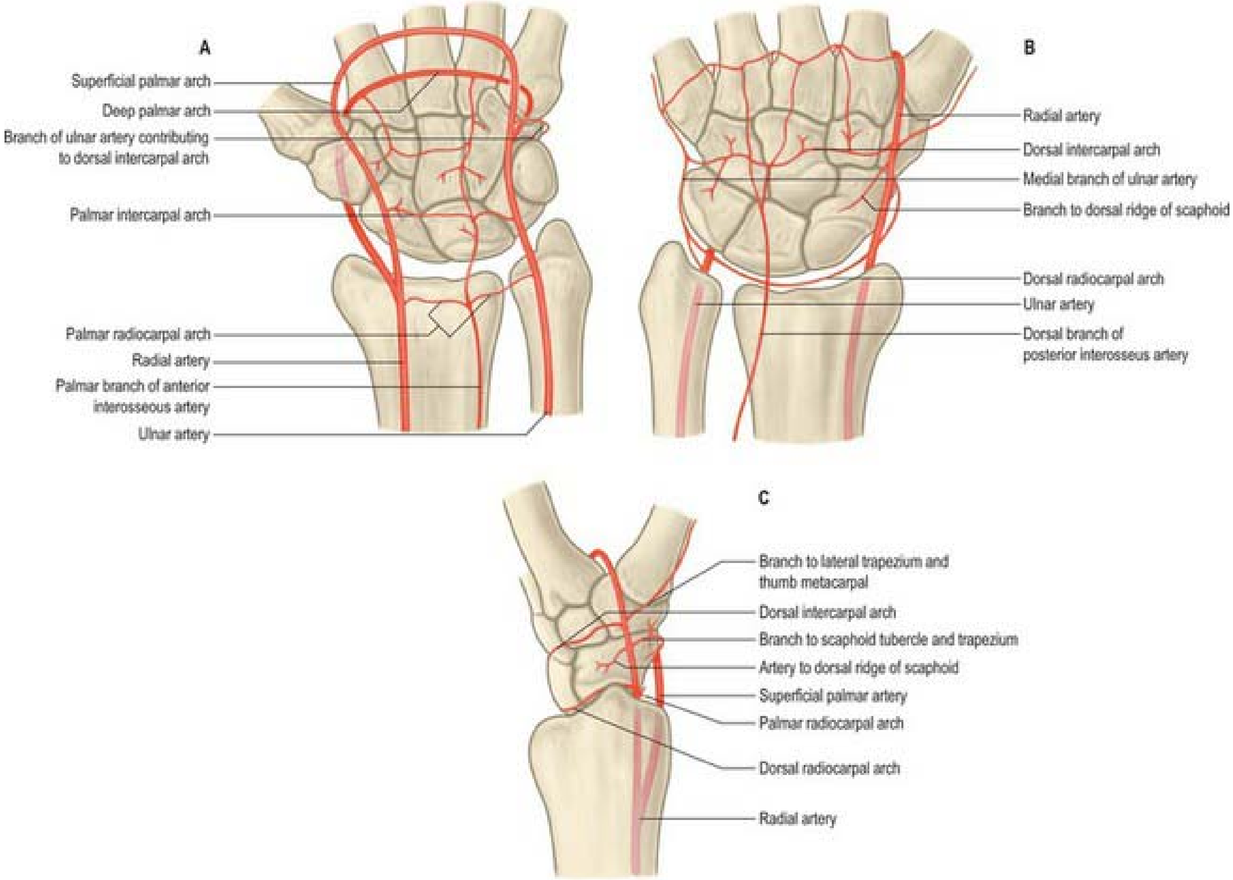
A
Superficial palmar arch
Deep palmar arch
Branch of ulnar artery contributing to dorsal intercarpal arch
Palmar intercarpal arch
Palmar radiocarpal arch
Radial artery
Palmar branch of anterior interosseous artery
Ulnar artery
B
Radial artery
Dorsal intercarpal arch
Medial branch of ulnar artery
Branch to dorsal ridge of scaphoid
Dorsal radiocarpal arch
Ulnar artery
Dorsal branch of posterior interosseus artery
C
Branch to lateral trapezium and thumb metacarpal
Dorsal intercarpal arch
Branch to scaphoid tubercle and trapezium
Artery to dorsal ridge of scaphoid
Superficial palmar artery
Palmar radiocarpal arch
Dorsal radiocarpal arch
Radial artery

Fig. 50.40 The extraosseous blood supply to the carpus. **A**, Palmar aspect; **B**, dorsal aspect; **C**, lateral aspect viewed from the radial side.

Superficial palmar branch

The superficial palmar branch arises from the radial artery just before it curves round the carpus. It passes through, and occasionally over, the thenar muscles, which it supplies, sometimes anastomosing with the end of the ulnar artery to complete a superficial palmar arch (Fig. 50.39).

Dorsal carpal branch

The dorsal carpal branch arises deep to the thumb extensor tendons. It runs medially across the dorsal carpal surface under them and anastomoses with the ulnar dorsal carpal branch and also with the anterior and posterior interosseous arteries to form a dorsal carpal arch. The carpal arches are both close to bone and supply the distal epiphysial parts of the radius and ulna.

From the dorsal arch three dorsal metacarpal arteries descend on the second to fourth dorsal interossei and bifurcate into the dorsal digital branches to supply the adjacent sides of all four fingers.

First dorsal metacarpal artery

The first dorsal metacarpal artery arises from the radial artery just before it passes between the heads of the first dorsal interosseous (Fig. 50.2). It divides almost at once into two branches which supply the adjacent sides of the thumb and index finger as far distally as the proximal interphalangeal joint. The radial side of the thumb receives a branch direct from the radial artery proper.

In the majority of cases the first dorsal metacarpal artery follows a fascial course overlying the first dorsal interosseous and parallel to the second metacarpal bone. Occasionally it may follow an intramuscular course. Distally, over the proximal phalanx, it anastomoses with the dorsal branches of the radiopalmar digital artery of the index finger. In a small number of cases, the first dorsal interosseous artery either arises from, or gives rise to, an ulnodorsal digital artery of the thumb. Occasionally it gives rise to the ulnopalmar digital artery of the thumb, and rarely may give rise to the second dorsal metacarpal artery.

The usual anatomical arrangement allows a flap of skin over the dorsum of the proximal phalanx of the index finger to be raised on this artery and its accompanying venae comitantes. This is particularly useful undercertain circumstances for reconstruction of the thumb following injury.

Second, third and fourth dorsal metacarpal arteries

The second to fourth dorsal metacarpal arteries arise from the dorsal carpal arch. Near their origins they anastomose with the deep palmar arch by proximal perforating arteries and, near their bifurcation, with dorsal perforating branches from the palmar metacarpal arteries which pass between the metacarpal necks. They also anastomose distally at the level of the web spaces with dorsal perforating branches from the palmar digital arteries from the superficial palmar arch. The third and fourth dorsal metacarpal arteries are much smaller than the first and second.

Cutaneous branches from the dorsal metacarpal arteries supply the dorsal skin as far distally as the proximal interphalangeal joint. At the level of the neck of the second, third and fourth metacarpals, a direct cutaneous branch is given off which passes proximally and supplies an area of skin between the two adjacent metacarpals (Fig. 50.41).

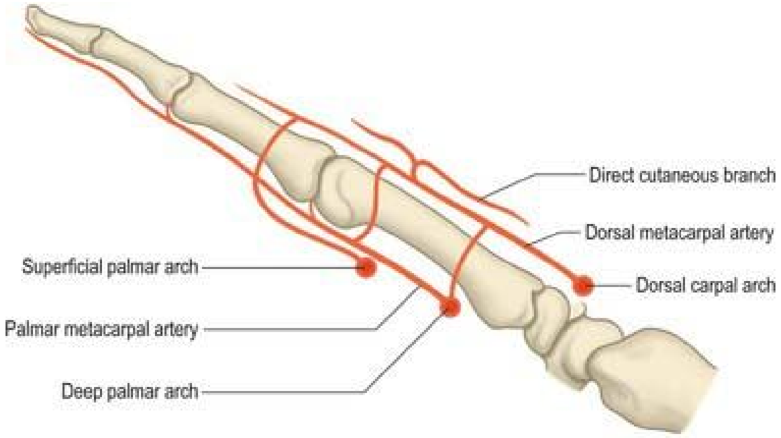

Fig. 50.41 Sagittal view showing communication between the palmar and dorsal metacarpal arteries and the direct cutaneous branch given off the dorsal metacarpal artery approximately 0.5–1.0 cm proximal to the metacarpophalangeal joint.

These anatomical arrangements permit the surgical elevation of flaps of dorsal skin to be based either proximally on the dorsal metacarpal arteries proper, or distally on the direct cutaneous branch. These flaps may be used for reconstructing areas of missing tissue elsewhere in the hand.

Arteria princeps pollicis

The arteria princeps pollicis arises from the radial artery as it turns into the palm to form the deep palmar arch. It descends on the palmar aspect of the first metacarpal under the oblique head of adductor pollicis lateral to the first palmar interosseous. At the base of the proximal phalanx, deep to the tendon of flexor pollicis longus, the artery divides into two branches. It appears between the medial and lateral attachments of the oblique head of adductor pollicis to run along both sides of the thumb. On the palmar surface of its distal phalanx it forms a pollicial arch which supplies the skin and subcutaneous tissue. The arteria princeps pollicis is the usual nutrient of supply to the first metacarpal bone.

Arteria radialis indicis

The arteria radialis indicis is often a proximal branch of the arteria princeps pollicis. It descends between the first dorsal interosseous and transverse head of adductor pollicis, and along the lateral side of the index finger to its end (Fig. 50.37). It anastomoses with the indicial medial digital artery. At the distal border of the transverse head of adductor pollicis it anastomoses with the arteria princeps pollicis and links with the superficial palmar arch. It may arise from the superficial arch or from the first dorsal metacarpal artery.

The arteria princeps pollicis and radialis indicis may be combined as the first palmar metacarpal artery.

Deep palmar arch

The deep palmar arch is formed by anastomosis of the end of the radial artery with the deep palmar branch of the ulnar artery (Fig. 50.39 and Fig. 50.42A). It crosses the bases of the metacarpal bones and interossei, covered by the oblique head of adductor pollicis, the digital flexor tendons and lumbricals. In its concavity, running laterally, is the deep branch of the ulnar nerve. Rarely the arch is incomplete. There are variations in the size of contribution from the ulnar artery.

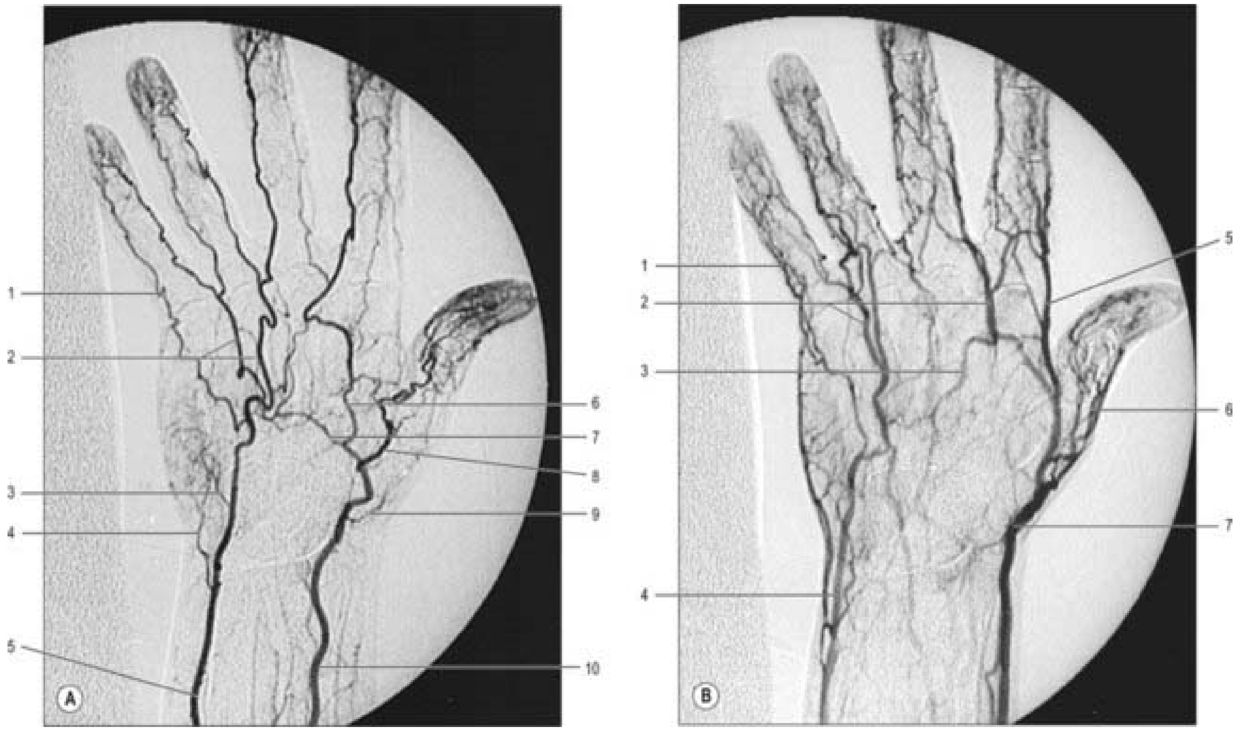

Fig. 50.42 **A**, Digitally subtracted hand arteriogram, dorsopalmar projection. Note that this patient has an incomplete superficial palmar arch. **B**, Venous phase of hand arteriogram. **A, 1**. Proper palmar digital artery. **2**. Common palmar digital artery. **3**. Palmar carpal branch of ulnar artery. **4**. Deep palmar branch of ulnar artery. **5**. Ulnar artery. **6**. Palmar metacarpal artery. **7**. Deep palmar arch. **8**. Princeps pollicis artery. **9**. Artery to radial aspect of thumb. **10**. Radial artery. **B, 1**. Palmar digital vein. **2**. Common palmar digital vein. **3**. Superficial palmar arch. **4**. Basilic vein. **5**. Radialis indicis vein. **6**. Princeps pollicis vein. **7**. Cephalic vein.

(By permission from Weir J, Abrahams PH 2003 Imaging Atlas of Human Anatomy, 3rd edn, London: Mosby, and contributions from Anna-Maria Belli, Margaret Hourihan, Niall Moore and Philip Owen.)

Palmar metacarpal artery

The three palmar metacarpal arteries run distally from the convexity of the deep palmar arch on the interossei of the second to fourth spaces, and join the common digital branches of the superficial arch at the digital clefts (Fig. 50.39). They supply nutrient branches to the medial four metacarpals.

Perforating branches

Three perforating branches from the deep palmar arch cross the second to fourth interosseous spaces between the heads of the corresponding dorsal interossei and anastomose with the dorsal metacarpal arteries.

Recurrent branches

Recurrent branches ascend proximally from the deep palmar arch anterior to the carpus to supply the carpal bones and intercarpal articulations. They end in the palmar carpal arch.

Ulnar artery

At the wrist the ulnar artery (Figs 50.37 and 50.39) is covered by skin, fasciae and palmaris brevis. It lies between the superficial and main parts of the flexor retinaculum, lateral to the ulnar nerve and pisiform.

Dorsal cutaneous branch

A constant dorsoulnar perforator vessel is given off distally. It arises 2–5 cm proximal to the pisiform and accompanies the dorsal cutaneous branch of the ulnar nerve. It emerges between flexor carpi ulnaris and extensor carpi ulnaris. The cutaneous perforator can support a flap of skin on the medial aspect of the distal forearm just proximal to the wrist and is useful in reconstructing areas of missing skin in this region.

Palmar carpal branch

A small palmar carpal branch crosses the distal ulna deep to the tendons of flexor digitorum profundus (Fig. 50.40), and anastomoses with a palmar carpal branch of the radial artery to make a palmar carpal arch.

Dorsal carpal branch

A dorsal carpal branch arises just proximal to the pisiform (Fig. 50.40). It curves deep to the tendon of flexor carpi ulnaris to reach the carpal dorsum, which it crosses laterally beneath the extensor tendons. It anastomoses with the dorsal carpal branch of the radial artery to complete the dorsal carpal arch. Near its origin it sends a small digital branch along the ulnar side of the fifth metacarpal to supply the medial side of the dorsal surface of the fifth finger.

Deep palmar branch

The deep palmar branch is often double (Fig. 50.40). It passes between abductor and flexor digiti minimi, through or deep to opponens digiti minimi. It anastomoses with the radial artery, completing the deep palmar arch. The deep palmar branch accompanies the deep branch of the ulnar nerve.

Superficial palmar arch

The superficial palmar arch is an anastomosis fed mainly by the ulnar artery (Figs 50.2 and 50.39). The latter enters the palm with the ulnar nerve, anterior to the flexor retinaculum and lateral to the pisiform. It passes medial to the hook of the hamate, then curves laterally to form an arch that is convex distally and level with a transverse line through the distal border of the fully extended pollicial base. About a third of the superficial palmar arches are formed by the ulnar artery alone; a further third are completed by the superficial palmar branch of the radial artery; and a third by the arteria radialis indicis, a branch of either arteria princeps pollicis or the median artery. The superficial palmar arch is covered by palmaris brevis and the palmar aponeurosis and it is superficial to flexor digiti minimi, branches of the median nerve and the long flexor tendons and lumbricals.

Common and proper palmar digital arteries

Three common palmar digital arteries arise from the convexity of the superficial palmar arch (Fig. 50.39). They pass distally on the second to fourth lumbricals, each joined by a corresponding palmar metacarpal artery from the deep palmar arch, and divide into two proper palmar digital arteries. These run along the contiguous sides of all four fingers, dorsal to the digital nerves, between Grayson’s and Cleland’s ligaments, anastomosing in the subcutaneous tissue of the finger tips and near the interphalangeal joints. Each digital artery has two dorsal branches which anastomose with the dorsal digital arteries and supply the soft parts dorsal to the middle and distal phalanges, including the matrices of the nails. The palmar digital artery for the medial side of the little finger leaves the arch under palmaris brevis. Palmar digital arteries supply the metacarpophalangeal and interphalangeal joints and nutrient rami to the phalanges. They are the main digital supply, because the dorsal digital arteries are minute.

The origins of the palmar digital arteries of the thumb are quite variable. Both may arise from a single princeps pollicis, or they may arise separately from the superficial palmar arch. The ulnar digital artery may arise from the first dorsal metacarpal artery.

The terminal branches of the digital arteries contribute to a number of vascular arcades which provide a rich vascular supply for the distal elements of each digit (Fig. 50.43). Three distal phalangeal dorsal arterial arcades anastomose with each other and with those from the other side of the digit. The superficial arcade occurs at the level of the proximal nailfold and is supplied primarily by a dorsal branch from the palmar digital artery, which is given off at the level of the middle phalanx. The proximal subungual arcade is at the level of the lunula and is supplied by a terminal branch of the digital artery, which passes dorsally. The distal subungual arcade occurs more distally in the nail bed. It is supplied by a dorsal vessel which emerges from the point of confluence of the ‘H’-shaped anastomosis between the terminal portions of both digital arteries, and passes from volar to dorsal aspect of the digit under the interosseous ligament which connects the proximal and distal parts of the distal phalanx (Fig. 50.43).

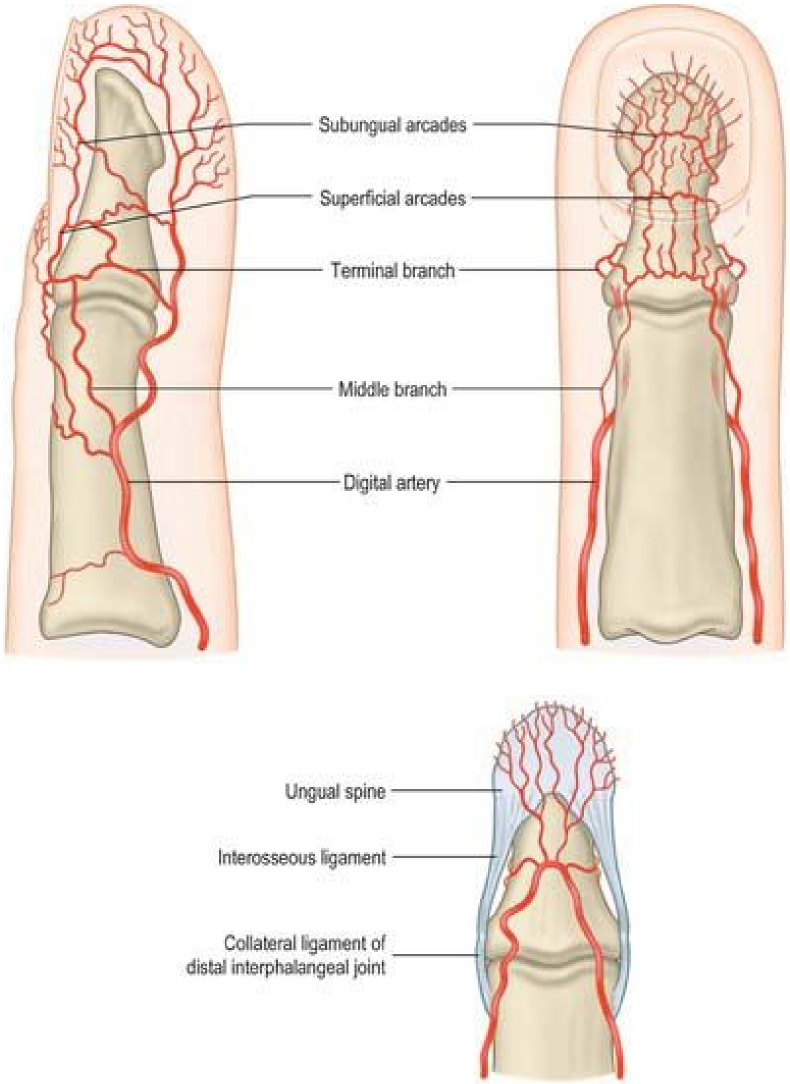
Subungual arcades
Superficial arcades
Terminal branch
Middle branch
Digital artery
Ungual spine
Interosseous ligament
Collateral ligament of distal interphalangeal joint

Fig. 50.43 Terminal vascular arcades over the distal phalanx.

(By permission from Flint MH 1956 Some observations on the vascular supply of the nail bed and terminal segments of the fingers. BJPS 8: 186–95.)

Glomus tumours

Glomus tumours are very painful (often tiny and sometimes difficult to identify) tumours of the glomus bodies (small AV anastomoses involved in the regulation of peripheral skin temperature control; see Fig. 6.16). These typically occur in the proximal nailfold/subungual regions of the finger tips in association with the dorsal digital arterial arcades, although they can occur anywhere. They are diagnosed by exquisite point tenderness over the swelling with reduction of tenderness when the finger is exsanguinated. If the tumour is not visible (as is often the case) then the best way surgically to explore the dorsal fingertip region to look for the tumour is to incise the lateral nailfold and hyponychium and raise this as a flap along with the underlying periosteum pedicled on the blood supply from the opposite nailfold. The dorsal distal phalangeal digital arterial arcades are then identified from their deep surface and any glomus tumour identified.

VEINS

Superficial veins of the hand

Dorsal and palmar digital veins

Dorsal digital veins pass along the sides of the fingers, joined by oblique branches. They unite from the adjacent sides of the digits into three dorsal metacarpal veins (Fig. 50.44), which form a dorsal venous network over the metacarpus. This is joined laterally by a dorsal digital vein from the radial side of the index finger and both dorsal digital veins of the thumb, and is prolonged proximally as the cephalic vein (Fig. 50.42). Medially a dorsal digital vein from the ulnar side of minimus joins the network, which ultimately drains proximally into the basilic vein. A vein often connects the central parts of the network to the cephalic vein near the midforearm.

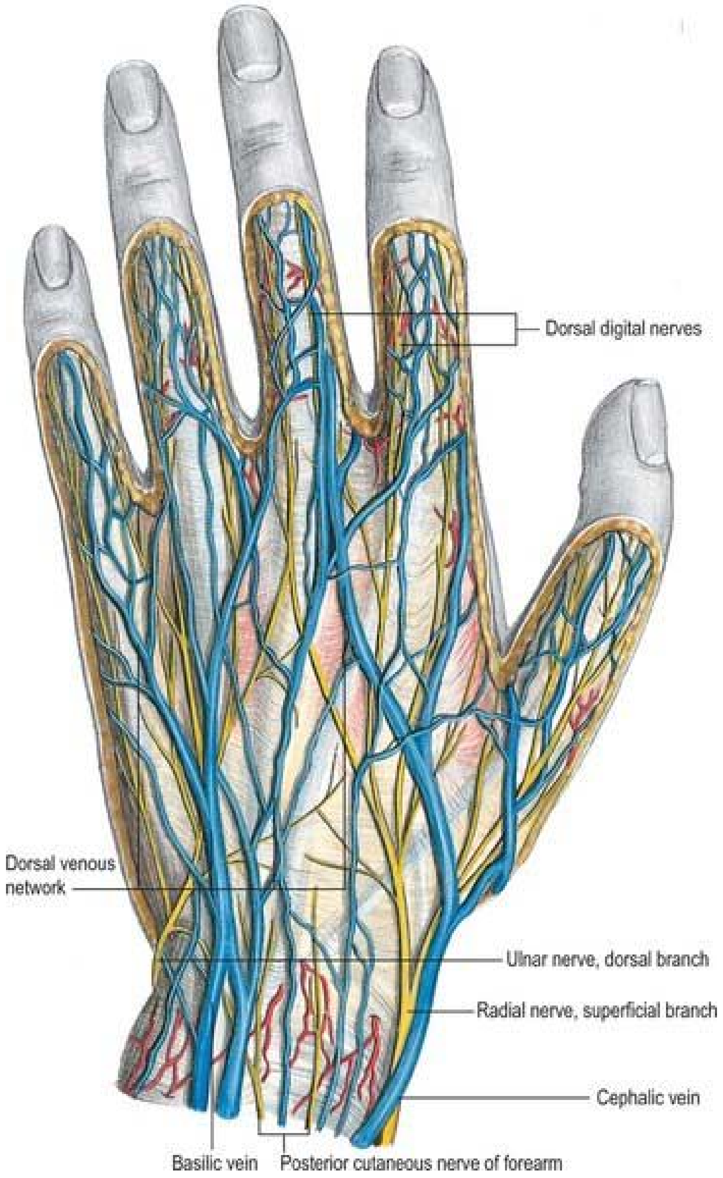
Dorsal digital nerves
Dorsal venous network
Ulnar nerve, dorsal branch
Radial nerve, superficial branch
Cephalic vein
Basilic vein
Posterior cutaneous nerve of forearm

Fig. 50.44 The veins of the dorsum of the hand.

(From Sobotta 2006.)

Palmar digital veins connect to their dorsal counterparts by oblique intercapitular veins which pass between metacarpal heads. They also drain to a plexus superficial to the palmar aponeurosis, extending over both thenar and hypothenar regions.

Cephalic vein

The cephalic vein forms over the anatomical snuff-box from the radial extremity of the dorsal venous plexus. It runs proximally over the distal lateral aspect of the radius, where it is easily visible.

Deep veins of the hand

Superior and deep palmar venous arches

Superficial and deep palmar venous arches accompany their arterial counterparts and receive the corresponding branches. Thus common palmar digital veins join the superficial arch, and palmar metacarpal veins join the deep arch.

Palmar and dorsal metacarpal veins

Deep veins accompanying the dorsal metacarpal arteries receive perforating branches from the palmar metacarpal veins. They end in the radial veins and the dorsal venous network over the metacarpus. This network is joined laterally by a dorsal digital vein from the radial side of the index finger and by both digital veins of the thumb, and is prolonged proximally as the cephalic vein.

INNERVATION

Median nerve

The median nerve proximal to the flexor retinaculum is lateral to the tendons of flexor digitorum superficialis and lies between the tendons of flexor carpi radialis and palmaris longus (Fig. 50.45A). It passes under the retinaculum in the ‘carpal tunnel’ where it may be compressed in the carpal tunnel syndrome (see p. 897). Distal to the retinaculum the nerve enlarges and flattens, and usually divides into five or six branches: the mode and level of division are variable.

Palmar cutaneous branch

The palmar cutaneous branch starts about 3 cm proximal to the flexor retinaculum. It runs in a small tunnel in the sheath of flexor carpi radialis before piercing the deep fascia where it divides into lateral branches that supply the thenar skin and connect with the lateral cutaneous nerve of the forearm. Medial branches supply the central palmar skin and connect with the palmar cutaneous branch of the ulnar nerve.

Communicating branches, which may be multiple, often arise in the proximal forearm, sometimes from the anterior interosseous branch. They pass medially between flexores digitorum superficialis and profundus and behind the ulnar artery to join the ulnar nerve. This communication is a factor in explaining anomalous muscular innervation in the hand (see below).

Muscular branch (motor or recurrent branch)

The muscular branch is short and thick, and arises from the lateral side of the nerve; it may be the first palmar branch or a terminal branch which arises level with the digital branches. It runs laterally, just distal to the flexor retinaculum, with a slight recurrent curve beneath the part of the palmar aponeurosis covering the thenar muscles (Fig. 50.45A). It turns round the distal border of the retinaculum to lie superficial to flexor pollicis brevis, which it usually supplies, and continues either superficial to the muscle or traverses it. It gives a branch to abductor pollicis brevis, which enters the medial edge of the muscle, and then passes deep to it to supply opponens pollicis, entering its medial edge. Its terminal part occasionally gives a branch to the first dorsal interosseous, and may be its sole or partial supply. The muscular branch may arise in the carpal tunnel and pierce the flexor retinaculum, a point of surgical importance.

Palmar digital branches

The median nerve usually divides into four or five digital branches (Fig. 50.45A). It often divides first into a lateral ramus which provides digital branches to the thumb and the radial side of the index finger, and a medial ramus, which supplies digital branches to adjacent sides of the index, middle and ring fingers. Other modes of termination can occur.

Digital branches are commonly arranged as follows. They pass distally, deep to the superficial palmar arch and its digital vessels, at first anterior to the long flexor tendons. Two proper palmar digital nerves, sometimes from a common stem, pass to the sides of the thumb: the nerve supplying its radial side crosses in front of the tendon of flexor pollicis longus. The proper palmar digital nerve to the lateral side of the index also supplies the first lumbrical. Two common palmar digital nerves pass distally between the long flexor tendons. The lateral divides in the distal palm into two proper palmar digital nerves which traverse adjacent sides of the index and middle finger. The medial divides into two proper palmar digital nerves which supply adjacent sides of the middle and ring fingers. The lateral common digital nerve supplies the second lumbrical, and the medial receives a communicating twig from the common palmar digital branch of the ulnar nerve and may supply the third lumbrical. In the distal part of the palm the digital arteries pass deeply between the divisions of the digital nerves: the nerves lie anterior to the arteries on the sides of the digits. The median nerve usually supplies palmar cutaneous digital branches to the radial three and one-half digits (thumb, index, middle and the lateral side of the ring): sometimes the radial side of the ring finger is supplied by the ulnar nerve. Occasionally, there is a communicating branch between the common digital nerve to the middle and ring fingers (derived from the median nerve) and the common digital nerve to the ring and little fingers (derived from the ulnar nerve): this can explain variations in sensory patterns that do not conform to the classic pattern.

The proper palmar digital nerves pass along the medial side of the index finger, and both sides of the middle and the lateral side of the ring finger. They enter these digits in fat between slips of the palmar aponeurosis. Together with the lumbricals and palmar digital arteries, they pass dorsal to the superficial transverse metacarpal ligament and ventral to the deep transverse metacarpal ligament. In the digits, the nerves run distally beside the long flexor tendons (outside their fibrous sheaths), level with the anterior phalangeal surfaces and anterior to the digital arteries, between Grayson's and Cleland's ligaments. Each nerve gives off several branches to the skin on the front and sides of the digit (where many end in Pacinian corpuscles), and sends branches to the metacarpophalangeal and interphalangeal joints.

The digital nerves supply the fibrous sheaths of the long flexor tendons, digital arteries (vasomotor) and sweat glands (secretomotor). Distal to the base of the distal phalanx each digital nerve gives off a branch which passes dorsally to the nail bed. The main nerve frequently trifurcates to supply the pulp and skin of the terminal part of the digit. Distal to the base of the proximal phalanx, each proper digital nerve also gives off a dorsal branch to supply the skin over the back of the middle and distal phalanges. The proper palmar digital nerves to the thumb and the lateral side of the index finger emerge with the long flexor tendons from under the lateral edge of the palmar aponeurosis. They are arranged in the digits as described above, but in the thumb small distal branches supply the skin on the back of the distal phalanx only.

Other branches

In addition to the branches of the median nerve described above, variable vasomotor branches supply the radial and ulnar arteries and their branches. Some of the intercarpal, carpometacarpal and intermetacarpal joints are said to be supplied by the median nerve or its anterior interosseous branch: the precise details are uncertain.

Carpal tunnel syndrome

Carpal tunnel syndrome is the most common entrapment mononeuropathy. It is caused by compression of the median nerve as it passes through the fibro-osseous tunnel beneath the flexor retinaculum. The carpal tunnel may be narrowed by arthritic changes in the wrist joint, particularly rheumatoid arthritis; soft tissue thickening as may occur in myxoedema and acromegaly; and may also be associated with oedema, obesity or pregnancy. Usually the condition is idiopathic. Normally the median nerve slides smoothly in and out of the carpal tunnel during flexion and extension of the wrist: when the nerve is compressed, additional damage may be produced during these movements. The dominant hand is usually affected first, probably because this hand is used more frequently and more vigorously. Typically, the syndrome produces pain, paraesthesia and numbness in the thumb, index, middle and medial side of the ring finger, which is worse at night and on gripping objects. The palmar branch of the median nerve is spared since it does not pass through the carpal tunnel. With time, the compression leads to wasting and weakness of abductor pollicis brevis. Treatment is usually surgical decompression of the nerve by dividing the flexor retinaculum.

Median nerve division at the wrist

The median nerve is vulnerable to division from lacerations at the wrist. Division leads to paralysis of the lumbricals to the index and middle fingers and the thenar muscles (apart from flexor pollicis brevis and adductor pollicis), as well as loss of sensation to the thumb, index, middle and radial half of the ring fingers. The radial half of the hand becomes flattened as a result of wasting of the thenar muscles and the adducted posture of the thumb.

Ulnar nerve

At the wrist, the ulnar nerve passes under the superficial part of the flexor retinaculum (in Guyon’s canal) with the ulnar artery, and divides into superficial and deep terminal branches.

Dorsal branch

The dorsal branch arises approximately 5 cm proximal to the wrist. It passes distally and dorsally, deep to flexor carpi ulnaris, perforates the deep fascia, descends along the medial side of the back of the wrist and hand and then divides into two, or often three, dorsal digital nerves. The first supplies the medial side of the little finger, the second, the adjacent sides of the little and ring fingers, while the third, when present, supplies adjoining sides of the ring and middle fingers. The latter may be replaced, wholly or partially, by a branch of the radial nerve, which always communicates with it on the dorsum of the hand (Fig. 50.45A). In the little finger, the dorsal digital nerves extend only to the base of the distal phalanx, and in the ring finger they extend only to the base of the middle phalanx. The most distal parts of the little finger and of the ulnar side of the ring finger are supplied by dorsal branches of the proper palmar digital branches of the ulnar nerve. The most distal part of the lateral side of the ring finger is supplied by dorsal branches of the proper palmar digital branch of the median nerve.

Superficial and deep terminal branches

Superficial terminal branch

The superficial terminal branch supplies palmaris brevis and the medial palmar skin. It divides into two palmar digital nerves, which can be palpated against the hook of the hamate bone. One supplies the medial side of the little finger, the other (a common palmar digital nerve) sends a twig to the median nerve and divides into two proper digital nerves to supply the adjoining sides of little and ring fingers. The proper digital branches are distributed like those derived from the median nerve.

Deep terminal branch

The deep terminal branch accompanies the deep branch of the ulnar artery as it passes between abductor digiti minimi and flexor digiti minimi and then perforates opponens digiti minimi to follow the deep palmar arch dorsal to the flexor tendons (Fig. 50.46). At its origin it supplies the three short muscles of the little finger. As it crosses the hand, it supplies the interossei and the third and fourth lumbricals. It ends by supplying adductor pollicis, the first palmar interosseous and usually flexor pollicis brevis. It sends articular filaments to the wrist joint.

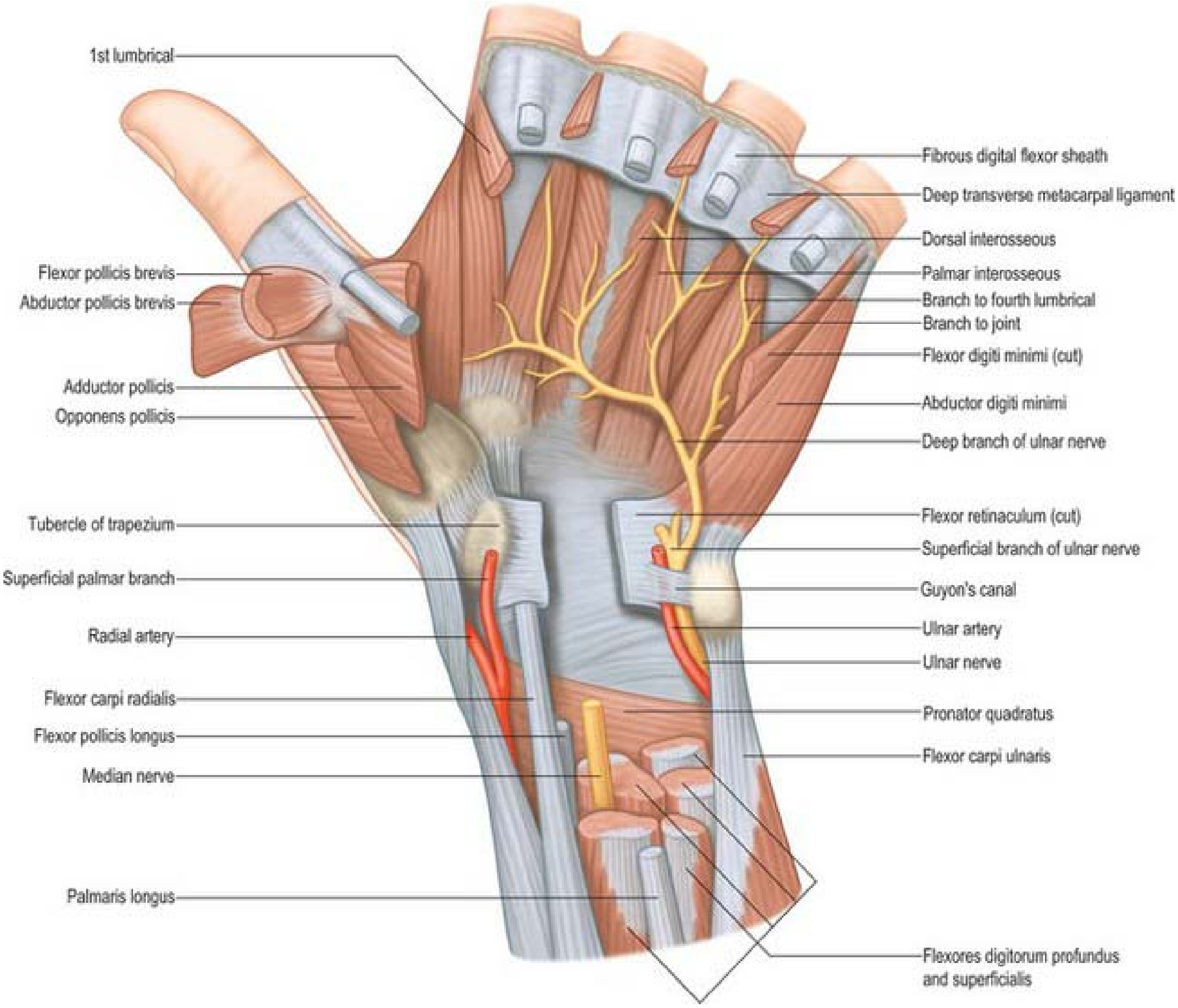
1st lumbrical
Flexor pollicis brevis
Abductor pollicis brevis
Adductor pollicis
Opponens pollicis
Tubercle of trapezium
Superficial palmar branch
Radial artery
Flexor carpi radialis
Flexor pollicis longus
Median nerve
Palmaris longus
Fibrous digital flexor sheath
Deep transverse metacarpal ligament
Dorsal interosseous
Palmar interosseous
Branch to fourth lumbrical
Branch to joint
Flexor digiti minimi (cut)
Abductor digiti minimi
Deep branch of ulnar nerve
Flexor retinaculum (cut)
Superficial branch of ulnar nerve
Guyon's canal
Ulnar artery
Ulnar nerve
Pronator quadratus
Flexor carpi ulnaris
Flexores digitorum profundus and superficialis

Fig. 50.46 Deep structures in the left palm and wrist showing the deep branch of the ulnar nerve.

The medial part of flexor digitorum profundus is supplied by the ulnar nerve, as are the third and fourth lumbricals which are connected with the tendons of this part of the muscle. Similarly, the lateral part of flexor digitorum profundus and the first and second lumbricals are supplied by the median nerve. The third lumbrical is often supplied by both nerves. The deep terminal branch is said to give branches to some intercarpal, carpometacarpal and intermetacarpal joints: precise details are uncertain. Vasomotor branches, arising in the forearm and hand, supply the ulnar and palmar arteries.

Ulnar tunnel syndrome

Ulnar tunnel syndrome is an entrapment neuropathy of the ulnar nerve as it passes through Guyon's canal at the wrist. Causes of compression at this site include a ganglion, trauma, and proximity of aberrant or accessory muscles. The symptoms include pain in the hand or forearm and sensory changes in the palmar aspect of the little and ulnar half of the ring fingers, however sensation on the ulnar aspect of the dorsum of the hand is normal. In addition there may be weakness and wasting of the intrinsic muscles of the hand supplied by the ulnar nerve, with clawing posture in extreme cases.

Surgical treatment involves decompression of the nerve by division of the roof of Guyon's canal and removal of the causative lesion, e.g. ganglion.

Ulnar nerve division at the wrist

Division of the ulnar nerve at the wrist paralyses all the intrinsic muscles of the hand (apart from the radial two lumbricals). The intrinsic muscle action of flexing the metacarpophalangeal joint and extending the interphalangeal joints is therefore lost. The unopposed action of the long extensors and flexors of the fingers cause the hand to assume a clawed appearance with extension of the metacarpophalangeal joints and flexion of the interphalangeal joints. The clawing is less intense in the index and middle fingers because of their intact lumbricals, supplied by the median nerve. (For a detailed account of the hand posture adopted in ulnar nerve lesions, see Smith 2002.)

There is sensory loss over the little finger and the ulnar half of the ring finger. In comparison to an ulnar nerve division at the elbow, the skin over the ulnar aspect of the dorsum of the hand is spared because the dorsal branch of the ulnar nerve is given off approximately 5 cm proximal to the wrist joint.

A combined median and ulnar nerve palsy at the wrist results in a full claw hand with thenar and hypothenar flattening, and thumb adduction and flexion. This posture is known as a simian hand because of the similarity to the appearance of the hand of an ape.

Radial nerve

Branches of the superficial branch of the radial nerve reach the hand by curving around the wrist over the tendons of abductor pollicis longus and extensor pollicis brevis. They divide into dorsal digital nerves. On the dorsum of the hand they usually communicate with the posterior and lateral cutaneous nerves of the forearm.

Dorsal digital nerves

There are usually four or five small dorsal digital nerves. The first supplies the skin of the radial side of the thumb and the adjoining thenar eminence, and communicates with branches of the lateral cutaneous nerve of the forearm. The second supplies the medial side of the thumb; the third, the lateral side of the index finger; the fourth, the adjoining sides of the index and middle fingers; the fifth communicates with a ramus of the dorsal branch of the ulnar nerve and supplies the adjoining sides of the middle and ring fingers, but is frequently replaced by the dorsal branch of the ulnar nerve. The pollicial digital nerves reach only to the root of the nail, those in the index finger, midway along the middle phalanx, those to the middle and the lateral part of the ring finger may reach no further than the proximal interphalangeal joints. The remaining distal dorsal areas of the skin in these digits are supplied by palmar digital branches of the median and ulnar nerves. The superficial terminal branch of the radial nerve may supply the whole dorsum of the hand.

REFERENCES

ı K-N, Berger RA, Cooney WP. Biomechanics of the Wrist Joint. New York: Springer-Verlag, 1991.

ndz P. The functional significance of the oblique retinacular ligament of Landsmeer. A review and new proposals. *J Hand Surg*. 1985;10:25-29.

owers WH, Wolf JWJr, Nehil JL, Bittinger S. The proximal interphalangeal joint volar plate. I. An anatomical and biochemical study. *J Hand Surg [Am]*. 1980;5:79-88.

ormack GC, Lamberty BGH. The Arterial Anatomy of Skin Flaps, 2nd edn. Edinburgh: Churchill Livingstone, 1994.

oyle JR, Blythe WF. The finger flexor tendon sheath and pulleys: anatomy and reconstruction. In: *AAOS Symposium on Tendon Surgery in the Hand*. St Louis: Mosby; 1975:81-88.

ırcia-Elias M. Carpal kinetics. In: Büchler V, editor. *Wrist Instability*. London: Martin Dunitz, 1996. Chapter 2.

reen D, Hotchkiss R, Pederson W. Green’s Operative Hand Surgery, 4th edn. New York: Churchill Livingstone, 1999.

ıuer JMG. The functional anatomy of the carpal joint: the whole and its components. In: *Wrist Instability*. London: Martin Dunitz; 1996.

ırk Watson H, Weinzweig J. The Wrist. Philadelphia: Lippincott, Williams & Wilkins, 2001.

cGrouther D. The microanatomy of Dupuytren’s contracture. *The Hand*. 1982;14:215-236.

ılmon M. Anatomic studies. In: Taylor GI, Razaboni RM. *Book 1: Arteries of the muscles of the extremities and the trunk. Book 2: Arterial anastomotic pathways of the extremities*. St Louis: Quality Medical Publishing, 1994.

nith PJ. Lister’s The Hand. Diagnosis and Indications. 4th edn.. Edinburgh: Churchill Livingstone; 2002.

inner MJB. Kaplan’s Functional and Surgical Anatomy of the Hand, 3rd edn. Philadelphia: Lippincott, Williams & Wilkins, 1984.

anley J, Saffar P. Anatomy. In: *Wrist Arthroscopy*. London: Martin Dunitz; 1994.

atson HK, Weinzweig J. The Wrist. Philadelphia: Lippincott Williams and Wilkins, 2001.

In particular the following chapters in this book: Garcia-Elias M, Anatomy of the wrist; and Ryu J, Biomechanics of the wrist..

CHAPTER 51

Development of the limbs

Development of the limb depends on a series of complex cell–cell interactions that have been identified in experiments on amphibian, avian and reptilian species; the range demonstrates the remarkable conservation of developmental processes. Fate maps have revealed which structures in the limb arise from particular cells or groups of cells in the embryo and considerable progress has been made in identifying the genetic basis of limb development. The finding that the same molecules are involved in developing embryos of both model organisms and humans has promoted an increasing convergence between developmental biology and clinical genetics.

The limbs develop from somatopleuric mesenchyme in the lateral body wall. Regions of the somatopleuric mesenchyme at specific positions along the main body axis proliferate extensively to give rise to limb buds. These buds are the first visible signs of limb development and are rimmed by a longitudinal ridge of high columnar epithelial cells, the apical ectodermal ridge (Fig. 51.1).

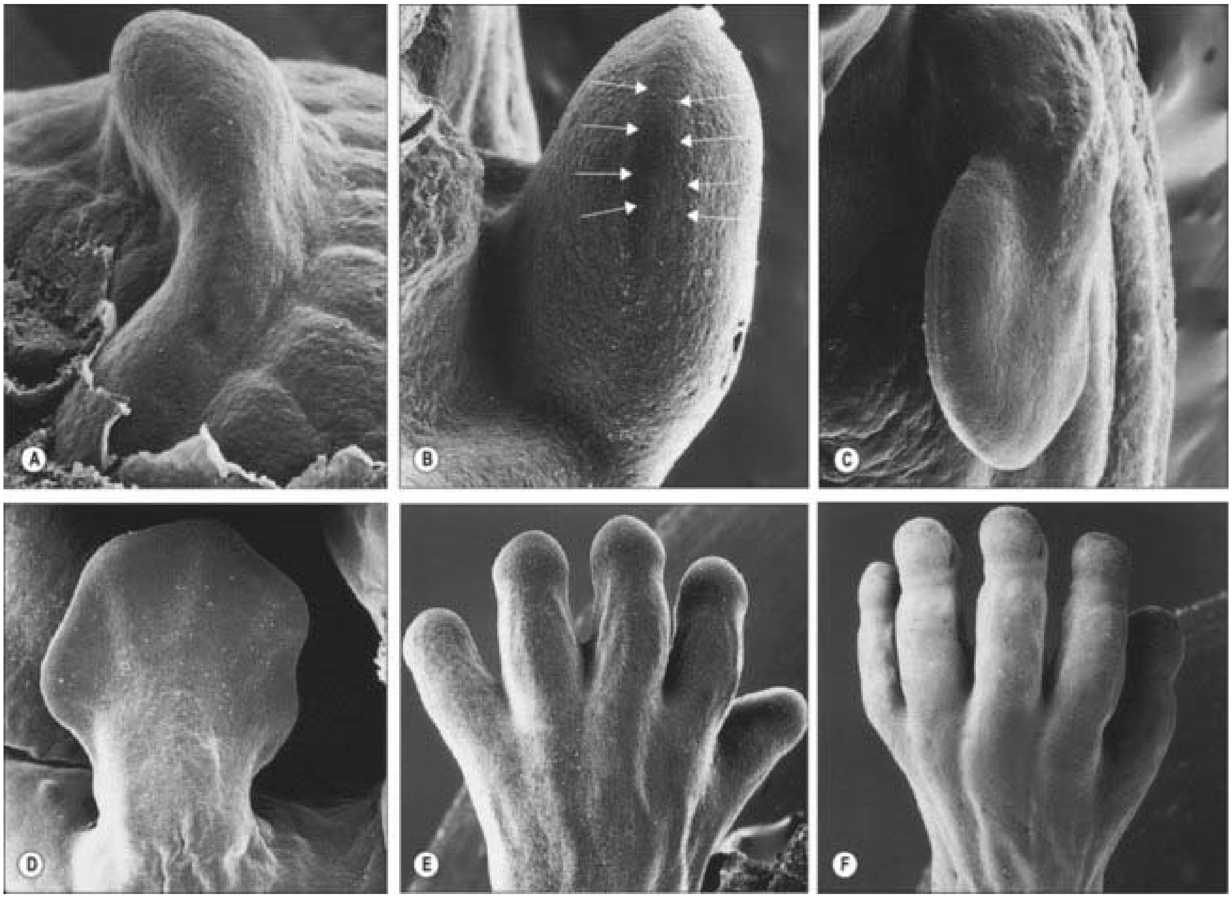

Fig. 51.1 Scanning electron micrographs to show the development of the upper limb. **A**, An early limb bud viewed from the postaxial border. **B**, Limb bud viewed from postaxial border; the apical ectodermal ridge (arrowed) can be seen. **C**, Limb bud, dorsolateral view; the shoulder and elbow region can be discerned, and a hand plate has formed. The apical ectodermal ridge is still obvious at the margin of the hand plate. **D**, Digital rays are present in the hand plate and the margin of the plate is becoming notched. **E**, The fingers are nearly separated and proliferation is commencing at the distal end of each digit to form the nail bed. **F**, The fingers each have tactile pads distally, and nail development continues.

(Photographs by P Collins; printed by S Cox, Electron Microscopy Unit, Southampton General Hospital.)

The early limb bud contains a mixed population of mesenchymal cells: somatopleuric mesenchyme gives rise to the connective tissues of the limb, including cartilage, bone, tendon and loose connective tissue, paraxial mesenchyme from the somites gives rise to the myogenic cells of the muscles, and angiogenic mesenchyme produces an extensive vascular network in the early limb bud. Motor and sensory nerves and the neural crest derived Schwann cells and melanocytes of the skin, migrate into the developing limb somewhat later.

AXES OF LIMBS

For descriptive, experimental and conceptual purposes, it has been necessary to define and name various ‘axes’, borders, surfaces and lines in relation to the developing limb bud (Fig. 51.2). An imaginary line from the centre of the elliptical base of the bud, through the centre of its mesenchymal core, to the centre of the apical ectodermal ridge, defines the proximodistal axis of the limb bud (previously known in descriptive embryology simply as the axis). Named in relation to the latter, the cranially placed limb border is the preaxial border, and the caudally placed limb border is the postaxial border. (In tetrapods and birds, the last two are termed anterior and posterior borders, respectively.) Any line that passes through the limb bud from preaxial to postaxial border, orthogonal to the proximodistal axis, constitutes a craniocaudal axis. The dorsal and ventral ectodermal surfaces thus clothe their respective aspects from preaxial to postaxial borders, and any line that passes from dorsal to ventral aspect, orthogonal to both proximodistal and craniocaudal axes, constitutes a dorsoventral axis. It should be noted here that the terms dorsal and ventral axial lines are to be used exclusively in relation to developing and definitive patterns of cutaneous innervation of the limbs and their associated levels of the trunk.

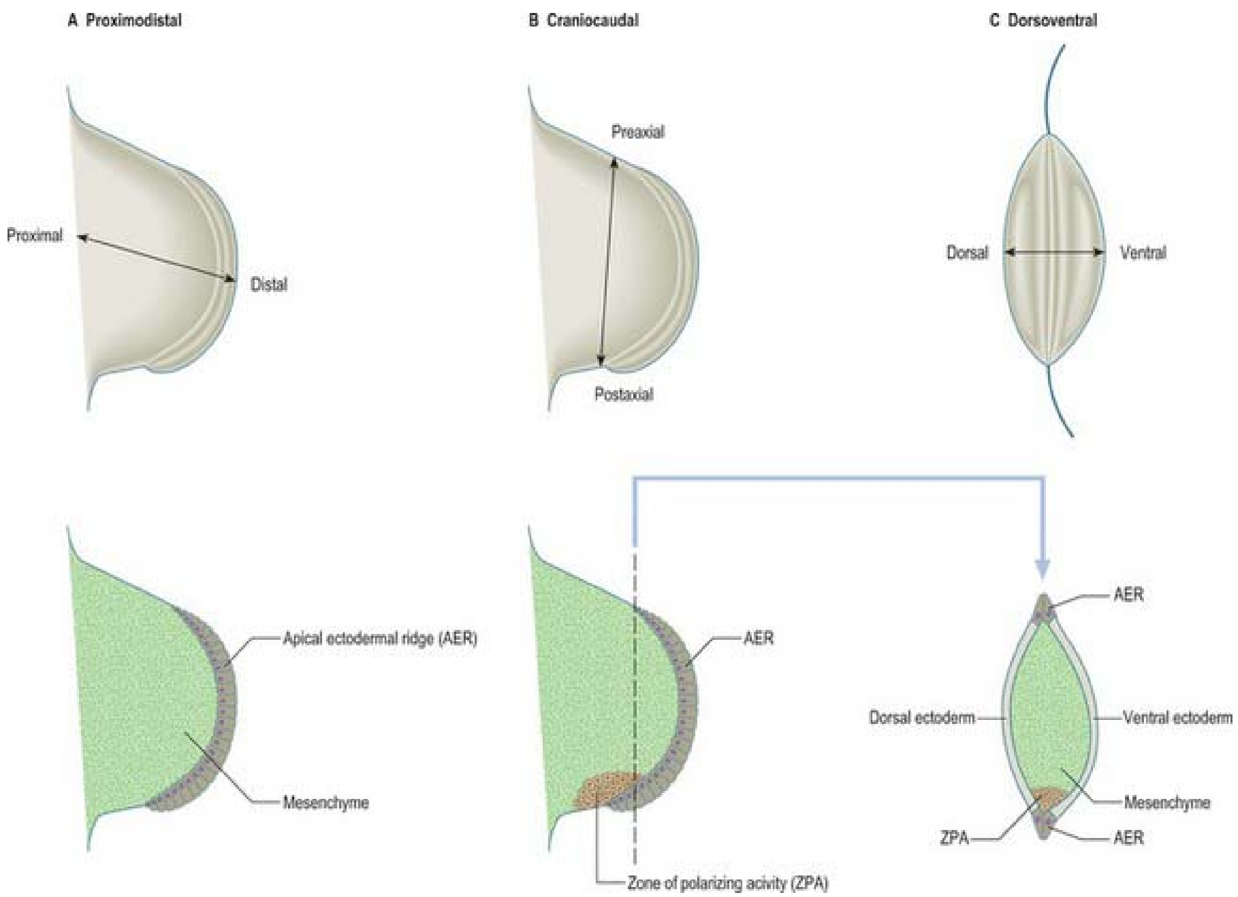
A Proximodistal
B Craniocaudal
C Dorsoventral
Proximal
Distal
Preaxial
Postaxial
Dorsal
Ventral
Apical ectodermal ridge (AER)
Mesenchyme
AER
Zone of polarizing acivity (ZPA)
AER
Dorsal ectoderm
Ventral ectoderm
Mesenchyme
ZPA
AER

Fig. 51.2 Axes of the developing limb and specification of structures along the different axes. **A**, Proximodistal and **B**, craniocaudal; limb bud (approximately stage 14) viewed from dorsal side; **C**, dorsoventral; limb bud viewed from distal end. The pattern of development of limb structures and the ectodermal specializations are controlled by the limb mesenchyme. Outgrowth of limb development is controlled by the apical ectodermal ridge and this is accompanied by the laying down of structures along the proximodistal axis; craniocaudal pattern is controlled by zone of polarizing activity (polarizing region); dorsoventral pattern is controlled by signals from dorsal and ventral ectoderm, shown in cross section, section taken in plane shown by dotted line.

The three developmental axes (proximodistal, craniocaudal, and dorsoventral) can be identified in the developing limb bud by stage 13. Experiments in chick embryos have shown that development of structures in relation to each of these three principal axes seem to be specified by different mechanisms (Fig. 51.2). Outgrowth along the proximodistal axis is controlled by the apical ectodermal ridge and subjacent somatopleuric mesenchyme; outgrowth of the limb bud is accompanied by the sequential formation of limb structures along the proximodistal axis. The craniocaudal axis is controlled by a small population of mesenchymal cells on the postaxial border of the limb bud; this region of mesenchyme is termed the zone of polarizing activity or polarizing region. The dorsoventral axis of the limb appears to be controlled by the surface ectodermal covering of the limb bud.

Early differential growth of parts of the limb bud results in two main changes to the originally symmetrical axes of the limb. The dorsal aspect of the limb grows faster than the ventral, which causes the limb bud to curve around the body wall. The ventral surface of the limb (closest to the body wall) remains relatively flat, but the dorsal surface bulges into the amniotic cavity. The originally laterally facing apical ectodermal ridge becomes increasingly directed ventrally.

APICAL ECTODERMAL RIDGE

The outgrowth of a limb bud is controlled by the apical ectodermal ridge. For many years it was thought that a timing mechanism that specified proximodistal pattern operated in the zone of proliferating undifferentiated mesenchyme cells at the tip of a developing limb bud. This zone was therefore called the progress zone. It was assumed that as cells left the progress zone their proximal distal value became fixed. Cells that spent a short time at the tip of the limb bud would form proximal structures, while cells that spent a longer time at the tip of the limb bud would form distal structures. However, it has been suggested more recently that proximodistal pattern is specified in the very early limb bud and that structures are elaborated as the bud grows out.

The fundamental epithelial–mesenchymal interactions seen in limb development are discussed in detail in Hinchcliffe & Johnson (1980) and the more recently discovered genetic basis of these interactions in Ferretti & Tickle (2006). The knowledge of limb embryology gained from studying chicks may be summarized as follows (Fig. 51.3). The apical ectodermal ridge provides the orientating influence for limb bud outgrowth. Its removal results in cessation of limb development, whereas grafting a second apical ectodermal ridge results in two axes of development, and duplication of distal structures (Fig. 51.3). There is evidence that the limb mesenchyme beneath the apical ectodermal ridge provides an apical ectodermal ridge maintenance factor that is essential to the function of the ridge. Thus, when leg bud cells are grafted to the tip of a wing bud beneath the apical ectodermal ridge, the ridge is maintained and bud outgrowth continues (it should be noted that the leg cells, even though placed in a wing bud, still form distal leg structures) (Fig. 51.3). In addition, the leg mesenchyme will pass information to the local ectoderm eliciting the appropriate epidermal development, which in this case is the formation of scales rather than feathers.

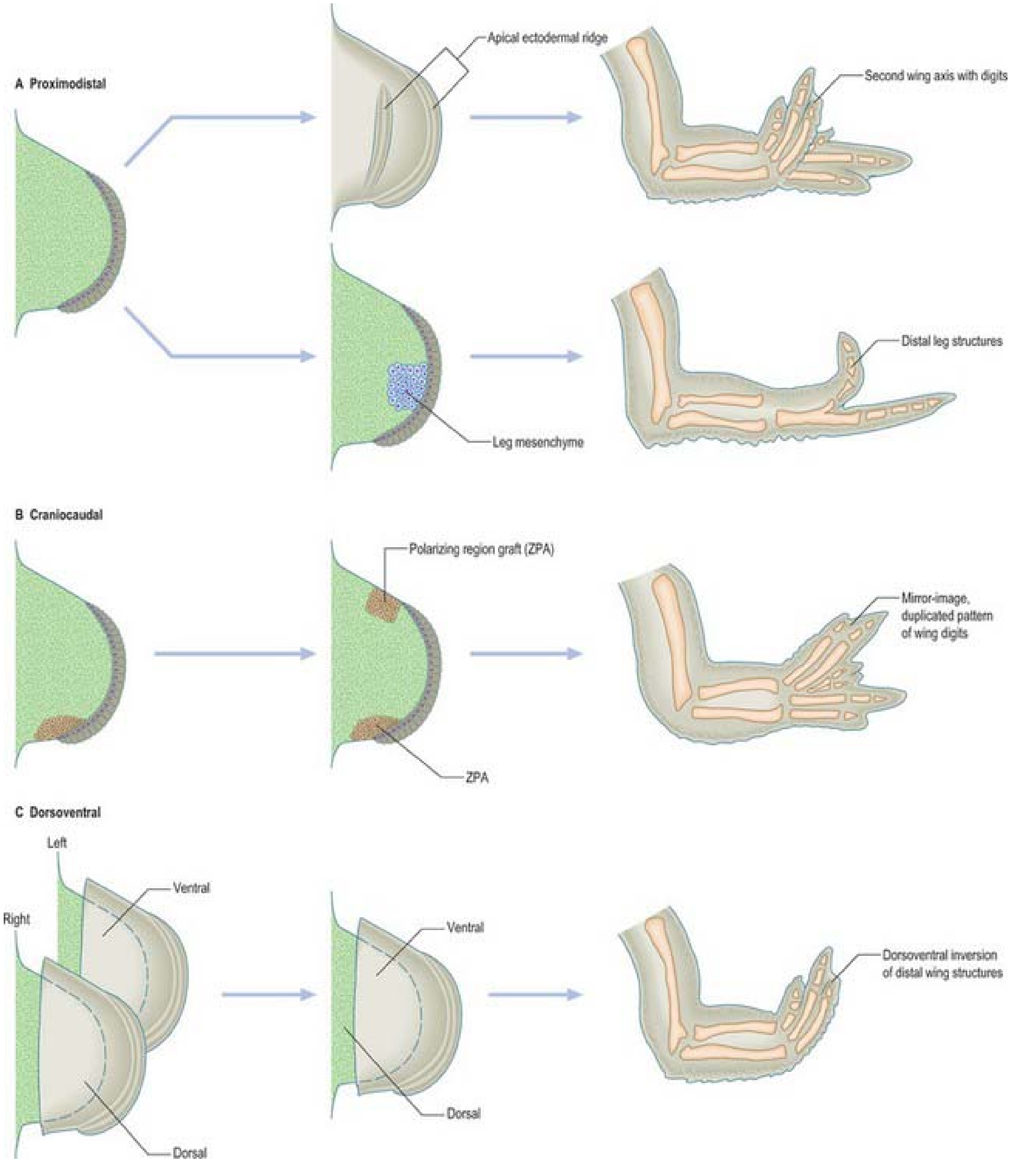
A Proximodistal
Apical ectodermal ridge
Second wing axis with digits
Distal leg structures
Leg mesenchyme
B Craniocaudal
Polarizing region graft (ZPA)
Mirror-image, duplicated pattern of wing digits
ZPA
C Dorsoventral
Left
Right
Ventral
Dorsal
Ventral
Dorsal
Dorsoventral inversion of distal wing structures

Fig. 51.3 **A–C**, Experimental manipulations that identified fundamental interactions involved in patterning the three main axes of the limb in the chick.

ZONE OF POLARIZING ACTIVITY

The zone of polarizing activity is a small region of somatopleuric mesenchyme on the postaxial border of the limb. When a second zone of polarizing activity is grafted beneath or adjacent to the apical ectodermal ridge at the preaxial border of a chick wing bud, duplication of distal limb structures occurs, generating a mirror-image pattern of six digits (Fig. 51.3). The digit closest to the zone of polarizing activity is always the most postaxial digit (in the chick wing this is digit 4), while more preaxial digits develop further away from the zone of polarizing activity. Thus signalling from the zone of polarizing activity appears to control both digit number and digit pattern. It has been suggested that digit number is controlled by regulation of the production of the apical ectodermal ridge maintenance factor, while digit pattern is regulated by production of a diffusible morphogen that acts in a concentration dependent fashion.

ECTODERMAL INTERACTION

It is possible to remove the mesenchymal core of an early chick limb bud leaving the surface ectodermal epithelium. When the ectodermal epithelium from a left limb bud is recombined with the mesenchymal core from a right limb bud, keeping the cranio-caudal axis in register, the distal part of the limb that subsequently develops conforms to the polarity of the ectoderm rather than that of the mesenchyme (Fig. 51.3). This can be seen in the pattern of muscles, orientation of the joints and eventual characteristic differentiation of the epidermis. Thus signals from the ectoderm control the pattern along the dorso-ventral axis.

MOLECULAR BASIS OF CELL–CELL INTERACTIONS

The apical ectodermal ridge secretes fibroblast growth factors that act on the underlying mesenchyme and maintain the zone of polarizing activity. The latter expresses *Sonic hedgehog* (*Shh*), a gene encoding another class of secreted protein that mediates cell–cell signalling. Sonic Hedgehog protein acts on adjacent mesenchyme cells and maintains the expression of the gene encoding Gremlin (an extracellular bone morphogenetic protein antagonist), which functions as an apical ectodermal ridge maintenance factor. Sonic hedgehog also plays a pivotal role in digit patterning: it diffuses across the limb bud and responding cells transduce the signal through the Gli family of transcription factors. (The Gli proteins are bifunctional effectors of Shh signalling and can lead to either activation or repression of expression of gene targets.) Dorsal limb ectoderm expresses *Wnt7a*, which acts as a dorsalizing signal.

Among the genes expressed in response to these cell–cell signalling molecules are 5′ members of two *Hox* gene complexes. *Hox-d* gene expression in the distal limb bud shows a nested arrangement similar to that of Russian dolls: the postaxial border of the limb bud tip expresses five *Hox-d* genes (*d*-13, *d*-12, *d*-11, *d*-10 and *d*-9), while in the next preaxial portion only four genes are expressed (*d*-12, *d*-11, *d*-10 and *d*-9), this sequential loss of expression of *Hox-d* genes is repeated until only *d*-9 is expressed in the most preaxial regions of the limb bud. The fact that five different *Hoxd* expression domains can be distinguished has prompted the suggestion that this may be why we have five fingers (and toes), but the explanation is unlikely to be so simple.

SKELETAL ELEMENTS OF THE LIMB

It has been suggested that formation of the cartilaginous elements of a limb is related to the shape of the limb and the conditions necessary for chondrogenesis. An antichondrogenic zone beneath the ectoderm of a developing limb prevents chondrogenesis within the dermis and myogenic zones. Foci of chondrogenesis occur in the centre of the limb bud where cell density is greatest. One centre of chondrogenesis forms in the proximal region of an early limb bud. As the limb bud lengthens it also widens, forming next two centres of chondrogenesis and five centres that appear further distally. The Sox9 transcription factor is essential for chondrocyte differentiation: expression of the *Sox9* gene is coincident with expression of the gene that encodes collagen type II, the collagen characteristic of cartilage extracellular matrix. *Sox9* gene transcripts are expressed in the humeral and forearm skeletal elements of human embryos at approximately 44 days, and in carpals, metacarpals and phalanges, in addition to more proximal elements, at approximately 52 days (Fig. 51.4).

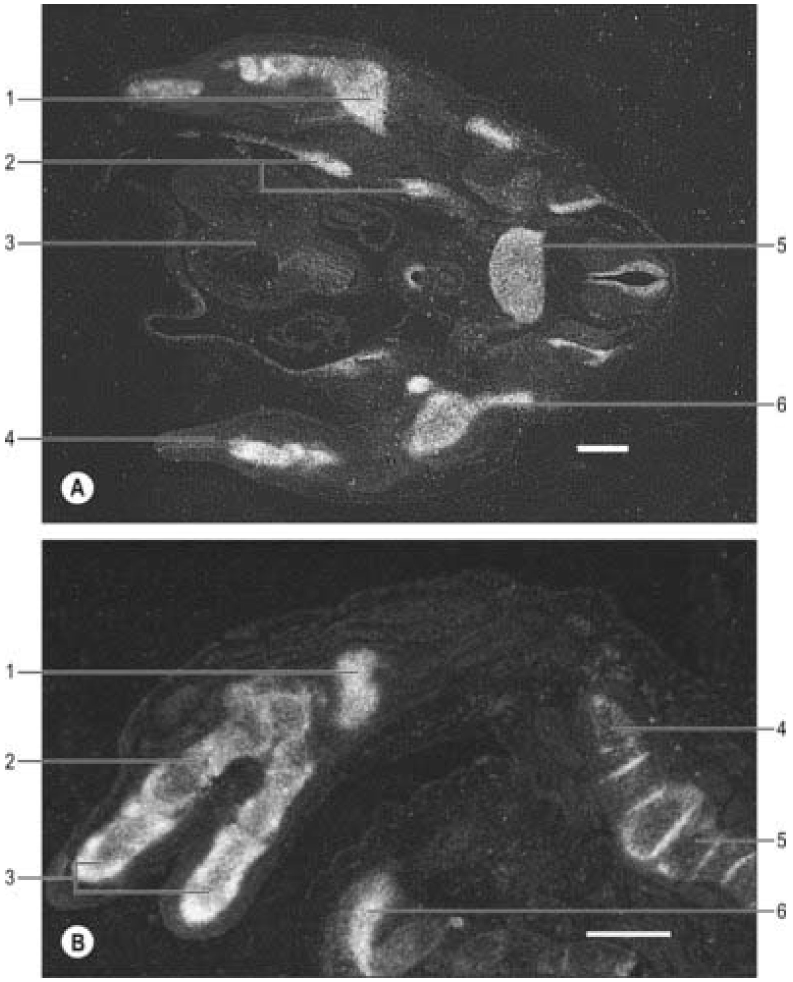

Fig. 51.4 *Sox9* expression in the skeleton of developing limbs of human embryos. **A**, Stage 18; approximately 44 days postovulation. **1**. Humerus. **2**. Ribs. **3**. Heart. **4**. Forearm. **5**. Vertebral body. **6**. Scapula. **B**, Stage 21; approximately 52 days postovulation. **1**. Carpal bone. **2**. Metacarpal bone. **3**. Phalanges. **4**. Humerus. **5**. Scapula. **6**. Rib. *Sox9* transcripts detected in sections with radioactively labelled probes followed by autoradiography, positive signal represented by silver grains that show up as white areas. Scale bars represent 500 µm in both **A** and **B**.

*(The human tissue was provided by the joint MRC-Wellcome Human Developmental Biology Resource (*http://www.hdbr.org*) at the Institute of Human Genetics, Newcastle upon Tyne, UK. By courtesy of Dr Susan Lindsay, Institute of Human Genetics, University of Newcastle upon Tyne, UK.)*

The apical ectodermal ridge controls the width of the digital plate, and the number of digits that develop is related to the width of the limb bud. Zones of preprogrammed cell death can be identified on the preaxial and postaxial borders of the limb which limit the length of the apical ectodermal ridge. (It should be noted that in the literature relating to work on animal embryos, pre- and post-axial borders are termed anterior and posterior borders respectively, and therefore the regions in which programmed cell death occurs are termed the anterior and posterior necrotic zones.) If the length of the apical ectodermal ridge is reduced, fewer digits will form (oligodactyly), whereas if the apical ectodermal ridge becomes longer, more digits will form (polydactyly). Supernumerary digits may develop on either the pre- or postaxial borders. Other regions of apoptotic cell death occur between the digits and result in digital separation, but these appear later than the anterior and posterior necrotic zones: the resultant debris in all of the necrotic zones is removed by macrophages.

The first evidence of bone formation is seen at the mid section of the diaphyses of long bones at 7–8 weeks in human embryos. Vascular invasion of the cartilage matrix precedes the formation of a periostial collar, and subsequently extends proximally and distally until it reaches the future epiphysial level, where a growth plate will be established. By 10 weeks, columns of chondrocytes can be seen at the epiphysial level of most bones. However, only the lower end of the femur and upper end of the tibia develop secondary ossification centres before birth.

For further details describing the development of cartilage see page 81, and the development of bone see page 92. For further details about the development of specific limb bones see the appropriate regional chapter.

DEVELOPMENT OF JOINTS

Regions of developing cartilage are easily recognized histologically in the developing limb because they consist of widely spaced cells surrounded by matrix. Somatopleuric mesenchymal cells are more condensed between the developing skeletal elements, and form plates of interzonal mesenchyme which mark the sites of future joints. Their subsequent development varies according to the type of joint that is formed.

In fibrous joints, the interzone is converted into collagen, which is the definitive medium connecting the bones involved. In synchondroses it becomes (growth) cartilage of the modified hyaline type, and in symphyses it is predominantly fibrocartilage. The interzonal mesenchyme of developing synovial joints becomes trilaminar when a more tenuous intermediate zone appears splitting the mesenchyme into two dense strata. As the skeletal elements chondrify, and in part ossify, the dense strata of the interzonal mesenchyme also become cartilaginous; subsequent cavitation of the intermediate zone establishes the cavity of the joint. The loose mesenchyme around the cavity forms the synovial membrane and probably also gives rise to all other intra-articular structures, such as tendons, ligaments, discs and menisci. In joints containing discs or menisci, and in compound articulations, more than one cavity may appear initially, sometimes merging later into a complex single cavity. As development proceeds, thickenings in the fibrous capsule can be recognized as the specializations peculiar to a particular joint. (In some joints, such accessions to the fibrous capsule are derived from neighbouring tendons, muscles or cartilaginous elements.) Although the initial stages in the process of cavitation of joints is independent of movements, a true joint cavity can form only in the presence of movements (Pitsillides 2006). The literature suggests that all musculoskeletal elements are in their appropriate positions by 10 weeks. For detailed accounts of the process, consult O’Rahilly & Gardner (1975) and Uhthoff (1990).

Musculature of the limb

It is now well established that all limb myogenic precursor cells originate from the somites. These cells are committed at an early stage and can be identified in the lateral halves of the somites. After the mesenchymal sclerotome cells have migrated from the epithelial somite, the remaining dorsolateral portion is termed the epithelial plate or dermomyotome of the somite (Fig. 44.3). Cells from the dorsomedial edge of the dermomyotomes form the axial musculature, whereas at limb levels cells de-epithelialize and migrate from the ventrolateral edges of the dermomyotome into the limb bud. These precursor limb myoblasts migrate through a non-random, structured network of extracellular fibrils. At their leading ends the migrating cells exhibit filopodia which are in contact with the extracellular fibrils or with other cells: it is believed that the orientation of the extracellular fibrils may direct the migration of the cells. The precursor muscle cells do not differentiate into muscle before their migration into the limb, probably in response to inhibitory signals produced by the somatopleuric mesenchyme.

The myogenic cells colonize the limb bud in a proximodistal direction, but never reach the most distal portion of the limb, where there seems to be a distal boundary for the muscle cells. Myogenic cells are still indifferent regarding their region-specific determination when they first enter the limb. When brachial or pelvic level somites are grafted opposite the leg-forming region instead of the wing, or opposite the wing instead of the leg, the precursor cells will give rise to normal leg or wing musculature respectively, i.e. the muscle cells, unlike the somatopleuric mesenchyme, have no ‘limbness’. Further, the muscle pattern developed in the limb reflects the pattern of the skeletal elements: duplication or lack of digits is accompanied by the duplication or lack of the corresponding muscles.

Two subpopulations of myogenic cells can be discerned in the limb bud. In the early buds, there are mainly replicating presumptive myoblasts, considered to be premitotic, whereas in later stages there are also postmitotic myoblasts. It is interesting that the invading myoblasts are still replicating; this may be a prerequisite for the formation of the considerable amount of skeletal muscular tissue that will develop in the limbs.

The first myogenic cells to arrive in the limb form the principal dorsal and ventral premuscle masses. It is believed that all classes of tetrapods begin limb muscle development with these blocks, which produce all the skeletal muscle in the limb. The blocks of premuscle undergo a spatiotemporal sequence of divisions and subdivisions as the limb lengthens, and this leads to the individualization of about 19 muscles in the upper limb and 14 muscles in the lower limb. The mechanisms that create gaps that lead to these divisions of the muscle masses are not known. In the upper limb, the premuscle masses first divide into three masses, the next division gives rise to the muscles attached to the carpus, and the final division produces the long muscles of the digits. A similar pattern is seen in the lower limb. Thus the patterning of the musculature of the limb is controlled by the somatopleuric mesenchyme.

Each anatomical muscle appears as a composite structure. The muscle cells and myosatellite cells are of somitic origin, and the connective tissue envelopes and the tendons are of somatopleuric origin. The precise way in which the muscles become anchored to the developing bones by the tendons is not clear.

For further development of skeletal muscle, see page 115.

EMBRYONIC MOVEMENTS

Embryonic movements are vital for development of the musculoskeletal system (reviewed by Pitsillides, 2006). They have effects on the developing muscle, and are necessary to align trabeculae within bones, and to ensure the correct attachments of the tendons and the appropriate coiling of the constituent collagen fibres within the tendons. Simple movements of an extremity have been observed sporadically as early as the seventh week of gestation. Combined movements of limb, trunk and head commence between 12 and 16 weeks of gestation in human embryos. Movements of the embryo and fetus encourage normal skin growth and flexibility, in addition to the progressive maturation of the musculoskeletal system.

FETAL MOVEMENTS

Fetal movements have been detected by ultrasonography in the second month of gestation. Those related to trunk and lower limb movements are perceived consistently by the mother from about 16 weeks' gestation (quickening). Movements of the fetus often involve slow and asymmetric twisting and stretching movements of the trunk and limbs which resemble athetoid movements. There may also be rapid, repetitive, wide-amplitude limb movements, similar to myoclonus.

By 32 weeks' gestation, symmetric flexor movements are most frequent. By term, the quality of the movements has generally matured to smooth alternating movement of the limbs, with medium speed and intensity. The reduced effect of gravity *in utero* may cause certain fetal movements to appear, on ultrasonography, more fluent than the equivalent movements observed postnatally. The number of spontaneous movements decreases after the 35th week of gestation, and from this time there is an increase in the duration of fixed postures. This restriction of normal fetal movements in late gestation reflects the degree of compliance of the maternal uterus: there is a slowing of growth at this time.

In addition to promoting normal musculoskeletal development, movements of the fetus encourage skin growth and flexibility indirectly. Fetuses with *in utero* muscular dystrophies, or other conditions that result in small or atrophied muscles, have webs of skin, pterygia, which pass across the flexor aspect of the joints and severely limit movement. Multiple pterygium syndrome is characterized by webbing across the neck, the axillae and antecubital fossae. Usually, the legs are maintained straight and webbing is not seen at the hip and knee. A group of congenital disorders, collectively termed 'multiple congenital contractures', may result from genetic causes, or limitations of embryonic and fetal joint mobility, or may be secondary to muscular, connective tissue, skeletal or neurological abnormalities. These conditions may be recognized on prenatal ultrasound examination by the appearance of fixed, immobile limbs in bizarre positions, or by webbing in limb flexures. Specific syndromes, lethal multiple pterygium syndrome, and congenital muscular dystrophy, have been described.

The workload undertaken by the musculoskeletal system before birth is relatively light because the fetus is supported by the amniotic fluid and therefore under essentially weightless conditions. The load on the muscles and bones is generated by the fetus itself, with little gravitational effect. The reduction of gravitational force afforded by the supporting fluid means that all parts of the fetus are subject to relatively equal forces, and that the position assumed by the fetus relative to gravity is of little consequence. This is important to ensure the normal modelling of fetal bones, especially the skull. Skulls of premature babies may become distorted as a result of the weight of the head on the mattress, despite regular changes in position, and the application of oxygen therapy via a mask attached by a band around the head can cause dysostosis of the occipital bone.

VASCULATURE OF THE LIMB

ARTERIES

The early limb bud receives blood via intersegmental arteries that contribute to a primitive capillary plexus. At the tip of the limb bud, there is a terminal plexus which is constantly renewed in a distal direction as the limb grows (see Figs 52.1, 85.1). Later, one main vessel, the axial artery, supplies the limb and the terminal plexus.

The development of the vasculature in the limb precedes the morphological and molecular changes that occur within the limb mesenchyme. The differentiation of cartilage within the limb occurs only after local vascular regression begins, and only in areas with few or no capillaries. Regions of mesenchyme free of capillaries and at high cell density are the sites of chondrogenesis. It is not known whether the presence, or lack, of blood vessels affords different local environmental stimuli for mesenchymal cells (by varying the supply of nutrients to the tissue), or whether the local environment is controlled by the endothelial cells. Similarly, it is not clear whether inductive factors from the limb mesenchyme cause the changes that occur in the pattern of blood vessels.

VEINS

At the tip of the early limb bud, blood in the terminal capillary plexus returns to the body via a marginal vein that develops along the pre- and postaxial borders of the limb. As the limb enlarges, the marginal vein can be subdivided into pre- and postaxial veins, which run along their respective borders and which are the precursors of the superficial veins of the limb. Generally, the preaxial (superficial) veins join the deep veins at the proximal joint, and the postaxial (superficial) veins join the deep veins at the distal joint of the limb. Deep veins develop *in situ* alongside the arteries.

REFERENCES

rretti P, Tickle C. The limbs. In: Ferretti P, Copp A, Tickle C, Moore G. *Embryos. Genes and Birth Defects*. 2nd edn. Chichester: Wiley; 2006:123-166.

Presents the most recently identified genes involved in the control of limb development..

nchcliffe JR, Johnson DR. The Development of the Vertebrate Limb. In: *An Approach through Experiment, Genetics and Evolution*. Oxford: Clarendon Press; 1980.

Presents the classic experiments on limb development..

ne EB, Tickle C. How to make a hand: a 3 day symposium held at the University of Dundee. *J Anat*. 202(1), 2003.

Includes reviews on limb development and human limb malformations..

Rahilly R, Gardner E. The timing and sequence of events in the development of the limbs in the human embryo. *Anat Embryol*. 1975;148:1-23.

tsillides AA. Early effects of embryonic movement: ‘a shot out of the dark’. *J Anat*. 2006;208:417-431.

Reviews recent work using chicken embryos to explore the importance of movement in development of the locomotor apparatus..

nthoff HK. The Embryology of the Human Locomotor System. Berlin: Springer-Verlag, 1990.

CHAPTER 52

Development of the pectoral girdle and upper limb

STAGES OF UPPER LIMB DEVELOPMENT

The upper limb bud is first visible as a ridge along the lateral longitudinal axis of the body wall opposite somites 8–10, at the level of the entrance to the cranial intestinal portal during stage 12. It enlarges, protruding laterally from its elliptical base at the body wall as a flattened plate, with a curved border and an apical ectodermal ridge forming its distal tip. It also has initially equal and relatively flat dorsal and ventral ectodermal surfaces, and a somatopleuric mesenchymal core.

By stage 13 the upper limb bud is curved ventrally. In stage 14 the bud has elongated and the preaxial border has started to lengthen. At this stage the limb bud is opposite the developing ventricles of the heart. In stage 15, the upper limb can be subdivided into definite regions. The proximal portion of the limb which still shows the dorsal bulge and ventral curve is the shoulder and upper arm region; the next distal portion (which was derived from the increase in the length of the preaxial border) can now be identified as the forearm; the most distal portion is now expanded into a flattened hand plate.

At stage 16, the upper limb appears much more substantial. It is sometimes close to the body wall and sometimes abducted. The hand plate has the first indications of digit rays. By stage 17, the upper limb has an elbow region and digit rays; in advanced members of this stage, the hand plate has a crenated rim indicating the beginning of tissue removal between the digits (see Fig. 51.1). In stage 18 embryos (44 days), there is further crenation of the hand plate between the digit rays. Changes during stages 19–23 are concerned with growth of the limb and separation of the digits. The hands now curve over the cardiac region. The distal phalangeal portions of the fingers enlarge at stage 21, forming the nail beds.

Most of the bones in the appendicular skeleton are derived from somatopleuric mesenchyme. Within the upper limb although the clavicle and coracoid portion of the scapula arise from somatopleuric mesenchyme, the body and spine of the scapula are derived from the somites. Prechondroblasts are present in the upper limb at stage 13, and condensations of cartilage can be detected at stage 16, when the humeral anlage can be recognized. Cavitation of the shoulder and elbow joints occurs at 7–8 weeks. By stage 17, when the radius and ulna chondrify, the branched tips of the radial, median and ulnar nerves have migrated to the distal hand plate. The carpal bones chondrify at stage 18, when the hand plate shows notching of the digital rays.

VESSELS IN THE UPPER LIMB

In the upper limb, usually only one arterial trunk, the subclavian, persists; it probably represents the lateral branch of the seventh intersegmental artery. Its main continuation (axis artery) to the upper limb (Fig. 52.1), later the axillary and brachial arteries, passes into the forearm deep to the flexor muscle mass and terminates as a deep plexus in the developing hand. The original axial vessel ultimately persists as the anterior interosseous artery and the deep palmar arch. A branch from the main trunk passes dorsally between the early radius and ulna as the posterior interosseous artery; a second branch accompanies the median nerve into the hand, where it ends in a superficial capillary plexus. The radial and ulnar arteries are the latest arteries to appear in the forearm. Initially the radial artery arises more proximally than the ulnar artery, crosses in front of the median nerve, and supplies biceps. Later, the radial artery establishes a new connection with the main trunk at or near the level of origin of the ulnar artery and the upper portion of its original stem usually disappears. On reaching the hand, the ulnar artery links up with the superficial palmar plexus, from which the superficial palmar arch is derived, while the median artery commonly loses its distal connections and is reduced to a small vessel. The radial artery passes to the dorsal surface of the hand; after giving off dorsal digital branches, it traverses the first intermetacarpal space and joins the deep palmar arch.

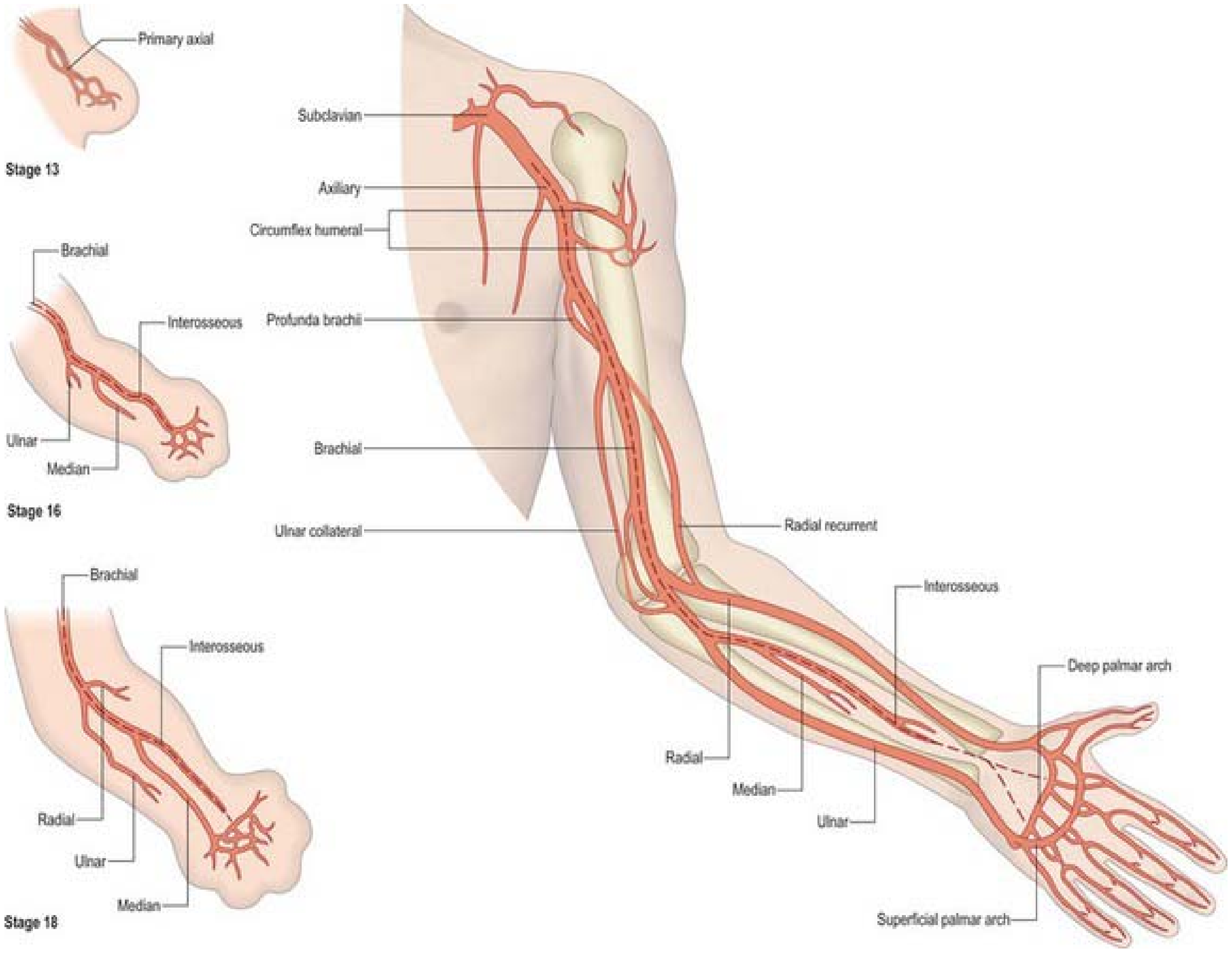
Primary axial
Stage 13
Brachial
Interosseous
Ulnar
Median
Stage 16
Brachial
Interosseous
Radial
Ulnar
Median
Stage 18
Subclavian
Axillary
Circumflex humeral
Profunda brachii
Brachial
Ulnar collateral
Radial recurrent
Interosseous
Deep palmar arch
Radial
Median
Ulnar
Superficial palmar arch

Fig. 52.1 Stages in the development of the arteries of the arm. The original path of the axis artery is indicated by an interrupted line.

For a number of reasons, anomalies of the forelimb arterial tree are fairly common. These arteries have multiple and plexiform sources; display a temporal succession of the emergence of principal arteries, anastomoses and periarticular networks; and some paths that are initially functionally dominant subsequently regress. In general, anomalous patterns may present as differences in the mode and proximodistal level of branching; the presence of unusual compound arterial segments; aberrant vessels that connect with other principal vessels, arcades or plexuses; vessels that occupy exceptional tissue planes (e.g. superficial fascia instead of the usual subfascial route), or which have unexpected neural, myological or osteoligamentous relationships.

In the upper limb, the preaxial vein becomes the cephalic vein, and drains into the axillary vein at the shoulder. The postaxial vein becomes the basilic vein, which passes deep in the arm to continue as the axillary vein.

NEONATAL UPPER LIMB

In general, the upper limbs in the neonate are proportionately shorter than they are in the adult. They are long compared with the neonatal trunk and lower limbs, and extend to the upper thigh as they do in the adult, but the trunk is much shorter in the neonate (see Fig. 14.6). At birth, the upper limbs are about the same length as the lower limbs, but much more developed. When the proportions of parts of the upper limb are examined, the forearm is longer than the upper arm in the newborn, more so in boys than girls. Only primary centres of ossification are present in the upper limb, apart from a centre in the head of the humerus. The elbow of the newborn cannot achieve full extension, being some 10–15% short; it can flex to 145°. The neonate has a relatively strong grasp within the first few days. The fingernails of the upper limb usually extend to the finger tips or just beyond. They are soft at birth but soon dry and become quite firm and sharp.

PERIPHERAL ARTERIAL PUNCTURE IN THE NEONATE

It is common practice to insert a small-bore cannula into a peripheral artery in neonates receiving intensive care when either the umbilical artery is not accessible or there are clinical reasons to avoid cannulation of the umbilical vessels. Transillumination can be used to provide an outline of the artery to be cannulated. The peripheral arteries that are most commonly used are the radial artery, just above the anterior surface of the wrist and the posterior tibial artery, posterior to the medial malleolus. The proximity of the ulnar nerve to the ulnar artery increases the risk of nerve damage associated with arterial cannulation of the ulnar artery, and the relatively poor collateral circulation associated with the dorsalis pedis artery means that this artery is used only as a last resort. The brachial artery at the antecubital fossa also has a poor collateral circulation and the median nerve is in close proximity; it is generally considered, therefore, that cannulation of this artery is not justified.

Confirmation that an adequate collateral circulation is present when cannulating the radial artery can be obtained by performing Allen’s test, in which both the radial and ulnar arteries are compressed at the wrist after exsanguination of the hand; release of pressure on the ulnar artery while maintaining occlusion of the radial artery should result in reperfusion of the hand if an adequate collateral ulnar arterial supply is present. Alternatively, intact arterial flow can usually be confirmed, particularly in the preterm infant, by direct visualization of the arteries using transillumination. A cold light source is placed on the posterior aspect of the lower forearm and the shadow of the pulsating arteries can be seen on the anterior surface of the forearm.

UPPER LIMB ANOMALIES

Approximately 1 in 600 neonates will have a congenital anomaly of the hand or forearm, 30% of which will be bilateral, and will occur with an approximately equal frequency in males and females. A defect is twice as likely to occur in the upper limb than in the lower limb.

A classification of congenital limb malformation uses seven subgroups (Swanson 1976). These describe a clinical picture and do not always relate accurately to the developmental process occurring in the limb. Failure of formation of parts of a limb is caused by developmental arrest affecting the long bones. The second subgroup, failure of differentiation, includes unsuccessful separation of parts, and so includes the range of syndactylies. Groups three to five include limb duplication, overgrowth and undergrowth. Group six includes limb amputations, mainly by adherent amniotic bands, and the last group includes all other generalized skeletal anomalies.

LIMB REDUCTION DEFECTS

Limb reduction defects are categorized as failures of development. The basis of limb reductions seen in infants whose mothers took thalidomide during their pregnancy seems likely to be due to death of mesenchyme cells in the early limb bud causing phocomelia. Proximal segments of the limb were lost although, in some cases, normal distal segments still formed. Similar defects can be produced by X-irradiation of chick embryo limb buds and there is now evidence that thalidomide interferes with vascularization and this could lead to cell death. In congenital absence of the radius, the ulna is usually shortened and curved towards the radial side. If the thumb is present, it is usually hypoplastic and the first metacarpal is absent.

Inheritance of autosomal dominant genes may cause anomalies of the hand. This could, for example, result in absence of the central digit ray of the distal hand plate and subsequent absence of the middle or ring finger and its metacarpals. Extra digits, preaxially, could result from ectopic polarizing activity due to mutations in regulatory regions that control expression of the Shh gene specifically in the developing limb bud. Other changes in digit number may be the result of alterations in limb bud width and the length of the apical ectodermal ridge.

ANOMALIES OF THE DIGITS

Webbing of the fingers is the most common congenital anomaly of the hand. It occurs because of failure to remove cells between the digit rays during stages 19–23, or because of a dominantly inherited disorder.

Clinodactyly is a congenital condition in which the little finger is curved towards the ring finger. It can occur in isolation, or in association with chromosomal abnormalities like Down's syndrome. Camptodactyly is a congenital condition in which the little finger, and sometimes the ring finger, is held in a fixed flexed position. Symphalangism is a rare congenital disorder in which there is fusion of the interphalangeal joints. The affected finger is stiff, skin creases are absent over the affected joint, there is minimal joint space, and sometimes the digit is shorter than normal. Several different types of brachydactyly, shortening of the digits, can be recognized according to which digits and which parts of these digits are affected. The genetic basis of four different types of brachydactyly has now been determined, which is particularly gratifying because brachydactyly was the first condition in humans to be recognized as a dominant Mendelian condition.

REFERENCES

vanson AB. A classification for congenital limb malformations. *J Hand Surg*. 1976;1:8-22.

ıpta A, Kay SPJ, Scheker LR. The Growing Hand. London: Harcourt Publishers Ltd., 2000.

Section 7
THORAX

CHAPTER 53

Thorax: overview and surface anatomy

The thorax is the upper part of the trunk. It consists of an external musculoskeletal cage, the thoracic wall, and an internal cavity that contains the heart, lungs, oesophagus, trachea, thymus, the vagus and phrenic nerves and the right and left sympathetic trunks, the thoracic duct and major systemic and pulmonary blood vessels. Inferiorly the thorax is separated from the abdominal cavity by the diaphragm, superiorly it communicates with the neck and the upper limbs. The thoracic wall also offers protection to some of the abdominal viscera: the greater part of the liver lies under the right dome of the diaphragm; the stomach and spleen lie under the left dome of the diaphragm; the posterior aspects of the superior poles of the kidneys lie on the diaphragm and are anterior to the twelfth rib on the right, and to the eleventh and twelfth ribs on the left (Fig. 53.1).

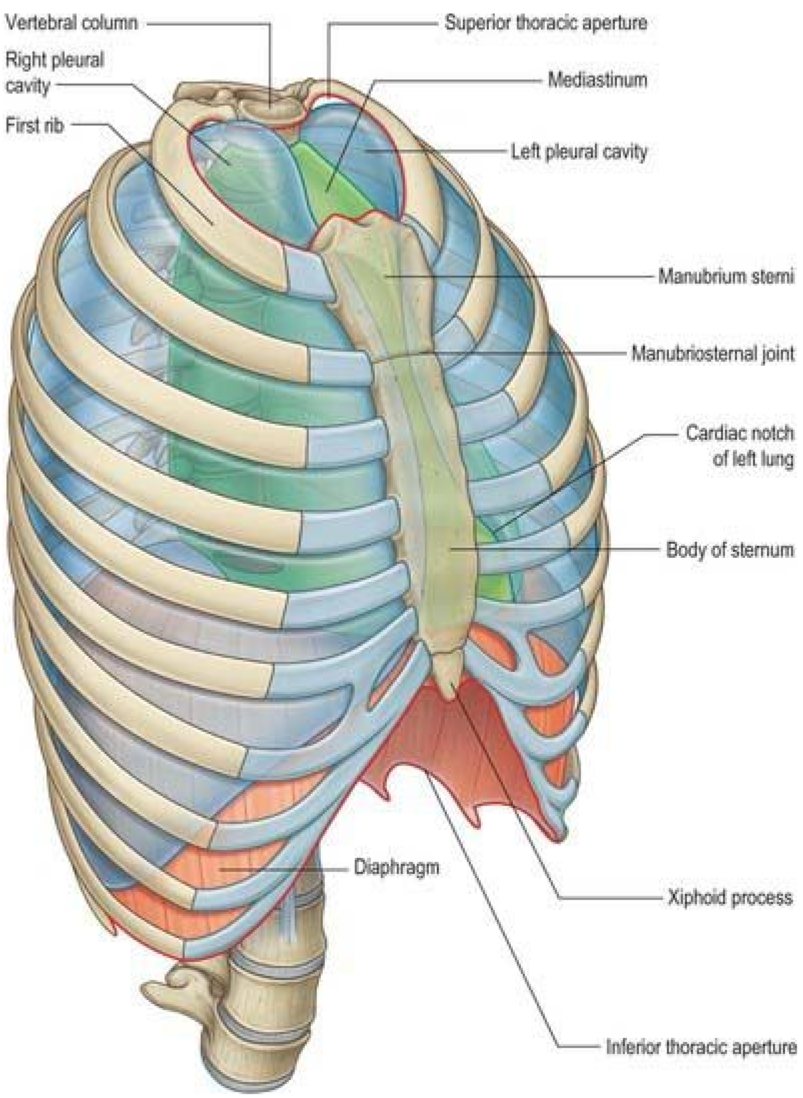
Vertebral column
Right pleural cavity
First rib
Superior thoracic aperture
Mediastinum
Left pleural cavity
Manubrium sterni
Manubriosternal joint
Cardiac notch of left lung
Body of sternum
Diaphragm
Xiphoid process
Inferior thoracic aperture

Fig. 53.1 Thoracic wall and cavity.

(From Drake, Vogl and Mitchell 2005.)

Variations in thoracic dimensions and proportions are partly individual and also linked to age, sex and race. At birth, the transverse diameter is relatively less than it is in the adult, but adult proportions develop as walking begins. Thoracic capacity is less in females than it is in males, both absolutely and proportionately: the female sternum is shorter, the thoracic inlet more oblique, and the suprasternal notch is level with the third thoracic vertebra (whereas it is level with the second in males). In all individuals, the size of the thoracic cavity changes continuously, according to the movements of the ribs and diaphragm during respiration (see Ch. 58), and the degree of distension of the abdominal viscera.

MUSCULOSKELETAL FRAMEWORK

BONES AND JOINTS

The thoracic skeleton consists of twelve thoracic vertebrae and their intervening intervertebral discs (midline, posterior), twelve pairs of ribs and their costal cartilages (predominantly lateral) and the sternum (midline, anterior). When articulated, they form an irregularly shaped osteocartilaginous cylinder, reniform in horizontal section, which is narrow above, broad below, flattened anteroposteriorly and longer behind (see Fig. 54.7). Laterally the thoracic cage is convex and is formed by the ribs, and anteriorly it is slightly convex and is formed by the sternum and the distal parts of the ribs and their costal cartilages. The first seven pairs of ribs are connected to the sternum by costal cartilages, the costal cartilages of the eighth to tenth ribs usually join the superjacent cartilage, and the eleventh and twelfth ribs are free (floating) at their anterior ends. The posterolateral curvature of the ribs, from their vertebral ends to their angles, produces a deep internal groove, the paravertebral gutter, on either side of the vertebral column. The ribs and costal cartilages are separated by intercostal spaces, which are deeper anteriorly and between the upper ribs. Each space is occupied by three layers of flat muscles and their aponeuroses, neurovascular bundles and lymphatic channels.

The narrow thoracic inlet (superior thoracic aperture) typically measures 5 cm anteroposteriorly and 10 cm transversely. It is bounded by the first thoracic vertebral body posteriorly, the medial border of the first ribs on each side, and the superior border of the manubrium sterni anteriorly. It slopes down and forwards, so that the apex of the lung extends upwards into the neck behind the anterior end of the first rib: structures that pass between the thorax and the upper limb therefore pass over the first rib and the apices of the lungs and the apical pleurae.

The broad thoracic outlet (inferior thoracic aperture) is limited posteriorly by the twelfth thoracic vertebral body, posterolaterally by the twelfth rib and the distal end of the eleventh rib, anterolaterally by the distal cartilaginous ends of the seventh to tenth ribs (which unite and ascend to form the costal margin), and anteriorly by the xiphoid process. It is wider in the transverse plane than in the sagittal plane and slopes obliquely downward and backward, so that the thoracic cavity is deeper posteriorly than anteriorly.

The horizontal plane that passes through the intervertebral disc between the fourth and fifth thoracic vertebrae posteriorly and the manubriosternal joint (sternal angle or angle of Louis) at the level of the second costal cartilage anteriorly is a useful aid to orientation in the thorax. It separates the superior mediastinum from the inferior mediastinum and also marks the positions of the superior limits of the pericardium and of the pulmonary trunk, the origin of the arch of the aorta, the level at which the trachea bifurcates into right and left main bronchi, and the site where the superior vena cava penetrates the pericardium to enter the right atrium.

MUSCLES

Intrinsic and extrinsic muscles

The intrinsic muscles of the chest wall are the intercostal muscles, subcostalis, transversus thoracis, levatores costarum, serratus posterior superior and serratus posterior inferior. The intercostal muscles occupy each of the intercostal spaces and are named according to their surface relations, i.e. external, internal and innermost. All except levatores costarum are innervated by the adjacent intercostal nerves derived from the ventral rami of the thoracic spinal nerves; levatores costarum are innervated by the dorsal rami of the thoracic spinal nerves. The intrinsic muscles can elevate or depress the ribs, and are active during respiration, particularly forced respiration: their primary action is believed to be to stiffen the chest wall, preventing paradoxical movement during inspiration (see Ch. 58).

The skeletal framework of the thoracic wall provides extensive attachment sites for muscles associated functionally with the neck, abdomen, back, and upper limbs. Some of them (scalenes, infrahyoid strap muscles, sternocleidomastoid, serratus anterior, pectoralis major and minor, external and internal obliques, and rectus abdominis) function as accessory muscles of respiration and are usually active only during forced respiration; scalenus medius is active in quiet inspiration. Scalenus anterior, medius and posterior are described in Chapter 28. Trapezius, latissimus dorsi, rhomboid major, rhomboid minor, levator scapulae, pectoralis major, pectoralis minor, subclavius, serratus anterior, deltoid, subscapularis, supraspinatus, infraspinatus, teres minor and teres major are described in Chapter 46. Rectus abdominis, external oblique and internal oblique are described in Chapter 61.

Diaphragm

The diaphragm is a curved musculotendinous sheet attached to the circumference of the thoracic outlet and to the upper lumbar vertebrae. It forms the floor of the thoracic cavity, and separates it from the abdominal cavity (see Ch. 58). The diaphragm is relatively flat centrally and domed peripherally, rising higher on the right side than on the left, an asymmetry that reflects the relative densities of the underlying liver and gastric fundus respectively. From its highest point on each side the diaphragm slopes downward to its costal and vertebral attachments: this slope is most marked posteriorly, where the space between the diaphragm and the posterior wall of the thorax is very narrow.

Diaphragmatic openings

The inferior vena cava passes through an opening in the central tendon of the diaphragm to enter the right side of the mediastinum at the level of the eighth thoracic vertebra; the oesophagus passes through the muscular part of the diaphragm and enters the abdomen just to the left of the midline at the level of the tenth thoracic vertebra; and the descending thoracic aorta passes posterior to the diaphragm in the midline at the level of the twelfth thoracic vertebra (see Fig. 58.1A,B). Other structures which pass between the thorax and abdomen include the right and left vagi, phrenic and subcostal nerves, the thoracic duct, the sympathetic trunks and the thoracic splanchnic nerves, the right and left superior epigastric arteries and the hemiazygos and accessory hemiazygos veins.

THORACIC CAVITY

PLEURAL CAVITIES

The right and left pleural cavities are separate compartments on either side of the mediastinum. Each encloses a lung and its associated bronchial tree and vessels, nerves and lymphatics (see Ch. 57). The walls are formed by a serous membrane, the pleura, arranged as a closed sac. The outer layer of the sac, the parietal pleura, lines the corresponding half of the thoracic wall and covers much of the diaphragm and structures occupying the middle region of the thorax. The inner or visceral layer is more delicate and adheres closely to the pulmonary surface, following the interlobar fissures. The two layers are continuous with each other around the structures at the hila of the lungs. They remain in close, though sliding, contact at all phases of respiration. The potential space between them is the pleural cavity, which is maintained at a negative pressure by the inward elastic recoil of the lung and the outward pull of the chest wall. The lungs do not fill this space in quiet respiration, but move into recesses such as the costodiaphragmatic recess, which separates the costal and diaphragmatic pleura, in deep breathing.

The left pleural cavity is the smaller of the two pleural cavities because the heart extends further to the left.

MEDIASTINUM

The mediastinum lies between the right and left pleural sacs in and near the median sagittal plane of the chest (see Ch. 55). It extends from the sternum anteriorly to the vertebral column behind. A horizontal plane passing through the manubriosternal joint and the intervertebral disc between the fourth and fifth thoracic vertebrae separates the mediastinum into superior and inferior portions.

Superior mediastinum

The superior mediastinum lies between the manubrium sterni anteriorly, and the upper thoracic vertebrae posteriorly, and is limited laterally by the pleurae. Its inferior boundary is a slightly oblique plane that passes backward from the manubriosternal joint to the lower part of the body of the fourth thoracic vertebra. It contains the lower ends of sternohyoid, sternothyroid and longus colli on each side; the aortic arch; the brachiocephalic artery and the thoracic portions of the left common carotid and left subclavian arteries; the brachiocephalic veins and the upper half of the superior vena cava; the left highest intercostal vein; the vagus, cardiac, phrenic and left recurrent laryngeal nerves; the trachea, oesophagus, and thoracic duct; the remains of the thymus, and lymph nodes.

Inferior mediastinum

The inferior mediastinum may be divided into three parts: anterior, in front of the pericardium; middle, containing the pericardium and its contents (see Ch. 56); posterior, behind the pericardium.

Anterior mediastinum

The anterior mediastinum exists only on the left side where the left pleura diverges from the midsternal line. It is bounded anteriorly by the sternum, laterally by the pleurae, and posteriorly by the pericardium. It is narrow above, but widens a little below. Its anterior wall is formed by the left transversus thoracis and the fifth to seventh left costal cartilages. It contains a quantity of loose areolar tissue, lymphatic vessels which ascend from the convex surface of the liver, two or three anterior mediastinal lymph nodes, and the small mediastinal branches of the internal thoracic artery.

Middle mediastinum

The middle mediastinum is the broadest part of the interpleural space; it contains the heart enclosed in the pericardium, the ascending aorta, the lower half of the superior vena cava with the azygos vein opening into it, the bifurcation of the trachea and the right and left principal bronchi, the pulmonary artery dividing into its two branches, the right and left pulmonary veins and phrenic nerves, and some bronchial lymph nodes.

Posterior mediastinum

The posterior mediastinum is an irregular triangular space, bounded anteriorly by the pericardium above and the posterior surface of the diaphragm below, posteriorly by the vertebral column from the lower border of the fourth to the twelfth thoracic vertebrae, and laterally by the mediastinal pleura. It contains the thoracic part of the descending aorta, the azygos and hemiazygos veins, the vagus and splanchnic nerves, oesophagus, thoracic duct, and lymph nodes.

VASCULAR SUPPLY AND LYMPHATIC DRAINAGE

ARTERIAL SUPPLY

The skin of the thorax is supplied by direct cutaneous vessels and musculocutaneous perforators which reach the skin primarily via the intercostal muscles, pectoralis major, latissimus dorsi and trapezius. Branches from the thoracoacromial axis, lateral thoracic, internal thoracic, anterior and posterior intercostal, thoracodorsal, transverse cervical, dorsal scapular and circumflex scapular arteries are the major contributing vessels (see Figs 42.4, 54.1, 54.2).

Muscles of the thoracic wall receive their blood supply from the internal thoracic artery (either directly or via the musculophrenic artery), the superior intercostal artery (from the costocervical trunk), superior thoracic artery (from the axillary artery), descending thoracic aorta, and the subcostal artery (Fig. 53.2). Additional contributions come from vessels that supply the proximal muscles of the upper limb, namely suprascapular, superficial cervical, thoracoacromial, lateral thoracic and subscapular arteries.

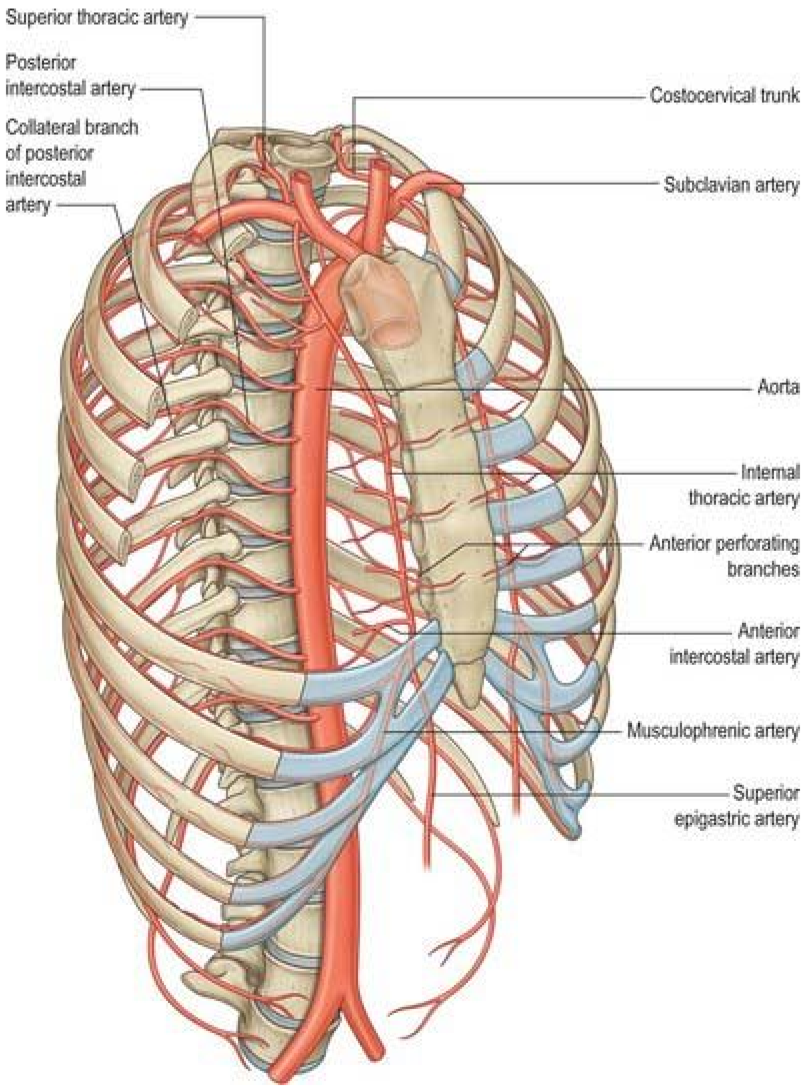
Superior thoracic artery
Posterior intercostal artery
Collateral branch of posterior intercostal artery
Costocervical trunk
Subclavian artery
Aorta
Internal thoracic artery
Anterior perforating branches
Anterior intercostal artery
Musculophrenic artery
Superior epigastric artery

Fig. 53.2 Arteries of the thoracic wall and thoracic aorta.

(From Drake, Vogl, Mitchell, Tibbitts and Richardson 2008.)

The detailed arterial supply of the thoracic viscera is described with the viscera.

VENOUS DRAINAGE

The intercostal veins accompany the similarly named arteries in the intercostal spaces (Fig. 53.3). The small anterior intercostal veins are tributaries of the internal thoracic and musculophrenic veins: the internal thoracic veins drain into the appropriate brachiocephalic vein. The posterior intercostal veins drain backwards and most drain directly or indirectly into the azygos vein on the right and the hemiazygos or hemiazygos veins on the left. The azygos veins exhibit great variation in their origin, course, tributaries, anastomoses and termination.

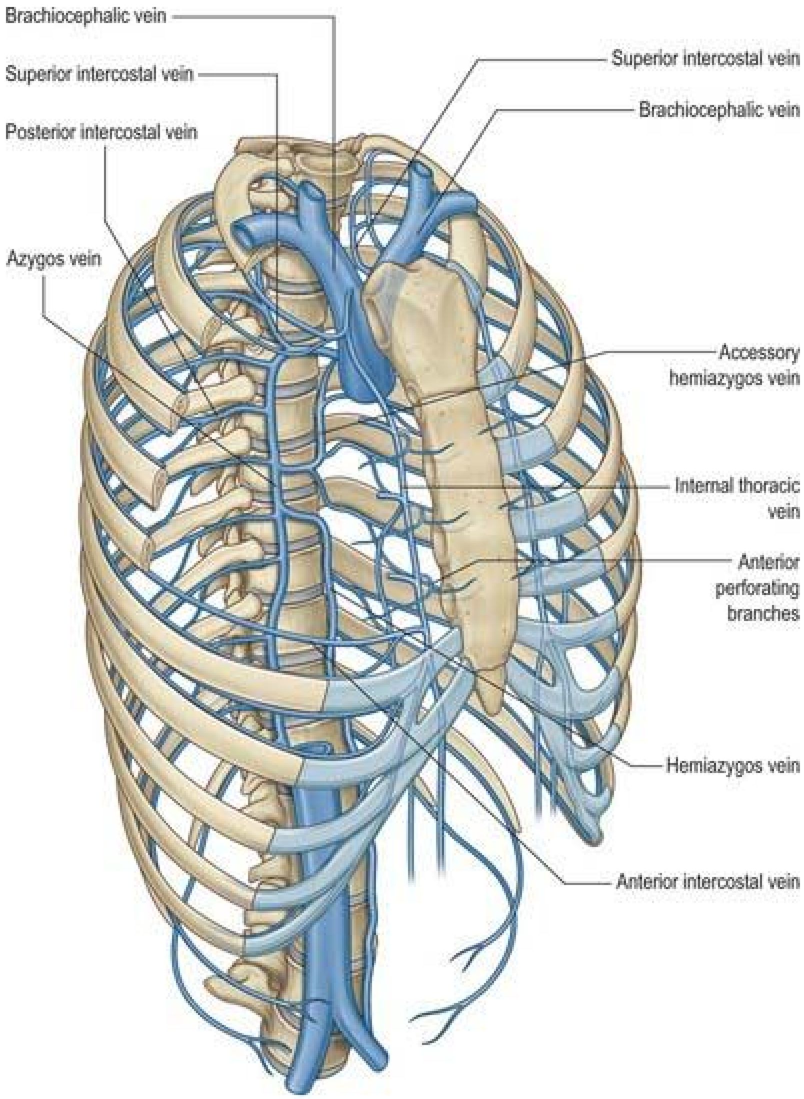
Brachiocephalic vein
Superior intercostal vein
Posterior intercostal vein
Azygos vein
Superior intercostal vein
Brachiocephalic vein
Accessory hemiazygos vein
Internal thoracic vein
Anterior perforating branches
Hemiazygos vein
Anterior intercostal vein

Fig. 53.3 Veins of the thoracic wall and azygos system.

(From Drake, Vogl, Mitchell, Tibbitts and Richardson 2008.)

LYMPHATIC DRAINAGE

Superficial lymphatic vessels of the thoracic wall ramify subcutaneously and converge on the axillary nodes (see Fig. 54.19). Lymph vessels from deeper tissues of the thoracic walls drain mainly to the parasternal, intercostal and diaphragmatic lymphatic nodes.

INNERVATION

THORACIC SPINAL NERVES

There are twelve pairs of thoracic spinal nerves. The ventral rami, unlike their cervical and lumbar counterparts, have retained a largely segmental distribution to the body wall (see Figs 15.12, 54.3, 54.20). The upper eleven lie between the ribs (intercostal nerves), and the twelfth lies below the last rib (subcostal nerve). Each is connected with the adjoining ganglion of the sympathetic trunk by pre- and postganglionic branches (white and grey rami communicantes respectively). Intercostal nerves are distributed primarily to the thoracic and abdominal walls. The greater part of the first thoracic ventral ramus passes into the brachial plexus, together with a variable proportion of the second. The next four ventral supply only the thoracic wall, and the lower five supply both thoracic and abdominal walls. The subcostal nerve is distributed to the abdominal wall and the gluteal skin. Communicating branches link the intercostal nerves posteriorly in the intercostal spaces, and the lower five nerves communicate freely in the abdominal wall. Thoracic dorsal rami divide into medial and lateral branches that supply the intrinsic muscles of the back and the overlying postvertebral skin on a segmental basis (see Ch. 42).

The supraclavicular branches of C4 from the cervical plexus innervate the skin over the clavicle and may communicate with the anterior cutaneous branches of the second thoracic ventral ramus (see Ch. 28).

AUTONOMIC INNERVATION

The autonomic nervous system in the thorax consists of right and left sympathetic trunks and vagus nerves and the cardiac, oesophageal and pulmonary plexuses.

Sympathetic trunks

The ganglionated sympathetic trunks lie anterior to the heads of the ribs; the ganglia are arranged segmentally (see Fig. 55.7). Preganglionic sympathetic axons originate from neurones in the lateral grey column of the spinal cord from T1 to L2, and leave the spinal cord with the corresponding ventral roots as white rami communicantes. Their targets vary. Some enter the sympathetic trunk, where they either synapse in their segmental ganglion or ascend or descend in the trunk to synapse in cervical or lumbar ganglia. Many of the preganglionic axons which originate in the lower thoracic spinal segments (T5–12) do not synapse locally but enter the abdominal cavity as the thoracic splanchnic nerves and synapse either in prevertebral ganglia, especially the coeliac ganglion, or around the medullary chromaffin cells of the suprarenal gland (see Ch. 72). Axons destined for the cervical ganglia are derived from preganglionic neurones in T1.

Vagus nerves in the thorax

Preganglionic parasympathetic fibres arise from neuronal cell bodies in the dorsal motor nucleus of the vagus in the medulla. Those destined for the thoracic viscera travel in the pulmonary, cardiac and oesophageal branches of the vagus and synapse in minute ganglia in the visceral walls. Axons traveling in cardiac branches join the cardiac plexuses and synapse in ganglia distributed over both atria: when stimulated, they slow the cardiac cycle (see Ch. 60). Pulmonary branches contain axons which relay in ganglia of the pulmonary plexuses and are motor (bronchoconstrictor) to the circular non-striated muscle fibres of the bronchi and bronchioles and secretomotor to the mucous glands of the respiratory epithelium.

Autonomic plexuses in the thorax

Cardiac plexus

The cardiac plexus has a superficial component inferior to the aortic arch, lying between it and the pulmonary trunk, and a deep part between the aortic arch and tracheal bifurcation (see Ch. 56). The superficial part is formed by the cardiac branch of the left superior cervical sympathetic ganglion and the lower of the two cervical cardiac branches of the left vagus. The deep part is formed by the cardiac branches of the cervical and upper thoracic sympathetic ganglia and of the vagus and recurrent laryngeal nerves. The only cardiac nerves which do not join it are those that join the superficial part of the plexus. Branches from the cardiac plexuses also form the left and right coronary plexuses and the atrial plexuses.

Pulmonary plexus

The pulmonary plexuses are anterior and posterior to the other structures at the hila of the lungs (see Ch. 57). They are formed by cardiac branches from the second to fifth (or sixth) thoracic sympathetic ganglia and from the vagus, and from cervical sympathetic cardiac nerves. The left plexus also receives branches from the left recurrent laryngeal nerve.

Oesophageal plexus

The oesophageal plexus surrounds the oesophagus below the level of the lung roots (see Ch. 55). Vagal fibres either pass through the plexus or are given off directly by the vagus in the thorax. All fibres relay in the oesophageal wall and are motor to the smooth muscle in the lower oesophagus and secretomotor to mucous glands in the oesophageal mucosa. Vasomotor sympathetic fibres arise from the upper six thoracic spinal cord segments. Those from the upper segments synapse in cervical ganglia; postganglionic axons innervate the vessels of the cervical and upper thoracic oesophagus. Fibres from the lower segments pass directly to the oesophageal plexus or to the coeliac ganglion, where they synapse; postganglionic axons innervate the vessels of the distal oesophagus.

SURFACE ANATOMY

BREAST

In females, the site of the nipple is dependent on the size and shape of the breasts. In the male, the nipple is usually sited in the fourth intercostal space in the midclavicular line. In the young adult of either sex, the nipples are usually positioned 20–23 cm from the jugular notch in the midclavicular line and 20–23 cm apart in the horizontal plane.

SKELETAL LANDMARKS

Anteriorly, the clavicle and sternoclavicular joint are not only palpable, but also visible in all but the most obese individuals (Fig. 53.4). The sternum can be felt throughout its length in the midline, but laterally it may be obscured by pectoralis major. The jugular notch (suprasternal notch) at the superior end of the sternum is easily found, and the trachea may be felt deep to it. The cartilaginous rings are usually palpable: by rolling one’s finger over the trachea, or by using two fingers within the notch, it is possible to assess whether the trachea is in the midline or deviated to one side. The jugular notch lies at the level of the junction between the second and third thoracic vertebrae. The manubriosternal angle is more pronounced in the male than in the female, and is felt at the junction of the manubrium with the body of the sternum. It is a particularly useful landmark because it indicates the medial ends of the second costal cartilages, and is level with the junction of the fourth and fifth thoracic vertebrae. The xiphisternal joint and xiphoid process may be felt at the inferior end of the sternum. The joint usually lies at the level of the ninth thoracic vertebra. Lateral to this, may be felt the costal margin, formed here by the anterior ends of the seventh costal cartilages. The rest of the costal margin is formed by the fused anterior ends of the eighth, ninth and tenth costal cartilages, whereas posteriorly the free ends of the eleventh and twelfth ribs may be palpable. In thin individuals, it is possible to palpate all the ribs from the first down to the costal margin. However, well-developed musculature or the female breast will obscure the ribs anteriorly and the shaft of the first rib (which lies predominantly behind the clavicle).

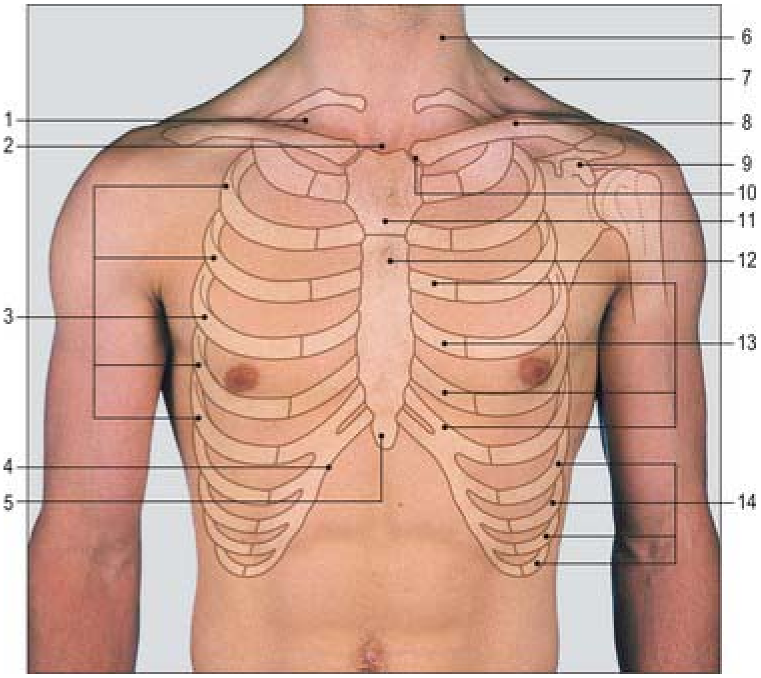

Fig. 53.4 Frontal view of the trunk demonstrating bony and soft tissue structures. **1**. Supraclavicular fossa. **2**. Jugular notch. **3**. True ribs. **4**. Costal margin. **5**. Xiphisternum. **6**. Sternocleidomastoid. **7**. Trapezius. **8**. Clavicle. **9**. Coracoid process. **10**. Sternoclavicular joint. **11**. Manubrium. **12**. Body of sternum. **13**. Costal cartilages. **14**. False ribs.

(Photo by permission from Lumley JSP 2002 Surface Anatomy, 3rd edn. Edinburgh: Churchill Livingstone.)

Posteriorly (Fig. 53.5), the spinous processes of the thoracic vertebrae are easily palpable; the posterior angles of the ribs can be felt lateral to the spinous processes. The surface anatomy of the back and skeletal surface landmarks are described in Chapters 42 and 43.

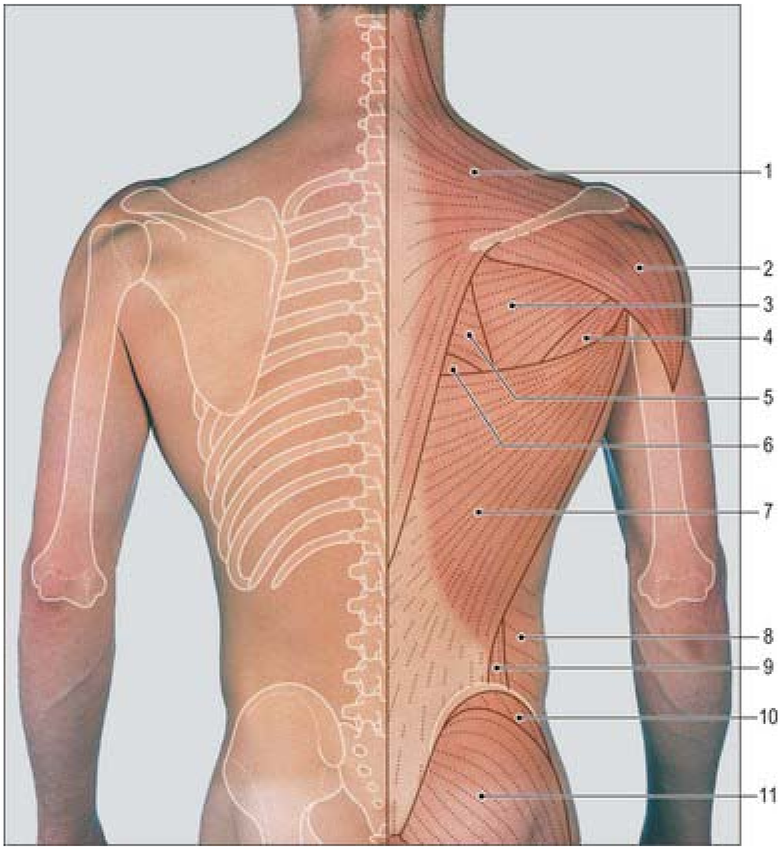

Fig. 53.5 Posterior view of the trunk demonstrating surface anatomy, bony and soft tissue structures. **1**. Trapezius. **2**. Deltoid. **3**. Infraspinatus. **4**. Teres major. **5**. Rhomboid major. **6**. Auscultatory triangle. **7**. Latissimus dorsi. **8**. External oblique. **9**. Lumbar triangle. **10**. Gluteus medius. **11**. Gluteus maximus.

(Photo by permission from Lumley JSP 2002 Surface Anatomy, 3rd edn. Edinburgh: Churchill Livingstone.)

MUSCULOTENDINOUS LANDMARKS

In a muscular subject, pectoralis major, the slips of serratus anterior, and latissimus dorsi, trapezius, external oblique and rectus abdominis are all easily visible. The anterior chest wall of females may be largely obscured by the breasts.

INTRATHORACIC VISCERA

Anteriorly, the manubriosternal joint overlies the concavity of the aortic arch and marks the level at which the trachea bifurcates and the azygos vein enters the superior vena cava. The costal cartilages of the second ribs meet the sternum here, and so the joint offers an accurate point at which to start counting ribs. The transverse thoracic plane, which includes the sternal angle, demarcates the lower border of the superior mediastinum and the point at which the aortic arch receives the ascending aorta (anteriorly) and becomes the descending aorta (posteriorly). At this point, the right and left pleurae are in contact with each other; it is therefore a useful starting point when delineating the surface markings of the parietal pleura (Fig. 53.6A,B).

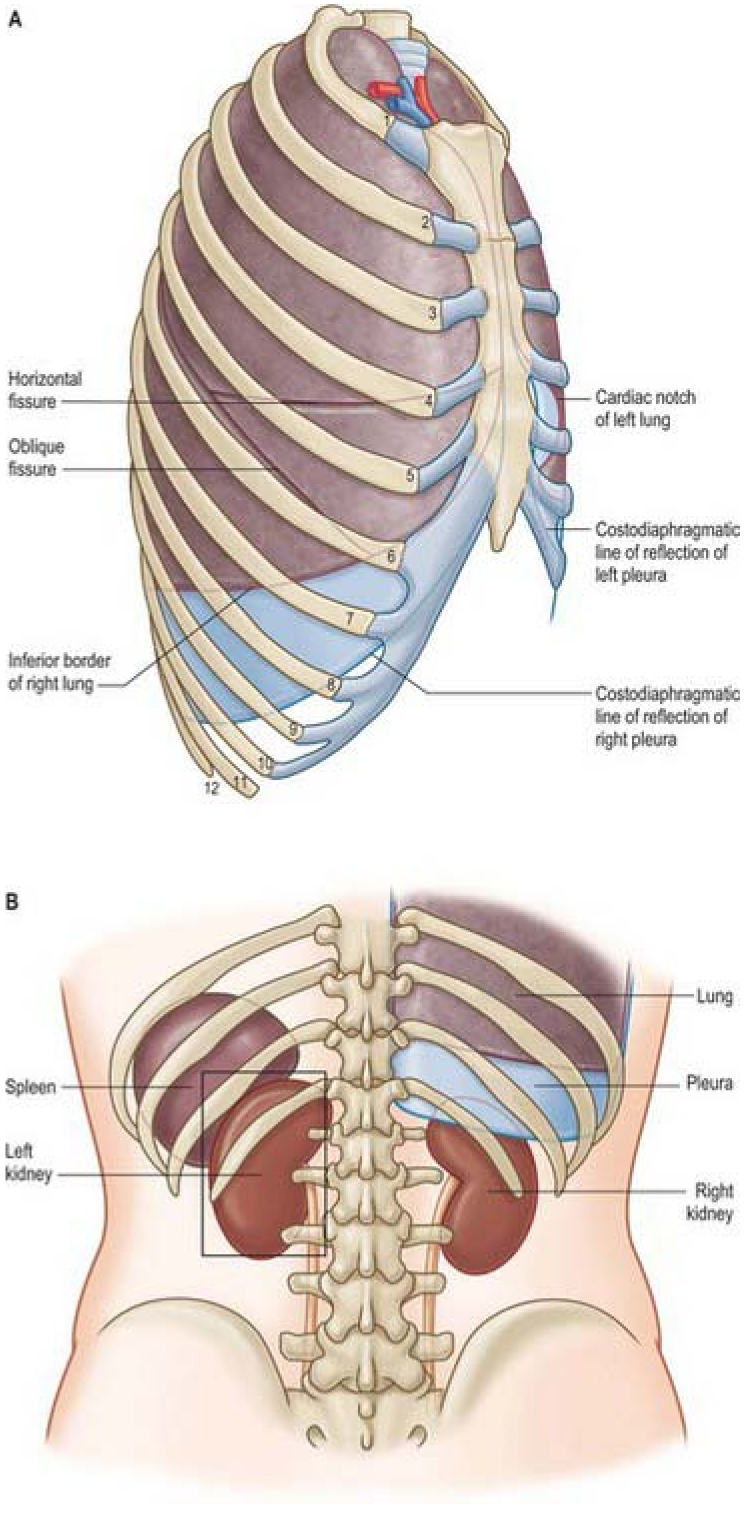
A
1
2
3
4
5
6
7
8
9
10
11
12
Horizontal fissure
Oblique fissure
Inferior border of right lung
Cardiac notch of left lung
Costodiaphragmatic line of reflection of left pleura
Costodiaphragmatic line of reflection of right pleura
B
Spleen
Left kidney
Lung
Pleura
Right kidney

Fig. 53.6 **A**, Relation of the pleura and lungs to the chest wall: right lateral aspect. **B**, Lower limits of the lung and pleura: posterior view. The lower portions of the lung and the pleura are shown on the right side.

Heart

The surface projections to be described below apply to an average adult. It must be appreciated that they are considerably modified by age, sex, stature and proportions, ventilation and posture. The projections of the position of the valves on the surface are not the best sites for their auscultation. The cardiac apex almost corresponds to the apex beat, which is usually visible and always palpable in the fifth intercostal space, slightly medial to the midclavicular line, 9 cm from the midline in average adult males. The apex beat is the most inferolateral point at which a pulsation can be felt; however, the true cardiac apex is a short distance further inferolaterally and does not contact the thoracic wall in systole.

The cardiac sternocostal surface, projected onto the anterior thoracic wall, is a trapezoid. The area of superficial cardiac dullness as mapped out by light percussion is roughly triangular and corresponds to the area of the heart not covered by lung. The borders of the heart, although frequently given as being fixed, are in fact variable and depend largely on the position of the diaphragm and the obesity and build of the patient.

The following borders are usually recognized. The upper border forms a gently sloping line from the second left costal cartilage to the third right costal cartilage. The right border is a gently curved line, convex to the right from the third right to the sixth right costal cartilage, usually 1–2 cm lateral to the sternal edge. The inferior or acute border runs from the sixth right costal cartilage to the apex of the heart, which lies in the fifth left intercostal space approximately in the midclavicular line. The left (‘obtuse’) border extends superomedially, convex laterally, from the apex to meet the second left costal cartilage 1 cm from the left sternal edge. An oblique line joining the sternal end of the third left and sixth right costal cartilages represents the anterior part of the coronary sulcus, which separates the right atrium from the right ventricle (the left atrium lies behind the heart). The left and right borders can be identified by heavy percussion.

The surface projection of the anterior part of the atrioventricular groove is an oblique line that joins the sternal ends of the third left and sixth right costal cartilages and separates the atrial and ventricular areas. Although in different planes, the projections of the cardiac valves are also sited along or close to this line (see Fig. 56.6).

The pulmonary orifice lies partly behind the superior border of the third left costal cartilage, and partly behind the left third of the sternum. It is represented by a horizontal line, 2.5 cm long, which crosses cartilage and sternum. Parallel lines from the ends of this line, up to the second left costal cartilage, indicate the site of the pulmonary trunk.

The aortic orifice is below and a little right of the pulmonary, and is marked by a line, 2.5 cm long, running from the medial end of the third left intercostal space downward to the right. Two parallel lines from the ends of this line, slanting up to the right half of the manubrio-sternal joint, outline the location of the ascending aorta.

The tricuspid valvar orifice is represented by a line, 4 cm long, starting near the midline just below the level of the fourth right costal cartilage, and passing down and slightly to the right. The centre of this line should be level with the middle of the fourth right intercostal space.

The mitral orifice is behind the left half of the sternum opposite the fourth left costal cartilage, and is represented by a line, 3 cm long, descending to the right.

The sites of auscultation for the cardiac valves do not correspond directly to the surface anatomy of the valves, because the intensity of the sounds is influenced by direction of blood flow, which carries the sound with it. Thus, convenient sites at which to apply the stethoscope bell or diaphragm are: the sternal end of the second left intercostal space (pulmonary area); the sternal end of the second right intercostal space (aortic area); near the cardiac apex (mitral area); and over the left lower sternal border, at the level of the fifth intercostal spaces (tricuspid area) (see Fig. 56.6).

Great vessels

The aortic arch lies predominantly behind the manubrium sterni. Starting at the aortic valve (behind the lower border of the third left costal cartilage), the ascending aorta curves forwards, upwards and to the right, to become the aortic arch behind the right half of the manubrium at the level of the second right costal cartilage. It continues to ascend behind the right side of the manubrium sterni, arching over the transthoracic plane and descending such that the aortic knuckle protrudes just to the left of the manubrium sterni in the first intercostal space. The pulmonary trunk and tracheal bifurcation lie within its concavity. The brachiocephalic artery arises approximately behind the centre point of the manubrium and ascends to the right sternoclavicular joint. The superior vena cava descends predominantly behind, but also just to the right of, the right manubrial border and enters the right atrium at the level of the third right costal cartilage. The short right brachiocephalic vein descends almost vertically from behind the medial end of the clavicle just lateral to the right sternoclavicular junction, whereas the much longer left brachiocephalic vein passes almost horizontally behind the superior portion of the manubrium sterni. Both join behind the first right costal cartilage to form the superior vena cava, which descends as a band, 2 cm wide, along the right sternal margin, reaching the right atrium at the level of the third right costal cartilage.

Lungs and pleurae

Anteriorly, the apex of the lung is approximately 2.5 cm above the centre of the medial one-third of the clavicle; posteriorly, it lies at the level of the seventh cervical vertebra. The surface markings of the apical dome and costovertebral border of the lung correspond to those of the parietal pleura. The anterolateral surface projection of the lung may be represented by a curved line that crosses the midclavicular line at the level of the sixth rib, and the midaxillary line at the level of the eighth rib. On inspiration, the lower border of the lung moves downwards, from the level of the tenth thoracic vertebra to the level of the twelfth thoracic vertebra (these levels are approximate). In full expiration, the lower border of the lung retreats anteriorly a short distance from the retrosternal costomediastinal recess; laterally, the lower margin of the lung may rise 5 cm above the parietal pleural reflection (the costodiaphragmatic recess).

Trachea, bronchi

The trachea originates at the level of the cricoid cartilage (C6), and usually runs in the midline. It is palpable within the suprasternal notch, where it may be felt either by rolling one finger over its convex surface or by defining its lateral extent with two fingers. A shift to one side indicates that the mediastinum has either been pulled over to that side by loss of lung volume, or pushed over, e.g. by a large pneumothorax or pleural effusion. The trachea bifurcates at the level of the sternal angle; the posterior landmark for the bifurcation is the fourth thoracic vertebra.

Fissures

On either side, the upper and lower lobes of the lung are separated by the oblique fissure. This may be marked by a line running from the posterior end of the third rib downwards and forwards to cross the fifth rib in the midaxillary line and then to the sixth costal cartilage at the midclavicular line (7–8 cm lateral to the midline). As a convenient approximation, the oblique fissure follows the medial border of the scapula when the arm is in full abduction. The left oblique fissure is slightly more vertical than the right.

The horizontal fissure, between the middle and upper lobes, lies at the level of the fourth costal cartilage on the right. It starts from the anterior border of the lung and passes posterolaterally to meet the oblique fissure: the horizontal fissure therefore extends from the fifth rib in the midaxillary line to the fourth rib at the right sternal border. The upper and middle lobes lie anterior to the oblique fissure and so are best examined from the front of the chest, whereas the lower lobes lie posteriorly and should be examined from the back of the chest. The right middle lobe may be projected onto the chest wall as a triangular surface, where the three points of the triangle are represented by the fourth rib at the right parasternal edge, the fifth rib at the midaxillary line, and the sixth rib at the midclavicular line.

Pleural reflections

Starting in the midline at the manubriosternal joint, the anterior reflections of the parietal pleura may be traced superiorly along a line that diverges from the midline and extends up and outwards to the apex of the pleural cavity. This point lies 3–4 cm above the anterior end of the first rib, on a level with the posterior end of the rib; its surface marking is usually 2.5 cm above the centre of the medial one-third of the clavicle. The parietal pleura is intimately fused with the inner aspect of the thoracic cavity, and it can be followed laterally and inferiorly down the inner aspect of the chest wall to the level of the tenth rib in the midaxillary line. Followed medially, the pleura covers the diaphragm; its position will therefore vary according to the phase of ventilation.

The costodiaphragmatic reflections of the pleurae can be followed anteriorly from the midaxillary line towards the midline. On the right, the pleura crosses the eighth rib in the midclavicular line, passes to the xiphisternum and then ascends to the manubriosternal joint. On the left, the pleura does not reach the midline, but turns superiorly at the anterior end of the sixth rib, 3–5 cm from the midline, and passes up to the level of the fourth costal cartilage. This deviation produces an area between the heart and the sternum that is free of pleura; a needle puncture of the heart may be performed at this site without risk of damaging the pleura. The right and left pleurae meet at the level of the fourth costal cartilage and maintain contact up to the level of the second costal cartilage.

Viewed from the back, the medial edge of the pleura may be followed along a line joining the transverse processes of the second to the twelfth thoracic vertebrae. It extends horizontally laterally, and crosses the twelfth and eleventh ribs to meet the tenth rib in the midaxillary line (Fig. 53.6A,B).

CHAPTER 54

Chest wall and breast

The chest wall surrounds the thoracic cavity. The skin and soft tissue cover a musculoskeletal frame consisting of 12 pairs of ribs which articulate with 12 thoracic vertebrae posteriorly, and (except for the last two pairs of ribs) with the sternum anteriorly, via their costal cartilages; intrinsic muscles and muscles which connect the chest wall with the upper limb and the vertebral column; numerous blood and lymphatic vessels and nerves which supply the components of the musculoskeletal frame and the overlying skin and breast tissue.

SKIN AND SOFT TISSUE

SKIN

Vascular supply

Arteries

The skin of the thorax is supplied by a combination of direct cutaneous vessels and musculocutaneous perforators which reach the skin primarily via the intercostal muscles, pectoralis major, latissimus dorsi and trapezius. Branches from the thoracoacromial axis, lateral thoracic artery, internal thoracic artery, anterior and posterior intercostal arteries, thoracodorsal, transverse cervical/dorsal scapular and circumflex scapular arteries are the major contributing vessels (Figs 54.1, 54.2; see Fig. 42.4).

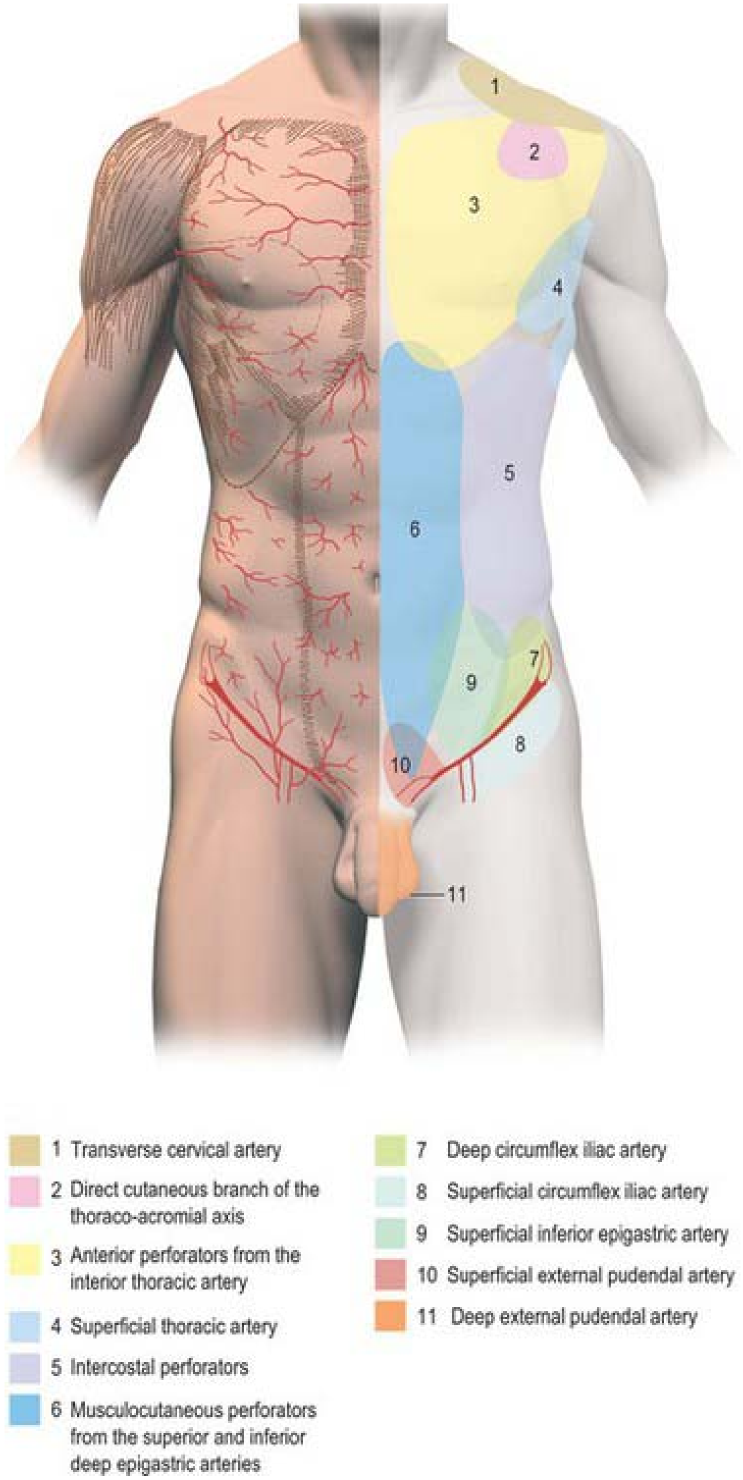
1
2
3
4
5
6
7
9
8
10
11
1 Transverse cervical artery
2 Direct cutaneous branch of the thoraco-acromial axis
3 Anterior perforators from the interior thoracic artery
4 Superficial thoracic artery
5 Intercostal perforators
6 Musculocutaneous perforators from the superior and inferior deep epigastric arteries
7 Deep circumflex iliac artery
8 Superficial circumflex iliac artery
9 Superficial inferior epigastric artery
10 Superficial external pudendal artery
11 Deep external pudendal artery

Fig. 54.1 Anatomical territories of cutaneous blood vessels on the anterior trunk.

(By permission from Cormack GC, Lamberty BGH 1994 The Arterial Anatomy of Skin Flaps, 2nd edn. Edinburgh: Churchill Livingstone.)

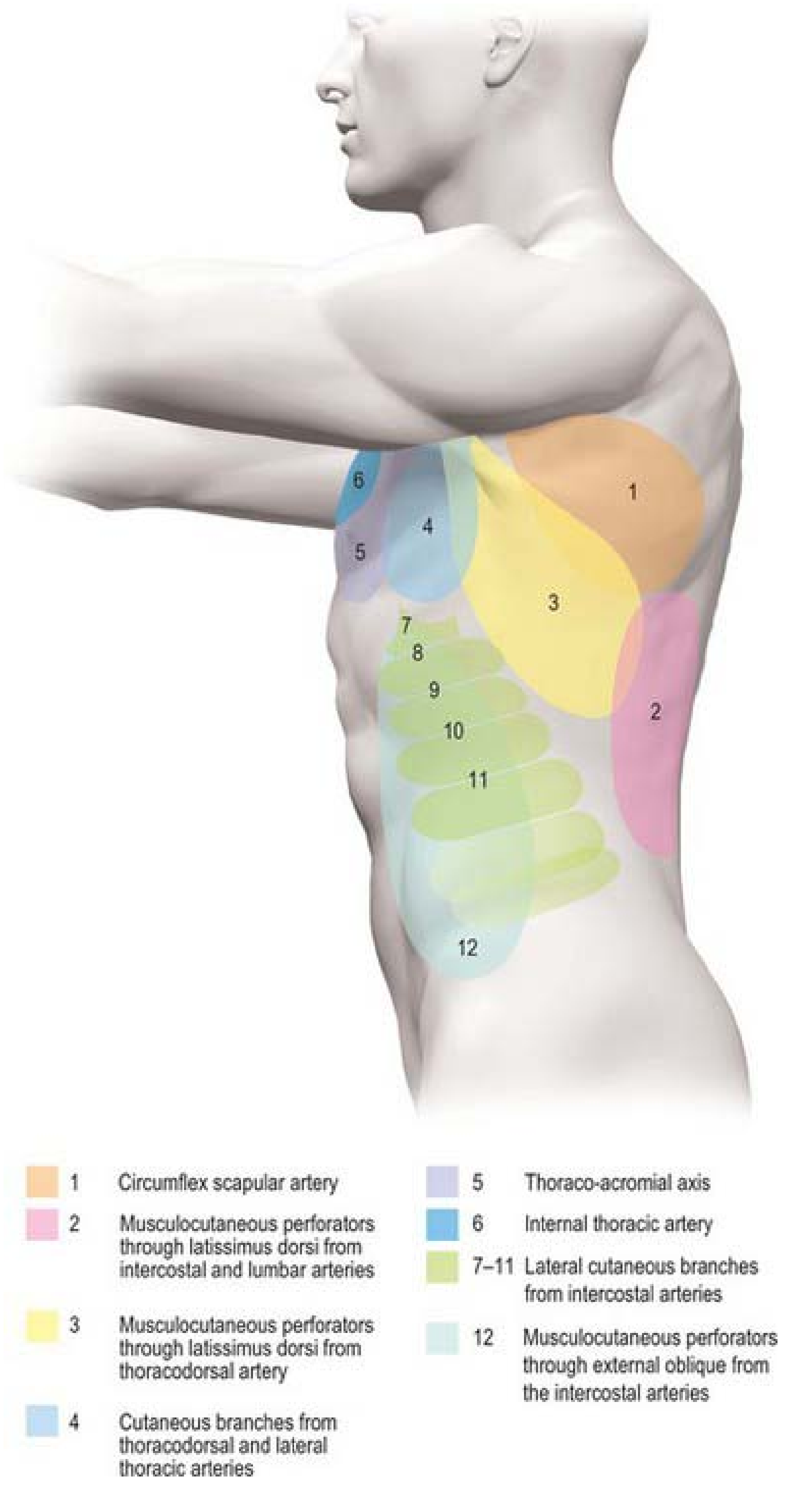
6
4
5
1
3
7
8
9
10
11
2
12
1 Circumflex scapular artery
2 Musculocutaneous perforators through latissimus dorsi from intercostal and lumbar arteries
3 Musculocutaneous perforators through latissimus dorsi from thoracodorsal artery
4 Cutaneous branches from thoracodorsal and lateral thoracic arteries
5 Thoraco-acromial axis
6 Internal thoracic artery
7–11 Lateral cutaneous branches from intercostal arteries
12 Musculocutaneous perforators through external oblique from the intercostal arteries

Fig. 54.2 Anatomical territories of cutaneous blood vessels on the lateral trunk.

(By permission from Cormack GC, Lamberty BGH 1994 The Arterial Anatomy of Skin Flaps, 2nd edn. Edinburgh: Churchill Livingstone.)

The anterior aspect of the thoracic skin is supplied by the thoracoacromial axis, the internal thoracic arteries, perforating branches from the intercostal arteries and branches from the lateral thoracic and superficial thoracic arteries. The thoracoacromial axis supplies the skin primarily via musculocutaneous perforators from its pectoral branch, which reach the skin through pectoralis major. In addition, direct cutaneous branches arise from the acromial and deltoid branches. The internal thoracic artery sends direct perforating branches to the skin of the upper six intercostal spaces, accompanied by the cutaneous branches of the anterior intercostal nerves. The branches reach the skin after passing through pectoralis major and travelling laterally in the subcutaneous fat as direct cutaneous vessels: the second intercostal perforator is usually the largest.

The lateral aspect of the thoracic skin is supplied by the lateral thoracic, superficial thoracic and lateral cutaneous branches of the intercostal arteries. The lateral thoracic artery gives off direct cutaneous branches to the lateral chest wall in addition to musculocutaneous branches that pass through pectoralis major.

The posterior aspect of the thoracic skin is supplied by the medial and lateral dorsal cutaneous branches of the posterior intercostal arteries (which reach the skin by passing through erector spinae and latissimus dorsi), musculocutaneous perforating branches from the superficial cervical artery and the transverse cervical/dorsal scapular artery (via trapezius), musculocutaneous perforating branches from the thoracodorsal artery and the intercostal arteries (via latissimus dorsi), and direct cutaneous branches from the circumflex scapular artery.

Veins

The intercostal veins accompany the similarly named arteries in the intercostal spaces (see Fig. 53.3). The small anterior intercostal veins are tributaries of the internal thoracic and musculophrenic veins; the internal thoracic veins drain into the appropriate brachiocephalic vein. The posterior intercostal veins drain backwards and most drain directly or indirectly into the azygos vein on the right and the hemiazygos or accessory hemiazygos veins on the left. The azygos veins exhibit great variation in their origin, course, tributaries, anastomoses and termination (see Ch. 55).

Lymphatic drainage

Superficial lymphatic vessels of the thoracic wall ramify subcutaneously and converge on the axillary nodes (see p. 928, Figs 54.19, 54.21). Lymph vessels from the deeper tissues of the thoracic walls drain mainly to the parasternal, intercostal and diaphragmatic lymphatic nodes.

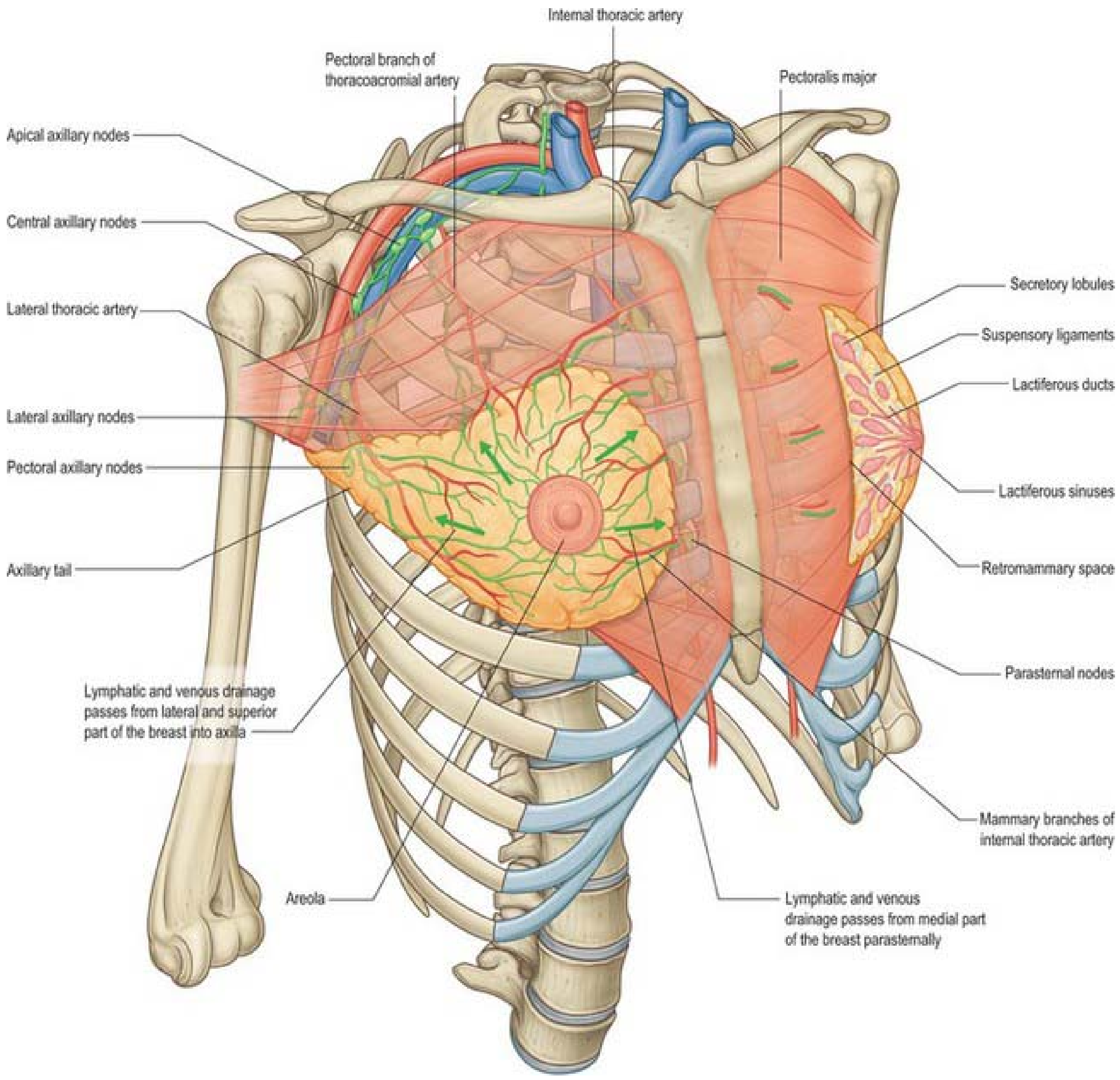
Internal thoracic artery
Pectoral branch of thoracoacromial artery
Pectoralis major
Apical axillary nodes
Central axillary nodes
Lateral thoracic artery
Lateral axillary nodes
Pectoral axillary nodes
Axillary tail
Secretory lobules
Suspensory ligaments
Lactiferous ducts
Lactiferous sinuses
Retromammary space
Parasternal nodes
Lymphatic and venous drainage passes from lateral and superior part of the breast into axilla
Mammary branches of internal thoracic artery
Areola
Lymphatic and venous drainage passes from medial part of the breast parasternally

Fig. 54.19 The relations of the breast.

(From Drake, Vogl and Mitchell 2005.)

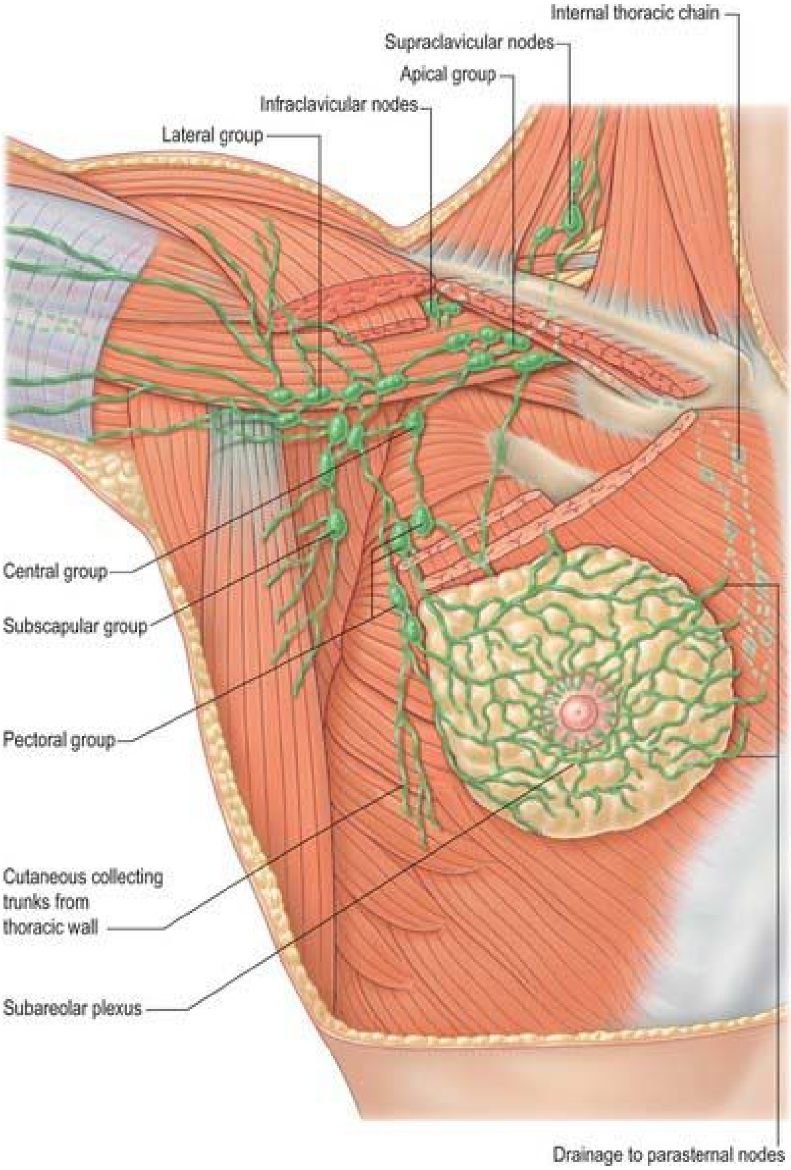
Internal thoracic chain
Supraclavicular nodes
Apical group
Infraclavicular nodes
Lateral group
Central group
Subscapular group
Pectoral group
Cutaneous collecting trunks from thoracic wall
Subareolar plexus
Drainage to parasternal nodes

Fig. 54.21 Lymph vessels of the breast and the axillary lymph nodes.

Innervation

The skin of the thorax is supplied by cutaneous branches of cervical and thoracic nerves in consecutive, curved zones, the upper almost horizontal and the lower oblique. On the upper ventral thoracic aspect, the third and fourth cervical areas adjoin the first and second thoracic areas (Fig. 54.3; see Fig. 42.3) because the intervening nerves provide the sensory and motor supply to the upper limb. There is a similar, but less extensive, posterior ‘gap’: most of the skin of the back of the thorax is supplied by the dorsal rami of the thoracic nerves. The subcostal margin is supplied by the seventh thoracic nerve.

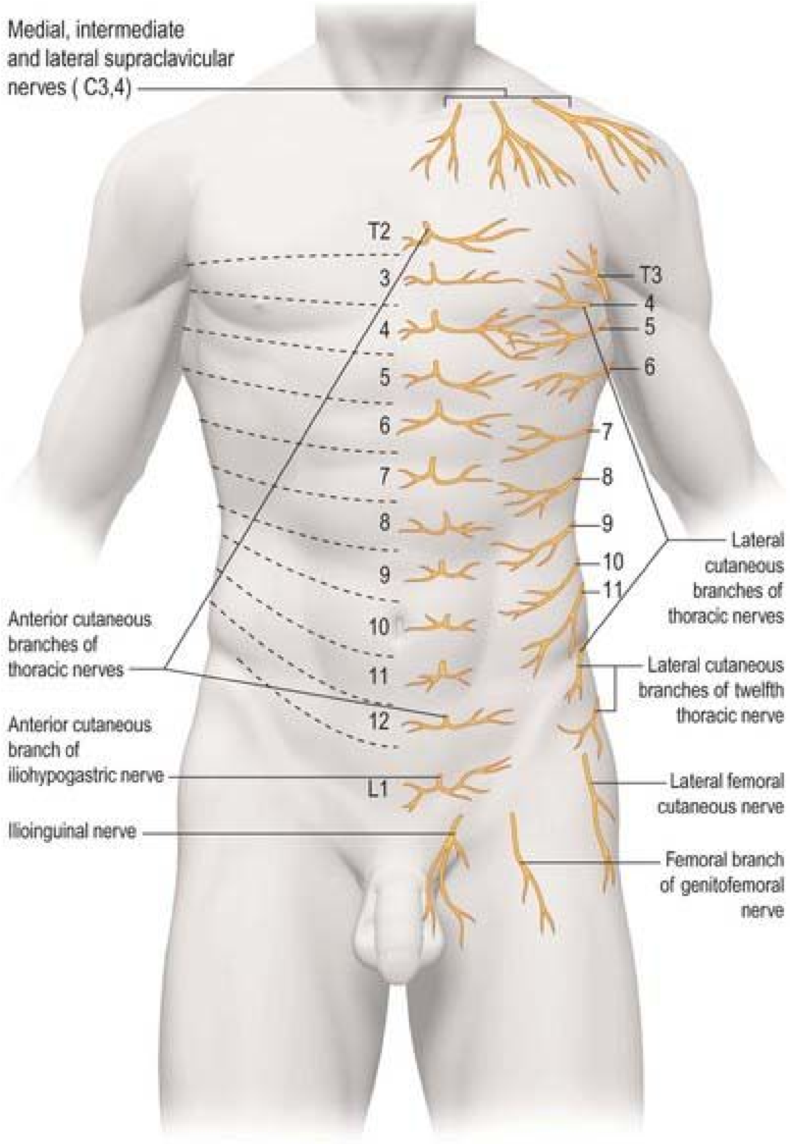
Medial, intermediate and lateral supraclavicular nerves (C3,4)
T2
3
4
5
6
7
8
9
10
11
12
L1
T3
4
5
6
7
8
9
10
11
Lateral cutaneous branches of thoracic nerves
Anterior cutaneous branches of thoracic nerves
Lateral cutaneous branches of twelfth thoracic nerve
Anterior cutaneous branch of iliohypogastric nerve
Lateral femoral cutaneous nerve
Ilioinguinal nerve
Femoral branch of genitofemoral nerve

Fig. 54.3 The approximate segmental distribution of the cutaneous nerves on the front of the trunk. The contribution from the first thoracic spinal

nerve is not shown and the considerable overlap that occurs between adjacent segments is not indicated.

The ventral rami of the first to the eleventh thoracic nerves pass into the intercostal spaces. Each intercostal nerve gives off a lateral cutaneous branch, which arises beyond the angle of the ribs and divides into anterior and posterior branches, and terminates near the sternum in an anterior cutaneous branch (see Fig. 54.18).

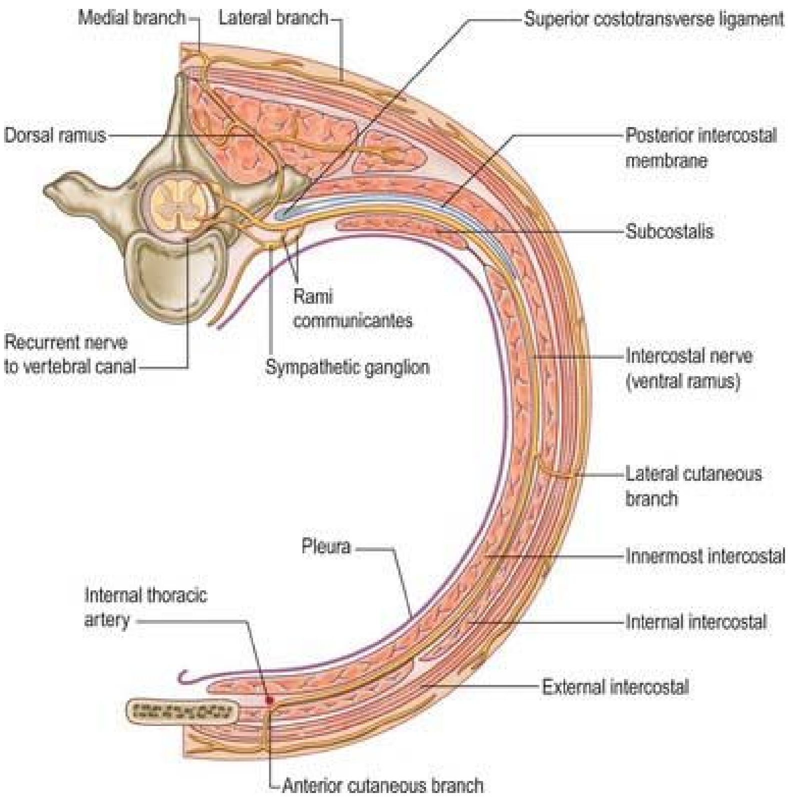
Medial branch
Lateral branch
Superior costotransverse ligament
Dorsal ramus
Posterior intercostal membrane
Subcostalis
Rami communicantes
Recurrent nerve to vertebral canal
Sympathetic ganglion
Intercostal nerve (ventral ramus)
Lateral cutaneous branch
Pleura
Innermost intercostal
Internal thoracic artery
Internal intercostal
External intercostal
Anterior cutaneous branch

Fig. 54.18 The course of a typical intercostal nerve. The muscular and the collateral branches are not shown.

Branches of the supraclavicular nerve, which originates from the third and fourth cervical nerve roots, supply the skin in the upper pectoral region. Most of the first thoracic nerve joins the brachial plexus: it gives off a small inferior branch, which becomes the first intercostal nerve. The lateral cutaneous branch of the second intercostal nerve supplies the skin of the axilla and is known as the intercostobrachial nerve. The costal margin is supplied by a branch from the seventh thoracic nerve, and the tenth thoracic nerve supplies the skin of the abdomen at the level of the umbilicus. The seventh to eleventh thoracic nerves supply the skin of the thoracic wall as they pass anteriorly and inferiorly; they continue beyond the costal cartilages and supply the skin and subcutaneous tissues of the abdominal wall. The subcostal nerve follows the inferior border of the twelfth rib and supplies the skin of the lower abdominal wall (Fig. 54.3).

SOFT TISSUE

Superficial fascia

The superficial fascia lies below the skin. It consists primarily of fat and is only loosely attached to the skin, an arrangement that allows some movement of the underlying structures. Small blood vessels and nerves perforate the superficial fascia to supply the skin.

The breast lies within the superficial fascia and is described later in this chapter.

Deep fascia

The deep fascia is a tough and fibrous membrane that allows some movement of structures over one another.

Clavipectoral fascia

The clavipectoral fascia is a sheet of deep fascia that extends between the clavicle and pectoralis minor, surrounds subclavius and extends medially to the first rib.

BONE AND CARTILAGE

The 12 thoracic vertebrae and their associated intervertebral discs are described in detail in Chapter 42.

STERNUM

The sternum consists of a cranial manubrium, an intermediate body (mesosternum) and a caudal xiphoid process (Figs 54.4, 54.5). Until puberty, the mesosternum consists of four sternebrae, which, from their costal relations, appear to be intersegmental. The total length of the sternum is approximately 17 cm in males, less in females. The ratio between manubrial and mesosternal lengths differs between the sexes. Growth may continue beyond the third decade and possibly throughout life.

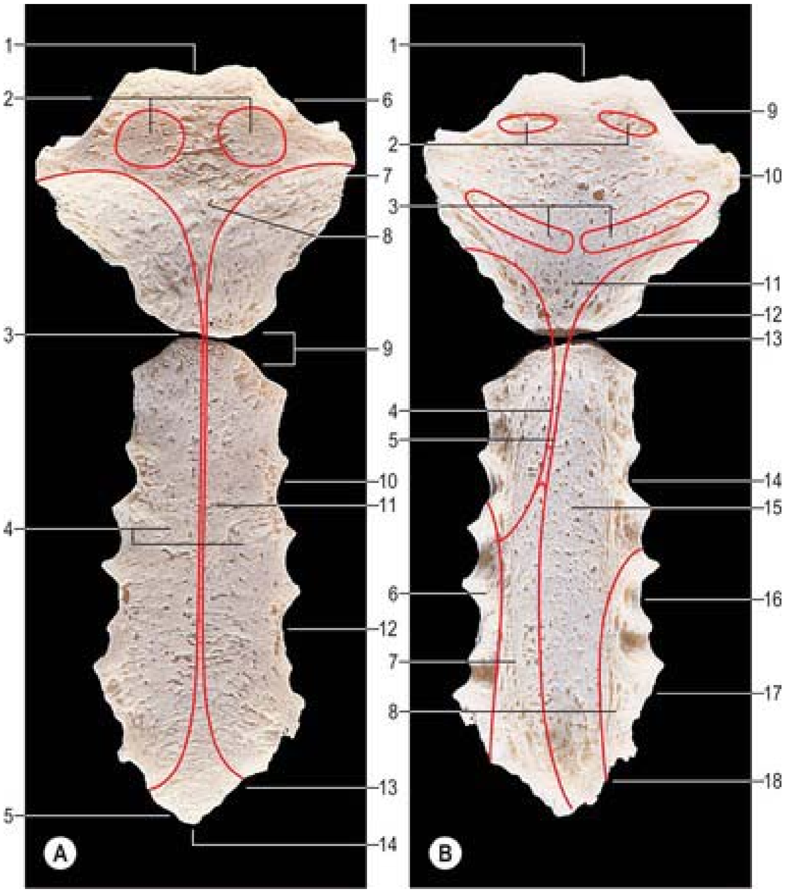

Fig. 54.4 The sternum. **A**, Anterior aspect. **B**, Posterior aspect.
Part A: 1. Jugular notch. **2**. Attachment for sternocleidomastoid. **3**. Sternal angle and manubriosternal joint. **4**. Attachment for pectoralis major. **5**. Notch for seventh costal cartilage. **6**. Clavicular notch. **7**. Notch for first costal cartilage **8**. Manubrium. **9**. Notch for second costal cartilage. **10**.

Notch for third costal cartilage. **11**. Body of sternum. **12**. Notch for fourth costal cartilage. **13**. Notch for sixth costal cartilage. **14**. Xiphisternal joint.

Part B: 1. Jugular notch. **2**. Attachment for sternohyoid. **3**. Attachment for sternothyroid. **4**. Edge of area covered by left pleura. **5**. Edge of area covered by right pleura. **6**. Attachment for transversus thoracis. **7**. Area in contact with pericardium. **8**. Attachment for transversus thoracis. **9**. Clavicular notch. **10**. Notch for first costal cartilage. **11**. Manubrium. **12**. Notch for second costal cartilage. **13**. Sternal angle and manubriosternal joint. **14**. Notch for third costal cartilage. **15**. Body of sternum. **16**. Notch for fourth costal cartilage. **17**. Notch for fifth costal cartilage. **18**. Notch for seventh costal cartilage.

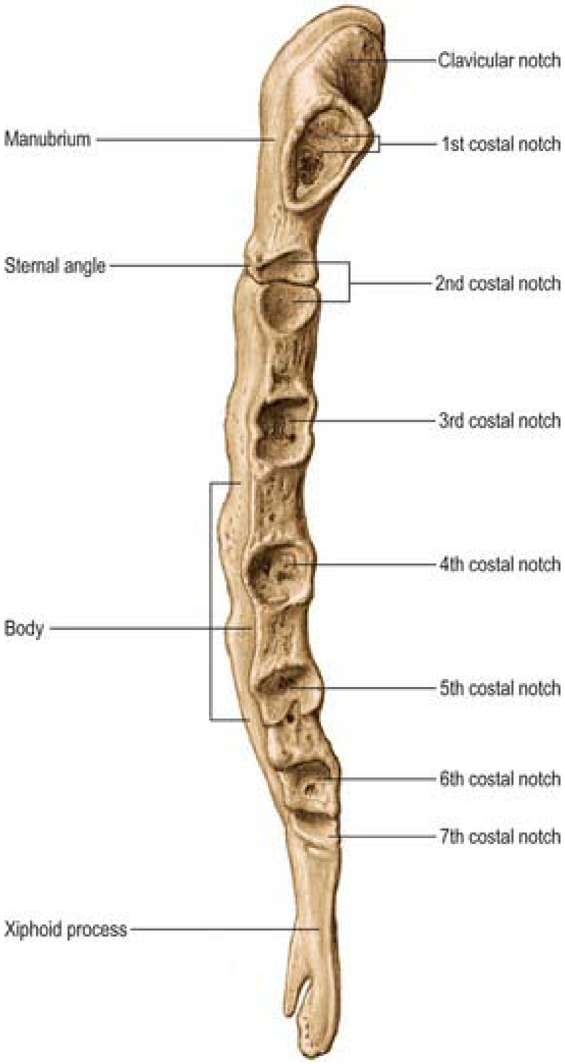
Clavicular notch
Manubrium
1st costal notch
Sternal angle
2nd costal notch
3rd costal notch
4th costal notch
Body
5th costal notch
6th costal notch
7th costal notch
Xiphoid process

Fig. 54.5 The sternum, left lateral aspect.

(From Sobotta 2006.)

In natural stance, the sternum slopes down and slightly forwards. It is convex in front, concave behind, and broadest at the junction with the first costal cartilages. It is narrow at the manubriosternal joint, below which it widens to its articulation with the fifth cartilages, and narrows again below this.

The sternum contains highly vascular trabecular bone enclosed by a compact layer that is thickest in the manubrium between the clavicular notches. Centrally, the bone is lightly constructed, whereas laterally the trabeculae are thicker and wider. The medulla contains haemopoietic bone marrow.

Manubrium

The manubrium is level with the third and fourth thoracic vertebrae. It is broad and thick above, and narrows to its junction with the body. The anterior surface is smooth, transversely convex and vertically concave, and the posterior surface is concave and smooth. The superior border is thick, and contains a central jugular (suprasternal) notch between two oval fossae, the clavicular notches, which are directed up and posterolaterally for articulation with the sternal ends of the clavicles. Fibres of the interclavicular ligament are attached to the jugular notch. The inferior border, oval and rough, carries a thin layer of cartilage for articulation with the body. The lateral borders are marked above by a depression for the first costal cartilage and below by a small articular demifacet, which articulates with part of the second costal cartilage. The narrow curved edge descends medially between these facets.

Unlike all the other sternocostal joints, the manubriocostal joint between the manubrium and the first costal cartilage is an unusual form of synarthrosis.

Body

The body is level with the fifth to ninth thoracic vertebrae. It is longer, narrower and thinner than the manubrium, and is broadest near its lower end. The anterior surface is nearly flat and faces slightly upwards. It bears three variable transverse ridges, which mark the levels of fusion of its four sternebrae. A sternal foramen, of varying size and form, may occur between the third and fourth sternebrae. The posterior surface, slightly concave, also displays three less distinct transverse lines. The oval upper end articulates with the manubrium at the level of the sternal angle (manubriosternal joint), which lies opposite the inferior border of the fourth vertebral body. The manubriosternal joint is marked by a posterior transverse groove and is palpable anteriorly as a ridge (Fig. 54.5).

The lower end of the body is narrow and continuous with the xiphoid process. On each lateral border, at its superior angle, a small notch articulates with part of the second costal cartilage (Fig. 54.4). Below this, four costal notches articulate with the third to sixth costal cartilages. The inferior angle bears a small facet which, together with the xiphoid process, articulates with the seventh costal cartilage. Between these articular depressions, a series of curved edges diminish in length downwards and form the anterior limits of the intercostal spaces.

Xiphoid process (xiphisternum)

The xiphoid process is in the epigastrium. It is the smallest and most variable sternal element, and may be broad and thin, pointed, bifid, perforated, curved or deflected. The xiphoid is cartilaginous in youth, but more or less ossified in adults. It is continuous with the lower end of the body at the xiphisternal joint. Anterior to its superolateral angles there are demifacets that articulate with parts of the seventh costal cartilages (Fig. 54.5).

Muscle attachments

The sternal ends of pectoralis major and sternocleidomastoid are attached to the anterior surface of the manubrium. Sternothyroid is attached to the posterior surface, opposite the first costal cartilage, and the most medial fibres of sternohyoid are attached above sternothyroid. The articular capsules of the sternocostal joints and sternal fibres of pectoralis major are attached to the anterior surface of the body. Transversus thoracis (sternocostalis) is attached to its posterior surface. The external intercostal membranes are attached to the borders of the body between the costal facets. The most medial fibres of rectus abdominis and the aponeuroses of external and internal oblique are attached to the anterior surface of the xiphoid. The linea alba is attached to its lower end, and the aponeuroses of internal oblique and transversus abdominis are attached to its borders. Slips of the diaphragm are attached to its posterior aspect, and the sternum is here related to the liver.

Vascular supply

The internal thoracic artery provides the main blood supply for the sternum. A sternal network of vessels derived from the internal thoracic arteries provides a network of perforating arteries at the level of each intercostal space. An anterior network formed by anastomoses between anterior superior and anterior inferior sternal branches and laterosternal and anterosternal arches provides branches that go directly into the sternum. A similar network of vessels exists posteriorly and is formed by anastomoses between posterior superior and posterior inferior vessels and laterosternal and retrosternal arches. The posterior network is more highly developed than the anterior system; these networks are particularly developed at the level of the fourth and fifth intercostal spaces.

The venous network is less developed and formed mainly by large vessels. The inframedullary network of sinuses form a network in the bone and then drain into the venous system. They are transcortical veins, and drain either into the peripheral sternal networks or into the internal thoracic vein.

Innervation

The manubrium is supplied by the anterior branch of the supraclavicular nerve and the anterior cutaneous branch of the first intercostal nerve, whereas the body of the sternum is supplied largely by anterior branches of the intercostal nerves. The anterior branch of the phrenic nerve runs anteromedially from the diaphragm and supplies the lower portion of the sternum with its contralateral counterpart.

Ossification

The sternum is formed by fusion of two cartilaginous sternal plates flanking the median plane. The arrangement and number of centres of ossification vary according to the level of completeness and time of fusion of the sternal plates, and to the width of the adult bone. Incomplete fusion leaves a sternal foramen. The manubrium is ossified from one to three centres appearing in the fifth fetal month. The first and second sternebrae usually ossify from single centres that appear at about the same time (Fig. 54.6A). Centres in the third and fourth sternebrae are commonly paired, and appear in the fifth and sixth months, respectively, but one of either pair may be delayed until the seventh or even eighth month, and the fourth sternebral centre may be absent. The xiphoid process begins to ossify in the third year or later. In some sterna, all centres are single and median; in others, the manubrial centre is single and the sternebral centres are all paired, symmetric or asymmetric. Union between mesosternal centres begins at puberty and proceeds from below upwards: by the age of 25 years, they are all united (Fig. 54.6B).

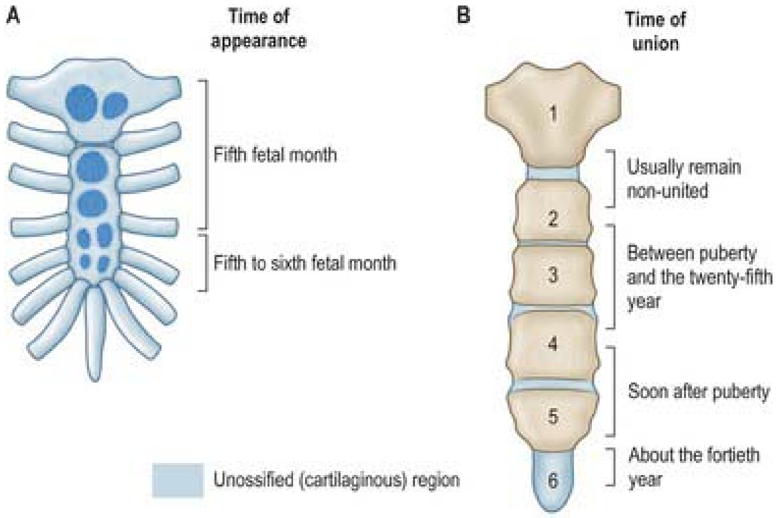
A
Time of appearance
Fifth fetal month
Fifth to sixth fetal month
Unossified (cartilaginous) region
B
Time of union
1
2
3
4
5
6
Usually remain non-united
Between puberty and the twenty-fifth year
Soon after puberty
About the fortieth year

Fig. 54.6 The ossification of the sternum. **A**, Before birth. **B**, After birth.

Suprasternal ossicles, paired or single, occur sometimes. They may fuse to the manubrium or articulate posteriorly at the lateral border of the jugular notch. When well formed, they are pyramidal, and their base is articular. The ossicles are cartilaginous at birth, and ossify during adolescence.

Pectus excavatum and carinatum

Pectus excavatum occurs to some extent in about 1 in 500 live births. It is a depression of the sternum and costal cartilage that results in a funnel-shaped chest. The lower costal cartilages and the body of the sternum are depressed and there is some asymmetric curving of the ribs posteriorly. There is frequently an abnormal posture with dorsal lordosis, and some patients also develop a scoliosis. The deformity is either found at birth or occurs early in life: the majority of affected individuals show signs of the abnormality in the first 12 months of life. The aetiology is unknown, but some cases are associated with conditions such as Marfan’s syndrome, in which the connective tissue is abnormal.

Pectus carinatum is the anterior protrusion of the sternum or a pigeon chest. The deformity is less common than pectus excavatum, and although present in early childhood, it usually progresses during adolescence and then remains the same from age 18 throughout adulthood.

CLAVICLE

The clavicle is described in Chapter 46.

RIBS

The ribs are 12 pairs of elastic arches (Fig. 54.7). They articulate posteriorly with the vertebral column and form the greater part of the thoracic skeleton. Their number may be increased by cervical or lumbar ribs or reduced by the absence of the twelfth pair. The first seven pairs are connected to the sternum by costal cartilages, and are referred to as the true ribs. The remaining five are the so-called false ribs: the cartilages of the eighth to tenth usually join the superjacent costal cartilage, whereas the eleventh and twelfth ribs, which are free at their anterior ends, are sometimes termed the ‘floating’ ribs. The tenth rib may also be a floating rib; the incidence varies from 35% to 70% in different races.

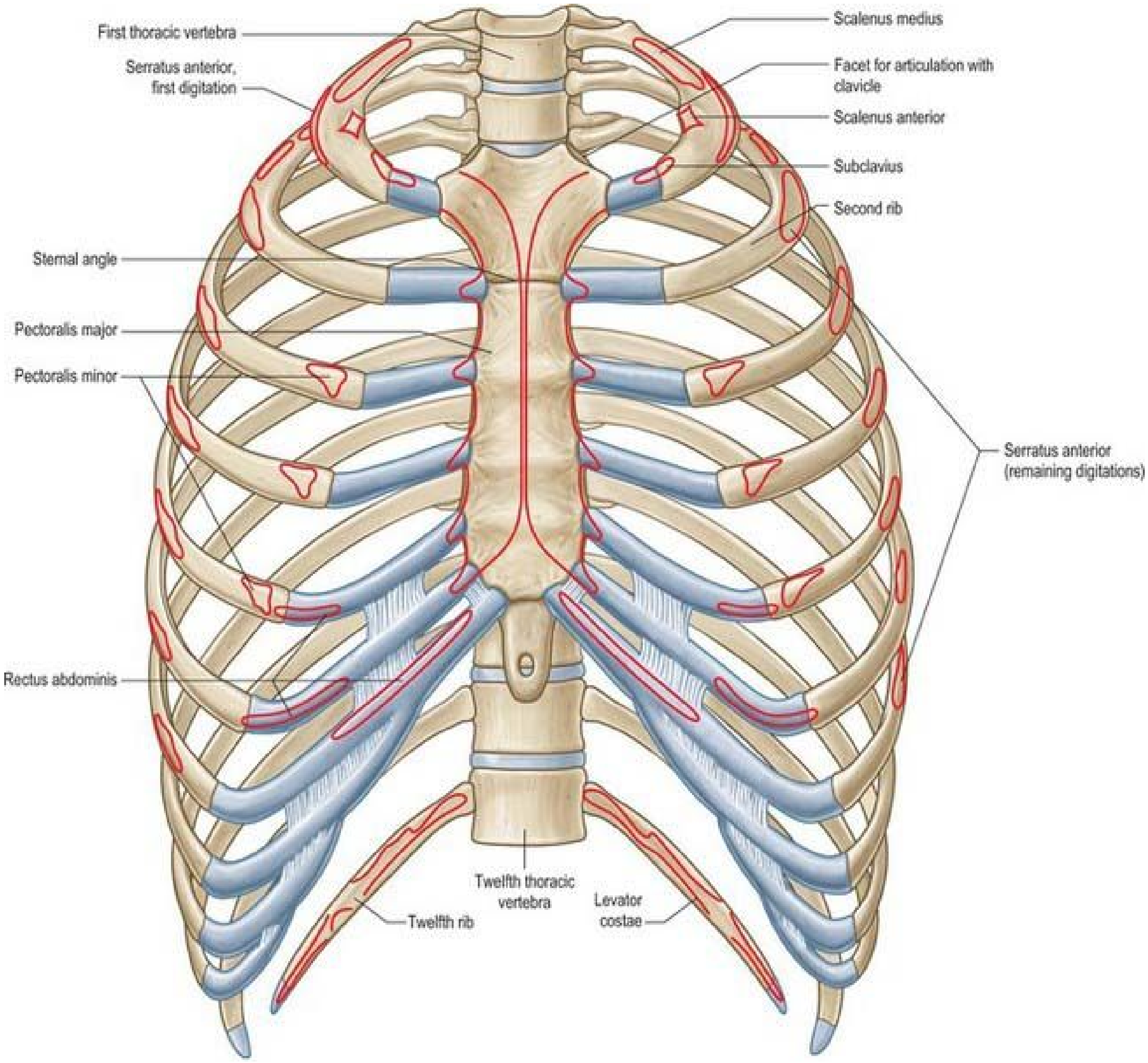
First thoracic vertebra
Serratus anterior, first digitation
Sternal angle
Pectoralis major
Pectoralis minor
Rectus abdominis
Scalenus medius
Facet for articulation with clavicle
Scalenus anterior
Subclavius
Second rib
Serratus anterior (remaining digitations)
Twelfth thoracic vertebra
Twelfth rib
Levator costae

Fig. 54.7 The skeleton of the thorax, anterior aspect, showing muscle attachments.

The ribs are separated by the intercostal spaces, which are deeper in front and between the upper ribs. The latter are less oblique than the lower ribs; obliquity is maximal at the ninth rib and decreases to the twelfth. Ribs increase in length from the first to seventh, and thereafter diminish to the twelfth. They decrease in breadth downwards; in the upper ten, the greatest breadth is anterior. The first two and last three ribs present special features, whereas the remainder conform to a common plan.

Ribs consist of highly vascular trabecular bone, enclosed in a thin layer of compact bone and containing large amounts of red marrow.

Typical rib

A typical rib has a shaft with anterior and posterior ends (Fig. 54.8). The anterior, costal, end has a small concave depression for the lateral end of its cartilage. The shaft has an external convexity and is grooved internally near its lower border, which is sharp, whereas its upper border is rounded. The posterior, vertebral, end has a head, neck and tubercle. The head presents two facets, separated by a transverse crest. The lower and larger facet articulates with the body of the corresponding vertebra, its crest attaching to the intervertebral disc above it. The neck is the flat part beyond the head, anterior to the corresponding transverse process. It is oblique, and faces anterosuperiorly. Its posteroinferior surface is rough and pierced by foramina. Its upper border is the sharp crest of the neck, its lower border rounded. The tubercle, which is more prominent in upper ribs, is posteroexternal at the junction of the neck and shaft and is divided into medial articular and lateral non-articular areas. The articular part bears a small, oval facet for the transverse process of the corresponding vertebra. The nonarticular area is roughened by ligaments. The shaft is thin and flat and has external and internal surfaces, and superior and inferior borders. It is curved, bent at the posterior angle (5–6 cm from the tubercle), and twisted about its long axis. The part behind the angle inclines superomedially, and so its external surface is posteroinferior. In front of the angle it faces slightly up. It is convex and smooth, and near the tubercle is crossed by a rough line, directed inferolaterally, towards the posterior angle. The smooth internal surface is marked by a costal groove, bounded below by the inferior border. The superior border of the groove continues behind the lower border of the neck, but terminates anteriorly at the junction of the middle and anterior thirds of the shaft, anterior to which the groove is absent.

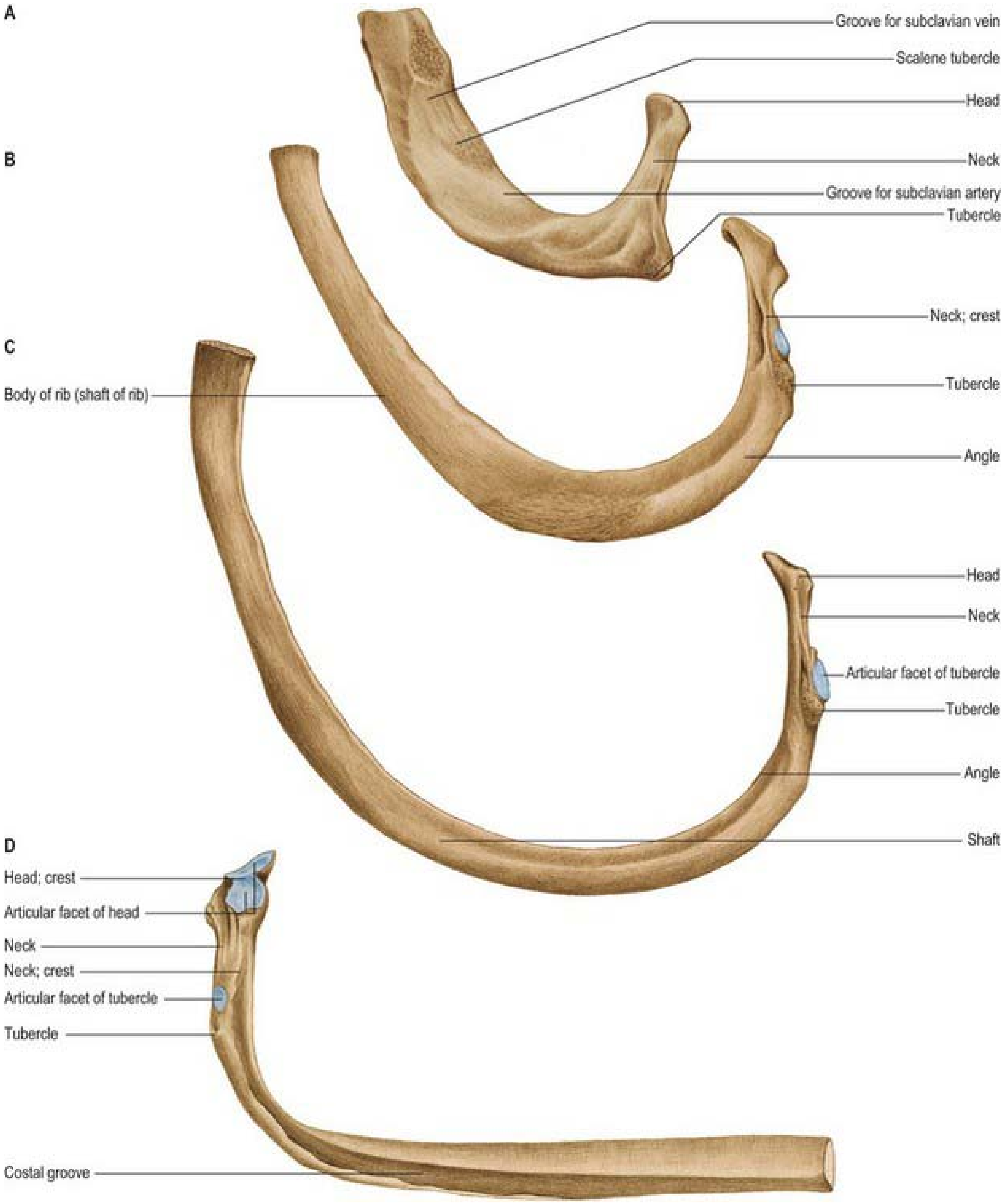
A
Groove for subclavian vein
Scalene tubercle
Head
B
Neck
Groove for subclavian artery
Tubercle
Neck; crest
C
Body of rib (shaft of rib)
Tubercle
Angle
Head
Neck
Articular facet of tubercle
Tubercle
Angle
Shaft
D
Head; crest
Articular facet of head
Neck
Neck; crest
Articular facet of tubercle
Tubercle
Costal groove

Fig. 54.8 Superior surfaces of a first rib (**A**) and of second (**B**) and third (**C**) ribs, and the inferior surface of an eighth (**D**) rib, left side.

(From Sobotta 2006.)

Attachments and relations

A radiate ligament is attached along the anterior border of the head and an intra-articular ligament is attached to the crest of the head. The anterior surface of the head is related to costal pleura and, in lower ribs, to the sympathetic trunk. The anterior surface of the neck is divided by a faint transverse ridge for the internal intercostal membrane and is continuous with the inner lip of the superior border of the shaft. The area above the ridge, which is more or less triangular, is separated from the membrane by fatty tissue. The lower, smooth area is covered by costal pleura. The posterior surface of the neck gives attachment to the costotransverse ligament and is pierced by vascular foramina. The superior costotransverse ligament is attached to the crest of the neck, which extends laterally into the outer lip of the superior border of the shaft. The rounded inferior border of the neck continues laterally into the upper border of the costal groove, and gives attachment to the internal intercostal membrane. The articular area of the tubercle in the upper six ribs is convex and faces posteromedially. In the succeeding three or four ribs it is almost flat, and faces down, back and slightly medially. The lateral costotransverse ligament is attached to the non-articular area.

The ridge on the external surface of the shaft (near its posterior angle) gives attachment to an upward continuation of the thoracolumbar fascia and lateral fibres of iliocostalis thoracis. From the second to the tenth ribs, the distance between angle and tubercle increases. Medial to the angle, the external surface gives attachment to a levator costae and is covered by erector spinae. Near the sternal end of this surface an indistinct oblique line, the anterior ‘angle’, separates the attachments of external oblique and serratus anterior (or latissimus dorsi, in the case of the ninth and tenth ribs). The internal intercostal muscle is attached to the costal groove on the internal surface, and separates the bone and the intercostal neurovascular bundle. At its vertebral end, the groove faces down, its borders in the same plane. The shaft broadens near the posterior angle, and the groove reaches its internal surface. The innermost intercostal is attached to the superior rim of the groove, and this attachment occasionally extends to the anterior quarter of the rib. Posteriorly, the superior rim meets the lower border of the neck. The external intercostal muscle is attached to the sharp inferior costal border. The superior border has two lips posteriorly: an inner and an outer lip. The internal intercostal muscles and the innermost intercostal muscles are attached to the inner lip. The external intercostal muscle is attached to the outer lip.

Vascular supply and innervation

Typical ribs receive their blood supply anteriorly via branches from the internal thoracic artery (first six intercostal spaces) or musculophrenic artery (subsequent spaces), and posteriorly from intercostal arteries derived directly from the aorta. Venous drainage is into the corresponding intercostal vein and then into the azygos system. Typical ribs are innervated segmentally by branches from the corresponding intercostal nerves.

Cervical rib

A cervical rib, the costal element of the seventh cervical vertebra, may be a mere epiphysis on its transverse process, but more often it has a head, neck and tubercle. When a shaft is present, it is of variable length, and extends anterolaterally into the posterior triangle of the neck, where it may end freely or join the first rib or costal cartilage, or even the sternum. A cervical rib may be partly fibrous, but its effects are not related to the size of its osseous part. If it is long enough, its relations are those of a first thoracic rib: the brachial plexus (usually lower trunk) and subclavian vessels are superior and apt to suffer compression in a narrow angle between the rib and scalenus anterior. Hence, cervical ribs may first be revealed by nervous and vascular symptoms, particularly those caused by pressure on the eighth cervical and first thoracic spinal nerves.

A cervical rib or pleurapophysis may show synostosis or diarthrosis with either the anterior (parapophysial) or posterior (diapophysial) ‘roots’ of the so-called seventh cervical transverse process or, more usually, with both.

First rib

Most acutely curved and usually shortest, the first rib is broad and flat, its surfaces are superior and inferior, and its borders are internal and external (Fig. 54.8). It slopes obliquely down and forwards to its sternal end. The obliquity of the first ribs accounts for the appearance of pulmonary and pleural apices in the neck.

The head of the first rib is small and round. It bears an almost circular facet, and articulates with the body of the first thoracic vertebra. The neck is rounded and ascends posterolaterally. The tubercle, wide and prominent, is directed up and backwards; medially, an oval facet articulates with the transverse process of the first thoracic vertebra. At the tubercle, the rib is bent, its head turned slightly down, and so the angle and tubercle coincide. The superior surface of the flattened shaft is crossed obliquely by two shallow grooves, separated by a slight ridge, which usually ends at the internal border as a small pointed projection, the scalene tubercle, to which scalenus anterior is attached. The groove anterior to the scalene tubercle forms a bed for the subclavian vein, and the rough area between this and the first costal cartilage gives attachment to the costoclavicular ligament and, more anteriorly, to subclavius. The subclavian artery and (usually) the lower trunk of the brachial plexus pass in the groove behind the tubercle. Behind this, scalenus medius is attached as far as the costal tubercle.

The external border is convex, thick posteriorly and thin anteriorly. It is covered behind by scalenus posterior descending to the second rib. The first digitation of serratus anterior is, in part, attached to it, behind the subclavian (arterial) groove. The internal border is concave and thin, and the scalene tubercle is near its midpoint. The suprapleural membrane, which covers the cervical dome of the pleura, is attached to the internal border. The inferior surface is smooth. The anterior end is larger than in any other rib.

Vascular supply and innervation

The first rib is supplied by the internal thoracic artery and the superior intercostal artery. Venous drainage is via the intercostal vein. The rib is innervated by the first intercostal nerve.

Ossification

The first rib has a primary centre for the shaft, and secondary ossification centres for the head of the rib and the tubercle.

Second rib

The second rib is twice the length of the first rib, and has a similar curvature. The non-articular area of the tubercle is small. The angle is slight and near the tubercle. The shaft is not twisted, but at the tubercle is convex upwards, as in the first rib, but less so. The external surface of the shaft is convex and superolaterally is marked centrally by a rough, muscular impression that continues posteromedially towards the tubercle as a narrow, roughened ridge. The internal surface, smooth and concave, faces inferomedially and there is a short costal groove posteriorly.

The lower parts of the first and second digitations of serratus anterior are attached to a rough prominence that extends from just behind the midpoint of the external surface (Fig. 54.8). The distinct lips of the upper border are widely separated behind; scalenus posterior and serratus posterior superior are attached to the outer lip in front of the angle.

Vascular supply and innervation

The blood supply of the second rib is the internal thoracic artery and the superior intercostal artery. Venous drainage is via the superior intercostal vein, which drains into the brachiocephalic vein, and the anterior intercostal veins, which drain into the internal thoracic vein. The bone is innervated by branches of the first intercostal nerve.

Ossification

The second rib is ossified from a primary centre for the shaft, which appears near the angle, late in the second month. The secondary centres for the head and articular and non-articular parts of the tubercle appear about puberty, uniting to the shaft soon after the age of 20 years.

Tenth, eleventh and twelfth ribs

The tenth rib has a single facet on its head that may articulate with the intervertebral disc above, in addition to the upper border of the tenth thoracic vertebra near its pedicle. The ninth and tenth ribs are usually united anteriorly by a fibrous joint. However, the tenth rib may be free, in which case it is pointed like the eleventh and twelfth ribs.

The eleventh and twelfth ribs each have one large, articular facet on the head, but no neck or tubercle. Their pointed anterior ends are tipped with cartilage. The eleventh rib has a slight angle and shallow costal groove. The twelfth rib has neither, is much shorter and slopes cranially at its vertebral end. The internal surfaces of both ribs face slightly upwards, more so in the twelfth.

Numerous muscles and ligaments are attached to the twelfth rib (Fig. 54.9). Quadratus lumborum and its anterior covering layer of thoracolumbar fascia are attached to the lower part of its anterior surface in its medial one-half to two-thirds; the upper part is related to the costodiaphragmatic pleural recess. The internal intercostal muscle (medially) and the diaphragm (laterally) are attached at or near the upper border. The lower border gives attachment to the middle lamella of the thoracolumbar fascia and, lateral to quadratus lumborum, to the lateral arcuate ligament and posterior lamella of the thoracolumbar fascia. The lumbocostal ligament is attached posteriorly, close to the head, connecting it to the first lumbar transverse process. The lowest levator costae, longissimus thoracis and iliocostalis are attached to the medial half of the external surface, and serratus posterior inferior, latissimus dorsi and external oblique are attached to its lateral half. The external intercostal muscle is attached along the upper border. These attachments vary: those of the internal intercostal, levator costae and erector spinae merge and those of latissimus dorsi, diaphragm and external oblique may reach the costal cartilage. The lower limit of the pleural sac crosses in front of the rib, approximately at the point where it is crossed by the lateral border of iliocostalis. Its lateral end is usually below the line of costodiaphragmatic pleural reflection and is therefore not covered by pleura.

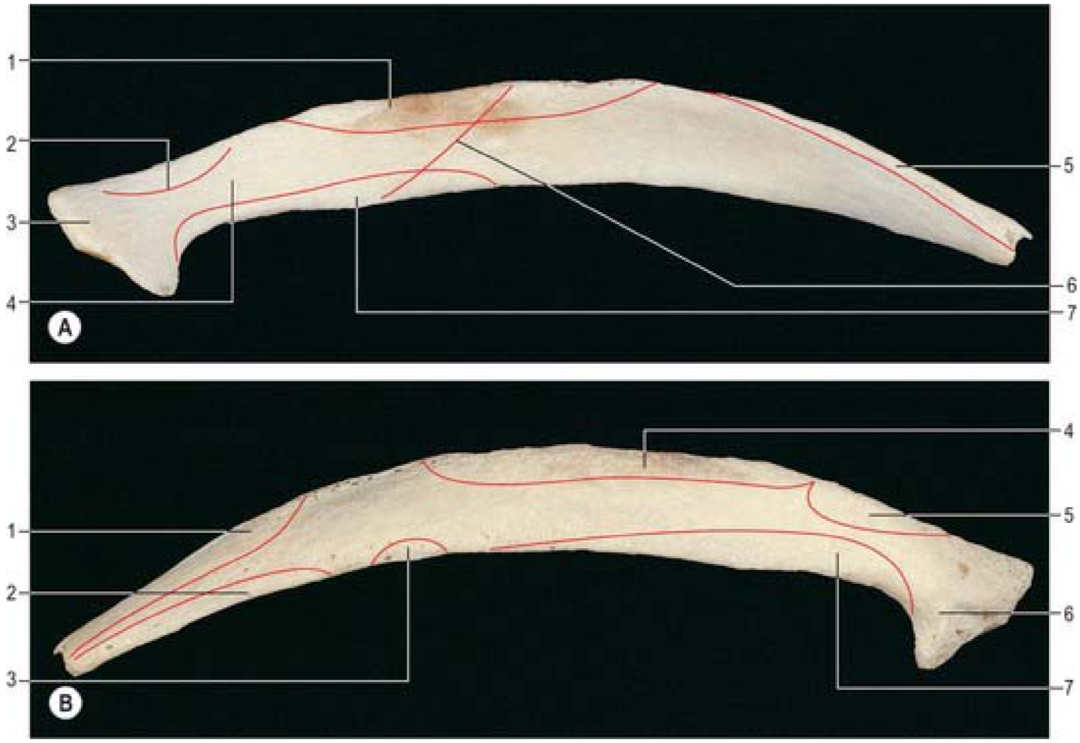

Fig. 54.9 The twelfth rib of the left side. **A**, Anterior aspect. **B**, Posterior aspect. **A: 1**. Attachment of internal intercostal muscle. **2**. Attachment of costotransverse ligament. **3**. Head. **4**. Area covered by pleura. **5**. Attachment of diaphragm. **6**. Line of pleural reflection. **7**. Attachment of quadratus lumborum. **B: 1**. Attachment of latissimus dorsi. **2**. Attachment of external oblique. **3**. Attachment of serratus posterior inferior. **4**. Attachment of external intercostal muscle. **5**. Attachment of levator costae. **6**. Head. **7**. Attachment of erector spinae.

Vascular supply and innervation

The tenth and eleventh ribs are supplied by the posterior intercostal artery and branches from the musculophrenic artery. The twelfth rib is supplied by the subcostal artery. Venous drainage is via the posterior intercostal and subcostal veins, which in turn drain into the azygos system. There is additional drainage via the anterior intercostal veins (branches of the musculophrenic vein). The tenth and eleventh ribs are innervated by the corresponding intercostal nerve, and the twelfth rib is innervated by the subcostal nerve.

Ossification

The tenth rib ossifies from a primary centre in the shaft and secondary centres for the head and articular parts of the tubercle. The eleventh and twelfth ribs, without tubercles, have two centres each.

Costal cartilages

Costal cartilages are the persistent, unossified anterior parts of the cartilaginous models in which the ribs develop. They are flat bars of hyaline cartilage that extend from the anterior ends of the ribs, and contribute greatly to thoracic mobility and elasticity (Fig. 54.7). The upper seven pairs join the sternum; the eighth to tenth articulate with the lower border of the cartilage above; the lowest two have free, pointed ends in the abdominal wall. They increase in length from the first to the seventh, and then decrease to the twelfth. They diminish in breadth from first to last, like the intercostal spaces. The costal cartilages are broad at their costal continuity and taper as they pass forward. The first and second are of even breadth and the sixth to eighth enlarge where their margins are in contact. The first descends a little, the second is horizontal and the third ascends slightly; the others are angulated and incline up towards the sternum or cartilage above, a little anterior to their ribs.

Each costal cartilage has two surfaces, borders and ends. The anterior surface is convex, facing anterosuperiorly. The sternoclavicular articular disc, costoclavicular ligament and subclavius are attached to the first costal cartilage. Pectoralis major is attached to the medial aspect of the first six cartilages and the others are covered by the partial attachments of the anterior abdominal muscles. The posterior surface is concave, and really posteroinferior. Sternothyroid is attached to the first cartilage, transversus thoracis is attached to the second to sixth, and transversus abdominis is attached to the lower six. The internal intercostal muscles and external intercostal membranes are attached to the concave superior and convex inferior borders. The inferior borders of the fifth (sometimes), and sixth to ninth cartilages project at points of greatest convexity. Oblong facets on these projections articulate with facets on slight projections from the superior borders of subjacent cartilages. The lateral end of each cartilage is continuous with its rib. The medial end of the first is continuous with the sternum; those of the six succeeding cartilages are round and articulate with shallow costal notches on the lateral margins of the sternum; those of the eighth to tenth are pointed, each connected with the cartilage above; those of the eleventh and twelfth are pointed and free. With the exception of the synarthrosis between the first rib and sternum, all these articulations are synovial.

In old age the costal cartilages tend to ossify superficially, lose their pliability and become brittle.

Rib fractures

Elastic recoil of the ribs which suspend the sternum may explain the rarity of sternal fractures. Despite their pliability, the ribs are much more frequently broken, the middle ribs being the most vulnerable. Because traumatic stress is often the result of compression of the thorax, the usual site of fracture is just in front of the angle, which is the weakest point of the rib. Direct impact may fracture a rib at any point; the ends of the broken bone may be driven inwards, and potentially may injure thoracic or upper abdominal viscera.

JOINTS

MANUBRIOSTERNAL JOINT

The manubriosternal joint lies between the manubrium and sternal body, and is usually a symphysis. The bony surfaces are covered by hyaline cartilage and connected by a fibrocartilage, which may ossify in the aged. Sometimes, the central part of the disc is absorbed and the joint appears synovial. The manubriosternal joint is connected by a fibrous membrane enveloping the entire bone. In occasional individuals over the age of 30 years, the manubrium is joined to the sternal body by bone, but the intervening cartilage may be only superficially ossified; ossification becomes complete only in the aged. Early synostosis has been attributed to a persistent synchondrosis in place of a symphysis. In the newborn, union is by collagenous and elastic fibres, without chondrocytes.

Movements

The symphysis permits a small range of angulation between the longitudinal axes of the manubrium and body of the sternum, and also limited anteroposterior displacement. A study of these movements in 62 male athletes yielded (standing position) mean values of 162.7° (full inspiration) and 164.7° (full expiration) for the manubriosternal angle: both movements contribute to respiratory excursions of the sternum.

XIPHISTERNAL JOINT

The joint between the xiphoid process and the body of the sternum process is a symphysis. It is usually transformed to a synostosis by the fortieth year, but sometimes remains unchanged even in old age.

STERNOCLAVICULAR JOINT

The sternoclavicular joint is described in Chapter 46.

COSTOVERTEBRAL, STERNOCOSTAL AND INTERCHONDRAL JOINTS

The heads of the ribs articulate with vertebral bodies (costocorporeal joints); their necks and tubercles articulate with transverse processes (costotransverse joints).

Joints of costal heads

Heads of typical ribs articulate with facets (often termed demifacets) on the margins of adjacent thoracic vertebral bodies and with the intervertebral discs between them (Fig. 54.10). The first and tenth to twelfth ribs articulate with a single vertebra by a simple synovial joint. In the others, an intra-articular ligament bisects the joint, producing a double synovial compartment, so the joint is classified as both compound and complex. Often inaccurately described as plane, their articular surfaces are slightly ovoid and the upper and lower synovial articulations are obtusely angled to each other. The ligaments are capsular, radiate and intra-articular.

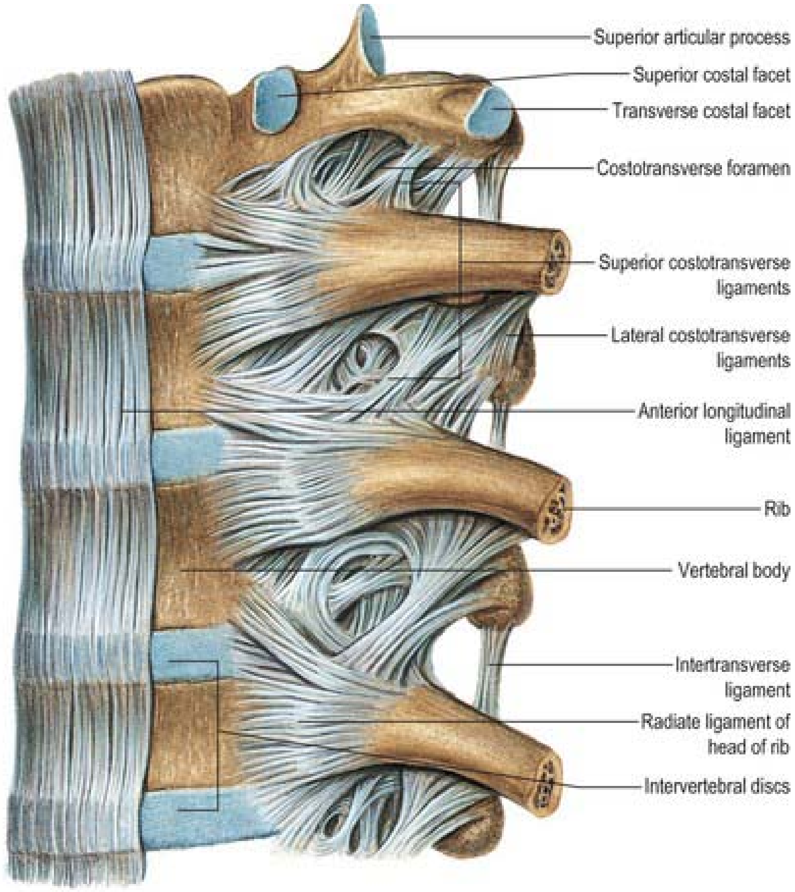
Superior articular process
Superior costal facet
Transverse costal facet
Costotransverse foramen
Superior costotransverse ligaments
Lateral costotransverse ligaments
Anterior longitudinal ligament
Rib
Vertebral body
Intertransverse ligament
Radiate ligament of head of rib
Intervertebral discs

Fig. 54.10 Ligaments of the vertebral column and costovertebral joints, lateral parts of the anterior longitudinal ligament removed, left lateral aspect.

(From Sobotta 2006.)

Fibrous capsules

The fibrous capsule connects the costal head to the circumference of the articular surface formed by an intervertebral disc and the demifacets of two adjacent vertebrae. Some of the upper fibres traverse their intervertebral foramina to blend with the posterior aspects of the intervertebral discs; the posterior fibres are continuous with the costotransverse ligaments.

Radiate ligaments

Radiate ligaments connect the anterior parts of each costal head to the bodies of two vertebrae and their intervening intervertebral disc. Each is attached to the head just beyond its articular surface. Superior fibres ascend to the vertebral body above, inferior to the body below. Intermediate fibres, shortest and least distinct, are horizontal and attached to the disc. The radiate ligament associated with the first rib is attached to the seventh cervical and first thoracic vertebrae. In the joints of the tenth to twelfth ribs, which articulate with single vertebrae, the radiate ligament is attached to the numbered vertebra and the one above.

Intra-articular ligament

The intra-articular ligament is a short, flat band, attached laterally to the crest between the costal articular facets and medially to the intervertebral disc, dividing the joint. The ligament is absent from the first and tenth to twelfth joints.

Costotransverse joints

The facet of a costal tubercle articulates reciprocally with the transverse process of its corresponding vertebra (Fig. 54.11). The eleventh and twelfth ribs lack this articulation. In the upper five or six joints, articular surfaces are reciprocally curved, but below this they are flatter (Fig. 54.12). Their ligaments are capsular, costotransverse, superior and lateral costotransverse, and accessory.

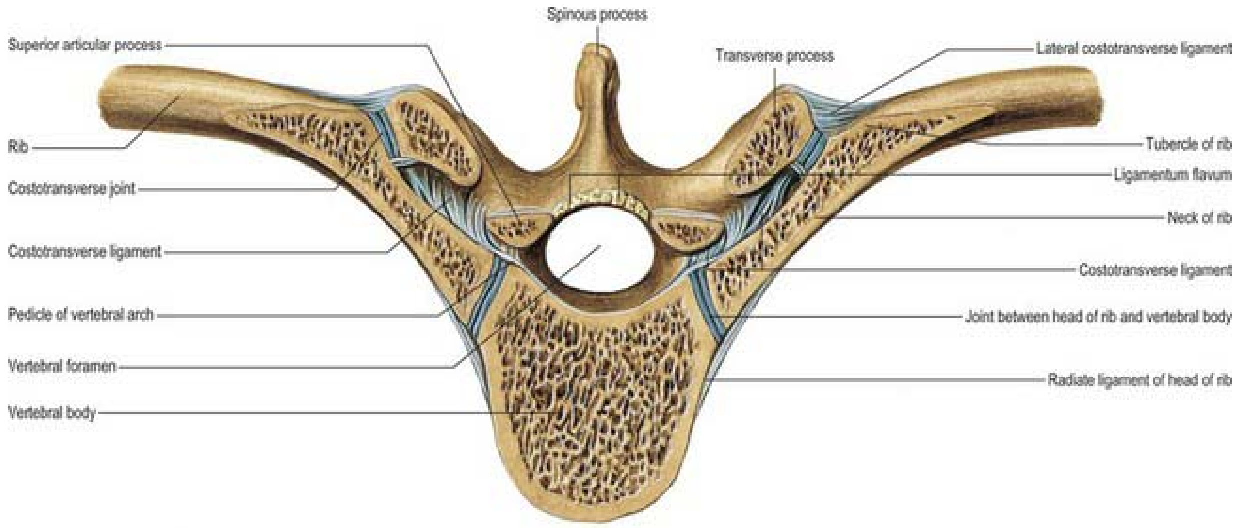
Spinous process
Superior articular process
Transverse process
Lateral costotransverse ligament
Rib
Tubercle of rib
Costotransverse joint
Ligamentum flavum
Neck of rib
Costotransverse ligament
Costotransverse ligament
Pedicle of vertebral arch
Joint between head of rib and vertebral body
Vertebral foramen
Radiate ligament of head of rib
Vertebral body

Fig. 54.11 Costovertebral joints, superior aspect.

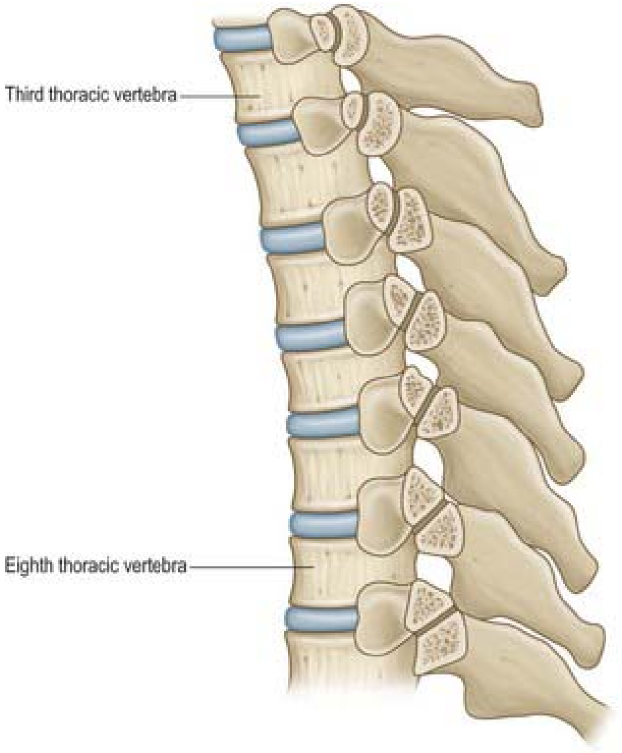

Fig. 54.12 Section through the costotransverse joints from the third to the ninth inclusive. Contrast the concave facets on the upper transverse processes with the less curved facets on the lower transverse processes.

Fibrous capsule

The fibrous capsule is thin and attached to articular peripheries, and has a synovial lining.

Costotransverse ligament

The costotransverse ligament fills the costotransverse foramen between the neck of the rib and its adjacent corresponding transverse process. Its numerous short fibres extend back from the posterior rough surface on the neck to the anterior surface of the transverse process. A costotransverse ligament is rudimentary or absent in the eleventh and twelfth ribs.

Superior costotransverse ligament

The superior costotransverse ligament has anterior and posterior layers. The anterior layer is attached between the crest of the costal neck and lower aspect of the transverse process above, and blends laterally with the internal intercostal membrane; it is crossed by the intercostal vessels and nerve. The posterior layer is attached posteriorly on the costal neck, ascending posteromedially to the transverse process above, and blends laterally with the external intercostal muscle. The first rib has no such ligament. The shaft of the twelfth rib, near its head, is connected to the base of the first lumbar transverse process by a lumbocostal ligament in series with the superior costotransverse ligaments.

Accessory ligament

An accessory ligament is usually present. It lies medial to the superior costotransverse ligament, and is separated from it by the dorsal ramus of a thoracic spinal nerve and accompanying vessels. These bands are variable in their attachments, but usually pass from a depression medial to a costal tubercle to the inferior articular process immediately above. Some fibres also pass to the base of the transverse process.

Lateral costotransverse ligament

The lateral costotransverse ligament is short, thick and strong and passes obliquely from the apex of the transverse process to the rough non-articular part of the adjacent costal tubercle. The ligaments of upper ribs ascend from their transverse processes, and are shorter and more oblique than those of the lower ribs, which descend.

Movements

Costal heads are so firmly tied to vertebral bodies by radiate and intra-articular ligaments that only slight gliding can occur. Strong ligaments binding costal necks and tubercles to transverse processes also limit movements at costotransverse joints to slight gliding, guided by the shape and direction of the articular surfaces (Fig. 54.12). The facets on the tubercles of the upper six ribs are oval and vertically convex, and fit corresponding concavities on the anterior surfaces of transverse processes; consequently, up and down movements of tubercles involve rotation of costal necks about their long axes. The facets on the seventh to tenth tubercles are almost flat, and face down, medially and backwards; their opposing surfaces are on the upper aspects of transverse processes, and so when these tubercles ascend they also move posteromedially. Both sets of joints move simultaneously and in the same directions: the costal neck therefore moves as if at a single joint in which the two articulations form its ends.

In the upper six ribs, the neck moves slightly up and down but its chief movement is one of rotation about its long axis, which means that downward rotation of its anterior aspect is associated with depression, and upward rotation with elevation, of the shaft and anterior end of the rib. In the seventh to tenth ribs, the neck ascends posteromedially or descends anterolaterally, increasing or diminishing the infrasternal angle respectively; slight rotation accompanies these movements.

Sternocostal joints

Costal cartilages articulate with small concavities on the lateral sternal borders (chondrosternal articulations) (Fig. 54.13). Perichondrium and periosteum are continuous. The first sternocostal joint is an unusual variety of synarthrosis, and is often inaccurately called a synchondrosis. The second to seventh costal cartilages articulate by synovial joints, although articular cavities are often absent, particularly in the lower joints. Fibrocartilage covers the articular surfaces and also unites the costal cartilages and the sternum in those joints where cavities are absent. The seventh costosternal joint may be synovial or ‘symphysial’. Ligaments involved are capsular, radiate sternocostal, intra-articular and costoxiphoid.

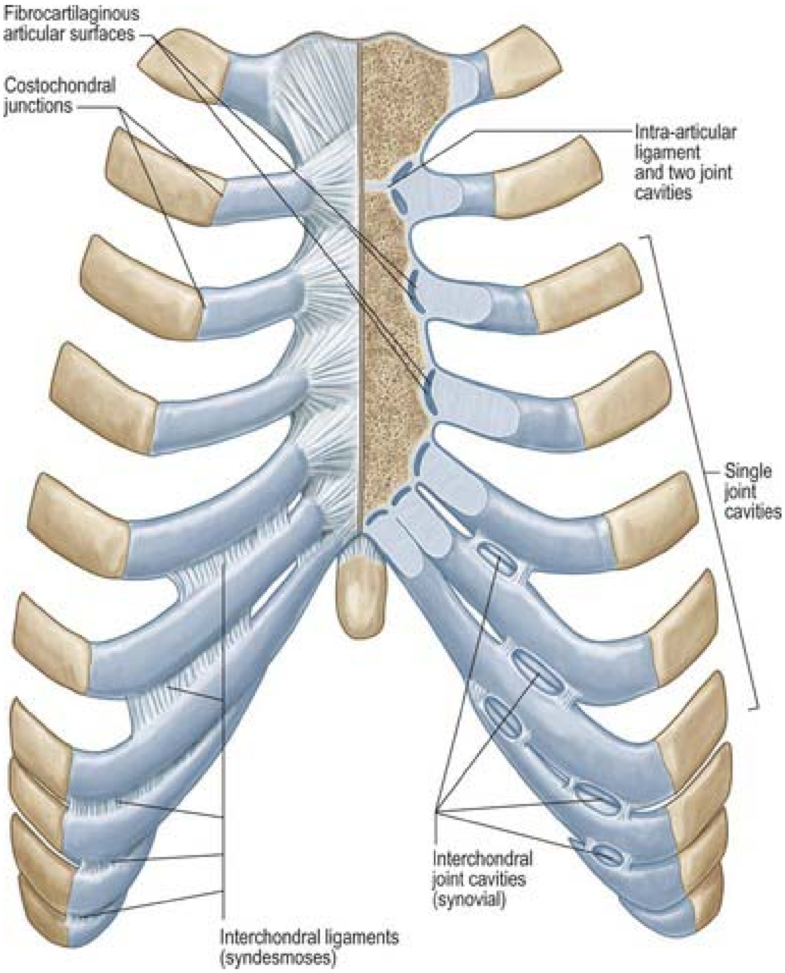
Fibrocartilaginous articular surfaces
Costochondral junctions
Intra-articular ligament and two joint cavities
Single joint cavities
Interchondral joint cavities (synovial)
Interchondral ligaments (syndesmoses)

Fig. 54.13 Sternocostal and interchondral joints, anterior aspect.

Fibrous capsules

Fibrous capsules surround the second to seventh sternocostal joints. They are thin, blended with the sternocostal ligaments and are strengthened above and below by fibres that connect the costal cartilages to the sternum.

Radiate sternocostal ligaments

The radiate sternocostal ligaments are broad, thin bands which radiate from the anterior and posterior surfaces of the sternal ends of the costal cartilages of the true ribs to the corresponding sternal surfaces. Their superficial fibres intermingle with adjacent ligaments above and below, with those of the opposite side and with tendinous fibres of pectoralis major; collectively, these tissues form a thick fibrous membrane around the sternum that is more marked inferiorly.

Intra-articular ligaments

Intra-articular ligaments are constant only between the second costal cartilages and sternum. The ligament associated with the second costal cartilage extends from the costal cartilage to the fibrocartilage uniting the manubrium and sternal body and is therefore intra-articular. Occasionally, the third sternal cartilage is connected with the first and second sternal segments by a similar ligament. Fibrocartilaginous strands may occur in the third and lower joints. Articular cavities may be absent at any age.

Costoxiphoid ligaments

Costoxiphoid ligaments connect the anterior and posterior surfaces of the seventh (and sometimes sixth) costal cartilage to the same surfaces of the xiphoid process. They vary in length and breadth, and the posterior is less distinct.

Movements

Slight gliding movements, sufficient for ventilation, occur at sternocostal joints.

Interchondral joints

Contiguous borders of the sixth to ninth costal cartilages articulate by apposition of small oblong facets. Each articulation is enclosed in a thin fibrous capsule, lined by synovial membrane, with lateral and medial interchondral ligaments. Sometimes the fifth cartilage, and less commonly the ninth cartilage, articulate at their inferior borders with adjoining cartilages; this connection is usually effected by ligamentous fibres. Articulation between the ninth and tenth cartilages is never synovial and sometimes absent.

Costochondral junctions

Artificially separated from its rib, a costal cartilage has a rounded end that fits a reciprocal depression in the rib. Periosteum and perichondrium are continuous across the costochondral junctions, and the collagen of the osseous and cartilaginous matrices blend. No movement occurs at costochondral junctions.

MUSCLES

The intrinsic muscles of the chest wall are the intercostals, subcostales, transversus thoracis, levatores costarum and serratus posterior. Scapular muscles and muscles connecting the upper limb, chest wall and vertebrae, i.e. trapezius, latissimus dorsi, rhomboids major and minor, levator scapulae, pectorales major and minor, subclavius, supra- and infraspinatus, teres major and teres minor, are described in detail in Chapter 46.

INTRINSIC CHEST WALL MUSCLES

Intercostal muscles

The intercostal muscles are thin multiple layers of muscular and tendinous fibres that occupy the intercostal spaces; their names are derived from their spatial relationship, i.e. the external, internal and innermost intercostals (Fig. 54.14).

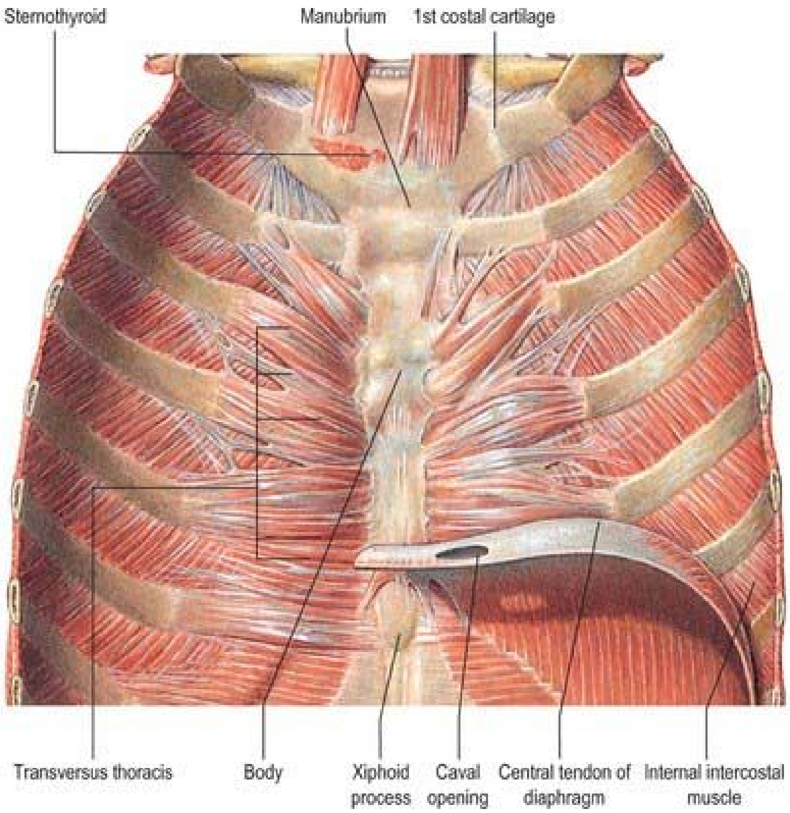
Sternothyroid
Manubrium
1st costal cartilage
Transversus thoracis
Body
Xiphoid process
Caval opening
Central tendon of diaphragm
Internal intercostal muscle

Fig. 54.14 The left transversus thoracis, exposed and viewed from its posterior aspect. Note that the lower border of transversus thoracis is in contact with the upper border of transversus abdominis in the interval between the sternal and costal origins of the diaphragm.

(From Sobotta 2006.)

External intercostals

Eleven pairs of external intercostals extend from the tubercles of the ribs, where they blend with the posterior fibres of the superior costotransverse ligaments, almost to the costal cartilages, where each continues forwards to the sternum as an aponeurotic layer, the external intercostal membrane. Each muscle passes from the lower border of one rib to the upper border of the rib below: their fibres are directed obliquely downwards and laterally at the back of the thorax, and downwards, forwards and medially at the front. In the upper two or three spaces, they do not quite reach the ends of the rib, and in the lower two spaces they extend to the free ends of the costal cartilages. The external intercostals are thicker than the internal intercostals.

Innervation

External intercostals are supplied by the adjacent intercostal nerves.

Action

External intercostals are believed to act with the internal intercostals (see Ch. 58).

Internal intercostals

Eleven pairs of internal intercostals begin anteriorly at the sternum, in the interspaces between the cartilages of the true ribs, and at the anterior extremities of the cartilages of the ‘false’ ribs. Their greatest thickness lies in this intercartilaginous or parasternal part. They continue back as far as the posterior costal angles, where each is replaced by an aponeurotic layer, the internal intercostal membrane, that is continuous posteriorly with the anterior fibres of a superior costotransverse ligament, and anteriorly with the fascia between the internal and external intercostal muscles. Each muscle descends from the floor of a costal groove and adjacent costal cartilage, and inserts into the upper border of the rib below: their fibres are directed obliquely, nearly at right angles to those of the external intercostal muscles.

Innervation

Internal intercostals are supplied by the adjacent intercostal nerves.

Action

Internal intercostals are believed to act with the external intercostals (see Ch. 58).

Innermost intercostals

The innermost intercostals were once regarded as internal laminae of the internal intercostal muscles, and fibres in the two layers do coincide in direction. Each muscle is attached to the internal aspects of two adjoining ribs. They are insignificant, and sometimes absent, at highest thoracic levels, but become progressively more substantial below this, typically extending through the middle two quarters of the lower intercostal spaces. Posteriorly, the innermost intercostals, in those spaces where they are well developed, may come together with the corresponding subcostales. The innermost intercostals are related internally to the endothoracic fascia and parietal pleura, and externally to the intercostal nerves and vessels.

Innervation

Innermost intercostals are supplied by the adjacent intercostal nerves.

Action

Innermost intercostals are believed to act with the internal intercostals (see Ch. 58).

Subcostales

Subcostales consist of muscular and aponeurotic fasciculi, and are usually well developed only in the lower part of the thorax. Each descends from the internal surface of one rib, near its angle, to the internal surface of the second or third rib below. Their fibres run parallel to those of the internal intercostals and, like the innermost intercostals, they lie between the intercostal vessels and nerves and the pleura.

Innervation

Subcostales are supplied by the adjacent intercostal nerves.

Action

Subcostales depress the ribs.

Transversus thoracis

Transversus thoracis (triangularis sternae, sternocostalis) spreads over the internal surface of the anterior thoracic wall (Fig. 54.14). It arises from the lower one-third of the posterior surface of the sternum, the xiphoid process and the costal cartilages of the lower three or four true ribs near their sternal ends. The fibres diverge and ascend laterally as slips that pass into the lower borders and inner surfaces of the costal cartilages of the second, third, fourth, fifth and sixth ribs. The lowest fibres are horizontal, and are contiguous with the highest fibres of transversus abdominis, the intermediate fibres are oblique, and the highest are almost vertical. Transversus thoracis varies in its attachments, not only between individuals but even on opposite sides of the same individual. Like the innermost intercostals and subcostales, transversus thoracis separates the intercostal nerves from the pleura.

Innervation

Transversus thoracis is supplied by the adjacent intercostal nerves.

Action

Transversus thoracis draws down the costal cartilages to which it is attached.

Levatores costarum

Levatores costarum are strong bundles, 12 on each side, that arise from the tips of the transverse processes of the seventh cervical and first to eleventh thoracic vertebrae. They pass obliquely downwards and laterally, parallel with the posterior borders of the external intercostals. Each is attached to the upper edge and external surface of the rib immediately below the vertebra from which it takes origin, between the tubercle and the angle (levatores costarum breves). Each of the four lower muscles divides into two fasciculi: one is attached as already described, and the other descends to the second rib below its origin (levatores costarum longi).

Innervation

Levatores costarum are supplied by the lateral branches of the dorsal rami of the corresponding thoracic spinal nerves.

Action

Levatores costarum elevate the ribs, but their importance in ventilation is disputed. They are also said to act from their costal attachments as rotators and lateral flexors of the vertebral column.

Serratus posterior

Serratus posterior superior

Serratus posterior superior (Fig. 54.15) is a thin quadrilateral muscle, external to the upper posterior part of the thorax. It arises by a thin aponeurosis from the lower part of the nuchal ligament, the spines of the seventh cervical and upper two or three thoracic vertebrae and their supraspinous ligaments. It descends laterally, and ends in four digitations attached to the upper borders and external surfaces of the second, third, fourth and fifth ribs, just lateral to their angles. It is superficial to the thoracic part of the thoracolumbar fascia and deep to the rhomboids. The number of digitations can vary from three to six, and the muscle may even be absent.

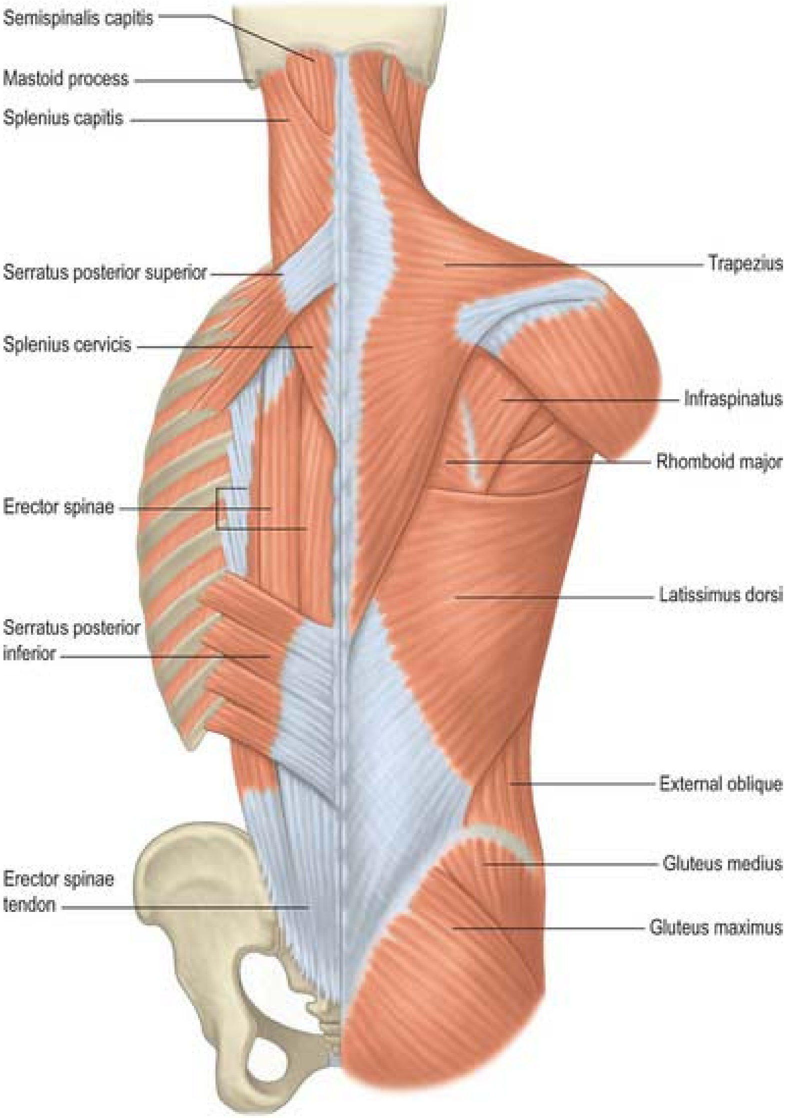
Semispinalis capitis
Mastoid process
Splenius capitis
Serratus posterior superior
Splenius cervicis
Erector spinae
Serratus posterior inferior
Erector spinae tendon
Trapezius
Infraspinatus
Rhomboid major
Latissimus dorsi
External oblique
Gluteus medius
Gluteus maximus

Fig. 54.15 Superficial (extrinsic) muscles of the back.

Innervation

Serratus posterior superior is innervated by the second, third, fourth and fifth intercostal nerves.

Action

The attachments of serratus posterior superior clearly indicate that it could elevate the ribs: its role in man is uncertain.

Serratus posterior inferior

Serratus posterior inferior is a thin, irregularly quadrilateral muscle at the junction of the thoracic and lumbar regions. It arises from the spines of the lower two thoracic and upper two or three lumbar vertebrae and their supraspinous ligaments by a thin aponeurosis that blends with the lumbar part of the thoracolumbar fascia. It ascends laterally, and its four digitations pass into the inferior borders and outer surfaces of the lower four ribs, a little lateral to their angles. There may be fewer digitations and in rare cases the entire muscle may be absent.

Innervation

Serratus posterior inferior is innervated by ventral rami of the ninth, tenth, eleventh and twelfth thoracic spinal nerves.

Action

Serratus posterior inferior draws the lower ribs downwards and backwards, although possibly not in ventilation.

Mechanism of thoracic cage movement

Breathing involves changing the thoracic volume by altering the vertical, transverse and anteroposterior dimensions of the thorax (see Ch. 58). The diaphragm is the key muscle in this process. Its muscle fibres descend from their relatively ‘high’ anterior sternocostal attachments steeply to the central tendon and obliquely to their complex ‘low’ posterior attachments (see Fig. 58.1). The central tendon is fixed: when the diaphragm contracts, it allows the lower ribcage to move inferiorly and anteriorly without any change to the curvature of the diaphragm. The intercostal muscles maintain the rigidity of the chest wall. The external and internal intercostals, transversus thoracis, subcostales, levatores costarum, serratus posterior superior and serratus posterior inferior can elevate or depress the ribs, and hence can act as accessory muscles of ventilation.

VASCULAR SUPPLY AND LYMPHATIC DRAINAGE OF THE CHEST WALL

ARTERIES

Muscles of the thoracic wall receive their blood supply from the internal thoracic artery, either directly or via the musculophrenic artery, the superior intercostal artery, descending thoracic aorta, and the subcostal and superior thoracic arteries. Additional contributions come from vessels that supply the proximal muscles of the upper limb, namely the suprascapular, superficial cervical, thoracoacromial, lateral thoracic and subscapular arteries.

Internal thoracic artery

The internal thoracic artery arises inferiorly from the first part of the subclavian artery, approximately 2 cm above the sternal end of the clavicle, opposite the root of the thyrocervical trunk (see Figs 53.2, 53.3). It descends behind the first six costal cartilages 1 cm from the lateral sternal border and divides at the level of the sixth intercostal space into musculophrenic and superior epigastric branches.

Relations

At first, the internal thoracic artery descends anteromedially behind the sternal end of the clavicle, the internal jugular and brachiocephalic veins and the first costal cartilage. As it enters the thorax, the phrenic nerve crosses it obliquely from its lateral side, usually in front. The artery then descends almost vertically to its bifurcation, lying behind pectoralis major, the first six costal cartilages, external intercostal membranes, internal intercostals and terminations of the upper six intercostal nerves. It is separated from the pleura, down to the second or third cartilage, by a strong layer of fascia, and below this by transversus thoracis. The artery is accompanied by a chain of lymph nodes and by venae comitantes that unite at about the third costal cartilage into a single vein medial to the artery. Its intermediate branches are sternal, anterior intercostal and perforating.

Sternal branches

Sternal branches are distributed to transversus thoracis, the periosteum of the posterior sternal surface and the sternal red bone marrow. These branches, together with small branches of the pericardiacophrenic artery, anastomose with branches of the posterior intercostal and bronchial arteries to form a subpleural mediastinal plexus.

Anterior intercostal branches

Anterior intercostal arteries are distributed to the upper six intercostal spaces. They pass laterally along the borders of the space and anastomose with the posterior intercostal arteries and their collateral branches. The anterior intercostals usually arise from the internal thoracic artery as single vessels that promptly divide into two branches, one passing to the superior, and one to the inferior, part of each intercostal space. Occasionally, one branch passes to the space above, and one to the space below. (The anterior intercostals may sometimes arise as two separate branches from the internal thoracic artery.) The arteries lie at first between the pleura and the internal intercostals, then between the innermost and the internal intercostals. They supply the intercostal muscles and send branches through them to the pectoral muscles, breast and skin.

Perforating branches

Perforating branches traverse the upper five or six intercostal spaces with the anterior cutaneous branches of the corresponding intercostal nerves. They pierce and supply pectoralis major, and then curve laterally to become direct cutaneous vessels that supply the skin. These cutaneous vessels provide the anatomical basis for surgically raising a skin flap in this region, the deltopectoral flap, that is used for reconstructing areas of missing tissue in the head and neck. The second to fourth branches supply the breast, and become enlarged during lactation.

Musculophrenic artery

The musculophrenic artery passes inferolaterally behind the seventh to ninth costal cartilages, traverses the diaphragm near the ninth, and ends near the last intercostal space. It anastomoses with the inferior phrenic and lower two posterior intercostal arteries and ascending branches of the deep circumflex iliac arteries. Two anterior intercostal arteries branch from it for each of the seventh to ninth intercostal spaces, and are distributed similarly to their counterparts in the higher spaces. The musculophrenic artery also supplies the lower part of the pericardium and the abdominal muscles.

Superior intercostal artery

The superior intercostal artery arises from the costocervical trunk. It descends between the pleura and the necks of the first and second ribs and anastomoses with the third posterior intercostal artery. Crossing the neck of the first rib, it lies medial to the ventral branch of the first thoracic spinal nerve, which it crosses at a lower level, and lateral to the stellate ganglion. In the first space it gives off the first posterior intercostal artery, which has a similar distribution to the lower posterior intercostal arteries. It descends to become the second posterior intercostal artery, usually joining a branch from the third. The artery is not constant, and is more common on the right; when absent, it is replaced by a direct branch from the aorta.

Posterior intercostal arteries

There are usually nine pairs of posterior intercostal arteries (Fig. 54.16). They arise from the posterior aspect of the descending thoracic aorta and are distributed to the lower nine intercostal spaces. Right posterior intercostal arteries are longer, because the aorta deviates to the left: they cross the vertebral bodies behind the oesophagus, thoracic duct and azygos vein, right lung and pleura. Left posterior intercostal arteries turn backwards on the vertebral bodies in contact with the left lung and pleura; the upper two are crossed by the left superior intercostal vein, and the lower by the hemiazygos and accessory hemiazygos veins. The further course of the arteries is the same on both sides. The sympathetic trunk lies anterior to all of the arteries, and the splanchnic nerves descend in front of the lower arteries.

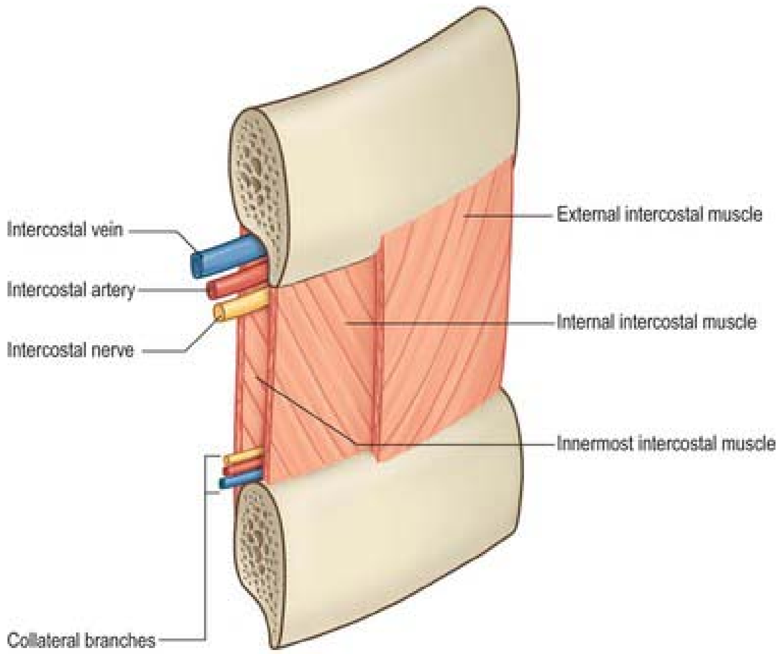
Intercostal vein
Intercostal artery
Intercostal nerve
Collateral branches
External intercostal muscle
Internal intercostal muscle
Innermost intercostal muscle

Fig. 54.16 Dissection of part of an intercostal space, showing the position of the intercostal vessels and nerve relative to the intercostal muscles.

Each artery crosses its intercostal space obliquely towards the angle of the rib above and continues forward in its costal groove. At first between the pleura and internal intercostal membrane as far as the costal angle, it passes between the internal intercostal and innermost intercostal muscles (Fig. 54.17), anastomosing with an anterior intercostal branch from either the internal thoracic or musculophrenic artery. Each artery has a vein above and a nerve below, except in the upper spaces, where the nerve at first lies above the artery. The third posterior intercostal artery anastomoses with the superior intercostal artery and may provide the major supply to the second space. The lower two arteries continue anteriorly into the abdominal wall, where they anastomose with the subcostal, superior epigastric and lumbar arteries. Each posterior intercostal artery has dorsal, collateral, muscular and cutaneous branches.

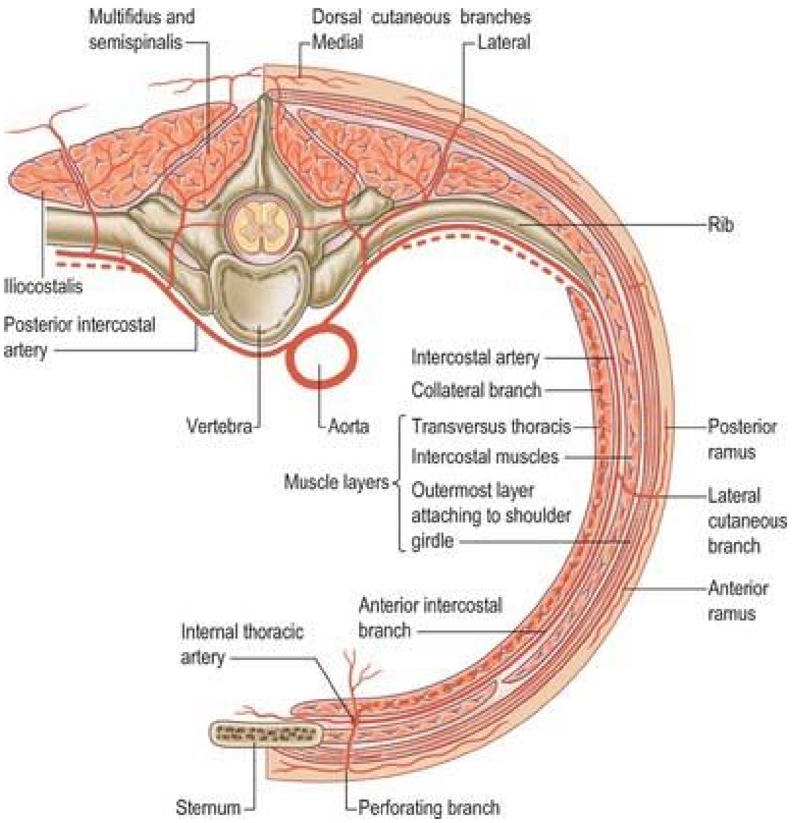
Multifidus and semispinalis
Dorsal cutaneous branches
Medial
Lateral
Rib
Iliocostalis
Posterior intercostal artery
Vertebra
Aorta
Intercostal artery
Collateral branch
Transversus thoracis
Intercostal muscles
Outermost layer attaching to shoulder girdle
Muscle layers
Posterior ramus
Lateral cutaneous branch
Anterior ramus
Anterior intercostal branch
Internal thoracic artery
Sternum
Perforating branch

Fig. 54.17 Schematic transverse section through one half of a lower intercostal space to show the branches of a typical intercostal artery. The usual branching arrangement of the dorsal cutaneous branch is shown to the right of the spine and a common variant is shown to the left.

(By permission from Cormack GC, Lamberty BGH 1994 The Arterial Anatomy of Skin Flaps, 2nd edn. Edinburgh: Churchill Livingstone.)

Dorsal branch

Each dorsal branch runs dorsally between the necks of adjoining ribs; a vertebral body and superior costotransverse ligament lie medial and lateral, respectively. Each dorsal branch gives off a spinal branch which enters the vertebral canal via the intervertebral foramen and supplies the vertebrae, spinal cord and meninges, and anastomoses with the spinal arteries above and below and with its contralateral fellow. It then divides into a medial and a lateral dorsal musculocutaneous branch (occasionally these arise separately from the posterior intercostal artery rather than from a common trunk). The medial branch crosses a transverse process with the medial dorsal branch of a thoracic spinal nerve to supply spinalis and longissimus thoracis and an area of overlying skin. The lateral branch supplies longissimus thoracis and iliocostalis, and the medial aspects of latissimus dorsi and trapezius, in addition to an area of overlying skin.

Collateral intercostal branch

A collateral intercostal branch arises near the costal angle and descends to the upper border of the subjacent rib, along which it courses to anastomose with an anterior intercostal branch of the internal thoracic or musculophrenic artery.

Muscular branches

Muscular branches supply intercostal and pectoral muscles and serratus anterior, and anastomose with the superior and lateral thoracic branches of the axillary artery. Lateral cutaneous branches accompany the same branches of the thoracic spinal nerves. Mammary branches from the vessels in the second to fourth spaces supply the pectoral muscles, breast tissue and skin: they enlarge during lactation.

Lateral cutaneous branch

The lateral cutaneous branch is given off in the posterior part of the intercostal space and travels anteriorly for a few centimetres with an accompanying vein and the lateral cutaneous branch of the equivalent intercostal nerve. This neurovascular bundle pierces the intercostal muscles and emerges lower down between the interdigitations of serratus anterior and external oblique. It divides into anterior and posterior rami, which contribute to the blood supply of the skin of the lateral trunk; these vessels are less significant in the upper three intercostal spaces.

Unnamed branches

Other unnamed branches supply tissues of the thoracic wall, e.g. costal periosteum, bone and bone marrow of the ribs, tissues of synovial and synarthrodial joints and the parietal pleura.

VEINS

Internal thoracic veins

The internal thoracic veins are venae comitantes of the inferior half of the internal thoracic artery. Near the third costal cartilages, the veins unite and ascend medial to the artery to end in their appropriate brachiocephalic vein (see Fig. 28.14). Tributaries correspond to branches of the artery, and include a pericardiacophrenic vein. The internal thoracic veins have several valves.

Left superior intercostal vein

The left superior intercostal vein drains the second and third (sometimes fourth) left posterior intercostal veins. It ascends obliquely forwards across the left aspect of the aortic arch, lateral to the left vagus and medial to the left phrenic nerve, to open into the left brachiocephalic vein (see Fig. 28.14). It usually receives the left bronchial veins, sometimes the left pericardiacophrenic vein, and connects inferiorly with the accessory hemiazygos vein.

Posterior intercostal veins

The posterior intercostal veins accompany their arteries in 11 pairs. Approaching the vertebral column, each vein receives a posterior tributary that returns blood from the dorsal muscles and skin and the vertebral venous plexuses (see Fig. 55.4A,B). On both sides, the first posterior intercostal vein ascends anterior to the neck of the first rib, arching forward above the pleural dome to end in the ipsilateral brachiocephalic or vertebral vein. On the right side, the second, third and often fourth veins form a right superior intercostal vein that joins the arch of the azygos vein. Veins from the lower spaces drain directly to the azygos. On the left side, the second, third and sometimes fourth veins form a left superior intercostal vein. Veins from the fourth or fifth to eighth intercostal spaces end in the accessory hemiazygos vein, and veins from the ninth to the eleventh intercostal spaces end in the hemiazygos vein.

Posterior intercostal veins are so called to distinguish them from small anterior intercostal veins, which are tributaries of the internal thoracic and musculophrenic veins.

LYMPHATIC DRAINAGE

Superficial lymphatic vessels of the thoracic wall ramify subcutaneously and converge on the axillary nodes (see Fig. 54.19). Those superficial to trapezius and latissimus dorsi unite to form 10 or 12 trunks which end in the subscapular nodes. Those in the pectoral region, including vessels from the skin covering the periphery of the breast and its subareolar plexus, run back, collecting those superficial to serratus anterior, to reach the pectoral nodes. Vessels near the lateral sternal margin pass between the costal cartilages to the parasternal nodes, but also anastomose across the sternum. A few vessels from the upper pectoral region ascend over the clavicle to the inferior deep cervical nodes. Lymph from the deeper tissues of the thoracic walls drains mainly to the parasternal, intercostal or diaphragmatic nodes.

Parasternal (internal thoracic) nodes

There are four or five parasternal nodes along each internal thoracic artery, at the anterior ends of the intercostal spaces. They drain afferents from the breast, deeper structures of the supraumbilical anterior abdominal wall, the superior hepatic surface (through a small group of nodes behind the xiphoid process) and deeper parts of the anterior thoracic wall. Their efferents usually unite with those from the tracheobronchial and brachiocephalic nodes to form the bronchomediastinal trunk. The latter may open, on either side, directly into the jugulosubclavian junction or into either great vein near the junction or may join the right subclavian trunk or right lymphatic duct, or the thoracic duct on the left.

Intercostal nodes

Intercostal nodes occupy the intercostal spaces near the heads and necks of the ribs. They receive deep lymph vessels from the posterolateral aspects of the chest and the breast, some of which are interrupted by small lateral intercostal nodes. Efferents of nodes in the lower four to seven spaces unite into a trunk that descends to the abdominal confluence of lymph trunks or to the start of the thoracic duct. Efferents of nodes in the left upper spaces end in the thoracic duct; those of the right upper spaces end in one of the right lymph trunks.

Diaphragmatic nodes

Located on the thoracic surface of the diaphragm, these nodes are arranged in anterior, right and left lateral, and posterior groups.

Anterior group

The anterior group consists of two or three small nodes behind the base of the xiphoid process, draining the convex hepatic surface, and one or two nodes on each side near the junction of the seventh rib and cartilage, which receive anterior lymph vessels from the diaphragm. The anterior group drains to the parasternal nodes.

Lateral groups

The lateral groups each contain two or three nodes, and lie close to the point where the phrenic nerves enter the diaphragm. On the right, some nodes lie within the fibrous pericardium anterior to the intrathoracic end of the inferior vena cava. Their afferents drain the central diaphragm; those on the right also drain the convex surface of the liver, and their efferents pass to the posterior mediastinal, parasternal and brachiocephalic nodes.

Posterior group

The posterior group consists of a few nodes that lie on the posterior aspect of the crura and connect with the lateral aortic and posterior mediastinal nodes.

Lymphatic drainage of deeper tissues

Collecting vessels of the deeper thoracic tissues include lymphatics that drain the muscles attached to the ribs. Most end in axillary nodes, and some from pectoralis major also drain to the parasternal nodes. Intercostal vessels drain the intercostal muscles and parietal pleura; those from the anterior thoracic wall and pleura end in the parasternal nodes, and their posterior counterparts drain to intercostal nodes.

Vessels from the diaphragm form two plexuses, thoracic and abdominal, which anastomose freely, especially in areas covered by pleurae and peritoneum respectively. The thoracic plexus unites with lymph vessels draining the costal and mediastinal pleura. Its efferents are anterior, draining to the anterior diaphragmatic nodes near the junctions of the seventh ribs and cartilages; middle, draining to nodes on the oesophagus and around the end of the inferior vena cava; posterior, draining to nodes around the aorta at the point where it leaves the thorax. The abdominal plexus anastomoses with the hepatic lymphatics and peripherally with those of the subperitoneal tissue. Efferents from its right half end in a group of nodes on the inferior phrenic artery, or in the right lateral aortic nodes. Those from the left half of the abdominal diaphragmatic plexus pass to the pre-aortic and lateral aortic nodes and to nodes near the terminal oesophagus.

INNERVATION OF THE CHEST WALL

THORACIC VENTRAL SPINAL RAMI

There are 12 pairs of thoracic ventral rami. The upper 11 lie between the ribs (intercostal nerves), and the twelfth lies below the last rib (subcostal nerve) (Figs 54.3, 54.18). Each is connected with the adjoining ganglion of the sympathetic trunk by grey and white rami communicantes; the grey ramus joins the nerve proximal to the point at which the white ramus leaves it. Intercostal nerves are distributed primarily to the thoracic and abdominal walls. The first two nerves supply fibres to the upper limb in addition to their thoracic branches, the next four supply only the thoracic wall, and the lower five supply both thoracic and abdominal walls. The subcostal nerve is distributed to the abdominal wall and the gluteal skin. Communicating branches link the intercostal nerves posteriorly in the intercostal spaces, and the lower five nerves communicate freely in the abdominal wall.

First to sixth thoracic ventral rami

The first thoracic ventral ramus divides unequally. A large branch ascends across the neck of the first rib, lateral to the superior intercostal artery, and enters the brachial plexus. The smaller branch is the first intercostal nerve; it runs in the first intercostal space and ends on the front of the chest as the first anterior cutaneous nerve of the thorax. It gives off a lateral cutaneous branch, which pierces the chest wall in front of serratus anterior and supplies the axillary skin; it may communicate with the intercostobrachial nerve and sometimes joins the medial cutaneous nerve of the arm. The first thoracic ramus often receives a connecting ramus from the second, which ascends in front of the neck of the second rib.

The second to sixth thoracic ventral rami pass forwards in their intercostal spaces below the intercostal vessels. Posteriorly they lie between the pleura and external intercostal membranes, but in most of their course they run between the internal intercostals and the subcostales and innermost intercostals. Near the sternum, they cross anterior to the internal thoracic vessels and transversus thoracis, pierce the internal intercostals, the external intercostal membranes and pectoralis major, and end as the anterior cutaneous nerves of the thorax, supplying the skin on the anterior chest wall. The second anterior cutaneous nerve may be connected to the medial supraclavicular nerves of the cervical plexus, and twigs from the sixth intercostal nerve supply abdominal skin in the upper part of the infrasternal angle.

Branches

Numerous slender muscular filaments supply the intercostals, serratus posterior superior and transversus thoracis. Anteriorly, some cross the costal cartilages from one intercostal space to another.

Each intercostal nerve gives off a collateral and a lateral cutaneous branch before it reaches the angle of the adjoining ribs (Fig. 54.18). The collateral branch follows the inferior border of its space in the same intermuscular place as the main nerve, which it may rejoin before it is distributed as an additional anterior cutaneous nerve. The lateral cutaneous branch accompanies the main nerve a little way and then pierces the intercostal muscles obliquely. With the exception of the lateral cutaneous branches of the first and second intercostal nerves, each divides into anterior and posterior rami that subsequently pierce serratus anterior. Anterior branches run forwards over the border of pectoralis major to supply the overlying skin; those of the fifth and sixth also supply twigs to a variable number of upper digitations of external oblique. Posterior branches run backwards and supply the skin over the scapula and latissimus dorsi.

The lateral cutaneous branch of the second intercostal nerve is the intercostobrachial nerve (see Fig. 46.30). It crosses the axilla to gain the medial side of the arm and joins a branch of the medial cutaneous nerve of the arm. It then pierces the deep fascia of the arm, and supplies the skin of the upper half of the posterior and medial parts of the arm, communicating with the posterior cutaneous branch of the radial nerve. Its size is in inverse proportion to the size of the medial cutaneous nerve. A second intercostobrachial nerve often branches off from the anterior part of the third lateral cutaneous nerve and sends filaments to the axilla and the medial side of the arm.

Seventh to eleventh thoracic ventral rami

The ventral rami of the seventh to eleventh thoracic nerves are continued anteriorly from the intercostal spaces into the abdominal wall; their further course is described in Chapter 62.

Lesions of the intercostal nerves

Subluxation of the interchondral joints between the lower costal cartilages may trap the intercostal nerves, causing referred abdominal pain. The dorsal cutaneous branch of an intercostal nerve can become entrapped as it penetrates the fascia of erector spinae. This produces an area of numbness, usually with painful paraesthesiae, which extends approximately 10 cm from the midline laterally and 10 cm in length (notalgia paraesthetica); the area between the medial edge of the scapula and the spine is commonly affected. The anterior cutaneous branches of the intercostal nerves can become entrapped as they penetrate the fascia of rectus abdominis, and this produces an area of numbness on the abdomen, usually with painful paraesthesiae, which extends from the midline laterally 10 or 12 cm (rectus abdominis syndrome).

Twelfth thoracic ventral ramus (subcostal nerve)

The ventral ramus of the twelfth thoracic nerve (subcostal nerve) is larger than the others and gives a communicating branch to the first lumbar ventral ramus (sometimes termed the dorsolumbar nerve). Like the intercostal nerves, it soon gives off a collateral branch and then accompanies the subcostal vessels along the inferior border of the twelfth rib, passing behind the lateral arcuate ligament and kidney and in front of the upper part of quadratus lumborum. It perforates the aponeurosis of the origin of transversus abdominis and passes forwards between that muscle and internal oblique, to be distributed in the same manner as the lower intercostal nerves. The subcostal nerve connects with the iliohypogastric nerve of the lumbar plexus and sends a branch to pyramidalis. Its lateral cutaneous branch pierces the internal and external oblique muscles and supplies the lowest slip of the latter. It usually descends over the iliac crest 5 cm behind the anterior superior iliac spine (see Fig. 61.4) and is distributed to the anterior gluteal skin; some filaments reach as low as the greater trochanter of the femur.

THORACIC DORSAL SPINAL RAMI

Thoracic dorsal rami pass backwards close to the vertebral zygapophysial joints and divide into medial and lateral branches. The medial branch emerges between the joint and the medial edge of the superior costotransverse ligament and intertransverse muscle. The lateral branch runs in the interval between the ligament and the muscle before inclining posteriorly on the medial side of levator costae.

Medial branches of the upper six thoracic dorsal rami pass between and supply semispinalis thoracis and multifidus; they then pierce the rhomboids and trapezius, and reach the skin near the vertebral spines (see Fig. 43.6). Medial branches of the lower six thoracic dorsal rami are distributed mainly to multifidus and longissimus thoracis; occasionally they give filaments to the skin in the median region. Lateral branches increase in size from above downwards. They run through or deep to longissimus thoracis to the interval between it and iliocostalis cervicis, and supply these muscles and levatores costarum; the lower five or six also give off cutaneous branches, which pierce serratus posterior inferior and latissimus dorsi in line with the costal angles (see Fig. 43.6). The lateral branches of a variable number of the upper thoracic rami also supply the skin. The lateral branch of the twelfth sends a filament medially along the iliac crest, then passes down to the skin of the anterior part of the gluteal region.

Medial cutaneous branches of the thoracic dorsal rami descend for some distance close to the vertebral spines before reaching the skin. Lateral branches descend for a considerable distance, which may be as much as the breadth of four ribs, before they become superficial, e.g. the branch of the twelfth thoracic ramus reaches the skin only a little way above the iliac crest.

BREAST

The breasts form a secondary sexual feature of females and are the source of nutrition for the neonate. They are also present in a rudimentary form in males. The breasts are the site of malignant change in as many as one in ten women. For reviews of normal breast structure, consult Ellis et al (1993).

In young adult females, each breast is a rounded eminence lying within the superficial fascia, largely anterior to the upper thorax but spreading laterally to a variable extent (Figs 54.19, 54.20B). Breast shape and size depend upon genetic, racial and dietary factors, and the age, parity and menopausal status of the individual. Breasts may be hemispherical, conical, variably pendulous, piriform or thin and flattened. In the adult female, the base of the breast, i.e. its attached surface, extends vertically from the second or third to the sixth rib, and in the transverse plane from the sternal edge medially almost to the midaxillary line laterally. The superolateral quadrant is prolonged towards the axilla along the inferolateral edge of pectoralis major, from which it projects a little, and may extend through the deep fascia up to the apex of the axilla (the axillary tail of Spence). The trunk superficial fascial system splits to enclose the breast to form the anterior and posterior lamellae. Posterior extensions of the superficial fascial system connect the breast to the pectoralis fascia, part of the deep fascial system. The inframammary crease is a zone of adherence of the superficial fascial system to the underlying chest wall at the inferior crescent of the breast.

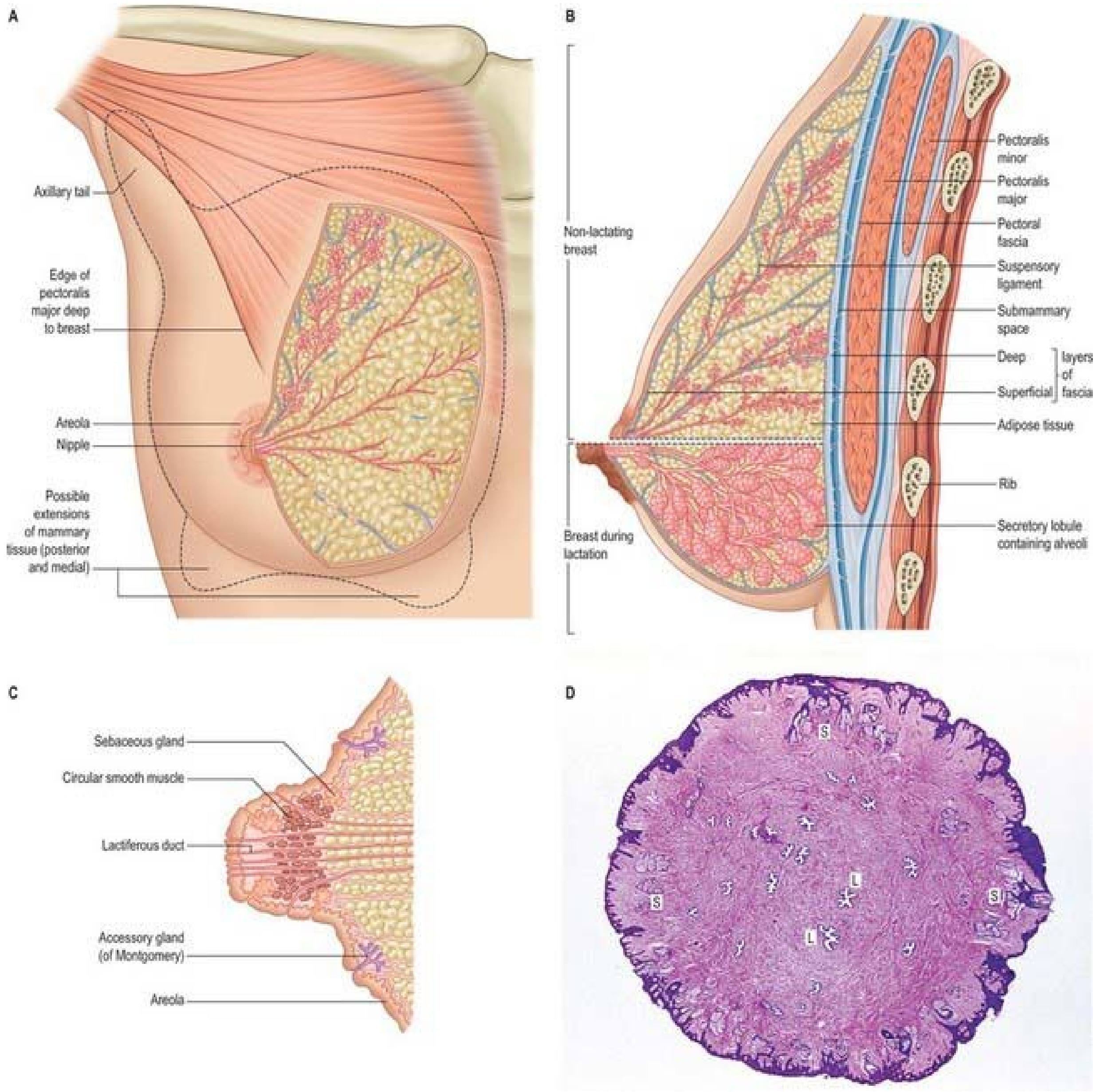
A
Axillary tail
Edge of pectoralis major deep to breast
Areola
Nipple
Possible extensions of mammary tissue (posterior and medial)
B
Non-lactating breast
Breast during lactation
Pectoralis minor
Pectoralis major
Pectoral fascia
Suspensory ligament
Submammary space
Deep
Superficial
layers of fascia
Adipose tissue
Rib
Secretory lobule containing alveoli
C
Sebaceous gland
Circular smooth muscle
Lactiferous duct
Accessory gland (of Montgomery)
Areola
D
S
L
L
S
S

Fig. 54.20 **A**, Structure of the breast. **B**, Changes in the breast during lactation. **C**, Section of the nipple. **D**, Cross-section of the nipple. There is a corrugated layer of stratified squamous keratinized epithelium over the nipple surface; 20 or more lactiferous ducts (L) open onto the surface; sebaceous glands (S) are deep to the epidermis.

*(**D**, By permission from Dr JB Kerr, Monash University, from Kerr JB 1999 Atlas of Functional Histology. London: Mosby.)*

The breast lies upon the deep pectoral fascia, which in turn overlies pectoralis major and serratus anterior superiorly and external oblique and its aponeurosis (as the latter forms the anterior wall of the sheath of rectus abdominis) inferiorly. Between the breast and the deep fascia the loose connective tissue in the ‘submammary space’ allows the breast some degree of movement on the deep pectoral fascia. Advanced mammary carcinoma may, by invasion, cause tethering or fixation of the breast to the underlying musculature. Occasionally, small projections of glandular tissue may pass through the deep fascia into the underlying muscle in normal subjects.

The nipple projects from the centre of the breast anteriorly (Fig. 54.20C,D). Its shape and projection varies from cylindrical and rounded at the top, to hemispherical, to flattened, depending on nervous, hormonal, developmental and other factors. The level of the nipple varies widely. In females, its site is dependent on the size and shape of the breasts, but it overlies the fourth intercostal space in most young women. In the male, the nipple is usually sited in the fourth intercostal space in the midclavicular line. In the young adult of either sex, the nipples are usually positioned 20–23 cm from the suprasternal notch in the midclavicular line and 20–23 cm apart in the horizontal plane. With increasing age and parity, female breasts adopt a more ptotic shape and the nipple position drops either to the level of the inframammary crease or lies below this surface landmark. In the nulliparous, it is pink, light brown or darker, depending on the general melanization of the body. Occasionally, the nipple may not evert during prenatal development, in which case it remains permanently retracted and so causes difficulty in suckling.

NIPPLE AND AREOLA

The skin covering the nipple and the surrounding areola (the disc of skin that circles the base of the nipple) has a convoluted surface (Fig. 54.20C). It contains numerous sweat and sebaceous glands which open directly onto the skin surface. The oily secretion of these specialized sebaceous glands acts as a protective lubricant and facilitates latching of the neonate during lactation: the glands are often visible in parous women, arranged circumferentially as small elevations, Montgomery’s tubercles, around the areola close to the margin. Other areolar glands, which are intermediate in structure between mammary and sweat glands, become enlarged in pregnancy and lactation as subcutaneous tubercles. The sebaceous glands of the areola usually lack hair follicles. The skin of the nipple and areola is rich in melanocytes and is therefore typically darker than the skin covering the remainder of the breast: further darkening occurs during the second month of pregnancy, and subsequently persists to a variable degree.

SOFT TISSUE

The breasts are composed of lobes which contain a network of glandular tissue consisting of branching ducts and terminal secretory lobules in a connective tissue stroma (see Fig. 54.26A). The terminal duct lobular unit is the functional milk secretory component of the breast and pathologically gives rise to primary malignant lesions within the breast. Although the lobes are usually described as discrete territories, they intertwine in three dimensions and merge at their edges; they cannot be distinguished during surgery. The connective tissue stroma that surrounds the lobules is dense and fibrocollagenous, whereas intralobular connective tissue has a loose texture that allows the rapid expansion of secretory tissue during pregnancy (see Fig. 54.26B). Fibrous strands or sheets consisting of condensations of connective tissue extend between the layer of deep fascia that covers the muscles of the anterior chest wall and the dermis. These suspensory ligaments (of Astley Cooper) are often well developed in the upper part of the breast and support the breast tissue, helping to maintain its non-ptotic form. Elsewhere in the normal breast, fibrous tissue surrounds the glandular components and extends to the skin and nipple, assisting the mechanical coherence of the gland. The interlobar stroma contains variable amounts of adipose tissue which is responsible for much of the increase in breast size at puberty.

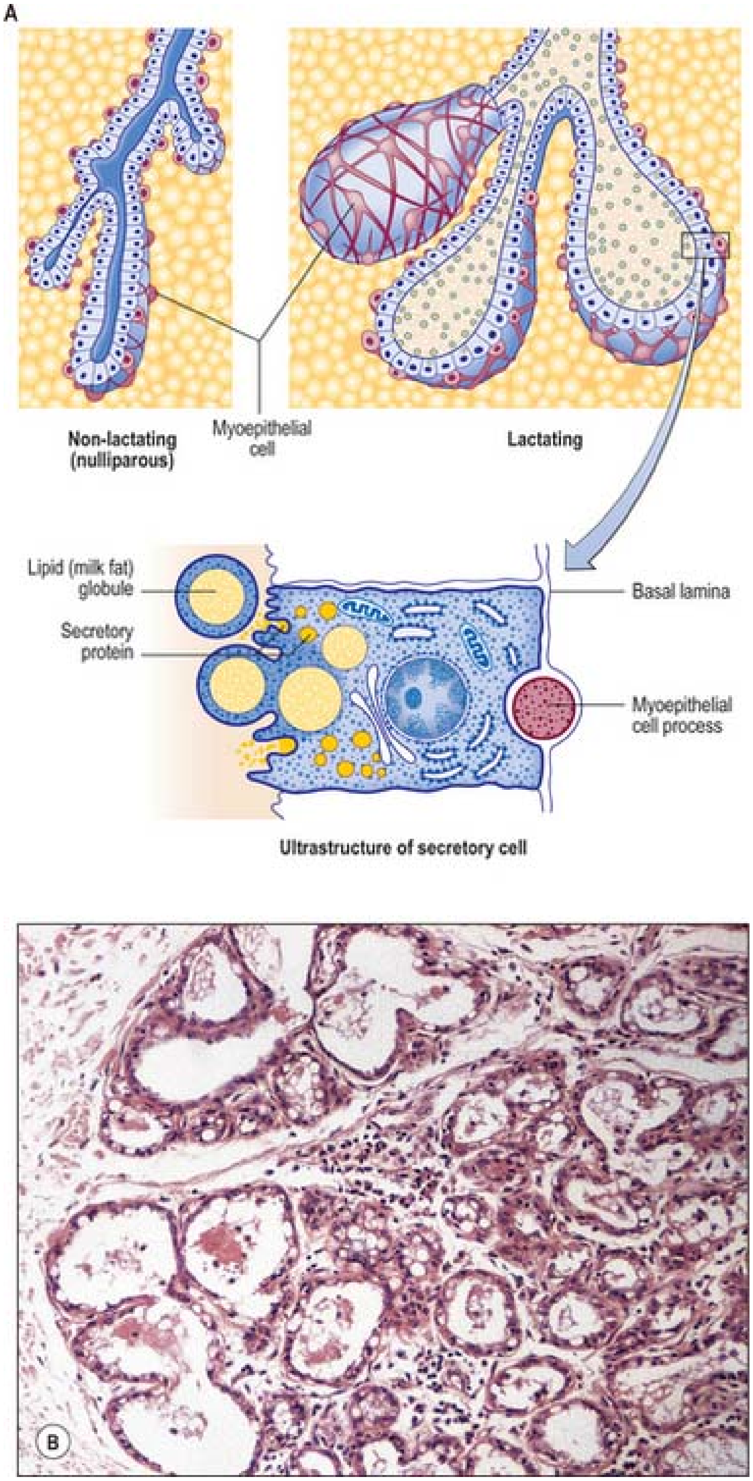
A
Non-lactating
(nulliparous)
Myoepithelial
cell
Lactating
Lipid (milk fat)
globule
Secretory
protein
Basal lamina
Myoepithelial
cell process
Ultrastructure of secretory cell
B

Fig. 54.26 Microstructure of breast epithelium. **A**, Note that the myoepithelial process is actually about half the relative size shown in the lower diagram. **B**, The peripheral part of a lactating breast lobule enclosed by a connective tissue septum (left). The alveoli are distended by milk

secretion. Milk protein appears as eosinophilic material in the lumen and milk fat as pale cytoplasmic vacuoles in the flattened alveolar epithelium. Intralobular connective tissue between the alveoli contains a prominent lymphocytic infiltration, including plasma cells secreting IgA.

VASCULAR SUPPLY AND LYMPHATIC DRAINAGE

Arteries

The breasts are supplied by branches of the axillary artery, the internal thoracic artery, and some intercostal arteries. The axillary artery supplies blood via the superior thoracic artery, the pectoral branches of the thoracoacromial artery, the lateral thoracic artery (via branches which curve around the lateral border of pectoralis major to supply the lateral aspect of the breast) and the subscapular artery. The internal thoracic artery supplies perforating branches to the anteromedial part of the breast. The second to fourth anterior intercostal arteries supply perforating branches more laterally in the anterior thorax: the second perforating artery is usually the largest, and supplies the upper region of the breast, and the nipple, areola and adjacent breast tissue.

Veins

Blood drains from the circular venous plexus around the areola and from the glandular tissue of the breast into the axillary, internal thoracic and intercostal veins via veins that accompany the corresponding arteries. Individual variation is common.

Lymphatic drainage

The lymphatic flow of the breast is of great clinical significance because metastatic dissemination occurs principally by the lymphatic routes. The dominant lymphatic drainage of the breast is derived from the dermal network. The breast lymphatics branch extensively and do not contain valves: lymphatic blockage through tumour occlusion may therefore result in reverse blood flow through the lymphatic channels. The direction of lymphatic flow within the breast parallels the major venous tributaries and enters the regional lymph nodes via the extensive periductal and perilobular network of lymphatic channels. Most of these lymphatics drain into the axillary group of regional lymph nodes either directly or through the retroareolar lymphatic plexus (see Fig. 46.28). Dermal lymphatics also penetrate pectoralis major to join channels that drain the deeper parenchymal tissues, and then follow the vascular channels to terminate in the subclavicular lymph nodes. Lymphatics from the left breast ultimately terminate in the thoracic duct and subsequently the left subclavian vein. On the right, the lymphatics ultimately drain into the right subclavian vein near its junction with the internal jugular vein. Part of the medial side of the right breast drains towards the internal thoracic group of lymph nodes. The internal thoracic chain may drain inferiorly via the superior and inferior epigastric lymphatic routes to the groin. Connecting lymphatics across the midline may provide access of lymphatic flow to the opposite axilla.

Axillary nodes receive more than 75% of the lymph from the breast (Fig. 54.21). There are 20–40 nodes, grouped artificially as pectoral (anterior), subscapular (posterior), central and apical. Surgically, the nodes are described in relation to pectoralis minor. Those lying below pectoralis minor are the low nodes (level 1), those behind the muscle are the middle group (level 2), while the nodes between the upper border of pectoralis minor and the lower border of the clavicle are the upper or apical nodes (level 3). There may be one or two other nodes between pectoralis minor and major; this interpectoral group of nodes are also known as Rotter’s nodes. Efferent vessels directly from the breast pass round the anterior axillary border through the axillary fascia to the pectoral lymph nodes; some may pass directly to the subscapular nodes. A few vessels pass from the superior part of the breast to the apical axillary nodes, sometimes interrupted by the infraclavicular nodes or by small, inconstant, interpectoral nodes. Most of the remainder drains to parasternal nodes from the medial and lateral parts of the breast; they accompany perforating branches of the internal thoracic artery. Lymphatic vessels occasionally follow lateral cutaneous branches of the posterior intercostal arteries to the intercostal nodes.

Axillary surgery in breast cancer

Axillary lymph node dissection may be performed because the presence of metastases within axillary lymph nodes has strong prognostic significance and might influence decisions on adjuvant therapy. However, axillary lymph node dissection can lead to chronic postoperative problems such as pain, seroma formation, reduced mobility of the arm, impaired sensation and lymphoedema The vessels and nerves have to be carefully identified at surgery as anatomical landmarks.

Lymphatic drainage in breast cancer and role of sentinel lymph node biopsy

Lymphatic mapping with sentinel lymph node biopsy has become an important technique in the staging of patients with early breast cancer. A radiolabelled colloid is injected into either the subareolar tissue of the index quadrant of the breast or the peritumoural tissue and intradermal tissue overlying the primary breast cancer. At the time of surgery, a vital blue dye is injected after general anaesthesia is established. The combination of radioisotope and dye provides the most accurate means of localizing the sentinel node (Rubio & Klimberg 2001, Tanis et al 2001). The sentinel node represents the first draining node of the axilla and is surgically removed for careful histopathological analysis to detect the presence of metastases. The sentinel node procedure seeks to identify this first draining node, and, if negative for cancer metastases, avoids more radical surgery in women who have no cancer spread, thus reducing morbidity associated with axillary dissection. In women who are found to have metastases to the axillary node, selective treatment to the axilla by completion axillary dissection or radiotherapy is offered. The majority of sentinel nodes are found in the low axilla within the level I group of nodes but can sometimes be found in higher echelon axillary nodes. This occurs in 5–10% of cases; the nodes are termed skip-metastases. Occasionally, the sentinel node is identified in an extra-axillary position, either within the breast parenchyma in an intramammary lymph node, the internal thoracic lymph node chain, or in the supraclavicular fossa.

INNERVATION

The breast is innervated by anterior and lateral branches of the fourth to sixth intercostal nerves, which carry sensory and sympathetic efferent fibres. The nipple is supplied from the anterior branch of the lateral cutaneous branch of T4 which forms an extensive plexus within the nipple; its sensory fibres terminate close to the epithelium as free endings, Meissner corpuscles and Merkel disc endings. These are essential in signalling suckling to the central nervous system. Secretory activities of the gland are largely controlled by ovarian and hypophysial hormones rather than by efferent motor fibres. The areola has fewer sensory endings.

MICROSTRUCTURE

The microstructure of breast tissue varies with age, time in the menstrual cycle, pregnancy and lactation. The following description relates to the mature, resting breast. For most of their lengths, the ducts are lined by columnar epithelium (Fig. 54.22). In the larger ducts, this is two cells thick, but, in the smaller ones, only a single layer of columnar or cuboidal cells is present. The bases of these cells are in close contact with numerous myoepithelial cells of ectodermal origin, similar to those of certain other glandular epithelia (see Figs 2.3, 54.26A). Myoepithelial cells are so numerous that they form a distinct layer surrounding the ducts and presumptive alveoli and give the epithelium a bilayered appearance.

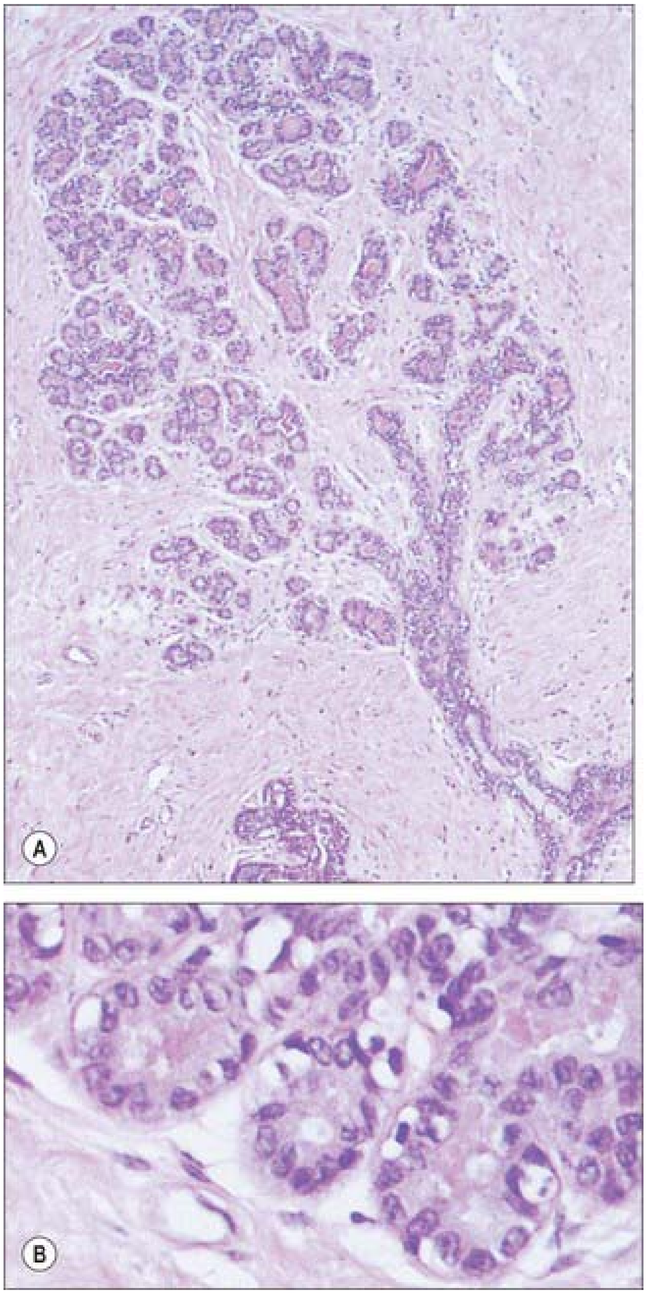

Fig. 54.22 **A**, A glandular lobule surrounded by collagenous interlobular connective tissue in the mature resting breast. A terminal duct (bottom right) branches extensively to terminate in rudimentary acini, which are shown at higher magnification in the lower panel (**B**).

(By permission from Young B, Heath JW 2000 Wheater's Functional Histology. Edinburgh: Churchill Livingstone.)

Lactiferous ducts draining each lobe of the breast pass through the nipple and open onto its tip as 15–20 orifices. Near its orifice, each of these ducts is slightly expanded as a lactiferous sinus, which, in the lactating breast, is further dilated by the presence of milk. Each lactiferous duct is therefore connected to a system of ducts and lobules, surrounded by connective tissue stroma, collectively forming a lobe of the breast. Lobules consist of the portions of the glands that have secretory potential. Their structure varies according to hormonal status. In the mature resting breast, each lobule consists of a cluster of blind-ended, branched ductules whose termini lack terminal alveoli (acini), which are the sites of milk secretion in the lactating breast (see Fig. 54.26B). The stratified cuboidal lining is replaced by keratinized stratified squamous epithelium, continuous with the epidermis, close to the openings of the lactiferous ducts on the nipple. Shed squames may sometimes block the duct apertures in the non-pregnant breast.

Internally, the nipple is composed mostly of collagenous dense connective tissue and contains numerous elastic fibres which wrinkle the overlying skin. Deep to the nipple and areola, bundles of smooth muscle cells are arranged radially and circumferentially within the connective tissue. Their contraction, induced by cold or tactile stimuli (e.g. in suckling), causes erection of the nipple and wrinkling of the surrounding areola.

BREAST CANCER

Breast cancer is a common disease, particularly in postmenopausal women (see Fentiman 1993). Each year in the United Kingdom, there are approximately 40,000 new cases diagnosed and 14,000 deaths. Male breast cancers make up 1% of all mammary malignancies and may include tissue beyond the areolar boundary.

Breast cancers arise within the epithelia of lobules or ducts. As they increase in size and infiltrate the stroma they often lead to a fibrous tissue reaction. Breast lumps may be classified as benign or malignant masses. Malignant breast lumps may have the clinical signs of infiltrating adjacent structures, leading to a hard and irregular mass with skin-tethering, muscle fixation, skin infiltration or oedema of the overlying skin (peau d'orange). Standard radiological imaging investigations of the breast include mammography and ultrasonography. Mammography is useful in detecting the presence of malignant masses as a stellate opacity with architectural distortion of the surrounding parenchyma. Early stages of preinvasive breast cancer, ductal cancer *in situ*, may appear as microcalcification on the mammogram. An ultrasound scan of the breast is helpful to distinguish solid from cystic (or fluid-filled) masses, and can also aid in the distinction of breast cancer from benign lumps by the different attenuation characteristics of the ultrasound waves and blood flow patterns. Magnetic resonance imaging is also useful in diagnosis, particularly in women with younger, more dense breasts, achieving higher sensitivity of breast cancer detection but with lower specificity. A cytological diagnosis of a breast lump can be achieved using fine needle aspiration (FNA) to evaluate the cellular component of a lump. FNA is also useful to drain symptomatic breast cysts. A wide bore needle biopsy is a procedure performed under local anaesthetic to obtain several pieces of specimen for a histological diagnosis with the tissue architecture maintained. This permits distinction between *in situ* and invasive cancer and provides an indication of tumour subtype by evaluation of the pathological characteristics. Vacuum-assisted mammotome biopsies based on the wide bore needle enables some benign and indeterminate lesions to be excised for full histological analysis and in some patients can avoid the need for conventional open surgery.

If a breast lump has to be surgically removed, the incision should be based, whenever possible, in the relaxed skin tension lines, for the best cosmetic results. In women with sizeable malignant lesions where breast conservation surgery is to be attempted, the skin incision should be planned with consideration of the possible requirement of the need for a subsequent mastectomy if the margins of excision are incompletely excised by pathological criteria. Most women with single breast cancers up to 4 cm in diameter are treated by breast conservation rather than mastectomy. This is a combination of surgery (tumour excision and axillary lymph node sampling or clearance) together with external beam radiotherapy. Patients with larger tumours are treated by modified radical mastectomy with axillary lymph node clearance. During axillary dissection to clear the axillary lymph nodes, the nerve to serratus anterior, the thoracodorsal vessels, the nerve to latissimus dorsi, and the medial and lateral pectoral nerves are all identified and carefully preserved. The boundaries of the axillary dissection are the nerve to serratus anterior medially, the thoracodorsal pedicle laterally and the axillary vein superiorly (see Fig. 46.30). The posterior limit of the dissection is the ventral surface of subscapularis. The superomedial limit of a level I axillary dissection extends to the lateral border of pectoralis minor at the apex of the axilla, a level II dissection extends to the medial border of pectoralis minor, and a level III dissection extends beyond the medial border until it reaches the point where the axilla is limited by the first rib (the latter is easily distinguished by its flat lateral surface, easily palpable at surgery). Failure to preserve the nerve to serratus anterior will result in winging of the scapula. The intercostobrachial nerve is often sacrificed in an axillary lymph node clearance operation, and this may result in anaesthesia of a narrow strip of sensation in the upper medial border of the arm.

Reconstructive surgery for breast cancer disease

Breast reconstruction may be performed at the time of mastectomy for breast cancer, or at a later stage (Serletti & Moran 2000). During a mastectomy where an immediate breast reconstruction is planned, the glandular breast tissue is removed either through a conventional mastectomy skin incision or in association with preservation of the native breast skin, a form of mastectomy termed a skin-sparing mastectomy. Patient selection is important to minimize risks of breast cancer recurrence in the skin of the reconstructed breast mound or associated lymph nodes. In an implant-based immediate breast reconstruction, a tissue expander is placed beneath the submusculofascial plane consisting of pectoralis major, in continuity laterally under serratus anterior with the intervening fascia, and the abdominal fascia inferiorly. The lower fibres of the attachment of pectoralis major to the sixth rib need to be detached, otherwise the implant will be placed too high on the chest wall. The tissue expander has to stretch the potential space below this musculofascial plane to match the space created by the removed breast beneath the subcutaneous plane and the deep fascia overlying pectoralis major. The tissue expander is subsequently replaced by a silicone or saline breast implant.

The skin and volume component of the breast can also be replaced by the latissimus dorsi musculocutaneous flap with or without an underlying silicone or saline breast implant. Latissimus dorsi and an overlying paddle of skin is raised on its dominant vascular pedicle, namely the thoracodorsal artery and vein, which enter the muscle on its deep surface and send perforating branches through the muscle to the overlying skin. The flap is transferred in an arc from the back to the front of the chest and fashioned to make a new breast. An implant is usually required to provide additional volume replacement, in which case it is placed beneath the flap. The donor defect on the back is directly sutured and there is minimal functional disability following transfer of latissimus dorsi. In suitable women, subcutaneous fat harvested in conjunction with the latissimus dorsi muscle may contain sufficient material to avoid the need for an implant as an autologous tissue breast reconstruction.

The skin and volume component of the breast can be replaced by a pedicled transverse rectus abdominis musculocutaneous flap (TRAM flap). In a pedicled TRAM flap, rectus abdominis and a transverse ellipse of skin from the lower abdomen are raised on the superior epigastric artery, which enters the deep surface of the muscle below the costal cartilage. Women suitable for an abdominal-based procedure have a sufficient abdominal panniculus to form the donor tissue in order to recreate the breast mound without an implant. Microvascular surgical techniques now permit the free transfer of the lower abdominal panniculous skin and subcutaneous fat based upon the cutaneous supply of the deep inferior epigastric artery with minimal disruption to rectus abdominis. Cutaneous perforators near the level of the umbilicus pass to the skin in two rows (a medial and a lateral row). If the superior epigastric artery is used as the pedicle for the flap, the deep inferior epigastric artery is ligated and the flap is swung on the pedicle and tunnelled up into the chest where it is fashioned into a new breast. If the deep inferior epigastric artery is used as the pedicle, the superficial epigastric artery is divided and the flap is transferred as a free flap; the deep inferior epigastric artery and vein are anastomosed to recipient vessels either in the chest (usually the internal thoracic vessels, accessed by removing the third costal cartilage) or to the dominant anterior intercostal perforator in the second (or third) intercostal space. A deep inferior epigastric artery perforator flap (DIEP flap) can be raised by dissecting a single cutaneous perforator through rectus abdominus to its origin from the deep inferior epigastric artery, a procedure that obviates the need to sacrifice the muscle.

The advantage of the TRAM flap over the latissimus dorsi flap is that there is sufficient volume to reconstruct even a large breast without the need for an implant. The donor defect in the abdominal wall is sutured directly; where the muscle has been harvested in the pedicled TRAM flap, a mesh may be incorporated into the repair of the rectus sheath to reduce the potential risk of muscle weakness caused by surgical disruption of rectus abdominis, which could produce a bulge of the abdominal contents or a hernia.

DEVELOPMENT

The epithelial/mesenchymal interactions that will give rise to the glandular tissue of the breast, in both sexes, can first be seen at about the fifth or sixth week, when two ventral bands of thickened ectoderm, the mammary ridges or milk lines, extend from the axilla to the inguinal region. Usually, invagination of the thoracic mammary bud occurs by day 49, and the remaining mammary line involutes.

The thoracic ectodermal ingrowths branch into 15–20 solid buds of ectoderm which will become the lactiferous ducts and their associated lobes of alveoli in the fully formed gland. They are surrounded by somatopleuric mesenchyme which forms the connective tissue, fat and vasculature which is invaded by the mammary nerves. Continued cell proliferation, elongation and further branching produces the alveoli and defines the duct system. Nipple formation begins at day 56, primitive ducts (mammary sprouts) develop at 84 days and canalization occurs at about the 150th day. During the last 2 months of gestation the ducts become canalized; the epidermis at the point of original development of the gland forms a small mammary pit, into which the lactiferous tubules open (Fig. 54.23). Perinatally the nipple is formed by mesenchymal proliferation. Should this process fail, the ducts open into shallow pits. Rarely, the nipple may not develop (athelia), a phenomenon that occurs more commonly in accessory breast tissue.

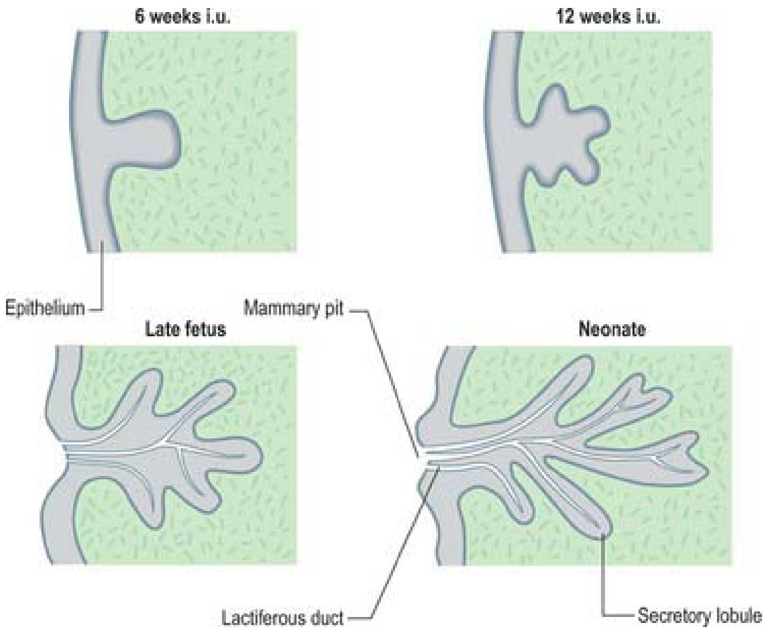

Fig. 54.23 Early development of breast epithelium.

At birth the breasts have reached a similar developmental stage in both sexes: the combination of fetal prolactin and maternal oestrogen may give rise to transient hyperplasia and secretion of ‘witch’s milk’. In males, the breasts normally remain undeveloped, whereas in females at puberty, in late pregnancy and during the period of lactation, they undergo further, hormone-dependent, developmental changes. The female breast is a unique organ in that it remains in a rudimentary (i.e. fetal) form until puberty, at which time its development continues under the influence of sex hormones. The adult form is reached in late adolescence, i.e. the breast is then able to function as a milk-producing organ. At menopause, the breast involutes into a predominantly fatty organ with minimal glandular parenchyma.

Accessory breast tissue and nipples

Polymastia (supernumerary breasts) and polythelia (supernumerary nipples) may develop in males and females anywhere along the length of the mammary ridges (milk lines; Fig. 54.24). Conversely, breast tissue may not develop at all (amastia) or there may be nipple development but no breast tissue (amazia). Supernumerary breast development occurs in most cases in the thoracic region, just inferior to the normal breast (90%), but may also occur in the axillary (5%) and abdominal regions (5%). Polythelia occurs along the same mammary line but no underlying glandular tissue develops. About 1% of the female population has this condition, but it is more common in males, where the accessory nipple may be mistaken for a mole.

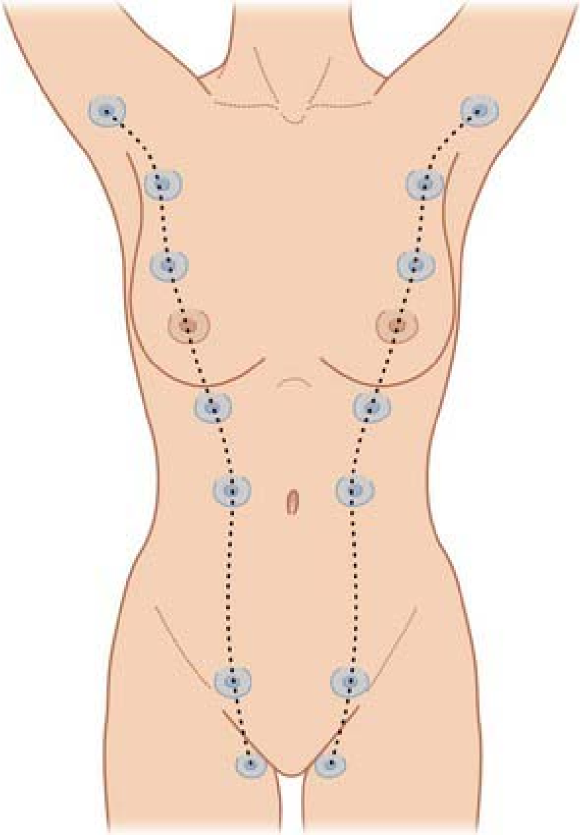

Fig. 54.24 The milk lines.

Congenital inversion of nipple

Congenital inversion of the nipples occurs in about 3% of the female population. The condition is almost always bilateral. The majority of the cases are umbilicated, i.e. the nipple can be easily pulled forward from its depressed position underneath the areolar surface. The condition is thought to be due to failure of proliferation of the mesenchymal tissue, which fails to push the nipple out. The remaining cases are due to invagination of the nipple. Apart from psychological implications, inversion of the nipple may cause recurrent mastitis and difficulty with breast feeding. The abnormality may be corrected surgically.

AGE-RELATED CHANGES

Prepuberty

The neonatal breast contains lactiferous ducts but no alveoli. Until puberty, little branching of the ducts occurs, and any slight mammary enlargement reflects the growth of fibrous stroma and fat.

Puberty

In the postpubertal female, the ducts, stimulated by ovarian oestrogens, become branched. The ends of the branches form solid, spheroidal masses of granular polyhedral cells, the potential alveoli. Oestrogens also promote adipocyte differentiation from mesenchymal cells in the interlobar stroma: breast enlargement at puberty is largely a consequence of lipid accumulation by these adipocytes.

From puberty onwards, externally recognizable breast development (thelarche) can be divided into five separate phases (Fig. 54.25): elevation of the breast bud (phase I); glandular subareolar tissue is present and both nipple and breast project from the chest wall as a single mass (phase II); the areola increases in diameter and becomes pigmented, and there is proliferation of palpable breast tissue (phase III); further pigmentation and enlargement occurs in the areola, so that the nipple and areola form a secondary mass anterior to the main part of the breast (phase IV); a smooth contour to the breast develops (phase V).

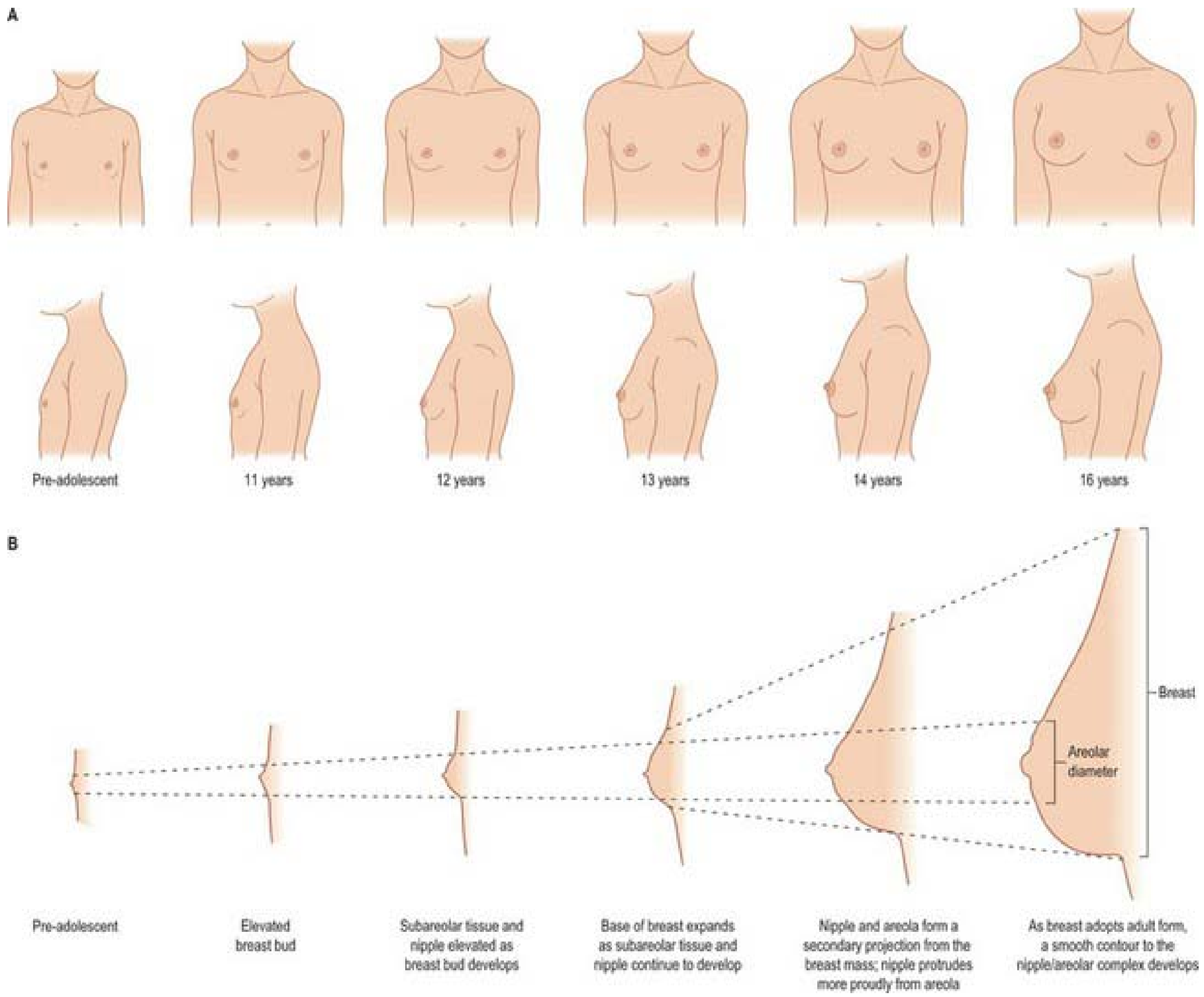
A
Pre-adolescent
11 years
12 years
13 years
14 years
16 years
B
Breast
Areolar diameter
Pre-adolescent
Elevated breast bud
Subareolar tissue and nipple elevated as breast bud develops
Base of breast expands as subareolar tissue and nipple continue to develop
Nipple and areola form a secondary projection from the breast mass; nipple protrudes more proudly from areola
As breast adopts adult form, a smooth contour to the nipple/areolar complex develops

Fig. 54.25 Pre- and postpubertal development and structure of the female breast, demonstrating changes in the contour of the breast.

Changes during the menstrual cycle

Changes occur in the breast tissues in the menstrual cycle. In the follicular phase (days 3–14), the stroma becomes less dense. Various changes including luminal expansion take place in the ducts; there are occasional mitoses but no secretion. In the luteal phase (days 15–28), there is a progressive increase in stromal density and the ducts have an open lumen that contains secretion, associated with flattening of the epithelial cells. Cell proliferation is maximal on day 26 and thereafter the ductal system undergoes reduction; epithelial cell apoptosis is greatest on day 28 of the cycle. There are also changes in blood flow, which are greatest at midcycle, and an increase in the water content of the stroma in the second half of the menstrual cycle.

Postmenopausal

Progressive atrophy of lobules and ducts occurs after the menopause, and there is fatty replacement of glandular breast tissue. A few ducts may remain. The stroma becomes much less cellular and collagenous fibres decrease. The amount of adipose tissue varies widely between individuals, and the breast may return to a condition similar to the prepubertal state.

CHANGES ASSOCIATED WITH PREGNANCY AND LACTATION

Pregnancy

As the output of oestrogen and progesterone produced first by the corpus luteum and later by the placenta rises during pregnancy, the intralobular ductal epithelium proliferates and the cells increase in size: the number and length of the ductal branches therefore increase. Alveoli develop at their termini and expand as their cells and lumina fill with newly synthesized and secreted milk. The myoepithelial cells, which are initially spindle-shaped, become highly branched stellate cells, especially around the alveoli. Adjacent myoepithelial cells intermesh to form a basket-like network around the alveoli and ducts, interposed between the basal lamina and the luminal cells. Their cytoplasm contains actin and myosin filaments and they are contractile. There is a concomitant reduction in adipose tissue in the stroma. The numbers of lymphocytes, including plasma cells, and eosinophils increase greatly. Blood flow through the breast increases.

Secretory activity in the alveolar cells rises progressively in the latter half of pregnancy. In late pregnancy, and for a few days after parturition, their product is different from later milk and is known as colostrum, which is low in lipid but rich in protein and immunoglobulins. Colostrum confers a measure of passive immunity to the neonatal alimentary tract; it also has laxative properties. Proliferation of the glandular breast parenchyma results in an overall increase in breast size through gestation.

Lactation

True milk secretion begins a few days after parturition as a result of a reduction in circulating oestrogen and progesterone, a change which appears to stimulate production of prolactin by the anterior hypophysis.

Milk distends the alveoli so that the cells flatten as secretion increases (Figs 54.20B, 54.26B,C). The alveolar cell cytoplasm accumulates membrane-bound granules of casein and other milk proteins, and these are released from the apical plasma membrane by membrane fusion (merocrine secretion; see Ch. 2). Lipid vacuoles are formed directly in the apical cytoplasm as small lipid droplets which fuse with each other to create large ‘milk vacuoles’ up to 10 μm across, that frequently protrude from the cell surface. These are released as intact lipid droplets with a thin surround of apical plasma membrane and adjacent cytoplasm (apocrine secretion). On hormonal stimulation by oxytocin, myoepithelial cells contract to expel alveolar secretions into the ductal system in readiness for suckling.

After the onset of lactation there is a gradual reduction in the numbers of lymphocytes and eosinophils in the stroma, although plasma cells continue to synthesize IgA for secretion into the milk. Alveolar cells take up IgA synthesized by adjacent plasma cells by endocytosis at their basal surfaces and secrete it apically, as dimers complexed to epithelial secretory component.

Postlactation

When lactation ceases, which may be as long as 3½ years, or even longer if frequent suckling is maintained, the secretory tissue undergoes some involution, but the ducts and alveoli never return completely to the pre-pregnant state. Two major processes are responsible for the regression of the alveolar–ductal system: a reduction in epithelial cell size and a reduction in cell numbers mediated via apoptosis (see Ch. 1). Gradually the breast tissue reverts to its resting state. If another pregnancy occurs, the resting glandular tissue is reactivated, and the process outlined above recurs. Up to the age of 50 years, increasing amounts of elastic tissue tend to be laid down around vessels and ducts (elastosis), and also in the stroma. Elastosis does not normally continue into later life.

MALE BREAST

The male breast remains rudimentary throughout life. It is formed of small ducts (without lobules or alveoli) or solid cellular cords and a little supporting fibroadipose tissue (see Ellis et al 1993). Slight temporary enlargement may occur in the newborn, reflecting the influence of maternal hormones, and again at puberty. The areola is well developed, although limited in area, and the nipple is relatively small. It is usually stated that the ducts do not extend beyond the areola in a male breast, but glandular tissue can be more extensive.

Gynaecomastia

Gynaecomastia is a benign proliferation of subareolar breast tissue or excessive growth of breast tissue. It is usually bilateral but may be unilateral, and is commonly associated with pain or tenderness, which is thought to be due to accumulation of fluid in the glandular ducts. Histological changes are fibrosis, followed by hyalinization. It is sometimes due to a biochemical imbalance in the ratio of free oestrogens, androgens and sex hormone-binding globulin. Hence it is commonly seen after antiandrogen therapy for conditions such as prostatic cancer, but other drugs such as spironolactone, cimetidine, anabolic steroids and cannabinoids have been implicated. Gynaecomastia may have a hormonal basis during puberty and senescence, or in liver failure where normal hepatic function is associated with sex steroid hormone metabolism. However, the majority of cases have no known cause and are termed idiopathic gynaecomastia.

SURGICAL ACCESS TO THORACIC VISCERA

Thoracocentesis (pleural aspiration)

Thoracocentesis or pleural aspiration is an essential step in the assessment of pleural effusions. A chest radiograph will confirm the location and extent of the effusion and clinical examination will identify the best position for aspiration: the posterior midscapular line is a common site. The skin of the desired interspace is cleaned and anaesthetized, and the aspiration needle is inserted at the lower margin of the interspace. The needle is not inserted in the middle of the interspace because the intercostal vessels run along the middle of the interspace posteriorly, and from the axilla forwards onto the anterior chest wall they are protected only by the lower border of the rib. After appropriate local analgesia has been applied, the needle is carefully advanced in a perpendicular direction in the lower portion of the interspace until it enters the pleural space. More complex or small effusions should be aspirated under ultrasound guidance.

Needle thoracocentesis

Needle thoracocentesis is performed in patients in whom a life-threatening tension pneumothorax is suspected. A needle is inserted into the second intercostal space in the midclavicular line on the side of the tension pneumothorax, with the patient in an upright position. A sudden escape of air is heard when the needle enters the parietal pleura. A chest tube must be inserted after this procedure.

Chest drain insertion

The insertion site for a chest drain is usually the fifth intercostal space, just anterior to the midaxillary line on the affected side. A 2 cm horizontal incision is followed by blunt dissection through the subcutaneous tissues to the top of the rib. The parietal pleura is punctured with the tip of a clamp and a gloved finger inserted into the pleural space to free up any adhesions. The chest drain (thoracostomy tube) is then inserted into the pleural space and attached to an underwater sealed container placed below the level of the lungs: the water level rises and falls in the tube with ventilation.

Pericardiocentesis

Pericardiocentesis is performed to aspirate a pericardial effusion or, in an emergency, to decompress a cardiac tamponade, where pressure from blood in the pericardial space prevents the heart chambers from filling during the cardiac cycle, and seriously impairs cardiac output.

Pericardial puncture can be performed in either the fifth or sixth left intercostal space near the sternum (to avoid the internal thoracic artery), or at the left costoxiphoid angle. The needle is passed 1–2 cm to the left of the costoxiphoid angle at 45° to the skin, and then up and backwards towards the tip of the scapula until it enters the pericardial sac.

Placement of electrocardiograph leads

The 12-lead electrocardiograph (ECG) provides three-dimensional information on the electrical activity of the heart. The limb leads provide information about the electrical activity in the frontal plane. They are placed on the left and right wrists, and the left foot, with the right foot acting as a neutral grounding point. The chest leads provide information about the electrical activity in the horizontal plane. They are placed as follows: V1, right fourth intercostal space, parasternal position; V2, left fourth intercostal space, parasternal position; V3, midpoint of V2 and V4 on the left; V4, fifth intercostal space, midclavicular line on the left; V5, fifth intercostal space, anterior axillary line on the left; V6, fifth intercostal space, midaxillary line on the left.

Thoracotomy incisions

Thoracotomy incisions may be posterolateral, anterolateral or involve a transverse thoracosternotomy.

Posterolateral

A posterolateral incision is most commonly used in thoracic surgery for unilateral pulmonary resections, bullectomy, unilateral lung volume reduction surgery, chest wall resection and oesophageal surgery (Fry 2000). The patient is placed in a lateral decubitus position with adequate support of the elbow, axilla and knee with padding. The standard approach is via an incision from the anterior axillary line which curves about 4 cm below the tip of the scapula and then vertically between the posterior midline and medial edge of the scapula. The incision is usually extended to the level of the spine of scapula. Overall, the incision forms an S-shape in the fifth intercostal space. The sixth or seventh intercostal space is used in oesophageal surgery.

The lower portions of trapezius and latissimus dorsi are divided. Serratus anterior is retracted, and may be divided in a high thoracotomy. The costal muscle and pleura are dissected along the inferior margin of the intercostal space to avoid damaging the neurovascular bundle. A small section of rib is removed at the costovertebral angle to reduce the risk of fracture, particularly in patients older than 40 years. This technique provides good access to the thoracic contents; the main problem is postoperative pain as a consequence of intraoperative musculoskeletal traction.

Anterolateral

Using an anterolateral approach, the patient is placed in the supine position with their arms by their sides. A roll is placed vertically under the back and hips so as to raise the operative side by approximately 45°. The incision is from the midaxillary line over the fifth intercostal space along the inframammary fold, and curves upwards parasternally. The pectoral muscles are divided, and subsequent access to the thorax is similar to that used in the posterolateral approach. However, access is limited, and may be improved by dividing costal cartilages.

‘Clam shell’

The transverse thoracosternotomy is known as the ‘clam shell’ incision. It provides excellent exposure to both sides of the chest and is therefore used in bilateral lung transplantation and in lung volume reduction surgery with bilateral lung resections. The patient is placed in the supine position with a roll vertically along the upper thoracic spine. Bilateral anterolateral incisions are made in the inframammary fold, and the sternum is transected. This allows the upper portion of the thorax to be displaced upwards with a rib-spreader, hence the name clam shell. The main disadvantage of the clam shell procedure is the need to transect the sternum: even after careful repair with sternal wires, there is a risk of sternal instability.

Sternotomy

Sternotomy is commonly needed in cardiac surgery. The patient is placed in the supine position with both arms extended by the side. A vertical incision is made in the midline from the suprasternal notch to a point just below the xiphoid process. The tissues around the manubrium and the xiphoid process are mobilized. The pectoral fascia in the midline is incised and the sternum is split and its two edges retracted. The sternum is closed using interosseous wire sutures.

Axillary thoracotomy

The patient is placed in the lateral decubitus position, with arms abducted at 90° and supported on an arm rest. The incision is based along the desired intercostal space, which, for upper thoracic lesions, is the second or third space. Latissimus dorsi is elevated and retracted, whereas serratus anterior is divided in the direction of its fibres. The anterior aspect of serratus anterior is divided to expose the intercostal muscles, which are divided in turn. The overall size of the incision is limited and it provides good access to the upper thorax. Postoperative pain is less than with some other approaches, but the long thoracic nerve (nerve of Bell) may be damaged if serratus anterior is divided too posteriorly.

Thoracoscopic access

Occasionally, video-assisted thoracoscopic surgery is required to assess the mediastinum. The thoracoscope is usually introduced via the fifth intercostal space in the midclavicular line, with additional ports at the third and sixth intercostal spaces to assess the anterior mediastinum. To assess the posterior mediastinum, the thoracoscope is inserted into the seventh intercostal space in the midclavicular line.

REFERENCES

lis H, Colborn GL, Skandalakis JE. Surgical embryology and anatomy of the breast and its related anatomic structures. *Surg Clin North Am*. 1993;73:611-632.

ntiman IS. Detection and Treatment of Early Breast Cancer. London: Martin Dunitz, 1993.

y WA. Thoracic incisions. Shields TW, LoCicero JIII, Ponn RB. General Thoracic Surgery. 5th edn.. Philadelphia: Lippincott Williams & Wilkins; 2000:367-374.

ırihara Y, Yakushiji YK, Matsumoto J, Ishikawa T, Hirata K. The ribs: anatomic and radiologic considerations. *Radiographics*. 1999;19:105-119.

Includes some chest wall and ribcage abnormalities..

ıbio IT, Klimberg S. Techniques of sentinel lymph node biopsy. *Semin Surg Oncol*. 2001;20:214-223.

rletti JM, Moran SL. Microvascular reconstruction of the breast. *Semin Surg Oncol*. 2000;19:264-271.

nis PJ, Nieweg OE, Valdes Olmos RA, Kroon BB. Anatomy and physiology of lymphatic drainage of the breast from the perspective of sentinel node biopsy. *J Am Coll Surg*. 2001;192:399-409.

ıp LH, Whiten SC, Forster A, Stevenson JH. The anatomical and neurophysiological basis of the sensate free TRAM and DIEP flaps. *Br J Plast Surg*. 2002;55:35-45.

CHAPTER 55

Mediastinum

Strictly speaking, the mediastinum is the partition between the lungs and includes the mediastinal pleura. However, the term is commonly applied to the region between the two pleural sacs bounded anteriorly by the sternum and posteriorly by the thoracic vertebral column and extending vertically from the thoracic inlet to the diaphragm. For descriptive purposes, this region is arbitrarily divided into superior and inferior mediastina, and the latter is subdivided into anterior, middle and posterior parts. The plane of division into superior and inferior mediastina crosses the manubriosternal joint and the lower surface of the fourth thoracic vertebra (Fig. 55.1). Detailed accounts of some mediastinal contents are also included with descriptions of the respiratory organs (see Ch. 57) and the heart (see Ch. 56).

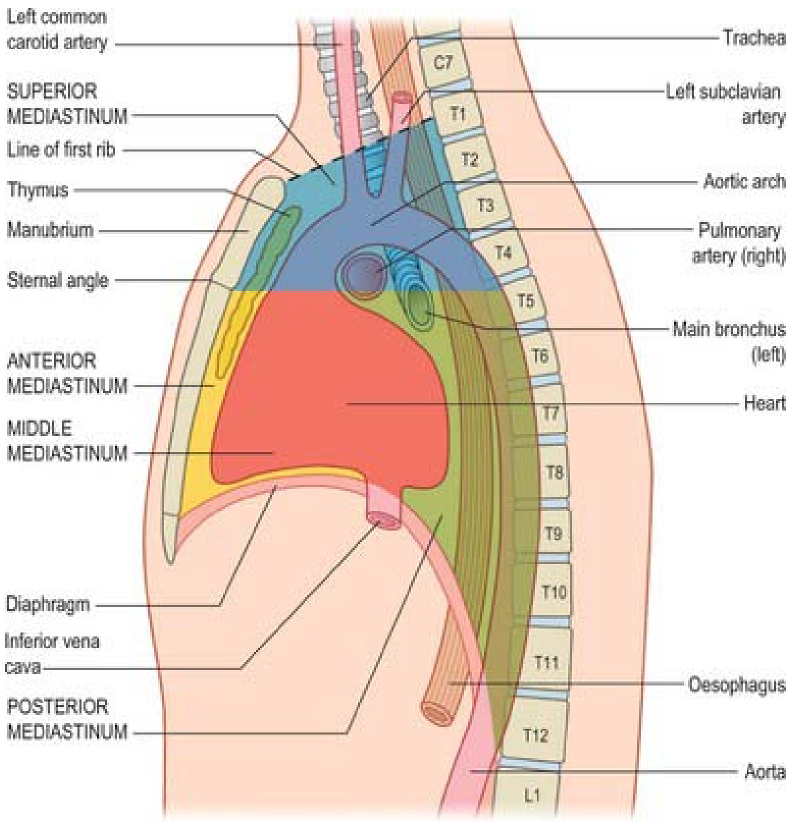
Left common carotid artery
SUPERIOR MEDIASTINUM
Line of first rib
Thymus
Manubrium
Sternal angle
ANTERIOR MEDIASTINUM
MIDDLE MEDIASTINUM
Diaphragm
Inferior vena cava
POSTERIOR MEDIASTINUM
Trachea
Left subclavian artery
Aortic arch
Pulmonary artery (right)
Main bronchus (left)
Heart
Oesophagus
Aorta
C7
T1
T2
T3
T4
T5
T6
T7
T8
T9
T10
T11
T12
L1

Fig. 55.1 The major divisions of the mediastinum (see text for further details). Note that not all mediastinal contents are depicted.

SUBDIVISIONS OF THE MEDIASTINUM

SUPERIOR MEDIASTINUM

The superior mediastinum lies between the manubrium sterni and the upper four thoracic vertebrae (see Fig. 55.19A–C). It is bounded below by the sternal plane, above by the plane of the thoracic inlet, and laterally by the mediastinal pleurae. It contains the lower ends of sternohyoid, sternothyroid and longus colli; thymic remnants; the internal thoracic arteries and veins, the brachiocephalic veins and the upper half of the superior vena cava, the aortic arch, the brachiocephalic, left common carotid and subclavian arteries and the left superior intercostal vein; the right and left vagi and phrenic nerves, the left recurrent laryngeal nerve, the cardiac nerves and the superficial part of the cardiac plexus; the trachea, oesophagus and thoracic duct. It also contains the paratracheal, brachiocephalic and tracheobronchial lymph nodes associated with their named structures.

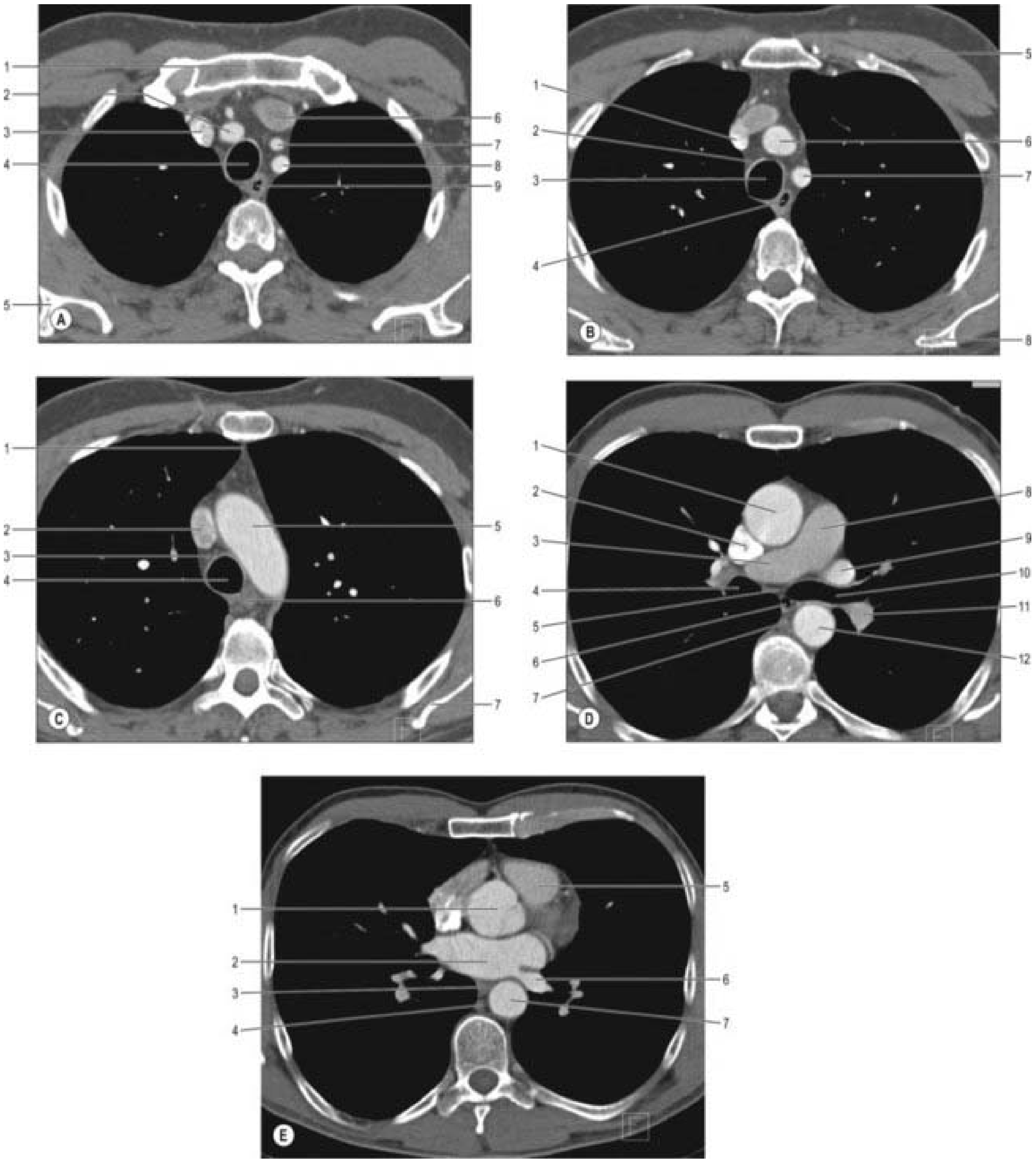
1
2
3
4
5
A
6
7
8
9
1
2
3
4
B
5
6
7
8
1
2
3
4
C
5
6
7
1
2
3
4
5
6
7
D
8
9
10
11
12
1
2
3
4
E
5
6
7

Fig. 55.19 Transverse section of the thorax, obtained by CT. **A**, At the level of the junction of the first rib. **1**. Manubrium. **2**. Right brachiocephalic artery. **3**. Right brachiocephalic vein. **4**. Trachea. **5**. Scapula. **6**. Left brachiocephalic vein. **7**. Left common carotid artery. **8**. Left subclavian artery. **9**. Oesophagus. **B**, Through the lower portion of the third thoracic vertebra. **1**. Brachiocephalic vein. **2**. Pretracheal space. **3**. Trachea. **4**.

Oesophagus. **5**. Pectoralis major. **6**. Combined brachiocephalic artery and left subclavian artery (normal variant). **7**. Left subclavian artery. **8**. Scapula. **C**, Through the middle of the fourth thoracic vertebra and aortic arch. **1**. Anterior junction. **2**. Superior vena cava. **3**. Pretracheal space. **4**. Trachea. **5**. Arch of aorta. **6**. Oesophagus. **7**. Scapula. **D**, At the upper border of the sixth thoracic vertebra, below the carina at the level of the pulmonary trunk and the right main pulmonary artery. **1**. Ascending aorta. **2**. Superior vena cava. **3**. Right pulmonary artery. **4**. Right main bronchus. **5**. Subcarinal space. **6**. Oesophagus **7**. Azygos vein. **8**. Trunk of pulmonary artery. **9**. Superior branch of left pulmonary vein. **10**. Left main bronchus. **11**. Inferior branch of left pulmonary artery. **12**. Descending aorta. **E**, Through the lower portion of the seventh thoracic vertebra, passing through the aortic root. **1**. Aortic root. **2**. Left atrium. **3**. Oesophagus. **4**. Azygos vein. **5**. Right ventricular outflow tract. **6**. Left inferior pulmonary vein. **7**. Descending aorta.

INFERIOR MEDIASTINUM

Anterior mediastinum

The anterior mediastinum lies between the sternal body and pericardium (see Fig. 55.19D,E). It narrows above the fourth costal cartilages, where the pleural sacs come close to each other, and contains loose connective tissue, the sternopericardial ligaments, a few lymph nodes and the mediastinal branches of the internal thoracic artery. The anterior mediastinum may sometimes contain part of the thymus gland or its degenerated remains.

Middle mediastinum

The middle mediastinum is the broadest part of the inferior mediastinum (see Fig. 55.19D,E). It contains the pericardium, the heart and the ascending aorta; the lower half of the superior vena cava receiving the azygos venous arch posteriorly; the tracheal bifurcation and both main bronchi; the pulmonary trunk and right and left pulmonary arteries and veins; the right and left phrenic nerves; the deep part of the cardiac plexus; the tracheobronchial lymph nodes.

Posterior mediastinum

The posterior mediastinum is bounded anteriorly by the bifurcation of the trachea, pulmonary vessels, pericardium and the posterior part of the upper surface of the diaphragm (see Fig. 55.19D,E). Posteriorly, it is bounded by the vertebral column, from the lower border of the fourth to the twelfth thoracic vertebrae, and on each side by the mediastinal pleura. It contains the descending thoracic aorta and the azygos, hemiazygos and accessory azygos veins; the right and left sympathetic chains, the splanchnic nerves and the right and left vagi; the oesophagus; the thoracic duct and posterior mediastinal lymph nodes.

MEDIASTINAL COMMUNICATIONS WITH THE NECK

Anatomical pathways exist between the oral cavity and the thorax via the parapharyngeal space and other fascial planes of the neck. The parapharyngeal space is more likely to be infected than any of the other potential tissue spaces in the head and neck: infection can pass from this space to the retropharyngeal and pretracheal spaces and so reach the superior mediastinum, from where it can track down into the anterior part of the inferior mediastinum (see Ch. 28).

VASCULAR SUPPLY AND LYMPHATIC DRAINAGE

The mediastinum contains the great vessels (i.e. the aortic arch and its branches, the descending thoracic aorta, the pulmonary trunk and the superior vena cava), the pulmonary, internal thoracic and posterior intercostal arteries and veins, and the azygos venous system.

Great vessels of the superior mediastinum

The aortic arch, descending thoracic aorta, pulmonary trunk and superior vena cava are described in Chapter 56.

Azygos venous system

Azygos vein

The azygos vein (Gr. *azygos* = ‘unpaired’) typically starts from the posterior aspect of the inferior vena cava, at or below the level of the renal veins, although the origin is not constant (Figs 55.2, 55.3; see Fig. 55.14B). When present, the lumbar azygos ascends anterior to the upper lumbar vertebrae. It may pass behind the right crus of the diaphragm or pierce it, or it may traverse the aortic hiatus to the right of the cisterna chyli. Anterior to the twelfth thoracic vertebral body, the azygos is joined by a large vessel formed by the right ascending lumbar and subcostal veins that passes forward and to the right of the twelfth thoracic vertebra behind the right crus: in the absence of a lumbar azygos, this common trunk may form the azygos vein itself. Whatever its origin, the azygos vein ascends in the posterior mediastinum to the level of the fourth thoracic vertebra, where it arches forward above the right pulmonary hilum. It ends in the superior vena cava, before the latter pierces the pericardium. The azygos lies anterior to the bodies of the lower eight thoracic vertebrae, anterior longitudinal ligament and right posterior intercostal arteries. The right greater splanchnic nerve, lung and pleura are right lateral relations. The thoracic duct and aorta and, where the vein arches forward, the oesophagus, trachea and right vagus, are left lateral relations. In the lower thorax the azygos is covered anteriorly by a recess of the right pleural sac and by the oesophagus; it emerges from behind the oesophagus to ascend behind the right hilum. The azygos vein lies close to the right posterolateral aspect of the descending thoracic aorta: aortic pulsations may assist venous return in the azygos and hemiazygos veins.

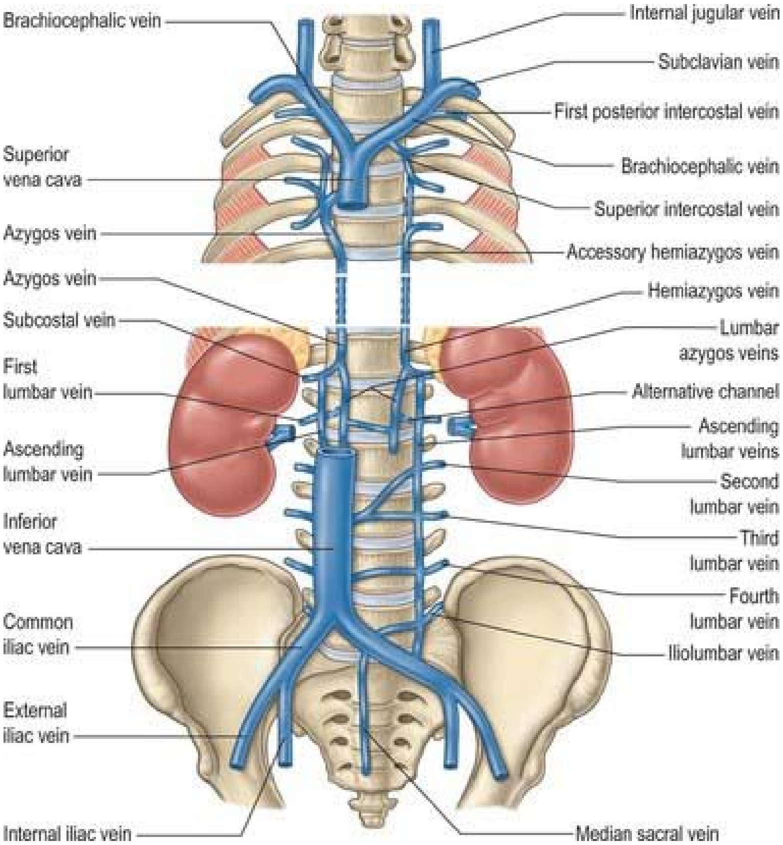
Brachiocephalic vein
Internal jugular vein
Subclavian vein
First posterior intercostal vein
Superior vena cava
Brachiocephalic vein
Superior intercostal vein
Azygos vein
Accessory hemiazygos vein
Azygos vein
Hemiazygos vein
Subcostal vein
Lumbar azygos veins
First lumbar vein
Alternative channel
Ascending lumbar vein
Ascending lumbar veins
Second lumbar vein
Inferior vena cava
Third lumbar vein
Fourth lumbar vein
Common iliac vein
Iliolumbar vein
External iliac vein
Internal iliac vein
Median sacral vein

Fig. 55.2 The superior and inferior extremities of the azygos system of veins and their principal associated veins. The intervening parts have been omitted because diagrams are often topographically misleading. There is considerable variation in the transthoracic parts of the azygos and hemiazygos veins in terms of numbers of radicles, levels of transmedian crossing, etc.

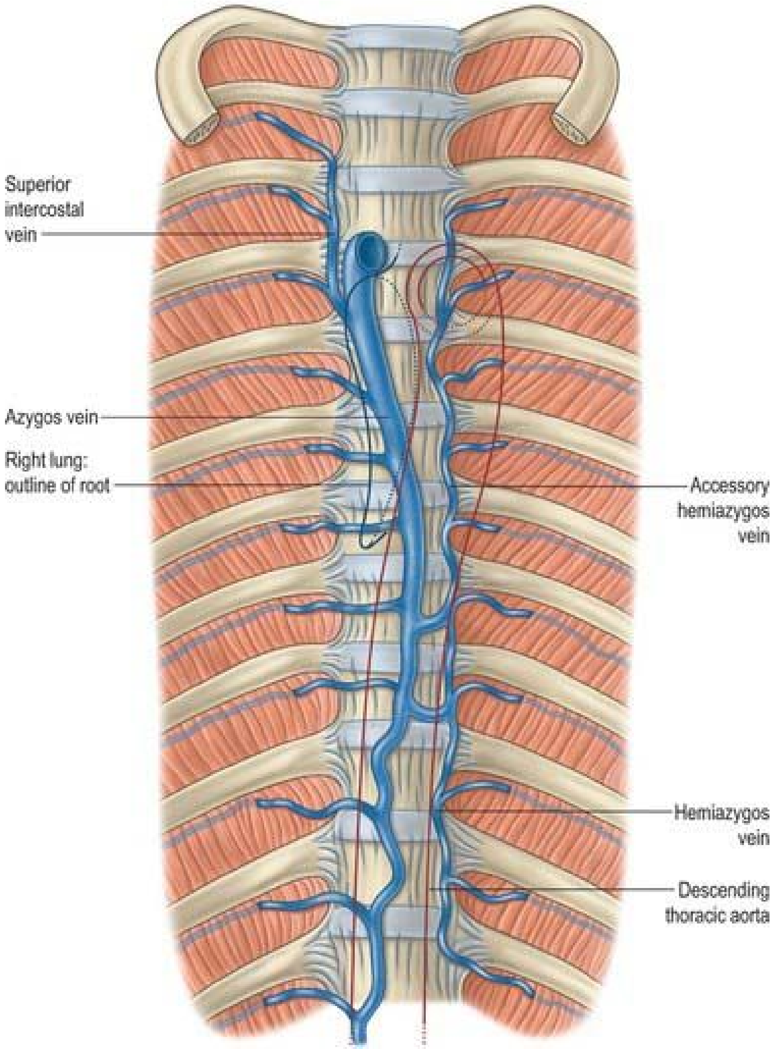
Superior intercostal vein
Azygos vein
Right lung: outline of root
Accessory hemiazygos vein
Hemiazygos vein
Descending thoracic aorta

Fig. 55.3 A frequent (perhaps the most common) course followed by the intrathoracic azygos, hemiazygos and accessory azygos veins. Outlines of the root of the right lung and ascending thoracic aorta are included.

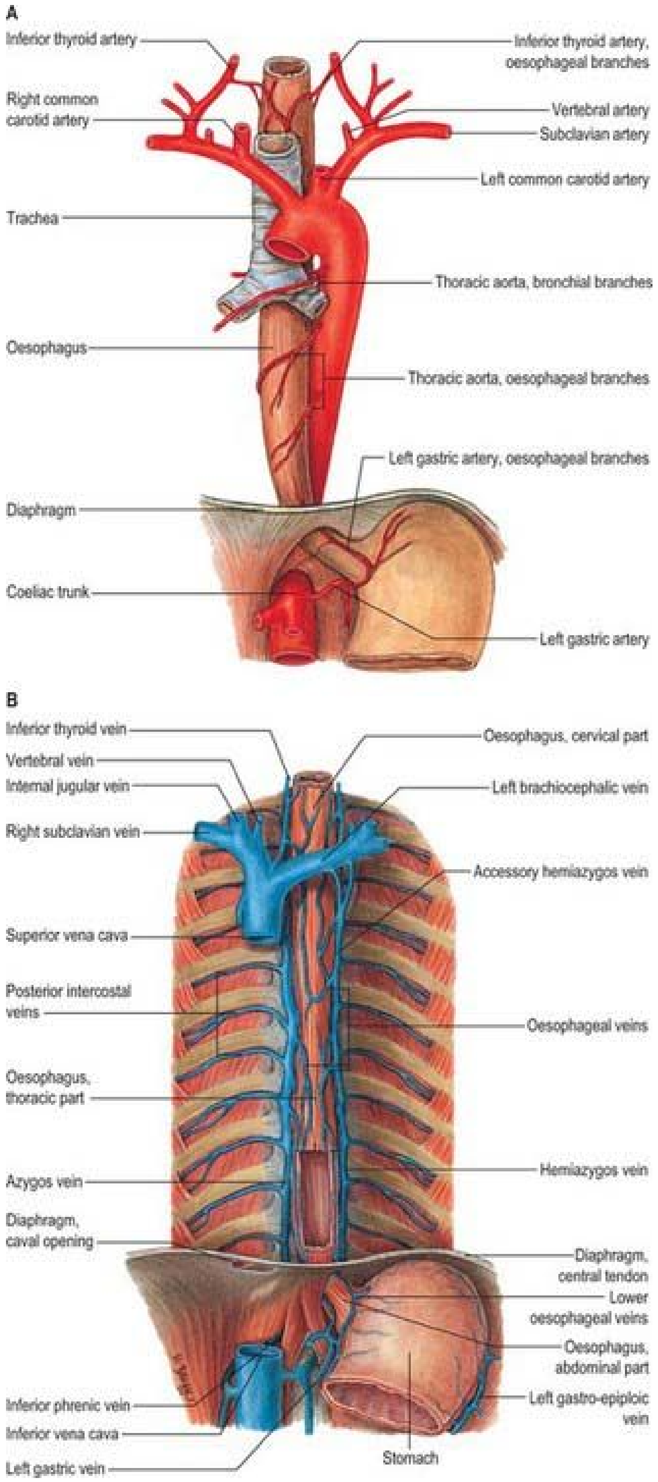
A
Inferior thyroid artery
Right common carotid artery
Trachea
Oesophagus
Diaphragm
Coeliac trunk
Inferior thyroid artery, oesophageal branches
Vertebral artery
Subclavian artery
Left common carotid artery
Thoracic aorta, bronchial branches
Thoracic aorta, oesophageal branches
Left gastric artery, oesophageal branches
Left gastric artery
B
Inferior thyroid vein
Vertebral vein
Internal jugular vein
Right subclavian vein
Superior vena cava
Posterior intercostal veins
Oesophagus, thoracic part
Azygos vein
Diaphragm, caval opening
Inferior phrenic vein
Inferior vena cava
Left gastric vein
Oesophagus, cervical part
Left brachiocephalic vein
Accessory hemiazygos vein
Oesophageal veins
Hemiazygos vein
Diaphragm, central tendon
Lower oesophageal veins
Oesophagus, abdominal part
Left gastro-epiploic vein
Stomach

Fig. 55.14 Oesophagus. **A**, Arterial blood supply. **B**, Venous drainage.

(From Sobotta 2006.)

Hemiazygos vein

The hemiazygos vein is formed on the left side from the lower three posterior intercostal veins, a common trunk formed by the left ascending lumbar and subcostal veins, and by oesophageal and mediastinal tributaries (Fig. 55.2). It ascends anterior to the level of the vertebral column to the eighth thoracic level then crosses the vertebral column posterior to the aorta, oesophagus and thoracic duct, and ends in the azygos vein (Fig. 55.3). Its lower end is often connected to the left renal vein.

Accessory hemiazygos vein

The accessory hemiazygos vein descends to the left of the vertebral column, and receives veins from the fourth or fifth to eighth left intercostal spaces; it crosses the seventh thoracic vertebra to join the azygos vein (see Figs 55.5 and 55.6). The accessory hemiazygos vein sometimes receives the left bronchial veins, and it may join the hemiazygos vein, in which case their common trunk opens into the azygos vein.

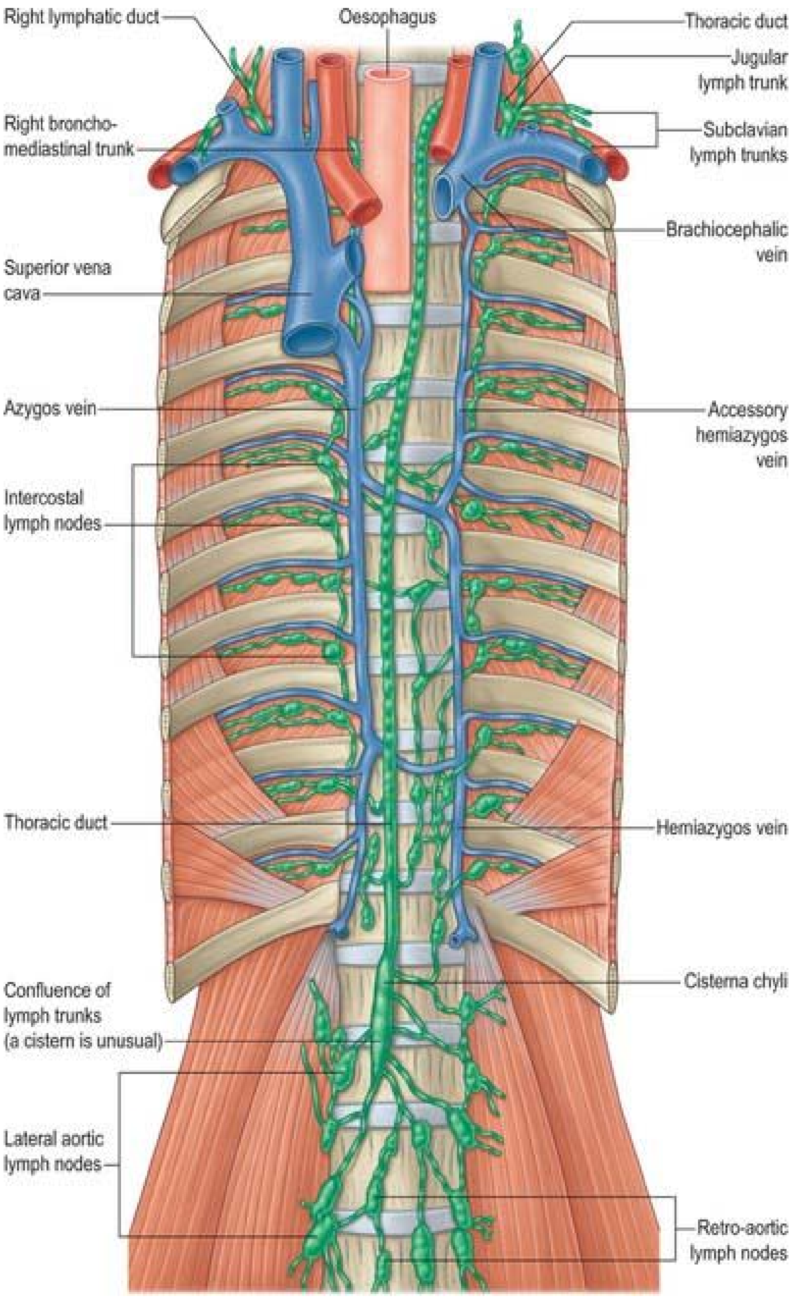
Right lymphatic duct
Oesophagus
Thoracic duct
Jugular lymph trunk
Right broncho-mediastinal trunk
Subclavian lymph trunks
Brachiocephalic vein
Superior vena cava
Azygos vein
Accessory hemiazygos vein
Intercostal lymph nodes
Thoracic duct
Hemiazygos vein
Cisterna chyli
Confluence of lymph trunks (a cistern is unusual)
Lateral aortic lymph nodes
Retro-aortic lymph nodes

Fig. 55.5 The thoracic and right lymphatic ducts. The accessory hemiazygos vein is crossing the median plane lower and the hemiazygos higher than usual. Note also the comments concerning the more common course of the azygos vein made in Fig. 55.2.

Variations of the azygos veins

The azygos veins vary greatly in their mode of origin, course, tributaries, anastomoses and termination. The accessory hemiazygos is the most variable, and may drain into the left brachiocephalic, azygos or hemiazygos vein. The arrangement shown in Fig. 55.3 represents a common pattern. Commonly, there is a main ‘right-sided’ azygos and at least some representative of the hemiazygos veins. The latter vary, and one or other may be absent or poorly developed. Very occasionally, independent left and right azygos veins (the early embryonic form) persist, or a single azygos vein may occur in a midline position without hemiazygos tributaries. Retro-aortic transvertebral connections from hemiazygos and accessory hemiazygos veins to the azygos are also extremely variable: there may be up to five connections. When either of the hemiazygos veins is absent, the relevant intercostal veins cross the vertebral bodies and end in the azygos. These transvertebral routes are often very short, because the azygos vein is more commonly anterior to the vertebral column and often passes to the left of the midline for part of its course. When there is congenital interruption of the inferior vena cava (IVC), the azygos vein can become as large as the IVC that it has replaced. Rarely, the azygos arch in the right tracheobronchial angle can be placed more superolaterally in a diagonal accessory azygos fissure in the right upper lobe of the lung as a consequence of failure of embryonic descent.

Internal thoracic arteries and veins

The internal thoracic vessels are described in Chapter 54.

Pulmonary arteries and veins

The pulmonary vessels are described in Chapter 57.

Posterior intercostal arteries and veins

The posterior intercostal veins accompany their arteries in 11 pairs; they are described in Chapter 54.

MEDIASTINAL LYMPH NODES

The mediastinal lymph nodes (Fig. 55.4; see Fig. 56.3) are classified into regional lymph node stations by thoracic surgeons for the purposes of staging lung cancer. The stations are defined as follows: **Station 1**: highest mediastinal nodes lie above a horizontal line of the level at which the left brachiocephalic vein crosses the trachea. **Station 2**: upper paratracheal nodes lie below the line of the highest mediastinal nodes and above a line drawn horizontally at the level of the upper border of the aortic arch. **Station 3**: prevascular and retrotracheal nodes lie behind the trachea but in front of the great vessels. **Station 4**: lower paratracheal nodes lie below the upper margin of the aortic arch and down to the upper margin of the corresponding upper lobe bronchus. On the right side, this is the upper margin of the right upper lobe bronchus; the majority of nodes in this area tend to be positioned anterolateral to the trachea. On the left side, the nodes are located below the upper margin of the aortic arch and above the margin of the left upper lobe bronchus. They lie medial to the ligamentum arteriosum and are usually lateral to the trachea. **Station 5**: subaortic nodes lie in the aortopulmonary window and are situated lateral to the ligamentum arteriosum or aorta or left pulmonary artery, but proximal to the first division of the left pulmonary artery. **Station 6**: para-aortic nodes lie between the upper margin of the aortic arch and lateral to the ascending aorta and aortic arch. **Station 7**: subcarinal nodes lie below the carina of the trachea, but are not associated with the lower lobe bronchi. **Station 8**: para-oesophageal nodes lie at either side of the oesophagus, well below the level of the subcarinal nodes. **Station 9**: pulmonary ligament nodes lie within the pulmonary ligament.

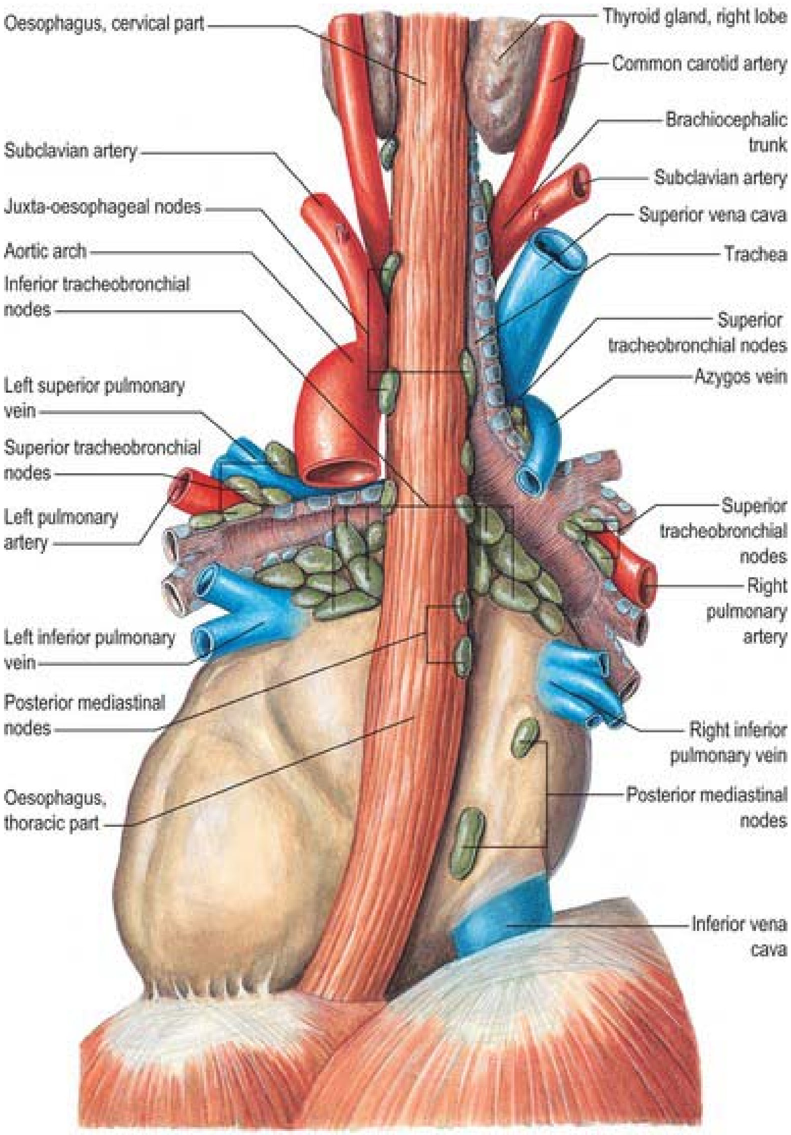
Oesophagus, cervical part
Subclavian artery
Juxta-oesophageal nodes
Aortic arch
Inferior tracheobronchial nodes
Left superior pulmonary vein
Superior tracheobronchial nodes
Left pulmonary artery
Left inferior pulmonary vein
Posterior mediastinal nodes
Oesophagus, thoracic part
Thyroid gland, right lobe
Common carotid artery
Brachiocephalic trunk
Subclavian artery
Superior vena cava
Trachea
Superior tracheobronchial nodes
Azygos vein
Superior tracheobronchial nodes
Right pulmonary artery
Right inferior pulmonary vein
Posterior mediastinal nodes
Inferior vena cava

Fig. 55.4 Thoracic lymph nodes.

(From Sobotta 2006.)

Involvement of these lymph nodes by cancer cells has important prognostic implications and influences the choice of treatment (Mountain & Dresler 1997). The staging system for lung cancer classifies involvement of ipsilateral hilar lymph nodes as N1, ipsilateral mediastinal lymph nodes as N2, contralateral mediastinal/hilar nodes as N3 and supraclavicular/scalene nodes as M1 (distant metastases).

These groups are not sharply demarcated. Pulmonary nodes become continuous with the bronchopulmonary nodes, and these in turn merge with the inferior and superior tracheobronchial nodes, which are continuous with the paratracheal group. Afferents of tracheobronchial nodes drain the lungs and bronchi, the thoracic part of the trachea, the heart and some efferents of the posterior mediastinal nodes. Their efferent vessels ascend on the trachea to unite with efferents of the parasternal and brachiocephalic nodes as the right and left bronchomediastinal trunks. The right trunk may occasionally join a right lymphatic duct or another right-sided lymph trunk and the left trunk may join the thoracic duct, but usually they open independently in or near the ipsilateral jugulosubclavian junction (see Ch. 28).

Mediastinoscopy

In cervical mediastinoscopy, a transverse incision is made in the suprasternal notch through the deep lamina of the deep cervical fascia after retraction of sternohyoid and sternothyroid which lie within its superficial lamina. The pretracheal plane is dissected along the anterior surface of the trachea and a space is created between the trachea and the brachiocephalic artery anteriorly down to the level of the carina and along both sides of the trachea and main bronchi. This allows insertion of the endoscope to inspect and biopsy lymph node masses in the upper paratracheal (station 2), lower paratracheal (station 4) and subcarinal nodes (station 7). The anterior part of the superior mediastinum is more difficult to assess by mediastinoscopy and usually requires an anterior mediastinotomy, where the mediastinoscope is inserted retrosternally along the prevascular plane. The nodes at stations 5 and 6 of the mediastinum can be accessed by this technique.

THORACIC DUCT

In adults, the thoracic duct, including the confluence of lymph trunks (or the cisterna chyli in the small proportion of individuals in whom the latter is saccular), is 38–45 cm in length and extends from the second lumbar vertebra to the base of the neck (Fig. 55.5). Starting from the superior pole of the confluence near the lower border of the twelfth thoracic vertebra (see Ch. 62), the thoracic duct traverses the retrocrural space of the diaphragm with the aorta, azygos and hemiazygos veins, then ascends in the posterior mediastinum, on the right of the midline, between the descending thoracic aorta (on its left) and the azygos vein (on its right). The vertebral column, the right aortic intercostal arteries and terminal segments of the hemiazygos and accessory hemiazygos veins are posterior relations. The diaphragm and oesophagus are anterior; a recess of the right pleural cavity may separate the duct and oesophagus. At the level of the body of the fifth thoracic vertebra, the duct gradually inclines to the left, enters the superior mediastinum and then ascends to the thoracic inlet along the left border of the oesophagus. In this part of its course the duct is first crossed anteriorly by the aortic arch and then runs posterior to the initial segment of the left subclavian artery, in close contact with the left mediastinal pleura. Passing into the neck, it arches laterally at the level of the transverse process of the seventh cervical vertebra. Its arch rises 3 or 4 cm above the clavicle and curves anterior to the vertebral artery and vein, the left sympathetic trunk, the thyrocervical trunk or its branches, the left phrenic nerve and the medial border of scalenus anterior. It passes posterior to the left common carotid artery, vagus nerve and internal jugular vein. Finally, the duct descends anterior to the arched cervical first part of the left subclavian artery and ends by opening into the junction of the left subclavian and internal jugular veins (see Fig. 28.16A). It may also open into either of the great veins, near the junction, or it may divide into a number of smaller vessels before terminating. In rare individuals there is no apparent thoracic duct on the left. Several terminal openings sometimes occur. Patterns vary greatly in different studies, but the commonly reported sites of termination are the internal jugular vein, jugulosubclavian junction and subclavian vein. Termination in the left brachiocephalic vein occurs occasionally.

At its abdominal origin, the thoracic duct is usually 5 mm in diameter, diminishing in calibre at midthoracic level, and then in approximately half of individuals is again slightly dilated before its termination. It is slightly sinuous, constricted at intervals and appears varicose. It may divide in its mid course into two unequal vessels that soon reunite, or into several small branches that form a plexus before continuing as a single duct. At a higher level it occasionally bifurcates, the left branch ending as usual, the right branch diverging to join one of the right lymph trunks or, when present, a right lymphatic duct. The combined vessel usually opens into the right subclavian vein. The thoracic duct has several valves corresponding to sites exposed to pressure. At its termination a bicuspid valve faces into the vein to prevent or reduce reflux of blood: post mortem, blood regurgitates freely into the duct.

Anomalies of the thoracic duct may be delineated by dissection into the inguinal lymphatics followed by cannulation and subsequent injection of an oily contrast medium (lipiodol) followed by plain films or CT.

TRIBUTARIES

Bilateral descending thoracic lymph trunks from intercostal lymph nodes of the lower six or seven intercostal spaces of both sides traverse the retrocrural space and join the lateral aspects of the thoracic duct in the abdomen immediately after its origin. Bilateral ascending lumbar lymph trunks from the upper lateral aortic nodes ascend and pierce their corresponding diaphragmatic crus, and then join the thoracic duct at a variable level within the thorax. The upper intercostal trunks drain the intercostal nodes in the upper five or six left intercostal spaces. The mediastinal trunks drain various nodal groups and provide paths to the thoracic duct from the convex diaphragmatic aspect of the liver, the diaphragm, the pericardium, heart and oesophagus. The left subclavian trunk usually joins the thoracic duct, but may open independently into the left subclavian vein. The left jugular trunk usually joins the thoracic duct, but may open independently into the left internal jugular vein. The left bronchomediastinal trunk occasionally joins the thoracic duct, but usually has an independent venous opening.

Many of the trunks listed above are described as possessing terminal bicuspid valves, which possibly prevent reflux of lymph.

INJURY DURING OESOPHAGEAL SURGERY

The thoracic duct is vulnerable to damage after thoracic, particularly oesophageal, surgery (Wemyss-Holden et al 2001). The incidence is between 0.2% and 3% and increases with transhiatal and thoracoscopic procedures. Thoracic duct laceration is a potentially life-threatening complication: mortality rates are more than 50% with conservative management and as high as 10–16% even after early surgical duct ligation. Rupture of the thoracic duct leads to leakage of chyle, which is rich in lipid, protein and lymphocytes, and hence a progressive nutritional and immune deficit occurs. Fortunately, the incidence of true thoracic duct transection is rare, and cases in which there are some postoperative chylous effusions are usually the result of damage to some of the tributaries of the thoracic duct, rather than to the duct itself. These are usually self-limiting and respond to conservative treatment.

The variable course of the thoracic duct, coupled with failure to identify it at surgery, may lead to its inadvertent incision or transection. The greater incidence of injury with transhiatal resection may be attributable to shear forces during the mobilization of the distal oesophagus, whereas the limited field of view probably contributes to the greater incidence of thoracic duct injury during thoracoscopic surgery. Injury should be suspected in the postoperative period if there is an enlarging mediastinal silhouette on serial chest radiographs, or if there is significant drainage of a cream-coloured liquid from the chest or abdominal drains. In cases of uncertainty, an electrophoretic confirmation for the presence of chylomicrons in the pleural fluid is diagnostic.

DEVELOPMENT

The development of the thoracic duct is described in Chapter 59.

RIGHT LYMPHATIC TRUNK

The right lymphatic trunk (Fig. 55.5) has a variable anatomy, which includes doubling of the duct, left-sided, right or bilateral termination. The plexiform nature of the trunks from which the thoracic duct develops leads to a number of possible abnormalities. The most common is duplication of the duct for a variable part of its course and subsequent merging to form a single duct which drains into the left internal jugular trunk. Occasionally the duct has dual terminations in the right and left internal jugular veins, and rarely it terminates only into the right internal jugular vein.

AUTONOMIC NERVOUS SYSTEM

The autonomic nervous system in the thorax consists of right and left ganglionated sympathetic chains and vagi and the cardiac, pulmonary and oesophageal plexuses. The cardiac plexus is described in Chapter 56, the pulmonary plexus is described in Chapter 57, and the oesophageal plexus is described below.

THORACIC SYMPATHETIC TRUNK

The thoracic sympathetic trunk (Fig. 55.7; see Fig. 15.13) contains ganglia almost equal in number to those of the thoracic spinal nerves (usually 11, occasionally 12, rarely 10 or 13). Almost always, the first thoracic ganglion is fused with the inferior cervical ganglion, forming the cervicothoracic ganglion. Occasionally, the second thoracic ganglion may be included in this fusion, in which case the succeeding ganglion is counted as the second in order to make the other ganglia correspond numerically with other segmental structures. Except for the second and lowest two or three, the thoracic ganglia lie against the costal heads, posterior to the costal pleura. The second thoracic sympathetic ganglion is commonly located in the second intercostal space, and the lowest two or three ganglia lie lateral to the bodies of the corresponding vertebrae. Caudally, the thoracic sympathetic trunk passes dorsal to the medial arcuate ligament (or through the crus of the diaphragm) to become the lumbar sympathetic trunk.

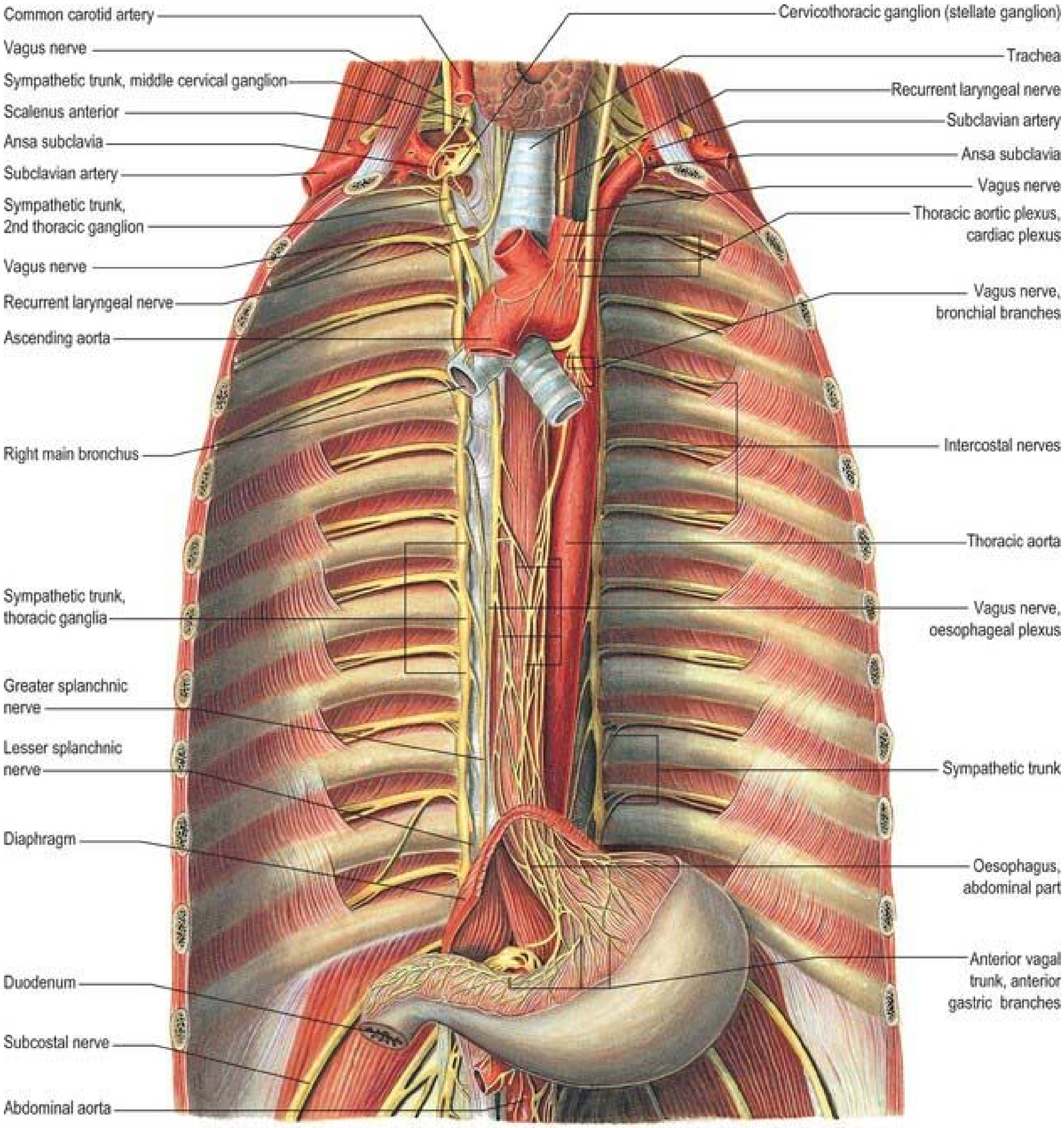
Common carotid artery
Vagus nerve
Sympathetic trunk, middle cervical ganglion
Scalenus anterior
Ansa subclavia
Subclavian artery
Sympathetic trunk, 2nd thoracic ganglion
Vagus nerve
Recurrent laryngeal nerve
Ascending aorta
Right main bronchus
Sympathetic trunk, thoracic ganglia
Greater splanchnic nerve
Lesser splanchnic nerve
Diaphragm
Duodenum
Subcostal nerve
Abdominal aorta
Cervicothoracic ganglion (stellate ganglion)
Trachea
Recurrent laryngeal nerve
Subclavian artery
Ansa subclavia
Vagus nerve
Thoracic aortic plexus, cardiac plexus
Vagus nerve, bronchial branches
Intercostal nerves
Thoracic aorta
Vagus nerve, oesophageal plexus
Sympathetic trunk
Oesophagus, abdominal part
Anterior vagal trunk, anterior gastric branches

Fig. 55.7 The thoracic autonomic nervous system.

(From Sobotta 2006.)

The ganglia are small and interconnected by intervening segments of the trunk. The classic description is that two or more rami communicantes, named white and grey, connect each ganglion with its corresponding spinal nerve, the white rami joining the nerve distal to the grey. Variation in this pattern is not uncommon, especially in the upper thoracic levels: these variations are rarely bilaterally symmetrical. Additional ascending and descending rami to higher and lower levels respectively issue from the second sympathetic ganglion (54% and 46% respectively), from the third ganglion (6% and 25%), and from the fourth ganglion (5% and 8%) (Cho et al 2005). The ascending ramus from the second ganglion is sometimes called the nerve of Kuntz. The anatomical variations displayed by the communicating rami and in the location of the second sympathetic ganglion might explain some surgical failures and symptom recurrences). Occasionally, a grey and a white ramus fuse to form a ‘mixed’ ramus.

The medial branches from the upper five ganglia are very small, and supply filaments to the thoracic aorta and its branches; they form a fine thoracic aortic plexus on the aorta with filaments from the greater splanchnic nerve. Rami of the second to fifth or sixth ganglia enter the posterior pulmonary plexus. Others, from the second to fifth ganglia, pass to the deep (dorsal) part of the cardiac plexus. Small branches of these pulmonary and cardiac nerves pass to the oesophagus and trachea. The medial branches from the lower seven ganglia are large; they supply the aorta and unite to form the greater, lesser and lowest splanchnic nerves (the last two are not always identifiable).

The greater splanchnic nerve consists mainly of myelinated preganglionic efferent and visceral afferent fibres, and is formed by branches from the fifth to ninth or tenth thoracic ganglia; fibres in the upper branches may be traced to the first or second thoracic ganglia. Its roots vary from one to eight, four being the most usual number. It descends obliquely on the vertebral bodies, supplies branches to the descending thoracic aorta and perforates the ipsilateral crus of the diaphragm to end mainly in the coeliac ganglion, but partly in the aorticorenal ganglion and suprarenal (adrenal) gland. A splanchnic ganglion exists on the nerve opposite the eleventh or twelfth thoracic vertebra in a majority of individuals.

The lesser splanchnic nerve, formed by rami of the ninth and tenth (sometimes the tenth and eleventh) thoracic ganglia and the trunk between them, pierces the diaphragm with the greater splanchnic nerve and joins the aorticorenal ganglion.

The lowest (least) splanchnic nerve (or renal nerve) from the lowest thoracic ganglion enters the abdomen with the sympathetic trunk to end in the renal plexus.

The greater splanchnic nerve is always present, the lesser is usually present, and the least is often present. A fourth (accessory) splanchnic nerve has been described.

Thoracic sympathectomy

Endoscopic thoracic sympathectomy (ETS) is the method of choice to cure moderate and severe hyperhidrosis of the palms, phobic facial blushing, endstage severe Raynaud's disease with peripheral ulcers, and severe reflex sympathetic dystrophy. The treatment of the last two disorders by ETS is controversial because the effect is usually transitory. ETS is very successful in curing patients with hyperhidrosis and phobic facial blushing: pain syndromes have a significantly poorer outcome.

The operation involves making tiny incisions behind the anterior pectoral fold in the axilla, and insufflating a small amount of carbon dioxide into the thoracic cavity to allow access with a modified thoracoscope. In the treatment of phobic facial blushing, it is sufficient to divide the fibres that run superiorly from the second thoracic ganglion over the neck of the second rib, leaving the second ganglion almost intact. Treatment of palmar hyperhidrosis requires ablation thermocoagulation of the sympathetic trunk over the necks of the third and fourth ribs, taking care to avoid any spreading of thermal energy along the trunk to avoid damaging the more superior stellate ganglion (see 'Horner's syndrome' paragraph below). The risk of compensatory sweating is greatly reduced, though not completely excluded, by limiting the number of ganglia treated to an absolute minimum. As an additional procedure, dividing the inconstant sympathetic pathways (nerve of Kuntz, ascending or descending additional rami communicantes) on the second, third and fourth ribs may improve surgical outcomes.

The effect is immediately evident: the patient awakes from anaesthesia with dry and warm hands. In many cases, even hyperhidrosis of the feet improves, but the underlying anatomical/physiological mechanisms are not yet properly understood (Gofeld & Faclier 2006). Surgical complications are very rare: Horner's syndrome is the most feared, and is caused by damage to the stellate ganglion and interruption of the sympathetic fibres from T1 which ascend around the arteries supplying the head and neck (see Ch. 28).

Side effects include compensatory sweating (ranging from barely noticeable to quite disturbing) in other locations of the body on exercise or from exposure to high temperatures in up to 70% of patients. This is severe in 5% of patients and may be more frequent in those operated on for axillary hyperhidrosis (when two more inferior ganglia have to be divided): some surgeons do not now consider isolated axillary hyperhidrosis as an indication for this procedure. Gustatory or olfactory sweating may also occur in up to a third of patients, but is rarely considered a problem. Other documented side effects are the inability to raise the heart rate when working-out physically, and in some cases this has led to decreased ability to perform work and daily activities. Some patients also experience an uncomfortable sensation of not being able to control their body temperature.

VAGUS NERVE IN THE MEDIASTINUM

The vagus nerve contains preganglionic parasympathetic fibres that arise in its dorsal nucleus and travel in the nerve and in its pulmonary, cardiac, oesophageal, gastric, intestinal and other branches. Some cardiac parasympathetic fibres may originate from neurones in or near the nucleus ambiguus. The proportion of efferent parasympathetic fibres in the vagus varies at different levels, but is small relative to its sensory and sensorimotor content. Efferent fibres relay in minute ganglia in the visceral walls.

Cardiac branches join the cardiac plexuses and relay in ganglia that are distributed freely over both atria in the subepicardial tissue. The terminal fibres are distributed to the atria and the atrioventricular bundle; they are concentrated around the sinuatrial and, to a lesser extent, the atrioventricular nodes (see Ch. 56). Cardiac branches slow the cardiac cycle and diminish the force of contraction. It has been claimed that the vagi can only influence ventricular muscle via their effect on the atrioventricular node, even though postganglionic parasympathetic innervation of the ventricles is sparse. The smaller branches of the coronary arteries are innervated mainly via the vagus, whereas larger arteries, with a dual innervation, are chiefly supplied by sympathetic fibres. Pulmonary branches are motor to the circular smooth muscle fibres of the bronchi and bronchioles and are therefore bronchoconstrictor; synaptic relays occur in the ganglia of the pulmonary plexuses.

The distribution of the vagi to the abdominal viscera is described in relevant chapters in the section on Abdomen and Pelvis.

Right vagus

The right vagus nerve descends posterior to the internal jugular vein and crosses the first part of the subclavian artery to enter the thorax. It descends through the superior mediastinum, at first behind the right brachiocephalic vein, and then to the right of the trachea and posteromedial to the right brachiocephalic vein and superior vena cava. The right pleura and lung are lateral to it above and are separated from it below by the azygos vein, which arches forwards above the right pulmonary hilum (Fig. 55.6). It passes behind the right main bronchus and lies on the posterior aspect of the right hilum, where it divides into the posterior pulmonary (or bronchial) branches. The latter unite with rami from the second to fifth or sixth thoracic sympathetic ganglia to form the right posterior pulmonary plexus. Two or three branches descend from the caudal part of this plexus on the posterior surface of the oesophagus and join a left vagal branch to form the posterior oesophageal plexus. A vagal trunk containing fibres from both right and left vagi leaves the plexus and runs down on the posterior surface of the oesophagus. It enters the abdomen by passing through the diaphragmatic oesophageal opening.

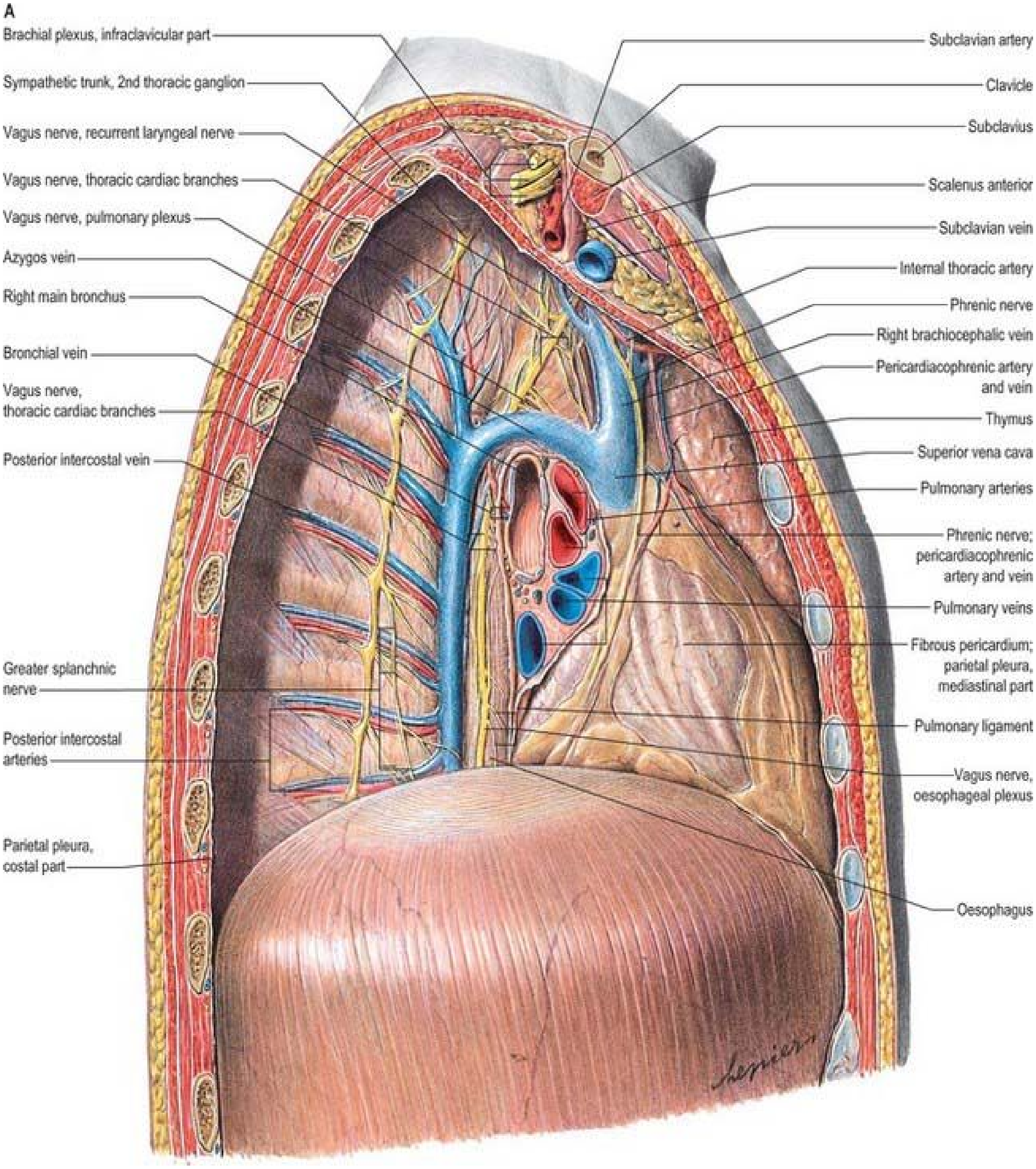
A
Brachial plexus, infraclavicular part
Sympathetic trunk, 2nd thoracic ganglion
Vagus nerve, recurrent laryngeal nerve
Vagus nerve, thoracic cardiac branches
Vagus nerve, pulmonary plexus
Azygos vein
Right main bronchus
Bronchial vein
Vagus nerve, thoracic cardiac branches
Posterior intercostal vein
Greater splanchnic nerve
Posterior intercostal arteries
Parietal pleura, costal part
Subclavian artery
Clavicle
Subclavius
Scalenus anterior
Subclavian vein
Internal thoracic artery
Phrenic nerve
Right brachiocephalic vein
Pericardiacophrenic artery and vein
Thymus
Superior vena cava
Pulmonary arteries
Phrenic nerve; pericardiacophrenic artery and vein
Pulmonary veins
Fibrous pericardium; parietal pleura, mediastinal part
Pulmonary ligament
Vagus nerve, oesophageal plexus
Oesophagus

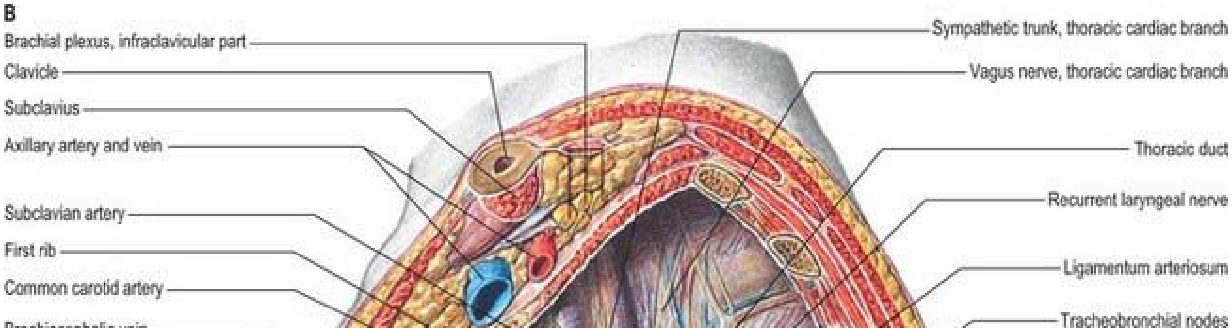
B
Brachial plexus, infraclavicular part
Clavicle
Subclavius
Axillary artery and vein
Subclavian artery
First rib
Common carotid artery
Sympathetic trunk, thoracic cardiac branch
Vagus nerve, thoracic cardiac branch
Thoracic duct
Recurrent laryngeal nerve
Ligamentum arteriosum
Tracheobronchial nodes

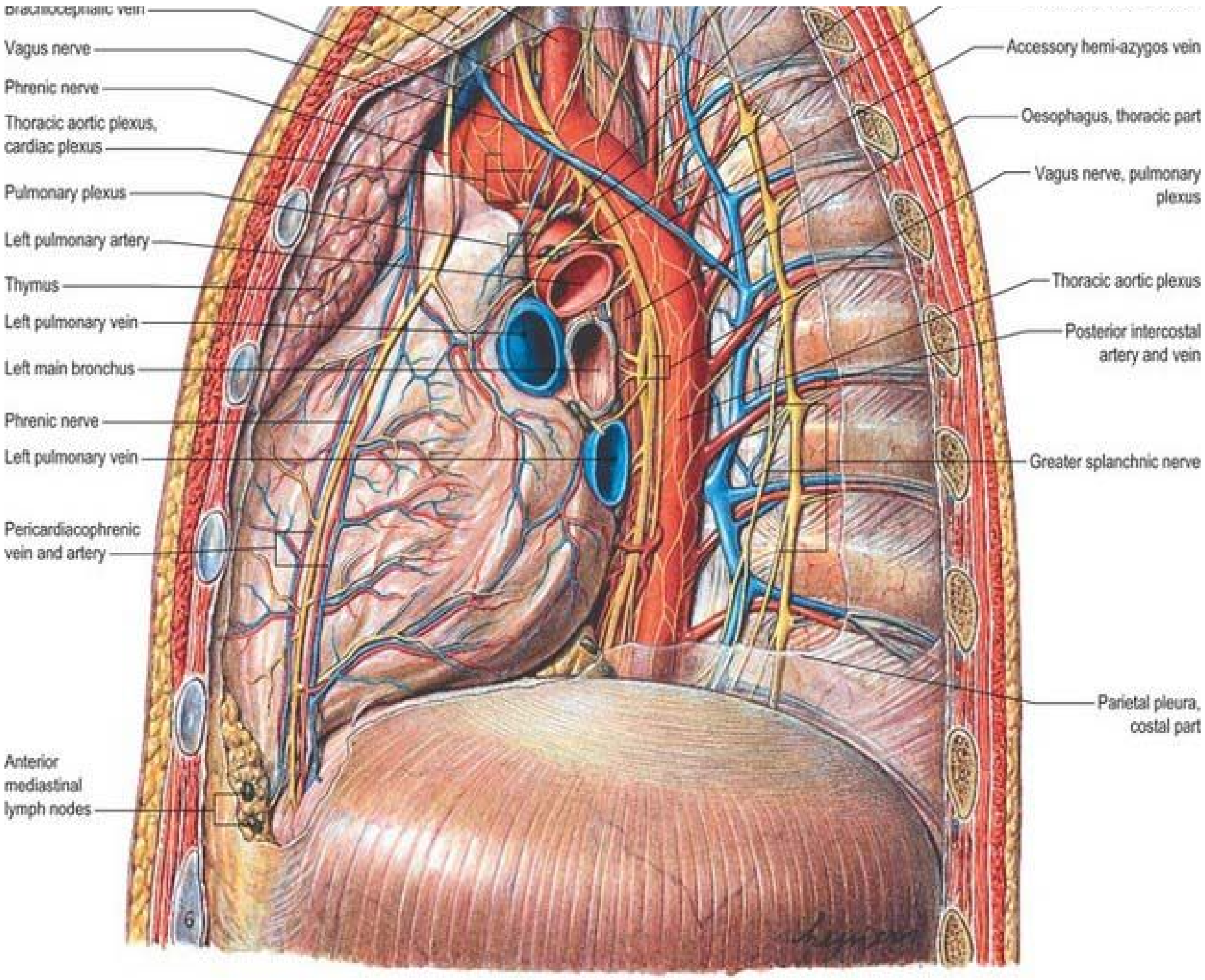
Brachiocephalic vein
Vagus nerve
Phrenic nerve
Thoracic aortic plexus, cardiac plexus
Pulmonary plexus
Left pulmonary artery
Thymus
Left pulmonary vein
Left main bronchus
Phrenic nerve
Left pulmonary vein
Pericardiacophrenic vein and artery
Anterior mediastinal lymph nodes
Accessory hemi-azygos vein
Oesophagus, thoracic part
Vagus nerve, pulmonary plexus
Thoracic aortic plexus
Posterior intercostal artery and vein
Greater splanchnic nerve
Parietal pleura, costal part

Fig. 55.6 The mediastinum. **A**, Right lateral aspect. **B**, Left lateral aspect.

(From Sobotta 2006.)

Left vagus

The left vagus enters the thorax between the left common carotid and subclavian arteries and behind the left brachiocephalic vein. It descends through the superior mediastinum and crosses the left side of the aortic arch to pass behind the left pulmonary hilum (Fig. 55.6). Above the aortic arch, it is crossed anterolaterally by the left phrenic nerve, and on the arch by the left superior intercostal vein. Behind the hilum it divides into the posterior pulmonary (or bronchial) branches, which unite with rami of the second to fourth thoracic sympathetic ganglia to form the left posterior pulmonary plexus. Two or three branches descend anteriorly on the oesophagus and join with a ramus from the right posterior pulmonary plexus to form the anterior oesophageal plexus. A trunk containing fibres from both vagi descends anterior to the oesophagus and enters the abdomen through the oesophageal diaphragmatic opening.

THYMUS

The thymus (Figs 55.8, 55.9) is one of the two primary lymphoid organs, the other being the bone marrow. It is an encapsulated soft, bilobed organ, the two parts being joined in the midline by connective tissue that merges with the capsule of each lobe. The latter may normally have adhesions to the fibrous pericardium that necessitate limited pericardiectomy during thymectomy. The thymus is visible on CT and MRI axial sections just anterior to the ascending aorta and inferior to the left brachiocephalic vein; the CT attenuation in younger individuals is homogeneous and similar to or greater than that of muscle, and the signal intensity with MRI on T_2-weighted images is similar to or greater than that of fat.

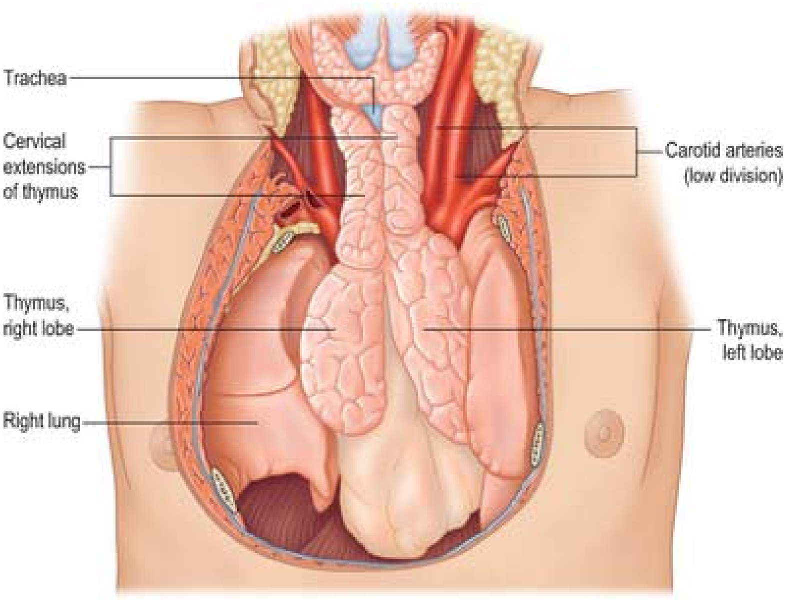
Trachea
Cervical extensions of thymus
Thymus, right lobe
Right lung
Carotid arteries (low division)
Thymus, left lobe

Fig. 55.8 The neonatal thymus.

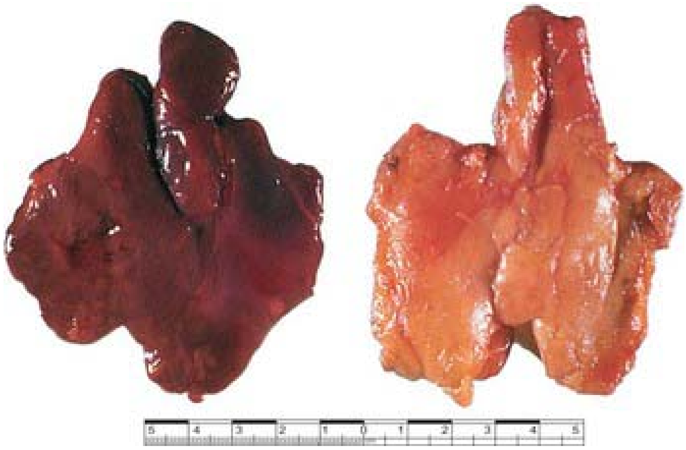

Fig. 55.9 Thymus from a 9-year-old girl (left) and an 80-year-old man (right). Note the fibrofatty infiltration of the older thymus.

(By courtesy of Professor M Kendall, Department of Physiology, GKT School of Medicine, London.)

RELATIONS

The thymus is largest in the early part of life, particularly around puberty, and persists actively into old age despite considerable fibrofatty degeneration which sometimes hides the existence of thymic tissue. The greater part of the thymus lies in the superior mediastinum and anterior part of the inferior mediastinum, and the lower border of the thymus reaches the level of the fourth costal cartilages. Superiorly, extensions into the neck are common, reflecting the (bilateral) embryonic origins of the thymus from the third pharyngeal pouch. Its upper poles join at, and extend above, the level of the suprasternal notch; the left usually extends higher and is seen first behind the strap muscles during the initial stages of transcervical thymectomy (see p. 949). It sometimes reaches the inferior poles of the thyroid gland or even higher, and is connected to the thyroid gland by the thyrothymic ligament. Its shape is largely moulded by adjacent structures. Inferiorly, the lower end of the right lobe commonly lies between the right side of the ascending aorta and the right lung, anterior to the superior cava. Anteriorly lie sternohyoid, sternothyroid and fascia (in the neck), and the manubrium sterni, internal thoracic vessels and upper three costal cartilages (in the thorax). The pleurae lie laterally and the phrenic nerves are anterolateral and inferior. Posteriorly, the thymus is in contact with the vessels of the superior mediastinum (the left brachiocephalic vein may be partly embedded in the gland), the upper part of the thoracic trachea and the anterior surface of the heart. Thoracic surgeons performing thymectomies must be aware of the anatomic variation where the upper poles may lie posterior to the left brachiocephalic vein.

Separated thymic tissue is often found scattered around the gland, and ectopic thymic rests are sometimes discovered in unusual mediastinal locations. Small accessory nodules may occur in the neck; they represent portions that have become detached during their embryological descent. Thin strands of thymic tissue may occur along the line of descent, and may reach as high as the thyroid cartilage or above. Connective tissue marking the embryological pathway may run between the thymus and the parathyroids.

VASCULAR SUPPLY AND LYMPHATIC DRAINAGE

Arteries

The thymus is supplied mainly from branches of the internal thoracic and inferior thyroid arteries, which also supply the surrounding mediastinal connective tissue. A branch from the superior thyroid artery is sometimes present. There is no main hilum, but arterial branches pass either directly through the capsule or, more often, into the depths of the interlobar septa before entering the thymus at the junction of the cortex and medulla.

Veins

Thymic veins drain to the left brachiocephalic, internal thoracic and inferior thyroid veins and occasionally directly into the superior vena cava. One or more veins often emerge medially from each lobe of the thymus to form a common trunk opening into the left brachiocephalic vein.

Lymphatic drainage

The thymus has no afferent lymphatics. Efferent lymphatics arise from the medulla and corticomedullary junction and drain through the extravascular spaces in company with the arteries and veins that supply the thymus. Thymic lymphatic vessels end in the brachiocephalic, tracheobronchial and parasternal nodes.

INNERVATION

The thymus is innervated from the sympathetic chain via the cervicothoracic (stellate) ganglion or ansa subclavia and from the vagus. Branches from the phrenic and descending cervical nerves are distributed mainly to the capsule. The two lobes are innervated separately through their dorsal, lateral and medial aspects. During development and before its descent into the thorax, the thymus is innervated by the vagus in the neck. After its descent, the thymus receives a sympathetic innervation via fibres that travel along the vessels: postganglionic sympathetic terminations branch radially and form a plexus with the vagal fibres at the corticomedullary junction.

Innervation is complete by the onset of thymic function. Many of the autonomic nerves are doubtless vasomotor, but other terminal branches (at least in rodents) ramify among the cells of the thymus, particularly the medulla, suggesting that they may have other roles. The medulla contains a number of different types of non-lymphoid cells, including cells positive for vasoactive intestinal polypeptide and acetylcholinesterase, large non-myoid cells, and cells containing oxytocin, vasopressin and neurophysin, of possible neural crest origin. The roles of the nervous system and other neuroendocrine elements in the overall biology of the thymus are little understood.

MICROSTRUCTURE

The thymus is responsible for the provision of thymus-processed (T) lymphocytes to the entire body, and provides a unique microenvironment in which T-cell precursors (thymocytes) undergo development, differentiation and clonal expansion to deliver the exquisitely specific T-cell response, simultaneously acquiring immune tolerance to the body's own components. These steps involve intimate interactions between thymocytes and other cells (mainly epithelial cells and antigen-presenting cells) and chemical factors in the thymic environment. The thymus is also part of the neuroimmunological and neuroendocrine axes of the body, and it both influences and is influenced by the products of these axes. Its activity therefore varies throughout life under the influence of different physiological states, disease conditions and chemical insults, such as hormones, drugs and pollutants.

General architecture

It is useful to consider the embryological origins of the thymus in order to understand its cellular organization. The thymus is derived from a number of sources, including epithelial derivatives of the pharyngeal pouches, mesenchyme, haemolymphoid cells and vascular tissue. In section, the thymus can be seen to consist of an outer cortex of densely packed cells mainly of the T-lymphocyte lineage (thymocytes) and an inner medulla with fewer lymphoid cells (Fig. 55.10).

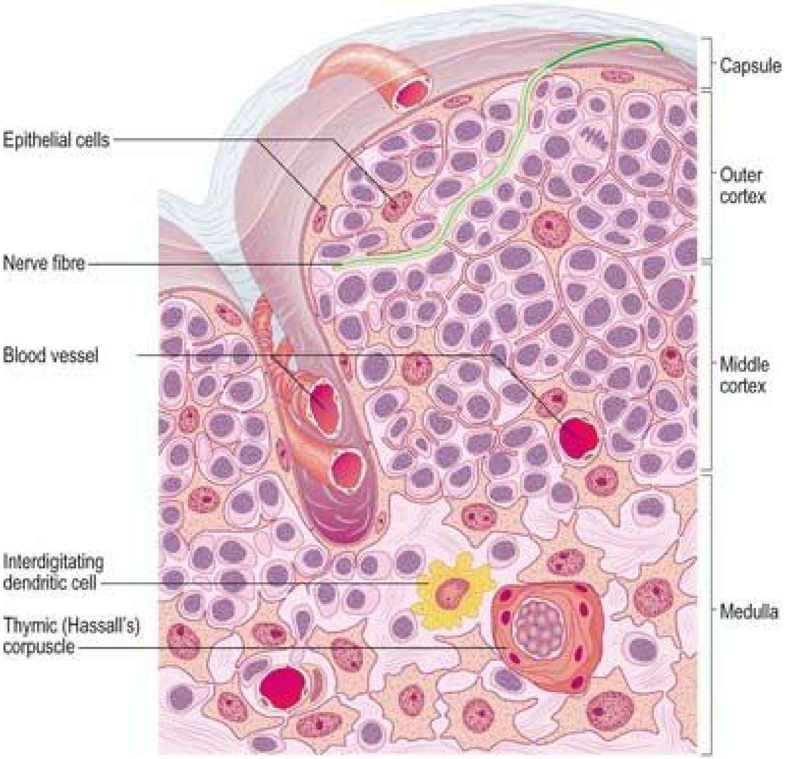
Capsule
Epithelial cells
Outer cortex
Nerve fibre
Blood vessel
Middle cortex
Interdigitating dendritic cell
Thymic (Hassall's) corpuscle
Medulla

Fig. 55.10 Thymic structure and cellular organization, showing an interlobular septum, the cortical circulation, and thymocytes within an epithelial framework.

Both thymic lobes have a loose fibrous connective tissue capsule, from which septa penetrate to the junction of the cortex and medulla, and partially separate the irregular lobules (see Fig. 55.12), which are each 0.5–2.0 mm in diameter. The connective tissue septa form a route of entry and exit for blood vessels and nerves and carry efferent lymphatics. Most migrant cells enter or leave the thymus by this route.

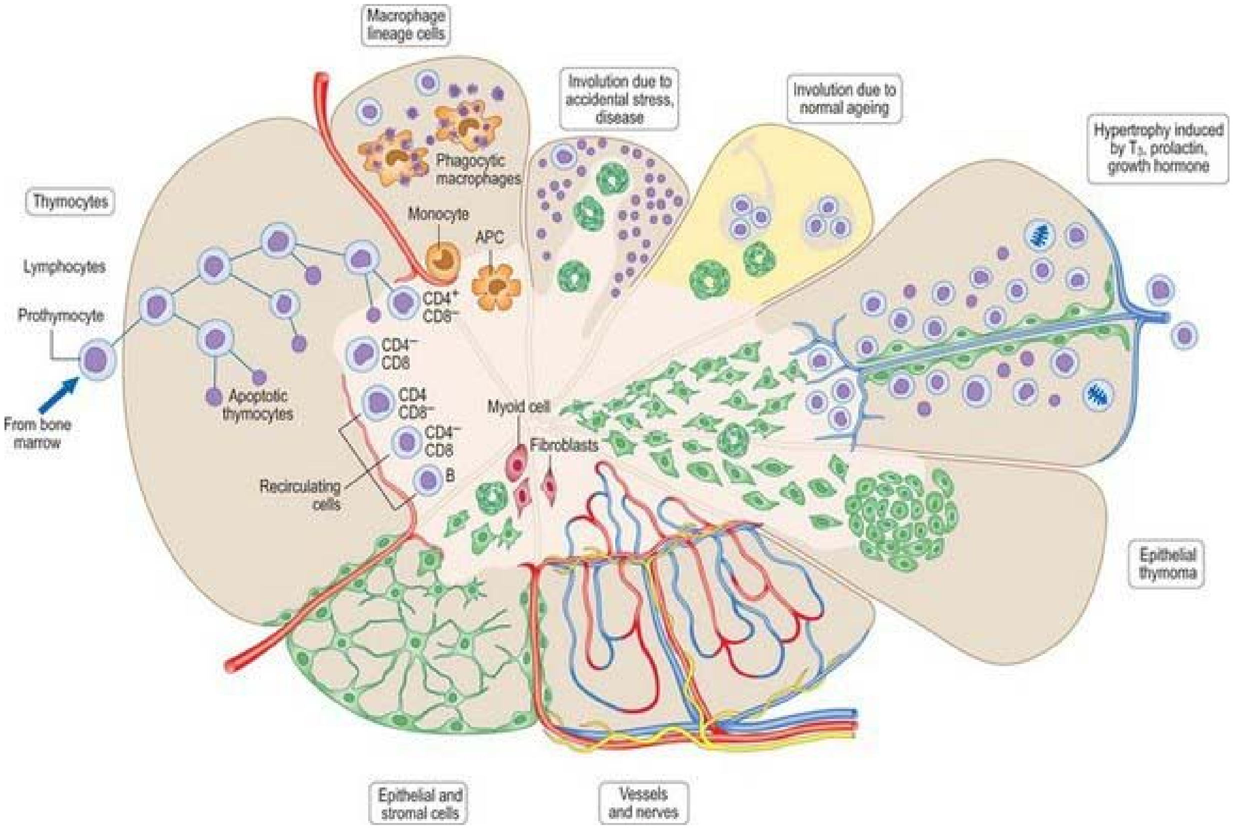
Macrophage lineage cells
Involution due to accidental stress, disease
Involution due to normal ageing
Hypertrophy induced by T3, prolactin, growth hormone
Thymocytes
Lymphocytes
Prothymocyte
From bone marrow
Phagocytic macrophages
Monocyte
APC
CD4+ CD8−
CD4− CD8
CD4 CD8−
CD4− CD8
B
Apoptotic thymocytes
Recirculating cells
Myoid cell
Fibroblasts
Epithelial thymoma
Epithelial and stromal cells
Vessels and nerves

Fig. 55.12 The microscopic organization of the thymus at various stages of life and under different conditions. APC, antigen-presenting cell; T_3, thyroid hormone (tri-iodothyronine).

In each lobule, the cortex is composed of a superficial subcapsular cortex (a narrow band of cells immediately beneath the capsule), and the main cortex, which is much more extensive. The central medulla of both thymic lobes is continuous from one lobule to the next.

Epithelial framework

Unlike other lymphoid structures, in which the supportive framework is chiefly collagenous reticular tissue, the thymus contains a network of interconnected epithelial cells (Fig. 55.10) which create an appropriate microenvironment, by cell–cell contact and the release of paracrine factors, in which thymic lymphocytes (T cells) develop and mature. Although differing in morphology, all the epithelial cells of the thymus share a common origin from pharyngeal endoderm. They vary in size and shape according to their positions within the thymus. Typically they have pale, oval nuclei, a rather eosinophilic cytoplasm and intercellular desmosomal attachments. Intermediate filament bundles of cytokeratin lie within their cytoplasm. The subcapsular cells form a continuous external lining to the thymus beneath its fibrous capsule, and follow its lobulated profile, ensheathing the vessels that pass into it, and contributing to the functional blood–thymus barrier. Other cortical epithelial cells form a loose mesh of long cytoplasmic processes, whereas medullary epithelial cells tend to form more solid cords as well as thymic or Hassall's corpuscles: lymphocytes lie within the interstices of the mesh or between the cords. Large epithelial cells may be associated with around 50 or more thymocytes and are sometimes called thymic nurse cells.

Hassall's corpuscles are whorls of flattened, concentrically layered medullary epithelial cells, from 30 to 100 μm in diameter, and are characteristic features of the thymic medulla (Figs 55.10, 55.11). They start to form before birth and their numbers increase throughout life. Their function is not clear, although they may represent a site for removal of dying, apoptotic thymocytes, because their centres are eosinophilic, partly keratinized and often contain cellular debris. Corpuscles with a similar appearance have been described in the palatine tonsil.

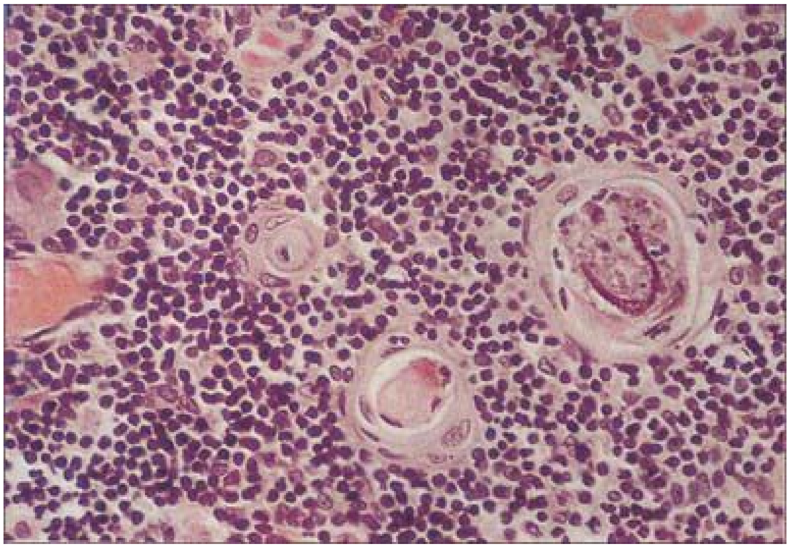

Fig. 55.11 The medulla of a neonatal thymus, showing three concentric Hassall's corpuscles of varying degrees of maturity, surrounded by closely packed lymphocytes and a few epithelial cells with larger nuclei.

Other non-lymphocytic thymic cells

The thymus also contains cells of the myeloid lineage, fibroblasts and myoid cells. Myeloid lineage cells include monocytes at the corticomedullary junction; mature macrophages throughout, but particularly in the cortex; and interdigitating dendritic (antigen-presenting) cells at the corticomedullary junction and in the medulla. Some dendritic cells are of lymphoid rather than myeloid origin. Fibroblasts are found in the capsule, perivascular spaces and medulla, but are infrequent in the cortex, except in the involuted thymus. Myoid cells, which are relatively rare, are situated mainly in the medulla and at the corticomedullary junction. They are large, rounded cells, and possess a central nucleus surrounded by irregularly arranged bundles of myofilaments. Their functions are unknown, although it has been suggested that their contractions might aid the movement of lymphoid cells across or out of the thymus.

Thymocytes

The cortex is densely packed with small thymocytes (thymic lymphocytes, presumptive T cells). They occupy the interstices of the epithelial reticulum, which in histological sections they largely obscure, and form 90% of the total weight of the neonatal thymus. A distinct subcapsular zone houses the thymic stem cells and lymphoblasts undergoing mitotic division. The first stem cells to enter the thymus in the embryo come from the yolk sac and liver during their haemopoietic phases. During later developmental periods, it is probable that all thymic lymphocytes originate in the bone marrow before passing in the blood stream to the thymus.

Thymocytes undergo mitosis in all cortical zones as the differentiating T cells mature, gradually moving deeper into the cortex (Fig. 55.12). The processes of thymocyte development and maturation to generate T cells depend on the microenvironment provided by epithelial cells, dendritic cells, macrophages and fibroblasts. T cells which either fail to recognize self-MHC (histocompatibility) molecules or which recognize self-antigens die by apoptosis, in order to achieve functional immune reactivity and maintain self-tolerance, respectively. Over 95% of cortical thymocytes die within the thymus; the surviving T cells migrate through the walls of venules and efferent lymphatics to enter the circulation and populate secondary lymphoid tissues.

Microcirculation

Cortex

The pattern of blood flow differs in the cortex and medulla. Major blood vessels enter the gland at the corticomedullary junction and pass within each lobe, giving off small capillaries to the cortex and larger vessels to the medulla. Most cortical capillaries loop around at different depths in the cortex and join venules at the corticomedullary junction; some continue through the cortex and join larger venules running in the capsule which leave the thymus. These smaller cortical capillaries usually have a narrow perivascular space, which sometimes contains pericytes and other cells, but rarely nerves. Sheaths of thymic epithelial cells of the blood–thymus barrier lie between the perivascular space and cortical thymocytes.

Medulla

Medullary blood vessels are not as well protected by epithelial cells, and those of the corticomedullary junction are only partially ensheathed, usually on their cortical aspect. Medullary vessels are very variable in size, and some may have short lengths of cuboidal endothelium similar to those in lymph nodes and mucosa-associated lymphoid tissue.

DEVELOPMENT

The embryology and prenatal development of the thymus are described in Chapter 35.

Thymic changes during postnatal life

At birth the thymus is most often bilobar. It is 4–6 cm long, 2.5–5 cm wide and 1 cm thick. The thickest part of the gland at birth is not at the thoracic inlet, but immediately above the base of the heart. During childhood the thymus narrows and lengthens and the cervical portion becomes less noticeable. CT and imaging studies of the thorax reveal that the right lobe of the thymus typically measures 9 mm in thickness, and the left 11 mm, in normal children. After the age of 20 years, it decreases to 5–6 mm in thickness (Fig. 55.12).

The thymus is largest relative to the body at birth, with a mass of 10–15 g. It rapidly increases to 20 g, and subsequently remains at that mass. Studies of thymic mass after sudden death have recorded a wide variation at all ages, but the general pattern is that, after the first year of life, when there is an increase, the mean mass is fairly constant at 20 g until the sixth decade, when a reduction occurs. However, although the mass of the thymus may be fairly constant, it becomes increasingly infiltrated by adipose tissue and so the total amount of active lymphoid tissue becomes progressively smaller with time. At birth, individual adipocytes may be seen in connective tissue septa, and increased numbers are found within the cortex in the second and third decades. Fatty infiltration is usually complete by the fourth decade, when only the medulla and small patches of associated cortex are spared. This process is independent of the level of obesity of the individual.

In children the gland is more pyramidal in shape and firmer than in later life, when the amount of lymphoid tissue is greatly reduced. In the fresh state it is deep red, reflecting its rich blood supply (Fig. 55.9). With age it becomes thinner and greyer, and infiltrated by yellow adipose tissue. Each of the two lobes is partially divided by the ingrowth of shallow septa, so that, superficially, the gland appears lobulated. As fatty atrophy proceeds, this lobulation becomes more distinct. The older thymus can be distinguished from the surrounding mediastinal fat only by the presence of its capsule. However, even within greatly atrophied glands there are usually greyer areas around blood vessels formed by persistent lymphoid tissue. Thymocyte production and differentiation persist throughout life: T cells from the thymus continue to populate the peripheral lymphoid tissue, blood and lymph.

Thymoma and myasthenia gravis

Thymic tumours may compress the trachea, oesophagus and large veins in the neck, causing hoarseness, cough, dysphagia and venous engorgement of the head and neck. Thymomas tend to have an inhomogeneous signal intensity on MRI. They may develop in one lobe of the thymus without affecting the other. Many affected patients also have myasthenia gravis and other autoimmune conditions. Myasthenia gravis, a chronic autoimmune disease of adults, presents as a diminution in power of repetitive contraction in certain voluntary muscles. Although there may be more than one condition with these signs, myasthenia gravis is essentially an autoimmune disease in which acetylcholine receptor proteins of neuromuscular junctions are attacked by autoantibodies. Muscles commonly involved are levator palpebrae superioris (leading to ptosis) and the extraocular muscles (leading to diplopia). Other muscles in the face, jaws, neck and limbs may be involved, and in severe cases the ventilatory muscles are compromised. About 10% of Caucasian individuals with myasthenia gravis have a thymoma and 50% have medullary follicular hyperplasia, the latter predominantly females younger than 40 years of age with strong expression of HLA-B8-DR3 in whom thymectomy often results in symptomatic improvement. In the absence of a thymoma, the onset of myasthenia gravis occurs after 40 years of age in patients with an HLA-B7-DR2 phenotype, except for a group in whom weaknesses are restricted to eye and eyelid movements.

Thymectomy

In myasthenia gravis, patient selection for thymectomy begins with a referral from a neurologist. The strongest association between thymectomy and an improved clinical course has been seen in female myasthenics with systemic weakness; controversial groups include the elderly and those with only ocular symptoms. A new transcervical approach for thymectomy is being performed more commonly, but the traditional sternal splitting approach is still the commonest technique. After a lower transverse neck incision, the ligamentous insertions of the sternocleidomastoids are divided vertically with electrocautery to allow improved exposure into the substernal plane. The upper edge of the skin flap is elevated in the subplatysmal plane to the level of the inferior border of the thyroid gland. The strap muscles are separated longitudinally along their midline raphae and the upper poles of the thymus gland are detected behind. Typically, the larger left superior pole is identified first and dissected free down towards the point at which it merges with the right superior pole just above the jugular notch. The prethymic plane is created by blunt finger dissection anterior then below the left brachiocephalic vein into the substernal location. The thymus is then gently retracted forward and upward to display the veins draining the thymus directly into the left brachiocephalic vein, which are divided. The dissection is then carried along the posterior aspect of the thymus into the mediastinum. The thymus generally remains completely encapsulated and is separated without difficulty from the pericardium (occasionally adhesions necessitate a limited pericardiectomy). Further inferiorly, depression of the great vessels allows direct visualization into the aortopulmonary window for complete removal of the thymus in this vicinity. Some directly contributing blood vessels may be encountered in the form of veins draining into the superior vena cava on the right, or small branches from either of the internal thoracic arteries. These can be dealt with using electrocautery, although care should be taken to avoid injury to the phrenic nerves (for this reason, patients are generally not given a paralytic agent during the course of the anaesthetic, so that the phrenic nerve may be identified intraoperatively).

In most cases the thymus gland is removed completely with both upper and lower poles intact. Careful inspection of the remaining tissue in the mediastinum is performed to identify any possible anatomic anomalies that might result in retained thymic tissue after the operation. The most common anomaly is the unanticipated location of the upper poles of the thymus behind the brachiocephalic vein. The aortopulmonary window is also a common location for thymic tissue and this area is sometimes difficult to expose with a transcervical approach. Any suspicious foci of fat in the mediastinum are removed, and, if necessary, sent for frozen section to ascertain whether or not they contain thymic tissue.

The thymus is essential to the normal development of lymphoid tissues during neonatal and early postnatal life. Thymectomy during this period leads to a progressively fatal condition, with hypoplasia of the peripheral lymphoid organs, wasting and an inability to mount an effective immune response. By puberty, when the main lymphoid tissues are fully developed, thymectomy is less debilitating, but a reduction in effective responses to novel antigens ultimately ensues.

Congenital anomalies of the thymus

Undescended thymus, accessory thymic bodies and rare cysts of the third branchial pouch are of no clinical significance (except where thymectomy is indicated). Patients with thymic agenesis, aplasia and hypoplasia, as in severe combined immune deficiency disease, have reduced lymphocyte numbers, and early death from infection is common. Most cases are familial, with autosomal recessive genes. In young children, a large normal thymus may press on the trachea, causing attacks of ventilatory stridor.

Mediastinal parathyroid adenoma

When primary hyperparathyroidism is diagnosed, surgical excision of the causative parathyroid adenoma (occasionally multiple) is usually performed whether or not symptoms are present. Approximately 3% of parathyroid tumours are found in glands in the mediastinum; 80% of these ectopic adenomas are found in the superior or anterior part of the inferior mediastinum, derived from inferior glands that descend with the thymus in the embryo, and the remainder are found in the posterior mediastinum.

Preoperative localization may help decrease surgical exploration time and morbidity: the sensitivity of technetium-99m sestamibi imaging for identification of parathyroid adenomas exceeds 90%. MRI has a sensitivity of up to 75%, while CT and suprasternal sonography are less sensitive (Iyer et al 1999). Venous sampling may also be used in cases of diagnostic difficulty.

Congenital mediastinal cysts

These form up to 30% of all mediastinal masses and include, in order of frequency, bronchogenic cysts, thymic cysts, pericardial and pleural cysts, oesophageal duplication cysts, meningoceles and thoracic duct cysts. Overall, just over one-third become symptomatic, either directly, as a result of pressure effects on surrounding structures (especially oesophageal and thymic cysts), or indirectly, as a result of secondary infection (bronchogenic cysts).

OESOPHAGUS

The oesophagus (Figs 55.13, 55.14; see also Figs 55.4, 55.7) is a muscular tube, typically 25 cm long, which connects the pharynx to the stomach. It begins in the neck, level with the lower border of the cricoid cartilage and the sixth cervical vertebra, and descends largely anterior to the vertebral column through the superior and posterior mediastina, passes through the diaphragm, level with the tenth thoracic vertebra, and ends at the gastric cardiac orifice level with the eleventh thoracic vertebra. Generally vertical in its course, the oesophagus has two shallow curves. It starts in the median plane, but inclines to the left as far as the root of the neck, gradually returns to the median plane near the fifth thoracic vertebra, and at the seventh thoracic vertebra deviates left again, before it pierces the diaphragm. The oesophagus also bends in an anteroposterior plane to follow the cervicothoracic curvatures of the vertebral column; it can also bend slightly to the right as it is pushed by the aorta before bending to the left to reach the oesophageal hiatus. It is the narrowest part of the alimentary tract (except for the vermiform appendix) and is constricted at the beginning (15 cm from the incisor teeth), where it is crossed by the aortic arch (22.5 cm from the incisor teeth), where it is crossed by the left principal bronchus (27.5 cm from the incisors) and as it passes through the diaphragm (40 cm from the incisors). These measurements are important clinically with regard to the passage of instruments along the oesophagus.

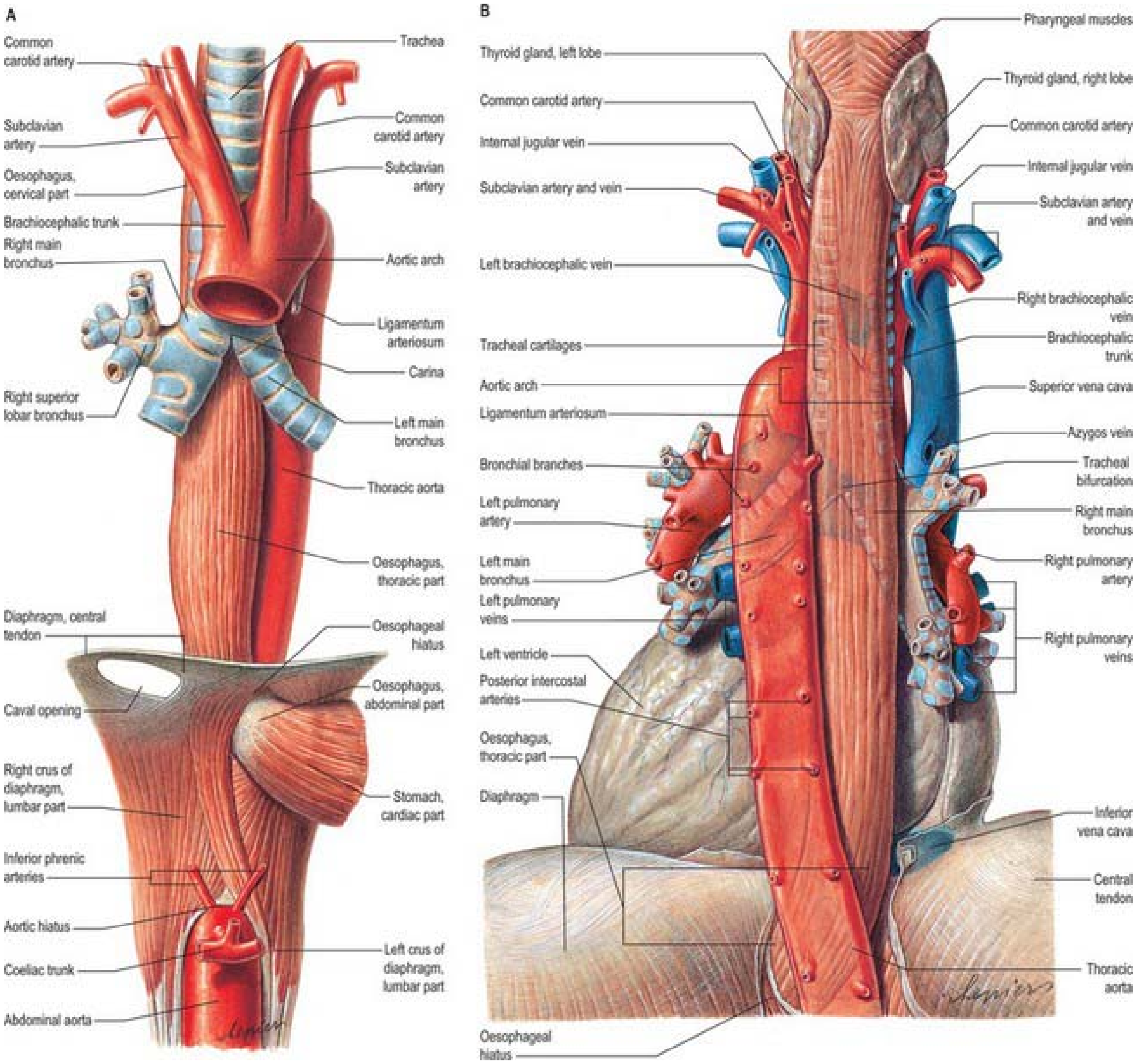
A
Common carotid artery
Subclavian artery
Oesophagus, cervical part
Brachiocephalic trunk
Right main bronchus
Right superior lobar bronchus
Diaphragm, central tendon
Caval opening
Right crus of diaphragm, lumbar part
Inferior phrenic arteries
Aortic hiatus
Coeliac trunk
Abdominal aorta
Trachea
Common carotid artery
Subclavian artery
Aortic arch
Ligamentum arteriosum
Carina
Left main bronchus
Thoracic aorta
Oesophagus, thoracic part
Oesophageal hiatus
Oesophagus, abdominal part
Stomach, cardiac part
Left crus of diaphragm, lumbar part
B
Thyroid gland, left lobe
Common carotid artery
Internal jugular vein
Subclavian artery and vein
Left brachiocephalic vein
Tracheal cartilages
Aortic arch
Ligamentum arteriosum
Bronchial branches
Left pulmonary artery
Left main bronchus
Left pulmonary veins
Left ventricle
Posterior intercostal arteries
Oesophagus, thoracic part
Diaphragm
Oesophageal hiatus
Pharyngeal muscles
Thyroid gland, right lobe
Common carotid artery
Internal jugular vein
Subclavian artery and vein
Right brachiocephalic vein
Brachiocephalic trunk
Superior vena cava
Azygos vein
Tracheal bifurcation
Right main bronchus
Right pulmonary artery
Right pulmonary veins
Inferior vena cava
Central tendon
Thoracic aorta

Fig. 55.13 Oesophagus. **A**, Anterior view. **B**, Posterior view.

(From Sobotta 2006.)

CERVICAL OESOPHAGUS

The cervical oesophagus (see Fig. 55.4) is posterior to the trachea and attached to it by loose connective tissue. The recurrent laryngeal nerves ascend on each side in or near the tracheo-oesophageal groove. Posteriorly are the vertebral column, longus colli and prevertebral layer of deep cervical fascia. Laterally on each side are the common carotid arteries and posterior part of the thyroid gland. In the lower neck, where the oesophagus deviates to the left, it is closer to the left carotid sheath and thyroid gland than it is on the right. The thoracic duct ascends for a short distance along its left side (see Fig. 55.5).

THORACIC OESOPHAGUS

The thoracic oesophagus (Figs 55.13, 55.14) is situated a little to the left in the superior mediastinum between the trachea and the vertebral column. It passes behind and to the right of the aortic arch to descend in the posterior mediastinum along the right side of the descending thoracic aorta. Below, as it inclines left, it crosses anterior to the aorta and enters the abdomen through the diaphragm at the level of the tenth thoracic vertebra. From above downwards, the trachea, right pulmonary artery, left main bronchus, pericardium (separating it from the left atrium) and the diaphragm are anterior. The vertebral column, longus colli, right posterior intercostal arteries, thoracic duct, azygos vein and the terminal parts of the hemiazygos and accessory hemiazygos veins, and, near the diaphragm, the aorta are posterior. A long recess of the right pleural sac lies between the oesophagus (in front) and the azygos vein and vertebral column (behind) in the posterior mediastinum.

In the superior mediastinum, the terminal part of the aortic arch, the left subclavian artery, thoracic duct, the left pleura and the recurrent laryngeal nerve are left lateral relations. In the posterior mediastinum, the oesophagus is related to the descending thoracic aorta and left pleura. The right pleura, and the azygos vein as it arches forwards above the right main bronchus to join the superior vena cava, are right lateral relations. Below the pulmonary roots, the vagus nerves descend in contact with the oesophagus, the right mainly behind and the left in front; the vagi subsequently unite to form a plexus around the oesophagus. Low in the posterior mediastinum, the thoracic duct is behind and to the right of the oesophagus; at higher levels the duct is posterior, crossing to the left of the oesophagus at about the level of the fifth thoracic vertebra and then ascending on the left. On the right of the oesophagus, just above the diaphragm, a small serous infracardiac bursa may occur; it represents the detached apex of the right pneumatoenteric recess.

ABDOMINAL OESOPHAGUS

The abdominal oesophagus is described in the section on Abdomen and Pelvis.

VASCULAR SUPPLY AND LYMPHATIC DRAINAGE

Arteries

The cervical oesophagus is supplied by the inferior thyroid artery (see Ch. 28). The thoracic oesophagus is supplied by bronchial and oesophageal branches of the thoracic aorta (Fig. 55.14A). Four or five oesophageal branches arise from the anterior surface of the aorta and descend obliquely to the oesophagus, where they form a vascular chain that anastomoses above with the oesophageal branches of the inferior thyroid arteries, and below with ascending branches from the left phrenic and left gastric arteries.

Veins

Blood from the oesophagus drains into a submucous plexus and thence into a peri-oesophageal venous plexus from which oesophageal veins arise. Those from the thoracic oesophagus drain predominantly into the azygos veins and, to a lesser extent, the hemiazygos, intercostal and bronchial veins (Fig. 55.14B). Those from the cervical oesophagus drain into the inferior thyroid vein. The left gastric vein meets the lower oesophageal veins at the oesophageal opening in the lesser curvature and then drains into the portal vein.

Oesophageal varices

Cirrhosis or fibrosis of the liver affects the vascular tree within the liver and results in a decrease in hepatic vascular compliance. There is also an increased vascular tone, possibly reflecting a reduction in endothelial vasodilators such as nitric oxide. The portal resistance increases, leading to the formation of a collateral circulation, and there is a concomitant increase in the systemic and splanchnic blood flow. Portosystemic shunting of blood occurs between the short gastric coronary veins and the oesophageal veins, largely as the result of the dilatation of pre-existing embryonic channels.

Varices in the distal oesophagus are easily visible at endoscopy, because they are situated superficially in the lamina propria. The blood from the superficial veins drains into a superficial venous plexus, then into a deeper intrinsic venous plexus and finally into the perioesophageal veins via perforating veins. Bidirectional flow is normally possible in this region, a phenomenon that permits pressure changes during breathing and Valsalva manoeuvres. However, in portal hypertension, the valves within the perforating vessels become incompetent and blood flow is retrograde, causing dilatation of the deep intrinsic veins. The greater pressure within this region predisposes the varices to brisk and life-threatening bleeding. Treatment is directed towards controlling the formation of a collateral circulation and the obliteration of varices that are susceptible to bleeding, and is achieved by paravariceal endoscopic injection of a sclerosant, which causes obliteration of the varices as a result of thrombus formation. Fibrosis is also induced within the mucosa, which reduces the formation of new collateral vessels. Alternatively, rubber bands may be applied in an attempt to ligate the varices. Bleeding from varices is associated with a mortality rate of 25%, reflecting the problems of rebleeding and underlying comorbidity.

Lymphatic drainage

The oesophagus has an extensive, longitudinally continuous submucosal lymphatic system, which presumably explains remote para-oesophageal lymphadenopathy in oesophageal carcinoma. Efferent vessels from the cervical oesophagus drain to the deep cervical nodes either directly or through the paratracheal nodes. Vessels from the thoracic oesophagus drain to the posterior mediastinal nodes and those from the abdominal oesophagus drain to the left gastric lymph nodes. Some may pass directly to the thoracic duct.

INNERVATION

The upper oesophagus is supplied by the branches of the recurrent laryngeal nerve and by postganglionic sympathetic fibres that reach it by travelling along the inferior thyroid arteries (Fig. 55.7) (see Ch. 28). The lower oesophagus is supplied by the oesophageal plexus, a wide-meshed autonomic network that surrounds the oesophagus below the level of the lung roots, and which contains a mixture of parasympathetic and sympathetic fibres.

Motor fibres to the striated and smooth muscle of the oesophageal wall travel in the vagus. Axons derived from neuronal cell bodies in the nucleus ambiguus travel via the recurrent laryngeal nerve and supply cricopharyngeus and the striated muscle of the upper one-third of the oesophagus. Axons with cell bodies in the dorsal nucleus of the vagus pass through the oesophageal plexus and supply the smooth muscle that makes up the lower two-thirds of the oesophagus, after local relay in the oesophageal wall. Other branches are given off by the vagus as it travels through the mediastinum, and pass directly to the oesophagus. The vagus also carries secretomotor fibres to mucous glands in the oesophageal mucosa, and visceral afferent (sensory) fibres to cell bodies in its inferior ganglion.

Vasomotor sympathetic fibres destined for the oesophagus arise from the upper four to six thoracic spinal cord segments. Those from the upper ganglia pass to the middle and inferior cervical ganglia, where they synapse on postganglionic neurones that give rise to axons which innervate the vessels of the cervical and upper thoracic oesophagus. Those from the lower ganglia pass either directly to the oesophageal plexus or to the coeliac ganglion (via the greater splanchnic nerve), where they synapse; postganglionic axons innervate the distal oesophagus. Afferent visceral pain fibres travel via the sympathetic fibres to the first four segments of the thoracic spinal cord: because these segments also receive afferents from the heart, it is sometimes difficult to distinguish between oesophageal and cardiac pain.

MICROSTRUCTURE

The tissues forming the thoracic oesophageal wall, from lumen outwards, are the mucosa (consisting of epithelium, lamina propria and muscularis mucosae), submucosa, muscularis externa and adventitia (Fig. 55.15; see Fig. 60.9).

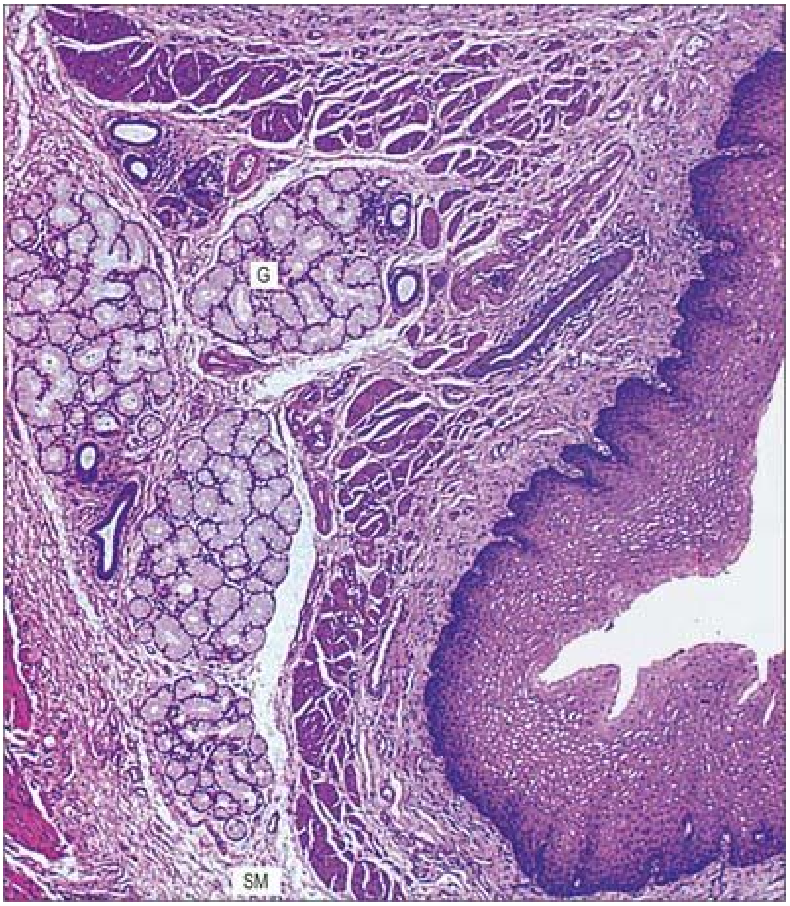

Fig. 55.15 The wall of the oesophagus. A stratified squamous, non-keratinizing epithelium lines the lumen (right), and submucosal glands (G) in the submucosa (SM) secrete mucus that lubricates the passage of food.

(By permission from Dr JB Kerr, Monash University, from Kerr JB 1999 Atlas of Functional Histology. London: Mosby.)

Mucosa

The mucosa is thick. At the gastro-oesophageal junction, a jagged boundary line separates the greyish-pink, smooth, oesophageal mucosa from the reddish-pink gastric mucosa, which is covered by minute bulges and depressions. Throughout its length, the oesophageal lumen is marked by deep longitudinal grooves and ridges, which disappear when the lumen is distended, but obliterate the lumen at all other times.

Epithelium

The epithelium is a non-keratinized, stratified squamous epithelium, continuous with that of the oropharynx. In humans this protective layer is quite thick (300–500 µm) (Fig. 55.15), and is not affected by oesophageal distension. The boundary between the oesophageal epithelium and its lamina propria is distinct but markedly uneven, because tall connective tissue papillae invaginate the epithelial base, assisting in the anchorage of the epithelium to underlying tissues (Fig. 55.15). These papillae are permanent structures, also unaffected by oesophageal distension, and they are rich in blood vessels and nerve fibres. At the base of the epithelium there is a basal lamina, to which epithelial cells are attached by hemidesmosomes, as occurs in the oral mucosa.

Oesophageal epithelium is similar to other stratified squamous epithelia. It can be divided into a basal, proliferative layer, a parabasal layer of cells undergoing terminal differentiation, and a flattened layer of superficial cells or squames which retain their nuclei. The most superficial strata of cells contain a few keratohyalin granules, in addition to keratin filaments. The epithelial cell population is constantly renewed by mitosis in the cuboidal basal cells and the deepest parabasal cells. As they migrate towards the lumen, they become progressively polygonal and then more flattened, and are eventually desquamated at the epithelial surface. This sequence of events normally takes 2–3 weeks, and is markedly slower than in the stomach and intestine.

The epithelium is an effective protection against mechanical injury during swallowing because of its thickness and the presence of mucus at its surface. However, protection is limited by repeated exposure to the strongly acidic, protease-rich secretions of the stomach, as occurs abnormally during reflux. Normally, the lower oesophageal sphincter prevents reflux, but if reflux does occur, ulceration and fibrosis of the oesophageal wall, accompanied by considerable pain and difficulties in swallowing may ensue. Exposure to acid may also cause oesophageal epithelial metaplasia to a gastric-like mucosa (Barrett's mucosa), or to more overt neoplastic changes.

Langerhans cells

Langerhans cells are present in the oesophageal epithelium. They are immature dendritic cells and resemble those found in the epidermis. They perform similar antigen-processing and antigen-presenting roles, which are important in immunostimulation of naive T cells and mucosal defence.

Lamina propria

The oesophageal lamina propria contains scattered groups of lymphoid follicles (mucosa-associated lymphoid tissue), which are especially prominent near the gastro-oesophageal junction. Small tubular mucous glands occur in this region, and in the upper part of the oesophagus close to the pharynx.

Muscularis mucosae

The muscularis mucosae is composed mainly of longitudinal smooth muscle, and forms a thin sheet near the epithelium, the contours of which it follows closely. At the pharyngeal end of the oesophagus it may be absent or represented only by sparse, scattered bundles; below this it becomes progressively thicker. The longitudinal orientation of its cells changes to a more plexiform arrangement near the gastro-oesophageal junction.

Submucosa

The submucosa loosely connects the mucosa and the muscularis externa, and penetrates the longitudinal ridges of the oesophageal lumen. It contains larger blood vessels, nerves and mucous glands. Its elastic fibres are important in the reclosure of the oesophageal lumen after peristaltic dilatation.

Oesophageal glands

Oesophageal glands are small tubuloacinar glands lying in the submucosa, each group sending a single long duct through the intervening layers of the gut wall to the surface. They are composed mostly of mucous cells, although they also contain serous cells that secrete lysozyme. In the region close to the pharynx, and at the lower end close to the stomach, the glands are simpler in form and restricted to the lamina propria of the mucosa. The mucosal mucous glands of the abdominal oesophagus closely resemble the cardiac glands of the stomach, and are therefore called oesophageal cardiac glands.

Muscularis externa

The muscularis externa is up to 300 µm thick, and consists of the outer longitudinal and inner circular layers typical of the intestine. The longitudinal fibres form a continuous coat around almost the entire length of the oesophagus, except that, posterosuperiorly, 3–4 cm below the cricoid cartilage, they diverge as two fascicles that ascend obliquely to the anterior aspect of the oesophagus. Here, they pass deep to the lower border of the inferior constrictor, and end in a tendon that is attached to the upper part of the ridge on the back of the cricoid lamina. The V–shaped space between these fascicles is filled by the circular muscle fibres of the oesophagus, which are thinly covered below by some decussating longitudinal fibres and above by the overlapping inferior constrictor. The longitudinal layer is generally thicker than the circular layer. Accessory slips of smooth muscle sometimes pass between the oesophagus and left pleura or the root of the left principal bronchus, trachea, pericardium or aorta, and are sometimes considered to fix the oesophagus to these structures. Superiorly, the circular fibres are continuous behind with the inferior pharyngeal constrictor. In front, the uppermost fibres are attached to the lateral margins of the tendon of the two longitudinal fasciculi of the oesophagus. Inferiorly, the circular muscle is continuous with the oblique layer of muscle fibres in the stomach wall. In the upper one-third of the oesophagus, the muscularis externa is formed by skeletal muscle; in the middle one-third, smooth muscle fascicles intermingle with striated muscle, and this increases distally such that the lower one-third contains only smooth muscle.

OESOPHAGOSCOPY AND TRANSOESOPHAGEAL ULTRASOUND

The oesophagus can be inspected visually by oesophagoscopy. This may be indicated in patients with persistent oesophageal symptoms such as atypical chest pain, dysphagia, odynophagia (painful swallowing) or symptoms of reflux. The procedure is performed with or without sedation. The endoscope is passed orally under direct vision with the patient in a lateral decubitus position. The endoscope is manoeuvred into the oesophageal inlet and the patient asked to swallow. Once the endoscope passes the oesophageal inlet, it is advanced slowly under direct vision and the mucosa carefully inspected. The mucosa normally appears whitish pink and changes at the lower oesophagus to a reddish mucosa at the squamocolumnar junction (Z line): this is closely related to the diaphragmatic hiatus, and displacement by more than 2 cm is indicative of a hiatus hernia. There may be slight extrinsic compression at the level of the aorta and occasionally at the left main bronchus.

Endoscopic transoesophageal ultrasound permits assessment of the oesophageal wall and para-oesophageal structures such as lymph nodes. This technique is more sensitive than CT scanning in detecting metastases in mediastinal lymph nodes, because it allows lymph nodes less than 10 mm in size to be assessed for possible malignant involvement. Normal lymph nodes cannot be easily identified by endoscopic ultrasound, because they have the same echogenicity characteristics as surrounding tissue; a hypoechoic or inhomogeneous pattern on ultrasound is considered more suspicious of malignancy. Endoscopic ultrasound-guided fine needle aspiration allows accurate diagnosis of lymph nodes, but only mediastinal nodes adjacent to the oesophagus can be fully evaluated. Transbronchial fine needle aspiration is an alternative approach for sampling mediastinal nodes, with lymph node choice based on CT findings. PET CT scanning is rapidly becoming the modality of choice for mediastinal nodal staging.

Oesophageal rupture

The majority of oesophageal ruptures are iatrogenic, and occur during the instrumentation of the oesophagus during simple endoscopy, endoscopic intervention and nasogastric tube placement. Other causes are traumatic, barotrauma, foreign bodies and oesophageal carcinoma. Barotrauma usually occurs with intense retching and vomiting. It usually causes a longitudinal tear in the posterior wall of the thoracic oesophagus. Overall, almost 60% of the perforations are located in the thoracic oesophagus, 25% in the cervical oesophagus and 15% in the abdominal oesophagus. Perforation in the cervical oesophagus occurs in the posterior wall, where it is at its thinnest, and often corresponds to an area of mucosa where there is no covering with muscle, and which is bordered by the pharyngeal inferior constrictor and cricopharyngeus. Mortality from oesophageal perforations is 20% and results from mediastinitis and necrotizing infection. Presenting symptoms include thoracic pain, odynophagia, haematemesis, subacute surgical emphysema, tachycardia and breathlessness and, in the advanced case, septic shock. Early diagnosis (within 24 hours) and repair are associated with a better prognosis and a mortality rate of between 10% and 15%, whereas late diagnosis has a much greater mortality rate. For a perforation in the upper two-thirds of the thoracic oesophagus, a right thoracotomy in the fifth and sixth intercostal space is performed. The lower one-third of the oesophagus is approached through a left thoracotomy in the sixth and seventh intercostal space. The perforation is closed in layers after any necrotic tissue has been debrided.

BARIUM STUDIES

A double-contrast barium swallow with fluoroscopy enables anatomical and functional assessment of the oesophagus (see Fig. 55.18). A standard examination involves the patient swallowing a barium solution and gas granules, and images be taken in the erect, supine and prone recumbent positions. The upright posture fully dilates the oesophagus and is useful in evaluating any constrictions. The narrow tubular lumen of the oesophagus is slightly indented by the aortic arch and the left main bronchus. The supine view allows better evaluation of any motor dysfunction and varices, and moving into the prone position provokes underlying gastro-oesophageal reflux. Both repeating single digital images and cine loops of fluoroscopy can be obtained. The fluoroscopic images demonstrate defective opening of the pharyngeal oesophageal sphincter and the nature of the contractions in the body of the oesophagus. The cardio-oesophageal sphincter can be assessed in achalasia. Other abnormalities such as hiatus hernia and areas of narrowing or dilatation of the oesophagus may be demonstrated. Mucosal relief images are obtained once the bulk of the contrast media has passed into the stomach, and this provides fine mucosal detail. Cross-sectional imaging is usually used for the preoperative planning and staging of oesophageal tumours, and is of value in radiotherapy planning.

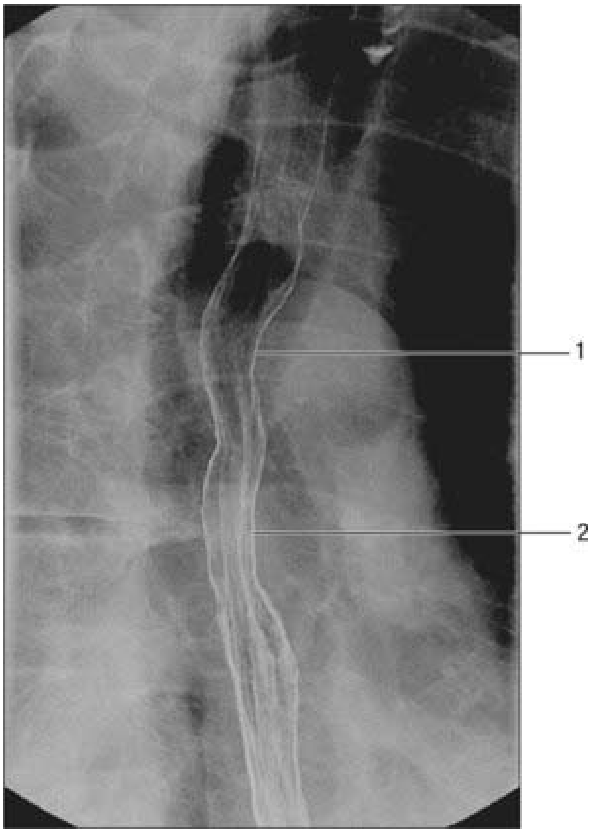

Fig. 55.18 Oblique radiograph of the thorax during the oesophageal transit of part of a ‘meal’ of barium sulphate paste. **1**. Indentation from aortic arch. **2**. Indentation from left main bronchus.

DEVELOPMENT

The development of the oesophagus is described in Chapter 35.

Tracheo-oesophageal fistula

Tracheo-oesophageal fistula is described in Chapter 59.

Oesophageal atresia

The vast majority of cases of oesophageal atresia occur in conjunction with a tracheo-oesophageal fistula, with an incidence of 1 : 3000–4000 births. There is a high incidence of associated congenital abnormalities such as cardiac, genitourinary, skeletal and other gastrointestinal anomalies. Prenatal diagnosis is unusual because of the lack of specific ultrasound features. The only prenatal indicators are polyhydramnios and, rarely, an absence of stomach gas; other clinical signs are the presence of a pharyngeal pouch on ultrasound. Postnatal clinical features are regurgitation of feeds; other symptoms, such as recurrent cough and choking spells, are related to the presence of a tracheo-oesophageal fistula. Corrective surgery is essential; overall survival is heavily influenced by the presence of associated cardiac anomalies.

OESOPHAGEAL SPHINCTERIC MECHANISMS

Radiological studies show that swallowed food stops momentarily in the gastric end of the oesophagus, before entering the stomach (see Fig. 55.18), suggesting the presence of a sphincter at this point. In the past there was much controversy as to the reason for this behaviour, because only slight thickening of the muscle coat has been found in humans. There is now ample physiological and clinical evidence that closure depends on two major mechanisms. The more important of these is the lower oesophageal sphincter, a specialized zone of circular smooth muscle surrounding the oesophagus at its transit through the diaphragm and for much of its short abdominal course. This region of the oesophagus is maintained under tonic contraction, except during swallowing, when it relaxes briefly to admit ingesta to the stomach, and during vomiting (see p. 954). It is controlled by the intramural plexuses of the enteric nervous system; in addition, the neural release of nitric oxide contributes to its relaxation. The second mechanism is a functional external sphincter provided by the crural diaphragm (usually the right crus), which encircles the oesophagus as it passes into the abdomen and is attached to it by the phreno-oesophageal ligament. Radiological, electromyographic and manometric analyses have shown that its muscular fibres contract around the oesophagus during inspiration and when intra-abdominal pressure is increased, thus helping to prevent gastro-oesophageal reflux, even when the lower oesophageal sphincter is inhibited experimentally with atropine. The relative importance of these two agents in the prevention of oesophageal reflux is still a matter for debate. Clinically, there is a good correlation between this condition and lower oesophageal sphincter dysfunction in some cases, whereas in others, failure of the diaphragmatic component, as seen in hiatus hernia, appears to be a major factor. The anatomical configuration of the gastro-oesophageal orifice may also play some part in these processes (see p. 954).

Swallowing

The oesophageal phase of swallowing is described in Chapter 33.

Vomiting

The lower oesophageal sphincter relaxes in the initial phase of vomiting at the same time as the crural fibres around the oesophagus relax. There is a subsequent rapid contraction of the diaphragm and abdominal muscles, with a resultant increase in intra-abdominal pressure.

OESOPHAGEAL DYSMOTILITY

The main disorders of oesophageal motility relate to disorders of the upper or lower oesophageal sphincters (discussed in detail in the section on upper gastro-oesophageal reflux) and achalasia. Problems with the upper oesophageal sphincter usually have a neurological aetiology. Brainstem disease impairs relaxation of cricopharyngeus (the lower oesophageal sphincter), leading to dysphagia of solids and liquids, with a tendency to aspirate; videofluoroscopy may demonstrate the abnormality.

Achalasia of the cardia is a primary motor disorder of the oesophagus in which there is failure of relaxation of the cardio-oesophageal sphincter and loss of peristalsis in the oesophageal body with degeneration of neuronal cell bodies in the myenteric nerve plexus. The clinical presentation is dysphagia, regurgitation of undigested food, retrosternal chest pain and occasional weight loss. A simple chest radiograph may show dilatation of the oesophagus and retention of food products as a mottled double-contoured mediastinal widening. Barium swallow shows a classical bird-beak appearance as a result of failure of relaxation of the lower oesophageal sphincter and an absence of peristalsis. Oesophageal manometry with pressure measurements confirms the diagnosis and demonstrates absent or impaired relaxation of the lower oesophageal sphincter. Treatment consists of pneumatic balloon dilatation during endoscopy or minimal-access surgical myotomy of the cardia. An alternative in frail patients is intrasphincteric injection of botulinum toxin. The advantages are lower morbidity and mortality, with a much lower risk of oesophageal perforation.

Diffuse oesophageal spasm may present with dysphagia and chest pain. It is characterized by abnormal oesophageal contractions on barium swallow, and produces simultaneous segmental contractions that obliterate the oesophageal lumen to produce a ‘corkscrew oesophagus’. Manometry also demonstrates titanic contractions of the oesophagus. Non-specific oesophageal motility disorder occurs with ageing (presbyoesophagus) and is characterized by a decreased incidence of normal, or even absent, peristalsis after swallowing. This may be accompanied by repetitive (tertiary) contractions and failure of relaxation of the lower oesophageal sphincter. Oesophageal dysmotility also includes oesophageal spasm and disorders caused by scleroderma or other connective tissue diseases, in which there is atrophy of smooth muscle and fibrous replacement in the submucosa and lamina propria.

GASTRO-OESOPHAGEAL REFLUX

Gastro-oesophageal reflux is described in Chapter 65, p. 1114.

HIATUS HERNIA

Hiatus hernia is described in Chapter 58.

MEDIASTINAL IMAGING

Mediastinal structures may be viewed using X-rays, CT and MRI.

NORMAL MEDIASTINAL CONTOURS ON FRONTAL CHEST RADIOGRAPH

In a standard posteroanterior chest radiograph the X-ray beam passes from back to the front of the chest. The standing patient breath-holds in full inspiration, and elevates and abducts the arms over the radiographic plate, movements which protract the scapulae and depress the medial ends of the clavicles to clear the peripheral lung fields and apices respectively. In this view the heart and large blood vessels appear as the ‘mediastinal silhouette’ (Fig. 55.16). Forming its left border, from above down, are the aortic arch (‘aortic knuckle’), sometimes with the left superior intercostal vein (‘aortic nipple’) visible, the pulmonary trunk and left ventricle. The descending aorta is projected as a continuous left paravertebral border all the way down to the diaphragm. The right border is delineated by the right brachiocephalic vein, superior vena cava, right atrium and thoracic inferior vena cava. A right paratracheal stripe (normally under 3 mm) is usually seen with the oval silhouette of the azygos arch at its lower margin. An accessory lung fissure, the azygos fissure, is seen rarely and extends from the apex of the lung to the right tracheobronchial angle. The azygos arch width should be no more than 5 mm, but may measure up to 10 mm in the third trimester of pregnancy as a result of a physiological blood volume increase. Enlargements or displacements of any of these structures accentuate the normal bulges on the borders of the mediastinal silhouette, thus an enlarged left auricle is seen between the pulmonary trunk and left ventricle. On both sides, opacities caused by pulmonary vessels associated with the roots of the lungs form hilar contours. In the upper thorax, the less dense projection of the trachea is visible in the median plane. The anterior junctional line, where the two lungs approximate above the heart, is sometimes visible. The posterior junctional line, which represents pleural apposition behind the oesophagus, is also sometimes seen: it projects up into the neck because of the obliquity of the thoracic inlet. The azygo-oesophageal recess is an area where a portion of the right lung is in contact with the azygos vein and the lateral wall line. The paraspinal lines are also visible parallel to the right and left margins of the thoracic spine.

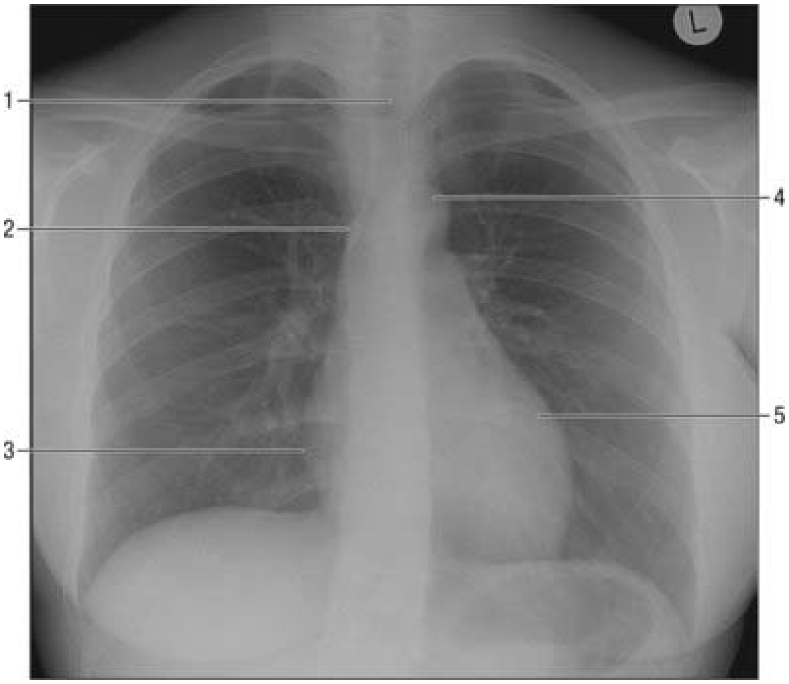

Fig. 55.16 Radiograph of chest of adult female, posteroanterior view. **1**. Trachea. **2**. Azygos vein. **3**. Right atrial border. **4**. Aortic arch. **5**. Left ventricular border.

NORMAL MEDIASTINAL CONTOURS ON A LATERAL CHEST RADIOGRAPH

On a lateral view, the cardiac silhouette is seen above the anterior part of the diaphragm (Fig. 55.17). The anterior and posterior cardiac silhouettes are formed by the right ventricle and left atrium respectively. Behind is the retrocardiac space (posterior mediastinum) containing the descending thoracic aorta and the oesophagus: the oesophagus can be visualized with swallowed air or barium on a chest radiograph or fluoroscopically in the barium swallow examination (Fig. 55.18). Above, the less dense trachea and main bronchi are recognizable.

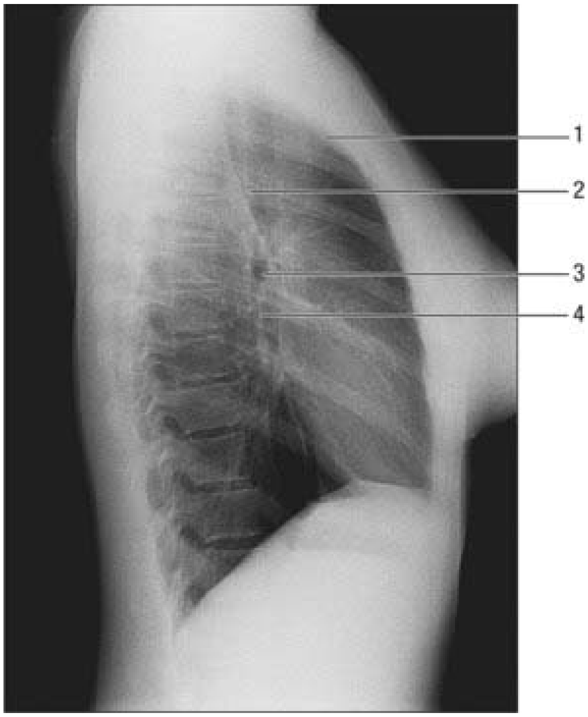

Fig. 55.17 Radiograph of chest of adult female, lateral view. **1**. Retrosternal line (fat). **2**. Posterior tracheal line. **3**. Right main bronchus. **4**. Bronchus intermedius.

The aortic arch and large vessels anterior to the trachea produce faint shadows in the superior mediastinum. The brachiocephalic veins are visible as an extrapleural bulge directly behind the manubrium. The oesophagus is directly behind the trachea; the posterior paratracheal line, seen in the majority of lateral radiographs, represents the juxtaposition of the anterior oesophageal and posterior tracheal walls. The inferior vena cava is visible in the majority of patients as it drains into the right atrium.

COMPUTED TOMOGRAPHY AND MAGNETIC RESONANCE IMAGING OF THE MEDIASTINAL SPACES

CT scans provide excellent cross-sectional views of the anatomy of the mediastinum and are complemented by MRI (Figs 55.19, 55.20). Intravenous contrast enhancement of the vessels improves the detail of the scan and improves distinction of blood vessels from lymph nodes and soft tissue opacities. Cross-sectional CT scanning is very useful in evaluating the mediastinal spaces, which include the pretracheal, subcarinal, right paratracheal and posterior tracheal spaces and aortopulmonary window: these areas are where mediastinal lymph node masses are located and hence of importance in the staging of lung cancer.

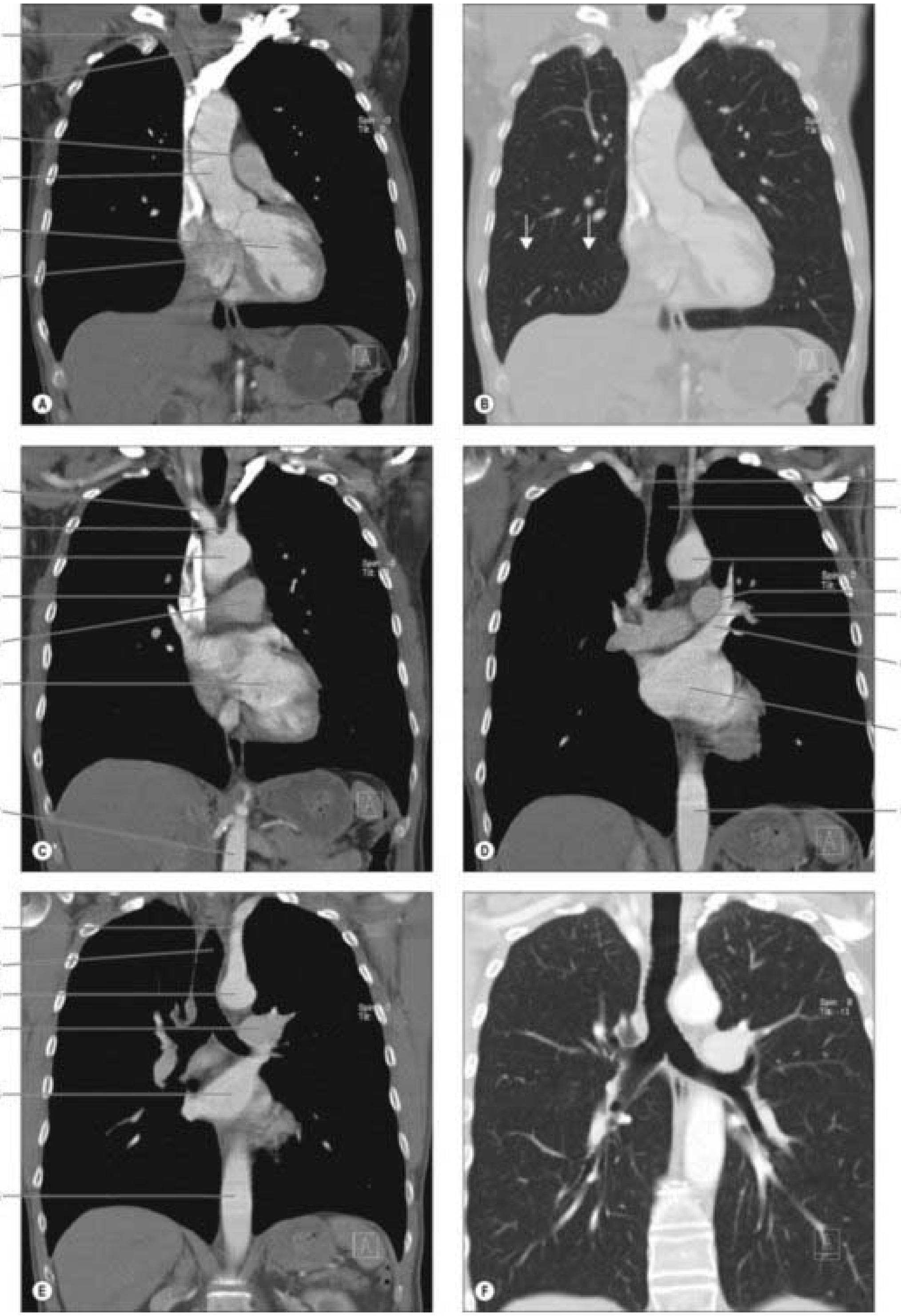
1
2
3
4
5
6
A
B
1
2
3
4
5
6
7
C
1
2
3
4
5
6
7
8
D
1
2
3
4
5
6
E
F

Fig. 55.20 Coronal sections of the mediastinum. **A**, At the level of the aortic valve. **1**. Right brachiocephalic vein. **2**. Left brachiocephalic vein. **3**. Pulmonary trunk. **4**. Ascending aorta. **5**. Left ventricle. **6**. Right atrium. **B**, As **A**, with lung window settings; horizontal (minor) fissure arrowed. **C**, At

the level of the anterior aortic arch. **1**. Brachiocephalic artery. **2**. Left common carotid. **3**. Aortic arch. **4**. Superior vena cava. **5**. Pulmonary trunk. **6**. Left ventricle. **7**. Abdominal aorta. **D**, At the level of the left atrium and mid arch. **1**. Right subclavian. **2**. Trachea. **3**. Aortic arch. **4**. Left main pulmonary artery. **5**. Right main pulmonary artery. **6**. Left superior pulmonary vein. **7**. Left atrium. **8**. Descending thoracic aorta. **E**, At the level of the posterior arch and tracheal carina. **1**. Left subclavian artery. **2**. Trachea. **3**. Posterior aortic arch. **4**. Left main pulmonary artery. **5**. Left atrium. **6**. Descending thoracic aorta. **F**, As **E**, with lung window settings.

The pretracheal space, as seen in cross-section, is bordered by the trachea posteriorly, the superior vena cava and right brachiocephalic vein anteriorly, and the descending aorta and the superior pericardial sinus to the left. The aortopulmonary window is located underneath the aortic arch and above the left pulmonary artery. The trachea forms its medial border and the lungs its lateral border. The right paratracheal space is in between the lung and the trachea on the anterolateral aspects, whereas the posterior tracheal space is formed between the lung and the posterior lateral aspect of the trachea. The subcarinal space is located below the carina and bounded by the two bronchi. On the right, the azygo-oesophageal recess is located posterior to the subcarinal space and on the left side is the oesophagus. All these areas are in direct continuity with each other and are traversed during cervical mediastinoscopy.

The junctional areas are where the two lungs approach each other. The anterior or prevascular junction is anterior to the great vessels and posterior to the chest wall, and between the two lungs. The left brachiocephalic vein, highest mediastinal nodes, thymus and phrenic nerves are located in the anterior junction. The posterior junction is an area posterior to the trachea and is where the lungs lie close to each other. The paraspinal area is a space between the lateral margins of the spine and the lungs. The intercostal vessels, sympathetic chain and ganglia, and small lymph nodes are located within the paraspinal space. The retrocrural space, between the diaphragmatic crura and the vertebral bodies, is traversed by the aorta, azygos and hemiazygos veins, the thoracic duct, intercostal arteries, sympathetic chains and splanchnic nerves.

REFERENCES

mstrong P. The normal chest. In: Armstrong P, Wilson AG, Dee P, Hansell DM. *Imaging of Diseases of the Chest*. 3rd edn. London: Mosby; 2000:21-62.

o HM, Lee DY, Sung SW. Anatomical variations of rami communicantes in the upper sympathetic trunk. *Eur J Cardiothoracic Surg*. 2005;27:320-324.

feld M, Faclier G. Bilateral pain relief after unilateral thoracic percutaneous sympathectomy. *Can J Anaesth*. 2006;53:258-262.

er RB, Whitman GJ, Sahin AA. Parathyroid adenoma of the mediastinum. *Am J Radiol*. 1999;173:94.

retzki A, Wolff M. ‘Maximal’ thymectomy for myasthenia gravis: surgical anatomy and operative technique. *J Thorac Cardiovasc Surg*. 1988;96:711-716.

asaoka A, Yamakawa Y, Niwa H, et al. Extended thymectomy for myasthenia gravis patients: a 20-year review. *Ann Thorac Surg*. 1996;62:853-859.

eyers BF, Cooper JD. Transcervical thymectomy for myasthenia gravis. *Chest Surg Clin N Am*. 2002;11:363-368.

ountain CF, Dresler CM. Regional lymph node classification for lung cancer staging. *Chest*. 1997;111:1718-1723.

quet K-J. Causes and pathomechanisms of oesophageal varices development. *Med Sci Monit*. 2000;6:915-928.

ngh TP, Bala Sanju, Kalsey G, Singla Rajan K. Applied anatomy of fascial spaces in the head and neck. *J Anat Soc India*. 2000;49:78-88.

itz L. Esophageal atresia: past, present and future. *J Paediatr Surg*. 1996;31:19-25.

emyss-Holden SA, Launois B, Maddern GJ. Management of thoracic duct injuries after oesophagectomy. *Br J Surg*. 2001;88:1442-1448.

CHAPTER 56

Heart and great vessels

PERICARDIUM

The pericardium contains the heart and the juxtacardiac parts of its great vessels. It consists of two components, the fibrous and the serosal pericardium. The fibrous pericardium is a sac made of tough connective tissue, completely surrounding the heart without being attached to it. This fibrous sac develops by a sequential process of cavitation of the embryonic body wall by expansion of the secondary pleural cavity. Thus its lateral walls are clothed externally by parietal mediastinal pleura. The serosal pericardium consists of two layers of serosal membrane, one inside the other: the inner (visceral) one adheres to the heart and forms its outer covering known as the epicardium, whereas the outer (parietal) one lines the internal surface of the fibrous pericardium. The two serosal surfaces are apposed and separated by a film of fluid. This allows movement of the inner membrane and the heart adhering to it, except at the arterial and venous areas of the pericardium where the two serosal membranes merge. These last constitute two parietovisceral lines of serosal reflexion. The separation of the two membranes of the serosal pericardium creates a narrow space, the pericardial cavity, which provides a complete cleavage between the heart and its surroundings and so allows it some freedom to move and change shape.

FIBROUS AND SEROSAL PERICARDIUM

The fibrous pericardium is compact collagenous fibrous tissue. The serosal pericardium is a single layer of flat cells on a thin subserosal layer of connective tissue, which blends with the fibrous pericardium in the parietal membrane and with the interstitial myocardial tissue in the visceral membrane. On the cardiac side, the subserosal layer contains fat, especially along the ventricular side of the atrioventricular groove, the inferior cardiac border and the interventricular grooves. The main coronary vessels and their larger branches are embedded in this fat; the amount is related to the general extent of body fat and gradually increases with age.

Fibrous pericardium

The fibrous pericardium is roughly conical and clothes the heart. Superiorly, it is continuous exteriorly with the adventitia of the great vessels; inferiorly it is attached to the central tendon of the diaphragm and a small muscular area of its left half. Above, the fibrous pericardium not only blends externally with the great vessels, but is continuous with the pretracheal fascia. Anteriorly, it is also attached to the posterior surface of the sternum by superior and inferior sternopericardial ligaments, although the extent of these ‘ligaments’ is extremely variable, and the superior one is often undetectable. The pericardium is securely anchored by these connections and maintains the general thoracic position of the heart, serving as the ‘cardiac seat belt’.

Anteriorly, the fibrous pericardium is separated from the thoracic wall by the lungs and the pleural coverings. However, in a small area behind the lower left half of the body of the sternum and the sternal ends of left fourth and fifth costal cartilages, the pericardium is in direct contact with the thoracic wall. Until it regresses, the lower end of the thymus is also anterior to the upper pericardium. The principal bronchi, oesophagus, oesophageal plexus, descending thoracic aorta and posterior parts of the mediastinal surface of both lungs are posterior relations. Laterally are the pleural coverings of the mediastinal surface of the lungs. The phrenic nerve, with its accompanying vessels, descends between the fibrous pericardium and mediastinal pleura on each side. Inferiorly, the pericardium is separated by the diaphragm from the liver and fundus of the stomach.

The aorta, superior vena cava, right and left pulmonary arteries and the four pulmonary veins all receive extensions of the fibrous pericardium. The inferior vena cava, which traverses the central tendon, has no such covering.

Serosal pericardium

The serosal pericardium is a closed sac within the fibrous pericardium, and has a visceral and a parietal layer. The visceral layer, or epicardium, covers the heart and great vessels and is reflected into the parietal layer, which lines the internal surface of the fibrous pericardium. The reflections of the serosal layer are arranged as two complex ‘tubes’: the aorta and pulmonary trunk are enclosed in one, and the superior and inferior venae cavae and the four pulmonary veins in the other. The tube surrounding the veins has the shape of an inverted J. The cul-de-sac within its curve is behind the left atrium and is termed the oblique sinus. The transverse sinus is a passage between the two pericardial ‘tubes’ (Fig. 56.1). It has the aorta and pulmonary trunk in front and the atria and great veins behind (see Fig. 56.2B,D). The arrangement of the oblique and transverse sinuses, along with that of the main ‘principal’ cavity, is further affected by the development of complex three-dimensional pericardial recesses between adjacent structures. These recesses can be grouped according to the siting of their orifices or ‘mouths’. From the principal pericardial cavity, the postcaval recess projects towards the left behind the atrial termination of the superior vena cava. It is limited above by the right pulmonary artery and below by the upper right pulmonary vein. Its mouth opens superolaterally to the right. The right and left pulmonary venous recesses each project medially and upwards on the back of the left atrium between the superior and inferior pulmonary veins on each side, indenting the side walls of the oblique sinus. The superior aortic recess extends from the transverse sinus. From its mouth, located inferiorly, it ascends posterior to, then to the right of, the ascending aorta and ends at the level of the sternal angle. The inferior aortic recess, also extending from the transverse sinus, is a diverticulum descending from a superiorly located mouth to run between the lower ascending part of the aorta and the right atrium. The left pulmonary recess, with its mouth under the fold of the left vena cava, passes to the left between the inferior aspect of the left pulmonary artery and the upper border of the superior left pulmonary vein. The right pulmonary recess lies between the lower surface of the proximal part of the right pulmonary artery and the upper border of the left atrium.

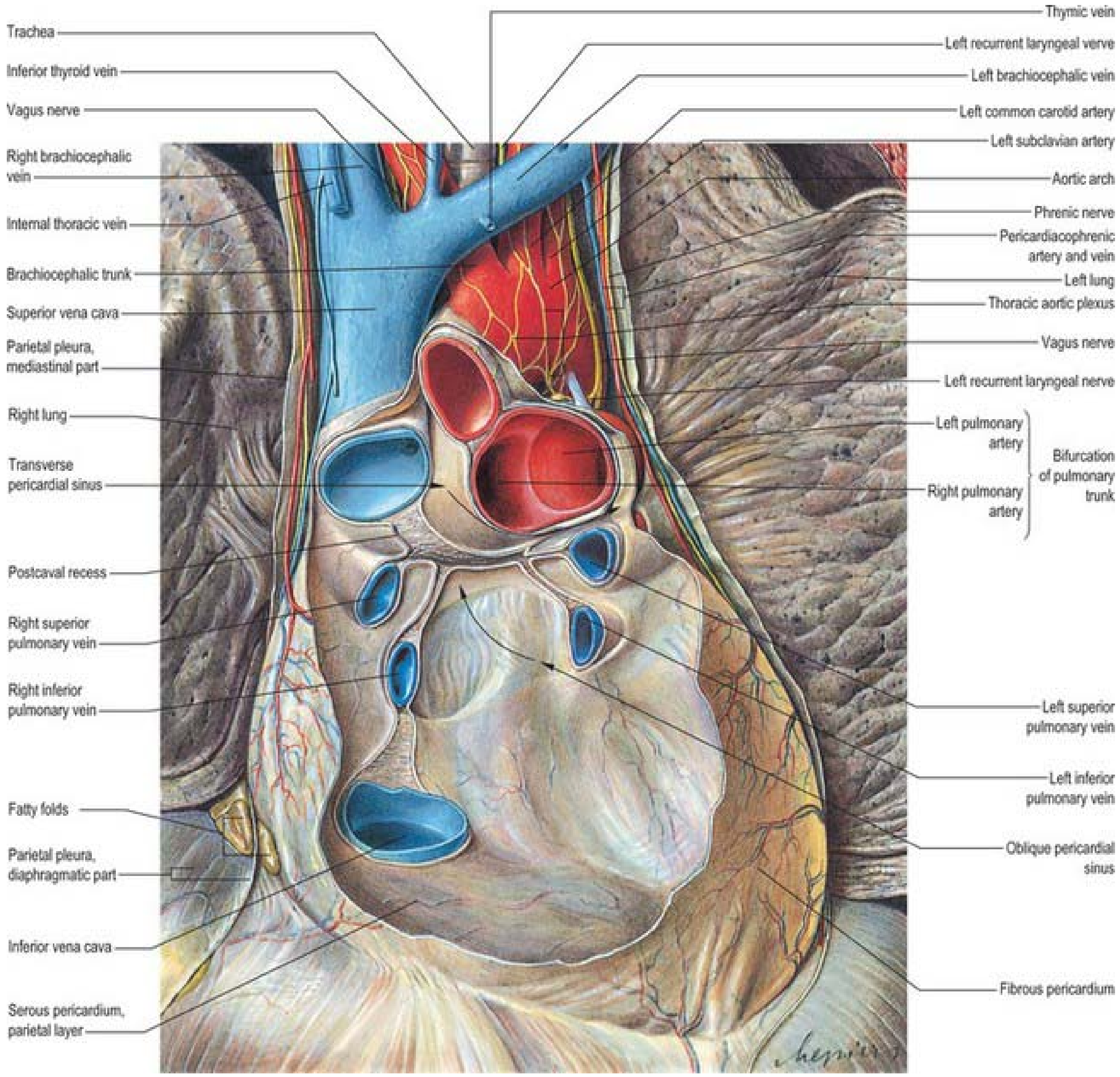
Trachea
Inferior thyroid vein
Vagus nerve
Right brachiocephalic vein
Internal thoracic vein
Brachiocephalic trunk
Superior vena cava
Parietal pleura, mediastinal part
Right lung
Transverse pericardial sinus
Postcaval recess
Right superior pulmonary vein
Right inferior pulmonary vein
Fatty folds
Parietal pleura, diaphragmatic part
Inferior vena cava
Serous pericardium, parietal layer
Thymic vein
Left recurrent laryngeal verve
Left brachiocephalic vein
Left common carotid artery
Left subclavian artery
Aortic arch
Phrenic nerve
Pericardiacophrenic artery and vein
Left lung
Thoracic aortic plexus
Vagus nerve
Left recurrent laryngeal nerve
Left pulmonary artery
Right pulmonary artery
Bifurcation of pulmonary trunk
Left superior pulmonary vein
Left inferior pulmonary vein
Oblique pericardial sinus
Fibrous pericardium

Fig. 56.1 Interior of the serosal pericardial sac after section of the large vessels at their cardiac origin and removal of the heart (seen from the front).

See text for additional named recesses of the general serosal pericardial cavity and its transverse sinus.

(From Sobotta 2006.)

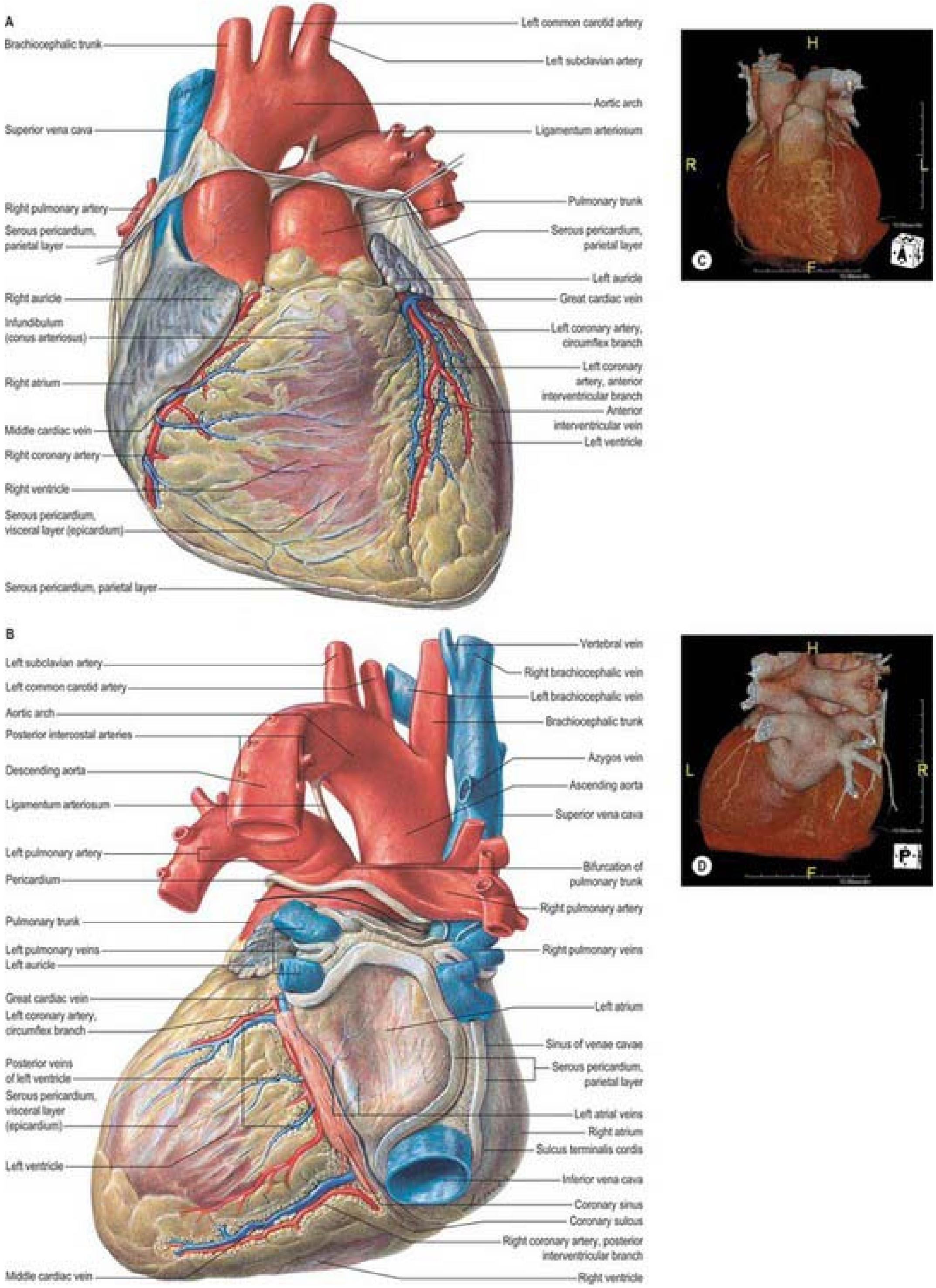
A
Brachiocephalic trunk
Superior vena cava
Right pulmonary artery
Serous pericardium, parietal layer
Right auricle
Infundibulum (conus arteriosus)
Right atrium
Middle cardiac vein
Right coronary artery
Right ventricle
Serous pericardium, visceral layer (epicardium)
Serous pericardium, parietal layer
Left common carotid artery
Left subclavian artery
Aortic arch
Ligamentum arteriosum
Pulmonary trunk
Serous pericardium, parietal layer
Left auricle
Great cardiac vein
Left coronary artery, circumflex branch
Left coronary artery, anterior interventricular branch
Anterior interventricular vein
Left ventricle
H
R
L
C
F
A
B
Left subclavian artery
Left common carotid artery
Aortic arch
Posterior intercostal arteries
Descending aorta
Ligamentum arteriosum
Left pulmonary artery
Pericardium
Pulmonary trunk
Left pulmonary veins
Left auricle
Great cardiac vein
Left coronary artery, circumflex branch
Posterior veins of left ventricle
Serous pericardium, visceral layer (epicardium)
Left ventricle
Middle cardiac vein
Vertebral vein
Right brachiocephalic vein
Left brachiocephalic vein
Brachiocephalic trunk
Azygos vein
Ascending aorta
Superior vena cava
Bifurcation of pulmonary trunk
Right pulmonary artery
Right pulmonary veins
Left atrium
Sinus of venae cavae
Serous pericardium, parietal layer
Left atrial veins
Right atrium
Sulcus terminalis cordis
Inferior vena cava
Coronary sinus
Coronary sulcus
Right coronary artery, posterior interventricular branch
Right ventricle
H
L
R
D
F
P

Fig. 56.2 The heart and great vessels: **A**, Anterior and **B**, posterior views with corresponding three-dimensional reconstructions from multislice CT scanning (**C**, **D**). (Main figures from Sobotta 2006.)

A triangular fold of serosal pericardium is reflected from the left pulmonary artery to the subjacent upper left pulmonary vein as the fold of the left superior vena cava. It contains a fibrous ligament, a remnant of the obliterated left common cardinal vein (left duct of Cuvier). This ligament descends anterior to the left pulmonary hilum from the upper part of the left superior intercostal vein to the back of the left atrium, where it is continuous with the oblique vein of the left atrium. The left common cardinal vein may persist as a left superior vena cava which then replaces the oblique vein of the left atrium and empties into the coronary sinus. When both common cardinal veins persist as right and left superior venae cavae, the transverse anastomosis between them, which normally forms the left brachiocephalic vein, may be small or absent. When there is a left superior vena cava, it is joined by the left superior intercostal vein.

VASCULAR SUPPLY AND LYMPHATIC DRAINAGE

The arteries of the pericardium are derived from the internal thoracic and musculophrenic arteries and the descending thoracic aorta. The veins are tributaries of the azygos system.

INNERVATION

The pericardium is innervated by the vagus, together with phrenic nerves and the sympathetic trunks (see Fig. 56.20; see Fig. 58.3). Pericardial pain is typically a sharp severe substernal pain. It may be exacerbated by lying back or on the left side and relieved by leaning forward. It occasionally radiates to the upper border of trapezius.

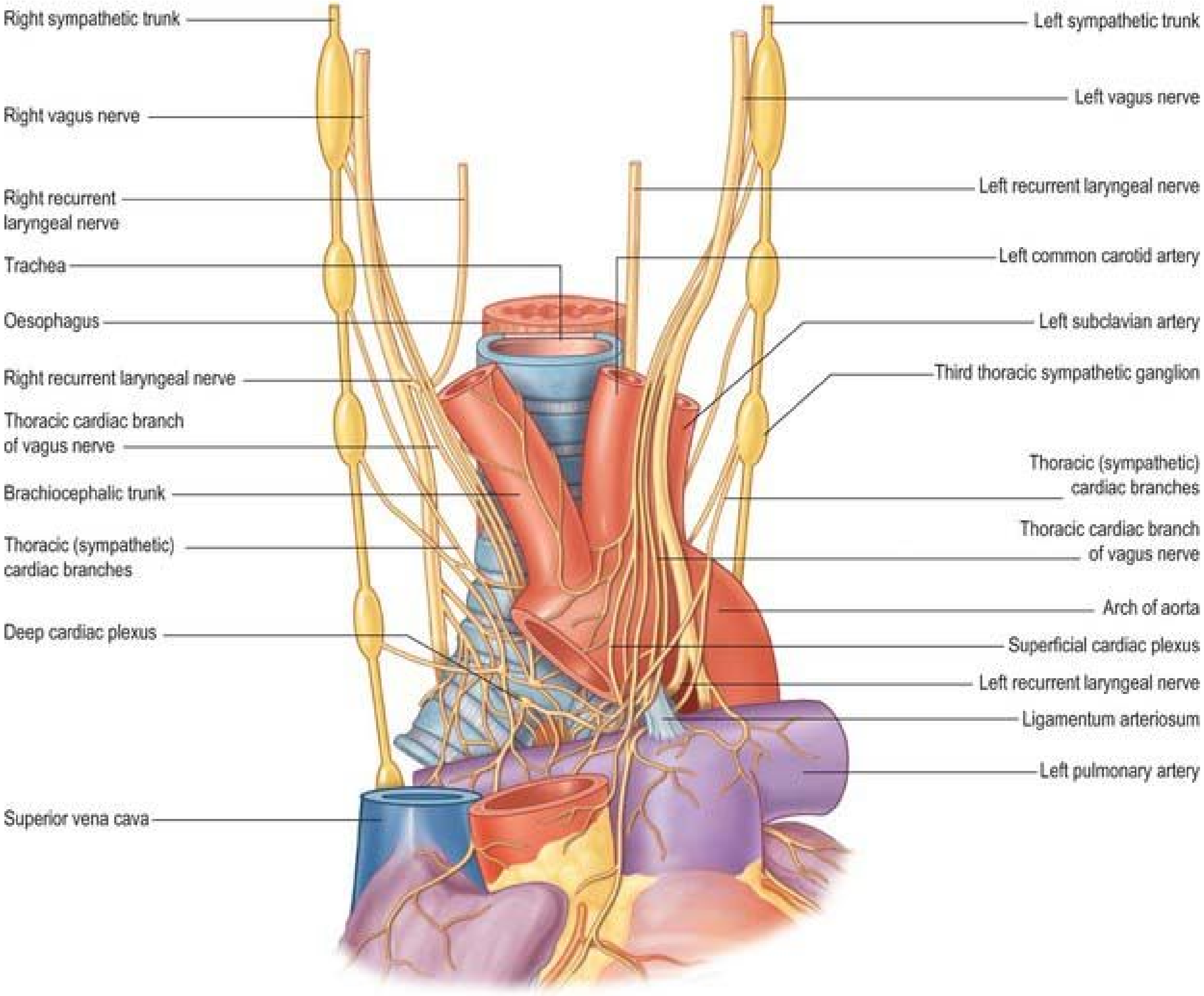
Right sympathetic trunk
Right vagus nerve
Right recurrent laryngeal nerve
Trachea
Oesophagus
Right recurrent laryngeal nerve
Thoracic cardiac branch of vagus nerve
Brachiocephalic trunk
Thoracic (sympathetic) cardiac branches
Deep cardiac plexus
Superior vena cava
Left sympathetic trunk
Left vagus nerve
Left recurrent laryngeal nerve
Left common carotid artery
Left subclavian artery
Third thoracic sympathetic ganglion
Thoracic (sympathetic) cardiac branches
Thoracic cardiac branch of vagus nerve
Arch of aorta
Superficial cardiac plexus
Left recurrent laryngeal nerve
Ligamentum arteriosum
Left pulmonary artery

Fig. 56.20 The human cardiac plexus: its source from the cervical parts of the vagus nerves and sympathetic trunks and its extensions, the pulmonary, atrial and coronary plexuses. Note the numerous junctions between sympathetic and parasympathetic (vagal) branches that form the plexus.

CARDIAC TAMPONADE

Cardiac tamponade is external compression of the heart usually caused by accumulation of fluid in the pericardial space. This causes compression of the right atrium and reduces venous return, which reduces cardiac output. It may occur after trauma, proximal extension from a dissecting aortic aneurysm or cardiac surgery. Patients develop hypotension and circulatory collapse. Emergency treatment involves first relieving the tamponade by percutaneous pericardial aspiration, followed by surgery to address the underlying cause. Echocardiography can be useful in assessing tamponade and is also useful in guiding percutaneous pericardial aspiration. Surgery is via a subxiphoid incision or a left anterior thoracotomy.

HEART

The microstructure of cardiac muscle is described in detail in Chapter 6.

GENERAL ORGANIZATION

The heart is a pair of valved muscular pumps combined in a single organ (Fig. 56.2A–D). Although the fibromuscular framework and conduction tissues of these pumps are structurally interwoven, each pump (the so-called ‘right’ and ‘left’ hearts) is physiologically separate, and is interposed in series at different points in the double circulation. Despite this functional disposition in series, the two pumps are usually described topographically in parallel.

Of the four cardiac chambers, the two atria receive venous blood as weakly contractile reservoirs for final filling of the two ventricles, which then provide the powerful expulsive contraction that forces blood into the main arterial trunks.

The right heart starts at the right atrium, and receives the superior and inferior venae cavae together with the main venous inflow from the heart itself via the coronary sinus. This systemic venous blood traverses the right atrioventricular orifice, guarded by the tricuspid valve, to enter the inlet component of the right ventricle. Contraction of the ventricle, particularly its apical trabecular component, closes the tricuspid valve and, with increasing pressure, ejects the blood through the muscular right ventricular outflow tract into the pulmonary trunk. The blood then flows through the pulmonary vascular bed, which has a relatively low resistance. Changes in pressure, time relations and valvular events are described below. Many structural features of the ‘right heart’, including its overall geometry, myocardial architecture and the construction and the relative strengths of the tricuspid and pulmonary valves, accord with this low resistance, being associated with comparatively low changes in pressure.

The left heart starts at the left atrium, which receives all the pulmonary inflow of oxygenated blood and some coronary venous inflow. It contracts to fill the left ventricle through the left atrioventricular orifice guarded by its mitral valve. The valve is the entry to the inlet of the left ventricle. Ventricular contraction rapidly increases the pressure in the apical trabecular component, closing the mitral valve and opening the aortic valve, enabling the ventricle to eject via the left ventricular outflow tract into the aortic sinuses and the ascending aorta, and thence to the entire systemic arterial tree, including the coronary arteries. This vast vascular bed presents a high peripheral resistance that, with large metabolic demands (especially the sustained requirements of the cerebral tissues), explains the more massive structural organization of the ‘left heart’. The ejection phase of the left ventricle is shorter than that of the right, but its fluctuations in pressure are very much greater. Because of its contrasting functional demands, the heart is far from a simple pair of (structurally combined) parallel pumps, even though the right and left ventricles must deliver more or less the same volume with each contraction. The heart has a complicated, spiral, three-dimensional organization which is markedly skewed when compared with the planes of the body. Terms such as ‘left’ and ‘right’, ‘anterior’ and ‘posterior’, ‘superior’ and ‘inferior’, therefore, do not always assist the descriptions of cardiac anatomy. Another potential source of confusion is the usual study of isolated whole or dissected hearts, with the subsequent difficulty in relating details to the heart as it is positioned within the body. The following preliminary description emphasizes such difficulties in order to circumvent certain misconceptions, before proceeding to an account of more detailed structure.

The right heart, while forming the right aspect or ‘border’, follows a gentle curve and covers most of the anterior aspect of the left heart (except for a left-sided strip including the apex). Thus the right heart forms the largest part of the anterior surface, its outflow tract ascending until it terminates on the left side of the outflow tract from the left ventricle. The sites of the tricuspid and pulmonary valves are widely separated and on different planes, the flat cavity of the right ventricle, which is crescentic in its section, splaying out between them. Conversely, the left heart (except the left-sided strip mentioned above) is largely posterior in position and when viewed from the front is obscured by the chambers of the right heart. The inlet to the left ventricle, which contains the mitral valve, is very close to its outlet (the aortic valve), the two being embraced by the wide tract linking inlet and outlet components of the right ventricle. The planes of the left ventricular orifices, although relatively inclined, are more nearly co-planar than those of the right. The left ventricular cavity is narrow and conical, and its tip occupies the cardiac apex. Most of the base of the heart is made up of the left atrium.

Cardiac size, shape and external features

The heart is a hollow, fibromuscular organ of a somewhat conical or pyramidal form, with a base, apex and a series of surfaces and 'borders'. Enclosed in the pericardium, it occupies the middle mediastinum between the lungs and their pleural coverings (Fig. 56.1). It is placed obliquely behind the body of the sternum and the adjoining costal cartilages and ribs. Approximately one-third of the mass lies to the right of the midline.

An average adult heart is 12 cm from base to apex, 8–9 cm at its broadest transverse diameter and 6 cm anteroposteriorly. Its weight varies from 280 to 340 g (average 300 g) in males and from 230 to 280 g (average 250 g) in females. Cardiac weight is 0.45% of body weight in males and 0.40% in females. Adult weight is achieved between the ages of 17 and 20 years. The oblique position of the heart may be emphasized by comparing it to a rather deformed pyramid, with the base facing posteriorly and to the right, and the apex anteriorly and to the left. A line from the apex to the approximate centre of the base, projected posterolaterally, emerges near the right midscapular line. Some surfaces of the cardiac 'pyramid' are flat, others more or less convex, these aspects merging along rather ill-defined 'borders'. Precise definition of surfaces and intervening 'borders' is, therefore, difficult. In the account that follows, official nomenclature (Terminologia Anatomica 1998) and more generally used terms from clinical practice are given as alternatives. The heart is described as having a base and apex, its surfaces being designated as sternocostal (anterior), diaphragmatic (inferior) and right and left (pulmonary). Its borders are termed upper, inferior ('acute' margin or border) and left ('obtuse' margin or border). Some name the right surface a 'border', despite its extent. One avoidable source of confusion is the use of 'posterior', which can be replaced with the unambiguous term 'diaphragmatic'. If posterior is to be used for a cardiac surface, it should be reserved for the base. (However, compounding this difficulty, there are a number of different usages of the term ‘cardiac base’.)

The heart is placed obliquely in the thorax. The atrial and ventricular septal structures are virtually in line, but inclined forwards and to the left at 45° to a sagittal plane. The planes of the mitral and tricuspid valves, although vertical and not precisely co-planar, are broadly at right angles to the septal plane. The right atrium, therefore, is not only to the right, but also anterior and inferior to the left atrium. It is also partly anterior to the left ventricle, an important atrioventricular septum intervening. The right ventricle forms most of the anterior aspect of the ventricular mass (Fig. 56.3), only its inferior end is to the right of the left ventricle, its upper left extremity (pulmonary orifice) is to the left and superior relative to the aortic valve. The left atrium forms most of the posterior aspect of the heart, whereas the left ventricle is only prominent inferiorly, running along the left margin to reach the apex. The atria are essentially right of and posterior to their respective ventricles. These general dispositions are of the greatest importance in planning or interpreting radiographs, scans, angiocardiograms and echocardiograms.

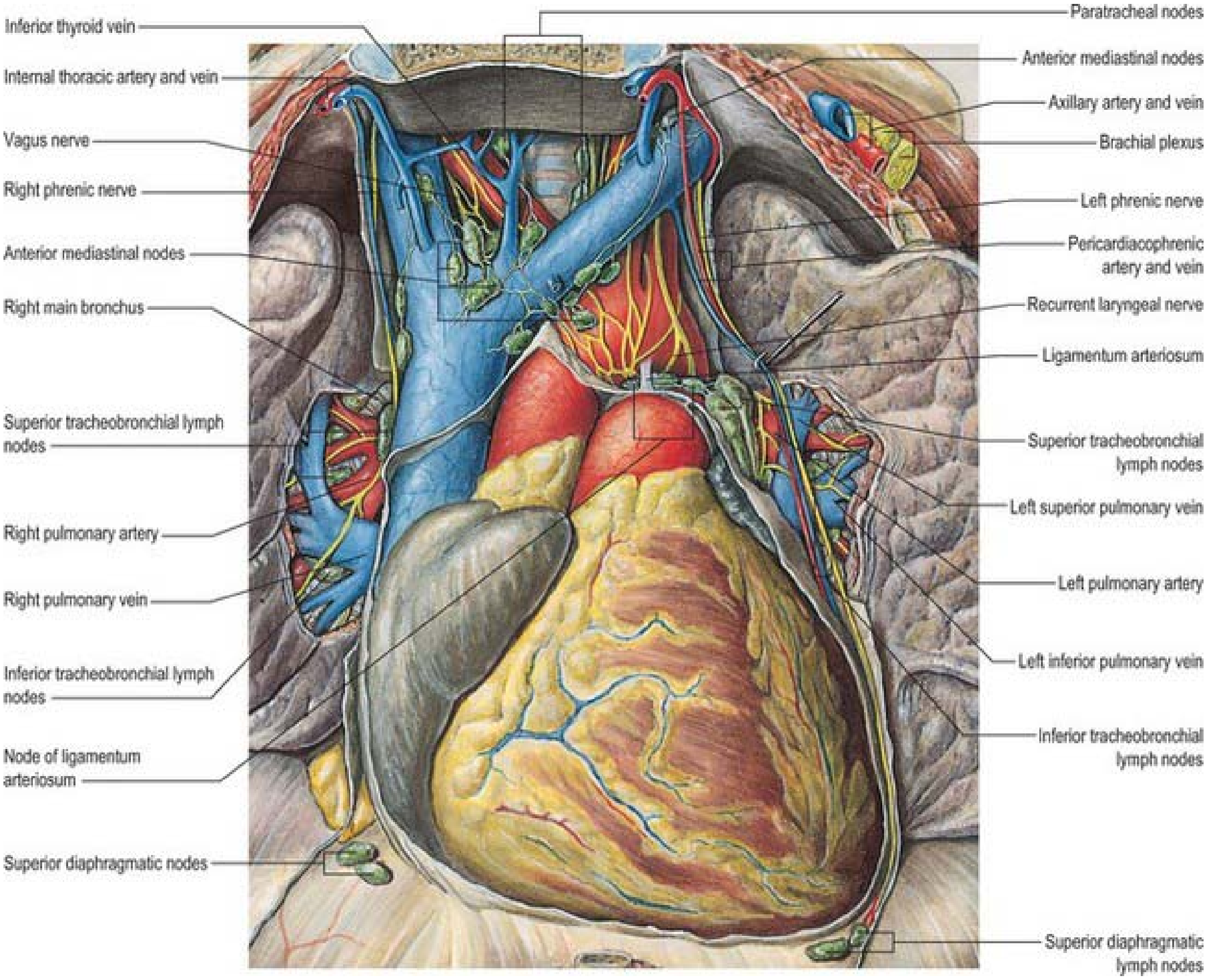
Inferior thyroid vein
Internal thoracic artery and vein
Vagus nerve
Right phrenic nerve
Anterior mediastinal nodes
Right main bronchus
Superior tracheobronchial lymph nodes
Right pulmonary artery
Right pulmonary vein
Inferior tracheobronchial lymph nodes
Node of ligamentum arteriosum
Superior diaphragmatic nodes
Paratracheal nodes
Anterior mediastinal nodes
Axillary artery and vein
Brachial plexus
Left phrenic nerve
Pericardiacophrenic artery and vein
Recurrent laryngeal nerve
Ligamentum arteriosum
Superior tracheobronchial lymph nodes
Left superior pulmonary vein
Left pulmonary artery
Left inferior pulmonary vein
Inferior tracheobronchial lymph nodes
Superior diaphragmatic lymph nodes

Fig. 56.3 Dissection that displays the heart, the great vessels and the lungs *in situ*: the manubrium sterni has been retracted cranially and the thymus has been removed totally. The pericardium has been partially removed and the hilum of the lung has been dissected to expose the tracheobronchial lymph nodes.

(From Sobotta 2006.)

Grooves on the cardiac surface

The division of the heart into four chambers produces boundaries that are visible externally as grooves (sulci). Some are deep and obvious and contain prominent structures. Others are less distinct, even barely perceptible, and are sometimes obscured, in part, by the major structures that cross them. The interatrial groove is a shallow groove separating the two atria. The lateral limits are defined by the borders of the atria. The atrioventricular (coronary) groove (or sulcus) separates the atria from the ventricles. This groove, containing the main trunks of the coronary arteries, is oblique. It descends to the right on the sternocostal surface, separating the right atrium (and its auricle or appendage) from the oblique right margin of the right ventricle and its infundibulum. Its upper left part is obliterated where it is crossed by the pulmonary trunk and, behind this, the aorta, from which the coronary arteries originate. Continuing to the left, the groove curves around the ‘obtuse’ margin and descends to the right, separating the atrial base from the diaphragmatic surface of the ventricles (Fig. 56.2A,D). This diaphragmatic part of the atrioventricular groove then curves around the ‘acute’ margin at its lower right end to become confluent with the sternocostal part. Thus the groove passes from high on the left to low on the right, with the diaphragmatic part being a little to the left of the sternocostal. A section that includes the atrioventricular groove is at 45° to the sagittal plane and at a greater but variable angle to the transverse and coronal planes. It approximately traverses the lines of attachment of the atrioventricular valves and (even less precisely) those of the aortic and pulmonary valves. A line at right angles to the centre of this plane will descend forwards and leftwards to the cardiac apex.

Internally, the ventricles are separated by the septum. The mural margins of the septum correspond to the anterior and inferior (diaphragmatic) interventricular grooves. The anterior groove, seen on the sternocostal cardiac surface, is near and almost parallel to the left ventricular obtuse margin. On the diaphragmatic surface, the groove is closer to the midpoint of the ventricular mass. The interventricular grooves extend from the atrioventricular groove to the apical notch on the acute margin, which is a little to the right of the true cardiac apex.

Cardiac base, apex, surfaces and borders

Posterior aspect of the heart

The true cardiac base is somewhat quadrilateral, with curved lateral extensions. It faces back and to the right, separated from the thoracic vertebrae (fifth to eighth in the recumbent, sixth to ninth in the erect posture) by the pericardium, right pulmonary veins, oesophagus and aorta. It is formed mainly by the left atrium, and only partly by the posterior part of the right atrium (Fig. 56.2B,D). It extends superiorly to the bifurcation of the pulmonary trunk and inferiorly to the posterior part of the atrioventricular groove, which contains the coronary sinus and branches of the coronary arteries. It is limited to the right and left by the rounded surfaces of the corresponding atria. These are separated by the shallow interatrial groove. The point of junction of the atrioventricular, interatrial and posterior interventricular grooves is termed the crux of the heart. Two pulmonary veins on each side open into the left atrial part of the base, whereas the superior and the inferior vena cava open into the upper and lower parts of the right atrial basal region. The area of the left atrium between the openings of right and left pulmonary veins forms the anterior wall of the oblique pericardial sinus (Fig. 56.1). This description of the anatomical base reflects the usual position of the heart in the thorax. Some confusion is produced by other current usages of the term ‘base’. It is often applied to the segment of the atrioventricular and ventriculoarterial junctions seen after dissections through the atrioventricular groove. This area is better termed the base of the ventricles. In clinical practice, auscultation in or near the parasternal parts of the second intercostal spaces is often described as occurring at the clinical ‘base’, to make the contrast with the clinical ‘apex’. Such descriptions, while less than perfect anatomically, will almost certainly persist.

Anatomical apex of the heart

This is the apex of the conical left ventricle, which is directed down, forwards and to the left. It is overlapped by the left lung and pleura. The apex is located most commonly behind the fifth left intercostal space, near or a little medial to the midclavicular line.

Anterior, sternocostal surface of the heart

Facing forwards and upwards, the anterior surface has an acute right and a more gradual left convexity (Fig. 56.3). It consists of an atrial area above and to the right, and a ventricular part below and to the left of the atrioventricular groove. The atrial area is occupied almost entirely by the right atrium. The left atrium is largely hidden by the ascending aorta and pulmonary trunk. Only a small part of the left appendage projects forwards to the left of the pulmonary trunk. Of the ventricular region, about one-third is made up by the left and two-thirds by the right ventricle. The site of the septum between them is indicated by the anterior interventricular groove. The sternocostal surface is separated by the pericardium from the body of the sternum, the sternocostal muscles and the third to the sixth costal cartilages. Because of the bulge of the heart to the left, more of this surface is behind the left costal cartilages than behind the right ones. It is also covered by the pleural membranes and by the thin anterior edges of the lungs, except for a triangular area at the cardiac incisure of the left lung. The lungs and their pleural coverings are variable in their degree of overlap of the heart.

Inferior, diaphragmatic surface of the heart

Largely horizontal, the inferior surface of the heart slopes down and forwards a little towards the apex (Fig. 56.2B,D). It is formed by the ventricles (chiefly the left) and rests mainly upon the central tendon but also, apically, on a small area of the left muscular part of the diaphragm. It is separated from the anatomical base by the atrioventricular groove and is traversed obliquely by the posterior interventricular groove.

Left surface of the heart

Facing up, back and to the left, the left surface consists almost entirely of the obtuse margin of the left ventricle, but a small part of the left atrium and its auricle contribute superiorly. Convex and widest above, where it is crossed by the atrioventricular groove, it narrows to the cardiac apex. It is separated by the pericardium from the left phrenic nerve and its accompanying vessels, and by the left pleura from the deep concavity of the left lung.

Right surface of the heart

The right surface is rounded and formed by the right atrial wall. It is separated from the mediastinal aspect of the right lung by the pericardium and the pleural coverings. Its convexity merges below into the short intrathoracic part of the inferior vena cava and above into the superior vena cava. The sulcus terminalis (terminal groove) is a prominent landmark between the true atrial and the venous components of the right atrium, curving approximately along the junction of the sternocostal and right surfaces.

Upper border of the heart

This is atrial (mainly the left atrium). Anterior to it are the ascending aorta and the pulmonary trunk (Fig. 56.1). At its extremity, the superior vena cava enters the right atrium.

Right border of the heart

Corresponding to the right atrium, the profile of the right border is slightly convex to the right and it approaches the vertical.

Inferior border of the heart

Also known as the acute margin of the heart, the inferior border is sharp, thin and nearly horizontal. It extends from the lower limit of the right border to the apex and it is formed mainly by the right ventricle, with a small contribution from the left ventricle near the apex.

Left border of the heart

Also known as the obtuse margin, the left border separates the sternocostal and left surfaces. It is round and mainly formed by the left ventricle but, to a slight extent superiorly, is formed by the auricle of the left atrium. It descends obliquely, convex to the left, from the auricle to the cardiac apex.

Right atrium

General and external features

The interatrial septum (or atrial septum) is oblique, so the right atrium is both anterior and to the right of the left atrium (Fig. 56.2A–D), also extending inferior to it. Its walls form the right upper sternocostal surface, the convex right (pulmonary surface) and a little of the right side of the anatomical base. The superior vena cava opens into its dome and the inferior vena cava into its lower posterior part (Fig. 56.2B,D). An extensive muscular pouch, the auricle, projects anteriorly to overlap the right side of the ascending aorta. The auricle is a broad, triangular structure and has a wide junction with the true atrial component of the atrium (Fig. 56.2A,C). The junction between the venous part (sinus venosus) and the atrium proper is marked externally by a shallow groove, the sulcus terminalis, extending between the right sides of the openings of the two venae cavae. The sulcus terminalis corresponds, internally, to the terminal crest (crista terminalis) which is the site of origin of the extensive pectinate muscles that arise serially at right angles from the crest. Posteriorly, the vertical interatrial groove descends to the crux.

Anteriorly, the right atrium is related to the anterior part of the mediastinal surface of the right lung, from which it is separated by pleura and pericardium. Laterally, the atrium is also related to the mediastinal surface of the right lung, but anterior to its hilum and separated from it by the pleura, right phrenic nerve and pericardiacophrenic vessels and pericardium. Posteriorly and to the left, the atrial septum and the surrounding infolded atrial walls separate the right from the left atrium (the mural infolding is indicated by an extensive interatrial groove). Posteriorly and to the right are the right pulmonary veins. Medially are the ascending aorta and, to a lesser extent, the root of the pulmonary trunk and its bifurcation.

Interior surface

The interior surface of the right atrium can be divided into three regions: a smooth-walled venous component posteriorly that leads, anteriorly, to the vestibule of the tricuspid valve and the auricle (Fig. 56.4A,B). The wall of the vestibule is smooth, but its junction with the auricle is ridged all around the atrioventricular junction. The smooth-walled part receives the opening of the venae cavae and the coronary sinus. It represents the venous component (sinus venosus) of the developing heart. The wall of the vestibule has a ridged surface and that of the auricle is trabeculated. Both are derived from the embryonic atrium proper.

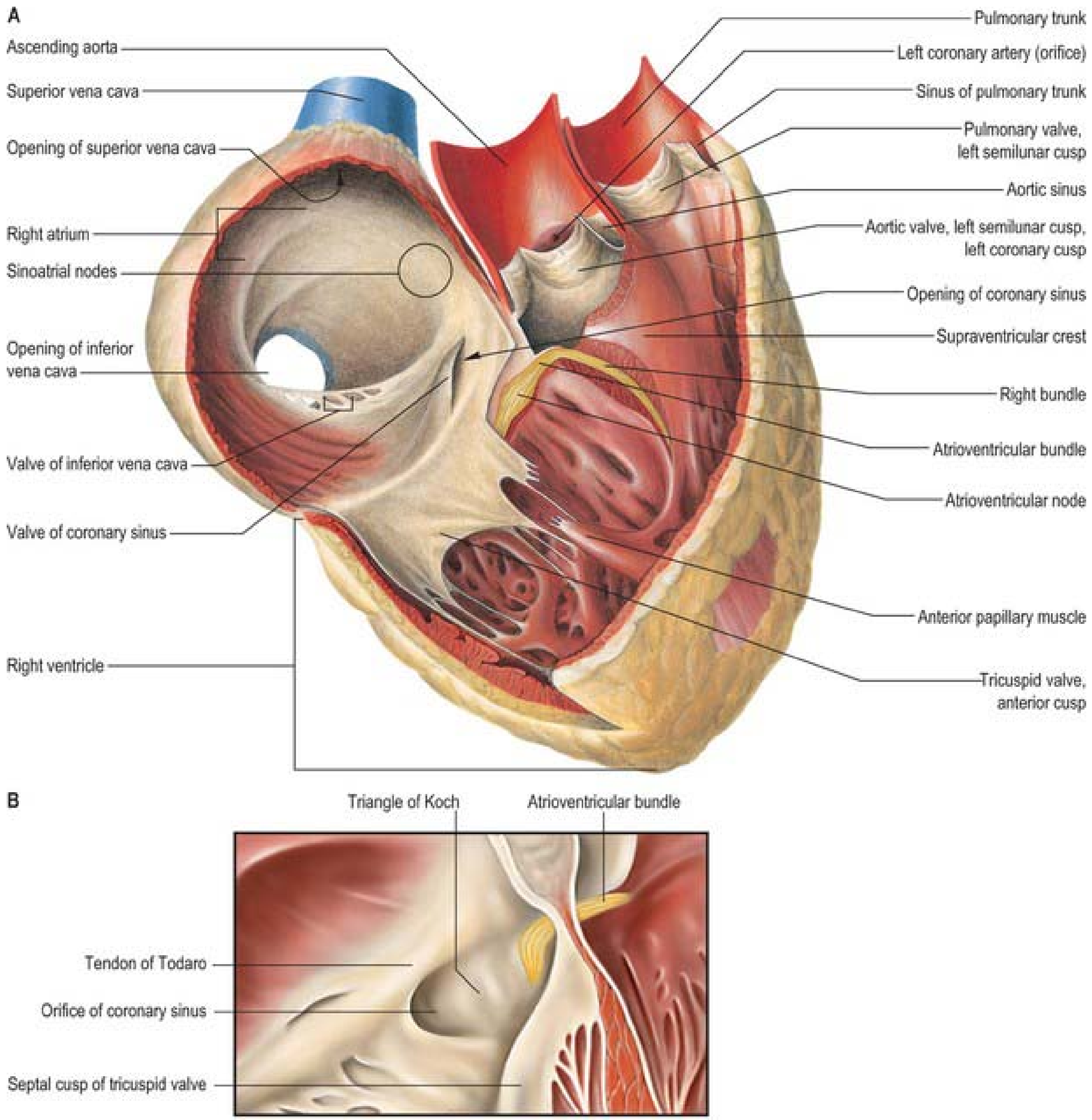
A
Ascending aorta
Superior vena cava
Opening of superior vena cava
Right atrium
Sinoatrial nodes
Opening of inferior vena cava
Valve of inferior vena cava
Valve of coronary sinus
Right ventricle
Pulmonary trunk
Left coronary artery (orifice)
Sinus of pulmonary trunk
Pulmonary valve, left semilunar cusp
Aortic sinus
Aortic valve, left semilunar cusp, left coronary cusp
Opening of coronary sinus
Supraventricular crest
Right bundle
Atrioventricular bundle
Atrioventricular node
Anterior papillary muscle
Tricuspid valve, anterior cusp
B
Triangle of Koch
Atrioventricular bundle
Tendon of Todaro
Orifice of coronary sinus
Septal cusp of tricuspid valve

Fig. 56.4 **A**, The interior of the heart, revealed by incising it along its right and part of the lower surface. The rest of the heart has been turned over to the left. **B**, The triangle of Koch, which is defined by the tendon of

Todaro, orifice of the coronary sinus and the septal cusp of the tricuspid valve.

*(**A** from Sobotta 2006.)*

The superior and inferior venae cavae open into the venous component. The superior vena cava returns blood from head, neck and upper limb through an orifice that faces inferoanteriorly and has no valve, and also receives blood from the chest wall and the oesophagus via the azygos system. The inferior vena cava is larger than its superior counterpart: it drains blood from all structures below and including the diaphragm into the lowest part of the atrium near the septum. Anterior to its orifice is a flap-like valve, the Eustachian valve or valve of the inferior vena cava (Fig. 56.4A,B). Of varying size, this valve is found along the lateral, or right, margin of the vein. When traced inferiorly, it runs into the sinus septum (see below), where it is contiguous with the valve of the coronary sinus. The lateral part of the Eustachian valve becomes continuous with the lower end of the terminal crest. The valve is a fold of endocardium enclosing a few muscular fibres. It is large during fetal life, when it serves to direct richly oxygenated blood from the placenta through the foramen ovale of the atrial septum into the left atrium. The valve varies markedly in size in postnatal life; it is sometimes cribriform or filamentous but often is absent. A particularly prominent recess, behind the Eustachian valve, is seen posteroinferiorly relative to the ostium of the coronary sinus.

The coronary sinus opens into the venous atrial component between the orifice of the inferior vena cava, the fossa ovale and the vestibule of the atrioventricular opening (Fig. 56.4A,B). The coronary sinus is often guarded by a thin, semicircular valve that covers the lower part of the orifice (Thebesius’ valve, also known as the Thebesian valve). The upper limb of this valve joins the Eustachian valve; a tendinous structure, the tendon of Todaro, runs from this commissure into the sinus septum, which is the septum between the coronary sinus and the fossa ovale. The tendon of Todaro runs forwards to insert into the central fibrous body and is one of the landmarks of the triangle of Koch (see below). The ostium of the coronary sinus forms a prominent landmark in the right atrium. The sinus itself lies within the left atrioventricular groove (Fig. 56.2B,D), and is the conduit for return of most of the venous blood from the heart, although some atrial veins drain directly to the right or left atrial chambers. The coronary sinus begins at the point where the oblique vein of the left atrium joins the great cardiac vein. The sinus receives the middle and small cardiac veins close to its junction with the right atrium.

Several small venous ostia, draining the minimal atrial veins, are found scattered around the atrial walls. They return a small fraction of blood from the heart, and are most numerous on the septal aspect. The anterior cardiac veins and, sometimes, the right marginal vein may enter the atrium through larger ostia.

The atrium proper and the auricle are separated from the venous sinus by the crista terminalis. This smooth, muscular ridge begins on the upper part of the septal surface and, passing anterior to the orifice of the superior vena cava, skirts its right margin to reach the right side of the orifice of the inferior vena cava. It marks the site of the right venous valve of the embryonic heart, and corresponds externally to the terminal groove. The sinu-atrial node is located within the superior part of the groove, lateral to and extending below the orifice of the superior vena cava (Fig. 56.4A,B).

The pectinate muscles (musculi pectinati), almost parallel muscular ridges, extend anterolaterally from the terminal crest and reach into the auricle, where they form several trabeculations.

The septal wall presents the fossa ovale, an oval depression above and to the left of the orifice of the inferior vena cava. Its floor is the primary atrial septum, the septum primum. The rim of the fossa is prominent and, although often said to represent the edge of the so-called septum secundum, in reality it is merely the infolded walls of the atrial chambers. It is most distinct above and in front of the fossa, and is usually deficient inferiorly. A small slit is sometimes found at the upper margin of the fossa, ascending beneath the rim to communicate with the left atrium. This represents failure of obliteration of the fetal foramen ovale, which remains patent in up to one-third of all normal hearts.

Anteroinferior in the right atrium is the large, oval vestibule leading to the orifice of the tricuspid valve. A triangular zone, the triangle of Koch, is defined between the attachment of the septal cusp of the tricuspid valve, the anteromedial margin of the ostium of the coronary sinus, and the round, collagenous, palpable, subendocardial tendon of Todaro (Fig. 56.4A,B). The triangle is a landmark of particular surgical importance, indicating the site of the atrioventricular node and its atrial connections. Anterosuperior to the insertion of the tendon of Todaro, the septal wall is formed by the atrioventricular component of the membranous septum, intervening between the right atrium and subaortic outlet of the left ventricle (Fig. 56.5). The atrial wall bulges anterosuperiorly above the membranous septum. This area is the aortic mound (torus aorticus) and marks the location of the non-coronary sinus of the aorta with its enclosed valvular cusp.

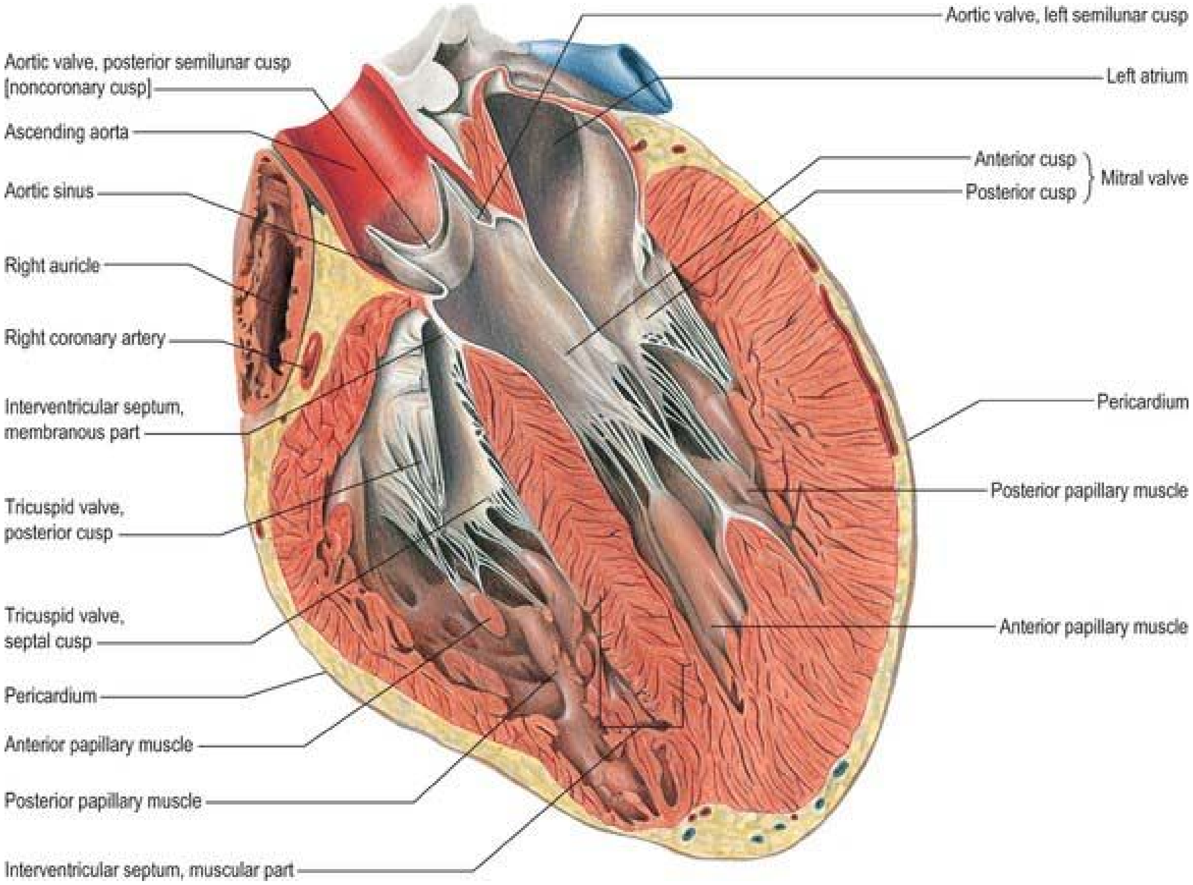
Aortic valve, left semilunar cusp
Aortic valve, posterior semilunar cusp [noncoronary cusp]
Left atrium
Ascending aorta
Anterior cusp
Posterior cusp
Mitral valve
Aortic sinus
Right auricle
Right coronary artery
Pericardium
Interventricular septum, membranous part
Posterior papillary muscle
Tricuspid valve, posterior cusp
Anterior papillary muscle
Tricuspid valve, septal cusp
Pericardium
Anterior papillary muscle
Posterior papillary muscle
Interventricular septum, muscular part

Fig. 56.5 A dissection opening the ventricles, viewed from the front.

(From Sobotta 2006.)

Right ventricle

The right ventricle extends from the right atrioventricular (tricuspid) orifice nearly to the cardiac apex. It then ascends to the left to become the infundibulum, or conus arteriosus, reaching the pulmonary orifice and supporting the cusps of the pulmonary valve. Topographically, the ventricle possesses an inlet component which supports and surrounds the tricuspid valve; a coarsely trabeculated apical component; and a muscular outlet or infundibulum, which surrounds the attachments of the cusps of the pulmonary valve.

External features

The convex anterosuperior surface of the right ventricle makes up a large part of the sternocostal aspect of the heart, and is separated from the thoracic wall only by the pericardium (Fig. 56.2A–D). The left pleura and, to a lesser extent, the anterior margin of the left lung are interposed above and to the left. The inferior surface is flat and is related mainly, with the interposition of the pericardium, to the central tendon and a small adjoining muscular part of the diaphragm. The left and posterior wall is the ventricular septum. This is slightly curved and bulges into the right ventricle so that, in sections across the cardiac axis, the outline of the right ventricle is crescentic. A delicate collagenous band, the tendon of the infundibulum (conus ligament), is believed by some to connect the pulmonary muscular infundibulum posteriorly to the root of the aorta. The wall of the right ventricle is significantly thinner (3–5 mm on average) than that of the left, the ratio of the thickness of the two walls usually being 1 : 3.

Internal features

The inlet and outlet components of the ventricle, supporting and surrounding the cusps of the tricuspid and pulmonary valves respectively, are separated in the roof of the ventricle by the prominent supraventricular crest (crista supraventricularis) (Fig. 56.4A). The crest is a thick, muscular, highly arched structure, extending obliquely forwards and to the right from a septal limb high on the interventricular septal wall to a mural or parietal limb on the anterolateral right ventricular wall. The posterolateral aspect of the crest provides a principal attachment for the anterosuperior cusp of the tricuspid valve. The septal limb of the crest may be continuous with, or embraced by, the septal limbs of the septomarginal trabecula. The inlet and outlet regions extend apically into and from the prominent coarsely trabeculated component of the ventricle. The inlet component is itself also trabeculated, whereas the outlet component (or infundibulum) has predominantly smooth walls. The trabeculated appearance is caused by a myriad of irregular muscular ridges and protrusions, which are known collectively as trabeculae carneae, and are lined by endocardium. These protrusions and intervening grooves impart great variation in wall thickness; the protrusions vary in extent from mere ridges to trabeculae, which are fixed at both ends but otherwise free. Other conspicuous protrusions are the papillary muscles, which are inserted at one end onto the ventricular wall and are continuous at the other end with collagenous cords, the chordae tendineae, inserted on the free edge and elsewhere on the free aspect of the atrioventricular valves. One protrusion in the right ventricle, the septomarginal trabecula or septal band, is particularly prominent. It reinforces the septal surface where, at the base, it divides into limbs that embrace the supraventricular crest. Towards the apex, it supports the anterior papillary muscle of the tricuspid valve and, from this point, crosses to the parietal wall of the ventricle as the ‘moderator band’ (this alternative name records an old idea that the septomarginal trabecula prevents overdistension of the ventricle). A further series of prominent trabeculae, the septoparietal trabeculations, extend from its anterior surface and run onto the parietal ventricular wall. The smooth-walled outflow tract, or infundibulum (conus arteriosus), ascends to the left above the septoparietal trabeculations and below the arch of the supraventricular crest to the pulmonary orifice.

Tricuspid valve

The atrioventricular valvular complex, in both right and left ventricles, consists of the orifice and its associated anulus, the cusps, the supporting chordae tendineae of various types and the papillary muscles.

Harmonious interplay of all these, together with the atrial and ventricular myocardial masses, depends on the conduction tissues and the mechanical cohesion provided by the fibroelastic cardiac skeleton. All parts change substantially in position, shape, angulation and dimensions during a single cardiac cycle.

Tricuspid valvular orifice

The tricuspid valve orifice is best seen from the atrial aspect and measures on average 11.4 cm in circumference in males and 10.8 cm in females. It has a clear line of transition from the atrial wall or septum to the lines of attachment of the valvular cusps. Its margins are not precisely in a single plane. It is almost vertical, but at 45° to the sagittal plane and slightly inclined to the vertical, such that it ‘faces’ (on its ventricular aspect) anterolaterally to the left and somewhat inferiorly (Fig. 56.6). Roughly triangular, its margins are described as anterosuperior, inferior and septal, corresponding to the lines of attachment of the valvular cusps.

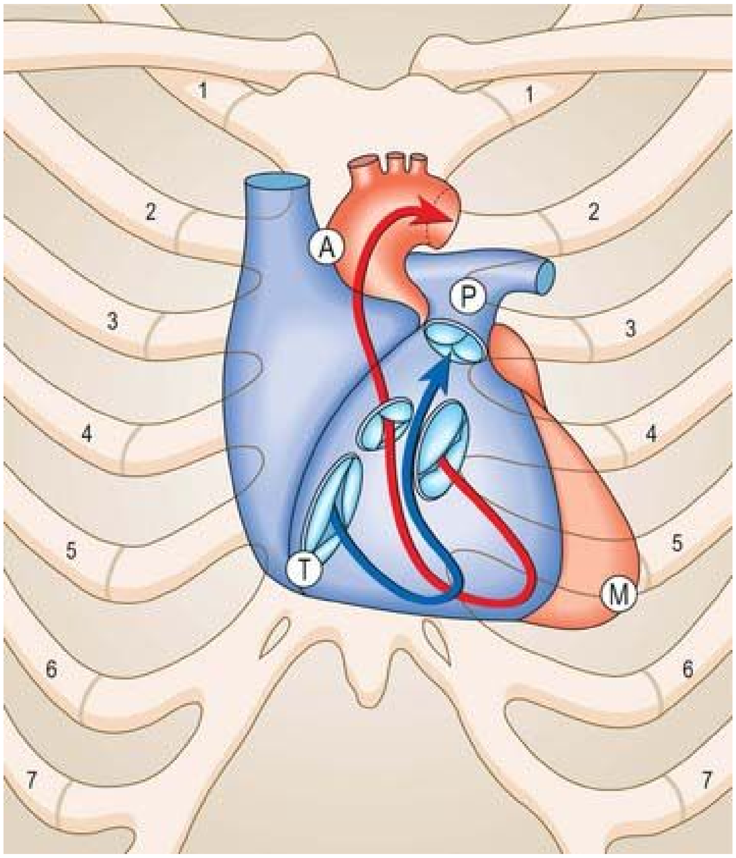

Fig. 56.6 Relation of the sternocostal surface and valves of the heart to the thoracic cage. The right heart is blue, the arrow denotes the inflow and outflow channels of the right ventricle; the left heart is treated similarly in red. The positions, planes and relative sizes of the cardiac valves are shown. The position of the letters A, P, T and M indicate respectively the aortic, pulmonary, tricuspid and mitral auscultation areas of clinical practice. Note that, for the purpose of illustration, the orifices of the aortic, mitral and tricuspid valves are shown with some separation between them. In reality, the cusps of the three valves are in fibrous continuity (see **Fig. 56.10**).

The connective tissues around the orifice of the atrioventricular valves separate the atrial and ventricular myocardial masses completely, except at the point of penetration of the atrioventricular bundle, and vary in density and disposition around the valvular circumference. Extending from the right fibrous trigone component of the central fibrous body are a pair of curved, tapered, subendocardial tendons, or 'prongs' (fila coronaria) that partly encircle the circumference. The latter is completed by more tenuous, deformable fibroblastic sulcal areolar tissue. Although the extent of fibrous tissue varies with sex and age, the tissue within the atrioventricular junction around the tricuspid orifice is always less robust than similar elements found at the attachments of the mitral valve. The topographical ‘attachment’ of the free valvular cusps in the tricuspid valve does not wholly correspond to the internal level of attachment of the fibrous core of the valve to the junctional atrioventricular connective tissue: the line of attachment of the cusp is best appreciated in the heart when examined grossly, and this feature is also more readily discerned clinically.

Tricuspid valve cusps

It is usually possible to distinguish three cusps in the tricuspid valve, hence the name. They are located anterosuperiorly, septally and inferiorly, corresponding to the marginal sectors of the atrioventricular orifice so named. Each is a reduplication of endocardium enclosing a collagenous core, continuous marginally and on its ventricular aspect with diverging fascicles of chordae tendineae (see below) and basally confluent with the anular connective tissue. All cusps of the atrioventricular valves display, passing from the free margin to the inserted margin, rough, clear and basal zones. The rough zone is relatively thick, opaque and uneven on its ventricular aspect where most chordae tendineae are attached. The atrial aspect of the rough zone makes contact with the comparable surface of the adjacent cusps during full closure of the valve. The clear zone is smooth and translucent, receives few chordae tendineae and has a thinner fibrous core. The basal zone, extending 2–3 mm from the circumferential attachment of the cusps, is thicker, contains more connective tissue and is vascularized and innervated. It contains the insertions of the atrial myocardium.

The anterosuperior cusp is the largest component of the tricuspid valve. It is attached chiefly to the atrioventricular junction on the posterolateral aspect of the supraventricular crest, but extends along its septal limb to the membranous septum, ending at the anteroseptal commissure. One or more notches often indent its free margin. The attachment of the septal cusp passes from the inferoseptal commissure on the posterior ventricular wall across the muscular septum and then angles across the membranous septum to the anteroseptal commissure. The septal cusp defines one of the borders of the triangle of Koch, thereby aiding location of the atrioventricular node, which lies at the apex of the triangle, and ensuring that this area can be avoided when operating on the tricuspid valve (Figs 56.4A,B; 56.5).

The inferior cusp is wholly mural in attachment and guards the diaphragmatic surface of the atrioventricular junction. Its limits are the inferoseptal and anteroinferior commissures.

Chordae tendineae (tendinous cords)

The chordae tendineae are fibrous collagenous structures supporting the cusps of the atrioventricular valves. False chordae connect papillary muscles to each other or to the ventricular wall including the septum, or pass directly between points on the wall (or septum, or both); they are irregular in numbers and dimensions in the right ventricle. The true chordae usually arise from small projections on the tips or margins of the apical one-thirds of papillary muscles, but sometimes arise from the bases of papillary muscles or directly from the ventricular walls and the septum. They are attached to various parts of the ventricular aspects or the free margins of the cusps. They have been classified into first-, second- and third-order chordae according to the distance of the attachment from the margins of the cusps; this scheme has little functional or morphological merit.

Fan-shaped chordae have a short stem from which branches radiate to attach to the margins (or the ventricular aspect) of the zones of apposition between cusps and to the ends of adjacent cusps. Rough zone chordae arise from a single stem which usually splits into three components that attach to the free margin, the ventricular aspect of the rough zone and to some intermediate point on the cusp, respectively. Free-edge chordae are single, thread-like and often long, passing from either the apex or the base of a papillary muscle into a marginal attachment, usually near the midpoint of a cusp or one of its scallops. Deep chordae, also long, pass beyond the margins and, branching to various extents, reach the more peripheral rough zone or even the clear zone. Basal chordae are round chordae or flat ribbons, long and slender, or short and muscular. They arise from the smooth or trabeculated ventricular wall and attach to the basal component of a cusp.

Papillary muscles

The two major papillary muscles in the right ventricle are located in anterior and posterior positions. A third, smaller muscle has a medial position together with several smaller, and variable, muscles attached to the ventricular septum. The anterior papillary muscle is largest. Its base arises from the right anterolateral ventricular wall below the anteroinferior commissure of the inferior cusp and it also blends with the right end of the septomarginal trabecula. The posterior, or inferior, papillary muscle arises from the myocardium below the inferoseptal commissure and is frequently bifid or trifid. The septal, or medial, papillary muscle is small but typical, and arises from the posterior septal limb of the septomarginal trabecula. All the major papillary muscles supply chordae to adjacent components of the cusps they support. A feature of the right ventricle is that the septal cusp is tethered by individual chordae tendineae directly to the ventricular septum; such septal insertions are never seen in the left ventricle. When closed, the three cusps fit snugly together, the pattern of the zones of apposition confirming the trifoliate arrangement of the tricuspid valve.

Opening of the tricuspid valve

Despite its name, the tricuspid valve acts more like a bicuspid valve, because the septal cusp, the smallest of the three cusps, is fixed between the right and left fibrous trigones and the atrial and ventricular septa. The remainder of the tricuspid anulus is muscular. During diastole the right ventricle relaxes, the anulus dilates and the large anterior and posterior cusps move away from the plane of the anulus into the right ventricle. During systole the anulus constricts as the right ventricle contracts, and the two major cusps move like sails to abut a relatively immobile septal cusp and the septum itself (Fig. 56.7).

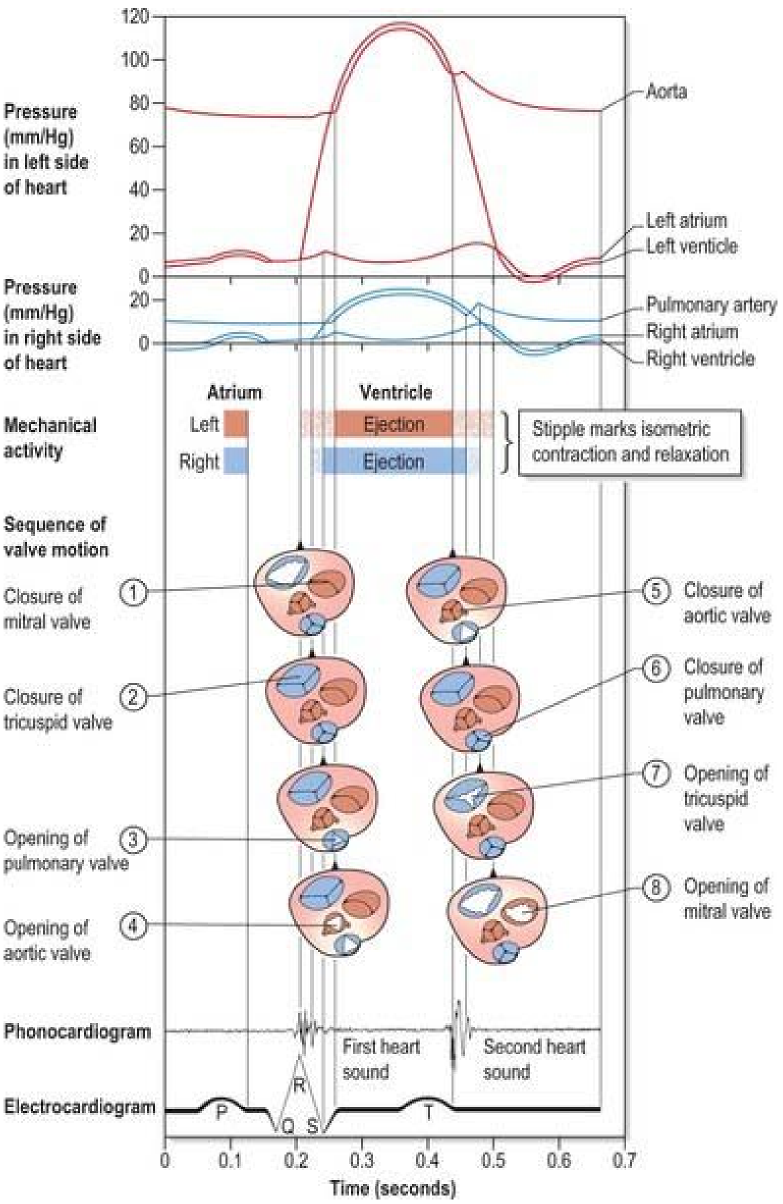
Pressure (mm/Hg) in left side of heart
120
100
80
60
40
20
0
Aorta
Left atrium
Left venticle
Pressure (mm/Hg) in right side of heart
20
0
Pulmonary artery
Right atrium
Right ventricle
Mechanical activity
Atrium
Ventricle
Left
Right
Ejection
Ejection
Stipple marks isometric contraction and relaxation
Sequence of valve motion
① Closure of mitral valve
② Closure of tricuspid valve
③ Opening of pulmonary valve
④ Opening of aortic valve
⑤ Closure of aortic valve
⑥ Closure of pulmonary valve
⑦ Opening of tricuspid valve
⑧ Opening of mitral valve
Phonocardiogram
First heart sound
Second heart sound
Electrocardiogram
P
R
Q
S
T
0
0.1
0.2
0.3
0.4
0.5
0.6
0.7
Time (seconds)

Fig. 56.7 Summary of some of the principal events that occur in the cardiac cycle and which are mentioned at various points throughout the chapter. Systole begins at the onset of the first heart sound (see phonocardiogram) and ends at the onset of the second heart sound, when diastole begins and this cycle repeats itself.

Pulmonary valve

The pulmonary valve, guarding the outflow from the right ventricle, surmounts the infundibulum and is situated at some distance from the other three cardiac valves (Figs 56.8, 56.9, 56.10). Its general plane faces superiorly to the left and slightly posteriorly. It has three semilunar cusps attached by convex edges partly to the infundibular wall of the right ventricle and partly to the origin of the pulmonary trunk. The line of attachments is curved, rising at the periphery of each cusp near their zones of apposition (the commissures) and reaching the sinutubular ridge of the pulmonary trunk (Fig. 56.11A–C). Removal of the cusps shows that the fibrous semilunar attachments enclose three crescents of infundibular musculature within the pulmonary sinuses, whereas three roughly triangular segments of arterial wall are incorporated within the ventricular outflow tract beneath the apex of each commissural attachment. There is, thus, no proper circular ‘anulus’ supporting the cusps of the valve, and the fibrous semilunar attachment is an essential requisite for snug closure of the nodules and lunules of the cusps (see below) during ventricular diastole. It is difficult to name the cusps and corresponding sinuses of the pulmonary valve and trunk precisely according to the coordinates of the body, because the valvular orifice is obliquely positioned. The official nomenclature (Terminologia Anatomica 1998) refers to an anterior, a posterior and a septal cusp, based on their position in the fetus. The position changes with development and in the adult there is one anterior semilunar cusp, and right and left semilunar cusps.

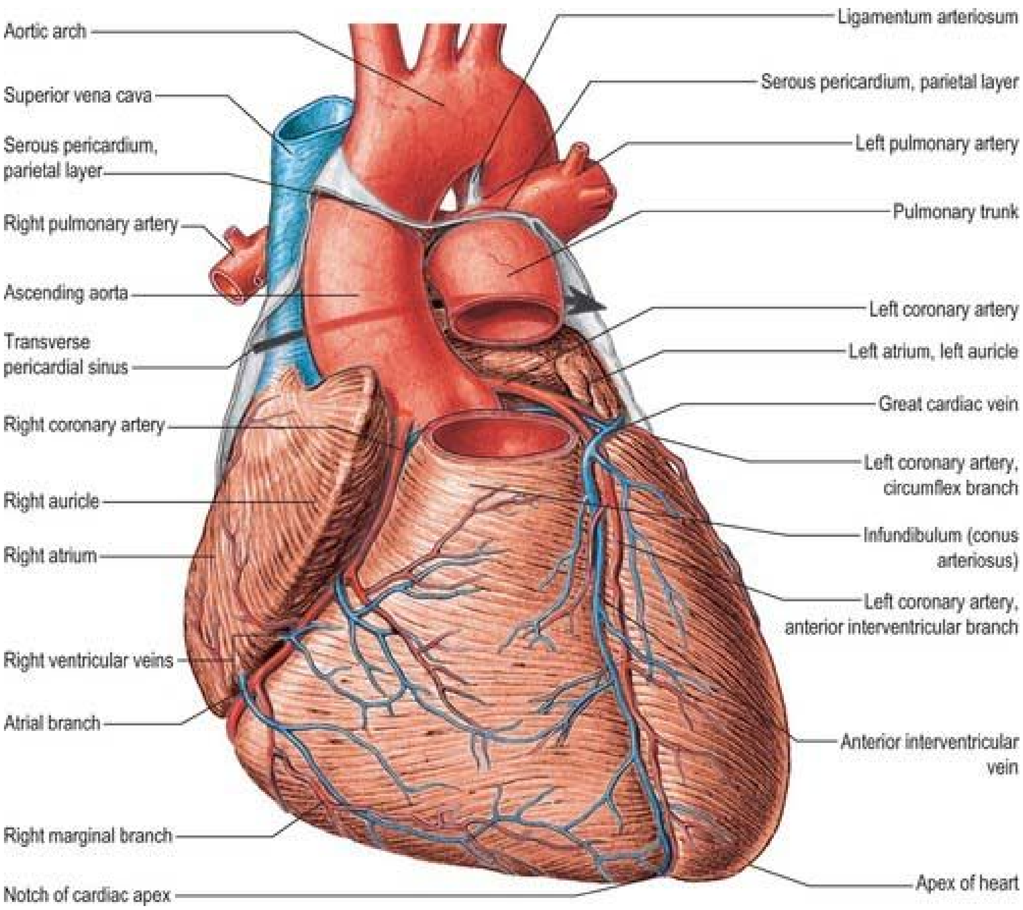
Aortic arch
Superior vena cava
Serous pericardium, parietal layer
Right pulmonary artery
Ascending aorta
Transverse pericardial sinus
Right coronary artery
Right auricle
Right atrium
Right ventricular veins
Atrial branch
Right marginal branch
Notch of cardiac apex
Ligamentum arteriosum
Serous pericardium, parietal layer
Left pulmonary artery
Pulmonary trunk
Left coronary artery
Left atrium, left auricle
Great cardiac vein
Left coronary artery, circumflex branch
Infundibulum (conus arteriosus)
Left coronary artery, anterior interventricular branch
Anterior interventricular vein
Apex of heart

Fig. 56.8 The anterior or sternocostal surface of the heart.

(From Sobotta 2006.)

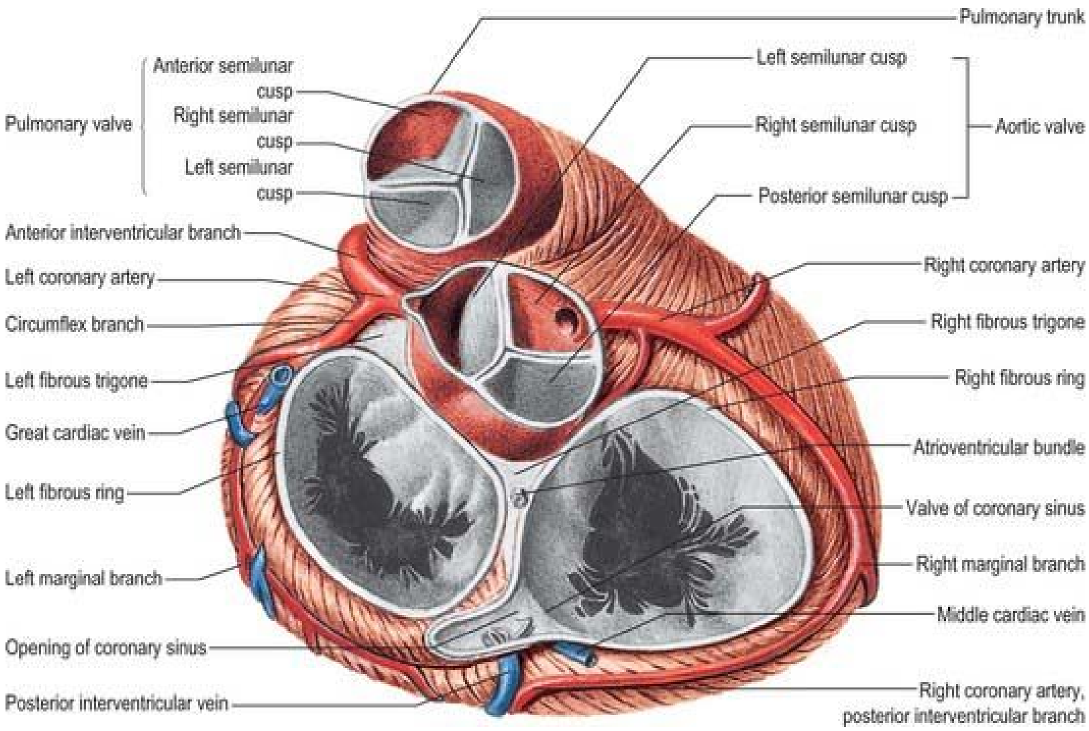
Pulmonary trunk
Left semilunar cusp
Right semilunar cusp
Posterior semilunar cusp
Aortic valve
Pulmonary valve
Anterior semilunar cusp
Right semilunar cusp
Left semilunar cusp
Anterior interventricular branch
Left coronary artery
Circumflex branch
Left fibrous trigone
Great cardiac vein
Left fibrous ring
Left marginal branch
Opening of coronary sinus
Posterior interventricular vein
Right coronary artery
Right fibrous trigone
Right fibrous ring
Atrioventricular bundle
Valve of coronary sinus
Right marginal branch
Middle cardiac vein
Right coronary artery, posterior interventricular branch

Fig. 56.9 The base of the ventricles, after removal of the atria and the pericardium. Coronary arteries and cardiac veins can be seen. Contrast the planes and positions of the aortic and pulmonary valves. Contrast with **Fig. 56.10**.

(From Sobotta 2006.)

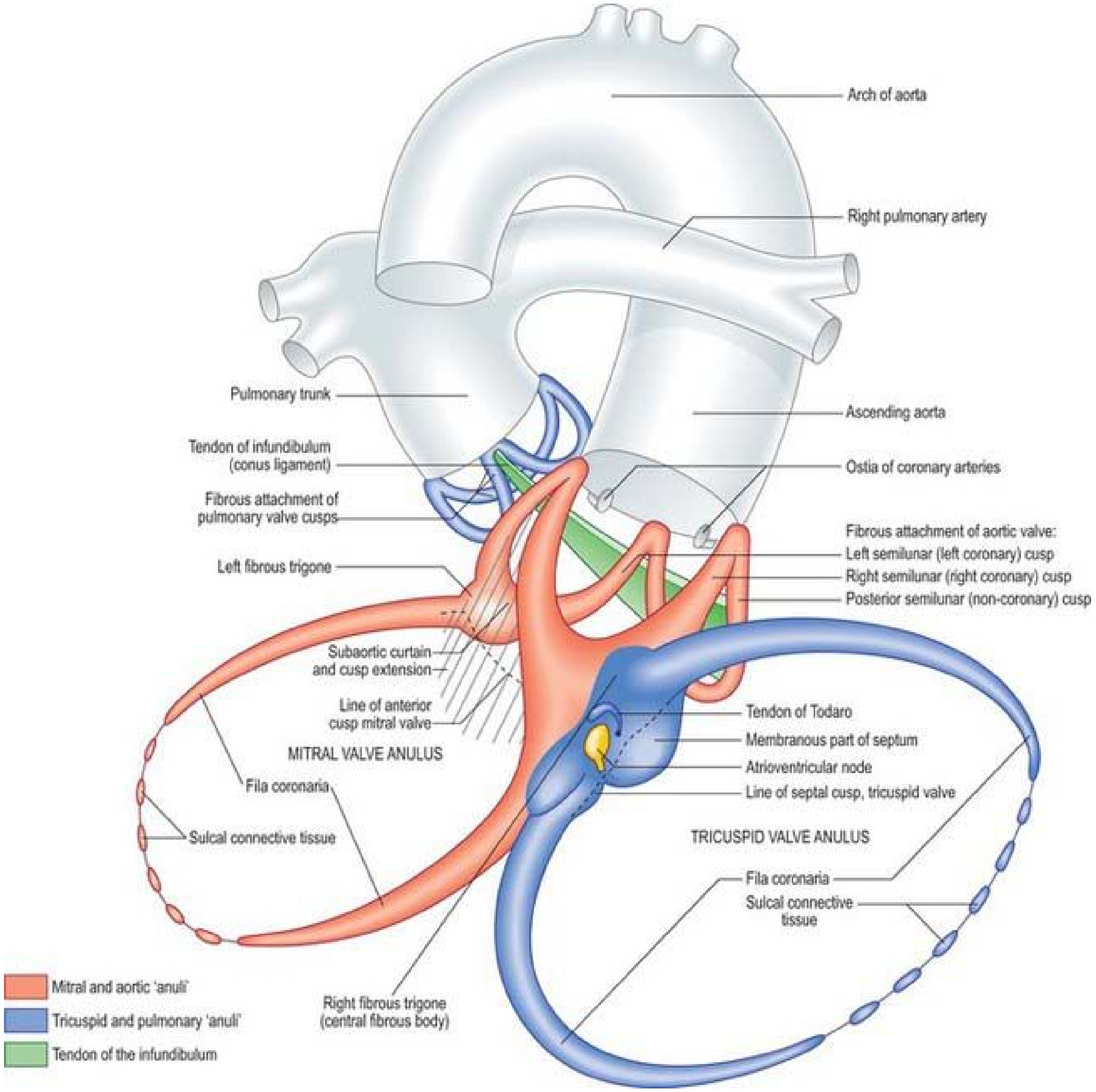
Arch of aorta
Right pulmonary artery
Pulmonary trunk
Ascending aorta
Tendon of infundibulum (conus ligament)
Ostia of coronary arteries
Fibrous attachment of pulmonary valve cusps
Fibrous attachment of aortic valve:
Left semilunar (left coronary) cusp
Right semilunar (right coronary) cusp
Posterior semilunar (non-coronary) cusp
Left fibrous trigone
Subaortic curtain and cusp extension
Line of anterior cusp mitral valve
Tendon of Todaro
Membranous part of septum
Atrioventricular node
Line of septal cusp, tricuspid valve
MITRAL VALVE ANULUS
Fila coronaria
Sulcal connective tissue
TRICUSPID VALVE ANULUS
Fila coronaria
Sulcal connective tissue
Right fibrous trigone (central fibrous body)
Mitral and aortic 'anuli'
Tricuspid and pulmonary 'anuli'
Tendon of the infundibulum

Fig. 56.10 Principal elements of the fibrous skeleton of the heart. For clarity, the view is from the right posterosuperior aspect. Perspective causes the pulmonary anulus to appear smaller than the aortic anulus, whereas in fact the reverse is the case. Consult text for an extended discussion.

(Copyright from The Royal College of Surgeons of England. Reproduced with permission.)

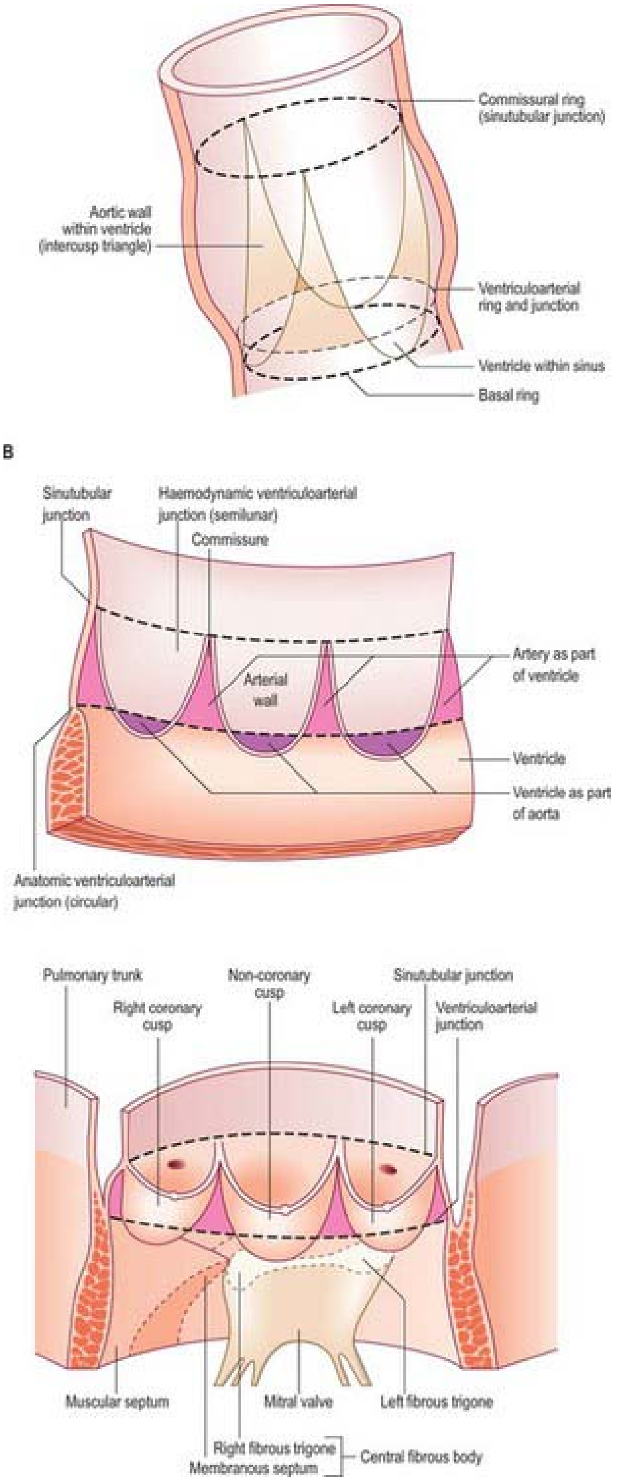
Commissural ring (sinutubular junction)
Aortic wall within ventricle (intercusp triangle)
Ventriculoarterial ring and junction
Ventricle within sinus
Basal ring
B
Sinutubular junction
Haemodynamic ventriculoarterial junction (semilunar)
Commissure
Arterial wall
Artery as part of ventricle
Ventricle
Ventricle as part of aorta
Anatomic ventriculoarterial junction (circular)
Pulmonary trunk
Right coronary cusp
Non-coronary cusp
Left coronary cusp
Sinutubular junction
Ventriculoarterial junction
Muscular septum
Mitral valve
Left fibrous trigone
Right fibrous trigone
Membranous septum
Central fibrous body

Fig. 56.11 The structure of the aortic root is best conceptualized in terms of a three-pronged coronet (**A**): there are at least three rings within this coronet, but none supports the entirety of the attachments of the valvular cusps (compare with **C**). In **B**, the cusps have been resected at their

attachment to the aortic wall. Note the relationship of the cusp insertions and the ventriculo-arterial junction. In **C**, the root of the aorta has been cut open and distended, in order to show the insertion of the semilunar cusps. Note the zone of fibrous continuity between the cusps of the aortic and mitral valves and their relationship to the fibrous trigones, and the semilunar attachment of the cusps (compare with **B**).

(Redrawn by courtesy of Professor RH Anderson, Institute of Child Health, University College, London.)

Each cusp is a fold of endocardium, with an intervening, and variably developed, fibrous core. The core is substantial along both the free edge and the semilunar attached border; the latter is particularly thickened at the deepest central part (nadir) of the base of each cusp (thus never forming a simple complete fibrous ring). The free margin of each cusp contains a central localized thickening of collagen, the nodule of the semilunar 'cusp' (nodule of Arantius). Perforations within the cusps close to the free margin and near the commissures are frequently present, but are of no functional significance. Each semilunar cusp is contained within one of the three sinuses of the pulmonary trunk.

Opening of the pulmonary valve

During diastole, the pulmonary valve is closed and all three cusps of the valve are tightly apposed. The pulmonary valve is difficult to visualize at echocardiography and usually only the posterior cusp is visible when the valve is closed; atrial systole may cause a slight posterior movement of the valve cusps. The pulmonary valve opens passively during ventricular systole and then closes rapidly at the end of systole (Fig. 56.7).

Left atrium

Although smaller in volume than the right, the left atrium has thicker walls (3 mm on average). Its cavity and walls are formed largely by the proximal parts of the pulmonary veins, which are incorporated into the atrium during development. The only clear derivative of the left part of the embryonic atrium is the auricle, together with the vestibule of the mitral valve. The left atrium is roughly cuboidal and extends behind the right atrium, separated from it by the obliquely positioned septum, thus the right atrium is in front and anterolateral to the right part of the left atrium. The left part is concealed anteriorly by the initial segments of the pulmonary trunk and aorta: part of the transverse pericardial sinus lies between it and these arterial trunks. Anteroinferiorly, and to the left, it adjoins the base of the left ventricle at the orifice of the mitral valve. Its posterior aspect forms most of the anatomical base of the heart and is approximately quadrangular, receiving the terminations of (usually) two pulmonary veins from each lung. It forms the anterior wall of the oblique pericardial sinus (Fig. 56.1). This surface ends at the shallow vertical interatrial groove, which descends to the cardiac crux. The left atrial auricle is constricted at its atrial junction and all the pectinate muscles of the left atrium are contained within it. It is characteristically longer, narrower and more hooked than the right auricle, its margins being more deeply indented. It turns forwards to the left of the pulmonary trunk, overlapping its origin (Fig. 56.8). Interiorly, the four pulmonary veins open into the upper posterolateral surfaces of the left atrium, two on each side. Their orifices are smooth and oval, the left pair frequently opening via a common channel. Some minimal cardiac veins return blood directly from the myocardium to the cavity of the left atrium. The left atrial aspect of the septum has a characteristically rough appearance, bounded by a crescentic ridge, concave upwards, which marks the site of the foramen ovale.

Left ventricle

General and external features

The left ventricle is constructed in accordance with its role as a powerful pump that sustains pulsatile flow in the high-pressured systemic arteries. Variously described as half-ellipsoid or cone-shaped, it is longer and narrower than the right ventricle, extending from its base in the plane of the atrioventricular groove to the cardiac apex. Its long axis descends forwards and to the left. In transverse section, at right angles to the axis, its cavity is oval or nearly circular, with walls about three times thicker (8–12 mm) than those of the right ventricle (Fig. 56.12). It forms part of the sternocostal, left and inferior (diaphragmatic) cardiac surfaces. Except where obscured by the aorta and pulmonary trunk, the base of the ventricular cone is superficially separated from the left atrium and atrial auricle by part of the atrioventricular groove; the coronary sinus runs in the posterior aspect of the groove to reach the right atrium (Fig. 56.2B,D). The anterior and posterior interventricular grooves indicate the lines of mural attachment of the ventricular septum and the limits of the left and right ventricular territories. The sternocostal surface of the ventricle curves bluntly into its left surface at the obtuse margin.

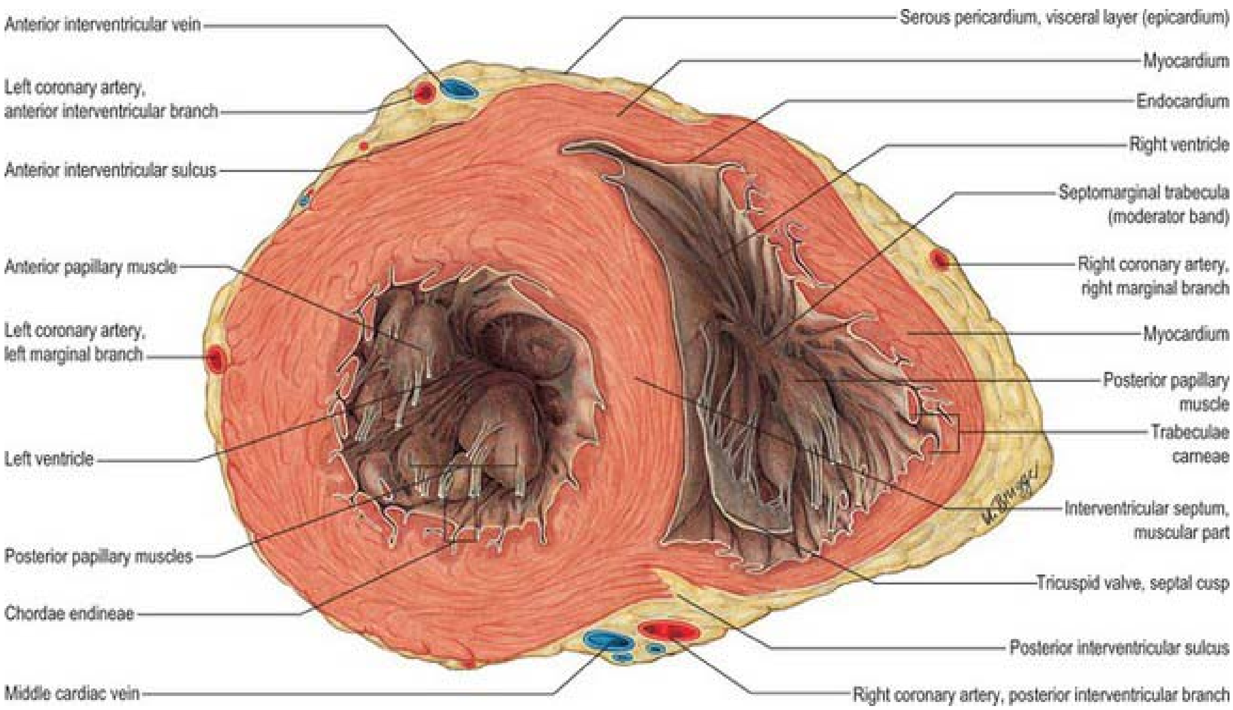
Anterior interventricular vein
Left coronary artery, anterior interventricular branch
Anterior interventricular sulcus
Anterior papillary muscle
Left coronary artery, left marginal branch
Left ventricle
Posterior papillary muscles
Chordae endineae
Middle cardiac vein
Serous pericardium, visceral layer (epicardium)
Myocardium
Endocardium
Right ventricle
Septomarginal trabecula (moderator band)
Right coronary artery, right marginal branch
Myocardium
Posterior papillary muscle
Trabeculae carneae
Interventricular septum, muscular part
Tricuspid valve, septal cusp
Posterior interventricular sulcus
Right coronary artery, posterior interventricular branch

Fig. 56.12 Left and right ventricles: cross section perpendicular to axis of the heart; superior aspect.

(From Sobotta 2006.)

Internal features

The left ventricle has an inlet region, guarded by the mitral valve (ostium venosum), an outlet region, guarded by the aortic valve (ostium arteriosum), and an apical trabecular component. The left atrioventricular orifice admits atrial blood during diastole, flow being towards the cardiac apex. After closure of the mitral cusps, and throughout the ejection phase of systole, blood is expelled from the apex through the aortic orifice. In contrast to the orifices within the right ventricle, those of the left ventricle are in close contact, with fibrous continuity between the cusps of the aortic and mitral valves (the subaortic curtain; Fig. 56.13). The inlet and outlet turn sharply round this fibrous curtain (Fig. 56.9).

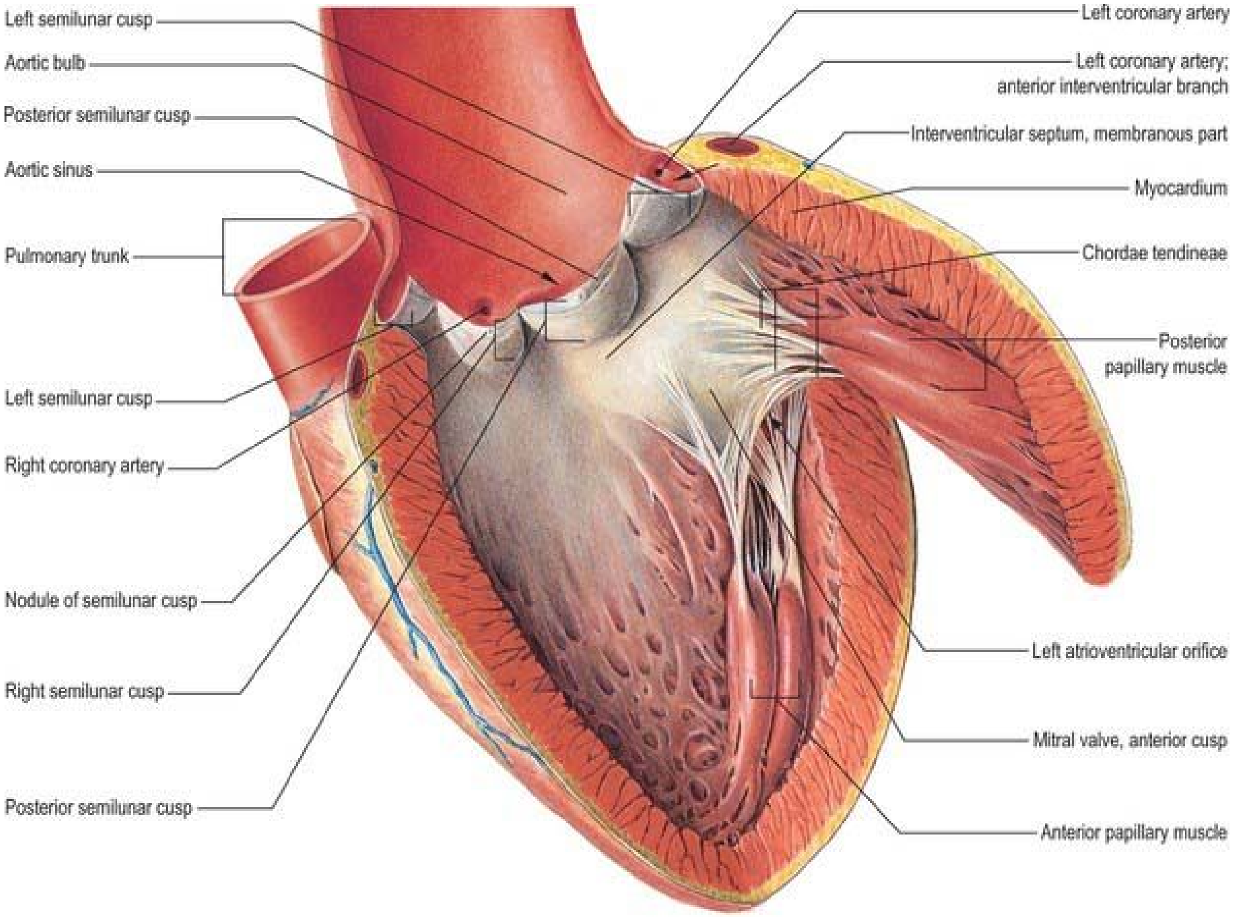
Left semilunar cusp
Aortic bulb
Posterior semilunar cusp
Aortic sinus
Pulmonary trunk
Left semilunar cusp
Right coronary artery
Nodule of semilunar cusp
Right semilunar cusp
Posterior semilunar cusp
Left coronary artery
Left coronary artery; anterior interventricular branch
Interventricular septum, membranous part
Myocardium
Chordae tendineae
Posterior papillary muscle
Left atrioventricular orifice
Mitral valve, anterior cusp
Anterior papillary muscle

Fig. 56.13 The aortic orifice opened from the front to show the cusps of the aortic valves, their nodules, lunules, commissures and the triple-scalloped line of anular attachment. Also shown is the continuity of the subaortic curtain with the mitral anterior cusp (i.e. 'aortic baffle') and the

coronary ostia, and the spatial relationship of the aortic orifice to the pulmonary orifice and to the left ventricle.

(From Sobotta 2006.)

The anterolateral wall is the concavo-convex ventricular septum, a muscular wall the convexity of which is the posteromedial profile of the right ventricle as seen in section. It thus completes the circular outline of the left ventricle (Fig. 56.12). Towards the aortic orifice, the septum becomes the thin, collagenous interventricular component of the membranous septum, an oval or round area below and confluent with the fibrous triangle separating the right and the non-coronary cusps of the aortic valve.

Between the lower limits of the free margins of the cusps of the mitral valve and the apex of the ventricle, the muscular walls are deeply trabeculated. These trabeculae carneae are finer and more intricate than those of the right ventricle, but similar in structure. Trabeculation is characteristically well developed near the apex, whereas the upper reaches of the septal surface are smooth (Fig. 56.13).

Hypertrophy of heart muscle

In hypertrophic cardiomyopathy, there is an increase in the thickening of the myocardial walls, particularly the interventricular septum, which is disproportionately thickened in comparison with the posterior wall. Echocardiography allows accurate assessment of the thickening and of systolic function. Other features in hypertrophic cardiomyopathy are dynamic left ventricular outflow obstruction, systolic anterior motion of the anterior mitral valve cusp, and midsystolic closure of the aortic valve. A degree of diastolic dysfunction is also present in some cases of hypertrophic cardiomyopathy. Serial short-axis magnetic resonance imaging (MRI) allows accurate measurement of wall thickness and is particularly useful in assessing hypertrophy confined to the apex. Gradient-echo MRI also allows some functional assessment of the hypertrophy. A number of histological changes are observed, including disarray of the cardiac myocytes with replacement fibrosis, and expansion of the collagen component. Treatment is usually medical, except for refractory cases and those in whom the left ventricular outflow tract obstruction has a gradient of greater than 50 mmHg. Ventricular septal myotomy and myectomy are performed in such cases. More recently, catheter alcohol septal ablation has been introduced as a non-surgical alternative. A number of patients may also require implantation of cardiac defibrillators to prevent sudden cardiac death.

An athlete’s heart may also hypertrophy and may require differentiation from hypertrophic cardiomyopathy. However, in athletes there is uniform hypertrophy, the left ventricle cavity is usually less than 55 mm in size, and the thickness decreases with deconditioning. Hypertrophic cardiomyopathy, in contrast, may show unusual patterns of left ventricular hypertrophy, which is often asymmetric with sharp transitions between segments, left atrial enlargement and bizarre electrocardiographic patterns. Furthermore, there is an autosomal dominant inheritance pattern of abnormalities in genes coding for myocardial proteins associated with hypertrophic cardiomyopathy. Individuals with mutations of the β-MHC (major histocompatibility complex) gene usually develop the classical form of hypertrophy, whereas those with cardiac troponin T gene mutations generally have only mild or clinically undetectable hypertrophy. Rare forms of hypertrophy include localized left ventricular apical hypertrophy as a result of cardiac troponin I mutations, and isolated midcavity hypertrophy caused by cardiac actin and MLC (myosin light chain) gene mutations.

Mitral valve

The general comments already made in respect to the tricuspid valve apply equally to the mitral. The valve has an orifice with its supporting anulus, cusps and a variety of chordae tendineae and papillary muscles.

Mitral valvular orifice

The mitral orifice is a well-defined transitional zone between the atrial wall and the bases of the cusps. It is smaller than the tricuspid orifice (mean circumference is 9.0 cm in males, 7.2 cm in females). The approximately circular orifice is almost vertical in diastole and at 45° to the sagittal plane, but with a slight forward tilt. Its ventricular aspect faces anterolaterally to the left and a little inferiorly towards the left ventricular apex. It is almost co-planar with the tricuspid orifice but posterosuperior to it, whereas it is posteroinferior and slightly to the left of the aortic orifice. The mitral, tricuspid and aortic orifices are intimately connected centrally at the central fibrous body. When the cusps of the mitral valve close, they form a single zone of coaptation, sometimes termed the commissure.

The anulus of the valve is not a simple fibrous ring, but is made up of fibrocollagenous elements of varying consistency from which the fibrous core of the cusps take origin. These variations allow major changes in the shape and dimensions of the anulus at different stages of the cardiac cycle and ensure optimal efficiency in valvular action.

The anulus is strongest at the internal aspects of the left and right fibrous trigones. Extending from these structures, the anterior and posterior coronary prongs (which are tapering, fibrous, subendocardial tendons) partly encircle the orifice at the atrioventricular junction (Figs 56.9, 56.10). Between the tips of the prongs, the atrial and ventricular myocardial masses are separated by a more tenuous sheet of deformable fibroelastic connective tissue. Spanning anteriorly between the trigones, the fibrous core of the central part of the anterior aortic cusp of the mitral valve is a continuation of the fibrous subaortic curtain that descends from the adjacent halves of the left and non-coronary cusps of the aortic valve (Fig. 56.13).

Mitral valve cusps

Since the earliest descriptions, the mitral valvular cusps have been described as paired structures. Hence, the name ‘bicuspid valve’ is more explicit, although erroneous (the cusps are not cuspid, or ‘peaked’, in form) and surely less picturesque than the clinical term ‘mitral’. Confusion, controversy and difficulties in quantitation have arisen, however, because small accessory cusps are almost always found between the two major cusps. These problems can be resolved if the mitral valve is described as consisting of a continuous veil attached around the entire circumference of the mitral orifice. Its free edge bears several indentations; two are sufficiently deep and regular to be nominated as the ends of a solitary and oblique zone of apposition, or commissure. It is more usual, however, for these anteromedial and posterolateral extremities to be designated as two independent commissures, each positionally named as indicated. The official names for these cusps, anterior and posterior, although simple, are somewhat misleading because of the obliquity of the valve.

When the valve is laid open, the anterior cusp (aortic, septal, 'greater' or anteromedial) is seen to guard one-third of the circumference of the orifice and to be semicircular or triangular, with few or no marginal indentations. Its fibrous core (lamina fibrosa) is continuous, on the outflow aspect, beyond the margins of the fibrous subaortic curtain, with the right and left fibrous trigones (Figs 56.5, 56.9, 56.11C). Between these, it is continuous with the fibrous curtain itself and, beyond the trigones, with the roots of the anular fibrous prongs (Fig. 56.10). The cusp has a deep crescentic rough zone, which receives various chordae tendineae. The ridge limiting the outer margin of the rough zone indicates the maximal extent of surface contact with the mural cusp in full closure. A clear zone is seen between the rough zone and the valvular anulus, which is devoid of attachments of chordae, although its fibrous core carries extensions from chordae attached in the rough zone. The anterior cusp has no basal zone, continuing instead into the valvular curtain. Hinging on its anular attachment, and continuous with the subaortic curtain, it is critically placed between the inlet and the outlet of the ventricle. During passive ventricular filling and atrial systole, its smooth atrial surface is important in directing a smooth flow of blood towards the body and apex of the ventricle. After the onset of ventricular systole and closure of the mitral valve, the ventricular aspect of its clear zone merges into the smooth surface of the subaortic curtain which, with the remaining fibrous walls of the subvalvular aortic vestibule, forms the smooth boundaries of the ventricular outlet.

The posterior cusp (mural, ventricular, 'smaller' or posterolateral) usually has two or more minor indentations. Lack of definition of major intervalvular commissures has previously led to disagreement and confusion concerning the territorial extent of this cusp and the possible existence of accessory ‘scallops’. Examination of the valve in the closed position, however, shows that the posterior cusp can conveniently be regarded as all the valvular tissue posterior to the anterolateral and posteromedial ends of the major zone of apposition with the aortic cusp. Thus defined, it has a wider attachment to the anulus than does the anterior cusp, guarding two-thirds of the circumferential attachments. Further indentations usually divide the mural cusp into a relatively large middle scallop and smaller anterolateral and posteromedial commissural scallops. Each scallop has a crescentic, opaque rough zone, receiving on its ventricular aspect the attachments of the chordae that define the area of valvular apposition in full closure. From the rough zone to within 2–3 mm of its anular attachment, there is a membranous clear zone devoid of chordae. The basal 2–3 mm is thick and vascular, and receives basal chordae. The ratio of rough to clear zone in the anterior cusp is 0.6; in the middle scallop of the posterior cusp it is 1.4. Much more of the mural cusp is in apposition with the aortic cusp during closure of the mitral valve.

Mitral chordae tendineae (tendinous cords)

The chordae tendineae resemble those supporting the tricuspid valve. False chordae (trabeculae carneae; Fig. 56.13) are also irregularly distributed as in the right ventricle. They occur in about 50% of all human left ventricles, and often cross the subaortic outflow. Many contain extensions from the ventricular conducting tissues. These left ventricular bands can often be identified by cross-sectional echocardiography. Their role, if any, has still to be determined. True chordae of the mitral valve may be divided into intercusp (or commissural) chordae, rough zone chordae, including the special strut chordae, so-called ‘cleft’ chordae and basal chordae. Most true chordae divide into branches from a single stem soon after their origin from the apical one-third of a papillary muscle, or proceed as single chordae that divide into several branches near their attachment. Basal chordae, in contrast, are solitary structures passing from the ventricular wall to the mural cusp.

There is such marked variation between the arrangement of the chordae in individual normal hearts that any detailed classification loses much of its clinical significance. Suffice it to say that, in the majority of hearts, the chordae support the entire free edges of the valvular cusps, together with varying degrees of their ventricular aspects and bases. There is some evidence to suggest that those valves with unsupported areas of the free edge become prone to prolapse in later life.

Papillary muscles

The two muscles supporting the cusps of the mitral valve also vary in length and breadth and may be bifid. The anterolateral muscle arises from the sternocostal mural myocardium, the posteromedial from the diaphragmatic region (Fig. 56.12). Chordae tendineae arise mostly from the tip and apical one-third of each muscle, but sometimes take origin near their base. The chordae from each papillary muscle diverge and are attached to corresponding areas of closure on both valvular cusps.

Opening of the mitral valve

At the onset of diastole, opening is passive but rapid, the cusps parting and projecting into the ventricle as left atrial pressure exceeds left ventricular diastolic pressure. Passive ventricular filling proceeds as atrial blood pours to the apex, directed by the pendant aortic cusp of the valve. The cusps begin to float passively together, hinging on their anular attachments, partially occluding the ventricular inlet. Atrial systole now occurs, jetting blood apically and causing re-opening of the cusps. As maximal filling is achieved, the cusps again float rapidly together. Closure is followed by ventricular systole, which starts in the papillary muscles and continues rapidly as a general contraction of the walls and septum. Coordinated contraction of the papillary muscles increases the tension in the chordae and promotes joining of the corresponding points on opposing cusps, preventing their eversion. With general mural and septal excitation and contraction, left ventricular pressure increases rapidly (Fig. 56.7). The cusps ‘balloon’ towards the atrial cavity and the atrial aspects of the rough zones come into maximal contact.

Precise papillary contraction, and increasing tension in the chordae, continue to prevent valvular eversion and maintain valvular competence.

The orifices and the cusps of both atrioventricular valves undergo considerable changes in position, form and area during a cardiac cycle. Both valves move anteriorly and to the left during systole, and reverse their motion in diastole. The mitral valve reduces its orificial (anular) area by as much as 40% in systole. Its shape also changes from circular to crescentic at the height of systole, the anular attachment of its aortic cusp being the concavity of the crescent. The attachment of its mural cusp, although remaining convex, contracts towards the anterior wall of the heart.

Aortic valve

The smooth left ventricular outflow tract, or aortic vestibule, ends at the cusps of the aortic valve. Although stronger in construction, the aortic valve resembles the pulmonary (Figs 56.9, 56.11, 56.13) in possessing three semilunar cusps, supported within the three aortic sinuses of Valsalva. Although the aortic valve, like the pulmonary valve, is often described as possessing an anulus in continuity with the fibrous skeleton, there is no complete collagenous ring supporting the attachments of the cusps. As with the pulmonary valve, the anatomy of the aortic valve is dominated by the fibrous semilunar attachment of the cusps (Fig. 56.11C).

Aortic valve cusps

The cusps are attached in part to the aortic wall and in part to the supporting ventricular structures. The situation is more complicated than in the pulmonary valve, because parts of the cusps also take origin from the fibrous subaortic curtain, and are continuous with the aortic cusp of the mitral valve (Fig. 56.13). This area of continuity is thickened at its two ends to form the right and left fibrous trigones (Fig. 56.9). However, as with the pulmonary valve, the semilunar attachments incorporate segments of ventricular tissue within the base of each aortic sinus. These sinuses and cusps are conveniently named as right, left and non-coronary, according to the origins of the coronary arteries (Fig. 56.11C). The semilunar attachments also incorporate three triangular areas (trigones) of aortic wall within the apex of the left ventricular outflow tract. As these triangular areas are part of the wall of the aorta rather than of the left ventricle, and are interposed between the bulbous aortic sinuses, they separate the cavity of the left ventricle from the pericardial space. Removal of the trigones in an otherwise intact heart is instructive in demonstrating the relationships of the aortic valve, which can justly be considered as the keystone of the heart. The base of the triangle between the non-coronary and the left coronary cusps is continuous inferiorly with the fibrous aortic-mitral curtain. The apex of this triangle 'points' into the transverse pericardial space. The triangle between right and non-coronary cusps has, as its base, the membranous components of the interventricular septum and thus 'faces' the right ventricle, whereas its apex 'points' towards the transverse pericardial space behind the origin of the right coronary artery. The third triangle, between the two coronary cusps, has its base on the muscular ventricular septum. Its apex 'points' to the plane of space found between the aortic wall and the free-standing sleeve of right ventricular infundibular musculature that supports the cusps of the pulmonary valve. Although the basal attachments of each cusp are thickened and collagenous at their ventricular origins, there is no continuous collagenous skeleton supporting, in circular fashion, all the attachments of the cusps of the aortic valve. Valvular function depends primarily upon the semilunar attachments of the cusps.

The cusps themselves are folds of endocardium with a central fibrous core. With the valve half open, each equals slightly more than a quarter of a sphere, an approximate hemisphere being completed by the corresponding sinus. Each cusp has a thick basal border, deeply concave on its aortic aspect, and a horizontal free margin. The latter is only slightly thickened, except at its midpoint, where there is an aggregation of fibrous tissue, the valvular nodule of the semilunar cusp. The fibrous core that flanks each nodule is tenuous, forming the lunules of translucent and occasionally fenestrated valvular tissue: fenestrations are of no functional significance. The aortic surface of each cusp is rougher than its ventricular aspect.

Currently, three sets of names are used to describe the aortic cusps. Posterior, right and left refer to presumed fetal positions before full cardiac rotation has occurred (Ch. 59). Corresponding terms based on the approximate positions in maturity are anterior, left posterior and right posterior. However, as already indicated, widespread clinical terminology links both cusps and sinuses to the origins of the coronary arteries. Thus, the anterior is termed the right coronary cusp, the left posterior is the left coronary, and the right posterior is the noncoronary: these clinical terms are preferable, in the normal heart, because they are simple and unambiguous.

Aortic sinuses (of Valsalva)

The aortic sinuses are more prominent than those in the pulmonary trunk. The upper limit of each sinus reaches considerably beyond the level of the free border of the cusp and forms a well-defined complete circumferential sinotubular ridge when viewed from the aortic aspect (Fig. 56.11C). Coronary arteries usually open near this ridge within the upper part of the sinus, but are markedly variable in their origin. The walls of the sinuses are largely collagenous near the attachment of the cusps, but the amount of lamellated elastic tissue increases with distance from the zone of attachment. Strands of myocardium may enter this fibroelastic wall. At the mid level of each sinus, its wall is about half the thickness of the supravalvular aortic wall and less than one-quarter of the thickness of the sinutubular ridge. At this level, the mean luminal diameter of the beginning of the aortic root is almost double that of the ascending aorta. These details are functionally significant in the mechanism of valvular motion.

Opening of the aortic valve

During diastole, the closed aortic valve supports an aortic column of blood at high but slowly diminishing pressure (Fig. 56.7). Each sinus and its cusp form a hemispherical chamber. The three nodules are apposed and the margins and lunular parts of adjacent cusps are tightly apposed on their ventricular aspects. From the aortic aspect, the closed valve is triradiate, three pairs of closely compressed lunules radiating from their nodules to their peripheral commissural attachments at the sinutubular junction (Fig. 56.9). As ventricular systolic pressure increases, it exceeds aortic pressure and the valve is passively opened. The fibrous wall of the sinuses nearest the aortic vestibule is almost inextensible but, in the upper parts of sinuses, the wall is fibroelastic. Under left ventricular ejection pressure, the radius here increases 16% in systole. Hence the commissures move apart, making the orifice triangular when fully open. The free margins of the cusps then become almost straight lines between peripheral attachments. However, they do not flatten against the sinus walls, even at maximal systolic pressure, which is probably an important factor in subsequent closure. During ejection, most blood enters the ascending aorta, but some enters the sinuses, forming vortices that help to maintain the triangular 'mid position' of the cusp during ventricular systole and probably initiate their approximation with the end of systole. Tight and full closure ensues, with the rapid decrease in ventricular pressure in diastole. Commissures narrow, nodules aggregate and the valve reassumes its triradiate form. Experiments indicate that 4% of ejected blood regurgitates through a valve with normal sinuses, whereas 23% regurgitates through a valve without them. The normal structure of the aortic sinuses also promotes non-turbulent flow into the coronary arteries.

Echocardiography

The gross anatomy of the heart can be evaluated by two-dimensional echocardiography in the para-sternal, apical, suprasternal and subcostal positions (Fig. 56.14). The standardized planes used are long axis, short axis and four-chamber. Echocardiography allows a detailed assessment of the functional anatomy of the heart. The long-axis view is obtained by placing the ultrasound transducer in the left apicosternal position and provides detailed images of the left ventricle, aorta, left atrium, and mitral and aortic valves (Fig. 56.14C). Angling the beam towards the right also allows assessment of the right atrium, right ventricle and tricuspid valves. Rotating the transducer by 90° in the clockwise direction produces the short-axis view, which allows assessment of the left ventricle, papillary muscles, chordae tendineae and mitral valves (Fig. 56.14B). The four-chamber view demonstrates the ventricles, atria, and mitral and tricuspid valves (Fig. 56.14A). Rotation of the transducer allows two-chamber views of the heart and more detailed assessment of the aorta and aortic valves. Cardiac magnetic resonance and computer tomography provide similar information on cardiac structure and function (Fig. 56.14D–F), together with complementary information on great vessels and other extracardiac intrathoracic stuctures.

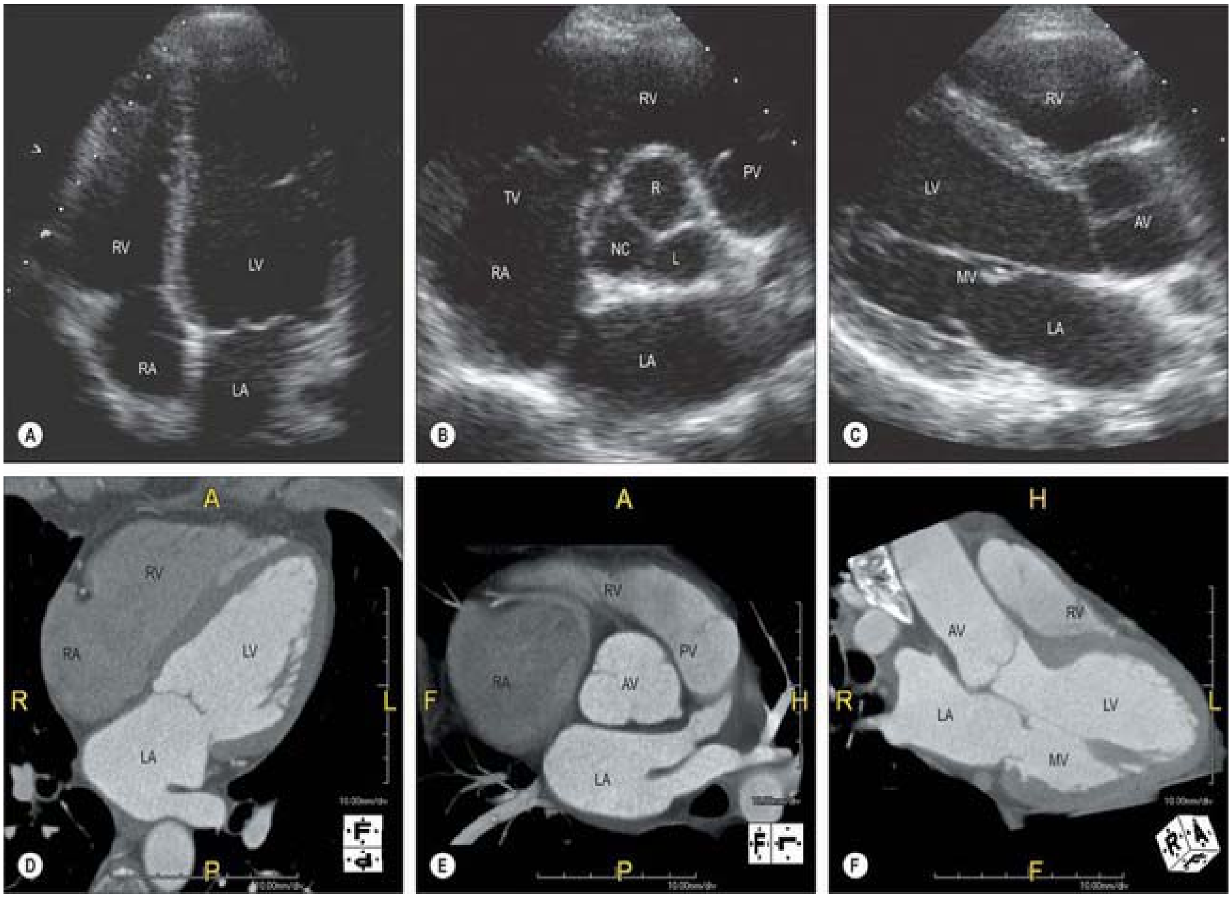

Fig. 56.14 Cardiac anatomy shown by transthoracic echocardiography and computed tomography. **A**, Four-chamber view. LA, left atrium; LV, left ventricle; RA, right atrium; RV, right ventricle. **B**, Short-axis view at aortic valve level. Note three aortic cusps R, right; L, left; and NC, non-coronary; and central position of the aorta; LA, left atrium; PV; pulmonary valve, RA, right atrium; RV; right ventricle; TV, tricuspid valve. **C**, Parasternal long-axis view; AV, aortic valve; LA, left atrium; LV, left ventricle; RV, right

ventricle; MV; mitral valve. **D**, **E** and **F**, Corresponding images by computed tomography. Note different orientation compared with transthoracic echocardiography (looked at from below, foot-to-head). R, right; L, left; A, anterior; P, posterior; H, head; F, foot.

(Images courtesy of Dr Konstantinos Dimopoulos, Royal Brompton and Chelsea and Westminster Hospitals, London.)

CONNECTIVE TISSUE AND FIBROUS SKELETON OF THE HEART

From epicardium to endocardium, and from the orifices of the great veins to the roots of the arterial trunks, the intercellular spaces between contractile and conduction elements are everywhere permeated by connective tissue. The amount varies greatly in arrangement and texture in different locations.

A fine layer of areolar tissue is found beneath the mesothelium of the serosal visceral epicardium over much of the heart. This accumulates subepicardial fat which becomes concentrated along the acute margin, the atrioventricular and interventricular grooves and their side channels. The coronary vessels and their main branches are embedded in this fat; the amount increases with age. The endocardium also lies on a fine areolar tissue rich in elastic fibres. Fibrocellular components of these subepicardial and subendocardial layers blend on their mural aspects with the endomysial and perimysial connective tissue on the myocardium. Each cardiac myocyte is invested by a delicate endomysium composed of fine reticular fibres, collagen and elastin fibres embedded in ground substance. This matrix is lacking only at desmosomal and gap junctional contacts of intercalated discs. Similar arrangements apply to myocytes of the ventricular conduction tissues and their extensive contacts with the working myocardium. The connective tissue matrix itself is interconnected laterally to form bundles, strands or sheets of macroscopic proportions showing a complex geometric pattern. The larger myocardial bundles are surrounded by, and attached to, stronger perimysial condensations. The overall pattern is described in terms of struts and weaves.

The myocardial matrix, despite its importance, cannot be dissected grossly. Running at the ventricular base, and intimately related to atrioventricular valves and the aortic orifice, is a complex framework of dense collagen with membranous, tendinous and fibroareolar extensions. The whole is sufficiently distinct to be termed the fibrous skeleton of the heart.

Although it is often stated that all four valves are contained within this skeleton, this is not the case. The cusps of the pulmonary valve are supported on a free-standing sleeve of right ventricular infundibulum which can easily be removed from the heart without disturbing either the fibrous skeleton or the left ventricle. The fibrous skeleton is strongest at the junction of the aortic, mitral and tricuspid valves, the so-called central fibrous body (see below) (Figs 56.9, 56.10). Two pairs of curved, tapering, collagenous prongs, fila coronaria, extend from the central fibrous body. They are stronger on the left, passing partially around the mitral and tricuspid orifices, which are almost co-planar and incline to face the cardiac apex. The aortic valve, in contrast, faces up, right and slightly forwards. It is anterosuperior and to the right of the mitral orifice. Two of the cusps of the aortic valve are in fibrous continuity with the aortic cusp of the mitral valve: this aortic-mitral or subaortic curtain is also an integral part of the fibrous skeleton (Figs 56.9, 56.11C). The two ends of the curtain are strengthened as the right and left fibrous trigones, which are the strongest part of the skeleton. The right trigone, together with the membranous septum, constitutes the central fibrous body, which is penetrated by the bundle of His, or atrioventricular bundle, i.e. by the mechanism for atrioventricular conduction. The membranous septum is crossed on its right aspect by the attachment of the tricuspid valve, which divides the septum into atrioventricular and interventricular components.

The fibrous skeleton has two functions. It ensures electrophysiological discontinuity between the atrial and ventricular myocardial masses (except at the site of penetration of the conduction tissue), and it also functions as a stable but deformable base for the attachments of the fibrous cores of the atrioventricular valves.

The aortic root is central within the fibrous skeleton and is often described in terms of an ‘anulus’ integrated within the fibrous skeleton. However, as with the pulmonary valve, the structure of the aortic root corresponds to the triple fibrous semilunar attachments of its cusps. Within this complex circumferential zone there are three crucially important triangular areas that separate, on the ventricular aspect, the aortic bulbous sinuses which house the valvular cusps. As a whole, these three triangles can be conceptualized in terms of a three-pointed coronet and are known as the subaortic spans. Their triangular apices correspond to the tips of the valvular commissures. Their walls, which are significantly thinner than those of the sinuses, variously consist of collagen or admixed muscle strands and fibroelastic tissue. They form the subvalvular extensions of the aortic vestibule. The interval between the non-coronary and left coronary sinuses is filled with the deformable subaortic curtain. The span between the non-coronary and right coronary sinuses is continuous with the anterior surface of the membranous septum. The third subaortic span, between the two coronary aortic sinuses, is filled with fibroelastic tissue, which separates the extension of the subaortic root from the wall of the free-standing subpulmonary infundibulum. Previously, this was thought to be the location of the tendon of the infundibulum (conus ligament). Similar fibrous triangles are found separating the sinuses of the pulmonary trunk, but these are significantly less robust.

The mitral and tricuspid rings (anuli) are not simple and rigid collagenous structures but dynamic, deformable lines of valvular attachment that vary greatly at different peripheral points and change considerably with each phase of the cardiac cycle and with increasing age. The tricuspid attachments are even less robust than those of the mitral valve. At several sites only fibroareolar tissue separates the atrial and ventricular muscular masses.

CONGENITAL CARDIAC MALFORMATIONS

Congenital malformations of the heart are common, amounting to about one-quarter of all developmental abnormalities. Their incidence is estimated at eight per 1000 live births, but they are found in up to 2% of stillbirths. Only a small proportion of the anomalies are directly attributable to genetic or environmental factors; the majority are the result of multifactorial events.

Abnormalities of cardiac position

The most severe abnormality of position is an extrathoracic heart, so-called ectopia cordis. The heart usually projects to the surface through the lower thoracic and upper abdominal wall, remaining covered, in most instances, by the fibrous pericardium. There is usually additional herniation of the abdominal contents. Another abnormality of cardiac position is a mirror-image i.e. reversal in shape and position of the heart: the heart is predominantly positioned in the right hemithorax (dextroposition) with its apex directed to the right instead of the left (dextrocardia). This arrangement may be part of ‘situs inversus’, where the heart, great vessels and abdominal organs occupy mirror-image positions. Dextrocardia may be associated with Kartagener’s syndrome (a subgroup of ciliary dyskinesias). More usually, an abnormal location of the heart occurs in cases of isomerism, in which both sides of the thorax, including the main bronchi and the atrial appendages, retain features of either morphological rightness or leftness. Isomerism is also commonly associated with anomalous arrangement of the abdominal organs, right isomerism is associated with ‘absence’ of the spleen (so called asplenia) and left isomerism with multiple spleens (polysplenia). The intracardiac anatomy in cases of isomerism is almost universally abnormal, and there is a range of heart defects (the defects are usually more simple in left atrial isomerism, and more complex in right atrial isomerism). These intrathoracic abnormal arrangements, with or without abdominal abnormalities, may first manifest themselves following ‘routine’ chest radiography. Reversal of normal anatomy has obvious clinical implications, a typical example being a patient with mirror-image arrangements and appendicitis, who presents with an acute left lower quadrant pain.

Most congenital heart abnormalities can be detected during antenatal ultrasound screening. Neonates with severe congenital heart disease may present with tachypnoea, difficulty in feeding, cyanosis and/or cardiovascular collapse. There may be audible murmurs on auscultation. The vast majority of abnormalities may be detected by postnatal echocardiography; in a very few cases, cardiac catheterization and direct measurements of pressure, oxygen saturations and angiography may be required.

Acyanotic cardiac defects

Acyanotic heart defects are the result of either left to right cardiac shunting through heart defects (intra- or extra-cardiac), or of obstruction. Left to right shunting leads to an increased workload and stress on the heart and the lungs as a consequence of increased pulmonary blood flow and, in turn, increased pulmonary venous return. Depending on the location of the shunt and the magnitude of left to right shunting, patients are at risk of developing pulmonary arterial hypertension, unless timely heart surgery is undertaken. Examples of defects leading to left to right shunting are simple septal defects such as atrial or ventricular septal defects or patent ductus arteriosus, or more complex cardiac defects, including atrioventricular septal defects, and/or a combination of any of these defects with abnormal atrioventricular or ventriculoarterial connections (e.g. a double outlet right ventricle, where more than 50% of both the aorta and the pulmonary artery originate from the right ventricle) (Ch. 59). Obstructive lesions may involve the atrioventricular or semilunar valves (mitral, aortic or pulmonary valve stenosis), or narrow vessels (e.g. coarctation of the aorta or interrupted aortic arch). Depending on the level and severity of the obstruction, patients may have a range of clinical presentations from an asymptomatic heart murmur (common) to cardiovascular collapse (uncommon). Treatment in all cases is directed towards normalizing heart workload, systemic and pulmonary blood flow, and cardiac output, and may be surgical and/or catheter-based.

Cyanotic cardiac defects

Cyanotic cardiac defects may be attributable to a right to left intra- or extra-cardiac shunt or to a severe reduction in pulmonary blood flow. They may be caused by simple lesions such as severe pulmonary stenosis with an atrial septal defect and right to left shunting; moderate lesions including Fallot's tetralogy, in which there is a ventricular septal defect, right ventricular outflow obstruction, right ventricular hypertrophy and an over-riding aorta; or more complex lesions including transposition of the great arteries (Fig. 56.15A,B) and tricuspid and pulmonary atresia (often in the setting of hypoplastic right ventricle and 'single' ventricular physiology). Neonates with severe cyanotic congenital heart defects may be dependent on the patency of the ductus arteriosus: early diagnosis, treatment with intravenous prostaglandin infusion and timely transfer to a tertiary centre for more definitive therapy, is key to survival and good long-term outcomes.

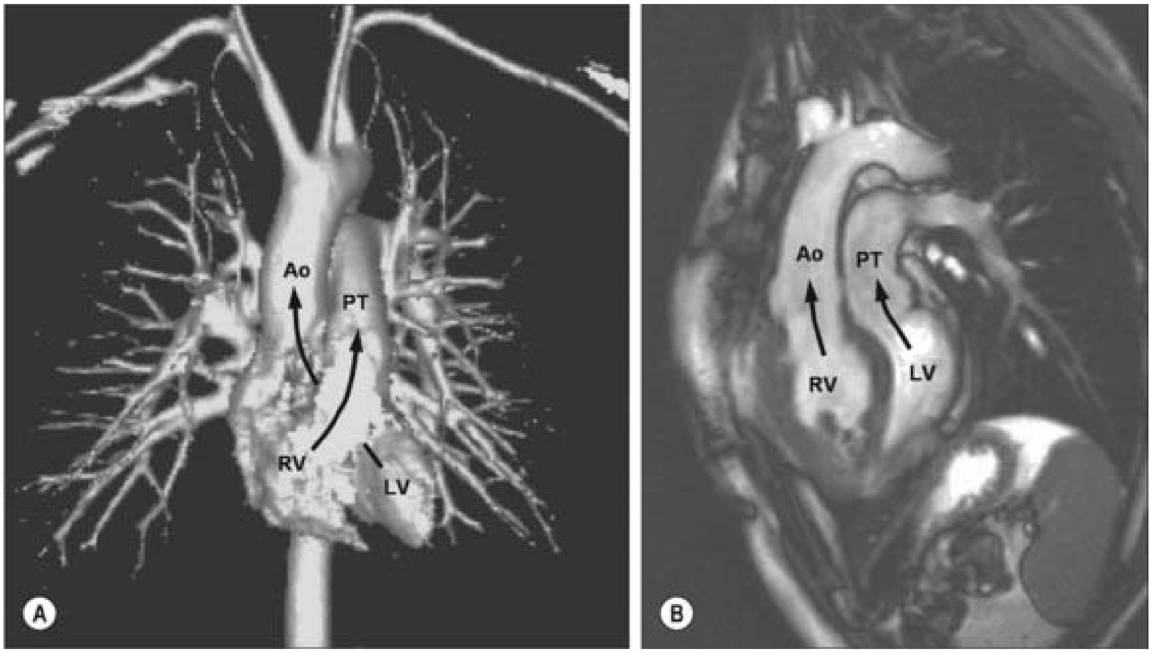

Fig. 56.15 **A**, Cardiac magnetic resonance angiography in a patient with a normal heart. Note the criss-cross relationship of the great arteries; the aorta arises from the left ventricle and runs to the right and posteriorly to the pulmonary trunk (at its origin) and towards the head. The pulmonary artery arises from the right and anterior right ventricle, crosses over and then runs

to the left of the aorta and towards the back (where it bifurcates into the right and left pulmonary arteries at the underside of the aortic arch). **B**, Cardiac magnetic resonance angiogram from a patient with transposition of the great arteries. Note the parallel or side by side relationship of the great vessels and loss of their normal criss-cross relationship. The aorta runs anteriorly and comes off the right ventricle. The hypertrophied right ventricle, supports the systemic circulation, and the ventricular septum bows from right to left. Ao, aorta; PT, pulmonary trunk; RV, right ventricle; LV, left ventricle.

(By courtesy of Dr Philip Kilner, Royal Brompton Hospital, London.)

In recent years, major advances in the diagnosis and management of infants with congenital cardiac malformations have resulted in an increased number of adolescents and adults with palliated or repaired, but not cured, congenital heart disease. This is an area that poses multiple challenges to both cardiovascular and other medical disciplines.

CONDUCTION TISSUE

The cells of cardiac muscle differ from those of skeletal muscle in having the inherent ability to contract and relax spontaneously. This myogenic rhythm is shown by small pieces of cardiac tissue, and even isolated myocytes. The underlying mechanism appears to be based on a further specialization of the sarcolemma that permits a slow inward leakage of sodium ions. Ventricular cells contract and relax at a lower frequency than atrial cells, but in the intact heart both are synchronized to a more rapid rhythm, generated by pacemaker tissue and conveyed to them by a system of fibres specialized for conduction. The anatomical arrangement of these tissues is described in the context of the heart. Here, consideration is restricted to the cells that make up the impulse-generating and conduction system. All are modified cardiac cells. Three types may be distinguished morphologically from normal working cardiac cells: P (=pale-staining = primitive = pacemaker) cells; transitional cells; and Purkinje fibres.

Although these terms will be used in the following account, it is important to recognize that there is a continuum of morphology between P cells, transitional cells, Purkinje fibres and working cardiac muscle cells.

Overview of the conduction system

Of all the cells in the heart, those of the sinu-atrial node generate the most rapid rhythm, and therefore function as the pacemaker of the heart. The impulse, believed to be generated in the P cells, is transmitted over preferentially conducting pathways to right and left atria and to the atrioventricular node. At the atrioventricular node, the impulse is delayed by 40 ms. This delay allows the atria to eject their contents fully before contraction of the ventricles begins. It also places an upper limit on the frequency of signals that can be transmitted to the ventricles. Slender transitional cells, closer in morphology to normal cardiac cells, extend from the node into the stem and principal branches of the atrioventricular bundle (of His). Here, they become continuous with cells of more distinctive appearance, the Purkinje fibres. Conduction of the impulse is rapid in the bundle and its branches (2–3 metres per second, as opposed to 0.6 metres per second in normal myocardium). The cardiac impulse therefore arrives at the apex of the heart before spreading through the ventricular walls, producing a properly coordinated ventricular ejection.

The human heart beats ceaselessly at 70 cycles every minute for many decades, maintaining perfusion of pulmonary and systemic tissues. The rate and stroke volume fluctuate in response to prevailing physiological demands. Figure 56.7 summarizes the principal events in a cardiac cycle, including: the electrical events recorded in the electrocardiogram; the mechanical sequences of diastole, atrial systole, isovolumetric contraction, ejection and isovolumetric relaxation in ventricular systole; the acoustic phenomena recorded in the phonocardiogram; the pressure profiles of right and left hearts and arterial trunks: the sequences of valvular events. Cardiac efficiency depends on precise timing of the operation in interdependent structures. Passive diastolic filling of the atria and ventricles is followed by atrial systole, stimulated by discharge from the sinu-atrial node, which completes ventricular filling. Excitation and contraction of the atria must be synchronous and finish before ventricular contraction. This is effected by a delay in the conduction of excitation from atria to ventricles. Thereafter, ventricular contraction proceeds in a precise manner. A specialized ventricular conduction system ensures that closure of atrioventricular valves is followed rapidly by a wave of excitation and contraction, which spreads from the ventricular apices towards the outflow tracts and orifices, rapidly accelerating the blood during ejection.

Cardiac contraction originates unequivocally in specialized myocytes, but neural influences are important in adapting the intrinsic cardiac rhythm to functional demands from the entire body. All cardiac myocytes are excitable, and display autonomous rhythmic depolarization and repolarization of the cell membrane, conduction of waves of excitation via gap junctions to adjacent myocytes, and excitationcontraction coupling to their actomyosin complexes. These properties are developed to different degrees in different sites and in different types of myocyte (see Ch. 6). The rate of depolarization and repolarization is slowest in the ventricular myocardium, intermediate in the atrial muscle and fastest in the myocytes of the sinoatrial node. These last over-ride those generating slower rhythms and, in the normal heart, are the locus for the rhythmic initiation of cardiac cycles. Conversely, conduction velocity is slow in nodal myocytes, intermediate in general ‘working’ cardiac myocytes and fastest in the myocytes of the ventricular conduction system.

The nodes and networks of the so-called specialized myocardial cells constitute the cardiac conduction system (Figs 56.4A, 56.16A,B and 56.17). The components of this system are the sinu-atrial and atrioventricular nodes, the atrioventricular bundle with its left and right bundle branches and the subendocardial plexus of ventricular conduction cells (Purkinje fibres). Within the system, the main pacemaker rhythm of the heart is generated (sinus), is influenced by nerves (sinus and its innervation) and is transmitted specifically from atria to ventricles (atrioventricular node and bundle) and, within the ventricles, to all their musculature. The spread of excitation is very rapid, but not instantaneous. Different parts of the ventricles are excited at slightly different times, with important functional consequences. Failure of the conduction system will not block cardiac contraction, but the system will become poorly coordinated or uncoordinated. The rhythm will be slower because it originates from a spontaneous (myogenic) activity in the working cardiac myocytes or in a subsidiary pacemaker in a more distal part of the diseased or disrupted conduction system.

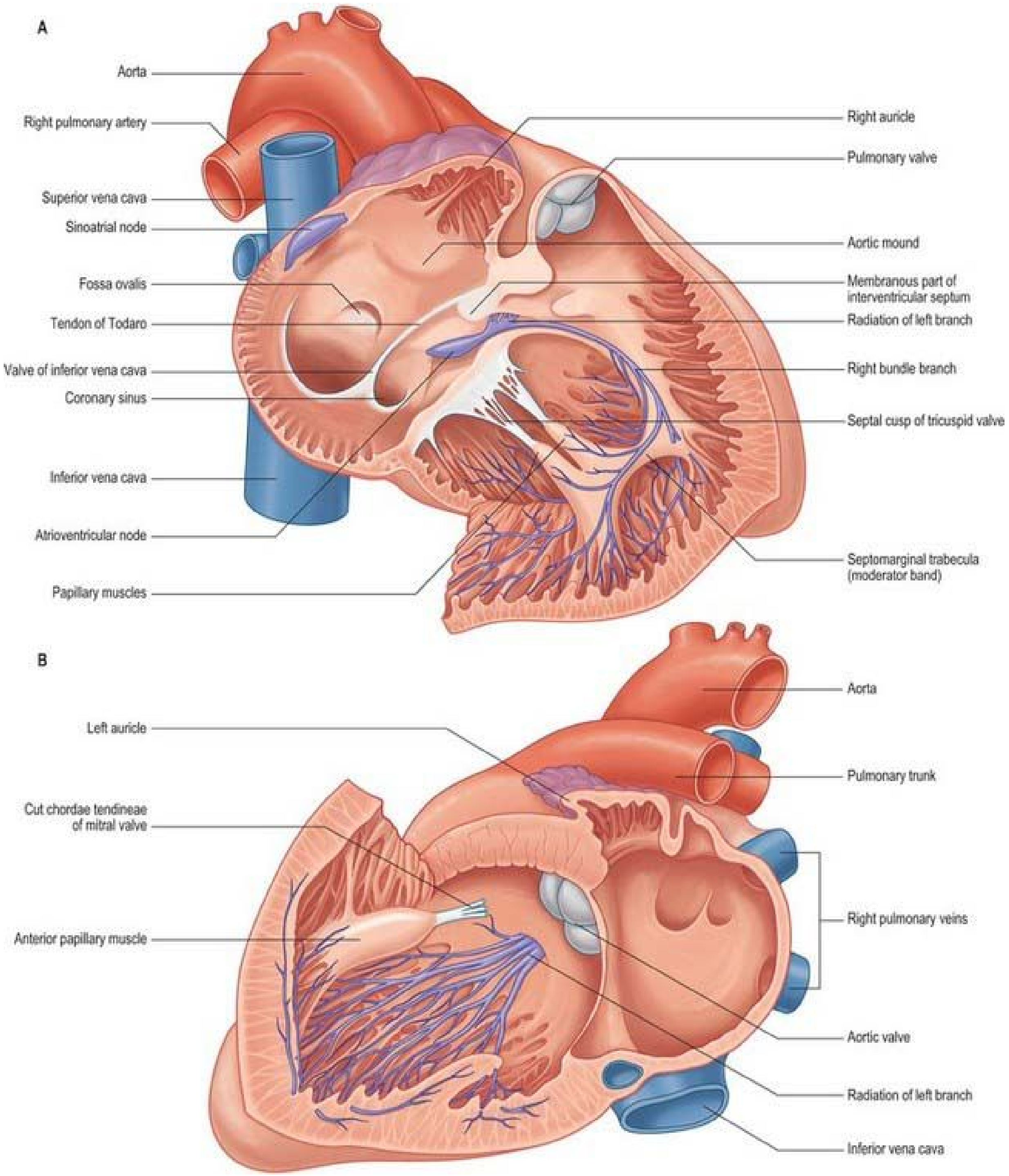
A
Aorta
Right pulmonary artery
Superior vena cava
Sinoatrial node
Fossa ovalis
Tendon of Todaro
Valve of inferior vena cava
Coronary sinus
Inferior vena cava
Atrioventricular node
Papillary muscles
Right auricle
Pulmonary valve
Aortic mound
Membranous part of interventricular septum
Radiation of left branch
Right bundle branch
Septal cusp of tricuspid valve
Septomarginal trabecula (moderator band)
B
Left auricle
Cut chordae tendineae of mitral valve
Anterior papillary muscle
Aorta
Pulmonary trunk
Right pulmonary veins
Aortic valve
Radiation of left branch
Inferior vena cava

Fig. 56.16 The conduction tissue of the heart: **A**, right aspect; **B**, left aspect. The elements of the conduction system are shown in purple. Note the conduction tissue accompanying fine trabeculae carneae and false chordae. In reality, the radiation of the left bundle branch is directly related to the cusps of the aortic valve.

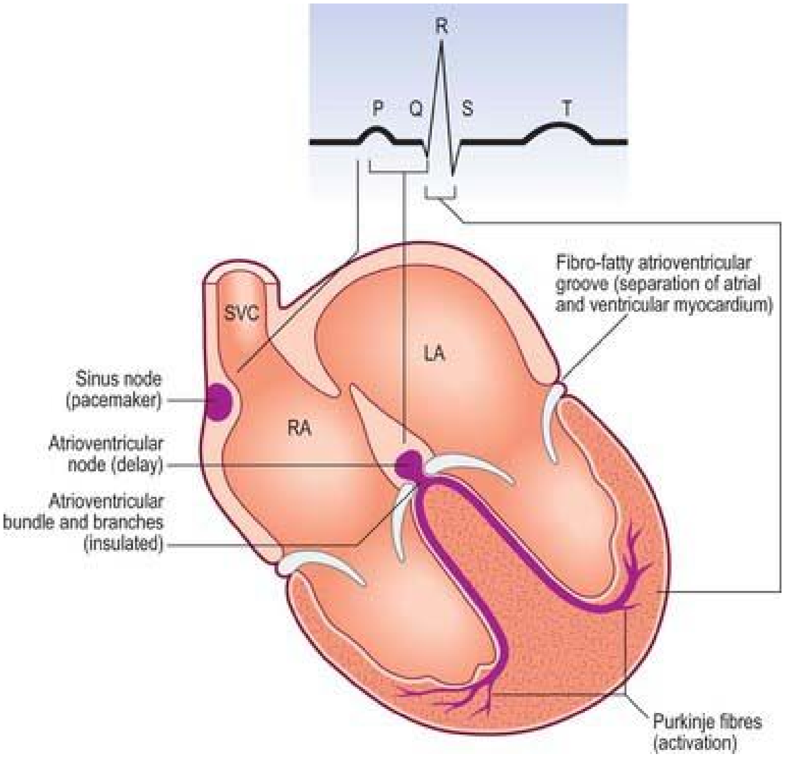
R
P
Q
S
T
Fibro-fatty atrioventricular groove (separation of atrial and ventricular myocardium)
SVC
LA
Sinus node (pacemaker)
RA
Atrioventricular node (delay)
Atrioventricular bundle and branches (insulated)
Purkinje fibres (activation)

Fig. 56.17 The basic structure of the conduction system, and its relationship with the electrocardiogram. Note foramen ovale allowing for communication between the right atrium (RA) and the left atrium (LA). SCV, superior vena cava.

(Redrawn by courtesy of Professor RH Anderson, Institute of Child Health, University College, London.)

There are no specialized internodal and interatrial conduction pathways. The excitation emanating from the sinoatrial node spreads to the atrial musculature and to the atrioventricular node through ordinary atrial working myocardium. The geometric arrangement of fibres along well-organized atrial muscle bundles, e.g. the terminal crest and the rims of the fossa ovale, ensure that conduction is marginally more rapid than elsewhere within the atrium.

Sinoatrial node

The sinoatrial node is an elliptical structure, 10–20 mm long. It is located at the junction between parts of the right atrium derived from the embryonic venous sinus and the atrium proper (Figs 56.4A, 56.17). The node is often covered by a plaque of subepicardial fat, making it visible in some instances to the naked eye. It extends between 1 and 2 cm on the right from the crest of the right auricle and runs posteroinferiorly into the upper part of the terminal groove. In a small proportion of individuals, about 1 in 10, it extends in horseshoe fashion across the crest of the auricle. Nodal tissue does not occupy the full thickness of the right atrial wall from epicardium to endocardium in humans, but rather sits as a wedge of specialized tissue subepicardially within the terminal groove. Its location is marked consistently by a large central artery, which is a branch of either the left circumflex or posterior descending branch of the right coronary artery. Nodal cells are grouped circumferentially around this artery and interwoven into its dense collagenous adventitia. These cells are now considered the ‘pacemakers’, although the functional implications of this relationship are not fully understood. Many nerve fibres are present, although none appears to terminate on cells. There are no autonomic ganglion cells within the node, although many border it anteriorly and posteriorly. P cells are most abundant in the central region. They are small, empty-looking cells, 5–10 μm in greatest diameter, with a large central nucleus. Their pale appearance is attributable to the sparsity of organelles: myofibrils are few and irregularly arranged, and there is no proper sarcotubular system and little glycogen. P cells are less abundant in the periphery of the node, where they mix with slender fusiform transitional cells which are part of a heterogeneous group that is intermediate in appearance between P cells and normal working cardiac cells, and which link P cells to other cells.

Atrioventricular node

The atrioventricular node is an atrial structure that lies at the root of an extensive tree of conduction tissue reaching the apex of the ventricles, the papillary muscles and other regions of the ventricles (Fig. 56.17). The node, with its transitional zones, is located within the atrial component of the muscular atrioventricular septum. Its anatomical landmarks are the boundaries of the triangle of Koch (the attachment of the septal cusp of the tricuspid valve inferiorly, the ostium of the coronary sinus basally, and the tendon of Todaro superiorly) (Fig. 56.4A,B). The compact node is a half oval set against the central fibrous body towards the apex of this triangle. Its atrial aspect is convex, and is overlain by atrial myocardium. Its left margin is concave and abuts on the superior aspect of the central fibrous body. Its basal end projects into the atrial muscle and its anteroinferior end enters the central fibrous body to become the penetrating atrioventricular bundle. The node is pervaded by an irregular collagenous reticulum enmeshing the myocytes, but this is less dense than in the sinu-atrial node. Its arterial supply is from a characteristic vessel that originates from the dominant coronary artery at the crux of the heart. The node has a well-formed compact zone made up of interlocking nodal cells, which frequently show stratification. The transitional cell zones are found superficially and posteriorly. The larger component of atrioventricular delay is probably produced in these transitional zones of the node.

Internodal conduction pathways converge on the atrioventricular node. This is similar in general appearance to the sinoatrial node, although the collagenous component is less dense. The majority of cells are of the transitional type, but P cells resembling those of the sinuatrial node are found in a more fibrous central region. Autonomic ganglia are present between the node and the coronary sinus. In both sinoatrial and atrioventricular nodes, the intercellular contacts between P cells, and between P cells and transitional cells, are much less specialized than the intercalated discs between normal cardiac cells. A sparsity of gap junctions is consistent with the absence from these areas of connexin-43, which is a major protein component of mammalian gap junctions. This probably accounts for the observed difficulty in exciting these cells from adjacent cells. The atrioventricular delay may owe much to this relative inexcitability of the P cells, which appears to disturb the spread of potential in a manner that delays propagation. The narrow diameter of the transitional cells may contribute to the conduction delay.

Atrioventricular bundle

The atrioventricular bundle is the direct continuation of the atrioventricular node, becoming oval, quadrangular or triangular in transverse sectional profile as it enters the central fibrous body (Fig. 56.4A). Traversing the fibrous body, it branches on the crest of the muscular interventricular septum, the branching tract being sandwiched between the muscular and the membranous components of the septum. The right branch of the bundle (crus dextrum) is a narrow, discrete round group of fascicles that courses at first within the myocardium and then subendocardially towards the apex of the ventricle, entering the septomarginal trabecula to reach the anterior papillary muscle. It gives few branches to the ventricular walls in its septal course. At the origin of the anterior papillary muscle, it divides profusely into fine subendocardial fascicles that diverge and, first, embrace the papillary muscle, and then recurve sub-endocardially to be distributed to the remaining ventricular walls. The left branch (crus sinistrum) arises as numerous fine intermingling fascicles that leave the left margin of the branching bundle through much of its course along the crest of the muscular ventricular septum (Fig. 56.16A,B). These fascicles form a flattened sheet down the smooth left ventricular septal surface. The sheet diverges apically and subendocardially across the left aspect of the ventricular septum, separating into anterior, septal and posterior divisions. Fine branches leave the sheets, forming subendocardial networks, which first surround the papillary muscles and then curve back subendocardially to be distributed to all parts of the ventricle.

The principal branches of the bundle are insulated from the surrounding myocardium by sheaths of connective tissue. Functional contacts between ventricular conduction and working myocytes become numerous only in the subendocardial terminal ramifications. Hence, papillary muscles contract first, followed by a wave of excitation and ensuing contraction that travels from the apex of the ventricle to the arterial outflow tract. Because the Purkinje network is subendocardial, muscular excitation proceeds from the endocardial to the epicardial aspect. In the developing heart, it can be shown that the bundle responsible for atrioventricular conduction is a much more extensive structure. Immunohistochemical analysis has revealed that the precursor of the system is a ring of cells that surrounds the inlet and outlet components of the developing ventricular loop (Ch. 59). This ring becomes modified after septation of the ventricles, so that it encircles the right atrioventricular orifice and the aortic outlet from the left ventricle. With subsequent growth, only the septal components of this ‘figure of eight’ persist as the atrioventricular conduction tract. However, remnants of the aortic ring can persist as a ‘dead-end tract’.

The Wolff–Parkinson–White syndrome is caused by abnormal small strands of otherwise unremarkable ventricular myocardium, which connect the atrial and ventricular myocardial masses at some point around the atrioventricular junctions. Histologically, they are strands of working myocardium running through the fibroareolar tissue of the atrioventricular groove.

Cardiac pacing

Temporary pacing wires are usually inserted by cannulation of either the internal jugular vein or the subclavian vein. The subclavian vein approach carries a slightly greater risk of a pneumothorax because of the proximity of the pleural cavity. Other potential risks are brachial plexus injury if the entry site is too posterior, and thoracic duct injury if the left subclavian vein is cannulated. With permanent pacemakers, the most common site at which to locate the device is in a subcutaneous pocket on the anterior chest wall. Access to the heart and the endocardium of the right ventricle and right atrium is gained via the cephalic vein as it lies in the deltopectoral groove.

Cardiac conduction studies

Intracardiac electrocardiography and electrophysiology are used to assess cardiac conduction and rhythm abnormalities. A catheter is inserted via the femoral, subclavian or internal jugular veins using a guidewire technique. Fluoroscopy, echocardiography, and more recently cardiac magnetic resonance, are used to guide accurate placement of the catheters in the appropriate position. The sites of study are high right atrium (for assessing the atrioventricular bundle and right bundle branch) and the coronary sinus (for evaluating atrioventricular junctional arrhythmias and accessory pathways). The multipolar electrodes provide detailed electroanatomical mapping of the sequence of excitation from the atria, atrioventricular junction and ventricles. The origin of supraventricular arrhythmias, ventricular tachycardias, accessory conduction pathways and re-entrant pathways can be identified and used to guide radiofrequency ablation.

Congenital conduction abnormalities

The majority of congenital conduction abnormalities used to have an anatomical basis for their origin, being the product of either accessory pathways or abnormal morphogenesis within the conduction tissue at any point from the atrioventricular node through the atrioventricular bundle. However today, conduction abnormalities are increasingly likely to relate to either long-standing haemodynamic problems and/or the effects of previous surgery for patients with congenital heart defects. This reflects the fact that although surgery for most of these defects has been available for the past four decades, surgery itself has not been curative and patients more often than not develop conduction abnormalities (and arrhythmia) secondary to haemodynamic problems (chamber dilation and/or hypertrophy), due to surgical scars. Very occasionally, conduction abnormalities are caused by tumours such as multifocal Purkinje cell tumours, or benign congenital polycystic tumours of the atrioventricular node.

VASCULAR SUPPLY AND LYMPHATIC DRAINAGE

Coronary arterial supply

The right and left coronary arteries arise from the ascending aorta in its anterior and left posterior sinuses (Figs 56.8, 56.9, 56.18A-E). The levels of the coronary ostia are variable. The two arteries, as indicated by their name, form an oblique inverted crown, in which an anastomotic circle in the atrioventricular groove is connected by marginal and interventricular (descending) loops intersecting at the cardiac apex (Fig. 56.18A–E). This is, of course, only an approximation. The degree of anastomosis varies and is usually insignificant. The main arteries and major branches are usually subepicardial, but those in the atrioventricular and interventricular grooves are often deeply sited, and occasionally hidden by overlapping myocardium or embedded in it.

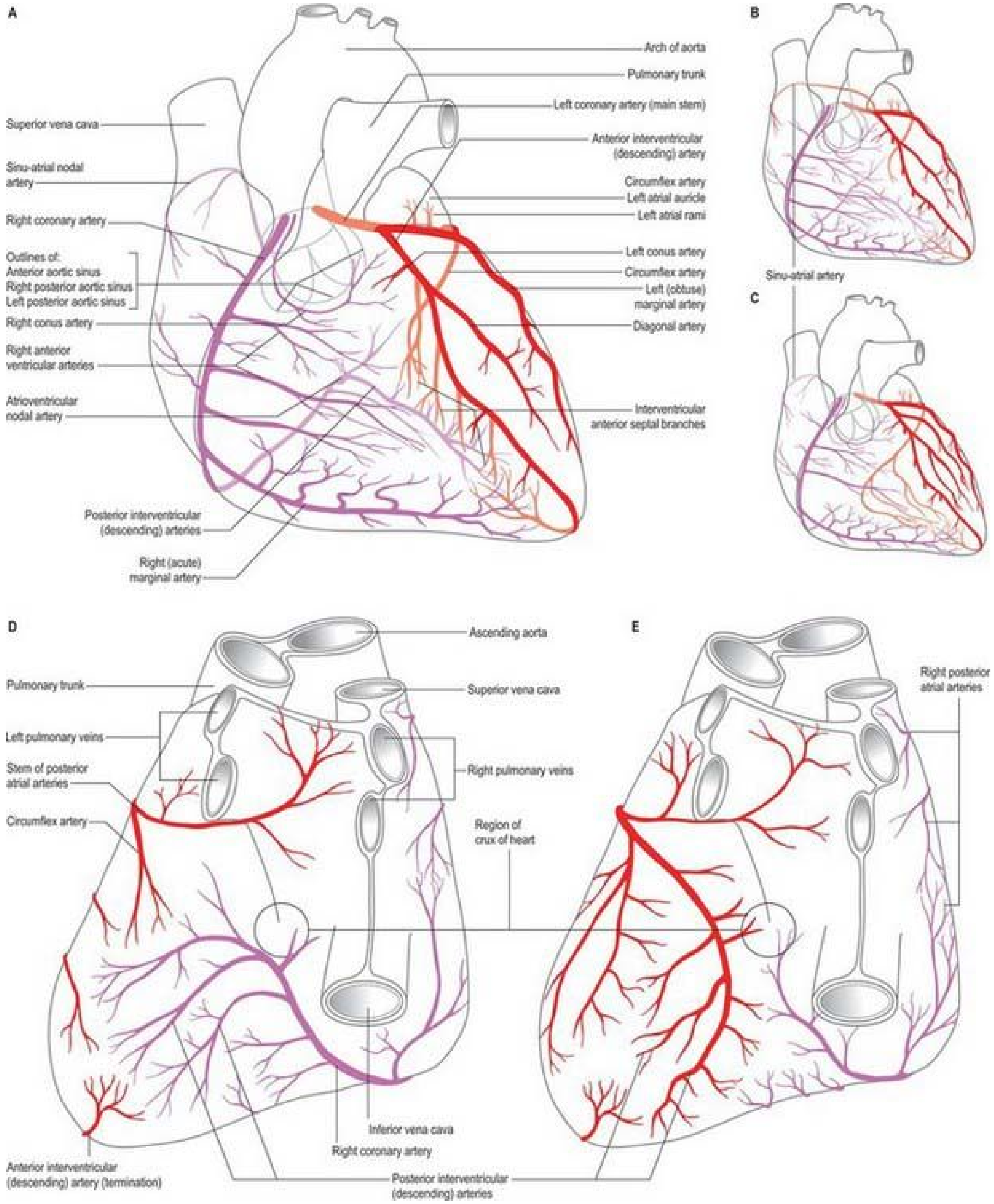
A
Arch of aorta
Pulmonary trunk
Left coronary artery (main stem)
Anterior interventricular (descending) artery
Circumflex artery
Left atrial auricle
Left atrial rami
Left conus artery
Circumflex artery
Left (obtuse) marginal artery
Diagonal artery
Interventricular anterior septal branches
Superior vena cava
Sinu-atrial nodal artery
Right coronary artery
Outlines of:
Anterior aortic sinus
Right posterior aortic sinus
Left posterior aortic sinus
Right conus artery
Right anterior ventricular arteries
Atrioventricular nodal artery
Posterior interventricular (descending) arteries
Right (acute) marginal artery
B
Sinu-atrial artery
C
D
Ascending aorta
Pulmonary trunk
Superior vena cava
Left pulmonary veins
Right pulmonary veins
Stem of posterior atrial arteries
Circumflex artery
Region of crux of heart
Inferior vena cava
Right coronary artery
Anterior interventricular (descending) artery (termination)
Posterior interventricular (descending) arteries
E
Right posterior atrial arteries

Fig. 56.18 Anterior views of the coronary arterial system, with the principal variations. The right coronary arterial tree is shown in magenta, the left in full red. In both cases posterior distribution is shown in a paler shade. **A**, The most common arrangement. **B**, A common variation in the

origin of the sinoatrial nodal artery. **C**, An example of left ‘dominance’ by the left coronary artery, showing also an uncommon origin of the sinu-atrial artery. Posteroinferior views of the coronary arterial system. The right coronary arterial tree is shown in magenta, the left in full red. **D**, An example of the more normal distribution in right ‘dominance’. **E**, A less common form of left ‘dominance’. In these ‘posterior’ views, the diaphragmatic (inferior) surface of the ventricular part of the heart has been artificially displaced and foreshortening ignored, to clarify the details of the so-called posterior (inferior) distribution of the coronary arteries.

The term ‘dominant’ is used to refer to the coronary artery giving off the posterior interventricular (descending) branch, which supplies the posterior part of the ventricular septum and often part of the posterolateral wall of the left ventricle. The dominant artery is usually the right (60%). Anastomoses between right and left coronary arteries are abundant during fetal life, but are much reduced by the end of the first year of life. Anastomoses providing collateral circulation may become prominent in conditions of hypoxia and in coronary artery disease. An additional collateral circulation is provided by small branches from mediastinal, pericardial and bronchial vessels.

The calibre of coronary arteries, both main stems and larger branches, based on measurements of arterial casts or angiograms, ranges between 1.5 and 5.5 mm for the coronary arteries at their origins. The left exceed the right in 60% of hearts, the right being larger in 17%, and both vessels being approximately equal in 23%. The diameters of the coronary arteries may increase up to the 30th year.

Right coronary artery

The right coronary artery arises from the anterior (‘right coronary’) aortic sinus: the ostium is below the margin of the cusps in 10%. The artery is usually single, but as many as four right coronary arteries have been observed. It passes at first anteriorly and slightly to the right between the right auricle and pulmonary trunk, where the sinus usually bulges. It reaches the atrioventricular groove and descends in this almost vertically to the right (acute) cardiac border, curving around it into the posterior part of the groove, where the latter approaches its junction with both interatrial and interventricular grooves, a region appropriately termed the crux of the heart. The artery reaches the crux and ends a little to the left of it, often by anastomosing with the circumflex branch of the left coronary artery. In a minority of individuals, the right coronary artery ends near the right cardiac border (10%), or between this and the crux (10%); more often (20%) it reaches the left border, replacing part of the circumflex artery.

Branches of the right coronary supply the right atrium and ventricle and, variably, parts of the left chambers and atrioventricular septum. The first branch (arising separately from the anterior aortic sinus in 36% of individuals) is the arteria coni arteriosi or conus artery. This is sometimes termed a ‘third coronary’ artery, but as a similar vessel comes from the left coronary, it is more correctly named the right conus artery. It ramifies anteriorly on the lowest part of the pulmonary conus and upper part of the right ventricle. It may anastomose with a similar left coronary branch from the left anterior descending artery to form the ‘anulus of Vieussens’, which is a tenuous anastomotic ‘circle’ around the right ventricular outflow tract.

The first segment of the right coronary artery (between its origin and the right margin of the heart) gives off anterior atrial and ventricular branches. These vessels diverge widely, approaching a right angle in the case of ventricular arteries, which is in marked contrast to the more acute origins of the left coronary ventricular branches. The anterior ventricular branches, usually two or three, ramify towards the cardiac apex, which they rarely reach unless the right marginal artery is included in this group of branches, as it is by some authors. The right marginal artery is greater in calibre than the other anterior ventricular arteries and long enough to reach the apex in most hearts (93%). When it is very large, the remaining anterior ventricular branches may be reduced to one, or may be absent. Up to three small posterior ventricular branches, commonly two, arise from the second segment of the right coronary artery between the right border and crux and supply the diaphragmatic aspect of the right ventricle. Their size is inversely proportional to that of the right marginal artery, which usually extends to the diaphragmatic surface of the heart. As the right coronary approaches the crux, it normally produces one to three posterior interventricular branches (occasionally there are none). One, the posterior interventricular artery, lies in the interventricular groove. It is usually single (70%), and flanked either to the right or left or bilaterally by parallel branches from the right coronary artery. When these flanking vessels exist, branches of the posterior interventricular artery are small and sparse. The posterior interventricular artery is replaced by a left coronary branch in 10% of individuals.

Although the atrial branches of the right coronary artery are sometimes described as anterior, lateral (right or marginal) and posterior groups, they are usually small single vessels 1mm in diameter. The right anterior and lateral branches are occasionally double, very rarely triple, and mainly supply the right atrium. The posterior branch is usually single and supplies the right and left atria. The artery of the sinoatrial node is an atrial branch, distributed largely to the myocardium of both atria, mainly the right. Its origin is variable: it comes from the circumflex branch of the left coronary in 35%. However, more commonly it arises from the anterior atrial branch of the right coronary artery, less often from its right lateral part, least often from its posterior atrioventricular part. This ‘nodal’ artery thus usually passes back in the groove between the right auricular appendage and aorta. Whatever its origin, it usually branches around the base of the superior vena cava, typically as an arterial loop from which small branches supply the right atrium. A large ‘ramus cristae terminalis’ traverses the sinu-atrial node (Fig. 56.18A–C); it would seem more appropriate to name this branch the ‘nodal artery’, as most of the currently named vessel actually supplies the atria and serves as the ‘main atrial branch’.

Septal branches of the right coronary artery are relatively short, and leave the posterior interventricular branch to supply the posterior interventricular septum. They are numerous, but do not usually reach the apical parts of the septum. The largest posterior septal artery, usually the first, commonly arises from the inverted loop which is said to characterize the right coronary artery at the crux. It supplies the atrioventricular node in 80% of hearts.

Small recurrent atrioventricular branches are given off from the ventricular branches of the right coronary artery as they cross the atrioventricular groove; they supply the adjoining atrial myocardium.

Left coronary artery

The left coronary artery is larger in calibre than the right, and supplies a greater volume of myocardium, including almost all the left ventricle and atrium, except in so-called ‘right dominance’, when the right coronary artery partly supplies a posterior region of the left ventricle (Fig. 56.18A-C). The left coronary artery usually supplies most of the interventricular septum. It arises from the left posterior (left ‘coronary’) aortic sinus; the ostium is below the margin of the cusps in 15%, and may be double, leading into major initial branches, usually the circumflex and anterior interventricular (descending) arteries. Its initial portion, between its ostium and its first branches, varies in length from a few millimetres to a few centimetres. The artery lies between the pulmonary trunk and the left atrial auricle, emerging into the atrioventricular groove, in which it turns left. This part is loosely embedded in subepicardial fat and usually has no branches, but may give off a small atrial ramus and, rarely, the sinu-atrial nodal artery.

Reaching the atrioventricular groove, the left coronary divides into two or three main branches: the anterior interventricular artery is commonly described as its continuation. This artery descends obliquely forward and to the left in the interventricular groove, sometimes deeply embedded in or crossed by bridges of myocardial tissue, and by the great cardiac vein and its tributaries. Almost invariably, it reaches the apex. It terminates there in one-third of specimens, but more often it turns round the apex into the posterior interventricular groove, and passes one-third to one-half of the way along its length, where it meets the terminal twigs of the posterior interventricular branches of the right coronary artery.

The anterior interventricular artery produces right and left anterior ventricular and anterior septal branches, and a variable number of corresponding posterior branches. Anterior right ventricular branches are small and rarely number more than one or two; the right ventricle is supplied almost wholly by the right coronary artery.

From two to nine large left anterior ventricular arteries branch at acute angles from the anterior interventricular artery and cross the anterior aspect of the left ventricle diagonally; larger terminals reach the rounded (obtuse) left border. One is often large and may arise separately from the left coronary trunk, which then ends by trifurcation. This left diagonal artery, reported in 33–50% or more individuals, is sometimes duplicated (20%). A small left conus artery frequently leaves the anterior interventricular artery near its origin, and anastomoses on the conus with its counterpart from the right coronary artery and with the vasa vasorum of the pulmonary artery and aorta. The anterior septal branches leave the anterior interventricular artery almost perpendicularly, and pass back and down in the septum, usually supplying its ventral two-thirds. Small posterior septal branches from the same source supply the posterior one-third of the septum for a variable distance from the cardiac apex.

The circumflex artery, comparable to the anterior interventricular artery in calibre, curves left in the atrioventricular groove, continuing round the left cardiac border into the posterior part of the groove and ending left of the crux in most hearts, but sometimes continuing as a posterior interventricular artery. Proximally, the left atrial auricle usually overlaps it. In 90%, a large ventricular branch, the left marginal artery, arises perpendicularly from the circumflex artery and ramifies over the rounded ‘obtuse’ margin, supplying much of the adjacent left ventricle, usually to the apex. Smaller anterior and posterior branches of the circumflex artery also supply the left ventricle. Anterior ventricular branches (from one to five, commonly two or three) course parallel to the diagonal artery, when it is present, and replace it when it is absent. Posterior ventricular branches are smaller and fewer; the left ventricle is partly supplied by the posterior interventricular artery. When this is small or absent, it is accompanied or replaced by an interventricular continuation of the circumflex artery, which is frequently double or triple. The circumflex artery may supply the left atrium via anterior, lateral and posterior atrial branches.

The circumflex artery has inconstant branches. The artery to the sinoatrial node (35%) is usually derived from the anterior circumflex segment, less often from the circum-marginal. It passes over and supplies the left atrium, encircling the superior vena cava like a right coronary nodal branch. It sends a large branch to (and through) the node, but is predominantly atrial in distribution. The artery to the atrioventricular node, the terminal branch in 20%, arises near the crux, in which case the circumflex usually supplies the posterior interventricular artery, an example of so-called ‘left dominance’. Kugel’s anastomotic artery (‘arteria anastomotica auricularis magna’) has been described as a constant circumflex branch, usually from its anterior part, which traverses the interatrial septum (near its ventricular border) to establish direct or indirect anastomosis with the right coronary; its existence has been questioned.

Coronary distribution

Details of coronary distribution require integration into a concept of total cardiac supply. Most commonly, the right coronary artery supplies all of the right ventricle (except a small region to the right of the anterior interventricular groove); a variable part of the diaphragmatic aspect of the left ventricle; the posteroinferior one-third of the intraventricular septum; the right atrium and part of the left atrium; the conduction system as far as the proximal parts of the right and left crura. Left coronary distribution is reciprocal, and includes most of the left ventricle; a narrow strip of right ventricle; the anterior two-thirds of the interventricular septum; most of the left atrium. As noted previously (Fig. 56.18A–E), variations in the coronary arterial system mainly affect the diaphragmatic aspect of the ventricles and reflect the relative ‘dominance’ of supply by the left or the right coronary artery. The term is misleading, because the left artery almost always supplies a greater volume of tissue than the right. In ‘right dominance’, the posterior interventricular artery is derived from the right coronary artery; in ‘left dominance’ it is derived from the left coronary artery. In the so-called ‘balanced’ pattern, branches of both arteries run in or near the posterior interventricular groove.

Less is known about variations in atrial supply because the small vessels involved are not easily preserved in the corrosion casts that are used for analysis. In more than 50% of individuals, the right atrium is supplied only by the right coronary artery, and in the remainder the supply is dual. More than 62% of left atria are supplied mainly by the left coronary artery, 27% by the right coronary artery (in each group a small accessory supply from the other coronary artery exists), and 11% are supplied almost equally by both arteries. Sinu-atrial and atrioventricular supplies also vary. The sinu-atrial node is supplied by the right (51–65%) or left (35–45%) coronary arteries, and fewer than 10% of nodes receive a bilateral supply. The atrioventricular node is supplied by the right (80–90%) or left (10–20%) coronary arteries.

Coronary anastomosis

Anastomoses between branches of the coronary arteries, both subepicardial and myocardial, and between these arteries and extracardiac vessels, are of prime medical importance. Clinical experience suggests that anastomoses cannot rapidly provide collateral routes sufficient to circumvent sudden coronary obstruction, and the coronary circulation is assumed to be end-arterial. Nevertheless, it has long been established that anastomoses do occur, particularly between fine subepicardial branches, and they may increase during individual life. Analyses of coronary radiographs and resin corrosion casts, and the results of radio-opaque perfusion studies, have revealed intra- and inter-coronary anastomoses in vessels up to 100–200 μm in calibre. The most frequent sites of extramural anastomoses are the apex, the anterior aspect of the right ventricle, the posterior aspect of the left ventricle, crux, interatrial and interventricular grooves, and between the sinoatrial nodal and other atrial vessels. The functional value of such anastomoses must vary, but they appear to become more effective in slowly progressive pathological conditions. Their structure is uncertain: most observations that have been made on corrosion casts suggest that anastomotic vessels are relatively straight in normal hearts, but greatly coiled in hearts that have been subject to coronary occlusion. Little has been recorded of their microscopic structure;

they appear little more than endothelial tubes, without muscles or elastic tissue.

Extracardiac anastomoses may connect various coronary branches with other thoracic vessels via the pericardial arteries and arterial vasa vasora of vessels which link the heart with the systemic and pulmonary circulations. The effectiveness of these connections as collateral routes in coronary occlusion is unpredictable.

Coronary arteriovenous anastomoses and numerous connections between the coronary circulation and cardiac cavities, producing so-called ‘myocardial sinusoids’ and ‘arterioluminal’ vessels, have been reported; their importance in coronary disease is uncertain.

Coronary artery disease

Atherosclerosis is characterized by deposition of lipid and accumulation of macrophages in the intima. Endothelial dysfunction leads to the recruitment of inflammatory cells into the vascular wall and the release of various cytokines and adhesion molecules which propagate the process of atherosclerosis. Lipid accumulation and smooth muscle proliferation lead to the formation of an atheromatous plaque. The formation of the plaque itself may cause stenosis of the coronary arteries, and reduces coronary blood flow (classically on exertion). The plaques are also susceptible to rupture with concomitant thrombus formation, which leads to acute occlusion of one of the coronary arteries and may cause myocardial infarction. Plaques may rupture as a result of fatigue within the fibrous cap, but are also more vulnerable when the lipid content is greater than 40% of the composition of the plaque. Superficial erosion of the plaque may also promote critical thrombus formation.

Assessment of coronary artery disease is possible via a number of radiological techniques, including MRI, positron emission tomography, scintigraphy and ultrasound, and invasively by coronary arteriography (which displays the anatomy and delineates regions of stenosis).

Coronary angiography

Coronary angiography may be performed by introducing a catheter through the femoral, radial or brachial arteries. The femoral artery is punctured with a needle 3 cm below the inguinal ligament while the leg is held adducted and slightly externally rotated. The exact position is guided by palpation of the femoral arterial pulse, and the needle is inserted at an angle of 45°. After arterial puncture, a fine guidewire is inserted through the needle and fed into the artery. The catheter is then inserted over the guidewire and manipulated via the iliac artery into the aorta, up the aortic arch and located in the ascending aorta. The brachial or radial artery may be used for percutaneous access to the circulation. Once the catheter is located in the ascending aorta, a variety of guidewires (straight tip, left and right curved catheters, and pigtail catheters) are used to enter the coronary vessels for selective arteriography and interventions. Angiography is performed with standard high osmolality contrast medium with cineangiography. In selected patients, new-generation low osmolality contrast medium may also be used. All the coronary arteries are catheterized and evaluated in a variety of views to obtain a full evaluation of their anatomy and to determine the location and degree of any stenoses. The ostium of the left coronary artery arises from the left sinus and is best viewed in the direct frontal and left anterior oblique directions. The right anterior oblique view is useful in demonstrating the diagonal branches and anterior interventricular (descending) coronary artery. The right coronary artery originates from the right sinus of Valsalva and is usually visualized in the right anterior oblique and left anterior oblique views. Pressure and oxygen saturations can be measured via the catheter. Changes in pressure across valves allow the degree of stenosis to be measured. Coronary blood flow and relative flow reserve can also be calculated. Significant stenosis may be treated initially by balloon angioplasty followed by insertion of stents. The balloon exerts pressure against the plaque in the arterial wall and fractures and splits the plaque. The splinting effect of the plaque and elastic recoil are reduced, resulting in an increase in the arterial lumen. Insertion of a stent reduces the rate of re-stenosis.

Coronary revascularization

Atherosclerosis causing greater than 60% stenosis of the terminal diameter of the coronary arteries is likely to cause a significant reduction in myocardial perfusion. Patients with high-grade lesions or left main-stem coronary artery or triple-vessel disease with impaired left ventricular function are usually considered for coronary artery bypass grafting. The common grafts that are used are the saphenous veins and internal thoracic (mammary) arteries. Other grafts that are occasionally used are the radial, ulnar, gastroepiploic and inferior epigastric arteries.

The left internal thoracic artery grafts have a greater patency rate than saphenous vein grafts. Approximately 15% of saphenous vein grafts occlude in 1 year and from then on at an annual rate of 1–2% in the first 6 years and 4% thereafter; 40–50% of saphenous vein grafts have occluded by 10 years. In contrast, only about 10% of left internal thoracic artery grafts will have occluded at 10 years.

The common surgical approach is via a midline sternotomy. If the internal thoracic artery is used as a donor graft, it is divided distally (maintaining its proximal origin from the subclavian artery) and anastomosed to the coronary artery distal to the stenosis. If saphenous vein grafts are used, they must be anastomosed both proximal and distal to the coronary artery, to bridge the site of the stenosis.

In selected cases, minimally invasive direct coronary artery bypass grafting is performed, but the approach is dependent on the vessel being grafted. The anterior approach is via mini-thoracotomy over the fourth intercostal space underneath the nipple for grafting the mid-left anterior interventricular (descending) and diagonal branches. The anterolateral approach is via an incision in the third intercostal space from the midclavicular line to the anterior axillary line and is used for grafting early marginal branches of the circumflex system. The lateral approach allows grafting of the circumflex vessels via a lateral thoracotomy measuring only 10 cm in size through the fifth or sixth intercostal space. Extrathoracic approaches that are occasionally used include the subxiphoid approach for the distal right coronary artery and posterior interventricular (descending) artery. Port access surgery allows for full re-vascularization with cardiopulmonary bypass, but obviates the need for midline sternotomy.

Cardiac veins

The heart is drained by the coronary sinus and its tributaries, the anterior cardiac veins and the small cardiac veins. The coronary sinus and its tributaries return blood to the right atrium from the entire heart (including its septa) except for the anterior region of the right ventricle and small, variable parts of both atria and the left ventricle. The anterior cardiac veins drain an anterior region of the right ventricle and, when the right marginal vein joins this group, a region around the right cardiac border, and end principally in the right atrium. The small cardiac veins (Thebesius' veins) open into the right atrium and ventricle and, to a lesser extent, the left atrium and sometimes the left ventricle.

Variation in cardiac veins

Attempts to categorize variations in cardiac venous circulation into 'types' have not produced any accepted pattern. There are major variations concerning the general directions of drainage. The coronary sinus may receive all the cardiac veins (except the small veins), including the anterior cardiac veins (33%), which may be reduced by diversion of some into the small cardiac vein and then to the coronary sinus (28%). The remainder (39%) represents the 'normal' pattern, as described above.

Coronary sinus

The large majority of cardiac veins drain into the wide coronary sinus, 2 or 3 cm long, lying in the posterior atrioventricular groove between the left atrium and ventricle (Fig. 56.2B,D; Fig. 56.19). The sinus opens into the right atrium between the opening of the inferior vena cava and the right atrioventricular orifice; the opening is guarded by an endocardial fold (semilunar valve of the coronary sinus; Fig. 56.4A). Its tributaries are the great, small and middle cardiac veins, the posterior vein of the left ventricle and the oblique vein of the left atrium; all except the last have valves at their orifices.

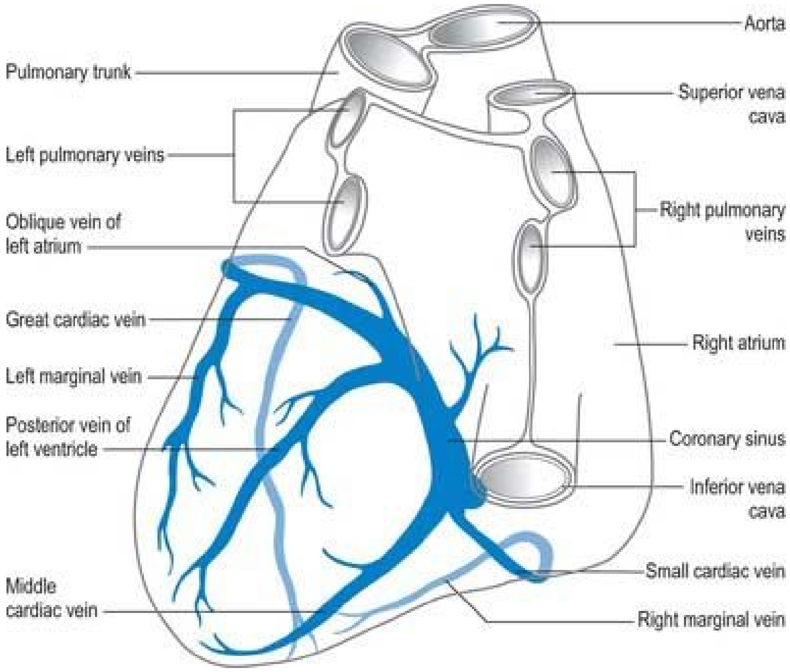
Pulmonary trunk
Left pulmonary veins
Oblique vein of left atrium
Great cardiac vein
Left marginal vein
Posterior vein of left ventricle
Middle cardiac vein
Aorta
Superior vena cava
Right pulmonary veins
Right atrium
Coronary sinus
Inferior vena cava
Small cardiac vein
Right marginal vein

Fig. 56.19 The principal veins of the heart.

Great cardiac vein

The great cardiac vein begins at the cardiac apex, ascends in the anterior interventricular groove to the atrioventricular groove and follows this, passing to the left and posteriorly to enter the coronary sinus at its origin (Fig. 56.19). It receives tributaries from the left atrium and both ventricles, including the large left marginal vein that ascends the left aspect (obtuse border) of the heart.

Small cardiac vein

The small cardiac vein lies in the posterior atrioventricular groove between the right atrium and ventricle and opens into the coronary sinus near its atrial end (Fig. 56.19). It receives blood from the posterior part of the right atrium and ventricle. The right marginal vein passes right, along the inferior cardiac margin (acute border). It may join the small cardiac vein in the atrioventricular groove, but more often opens directly into the right atrium.

Middle cardiac vein

The middle cardiac vein (Fig. 56.19) begins at the cardiac apex, and runs back in the posterior interventricular groove to end in the coronary sinus near its atrial end.

Posterior vein of the left ventricle

The posterior vein of the left ventricle (Fig. 56.19) is found on the diaphragmatic surface of the left ventricle a little to the left of the middle cardiac vein. It usually opens into the centre of the coronary sinus, but sometimes opens into the great cardiac vein.

Oblique vein of the left atrium

The small vessel that is the oblique vein of the left atrium (Fig. 56.19) descends obliquely on the back of the left atrium to join the coronary sinus near its end. It is continuous above with the ligament of the left vena cava. The two structures are remnants of the left common cardinal vein.

Anterior cardiac veins

The anterior cardiac veins drain the anterior part of the right ventricle (Figs 56.2A,C; 56.8). Usually two or three, sometimes even five, they ascend in subepicardial tissue to cross the right part of the atrioventricular groove, passing deep or superficial to the right coronary artery. They end in the right atrium, near the groove, separately or in variable combinations. A subendocardial collecting channel, into which all may open, has been described. The right marginal vein courses along the inferior (acute) cardiac margin, draining adjacent parts of the right ventricle, and usually opens separately into the right atrium. It may join the anterior cardiac veins or, less often, the coronary sinus. Because it is commonly independent, it is often grouped with the small cardiac veins, but it is larger in calibre, being comparable to the anterior cardiac veins or even wider.

Small cardiac veins

The existence of small cardiac veins, opening into all cardiac cavities, has been confirmed, but they are more difficult to demonstrate than larger cardiac vessels. Their numbers and size are highly variable: up to 2 mm in diameter opening into the right atrium and 0.5 mm into the right ventricle. Numerous small cardiac veins have been identified in the right atrium and ventricle, but they are rare in the left atrium and left ventricle.

Cardiac venous anastomosis

There are widespread anastomoses at all levels of the cardiac venous circulation, on a scale exceeding that of the arteries and amounting to a veritable venous plexus. Not only are adjacent veins often connected, but connections also exist between tributaries of the coronary sinus and those of the anterior cardiac veins. Abundant anastomoses occur at the apex and its anterior and posterior aspects. Like coronary arteries, cardiac veins connect with extracardiac vessels, chiefly the vasa vasorum of the large vessels continuous with the heart.

Lymphatic drainage of the heart

Cardiac lymphatic vessels form subendocardial, myocardial and subepicardial plexuses, the first two draining into the third. Efferents from the subepicardial plexuses form the left and right cardiac collecting trunks. Two or three left trunks ascend the anterior interventricular groove, receiving vessels from both ventricles. On reaching the atrioventricular groove, they are joined by a large vessel from the diaphragmatic surface of the left ventricle, which first ascends in the posterior interventricular groove and then turns left along the atrioventricular groove. The vessel formed by this union ascends between the pulmonary artery and the left atrium, and usually ends in an inferior tracheobronchial node. The right trunk receives afferents from the right atrium and the right border and diaphragmatic surface of the right ventricle. It ascends in the atrioventricular groove, near the right coronary artery, and then anterior to the ascending aorta to end in a brachiocephalic node, usually on the left.

INNERVATION

Initiation of the cardiac cycle is myogenic, originating in the sinu-atrial node. It is harmonized in rate, force and output by autonomic nerves which operate on the nodal tissues and their prolongations, on coronary vessels and on the working atrial and ventricular musculature. All the cardiac branches of the vagus (parasympathetic) and all the sympathetic branches (except the cardiac branch of the superior cervical sympathetic ganglion) contain both afferent and efferent fibres; the cardiac branch of the superior cervical sympathetic ganglion is entirely efferent. Sympathetic fibres accelerate the heart and dilate the coronary arteries when stimulated, whereas vagal fibres slow the heart and cause constriction of the coronary arteries.

Preganglionic cardiac sympathetic axons arise from neurones in the intermediolateral column of the upper four or five thoracic spinal segments. Some synapse in the corresponding upper thoracic sympathetic ganglia, others ascend to synapse in the cervical ganglia; postganglionic fibres from these ganglia form the sympathetic cardiac nerves.

Preganglionic cardiac parasympathetic axons arise from neurones in either the dorsal vagal nucleus or near the nucleus ambiguus; they run in vagal cardiac branches to synapse in the cardiac plexuses and atrial walls. In man (like most mammals) intrinsic cardiac neurones are limited to the atria and interatrial septum, and are most numerous in the subepicardial connective tissue near the sinu-atrial and atrioventricular nodes. There is evidence that these intrinsic ganglia are not simple nicotinic relays, but may act as sites for integration of extrinsic nervous inputs and form complex circuits for the local neuronal control of the heart, and perhaps even local reflexes.

Cardiac plexus

Nearing the heart, the autonomic nerves form a mixed cardiac plexus, usually described in terms of a superficial component inferior to the aortic arch lying between it and the pulmonary trunk, and a deep part between the aortic arch and tracheal bifurcation. The cardiac plexus is also described by regional names for its coronary, pulmonary, atrial and aortic extensions (Fig. 56.20). These plexuses contain ganglion cells. Ganglion cells, confined to the atrial tissues, and with a preponderance adjacent to the sinu-atrial node, are also found in the heart along the distribution of branches of the plexus. Their axons are considered to be largely, if not exclusively, postganglionic parasympathetic. Cholinergic and adrenergic fibres, arising in or passing through the cardiac plexus, are distributed most profusely to the sinu-atrial and atrioventricular nodes; the supply to the atrial and ventricular myocardium is much less dense. Adrenergic fibres supply the coronary arteries and cardiac veins. Rich plexuses of nerves containing cholinesterase, adrenergic transmitters and other peptides, e.g. neuropeptide Y, are found in the subendocardial regions of all chambers and in the cusps of the valves.

Superficial (ventral) part of the cardiac plexus

The superficial (ventral) part of the cardiac plexus lies below the aortic arch and anterior to the right pulmonary artery. It is formed by the cardiac branch of the left superior cervical sympathetic ganglion and the lower of the two cervical cardiac branches of the left vagus. A small cardiac ganglion is usually present in this plexus immediately below the aortic arch, to the right of the ligamentum arteriosum. This part of the cardiac plexus connects with the deep part, the right coronary plexus and the left anterior pulmonary plexus.

Deep (dorsal) part of the cardiac plexus

The deep (dorsal) part of the cardiac plexus is anterior to the tracheal bifurcation, above the point of division of the pulmonary trunk and posterior to the aortic arch. It is formed by the cardiac branches of the cervical and upper thoracic sympathetic ganglia and of the vagus and recurrent laryngeal nerves. The only cardiac nerves that do not join it are those that join the superficial part of the plexus.

Branches from the right half of the deep part of the cardiac plexus pass in front of and behind the right pulmonary artery. Those anterior to it, the more numerous, supply a few filaments to the right anterior pulmonary plexus and continue on to form part of the right coronary plexus. Those behind the pulmonary artery supply a few filaments to the right atrium and then continue into the left coronary plexus. The left half of the deep part of the cardiac plexus is connected with the superficial, and supplies filaments to the left atrium and left anterior pulmonary plexus. It forms much of the left coronary plexus.

Left coronary plexus

The left coronary plexus is larger than the right, and is formed chiefly by the prolongation of the left half of the deep part of the cardiac plexus and a few fibres from the right. It accompanies the left coronary artery to supply the left atrium and ventricle.

Right coronary plexus

The right coronary plexus is formed from both superficial and deep parts of the cardiac plexus, and accompanies the right coronary artery to supply the right atrium and ventricle.

Atrial plexuses

The atrial plexuses are derivatives of the right and left continuations of the cardiac plexus along the coronary arteries. Their fibres are distributed to the corresponding atria, overlapping those from the coronary plexuses.

MAJOR BLOOD VESSELS

The major blood vessels comprise the pulmonary trunk, the thoracic aorta and its branches, the superior and inferior venae cavae and their tributaries.

ARTERIES

Pulmonary trunk

The pulmonary trunk, or pulmonary artery, conveys deoxygenated blood from the right ventricle to the lungs (Fig. 56.2A,C; see Fig. 57.8). About 5 cm in length and 3 cm in diameter, it is the most anterior of the cardiac vessels and arises from the base of the right ventricle (from the pulmonary anulus surmounting the conus arteriosus) above and to the left of the supraventricular crest. It slopes up and back, at first in front of the ascending aorta, then to its left. Below the aortic arch it divides, level with the fifth thoracic vertebra and to the left of the midline, into right and left pulmonary arteries of almost equal size. The pulmonary trunk bifurcation lies below, in front and to the left of the tracheal bifurcation (which is also associated with the inferior tracheobronchial lymph nodes and the deep cardiac nerve plexus). In the fetus, at the level of the bifurcation the pulmonary artery is connected to the aortic arch by the ductus arteriosus, which lies in the same direction as the pulmonary artery.

Relations

The pulmonary artery is entirely within the pericardium, enclosed with the ascending aorta in a common tube of visceral pericardium. The fibrous pericardium gradually disappears within the adventitia of the pulmonary arteries. Anteriorly, it is separated from the sternal end of the left second intercostal space by the pleura, left lung and pericardium. Posterior are the ascending aorta and left coronary artery initially, then the left atrium. The ascending aorta ultimately lies on its right. An auricle and coronary artery lie on each side of its origin. The superficial cardiac plexus is between the pulmonary bifurcation and the aortic arch. The tracheal bifurcation, lymph nodes and nerves are above, bilateral and right.

During fetal life, when blood pressure is similar in the pulmonary artery and the aorta, the structure of the vessels is similar. After birth, the lungs expand and pulmonary arterioles dilate, and so pulmonary vascular resistance decreases, whereas blood flow increases. The systolic pressure in the pulmonary artery consequently decreases and this is accompanied by a structural remodelling of its wall. The elastic material, which originally had a lamellar structure, becomes aggregated into star-shaped units linked to many muscle cells. The amount of muscular tissue grows extensively after birth and exceeds that found in the aorta. The thickness of the wall of the aorta is about twice that of the pulmonary artery.

Right and left pulmonary arteries

The pulmonary arteries are described on page 996.

Thoracic aorta

Ascending aorta

The ascending aorta is typically 5 cm long and begins at the base of the left ventricle, level with the lower border of the third left costal cartilage; it ascends obliquely, curving forwards and to the right, behind the left half of the sternum to the level of the upper border of the second left costal cartilage (Figs 56.2A, B, 56.8, 56.18A-C; see Figs 53.2, 57.8). At its origin, proximal to the aortic anulus, the sectional profile is larger and not circular because of three almost hemispherical outward bulges (sinuses of Valsalva), one posterior (non-coronary), one left and one right, which correspond to the three cusps of the aortic valve (see above). Distal to the aortic anulus there are three aortic sinuses, beyond which the calibre of the vessel is slightly increased by a bulging of its right wall. This aortic bulb gives the vessel an oval section.

Relations

The ascending aorta is within the fibrous pericardium, enclosed in a tube of serosal pericardium with the pulmonary trunk (Figs 56.1, 56.2A,C). Anterior to its lower part are the infundibulum, the initial segment of the pulmonary trunk and the right auricle. Superiorly, it is separated from the sternum by the pericardium, right pleura, anterior margin of the right lung, loose areolar tissue and the remains of the thymus gland. Posterior are the left atrium, right pulmonary artery and principal bronchus. Right lateral are the superior vena cava and right atrium, the former partly posterior, and left lateral are the left atrium and, at a higher level, the pulmonary trunk. At least two structures, aorticopulmonary bodies (reminiscent of the carotid arterial chemoreceptors and baroreceptors), lie between the ascending aorta and the pulmonary trunk. The inferior aorticopulmonary body is near the heart and anterior to the aorta, and the middle aorticopulmonary body is near the right side of the ascending aorta.

Aortic arch

The aortic arch continues from the ascending aorta (Figs 56.1, 56.2A,C). Its origin, slightly to the right, is level with the upper border of the second right sternocostal joint. The arch first ascends diagonally back and to the left over the anterior surface of the trachea, then back across its left side and finally descends to the left of the fourth thoracic vertebral body, continuing as the descending thoracic aorta. It ends level with the sternal end of the second, left costal cartilage. Thus the aortic arch lies wholly in the superior mediastinum. It curves around the hilum of the left lung, and extends upwards to the mid level of the manubrium of the sternum. The shadow of the arch is easily identified in anteroposterior radiographs and its left profile is sometimes called the ‘aortic knuckle’ (see Fig. 55.16). The arch may also be visible in left anterior oblique views enclosing a pale space, ‘the aortic window’, in which shadows of the pulmonary trunk and its left branch may be discerned. Its diameter at the origin is the same as in the ascending aorta, 28 mm, but it is reduced to 20 mm at the end, after the issue of its large collateral branches. At the border with the thoracic aorta, a small stricture (aortic isthmus), followed by a dilatation, can be recognized. In fetal life the isthmus lies between the origin of the left subclavian artery and the opening of the ductus arteriosus.

Relations

Anteriorly and to the left of the aortic arch is the left mediastinal pleura. Deep to the pleura it is crossed, in anteroposterior order by: the left phrenic nerve, left lower cervical cardiac branch of the vagus, left superior cervical cardiac branch of the sympathetic and left vagus (Figs 56.1, 56.20). As the left vagus crosses the arch, its recurrent laryngeal branch hooks below the vessel left and behind (developmentally caudal to) the ligamentum arteriosum and then ascends on the right of the arch. The left superior intercostal vein ascends obliquely forwards on the arch, superficial to the left vagus, deep to the left phrenic nerve. The left lung and pleura separate all these from the thoracic wall. Posterior and to the right are the trachea and deep cardiac plexus, the left recurrent laryngeal nerve, oesophagus, thoracic duct and vertebral column. Above, the brachiocephalic, left common carotid and left subclavian arteries arise from its convexity, and are crossed anteriorly near their origins by the left brachiocephalic vein. Below are the pulmonary bifurcation, left principal bronchus, ligamentum arteriosum, superficial cardiac plexus and left recurrent laryngeal nerve. Best viewed from the left, the concavity of the aortic arch is the upper curved limit through which structures gain access to or leave the hilum of the left lung.

Variations of the arch and its branches

The summit of the arch is usually about 2.5 cm below the superiosternal border, but may diverge from this. In the infant it is closer to the upper border of the sternum; the same is often the case in old age, because of the dilatation of the vessel. Sometimes the aorta curves over the right pulmonary hilum and descends to the right of the vertebral column. This is usually accompanied by transposition of thoracic and abdominal viscera. Less often, after arching over the right hilum, it passes behind the oesophagus to gain its usual position (this is not accompanied by visceral transposition). The aorta may divide into ascending and descending trunks, the former dividing into three branches to supply the head and upper limbs. Sometimes it divides near its origin, the two branches soon reuniting, and the oesophagus and trachea usually pass through the interval between them.

Branches

Three branches arise from the convex aspect of the arch: the brachiocephalic trunk, left common carotid and left subclavian arteries (Figs 56.1, 56.2A-D).

They may branch from the beginning of the arch or the upper part of the ascending aorta. The distance between these origins varies, the most frequent being approximation of the left common carotid artery to the brachiocephalic trunk.

Primary branches from the aortic arch may be reduced to one, but more commonly two. The left common carotid may arise from the brachiocephalic trunk (7%). More rarely, the left common carotid and subclavian arteries may arise from a left brachiocephalic trunk, or the right common carotid and right subclavian may arise separately, in which case the latter more often branches from the left end of the arch and passes behind the oesophagus. The left vertebral artery may arise between the left common carotid and the subclavian arteries. Very rarely, external and internal carotid arteries arise separately, the common carotid being absent on one or both sides, or both carotids and one or both vertebral arteries may be separate branches. When a ‘right aorta’ occurs, the arrangement of its three branches is reversed. The common carotids may have a single trunk. Other arteries may branch from it, most commonly one or both bronchial arteries and the thyroid ima artery.

An analysis of variation in branches from 1000 aortic arches showed the usual pattern in 65%; a left common carotid shared the brachiocephalic trunk in 27% (contrast percentage quoted above) and the four large arteries branched separately in 2.5%. The remaining 5% showed a great variety of patterns, the most common (1.2%) being symmetric right and left brachiocephalic trunks.

Coarctation of the aorta

The aortic lumen is occasionally partly or completely obliterated, either above (preductal or infantile type), opposite, or just beyond (postductal or adult type), the entry of the ductus arteriosus. In the preductal type, the length of coarctation is variable, aortic arch hypoplasia is common and the left subclavian and even the brachiocephalic artery may be involved. Severe forms of infantile coarctation and its extreme form (aortic interruption) may be patent ductus arteriosus dependent, as there is no time for effective collateral circulation to develop. Prostaglandin infusion prior to transfer, and surgery at a tertiary centre, often provide a very good mid- to long-term outlook for such infants.

The postductal type of coarctation has been attributed to abnormal extension of the ductal tissue into the aortic wall, stenosing both vessels as the duct contracts after birth. This form can permit years of normal life, allowing the development of an extensive collateral circulation to the aorta distal to the stenosis (Fig. 56.21). High vascularity of the thoracic wall is important and clinically characteristic; many arteries arising indirectly from the aorta, proximal to the coarctation segment, anastomose with vessels connected with it distal to the block, and all of these vessels become greatly enlarged. Thus, in the anterior thoracic wall, the thoraco-acromial, lateral thoracic and subscapular arteries (from the axillary artery), the suprascapular artery (from the subclavian artery), and the first and second posterior intercostal arteries (from the costocervical trunk), anastomose with other posterior intercostal arteries, and the internal thoracic artery and its terminal branches anastomose with the lower posterior intercostal and inferior epigastric arteries. Posterior intercostal arteries are always involved, and enlargement of their dorsal branches may eventually groove (‘notch’) the inferior margins of the ribs. The radiographic shadow of the enlarged left subclavian artery is also increased. Enlargement of the scapular vessels and anastomoses may lead to widespread interscapular pulsation (easily appreciated with the palm of the hand, and sometimes heard on auscultation).

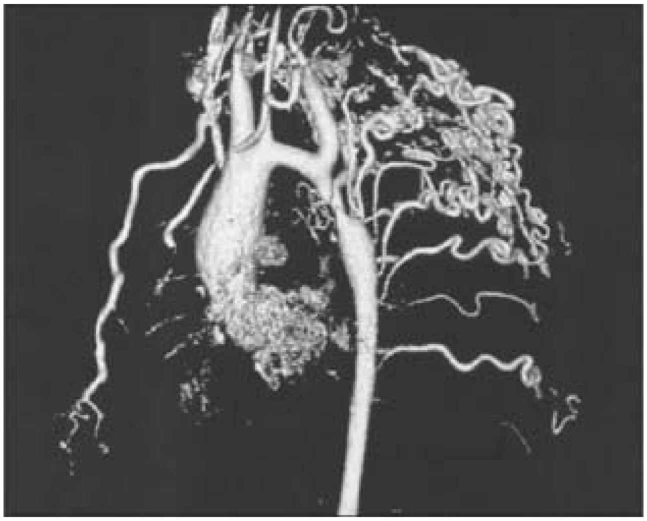

Fig. 56.21 Cardiac magnetic resonance angiography showing 3D reconstruction of native aortic coarctation in an adult patient with extensive collateral flow. Note the marked dilatation of the left subclavian artery, supplying most of the collateral vessels and mild aortic arch hypoplasia.

(By courtesy of Dr Raad Mohiaddin, Royal Brompton Hospital, London.)

Aortic aneurysm formation

An aneurysm (abnormal dilatation) may form in any part of the aorta. Degeneration of the medial wall of the aorta and intimal dissection occur in the majority of thoracic aneurysms, particularly affecting the ascending aorta and aortic arch. These are often the result of abnormalities of connective tissue such as occur in Marfan’s syndrome, homocysteinuria and Ehlers–Danlos syndrome, or may relate to a bicuspid aortic valve or be secondary to syphilis. Descending aortic aneurysms are generally caused by atherosclerosis (90%); the remainder result from mycotic disease or trauma. Some aortic aneurysms are incidental findings on chest X-rays or computed tomography scans. Symptomatic cases present with breathlessness, chest pain, back pain, hoarse voice, cough and haemoptysis. Early diastolic murmurs may be audible on cardiac auscultation and are caused by aortic regurgitation. Repair is carried out in patients with symptoms or fusiform dilatation measuring more than 5 cm in diameter.

Aortic dissection

Aortic dissection occurs as a result of degeneration of the medial aspect of the aortic wall as a result of ageing, persistent hypertension or in fibrillin diseases such as Marfan’s disease. An intimal tear may occur, producing a split into the medial wall, which creates a false lumen. These cases present acutely with severe retrosternal or intrascapular chest pain. Depending on the extent of the dissection, they may be associated with neurological signs, diarrhoea or leg weakness. Extension into the pericardium causes cardiac tamponade and circulatory collapse. Diagnosis is established by echocardiography and on contrast-enhanced computed tomography or magnetic resonance scans. Surgical repair is essential for ascending aortic or aortic arch dissection.

Brachiocephalic artery

The brachiocephalic (innominate) artery, the largest branch of the aortic arch, is 4–5 cm in length (Fig. 56.2A,C; see Fig. 28.14). It arises from the convexity of the arch posterior to the centre of the manubrium of sternum, and ascends posterolaterally to the right, at first anterior to the trachea, then on its right. Level with the upper border of the right sternoclavicular joint, it divides into the right common carotid and right subclavian arteries.

Relations

Sternohyoid and sternothyroid, the remains of the thymus, left brachiocephalic and right inferior thyroid veins, crossing its root, and sometimes the right cardiac branches of the vagus, all separate the brachiocephalic artery from the manubrium. Posterior are the trachea (superiorly) and the right pleura (inferiorly). The right vagus is posterolateral before passing lateral to the trachea. Right lateral are the right brachiocephalic vein, the upper part of the superior vena cava and pleura, and left lateral are the thymic remains, the origin of the left common carotid artery, the inferior thyroid veins and the trachea.

Branches

The brachiocephalic artery usually has only terminal branches, the right common carotid and right subclavian artery. Occasionally a thymic or bronchial branch, or a thyroidea ima artery, arises from it. The thyroidea ima artery is a small and inconstant artery which may arise from the aorta, right common carotid, subclavian or internal thoracic arteries; it ascends on the trachea to the thyroid isthmus, where it terminates.

Descending thoracic aorta

The thoracic aorta is the segment of descending aorta confined to the posterior mediastinum (see Fig. 55.4B). It begins level with the lower border of the fourth thoracic vertebra, continuous with the aortic arch, and ends anterior to the lower border of the 12th thoracic vertebra in the diaphragmatic aortic aperture. At its origin it is left of the vertebral column, as it descends it approaches the midline, and at its termination is directly anterior to it.

Relations

Anterior to the descending thoracic aorta, from above down, are the left pulmonary hilum, the pericardium separating it from the left atrium, oesophagus and diaphragm. Posterior are the vertebral column and hemiazygos veins. Right lateral are the azygos and thoracic duct and below, the right pleura and lung, and left lateral are the pleura and lung. The oesophagus, with its plexus of nerves, is right lateral above, but becomes anterior in the lower thorax, and close to the diaphragm it is left anterolateral. To a limited degree, the descending aorta and oesophagus are mutually spiralized.

Surface anatomy

The descending thoracic aorta may be projected as a 2.5 cm broad band from the sternal end of the second left costal cartilage to a median position 2 cm above the transpyloric plane.

Branches

The thoracic aorta provides visceral branches to the pericardium, lungs, bronchi and oesophagus, and parietal branches to the thoracic wall.

Pericardial branches

A few small vessels are distributed to the posterior aspect of the pericardium.

Bronchial arteries

Bronchial arteries vary in number, size and origin. There is usually only one right bronchial artery which arises either from the third posterior intercostal or upper left bronchial artery, and runs posteriorly on the right bronchus. Its branches supply these structures, in addition to the pulmonary areolar tissue and the bronchopulmonary lymph nodes, pericardium and oesophagus. The left bronchial arteries, usually two, arise from the thoracic aorta, the upper near the fifth thoracic vertebra, the lower below the left bronchus, and run posteriorly to the left bronchus; they are distributed as on the right.

Mediastinal branches

Numerous small vessels supply lymph nodes and areolar tissue in the posterior mediastinum.

Phrenic branches

Phrenic branches arise from the lower thoracic aorta and are distributed posteriorly to the superior diaphragmatic surface. They anastomose with the musculophrenic and pericardiacophrenic arteries.

Posterior intercostal arteries

The posterior intercostal arteries and their branches are described in Chapter 54.

Subcostal arteries

Subcostal arteries are the last paired branches of the thoracic aorta, in series with the posterior intercostal arteries, and below the twelfth ribs. Each runs laterally anterior to the twelfth thoracic vertebral body and posterior to the splanchnic nerves, sympathetic trunk, pleura and diaphragm. The right is also posterior to the thoracic duct and azygos vein, the left is posterior to the accessory hemiazygos vein. Each then enters the abdomen at the lower border of the 12th rib, accompanied by the 12th thoracic (subcostal) nerve, lying posterior to the lateral arcuate ligament and kidney, and anterior to quadratus lumborum. The right artery courses posterior to the ascending colon, the left posterior to the descending colon. Piercing the aponeurosis of transversus abdominis, each proceeds between this and internal oblique, and anastomoses with the superior epigastric, lower posterior intercostal and lumbar arteries. Each has a dorsal branch, distributed like those of the posterior intercostal arteries.

Aberrant artery

A small artery sometimes leaves the thoracic aorta on its right near the right bronchial artery origin. It ascends to the right behind the trachea and oesophagus and may anastomose with the right superior intercostal. It is a vestige of the right dorsal aorta; occasionally it is enlarged as the first part of a right subclavian artery.

Aortic rupture in trauma

Aortic rupture resulting from blunt trauma is a life-threatening injury. It commonly occurs in road traffic accidents and has a poor survival rate of 20%. There is usually a transverse tear in the wall of the aorta, which may involve the intima through to the media of the aorta. The pressure within the systemic circulation may itself cause the formation of a false aneurysm. Rupture of the isthmus region of the descending aorta is more common, probably because the isthmus tends to be the junction between the mobile and fixed portions of the aorta. Other sites include the ascending aorta proximal to the origin of the brachiocephalic artery, the aortic arch and the abdominal aorta. Rupture is likely to be the result of a number of factors, including torsion and shear and stretching forces, and is possibly compounded by hydrostatic pressure.

Aortic atherosclerosis or calcification

Aortic sclerosis or calcification may be implicated in embolic events and strokes. Echocardiography, and particularly transoesophageal echocardiography, allows very detailed assessment of the proximal aorta. The extent of turbulent flow appears as signal loss in the ascending aorta using MRI, and can be used to assess any functional narrowing. MRI also allows an accurate assessment of the composition and size of atherosclerotic plaques, which permits assessment of the risk of plaque rupture and thrombus formation.

Aortic bodies

Aortic bodies develop progressively during fetal life. They attain maximum size in the first three postnatal years, when the largest are two brownish bodies, 1 cm long, which flank the abdominal aorta and are usually united anterior to it by a horizontal mass immediately above the inferior mesenteric artery, thereby forming an inverted crescentic or H-shaped arrangement which is intimately related to the intermesenteric and superior hypogastric plexuses (see Fig. 15.16). Their constituent cells disperse and atrophy and by 14 years they may have disintegrated completely. When well developed, they consist of masses of polygonal chromaffin cells embedded in wide-meshed capillary plexuses and secreting noradrenaline (norepinephrine). Other small chromaffin bodies are also widespread in the fetus in the abdominal and pelvic prevertebral sympathetic plexuses. They reach a maximum size between the fifth and eighth fetal months, and survive in adults mainly near the coeliac and superior mesenteric arteries and as microscopic collections of cells that persist in the lower parts of the intermesenteric plexus.

Subclavian arteries

Right subclavian artery

The right subclavian artery arises from the brachiocephalic trunk. The right subclavian artery is formed behind the upper border of the right sternoclavicular joint. It ascends above the clavicle superomedial and then posterior to scalenus anterior. It next descends laterally to scalenus anterior, to the outer border of the first rib, where it becomes the axillary artery.

Left subclavian artery

In the majority of individuals, the left subclavian artery originates independently from the aortic arch after the origin of the brachiocephalic trunk and left common carotid artery. The left subclavian artery arises from the aortic arch below the left common carotid artery and rises into the neck lateral to the medial border of scalenus anterior, crosses behind this muscle and then descends towards the outer border of the first rib, where it becomes the axillary artery. A common origin exists occasionally between the left subclavian artery and left vertebral artery. Rarely, there are bilateral brachiocephalic trunks, which subsequently divide on both sides into common carotid and subclavian arteries.

Relations

In the thorax the left subclavian artery is related anteriorly to the left common carotid artery and left brachiocephalic vein, from which it is separated by the left vagus, cardiac and phrenic nerves. More superficially, the anterior pulmonary margin, pleura, sternothyroid and sternohyoid lie between the vessel and the upper left area of the manubrium of sternum. The left side of the oesophagus, the thoracic duct and longus colli are posterior. The left subclavian artery is in contact posterolaterally with the left lung and pleura. The trachea, the left recurrent laryngeal nerve, oesophagus and thoracic duct are medial. Laterally, the artery grooves the mediastinal surface of the left lung and pleura, which also encroach on its anterior and posterior aspects.

Common carotid arteries

The right and left carotid arteries differ in length and origin. The right carotid is exclusively cervical, and arises from the brachiocephalic trunk behind the right sternoclavicular joint. The left carotid originates directly from the aortic arch immediately posterolateral to the brachiocephalic trunk and therefore has both thoracic and cervical parts.

Right common carotid artery

The right common carotid artery and its relations are described in Chapter 28.

Left common carotid artery

The left common carotid artery (see Fig. 28.14) ascends until level with the left sternoclavicular joint, where it enters the neck. It is 20–25 mm long and it lies at first in front of the trachea, then it inclines to the left. The further course of the artery is described in Chapter 28.

Relations

Sternohyoid and sternothyroid, the anterior parts of the left pleura and lung, the left brachiocephalic vein and the thymic remnants are anterior and separate the left common carotid artery from the manubrium. The trachea, left subclavian artery, left border of the oesophagus, left recurrent laryngeal nerve and thoracic duct are posterior. To the right are the brachiocephalic trunk (below) and the trachea, inferior thyroid veins and thymic remains (above). To the left are the left vagus and phrenic nerves, left pleura and lung.

VEINS

Superior vena cava

The superior vena cava returns blood to the heart from the tissues above the diaphragm. It is approximately 7 cm in length, and is formed by the junction of the brachiocephalic veins behind the lower border of the first right costal cartilage near the sternum. It descends vertically behind the first and second intercostal spaces, and ends in the upper right atrium behind the third right costal cartilage. Its inferior half is within the fibrous pericardium, which it pierces level with the second costal cartilage. Covered anterolaterally by serous pericardium (from which a retrocaval recess projects), it is slightly convex to the right (Figs 56.1, 56.3; see Fig. 28.14). The superior vena cava has no valves.

Relations

The anterior margins of the right lung and pleura are anterior and the pericardium intervenes below: these structures separate the superior vena cava from the internal thoracic artery, first and second intercostal spaces, and second and third costal cartilages. The trachea and right vagus are posteromedial, the right lung and pleura are posterolateral, and the right pulmonary hilum is posterior. The right phrenic nerve and pleura are right lateral and the brachiocephalic artery and ascending aorta are left lateral, the aorta overlapping the superior vena cava (see Fig. 58.3).

Variations

The brachiocephalic veins may enter the right atrium separately, the right vein descending like a normal superior vena cava. A left superior vena cava may have a slender connection with the right and then cross the left side of the aortic arch to pass anterior to the left pulmonary hilum before turning to enter the right atrium. It replaces the oblique atrial vein and coronary sinus and receives all the tributaries of the coronary sinus. The left brachiocephalic vein sometimes projects above the manubrium (more frequently in childhood), and crosses the suprasternal fossa in front of the trachea.

Tributaries

Tributaries of the superior vena cava are the azygos vein and small veins from the pericardium and other mediastinal structures (see Fig. 55.6).

Superior vena caval obstruction

Superior vena caval obstruction is characterized by headaches, facial congestion and facial oedema, reflecting impaired venous drainage of the head, neck and upper arms. It is often caused by bronchial carcinoma involving the right upper lobe of the lung, or by metastatic involvement of the right paratracheal lymph nodes resulting in circumferential narrowing or complete obstruction of the superior vena cava. This is usually considered to be an oncological emergency and symptoms may be relieved by insertion of a vascular stent or by radiotherapy to the affected region after a tissue diagnosis is established.

Inferior vena cava

The inferior vena cava returns blood to the heart from the tissues below the diaphragm. It passes through the diaphragm between the right leaf and central area of the central tendon of the diaphragm at the level of the eight and ninth thoracic vertebrae, and drains into the inferoposterior part of the right atrium (see Fig. 58.1). The thoracic part is very short, and is partly inside and partly outside the pericardial sac. The extrapericardial part is separated from the right pleura and lung by the right phrenic nerve, and the intrapericardial part is covered, except posteriorly, by inflected serous pericardium. The abdominal course of the inferior vena cava is described in Chapter 62.

Collateral venous channels

In obstruction of the upper inferior vena cava, the azygos and hemiazygos veins and vertebral venous plexuses are the main collateral channels maintaining venous circulation. They connect the superior and inferior venae cavae and communicate with the common iliac vein by the ascending lumbar veins and with many tributaries of the inferior vena cava.

Brachiocephalic veins

The right and left brachiocephalic veins join to form the superior vena cava.

Right brachiocephalic vein

The right brachiocephalic vein is about 2.5 cm long, and begins posterior to the sternal end of the right clavicle. It descends almost vertically to join the left brachiocephalic vein, forming the superior vena cava posterior to the lower border of the first right costal cartilage, near the right sternal border. It is anterolateral to the brachiocephalic artery and right vagus nerve; the right pleura, phrenic nerve and internal thoracic artery are posterior to it above, and become lateral below (see Fig. 28.14). Its tributaries are the right vertebral, internal thoracic, inferior thyroid and sometimes the first right posterior intercostal veins.

Left brachiocephalic vein

The left brachiocephalic vein is longer than the right, being some 6 cm long. It begins posterior to the sternal end of the left clavicle, anterior to the cervical pleura, and descends obliquely to the right, posterior to the upper half of the manubrium sterni, to the sternal end of the first right costal cartilage, where it joins the right brachiocephalic vein to form the superior vena cava. It is separated from the left sternoclavicular joint and manubrium by sternohyoid and sternothyroid, the thymus or its remains, and areolar tissue; terminally it is overlapped by the right pleura. It crosses anterior to the left internal thoracic, subclavian, brachiocephalic and common carotid arteries, left phrenic and vagus nerves, and the trachea. The aortic arch is inferior to it. Its tributaries are the left vertebral, internal thoracic, inferior thyroid, superior intercostal, sometimes the first left posterior intercostal, thymic and pericardial veins.

REFERENCES

nderson RH, Ho SY, Becker AE. The surgical anatomy of the conduction tissues. *Thorax*. 1983;38:408-420.

arvalho JS, Moscoso G, Ville Y. First-trimester transabdominal fetal echocardiography. *Lancet*. 1998;351:1023-1027.

ederative Committee on Anatomical Terminology. Terminologia Anatomica. Stuttgart: Thieme, 1998.

o SY, McCarthy KP, Josen M, Rigby ML. Anatomic-echocardiographic correlates: an introduction to normal and congenitally malformed hearts. *Heart*. 2001;86:3-11.

mes TN. Congenital disorders of cardiac rhythm and conduction. *J Cardiovasc Electrophysiol*. 1993;4:702-718.

izeres NJ. The cardiac plexus in man. *Am J Anat*. 1963;112:141-151.

CHAPTER 57

Pleura, lungs, trachea and bronchi

The lungs are the essential organs of respiration and are responsible for the uptake of oxygen into the blood and the removal of carbon dioxide. The functional design of the thorax facilitates this complex process. The muscles of respiration and the diaphragm, acting together, increase the intrathoracic volume, creating a negative pressure within the pleural space which surrounds the lung and causing expansion of the lung (see Ch. 58). The resultant reduction in intra-alveolar pressure prompts the conduction of air through the upper respiratory tract into the trachea and airways and thence into the alveoli, where gaseous exchange occurs. The process of breathing exposes the lung to noxious agents, including gases, dust particles, bacteria and viruses; the mucous barrier, mucociliary escalator, branching pattern of the airways and the cough reflex are all anatomical defences against these insults. Anatomical defects may compromise respiratory function; for example, chest wall abnormalities may cause restrictive lung disease. Similarly, ultrastructural abnormalities such as ciliary dysfunction (as seen in Kartagener’s syndrome) lead to recurrent respiratory infections and airway damage.

PLEURA

Each lung is covered by pleura, a serous membrane arranged as a closed invaginated sac. The visceral or pulmonary pleura adheres closely to the pulmonary surface and its interlobar fissures. Its continuation, the parietal pleura, lines the corresponding half of the thoracic wall and covers much of the diaphragm and structures occupying the middle region of the thorax. The visceral and parietal pleurae are continuous with each other around the hilar structures, and they remain in close, though sliding, contact at all phases of respiration. The potential space between them is the pleural cavity, which is maintained at a negative pressure by the inward elastic recoil of the lung and the outward pull of the chest wall.

The right and left pleural sacs form separate compartments and touch only behind the upper half of the sternal body (see Fig. 53.6A,B), although they are also close to each other behind the oesophagus at the midthoracic level. The region between them is the mediastinum (interpleural space). The left pleural cavity is the smaller of the two, because the heart extends further to the left. The upper and lower limits of the pleurae are about the same on the two sides, but the left sometimes descends lower in the midaxillary line.

The interlobar fissures and posterior azygo-oesophageal and retrosternal pleural reflections are the only aspects of the normal pleura that can be visualized on a chest radiograph or CT scan (Fig. 57.1A–D; see Figs 55.16, 55.17). Demonstration of significant pleural shadowing in any other regions usually implies pathological abnormalities of the pleura. Thoracoscopy allows the direct inspection of both the parietal and visceral surfaces. The parietal pleura is translucent and at thoracoscopy the underlying muscles and blood vessels are visible. The visceral pleura is also translucent and has a grey variegated appearance due to the underlying lung and the vascular network in the subpleural layer.

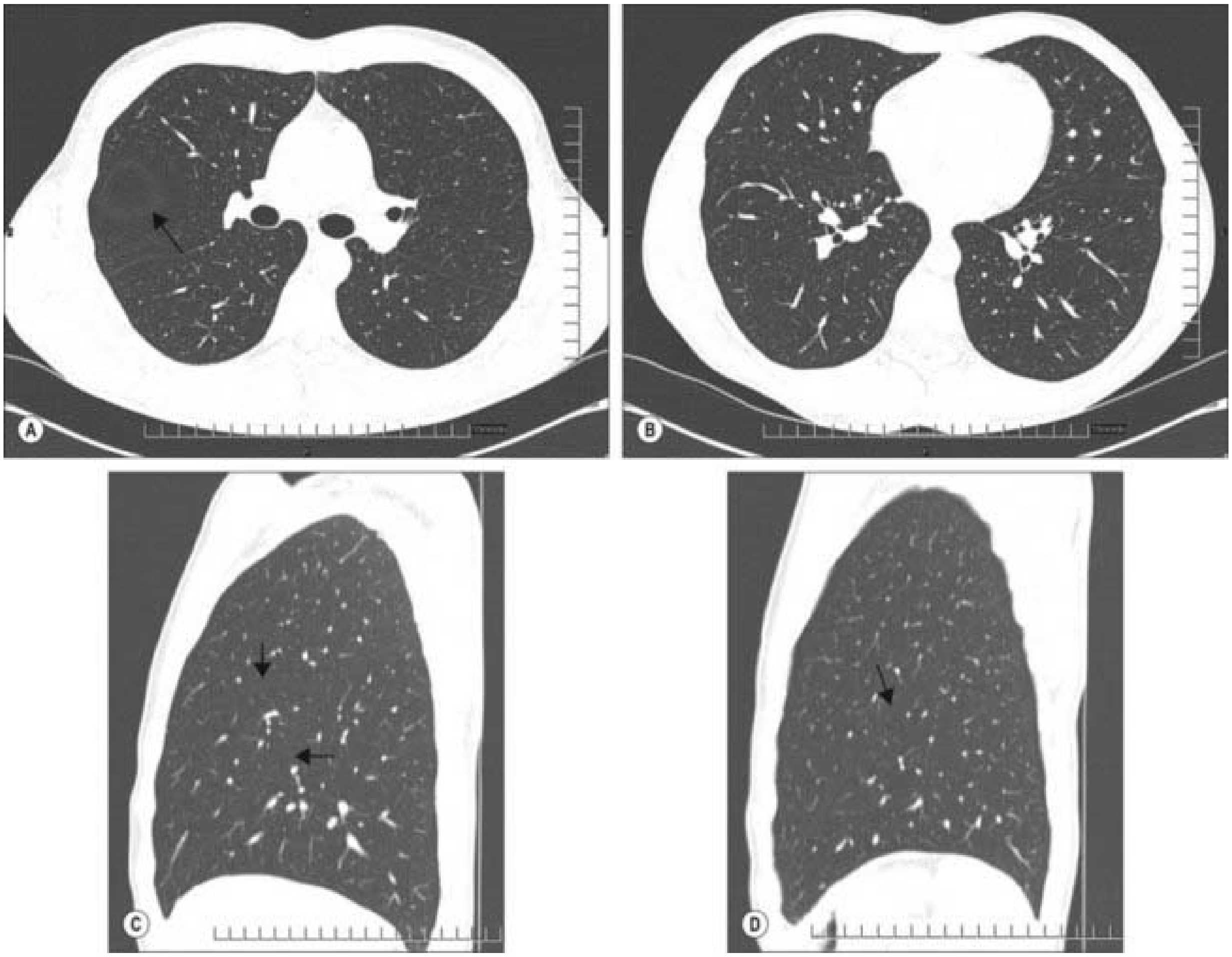

Fig. 57.1 **A**, Axial section through the lungs below the carina demonstrates the left and right major fissures. The circular avascular area anterior to the right major fissure and surrounded by a halo of white (arrow) is due to the horizontal (minor) fissure. In this subject the fissure is slightly domed and passing through the plane of the section. **B**, Axial section through the lungs at the mid left atrial level demonstrating the left and right major fissures as they pass more anteriorly and separate the lower lobes from the lingula and middle lobes. **C**, Sagittal section through the right lung demonstrating the major and minor fissures (arrows). **D**, Sagittal section through the left lung demonstrating the major fissure (arrow).

PARIETAL PLEURA

Different regions of parietal pleura are customarily distinguished by name, thus the costovertebral pleura lines the internal surface of the thoracic wall and the vertebral bodies, the diaphragmatic pleura lies on the thoracic surface of the diaphragm, the cervical pleura lies over the pulmonary apices (and is therefore also called the dome of the pleura), and the mediastinal pleura is applied to the structures between the lungs.

Costovertebral pleura

Costovertebral pleura lines the sternum, ribs, transversus thoracis and intercostal muscles and the sides of the vertebral bodies; normally it is easily separated from these structures. External to the pleura is a thin layer of loose connective tissue, the endothoracic fascia, which corresponds to the transversalis fascia of the abdominal wall. Anteriorly, the costal pleura begins behind the sternum, where it is continuous with the mediastinal pleura along a junction extending from behind the sternoclavicular joint down and medially to the midline behind the sternal angle. From here, the right and left costal pleurae descend in contact with each other to the level of the fourth costal cartilages and then diverge. On the right side, the line descends to the back of the xiphisternal joint, while on the left the line diverges laterally and descends at a distance of 2–2.5 mm from the sternal margin to the sixth costal cartilage, forming the cardiac notch. On each side, the costal pleura sweeps laterally, lining the internal surfaces of the costal cartilages, ribs, transversus thoracis and intercostal muscles. Posteriorly, it passes over the sympathetic trunk and its branches to reach the sides of the vertebral bodies, where it is again continuous with the mediastinal pleura. The costovertebral pleura is continuous with the cervical pleura at the inner margin of the first rib and below it becomes continuous with the diaphragmatic pleura along a line which differs slightly on the two sides. On the right, this line of costodiaphragmatic reflection begins behind the xiphoid process, passes behind the seventh costal cartilage to reach the eighth rib in the midclavicular line, the tenth rib in the midaxillary line, and then ascends slightly to cross the twelfth rib level with the upper border of the twelfth thoracic spine (see Fig. 53.6A,B). On the left, the line initially follows the ascending part of the sixth costal cartilage, but then follows a course similar to that on the right, although it may be slightly lower.

Diaphragmatic pleura

The diaphragmatic pleura is a thin, tightly adherent layer which covers most of the upper surface of the diaphragm. It is continuous with the costal pleura and on its medial aspect is continuous with the mediastinal pleura along the line of attachment of the pericardium to the diaphragm.

Cervical pleura

The cervical pleura is a continuation of the costovertebral pleura over the pulmonary apex (Fig. 57.2). It ascends medially from the internal border of the first rib to the apex of the lung, as high as the lower edge of the neck of the first rib, and then descends lateral to the trachea to become the mediastinal pleura. As a result of the obliquity of the first rib, the cervical pleura extends 3–4 cm above the first costal cartilage, but not above the neck of the first rib. The cervical pleura is strengthened by a fascial suprapleural membrane, which is attached in front to the internal border of the first rib, and behind to the anterior border of the transverse process of the seventh cervical vertebra. It contains a few muscular fibres, which spread from the scaleni. Scalenus minimus extends from the anterior border of the transverse process of the seventh cervical vertebra to the inner border of the first rib behind its subclavian groove, and also spreads into the pleural dome, which it therefore tenses: it has been suggested that the suprapleural membrane is the tendon of scalenus medius. The cervical pleura (like the pulmonary apex) reaches the level of the seventh cervical spine approximately 2.5 cm from the midline. Its projection is a curved line from the sternoclavicular joint to the junction of the medial and middle thirds of the clavicle, its summit being 2.5 cm above it. The subclavian artery ascends laterally in a furrow below the summit of the cervical pleura (Fig. 57.2).

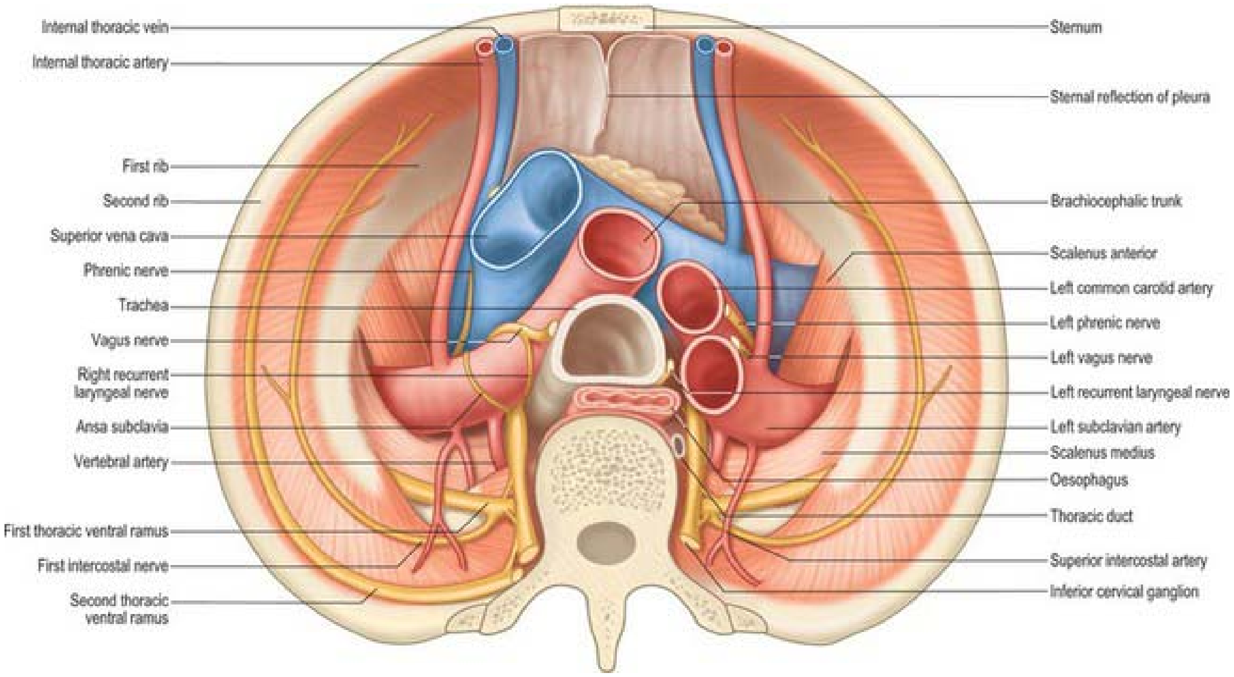
Internal thoracic vein
Internal thoracic artery
First rib
Second rib
Superior vena cava
Phrenic nerve
Trachea
Vagus nerve
Right recurrent laryngeal nerve
Ansa subclavia
Vertebral artery
First thoracic ventral ramus
First intercostal nerve
Second thoracic ventral ramus
Sternum
Sternal reflection of pleura
Brachiocephalic trunk
Scalenus anterior
Left common carotid artery
Left phrenic nerve
Left vagus nerve
Left recurrent laryngeal nerve
Left subclavian artery
Scalenus medius
Oesophagus
Thoracic duct
Superior intercostal artery
Inferior cervical ganglion

Fig. 57.2 Structures related to the cervical pleura, as seen from below.

Mediastinal pleura

The mediastinal pleura is the lateral boundary of the mediastinum and forms a continuous surface above the hilum of the lung from sternum to vertebral column. On the right it covers the right brachiocephalic vein, the upper part of the superior vena cava, the terminal part of the azygos vein, the right phrenic and vagus nerves, the trachea and oesophagus. On the left it covers the aortic arch, left phrenic and vagus nerves, left brachiocephalic and superior intercostal veins, left common carotid and subclavian arteries, thoracic duct and oesophagus. At the hilum of the lung it turns laterally to form a tube that encloses the hilar structures and is continuous with the pulmonary pleura.

VISCERAL PLEURA

The pulmonary pleura is inseparably adherent to the lung over all its surfaces, including those in the fissures, except at the root or hilum of the lung and along a line descending from this, which marks the attachment of the pulmonary ligament (Figs 57.3, 57.4).

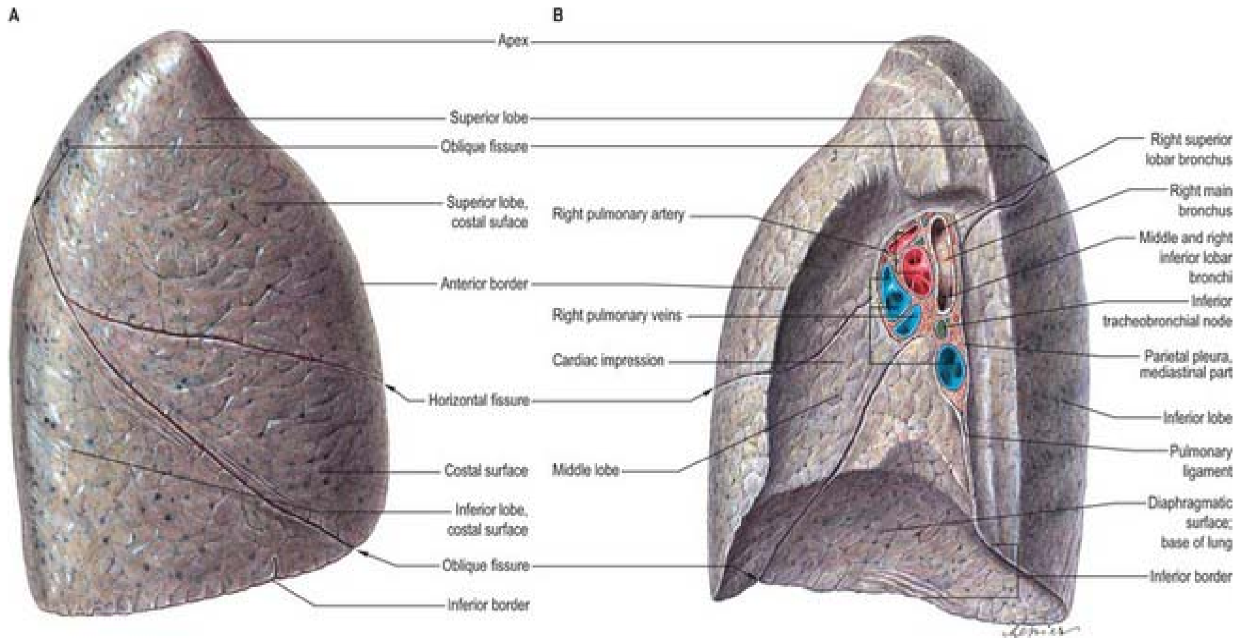
A
B
Apex
Superior lobe
Oblique fissure
Superior lobe, costal suface
Anterior border
Horizontal fissure
Costal surface
Inferior lobe, costal surface
Oblique fissure
Inferior border
Right pulmonary artery
Right pulmonary veins
Cardiac impression
Middle lobe
Right superior lobar bronchus
Right main bronchus
Middle and right inferior lobar bronchi
Inferior tracheobronchial node
Parietal pleura, mediastinal part
Inferior lobe
Pulmonary ligament
Diaphragmatic surface; base of lung
Inferior border

Fig. 57.3 The right lung. **A**, Lateral surface. **B**, Medial surface.

(From Sobotta 2006.)

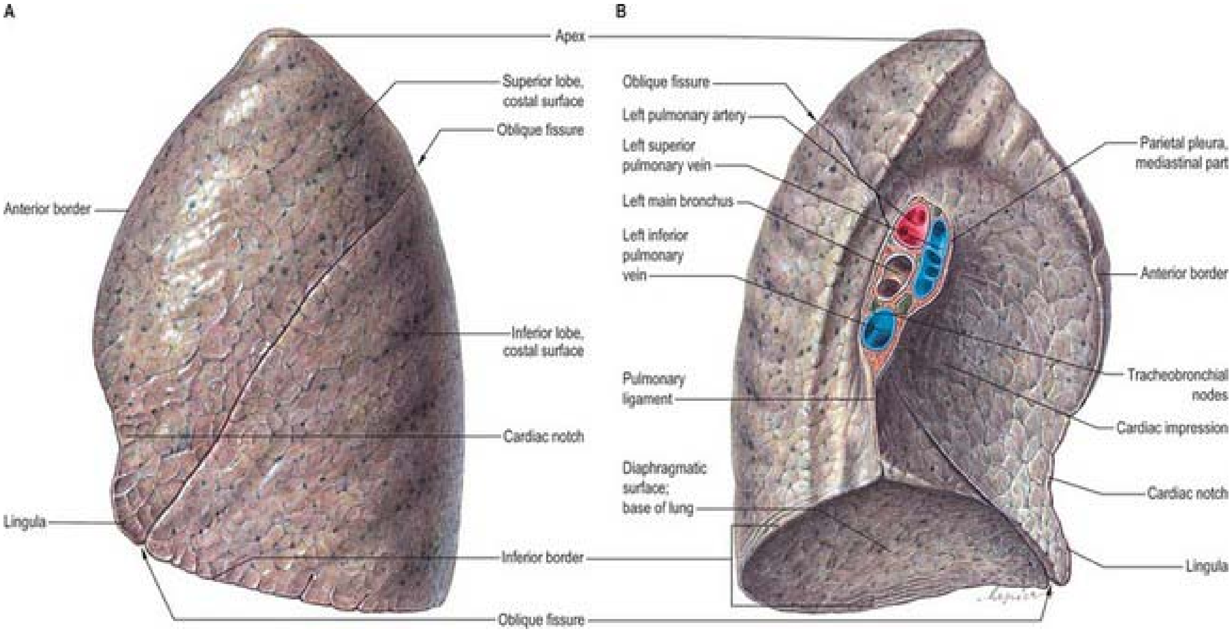
A
B
Apex
Superior lobe, costal surface
Oblique fissure
Anterior border
Inferior lobe, costal surface
Cardiac notch
Lingula
Inferior border
Oblique fissure
Oblique fissure
Left pulmonary artery
Left superior pulmonary vein
Left main bronchus
Left inferior pulmonary vein
Pulmonary ligament
Diaphragmatic surface; base of lung
Parietal pleura, mediastinal part
Anterior border
Tracheobronchial nodes
Cardiac impression
Cardiac notch
Lingula

Fig. 57.4 The left lung. **A**, Lateral surface. **B**, Medial surface.

(From Sobotta 2006.)

INFERIOR PULMONARY LIGAMENTS

Below the hilum the mediastinal pleura extends as a double layer, the pulmonary ligament, from the lateral surface of the oesophagus to the mediastinal surface of the lung, where it is continuous with the parietal pleura (Figs 57.3, 57.4). It is continuous above with the pleura around the hilar structures and below it ends in a free sickle-shaped border.

PLEURAL RECESSES

The pleura extends considerably beyond the inferior border of the lung, but not as far as the attachment of the diaphragm, which means that the diaphragm is in contact with the costal cartilages and intercostal muscles below the line of pleural reflection from the thoracic wall to the diaphragm. In quiet inspiration the inferior margin of the lung does not reach this reflection, and the costal and diaphragmatic pleurae are separated merely by a narrow slit, the costodiaphragmatic recess. In quiet inspiration the lower limit of the lung is normally 5 cm above the lower pleural limit. A similar costomediastinal recess exists behind the sternum and the costal cartilages, where the thin anterior margin of the lung falls short of the line of pleural reflection. The extent of this recess, the anterior costomediastinal line of pleural reflection, and the position of the anterior margin of the lung all exhibit individual variation.

The inferior border of the right costodiaphragmatic recess is an important consideration in the surgical posterior approach to the kidney. Usually the pleura crosses the twelfth rib at the lateral border of erector spinae, so that the medial region of the kidney is above the pleural reflection (see Fig. 53.6B). However, if the twelfth rib does not project beyond the muscle, the eleventh rib may be mistaken for the twelfth in palpation, and an incision prolonged to this level will damage the pleura. Whether the lowest palpable rib is the eleventh or twelfth can be ascertained by counting from the second rib (identified at its junction with the sternal angle).

VASCULAR SUPPLY AND LYMPHATIC DRAINAGE

The parietal and visceral pleurae are developed from somatopleural and splanchnopleural layers of the lateral plate mesoderm respectively, which means that the parietal pleura is supplied by arteries from somatic sources. The costovertebral pleura is supplied by branches of intercostal and internal thoracic arteries; the mediastinal pleura is supplied by branches from bronchial, upper diaphragmatic, internal thoracic and mediastinal arteries; the cervical pleura is supplied by branches from the subclavian artery; and the diaphragmatic pleura is supplied by the superficial part of the microcirculation of the diaphragmatic muscle. The veins join systemic veins in the thoracic wall which drain into the superior vena cava. Lymph from the costovertebral parietal pleura drains into the internal thoracic chain anteriorly and intercostal chains posteriorly, while that from the diaphragmatic pleura drains into the mediastinal, retrosternal and coeliac axis nodes.

The visceral pleura forms an integral part of the lung and accordingly its arterial supply and venous drainage are provided by the bronchial vessels. The bronchial arteries at the hilum form an anulus that surrounds the main bronchus, and pleural branches from this anulus supply the visceral pleura facing the mediastinum, interlobar surfaces, apical surface and part of the diaphragmatic surface. The visceral pleura is drained by pulmonary veins, apart from an area around the hilum that drains into bronchial veins. The lymphatic drainage of the visceral pleura is to the deep pulmonary plexus within the interlobar and peribronchial spaces.

INNERVATION

The costal and peripheral diaphragmatic parietal pleurae are innervated by intercostal nerves, and the mediastinal and central diaphragmatic parietal pleurae are innervated by the phrenic nerve. Irritation of the former results in pain that is referred along the intercostal nerves to the appropriate part of the thoracic or abdominal wall, whereas irritation of the central diaphragmatic pleura causes pain that is referred to the lower neck and shoulder tip, i.e. to the C3, 4 dermatomes. The visceral pleura is innervated by visceral afferents that reach it by travelling along the bronchial vessels with the autonomic fibres.

PNEUMOTHORAX

Any breach of the chest wall and parietal pleura or visceral pleura leads to the accumulation of air within the pleural cavity (pneumothorax). Fluid (hydrothorax), blood (haemothorax) and rarely lymph (chylothorax) can also accumulate in this space. Pneumothoraces may occur spontaneously or following trauma (e.g. rib fractures, penetrating injuries from sharp instruments, iatrogenic injury). Significant air in the pleural space is visible on a chest radiograph: there is separation of the parietal and visceral pleurae and an absence of pulmonary vascular markings in the corresponding area. Occasionally, a ball valve-like effect occurs, so that air enters the pleural space during inspiration but cannot escape in expiration. This tension pneumothorax can be life-threatening and should be suspected whenever there are unilateral decreased breath sounds and hyperresonance on percussion, hypotension, jugular venous distension and contralateral tracheal deviation. A tension pneumothorax requires immediate decompression by the insertion of an intercostal drain or wide bore catheter. Fluid collection in the pleural space may be due to congestive cardiac failure, hypoalbuminaemia, inflammatory, infective or neoplastic conditions. A pleural effusion causes obliteration of the costophrenic angle and the diaphragm, and a lateral meniscus is visible on a frontal chest radiograph. Drainage of the fluid and subsequent analysis is required for diagnostic purposes. Where there is a collection of pus (empyema) or blood, pleural drainage is essential for therapeutic purposes. Ultrasonography is useful in assessing the size and characteristics of an effusion, such as the presence of loculation and debris. It may even demonstrate underlying consolidated lung. Computed tomography is utilized to assess the underlying hidden lung parenchyma and mediastinal glands. For further review of the radiology of the pleurae and lungs, see Armstrong (2000).

MICROSTRUCTURE

The pleural surface is smooth and moistened by serous fluid. It consists of a single layer of flat mesothelial cells separated by a basal lamina from an underlying lamina propria of loose connective tissue. Ultrastructurally, pleural mesothelial cells are like those of the peritoneum in that they have highly folded basal plasma membranes, their adjacent cell surfaces interdigitate and are joined by desmosomes, and their luminal surfaces bear numerous microvilli and some cilia. Pinocytotic vesicles are common in their cytoplasm.

The deeper layers of the lamina propria are continuous with the tissue surrounding the pulmonary lobules. Blood and lymph vessels and nerves all travel within the pleura.

Serosa

The serosa is formed by the visceral pleura, which is a transparent single sheet of mesothelium covering a thin lamina propria of connective tissue, and is closely attached to the various structures of the lung, except at the hilum. Beneath the serosa, loose connective tissue covers the entire pulmonary surface: it extends from the hilum along the conducting tubes and blood vessels within the substance of the lung. The connective tissue partitions the lung into numerous lobules, small polyhedral tissue masses which each receives a lobular bronchiole and the terminal branches of arterioles, venules, lymphatics and nerves. Lobules vary in size, the superficial ones are the largest, and are visible as polygonal areas 5–15 mm across.

LUNGS

The lungs are the essential organs of respiration. They are situated on either side of the heart and other mediastinal contents (Figs 57.3, 57.4). Each lung is free in its pleural cavity, except for its attachment to the heart and trachea at the hilum and pulmonary ligament respectively. When removed from the thorax, a fresh lung is spongy, can float in water, and crepitates when handled, because of the air within its alveoli. It is also highly elastic and so it retracts on removal from the thorax. Its surface is smooth and shiny and is separated by fine, dark lines into numerous small polyhedral domains, each crossed by numerous finer lines, indicating the areas of contact between its most peripheral lobules and the pleural surface.

At birth the lungs are pink, but in adults they are dark grey and patchily mottled. As age advances, this maculation becomes black, as granules of inhaled carbonaceous material are deposited in the loose connective tissue near the lung surface. Darkening is often more marked in men than women, in those who have dwelt in industrial areas and in smokers. The posterior pulmonary border is usually darker than the anterior. In the upper, less movable parts of the lung, this surface pigmentation tends to be concentrated opposite the intercostal spaces. Lungs from fetuses or stillborn infants who have not respired differ from those of infants who have taken a breath in that they are firm, non-crepitant and do not float in water.

The adult right lung usually weighs 625 g, and the left 565 g, but the range of wet weights is considerable, not least because it reflects the amount of blood or serous fluid contained within the lungs when weighed. In proportion to body stature, the lungs are heavier in men than in women.

PULMONARY SURFACE FEATURES

Each lung has an apex, base, three borders and two surfaces (Figs 57.3, 57.4). In shape, each lung approximates to half a cone.

Apex

The apex, the rounded upper extremity, protrudes above the thoracic inlet where it contacts the cervical pleura, and is covered in turn by the suprapleural membrane. As a consequence of the obliquity of the inlet, the apex rises 3–4 cm above the level of the first costal cartilage; it is level posteriorly with the neck of the first rib. Its summit is 2.5 cm above the medial third of the clavicle. The apex is therefore in the root of the neck (see Fig. 35.5A). It has been claimed that, because the apex does not rise above the neck of the first rib, it is really intrathoracic, and that it is the anterior surface that ascends highest in inspiration. The subclavian artery arches up and laterally over the suprapleural membrane, grooves the anterior surface of the apex near its summit and separates it from scalenus anterior. The cervicothoracic (stellate) sympathetic ganglion, the ventral ramus of the first thoracic spinal nerve and the superior intercostal artery all lie posterior to the apex. Scalenus medius is lateral, the brachiocephalic artery, right brachiocephalic vein and trachea are adjacent to the right medial surface of the lung, and the left subclavian artery and left brachiocephalic vein are adjacent to the left medial surface of the apex of the lung.

Base

The basal surface is semilunar and concave, and rests upon the superior surface of the diaphragm, which separates the right lung from the right lobe of the liver and the left lung from the left lobe of the liver, the gastric fundus and spleen. Since the diaphragm extends higher on the right than on the left, the concavity is deeper on the base of the right lung. Posterolaterally, the base has a sharp margin that projects a little into the costodiaphragmatic recess.

Costal surface

The costal surface of the lung is smooth and convex, and its shape is adapted to that of the thoracic wall, which is vertically deeper posteriorly. It is in contact with the costal pleura; in specimens that have been preserved *in situ*, this surface exhibits grooves that correspond with the overlying ribs.

Medial surface

The medial surface has a posterior vertebral and anterior mediastinal part. The vertebral part lies in contact with the sides of the thoracic vertebrae and intervertebral discs, the posterior intercostal vessels and the splanchnic nerves. The mediastinal area is deeply concave, because it is adapted to the heart at the cardiac impression, which is much larger and deeper on the left lung where the heart projects more to the left of the median plane. Posterosuperior to this concavity is the somewhat triangular hilum, where various structures enter or leave the lung, collectively surrounded by a sleeve of pleura that also extends below the hilum and behind the cardiac impression as the pulmonary ligament.

Other impressions on the lung surface

In addition to these pulmonary features, cadaveric lungs that have been preserved *in situ* can show a number of other impressions that indicate their relations with surrounding structures (Figs 57.3, 57.4). On the right lung the cardiac impression is related to the anterior surface of the right auricle, the anterolateral surface of the right atrium and partially to the anterior surface of the right ventricle. The impression ascends anterior to the hilum as a wide groove for the superior vena cava and the terminal portion of the right brachiocephalic vein. Posteriorly this groove is joined by a deep sulcus which arches forwards above the hilum and is occupied by the azygos vein. The right side of the oesophagus makes a shallow vertical groove behind the hilum and the pulmonary ligament. Towards the diaphragm it inclines left and leaves the right lung, and therefore does not reach the lower limit of this surface. Posteroinferiorly the cardiac impression is confluent with a short wide groove adapted to the inferior vena cava. Between the apex and the groove for the azygos, the trachea and right vagus are close to the lung, but do not mark it.

On the left lung (Fig. 57.4) the cardiac impression is related to the anterior and lateral surfaces of the left ventricle and auricle. The anterior infundibular surface and adjoining part of the right ventricle is also related to the lung as it ascends in front of the hilum to accommodate the pulmonary trunk. A large groove arches over the hilum, and descends behind it and the pulmonary ligament, corresponding to the aortic arch and descending aorta. From its summit a narrower groove ascends to the apex for the left subclavian artery. Behind this, above the aortic groove, the lung is in contact with the thoracic duct and oesophagus. In front of the subclavian groove there is a faint linear depression for the left brachiocephalic vein. Inferiorly, the oesophagus may mould the surface in front of the lower end of the pulmonary ligament.

Pulmonary borders

The inferior border is thin and sharp where it separates the base from the costal surface and extends into the costodiaphragmatic recess, and is more rounded medially where it divides the base from the mediastinal surface. It corresponds, in quiet respiration, to a line drawn from the lowest point of the anterior border which passes to the sixth rib at about the midclavicular line, then to the eighth rib in the midaxillary line (usually 10 cm above the costal margin), and then continues posteriorly, medially and slightly upwards to a point 2 cm lateral to the tenth thoracic spine (see Fig. 53.5A,B). The diaphragm rises higher on the right to accommodate the liver, and so the right lung is vertically shorter (by approximately 2.5 cm) than the left. However, cardiac asymmetry means that the right lung is broader, and has a greater capacity and weight than the left. The posterior border separates the costal surface from the mediastinal surface, and corresponds to the heads of the ribs. It has no recognizable markings and is really a rounded junction of costal and vertebral (medial) surfaces. The thin, sharp, anterior border overlaps the pericardium. On the right it corresponds closely to the costomediastinal line of pleural reflection, and is almost vertical. On the left it approaches the same line above the fourth costal cartilage; below this point it shows a variable cardiac notch, the edge of which passes laterally for 3.5 cm before curving down and medially to the sixth costal cartilage 4 cm from the midline. It therefore does not reach the line of pleural reflection here (see Fig. 53.5A) and so the pericardium is covered only by a double layer of pleura (area of superficial cardiac dullness). However, surgical experience suggests that the line of pleural reflection, the anterior pulmonary margin and the costomediastinal pleural recess are all variable.

PULMONARY FISSURES AND LOBES

Right lung

The right lung is divided into superior, middle and inferior lobes by an oblique and a horizontal fissure (Fig. 57.3). The upper, oblique fissure separates the inferior from the middle and upper lobes, and corresponds closely to the left oblique fissure, although it is less vertical, and crosses the inferior border of the lung approximately 7.5 cm behind its anterior end. On the posterior border it is either level with the spine of the fourth thoracic vertebra or slightly lower. It descends across the fifth intercostal space and follows the sixth rib to the sixth costochondral junction. The short horizontal fissure separates the superior and middle lobes. It passes from the oblique fissure, near the midaxillary line, horizontally forwards to the anterior border of the lung, level with the sternal end of the fourth costal cartilage, then passes backwards to the hilum on the mediastinal surface. The horizontal fissure is usually visible on a frontal chest radiograph. The oblique fissure is usually visible on a lateral radiograph and on a high resolution CT scan as a curvilinear band from the lateral aspect to the hilum (Fig. 57.1A–D). The small middle lobe is cuneiform and includes some of the costal surface, the lower part of the anterior border and the anterior part of the base of the lung. Sometimes the medial part of the upper lobe is partially separated by a fissure of variable depth which contains the terminal part of the azygos vein, enclosed in the free margin of a mesentery derived from the mediastinal pleura, and forming the ‘lobe of the azygos vein’. This varies in size, and sometimes includes the apex of the lung. It is always supplied by one or more branches of the apical bronchus. Radiographically, a pleural effusion may be limited to the azygos fissure. Less common variations are the presence of an inferior accessory fissure, which separates the medial basal segment from the remainder of the lower lobe, and a superior accessory fissure, which separates the apical segment of the lower lobe from the basal segments. The identification of the completeness of the fissures is important prior to lobectomy, because individuals with incomplete fissures are more prone to develop postoperative air leaks, and may require further procedures such as stapling and pericardial sleeves (see Venuta et al 1998).

Left lung

The left lung is divided into a superior and an inferior lobe by an oblique fissure (Fig. 57.4) which extends from the costal to the medial surfaces of the lung both above and below the hilum. Superficially this fissure begins on the medial surface at the posterosuperior part of the hilum. It ascends obliquely backwards to cross the posterior border of the lung 6 cm below the apex, then descends forwards across the costal surface, to reach the lower border almost at its anterior end. It finally ascends on the medial surface to the lower part of the hilum. At the posterior border of the lung the fissure usually lies opposite a surface point 2 cm lateral to the midline between the spines of the third and fourth thoracic vertebrae, but it may be above or below this level. Traced around the chest, the fissure reaches the fifth intercostal space (at or near the midaxillary line) and follows this to intersect the inferior border of the lung close to, or just below, the sixth costochondral junction (7.5 cm from the midline). The left oblique fissure is usually more vertical than the right, and is indicated approximately by the medial border of the scapula when the arm is fully abducted above the shoulder. A left horizontal fissure is a normal variant found occasionally.

The superior lobe, which lies anterosuperior to the oblique fissure, includes the apex, anterior border, much of the costal and most of the medial surfaces of the lung. At the lower end of the cardiac notch a small process, the lingula, is usually present. The larger inferior lobe lies behind and below the fissure, and contributes almost the whole of the base, much of the costal surface and most of the posterior border of the lung.

Bronchopulmonary segments

Each of the principal bronchi divides into lobar bronchi. Primary branches of the right and left lobar bronchi are termed segmental bronchi because each ramifies in a structurally separate, functionally independent, unit of lung tissue called a bronchopulmonary segment (Figs 57.5-57.7).

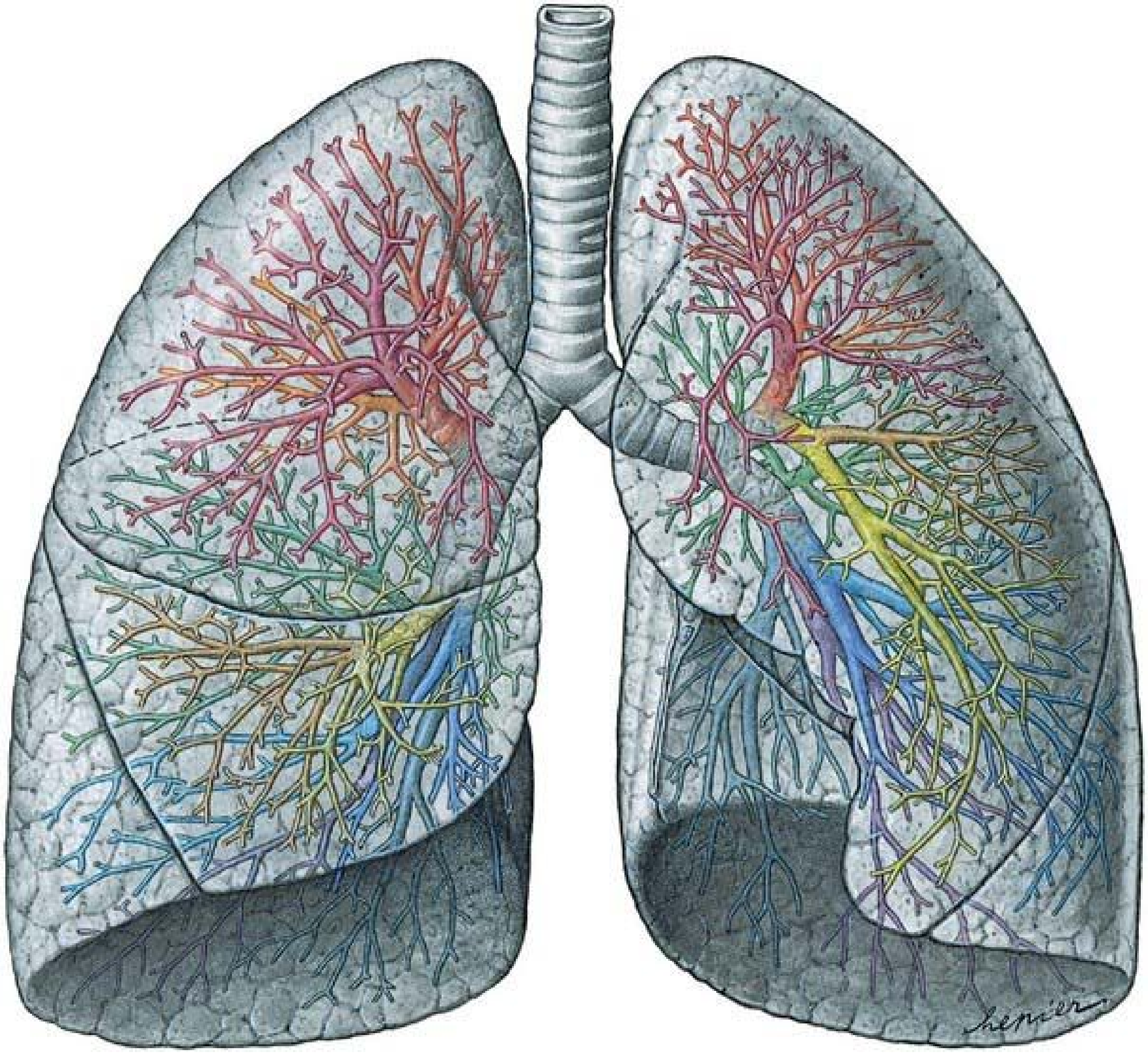

Fig. 57.5 Lungs and bronchi, ventral aspect. The lobar and segmental bronchi are projected onto the lung in different colours (compare with **Fig. 57.6**).

(From Sobotta 2006.)

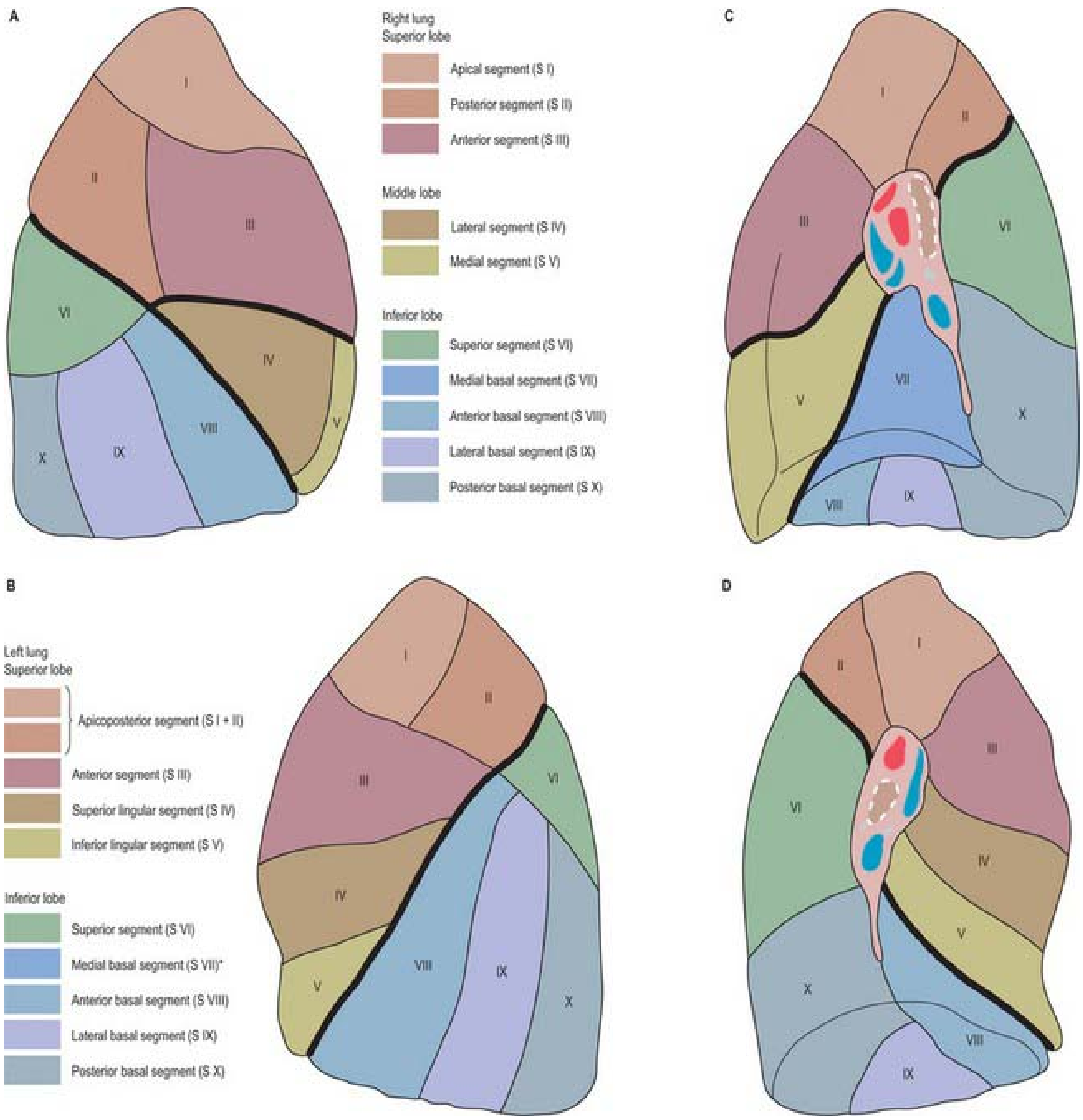
A
I
II
III
IV
V
VI
VIII
IX
X
Right lung
Superior lobe
Apical segment (S I)
Posterior segment (S II)
Anterior segment (S III)
Middle lobe
Lateral segment (S IV)
Medial segment (S V)
Inferior lobe
Superior segment (S VI)
Medial basal segment (S VII)
Anterior basal segment (S VIII)
Lateral basal segment (S IX)
Posterior basal segment (S X)
C
I
II
III
VI
VII
V
X
VIII
IX
B
Left lung
Superior lobe
Apicoposterior segment (S I + II)
Anterior segment (S III)
Superior lingular segment (S IV)
Inferior lingular segment (S V)
Inferior lobe
Superior segment (S VI)
Medial basal segment (S VII)*
Anterior basal segment (S VIII)
Lateral basal segment (S IX)
Posterior basal segment (S X)
I
II
III
VI
IV
V
VIII
IX
X
D
II
I
III
VI
IV
V
X
VIII
IX

Fig. 57.6 Bronchopulmonary segments of the right and left lungs, coloured to indicate the different territories. **A**, Right lung, lateral aspect. **B**, Left lung, lateral aspect. **C**, Right lung, medial aspect. **D**, Left lung, medial aspect. *Generally, this segment is not a separate unit, but is fused with the anterior basal segment.

(From Sobotta 2006.)

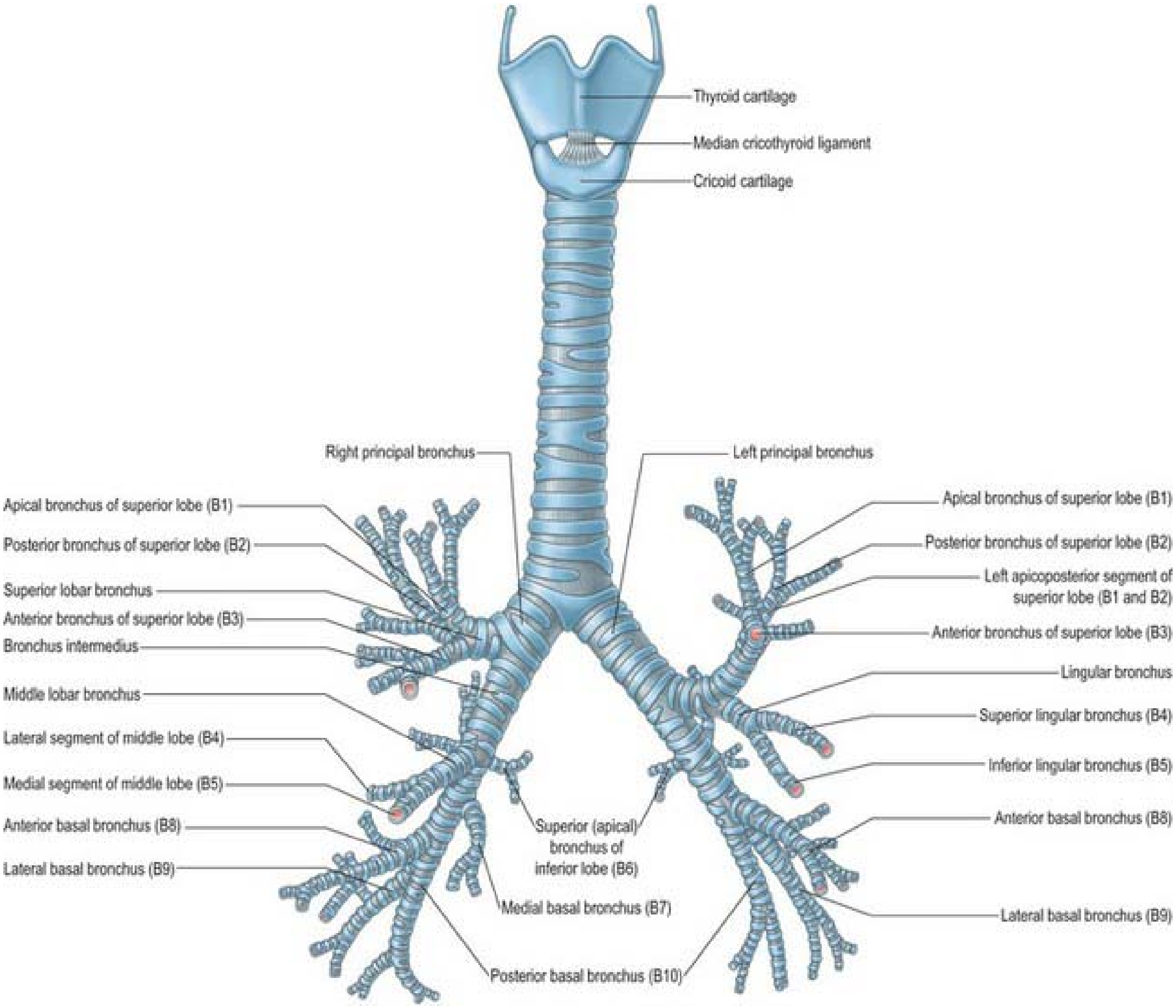
Thyroid cartilage
Median cricothyroid ligament
Cricoid cartilage
Right principal bronchus
Left principal bronchus
Apical bronchus of superior lobe (B1)
Posterior bronchus of superior lobe (B2)
Superior lobar bronchus
Anterior bronchus of superior lobe (B3)
Bronchus intermedius
Middle lobar bronchus
Lateral segment of middle lobe (B4)
Medial segment of middle lobe (B5)
Anterior basal bronchus (B8)
Lateral basal bronchus (B9)
Superior (apical) bronchus of inferior lobe (B6)
Medial basal bronchus (B7)
Posterior basal bronchus (B10)
Apical bronchus of superior lobe (B1)
Posterior bronchus of superior lobe (B2)
Left apicoposterior segment of superior lobe (B1 and B2)
Anterior bronchus of superior lobe (B3)
Lingular bronchus
Superior lingular bronchus (B4)
Inferior lingular bronchus (B5)
Anterior basal bronchus (B8)
Lateral basal bronchus (B9)

Fig. 57.7 The cartilages of the larynx, trachea and bronchi: anterior aspect. The bronchopulmonary segments are shown in brackets.

(Redrawn from an original figure drawn from a metal cast made by the late Lord Russell Brock, GKT School of Medicine, London.)

The main segments are named and numbered as follows:

Right lung	
Superior lobe:	I, apical; II, posterior; III, anterior

Middle lobe:	IV, lateral; V, medial
Inferior lobe:	VI, superior (apical); VII, medial basal; VIII, anterior basal; IX, lateral basal; X, posterior basal
Left lung	
Superior lobe:	I, apical; II, posterior; III, anterior; IV, superior lingular; V, inferior lingular
Inferior lobe:	VI, superior (apical); VIII, anterior basal; IX, lateral basal; X, posterior basal

Each segment is surrounded by connective tissue that is continuous with the visceral pleura, and is a separate respiratory unit. The vascular and lymphatic arrangements of the segments are described on pages 996–998.

PULMONARY HILA

The pulmonary root connects the medial surface of the lung to the heart and trachea and is formed by a group of structures which enter or leave the hilum (Figs 57.3, 57.4; see also Fig. 55.4B). These are the principal bronchus, pulmonary artery, two pulmonary veins, bronchial vessels, a pulmonary autonomic plexus, lymph vessels, bronchopulmonary lymph nodes and loose connective tissue, all of which are enveloped by a sleeve of pleura. The pulmonary roots, or pedicles, lie opposite the bodies of the fifth to seventh thoracic vertebrae. The phrenic nerve, pericardiacophrenic artery and vein, and anterior pulmonary plexus are common anterior relations of both hila, and the vagus nerve and posterior pulmonary plexus are common posterior relations. The pulmonary ligament is a common inferior relation. The major structures in both roots are similarly arranged, so that the upper of the two pulmonary veins is anterior, the pulmonary artery and principal bronchus are more posterior, and the bronchial vessels are most posterior. The arrangement of bronchopulmonary segments and the pulmonary hila permit the resection of abscesses and localized lesions caused by lung cancer.

Right hilum

The right root is situated behind the superior vena cava and right atrium and below the terminal part of the azygos vein. The usual sequence of hilar structures from above downwards is: superior lobar bronchus, pulmonary artery, principal bronchus, and lower pulmonary vein (Fig. 57.3).

Left hilum

The left root lies below the aortic arch and in front of the descending thoracic aorta. The usual vertical sequence of structures at the left hilum is pulmonary artery, principal bronchus, and lower pulmonary vein (Fig. 57.4). The pulmonary artery is longer on the left side, and each of its branches from the hilum to the oblique fissure must be identified in pulmonary resections.

SECONDARY PULMONARY LOBULES

Each segmental bronchus supplies a bronchopulmonary segment. Progressive subdivisions of the bronchus occur within each segment and the bronchi become increasingly narrow. All intrapulmonary bronchi are kept patent by cartilaginous plates, which decline in size and number and finally disappear when the tubes are less than 1 mm in diameter (bronchioles). The terminal bronchiole is the most peripheral bronchiole not to have alveoli in its wall. Distal to each terminal bronchiole is an acinus, which consists of three to four orders of respiratory bronchioles, leading to three to eight orders of alveolar ducts. The walls of these ducts consist of alveolar sacs or the mouths of alveoli. The primary lobule is the lung distal to the respiratory bronchiole. The secondary lobule is the smallest subsection of the peripheral lung bounded by connective tissue septa and consists of approximately six terminal bronchioles. The connective tissue septa are uneven in both size and shape.

VASCULAR SUPPLY AND LYMPHATIC DRAINAGE

The lungs have two functionally distinct circulatory pathways. The pulmonary vessels convey deoxygenated blood to the alveolar walls and drain oxygenated blood back to the left side of the heart, and the much smaller bronchial vessels, which are derived from the systemic circulation, provide oxygenated blood to lung tissues that do not have close access to atmospheric oxygen, i.e. those of the bronchi and larger bronchioles.

The pulmonary artery bifurcates into right and left pulmonary arteries which pass to the hila of the lungs. On entering the lung tissue, both arteries divide into branches that accompany segmental and subsegmental bronchi and lie mostly dorsolateral to them. The pulmonary capillaries form plexuses immediately outside the epithelium in the walls and septa of alveoli and alveolar sacs. The plexus forms a single layer in the interalveolar septa, with meshes smaller than the capillaries, and exceedingly thin walls. Pulmonary veins, two from each lung, drain the pulmonary capillaries. Their radicles coalesce into larger branches which traverse the lung independently of the pulmonary arteries and bronchi. Communicating freely, they form large vessels that ultimately accompany the arteries and bronchial tubes to the pulmonary hilum, where the bronchi often separate the dorsolateral artery and the ventromedial vein. The pulmonary veins open into the left atrium and convey oxygenated blood for systemic distribution by the left ventricle.

At the hilum, the pulmonary vessels accompany the main bronchial divisions. This is not the case in the bronchopulmonary segments, where a segmental bronchus, its branches and associated arteries occupy a central position in each segment, but the many tributaries of the pulmonary veins run between segments, serving adjacent segments (which therefore drain into more than one vein). Some veins also lie beneath the visceral pleura, including the pleura in the interlobar fissures. It follows from this that a bronchopulmonary segment is not a complete vascular unit with an individual bronchus, artery and vein. During resection of segments, it is obvious that the planes between them are not avascular but are crossed by pulmonary veins and sometimes by branches of arteries. This pattern of bronchi, arteries and veins exhibits considerable variation: veins are the most variable, and arteries are more variable than bronchi.

Pulmonary arteries

The right pulmonary artery divides into two large branches as it emerges behind the superior vena cava (Fig. 57.8). A lymph node usually occupies the bifurcation. The superior branch, which is the smaller of the two, goes to the superior lobe and usually divides into two further branches, which supply the majority of that lobe. The inferior branch descends anterior to the intermediate bronchus and immediately posterior to the superior pulmonary vein. It provides a small recurrent branch to the superior lobe, then at the point where the horizontal fissure meets the oblique fissure, it gives off the branch to the middle lobe anteriorly, and the branch to the superior segment of the inferior lobe posteriorly. It then continues a short distance before dividing to supply the rest of the inferior lobe segments.

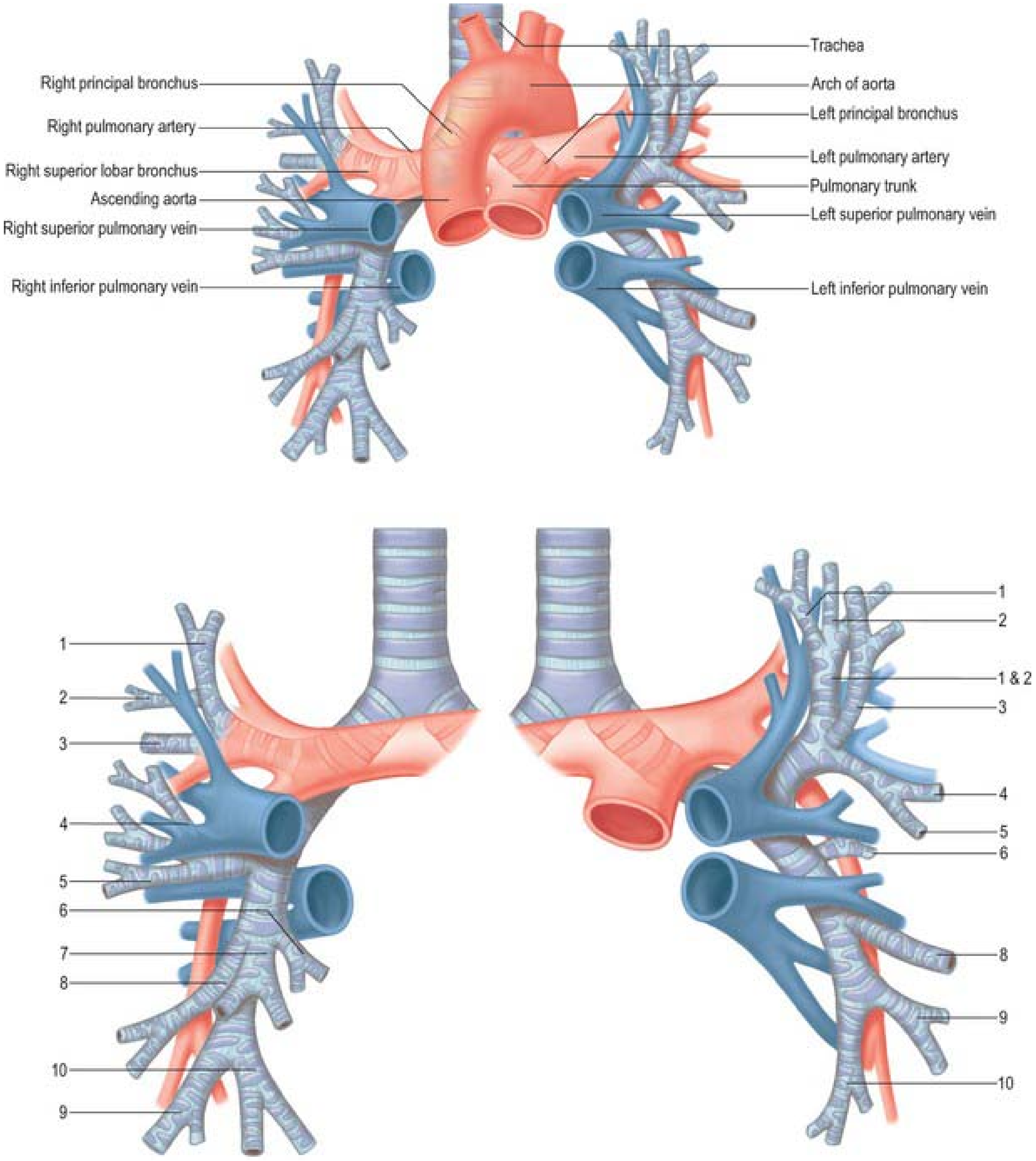
Right principal bronchus
Right pulmonary artery
Right superior lobar bronchus
Ascending aorta
Right superior pulmonary vein
Right inferior pulmonary vein
Trachea
Arch of aorta
Left principal bronchus
Left pulmonary artery
Pulmonary trunk
Left superior pulmonary vein
Left inferior pulmonary vein
1
2
3
4
5
6
7
8
10
9
1
2
1 & 2
3
4
5
6
8
9
10

Fig. 57.8 The relationship between the central airways and the pulmonary vessels. The numbers in the lower figure denote the numbers of the bronchopulmonary segments.

The left pulmonary artery emerges from within the concavity of the aortic arch and descends anterior to the descending aorta to enter the oblique fissure (Fig. 57.8). The branches of the left pulmonary artery are extremely variable. The first and largest branch is usually given off to the anterior segment of the left superior lobe. Before reaching the oblique fissure, the artery gives off a variable number of other branches to the superior lobe, and as it enters the fissure it usually supplies a large branch to the superior segment of the inferior lobe. Lingular branches arise within the fissure, and the rest of the lower lobe is supplied by many varied branching patterns: it was a surgical aphorism of the late Lord Brock that when performing a left upper lobectomy, … 'there was always one more branch of the pulmonary artery than you thought!'.

Pulmonary sequestration

When a portion of lung exists without the appropriate bronchovascular connections, it is usually supplied by the systemic vasculature. Extralobar pulmonary sequestration segments are covered by visceral pleura and usually found below the left lower lobe, whereas intralobar abnormalities are usually embedded in normal lung, classically the posterior basal segment of the left lower lobe. Extralobar pulmonary sequestration *per se* is asymptomatic, but is often associated with other congenital abnormalities.

Pulmonary arteriography and embolization

A thrombus that forms in the legs or pelvic veins may embolize and travel in the right side of the circulation through the right atrium and right ventricle and then lodge in the pulmonary vasculature. The clinical abnormalities observed depend on the size of the embolus. Large emboli may lodge in the main pulmonary artery branches and cause right ventricular dysfunction and hypoxia. Smaller emboli may lodge in segmental pulmonary arteries and cause pleuritic chest pain, shortness of breath and haemoptysis. Pulmonary emboli cause a ventilation/perfusion mismatch that can have serious physiological implications leading to a significant reduction in the oxygenation of blood. Ventilation/perfusion scans with radiolabelled xenon and technetium usually demonstrate segmental abnormalities in perfusion with normal ventilation in the corresponding regions. Pulmonary emboli may also be evaluated by contrast-enhanced spiral CT or pulmonary angiograms and appear as filling defects.

Pulmonary veins

There are usually four pulmonary veins, two from each lung. They originate from capillary networks in the alveolar walls and return oxygenated blood to the left atrium. All the main tributaries of the pulmonary veins receive smaller tributaries, both intra- and inter-segmental; by repeated junctions, tributary veins finally form a single trunk in each lobe, i.e. three in the right lung, and two in the left. The right middle and superior lobar veins usually join and so two veins, superior and inferior, leave each lung.

In the pulmonary hilum, the usual distribution of veins is as follows. The superior pulmonary vein is anteroinferior to the pulmonary artery, and the inferior is the most inferior hilar structure and also slightly posterior. On the right, the union of apical, anterior and posterior veins (draining the upper lobe) with a middle lobar vein (formed by lateral and medial tributaries; Fig. 57.8) forms the superior right pulmonary vein. The inferior right pulmonary vein is formed by the hilar union of superior (apical) and common basal veins from the lower lobe. The union of superior and inferior basal tributaries forms the common basal vein. Occasionally the three right lobar veins remain separate. The right superior pulmonary vein passes posterior to the superior vena cava, the inferior behind the right atrium. On the left, the superior left pulmonary vein, which drains the upper lobe, is formed by the union of apicoposterior (draining the apical and posterior segments), anterior and lingular veins (Fig. 57.8). The inferior left pulmonary vein, which drains the lower lobe, is formed by the hilar union of two veins, superior (apical) and common basal, the latter formed by the union of a superior and an inferior basal vein. Both superior and inferior left pulmonary veins pass anterior to the descending thoracic aorta. Sometimes the two left pulmonary veins form a single trunk, or they may be augmented by an accessory lobar vein from each lobe, which unite to form a third left pulmonary vein.

The right and left pulmonary veins perforate the fibrous pericardium and open separately in the posterosuperior aspect of the left atrium (see Figs 56.1, 56.2B). Their terminations are separated centrally by the oblique pericardial sinus, and laterally by smaller and variable pulmonary venous pericardial recesses that are directed medially and upwards. The pulmonary veins are devoid of valves.

Lymphatics

Pulmonary lymphatic vessels originate in a superficial subpleural plexus. A deep plexus accompanies the branches of the pulmonary vessels and bronchi. Superficial efferents turn round lung borders and the margins of fissures to converge in the bronchopulmonary nodes. There is little anastomosis between the superficial and deep lymphatics, except in the hilar regions. In peripheral parts of the lungs, small channels connect superficial and deep lymphatic vessels, and are capable of dilatation to direct lymph from the deep to the superficial channels when outflow from deep vessels is obstructed by pulmonary disease. There is a tendency for vessels from the upper lobes to pass to the superior tracheobronchial nodes, and those from lower lobes to the inferior tracheobronchial group; however, lymphatic vessels of adjoining lobes connect deep in the fissures and so these connections are not exclusive. At the level of pulmonary lobation, the arrangement of lymphatic vessels follows the central artery of a lobule and its peripheral veins. Lymphoid aggregations, non-follicular in appearance, occur in peribronchial sites and in ‘placoid’ formations adjoining pulmonary pleura.

INNERVATION

The autonomic nervous system controls many aspects of airway function, including regulation of airway smooth muscle tone, mucus secretion from submucosal glands and surface epithelial goblet cells, vascular permeability and blood flow (see Belvisi 2002).

Pulmonary plexuses

The pulmonary plexuses lie anterior and posterior to the other hilar structures of the lungs (see Fig. 56.20). The anterior plexus is small and is formed by rami from vagal and sympathetic cervical cardiac nerves via connections with the superficial cardiac plexus. The posterior pulmonary plexus is formed by the rami of vagal and sympathetic cardiac branches from the second to fifth or sixth thoracic sympathetic ganglia. The left plexus also receives branches from the left recurrent laryngeal nerve. Further details of the pulmonary plexuses are given in the description of the cardiac plexuses in Chapter 56.

MICROSTRUCTURE OF RESPIRATORY SURFACES

Thin-walled respiratory surfaces (alveoli) are distributed as isolated patches within the walls of respiratory bronchioles, and as tube-like alveolar ducts and balloon-like alveolar sacs which contain groups of adjacent alveoli.

Alveolar area

Normal adult human alveoli have a mean total surface area of 143 m^2: an adult respiratory system contains of the order of 300 million alveoli. Their inflated diameter varies with lung position, and is greater in the upper regions than in the lower, because of the increased gravitational pressure at the lung base. These values vary considerably between normal young individuals; the differences become even more marked with age as a consequence of degenerative changes.

Alveolar structure

The alveoli are thin-walled pouches which provide the respiratory surface for gaseous exchange (Figs 57.9-57.11). Their walls contain two types of epithelial cell (pneumocytes) and cover a delicate connective tissue within which a network of capillaries ramifies. Since the walls are extremely thin, they present a minimal barrier to gaseous exchange between the atmosphere and the blood in the capillaries. Adjacent alveoli are frequently in close contact and then the intervening connective tissue forms the central part of an interalveolar septum. Alveolar macrophages are present within the alveolar lumen, and migrate over the epithelial surface.

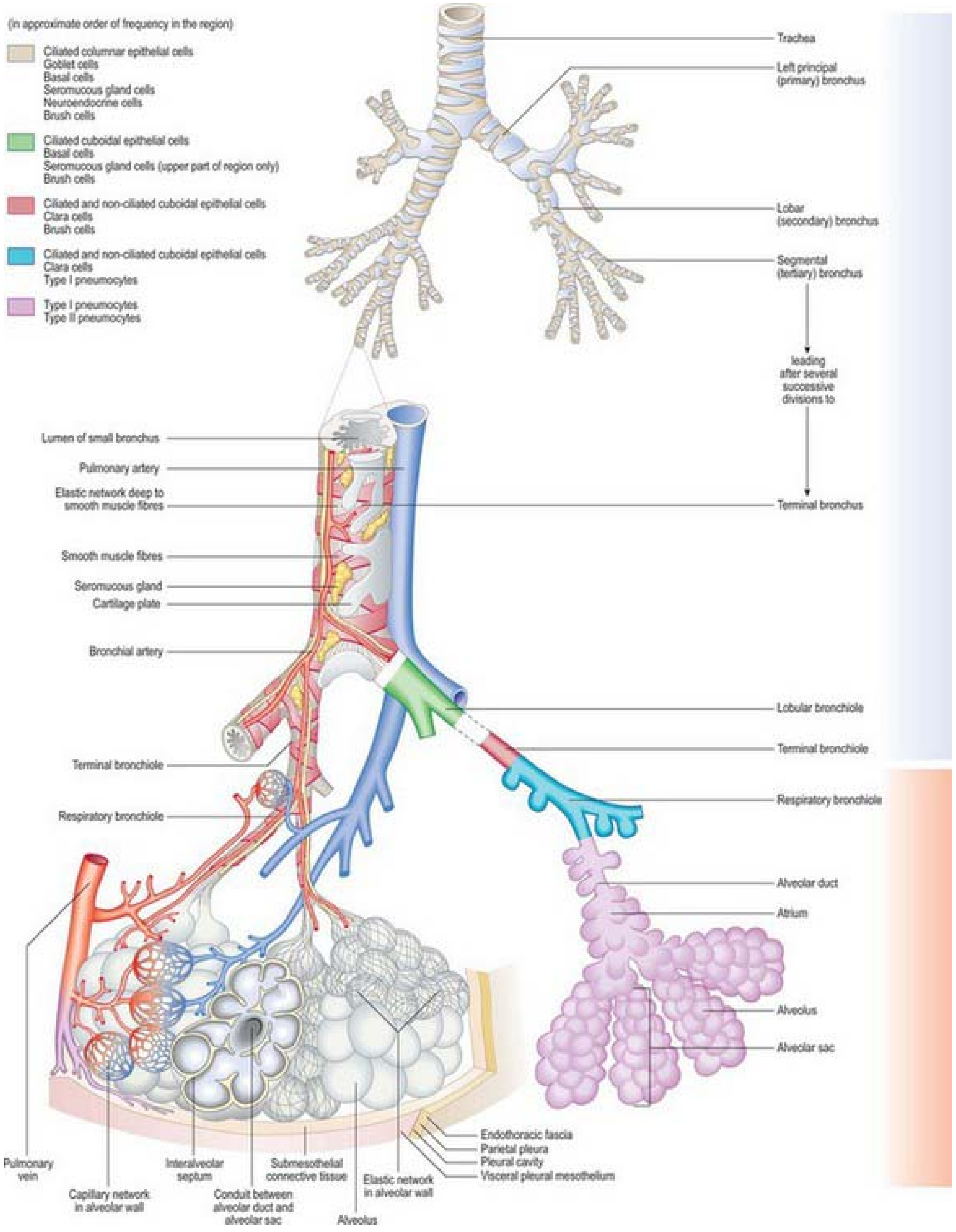
(in approximate order of frequency in the region)
Ciliated columnar epithelial cells
Goblet cells
Basal cells
Seromucous gland cells
Neuroendocrine cells
Brush cells
Ciliated cuboidal epithelial cells
Basal cells
Seromucous gland cells (upper part of region only)
Brush cells
Ciliated and non-ciliated cuboidal epithelial cells
Clara cells
Brush cells
Ciliated and non-ciliated cuboidal epithelial cells
Clara cells
Type I pneumocytes
Type I pneumocytes
Type II pneumocytes
Trachea
Left principal (primary) bronchus
Lobar (secondary) bronchus
Segmental (tertiary) bronchus
leading after several successive divisions to
Terminal bronchus
Lumen of small bronchus
Pulmonary artery
Elastic network deep to smooth muscle fibres
Smooth muscle fibres
Seromucous gland
Cartilage plate
Bronchial artery
Lobular bronchiole
Terminal bronchiole
Terminal bronchiole
Respiratory bronchiole
Respiratory bronchiole
Alveolar duct
Atrium
Alveolus
Alveolar sac
Endothoracic fascia
Parietal pleura
Pleural cavity
Visceral pleural mesothelium
Pulmonary vein
Capillary network in alveolar wall
Interalveolar septum
Conduit between alveolar duct and alveolar sac
Submesothelial connective tissue
Alveolus
Elastic network in alveolar wall

Fig. 57.9 The respiratory tree and its blood supply and drainage, lymphatic drainage and nerve supply. The distribution of the different epithelial cells is shown. Blue = vessels which contain deoxygenated blood; red = vessels which contain oxygenated blood.

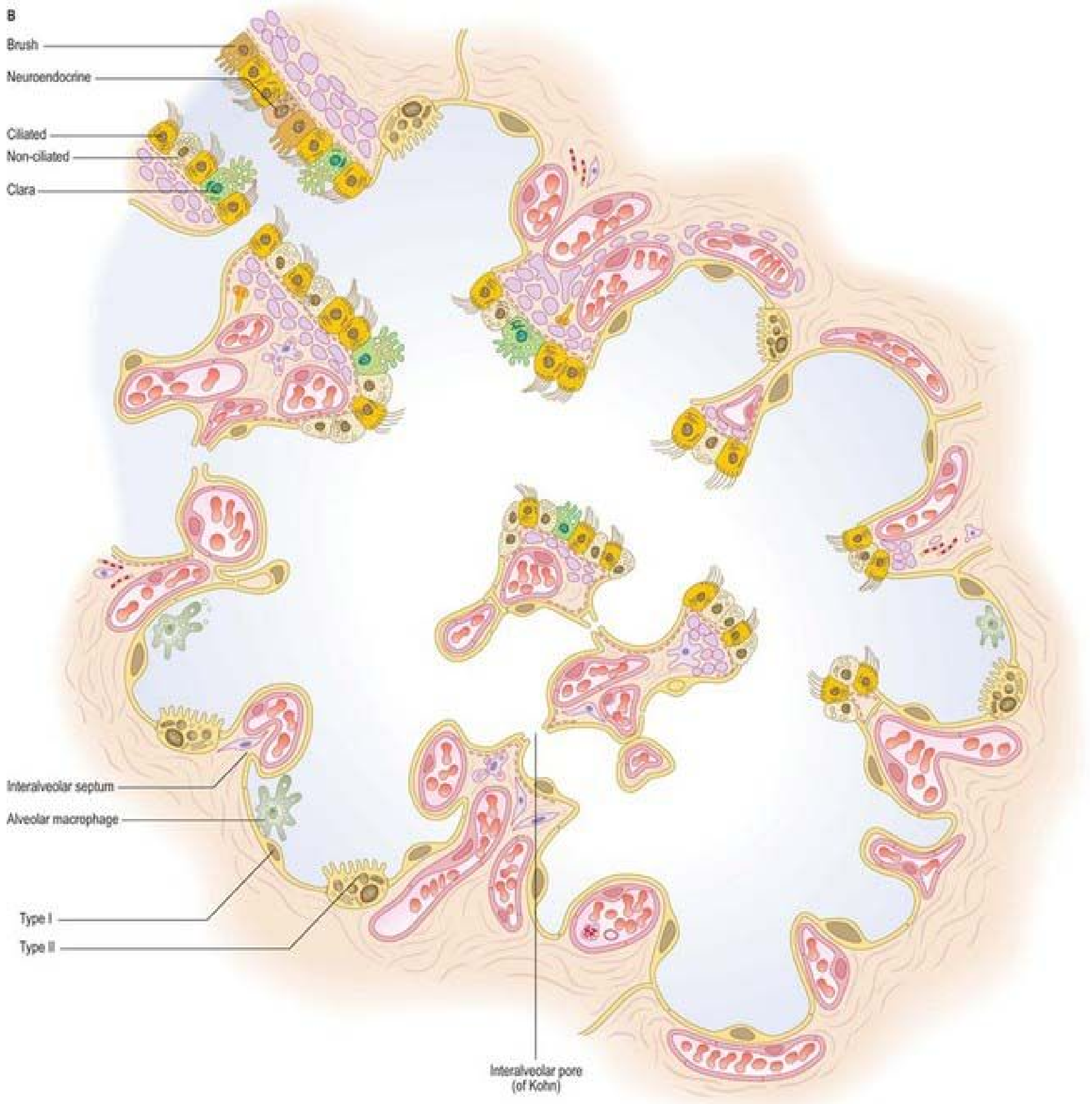
B
Brush
Neuroendocrine
Ciliated
Non-ciliated
Clara
Interalveolar septum
Alveolar macrophage
Type I
Type II
Interalveolar pore
(of Kohn)

Fig. 57.10 The respiratory portion of the lung and its cell types.

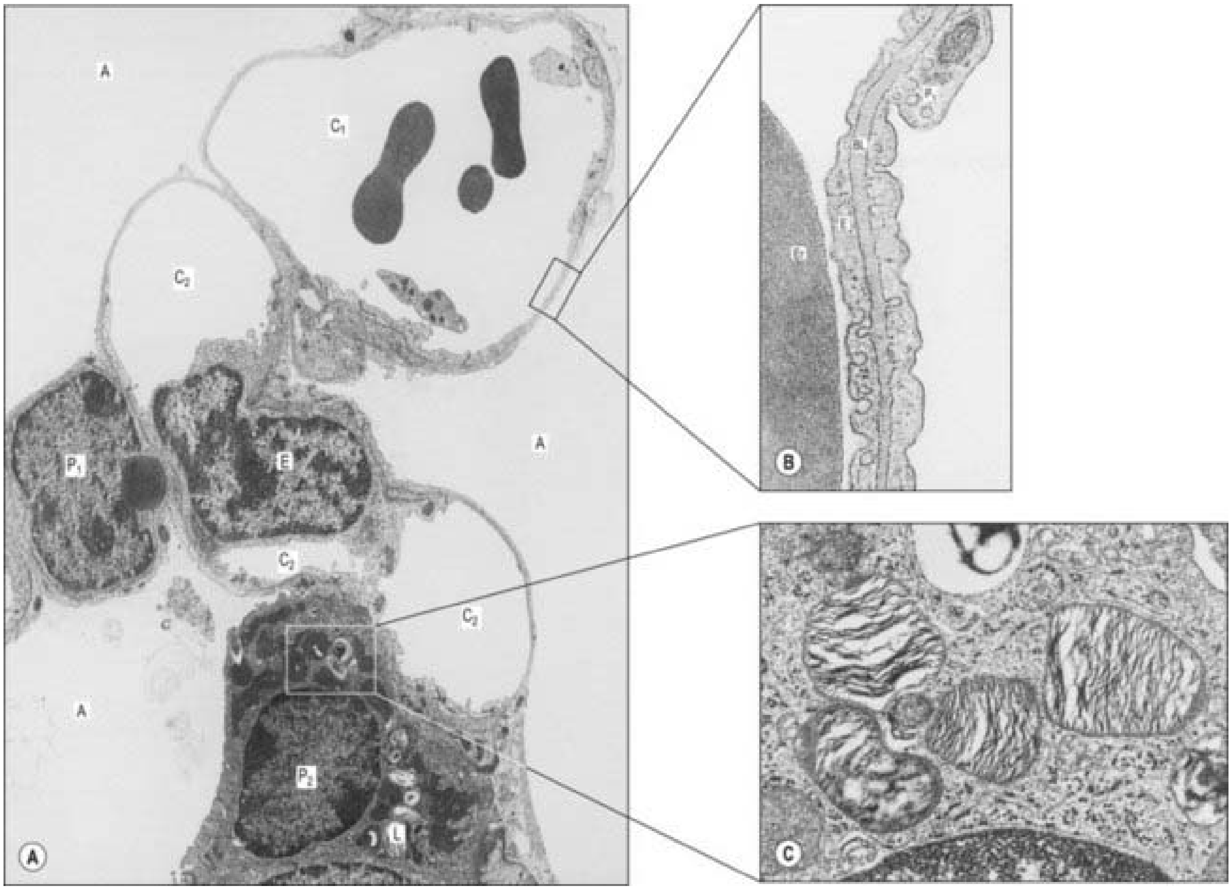

Fig. 57.11 **A**, Electron micrograph showing the septum between three adjacent alveoli (A). The septum contains two capillaries (C_1 and C_2) in section; the lower one is cut obliquely through the nucleus of an endothelial cell (E). Type I pneumocytes (P_1) line the alveolar airspaces except where a type II pneumocyte (P_2), with cytoplasmic lamellar bodies (L), is located. **B**, The thin portion of an interalveolar septum. Part of an erythrocyte (Er) is shown in the capillary lumen, lined by endothelium (E). The alveolar airspace (right) is lined by a type I pneumocyte (P_1). Between these two cells is a shared basal lamina (BL). **C**, Cytoplasmic lamellar bodies in a type II pneumocyte are composed mainly of phospholipids which contribute to the surfactant secreted by these pneumocytes and Clara cells of the respiratory bronchioles.

(By permission from Young B, Heath JW 2000 Wheater's Functional Histology. Edinburgh: Churchill Livingstone.)

Interalveolar septum

The alveolar lining epithelium varies in thickness, but extensive areas of it are as little as 0.05 µm thick (see Fig. 57.11). The epithelium lies on a basal lamina, which, in the thin portions of a septum, is fused with the basal lamina surrounding the adjacent capillaries. The total barrier to diffusion between air and blood in these thin portions may be as little as 0.2 µm. The thick portions of a septum contain connective tissue elements, including elastic fibres, collagen type III fibres, resident and migratory cells (Fig. 57.10).

Alveolar epithelial cells (pneumocytes)

The alveolar epithelium is a mosaic of types I and II pneumocytes. Type I pneumocytes are simple squamous epithelial cells and form over 90% of the alveolar area. Their basal laminae fuse with the basal laminae of the adjacent capillary endothelium to form the thin portions of interalveolar septa. Their cytoplasm is thin (0.05–0.2 µm) which facilitates gaseous diffusion between the lumen of the alveolus and its capillaries. The edges of adjacent cells overlap; they are joined by tight junctions, creating a strict diffusion barrier between the alveolar surface and underlying tissues. Together with a similar endothelial barrier, this arrangement limits the movement of fluid from blood and interstitial spaces into the alveolar lumen (the blood–air barrier). If damaged, type I cells, which do not divide, are replaced by type II cells, which proliferate and differentiate into type I pneumocytes.

The smaller type II cells are often more numerous than type I cells, but they contribute less than 10% of the alveolar surface area. They are rounded cells and protrude from the alveolar surface, particularly at the angles between alveolar profiles. In the human lung they are often associated with interalveolar pores of Kohn. Their cytoplasm contains numerous characteristic secretory lamellar bodies consisting of concentric whorls of phospholipid-rich membrane, the precursors of alveolar surfactant (Fig. 57.11C), which they can recycle.

Interalveolar pores (of Kohn)

These are small pores lined by epithelium (usually type II alveolar cells), which cross interalveolar septa to link adjacent alveolar airspaces. Humans have up to seven pores per alveolus, ranging in size from 2 to 13 μm. These small passages may sustain the flow of air in the event of blockage of one of the alveolar ducts and also provide routes of migration for alveolar macrophages.

Alveolar macrophages

Alveolar macrophages are derived from circulating monocyte precursors. They originate in haemopoietic tissue in the bone marrow, migrate into the alveolar lumen from adjacent blood vessels and connective tissue, and wander about on the epithelial surfaces. They clear the respiratory spaces of inhaled particles which are small enough to reach the alveoli (hence their alternative name of ‘dust cells’). Most of them migrate with their phagocytosed load to the bronchioles, where they are swept into the mucociliary rejection current and removed from the lung. Others migrate through the epithelium of the alveoli into the lymphatics which drain the connective tissue of the lung, and so pass into lymphoid tissue around the pulmonary lobules. Under normal conditions alveolar macrophages have a granular cytoplasm because they contain phagocytosed particles: in smokers the particles have a characteristic appearance, and are called tar bodies. When actively phagocytic, macrophages release proteases: if antiproteases (e.g. $\alpha_1$antitrypsin) that are normally present in the alveolar lining are deficient, macrophage activity may damage the lung. Alveolar macrophages are involved in the turnover of surfactant.

Alveolar macrophages can be recovered from sputum, and are of diagnostic importance if they appear abnormal. For instance, whenever erythrocytes leak from pulmonary capillaries, the macrophages that engulf the extravasated cells become brick red, and are detectable in ‘rusty’ sputum. They are typical of congestive heart failure, and often termed heart-failure cells. Macrophages that migrate back into the connective tissue of the lung settle in patches that are visible beneath the visceral pleura, e.g. carbon-filled cells give the lungs a mottled appearance. However, if the inhaled particles are abrasive or chemically active, they may elude macrophage removal and damage the respiratory surface, producing fibrosis and a concomitant reduction in the respiratory area. This occurs in many industrial diseases, e.g. pneumoconiosis, caused by coal dust, or asbestosis, where the long thin fibres of asbestos can cause considerable damage and may trigger fatal mesothelioma in the pleural lining.

Alveolar surfactant

The alveolar surface is normally covered by a film of pulmonary surfactant, which is a complex mixture, mainly of phospholipids (particularly dipalmitoylphosphatidylcholine and phosphatidylglycerol), with some protein and neutral lipid (Devendra & Spragg 2002). Surfactant is stored in lamellar bodies and secreted in the form of tubular myelin (unrelated to myelin of the nervous system) by type II pneumocytes. It is recycled by type II pneumocytes, or cleared (i.e. phagocytosed) by alveolar macrophages. Clara cells of the bronchiolar epithelium are believed to secrete surfactant of a different composition.

Surface tension at the alveolar surface is very high, because the alveoli are minute. This opposes expansion during inspiration, and tends to collapse the alveoli in expiration. The detergent-like properties of pulmonary surfactant greatly reduce the surface tension, and make ventilation of the alveoli much more efficient.

TRACHEA AND BRONCHI

The trachea is a tube formed of cartilage and fibromuscular membrane, lined internally by mucosa. The anterolateral portion is made up of incomplete rings of cartilage, and the posterior aspect by a flat muscular wall. It is 10–11 cm long, and descends from the larynx (Fig. 57.7) from the level of the sixth cervical vertebra to the upper border of the fifth thoracic vertebra, where it divides into right and left principal (pulmonary) bronchi. It lies approximately in the sagittal plane, but its point of bifurcation is usually a little to the right. The trachea is mobile and can rapidly alter in length; during deep inspiration, the bifurcation may descend to the level of the sixth thoracic vertebra. Its external transverse diameter is typically 2 cm in adult males, and 1.5 cm in adult females. In children it is smaller, more deeply placed and more mobile. The lumen in live adults has an average transverse diameter of 12 mm, although this increases after death because the smooth muscle making up its posterior aspect relaxes. In the first postnatal year, the tracheal diameter does not exceed 4 mm, while during later childhood its diameter in millimetres is approximately equal to age in years. The transverse shape of the lumen is variable, especially in the later decades of life, and may be round, lunate or flattened. At bronchoscopy the posterior wall of the trachea bulges into the lumen and this is exaggerated in expiration and coughing. The distal end of the trachea is visible as a concave spur. A tracheal bronchus may occasionally arise from the lateral wall of the trachea, more frequently from the right side: it may be supernumerary or it may represent a displaced upper lobe airway.

TRACHEAL RELATIONS

Cervical part of the trachea

Anterior relations

The cervical trachea is crossed anteriorly by skin and by the superficial and deep cervical fasciae. It is also crossed by the jugular arch and overlapped by sternohyoid and sternothyroid. The second to fourth tracheal cartilages are crossed by the isthmus of the thyroid gland, above which an anastomotic artery connects the bilateral superior thyroid arteries; below this and in front are the pretracheal fascia, inferior thyroid veins, thymic remnants and the thyroid ima artery (when it exists). In children the brachiocephalic artery crosses obliquely in front of the trachea at, or a little above, the upper border of the manubrium; the left brachiocephalic vein may also rise a little above this level.

Posterior relations

The oesophagus lies behind the cervical trachea, separating it from the vertebral column and the prevertebral fascia.

Lateral relations

The paired lobes of the thyroid gland, which descend to the fifth or sixth tracheal cartilage, and the common carotid and inferior thyroid arteries are lateral relations. The recurrent laryngeal nerves ascend on each side, in or near the grooves between the sides of the trachea and the oesophagus.

Thoracic part of the trachea

Anterior relations

As it descends through the superior mediastinum, the thoracic trachea lies behind the manubrium sterni, the attachments of sternohyoid and sternothyroid, the thymic remnants and the inferior thyroid vein. The brachiocephalic and left common carotid arteries come to lie on the right and left respectively of the trachea as they diverge upwards into the neck. At a lower level, the aortic arch, the brachiocephalic and left common carotid arteries, left brachiocephalic veins, deep cardiac plexus and some lymph nodes are all anterior to the trachea.

Posterior relations

The oesophagus is posterior to the trachea and separates it from the vertebral column.

Lateral relations

Laterally and on the right are the right lung and pleura, right brachiocephalic vein, superior vena cava, right vagus nerve and azygos vein. On the left are the arch of the aorta, and the left common carotid and left subclavian arteries. The left recurrent laryngeal nerve is at first situated between the trachea and aortic arch, and then lies in, or just in front of, the groove between the trachea and the oesophagus.

RIGHT MAIN BRONCHUS

The right principal bronchus is approximately 2.5 cm long, and is wider, shorter and more vertical than the left (Figs 57.7, 57.8, 57.12). These differences explain why inhaled foreign bodies enter the right principal bronchus more often than the left (these events are more common in children and they may present with breathlessness, unilateral wheeze or recurrent aspirations: a chest radiograph may show air trapping in the affected lobe). The right main bronchus gives rise to its first branch, the superior lobar bronchus, then enters the right lung opposite the fifth thoracic vertebra. The azygos vein arches over it, and the right pulmonary artery lies at first inferior, then anterior, to it. After giving off the superior lobar bronchus, which arises posterosuperior to the right pulmonary artery, the right main bronchus crosses the posterior aspect of the artery, enters the pulmonary hilum posteroinferior to it, and divides into a middle and an inferior lobar bronchus. Normal variants in the bronchial anatomy are occasionally seen and consist of either displaced or supernumerary airways (see Ghaye et al 2001). Abnormalities include a common origin of the right upper and middle lobe bronchi; an accessory cardiac bronchus; and a right lower lobe bronchus that may arise from the left main stem bronchus. These anatomical variants are largely asymptomatic, but occasionally may cause haemoptysis, recurrent infection and development of bronchiectasis of the airway.

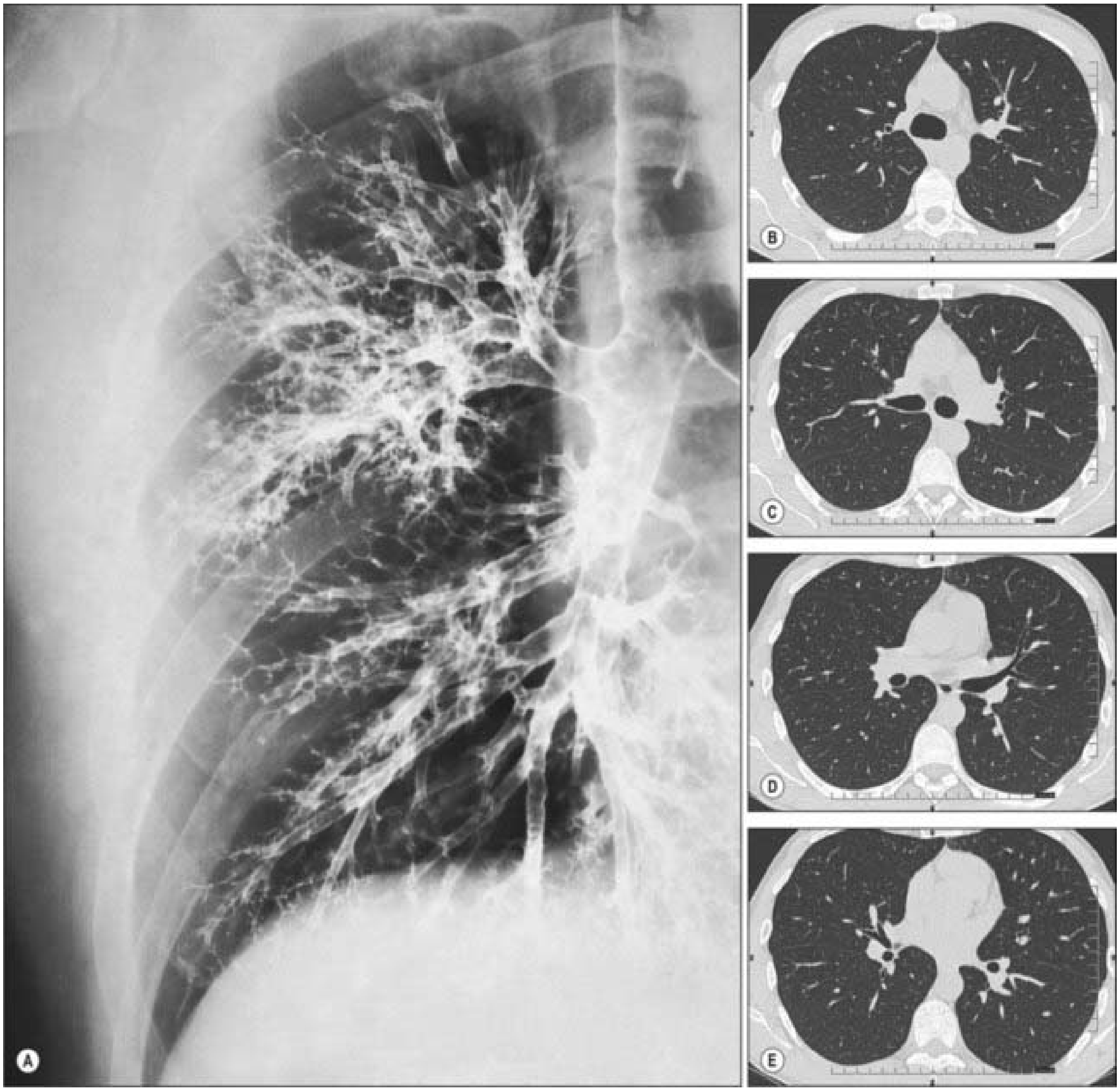

Fig. 57.12 **A**, Bronchogram showing the branching pattern of the trachea and bronchi of the right lung, in a slightly oblique anteroposterior view. In this procedure, a radiopaque contrast medium has been introduced into the respiratory tract to coat the walls of the respiratory passages. For identification of the major branches (compare with Fig. 57.5. **B–E** and Fig. 57.6) CT images demonstrating lobar and segmental bronchial branching. (**B–E** correspond to the 1st, 2nd, 3rd and 4th intercostal spaces, respectively.)

Right superior lobar bronchus

The right superior lobar bronchus arises from the lateral aspect of the parent bronchus and runs superolaterally to enter the hilum; 1 cm from its origin it divides into three segmental bronchi.

Segmental anatomy

The apical segmental bronchus continues superolaterally towards the apex of the lung, which it supplies, and divides near its origin into apical and anterior branches. The posterior segmental bronchus serves the posteroinferior part of the superior lobe, passes posterolaterally and slightly superiorly, and soon divides into a lateral and a posterior branch. The anterior segmental bronchus runs anteroinferiorly to supply the rest of the superior lobe, and divides near its origin into a lateral and an anterior branch of equal size (Figs 57.5, 57.6).

Right middle lobar bronchus

The right middle lobar bronchus normally starts 2 cm below the superior lobar bronchus, from the front of right bronchus intermedius, and descends anterolaterally.

Segmental anatomy

The right middle lobar bronchus soon divides into a lateral and a medial segmental bronchus: these pass to the lateral and medial parts of the middle lobe respectively (Figs 57.5, 57.6).

Right inferior lobar bronchus

The right inferior lobar bronchus is the continuation of the principal bronchus beyond the origin of the middle lobar bronchus.

Segmental anatomy

At or a little below its origin from the principal bronchus, the right inferior lobar bronchus gives off a large superior (apical) segmental bronchus posteriorly. This runs posteriorly to the upper part of the inferior lobe, and then divides into medial, superior and lateral branches; the first two usually arise from a common stem. After giving off the superior segmental branch, the right inferior lobar bronchus descends posterolaterally. The medial basal segmental bronchus branches from its anteromedial aspect, and runs inferomedially to serve a small region below the hilum. The inferior lobar bronchus continues downwards and then divides into an anterior basal segmental bronchus, which descends anteriorly, and a trunk that soon divides into a lateral basal segmental bronchus, which descends laterally, and a posterior basal segmental bronchus, which descends posteriorly. In more than half of all right lungs a subsuperior (subapical) segmental bronchus arises posteriorly from the right inferior lobar bronchus 1–3 cm below the superior segmental bronchus, and is distributed to the region of lung between the superior and posterior basal segments (Figs 57.5, 57.6).

LEFT MAIN BRONCHUS

The left principal bronchus, which is narrower and less vertical than the right, is 5 cm long. Passing to the left inferior to the aortic arch, it crosses anterior to the oesophagus, thoracic duct and descending aorta; the left pulmonary artery is at first anterior and then superior to it. It enters the hilum of the left lung at the level of the sixth thoracic vertebra and divides into a superior and an inferior lobar bronchus.

Left superior lobar bronchus

The left superior lobar bronchus arises from the anterolateral aspect of its parent stem, curves laterally, and soon divides into two bronchi which correspond to the branches of the right principal bronchus as it supplies the right superior and middle lobes, except that on the left side both are distributed to the left superior lobe because there is no separate middle lobe.

Segmental anatomy

The superior division of the left superior lobar bronchus ascends 1 cm, gives off an anterior segmental bronchus, continues a further 1 cm as the apicoposterior segmental bronchus, and then divides into apical and posterior branches. The apical, posterior and anterior segmental bronchi are largely distributed as they are in the right superior lobe. The inferior division descends anterolaterally to the anteroinferior part of the left superior lobe (the lingula) and forms the lingular bronchus, which divides into superior and inferior lingular segmental bronchi. This is different from the pattern in the right middle lobe, where the corresponding distribution is lateral and medial (Figs 57.5, 57.6).

Left inferior lobar bronchus

The left inferior bronchus descends posterolaterally and divides to supply territories of the lung that are distributed in essentially the same manner as they are in the right lung.

Segmental anatomy

The superior (apical) segmental bronchus arises from the inferior lobar bronchus posteriorly 1 cm from its origin. After a further 1–2 cm, the inferior lobar bronchus divides into an anteromedial and a posterolateral stem. The latter divides into lateral and posterior basal segmental bronchi. The anterior basal segmental bronchus is an independent branch of the inferior lobar bronchus occasionally. A subsuperior (subapical) segmental bronchus arises posteriorly from the left inferior lobar bronchus sometimes (Figs 57.5, 57.6).

VASCULAR SUPPLY AND LYMPHATIC DRAINAGE

Trachea

The trachea is supplied with blood mainly by branches of the inferior thyroid arteries. The thoracic portion of the trachea is also supplied by branches of the bronchial arteries that ascend to anastomose with the tracheal branches of the inferior thyroid arteries. Veins draining the trachea end in the inferior thyroid venous plexus. The lymph vessels pass to the pretracheal and paratracheal lymph nodes.

Bronchi

Bronchial arteries

The bronchial arteries supply oxygenated blood to maintain the pulmonary tissues. They are derived from the descending thoracic aorta either directly or indirectly (Baile 1996). The right bronchial artery is usually a branch of the third posterior intercostal artery. There are normally two left bronchial arteries (upper and lower) that branch separately from the thoracic aorta. The bronchial arteries accompany the bronchial tree and supply bronchial glands, the walls of the bronchial tubes and larger pulmonary vessels. The bronchial branches form a capillary plexus in the muscular tunic of the air passages which supports a second, mucosal plexus that communicates with branches of the pulmonary artery and drains into the pulmonary veins. Other arterial branches ramify in interlobular loose connective tissue and most end in either deep or superficial bronchial veins; some also ramify on the surface of the lung, forming subpleural capillary plexuses. Bronchial arteries supply the bronchial wall as far as the respiratory bronchioles, and anastomose with branches of the pulmonary arteries in the walls of the smaller bronchi and in the visceral pleura. These bronchopulmonary anastomoses may be more numerous in the newborn and are subsequently obliterated to a marked degree. In addition to the main bronchial arteries, smaller bronchial branches arise from the descending thoracic aorta: one of these may lie in the pulmonary ligament and may cause bleeding during inferior lobectomy.

Bronchial veins

Usually two on each side, the bronchial veins drain blood from larger bronchi and from hilar structures. They form two distinct systems. Deep bronchial veins commence as intrapulmonary bronchiolar plexuses that communicate freely with the pulmonary veins and eventually join a single trunk that ends in a main pulmonary vein or in the left atrium. Superficial bronchial veins drain extrapulmonary bronchi, visceral pleura and the hilar lymph nodes. They also communicate with the pulmonary veins and end in the azygos vein on the right and in the left superior intercostal or the accessory hemiazygos veins on the left. Bronchial veins do not receive all the blood conveyed by bronchial arteries, some enters the pulmonary veins (see pp. 996–997). The main bronchial arteries and veins run on the dorsal aspect of the extrapulmonary bronchi.

Lymphatic drainage

The deep lymphatic plexus reaches the hilum by travelling along the pulmonary vessels and bronchi. In larger bronchi the deep plexus has submucosal and peribronchial parts, but in smaller bronchi there is only a single plexus that extends to the bronchioles. The walls of the alveoli have no lymphatic vessels.

INNERVATION

The anterior and posterior pulmonary plexuses innervate the trachea and the bronchi. The two plexuses are interconnected. The trachea is innervated by branches of the vagi, recurrent laryngeal nerves and sympathetic trunks. The nerves enter the lung as networks that travel along branches of the bronchi and pulmonary and bronchial vessels as far as the visceral pleura. Efferent vagal preganglionic axons synapse on small ganglia within the walls of the tracheobronchial tree: these may act as sites of integration and/or modulation of the input from extrinsic nerves, or permit some local control of aspects of airway function by local reflex mechanisms. The parasympathetic nervous system is the dominant neuronal pathway in the control of airway smooth muscle tone. Stimulation of cholinergic nerves causes bronchoconstriction, mucus secretion and bronchial vasodilation. Sympathetic nerves may control tracheobronchial blood vessels, but innervation of human airway smooth muscle by sympathetic-adrenergic fibres has yet to be convincingly demonstrated.

MICROSTRUCTURE OF THE CONDUCTING AIRWAYS

The conducting airways are lined internally by a mucosa, and the epithelium lies on a thin connective tissue lamina propria. External to this is a submucosa, also composed of connective tissue, in which are embedded airway smooth muscle, glands, cartilage plates (depending on the level in the respiratory tree), vessels, lymphoid tissue and nerves. Cartilage is present from the trachea to the smallest bronchi, but is absent (by definition) from bronchioles.

Epithelium

The epithelia of the trachea, bronchi and bronchioles are, in general, similar to each other, with graded variations in the numbers of different cell types. The extrapulmonary and larger intrapulmonary passages are lined with respiratory epithelium, which is pseudostratified, predominantly ciliated, and contains interspersed mucus-secreting goblet cells. There are fewer cilia in terminal and respiratory bronchioles, and the cells are reduced in height to low columnar or cuboidal. The epithelium of smaller bronchi and bronchioles is folded into conspicuous longitudinal ridges, which allow for changes in luminal diameter (Fig. 57.9). The epithelium in the respiratory bronchioles progressively reduces in height towards the alveoli, and is eventually composed of cuboidal, non-ciliated cells. Respiratory bronchioles have lateral pouches in their walls, which are lined with squamous cells, so providing an accessory respiratory surface.

Six distinct types of epithelial cell have been described in the conducting airways, namely, ciliated columnar, goblet, Clara, basal, brush and neuroendocrine. Lymphocytes and mast cells migrate into the epithelium from the underlying connective tissue.

Ciliated columnar cells

Ciliated columnar cells are the driving force of the mucociliary rejection current (escalator) in the bronchial tree. They vary from low to tall columnar, and each has up to 300 cilia projecting from the apical surface. The cilia extend into a watery fluid secreted by serous cells of the submucosal glands, but their tips are in contact with a more superficial layer of thicker mucus secreted by surface goblet cells and mucous cells in the submucosal glands. The rate of ciliary beating is usually 12–16 per second, although mechanical stimulation of the epithelial surface, and inflammatory mediators, increase the rate. In addition to tight junctions which seal the apical intercellular space from the airway lumen, the ciliated cells are coupled by gap junctions which allow a change in rate of beating to spread from stimulated cells to their neighbours (probably via calcium signalling) so that their metachronal coordination remains intact.

Goblet cells

Goblet cells are present from the trachea (6000–7000 per mm^2) down to the smaller bronchi, but are normally absent from bronchioles. They contain an apical region full of large secretory vacuoles filled with mucinogen. When the epithelium is irritated, e.g. by tobacco smoke, there is an overall increase in the number of goblet cells, and they also extend into the bronchioles.

Clara cells

Clara cells are cuboidal non-ciliated cells with apices which bulge into the lumen. They contain numerous electron-dense secretory granules and many lysosomes. Clara cells produce surfactant lipoprotein and thus share functional similarities with the type II alveolar cell of pulmonary alveoli, although their secretory granules differ in structure and composition. They may also regulate ion transport.

Basal cells

Basal cells are small rounded cells that occur in parts of the airway lined by pseudostratified respiratory epithelium; they are mitotic stem cells for other epithelial cell types. Basal cells contact the basal lamina and are most frequent in the larger conducting passages.

Brush cells

Brush cells are slender, non-ciliated cells with characteristically long, stiff apical microvilli from which they derive their name. Although infrequent, they are present throughout all parts of the conducting airway passages, including the respiratory epithelium of the nasopharynx. They are in contact with afferent nerve fibres basally and are presumed to have a sensory receptor function.

Neuroendocrine cells

Neuroendocrine cells, also termed dense-core or small granule (Kulchitsky) cells, are found mainly in the basal part of the epithelium. They have a rounded shape and the cytoplasm basal to their nuclei contains numerous small dense-cored vesicles, approximately 150 nm diameter. They form part of the dispersed neuroendocrine system of amine precursor uptake and decarboxylation (APUD) cells. Neuroendocrine cells are most numerous in fetal lungs and their number decreases dramatically after birth. There appears to be little further change in their frequency during adult life, although they may proliferate in certain pulmonary diseases.

Lymphocytes

Small lymphocytes, mainly T cells derived from mucosa-associated lymphoid tissue in the walls of the passages, occur within the epithelium throughout the conducting airway tissues, particularly in the extrapulmonary portion: they are concerned with the immune surveillance of the epithelium. Clusters of lymphocytes sometimes lie beneath non-ciliated epithelial cells of the microfold (M-cell) type.

Mast cells

Mast cells are present within the basal regions of the epithelium. They resemble connective tissue mast cells, and their cytoplasmic histamine-containing granules are released in response to irritants, including inhaled allergens.

Submucosal glands

Tubuloacinar, seromucous glands are present in the submucosa of the trachea and bronchi and, to a lesser extent, in the larger bronchioles. They contain separate mucous and serous cells, and are an important source of the mucous layer at the surface of the ciliated respiratory epithelium. Their secretions include mucins; the bacteriostatic substances lysozyme and lactoferrin; secretory antibodies (IgA) produced by plasma cells in the submucosal connective tissue; and protease inhibitors (e.g. α_1-antitrypsin) important for neutralizing leukocyte-derived proteases, particularly elastase, in the respiratory tract. The secretory acini and tubules are surrounded by myoepithelial cells, which are innervated by autonomic fibres.

Connective tissue and muscle

Broad, longitudinal bands of elastin (Fig. 57.13) within the submucosa follow the course of the respiratory tree and connect with the elastin networks of the interalveolar septa (see Fig. 57.9). This elastic framework is a vital mechanical element of the lung, and is responsible for elastic recoil during expiration.

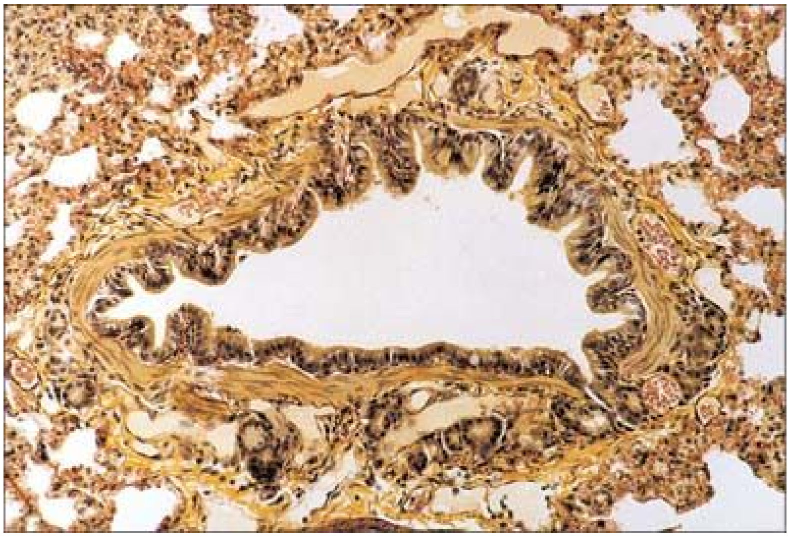

Fig. 57.13 Large bronchiole stained for elastin, showing smooth muscle in the bronchiolar wall and a few small seromucous glands (below).

In the trachea and extrapulmonary bronchi, the smooth muscle is mainly confined to the posterior, non-cartilaginous part of the tracheal tube (Fig. 57.14). Along the entire intrapulmonary bronchial tree, smooth muscle forms two opposed helical tracts which become thinner and finally disappear at the level of the alveoli. The tone of these muscle fibres is under nervous and hormonal control: groups of muscle cells are coupled by gap junctions to spread excitation within fascicles.

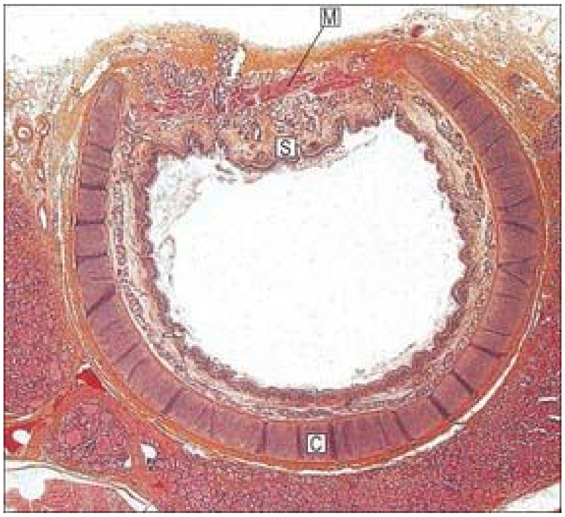

Fig. 57.14 Micrograph of the trachea of a child, sectioned transversely, showing an incomplete cartilage ring (C), joined posteriorly by muscular tissue (M). Seromucous submucosal glands (S) are concentrated in this region and between adjacent cartilages. Note thyroid tissue (bottom).

(By permission from Stevens A, Lowe JS 1996 Human Histology, 2nd edn. London: Mosby.)

Muscle cell contraction narrows the airway, while relaxation permits bronchodilation. Some tone normally exists in the muscular bands, which relax slightly during inspiration and contract during expiration, thereby assisting the tidal flow of air. Abnormal contraction may be caused by circulating smooth muscle stimulants or by local release of excitants such as serotonin, histamine and leukotrienes, which produces bronchospasm. Numerous mast cells are present in the connective tissue of the respiratory tree, especially towards the bronchioles.

Cartilaginous support

The trachea and extrapulmonary bronchi contain a framework of incomplete rings of hyaline cartilage which are united by fibrous tissue and smooth muscle (Fig. 57.14). Intrapulmonary bronchi contain discontinuous plates or islands of hyaline cartilage in their walls.

Tracheal cartilages

Tracheal cartilages vary from 16 to 20 in number. Anteriorly, each cartilage takes the form of an incomplete ring which surrounds approximately two-thirds of the tracheal circumference. Posteriorly, where the cartilages are deficient, the tube is flat and is completed by fibroelastic tissue and smooth muscle. The cartilages are horizontally stacked and separated by narrow intervals. They are typically 4 mm vertically, and 1 mm thick. Their external surfaces are vertically flat, and their internal surfaces are convex. Two or more cartilages often unite, partially or completely, and sometimes bifurcate at their ends. They may become calcified in the elderly. The cartilages are shorter, narrower and less regular in extrapulmonary bronchi, but they are generally similar in shape and arrangement.

The first and last tracheal cartilages differ from the rest (Fig. 57.7). The first cartilage is the broadest. It often bifurcates at one end and is connected by the cricotracheal ligament to the inferior border of the cricoid cartilage, with which it may blend. It may also blend with the second cartilage. The last cartilage is centrally thick and broad and its lower border, the carina, is a triangular hook-shaped process which curves down and backwards between the bronchi (Fig. 57.9). It forms an incomplete ring on each side, and encloses the start of a principal bronchus.

Bronchial cartilages

The irregularity of the cartilaginous plates in the extrapulmonary bronchi increases as they are traced distally, and as the major bronchi approach their lungs and lobes, the plates surround their dorsal aspects. In intrapulmonary bronchi, discontinuous plates of cartilage progressively form less and less of the bronchial wall, and they are not present in the bronchioles.

PULMONARY DEFENSIVE MECHANISMS

The respiratory tract presents a huge surface area that is vulnerable to desiccation, microbial invasion and the mechanical and chemical effects of inhaled particles. Inhaled air is humidified chiefly in the upper respiratory tract where it passes, with some turbulence, over the nasal and buccopharyngeal mucosae. The secretions of the various glands of the bronchial tree also help to prevent desiccation. Goblet cells secrete sulphated acid mucosubstances; cells in mucous glands beneath the epithelial surface contain mainly carboxylated mucosubstances, particularly those associated with sialic acid, although sulphated groups also occur; cells of serous glands contain neutral mucosubstances. Goblet cells respond mainly to local irritation, while tubular glands, both mucous and serous, are mainly under neural and hormonal control. Excessive or altered secretions may obstruct the flow of air. In addition to mucosubstances secreted by bronchial glands, antibacterial and antiviral substances, e.g. lysozyme, antibodies of the IgA type and possibly interferon, also appear in the secreted fluid.

Inhaled particles may be removed via the mucociliary rejection current. Cilia sweep the fluid overlying the surfaces of bronchioles, bronchi and trachea upwards at 1 cm/min, and much of the inhaled matter trapped in the viscous fluid may be removed in this way. Particles small enough to reach the alveoli may be removed by alveolar phagocytes (see p. 998). Alveolar epithelium has limited powers of regeneration but normally is continually replaced. The lifespan of alveolar squamous cells is approximately 3 weeks, and that of alveolar phagocytes is 4 days. Inhaled particles may also be cleared by the cough reflex.

Numerous lymphoid nodules occur in the bronchial lining. They provide foci for the production of lymphocytes and give local immunological protection against infection both by cell-mediated (T-cell) activities, and by the production of immunoglobulins (mainly IgA) from B cells, which are passed on to gland cells for secretion to the epithelial surface.

Anatomy of coughing

Coughing involves an initial deep inspiration, followed by forceful contraction of the expiratory muscles and diaphragm against a closed glottis. This leads to an abrupt rise in pleural pressure (6.5 to 13 kPa) and intra-alveolar pressure. Subsequent glottal opening causes a rapid peak expiratory flow of air, followed by some collapse of the trachea and central airways, which is responsible for the post-peak plateau in flow.

Coughing is initiated when mechanically and chemically sensitive vagal afferents innervating the airways are activated. Data from experimental studies suggest that the receptors innervated by these afferents may be broadly divided into three groups: slowly (SAR) and rapidly (RAR) adapting stretch receptors and bronchopulmonary C fibres. The vagal afferents terminate centrally in largely nonoverlapping regions of the caudal half of the nucleus of the solitary tract; second order neurones from this nucleus terminate in respiratory-related regions of the medulla, pons and spinal cord. Afferent nerves innervating other viscera, and somatosensory nerves innervating the chest wall, diaphragm and anterior abdominal musculature are also likely be involved in regulating cough.

The identity of the afferent terminals in the airways is uncertain; receptors similar to taste buds are considered to be responsible at the laryngeal aditus, and some of the ‘brush cells’ of the respiratory epithelium appear to have neural contacts, and may therefore represent sensory cells with basal synaptic outputs (Widdicombe 2002). Other than the larynx, the carina and branching points of the tracheobronchial tree appear to be the most sensitive areas of the epithelium lining the airways.

For further details, see Kubin et al (2006) and Canning (2006).

BRONCHOSCOPY

Bronchoscopy allows the direct visualization of the vocal cords, trachea and major airways as far as the first division of the subsegmental airway. Occasionally bronchoscopy can also provide some information about structures adjacent to the airways, for example, significant subcarinal lymphadenopathy may cause splaying or widening of the carina. Bronchoscopy enables the acquisition of samples (e.g. bronchial lavage, bronchial brushings, bronchial and transbronchial biopsies), provides information about staging in lung cancer, and facilitates therapeutic procedures (e.g. foreign body removal, ablation of tumours and insertion of airway stents). The information obtained by continuous (spiral) volume CT scanning can be reconstructed to provide three-dimensional images which can be used to create endobronchial views (virtual bronchoscopy, Fig 57.15) or to demonstrate the pulmonary arteries.

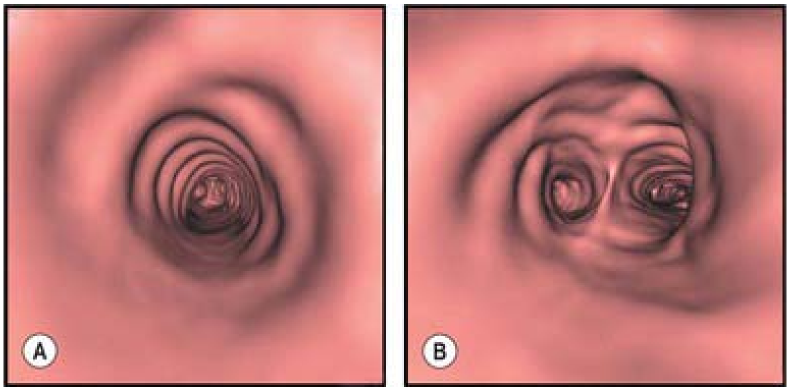

Fig. 57.15 Virtual CT bronchoscopic view obtained by planar reconstruction of spiral CT. **A**, Left main bronchus. **B**, Carina.

(By courtesy of GE Medical Systems.)

REFERENCES

mstrong P. The normal chest. In: Armstrong P, Wilson AG, Dee P, Hansell DM. *Images of the Diseases of the Chest*. London: Mosby; 2000:21-62.

ile EM. The anatomy and physiology of the bronchial circulation. *J Aerosol Med*. 1996;9:1-6.

lvisi MG. Overview of the innervation of the lung. *Curr Opin Pharmacol*. 2002;2:211-215.

nning BJ. Anatomy and neurophysiology of the cough reflex: ACCP evidence-based clinical practice guidelines. *Chest*. 2006;129:33S-47S.

vendra G, Spragg RG. Lung surfactant in subacute pulmonary disease. *Respir Res*. 2002;3:19-22.

aye B, Szapiro D, Fanchamps JM, Dondelinger RF. Congenital bronchial abnormalities revisited. *Radiographics*. 2001;21:105-119.

ffery PK. Microscopic structure of the lung. In: Gibson GJ, Geddes DM, Costabel U, Sterk PJ, Corrin B. *Respiratory Medicine*. 3rd edn. London: Elsevier Science; 2003:34-50.

bin L, Alheid GF, Zuperku EJ, McCrimmon DR. Central pathways of pulmonary and lower airway vagal afferents. *J Appl Physiol*. 2006;101:618-627.

nuta F, Rendina EA, De Giacoma T, et al. Technique to reduce air leaks after pulmonary lobectomy. *Eur J Cardiothorac Surg*. 1998;13:361-364.

iddicombe J. Neuroregulation of cough: implications for drug therapy. *Curr Opin Pharmacol*. 2002;2:256-263.

CHAPTER 58

Diaphragm

The diaphragm is a curved musculofibrous sheet that separates the thoracic from the abdominal cavity (Figs 58.1, 58.2). Its mainly convex upper surface faces the thorax, and its concave inferior surface is directed towards the abdomen. The positions of the domes or cupolae of the diaphragm are extremely variable because they depend on body build and the phase of ventilation. Thus the diaphragm will be higher in short, fat people than in tall, thin people, and overinflation of the lung, as occurs for example in emphysema, causes marked depression of the diaphragm. Usually, after forced expiration the right cupola is level anteriorly with the fourth costal cartilage and therefore the right nipple, whereas the left cupola lies approximately one rib lower. With maximal inspiration, the cupola will descend as much as 10 cm, and on a plain chest radiograph the right dome coincides with the tip of the sixth rib. In the supine position, the diaphragm will be higher than in the erect position, and when the body is lying on one side, the dependent half of the diaphragm will be considerably higher than the uppermost one.

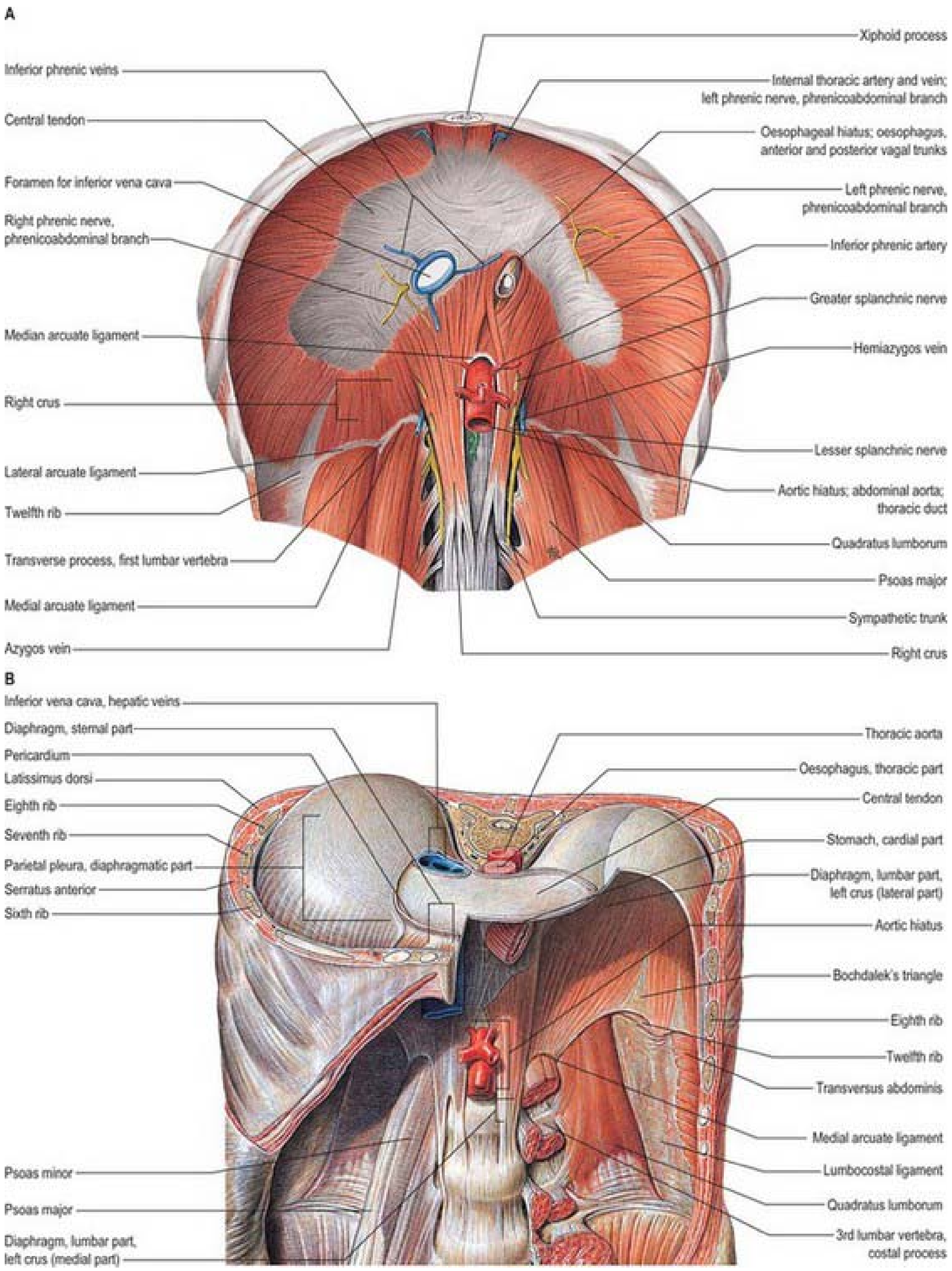
A
Inferior phrenic veins
Central tendon
Foramen for inferior vena cava
Right phrenic nerve, phrenicoabdominal branch
Median arcuate ligament
Right crus
Lateral arcuate ligament
Twelfth rib
Transverse process, first lumbar vertebra
Medial arcuate ligament
Azygos vein
Xiphoid process
Internal thoracic artery and vein; left phrenic nerve, phrenicoabdominal branch
Oesophageal hiatus; oesophagus, anterior and posterior vagal trunks
Left phrenic nerve, phrenicoabdominal branch
Inferior phrenic artery
Greater splanchnic nerve
Hemiazygos vein
Lesser splanchnic nerve
Aortic hiatus; abdominal aorta; thoracic duct
Quadratus lumborum
Psoas major
Sympathetic trunk
Right crus
B
Inferior vena cava, hepatic veins
Diaphragm, sternal part
Pericardium
Latissimus dorsi
Eighth rib
Seventh rib
Parietal pleura, diaphragmatic part
Serratus anterior
Sixth rib
Psoas minor
Psoas major
Diaphragm, lumbar part, left crus (medial part)
Thoracic aorta
Oesophagus, thoracic part
Central tendon
Stomach, cardial part
Diaphragm, lumbar part, left crus (lateral part)
Aortic hiatus
Bochdalek's triangle
Eighth rib
Twelfth rib
Transversus abdominis
Medial arcuate ligament
Lumbocostal ligament
Quadratus lumborum
3rd lumbar vertebra, costal process

Fig. 58.1 **A**, Abdominal aspect of the diaphragm. Note the apertures for the oesophagus and inferior vena cava and the aortic hiatus. The medial part of the right crus frequently consists of three components and extends further

distally than the left crus. **B**, Trunk sectioned at the level of the tenth thoracic vertebra.

(From Sobotta 2006.)

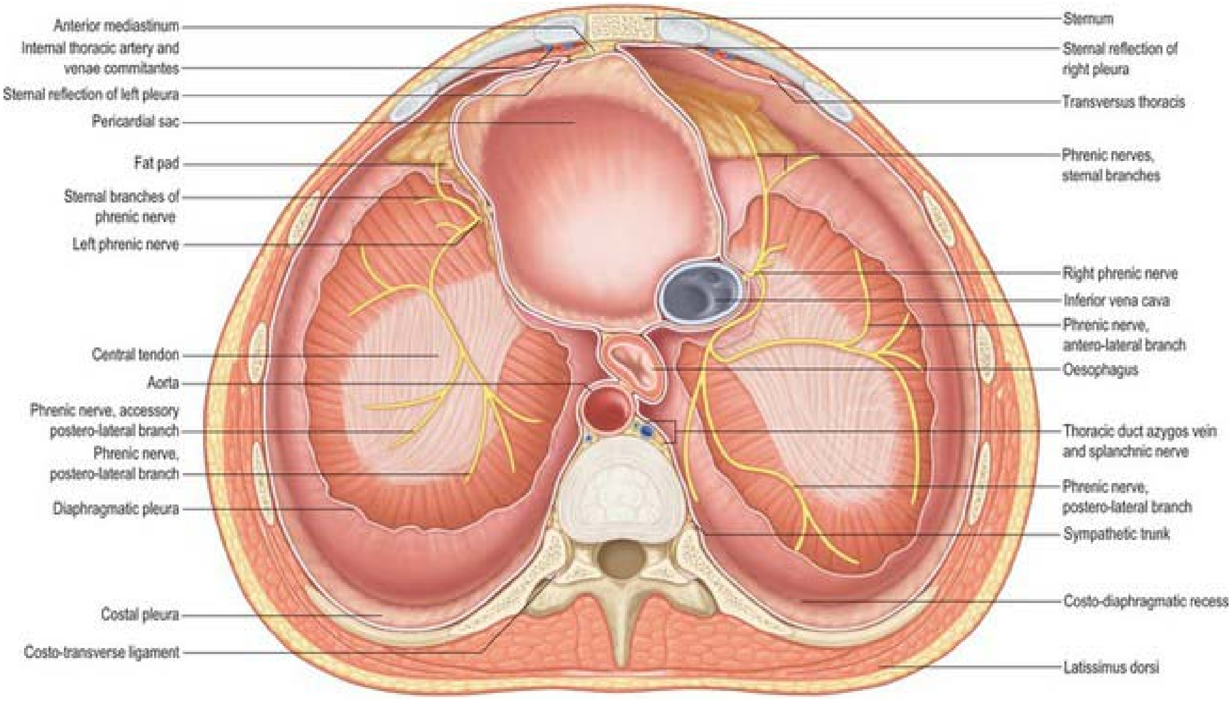
Anterior mediastinum
Internal thoracic artery and venae commitantes
Sternal reflection of left pleura
Pericardial sac
Fat pad
Sternal branches of phrenic nerve
Left phrenic nerve
Central tendon
Aorta
Phrenic nerve, accessory postero-lateral branch
Phrenic nerve, postero-lateral branch
Diaphragmatic pleura
Costal pleura
Costo-transverse ligament
Sternum
Sternal reflection of right pleura
Transversus thoracis
Phrenic nerves, sternal branches
Right phrenic nerve
Inferior vena cava
Phrenic nerve, antero-lateral branch
Oesophagus
Thoracic duct azygos vein and splanchnic nerve
Phrenic nerve, postero-lateral branch
Sympathetic trunk
Costo-diaphragmatic recess
Latissimus dorsi

Fig. 58.2 Thoracic aspect of the diaphragm. Note that the fibres descend from their relatively ‘high’ anterior sternocostal attachments steeply and obliquely to their complex ‘low’ posterior attachments. The phrenic nerves are demonstrated on the diaphragmatic surfaces.

ATTACHMENTS AND COMPONENTS

The muscle fibres of the diaphragm arise from the highly oblique circumference of the thoracic outlet: the attachments are low posteriorly and laterally, but high anteriorly. Although it is a continuous sheet, the muscle can be considered in three parts, sternal, costal and lumbar, which are based on the regions of peripheral attachment. The sternal part arises by two fleshy slips from the back of the xiphoid process, and is not always present. The costal part arises from the internal surfaces of the lower six costal cartilages and their adjoining ribs on each side, and interdigitates with transversus abdominis (see Fig. 54.14). The lumbar part arises from two aponeurotic arches, the medial and lateral arcuate ligaments (sometimes termed lumbocostal arches) and from the lumbar vertebrae by two pillars or crura.

The lateral arcuate ligament is a thickened band in the fascia that covers quadratus lumborum, and it arches across the upper part of that muscle. It is attached medially to the front of the transverse process of the first lumbar vertebra, and laterally to the lower margin of the twelfth rib near its midpoint. The medial arcuate ligament is a tendinous arch in the fascia that covers the upper part of psoas major. Medially, it is continuous with the lateral tendinous margin of the corresponding crus, and is thus attached to the side of the body of the first or second lumbar vertebra. Laterally, it is fixed to the front of the transverse process of the first lumbar vertebra.

The crura are tendinous at their attachments, and blend with the anterior longitudinal ligament of the vertebral column. The right crus is broader and longer than the left, and arises from the anterolateral surfaces of the bodies and intervertebral discs of the upper three lumbar vertebrae. The left crus arises from the corresponding parts of the upper two lumbar vertebrae. The medial tendinous margins of the crura meet in the midline to form an arch, the median arcuate ligament, which crosses the front of the aorta at the level of the thoracolumbar disc; it is often poorly defined.

From these circumferential attachments, the fibres of the diaphragm converge into a central tendon. Fibres from the xiphoid process are short, run almost horizontally and are occasionally aponeurotic. Fibres from the medial and lateral arcuate ligaments, and more especially those from the ribs and their cartilages, are longer. They rise almost vertically at first and then curve towards their central attachment. Fibres from the crura diverge, and the most lateral become even more lateral as they ascend to the central tendon. Medial fibres of the right crus embrace the oesophagus where it passes through the diaphragm, the more superficial fibres ascend on the left, and deeper fibres cover the right margin. Sometimes, a fleshy fasciculus from the medial side of the left crus crosses the aorta and runs obliquely through the fibres of the right crus towards the vena caval opening, but this fasciculus does not continue upwards around the oesophageal passage on the right side.

The central tendon of the diaphragm is a thin but strong aponeurosis of closely interwoven fibres situated near the centre of the muscle, but closer to the front of the thorax, so that the posterior muscular fibres are longer. In the centre it lies immediately below the pericardium, with which it is partially blended. Its shape is trifoliate. The middle, or anterior, leaf has the form of an equilateral triangle with the apex directed towards the xiphoid process. The right and left folia are tongue-shaped and curve laterally and backwards, the left being a little narrower. The central area of the tendon consists of four well-marked diagonal bands fanning out from a thick central node where compressed tendinous strands decussate in front of the oesophagus and to the left of the vena cava.

RELATIONS

The upper surface of the diaphragm is related to three serous membranes. On each side, the pleura separates it from the base of the corresponding lung, and the pericardium is interposed between the middle folium of the central tendon and the heart. This latter area, which is almost flat, is referred to as the cardiac plateau and extends more to the left than the right. In anteroposterior view, the superior profile of the diaphragm rises on either side of the cardiac plateau to a smooth convex dome or cupola, the cupola on the right being higher and slightly broader than that on the left. Most of the inferior surface is covered by peritoneum. The right side is accurately moulded over the convex surface of the right lobe of the liver, the right kidney and right suprarenal gland. The left side conforms to the left lobe of the liver, the fundus of the stomach, the spleen, the left kidney and the left suprarenal (adrenal) gland. In view of these differences in the profile and anatomical relationships of the right and left sides of the diaphragm, the side should always be specified in clinical descriptions. At full inspiration, the right hemidiaphragm is found at the anterior sixth rib on a posteroanterior chest radiograph; the left hemidiaphragm is 1.5–2.5 cm lower than the right (see Fig. 55.16). Unilateral paralysis may be seen as a raised hemidiaphragm on a chest radiograph, but this sign should not be relied upon uncritically in clinical practice.

APERTURES

A number of structures pass between the thorax and abdomen via apertures in the diaphragm. There are three large openings, for the aorta, oesophagus and inferior vena cava, and a number of smaller ones (Fig. 58.2).

The aortic aperture is the lowest and most posterior of the large openings, and is found at the level of the lower border of the twelfth thoracic vertebra and the thoracolumbar intervertebral disc, slightly to the left of the midline. It is an osseo-aponeurotic opening defined by the diaphragmatic crura laterally, the vertebral column posteriorly and the diaphragm anteriorly. Strictly speaking, it lies behind the diaphragm and its median arcuate ligament (when present). Occasionally, some tendinous fibres from the medial parts of the crura also pass behind the aorta, converting the opening into a fibrous ring. The aortic opening transmits the aorta, thoracic duct, lymphatic trunks from the lower posterior thoracic wall and, sometimes, the azygos and hemiazygos veins.

The oesophageal aperture is located at the level of the tenth thoracic vertebra, above, in front and a little to the left of, the aortic opening. It transmits the oesophagus, gastric nerves, oesophageal branches of the left gastric vessels and some lymphatic vessels. The elliptical opening has a slightly oblique long axis, and is bounded by muscle fibres that originate in the medial part of the right crus and cross the midline, forming a ‘chimney’ approximately 2.5 cm long, which accommodates the terminal portions of the oesophagus. The outermost fibres run in a craniocaudal direction, and the innermost fibres are arranged circumferentially. There is no direct continuity between the oesophageal wall and the muscle around the oesophageal opening. The fascia on the inferior surface of the diaphragm is continuous with the transversalis fascia and is rich in elastic fibres. It extends upwards into the opening as a flattened cone to blend with the wall of the oesophagus 2–3 cm above the oesophago-gastric (squamocolumnar) junction. Some of its elastic fibres penetrate to the submucosa of the oesophagus. This peri-oesophageal areolar tissue is referred to as the phreno-oesophageal ligament. It connects the oesophagus flexibly to the diaphragm, permitting some freedom of movement during swallowing and ventilation while at the same time limiting upward displacement of the oesophagus.

The vena caval aperture, the highest of the three large openings, lies at about the level of the disc between the eighth and ninth thoracic vertebrae. It is quadrilateral, and located at the junction of the right leaf with the central area of the tendon, and so its margins are aponeurotic. It is traversed by the inferior vena cava, which adheres to the margin of the opening, and by some branches of the right phrenic nerve.

There are two lesser apertures in each crus: one transmits the greater, and the other the lesser, splanchnic nerve. The ganglionated sympathetic trunks usually enter the abdominal cavity behind the diaphragm, deep to the medial arcuate ligament. Openings for minute veins frequently occur in the central tendon.

On each side of the diaphragm there are small areas where the muscle fibres are replaced by areolar tissue. One, between the sternal and costal parts, contains the superior epigastric branch of the internal thoracic artery and some lymph vessels from the abdominal wall and convex surface of the liver. The other, between the costal part and the fibres that spring from the lateral arcuate ligament, is less constant; when it is present, the posterosuperior surface of the kidney is separated from the pleura only by areolar tissue.

Oesophageal reflux

Reflux of gastric contents into the oesophagus, with risk of inhalation into the lungs, is normally prevented by a physiological antireflux barrier located at the gastro-oesophageal junction. The major components of this barrier are the specialized smooth muscle of the wall of the lower oesophagus and the encircling fibres of the crural diaphragm. See also Chapter 65.

Hiatus hernia

The diaphragm lends additional power to all expulsive efforts: sneezing, coughing, laughing, crying, urinating, defecating, and expelling the fetus from the uterus are all preceded by a deep inspiration. Similarly, a deep inspiration followed by closure of the glottis is a common preliminary to powerful recruitment of the trunk muscles, e.g. in lifting heavy weights, because the increased intra-abdominal pressure provides pneumatic bracing of the vertebral column. Repeated stress may eventually compromise the integrity of the hiatus, so that the muscular hiatal tunnel widens. Concomitant laxity of the phreno-oesophageal membrane allows the gastro-oesophageal junction to slide into the thorax; this is usually termed a sliding, or type I, hiatus hernia (Kahrilas 2001). Sliding hernias are typically acquired. They commonly occur in the fifth decade of life and are found in more than 50% of patients with gastro-oesophageal reflux, a condition that induces tonic contraction of the longitudinal oesophageal muscle, which further exacerbates the hiatus hernia. When the stomach herniates into the thorax alongside the oesophagus, it is termed a para-oesophageal, or type II, hiatus hernia.

Congenital hernias/eventration

Abdominal organs, usually the stomach, may herniate through the diaphragm into the thorax. There are three sites at which such hernias can occur: posterolateral (Bochdalek), subcostosternal (Morgagni) and oesophageal.

The most common is a posterolateral (Bochdalek) hernia, which occurs as a result of a defect in the posterior diaphragm in the region of the tenth or eleventh ribs. It is more common on the left, and presents with abdominal contents in the left hemithorax at birth; clinically significant cases develop hypoxaemia and respiratory failure at birth. A chest radiograph demonstrates mediastinal shift to the contralateral side and the presence of the gastrointestinal contents in the thorax; the diagnosis should be made at routine prenatal ultrasound. Treatment involves decompression of the gastrointestinal contents and cardiopulmonary stabilization. Surgical repair is performed when the patient is stable, but prognosis is determined by the degree of accompanying pulmonary hypoplasia, severity of pulmonary vascular abnormalities and any associated congenital heart defects.

Subcostosternal hernia, first described by Morgagni, is uncommon and occurs through a defect in the anterior diaphragm just lateral to the xiphoid process. It is frequently asymptomatic.

Oesophageal hernia occurs as a result of a defect in the oesophageal aperture, so that part of the stomach herniates into the thorax. It is rarely congenital in origin, usually develops later in life, and is believed to be acquired.

Diaphragmatic trauma

Closed and penetrating thoracoabdominal injuries may result in rupture or laceration of the diaphragm. With closed injuries and diaphragmatic rupture, there may be subsequent herniation of the abdominal contents into the thorax. Spiral CT with planar reformation should be the primary investigation (Shanmuganathan et al 2000): MRI is usually performed when other imaging modalities have produced equivocal findings. Early operative repair is recommended in diaphragmatic trauma, because untreated cases are at risk of developing gastrointestinal obstruction or perforation. Patients with penetrating injuries may require additional assessment by thoracoscopy (Lowdermilk & Naunheim 2000).

VASCULAR SUPPLY

ARTERIES

The lower five intercostal and subcostal arteries supply the costal margins of the diaphragm while the phrenic arteries supply the main central portion of the diaphragm. The anastomotic arrangement (see p. 1010) ensures profuse blood supply.

Phrenic arteries

Two small phrenic vessels help to supply the diaphragm via the abdominal surface. They may arise separately from the aorta, just above its coeliac trunk, or by a common aortic stem, or from the coeliac trunk. Occasionally, one is from the aorta, the other from a renal artery. Each artery ascends laterally anterior to a crus of the diaphragm, near the medial border of the suprarenal gland. The left passes behind the oesophagus and then runs forwards on the left side of its diaphragmatic opening. The right phrenic artery passes posterior to the inferior vena cava, and then along the right side of its opening. Each phrenic artery divides into medial and lateral branches near the posterior border of the central tendon. The medial branch curves forwards to anastomose with its contralateral fellow in front of the central tendon and with the musculophrenic and pericardiacophrenic arteries. The lateral branch approaches the thoracic wall, and anastomoses with the lower posterior intercostal and musculophrenic arteries. The lateral branch of the right artery supplies the inferior vena cava, whereas the left sends ascending branches to the oesophagus. Invariably there is a communicating artery between the left gastric and inferior phrenic arteries.

VEINS

Phrenic veins

The phrenic veins follow the corresponding arteries on the inferior diaphragmatic surface. The right phrenic vein ends in the inferior vena cava. The left phrenic vein is often double: one branch ends in the left renal or suprarenal vein, the other passes anterior to the oesophageal opening to join the inferior vena cava.

INNERVATION

The diaphragm receives its motor supply via the phrenic nerves (Fig. 58.3). Sensory fibres are distributed to the peripheral part of the muscle by the lower six or seven intercostal nerves. The right crus of the diaphragm, the fibres of which divide to the right and left of the oesophageal opening, is innervated by both right and left phrenic nerves. There is some evidence that the crural fibres contract slightly before the costal part, and this may be functionally significant for non-respiratory tasks (Sharshar et al 2005).

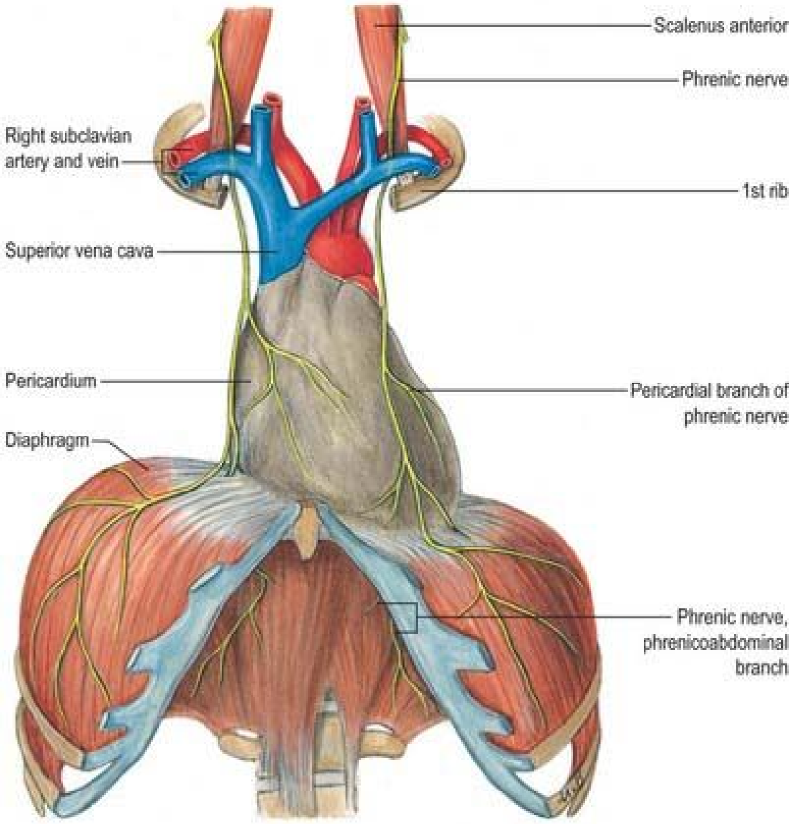
Scalenus anterior
Phrenic nerve
Right subclavian artery and vein
1st rib
Superior vena cava
Pericardium
Pericardial branch of phrenic nerve
Diaphragm
Phrenic nerve, phrenicoabdominal branch

Fig. 58.3 The distribution of the right and left phrenic nerves.

(From Sobotta 2006.)

Phrenic nerve

The phrenic nerve is a mixed nerve that provides the sole motor supply to the diaphragm. It is derived mostly from the fourth cervical ramus, but also receives contributions from the third and fifth cervical rami (see Fig. 43.6). The course of the cervical part of the phrenic nerve is described on page 456. Within the thorax, the phrenic nerve descends anterior to the pulmonary hilum, between the fibrous pericardium and mediastinal pleura, to the diaphragm, accompanied by the pericardiophrenic vessels. In its thoracic course, each phrenic nerve supplies sensory branches to the mediastinal pleura, fibrous pericardium and parietal serous pericardium. The right and left phrenic nerves differ in their intrathoracic relationships (Rajanna 1947).

Right phrenic nerve

The right phrenic nerve is shorter and more vertical than the left, and is separated at the root of the neck from the second part of the right subclavian artery by scalenus anterior. It subsequently descends lateral to the right brachiocephalic vein, the superior vena cava and the fibrous pericardium that covers the right surface of the right atrium and inferior vena cava, and divides just above or at the level of the diaphragm (Fig. 58.2).

Left phrenic nerve

At the root of the neck, the left phrenic nerve is commonly stated to leave the medial edge of scalenus anterior and to pass anterior to the first part of the left subclavian artery and behind the thoracic duct. However, sometimes the right and left nerves are symmetric in their cervical course, and so the left phrenic nerve may cross anterior to the second part of the left subclavian artery, separated from it by scalenus anterior at the level of the thoracic inlet. Thereafter, the left phrenic nerve crosses anterior to the left internal thoracic artery, descending across the medial aspect of the apex of the left lung and its pleura to the first part of the subclavian artery, which it crosses obliquely to reach a groove between the left common carotid and subclavian arteries. It passes anteromedially, superficial to the left vagus nerve just above the aortic arch and behind the left brachiocephalic vein, and then passes superficial to the aortic arch and the left superior intercostal vein, anterior to the left pulmonary hilum, to lie between the fibrous pericardium covering the surface of the left ventricle and the mediastinal pleura (see Fig. 56.1).

Diaphragmatic relationships

The right phrenic nerve passes through the central tendon of the diaphragm, either by the caval aperture or just lateral to it. The left phrenic nerve passes through the muscular part of the diaphragm anterior to the central tendon, just lateral to the left cardiac surface and more anterior than the right phrenic nerve (Fig. 58.2). At the diaphragm or slightly above it, each phrenic nerve supplies fine branches to the parietal pleura above, and the parietal peritoneum below, the central diaphragm. Typically, the trunk of each nerve then divides into three branches as it passes through the diaphragm. These are commonly arranged as follows (with some variation): an anterior (sternal) branch, which runs anteromedially towards the sternum and connects with its fellow; an anterolateral branch, which runs laterally anterior to the lateral leaf of the central tendon; a short posterior branch, which divides into a posterolateral ramus coursing behind the lateral leaf and a posterior (crural) ramus which supplies the crural fibres. Posterolateral and crural branches may arise separately from the phrenic nerve. These main branches may be submerged in diaphragmatic muscle or lie below it. They supply motor fibres to the muscle and sensory fibres to the peritoneum and pleura related to the central part of the diaphragm. They also relay proprioceptive fibres from the musculature. The right phrenic nerve supplies the part of the right crus to the right of the oesophagus, and the left phrenic nerve supplies the left crus and the part of the right crus that lies on the left of the oesophagus. Phrenic rami connect with branches of the coeliac plexuses on the inferior surface of the diaphragm, and there is a small phrenic ganglion on the right, at the junction of the plexuses. Rami from the plexuses supply the suprarenal glands and, on the right, the hepatic falciform and coronary ligaments, the inferior vena cava and, possibly (via connections with coeliac and hepatic plexuses), the gallbladder.

Lesions of the phrenic nerve

An appreciation of the location of the main branches of the phrenic nerves is important to avoid iatrogenic surgical damage. Radial incisions in the diaphragm from the costal margin to the oesophageal hiatus lead to diaphragmatic paralysis, whereas thoracoabdominal incisions in a circumferential manner in the periphery of the diaphragm do not involve any significant branches of the phrenic nerves and preserve diaphragmatic function. Similarly, incisions of the central tendon are safe.

Division of the phrenic nerve in the neck completely paralyses the corresponding half of the diaphragm, which atrophies. If an accessory phrenic nerve exists, section or crushing of the main nerve as it lies on scalenus anterior will not produce complete paralysis. The phrenic nerve may be involved with traumatic lesions of the upper brachial plexus. Historically, it was deliberately injured in order to collapse, and hence rest, the lung in patients with pulmonary tuberculosis. Cardiac surgery is one of the most common medical causes of phrenic nerve injury, especially as a result of the instillation of saline slush for myocardial preservation. Other causes include thoracic surgery, tumours of the lung or mediastinum, and infections such as polio. Respiratory muscle weakness of rapid onset is a feature of Guillain–Barré syndrome.

Phrenic nerve damage leads to paradoxical movement of the diaphragm that is best observed fluoroscopically, with the patient first in the upright position (diaphragm unloaded), and then supine with a small weight on the abdomen (diaphragm loaded). Diaphragmatic paralysis can also be assessed by ultrasound examination with a sniff manoeuvre. The ‘gold standard’ for assessment of the phrenic nerve/diaphragm unit is electrical or magnetic stimulation of the phrenic nerve with recording of the compound muscle action potential and/or the transdiaphragmatic pressure. Electrical stimulation of the diaphragm, by ‘pacing’ of one or both phrenic nerves, has been used with some success in infants with central alveolar hypoventilatory syndrome (‘Ondine’s curse’) and in patients with high cervical lesions of the spinal cord, in whom the diaphragm is paralysed but the lower motor neurones are intact. Electrodes are placed adjacent to the nerves, sometimes in the neck but more usually in the chest, and a ventilatory rhythm is established by trains of stimuli delivered by an implanted device. Because this is an unphysiological way of recruiting the muscle, the fibres must be ‘conditioned’ during the initial period of stimulation, so that they acquire the necessary resistance to fatigue.

Referred pain

Diaphragmatic pain is frequently felt at the tip of the shoulder, reflecting common nerve root origins in the neck. It usually occurs when there is inflammation of the diaphragmatic pleura, e.g. in basal pneumonia, pleural effusions or malignant disease.

Accessory phrenic nerve

The accessory phrenic nerve is described in Chapter 28.

ANATOMY OF BREATHING

Breathing is a highly coordinated abdominal and thoracic process. The diaphragm is the major muscle of inspiration, responsible for approximately two-thirds of quiet breathing in healthy humans. The external intercostal muscles are most active in inspiration, and the internal intercostals, which are not as strong, are most active in expiration. Increasing the vertical, transverse and anteroposterior dimensions of the chest increases the volume of the pleural space, and the resulting decrease in intrapleural pressure draws air into the lungs. During expiration, the diaphragm relaxes and moves superiorly. Air is expelled from the lungs and the elastic recoil of the lung creates a subatmospheric pressure that returns the lateral and anteroposterior dimensions of the thorax to normal (De Troyer & Estenne 1988, Celli 1998).

During inspiration, the lowest ribs are fixed, and contraction of the diaphragm draws the central tendon downwards. In this movement, the curvature of the diaphragm is scarcely altered. The cupolae move downwards and a little forwards almost parallel to their original positions. The associated downward displacement of the abdominal viscera is permitted by the extensibility of the abdominal wall, but the limit of this extensibility is soon reached. The central tendon, its motion arrested by the abdominal viscera, then becomes a fixed point from which the fibres of the diaphragm continue to contract. This causes the second to tenth ribs to be elevated and the inferior portions of the ribs are turned outwards as a result of direct transmission of pressure through the zone of apposition (Fig. 58.4). The medial aspect of the rib is elevated and this increases the transverse dimension of the chest in the same manner as a bucket handle swinging outwards (Fig. 58.5A). This effect is most evident in the lower ribs (seventh to tenth ribs). Movements at the costovertebral joints cause elevation of the anterior ends of the ribs that push the body of the sternum and the upper ribs forwards. This ‘pump handle’ movement is most evident in the superior ribs (second to sixth ribs) and increases the anteroposterior dimension of the thorax (Fig. 58.5B). The right cupola of the diaphragm, which lies on the liver, has a greater resistance to overcome than the left, which lies over the stomach, and so the right crus and the fibres of the right side are more substantial than those of the left. The balance between descent of the diaphragm, protrusion of the abdominal wall (‘abdominal’ breathing), and elevation of the ribs (‘thoracic’ breathing) varies in different individuals and with the depth of ventilation. The thoracic element is usually more marked in females, but increases in both sexes during deep inspiration.

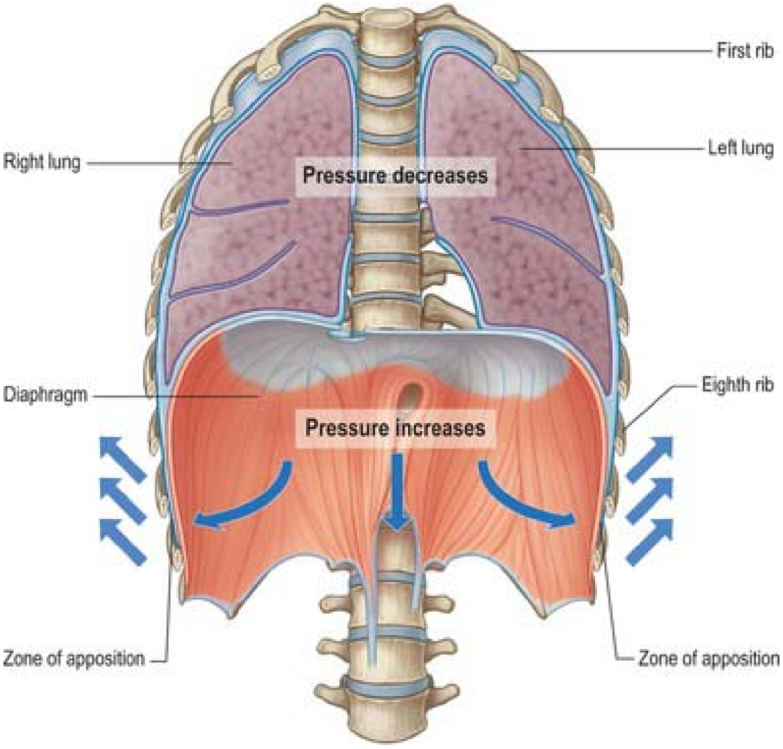
First rib
Right lung
Left lung
Pressure decreases
Diaphragm
Eighth rib
Pressure increases
Zone of apposition
Zone of apposition

Fig. 58.4 Inspiratory movements: pressure changes during inspiration.

(Adapted from Drake, Vogl and Mitchell 2005.)

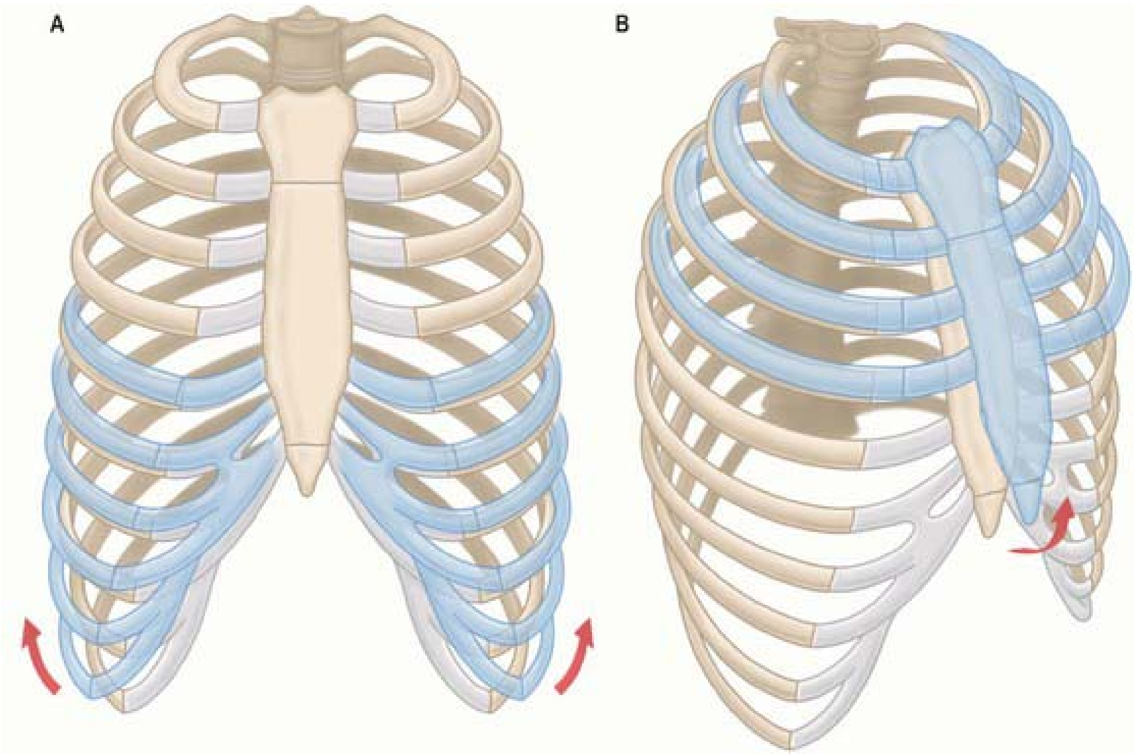

Fig. 58.5 Movements of the ribs during inspiration (**A**) increase the transverse diameter of the chest by the ‘bucket handle’ movement, and (**B**) increase the anteroposterior dimension of the thorax by the ‘pump handle’ movement.

Diaphragmatic excursion is typically 1.5 cm in quiet breathing. During deep ventilation, the maximum movement ranges from 6 to 10 cm. After a forced inspiration, e.g. when breathing is partially obstructed, the right cupola of the diaphragm can descend to about the level of the eleventh thoracic vertebra, while the left cupola may reach the level of the body of the twelfth thoracic vertebra. After a forced expiration, the right cupola of the diaphragm is level anteriorly with the fourth costal cartilage, laterally with the fifth, sixth and seventh ribs, and posteriorly with the eighth rib, and the left cupola is a little lower.

The level of the diaphragm is affected by the phase and depth of ventilation, and by the degree of distension of the stomach and intestines and the size of the liver. Radiographs show that the height of the diaphragm within the thorax also varies considerably with posture. It is highest when the body is supine, and in this position it performs the greatest ventilatory excursions with normal breathing. When the body is erect, the diaphragm is lower, and its ventilatory movements become smaller. The diaphragmatic profile is still lower in the sitting posture, and ventilatory excursions are smallest under these conditions. When the body is horizontal and on one side, the two halves of the diaphragm do not behave in the same way. The uppermost half sinks to a lower level than that seen when sitting, and moves little with ventilation. The lower half rises higher in the thorax than it does even in the supine position, and its ventilatory excursions are considerably greater. Changes in the level of the diaphragm with alterations in posture explain why patients with severe dyspnoea are most comfortable, and least short of breath, when sitting up.

The primary role of the intercostal muscles is to stiffen the chest wall, preventing paradoxical motion during descent of the diaphragm in inspiration. This becomes most obvious immediately after high spinal injury, when there is flaccid paralysis of the entire trunk and only the diaphragm is left functioning. In a healthy adult with a vital capacity of 4.5 L, some 3 L is accounted for by diaphragmatic excursion. Immediately after high spinal injury, the vital capacity decreases to about 300 mL, even though the diaphragm is moving maximally, because some 2.7 L is lost by paradoxical incursion of the flaccid chest wall as the diaphragm descends. With time (usually several weeks), the paralysis becomes spastic, stiffening the chest wall, and the vital capacity increases towards its phrenic limit of about 3 L.

In the same way, high spinal injury reveals the role of the abdomen in inspiration and expiration. The abdominal musculature plays a major role in active expiration in man. During the flaccid stage of high spinal paralysis, the only mechanisms available for returning the relaxed diaphragm into the thorax on expiration are passive recoil of the lungs and chest wall, and the weight of the abdominal viscera. The latter is the most important, and operates only when patients are lying down. If they are sat up or raised upright, they are unable to breathe out. Trussing the abdomen with an elastic binder can help such patients. Conversely, when paralysis becomes spastic, the stiff abdominal wall opposes inspiration.

The role of the abdomen in breathing is often underestimated. If, for example, the anterolateral wall were made of steel and linked the pelvic rim rigidly to the costal margins, inspiration would be impossible. The diaphragm could not descend (because the abdominal contents are incompressible), and the ribs could not rise (because the links to the pelvis would be inextensible). During normal breathing, the abdomen relaxes as the diaphragm contracts. It is possible to oppose this motion by tensing the abdomen, as in the ‘beach posture’ adopted to exaggerate the size of the chest. In this case, the abdominal contents fix the central tendon of the diaphragm, so that it raises the ribcage as it contracts, but it is a condition of that manoeuvre that the gap between the ribs and the pelvic rim widens.

The ventilatory muscles must also work during sleep, when the pharyngeal muscles relax and upper airway resistance increases. It is now appreciated that in some people, particularly the obese, this relaxation can lead to periodic apnoea and marked hypoxia during sleep, implying that the pharyngeal muscles play an important ventilatory role in waking life. It is also clear that although ventilatory muscles rarely tire in normal life, they do fatigue when placed under abnormal loads, e.g. in chronic obstructive pulmonary disease.

The different pulmonary regions do not all move equally in ventilation. In quiet ventilation, the juxtahilar part of the lung scarcely moves and the middle region moves only slightly. The superficial parts of the lung expand the most, and the mediastinal surface, posterior border and apex move less, because they are related to less movable structures. The diaphragmatic and costomediastinal regions expand most of all. Most of the volumetric change during ventilation occurs in the alveoli.

REFERENCES

ohn D. Congenital diaphragmatic hernia. *Am J Respir Crit Care Med*. 2002;166:911-915.

Reviews the epidemiology, diagnosis and treatment of congenital diaphragmatic hernia..

elli B. The diaphragm and respiratory muscles. *Chest Surg Clin N Am*. 1998;8:207-224.

e Troyer A, Estenne M. Functional anatomy of the respiratory muscles. *Clin Chest Med*. 1988;9:175-193.

ahrilas PJ. Supraesophageal complications of reflux disease and hiatal hernia. *Am J Med*. 2001;111(suppl 8A):51-55.

Reviews gastro-oesophageal reflux and type I sliding hiatus hernia..

owdermilk GA, Naunheim KS. Thoracoscopic evaluation and treatment of thoracic trauma. *Surg Clin North Am*. 2000;80:1535-1542.

Discusses the additional benefit and role of video-assisted thoracoscopy in thoracic trauma..

tterson WG. The normal antireflux mechanism. *Chest Surg Clin N Am*. 2001;11:473-483.

Describes how the normal anatomy of the distal oesophagus, proximal stomach and the diaphragm serves as an antireflux barrier..

ajanna MJ. Anatomical and surgical considerations of the phrenic and accessory phrenic nerves. *J Int Coll Surg*. 1947;60:42-52.

Describes the anatomical course of the phrenic nerve in 203 cadaveric dissections..

hanmuganathan K, Killeen K, Mirvis SE, White CS. Imaging of diaphragmatic injuries. *J Thorac Imaging*. 2000;15:104-111.

Reviews the radiological techniques available in the assessment of the diaphragm after trauma, and the extent and anatomical sites of coexisting thoracoabdominal injuries..

harshar T, Hopkinson NS, Ross ET, et al. Motor control of the costal and crural diaphragm – insights from transcranial magnetic stimulation in man. *Respir Physiol Neurobiol*. 2005;146:5-19.

Evaluates the neural control of the diaphragm..

CHAPTER 59

Development of the thorax

THORACIC WALL AND DIAPHRAGM

The thorax as an entity is not apparent in embryos until the end of the embryonic stage of development (stage 23). It develops around the early pericardial cavity and the associated pericardioperitoneal canals (Fig. 59.1A; see Fig. 59.3A). The pericardioperitoneal canals give rise to the pleural cavities surrounding the lungs and that part of the peritoneal cavity surrounding the lower end of the foregut, which becomes the oesophagus, stomach and duodenum within the thoracic cage. Later these portions of peritoneal cavity are sequestered into the abdominal cavity by the development of the diaphragm.

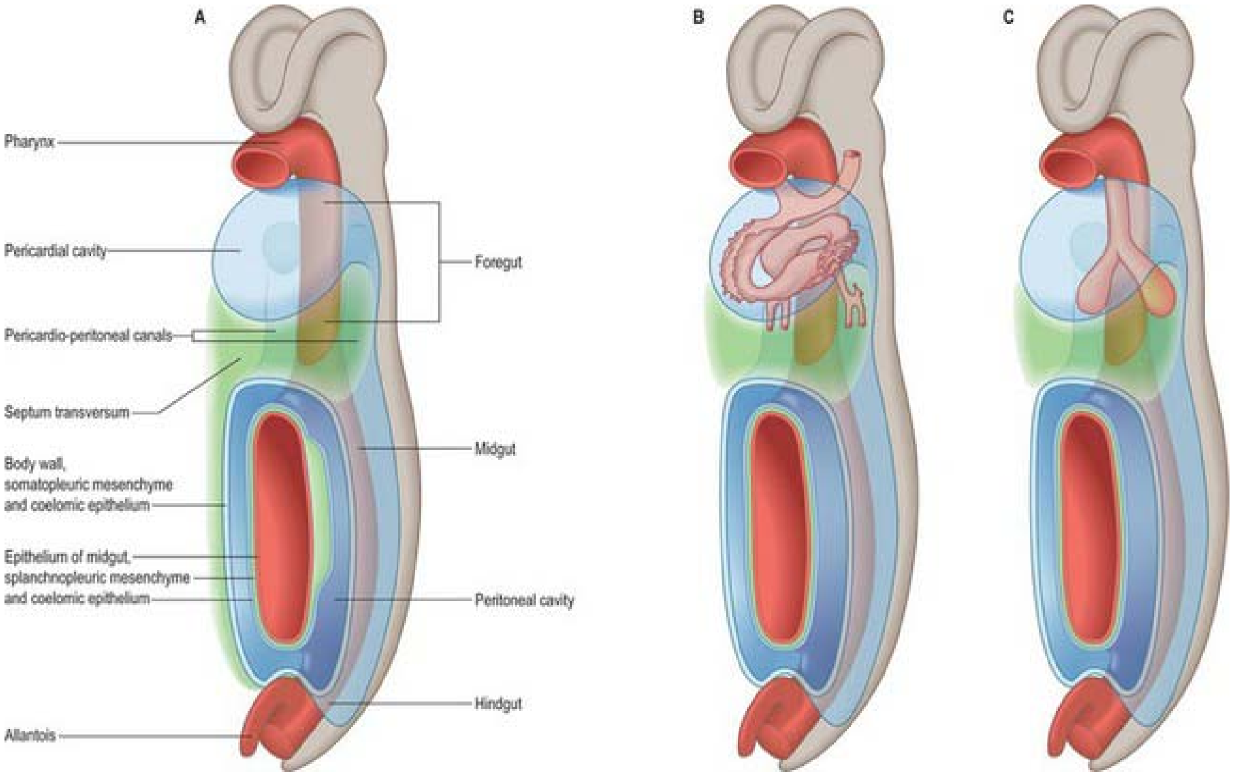
A
B
C
Pharynx
Pericardial cavity
Pericardio-peritoneal canals
Septum transversum
Body wall, somatopleuric mesenchyme and coelomic epithelium
Epithelium of midgut, splanchnopleuric mesenchyme and coelomic epithelium
Allantois
Foregut
Midgut
Peritoneal cavity
Hindgut

Fig. 59.1 **A**, The arrangement of the epithelial populations in an embryo at about stage 11. The future thoracic region lies caudal to the pharynx and extends to the upper part of the septum transversum. **B**, The heart is shown *in situ* within the pericardial cavity. Venous tributaries return blood from the body, yolk sac and placenta and arterial trunks pass each side of the pharynx. **C**, The respiratory diverticulum arises in the midline from the

lower portion of the pharynx and lung buds extend dorsally into the pericardio-peritoneal canals.

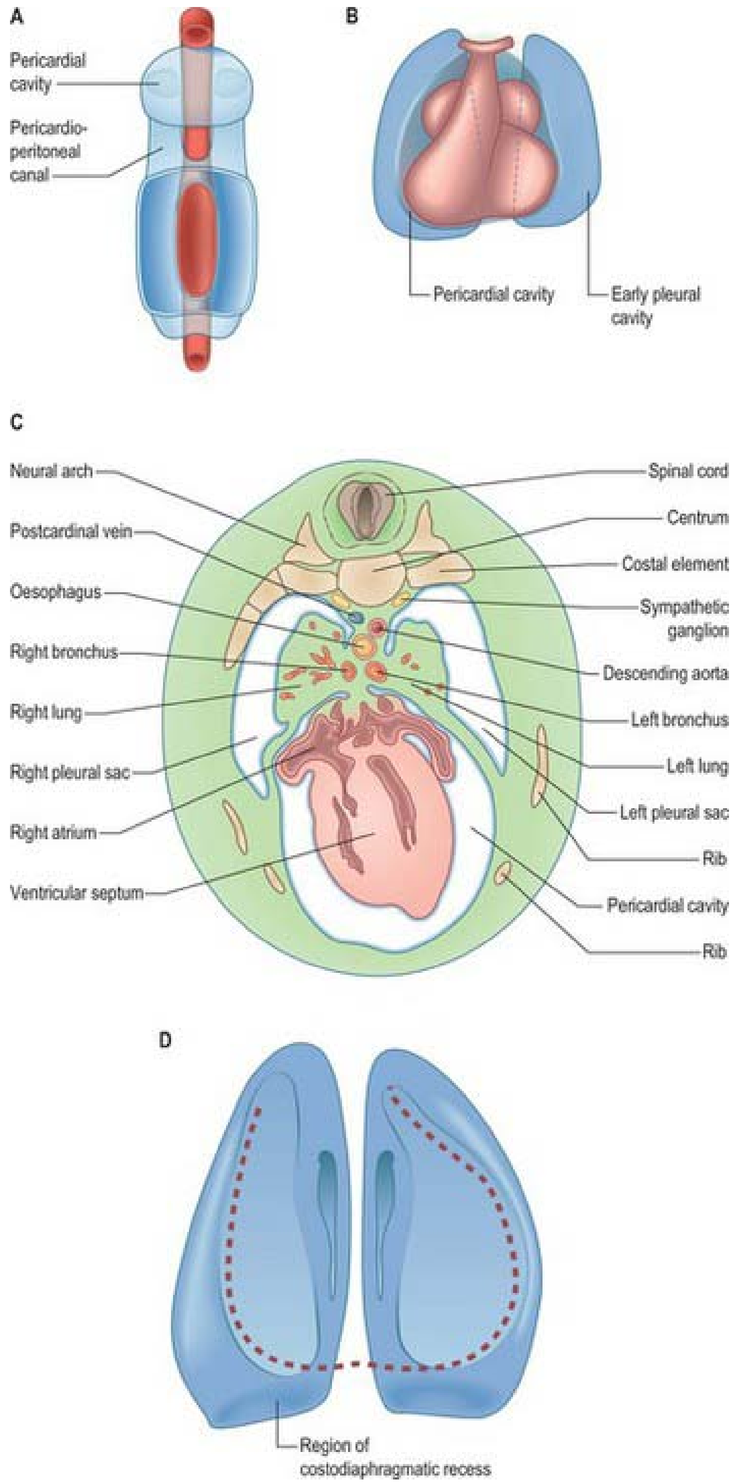
A
Pericardial cavity
Pericardio-peritoneal canal
B
Pericardial cavity
Early pleural cavity
C
Neural arch
Postcardinal vein
Oesophagus
Right bronchus
Right lung
Right pleural sac
Right atrium
Ventricular septum
Spinal cord
Centrum
Costal element
Sympathetic ganglion
Descending aorta
Left bronchus
Left lung
Left pleural sac
Rib
Pericardial cavity
Rib
D
Region of costodiaphragmatic recess

Fig. 59.3 **A**, Ventral view of the intraembryonic coelom forming early body cavities. **B**, The parietal pericardium is shown surrounding the developing heart ventrally with the parietal pleura of the lungs dorsal and lateral on each side. **C**, A transverse section through the thoracic region showing the ventral extensions of the pleural sacs on each side of the pericardium which split the body wall mesenchyme. **D**, Anterior view of the pleural sacs. The position of the pericardium is shown by a dotted line. Dorsolateral growth of the pleural sacs also split the body wall dorsocaudally defining the costodiaphragmatic recess.

In stage 14 embryos, the heart is at the level of the upper cervical somites and above the upper limb buds. The thoracic somites are opposite the midgut. The putative thoracic region contains the pericardial cavity ventrally and the pericardioperitoneal canals posteriorly, on each side of the foregut. The future pleural cavities are as yet undefined regions of the pericardioperitoneal canals. Below the heart, septum transversum mesenchyme (see Fig. 73.5A) that has arisen from the caudal pericardial wall is being invaginated by endodermal epithelial cells from the foregut hepatic primordium.

The heart and pericardial cavity are relatively large in the early embryo (Fig. 59.1B; see Fig. 59.3A). Throughout development the lungs remain unexpanded and do not achieve their full size within the thorax, reflecting the fact that the placenta, and not the lungs, is the organ of fetal respiration. The lower partition of the thorax, the diaphragm, can be identified in stage 13 embryos; it migrates caudally in line with the craniocaudal progression of development and the elongation of the neck. The parietal pericardium remains attached to the diaphragm as it descends.

For the lungs to inflate and deflate, they must be surrounded by a complete pleural cavity slightly larger than the capacity of the lungs. The synchronous development of the thoracic cage, diaphragm and the pleural cavities is therefore of vital importance for the normal development of the lungs and postnatal functioning of the respiratory system. Before birth, fetal breathing movements may be observed using ultrasonography. These can have no respiratory function, but it is thought that these phasic changes lead to the release of growth factors which promote normal lung development. These movements require an intact thoracic and abdominal cavity, so that the diaphragm can descend towards the rigid pelvic bowl, pushing out the abdominal wall. In conditions where this is not the case, for example omphalocele, the lungs may be smaller than normal. Other causes of interference with these movements include neuromuscular disorders of antenatal onset, such as severe spinal muscular atrophy and myotonic dystrophy inherited from the mother, and reduced volume of amniotic fluid, for example in Potter's syndrome (bilateral renal agenesis, oligohydramnios sequence).

The lung buds are invested by splanchnopleuric mesenchyme derived from the medial walls of the pericardioperitoneal canals, whereas the lateral walls produce somatopleuric mesenchyme, which contributes to the body wall. This latter mesenchyme is penetrated by the developing ribs which arise from the thoracic sclerotomes. In the midline, the somatopleuric mesenchyme gives rise to the sternum and costal cartilages. The bony and cartilaginous cage provides insertions for the intercostal muscles, which arise from the ventrolateral edge of the epithelial plate of the somites. The somatopleuric coelomic epithelium, after its proliferative phase, gives rise to the mesothelium of the parietal layer of pleura.

As the lung buds project into the pericardioperitoneal canals (Figs 59.1C, 59.2A), they subdivide them into primary pleural coeloms around the lung buds cranially, and paired peritoneal coeloms caudally, which are continuous with the wider peritoneal coelom around the mid- and hindguts. The communications with the pericardial and peritoneal coeloms become termed the pleuropericardial and pleuroperitoneal canals, respectively. When separation between these fluid-filled major coelomic regions is advancing towards completion, they are named the pericardial, pleural and peritoneal cavities. In early embryos, the cavities retain substantial volumes of fluid and their walls are separate: they provide the route for a primitive type of circulation until superseded by the blood vascular system. In later fetal and postnatal life, the cavity walls are coapted, so that a mere microscopic film of serous fluid intervenes between them.

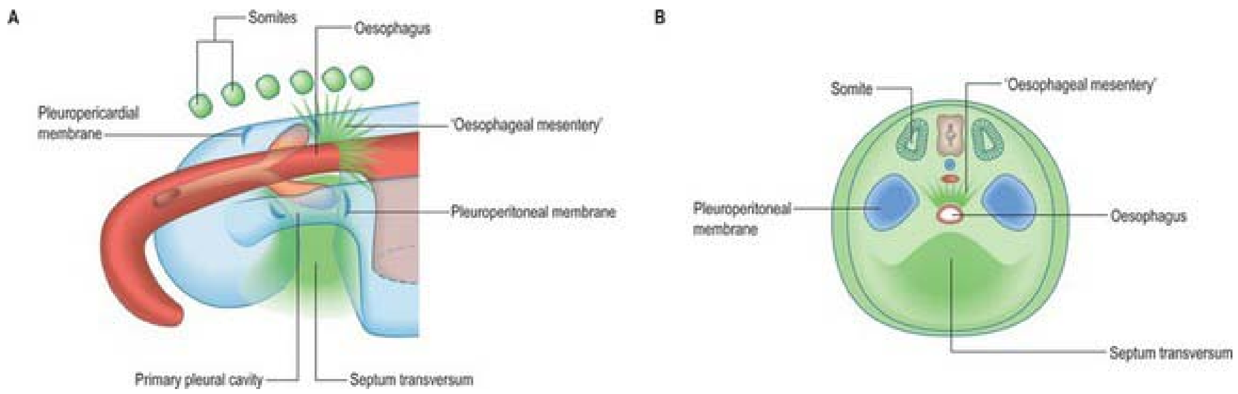
A
Somites
Oesophagus
Pleuropericardial membrane
'Oesophageal mesentery'
Pleuroperitoneal membrane
Primary pleural cavity
Septum transversum
B
Somite
'Oesophageal mesentery'
Pleuroperitoneal membrane
Oesophagus
Septum transversum

Fig. 59.2 **A**, Dorsolateral view of the foregut between the pericardio-peritoneal canals. The respiratory diverticulum arises from the ventral side of the pharynx and grows caudally. Bilateral lung buds extend dorsally into the pericardio-peritoneal canals dorsolaterally. Later changes in position of the common cardinal veins contribute to the formation of the pericardio-pleural membranes cranial to the developing lungs whereas folds of coelomic epithelium, pleuroperitoneal membranes, separate the pleural cavities from the peritoneal cavity. **B**, Components of the diaphragm.

A curved elevation of tissue, the pulmonary ridge, develops on the lateral wall of the pleural coelom and partly encircles the pleuropericardial canal. The ridge is continuous with the dorsolateral edge of the septum transversum. The developing lung bud abuts on the ridge, which as a result divides into two diverging membranes meeting at the septum transversum. One is cranially placed and termed the pleuropericardial membrane (Fig. 59.2A); embedded within it are the common cardinal vein and phrenic nerve, which reach the septum transversum by this route. The other membrane, caudally placed, is termed the pleuroperitoneal membrane (Fig. 59.2A,B). As the apical part of the lung forms, it invades and splits the body wall and extends cranially on the lateral aspect of the common cardinal vein, preceded by an extension from the primary pleural coelom to form part of the secondary, definitive, pleural sac. In this way the common cardinal vein and the phrenic nerve come to lie medially in the mediastinum. The pleuropericardial canal, which lies medial to the vein, is gradually narrowed to a slit, which is soon obliterated by the apposition and fusion of its margins. Closure occurs early and is mainly effected by the growth and expansion of the surrounding viscera (heart and great vessels, lungs, trachea and oesophagus), and not by active growth of the pleuropericardial membrane across the opening to the root of the lung.

In addition to its extension in a cranial direction, the lung and its associated visceral and parietal pleurae also enlarge ventromedially and caudodorsally. With the ventromedial extension, the lungs and pleurae therefore excavate and split the somatopleuric mesenchyme over the pericardium, separating the latter from the ventral and lateral thoracic walls (Fig. 59.3B–D). The ventrolateral fibrous pericardium, parietal serous pericardium and mediastinal parietal pleura, although topographically deep, are therefore somatopleuric in origin.

Congenital disorders of the chest wall

The dorsal portion of the thorax is derived from somites, the sclerotomal portions of which form the thoracic vertebrae and ribs (Ch. 44). Vertebral anomalies, including formation of hemivertebrae and block vertebrae (where cranial and caudal sclerotomal halves do not separate), may contribute to scoliosis. Five percent of scoliosis is congenital; it may be associated with multiple other anomalies, e.g. the VACTERL (**V**ertebral; **A**norectal; **C**ardiac; **T**racheal; **E**sophageal; **R**enal; **L**imb) association or with congenital syndromes such as Marfan’s and congenital neurofibromatosis. The diagnosis may be missed at birth. There are a number of syndromes in which the chest wall does not develop properly, and the lungs are consequently hypoplastic. These include Jeune’s syndrome, asphyxiating thoracic dystrophy (an autosomal recessive condition which may be associated with short limb dwarfism and polydactyly). Rib cage abnormalities also occur in thanatrophic dwarfism, achondroplasia, chondroectodermal dysplasia and giant exomphalos. Many of these conditions are fatal soon after birth; milder forms may improve with time, but affected individuals may need prolonged respiratory support.

DIAPHRAGM

The separation of the pleural and peritoneal cavities is effected by development of the diaphragm, which forms from a portion of the septum transversum mesenchyme above the developing liver (Fig. 59.2A,B). The septum transversum is a population of mesenchymal cells which arises from the coelomic wall of the caudal part of the pericardial cavity. As the population proliferates, it forms a condensation of mesenchyme, caudal to the pericardial cavity and extending from the ventral and lateral regions of the body wall to the foregut. Dorsal to it on each side are the relatively narrow pleuroperitoneal canals. The endodermal hepatic bud grows into the caudal part of the septum transversum, whereas the cranial portion will form the diaphragm.

The oesophagus and stomach are medial to the pleuroperitoneal canals. As development proceeds, the lower portion of the oesophagus inclines ventrally anterior to the descending thoracic aorta. Although the oesophagus has no true ventral or dorsal mesentery, in descriptions of diaphragmatic development the portion of mesenchyme between the oesophagus and aorta at the level of the forming diaphragm is often homologized with part of a dorsal meso-oesophagus. The pleuroperitoneal membranes, which remain small, are dorsolateral to the canals, and the mesonephric ridges, suprarenal glands and gonads are dorsal. Just as the enlargement of the pleural cavity cranially and ventrally is effected by a process of burrowing into the body wall, so is its caudodorsal enlargement. The expanding pleural cavities extend into the mesenchyme dorsal to the suprarenal glands, the gonads and (degenerating) mesonephric ridges. Thus somatopleuric mesenchyme is peeled off the dorsal body wall to form a substantial portion of the dorsolumbar part of the diaphragm (Fig. 59.3C). The pleuroperitoneal canal is closed by the fusion of its edges, which are carried together from posterolaterally to anteromedially by growth of the organs surrounding it, in particular by growth of the suprarenal gland. The right pleuroperitoneal canal closes earlier than the left, which presumably explains why an abnormal communication persisting between the pleural and peritoneal cavities is more frequently encountered on the left.

While these changes are occurring, the septum transversum undergoes a progressive alteration in relative position. The dorsal border of the septum transversum which initially lies opposite the second cervical segment, migrates caudally as the embryo grows and the heart enlarges. At first the ventral border moves more rapidly than the dorsal, but after the embryo has attained a length of 5 mm, the dorsal border migrates more rapidly. When the dorsal border of the septum transversum lies opposite the fourth cervical segment, the phrenic nerve (C3, 4 and 5) and portions of the corresponding myotomes, grow into it and accompany it in its later migrations. The dorsal border of the septum transversum does not come to lie opposite the last thoracic and first lumbar segments, the final position occupied by some of the dorsal attachments of the diaphragm, until the end of the second month. The main derivatives of the central part of the diaphragm lie at considerably more cranial levels.

The diaphragm is therefore composed of the dorsal mesooesophagus and paired pleuroperitoneal membranes (posteriorly); septum transversum mesenchyme (ventrally); and excavated body wall (posteriorly and laterally).

Diaphragmatic herniae

Diaphragmatic herniae may result from failure of fusion of the component parts or from a primary defect. Posterolateral defects (Bochdalek’s hernia) are the most common (85–90%) and may be bilateral (5%) or unilateral. Of the unilateral defects, the left side is more commonly affected (80%). Although these hernias have been attributed to failure of fusion of the pleuroperitoneal membrane, there is increasing evidence that the primary abnormality is lung hypoplasia, and the herniation of the abdominal contents is secondary, which has important implications for treatment (Jesudason 2002). A non-muscular membranous sac, possibly derived from the pleuroperitoneal canal wall is present in 10–15% of cases, signifying the early occurrence of this lesion prior to closure of the pleuroperitoneal canal. Hernias between the costal and sternal origins (Morgagni hernia) are rare (1–

2%). Midline defects in the central tendon arise from septum transversum defects. The incidence of congenital diaphragmatic hernias is about 1 : 3000 to 1 : 5000 in neonates, with a prenatal incidence of 1 : 2000.

Diaphragmatic hernias can usually be diagnosed by antenatal ultrasound examination. The presence of bowel in the thorax and mediastinal shift may be seen. The main causes of death in babies with diaphragmatic hernias are pulmonary hypoplasia and hypertension. Pulmonary hypoplasia is related to the abnormal branching of the airways both ipsilaterally and contralaterally, resulting in the formation of reduced numbers of alveoli. Pulmonary hypertension is related to pulmonary hypoplasia, and also to the increased muscularization and reactivity of the pulmonary circulation. There may be associated abnormalities, including trisomy 13 and 18, and diaphragmatic hernia may be part of a number of syndromes, many of which may lead to termination of the pregnancy or to death of the neonate.

Diaphragmatic eventration is a condition in which a (usually) right-sided abnormal diaphragmatic silhouette is seen on X-ray with an abnormal medial bulge into the thorax. This is a benign condition, often a chance finding, and usually requiring no treatment: it is occasionally associated with rib and cardiac abnormalities.

OESOPHAGUS

The development of the oesophagus is described in Chapters 35 and 73. Failure of separation of the oesophagus and trachea is described on page 1036. Oesophageal atresia and tracheo-oesophageal fistula may present antenatally with polyhydramnios due to failure of fetal swallowing, and choking and inability to swallow saliva in the neonatal period.

Neonatal thorax and diaphragm

A number of differences between the neonatal and adult thorax and diaphragm are significant in early postnatal life, especially in the preterm infant. The full-term neonatal thorax has a rounded circumference whereas the adult profile is dorsoventrally flattened. The compliance of the adult chest wall and lung are approximately equal, but the neonatal chest wall is up to five times more compliant than the lungs and so is easily deformable: indrawing of the chest wall is an important sign of increased work of breathing in the neonate. The diaphragm is relatively flat at birth and gains its dome shape as the thorax and abdominal viscera grow. The arrangement of the ribs and diaphragm in the neonate means that contraction of the diaphragm pulls the compliant ribs inwards, which does not contribute to inspiration and leads to chest distortion, and which may be opposed by the stabilizing action of the expiratory muscles. The neonatal diaphragm exhibits an exaggerated asymmetric movement: the posterior portion shows a considerably greater excursion than the anterior portion.

A neonate undertakes relatively greater work in order to breathe, and is much more vulnerable to developing respiratory muscle fatigue and respiratory muscle failure than an adult. Experimental animal studies suggest that neonates may be especially vulnerable to respiratory muscle failure because of the initial immaturity of synapses. Moreover, myosin isoforms are developmentally regulated in the diaphragm: the reduced power output and work performance of the newborn diaphragm may reflect these molecular differences.

In expiration, there may be active braking of airflow, caused by inspiratory muscle activity and partial constriction of the larynx: this produces grunting on expiration especially if the lungs are stiff, for example in neonatal respiratory distress. A very preterm neonate is difficult to study, but respiration is likely to be even more compromised by the compliant chest wall and lack of reserve than it is in the term newborn (Mortola 2002).

At all ages, there is a reduction, if not loss, of tonic intercostal activity during rapid eye movement (REM) sleep. The mechanism is believed to be related to a descending spinal inhibition of the muscle spindle system. In addition, although during REM sleep the diaphragm descends further, this inspiratory effort is dissipated in sucking in the ribs and enlarging the abdomen, thus the rib cage and abdominal ventilatory movements become out of phase. The neonate is at particular risk in this respect, because the chest wall is flexible, and much of the infant sleep activity is of the REM type. Furthermore, the upper airway musculature may lose tone during REM sleep, so that the soft tissues of the pharynx are sucked in during inspiration, limiting the cross-sectional area of the upper airway, and further increasing the work of breathing.

HEART AND GREAT VESSELS

Cardiac differentiation and morphogenesis are intimately related processes, achieved by a highly complicated transcriptional network. The cardiac transcription factor Nkx2–5, which has a homogeneous distribution over the embryonic heart tube, is generally important for cardiac-specific gene expression. In the human, mutations in this factor cause atrial septal defects and disturbances of atrioventricular conduction; in *Drosophila* the heart will not form in its absence. The recent discovery of the involvement of the role of T-box transcription factors, which are locally expressed, provides some evidence of the further complexity of patterning the heart. Whereas Tbx5 confers caudo-cranial positional information over the heart tube, thereby determining the regional development of the cardiac chambers along these axes, Tbx2 and 3 prevent regional formation of the cardiac chambers, permitting the myocardium in these regions to differentiate into the conduction system. Tbx18 is involved in the development of the sinus venosus and Tbx1 in the development of the outflow tract of the heart.

A number of terms must be specified before development of the heart and discussion of the cardiac chambers can be described. The inflow tract of the heart starts at the transition of the systemic tributaries (sinus venosus) into the primary heart tube. Within the straight heart tube, one atrial and one ventricular chamber are initially discerned, separated by an atrioventricular canal. The inflow tract thus connects the sinus venosus with the forming atrium, whereas the outflow tract connects the ventricle with the aortic sac; a proximal portion (close to the ventricle) and a distal portion can be defined within the outflow tract.

CELLS THAT GIVE RISE TO THE HEART

The heart is formed from tissues derived from the midline splanchnopleuric coelomic epithelium with later contributions from neural crest mesenchyme. The splanchnopleuric coelomic epithelium gives rise to the myocardium, including the conduction system of the heart, and the endocardium, including its derived cardiac mesenchymal population which produces the valvular tissues of the heart. Splanchnopleuric coelomic epithelium is also the source of the epicardium, coronary arteries and interstitial fibroblasts.

Primitive cardiac myocytes can first be seen in embryos at stage 9. During the onset of neurulation and somitogenesis, the intraembryonic coelom forms across the midline, initially above the endoderm, in a horse shoe-shaped area termed the cardiac crescent (Fig. 59.4). As the head fold emerges, the coelom undergoes a reversal, so that the future pericardial cavity comes to lie ventral to the endodermal foregut (Figs 59.1, 59.5). The splanchnopleuric wall of the pericardial coelom, subjacent to the endoderm, provides a germinal epithelium that produces early cardiac myocytes. It is characterized by the expression of myocardial specific markers, such as cardiac myosin heavy chain. This initial origin of myocardial cells is termed the primary heart-forming field, distinguishing it from later myocardial additions from mesenchyme localized central and peripheral to the cardiac crescent on the embryonic disc, termed the second heart-forming field (Fig. 59.4). It is not yet known whether these two sources of myocardium represent distinct myocardial lineages, or a single part which develops into separate components later on.

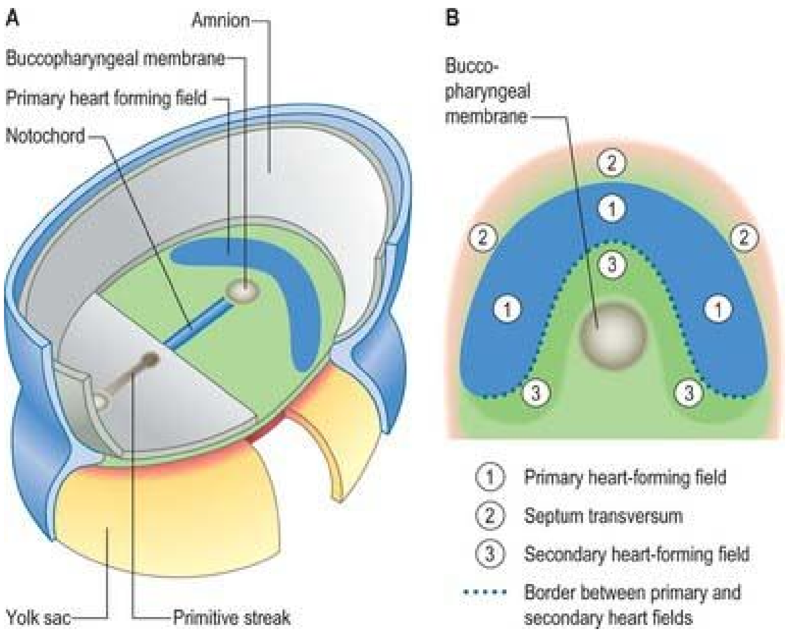
A
Amnion
Buccopharyngeal membrane
Primary heart forming field
Notochord
Yolk sac
Primitive streak
B
Bucco-
pharyngeal
membrane
② ① ② ③ ① ① ③ ③ ②
① Primary heart-forming field
② Septum transversum
③ Secondary heart-forming field
Border between primary and
secondary heart fields

Fig. 59.4 **A**, The early embryonic disc viewed from a dorsolateral aspect showing the position of the primary heart-forming field relative to the surface ectoderm of the trilaminar disc; **B**, The rostral end of the unfolded embryonic disc from a dorsal aspect showing the position of the mesenchymal populations which will give rise to the primary heart-forming field, septum transversum mesenchyme and second heart-forming field.

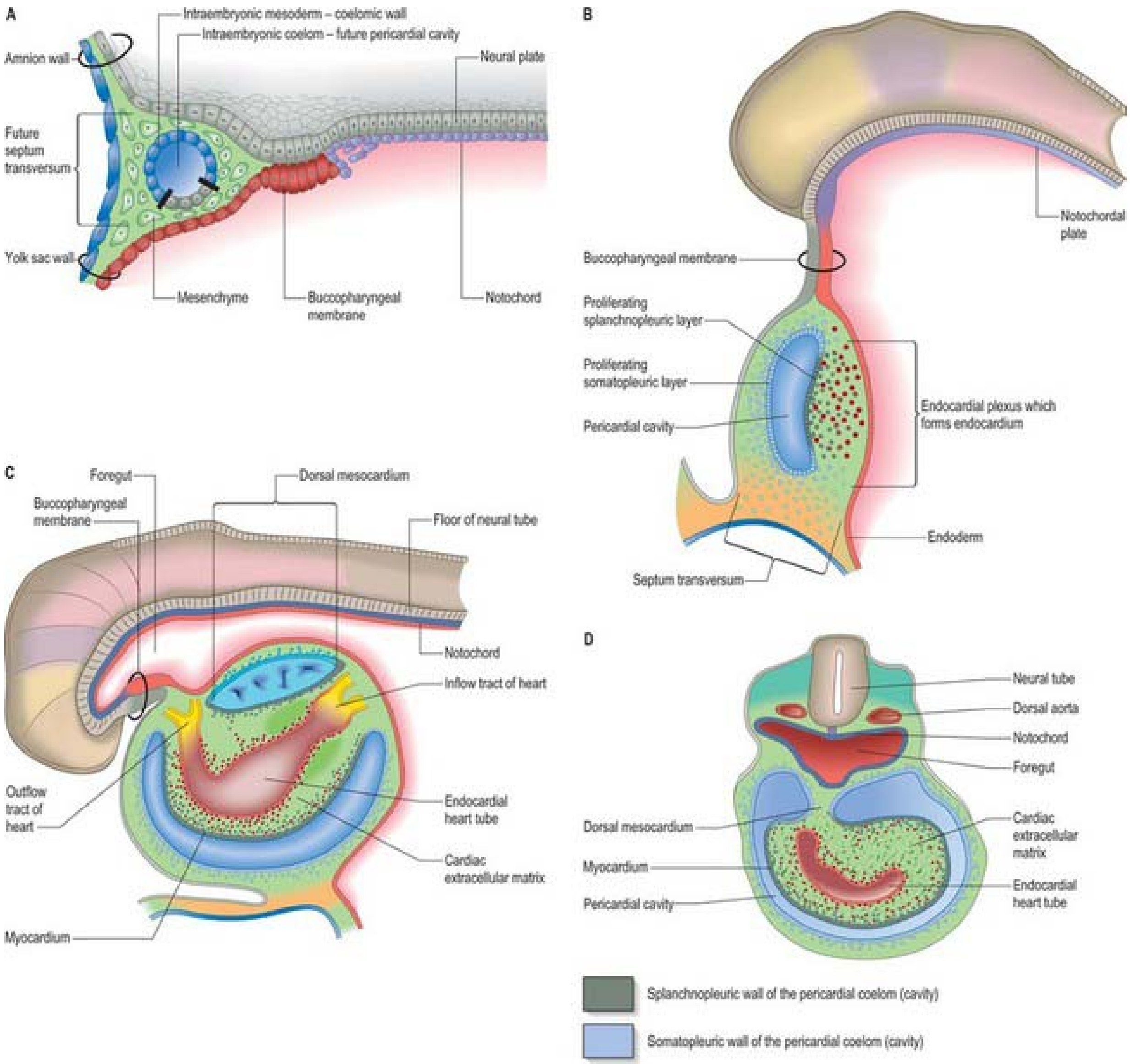
A
Intraembryonic mesoderm – coelomic wall
Intraembryonic coelom – future pericardial cavity
Amnion wall
Neural plate
Future septum transversum
Yolk sac wall
Mesenchyme
Buccopharyngeal membrane
Notochord
B
Notochordal plate
Buccopharyngeal membrane
Proliferating splanchnopleuric layer
Proliferating somatopleuric layer
Pericardial cavity
Endocardial plexus which forms endocardium
Endoderm
Septum transversum
C
Foregut
Dorsal mesocardium
Buccopharyngeal membrane
Floor of neural tube
Notochord
Inflow tract of heart
Outflow tract of heart
Endocardial heart tube
Cardiac extracellular matrix
Myocardium
D
Neural tube
Dorsal aorta
Notochord
Foregut
Dorsal mesocardium
Cardiac extracellular matrix
Myocardium
Endocardial heart tube
Pericardial cavity
Splanchnopleuric wall of the pericardial coelom (cavity)
Somatopleuric wall of the pericardial coelom (cavity)

Fig. 59.5 **A**, Median section through part of the embryonic disc to show the position of the future pericardial cavity before head folding. **B**, Median section through the cranial end of a human embryo during early head folding showing its reversal effect on the position of the pericardium. **C**, Median section through the cranial end of a human embryo after head folding showing the pericardial cavity and endothelial heart tube now ventral to the foregut. **D**, Horizontal section through the pericardium and endothelial heart tube shown in **C**. The position of the dorsal mesocardium which is a source of secondary heart field mesenchyme is indicated.

The endocardium also develops during stage 9 from the coelomic splanchnopleuric epithelium. Cells arise singly close to the ventro-lateral edges of the cranial intestinal portal and form an endocardial plexus between the splanchnopleuric coelomic epithelium and the foregut endoderm. These groups of cells are now termed angioblastic mesenchyme; they are amongst the earliest intraembryonic vascular precursors to appear and express markers for the endothelial cell lineage. The cells aggregate to form an epithelium, the endocardium, which encloses small cavities which coalesce in the vicinity of the developing foregut to establish bilateral, hollow endocardial tubes. The latter fuse across the midline progressively, commencing at the outflow tract, or arterial pole, and extending to the inflow tract, or venous pole (Fig. 59.5). By stage 10 a single endocardial tube is present and is almost completely surrounded by myocardial cells. This arrangement of an outer myocardial sleeve containing an inner endocardial tube constitutes the primary heart tube. The inner endocardial epithelium induces the myocardial cells to synthesize specific extracellular matrix proteins which form a fine extracellular reticulum that holds the endocardial tube apart from the developing myocardium. Close to the foregut endoderm, the myocardial cells at the reflections of the pericardial splanchnopleuric epithelium form the dorsal mesocardium, which may stabilize the developing endothelium and promote the fusion of the bilateral endocardial tubes. The dorsal mesocardium encompasses a mesenchymal population specifically referred to as mediastinal mesenchyme, and is contiguous with the splanchnopleuric mesenchyme surrounding the embryonic foregut.

Much later in heart development, neural crest cells, arising from the region between the otic vesicle and the caudal limit of somite three, grow into the outflow tract of the heart. They are believed to play a role in the spatio-temporal regulation of the division of the outflow tract into the aortic and pulmonary pathways, and the development of the muscular sub-pulmonary infundibulum.

The epicardium, sometimes included in descriptions of the myocardium as ‘epimyocardium’, is not present at the early stages of heart development (but see p. 1027).

Endocardial cushions

The extracellular matrix of the heart, historically termed cardiac jelly, promotes occlusion of the endocardial tubular lumen during myocardial contraction, thus providing mechanical assistance for the generation of the flow of blood. It also acts as a site for the deposition of inductive factors from the myocardial cells, which, in turn, modify the differentiation of specific endocardial cells. It has been called a gelatinoreticulum, a myoepicardial reticulum (Fig. 59.5C,D) and, more recently, the myocardial basement membrane. Here, the term cardiac extracellular matrix will be used. It is composed of, among other things, hyaluronic acid, hyaluronidase and fibronectin. Inductive signals originating from the myocardial cells cause a subset of endocardial cells lining the atrioventricular canal and the proximal outflow tract to transform into mesenchyme (cardiac mesenchyme); the endocardial cells in other regions of the heart tube, such as those in the ventricle, do not undergo such a transition. When activated by myocardial inductive factors, the endocardial cells lose their cell-to-cell associations, show decreased expression of neural cell adhesion molecule, and increased expression of substrate adhesion molecules such as chondroitin sulphate and fibronectin. They undergo rearrangement of their cytoskeleton necessary for migration, and they express type I procollagen. Uniquely, they retain their expression of endothelial markers. This epithelial to mesenchymal transition may, perhaps, be the only example of a mesenchymal population that is derived from an endothelial lineage.

Formation of cardiac mesenchymal cells at the atrioventricular canal and the proximal myocardial outflow tract is followed by their migration into the cardiac extracellular matrix. These cells proliferate between the endocardium and myocardium and, with local accumulation of extracellular matrix molecules, produce protrusions, termed endocardial or cardiac cushions, which bulge into the primary heart tube and initially provide the valvular mechanisms required in the atrioventricular canal and outflow tract. Their position corresponds to the future positions of the definitive cardiac valves. In the distal part of the outflow tract, which initially has myocardial walls, cells which are derived from the neural crest subsequently make significant contributions to the mesenchyme of the endocardial cushions. Although proper migration of these cells from the neural crest is crucial for normal development of the outflow tract and formation of the leaflets and sinuses of the arterial valves, their function is largely obscure. They are no longer found in the leaflets of the arterial valves in the formed heart, or in the muscular subpulmonary infundibulum, which is also derived from the outflow cushions. The endocardial cushions themselves ultimately fuse, forming a wedge of mesenchyme that serves to guide the union of the internal muscular septal structures (see p. 1024). At their time of fusion, the atrioventricular endocardial cushions are large relative to the size of the atrioventricular orifices; they will provide the scaffold for formation of the leaflets of the tricuspid and mitral valves.

Cardiac myocytes – contraction, conduction and automaticity

Cardiac myocytes share a number of characteristic features that distinguish them from other cells. All cardiac myocytes have sarcomeres and a sarcoplasmic reticulum and, in principle, share the capacity of producing an intrinsic cycle of electrical activity resulting in contraction. This phenomenon is called automaticity, or pacemaker activity. An absolute requirement for effective pacemaking is poor electrical coupling of the cells, which also implies slow conduction. It allows the cells to build up sufficient electrical charge which is then propagated through the surrounding myocardium. Thus ‘a small node can drive a large heart’ (see p. 1021).

Varying degrees of differentiation are seen in early populations of cardiac myocytes which can be categorized as forming working, nodal, conducting and primary myocardium (Table 59.1). Cells of the atrial and ventricular working myocardium display virtually no automaticity, but are well coupled and have well developed sarcomeres and sarcoplasmic reticular structures. The development of the synchronously (fast) contracting working myocardium requires fast conduction of the depolarizing impulse, and so the cells possess well-developed gap junctions. In marked contrast, the cells forming the nodes of the cardiac conduction system have the opposite phenotype, and resemble the myocytes which are found initially in the primary heart tube. The cells of the putative atrioventricular and peripheral ventricular conduction system have an ambiguous phenotype: the cells are well-coupled, thus allowing fast conduction of the depolarizing impulse, but otherwise retain an embryonic phenotype. The division does not imply that the cells belonging to one group are identical, but rather that they share distinguishing features developed to variable degrees.

Table 59.1 Basic phenotypes of cardiac myocytes.

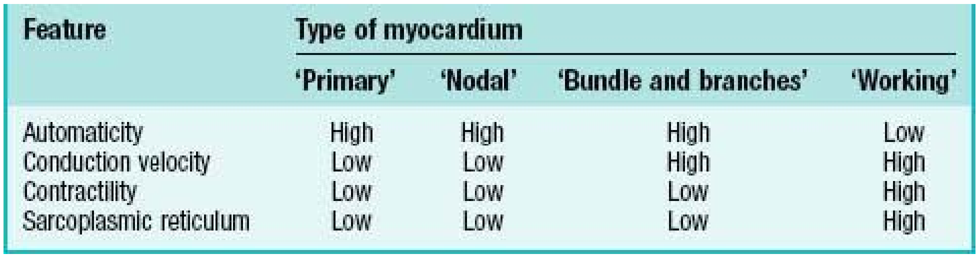

Feature	Type of myocardium			
	'Primary'	'Nodal'	'Bundle and branches'	'Working'
Automaticity	High	High	High	Low
Conduction velocity	Low	Low	High	High
Contractility	Low	Low	Low	High
Sarcoplasmic reticulum	Low	Low	Low	High

Automaticity and slow conduction are features of the myocardium of the primary heart tube. The slow conduction of the depolarizing impulse over the heart tube causes a peristaltic wave of contraction, by means of which the blood is pushed towards the arterial pole. During the waves of contraction, the accumulated cardiac extracellular matrix closes the endocardial tube and prevents the backward flow of blood. Unambiguous morphologic markers are often lacking in the early embryonic heart, which means that it is not possible to distinguish the various cells phenotypically; automaticity and the speed of conduction have therefore become important functional parameters with which to describe the development of the different parts of the heart.

HEART TUBE

During the process of embryonic folding, the midline splanchopleuric coelomic epithelium, which is derived from the primary heart field (cardiac crescent) becomes positioned ventral to the foregut. The splanchopleuric epithelium is proliferative and gives rise to mesenchymal populations and particularly early cardiac myocytes which arise from the coelomic wall adjacent to the endoderm of the foregut (Fig. 59.5). After folding, the second heart field contributes cells to both the arterial and venous poles of the heart. It has been suggested that the secondary heart field may contribute cells only to those cardiac components that are required for the pulmonary circulation, namely the right ventricle and outflow tract at the arterial pole, and the atrial septum and the dorsal atrial wall at the venous pole. Extending this suggestion, the original primary heart-forming field would give rise to those components that are required for the systemic circulation, namely the systemic venous sinus and its tributaries, the initial atrium, the left ventricle, and the arterial conus, as seen in the outflow tract of primitive fishes, although this latter structure has no homologue in mammalian hearts.

During the process of folding, the pericardial cavity and concomitantly the myocardium, gradually extend around the forming endocardial tube, leaving the dorsal mesocardium, a transient connection that is analogous to the mesentery of the intestines (Fig. 59.5C,D). The persisting stalk of the dorsal mesocardium connects the venous pole of the heart with the splanchnopleuric mesenchyme around the developing lung buds and with the septum transversum mesenchyme, which will give rise to the liver. The dorsal mesocardium is the site of early mediastinal mesenchyme production. It disappears as a mesenteric entity during the third week of development, when the embryo has from 4 to 12 somites; at the same time, the endocardial heart tube becomes entirely surrounded by the myocardium, and enclosed within the pericardial cavity. The breakdown of the dorsal mesocardium establishes a passage across the pericardial cavity, from side to side dorsal to the heart, which persists as the transverse sinus of the pericardium.

At this stage, the heart is bilaterally symmetrical and has the form of an inverted ‘Y’. The legs of the Y are positioned caudal to each side of the cranial intestinal portal, where they form the venous pole of the heart (59.6A,B). The stem of the Y connects cranially with the great arteries, forming the arterial pole of the heart. From the outset, both poles are connected with the systemic vessels running from the embryo, the yolk sac, and the placenta. The pulmonary veins form later, during the fifth week of development, the initial venous primordium becoming evident in the mesenchyme derived from the dorsal mesocardium caudally. Also at this site, mediastinal myocardium continues to be added to the heart, forming the smooth dorsal wall of the left atrium, and providing the site of formation of the primary atrial septum.

Recent fate maps have shown that the primary heart tube contains cell lines which will contribute to only two compartments. The myocardium of the stem of the inverted Y contains only precursor cells of the left ventricle, and both legs of the inverted Y contain precursor cells of the atrioventricular canal and parts of both atrial chambers. There is no evidence to support the previous, traditional concept of heart development, i.e. that all the putative cardiac segments are already present in the straight heart tube and develop to contribute to the various parts of the definitive cardiac chambers. This hypothesis has now been disproved by elegant experimental studies which have shown that the definitive cardiac chambers are formed by local differentiation and expansion, or ‘ballooning’, of the myocardial walls of the primary heart tube.

Looping of the heart tube

Cranial and caudal recruitment of myocardium and endocardium produces considerable lengthening of the primary heart tube. Recent studies of the mechanism of proliferation in the avian heart have shown that cardiac myocytes stop dividing after overt differentiation. The tube continues to elongate, largely as a result of the recruitment of additional myocytes to the tube, as shown by studies of both morphology and molecular lineages, and to a lesser extent because of an increase in the size of the myocytes which form the walls of the tube. The lengthening heart tube bends ventrally and rightwards, concomitant with the breakdown of the dorsal mesocardium. The bend is called the ventricular loop, since the left ventricle subsequently balloons and expands at its outer curvature, which is the original ventral side of the straight tube. The inner curvature of this loop was originally its dorsal side.

It is often stated that looping of the tube is the first visual evidence of asymmetry in the embryo, although careful examination reveals that the atrioventricular canal has become asymmetric prior to the start of looping. Although the sense of laterality of the developing organs of the body, including the atrial appendages, develops during gastrulation, the pathway of signalling that governs rightward looping of the heart tube remains unknown. However, it is now well established that signalling pathways including *Pitx2*, *nodal*, *lefty*, and *cited-2*, determine the formation of the morphologically left-sided or right-sided features seen in organs such as the lungs, the bronchial tree, the liver and spleen, and the atrial appendages.

By the time the primary heart tube has formed its ventricular loop, it is possible to distinguish the atrial and ventricular components of the developing heart (Figs 59.6D-G, 59.7A,B) and to recognize an outflow tract connected with the aortic sac and developing pharyngeal arch arteries. The cells which, at this stage, make up the outflow tract, will, at later stages, be found within the right ventricle. At the proximal side of the outflow tract, cells are recruited to the developing right ventricle and, contemporaneously, new cells are recruited to the outflow tract from the second heart-forming field. The atrial and ventricular components are separated one from another by the atrioventricular canal, which at this stage has significant length. The systemic venous tributaries drain directly to the atrial cavity.

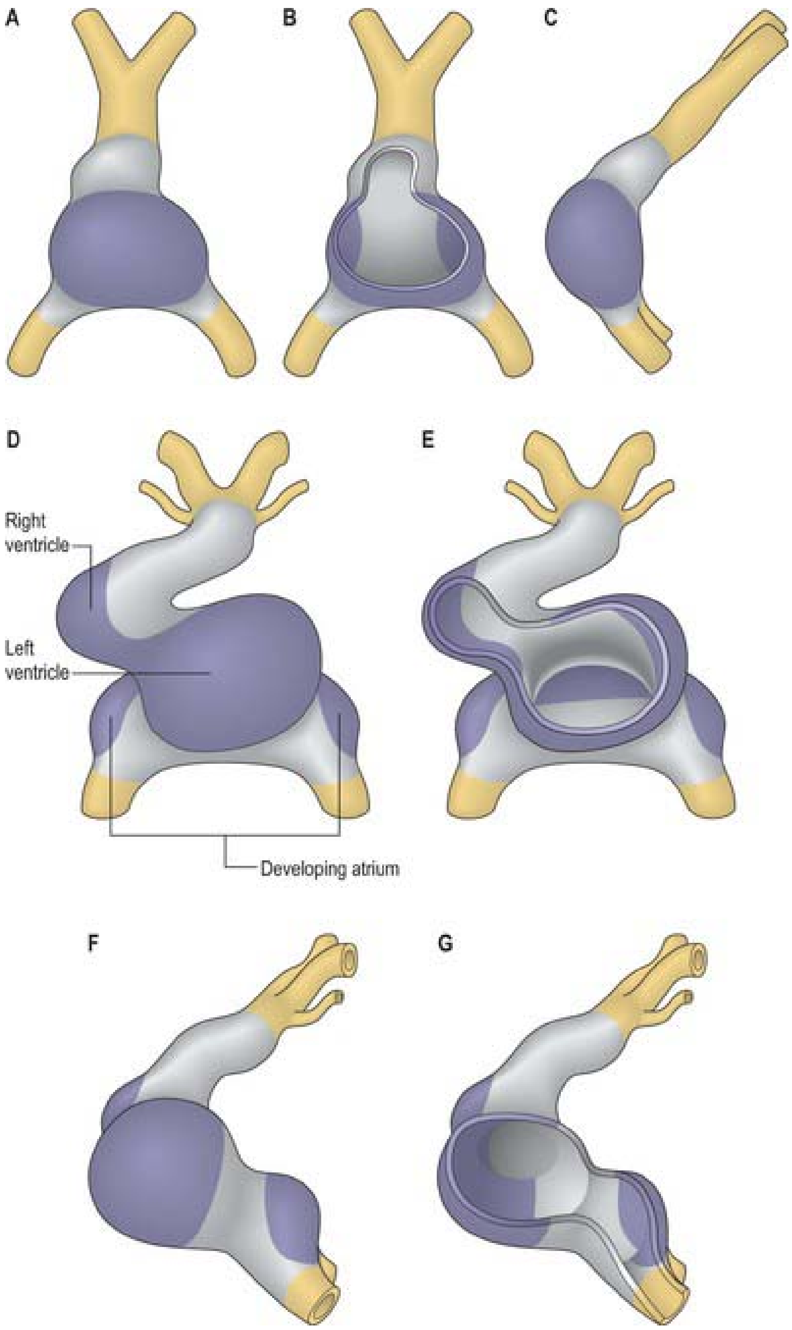
A
B
C
D
E
Right ventricle
Left ventricle
Developing atrium
F
G

Fig. 59.6 Local expansion of the myocardial wall of the early heart tube and heart tube looping **A**, ventral view; **B**, ventral wall removed to show inner aspect of the early heart tube; **C**, left lateral view. The early heart tube is shaped like an inverted ‘Y’. The legs of the Y pass caudal to each side of the cranial intestinal portal. In the early heart tube the myocardium of the stem of the Y (purple) contains only precursor cells for the left ventricle. The remaining myocardium (grey) contains only precursor cells for the

atrioventricular canal and atria. The precursor left ventricular cells expand first. **D–G**: Later heart tube showing looping. **D**, Ventral view. **E**, Ventral wall removed to show inner aspect of the folding heart tube. **F**, Left lateral view. **G**, Lateral wall removed to show the inner aspect of the heart from the left. In **D** and **E** the expansion of the right ventricle can be seen and the heart tube has elongated to the right. The developing atrium can be seen dorsolaterally in **D–G**.

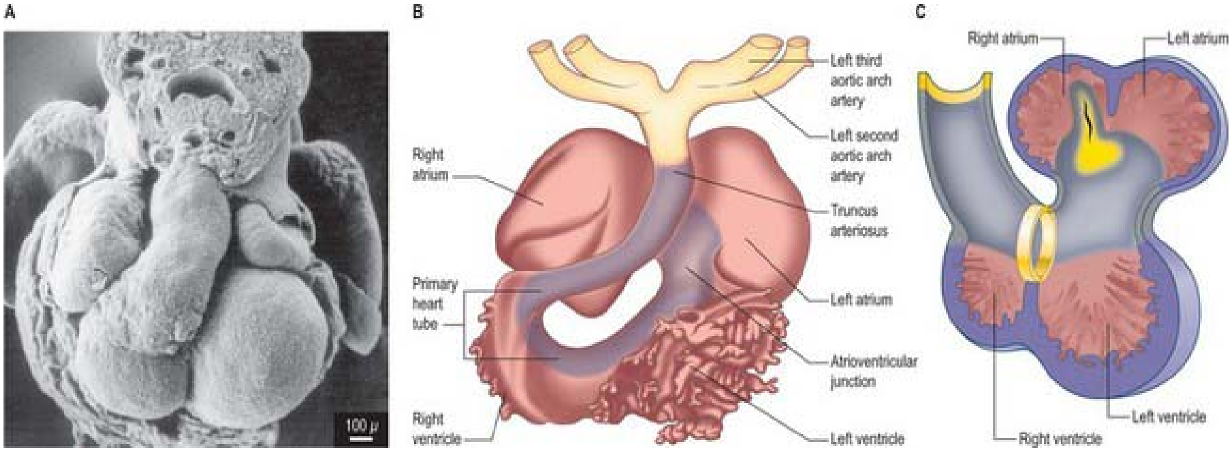
A
100 μ
B
Left third aortic arch artery
Left second aortic arch artery
Right atrium
Truncus arteriosus
Primary heart tube
Left atrium
Atrioventricular junction
Right ventricle
Left ventricle
C
Right atrium
Left atrium
Left ventricle
Right ventricle

Fig. 59.7 **A**, SEM of early developing human heart showing external appearance of the myocardium of the right and left ventricles, and right and left atrial appendages. The truncus arteriosus passes between the atria. **B**, Reconstruction of heart tube at stage 13 showing the endocardium. At the left and right ventricles the endocardium interdigitates with the myocardium and appears trabeculated; elsewhere it is separated from the myocardium by the cardiac extracellular matrix. **C**, The heart at stage 13 with the truncus arteriosus reflected to the right. The opening of the sinus venosus into the right atrium can be seen (yellow). The region of the primary heart tube is indicated by a ring.

*(**A** With permission from Oostra RJ, Steding G, Lamers WH, Moorman AFM. Steding’s and Virágh’s scanning electron microscopy atlas of the developing human heart. New York: Springer-Verlag, 2006. **B** Modified from O’Rahilly and Müller. Developmental Stages in Human Embryos 1987 Carnegie Institution of Washington. Pub 637.)*

The sinus venosus with right and left sinus horns, which forms at the confluence of the systemic venous tributaries, is a prominent structure in lower vertebrates. In mammals, it does not become recognizable as a morphologic entity until the systemic veins have excavated themselves from the mesenchyme of the body and been surrounded by myocardium. It then becomes incorporated into the pericardial cavity so that the sinus horns become part of the heart. All of these processes occur up to the 25th day of development in humans: only after this stage is it possible to consider development of the definitive atrial and ventricular chambers.

INFLOW TRACT

The working myocardium of the atrium differentiates locally at the dorsolateral sides of the heart tube (59.6D–G). The developing atrium then expands enormously, in dorsal, lateral and, most prominently, in a cranial direction. The cranial expansion is seen as pouches which become the left and right atrial appendages (Fig. 59.7A,B). The floor of the atrium, including the sinus venosus, and the atrioventricular canal, are made of primary myocardium. Less cellular proliferation occurs in these parts than in the expanding atrial chambers: the primary myocardium marks the inflow to, and the outflow from, the initial atrial chambers as ‘rings’ which are also associated with the formation of the conduction system (see p. 1021). The ring at the inflow defines the sinu-atrial junction, whilst the atrioventricular canal, which forms the atrial outlet during development, will eventually be incorporated into the definitive right and left atrial chambers as the atrial vestibules. Although it is possible to recognize the forming left and right atrial appendages at this stage, the right being more extensive than the left, the atrium itself has a single cavity and there is no evidence of septum formation. The myocardium of the sinus venosus and the newly forming mediastinal myocardium are smooth-walled, whereas the myocardium of the appendages shows ridges, the pectinate muscles, on the inner surface. The formation of the different appendages is under control of the *Pitx2* signalling pathway. The myocardium of the appendages has a chamber phenotype, or is working myocardium; it expresses atrial natriuretic factor and connexin40 among other markers.

Right atrium

The further development of the right atrium is characterized by the incorporation of the sinus venosus into the right part of the primary atrium. This process is under control of the T-box transcription factor Tbx18. At about 4 weeks of development, the sinuatrial junction of the looping primary heart tube is positioned symmetrically in the midline (Fig. 59.8; see also Figs 13.1B, 73.8). The left and right common cardinal veins drain directly into the cavity of the primary atrium. The atrial myocardium extends to the margins of the pericardial cavity, and strictly speaking the sinus venosus is not yet formed, because the systemic venous tributaries are embedded within the mesenchyme of the septum transversum.

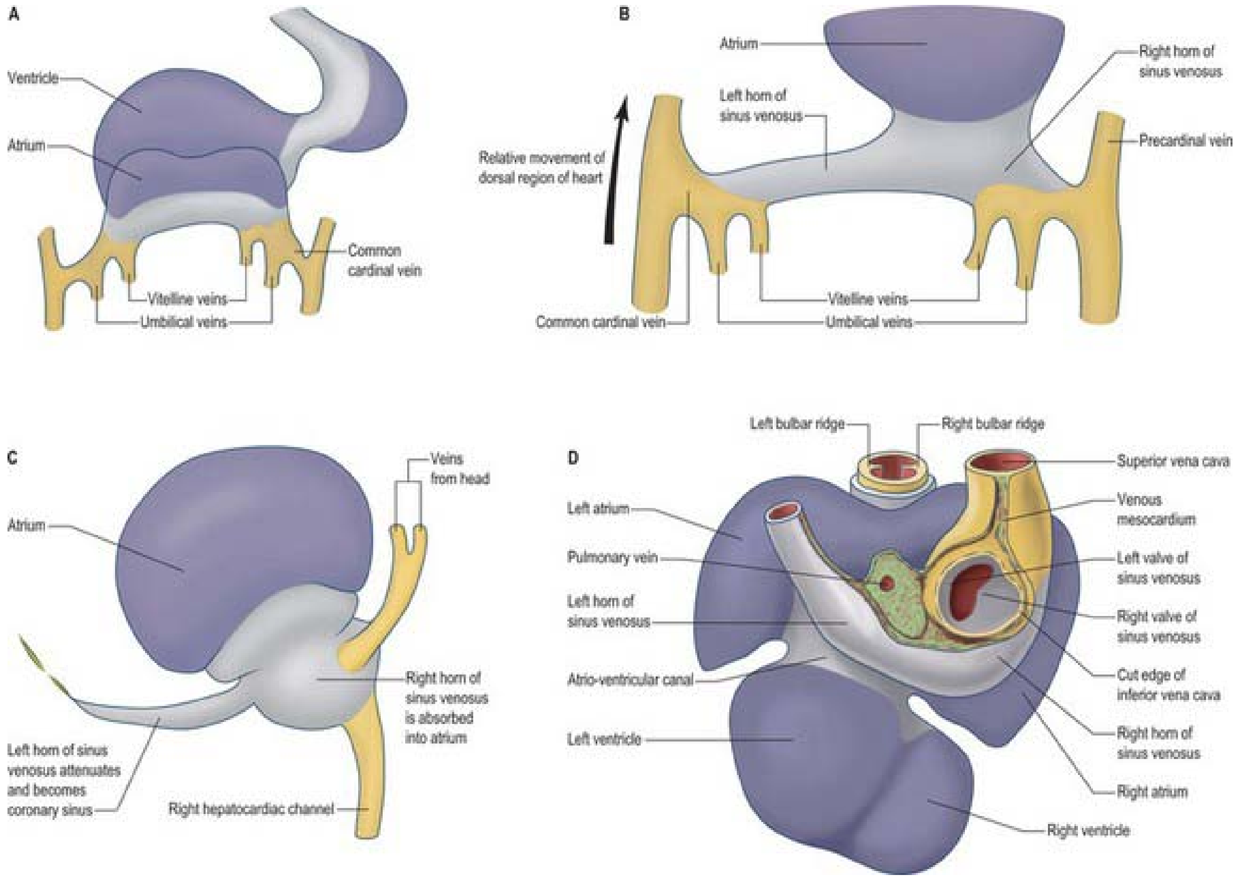
A
Ventricle
Atrium
Common cardinal vein
Vitelline veins
Umbilical veins
B
Atrium
Left horn of sinus venosus
Right horn of sinus venosus
Precardinal vein
Relative movement of dorsal region of heart
Common cardinal vein
Vitelline veins
Umbilical veins
C
Veins from head
Atrium
Right horn of sinus venosus is absorbed into atrium
Left horn of sinus venosus attenuates and becomes coronary sinus
Right hepatocardiac channel
D
Left bulbar ridge
Right bulbar ridge
Superior vena cava
Venous mesocardium
Left atrium
Pulmonary vein
Left valve of sinus venosus
Left horn of sinus venosus
Right valve of sinus venosus
Atrio-ventricular canal
Cut edge of inferior vena cava
Left ventricle
Right horn of sinus venosus
Right atrium
Right ventricle

Fig. 59.8 The changes to the sinus venosus. **A**, Dorsal view of the early heart tube shown in **Fig. 59.6D**. **B**, Changes to the circulation brings the venous circulation to the right. This causes enlargement of the right horn of the sinus venosus and atrium and attenuation of the left horn of the sinus venosus. **C**, The right horn of the sinus venosus becomes absorbed into the atrium. The left horn of the sinus venosus becomes the coronary sinus. **D**, Dorsal view of the embryonic heart showing the relative changes to the sinus venosus.

During subsequent development, the pericardial cavity expands to enclose the terminal segments of the systemic venous tributaries, and at the same time their walls differentiate as myocardium. They can now be termed the left and right horns of the sinus venosus; each horn receives the union of the corresponding umbilical vein, vitelline radicles, and common cardinal vein (Fig. 59.8; see also Fig. 73.8). Concomitantly, the constriction between the left horn and the atrium becomes more pronounced. As the dorsal wall of the left atrium is formed from additions of mediastinal myocardium, the left horn becomes incorporated into the developing left atrioventricular junction, its orifice draining to the newly formed right atrium. At the same time, the left-sided venous tributaries diminish in size; the left common cardinal vein forms the oblique vein of the left atrium, and the left sinus horn forms the coronary sinus (Fig. 59.8), maintaining its own myocardial wall as it becomes incorporated into the atrioventricular junction.

The right sinus horn increases rapidly in size with growth of the liver (see Figs 73.8, 73.9). The vitello-umbilical blood flow enters the right horn through a wide but short hepatocardiac channel, which becomes the cranial end of the inferior vena cava. The right horn also receives the right common cardinal vein, draining the blood from the right side of the body (Fig. 59.8B,C). Later, when transverse connections are established between the cardinal veins, the blood from the left side of the body also reaches the heart via the veins draining the right side (see Fig. 13.4). As these changes take place, the right sinus horn, including the proximal parts of the superior and inferior cardinal veins, becomes incorporated into the right atrium, forming the smooth-walled systemic venous sinus, also known as the sinus venarum.

The right sinus horn opens into the right atrium through its dorsal and caudal walls (Fig. 59.8; see Fig. 59.12). The sinuatrial orifice becomes elongated and slit-like, guarded by two muscular folds, the left and right sinuatrial (venous) valves. These two valves meet cranially and become continuous with a fold that projects from the atrial roof, the septum spurium. The valves also meet caudally, and merge with the inferior atrioventricular cushion. With ongoing development, the cranial part of the right sinu-atrial valve loses its fold-like form, but its position is indicated in the adult heart by the site of the crista terminalis of the right atrium. Its caudal part forms the valve of the coronary sinus, also known as the Thebesian valve, and most of the valve of the inferior vena cava (Eustachian valve). The union of the two valvular remnants then passes through the tissue which separates the orifice of the coronary sinus from the fossa ovalis. This area is known as the ‘sinus septum’, but in reality this ‘septum’ is no more than a muscular fold in the dorsal wall of the right atrium. The continuation of the venous valves persists as the tendon of Todaro, an important landmark to the location of the atrioventricular node in the definitive heart. The left venous valve blends with the right side of the atrial septum; there is usually no trace of it in the postnatal heart.

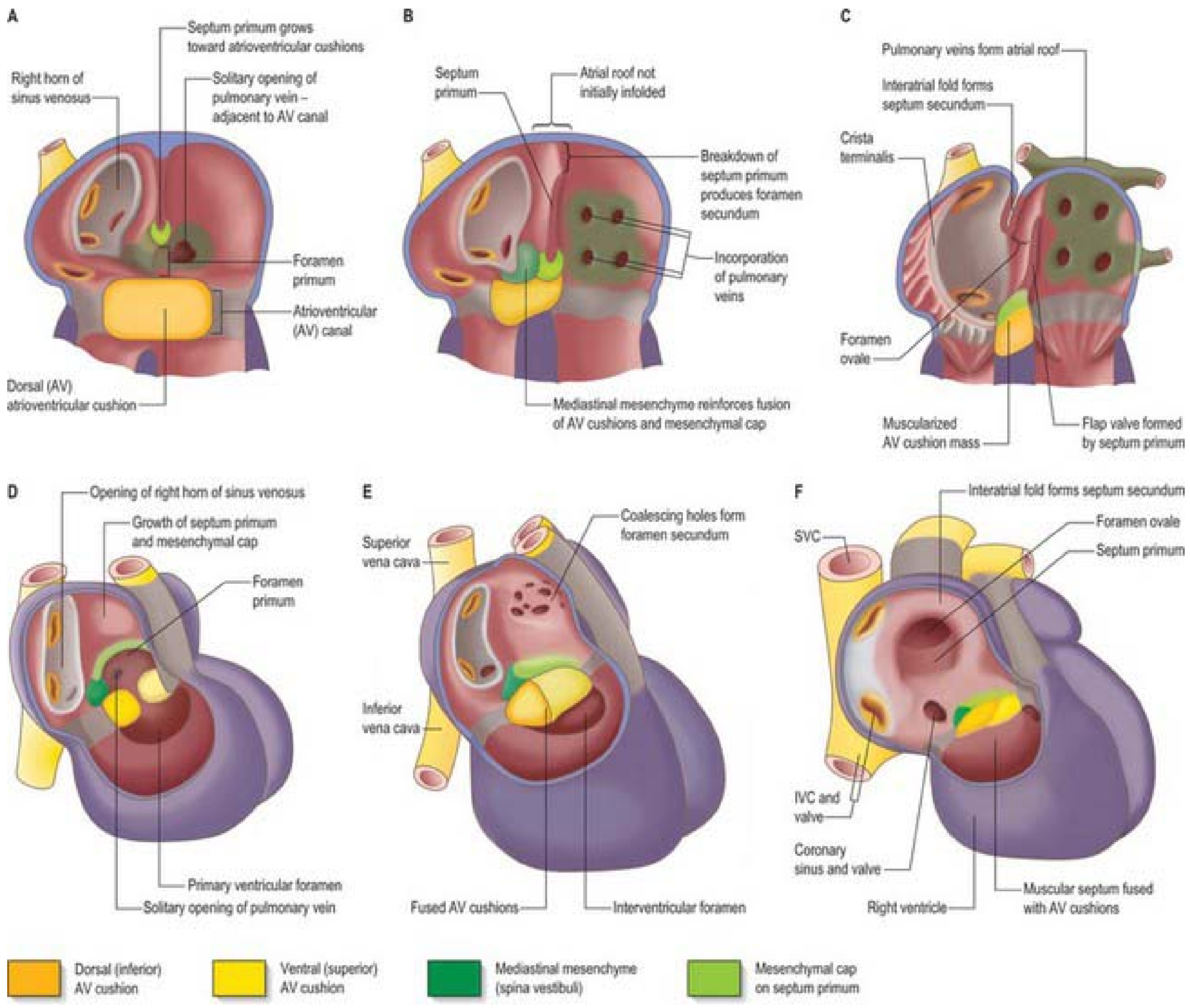
A
Septum primum grows toward atrioventricular cushions
Right horn of sinus venosus
Solitary opening of pulmonary vein – adjacent to AV canal
Foramen primum
Atrioventricular (AV) canal
Dorsal (AV) atrioventricular cushion
B
Septum primum
Atrial roof not initially infolded
Breakdown of septum primum produces foramen secundum
Incorporation of pulmonary veins
Mediastinal mesenchyme reinforces fusion of AV cushions and mesenchymal cap
C
Pulmonary veins form atrial roof
Interatrial fold forms septum secundum
Crista terminalis
Foramen ovale
Muscularized AV cushion mass
Flap valve formed by septum primum
D
Opening of right horn of sinus venosus
Growth of septum primum and mesenchymal cap
Foramen primum
Primary ventricular foramen
Solitary opening of pulmonary vein
E
Superior vena cava
Coalescing holes form foramen secundum
Inferior vena cava
Fused AV cushions
Interventricular foramen
F
Interatrial fold forms septum secundum
SVC
Foramen ovale
Septum primum
IVC and valve
Coronary sinus and valve
Right ventricle
Muscular septum fused with AV cushions
Dorsal (inferior) AV cushion
Ventral (superior) AV cushion
Mediastinal mesenchyme (spina vestibuli)
Mesenchymal cap on septum primum

Fig. 59.12 Three representative stages in the development of the atrial septum. **A–C**, Coronal views from the front; **D–F**, lateral views from the right side. **A** and **D**, The septum primum has not yet obliterated the original communication between the two atria (foramen primum) and the atrioventricular endocardial cushions have not yet fused. **B** and **E**, the atrioventricular endocardial cushions have fused with each other and with the septum primum, which has broken down in its dorsal part to form the foramen secundum. **C** and **F**, The septum secundum is forming on the right side of the foramen secundum from an interatrial fold.

Left atrium

Following the formation of the primary atrium and the left atrial appendage, the left atrium takes shape by the formation and incorporation of mediastinal myocardium. While the tributaries of the sinus venosus approach the atrium caudally, the differentiating pulmonary veins gain their entrance to the atrial cavity through the dorsal mesocardium (Fig. 59.5). The topographical relationships seen in the postnatal heart are thus established as soon as differentiation of the pulmonary venous portal occurs.

Early in the development of the atrium, the pulmonary vein develops as a solitary channel from angiogenic cells derived from the dorsal mesocardium, and establishes continuity with the vascular plexus formed in the mediastinal mesenchyme around the developing lung buds. The solitary pulmonary vein opens into the caudo-dorsal wall of the atrium adjacent to the developing atrioventricular junction, its atrial orifice being flanked by two prominent ridges. The primary atrial septum develops from the right ridge, following incorporation of the left sinus horn into the right side of the primary atrium, thus confining the pulmonary venous orifice to the developing left atrium (Fig. 59.12). The pulmonary vein initially branches within the dorsal mediastinal mesenchyme, its tributaries draining blood from the developing lung. With continuing development, the walls of the venous channels become surrounded by myocardium, this process occurring to the level of the second bifurcation. The veins then expand, and are incorporated into the roof of the left atrium, eventually forming the greater part of its cavity. However, all four pulmonary veins do not achieve their separate opening into the atrial roof until well after the completion of atrial septation, and probably not until the 10th or 11th week of development. Variations in the precise pattern of pulmonary venous drainage are quite common. With these changes, the left half of the primary atrium becomes progressively restricted to the mature appendage. The myocardial sleeves surrounding the pulmonary orifices taper off, and become intermingled with fibrous tissue. In later life, it is likely that this intermingling of myocardial and fibrous tissues forms the substrate for some forms of atrial fibrillation. The opening of the solitary pulmonary vein to the left of the right pulmonary ridge is an essential pre-requisite for atrial septation.

VENTRICLES

The ventricles develop at the ventral side of the looping primary heart tube during the fourth week of development (Figs 59.6, 59.7). The left ventricle develops from the stem of the Y-shaped heart, the right ventricle develops later, downstream relative to the left ventricle, when more myocardium has been added to the cardiac tube. As a result of the looping of the heart tube, the right ventricle is positioned at the right of the left ventricle, which is a prerequisite for the appropriate connection with the expanding atrial component of the heart. Unlike the atrial chambers, the morphological differences between the right and left ventricles are not part of the general asymmetry between the right- and left-sided organs of the body, but rather are under control of the signalling pathways which determine caudo-cranial differentiation. Retinoic acid, and its downstream transcription factor Tbx5, play a crucial role in this process.

The myocardium at the inner curvature, the original dorsal side of the cardiac tube, remains smooth-walled and maintains its molecular phenotype, whereas the myocardium at the outer curvature of the myocardial tube displays trabeculations in the fifth week of development (Fig. 59.7B). By stage 17, the trabeculations have achieved a typical spatial orientation, giving a sponge-like appearance to the internal aspect of both ventricles (Fig. 59.9). The definitive trabeculations, coarse in the right ventricle but much finer in the left, are first observed about the 40th day of gestation: they appear initially in the walls of both ventricles at the level of the atrioventricular junction and develop towards the apex of the heart. By the time the fetus is 10 weeks old, the trabeculations are much sparser, and are confined to the apical regions. This process of remodeling is accomplished without the intervention of macrophages or inflammatory cells in the immediate interstitium. The ventricular myocardium, encompassing the trabeculations and exterior wall, possesses a chamber phenotype, the myocytes expressing, among other proteins, the gap-junctional protein Cx40 and atrial natriuretic peptide. This myocardium stops proliferating and differentiates into the fast-conducting peripheral ventricular conduction system, whereas the outer layer becomes highly proliferative and forms the compact layer of the ventricular wall.

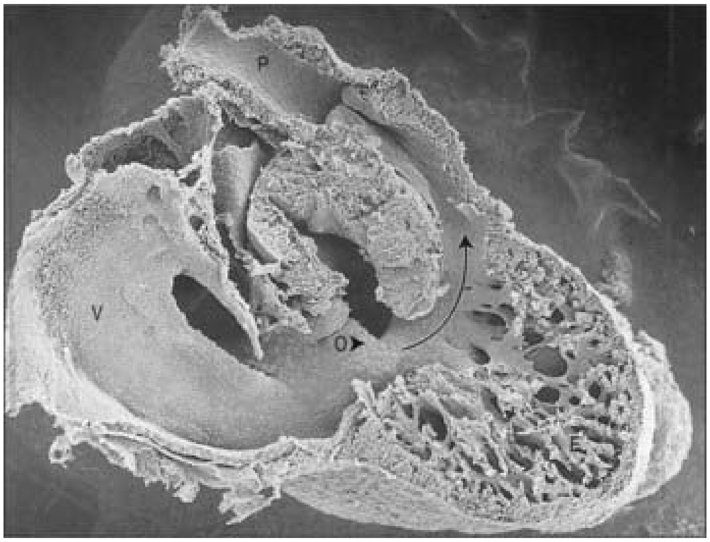

Fig. 59.9 SEM of human heart at 42 days' gestation. The right lateral wall of the right atrium, right ventricle and the outflow tract have been removed. The valve of the sinus venosus (V) is prominent. There is no septal cusp of the tricuspid valve guarding the inlet portion of the right ventricle. The parietal cusp has been removed. The atrioventricular cushions are fused. Note the adjacent right lateral tubercles (O). A small interventricular foramen (secundum, see text) is indicated (small arrowhead). There is a well developed right ventricular outflow tract (curved arrow). E, embryonic trabeculae; P, pulmonary trunk

OUTFLOW TRACT

Initially the outflow tract possesses myocardial walls up to the pericardial reflections. It displays a characteristic bend, which has a proximal part arising from the developing right ventricle and a distal part which becomes continuous with the aortic sac beyond the pericardial reflections. Although this bend is a conspicuous morphologic feature, it is highly unlikely that the cells to either side of it retain their position during subsequent development. Instead, it seems probable that cells are recruited from the second heart-forming field, and pass through the outflow tract to contribute to the definitive right ventricle. Subsequently, still more cells are recruited from pharyngeal mesenchyme, passing proximal to the pericardial reflections and forming the intrapericardial components of the arterial trunks. There remains much disagreement as how best to describe these morphological parts of the outflow tract. Some authors have labeled the proximal myocardial part the *conus*, calling the distal part the *truncus*, and the intrapericardial portion of the outflow tract the *aortic sac*. Others have called the entire myocardial outflow tract the *bulbus*, since the myocardial outflow tract of primitive vertebrates, called the *conus arteriosus* in primitive fish, and the *bulbus cordis* in amphibia, is presumed to develop into the right ventricle in higher vertebrates. Because the terms conus and truncus have been inconsistently used in literature, we prefer simply to describe proximal and distal parts of the myocardial outflow tract, and to describe, when it appears, an intrapericardial arterial portion of the outflow tract, this part interposing between the muscular component and the ventral aorta, the distal junction occurring at the pericardial reflections.

Given that different authors use different terminologies, it is not surprising that formation of the outflow tract remains one of the most confusing areas of cardiac development. The recent finding that the stem of the heart tube contains precursor cells exclusively for the left ventricle makes it essential to adopt descriptions which follow dynamic events, rather than continuing to use static names. Thus, as soon as the primary heart tube bends to produce its ventral ventricular expansion, by definition the developing ventricle achieves inlet and outlet components, even though these structures are not the definitive ventricular inlets and outlets. Cells that, initially, are found in the ventricular outflow tract subsequently become cells of the right ventricle. Furthermore, working myocytes can easily be distinguished from the primary myocytes of the straight heart tube. The primary myocardium is smooth-walled, whereas the developing myocardium of the ventricles is trabeculated, and expresses specific markers such as atrial natriuretic peptide and connexin40. Thus, that part of the primary heart tube downstream of the developing ventricular loop is termed the outflow tract, irrespective of the fact that eventually it will largely become incorporated within the definitive right ventricle (Figs 59.6, 59.7). Moreover, within the inner curvature of the ventricular loop, the walls of the outflow tract and atrioventricular canal fade into one another without a clear boundary. Indeed, ventricular working myocardium never develops at the inner curvature. It is within this ventricular part of the primary heart tube that the cushions of the atrioventricular canal and the outflow tract must achieve appropriate connections with the muscular ventricular septum in order to divide this part of the tube into left and right compartments. The cavity of the tube within which these events take place has been called ‘interventricular foramen’. This is incorrect, since it is rather the region between adjacent parts of the primary heart tube. It is, nonetheless, the remodelling of this inner curvature that sets the scene for the completion of cardiac septation.

CARDIAC FUNCTION AND THE CONDUCTION SYSTEM

Although only mammalian hearts have a well-defined conduction system, an essentially similar electrocardiogram can be recorded from animals as diverse as fish and man, indicating that the electrical connections between the cardiac components have been conserved during vertebrate evolution. Indeed, the development of the conduction system of the heart is inextricably associated with the development of the basic building plan for the heart. The conduction system is best defined as the system that initiates and conducts the sinus impulse. In mammals, it encompasses the sinu-atrial node, the atrioventricular node, the atrioventricular bundle, the bundle branches and their terminal ramifications. The nodes and the atrioventricular bundle can be considered the central conduction system, while the bundle branches and their ramifications represent the peripheral ventricular conduction system. The sinus impulse is generated in the sinus node, whence it is rapidly propagated through the atrial myocardium towards the atrioventricular node, where propagation is delayed. After an essential period of atrioventricular delay, the impulse travels rapidly through the atrioventricular conduction axis and the peripheral ramifications to reach the ventricular myocardium, which is then rapidly depolarized. Following repolarization, the sequence recurs in endless fashion throughout the life of the individual. The term ‘conduction system’, as opposed to the working myocardium of the chambers, may suggest that the working myocardium does not conduct, while the conduction system conducts rapidly. In order to produce powerful synchronous contractions, the working myocardium of the chambers must also, of necessity, conduct rapidly, whereas to act as a pacemaker, the cells of the nodes need to be poorly coupled, and hence display slow conduction.

The vertebrate heart is myogenic, implying that all cardiomyocytes have the capacity to generate and conduct the depolarizing impulse. Because cardiac myocytes are electrically coupled, the cells with the highest pacemaking activity take the lead. In the formed normal heart, the leading pacemaker is always within the sinus node. In embryonic hearts, the leading pacemaker is always found at the venous pole. Thus, it is the most recently recruited cells at the venous pole which always have the highest pacemaking activity. All regions of the early embryonic heart tube possess poorly coupled cells and display intrinsic automaticity, thus permitting slow propagation of the depolarizing impulses along the cardiac tube, and producing matching peristaltic waves of contraction which push the blood in an antegrade direction. The myocytes of a developing heart do not have well-developed sarcomeric structures, and have a poorly developed sarcoplasmic reticulum. This tissue has been called primary myocardium, distinguishing it from the rapidly conducting and well-developed working myocardium of the atrial and ventricular chambers.

As development proceeds, the ventricular chambers develop in the cranial part of the heart tube, by ventral expansion, and the atrial chambers in the caudal part by dorso-lateral expansion (Fig. 59.6). An adult type of electrocardiogram can be recorded from such hearts, showing rapid atrial depolarization, a period of atrioventricular delay, and rapid ventricular depolarization. The electrocardiographic tracings reflect the development of fast-conducting components within a slowly conducting heart tube, i.e. the development of a morphologic conduction system. The newly developed working myocardium expresses atrial natriuretic factor, along with the gap junctional proteins connexin40 and 43, which permit fast conduction.

Like the early peristaltic heart, flow through the developing chambered heart remains directional because the dominant pacemaking activity is still at the inlet of the heart. Peristaltic hearts do not need valves, whereas chambered hearts require the presence of one-way valves at the inlets to, and the outlets from, the chambers. The slowly conducting atrioventricular canal, interposed between the atrium and the ventricle, and the outflow tract positioned between the ventricle and the great arteries, are the parts which contain the endocardial cushions. These are able to function as sphincteric valves, as a result of their prolonged duration of contraction. These components retain their function until the definitive leaflets of the one-way valves have been sculpted from the cushions. The primary myocardium of the outflow tract does not regress until the arterial valves have been formed, and does not disappear in its entirety until around the twelfth week of human development. The primary myocardium of the atrioventricular canal is eventually incorporated into the atrial vestibules at the same time as the formation of the atrioventricular valves, becoming sequestrated on the atrial side of the atrioventricular junctions between 6 and 12 weeks of development (Fig. 59.10). An important part of the canal persists dorsally, where it differentiates into the slowly conducting atrioventricular node.

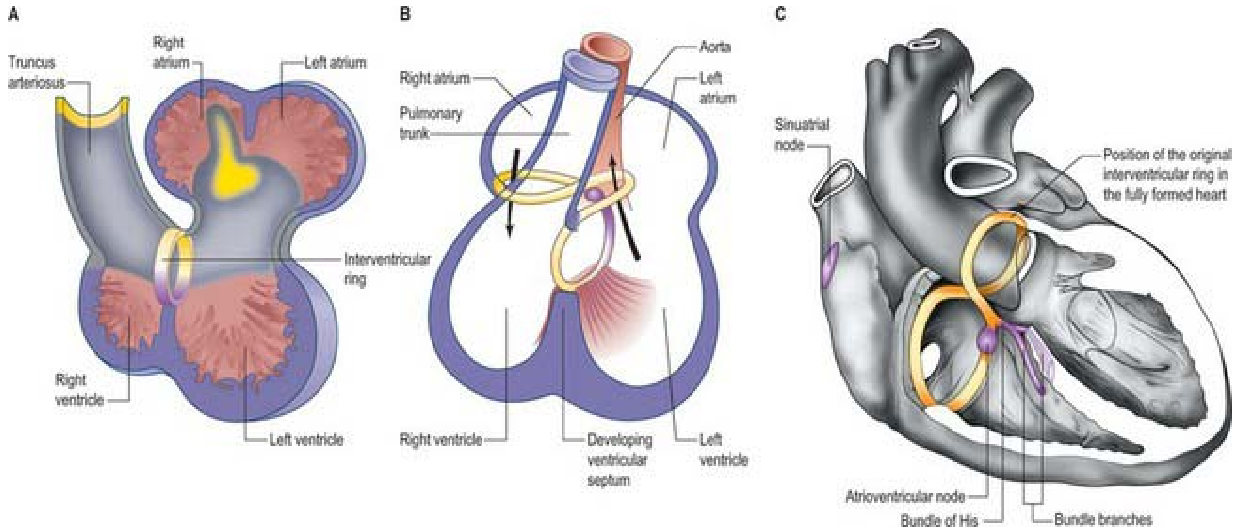
A
Truncus arteriosus
Right atrium
Left atrium
Interventricular ring
Right ventricle
Left ventricle
B
Right atrium
Pulmonary trunk
Aorta
Left atrium
Right ventricle
Developing ventricular septum
Left ventricle
C
Sinuatrial node
Position of the original interventricular ring in the fully formed heart
Atrioventricular node
Bundle of His
Bundle branches

Fig. 59.10 Development of the conduction system of the heart. **A**, At stage 13 with the truncus arteriosus reflected to the right, the interventricular ring marks the region of the primary heart tube. The purple part of the interventricular ring will give rise to the atrioventricular bundle and bundle branches, whereas the yellow part of the interventricular ring will not participate in the formation of the adult conducting system. **B**, The truncus arteriosus, now divided into the pulmonary trunk and aorta, is presented between the right and left atria which expand lateral to it The right atrium is now positioned entirely above the right ventricle and the outflow tract has expanded to the left; the left ventricle has access to the aorta. **C**, The position of the original primary heart tube ring indicated in the formed heart. The pulmonary trunk has been removed.

Considerable progress has been made over recent years in deciphering the pathways involved in establishing the building plan of the heart (Fig. 59.11). The combined action of the transcription factors Tbx5 and Nkx2–5 is required for the formation of the myocardium of the atrial and ventricular chambers. Tbx5 is expressed in a gradient over the heart tube, decreasing in concentration from caudal to cranial and may impose positional information. However, its pattern cannot explain the localized formation of the chambers and the conduction system. Localized expression of the transcriptional repressors Tbx2 and Tbx3 in the inflow tract, the floor of the atrium, the atrioventricular canal, the inner curvature of the ventricular region, and the outflow tract prevents the differentiation of primary into working myocardium. Tbx2 and Tbx3 effectively compete for binding to the promoters of the chamberspecific genes, such as atrial natriuretic factor and connexin40. The remaining primary myocardium of these regions initially induces the endocardium to undergo epithelial-to-mesenchymal transition, by which process the cardiac cushions become filled with mesenchyme. The myocardium also participates in the alignment of the atrial and ventricular chambers (which is essential for proper cardiac septation, and which is guided by the fusing cardiac cushions), and it forms the conduction system, including the sinus and atrioventricular nodes, the atrioventricular bundle, the floor of the developing right atrium (the internodal region), and the entirety of the atrioventricular canal. In the early chamber-forming heart of the mouse, Tbx3 is expressed in the atrioventricular canal, the floor of the atrium and around the orifices of the systemic venous tributaries, but not in the dorsal mesocardium surrounding the entrance of the pulmonary vein. During subsequent development, the domain of expression of Tbx3 expands from the atrioventricular canal to form a crescent on the crest of the ventricular septum. The dorsal aspect of this crescent develops into the atrioventricular bundle, while the atrioventricular node is formed at the dorsal junction with the atrioventricular canal. The ventral parts subsequently disappear during development.

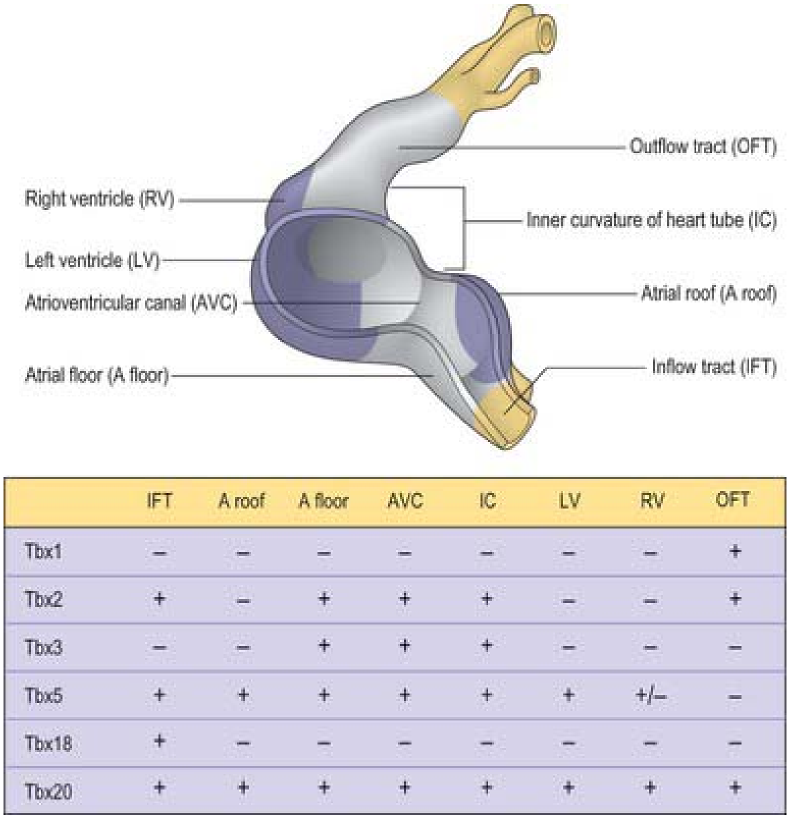
Outflow tract (OFT)
Right ventricle (RV)
Inner curvature of heart tube (IC)
Left ventricle (LV)
Atrioventricular canal (AVC)
Atrial roof (A roof)
Atrial floor (A floor)
Inflow tract (IFT)

	IFT	A roof	A floor	AVC	IC	LV	RV	OFT
Tbx1	–	–	–	–	–	–	–	+
Tbx2	+	–	+	+	+	–	–	+
Tbx3	–	–	+	+	+	–	–	–
Tbx5	+	+	+	+	+	+	+/–	–
Tbx18	+	–	–	–	–	–	–	–
Tbx20	+	+	+	+	+	+	+	+

Fig. 59.11 The early heart: distribution of the T-box transcription factors involved in patterning the heart.

The fact that the ventricular conducting system originates from a single primary ring provides a solid base for understanding the disposition of the conducting system in a number of congenital malformations. The concept accounts particularly well for the morphology and disposition of the atrioventricular node and bundle in hearts with straddling tricuspid valves, with double inlet left ventricles, and with congenitally corrected transposition.

SEPTATION OF THE EMBRYONIC CARDIAC COMPARTMENTS

The flow of blood on the right and left sides does not intermingle even in the developing heart, because flow is laminar, and the pressures are similar at the right and left sides. It is only after birth that the pressures in the ‘left’ systemic circulation become higher than those in the ‘right’ pulmonary circulation, and therefore the different flows have to be separated physically in order to prevent admixture of oxygenated and deoxygenated blood. Prior to birth the lungs are not functioning and blood flow to them is small. Even so, normal development of the heart requires that all cardiac compartments receive an adequate amount of blood. To this end, even before birth, the systemic blood of the right atrium is guided to the left atrium so that the left half of the heart and the brain is provided with a normal flow of blood. The right ventricle, in contrast, drains to the dorsal aorta via the ductus arteriosus (see Fig. 35.8). The walls that separate the right and left sides of the heart are largely formed in the fourth and fifth week of development. Some time later, not only the components of the primary heart tube, specifically the atrioventricular canal and the outflow tract, but also the atrial and ventricular chambers, must be separated physically into right and left halves. However, each compartment is separated in markedly different fashion.

Septation of the atrial chambers

As a prelude to atrial septation, the right horn of the sinus venosus is incorporated into the right part of the atrium and the pulmonary vein arises as a midline structure within the dorsal mesocardium. Internal separation into right and left atria is mainly effected by growth of two septa coupled with remodelling of the venous compartments. At the end of the fourth week of development, a crescentic fold, the primary atrial septum or septum primum, grows by active proliferation from the dorso-cranial atrial roof into the direction of the atrioventricular canal, extending downwards just to the right of the entrance of the pulmonary vein (Fig. 59.12A,D). It is separated from the left sinu-atrial valve by the interseptovalvular space. The leading edge of the septum primum is covered by a mesenchymal cap in continuity dorsally with extracardiac mesenchyme (mediastinal mesenchyme) derived from the dorsal mesocardium which forms the vestibular spine, or spina vestibuli. The ventral horn of the septum primum reaches the ventral (cranial) atrioventricular cushion, while the dorsal horn reaches the dorsal (caudal) cushion. Thus the primary atrial foramen, the foramen or ostium primum, is entirely surrounded by mesenchyme derived from endocardium. Ventral and caudal to the advancing edge of the septum primum, the developing atrial chambers communicate through the foramen primum (Fig. 59.12A,D).

As the foramen primum diminishes in size, the upper margin of the septum primum perforates by apoptosis, and thus right to left shunting of blood continues through a secondary foramen, the foramen or ostium secundum. The latter is formed before the end of the fifth week of development. Initially it lacks an upper rim, since its upper border is the atrial roof. The foramen primum is finally occluded in the median plane, as the edge of the septum primum merges with the fusing atrioventricular cushions (Fig. 59.12B,E). The foramen secundum then enlarges to permit free passage of blood from the right to the left atrium.

The solitary opening of the pulmonary vein into the roof of the left atrium, which is originally adjacent to the atrioventricular junction, becomes incorporated into the atrial wall, ultimately forming four separate orifices at the corners of the atrial roof. As this development continues, the muscular atrial roof itself invaginates on the right side of the primary atrial septum (Fig. 59.12B,E), the invaginated fold constituting the septum secundum. The free edge of the septum secundum overlaps the foramen secundum. When left atrial pressure exceeds right atrial pressure in postnatal life, the septum primum closes against the septum secundum as a flap-valve (Fig. 59.12C,F). The passage taken by blood as it passes from the right atrium, under the crescentic edge of the septum secundum, then obliquely towards and through the foramen secundum to the left atrium, persists throughout intrauterine life as the foramen ovale. At first, the foramen ovale is sited cranio-dorsally relative to the atrial septum, but with remoulding of the venous components, it achieves a cranio-ventral position.

Septation and appropriate positioning of the atrioventricular canal

Extracellular matrix accumulates between the endocardium and myocardium of the primary heart tube. However, it mostly disappears in the regions of ballooning of the chamber myocardium of the developing atria and ventricles. The matrix becomes filled with mesenchyme in the persisting regions of the primary heart tube. In conventional accounts of the process, these regions are called the atrioventricular canal and the outflow tract, or conotruncus. The dorsal or inferior atrioventricular cushion continues into the floor of the atrium, which is made of primary myocardium. As the cushion extends dorsally, it meets the mediastinal mesenchyme in the region initially termed the spina vestibuli, where it continues as a mesenchymal cap running along the leading edge of the septum primum until it meets the ventral, or cranial, atrioventricular cushion (Fig. 59.12 and see Fig. 59.14). The dorsal cushion also has a significant ventricular extension in the inner curvature of the heart tube, which comes to lie on top of the developing muscular ventricular septum. The two atrioventricular cushions fuse in the sixth week of development, dividing the atrioventricular canal into its right and left components. The cushions are very large relative to the canal, leaving narrow right and left slits, which increase markedly in size during further development.

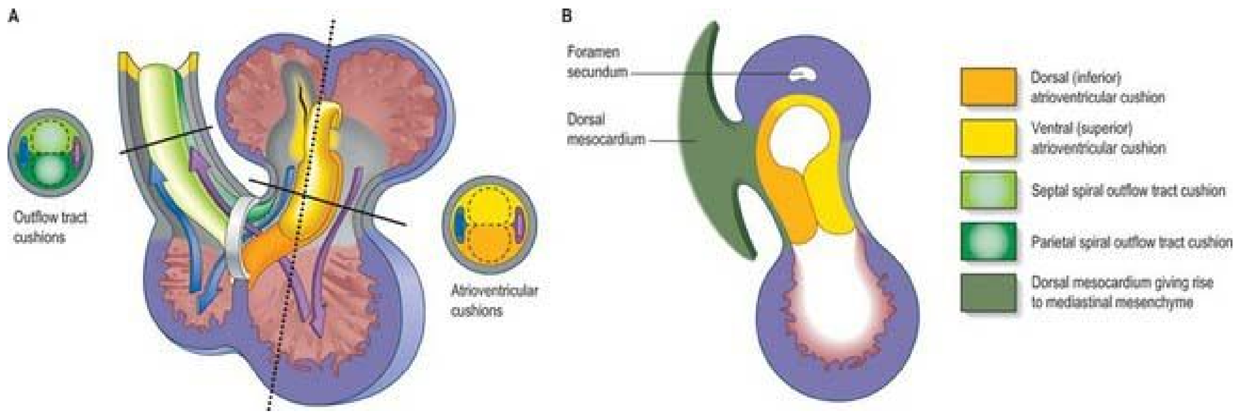
A
Outflow tract cushions
Atrioventricular cushions
B
Foramen secundum
Dorsal mesocardium
Dorsal (inferior) atrioventricular cushion
Ventral (superior) atrioventricular cushion
Septal spiral outflow tract cushion
Parietal spiral outflow tract cushion
Dorsal mesocardium giving rise to mediastinal mesenchyme

Fig. 59.14 Septation of ventricles and outflow tract. **A**, Frontal view of heart at stage 13 with the outflow tract reflected to the right. Lines show the

level of transverse sections of the atrioventricular cushions and outflow tract. Note that blood from both atria pass through the embryonic interventricular foramen at this stage. **B**, Sagittal section of heart along the dotted line in A showing the atrioventicular junctional region seen from the right side. The atrioventricular cushions extend onto the leading edge of the septum primum (although the mesenchymal cap on the atrial septum, see **Fig. 59.12**, probably has a different developmental origin).

At the start of stage 10, the venous pole, the atrioventricular canal, the developing left ventricle and the outflow tract are all positioned symmetrically around the midline (Fig. 59.13A). As a result of the subsequent rapid growth of the cardiac tube, the atrioventricular canal moves in its entirety to the left (Fig. 59.13B), as the ventricular part of the heart tube loops to the right, thus placing the developing left ventricle on the left, and the forming right ventricle on the right (Fig. 59.7). This ventricular loop is conspicuous throughout the fourth and fifth weeks of development, and it is at this stage that a deep interventricular groove appears externally. Over this period the atrial floor, including the developing systemic venous sinus (sinus venosus) and the atrioventricular canal, move to the right (Fig. 59.13C). The developing pulmonary vein remains anchored in the midline and, subsequent to these manoeuvres, the atrioventricular canal once more becomes positioned in the midline: this process facilitates the appropriate connections of the developing muscular septum with the atrioventricular and outflow cushions. The orifice of the sinus venosus is by now positioned to the right. From the outset, the muscular ventricular septum develops in line with the right side of the dorsal (inferior) atrioventricular cushion (Fig. 59.14), so that the separating right atrium always has direct access to the developing right ventricle. The process also ensures that space remains ventrally for incorporation of the subaortic component of the outflow tract into the left ventricle.

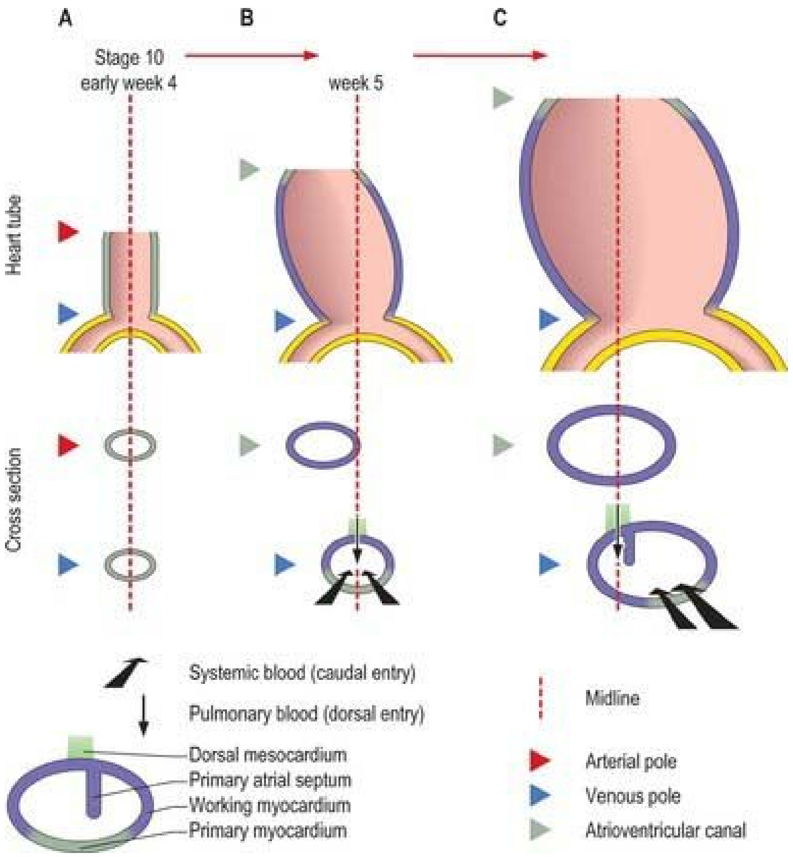
A
B
C
Stage 10
early week 4
week 5
Heart tube
Cross section
Systemic blood (caudal entry)
Pulmonary blood (dorsal entry)
Dorsal mesocardium
Primary atrial septum
Working myocardium
Primary myocardium
Midline
Arterial pole
Venous pole
Atrioventricular canal

Fig. 59.13 Movements of the atrioventricular canal relative to the midline during development.

Septation of the ventricles

After the looping of the heart tube, it is easy to gain the impression that the atrioventricular canal communicates exclusively with the developing left ventricle, while the outflow tract is supported exclusively by the developing right ventricle. In the definitive heart, blood entering the right ventricle passes in through the right atrial vestibule and exits through the muscular subpulmonary infundibulum, while blood entering the left ventricle passes in through the left atrial vestibule, and exits through the aortic root. The changes needed to produce the definitive connections between the cardiac components are complex. Three distinct structures contribute to the formation of the postnatal ventricular septum: the muscular ventricular septum, the proximal parts of the outflow cushions and the atrioventricular endocardial cushions. The latter two components separate those parts of the primary heart tube that are committed to the right and left ventricles, as opposed to the ballooned apical ventricular components. Inappropriate formation and connection of the cushions with the muscular ventricular septum underscores deficiencies of the definitive ventricular septum; such lesions account for about two-thirds of all cardiac septal defects.

Separation between the right and left ventricles is initially heralded by the appearance of a caudal crescentic ridge within the ventricular loop. The trabeculated parts of the ventricles contain less extracellular matrix than the walls of the primary heart tube, and it is these parts of the chambers that expand on each side of the ridge that remains between them. The crest of the developing septum, therefore, is its oldest portion. The more apical parts are added concomitant with enlargement of the chambers, as if they were expanding like balloons. The impression can be gained that the dorsal and ventral horns of the ventricular septum grow along the ventricular walls, meeting and fusing with the right extremities of the dorsal and ventral cushions of the atrioventricular canal. In reality, the crest of the septum marks the position of the original primary heart tube, and becomes the atrioventricular bundle. The septum has a free sickle-shaped margin that, together with the fused caudal surface of the endocardial cushions, bounds an ovoid foramen. Previously this foramen has erroneously been termed the interventricular, or bulboventricular foramen: it is no more than a locus within the cavity of the primary heart tube. The apical trabecular components of the ventricles balloon from the ventral side of the primary heart tube. At the dorsal side, or the inner curvature, there is no chamber myocardium, only the smooth walls of the primary heart tube. Therefore, from the outset of the process, the forming apical parts of the ventricles are separated by a muscular septum. The foramen marked caudally by the crest of the ventricular septum provides the initial inlet to the developing right ventricle, and the outlet for the developing left ventricle. Completion of ventricular septation requires division of this primary foramen, rather than its closure. It also demands appropriate connection between the muscular septum and the divided atrioventricular canal, including its cushions, and with the divided outflow tract, along with its cushions (Fig 59.14).

Use of inappropriate terminology means that the entire region upstream relative to the foramen has previously been called the primitive ventricle, the entire downstream region the bulbus, and the junction between them, the bulboventricular junction. In the account presented here, the area is termed the primary junction, initially marked by a distinct notch on the outside of the heart, and inside by the corresponding ridge of the developing ventricular septum. The ridge is positioned between the atrioventricular orifice, which is initially a common structure, and the caudal part of the forming right ventricle.

Appropriate connection with the separating atrioventricular and arterial junctions is essential for the development of a four-chambered heart. The serendipitous discovery of the expression of a ‘neural’ antigen in the primary junctional myocardium, surrounding the so-called primary interventricular foramen, has clarified the steps involved in the remodeling of this region at the inner curvature.

Septation and appropriate positioning of the outflow tract

The length of the myocardial portion of the outflow tract decreases markedly between the fourth and eighth weeks of development. In part, the myocardium becomes incorporated into the ventricles, and in part it disappears by apoptosis: in the definitive heart, there is no distinct myocardial outflow tract present within the left ventricle, because the myocardium which initially separated the developing mitral and aortic valves disappears, leaving the fibrous aortic-mitral continuity distinctive for the postnatal heart. In the right ventricle, the proximal myocardial outflow tract persists as the smooth-walled muscular subpulmonary infundibulum. Formation of the part adjacent to the aortic root requires muscularization of the most proximal parts of the outflow cushions to form the greater part of the supraventricular crest, or crista supraventricularis.

Key to separation of the outflow tract is the appearance of the two outflow ridges, or cushions, which spiral one round another as they run from the distal end of the right ventricle, where they are positioned septally and parietally, to the aortic sac (Figs 59.14, 59.15). Within the aortic sac, a transverse wedge of tissue, termed the aorto-pulmonary septum, separates the origins of the arteries traversing the fourth and sixth pharyngeal arteries. The septum is formed from dorsal mediastinal mesenchyme. Myocardial precursor cells and non-myocardial cells are added to the outflow tract, the latter forming the intra-pericardial components of the arterial trunks. Neural crest cells migrate from the pharyngeal mediastinal myocardium into the outflow cushions. They do not appear to populate the septum itself, but form the larger parts of the walls of the intrapericardial portions of the truncus arteriosus. The precise relationship between the outflow cushions and the newly formed aortic arch arteries, which never possess a septum between them, has still to be assessed.

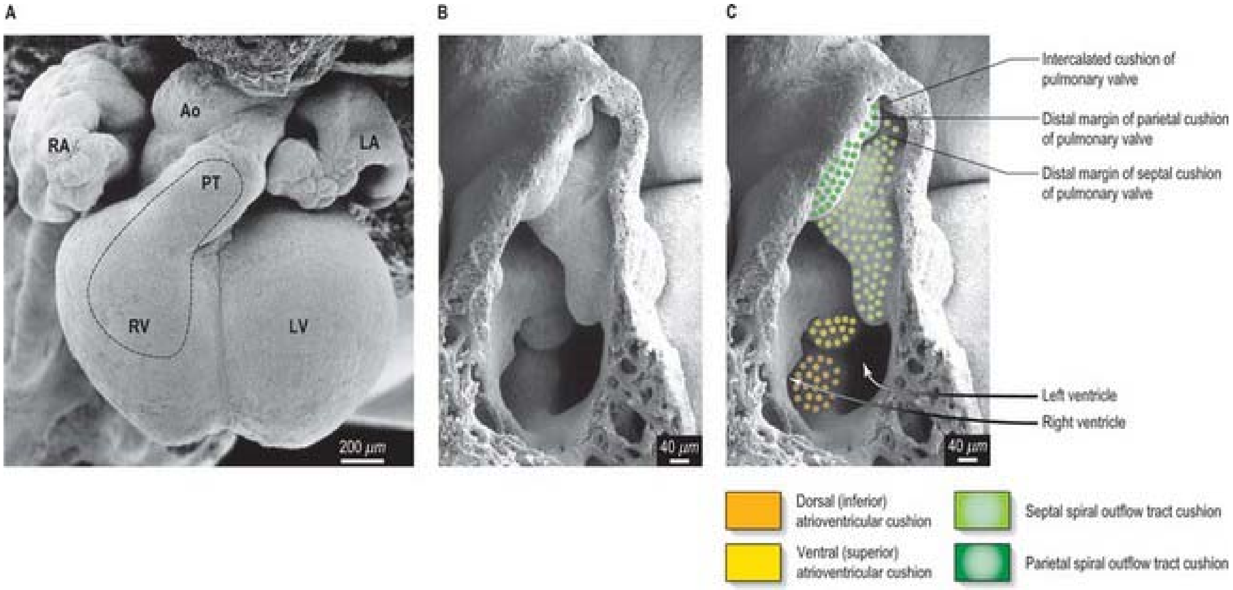
A
B
C
RA
Ao
LA
PT
RV
LV
200 µm
40 µm
40 µm
Intercalated cushion of pulmonary valve
Distal margin of parietal cushion of pulmonary valve
Distal margin of septal cushion of pulmonary valve
Left ventricle
Right ventricle
Dorsal (inferior) atrioventricular cushion
Ventral (superior) atrioventricular cushion
Septal spiral outflow tract cushion
Parietal spiral outflow tract cushion

Fig. 59.15 Septation of outflow tract. **A**, SEM of human heart at stage 18. The pulmonary trunk is separate from the aorta. **B**, SEM of human heart at stage 17 showing the luminal aspect of the right ventricle and the outflow tract. The anterior and parietal wall of the outflow tract has been removed along the dotted lines shown in **A**. **C**, SEM with added colour to show the structures in **B**. The outflow cushions are unfused; the distal margins of both outflow tract cushions are contributing to the developing pulmonary valve, the third leaflet and sinus of this valve are derived from the intercalated

cushion. The components of the aortic valve develop from the dorsal aspect of the outflow tract cushions.

(By courtesy of Prof G Steding, Göttingen, with permission from Oostra RJ, Steding G, Lamers WH, Moorman AFM. Steding’s and Virágh’s scanning electron microscopy atlas of the developing human heart. New York: Springer-Verlag, 2006.)

The spiral outflow ridges start to fuse from the sixth week onward, initially in the distal part of the outflow tract, and fusions continue gradually in the direction of the ventricular septum (Figs 59.15, 59.16A). The most proximal parts of the cushions remain unfused when the aorta and pulmonary trunk have gained their separate existence within the pericardial cavity. At this time, the proximal part of the outflow tract, upstream to the intrapericardial arterial trunks, remains encased in a myocardial sleeve. The arterial valves and sinuses then develop within the more distal part of this myocardial outflow tract; the outer myocardial wall does not disappear completely until well after the completion of septation. The most proximal parts of the cushions are the last ones to fuse, and they then muscularize and join the muscular ventricular septum, thereby joining the aorta into the left ventricle. The dorsal atrioventricular cushion maintains its mesenchymal character, becoming the membranous part of the interventricular septum in the formed heart. Formation of its interventricular and atrioventricular components does not become evident until the septal leaflet of the tricuspid valve delaminates from the surface of the ventricular septum.

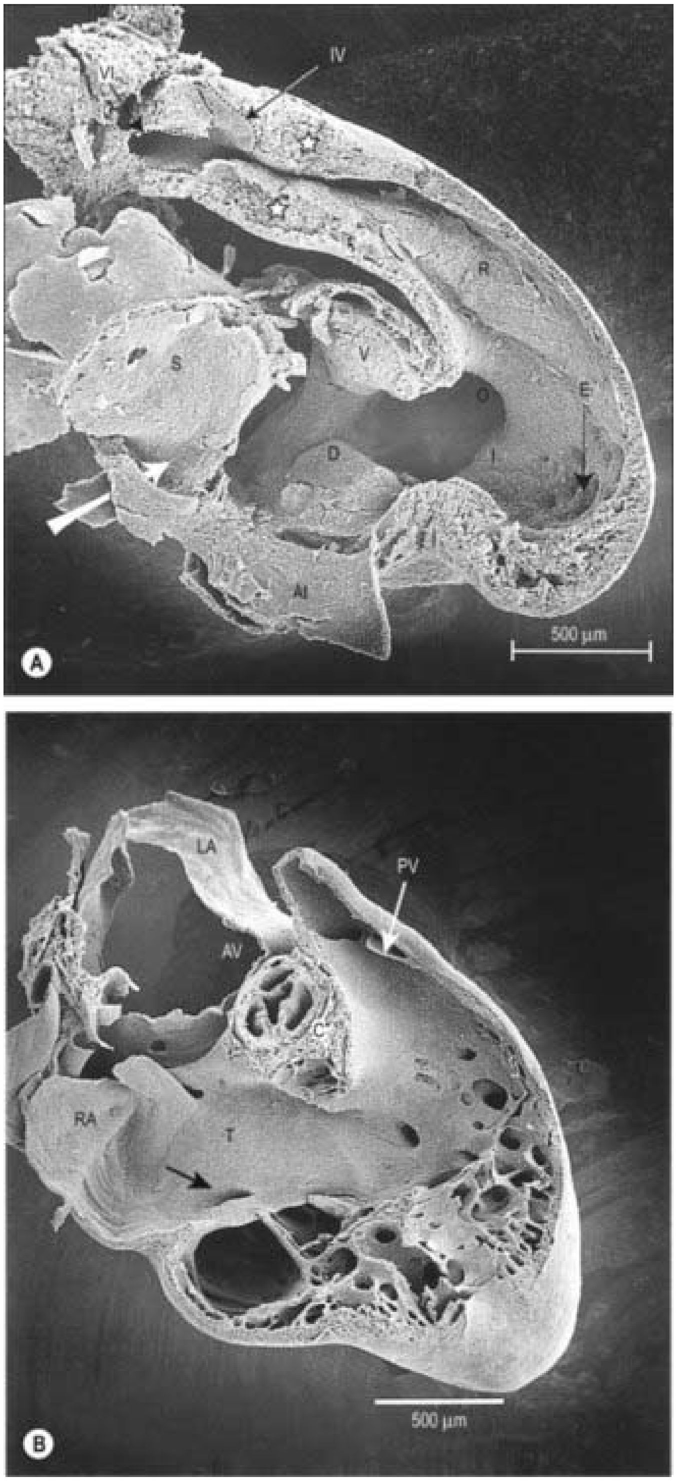
VI
IV
R
S
V
G
E
D
I
AI
500 µm
A
LA
PV
AV
C
RA
T
500 µm
B

Fig. 59.16 **A**, SEM of human heart at 32 days (stage 15). The right lateral wall of the right atrium, right ventricle and the outflow tract have been removed. The septum primum (S) and the developing valve of the sinus venosus (white arrow) are at a distance from the unfused ventral (V) and

dorsal (D) atrioventricular cushions. The interventricular foramen (primum) is open (O). Its lower margin is made up by the developing interventricular septum (I). Note the left anterolateral ridge (R) and, at the distal margins of the truncus arteriosus, the valve swellings (*) of the putative aorta and pulmonary trunk. IV, origin of IVth aortic arch; VI, origin of VIth aortic arch. At, atrium; E, embryonic trabeculae. **B**, Septal aspect of the right ventricle of a human heart at 8 weeks. Delamination of the septal cusp of the tricuspid valve (T) is taking place. A cleft (black arrow) has appeared, marking the posterior margin of the septal cusp. There are no clefts delineating the anterior margins in the region adjacent to the supraventricular crest (C), and the endocardium is continuous. No tension apparatus is present. AV, aortic valve; LA, left atrium; PV, pulmonary valve; RA, right atrium.

NON-MYOCARDIAL COMPONENTS OF THE HEART

The non-myocardial components of the heart are the epicardium, including the coronary vasculature, and the interstitial fibroblasts and the valvular apparatus, which are formed in their larger part from endocardially derived mesenchyme. From the outset, the atrioventricular valves, mitral and tricuspid, are formed at the site of the initial atrioventricular canal, whereas the aortic and pulmonary valves are initially developed within the myocardial outflow tract, and only later achieve the semilunar attachments of the leaflets, which cross the anatomic ventriculo-arterial junctions. All of the leaflets form initially as internal endocardial projections which enclose a myocardial basement membrane, matrix, and mesenchymal cells. The precise mechanisms involved in the formation of these areas have still to be determined.

Development of the epicardium and the coronary vasculature

The epicardium, coronary vascular bed, and interstitial fibroblasts develop from a mesothelially covered protrusion of mesenchymal cells, the pro-epicardium, which arises from the pericardium in the region of the sinus venosus during week 5. The base of the pro-epicardium encompasses bi-potential pericardial cells which are recruited either to the cardiac lineage to form the venous pole of the heart, or else to the epicardial lineage. Bone morphogenetic proteins and fibroblast growth factors influence which lineage is followed; the precise mechanism of specification is not yet clear. Cells detach from the pro-epicardium and spread over the myocardial tube from caudally to cranially, and from dorsally to ventrally. Thus, in successive stages, the pro-epicardial cells approach the myocardial surface of the developing atria, atrioventricular canal, ventricles, and the proximal part of the outflow tract. The distal part of the outflow tract, as it becomes arterialized with regression of the initial myocardial walls, is covered by an outgrowth of the pericardial mesothelium at the site of the initial pericardial reflections. After the formation of the epicardium, a space is formed between the developing epicardium and the outer myocardial layer, which is particularly pronounced at the atrioventricular and outflow regions of the heart tube. This is the subepicardial space, or subepicardium: it is subsequently populated by mesenchymal cells which are largely derived from the epicardium and which play an important role in the formation of the coronary vasculature. The precursors of coronary fibroblasts, smooth muscle cells and endothelium are all derived from these pluripotent cells, which possibly also play roles in the development of non-vascular tissues, including the mesenchyme of the atrioventricular cushions and some myocardial elements. The remnants of the pro-epicardium can be found in the area of the developing systemic venous tributaries up to stage 15.

The coronary arteries were previously assumed to form by means of angiogenesis, or sprouting from the aortic root. However, recent studies have demonstrated that the vessels develop prior to the formation of the arterial orifices in the aortic sinuses: it is now thought that the vessels arise by vasculogenesis, and that mesenchymal cells in the subepicardial space give rise to primitive vessels which invade the myocardium and spread over the myocardial surface. Sprouts of this plexus approach the base of the outflow tract, and connect to the sinuses of the aortic root. Ultimately only solitary right and left coronary arteries remain, although in up to one-third of human hearts small accessory branches of the coronary arteries take origin directly from the coronary sinuses. The vessels that remain acquire a medial wall and an adventitial covering, whereas those that do not form a medial wall are destined to regress. The coronary veins develop in a similar manner from a plexus of capillaries which sprouts subepicardially; they empty into the coronary sinus and directly to the atrial chambers. The mature coronary vascular pattern is established by remodeling of the capillary plexuses, and reduction in the number of arteriovenous anastomoses.

Atrioventricular valves

Initially, the atrial myocardium is continuous with the ventricular myocardium through the myocardium of the atrioventricular canal. The atrioventricular canal itself is characterized by the tissues of the atrioventricular groove on the epicardial side, and of the endocardial cushions on the endocardial side. As the atrioventricular valves develop, these tissues fuse at the ventricular margin of the canal, and so disrupt myocardial continuity. Molecular lineage studies in mouse have demonstrated that the valvular leaflets and their tendinous cords are subsequently derived in their entirety from the endocardium.

The atrioventricular valves develop as shelf-like projections from the margins of the atrioventricular orifices. They are directed as almost complete conical sheets towards the ventricles, their advancing edges continuing, initially as trabecular ridges, deep into the ventricular cavity. With continued differential growth and excavation on their ventricular aspects, each sheet develops major indentations forming the mitral and tricuspid orifices and defining their principal leaflets. Minor marginal indentations subdivide some leaflets into scallops. Each leaflet develops functionally significant regional variations in surface texture and its core condenses as a collagenous fibrous lamina, supported either by the fibro-fatty tissue of the atrioventricular groove, or by a fibrous anulus. The anterior leaflet of the tricuspid valve and the aortic and mural leaflets of the mitral valve all appear at about the time of fusion of the atrioventricular and outflow cushions. Delamination of the septal leaflet of the tricuspid valve occurs after the completion of ventricular septation, producing the interventricular and atrioventricular components of the membranous septum, and continuing until at least week 11 (Fig. 59.16B).

Aortic and pulmonary valves

The aortic and pulmonary valves form from endocardial cushions within the distal end of the myocardial outflow tract and become populated by neural crest cells, in addition to endocardial and pharyngeal derived mesenchyme. The fusing outflow cushions divide, providing two rudiments each for the developing aortic and pulmonary valves. The remaining leaflet for each valve is then produced from the newly appearing intercalated cushions (Fig. 59.15). Each cushion-derived intrusion grows, and is also excavated on its mural aspect to form a semilunar valvular leaflet. Similar events affect the adjacent wall. In this way, the pouches between the valves and the walls of the cushions gradually enlarge, the mural aspect of each cushion forming the valvular sinuses. The core of each leaflet forms a collagenous fibrous lamina, delicate and thin in each crescentic lunule, thick and compact in the central nodule, with marginal radiate and basal bands. The dynamic nature of cardiac development makes it difficult to describe the positions of the leaflets precisely in space and therefore it is best to describe the right, left, and non-coronary sinuses and leaflets of the aortic valve, and the adjacent and non-adjacent leaflets of the pulmonary valve.

FETAL CIRCULATION

As the cardiovascular system develops, the embryonic circulation (see Ch. 13) is modified into a fetal circulation which maintains a placental circulation and is also able to establish the pulmonary circulation at birth. Extensive remodeling of the early aortic arch arteries and (initially bilateral) dorsal aortae occurs (see Ch. 35). The dorsal aortae persist on the cranial side of the third aortic arches as continuations of the internal carotid arteries (see Fig. 35.8). The dorsal aorta between the third and fourth aortic arches, the carotid duct, diminishes and finally disappears. From the fourth arch to the origin of the seventh intersegmental artery, the right dorsal aorta becomes part of the right subclavian artery, and caudal to the seventh intersegmental artery, the right dorsal aorta disappears as far as the locus of fusion of the thoracic aortae. After disappearance of the left carotid duct, the remainder persists to form the descending part of the arch of the aorta. The fused right and left embryonic dorsal aortae persist as the definitive descending thoracic and abdominal aorta. A constriction, the aortic isthmus, is sometimes present in the aorta between the final site of origin of the left subclavian artery and the orifice of the arterial duct.

Concomitant changes also occur in the early venous system. The precardinal veins enlarge as the head and brain develop. They are further augmented by the subclavian veins from the upper limb buds, which become the chief tributaries of the common cardinal veins, gradually assuming an almost vertical position as the heart descends into the thorax (see Fig. 13.4). That part of the original precardinal vein rostral to the subclavian vein is now the internal jugular vein, and their confluence is the brachiocephalic vein of each side. The right and left common cardinal veins are originally of the same diameter: by the development of a large oblique transverse connection, the left brachiocephalic vein carries blood across from the left to the right (see Fig. 13.4). The part of the original right precardinal vein between the junction of the two brachiocephalic veins and the azygos veins forms the upper part of the superior vena cava. The caudal part of this vessel, below the entrance of the azygos vein, is formed by the right common cardinal vein.

The left precardinal and left common cardinal veins caudal to the transverse branching of the left brachiocephalic vein largely atrophy: the precardinal constitutes the terminal part of the left superior intercostal vein, while the common cardinal is represented by the ligament of the left superior vena cava and the oblique vein of the left atrium (see Fig. 13.4). The remainder of the left superior intercostal vein is developed from the cranial end of the postcardinal vein and drains the second, third and, on occasion, the fourth, intercostal veins. The oblique vein passes downwards across the back of the left atrium to open into the coronary sinus, which represents the persistent left horn of the systemic venous sinus.

The fetal circulation contains a number of relatively large vessels which permit the majority of the blood flow to bypass the liver and lungs. The placenta serves as the organ for fetal nutrition and excretion, receiving deoxygenated fetal blood and returning it oxygenated and detoxified. Fetal blood reaches the placenta via two umbilical arteries and in early fetal life returns by two umbilical veins (Fig. 59.17). The right umbilical vein later disappears, whereas the persisting left umbilical vein enters the abdomen at the umbilicus, traverses the edge of the falciform ligament to reach the hepatic surface, and then joins the left branch of the portal vein at the hepatic portal. Opposite the junction, a large vessel, the ductus venosus, arises and ascends posterior to the liver to join the left hepatic vein near its termination in the inferior vena cava. (For a detailed developmental account of the circumhepatic veins, see Ch. 73, Figs 73.8–73.10.) The portal vein is small in the fetus compared to the size of the umbilical vein. Parts of the left branch of the umbilical vein, proximal and distal to their junctions, function as branches of the portal vein, carrying oxygenated blood to the right and left parts of the liver. Blood in the left umbilical vein therefore reaches the inferior vena cava by three routes: some enters the liver directly and reaches the vena cava via the hepatic veins; a considerable quantity circulates through the liver with portal venous blood before also entering by the hepatic veins; the remainder is bypassed into the inferior vena cava by the ductus venosus.

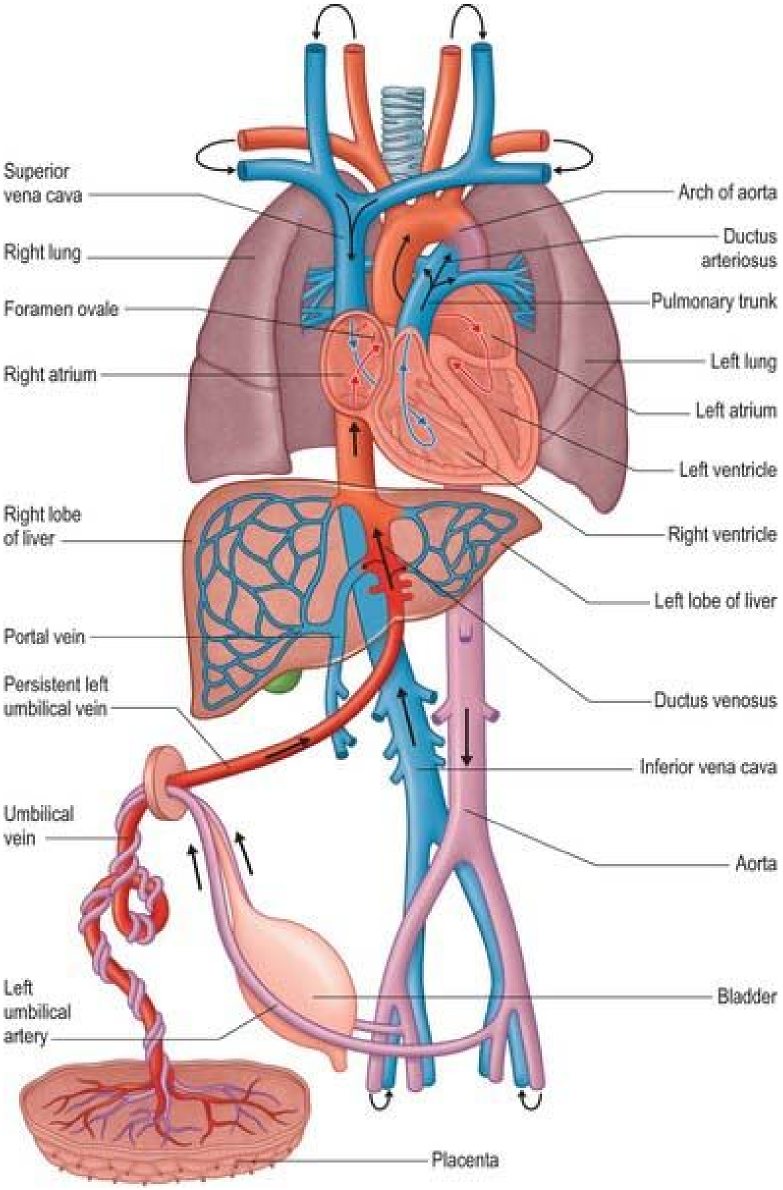
Superior vena cava
Right lung
Foramen ovale
Right atrium
Right lobe of liver
Portal vein
Persistent left umbilical vein
Umbilical vein
Left umbilical artery
Arch of aorta
Ductus arteriosus
Pulmonary trunk
Left lung
Left atrium
Left ventricle
Right ventricle
Left lobe of liver
Ductus venosus
Inferior vena cava
Aorta
Bladder
Placenta

Fig. 59.17 Plan of the fetal circulation. The arrows indicate the direction of blood flow. The placenta is drawn to a greatly reduced scale.

The refreshed placental blood passes almost directly to the aorta for distribution to the head and upper limbs. Blood from the ductus venosus and hepatic veins mixes in the inferior vena cava with blood from the lower limbs and abdominal wall and enters the right atrium. Because right atrial pressure is much greater than left atrial pressure, it forces the flap-like valve of the septum primum to the left, which permits passage of blood from the right to the left atrium. The valve of the inferior vena cava is so placed as to direct 75% of the richly oxygenated blood from the umbilical vein to the foramen ovale and left atrium, where it mingles with the limited venous return from the pulmonary veins. From the left atrium, blood enters the left ventricle and thence the aorta, by which it is probably distributed almost entirely to the heart, head and upper limbs, which means that little reaches the descending aorta.

Blood from the head and upper limbs returns to the right atrium via the superior vena cava, flows through the right atrioventricular orifice into the right ventricle (together with the small amount of blood that is returned via the inferior vena cava), and then passes into the pulmonary trunk. However, because the fetal lungs are largely inactive, only a little of the blood from the right ventricle flows through the right and left pulmonary arteries and returns to the left atrium via the pulmonary veins. The greater part of the outflow through the pulmonary trunk is carried by the ductus arteriosus directly to the aorta, where it mixes with the small quantity of blood that passes from the left ventricle into this part of the aorta. The mixture descends in the aorta and most is returned via the umbilical arteries to the placenta: some is distributed to the lower limbs and the organs of the abdomen and pelvis.

CHANGES IN THE FETAL CIRCULATION AND OCCLUSION OF FETAL VESSELS AFTER BIRTH

At birth, as pulmonary respiration begins, increased amounts of blood from the pulmonary trunk flow through the pulmonary arteries to the lungs and return by the pulmonary veins to the left atrium: pressure therefore increases within the left atrium. A decrease in pressure also occurs in the inferior vena cava as a result of the reduction of venous return concomitant with occlusion of the umbilical vein and ductus venosus. Atrial pressures become equal and the valvular foramen ovale is closed by apposition, and subsequent fusion, of the septum primum to the rims of the foramen. Contraction of the atrial septal muscle, synchronized with that in the superior vena cava, may assist this closure, which occurs after functional closure of the ductus arteriosus. Although the foramen ovale closes functionally after pulmonary respiration is established, it does not become structurally closed until some time later. It is obliterated in fewer than 3% of infants 2 weeks after birth, and in 87% by 4 months after birth. Fusion is sometimes incomplete and a potential atrial communication (atrial septal defect) persists throughout life. Almost always this has no functional effect, because the inequality of atrial pressures and the valve-like arrangement of the opening do not favour passage of blood.

Soon after birth, a number of fetal vessels occlude, although the majority remain patent. This differential constriction suggests that the walls of a population of fetal vessels are different to those of the remaining vessels. Bradykinin, one of the kinin polypeptide hormones which induce contraction or relaxation of smooth muscle, forms in the blood of the umbilical cord when the temperature of the cord decreases at or shortly after birth. It is also formed and released by granular leukocytes in the lungs of the neonate after exposure to adequate oxygen. Bradykinin is a potent constrictor of the umbilical arteries and veins and of the ductus arteriosus, and is also a potent inhibitor of contraction of the pulmonary vessels.

Ductus arteriosus

The ductus arteriosus shunts blood from the pulmonary trunk to the arch of the aorta, bypassing the fetal lungs (Figs 59.17, 59.18). It arises as a direct continuation of the pulmonary trunk at the point where it divides into right and left pulmonary arteries. It is 8–12 mm long, and joins the aorta at an angle of 30–35° on the left side, anterolaterally, below the origin of the left subclavian artery. The opening of the ductus arteriosus into the aorta is greatly elongated. Its diameter at its origin from the pulmonary trunk, when distended with blood, is 4–5 mm, which is nearly equal to the diameter of the adjacent ascending aorta (5–6 mm). Both arteries taper to a smaller diameter as they pass inferiorly and the aorta remains slightly larger (4 mm) (Fig. 59.19). In the neonate, the ductus arteriosus is closely related to the left primary bronchus inferiorly and the thymus gland anteriorly.

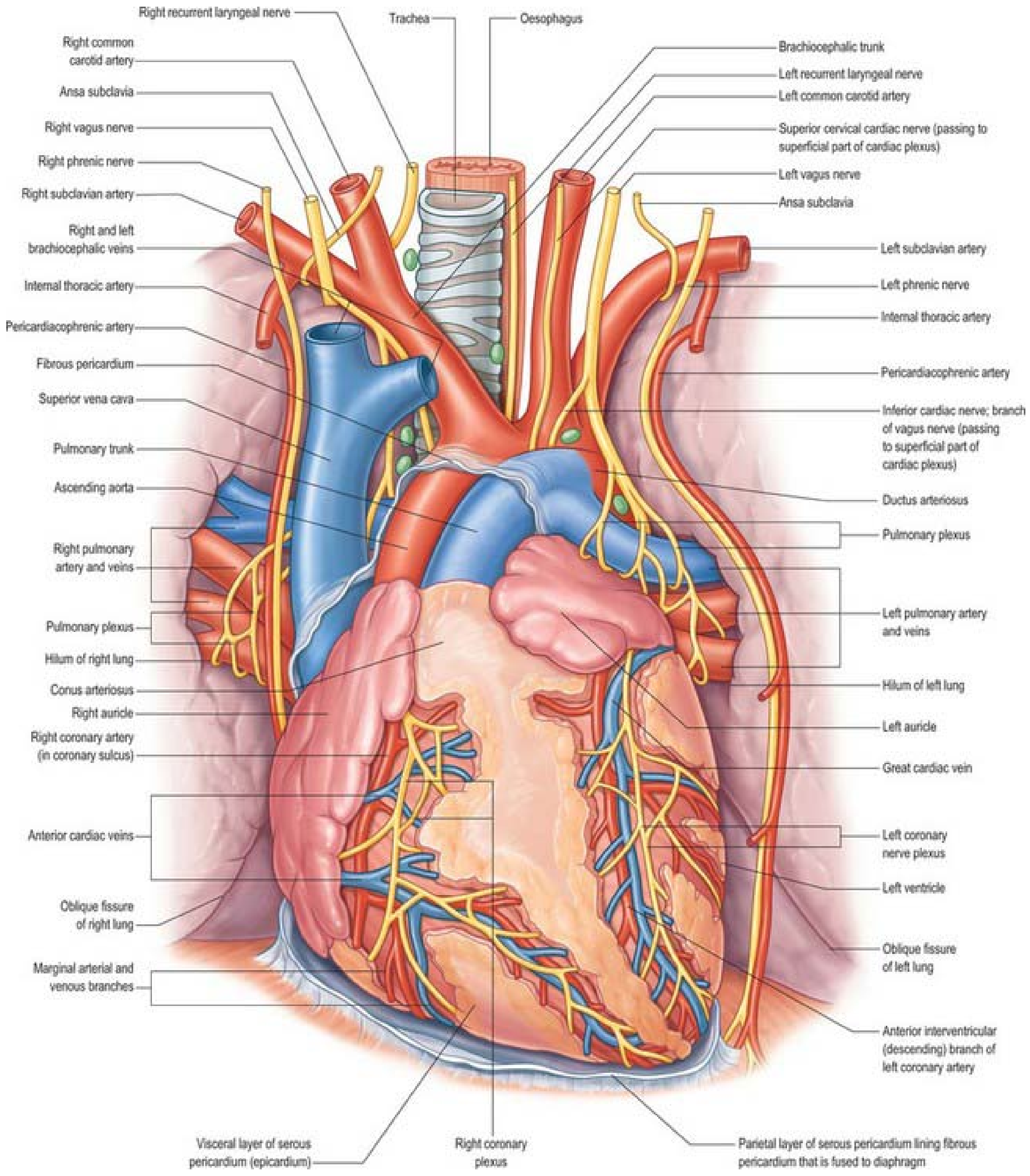
Right recurrent laryngeal nerve
Trachea
Oesophagus
Right common carotid artery
Ansa subclavia
Right vagus nerve
Right phrenic nerve
Right subclavian artery
Right and left brachiocephalic veins
Internal thoracic artery
Pericardiacophrenic artery
Fibrous pericardium
Superior vena cava
Pulmonary trunk
Ascending aorta
Right pulmonary artery and veins
Pulmonary plexus
Hilum of right lung
Conus arteriosus
Right auricle
Right coronary artery (in coronary sulcus)
Anterior cardiac veins
Oblique fissure of right lung
Marginal arterial and venous branches
Visceral layer of serous pericardium (epicardium)
Right coronary plexus
Brachiocephalic trunk
Left recurrent laryngeal nerve
Left common carotid artery
Superior cervical cardiac nerve (passing to superficial part of cardiac plexus)
Left vagus nerve
Ansa subclavia
Left subclavian artery
Left phrenic nerve
Internal thoracic artery
Pericardiacophrenic artery
Inferior cardiac nerve; branch of vagus nerve (passing to superficial part of cardiac plexus)
Ductus arteriosus
Pulmonary plexus
Left pulmonary artery and veins
Hilum of left lung
Left auricle
Great cardiac vein
Left coronary nerve plexus
Left ventricle
Oblique fissure of left lung
Anterior interventricular (descending) branch of left coronary artery
Parietal layer of serous pericardium lining fibrous pericardium that is fused to diaphragm

Fig. 59.18 Anterior view of heart and great vessels in a full-term neonate. The lungs have been displaced to expose the heart and the epicardium dissected off the heart and roots of the great vessels. Note that, after birth, blood flow reverses through the ductus arteriosus prior to its closure. (After Crelin ES 1969 Anatomy of the Newborn. Philadelphia: Lea and Febiger.)

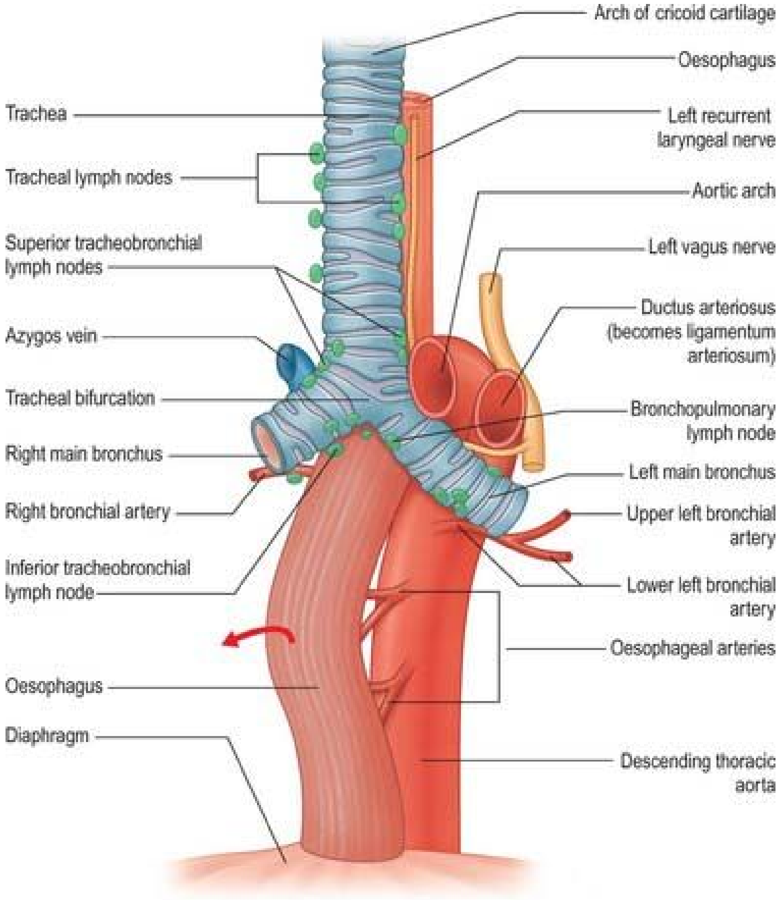
Arch of cricoid cartilage
Oesophagus
Trachea
Left recurrent laryngeal nerve
Tracheal lymph nodes
Aortic arch
Superior tracheobronchial lymph nodes
Left vagus nerve
Ductus arteriosus (becomes ligamentum arteriosum)
Azygos vein
Tracheal bifurcation
Bronchopulmonary lymph node
Right main bronchus
Left main bronchus
Right bronchial artery
Upper left bronchial artery
Inferior tracheobronchial lymph node
Lower left bronchial artery
Oesophageal arteries
Oesophagus
Diaphragm
Descending thoracic aorta

Fig. 59.19 Anterior view with the heart removed to show the relationship between the left primary bronchus, the aortic arch and the ductus arteriosus in a full-term fetus. (After Crelin ES 1969 Anatomy of the Newborn. Philadelphia: Lea and Febiger.)

The ductus arteriosus differs from the other great vessels which arise from the heart because its tunica media contains smooth muscle rather than layers of elastin. It has been suggested that the relationship between the recurrent laryngeal branch of the vagus nerve and the developing ductus arteriosus is responsible for this histological difference on the grounds that the left recurrent laryngeal nerve (which, in a stage 16 embryo, is very large in relation to the aortic arch system) supports the ductus arteriosus as it enwraps it, thereby permitting the ductus to develop as a muscular, and not an elastic, artery.

It is essential that the ductus arteriosus remains patent during intrauterine life. Prostaglandins appear to have a role in maintaining this patency. Fetal and neonatal ductal tissue can produce prostaglandins E_2, I_2 and F_2a, which inhibit the ability of the ductus to contract in response to oxygen.

Closure of the ductus arteriosus

The ductus arteriosus starts to close immediately after birth, although blood probably continues to flow intermittently through it for a week or so. The flow is reversed relative to that occurring in the fetal circulation, reflecting the increased systemic vascular resistance which follows exclusion of the placental circulation, and the decreased pulmonary resistance which follows expansion of the lungs. Initial constriction at birth has been attributed to increased oxygen tension. A neural factor may also be involved: the muscular wall has afferent and efferent nerve endings and responds to adrenaline and noradrenaline.

The first stage of ductal closure is completed within 10–15 hours and the second stage takes 2–3 weeks. The first stage consists of contraction of the smooth muscle cells and development of subendothelial oedema. Destruction of the endothelium and proliferation of the intima subsequently occurs, and leads to permanent closure. Diverse factors which may promote ductal closure have been identified. They include: increased oxygen tension; increased plasma catecholamine concentrations; suppression of prostaglandin I_2 production; switching off prostaglandin E receptors; a synergistic role of prostaglandin F_2a and oxygen concentrations; a decrease in plasma adenosine concentration. After birth, these interrelated events result in the closure of the ductus arteriosus. It has been proposed that the high oxygen tension of the reversed blood flow through the ductus initiates the synthesis of a hydroperoxy fatty acid which suppresses prostacyclin production, thus exposing the ductus to the contractile effects of prostaglandin endoperoxide. After closure, the duct becomes the ligamentum arteriosum, which connects the left pulmonary artery (near its origin) with the aortic arch.

FETAL AND NEONATAL HEART

At full term, the heart is situated midway between the crown of the head and the lower level of the buttocks (see Fig. 14.4). The anterior surface is formed mainly by the right atrium and right ventricle, as it is in the adult. This surface is usually covered by the thymus, which may extend over the base of the right ventricle. The heart is relatively large at birth, weighing around 20 grams. The cardiac output is around 550 ml per minute, and the blood pressure is 80/46 mmHg. The heart rate during fetal life, as term approaches, is around 150 beats per minute. It increases at birth to around 180 beats, decreases over the first 10 minutes after birth to 170 beats, and reaches 120–140 beats per minute from 15 minutes to 1 hour after birth. Any signs of fetal distress will increase this general basic level. The heart rate decreases further with increasing age: it is normally 113–127 beats per minute from 6 months to 1 year, and settles to around 100 beats per minute by the end of the first year.

Considered relative to the thoracic landmarks, the foramen ovale lies at the level of the third intercostal space, with its long axis in the median plane. It is 4–6 mm in vertical length and 3–4 mm wide (see Fig. 14.4). It is almost exactly in the coronal plane of the body, so that blood passes from the anterior, or ventral, right atrium posteriorly and upwards to reach the upper and posterior part of the left atrium. After birth, the intra-atrial pressures are equalized, and the free edge of the flap valve formed by the primary atrial septum is kept in contact with the left side of the rims of the fossa, promoting subsequent anatomic fusion, albeit that the foramen remains probe-patent in up to one-third of all individuals. The initially free crescentic margin of the infolded superior interatrial fold forms the border of the fossa after fusion; the flap valve formed by the primary septum accounts for its floor in the adult heart.

Functionally, the ventricular septum is often considered to be part of the left ventricle: while this is certainly true in terms of the orientation of the myocardial aggregates which make up the ventricular walls, it is not correct from a cellular lineage perspective. The ratio of cardiac weight is usually expressed as the weight of the right ventricle relative to that of the left ventricle and the septum. Calculated in this fashion, the left ventricle at birth weighs about 25% more than the right ventricle. However, the right ventricle has been working against the systemic pressure in the fetus, the pulmonary circulation not yet being active, and there is a preponderance of right ventricular function in the first 2 or 3 months after birth. With the establishment of the pulmonary circulation, the work of the right side of the heart decreases, and the left side of the heart, particularly the ventricle, grows rapidly to meet the demands of the active neonate. By the end of the second year, the left side weighs twice as much as the right, a ratio that continues to middle age. At birth, the average thicknesses of the lateral walls of the ventricles are approximately equal (5 mm). By the end of the third post natal month, the left ventricle has already become thicker than the right, it becomes twice as thick by the second year, and three times as thick by puberty.

CONGENITAL HEART DEFECTS

Defects of cardiac development may not come to light until after birth, although many, if not most, can now be observed on fetal ultrasonic examination. They may affect any part of the developing heart, and include more complex forms with inappropriate connections of cardiac components. They include anomalies such as double inlet ventricle; absence of one atrioventricular connection, commonly described as tricuspid or mitral atresia; and discordant atrioventricular and ventriculo-arterial connections, also known as congenitally corrected transposition.

Congenital cardiac malformations are often multiple, and probably occur more frequently in siblings and in children of consanguineous marriages: there is a low correlation among monozygotic twins. Ventricular septal defects are the most common lesions, making up around one-fifth of all cases, followed by persistent patency of the ductus arteriosus, coarctation, pulmonary stenosis, Fallot's tetralogy, transposition, aortic stenosis, and hypoplasia of the left heart.

Atrial septal defects

A persistent communication between the atrial chambers within the fossa ovale is common, and results from the failure of the flap valve of the primary atrial septum to fuse with the infolded muscular rims of the fossa. When the flap valve is still able to overlap the rims, the communication is of no functional significance as long as left atrial pressure is greater than right, which is usually the case. However, when the flap valve is smaller than the fossa ovale, or when it is perforate, there is a true atrial septal defect (Fig. 59.20A).

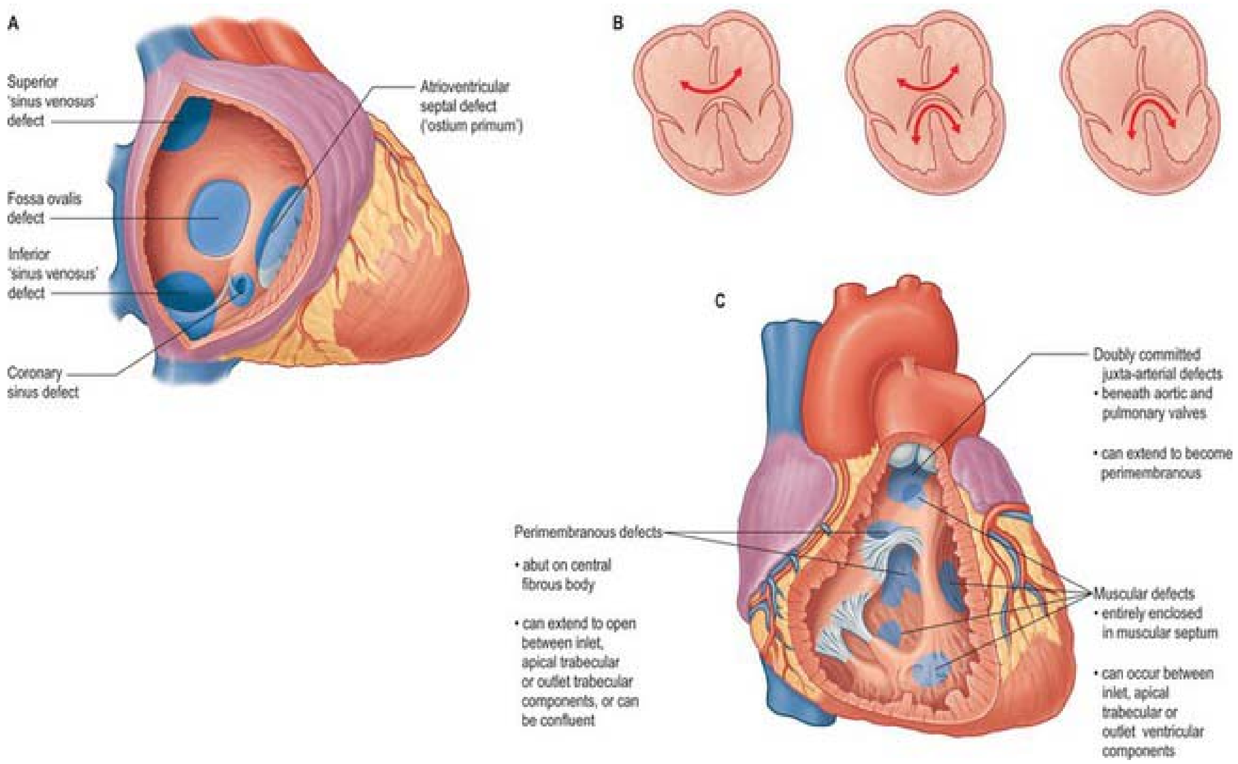
A
Superior 'sinus venosus' defect
Fossa ovalis defect
Inferior 'sinus venosus' defect
Coronary sinus defect
Atrioventricular septal defect ('ostium primum')
B
C
Doubly committed juxta-arterial defects
• beneath aortic and pulmonary valves
• can extend to become perimembranous
Perimembranous defects
• abut on central fibrous body
• can extend to open between inlet, apical trabecular or outlet trabecular components, or can be confluent
Muscular defects
• entirely enclosed in muscular septum
• can occur between inlet, apical trabecular or outlet ventricular components

Fig. 59.20 **A**, Location of the defects that produce an interatrial communication. Only defects within the fossa ovalis are true atrial septal defects. **B**, Shunting across an atrioventricular septal defect. This can be atrial (left), ventricular (right) or at both levels (middle), depending on the attachment of the bridging cusps. **C**, Ventricular septal defects. Depending on the structure of the anatomic borders seen from the right ventricle, these defects can be placed into perimembranous, muscular or doubly committed groups.

*(**B** and **C** by courtesy of Professor RH Anderson, Institute of Child Health, University College, London.)*

In normal development, the free leading edge of the septum primum merges with the atrioventricular endocardial cushions, permitting subsequent formation of the atrioventricular septum. When this does not happen, there is a common atrioventricular junction and an atrioventricular septal defect. This can occur when the leaflets of the atrioventricular valves are fused to the crest of the ventricular septum (Fig. 59.20A), producing an interatrial communication at the expected site of the atrioventricular septum. This is the so-called ostium primum defect, and in reality is an atrioventricular septal defect permitting exclusive atrial shunting. Other interatrial communications can be formed in the mouths of the vena cavae, most frequently the superior vena cava, and are usually associated with drainage of the right pulmonary veins into the cavo-atrial junction. Known as sinus venosus defects (Fig. 59.20A), their essential feature is a bi-atrial connection of the involved caval vein. An interatrial communication can also occur through the mouth of the coronary sinus when there is a deficiency or absence of the walls that usually separate the sinus from the left atrium.

Atrioventricular septal defects result from failure of fusion of the endocardial atrioventricular cushions, producing a common atrioventricular orifice and deficiencies of the adjacent septal structures (Fig. 59.20B). The common orifice is guarded by a basically common valve, with superior and inferior leaflets bridging the scooped-out ventricular septum and tethered in both right and left ventricles. Although the left component of the valve thus formed is often interpreted as a 'cleft mitral valve', in reality it bears no resemblance to the normally structured mitral valve, because it has three leaflets; the 'cleft' forms the zone of apposition between the left ventricular components of the bridging leaflets. Two major subgroups are identified. The more frequent pattern has a common atrioventricular orifice, and the potential for shunting through the septal defect at both atrial and ventricular levels (Fig. 59.20B). The less common form has separate right and left atrioventricular orifices, and shunting occurs only at atrial level. Occasionally, when the bridging leaflets are attached to the underside of the atrial septum, shunting is confined at ventricular level, and is typically small.

Ventricular septal defects

The most common defect of the ventricular septum occurs around the expected site of the membranous septum in the right wall of the aortic vestibule, below the zone of apposition between the non-coronary and right coronary leaflets of the aortic valve (Fig. 59.20C). The defect is closely related to the septal leaflet of the tricuspid valve, but can extend to open into the ventricular outlet beneath the supraventricular crest. It occurs because the ventricular septum is incompletely closed by its membranous component, and it is often associated with overriding of the crest of the muscular septum by the aortic orifice, together with pulmonary stenosis or atresia and hypertrophy of the right ventricle (this latter combination is known as Fallot's tetralogy). Rarely, the pulmonary trunk can be normal or even dilated with this combination of abnormalities (Eisenmenger complex). Peri-membranous defects, which retain the remnant of the membranous septum as part of their perimeter, can also occur with abnormal ventriculo–arterial connections, e.g. the pulmonary trunk may override the muscular septum, (the Taussig–Bing anomaly). In perimembranous ventricular septal defects, the atrioventricular bundle and its right and left branches are always found along the postero-inferior margin of the defect.

Less commonly, a septal defect can be found in the ventricular outflow tracts roofed by the conjoined facing leaflets of the aortic and pulmonary valves. Such juxta-arterial defects are doubly committed, in that they open beneath the orifices of both aortic and pulmonary valves. They are the result of the failure of formation of the free-standing subpulmonary muscular infundibulum, but with appropriate septation of the ventriculo-arterial junctions. They usually have a muscular postero-inferior rim, which protects the atrioventricular bundle, but can extend to become peri-membranous.

The third type of ventricular septal defect occurs within the musculature of the septum: defects may affect all parts of the septum, and can be multiple, producing a so-called 'Swiss-cheese' septum.

Defects within the inlet part of the septum are important, because the atrioventricular bundle passes in their upper border. Perimembranous defects open into the inlet of the right ventricle, where the atrioventricular bundle is postero-inferiorly located.

ABNORMAL CONNECTIONS OF THE GREAT ARTERIES AND VEINS

A number of outflow anomalies may occur should the outflow cushions either fail to develop, or fuse in inappropriate fashion. When the spiral septum cushions fail to fuse, the result is a common arterial trunk, represented by an undivided arterial channel, guarded by a common arterial valve, positioned above and astride the free margin of the muscular ventricular septum (Fig. 59.21). There is, therefore, a coexisting juxta-arterial deficiency of the ventricular septum. The right and left pulmonary arteries usually arise via a confluent segment, but can take independent origin from the common arterial trunk, which continues as the ascending aorta. The common valve usually has three leaflets, but may have two, four or more. The lesion is almost certainly linked to abnormal migration of cells into the heart from the neural crest.

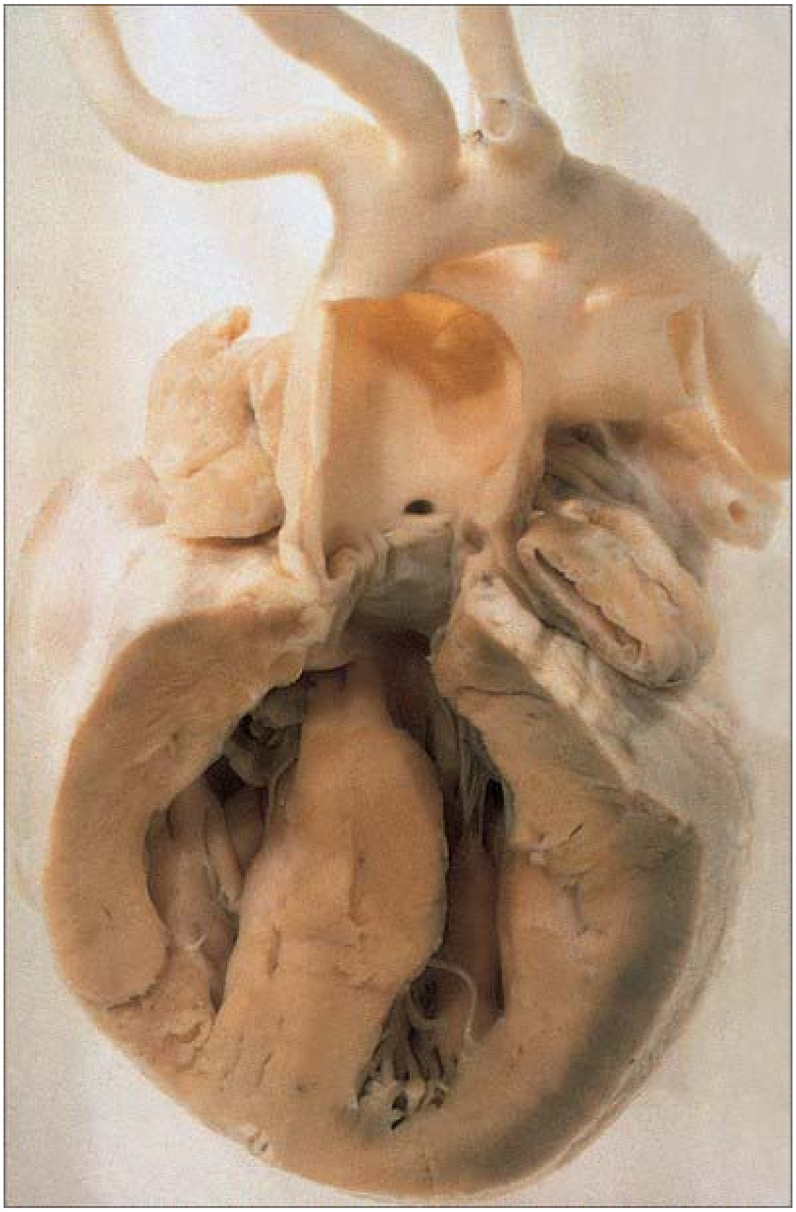

Fig. 59.21 This heart possesses a common arterial trunk, with a common truncal valve over-riding a juxta-arterial deficiency of the ventricular septum, the result of failure of septation of the arterial pole of the developing heart.

(By courtesy of Professor RH Anderson, Institute of Child Health, University College, London. Specimen prepared by Dr Leon M Gerlis.)

Transposition of the arterial trunks (also referred to as transposition of the great vessels) is the condition in which the aorta arises from the right ventricle and the pulmonary trunk from the left. Better described as having discordant ventriculo-arterial connections, such hearts can co-exist with deficiencies of cardiac septation. They can also be found with discordant connections at the atrioventricular junctions, producing congenitally corrected transposition. The developmental history of discordant connections remains unknown.

Double outlet ventricle exists when the greater parts of both arterial valves are attached within the same ventricle, almost always the right. For the circulation to continue, it is then necessary for the ventricular septum to be deficient, although the septal defect can rarely close as a secondary event. The position of the septal defect serves for subclassification. It is usually beneath the aorta or the pulmonary trunk, but can be doubly committed or even non-committed.

Either the systemic or pulmonary veins can be anomalously connected. Right and left superior vena cavae are present in some animals, and occasionally persist in mankind. The most common systemic anomaly is a persistent left superior vena cava draining into the right atrium through the enlarged orifice of the coronary sinus. More rarely, the persisting left-sided vena cava may connect directly with the superior aspect of the left atrium, usually associated with so-called ‘unroofing’ of the coronary sinus, so that the orifice of the sinus functions as an interatrial communication. The most common lesion of the inferior vena cava is when its abdominal course is interrupted, with drainage to the heart via the azygos or hemiazygos venous system. This lesion is found most frequently with isomerism of the left atrial appendages. The pulmonary veins can be connected to an anomalous site individually or in combination. Totally anomalous connection is of most significance. Usually, the veins form a confluence behind the left atrium that then connects to the superior vena cava, the coronary sinus, or the portal venous system after traversing the diaphragm.

A right aortic arch is found most frequently with Fallot’s tetralogy or with a common arterial trunk. It can also exist, together with a left arch, in various combinations known as arterial rings, which compress the oesophagus, giving so-called dysphagia lusoria. Persistent patency of the ductus arteriosus must be distinguished from delayed closure. The persistently patent ductus can be an obligatory part of the circulation when associated with aortic or pulmonary atresia. Coarctation of the aorta can be found as an isolated lesion when the ductus arteriosus is closed, or with an open duct, when it is more likely to be associated with additional lesions within the heart (see p. 984).

In the adult, the right subclavian artery occasionally arises from the arch of the aorta distal to the origin of the left subclavian artery, and then passes upwards and to the right, behind the trachea and oesophagus. This condition is possibly explained by the persistence of the embryonic right dorsal aorta and the obliteration of the fourth aortic arch of the right side.

NEONATAL ARTERIAL AND VENOUS VESSELS

In the neonate, the blood vessels of the trunk and their associated visceral branches are relatively larger than the vessels in the limbs, an arrangement which favours central pooling of blood. Neonatal peripheral vessels are nearly microscopic: their cannulation consequently poses much more of a problem than is the case with their adult counterparts. Large vessels are in the same relative positions as in the adult, but may correspond to different vertebral levels. Thus, although the bifurcation of the common carotid artery into internal and external carotid arteries occurs at the level of the upper border of the thyroid cartilage, in both neonate and adult, the thyroid cartilage is relatively higher in the neonatal neck than it is in the adult. The renal arteries also arise higher in the neonate, often between T12 and L1, whereas they arise at the upper border of L2 in the adult. The abdominal aorta bifurcates into common iliac arteries at the upper border of L4, rather than at the lower border of L4 as occurs in the adult.

Central venous catheterization

Small-bore catheters can be fed into large central veins or into the right atrium via needles or catheters inserted in the peripheral veins. Typically, the median cubital or basilic veins are used in the upper limb and the long saphenous vein at the medial malleolus in the lower limb. The tip of the catheter is sited at the entrance to the right atrium. The required catheter length is assessed from direct measurement of the distance between the point of surface entry in the limb to the right atrium, estimated at midsternal level. For details of umbilical catheterization, see Chapter 73.

RESPIRATORY TREE

The development of the respiratory system can be conceptualized as the growth of six intertwined trees: the bronchial tree of conducting airways and exchange spaces; the systemic arterial and venous trees supplying the airways; the pulmonary arterial and venous trees which will provide blood oxygenation after birth; the lymphatic tree. Development of each tree is related to the other and all proceed in proximal to distal growth and expansion.

The development of the respiratory diverticulum can first be seen at stage 12 (approximately 26 days), when there is a sharp onset of epithelial proliferation within the foregut at regions of the endoderm tube destined to become the lungs, stomach, liver and dorsal pancreas. The specialist respiratory epithelium forms from the endoderm; the other elements of the airway wall are of mesenchymal origin. The future respiratory epithelium bulges ventrally into the investing splanchnopleuric mesenchyme, then grows caudally as a bulb-shaped tube (Figs 59.1, 59.22; see Fig. 73.9). By stage 13, the caudal end of the tube has divided asymmetrically to form the future primary bronchi: with growth the right primary bronchus becomes orientated more caudally whereas the left extends more transversely. The trachea is clearly recognizable at stage 14. From this time the origin of the trachea remains close to its site of evagination from the future oesophagus, however, longitudinal growth of the trachea causes the region of the future carina to descend. Failure of complete separation between trachea and oesophagus will result in the baby being born with a tracheo-oesophageal fistula (see below). Lung development is controlled by groups of homeobox genes, transcription factors and growth factors (summarized in detail by Roth-Kleiner & Post 2005). The formation of the lung bud is dependent on the transcription factors hepatocyte nuclear factor-3β (*HNF-3* β), thyroid transcription factor (*TTF-1*) and sonic hedgehog (SHH). *Gli* proteins and retinoic acid receptors are implicated in the mesenchymal-epithelial cell interactions that are essential for lung branching morphogenesis.

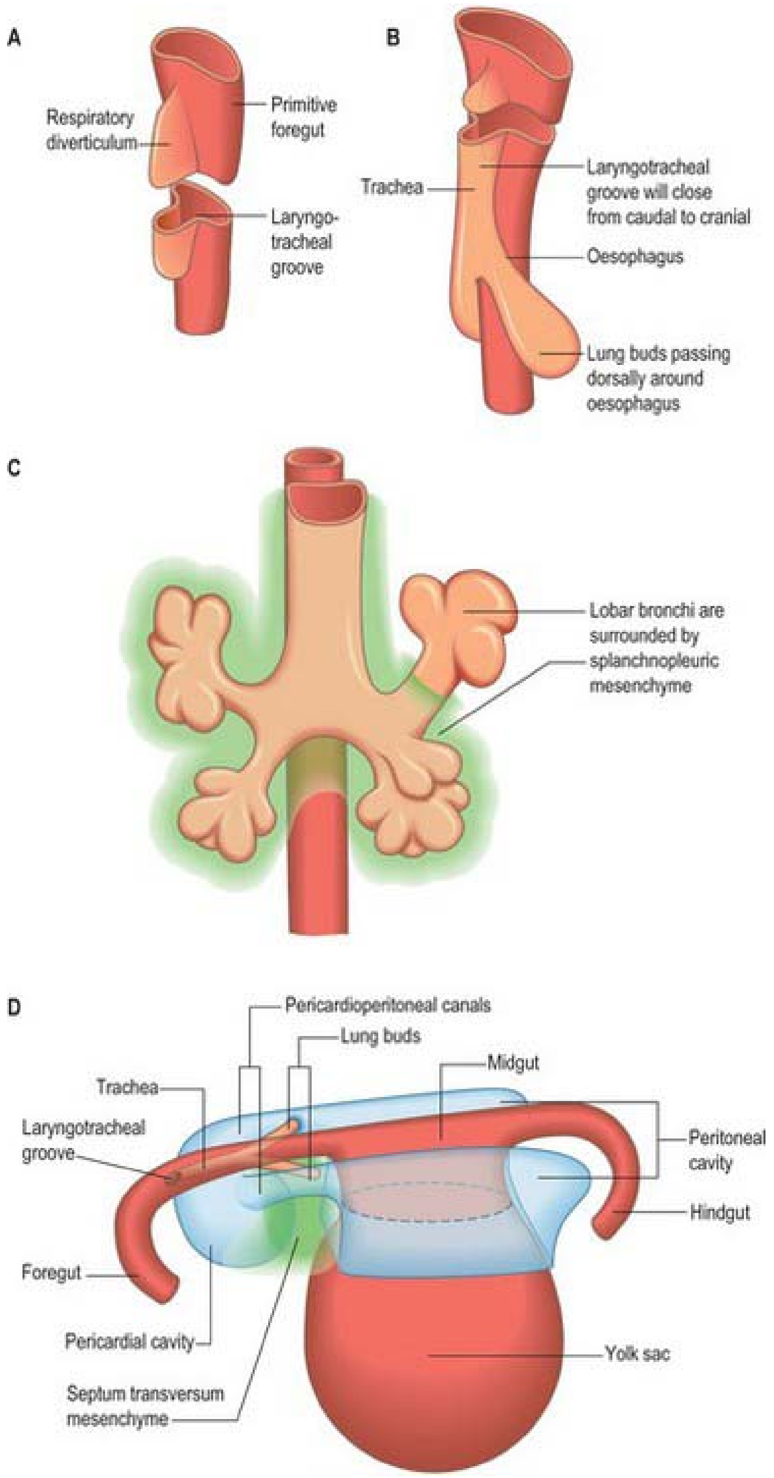
A
Respiratory diverticulum
Primitive foregut
Laryngo-tracheal groove
B
Trachea
Laryngotracheal groove will close from caudal to cranial
Oesophagus
Lung buds passing dorsally around oesophagus
C
Lobar bronchi are surrounded by splanchnopleuric mesenchyme
D
Pericardioperitoneal canals
Lung buds
Midgut
Trachea
Laryngotracheal groove
Peritoneal cavity
Hindgut
Foregut
Pericardial cavity
Septum transversum mesenchyme
Yolk sac

Fig. 59.22 Development of the respiratory tree and diaphragm. **A–C**, Development of the endodermal respiratory tree. **D**, Major epithelial populations in the early embryo from a left dorsolateral view. The lung buds are bulging into the laterally placed pericardioperitoneal canals.

There is a sexual dimorphism in lung development. Androgens delay fetal lung maturation while stimulating fetal lung growth: in males, type II cells are less mature than in females as they develop during the cannalicular phase, perhaps because androgens block the effects of cortisol on fibroblast–pneumocyte factor concentrations. It is possible that in male fetuses surfactant production is delayed. The clinical counterpart is the observation that preterm males may have worse respiratory distress than females after control for other risk factors such as degree of prematurity.

TRACHEA

The trachea starts to develop at stage 12, as a ventral outgrowth from the endodermal foregut into the mesenchyme surrounding the sinus venosus and inflow tract of the heart (Fig. 59.1B,C; see Figs 73.3, 73.5). The point at which the original respiratory diverticulum buds from the foregut, the laryngotracheal groove, remains at a constant level during the embryonic period, and the trachea lengthens distally as the bifurcation point descends. The respiratory diverticulum generally becomes surrounded by angiogenic mesenchyme which connects to the developing sixth aortic arch artery and which is essential for airway branching. By stage 17, the mesenchyme around the trachea is beginning to condense to form cartilage.

Initially, the tracheal mesenchyme is continuous with that surrounding the ventral wall of the oesophagus (Fig. 59.3). Progressive lengthening and continued division of the tracheal bud, together with deviation of the lung buds dorsally, isolates the oesophagus and trachea within tissue-specific mesenchyme and facilitates regional differentiation, not only between trachea and lungs, but also within the lungs themselves, i.e. the number of lobes, or the degree of growth and maturity of a particular lung. Each lung develops by a process of dichotomous branching. For branching to occur, a cleft must develop in the tip (or side) of the epithelial tube. The epithelium then evaginates each side of the cleft, forming new branches which lengthen, and the process is then repeated. At the tips of the developing epithelial buds, the mesenchyme is flattened and densely packed, whereas it forms an ordered row of cuboidal cells along the side of the bud and in the clefts. Cells in both arrangements send processes towards the epithelial basal lamina, which is thicker in the clefts, but so attenuated as to be almost indistinguishable on the tips of the buds where the epithelium and mesenchymal cells form intimate contacts. Tenascin, an extracellular matrix molecule, is present in the budding and distal tip regions, but absent in the clefts. Conversely, fibronectin, an extracellular matrix molecule found commonly in basal laminae, is found in the clefts and along the sides of the developing bronchi, but not on the budding and distal tips.

The control of the branching pattern of the respiratory tree resides with the splanchnopleuric mesenchyme. Experimental recombination of tracheal mesenchyme with bronchial respiratory endoderm results in inhibition of bronchial branching, whereas recombination of bronchial mesenchyme with tracheal epithelium will induce bronchial outgrowths from the trachea. Experimental exposure of rat fetal airway to chick mesenchyme produces a chick airway branching pattern. Broadly, receptor tyrosine kinases and their ligands positively modulate growth and branching morphogenesis, while transforming growth factor β (TGF β) family members have an inhibitory effect.

In the normal neonate, the trachea is relatively small in relation to the larynx (Fig. 14.4). The walls of the trachea are relatively thick and the tracheal cartilages are relatively closer together than in the adult. The trachea begins at the upper border of the sixth cervical vertebra, a relationship that is conserved with growth, and it bifurcates at the level of the third or fourth thoracic vertebra.

Endotracheal intubation in the neonate

The insertion of an endotracheal tube is a procedure that may be required for resuscitation of the newborn at birth and subsequently to enable artificial ventilation. The tube is introduced usually orally initially and guided through the vocal cords with the help of a laryngoscope. The length of the trachea in the neonate can be as short as 3.1 cm in premature infants, and the T1-to-carina distance ranges from 1.4 cm in babies weighing 500–1000 g, to 1.8 cm in those weighing 3001–3500 g. Once in place, the tip of the tube should be in the midtrachea, well above the carina.

The required length of the tube can be estimated according to birth weight. If a shouldered tube is used, only the distal, tapered portion of the tube is inserted beyond the vocal cords, and the shoulders should prevent the tube being advanced too far. Confirmation of correct positioning of the endotracheal tube is obtained from a chest X-ray. The anatomical reference points used for the X-ray to assess the position of the endotracheal tube are the clavicles, the bodies of the vertebrae and the carina (although the last of these is not always visible on X-ray). Previously, it was advised that the tip of the endotracheal tube should be placed just below the clavicles, at the level of the first rib or 1–2 cm above the carina. Recently, this has been revised because positioning of the clavicles can vary according to angulation and placement of the baby, and the carina cannot always be identified. It is now suggested that the body of the first thoracic vertebra (T1) is a more stable reference point as the target for the tip of the endotracheal tube.

LUNGS

Branching of the conducting airways is generally complete by week 16. Airways subsequently increase in size, but not in number. Alveolar development is largely (but not completely) a postnatal phenomenon. The development of pre-acinar blood vessels follows the conducting airway development, whereas development of intra-acinar blood vessels follows the development of the alveolar ducts and alveolar sacs. Lung development is described histologically as progressing through embryonic, pseudoglandular, canalicular, saccular and alveolar phases. (For further details see Rosenthal & Bush 2002; Bush 2005.)

Embryonic phase

The lung buds grow dorsally, passing each side of the relatively smaller oesophagus and bulge into the medial walls of the laterally situated pericardioperitoneal canals (Fig. 59.22; see Fig. 73.5A). The investing splanchnopleuric mesenchyme surrounding the lung buds contains a mixed population of cells. Further mesenchymal cells will differentiate into the smooth muscle cells that surround both the respiratory tubes and the blood vessels. In stage 13 embryos, proliferation of the adjacent splanchnopleuric coelomic epithelium (of the primary pleural cavities) is especially evident. The proliferative activity decreases in stage 14, and the mesenchyme becomes arranged in zones around the developing endoderm. Key molecules in airway branching include the fibroblast growth factors (FGF) especially FGF-10, and their four receptors. There is almost certainly redundancy in the system, since mice null for either FGF-1 or FGF-7 exhibit normal lung development, despite the potent *in vitro* effects of these mediators. The key receptor appears to be FGFR2IIIb, and those ligands that bind it. SHH is another gene important in lung development: it is tightly regulated and over-expression leads to the formation of excessive lung mesenchyme. The three members of the gli family of transcription factors are implicated in SHH signalling. SHH produced in distal epithelial cells appears to act on mesenchymal cells to suppress FGF-10 to limit budding. Other signals interacting with this process include bone morphogenetic protein 4 and TGF-β1.

At stage 15, angiogenetic mesenchyme is apparent around the primary bronchi. It forms an extensive capillary network around each lung bud, receiving blood from the developing sixth aortic arch artery and draining it into an anastomosis connected to the dorsal surface of the left atrium in the mediastinal mesenchyme. The pulmonary arteries arise from the sixth aortic arch arteries and the pulmonary veins develop from a solitary channel derived from the dorsal mesocardium which establishes continuity with the vascular plexus formed in the mediastinal mesenchyme. The pulmonary veins become surrounded by myocardium to the level of the second bifurcation; the veins themselves expand and are incorporated into the roof of the left atrium: cardiac muscle is therefore found in the central branches of the pulmonary venous tree (Hislop 2005).

The lung buds on each side of the oesophagus project dorsally into the pericardioperitoneal canals at stage 15. After this stage, the coelomic epithelium at the perimeter of the lung surface follows a differentiation pathway to form the visceral pleura. Lobar or secondary bronchi can be seen at stage 16, and the bronchopulmonary segments are present at stage 17 (see Fig. 73.3). Later stages of respiratory development involve the repeated division of the bronchial tree to form the subsegmental bronchi.

Pseudoglandular phase

By stage 17 (late sixth to early seventh week), the separation of the lungs from the digestive system is complete and the pseudoglandular phase of pulmonary development, which includes the development of the lower conducting airways and the appearance of the acinar structures, can be identified. During this period, virtually the complete branching structure of the future bronchial tree is laid down, giving rise to 20 generations.

The growth and branching of the endoderm epithelium is controlled by the local investing splanchnopleuric mesenchyme. The airways begin to differentiate during this stage. Primitive ciliated cells appear at about week 7, initially in the region of the membranous trachea, and in the cartilaginous region by week 12. The *in utero* function of these early ciliated cells in the trachea is obscure; elsewhere in the embryo, primary cilia have important developmental functions, e.g. in determining organ situs (nodal cilia). It is unclear whether airway ciliated cells develop from an undifferentiated precursor, or through the further development of a population of secretory cells. The epithelium differentiates into ciliated and goblet cells. The proximal airways develop basal cells from week 11, and ciliogenesis is complete at birth in humans. Mucous glands develop by 12 weeks and enlarge in the submucosa: secretory activity has been identified in the trachea at 14 weeks. The splanchnopleuric mesenchyme condenses around the epithelium and differentiates into connective tissue cell types and smooth muscle, which differentiates proximal to the tips of the developing airways as they develop, from week 6 onwards. Smooth muscle cells are innervated from as early as week 8 (see below). First trimester human tracheal smooth muscle cells have a fluctuating resting membrane potential which is associated with the spontaneous development of tone and peristalsis-like contractions of the airway of a myogenic nature, probably modified by neuro-humoral factors. These contractions are important in moving fluid from distal to proximal within the airways, which is essential for normal lung development, and may stimulate mediator release. Clara cells develop in the peripheral airways during the pseudoglandular period. They produce a 10-kDa protein (CC10) which has immuno-modulatory and anti-inflammatory activity as well as producing a surfactant apoprotein. Cartilage also develops during this period, and is found in the airways in an adult distribution by 24 weeks. By the end of this period, the airway branching and the pre-acinar vascular patterns are fully mature. A normal airway ‘template’ is essential for normal alveolar formation: in conditions characterized by an abnormal airway branching pattern (e.g. both ipsilateral and contralateral to a diaphragmatic hernia), a degree of pulmonary alveolar hypoplasia is inevitable.

Endothelial development is also seen in the pseudoglandular phase when capillary networks form around the developing lung buds. These networks will become capillary anastomoses around the future alveoli. The mesenchyme produces both the endothelium and the smooth muscle cells of the tunica media of the vessels. Vimentin occurs in the cells around developing vessels in the pseudoglandular stage, but is replaced by desmin in the saccular phase.

Canalicular phase

During the canalicular phase, about two to three generations of branching take place, after which the amount of mesenchyme around the branching tips of the dividing respiratory tree decreases and the distal airspaces widen. At 23 weeks, longitudinal sections of the future distal regions show a sawtooth margin, which may indicate the site of further acini. Peripheral growth is accompanied by an increase in the capillary network around the distal airspaces. In many places, the capillaries are in close contact with the respiratory cuboidal epithelium. The primitive cuboidal cells, which hitherto predominated in this part of the lung, differentiate into Type 2 epithelial cells (pneumocytes), containing lamellar bodies which form the intracellular storage bodies of surfactant, and Type 1 epithelial cells (pneumocytes). Type II pneumocytes are believed to be the stem cells of the alveolar epithelium. Apposition of the capillary networks to the thin pneumocytes (Type 1), and reduction of the interstitial tissue of the lung, are prerequisites for future effective gas exchange. By 24 weeks of gestation the histological characteristics of the airways are the same as in the adult.

Saccular phase

Thin walled terminal saccules are apparent at the saccular stage: they will become alveolar ducts as development proceeds. The expansion of the prospective respiratory airspaces which occurs during this period is accompanied by a further decrease in the amount of interstitial tissue, and the capillary networks become ever more closely opposed to the pneumocyte epithelium. Invaginations termed secondary crests develop from the saccule walls. As a crest protrudes into a saccule, part of the capillary network becomes drawn into it. After the later expansion of the saccules on each side of the crest, a double capillary layer becomes annexed between what are now alveolar walls. During the saccular stage, elastin is deposited beneath the epithelium (an important step for future alveolar formation), and surfactant production, from Type 2 pneumocytes, matures (essential for the survival of a preterm neonate).

Alveolar phase

Exactly when the saccular structure of the lung can be termed alveolar is not yet clear: opinions range from 28 to 32 weeks. The distal airspaces expand during late gestation and continue to do so after birth. This process is accompanied by fusion of adjacent capillary nets, so that shortly after birth there is an extensive double capillary net. Fusion of these layers is apparent at 28 days postnatally and extensive at 1.5 years; it is probably complete by 5 years. The alveolar stage continues into childhood, perhaps up to 8 years of age, although the balance of the evidence is that most alveoli are present by two years of age. The number of alveoli present at birth (variously estimated as between none to 5×10^7) and the age at end of alveolarization (estimated at between 2 and 20 years) is controversial. The process of forming new alveoli is rapid for six months, and by then mostly complete, with a plateau phase to two years with formation of alveoli largely complete at this time. Thereafter, probably growth of new alveoli is minimal.

The formation of millions of alveoli is accomplished by a complex process of folding and division. Existing walls of distal airspaces become thinner as pneumocyte epithelial cells flatten, and some cells undergo apoptosis. Ridges subsequently grow out from the sides of the saccule walls, forming primitive alveoli. The secondary septa contain a double capillary layer, and further new alveoli form by the infolding of one of these layers, further subdividing the air spaces. The double capillary networks then undergo remodeling to form the familiar single capillary sheet around each alveolus. Conducting airways also undergo profound postnatal changes, and exhibit increased smooth muscle and bronchoconstrictor responsiveness. Although the precise molecular signalling for these processes is unknown, it is acknowledged to be tightly developmentally regulated, thus dexamethasone treatment of rats during the alveolarization period permanently abrogates alveolar development. This finding implies that iatrogenic damage to the developing alveoli when ventilating a preterm baby with oxygen-enriched mixtures is probably irreversible.

It is becoming clear that elastin gene expression, possibly modulated through retinoic acid, is of pivotal importance in alveolar budding. Retinoic acid treatment of rats increases alveolarization, and salvages some alveoli in the steroid treatment model, whereas mice with a deletion in the retinoic acid receptor γ have impaired alveolarization. Retinoic acid regulates the expression of a number of growth signalling molecules, homeobox genes and lung epithelial genes; other gene groups involved in alveolarization probably include TGF-β, platelet-derived and fibroblast growth factors.

Development of the intrapulmonary vasculature and lymphatics

In an adult lung, the pulmonary arteries accompany the airways. The pulmonary veins have a similar number of branches but are separated from the airways by the alveoli: they have a different embryological origin deriving from the mediastinal mesenchyme proximally rather than splanchnopleuric mesenchyme around the bifurcating respiratory tree. The mesenchyme around the single lung bud contains a number of cells staining positively for CD34 and CD31, which are markers for endothelial cells. The earliest pulmonary vessels form in the mesenchyme by vasculogenesis: the capillaries coalesce to form small blood vessels alongside the airways. By 34 days of gestation, blood circulates from the aortic sac via pulmonary arteries into a capillary plexus around the two lung buds, and drains to the developing atrium. As each new airway forms in the mesenchyme, a new plexus forms as a halo around it, and coalesces with the vessels already alongside the previous airway. In this way, addition of the newly formed tubules to the existing vessels is sustained: the airways acting as a template for the development of blood vessels. Vessel formation occurs at least until the end of the pseudoglandular stage and is probably controlled by production of VEGF from the epithelial cells of the peripheral lung buds. As the arteries increase in size they acquire a muscular wall. Initially this arterial tunica media is derived from the bronchial smooth muscle of the adjacent airways, but as the vessels enlarge further, cells derived from the splanchnopleuric mesenchyme differentiate around the wall to form layers of smooth muscle cells. The muscular wall is thick relative to the lumen and this in part increases resistance to blood flow, although only 10% of blood flow goes through the pulmonary circulation of the lung during intra-uterine life. At 20 weeks, the structure of the pulmonary vessels is the same as it is in the adult. Vascular innervation follows muscularization; the vasoactive peptides in these nerves are predominantly vasoconstrictor.

As the pulmonary veins enlarge they become separated from the airways by lymphatic vessels which lie within connective tissue. At around week 12, the peripheral veins develop a single layer of smooth muscle cells in their walls. This layer is derived only from the splanchnopleuric mesenchyme and not from bronchial smooth muscle (as occurs in the arteries). The lumen of each vein is relatively large and the wall is relatively thin at all levels. Arteries and veins continue to develop in the canalicular phase, probably by angiogenesis; dividing cells are seen in the peripheral capillaries. The epithelium of the most peripheral conducting airways flattens when the developing capillaries come to lie immediately subjacent to it during this phase. (For a review of the development of the pulmonary circulation see Hislop 2005.)

Lymphatic capillaries and vessels run within bronchovascular bundles. Lymphatic channels develop from outgrowths of vascular endothelial cells. The molecular trigger for lymphatic sprouting is VEGF-C and D, acting through the VEGF receptor 3 (Janér et al 2006).

As well as developing a pulmonary circulation, the lung also develops a bronchial supply from the systemic circulation. Two or three bronchial arteries grow from the descending aorta from week 8 onwards, entering the lung at the hilum. These arteries extend down the intrapulmonary airways, eventually forming sub-epithelial and adventitial plexuses, which by birth have reached the distal portions of the bronchioli. The bronchial veins from the periphery of the lungs drain into the pulmonary veins. Bronchial arteries also supply the pleura near the hilum, and form vasa vasorum in the adventitia of the large arteries and veins. Post-natally, inflammatory lung conditions such as bronchiectasis cause hypertrophy of the bronchial circulation; these vessels may bleed, giving rise to massive haemoptysis in some cases.

Intra-uterine maturation of the lungs

There are more than 30 different cell types within the adult lung which mature during development. Only a few important changes which are relevant to human disease will be highlighted here.

Pulmonary surfactant is produced by Type 2 alveolar epithelial cells, and stored in lamellar bodies. It is crucial for maintaining the functional integrity of alveoli: the main morbidity of extreme prematurity reflects surfactant deficiency causing neonatal respiratory distress (treatment has been transformed by the availability of exogenous surfactant). Fetal breathing movements appear to be important in surfactant synthesis: the functional maturation of the surfactant system can be accelerated therapeutically by the administration of steroids to the mother.

Normal lung development requires sufficient intrathoracic space, normal fetal breathing movements and sufficient amniotic fluid. There is evidence that perturbation of fetal lung blood flow also affects lung growth, even though most of the right ventricular output of the heart is shunted away from the lungs through the ductus arteriosus: pulmonary valve stenosis is associated with pulmonary hypoplasia.

Although many fetal organs are able to grow to normal proportions even if they are in abnormal locations, this is not the case for the lungs. Lung growth becomes impaired by restricted expansion, and distension of the developing lung may provide a major stimulus to growth during normal development. Absence or impairment of fetal breathing movements, and defects affecting diaphragmatic activity, are all associated with pulmonary hypoplasia. It is believed that normal fetal breathing movements increase the lung volume and stimulate growth of the distal airspaces. Fetal breathing movements involve rhythmic activation of the diaphragm and the muscles of the upper respiratory tract. Even though such movements are necessarily very small compared with those seen after birth, because the fetal airways are filled with lung fluid, there is evidence that these phasic movements are important in the release of growth factors.

During development, the mucous glands of the trachea and bronchi secrete a chloride-rich fluid, which usually passes up the respiratory tract to mix with the amniotic fluid. The relationship between lung fluid and amniotic fluid is far more complex than was previously believed. Pulmonary hypoplasia at birth may be associated with severe congenital urinary obstruction and oligohydramnios (Potter’s syndrome). In renal agenesis, reduced bronchial branching occurs as early as 12–14 weeks of gestation (i.e. at a time before amniotic fluid is produced by the kidneys), which suggests that a direct renal factor supports lung development. Later, the presence of amniotic fluid is necessary for normal fetal lung development. The fetal lung is a net fluid secretor, the output of fluid reaching as high as 5 ml/kg shortly before birth. Most of the fluid produced within the lungs remains there because of the mechanical effect exerted by amniotic fluid pressure, and normally only a small amount of this fluid contributes to the amniotic fluid. The normal functioning of the kidneys regulates the volume and pressure of the lung airway fluid and may in turn provide the pressure needed for expansion and enlargement of the bronchial and pulmonary systems. Interestingly, obstruction to the fetal airway causes accelerated maturation of alveoli; this approach has been used therapeutically in congenital diaphragmatic hernia, where intermittent inflation and deflation of an intra-tracheal balloon in a lamb model resulted in better lung growth and maturation (Nelson et al 2005).

FUNCTIONAL CHANGES IN THE LUNG AROUND THE TIME OF BIRTH

Just prior to birth, the placenta is the organ of respiration. Virtually all the venous return to the right heart is shunted away from the lungs through the foramen ovale and the ductus arteriosus. Pulmonary vascular resistance (PVR) is maintained at a very high level by the muscular precapillary vessels. At birth, the umbilical cord is tied and cut, and within seconds the lungs must take over all respiratory function in order to maintain life. They also must convert from secreting fluid to absorbing it. The mechanisms that mediate these dramatic changes are obscure. However, it is clear that the first breath results in vasodilatation by at least two mechanisms. First, the mechanical effect of traction on the vasculature: as the chest wall expands, it pulls open the pulmonary vessels. Second, oxygen entering the lungs for the first time produces pulmonary vasodilatation. The experimental demonstration that PVR falls even if the fetus is delivered into an atmosphere of pure nitrogen, implies that other mediators, including cyclo-oxygenase metabolites, are undoubtedly important. The gene for cyclo-oxygenase 1 (but not 2) in endothelium and vascular smooth muscle shows enhanced expression in late fetal and early post-natal life. Endothelin receptor expression increases around the time of birth, implying a role for this system in postnatal adaptation. The role of nitric oxide in postnatal adaptation is controversial, and there are likely to be important species differences. Nitric oxide synthase (NOS) is more abundant in young compared with mature animals, and smooth muscle sensitivity to nitric oxide may be greater at birth than in older animals. The effects of mediators may differ ante- and postnatally, e.g. endothelin (ET)-1 causes vasodilatation in fetal sheep, but vasoconstriction postnatally.

Immediately after birth, and before structural remodeling has taken place, PVR may rise steeply if the baby becomes even minimally hypoxic or acidaemic. The fetal shunts (foramen ovale and ductus arteriosus) reopen and right to left shunting causes profound hypoxemia, ‘persistent fetal circulation’.

POSTNATAL LUNG DEVELOPMENT

The amount and type of connective tissue in the lung change after birth. The neonatal lung has abundant Type III and Type IV collagen, but little Type I collagen. Types III and IV collagen are not mechanically strong, suggesting that the neonatal lung has a phenotype that facilitates the changes in cell shape and orientation which characterize adaptation to extrauterine life. It is probable that the rapid deposition of Type I collagen postnatally contributes structural stiffness to the blood vessel walls.

Lung volume increases most rapidly during the first year of life and also increases more rapidly than airway calibre during this time, a finding which is consistent with the concept of dysanaptic lung growth, i.e. a dissociation between the growth of the lung parenchyma and the airways. Most of the alveoli have been formed by two years of age, and subsequent lung growth primarily results from an increase in the size of individual alveoli. Forced vital capacity is reported to be the same in male and female infants and very young children (Jones et al 2000), which is consistent with post mortem morphometric measurements. By the second year of life the rate of increase in forced vital capacity is similar to that reported in older children.

During childhood, lung volumes and flow rates increase linearly with height, with a greater intercept and more positive slope in boys compared to girls (Rosenthal et al 1993a & b). The linearity of these changes is interrupted by puberty, when important shape changes occur in the thorax, particularly in boys, and are mirrored by changes in the size of the underlying lung (and in particular the alveoli) as manifest by an abrupt increase in vital capacity, forced expired volume in one second, and total lung capacity. Thereafter, the change in lung size again proceeds in a linear fashion. High resolution computed tomographic scanning has been used to measure airway dimensions, although this technique should be used with caution because of the radiation exposure. Alveolar size can now be measured using hyperpolarized helium, using magnetic resonance imaging.

Normal postnatal pulmonary arterial development

Immediately after birth, dramatic remodelling of the pulmonary vasculature occurs to effect an abrupt reduction of pulmonary vascular resistance. This process continues at a rapid rate throughout the first 1–2 months, while the lungs adapt to extrauterine life, and then more slowly throughout childhood. Failure to remodel in the presence of an anatomically normal heart leads to persistent pulmonary hypertension. Normal postnatal pulmonary arterial development in the full-term neonate can be divided into three stages:

Stage one

lasts from birth to about postnatal day 4, and concerns the immediate adaptation to extrauterine life. At birth, the endothelial cells of the precapillary arteries are squat and have narrow bases on the subendothelium, a low surface : volume ratio and many surface projections. Five minutes after birth, the endothelial cells are thinner and gradually show less cell overlap, the surface : volume ratio increases, few cell projections are seen, the vessel wall becomes thinner and the lumen diameter increases (Fig. 59.23). The smooth muscle cells show a significant reduction in diameter during this time.

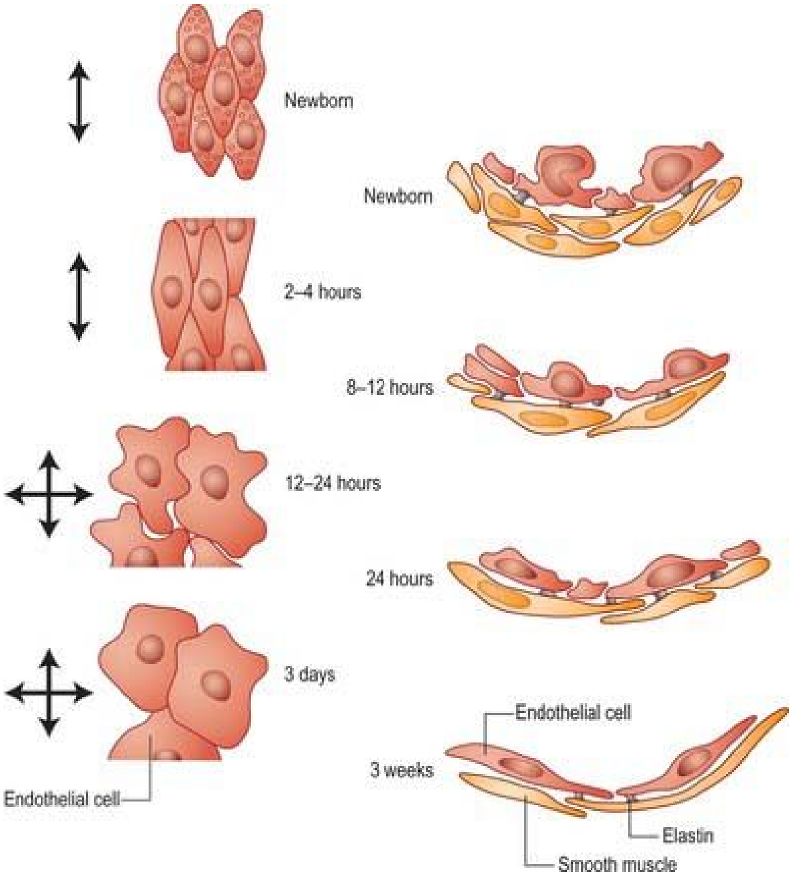
Newborn
Newborn
2–4 hours
8–12 hours
12–24 hours
24 hours
3 days
Endothelial cell
Endothelial cell
3 weeks
Elastin
Smooth muscle

Fig. 59.23 En face views (left) and transverse sections (right) showing the changes in the endothelial and smooth muscle cells of small muscular pulmonary arteries accompanying terminal bronchi from the neonatal period to 3 weeks after birth.

Stage two

lasts from around day 4 to 3–4 weeks, and is the time when the cells deposit matrix around themselves to fix their new positions. At birth, the internal elastic lamina of the small muscular arteries consists only of amorphous elastin in a basal lamina-like matrix. By 3 weeks of age, a definitive elastic lamina is evident, although it is heavily fenestrated, permitting contact between the endothelial cells and the smooth muscle cells.

Stage three

continues into adulthood. The intrapulmonary arteries increase in size and their walls increase in thickness. However, the maturation of all of the pulmonary vascular smooth muscle cells, from the hilum to the precapillary bed, is not advanced until 2 years. As the distal airspaces expand, the capillary nets fuse from one alveolus to another, forming, for a period, an extensive double capillary net: this process can be seen from postnatal day 28, becomes more extensive by 1.5 years, and it is believed to be complete by 5 years.

CONGENITAL MALFORMATIONS OF THE TRACHEA, BRONCHI AND LUNGS

This is an enormous topic and only a small number of abnormalities can be mentioned here (for further information, see Bush 2001; Abel et al 2006). The concept of the lung as six 'trees' has been mentioned earlier: all but the systemic venous tree may contribute to a congenital thoracic malformation (CTM). In addition, congenital abnormalities of the heart and great vessels, and of the chest and abdominal walls, including neuromuscular disease, may impact on lung development. It is somewhat artificial to describe airway malformations in isolation, and the possibility of associated vascular abnormalities must always be considered. Moreover, descriptions of what is seen clinically should be kept separate from speculations about the embryological origins of the abnormality.

Disorders of the proximal airways

Tracheomalacia and bronchomalacia

Abnormalities in cartilage development lead to the affected airways being 'floppy', and collapsing during inspiration or expiration, depending on whether they are outside or inside the bony thorax, respectively: these abnormalities are termed tracheomalacia when the trachea is affected, and bronchomalacia when the bronchi are involved. The abnormality may involve a small, localized area, or may be more generalized (e.g. Williams–Campbell syndrome – congenital deficiency of the airway cartilage – in which there is diffuse bronchomalacia from the second to the seventh generation of bronchi). Tracheobronchomalacia usually presents in early infancy with cough, tachypnoea, stridor and wheeze; it may also be associated with cardiac or respiratory abnormalities, such as absent pulmonary valve syndrome, or tracheo-oesophageal fistula, respectively. Patients with significant obstruction and apnoea may be treated by the insertion of airway stents if the disease is localized; generalized disease may mandate respiratory support, either with non-invasive mask ventilation during sleep, or via a tracheostomy, depending on severity. Surgical treatment by aortopexy is controversial.

Tracheo-oesophageal fistulae

Tracheo-oesophageal fistulae are the most common abnormalities of the lower respiratory tract, and occur in about 1 in 3000 births. They usually present in the newborn with recurrent respiratory distress and choking spells, although late presentation in adult life has been described. The anomaly may be associated with oesophageal atresia. Normally, the oesophagus lengthens with the rapid elongation of the embryo up to 7 weeks. The rapid proliferation of the oesophageal lumen partially obliterates the mucosa and recanalization is not complete until 8 weeks. The cellular processes that lead to separation of the trachea and oesophagus occasionally produce oesophageal atresia. Tracheo-oesophageal atresia is rare, with an incidence of 1 in 3000 to 1 in 4500 births. Five types of tracheo-oesophageal fistulae may be recognized (Fig. 59.24). In almost all cases, the oesophagus ends blindly and the stomach is connected to the lower end of the trachea. Because of this connection, the abdomen becomes rapidly distended with air once the baby is delivered and starts breathing. Prenatally, polyhydramnios may be a clinical feature, but may not be apparent until the third trimester. In two of the five types of tracheo-oesophageal fistulae there is no communication between the stomach and the upper gut. Such cases are identifiable on ultrasound, because the stomach should always be visible at a 20-week examination, and its absence on ultrasound should prompt further evaluation.

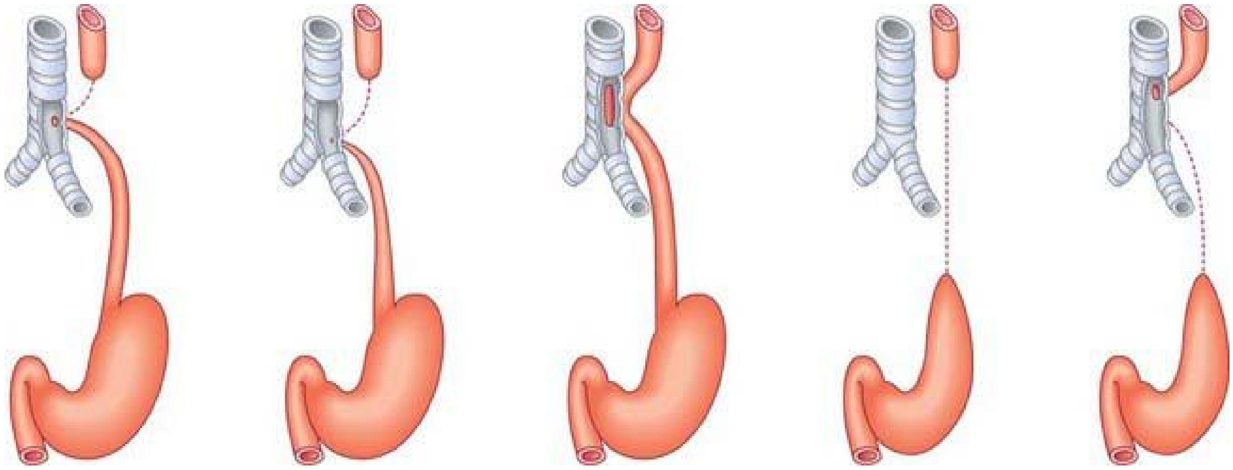

Fig. 59.24 Examples of tracheo-oesophageal fistulae and oesophageal atresia.

Tracheo-oesophageal fistula is commonly associated with other congenital anomalies, including cardiovascular defects (30%), anorectal (15%) and genitourinary anomalies (15%). These defects may be combined in the VATER syndrome, which involves vertebral, anorectal, cardiac and oesophageal anomalies, together with radial aplasia and the presence of a single umbilical artery.

Complete cartilage rings

The normal large airway cartilages are horseshoe shaped. Complete cartilage rings may develop in the trachea and large airways, and the posterior membranous part of the airway may be absent in a single cartilage or in long segments of the airway. This abnormality may be associated with vascular abnormalities such as pulmonary artery sling (where the left pulmonary artery originates from the right pulmonary artery, and not from the main pulmonary trunk). Extensive severe disease may present with neonatal respiratory distress; later presentations include apparently steroid-resistant asthma. Tracheal transplantation has been used to treat long segment tracheal stenosis.

Disorders of the distal airways

Agenesis and aplasia of the lungs

Agenesis/aplasia of the lungs are extremely rare congenital abnormalities, in which there may be unilateral or bilateral absence of the lung. In agenesis, the airway stump is absent, i.e. the trachea is absent in bilateral disease, or the primary bronchus is absent in unilateral disease. In aplasia, there is a rudimentary airway stump, but no distal lung; the contralateral lung is enlarged, with a greater number of alveoli, but has a normal bronchial pattern. Individuals with aplasia may present with recurrent infection, dyspnoea and reduced exercise capacity, and there may be pooling of bronchial secretions, with secondary infection and overspill of infected secretions into the contralateral normal lung.

Bronchogenic and other cysts

Cysts of various types, by order of frequency, may be found in the carinal (51%), right para-tracheal (19%), para-oesophageal (14%), hilar (9%) and pericardial, retrosternal and para-vertebral (7%) regions. Clinically they are part of the spectrum of congenital thoracic malformations, and can only be classified in more detail pathologically when the wall of the cyst is examined; they may have a systemic blood supply and venous drainage. Multicystic abnormalities, described as various types of congenital cystic adenomatous malformations (CCAM) and sequestrations (intra- and extra-pulmonary), are best considered generically as CTM spectrum, at least until examined pathologically. Presentation may be with a range of problems, from intractable newborn respiratory distress to a chance finding in adult life. Treatment is usually surgical if feasible, for all but the tiniest malformations.

Bronchial atresia

Bronchial atresia is a congenital condition in which a major bronchus or segmental airway ends blindly or with a thin membrane. Pulmonary development normally occurs distally, and over time this tissue becomes distended with debris and mucus (bronchocele), with adjacent over-inflated lung tissue. It characteristically affects the left upper lobe (64% of cases) and the chest radiographic findings are of a perihilar ovoid density with strands projecting into a localized area of hyperlucent lung. The left lower lobe is affected in 14% of cases and the right lower and right middle lobe in 8% of cases. The majority of cases are asymptomatic and are revealed as incidental findings on chest radiographs. However, many eventually become the seat of recurrent infection, and require operative removal. Some infants may show a congenital large hyperlucent pulmonary lobe (CLHL). This condition is termed ‘congenital lobar emphysema’ although it has nothing to do with adult emphysema. Presentation in severe cases is with newborn respiratory distress, in which case early surgery is required, otherwise, it may be a chance radiographic finding later in life, in which case no action is needed.

REFERENCES

el R, Bush A, Chitty L, Harcourt J, Nicholson A. Congenital lung disease. In: Chernick V, Boat T, Wilmott R, Bush A. *Kendig's Disorders of the Respiratory Tract in Children*. 7th edn. Edinburgh: Elsevier; 2006:280-316.

A review of all aspects of the diagnosis, nomenclature and management of congenital malformations of the airways, lung and chest wall..

len J, Gripp KW. Haddad GG, Abman SH, Chernick V. Development of the thoracic cage, Basic Mechanisms of Pediatric Respiratory Disease. 2nd edn.. Hamilton, Ont: BC Decker; 2002:124-138.

derson RH, Webb S, Brown NA, Lamers WH, Moorman AFM. Development of the heart. 2. Septation of the atriums and ventricles. *Heart*. 2003;89:949-958.

derson RH, Webb S, Brown NA, Lamers WH, Moorman AFM. Development of the Heart. 3. Formation of the ventricular outflow tracts, arterial valves, and intrapericardial arterial trunks. *Heart*. 2003;89:1110-1118.

derson RH, Christoffels VM, Moorman AFM. Controversies concerning the anatomical definition of the conduction tissues. *Anat Record B New Anat*. 2004;280:8-14.

nderson RH, Brown NA, Moorman AFM. Development and structures of the venous pole of the heart. *Dev Dyn*. 2006;235:2-9.

ckingham M, Meilhac S, Zaffran S. Building the mammalian heart from two sources of myocardial cells. *Nat Rev Genet*. 2005;6:826-837.

sh A. Congenital lung disease: a plea for clear thinking and clear nomenclature. *Pediatr Pulmonol*. 2001;32:328-337.

A new classification of congenital lung malformations..

sh A. Asthma research: The real action is in children. *Paediatr Respir Rev*. 2005;6:101-110.

A review of how early problems with lung growth and development impact on later lung disease..

ristoffels VM, Burch JBE, Moorman AFM. Architectural plan for the heart: Early patterning and delineation of the chambers and the nodes. *Trends in Cardiovasc Med*. 2004;14:301-307.

Lange FJ, Moorman AFM, Anderson RH, et al. Lineage and morphogenetic analysis of the cardiac valves. *Circ Res*. 2004;95:645-654.

slop A. Developmental biology of the pulmonary circulation. *Paediatr Respir Rev*. 2005;6:35-43.

nér J, Lassus P, Haglund C, Paavonen K, Alitalo K, Andersson S. Pulmonary vascular endothelial growth factor-C in development and lung injury in preterm infants. *Am J Respir Crit Care Med*. 2006;174:326-330.

The role of VEGF and its receptors in the development of the lymphatic system..

sudason EC. Challenging embryological theories on congenital diaphragmatic hernia: Future therapeutic implications for paediatric surgery. *Ann R Coll Surg Engl*. 2002;84:252-259.

nes M, Castile R, Davis S, et al. Forced expiratory flows and volumes in infants: Normative data and lung growth. *Am J Respir Crit Care Med*. 2000;161:353-359.

mers WH, Moorman AFM. Cardiac septation: A late contribution of the embryonic primary myocardium to heart morphogenesis. *Circ Res*.

2002;91:93-103.

ommersteeg MTM, Soufan AT, de Lange FJ, et al. Two distinct pools of mesenchyme contribute to the development of the atrial septum. *Circ Res*. 2006;99:351-353.

oorman AFM, Christoffels VM. Cardiac chamber formation: Development, genes and evolution. *Physiol Rev*. 2003;83:1223-1267.

oorman AFM, Webb S, Brown NA, Lamers WH, Anderson RH. Development of the heart: I. Formation of the cardiac chambers and arterial trunks. *Heart*. 2003;89:806-814.

oorman AFM, Christoffels VM. Development of the cardiac conduction system: A matter of chamber development. *Novartis Found Symp*. 2003;250:25-34.

ortola JP. Comparative aspects of neonatal respiratory mechanics. In: Haddad GG, Abman SH, Chernick V. *Basic Mechanisms of Pediatric Respiratory Disease*. 2nd edn. Hamilton, Ont: BC Decker; 2002:171-178.

elson SM, Hajivassiliou CA, Haddock G, et al. Rescue of the hypoplastic lung by prenatal cyclical strain. *Am J Respir Crit Care Med*. 2005;171:1395-1402.

How tracheal occlusion can be used in an animal model to improve lung growth and maturation..

osenthal M, Bain SH, Cramer D, Helms P, Denison D, Bush A, Warner JO. Lung function in white children aged 4–19 years: I. Spirometry. *Thorax*. 1993;48:794-802.

osenthal M, Cramer D, Bain SH, Denison D, Bush A, Warner JO. Lung function in white children aged 4–19 years: II. Single breath analysis and plethysmography. *Thorax*. 1993;48:803-808.

osenthal M, Bush A. The growing lung: Normal development, and the long-term effects of pre- and post-natal insults. *Eur Respir Monogr*. 2002;7:1-24. In: Bush A, Zach M, Carlsen K-H (eds) Growing up with lung disease: The lung in transition to adult life.

th-Kleiner M, Post M. Similarities and dissimilarities of branching and septation during lung development. *Pediatr Pulmonol*. 2005;40:113-134.

An account of the molecular mechanisms underlying normal lung development..

ufan AT, van den Hoff MJB, Ruijter JM. Reconstruction of the patterns of gene expression in the developing mouse heart reveals an architectural arrangement that facilitates the understanding of atrial malformations and arrhythmias. *Circ Res*. 2004;95:1207-1215.

Section 8

ABDOMEN AND PELVIS

CHAPTER 60

Abdomen and pelvis: overview and surface anatomy

GENERAL STRUCTURE AND FUNCTION OF THE ABDOMINOPELVIC CAVITY

Although often considered separately, the abdomen and pelvis form the largest effectively continuous visceral cavity of the body. They act together to provide multiple vital functions including: support and protection of the digestive and urinary tracts and internal reproductive organs and their associated neurovascular supplies; transmission of the neurovascular supply to and from the thorax and the lower limb; provision of support and attachment to the external genitalia and access to and from the internal reproductive and urinary organs; provision of accessory muscles of physiological actions such as respiration, defecation, and micturition; support for the spinal column in weight bearing and movement.

MUSCULOSKELETAL FRAMEWORK OF THE ABDOMEN AND PELVIS

The walls of the abdominopelvic cavity consist of five lumbar vertebrae and their intervening intervertebral discs (lying in the posterior midline); three layers of skeletal muscles (transversus abdominis, internal oblique and external oblique) with associated fasciae and skin (lying lateral and anterolateral); a single muscular layer (rectus abdominis) with its associated fascial coverings (lying anterior); the bony ‘bowl’ formed by the walls of the true and false pelvis (ilium, ischium and pubis on each side); the muscles of the pelvic floor and perineum (lying inferiorly); the diaphragm (lying superiorly) (Fig. 60.1).

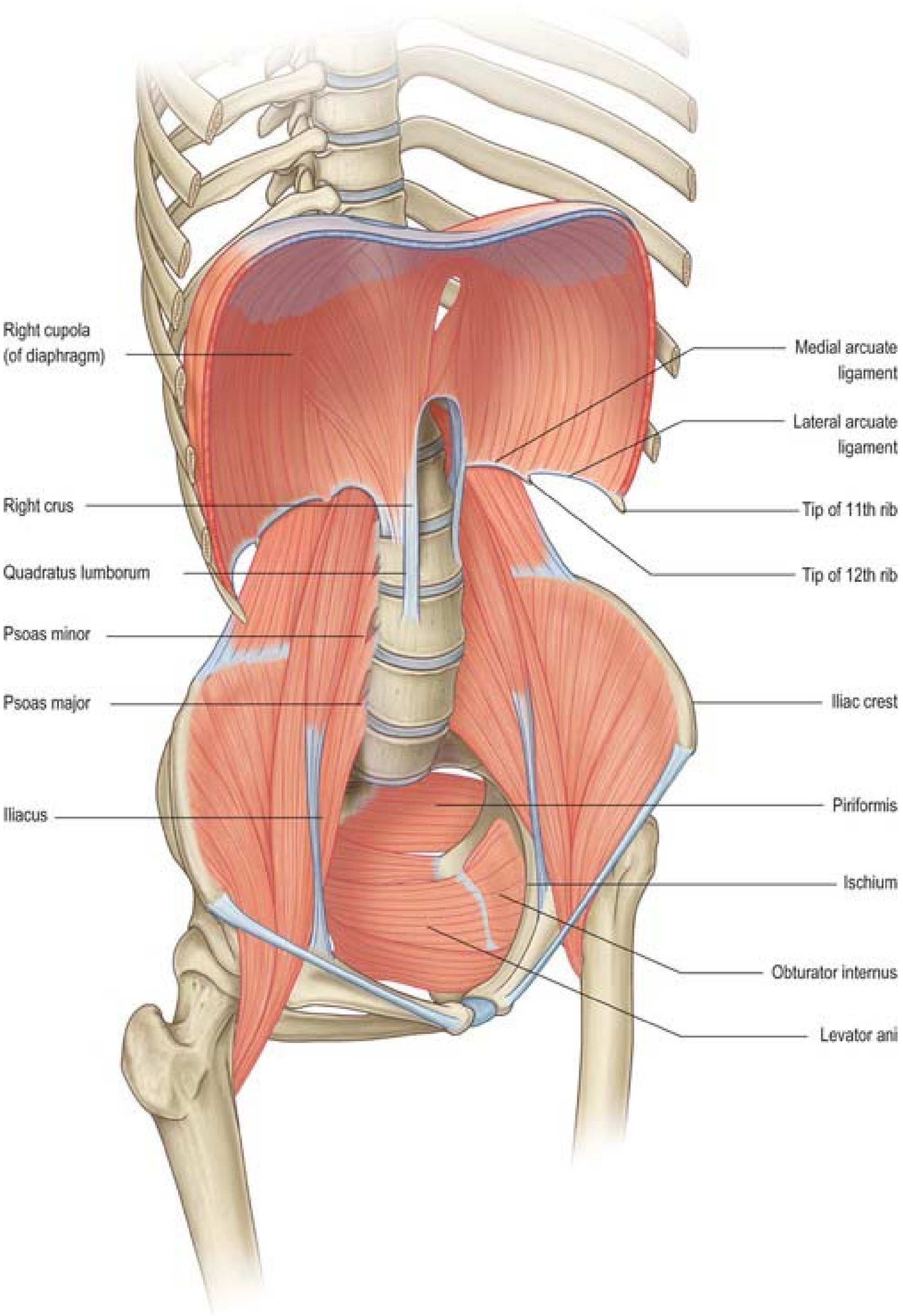
Right cupola (of diaphragm)
Right crus
Quadratus lumborum
Psoas minor
Psoas major
Iliacus
Medial arcuate ligament
Lateral arcuate ligament
Tip of 11th rib
Tip of 12th rib
Iliac crest
Piriformis
Ischium
Obturator internus
Levator ani

Fig. 60.1 The bony and muscular structures making up the abdominopelvic ‘cavity’. The anterolateral abdominal muscles have been removed for clarity.

The bony protection of the cavity is restricted to the pelvis (true and false) and the upper abdomen, which is partly enclosed by the anterolateral portions of the lower six ribs and their cartilages even though these structures are technically part of the thoracic wall. Between these two zones, the anterolateral abdominal wall is entirely musculofascial but of sufficient thickness and strength that it provides adequate protection for the viscera such that even direct blows can be resisted.

The abdominal wall and retroperitoneal structures play an important role in the function of the spinal column in both movement of the thorax in relation to the pelvis and in aiding support of the spine in weight bearing. The anterolateral muscles provide assistance with flexion and rotation of the thorax in relation to the pelvis (or vice versa if the thorax is fixed).

In the upright position, the pelvis lies at an angle such that the pelvic canal slopes posteriorly at an angle of 45° to the main abdominal visceral cavity. The main abdominal cavity is shaped by the spinal column and the posterior abdominal wall muscles. Although less pronounced than in the thorax, due to the presence of quadratus lumborum and psoas major, its prominence within the abdominal cavity produces two distinct paravertebral gutters on either side of the vertebral column. The lordosis of the lumbar spine in combination with the angle between the fifth lumbar vertebra and the sacrum produces the parabola shape of the sagittal section of each paravertebral gutter.

Thoracoabdominal interface

The thoracic and abdominal cavities interface with each other across the diaphragm. Six principle communications exist between the two cavities: the inferior vena cava, as it crosses between its short supra-hepatic portion and the intrathoracic portion below the right atrium, through the caval opening of the diaphragm (Ch. 62); the oesophagus passing inferiorly through the oesophageal opening of the diaphragm (Ch. 65); the aorta between the descending thoracic and abdominal portions, posterior to the median arcuate ligament of the diaphragm (Ch. 62); the lymphatics of the abdomen draining upwards to the thorax, mainly posterior to the median arcuate ligament via the thoracic duct lying posterolateral to the aorta, but also via peri-caval lymphatics and small vessels draining directly through and at the peripheral insertions of the diaphragm; the azygos and hemiazygos veins ascending behind the median arcuate ligament of the diaphragm into the thoracic azygos system (Ch. 62); the autonomic nervous system, both sympathetic and parasympathetic (see below) which cross between the two cavities behind the medial arcuate ligaments of the diaphragm, via the various diaphragmatic openings, and directly through the substance of the diaphragm itself (Ch. 54). Cutaneous neurovascular structures also cross between the thorax into the abdominal wall structures.

Pelvis–lower limb interface

The pelvis forms an integral part of the bony structure of both the abdominopelvic cavity and the lower limb. It transmits the weight of the upright body from the femoral heads to the lumbar spine as well as providing a stable platform about which movement of the hip joint can occur. Its bony surfaces give rise to extensive muscular attachments for the muscles of the buttock and thigh (Ch. 67) as well as for the muscles of the pelvic floor and perineal diaphragm (Ch. 63). The pelvis also transmits or gives origin to the neuro-lympho-vascular structures which supply the lower limb. The principle structures are as follows. The venous drainage includes the common femoral vein passing under the inguinal ligament to become the external iliac vein; the obturator veins passing through the obturator foramen; the superior and inferior gluteal veins draining from the buttock into the internal iliac vein via the greater and lesser sciatic foramina; multiple smaller venous channels. The arterial supply includes the external iliac artery passing under the inguinal ligament to become the common femoral artery; the obturator artery passing into the thigh via the obturator foramen; the superior and inferior gluteal arteries from the posterior division of the internal iliac artery passing out of the pelvis via the greater and lesser sciatic foramina. The lymphatic drainage principally passes under the inguinal ligament, via the femoral and obturator canals and via the sciatic foramina, to drain into the pelvic lymphatic chains (Ch. 63). The somatic neural structures include the femoral, obturator and sciatic nerves and other minor branches of the lumbosacral plexus (Ch. 62). The autonomic neural structures include those running with the arterial supply and with the branches of the lumbosacral plexus. Cutaneous neurovascular structures also cross between the lower abdomen and pelvis into the skin and superficial tissues of the lower limb.

GENERAL ARRANGEMENT OF ABDOMINOPELVIC NEUROVASCULAR STRUCTURES

It is useful to review here the overall arrangement of the neurovascular systems which cover several regions or multiple viscera of the abdominopelvic region. Descriptions of the neurovascular supply to individual organs are given in the relevant chapters.

AUTONOMIC SUPPLY

The autonomic supply to the abdominal and pelvic viscera is via the abdominopelvic part of the sympathetic chain and the greater, lesser and least splanchnic nerves (sympathetic), and the vagus and pelvic parasympathetic nerves (parasympathetic). Considerable ramification occurs between plexuses and ganglia, particularly in the major plexuses around the abdominal aorta, hence the descriptions tend to be simplifications based on the ‘main’ supply to each organ (Fig. 60.2). The details of the terminations of these fibres are given on page 1050.

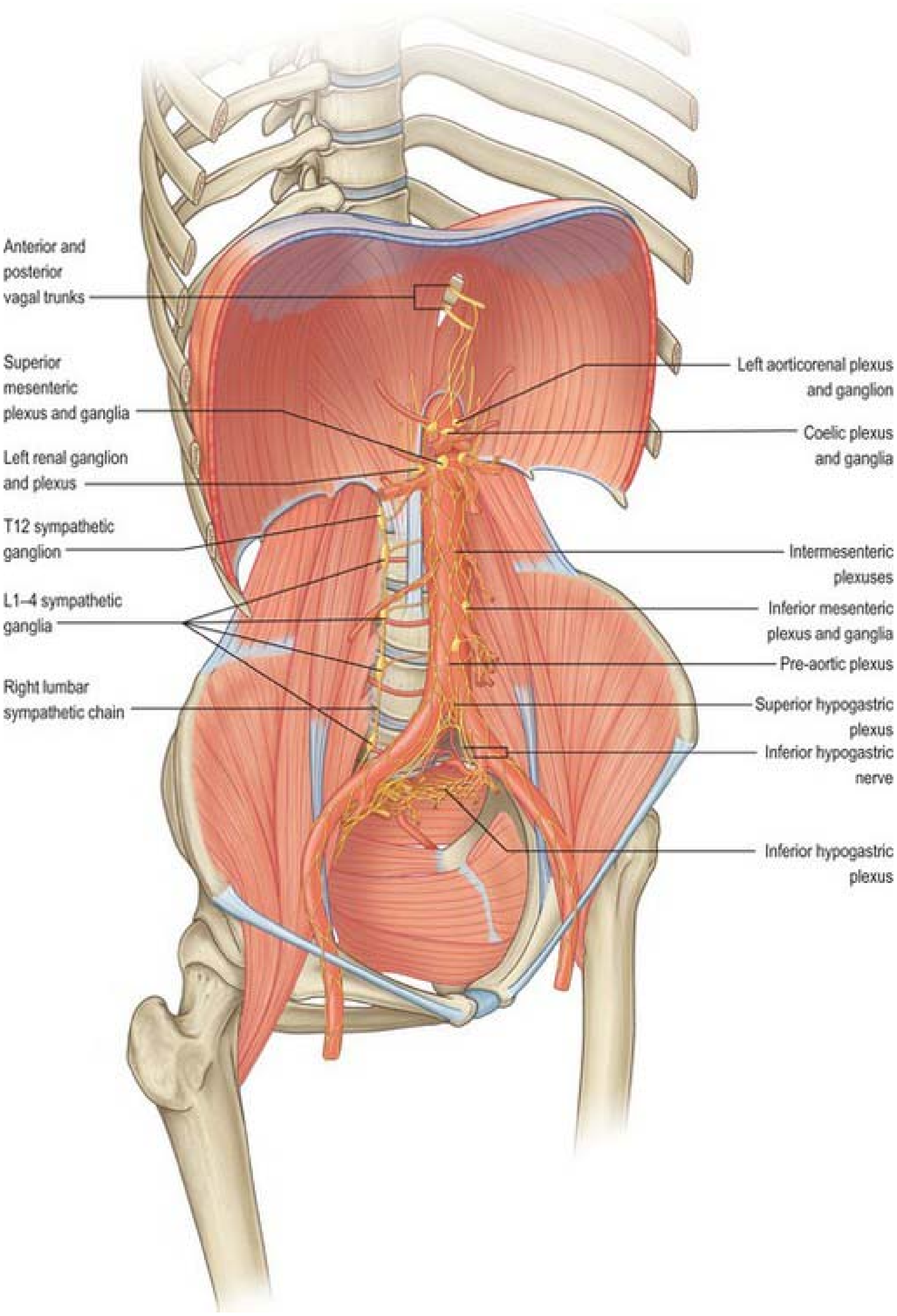
Anterior and posterior vagal trunks
Superior mesenteric plexus and ganglia
Left renal ganglion and plexus
T12 sympathetic ganglion
L1–4 sympathetic ganglia
Right lumbar sympathetic chain
Left aorticorenal plexus and ganglion
Coelic plexus and ganglia
Intermesenteric plexuses
Inferior mesenteric plexus and ganglia
Pre-aortic plexus
Superior hypogastric plexus
Inferior hypogastric nerve
Inferior hypogastric plexus

Fig. 60.2 The overall arrangement of the autonomic plexuses of the abdominal and pelvic viscera.

Sympathetic innervation

The cell bodies of neurones of the sympathetic supply of the abdomen and pelvis lie in the intermediolateral grey matter of the first to 12th thoracic and first two lumbar spinal segments. These neurones give rise to myelinated axons which travel in the ventral ramus of the spinal nerve of the same level, leaving it via the white ramus communicans to enter a thoracic or lumbar paravertebral ganglion. Visceral branches may exit at the same level or ascend or descend several levels before exiting but leave the ganglia without synapsing in medial (visceral) branches. These give rise to the greater, lesser and least splanchnic nerves, and the lumbar and sacral splanchnic nerves. Axons destined for supply to somatic structures always synapse in the ganglion of the same level and post-ganglionic, unmyelinated axons leave the ganglion via the grey ramus communicans to enter the spinal nerve of the same level.

Greater splanchnic nerve

The greater splanchnic nerve is derived from the medial, visceral branches of the fifth to ninth thoracic ganglia. It enters the abdomen running through the fibres of the ipsilateral crus of the diaphragm and lies on the crus as it runs anteroinferiorly. The main trunk of the nerve enters the superior aspect of the coeliac ganglion.

Lesser splanchnic nerve

The lesser splanchnic nerve is derived from the medial, visceral branches of the 10th and 11th thoracic ganglia. It enters the abdomen running through the lowermost fibres of the ipsilateral crus of the diaphragm or under the medial arcuate ligament and lies on the crus as it runs anteroinferiorly. The trunk of the nerve enters the aorticorenal ganglion and may give branches to the lateral aspect of the coeliac ganglion. It occasionally joins the greater and least splanchnic nerves as a single splanchnic nerve.

Least splanchnic nerve

The least splanchnic nerve is derived from the medial, visceral branches of the 12th thoracic ganglia. It enters the abdomen running with the sympathetic chain under the medial arcuate ligament and runs inferiorly to enter the renal plexus. The trunk of the nerve enters the aorticorenal ganglion and may give branches to the lateral aspect of the coeliac ganglion. It is sometimes part of the lesser splanchnic nerve, when it forms a twig which enters the renal plexus just below the aorticorenal ganglion.

Lumbar sympathetic system

The lumbar part of each sympathetic trunk usually contains four interconnected ganglia. The trunk runs in the extraperitoneal connective tissue anterior to the vertebral column and along the medial margin of psoas major. Superiorly, it is continuous with the thoracic trunk posterior to the medial arcuate ligament. Inferiorly, it passes posterior to the common iliac artery and is continuous with the pelvic sympathetic trunk. On the right side, it lies posterior to inferior vena cava, and on the left it is posterior to the lateral aortic lymph nodes. It is anterior to most of the lumbar vessels, but may pass behind some lumbar veins.

The first, second and sometimes third lumbar ventral spinal rami send white rami communicantes to the corresponding ganglia. Grey rami communicantes pass from all four lumbar ganglia to the lumbar spinal nerves. They are long, and accompany the lumbar arteries round the sides of the vertebral bodies, medial to the fibrous arches to which psoas major is attached. They supply the sympathetic innervation to the lumbar somatomes via these arteries. Four lumbar splanchnic nerves pass as medial branches from the ganglia to join the coeliac, inferior mesenteric (or occasionally abdominal aortic) and superior hypogastric plexuses. The first lumbar splanchnic nerve, from the first ganglion, gives branches to the coeliac, renal and inferior mesenteric plexuses. The second nerve joins the inferior part of the intermesenteric or inferior mesenteric plexus. The third nerve arises from the third or fourth ganglion and passes anterior to the common iliac vessels to join the superior hypogastric plexus. The fourth lumbar splanchnic nerve from the lowest ganglion passes above the common iliac vessels to join the lower part of the superior hypogastric plexus, or the inferior hypogastric ‘nerve’.

Vascular branches

Vascular branches from all the lumbar ganglia join the abdominal aortic plexus. Fibres of the lower lumbar splanchnic nerves pass to the common iliac arteries and form a plexus which extends along the internal and external iliac arteries. Many postganglionic fibres travel in the muscular, cutaneous and saphenous branches of the femoral nerve, supplying vasoconstrictor nerves to the femoral artery and its branches in the thigh. Other postganglionic fibres travel via the obturator nerve to the obturator artery. Considerable uncertainty persists regarding the exact path of the sympathetic nerve supply to the lower limb (Pick 1970). Sympathetic denervation of vessels in the lower limb can be effected by removing or ablating the upper three lumbar ganglia and the intervening parts of the sympathetic trunk; very rarely, this procedure is useful in treating vascular insufficiency of the lower limb.

Pelvic sympathetic system

The pelvic sympathetic trunk lies in the extraperitoneal tissue anterior to the sacrum beneath the presacral fascia. It lies medial or anterior to the anterior sacral foramina and has four or five interconnected sacral ganglia (they often merge to a greater or lesser extent). Above, it is continuous with the lumbar sympathetic trunk and receives preganglionic fibres descending via the lumbar chain from the lower lumbar spinal segments. Below the lowest ganglia, the two trunks converge to unite in the small ganglion impar anterior to the coccyx. Grey rami communicantes pass from the ganglia to the sacral and coccygeal spinal nerves but there are no white rami communicantes. Medial branches connect across the midline and twigs from the first two ganglia, referred to as sacral splanchnic nerves, join the inferior hypogastric plexus or the hypogastric ‘nerve’ to be distributed to the pelvic viscera via a fine network of pelvic nerves (the ‘pelvic plexus’). Small branches form a plexus on the median sacral artery.

Vascular branches

Postganglionic fibres pass through the grey rami communicantes to the roots of the sacral plexus. Those forming the tibial nerve are conveyed to the popliteal artery and its branches in the leg and foot whilst those in the pudendal and superior and inferior gluteal nerves accompany the same named arteries to the gluteal and perineal tissues. Branches may also supply the pelvic lymph nodes.

Preganglionic fibres for the rest of the lower limb are derived from the lower three thoracic and upper two or three lumbar spinal segments. They reach the lower thoracic and upper lumbar ganglia through white rami communicantes and descend through the sympathetic trunk to synapse in the lumbar ganglia.

Parasympathetic innervation

The parasympathetic neurones innervating the abdomen and pelvis lie either in the dorsal motor nucleus of the vagus nerve or in the intermediolateral grey matter of the second, third and fourth sacral spinal segments. The vagus nerves supply parasympathetic innervation to the abdominal viscera with the exception of the colon distal to the mid descending colon, rectum and upper anal canal. The nerves are derived from the oesophageal plexus and enter the abdomen via the oesophageal opening, closely related to the anterior and posterior walls of the abdominal oesophagus, from which they are separated by loose connective tissue. The anterior vagus is mostly derived from the left vagus and the posterior from the right vagus. The nerves supply the intra-abdominal oesophagus and stomach directly. The anterior nerve supplies branches to the hepatic plexus, which innervates the liver parenchyma and vasculature, the biliary tree including the gallbladder, and the structures in the free edge of the lesser omentum. The posterior nerve supplies branches to the coeliac plexus. These fibres frequently constitute the largest portion of the fibres derived from the plexus: they arise directly from the nerve and from the greater posterior gastric nerve and run beneath the peritoneum, deep to the posterior wall of the lesser sac, at the upper limit of the lesser omentum to reach the coeliac plexus. Their synaptic relays with postganglionic neurones are situated in the myenteric (Auerbach’s) and submucosal (Meissner’s) plexuses (see below).

Pelvic splanchnic nerves

Pelvic splanchnic nerves to the pelvic viscera travel in anterior rami of the second, third and fourth sacral spinal nerves. They leave the nerves as they exit the anterior sacral foramina and pass in the presacral tissue as a fine network of branches which are distributed to three locations. Most pass anterolaterally into the network which forms the inferior hypogastric plexus, whence most are distributed as a fine network of nerves (the ‘pelvic plexus’) to the pelvic viscera (alongside the sympathetic pelvic supply). Some join directly with the fibres forming the inferior hypogastric nerves and hence ascend out of the pelvis, some as far as the superior hypogastric plexus. A few run superolaterally in the presacral tissue, over the pelvic brim anterior to the iliac vessels. They pass directly into the tissue of the retroperitoneum and into the posterior aspect of the mesentery of the sigmoid and descending colon.

The pelvic splanchnic nerves are motor to the smooth muscle of the rectum, anus and bladder wall but inhibitory to the vesical sphincter. They supply vasodilator fibres to the erectile tissue of the penis and clitoris and are probably also vasodilator to the testes, ovaries, uterine tubes and uterus. They are visceromotor to the sigmoid and descending colon as far as the splenic flexure and distal transverse colon.

Abdominopelvic autonomic plexuses and ganglia

The abdominopelvic autonomic plexuses are somewhat variable and often fuse or are closely inter-related. The following descriptions recognize their main features (Figs 60.3, 60.4).

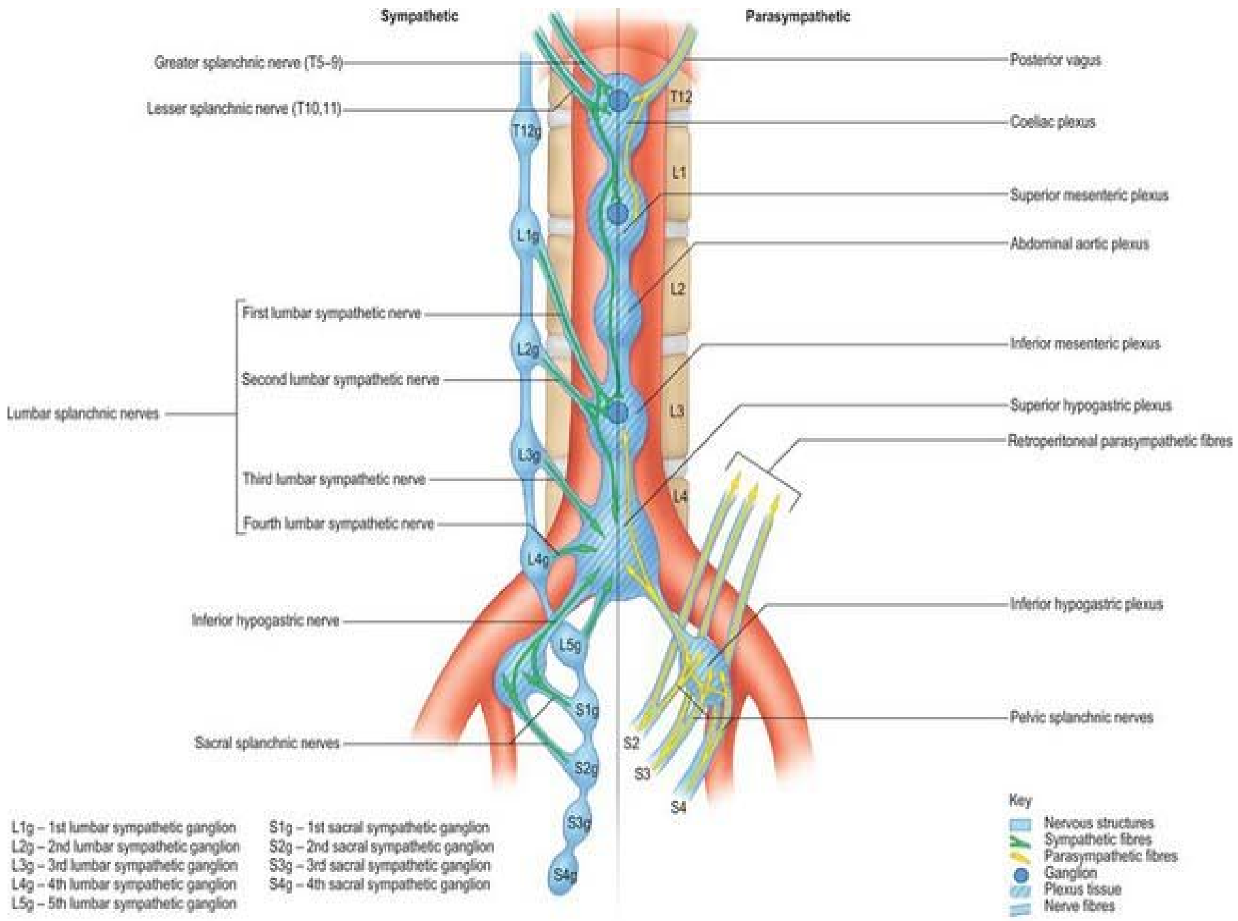
Sympathetic
Parasympathetic
Greater splanchnic nerve (T5–9)
Lesser splanchnic nerve (T10,11)
Posterior vagus
Coeliac plexus
T12
T12g
L1
L1g
Superior mesenteric plexus
Abdominal aortic plexus
L2
First lumbar sympathetic nerve
L2g
Inferior mesenteric plexus
Second lumbar sympathetic nerve
Lumbar splanchnic nerves
L3
Superior hypogastric plexus
Retroperitoneal parasympathetic fibres
L3g
Third lumbar sympathetic nerve
L4
Fourth lumbar sympathetic nerve
L4g
Inferior hypogastric nerve
Inferior hypogastric plexus
L5g
S1g
Pelvic splanchnic nerves
S2
Sacral splanchnic nerves
S2g
S3
S4
S3g
S4g
L1g – 1st lumbar sympathetic ganglion
L2g – 2nd lumbar sympathetic ganglion
L3g – 3rd lumbar sympathetic ganglion
L4g – 4th lumbar sympathetic ganglion
L5g – 5th lumbar sympathetic ganglion
S1g – 1st sacral sympathetic ganglion
S2g – 2nd sacral sympathetic ganglion
S3g – 3rd sacral sympathetic ganglion
S4g – 4th sacral sympathetic ganglion
Key
Nervous structures
Sympathetic fibres
Parasympathetic fibres
Ganglion
Plexus tissue
Nerve fibres

Fig. 60.3 The autonomic plexuses innervating the abdominal and pelvic viscera: schematic diagram.

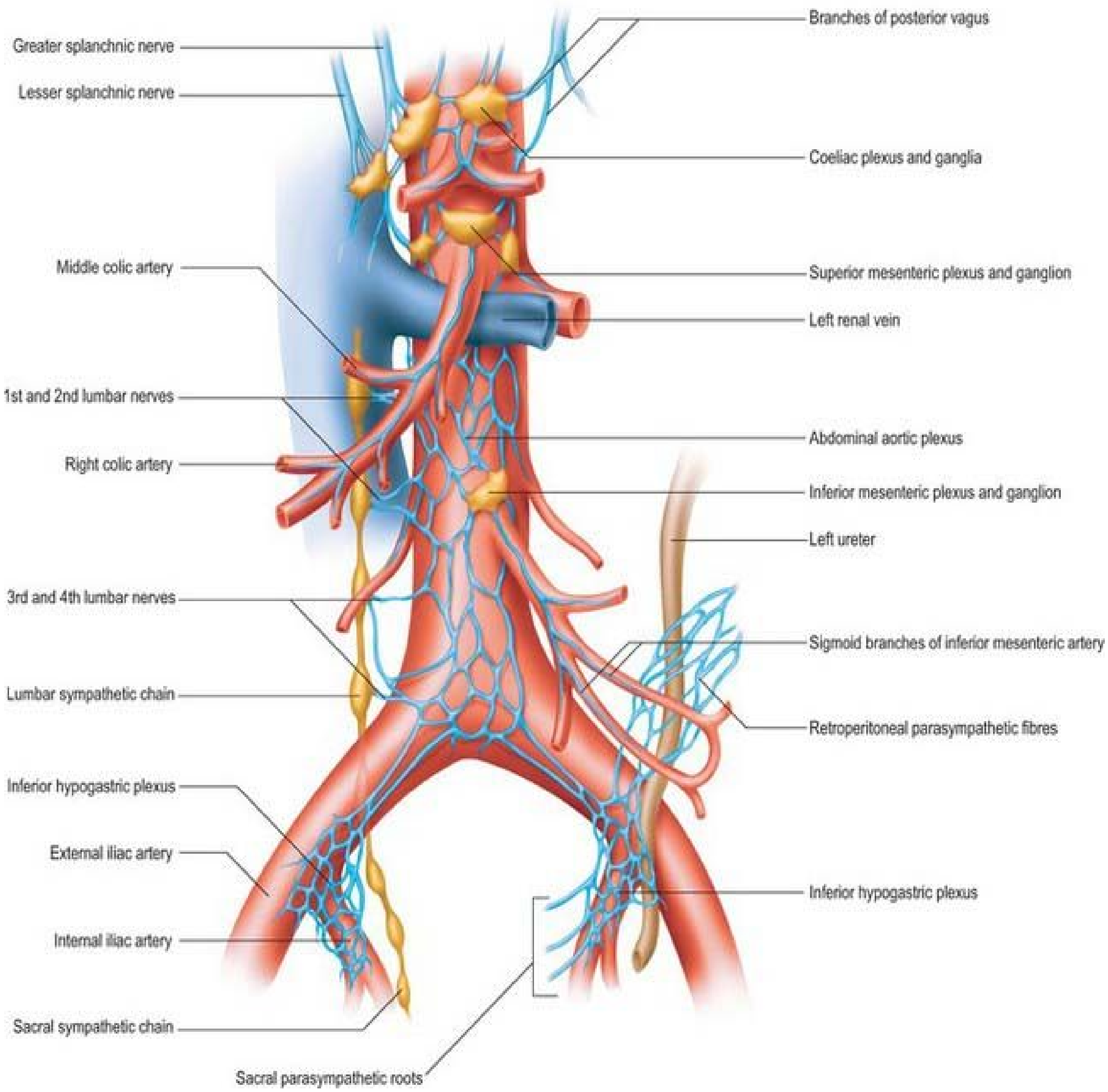
Greater splanchnic nerve
Lesser splanchnic nerve
Middle colic artery
1st and 2nd lumbar nerves
Right colic artery
3rd and 4th lumbar nerves
Lumbar sympathetic chain
Inferior hypogastric plexus
External iliac artery
Internal iliac artery
Sacral sympathetic chain
Sacral parasympathetic roots
Branches of posterior vagus
Coeliac plexus and ganglia
Superior mesenteric plexus and ganglion
Left renal vein
Abdominal aortic plexus
Inferior mesenteric plexus and ganglion
Left ureter
Sigmoid branches of inferior mesenteric artery
Retroperitoneal parasympathetic fibres
Inferior hypogastric plexus

Fig. 60.4 The autonomic plexuses of the abdominal and pelvic viscera.

Coeliac plexus

The coeliac plexus is the largest major autonomic plexus, sited at the level of the twelfth thoracic and first lumbar vertebrae. It is a dense network uniting two large coeliac ganglia and surrounds the coeliac artery and the root of the superior mesenteric artery. It is posterior to the stomach and lesser sac, anterior to the crura of the diaphragm and the beginning of the abdominal aorta, and lies between the suprarenal glands. The plexus and ganglia are joined by the greater and lesser splanchnic nerves and branches from the vagus and phrenic nerves. The plexus extends as numerous secondary plexuses along adjacent arteries. The coeliac plexus is connected to, or gives rise to, the phrenic, splenic, hepatic, superior mesenteric, suprarenal, renal and gonadal plexuses (Fig. 60.5).

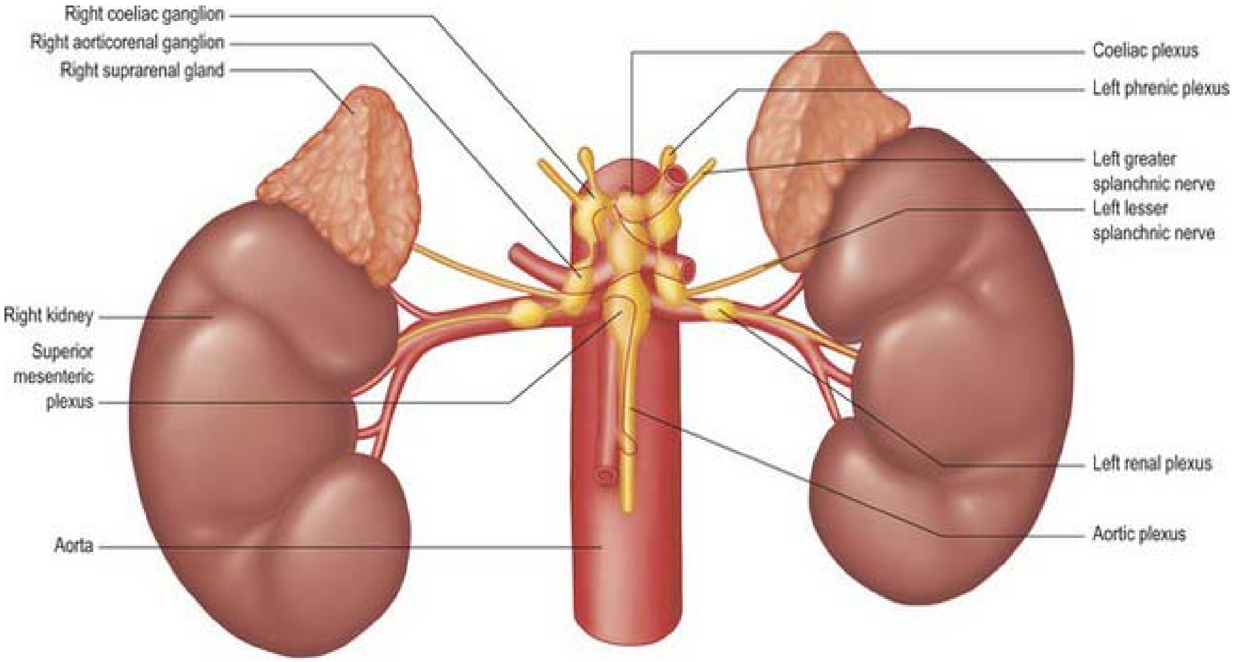
Right coeliac ganglion
Right aorticorenal ganglion
Right suprarenal gland
Right kidney
Superior mesenteric plexus
Aorta
Coeliac plexus
Left phrenic plexus
Left greater splanchnic nerve
Left lesser splanchnic nerve
Left renal plexus
Aortic plexus

Fig. 60.5 Distribution of the upper abdominal autonomic plexuses.

Coeliac and aorticorenal ganglia

The coeliac ganglia are irregular masses on each side of the coeliac trunk adjacent to the suprarenal glands and anterior to the crura of the diaphragm. The right ganglion is posterior to the inferior vena cava, the left ganglion posterior to the origin of the splenic artery. The ipsilateral greater splanchnic nerve joins the upper part of each ganglion. The lower part of each ganglion forms a distinct subdivision, usually termed the aorticorenal ganglion, which receives the ipsilateral lesser splanchnic nerve and gives origin to the majority of the renal plexus (which most commonly lies anterior to the origin of the renal artery).

Phrenic plexus

The phrenic plexus lies around the inferior phrenic arteries on the crura of the diaphragm. It arises as a superior extension of the coeliac ganglion and often receives one or two sensory branches from the phrenic nerve. The left phrenic plexus is usually larger than the right. On the left it supplies branches to the left suprarenal gland and the cardiac orifice of the stomach. The right phrenic plexus joins the phrenic nerve, forming a small phrenic ganglion which distributes branches to the inferior vena cava, suprarenal gland and hepatic plexus.

Superior mesenteric plexus and ganglion

The superior mesenteric plexus lies in the preaortic connective tissue posterior to the pancreas, around the origin of the superior mesenteric artery. It is an inferior continuation of the coeliac plexus, and includes branches from the posterior vagus nerve and the coeliac plexus. Its branches accompany the superior mesenteric artery and divide into secondary plexuses which are distributed along the branches of the artery. The superior mesenteric ganglion lies superiorly in the plexus, usually above the origin of the superior mesenteric artery.

Abdominal aortic plexus (intermesenteric plexus)

The abdominal aortic plexus lies on the sides and front of the aorta, between the origins of the superior and inferior mesenteric arteries. It consists of 4–12 intermesenteric nerves, connected by oblique branches. It is continuous above with the superior mesenteric plexus and below with the superior hypogastric plexus, and is formed by parasympathetic and sympathetic branches from the coeliac plexus. It receives rami from the first and second lumbar splanchnic nerves (which contain sympathetic fibres). The abdominal aortic plexus is connected to the gonadal, inferior mesenteric, iliac and superior hypogastric plexuses.

Inferior mesenteric plexus

The inferior mesenteric plexus lies around the origin of the inferior mesenteric artery and is distributed along its branches. It is formed predominantly from the aortic plexus and the first and second lumbar splanchnic nerves (sympathetic fibres), but it also receives connections from the superior hypogastric plexus (sympathetic and parasympathetic fibres). Disruption of the intermesenteric and inferior mesenteric plexuses rarely causes clinically significant disturbances of autonomic function.

Superior hypogastric plexus

The superior hypogastric plexus lies anterior to the aortic bifurcation, the left common iliac vein, medial sacral vessels, fifth lumbar vertebral body and sacral promontory, and between the common iliac arteries. It is occasionally termed the presacral nerve, but is seldom a single nerve and it is prelumbar rather than presacral. Most frequently found to the left side of the midline, it lies in extraperitoneal connective tissue from which the parietal peritoneum can easily be stripped. The breadth and condensation of its constituent nerves vary. The attachment of the sigmoid mesocolon and upper limit of the mesorectum containing the superior rectal vessels are anterior and to the left of the lower part of the plexus, and separated from it only by a thin sheet of loose connective tissue. The plexus is formed by branches from the aortic plexus and the third and fourth lumbar splanchnic nerves (which are mainly sympathetic). It may also contain parasympathetic fibres from the pelvic splanchnic nerves, which ascend from the two inferior hypogastric plexuses, via a series of filaments which are sometimes identified as the right and left hypogastric ‘nerves’. The latter lie in loose connective tissue just posterolateral to the start of the mesorectum and pass over the pelvic brim medial to the internal iliac vessels. The superior hypogastric plexus supplies fibres to the inferior mesenteric plexus and to the ureteric, gonadal and common iliac plexuses as well as small branches which turn abruptly forward into the upper mesorectum to supply the plexus around the superior rectal artery.

Inferior hypogastric plexus, pelvic plexus and nerves

The inferior hypogastric plexus lies in the thin extraperitoneal connective tissue on the pelvic side-wall anterolateral to the mesorectal fascia. It is directly related to the internal iliac vessels and the attachments of levator ani, coccygeus and obturator internus which lie laterally and the superior vesical and obliterated umbilical arteries superiorly. In males, the inferior hypogastric plexus lies posterolaterally on either side of the seminal vesicles, prostate and the posterior part of the urinary bladder. In females, each plexus lies lateral to the uterine cervix, vaginal fornix and the posterior part of the urinary bladder, and often extends into the broad ligaments of the uterus.

The inferior hypogastric plexus is formed mainly from the sacral splanchnic (sympathetic) and pelvic splanchnic (parasympathetic) branches; a small contribution is made from some sympathetic fibres (from the lower lumbar ganglia) which descend into the plexus via the inferior hypogastric nerves from the superior hypogastric plexus. It gives origin to a complex network of tiny pelvic branches, often referred to as the ‘pelvic plexus’, which supply the pelvic viscera either directly or via periarterial plexuses. The branches of the pelvic plexus supply the vas deferens, seminal vesicles, prostate, accessory glands and penis in males, the ovary, fallopian tubes, uterus, uterine cervix and vagina in females, and the urinary bladder and distal ureter in both sexes. The plexus also gives rise to the long branches of the parasympathetic pelvic splanchnic nerves.

Inferior hypogastric nerves

The inferior hypogastric ‘nerves’ are often double, multiple or form an extended plexus on each side. They contain mainly sympathetic and a few parasympathetic fibres. Most of these fibres are ascending from the inferior hypogastric plexus and so it is better to describe them running up out of the pelvis than down into it.

Other plexuses

Separate plexuses exist for organs within the abdomen and pelvis, for example, the hepatic, splenic and gonadal plexuses. Each tends to lie around the main arterial supply to the organ and is supplied with both sympathetic and parasympathetic fibres from one or more of the main plexuses.

Para-aortic bodies

The para-aortic bodies are condensations of chromaffin tissue which are found in close relation to the aortic autonomic plexuses and lumbar sympathetic chains. They are largest in the fetus, become relatively smaller in childhood and have largely disappeared by adulthood. They are most commonly found as a pair of bodies lying anterolateral to the aorta in the region of the intermesenteric, inferior mesenteric and superior hypogastric plexuses. They may lie as high as the coeliac plexus, as low as the inferior hypogastric plexus in the pelvis, or may be closely applied to the sympathetic ganglia of the lumbar chain. Scattered cells which persist into adulthood may, rarely, be the sites of development of a tumour of chromaffin tissue (phaeochromocytoma); these are much more commonly found arising from the cells of the suprarenal medulla. The wide variation in the site of persistent para-aortic body tissue accounts for the range of locations of such tumours.

MAJOR ABDOMINOPELVIC ARTERIAL AND VENOUS ARRANGEMENTS

The major vessels which occupy the abdomen and pelvis not only supply the viscera, retroperitoneal structures and much of the bony and soft tissue walls of the cavities, they also course through the cavities en route to supply the lower limbs. Both the arterial and systemic venous trees of the abdomen and pelvis lie predominantly posteriorly in the abdomen and postero-laterally in the pelvis; from the caval and aortic orifices in the diaphragm and the other points where smaller vessels cross the abdominothoracic interface, they follow the general parabolic shape of the lumbar spine. The pelvic divisions follow the contours of the brim and side wall of the true pelvis (Figs 60.6, 60.7). The individual parts of the aorto-iliac and iliocaval systems are described in the appropriate chapters.

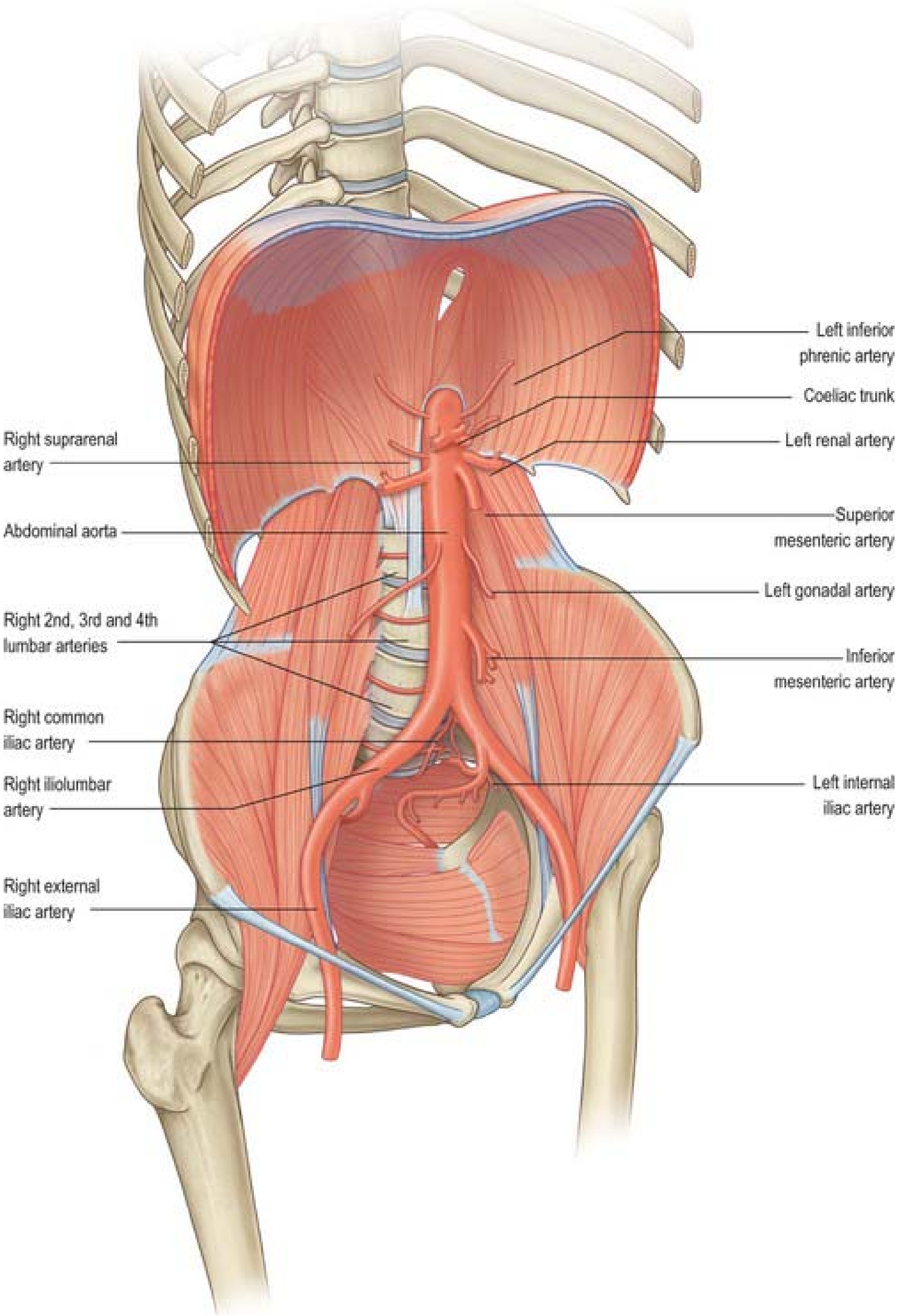
Left inferior phrenic artery
Coeliac trunk
Left renal artery
Superior mesenteric artery
Left gonadal artery
Inferior mesenteric artery
Left internal iliac artery
Right suprarenal artery
Abdominal aorta
Right 2nd, 3rd and 4th lumbar arteries
Right common iliac artery
Right iliolumbar artery
Right external iliac artery

Fig. 60.6 The overall arrangement of the aorto-iliac arterial tree of the abdomen and pelvis.

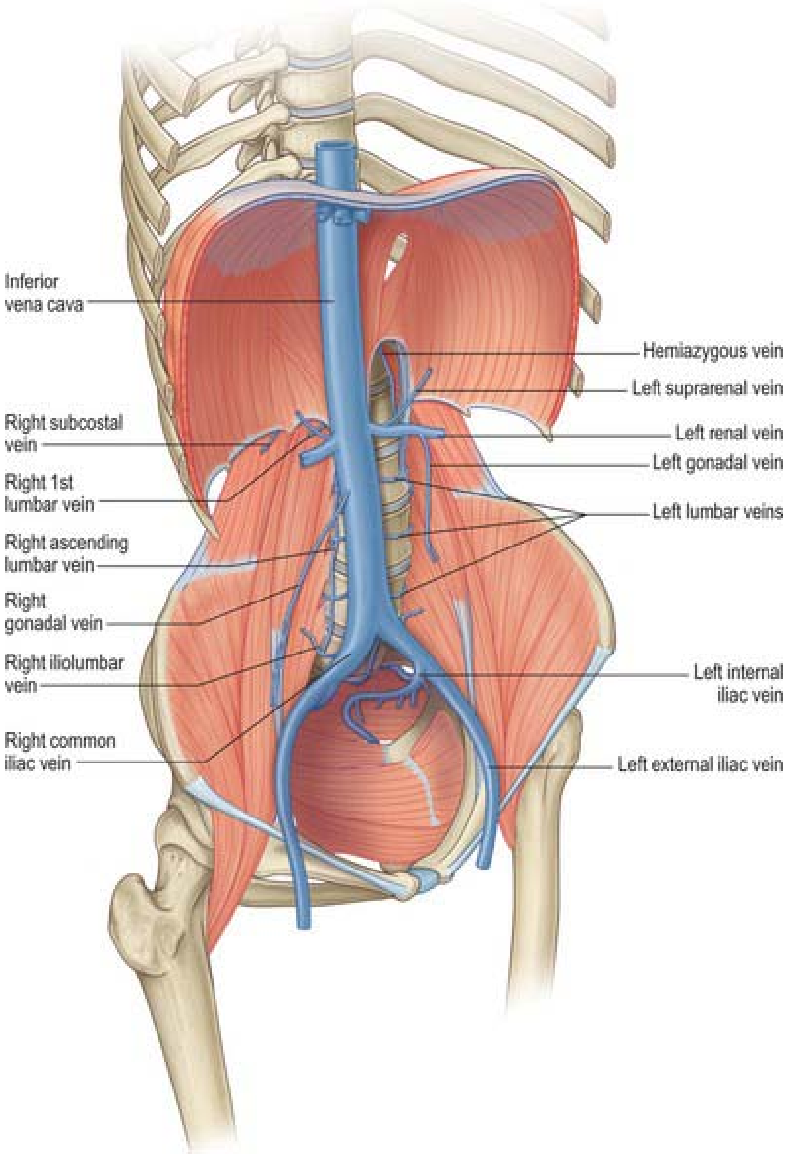
Inferior vena cava
Hemiazygous vein
Left suprarenal vein
Right subcostal vein
Left renal vein
Left gonadal vein
Right 1st lumbar vein
Left lumbar veins
Right ascending lumbar vein
Right gonadal vein
Right iliolumbar vein
Left internal iliac vein
Right common iliac vein
Left external iliac vein

Fig. 60.7 The overall arrangement of the iliocaval venous system of the abdomen and pelvis.

Arterial supply to the gastrointestinal tract

The arterial supply to the gastrointestinal tract is derived from the anterior midline visceral branches of the aorta. There are usually three anterior branches, the coeliac trunk and the superior and inferior mesenteric arteries. Variants in the origin of the arteries are very rare. The most common is a joint origin of the upper two branches as either a coeliacomesenteric trunk or a lienohepaticomesenteric trunk with a separate left gastric artery. Accessory or replaced branches to the upper abdominal viscera are more common (see Chs 65, 66, 67 and 68). Accessory anastomotic vessels between the origin of the coeliac trunk and superior mesenteric artery are rare. The inferior mesenteric artery always arises separately, however, replaced, accessory or anastomotic vessels occasionally arise from the proximal superior mesenteric artery or its branches and contribute to the arterial supply to the proximal territory of the inferior mesenteric artery.

The coeliac trunk and its branches supplies the gastrointestinal tract from the distal third of the oesophagus to the mid part of the duodenum and all derived adenexae (liver, biliary tree, spleen, dorsal pancreas, greater omentum and lesser omentum). The superior mesenteric artery supplies the tract from the mid second part of the duodenum to the distal third of the transverse colon (jejunum, ileum, caecum, appendix, ascending colon and ileal mesentery). The inferior mesenteric artery supplies the tract from the distal transverse colon to the upper anal canal. Other than accessory arteries, numerous medium calibre arteries form anastomoses between the vascular territories. The most profuse occurs around the head of the pancreas and the duodenum, where anastomoses form between the anterior and posterior superior pancreaticoduodenal arteries and the inferior pancreaticoduodenal arteries; the posterior superior pancreaticoduodenal artery and jejunal arteries; the greater pancreatic artery and jejunal arteries. The anastomoses between the territories of the superior and inferior mesenteric arteries are less pronounced and more variable: the most reliable is the pericolic marginal artery, which runs along the transverse colon. Additional anastomotic arcades may exist in the colic mesentery between the transverse and descending colon.

Portal venous system

The (hepatic) portal system, like all portal venous systems, connects two capillary beds: that of the abdominal part of the digestive tube, with the exception of the lower anal canal but including the abdominal part of the oesophagus, and all organs, except the liver, derived from it (i.e. the spleen, pancreas and gallbladder) and the hepatic sinusoidal ‘capillary’ bed. The intrahepatic portal vein ramifies like an artery, and ends in sinusoids from which vessels again converge to reach the inferior vena cava via the hepatic veins. In adults, the portal vein and its tributaries have no valves. In fetal life and for a short postnatal period, valves are demonstrable in its tributaries, but they usually atrophy; although some occasionally persist in an atrophic form into adulthood.

Portal vein

The portal vein begins at the level of the second lumbar vertebra and is formed from the convergence of the superior mesenteric and splenic veins (see Fig. 70.8). It is approximately 8 cm long and lies anterior to the inferior vena cava, posterior to the neck of the pancreas (Fig. 60.8) and obliquely to the right. It ascends behind the first part of the duodenum, the common bile duct and gastroduodenal artery. At this point it is directly anterior to the inferior vena cava. It enters the right border of the lesser omentum, ascends anterior to the epiploic foramen to reach the right end of the porta hepatis, and then divides into right and left main branches which accompany the corresponding branches of the hepatic artery into the liver. In the lesser omentum it lies posterior to both the common bile duct and hepatic artery. The portal vein is surrounded by the hepatic nerve plexus and accompanied by many lymph vessels and some lymph nodes.

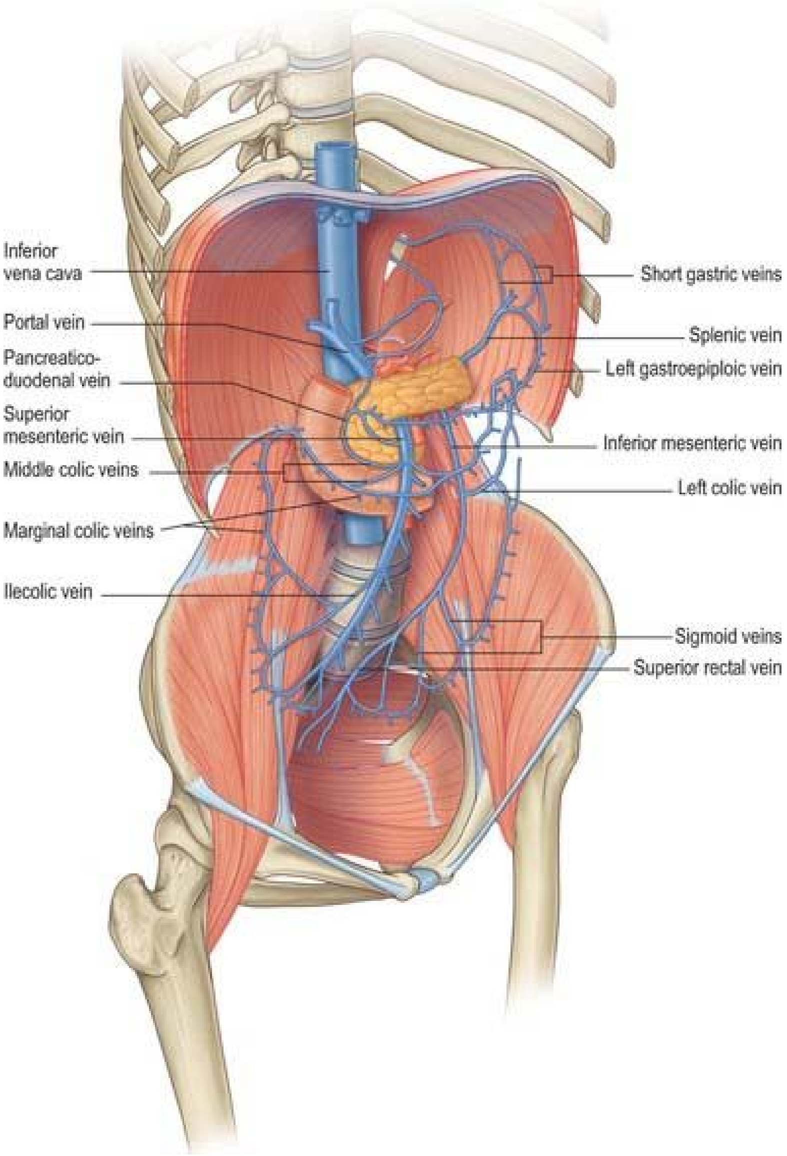
Inferior vena cava
Portal vein
Pancreatico-duodenal vein
Superior mesenteric vein
Middle colic veins
Marginal colic veins
Ilecolic vein
Short gastric veins
Splenic vein
Left gastroepiploic vein
Inferior mesenteric vein
Left colic vein
Sigmoid veins
Superior rectal vein

Fig. 60.8 The overall arrangement of the portal venous system draining the abdominal viscera.

Tributaries of the portal vein

The right branch of the portal vein usually receives the cystic vein and then enters the right lobe of the liver. The left branch receives only the obliterated umbilical vein via the ligamentum teres which connects to its vertical portion. The main extrahepatic tributaries of the main portal vein are the coronary or the left gastric vein which ends in the left margin of the portal vein, and the posterior superior pancreaticoduodenal vein nearer to the head of the pancreas.

GENERAL MICROSTRUCTURE OF THE GUT WALL

The gut wall displays a common structural plan which is modified regionally to take account of local functional differences. The general microstructure is best appreciated by reference to the development of the gut (Ch. 73). Much of the alimentary canal originates as a tube of endoderm enclosed in splanchnopleuric mesoderm. Its external surface faces the embryonic coelom, and the endodermal lining forms the epithelium of the canal and also the secretory and ductal cells of various glands which secrete into the lumen, including the pancreas and liver. The splanchnopleuric mesoderm forms the connective tissue, muscle layers, blood vessels and lymphatics of the wall, and its external surface becomes the visceral mesothelium or serosa. There is no serosa surrounding the cervical and thoracic portions of the gut, or where the hindgut traverses the pelvic floor: in these sites the gut tube is surrounded by a connective tissue adventitia. Neural elements invade the gut from neural crest tissue (Ch. 24). The smooth muscle of the muscularis externa layers of the alimentary canal is supplemented with striated muscle both cranially (from the branchial arches) and caudally. The mature gut wall has four main layers, namely mucosa, submucosa, muscularis externa and serosa (Fig. 60.9). The mucosa (mucous membrane) is the innermost layer and is subdivided into a lining epithelium, an underlying lamina propria (a layer of loose connective tissue, where many of the glands are also found) and a thin layer of smooth muscle, the muscularis mucosae. The submucosa is a strong and highly vascularized layer of connective tissue. The muscularis externa consists of inner circular and outer longitudinal layers which are present throughout the gut wall: a partial oblique layer is present only in the stomach. The external surface is bounded by a serosa or adventitia, depending on its position within the body.

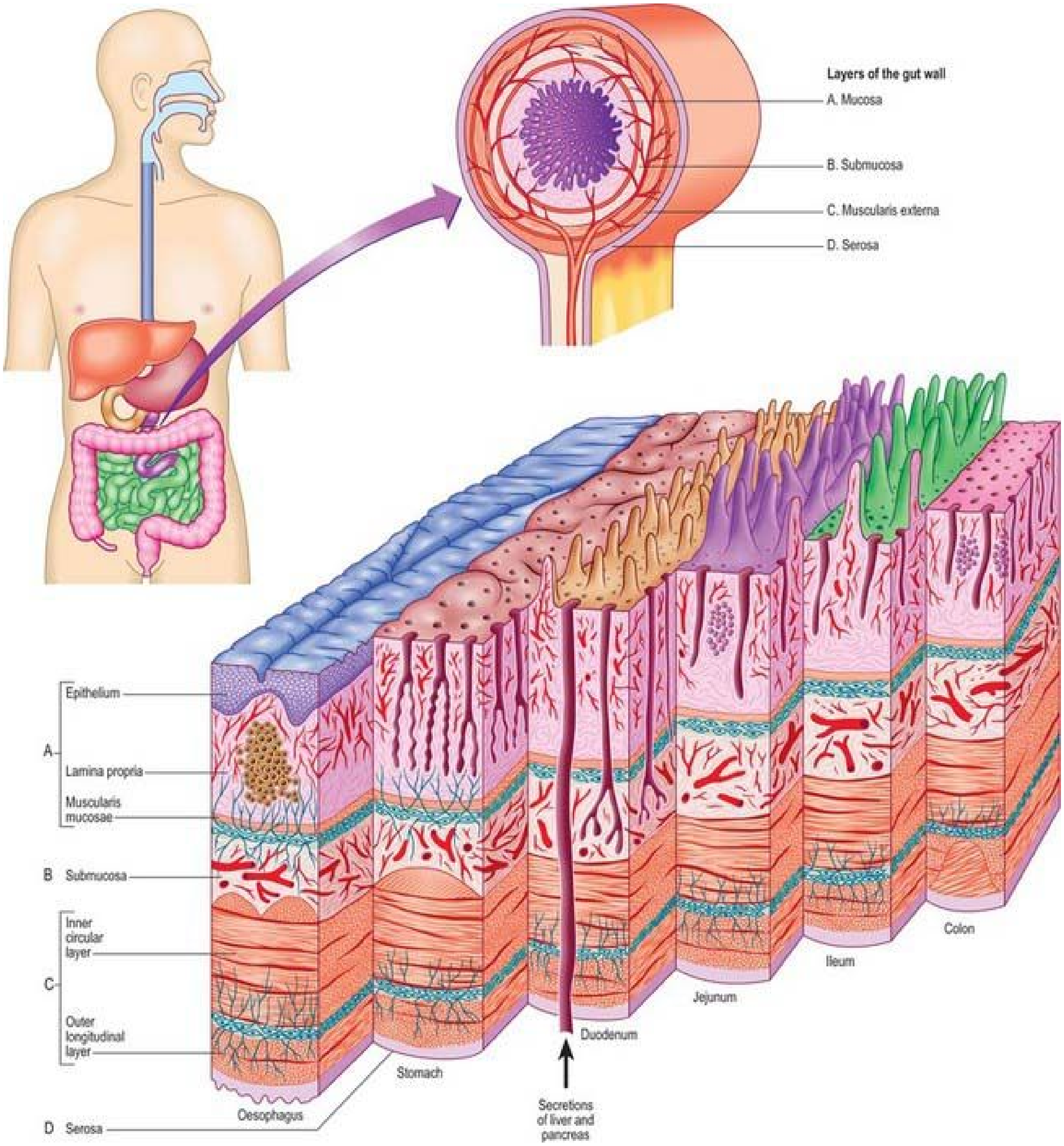
Layers of the gut wall
A. Mucosa
B. Submucosa
C. Muscularis externa
D. Serosa
Epithelium
A
Lamina propria
Muscularis mucosae
B Submucosa
Inner circular layer
C
Outer longitudinal layer
D Serosa
Oesophagus
Stomach
Secretions of liver and pancreas
Duodenum
Jejunum
Ileum
Colon

Fig. 60.9 The general arrangement of the alimentary canal to show the layers of the gut wall at the levels indicated.

Mucosa

Epithelium

The epithelium is a protective barrier and the site of secretion and absorption. Its protective function (against mechanical, thermal and chemical injury) is particularly evident in the oesophagus and in the terminal part of the rectum, where it is thick, stratified, and covered in mucus, which serves as a protective lubricant. Other than in these sites, the epithelium lining the gut wall is single-layered, and either cuboidal (in glands) or columnar. It contains cells modified for absorption as well as various types of secretory cell.

The barrier function and selectivity of absorption depend on tight junctions over the entire epithelium. The surface area of the lumen available for secretion or absorption is increased by the presence of mucosal folds, pits, crypts, villi and glands (Fig. 60.9). Microvilli on the surfaces of individual absorptive cells amplify the area of apical plasma membrane in contact with the contents of the gut. Some glands lie in the lamina propria, some in the submucosa, and others (the liver and pancreas) are totally external to the wall of the gut. All of these glands drain into the lumen of the gut through individual ducts. The epithelium also contains scattered neuroendocrine (enteroendocrine) cells.

Lamina propria

The lamina propria consists of compact connective tissue, often rich in elastin fibres, which supports the surface epithelium and provides nutrient vessels and lymphatics. Lymphoid follicles are present in many regions of the gut, most notably in Peyer’s patches. Cells within the lamina propria are the source of growth factors which regulate cell turnover, differentiation and repair in the overlying epithelium.

Muscularis mucosae

The muscularis mucosae is well developed in the oesophagus and in the large intestine, especially in the terminal part of the rectum. In addition, single muscle cells originating from the muscularis mucosae are found inside the villi or between the tubular glands of the stomach and large intestine. By its contraction, the muscularis mucosae can alter the surface configuration of the mucosa locally, allowing it to adapt to the shapes and mechanical forces imposed by the contents of the lumen, and in the intestinal villi, promoting vascular exchange and lymphatic drainage.

Submucosa

The submucosa contains large bundles of collagen and is the strongest layer of the gut wall. However, it is also pliable and deformable and can therefore adjust to changes in the length and diameter of the gut. It contains the largest arterial network of the wall, which supplies both the mucosa and the muscle coat. The submucosa invades the folds which project into the lumen of the oesophagus and rectum, the rugae of the gastric wall, and the plicae circulares of the small intestine, but does not enter the villi.

Muscularis externa

The muscularis externa usually consists of distinct inner circular and outer longitudinal layers whose antagonistic activities create waves of peristalsis responsible for the movement of ingested material through the lumen of the gut. In the stomach, where movements are more complex, there is a partial oblique layer, internal to the other two layers. The layer of circular muscle is invariably thicker than the longitudinal muscle, except in the colon, where the longitudinal muscle is gathered into three cords (taenia coli).

The muscularis externa is composed almost exclusively of smooth muscle, except in the upper oesophagus, where smooth muscle blends with striated muscle. Although the oesophageal musculature resembles that of the pharynx, it is entirely under involuntary control. For most of its length, the smooth muscle of the gut wall consists of ill-defined bundles of cells, typically visceral in type, and somewhat larger than vascular smooth muscle cells. They are approximately 500 µm long, regardless of body size, and are electrically and mechanically coupled. Their fasciculi lack a perimysium, but have sharp boundaries.

The arrangement of the musculature means that a segment of gut can change extensively in diameter (to virtual occlusion of the lumen) and also in length, although elongation is limited by the presence of mesenteries. The co-ordinated activity of the two muscle layers produces a characteristic motor behaviour which is mainly propulsive and directed anally (peristalsis), combined with a non-propulsive motor activity which either mixes the luminal contents, as occurs in the stomach, or partitions them, as occurs at the pyloric sphincter. The muscle maintains constant volume, so that shortening of a segment of the gut wall is accompanied by an increase in muscle layer circumference.

Intestinal smooth muscle exhibits variable and changing degrees of contraction on which rhythmic (or phasic) contractions are superimposed. Slow waves of rhythmic electrical activity, driven by changes in membrane potential in pacemaker cells (interstitial cells), spread throughout the thickness of the circular and longitudinal smooth muscle coats. After spreading circumferentially, slow waves can move in either oral or anal directions, causing segmental contraction. The distances of propagation and the patterns of this spontaneous activity vary between areas of the intestine. Neural regulation of slow and phasic contractions involves excitatory and inhibitory transmitters which are released from the myenteric plexus. This motor control is closely co-ordinated with mucosal absorption and secretion and is mediated via intrinsic nerves in the submucous plexus. The peristaltic reflex occurs during passage of luminal contents down the intestine. It involves ascending contraction and descending relaxation: the sensory limb is mediated by sensory neurones that respond to either mucosal stimulation (intrinsic primary afferents) or muscle stretch (extrinsic afferents).

Interstitial cells

Interstitial cells (of Cajal) are thought to act as pacemakers for the myogenic contraction of muscularis externa, establishing the rhythm of bowel contractions through their influence on electrical slow wave activity. They receive modulatory inputs from the enteric nervous system and from the extrinsic innervation of the gut.

Interstitial cells are thin, flat, and branched. They resemble smooth muscle cells because they contain actin and myosin filaments, and are linked by gap junctions to typical smooth muscle cells. However, they are phenotypically distinct from muscle cells because their intermediate filaments are vimentin rather than desmin, (which is typical of muscle cells). They lie in close apposition to varicose nerve endings of at least two types; one contains small, round clear vesicles (50 nm diameter), the other contains flat, discoidal vesicles (70 nm diameter).

The positions of the interstitial cell layers vary regionally. In general, they lie in the same layers as the enteric plexuses. They are scattered among the cells of the circular muscle layer in the oesophagus and stomach, lie between the inner and outer layers of circular smooth muscle in the small intestine, and colocalize with the myenteric plexus and the single layer of the submucosal plexus on the luminal side of the circular component of the muscularis externa, in the large intestine.

Serosa and adventitia

A layer of connective tissue, of variable thickness, lies external to the muscularis externa. In many places it contains adipose tissue. Where the gut is covered by visceral peritoneum, the external layer is a serosa, which consists of a thin connective tissue layer and an external coat of mesothelium. Elsewhere the connective tissue blends with that of the surrounding fasciae and is referred to as an adventitia. Where the alimentary tract is retroperitoneal, the surface facing the abdominal cavity is covered by serosa, and the other parts are covered by adventitia.

Vascular plexuses

Vascular plexuses are present at various levels of the wall, especially in the submucosa and mucosa: they connect with plexuses of vessels which supply the surrounding tissues or those entering through the mesentery, and accompany the ducts of outlying glands.

Innervation

The gut is densely innervated by the autonomic and enteric nervous systems, and is under extrinsic and intrinsic neuronal control. Neuronal cell bodies of the enteric nervous system lie between the circular and longitudinal components of the muscularis externa (myenteric plexus) and within the submucosa (submucosal plexus). They provide the intrinsic sensory and motor supply of the gut wall and connect with extrinsic sensory, motor and sensorimotor nerves of cranial or spinal origin.

Extrinsic innervation

The extrinsic innervation is derived from neurones outside the gut, and contains functional components from the sympathetic, parasympathetic and visceral sensory divisions of the peripheral nervous system (see p. 1041). Visceral sensory endings respond to excessive muscular contraction or distension: their cell bodies are situated in the nodose ganglion of the vagus nerve and in thoracic and lumbar spinal or dorsal root ganglia. The cell bodies of parasympathetic efferent axons lie in the vagal dorsal motor nucleus in the medulla oblongata. Sympathetic efferent fibres arise from the thoracic and lumbar spinal cord and relay in prevertebral sympathetic ganglia (coeliac, mesenteric and pelvic).

A subserosal plexus, which sometimes contains neuronal cell bodies, connects the extrinsic nerve fibres with the myenteric plexus and is particularly prominent near the mesentery. Fibres from this plexus run through the longitudinal muscle layer to reach the myenteric plexus.

Intrinsic innervation

The intrinsic innervation of the gut wall is derived from neurones which are located entirely within the wall in intramural ganglionated plexuses. The myenteric (Auerbach’s) plexus is a network of fine bundles of axons and small ganglia which lies within the muscularis externa, between the circular and longitudinal layers. It is often associated with secondary and tertiary plexuses of nerve fibres which sometimes contain isolated neuronal cell bodies. There are two or more submucosal plexuses, the most superficial of which is Meissner’s plexus.

Non-ganglionated nerve plexuses lie at various levels in the wall, notably in the lamina propria (mucosal plexus); at the interface between the submucosa and muscularis externa; between the circular and longitudinal muscles (the non-ganglionated part of the myenteric plexus); and within the serosa. An additional non-ganglionated plexus lies between the internal and external components of the circular muscle of the small intestine. All parts of the myenteric plexus are continuous not only with each other, but also with the nerve fibre bundles in the circular muscle. The latter are connected to the ganglionated and non-ganglionated plexuses of the submucosa, and these in turn are connected with the mucosal plexus by fibres which pass through the muscularis mucosa.

SURFACE AND DIAGNOSTIC ANATOMY OF THE ABDOMEN AND PELVIS

ABDOMINAL PLANES AND REGIONS

For descriptive purposes, the abdomen can be divided by a number of imaginary horizontal and vertical lines drawn using the skeletal landmarks of the thorax and abdomen (Fig.). Projection of these lines into the sagittal or transverse planes can then be used to define certain abdominal ‘planes’. Apart from dividing the abdomen into different regions for descriptive purposes, these planes are also of value in defining approximate vertebral levels and the positions of some relatively fixed intra-abdominal structures.

Vertical planes

In addition to the midline, which passes through the xiphisternal process and the pubic symphysis, there are two paramedian planes which are projected from the midclavicular line (also sometimes called the lateral or the mammary line). This line passes through the midpoint of the clavicle, crosses the costal margin just lateral to the tip of the ninth costal cartilage, and passes through a point mid way between the anterior superior iliac spine and the symphysis pubis. It approximates to, but does not exactly correspond to, the lateral border of rectus abdominis.

Horizontal planes

Several horizontal planes have been defined, but only the subcostal and transtubercular planes are in common clinical use.

The xiphisternal plane runs horizontally through the xiphoid processes at the level of the ninth thoracic vertebra. It demarcates the level of the cardiac plateau on the central part of the upper border of the liver.

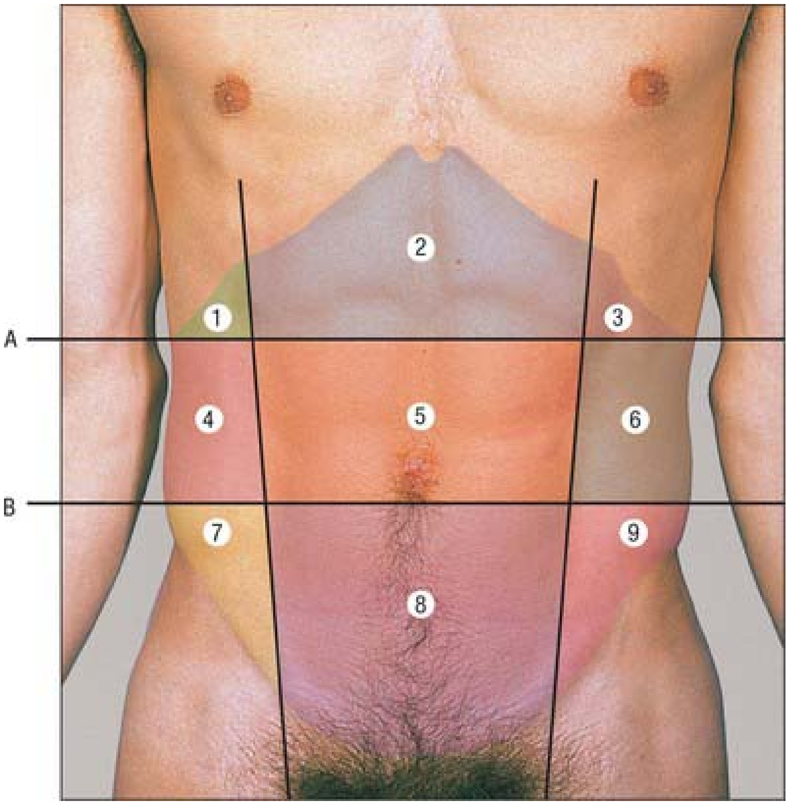

Fig. 60.10 Planes and regions of the abdomen. Key for planes: **A**, Subcostal plane. **B**, Transtubercular plane. Key for nine regions of the abdomen: **1**. Right hypochondrium. **2**. Epigastric. **3**. Left hypochondrium. **4**. Right lumbar. **5**. Central/umbilical. **6**. Left lumbar. **7**. Right iliac fossa. **8**. Suprapubic/hypogastrium. **9**. Left iliac fossa.

(Photograph by permission from Lumley JSP 2002 Surface Anatomy, 3rd edn. Edinburgh: Churchill Livingstone.)

The transpyloric plane lies midway between the suprasternal notch of the manubrium and the upper border of the pubic symphysis. It usually lies at the level of the body of the first lumbar vertebra near its lower border and meets the costal margins at the tips of the ninth costal cartilages, where a distinct ‘step’ may be felt at the costal margin. The linea semilunaris crosses the costal margin on the transpyloric plane. The hilum of both kidneys, the origin of the superior mesenteric artery, the termination of the spinal cord, the neck, adjacent body and head of the pancreas, and the confluence of the superior mesenteric and splenic veins as they form the hepatic portal vein may all lie in this plane. The pylorus may be found in the transpyloric plane, but is not a constant feature.

The subcostal plane is a line joining the lowest point of the costal margins, formed by the tenth costal cartilage on each side. It usually lies at the level of the body of the third lumbar vertebra, the origin of the inferior mesenteric artery from the aorta, and the third part of the duodenum, although this varies with posture.

The supracristal plane joins the highest point of the iliac crest on each side. It usually lies at the level of the body of the fourth lumbar vertebra, and marks the level of bifurcation of the abdominal aorta. On the posterior abdominal surface, it is a common level for the identification of the fourth lumbar vertebra, and is used to perform lumbar puncture at the L4–5 or L5–S1 intervertebral level, which is safely below the termination of the spinal cord.

The transtubercular plane joins the tubercles of the iliac crests and usually lies at the level of the body of the fifth lumbar vertebra near its upper border. It indicates, or is just above, the confluence of the common iliac veins and marks the origin of the inferior vena cava.

The interspinous plane joins the centres of the anterior superior spines of the iliac crests. It passes through either the lumbosacral disc, or the sacral promontory, or just below them, depending on the degree of lumbar lordosis, sacral inclination and curvature.

The plane of the pubic crest lies at the level of the inferior end of the sacrum or part of the coccyx, depending on the degree of lumbar lordosis, sacral inclination and curvature.

Abdominal regions

The abdomen can be divided into nine arbitrary regions by the subcostal and transtubercular planes and the two midclavicular planes projected onto the surface of the body. These regions are used in practice for descriptive localization of the position of a mass or the localization of a patient’s pain, and may also be used in the description of the location of the abdominal viscera. The nine regions thus formed are: epigastrium; right and left hypochondrium; central or umbilical; right and left lumbar; hypogastrium or suprapubic; right and left iliac fossa.

ANTERIOR ABDOMINAL WALL

Skeletal landmarks

The superior boundary of the anterior abdominal wall is formed by several clear landmarks (Fig. 60.11). In the midline superiorly lies the xiphoid process. From this point, the costal margins extend to either side from the seventh costal cartilage at the xiphisternal joint to the tip of the twelfth rib (the latter is often difficult to feel in the obese or if it is short). The lowest part of the costal margin lies in the midaxillary line and is formed by the inferior margin of the tenth costal cartilage. The tip of the lower border of the ninth costal cartilage can usually be defined as a distinct 'step' along the costal margin.

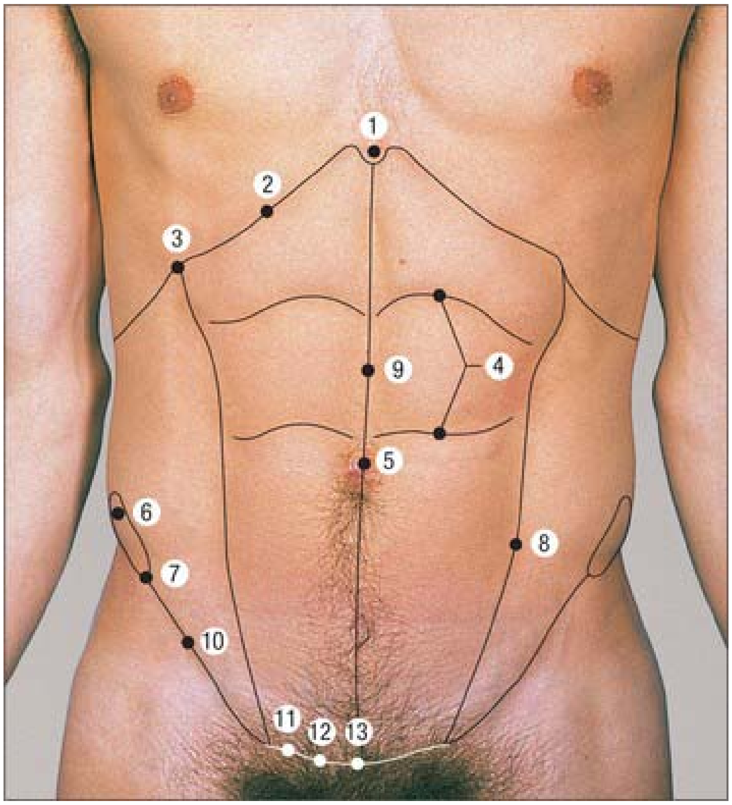

Fig. 60.11 Anterior abdominal wall landmarks. **1**. Xiphoid process. **2**. Costal margin. **3**. Tip of the ninth costal cartilage. **4**. Tendinous intersections. **5**. Umbilicus. **6**. Iliac crest. **7**. Anterior superior iliac spine. **8**.

Linea semilunaris. **9**. Linea alba. **10**. Inguinal ligament. **11**. Pubic tubercule. **12**. Pubic crest. **13**. Pubic symphysis.

(Photograph by permission from Lumley JSP 2002 Surface Anatomy, 3rd edn. Edinburgh: Churchill Livingstone.)

The inferior boundary of the anterior abdominal wall is formed, in order, by the iliac crest, which descends from the tubercle of the iliac crest to the anterior superior iliac spine; the inguinal ligament, which runs downwards and forwards to the pubic tubercle; and the pubic crest, which runs from the pubic tubercle laterally to the pubic symphysis in the midline. The pubic tubercle can be identified by direct palpation in thin individuals and can be detected, even in the obese, by palpation of the tendon of adductor longus, which runs up to its attachment on the pubis directly below the pubic tubercle. The tendon is best felt in tension with the hip flexed, abducted and externally rotated.

The posterolateral boundary is defined by the midaxillary line.

Soft tissue landmarks

Umbilicus

The umbilicus is an obvious but very inconstant landmark. In the supine adult, it usually lies at the level of the disc between the third and fourth lumbar vertebrae. The bifurcation of the abdominal aorta then lies about 2 cm caudal to the umbilicus. In the erect position, in children and in the obese, or in individuals with a pendulous abdomen, the umbilicus may lie at a lower level.

Rectus abdominis

In a thin and muscular individual, the tendinous intersections of rectus abdominis may be visible when the muscle is tensed by lifting the head against resistance or by sitting up: the intersections are usually situated at the level of the umbilicus, the level of the xiphoid process and mid way between these two points.

Linea alba

The linea alba is usually only visible in thin muscular individuals. It is wide and obvious above the umbilicus, but is almost linear and invisible below this level.

Linea semilunaris

The linea semilunaris lies along the lateral margin of the rectus sheath and is visible as a shallow curved groove in muscular individuals when the abdominal muscles are tensed, e.g. by sitting up from the lying position.

Inguinal region

The two commonly described surface markings in the inguinal region are the mid-inguinal point and the midpoint of the inguinal ligament.

Mid-inguinal point

The mid-inguinal point lies at the midpoint of the line between the symphysis pubis and the anterior superior iliac spine. It is superior to the point of palpation of the pulse of the femoral artery as it emerges from beneath the inguinal ligament. The approximate surface marking of the deep inguinal ring lies immediately above the mid-inguinal point, and is a useful landmark for palpation of the origin of an indirect inguinal herniae sac.

Midpoint of the inguinal ligament

The midpoint of the inguinal ligament lies halfway between the pubic tubercle and the anterior superior iliac spine, and is directly lateral to the origin of the inferior epigastric vessels as they lie on the posterior wall of the inguinal canal.

INTRA-ABDOMINAL VISCERA

The surface markings of the intra-abdominal viscera are variable and depend on age, body habitus, nutritional state, phase of ventilation and body position. The use of radiological imaging of the abdominal viscera means that the location of viscera by surface markings is almost obsolete in modern clinical practice. The following descriptions are at best regarded as the most common or approximate markings in a healthy supine individual (Fig. 60.12).

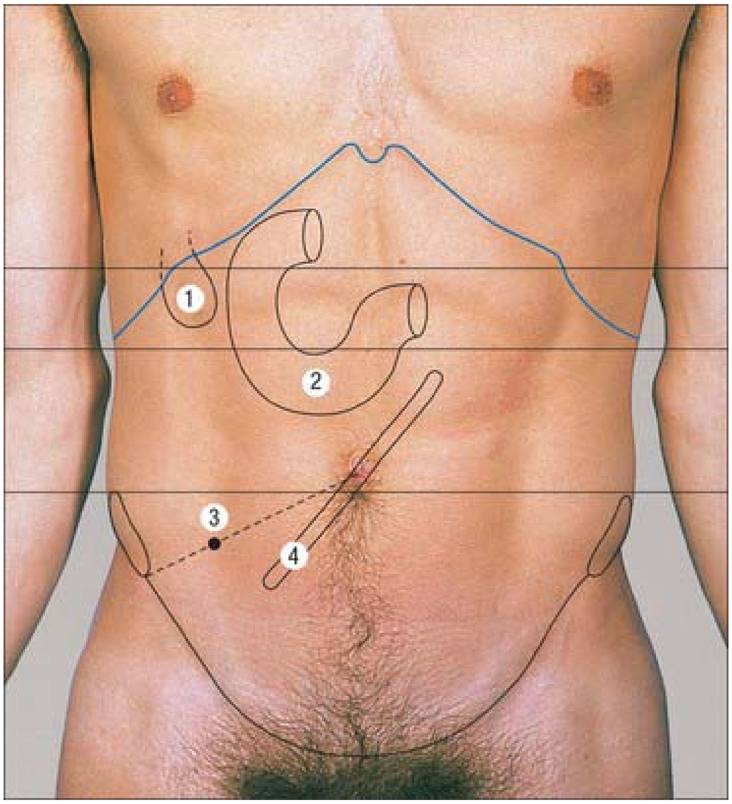

Fig. 60.12 Intra-abdominal visceral landmarks. **1**. Gallbladder. **2**. Duodenum. **3**. Appendix. **4**. Root of small bowel mesentery.

(Photograph by permission from Lumley JSP 2002 Surface Anatomy, 3rd edn. Edinburgh: Churchill Livingstone.)

Stomach

The stomach lies in a curve within the left hypochondrium and epigastrium although, when distended and pendulous, it may lie as far down as the central or hypogastric regions. The epigastrium is the usual place to auscultate for a ‘succussion splash’ caused by chronic gastric stasis in upper intestinal obstruction.

Duodenum

The first part of the duodenum sometimes lies just above the trans-pyloric plane, depending on its mobility and length. The second part usually lies in the transpyloric plane just to the right of the midline, and the third part usually lies in the subcostal plane across the midline. The fourth part often lies in the transpyloric plane to the left of the midline, although its position varies according to the length of its mesentery.

Small bowel and its mesentery

The small bowel is usually referred to as lying in the central umbilical region, but often occupies part of both iliac fossae, both lumbar regions and the hypogastrium. The small bowel mesentery runs obliquely in a line from a point 2 cm to the left of the body of the second lumbar vertebra above the subcostal plane, to a point just anterior to the right sacroiliac joint just below the interspinous plane.

Appendix

The appendix is highly variable both in its length and in its position. Its base is commonly referred to as lying beneath a point marked two-thirds of the way along a line joining the umbilicus to the anterior superior iliac spine.

Liver

The inferior border of the liver extends along a line that passes from the right 10th costal cartilage to the left fifth rib in the midclavicular line. The upper border of the liver follows a line that passes from the fifth rib in the midclavicular line on the right to the equivalent point on the left. This upper border curves slightly downwards at its centre and crosses the midline behind the xiphoid. The right border of the liver is curved to the right and joins the upper and lower right limits. The outline of the liver may be defined by the dull note it gives on percussion when compared with the resonance of the lungs above and the hollow abdominal viscera below.

The lower edge of a normal liver cannot usually be palpated, even in women and children, in whom the liver is at a slightly lower level. What is often mistaken for the liver in abdominal palpation is the bulge of rectus abdominis above its upper tendinous intersection.

Gallbladder

The fundus of the gallbladder is very variable in location. It is commonly identified with the tip of the ninth costal cartilage (in the transpyloric plane), near the junction of the linea semilunaris with the costal margin.

Spleen

The spleen lies beneath the ninth, 10th and 11th ribs on the left side. Its surface markings can be delineated on the lower posterior thoracic wall by defining its axis, which extends from a point 5 cm to the left of the midline at the level of the 10th thoracic spine, and passes laterally along the line of the tenth rib to the midaxillary line.

RETROPERITONEAL VISCERA

The surface projections of the retroperitoneal viscera are fairly reliable but have little clinical use since most interventions and procedures are guided by radiological imaging.

Pancreas

The surface projection of the head of the pancreas lies within the duodenal curve. The neck lies in the transpyloric plane, behind the pylorus in the midline. The body passes obliquely up and to the left for approximately 10 cm, its left part lying a little above the transpyloric plane. The tail lies a little above and to the left of the intersection of the transpyloric and left lateral planes.

Kidney

The anterior and posterior surface projections of the kidneys are related to anterior and posterior abdominal wall landmarks. In the description that follows, all measurements are approximate. The right kidney lies 1.25 cm lower than the left. On the anterior surface, the centre of the hilum lies in the transpyloric plane 5 cm from the midline and slightly medial to the tip of the ninth costal cartilage. From the hilum, the outline of the anterior surface can be drawn 11 cm long and 4.5 cm broad, the upper pole being 2.5 cm, and the lower 7.5 cm, from the midline: since the transverse axis is oblique, the width thus shown is 1.5 cm less than the actual width of the kidney. On the posterior surface, the centre of the hilum lies opposite the lower border of the spinous process of the first lumbar vertebra and 5 cm from the midline. The outline of the posterior surface can be traced similarly to the anterior surface. The lower pole is 2.5 cm above the summit of the iliac crest. The kidneys are 2.5 cm lower in the standing than in the supine individual; they ascend and descend a little with respiration, which is of particular importance in endoscopic renal surgery. The lower pole of the normal right kidney may occasionally be felt in the thin individual, especially the female, by bimanual palpation on full inspiration.

Ureter

The ureter starts on either side approximately at the transpyloric plane (the left higher than the right), approximately 5 cm from the midline. Each passes downwards and somewhat medially to enter the bladder at a point marked superficially by the position of the pubic tubercle.

Abdominal aorta

The abdominal aorta starts just to the left of the midline, at the level of the body of the 12th thoracic vertebra. It continues downwards for 10 cm as a band 2 cm wide, and bifurcates at the level of the fourth lumbar vertebra (which is marked by the transtubercular plane), 1.5 cm below and to the left of the umbilicus. The pulsations of the aorta can be felt in a thin individual in the supine position by pressing firmly in the midline backwards onto the vertebral column. An easily palpable aorta in an obese person should raise the suspicion of an aneurysm, to be checked by radiological imaging.

Visceral arteries

The coeliac trunk arises from the aorta immediately after it enters the abdomen at the level of the 12th thoracic vertebra. The origin of the superior mesenteric artery usually lies above the transpyloric plane, and that of the inferior mesenteric artery lies at the level of the body of the third lumbar vertebra, in the subcostal plane.

Renal arteries

The renal arteries can be projected as broad lines running laterally for 4 cm from the aorta just inferior to the transpyloric plane; the left inclines across the plane.

Iliac arteries

The surface projection of the common iliac artery corresponds to the superior one-third of a broad line, which is laterally slightly convex, from the aortic bifurcation to a point mid-way between the anterior superior iliac spine and the pubic symphysis. The external iliac artery corresponds to the inferior two-thirds of this line.

Superior gluteal artery

The surface marking of the exit of the superior gluteal artery from the pelvis corresponds to the junction of the upper and middle thirds of a line joining the posterior superior iliac spine to the apex of the greater trochanter.

Inferior gluteal artery

The surface marking of the exit of the inferior gluteal artery from the pelvis lies near the midpoint of a line joining the posterior superior iliac spine and the ischial tuberosity.

Inferior vena cava

The inferior vena cava starts at the level of the body of the fifth lumbar vertebra, usually in the transtubercular plane (2.5 cm below the supracristal plane). From this level it can be represented by a band, running vertically and 2.5 cm to the right of the midline. The inferior vena cava leaves the abdomen by traversing the diaphragm at the level of the eighth thoracic vertebra, directly behind the sternal extremity of the right sixth costal cartilage.

CLINICAL PROCEDURES

Pneumoperitoneum for laparoscopy

The establishment of a pneumoperitoneum is frequently performed by accessing the peritoneal cavity at the level of the umbilicus. Most commonly done just below the umbilicus, the incision through the linea alba allows access to the peritoneum at a point where there is relatively little extraperitoneal fat present and where the linea alba is relatively wide.

Surgical incisions

Most surgical incisions are performed according to surgical imperatives rather than anatomical constraints. The paramedian incision has been used to decrease the risk of incisional hernia. The skin and anterior fascial incision is made over the belly of rectus abdominis, at the level required. The muscle is displaced laterally, in order not to interfere with its neurovascular supply (which enters laterally), and the posterior rectus sheath is then incised in the paramedian plane. This approach allows rectus abdominis to lie between the two fascial incisions once the wound is closed.

Intestinal stomas (ileostomy, colostomy, caecostomy)

Where possible, intestinal stomas are usually formed through trans-rectus incisions. A cruciate incision is made in the anterior rectus sheath and the muscle fibres parted until the posterior sheath is reached. The latter is then incised without injury to the epigastric vessels (inferior or superior, depending on the level). This incision offers the advantage that fibres of rectus abdominis act to support the stoma: they provide a dynamic, contractile surround that tends to reduce the risk of herniation occurring around the stoma.

Suprapubic catheterization

The urinary bladder is commonly accessed for short- or long-term catheterization through the anterior abdominal wall. As the bladder fills, the upper part of its dome comes to lie in the preperitoneal space in the suprapubic region, and it can be relatively easily accessed via transcutaneous puncture in the midline (because there are no major neurovascular structures at this level and the linea alba is relatively thin).

REFERENCES

ck J. The Autonomic Nervous System. Philadelphia: Lippincott, 1970.

CHAPTER 61

Anterior abdominal wall

The anterior abdominal wall extends from the costal margins and xiphoid process superiorly to the iliac crests, pubis and pubic symphysis inferiorly. It overlaps and is connected to both the posterior abdominal wall and paravertebral tissues. It forms a continuous but flexible sheet of tissue across the anterior and lateral aspects of the abdomen. The anterior abdominal wall is composed of the integument, muscles and connective tissue lining the peritoneal cavity (Figs 61.1-61.5). It has an important role in maintaining the form of the abdomen and is involved in many physiological activities. Anterior abdominal wall tissues form the inguinal canal that connects the abdominal cavity to the scrotum in men or labia majora in women, and also form the umbilicus; both of these sites are of considerable clinical importance.

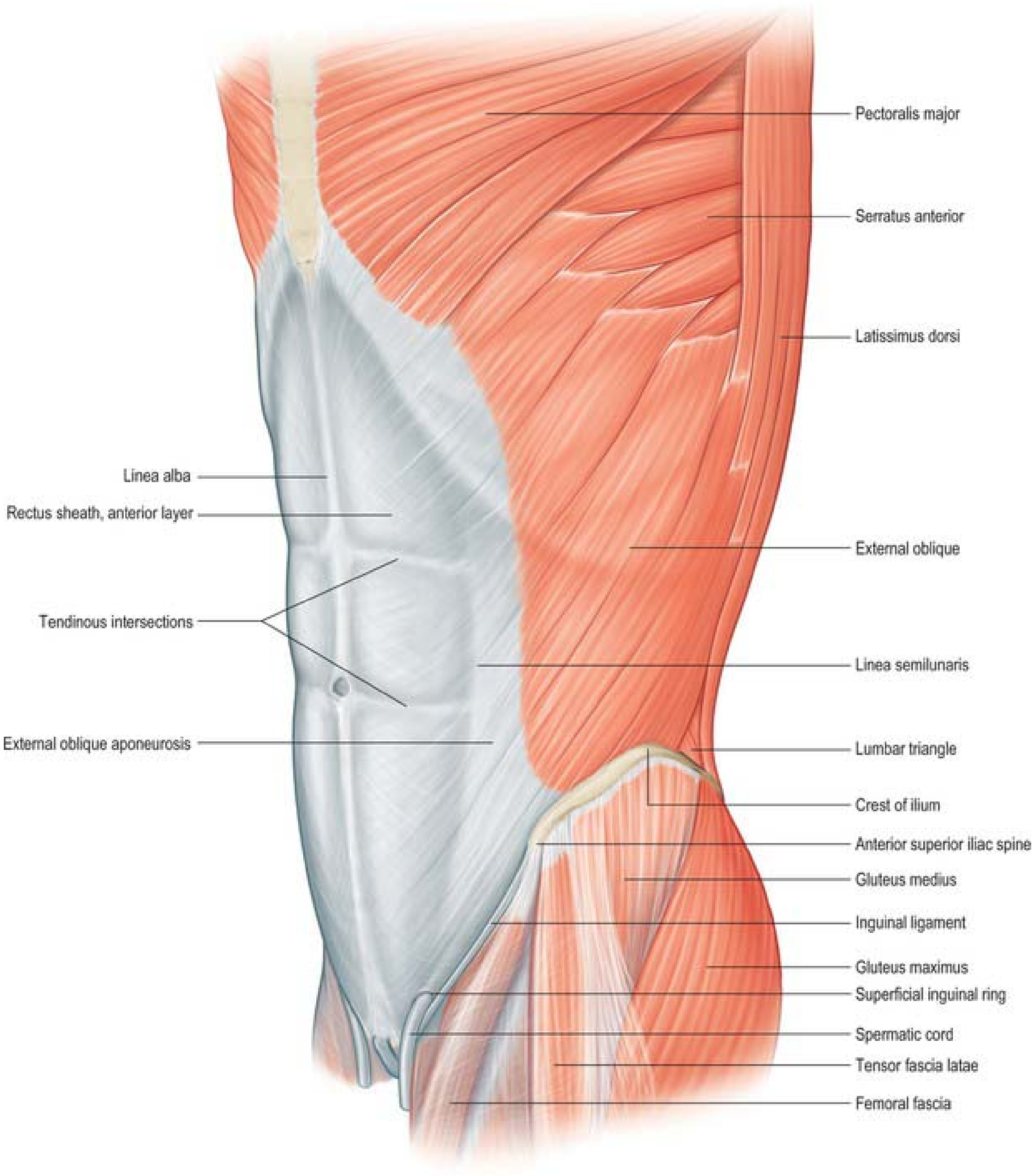
Pectoralis major
Serratus anterior
Latissimus dorsi
Linea alba
Rectus sheath, anterior layer
External oblique
Tendinous intersections
Linea semilunaris
External oblique aponeurosis
Lumbar triangle
Crest of ilium
Anterior superior iliac spine
Gluteus medius
Inguinal ligament
Gluteus maximus
Superficial inguinal ring
Spermatic cord
Tensor fascia latae
Femoral fascia

Fig. 61.1 The left anterolateral abdominal wall muscles.

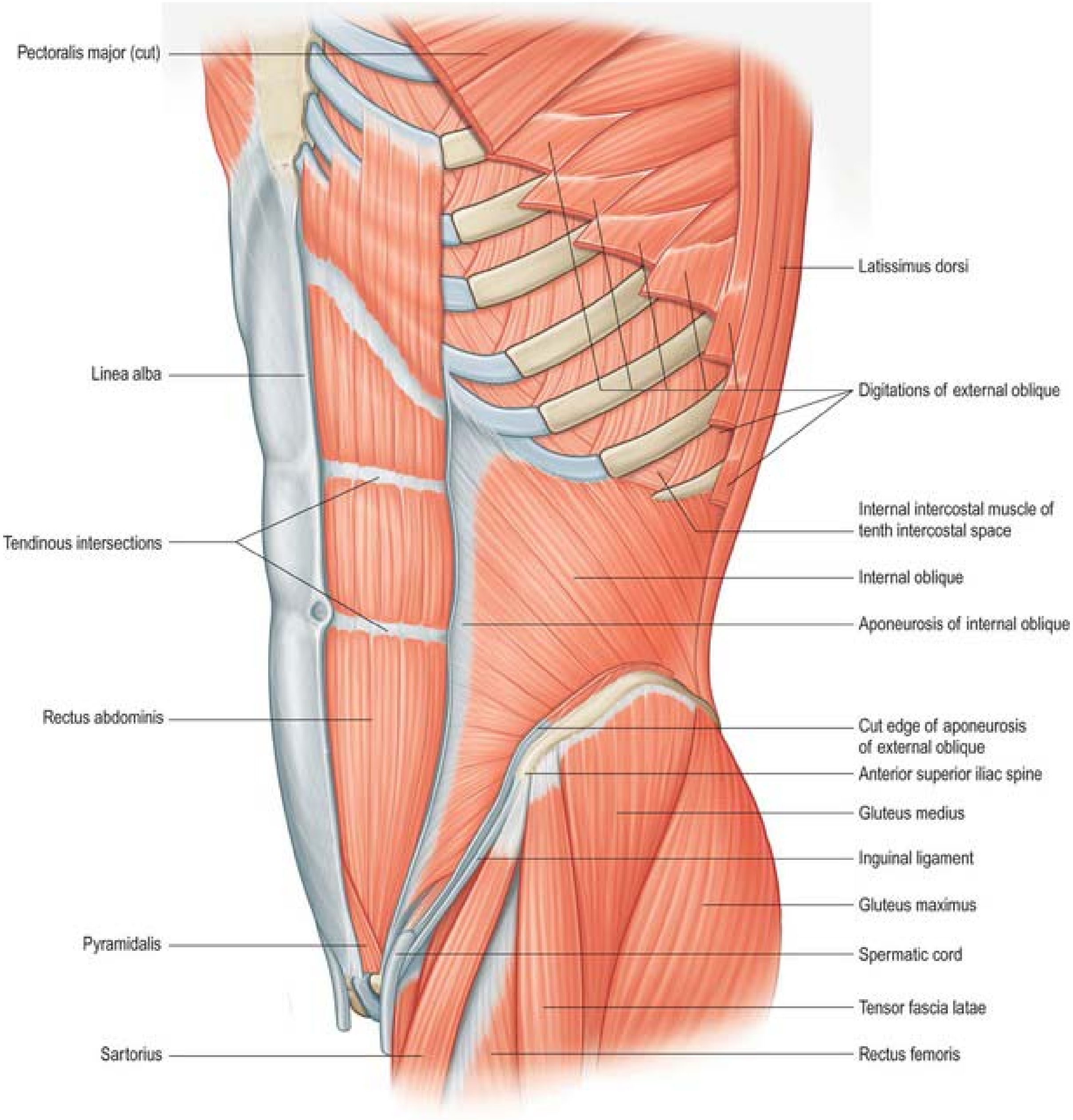
Pectoralis major (cut)
Linea alba
Tendinous intersections
Rectus abdominis
Pyramidalis
Sartorius
Latissimus dorsi
Digitations of external oblique
Internal intercostal muscle of tenth intercostal space
Internal oblique
Aponeurosis of internal oblique
Cut edge of aponeurosis of external oblique
Anterior superior iliac spine
Gluteus medius
Inguinal ligament
Gluteus maximus
Spermatic cord
Tensor fascia latae
Rectus femoris

Fig. 61.2 Muscles of the left side of the trunk. External oblique has been removed to show internal oblique, but its digitations from the ribs have been preserved. The sheath of rectus abdominis has been opened and its anterior lamina removed.

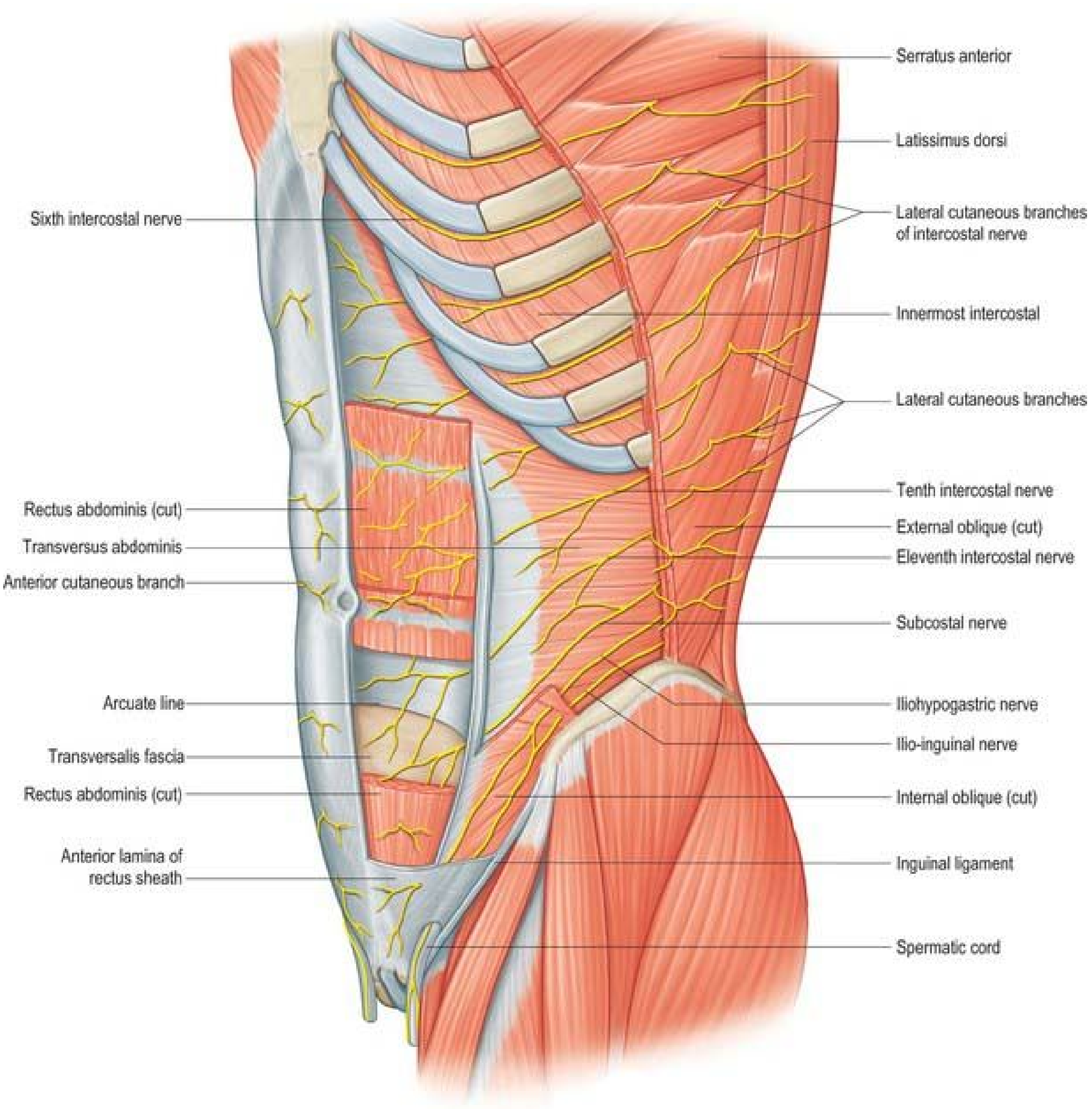
Serratus anterior
Latissimus dorsi
Sixth intercostal nerve
Lateral cutaneous branches of intercostal nerve
Innermost intercostal
Lateral cutaneous branches
Tenth intercostal nerve
Rectus abdominis (cut)
External oblique (cut)
Transversus abdominis
Eleventh intercostal nerve
Anterior cutaneous branch
Subcostal nerve
Arcuate line
Iliohypogastric nerve
Ilio-inguinal nerve
Transversalis fascia
Rectus abdominis (cut)
Internal oblique (cut)
Inguinal ligament
Anterior lamina of rectus sheath
Spermatic cord

Fig. 61.3 The cutaneous branches of the lower intercostal and lumbar nerves. Portions of the muscles of the anterior abdominal wall have been removed, including most of the anterior layer of the rectus sheath and parts of rectus abdominis.

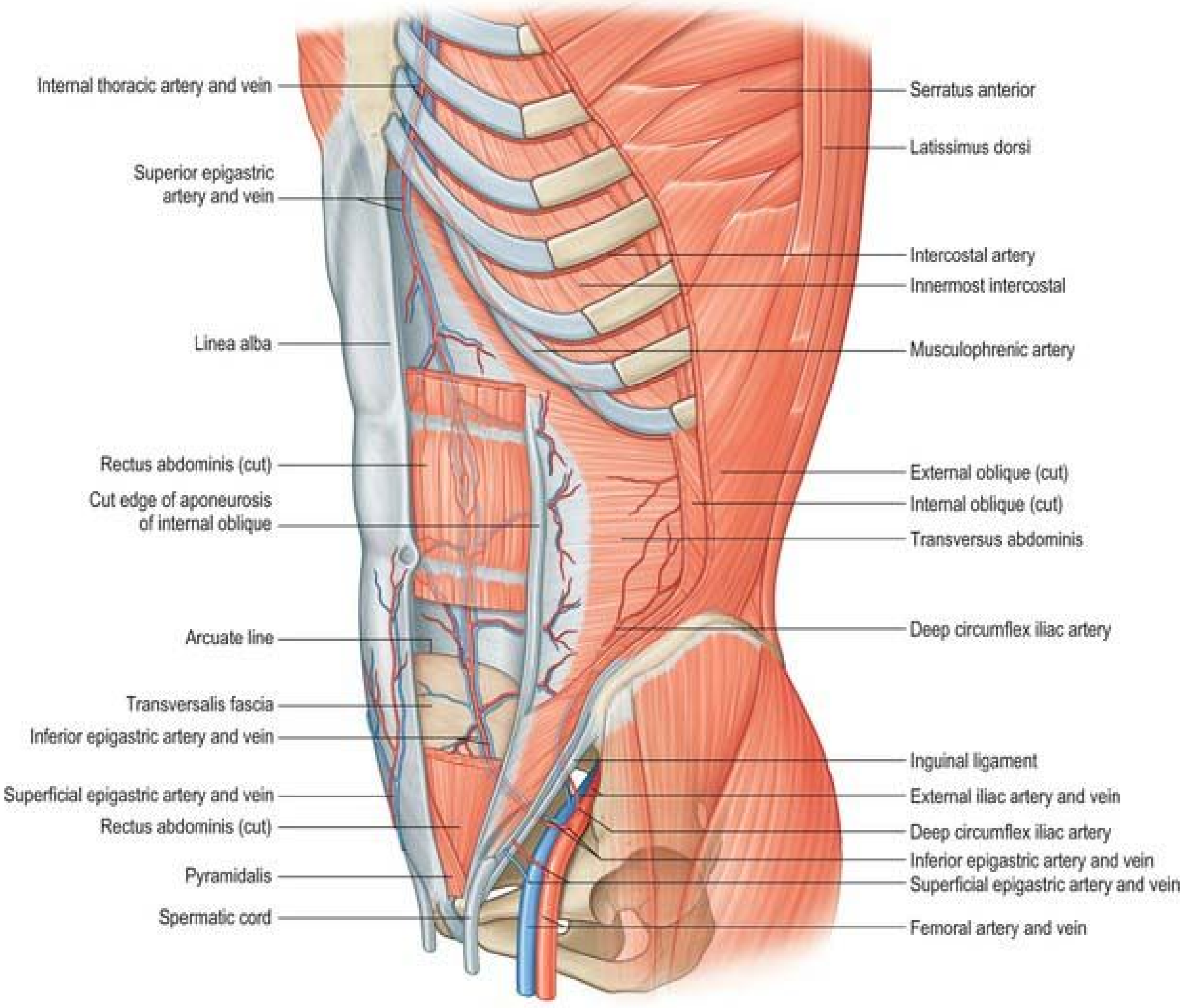
Internal thoracic artery and vein
Superior epigastric artery and vein
Linea alba
Rectus abdominis (cut)
Cut edge of aponeurosis of internal oblique
Arcuate line
Transversalis fascia
Inferior epigastric artery and vein
Superficial epigastric artery and vein
Rectus abdominis (cut)
Pyramidalis
Spermatic cord
Serratus anterior
Latissimus dorsi
Intercostal artery
Innermost intercostal
Musculophrenic artery
External oblique (cut)
Internal oblique (cut)
Transversus abdominis
Deep circumflex iliac artery
Inguinal ligament
External iliac artery and vein
Deep circumflex iliac artery
Inferior epigastric artery and vein
Superficial epigastric artery and vein
Femoral artery and vein

Fig. 61.4 Deep muscles and arterial supply of the anterolateral abdominal wall. The greater part of the left rectus abdominis has been removed to show the superior and inferior epigastric vessels.

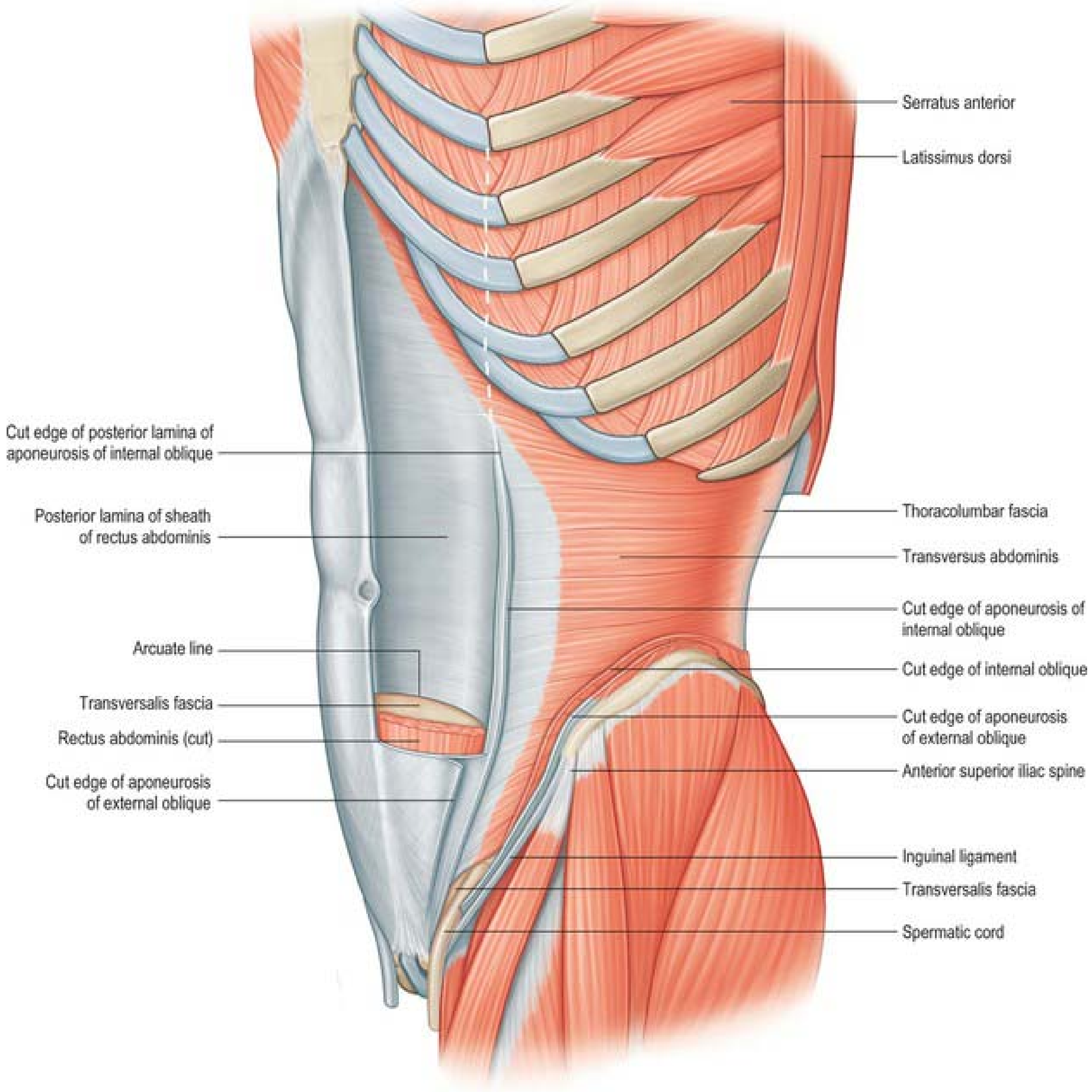
Cut edge of posterior lamina of aponeurosis of internal oblique
Posterior lamina of sheath of rectus abdominis
Arcuate line
Transversalis fascia
Rectus abdominis (cut)
Cut edge of aponeurosis of external oblique
Serratus anterior
Latissimus dorsi
Thoracolumbar fascia
Transversus abdominis
Cut edge of aponeurosis of internal oblique
Cut edge of internal oblique
Cut edge of aponeurosis of external oblique
Anterior superior iliac spine
Inguinal ligament
Transversalis fascia
Spermatic cord

Fig. 61.5 Left transversus abdominis. The aponeurosis of transversus abdominis fuses into the posterior layer of the rectus sheath above the arcuate line. The position of lateral border of rectus abdominis is shown by the white dotted line.

SKIN AND SOFT TISSUE

The integument of the anterior abdominal wall comprises skin, soft tissues, lymphatic and vascular structures, and segmental nerves. The outer layer is formed from the skin and subcutaneous fat. The skin is non-specialized and variably hirsute, depending on the sex and race. All post-pubertal individuals have some extension of the pubic hair onto the anterior abdominal wall skin, although this is commonly most pronounced in males, in whom the hair may extend almost up to the umbilicus in a triangular pattern. The subcutaneous fat of the abdominal wall is highly variable in thickness and is one of the areas where excess fat is stored during periods of obesity, particularly in males.

VASCULAR SUPPLY AND LYMPHATIC DRAINAGE

The anterior abdominal wall receives its blood supply from paired superior and inferior epigastric arteries running vertically through the tissues, and from paired posterior intercostal, subcostal and lumbar vessels running obliquely around the anterolateral aspects of the abdomen.

Superior epigastric artery and veins

The superior epigastric artery is a terminal branch of the internal thoracic artery. It descends between the costal and xiphoid slips of the diaphragm, accompanied by two or more veins (Fig. 61.4). The vessels pass anterior to the lower fibres of transversus thoracis and the upper fibres of transversus abdominis. The artery enters the rectus sheath behind rectus abdominis and runs down to anastomose with the inferior epigastric artery usually above the level of the umbilicus. Branches supply rectus abdominis and perforate the sheath to supply the abdominal skin. A branch given off in the upper rectus sheath passes anterior to the xiphoid process of the sternum and anastomoses with the same contralateral branch. This vessel may give rise to troublesome bleeding during surgical incisions that extend up to and alongside the xiphoid process. The superior epigastric artery supplies small branches to the anterior part of the diaphragm. On the right, small branches reach the falciform ligament, where they anastomose with branches arising from the hepatic artery.

Inferior epigastric artery and veins

The inferior epigastric artery originates from the external iliac artery posterior to the inguinal ligament (Fig. 61.6). Its accompanying veins, usually two, drain into the external iliac vein. It curves forwards in the anterior extraperitoneal tissue and ascends obliquely along the medial margin of the deep inguinal ring. It lies posterior to the spermatic cord, but is separated from it by the transversalis fascia. It pierces the transversalis fascia which forms the flimsy posterior support of rectus abdominis, and ascends between the muscle and the fascia and overlying pre-peritoneal connective tissue. In this part of its course, it raises the parietal peritoneum of the anterior abdominal wall as the lateral umbilical fold but has little supporting tissue posteriorly. Disruption of the artery, by surgical incisions e.g. for laparoscopic ports or drains, is not uncommon and the resulting haematoma may expand to considerable size because of the lack of tissue against which the bleeding is effectively compressed. The artery divides into numerous branches. Those which anastomose with branches of the superior epigastric artery do so posterior to rectus abdominis at a variable height above the umbilicus. The inferior epigastric vessels are usually significantly larger than the superior vessels and provide the ‘dominant’ supply to rectus abdominis. Preparatory ligation of the inferior epigastric artery is often performed for myo(cutaneous) flaps using the mid or lower rectus abdominis based on the superior epigastric artery to allow expansion of the superior arterial flow to improve viability of the flap. Branches anastomose with terminal branches of the lower six posterior intercostal arteries posterior to rectus abdominis at the lateral border close to the sheath. The artery is an important inferomedial relation of the deep inguinal ring, and may be damaged during extensive medial dissection of the deep ring during hernia repair, particularly when this is performed in the preperitoneal plane. The vas deferens in the male, or round ligament in the female, wind laterally round it. It has the following branches: the cremasteric artery, a pubic branch, and muscular and cutaneous branches.

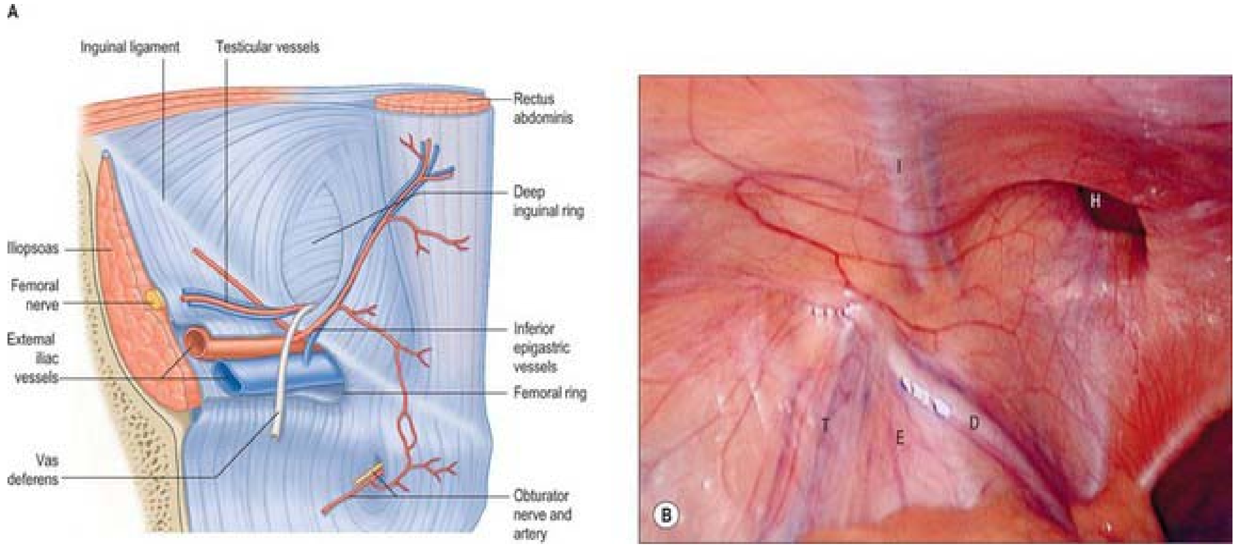
A
Inguinal ligament
Testicular vessels
Rectus abdominis
Deep inguinal ring
Iliopsoas
Femoral nerve
External iliac vessels
Inferior epigastric vessels
Femoral ring
Vas deferens
Obturator nerve and artery
I
H
T
E
D
B

Fig. 61.6 **A**, The deep aspect of the lower part of the abdominal wall of the left side with the thinner posterior wall of the rectus sheath. The femoral and deep inguinal rings are displayed, together with the vessels and other structures in relation to them and also the opening into the obturator canal. **B**, Laparoscopic view showing the parietal peritoneum covering the area. I, inferior epigastric vessels; H, hernia orifice; D, ductus deferens; T, testicular vessels; E, external iliac vessels.

*(**B** From Drake, Vogl and Mitchell 2005.)*

The cremasteric artery accompanies the spermatic cord in males and supplies the cremaster and other coverings of the cord. It anastomoses with the testicular artery. In females it is small and accompanies the round ligament. A pubic branch, near the femoral ring, descends posterior to the pubis and anastomoses with the pubic branch of the obturator artery. Occasionally, the pubic branch of the inferior epigastric artery is larger than the main obturator artery origin, and it supplies the majority of flow into the obturator artery in the thigh. It is then referred to as the aberrant obturator artery. It lies close to the medial border of the femoral ring and may be damaged in medial dissection of the ring during femoral hernia repair. Muscular branches supply the abdominal muscles and peritoneum, and anastomose with the circumflex iliac and lumbar arteries. Cutaneous branches perforate the aponeurosis of external oblique, supply the skin and anastomose with branches of the superficial epigastric artery.

Sometimes the inferior epigastric artery arises from the femoral artery. It then ascends anterior to the femoral vein into the abdomen to follow its course as above. It occasionally arises from the external iliac artery, in common with an aberrant obturator artery and, rarely, from the obturator artery.

The superior and inferior epigastric arteries are important sources for a potential collateral circulation between the internal thoracic artery and the external iliac artery in situations where flow in the thoracic or abdominal aorta is compromised. Small tributaries of the inferior epigastric vein drain the skin around the umbilicus and anastomose with the terminal branches of the umbilical vein, draining the inner surface of the umbilicus via the falciform ligament. These anastomoses may open widely in cases of portal hypertension, when portal venous blood may drain into the systemic circulation via the inferior epigastric vessels. The radiating dilated veins seen under the umbilical skin are referred to as the 'caput medusae'.

Posterior intercostal, subcostal and lumbar arteries

The 10th and 11th posterior intercostal arteries and the subcostal artery emerge from under the subcostal groove of their respective ribs and pass into the tissues of the anterior abdominal wall. They run through the aponeurosis of transversus abdominis and lie deep to the fibres of internal oblique. The lumbar arteries also cross the aponeurosis of transversus abdominis and lie deep to internal oblique. The arteries on either side run forward, giving off muscular branches to the overlying internal and external oblique, before anastomosing with the lateral branches of the superior and inferior epigastric arteries at the lateral border of the rectus sheath (Fig. 61.7). Perforating cutaneous vessels run vertically through the muscles to supply the overlying skin and subcutaneous tissue. A small contribution to the supply of the lower abdominal muscles comes from branches of the deep circumflex iliac arteries.

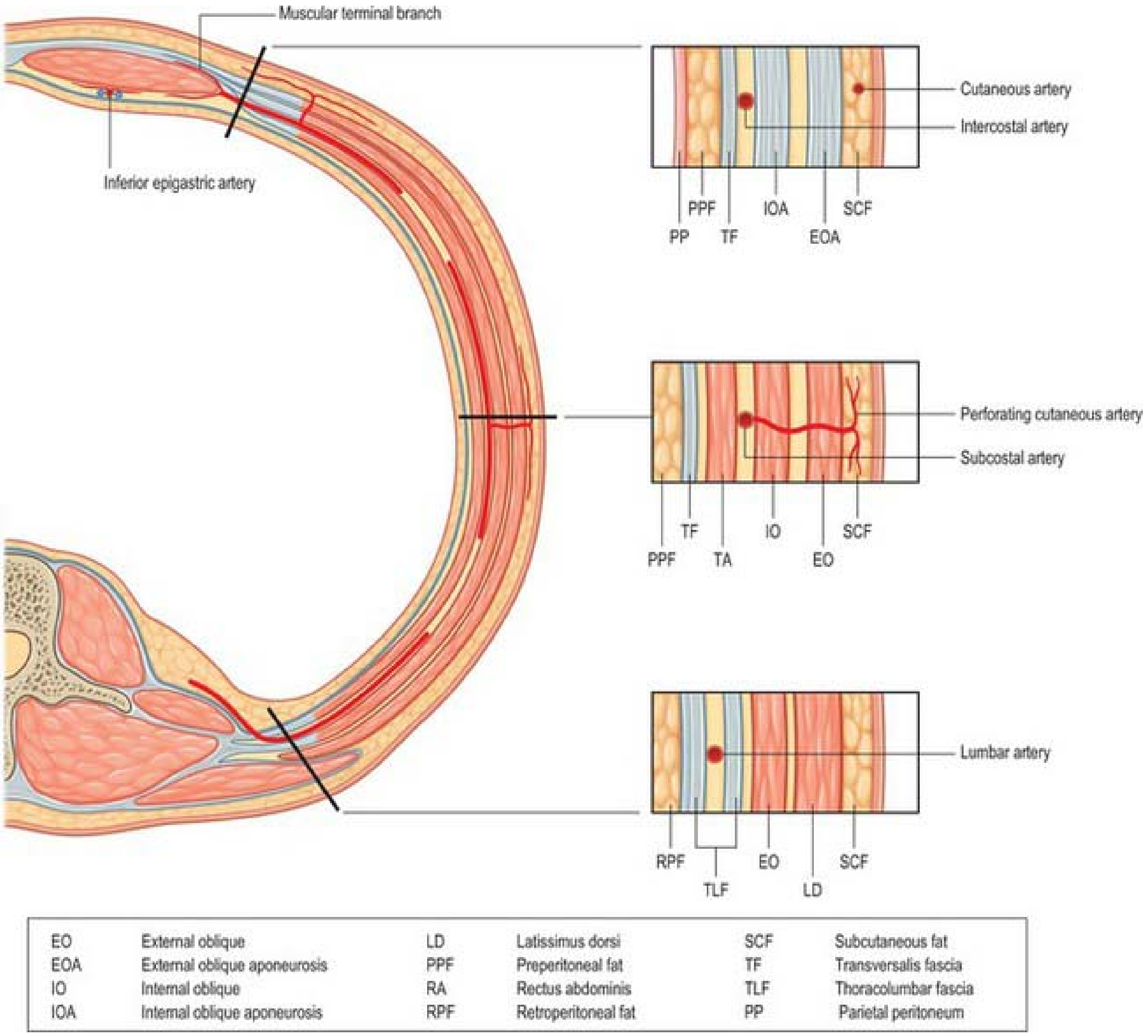
Muscular terminal branch
Inferior epigastric artery
Cutaneous artery
Intercostal artery
PPF
PP
TF
IOA
EOA
SCF
Perforating cutaneous artery
Subcostal artery
TF
PPF
TA
IO
EO
SCF
Lumbar artery
RPF
TLF
EO
LD
SCF
EO External oblique
EOA External oblique aponeurosis
IO Internal oblique
IOA Internal oblique aponeurosis
LD Latissimus dorsi
PPF Preperitoneal fat
RA Rectus abdominis
RPF Retroperitoneal fat
SCF Subcutaneous fat
TF Transversalis fascia
TLF Thoracolumbar fascia
PP Parietal peritoneum

Fig. 61.7 Arrangement of the anterolateral abdominal wall vessels at the level of the mid abdomen.

Lymphatic drainage

The lymphatic vessels of the anterior abdominal wall lie both superficial and deep to the deep fascia.

Superficial vessels

The superficial lymphatic vessels accompany the subcutaneous blood vessels. Vessels from the lumbar and gluteal regions run with the superficial circumflex iliac vessels. Those from the infra-umbilical skin run with the superficial epigastric vessels. Both drain into the superficial inguinal nodes. The supra-umbilical region is drained by vessels running obliquely up to the pectoral and subscapular axillary nodes, and there is some drainage to the parasternal nodes.

Deep vessels

The deep lymphatic vessels accompany the deep arteries. The vessels from the posterior portion of the abdominal wall pass with the lumbar arteries to drain into the lateral aortic and retro-aortic nodes. Vessels from the upper anterior abdominal wall run with the superior epigastric vessels to the parasternal nodes. Vessels of the lower abdominal wall drain into the circumflex iliac, inferior epigastric and external iliac nodes.

SEGMENTAL NERVES

The seventh to the 12th lower thoracic ventral rami continue anteriorly from the intercostal spaces into the abdominal wall (Fig. 61.3). Approaching the anterior ends of their respective spaces, the seventh and eighth nerves curve superomedially across the deep surface of the costal cartilages between the digitations of transverse abdominis. They reach the deep aspect of the posterior layer of the aponeurosis of internal oblique. Both the seventh and eighth nerves then run through this aponeurosis, pass posterior to rectus abdominis and supply branches to the upper portion of the muscle. They pass through the muscle near its lateral edge and pierce the anterior rectus sheath to supply the skin of the epigastrium.

The ninth to 11th intercostal nerves pass from their intercostal spaces between digitations of the diaphragm and transversus abdominis. They enter the layer between transversus abdominis and internal oblique. Here, the ninth nerve runs forwards almost horizontally, whereas the tenth and 11th pass inferomedially. At the lateral edge of rectus abdominis, the nerves pierce the posterior layer of the aponeurosis of internal oblique and pass behind the muscle to end, like the seventh and eighth intercostal nerves, with cutaneous branches. The ninth nerve supplies skin above the umbilicus, the tenth supplies skin, which includes the umbilicus, and the 11th supplies skin below the umbilicus (see Fig. 15.12 and Chapters 42, 45 and 79). The 12th thoracic nerve (subcostal nerve) connects with the first lumbar ventral ramus (dorsolumbar nerve). It accompanies the subcostal vessels along the inferior border of the 12th rib, passing behind the lateral arcuate ligament and kidney and anterior to the upper part of the quadratus lumborum. It perforates the transversus abdominis fascia, running deep to the internal oblique, to be distributed like the lower intercostal nerves. It supplies the anterior gluteal skin reaching down to the greater trochanter.

The seventh to 12th intercostal nerves supply the intercostal, subcostal and abdominal muscles. The tenth, 11th and 12th supply serratus posterior inferior. All six nerves also provide sensory fibres to the costal parts of the diaphragm and related parietal pleura and peritoneum. Like the upper intercostal nerves, they give off collateral and lateral cutaneous branches before they reach the costal angles. The collateral branch may rejoin its parent nerve but, if it does, it leaves it again near the lateral border of rectus abdominis. It then runs forward, through the muscle and its anterior sheath near the linea alba to supply the overlying skin. The lateral cutaneous branches pierce the intercostal muscles and external oblique and divide into anterior and posterior branches. These branches supply the skin of the abdomen and back. The anterior branches supply external oblique. The posterior branches pass back to supply the skin over latissimus dorsi. Each lateral cutaneous nerve descends as it pierces external oblique and the superficial fascia and reaches the skin on a level with the anterior and posterior cutaneous nerves of the segment.

Dermatomes

The dermatomes of the anterior abdominal wall are shown in Figure 15.12.

SOFT TISSUE

Superficial fascia

The superficial fascia of the abdominal wall consists mostly of a single layer that contains a variable amount of fat. It lies between the skin and muscles of the anterior abdominal wall. In the lower part, the fascia differentiates into superficial and deep layers between which lie superficial vessels and nerves and, in the region of the groin, superficial inguinal lymph nodes.

Superficial layer

Where present, the superficial layer is thick, areolar in texture and contains a variable amount of fat. It is often greatly thickened in obese individuals. Inferiorly, it lies superficial to the inguinal ligament and is continuous with the superficial fascia of the thigh. In the male, this layer continues over the penis and outer surface of the spermatic cord into the scrotum, where it changes its character. In this region it is generally thin, with very little adipose tissue present and is pale red in colour. In the scrotum it also contains smooth muscle fibres, which form the dartos muscle. From the scrotum it may be traced backwards into continuity with the superficial fascia of the perineum. In the female, it continues from the suprapubic skin of the abdomen into the labia majora and perineum.

Deep (membranous) layer

When present as a distinct entity, the deep layer of the fascia is more membranous than the superficial, and contains elastic fibres. It is loosely connected by areolar tissue to the aponeurosis of external oblique, but in the midline it is intimately adherent to the linea alba and symphysis pubis. In the male, it extends onto the dorsum of the penis and forms part of the superficial ligament of the penis. Superiorly, it is continuous with the superficial fascia over the remainder of the trunk. Inferiorly, it lies superficial to the inguinal ligament and fuses with the overlying superficial layer and the underlying fascia lata in the inguinal flexure line or skin crease of the thigh.

In the male, the deep layer of the fascia continues inferiorly and medially over the penis and spermatic cord to the scrotum, where it becomes continuous with the membranous layer of the superficial fascia of the perineum. In the female, it continues into the labia majora and is continuous with the fascia of the perineum.

In the child, the testis can frequently be retracted out of the scrotum into the loose areolar tissue between external oblique and the deep layer of superficial fascia over the inguinal canal. This ‘space’ is sometimes called the superficial inguinal pouch.

Transversalis fascia

The transversalis fascia is a thin layer of connective tissue lying between the inner surface of transversus abdominis and the extraperitoneal fat. It is part of the general layer of fascia between the peritoneum and the abdominal wall. Posteriorly, it is continuous with the anterior layer of the thoracolumbar fascia, and it forms a continuous sheet anteriorly. Inferiorly, it is continuous with the iliac and pelvic fasciae, and superiorly it blends with the fascial covering of the inferior surface of the diaphragm. It is attached to the entire length of the iliac crest between the origins of transversus abdominis and iliacus and to the posterior margin of the inguinal ligament between the anterior superior iliac spine and the femoral vessels. In the inguinal region it is thick and dense, and augmented by the aponeurosis of transversus abdominis. Medial to the femoral vessels it is thin and fused to the pubis behind the conjoint tendon. Anterior to the femoral vessels, fascia extends down from the fascia transversalis to form the anterior part of the femoral sheath. The fascia is strengthened here by fibres, which arch transversely. Some fibres spread laterally towards the anterior superior iliac spine, some fibres run medially behind rectus abdominis, and some descend to the pubis behind the conjoint tendon. These arched fibres constitute the deep crural arch. The curved fibres of the deep crural arch thicken the inferomedial part of the rim of the deep inguinal ring. The spermatic cord in the male, or the round ligament of the uterus in the female, pass through the transversalis fascia at the deep inguinal ring. This opening is not visible during dissection through the skin because the transversalis fascia is prolonged on these structures as the internal spermatic fascia, but it can be seen from within the abdomen once the peritoneum has been stripped off. The internal spermatic fascia surrounds the testis and blends with the areolar tissue on the parietal layer of the tunica vaginalis: it may contain smooth muscle fibres.

Extraperitoneal connective tissue

The extraperitoneal connective tissue is a layer of areolar tissue lying between the peritoneum and the fasciae lining the abdominal and pelvic cavities. The amount of extraperitoneal tissue varies: it is especially abundant on the posterior wall of the abdomen, particularly around the kidneys, where it contains much adipose tissue; variable in thickness on the anterolateral wall, where it is thin in children and normal adults but often thickened in the obese, particularly in males; scanty in the suprapubic region, above the iliac crest and in the pelvis. Extraperitoneal tissue is continuous with the epimysium of the muscles of the abdominal wall.

MUSCLES

ANTEROLATERAL MUSCLES OF THE ABDOMEN

Rectus abdominis, pyramidalis, external oblique, internal oblique and transversus abdominis constitute the anterolateral muscles of the abdomen. They act together to perform a range of functions, some of which involve the generation of a positive pressure within one or more body cavities. Although many of these activities may occur with no ‘forced assistance’, activities such as expiration, defecation and micturition may be aided by the generation of a positive intra-abdominal pressure. Parturition, coughing and vomiting always require such a positive pressure. Under resting conditions, the tone developed within the muscles provides support for the abdominal viscera and retains the normal contour of the abdomen. The consequences of lack of muscular support can be seen in conditions such as ‘prune belly syndrome’, where there is congenital absence of these muscles.

Active contraction of the muscles provides an important role in the maintenance of abdominal wall tone when the intra-abdominal pressure is increased. The compression of the abdominal cavity required to increase the internal pressure is brought about mainly by the contraction of the diaphragm. The bony pelvis and lower thoracic cage provide an almost incompressible structure to part of the abdominal wall. During the generation of positive intra-abdominal pressure, the abdominal wall acts to hold the position of the wall fixed, rather than to generate pressure directly: because the majority of the abdominal wall is muscular, the anterolateral abdominal wall muscles must be synchronously contracted to prevent displacement of the viscera and the resultant loss of pressure. The oblique muscles, acting through the anterior aponeurosis and the rectus sheath, provide the majority of this tension, although transversus abdominis and rectus abdominis also contribute.

The lateral muscles, external oblique, internal oblique and transversus abdominis, have the greatest roles in these functions, tensing the rectus sheath and linea alba. The anterolateral abdominal muscles contribute little to the movements of the trunk during normal sitting and standing, which are movements controlled predominantly by the paravertebral and spinal muscles. However, movements of the trunk against resistance or when the individual is supine require the anterolateral abdominal muscles. Rectus abdominis is the most important in these situations, causing anterior flexion of the trunk. If the pelvic girdle is fixed, flexion of the thorax and pectoral girdle occurs. With a fixed thoracic cage, contraction of rectus abdominis causes the pelvis to lift and tilt to lie more nearly in a horizontal plane. Lateral flexion and rotation of the trunk against resistance is provided by unilateral contraction of the oblique muscles.

Rectus abdominis

Rectus abdominis is a long, strap-like muscle that extends along the entire length of the anterior abdominal wall. It is widest in the upper abdomen and lies just to the side of the midline. The paired recti are separated in the midline by the linea alba (Fig. 61.4).

The muscle fibres of rectus abdominis are interrupted by three fibrous bands or tendinous intersections. One is usually situated at the level of the umbilicus, another opposite the free end of the xiphoid process and a third about midway between the other two. These intersections pass transversely or obliquely across the muscle in a zigzag manner. They are rarely full-thickness and may extend only half-way through the body of the muscle. They usually fuse with the fibres of the anterior lamina of the sheath of the muscle. Sometimes, one or two incomplete intersections are present below the umbilicus. The intersections may occur during development or may represent the myosepta delineating the myotomes that form the muscle.

The medial border of rectus abdominis is closely related to the linea alba. Its lateral border may be visible on the surface of the anterior abdominal wall as a curved groove, the linea semilunaris, which extends from the tip of the ninth costal cartilage to the pubic tubercle. In a muscular individual it is readily visible, even when the muscle is not actively contracting, but in many normal and obese individuals it may be completely obscured.

Attachments

Rectus abdominis arises by two tendons. The larger, lateral tendon is attached to the crest of the pubis and may extend beyond the pubic tubercle to the pectineal line. The medial tendon interlaces with the contralateral muscle and blends with the ligamentous fibres covering the front of the symphysis pubis. Additional fibres may arise from the lower part of the linea alba. Superiorly, rectus abdominis is attached by three slips of muscle to the fifth, sixth and seventh costal cartilages. The most lateral fibres are usually attached to the anterior end of the fifth rib. Sometimes this slip is absent, and occasionally it may extend to the fourth and third ribs. The most medial fibres are occasionally connected to the costoxiphoid ligaments and the side of the xiphoid process. In males, the pubic attachment of rectus abdominis may run over the anterior surface of the symphysis pubis and become continuous with the attachment of the gracilis and the fascia lata to the pubis.

Vascular supply

Rectus abdominis is supplied principally by the superior and inferior epigastric arteries. The inferior epigastric artery tends to be larger in calibre than the superior. Small terminal branches from the lower three posterior intercostal arteries, the subcostal artery, the posterior lumbar arteries and the deep circumflex artery may provide some contribution, particularly to the lateral edges and the lower attachments, and they form small anastomoses with the lateral branches of the epigastric arteries. Rectus abdominis provides an excellent myocutaneous flap, either pedicled or free, because of the excellent vascularity provided by the epigastric vessels and because the muscle belly is separated from surrounding tissue within the rectus sheath. The upper half of the muscle may be used for breast reconstruction or augmentation of tissue loss on the anterior thorax. The lower half may be used in the region of the thigh and may be rotated on its lower attachments, passed through the pelvis and delivered into the perineum for reconstruction after radical pelvic and perineal resections.

Innervation

Rectus abdominis is innervated by the terminal branches of the ventral rami of the lower six or seven thoracic spinal nerves via the lower intercostal and subcostal nerves.

Actions

The recti contribute to the flexion of the trunk. They also contribute to the maintenance of abdominal wall tone required during straining.

Rectus sheath

Rectus abdominis on each side is enclosed by a fibrous sheath. The anterior portion of this sheath extends the entire length of the muscle and fuses with the periosteum of the muscle attachments. Posteriorly, the sheath is complete in the upper two-thirds of the muscle. In the lower one-third, the posterior layer of the sheath stops approximately midway between the umbilicus and the pubis. In most individuals this is a clearly defined line, although the transition may not always be clear-cut in others. The lower border of the posterior sheath is called the arcuate line. Below this level, rectus abdominis is enclosed posteriorly by the transversalis fascia and extraperitoneal connective tissue (Figs 61.8 and 61.9). The rectus sheath is formed from decussating fibres from all three lateral abdominal muscles. External oblique, internal oblique and transversus abdominis each forms a bilaminar aponeurosis at their medial borders. The fibres from all three anterior leaves run obliquely upwards, whereas the posterior leaves run obliquely downwards at right angles to the anterior leaves.

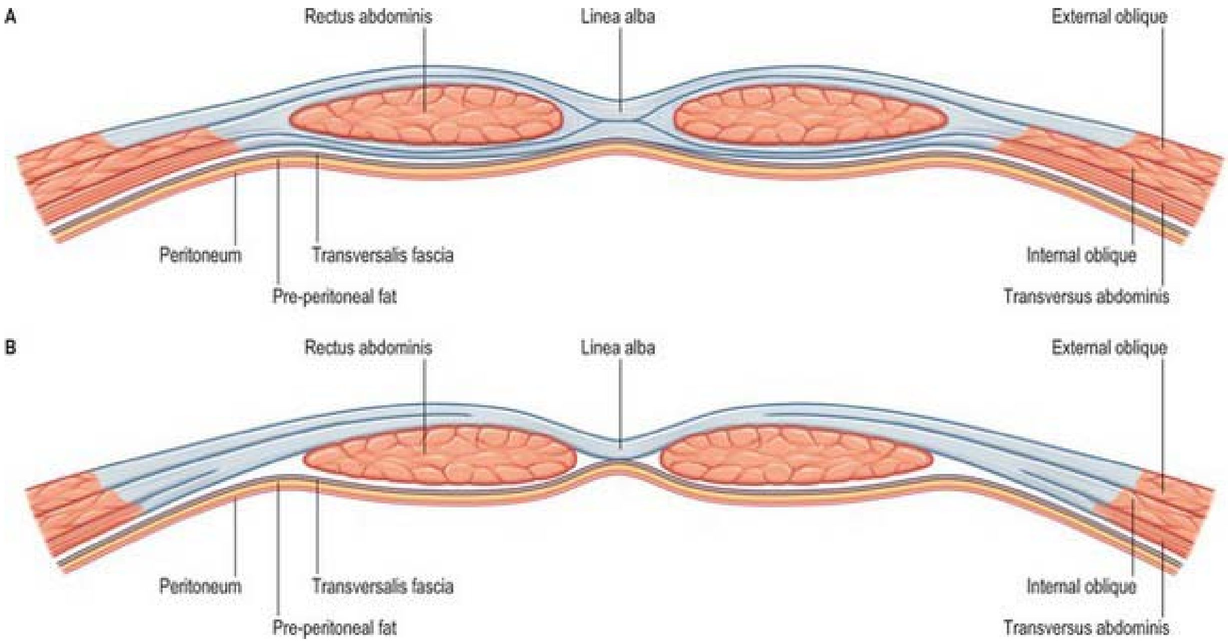
A
Rectus abdominis
Linea alba
External oblique
Peritoneum
Transversalis fascia
Pre-peritoneal fat
Internal oblique
Transversus abdominis
B
Rectus abdominis
Linea alba
External oblique
Peritoneum
Transversalis fascia
Pre-peritoneal fat
Internal oblique
Transversus abdominis

Fig. 61.8 Transverse sections through the anterior abdominal wall: **A**, immediately above the umbilicus; **B**, below the arcuate line. The bilaminar nature of each muscular aponeurosis is difficult to illustrate in cross-section. The fibres appear to fuse into a single sheet during formation of the rectus sheath. Note that rectus is supported directly by the transversalis fascia below the arcuate line.

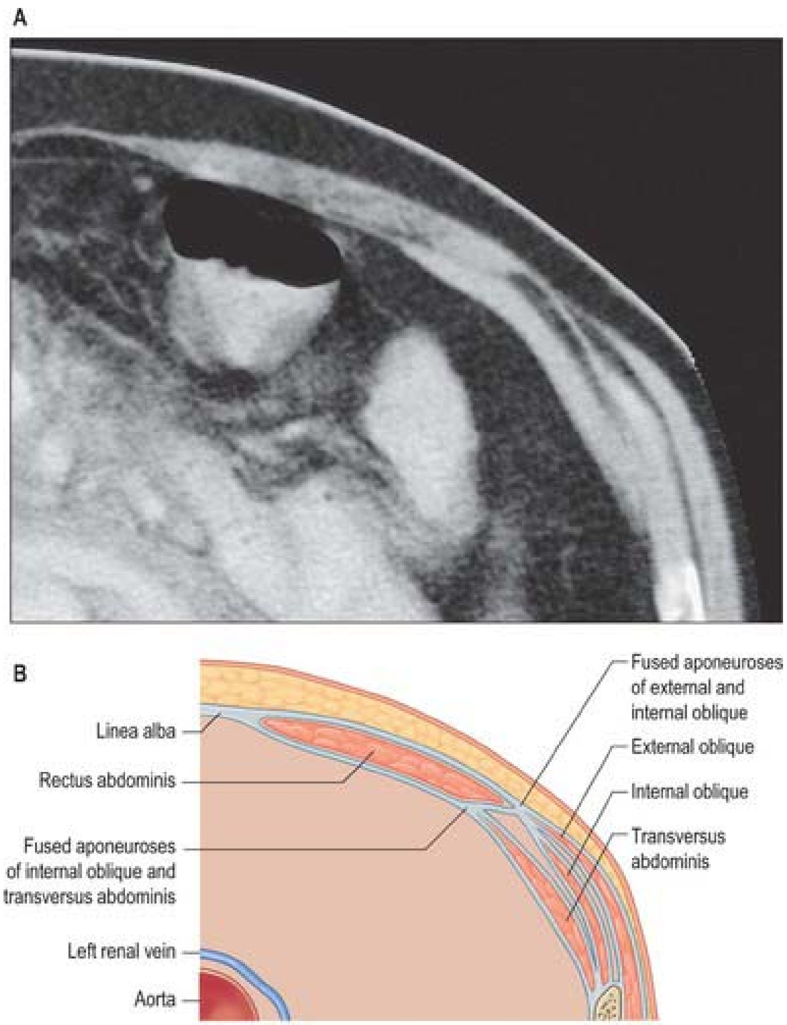
A
B
Fused aponeuroses of external and internal oblique
Linea alba
External oblique
Rectus abdominis
Internal oblique
Transversus abdominis
Fused aponeuroses of internal oblique and transversus abdominis
Left renal vein
Aorta

Fig. 61.9 Rectus sheath. Computed tomography scan (**A**) and diagram (**B**) of the anterior abdominal wall, demonstrating the formation of the rectus sheath above the umbilicus. The anterior rectus sheath is composed of both leaves of the aponeurosis of external oblique and the anterior leaf of the aponeurosis of internal oblique, fused together. The posterior rectus sheath is composed of the posterior leaf of the aponeurosis of internal oblique and both leaves of the aponeurosis of transversus abdominis.

The anterior rectus sheath is composed of both leaves of the aponeurosis of external oblique and the anterior leaf of the aponeurosis of internal oblique fused together. The posterior rectus sheath is composed of the posterior leaf of the aponeurosis of internal oblique and both leaves of the aponeurosis transversus abdominis (Fig. 61.10). Because of this arrangement, both the anterior and posterior layers of the rectus sheath consist of three layers of fibres with the middle layer running obliquely at right angles to the other two. At the midline, the anterior and posterior layers are closely approximated. Fibres of each layer decussate to the opposite side of the sheath, forming a continuous aponeurosis with the contralateral muscles (Fig. 61.11). Fibres also decussate anteroposteriorly, crossing from anterior sheath to posterior sheath. The dense fibrous line caused by this decussation is called the linea alba. The external oblique, internal oblique and transversus abdominis muscles can thus be regarded as paired, digastric muscles with a central tendon in the form of the linea alba. These decussating fibres maybe used to identify the midline during surgical incisions, since they can be seen as oblique fibres crossing at right angles. Below the level of the arcuate line, the fibres forming the posterior rectus sheath rapidly cease running behind the rectus and all leaves pass into the anterior rectus sheath.

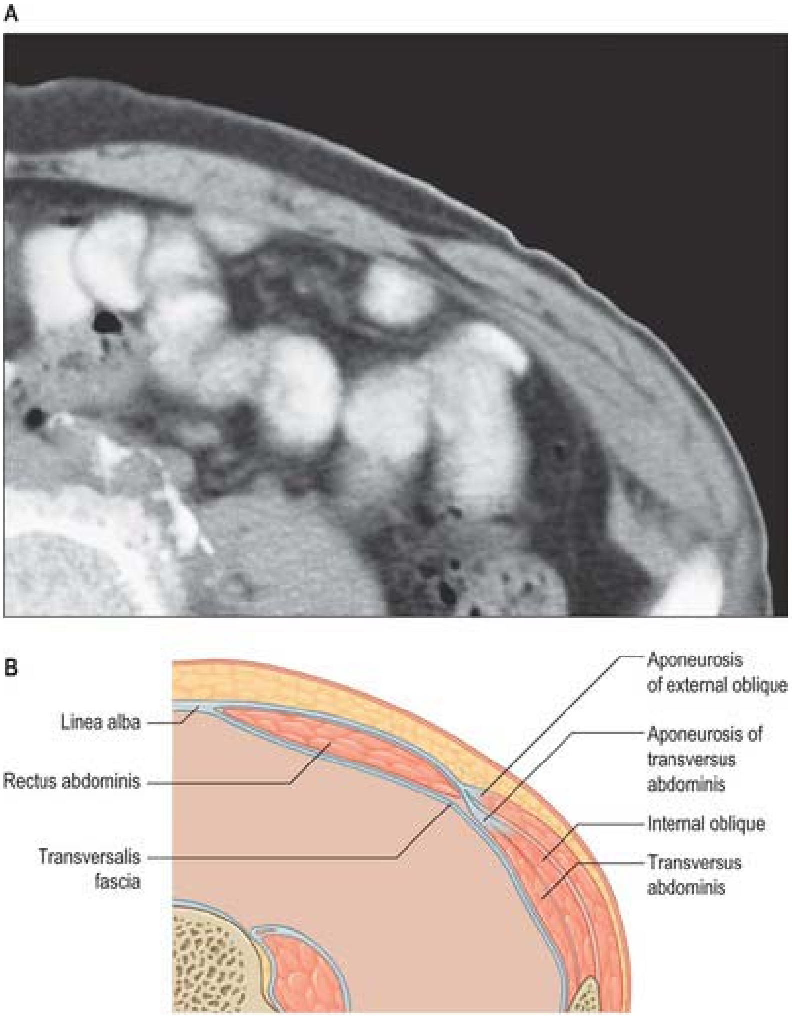
A
B
Linea alba
Rectus abdominis
Transversalis fascia
Aponeurosis of external oblique
Aponeurosis of transversus abdominis
Internal oblique
Transversus abdominis

Fig. 61.10 Rectus sheath. Computed tomography scan (**A**) and diagram (**B**) of the anterior abdominal wall, demonstrating the formation of the rectus sheath below the umbilicus. The posterior rectus sheath is formed by the transversalis fascia and extraperitoneal connective tissue.

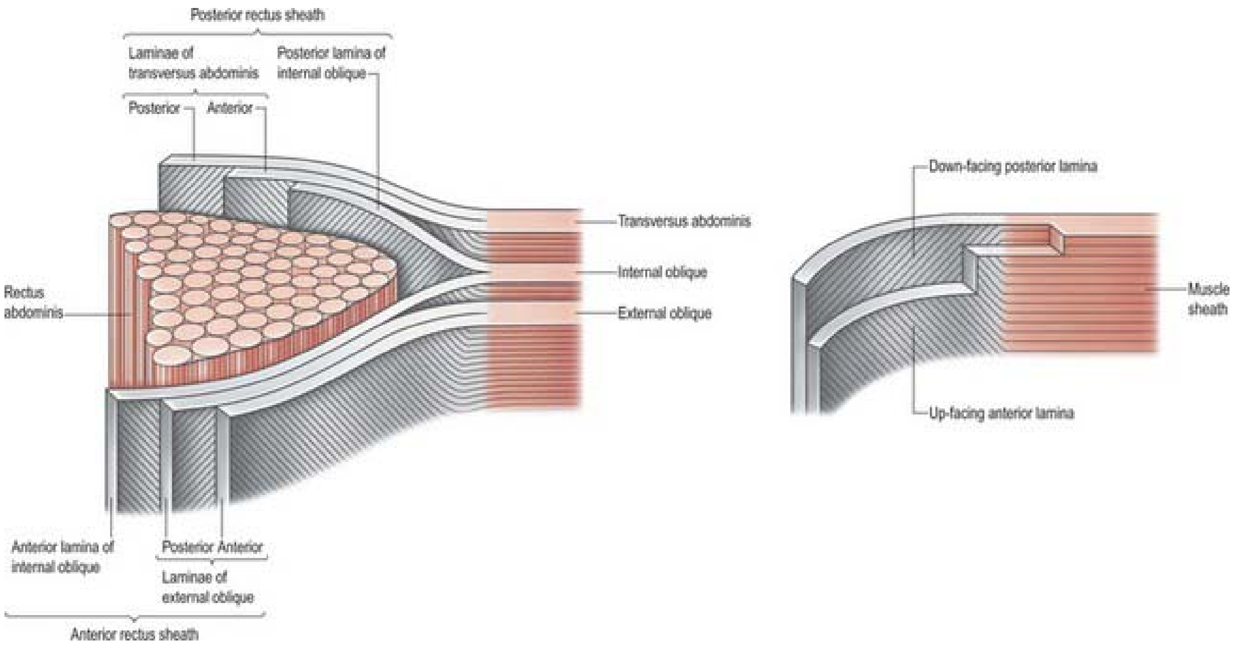
Posterior rectus sheath
Laminae of transversus abdominis
Posterior lamina of internal oblique
Posterior
Anterior
Transversus abdominis
Internal oblique
External oblique
Rectus abdominis
Anterior lamina of internal oblique
Posterior Anterior
Laminae of external oblique
Anterior rectus sheath
Down-facing posterior lamina
Muscle sheath
Up-facing anterior lamina

Fig. 61.11 The concept of bilaminar aponeuroses of the external oblique muscles. Note that the fibres of the superficial and deep layers are approximately at right angles; decussations occur as part of the linea alba.

Linea alba

The linea alba is a tendinous raphe extending from the xiphoid process to the symphysis pubis and pubic crest. It lies between the two recti and is formed by the interlacing and decussating aponeurotic fibres of external oblique, internal oblique and transversus abdominis. It is visible only in the lean and muscular, as a slight groove in the anterior abdominal wall. A fibrous cicatrix, the umbilicus, lies a little below the midpoint of the linea alba, and is covered by an adherent area of skin. Below the umbilicus, the linea alba narrows progressively as the rectus muscles lie closer together. Above the umbilicus, the rectus muscles diverge from one other and the linea alba is correspondingly broader. The linea alba has two attachments at its lower end: its superficial fibres are attached to the symphysis pubis, and its deeper fibres form a triangular lamella that is attached behind rectus abdominis to the posterior surface of the pubic crest on each side. This posterior attachment of linea alba is named the ‘adminiculum lineae albae’. The linea alba is crossed from side to side by a few minute vessels.

In the fetus, the umbilicus transmits the umbilical vessels, urachus and, up to the third month, the vitelline or yolk stalk. It closes a few days after birth, but the vestiges of the vessels and urachus remain attached to its deep surface. The remnant of the fetal left umbilical vein forms the round ligamentum of the liver. The obliterated umbilical arteries form the medial umbilical ligaments, enclosed in peritoneal folds of the same name. The partially obliterated remains of the urachus persist as the median umbilical ligament.

Divarication of the recti

Thinning and widening of the upper linea alba may occur, most commonly as a result of obesity or chronic straining. This process disrupts the arrangement of the fibres of the bilaminar aponeurosis. Contraction of the anterolateral abdominal muscles fails to be transmitted across the midline through the linea alba and increased intra-abdominal pressure causes the abdominal viscera to protrude beneath the thinned tissue as a broad midline bulge. The recti become widely separated or divaricated. This is not true herniation, as all the layers of the abdominal wall in that region are intact.

Umbilical hernia

There are three varieties of umbilical hernia. In true congenital herniation, a defect is present from birth. This is usually simply the result of failure of closure of the umbilicus after retraction of the umbilical gut loop. Less commonly, the gut loop does not retract and remains, in part, outside the abdominal cavity. An infantile umbilical hernia is caused by stretching of the umbilical scar tissue, associated with increased intra-abdominal pressure. An acquired umbilical or paraumbilical hernia actually occurs through small areas of weakness in the linea alba, above or below the umbilical scar.

Pyramidalis

Attachments

Pyramidalis is a triangular muscle that lies in front of the lower part of rectus abdominis within the rectus sheath. It is attached by tendinous fibres to the front of the pubis and to the ligamentous fibres in front of the symphysis. The muscle diminishes in size as it runs upwards, and ends in a pointed apex that is attached medially to the linea alba. This attachment usually lies midway between the umbilicus and pubis, but may occur higher. The muscle varies considerably in size. It may be larger on one side than on the other, absent on one or both sides, or even doubled.

Vascular supply

Pyramidalis is supplied by branches of the inferior epigastric artery, with some contribution from the deep circumflex iliac artery. A small artery frequently crosses the midline posterior to the belly of the muscle to anastomose with the contralateral vessel. This may cause troublesome bleeding during surgical incisions that run down as far as the lower rectus sheath above the symphysis pubis.

Innervation

Pyramidalis is supplied by the terminal branches of the subcostal nerve, which is the ventral ramus of the 12th thoracic spinal nerve.

Actions

Pyramidalis contributes to tensing the lower linea alba, but is of doubtful physiological significance.

External oblique

Attachments

External oblique is the largest and the most superficial of the three lateral abdominal muscles (Fig. 61.1). It curves around the lateral and anterior parts of the abdomen and is attached to the external surfaces and inferior borders of the lower eight ribs. The attachments rapidly become muscular and interdigitate with the lower attachment of serratus anterior and latissimus dorsi along an oblique line that extends downwards and backwards. The upper attachments are close to the cartilages of the corresponding ribs, the middle ones arise from the ribs at some distance from their cartilages and the lowest are close to the apex of the cartilage of the 12th rib. The fibres of external oblique diverge as they pass to their lower attachments. Those from the lower two ribs pass nearly vertically downwards and are attached to the anterior half or more of the outer lip of the anterior segment of the iliac crest. The middle and upper fibres pass downwards and forwards and end in the anterior aponeurosis, along a line drawn vertically from the ninth costal cartilage to a little below the level of the umbilicus. The muscle fibres rarely descend beyond a line from the anterior superior iliac spine to the umbilicus. The posterior border of the muscle is free.

The inguinal ligament is formed by the margin of the aponeurosis of external oblique extending between the anterior superior iliac spine and the pubic tubercle. The deep fibres of the aponeurosis of external oblique are not initially parallel to the long axis of the inguinal ligament: they approach the ligament obliquely at an angle of 10–20°. On reaching the ligament, fibres turns medially, and most run along the ligament to reach the pubic tubercle. The deepest fibres of the aponeurosis spread out posteromedially to insert into the pectineal line.

The upper and lower rib attachments of the muscle may be absent. Digitations or even the entire muscle may be reduplicated. The upper attachments of the muscle are sometimes continuous with pectoralis major or serratus anterior.

Vascular supply

External oblique is supplied by branches from the lower posterior intercostal and subcostal arteries, the superior and inferior epigastric arteries, the superficial and deep circumflex arteries and the posterior lumbar arteries.

Innervation

External oblique is innervated by the terminal branches of the lower five intercostal nerves and the subcostal nerve from the ventral rami of the lower six thoracic spinal nerves.

Actions

External oblique contributes to the maintenance of abdominal tone, increasing intra-abdominal pressure and lateral flexion of the trunk against resistance.

Inguinal ligament

The inguinal ligament is the thick, inrolled lower border of the aponeurosis of external oblique and stretches from the anterior superior iliac spine to the pubic tubercle. Its grooved abdominal surface forms the ‘floor’ of the inguinal canal. The ligament is not linear and has an inferior and an anterior convexity. At its lower border, it is continuous with the fascia lata. The lateral half is rounded and lies more obliquely than the medial half. The latter gradually widens towards its attachment to the pubis, where it becomes more horizontal and supports the spermatic cord. At the medial end, some fibres do not attach to the pubic tubercle but extend in two directions. Some expand posteriorly and laterally to attach to the pectineal line, forming the lacunar ligament complex. Other fibres pass upwards and medially behind the superficial inguinal ring and external oblique to join the rectus sheath and the linea alba. These constitute the reflected part of the inguinal ligament. Fibres from either side decussate in the linea alba, similarly to the aponeurosis of the abdominal muscles.

Internal oblique

Attachments

Internal oblique lies deep to external oblique for the majority of its course (Fig. 61.2). It is thinner and less bulky than external oblique. Its fibres arise from the lateral two-thirds of the grooved upper surface of the inguinal ligament, where they form a common attachment with the iliac fascia to the inguinal ligament. Laterally, internal oblique is also attached to the anterior two-thirds of the intermediate line of the anterior segment of the iliac crest, and posteriorly some fibres are attached to the thoracolumbar fascia. The fibres originating from the posterior end of the iliac attachment pass upwards and laterally and are attached to the inferior borders and tips of the lower three or four ribs and their cartilages. Here, the attachments merge with those of the internal intercostals. The uppermost of these fibres form a short, free superior border. The fibres attached to the anterior iliac crest diverge and end in the anterior aponeurosis, which gradually broadens from below upwards. The uppermost part of the aponeurosis is attached to the cartilages of the seventh, eighth and ninth ribs. The fibres that originate from the inguinal ligament arch downwards and medially across the spermatic cord in the male and the round ligament of the uterus in the female. They become tendinous, fuse with the corresponding part of the aponeurosis of transversus abdominis, and attach to the crest and medial part of the pectineal line, forming the conjoint tendon.

Vascular supply

Internal oblique is supplied by branches from the lower posterior intercostal and subcostal arteries, the superior and inferior epigastric arteries, the superficial and deep circumflex arteries and the posterior lumbar arteries.

Innervation

Internal oblique is innervated by the terminal branches of the lower five intercostal nerves and the subcostal nerve from the ventral rami of the lower six thoracic spinal nerves, in addition to a small contribution from the iliohypogastric and ilioinguinal nerves from the ventral ramus of the first lumbar spinal nerve.

Actions

Internal oblique contributes to the maintenance of abdominal tone, increasing intra-abdominal pressure, and enables lateral flexion of the trunk against resistance.

Cremaster

Attachments

Cremaster consists of loosely arranged muscle fasciculi lying along the spermatic cord. It is variable in thickness and is thickest in young men. It may form an incomplete coating around the cord, known as the cremasteric fascia, which extends around the testis but lies within the external spermatic fascia. The attachment of the muscle arises mainly from the inferomedial border of internal oblique and transversus abdominis. A separate tendinous attachment may also occur to the middle of the inguinal ligament, extending as far as the anterior superior iliac spine. The medial portion is attached to the pubic tubercle and lateral pubic crest. The fibres spread out over the lateral aspect of the spermatic cord as it approaches the superficial inguinal ring. The shortest and most superior fasciculi turn inwards in front of the cord to join the medial part. The longer, lateral fasciculi blend with the fascia over the cord and upper part of the tunica vaginalis. In the female, a few fibres descending on the round ligament of the uterus represent the lateral part of cremaster. The medial part of the muscle is variably developed, and may be absent. It is attached to the pubic tubercle and the lateral pubic crest, the conjoint tendon and lower border of transversus abdominis. These fasciculi loop on the posteromedial aspect of the cord, interlacing with those of the lateral part. The entire muscle appears to form continuous loops that pass from the middle of the inguinal ligament as far as the tunica vaginalis, and then return to attach to the pubic tubercle.

Vascular supply

Cremaster is supplied by the cremasteric artery, a branch of the inferior epigastric artery.

Innervation

Cremaster is innervated by the genital branch of the genitofemoral nerve, derived from the first and second lumbar spinal nerves.

Actions

Cremaster pulls the testis up towards the superficial inguinal ring. Although its fibres are striated, it is not usually under voluntary control. Stroking the skin of the medial side of the thigh evokes a reflex contraction of the muscle, the cremasteric reflex, which is most pronounced in children. It may represent a protective reflex, and the cremaster may also have a role in testicular thermoregulation.

Transversus abdominis

Attachments

Transversus abdominis is the deepest of the lateral abdominal muscles (Fig. 61.5). It is attached to the lateral one-third of the inguinal ligament and the associated iliac fascia, the anterior two-thirds of the inner lip of the anterior segment of the iliac crest, the thoracolumbar fascia between the iliac crest and the 12th rib, and the internal aspects of the lower six costal cartilages. The costal attachments interdigitate with the attachment of the diaphragm. The muscle ends in an anterior aponeurosis. The lower fibres curve downwards and medially, together with those of the aponeurosis of internal oblique, and insert into the pubic crest and pectineal line to form the conjoint tendon. A band of fibres, sometimes muscular, may run from the lower border of the muscle to the inguinal ligament and is called the inter-foveolar ligament. The remainder of the aponeurosis passes medially and the fibres decussate at, and blend with, the linea alba. The upper costal and anterior iliac fibres of transversus abdominis are short. The lower costal and posterior iliac fibres are longer, and the thoracolumbar fibres are longest. Near the xiphoid process, the aponeurosis is formed only 2–3 cm from the linea alba, so the muscular part of transversus abdominis extends behind rectus into the posterior layer of the rectus sheath. The medial edge of the muscle, at the start of the aponeurosis, curves first downwards and laterally, and is furthest from the lateral edge of the rectus sheath at the level of the umbilicus. It then curves downwards and medially towards the middle of the superior crus of the superficial inguinal ring.

Occasional defects filled with fascia may occur in the lower muscular and aponeurotic parts of both internal oblique and transversus abdominis. The two muscles are sometimes fused and, rarely, transversus abdominis may be absent.

Vascular supply

Transversus abdominis is supplied by branches from the lower posterior intercostal and subcostal arteries, the superior and inferior epigastric arteries, the superficial and deep circumflex arteries and the posterior lumbar arteries.

Innervation

Transversus abdominis is innervated by the terminal branches of the lower five intercostal nerves, the subcostal nerve and the iliohypogastric and ilioinguinal nerves. These arise from the ventral rami of the lower six thoracic and first lumbar spinal nerves.

Actions

Transversus abdominis contributes mainly to the maintenance of abdominal tone and increasing intra-abdominal pressure.

Conjoint tendon

The conjoint tendon is formed from the lower fibres of internal oblique and the lower part of the aponeurosis of transversus abdominis. It is attached to the pubic crest and pectineal line. It descends behind the superficial inguinal ring and acts to strengthen the medial portion of the posterior wall of the inguinal canal. The attachment to the pectineal line is frequently absent. Medially, the upper fibres of the tendon fuse with the anterior wall of the rectus sheath, and laterally some fibres may blend with the interfoveolar ligament.

Inguinal canal

The inguinal canal is a natural hiatus in the tissues of the anterior abdominal wall, and is formed from the various layers of the wall in the region of the groin (Figs 61.12, 61.13, 61.14, 61.15, and see Fig. 76.2). Its size and form vary with age, and although it is present in both sexes it is most well developed in the male. The canal is an oblique tunnel, with deep and superficial openings or rings. It contains the spermatic cord in males, the round ligament of the uterus in females, and the ilioinguinal nerve in both sexes.

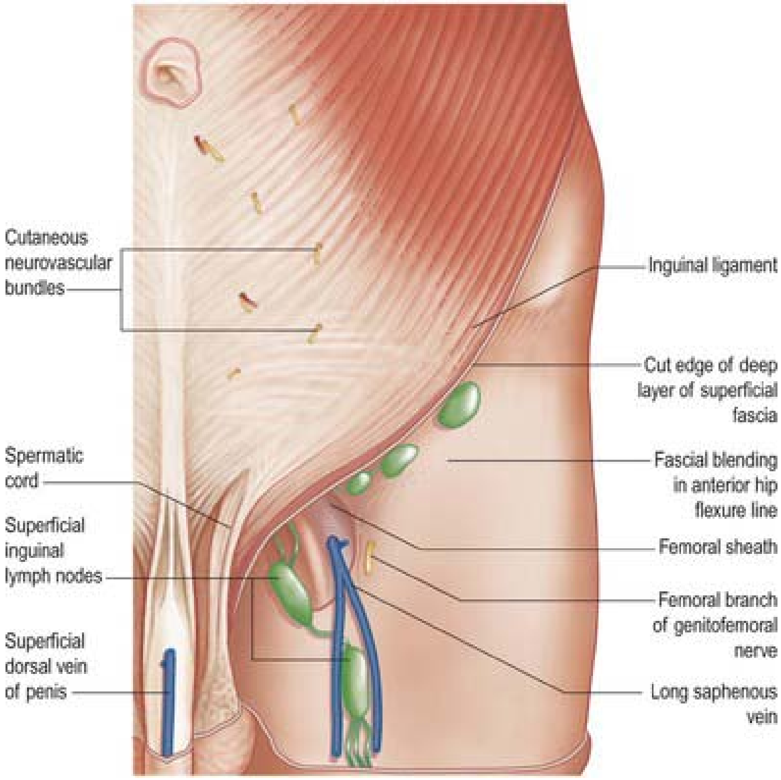
Cutaneous neurovascular bundles
Spermatic cord
Superficial inguinal lymph nodes
Superficial dorsal vein of penis
Inguinal ligament
Cut edge of deep layer of superficial fascia
Fascial blending in anterior hip flexure line
Femoral sheath
Femoral branch of genitofemoral nerve
Long saphenous vein

Fig. 61.12 Superficial structures of the inguinal region and lower part of the anterior abdominal wall on the left side.

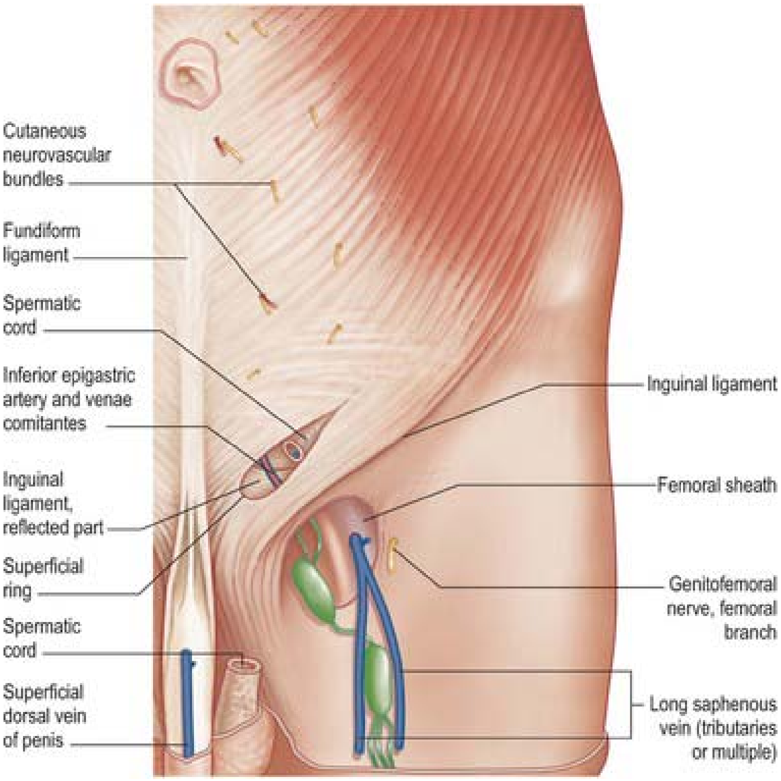
Cutaneous neurovascular bundles
Fundiform ligament
Spermatic cord
Inferior epigastric artery and venae comitantes
Inguinal ligament, reflected part
Superficial ring
Spermatic cord
Superficial dorsal vein of penis
Inguinal ligament
Femoral sheath
Genitofemoral nerve, femoral branch
Long saphenous vein (tributaries or multiple)

Fig. 61.13 Superficial structures of the inguinal region and lower part of the anterior abdominal wall on the left side: superficial aponeurotic layer removed.

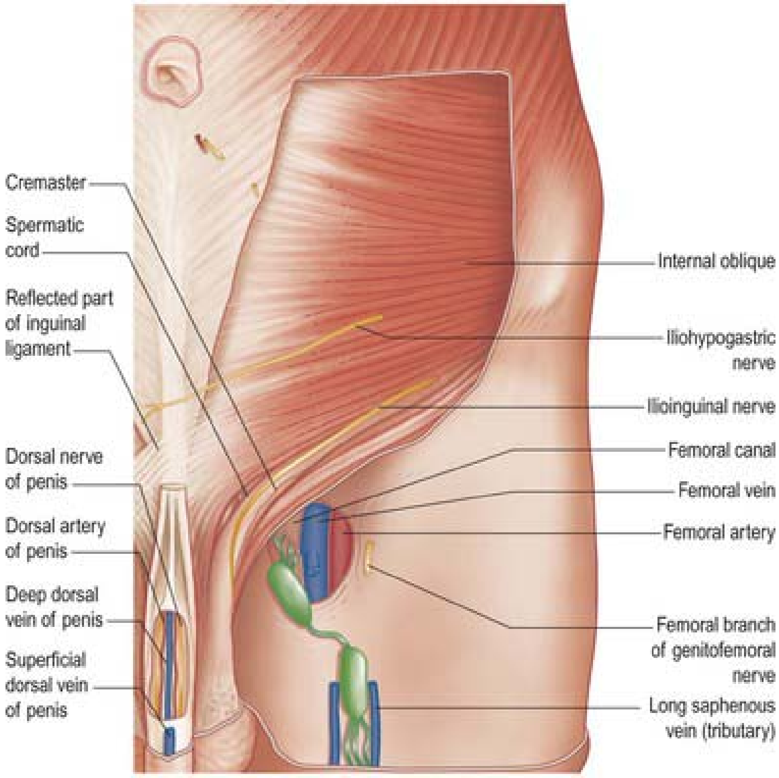
Cremaster
Spermatic cord
Reflected part of inguinal ligament
Dorsal nerve of penis
Dorsal artery of penis
Deep dorsal vein of penis
Superficial dorsal vein of penis
Internal oblique
Iliohypogastric nerve
Ilioinguinal nerve
Femoral canal
Femoral vein
Femoral artery
Femoral branch of genitofemoral nerve
Long saphenous vein (tributary)

Fig. 61.14 Dissection of the regions shown in Fig. 61.12, with part of external oblique removed.

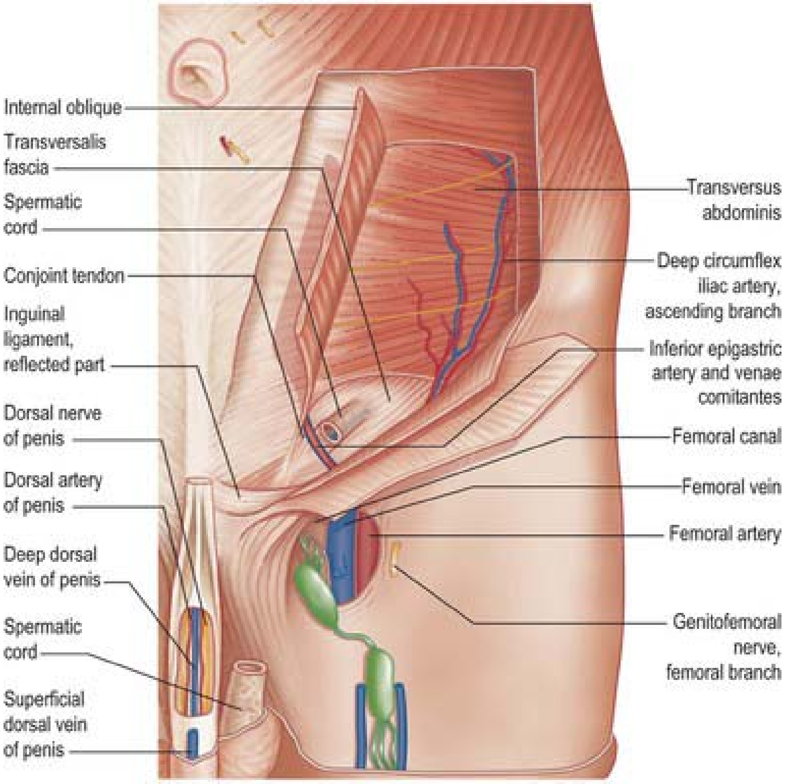
Internal oblique
Transversalis fascia
Spermatic cord
Conjoint tendon
Inguinal ligament, reflected part
Dorsal nerve of penis
Dorsal artery of penis
Deep dorsal vein of penis
Spermatic cord
Superficial dorsal vein of penis
Transversus abdominis
Deep circumflex iliac artery, ascending branch
Inferior epigastric artery and venae comitantes
Femoral canal
Femoral vein
Femoral artery
Genitofemoral nerve, femoral branch

Fig. 61.15 Dissection of the regions shown in Fig. 61.13, with parts of external and internal oblique muscles removed.

Superficial inguinal ring

The superficial inguinal ring is a hiatus in the aponeurosis of external oblique, just above and lateral to the crest of the pubis. The ring is actually triangular, and its apex points along the line of the deep fibres of the aponeurosis. Although it varies in size, it does not usually extend laterally beyond the medial one-third of the inguinal ligament – the ring is smaller in the female. The base lies along the crest of the pubis and its sides are the crura of the opening in the aponeurosis. The lateral crus is the stronger and is reinforced by fibres of the inguinal ligament inserted into the pubic tubercle. The medial crus is thin. The fibres attach to the front of the symphysis pubis and interlace with fibres from the opposite side. In the external layer of the investing fascia of external oblique, some fibres arch above the apex of the superficial inguinal ring as intercrural fibres. In the male, the lateral crus is curved to form a groove, in which the spermatic cord rests. Fibres from the aponeurosis of external oblique and overlying fascia continue downwards from the crura of the ring, and form a delicate tubular prolongation of fibrous tissue around the spermatic cord and testis. This is the external spermatic fascia and constitutes the outermost covering of the cord. The superficial inguinal ring is only a distinct aperture when the continuity of this fascia with the aponeurosis is interrupted.

Deep inguinal ring

The deep inguinal ring is situated in the transversalis fascia, midway between the anterior superior iliac spine and the symphysis pubis approximately 1.25 cm above the inguinal ligament. It is oval, with an almost vertical long axis. Its size varies between individuals, and it is always much larger in the male. It is related above to the arched lower margin of transversus abdominis, and medially to the inferior epigastric vessels and the interfoveolar ligament, when that is present. Traction on the fascial ring exerted by internal oblique may constitute a valve-like safety mechanism when intra-abdominal pressure is increased.

Boundaries

The inguinal canal is a virtual space lying between the various layers formed from the lower tissues of the anterior abdominal wall. It lies obliquely and slants downwards and medially, parallel with and a little above the inguinal ligament. It extends from the deep to the superficial inguinal rings: the length depends on the age of the individual, but in the adult is between 3 and 5 cm long. The canal is bounded anteriorly by the skin, superficial fascia and aponeurosis of external oblique. In its lateral one-third, the anterior wall is reinforced by the muscular fibres of the internal oblique just above their origin from the inguinal ligament. Posteriorly lie the reflected inguinal ligament, the conjoint tendon and the transversalis fascia, which separate it from extraperitoneal connective tissue and peritoneum. Superiorly lie the arched fibres of internal oblique and transversus abdominis, forming the conjoint tendon, and inferiorly is the union of the transversalis fascia with the inguinal ligament and, at the medial end, the lacunar ligament.

In the newborn, the deep and superficial rings are nearly superimposed and the canal is extremely short. This creates an approximately oval defect in the abdominal wall. As the child grows, the anterior abdominal wall muscles grow rapidly, causing the positions of the rings to separate and the canal to lengthen. The defect thus becomes progressively more oblique until, in adulthood, the presence of separate anterior and posterior canal walls forms a ‘flap valve’ effect. Increases in intra-abdominal pressure transmitted through the posterior wall and the deep ring are supported by the presence of the thickest part of the overlying anterior wall. At the superficial ring and medial end of the anterior wall, where it is weakest, the posterior wall is strengthened by the conjoint tendon and the reflected inguinal ligament. The fibres of internal oblique and transversus abdominis, which form the conjoint tendon, are constantly active in standing; this activity increases during episodes of increased intra-abdominal pressure.

Relations

The inferior epigastric vessels are important posterior relations of the medial end of the canal (Fig. 61.16). They lie on the transversalis fascia as they ascend obliquely behind the conjoint tendon into the posterior portion of the rectus sheath.

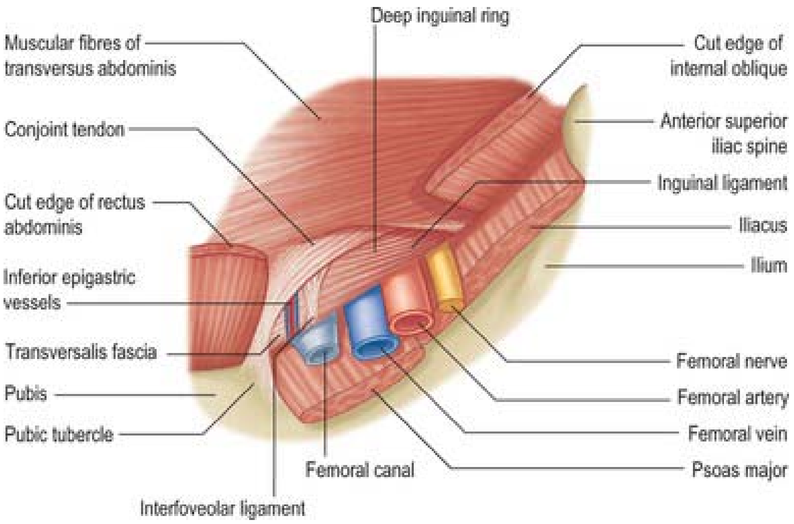
Deep inguinal ring
Muscular fibres of transversus abdominis
Cut edge of internal oblique
Anterior superior iliac spine
Conjoint tendon
Inguinal ligament
Cut edge of rectus abdominis
Iliacus
Ilium
Inferior epigastric vessels
Transversalis fascia
Femoral nerve
Pubis
Femoral artery
Pubic tubercle
Femoral vein
Femoral canal
Psoas major
Interfoveolar ligament

Fig. 61.16 Deep structures of the inguinal canal. The aponeurosis of external oblique has been removed. For clarity, the fibres of internal oblique

and rectus abdominis have been divided and the structures passing posteroinferiorly to the inguinal ligament have been excluded.

The inguinal triangle lies in the posterior wall of the canal. It is bounded inferiorly by the medial half of the inguinal ligament, medially by the lower lateral border of rectus abdominis and laterally by the inferior epigastric artery, and overlies the medial inguinal fossa and, in part, the supravesical fossa.

Lacunar ligament

The lacunar ligament is a thick triangular band of tissue lying mainly posterior to the medial end of the inguinal ligament. It measures approximately 2 cm from base to apex and is a little larger in the male. It is formed from fibres of the medial end of the inguinal ligament and fibres from the fascia lata of the thigh, which join the medial end of the inguinal ligament from below. The inguinal fibres run posteriorly and laterally to the medial end of the pectineal line and are continuous with the pectineal fascia. They form a near horizontal, triangular sheet with a curved lateral border which forms the medial border of the femoral canal. The apex of the triangle is attached to the pubic tubercle. A strong fibrous band, the pectineal ligament of Astley Cooper, extends laterally along the pectineal line from the pectineal attachment. The fibres from the fascia lata join the inferior/posterior border of the inguinal ligament; the latter, in combination with fibres from the transversalis fascia, fuses with the pectineal fascia as it joins the thickened periosteum of the pectineal line. This portion of the lacunar ligament forms the lower extension of the medial border of the femoral canal and femoral sheath.

HERNIAS OF THE ANTERIOR ABDOMINAL WALL

INGUINAL HERNIA

Although the inguinal canal is arranged such that the weaknesses in the anterior abdominal wall caused by the deep and superficial inguinal rings are supported, the region remains a potential cause of herniation. An inguinal hernia involves the protrusion of a viscus through the tissues of the inguinal region of the abdominal wall.

Indirect inguinal hernia

An indirect hernia is defined as arising lateral to the inferior epigastric vessels. Many indirect hernias are related to the congenital abnormal persistence of the vaginal process, others are acquired as a result of progressive weakening of the lateral and posterior walls of the canal. The hernia may pass through the deep ring or may expand the deep ring such that it is no longer a clear entity. Small indirect hernias tend to lie below and lateral to the fibres of the conjoint tendon, but larger hernias often distort and thin the tendon superiorly. Small hernias, which do not protrude beyond the inguinal canal, are covered by the same inner layers as the spermatic cord, including the internal spermatic fascia and cremaster. If the hernia extends through the superficial inguinal ring it is additionally covered by external spermatic fascia.

In hernias related to a persistent fully patent vaginal process, the hernia contents descend in front of the testis into the tunica vaginalis (complete congenital hernia) and the vaginal process and tunica form part of the hernial sac. Where the vaginal process is sealed off from the tunica vaginalis, the hernia contents descend to the top of the testis (incomplete congenital hernia). Although both types are related to a congenital abnormality, actual herniation into the potential sac may not occur until adult life, when it may happen as a consequence of increased intra-abdominal pressure or sudden muscular strain.

Direct inguinal hernia

A direct inguinal hernia is defined as arising medial to the inferior epigastric vessels. Direct hernias are always caused by an acquired weakness of the inguinal triangle in the medial posterior wall of the canal, and frequently extend through the anterior wall of the canal or superficial ring. The hernia may protrude through the transversalis fascia, between the conjoint tendon and the inferior epigastric vessels, and enter the inguinal canal. It may closely resemble an indirect hernia, in that the coverings are similar. Its clinical presentation can also mimic an indirect inguinal hernia. Other direct hernias arise either between the fibres of the conjoint tendon or by eventration of the tendon such that it forms a thin covering to the hernia. In either case, a hernia enters the lower end of the canal, protruding through the superficial ring medial to the cord, and is covered by external spermatic fascia.

Clinical features of inguinal hernias

Indirect hernias often descend from lateral to medial in the same oblique angle as the canal, because of their origin in the lateral end of the inguinal canal. This is particularly true for congenital hernias. Direct hernias arise from the medial end of the canal and tend to protrude more directly anteriorly. With the patient in the supine position and the hernia reduced, pressure applied over the region of the deep inguinal ring may prevent appearance of an indirect hernia on standing or straining. This method of determining the type of hernia is fraught with difficulties. Indirect hernias may have a wide neck, and occlusion of the deep ring may not be possible with simple digital pressure. An acquired indirect hernia may arise medial to the deep ring. The angle of the descent of the hernia is also an unreliable guide, as it depends on the size of the defect in the posterior wall of the canal, the length of the canal and whether the hernia protrudes through the anterior wall. Direct hernias are more likely to have a wide-necked origin, making strangulation less likely.

FEMORAL HERNIA

A femoral hernia protrudes through the femoral ring. The femoral ring is normally closed by a femoral septum of modified extraperitoneal tissue, and is therefore a weak spot. In females, the ring is relatively large and subject to profound changes during pregnancy, which explains why femoral hernias are more common in women. When a section of intestine bulges through the ring, it pushes out a hernial sac of peritoneum. It is covered by extraperitoneal tissue (the femoral septum) and descends along the femoral canal to the saphenous opening. It is prevented from descending further along the femoral sheath by the narrow saphenous opening, by the vessels and by the close attachment of the superficial fascia and sheath to the lower part of the rim of the saphenous opening. The hernia hence turns forwards, distending the cribriform fascia and curving upwards over the inguinal ligament and the lower part of the aponeurosis of external oblique. While in the canal the hernia is usually small, because of the resistance of surrounding tissues, but it enlarges as it escape into the inguinal loose connective tissue. A femoral hernia first descends and then ascends forwards: pressure to reduce it should therefore be directed in the reverse order, with the thighs passively flexed for greatest relaxation.

The coverings of a femoral hernia are, from within outwards: the peritoneum, femoral septum, femoral sheath, cribriform fascia, superficial fascia and skin. A fibrous covering, the fascia propria, may lie outside the peritoneal sac and is frequently separated from it by adipose tissue. It represents a femoral septum which has been thickened to form a membranous sheet by hernial pressure. The fascia propria may easily be mistaken for the sac, and its contained extraperitoneal fat for omentum; the fat may resemble a lipoma, but dissection will reveal the true hernial sac in its centre. The intestine reaches only to the saphenous opening in incomplete femoral hernia, in contradistinction to complete hernia, in which it passes through the opening. The small size of an incomplete hernia renders it difficult to detect and therefore dangerous, especially in the corpulent. The site of strangulation varies: it may be at the neck of the hernial sac, more often it is at the junction of the falciform margin of the saphenous opening with the free edge of the pectineal part of the inguinal ligament, or it may be at the saphenous opening. The site of narrowing should be divided superomedially for a distance of 4–6 mm to avoid all normally positioned vessels and other important structures. Occasionally the obturator artery is replaced by an enlarged pubic branch of the inferior epigastric artery descending almost vertically to the obturator foramen. This vessel sometimes curves along the edge of the lacunar part of the inguinal ligament, encircling the neck of a hernial sac, and may be inadvertently cut during enlargement of the femoral ring in reducing a femoral hernia.

The pubic tubercle is an important landmark in distinguishing inguinal from femoral hernias; the neck of the hernia is superomedial to it in inguinal hernia, but inferolateral in the femoral form.

LESIONS OF THE INTERCOSTAL NERVES

Lesions of individual intercostal nerves do not produce any appreciable clinical effects. The anterolateral muscles are innervated by a number of different nerves: injury to a single nerve will not reduce the tone of the muscle wall. The overlap between sequential dermatomes means that significant cutaneous anaesthesia is appreciated only after sectioning of at least two sequential nerves.

REFERENCES

rmack GC, George B, Lamberty H. The Arterial Anatomy of Skin Flaps, 2nd edn., London, Edinburgh: Churchill Livingstone; 1994:168-172.

tle WJ. Inguinal anatomy. *J Anat*. 1979;128:581-594.

zk NN. A new description of the anterior abdominal wall in man and mammals. *J Anat*. 1980;131:373-385.

afik A. The cremasteric muscle. In: Johnson AD, Gomes WR. *The Testis*. New York: Academic Press, 1977.

CHAPTER 62

Posterior abdominal wall and retroperitoneum

The posterior abdominal wall consists of fasciae, muscles and their vessels and spinal nerves; the overlying skin is continuous with that of the back. It is not easily defined, and is best described as that part of the abdominal wall lying between the two mid-dorsal lines, below the posterior attachments of the diaphragm and above the pelvis. It is continuous laterally with the anterolateral abdominal wall, superiorly with the posterior wall of the thorax behind the attachments of the diaphragm and inferiorly with the structures of the pelvis. The spinal column forms part of its structure and the muscles and fasciae of the back are closely related to it, especially posterolaterally.

The major vessels and lymphatic channels, in addition to the peripheral autonomic nervous systems of the abdomen, pelvis and lower limbs lie on the posterior abdominal wall. These structures, together with several viscera (including the kidneys [Ch. 74], suprarenal glands [Ch. 72], pancreas [Ch. 70], ureters [Ch. 74] and parts of the gut tube [Chs 66 and 67]), lie beneath the posterior parietal peritoneum. These tissues and their surrounding connective and fascial planes are collectively referred to as the retroperitoneum.

It has been suggested that the retroperitoneum can be divided into several spaces according to their relationships to the fascial layers that surround the kidneys and ureters. In this description, the layers of the perirenal fascia enclose a perirenal space containing the kidney, suprarenal gland, upper ureter and their neurovascular supply. The anterior layer of the perirenal fascia is continuous across the midline anterior to the main neurovascular structures of the retroperitoneum, and the right and left perirenal spaces communicate, although this channel is limited and contains many of the midline neurovascular structures of the retroperitoneum. Behind the posterior layer of the perirenal fascia lies the posterior pararenal space. Anterior to the anterior layer of the perirenal fascia lies the anterior pararenal space, in which lie several retroperitoneal parts of the gut tube, including the duodenum and pancreas. The anterior pararenal spaces are also continuous across the midline and are limited posteriorly by the anterior communicating layer of the perirenal fascia and anteriorly by the parietal peritoneum. This description helps to explain why moderate amounts of fluid, blood or pus collecting in the retroperitoneum tend to remain constrained within the space in which they are formed although, for pathological processes such as tumour invasion, the fascial planes provide a weak barrier to local spread (Figs 62.1, 62.2).

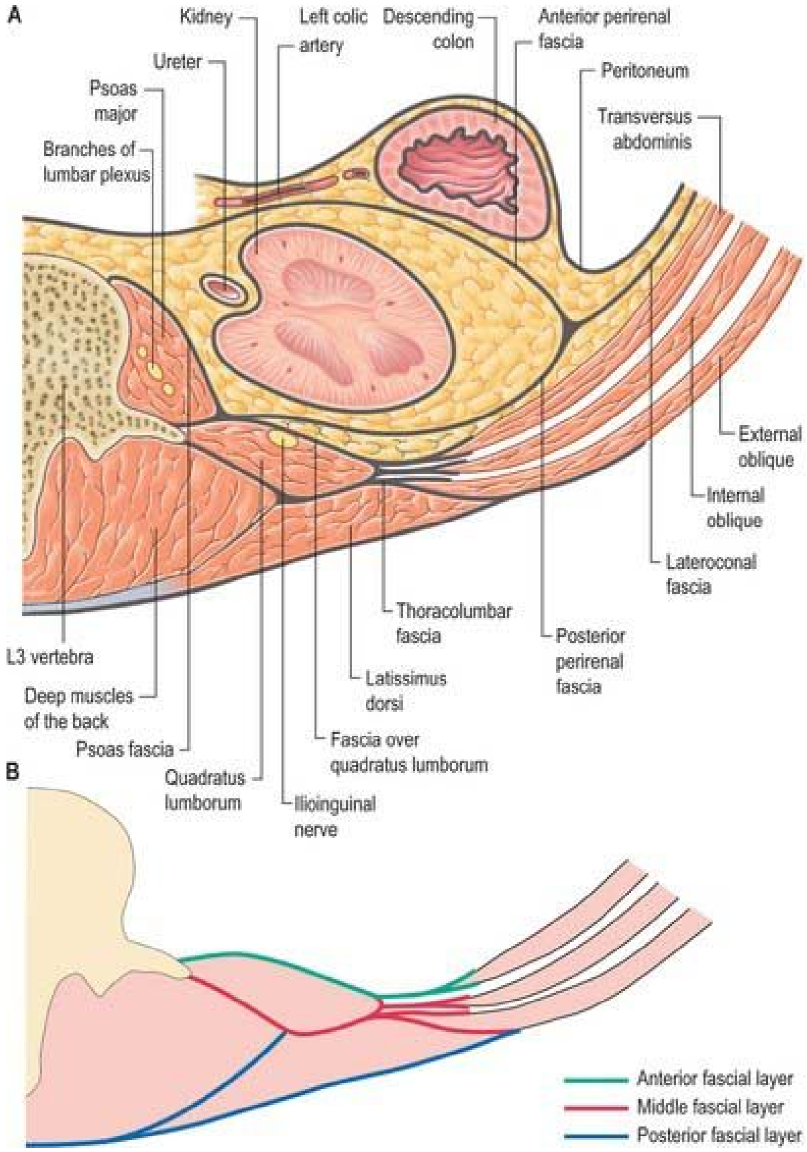
A
Kidney
Left colic artery
Descending colon
Anterior perirenal fascia
Ureter
Peritoneum
Psoas major
Transversus abdominis
Branches of lumbar plexus
External oblique
Internal oblique
Lateroconal fascia
Thoracolumbar fascia
Posterior perirenal fascia
L3 vertebra
Latissimus dorsi
Deep muscles of the back
Fascia over quadratus lumborum
Psoas fascia
B
Quadratus lumborum
Ilioinguinal nerve
Anterior fascial layer
Middle fascial layer
Posterior fascial layer

Fig. 62.1 Fascial layers of the upper posterior abdominal wall. **A**, Transverse section just below the level of the hilum of the kidney. For clarity, the deep muscles of the back have not been identified separately. **B**, The separate layers of the thoracolumbar fascia.

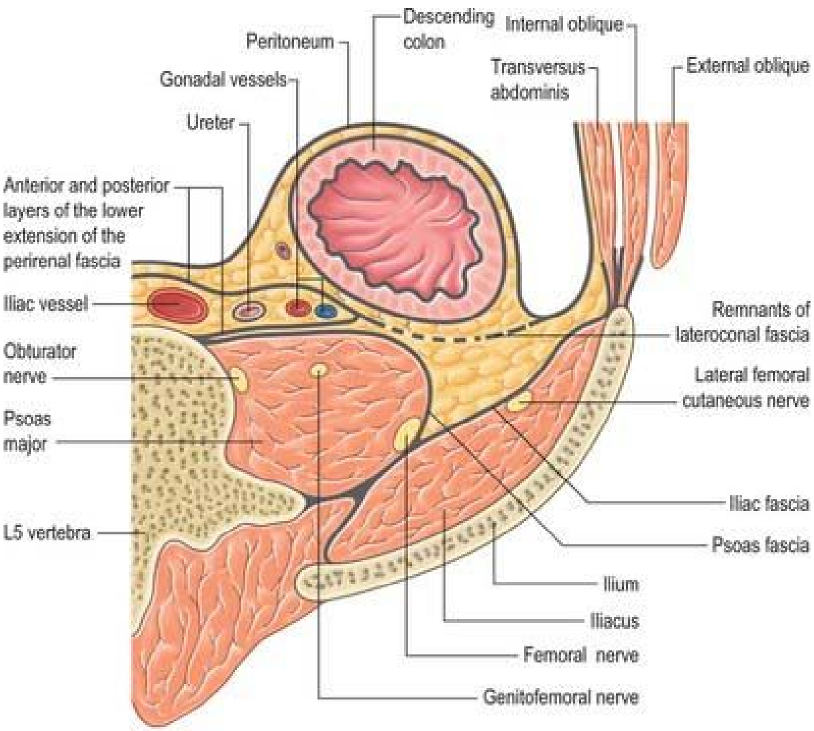
Descending colon
Internal oblique
Peritoneum
Transversus abdominis
External oblique
Gonadal vessels
Ureter
Anterior and posterior layers of the lower extension of the perirenal fascia
Iliac vessel
Remnants of lateroconal fascia
Obturator nerve
Lateral femoral cutaneous nerve
Psoas major
Iliac fascia
L5 vertebra
Psoas fascia
Ilium
Iliacus
Femoral nerve
Genitofemoral nerve

Fig. 62.2 Fascial layers of the lower posterior abdominal wall. Transverse section at the level of the fifth lumbar vertebra.

Several structures, such as the pancreas, are referred to as being retroperitoneal. Although they are derived embryologically from the gut tube, they are not readily separated from the other retroperitoneal structures. Several other structures, such as the descending colon, are also referred to as being retroperitoneal, but they remain separated from the other retroperitoneal structures by a clearly defined fascial plane, which corresponds with the plane of fusion of their mesentery during development. This is of relevance during surgical exposure of the retroperitoneal organs and in some pathological processes: those defined by clear fascial planes may be mobilized with little or no risk of bleeding, whereas mobilization of the pancreas, for example, is difficult and often very vascular.

SKIN AND SOFT TISSUES

The skin of the back in the region of the posterior abdominal wall is similar to that of the rest of the trunk. It is supplied by vessels from the musculocutaneous branches of the lumbar arteries and veins, and receives its innervation from the dorsal rami of the lumbar spinal and lower thoracic nerves.

The soft tissues of the posterior abdominal wall and retroperitoneum are composed of several distinct layers of fascia, which divide them into anatomically distinct compartments.

THORACOLUMBAR FASCIA

The thoracolumbar fascia in the lumbar region is in three layers (Figs 62.1, 62.2, 62.3). The posterior layer is attached to the spines of the lumbar and sacral vertebrae and to the supraspinous ligaments. The middle layer is attached medially to the tips of the transverse processes of the lumbar vertebrae and the intertransverse ligaments, inferiorly to the iliac crest, and superiorly to the lower border of the 12th rib and the lumbocostal ligament. The anterior layer covers quadratus lumborum and is attached medially to the anterior surfaces of the transverse processes of the lumbar vertebrae behind the lateral part of psoas major. Inferiorly, it is attached to the iliolumbar ligament and the adjoining part of the iliac crest. Superiorly, it is attached to the apex and inferior border of the 12th rib and then extends to the transverse process of the first lumbar vertebra, to form the lateral arcuate ligament of the diaphragm. The posterior and middle layers of the thoracolumbar fascia unite at the lateral margin of erector spinae. At the lateral border of quadratus lumborum they are joined by the anterior layer, to form the aponeurotic origin of transversus abdominis.

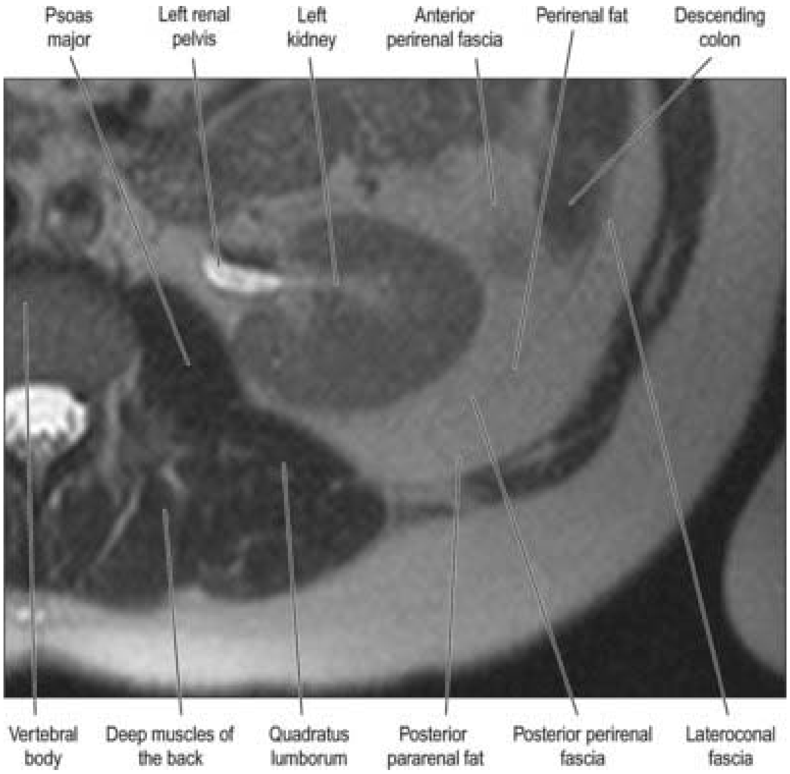
Psoas major
Left renal pelvis
Left kidney
Anterior perirenal fascia
Perirenal fat
Descending colon
Vertebral body
Deep muscles of the back
Quadratus lumborum
Posterior pararenal fat
Posterior perirenal fascia
Lateroconal fascia

Fig. 62.3 Axial T2 weighted MRI scan showing the fascial layers of the posterior abdominal wall at the level of the renal hilum.

(Courtesy of Dr Louise Moore, Chelsea & Westminster Hospital, London.)

OTHER FASCIAL LAYERS

Psoas fascia

Psoas major is enclosed within a layer of fascia over its anterior surface. The medial border is continuous with the attachments of the muscle to the transverse processes of the lumbar vertebrae, the bodies of the lumbar vertebrae and the tendinous arches. Superiorly, the fascia forms part of the medial arcuate ligament. Laterally, the fascia blends with the fascia over quadratus lumborum in the upper part of the muscle and is continuous with the iliac fascia lower down. It separates the anterior mass of psoas major from the retroperitoneal structures lying on it. The fascia extends down into the thigh. Inflammatory collections arising from the paraspinal tissues or the retroperitoneal tissues that penetrate through the fascia tend to be confined by it, and they may track down the length of the muscle, to appear in the groin where the fascia is thinnest.

Iliac fascia

The iliac fascia is continuous with and indistinguishable from the psoas fascia. The fascia blends with the anterior layer of the thoracolumbar fascia over quadratus lumborum in the upper retroperitoneum. Lower down, it is attached firmly to the inner aspect of the iliac crest and medially to the periosteum of the ilium at the pelvic brim. It is also attached in the abdomen to the iliopectineal eminence.

Perirenal fascia

The perirenal fascia is a multilaminated fascial layer that surrounds the kidney, suprarenal glands, upper ureter and associated fat, which all lie in the perirenal space (see Ch. 74). Although described as having anterior and posterior layers, these are continuous with each other laterally, and give rise to the lateroconal fascia at this point (Figs 62.1-62.3). The posterior layer of the renal fascia is adherent to the fascia over psoas major, the iliac fascia and the anterior layers of the thoracolumbar fascia. In the obese, there may be some loose adipose tissue between these layers, but it is rarely thick. The anterior part of the renal fascia separates the kidney and the perirenal space from the overlying anterior pararenal space and its associated viscera (on the right the duodenum, ascending colon and right colonic mesentery and on the left the duodenum, descending colon and left colonic mesentery). Inferiorly, the perirenal fascia continues down and encloses the ureter. It becomes progressively thinner towards the brim of the pelvis, where it is no longer distinguishable from the loose general connective tissue of the retroperitoneum.

Lateroconal fascia

The lateroconal fascia is formed from the lateral aspect of the perirenal fascia and extends anterolaterally to fuse with the fascia over transversus abdominis. It divides the anterior and posterior pararenal spaces from each other, but is thinnest in the inferior part of the retroperitoneum.

POSTERIOR EXTRAPERITONEAL CONNECTIVE TISSUE

The retroperitoneum usually contains loose connective tissue between the fascial layers. This is particularly true around the renal fascia and anterior to the psoas and iliac fascia. In all but the thinnest individuals, there is some adipose tissue present in these areas, and in the obese it may be markedly thickened. The retroperitoneal arteries and veins lie within this tissue, but the branches of the lumbar plexus of nerves lie deep to it, beneath the iliac and psoas fascia.

BONES

The posterior abdominal wall is supported by the bony structures of the vertebral column and bony pelvis. These include the lower two ribs, the 12th thoracic and five lumbar vertebrae, and the sacrum and ilium, in addition to their interconnecting ligaments.

MUSCLES

The majority of the muscles of the posterior abdominal wall are functionally part of the lower limb or vertebral column. They provide the surface against which the neurovascular structures of the retroperitoneum lie, and they are supported and separated from the majority of the retroperitoneal structures by fascial layers (Figs 62.4, 62.5; see Fig. 62.14).

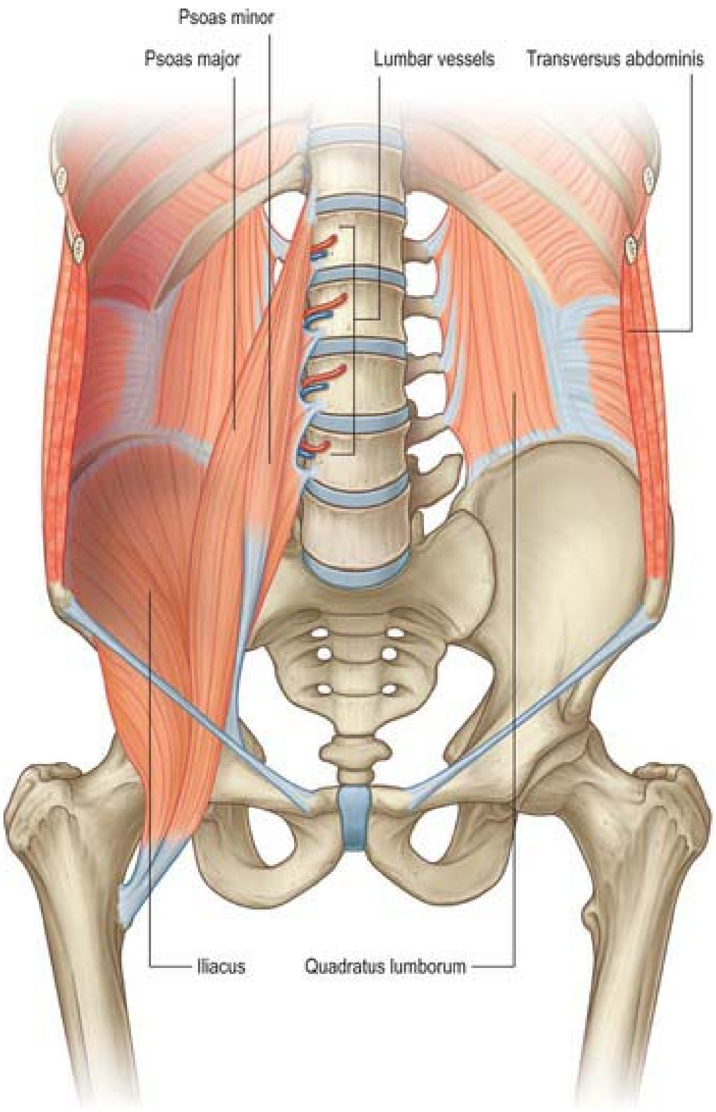
Psoas minor
Psoas major
Lumbar vessels
Transversus abdominis
Iliacus
Quadratus lumborum

Fig. 62.4 Bones and deep muscles of the posterior abdominal wall. Left psoas major and the diaphragm have been removed.

(Adapted from Drake, Vogl and Mitchell 2005.)

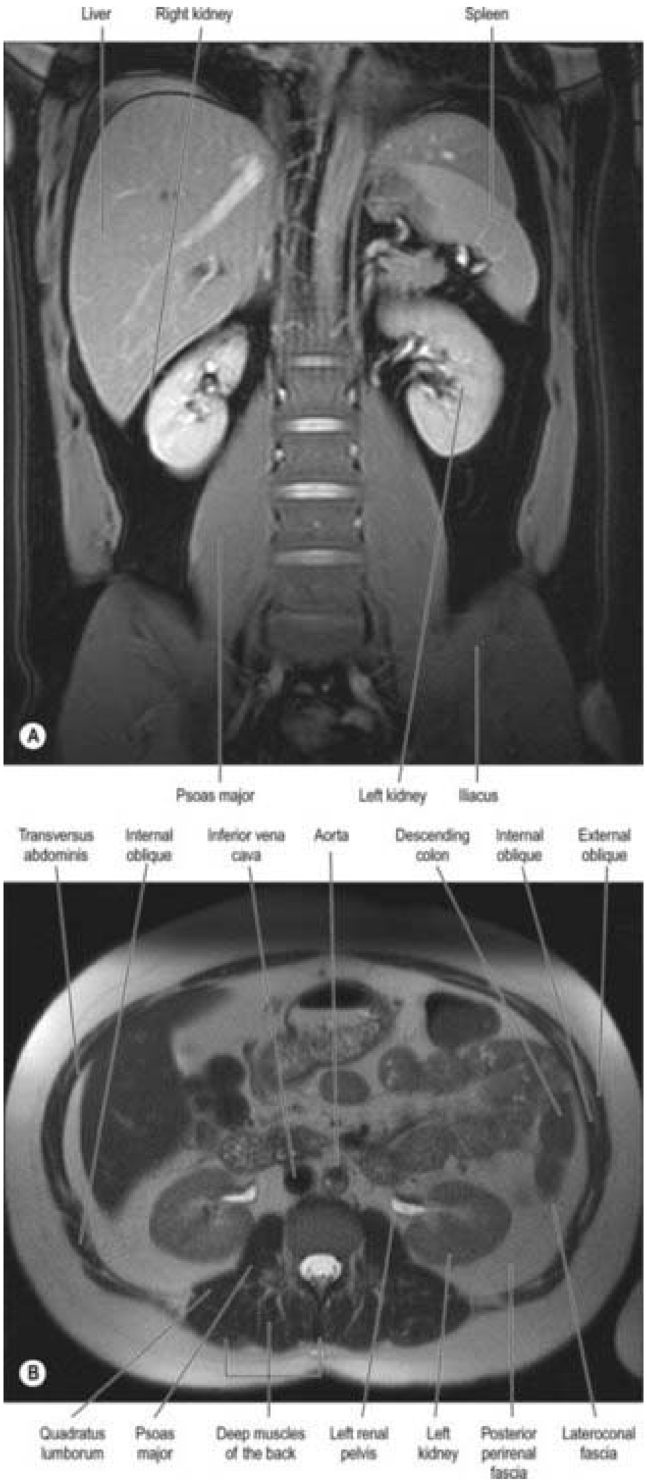
Liver
Right kidney
Spleen
A
Psoas major
Left kidney
Iliacus
Transversus abdominis
Internal oblique
Inferior vena cava
Aorta
Descending colon
Internal oblique
External oblique
B
Quadratus lumborum
Psoas major
Deep muscles of the back
Left renal pelvis
Left kidney
Posterior perirenal fascia
Lateroconal fascia

Fig. 62.5 Muscles of the posterior abdominal wall. **A**, Coronal True FISP MRI. **B**, Axial T2 weighted MRI. (Provided by Dr Louise Moore Chelsea & Westminster Hospital.)

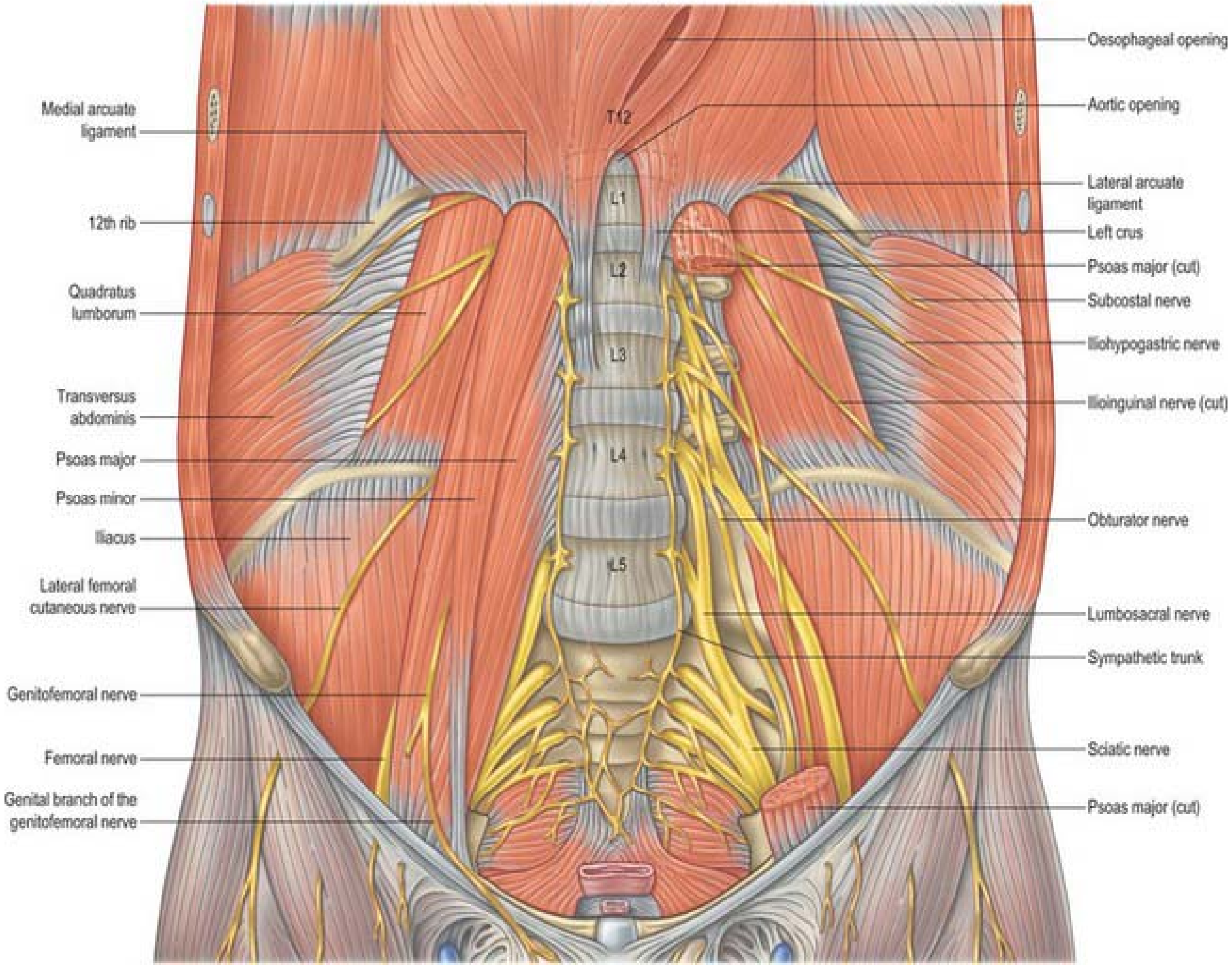
Medial arcuate ligament
12th rib
Quadratus lumborum
Transversus abdominis
Psoas major
Psoas minor
Iliacus
Lateral femoral cutaneous nerve
Genitofemoral nerve
Femoral nerve
Genital branch of the genitofemoral nerve
T12
L1
L2
L3
L4
L5
Oesophageal opening
Aortic opening
Lateral arcuate ligament
Left crus
Psoas major (cut)
Subcostal nerve
Iliohypogastric nerve
Ilioinguinal nerve (cut)
Obturator nerve
Lumbosacral nerve
Sympathetic trunk
Sciatic nerve
Psoas major (cut)

Fig. 62.14 Muscles and nerves of the posterior abdominal wall. The left psoas major has been removed to expose the origins of the lumbar plexus and quadratus lumborum.

Quadratus lumborum

Quadratus lumborum is an irregularly shaped quadrilateral muscle, which is broader at its inferior attachment than superiorly.

Attachments

Quadratus lumborum is attached below by aponeurotic fibres to the iliolumbar ligament and the adjacent portion of the iliac crest for approximately 5 cm. The superior attachment is to the medial half of the lower border of the 12th rib, and by four small tendons to the apices of the transverse processes of the upper four lumbar vertebrae. Sometimes it is also attached to the transverse process or body of the 12th thoracic vertebra. Occasionally, a second layer of this muscle is found in front of the first, attached to the upper borders of the transverse processes of the lower three or four lumbar vertebrae and to the lower margin and the lower part of the anterior surface of the 12th rib.

Relations

Anteriorly are the colon (ascending on the right, descending on the left), kidney, psoas major and minor, and diaphragm. The subcostal, iliohypogastric and ilioinguinal nerves lie on the fascia anterior to the muscle, but are bound down to it by the medial continuation of the transversalis fascia.

Vascular supply

Quadratus lumborum is supplied by branches of the lumbar arteries, the arteria lumbalis ima, the lumbar branch of the iliolumbar artery and branches of the subcostal artery.

Innervation

Quadratus lumborum is innervated by the ventral rami of the 12th thoracic and upper three or four lumbar spinal nerves.

Actions

Quadratus lumborum fixes the last rib, and acts as a muscle of inspiration by helping to stabilize the lower attachments of the diaphragm. It has been suggested that this action might also provide a fixed base for controlled relaxation of the diaphragm in the precise adjustment of expiration needed for speech and singing. With the pelvis fixed, quadratus acts upon the vertebral column, flexing it to the same side. When both muscles contract, they probably help to extend the lumbar part of the vertebral column.

Psoas major

Psoas major has several sites of abdominal attachment. Posteriorly, the attachments are to the anterior surfaces and lower borders of the transverse processes of all the lumbar vertebrae. The muscle arising from these attachments is referred to as the posterior mass. The muscle also has an anterior mass. It consists of two different sets of attachments. The first part is five slips of muscle attached to the bodies of two adjoining vertebrae and their intervertebral disc (from the 12th thoracic vertebra and the thoracolumbar disc to the body of the fifth lumbar vertebra). The second part is a series of tendinous arches extending across the narrow parts of the bodies of the five lumbar vertebrae between these slips. The upper four lumbar intervertebral foramina bear important relations to these attachments of the muscle. The foramina lie anterior to the transverse processes (the posterior attachments) and posterior to the vertebral bodies, discs and tendinous arches (anterior attachments). The roots of the lumbar plexus therefore enter the muscle directly between the two masses and the plexus is lodged within it. The branches then emerge from the borders and surfaces of psoas major.

Psoas minor

Psoas minor is often absent but, when present, lies anterior to psoas major. It arises from the sides of the bodies of the 12th thoracic and first lumbar vertebrae and from the disc between them, and ends in a long, flat tendon attached to the pectineal line and iliopectineal eminence and, laterally, to the iliac fascia.

Erector spinae

The muscles of the erector spinae group (see Ch. 42) do not form part of the posterior abdominal wall itself, but are closely associated with the fascial layers of the posterior wall.

Iliacus

Iliacus is a triangular sheet of muscle that arises from the superior two-thirds of the concavity of the iliac fossa, the inner lip of the iliac crest, the ventral sacroiliac and iliolumbar ligaments and the upper surface of the lateral part of the sacrum. It reaches as far as the anterior superior and anterior inferior iliac spines, and receives a few fibres from the upper part of the capsule of the hip joint. Most of its fibres converge into the lateral side of the strong tendon of psoas major. It lines the posterior wall of the lesser pelvis formed by the ilium.

Posterior abdominal wall hernias

Herniation through the posterior abdominal wall is extremely rare because the fascial layers usually provide an excellent protection against protrusion of the posterior abdominal viscera, which are relatively immobile. However, the posterior free border of external oblique and the inferior free border of latissimus dorsi create an area of potential weakness, referred to as the lumbar triangle. Spontaneous hernias through this tissue are very rare in the absence of previous surgical access such as a nephrectomy.

VASCULAR SUPPLY AND LYMPHATIC DRAINAGE

ABDOMINAL AORTA

The abdominal aorta begins at the median, aortic hiatus of the diaphragm, anterior to the inferior border of the 12th thoracic vertebra and the thoracolumbar intervertebral disc (Figs 62.6, 62.7). It descends anterior to the lumbar vertebrae to end at the lower border of the fourth lumbar vertebra, a little to the left of the midline, by dividing into two common iliac arteries. It diminishes rapidly in calibre from above downward, because its branches are large; however, the diameter of the vessel at any given height tends to increase slightly with age. The cadaveric superior and inferior calibres are between 9–14 mm and 8–12 mm, respectively, with little difference between the sexes. The angle of the aortic bifurcation varies widely, particularly in the elderly. It has been suggested that the relationship between aortic size and shape is a possible causative factor in the development of abdominal aortic aneurysm (Newman et al 1971). The reflection of transmitted pressure waves at junctions between vessels (of which the abdominal aorta has many) may focally weaken the intimal lining, e.g. at the aortic bifurcation, pressure oscillations and possibly turbulence may be set up as a result of differences in the luminal diameters of the common iliac arteries, producing reflected waves that may injure the intima of the distal abdominal aorta. The role of the relative calibres of the iliac arteries remains uncertain (Shah et al 1978).

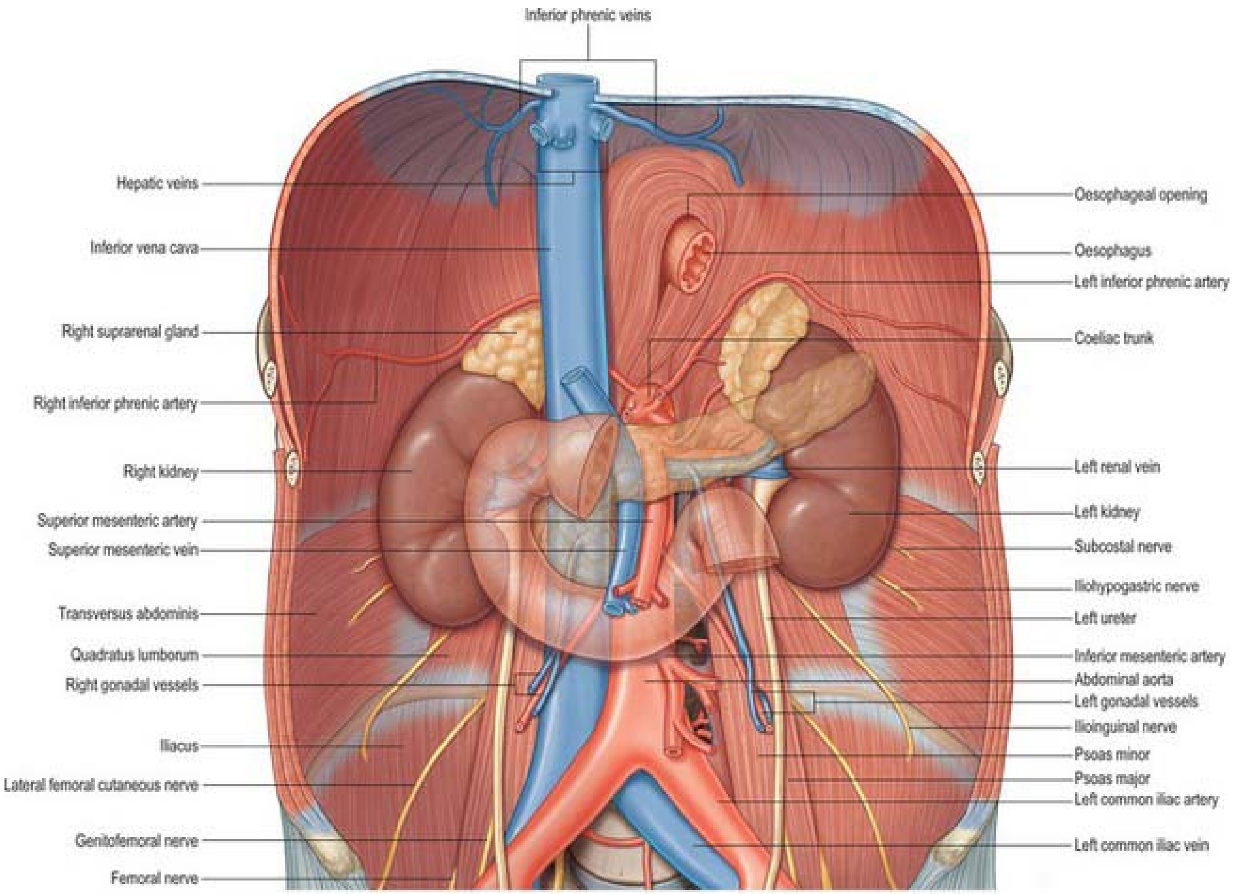
Inferior phrenic veins
Hepatic veins
Inferior vena cava
Right suprarenal gland
Right inferior phrenic artery
Right kidney
Superior mesenteric artery
Superior mesenteric vein
Transversus abdominis
Quadratus lumborum
Right gonadal vessels
Iliacus
Lateral femoral cutaneous nerve
Genitofemoral nerve
Femoral nerve
Oesophageal opening
Oesophagus
Left inferior phrenic artery
Coeliac trunk
Left renal vein
Left kidney
Subcostal nerve
Iliohypogastric nerve
Left ureter
Inferior mesenteric artery
Abdominal aorta
Left gonadal vessels
Ilioinguinal nerve
Psoas minor
Psoas major
Left common iliac artery
Left common iliac vein

Fig. 62.6 The abdominal aorta, inferior vena cava and their branches. The fasciae, lymphatics and connective tissue have been removed for clarity.

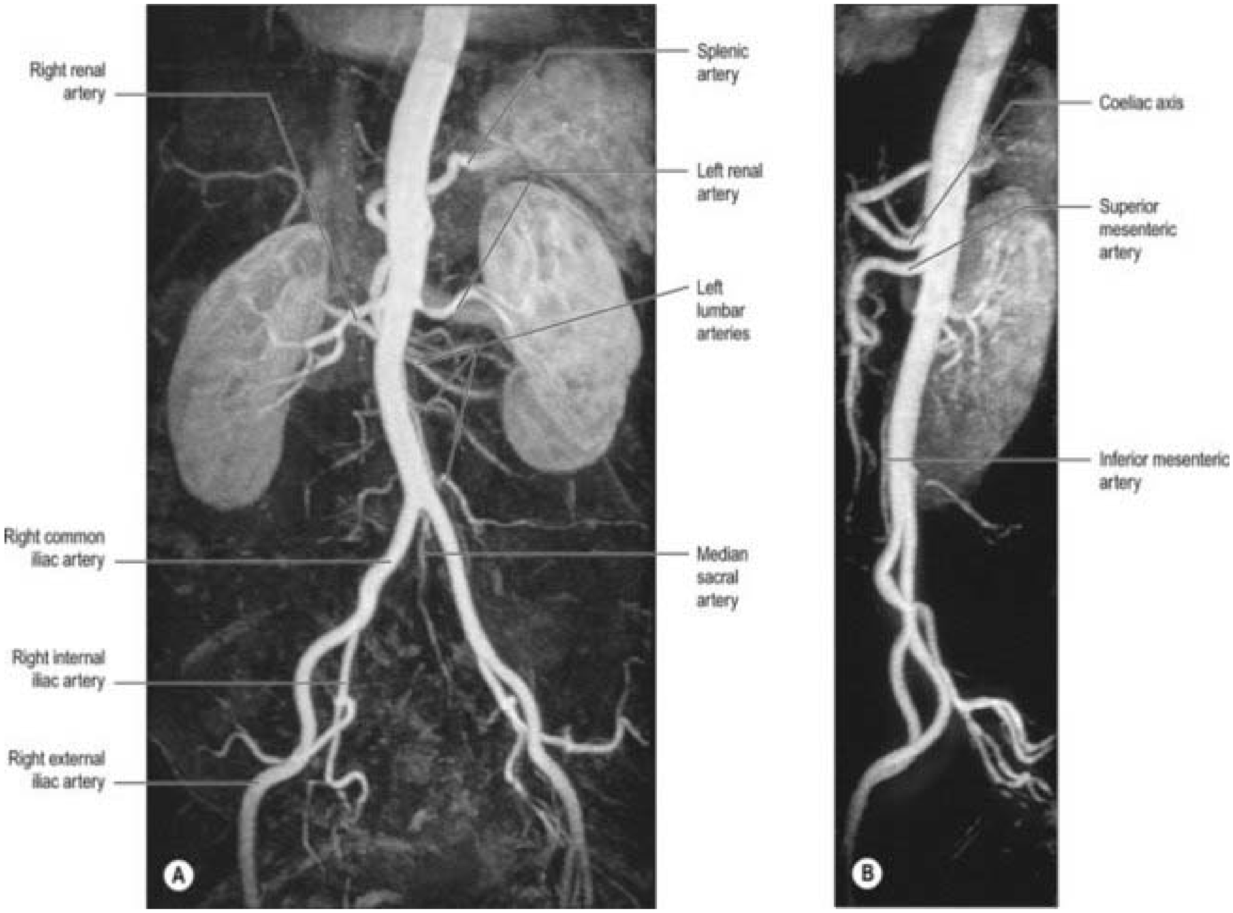
Right renal artery
Splenic artery
Left renal artery
Left lumbar arteries
Right common iliac artery
Median sacral artery
Right internal iliac artery
Right external iliac artery
A
Coeliac axis
Superior mesenteric artery
Inferior mesenteric artery
B

Fig. 62.7 Magnetic resonance aorto-iliac angiogram. **A**, Coronal reformat. **B**, Sagittal reformat.

Relations

The upper abdominal aorta is related anteriorly to the coeliac trunk and its branches. The coeliac plexus and the lesser sac lie between it and the left lobe of the liver and lesser omentum. Below this, the superior mesenteric artery leaves the aorta, crossing anterior to the left renal vein. The body of the pancreas, with the splenic vein on its posterior surface, extends obliquely up and to the left across the abdominal aorta, separated from it by the superior mesenteric artery and left renal vein. Below the pancreas, the proximal parts of the gonadal arteries, and the third part of the duodenum, lie anteriorly. In its lowest part it is covered by the posterior parietal peritoneum and crossed obliquely by the origin of the small intestinal mesentery.

The thoracolumbar intervertebral discs, the upper four lumbar vertebrae, intervening intervertebral discs and the anterior longitudinal ligament are all posterior to the abdominal aorta. Lumbar arteries arise from its dorsal aspect and cross posterior to it. The third and fourth (and sometimes second) left lumbar veins also cross behind it to reach the inferior vena cava. The aorta may overlap the anterior border of the left psoas major.

On the right, the aorta is related above to the cisterna chyli and thoracic duct, the azygos vein and the right crus of the diaphragm, which overlaps and separates it from the inferior vena cava and right coeliac ganglion. Below the second lumbar vertebra, it is closely applied to the left side of the inferior vena cava. This close relationship occasionally allows the formation of an aorto-caval fistula, particularly after surgery for aneurysmal disease or trauma to the aorta.

On the left, the aorta is related above to the left crus of the diaphragm and left coeliac ganglion. Level with the second lumbar vertebra, it is related to the duodenojejunal flexure and the left sympathetic trunk, the fourth part of the duodenum and the inferior mesenteric vein.

Branches

The branches of the aorta are described as anterior, lateral and dorsal (Fig. 62.8). The anterior and lateral branches are distributed to the viscera and the dorsal branches supply the body wall, vertebral column, vertebral canal and its contents. The aorta terminates by dividing into the right and left common iliac arteries.

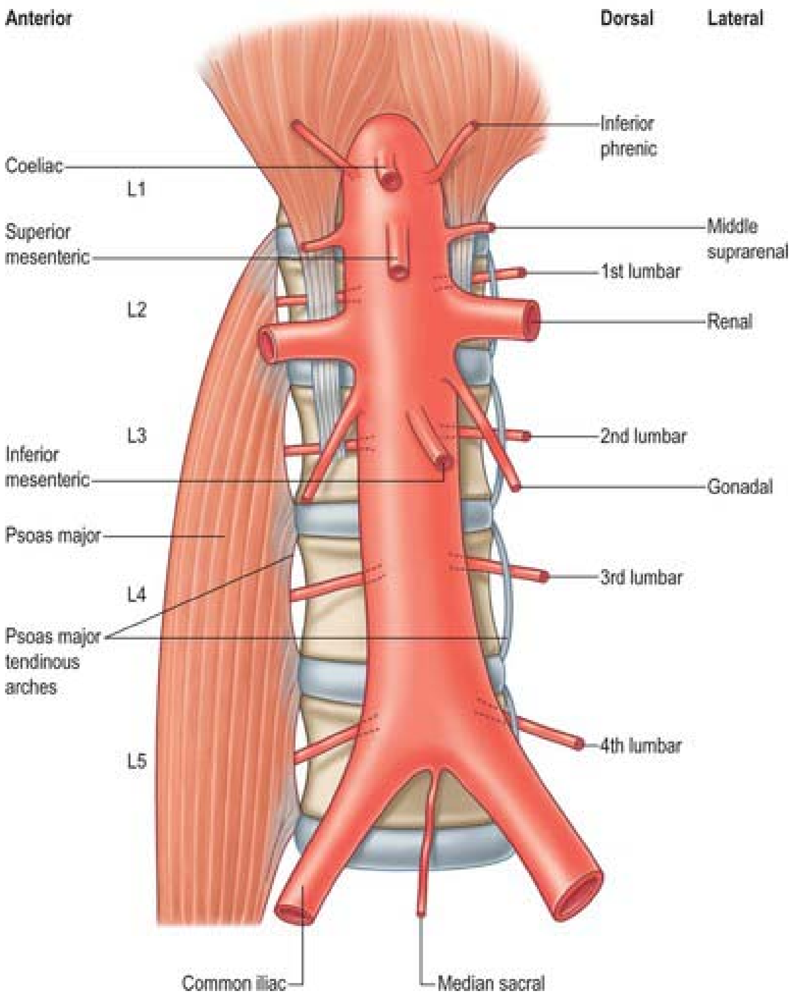
Anterior
Dorsal
Lateral
Coeliac
L1
Inferior phrenic
Superior mesenteric
Middle suprarenal
1st lumbar
L2
Renal
L3
2nd lumbar
Inferior mesenteric
Gonadal
Psoas major
3rd lumbar
L4
Psoas major tendinous arches
L5
4th lumbar
Common iliac
Median sacral

Fig. 62.8 The branches of the abdominal aorta.

Anterior group

Coeliac trunk

The coeliac trunk is the first anterior branch and arises just below the aortic hiatus at the level of T12/L1 vertebral bodies (Fig. 62.9). It is 1.5–2 cm long and passes almost horizontally forwards and slightly right above the pancreas and splenic vein. It divides into the left gastric, common hepatic and splenic arteries. The coeliac trunk may also give off one or both of the inferior phrenic arteries. The superior mesenteric artery may arise with the coeliac trunk as a common origin. One or more of the superior mesenteric branches may arise from the coeliac trunk. Anterior to the coeliac trunk lies the lesser sac. The coeliac plexus surrounds the trunk, sending extensions along its branches. On the right lie the right coeliac ganglion, right crus of the diaphragm and the caudate lobe of the liver. To the left lie the left coeliac ganglion, left crus of the diaphragm and the cardiac end of the stomach. The right crus may compress the origin of the coeliac trunk, giving the appearance of a stricture. The body of the pancreas and the splenic vein are inferior to the coeliac trunk.

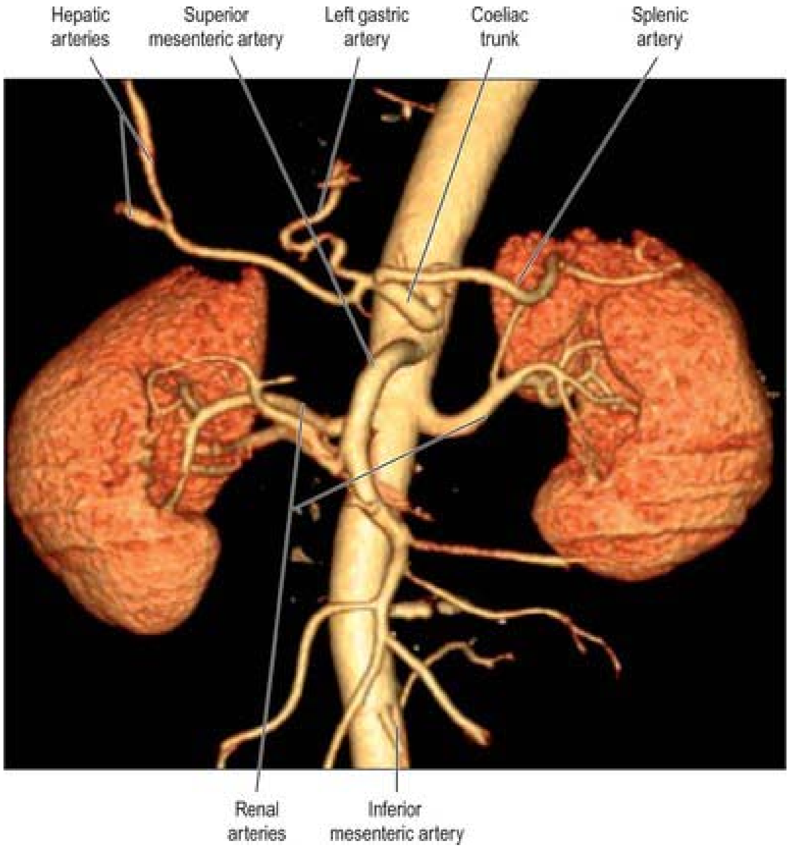
Hepatic arteries
Superior mesenteric artery
Left gastric artery
Coeliac trunk
Splenic artery
Renal arteries
Inferior mesenteric artery

Fig. 62.9 Volume rendered surface shaded CT angiogram of the major branches of the abdominal aorta (renal, coeliac and superior mesenteric arteries).

(Courtesy of Dr Nasir Khan, Chelsea & Westminster Hospital, London.)

Superior mesenteric artery

The superior mesenteric artery originates from the aorta approximately 1 cm below the coeliac trunk, at the level of the L1/2 intervertebral disc (Fig. 62.9). It lies posterior to the splenic vein and the body of the pancreas, and is separated from the aorta by the left renal vein. It runs inferiorly and anteriorly, anterior to the uncinate process of the pancreas and the third part of the duodenum.

Inferior mesenteric artery

The inferior mesenteric artery is usually smaller in calibre than the superior mesenteric artery. It arises from the anterior or left anterolateral aspect of the aorta at about the level of the third lumbar vertebra, 3 or 4 cm above the aortic bifurcation and posterior to the horizontal part of the duodenum (Figs 62.6, 62.9).

Lateral group

Suprarenal artery

The middle suprarenal artery arises from the lateral aspect of the abdominal aorta, level with the superior mesenteric artery. It ascends slightly, and runs over the crura of the diaphragm to the suprarenal glands, where it anastomoses with the suprarenal branches of the phrenic and renal arteries. The right middle suprarenal artery passes behind the inferior vena cava, near the right coeliac ganglion. The left middle suprarenal artery passes close to the left coeliac ganglion, splenic artery and the superior border of the pancreas.

Renal artery

The renal arteries are two of the largest branches of the abdominal aorta and arise laterally from the vessel just below the origin of the superior mesenteric artery. The right is longer and usually arises slightly higher than the left. It passes posterior to the inferior vena cava, right renal vein, head of the pancreas and second part of the duodenum. The left renal artery arises a little lower down and passes behind the left renal vein, the body of the pancreas and the splenic vein.

Gonadal artery

The gonadal arteries are two long, slender vessels that arise from the aorta a little inferior to the renal arteries. Each passes inferolaterally under the parietal peritoneum on psoas major.

Dorsal group

Inferior phrenic arteries

The inferior phrenic arteries usually arise from the aorta, just above the level of the coeliac trunk. Occasionally they arise from a common aortic origin with the coeliac trunk, from the coeliac trunk itself or from the renal artery. They contribute to the arterial supply of the diaphragm. Each artery ascends and runs laterally anterior to the crus of the diaphragm, near the medial border of the suprarenal gland. The left passes behind the oesophagus and forwards on the left side of its diaphragmatic opening. The right passes posterior to the inferior vena cava and then along the right of the diaphragmatic opening for the inferior vena cava. Near the posterior border of the central tendon of the diaphragm, each divides into medial and lateral branches (Fig. 62.6). The medial branch curves forwards to anastomose with its fellow in front of the central tendon and with the musculophrenic and pericardiacophrenic arteries. The lateral branch approaches the thoracic wall, and anastomoses with the lower posterior intercostal and musculophrenic arteries. The lateral branch of the right artery provides the arterial supply to the wall of the inferior vena cava, whereas the left sends ascending branches to the serosal surface of the abdominal oesophagus. Each inferior phrenic artery has two or three small suprarenal branches. The capsule of the liver and spleen may also receive a small supply from the arteries.

Lumbar arteries

There are usually four lumbar arteries on each side, in series with the posterior intercostal arteries. They arise from the posterolateral aspect of the aorta, opposite the lumbar vertebrae. A fifth, smaller, pair occasionally arise from the median sacral artery, but lumbar branches of the iliolumbar arteries usually take their place. The lumbar arteries run posterolaterally on the first to the fourth lumbar vertebral bodies, behind the sympathetic trunks, to intervals between the lumbar transverse processes. From here they continue into the muscles of the posterior abdominal wall. The right arteries pass posterior to the inferior vena cava. The upper two on the right side, and the first left lumbar arteries, lie posterior to the corresponding crus of the diaphragm. Arteries of both sides pass under tendinous arches, which span the lateral concavities of the vertebral bodies, and which form the attachment of psoas major. The arteries run posterior to the muscle and the lumbar plexus, then cross the anterior surface of quadratus lumborum. At the lateral border of quadratus lumborum they pierce the posterior aponeurosis of transversus abdominis, and run forwards between it and internal oblique. They anastomose with one another and the lower posterior intercostal, subcostal, iliolumbar, deep circumflex iliac and inferior epigastric arteries.

Dorsal branches

Each lumbar artery has a dorsal branch, which passes backwards between the adjacent transverse vertebral processes to supply the dorsal muscles of the back, the joints and skin of the back. This branch also has a spinal branch which enters the vertebral canal to supply its contents and adjacent vertebra, anastomosing with the arteries above and below it and across the midline (see Fig. 43.9). The spinal branch of the first lumbar artery supplies the terminal part of the spinal cord proper and the remainder supply the cauda equina, meninges and vertebral canal. Occlusion of all or most of these arteries by dissection or aneurysm of the abdominal aorta may cause ischaemia of the cauda equina, producing the so-called ‘cauda equina syndrome’. This is rare, however, even after infrarenal aortic graft surgery, because of the relatively good collateral circulation of the spinal cord arteries from the descending thoracic aorta. Branches of the lumbar arteries and their dorsal branches supply the adjacent muscles, fasciae, bones, haemopoeitic marrow, ligaments and joints of the vertebral column.

Median sacral artery

The median sacral artery is a small branch that arises from the posterior aspect of the aorta a little above its bifurcation. It descends in the midline, anterior to the fourth and fifth lumbar vertebrae, sacrum and coccyx, and ends in the coccygeal body. At the level of the fifth lumbar vertebra, it is crossed by the left common iliac vein and often gives off a small lumbar artery (arteria lumbalis ima), small branches of which reach the anorectum via the anococcygeal ligament. Anterior to the fifth lumbar vertebra the median sacral artery anastomoses with a lumbar branch of the iliolumbar artery. Anterior to the sacrum it anastomoses with the lateral sacral arteries and sends branches into the anterior sacral foramina.

INFERIOR VENA CAVA

The inferior vena cava conveys blood to the right atrium from all structures below the diaphragm (Fig. 62.10). The majority of its course is within the abdomen, but a small section lies within the fibrous pericardium in the thorax.

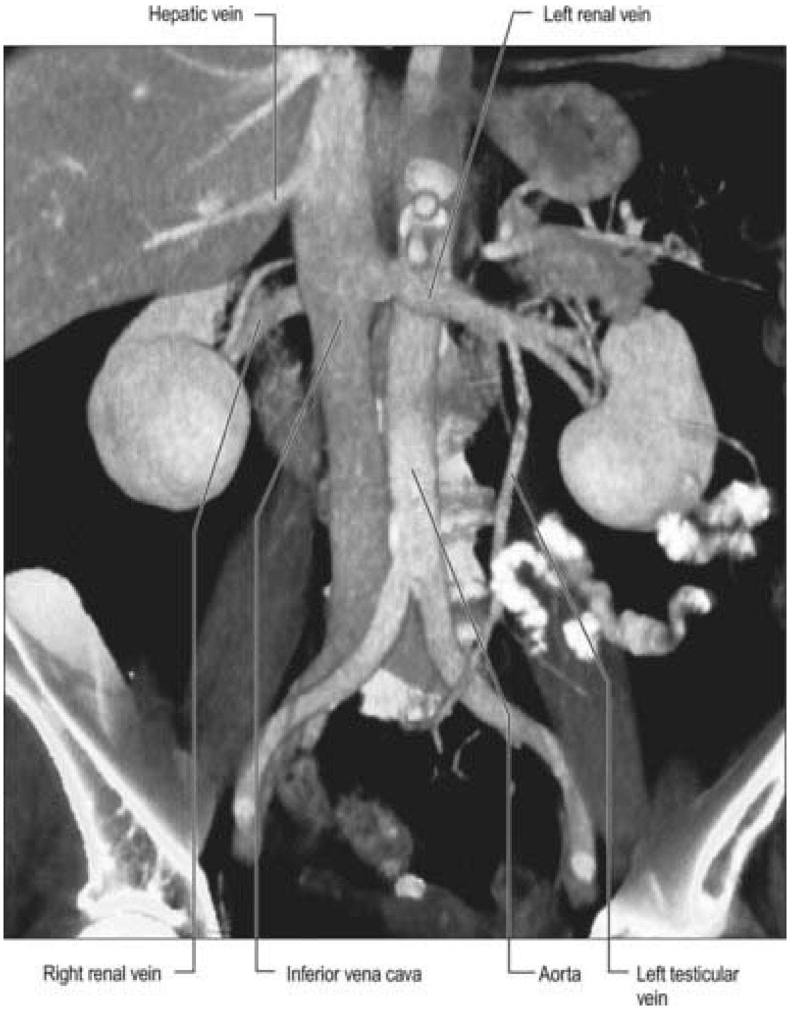
Hepatic vein
Left renal vein
Right renal vein
Inferior vena cava
Aorta
Left testicular vein

Fig. 62.10 Multislice computed tomography three-dimensional surface-shaded angiogram of the abdominal aorta and inferior vena cava.

The inferior vena cava is formed by the junction of the common iliac veins anterior to the fifth lumbar vertebral body, a little to its right. It ascends anterior to the vertebral column, to the right of the aorta, and is contained in a deep groove on the posterior surface of the liver, or sometimes in a tunnel completed by a band of liver tissue. It next crosses the tendinous part of the diaphragm between its median and right ‘leaves’, inclines slightly anteromedially and passes through the fibrous pericardium and a posterior inflexion of the serous pericardium to open into the inferoposterior part of the right atrium. The abdominal portion of the inferior vena cava is devoid of valves.

Relations of the abdominal part of the inferior vena cava

Anteriorly, the inferior vena cava is related to the right common iliac artery at its origin. It is crossed obliquely by the root of the mesentery and its contained vessels and nerves, and by the right gonadal artery. It lies behind the peritoneum of the posterior abdominal wall and the third part of the duodenum, and ascends behind the head of the pancreas and then the first part of the duodenum, separated from these structures by the common bile duct and portal vein. Above the duodenum it is again covered by the peritoneum of the posterior abdominal wall, which forms the posterior wall of the epiploic foramen and which separates the inferior vena cava from the right free border of the lesser omentum and its contents. Above this it is intimately related to the liver anteriorly.

The lower three lumbar vertebral bodies and their intervertebral discs, the anterior longitudinal ligament, right psoas major, sympathetic trunk and third and fourth lumbar arteries, are all posterior to the inferior vena cava. Superior to these structures, the inferior vena cava is related posteriorly to the right crus of the diaphragm, the medial part of the right suprarenal gland, the right coeliac ganglion and the right renal, middle suprarenal and inferior phrenic arteries.

The right ureter, the second part of the duodenum, medial border of the right kidney and the right lobe of the liver are all lateral to the right side of the inferior vena cava. The aorta, the right crus of the diaphragm and the caudate lobe of the liver are all lateral to the left side.

Numerous anomalies may occur in the anatomy of the inferior vena cava, mostly related to its complex formation. It is sometimes replaced, below the level of the renal veins, by two more or less symmetric vessels (Fig. 62.11), often associated with the failure of interconnection between the common iliac veins, and persistence on the left of a longitudinal channel (usually the supracardinal or subcardinal vein) that normally disappears in early fetal life. In complete visceral transposition, the inferior vena cava lies to the left of the aorta.

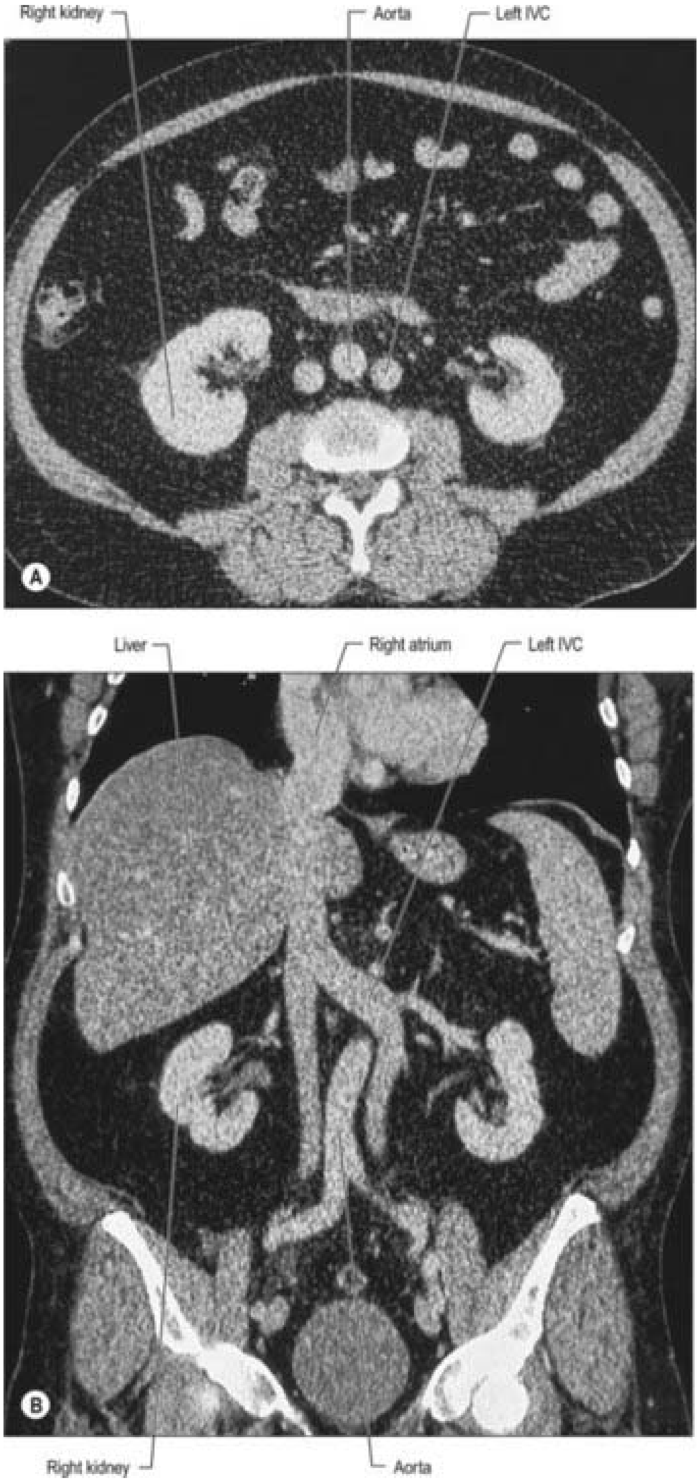
Right kidney
Aorta
Left IVC
A
Liver
Right atrium
Left IVC
B
Right kidney
Aorta

Fig. 62.11 Multislice computed tomography demonstrating a double inferior vena cava (IVC). **A**, Axial CT at the level of the renal hilum, showing an IVC on either side of the aorta. **B**, Coronal reformat showing bilateral IVC joining above the level of the renal veins.

Tributaries

The abdominal inferior vena cava usually receives the common iliac veins at its origin and the lumbar, right gonadal, renal, right suprarenal, inferior phrenic and hepatic veins during its course (Figs 62.6, 62.12).

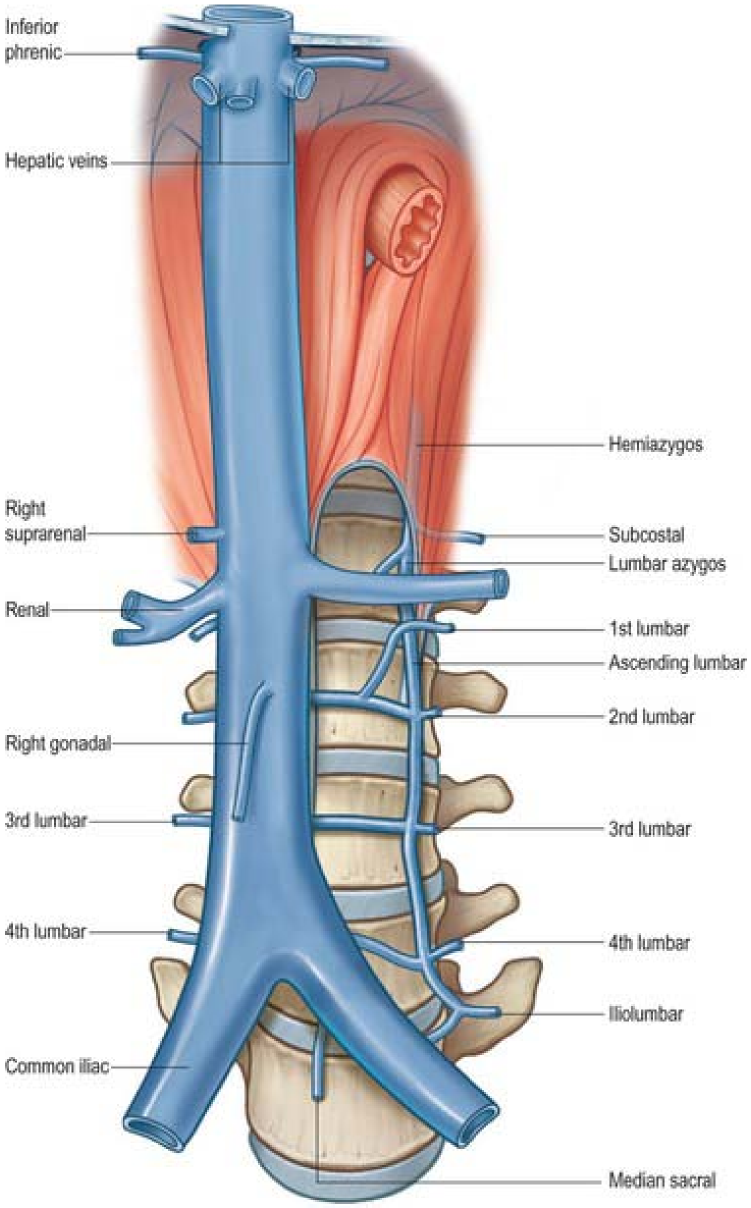
Inferior phrenic
Hepatic veins
Right suprarenal
Renal
Right gonadal
3rd lumbar
4th lumbar
Common iliac
Hemiazygos
Subcostal
Lumbar azygos
1st lumbar
Ascending lumbar
2nd lumbar
3rd lumbar
4th lumbar
Iliolumbar
Median sacral

Fig. 62.12 Tributaries of the inferior vena cava and lumbar veins. Only the left lumbar venous system is shown, for clarity.

Lumbar veins

Four pairs of lumbar veins collect blood by dorsal tributaries from the lumbar muscles and skin. These branches anastomose with tributaries of the lumbar origin of the azygos and hemiazygos veins. The abdominal tributaries to the lumbar veins drain blood from the posterior, lateral and anterior abdominal walls, including the parietal peritoneum. Anteriorly, the abdominal tributaries anastomose with branches of the inferior and superior epigastric veins. These anastomoses provide routes of continued venous drainage from the pelvis and lower limb to the heart in the event of inferior vena caval obstruction. The abdominal tributaries drain into the superior epigastric veins and hence via the internal thoracic veins to the superior vena cava, whereas the dorsal tributaries carry blood into the azygos and hemiazygos system and hence into the superior vena cava. Near the vertebral column, the lumbar veins drain the vertebral plexuses and are connected by the ascending lumbar vein, which is a vessel running longitudinally anterior to the roots of the transverse processes of the lumbar vertebrae. The third and fourth lumbar veins are fairly consistent in their course, and usually pass forward on the sides of the corresponding vertebral bodies to enter the posterior aspect of the inferior vena cava. The left lumbar veins pass behind the abdominal aorta and are therefore longer. First and second lumbar veins are much more variable; they may drain into the inferior vena cava, ascending lumbar vein, or lumbar azygos veins, and are often connected to each other. The first lumbar vein does not usually enter the inferior vena cava directly, but either turns down to join the second lumbar vein or, less commonly, may drain directly into the ascending lumbar vein or pass forward over the first lumbar vertebral body to join the lumbar azygos vein. The second lumbar vein may join the inferior vena cava at or near the level of the renal veins, or, less commonly, join the third lumbar or ascending lumbar vein.

Ascending lumbar vein

The ascending lumbar vein connects the common iliac, iliolumbar and lumbar veins. It lies between psoas major and the roots of the lumbar transverse processes. There is considerable variability in the course of this vein and the related lumbar azygos and first lumbar veins. Superiorly, it commonly joins the subcostal vein to form the azygos vein on the right and the hemiazygos on the left. These veins run forward over the 12th thoracic vertebral body, and pass deep to the crura of the diaphragm and into the thorax. The ascending lumbar vein is usually joined by a small vessel from the back of the inferior vena cava or left renal vein on the left. This little vein represents the azygos line and is referred to as the lumbar azygos vein. Sometimes the ascending lumbar vein ends in the first lumbar vein, which then skirts the first lumbar vertebra with the first lumbar artery, to join the lumbar azygos vein. In this circumstance the subcostal veins join the azygos vein on the right and the hemiazygos vein on the left.

Gonadal veins

Only the right gonadal vein joins the inferior vena cava directly. It opens into its right anterolateral aspect at an acute angle just inferior to the level of the left renal vein. It is often double all the way to the level of entry into the inferior vena cava.

Renal veins

The renal veins are large calibre vessels, which lie anterior to the renal arteries and open into the inferior vena cava almost at right angles (Fig. 62.10). The left is three times longer than the right in length (7.5 cm and 2.5 cm, respectively). The left vein lies on the posterior abdominal wall posterior to the splenic vein and body of the pancreas. Close to its opening into the inferior vena cava, it lies anterior to the aorta with the superior mesenteric artery just above it. The right renal vein lies posterior to the second part of the duodenum and sometimes the lateral part of the head of the pancreas.

Suprarenal vein

The right suprarenal vein drains directly into the inferior vena cava at the level of the 12th thoracic vertebra.

Inferior phrenic veins

The inferior phrenic veins run on the inferior surface of the central tendon of the diaphragm. They drain into the posterolateral aspect of the inferior vena cava around the level of the tenth thoracic vertebra. The left vein tends to drain at a slightly higher level than the right, and runs above the level of the oesophageal opening in the diaphragm. It may be double, with a branch draining into the left renal or suprarenal vein.

Collaterals in inferior vena caval occlusion

Occlusion of the inferior vena cava may follow thrombosis resulting from hypercoagulable conditions, or embolism from lower limb or pelvic thromboses. Collateral venous circulation is established through a wide range of anastomoses between branches that drain ultimately to the superior vena cava. The lumbar veins connect to branches of the superior and inferior epigastric, circumflex iliac, lateral thoracic, subcostal and posterior intercostal veins. They also anastomose with tributaries of the azygos, hemiazygos and lumbar azygos veins. The interconnecting vertebral venous plexuses provide an additional route of collateral circulation between the vena cavae.

Inferior vena caval filters

Recurrent embolization of clot from the pelvic or lower limbs veins may be a serious threat to life. In an effort to prevent life-threatening pulmonary embolism, a fenestrated filter may be placed within the inferior vena cava in an effort to trap the clot. These are most commonly inserted by radiological guidance via the internal jugular vein and superior vena cava and placed at a level below the origin of the renal veins. Progressive occlusion of the filter by clot may lead to symptoms of vena caval obstruction. Rarely, damage to the medial wall of the vena cava from the retaining hooks of the filter may lead to the development of an aorto-caval fistula as a result of the close proximity of the aorta at this level.

LYMPHATIC DRAINAGE

The lymphatic drainage of the muscles, deep tissues and integument of the posterior abdominal wall is broadly divided into four regions. The small upper left and upper right regions drain to the lateral aortic nodes and the ipsilateral axillary lymph nodes. The larger lower left and lower right portions drain to the lateral and retro-aortic lymph nodes, although some drainage also occurs to the left and right superficial inguinal nodes.

The lymphatic drainage of the abdominal viscera occurs almost exclusively through the cisterna chyli and the thoracic duct. Some lymphatic drainage may occur across the diaphragm from the bare area of the liver and the uppermost retroperitoneal tissues, but this is probably of little clinical consequence other than during obstruction of the thoracic duct. The lymph nodes of the retroperitoneum lie around the abdominal aorta and form pre-aortic, lateral aortic and retro-aortic groups (Fig. 62.13). Collectively, they are referred to as the para-aortic lymph nodes and clinically it is difficult to distinguish between them, either at operation or on cross-sectional imaging.

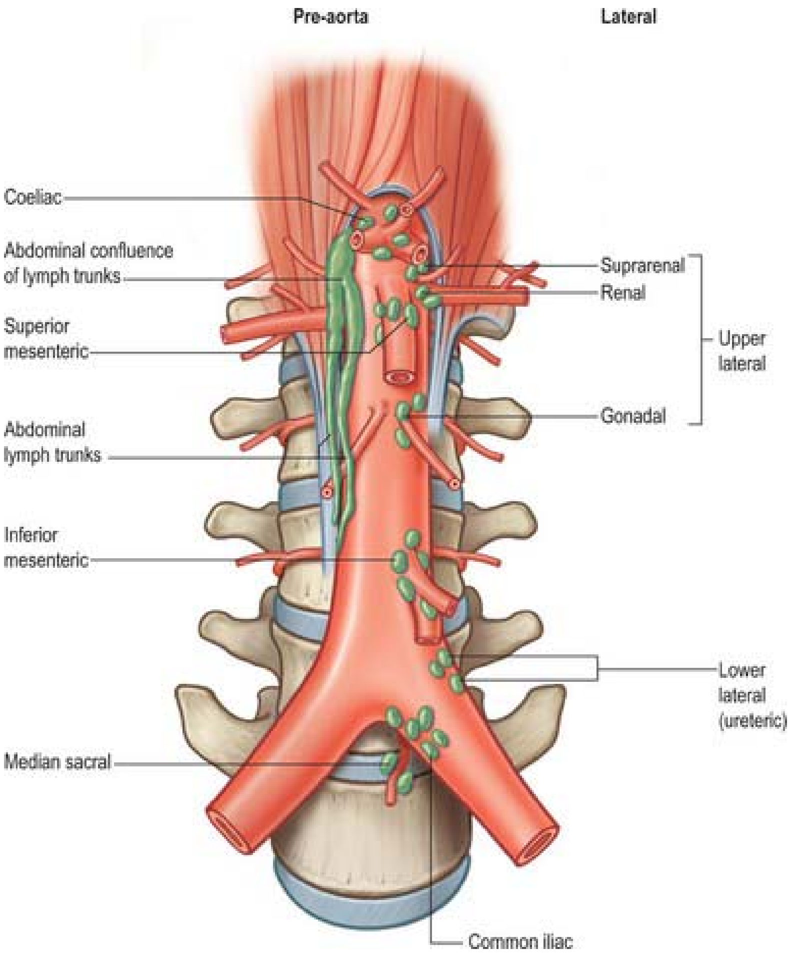
Pre-aorta
Lateral
Coeliac
Abdominal confluence of lymph trunks
Superior mesenteric
Abdominal lymph trunks
Inferior mesenteric
Median sacral
Suprarenal
Renal
Upper lateral
Gonadal
Lower lateral (ureteric)
Common iliac

Fig. 62.13 Para-aortic lymph node groups. The main pre-aortic groups are shown. Only the left-sided lateral nodes are shown, for clarity.

Cisterna chyli and abdominal lymph trunks

The abdominal origin of the thoracic duct lies to the right of the midline at the level of the lower border of the 12th thoracic vertebral body or the thoracolumbar intervertebral disc. It receives all the lymph delivered by the four main abdominal lymph trunks, which converge to an elongated arrangement of channels, referred to as the abdominal confluence of lymph trunks. The confluence may be a simple duct-like structure or be duplicated, triplicated or plexiform. When it is wider than the thoracic duct, its interior is sometimes irregular and bilocular or trilocular, and it may surround intercalated lymph nodes. Occasionally the confluence is a simple, fusiform, saccular dilatation; the widely used name ‘cisterna chyli’ best describes these simpler forms.

The abdominal confluence of lymph trunks extends from the beginning of the thoracic duct, vertically downwards for 5–7 cm, and lies anterolateral to the right of the first and second lumbar vertebral bodies and their intervening discs. It lies immediately to the right of the abdominal aorta. Along its length it lies between the territories containing the upper right lateral aortic lymph nodes and right-sided members of the coeliac and superior mesenteric pre-aortic groups, branches from which may drain directly into the various trunks. The upper two right lumbar arteries and the right lumbar azygos vein are between the confluence and the vertebral column. The medial edge of the right crus of the diaphragm lies anterior to the abdominal confluence of lymph trunks. The confluence receives the right and left lumbar and intestinal lymph trunks, although rarely these may drain directly into the thoracic duct.

The lumbar lymph trunks are formed by vessels draining from the lateral aortic nodes. Thus, either directly, or after traversing intermediary groups, the trunks carry lymph from the lower limbs, the full thickness of the pelvic, perineal and infra-umbilical abdominal walls, the deep tissues of most of the supra-umbilical abdominal walls, most of the pelvic viscera, gonads, kidneys and suprarenal glands. The intestinal lymph trunks receive vessels draining from coeliac nodes and, via these nodes, the superior and inferior mesenteric nodes, which are collectively the pre-aortic nodes. Either directly or via intermediary groups, they drain the entire abdominal gastrointestinal tract down to the anus.

The intimate relationship of the cisterna chyli and abdominal lymph trunks to the abdominal aorta may lead to problems after aortic surgery, particularly dissections carried out around the aorta above the level of the coeliac axis. The large calibre of the trunks, coupled with the volume of lymph flowing through them, means that they do not readily self-seal after injury, and this may lead to problematic recurrent chylous (lymphatic) ascites.

The thoracic duct leaves the superior end of the cisterna chyli or the abdominal confluence and immediately passes through the aortic aperture of the diaphragm posterolateral to the aorta.

Pre-aortic group

The pre-aortic groups tend to lie around the origins of the anterior (visceral) arteries and receive lymph from the gastrointestinal tract and its accessory structures (liver, spleen and pancreas) from the abdominal oesophagus to the level of the anus. They give rise to lymphatic vessels, which drain upwards to form the intestinal trunks that enter the abdominal confluence of lymph trunks. They are divisible into coeliac, superior mesenteric and inferior mesenteric groups, being near the origins of these arteries.

Coeliac nodes

The coeliac nodes lie anterior to the abdominal aorta around the origin of the coeliac artery. They are a terminal group and receive lymph draining from the regional lymph nodes around the branches of the coeliac artery (left gastric, hepatic and pancreaticosplenic nodes) and from the lower pre-aortic groups (the superior mesenteric and inferior mesenteric). The coeliac nodes give rise to right and left intestinal lymph trunks.

Gastric

There are numerous gastric lymph node groups. They drain the stomach, upper duodenum, abdominal oesophagus and the greater omentum into the coeliac group.

Hepatic

The hepatic nodes extend in the lesser omentum along the hepatic arteries and bile duct. They vary in number and site, but almost always occur at the junction of the cystic and common hepatic ducts (the cystic node), alongside the upper common bile duct and in the anterior border of the epiploic foramen. Hepatic nodes drain the majority of the liver, gallbladder and bile ducts, but also receive drainage from some parts of the stomach, duodenum and pancreas. They drain into the coeliac nodes and thence to the intestinal trunks.

Pancreaticosplenic

The pancreaticosplenic nodes drain the spleen, pancreas and part of the stomach into the coeliac nodes.

Superior mesenteric and inferior mesenteric nodes

The superior and inferior mesenteric nodes lie anterior to the aorta near the origins of their respective arteries. The superior and inferior mesenteric nodes are preterminal groups for the alimentary canal from the duodenojejunal flexure to the upper anal canal. They collect from outlying groups, including the mesenteric, ileocolic, colonic and pararectal nodes and drain into the coeliac nodes.

Lateral aortic group

The lateral aortic nodes lie on either side of the abdominal aorta anterior to the medial margins of psoas major, diaphragmatic crura and sympathetic trunks. On the right, some nodes lie lateral and anterior to the inferior vena cava near the end of the right renal vein. Nodes rarely lie between the aorta and inferior vena cava where they are closely related. The lateral aortic nodes drain the viscera and other structures supplied by the lateral and dorsal aortic branches. The upper lateral groups receive the lymph drainage directly from the suprarenal glands, kidneys, ureters, gonads, uterine tubes and upper uterus. They also receive lymph directly from the deeper tissues of the posterior abdominal wall. Lymphatics from the pelvis, most of the pelvic viscera, the perineum and the anterolateral abdominal wall pass first to regional nodes largely related to the iliac arteries and their branches. These include the common iliac, external iliac, internal iliac and circumflex iliac nodes, in addition to the inferior epigastric and sacral nodes. Lymph from the lower limbs passes through the pelvic lymph nodes via the iliac groups.

The lateral aortic group drains into the two lumbar lymph trunks, one on each side, which terminate in the confluence of lymph trunks. A few vessels may pass to the pre-aortic and retro-aortic nodes and others cross the midline to flow into the contralateral nodes, forming a loose plexus.

Retro-aortic group

The retro-aortic group is the smallest of all the para-aortic lymph nodes and has no particular areas of drainage, although it may receive some lymph directly from the paraspinal posterior abdominal wall. Retro-aortic nodes are effectively peripheral nodes of the lateral aortic groups and provide interconnections between surrounding groups.

INNERVATION

The posterior abdominal wall contains the origin of the lumbar plexus and numerous autonomic plexuses and ganglia, which lie close to the abdominal aorta and its branches (Fig. 62.14).

The lumbar ventral rami descend laterally into psoas major, and increase in size from first to last. The first three and most of the fourth form the lumbar plexus; the smaller moiety of the fourth joins the fifth as a lumbosacral trunk, which joins the sacral plexus. The fourth ramus is often termed the nervus furcalis, because it is divided between the two plexuses. Occasionally the third ramus is the nervus furcalis, and both third and fourth ventral rami may be furcal nerves, in which case the plexus is termed prefixed. More frequently, the fifth ventral ramus is furcal, and the plexus is then termed postfixed. These variations modify the sacral plexus.

The first and second, and sometimes the third, lumbar ventral rami are each connected with the lumbar sympathetic trunk by a white ramus communicans. All lumbar ventral rami are joined near their origins by long slender grey rami communicantes from the four lumbar sympathetic ganglia. The rami communicantes accompany the lumbar arteries round the sides of the vertebral bodies, behind psoas major. Their arrangement is irregular: one ganglion may give rami to two lumbar ventral rami, or one lumbar ventral ramus may receive rami from two ganglia, or grey rami often leave the sympathetic trunk between ganglia.

LUMBAR PLEXUS

The lumbar plexus lies within the substance of the posterior part of psoas major, anterior to the transverse processes of the lumbar vertebrae and in ‘line’ with the intervertebral foramina (Fig. 62.15). It is formed by the first three, and most of the fourth, lumbar ventral rami, with a contribution from the 12th thoracic ventral ramus. Although there may be minor variations, the most common arrangement of the plexus is described here.

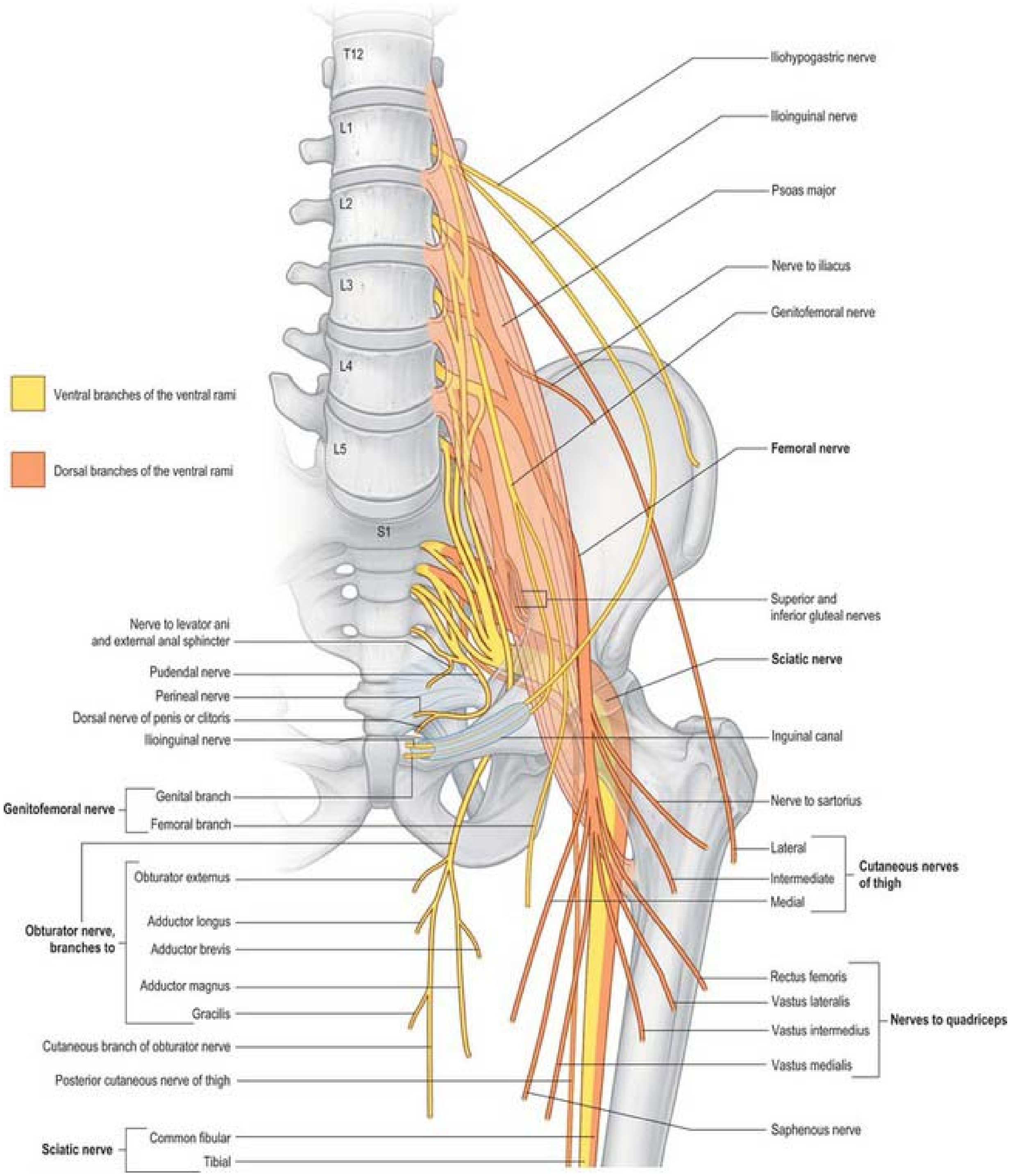
T12
L1
L2
L3
L4
L5
S1
🟨 Ventral branches of the ventral rami
🟧 Dorsal branches of the ventral rami
Iliohypogastric nerve
Ilioinguinal nerve
Psoas major
Nerve to iliacus
Genitofemoral nerve
Femoral nerve
Superior and inferior gluteal nerves
Sciatic nerve
Inguinal canal
Nerve to sartorius
Lateral
Intermediate
Medial
Cutaneous nerves of thigh
Rectus femoris
Vastus lateralis
Vastus intermedius
Vastus medialis
Nerves to quadriceps
Saphenous nerve
Nerve to levator ani and external anal sphincter
Pudendal nerve
Perineal nerve
Dorsal nerve of penis or clitoris
Ilioinguinal nerve
Genitofemoral nerve
Genital branch
Femoral branch
Obturator nerve, branches to
Obturator externus
Adductor longus
Adductor brevis
Adductor magnus
Gracilis
Cutaneous branch of obturator nerve
Posterior cutaneous nerve of thigh
Sciatic nerve
Common fibular
Tibial

Fig. 62.15 The lumbar plexus and its branches.

The first lumbar ventral ramus, joined by a branch from the 12th thoracic ventral ramus, bifurcates, and the upper and larger part divides again into the iliohypogastric and ilioinguinal nerves. The smaller lower part unites with a branch from the second lumbar ventral ramus to form the genitofemoral nerve. The remainder of the second, third, and part of the fourth, lumbar ventral rami join the plexus and divide into ventral and dorsal branches. Ventral branches of the second to fourth rami join to form the obturator nerve. The main dorsal branches of the second to fourth rami join to form the femoral nerve. Small branches from the dorsal branches of the second and third rami join to form the lateral femoral cutaneous nerve. The accessory obturator nerve, when it exists, arises from the third and fourth ventral branches. The lumbar plexus is supplied by branches from the lumbar vessels which supply psoas major.

The branches of the lumbar plexus are:

Muscular	T12, L1–4
Iliohypogastric	L1
Ilioinguinal	L1
Genitofemoral	L1, L2
Lateral femoral cutaneous	L2, L3
Femoral	L2–4 dorsal divisions
Obturator	L2–4 ventral divisions
Accessory obturator	L2, L3

Division of constituent ventral rami into ventral and dorsal branches is not as clear in the lumbar and lumbosacral plexuses as it is in the brachial plexus. Anatomically, the obturator and tibial nerves (via the sciatic) arise from ventral divisions, and the femoral and fibular nerves (via the sciatic) from dorsal divisions. Lateral branches of the 12th thoracic and first lumbar ventral rami are drawn into the gluteal skin, but otherwise these nerves are typical. The second lumbar ramus is difficult to interpret. It not only contributes substantially to the femoral and obturator nerves, but also has an anterior terminal branch (the genital branch of the genitofemoral) and a lateral cutaneous branch (lateral femoral cutaneous nerve and the femoral branch of the genitofemoral). Anterior terminal branches of the third to fifth lumbar and first sacral rami are suppressed, but the corresponding parts of the second and third sacral rami supply the skin, etc. of the perineum.

Inflammatory processes may occur in the posterior abdominal wall in the tissues anterior to psoas major, such as retrocaecal appendicitis on the right and diverticular abscess on the left. This may cause irritation of one or more of the branches of the lumbar plexus and lead to presenting symptoms of pain or dysaesthesia in the distribution of the affected nerves such as in the thigh, hip or buttock skin.

Muscular branches

Small branches from all five lumbar roots.

Iliohypogastric nerve

Distribution

The iliohypogastric nerve originates from the L1 ventral ramus. It emerges from the upper lateral border of psoas major, crosses obliquely behind the lower renal pole and in front of quadratus lumborum. Above the iliac crest, it enters the posterior part of transversus abdominis. Between transversus abdominis and internal oblique, it divides into lateral and anterior cutaneous branches, and also supplies both muscles. The lateral cutaneous branch runs through internal and external oblique above the iliac crest, a little behind the iliac branch of the 12th thoracic nerve, and is distributed to the posterolateral gluteal skin. The anterior cutaneous branch runs between and supplies internal oblique and transversus abdominis. It runs through internal oblique approximately 2 cm medial to the anterior superior iliac spine, and through the external oblique aponeurosis approximately 3 cm above the superficial inguinal ring, and is then distributed to the suprapubic skin. The iliohypogastric nerve connects with the subcostal and ilioinguinal nerves (see Fig. 61.4). The nerve is occasionally injured during an oblique surgical approach to the appendix, but there is rarely any detectable sensory loss because the suprapubic skin is innervated from several sources. Division of the iliohypogastric nerve above the anterior superior iliac spine may weaken the posterior wall of the inguinal canal and predispose to formation of a direct hernia.

Motor

The iliohypogastric nerve supplies a small motor contribution to transversus abdominis and internal oblique, including the conjoint tendon.

Sensory

The iliohypogastric nerve supplies sensory fibres to transversus abdominis, internal oblique and external oblique, and innervates the posterolateral gluteal and suprapubic skin.

Ilioinguinal nerve

Distribution

The ilioinguinal nerve originates from the L1 ventral ramus. It is usually smaller than the iliohypogastric nerve and arises with it from the first lumbar ventral ramus, to emerge from the lateral border of psoas major, with or just inferior to the iliohypogastric nerve. It passes obliquely across quadratus lumborum and the upper part of iliacus and enters transversus abdominis near the anterior end of the iliac crest, where it sometimes connects with the iliohypogastric nerve. At this point it can readily be affected by a relatively small volume of local anaesthetic to help anaesthetize the inguinal canal for surgery. It pierces internal oblique a little lower down, supplies it and then traverses the inguinal canal below the spermatic cord. It emerges with the cord from the superficial inguinal ring and supplies the proximal medial skin of the thigh and the skin over the root of the penis and upper part of the scrotum in males, or the skin covering the mons pubis and the adjoining labium majus in females. The ilioinguinal and iliohypogastric nerves are reciprocal in size. The ilioinguinal is occasionally very small and ends by joining the iliohypogastric, a branch of which then takes its place. Occasionally, the ilioinguinal nerve is completely absent, in which case the iliohypogastric nerve supplies its territory. The nerve may be injured during inguinal surgery, particularly for hernia, which produces paraesthesia over the skin of the genitalia. Entrapment of the nerve during surgery may cause troublesome recurrent pain in this distribution.

Motor

The ilioinguinal nerve supplies motor nerves to transversus abdominis and internal oblique.

Sensory

The ilioinguinal nerve supplies sensory fibres to transversus abdominis and internal oblique. It innervates the medial skin of the thigh and the skin over the root of the penis and upper part of the scrotum in males or the skin covering the mons pubis and the adjoining labium majus in females.

Genitofemoral nerve

Distribution

The genitofemoral nerve originates from the L1 and L2 ventral rami and is formed within the substance of psoas major. It descends obliquely forwards through the muscle to emerge on its abdominal surface near the medial border, opposite the third or fourth lumbar vertebra. It then descends beneath the peritoneum on psoas major, crosses obliquely behind the ureter and divides above the inguinal ligament into genital and femoral branches; it often divides close to its origin, in which case its branches emerge separately from psoas major. The genital branch crosses the lower part of the external iliac artery, enters the inguinal canal by the deep ring and supplies cremaster and the skin of the scrotum in males. In females, it accompanies the round ligament and ends in the skin of the mons pubis and labium majus. The femoral branch descends lateral to the external iliac artery, and sends a few filaments round it before crossing the deep circumflex iliac artery, passing behind the inguinal ligament and entering the femoral sheath lateral to the femoral artery. It pierces the anterior layer of the femoral sheath and fascia lata and supplies the skin anterior to the upper part of the femoral triangle. It connects with the femoral intermediate cutaneous nerve and supplies the femoral artery. Like the ilioinguinal nerve, the genital branch may be injured during inguinal surgery.

Motor

The genitofemoral nerve innervates cremaster via the genital branch.

Cutaneous

The genitofemoral nerve innervates the skin of the scrotum in males or mons pubis and labium majus in females via the genital branch, and the anteromedial skin of the thigh via the femoral branch.

Femoral nerve

The femoral nerve descends through psoas major and emerges low on its lateral border. It passes between psoas major and iliacus deep to the iliac fascia and runs posterior to the inguinal ligament into the thigh. It gives off branches which supply iliacus and pectineus and sends sensory fibres to the femoral artery. Posterior to the inguinal ligament, it lies lateral to the femoral artery and is separated from it by a part of psoas major. The further course and distribution of the femoral nerve is described in Chapter 80.

Lateral femoral cutaneous nerve of the thigh

The lateral femoral cutaneous nerve of the thigh emerges from the lateral border of psoas major and crosses iliacus obliquely towards the anterior superior iliac spine. It supplies sensory fibres to the parietal peritoneum in the iliac fossa. The right nerve passes posterolateral to the caecum, separated from it by the iliac fascia and peritoneum. The left nerve passes behind the lower part of the descending colon. Both nerves pass behind or through the inguinal ligament approximately 1 cm medial to the anterior superior iliac spine and anterior to, or through, sartorius into the thigh. The further course and distribution of the lateral femoral cutaneous nerve is described in Chapter 80.

Obturator nerve

The obturator nerve descends within the substance of psoas major to emerge from its medial border at the level of the pelvic brim. It passes posterior to the common iliac vessels and lateral to the internal iliac vessels. It then descends on the lateral wall of the pelvis attached to the fascia over obturator internus and lies anterosuperior to the obturator vessels before running into the obturator foramen to enter the thigh. It has no branches in the abdomen or pelvis. The further course and distribution of the obturator nerve is described in Chapter 80.

Accessory obturator nerve

When present, the accessory obturator nerve emerges from the medial border of psoas major and runs along this border over the posterior surface of the superior pubic ramus posterior to pectineus. It gives off branches here to supply pectineus and the hip joint, and it may join with the main obturator nerve.

LUMBOSACRAL PLEXUS

The lumbosacral plexus provides the nerve supply to the pelvis and lower limb, in addition to part of the autonomic supply to the pelvic viscera. It gives origin to the sciatic, inferior gluteal, superior gluteal and pudendal nerves and the nerves to quadratus femoris, obturator internus and the posterior cutaneous nerve of the thigh. The further course and distribution of these nerves is described in Chapter 80.

LUMBAR SYMPATHETIC SYSTEM

The lumbar part of each sympathetic trunk usually contains four interconnected ganglia lying on the extraperitoneal connective tissue anterior to the vertebral column and along the medial margin of psoas major. Superiorly, it is continuous with the thoracic trunk posterior to the medial arcuate ligament. Inferiorly, it passes posterior to the common iliac artery and is continuous with the pelvic sympathetic trunk. On the right side, it lies posterior to inferior vena cava, and on the left it is posterior to the lateral aortic lymph nodes. It is anterior to most of the lumbar vessels, but may pass behind some lumbar veins.

LUMBAR PARASYMPATHETIC SYSTEM

The parasympathetic supply to the abdominal viscera is provided by the vagus nerve to the coeliac and superior mesenteric plexuses, and from the pelvic splanchnic nerves to the inferior mesenteric, superior hypogastric and inferior hypogastric plexuses.

PARA-AORTIC BODIES

The para-aortic bodies are condensations of chromaffin tissue that are found in close relation to the aortic autonomic plexuses and lumbar sympathetic chains. They are largest in the fetus, become relatively smaller in childhood and have largely disappeared by adulthood. They are most commonly found as a pair of bodies lying anterolateral to the aorta in the region of the intermesenteric, inferior mesenteric and superior hypogastric plexuses. They may lie as high as the coeliac plexus, as low as the inferior hypogastric plexus in the pelvis, or may be closely applied to the sympathetic ganglia of the lumbar chain. Scattered cells that persist into adulthood may, rarely, be the sites of development of tumours of the chromaffin tissue (phaeochromocytoma), although these are much more commonly found arising from the cells of the suprarenal medulla. The wide variation in site of persistent para-aortic body tissue accounts for the range of locations of such tumours.

REFERENCES

rkhill GJC, Healy JC. Anatomy of the retroperitoneum. *Imaging*. 2000;12:10-20.

ewman DL, Gosling RG, Bowden R. Changes in aortic distensibility and area ratio with the development of atherosclerosis. *Atherosclerosis*. 1971;14:231-240.

ck J. The Autonomic Nervous System. Philadelphia: Lippincott, 1970.

ah PM, Scarton HA, Tsapogas MJ. Geometric anatomy of the aorto-common iliac bifurcation. *J Anat*. 1978;126:451-458.

Both this and the Newman reference describe the anatomical factors that may affect the development of aortoiliac atherosclerosis..

CHAPTER 63

True pelvis, pelvic floor and perineum

TRUE PELVIS AND PELVIC FLOOR

The true pelvis is a bowl-shaped structure formed from the sacrum, pubis, ilium, ischium, the ligaments which interconnect these bones and the muscles which line their inner surfaces. The true pelvis is considered to start at the level of the plane passing through the promontory of the sacrum, the arcuate line on the ilium, the iliopectineal line and the posterior surface of the pubic crest. This plane, or 'inlet' lies at an angle of between 35 and 50° up from the horizontal and above this the bony structures are sometimes referred to as the false pelvis. They form part of the walls of the lower abdomen. The floor or 'outlet' of the true pelvis is formed by the muscles of levator ani. Although the floor is gutter shaped, it generally lies in a plane between 5 and 15° up from the horizontal. This difference between the planes of the inlet and outlet is the reason why the true pelvis is said to have an axis (lying perpendicular to the plane of both inlet and outlet) which progressively changes through the pelvis from above downwards. The details of the topography of the bony and ligamentous pelvis are considered fully on page 1358.

MUSCLES AND FASCIAE OF THE PELVIS

Pelvic muscles

The muscles arising within the pelvis form two groups. Piriformis and obturator internus, although forming part of the walls of the pelvis, are considered as primarily muscles of the lower limb (Fig. 63.1). Levator ani and coccygeus form the pelvic diaphragm and delineate the lower limit of the true pelvis (Fig. 63.2). The fasciae investing the muscles are continuous with visceral pelvic fascia above, perineal fascia below and obturator fascia laterally.

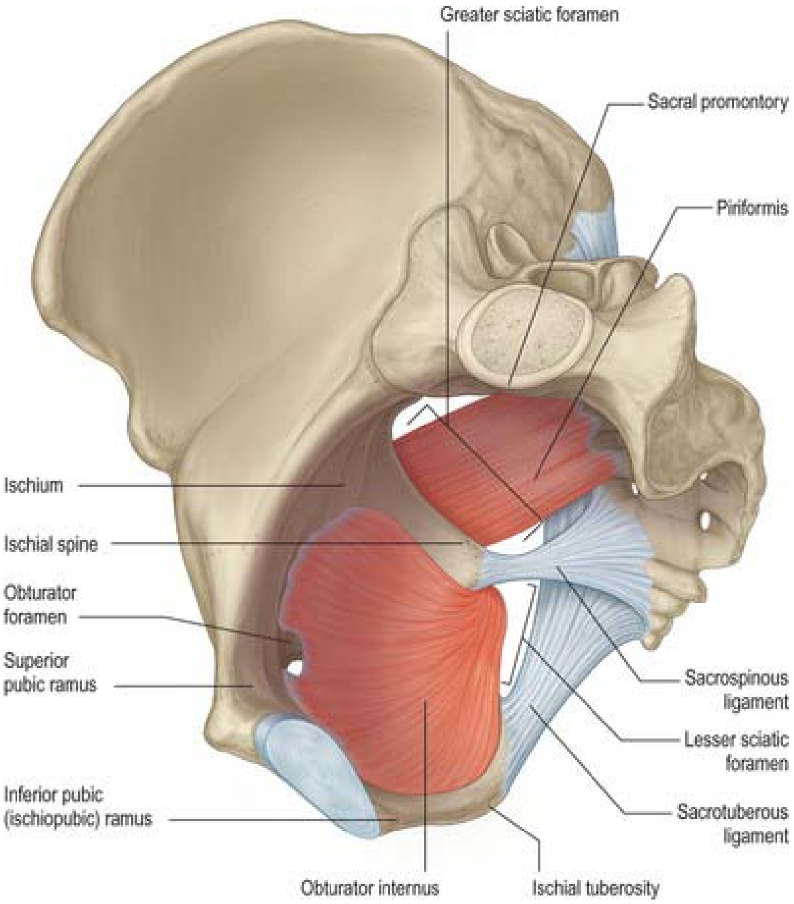
Greater sciatic foramen
Sacral promontory
Piriformis
Ischium
Ischial spine
Obturator foramen
Superior pubic ramus
Inferior pubic (ischiopubic) ramus
Obturator internus
Ischial tuberosity
Sacrospinous ligament
Lesser sciatic foramen
Sacrotuberous ligament

Fig. 63.1 Piriformis, obturator internus and the ligaments of the pelvis. Those muscles relating only to the pelvis or perineum have been omitted for clarity.

(*Adapted from Drake, Vogl and Mitchell 2005.*)

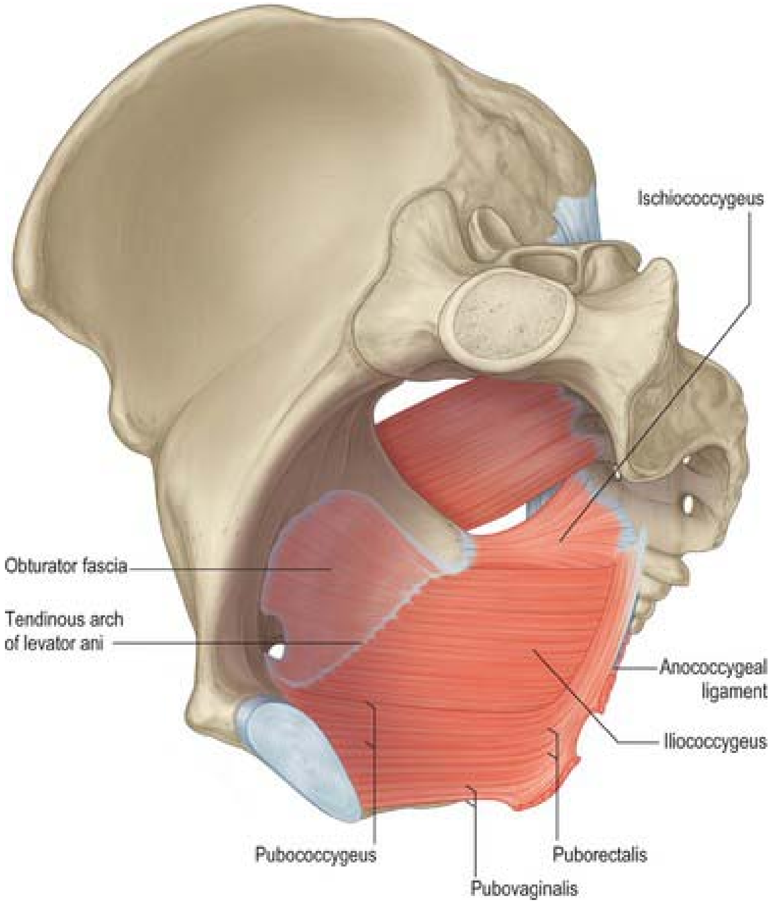
Ischiococcygeus
Obturator fascia
Tendinous arch of levator ani
Anococcygeal ligament
Iliococcygeus
Pubococcygeus
Puborectalis
Pubovaginalis

Fig. 63.2 Muscles of the female pelvis. The superior gluteal and obturator vessels and nerves as well as the pelvic viscera have been omitted for clarity.

(*Adapted from Drake, Vogl and Mitchell 2005.*)

Piriformis

The complete description of piriformis is in Chapter 80.

Piriformis (see p. 1371) forms part of the posterolateral wall of the true pelvis and is attached to the anterior surface of the sacrum, the gluteal surface of the ilium near the posterior inferior iliac spine, the capsule of the adjacent sacroiliac joint and sometimes to the upper part of the pelvic surface of the sacrotuberous ligament. It passes out of the pelvis through the greater sciatic foramen. Within the pelvis, the anterior surface of piriformis is related to the rectum (especially on the left), the sacral plexus of nerves and branches of the internal iliac vessels. The posterior surface lies against the sacrum.

Obturator internus

Obturator internus (see p. 1371) and the fascia over its upper inner (pelvic) surface form part of the anterolateral wall of the true pelvis. It is attached to the structures surrounding the obturator foramen, the inferior ramus of the pubis, the ischial ramus, the pelvic surface of the hip bone below and behind the pelvic brim, and the upper part of the greater sciatic foramen. It also attaches to the medial part of the pelvic surface of the obturator membrane. The muscle is covered by a thick fascial layer and the fibres themselves cannot be seen directly from within the pelvis. This fascia gives attachment to some of the fibres of levator ani and thus only the upper portion of the muscle lies lateral to the contents of the true pelvis, whilst the lower portion forms part of the boundaries of the ischio-anal fossa. In the male, the upper portion lies lateral to the bladder, the obturator and vesical vessels, and the obturator nerve. In the female, the attachments of the broad ligament of the uterus, the ovarian end of the uterine tubes, and the uterine vessels, also lie medial to obturator internus and its fascia.

Levator ani (ischiococcygeus, iliococcygeus, pubococcygeus)

Levator ani is a broad muscular sheet of variable thickness which is attached to the internal surface of the true pelvis and forms a large portion of the pelvic floor (Fig. 63.3). The muscle is subdivided into named portions according to their attachments and the pelvic viscera to which they are related. These parts are often referred to as separate muscles, but the boundaries between each part cannot be easily distinguished and they perform many similar physiological functions. The separate parts are referred to as ischiococcygeus, iliococcygeus and pubococcygeus. Pubococcygeus is often subdivided into separate parts according to the pelvic viscera to which they relate (puboperinealis, puboprostaticus or pubovaginalis, puboanalis, puborectalis). Levator ani arises from each side of the walls of the pelvis along the condensation of the obturator fascia (the tendinous arch of levator ani; see below). Fibres from ischiococcygeus attach to the sacrum and coccyx but the remaining parts of the muscle converge in the midline. The fibres of iliococcygeus join by a partly fibrous intersection and form a raphe posterior to the anorectal junction. Closer to the anorectal junction and elsewhere in the pelvic floor, the fibres are more nearly continuous with those of the opposite side and the muscle forms a sling (puborectalis and pubovaginalis or pubourethralis).

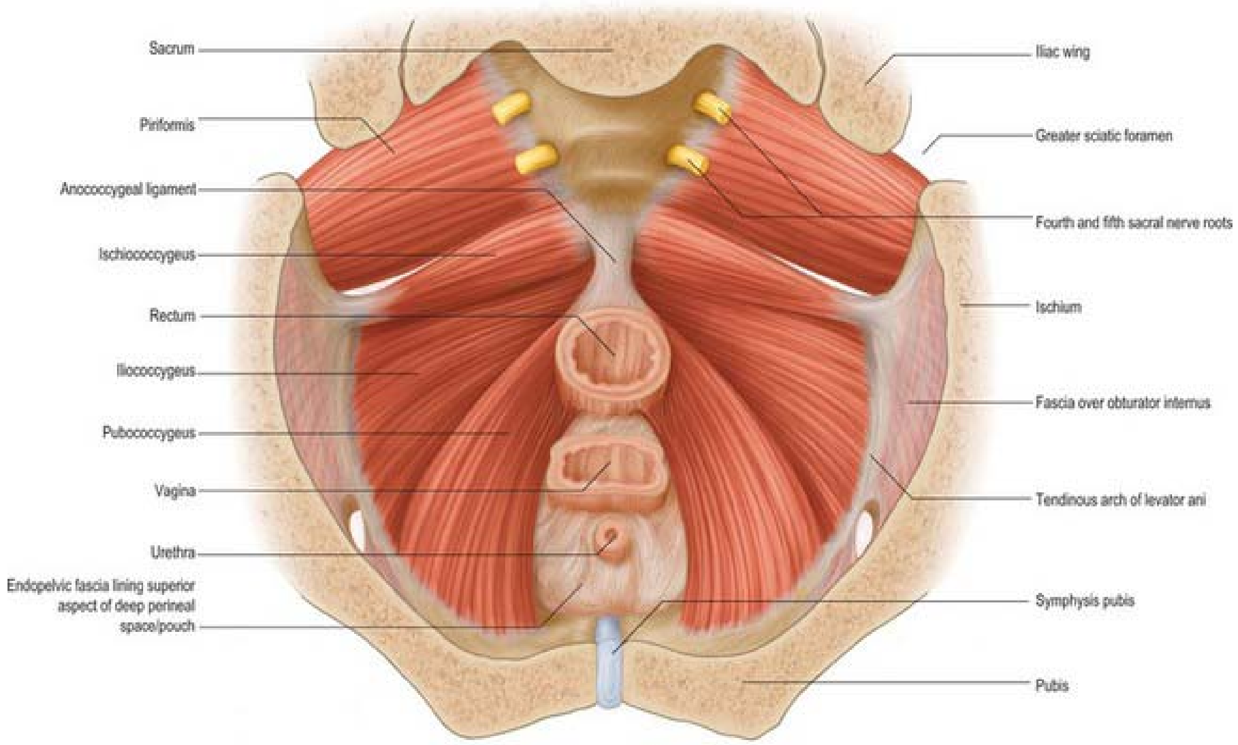
Sacrum
Piriformis
Anococcygeal ligament
Ischiococcygeus
Rectum
Iliococcygeus
Pubococcygeus
Vagina
Urethra
Endopelvic fascia lining superior aspect of deep perineal space/pouch
Iliac wing
Greater sciatic foramen
Fourth and fifth sacral nerve roots
Ischium
Fascia over obturator internus
Tendinous arch of levator ani
Symphysis pubis
Pubis

Fig. 63.3 Muscles of the female pelvis viewed from above. The sacral nerve roots have been divided close to the sacral foramina. The anorectal junction, vagina and urethra have been divided at the level of the pelvic floor.

Attachments

The attachments for the ischiococcygeus, iliococcygeus and pubococcygeus parts are as follows.

Ischiococcygeus

The ischiococcygeal part may be referred to as a separate muscle, sometimes named coccygeus. It lies as the most posterosuperior portion of levator ani and arises as a triangular musculotendinous sheet with its apex attached to the pelvic surface and tip of the ischial spine. The base of the muscle is attached to the lateral margins of the coccyx and the fifth sacral segment. Ischiococcygeus is rarely absent, but may be nearly completely tendinous rather than muscular. It lies on the pelvic aspect of the sacrospinous ligament and may be fused with it, particularly if it is mostly tendinous. The sacrospinous ligament may represent a degenerate part or an aponeurosis of the muscle since the muscle and ligament are coextensive.

Iliococcygeus

The iliococcygeal part is attached to the inner surface of the ischial spine below and anterior to the attachment of ischiococcygeus and to the tendinous arch as far forward as the obturator canal (Fig. 63.2). The most posterior fibres are attached to the tip of the sacrum and coccyx but most join with fibres from the opposite side to form a raphe. This raphe is effectively continuous with the fibroelastic anococcygeal ligament, which is closely applied to its inferior surface and some muscle fibres may attach into the ligament. The raphe provides a strong attachment for the pelvic floor posteriorly and must be divided to allow wide excisions of the anorectal canal during abdominoperineal excisions for malignancy. An accessory slip may arise from the most posterior part and is sometimes referred to as iliosacralis.

Pubococcygeus

The pubococcygeal part is attached to the back of the body of the pubis and passes back almost horizontally. The most medial fibres run directly lateral to the urethra and its sphincter as it passes through the pelvic floor; here the muscle is correctly called the puboperinealis, although due to its close relationship to the upper half of the urethra in both sexes it is often referred to as pubourethralis. The muscle fibres from both sides form part of the urethral sphincter complex together with the intrinsic striated and smooth musculature of the urethra; fibres decussate across the midline directly behind the urethra. In males some of these fibres lie lateral and inferior to the prostate and are referred to as puboprostaticus (levator prostatae). In females, some fibres form the pubourethralis, others run further back to form a sling around the posterior wall of the vagina where they are referred to as pubovaginalis. In both sexes, fibres from this part of pubococcygeus attach to the perineal body; a few elements also attach to the anorectal junction. Some of these fibres, sometimes called puboanalis, decussate and blend with the longitudinal rectal muscle and fascial elements to contribute to the conjoint longitudinal coat of the anal canal. Behind the rectum, some fibres of pubococcygeus form a tendinous intersection as part of the levator raphe, and a thick muscular sling, puborectalis, wraps around the anorectal junction. Some fibres blend with those of the external anal sphincter. Pubourethralis, pubovaginalis/puboprostaticus and puboanalis are sometimes collectively referred to as ‘pubovisceralis’.

Relations

The superior, pelvic surface of levator ani is separated only by fascia (superior pelvic diaphragmatic, visceral and extraperitoneal) from the urinary bladder, prostate or uterus and vagina, rectum and peritoneum. Its inferior, perineal, surface forms the medial wall of the ischio-anal fossa and the superior wall of the anterior recess of the fossa, both being covered by inferior pelvic diaphragmatic fascia. The posterior border is separated from the coccyx by areolar tissue. The medial borders of the two levator muscles are separated by the visceral outlet, through which pass the urethra, vagina, and anorectum.

Vascular supply

Levator ani is supplied by branches of the inferior gluteal, inferior vesical and pudendal arteries.

Innervation

Fibres which originate mainly in the second, third and fourth sacral spinal segments reach levator ani from below and above by a variety of routes (Wendell-Smith & Wilson 1991). Most commonly, pubococcygeus is supplied by second and third sacral spinal segments via the pudendal nerve, and ischiococcygeus and iliococcygeus by direct branches of the sacral plexus from the third and fourth sacral spinal segments.

Actions

Pubococcygeus is a lateral compressor of the various visceral canals which cross the pelvic floor. Puborectalis also reinforces the external anal sphincter, helps to create the anorectal angle, and reduces the anteroposterior dimension of the ano-urogenital hiatus. Iliococcygeus and, to a lesser extent, the less muscular ischiococcygeus, assist puborectalis in contributing to anorectal and urinary continence.

Levator ani must relax appropriately to permit expulsion of urine and particularly faeces, and it contracts with abdominal muscles and the abdominothoracic diaphragm to raise intra-abdominal pressure. It forms much of the basin-shaped muscular pelvic diaphragm, which supports the pelvic viscera. Like the abdominothoracic diaphragm, but unlike abdominal muscles, levator ani is also active in the inspiratory phase of quiet respiration. In the pregnant female, the shape of the pelvic floor may help to direct the fetal head into the anteroposterior diameter of the pelvic outlet.

Pelvic fasciae

The pelvic fasciae may be conveniently divided into the parietal pelvic fascia, which mainly forms the coverings of the pelvic muscles, and the visceral pelvic fascia, which forms the coverings of the pelvic viscera and their vessels and nerves (Fig. 63.4).

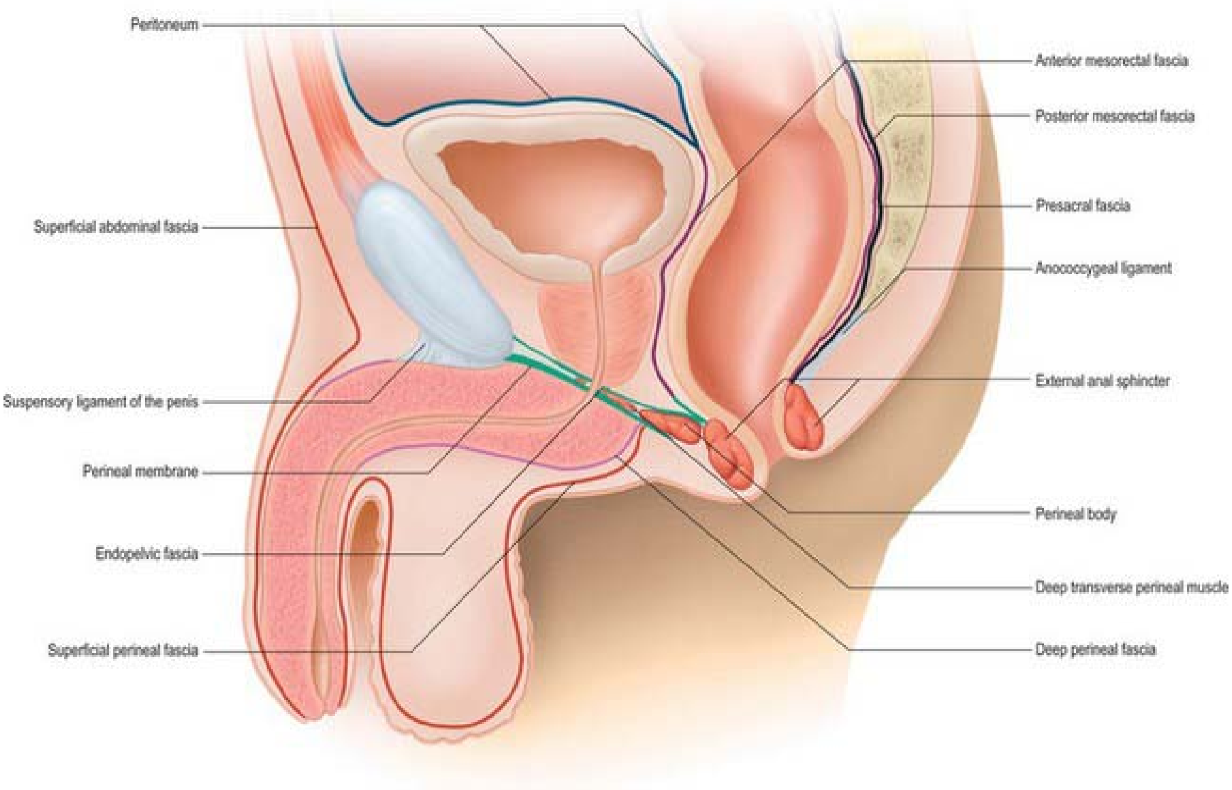
Peritoneum
Superficial abdominal fascia
Suspensory ligament of the penis
Perineal membrane
Endopelvic fascia
Superficial perineal fascia
Anterior mesorectal fascia
Posterior mesorectal fascia
Presacral fascia
Anococcygeal ligament
External anal sphincter
Perineal body
Deep transverse perineal muscle
Deep perineal fascia

Fig. 63.4 Fasciae of the pelvis and perineum. Median sagittal section in the male. The parietal pelvic fascia is shown in black, the mesorectal fascia in brown, the fascial boundaries of the deep perineal space/pouch in green, the peritoneum in blue, the deep abdominal fascia in purple and the subcutaneous abdominal and perineal fascia in red. The visceral perietal fasciae have been omitted for clarity.

Parietal pelvic fascia

The parietal pelvic fascia consists of the obturator fascia, the fasciae over piriformis, and over levator ani (the pelvic diaphragm), and the presacral fascia.

Obturator fascia

The parietal pelvic fascia on the pelvic (medial) surface of obturator internus is well differentiated. Although in humans it is derived from the degenerate upper portion of the attachment of levator ani, it is usually referred to as the obturator fascia. Above, it is connected to the posterior part of the arcuate line of the ilium, and is continuous with iliac fascia. Anterior to this, as it follows the line of origin of obturator internus, it is gradually separated from the attachment of the iliac fascia and a portion of the periosteum of the ilium and pubis spans between them. It arches below the obturator vessels and nerve, investing the obturator canal, and is attached anteriorly to the back of the pubis. Behind the obturator canal, the fascia is markedly aponeurotic and gives a firm attachment to levator ani, usually called the tendinous arch of levator ani (arcus tendineus musculi levatoris ani) (see Figs 63.3, 63.13, 63.14). Below the attachment of levator ani, the fascia is thin and is effectively composed only of the epimysium of the muscle and overlying connective tissue; posteriorly it forms part of the lateral wall of the ischio-anal fossa in the perineum, and anteriorly it merges with the fasciae of the muscles of the deep perineal space (see Fig. 63.14), which is continuous with the ischio-anal fossa. The obturator fascia is continuous with the pelvic periosteum and thus the fascia over piriformis.

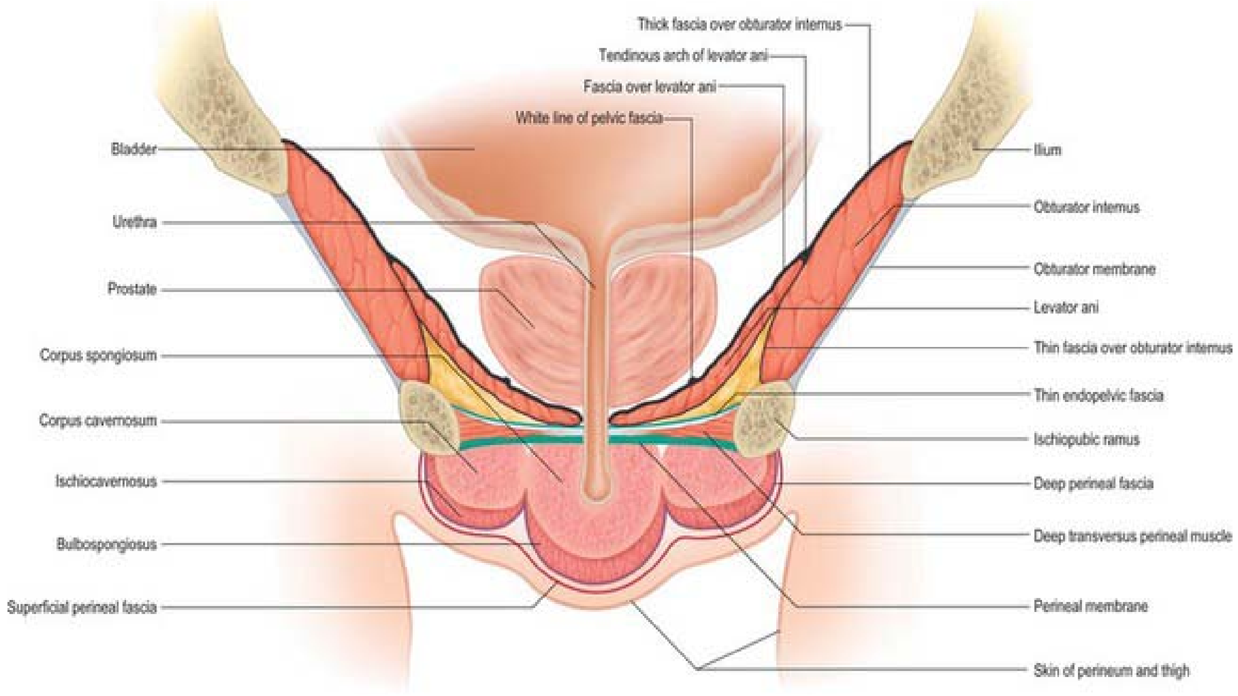
Thick fascia over obturator internus
Tendinous arch of levator ani
Fascia over levator ani
White line of pelvic fascia
Bladder
Urethra
Prostate
Corpus spongiosum
Corpus cavernosum
Ischiocavernosus
Bulbospongiosus
Superficial perineal fascia
Ilium
Obturator internus
Obturator membrane
Levator ani
Thin fascia over obturator internus
Thin endopelvic fascia
Ischiopubic ramus
Deep perineal fascia
Deep transversus perineal muscle
Perineal membrane
Skin of perineum and thigh

Fig. 63.13 Muscles and fasciae of the male perineum – coronal view. The section passes through the bulb of the penis at the level of the urethra. The

deep perineal space is continuous with the ischio-anal fossa posteriorly. The parietal pelvic fascia is shown in black, fascial boundaries of the deep perineal space/pouch in green, the deep perineal fascia in purple and the superficial perineal fascia in red. The visceral and parietal fasciae have been omitted for clarity. The pelvic fascia over the 'pelvic' aspect of the deep transverse perinei is very thin and does not form a distinct layer as such in places blending with the parietal pelvic fascia over the inferior aspect of levator ani.

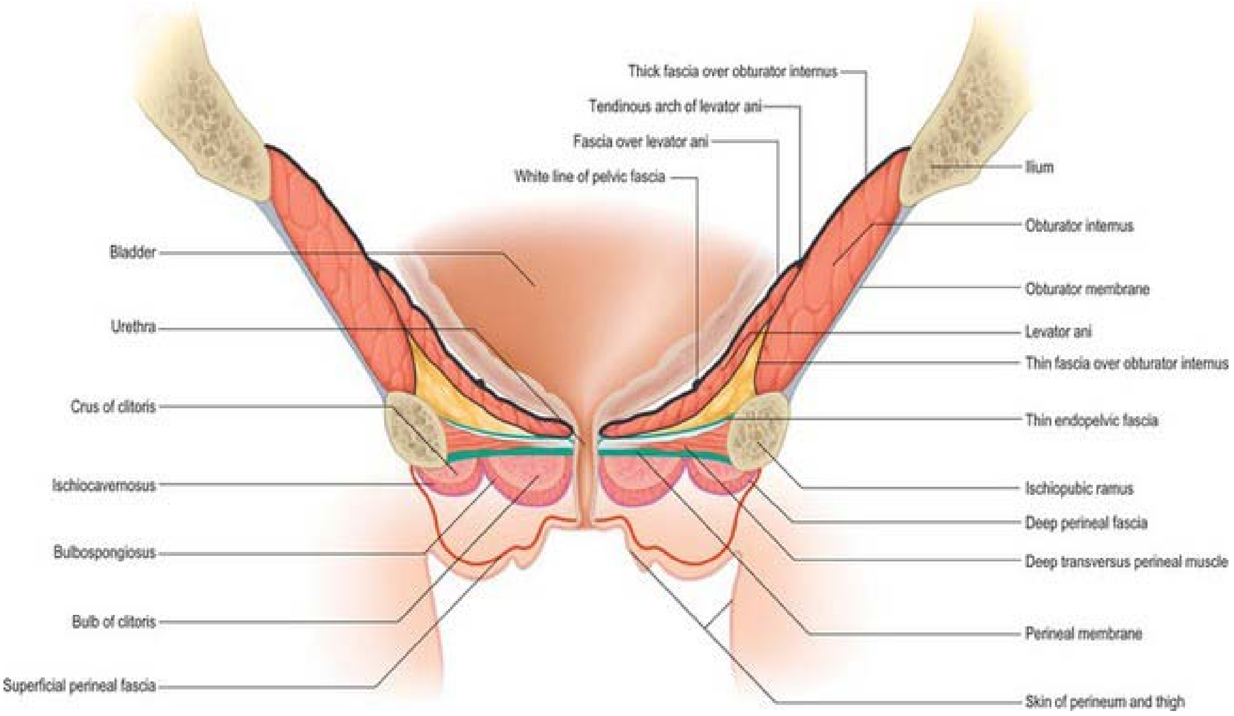
Thick fascia over obturator internus
Tendinous arch of levator ani
Fascia over levator ani
White line of pelvic fascia
Ilium
Obturator internus
Obturator membrane
Levator ani
Thin fascia over obturator internus
Thin endopelvic fascia
Ischiopubic ramus
Deep perineal fascia
Deep transversus perineal muscle
Perineal membrane
Skin of perineum and thigh
Bladder
Urethra
Crus of clitoris
Ischiocavernosus
Bulbospongiosus
Bulb of clitoris
Superficial perineal fascia

Fig. 63.14 Muscles and fasciae of the female perineum – coronal view. The section passes through the bulb of the clitoris at the level of the urethra. The deep perineal space is continuous with the ischio-anal fossa posteriorly. The parietal pelvic fascia is shown in black, fascial boundaries of the deep perineal space/pouch in green, the deep perineal fascia in purple and the superficial perineal fascia in red. The visceral and parietal fasciae have been omitted for clarity. The pelvic fascia over the 'pelvic' aspect of the deep transverse perinei is very thin and does not form a distinct layer as such in places blending with the parietal pelvic fascia over the inferior aspect of levator ani.

Fascia over piriformis

The fascia over the inner aspect of piriformis is very thin, and fuses with the periosteum on the front of the sacrum at the margins of the anterior sacral foramina. It ensheathes the sacral anterior primary rami which emerge from these foramina: the nerves are often described as lying behind the fascia. The internal iliac vessels lie in front of the fascia over piriformis; their branches draw out sheaths of the fascia and extraperitoneal tissue into the gluteal region, above and below piriformis.

Fascia over levator ani (pelvic diaphragm)

The fascia over levator ani covers both of the surfaces of the pelvic diaphragm. On the lower surface, the thin inferior fascia is continuous with the obturator fascia below the tendinous arch of levator ani laterally. It covers the medial wall of the ischio-anal fossa and blends below with fasciae on the urethral sphincter and the external anal sphincter. On the upper surface, the superior fascia of the pelvic diaphragm is markedly thicker than that over the inferior surface. It is attached anteriorly to the back of the body of the pubis, approximately 2 cm above its lower border, and extends laterally across the superior ramus of the pubis, blending with the obturator fascia and continuing along an irregular line to the spine of the ischium. It is continuous posteriorly with the fascia over piriformis and the anterior sacrococcygeal ligament. Medially, the superior fascia of the pelvic diaphragm blends with the visceral pelvic fascia forming part of the endopelvic fascia.

Arcus tendineus fascia pelvis/white line of the parietal pelvic fascia

Low on the superomedial aspect of the upper fascia over levator ani, a thick white band of condensed connective tissue extends from the lower part of the symphysis pubis to the inferior margin of the spine of the ischium (see Figs 63.4, 63.13, 63.14). Although often referred to as the tendinous arch of the pelvic fascia (arcus tendineus fasciae pelvis), it is really the remnant of the degenerate tendon of iliococcygeus in humans and is best referred to as the white line of the parietal pelvic fascia (Smith 1908). It provides attachment for the condensations of visceral pelvic fascia which provide support to the urethra, bladder and vagina in females (see below).

Presacral fascia

The presacral fascia forms a hammock-like structure posterior to the posterior portion of the mesorectal fascia. Laterally it extends to the origin of the fascia over piriformis and the fascia over levator ani (superior pelvic diaphragmatic fascia) with which it blends, and more inferiorly it extends between the white line of the parietal pelvic fascia on either side. Inferiorly, it extends to the anorectal junction, where it fuses with the posterior aspect of the mesorectal fascia and the anococcygeal ligament at the level of the anorectal junction. Superiorly, it can be traced to the origin of the superior hypogastric plexus, where it becomes progressively thinner over the promontory of the sacrum and becomes continuous with the retroperitoneal tissues. The right and left hypogastric nerves and inferior hypogastric plexuses lie on its surface and the presacral veins lie immediately posterior to it. It forms a distinct layer which can be seen both on magnetic resonance images of the pelvis and during surgery. The presacral fascia provides an important landmark because extension of rectal tumours through it significantly reduces the possibility of curative resectional surgery. Dissection in the plane posterior to the fascia may result in bleeding from the presacral veins: because the adventitia of the veins is partly attached to the posterior surface of the fascia, the haemorrhage may be severe (since the veins are unable to contract properly).

Visceral pelvic fascia

The visceral pelvic fascia is formed from condensations of connective tissue which are closely associated with the pelvic viscera to which it relates and with the neurovascular structures supplying or running near those organs. In its most inferior and lateral extent, the visceral pelvic fascia is closely related to, and effectively derived from, the superior fascia over the attachment of levator ani (see below), whereas more superiorly and posteriorly, it is derived from part of the fascia over piriformis. The condensations where these fasciae meet are sometimes collectively referred to as the ‘endopelvic fascia’. Further accounts are given of the paravisceral portions of the visceral pelvic fascia (e.g. parametrium, paracolpium) in the chapters describing the organs to which the fascia relates.

Several different condensations of endopelvic fascia are recognized both at operation and by MRI imaging. They provide important support to the pelvic viscera and play a role in continence in both sexes.

In the female, pubourethral ligaments form from periurethral connective tissue and attach to the white line of the parietal pelvic fascia close to its pubic end. A little more laterally, similar tissue exists which may be termed the urethropelvic ligaments, and which insert into the white line over levator ani. These condensations are effectively continuous with connective tissue which runs from the paravaginal tissue to the white line, and is sometimes referred to as the vaginolevator support or attachment. Since the normal angle of the urethra during standing is nearly 45° to the vertical, these two structures combined can be viewed as providing a ‘hammock-like’ support to the midurethra (DeLancey 1994); some fibres may even decussate across the midline between the urethra and the anterior vaginal wall. The upper portion of the pubourethral ligament blends with the pubovesical and vesicopelvic ligaments (connective tissue around the neck of the urinary bladder), and may contain cholinergically innervated smooth muscle fibres, sometimes referred to as pubovesicalis. In males, pubourethral structures are augmented by the puboprostatic ligament/puboprostaticus. In both sexes, these muscles may have a role in opening the upper urethra and bladder neck during micturition.

There is much less condensation of connective tissue around the rectum, and no similar rectopelvic ligaments exist. The connective tissue over the longitudinal muscles of the rectum is thickened just above the anal hiatus in levator ani and it fuses with the endopelvic fascia and the anococcygeal ligament, sometimes referred to as a rectosacral ligament.

VASCULAR SUPPLY AND LYMPHATIC DRAINAGE OF THE PELVIS

The true pelvis contains the internal iliac arteries and veins and the lymphatics which drain the majority of the pelvic viscera. The common and external iliac vessels and the lymphatics which drain the lower limb lie along the pelvic brim and in the lower retroperitoneum, but are conveniently discussed together with the vessels of the true pelvis.

Arteries of the pelvis

Common iliac arteries

The abdominal aorta bifurcates into the right and left common iliac arteries anterolateral to the left side of the fourth lumbar vertebral body. These arteries diverge as they descend and divide at the level of the sacroiliac joint into external and internal iliac arteries. The external iliac artery is the principal artery of the lower limb. The internal iliac artery provides the principal supply to the walls and viscera of the pelvis, the perineum and the gluteal region.

Right common iliac artery

The right common iliac artery is approximately 5 cm long. It passes obliquely across part of the fourth and the fifth lumbar vertebral bodies, and is crossed anteriorly by the sympathetic rami to the pelvic plexus and, at its division into internal and external iliac arteries, by the ureter. It is covered by the parietal peritoneum, which separates it from the coils of the small intestine. Posteriorly, it is separated from the fourth and fifth lumbar vertebral bodies and their intervening disc by the right sympathetic trunk, the terminal parts of the common iliac veins and the start of the inferior vena cava, the obturator nerve, lumbosacral trunk and iliolumbar artery. Laterally, the inferior vena cava and the right common iliac vein lie superiorly and the right psoas major lies inferiorly. The left common iliac vein is medial to the upper part of the right common iliac artery.

Left common iliac artery

The left common iliac artery is shorter than the right and is approximately 4 cm long. Lying anterior to it are the sympathetic rami to the pelvic plexus, the superior rectal artery and, at its terminal bifurcation, the ureter. The sympathetic trunk, the fourth and fifth lumbar vertebral bodies and intervening disc, the obturator nerve, lumbosacral trunk and iliolumbar artery are all posterior. The left common iliac vein is posteromedial, and the left psoas major lateral, to the left common iliac artery.

Branches

In addition to the external iliac and internal iliac branches, each common iliac artery also gives small branches to the peritoneum, psoas major, ureter, adjacent nerves and surrounding areolar tissue. The common iliac artery occasionally gives rise to the iliolumbar artery and accessory or replaced renal arteries if the kidney is low lying.

Internal iliac arteries

Each internal iliac artery, approximately 4 cm long, begins at the common iliac bifurcation, level with the lumbosacral intervertebral disc and anterior to the sacroiliac joint. It descends posteriorly to the superior margin of the greater sciatic foramen where it divides into an anterior trunk, which continues in the same line towards the ischial spine, and a posterior trunk, which passes back to the greater sciatic foramen. Anterior to the artery are the ureter and, in females, the ovary and fimbriated end of the uterine tube. The internal iliac vein, lumbosacral trunk and sacroiliac joint are posterior. Lateral is the external iliac vein, between the artery and psoas major, and the obturator nerve lying inferior to the vein. The parietal peritoneum is medial, separating it from the terminal ileum on the right and the sigmoid colon on the left. Tributaries of the internal iliac vein are also medial (Fig. 63.5).

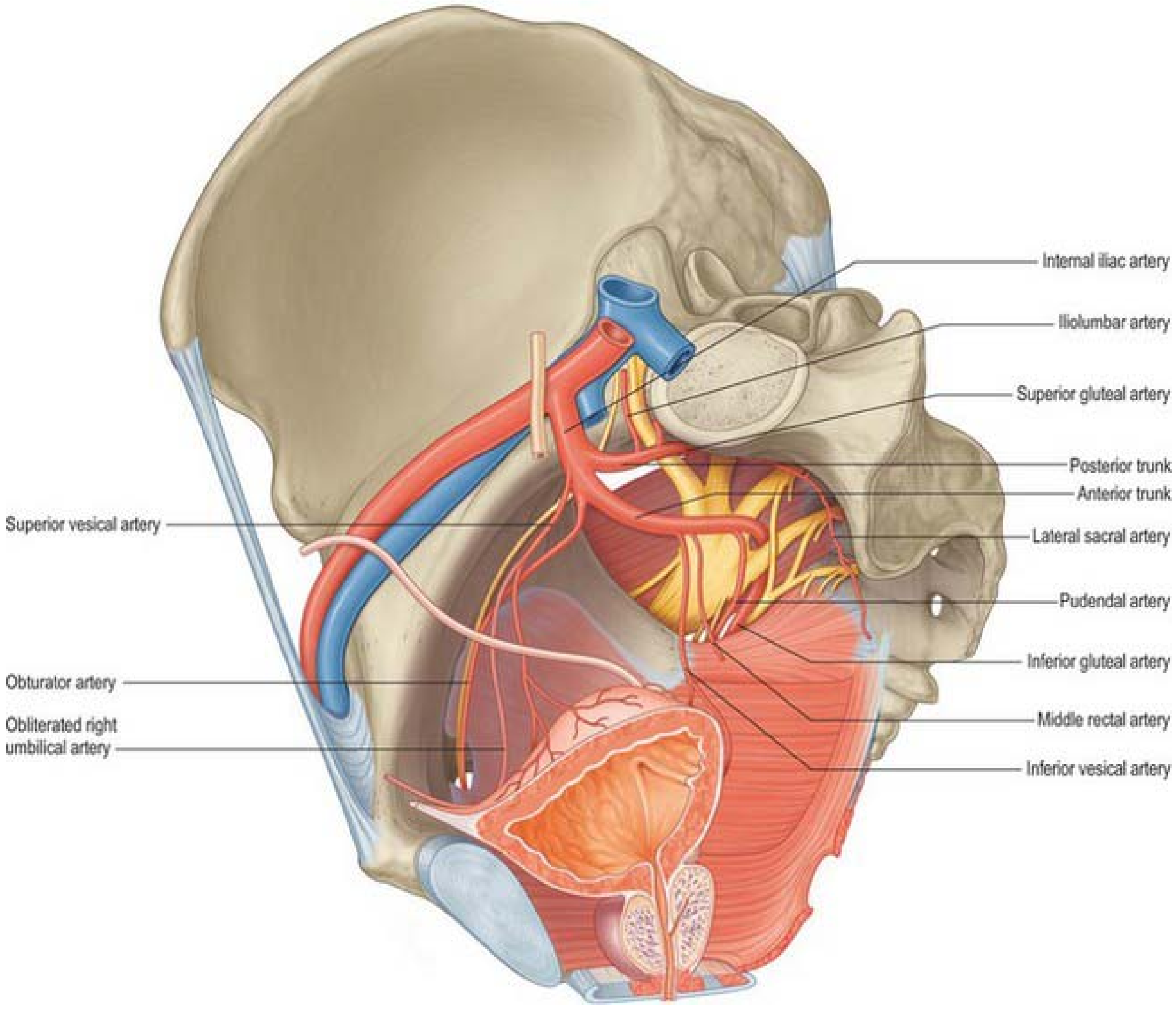
Internal iliac artery
Iliolumbar artery
Superior gluteal artery
Posterior trunk
Anterior trunk
Superior vesical artery
Lateral sacral artery
Pudendal artery
Inferior gluteal artery
Obturator artery
Obliterated right umbilical artery
Middle rectal artery
Inferior vesical artery

Fig. 63.5 Arteries of the male pelvis.

In the fetus, the internal iliac artery is twice the size of the external iliac artery and is the direct continuation of the common iliac artery. The main trunk ascends on the anterior abdominal wall to the umbilicus, converging on the contralateral artery, and the two arteries run through the umbilicus to enter the umbilical cord as the umbilical arteries. At birth, when placental circulation ceases, only the pelvic segment remains patent as the internal iliac artery and part of the superior vesical artery; the remainder becomes a fibrous medial umbilical ligament. In males, the patent part (usually the superior vesical artery) usually gives off an artery to the vas deferens.

Posterior trunk branches

The branches of the posterior trunk of the internal iliac artery are the iliolumbar, lateral sacral and superior gluteal arteries.

Iliolumbar artery

The iliolumbar artery is the first branch of the posterior trunk and ascends laterally anterior to the sacroiliac joint and lumbosacral nerve trunk. It lies posterior to the obturator nerve and external iliac vessels and reaches the medial border of psoas major, dividing behind it into the lumbar and iliac branches. The lumbar branch supplies psoas major and quadratus lumborum and anastomoses with the fourth lumbar artery. It sends a small spinal branch through the intervertebral foramen between the fifth lumbar and first sacral vertebrae, to supply the cauda equina. The iliac branch supplies iliacus; between the muscle and bone it anastomoses with the iliac branches of the obturator artery. A large nutrient branch enters an oblique canal in the ilium. Other branches runs around the iliac crest, contribute to the supply of the gluteal and abdominal muscles, and anastomose with the superior gluteal, circumflex iliac and lateral circumflex femoral arteries.

Lateral sacral arteries

The lateral sacral arteries are usually double, or if single, divide rapidly into superior and inferior branches. The superior and larger artery passes medially into the first or second anterior sacral foramen, supplies the sacral vertebrae and contents of the sacral canal, and then leaves the sacrum via the corresponding dorsal foramen to supply the skin and muscles dorsal to the sacrum. The inferior or lateral sacral artery crosses obliquely anterior to piriformis and the sacral anterior spinal rami, then descends lateral to the sympathetic trunk to anastomose with its fellow and the median sacral artery anterior to the coccyx. Its branches enter the anterior sacral foramina and are distributed in the same way as the branches of the superior artery.

Superior gluteal artery

The superior gluteal artery is the largest branch of the internal iliac artery and effectively forms the main continuation of its posterior trunk. It runs posteriorly between the lumbosacral trunk and the first sacral ramus or between the first and second rami, then turns slightly inferiorly, leaving the pelvis by the greater sciatic foramen above piriformis and dividing into superficial and deep branches. In the pelvis it supplies piriformis, obturator internus and a nutrient artery to the ilium. The superficial branch enters the deep surface of gluteus maximus. Its numerous branches supply the muscle and anastomose with the inferior gluteal branches while others perforate the tendinous medial attachment of the muscle to supply the skin over the sacrum, where they anastomose with the posterior branches of the lateral sacral arteries. The deep branch of the superior gluteal artery passes between gluteus medius and the bone, soon dividing into superior and inferior branches. The superior branch skirts the superior border of gluteus minimus to the anterior superior iliac spine and anastomoses with the deep circumflex iliac artery and the ascending branch of the lateral circumflex femoral artery. The inferior branch runs through gluteus minimus obliquely, supplies it and gluteus medius and anastomoses with the lateral circumflex femoral artery. A branch enters the trochanteric fossa to join the inferior gluteal artery and ascending branch of the medial circumflex femoral artery; other branches run through gluteus minimus to supply the hip joint.

The superior gluteal artery occasionally arises directly from the internal iliac artery with the inferior gluteal artery and sometimes from the internal pudendal artery.

Anterior trunk branches

The branches of the anterior trunk of the internal iliac artery are the superior and inferior vesical, middle rectal, vaginal, obturator, uterine, internal pudendal and inferior gluteal.

Superior vesical artery

The superior vesical arter is the first large branch of the anterior trunk. It lies on the lateral wall of the pelvis just below the brim and runs anteroinferiorly medial to the periosteum of the posterior surface of the pubis. It supplies the distal end of the ureter, the bladder, the proximal end of the vas deferens and the seminal vesicles. It also gives origin to the umbilical artery in the foetus, which remains as a fibrous cord, the medial umbilical ligament, in the adult. This vessel occasionally remains patent as a small artery supplying the umbilicus.

Inferior vesical artery

The inferior vesical artery may arise as a common branch with the middle rectal artery. In the female it is often replaced by the vaginal artery. It supplies the bladder, the prostate, the seminal vesicles and the vas deferens.

Middle rectal artery

The middle rectal artery is often multiple and may be small. It runs into the lateral fascial coverings of the mesorectum. It occasionally arises close to or in common with the origin of the inferior vesical artery in males.

Vaginal artery

In females the vaginal artery may replace the inferior vesical artery. It may arise from the uterine artery close to its origin (Fig. 63.6).

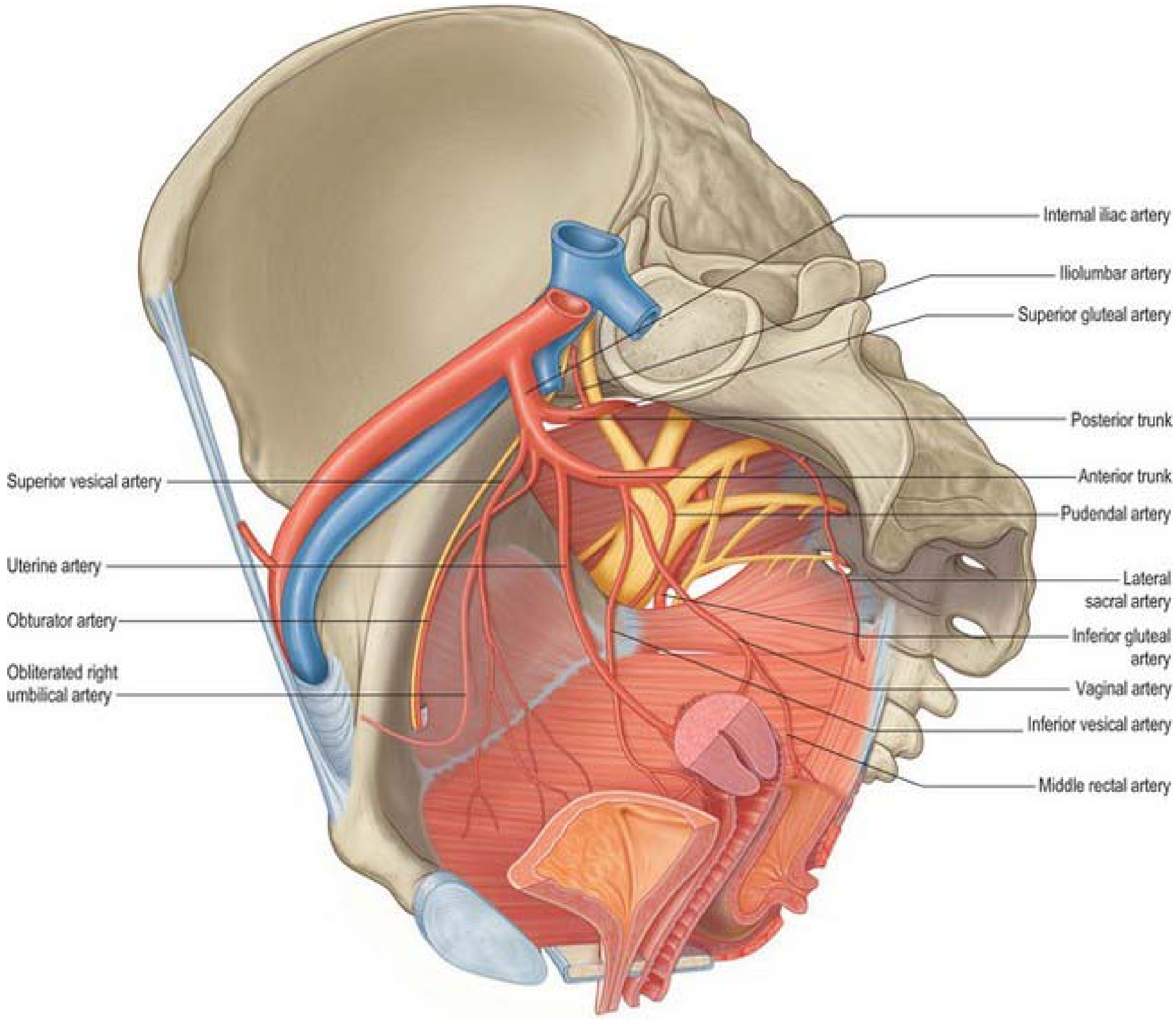
Internal iliac artery
Iliolumbar artery
Superior gluteal artery
Posterior trunk
Superior vesical artery
Anterior trunk
Pudendal artery
Uterine artery
Lateral sacral artery
Obturator artery
Inferior gluteal artery
Obliterated right umbilical artery
Vaginal artery
Inferior vesical artery
Middle rectal artery

Fig. 63.6 Arteries of the female pelvis.

Obturator artery

The obturator artery runs anteroinferiorly from the anterior trunk on the lateral pelvic wall to the upper part of the obturator foramen. It leaves the pelvis via the obturator canal and divides into anterior and posterior branches. In the pelvis it is related laterally to the fascia over obturator internus and is crossed on its medial aspect by the ureter and, in the male, by the vas deferens. In the nulliparous female the ovary lies medial to it. The obturator nerve is above the artery, the obturator vein below it. In the pelvis, the obturator artery provides iliac branches to the iliac fossa which supply the bone and iliacus and anastomose with the iliolumbar artery. A vesical branch runs medially to the bladder and sometimes replaces the inferior vesical branch of the internal iliac artery. A pubic branch usually arises just before the obturator artery leaves the pelvis, and ascends over the pubis to anastomose with the contralateral artery and the pubic branch of the inferior epigastric artery.

Outside the pelvis, the anterior and posterior terminal branches encircle the foramen between obturator externus and the obturator membrane. The anterior branch curves anteriorly on the membrane and then inferiorly along its anterior margin to supply branches to obturator externus, pectineus, the femoral adductors and gracilis. It anastomoses with the posterior branch and the medial circumflex femoral artery. The posterior branch follows the posterior margin of the foramen and turns anteriorly on the ischial part to anastomose with the anterior branch. It supplies the muscles attached to the ischial tuberosity and anastomoses with the inferior gluteal artery. An acetabular branch enters the hip joint at the acetabular notch, ramifies in the fat of the acetabular fossa and sends a branch along the ligament of the femoral head.

Occasionally the obturator artery is replaced by an enlarged pubic branch of the inferior epigastric artery which descends almost vertically to the obturator foramen. It usually lies near the external iliac vein, lateral to the femoral ring, and is rarely injured during inguinal or femoral hernia surgery. Sometimes it curves along the edge of the lacunar part of the inguinal ligament, partly encircling the neck of a hernial sac, and may be inadvertently cut during enlargement of the femoral ring in reducing a femoral hernia.

Uterine artery

The uterine artery is an additional branch in females. It is a large artery which arises below the obturator artery on the lateral wall of the pelvis and runs inferomedially into the broad ligament of the uterus.

Internal pudendal artery (in the pelvis)

The internal pudendal artery arises just below the origin of the obturator artery. It descends laterally to the inferior rim of the greater sciatic foramen, where it leaves the pelvis between piriformis and ischiococcygeus to enter the gluteal region. It then curves around the dorsum of the ischial spine to enter the perineum by the lesser sciatic foramen. This course effectively allows the nerve to wrap around the posterior limit of levator ani at its attachment to the ischial spine and so gain access to the perineum. In the pelvis the internal pudendal artery crosses anterior to piriformis, the sacral plexus and the inferior gluteal artery. Behind the ischial spine it is covered by gluteus maximus, with the pudendal nerve medial and the nerve to obturator internus lateral to it. The internal pudendal artery gives off several muscular branches in the pelvis and gluteal region which supply adjacent muscles and nerves.

Inferior gluteal artery

The inferior gluteal artery is the larger terminal branch of the anterior internal iliac trunk and principally supplies the buttock and thigh. It descends posteriorly, anterior to the sacral plexus and piriformis but posterior to the internal pudendal artery. It passes between the first and second, or second and third, sacral anterior spinal nerve rami, then between piriformis and ischiococcygeus and runs through the lower part of the greater sciatic foramen to reach the gluteal region. The artery runs inferiorly between the greater trochanter and ischial tuberosity with the sciatic and posterior femoral cutaneous nerves, deep to gluteus maximus. It continues down the thigh, supplying the skin and anastomosing with branches of the perforating arteries. The inferior gluteal and internal pudendal arteries often arise as a common stem from the internal iliac artery, sometimes with the superior gluteal artery. Inside the pelvis the inferior gluteal artery gives branches to piriformis, ischiococcygeus and iliococcygeus and occasionally contributes to the middle rectal arterial supply. In the male, it may supply vessels to the seminal vesicles and prostate.

External iliac arteries

The external iliac arteries are of larger calibre than the internal iliac arteries. Each artery descends laterally along the medial border of psoas major, from the common iliac bifurcation to a point midway between the anterior superior iliac spine and the symphysis pubis, and enters the thigh posterior to the inguinal ligament to become the femoral artery.

The parietal peritoneum and extraperitoneal tissue separate the right external iliac artery from the terminal ileum and, usually, the appendix, and the left external iliac artery from the sigmoid colon and coils of the small intestine anteromedially. At its origin, the external iliac artery may be crossed by the ureter and is also crossed by the gonadal vessels, the genital branch of the genitofemoral nerve, the deep circumflex iliac vein and the vas deferens (male) or round ligament (female). Posteriorly, the artery is separated from the medial border of psoas major by the iliac fascia. The external iliac vein lies partly posterior to its upper part, but is more medial below. Laterally, it is related to psoas major, which is covered by the iliac and psoas fascia. Numerous lymph vessels and nodes lie on its front and sides.

The external iliac artery is principally the artery of the lower limb and as such has few branches in the pelvis. Apart from very small vessels to psoas major and neighbouring lymph nodes, the artery has no branches until it gives off the deep circumflex iliac and inferior epigastric arteries, which arise near to the point at which it passes under the inguinal ligament.

Deep circumflex iliac artery

The deep circumflex iliac artery branches laterally from the external iliac artery almost opposite the origin of the inferior epigastric artery. It ascends and runs laterally to the anterior superior iliac spine behind the inguinal ligament in a sheath formed by the union of the transversalis and iliac fasciae. There it anastomoses with the ascending branch of the lateral circumflex femoral artery, pierces the transversalis fascia and skirts the internal lip of the iliac crest. About halfway along the iliac crest it runs through transversus abdominis and then between transversus abdominis and internal oblique to anastomose with the iliolumbar and superior gluteal arteries. It gives off a large ascending branch at the anterior superior iliac spine which runs between internal oblique and transversus abdominis, supplies both muscles, and anastomoses with the lumbar and inferior epigastric arteries.

Inferior epigastric artery

The inferior epigastric artery originates from the external iliac artery posterior to the inguinal ligament. It curves forwards in the anterior extraperitoneal tissue and ascends obliquely along the medial margin of the deep inguinal ring whence it continues as an artery of the anterior abdominal wall.

Veins of the pelvis

The true pelvis contains a large number of veins which drain the pelvic walls and most of the viscera contained within the pelvis, and which carry venous blood from the gluteal region, hip and thigh. The external iliac veins, which lie close to the brim of the pelvis, carry the venous drainage from most of the lower limb. There is considerable variation in the venous drainage of the pelvis: although the major veins frequently follow their named arterial counterparts, the small tributaries exhibit a great deal of variation between individuals.

Common iliac veins

The common iliac vein is formed by the union of the external and internal iliac veins, anterior to the sacroiliac joints. It ascends obliquely to end at the right side of the fifth lumbar vertebra, uniting at an acute angle with the contralateral vessel to form the inferior vena cava. The right common iliac vein is shorter and more nearly vertical, lying posterior and then lateral to its artery. The right obturator nerve passes posteriorly. The left common iliac vein is longer and more oblique, and lies first medial, then posterior, to its artery. It is crossed anteriorly by the attachment of the sigmoid mesocolon and superior rectal vessels. Each vein receives iliolumbar and sometimes lateral sacral veins. The left common iliac vein usually drains the median sacral vein. There are no valves in these veins.

The left common iliac vein occasionally ascends to the left of the aorta to the level of the kidney, where it receives the left renal vein and crosses anterior to the aorta to join the inferior vena cava: this vessel represents the persistent caudal half of the left postcardinal or supracardinal vein.

Median sacral veins

The right and left medial sacral veins accompany the corresponding arteries anterior to the sacrum, where they unite to form a single vein which usually ends in the left common iliac vein, but which sometimes ends at the common iliac junction.

Internal pudendal veins

The internal pudendal veins are venae comitantes of the internal pudendal artery and unite as a single vessel which ends in the internal iliac vein. They receive veins from the inferior rectal veins and either the penile bulb and scrotum (males) or the clitoris and labia (females).

Internal iliac vein

The internal iliac vein is formed by the convergence of several veins above the greater sciatic foramen. It does not have the predictable trunks and branches of the internal iliac artery but its tributaries drain the same territories. It ascends posteromedial to the internal iliac artery to join the external iliac vein, forming the common iliac vein at the pelvic brim, anterior to the lower part of the sacroiliac joint. It is covered anteromedially by parietal peritoneum. Its tributaries are the gluteal, internal pudendal and obturator veins, which originate outside the pelvis; the lateral sacral veins, which run from the anterior surface of the sacrum; and the middle rectal, vesical, uterine and vaginal veins, which originate in the venous plexuses of the pelvic viscera (Fig. 63.7).

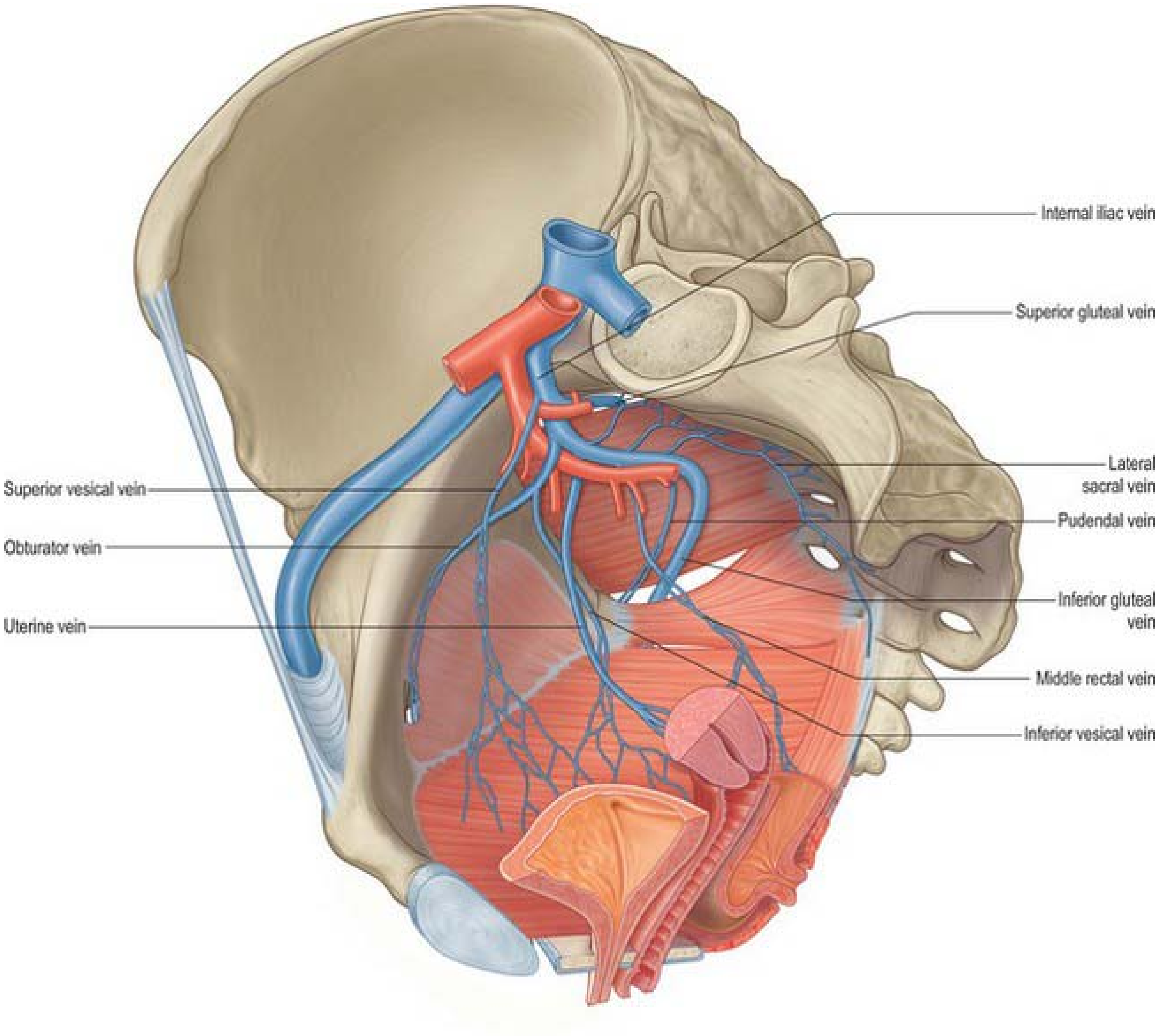
Internal iliac vein
Superior gluteal vein
Lateral sacral vein
Pudendal vein
Inferior gluteal vein
Middle rectal vein
Inferior vesical vein
Superior vesical vein
Obturator vein
Uterine vein

Fig. 63.7 Veins of the female pelvis.

The venous drainage of the leg may be blocked by thrombosis involving the external iliac systems and the inferior vena cava. Under these circumstances, the pelvic veins, particularly the internal iliac tributaries, enlarge and provide a major avenue of venous return from the femoral system. Surgical interference with these veins may seriously compromise venous drainage and precipitate oedema of one or both legs.

Superior gluteal veins

The superior gluteal veins are the venae comitantes of the superior gluteal artery. They receive tributaries which correspond to the branches of the superior gluteal artery and enter the pelvis via the greater sciatic foramen, above piriformis. They join the internal iliac vein, frequently as a single trunk.

Inferior gluteal veins

The inferior gluteal veins are venae comitantes of the inferior gluteal artery. They begin proximally and posterior in the thigh, where they anastomose with the medial circumflex femoral and first perforating veins, and enter the pelvis low in the greater sciatic foramen, joining to form a vessel opening into the distal (lower) part of the internal iliac vein. The inferior gluteal and superficial gluteal veins connect by perforating veins (Doyle 1970) which are analogous to the sural perforating veins. The gluteal veins probably have a venous ‘pumping’ role, and provide collaterals between the femoral and internal iliac veins.

Obturator vein

The obturator vein begins in the proximal adductor region and enters the pelvis via the obturator foramen. It runs posteriorly and superiorly on the lateral pelvic wall below the obturator artery and between the ureter and internal iliac artery and ends in the internal iliac vein. It is sometimes replaced by an enlarged pubic vein, which joins the external iliac vein.

Lateral sacral veins

The lateral sacral veins accompany the lateral sacral arteries, and are interconnected by a sacral venous plexus.

Middle rectal vein

The middle rectal vein begins in the rectal venous plexus and drains the rectum and mesorectum. Variable in size, it runs laterally on the pelvic surface of levator ani to end in the internal iliac vein. The middle rectal vein often receives tributaries from the bladder and either the prostate and seminal vesicle (males) or the posterior aspect of the vagina (females).

External iliac vein

The external iliac vein is the proximal continuation of the femoral vein. It begins posterior to the inguinal ligament, ascends along the pelvic brim and ends anterior to the sacroiliac joint by joining the internal iliac vein to form the common iliac vein. On the right it lies medial to the external iliac artery, gradually inclining behind it as it ascends. On the left it is wholly medial. Disease of the external iliac artery may cause it to adhere closely to the vein at the point where it is in contact, and, particularly on the right side, the walls of the vessels may become fused, making dissection hazardous. The external iliac vein is crossed medially by the ureter and internal iliac artery. In males it is crossed by the vas deferens, in females by the round ligament and ovarian vessels. Psoas major lies laterally, except where the artery intervenes. The vein is usually valveless, but may contain a single valve. It tributaries are the inferior epigastric, deep circumflex iliac and pubic veins.

Inferior epigastric vein

One or two inferior epigastric veins accompany the inferior epigastric artery and drain into the external iliac vein a little above the inguinal ligament.

Deep circumflex iliac vein

The deep circumflex vein is formed from venae comitantes of the corresponding artery. It joins the external iliac vein a little above the inferior epigastric vein after crossing anterior to the external iliac artery.

Pubic vein

The pubic vein connects the external iliac and obturator veins. It ascends on the pelvic surface of the pubis with the pubic branch of the inferior epigastric artery and sometimes replaces the normal obturator vein.

Lymphatic drainage of the pelvis

The lymph nodes in the pelvis are grouped around the common, external and internal iliac vessels, and are named accordingly.

Common iliac nodes

The common iliac nodes receive the entire lymphatic drainage of the lower limb because they drain both internal and external iliac nodes. They usually lie in medial, lateral and anterior chains around the common iliac artery, the lateral being the main route: one or two lie inferior to the aortic bifurcation and anterior to the fifth lumbar vertebra or sacral promontory. The common iliac nodes connect to the lateral aortic nodes.

External iliac nodes

The external iliac nodes usually form three subgroups which are lateral, medial and anterior to the external iliac vessels. The medial nodes are considered the main channel of drainage, collecting lymph from the lower limb via the inguinal nodes, the deeper layers of the infra-umbilical abdominal wall, the adductor region of the thigh, the glans penis or clitoris, the membranous urethra, prostate, fundus of the bladder, uterine cervix and upper vagina. Their efferents pass to the common iliac nodes.

Inferior epigastric and circumflex iliac nodes

The inferior epigastric and circumflex iliac nodes are associated with their similarly named vessels and drain the corresponding areas to the external iliac nodes.

Internal iliac nodes

The internal iliac nodes surround the branches of the internal iliac vessels. They receive afferents from most of the pelvic viscera (with the exception of the gonads and the majority of the rectum), the deeper parts of the perineum and the gluteal and posterior femoral muscles, and drain to the common iliac nodes. The individual groups are considered in the description of the viscera. There are frequent connections between the right and left groups particularly when they lie close to the anterior and posterior midlines (Fig. 63.8).

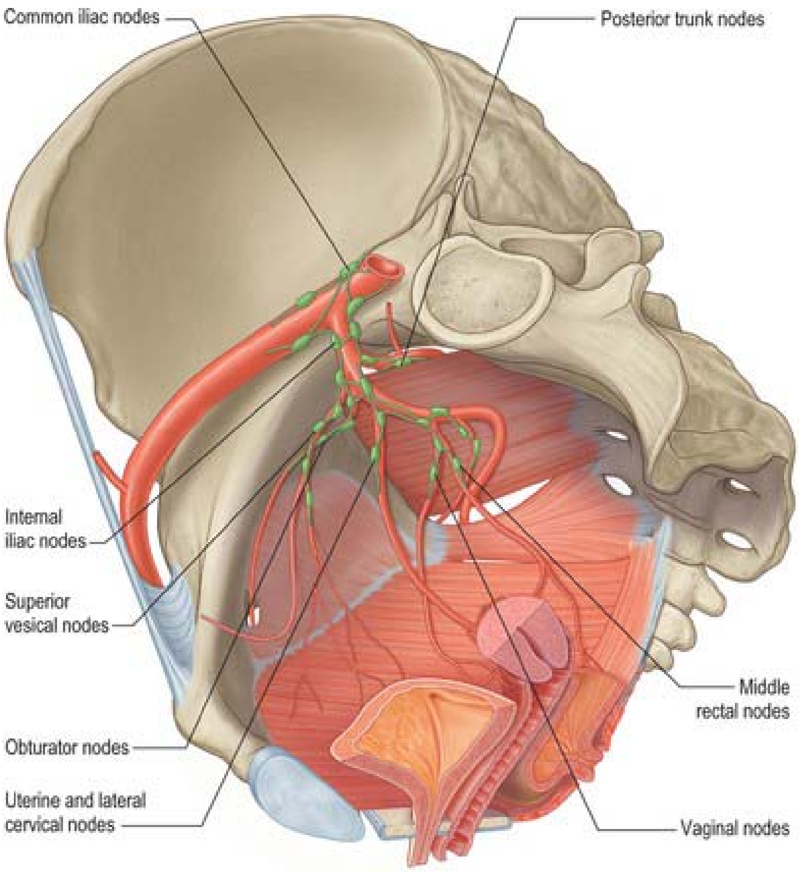
Common iliac nodes
Posterior trunk nodes
Internal iliac nodes
Superior vesical nodes
Obturator nodes
Uterine and lateral cervical nodes
Middle rectal nodes
Vaginal nodes

Fig. 63.8 Lymphatic drainage of the female pelvis and urinary bladder.

INNERVATION OF THE PELVIS

The pelvis contains the lumbosacral nerve trunk, the sacral and coccygeal plexuses and the pelvic parts of the sympathetic and parasympathetic systems. Collectively, these nerves carry the somatic and autonomic innervation to the majority of the pelvic visceral organs, the pelvic floor and perineum, the gluteal region and the lower limb.

The ventral rami of the sacral and coccygeal spinal nerves form the sacral and coccygeal plexuses (Fig. 63.9). The upper four sacral ventral rami enter the pelvis by the anterior sacral foramina, the fifth enters between the sacrum and coccyx, and the ventral ramus of the coccygeal nerve curves forwards below the rudimentary transverse process of the first coccygeal segment. The first and second sacral ventral rami are large, the third to fifth diminish progressively, and the coccygeal is the smallest. Each receives a grey ramus communicans from a corresponding sympathetic ganglion. Visceral efferent rami leave the second to fourth sacral rami as the pelvic splanchnic nerves, containing parasympathetic fibres to minute ganglia in the walls of the pelvic viscera.

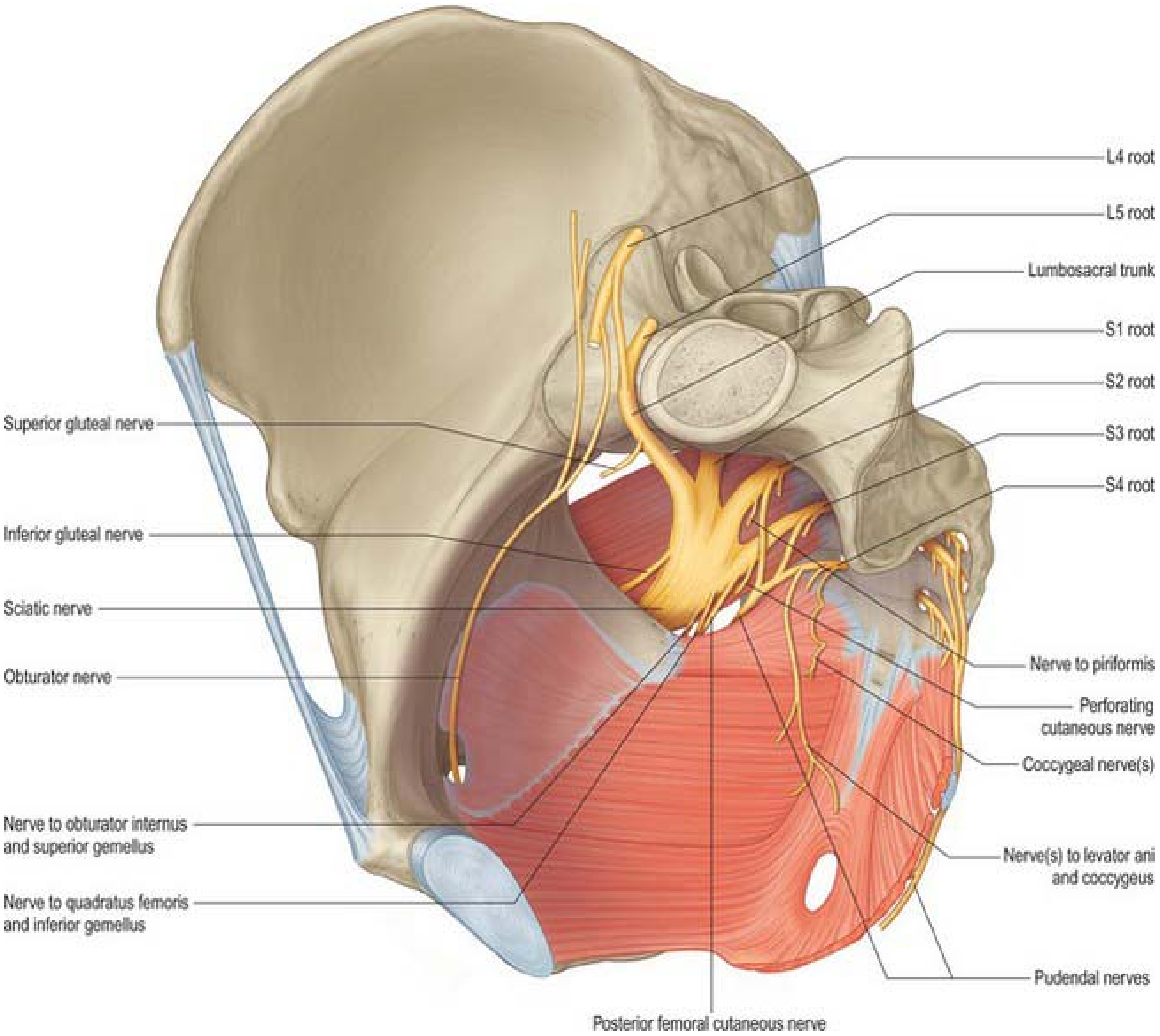
L4 root
L5 root
Lumbosacral trunk
S1 root
S2 root
S3 root
S4 root
Superior gluteal nerve
Inferior gluteal nerve
Sciatic nerve
Obturator nerve
Nerve to piriformis
Perforating cutaneous nerve
Coccygeal nerve(s)
Nerve to obturator internus and superior gemellus
Nerve(s) to levator ani and coccygeus
Nerve to quadratus femoris and inferior gemellus
Pudendal nerves
Posterior femoral cutaneous nerve

Fig. 63.9 The lumbosacral plexus in the pelvis.

Lumbosacral trunk and sacral plexus

The sacral plexus is formed by the lumbosacral trunk, the first to third sacral ventral rami and part of the fourth sacral ventral ramus (the remainder of the fourth sacral ventral ramus joins the coccygeal plexus).

The lumbar part of the lumbosacral trunk contains part of the fourth and all the fifth lumbar ventral rami; it appears at the medial margin of psoas major, and descends over the pelvic brim anterior to the sacroiliac joint to join the first sacral ramus. The greater part of the second and third sacral rami converge on the inferomedial aspect of the lumbosacral trunk in the greater sciatic foramen to form the sciatic nerve. The ventral and dorsal divisions of the nerves do not separate physically from each other, but their fibres remain separate within the rami; the ventral and dorsal divisions of each contributing root join within the sciatic nerve. The fibres of the dorsal divisions will go on to form the common fibular nerve and the fibres of the ventral division form the tibial nerve. The sciatic nerve occasionally divides into common fibular and tibial nerves inside the pelvis. In these cases the common fibular nerve usually runs through piriformis.

The sacral plexus lies against the posterior pelvic wall anterior to piriformis, posterior to the internal iliac vessels and ureter, and behind the sigmoid colon on the left. The superior gluteal vessels run either between the lumbosacral trunk and first sacral ventral ramus or between the first and second sacral rami, while the inferior gluteal vessels lie between either the first and second or second and third sacral rami (Fig. 63.9).

The sacral plexus is not commonly involved in malignant tumours of the pelvis because it lies behind the relatively dense presacral fascia, which resists all but locally very advanced malignant infiltration. When it occurs, there is intractable pain in the distribution of the branches of the plexus which may be very difficult to treat. The plexus may also be involved in the reticuloses or be affected by plexiform neuromas.

Branches of the sacral plexus

The branches of the sacral plexus are:

	Ventral divisions	**Dorsal divisions**
Nerve to quadratus femoris and gemellus inferior	L4,5, S1	
Nerve to obturator internus and gemellus superior	L5, S1,2	
Nerve to piriformis		S2 (S1)
Superior gluteal nerve		L4,5, S1
Inferior gluteal nerve		L5, S1,2

Posterior femoral cutaneous nerve	S2,3	S1,2
Tibial (sciatic) nerve	L4,5, S1,2,3	
Common fibular (sciatic) nerve		L4,5, S1,2
Perforating cutaneous nerve		S2,3
Pudendal nerve	S2,3,4	
Nerves to levator ani and external anal sphincter	S4	
Pelvic splanchnic nerves		S2,3 (S4)

The course and distribution of most of the branches of the sacral plexus are covered fully on page 1384.

Pudendal nerve (in the pelvis)

The pudendal nerve arises from the ventral divisions of the second, third and fourth sacral ventral rami and is formed just above the superior border of the sacrotuberous ligament and the upper fibres of ischiococcygeus. It leaves the pelvis via the greater sciatic foramen between piriformis and ischiococcygeus, enters the gluteal region and crosses the sacrospinous ligament close to its attachment to the ischial spine, where it lies medial to the internal pudendal vessels. It accompanies the internal pudendal artery through the lesser sciatic foramen into the pudendal (Alcock’s) canal on the lateral wall of the ischio-anal fossa. In the posterior part of the canal it gives rise to the inferior rectal nerve, the perineal nerve and the dorsal nerve of the penis or clitoris.

Sacral visceral branches

Visceral branches, the pelvic splanchnic nerves, arise from the second to fourth sacral ventral rami and innervate the pelvic viscera.

Sacral muscular branches

Several muscular branches arise from the fourth sacral ventral ramus to supply the superior surface of levator ani and the upper part of the external anal sphincter. The branches to levator ani enter the superior (pelvic) surface of the muscle whilst the branch to the external anal sphincter (also referred to as the perineal branch of the fourth sacral nerve) reaches the ischio-anal fossa by running either through ischiococcygeus or between ischiococcygeus and iliococcygeus. It supplies the skin between the anus and coccyx via its cutaneous branches.

Coccygeal plexus

The coccygeal plexus is formed by a small descending branch from the fourth sacral ramus and by the fifth sacral and coccygeal ventral rami. The fifth sacral ventral ramus emerges from the sacral hiatus, curves round the lateral margin of the sacrum below its cornu and pierces ischiococcygeus from below to reach its upper, pelvic surface. Here it is joined by a descending branch of the fourth sacral ventral ramus; the small trunk so formed descends on the pelvic surface of ischiococcygeus and joins the minute coccygeal ventral ramus which emerges from the sacral hiatus and curves round the lateral coccygeal margin to pierce coccygeus to reach the pelvis. The small trunk that is formed in this way is the coccygeal plexus. Anococcygeal nerves arise from it and form a few fine filaments which pierce the sacrotuberous ligament to supply the adjacent skin.

Pelvic part of the sympathetic system

The pelvic sympathetic trunk lies in the extraperitoneal tissue anterior to the sacrum beneath the presacral fascia (Fig. 63.10). It lies medial or anterior to the anterior sacral foramina and has four or five interconnected ganglia. Above, it is continuous with the lumbar sympathetic trunk. The right and left trunks converge below the lowest ganglia and unite in the small ganglion impar anterior to the coccyx. Grey rami communicantes pass from the ganglia to sacral and coccygeal spinal nerves but there are no white rami communicantes. Medial branches connect across the midline and twigs from the first two ganglia join the inferior hypogastric plexus or the hypogastric ‘nerve’. Other branches form a plexus on the median sacral artery.

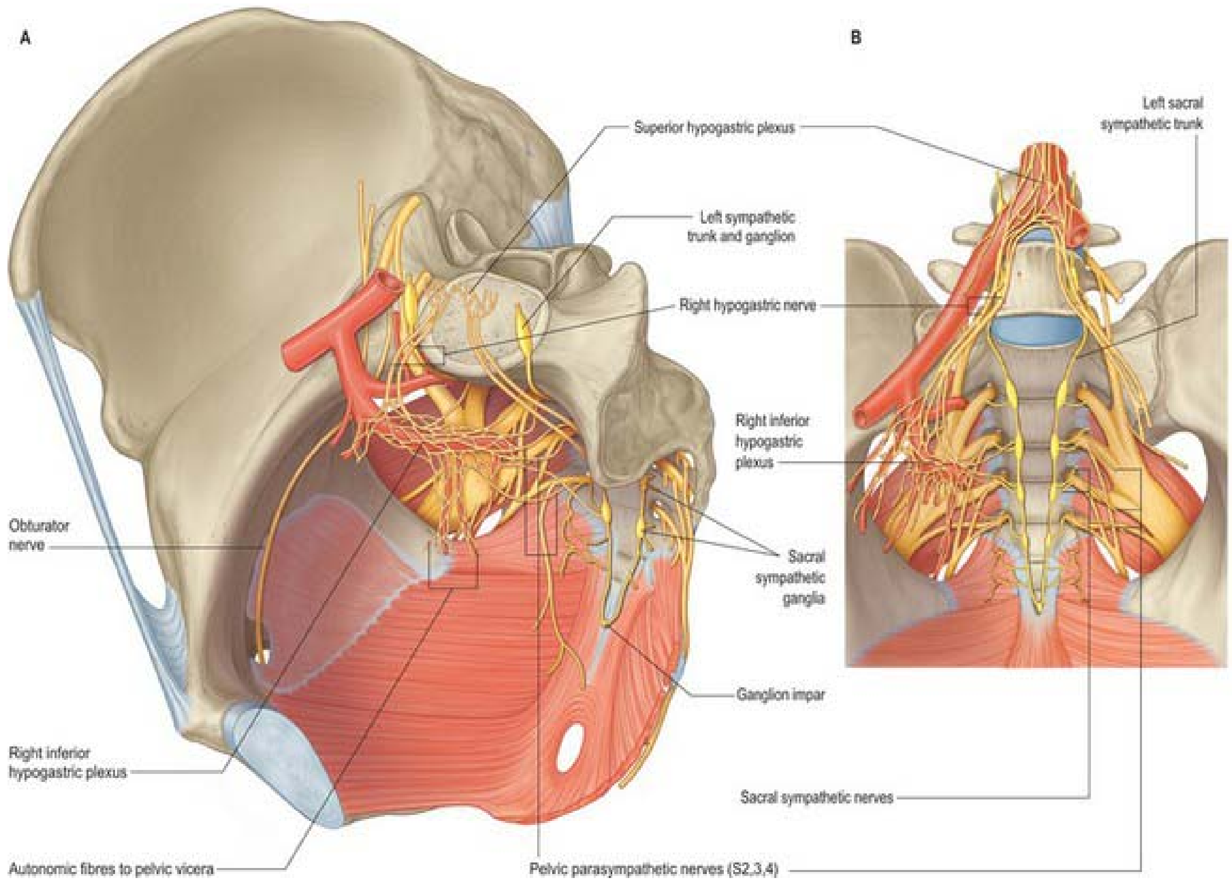
A
B
Superior hypogastric plexus
Left sacral sympathetic trunk
Left sympathetic trunk and ganglion
Right hypogastric nerve
Right inferior hypogastric plexus
Obturator nerve
Sacral sympathetic ganglia
Ganglion impar
Right inferior hypogastric plexus
Sacral sympathetic nerves
Autonomic fibres to pelvic vicera
Pelvic parasympathetic nerves (S2,3,4)

Fig. 63.10 Autonomic nerves of the pelvis.

Vascular branches

Preganglionic fibres for the vessels supplying the pelvis and lower limb are derived from the lower three thoracic and upper two or three lumbar spinal segments. They reach the lower thoracic and upper lumbar ganglia through white rami communicantes and descend through the sympathetic trunk to synapse in the lumbar ganglia. Postganglionic fibres pass from these ganglia via grey rami communicantes to the femoral nerve which carries them to the femoral artery and its branches. Some fibres descend through the lumbar ganglia to synapse in the upper two or three sacral ganglia, from which postganglionic axons pass through grey rami communicantes to the roots of the sacral plexus. Those in the pudendal and superior and inferior gluteal nerves accompany the arteries of the same name to the gluteal and perineal tissues; branches may also supply the pelvic lymph nodes. Those joining the tibial nerve are carried to the popliteal artery and distributed via its branches to the leg and foot.

Sympathetic denervation of vessels in the lower limb can be effected by removing or ablating the upper three lumbar ganglia and the intervening parts of the sympathetic trunk, which is used rarely in treating vascular insufficiency of the lower limb.

PERINEUM

MUSCLES AND FASCIAE OF THE PERINEUM

The perineum is an approximately diamond-shaped region which lies below the pelvic floor, between the inner aspects of the thighs and anterior to the sacrum and coccyx. It is usually described as if from the position of an individual lying supine with the hip joints in abduction and partial flexion. The surface projection of the perineum and the form of the skin covering it varies considerably depending on the position of the thighs whereas the deep tissues themselves occupy relatively fixed positions. The perineum is bounded anteriorly by the pubic symphysis and its arcuate ligament, posteriorly by the coccyx, anterolaterally by the ischiopubic rami and the ischial tuberosities, and posterolaterally by the sacrotuberous ligaments. The deep limit of the perineum is the inferior surface of the pelvic diaphragm and its superficial limit is the skin which is continuous with that over the medial aspect of the thighs and the lower abdominal wall. An arbitrary line joining the ischial tuberosities (the interischial line) divides the perineum into an anterior urogenital triangle and a posterior anal triangle. The urogenital triangle faces downwards and forwards, whereas the anal triangle faces downwards and backwards.

The male urogenital triangle contains the bulb and attachments of the penis (Fig. 63.11) (Ch. 76) and the female urogenital triangle contains the mons pubis, the labia majora, the labia minora, the clitoris and the vaginal and urethral orifices (Ch. 77).

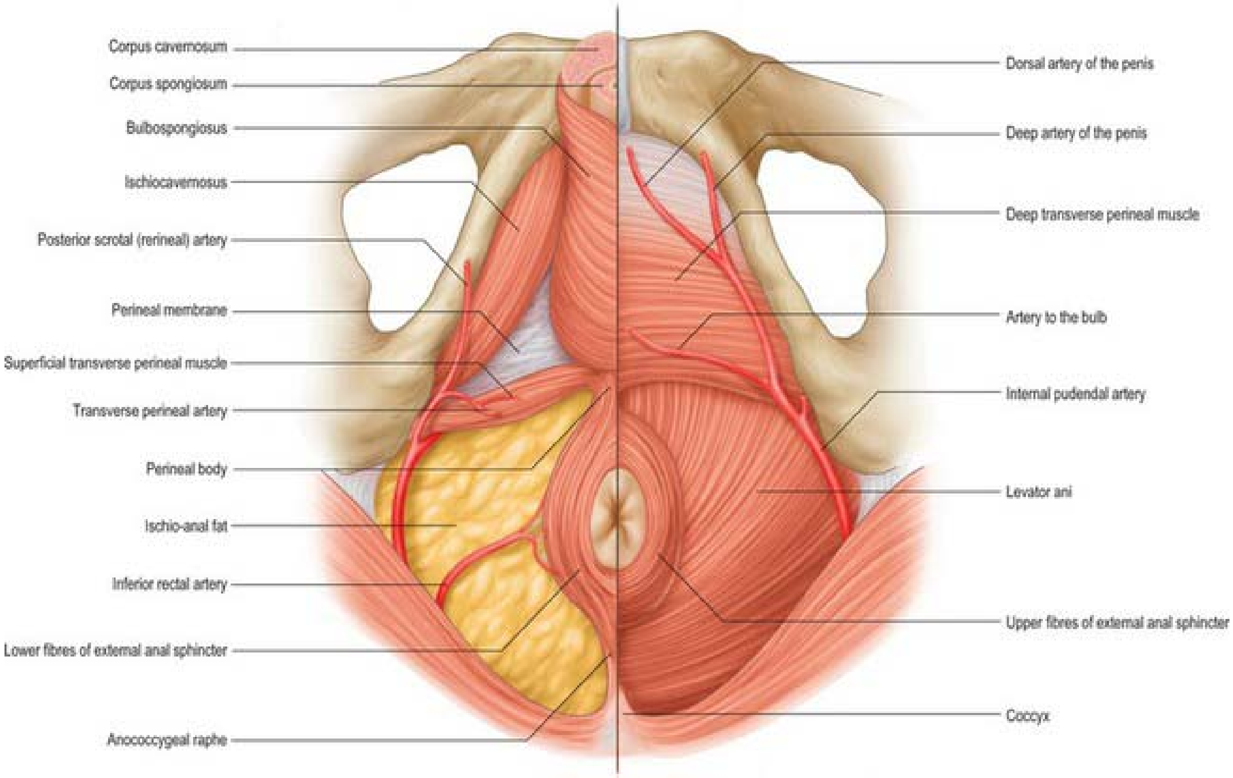
Corpus cavernosum
Corpus spongiosum
Bulbospongiosus
Ischiocavernosus
Posterior scrotal (perineal) artery
Perineal membrane
Superficial transverse perineal muscle
Transverse perineal artery
Perineal body
Ischio-anal fat
Inferior rectal artery
Lower fibres of external anal sphincter
Anococcygeal raphe
Dorsal artery of the penis
Deep artery of the penis
Deep transverse perineal muscle
Artery to the bulb
Internal pudendal artery
Levator ani
Upper fibres of external anal sphincter
Coccyx

Fig. 63.11 Muscles and fasciae of the male perineum. On the left side the skin and superficial fascia of the perineum only have been removed. The posterior scrotal (perineal) artery has been shown as it runs forward into the scrotal tissues. On the right side, the corpora cavernosa and corpus spongiosum and their associated muscles, the superficial perineal muscles and perineal membrane have been removed to reveal the underlying deep muscles and arteries of the perineum. All veins and nerves have been omitted for clarity.

Anal triangle

The structure of the anal triangle is similar in males and females, the main difference reflecting the wider transverse dimension of the triangle in females as a result of the larger size of the pelvic outlet. The anal triangle contains the anal canal and its sphincters, and the ischio-anal fossa and its contained nerves and vessels. It is lined by superficial and deep fascia.

Superficial fascia of the anal triangle

The superficial fascia of the region is thin and is continuous with the superficial/subcutaneous fascia of the skin of the perineum, thighs and buttocks (see p. 1095).

Deep fascia of anal triangle

The deep fascia lines the inferior surface of levator ani and is continuous at its lateral origin with the fascia over obturator internus below the attachment of levator ani. It lines the deep portion of the ischio-anal fossa and its lateral walls.

Ischio-anal fossa

The ischio-anal fossa is an approximately horse-shoe shaped region filling the majority of the anal triangle: although often referred to as a space, it is filled with loose adipose tissue and occasional blood vessels. The ‘arms’ of the horseshoe are triangular in cross section because levator ani slopes downwards towards the anorectal junction (see Fig. 67.43). The anal canal and its sphincters lie in the centre of the horseshoe. Above them the deep medial limit of the fossa is formed by the deep fascia over levator ani. The outer boundary of the fossa is formed anterolaterally by the deep fascia over obturator internus deeply and the periosteum of the ischial tuberosities more superficially. Posterolaterally, the outer boundary is formed by the lower border of gluteus maximus and the sacrotuberous ligament. Anteriorly, the superficial boundary of the fossa is formed by the posterior aspect of the transverse perineal muscles and the deep perineal pouch. Deep to this there is no fascial boundary between the fossa and the tissues deep to the perineal membrane as far anteriorly as the posterior surface of the pubis below the attachment of levator ani. Posteriorly, the fossa contains the attachment of the external anal sphincter to the tip of the coccyx: above and below this, the adipose tissue of the fossa is uninterrupted across the midline. These continuations of the ischio-anal fossa mean that infections, tumours and fluid collections within may not only enlarge relatively freely to the side of the anal canal, but may also spread with little resistance to the opposite side and deep to the perineal membrane. The internal pudendal vessels and accompanying nerves lie in the lateral wall of the ischio-anal fossa, enclosed in fascia forming the pudendal canal. The inferior rectal vessels and nerves cross the fossa from the pudendal canal and often branch within it.

The ischio-anal fossa is an important surgical plane during resections of the anal canal and anorectal junction for malignancy. It provides an easy, relatively bloodless, plane of dissection which encompasses all of the muscular structures of the anal canal and leads to the inferior surface of levator ani through which the dissection is carried.

External anal sphincter

The external anal sphincter is an oval tube of striated muscle which surrounds the lowest part of the anal canal. The uppermost (deepest) fibres blend with the lowest fibres of puborectalis; the two are seen to be continuous on endoanal ultrasound and magnetic resonance imaging. Anteriorly, some of these upper fibres decussate into the superficial transverse perineal muscles. Posteriorly, some fibres are attached to the anococcygeal raphe. The majority of the middle fibres of the external anal sphincter surround the lower part of the internal sphincter and are attached anteriorly to the perineal body and posteriorly to the coccyx via the anococcygeal ligament. Some fibres from each side of the sphincter decussate in these areas to form a sort of commissure in the anterior and posterior midline. The anterior and posterior attachments of the external anal sphincter give the muscular tube an oval profile lying anteroposteriorly. The lower fibres lie below the level of the internal anal sphincter and are separated from the lowest anal epithelium only by submucosa.

Anococcygeal ligament

The anococcygeal ligament is a layered musculotendinous structure running between the middle portion of the external anal sphincter and the coccyx. The lowest portion of the presacral fascia lies above the deep part of the ligament and the most posterior fibres of the raphe of iliococcygeus lie between the two: these three structures together are sometimes referred to as the postanal plate. Division of the anococcygeal raphe may cause descent of the anal canal and a lowering of the posterior part of the anal triangle, but does not demonstrably interfere with the process of defecation.

Urogenital triangle

The urogenital triangle is bounded posteriorly by the inter-ischial line which usually overlies the posterior border of the transverse perineal muscles. Anteriorly and laterally it is bounded deeply by the symphysis pubis and ischiopubic rami. In males, the urogenital triangle extends superficially to encompass the scrotum and the root of the penis. In females, it extends to the lower limit of the labia and mons pubis. The urogenital triangle is divided into two parts by a strong perineal membrane: the deep perineal space lies above the membrane and the superficial perineal space lies below it.

The female urogenital triangle includes muscles, fasciae and spaces similar to those in the male. There are some differences in size and disposition caused by the presence of the vagina and female external genitalia.

Deep perineal pouch (space)

The deep perineal pouch was long regarded as an anatomical region between the urogenital diaphragm and the perineal membrane containing the urethra and urethral sphincter. However, the urogenital diaphragm does not exist and the urethral sphincter, previously thought to be the principle content of the deep perineal space (where it was described as surrounding the urethra), is now recognized to be contained within the urethra. The deep perineal pouch is bounded deeply by the endopelvic fascia of the pelvic floor and superficially by the perineal membrane. Between these two fascial layers lie the deep transverse perinei, superficial to the urethral sphincter mechanism and pubourethralis, and in females superficial to the compressor urethrae and sphincter urethrovaginalis. These muscles do not form a true diaphragmatic sheet as such because fibres from several parts extend through the visceral outlet in the pelvic floor into the lower reaches of the pelvic cavity.

Perineal membrane (previously the inferior fascia of the urogenital diaphragm)

The perineal membrane is a triangular membrane which stretches almost horizontally across the deep perineal pouch. It is attached laterally to the periosteum of the ischiopubic rami and its apex is attached to the arcuate ligament of the pubis. It is particularly thick in this area and is here referred to as the transverse perineal ligament. The posterior border is fused with the deep part of the perineal body and is continuous with the fascia over the deep transverse perinei.

In the male, the perineal membrane is crossed by the urethra, 2–3 cm behind the inferior border of the symphysis pubis; the vessels and nerves to the bulb of the penis; the ducts of the bulbourethral glands, posterolateral to the urethral orifice; the deep dorsal vessels and dorsal nerves of the penis, behind the pubic arch in the midline; and the posterior scrotal vessels and nerves, anterior to the transverse perinei.

In the female, the perineal membrane is less well defined than in the male. It is divided almost into two halves by the vagina and urethra such that it forms a triangle on each side of these structures; the pubourethral ligament (the female equivalent of the transverse perineal ligament in males) links the two sides anteriorly behind the pubic arch. It is crossed by the urethra, 2–3 cm behind the inferior border of the symphysis pubis; the vagina, centrally; the ducts of Bartholin’s glands, posterolateral to the urethral orifice; the deep dorsal vessels and dorsal nerves of the clitoris, behind the pubic arch in the midline; the posterior labial vessels and nerves, anterior to the transverse perinei.

Deep transverse perinei

The deep transverse perinei form an incomplete sheet of muscle extending across the deep perineal pouch from the medial aspects of the ischiopubic rami. Posteriorly the sheet is attached to the perineal body where its fibres decussate with those of the opposite side. Anteriorly, the muscles are deficient and the visceral structures pass across the endopelvic fascia and the perineal membrane. Some fibres pass to the deep part of the external anal sphincter posteriorly and sphincter urethrae anteriorly. Together with the superficial transverse perinei, the muscles act to tether the perineal body in the median plane and may help to support the visceral canals which pass through them. They are supplied by the perineal branches of the pudendal vessels and nerves.

Urethral sphincter mechanism

The urethral sphincter mechanism consists of the intrinsic striated and smooth muscle of the urethra and the puboperinealis (pubourethralis) component of levator ani which surrounds the urethra at the point of maximum concentration of those muscles. It surrounds the membranous urethra in the male and the middle and lower thirds of the urethra in the female. In the male, fibres also reach up to the lowest part of the neck of the bladder and, between the two, lie on the surface of the prostate. The bulk of the fibres surround the membranous urethra and some fibres are attached to the inner surface of the ischiopubic ramus. In the female, the sphincter mechanism surrounds more than the middle third of the urethra. It blends above with the smooth muscle of the bladder neck and below with the smooth muscle of the lower urethra and vagina.

Actions

The urethral sphincter mechanism compresses the urethra, particularly when the bladder contains fluid. Its location around the region of highest urethral closing pressure suggests that it plays an important role in the continence of urine. Like bulbospongiosus, it is relaxed during micturition, but it contracts to expel final drops of urine, or of semen in the male, from the bulbar urethra. It may be stimulated via a vaginal tampon electrode, as has been used in the treatment of stress incontinence of urine in females.

Innervation

The urethral sphincter mechanism extends from the perineum through the urogenital hiatus into the pelvic cavity. It probably receives innervation via the perineal branch of the pudendal nerve from below and direct branches from the sacral plexus and the pelvic splanchnic nerves from above (Wendell-Smith & Wilson 1991). All these nerves originate in the second, third and fourth sacral spinal segments.

Compressor urethrae

Compressor urethrae exists in females and arises from the ischiopubic rami of each side by a small tendon. Fibres pass anteriorly to meet their contralateral counterparts in a flat band which lies anterior to the urethra, below sphincter urethrae (Fig. 63.12). A variable number of fibres from the same origin fan medially to reach the lower walls of the vagina, and may rarely reach as far posteriorly as the perineal body.

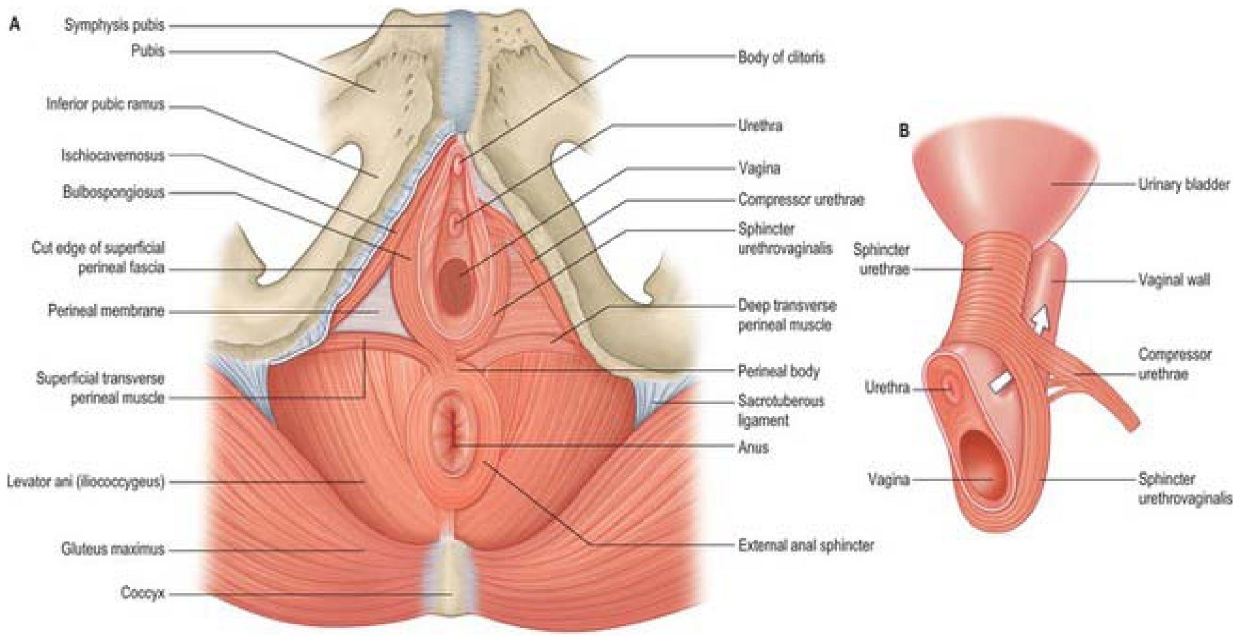
A
Symphysis pubis
Pubis
Inferior pubic ramus
Ischiocavernosus
Bulbospongiosus
Cut edge of superficial perineal fascia
Perineal membrane
Superficial transverse perineal muscle
Levator ani (iliococcygeus)
Gluteus maximus
Coccyx
Body of clitoris
Urethra
Vagina
Compressor urethrae
Sphincter urethrovaginalis
Deep transverse perineal muscle
Perineal body
Sacrotuberous ligament
Anus
External anal sphincter
B
Urinary bladder
Sphincter urethrae
Vaginal wall
Compressor urethrae
Urethra
Vagina
Sphincter urethrovaginalis

Fig. 63.12 Muscles of the female perineum. **A**, On the right side, the membranous layer of superficial fascia has been removed (note the cut edge). On the left side, superficial perineal muscles and overlying fascia have been removed to show the deep perineal muscles. **B**, The continuity of the deep perineal muscles with sphincter urethrae.

Sphincter urethrovaginalis

Sphincter urethrovaginalis exists in females and arises from the perineal body. Fibres pass forwards on either side of the vagina and urethra to meet their contralateral counterparts in a flat band, anterior to the urethra, below compressor urethrae.

Actions

The direction of the fibres of compressor urethrae and sphincter urethrovaginalis suggests that they produce elongation as well as compression of the membranous urethra and thus aid continence in females.

Superficial and deep perineal fasciae

Superficial perineal fascia

The tissue commonly referred to as the superficial fascia of the perineum (Colles' fascia) forms a clear, surgically recognizable plane beneath the skin of the anterior perineum. It is firmly attached posteriorly to the fascia over the superficial transverse perinei and the posterior limit of the perineal membrane. Laterally, it is attached to the margins of the ischiopubic rami as far back as the ischial tuberosities. From here it runs more superficially to the skin of the urogenital triangle, lining the skin of the external genitalia; in the male it is also continuous with the fascial layer in the skin of the scrotum which contains the dartos muscle. In females, the fascia follows the same limits but is much less extensive in the labia majora. This layer runs anteriorly and superiorly into the skin of the lower abdominal wall where it is continuous with the membranous fascia (Scarpa's fascia). These tissue layers are referred to in English as a 'superficial fascia' but this is really a misnomer since they are correctly referred to as the membranous layer of the subcutaneous tissue (the tela subcutanea).

Deep perineal fascia (investing fascia of the superficial perineal muscles)

The tissue commonly referred to as the deep perineal fascia is a layer of fascia overlying the superficial muscles of the perineum (bulbospongiosus, ischiocavernosus, superficial transverse perinei). It is in effect the investing fascia of the superficial perineal muscles and as such is firmly attached to the borders of the muscles at attachments to the ischiopubic rami, posterior margin of the perineal membrane and perineal body. In front it fuses with the suspensory ligament of the penis or clitoris and the fasciae of external oblique and the rectus sheath.

Superficial and subcutaneous perineal pouches

Subcutaneous perineal pouch

The subcutaneous perineal pouch lies between the deep perineal fascia and the superficial perineal fascia. Under normal circumstances these two layers are only separated by relatively thin subcutaneous connective tissue and the skin of the anterior perineum and genitals is relatively mobile over the deeper structures. This pouch is, however, capable of expanding considerably in the presence of fluid accumulation; blood, urine or fluid collecting in the subcutaneous pouch due to trauma or surgery on the urogenital triangle will spread throughout the tissues of the triangle including the scrotum or labia majora, but cannot pass posteriorly into the anal triangle or laterally into the medial thigh due to the firm tethering of the posterior attachments of the subcutaneous fascia. Since the superficial perineal fascia is in continuity with the fascia of the anterior abdominal wall, fluid, blood or pus may also track freely between the subcutaneous tissues of the anterior abdominal wall and the subcutaneous perineal pouch (e.g. post surgical haematomas of the abdominal wall readily cause discolouration of the perineal and genital skin).

Superficial perineal pouch

The superficial perineal pouch lies below the perineal membrane and is limited superficially by the deep perineal fascia (investing fascia of the superficial perineal muscles) (Fig. 63.13). It contains the corpora cavernosa and corpus spongiosum, ischiocavernosus, bulbospongiosus and the superficial transverse perinei, and branches of the pudendal vessels and nerves. In the female, it is crossed by the urethra and vagina and contains the clitoris. In the male, it contains the urethra as it runs in the root of the penis.

It is a fully confined space; injuries to the contents of the space (such as bleeding into the urethra in the penile root) do not communicate with the deep or subcutaneous pouches unless the fascial coverings are also lacerated or breached.

Perineal body

The perineal body is a poorly defined aggregation of fibromuscular tissue located in the midline at the junction between the anal and urogenital triangles. It is attached to many structures in both the deep and superficial urogenital spaces. Posteriorly, it merges with fibres from the middle part of the external anal sphincter and the conjoint longitudinal coat. Superiorly, it is continuous with the rectoprostatic or rectovaginal septum, including fibres from levator ani (puborectalis or pubovaginalis). Anteriorly, it receives a contribution from the deep transverse perinei, the superficial transverse perinei and bulbospongiosus (Fig. 63.4). The perineal body is continuous with the perineal membrane and the superficial perineal fascia. Since the superficial perineal fascia runs forward into the skin of the perineum, the perineal body is tethered to the central perineal skin, which is often puckered over it. In males, this is continuous with the perineal raphe in the skin of the scrotum. In females, the perineal body lies directly posterior to, and is attached to, the posterior commissure of the labia majora and the introitus of the vagina.

The anus can be surgically detached from the perineal body without any clinical consequences. However, spontaneous lacerations of the body sustained during childbirth are often associated with damage to the anterior fibres of the external anal sphincter. The deliberate division of the perineal body to facilitate delivery (episiotomy) is angled laterally to avoid such injuries. The perineal body is often used for the positioning of radiological markers used to determine the amount the perineum descends during straining in order to assess pelvic floor dysfunction.

Superficial transverse perinei

The superficial transverse perinei are narrow strips of muscle which run more or less transversely across the superficial perineal space anterior to the anus. The muscles are occasionally small and rarely absent. On each side the muscle is attached to the medial and anterior aspects of the ischial tuberosity. Medially, the fibres mostly run into the perineal body although some may also pass into the ipsilateral bulbospongiosus or external anal sphincter.

Bulbospongiosus

Bulbospongiosus differs between the sexes. In the male, it lies in the midline, anterior to the perineal body. It consists of two symmetrical parts united by a median fibrous raphe. The fibres attach to the perineal body, in which they decussate, and to the transverse superficial perinei and the external anal sphincter; they diverge like the sides of a feather from the median raphe. A thin layer of posterior fibres joins the posterior portion of the perineal membrane. The majority of the middle fibres encircle the bulb of the penis and adjacent corpus spongiosum and attach to an aponeurosis on the dorsal surfaces. The anterior fibres spread out over the sides of the corpora cavernosa, ending partly in them, anterior to ischiocavernosus, and partly in a tendinous expansion which covers the dorsal vessels of the penis. In the female, bulbospongiosus also attaches to the perineal body, but the muscle on each side is separate and covers the superficial parts of the vestibular bulbs and greater vestibular glands. Fibres run anteriorly on either side of the vagina to attach to the corpora cavernosa clitoridis, and a few fibres cross over the dorsum of the body of the clitoris.

Actions

Bulbospongiosus helps to empty the urethra of urine after the bladder has emptied. In the male, it may assist in the final stage of erection as the middle fibres compress the erectile tissue of the bulb and the anterior fibres contribute by compressing the deep dorsal vein of the penis. It contracts six or seven times during ejaculation, assisting in the expulsion of semen. In the female, bulbospongiosus acts to constrict the vaginal orifice and express the secretions of the greater vestibular glands. Anterior fibres contribute to erection of the clitoris by compressing its deep dorsal vein.

Ischiocavernosus

In the male, ischiocavernosus covers the crus penis. It is attached by tendinous and muscular fibres to the medial aspect of the ischial tuberosity behind, and to the ischial ramus on both sides of the crus. These fibres end in an aponeurosis which is attached to the sides and under surface of the crus penis. In the female, ischiocavernosus is related to a smaller crus clitoris and has a much smaller attachment to the ischiopubic ramus, but is otherwise similar to the corresponding muscle in the male (Figs 63.14, 63.15).

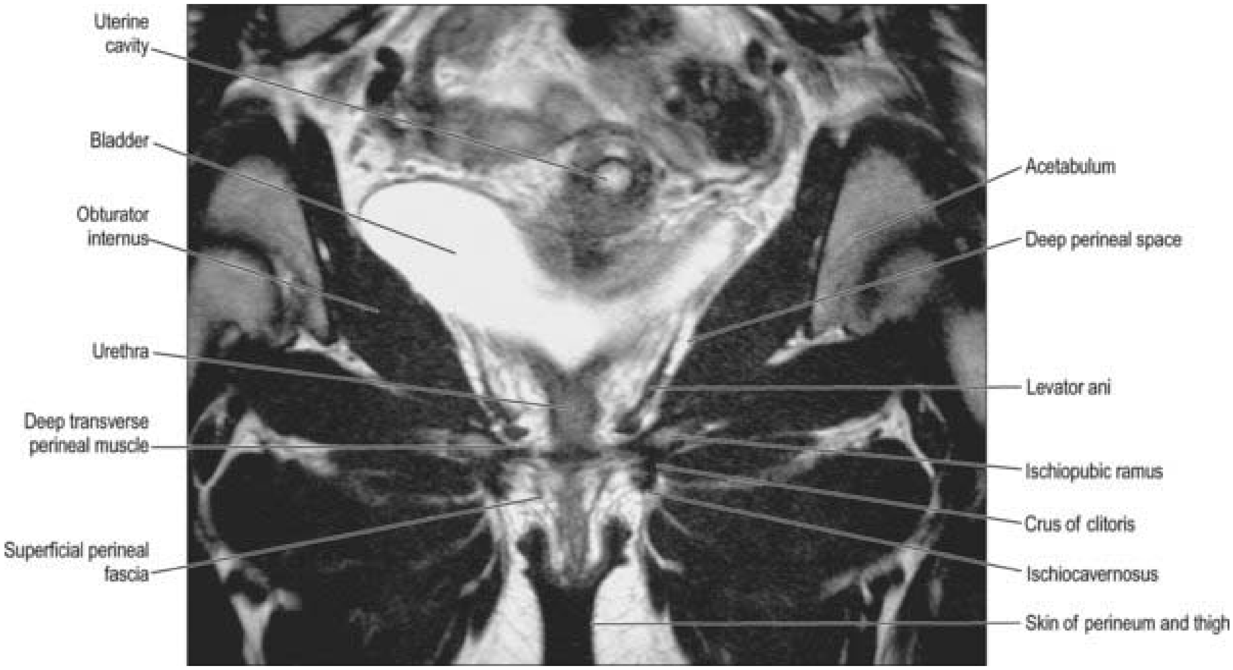
Uterine cavity
Bladder
Obturator internus
Urethra
Deep transverse perineal muscle
Superficial perineal fascia
Acetabulum
Deep perineal space
Levator ani
Ischiopubic ramus
Crus of clitoris
Ischiocavernosus
Skin of perineum and thigh

Fig. 63.15 Muscles and fasciae of the female perineum – coronal T2-weighted MRI.

(By courtesy of Dr J Lee and Ms K Wimpey, Chelsea and Westminster Hospital, London.)

Action

Ischiocavernosus compresses the crus penis in males and may help to maintain penile erection. The muscles form a triangle on each side of the midline with bulbospongiosus medially and the superficial transverse perinei posteriorly, attached to the perineal membrane: when contracted, the two ischiocavernosi act together to stabilize the erect penis. In the female, ischiocavernosus may help to promote clitoral erection.

VASCULAR SUPPLY AND LYMPHATIC DRAINAGE OF THE PERINEUM

Arteries of the perineum

Internal pudendal artery (in the perineum)

The internal pudendal artery enters the perineum around the posterior aspect of the ischial spine and runs on the lateral wall of the ischio-anal fossa in the pudendal (Alcock’s) canal with the pudendal veins and the pudendal nerve. The canal is formed by the connective tissue binding the vessels and nerve to the perineal surface of the obturator internus fascia and lies about 4 cm above the lower limit of the ischial tuberosity. As the artery approaches the margin of the ischial ramus, it proceeds above or below the perineal membrane, along the medial margin of the inferior pubic ramus and ends behind the inferior pubic ligament.

In the male, the internal pudendal artery distal to the perineal artery gives a branch to the bulb of the penis before it divides into the deep (cavernosal) and dorsal arteries of the penis (Fig. 63.11). Given its distribution, the internal pudendal artery distal to its perineal branch has been named the artery of the penis. The artery to the bulb supplies the corpus spongiosum and the deep artery to the penis supplies the corpus cavernosa on each side. The dorsal artery runs on the dorsal aspect of the penis, and supplies circumflex branches to the corpora cavernosa and corpus spongiosum which end by anastomosing in the coronal sulcus and supplying the glans penis and its overlying skin.

In the female, the artery to the bulb is distributed to the erectile tissue of the vestibular bulb and vagina. The cavernosal artery is much smaller and supplies the corpora cavernosa of the clitoris; the dorsal artery supplies the glans and prepuce of the clitoris (Fig. 63.11).

Branches of the internal pudendal artery are sometimes derived from an accessory pudendal artery, which is usually a branch of the pudendal artery before its exit from the pelvis; effectively the artery is double before it leaves the pelvis.

Inferior rectal artery

The inferior rectal artery arises just after the internal pudendal artery enters the canal on the lateral wall of the ischio-anal fossa and runs anteromedially through the adipose tissue of the ischio-anal fossa to reach the deep portion of the external anal sphincter. It often branches before reaching the sphincter. During dissections of the anal canal, particularly during perineal excisions of the anorectum, the inferior rectal vessels are encountered in the ischio-anal fossa and must be secured before division or they tend to retract laterally to the canal, where they can cause troublesome bleeding.

Perineal artery

The perineal artery is a branch of the internal pudendal artery near the anterior end of the pudendal canal, and runs through the perineal membrane. In the male, it approaches the scrotum in the superficial perineal space, between bulbospongiosus and ischiocavernosus. A small transverse branch passes medially, inferior to the superficial transverse perineal muscle, to anastomose with the contralateral artery and with the posterior scrotal and inferior rectal arteries. It supplies the transverse perinei, the perineal body and the posterior attachment of the bulb of the penis. The posterior scrotal arteries are usually terminal branches of the perineal artery but may also arise from its transverse branch. They are distributed to the scrotal skin and dartos muscle in the male and supply the perineal muscles. In the female, the perineal artery runs an almost identical course to that in the male, and gives off similar branches; the posterior scrotal arteries are replaced by posterior labial arteries.

Veins of the perineum: internal pudendal veins

The internal pudendal veins are venae comitantes of the internal pudendal artery and unite as a single vessel ending in the internal iliac vein. The perineal tributaries receive veins from the penile bulb and the scrotum (males) or clitoris and labia (females) and the inferior rectal veins join towards the posterior end of the pudendal canal.

Lymphatic drainage of the perineum

The lymphatics from the skin of the penis and scrotum (male) or skin of the clitoris and labia (female) drain together with lymphatics from the perineal skin to the superficial inguinal nodes and thence to the deep inguinal nodes. The glans, corpora cavernosa and corpus spongiosum of the penis or clitoris drain directly to the deep inguinal nodes.

INNERVATION OF THE PERINEUM: PUDENDAL NERVE (IN THE PERINEUM)

The pudendal nerve gives rise to the inferior rectal and perineal nerves and the dorsal nerves of the penis or clitoris.

The pudendal nerve occupies a very constant position over the ischial spine and is readily found. It may be ‘blocked’ by infiltration with a local anaesthetic applied via a needle passed through the lateral wall of the vagina to numb the perineal and anal skin. It may also be palpated over the ischial spine through the lateral wall of the rectum and motor terminal latencies measured.

Inferior rectal nerve

The inferior rectal nerve runs through the medial wall of the pudendal canal with the inferior rectal vessels. It crosses the ischio-anal fossa to supply the external anal sphincter, the lining of the lower part of the anal canal, and the circumanal skin. It frequently breaks into terminal branches just before reaching the lateral border of the sphincter. Its cutaneous branches distributed around the anus overlap the cutaneous branches of the perineal branch of the posterior femoral cutaneous nerve and of the scrotal or labial nerves. The inferior rectal nerve occasionally arises directly from the sacral plexus and crosses the sacrospinous ligament or reconnects with the pudendal nerve. In females, the inferior rectal nerve may supply sensory branches to the lower part of the vagina.

Perineal nerve

The perineal nerve is the inferior and larger terminal branch of the pudendal nerve in the pudendal canal. It runs forwards below the internal pudendal artery and accompanies the perineal artery, dividing into posterior scrotal or labial and muscular branches. The posterior scrotal or labial nerves are usually double and have medial and lateral branches which run over the perineal membrane and pass forwards in the lateral part of the urogenital triangle with the scrotal or labial branches of the perineal artery. They supply the skin of the scrotum or labia majora, overlapping the distribution of the perineal branch of the posterior femoral cutaneous and inferior rectal nerves. In females, the posterior labial branches also supply sensory fibres to the skin of the lower vagina.

Muscular branches arise directly from the pudendal nerve to supply the superficial transverse perinei, bulbospongiosus, ischiocavernosus, deep transverse perinei, sphincter urethrae and the anterior parts of the external anal sphincter and levator ani. In males, a nerve to the bulb of the urethra leaves the nerve to the bulbospongiosus, pierces this muscle to supply the corpus spongiosum penis and ends in the urethral mucosa.

Dorsal nerve of the penis or clitoris

The dorsal nerve of the penis or clitoris runs anteriorly above the internal pudendal artery along the ischiopubic ramus deep to the perineal membrane. It supplies the corpus cavernosum and accompanies the dorsal artery of the penis or clitoris between the layers of the suspensory ligament. In males, the dorsal nerve of the penis runs on the dorsum of the penis to end in the glans. In females the dorsal nerve of the clitoris is very small.

REFERENCES

yle JF. The perforating veins of the gluteus maximus. *Ir J Med Sci*. 1970;3:285-288.

nith GE. Studies in the anatomy of the human pelvis, with special reference to the fasciae and visceral supports. Part I. *J Anat Physiol*. 1908;42:198-218.

Lancey JO. Structural support of the urethra as it relates to stress urinary incontinence: the hammock hypothesis. *Am J Obstet Gynecol*. 1994;170:1713-1723.

endell-Smith CP, Wilson PM. The vulva, vagina and urethra and the musculature of the pelvic floor. In: Philipp E, Setchell M, Ginsburg J.

Scientific Foundations of Obstetrics and Gynaecology. Oxford: Butterworth-Heinemann; 1991:84-100.

CHAPTER 64

Peritoneum and peritoneal cavity

The peritoneum is the largest serous membrane in the body, and its arrangements are complex. In males it forms a closed sac, but in females it is open at the lateral ends of the uterine tubes. It consists of a single layer of flat mesothelial cells lying on a layer of loose connective tissue. The mesothelium usually forms a continuous surface, but in some areas may be fenestrated. Neighbouring cells are joined by junctional complexes, but probably permit the passage of macrophages. The submesothelial connective tissue may also contain macrophages, lymphocytes and adipocytes (in some regions). Mesothelial cells may transform into fibroblasts, which may play an important role in the formation of peritoneal adhesions after surgery or inflammation of the peritoneum.

The peritoneal cavity is a potential space between the parietal peritoneum, which lines the abdominal wall, and infoldings of visceral peritoneum, which suspend the abdominal viscera within the cavity. It contains a small amount of serous fluid, but is otherwise empty. The fluid lubricates the visceral peritoneum and allows the mobile viscera to glide freely on the abdominal wall and each other within the limits dictated by their attachments. It contains water, proteins, electrolytes and solutes derived from interstitial fluid in the adjacent tissues and from the plasma in the local blood vessels. It normally contains a few cells, including desquamated mesothelium, nomadic peritoneal macrophages, mast cells, fibroblasts, lymphocytes and other leukocytes. Some cells, particularly macrophages, migrate freely between the peritoneal cavity and the surrounding connective tissue. Lymphocytes provide both cellular and humoral immunological defence mechanisms within the peritoneal cavity. The intraperitoneal fluid is directed by gravity to dependent sites within the peritoneal cavity, and also flows in a cephalad direction as a consequence of the negative upper intra-abdominal pressures which are generated by respiration.

The peritoneal cavity never contains gas in normal circumstances, although the amount of fluid may be increased in inflammatory conditions of the viscera. In females blood or fluid may occasionally escape from the uterine tubes into the pelvic peritoneal cavity during menstruation.

Extraperitoneal connective tissue separates the parietal peritoneum from the muscular layers of the abdominal walls. The parietal peritoneum covering the anterior abdominal wall and pelvic walls is generally attached only loosely by this tissue, an arrangement which allows for considerable alteration in the size of the bladder and rectum. The extraperitoneal tissue on the inferior surface of the diaphragm and behind the linea alba is denser and more firmly adherent. The extraperitoneal tissue frequently contains large amounts of fat over the posterior abdominal wall, especially in obese males. The visceral peritoneum is firmly adherent to the underlying tissues and cannot be easily detached. Its connective tissue layer is often continuous with the fibrous matrix of the wall of the underlying viscera and rarely contains much loose connective or adipose tissue. The visceral peritoneum is often considered as part of the underlying viscus for clinical and pathological purposes such as the staging of carcinoma.

GENERAL ARRANGEMENT OF THE PERITONEUM

In utero, the alimentary tract develops as a single tube suspended in the coelomic cavity by ventral and dorsal mesenteries (see Ch. 73). Ultimately, the ventral mesentery is largely resorbed, although some parts persist in the upper abdomen and form structures such as the falciform ligament. The mesenteries of the intestines in the adult are the remnants of the dorsal mesentery. The migration and subsequent fixation of parts of the gastrointestinal tract produce the so-called ‘retroperitoneal’ segments of bowel (duodenum, ascending colon, descending colon, and rectum), and four separate intraperitoneal bowel loops suspended by mesenteries of variable lengths. These are all covered by visceral peritoneum which is continuous with the parietal peritoneum covering the posterior abdominal wall. The first intraperitoneal loop is formed by the intraperitoneal oesophagus, the stomach and first part of the duodenum. The second loop is made up of the duodenojejunal junction, jejunum, ileum and occasionally the caecum and proximal ascending colon. The third loop contains the transverse colon and the final loop contains the sigmoid colon and occasionally the distal descending colon.

Where the visceral peritoneum encloses or suspends organs within the peritoneal cavity, the peritoneum and related connective tissues are known as the peritoneal ligaments, omenta or mesenteries. All but the greater omentum are composed of two layers of visceral peritoneum separated by variable amounts of connective tissue. The greater omentum is folded back on itself and is therefore made up of four layers of closely applied visceral peritoneum, which are separated by variable amounts of adipose tissue. The mesenteries attach their respective viscera to the posterior abdominal wall: the attachment is referred to as the mesenteric root, and the peritoneum of the mesentery is continuous with that of the posterior abdominal wall in this area (Fig. 64.1).

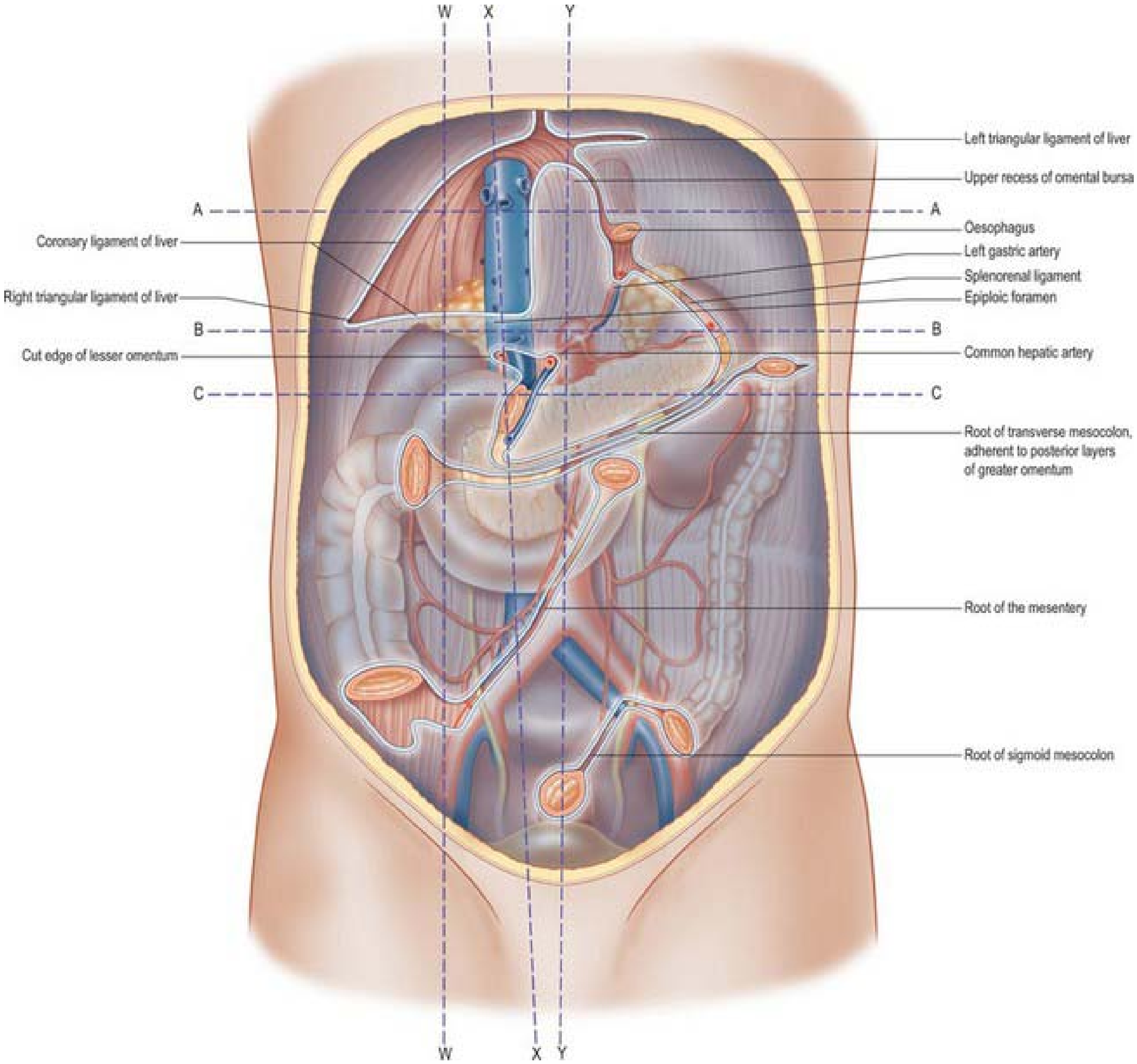
W
X
Y
Left triangular ligament of liver
Upper recess of omental bursa
A
A
Coronary ligament of liver
Oesophagus
Left gastric artery
Right triangular ligament of liver
Splenorenal ligament
Epiploic foramen
B
B
Cut edge of lesser omentum
Common hepatic artery
C
C
Root of transverse mesocolon, adherent to posterior layers of greater omentum
Root of the mesentery
Root of sigmoid mesocolon
W
X
Y

Fig. 64.1 The posterior abdominal wall, showing the lines of peritoneal reflection, after removal of the liver, spleen, stomach, jejunum, ileum, caecum, transverse colon and sigmoid colon. The various sessile (retroperitoneal) organs are seen shining through the posterior parietal peritoneum. Note: the ascending and descending colon, duodenum, kidneys, suprarenals, pancreas and inferior vena cava. Line W–W represents the plane of **Fig. 64.2**. Line X–X represents the plane of **Fig. 64.3**. Line Y–Y represents the plane of **Fig. 64.4**. Line A–A represents the plane of **Fig. 64.5A**. Line B–B represents the plane of **Fig. 64.5B**. Line C–C represents the plane of **Fig. 64.5C**.

Although they are described as intraperitoneal, strictly speaking the suspended organs do not lie within the peritoneal cavity because they are covered by visceral peritoneum. They are continuous with the extraperitoneal tissues, including the retroperitoneum, via subperitoneal tissue lying between the folds of visceral peritoneum. The loose areolar connective tissues of the extraperitoneal and subperitoneal tissues are sometimes conceptualized as ‘spaces’ because fluid or blood collects relatively easily within them. The subperitoneal tissues contain the neurovascular bundles and lymphatic channels which supply the suspended organs. In obese individuals, extensive adipose tissue within the mesenteries and omenta may obscure the neurovascular bundles. In contrast, in the very young, the elderly or the malnourished, the mesentery may contain very little adipose tissue and the neurovascular bundles are usually obvious.

PERITONEUM OF THE UPPER ABDOMEN

The abdominal oesophagus, stomach, liver and spleen all lie within a double fold of visceral peritoneum which runs from the posterior to the anterior abdominal wall. This fold has no recognized name, but has been referred to as the mesogastrium by Coakley & Hricak 1999 because it is derived from the fetal mesogastrium. It has a complex attachment to the wall of the abdominal cavity and gives rise to the falciform ligament, coronary ligaments, lesser omentum (gastrohepatic and hepatoduodenal ligaments), greater omentum (including gastrocolic ligament), gastrosplenic ligament, splenorenal ligament, and phrenicocolic ligament (Figs 64.2, 64.3, 64.4).

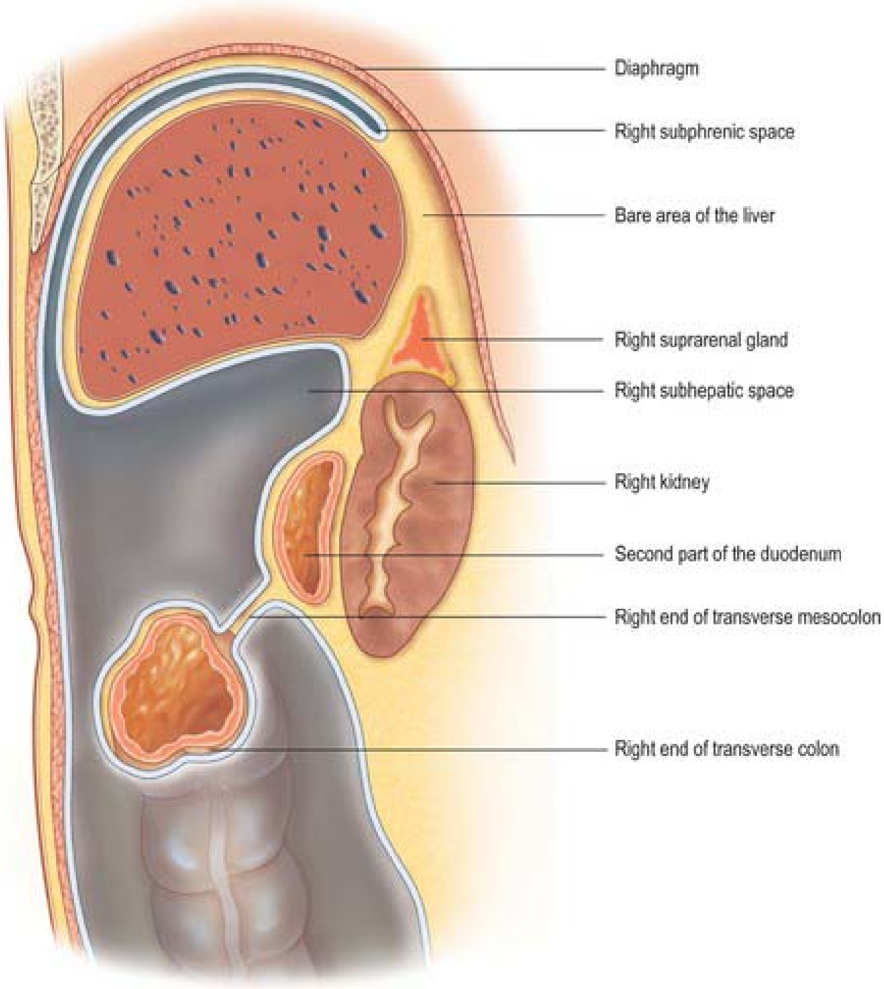
Diaphragm
Right subphrenic space
Bare area of the liver
Right suprarenal gland
Right subhepatic space
Right kidney
Second part of the duodenum
Right end of transverse mesocolon
Right end of transverse colon

Fig. 64.2 Sagittal section through the abdomen to the right of the epiploic foramen along one line of W–W in **Fig. 64.1**.

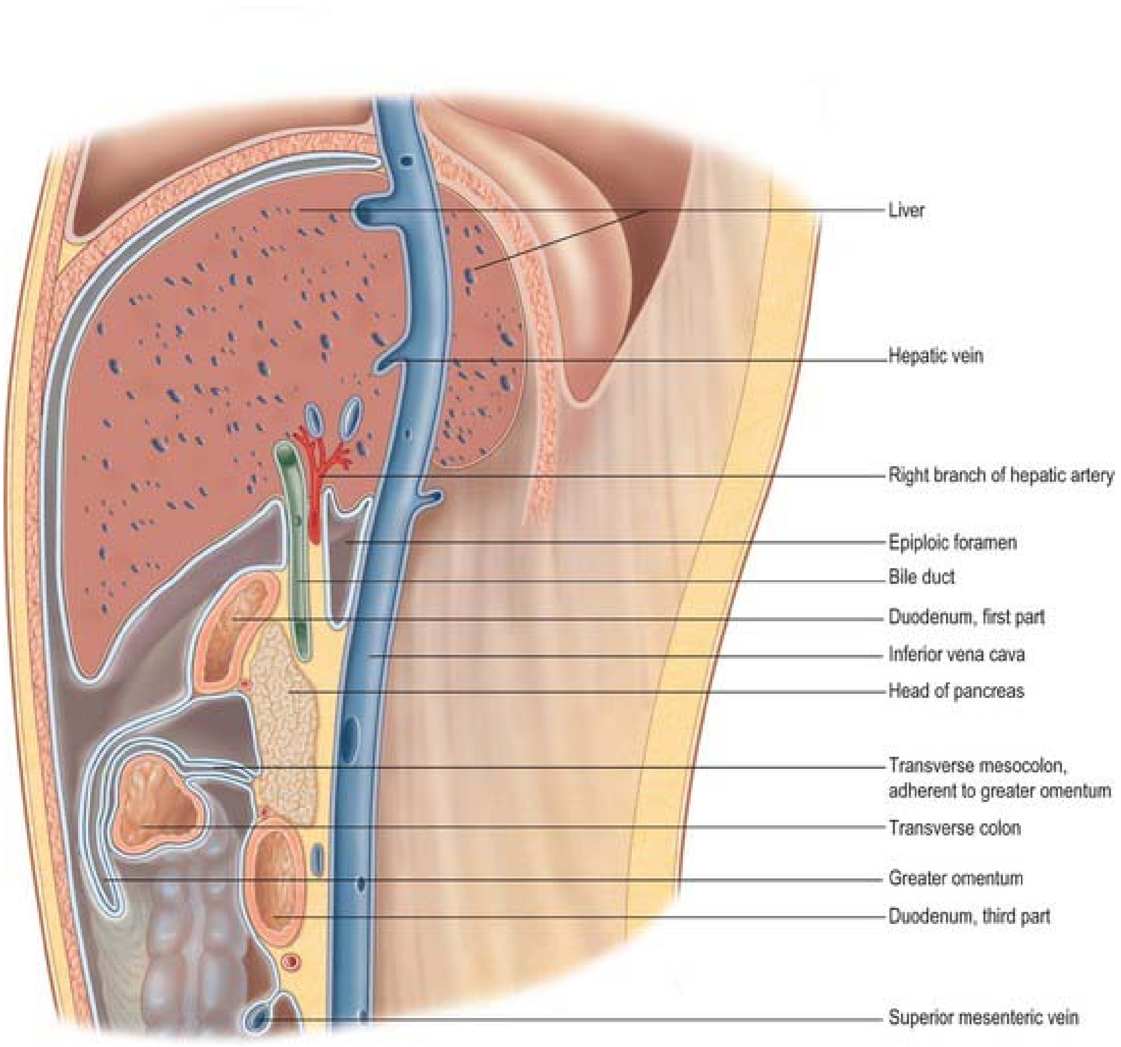
Liver
Hepatic vein
Right branch of hepatic artery
Epiploic foramen
Bile duct
Duodenum, first part
Inferior vena cava
Head of pancreas
Transverse mesocolon, adherent to greater omentum
Transverse colon
Greater omentum
Duodenum, third part
Superior mesenteric vein

Fig. 64.3 Section through the upper part of the abdominal cavity, along the line X–X in **Fig. 64.1**. The boundaries of the epiploic foramen are shown and a small recess of the lesser sac is displayed in front of the head of the pancreas. Note that the transverse colon and its mesocolon are adherent to the posterior two layers of the greater omentum.

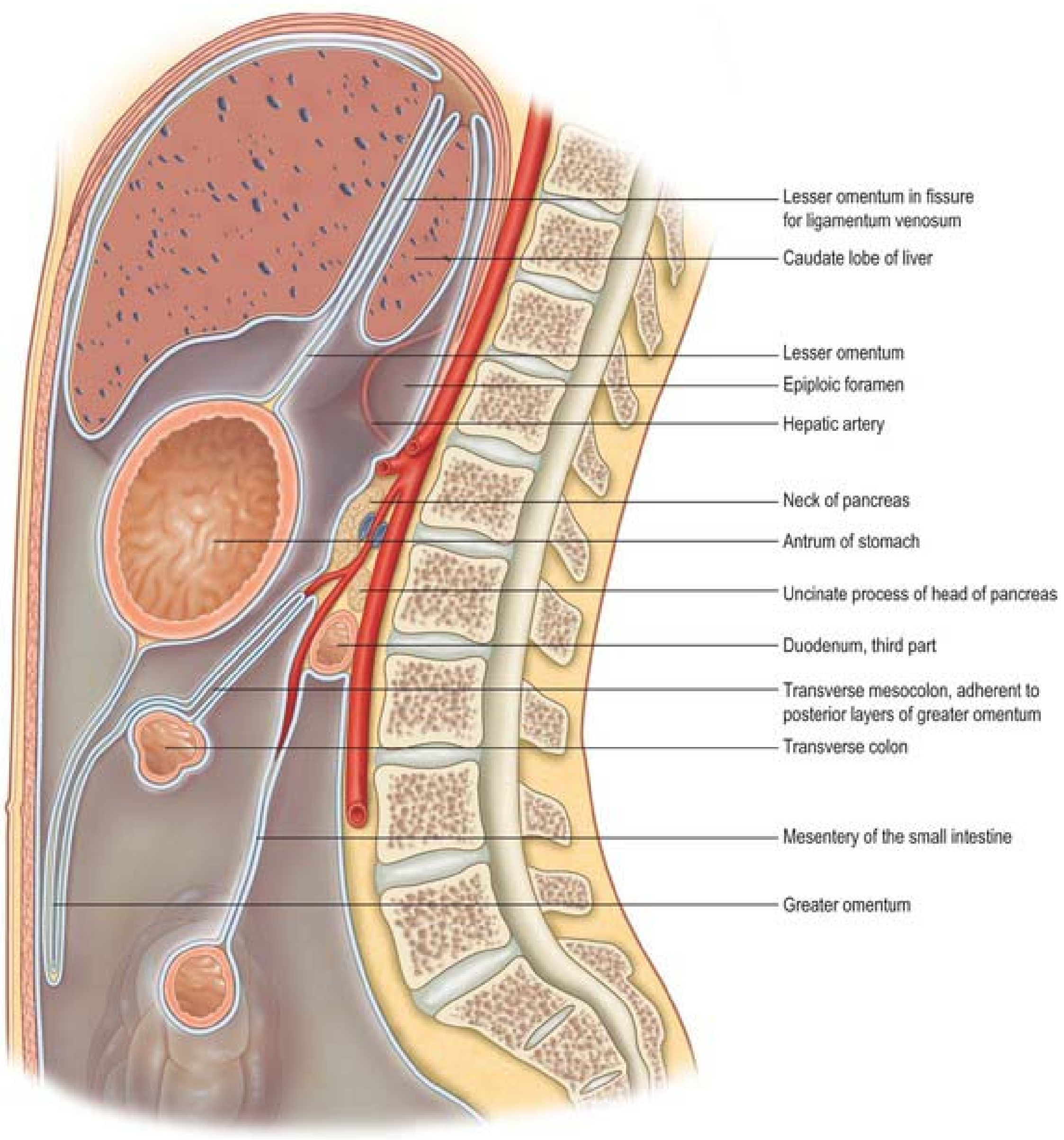
Lesser omentum in fissure for ligamentum venosum
Caudate lobe of liver
Lesser omentum
Epiploic foramen
Hepatic artery
Neck of pancreas
Antrum of stomach
Uncinate process of head of pancreas
Duodenum, third part
Transverse mesocolon, adherent to posterior layers of greater omentum
Transverse colon
Mesentery of the small intestine
Greater omentum

Fig. 64.4 Sagittal section through the abdomen, approximately in the median plane. Compare with **Fig. 64.1**. The section cuts the posterior abdominal wall along the line Y–Y in **Fig. 64.1**. The peritoneum is shown in blue except along its cut edges, which are left white.

The falciform ligament

The falciform ligament is a thin anteroposterior peritoneal fold which connects the liver to the posterior aspect of the anterior abdominal wall just to the right of the midline. It extends inferiorly to the level of the umbilicus, and is widest between the liver and umbilicus. The ligament narrows superiorly as the distance between the liver and anterior abdominal wall reduces and narrows to just a centimetre or so in height over the superior surface of the liver. Its two peritoneal layers divide to enclose the liver and are continuous with the visceral peritoneum that is adherent to the surface of the liver. Superiorly, they are reflected onto the inferior surface of the diaphragm and are continuous with the parietal peritoneum over the right dome. At the posterior limit, or apex, of the falciform ligament, the two layers are also reflected vertically left and right, and are continuous with the anterior layers of the left triangular ligament and the superior layer of the coronary ligament of the liver. The inferior aspect of the falciform ligament forms a free border where the two peritoneal layers become continuous with each other as they fold over to enclose the ligamentum teres. Because the peritoneum of the falciform ligament is continuous with that covering the posterior abdominal wall and the periumbilical anterior abdominal wall, blood arising from retroperitoneal haemorrhage (commonly acute haemorrhagic pancreatitis) may track between the folds of peritoneum and appear as haemorrhagic discolouration around the umbilicus (Cullen’s sign). Inflammatory change from the pancreas may spread via the gastrohepatic ligament (lesser omentum) and then via the falciform ligament to the umbilicus.

The peritoneal connections of the liver

The liver is almost completely covered in visceral peritoneum, and only the ‘bare area’ is in direct contact with the right dome of the diaphragm. Peritoneal folds, the ligaments of the liver, run from the liver to the surrounding viscera and to the abdominal wall and diaphragm (Fig. 64.5); they are described in detail in Chapter 68.

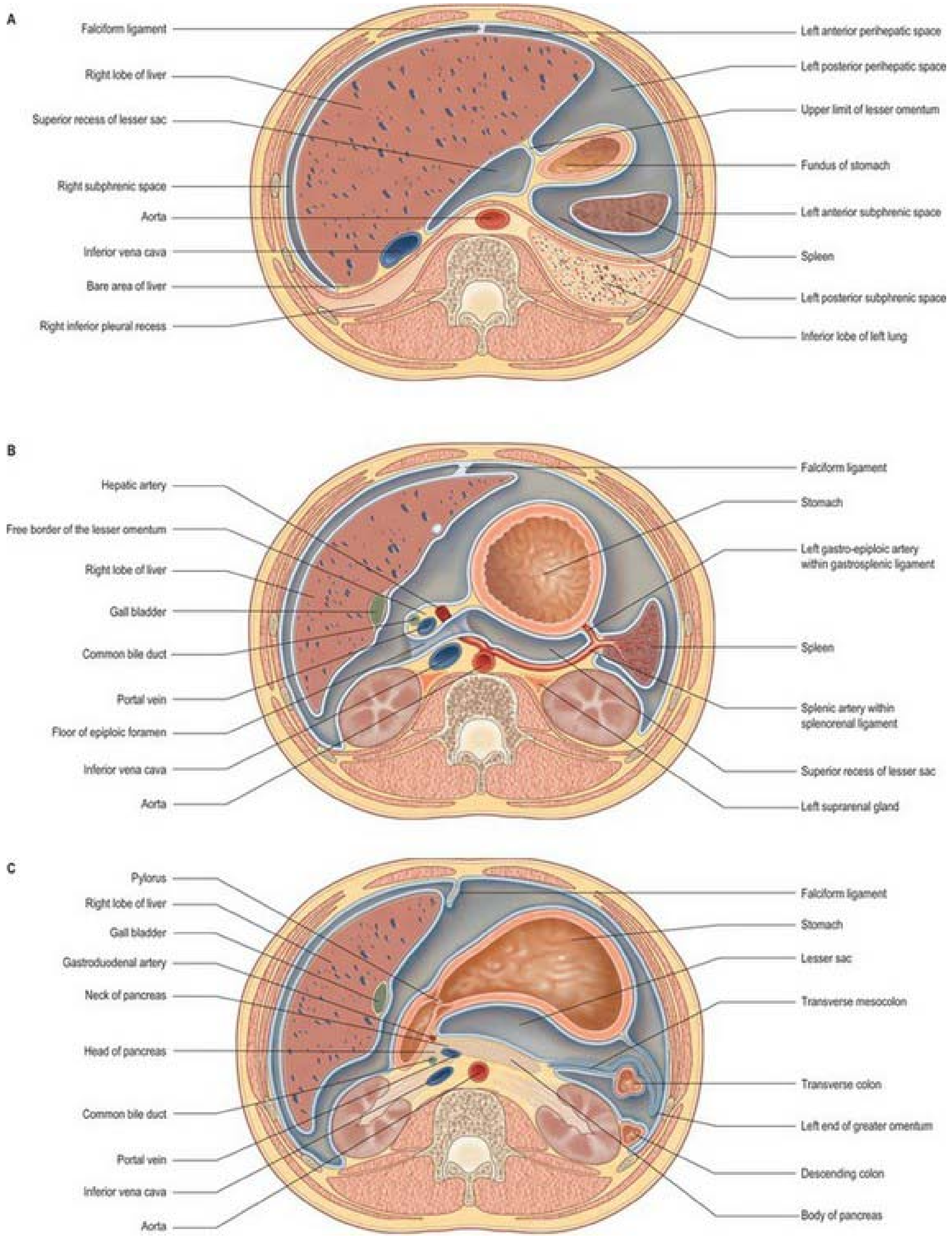
A
Falciform ligament
Right lobe of liver
Superior recess of lesser sac
Right subphrenic space
Aorta
Inferior vena cava
Bare area of liver
Right inferior pleural recess
Left anterior perihepatic space
Left posterior perihepatic space
Upper limit of lesser omentum
Fundus of stomach
Left anterior subphrenic space
Spleen
Left posterior subphrenic space
Inferior lobe of left lung
B
Hepatic artery
Free border of the lesser omentum
Right lobe of liver
Gall bladder
Common bile duct
Portal vein
Floor of epiploic foramen
Inferior vena cava
Aorta
Falciform ligament
Stomach
Left gastro-epiploic artery
within gastrosplenic ligament
Spleen
Splenic artery within
splenorenal ligament
Superior recess of lesser sac
Left suprarenal gland
C
Pylorus
Right lobe of liver
Gall bladder
Gastroduodenal artery
Neck of pancreas
Head of pancreas
Common bile duct
Portal vein
Inferior vena cava
Aorta
Falciform ligament
Stomach
Lesser sac
Transverse mesocolon
Transverse colon
Left end of greater omentum
Descending colon
Body of pancreas

Fig. 64.5 Transverse sections through the abdomen. **A**, At the level of the line A–A in **Fig. 64.1**. The line passes through the bare area of the liver at the superior end of the lesser omentum. The parts of the left subphrenic space are clearly seen although they are continuous with each other. **B**, At

the level of line B–B in **Fig. 64.1**, viewed from below. The peritoneal cavity is shown by a blue 'wash'; the peritoneum and its cut edges in pale blue. **C**, Transverse section through the abdomen at the level of the line C–C in **Fig. 64.1**, viewed from below. Colours as in **Fig. 64.1**.

The coronary ligament is formed by the reflection of the peritoneum from the diaphragm onto the posterior surfaces of the right lobe of the liver. Between the two layers of this ligament, a large area of liver, the bare area, is devoid of peritoneal covering. At this point the liver is attached to the diaphragm by areolar tissue and is in continuity inferiorly with the uppermost part of the anterior pararenal space. The layers of the coronary ligament are continuous on the right with the right triangular ligament.

The upper layer of the coronary ligament is continuous superiorly with the peritoneum over the inferior surface of the diaphragm and inferiorly with the peritoneum over the right and superior surfaces of the liver. At the lower margin of the bare area the lower layer of the coronary ligament becomes continuous inferiorly with the peritoneum of the posterior abdominal wall over the right suprarenal gland and upper pole of the right kidney, and superiorly with the peritoneum over the inferior surface of the liver.

The left triangular ligament is a double layer of peritoneum which extends over the superior border of the left lobe of the liver to a variable length. Medially, its anterior leaf is continuous with the left layer of the falciform ligament. The posterior layer is continuous with the left layer of the lesser omentum. The left triangular ligament lies in front of the abdominal part of the oesophagus, the upper end of the lesser omentum and part of the fundus of the stomach. Intraoperative division of the left triangular ligament permits mobilization of the left lobe of the liver in order to expose the abdominal oesophagus and crura of the diaphragm.

The right triangular ligament is a short V-shaped fold formed by the approximation of the two layers of the coronary ligament at its right lateral end, and is continuous with the peritoneum of the right posterolateral abdominal wall. The coronary ligament is reflected inferiorly and is directly continuous with the peritoneum over the upper pole of the right kidney. This fold is sometimes referred to as the hepatorenal ligament. The recess formed between the peritoneum of the inferior surface of the liver, the hepatorenal ligament and the peritoneum over the right kidney is known as the hepatorenal pouch (of Morison). In the supine position this is the most dependent part of the peritoneal cavity in the upper abdomen, and is a common site of pathological fluid accumulation.

The peritoneum is reflected inferolaterally from the posterior layer of the left triangular ligament onto the posterior abdominal wall above the oesophageal opening of the diaphragm. It lines the inferior surface of the left dome of the diaphragm and continues backwards onto the posterior abdominal wall. Inferiorly, it is reflected behind the spleen onto the most lateral part of the mesentery of the transverse colon and the splenic flexure. It continues down lateral to the descending colon into the pelvis, and forms the left paracolic ‘gutter’. Medially, the peritoneum covering the left upper posterior abdominal wall is reflected anteriorly to form the left layer of the upper end of the lesser omentum, the peritoneum over the left aspect of the abdominal oesophagus and the left layer of the splenorenal ligament.

From the inferior layer of the coronary ligament the peritoneum descends over the anterior surface of the right kidney to the front of the first part of the duodenum and hepatic flexure of the colon. Medially it passes in front of a short segment of the inferior vena cava between the duodenum and liver, forming as it does so the posterior wall of the epiploic foramen. This narrow strip broadens out as the peritoneum continues across the midline onto the posterior wall of the lesser sac.

The peritoneum lines the posterior abdominal wall over the diaphragmatic crura, the upper abdominal aorta, the coeliac axis, nodes and plexus and the upper border of the pancreas. Inferiorly, below the liver, it continues down on the posterior abdominal wall to the right of the ascending colon, forming the right paracolic ‘gutter’ between the anterolateral abdominal wall and colon.

The lesser omentum

The lesser omentum is formed of two layers of peritoneum separated by a variable amount of connective tissue and is derived from the ventral mesogastrium. It runs from the inferior visceral surface of the liver to the abdominal oesophagus, stomach, pylorus and first part of the duodenum. Superiorly, its attachment to the inferior surface of the liver forms an L-shape. The vertical component of the L is formed by the fissure for the ligamentum venosum. Inferiorly, the attachment turns and runs horizontally to complete the L in the portal fissure. The vertical and horizontal components of the lesser omentum run between the liver and the stomach and duodenum and are known as the gastrohepatic and hepatoduodenal ligaments, respectively. At the lesser curvature of the stomach, the layers of the lesser omentum split to enclose the stomach and are continuous with the visceral peritoneum covering the anterior and posterior surfaces of the stomach. The anterior layer of the lesser omentum descends from the fissure for the ligamentum venosum onto the anterior surface of the abdominal oesophagus, stomach and duodenum. The posterior layer descends from the posterior part of the fissure for the ligamentum venosum and runs onto the posterior surface of the stomach and pylorus. The lesser omentum forms the anterior surface of the lesser sac. The gastrohepatic ligament contains the right and left gastric vessels, branches of the vagus nerves, and gastrohepatic lymph nodes between its two layers near their attachment to the stomach. The right lateral border of the lesser omentum is thickened and extends from the junction between the first and second parts of the duodenum to the porta hepatis. This border is free and forms the anterior wall of the epiploic foramen. It contains the portal vein, common bile duct, hepatic artery, portocaval lymph nodes and lymphatics and the hepatic plexus of nerves ensheathed in a perivascular fibrous capsule. Occasionally the free margin extends to the right of the epiploic foramen, runs to the gallbladder and is referred to as the cystoduodenal ligament.

The left border of the lesser omentum is short and runs over the inferior surface of the diaphragm between the liver and medial aspect of the abdominal oesophagus. The lesser omentum is thinner on the left and may be fenestrated or incomplete: the variations in thickness are dependent upon the amount of connective tissue, especially fat.

The greater omentum

The greater omentum is the largest peritoneal fold and hangs inferiorly from the greater curvature of the stomach. It is a double sheet: each sheet consists of two layers of peritoneum separated by a scant amount of connective tissue. The two sheets are folded back on themselves and are firmly adherent to each other. The anterior sheet descends from the greater curvature of the stomach and first part of the duodenum. The most anterior layer is continuous with the visceral peritoneum over the anterior surface of the stomach and duodenum and the posterior layer is continuous with the peritoneum over the posterior wall of the stomach and pylorus. The anterior sheet descends a variable distance into the peritoneal cavity and then turns sharply on itself to ascend as the posterior sheet. The posterior sheet passes anterior to the transverse colon and transverse mesocolon. It is attached to the posterior abdominal wall above the origin of the small intestinal mesentery and anterior to the head and body of the pancreas. The anterior layer of the posterior sheet is continuous with the peritoneum of the posterior wall of the lesser sac. The posterior layer is reflected sharply inferiorly and is continuous with the anterior layer of the transverse mesocolon. The posterior sheet is adherent to the transverse mesocolon at its root and is often known as the gastrocolic ligament, which is the supracolic part of the greater omentum. In early fetal life the greater omentum and transverse mesocolon are separate structures, and this arrangement sometimes persists. During surgical mobilization of the transverse colon, the plane between the transverse mesocolon and greater omentum can be entered opposite the taenia omentalis, and the greater omentum can be separated entirely from the transverse colon and mesocolon if required. Access into the lesser sac can be obtained via this approach if the upper part of the posterior sheet of the greater omentum is then divided. This gives a relatively bloodless plane of entry for surgical access to the posterior wall of the stomach and to the anterior surface of the pancreas. The greater omentum is continuous with the gastrosplenic ligament on the left, and on the right it extends to the start of the duodenum. A fold of peritoneum, the hepatocolic ligament, may run from either the inferior surface of the right lobe of the liver or the first part of the duodenum to the right side of the greater omentum or hepatic flexure of the colon.

The right border of the greater omentum is occasionally adherent to the anterior surface of the ascending colon down as far as the caecum: its peritoneal layers are not continuous with the peritoneum over this part of the colon. A thin sheet of peritoneum referred to as Jackson’s membrane may run from the front of the ascending colon and caecum to the posterolateral abdominal wall and may merge with the greater omentum. It often contains several small blood vessels. Occasionally, a band passes from the right side of the ascending colon to the lateral abdominal wall near the level of the iliac crest. It has been called the ‘sustentaculum hepatis’ but plays no role in the support of the liver. Other folds between the ascending colon and posterolateral abdominal wall may divide the right lateral paracolic gutter into several small recesses. Less commonly the greater omentum is adherent to the anterior surface of the left colon; very occasionally it extends to the level of the sigmoid colon.

When the undisturbed abdomen is opened, the greater omentum is frequently wrapped around the upper abdominal organs. Only rarely is it evenly dependent anterior to the coils of the small intestine, although this is the disposition which is frequently illustrated. It is usually thin and cribriform, but it always contains some adipose tissue and is a common site for storage of fat in obese individuals, particularly males.

Between the two layers of the anterior fold of the greater omentum, close to the greater curvature of the stomach, the right and left gastroepiploic vessels form a wide anastomotic arc. Numerous vessels are given off from the arc and extend the full length of the omentum. This supply appears to exceed the metabolic requirements of the omentum, and perhaps reflect the role the greater omentum may play in peritoneal disease processes. The greater omentum is highly mobile and frequently becomes adherent to inflamed viscera within the abdominal cavity. This action may help to limit the spread of infection and the omentum may provide a source of well-vascularized tissue to take part in the early reparative process. It contains numerous fixed macrophages, which are easily mobilized when activated and may accumulate into dense, oval or round visible ‘milky-spots’.

The peritoneal connections of the spleen

The peritoneal connections of the spleen suspend the spleen in the left upper quadrant of the abdomen; they include the gastrosplenic, splenorenal and phrenicocolic ligaments. The gastrosplenic ligament runs between the greater curvature of the stomach and the hilum of the spleen and is in continuity with the left side of the greater omentum. The layers of the gastrosplenic ligament separate to enclose the spleen and then rejoin to form the splenorenal ligament and phrenicocolic ligaments. The splenorenal ligament extends from the spleen to the posterior abdominal wall and the phrenicocolic ligament extends to the anterolateral abdominal wall.

The splenorenal ligament is formed from two layers of peritoneum. The anterior layer is continuous medially with the peritoneum of the posterior wall of the lesser sac over the left kidney and runs up to the splenic hilum where it is continuous with the posterior layer of the gastrosplenic ligament. The posterior layer of the splenorenal ligament is continuous laterally with the peritoneum over the inferior surface of the diaphragm and runs onto the splenic surface over the renal impression. The splenic vessels lie between the layers of the splenorenal ligament: the tail of the pancreas is usually present in its lower portion. The gastrosplenic ligament also has two layers. The posterior layer is continuous with the peritoneum of the splenic hilum and the peritoneum over the posterior surface of the stomach. The anterior layer is formed from the peritoneum reflected off the gastric impression of the spleen and is continuous with the peritoneum over the anterior surface of the stomach. The short gastric and left gastroepiploic branches of the splenic artery, with their corresponding veins, pass between the layers of the gastrosplenic ligament. The phrenicocolic ligament extends from the splenic flexure of the colon to the diaphragm at the level of the eleventh rib. It extends inferiorly and laterally and is continuous with the peritoneum of the lateral end of the transverse mesocolon at the lateral margin of the pancreatic tail, and the splenorenal ligament at the hilum of the spleen.

A fan-shaped presplenic fold frequently extends from the anterior aspect of the gastrosplenic ligament near the greater curvature of the stomach below the inferolateral pole of the spleen and blends with the phrenicocolic ligament.

If the peritoneal attachments of the spleen are not recognized during surgery, the splenic capsule is at risk of injury and there may be subsequent serious bleeding. Downward traction on the phrenicocolic ligament during handling of the descending colon, especially during mobilization of the splenic flexure, may cause rupture of the splenic capsule. This is less likely if traction on the phrenicocolic ligament is made laterally or medially. The superior border and anterior diaphragmatic surface of the splenic capsule are often adherent to the peritoneum of the greater omentum. Medial traction on the omentum during surgery may cause splenic capsular injury: such injury is less likely, if any limited traction required is applied inferiorly.

PERITONEUM OF THE LOWER ABDOMEN

The posterior surface of the lower anterior abdominal wall is lined by parietal peritoneum, which extends from the linea alba centrally to the lateral border of quadratus lumborum. Here it is continuous with the peritoneum of the lateral paracolic gutter and is reflected over the sides and front of the ascending colon on the right and the descending colon on the left. Occasionally the ascending and descending colon are suspended by a short mesentery from the posterior abdominal wall. Between the ascending and descending colon, the peritoneum lines the posterior abdominal wall other than the oblique area, where it is reflected anteriorly to form the right and left layers of the small intestinal mesentery. Over the posterior abdominal wall it covers the left and right psoas major, inferior vena cava, duodenum, vertebral column and right and left ureters. At the upper extent of the posterior abdominal wall the peritoneum is reflected anteriorly and is continuous with the peritoneum of the posterior layer of the transverse mesocolon.

Transverse mesocolon

The mesentery of the transverse colon is a broad fold of visceral peritoneum reflected anteriorly from the posterior abdominal wall and suspends the transverse colon in the peritoneal cavity. The root of the transverse mesocolon lies along an oblique line passing from the anterior aspect of the second part of the duodenum, over the head and neck of the pancreas, above the duodenojejunal junction and over the upper pole of the left kidney to the splenic flexure (Fig. 64.1). It varies considerably in length but is shortest at either end. It contains the middle colic vessels and their branches together with branches of the superior mesenteric plexus, lymphatics and regional lymph nodes. Its two layers pass to the posterior surface of the transverse colon, where they separate to cover the colon. The upper layer of peritoneum is reflected from the posterior abdominal wall immediately anteriorly and inferiorly and becomes continuous with the posterior layer of the greater omentum to which it is adherent. The lower layer of peritoneum of the transverse mesocolon is continuous with the peritoneum of the posterior abdominal wall. Lateral extensions of the transverse mesocolon produce two shelf-like folds on the right and left sides of the abdominal cavity. On the right the duodenocolic ligament extends from the transverse mesocolon at the hepatic flexure to the second part of the duodenum. On the left the phrenicocolic ligament extends from the transverse mesocolon at the splenic flexure to the diaphragm at the level of the eleventh rib. The root of the transverse mesocolon is closely related to the upper limit of the root of the mesentery of the small intestine near the uncinate process of the pancreas.

Mesentery of the small intestine

The mesentery of the small intestine is arranged as a complex fan formed from two layers of peritoneum (anterosuperior and posteroinferior) separated by connective tissue and vessels. The root of the mesentery lies along a line running diagonally from the duodenojejunal flexure on the left side of the second lumbar vertebral body to the right sacroiliac joint (Fig. 64.1). The root crosses over the third part of the duodenum, aorta, inferior vena cava, right ureter and right psoas major. The average length of the root of the mesentery is 15 cm in adults; while along its intestinal attachment is the same length as the small intestine (approximately 5 m), and consequently the mesentery is usually thrown into multiple folds along its intestinal border. The average depth of the mesentery from the root to the intestinal border is 20 cm, but this varies along the length of the small intestine: it is shortest at the jejunum and terminal ileum and longest in the region of the mid ileum. Its two peritoneal layers contain the jejunum, ileum, jejunal and ileal branches of the superior mesenteric vessels, branches of the superior mesenteric plexus, lacteals and regional lymph nodes. Because of the length and mobility of the mesentery, identification of the proximal and distal ends of a loop of small intestine may be difficult through small surgical incisions. Tracing the continuity of the right peritoneal layer of the mesentery onto the posterior abdominal wall above the root towards the ascending colon, and the continuity of the left layer towards the descending and sigmoid colon, may be useful in helping to orientate an individual loop of ileum. The mesentery of the small intestine is sometimes joined to the transverse mesocolon at the duodenojejunal junction by a peritoneal band. Occasionally the fourth part of the duodenum possesses a very short mesentery which is continuous with the upper end of the root of the small bowel mesentery. Pronounced bands of peritoneum may extend to the posterior abdominal wall at the terminal ileum. The root of the mesentery of the small intestine is continuous with the peritoneum surrounding the appendix and caecum in the right iliac fossa.

Mesoappendix

The mesentery of the appendix is a triangular fold of peritoneum around the vermiform appendix, attached to the posterior surface of the lower end of the mesentery of the small intestine close to the ileocaecal junction. It usually reaches the tip of the appendix but sometimes fails to reach the distal third, in which case a vestigial low peritoneal ridge containing fat is present over the distal third. It encloses the blood vessels, nerves and lymph vessels of the vermiform appendix, and usually contains a lymph node.

Sigmoid mesocolon

The sigmoid mesocolon shows individual variation in length and depth. The root of the sigmoid colon forms a shallow inverted V with an apex near the division of the left common iliac artery but may vary from a very short straight line at the pelvic brim to a long curved attachment. The upper, left end of the attachment runs medially over the left psoas major. The lower, right end passes into the pelvis towards the midline at the level of the third sacral vertebra. The root extends for a variable distance over the brim of the pelvis and the lower posterior abdominal wall. The anteromedial peritoneal layer of the mesentery of the sigmoid colon is continuous with the peritoneum of the lower left posterior abdominal wall and its posterolateral layer is continuous with the peritoneum of the pelvis and lateral abdominal wall. The proximal and distal ends of the sigmoid colon are occasionally joined together by a fibrous band which is usually associated with a narrow based sigmoid mesentery and may predispose the sigmoid colon to volvulus. Pronounced bands of peritoneum may also be found running from the proximal sigmoid colon to the posterior abdominal wall. The sigmoid and superior rectal vessels run between its layers and the left ureter descends into the pelvis behind its apex.

PERITONEUM OF THE LOWER ANTERIOR ABDOMINAL WALL

The peritoneum of the lower anterior abdominal wall is raised into five ridges which diverge as they descend from the umbilicus. These are the median and right and left lateral and medial umbilical folds (Fig. 64.6). The median umbilical fold extends from the umbilicus to the apex of the bladder and contains the urachus or its remnant (Ch. 78). The obliterated umbilical artery lies under the medial umbilical fold which ascends from the pelvis to the umbilicus. The supravesical fossa lies between the medial and median umbilical folds on either side of the midline. The lateral umbilical fold covers the inferior epigastric artery and vein below their entry into the rectus sheath, and is separated from the medial umbilical fold by the medial inguinal fossa. The lateral inguinal fossa lies lateral to the lateral umbilical fold, and covers the deep inguinal ring. The femoral fossa lies inferomedial to the lateral inguinal fossa, from which it is separated by the medial end of the inguinal ligament. It overlies the femoral ring (see Ch. 61).

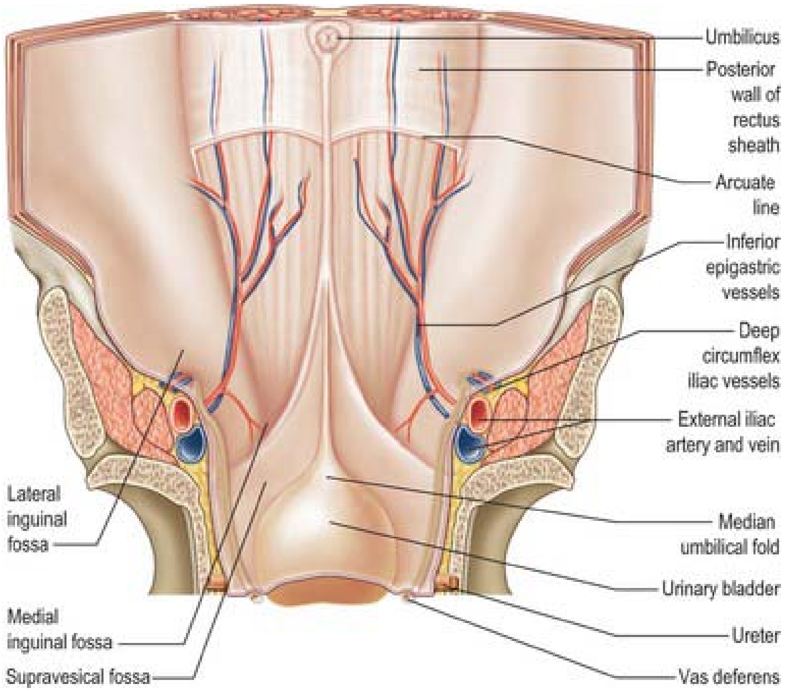
Umbilicus
Posterior wall of rectus sheath
Arcuate line
Inferior epigastric vessels
Deep circumflex iliac vessels
External iliac artery and vein
Median umbilical fold
Urinary bladder
Ureter
Vas deferens
Lateral inguinal fossa
Medial inguinal fossa
Supravesical fossa

Fig. 64.6 The infra-umbilical part of the anterior abdominal wall of a male subject: posterior surface, with the peritoneum *in situ*. Note the pelvic bones flanking the wide greater pelvis (middle) and narrower lesser pelvis (below) containing the bladder.

PERITONEUM OF THE PELVIS

The parietal peritoneum of the posterior surface of the anterior abdominal wall and that lining the posterior abdominal wall continue into the pelvis as the pelvic peritoneum. The pelvic peritoneum then follows the surfaces of the true pelvic viscera and pelvic side walls although there are important differences between the sexes.

Peritoneum of the male pelvis

In males, the peritoneum of the left lower abdominal wall is reflected from the junction of the sigmoid colon and anterolateral surface of the rectum to line the brim and upper inner surface of the true pelvis (Fig. 64.7). The peritoneum passes down into the true pelvis, lying over the anterior surface of the rectum, which then becomes an extraperitoneal organ. Laterally, the peritoneum is reflected to the pelvic side walls to form the right and left pararectal fossae: these vary in size according to the degree of distension of the rectum. The peritoneum is reflected anteriorly from the anterior surface of the rectum over the upper poles of the seminal vesicles and onto the posterior surface of the bladder, producing the rectovesical pouch. Anteriorly the rectovesical pouch is limited laterally by peritoneal folds, the sacrogenital folds, which extend from the sides of the bladder posteriorly to the anterior aspect of the sacrum. The peritoneum covers the superior surface of the bladder, and forms a paravesical fossa on each side limited laterally by a ridge of peritoneum which contains the ductus deferens. The size of the paravesical fossae depends on the volume of urine in the bladder. When the bladder is empty, a variable transverse vesical fold divides each fossa into two. The anterior ends of the sacrogenital folds may sometimes be joined by a ridge separating a middle fossa from the main rectovesical pouch. Between the paravesical and pararectal fossae the ureters and internal iliac vessels may cause slight elevations in the peritoneum. From the apex of the bladder the peritoneum extends superiorly along the posterior surface of the lower anterior abdominal wall to the umbilicus. When the bladder distends, the peritoneum is lifted from the lower anterior abdominal wall so that part of the anterior surface of the bladder is in direct contact with the posterior surface of the lower median area of the anterior abdominal wall. This relationship means that a well-distended bladder can be entered by direct puncture through the lower anterior abdominal wall without entering the peritoneal cavity (suprapubic puncture).

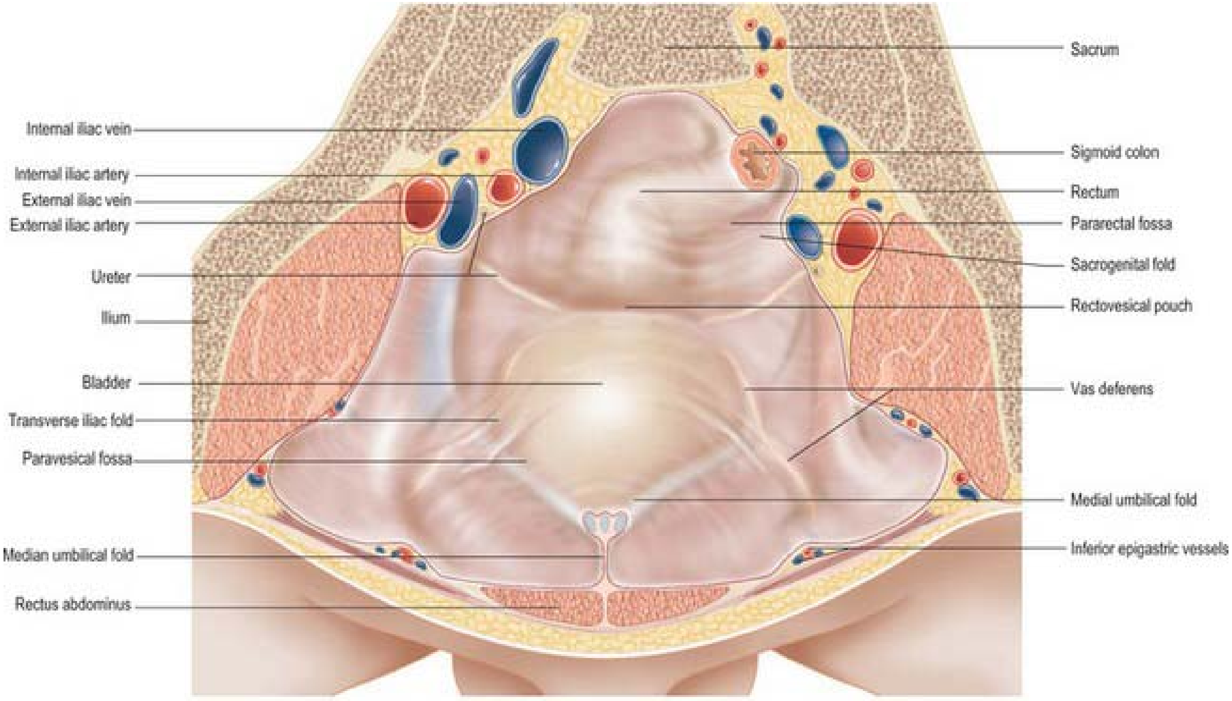
Internal iliac vein
Internal iliac artery
External iliac vein
External iliac artery
Ureter
Ilium
Bladder
Transverse iliac fold
Paravesical fossa
Median umbilical fold
Rectus abdominus
Sacrum
Sigmoid colon
Rectum
Pararectal fossa
Sacrogenital fold
Rectovesical pouch
Vas deferens
Medial umbilical fold
Inferior epigastric vessels

Fig. 64.7 The peritoneum of the male pelvis: anterosuperior view. The median umbilical fold contains both the unpaired median and the paired medial umbilical ligaments in the plane of section in this subject.

Peritoneum of the female pelvis

In females the peritoneum covers the upper rectum as it does in the male, but it descends further over the anterior surface of the rectum. The lateral limit of the pararectal and paravesical fossae is the peritoneum covering the round ligament of the uterus. The rectovesical pouch is occupied by the uterus and vagina. The peritoneum from the rectum is thus reflected anteriorly onto the posterior surface of the posterior fornix of the vagina and the uterus, producing the recto-uterine pouch (of Douglas). The peritoneum covers the fundus of the uterus to its anterior (vesical) surface as far as the junction of the body and cervix, from which it is reflected forwards to the upper surface of the bladder, forming a shallow vesico-uterine pouch. Peritoneum is reflected from the bladder to the posterior surface of the anterior abdominal wall as it is in males. Marginal recto-uterine folds correspond to the sacrogenital folds in males and pass back to the sacrum from the sides of the cervix, lateral to the rectum. Peritoneum is reflected from the anterior and posterior uterine surfaces to the lateral pelvic walls as the broad ligament of the uterus (see Fig. 77.18). This consists of anteroinferior and posterosuperior layers which are continuous at the upper border of the ligament. The broad ligament extends from the sides of the uterus to the lateral pelvic walls, and contains the uterine tubes in its free superior margins and the ovaries attached to its posterior layer. Below, it is continuous with the lateral pelvic parietal peritoneum. Between the ridges formed by the obliterated umbilical arteries and the ureter, the peritoneum forms a shallow depression on the lateral pelvic wall, the ovarian fossa, which lies behind the lateral attachment of the broad ligament. The ovary usually rests in the fossa in nulliparous females.

VASCULAR SUPPLY AND LYMPHATIC DRAINAGE

Parietal and visceral peritoneum develop from the somatopleural and splanchnopleural layers respectively of lateral plate mesoderm (see Ch. 73). Parietal peritoneum is therefore supplied by somatic blood vessels of the abdominal and pelvic walls and its lymphatics join those in the body wall and drain to parietal lymph nodes. Visceral peritoneum is best considered as an integral part of the viscera which it overlies; it derives its blood supply from the viscera, and its lymphatics join the visceral vessels to drain to the regional lymph nodes.

INNERVATION

The parietal peritoneum is innervated by branches from somatic efferent and afferent nerves that also supply the muscles and skin respectively of the overlying body wall. The visceral peritoneum is innervated by branches of visceral afferent nerves which travel with the autonomic supply to the underlying viscera. The different sensations arising from pathologies which affect either the parietal or visceral peritoneum reflect these differences in patterns of innervation. Well-localized pain is elicited by mechanical, thermal or chemical stimulation of the nocioceptors of the parietal peritoneum. The sensation is usually confined to one or two dermatomes for each area of peritoneum stimulated and is both lateralized and well localized. Somatic nerves that innervate the parietal peritoneum also supply the corresponding segmental areas of skin and muscles; when the parietal peritoneum is irritated, muscles tend to contract reflexly, causing localized hypercontractility (guarding) or even rigidity of the abdominal wall. The parietal diaphragmatic peritoneum is supplied with afferent fibres from the phrenic nerves (centrally) and by the lower six intercostal nerves and subcostal nerves (peripherally): peripheral irritation of the diaphragm may therefore result in pain, tenderness and muscular rigidity in the distribution of the lower thoracic spinal nerves, while central irritation may result in pain in the cutaneous distribution of the third to fifth cervical spinal nerves, i.e. the shoulder region.

The visceral peritoneum and viscera are not affected by these stimuli because the visceral afferent innervation provides a much more limited sensation of discomfort. When stimulated, the sensation of pain is of a less severe nature and is referred to the area of abdominal wall according to the region of the intestinal tract affected. Discomfort from structures derived from the foregut is felt in the region of the epigastrium, from midgut structures in the region of the umbilicus, and from hindgut structures in the suprapubic region: none of these sensations shows significant lateralization. However, stretch of the visceral peritoneum is a potent cause of certain sensations and responses. Various neural elements in the visceral walls, mesenteries and overlying peritoneum mediate poorly localized sensations of discomfort when stimulated by stretch, and may also elicit profound reflex autonomic reactions involving vasomotor and cardiac changes. This is of considerable clinical relevance. The effects of division of the parietal peritoneum may be rendered painless by local or regional local anaesthesia. In marked contrast, the direct central connections of the visceral afferents, particularly via the vagus, mean that stretching the visceral peritoneum may have profound effects, and may produce acute haemodynamic instability despite high spinal anaesthesia. Ischaemia of the underlying viscera causes poorly localized abdominal pain, probably due to the spasms of visceral smooth muscle.

GENERAL ARRANGEMENT OF THE PERITONEAL CAVITY

The peritoneal cavity is a single continuous space between the parietal peritoneum lining the abdominal wall and the visceral peritoneum enveloping the abdominal organs. It consists of a main region, termed the greater sac, which is equivalent to the main abdominal cavity surrounding the majority of the abdominal and pelvic viscera. The lesser sac, or omental bursa, is a small diverticulum lined with peritoneum, which is situated behind the stomach and lesser omentum and in front of the pancreas and retroperitoneum. These two areas communicate via the epiploic foramen.

For clinical purposes the peritoneal cavity can be divided into several spaces because pathological processes are often contained within these spaces and their anatomy may influence diagnosis and treatment. It is useful to divide the peritoneal cavity into two main compartments, supramesocolic and inframesocolic, which are partially separated by the transverse colon and its mesentery (the latter connects the transverse colon to the posterior abdominal wall). The pelvic peritoneal spaces are described above.

SUPRAMESOCOLIC COMPARTMENT

The supramesocolic space lies above the transverse mesocolon between the diaphragm and the transverse colon. It can be arbitrarily divided into right and left supramesocolic spaces. These regions can be further subdivided into a number of subspaces, which are normally in communication, but are frequently subdivided by inflammatory adhesions in disease. The right supramesocolic space can be divided into three subspaces; the right subphrenic space, the right subhepatic space, and the lesser sac. The left supramesocolic space can be divided into two subspaces; the left subphrenic space and the left perihepatic space.

Right subphrenic space

The right subphrenic space lies between the diaphragm and the anterior, superior and right lateral surfaces of the right lobe of the liver. It is bounded on the left side by the falciform ligament and behind by the upper layer of the coronary ligament. It is a relatively common site for collections of fluid after right sided abdominal inflammation.

Right subhepatic space (hepatorenal recess)

The right subhepatic space lies between the right lobe of the liver and the right kidney. It is bounded superiorly by the inferior layer of the coronary ligament, laterally by the right lateral abdominal wall, posteriorly by the anterior surface of the upper pole of the right kidney and medially by the second part of the duodenum, hepatic flexure, transverse mesocolon and part of the head of the pancreas. In the supine position the posterior right subhepatic space is more dependent than the right paracolic gutter: postoperative infected fluid collections are common in this location.

Lesser sac (omental bursa)

The lesser sac is a cavity lined with peritoneum and connected to the larger general peritoneal cavity (greater sac) by the epiploic foramen. It is considered part of the right supramesocolic space because embryologically the liver grows into the right peritoneal space and stretches the dorsal mesentery to form the lesser sac behind the stomach. The sac varies in size according to the size of the viscera making up its walls. It has posterior and anterior walls as well as superior, inferior, right and left borders.

The anterior wall is made up of the posterior peritoneal layer of the lesser omentum, the peritoneum over the posterior wall of the stomach and first part of the duodenum, and the uppermost part of the anterior layer of the greater omentum. At its right border, the anterior wall is mostly formed by the lesser omentum but moving towards the left, the lesser omentum becomes progressively shorter and more of the anterior wall is formed by the posterior aspect of the stomach and greater omentum.

The posterior wall is formed mainly by the peritoneum covering the posterior abdominal wall in this area. In the lower part, the posterior wall is made up of the anterior layer of the posterior sheet of the greater omentum as it lies on the transverse mesocolon. The posterior wall covers, from below upwards, a small part of the head and the whole neck and body of the pancreas, the medial part of the anterior aspect of the left kidney, most of the left suprarenal gland, the commencement of the abdominal aorta and coeliac artery and part of the diaphragm. The inferior phrenic, splenic, left gastric and hepatic arteries lie partly behind the bursa. Many of these structures form the ‘bed’ of the stomach and are separated from it only by the linings of the lesser sac.

The superior border of the lesser sac is narrow and lies between the right side of the oesophagus and the upper end of the fissure for the ligamentum venosum. Here peritoneum of the posterior wall of the lesser sac is reflected anteriorly from the diaphragm to join the posterior layer of the lesser omentum.

The inferior border of the lesser sac runs along the line of the fusion of the layers of the greater omentum. This runs from the gastrosplenic ligament to the peritoneal fold behind the first part of the duodenum. In cases where the layers are not completely adherent to each other, the lesser sac may extend as far as the bottom of the two sheets of the greater omentum. In adults, even in these circumstances of separation of the layers, the lowest extent of the inferior border is rarely below the level of the transverse colon.

The right border of the lesser sac is formed by the reflection of the peritoneum from the pancreatic neck and head onto the inferior aspect of the first part of the duodenum. The line of this reflection ascends to the left, along the medial side of the gastroduodenal artery. Near the upper duodenal margin the right border joins the floor of the epiploic foramen round the hepatic artery proper. The epiploic foramen thus forms a break in the right border. Above the epiploic foramen the right border is formed by the reflection of peritoneum from the diaphragm to the right margin of the caudate lobe of the liver and along the left side of the inferior vena cava, enclosing the hepatic recess.

The left border of the lesser sac runs from the left end of the root of the transverse mesocolon and is mostly formed by the inner layer of peritoneum of the splenorenal and gastrosplenic ligaments. The part of the lesser sac lying between the splenorenal and gastrosplenic ligaments is referred to as the splenic recess. Above the level of the spleen, the two ligaments are merged as the short gastrophrenic ligament, which passes forwards from the diaphragm to the posterior aspect of the fundus of the stomach and forms part of the upper left border of the lesser sac. The two layers of the gastrophrenic ligament diverge near the abdominal oesophagus, leaving part of the posterior gastric surface devoid of peritoneum. The left gastric artery runs forwards here into the lesser omentum.

The lesser sac is narrowed by two crescentic peritoneal folds produced by the hepatic and left gastric arteries. The left gastropancreatic fold overlies the left gastric artery as it runs from the posterior abdominal wall to the lesser curvature of the stomach. The right gastropancreatic fold overlies the hepatic artery as it runs from the posterior abdominal wall to the lesser omentum. The folds vary in size. When prominent, they divide the lesser sac into a smaller superior and a larger inferior recess. The superior recess lies posterior to the lesser omentum and liver, and encloses the caudate lobe of the liver, which is covered by peritoneum on both its anterior and posterior surfaces. It extends superiorly into the fissure for the ligamentum venosum and lies adjacent to the right crus of the diaphragm posteriorly. The inferior recess of the lesser sac lies between the stomach and pancreas and is contained in the double sheet of the greater omentum.

Epiploic foramen (of Winslow)

The epiploic foramen (foramen of Winslow, aditus to the lesser sac), is a short, vertical slit, usually 3 cm in height in adults, in the upper part of the right border of the lesser sac. It leads into the greater sac. The hepatoduodenal ligament, which is formed by the thickened right edge of the lesser omentum extending from the flexure between the first and second parts of the duodenum, forms the anterior margin of the foramen. The anterior border contains the common bile duct (on the right), portal vein (posteriorly) and hepatic artery (on the left) between its two layers. Superiorly the peritoneum of the posterior layer of the hepatoduodenal ligament runs over the caudate lobe of the liver which forms the roof of the epiploic foramen. This layer of peritoneum is then reflected onto the inferior vena cava which forms the posterior margin of the epiploic foramen. At the upper border of the first part of the duodenum the peritoneum runs forwards from the inferior vena cava, above the head of the pancreas, and is continuous with the posterior layer of the lesser omentum, forming the floor of the epiploic foramen. A narrow passage, the vestibule of the lesser sac, may be found to the left of the foramen between the caudate process and the first part of the duodenum. To the right, the rim of the foramen is continuous with the peritoneum of the greater sac. The roof is continuous with the peritoneum on the inferior surface of the right hepatic lobe. The anterior and posterior walls of the foramen are normally apposed.

Left subphrenic space

The left subphrenic space lies between the diaphragm, the anterior and superior surfaces of the left lobe of the liver, the anterosuperior surface of the stomach and the diaphragmatic surface of the spleen. It is bounded to the right by the falciform ligament and behind by the anterior layer of the left triangular ligament. It is much enlarged in the absence of the spleen and is a common site for fluid collection particularly after splenectomy. The left subphrenic space is substantially larger than the right and is sometimes described as being divided into anterior and posterior parts, although no obvious demarcation exists in the absence of disease. The left posterior subphrenic space is small and lies between the fundus of the stomach and the diaphragm above the origin of the splenorenal ligament. The left anterior subphrenic space is large and lies between the superior and anterolateral surfaces of the spleen and the left dome of the diaphragm. Inferiorly and medially, this space is bounded by the splenorenal, gastrosplenic, and phrenicocolic ligaments which produces a partial barrier to the left paracolic gutter. This may explain why left subphrenic collections are less frequent than right subphrenic collections following lower abdominal and pelvic surgery, but the left subphrenic space is the commonest site of fluid collection after upper abdominal, particularly splenic, surgery.

Left perihepatic space

The left perihepatic space is sometimes subdivided into anterior and posterior spaces. The posterior perihepatic space is also known as the left subhepatic space or gastrohepatic recess. The left anterior perihepatic space lies between the anterosuperior surface of the left lobe of the liver and diaphragm. The left posterior perihepatic space lies inferior to the left lobe of the liver, and extends into the fissure for the ligamentum venosum on the right, anterior to the main portal vein. Posteriorly, the lesser omentum separates this space from the superior recess of the lesser sac. On the left, the space is bounded by the lesser curvature of the stomach.

INFRAMESOCOLIC COMPARTMENT

The inframesocolic compartment lies below the transverse mesocolon and transverse colon are far as the true pelvis. It is divided in two unequal spaces by the root of the mesentery of the small intestine. It contains the right and left paracolic gutters lateral to the ascending and descending colon. As a consequence of the mobility of the transverse mesocolon and mesentery of the small intestine, disease processes are rarely well contained within these spaces, and fluid within the infracolic space tends to descend into the pelvis or the paracolic gutters.

Right infracolic space

The right infracolic space is a triangular space. It is smaller than its counterpart on the left, and lies posterior and inferior to the transverse colon and mesocolon and to the right of the small intestinal mesentery. The space is narrowest inferiorly because the attachment of the root of the mesentery of the small intestine lies well to the right of the midline. The vermiform appendix often lies in the lower part of the right infracolic space.

Left infracolic space

The left infracolic space is larger than its counterpart on the right and is in free communication with the pelvis to the right of the midline. It lies posterior and inferior to the transverse colon and mesocolon and to the left of the mesentery of the small intestine. The sigmoid colon and its mesentery may partially restrict the flow of fluid or blood into the pelvis to the left of the midline.

Paracolic gutters

The right and left paracolic gutters are peritoneal recesses on the posterior abdominal wall lying alongside the ascending and descending colon. The main paracolic gutter lies lateral to the colon on each side. A less obvious medial paracolic gutter may be formed, especially on the right side, if the colon possesses a short mesentery for part of its length. The right (lateral) paracolic gutter runs from the superolateral aspect of the hepatic flexure of the colon, down the lateral aspect of the ascending colon, and around the caecum. It is continuous with the peritoneum as it descends into the pelvis over the pelvic brim. Superiorly, it is continuous with the peritoneum which lines the hepatorenal pouch and, through the epiploic foramen, the lesser sac. Bile, pus or blood released from viscera anywhere along its length may run along the gutter and collect in sites quite remote from the organ of origin. In supine patients, infected fluid from the right iliac fossa may ascend in the gutter to enter the lesser sac. In patients nursed in a sitting position, fluid from the stomach, duodenum or gallbladder may run down the gutter to collect in the right iliac fossa or pelvis and may mimic acute appendicitis or form a pelvic abscess. The right paracolic gutter is larger than the left, which together with the partial barrier provided by the phrenicocolic ligament, may explain why right subphrenic collections are more common than left subphrenic collections.

Extraperitoneal subphrenic spaces

There are two potential ‘spaces’ which actually lie outside the peritoneal coverings of the abdomen, but are of clinical relevance because of the possibility that fluid collections will accumulate in them. The right extraperitoneal space is bounded by the two layers of the coronary ligament, the bare area of the liver and the inferior surface of the right dome of the diaphragm. The left extraperitoneal space lies anterior to the left suprarenal gland and upper pole of the left kidney. It contains extraperitoneal connective tissue.

RECESSES OF THE PERITONEAL CAVITY

Peritoneal folds may create fossae or recesses within the peritoneal cavity. These are of clinical interest because a length of intestine may enter one and be constricted by the fold at the entrance to the recess: it may subsequently become a site of internal herniation. The contents of the peritoneal fold may be important if surgical incision is required to reduce such a hernia. Although internal herniation may occur into the lesser sac via the epiploic foramen, the sac is not usually considered to be a peritoneal recess.

Duodenal recesses

Several folds of peritoneum may exist around the fourth part of the duodenum and the duodenojejunal junction forming a number of named recesses (Fig. 64.8).

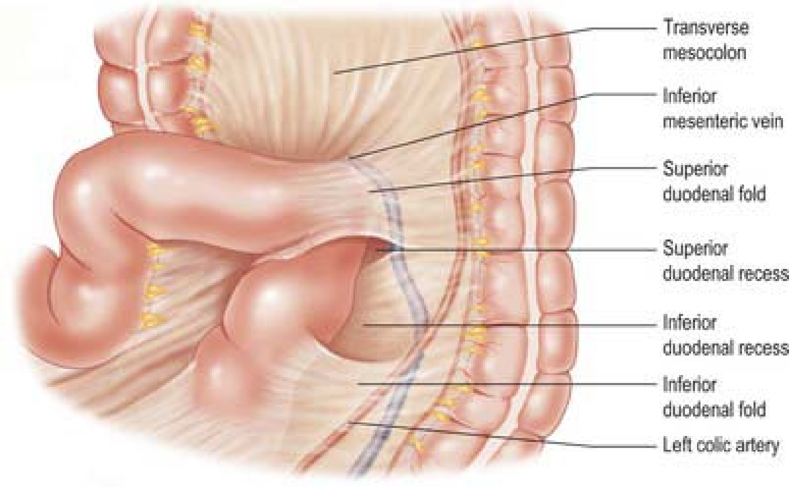
Transverse mesocolon
Inferior mesenteric vein
Superior duodenal fold
Superior duodenal recess
Inferior duodenal recess
Inferior duodenal fold
Left colic artery

Fig. 64.8 The superior and inferior duodenal recesses. The transverse colon and jejunum have been displaced.

Superior duodenal recess

The superior duodenal recess is occasionally present, usually in association with an inferior duodenal recess. It lies to the left of the end of the fourth part of the duodenum, opposite the second lumbar vertebra, and behind a crescentic superior duodenal fold (duodenojejunal fold). The fold has a semilunar free lower edge which merges to the left with the peritoneum anterior to the left kidney. The inferior mesenteric vein is directly behind the junction of the left (lateral) end of this fold and the posterior parietal peritoneum. The recess varies in size but is commonly 2 cm deep, admitting a fingertip. It opens downwards, its orifice being in the angle formed by the left renal vein as it passes across the abdominal aorta.

Inferior duodenal recess

The inferior duodenal recess is usually present often associated with a superior recess with which it may share an orifice. It lies to the left of the fourth part of the duodenum, opposite the third lumbar vertebra. It sits behind a non-vascular, triangular inferior duodenal fold (duodenomesocolic fold), which has a sharp upper edge. It is usually 3 cm deep, admits one or two fingers and opens upwards towards the superior duodenal recess. It sometimes extends behind the fourth part of the duodenum and to the left, in front of the ascending branch of the left colic artery and the inferior mesenteric vein.

Paraduodenal recess

The paraduodenal recess may occur in conjunction with superior and inferior duodenal recesses. It is rare in adults but is more commonly seen in newborn children. It lies a little to the left and slightly behind of the fourth part of the duodenum, behind a falciform paraduodenal fold. The free right edge of the fold contains the inferior mesenteric vein and ascending branch of the left colic artery, and represents part of the upper left colic mesentery. Its free edge lies in front of the wide orifice of the recess, which faces right.

Retroduodenal recess

The retroduodenal recess is the largest of the duodenal recesses, but is rarely present. It lies behind the third and fourth parts of the duodenum in front of the abdominal aorta. It ascends nearly to the duodenojejunal junction, is 8–10 cm deep, and bounded on both sides by duodenoparietal folds. It has a wide orifice which faces down and to the left.

Duodenojejunal recess

The duodenojejunal or mesocolic recess typically occurs in 20% of adults. When present, it is almost never associated with any other duodenal recesses. It is approximately 3 cm deep and lies to the left of the abdominal aorta, between the duodenojejunal junction and the root of the transverse mesocolon. It is bounded above by the pancreas, on the left by the kidney, and below by the left renal vein. It has a circular opening between two peritoneal folds, and faces down and to the right.

Mesentericoparietal recess

The mesentericoparietal recess is only rarely present. It lies just below the third part of the duodenum and invaginates into the upper part of the mesentery towards the right. Its orifice is large and faces left behind a fold of mesentery raised by the superior mesenteric artery.

Caecal recesses

Several folds of peritoneum may exist around the caecum and form recesses (Fig. 64.9). Paracaecal recesses are common sites for abscess formation following acute appendicitis.

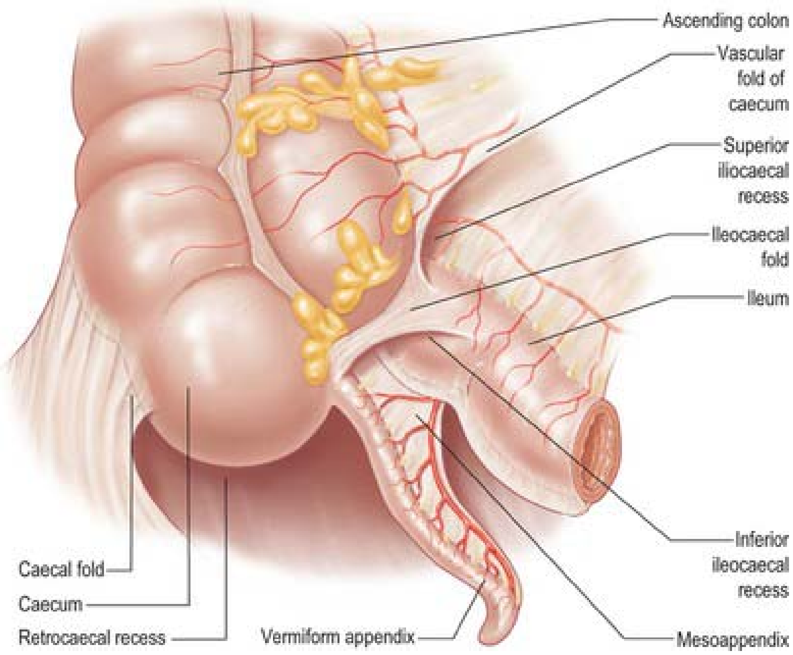
Ascending colon
Vascular fold of caecum
Superior iliocaecal recess
Ileocaecal fold
Ileum
Inferior ileocaecal recess
Mesoappendix
Caecal fold
Caecum
Retrocaecal recess
Vermiform appendix

Fig. 64.9 The peritoneal folds and recesses in the caecal region.

Superior ileocaecal recess

The superior ileocaecal recess is usually present and best developed in children. It is often reduced and absent in the aged, especially the obese. It is formed by the vascular fold of the caecum, which arches over the anterior caecal artery, supplying the anterior part of the ileocaecal junction, and its accompanying vein. It is a narrow slit bounded in front by the vascular fold, behind by the ileal mesentery, below by the terminal ileum and on the right by the ileocaecal junction. Its orifice opens downwards to the left.

Inferior ileocaecal recess

The inferior ileocaecal recess is well marked in youth but frequently obliterated by fat in adults. It is formed by the ileocaecal fold, which extends from the anteroinferior aspect of the terminal ileum to the front of the mesoappendix (or to the appendix or caecum). It is also known as the ‘bloodless fold of Treves’, although it sometimes contains blood vessels and will often bleed if divided during surgery. If inflamed, especially when the appendix and its mesentery are retrocaecal, it may be mistaken for the mesoappendix. The recess is bounded in front by the ileocaecal fold, above by the posterior ileal surface and its mesentery, to the right by the caecum, and behind by the upper mesoappendix. Its orifice opens downwards to the left.

Retrocaecal recess

The retrocaecal recess lies behind the caecum. It varies in size and extent and ascends behind the ascending colon, often being large enough to admit an entire finger. It is bounded in front by the caecum (and sometimes the lower ascending colon), behind by the parietal peritoneum and on each side by caecal folds (parietocolic folds) passing from the caecum to the posterior abdominal wall. The vermiform appendix frequently occupies this recess when in the retrocaecal position.

Intersigmoid recess

The intersigmoid recess is constant in fetal life and infancy, but may disappear during later development. It lies behind the apex of the V-shaped parietal attachment of the sigmoid mesocolon and is funnel shaped. It is directed upwards and opens downwards. It varies in size from a slight depression to a shallow fossa. Its posterior wall is formed by the parietal peritoneum of the posterior abdominal wall which covers the left ureter as it crosses the bifurcation of the left common iliac artery. Occasionally the recess is within the layers of the sigmoid mesocolon, and is nearer the bowel wall than the mesenteric root. It is probably produced by an imperfect blending of the mesocolon with the posterior parietal peritoneum.

CLINICAL MANAGEMENT OF FLUID COLLECTIONS IN THE PERITONEAL CAVITY

Fluid collections frequently occur within the peritoneal cavity as a result of a wide range of pathological processes. In the absence of any inflammation, peritoneal adhesions or previous surgery, serous fluid is almost always distributed freely between the peritoneal spaces and is not confined to any particular area. Simple ascites, for example, can therefore be drained freely from any convenient dependent part of the peritoneal cavity. This is most commonly performed by blind or ultrasound guided insertion of a catheter into the lower left or right paracolic gutters, which usually readily fill with fluid. The colon and some loops of small bowel may be present, but their relatively mobility ensures that they are very unlikely to be injured during this procedure.

Fluid collections caused by inflammatory processes are often much more viscid because they contain pus, fibrin or blood and are usually associated with peritoneal inflammation which results in, at least transient, peritoneal adhesions. These factors mean that collections may become localized if the flow of fluid is restricted by the partial compartmentalization of the peritoneum. Once collected in a particular ‘space’, this fluid often becomes further confined by ongoing inflammation and may even form a truly walled-off cavity over time. Any of the spaces of the peritoneum may develop a collection, but the subphrenic, subhepatic and pelvic spaces are the commonest since they are most well defined by the fixed peritoneal folds and organs forming their boundaries. These spaces are also the most dependent spaces within the peritoneum in the supine position and consequently any initially free fluid tends to gravitate to them.

Surgical access to the peritoneal spaces is rarely necessary today because of the great advances which have been made in radiologically guided drainage. When necessary, lateral subcostal or intercostal incisions may give adequate access to the subphrenic spaces and the anterior wall of the rectum is also a useful route to access the rectouterine or rectovesical space. Computerized tomography or ultrasound guided drainage offers a much more reliable and versatile method of accessing even difficult spaces such as subhepatic, perihepatic, paracolic or even intermesenteric collections. Posterolateral translumbar or trans-sciatic approaches can be used to access these more difficult areas.

Peritoneal dialysis

The mesothelium resembles vascular endothelium in being a dialysing membrane which fluids and small molecules may traverse. Numerous endocytic vesicles occur near the cell surfaces, and the remaining cytoplasm is poor in organelles, indicating low metabolic activity. Normally the volumes of fluid transmitted by peritoneal surfaces are small, but large volumes may be administered via the intraperitoneal route. Conversely, substances such as urea can be dialysed from blood into fluid circulated through the peritoneal cavity.

Ventriculoperitoneal shunts

The absorptive capabilities of the peritoneum can be used to absorb excess transitional fluids from several sites in the body. The commonest of these is the absorption of cerebrospinal fluid drained from the intracerebral ventricles or the intrathecal space via a fine calibre catheter. The catheter can be placed within the peritoneum with a one way valve preventing reflux of peritoneal fluid into the cerebrospinal fluid. The fluid is then continuously absorbed, maintaining a low pressure within the intrathecal or intraventricular space.

REFERENCES

akley FV, Hricak H. Imaging of peritoneal and mesenteric disease: key concepts for the clinical radiologist. *Clin Radiol*. 1999;54:563-574.

Explains the complex anatomy of the upper abdominal peritoneal fold suspending the stomach, liver and spleen.

ealy JC, Reznek RH. The anterior abdominal wall and peritoneum. In: Butler P, Mitchell A, Ellis H. *Applied Radiological Anatomy*. Cambridge:

Cambridge University Press; 1999:189-200.

Demonstrates the imaging anatomy of the peritoneal spaces and reflections using cross-sectional imaging..

eyers M. Dynamic Radiology of the Abdomen. In *Normal and Pathologic Anatomy*. New York: Springer; 1994.

Provides a systematic application of anatomic and dynamic principles to the understanding and diagnosis of intra-abdominal disease..

CHAPTER 65

Abdominal oesophagus and stomach

ABDOMINAL OESOPHAGUS

The abdominal oesophagus is 1–2.5 cm in length, and is slightly broader at the cardiac orifice than the diaphragmatic aperture. It lies to the left of the midline and enters the abdomen through the oesophageal aperture (formed by the two diaphragmatic crura) opposite the level of the tenth thoracic vertebra. It runs obliquely to the left and slightly posteriorly, and ends at the gastro-oesophageal junction/cardiac orifice of the stomach. The abdominal oesophagus lies posterior to the left lobe of the liver, which it grooves slightly, anterior to the left crus, the left inferior phrenic vessels and the left greater splanchnic nerve; its surface is covered in a thin layer of connective tissue and visceral peritoneum which contains the anterior and posterior vagi as well as the oesophageal branches of the left gastric vessels. The anterior vagus may be single or composed of multiple trunks, and is closely related to the outer fibres of the longitudinal muscle coat of the oesophagus. The posterior vagus is usually a single trunk and is less closely applied to the oesophageal muscle within the loose connective tissue, which makes its identification during surgery somewhat easier.

The abdominal oesophagus is effectively tethered to the diaphragm by connective tissue (Fig. 65.1); the phreno-oesophageal ligament. This is formed of two thickened bands of elastin-rich connective tissue; the inferior phreno-oesophageal ligament is effectively an extension of the transversalis fascia extending beneath the parietal peritoneum as it is reflected from the diaphragm onto the abdominal oesophagus. The fibres are only loosely attached to the adventitial tissues and a variable amount of fat often lies beneath it, between the oesophageal wall and the crural sling. This oesophageal fat pad tends to act to tether the oesophagus to the fibres of the crura but tends to regress with age. On the thoracic side of the diaphragm the superior phreno-oesophgeal ligament is similarly formed from an extension of the subpleural endothoracic fascia. It is denser than its inferior counterpart with more elastin present and is tethered much more firmly through the muscle fibres of the oesophageal wall into the submucosal tissues. It may well act to restore lower oesophageal position after the movement engendered by the peristalsis of swallowing (Kwok et al 1999). Anteriorly, the subperitoneal connective tissue is particularly dense and blends with both the outer layer of the oesophageal wall and the apex of the crural fibres of the diaphragm. On the posterior aspect the peritoneal reflection is extremely short since the crura lie steeply angled, and the posterior oesophageal wall has a much shorter 'effective length' than the anterior. This short reflection of peritoneum is sometimes referred to as the gastrophrenic ligament and, via the peritoneum over the oesophagus continues directly onto the posterior surface of the stomach. It covers the oesophageal branches of the left gastric vessels and the coeliac branches of the posterior vagus and can thus be said to form an extremely short, wide mesentery to the abdominal oesophagus. In all but the thinnest individuals a pad of adipose tissue is found beneath the peritoneum covering the anterior surface of the lower abdominal oesophagus and the adjacent gastric wall. It is a useful surgical marker for the external location of the gastro-oesophageal junction.

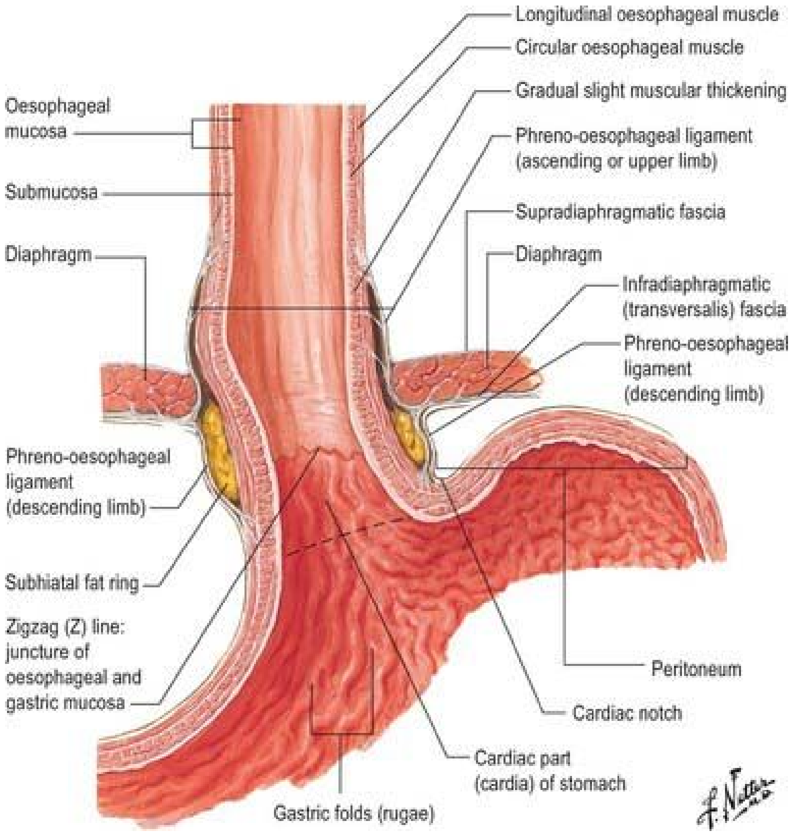
Longitudinal oesophageal muscle
Circular oesophageal muscle
Gradual slight muscular thickening
Phreno-oesophageal ligament (ascending or upper limb)
Supradiaphragmatic fascia
Diaphragm
Infradiaphragmatic (transversalis) fascia
Phreno-oesophageal ligament (descending limb)
Oesophageal mucosa
Submucosa
Diaphragm
Phreno-oesophageal ligament (descending limb)
Subhiatal fat ring
Zigzag (Z) line: juncture of oesophageal and gastric mucosa
Peritoneum
Cardiac notch
Cardiac part (cardia) of stomach
Gastric folds (rugae)

Fig. 65.1 The anatomical structures around the abdominal oesophagus.

(Reprinted from Netter Anatomy Illustration Collection, © Elsevier Inc. All Rights Reserved.)

VASCULAR SUPPLY AND LYMPHATIC DRAINAGE

Arteries

The abdominal oesophagus is supplied by oesophageal branches of the left gastric artery. These ascend as an anterior and posterior branch beneath the visceral peritoneum to supply perforating branches to the intramural and submucosal plexuses. The posterior surface usually receives an additional supply via branches of the upper short gastric arteries, the terminal branches of the oesophageal branches of the thoracic aorta and occasionally an ascending branch of the posterior gastric artery.

Veins

Veins drain via plexuses to the left gastric and upper short gastric veins (see Stomach veins below).

Lymphatic drainage

Lymphatic drainage occurs to the left gastric and left and right paracardial nodes and from the posterior surface directly to the uppermost para-aortic nodes (see Fig. 65.13).

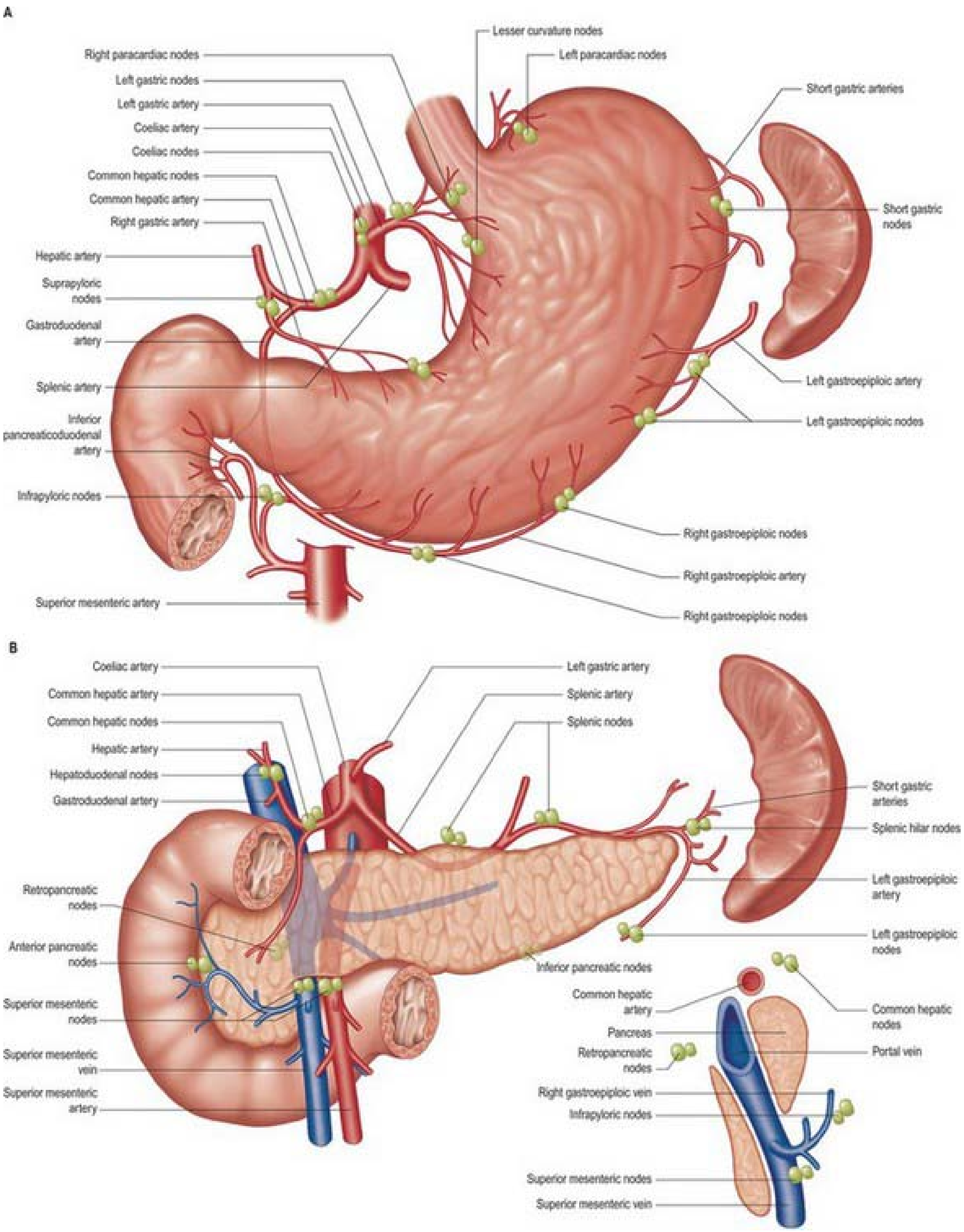
A
Lesser curvature nodes
Right paracardiac nodes
Left paracardiac nodes
Left gastric nodes
Left gastric artery
Coeliac artery
Coeliac nodes
Short gastric arteries
Common hepatic nodes
Common hepatic artery
Right gastric artery
Short gastric nodes
Hepatic artery
Suprapyloric nodes
Gastroduodenal artery
Splenic artery
Left gastroepiploic artery
Left gastroepiploic nodes
Inferior pancreaticoduodenal artery
Infrapyloric nodes
Right gastroepiploic nodes
Right gastroepiploic artery
Right gastroepiploic nodes
Superior mesenteric artery
B
Coeliac artery
Left gastric artery
Common hepatic artery
Splenic artery
Common hepatic nodes
Splenic nodes
Hepatic artery
Hepatoduodenal nodes
Gastroduodenal artery
Short gastric arteries
Splenic hilar nodes
Left gastroepiploic artery
Retropancreatic nodes
Left gastroepiploic nodes
Anterior pancreatic nodes
Inferior pancreatic nodes
Common hepatic artery
Common hepatic nodes
Superior mesenteric nodes
Pancreas
Portal vein
Superior mesenteric vein
Retropancreatic nodes
Superior mesenteric artery
Right gastroepiploic vein
Infrapyloric nodes
Superior mesenteric nodes
Superior mesenteric vein

Fig. 65.13 Main lymph node stations of the stomach and upper abdominal viscera. The sagittal relationships of the node groups around the neck of the pancreas are shown bottom right. The para-aortic nodes are

among the highest nodes for these viscera but have been removed for clarity (see **Ch. 66**).

INNERVATION

The abdominal oesophagus is innervated by sympathetic and parasympathetic fibres. The parasympathetic fibres are derived directly from the peri-oesophageal thoracic plexus and to a lesser extent from the anterior and posterior vagi. They are motor to the distal oesophagus and both stimulatory and inhibitory to the functional lower oesophageal sphincter (LOS), maintaining both background tone and co-ordinating distal oesophageal peristalsis with relaxation of the LOS during swallowing. The sympathetic supply originates from the fifth to 12th thoracic spinal segments and is mainly distributed via the greater and lesser splanchnic nerves and the coeliac plexus.

STOMACH

The stomach is the widest part of the alimentary tract and lies between the oesophagus and the duodenum. It is situated in the upper abdomen, extending from the left upper quadrant downwards, forwards and to the right, lying in the left hypochondriac, epigastric and umbilical areas. It occupies a recess beneath the diaphragm and anterior abdominal wall that is bounded by the upper abdominal viscera on either side. The mean capacity of the stomach increases from approximately 30 ml at birth, to 1000 ml at puberty, and approximately 1500 ml in adults. The peritoneal surface of the stomach is interrupted by the attachments of the greater and lesser omenta which define the greater and lesser curvatures that separate two surfaces.

PARTS OF THE STOMACH

For descriptive purposes, the stomach is divided by arbitrary lines drawn on its external surface into a fundus, body, pyloric antrum and pylorus (Fig. 65.2). The internal appearance and microstructure of these regions varies to some degree. The fundus is dome shaped and projects above and to the left of the cardiac orifice to lie in contact with the left dome of the diaphragm. It lies above a line drawn horizontally from the incisura cardiaca to the greater curvature. The body extends from the fundus to the incisura angularis, which is a constant external notch at the lower end of the lesser curvature. A line drawn from the incisura angularis to an indentation on the greater curvature defines the lower boundary of the body. The pyloric antrum extends from this line to the sulcus intermedius, where the stomach narrows to become the pyloric canal (1–2 cm long), which terminates at the pyloric orifice.

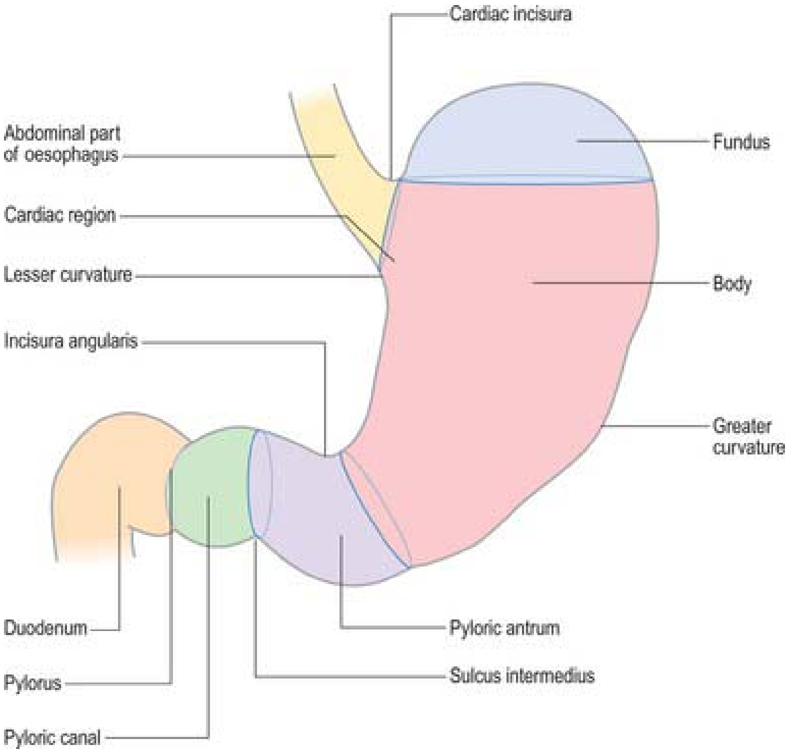
Cardiac incisura
Abdominal part of oesophagus
Fundus
Cardiac region
Lesser curvature
Body
Incisura angularis
Greater curvature
Duodenum
Pyloric antrum
Pylorus
Sulcus intermedius
Pyloric canal

Fig. 65.2 The parts of the stomach.

GASTRIC RELATIONS

Gastric curvatures

Lesser curvature

The lesser curvature extends between the cardiac and pyloric orifices and forms the medial (posterior and superior) border of the stomach. It descends from the medial side of the oesophagus in front of the decussating fibres of the right crus of the diaphragm, curves downwards and to the right and lies anterior to the superior border of the pancreas (Fig. 65.3). It ends at the pylorus just to the right of the midline. In the most dependent part there is typically a notch, the incisura angularis, whose position and appearance vary with gastric distension. The lesser omentum is attached to the lesser curvature and contains the right and left gastric vessels.

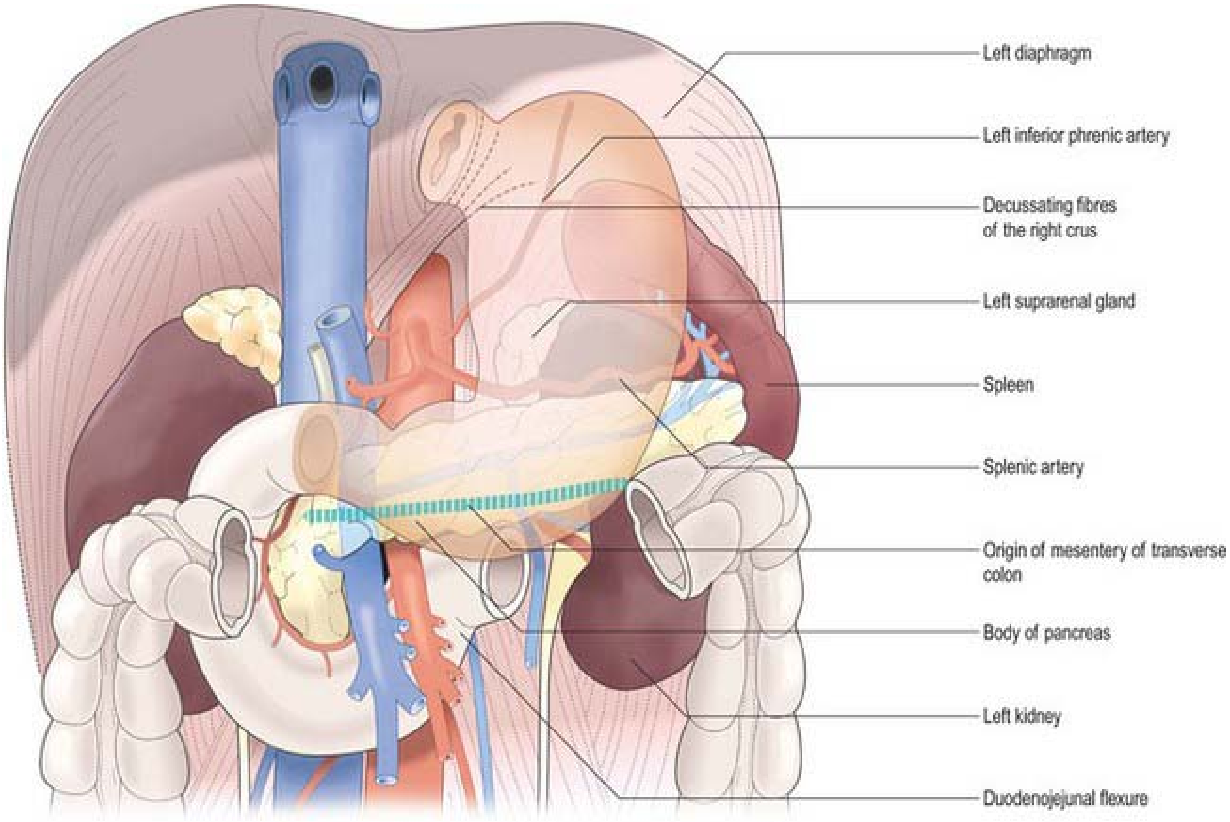
Left diaphragm
Left inferior phrenic artery
Decussating fibres of the right crus
Left suprarenal gland
Spleen
Splenic artery
Origin of mesentery of transverse colon
Body of pancreas
Left kidney
Duodenojejunal flexure

Fig. 65.3 Posterior relations of the stomach.

Greater curvature

The greater curvature is four or five times longer than the lesser. It starts from the incisura cardiaca formed between the lateral border of the abdominal oesophagus and the fundus of the stomach. It arches upwards, posterolaterally and to the left. Its highest convexity, the apex of the fundus, is approximately level with the left fifth intercostal space just below the left nipple in males, but varies with respiration. From this level it sweeps inferiorly and anteriorly, slightly convex to the left, almost as far as the tenth costal cartilage in the supine position, where it turns medially to end at the pylorus. There is frequently a groove, termed the sulcus intermedius, in the curvature close to the pyloric constriction. The start of the greater curvature is covered by peritoneum which continues over the anterior surface of the stomach. Laterally the greater curvature gives attachment to the gastrosplenic ligament and beyond this to the greater omentum, which contains the gastroepiploic vessels. The gastrosplenic ligament and the greater omentum, together with the gastrophrenic and splenorenal ligaments, are continuous parts of the original dorsal mesogastrium: their names merely indicate regions of the same continuous sheet of peritoneum and its associated connective tissue.

Gastric volvulus

Volvulus of the stomach is much less common than volvulus of either the sigmoid colon or caecum. Two types of gastric volvulus may occur. The first, organoaxial volvulus, occurs about a line of rotation running from below the cardiac orifice to the pylorus. The antrum, body and fundus rotate upwards, with the greater curvature coming to lie above the lesser curvature as the volvulus progresses. The second, mesenteroaxial volvulus, occurs about a line drawn ‘across’ the body of the stomach, usually just above the incisura angularis. This type of volvulus is perpendicular to the line of organoaxial volvulus. The distal body and antrum rotate anteriorly, superiorly and laterally while the upper body and fundus rotate posteriorly, medially and inferiorly. Although relatively mobile within the upper abdomen, the stomach is normally tethered to the oesophagus at the gastro-oesophageal junction (see above), to the duodenum at the pylorus, to the spleen by the gastrosplenic omentum, and to the liver by the lesser omentum. The attachment to the transverse colon via the gastrocolic omentum also restrains the stomach but is the most mobile of all. For either type of gastric volvulus to occur, it is necessary for some or all of these points of tethering to be loosened either by previous surgical division or by chronic lengthening and loosening of their connective tissue. Organoaxial volvulus is most common because the lesser omentum, gastrosplenic ligament and gastrocolic omentum are more likely to undergo chronic lengthening by traction than the other attachments of the stomach. Mesenteroaxial volvulus requires the gastro-oesophageal junction and pylorus to be sufficiently mobile as to come into close approximation. These structures are firmly tethered and consequently this form of gastric volvulus is much less common. Despite the profuse gastric arterial supply, either type of volvulus may compromise the vascularity of the stomach.

Gastric surfaces

When the stomach is empty and contracted, the two surfaces tend to lie facing almost superiorly and inferiorly, but with increasing degrees of distension they come to face progressively more anteriorly and posteriorly (Fig. 65.4).

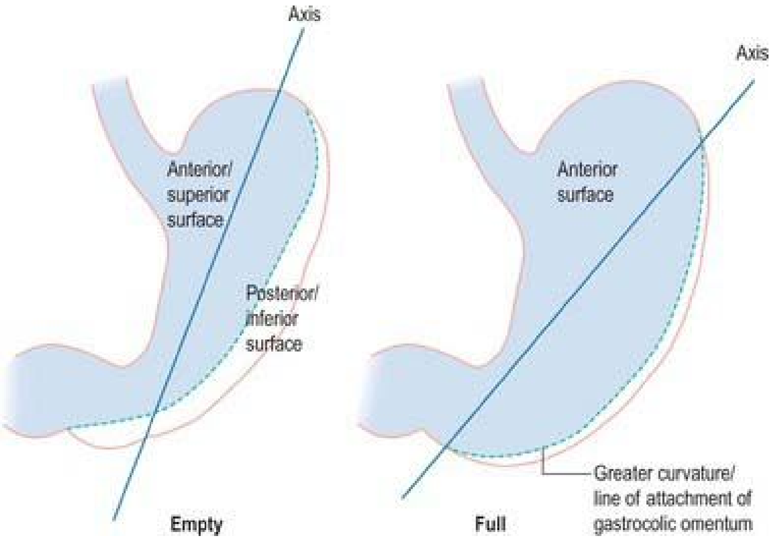
Axis
Anterior/
superior
surface
Posterior/
inferior
surface
Empty
Axis
Anterior
surface
Greater curvature/
line of attachment of
gastrocolic omentum
Full

Fig. 65.4 Axes of the empty and full stomach. As the stomach distends, the greater curvature 'rolls' downwards and the anterosuperior surface comes to lie almost completely vertical as the anterior surface.

Anterior (superior) surface

The lateral part of the anterior surface is posterior to the left costal margin and in contact with the diaphragm, which separates it from the left pleura, the base of the left lung, the pericardium and the left sixth to ninth ribs (Fig. 65.5). It lies posterior to the costal attachments of the upper fibres of transversus abdominis, which separate it from the seventh to ninth costal cartilages. The upper and left part of this surface curves posterolaterally and is in contact with the gastric surface of the spleen. The right half of the anterior surface is related to the left and quadrate lobes of the liver and the anterior abdominal wall. When the stomach is empty, the transverse colon may lie adjacent to the anterior surface. The entire anterior (superior) surface is covered by peritoneum.

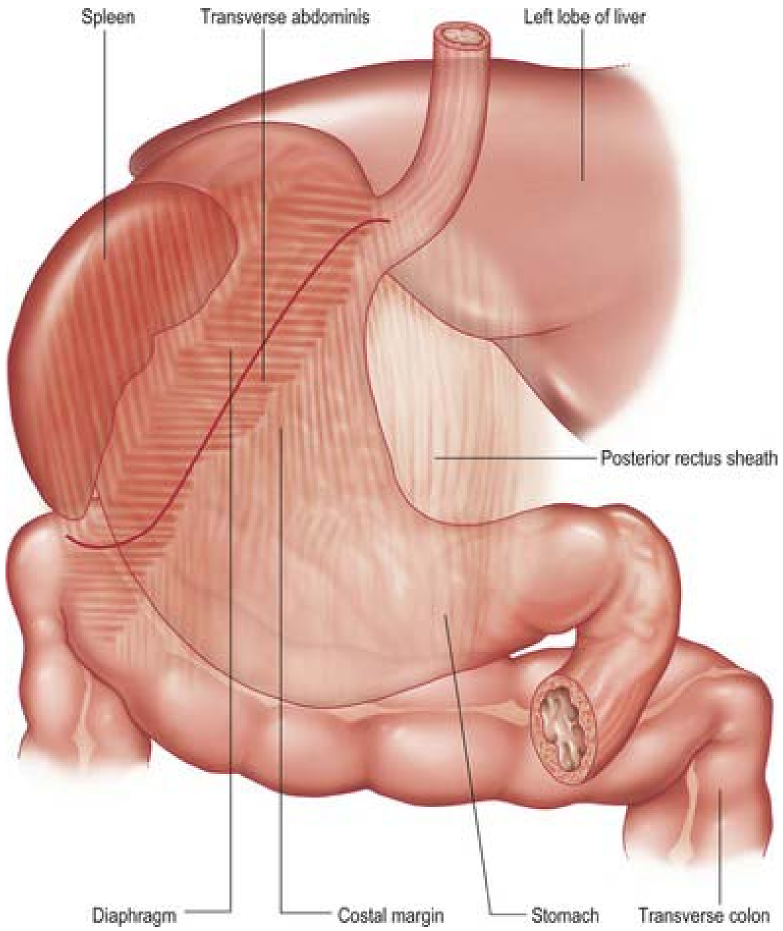
Spleen
Transverse abdominis
Left lobe of liver
Posterior rectus sheath
Diaphragm
Costal margin
Stomach
Transverse colon

Fig. 65.5 Anterior relations of the stomach, viewed from behind. The fibres of the diaphragm (oblique), transversus abdominis (transverse) and rectus abdominis (vertical) can be seen through the outlines of the stomach and its visceral relations.

Posterior (inferior) surface

The posterior surface lies anterior to the left crus and lower fibres of the diaphragm, the left inferior phrenic vessels, the left suprarenal gland, the superior pole of the left kidney, the splenic artery, the anterior pancreatic surface, the splenic flexure of the colon and the upper layer of the transverse mesocolon (Fig. 65.3). Together these form the shallow stomach bed: they are separated from the stomach by the lesser sac (over which the stomach slides as it distends). The upper left part of the surface curves anterolaterally and lies in contact with the gastric surface of the spleen. The greater omentum and the transverse mesocolon separate the stomach from the duodenojejunal flexure and ileum. The posterior surface is covered by peritoneum, except near the cardiac orifice, where a small, triangular area contacts the left diaphragmatic crus and sometimes the left suprarenal gland. The left gastric vessels reach the lesser curvature at the right extremity of this bare area in the left gastropancreatic fold. The gastrophrenic ligament passes from the lateral aspect of this bare area to the inferior surface of the diaphragm.

GASTRIC ORIFICES

Cardiac orifice and gastro-oesophageal junction

The opening from the oesophagus into the stomach is the cardiac orifice (Fig. 65.1). It is typically situated to the left of the midline behind the seventh costal cartilage at the level of the eleventh thoracic vertebra. It is typically 10 cm from the anterior abdominal wall and 40 cm from the incisor teeth. The abdominal oesophagus is continuous with the cardiac orifice; the right side is continuous with the lesser curvature, the left side with the greater curvature. There is no specific anatomically discernible cardiac sphincter related to the orifice.

Internally, the transition between oesophagus and stomach is difficult to define because mucosa of gastric fundal pattern extends a variable distance up into the abdominal oesophagus. It usually forms a ‘zig-zag’ squamo-columnar epithelial junction with the oesophageal epithelium above this Z line: for histological and endoscopic purposes, this is often referred to as the gastro-oesophageal junction. A sling of longitudinal and oblique gastric muscle fibres forms a loop on the superior, left, side of the gastro-oesophageal junction between the oesophagus and the lesser curvature, and this is taken as the external boundary of this junction. Bands of thickened circular smooth muscle in the upper wall of the greater curvature and the distal oesophagus are sometimes confusingly referred to as ‘clasp’ or ‘sphincter’ fibres.

Lower oesophageal sphincter and gastro-oesophageal reflux

At rest there is a gastro-oeosophageal pressure gradient due to the presence of negative intra-thoracic pressure (transferred to the thoracic oesophagus) and positive intra-abdominal pressure (transferred to the stomach and augmented by any contraction of the stomach wall itself). Several anatomical and physiological factors normally prevent gastro-oesophageal reflux. Minor factors include the folds of gastric mucosa present in the gastro-oesophageal junction, the mucosal rosette, which contribute to the formation of a fluid-

and gas-tight seal and also help to ensure that even low levels of tone within the lower oesophageal wall muscles may occlude the lumen of the junction against low pressures of gastric gas; the angle of the cardiac orifice, which is formed, in part, by the pull of the long oblique fibres of the inner layer of the gastric smooth muscle and may help to form a type of ‘flap valve’; and the length of the abdominal oesophagus, which is buttressed externally by pads of adipose connective tissue at and below the level of the diaphragmatic hiatus. However, the major anti-reflux mechanisms are the tonic contractions of the specialized smooth muscle of the wall lower oesophageal and the encircling fibres of the right diaphragmatic crus, which, together, exert a radial pressure that can be measured by electromyography or manometric testing (Paterson 2001, Mittal 2006), and form an effective high pressure zone (HPZ). At and just below the level of the entry of the abdominal oesophagus into the stomach, the circular fibres of the intermediate layer of the muscularis externa lying over the upper lesser curvature are particularly pronounced and sometimes referred to as ‘clasp’ fibres and exert fairly constant myogenic tone (Fig. 65.6). Since the oesophagus passes obliquely into the stomach, with increasing gastric distension the tone in the clasp fibres rises and they may act to draw the anterior and posterior surfaces together, increasing the tone at the gastro-oesophageal junction, contributing to the HPZ. These anatomical and physiological features are together referred to as the lower oesophageal sphincter (LOS). If reflux is to be prevented, the pressure within the HPZ must exceed the difference between the pressures on either side of the junction. The oesophageal part of the LOS is controlled by the intramural plexuses of the enteric nervous system via the neural release of nitric oxide which relaxes the smooth muscle of the LOS. Tone is reduced in advance of the oesophageal peristaltic wave during swallowing and raised again after the food bolus has passed. During inspiration, the greater negative intrathoracic pressure which increases the gastro-oesophageal pressure gradient is offset by increased pressure in the HPZ due to contraction of the peri-oesophageal fibres of the right diaphragmatic crus. Activation of the crural diaphragm slightly before the costal fibres ensures that this increase precedes the increase in the gradient.

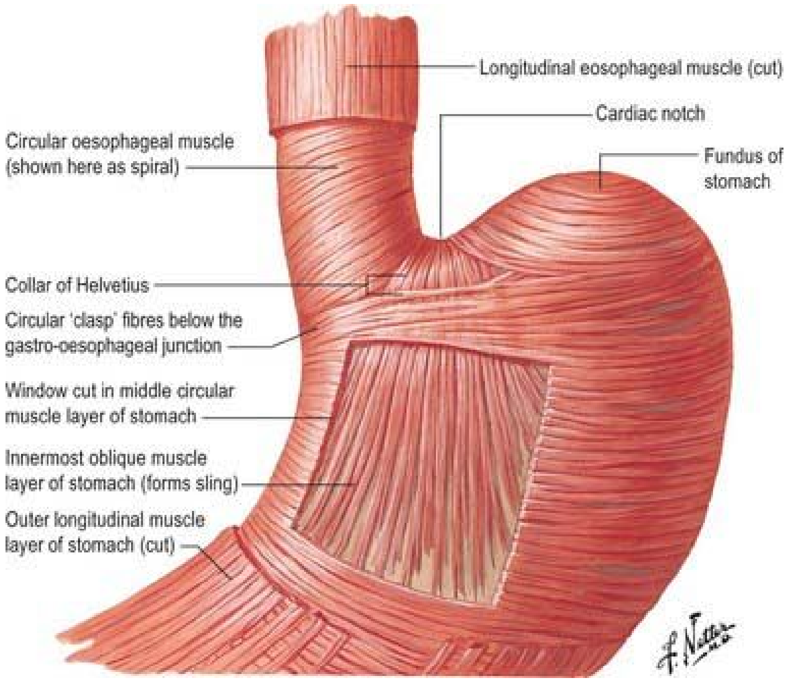
Longitudinal eosophageal muscle (cut)
Cardiac notch
Fundus of stomach
Circular oesophageal muscle (shown here as spiral)
Collar of Helvetius
Circular 'clasp' fibres below the gastro-oesophageal junction
Window cut in middle circular muscle layer of stomach
Innermost oblique muscle layer of stomach (forms sling)
Outer longitudinal muscle layer of stomach (cut)
F. Netter

Fig. 65.6 Detail of the arrangements of the muscle layers of the oesophageal and gastric walls.

(Reprinted from Netter Anatomy Illustration Collection, © Elsevier Inc. All Rights Reserved.)

Reflux of gastric contents into the abdominal and lower thoracic oesophagus as a result of transient relaxation of the LOS occurs as a normal event in most individuals for a small percentage of their daily life. It also occurs as a result of a weak LOS, or of hiatus hernia which disrupts the normal anatomical barriers. Surgical procedures to prevent excessive reflux mainly focus on the restoration of a normal length of intra-abdominal oesophagus, by reduction of any hiatus hernia which carries the gastro-oesophageal junction into the thorax, and an increase in the tonic contraction surrounding the intra-abdominal oesophagus, which is usually achieved by partial wrapping of the fundus of the stomach around the intra-abdominal oesophagus to provide greater tone, 'fundoplication'.

Barrett's oesophagus

The squamous epithelium lining the lower oesophagus may be pathologically replaced by islands, strips, or circumferential patches of columnar, gastric type epithelium. This process is most likely to be the result of chronic reflux of gastric contents, acid or alkali, into the oesophagus, inducing a change in mucosal cell type. The abnormal columnar type epithelium, which may extend for a variable length up the lower part of the oesophagus, is referred to as Barrett's epithelium.

Pyloric orifice

The pyloric orifice is the opening from the stomach into the duodenum, and typically lies 1–2 cm to the right of the midline in the transpyloric plane when the body is supine and the stomach empty. The pyloric sphincter is a muscular ring formed by a marked thickening of the circular gastric muscle interlaced with some longitudinal fibres. The circular pyloric constriction on the surface of the stomach usually indicates the location of the pyloric sphincter, and is often marked by a prepyloric vein which crosses the anterior surface vertically downwards.

GASTRIC FORM AND INTERNAL APPEARANCES

Numerous factors influence both the form and position of the stomach, including the posture and build of the individual, the extent of filling of the stomach, the position of the surrounding viscera, and the tone of the abdominal wall and gastric musculature. The empty stomach is most commonly J-shaped, the fundus usually contains gas, and, in the erect posture, the pylorus descends to the level of the second or the third lumbar vertebra. The lowest part of the antrum often lies below the level of the umbilicus, and the overall axis of the organ is slightly inclined from the vertical (Fig. 65.7). In short, obese individuals, the axis of the stomach lies more towards the horizontal as a ‘steer-horn’ shape.

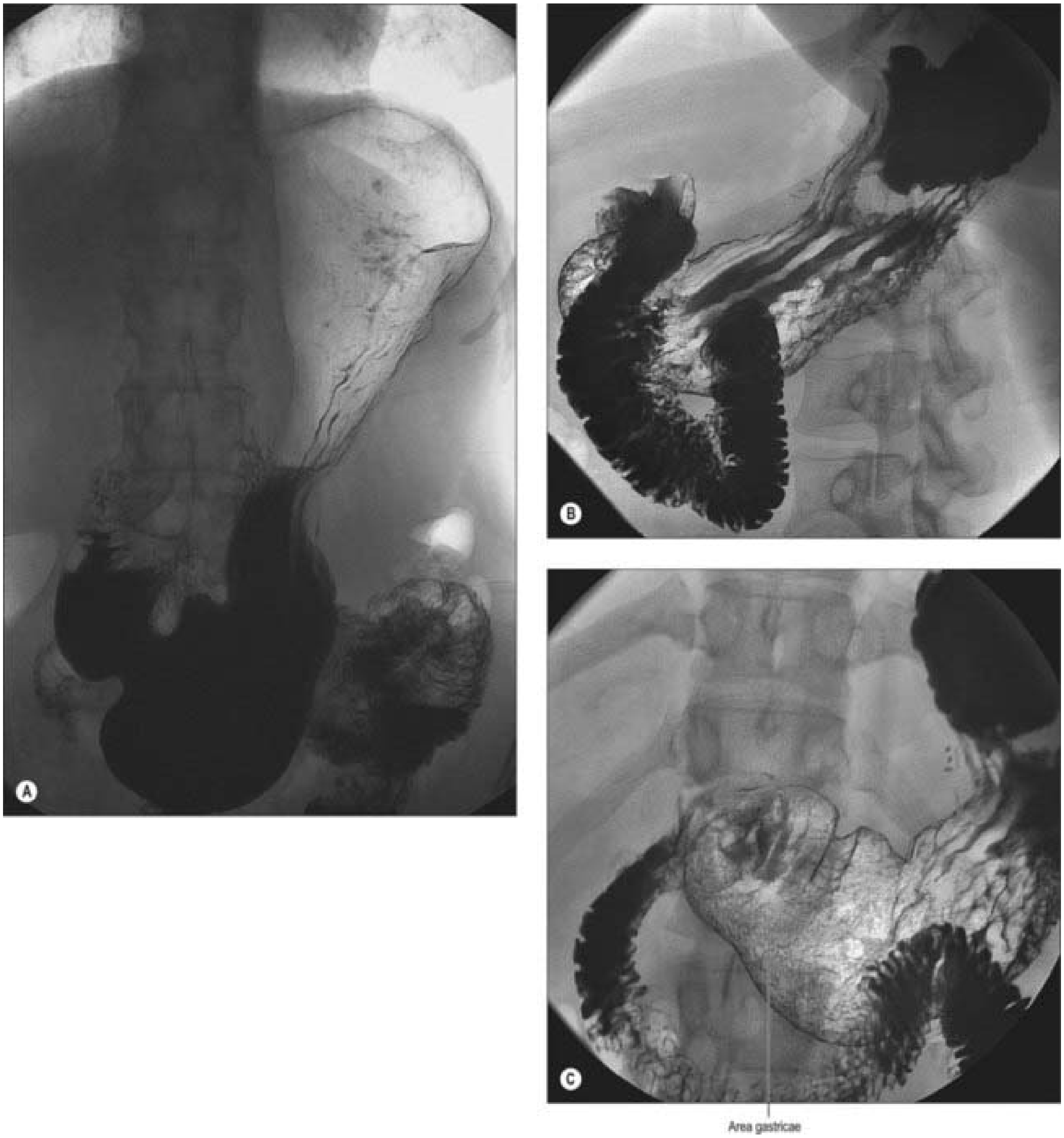

Fig. 65.7 Double contrast barium meal. **A**, In the erect position the stomach has a more ‘J’-shaped configuration. **B**, Initial stomach filling demonstrates a horizontally lying stomach with prominent gastric rugal folds. **C**, The area gastricae within the antrum are clearly identified on distension of the stomach.

The extent of filling mainly affects the shape and position of the body, because the pyloric part usually remains contracted during digestion. As the stomach fills, it expands forwards and downwards but, when the colon or small bowel is distended, the fundus enlarges towards the liver and diaphragm. As stomach capacity increases, the pylorus is displaced to the right and the axis of the whole organ lies in a more oblique direction. In this position the anterior and posterior surfaces tend to face forwards and backwards and the lowest part is the pyloric antrum, which extends below the umbilicus. When intestinal distension interferes with downward expansion of the body, the stomach retains a horizontal position.

Internal appearances

During endoscopic examination (Fig. 65.8), the stomach is typically at least partially distended by air. The cardiac orifice and the lowest portion of the abdominal oesophagus viewed from above are typically closed at rest by tonic contraction of the lower oesophageal musculature. The gastric mucosa lining the orifice is puckered into ridges and is present for a short but variable distance up the abdominal oesophagus; the transition between columnar and squamous epithelium is usually clearly visible. The presence of abnormal columnar epithelium within the oesophagus is referred to as Barrett's oesophagus but the precise definition of this condition is difficult (see above). From within the distended stomach, the cardiac orifice appears in the medial wall of the fundus and is asymmetrical. The medial edge of the cardiac orifice is continuous with the medial wall of the body of the stomach. The mucosa is slightly thickened at this point with a raised profile, forming part of the 'mucosal rosette' that lines the orifice. The 'rosette' aids closure of the cardiac orifice and helps prevent reflux of stomach contents into the oesophagus. The medial edge of the orifice is more clearly visible than the lateral edge because it forms a more acute angle with the mucosal lining of the abdominal oesophagus.

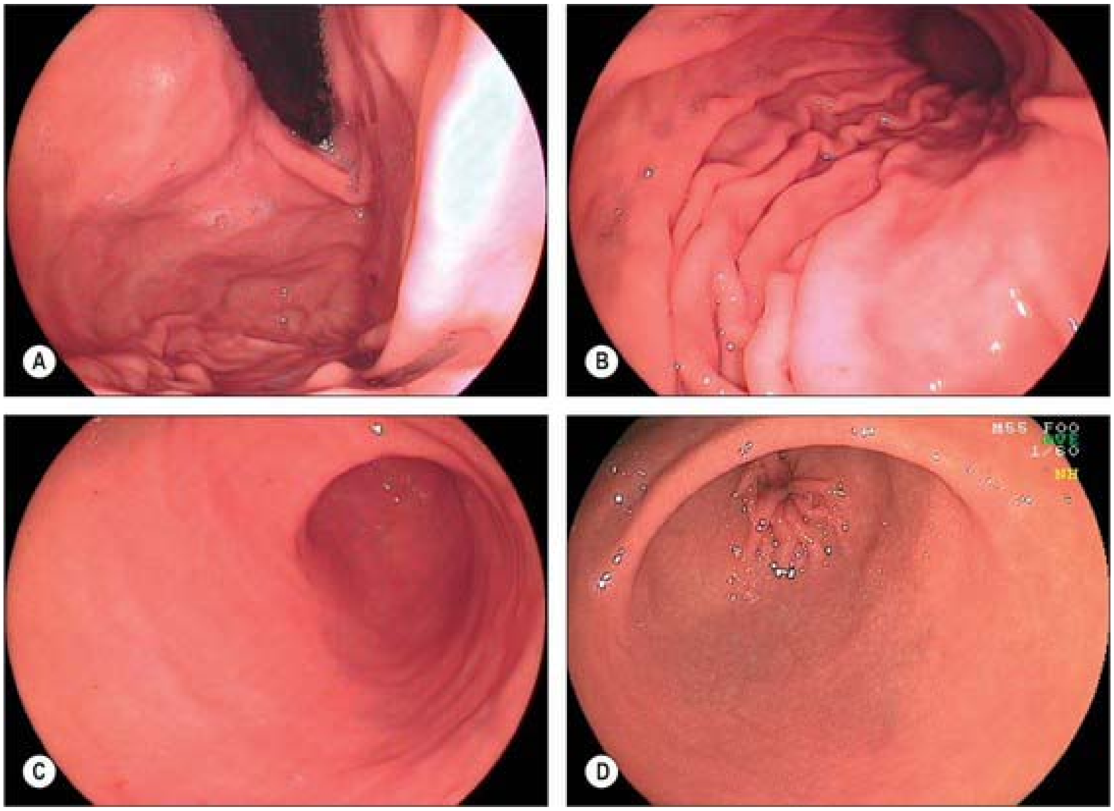

Fig. 65.8 Endoscopic appearances of the stomach. **A**, Cardiac orifice and fundus from below showing the pronounced lateral mucosal fold at the cardiac orifice; **B**, Body and greater curvature showing mucosal folds (‘magenstrasse’); **C**, Antrum showing the internal appearance of the incisura angularis; **D**, Prepyloric antrum and opening of the pyloric canal.

In the partly distended stomach, the mucosa of the fundus is thrown into gentle folds with no particular pattern (rugae). As the stomach fills towards capacity, these folds rapidly become less pronounced, and the wall is nearly smooth when the stomach is over-inflated. The body of the stomach has the most pronounced mucosal folds. Even in moderate distension, they appear as long, broad mucosal ridges running in sinuous strips from fundus to pyloric antrum (Fig. 65.7). They are seen on all mucosal surfaces of the body but are most obvious on the anterolateral, lateral and posterolateral parts (which correspond to the inner surface of the anterior and posterior external surfaces and to the greater curvature). Here they are occasionally called the *magenstrasse*, a reference to their possible role in directing liquid entering the stomach immediately down into the pyloric antrum. These folds are least prominent on the medial surface (corresponding to the inner surface of the lesser curvature), which is much smoother, particularly when the stomach distends.

The areae gastricae within the antrum are small elevations or puckerings of the mucosal surface that are readily seen on double contrast barium meal (Fig. 65.7). The few folds present in the antrum when the stomach is relaxed disappear with distension. The antrum adjacent to the pyloric canal, the prepyloric antrum, has a smooth mucosal surface that culminates in a slight puckering of the mucosa at the pyloric orifice caused by the contraction of the pyloric sphincter.

Gastrostomy

Since the lower body and antrum of the stomach is related to the posterior aspect of the left anterior abdominal wall, it may usefully be accessed to form a gastrostomy. Its mobility enables the anterior surface of the stomach to be readily approximated to the parietal peritoneum on the posterior surface of the abdominal wall, and a communication to be established between the lumen of the stomach and the surface of the skin. Although this may be performed as a direct open surgical procedure under general anaesthetic, it is much more commonly performed using a percutaneous puncture guided by either endoscopic visualization of the stomach or radiological imaging. The procedure is made easier by the fact that the anterior surface of the stomach lies most nearly in the vertical plane when the stomach is distended. One of the main hazards of the procedure results from the occasional interposition of the transverse colon between the stomach and anterior abdominal wall, which may lead to inadvertent transfixion of the colon by the needle puncture system. The variable length of the transverse colonic mesentery means that it may sometimes lie adjacent to the anterior gastric surface when a subject is recumbent. These risks may be reduced by radiological guidance.

VASCULAR SUPPLY AND LYMPHATIC DRAINAGE

Arteries

The arterial supply to the stomach comes predominantly from the coeliac axis although intramural anastomoses exist with vessels of other origins at the two ends of the stomach (Figs 65.9, 65.10, 65.11). The left gastric artery arises directly from the coeliac axis. The splenic artery gives origin to the short gastric arteries as well as the left gastroepiploic artery and may occasionally give origin to a posterior gastric artery. The hepatic artery gives origin to the right gastric artery and to the gastroduodenal artery, which in turn gives origin to the right gastroepiploic artery.

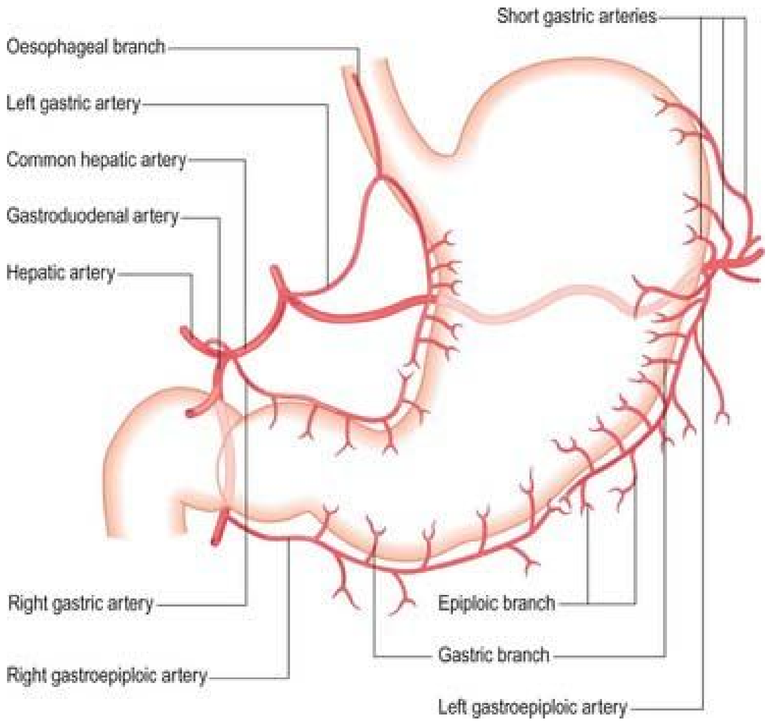
Short gastric arteries
Oesophageal branch
Left gastric artery
Common hepatic artery
Gastroduodenal artery
Hepatic artery
Right gastric artery
Right gastroepiploic artery
Epiploic branch
Gastric branch
Left gastroepiploic artery

Fig. 65.9 Arterial supply of the stomach.

Rights were not granted to include this figure in electronic media.
Please refer to the printed publication.

Fig. 65.10 Coeliac axis and its branches. Demonstrated on digital subtraction angiography (**A**) and digital reformatted multislice CT angiogram

*(**B** and **C**). **B** and **C** by courtesy of GE Worldwide Medical Systems. (by courtesy of Dr James McCall, Chelsea & Westminster Hospital, London)*

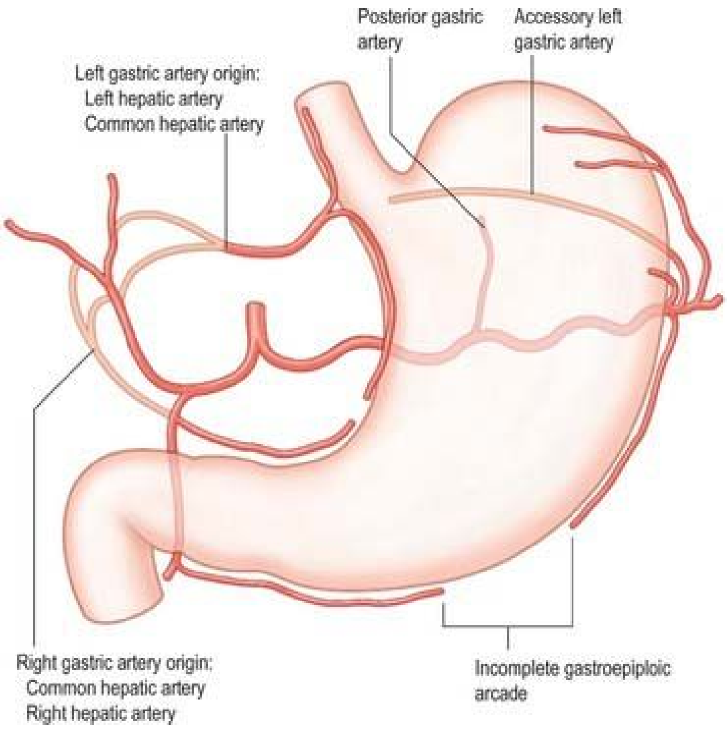
Posterior gastric artery
Accessory left gastric artery
Left gastric artery origin:
Left hepatic artery
Common hepatic artery
Right gastric artery origin:
Common hepatic artery
Right hepatic artery
Incomplete gastroepiploic arcade

Fig. 65.11 Principle variations in the gastric arterial supply. Accessory vessels or possible replaced origins of vessels are shown by pale pink lines.

Left gastric artery

The left gastric artery is the smallest branch of the coeliac axis. It ascends to the left of the midline and crosses either just over the lower end of or below the level of the origin of the left crus of the diaphragm beneath the peritoneum of the upper posterior wall of the lesser sac. Here it lies adjacent to the left inferior phrenic artery and medial or anterior to the left suprarenal gland. It runs forwards into the superior portion of the lesser omentum adjacent to the superior end of the lesser curvature, and turns anteroinferiorly to run along the lesser curvature between the two peritoneal leaves of the lesser omentum. At the highest point of its course, it gives off one or more oesophageal branches. In its course along the lesser curvature, it gives off multiple branches that run onto the anterior and posterior surfaces of the stomach and anastomose with the right gastric artery in the region of the incisura angularis.

The left gastric artery rarely arises from the common hepatic artery or its branches. The most common of these rare variations is an origin from the left hepatic artery, when the left gastric artery passes between the peritoneal layers of the superior lesser omentum to reach the lesser curvature of the stomach. Other variants include a common origin with the common hepatic artery. (A replaced/accessory left hepatic artery origin from the left gastric artery is more common than a replaced/accessory left gastric origin.)

Short gastric arteries

There is no universally accepted definition of what constitutes the short gastric arteries but a practical definition is ‘vessels which supply the fundus of the stomach above the level of the splenic artery and which arise to the left of the greater curvature of the stomach’. The short gastric arteries are variable in number, commonly between five and seven. They arise from the splenic artery or its divisions, or from the proximal left gastroepiploic artery, and pass between layers of the gastrosplenic ligament to supply the cardiac orifice and gastric fundus. They anastomose with branches of the left gastric and left gastroepiploic arteries. An accessory left gastric artery may arise with these vessels from the distal splenic artery.

Left gastroepiploic artery

The left gastroepiploic artery is the largest branch of the splenic artery. It arises near the splenic hilum and runs anteroinferiorly between the layers of the gastrosplenic ligament into the upper gastrocolic omentum. It lies between the layers of peritoneum close to the greater curvature, running inferiorly to anastomose with the right gastroepiploic artery. It gives off gastric branches to the fundus of the stomach through the gastrosplenic ligament, and to the body of the stomach through the gastrocolic omentum. These are necessarily longer than the gastric branches of the right gastroepiploic artery and may be 8–10 cm long. Epiploic (omental) branches arise along the course of the vessel and descend between the layers of the gastrocolic omentum into the greater omentum. A particularly large epiploic branch commonly originates close to the origin of the left gastroepiploic artery, descends in the lateral portion of the greater omentum and provides a large arterial supply to the lateral half of the omentum.

Posterior gastric artery

A distinct posterior gastric artery may occur. When present, it arises from the splenic artery in its middle section posterior to the body of the stomach (Fig. 65.11). It ascends behind the peritoneum of the lesser sac towards the fundus and reaches the posterior surface of the stomach in the gastrophrenic fold.

Right gastric artery

The right gastric artery arises from the hepatic artery as it passes forwards from the posterior wall of the lesser sac into the lower border of the lesser omentum above the first part of the duodenum. It runs between the peritoneal layers of the lesser omentum just above the medial end of the lesser curvature, passes superiorly along the lesser curvature, giving off multiple branches onto the anterior and posterior surfaces of the stomach, and anastomoses with the left gastric artery.

The origin of the right gastric artery often varies: the most common alternative origins are from the common hepatic, left hepatic, gastroduodenal or supraduodenal arteries.

Gastroduodenal artery

The gastroduodenal artery arises from the common hepatic artery posterior and superior to the first part of the duodenum. It gives origin to the right gastroepiploic and superior pancreaticoduodenal arteries at the lower border of the first part of the duodenum. (For details of the gastroduodenal artery and its relevance to clinical situations, see Chapter 66.)

Right gastroepiploic artery

The right gastroepiploic artery originates from the gastroduodenal artery behind the first part of the duodenum, anterior to the head of the pancreas. It passes inferiorly towards the midline between the layers of the gastrocolic omentum, lies inferior to the pylorus, then runs laterally along the greater curvature and ends by anastomosing with the left gastroepiploic artery. It is adjacent to the pylorus but, more distally, lies approximately 2 cm from the greater curvature of the stomach. The right gastroepiploic artery gives off gastric branches that ascend onto the anterior and posterior surfaces of the antrum and lower body of the stomach, epiploic branches that descend into the greater omentum, and branches that contribute to the supply of the inferior aspect of the first part of the duodenum.

Arterial anastomoses of the stomach

There is an anastomosis between the oesophageal arteries originating from the thoracic aorta and the vessels that supply the fundus in the region of the cardiac orifice. At the pyloric orifice the extensive network of vessels supplying the duodenum allows for some anastomosis between vessels of superior mesenteric artery origin and the pyloric vessels. The major named vessels supplying the stomach form extensive arterial anastomoses both on the serosal surface and around the curvatures. The right and left gastroepiploic arteries and the left and right gastric arteries anastomose freely with each other along the greater and lesser curvatures respectively. Anastomoses also form between the short gastric and left gastric arteries in the region of the fundus, and between the right gastric and right gastroepiploic arteries in the region of the antrum. In addition to the extensive serosal anastomoses, networks form within the stomach wall at intramuscular, submucosal and mucosal levels. A true plexus of small arteries and arterioles is present within the submucosa: it supplies the mucosa and shows considerable regional variation both in the gastric wall and in the proximal duodenum. The rich arterial supply to the stomach ensures that the high mucosal blood flow required for physiological functioning is maintained even if one or more vessels become occluded: the stomach exhibits considerable resistance to ischaemia even when multiple arterial supplies are lost.

The pyloric arteries are rami of the right gastric and right gastroepiploic arteries. They pierce the duodenum distal to the sphincter around its entire circumference and pass through the muscular layer to the submucosa where they divide into two or three rami. The latter turn back into the pyloric canal beneath the mucosa and run to the end of the pyloric antrum: they supply the entire mucosa of the pyloric canal (Fig. 65.12). Branches of the pyloric submucosal arteries may anastomose close to their origin with the duodenal submucosal arteries, and their terminal rami also anastomose with gastric arteries from the prepyloric antrum. The pyloric sphincter is supplied by the gastric and pyloric arteries via rami that leave their parent vessels in the subserosal and submucosal levels to penetrate the sphincter.

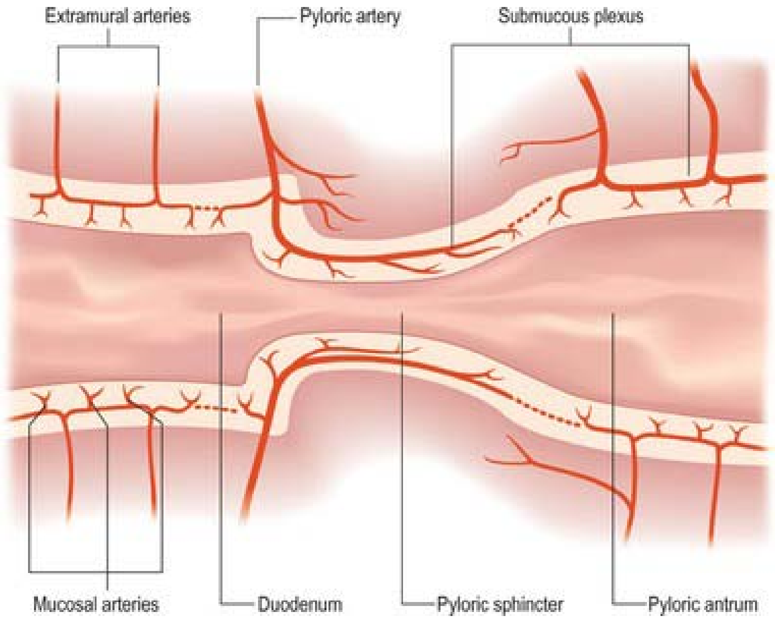

Fig. 65.12 Blood supply of the stomach and the proximal duodenum. A scheme of arterial arrangements at the gastroduodenal junction. Dotted lines indicate sites where the submucous plexus may be non-continuous. Shaded areas represent the muscular layer of the visceral wall.

(Redrawn courtesy of C Piasecki, Department of Anatomy, Royal Free Hospital School of Medicine, London and the Journal of Anatomy.)

Dieu la Foy lesions

Abnormalities of the intramural vascularity of the stomach are a rare cause of bleeding from the upper gastrointestinal tract. So-called ‘Dieu la Foy’ lesions commonly occur in the proximal body or fundus. Originally thought to be small arteriovenous malformations of the submucosal plexus, they are now considered to be caused by a larger than normal penetrating arterial vessel running through the muscular coat of the stomach into the submucosa before branching into the submucosal plexus.

Veins

The veins draining the stomach ultimately empty into the portal vein. A rich submucosal and intramural venous network gives rise to veins that usually accompany the corresponding named arteries and drain into either the splenic or superior mesenteric veins, although some pass directly into the portal vein. The course and distribution of the veins is highly variable even up to the level of the major named vessels.

Short gastric veins

Four or five short gastric veins drain the gastric fundus and the upper part of the greater curvature into the splenic vein or one of its large tributaries.

Left gastroepiploic vein

The left gastroepiploic vein drains both anterior and posterior surfaces of the body of the stomach and the adjacent greater omentum via multiple tributaries. It runs superolaterally along the greater curvature, between the layers of the gastrocolic omentum, and drains into the splenic vein within the gastrosplenic ligament.

Right gastroepiploic vein

The right gastroepiploic vein drains the greater omentum, distal body and antrum of the stomach. It passes medially, inferior to the greater curvature, in the upper portion of the gastrocolic omentum. Just proximal to the pyloric constriction it passes posteriorly to drain into the superior mesenteric vein below the neck of the pancreas. The right gastroepiploic vein may receive the superior pancreaticoduodenal vein close to its entry into the superior mesenteric vein.

Left gastric vein

The left gastric vein drains the upper body and fundus of the stomach. It ascends along the lesser curvature to the oesophageal opening where it receives several lower oesophageal veins, then curves posteriorly and medially behind the posterior peritoneal surface of the lesser sac. It drains into the portal vein directly at the level of the upper border of the first part of the duodenum.

Right gastric vein

The right gastric vein is typically small and runs along the medial end of the lesser curvature, passing under the peritoneum as it is reflected from the posterior aspect of the pylorus and first part of the duodenum onto the posterior wall of the lesser sac. It drains directly into the portal vein at the level of the first part of the duodenum. It receives the prepyloric vein as it ascends anterior to the pylorus at the level of the pyloric opening.

Posterior gastric veins

Distinct posterior gastric veins may occur, sometimes as multiple small vessels. When present, they accompany the posterior gastric artery from the middle of the posterior surface of the stomach and drain into the splenic vein.

Oesophageal and gastric varices

Blood from the mucosa normally drains into a superficial venous plexus, then into a deeper intrinsic venous plexus and finally into the peri-oesophageal veins via perforating veins. In the abdominal oesophagus the perforating veins drain into tributaries of the left gastric veins; in the lower thoracic oesophagus they form tributaries of the azygos and hemiayzgos systems. Bidirectional flow is possible in this region, and accommodates pressure changes that occur during breathing and Valsalva manoeuvres.

Varices are progressive dilatations which occur predominantly in the submucosal plexus of the distal abdominal oesophagus and occasionally on the gastric side of the gastric orifice at portal venous pressures above 15 mmHg. Portal venous hypertension, of any cause, predisposes to the opening up of pre-existing embryonic venous channels between venous tributaries of the portal system and the systemic venous circulation (Paquet 2000), such as the venous plexuses which exist in the lower abdominal oesophagus and gastric orifice. In portal hypertension, the valves within the perforating vessels become incompetent, permitting retrograde flow, and this causes variceal dilatation of the deep and superficial veins. Varices in the distal oesophagus are often easily visible at endoscopy, because they are situated superficially in the lamina propria and protrude into the oesophageal lumen; they are a frequent cause of substantial upper gastrointestinal bleeding. Spontaneous cessation of the bleeding is less common than at other sites, in part because the pressure and the flow rate within the veins is high, but also because there is a relative lack of submucosal supporting connective tissue to allow for venous contraction and thrombosis. Gastric varices are often present on the inferior aspect of the gastric orifice. They present less commonly in clinical practice than oesophageal varices, are less easy to diagnose because of their location, and occasionally exist without the presence of oesophageal varices. In these circumstances, it may be that the embryonal ‘point of meeting’ between portal and systemic venous systems is lower than usual and occurs in the upper stomach rather than the lower oesophagus.

Lymphatic drainage

The stomach has a rich network of lymphatics that connect with lymphatics draining the other visceral organs of the upper abdomen. At the gastro-oesophageal junction the lymphatics are continuous with those draining the lower oesophagus, and in the region of the pylorus they are continuous with those draining the duodenum. In general, they follow the course of the arteries supplying the stomach. However, many separate groups of nodes are now recognized (Fig. 65.13), and their relationship to the regions of the stomach and the vascular territories supplied, is of great importance during resection of the stomach, particularly for malignancy. Pancreatic and hepatic lymphatics play a significant role in draining areas of the stomach during disease.

Gastrectomy and gastric lymphadenectomy

Surgery for gastro-oesophageal malignancy involves varying degrees of radical resection of the associated lymph nodes that potentially drain the tumour area. The wide ramification of the gastro-oesophageal lymph node drainage and the multiple possible nodes which may be involved in a tumour inevitably mean that the extent of lymphadenectomy undertaken may be wide. The extent of possible/actual nodal involvement by the tumour is classified as N1 (loco-regional nodes specific to the tumour site), N2 (regional and major named vessel nodes draining the tumour) and N3 (wider draining nodes including para-aortic nodes). Gastrectomies can be classified according to the node groups excised for the tumour: D1 (e.g. removal of the portion of the stomach involved and the local lymph nodes directly related to the arteries ligated), D2 (e.g. total gastrectomy including all gastric lymph node groups often including the spleen) and D3 (e.g. total gastrectomy plus extensive lymphadenectomy that includes the associated upper abdominal lymph nodes, namely pancreatic, superior mesenteric, coeliac, hepatic and transverse colic). (For details of the lymph node stations relevant to surgical gastric resection, see Japanese Gastric Cancer Association 1998 and UICC 1997.)

INNERVATION

The stomach is innervated by sympathetic and parasympathetic fibres.

Sympathetic innervation

The sympathetic supply to the stomach originates from the fifth to 12th thoracic spinal segments, and is mainly distributed to the stomach via the greater and lesser splanchnic nerves via the coeliac plexus. Periarterial plexuses form along the arteries and supply the stomach from the coeliac axis. Additional innervation comes from fibres of the hepatic plexus, which pass to the upper body and fundus via the upper limit of the lesser omentum and via direct branches from the greater splanchnic nerves.

The gastric sympathetic nerves are vasoconstrictor to the gastric vasculature and inhibitory to gastric musculature. The sympathetic supply to the pylorus is motor, and brings about pyloric constriction. The sympathetic supply also conducts afferent impulses that mediate sensations, including pain.

Parasympathetic innervation

The parasympathetic supply to the stomach is from the anterior and posterior vagus nerves (Fig. 65.14). The anterior vagus (formed mainly from fibres from the left vagus originating from the oesophageal plexuses) is often double or even triple and supplies filaments to the cardiac orifice. The nerve lies very closely applied to the outer muscle of the abdominal oesophagus and divides near the oesophageal end of the lesser curvature into gastric and pyloric/hepatic branches. The upper anterior gastric branches radiate on the anterior surface of the upper body and fundus. The main gastric branch is termed the greater anterior gastric nerve and lies in the lesser omentum near the lesser curvature; branches from this nerve pass to the body and antrum with the gastric arterial supply branches. Hepatic/pyloric branches (generally one main and possibly one accessory) originate below the cardiac orifice. The main hepatic/pyloric nerve runs between the peritoneal layers of the lesser omentum almost horizontally towards its free edge to reach the hilum of the liver where hepatic branches ramify and pyloric branches turn down on the left side of the hepatic artery to reach the pylorus. The second nerve usually arises from the greater anterior gastric nerve during its course and runs inferomedially to the pyloric antrum where pyloric (and antral) branches form and hepatic branches (one or two) run superiorly to contribute to the hepatic plexus. Variations in the anterior nerve include accessory pyloric branches, long gastric branches with a high lying nerve trunk and a low origin of the pyloric branch with a low lying nerve trunk.

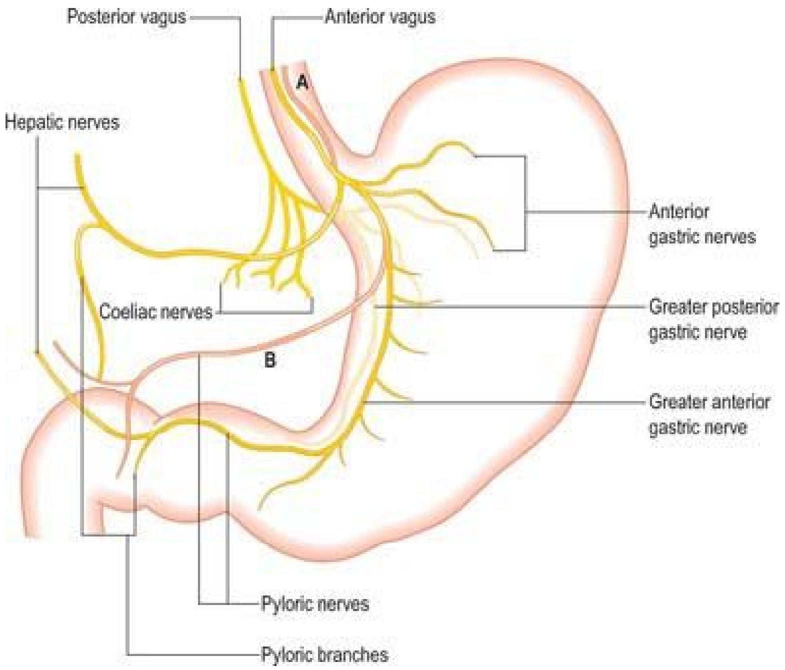
Posterior vagus
Anterior vagus
A
Hepatic nerves
Anterior gastric nerves
Coeliac nerves
Greater posterior gastric nerve
B
Greater anterior gastric nerve
Pyloric nerves
Pyloric branches

Fig. 65.14 Distribution of the vagal nerves to the stomach. The two commonest variations in the anterior vagus are shown in pink. **A**, Multiple main trunks. **B**, Low origin of the hepatic/pyloric branch lying close to the lesser curvature.

The posterior nerve tends to lie more medial than the anterior and is often a short distance from the wall of the abdominal oesophagus. It produces two main groups of branches, gastric and coeliac. Gastric branches arise and then run behind the cardiac orifice and upper body of the stomach. They extend over the posterior surface of the body and fundus to the proximal antrum but do not normally reach the pyloric sphincter. The largest is termed the greater posterior gastric nerve and runs posteriorly along the lesser curvature. Large coeliac branches (one or more) arise from the posterior nerve as thick bundles which carry the majority of fibres forming the nerve to the coeliac plexus (and onwards). Hepatic branches (one or two) are often small and originate from the coeliac branches. No true plexus occurs on either the anterior or posterior gastric surfaces, but plexuses are present in the submucosa and between the layers of the muscularis externa.

The parasympathetic gastric supply is secretomotor to the gastric mucosa and motor to the gastric musculature. It is responsible for coordinated relaxation of the pyloric sphincter during gastric emptying.

Referred pain

The majority of the sensation of pain arising from the stomach is poorly localized, and in common with other structures of foregut origin, is referred to the central epigastrium. Pain arising from the region of the gastro-oesophageal junction is commonly referred to the lower retrosternal and subxiphoid areas.

MICROSTRUCTURE

The gastric wall consists of the major layers found elsewhere in the gut, i.e. mucosa, submucosa, muscularis externa and serosa, together with gastric vessels and nerves (Figs 65.15, 65.16). The microstructure reflects the functions of the stomach as an expandable muscular sac lined by secretory epithelium, although there are local structural and functional variations in this pattern.

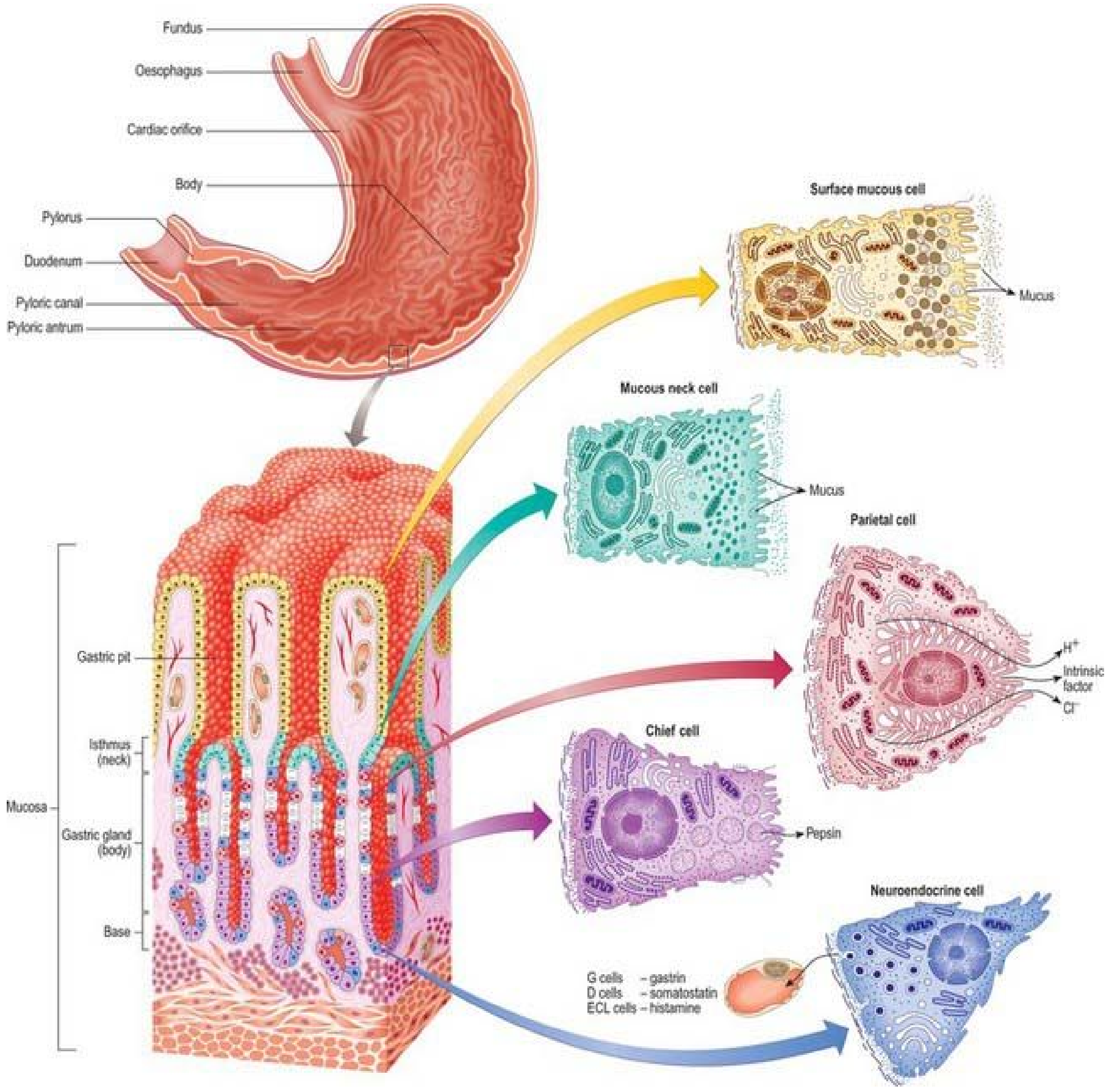
Fundus
Oesophagus
Cardiac orifice
Body
Pylorus
Duodenum
Pyloric canal
Pyloric antrum
Surface mucous cell
Mucus
Mucous neck cell
Mucus
Parietal cell
H^+
Intrinsic factor
Cl^-
Chief cell
Pepsin
Neuroendocrine cell
G cells – gastrin
D cells – somatostatin
ECL cells – histamine
Gastric pit
Isthmus (neck)
Mucosa
Gastric gland (body)
Base

Fig. 65.15 Principal regions of the interior of the stomach and the microstructure of tissues and cells within its wall. Undifferentiated, dividing cells are shown in white.

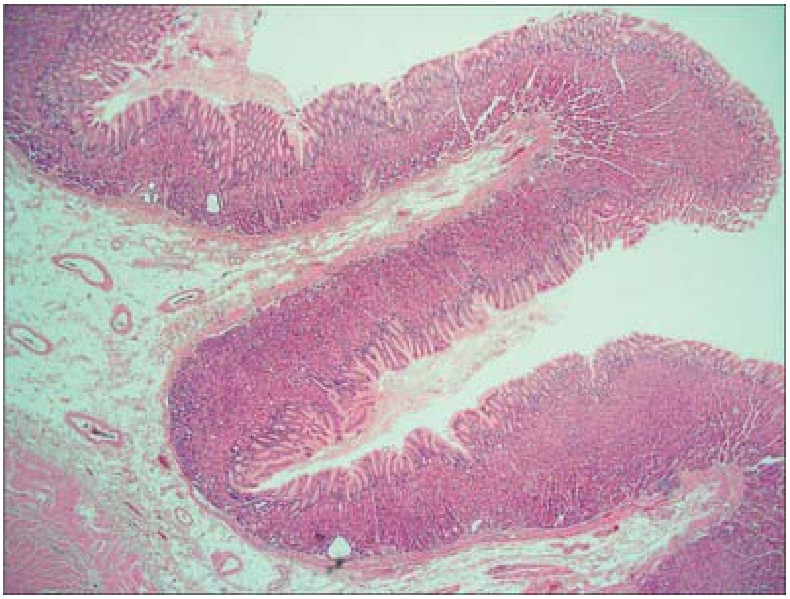

Fig. 65.16 Low power micrograph showing the stomach wall, thrown into longitudinal folds or rugae which are visible macroscopically. The surface epithelium is infolded microscopically to form gastric pits. Gastric glands extend through the thickness of the mucosal lamina propria and open into the bases of the gastric pits. A muscularis mucosae layer and submucosa follow the contours of the rugae. Part of the external muscularis layers is seen below left.

(By courtesy of Mr Peter Helliwell and Dr Joseph Mathew, Department of Histopathology, Royal Cornwall Hospitals Trust, UK.)

Mucosa

The mucosa is a thick layer with a soft, smooth surface that is mostly reddish brown in life but pink in the pyloric region. In the contracted stomach the mucosa is folded into numerous folds or rugae, most of which are longitudinal. They are most marked towards the pyloric end and along the greater curvature. The rugae represent large folds in the submucosal connective tissue (see below) rather than variations in the thickness of the mucosa covering them, and they are obliterated when the stomach is distended. As elsewhere in the gut, the mucosa is composed of a surface epithelium, lamina propria and muscularis mucosae.

Epithelium

When viewed microscopically at low magnification, the internal surface of the stomach wall appears honeycombed by small, irregular gastric pits approximately 0.2 mm in diameter (Figs 65.15, 65.16). The base of each gastric pit receives several long, tubular gastric glands that extend deep into the lamina propria as far as the muscularis mucosae. Simple columnar mucus-secreting epithelium covers the entire luminal surface including the gastric pits, and is composed of a continuous layer of surface mucous cells which release gastric mucus from their apical surfaces to form a thick protective, lubricant layer over the gastric lining. This epithelium commences abruptly at the cardiac orifice, where there is a sudden transition from oesophageal stratified squamous epithelium.

Gastric glands

Although all gastric glands are tubular, they vary in form and cellular composition in different parts of the stomach. They can be divided into three groups – cardiac, principal and pyloric. The most highly specialized are the principal glands.

Principal gastric glands

The principal glands are found in the body and fundus, three to seven opening into each gastric pit. Their junction with the base of the pit is the isthmus, immediately basal to this is the neck, and the remainder is the base. The walls of the gland contain at least five distinct cell types: chief, parietal, mucous neck, stem and neuroendocrine.

Chief (peptic) cells (Fig. 65.15) are the source of the digestive enzymes pepsin and lipase. They are usually basal in position and cuboidal in shape, and their nuclei are rounded and euchromatic. They contain secretory zymogen granules and their abundant cytoplasmic RNA renders them strongly basophilic. Parietal (oxyntic) cells are the source of gastric acid and of intrinsic factor, a glycoprotein necessary for the absorption of vitamin B_{12}. They are large, oval and strongly eosinophilic, and have centrally placed nuclei. Parietal cells occur intermittently along the walls of the more apical half of the gland, but can reach as far as the isthmus; they bulge laterally into the surrounding connective tissue. They have a unique ultrastructure related to their ability to secrete hydrochloric acid. The luminal side of the cell is deeply invaginated to form a series of blind-ended channels (canaliculi) that bear numerous irregular microvilli covered by a plasma membrane rich in H^+/K^+ ATPase antiporter channels. The latter actively secrete hydrogen ions into the lumen; chloride ions follow along the electrochemical gradient. The mitochondria-rich cytoplasm facing these channels contains a tubulo-vesicular system of abundant fine membranous tubules directed towards the canalicular surface. The precise structure of the cell varies with its secretory phase: when stimulated, the number and surface area of the microvilli increases up to five-fold, probably as a result of the rapid fusion of the tubulo-vesicular system with the plasma membrane. This process is reversed at the end of stimulated secretion, when the excess membrane retreats back into the tubulo-alveolar system and microvilli are lost.

Mucous neck cells are numerous at the necks of the glands and are scattered along the walls of the more basal regions. They are typical mucus-secreting cells, displaying apical secretory vesicles containing mucins, and basally displaced nuclei: their products are distinct histochemically from those of the superficial mucous cells.

Stem cells are relatively undifferentiated mitotic cells from which the other types of gland cell are derived. They are relatively few in number, and are situated in the isthmus of the gland and the bases of the gastric pits. Stem cells are columnar and possess a few short apical microvilli. They periodically undergo mitosis; their progeny migrate either apically, to differentiate into new surface mucous cells, or basally, to form mucous neck, parietal, chief or neuroendocrine cells. All of these cells have a limited lifespan, especially the mucus-secreting types, and so they are constantly replaced. The typical replacement period for surface mucous cells is 3 days, and for mucous neck cells is 1 week. Other cell types appear to live much longer.

Neuroendocrine (enteroendocrine) cells occur in all types of gastric gland, but more frequently in the body and fundus of the stomach. They are situated mainly in the deeper parts of the glands, among the chief cells. They are basally situated, pleomorphic cells and display irregular nuclei surrounded by granular cytoplasm that contains clusters of large (0.3 μm) secretory granules. Neuroendocrine cells synthesize a number of biogenic amines and polypeptides that are important in the control of gut motility and glandular secretion. They are part of the system of dispersed neuroendocrine cells: in the stomach they include G cells, which secrete gastrin; D cells, which secrete somatostatin; and ECL (enterochromaffin-like) cells, which secrete histamine.

Cardiac glands

Cardiac glands are confined to a small area near the cardiac orifice: some are simple tubular glands, others are compound branched tubular. Mucus-secreting cells predominate; parietal and chief cells are present, but sparse.

Pyloric glands

Pyloric glands empty via groups of two or three short convoluted tubes into the bases of the deep gastric pits of the pyloric antrum: the pits occupy about two-thirds of the mucosal depth (Fig. 65.17). The glands are populated mainly by mucus-secreting cells, but they also contain neuroendocrine cells, especially G cells, which secrete gastrin when activated by appropriate mechanical stimulation (causing increased gastric motility and secretion of gastric juices). Although parietal and chief cells are scarce, parietal cells are always present in both fetal and postnatal pyloric glands, and may also appear in the duodenal mucosa, proximally near the pylorus, in adult tissue.

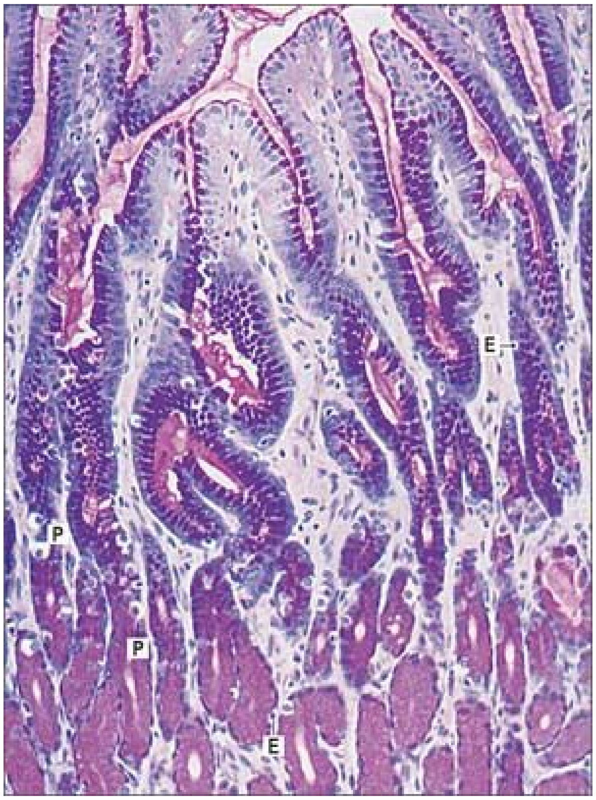

Fig. 65.17 Micrograph showing the pyloric region of the stomach. Pyloric glands are stained with the periodic acid-Schiff (PAS) technique to show mucin (magenta) in the gastric pits and glands. Pale staining cells are the larger parietal cells (P) and smaller enteroendocrine cells (E).

(By permission from Dr JB Kerr, Monash University, from Kerr JB 1999 Atlas of Functional Histology. London: Mosby.)

Lamina propria

The lamina propria forms a connective tissue framework between the glands. It contains small masses of lymphoid tissue, gastric lymphatic follicles, which resemble solitary intestinal follicles (especially in early life). It also contains a complex periglandular vascular plexus involved in the maintenance of the mucosal environment, e.g. the removal of bicarbonate produced in the tissues as a counterpart to acid secretion, and neural plexuses rich in both sensory and motor terminals.

Muscularis mucosae

The muscularis mucosae is a thin layer of smooth muscle fibres lying external to the layer of glands, arranged as continuous inner circular and outer longitudinal layers, and a discontinuous external circular layer. The inner layer sends strands of smooth muscle cells between the glands: their contraction probably assists in emptying into the gastric pits.

Submucosa

The submucosa is a variable layer of loose connective tissue. It contains thick bundles of collagen, numerous elastin fibres, blood vessels and nervous plexuses, including the ganglionated submucosal (Meissner's) plexus.

Muscularis externa

The muscularis externa is a thick muscle coat immediately under the serosa, with which it is closely connected by subserous loose connective tissue. From innermost outwards, it contains oblique, circular and longitudinal layers of smooth muscle fibres. The layers are not always easily separated: the circular layer is poorly developed in the oesophageal region, but is thickened at the distal pyloric antrum to form the anular pyloric sphincter; the outer longitudinal layer is most pronounced in the upper two-thirds of the stomach; the inner oblique layer is most obvious in the lower half.

The actions of the muscularis externa of the stomach produce a churning movement that mixes food with the gastric secretions. When the muscles contract, they reduce the volume of the stomach and throw the mucosa into longitudinal folds or rugae (see above). The folds flatten as the stomach distends with food and the musculature relaxes and thins. Muscle activity is controlled by a network of unmyelinated autonomic nerve fibres and their ganglia which lie between the muscle layers in the myenteric (Auerbach's) plexus.

Serosa or visceral peritoneum

The serosa is an extension of the visceral peritoneum. It covers the entire surface of the stomach other than along the attachments of the greater and lesser omenta to the greater and lesser curvatures respectively, where the peritoneal layers are separated by vessels and nerves, and over a small posteroinferior area near the cardiac orifice, where the stomach contacts the diaphragm at the reflections of the gastrophrenic and left gastropancreatic folds.

REFERENCES

Dio LJ, Anderson MC. The ‘Sphincters’ of the Digestive System. Baltimore: Williams and Wilkins, 1968.

panese Gastric Cancer Association. Japanese classification of gastric carcinoma. *Gastric Cancer*. 1998;1:10-24. 2nd English edition.

panese Research Society for Gastric Cancer. Japanese Classification of Gastric Carcinoma. Tokyo: Kanehara & Co Ltd, 1998. and Gastric Cancer 1: 10–24, 25–30

A detailed, widely accepted, description of the lymph node fields of the upper abdominal viscera, particularly in relation to malignancy..

wok H, Marriz Y, Al-Ali S, Windsor JA. Phrenoesophageal ligament revisited. *Clin Anat*. 1999;12:164-170.

ittal RK, Goyal RK 2006 Sphincter mechanisms at the lower end of the esophagus. GI Motility online.

quet KJ. Causes and mechanisms of oesophageal varices development. *Med Sci Monit*. 2000;6:915-928.

terson WG. The normal anti-reflux mechanism. *Chest Surg Clin N Am*. 2001;11:473-483.

lverstein FE, Tytgat GNJ. Atlas of Gastrointestinal Endoscopy, 2nd edition. New York: Gower Medical Publishing, 1991.

CC, Sobin LH, Wittekind CH. TNM classification of malignant tumours, 5th edition, Berlin: Springer-Verlag, 1997.

CHAPTER 66

Small intestine

OVERVIEW

The small intestine consists of the duodenum, jejunum and ileum. It extends from the distal end of the pyloric canal to the ileocaecal valve, an overall length of 5 metres (3–7 metres) in the living adult. The duodenum extends up to the duodenojejunal junction, and the remaining small intestine is often referred to as the 'small bowel', of which the proximal two-fifths is referred to as the jejunum and the distal three-fifths as the ileum. There is no clear distinction between the two parts, but there is a gradual change in morphology from the proximal to distal ends of the small bowel. The distal 30 cm or so of the ileum is often referred to as the terminal ileum, which has some specialized physiological functions.

The duodenum lies mostly in the upper retroperitoneum. The jejunum and ileum occupy the central and lower parts of the abdominal cavity and usually lie within the boundary formed by the abdominal colon; they are attached to the posterior abdominal wall by a mesentery which allows considerable mobility of the loops of small bowel. In the supine position, loops of jejunum may be found anterior to the transverse colon, stomach and even lesser omentum, whereas in the upright position, loops of ileum may descend into the pelvis anterior to the rectum and, in women, may occupy the rectouterine pouch. The upper jejunum and some ileum are often covered anteriorly by the greater omentum. The jejunum and ileum are covered by peritoneum on all but their mesenteric borders, here the adipose connective tissue of the mesentery abuts the muscular wall. The serosal peritoneum is continuous with the peritoneum enclosing the tissues of the mesentery. Mesenteric fat covers 20% of the circumference wall of the ileum and somewhat less of the jejunum.

DUODENUM

The adult duodenum is 20–25 cm long and is the shortest, widest and most predictably placed part of the small intestine. It is only partially covered by peritoneum, although the extent of the peritoneal covering varies along its length: the proximal 2.5 cm is intraperitoneal, and the remainder is retroperitoneal. The duodenum forms an elongated ‘C’ that lies between the level of the first and third lumbar vertebrae in the supine position. The lower ‘limb’ of the C extends further to the left of the midline than the upper limb. The head and uncinate process of the pancreas lie within the concavity of the duodenum which is ‘draped’ over the prominence formed from the lumbar spine, the duodenum therefore bends in an antero-posterior direction as well as following the form of a ‘C’. The duodenum lies entirely above the level of the umbilicus and is described as having four parts (Figs 66.1, 66.2).

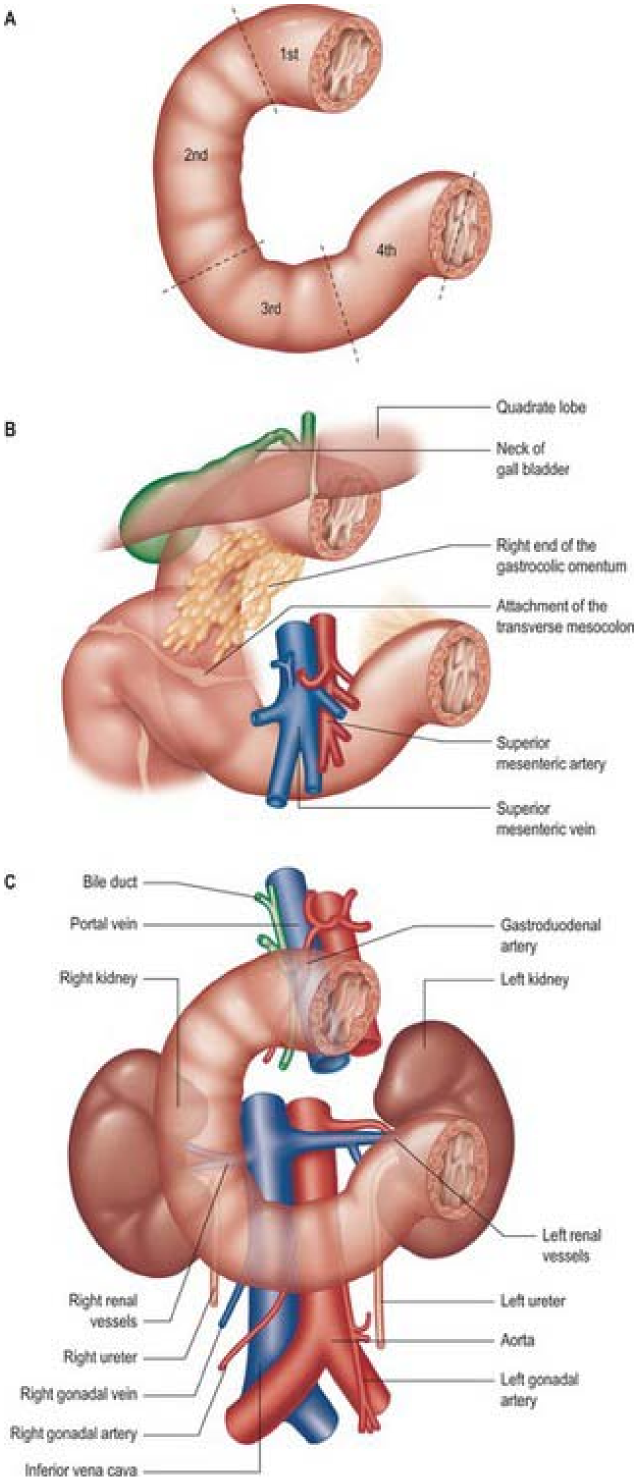
A
1st
2nd
3rd
4th
B
Quadrate lobe
Neck of gall bladder
Right end of the gastrocolic omentum
Attachment of the transverse mesocolon
Superior mesenteric artery
Superior mesenteric vein
C
Bile duct
Portal vein
Right kidney
Gastroduodenal artery
Left kidney
Left renal vessels
Right renal vessels
Right ureter
Right gonadal vein
Right gonadal artery
Inferior vena cava
Left ureter
Aorta
Left gonadal artery

Fig. 66.1 **A**, The four parts of the duodenum. **B&C**, The relations of the duodenum: **B**, anterior surface; **C**, posterior surface.

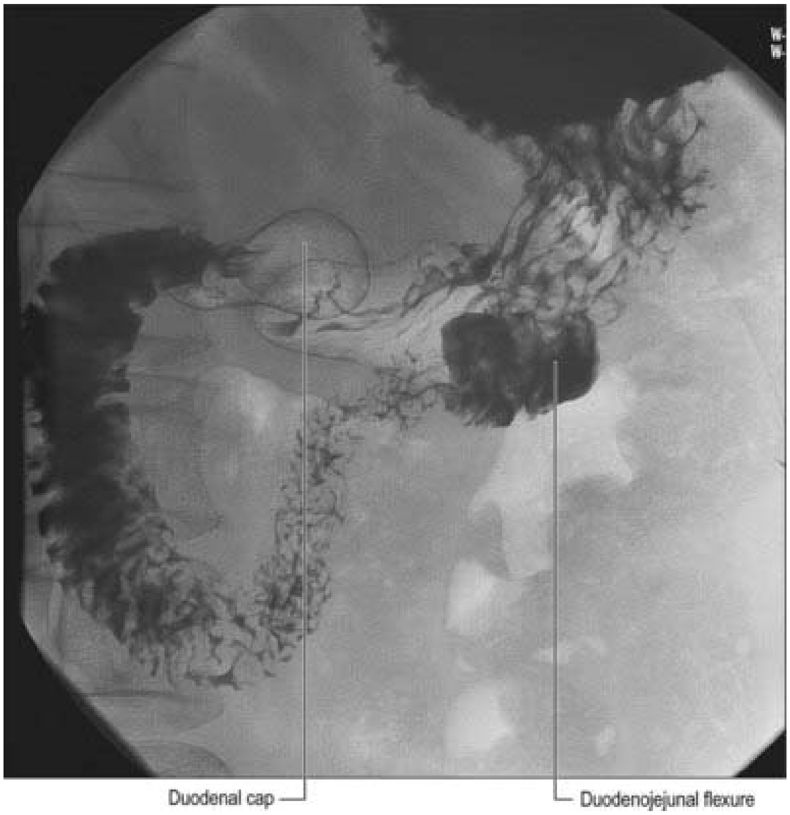
Duodenal cap
Duodenojejunal flexure

Fig. 66.2 Contrast radiographic appearance of the duodenum showing a distended duodenal cap and the remainder of the duodenum up to the duodenojejunal flexure.

FIRST (SUPERIOR) PART

The first, and most mobile, part of the duodenum is about 5 cm long. It starts as a continuation of the duodenal end of the pylorus and ends at the superior duodenal flexure. Peritoneum covers the anterior and superior part of its posterior aspect close to the pylorus, where the duodenum forms part of the anterior wall of the epiploic foramen. Here the lesser omentum is attached to its upper border and the greater omentum to its lower border. The first 2 or 3 cm have a bland internal mucosal appearance and readily distend on insufflation during endoscopy. This part is frequently referred to as the duodenal ‘cap’. It has a triangular, homogeneous appearance during contrast radiology, shows the same pattern of internal rugae as the pylorus, and is often visible on plain radiographs of the abdomen as an isolated triangular gas shadow to the right of the first or second lumbar vertebra. The duodenum next passes superiorly, posteriorly and laterally for 5 cm before curving sharply inferiorly into the superior duodenal flexure: it rapidly becomes more retroperitoneal during this part of its course, until peritoneum only covers its anterior aspect. From the end of the duodenal cap, its internal appearance is characterized by extensive, deep mucosal folds that involve up to half of the circumference of the lumen. Even during endoscopic insufflation, these folds are pronounced (Fig. 66.3) and they are readily seen on contrast radiographs. The section from the duodenal cap to the superior duodenal flexure lies posterior and inferior to the quadrate lobe of the liver.

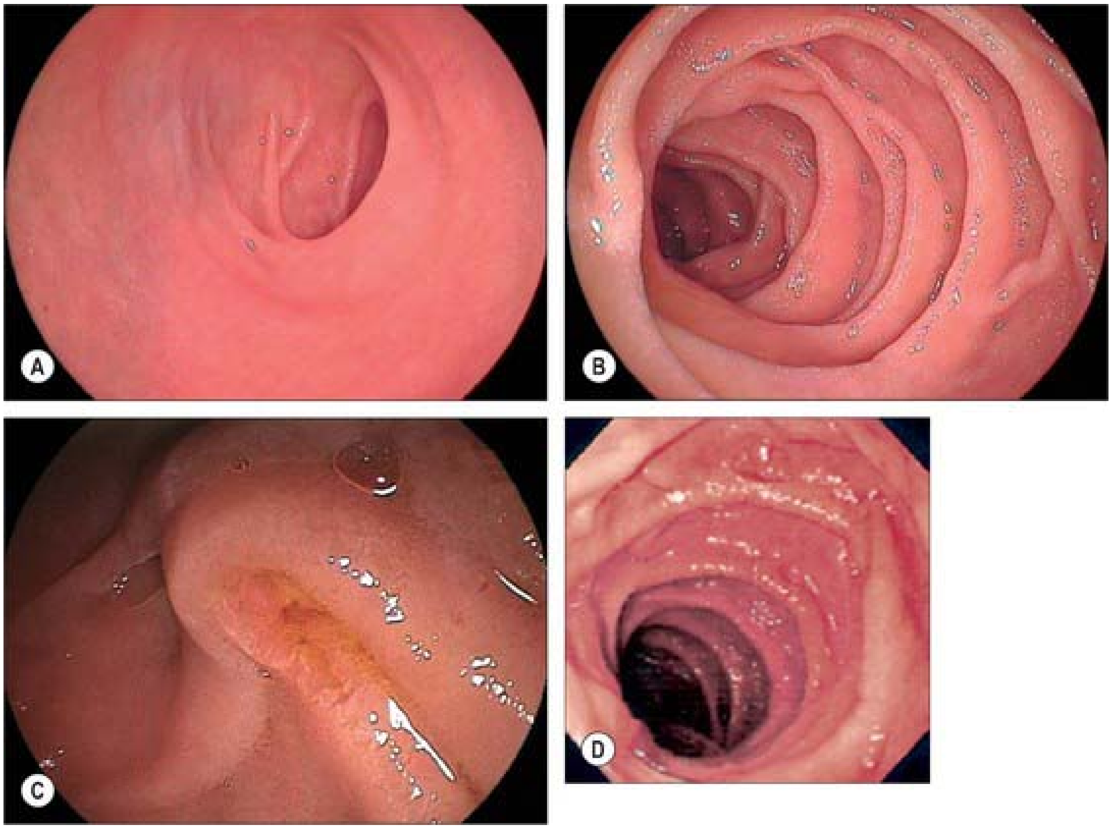

Fig. 66.3 Endoscopic appearance of the duodenum: **A**, Duodenal cap (first part). **B**, Second part showing the pronounced, ‘branched’ mucosal folds. **C**, Major duodenal papilla. **D**, Third part.

The first part of the duodenum lies anterior to the gastroduodenal artery, common bile duct and portal vein and anterosuperior to the head and neck of the pancreas. It is posterior to the neck of the gallbladder. The gastroduodenal artery lies immediately posterior to the posterior wall of the duodenum: penetrating peptic ulceration in the posterior wall and subsequent erosion of the gastroduodenal artery may lead to dramatic haemorrhage. Penetrating peptic ulceration in the anterior wall may lead to free perforation into the peritoneal cavity because the anterior surface of the first part is covered only by peritoneum.

The common hepatic and hepatoduodenal lymph nodes lie close to the first part of the duodenum and can be visualized using endoscopic ultrasound. This may be important in the staging of gastric, pancreatic or bile duct tumours. The proximity of the common bile duct to the first part of the duodenum allows endoscopic ultrasound examination of the distal common bile duct and the formation of a surgical anastomosis between bile duct and duodenum (choledochoduodenostomy) when required.

The junction of the first and second parts of the duodenum lies posterior to the neck of the gallbladder.

SECOND (DESCENDING) PART

The second part of the duodenum is 8–10 cm long. It starts at the superior duodenal flexure and runs inferiorly in a gentle curve, convex to the right side of the vertebral column and extending to the lower border of the third lumbar vertebral body. It then turns sharply medially into the inferior duodenal flexure which marks its junction with the third part of the duodenum. It is covered by peritoneum only on its upper anterior surface, lies posterior to the neck of the gallbladder and the right lobe of the liver at its start, and is crossed anteriorly by the transverse colon. The medial end of the gastrocolic omentum and the origin of the transverse mesocolon are attached to the anterior surface of the duodenum by loose connective tissue. Below the attachment of the transverse mesocolon, the connective tissue and vessels forming the mesentery of the upper ascending colon and hepatic flexure are loosely attached to its anterior surface. This section of duodenum is at risk of injury during surgical mobilization of the ascending colon.

The second part lies anterior to the hilum of the right kidney, the right renal vessels, the edge of the inferior vena cava and the right psoas major. The head of the pancreas and the common bile duct are medial and the hepatic flexure is above and lateral. A small part of the pancreatic head is sometimes embedded in the medial duodenal wall, and pancreatic ‘rests’ in the duodenal wall may produce small filling defects on contrast radiology. The internal appearance is similar to that of the distal portion of the first part of the duodenum, with pronounced mucosal folds (Fig. 66.3). The common bile duct and pancreatic duct enter the medial wall obliquely and usually unite to form the common hepatopancreatic ampulla. The narrow distal end opens on the summit of the major duodenal papilla (ampulla of Vater), which is situated on the posteromedial wall of the second part, 8–10 cm distal to the pylorus. There are variants of the ductal anatomy. The most common is a second, accessory pancreatic duct which may open 2 cm above the major papilla on a minor duodenal papilla. Peptic ulceration of the second part of the duodenum is less common than that of the first part, and tends to occur on the anterior or lateral wall.

Duodenal diverticula

The duodenum is the most common site for a diverticulum in the small intestine. Diverticula are congenital and usually solitary. They almost always arise in the medial wall of the second part of the duodenum, intimately related to the head of the pancreas, such that the major duodenal papilla may frequently be found either on the mucosal fold at the mouth of a diverticulum or arising from the mucosa within the body of a diverticulum, particularly on the superomedial wall. This may complicate interpretation of contrast radiographs of the duodenum or biliary system, and may cause difficulties during attempted endoscopic cannulation of the papilla because the diverticulum may restrict access. If the papilla is located on or close to the anterior wall of a diverticulum, the procedure of opening the ampulla with an electrocautery current during attempted cannulation (sphincterotomy) is made more hazardous because the wall is thin at this point and so there is a risk of free perforation into the peritoneal cavity.

THIRD (HORIZONTAL) PART

The third part of the duodenum starts at the inferior duodenal flexure and is approximately 10 cm long. It runs from the right side of the lower border of the third lumbar vertebra, angled slightly superiorly, across to the left, anterior to the inferior vena cava, becoming continuous with the fourth part in front of the abdominal aorta. It lies posterior to the transverse mesocolon, the origin of the small bowel mesentery and the superior mesenteric vessels. The lower portion of its anterior aspect is covered by peritoneum which is reflected anteriorly to form the posterior layer of the origin of the small bowel mesentery. The anterior surface of the left lateral end, close to the junction with the fourth part, is also covered with peritoneum.

The third part is anterior to the right ureter, right psoas major, right gonadal vessels, inferior vena cava and abdominal aorta (at the origin of the inferior mesenteric artery), and inferior to the head of the pancreas. Anteroinferiorly, loops of jejunum lie in the right and left infracolic compartments. The mid portion of the third part lies in the angle between the superior mesenteric vessels, just below their origin, anteriorly, and the abdominal aorta posteriorly: very rarely, this arrangement is associated with intermittent symptoms of obstruction of the duodenum at this point.

FOURTH (ASCENDING) PART

The fourth part of the duodenum is 2.5 cm long. It starts just to the left of the aorta, runs superiorly and laterally to the level of the upper border of the second lumbar vertebra, then turns sharply anteroinferiorly at the duodenojejunal flexure to become continuous with the jejunum. The main trunk of the inferior mesenteric vein lies either posterior to the duodenojejunal flexure or beneath the adjacent peritoneal fold. (The duodenojejunal flexure is a useful landmark to locate the vein radiologically or surgically.) The aorta, left sympathetic trunk, left psoas major, left renal and left gonadal vessels are all posterior relations, the left kidney and left ureter are posterolateral, and the upper part of the root of the small bowel mesentery, the left lateral transverse mesocolon and transverse colon, which separate it from the stomach, are anterior. The peritoneum of the root of the small bowel mesentery continues over its anterior surface. The lower border of the body of the pancreas is superior.

At its left lateral end, the fourth part becomes progressively covered in peritoneum on its superior and inferior surfaces, such that it is suspended from the retroperitoneum by a double fold of peritoneum, the ligament of Treitz, at the start of the duodenojejunal flexure. The ligament of Treitz may contain a small slip of muscle, the suspensory muscle of the duodenum. When present, the suspensory muscle contains skeletal muscle fibres that run from the left crus of the diaphragm to connective tissue around the coeliac axis, and smooth muscle fibres that run from the coeliac axis: its function is unknown. It is an important landmark in the radiological diagnosis of incomplete rotation and malrotation of the small intestine (see Ch. 73). The ligament of Treitz does not form part of the duodenal mesentery because the vascular supply to the fourth part of the duodenum continues to enter its wall from the posteromedial aspect.

VASCULAR SUPPLY AND LYMPHATIC DRAINAGE

Arteries

The main vessels supplying the duodenum are the superior and inferior pancreaticoduodenal arteries. The first and second parts also receive contributions from several sources including the right gastric, supraduodenal, right gastroepiploic, hepatic and gastroduodenal arteries. Branches of the superior pancreaticoduodenal artery may contribute to the supply of the pyloric canal, with a minor degree of anastomosis to the gastric arteries in the muscular layer across the pyloroduodenal junction (Fig. 66.4).

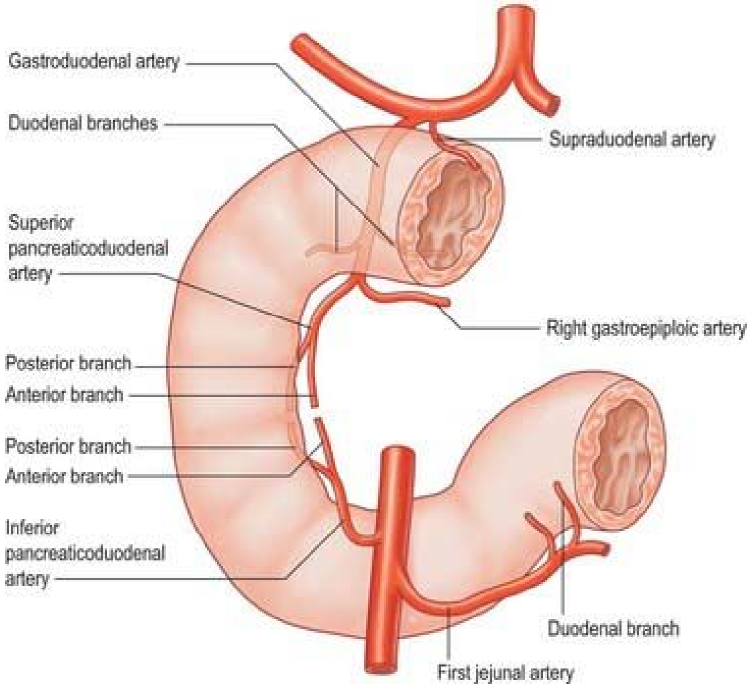
Gastroduodenal artery
Duodenal branches
Supraduodenal artery
Superior pancreaticoduodenal artery
Right gastroepiploic artery
Posterior branch
Anterior branch
Posterior branch
Anterior branch
Inferior pancreaticoduodenal artery
Duodenal branch
First jejunal artery

Fig. 66.4 The arterial supply of the duodenum. Only representative branches of the small vessels, which may be multiple, are shown.

Gastroduodenal artery

The gastroduodenal artery usually arises from the common hepatic artery behind, or sometimes above, the first part of the duodenum. It descends between the first part of the duodenum and the neck of the pancreas, immediately to the right of the peritoneal reflection from the posterior surface of the duodenum. It usually lies to the left of the common bile duct but occasionally is anterior. At the lower border of the first part of the duodenum it divides into the right gastroepiploic and superior pancreaticoduodenal arteries. Before its division, the lowest part of the artery gives rise to small branches that supply the pyloric end of the stomach and the pancreas, and retroduodenal branches that supply the first part and the proximal portion of the second part of the duodenum directly. Although the gastroduodenal artery usually branches from the common hepatic artery, it may also arise as a trifurcation with the right and left hepatic arteries, or from the superior mesenteric artery or the left hepatic artery (occasionally), or from the coeliac axis or right hepatic artery (rarely).

The supraduodenal artery often arises from the gastroduodenal artery behind the upper border of the first part of the duodenum and supplies the superior aspect of the first part; it may occasionally arise from the common hepatic artery or right gastric artery. Because of its close relationship to the posteromedial wall of the second part of the duodenum, deeply penetrating ulcers or tumours of the duodenum may cause torrential bleeding from the gastroduodenal ‘artery of haemorrhage’, not least because of the profuse arterial network in the region ensures a high flow rate in the vessel.

Superior pancreaticoduodenal arteries

The superior pancreaticoduodenal artery is usually double. The anterior artery is a terminal branch of the gastroduodenal artery and descends in the anterior groove between the second part of the duodenum and the head of the pancreas. It supplies branches to the first and second parts of the duodenum and to the head of the pancreas, and anastomoses with the anterior division of the inferior pancreaticoduodenal artery. The posterior artery is usually a separate branch of the gastroduodenal artery and is given off at the upper border of the first part of the duodenum. It descends to the right, anterior to the portal vein and common bile duct as the latter lies behind the first part of the duodenum. It then runs behind the head of the pancreas, crosses posterior to the common bile duct (which is embedded in the head of the pancreas), enters the duodenal wall and anastomoses with the posterior division of the inferior pancreaticoduodenal artery. The posterior artery supplies branches to the head of the pancreas, the first and second parts of the duodenum, and several branches to the lowest part of the common bile duct.

Inferior pancreaticoduodenal artery

The inferior pancreaticoduodenal artery usually arises from the superior mesenteric artery or its first jejunal branch, near the superior border of the third part of the duodenum. It crosses behind the superior mesenteric vein and divides directly into anterior and posterior branches. The anterior branch passes to the right, anterior to the lower border of the head of the pancreas, and runs superiorly to anastomose with the anterior superior pancreaticoduodenal artery. The posterior branch runs posteriorly and superiorly to the right, lying posterior to the lower border of the head of the pancreas, and anastomoses with the posterior superior pancreaticoduodenal artery. Both branches supply the pancreatic head, its uncinate process and the second and third parts of the duodenum. Occasionally the anterior and posterior branches arise separately from the superior mesenteric or first jejunal artery.

Jejunal artery branches

Branches from the first jejunal branch of the superior mesenteric artery supply the fourth part of the duodenum and frequently form an anastomosis with the terminal branch of the anterior inferior pancreaticoduodenal artery (which arises from the superior mesenteric artery). The fourth part of the duodenum therefore receives a potential collateral supply from the coeliac axis and superior mesenteric artery, which means that it is not commonly affected by ischaemia.

Veins

The duodenal veins drain ultimately into the portal vein. Submucosal and intramural veins give rise to pancreaticoduodenal veins that usually accompany the corresponding named arteries. The superior pancreaticoduodenal vein is formed medial to the mid point of the second part of the duodenum. It runs superomedially on the posterior surface of the head of the pancreas, passes posterior to the distal common bile duct and drains into the portal vein behind the neck of the pancreas. The inferior pancreaticoduodenal vein runs from the anteromedial aspect of the second part of the duodenum inferiorly in the groove between the second and third parts of the duodenum and the head of the pancreas. It usually drains into the superior mesenteric vein but may drain into the right gastroepiploic vein. Small veins from the first and upper second part of the duodenum may drain into the prepyloric vein and veins from the third and fourth parts may drain directly into the superior mesenteric vein.

Lymphatics

Duodenal lymphatics run to anterior and posterior pancreatic nodes that lie in the anterior and posterior grooves between the head of the pancreas and the duodenum: these nodes drain widely into the supra-pyloric, infrapyloric, hepatoduodenal, common hepatic and superior mesenteric nodes.

INNERVATION

The duodenum is innervated by both parasympathetic and sympathetic neurones.

Preganglionic sympathetic axons originate from neurones in the intermediolateral columns of the grey matter in the fifth to the 12th thoracic spinal segments. They travel via the greater and lesser splanchnic nerves to the coeliac plexus where they synapse on neurones in the coeliac ganglion: postganglionic axons are distributed to the duodenal wall via periarterial plexuses on the branches of the coeliac axis and superior mesenteric artery. The sympathetic nerves are vasoconstrictor to the duodenal vasculature and inhibitory to duodenal musculature.

The preganglionic parasympathetic supply is carried by vagal axons that are distributed via the coeliac plexus and which synapse on neurones in the duodenal wall. The parasympathetic supply is secretomotor to the duodenal mucosa and motor to the duodenal musculature. The sympathetic nerves are vasoconstrictor to the duodenal vasculature and inhibitory to duodenal musculature.

Referred pain

In common with other structures derived from the foregut, the visceral sensation of pain arising from the duodenum is poorly localized and referred to the central epigastrium.

JEJUNUM

The jejunum has a median external diameter of 4 cm and an internal diameter of 2.5 cm. It has a thicker wall than the ileum, and an extensive arterial blood supply that makes it appear redder than the ileum in the living. The plicae circulares are most pronounced in the proximal jejunum, where they are more numerous and deeper than elsewhere in the small bowel (Fig. 66.5A). They frequently ‘branch’ around the lumen and may appear to be ranged one on top of another, giving the jejunum a characteristic appearance during single contrast radiography (Fig. 66.6). Lymphoid aggregates are almost absent from the proximal jejunum, but are present distally, although they are fewer in number and smaller than in the ileum. Where present, they are usually discoid in shape and impalpable.

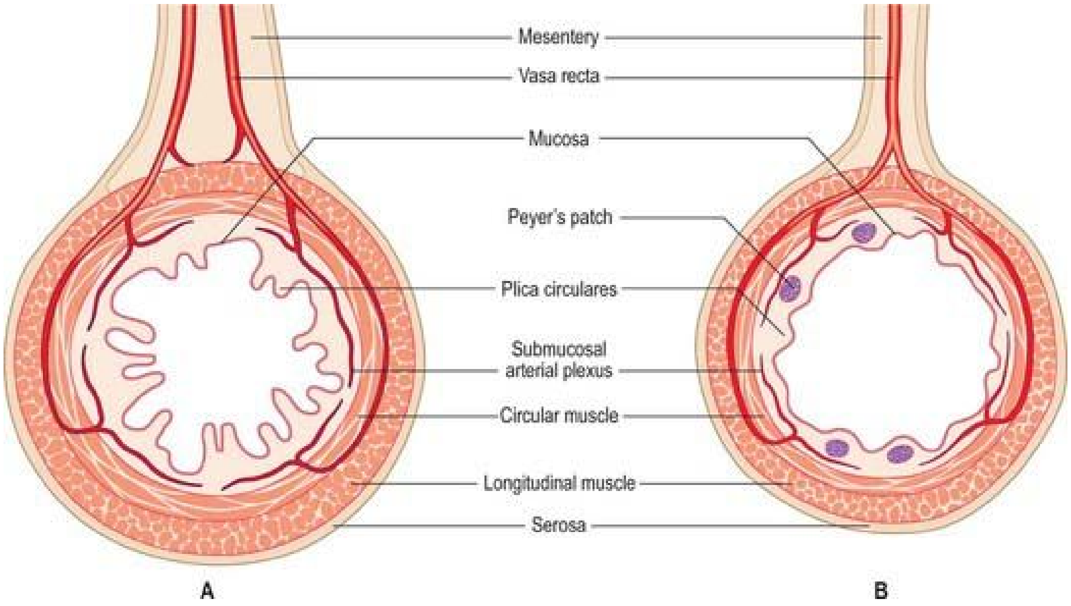
Mesentery
Vasa recta
Mucosa
Peyer's patch
Plica circulares
Submucosal arterial plexus
Circular muscle
Longitudinal muscle
Serosa
A
B

Fig. 66.5 Typical cross sections through the proximal jejunum (**A**) and terminal ileum (**B**). The mesenteric attachment is wider in the jejunum, and two leaves of vessels enter the bowel wall. The latter is also thicker in the jejunum.

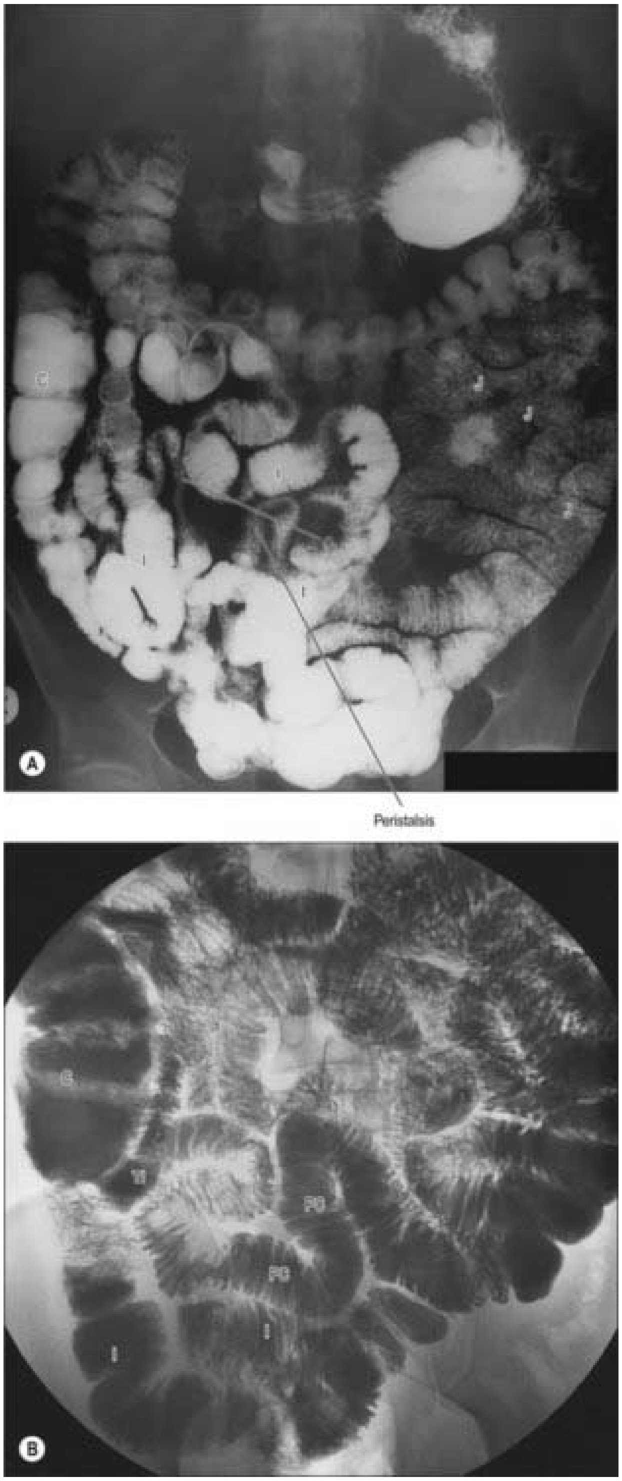

Fig. 66.6 Barium studies of the jejunum and ileum. **A**, Barium follow-through. The feathery appearance of the small intestine is due to the plicae circulares and is most prominent in the jejunum. The constrictions are the result of peristalsis. **B**, Small bowel enema (enteroclysis). The plicae

circulares are clearly demonstrated by this technique. C, caecum; I, ileum; J, jejunum; PC, plicae circulares; TI, terminal part of ileum.

In the supine position the jejunum usually occupies the upper left infracolic compartment, extending down to the umbilical region. The first one or two loops often occupy a recess between the left part of the transverse mesocolon and the left kidney. On supine radiological examination, the jejunal loops are characteristically situated in the upper abdomen, to the left of the midline, whereas the ileal loops tend to lie in the lower right part of the abdomen and pelvis. This distribution can be reversed during paralytic ileus or small bowel obstruction due to rotation around the mesenteric attachment following bowel distension.

Jejunal feeding

In situations where the stomach and duodenum are either unsuitable or unavailable for receiving oral nutrition, delivery of prepared feed to the jejunum is possible using either a surgically created jejunostomy or by insertion of a feeding tube. Because the jejunum is highly mobile, it is possible to bring the first or second loop of jejunum into contact with the abdominal wall to create a surgical jejunostomy. Insertion of a fine-bore feeding tube via the nose as far as the jejunum is also possible: the end of the feeding tube must lie beyond the duodenojejunal flexure to prevent reflux of the feed into the duodenum and stomach, and this is usually confirmed by radiological monitoring of the progress of the tube through the duodenum.

ILEUM

The ileum has a median external diameter of 3.5 cm and an internal diameter of 2 cm, and tends to have a thinner wall than the jejunum (Fig. 66.5B). The plicae circulares become progressively less obvious in the distal mucosa in the ileum; they tend to be single and flatter with less pronounced crests (Figs 66.6, 66.7), and the mucosa of the terminal ileum immediately proximal to the ileocaecal valve may appear almost flat. Lymphoid aggregates are larger and more numerous than in the jejunum and may be easily palpable in the terminal ileum. They are most prominent in early childhood and, when enlarged in viral infections, may form the apex of an ileo-ileal intussusception. They become less prominent prior to puberty, and attain adult morphology by late teenage years. In the supine position, the ileum lies mainly in the hypogastric region and right iliac fossa. The terminal ileum frequently lies in the pelvis, whence it ascends over the right psoas major and right iliac vessels, to end by opening into the ileocaecal valve in the right iliac fossa.

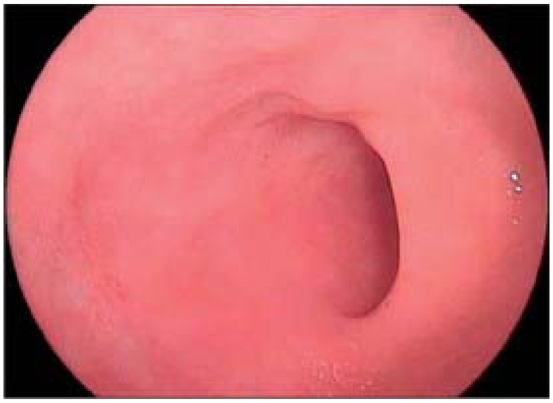

Fig. 66.7 Endoscopic appearance of the terminal ileum.

Meckel's diverticulum

An ileal diverticulum (of Meckel) exists in 3% of adults and represents the remnant of the proximal part of the intestino-vitelline duct. It projects from the antimesenteric border of the terminal ileum and is commonly located between 50 and 100 cm from the ileocaecal valve. It is variable in length (median 5 cm), often possessing a short ‘mesentery’ of adipose tissue that extends from the ileal mesentery up to its base. The lumen of the diverticulum usually has a calibre similar to that of the ileum. The tip is normally free but occasionally it may be connected to the anterior abdominal wall near the umbilicus by a fibrous band. The mucosa is typically ileal, but small heterotopic areas of gastric body type epithelium, pancreatic, colonic or other tissues may also occur in the wall of a diverticulum. Unopposed acid secretion by heterotopic gastric body type epithelium may occasionally give rise to bleeding in the adjacent normal ileal mucosa. Diverticular inflammation may mimic acute appendicitis; since Meckel’s diverticulum and the appendix are both derived from midgut structures, pain from either structure is referred to the periumbilical region.

VASCULAR SUPPLY AND LYMPHATIC DRAINAGE

Arteries

Branches from the superior mesenteric artery supply the jejunum and ileum. The arteries divide as they approach the mesenteric border, giving off numerous branches which extend between the serosal and muscular layers, supplying the muscle and forming an intricate sub-mucosal plexus that supplies the glands and villi. Although there is a profuse anastomotic network of arteries within the mesentery, anastomoses between the terminal branches close to the intestinal wall are few (Fig. 66.8). The intramural and submucosal arterial networks are not of large calibre, which means that flow along lengths of small bowel is limited to a few centimetres, and division or occlusion of several consecutive vasa recta may produce segmental, focal ischaemia. Division of more proximal vessels allows flow to continue in the arcades for moderately long lengths of intestine.

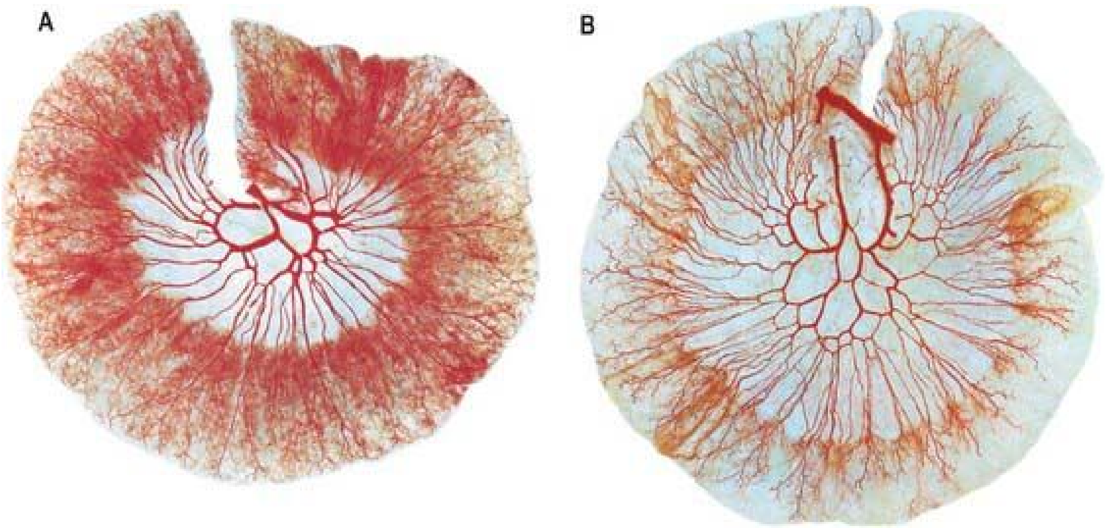

Fig. 66.8 Specimens of the jejunum (**A**) and ileum (**B**) from a cadaver where the superior mesenteric artery was injected with a red coloured mass of gelatin before fixation. Subsequently the specimens were dehydrated and then cleared in benzene followed by methyl salicylate. The largest vessels present are the jejunal and ileal branches of the superior mesenteric artery

and these are succeeded by anastomotic arterial arcades, which are relatively few in number (1–3) in the jejunum, becoming more numerous (5–6) in the ileum. From the arcades, straight arteries pass towards the gut wall; frequently, successive straight arteries are distributed to opposite sides of the gut. Note the denser vascularity of the jejunal wall.

(Specimens prepared by MCE Hutchinson; photographs by Kevin Fitzpatrick on behalf of GKT School of Medicine, London.)

Superior mesenteric artery

The superior mesenteric artery originates from the aorta 1 cm below the coeliac trunk, at the level of the intervertebral disk between the first and second lumbar vertebrae (Figs 66.9, 66.10). The angle of its origin from the aorta is acute, which makes cannulation via the transfemoral route somewhat difficult. The artery runs inferiorly and anteriorly, anterior to the uncinate process of the pancreas and the third part of the duodenum, and posterior to the splenic vein and the body of the pancreas. The left renal vein lies behind it and separates it from the aorta (Fig. 66.11). The artery crosses anterior to the inferior vena cava, right ureter and right psoas major as it descends in the root of the small bowel mesentery. Its calibre progressively decreases as successive branches are given off to loops of jejunum and ileum, and its terminal branch anastomoses with the ileocolic artery.

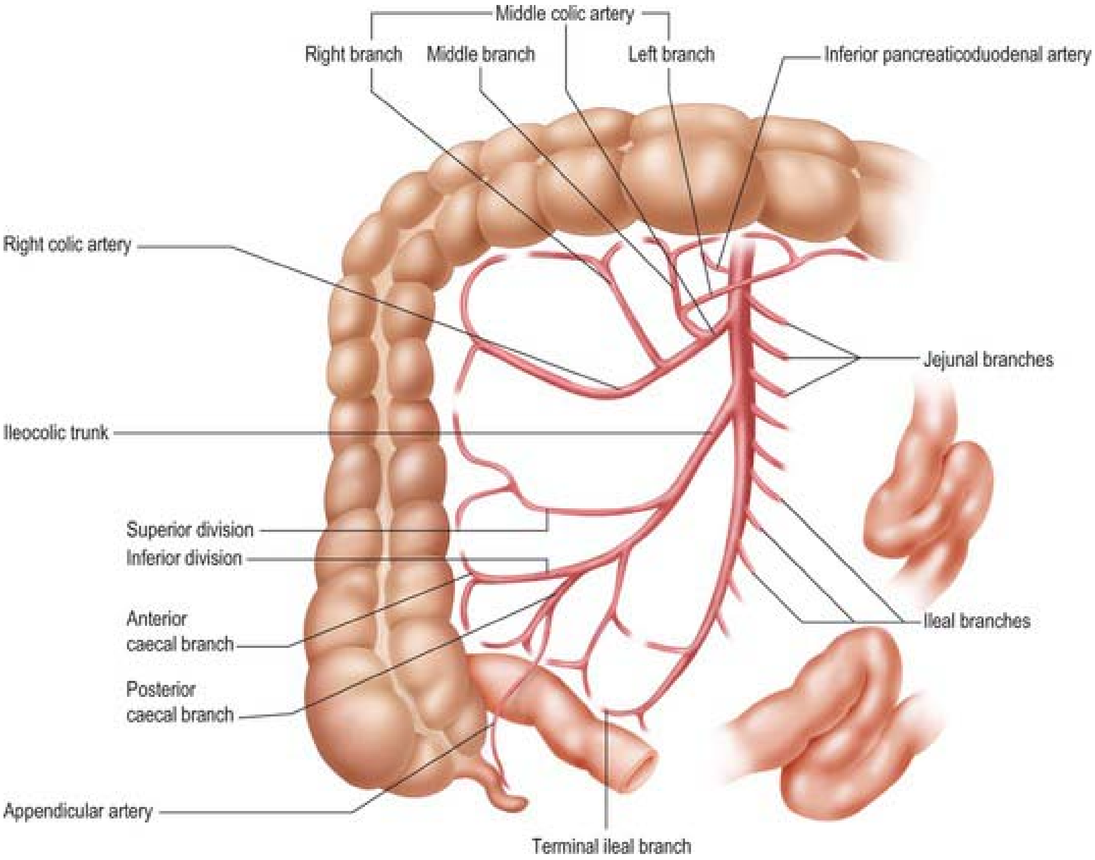
Middle colic artery
Right branch
Middle branch
Left branch
Inferior pancreaticoduodenal artery
Right colic artery
Jejunal branches
Ileocolic trunk
Superior division
Inferior division
Anterior caecal branch
Posterior caecal branch
Ileal branches
Appendicular artery
Terminal ileal branch

Fig. 66.9 The superior mesenteric artery and its branches. The outlines of representative ileal and jejunal loops, appendix, caecum, ascending and transverse colon are shown for reference. Only the origin of jejunal and ileal branches are shown. For details of arcades see **Fig. 66.8**.

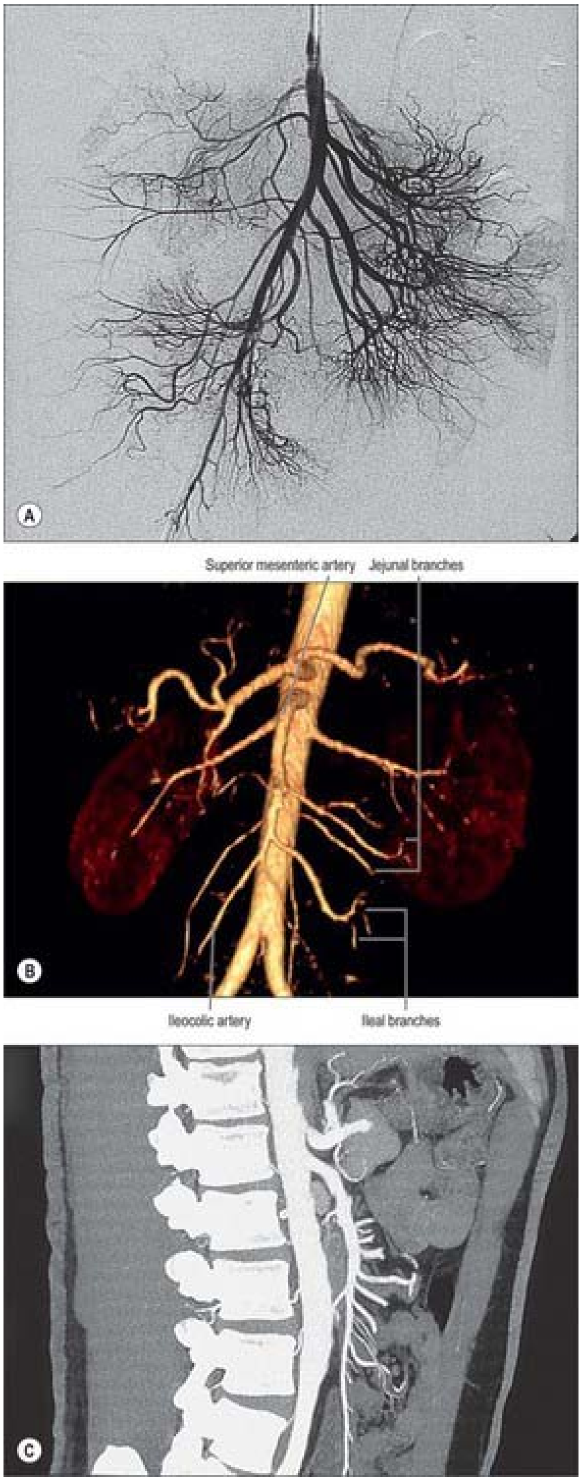
A
Superior mesenteric artery
Jejunal branches
B
Ileocolic artery
Ileal branches
C

Fig. 66.10 The superior mesenteric artery and its branches. **A**, Digital subtraction angiogram. **C**, Sagittal reformat of multislice CT angiogram.

(by courtesy of Dr Adam Mitchell, Charing Cross Hospital, London). ***B****, Surface shaded, volume rendered CT angiogram (by courtesy of Dr Nasir Khan, Chelsea and Westminster Hospital, London)*

(by courtesy of GE Worldwide Medical Systems)

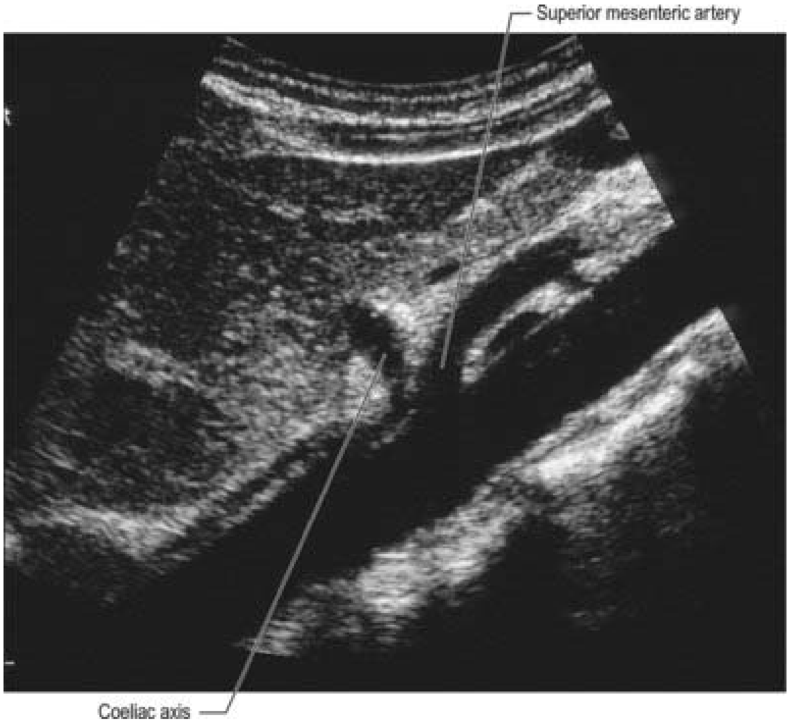

Fig. 66.11 Ultrasound image through the origin of the superior mesenteric artery, sagittal plane.

The superior mesenteric artery gives off middle colic, right colic (sometimes), ileocolic, jejunal and ileal branches. It may be the source of the common hepatic, gastroduodenal, accessory right hepatic, accessory pancreatic or splenic arteries, and may arise from a common coeliacomesenteric trunk. Its jejunal and ileal branches form arcades within the mesentery to a varying extent. The last of these arcades is said to form a 'marginal artery' of the small intestine, although the latter is irregular and not a single definable vessel. Straight arteries, the vasa recta, which supply the small intestine directly without further branches, are given off from this lowest arcade.

The remnant of the vitellointestinal artery (the embryonic artery which originally connected the intestinal circulation to the yolk sac) is usually obliterated; when present, it forms the artery supplying a Meckel's diverticulum. It is occasionally represented in the mesentery by a fibrous strand from the region of the last ileal branch.

Jejunal branches

There are usually five to ten jejunal branches which arise from the left side of the upper portion of the superior mesenteric artery (Figs 66.9, 66.10). They are distributed to the jejunum as a series of short arcades which form a single (occasionally double) tier of anastomotic arcs before giving rise to multiple vasa recta (Fig. 66.8). These vessels run almost parallel in the mesentery and are distributed alternately to opposite aspects of its wall where the two series of vessels form distinct ‘leaves’ within the mesentery. Small twigs supply regional lymph nodes and other structures in the mesentery.

Ileal branches

Ileal branches are more numerous than the jejunal branches but smaller in calibre. They arise from the left and anterior aspects of the superior mesenteric artery. The length of the mesentery is greater in the ileum and the branches form three, four or sometimes five tiers of arcs within the mesentery before giving rise to multiple vasa recta that run directly towards the ileal wall. The ileal branches run parallel in the mesentery and are distributed to alternate aspects of the ileum. They are longer and smaller than similar jejunal vessels, particularly in the distal ileum, and do not form such definite parallel ‘leaves’ of vessels. The vascular supply in the last loop of the terminal ileum is limited. There are usually only two separate arcades, peri-serosal and in the mid-zone of the mesentery. They each receive a contribution from the ileal branch of the ileocolic artery and the last ileal branch of the superior mesenteric artery and are often larger in calibre than the mid-ileal vessels. Other than this connection, few if any vessels connect the ileocolic and superior mesenteric arteries, which makes surgical exposure of the ileocolic artery up to its origin relatively simple.

Veins

Superior mesenteric vein

The superior mesenteric vein drains the small intestine, caecum, ascending and transverse parts of the colon (Fig. 66.12; see Fig. 60.8). It is formed in the right lower mesentery of the small bowel by the union of tributaries from the terminal ileum, caecum and vermiform appendix. It ascends in the mesentery to the right of the superior mesenteric artery, passes anterior to the right ureter, inferior vena cava, third part of the duodenum and uncinate process of the pancreas, and finally joins the splenic vein behind the neck of the pancreas to form the portal vein.

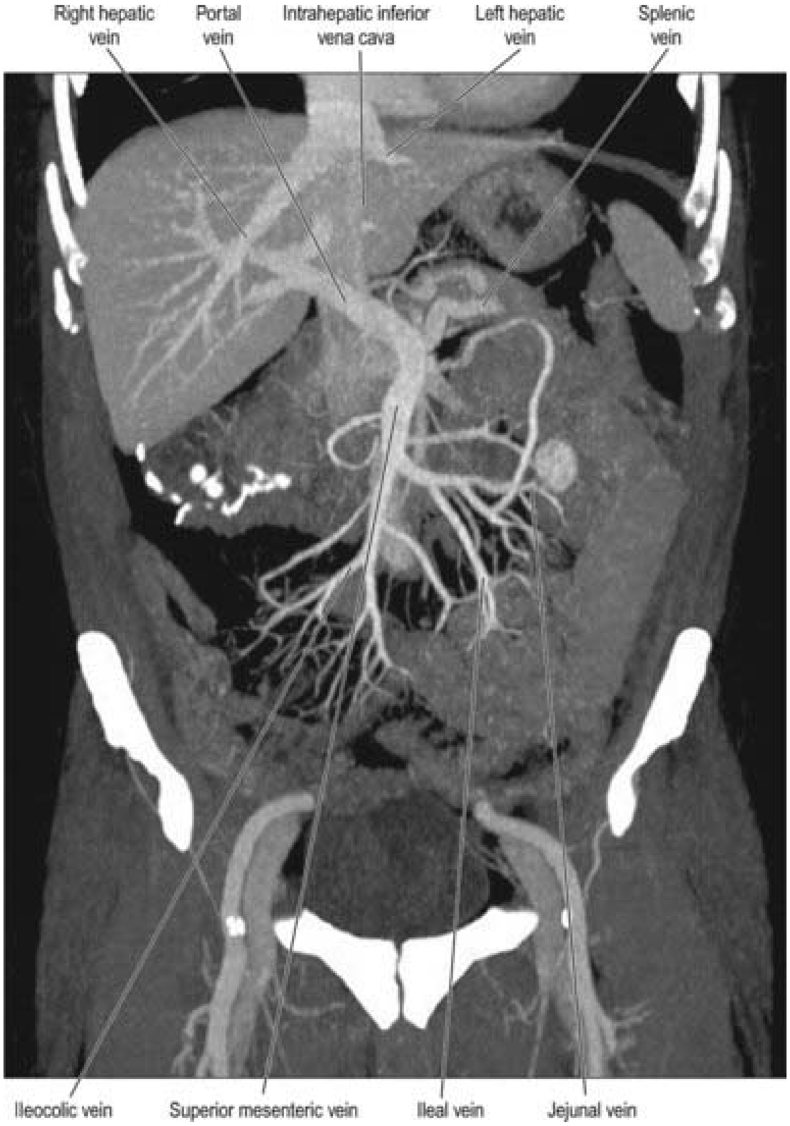
Right hepatic vein
Portal vein
Intrahepatic inferior vena cava
Left hepatic vein
Splenic vein
Ileocolic vein
Superior mesenteric vein
Ileal vein
Jejunal vein

Fig. 66.12 The superior mesenteric vein and its branches, CT venogram, coronal plane.

(Courtesy of Dr Nasir Khan, Chelsea and Westminster Hospital, London.)

Tributaries

The superior mesenteric vein receives jejunal, ileal, ileocolic, right colic (when present), middle colic, right gastroepiploic and pancreaticoduodenal veins in a similar distribution to the corresponding arteries.

Lymphatics

Lymph vessels, lacteals, are found in the mucosa and muscular coat of the small bowel. Lacteals from the villi arise from an intricate plexus in the mucosa and submucosa and are joined by vessels from lymph spaces at the bases of solitary lymphoid follicles. They drain to larger vessels at the mesenteric border of the gut. The lacteals of the muscular tunic form a close plexus that runs mostly between the two muscle layers; they communicate freely with mucosal vessels and open into vessels at the mesenteric border. Mesenteric lacteals pass between the layers of the mesentery and drain into a series of mesenteric lymph nodes which are arranged in tiers within the mesentery and which follow the same distribution as the regional arterial supply; they may form ‘chains’ along the major arteries. Elsewhere in the ileal and jejunal mesenteries the lacteals form an extensive network that affords a relatively wide field of lymph node drainage. This arrangement makes radical surgical resection of lymph nodes difficult if the vessels to the remaining unaffected small bowel are to be preserved. The mesenteric nodes drain into superior mesenteric nodes around the root of the superior mesenteric artery.

INNERVATION

The ileum and jejunum are innervated by parasympathetic and sympathetic fibres via the superior mesenteric plexus (see Figs 60.2–60.4). Preganglionic sympathetic axons originate from neurones in the intermediolateral grey matter of the mid-thoracic spinal segments and travel in the greater and lesser splanchnic nerves to the superior mesenteric ganglion where they synapse. Postganglionic axons accompany the superior mesenteric artery into the mesentery and are distributed along branches of the artery. The sympathetic nerves are vasoconstrictor to the vasculature and inhibitory to the musculature of the jejunum and ileum.

Preganglionic parasympathetic axons travel in the anterior and right vagus nerve and are secretomotor to the mucosa and motor to the musculature of the jejunum and ileum.

Referred pain

In common with other structures derived from the midgut, the visceral sensation of pain arising from the jejunum or ileum is poorly localized, and is usually referred to the periumbilical region or central epigastrium.

MICROSTRUCTURE

The intestinal wall is composed of mucosa, submucosa, muscularis externa and serosa or adventitia. The mucosa is thick and very vascular in the proximal small intestine, but thinner and less vascular distally. In places it is ridged by the underlying submucosa to form circular folds, plicae circulares, which protrude into the lumen; mucosal finger- or leaf-like intestinal villi cover the whole surface (Fig. 66.13). There are numerous simple tubular intestinal glands or crypts between the bases of the villi, and additional submucosal glands in the duodenum. The submucosa contains aggregates of lymphoid tissue, most numerous in the ileum.

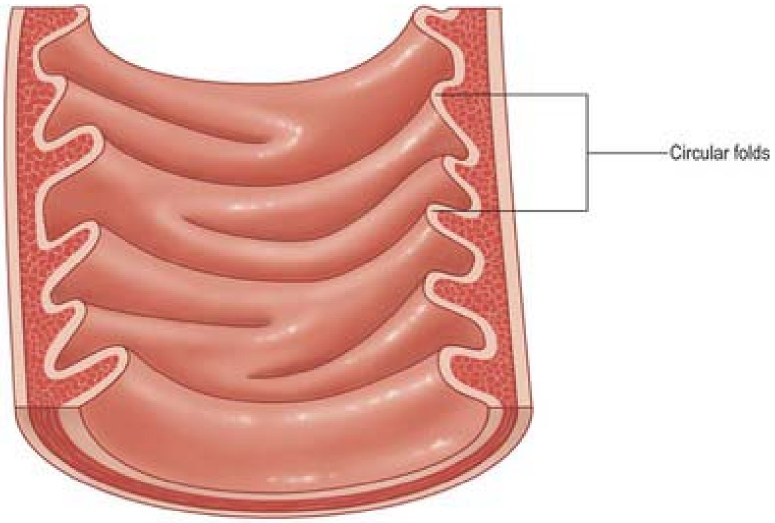

Fig. 66.13 Internal aspect of a representative sample of the proximal jejunum, showing circular folds.

Circular folds

Other than in the first part of the duodenum, large crescentic folds of mucosa project into the lumen of the small intestine, lying either transversely or slightly obliquely to its long axis (Fig. 66.14). Unlike gastric folds they are not lost during physiological distension of the intestine. Most extend round half or two-thirds of the luminal circumference, some are complete circles, some bifurcate and join adjacent folds, yet others are spiral but extend only once (occasionally two or three times) round the lumen. Larger folds are up to 8 mm deep at their broadest, but most are smaller than this, and larger folds often alternate with smaller ones. Folds begin to appear 2.5–5 cm beyond the pylorus. Distal to the major duodenal papilla they are large and close together, as they also are in the proximal half of the jejunum. From here to midway along the ileum they diminish, and they disappear almost completely in the distal ileum, which accounts for the thinness of this part of the intestinal wall. The circular folds slow the passage of the intestinal contents and increase the absorptive surface. They are visible in contrast and occasionally plain radiographs.

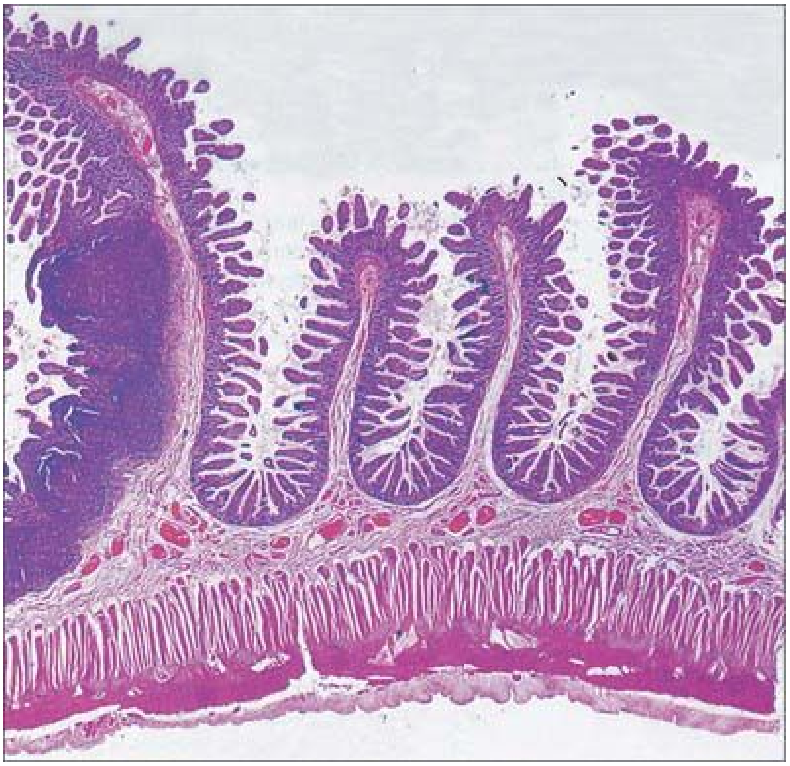

Fig. 66.14 Low-power micrograph showing several circular folds in the wall of the ileum. The folds are covered with villi projecting into the lumen and the submucosa extends into the core of each fold. Circular (innermost) and longitudinal smooth muscle layers form the underlying muscularis externa. Large masses of lymphoid tissue (Peyer’s patches) occupy the mucosa at the left of the field.

(By permission from Young B, Heath JW 2000 Wheater's Functional Histology. Edinburgh: Churchill Livingstone.)

Intestinal villi

Intestinal villi are highly vascular projections of the mucosal surface, just visible to the naked eye (Figs 66.15-66.17). They cover the entire intestinal mucosa, increase the surface area of the lumen about eight-fold, and give it a velvety texture. Villi are large and numerous in the duodenum and jejunum, and smaller and fewer in the ileum. In the first part of the duodenum they appear as broad ridges, become tall and foliate in the distal duodenum and proximal jejunum, and then gradually shorten to a finger-like form in the distal jejunum and ileum. Villi vary in density from 10 to 40 per square millimetre and from 0.5–1.0 mm in height (Fig. 66.15). Infoldings of the mucosa dip down from the base of the villi for a short distance into the lamina propria. These crypts (of Lieberkühn), are most prominent in the proximal small intestine (Fig. 66.16).

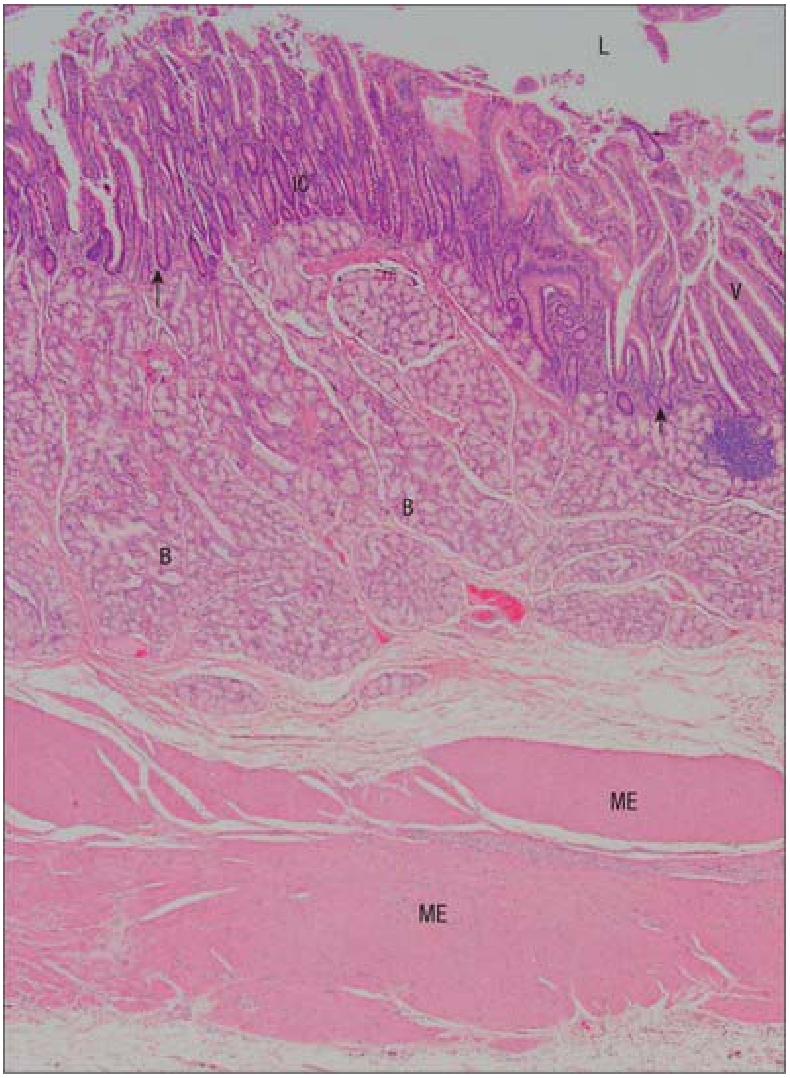

Fig. 66.15 Low power micrograph showing the wall of the duodenum, with villi (V) projecting into the lumen (L); intestinal crypts (IC) of Lieberkühn in the mucosa, seen mainly in transverse section; muscularis mucosae (arrows); submucosal seromucous (Brunner's) glands (B) and muscularis externa (ME).

(By courtesy of Mr Peter Helliwell and Dr Joseph Mathew, Department of Histopathology, Royal Cornwall Hospitals Trust, UK.)

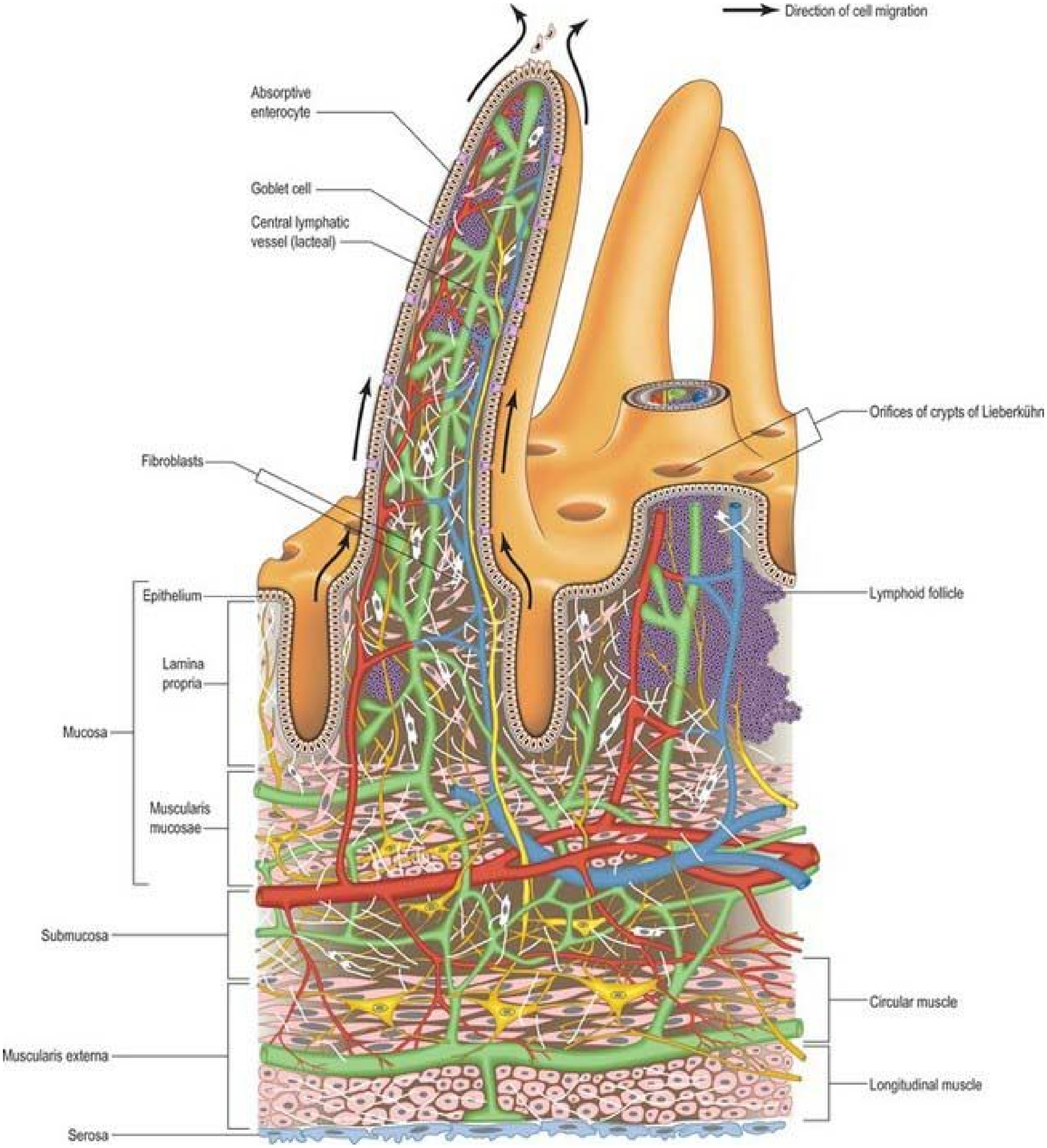
Direction of cell migration
Absorptive enterocyte
Goblet cell
Central lymphatic vessel (lacteal)
Fibroblasts
Orifices of crypts of Lieberkühn
Epithelium
Lamina propria
Mucosa
Muscularis mucosae
Lymphoid follicle
Submucosa
Circular muscle
Muscularis externa
Longitudinal muscle
Serosa

Fig. 66.16 The architecture of an intestinal villus. The various layers and cells are not drawn to scale.

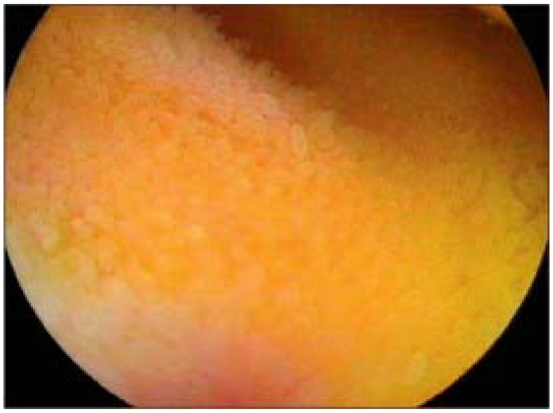

Fig. 66.17 Endoscopic appearance of the terminal villi (magnified).

Mucosa

The mucosa consists of epithelium, lamina propria and muscularis mucosae.

Epithelium

A single-layered epithelium covers the intestinal villi (Figs 66.15, 66.16) and also lines the intestinal glands (crypts) that open between the bases of villi. Two types of cell, enterocytes and goblet cells, cover the surfaces of the villi, whereas microfold cells (M cells) are restricted to the dome epithelium that covers localized accumulations of lymphoid tissues. These cell types are all in contact basally with a basal lamina to which they adhere, and all are derived from a common stem cell in the intestinal crypts.

Enterocytes

Enterocytes are columnar absorptive cells, approximately 20 µm tall. They are the most numerous type of cell in the small intestinal lining, and are responsible for nutrient absorption. Their surfaces bear up to 3000 microvilli, which greatly increase the surface area for absorption. Collectively, microvilli are visible by light microscopy as a brush (striated) border 1 µm thick: individual microvilli can be resolved only by electron microscopy. Enterocyte nuclei are elongated vertically, mainly euchromatic and located just below the centre of the cell.

The apical cell surface is resistant to protease attack because microvilli possess a specialized glycoprotein-rich surface coat (glycocalyx) which, with an overlying layer of mucus, protects the epithelium against pancreatic enzymes in the intestinal lumen. The cell coat also contains a number of digestive enzymes as integral membrane proteins. These include enzymes that degrade disaccharides and oligopeptides prior to absorption. Further details of the structure of microvilli are given on page 18).

The luminal surface is an important barrier to diffusion. Nutrients generally have to pass through enterocytes (transcellular absorption) before they reach the underlying lamina propria and its blood vessels and lymphatics (lacteals). Classical epithelial junctional complexes encircle the apical plasma membranes of adjacent enterocytes: their tight junctions form an effective barrier to non-selective diffusion between the gut lumen and the body as a whole. The lateral plasma membranes of enterocytes are highly folded, interdigitating with each other to form complex intercellular boundaries, anchored periodically by desmosomes, and making contact at gap junctions. The lateral intercellular space expands during active absorption and is an additional conduit (supplementing transport across the basal cell surface) for the passage of fluids, nutrients and other solutes to the vessels of the lamina propria.

Enterocytes have a lifespan after differentiation of about 5 days. Their position on the villus wall reflects their stage in the life cycle: at the tips of intestinal villi they undergo programmed, apoptotic, cell death and are shed from the epithelium. They are replaced at the base of the villus by stem cell mitosis.

Goblet cells

Goblet cells are most numerous in the distal small intestine, increasing in number from the duodenum to their highest density in the terminal ileum. They have elongated basal nuclei, an apical region containing many membrane-bound mucinogen granules, and apical surfaces that bear a few short microvilli. Goblet cell mucins contribute to protection against microorganisms and toxins in the gut lumen, and also provide lubrication and mechanical protection from the intestinal contents.

Microfold (M) cells

Microfold cells are present where the epithelium covers lymphoid aggregates in the intestinal wall (p. 74). They are cuboidal or flattened in shape and have long, widely spaced microfolds rather than microvilli on their apical surfaces. They sample luminal antigens by endocytosis, and transport antigen to lymphocytes lying within intercellular pockets formed by deep invaginations of the M-cell basolateral plasma membranes. See page 78 for details of antigen processing and presentation.

Lymphocytes

Intraepithelial lymphocytes are found in close association with M cells and also between the basolateral regions of enterocytes and goblet cells. They are migratory cells derived from the underlying lymphoid tissue and constitute an important means of immune defence.

Intestinal glands or crypts

Intestinal glands or crypts (of Lieberkühn) are tubular pits that open into the lumen throughout the intestinal mucosa via small circular apertures between the bases of the villi (Figs 66.14-66.16). Their thin walls are composed of columnar enterocytes supplemented by mucous cells, Paneth cells, stem cells and neuroendocrine cells. They are separated by a basement membrane from a rich capillary plexus within the lamina propria.

Enterocytes

Enterocytes in the crypts secrete ions and alkaline fluid to dilute chyme and aid absorption by structurally similar cells that cover the villi.

Mucous cells

The mucous cells in the crypts are similar to the goblet cells of the villi.

Paneth cells

Paneth cells are numerous in the deeper parts of the intestinal crypts, particularly in the duodenum. They are rich in zinc and contain large acidophilic granules that stain strongly with eosin or phosphotungstic haematoxylin. Paneth cells secrete lysozyme, a highly specific antibacterial enzyme, and other defensive proteins (defensins) such as tumour necrosis factor alpha (TNF-α), which protect the intestinal luminal surface.

Stem cells

Stem cells occur in a zone just above the basal region of the crypts and are the source of most of the cell types of the intestinal epithelium. Their progeny, transit (transient) amplifying cells, have one of the most rapid proliferation rates in the body. They migrate out of the intestinal crypts along the sides of the villi, where they differentiate mainly into the short-lived columnar enterocytes or goblet cells (which are thus continually replaced). When not dividing, their apical surfaces have fewer and more irregular microvilli than the differentiated enterocytes.

Neuroendocrine cells

Several types of neuroendocrine cell are scattered among the walls of the intestinal crypts, and less commonly over the villi. They secrete bioactive peptides, such as gastrin, cholecystokinin and secretin, basally into the surrounding lamina propria. Crypt neuroendocrine cells are derived from stem cells, which also give rise to enterocytes and other epithelial elements. For further details of the dispersed neuroendocrine system, see page Chapter 60.

Lamina propria

The lamina propria is composed of connective tissue and provides mechanical support for the epithelium. It has a rich vascular plexus, receives nutrients absorbed by the enterocytes, and forms the cores of the villi. It contains lymphoid tissue, fibroblasts and connective tissue extracellular matrix fibres, smooth muscle cells, eosinophils, macrophages, mast cells, capillaries, lymphatic vessels and unmyelinated nerve fibres. Plasma cells are numerous. Lymphocytes may be clustered in solitary or aggregated follicles, some of which extend through the muscularis mucosae into the submucosa.

Core of the villus

Each villus has a core of delicate connective tissue that contains a large blind-ending lymphatic vessel or lacteal (so called because of its content of suspended chylomicrons, the droplets of apoprotein–lipid complex elaborated by enterocytes from absorbed dietary fats). The core also contains blood vessels, nerves and smooth muscle cells derived from fine extensions of the muscularis mucosae. Each lacteal, usually single but occasionally double, starts in a closed dilated extremity near the tip of a villus, and extends through the core to the base of the villus, where it joins a narrower lymphatic plexus in the deeper lamina propria. Its wall is a single layer of endothelial cells. Smooth muscle cells surround the lacteal throughout the villus and their contraction propels its contents into the underlying lymphatic plexus. Capillaries within the core are lined by fenestrated endothelium to facilitate the rapid intake of nutrients diffusing from the covering absorptive epithelium.

Mucosa-associated lymphoid tissue

Mucosa-associated lymphoid tissue (MALT) consists of lymphoid follicles covered by follicle-associated intestinal epithelium which includes scattered M cells. It is found mainly in the lamina propria, but sometimes expands into the submucosa, and is the source of B and T lymphocytes and other related cells involved in the immune defence of the gut wall.

Solitary lymphoid follicles are scattered along the length of the intestinal mucosa, and are most numerous in the distal ileum. Aggregated lymphoid follicles, Peyer’s patches, are circular or oval masses containing 10–260 follicles. They vary in length from 2 to 10 cm, are visible macroscopically as dome-like elevations, and usually situated in the intestinal wall opposite the mesenteric attachment. They are largest and most numerous in the ileum; small, circular and few in the distal jejunum; and rare in the duodenum. Villi are small or absent over the larger follicular groups.

Like other masses of MALT (except lymph nodes), solitary and aggregated lymphoid follicles are most prominent around the age of puberty, after which they diminish in number and size, although many persist into old age. For further details of intestinal MALT and its function, including Peyer's patches, see Didierlaurent, Simonet & Sira (2006).

Muscularis mucosae

The muscularis mucosae forms the base of the mucosa, and has external longitudinal and internal circular layers of smooth muscle cells. It follows the surface profiles of the circular folds and sends fine fascicles of smooth muscle cells into the cores of the villi.

Submucosa

The submucosa is composed of loose connective tissue and contains blood vessels, lymphatics and nerves. Its ridged elevations form the cores of the circular folds. The geometry of its collagen and elastin fibres permits the considerable changes in transverse and longitudinal dimensions that accompany peristalsis, whilst still providing adequate support, elasticity and strength.

Submucosal (Brunner's) glands

Submucosal glands are limited to the submucosa of the duodenum and often referred to as 'Brunner's glands' (see Fig. 66.15). Their ducts traverse the muscularis mucosae to enter the bases of the mucosal crypts. They are largest and most numerous near the pylorus and form an almost complete layer in the proximal half of the descending duodenum, thereafter they gradually diminish in number and disappear at the duodenojejunal junction. They are small, branched tubuloacinar glands: each has several secretory acini lined by low columnar epithelial cells that produce an alkaline (pH 9) mucoid secretion which effectively neutralizes acidic chyme from the stomach. Many neuroendocrine cells are present among the acinar cells.

Muscularis externa

The muscularis externa consists of a thin external longitudinal layer and a thick internal circular layer of smooth muscle cells. It is thicker in the proximal small intestine and is mainly responsible for the differential appearance of proximal jejunum and distal ileum of CT scanning.

Serosa

Serosa is visceral peritoneum and consists of a subserous stratum of loose connective tissue covered by mesothelium. It covers the majority of the muscularis externa, the only exceptions are the part adjacent to mesenteric adipose tissue and the retroperitoneal portions of the duodenum, both of which are covered mainly by a connective tissue adventitia rather than by serosa.

REFERENCES

dierlaurent A, Simonet M, Sira J-C. Innate and acquired plasticity of the intestinal immune system. *Cell Mol Life Sci*. 2006;62:1285-1287.

ckson JE. Vascular anatomy of the gastrointestinal tract. In: Butler P, Mitchell AWM, Ellis H. *Applied Radiological Anatomy*. Cambridge: Cambridge University Press, 1999.

adir S. Atlas of Normal and Variant Angiographic Anatomy. Philadelphia: WB Saunders, 1991.

aehenbuhl JP, Neutra MR. Molecular and cellular basis of immune protection of mucosal surfaces. *Physiol Rev*. 1992;72:853-879.

derhill BML. Intestinal length in man. *Br Med J*. 1955;2:1243-1246.

CHAPTER 67

Large intestine

OVERVIEW

The large intestine extends from the ileocaecal valve to the anus. Broadly speaking, it lies in a curve which tends to form a border around the loops of small intestine that are located centrally within the abdomen (Figs 67.1, 67.2). The large intestine begins in the right iliac fossa as the caecum, from which the vermiform appendix arises. The caecum becomes the ascending colon which passes upwards in the right lumbar region and hypochondrium to the inferior aspect of the liver where it bends to the left forming the hepatic flexure (right colic flexure) and becomes the transverse colon. This loops across the abdomen with an anteroinferior convexity until it reaches the left hypochondrium, where it curves inferiorly to form the splenic flexure (left colic flexure) and becomes the descending colon, which proceeds through the left lumbar and iliac regions to become the sigmoid colon in the left iliac fossa. The sigmoid colon descends deep into the pelvis and becomes the rectum which ends in the anal canal at the level of the pelvic floor. The large intestine is approximately 1.5 m long in adults, although there is considerable variation in its length. Its calibre is greatest near the caecum and gradually diminishes to the level of the sigmoid colon. The rectum is largest in calibre in its lower third and forms the rectal ampulla above the anal canal.

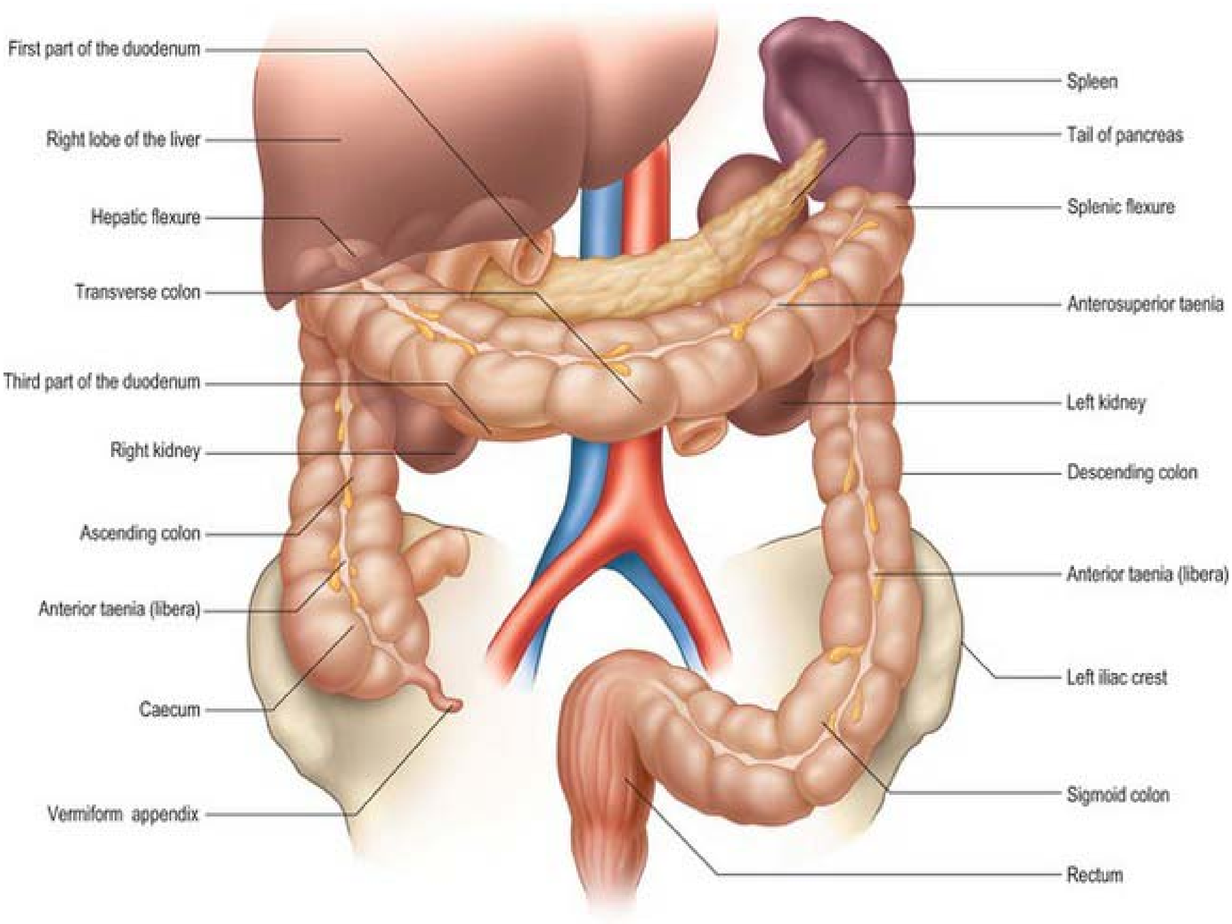
First part of the duodenum
Right lobe of the liver
Hepatic flexure
Transverse colon
Third part of the duodenum
Right kidney
Ascending colon
Anterior taenia (libera)
Caecum
Vermiform appendix
Spleen
Tail of pancreas
Splenic flexure
Anterosuperior taenia
Left kidney
Descending colon
Anterior taenia (libera)
Left iliac crest
Sigmoid colon
Rectum

Fig. 67.1 Overview of the abdominal colon and its relations.

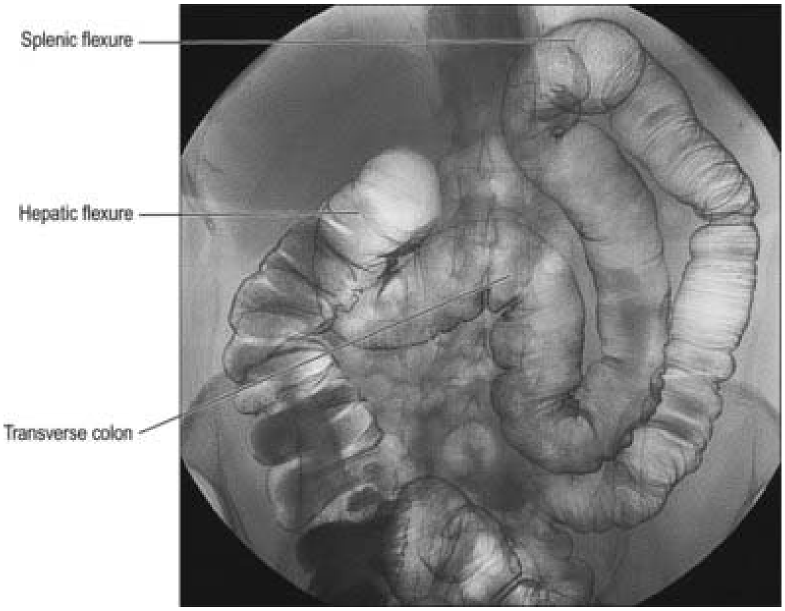
Splenic flexure
Hepatic flexure
Transverse colon

Fig. 67.2 Appearance of the abdominal colon on double contrast barium enema examination demonstrating the transverse colon, hepatic and splenic flexures.

The large intestine differs from the small intestine in several ways: it has a greater calibre; for most of its course it is more fixed in position; its longitudinal muscle, though a complete layer, is concentrated into three longitudinal bands, taeniae coli, in all but the distal sigmoid colon and rectum; small adipose projections, appendices epiploicae, are scattered over the free surface of the whole colon (they tend to be absent from the caecum, vermiform appendix and rectum); the colonic wall is puckered into sacculations (haustrations), which may partly be due to the presence of the taeniae coli, and which may be demonstrated on plain radiographs as incomplete septations arising from the bowel wall.

The large intestine develops as a fully mesenteric organ. However, after the rotation of the gut tube *in utero*, large portions of it come to lie adherent to the retroperitoneum, which means that some parts of the colon are fixed within the retroperitoneum, and other parts are suspended by a mesentery within the peritoneal cavity. Those portions of the colon within the retroperitoneum are separated from other retroperitoneal structures by a thin layer of connective tissue which forms an avascular field during surgical dissection, but which offers little or no barrier to the spread of disease within the retroperitoneum.

The caecum may be within the retroperitoneum, but more frequently is suspended by a short mesentery. The ascending colon is usually a retroperitoneal structure although the hepatic flexure may be suspended by a mesentery. The transverse colon emerges from the retroperitoneum on a rapidly elongating mesentery and lies, often freely mobile, in the upper abdomen. The transverse mesocolon shortens to the left of the upper abdomen and may become retroperitoneal at the splenic flexure. Occasionally the splenic flexure is suspended by a short mesentery. The descending colon is retroperitoneal usually to the level of the left iliac crest. As the colon enters the pelvis it becomes increasingly more mesenteric again at the origin of the sigmoid colon, although the overall length of the sigmoid mesentery is highly variable. The distal sigmoid colon lies on a rapidly shortening mesentery as it approaches the pelvis; by the level of the rectosigmoid junction the mesentery has all but disappeared, so that the rectum enters the pelvis as a retroperitoneal structure. The caecum and proximal ascending colon are often more mobile on a longer mesentery in the neonate and infant than they are in the adult.

The mesenteries of the colon consist of visceral peritoneum enclosing connective and adipose tissues which envelop the vessels, nerves and lymphatics as they course from the retroperitoneum. Where the colonic mesenteries lie in contact with the retroperitoneum, the (potential) space between the retroperitoneum and mesentery is referred to as the subperitoneal space, which allows free tracking of pathological processes in either direction.

EXTERNAL APPEARANCE

The haustrations of the colon are often absent in the caecum proximal to the origin of the ascending colon and are often relatively sparse in the ascending and proximal transverse colon. In these regions the taeniae coli are usually thin and occupy only a small percentage of the circumference of the colon. There are few if any appendices epiploicae on the serosal surface of the caecum, and only a limited number on the surface of the ascending colon. The haustrations become more pronounced from the middle of the transverse colon to the distal portion of the descending colon: the sigmoid colon is often characterized by marked sacculation. The width of the taeniae coli remains fairly constant throughout the length of colon but the number of appendices epiploicae usually increases, becoming in the sigmoid colon where they can be large in the obese individual. The taeniae are located in fairly constant positions beneath the serosal surface of the colon except in the transverse colon. They are oriented anteriorly on the anti-mesenteric aspect of the colon opposite the midline of the mesenteric attachment (taenia libera), posterolaterally (taenia omentalis) and posteromedially (taenia mesocolica) midway between the taenia libera and the mesentery (Fig. 67.3). In the caecum and descending colon, which are partly retroperitoneal structures, the posterolateral taenia is often obscured from view by the peritoneal reflection onto the colonic wall. In the transverse colon, the taeniae are rotated through 90° as a consequence of the mobility and dependent position of this part of the colon, thus anterior becomes inferior, posteromedial becomes posterior and posterolateral becomes superior. The taeniae coli broaden to occupy more of the circumference of the sigmoid colon in its distal portion and by the level of the rectosigmoid junction they form distinct anterior and posterior bands. These bands subsequently unite to form a complete longitudinal muscle covering for the rectum which therefore has no external sacculation. The rectum also lacks serosal appendices epiploicae.

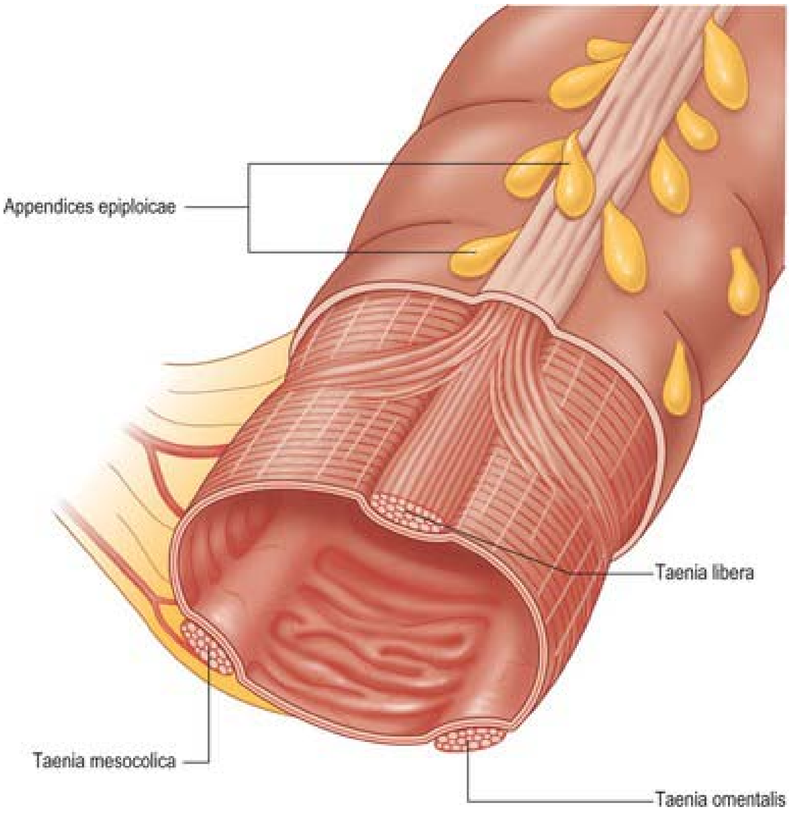
Appendices epiploicae
Taenia libera
Taenia mesocolica
Taenia omentalis

Fig. 67.3 Layers of the colonic wall.

INTERNAL APPEARANCE

Throughout its length, the internal aspect of the colon is characterized by the presence of haustrations. These infoldings of the wall consist of mucosa and submucosa, and may partially span the lumen, but they never form a complete, circumferential ring. The pattern of the haustrations and appearance of the colonic mucosa help the clinician appreciate the level reached during flexible endoscopic examinations of the colon. In the portion of the caecum where haustrations occur, the three longitudinal taeniae coli converge to form a characteristic ‘trefoil’ pattern on the caecal wall (Fig. 67.4). Elsewhere, the wall of the lower pole of the caecum is usually devoid of haustrations, although a spiral mucosal pattern is often seen in the region of the appendix orifice (see Fig. 67.19). The upper caecum and ascending colon possess shallow but long haustrations which may extend across one-third of the lumen (Fig. 67.5). This pattern is most pronounced in the transverse colon where the long haustrations often confer a triangular appearance to the cross section of the lumen when viewed along the axis (such as at colonoscopy) (Fig. 67.6). The wall of the colon is thinnest in the region of the caecum and ascending colon and is most at risk of perforation during therapeutic endoscopic procedures. The haustrations of the descending and sigmoid colon tend to be thicker and shorter than those of the transverse colon, and this gives a more circular cross-section to the lumen. The overall luminal diameter is often smallest in the descending colon (Fig. 67.7). During endoscopy, the pattern of the submucosal vessels becomes more conspicuous in the sigmoid colon (Fig. 67.8). The mobility of the sigmoid colon on its mesentery means that shorter lengths of colon tend to be visible during endoscopy than anywhere else in the colon. The haustrations of the rectum tend to form consistent and recognizable folds: the pattern of the submucosal vessels is the most pronounced in the colon being of largest calibre with multiple visible veins (Fig. 67.9). Distinct veins are usually visible during endoscopy, and they are most marked above the anorectal junction.

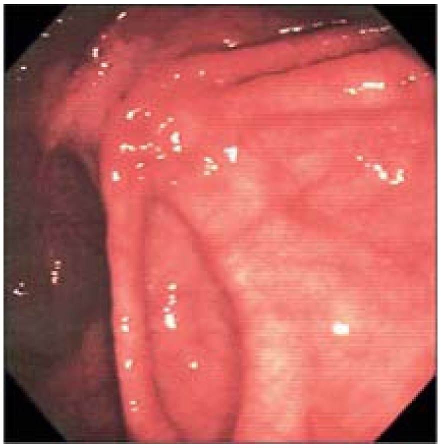

Fig. 67.4 Endoscopic appearance of the caecum. The characteristic trefoil appearance of the confluence of the three taeniae is usually obvious.

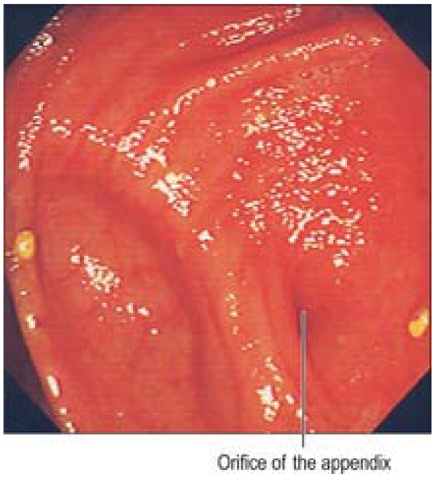

Fig. 67.19 Endoscopic appearance of the orifice of the appendix. The orifice varies from a small depression to an obvious lumenal structure.

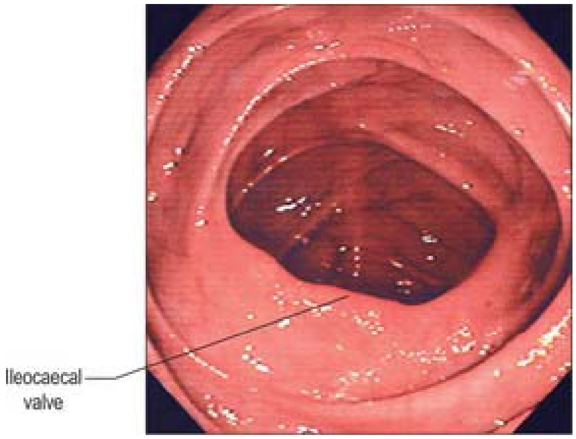

Fig. 67.5 Endoscopic appearance of the ascending colon.

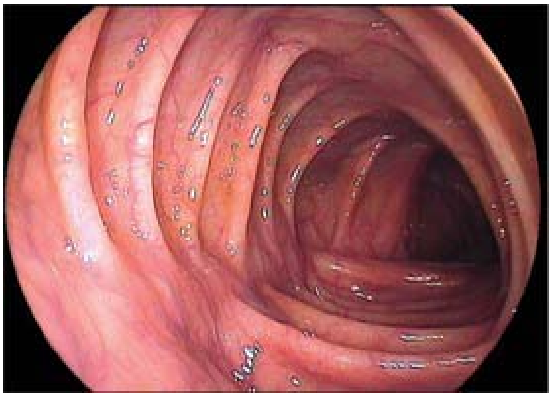

Fig. 67.6 Endoscopic appearance of the transverse colon. Note the characteristic triangular appearance of the haustrations when viewed collectively (see also Fig. 67.10C).

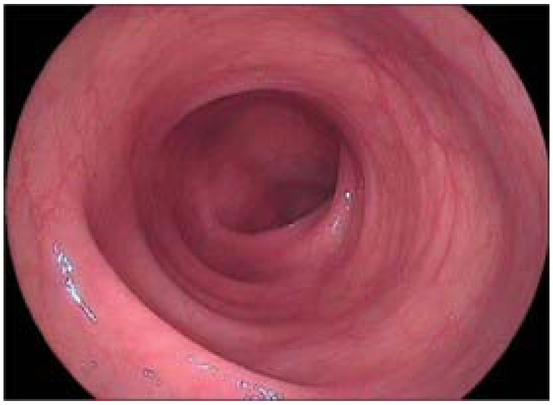

Fig. 67.7 Endoscopic appearance of the descending colon. The lumen tends to look rather more featureless than the more proximal colon.

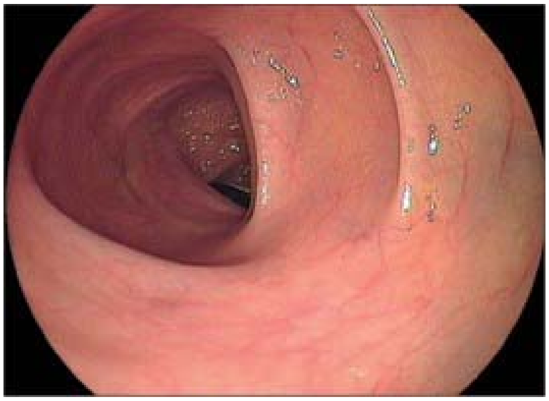

Fig. 67.8 Endoscopic appearance of the sigmoid colon. Multiple large mucosal folds are characteristic.

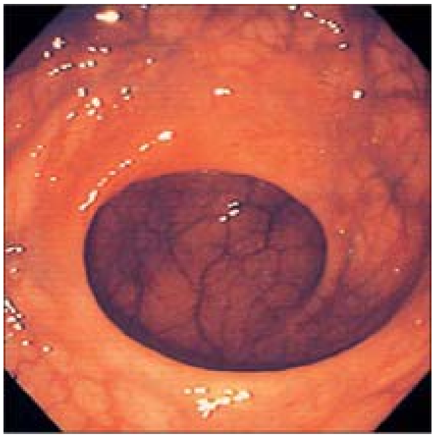

Fig. 67.9 Endoscopic appearance of the rectum. Note the large transverse folds, with little else in the way of mucosal folds, characterizes the rectum. Prominent veins are often seen, particularly in the lower third.

RADIOGRAPHIC APPEARANCES

Cross-sectional imaging of the colon can be performed with computerized tomography (CT) and magnetic resonance imaging (MRI). On axial imaging the colon may be filled with particulate faeces and air (Fig. 67.10). The wall in normal individuals is thin. The caecum and ascending colon often contain faecal residue and are easily identified in the right retroperitoneum. The transverse colon may contain faeces or gas, but lies in a variable position suspended by its mesentery. The descending colon in the left retroperitoneum is frequently collapsed and contains little faecal residue.

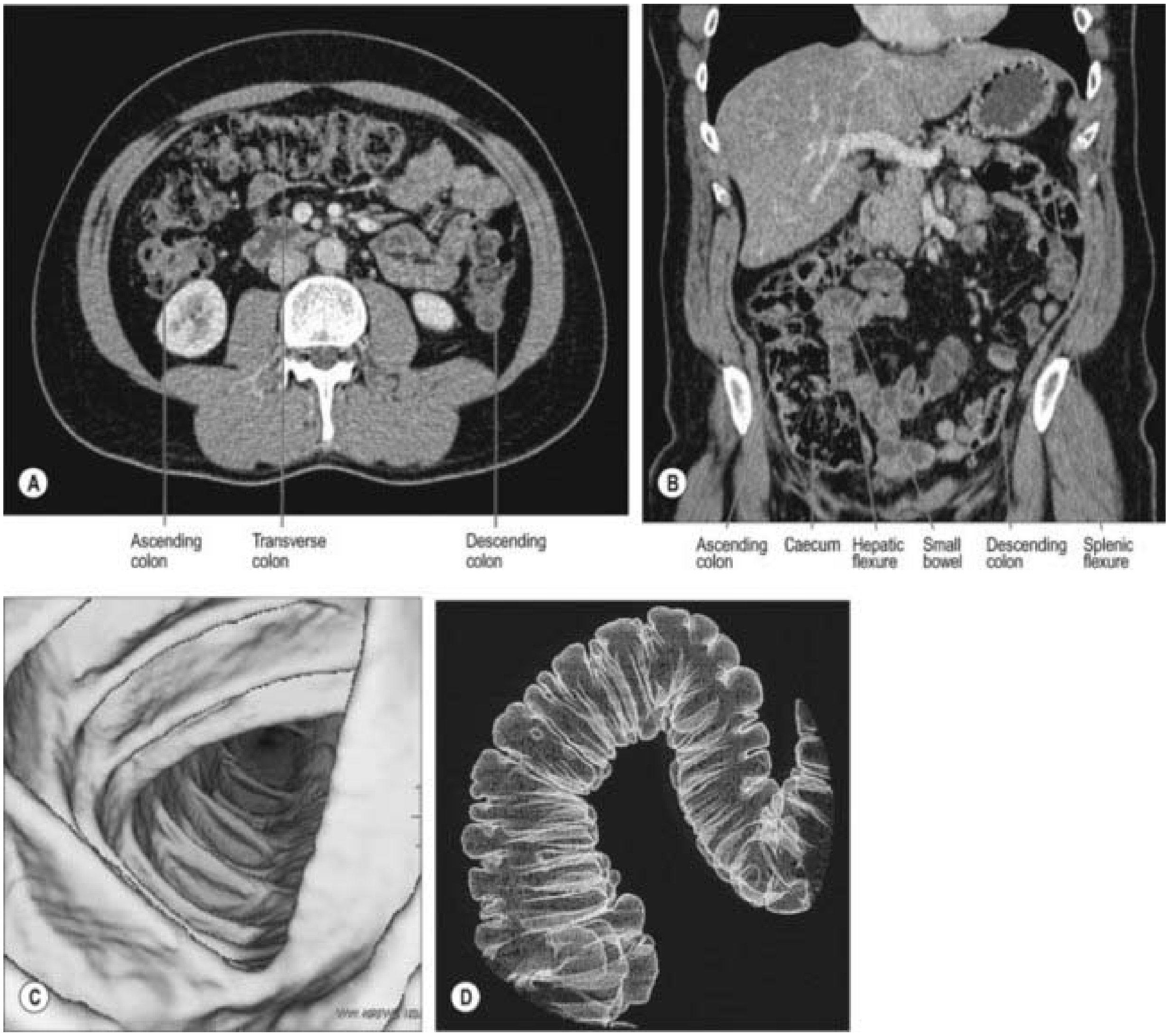
A
Ascending colon
Transverse colon
Descending colon
B
Ascending colon
Caecum
Hepatic flexure
Small bowel
Descending colon
Splenic flexure
C
D

Fig. 67.10 Appearance of the colon on multislice computerized tomographic examination. **A**, Axial CT. **B**, Coronal reformat showing normal calibre and distribution of the abdominal colon (ascending, transverse and descending). **C**, Volume-rendering of the colonic wall using the axial data set to produce virtual colonoscopic views, showing the triangular lumen of the transverse colon. **D**, Volume-rendering of the air-filled colon using the axial data set to give an image similar to a double contrast barium enema demonstrating haustrations.

*(**A** and **B** by courtesy of Dr Louise Moore, Chelsea and Westminster Hospital.) (**C** and **D** by courtesy of GE Worldwide Medical Systems.)*

The volume data sets produced by modern multislice CT can now produce virtual colonoscopic mucosal images in the distended and cleaned colon, and surface-rendered images of the internal surface of the bowel.

VASCULAR SUPPLY AND LYMPHATIC DRAINAGE

Arteries

The arterial supply of the large intestine is derived from both the superior and inferior mesenteric arteries (Fig. 67.11). The caecum, appendix, ascending colon and right two-thirds of the transverse colon (derived from the midgut) are supplied from ileocolic, right colic and middle colic branches of the superior mesenteric artery. The left part of the transverse, descending and sigmoid colon, rectum and upper anal canal (hindgut derivatives) are supplied predominantly from the inferior mesenteric artery via the left colic, sigmoid and superior rectal arteries, with small contributions from branches of the internal iliac artery (the middle and inferior rectal arteries). The larger unnamed branches of these vessels ramify between the muscular layers of the colon which they supply. They subdivide into smaller submucosal rami and enter the mucosa. The terminal branches divide into vasa brevia and vasa longa which either enter the colonic wall directly or run through the subserosa for a short distance before crossing the circular smooth muscle to give off branches to the appendices epiploicae (Fig. 67.12).

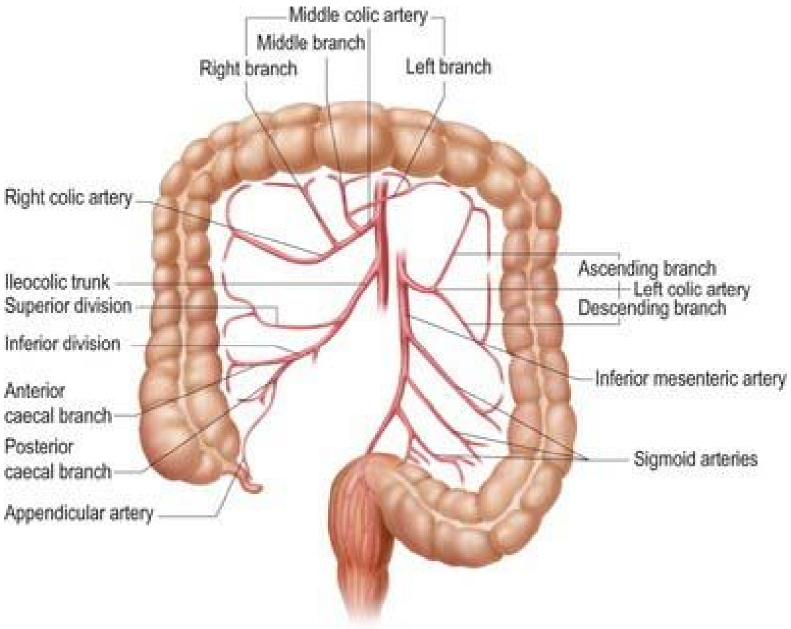
Middle colic artery
Middle branch
Right branch
Left branch
Right colic artery
Ileocolic trunk
Superior division
Inferior division
Anterior caecal branch
Posterior caecal branch
Appendicular artery
Ascending branch
Left colic artery
Descending branch
Inferior mesenteric artery
Sigmoid arteries

Fig. 67.11 The main branches of the superior and inferior mesenteric arteries.

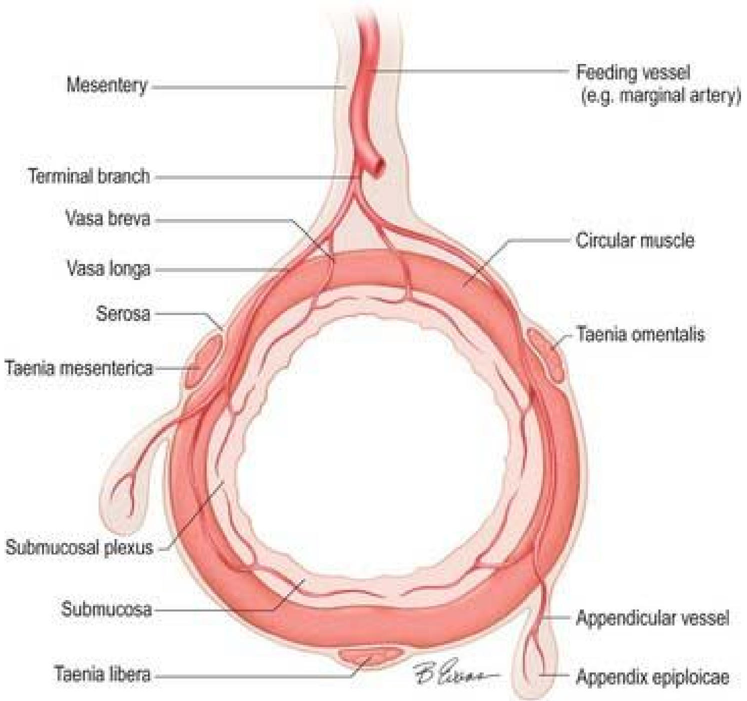
Mesentery
Feeding vessel (e.g. marginal artery)
Terminal branch
Vasa breva
Circular muscle
Vasa longa
Serosa
Taenia omentalis
Taenia mesenterica
Submucosal plexus
Submucosa
Appendicular vessel
Taenia libera
Appendix epiploicae

Fig. 67.12 Typical pericolic arrangement of arterial vasculature.

Arterial anastomoses and the marginal artery of the colon

The arterial supply to the large intestine has less profuse anastomoses and ‘cross-over’ of arterial territories than the small intestine but there are several areas and anastomoses which provide for some degree of anatomical collateral supply to areas of the large intestine.

The marginal artery (of Drummond) of the colon is the name given to the vessel which lies closest to and parallels the wall of the large intestine. It is formed by the main trunks, and the arcades arising from, the ileocolic and right colic, middle colic and left colic arteries. It is most apparent in the ascending, transverse and descending colons (Fig. 67.13). The sigmoid colon has little if any marginal artery. Anastomoses form between the main terminal branches which run parallel to the colon within the mesentery and give rise to vasa recta and vasa brevia to supply the colon. The marginal artery in the region of the splenic flexure may be absent or of such small calibre as to be of little clinical relevance. It may hypertrophy significantly when one of the main visceral arteries is compromised, e.g. following stenosis or occlusion of the inferior mesenteric artery, and it then provides a vessel of collateral supply.

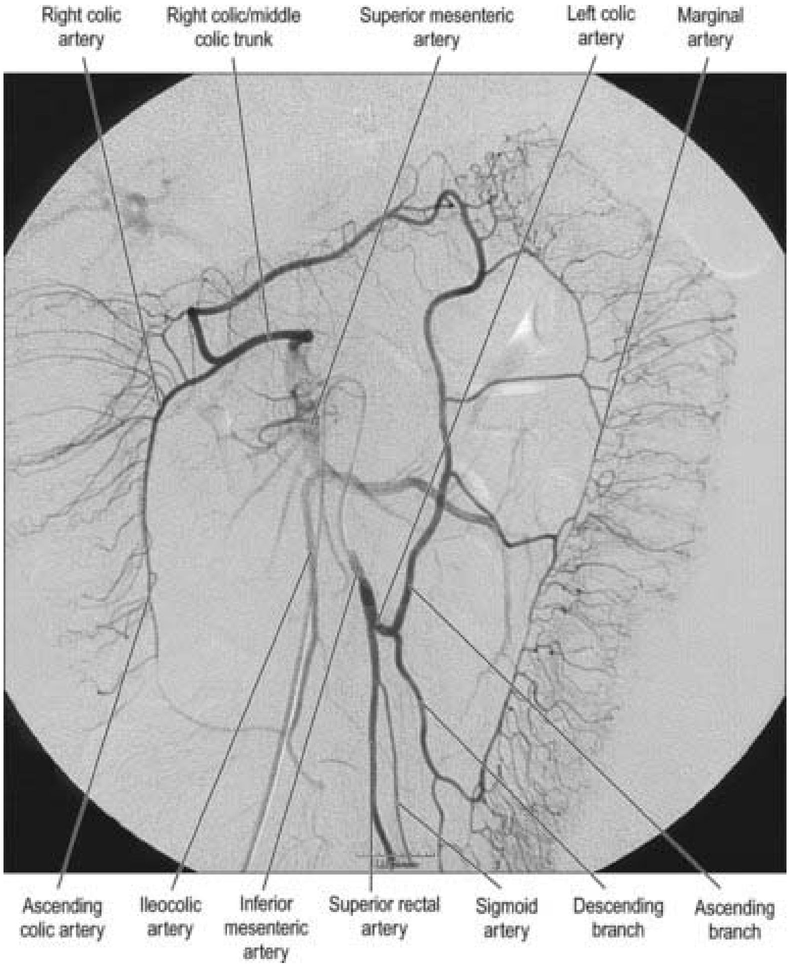
Right colic artery
Right colic/middle colic trunk
Superior mesenteric artery
Left colic artery
Marginal artery
Ascending colic artery
Ileocolic artery
Inferior mesenteric artery
Superior rectal artery
Sigmoid artery
Descending branch
Ascending branch

Fig. 67.13 The marginal artery running parallel to the colon and anastomosing with the branches of the superior mesenteric artery supplying the right side of the colon, digital subtraction arteriogram.

(By courtesy of Dr J Jackson, Hammersmith Hospital, London.)

The arc of Riolan is the name given to the arterial anastomosis which is sometimes present in the mesentery between the right side of the transverse colon and the upper descending colon. When present it is formed from a large branch of the middle colic artery which runs parallel and posterior to the middle colic artery in the transverse mesocolon and anastomoses with an ascending branch of the left colic artery close to its origin in the root of the mesentery. This provides a direct communication between the superior and inferior mesenteric arteries.

Colonic vascular occlusion

The marginal artery of the colon may become massively dilated when there is chronic, progressive occlusion of the superior mesenteric artery, because under these conditions it is required to supply the majority of the midgut (except the proximal portion which is supplied by collateral vessels from the coeliac artery). Occlusion of the aorta or common iliac arteries may also result in dilatation of the marginal and inferior mesenteric arteries, which become an important collateral supply to the legs via dilated middle rectal vessels arising from the internal iliac artery.

Occlusion of the inferior mesenteric artery does not always result in irreversible ischaemia of the descending and sigmoid colon, because the marginal artery of the colon usually receives an adequate supply from the left branch of the middle colic artery. Moreover, the sigmoid arteries may be supplied by the superior rectal artery, which anastomoses with the middle and inferior rectal arteries. When ischaemia does occur, it is usually maximal in the proximal descending colon because this region is furthest from the collateral arterial supplies.

Veins

The venous drainage of the large intestine is primarily into the hepatic portal vein via the superior mesenteric and inferior mesenteric veins, although a small amount of drainage from the rectum occurs via middle rectal veins into the internal iliac veins and via inferior rectal veins into the pudendal vein. Those parts of the colon derived from the midgut (caecum, appendix, ascending colon and right two-thirds of the transverse colon) drain into colic branches of the superior mesenteric vein, while hindgut derivatives (left part of the transverse, descending and sigmoid colon, rectum and upper anal canal) drain into the inferior mesenteric vein (Fig. 67.14).

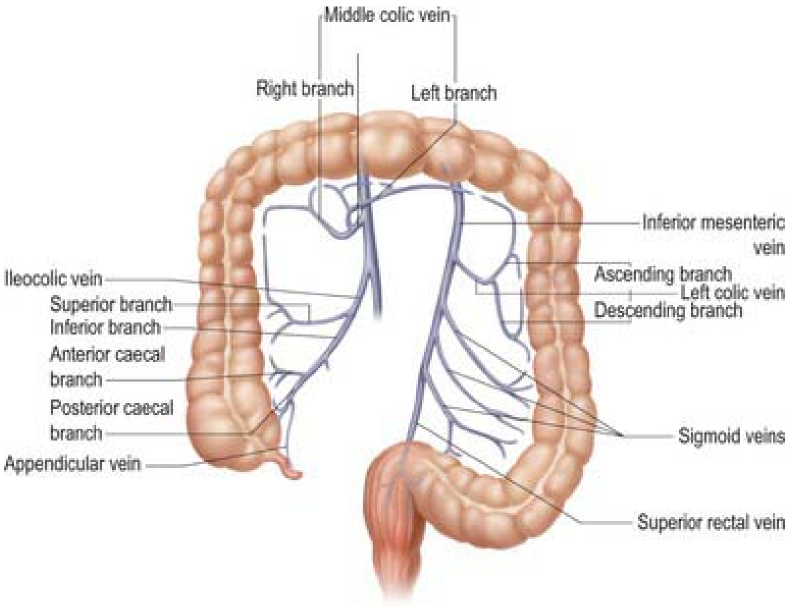
Middle colic vein
Right branch
Left branch
Inferior mesenteric vein
Ascending branch
Left colic vein
Descending branch
Ileocolic vein
Superior branch
Inferior branch
Anterior caecal branch
Posterior caecal branch
Appendicular vein
Sigmoid veins
Superior rectal vein

Fig. 67.14 The main branches of the superior and inferior mesenteric veins.

Lymphatics

Lymphatic vessels of the caecum, ascending and proximal transverse colon drain ultimately into lymph nodes related to the superior mesenteric artery, while those of the distal transverse colon, descending colon, sigmoid colon and rectum drain into nodes following the course of the inferior mesenteric artery (Fig. 67.15). In cases where the distal transverse colon or splenic flexure is predominantly supplied by vessels from the middle colic artery, the lymphatic drainage of this area may be predominantly to superior mesenteric nodes.

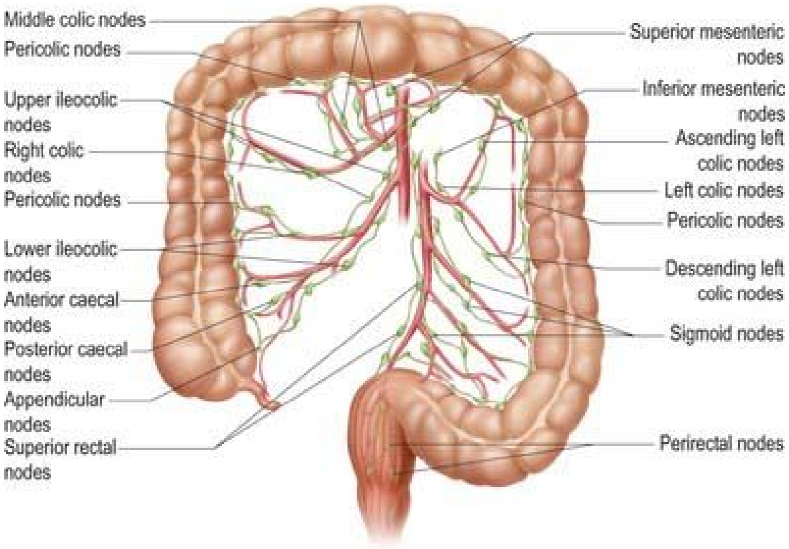
Middle colic nodes
Pericolic nodes
Upper ileocolic nodes
Right colic nodes
Pericolic nodes
Lower ileocolic nodes
Anterior caecal nodes
Posterior caecal nodes
Appendicular nodes
Superior rectal nodes
Superior mesenteric nodes
Inferior mesenteric nodes
Ascending left colic nodes
Left colic nodes
Pericolic nodes
Descending left colic nodes
Sigmoid nodes
Perirectal nodes

Fig. 67.15 The lymph vessels and nodes during the large intestine.

Colic nodes

Lymph nodes related to the colon form four groups, namely epicolic, paracolic, intermediate colic and preterminal colic nodes. Epicolic nodes are minute nodules on the serosal surface of the colon, sometimes in the appendices epiploicae. Paracolic nodes lie along the medial borders of the ascending and descending colon and along the mesenteric borders of the transverse and sigmoid colon. Intermediate colic nodes lie along the named colic vessels (the ileocolic, right colic, middle colic, left colic, sigmoid and superior rectal arteries). Preterminal colic nodes lie along the main trunks of the superior and inferior mesenteric arteries and drain into para-aortic nodes at the origin of these vessels. These are commonly referred to as the highest nodes of the territory which they drain.

Lymph node clearance in colorectal cancer resections

Radical lymphadenectomy during resection for colorectal cancer requires removal of the highest possible lymph node draining the area of colon in which the tumour is located. In cases of cancer involving the rectum and sigmoid colon, this usually involves resection of the preterminal colic nodes of the inferior mesenteric artery and thus ligation of the inferior mesenteric artery at its root or just below the origin of the left colic artery. A detailed description of the classification of the lymph nodes with regard to the site of the primary tumour within the colon has been suggested by the Japanese Society for the Cancer of the Colon and Rectum.

INNERVATION

The colon and rectum are innervated by the sympathetic and parasympathetic systems (see Ch. 60; see Figs 60.2–60.4).

The sympathetic supply to the caecum, appendix, ascending colon and right two-thirds of the transverse colon originates in the fifth to the 12th thoracic spinal segments and are conveyed to the coeliac and superior mesenteric plexuses via the greater and lesser splanchnic nerves where they and synapse on ganglionic neurones. Postganglionic axons travel along branches of the superior mesenteric artery, and are distributed to the colon from periarterial plexuses. The parasympathetic supply is derived from the vagus nerve via the coeliac and superior mesenteric plexuses.

The sympathetic supply of the left third of the transverse colon, the descending and sigmoid colon, rectum and upper anal canal originates in the first and second lumbar spinal segments. The fibres are distributed via the lumbar splanchnic nerves through the abdominal aortic and the inferior mesenteric plexuses and via the sacral splanchnic nerves through the superior and inferior hypogastric plexuses. Postganglionic axons reach the gut wall via periarterial plexuses on branches of the inferior mesenteric artery. The parasympathetic supply travels via the pelvic splanchnic nerves (nervi erigentes) from cell bodies in the second to the fourth sacral spinal segments. Those distributed to the rectum and upper anal canal run through the inferior and superior hypogastric plexuses to branches of the inferior mesenteric artery. Some of those distributed to the descending and sigmoid colon run via these plexuses; however, a large number of fibres pass directly through the retroperitoneal tissues to the splenic flexure, descending and sigmoid colon independently of the inferior mesenteric artery.

The ultimate distribution within the wall of the large intestine is similar to the small intestine. The colic sympathetic nerves are motor to the ileocaecal valve musculature and inhibitory to mural muscle in the colon and rectum. Some fibres are vasoconstrictor to the colic vasculature. Parasympathetic nerves are secretomotor to colorectal glands, motor to the colic and rectal musculature and inhibitory to the internal anal sphincter.

Afferent impulses mediating sensations of distension are carried by visceral afferent fibres which travel with the parasympathetic nerves; pain impulses pass in visceral afferents travelling with the sympathetic and parasympathetic nerves supplying the rectum and the upper part of the anal canal.

CAECUM, VERMIFORM APPENDIX AND ASCENDING COLON

CAECUM

The caecum is a large blind pouch lying in the right iliac fossa below the ileocaecal valve, continuous proximally with the distal ileum and distally with the ascending colon. The blind-ending vermiform appendix usually arises on its medial side at the level of the ileal opening. Its average axial length is 6 cm and its breadth 7.5 cm. It rests posteriorly on the right iliacus and psoas major, with the lateral cutaneous nerve of the thigh interposed. Posteriorly lies the retrocaecal recess which frequently contains the vermiform appendix. The anterior abdominal wall is immediately anterior to the caecum except when it is empty, in which case the greater omentum and some loops of the small intestine may be interposed. Usually the caecum is entirely covered by peritoneum, but occasionally this is incomplete posterosuperiorly where it lies over the iliac fascia only separated from it by loose connective tissue.

In early fetal life the caecum is usually short, conical and broad based, with an apex turned superomedially towards the ileocaecal junction. As the fetus grows, the caecum increases initially in length more than in breadth, still with the apex turned superomedially; in the later stages of intrauterine growth, the proximal part of the caecum widens so that the caecum is still a conical shape, but the apex (from which the appendix arises) comes to point inferomedially. This infantile form persists throughout life in only a very small percentage of individuals. Occasionally the originally conical caecum becomes quadrate as a result of the outgrowth of a saccule on each side of the anterior taenia: the saccules are of equal size and the appendix arises from the depression between them instead of from the apex of a cone. In the normal adult form, the right saccule grows more rapidly than the left, forming a new ‘apex’. The original apex, with the appendix attached, is pushed towards the ileocaecal junction (Fig. 67.16).

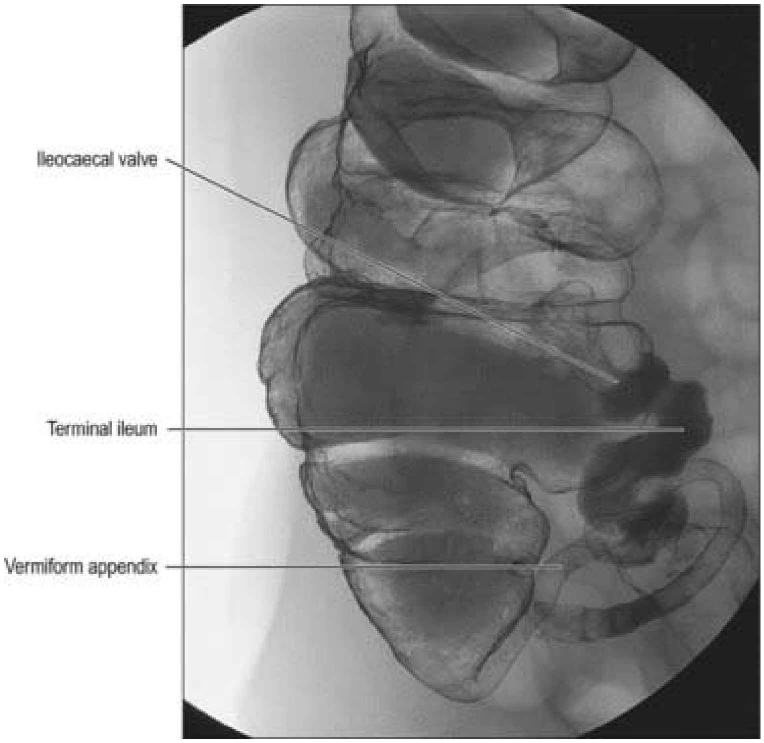

Fig. 67.16 The caecum and ileocaecal valve, double contrast barium enema appearance.

The process of fluid and electrolyte reabsorption starts in the caecum but takes place largely in the ascending and transverse colon. The distensible nature and ‘sac-like’ morphology of the caecum permit storage of large volumes of semi-liquid chyme that enters from the small bowel via the ileocaecal valve. The large resting diameter of the caecum makes it most liable to distension during periods of increased intracolonic pressure and thus it is the most vulnerable portion of the large intestine to perforation secondary to dilatation (obstructed or otherwise).

Ileocaecal valve

The ileum opens into the posteromedial aspect of the large intestine at the junction of the caecum and colon via the ileocaecal ‘valve’. The orifice has two flaps which project into the lumen of the large intestine (Fig. 67.17). The precise shape and form of the valve varies; in the cadaveric caecum the flaps are often semilunar, but in life they can often be seen to form a rosette or trefoil pattern of mucosa. The upper flap, approximately horizontal, is attached to the junction of the ileum and colon; the lower flap is longer and more concave, and is attached to the junction of the ileum and caecum. At their ends the flaps fuse, continuing as narrow membranous ridges, the frenula of the valve. The orifice may appear in many different shapes depending on the state of contraction or distension of the caecum; it is commonly either a slit or an oval.

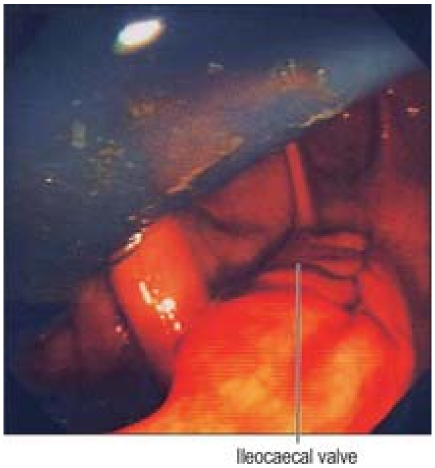

Fig. 67.17 Endoscopic appearance of the ileocaecal valve.

The margin of the ileocaecal valve is formed by a reduplication of the intestinal mucosa and circular muscle. Longitudinal muscle fibres are partly reduplicated as they enter the valve, but the more superficial fibres and the peritoneum continue from the small to the large intestine without interruption. The valve may prevent reflux of chyme from the caecum to the ileum, and may slow the passage of ileal contents into the caecum when the circular muscle of the valve is contracted by sympathetic stimulation. Although circular and longitudinal muscle layers of the terminal ileum continue into the valve, there is little evidence that it constitutes a true functional sphincter.

The ileal valvular surfaces are covered with villi and have the structure of the small intestinal mucosa, whereas their caecal surfaces have no villi but display numerous orifices of tubular glands peculiar to the colonic mucosa.

Caecal volvulus

Because the caecum and ascending colon may possess a mesentery to a variable degree, it is possible for the caecum (and lower portion of the ascending colon) to rotate about their mesenteric attachment (mesentero-axial volvulus) such that the lower pole of the caecum comes to lie in the left or right upper quadrant of the abdomen. The fixed apex of this rotation is formed by the attachment of the caecal mesentery to the retroperitoneum. Volvulus occurs most commonly in those individuals where a large portion of the ascending colon lies on a mesentery and the common origin of the caecal and ascending colic mesentery is narrow. It is extremely unlikely in individuals where the caecum and ascending colon possess a short broadly attached mesentery. True isolated volvulus of the caecum is extremely rare.

VERMIFORM APPENDIX

The vermiform appendix is a narrow, vermiform (worm-like) tube which arises from the posteromedial caecal wall, approximately 2 cm below the end of the ileum. It may occupy one of several positions (Fig. 67.18). The commonest positions seen in clinical practice are retrocaecal or retrocolic (behind the caecum or lower ascending colon respectively), pelvic, or descending (when the appendix hangs dependently over the pelvic brim, in close relation to the right uterine tube and ovary in females). Other positions, including subcaecal (below the caecum), and pre- or post-ilial (anterior or posterior to the terminal ileum respectively), are occasionally seen, especially when there is a long appendicular mesentery which allows greater mobility.

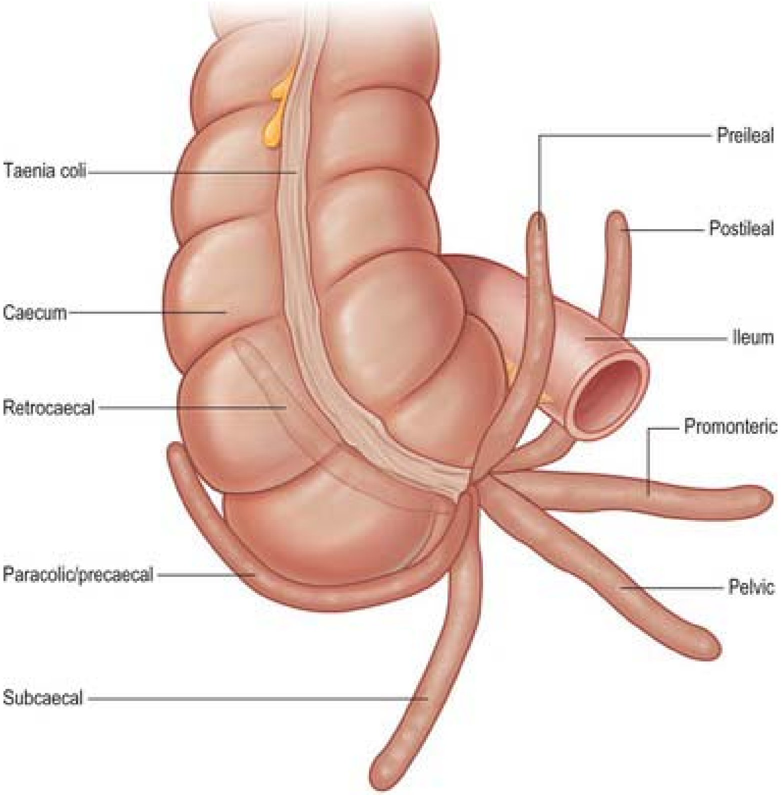
Taenia coli
Caecum
Retrocaecal
Paracolic/precaecal
Subcaecal
Preileal
Postileal
Ileum
Promonteric
Pelvic

Fig. 67.18 The major positions of the appendix encountered at surgery or postmortem.

The three taeniae coli on the ascending colon and caecum converge on the base of the appendix, and merge into its longitudinal muscle. The anterior caecal taenia is usually distinct and can be traced to the appendix, which affords a guide to its location intra-operatively. The appendix varies from 2–20 cm in length: it is often relatively longer in children and may atrophy and shorten after mid-adult life. It is connected by a short mesoappendix to the lower part of the ileal mesentery. This fold is usually triangular, extending almost to the appendicular tip along the whole viscus.

The lumen of the appendix is small and opens into the caecum by an orifice lying below and slightly posterior to the ileocaecal opening. The orifice is sometimes guarded by a straight mucosal fold forming an asymmetrical 'valve' which gives the appendix orifice the appearance of a 'strung bow' (Fig. 67.19). This fold tends to lie parallel to the medial wall of the caecum and ileocaecal valve and an imaginary 'arrow' placed in the bow usually points in the direction of the ileocaecal valve; this is a useful sign during colonoscopic examinations. The lumen may be widely patent in early childhood but is often partially or wholly obliterated in the later decades of life.

Microstructure

The layers of the wall of the appendix are essentially those of the rest of the large intestine (see below) but some features are notably different and are described here. The serosa forms a complete covering, except along the mesenteric attachment. The longitudinal muscular fibres form a complete layer of uniform thickness, except over a few small areas where both muscular layers are deficient, so that the serosa and submucosa are in contact. At the base of the appendix, the longitudinal muscle thickens to form rudimentary taeniae that are continuous with those of the caecum and colon.

The submucosa typically contains many large lymphoid aggregates that extend from the mucosa and obscure the muscularis mucosae layer, which consequently is discontinuous. These aggregates also cause the mucosa to bulge into the lumen of the appendix, so that it narrows irregularly (Fig. 67.20). The mucosa is covered by a columnar epithelium as it is elsewhere in the large intestine, and the epithelium that overlies the mucosal lymphoid tissue contains M cells. Glands (crypts) are similar to those of the colon but are fewer in number and so are less densely packed. They penetrate deep into the lymphoid tissue of the mucosal lamina propria. The submucosal lymphoid tissue frequently exhibits germinal centres within its follicles, indicative of B-cell activation, as occurs in secondary lymphoid tissue elsewhere. Lymphoid follicles are absent at birth but accumulate over the first 10 years of life to become a prominent feature of the appendix. In adults, the normal layered structure of the appendix is lost and the lymphoid follicles atrophy and are replaced by collagenous tissue, and in the elderly, the appendix may be filled with fibrous scar tissue.

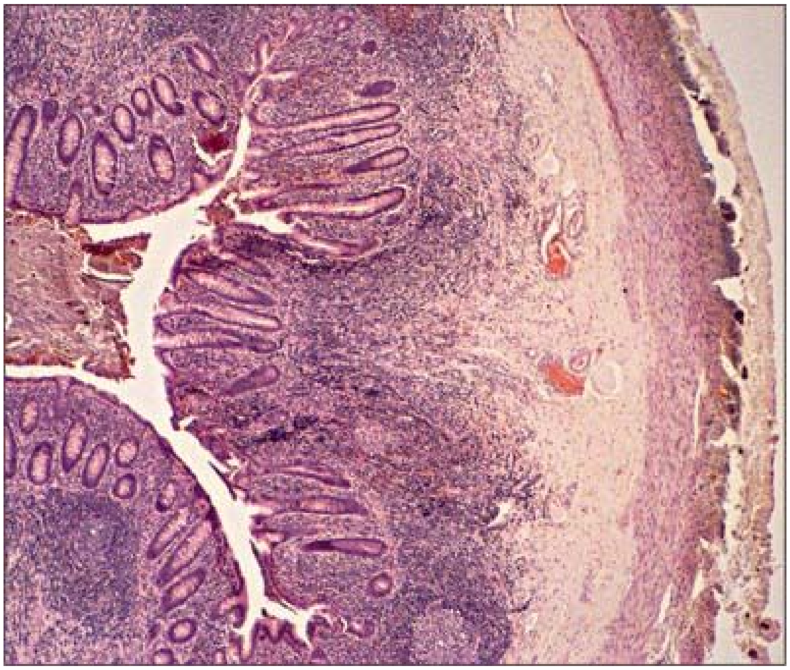

Fig. 67.20 Low-power micrograph of the appendix in transverse section, showing part of its circumference and a faecal pellet lodged in its lumen. Lymphoid tissue (basophilic staining) occupies much of the mucosa between crypts, and part of the submucosa. The muscularis externa and outermost serosal layer are seen at the right of the field.

Acute appendicitis

The genesis of acute appendicitis varies between individuals. It may follow obstruction of the lumen, when it is a consequence of increased intraluminal pressure and retention of (infected) contents which allows acute suppuration to occur. The size of the orifice of the appendix in some individuals may contribute to the risk that this will happen. Appendicoliths may be visible on plain radiographs in 7–15% of the normal population: in those patients with acute abdominal pain, their presence indicates a high risk of appendicitis being present. The increased size of the orifice and lumen at the extremes of life may be a reason why acute appendicitis is relatively uncommon in these age groups. Acute appendicitis may also present as a primary suppuration of the tissues of the appendix itself: the reduction in appendicular lymphoid tissue that occurs in later life may be another reason why the disease is infrequent in the elderly. Although the appendix is well supplied by arterial anastomoses at its base, the appendicular artery is an end artery from the midpoint upwards and its close proximity to the wall makes it susceptible to thrombosis during episodes of acute inflammation. This may render the distal appendix ischaemic and explains the frequency of gangrenous perforation seen in the disease.

The appendix and overlying visceral peritoneum are innervated by sympathetic and parasympathetic nerves from the superior mesenteric plexus. Visceral afferent fibres carrying sensations of distension and pressure mediate the symptoms of ‘pain’ felt during the initial stages of appendicular inflammation. In keeping with other structures derived from the midgut, these sensations are poorly localized initially, and referred to the central (periumbilical) region of the abdomen. It is not until parietal tissues adjacent to the appendix become involved in any inflammatory process that somatic nociceptors are stimulated, and there is an associated change in the nature and localization of pain. The caecum and proximal ascending colon share a common innervation with the appendix (sympathetic and parasympathetic nerves via the superior mesenteric plexus), which means that early inflammation in the caecum (typhlitis) results in similar visceral pain symptoms to those experienced in appendicitis.

ASCENDING COLON

The ascending colon is approximately 15 cm long and narrower than the caecum. It ascends to the inferior surface of the right lobe of the liver, on which it makes a shallow depression, and then turns abruptly forwards and to the left, at the hepatic flexure. It is a retroperitoneal structure covered anteriorly and on both sides by peritoneum. Its posterior surface is separated by loose connective tissue from the iliac fascia, the iliolumbar ligament, quadratus lumborum, the aponeurosis of transversus abdominis, and the anterior peri-renal fascia inferolateral to the right kidney. The lateral femoral cutaneous nerve, usually the fourth lumbar artery, and sometimes the ilioinguinal and iliohypogastric nerves, lie posteriorly as they cross quadratus lumborum. Laterally the peritoneum forms the lateral paracolic gutter and medially the medial paracolic gutter (Fig. 67.21). The ascending colon possesses a narrow mesocolon for part of its course in up to one-third of cases. Anteriorly it is in contact with loops of ileum, the greater omentum and the anterior abdominal wall.

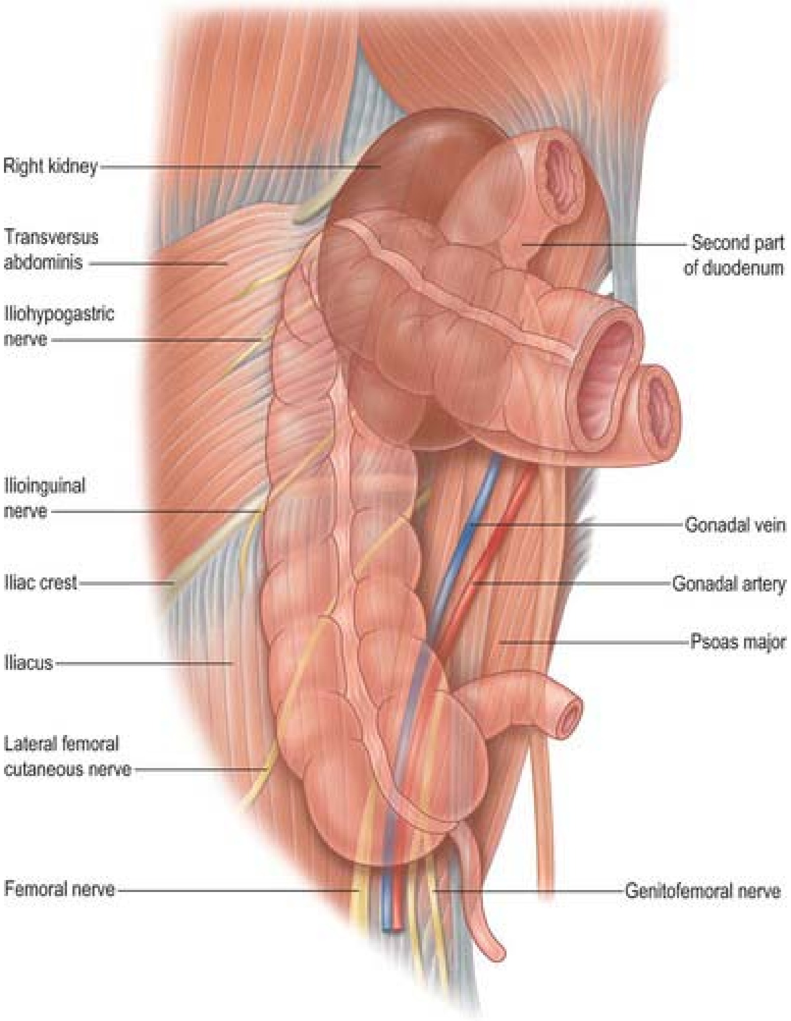
Right kidney
Transversus abdominis
Iliohypogastric nerve
Ilioinguinal nerve
Iliac crest
Iliacus
Lateral femoral cutaneous nerve
Femoral nerve
Second part of duodenum
Gonadal vein
Gonadal artery
Psoas major
Genitofemoral nerve

Fig. 67.21 Posterior relations of the ascending colon.

Hepatic flexure

The hepatic flexure forms the junction of the ascending and transverse colon as the latter turns down, forwards and to the left. It is variable in position and usually has a less acute angle than the splenic flexure. The anterior surface of the lower pole of the right kidney is posterior, the right lobe of the liver is superior and anterolateral (Fig. 67.22), the descending (second) part of the duodenum is medial and the fundus of the gallbladder is anteromedial. The posterior aspect of the hepatic flexure is not covered by peritoneum and the gut wall is in direct contact with pararenal fascia. The hepatic flexure is often covered in the greater omentum which may be attached to the anterior surface both of the upper ascending colon and the proximal (right) end of the transverse colon.

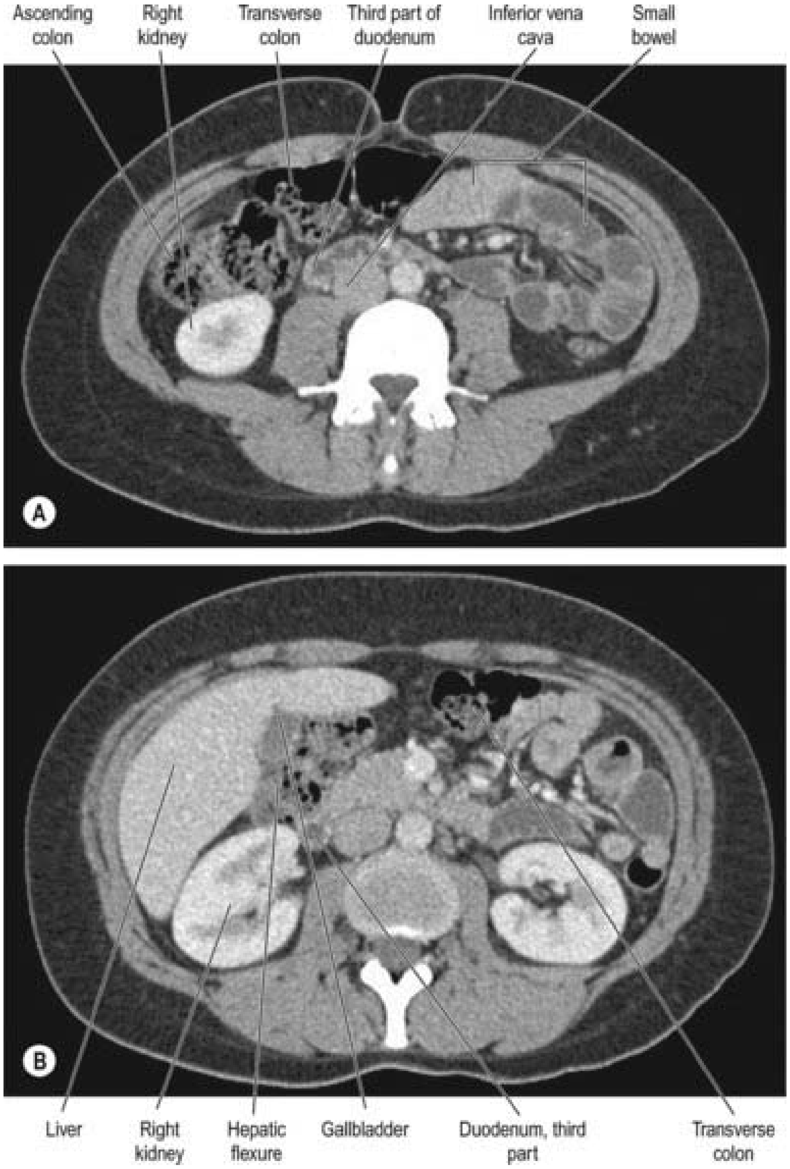
Ascending colon
Right kidney
Transverse colon
Third part of duodenum
Inferior vena cava
Small bowel
A
B
Liver
Right kidney
Hepatic flexure
Gallbladder
Duodenum, third part
Transverse colon

Fig. 67.22 Axial CT images of the ascending colon obtained (**A**) at the level of the mid ascending colon and (**B**) at the level of the hepatic flexure, showing the relationship of the ascending colon and hepatic flexure to the right lobe of the liver, the right and left kidneys, the second part of the duodenum, and the gallbladder (supplied by Dr Louise Moore, Chelsea and Westminster Hospital, London).

VASCULAR SUPPLY AND LYMPHATIC DRAINAGE

Arteries

Superior mesenteric artery

The arteries to the caecum, appendix and ascending colon are somewhat variable, but all are derived from the superior mesenteric artery via the ileocolic and right colic (when present) arteries (see Figs 67.11, 67.13).

Ileocolic artery

The ileocolic artery arises from the right side of the superior mesenteric artery in its upper half in the root of the mesentery. It descends to the right beneath the parietal peritoneum towards the caecum and crosses anterior to the right ureter, gonadal vessels and psoas major to enter the right iliac fossa. Although the terminal distribution varies, the artery usually divides into a superior division which runs superolaterally towards the ascending colon where it anastomoses with the right colic artery (or right branch of the middle colic artery), and an inferior division which anastomoses with the final ileal branch of the distal superior mesenteric artery. The inferior division approaches the superior border of the ileocolic junction. It usually gives rise to the following branches: ascending colic (which passes up on the ascending colon to anastomose with the superior division), anterior caecal, posterior caecal (which usually gives rise to the appendicular artery) and ileal (which ascends to the left on the lower ileum, supplies it and anastomoses with the last ileal branch of the superior mesenteric artery (Fig. 67.23). The caecum is supplied almost entirely from the ileocolic artery.

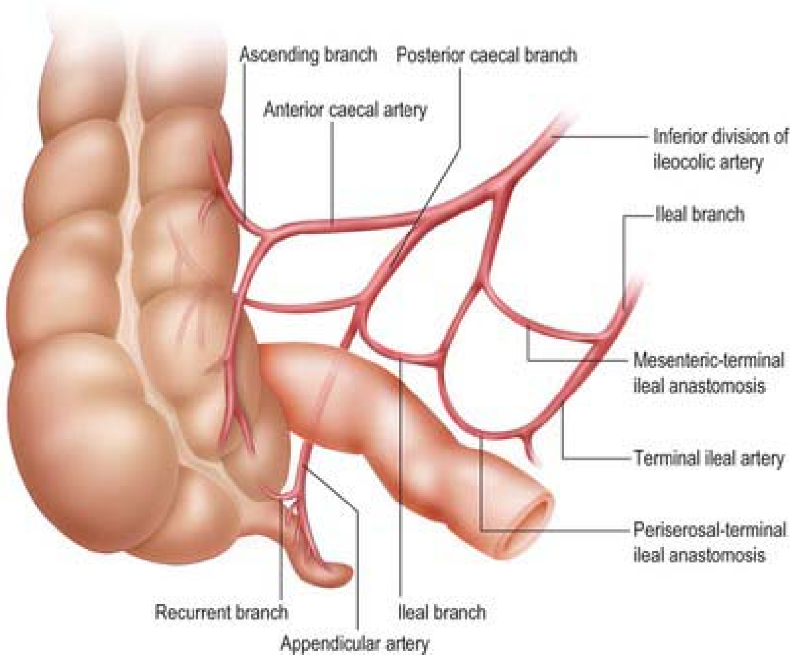
Ascending branch
Posterior caecal branch
Anterior caecal artery
Inferior division of ileocolic artery
Ileal branch
Mesenteric-terminal ileal anastomosis
Terminal ileal artery
Periserosal-terminal ileal anastomosis
Recurrent branch
Ileal branch
Appendicular artery

Fig. 67.23 The arteries of the caecum, vermiform appendix and ascending colon.

The ileocolic artery is the most prominent vessel in the lower right colic mesentery and traction on the caecum in the direction of the anterior superior iliac crest will readily cause the vessel to ‘tent’ the mesentery due to its direct course towards the caecum. This allows easy identification of the vessel during laparoscopic surgery.

The appendicular artery descends behind the terminal ileum to enter the mesoappendix a short distance from the appendicular base (Fig. 67.23). Here it gives off a recurrent branch, which anastomoses at the base of the appendix with a branch of the posterior caecal artery: the anastomosis is sometimes extensive. The main appendicular artery approaches the tip of the organ, at first near to, and then in the edge of, the mesoappendix. The terminal part of the artery lies on the wall of the appendix and may be thrombosed in appendicitis, which results in distal gangrene or necrosis. Accessory arteries are common, and many individuals possess two or more arteries of supply to the appendix.

The arcades of the terminal ileal artery provide a collateral supply to the caecum via anastomoses with the ileal branch of the ileocolic artery.

Right colic artery

The right colic artery is a small vessel that is highly variable in its anatomy (Fig. 67.24). Most commonly it arises as a common trunk with the middle colic artery. Alternatively it may arise as a separate branch from the right side of the superior mesenteric artery, or from the ileocolic artery (when it is referred to as an accessory right colic artery), and occasionally it may be absent. From its origin in common with the middle colic artery it passes towards the ascending colon, deep to the parietal peritoneum and anterior to the right gonadal vessels, right ureter and psoas major. Sometimes it arises more superiorly and crosses the second part of the duodenum and inferior pole of the right kidney. Near the colon it divides into a descending branch, which anastomoses with the ileocolic artery, and an ascending branch which anastomoses with the right branch of the middle colic artery. These form the marginal artery in the area of the hepatic flexure from which vessels are distributed to the upper third of the ascending colon, and the right side of the transverse colon.

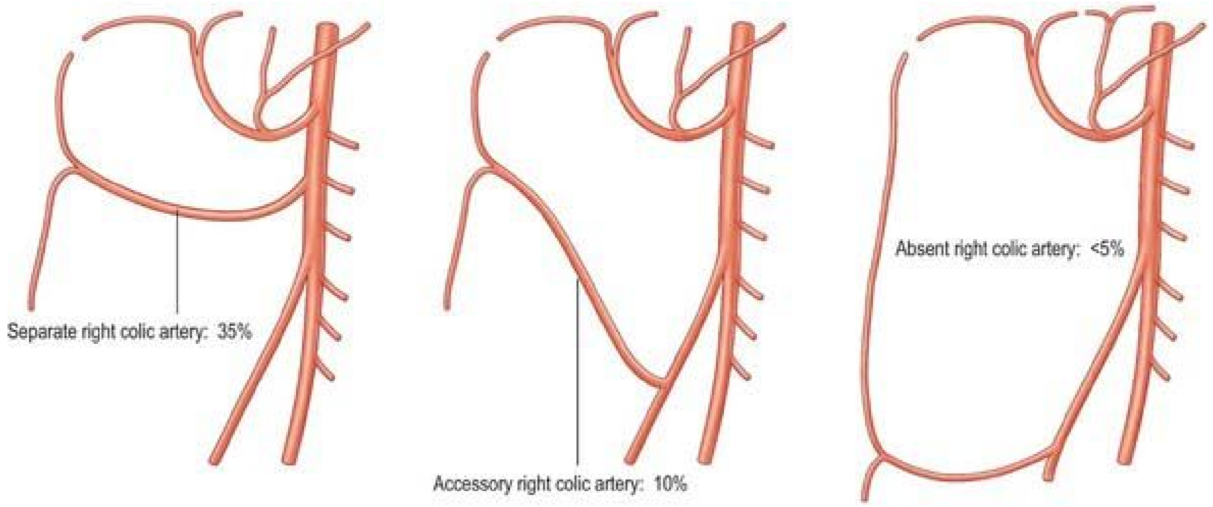
Separate right colic artery: 35%
Accessory right colic artery: 10%
Absent right colic artery: <5%

Fig. 67.24 Anatomical variants of the right colic artery.

Veins

Venous blood from the wall of the caecum, appendix and ascending colon drains into mesenteric arcades and subsequently into segmental veins, which accompany their respective arteries and tend to follow variations in arterial drainage. The segmental veins drain into the superior mesenteric vein, which lies to the right of the mesenteric artery.

Superior mesenteric vein

The superior mesenteric vein receives one or more middle colic veins, the right colic vein and the ileocolic vein and drains into the portal vein (see Figs 67.31, 66.12).

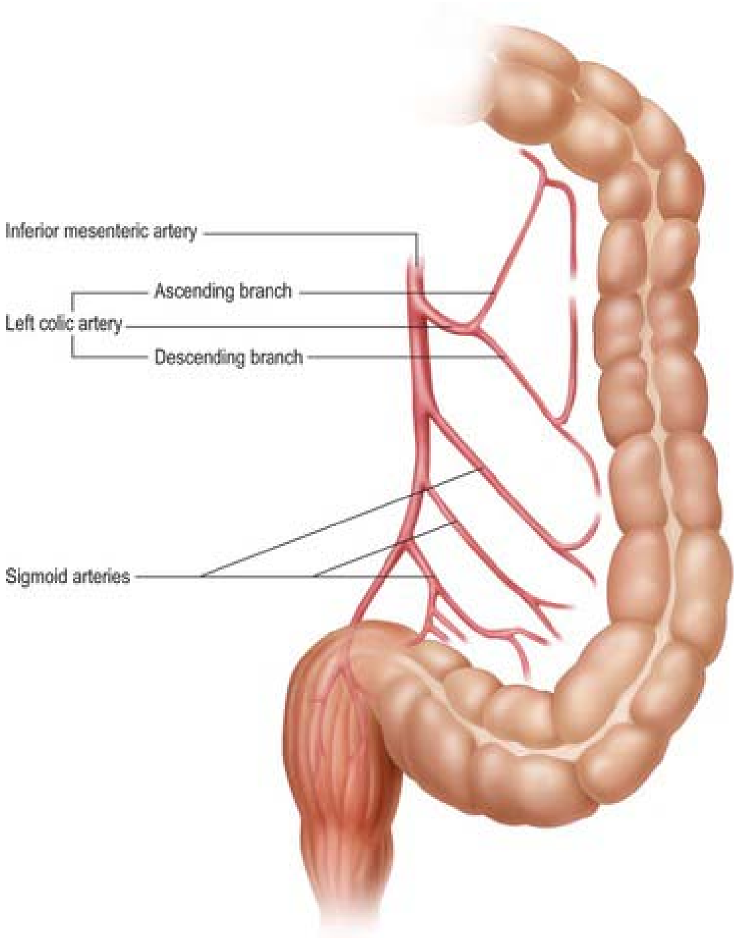
Inferior mesenteric artery
Ascending branch
Left colic artery
Descending branch
Sigmoid arteries

Fig. 67.31 The inferior mesenteric artery.

Ileocolic vein

The tributaries of the ileocolic vein follow a broadly similar pattern to the branches of the ileocolic artery, and are formed from superior and inferior tributaries. The vein ascends alongside the ileocolic artery beneath the peritoneum of the ileocaecal mesentery and drains into the superior mesenteric vein. The inferior tributary receives appendicular veins (via the posterior caecal or ileocolic veins) and anterior and posterior caecal and ileal veins, and the superior tributary drains the ascending colic veins.

Ascending tributaries of the ileocolic and right colic veins accompany their respective arteries into the root of the mesentery and drain via the ileocolic vein into the superior mesenteric vein.

Right colic vein

The right colic vein is highly variable and may drain into the superior mesenteric vein directly, or the right gastroepiploic or inferior pancreaticoduodenal vein to form a ‘gastrocolic trunk’ which drains into the superior mesenteric vein, or it may be absent entirely.

Lymphatics

Lymphatic vessels originate from both anterior and posterior aspects of the colon and drain into nodes located along the branches of the ileocolic and the right colic arteries. Lymphatic drainage from the distal ascending colon and hepatic flexure may be predominantly to the nodes of the right colic artery. The lymphatic anastomoses are rich and the preterminal nodes for both routes of drainage are the ileocolic nodes, located close to the superior mesenteric artery (Fig. 67.15).

Lymphatic vessels in the appendix are numerous and there is abundant lymphoid tissue in its walls. From the body and apex of the appendix, 8–15 vessels ascend in the mesoappendix, occasionally interrupted by one or more nodes. They unite to form three or four larger vessels which run into the lymphatic vessels that drain the ascending colon, and end in the inferior and superior nodes of the ileocolic chain.

INNERVATION

The sympathetic supply to the caecum, appendix and ascending colon originates in the intermediolateral grey matter of the fifth to the 12th thoracic spinal segments. Preganglionic axons travel via the greater and lesser splanchnic nerves to the coeliac and superior mesenteric plexuses where they synapse on neurones in the coeliac and superior mesenteric ganglia; postganglionic axons form periarterial plexuses along the branches of the superior mesenteric artery, whence they are distributed to the walls of the colon.

The parasympathetic supply to the caecum, appendix and ascending colon is derived from the vagus nerve via the coeliac and superior mesenteric plexuses.

Referred pain

The appendix and overlying visceral peritoneum are innervated by sympathetic and parasympathetic nerves from the superior mesenteric plexus. Visceral afferent fibres carrying sensations of distension and pressure mediate the symptoms of ‘pain’ felt during the initial stages of appendicular inflammation. In keeping with other structures derived from the midgut, these sensations are poorly localized initially, and referred to the central (periumbilical) region of the abdomen. It is not until parietal tissues adjacent to the appendix become involved in any inflammatory process that somatic nociceptors are stimulated, and there is an associated change in the nature and localization of pain. The caecum and proximal ascending colon share a common innervation to the appendix (sympathetic and parasympathetic nerves via the superior mesenteric plexus); early inflammation in the caecum (typhlitis) results in similar visceral pain symptoms to appendicitis.

TRANSVERSE COLON

The transverse colon is approximately 50 cm long, and extends from the hepatic flexure in the right lumbar region across into the left hypochondriac region, where it curves posteroinferiorly below the spleen as the splenic flexure. It is highly variable in length and position, as may be confirmed by radiological assessment, but it often describes an inverted arch, with its concavity directed posteriorly and superiorly. Near the splenic flexure an abrupt U-shaped curve may descend lower than the main arch. The posterior surface at the hepatic flexure is devoid of peritoneum and is attached by loose connective tissue to the front of the descending part of the duodenum and the head of the pancreas. The transverse colon from here to the splenic flexure is almost completely invested by peritoneum. It is suspended from the anterior border of the body of the pancreas by the transverse mesocolon which is attached from the inferior part of the right kidney, across the second part of the duodenum and pancreas, to the inferior pole of the left kidney. The transverse colon hangs down between the flexures to a variable extent, and sometimes reaches the pelvis. Above it are the liver and gallbladder, the greater curvature of the stomach and the body of the spleen. The transverse colon is usually attached to the greater curvature of the stomach by the gastrocolic ligament, which is in continuity with the greater omentum, lying anteriorly and extending inferiorly. Behind and below the transverse colon lie the descending part of the duodenum, the head of the pancreas, the upper end of the small bowel mesentery, the duodenojejunal flexure and loops of the jejunum and ileum.

The transverse mesocolon permits considerable mobility of the transverse colon: occasionally the colon may be interposed between the liver and the diaphragm (Chilaiditi syndrome), and may be mistaken for free intraperitoneal gas.

SPLENIC FLEXURE

The splenic flexure forms the junction of the transverse and descending colon and lies in the left hypochondrium, inferomedial to the lower pole of the spleen (Fig. 67.25). It is anterior to the pancreatic tail, and also to the left kidney, from which it is separated by the anterior perirenal fascia. The splenic flexure often adopts a very acute angle such that the end of the transverse colon overlaps the beginning of the descending colon; there may be peritoneal and omental adhesions between the two structures. It lies more superiorly and posteriorly than the right hepatic flexure; the visceral peritoneum covering its lateral aspect is often attached to the diaphragm at the level of the 10th and 11th ribs by the phrenicocolic ligament, which lies below the anterolateral pole of the spleen. Its position with respect to the spleen in variable: it usually lies directly inferomedial to the lower pole, forming the colic impression, but it may lie anterior to the splenic hilum, and even a little above. In these cases, the visceral peritoneum is often adherent to the splenic capsule or hilar connective tissue; inadvertent, downwards traction on the splenic flexure during surgery may tear the capsule or hilar vessels. It may lie ‘low’ in the splenorenal recess with no direct attachment to the splenic capsule.

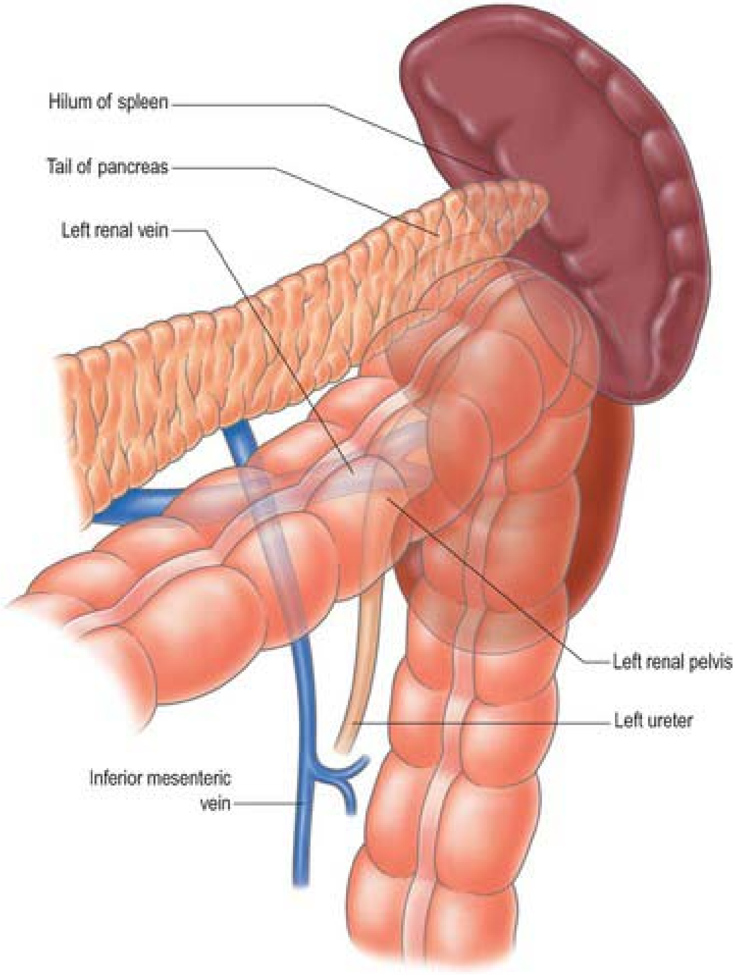
Hilum of spleen
Tail of pancreas
Left renal vein
Left renal pelvis
Left ureter
Inferior mesenteric vein

Fig. 67.25 Relations of the splenic flexure.

VASCULAR SUPPLY AND LYMPHATIC DRAINAGE

Arteries

The proximal two-thirds of the transverse colon is supplied by the superior mesenteric artery via the middle colic artery (Fig. 67.11). The distal third is usually supplied by the ascending branch of the left colic artery via the marginal artery of the colon, although this is somewhat variable.

Middle colic artery

The middle colic artery usually arises from the anterolateral aspect of the superior mesenteric artery, either separately or as a common trunk with the right colic artery, just inferior to the uncinate process of the pancreas and anterior to the third part of the duodenum. Initially it passes inferiorly, then turns to run anteriorly and superiorly within the root of the transverse mesocolon, just to the right of the midline, and usually divides into a right and left branch. The right branch anastomoses with the right colic artery, and the left branch anastomoses with the left colic artery. The arterial arches thus formed lie 3 or 4 cm from the transverse colon, which they supply. Sometimes the middle colic artery divides into three or more branches within the transverse mesocolon, in which case the most lateral branches form the arterial anastomoses. An accessory or rarely a replaced middle colic artery may arise from the dorsal pancreatic, hepatic, inferior mesenteric or left colic arteries (Fig. 67.26). In the latter two instances the left half or more of the transverse colon will derive its arterial supply from the inferior mesenteric artery.

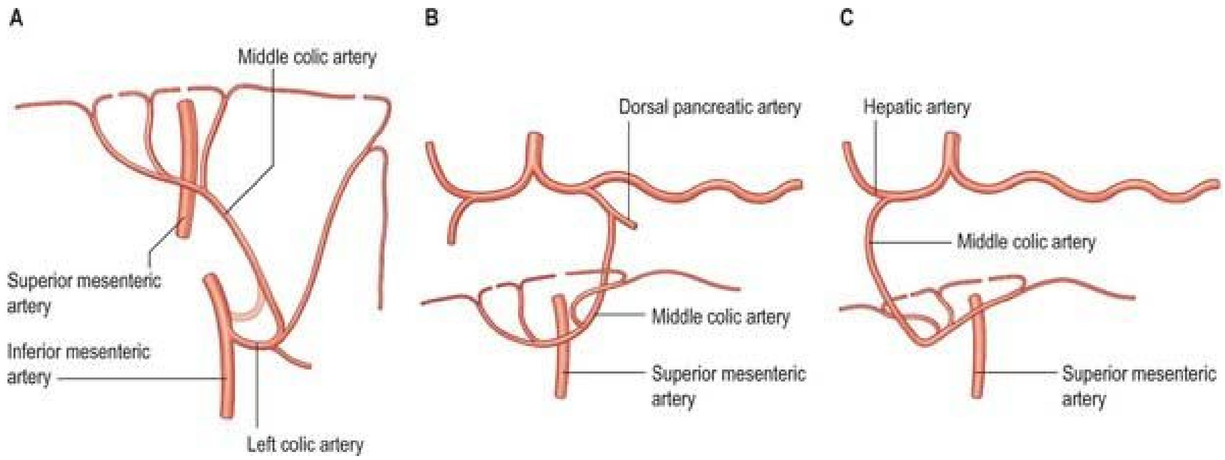
A
Middle colic artery
Superior mesenteric artery
Inferior mesenteric artery
Left colic artery
B
Dorsal pancreatic artery
Middle colic artery
Superior mesenteric artery
C
Hepatic artery
Middle colic artery
Superior mesenteric artery

Fig. 67.26 Variants in the origin of the middle colic artery: only replaced arteries have been illustrated for simplicity. Accessory arteries are more common in each case than complete replacement of the origin. **A**, Left colic artery or inferior mesenteric artery (<5%). **B**, The dorsal pancreatic artery (<5%). **C**, Hepatic artery (<5%).

Veins

Superior mesenteric vein

The superior mesenteric vein receives one or more middle colic veins and the ileocolic vein (see Figs. 67.31, 66.12). The right colic vein is often absent or drains as a tributary to the right branch of the middle colic vein.

Middle colic veins

Several tributaries drain into one or more middle colic veins which are highly variable in extent and position. The middle colic veins drain either into the superior mesenteric vein, just before its junction with the splenic vein, or directly into the hepatic portal vein.

Lymphatics

Lymph vessels drain into nodes along the middle colic arteries and then into the superior mesenteric nodes. The predominant lymphatic drainage of the splenic flexure is usually via nodes along the left colic artery which drain into the inferior mesenteric nodes: this arrangement is dependent on the arterial supply to the distal third of the transverse colon.

INNERVATION

The proximal two-thirds of the transverse colon is innervated by sympathetic and parasympathetic nerves via the superior mesenteric plexus. The distal third usually receives a sympathetic supply from the inferior mesenteric plexus and a parasympathetic supply that is derived partly from the inferior mesenteric plexus and partly from retroperitoneal fibres which travel in the pelvic splanchnic nerves that arise from neurones in the second, third and fourth sacral spinal segments. The sympathetic nerves are inhibitory to mural muscle in the transverse colon; some fibres are vasoconstrictor to the colic vasculature. Parasympathetic nerves are secretomotor to colic glands and motor to the colic musculature.

DESCENDING COLON

The descending colon is approximately 25 cm long. It descends through the left hypochondrium and lumbar region, initially following the lateral border of the lower pole of the left kidney, and then descending in the angle between psoas major and quadratus lumborum to the iliac crest. It then curves inferomedially, lying anterior to iliacus and psoas major, to become the sigmoid colon below the level of the iliac crest (inlet of the lesser pelvis). It lies on the retroperitoneum covered anteriorly and on both sides by peritoneum. Its posterior surface is separated by loose connective tissue from the anterior peri-renal fascia inferolateral to the left kidney, the aponeurosis of transversus abdominis, quadratus lumborum, iliacus and the most superolateral part of psoas major. The subcostal vessels and nerves, iliohypogastric, ilio-inguinal, lateral femoral cutaneous, femoral and genitofemoral nerves, and the fourth lumbar artery (usually), all lie posterior to the descending colon (Fig. 67.27). Loops of jejunum lie anteriorly. If the anterior abdominal walls are relaxed, the most inferior part of the descending colon may be directly palpated transabdominally. The descending colon is smaller in calibre, more deeply placed, and more frequently covered posteriorly by peritoneum, than the ascending colon.

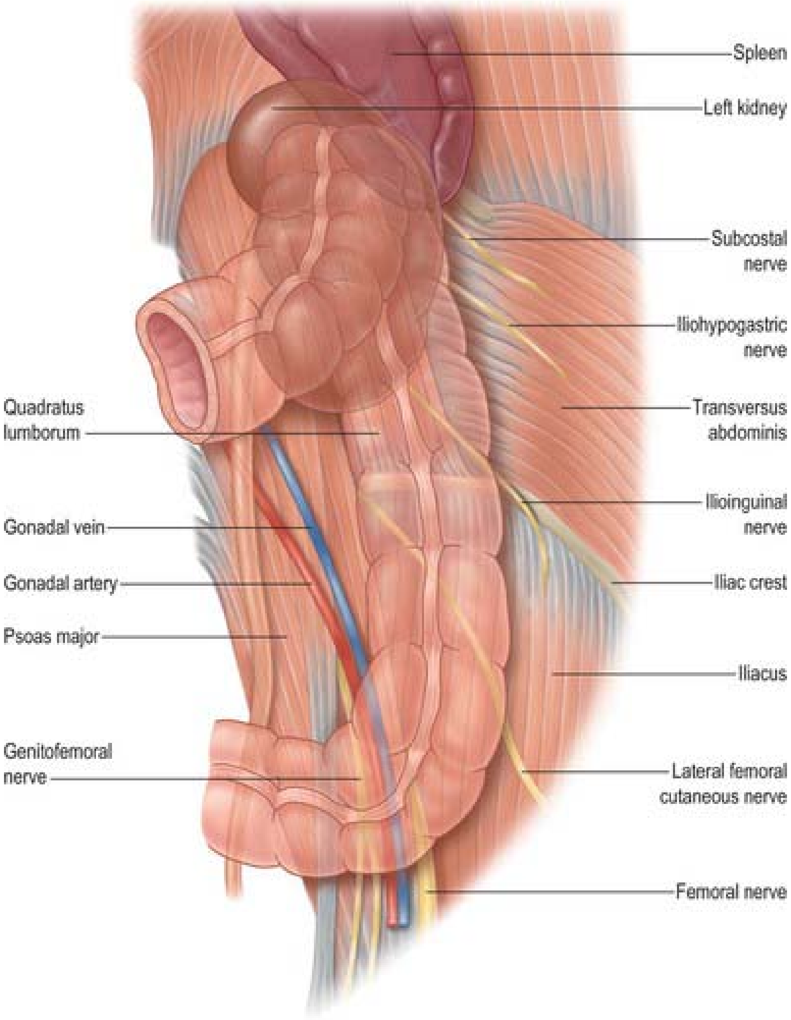
Spleen
Left kidney
Subcostal nerve
Iliohypogastric nerve
Quadratus lumborum
Transversus abdominis
Ilioinguinal nerve
Gonadal vein
Gonadal artery
Iliac crest
Psoas major
Iliacus
Genitofemoral nerve
Lateral femoral cutaneous nerve
Femoral nerve

Fig. 67.27 Posterior relations of the descending colon.

SIGMOID COLON

The sigmoid colon begins below the pelvic inlet and ends at the rectum. Characteristically it forms a mobile loop which normally lies in the lesser pelvis, but its length and form are the most variable of all colonic segments. It is usually completely invested in peritoneum and is attached to the lower posterior abdominal wall and the posterior wall of the false pelvis by the fan-shaped sigmoid mesocolon. The root of the sigmoid mesocolon has an inverted ‘V’ attachment to the posterior abdominal wall.

The sigmoid colon initially descends over the iliac crest into the false pelvis but thereafter its position is extremely variable. It may remain folded and principally in contact with, or adherent to, the peritoneum overlying iliacus, or it may cross the pelvic cavity between the rectum and bladder in males, or the rectum and uterus in females, and it may even reach the right pelvic wall. If long, the sigmoid loop may rise out of the pelvis into the abdominal cavity and lie in contact with loops of ileum. The sigmoid loop ends in a relatively constant position lying just to the left of the midline at the level of the third sacral body, where it bends inferiorly and is continuous with the rectum. The sigmoid loop is fixed at its junctions with the descending colon and rectum but quite mobile between them. Its relations are therefore variable (Fig. 67.28). Laterally are the left external iliac vessels, the obturator nerve, ovary or vas deferens and the lateral pelvic wall; posteriorly lie the left external and internal iliac and gonadal vessels, ureter, piriformis and sacral plexus; anteroinferiorly lie the bladder in males, or uterus and bladder in females; superiorly and to the right the sigmoid colon is in contact with loops of the ileum. The gonadal vessels and ureter lie in a distinct fascial plane which is the inferior extension of the anterior and posterior peri-renal fascia in the lower retroperitoneum and which is separate from the thin fascial coverings of the mesosigmoid. The plane between the two layers can be recognized during surgical dissection of the mesentery of the sigmoid colon because it does not contain the numerous small vessels which are often present in the loose connective tissue surrounding the ureter and gonadal vessels.

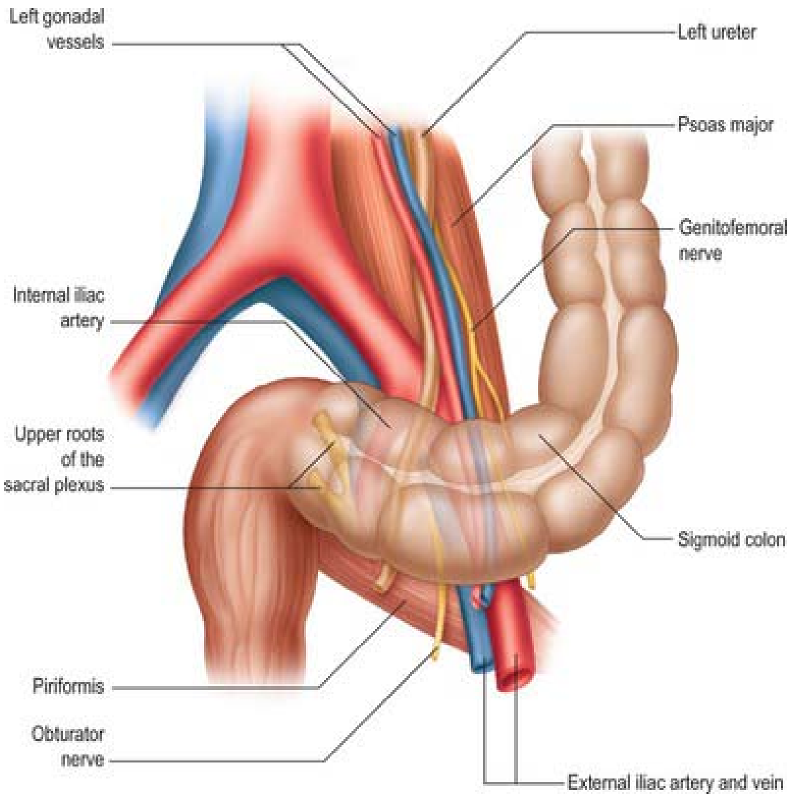
Left gonadal vessels
Left ureter
Psoas major
Genitofemoral nerve
Internal iliac artery
Upper roots of the sacral plexus
Sigmoid colon
Piriformis
Obturator nerve
External iliac artery and vein

Fig. 67.28 Posterior relations of the sigmoid colon.

The position and shape of the sigmoid colon vary according to the length of the colon; the length and mobility of its mesocolon; the degree of distension (when distended the sigmoid colon rises into the abdominal cavity, and it sinks again into the lesser pelvis when empty); the condition of the rectum, bladder and uterus (the sigmoid colon tends to rise when these are distended, and to fall when they are empty). The length and diameter of the sigmoid colon vary in different races.

SIGMOID VOLVULUS

Rotation or volvulus may occur around the mesenteric attachment of the sigmoid colon, similar to the rotation of the caecum around its mesentery. Only the sigmoid colon is affected, because the descending colon rarely possesses sufficient mesentery to become involved in the rotation. Rotation usually involves at least 270°. Volvulus is more common when the length of the sigmoid colon increases, since this is associated with a ‘fan-like’ mesentery with a short retroperitoneal attachment. Volvulus does not occur in individuals where the sigmoid colon is short or where the mesentery is short and its attachment runs over the brim of the pelvis. The combination of anatomical features predisposing to sigmoid volvulus is most commonly found in sub-Saharan Africans and chronically institutionalized patients.

DIVERTICULAR DISEASE

The development of acquired diverticula occurs commonly in the sigmoid colon, particularly in white Caucasian populations. Their location appears to be related to the underlying anatomy of the wall of the colon. Thus, diverticula commonly occur midway between the anti-mesenteric and lateral taeniae, i.e. where the colonic wall is potentially weak, not only because the circular muscle lacks the support of the longitudinal muscle, but also because it is traversed here by arteries as they access the submucosal vascular plexus. The predilection of the diverticula for the sigmoid colon probably relates to causative factors rather than intrinsic differences in the structure of its walls. In marked contrast, congenital diverticula may occur anywhere throughout the colon, and are often found adjacent to the mesenteric attachment of the colon.

VASCULAR SUPPLY AND LYMPHATIC DRAINAGE

Arteries

The arterial supply of the descending colon is from the inferior mesenteric artery via its left colic branch, which also anastomoses with the marginal artery of the colon (in the region of the splenic flexure), and the sigmoid arteries (in the region of the junction with the sigmoid colon) (Figs 67.29-67.31).

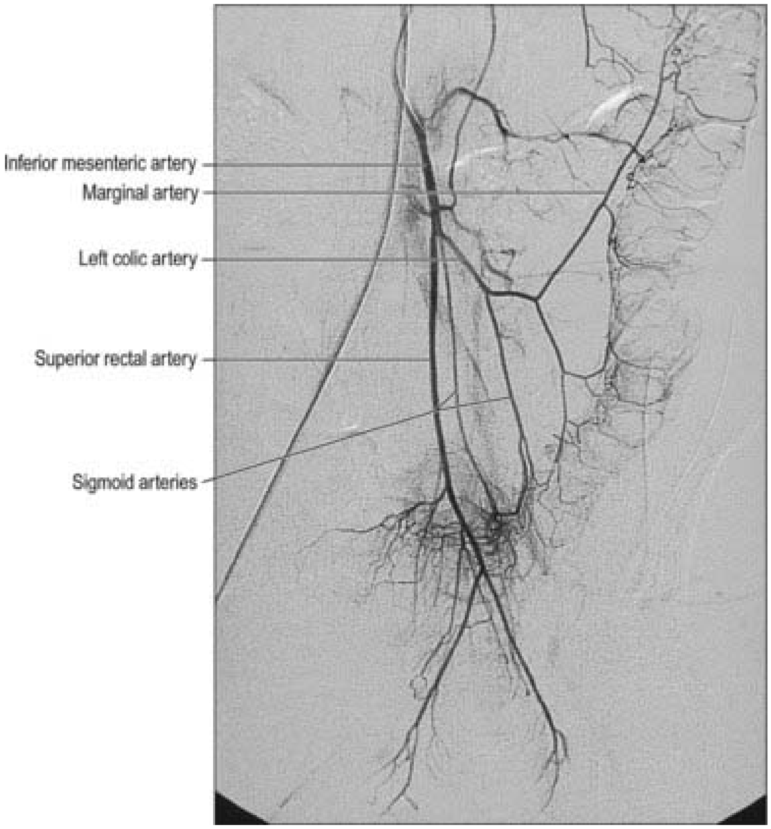
Inferior mesenteric artery
Marginal artery
Left colic artery
Superior rectal artery
Sigmoid arteries

Fig. 67.29 Digital subtraction arteriogram showing the inferior mesenteric artery and its branches.

(By kind permission from Dr Adam Mitchell, Charing Cross Hospital, London.)

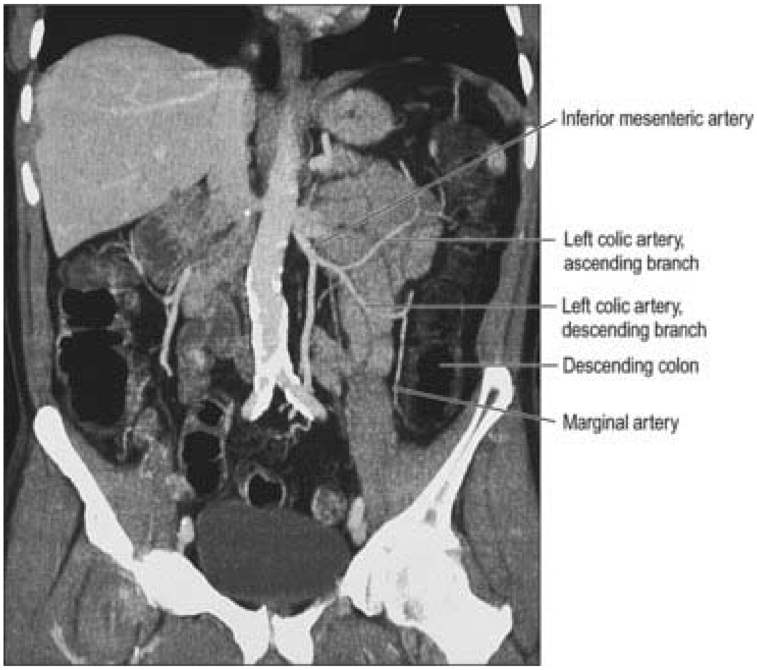
Inferior mesenteric artery
Left colic artery, ascending branch
Left colic artery, descending branch
Descending colon
Marginal artery

Fig. 67.30 The vascular supply of the descending colon from the inferior mesenteric artery via the ascending and descending branches of the left colic artery, coronal reformat CT.

(By kind permission from Dr Louise Moore, Chelsea and Westminster Hospital, London.)

Inferior mesenteric artery

The inferior mesenteric artery is usually smaller in calibre than the superior mesenteric artery. It arises from the anterior or left anterolateral aspect of the aorta at about the level of the third lumbar vertebra, 3 or 4 cm above the aortic bifurcation and below the third part of the duodenum. It descends in the root of the left colic mesentery initially anterior and then to the left of the aorta, crosses the origin of the left common iliac artery medial to the left ureter, and then enters, and continues in, the root of the sigmoid mesocolon as the superior rectal artery. The inferior mesenteric vein lies on its lateral side in its distal course. The principal branches of the inferior mesenteric artery are the left colic, sigmoid and superior rectal arteries (see Figs 67.11, 67.29).

Left colic artery

The left colic artery arises from the inferior mesenteric artery shortly after its origin, ascends within the left colic mesentery anterior to the left psoas major, and bifurcates into ascending and descending branches (this division may occur soon after its origin). The artery or its branches cross the left ureter and gonadal vessels. The ascending branch passes anterior to the left kidney and anastomoses with the left branch of the middle colic artery in the subperitoneal space within the transverse mesocolon. The descending branch passes laterally in the retroperitoneum and approaches the descending colon, where it forms part of the marginal artery and anastomoses with the highest sigmoid artery. The arterial arches thus formed supply the distal third of the transverse and the descending colon. Occasionally an accessory, or rarely a replaced, left colic artery may originate from the trunk of the superior mesenteric artery or the first jejunal branches. When present, it runs laterally in the upper left colic mesentery just below the level of the duodenojejunal junction to supply the upper descending colon and form part or all of the marginal artery and the arterial anastomosis in the region of the distal transverse colon (Fig. 67.32). The left colic artery may itself give rise to an accessory left middle colic artery. Occasionally the left colic artery gives rise to a branch shortly after its origin which ascends in the mesentery and anastomoses directly with a similar descending branch of the left branch of the middle colic artery (the arc of Riolan).

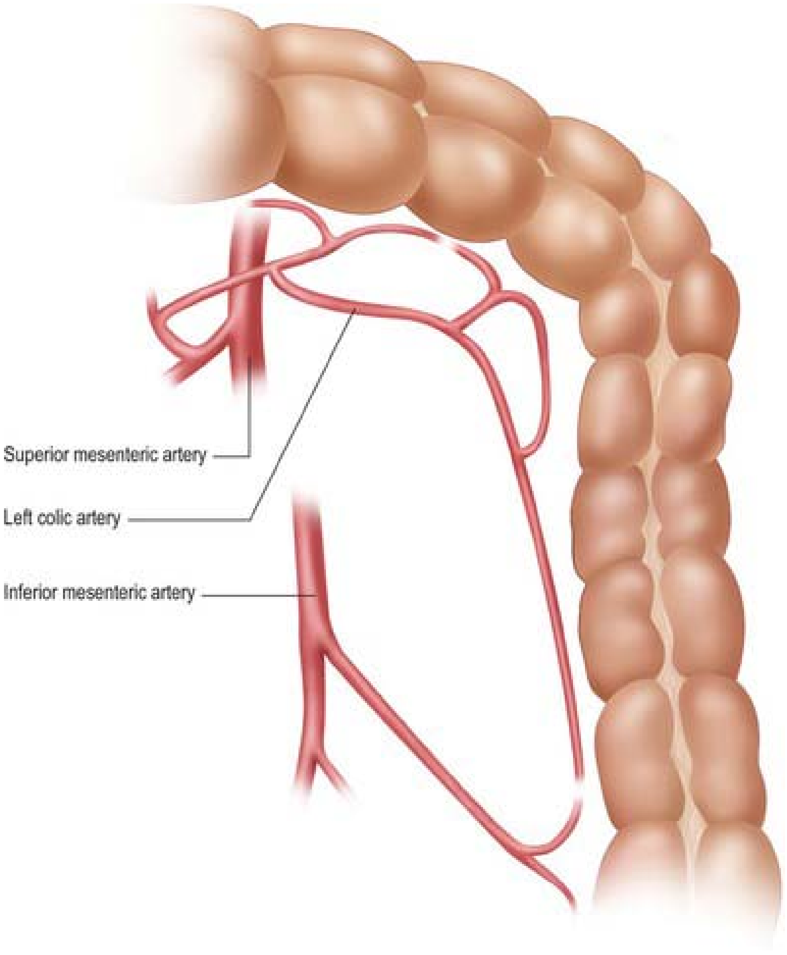

Fig. 67.32 Replaced left colic artery arising from the superior mesenteric artery.

Sigmoid (inferior left colic) arteries

There are between two and five sigmoid arteries, which are branches of the inferior mesenteric artery. They descend obliquely within the subperitoneal space in the sigmoid mesentery, anterior to the left psoas major, ureter and gonadal vessels. They supply the distal descending colon and sigmoid colon, and anastomose superiorly with the left colic artery and inferiorly with the superior rectal artery. Unlike the small intestine, arterial arcades do not form until the arteries are close to the wall of the colon, when small branches arise which supply the sigmoid colon directly. The formation of a true marginal artery is less pronounced in the region of the sigmoid colon than in the region of the descending colon. A significant space often exists in the mesentery between the highest sigmoid artery and the descending branch of the left colic artery: this is a useful guide to the arterial territories during surgical dissection.

In the region of the splenic flexure the marginal artery receives contributions from the left branch of the middle colic artery which anastomoses with an ascending branch of the left colic artery to supply the upper descending colon. The descending branch of the left colic artery anastomoses with upper branches of the highest sigmoid artery to supply the descending colon. The origin of the primary arterial supply for the splenic flexure and distal third of the transverse colon is usually via the left colic artery but may be from the left branch of the middle colic artery. The marginal artery in the region of the splenic flexure may be absent or of such small calibre as to be of little clinical relevance. It may, however, hypertrophy significantly when one of the main visceral arteries is compromised, e.g. following stenosis or occlusion of the inferior mesenteric artery, and it then provides a vessel of collateral supply.

Vascular ligation in left colonic resections

During resection of the distal descending and sigmoid colon, ligation of the inferior mesenteric artery close to its origin preserves the bifurcation of the left colic artery. The arterial supply to the proximal descending colon is maintained via the anastomosis between the ascending branch of the left colic artery and the left branch of the middle colic artery. Less radical resection, involving ligation of the left colic artery close to its bifurcation, may interfere with or obliterate this supply and render the descending colon more likely to become ischaemic. The same is true for ligation of the left colic vein. If the inferior mesenteric vein is ligated, then the bifurcation of the vein forms the route of venous drainage for the descending colon to the middle colic vein territory. Ligation of the branches separately will impair the venous drainage.

Veins

Inferior mesenteric vein

The inferior mesenteric vein drains the rectum, sigmoid, descending and distal transverse colon (Fig. 67.33; see also Fig. 67.14). It begins as the superior rectal vein, from the rectal plexus, through which it connects with middle and inferior rectal veins. The inferior mesenteric vein lies to left of the inferior mesenteric artery, ascends deep to the peritoneum and anterior to the left psoas major and may cross the testicular or ovarian vessels or ascend medial to them. It usually lies lateral to or occasionally posterior to the duodenojejunal flexure and the peritoneal fold directly lateral to the flexure is a useful guide to locating the vein surgically. It usually drains into the splenic vein, but occasionally drains into the confluence of the splenic and superior mesenteric veins or directly into the superior mesenteric vein. If a duodenal or paraduodenal fossa exists, the vein is usually in its anterior wall. The inferior mesenteric vein receives tributaries from several sigmoid veins, the middle and the left colic veins.

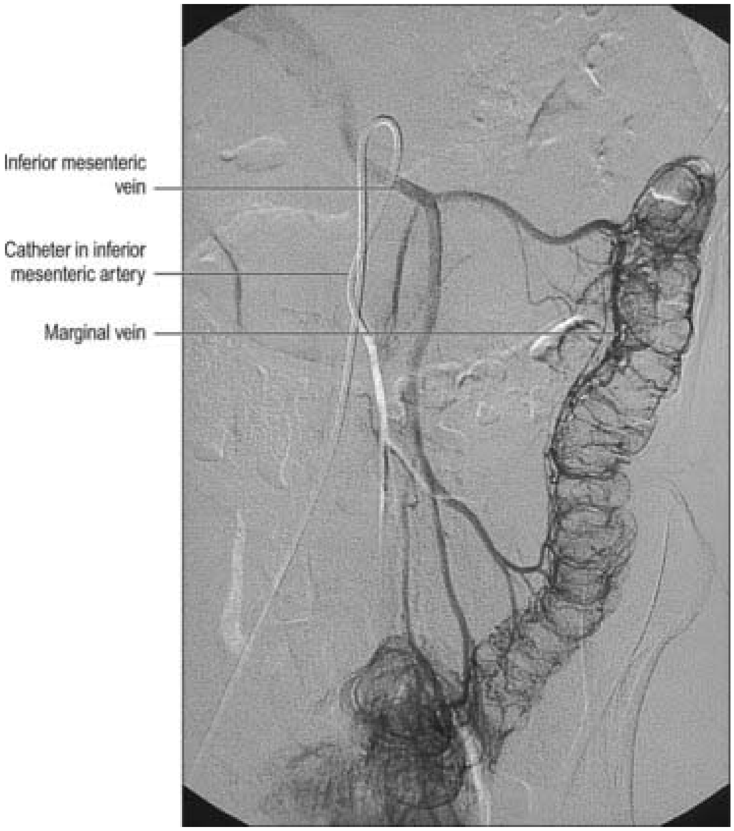

Fig. 67.33 The inferior mesenteric vein and its tributaries, digital subtraction arteriogram.

(By kind permission from Dr Adam Mitchell, Charing Cross Hospital, London.)

Left colic vein

The left colic vein is formed from several tributaries including ascending and descending branches which correspond to the equivalent arteries. These tributaries may not form a discrete vein until they drain into the inferior mesenteric vein, and occasionally there may be two distinct veins which both run into the inferior mesenteric vein. The left colic vein usually lies more superiorly in the left colon mesentery than its equivalent artery, and has a shorter course because the inferior mesenteric vein lies more laterally than the inferior mesenteric artery.

Several sigmoid veins drain the sigmoid colon and run superiorly alongside their respective arteries to drain into the inferior mesenteric vein.

Lymphatics

Lymph vessels drain from the descending colon into nodes along the left colic artery, and from the sigmoid colon into sigmoid nodes in the sigmoid mesocolon which then join superior rectal and left colic vessels. All of these nodes drain into the inferior mesenteric nodes.

INNERVATION

The sympathetic supply to the left third of the transverse colon and the descending and sigmoid colon originates in the first and second lumbar spinal segments, and runs in the upper lumbar splanchnic nerves: preganglionic axons synapse on neurones in the abdominal aortic and the inferior mesenteric plexuses, whence postganglionic axons reach the gut wall via periarterial plexuses on branches of the inferior mesenteric artery. These axons are inhibitory to the mural muscle of the colon and some fibres are vasoconstrictor to the colic vasculature.

The parasympathetic supply is via the pelvic splanchnic nerves. Some fibres run through the inferior and superior hypogastric plexuses and along branches of the inferior mesenteric artery, but many more pass directly through the retroperitoneal tissues, independent of the inferior mesenteric artery, to reach the splenic flexure and descending and sigmoid colon. Parasympathetic nerves are secretomotor to colic glands and motor to the colic musculature. Afferent impulses mediating sensations of distension are carried by visceral afferent fibres which travel with the parasympathetic nerves.

RECTUM

The rectum is continuous with the sigmoid colon at the level of the third sacral vertebra and terminates at the upper end of the anal canal. It descends along the sacrococcygeal concavity as the sacral flexure of the rectum, initially inferoposteriorly and then inferoanteriorly, to join the anal canal by passing through the pelvic diaphragm. The anorectal junction is 2–3 cm in front of and slightly below the tip of the coccyx, which is opposite the apex of the prostate in males. From this level the anal canal passes inferiorly and posteriorly from the lower end of the rectum. The posterior bend is termed the perineal flexure of the rectum and the angle it forms with the upper anal canal is the anorectal angle. The rectum also deviates in three lateral curves: upper, convex to the right; middle (the most prominent), convex to the left; lower, convex to the right. Both ends of the rectum are in the median plane (Fig. 67.34).

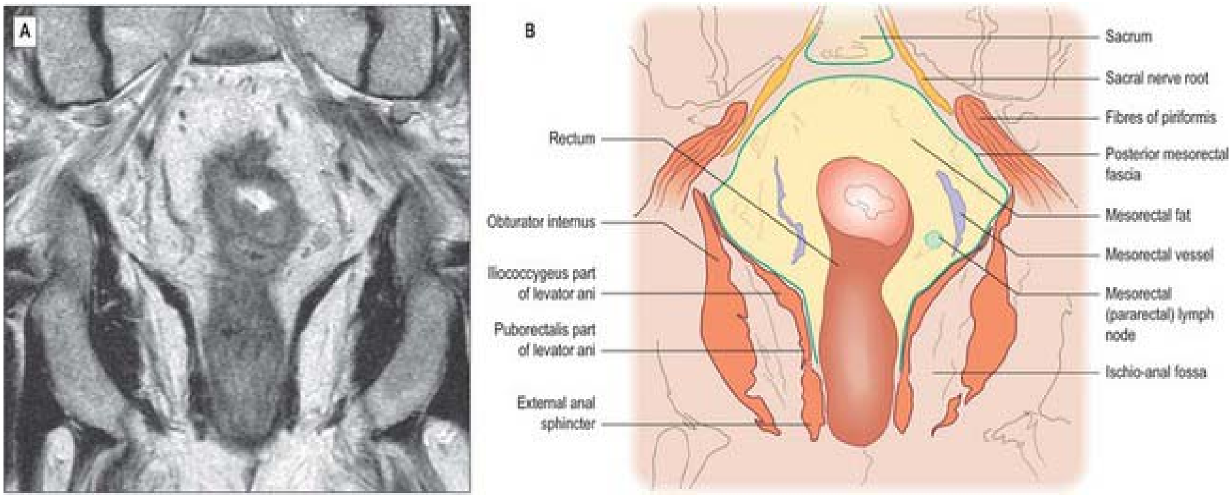
A
B
Sacrum
Sacral nerve root
Fibres of piriformis
Posterior mesorectal fascia
Rectum
Mesorectal fat
Obturator internus
Mesorectal vessel
Iliococcygeus part of levator ani
Mesorectal (pararectal) lymph node
Puborectalis part of levator ani
Ischio-anal fossa
External anal sphincter

Fig. 67.34 **A**, Coronal T2-weighted MRI of the rectum. **B**, Line diagram illustrating main features in **A**.

Although variable in absolute length, a common landmark used in clinical practice to define the rectum is a length of 15 cm above the external anal margin. The initial diameter is similar to that of the sigmoid colon, but more inferiorly it becomes dilated as the rectal ampulla. The rectum differs from the sigmoid colon in having no sacculations or appendices epiploicae. The taeniae blend approximately 5 cm above the rectosigmoid junction, forming two wide muscular bands which descend anteriorly and posteriorly in the rectal wall. These then fuse to form an encircling layer of longitudinal muscle, which invests the entire length of the rectum. At the rectal ampulla a few strands of the anterior longitudinal fibres pass forwards to the perineal body as the musculus recto-urethralis. In addition, two fasciculi of smooth muscle may pass anteroinferiorly from the anterior surfaces of the bodies of the second and third coccygeal vertebrae to blend with the longitudinal muscle fibres on the posterior wall of the anal canal, forming the rectococcygeal muscles.

The upper third of the rectum is covered by peritoneum on its anterior and lateral aspects. It is related anteriorly to the sigmoid colon or loops of ileum if these lie in the pelvis, otherwise it is related to the urinary bladder in males, or the cervix and body of the uterus in females. The middle third of the rectum is covered by peritoneum only on its anterior aspect. The peritoneum is reflected superiorly onto the urinary bladder in males to form the rectovesical pouch, or onto the posterior vaginal wall in females to form the recto-uterine pouch (pouch of Douglas). The level of this reflection is higher in males; the rectovesical pouch is approximately 7.5 cm (about the length of the index finger) from the anorectal junction. In females the recto-uterine pouch is approximately 5.5 cm from the anorectal junction. In the male neonate, peritoneum extends on to the front of the rectum as far as the lower limit of the prostate. Superiorly the peritoneum is firmly attached to the muscle layer of the sigmoid colon by fibrous connective tissue, but as it descends onto the rectum it is more loosely attached by fatty connective tissue, which allows for considerable expansion of the upper half of the rectum (Figs 67.35, 67.36).

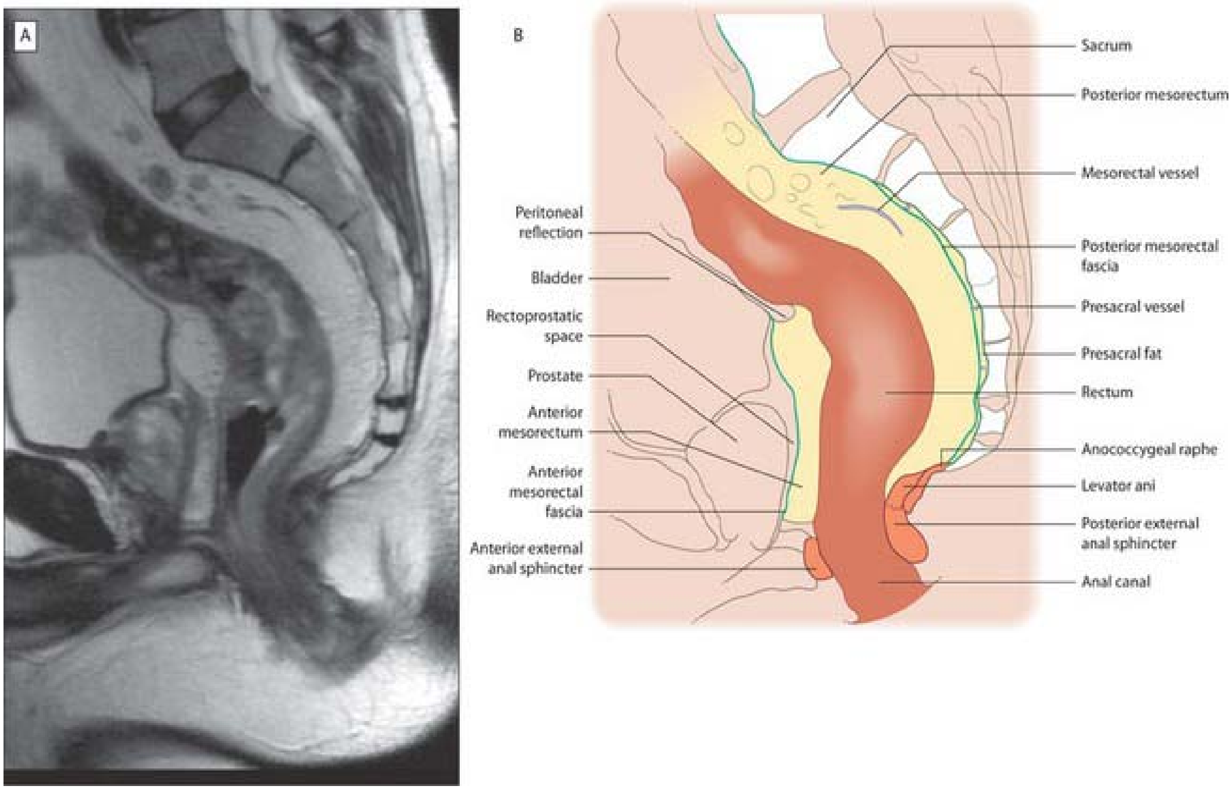
A
B
Sacrum
Posterior mesorectum
Mesorectal vessel
Peritoneal reflection
Posterior mesorectal fascia
Bladder
Presacral vessel
Rectoprostatic space
Presacral fat
Prostate
Rectum
Anterior mesorectum
Anococcygeal raphe
Levator ani
Anterior mesorectal fascia
Posterior external anal sphincter
Anterior external anal sphincter
Anal canal

Fig. 67.35 **A**, Sagittal T2-weighted MRI of the rectum in a male. **B**, Line diagram illustrating main features in **A**.

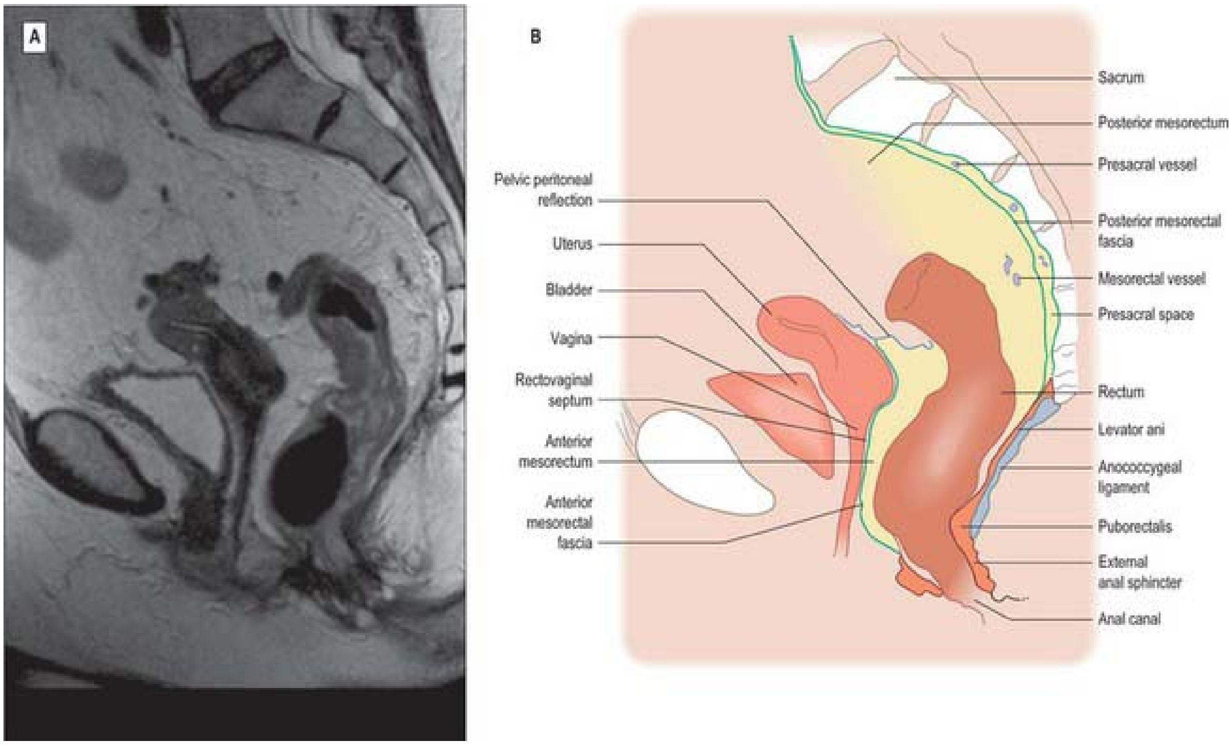
A
B
Pelvic peritoneal reflection
Uterus
Bladder
Vagina
Rectovaginal septum
Anterior mesorectum
Anterior mesorectal fascia
Sacrum
Posterior mesorectum
Presacral vessel
Posterior mesorectal fascia
Mesorectal vessel
Presacral space
Rectum
Levator ani
Anococcygeal ligament
Puborectalis
External anal sphincter
Anal canal

Fig. 67.36 **A**, Sagittal T2-weighted MRI of the rectum in a female. **B**, Line diagram illustrating main features in **A**.

There are no haustra in the rectum. When empty the mucosa forms a number of longitudinal folds in its lower part which become effaced during distension. The rectum commonly has three permanent semi-lunar transverse or horizontal folds (although the number can vary), which are most marked in rectal distension (Fig. 67.9). Two forms of horizontal fold have been recognized. One consists of the mucosa, a circular muscle layer and part of the longitudinal muscle, and is marked externally by an indentation. The other is devoid of longitudinal muscle and has no external marking. The most superior fold at the beginning of the rectum may be either on the left or right and occasionally encircles the rectal lumen. The middle fold is largest and most constant. It lies immediately above the rectal ampulla, projecting from the anterior and right wall just below the level of the anterior peritoneal reflection; the circular muscle is more marked in this fold than in the others. The most inferior and variable fold is found on the left below the middle fold. Sometimes a fourth fold is found on the left a little above the middle fold.

MESORECTUM, RECTAL FASCIAE AND ‘SPACES’

The mesorectum (mesentery of the rectum) and its contents are intimately related to the rectum down to the level of levator ani (Figs 67.37-67.39). It is a distinct compartment derived from the embryological hindgut. It contains the superior rectal artery and its branches, the superior rectal vein and its tributaries, the lymphatic vessels and nodes that lie along the superior rectal artery, branches from the inferior mesenteric plexus which descend to innervate the rectum, and loose adipose connective tissue.

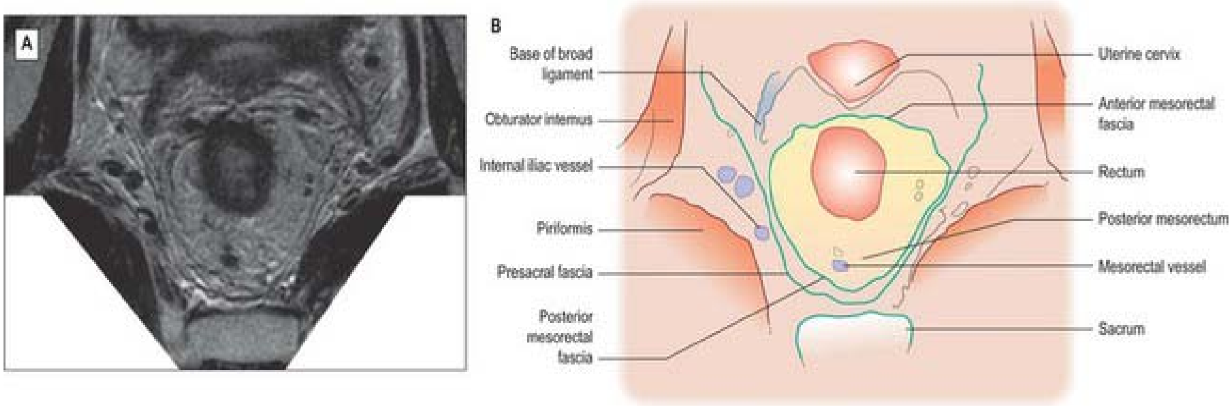
A
B
Base of broad ligament
Obturator internus
Internal iliac vessel
Piriformis
Presacral fascia
Posterior mesorectal fascia
Uterine cervix
Anterior mesorectal fascia
Rectum
Posterior mesorectum
Mesorectal vessel
Sacrum

Fig. 67.37 **A**, Axial T2-weighted MRI of the upper rectum in a female. **B**, Line diagram illustrating main features in **A**.

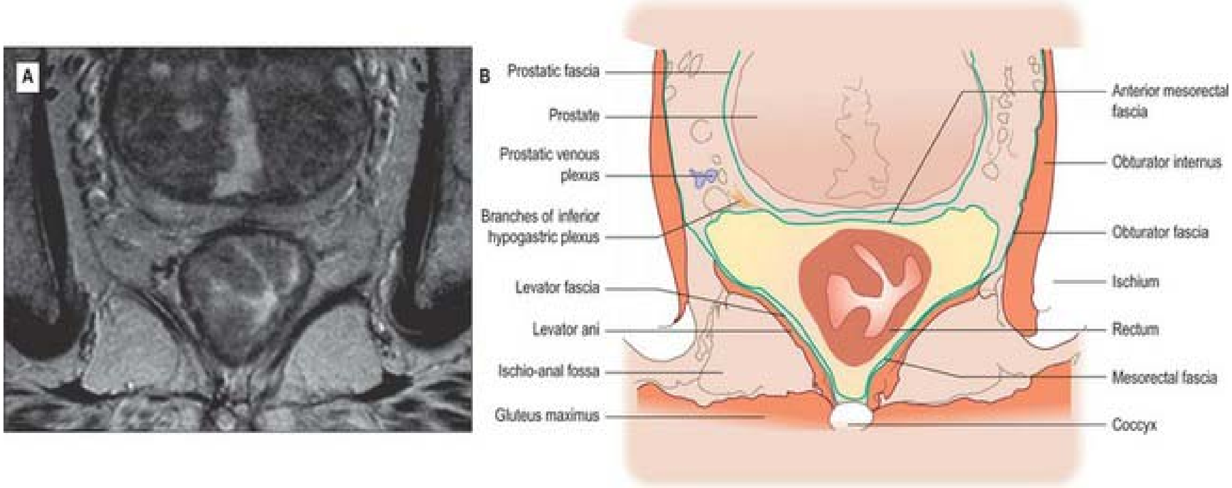
A
B
Prostatic fascia
Prostate
Prostatic venous plexus
Branches of inferior hypogastric plexus
Levator fascia
Levator ani
Ischio-anal fossa
Gluteus maximus
Anterior mesorectal fascia
Obturator internus
Obturator fascia
Ischium
Rectum
Mesorectal fascia
Coccyx

Fig. 67.38 **A**, Axial T2-weighted MRI of the mid rectum below the peritoneal reflection in a male. **B**, Line diagram illustrating main features in **A**.

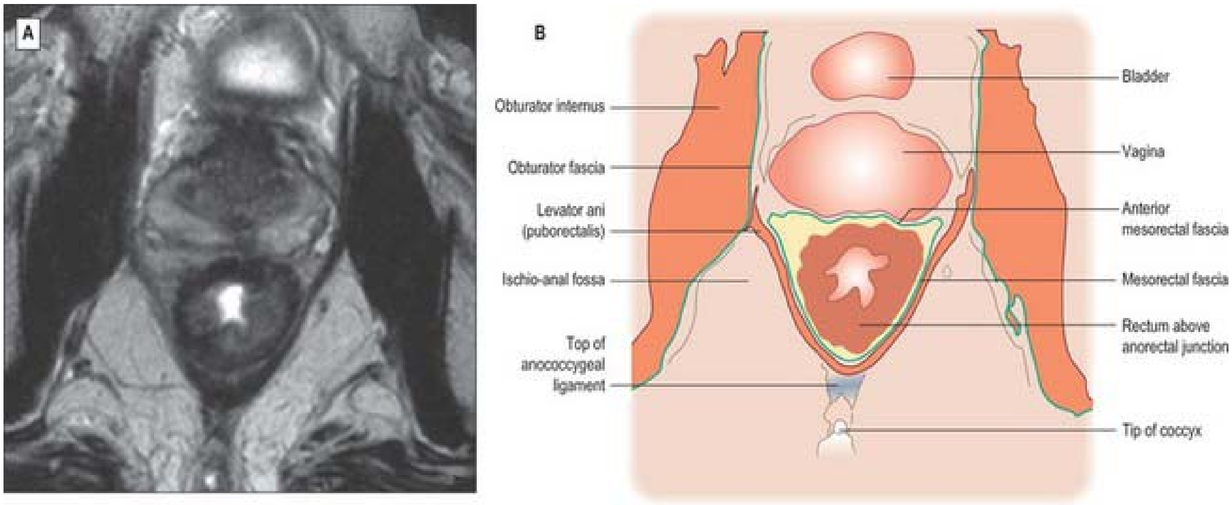
A
B
Obturator internus
Obturator fascia
Levator ani (puborectalis)
Ischio-anal fossa
Top of anococcygeal ligament
Bladder
Vagina
Anterior mesorectal fascia
Mesorectal fascia
Rectum above anorectal junction
Tip of coccyx

Fig. 67.39 **A**, Axial T2-weighted MRI of the low rectum below the peritoneal reflection in a female. **B**, Line diagram illustrating main features in **A**.

The mesorectum is enclosed by mesorectal fascia, a distinct covering derived from the visceral peritoneum that is also called the visceral fascia of the mesorectum, fascia propria of the rectum or the presacral wing of the hypogastric sheath. The fascia bounds the mesorectum posteriorly and thus lies anterior to the retrorectal space and the pre-sacral fascia. The mesorectal fascia is surrounded by a very thin layer of loose areolar tissue which separates it from the posterior and lateral walls of the true pelvis. Superiorly, the mesorectal fascia blends with the connective tissue bounding the sigmoid mesentery. Laterally, it extends around the rectum and mesorectum and becomes continuous with a denser condensation of fascia anteriorly. In males this anterior fascia is known as the rectovesical fascia of Denonvillier, and in females it forms the fascia of the rectovaginal septum.

On MRI scanning, the mesorectum appears as a fat-containing envelope in which vessels are depicted as low signal due to signal void produced by blood flow. Lymph nodes appear as high signal ovoid structures. Small nerves within the mesorectum are not visualized, but interlacing connective tissue within the mesorectum can be seen as low signal intensity strands. The mesorectal fascia is demonstrated on axial views as a low signal layer that surrounds the mesorectum, and which corresponds to the distinct condensation of fascia seen on histological sections containing the mesorectum (Brown et al 1999). Identification of the involvement of this layer by malignant tumours of the rectum on MRI scanning may help plan preoperative radiotherapy, and predict the chance of successful surgical resection.

Anterolaterally, branches of the inferior hypogastric plexus and branches of the middle rectal artery and veins run into the mesorectum. They are ensheathed by fascia and are sometimes jointly referred to as the ‘lateral rectal ligaments’. The number and calibre of the middle rectal vessels are highly variable; they may be very small or even absent (Sato & Sato 1991). The ‘lateral ligaments’ are not seen on MRI or CT scanning, and only appear as an identifiable structure with surgical traction on the rectum. The fascia of the ‘ligaments’ is flimsy and they probably play very little role in support of the rectum.

The parietal fascia that covers levator ani and the muscles of the side-wall of the pelvis forms a denser condensation of fascial tissue overlying the sacrum (Fig. 67.40).

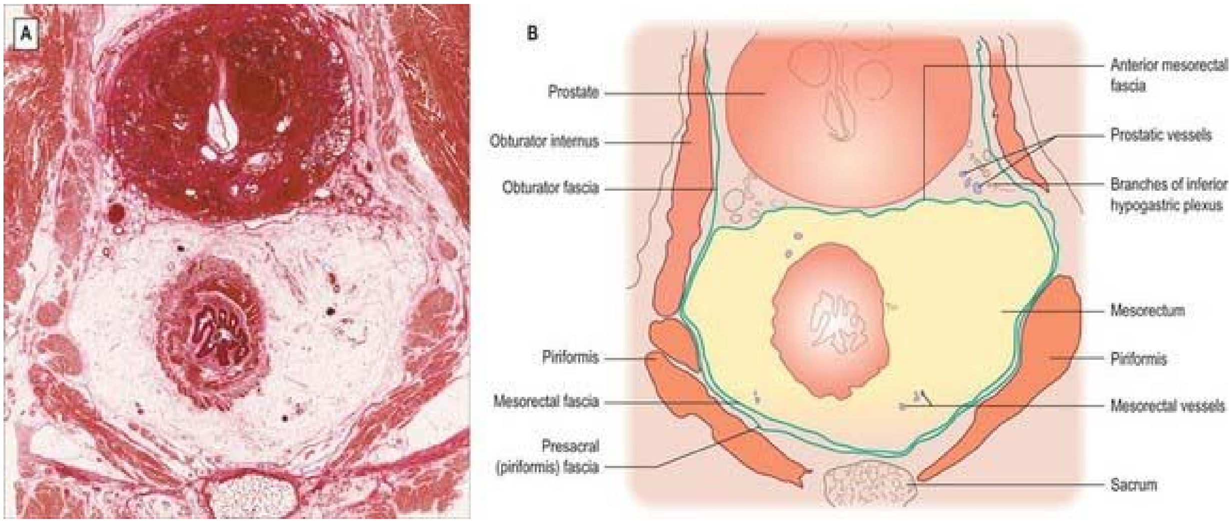
A
B
Prostate
Obturator internus
Obturator fascia
Piriformis
Mesorectal fascia
Presacral (piriformis) fascia
Anterior mesorectal fascia
Prostatic vessels
Branches of inferior hypogastric plexus
Mesorectum
Piriformis
Mesorectal vessels
Sacrum

Fig. 67.40 **A**, Light microscope transverse section of the mid rectum (male, cadaveric specimen). **B**, Line diagram illustrating main features in **A**.

RELATIONS OF THE RECTUM

Posterior to the rectum and mesorectum, and separated from them by the presacral fascia, in the median plane are the lower three sacral vertebrae, coccyx, median sacral vessels, and the lowest portion of the sacral sympathetic chain. Laterally, the upper part of the rectum is related to the pararectal fossa and its contents (sigmoid colon or terminal ileum), while below the peritoneal reflection lie piriformis, the anterior rami of the lower three sacral and coccygeal nerves, the sympathetic trunk, lower lateral sacral vessels, and coccygei and levatores ani. Anteriorly, above the level of the peritoneal reflection, lie loops of sigmoid colon or terminal ileum (if these lie in the pelvis), otherwise the rectum is related to the upper parts of the base of the bladder in males, or to the cervix/body of the uterus and upper vagina in females. The lower parts of the base of the bladder, the seminal vesicles, vas deferens, terminal parts of the ureters, and the prostate in males (Figs 67.38, 67.39), or the lower part of the vagina in females, lie below the reflection. In females, the rectovaginal septum is composed of a condensation of connective tissue which is continuous with the connective tissue of the outer layers of the rectal and vaginal walls. In postmenopausal females, and following childbirth, the connective tissue of the rectovaginal septum may atrophy or be thinned, reducing the support for the anterior rectal and posterior vaginal walls.

RECTAL PROLAPSE

Prolapse of the rectum involving all layers of the rectal wall may occur: the precise aetiology is not known. During prolapse, the mid and upper rectum descends towards the pelvic floor on straining. This descent tends to occur within the lumen of the rectum as a form of intussusception, and may be a consequence of the large diameter of the lower rectal ampulla and relative fixation of the anorectal junction and anal canal. The upper mesorectum is formed by relatively loose adipose connective tissue, and so relatively little tissue actually fixes the mid and upper rectum in position within the pelvis. The 'lateral ligaments' are composed mainly of vascular structures and offer only limited support against rectal descent. Chronic enlargement of the anorectal space bound by levatores ani commonly occurs in patients suffering rectal prolapse, but it is thought to be a consequence rather than a cause of the prolapse. During prolapse, the recto-uterine pouch in females also descends with the anterior rectal wall, and in extreme cases may become everted through the anus between the layers of rectal wall. This rarely happens to the rectovesical pouch in males.

RECTOCELE

When the rectovaginal septum is grossly effaced, especially in postmenopausal females, the pressure of defecation transmitted forward along the sacral flexure of the rectum can eventually cause bulging of the rectal wall into the posterior vagina, and, in extreme cases, through the vaginal introitus. Failure of support of the rectum and perineum by the puborectalis and pubovaginalis muscles contributes to this prolapse by allowing descent of the posterior perineum during straining.

MESORECTAL EXCISION IN RECTAL CANCER

An important concept in the oncological treatment of adenocarcinoma of the rectum is the integrity of the rectum and its mesorectal tissue. The epirectal and pararectal lymphatic tissues are located throughout the mesorectum. If the mesorectum is divided or disrupted during surgical excision of rectal carcinoma, involved nodes may be left *in situ*, which may predispose to local recurrence of tumour (Heald et al 1982). Oncological excision of the rectum involves mobilization of the rectum in the plane formed by the mesorectal fascia posterolaterally around the mesorectum. This plane allows the rectum and mesorectum to be removed as a whole without disruption of the presacral fascia and its underlying venous plexus. It is continuous with the plane between the mesentery surrounding the origin of the superior rectal artery and the presacral fascia over the sacral promontory, which is opened during mobilization of the origin of the inferior mesenteric artery prior to ligation. The mesorectal plane extends laterally and anteriorly, disrupted only by small branches of the middle rectal vessels, and is continuous with the rectovesical or rectovaginal fascia, which provides a similar oncological plane of dissection. Since the inferior hypogastric nerves are closely related to the plane of the mesorectal fascia in its upper third, dissection must spare the nerves if a degree of pelvic autonomic disturbance (bladder dysfunction and erectile dysfunction in males) is to be avoided following surgery. Complete excision of the rectum – total mesorectal excision – involves mobilization of this plane to the level of levatores ani. During the excision it is important to follow the sacral curve of the rectum to prevent entry into the presacral fascia or anococcygeal ligament with subsequent bleeding from presacral vessels.

ABDOMINOPERINEAL EXCISION IN RECTAL CANCER

The posterior mesorectum is thinnest at its lowest extremity, where the mesorectal fascia becomes continuous with the periserosal tissues which condense on the outer muscle layer as it passes inside the fibres of puborectalis and it lies directly on the fascia of levator ani (endopelvic fascia) (see Fig. 63.4). Tumours penetrating through the rectal wall at this point may therefore lie in extremely close proximity to the mesorectal margin. Conventional dissection in the mesorectal plane as far as the pelvic floor may open this fascial space close to the tumour and abdominoperineal excision of the rectum should be conducted through the ischio-anal fossa, vertically through levator ani outside the puborectalis sling and into the mesorectal plane well above the area of contact with the pelvic floor to avoid opening this potential tumour plane.

LOCAL EXCISION OF THE RECTUM

Full thickness excision of lesions of the rectal wall is possible in those parts of the rectum lying in the extraperitoneal compartment, i.e. below the peritoneal reflections. The mesorectal adipose tissue contains any leakage of contents and provides support to the closure of the defect in the rectal wall. Since only the lower third of the rectum is wholly extraperitoneal, full thickness local excisions of the rectum should be avoided on the anterior wall of the middle third and anterolateral walls of the upper third of the rectum. The height to which such excision can be performed anteriorly in females is lower than in males, because the lower level of the peritoneal reflection makes entry into the peritoneal cavity more likely.

VASCULAR SUPPLY AND LYMPHATIC DRAINAGE

Arteries

The principal arterial supply to the upper two-thirds of the rectum is the superior rectal artery. Branches of the middle rectal artery provide some additional supply to the middle third, and ascending branches of the inferior rectal artery supply the distal third. The median sacral artery (the terminal midline branch of the aorta), contributes a small branch which enters the posterior wall of the anorectal junction on the sacrorectal fascia (Fig. 67.41).

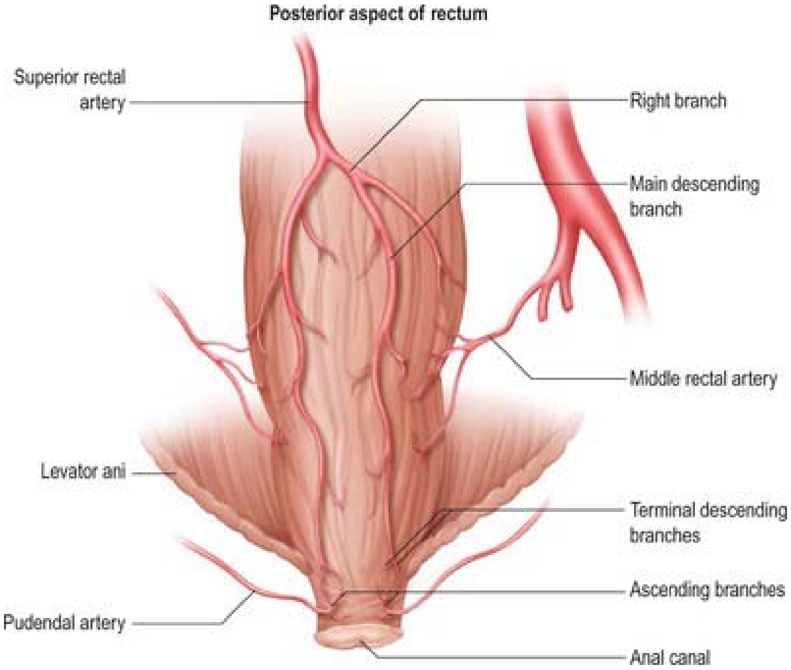
Posterior aspect of rectum
Superior rectal artery
Right branch
Main descending branch
Middle rectal artery
Levator ani
Terminal descending branches
Ascending branches
Pudendal artery
Anal canal

Fig. 67.41 The arterial supply of the rectum.

Superior rectal artery

The superior rectal artery is the principal continuation of the inferior mesenteric artery (Fig. 67.31). It descends into the pelvis in the sigmoid mesocolon, crosses the left common iliac vessels and passes over the sacral promontory usually just to the left of the midline. It is straddled by the inferior hypogastric nerves on either side. It lies anterior to the upper sacral vertebrae and passes into the upper mesorectum, then descends, initially in the midline, and divides into two branches at the level of the third sacral vertebra. These lie initially posterolateral, then lateral, to the rectal wall as they descend one on each side of the rectum. Terminal branches pierce the muscle wall from the level of the upper mesorectum to enter the rectal submucosa, where they anastomose with ascending branches of the inferior rectal arteries.

Middle rectal arteries

The middle rectal arteries arise either directly from the anterior division of the internal iliac artery or from the inferior vesical artery (vaginal artery in females). They enter the mesorectum anterolaterally in the ‘lateral rectal ligaments’, and are frequently either absent or may be very small in calibre (Sato & Sato 1991). When present, they provide an arterial supply to the muscle of the mid and lower rectum, but form only poor anastomoses with the superior and inferior rectal arteries.

Inferior rectal arteries

The inferior rectal arteries are terminal branches of the internal pudendal arteries. They cross the ischio-anal fossa to enter the upper anal canal laterally where they branch. They supply the internal and external anal sphincters, the anal canal and the perianal skin. Ascending branches pass superiorly in the submucosal plain, and anastomose with the terminal branches of the superior rectal artery.

Veins

Rectal venous plexus

The rectal venous plexus surrounds the rectum, and connects anteriorly with the vesical plexus in males or the uterovaginal plexus in females. It consists of an internal part, beneath the rectal and anal epithelium, and an external part outside the muscular wall. In the anal canal the internal plexus displays longitudinal dilatations, connected by transverse branches in circles immediately above the anal valves. The dilatations are most prominent in the left lateral, right anterolateral and right posterolateral sectors. The internal plexus drains mainly to the superior rectal vein but connects widely with the external plexus. The inferior portion of the external plexus is drained by the inferior rectal vein into the internal pudendal vein, the middle portion by one or more middle rectal veins into the internal iliac vein, and its superior part by the superior rectal vein, which drains into the inferior mesenteric vein. Communication between portal and systemic venous systems is thus established in the rectal plexus.

Superior rectal veins

The superior rectal veins are formed from the internal rectal plexus. The tributaries of the superior rectal vein ascend in the rectal submucosa as about six vessels of considerable size which pierce the rectal wall approximately 7.5 cm above the anus. The branches unite to form the superior rectal vein, which runs along the superior rectal artery in the root of the mesorectum and mesosigmoid, crosses the left common iliac vessels with the superior rectal artery, and continues upwards as the inferior mesenteric vein to the left of the midline (see Figs 67.14 and 67.43A).

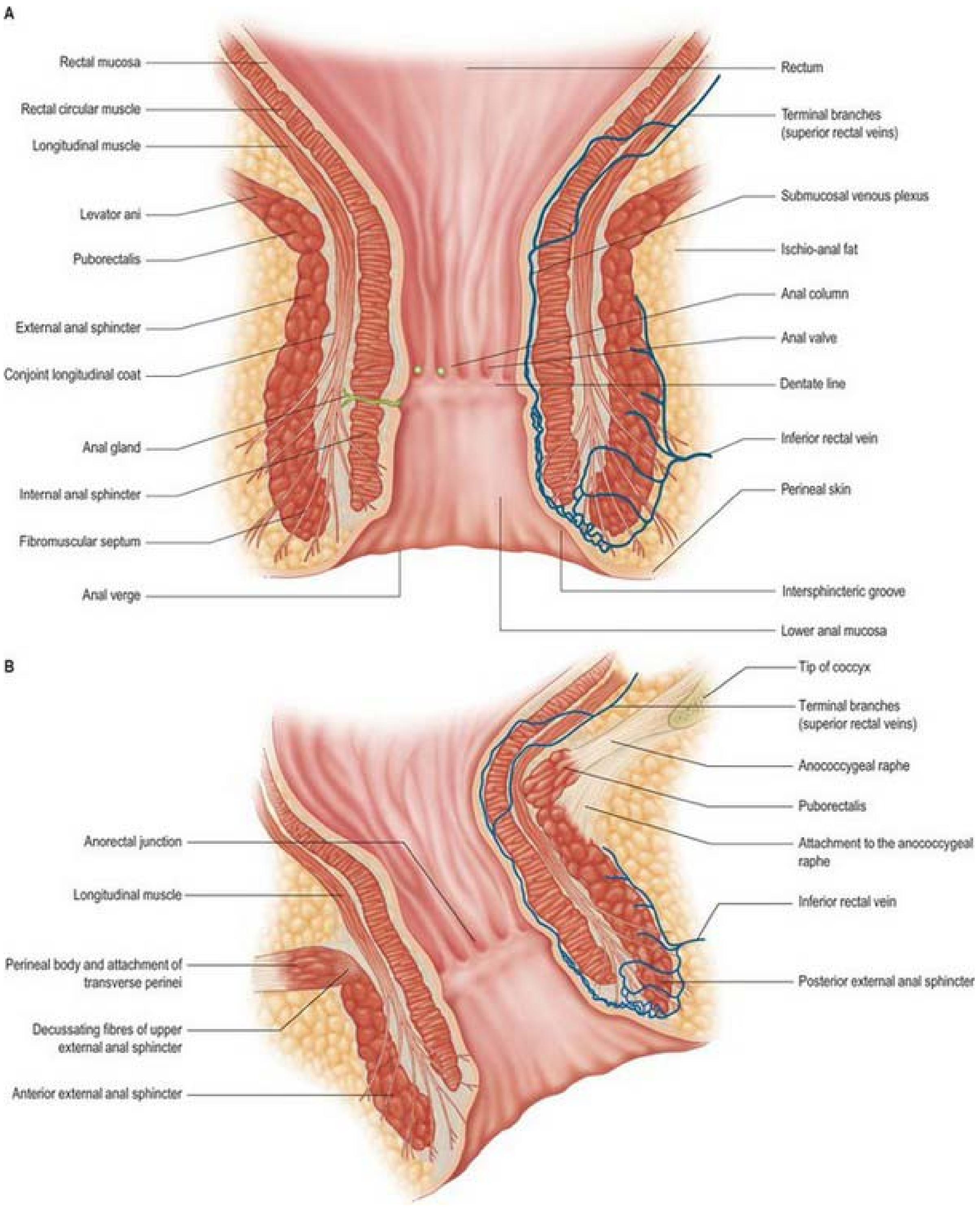
A
Rectal mucosa
Rectal circular muscle
Longitudinal muscle
Levator ani
Puborectalis
External anal sphincter
Conjoint longitudinal coat
Anal gland
Internal anal sphincter
Fibromuscular septum
Anal verge
Rectum
Terminal branches (superior rectal veins)
Submucosal venous plexus
Ischio-anal fat
Anal column
Anal valve
Dentate line
Inferior rectal vein
Perineal skin
Intersphincteric groove
Lower anal mucosa
B
Anorectal junction
Longitudinal muscle
Perineal body and attachment of transverse perinei
Decussating fibres of upper external anal sphincter
Anterior external anal sphincter
Tip of coccyx
Terminal branches (superior rectal veins)
Anococcygeal raphe
Puborectalis
Attachment to the anococcygeal raphe
Inferior rectal vein
Posterior external anal sphincter

Fig. 67.43 **A**, Coronal section through the anal canal: glandular and vascular structures are shown unilaterally for clarity. **B**, Sagittal section through the anal canal: the anal canal is angled posteriorly and so anterior sphincteric structures appear to be lower than posterior structures. The

glandular, vascular and fibromuscular structures and the conjoint longitudinal coat have been omitted for clarity.

Middle rectal veins

The middle rectal veins pass alongside the middle rectal arteries to drain into the anterior division of the internal iliac vein on the lateral wall of the pelvis.

Lymphatics

Lymphatics draining the rectum and the upper anal canal above the level of the dentate line pass superiorly, initially through the rectal wall, and then as a fine network over the surface of the rectum, before draining into nodes which lie in the loose adipose connective tissue of the mesorectum. Epirectal nodes lie very close to the outer fibres of the rectal longitudinal muscle while pararectal nodes lie within the mesorectum, a variable distance from the rectal wall. The overall direction of drainage is upwards along the branches of the superior rectal artery. Drainage to intermediate groups occurs up to the nodes near the origin of the inferior mesenteric artery (Fig. 67.42).

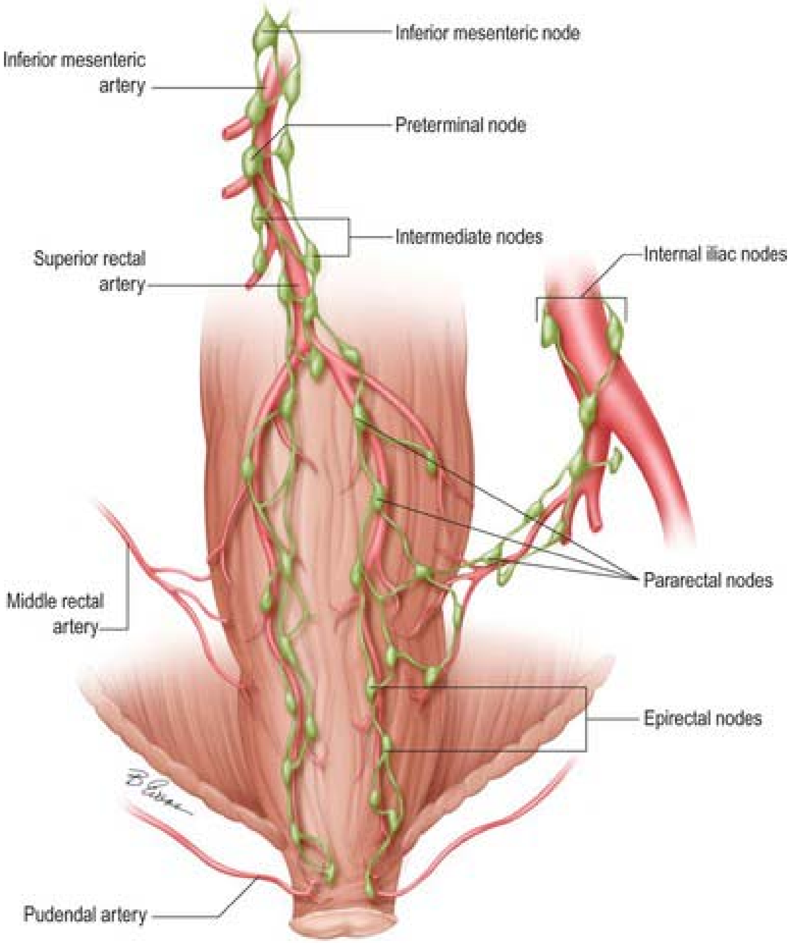
Inferior mesenteric node
Inferior mesenteric artery
Preterminal node
Intermediate nodes
Superior rectal artery
Internal iliac nodes
Pararectal nodes
Middle rectal artery
Epirectal nodes
B Gibbs
Pudendal artery

Fig. 67.42 Lymph nodes of the rectum and upper anal canal (viewed from behind).

INNERVATION

The sympathetic supply to the rectum and upper anal canal originates in the first and second lumbar spinal segments. The fibres are distributed via the lumbar splanchnic nerves through the inferior mesenteric plexuses and via the sacral splanchnic nerves through the superior and inferior hypogastric plexuses: postganglionic axons reach the gut wall via periarterial plexuses on branches of the superior and middle rectal arteries, and are inhibitory to the muscle of the rectal wall.

The preganglionic parasympathetic supply to the rectum and upper anal canal is mediated via the pelvic splanchnic nerves, which travel through the inferior and superior hypogastric plexuses and along the nerve plexuses on the branches of the inferior mesenteric artery. Parasympathetic nerves are secretomotor to the colorectal glands, and motor to the rectal musculature, causing relaxation of the internal anal sphincter. Afferent impulses mediating sensations of distension are carried by visceral afferent fibres which travel with the parasympathetic nerves. Pain impulses pass in visceral afferents travelling with the sympathetic and parasympathetic nerves that supply the rectum and the upper part of the anal canal.

The role of rectal innervation in anorectal function and continence is described below.

ANAL CANAL

The anal canal begins at the anorectal junction and ends at the anal verge (Figs 67.43-67.45). It is angulated in relation to the rectum because the pull of the sling-like puborectalis produces the anorectal angle. It lies 2–3 cm in front of and slightly below the tip of the coccyx, which is opposite the apex of the prostate in males. The anal verge is marked by a sharp turn where the squamous epithelium which lines the lower anal canal becomes continuous with the skin of the perineum. The pigmentation of skin around the anal verge approximately corresponds to the extent of the external sphincter. Identification of the anal verge may be difficult, particularly in males in whom the perineum may ‘funnel’ upwards into the lower anal canal, however, the characteristic puckering of the external epithelium caused by the penetrating fibres of the conjoint longitudinal layer makes a useful landmark. The functional anal canal is represented by a zone of high pressure which roughly equates to the anatomical canal. The anal canal consists of an inner epithelial lining, a vascular subepithelium, the internal and external anal sphincters and fibromuscular supporting tissue as well as dense neuronal networks of both autonomic and somatic origin. It is between 2.5 and 5 cm long in adults although the anterior wall is slightly shorter than the posterior. It is usually shorter in females. At rest it forms an oval slit in the anteroposterior plane rather than a circular canal: the arrangement of the external anal sphincter and its attachments to the perineal body and coccyx create sites of maximum pressure within the anal canal in the anterior and posterior midline.

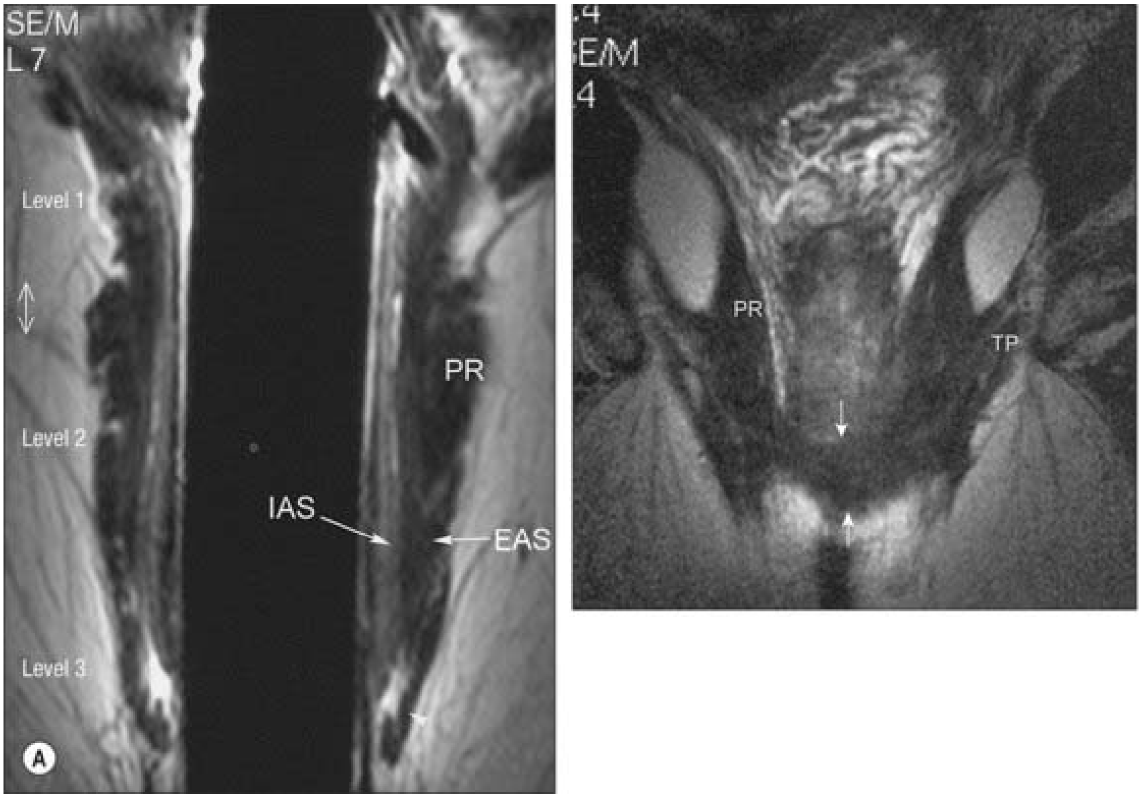
SE/M
L 7
Level 1
Level 2
Level 3
PR
IAS
EAS
A
E/M
4
PR
TP

Fig. 67.44 **A**, Mid-coronal MRI endocoil image of the anal canal. **B**, Anterior coronal MRI endocoil section in a woman showing the transverse perineii (TP) joining the external anal sphincter anteriorly (between arrows). EAS, external anal sphincter; IAS, internal anal sphincter; PR, puborectalis.

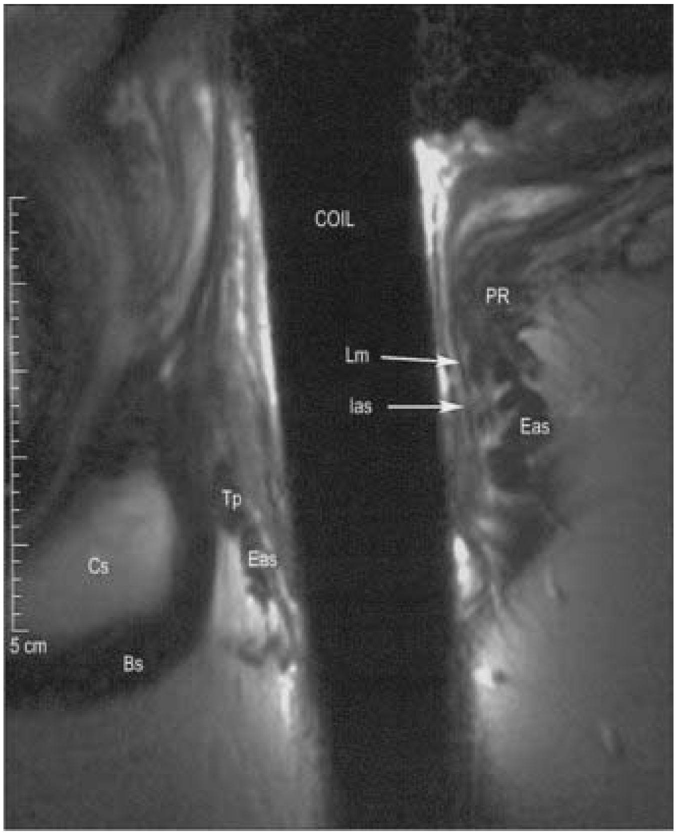

Fig. 67.45 MRI endocoil mid sagittal view of the anal canal in a man. Cs, corpus spongiosus; Tp, transverse perineii; Eas, external anal sphincter; Lm, longitudinal muscle; Ias, internal anal sphincter; PR, puborectalis; Bs, bulbospongiosus.

Anteriorly, the middle third of the anal canal is attached by dense connective tissue to the perineal body, which separates it from the membranous urethra and penile bulb in males or from the lower vagina in females. Laterally and posteriorly, the anal canal is surrounded by loose adipose tissue within the ischio-anal fossae; this offers a potential pathway for the spread of perianal sepsis from one side to the other (see Ch. 63). Posteriorly, the anal canal is attached to the coccyx by the anococcygeal ligament, a midline fibroelastic structure which may possess some skeletal muscle elements, and which runs between the posterior aspect of the middle portion of the external sphincter and the coccyx. Just above this is the raphe of the levator ani ‘plate’, the fusion of the two halves of iliococcygeus, which merges anteriorly with puborectalis. Between these two structures is a potential ‘postanal’ space.

The ischial spines may be palpated laterally by an examining finger in the upper anal canal. The pudendal nerves pass over the ischial spines at this point and pudendal nerve motor terminal latency may be measured digitally using a modified electrode worn on the examining glove.

LINING OF THE ANAL CANAL

The upper portion of the anal canal is lined by columnar epithelium similar to that of the rectum. It contains secretory and absorptive cells with numerous tubular glands or crypts. The subepithelial tissues are mobile and relatively distensible and possess profuse submucosal arterial and venous plexuses. Terminal branches of the superior rectal vessels pass downwards towards the anal columns. The submucosal veins drain into the submucosal rectal venous plexus and also through the fibres of the upper internal anal sphincter into an intermuscular venous plexus.

There are 6–10 vertical folds, the anal columns, in the mid anal canal. They tend to be obvious in children but less well-defined in adults. Each column contains a terminal radicle of the superior rectal artery and vein: the vessels are largest in the left-lateral, right-posterior and right-anterior quadrants of the wall of the canal where the subepithelial tissues expand into three ‘anal cushions’ (Fig. 67.46). The cushions help to seal the anal canal, to maintain continence to flatus and fluid, and are also important in the pathogenesis of haemorrhoids. The lower ends of the columns may form small crescentic folds, called the anal valves, between which lie small recesses referred to as anal sinuses. The anal valves and sinuses together form the dentate (or pectinate) line. About six anal glands open into small depressions, anal crypts, in the anal valves. The glands are branched and lined by stratified columnar epithelium. Cystic dilatations in the glands may extend through the internal sphincter and even into the external sphincter (Seow-Cheon & Ho 1994).

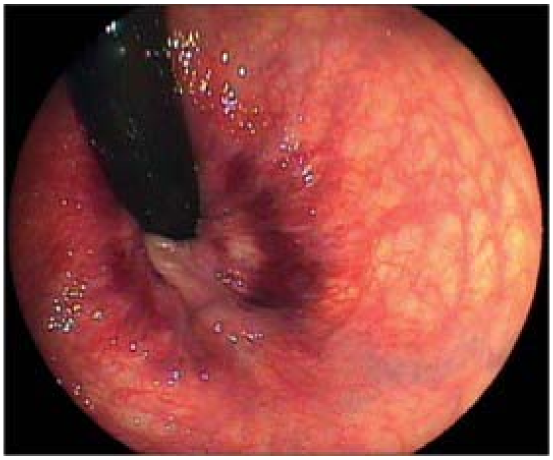

Fig. 67.46 Endoscopic appearance of the anorectal junction.

The mucosa below the dentate line is smooth, and termed the pectin. It is non-keratinized stratified squamous epithelium which lacks sweat and sebaceous glands and hair follicles, but contains numerous somatic nerve endings. It extends down to the intersphincteric groove, a depression at the lower border of the internal sphincter. The canal below the intersphincteric groove is lined by hair-bearing, keratinizing, stratified epithelium which is continuous with the perianal skin. The submucosa in this region contains profuse arterial and venous plexuses and has more connective tissue than the upper canal. It may be tethered to fibres of the conjoint longitudinal layer in the region of the intersphincteric groove.

The junction between the columnar and squamous epithelia is referred to as the anal transition zone (ATZ). It is variable in height and position and often contains islands of squamous epithelium extending up into the columnar mucosa; it is not the same as the dentate line which is an indistinct line observed in the anal canal. Nerve endings including thermoreceptors exist in the submucosa around the upper ATZ; they probably play a role in continence by providing a highly specialized ‘sampling’ mechanism to identify the contents of the lower rectum when the upper anal canal relaxes to allow rectal contents to come into contact with the upper anal canal epithelium (Duthie & Gairns 1960).

The well-defined muscularis mucosae of the rectum continues into the upper canal. Fibres from the longitudinal muscle pass through the internal sphincter and surround the submucosal venous plexus before turning upwards to merge with the muscularis mucosae and form the musculus submucosae ani.

Haemorrhoids

Haemorrhoids represent abnormal enlargement of the anal cushions. The partial drainage of the venous plexus into the intermuscular plane may play a role in this chronic engorgement as a result of obstruction of the venous flow during prolonged straining and defecation. Since the subepithelial vascular cushions of the upper, mid and lower anal canal form a continuous plexus, the differentiation of haemorrhoids into ‘internal’ and ‘external’ is somewhat arbitrary. The laxity of the upper anal canal submucosa is probably responsible for the fact that internal haemorrhoids may form more easily, although engorgement of the plexus deep to the lower anal epithelium may also occur. Since the epithelium in the lower canal is well supplied with sensory nerve endings, acute distension or invasive treatment to haemorrhoids in this area causes profound discomfort, whereas invasive or destructive therapy with relatively few symptoms is possible in the upper canal because the latter is lined with insensate columnar mucosa.

Anal fissures

Acute, transient, vertical breaks in the anal epithelium are not uncommon. The development of chronic, non-healing fissures is less common. They are more likely to develop in the anterior, and particularly the posterior, midline of the anus, possibly because stress within the anal canal is concentrated in these regions by the arrangement of the fibres of the external sphincter: the relative paucity of the arterial supply in these regions probably contributes to poor healing. Persistent hypertonicity of the anal sphincter is a primary pathogenic factor, possibly developing as a consequence of disordered local reflex mechanisms between the lower rectum and internal anal sphincter.

Cryptoglandular sepsis and fistula in ano

Infection of the anal glands is the main cause of anal sepsis and cryptogenic fistula formation (Parks et al 1976). Because many of these glands extend into the intersphincteric plane, so-called cryptoglandular sepsis may readily spread into the same plane. The commonest route of drainage of this sepsis is downwards between the internal and external anal sphincters, appearing beneath the skin at the anal verge. Rupture or drainage of the sepsis at this point will form a fistula *in ano* in the intersphincteric plane. Less commonly, the infection drains outwards from the intersphincteric plane and passes through the fibres of the external anal sphincter, possibly along the spreading septa of the conjoint longitudinal coat, and appears in the perianal skin outside the external anal sphincter as a transphincteric fistula. If the sepsis does not originate in the intersphincteric plane, drainage is likely to be beneath the anal mucosa alone and a submucous fistula forms. Sepsis within the ischio-anal fossa surrounding the lower anal canal can spread with relative ease because the connective tissue is mostly loose adipose tissue. Pus may spread posteriorly, behind the lower anal canal into the contralateral ischio-anal fossa, because the lower anal canal lacks any ligamentous attachments (Parkes 1961).

MUSCLES OF THE ANAL CANAL

The anal canal is encircled by internal and external anal sphincters, separated by the longitudinal layer, and has connections superiorly to puborectalis and the transverse perineii (Fig. 67.47).

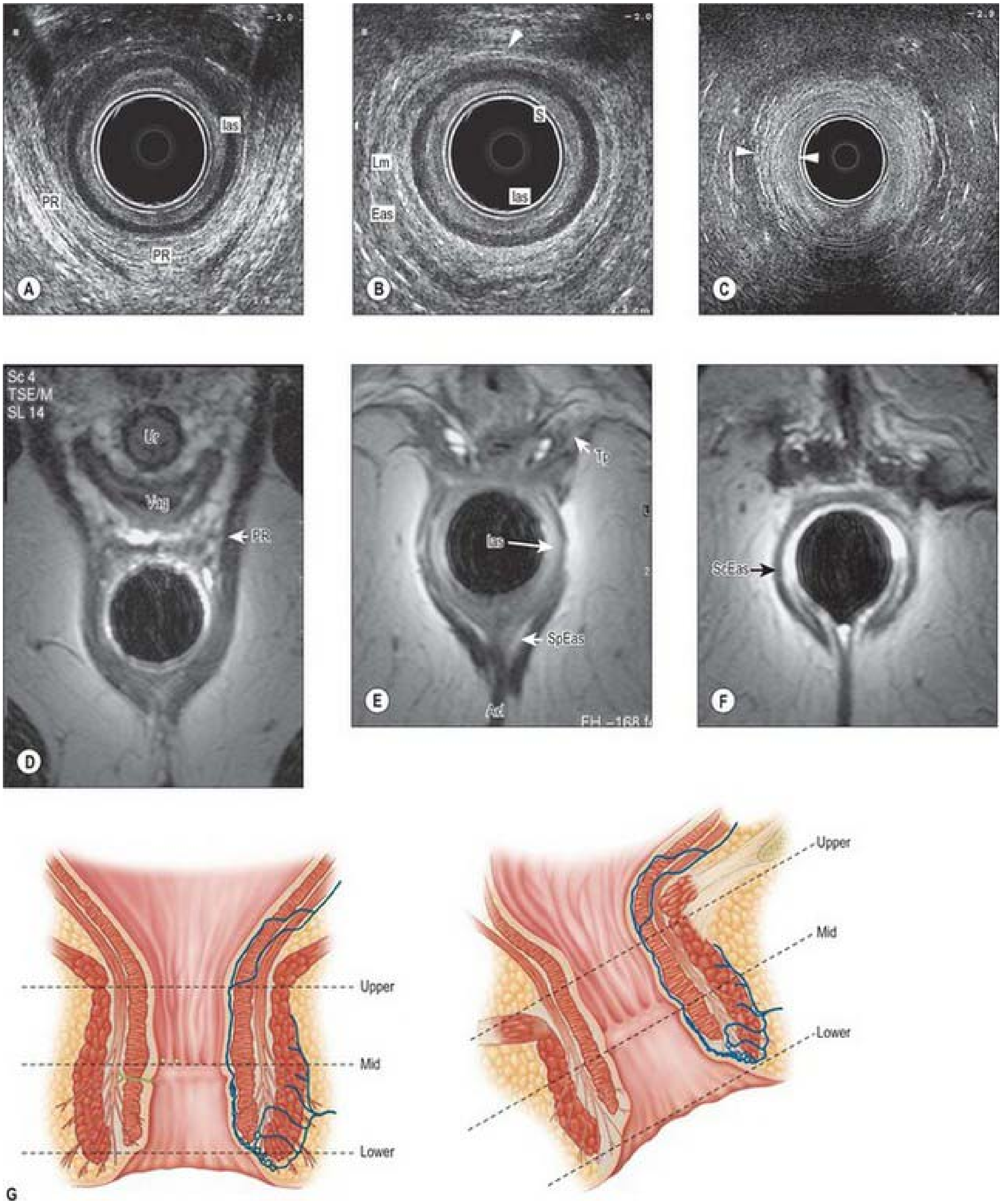
Ias
PR
PR
A
S
Lm
Eas
Ias
B
C
Sc 4
TSE/M
SL 14
Ur
Vag
PR
D
Tp
Ias
SpEas
Ad
E
ScEas
F
Upper
Mid
Lower
Upper
Mid
Lower
G

Fig. 67.47 **A–C**, Axial views of the anal canal at three levels on endoanal ultrasound in a woman. The endoanal ultrasound probe is the central black structure. **A**, Upper anal canal. The ‘U’ shape of puborectalis (PR) is visible. Ias, internal anal sphincter. **B**, Middle anal canal. The external anal

sphincter (Eas) is now a complete ring anteriorly (arrowhead). Lm, longitudinal muscle; S, subepithelial tissues. **C**, Lower anal canal. Below the termination of the internal anal sphincter, the longitudinal layer extends through the subcutaneous external anal sphincter (between arrowheads). **D–F**, MRI of the anal canal. **D**, At upper anal canal level, the sling of puborectalis (PR) extends anteriorly to the pubic bones. Vag, vagina; Ur, urethra. **E**, At mid anal canal level, the transverse perineii (Tp) fuse into the external anal sphincter anteriorly. The superficial (middle) external anal sphincter (SpEas) is attached either side of the anococcygeal ligament (Acl). Ias, internal anal sphincter. **F**, Low anal canal level, below the internal anal sphincter. ScEas, subcutaneous (lower) part of the external anal sphincter. **G**, Key for levels of the anal canal.

Internal anal sphincter

The internal anal sphincter is a well-defined ring of obliquely orientated smooth muscle fibres that is continuous with the circular muscle of the rectum, and which terminates at the junction of the superficial and subcutaneous components of the external sphincter. Its thickness varies between 1.5 and 3.5 mm, depending upon the height within the anal canal and whether the canal is distended. It is usually thinner in females and becomes thicker with age. It may also be thickened in disease processes such as rectal prolapse and chronic constipation. The lower portion of the sphincter is crossed by fibres from the conjoint longitudinal coat which pass into the submucosa of the lower canal.

Vascular supply

The internal anal sphincter is supplied from the terminal branches of the superior rectal vessels and branches of the inferior rectal vessels.

Innervation

The internal anal sphincter is supplied by the sympathetic and parasympathetic systems by fibres that extend down from the lower rectum. Sympathetic fibres originate in the lower two lumbar spinal segments, are distributed via the inferior hypogastric plexus, and cause contraction of the sphincter. Parasympathetic fibres originate in the second to fourth sacral spinal segments, are distributed via the inferior hypogastric plexus, and cause relaxation of the sphincter.

External anal sphincter

The external anal sphincter is an oval tube-shaped complex of striated muscle, composed mainly of type 1 (slow twitch) skeletal muscle fibres, which are well suited to prolonged contraction. It has been described as consisting of deep, superficial and subcutaneous parts but the external anal sphincter should be considered as a single functional and anatomical entity although the upper middle and lower thirds show different features and attachments. Endoanal ultrasound and magnetic resonance imaging reveal that the uppermost fibres blend with the lowest fibres of puborectalis. In the upper third some of these upper fibres decussate anteriorly into the superficial transverse perineal muscles and posteriorly some fibres are attached to the anococcygeal raphe. The majority of the fibres of the middle third of the external anal sphincter surround the lower part of the internal sphincter. The middle third is attached anteriorly to the perineal body and posteriorly to the coccyx via the anococcygeal ligament: some fibres from each side of the sphincter decussate in these areas to form a commissure in the anterior and posterior midline. The fibres of the lower third lie below the level of the internal anal sphincter and are separated from the lowest anal epithelium by submucosa.

The length and thickness of the external anal sphincter varies between the sexes. In females, the anterior portion tends to be shorter, the wall may be slightly thinner, and the tube may take the form of an asymmetrical cone (Rociu et al 2000) and the transverse perineii and bulbospongiosus fuse with the external sphincter in the lower part of the perineum. In males, the external sphincter is more anular and is separate from the central point of the perineum into which the transverse perineii and bulbospongiosus fuse, so that there is a surgical plane of cleavage between the external sphincter and perineum (Fig. 67.48).

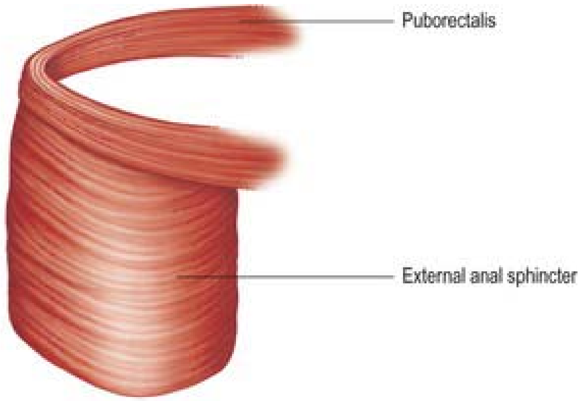
Puborectalis
External anal sphincter

Male

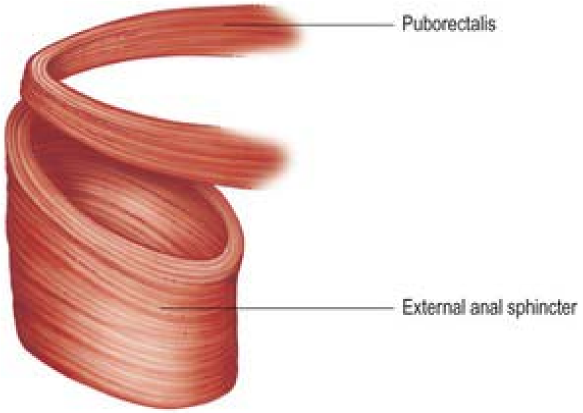
Puborectalis
External anal sphincter

Female

Fig. 67.48 Typical anatomy of male and female external anal sphincters. Puborectalis is shown in isolation with the external anal sphincter viewed from the superolateral aspect. The anterior portion of the external anal sphincter is typically shorter and thinner in females.

Vascular supply

The external anal sphincter is supplied from the terminal branches of the inferior rectal vessels with a small contribution from the median sacral artery.

Innervation

The external anal sphincter is innervated mainly by the inferior rectal branch of the pudendal nerve (anterior divisions of the second, third and fourth sacral spinal nerves). It may also receive some direct supply via fibres which leave the ventral rami of these nerves as they exit the sacral foramina and run beneath the fascia over levator ani to reach the anorectal junction.

FIBROMUSCULAR STRUCTURES OF THE ANAL CANAL

Longitudinal layer and conjoint longitudinal coat

The longitudinal layer is situated between the internal and external sphincters. It contains a fibromuscular layer, the conjoint longitudinal coat, and the intersphincteric space with its connective tissue components (Lunniss & Phillips 1992). The longitudinal layer has muscular and fibroelastic components. The muscular element is formed by fusion of striated muscle fibres from puboanalis, which is the innermost part of puborectalis, with smooth muscle from the longitudinal muscle of the rectum. Endoanal ultrasound and magnetic resonance imaging demonstrate either bundles or incomplete sheets of muscle extending down between the sphincters in the upper canal in both sexes: in men these often end just above the lower border of the internal sphincter. The layer then becomes completely fibroelastic, and splits into septa running between bundles of the subcutaneous external sphincter to terminate in the perianal skin. The area bounded by these septa is generally referred to as the perianal space. The most peripheral of the septa extend between the fibres of the external sphincter into the ischio-anal fat. The most central septa pass through the fibres of the internal sphincter to reach the anal lining and may help to form the intersphincteric groove. The conjoint longitudinal coat is innervated by autonomic fibres that share an origin with the fibres that innervate the internal sphincter.

Other fibromuscular structures

A layer of smooth muscle, yellow elastic fibres, and collagenous connective tissue is found in the anal submucosa, inferior to the anal sinuses. It is derived mainly from strands of the conjoint longitudinal coat, which descend inwards between the fibres of the internal sphincter. Some of the strands end by turning outwards around the lower edge of the internal sphincter to rejoin the main longitudinal layer. Most continue obliquely downwards and insert into the dermis below the intersphincteric groove. These attachments may help to form the corrugations seen in the perianal skin. The septa end in a honeycomb-like arrangement of fibres, which prevents easy distension of the lowest anal lining. This may explain the severe pain produced by pus or blood which collects here, since small volumes of fluid rapidly produce high pressure within the subepithelium.

VASCULAR SUPPLY AND LYMPHATIC DRAINAGE

Arteries

The arterial supply to the anal canal is derived from terminal branches of the superior rectal artery, the inferior rectal branch of the pudendal artery and branches of the median sacral artery. The supply to the anal canal lining is not distributed uniformly. The arterial supply of the anterior and, more particularly, the posterior, midline epithelia is less good than that lining the lateral portions of the canal (Klosterhalfen et al 1989), which is relevant to the perpetuation of chronic anal fissures.

Veins

The venous drainage of the upper anal canal mucosa, internal anal sphincter and conjoint longitudinal coat passes via the terminal branches of the superior rectal veins into the inferior mesenteric vein. The lower anal canal and external sphincter drain via the inferior rectal branch of the pudenal vein into the internal iliac vein.

Lymphatics

Lymphatics from the upper anal mucosa, internal anal sphincter and conjoint longitudinal coat drain upwards into the submucosal and intramural lymphatics of the rectum. The lower anal canal epithelium and external anal sphincter lymphatics drain downwards via perianal plexuses into vessels that drain into the external inguinal lymph nodes. The lymphatics of puborectalis drain into the internal iliac lymph nodes. This arrangement has considerable importance for tumours of the lower rectum and upper anal canal. If the tumour is confined to the tissue of origin, malignant spread is confined to the mesorectal lymph nodes. However, if the tumour involves puborectalis or tissues associated with the external anal sphincter, the possibility of lymph node spread to these other groups may require radical excision and much more extensive surgery.

INNERVATION

The anal canal is innervated by both autonomic and somatic nervous systems. Preganglionic sympathetic fibres originate in the lower two lumbar segments, run via the lumbar sympathetic chain into the upper two sacral sympathetic ganglia, and into the inferior hypogastric plexus via the sacral splanchnic nerves. Parasympathetic fibres originate in the second to fourth sacral spinal segments and also run to the inferior hypogastric plexus via the pelvic splanchnic nerves. From the inferior hypogastric plexus both sympathetic and parasympathetic fibres run together in nerves of the ‘pelvic plexus’ and enter the lower rectal wall via the ‘lateral ligaments’ of the rectum and anorectal junction via the endopelvic fascia over levator ani. They are distributed to the submucosal and myenteric plexuses where most fibres terminate on interstitial cells (of Cajal).

The autonomic supply to the anus innervates the upper anal mucosa (rich in thermoreceptors), the internal anal sphincter and the conjoint longitudinal coat. Sympathetic fibres cause relaxation of the lower rectal muscle but contraction of the conjoined longitudinal coat and internal anal sphincter fibres via α-adrenergic receptors. Parasympathetic fibres cause relaxation of the internal sphincter via muscarinic receptors which stimulate release of nitric oxide from intramural nitrergic neurones (Brading & Ramalingam 2006).

The external anal sphincter and lower half of the anal mucosa and perianal skin (which are both rich in nocioceptors and pressure receptors) receive a somatic innervation from the anterior divisions of the second, third and fourth sacral spinal nerves which is mainly distributed via the inferior rectal branch of the pudendal nerve. There may also be some direct supply via fibres which leave the ventral rami of the second to fourth sacral nerves as they exit the sacral foramina and run beneath the fascia over levator ani to reach the anorectal junction (because some somatic reflexes are not abolished by division of the pudendal nerves).

Referred pain

Pain in the lower two thirds of the anus is usually felt with a high degree of acuity and is well localized to the perineum and anal canal itself.

Reflexes, control of anorectal function and continence

Local reflex arcs exist within the anorectal intramural plexuses and also within the sacral segments of the spinal cord a spinal centre for co-ordination of anorectal function has not yet been identified. These reflex arcs involve both autonomic and somatic elements because the co-ordination of continence and the initiation of defecation requires that the lower rectum, internal and external anal sphincters act together.

The internal anal sphincter often relaxes following distension of the rectum (Recto-Anal Inhibitory Reflex or 'RAIR'), suggesting that local reflex pathways exist between the lower rectal sensory fibres and sphincteric motor fibres. This relaxation also occurs on stimulation of somatic sensory nerves, even after the rectum has been excised completely, and is presumably mediated via proprioceptors present in the pelvic floor and an additional reflex pathway via the sacral spinal segments. Integrating the sensory input from the anal canal so as to control the activity of the anal musculature occurs at many levels in the nervous system, including the spinal cord, brain stem, thalamus and cortex. Neural activity not only monitors and regulates defecation, but also other more subtle behaviours within the rectum and anal canal, such as the separation of faeces from rectal gas; local adjustments to faecal consistency and quantities; self-cleansing movements in the rectum and anal canal; coordination with other actions of the perineal and abdominal muscles.

To keep the anal canal closed, the pressure within the anal canal has to be higher than that in the rectum. The resting pressure in the canal is maintained mainly by tonic activity of the internal sphincter as a result of sympathetic tone: sudden increases of intrarectal pressure, e.g. during coughing or exertion, are compensated for by rapid contraction of the external sphincter and puborectalis via spinal reflexes. Angulation of the anorectal junction and the 'flap valve' theory is no longer considered important in continence since dynamic imaging of the process of defecation (proctography) has demonstrated that there is a wide range of angulation which does not correlate with function. The internal sphincter does not close the canal completely; the gap (approximately 7 mm) is sealed by the distensible, vascular subepithelial tissues.

Defecation

Defecation is a conscious physiological act in response to feeling the need to pass stool in the rectum: it requires coordinated relaxation of the pelvic floor muscles and anal sphincter. The dynamics have been studied using pressure measurements in the colon, rectum and anus (Herbst et al 1997), and by various imaging techniques including fluoroscopy, ultrasonography and magnetic resonance imaging (Kruyt et al 1991). The process is initiated by mass colonic contractions which drive faeces into the rectum. Rectal distension occurs progressively; there is little increase in intra-rectal pressure because the rectal musculature relaxes as a result of either local intramural or spinal reflexes mediated via sympathetic and parasympathetic fibres. The RAIR is probably involved in allowing the descent of rectal contents into the upper anal canal where it can be ‘sampled’ by contact with the mucosal receptors (particularly thermoreceptors). Defecation may be deferred by conscious contraction of the external anal sphincter until contractions cease and retrograde rectal peristalsis moves stool out of the distal rectum, so that the sensation to defecate passes off. Initiation of defecation involves conscious relaxation of the pelvic floor muscles and external sphincter, so that the pelvic floor descends slightly allowing the anorectal angle to straighten. Reflex relaxation of the internal anal sphincter and conjoint longitudinal coat allows the anal canal to open. Abdominal muscle contraction will aid expulsion from the rectum, but continuing mass colonic contractions push more faeces down into the rectum, so that the entire left colon may be emptied.

Anorectal incontinence

Anal incontinence is common and may occur for a variety of reasons. Abnormally high rectal pressures, as occur in severe diarrhoea, may overcome a normal sphincter, and autonomic disorders may produce abnormal motor activity or loss of normal sensation, so that there is no awareness of the presence of stool. Damage to the anal sphincter may result from vaginal delivery due to stretch, instrumentation or surgical procedures. Atrophy of the external sphincter may occur secondary to pudendal nerve damage during delivery (and may also occur in diabetics, neurological disease and the elderly) A damaged sphincter will not be able to overcome normal fluctuations of intrarectal pressures, or there may be a combination of damage and rectal dysfunction resulting in anal incontinence.

MICROSTRUCTURE

The layers of tissue in the large intestinal wall (see Fig. 67.3; Fig. 67.49) resemble those in the small intestine (Ch. 66), except that villi and circular folds are absent and the glands (crypts) are longer.

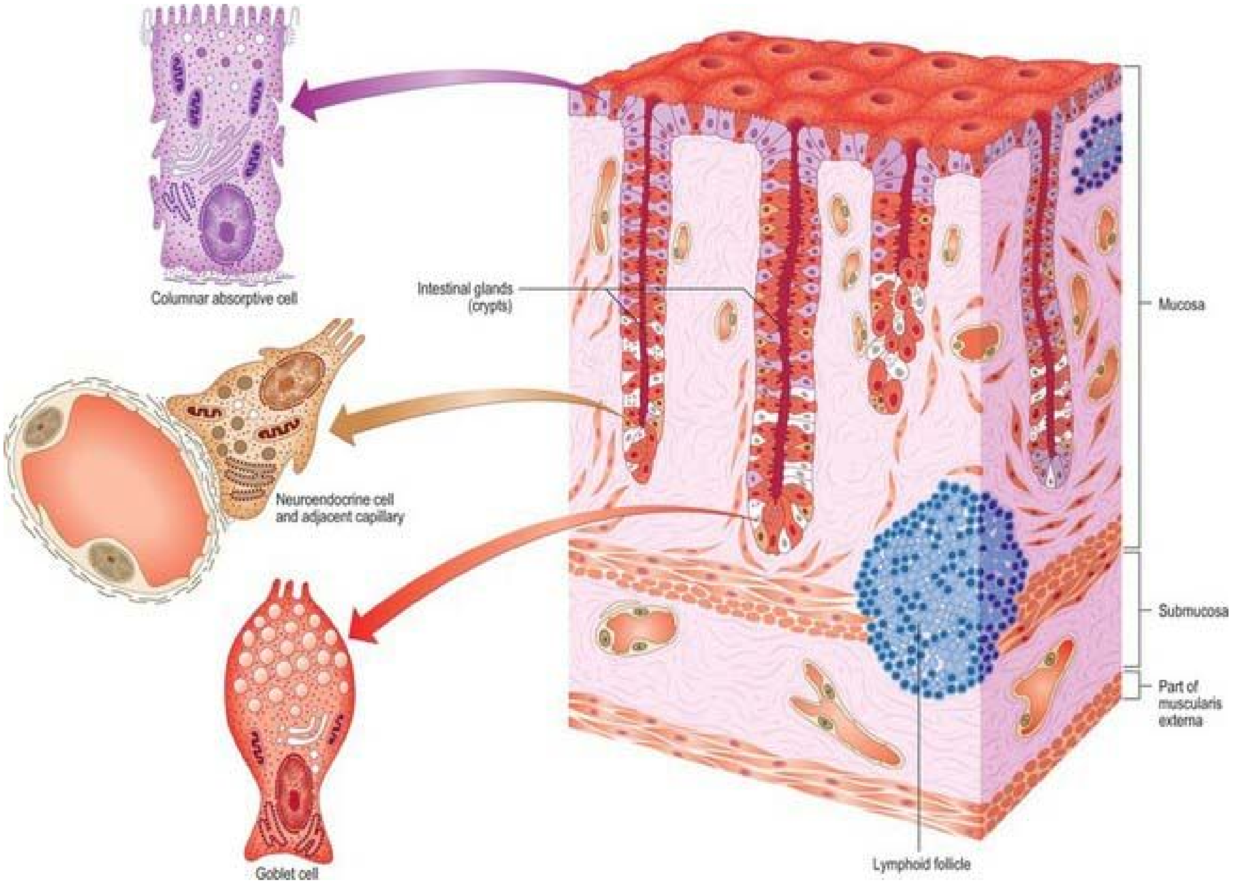

Columnar absorptive cell
Intestinal glands (crypts)
Mucosa
Neuroendocrine cell and adjacent capillary
Submucosa
Part of muscularis externa
Goblet cell
Lymphoid follicle

Fig. 67.49 The microstructure of the colonic wall and its epithelial cells. Note the aggregations of lymphocytes (blue) and undifferentiated epithelial cells (white).

Mucosa

The mucosa is pale, smooth, and, in the colon, raised into numerous crescent-shaped folds between the sacculi. In the rectum it is thicker, darker, more vascular, and more loosely attached to the submucosa.

Epithelium

The luminal surface of all but the anorectal junction is lined by columnar cells, mucous (goblet) cells, and occasional microfold (M) cells that are restricted to the epithelium overlying lymphoid follicles. Columnar and mucous cells are also present in the intestinal glands (crypts) which additionally contain stem cells and neuroendocrine cells. In general, the glands lack Paneth cells, but some may be present in the caecum.

Columnar (absorptive) cells

Columnar (absorptive) cells are the most numerous of the epithelial cell types. They are responsible for ion exchange and other transepithelial transport functions including water resorption, particularly in the colon. Although there is some variation in their structure, they all bear apical microvilli, which are shorter and less regular than those on enterocytes in the small intestine. All cells have typical junctional complexes around their apices, and these limit extracellular diffusion from the lumen across the intestine wall.

Mucous (goblet) cells

Mucous cells have a similar structure to those of the small intestine, but are more numerous. They are outnumbered by absorptive cells for most of the length of the colon, but they are equally frequent towards the rectum, where their numbers increase further.

Microfold (M) cells

Microfold cells are similar to those of the small intestine: they are flattened or cuboidal cells with long, blunt microfolds rather than typical microvilli, and they are restricted to epithelium overlying lymphoid follicles.

Stem cells

Stem cells are the source of the other epithelial cell types in the large intestine. They are located at or near the bases of the intestinal glands, where they divide by mitosis. They provide cells that migrate towards the luminal surface of the intestine: their progeny differentiate, undergo apoptosis and are shed after approximately 5 days.

Neuroendocrine cells

Neuroendocrine cells are situated mainly at the bases of the glands, and secrete basally into the lamina propria.

Intestinal glands (crypts)

The crypts are narrow perpendicular tubular glands which are longer, more numerous and closer together than those of the small intestine. Their openings give a cribriform appearance to the mucosa in surface view. The glands are lined by low columnar epithelial cells, mainly goblet cells, between which are columnar absorptive cells and neuroendocrine cells. Epithelial stem cells at their bases give rise to all three cell types.

Lamina propria

The lamina propria is composed of connective tissue that supports the epithelium. It forms a specialized pericryptal myofibroblast sheath around each intestinal gland. Solitary lymphoid follicles within the lamina propria are most abundant in the caecum, appendix and rectum, but are also present scattered along the rest of the large intestine. They are similar to those of the small intestine; efferent lymphatic vessels originate within them. Lymphatic vessels are absent from the lamina propria core between crypts.

Muscularis mucosae

The muscularis mucosae of the large intestine is essentially similar to that of the small intestine: it has prominent longitudinal and circular layers.

Submucosa

The submucosa of the large intestine is similar to that of the small intestine.

Muscularis externa

The muscularis externa has outer longitudinal and inner circular layers of smooth muscle. The longitudinal fibres form a continuous layer but, with the exception of the uniform outer muscle layer of most of the appendix, macroscopically these are aggregated as longitudinal bands or taeniae coli (see Figs 67.3 and 67.12). Between the taeniae coli the longitudinal layer is much thinner, less than half the circular layer in thickness. The circular fibres form a thin layer over the caecum and colon, and are aggregated particularly in the intervals between the sacculi. In the rectum they form a thick layer and in the anal canal they form the internal anal sphincter. There is an interchange of fascicles between circular and longitudinal layers, especially near the taeniae coli. Deviation of longitudinal fibres from the taeniae to the circular layer may, in some instances, explain the haustration of the colon.

Serosa

The serosa or visceral peritoneum is variable in extent. Along the colon the peritoneum forms small fat-filled appendices epiploicae which are most numerous on the sigmoid and transverse colon but generally absent from the rectum. Subserous loose connective tissue attaches the peritoneum to the muscularis externa.

REFERENCES

ading A, Ramalingam T. Mechanisms controlling normal defecation and the potential effects of spinal cord injury. *Prog Brain Res*. 2006;152:345-358.

oden B, Snellman B. Procidentia of the rectum studied with cineradiography. A contribution to the discussion of causative mechanisms. *Dis Colon Rectum*. 1968;11:330-347.

own G, Richards CJ, Newcombe RG, et al. Rectal carcinoma: thin-section MR imaging for staging in 28 patients. *Radiology*. 1999;211(1):215-222.

schard K, Kjaeldgaard A. Investigations and analysis of the positions, fixation, length and embryology of the vermiform appendix. *Acta Chir Scand*. 1973;139:293-298.

uthie HL, Gairns FW. Sensory nerve-endings and sensation in the anal region of man. *Br J Surg*. 1960;47:585-595.

nlon HM. Virtual colonoscopy. *Br J Surg*. 2002;89(1):1-3.

Describes and reviews the use of multislice CT to image the colon..

sher DFJr, Fry WJ. Collateral mesenteric circulation. *Surg Gynecol Obstet*. 1987;164(5):487-492.

Reviews collateral mesenteric circulations that develop during disease processes..

eald RJ, Husband EM, Ryall RDH. The mesorectum in rectal cancer surgery: the clue to pelvic recurrence? *Br J Surg*. 1982;69:613-616.

Original description of the mesorectal plane and its relevance to the surgical excision of rectal tumours..

erbst F, Kamm MA, Morris GP, Britton K, Woloszko J, Nicholls RJ. Gastrointestinal transit and prolonged ambulatory colonic motility in health and faecal incontinence. *Gut*. 1997;41:381-389.

ckson JE. Vascular anatomy of the gastrointestinal tract. In: Butler P, Mitchell AWM, Ellis H. *Applied Radiological Anatomy*. Cambridge: Cambridge University Press, 1999.

panese Society for the Cancer of the Colon and Rectum. Japanese Classification of Colorectal Carcinoma. Tokyo: Kanehara, 1997.

Describes the topography of colonic mesenteric lymph nodes with particular reference to radical excision for carcinoma..

osterhalfen B, Vogel P, Rixen H, Mittermayer C. Topography of the inferior rectal artery: a possible cause of chronic primary anal fissure. *Dis Colon Rectum*. 1989;32:43-52.

A detailed postmortem angiographic study demonstrating the arrangement of anal arterial supply..

uyt RH, Delemarre JB, Doornbos J, Vogel HJ. Normal anorectum: dynamic MR imaging anatomy. *Radiology*. 1991;179(1):159-163.

Describes the MR anatomy of the anorectum in relation to surrounding structures and the anorectal angle at rest, during perineal contraction, and during straining, in asymptomatic subjects..

ınniss PJ, Phillips RK. Anatomy and function of the anal longitudinal muscle. *Br J Surg*. 1992;79:882-884.

urphy JM, Maibaum A, Alexander G, Dixon AK. Chilaiditi's syndrome and obesity. *Clin Anat*. 2000;13(3):181-184.

ıiphant M, Berne AS, Meyers MA. The subperitoneal space of the abdomen and pelvis: planes of continuity. *Am J Roentgenol*. 1996;167(6):1433-1439.

ırkes AG. The pathogenesis and treatment of fistula in ano. *Br Med J*. 1961;1:463-469.

An early, full description of the relationship between the anatomy of anal glands and cryptoglandular sepsis..

ırks AG, Gordon PH, Hardcastle JD. A classification of fistula-in-ano. *Br J Surg*. 1976;63(1):1-12.

A classification of anal fistulas based on the pathogenesis of the disease and the normal muscular anatomy of the pelvic floor..

ɔciu E, Stoker J, Eijkemans MJ, Lameris JS. Normal anal sphincter anatomy and age- and sex-related variations at high-spatial-resolution endoanal MR imaging. *Radiology*. 2000;217:395-401.

ıto K, Sato T. The vascular and neuronal composition of the lateral ligament of the rectum and the rectosacral fascia. *Surg Radiol Anat*. 1991;13(1):17-22.

ɛow-Choen F, Ho JM. Histoanatomy of anal glands. *Dis Colon Rectum*. 1994;37:1215-1218.

lverstein FE, Tytgat GNJ. Atlas of Gastrointestinal Endoscopy, 2nd edn. London: Gower Medical Publishing, 1991.

ımaguchi S, Kuroyanagi H, Milson JW, Sim R, Shimada H. Venous anatomy of the right colon: precise structure of the major veins and gastrocolic trunk in 58 cadavers. *Dis Colon Rectum*. 2002;45:1337-1340.

CHAPTER 68

Liver

The liver is the largest of the abdominal viscera, occupying a substantial portion of the upper abdominal cavity. It occupies most of the right hypochondrium and epigastrium, and frequently extends into the left hypochondrium as far as the left lateral line (Fig. 68.1). As the body grows from infancy to adulthood the liver rapidly increases in size. This period of growth reaches a plateau around 18 years and is followed by a gradual decrease in the liver weight from middle age. The ratio of liver to body weight decreases with growth from infancy to adulthood. The liver weighs approximately 5% of the body weight in infancy and it decreases to approximately 2% in adulthood. The size of the liver also varies according to sex, age and body size. It has an overall wedge shape, which is in part determined by the form of the upper abdominal cavity into which it grows. The narrow end of the wedge lies towards the left hypochondrium, and the anterior edge points anteriorly and inferiorly. The superior and right lateral aspects are shaped by the anterolateral abdominal and chest wall as well as the diaphragm. The inferior aspect is shaped by the adjacent viscera. The capsule is no longer thought to play an important part in maintaining the integrity of the shape of the liver.

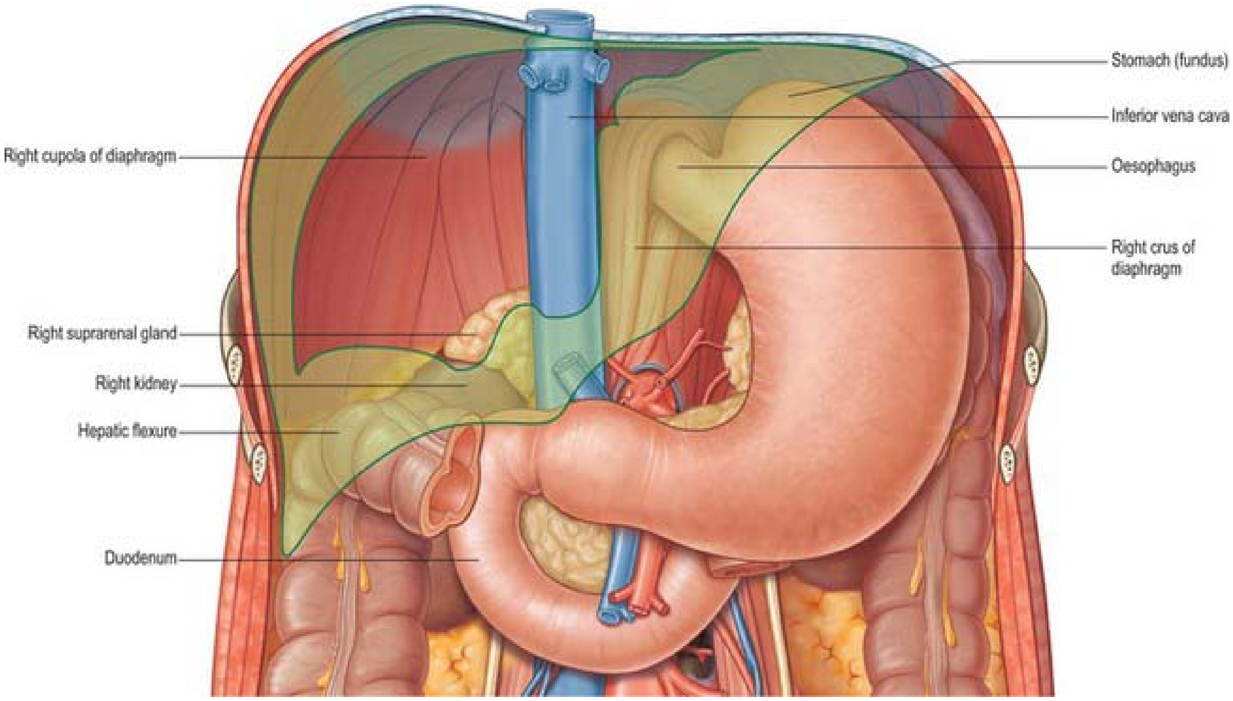
Stomach (fundus)
Inferior vena cava
Oesophagus
Right crus of diaphragm
Right cupola of diaphragm
Right suprarenal gland
Right kidney
Hepatic flexure
Duodenum

Fig. 68.1 The ‘bed’ of the liver. The outline of the liver is shaded green. The central bare area is unshaded.

Throughout life the liver is reddish brown in colour, although this can vary depending upon the fat content. Obesity is the most common cause of excess fat in the liver (also known as steatosis): the liver assumes a more yellowish tinge as its fat content increases. The texture is usually soft to firm, although it depends partly on the volume of blood the liver contains and the fat content.

The liver performs a wide range of metabolic activities required for homeostasis, nutrition and immune defence. For example, it is important in the removal and breakdown of toxic, or potentially toxic, materials from the blood and the regulation of blood glucose and lipids, the storage of certain vitamins, iron, and other micronutrients, and in breaking down or modifying amino acids. It is involved in a plethora of other biochemical reactions. Since the majority of these processes are exothermic, a substantial part of the thermal energy production of the body, especially at rest, is provided by the liver. The liver is populated by phagocytic macrophages, components of the mononuclear phagocyte system capable of removing particulates from the blood stream. It is an important site of haemopoiesis in the fetus.

SURFACES OF THE LIVER

The liver is usually described as having superior, anterior, right, posterior and inferior surfaces, and has a distinct inferior border (Figs 68.2, 68.3). However, the superior, anterior and right surfaces are continuous and no definable borders separate them. It would be more appropriate to group them as the diaphragmatic surface, which is mostly separated from the inferior, or visceral surface, by a narrow inferior border. At the infrasternal angle the inferior border is related to the anterior abdominal wall and is accessible to examination by percussion, but is not usually palpable. In the midline, the inferior border of the liver is near the transpyloric plane, about a hand's breadth below the xiphisternal joint. In women and children the border often projects a little below the right costal margin.

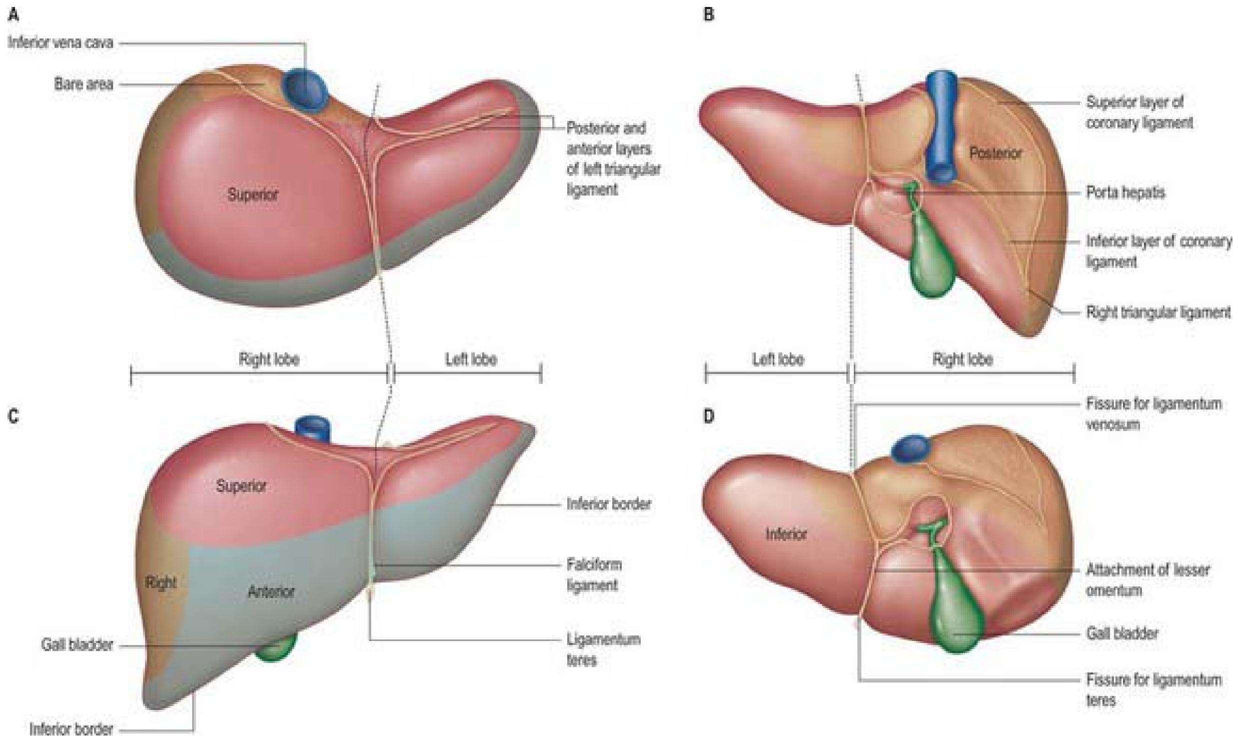
A
Inferior vena cava
Bare area
Superior
Posterior and anterior layers of left triangular ligament
Right lobe
Left lobe
B
Superior layer of coronary ligament
Posterior
Porta hepatis
Inferior layer of coronary ligament
Right triangular ligament
Left lobe
Right lobe
C
Superior
Right
Anterior
Inferior border
Falciform ligament
Ligamentum teres
Gall bladder
Inferior border
D
Fissure for ligamentum venosum
Inferior
Attachment of lesser omentum
Gall bladder
Fissure for ligamentum teres

Fig. 68.2 The surfaces and external features of the liver. **A**, superior view; **B**, posterior view; **C**, anterior view; **D**, inferior view.

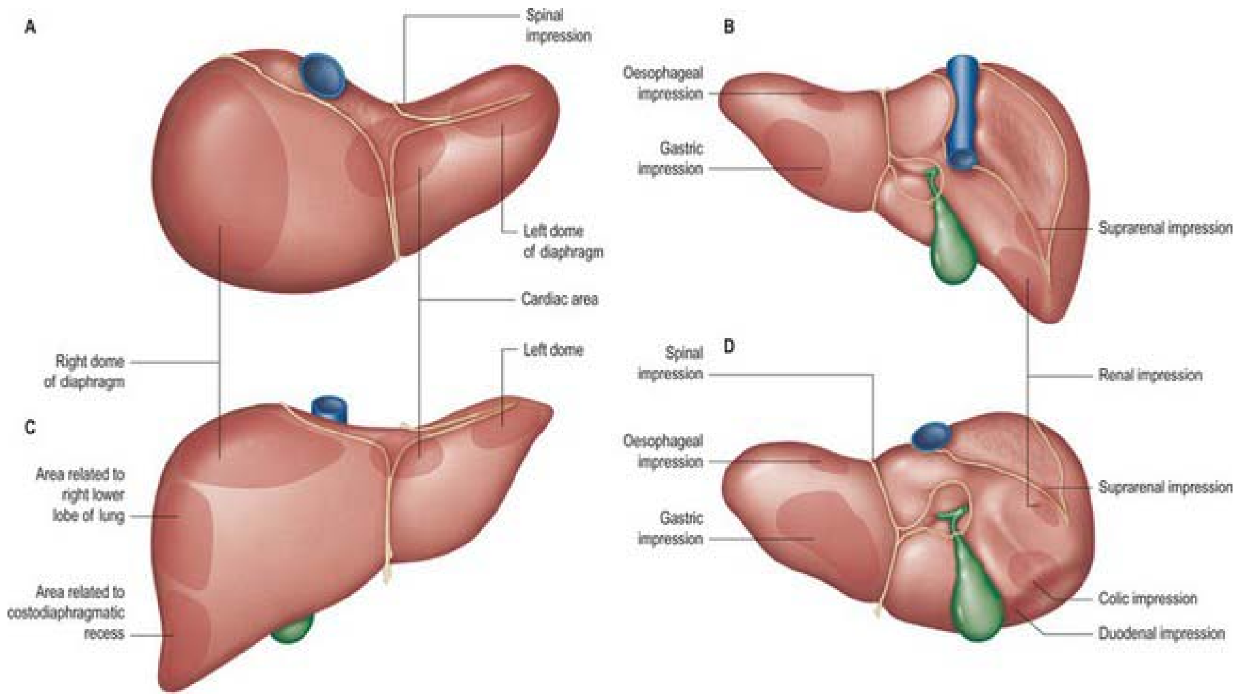
A
Spinal impression
B
Oesophageal impression
Gastric impression
Left dome of diaphragm
Suprarenal impression
Cardiac area
Right dome of diaphragm
Left dome
Spinal impression
D
Renal impression
C
Oesophageal impression
Area related to right lower lobe of lung
Gastric impression
Suprarenal impression
Area related to costodiaphragmatic recess
Colic impression
Duodenal impression

Fig. 68.3 Relations of the liver. **A**, superior view; **B**, posterior view; **C**, anterior view; **D**, inferior view.

Superior surface

The superior surface is the largest surface and lies immediately below the diaphragm, separated from it by peritoneum except for a small triangular area where the two layers of the falciform ligament diverge. The majority of the superior surface lies beneath the right dome, but there is a shallow cardiac impression centrally that corresponds to the position of the heart above the central tendon of the diaphragm. The left side of the superior surface lies beneath part of the left dome of the diaphragm.

Anterior surface

The anterior surface is approximately triangular and convex and is covered by peritoneum except at the attachment of the falciform ligament. Much of it is in contact with the anterior attachment of the diaphragm. On the right the diaphragm separates it from the pleura and sixth to tenth ribs and cartilages, and on the left from the seventh and eighth costal cartilages.

Right surface

The right surface is covered by peritoneum and lies adjacent to the right dome of the diaphragm which separates it from the right lung and pleura and the seventh to 11th ribs. The right lung and basal pleura both lie above and lateral to its upper third, between the diaphragm and the seventh and eighth ribs. The diaphragm, the costodiaphragmatic recess lined by pleura, and the ninth and tenth ribs all lie lateral to the middle third of the right surface. Lateral to the lower third, the diaphragm and thoracic wall are in direct contact. Rarely, the hepatic flexure and proximal transverse colon may lie on a long mesentery over the right and superior surfaces of the liver, referred to as Chilaiditi syndrome.

Posterior surface

The posterior surface is convex, wide on the right, but narrow on the left. A deep median concavity corresponds to the forward convexity of the vertebral column close to the attachment of the ligamentum venosum. Much of the posterior surface is attached to the diaphragm by loose connective tissue, forming the triangular ‘bare area’. The inferior vena cava lies in a groove or tunnel in the medial end of the ‘bare area’. To the left of the caval groove the posterior surface of the liver is formed by the caudate lobe, and covered by a layer of peritoneum continuous with that of the inferior layer of the coronary ligament and the layers of the lesser omentum. The caudate lobe is related to the diaphragmatic crura above the aortic opening and the right inferior phrenic artery, and separated by these structures from the descending thoracic aorta.

The fissure for the ligamentum venosum separates the posterior aspect of the caudate lobe from the main part of the left lobe. The fissure cuts deeply in front of the caudate lobe and contains the two layers of the lesser omentum. The posterior surface over the left lobe bears a shallow impression near the upper end of the fissure for the ligamentum venosum that is caused by the abdominal part of the oesophagus. The posterior surface of the left lobe to the left of this impression is related to part of the fundus of the stomach. Together these posterior relations make up what is sometimes referred to as the ‘bed’ of the liver (Fig. 68.1).

Inferior surface

The inferior surface is bounded by the inferior edge of the liver. It blends with the posterior surface in the region of the origin of the lesser omentum, the porta hepatis and the lower layer of the coronary ligament, and is marked near the midline by a sharp fissure which contains the ligamentum teres (the obliterated fetal left umbilical vein). The gallbladder usually lies in a shallow fossa, but this is variable: it may have a short mesentery or be completely intrahepatic and lie within a cleft in the liver parenchyma. The quadrate lobe lies between the fissure for the ligamentum teres and the gallbladder.

The inferior surface of the left lobe is related inferiorly to the fundus of the stomach and the upper lesser omentum. The quadrate lobe lies adjacent to the pylorus, first part of the duodenum and the lower part of the lesser omentum. Occasionally the transverse colon lies between the duodenum and the quadrate lobe. To the right of the gallbladder, the inferior surface is related to the hepatic flexure of the colon, the right suprarenal gland and right kidney, and the first part of the duodenum.

GROSS ANATOMICAL LOBES

Historically, the liver has been considered to be divided into right, left, caudate and quadrate lobes by the surface peritoneal and ligamentous attachments.

Right lobe

The right lobe is the largest in volume and contributes to all surfaces of the liver. It is divided from the left lobe by the falciform ligament superiorly and the ligamentum venosum inferiorly. On the inferior face to the right of the groove formed by the ligamentum venosum there are two prominences separated by the porta hepatis: the caudate lobe lies posterior, and the quadrate lobe anterior, to the porta hepatis. The gallbladder lies in a shallow fossa to the right of the quadrate lobe.

Left lobe

The left lobe is the smaller of the two main lobes, although it is nearly as large as the right lobe in young children.

It lies to the left of the falciform ligament with no subdivisions, and is substantially thinner than the right lobe, having a thin apex that points into the left upper quadrant.

Quadrate lobe

The quadrate lobe is visible as a prominence on the inferior surface of the liver, to the right of the groove formed by the ligamentum venosum (and thus is incorrectly said to arise from the right lobe although it is functionally related to the left lobe). It lies anterior to the porta hepatis and is bounded by the gallbladder fossa to the right, a short portion of the inferior border anteriorly, the fissure for the ligamentum teres to the left, and the porta hepatis posteriorly.

Caudate lobe

The caudate lobe is visible as a prominence on the inferior and posterior surfaces to the right of the groove formed by the ligamentum venosum: it lies posterior to the porta hepatis. To its right is the groove for the inferior vena cava. Above, it continues into the superior surface on the right of the upper end of the fissure for the ligamentum venosum. In gross anatomical descriptions this lobe is said to arise from the right lobe, but it is functionally separate.

FUNCTIONAL ANATOMICAL DIVISIONS

Current understanding of the functional anatomy of the liver is based on Couinaud's division of the liver into eight (subsequently nine) functional segments, based upon the distribution of portal venous branches and the location of the hepatic veins in the parenchyma (Couinaud 1957). Further understanding of the intrahepatic biliary anatomy, especially of the right ductal system, was enhanced by contributions from Hjortsjo (1948) and Healey & Schroy (1953) using the biliary system as the main guide for division of the liver (Fig. 68.4).

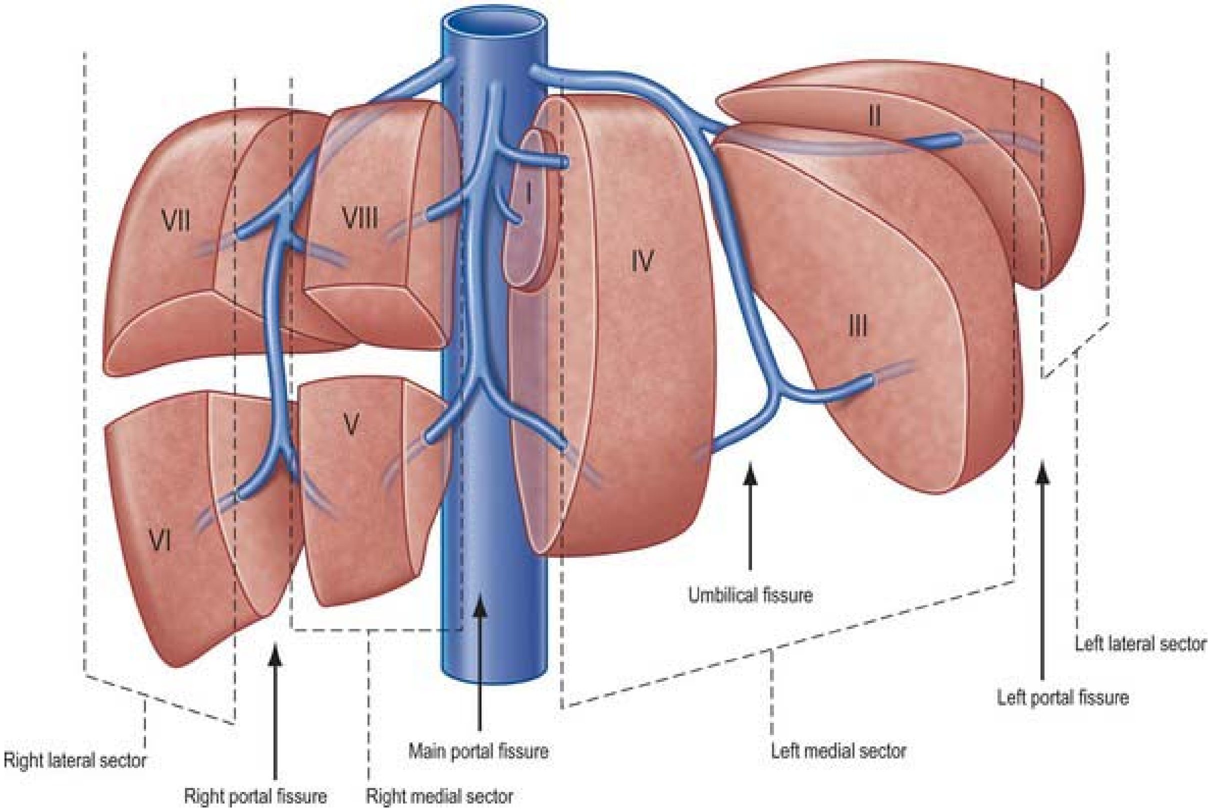
II
VII
VIII
I
IV
III
V
VI
Umbilical fissure
Left lateral sector
Left portal fissure
Right lateral sector
Main portal fissure
Left medial sector
Right portal fissure
Right medial sector

Fig. 68.4 The fissures and sectors of the liver. (Right lateral = right posterior; right medial = right anterior.)

The liver is divided into four portal sectors by the four main branches of the portal vein. These are right lateral, right medial, left medial and left lateral (sometimes the term posterior is used in place of lateral and anterior in place of medial). The three main hepatic veins lie between these sectors as intersectorial veins. These intersectoral planes are also called portal fissures (scissures). The fissures containing portal pedicles are called hepatic fissures. Each sector is sub-divided into segments (usually two) based on their supply by tertiary divisions of the vascular biliary sheaths.

Fissures of the liver

Knowledge of the fissures of the liver is essential for understanding liver surgery. Three major fissures, not visible on the surface, run through the liver parenchyma and harbour the three main hepatic veins (main, left and right portal fissures). Three minor fissures are visible as physical clefts of the liver surface (umbilical, venous and fissure of Gans).

Main portal fissure

The main fissure extends from the tip of the gallbladder back to the midpoint of the inferior vena cava and contains the middle (main) hepatic vein. It separates the liver into right and left hemi-livers. Segments V and VIII lie to the right and segment IV to the left of the fissure.

Left portal fissure

The left fissure divides the left hemi-liver into medial (anterior) and lateral (posterior) sectors. It extends from the mid point of the anterior edge of the liver between the falciform ligament and the left triangular ligament to the point which marks the confluence of the left and middle hepatic veins. It contains the left hepatic vein and separates the left anterior and left posterior sectors: segment III lies anteriorly and segment II posteriorly.

Right portal fissure

The right portal fissure divides the right hemi-liver into lateral (posterior) and medial (anterior) sectors. The plane of the right fissure is the most variable amongst the main fissures and runs approximately diagonally through the gross right lobe from the lateral end of the anterior border to the confluence of the left and middle hepatic veins. The fissure divides the right anterior sector to its left (segments V and VIII) from the right posterior sector to its right (segments VI and VII), and contains the right hepatic vein. The right fissure marks the thickest point of liver parenchyma which is commonly transected during liver resection.

Umbilical fissure

The umbilical fissure separates segment III from segment VI within the left anterior sector and contains a main branch of the left hepatic vein (the umbilical fissure vein). It is marked by the attachment of the falciform ligament and sometimes covered by a ridge of liver tissue extending between the segments: it is often avascular and can be divided safely with diathermy during a surgical approach. It contains the umbilical portion of the left portal vein and the final divisions of the left hepatic duct and the left hepatic artery branches. The umbilical portion of the left portal vein is an important landmark: access to this vein and mobilization of the left portal vein are essential steps in surgery for hilar cholangiocarcinoma. A knowledge of the arrangement of the portal vein, hepatic artery and bile duct within the umbilical fissure is also essential when splitting the liver for an adult and paediatric recipient and for live donor liver transplantation for a child recipient.

Venous fissure

The venous fissure is a continuation of the umbilical fissure on the under surface of the liver and contains the ligamentum venosum. It lies between the caudate lobe and segment IV. The deeper continuation of this plane is the dorsal fissure.

Fissure of Gans

The fissure of Gans lies on the undersurface of the right lobe of the liver behind the gallbladder fossa. It often contains the portal pedicle to the right posterior sector and is thought to correspond to the right fissure as it relates to the separation of the sectors of the liver.

Sectors and segments of the liver

Sectors

The sectors of the liver are made up of between one and three segments: right lateral sector = segments VI and VII; right medial sector = segments V and VIII; left medial sector = segments III and IV (and part of I); left lateral sector = segment II (Fig. 68.5). Segments are numbered in an ante-clockwise spiral centered on the portal vein with the liver viewed from beneath, starting with segment I up to segment VI, and then back clockwise for the most cranial two segments VII and VIII (Fig. 68.6).

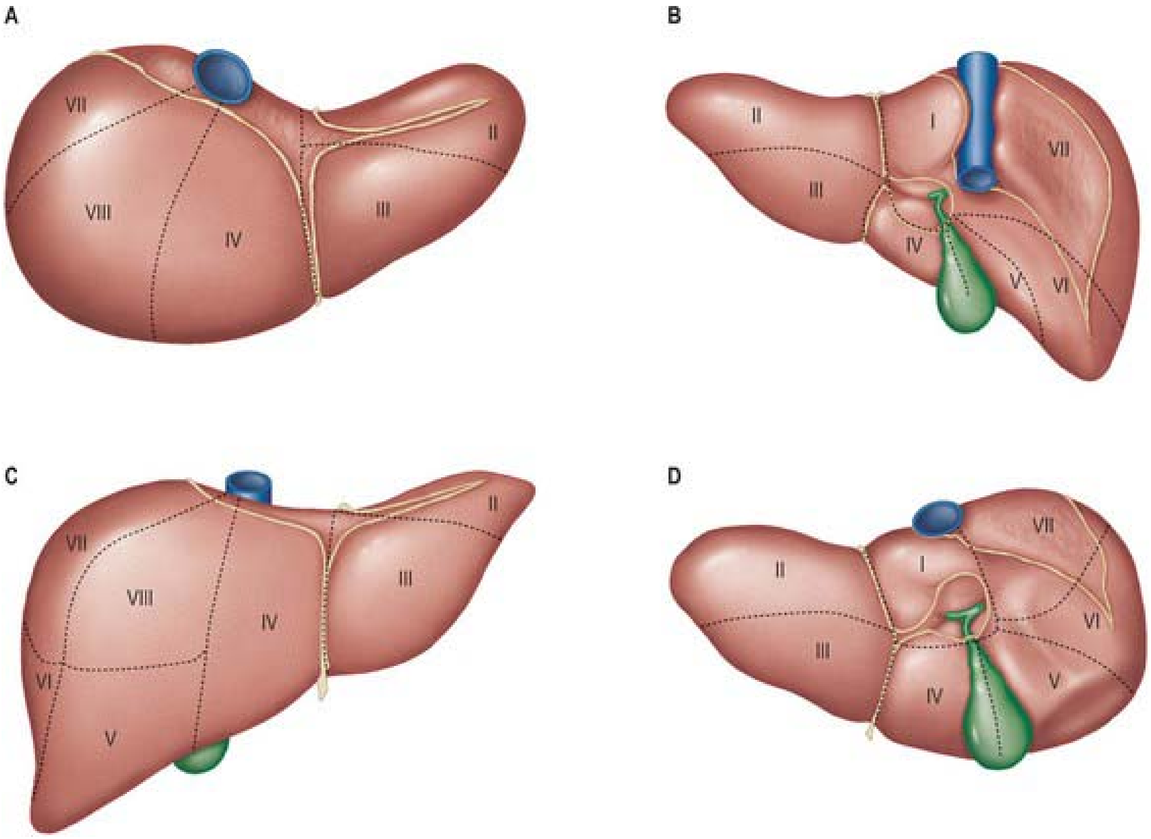

Fig. 68.5 Segments of the liver (after Couinaud). **A**, superior view; **B**, posterior view; **C**, anterior view; **D**, inferior view. The segments are sometimes referred to by number (name) – I (caudate) (sometimes subdivided into left and right parts called segment IX); II (left lateral superior); III (left medial inferior); IV (left medial superior) (sometimes subdivided into superior and inferior parts); V (right medial inferior); VI

(right lateral inferior); VII (right lateral superior); VIII (right medial superior).

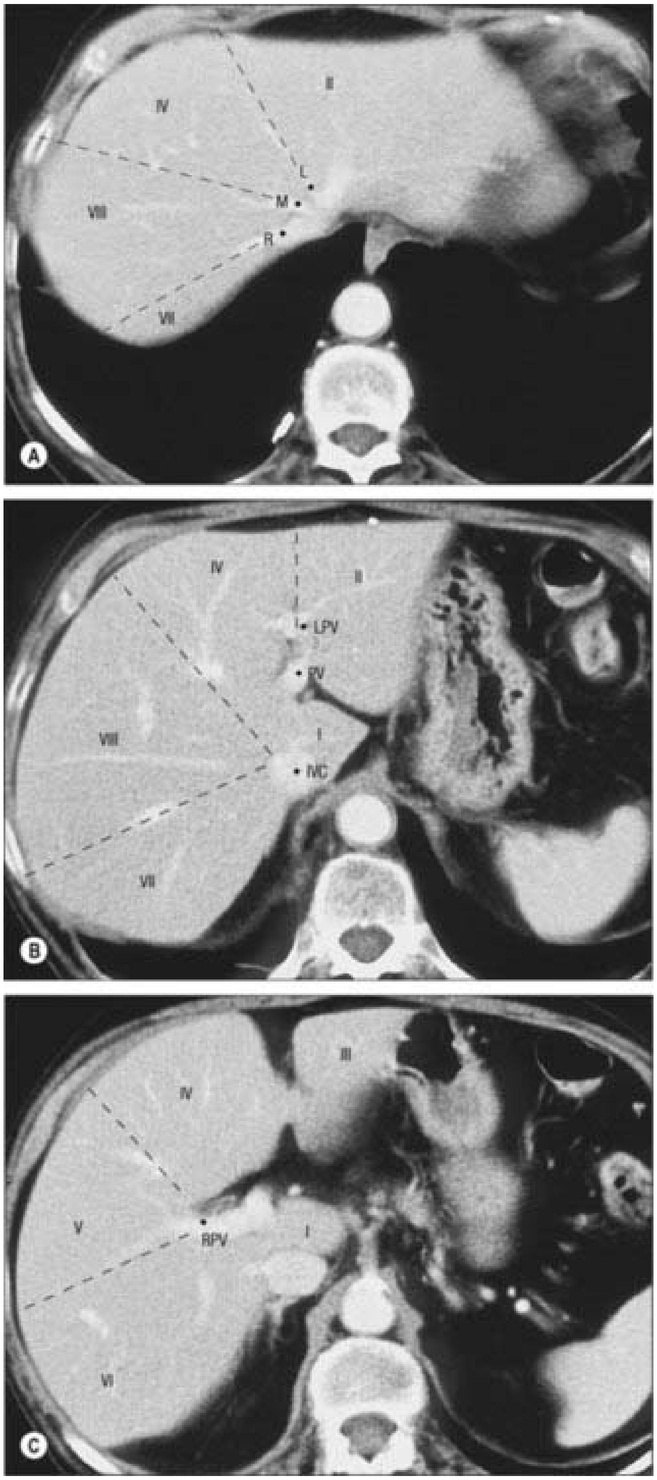
II
IV
L
M
VIII
R
VII
A
IV
II
LPV
PV
I
VIII
IVC
VII
B
III
IV
V
RPV
I
VI
C

Fig. 68.6 Segments of the liver seen on axial CT scan. **A**, Contrast enhanced CT shows the left (L), middle (M), and right (R) hepatic veins at the superior aspect of the liver marking the left main and right portal fissures. **B**, Inferior to this the caudate lobe (segment I) lies between the inferior vena cava (IVC) and the main portal vein (PV). The left portal vein (LPV) separates segment II superiorly from segment III inferiorly. **C**, The right portal vein (RPV) divides segments V and VI inferiorly (**C**) from segments VII and VIII superiorly (**B**).

Segment I

Segment I corresponds to the anatomical caudate lobe and lies posterior (dorsal) to segment IV with its left half directly posterior to segments II and II and its medial half surrounded by major vascular branches. The Glissonian sheaths to segment I arise from both right and left main sheaths: the segment therefore receives vessels independently from the left and right portal veins and hepatic arteries, and it drains independently into the inferior vena cava by multiple small branches (referred to as the lower group). They nearly always arise in the lower and occasionally from the middle third, but never from the upper third of the segment. The bile ducts draining the segment are closely related to the confluence of the right and left hepatic ducts such that excision of central bile duct tumours usually requires removal of segment IV.

Segment II

Segment II is the only segment in the left lateral sector of the liver and lies postero-lateral to the left fissure. It often has only one Glissonian sheath and drains into the left hepatic vein. Rarely, a separate vein drains directly into the inferior vena cava.

Segment III

Segment III lies between the umbilical fissure and the left fissure and is often supplied by one to three Glissonian sheaths: it drains into the left hepatic vein. The vein of the falciform ligament can provide an alternative drainage route for segment III.

Segment IV

Segment IV lies between the umbilical fissure and the main fissure, anterior to the dorsal fissure and segment I. Segment IV is supplied by three to five Glissonian sheaths, of which the majority arise in the umbilical fissure; their origins are often close to those that supply to segments II and III. Occasionally segment IV is supplied by branches from the main left pedicle. The main venous drainage segment is into the middle hepatic vein; the segment can also drain into the left hepatic vein through the vein of the falciform ligament.

Segment V

Segment V is the inferior segment of the right medial sector and lies between the middle and the right hepatic veins. Its size is variable, as are the number of Glissonian sheaths that supply it. Venous drainage is into the right and middle hepatic veins.

Segment VI

Segment VI forms the inferior part of the right lateral sector posterior to the right portal fissure. It is often supplied by two to three branches from the right posterior Glisson’s sheath, but occasionally the Glisson’s sheath to segment VI can arise directly from the right pedicle. Venous drainage is normally into the right hepatic vein, but may be via the right inferior hepatic vein directly into the inferior vena cava.

Segment VII

Segment VII forms the superior part of the posterior sector and lies behind the right hepatic vein. The sheaths to segment VII are often single. The venous drainage is into the right hepatic vein; occasionally the segment can drain through the right middle hepatic vein directly into the inferior vena cava.

Segment VIII

Segment VIII is the superior part of the right anterior sector. The right anterior sectoral sheaths end in segment VIII and supply it after giving off branches to segment V. The venous drainage is to the right and middle hepatic veins.

Segment IX

Segment IX is a recent subdivision of segment I, and describes that part of the segment that lies posterior to segment VIII.

Supports of the liver

The liver is stabilized and maintained in its position in the right upper quadrant of the abdomen by both static and dynamic factors. Richelme & Bourgeon (1973) suggested a three-tier classification of the anatomical factors: the suspensory attachments at the posterior abdominal wall to the inferior vena cava, hepatic veins, coronary and triangular ligaments (primary factors); the support provided by the right kidney, right colonic angle and duodenopancreatic complex (secondary factors); the attachment to the anterior abdominal wall and diaphragm by the falciform ligament (tertiary factors).

The surgical implications of these different factors are important for traumatologists in terms of achieving a better understanding of the pathophysiology of liver trauma. The inferior vena cava and the supra-hepatic veins, especially the right hepatic vein, appear to be the most important anatomical structures that support the bulk of the liver. Other factors which are responsible for the maintenance of the position of the liver within the abdominal cavity include positive intra-abdominal pressure and the movement of the diaphragm during respiration.

Peritoneal attachments and ligaments of the liver

The liver is attached to the anterior abdominal wall, diaphragm and other viscera by several ligaments which are formed from condensations of the peritoneum.

Falciform ligament

The liver is attached in front to the anterior abdominal wall by the falciform ligament. The two layers of this ligament descend from the posterior surface of the anterior abdominal wall and diaphragm and turn onto the anterior and superior surfaces of the liver. On the dome of the superior surface, the right leaf runs laterally and is continuous with the upper layer of the coronary ligament. The left layer of the falciform ligament turns medially and is continuous with the anterior layer of the left triangular ligament. The ligamentum teres, which represents the obliterated left umbilical vein, runs in the lower free border of the falciform ligament and continues into a fissure on the inferior surface of the liver. In fetal life the left umbilical vein opens into the left portal vein: it is supposed to be obliterated in adult life, but frequently remains partially patent. This lumen may open up in conditions such as portal hypertension to form a collateral channel. The ligamentum teres has importance in abdominal surgery for several reasons. It is quite often divided in upper abdominal surgery to optimize access to the upper abdominal viscera or as the first step in the mobilization of the liver. The ligament is vascularized by numerous arterial branches, mainly from the segment IV artery, and these form an anastomotic connection with the branches of the internal thoracic artery: it is therefore important to ligate or coagulate the ligament during its division. The ligamentum teres is a landmark and guide to the segment III hepatic duct used in hepatocojejunostomy formation, and to the left portal vein lying in the umbilical fissure during creation of a mesentericoportal shunt.

Coronary ligament

The coronary ligament is formed by the reflection of the peritoneum from the diaphragm onto the posterior surfaces of the right lobe of the liver. A large triangular area of liver devoid of peritoneal covering, the ‘bare area’ of the liver, is defined between the two layers of the coronary ligament. Here the liver is attached to the diaphragm by areolar tissue and is in continuity inferiorly with the anterior pararenal space. The coronary ligament is continuous on the right with the right triangular ligament. On the left, the two layers become closely applied, and form the left triangular ligament. The upper layer of the coronary ligament is reflected superiorly onto the inferior surface of the diaphragm and inferiorly onto the right and superior surface of the liver. The lower layer of the coronary ligament is reflected inferiorly over the right suprarenal gland and right kidney, and superiorly onto the inferior surface of the liver. Surgical division of the right triangular and coronary ligaments allows the right lobe of the liver to be brought forward, and exposes the lateral aspect of the inferior vena cava behind the liver.

Triangular ligaments

The left triangular ligament is a double layer of peritoneum which extends to a variable length over the superior border of the left lobe of the liver. Medially the anterior leaf is continuous with the left layer of the falciform ligament and the posterior layer is continuous with the left layer of the lesser omentum. The left triangular ligament lies in front of the abdominal part of the oesophagus, the upper end of the lesser omentum and part of the fundus of the stomach. Division of the left triangular ligament allows the left lobe of the liver to be mobilized for exposure of the abdominal oesophagus and crura of the diaphragm. The left triangular ligament is an important stabilizing factor for the left lobe in operations involving removal of the right lobe of the liver. Its division will result in the left lobe being unstable to the extent that it can rotate and displace into the space vacated under the right hemidiaphragm: this extreme degree of rotation can compromise the venous outflow of the liver with consequent liver dysfunction. If it is divided, the left triangular ligament must be fixed at the end of the surgery, in addition to fixing back the falciform ligament.

The right triangular ligament is a short structure which lies at the apex of the ‘bare area’ of the liver and is continuous with the layers of the coronary ligament.

Lesser omentum

The lesser omentum is a fold of peritoneum which extends from the lesser curve of the stomach and proximal duodenum to the inferior surface of the liver. Its attachment to the inferior surface of the liver is L-shaped. The vertical component follows the line of the fissure for the ligamentum venosum, the fibrous remnant of the ductus venosus. More inferiorly the attachment runs horizontally to complete the L in the porta hepatis. At its upper end, the superior layer of the lesser omentum is continuous on the left with the posterior layer of the left triangular ligament, and the inferior layer is continuous on the right with the coronary ligament as it encloses the inferior vena cava. At its lower end, the two layers diverge to surround the structures of the porta hepatis. A thin fibrous condensation of fascia usually runs from the medial end of the porta hepatis into the fissure in the inferior surface which contains the ligamentum teres. This fascia is continuous with the lower border of the falciform ligament when the ligamentum teres re-emerges at the inferior border of the liver. Care should be taken when dividing the lesser omentum, because an aberrant left hepatic artery may run in the medial end: when present, it invariably extends to the liver at the base of the umbilical fissure, and may be identified by a pulsation in the lesser omentum close to the umbilical fissure.

Ligamentum venosum

The ligamentum venosum represents the obliterated venous connection that existed between the left portal vein and the left hepatic vein in fetal life. It is used as a guide and aid to control the left hepatic vein extrahepatically during surgery. By dividing the ligament close to its insertion into the left hepatic vein and retracting it laterally, the angle between the left and the middle hepatic veins, required for dissection and control of the left hepatic vein, may be accessed.

Porta hepatis, hepatoduodenal ligament and hilar plate

The porta hepatis is a deep fissure on the inferior surface of the liver. It is situated between the quadrate lobe in front and the caudate process behind, and contains the portal vein, hepatic artery and hepatic nervous plexuses as they ascend into the parenchyma of the liver, and the right and left bile ducts and some lymph vessels as they emerge from the liver. The hepatic ducts lie anterior to the portal vein and its branches, and the hepatic artery with its branches lies between the two (Fig. 68.7). All these structures are enveloped in the perivascular fibrous capsule, the hepatobiliary capsule of Glisson, a sheath of loose connective tissue which surrounds the vessels as they course through the portal canals in the liver and is also continuous with the fibrous hepatic capsule. The dense aggregation of vessels, supporting connective tissue, and liver parenchyma just above the porta hepatis is often referred to as the 'hilar plate' of the liver (Fig. 68.8). Understanding of the concept of hilar plate is important in surgical approaches to the hilar structures. Division or lowering of the hilar plate are essential for surgical access to the left hepatic duct. The hepatic artery, bile duct and portal vein extend from the porta hepatis towards the duodenum in the free edge of the hepatoduodenal ligament, which forms the anterior boundary of the epiploic foramen. Rapid control of the vessels entering the porta hepatis can be obtained by dividing the lesser omentum to the left of these structures and passing a tape around them from left to right through the epiploic foramen (a 'Pringle' manoeuvre).

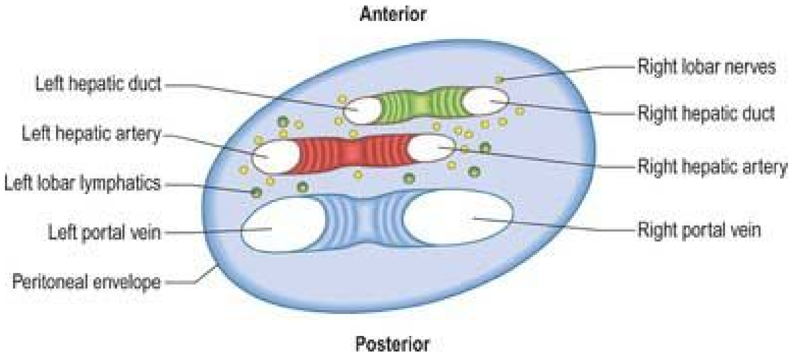
Anterior
Left hepatic duct
Left hepatic artery
Left lobar lymphatics
Left portal vein
Peritoneal envelope
Right lobar nerves
Right hepatic duct
Right hepatic artery
Right portal vein
Posterior

Fig. 68.7 Cross-section of the structures at the porta hepatis.

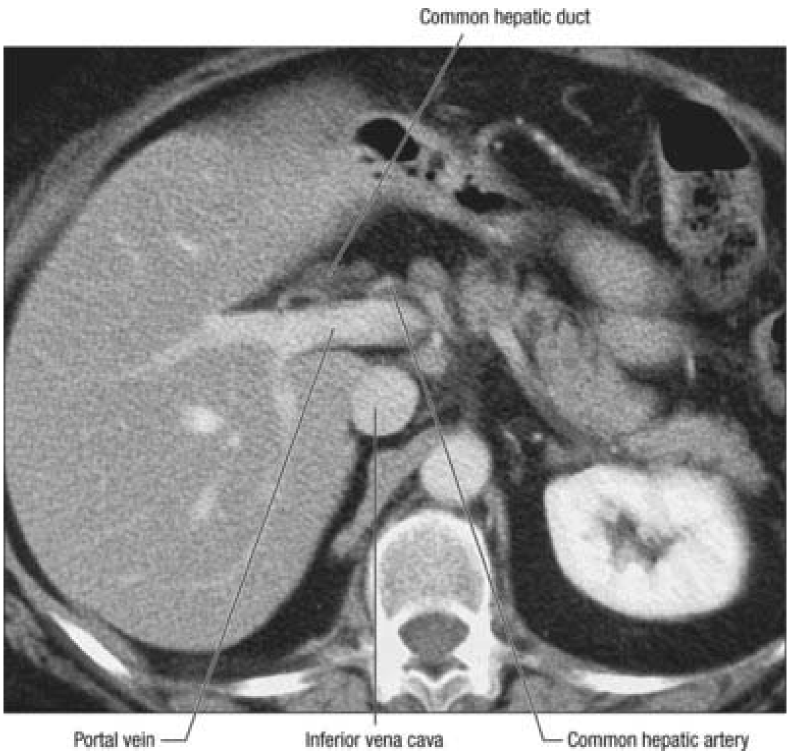

Fig. 68.8 Axial CT of the porta hepatis. The hepatic ducts lie anteriorly, the portal vein posteriorly, and hepatic artery between the two.

The left hepatic duct remains extrahepatic as it runs down to the bifurcation along the base of segment IV (the quadrate lobe). This extrahepatic length of duct is particularly useful when performing high biliary duct reconstructions where a length of jejunum is anastomosed to form a biliary-enteric bypass, to treat strictures of the common hepatic duct.

Glisson’s sheath

Glisson’s capsule condenses around the branches of the portal triad structures as Glissonian sheaths as they enter the liver parenchyma and extends as far the individual segments of the liver. This arrangement facilitates surgical control of both the main right and left pedicles of the liver as well as all the structures (biliary, autonomic and lymphatic elements) that supply individual sectors and segments in liver complex resectional surgery.

VASCULAR SUPPLY AND LYMPHATIC DRAINAGE

The vessels connected with the liver are the portal vein, hepatic artery and hepatic veins. The portal vein and hepatic artery ascend in the lesser omentum to the porta hepatis, where each bifurcates. The hepatic bile duct and lymphatic vessels descend from the porta hepatis in the same omentum (Figs 68.7 and 68.8). The hepatic veins leave the liver via its posterior surface and run directly into the inferior vena cava.

Hepatic artery

In adults the hepatic artery is intermediate in size between the left gastric and splenic arteries. In fetal and early postnatal life it is the largest branch of the coeliac axis. The hepatic artery gives off right gastric, gastroduodenal and cystic branches as well as direct branches to the bile duct from the right hepatic and sometimes the supraduodenal artery (Fig. 68.9A). After its origin from the coeliac axis, the hepatic artery passes anteriorly and laterally below the epiploic foramen to the upper aspect of the first part of the duodenum. It may be subdivided into the common hepatic artery, from the coeliac trunk to the origin of the gastroduodenal artery, and the hepatic artery ‘proper’, from that point to its bifurcation. It passes anterior to the portal vein and ascends anterior to the epiploic foramen between the layers of the lesser omentum. Within the free border of the lesser omentum the hepatic artery is medial to the common bile duct and anterior to the portal vein. At the porta hepatis it divides into right and left branches before these run into the parenchyma of the liver. The right hepatic artery usually crosses posterior (occasionally anterior) to the common hepatic duct (Fig. 68.9B). This close proximity often means that the right hepatic artery is involved in bile duct cancer earlier than the left hepatic artery. Occasionally the right hepatic artery crosses in front of the common bile duct and may be injured in surgery of the common bile duct. It almost always divides into an anterior branch supplying segments V and VIII, and a posterior branch supplying segments VI and VII. The anterior division often supplies a branch to segment I and the gallbladder. The segmental arteries are macroscopically end-arteries although some collateral circulation occurs between segments via fine terminal branches.

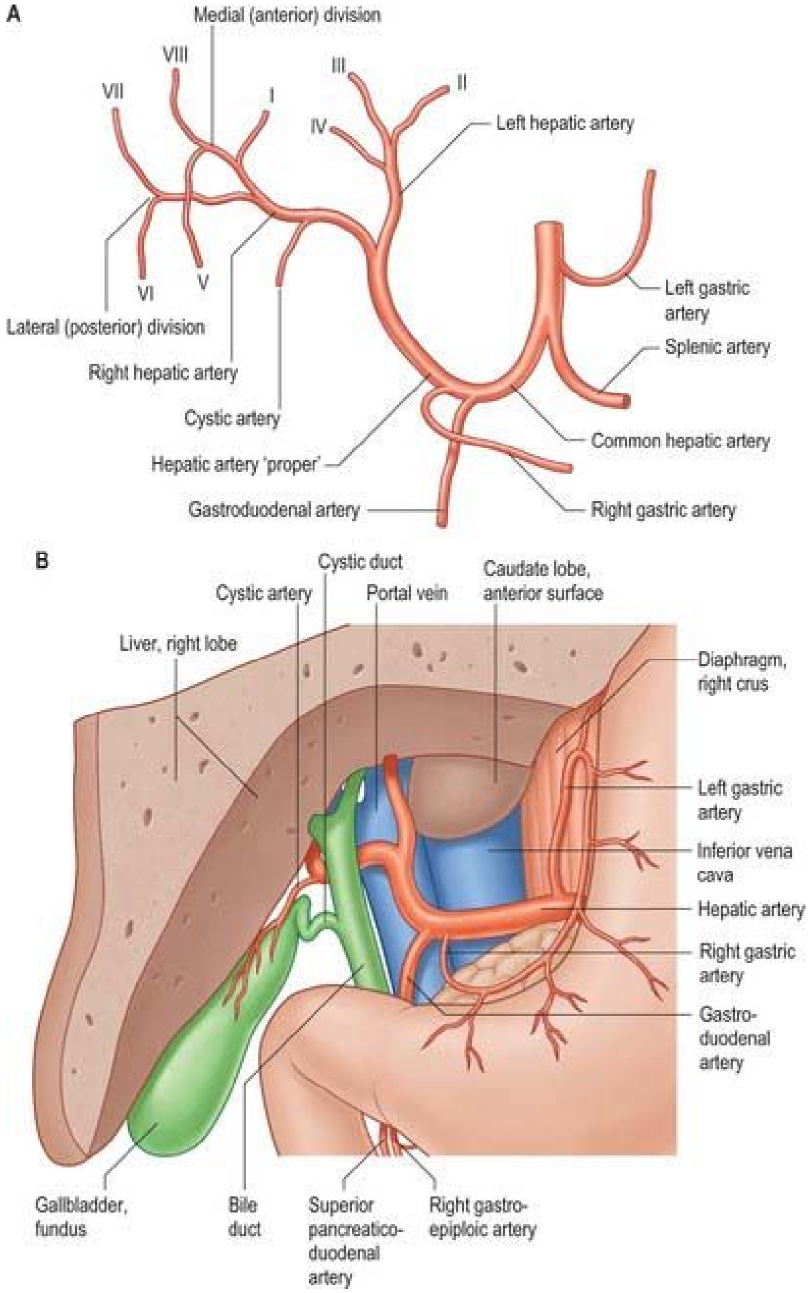
A
Medial (anterior) division
VIII
VII
I
III
II
IV
Left hepatic artery
VI
V
Lateral (posterior) division
Right hepatic artery
Cystic artery
Hepatic artery 'proper'
Gastroduodenal artery
Left gastric artery
Splenic artery
Common hepatic artery
Right gastric artery
B
Cystic duct
Cystic artery
Portal vein
Caudate lobe, anterior surface
Liver, right lobe
Diaphragm, right crus
Left gastric artery
Inferior vena cava
Hepatic artery
Right gastric artery
Gastro-duodenal artery
Gallbladder, fundus
Bile duct
Superior pancreatico-duodenal artery
Right gastro-epiploic artery

Fig. 68.9 The hepatic artery. **A**, Branches. **B**, Relations of the hepatic artery, bile duct and portal vein to each other in the lesser omentum: anterior aspect, portion of the liver removed.

A small number of normal variants are important to demonstrate angiographically because they may influence surgical and interventional radiological procedures. A vessel that supplies a lobe in addition to its normal vessel is defined as an accessory artery. A replaced hepatic artery is a vessel that does not originate from an orthodox position and provides the sole supply to that lobe. Rarely a replaced common hepatic artery arises from the superior mesenteric artery (Fig. 68.10) and is identified at surgery by a relatively superficial portal vein (reflecting the absence of a common hepatic artery that would normally cross in front of the vein). More commonly a replaced right hepatic artery or an accessory right hepatic artery arises from the superior mesenteric artery (Fig. 68.11). In this case they run behind the portal vein and bile duct in the lesser omentum and can be identified at surgery by pulsation behind the portal vein. The accessory right hepatic artery may be injured during resections of the pancreatic head because the artery lies in close proximity to the portal vein. Occasionally, a replaced left hepatic artery or an accessory branch arises from the left gastric artery: these vessels provides a source of collateral arterial circulation in cases of occlusion of the vessels in the porta hepatis but may also be injured during mobilization of the stomach as it lies in the upper portion of the lesser omentum. Rarely, accessory left or right hepatic arteries may arise from the gastroduodenal artery or aorta. The presence of replaced arteries can be lifesaving in patients with bile duct cancer: because they are further away from the bile duct they tend to be spared from the cancer, making excision of the tumour feasible. Knowledge of these variations is also important in planning whole and split liver transplantation.

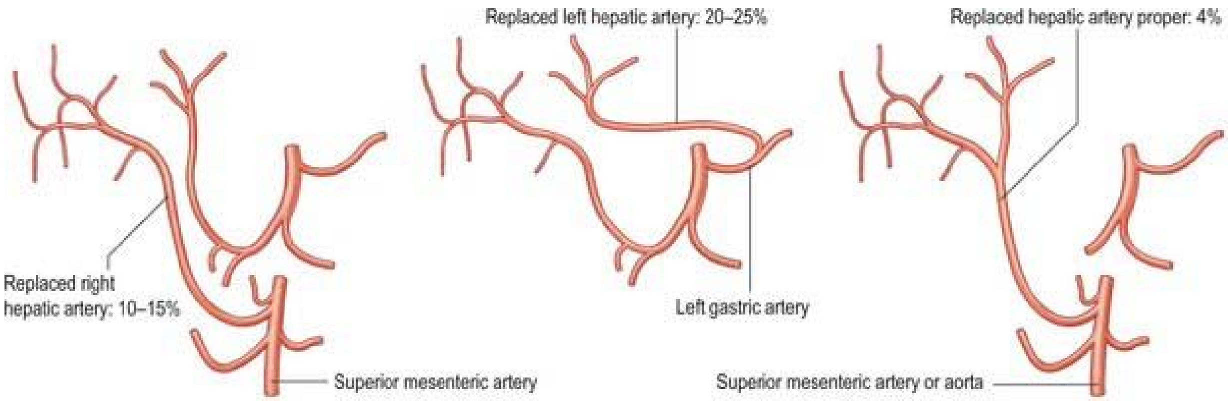
Replaced left hepatic artery: 20–25%
Replaced hepatic artery proper: 4%
Replaced right hepatic artery: 10–15%
Left gastric artery
Superior mesenteric artery
Superior mesenteric artery or aorta

Fig. 68.10 Most common variants of the main hepatic artery.

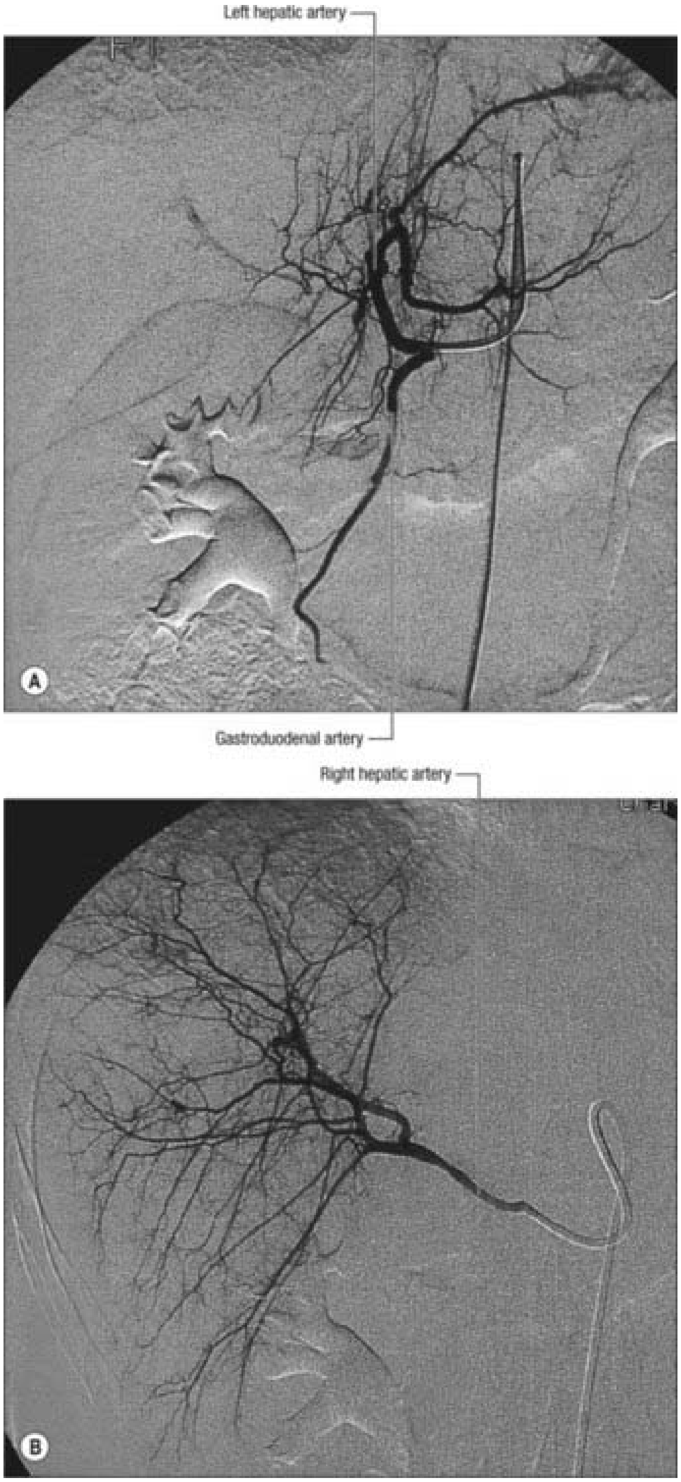
Left hepatic artery
A
Gastroduodenal artery
Right hepatic artery
B

Fig. 68.11 Hepatic arteriogram. **A**, A selective hepatic arteriogram shows normal left hepatic artery branches and small right hepatic artery branches. **B**, The right hepatic artery is arising from the origin of the superior mesenteric artery.

Variations in the intrahepatic arteries are common and may be surgically important. For example, the segment VI artery most commonly arises from the left hepatic artery, but in about 10–20% of cases it arises from the right hepatic artery or the main hepatic artery. Failure to recognize this variation may compromise the blood supply to segment IV following right hepatectomy, and is especially important following right lobe donation for live donor liver transplantation.

Veins

The liver has two venous systems. The portal system conveys venous blood from the majority of the gastrointestinal tract and its associated organs to the liver (see Ch. 60). The hepatic venous system drains blood from the liver parenchyma into the inferior vena cava.

Portal vein

The portal vein begins at the level of the second lumbar vertebra and is formed from the convergence of the superior mesenteric and splenic veins (Fig. 68.12; see also Fig. 71.4 and Fig. 60.8. It is approximately 8 cm long and lies anterior to the inferior vena cava and posterior to the neck of the pancreas. It lies obliquely to the right and ascends behind the first part of the duodenum, the common bile duct and gastroduodenal artery. At this point it is directly anterior to the inferior vena cava. It enters the right border of the lesser omentum, ascends anterior to the epiploic foramen to reach the right end of the porta hepatis and then divides into right and left main branches which accompany the corresponding branches of the hepatic artery into the liver. In the lesser omentum the portal vein lies posterior to both the common bile duct and hepatic artery. It is surrounded by the hepatic nerve plexus and accompanied by many lymph vessels and some lymph nodes.

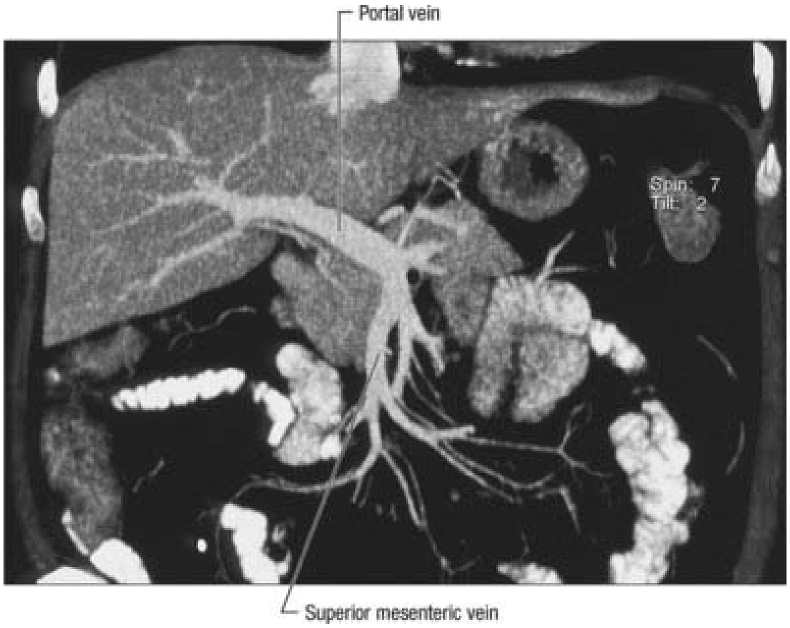

Fig. 68.12 Coronal CT of the portal vein and superior mesenteric vein.

The main extrahepatic tributaries of the portal vein are the coronary or the left gastric vein, which ends in the left margin of the portal vein, and the posterior superior pancreatoduodenal vein nearer to the head of the pancreas. The portal vein divides into right and left branches at the hilum (Fig. 68.13). The left portal vein has a longer extraparenchymal course (4–5 cm) and tends to lie slightly more horizontally than the right portal vein, but is often of smaller calibre. It has horizontal and vertical portions. The horizontal portion runs along the base of segment VI and often gives branches to segment I and sometimes to segment VI in this part of its course. The branch to segment II continues laterally but the main left portal vein takes a more anterior and vertical course in the umbilical fissure (the vein of the umbilical fissure) where it gives branches to segments III and IV and receives the obliterated left umbilical vein (ligamentum teres). The majority of the supply to segment IV comes from the left portal vein, and only occasionally from the right via proximal branches of the main vein or branches from veins to segments V or VIII. The right portal vein is only 2–3 cm in length and usually divides into a right medial (anterior) sectoral division supplying segments V and VIII, and a right lateral (posterior) sectoral division supplying segments VI and VII. The medial division may give a branch to segment I.

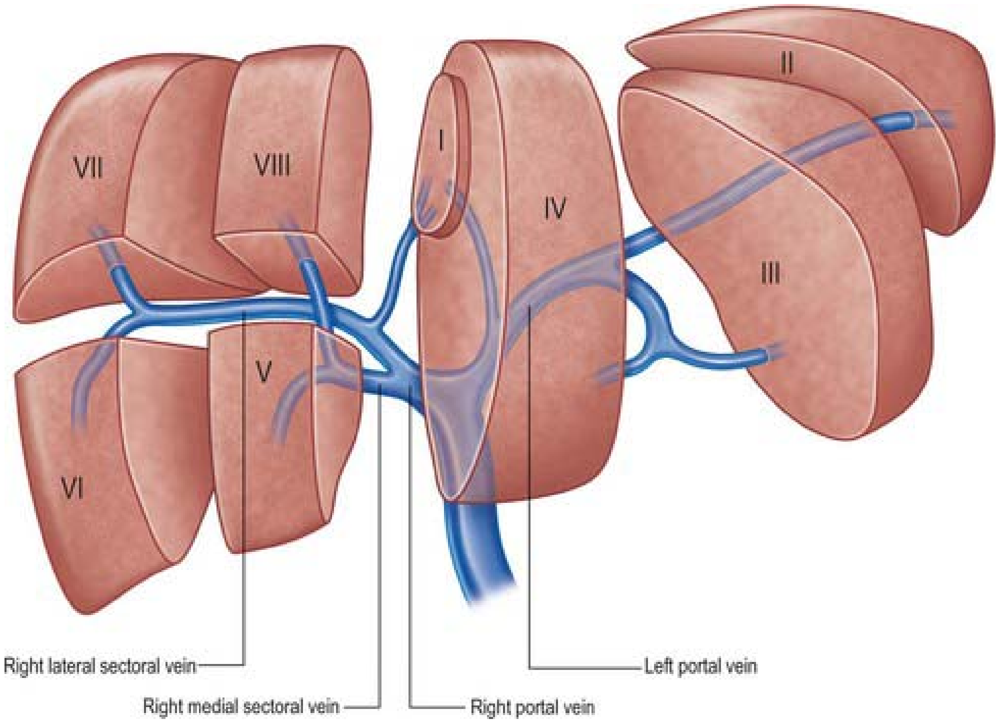

Fig. 68.13 The main portal vein and its intraheptic branches. (Right lateral = right posterior; right medial = right anterior.)

Variations usually involve the right portal vein: absence of a right portal vein with the resulting portal trifurcation in the form of left portal vein, right medial and right lateral portal veins, is present in 10–15% of livers. Occasionally the right medial vein arises from the left portal vein, a variant which is important to remember during left sided liver resection. The portal trifurcation has implications for split liver and live donor liver transplantation, where its presence might be considered as a relative contra-indication. On rare occasions, the portal bifurcation is absent, in which case the main portal vein enters the liver giving off the right segmental branches and then turns left to supply the left lobe of the liver (a contraindication to major liver surgery). Occasionally one or more of the segmental branches of the right lobe (especially segment IV) arises proximally.

Porto-systemic shunts

Increased pressure within the portal venous system may result in dilatation of the portal venous tributaries: a reversal of flow may occur where these veins form anastomoses with veins which drain into the systemic venous circulation. The common sites where porto-systemic shunts may occur, and the associated clinical implications, are listed in Table 68.1.

Table 68.1 Common sites of occurrence of porto-systemic shunts, and associated clinical implications.

Portal veins	**Systemic veins**	**Clinical presentations**
Left gastric and lower oesophageal veins	Lower branches of oesophageal veins that drain into azygos and accessory hemiazygos veins	Oesophageal or gastric varices
Superior rectal veins	Middle and inferior rectal veins that drain into internal iliac and pudendal veins	Rectal varices
Persistent tributaries of left branch of portal vein, running in ligamentum teres	Peri-umbilical branches of superior and inferior epigastric veins	‘Caput medusae’
Intraparenchymal branches of right branch of portal vein, lying in liver tissue exposed in ‘bare area’	Retroperitoneal veins that drain into lumbar, azygos and hemiazygos veins	Retroperitoneal dilated veins are at risk during surgery or interventional procedures
Omental and colonic veins in the region of the hepatic and splenic flexure	Retroperitoneal veins in the region of the hepatic and splenic flexure	
Patent ductus venosus connected to the left branch of the portal vein	Inferior vena cava	Is rare

Hepatic veins

The liver is drained by three major hepatic veins into the suprahepatic part of the inferior vena cava and a multitude of minor hepatic veins that drain into the intrahepatic inferior vena cava. The three major veins are located between the four major sectors of the liver (Figs 68.6A, 68.14 and 68.15).

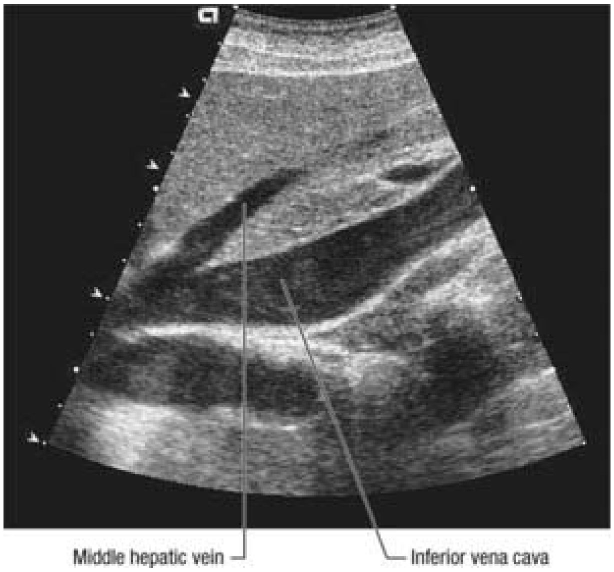

Fig. 68.14 Sagittal ultrasound of the middle hepatic vein. Middle hepatic vein draining into the inferior vena cava.

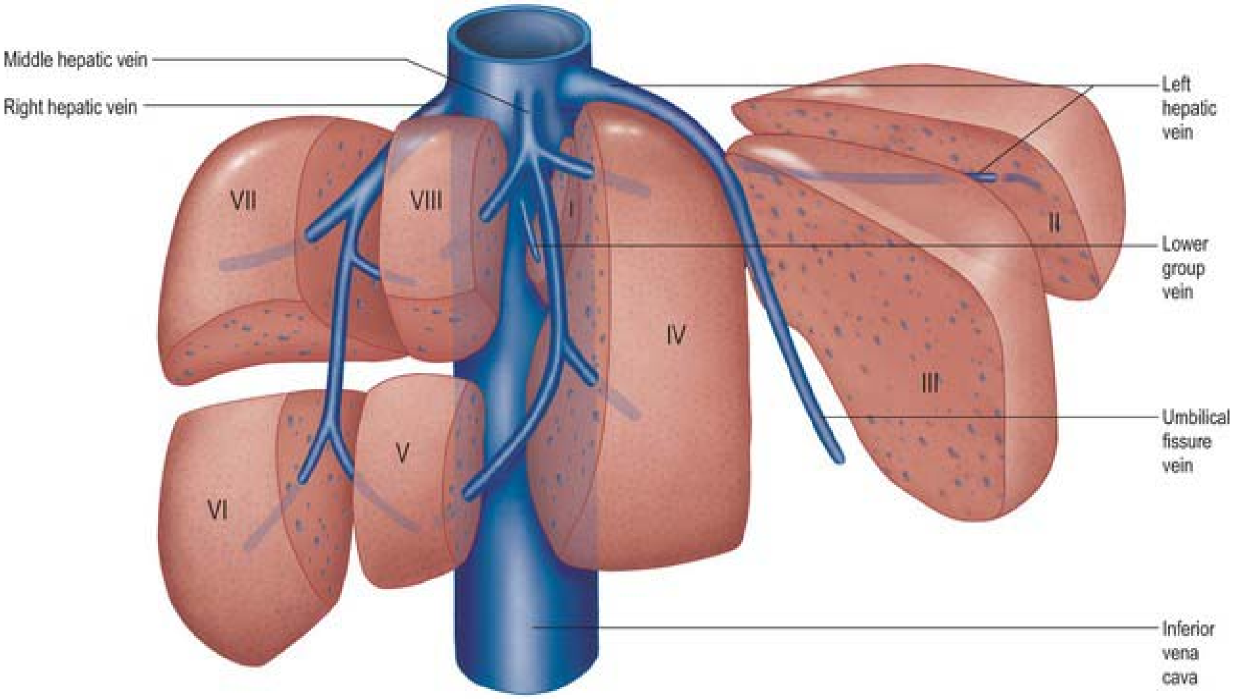
Middle hepatic vein
Right hepatic vein
Left hepatic vein
VII
VIII
I
II
Lower group vein
IV
III
Umbilical fissure vein
V
VI
Inferior vena cava

Fig. 68.15 Arrangement of the hepatic venous territories. Multiple lower group veins may be present. Individual segments may drain into more than one hepatic venous territory.

Right hepatic vein

This is the longest and the largest vein and also the most variable. It is usually single, but occasionally it remains as two trunks until it terminates by draining into the inferior vena cava. The right hepatic vein runs into the intersectoral plane between the right medial and right lateral sectors. It drains the whole of segments VI and VII and parts of segments V and VIII. The extent of its contribution to the drainage of segments V and VIII is variable, and depends upon the size of the veins that drain these segments into the middle hepatic vein. The right hepatic vein is formed near the anterior and inferior edge of the liver and lies in a coronal plane through most of its course. It drains into the inferior vena cava near the upper border of the caudate lobe. Of all the three major veins the right hepatic vein is the one which is the most variable in its size not only due to the differential contribution to segments V and VIII drainage along with the middle hepatic vein but also due to the occasional presence of an accessory right middle and right inferior veins.

Middle hepatic vein

The middle hepatic vein lies along the plane between the right medial and the left medial sectors of the liver. It usually joins with the left hepatic vein and terminates into the inferior vena cava as a common trunk. It drains the central part of the liver receiving constant branches from segments IV, V and VIII. The sizes of the branches draining segments V and VIII are variable and are of surgical importance in terms of right lobe living donation.

Left hepatic vein

The left hepatic vein lies between the left medial and left lateral sectors of the liver. It drains segments II, III and occasionally IV. Small veins draining segment II and occasionally the superior part of segment IV may drain directly into the inferior vena cava in the minority of livers. Usually a major tributary of the left hepatic vein, the umbilical fissure vein runs in the intersegmental plane between segments III and IV and contributes to their drainage. Occasionally the vein draining segment III ends separately in the confluence of the left and middle hepatic veins. These variations in the venous drainage are of significance in terms of split liver transplantation and live donor liver transplantation.

Minor veins

Segment I veins drain directly into the inferior vena cava and vary in number from one to five. Since it has an independent drainage from the rest of the liver in patients with Budd–Chiari syndrome, where all the major hepatic veins are blocked, segment I often continues to drain effectively and undergoes compensatory hypertrophy. Rarely there is an accessory right middle or inferior hepatic vein. When they are present they are of surgical importance especially if they are of more than 5 mm in diameter; they drain segments V and VI independently of the three major veins and therefore any tumour involving the three major veins can be safely resected as long as venous drainage from the accessory veins is ensured. In live donor and split liver transplantation these veins must be individually anastomosed to the recipient inferior vena cava to ensure adequate venous drainage.

Transjugular intraparenchymal porto-systemic shunt (TIPS) procedure for portal hypertension

In extreme cases of chronic portal hypertension, large calibre anastomoses between portal and systemic circulations may be formed within the liver parenchyma using a balloon catheter, introduced via the internal jugular vein and under radiological control, to puncture across and rupture through a thinned strip of liver parenchyma between hepatic veins and dilated portal branches.

Lymphatics

Lymph from the liver has abundant protein content. Lymphatic drainage from the liver is wide and may pass to nodes above and below the diaphragm. Obstruction of the hepatic venous drainage increases the flow of lymph in the thoracic duct. Hepatic collecting vessels are divided into superficial and deep systems.

Superficial hepatic vessels

The superficial vessels run in subserosal areolar tissue over the whole surface of the liver and drain in four directions. Lymph vessels from the majority of the posterior surface, the surface of the caudate lobe, and the posterior part of the inferior surface of the right lobe, accompany the inferior vena cava and drain into pericaval nodes. Vessels in the coronary and right triangular ligaments may directly enter the thoracic duct without any intervening node. Vessels from the majority of the inferior surface, anterior surface and most of the superior surface all converge on the porta hepatis to drain into the hepatic nodes. A few lymph vessels from the posterior surface of the lateral end of the left lobe pass towards the oesophageal opening to drain into the para-cardiac nodes. One or two lymph trunks from the right surface and right end of the superior surface accompany the inferior phrenic artery across the right crus to drain into the coeliac nodes.

Deep hepatic vessels

The great majority of the liver parenchyma is drained by lymphatic vessels within the substance of the liver. Fine lymphatic vessels merge to form larger vessels. Some run superiorly through the parenchyma to form the ascending trunks which accompany the hepatic veins and pass through the caval opening in the diaphragm to drain into nodes around the end of the inferior vena cava. Vessels from the lower portion of the liver form descending trunks which emerge from the porta hepatis and drain into the hepatic nodes.

INNERVATION

The liver has a dual innervation. The parenchyma is supplied by hepatic nerves which arise from the hepatic plexus and contain sympathetic and parasympathetic (vagal) fibres. They enter the liver at the porta hepatis and most accompany the hepatic arteries and bile ducts. A very few may run directly within the liver parenchyma. The capsule is supplied by some fine branches of the lower intercostal nerves, which also supply the parietal peritoneum, particularly in the area of the ‘bare area’ and superior surface: distension or disruption of the liver capsule causes quite well localized sharp pain.

Hepatic plexus

The hepatic plexus is the largest derivative of the coeliac plexus and receives branches from the anterior and posterior vagi. It accompanies the hepatic artery and portal vein and their branches into the liver, where its fibres run close to the branches of the vessels, supplying vasomotor fibres to the hepatic vessels and biliary tree, and innervating the hepatocytes directly. Multiple fine branches from the plexus supply the common and hepatic bile ducts directly; branches to the gallbladder form a delicate cystic plexus. The vagal fibres are motor to the musculature of the gallbladder and bile ducts and inhibitory to the sphincter of the bile duct.

Nerves from the hepatic plexus run with the branches of the common hepatic artery to supply, or contribute to the supply of, foregut derivatives. Branches run inferiorly from the plexus with the right gastric artery to contribute to the supply of the pylorus, with the gastroduodenal artery and its branches to reach the pylorus and the first part of the duodenum, and with the right gastroepiploic artery to provide a small contribution to the supply the right side of the stomach and the greater curvature. The superior pancreaticoduodenal extension supplies the descending part of the duodenum, the pancreatic head and the intrapancreatic part of the common bile duct.

Referred pain

Pain arising from the parenchyma of the liver is poorly localized. In common with other structures of foregut origin, pain is referred to the central epigastrium. Stretch of or involvement of the liver capsule by inflammatory or neoplastic processes rapidly produces well-localized pain of a ‘somatic’ nature.

MICROSTRUCTURE

The liver is essentially an epithelial-mesenchymal outgrowth of the caudal part of the foregut, with which it retains its connection via the biliary tree. The surface of the liver facing the peritoneal cavity is covered by a typical serosa, the visceral peritoneum. Beneath this, and enclosing the whole structure, is a thin (50–100 µm) layer of connective tissue from which extensions pass into the liver as connective tissue septa and trabeculae. Branches of the hepatic artery and hepatic portal vein, together with bile ductules and ducts, run within these connective tissue trabeculae which are termed portal tracts (portal canals). The combination of the two types of vessel and a bile duct is termed a portal triad (Fig. 68.16); these structures are usually accompanied by one or more lymphatic vessels.

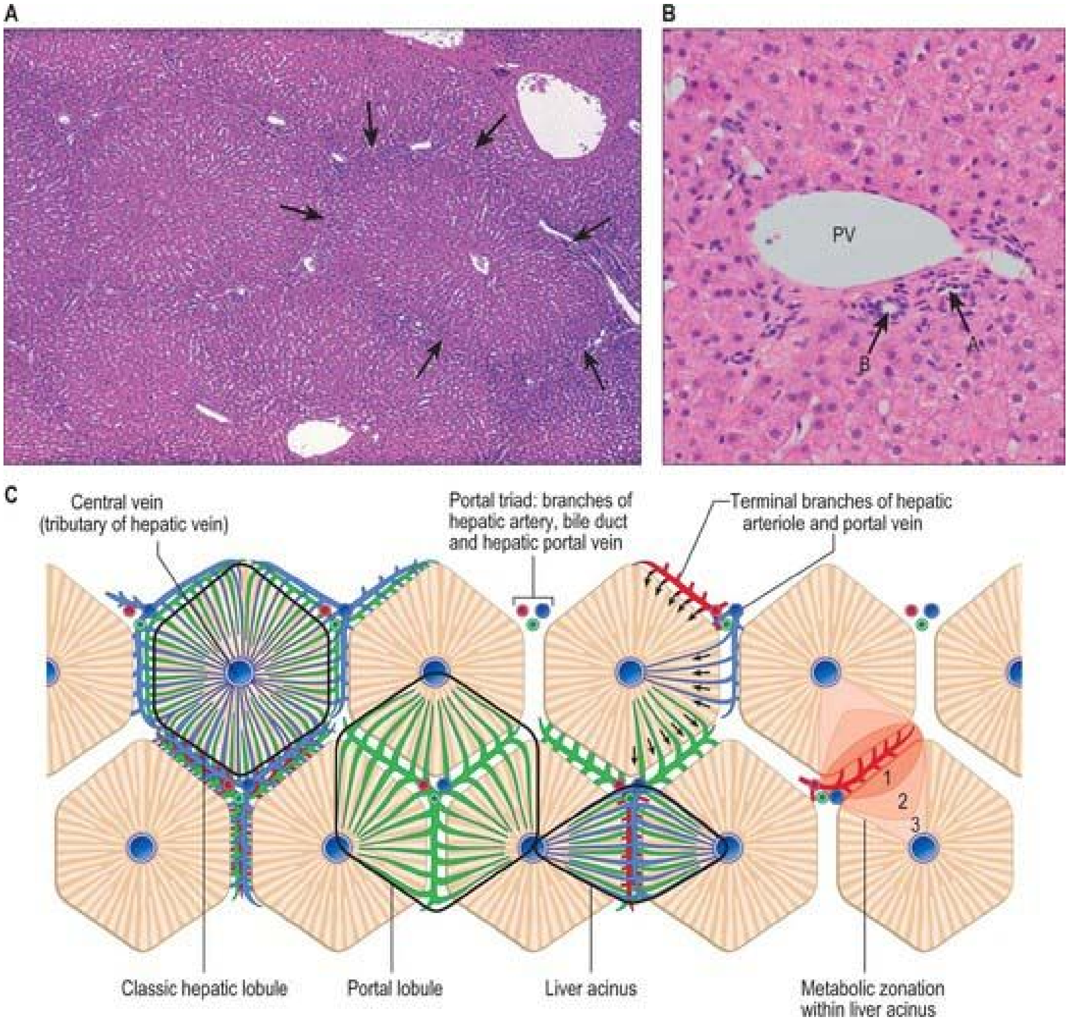
A
B
PV
B
A
C
Central vein
(tributary of hepatic vein)
Portal triad: branches of hepatic artery, bile duct and hepatic portal vein
Terminal branches of hepatic arteriole and portal vein
1
2
3
Classic hepatic lobule
Portal lobule
Liver acinus
Metabolic zonation within liver acinus

Fig. 68.16 The structural organization of human liver tissue. **A**, Lobules bordered by delicate connective tissue septa (arrows) in which run branches of the hepatic portal vein, hepatic artery and bile duct, grouped as portal triads. A central vein drains each lobule. **B**, A portal triad containing branches of the hepatic portal vein (PV; generally the largest profile), the hepatic artery (A) and a bile duct (B), with typical round epithelial nuclei. Other small bile ductule and arteriolar branches are also visible. **C**, A functional view in which the territories of the hepatic lobules are shown as regular hexagons (unlike their real appearance, which is highly variable). The different functions, such as blood flow from the territory of the acinus to sectors of adjacent hepatic lobules, are shown in different lobules, though in reality all occur in each lobule.

(By permission from Dr JB Kerr, Monash University, from Kerr JB 1999 Atlas of Functional Histology. London: Mosby.) (By courtesy of Mr Peter Helliwell and Dr Joseph Mathew, Department of Histopathology, Royal Cornwall Hospitals Trust, UK.)

The liver parenchyma consists of a complex network of epithelial cells, supported by connective tissue, and perfused by a rich blood supply from the hepatic portal vein and hepatic artery. The epithelial cells, hepatocytes, carry out the major metabolic activities of this organ, but additional cell types possess storage, phagocytic and mechanically supportive functions. In the mature liver, hepatocytes are arranged mainly in plates (or cords, as seen in two-dimensional sections) that are usually only one cell thick and separated by venous sinusoids which anastomose with each other via gaps in the plates. Until about seven years of age, plates are normally two cells thick.

Bile secreted by the hepatocytes is collected in a network of minute tubes (canaliculi). The hepatocytes can therefore be regarded as exocrine cells, secreting bile into the alimentary tract via the hepatic ducts and bile duct. Their other metabolic functions involve complex biochemical exchanges with the blood.

The fetal liver is a major haemopoietic organ: erythrocytes, leukocytes and platelets develop from the mesenchyme covering the sinusoidal endothelium.

Lobulation of the liver

The structural unit of the liver is the lobule: a roughly hexagonal arrangement of plates of hepatocytes, separated by intervening sinusoids which radiate outward from a central vein, with portal triads at the vertices of each hexagon (Fig. 68.16). The central vein is a tributary of the hepatic vein that drains the tissue. In some species, the classic lobular units are delimited microscopically by distinct connective tissue septa. However, the lobular organization of the human liver is not immediately evident in histological sections: the lobules do not have distinct boundaries, and connective tissue is sparse. The plates do not pass straight to the periphery of a lobule like the spokes of a wheel but run irregularly as they anastomose and branch.

Detailed studies of human liver, using three-dimensional reconstruction and morphometric analysis combined with histopathological observations, have revealed a highly ordered arrangement of functional units, the hepatic (portal) acini. Each acinus is an approximately oval mass of tissue, oriented around the afferent vascular system, i.e. a terminal branch of a hepatic arteriole and portal venule, and with its long axis defined by the territory between two adjacent central veins. It includes the hepatic tissue served by these afferent vessels, and is bounded by the territories of other acini.

The acinar definition of hepatic micro-organization has clarified important problems of liver histopathology, especially the development of zones of anoxic damage, glycogen deposition and removal, and of toxic trauma, which are all related to the direction of blood flow and thus tend to follow the acinar pattern. There are also real metabolic differences between hepatocytes within the acini, and they have been divided into three zones: zone 1 (periportal) is nearest to the terminal branches of afferent vessels; zone 2 is the intermediate zone; and zone 3 is the area closest to the central venous drainage.

Blood supply

Preterminal hepatic arterioles in the portal canals branch to convey arterial blood to the sinusoids by several routes. The main pattern is via a fine capillary plexus which drains to branches of the portal veins. Some arterial blood passes directly to the hepatic sinusoids, bypassing these capillary plexuses, but this represents only a small part of the total flow. Sinusoids thus contain mixed venous and arterial blood. Central veins from adjacent lobules form interlobular veins which unite as hepatic veins and drain to the inferior vena cava. Hepatic veins draining the tissue run quite separately with respect to the portal triad system, freely crossing the boundaries of triad territories.

Hepatic plates (cords)

The endothelial linings of the sinusoids are separated from hepatocytes forming the hepatic plates by a narrow gap, the perisinusoidal space of Disse, which is normally about 0.2–0.5 μm wide, but which distends in anoxic conditions. The space contains fine collagen fibres (mostly type III, with some types I and IV), the microvilli of adjacent hepatocytes, and occasional non-myelinated nerve terminals. There is no basal lamina within the space of Disse.

Minute bile canaliculi form nets with polygonal meshes in the hepatic plates. Each polygonal hepatocyte is surrounded by canaliculi (see below) except on the surfaces, at least two per cell, that face sinusoids. Hepatic plates thus enclose a network of canaliculi that pass to the lobular periphery, where they join to form narrow intralobular ductules (terminal ductules or the canals of Hering) lined by squamous or cuboidal epithelium. The intralobular ductules enter bile ductules, lined by cuboidal or columnar cells, in the portal canals. The flow of bile is thus towards the periphery of lobules, in the opposite direction to the blood flow, which is centripetal.

Cells of the liver

Cells of the liver include hepatocytes, hepatic stellate cells (also known as perisinusoidal lipocytes, or Ito cells), sinusoidal endothelial cells, macrophages (Kupffer cells), the cells of the biliary tree (cuboidal to columnar epithelium) and connective tissue cells of the capsule and portal tracts (Figs 68.16B and 68.17).

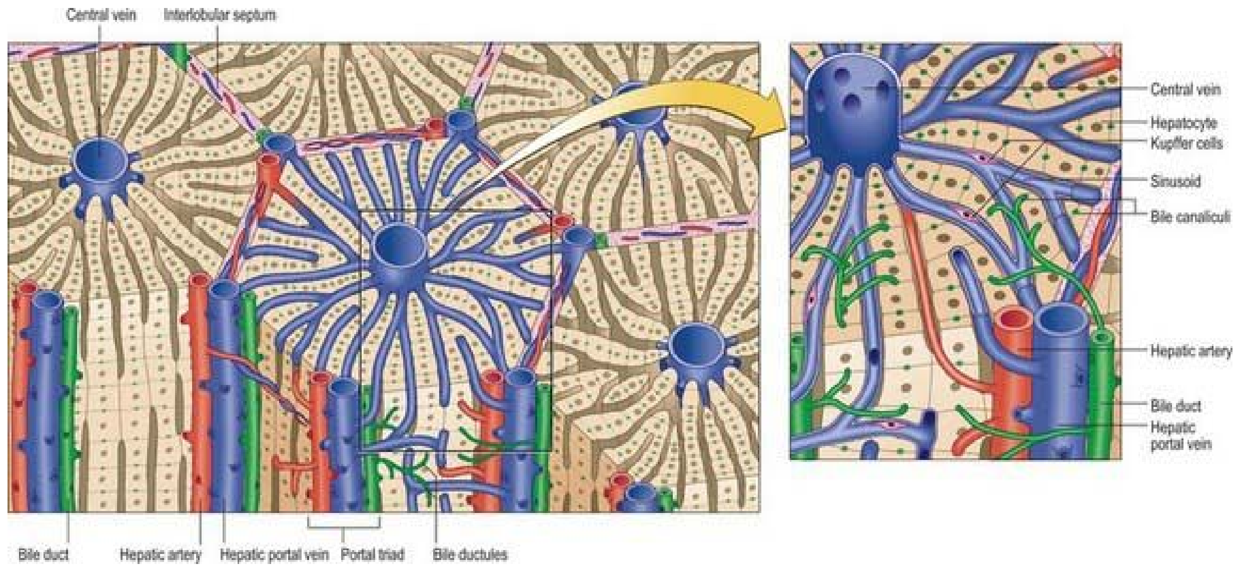
Central vein
Interlobular septum
Central vein
Hepatocyte
Kupffer cells
Sinusoid
Bile canaliculi
Hepatic artery
Bile duct
Hepatic portal vein
Bile duct
Hepatic artery
Hepatic portal vein
Portal triad
Bile ductules

Fig. 68.17 Hepatic microstructure. Sinusoidal endothelial cells are not shown.

Hepatocytes

About 80% of the liver volume and 60% of its cell number are formed by hepatocytes (parenchymal cells) (Fig. 68.17). They are polyhedral, with 5–12 sides and are from 20 to 30 μm across. Their nuclei are round, euchromatic and often tetraploid, polyploid or multiple, with two or more in each cell. Their cytoplasm typically contains a considerable amount of rough and smooth endoplasmic reticulum, many mitochondria, lysosomes and well-developed Golgi apparatus, which are all features that indicate a high metabolic activity. Glycogen granules and lipid vacuoles are usually prominent. Numerous large peroxisomes and vacuoles containing enzymes, e.g. urease in distinctive crystalline forms, indicate the complex metabolism of these cells. Their role in iron metabolism is reflected by the presence of storage vacuoles containing crystals of ferritin and haemosiderin.

The surfaces of hepatocytes facing the sinusoids exhibit numerous microvilli, approximately 0.5 μm long, creating a large area of membrane, 70% of the hepatocyte surface, exposed to blood plasma. Elsewhere, hepatocytes are linked by numerous gap junctions and desmosomes. Lateral plasma membranes of adjacent hepatocytes form microscopic channels, the bile canaliculi, which are specialized regions of intercellular space formed by apposing grooves in hepatocyte plasma membranes, sealed from extraneous interstitial space by tight junctions. Numerous membrane-bound exocytotic vesicles cluster near the lumen of the canaliculi because the secretion of bile components is targeted to the canalicular plasma membrane. These canaliculi form the origins of the biliary tree and their tight junctions prevent bile from entering interstitial fluid or blood plasma: this is the blood–bile barrier.

Hepatic stellate cells

Hepatic stellate cells are much less numerous than hepatocytes. They are irregular in outline and lie within the hepatic plates, between the bases of hepatocytes. They are thought to be mesenchymal in origin and are characterized by numerous cytoplasmic lipid droplets. These cells secrete most of the intralobular matrix components, including collagen type III (reticular) fibres. They store the fat-soluble vitamin A in their lipid droplets and are a significant source of growth factors active in liver homeostasis and regeneration. Hepatic stellate cells also play a major role in pathological processes. In response to liver damage, they become activated and predominantly myofibroblast-like. They are responsible for the replacement of toxically damaged hepatocytes with collagenous scar tissue, a process called hepatic fibrosis, that is seen initially in zone 3, around central veins. Fibrosis can progress to cirrhosis, where the parenchymal architecture and pattern of blood flow are destroyed, with major systemic consequences.

Sinusoidal endothelial cells

Hepatic venous sinusoids are generally wider than blood capillaries and are lined by a thin but highly fenestrated endothelium that lacks a basal lamina. The endothelial cells are typically flattened, each with a central nucleus and joined to each other by junctional complexes. The fenestrae are grouped in clusters with a mean diameter of 100 nm, allowing plasma direct access to the basal plasma membranes of hepatocytes. Their cytoplasm contains numerous typical transcytotic vesicles.

Kupffer cells

Kupffer cells are hepatic macrophages derived from circulating blood monocytes and originate in the bone marrow. They are long-term hepatic residents and lie within the sinusoidal lumen attached to the endothelial surface. Kupffer cells are irregular in shape, and have long processes that extend into the sinusoidal lumen. They form a major part of the mononuclear phagocyte system which is responsible for removing cellular and microbial debris from the circulation, and for secreting cytokines involved in defence. They remove aged and damaged red cells from the hepatic circulation, a function normally shared with the spleen, but fulfilled entirely by the liver after splenectomy.

REFERENCES

ouinaud C. Le foié: etudes anatomique et chirurgicules. Paris: Masson, 1957.

The original description of hepatic segmentation by Couinaud..

ealey JE, Schroy PC. Anatomy of the biliary ducts within the human liver; analysis of the prevailing pattern of branchings and the major variations of the biliary ducts. *Arch Surg*. 1953;66:599-616.

itchell AWM, Dick R. Liver, gall-bladder, pancreas and spleen. In: Butler P, Mitchell AWM, Ellis H. *Applied Radiological Anatomy*. Cambridge: Cambridge University Press; 1999:239-258.

CHAPTER 69

Gallbladder and biliary tree

The biliary tree consists of the system of vessels and ducts which collect and deliver bile from the liver parenchyma to the second part of the duodenum. It is conventionally divided into intrahepatic and extrahepatic biliary trees. The intrahepatic ducts are formed from the larger bile canaliculi which come together to form segmental ducts. These fuse close to the porta hepatis into right and left hepatic ducts. The extrahepatic biliary tree consists of the right and left hepatic ducts, the common hepatic duct, the cystic duct and gallbladder and the common bile duct (Fig. 69.1).

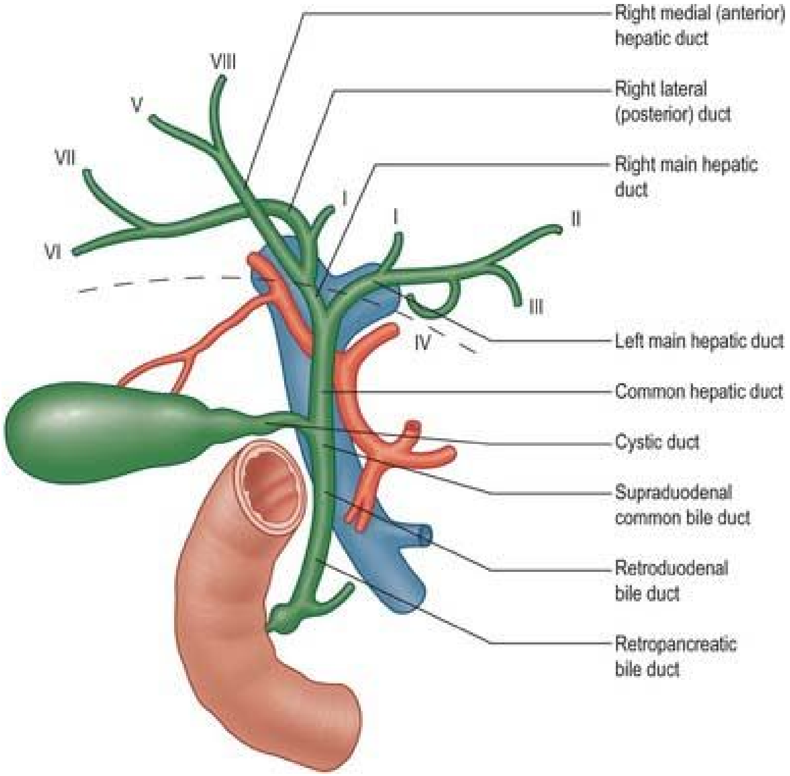
Right medial (anterior) hepatic duct
VIII
V
Right lateral (posterior) duct
VII
Right main hepatic duct
I
I
II
VI
III
IV
Left main hepatic duct
Common hepatic duct
Cystic duct
Supraduodenal common bile duct
Retroduodenal bile duct
Retropancreatic bile duct

Fig. 69.1 Overall arrangement of the intrahepatic and extrahepatic biliary tree. The segmental ducts often branch just before, or are multiple, as they enter the main ducts, but for clarity are shown here as single ducts. Note that segment I usually has drainage from both right and left hepatic ducts. The level of the liver parenchyma at the porta hepatis is shown by the dashed brown line.

GALLBLADDER

The gallbladder is a flask-shaped, blind-ending diverticulum attached to the common bile duct by the cystic duct. In life, it is grey-blue in colour and usually lies attached to the inferior surface of the right lobe of the liver by connective tissue (Fig. 69.2). In the adult the gallbladder is between 7 and 10 cm long with a capacity of up to 50 ml. It usually lies in a shallow fossa in the liver parenchyma covered by peritoneum continued from the liver surface. This attachment can vary widely. At one extreme the gallbladder may be almost completely buried within the liver surface, having no peritoneal covering (intraparenchymal pattern); at the other extreme it may hang from a short mesentery formed by the two layers of peritoneum separated only by connective tissue and a few small vessels (mesenteric pattern). The gallbladder is described as having a fundus, body and neck. The neck lies at the medial end close to the porta hepatis, and almost always has a short peritoneal-covered attachment to the liver (mesentery); this mesentery usually contains the cystic artery. The mucosa at the medial end of the neck is obliquely ridged, forming a spiral groove continuous with the spiral valve of the cystic duct. At its lateral end the neck widens out to form the body of the gallbladder and this widening is often referred to in clinical practice as ‘Hartmann’s pouch’. The neck lies anterior to the second part of the duodenum.

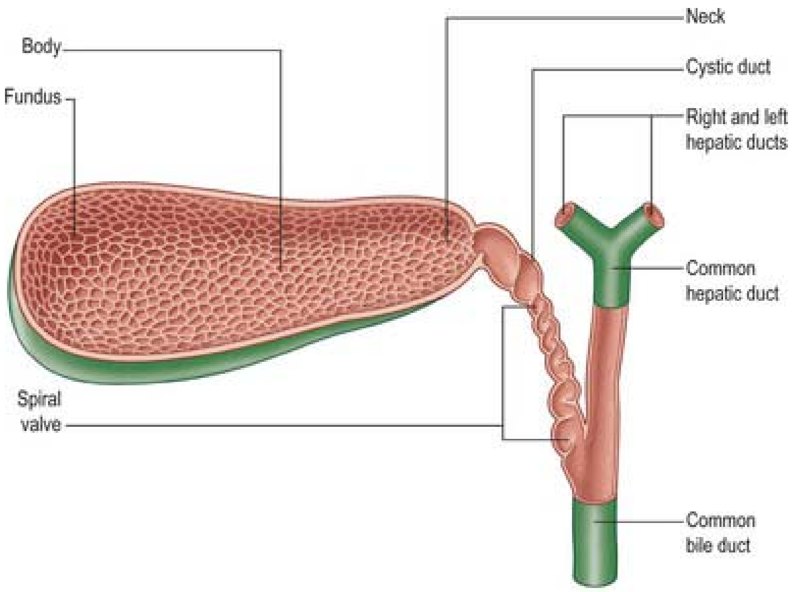

Fig. 69.2 Interior of the gallbladder and bile ducts.

The body of the gallbladder normally lies in contact with the liver surface. When the neck possesses a mesentery, this rapidly shortens along the length of the body as it comes to lie in the gallbladder fossa. It lies anterior to the second part of the duodenum and the right end of the transverse colon. The fundus lies at the lateral end of the body and usually projects past the inferior border of the liver to a variable length. It often lies in contact with the anterior abdominal wall behind the ninth costal cartilage where the lateral edge of the right rectus abdominis crosses the costal margin. This is the location where enlargement of the gallbladder is best sought on clinical examination. The fundus commonly lies adjacent to the transverse colon.

The gallbladder varies in size and shape. The fundus may be elongated and highly mobile. Rarely, the fundus is folded back upon the body of the gallbladder, the so-called Phrygian cap: on ultrasound, this may be wrongly interpreted as an apparent septum within an otherwise normal gallbladder. Again, rarely, the gallbladder may be bifid or completely duplicated, usually with a duplicated cystic duct.

INTRAHEPATIC BILIARY TREE

SEGMENTAL AND SECTORAL DUCTS

The segmental ducts of the left liver have a relatively constant pattern, although several segmental ducts may drain each particular segment. The left hepatic duct is formed by the union of segment II and III ducts behind the umbilical portion of the left portal vein (Fig. 69.1). The segment IV duct is more variable, but usually drains into the left hepatic duct. The right hepatic duct is formed by the union of the right medial (anterior) and lateral (posterior) sectoral ducts. These sectoral ducts in turn are formed by the segmental ducts: VII and VI from the lateral, and VIII and V from the medial duct. The right lateral sectoral duct is often identified on a cholangiogram as curving around the right medial duct before joining the medial side of the medial sectoral duct: this is often described as Hjortsjo’s crook, and has surgical importance for liver resections. The right hepatic duct and its branches are subject to more variations than the left ductal system, and these variations have been classified by Blumgart into six main types (Table 69.1).

Table 69.1 Variations of the right hepatic duct and its branches

Type	Percentage of population	Description
A	55	Anatomy is normal.
B	15	There is no right hepatic duct and the common hepatic duct is formed by the right anterior, right posterior and left hepatic ducts as a trifurcation.
C	20	There is a low drainage of one the right sectoral ducts into the common hepatic duct.
D	5	One of the right sectoral ducts joins the left hepatic duct.
E	5	The common hepatic duct is formed by the union of two or more ducts from either lobe.
F	5	The right posterior sectoral duct drains into the cystic duct.

EXTRAHEPATIC BILIARY TREE

CYSTIC DUCT

The cystic duct drains the gallbladder into the common bile duct. It is between 3 and 4 cm long, passes posteriorly to the left from the neck of the gallbladder, and joins the common hepatic duct to form the common bile duct. It almost always runs parallel to, and is adherent to, the common hepatic duct for a short distance before joining it. The junction usually occurs near the porta hepatis but may be lower down in the free edge of the lesser omentum. The cystic duct may have several important variations in its anatomy (Fig. 69.3). Rarely, the cystic duct lies along the right edge of the lesser omentum all the way down to the level of the duodenum before the junction is formed, but in these cases the cystic and common bile ducts are usually closely adherent. The cystic duct occasionally drains into the right hepatic duct, in which case it may be elongated, lie anterior or posterior to the common hepatic duct, and join the right hepatic duct on its left border. Rarely, the duct is double or even absent, in which case the gallbladder drains directly into the common bile duct. One or more accessory hepatic ducts occasionally emerge from segment V of the liver and join either the right hepatic duct, the common hepatic duct, the common bile duct, the cystic duct, or the gallbladder directly. These variations in cystic duct anatomy are of considerable importance during surgical excision of the gallbladder. Ligation or clip occlusion of the cystic duct must be performed at an adequate distance from the common bile duct to prevent angulation or damage to it. Accessory ducts must not be confused with the right hepatic or common hepatic ducts.

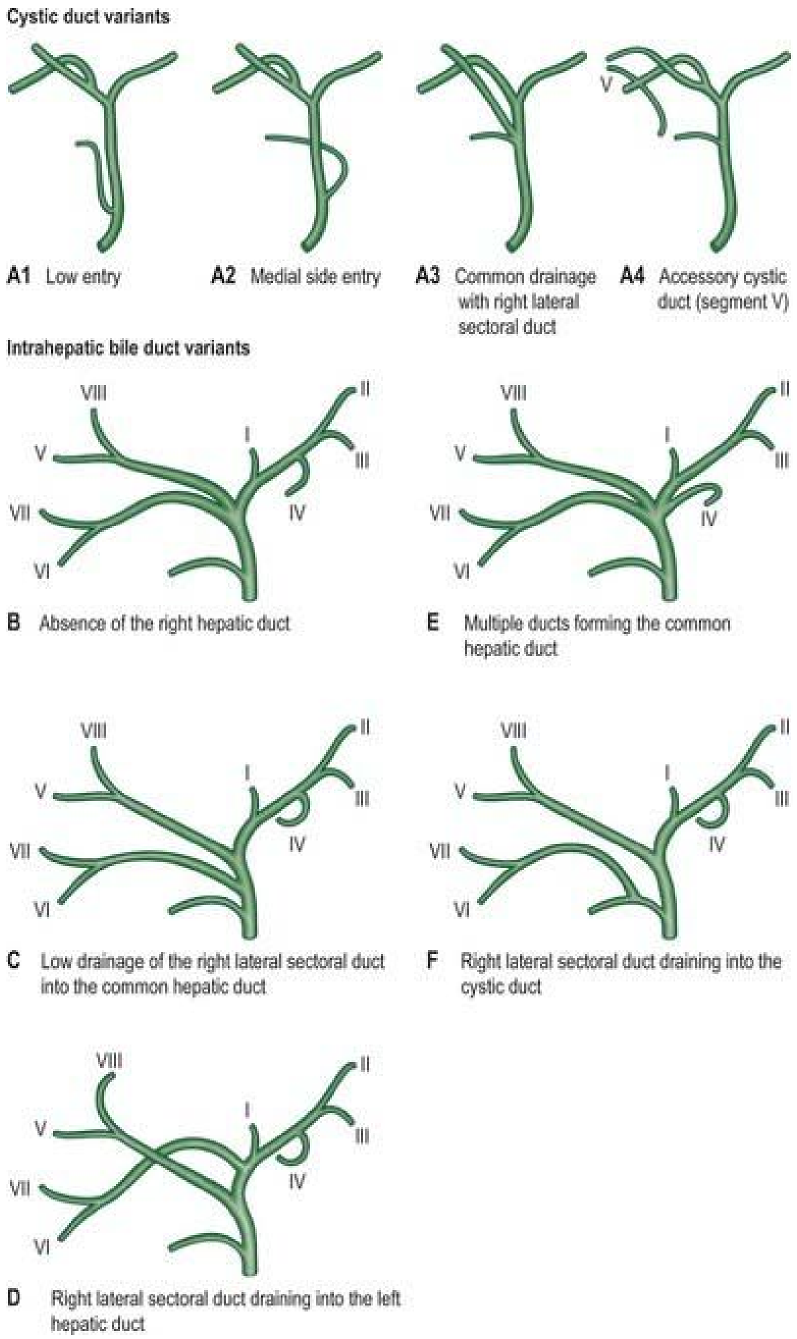

Cystic duct variants
V
A1 Low entry
A2 Medial side entry
A3 Common drainage with right lateral sectoral duct
A4 Accessory cystic duct (segment V)
Intrahepatic bile duct variants
VIII
II
I
V
III
VII
IV
VI
B Absence of the right hepatic duct
E Multiple ducts forming the common hepatic duct
C Low drainage of the right lateral sectoral duct into the common hepatic duct
F Right lateral sectoral duct draining into the cystic duct
D Right lateral sectoral duct draining into the left hepatic duct

Fig. 69.3 Variations in the anatomy of the cystic and intrahepatic bile ducts. The cystic duct variations are labelled A1–A3 and the letters B–F are used for the variants of the intrahepatic ducts to ensure consistency with the Blumgart nomenclature.

The mucosa of the cystic duct bears 5–12 crescentic folds, continuous with those in the neck of the gallbladder. They project obliquely in regular succession, appearing to form a spiral valve when the duct is cut in longitudinal section. When the duct is distended, the spaces between the folds dilate and externally it appears twisted like the neck of the gallbladder.

HEPATIC BILE DUCTS

The main right and left hepatic ducts emerge from the liver and unite near the right end of the porta hepatis as the common hepatic duct. The extrahepatic right duct is short and nearly vertical while the left is more horizontal and lies along the base of segment IV. The common hepatic duct descends approximately 3 cm before being joined on its right at an acute angle by the cystic duct to form the common bile duct. The common hepatic duct lies to the right of the hepatic artery and anterior to the portal vein in the free edge of the lesser omentum.

COMMON BILE DUCT

The common bile duct is formed near the porta hepatis, by the junction of the cystic and common hepatic ducts (Figs 69.4 and 69.5), and is usually between 6 and 8 cm long. Its diameter tends to increase somewhat with age but is usually around 6 mm in adults. It descends posteriorly and slightly to the left, anterior to the epiploic foramen, in the right border of the lesser omentum, where it lies anterior and to the right of the portal vein and to the right of the hepatic artery. It passes behind the first part of the duodenum with the gastroduodenal artery on its left, and then runs in a groove on the superolateral part of the posterior surface of the head of the pancreas. The duct lies anterior to the inferior vena cava and is sometimes embedded in the pancreatic tissue. It may lie close to the medial wall of the second part of the duodenum or as much as 2 cm from it: even when it is embedded in the pancreas, a groove in the gland marking its position can be palpated behind the second part of the duodenum.

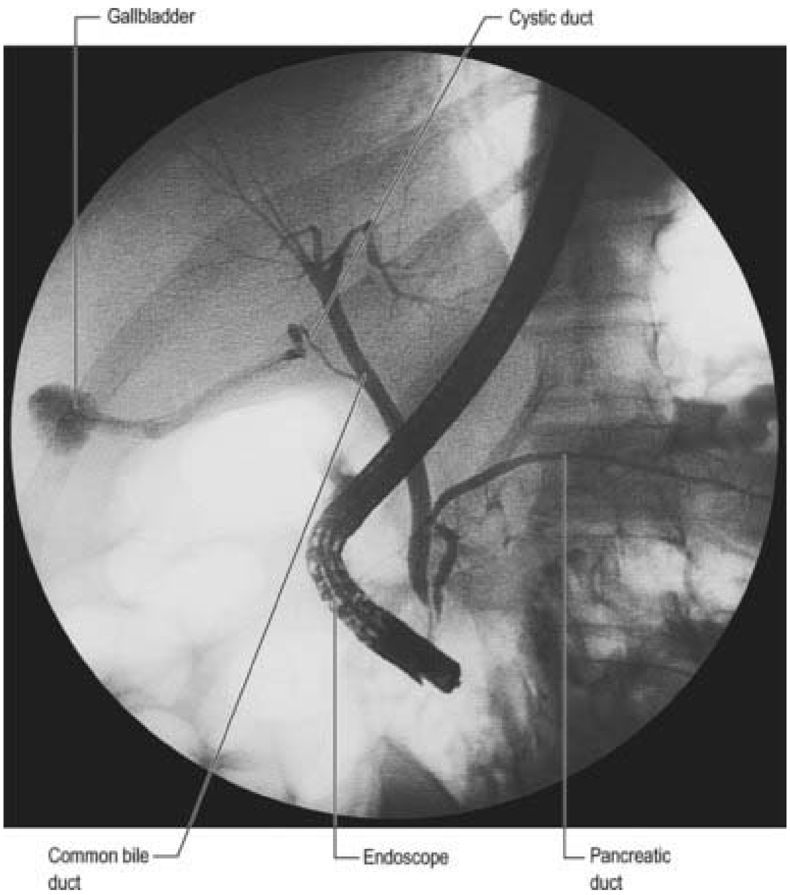
Gallbladder
Cystic duct
Common bile duct
Endoscope
Pancreatic duct

Fig. 69.4 Endoscopic retrograde cholangiopancreatogram.

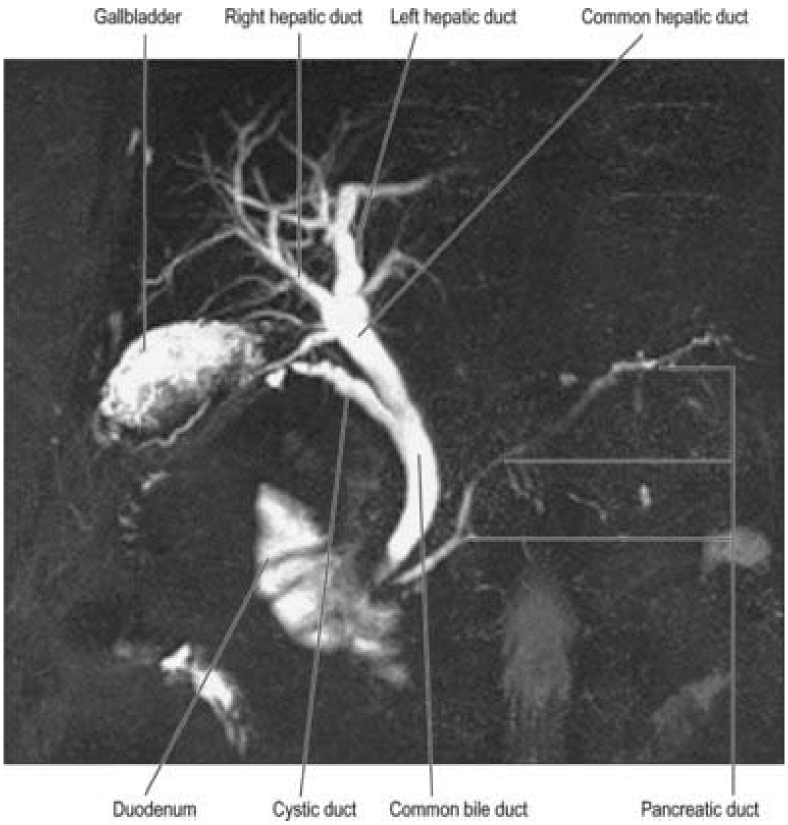
Gallbladder
Right hepatic duct
Left hepatic duct
Common hepatic duct
Duodenum
Cystic duct
Common bile duct
Pancreatic duct

Fig. 69.5 Magnetic resonance cholangiopancreatogram.

Hepatopancreatic ampulla (of Vater)

As it lies medial to the second part of the duodenum, the common bile duct approaches the right end of the pancreatic duct. The ducts enter the duodenal wall together, and usually unite to form the hepatopancreatic ampulla. Rarely the common bile duct and pancreatic duct drain into the duodenum separately. Circular muscle usually surrounds the lower part of the common bile duct (bile duct sphincter) and frequently also surrounds the terminal part of the main pancreatic duct (pancreatic duct sphincter) and the hepatopancreatic ampulla (sphincter of Oddi). When all elements are present, this arrangement may allow for separate control of pancreatic and common bile duct emptying. Division of the upper part of the ampulla and ampullary sphincter (sphincterotomy) may be required to allow access to the common bile duct during endoscopic retrograde cholangiography.

Calot’s triangle

The near triangular space formed between the cystic duct, the common hepatic duct and the inferior surface of segment V of the liver (Suzuki et al 2000), is commonly referred to as Calot’s triangle. It is enclosed by the double layer of peritoneum which forms the short mesentery of the cystic duct. Since the two layers are not closely opposed, there is an appreciable amount of loose connective tissue within the triangle. It is perhaps better described as a pyramidal ‘space’ with one apex lying at the junction of the cystic duct and fundus of the gallbladder, one at the porta hepatis, and two closer apices at the attachments of the gallbladder to the liver bed. The base of the triangle thus lies on the inferior surface of the liver. This space usually contains the cystic artery as it approaches the gallbladder, the cystic lymph node and lymphatics from the gallbladder, one or two small cystic veins, the autonomic nerves running to the gallbladder, and some loose adipose tissue. It may contain any accessory ducts which drain into the gallbladder from the liver. Appreciation of the variations in ductal and arterial anatomy as they relate to the triangle are of considerable importance during excision of the gallbladder in order to avoid mistakenly ligating the common hepatic or common bile duct.

BILIARY STONES

Gallstones usually form in the gallbladder. As the gallbladder empties, gallstones move towards the cystic duct. When small stones enter the cystic duct they may irritate the columnar mucosa, this leads to spasm of the smooth muscle in the cystic duct wall, and the spasm generates pain known as biliary colic, which is often very severe. The mucosal folds in the neck of the gallbladder and the cystic duct provide a common site of entrapment of gallstones. Stones occluding the neck of the gallbladder may cause a sterile distension of the gallbladder: providing the gallbladder has not undergone acute inflammation previously it remains non-fibrotic and readily distensible, and an enlarged fundus often becomes palpable below the costal margin. Stones lodged in the distal cystic duct may cause swelling in the tissues around the duct. The close relationship of the distal cystic duct to the common hepatic duct means that this swelling may cause secondary compression of the common hepatic duct, resulting in partial obstruction to the flow of bile and the appearance of mild jaundice, the so called ‘Mirizzi syndrome’. Once stones have passed through the cystic duct they often become impacted at the junction of the common bile duct and pancreatic duct just proximal to the hepatopancreatic ampulla, producing obstructive jaundice and/or acute pancreatitis.

ENDOSCOPIC CHOLANGIOGRAPHY

The common bile duct may be accessed endoscopically from the duodenum for diagnostic cholangiography and therapeutic interventions. The angled relationship of the distal common bile duct and pancreatic duct may make direct cannulation of the bile duct difficult. When the duct lies in a more vertical position, embedded within the wall of the duodenum, a direct incision in the base of the hepatopancreatic ampulla and the adjacent wall of the duodenum (pre-cut sphincterotomy) may expose the duct to allow cannulation. This is occasionally associated with haemorrhage from the duodenal wall vessels. Division of the smooth muscle fibres of the common bile duct sphincter may be necessary for endoscopic access to the bile duct, but it often results in uncontrolled reflux of duodenal contents into the distal common bile duct, and this may result in recurrent biliary infections.

BILIARY DRAINAGE

The proximity of the fundus of the gallbladder to the anterior abdominal wall provides a useful route of access for percutaneous drainage of a distended, obstructed gallbladder. It is rarely obscured by liver tissue, can often be accessed below the costal margin, and is most often performed under ultrasound guidance. Because of the small calibre and spiral conformation of the cystic duct, drainage of the gallbladder is rarely adequate to decompress the biliary tree if it is blocked, and this must be achieved endoscopically, surgically or by a percutaneous, transhepatic approach. This latter technique requires the identification of dilated intrahepatic bile ducts, usually by ultrasound imaging with direct guided puncture via a right subcostal approach. Percutaneous access is obtained via segment III in the left lobe of the liver and via segments V and VI in the right lobe of the liver.

VASCULAR SUPPLY AND LYMPHATIC DRAINAGE

Cystic artery

The cystic artery usually arises from the right hepatic artery (Fig. 69.6). It usually passes posterior to the common hepatic duct and anterior to the cystic duct to reach the superior aspect of the neck of the gallbladder and divides into superficial and deep branches. The superficial branch ramifies on the inferior aspect of the body of the gallbladder, the deep branch on the superior aspect. These arteries anastomose over the surface of the body and fundus. The origin of the cystic artery frequently varies (Fig. 69.7). The most common variant is an origin from the common hepatic artery (occasionally low down), sometimes from the left hepatic or gastroduodenal artery, and rarely from the superior pancreaticoduodenal, coeliac, right gastric or superior mesenteric arteries. In these cases, it crosses anterior (or less commonly posterior) to the common bile duct or common hepatic duct to reach the gallbladder. An accessory cystic artery may arise from the common hepatic artery or one of its branches and the cystic artery often bifurcates close to its origin, giving rise to two vessels which approach the gallbladder. Multiple fine arterial branches may arise from the parenchyma of segments IV or V of the liver and contribute to the supply of the body, particularly when the gallbladder is substantially intrahepatic. This makes the gallbladder relatively resistant to necrosis during inflammation which otherwise occludes the cystic artery.

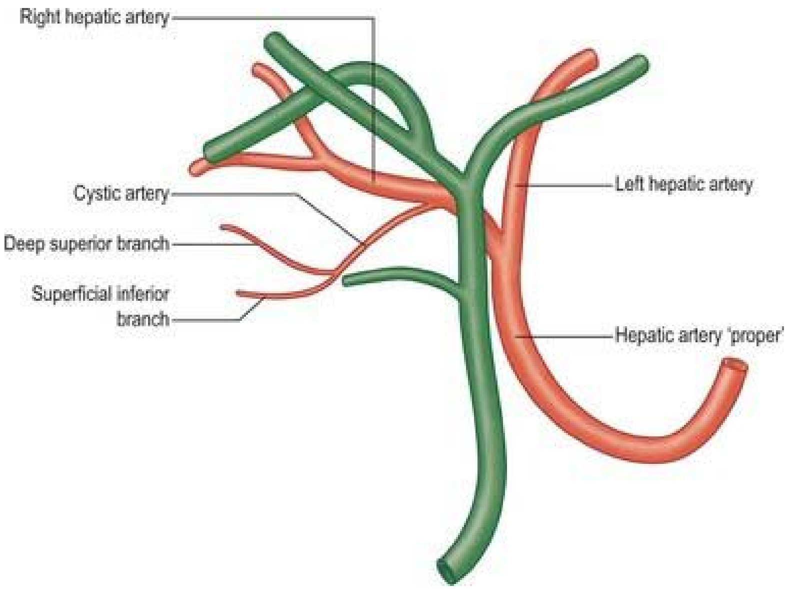
Right hepatic artery
Cystic artery
Deep superior branch
Superficial inferior branch
Left hepatic artery
Hepatic artery 'proper'

Fig. 69.6 Normal anatomy of the cystic artery.

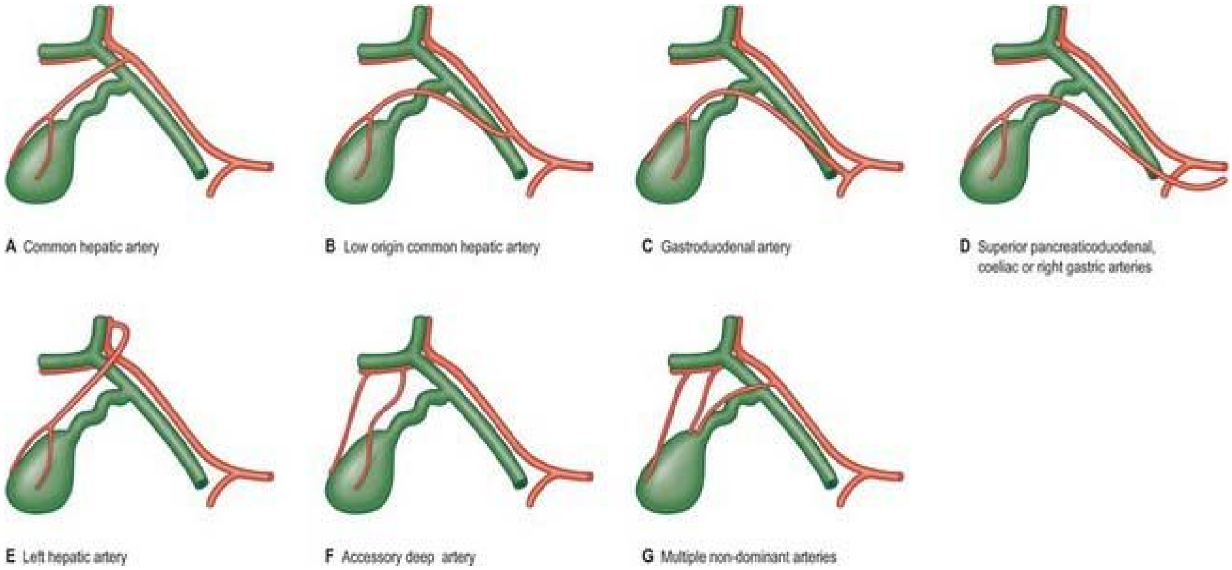
A Common hepatic artery
B Low origin common hepatic artery
C Gastroduodenal artery
D Superior pancreaticoduodenal, coeliac or right gastric arteries
E Left hepatic artery
F Accessory deep artery
G Multiple non-dominant arteries

Fig. 69.7 Variant anatomy of the cystic artery origin and distribution.

The cystic artery gives rise to multiple fine branches which supply the common and lobar hepatic ducts and upper part of the common bile duct. These fine branches form a network which anastomoses with the vessels ascending around the common bile duct and with the vessels from the liver parenchyma which descend with the right and left hepatic ducts.

Ductal arteries

The common bile duct and hepatic ducts are supplied by a fine network of vessels which usually receives contributions from several sources, and which lies in close proximity to the ducts. Disruption of the network during surgical exposure of the bile ducts over a long length frequently causes chronic ischaemia and resultant stenosis of the duct. Approaches which spare the network are necessary to avoid this complication.

The common bile duct is fairly consistently supplied by two to four ascending and descending arteries which form long narrow anastomotic channels along the length of the duct: the most prominent of these are disposed into medial and lateral ‘trunks’, although they may lie more anterolateral and posteromedial. The largest contributions usually arise as one or two branches from the retroduodenal branch of the gastroduodenal artery as it crosses the anterior surface of the duct at the upper border of the duodenum. Three or four descending branches supply this network from the right hepatic and cystic arteries as these vessels pass close to the lower common hepatic duct: occasionally they are the dominant supply to the common bile duct.

Posteriorly, a retroportal artery often arises from the coeliac axis, superior mesenteric artery or one of their major branches close to the origin from the aorta, and runs upwards on the posterior surface of the portal vein. It usually ends by joining the retroduodenal artery close to the lower end of the supraduodenal bile duct, but occasionally it passes up behind the bile duct to join the right hepatic artery. When present, the retroportal artery contributes to the arterial network supplying the supraduodenal bile duct system.

The hilar and intrahepatic ducts are supplied by a fine network of periductal arteries that arise from the segmental arteries within the Glissonian sheaths.

Cystic veins

The venous drainage of the gallbladder is rarely by a single cystic vein. There are usually multiple small veins. Those arising from the superior surface of the body and neck lie in areolar tissue between the gallbladder and liver and enter the liver parenchyma to drain into the segmental portal veins. The remainder form one or two small cystic veins, which enter the liver either directly or after joining the veins that drain the hepatic ducts and upper bile duct. Only rarely does a single or double cystic vein drain into the right portal branch.

Lymphatics

Numerous lymphatic vessels run from the submucosal and subserosal plexuses on all aspects of the gallbladder and cystic duct. Those on the hepatic aspect of the gallbladder connect with the intrahepatic lymph vessels. The remainder drain into the cystic node, which usually lies above the cystic duct in the tissue of Calot’s triangle. This node, and some lymphatic channels which bypass the cystic node, drain into a node lying in the anterior border of the free edge of the lesser omentum. Hepatic nodes lying in the porta hepatis collect lymph from vessels that accompany the hepatic ducts and the upper part of the bile duct. Lymphatics from the lower part of the common bile duct drain into the inferior hepatic and upper pancreaticosplenic nodes.

INNERVATION

The gallbladder and the extrahepatic biliary tree are innervated by branches from the hepatic plexus. The retroduodenal part of the common bile duct and the smooth muscle of the hepatopancreatic ampulla are also innervated by twigs from the pyloric branches of the vagi.

Referred pain

In common with other structures of foregut origin, pain caused by stretch of the common bile duct or gallbladder is referred to the central epigastrium. Involvement of the overlying somatic peritoneum produces pain which is more localized to the right upper quadrant.

MICROSTRUCTURE

GALLBLADDER

The fundus of the gallbladder is completely covered by a serosa, and the inferior surfaces and sides of the body and neck of the gallbladder are usually covered by a serosa. If the gallbladder possesses a mesentery the serosa extends around the sides of the body and neck onto the superior surface and continues into the serosa of the mesentery, whereas the serosa is limited to the inferior surfaces only if the gallbladder is intrahepatic. Beneath the serosa is subserous loose connective and adipose peritoneal tissue. The gallbladder wall microstructure generally resembles that of the small intestine. The mucosa is yellowish-brown and elevated into minute rugae with a honeycomb appearance (Fig. 69.2). In section, projections of the mucosa into the gallbladder lumen resemble intestinal villi, but they are not fixed structures and the surface flattens as the gallbladder fills with bile. The epithelium is a single layer of columnar cells with apical microvilli; basally, the spaces between epithelial cells are dilated (Fig. 69.8). Many capillaries lie beneath the basement membrane. The epithelial cells actively absorb water and solutes from the bile and concentrate it up to ten-fold. There are no goblet cells in the epithelium. The thin fibromuscular layer is composed of fibrous tissue mixed with smooth muscle cells arranged loosely in longitudinal, circular and oblique bundles.

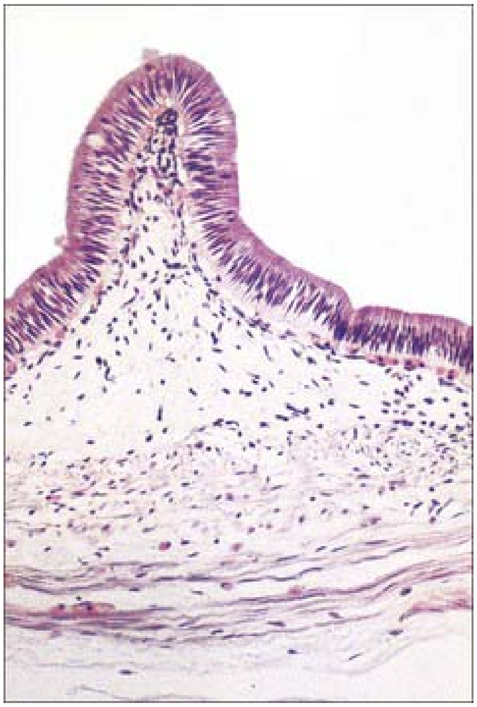

Fig. 69.8 Low power micrograph showing the gallbladder wall, with a mucosal projection which flattens in the full gallbladder, and the thin muscular layer.

BILE DUCTS

The walls of the large biliary ducts consist of external fibrous and internal mucosal layers (Fig. 69.9). The outer layer is fibrous connective tissue containing a variable amount of longitudinal, oblique and circular smooth muscle cells. The mucosa is continuous with that in the hepatic ducts, gallbladder and duodenum. The epithelium is columnar and there are numerous tubuloalveolar mucous glands in the duct walls.

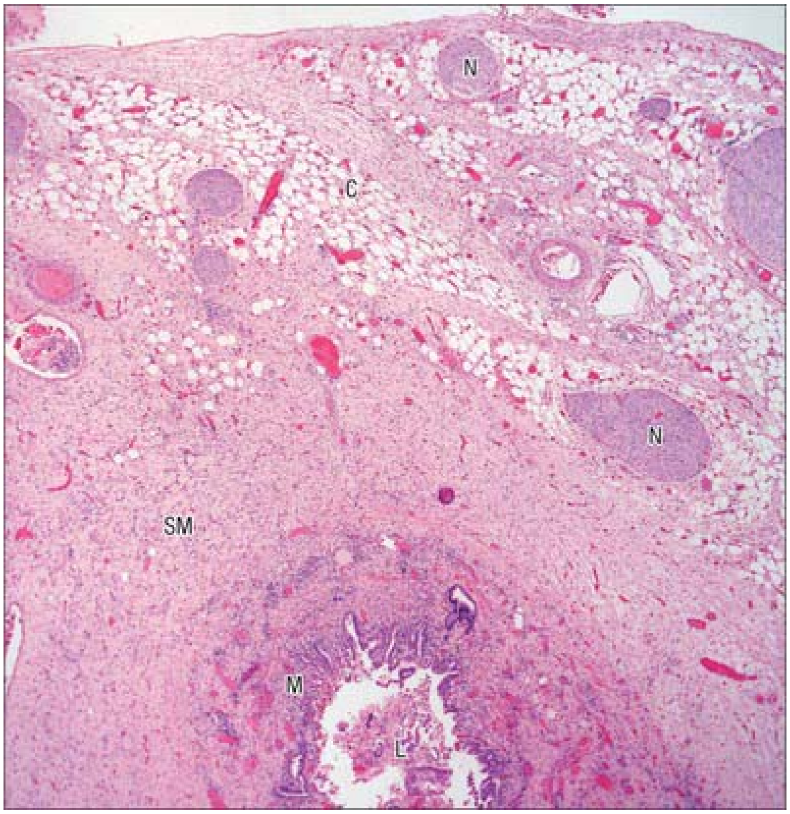

Fig. 69.9 Low power micrograph showing the human common bile duct structure. Shown are the lumen (L), mucosal lining (m), smooth muscle coat (SM) and outer connective tissue (C), with numerous nerve fibre bundles (N).

(By courtesy of Mr Peter Helliwell and Dr Joseph Mathew, Department of Histopathology, Royal Cornwall Hospitals Trust, UK.)

Expulsion of gallbladder contents is under neuroendocrine control. Fat in the duodenum causes the release of cholecystokinin (CCK), which stimulates the gallbladder to contract because muscle cells in its walls bear surface receptors for CCK. When the pressure exceeds 100 mm H_2O of bile, the sphincter of Oddi relaxes and bile enters the duodenum. The termination of the united bile and pancreatic ducts is packed with villous, valvular folds of mucosa that contain muscle cells in their connective tissue cores. Contraction is thought to result in retraction and clumping of these folds, so preventing reflux of duodenal contents and controlling the exit of bile.

REFERENCES

zuki M, Akaishi S, Rikiyama T, Naitoh T, Rahman MM, Matsuno S. Laparoscopic cholecystectomy, Calot’s triangle, and variations in cystic arterial supply. *Surgical Endoscopy*. 2000;14:141-144.

PBA Brisbane 2000 Terminology of Liver Anatomy and Resections.

CHAPTER 70

Pancreas

The pancreas is the largest of the digestive glands and performs a range of both endocrine and exocrine functions. The major part of the gland is exocrine, secreting a range of enzymes involved in the digestion of lipids, carbohydrates and proteins. The endocrine function of the pancreas is derived from cells scattered throughout the substance of the gland: they take part in glucose homeostasis and are also involved in the control of upper gastrointestinal motility and function.

The pancreas is salmon pink in colour with a firm, lobulated smooth surface. The main portion is divided into four parts, head, neck, body and tail, purely on the basis of anatomical relations: there are only very minor functional or anatomical differences between each part (Figs 70.1 and 70.2). The pancreas also possesses one accessory lobe (the uncinate process), which is anatomically and embryologically distinct. In adults the pancreas measures between 12 and 15 cm long and is shaped as a flattened ‘tongue’ of tissue, thicker at its medial end (head) and thinner towards the lateral end (tail). With age, the amount of exocrine tissue tends to decline, as does the amount of fatty connective tissue within the substance of the gland, and this leads to a progressive thinning atrophy which is particularly noticeable on CT scanning. The pancreas lies within the curve of the first, second and third parts of the duodenum, and extends transversely and slightly upwards across the posterior abdominal wall to the hilum of the spleen, behind the stomach. It does not lie in one plane but is effectively ‘draped’ over the other structures in the retroperitoneum and the vertebral column and so forms a distinct shallow curve, of which the neck and medial body are the most anterior parts. Because of its flattened shape, the parts of the pancreas, particularly the body, are often referred to as having surfaces and borders.

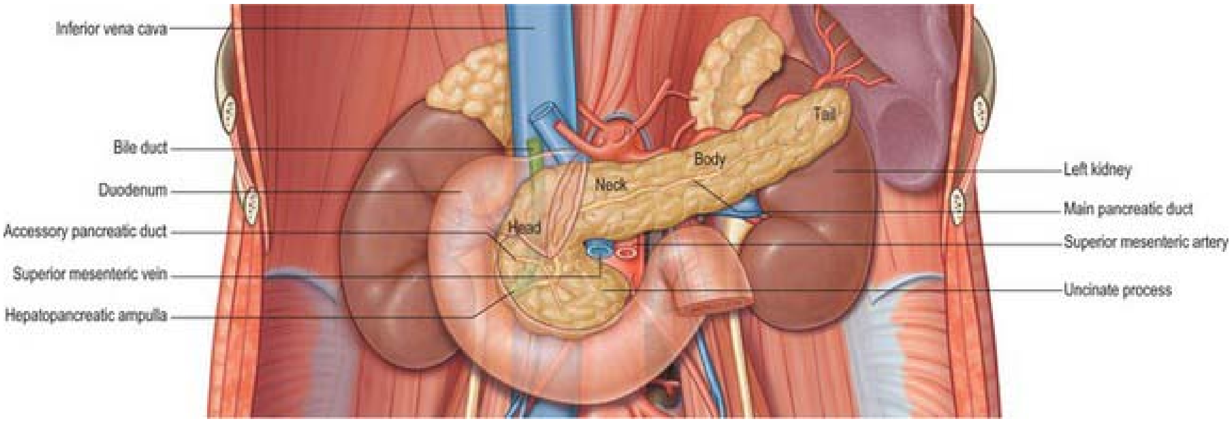
Inferior vena cava
Bile duct
Duodenum
Accessory pancreatic duct
Superior mesenteric vein
Hepatopancreatic ampulla
Tail
Body
Neck
Head
Left kidney
Main pancreatic duct
Superior mesenteric artery
Uncinate process

Fig. 70.1 Relations of the pancreas.

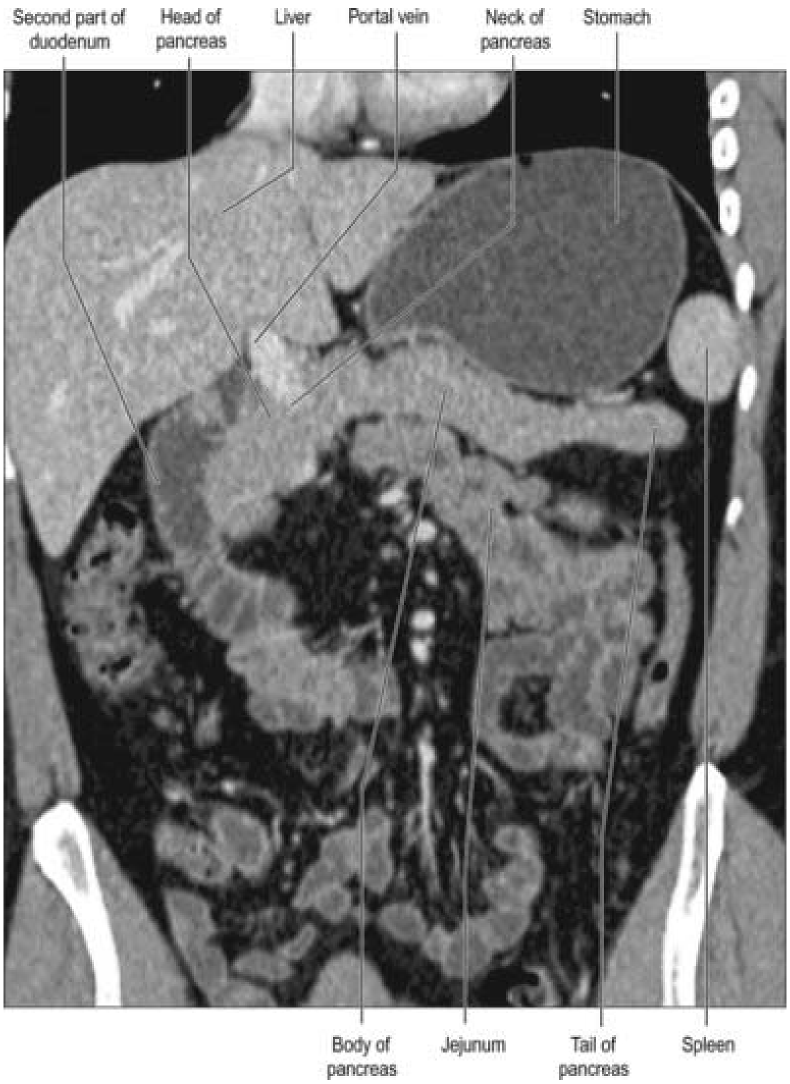
Second part of duodenum
Head of pancreas
Liver
Portal vein
Neck of pancreas
Stomach
Body of pancreas
Jejunum
Tail of pancreas
Spleen

Fig. 70.2 Coronal reformat CT of the pancreas

(by courtesy of Dr Louise Moore, Chelsea and Westminster Hospital).

HEAD

The head of the pancreas lies to the right of the midline, anterior and to the right side of the vertebral column, within the curve of the duodenum. It is the thickest and broadest part of the pancreas but is still flattened in the anteroposterior plane. Superiorly it lies adjacent to the first part of the duodenum, but close to the pylorus the duodenum is on a short mesentery, and here the duodenum lies anterior to the upper part of the head. The duodenal border of the head is flattened and slightly concave, and is firmly adherent to the second part of the duodenum; occasionally a small part of the head is actually embedded in the wall of the second part of the duodenum. The superior and inferior pancreaticoduodenal arteries lie between the head and the duodenum in this area. The inferior border lies superior to the third part of the duodenum and is continuous with the uncinate process. Close to the midline, the head is continuous with the neck. The boundary between head and neck is often marked anteriorly by a groove for the gastroduodenal artery and posteriorly by a similar but deeper deep groove that contains the union of the superior mesenteric and splenic veins as they form the portal vein.

Anterior surface

The anterior surface of the head (Fig. 70.3) is covered in peritoneum and is related to the origin of the transverse mesocolon.

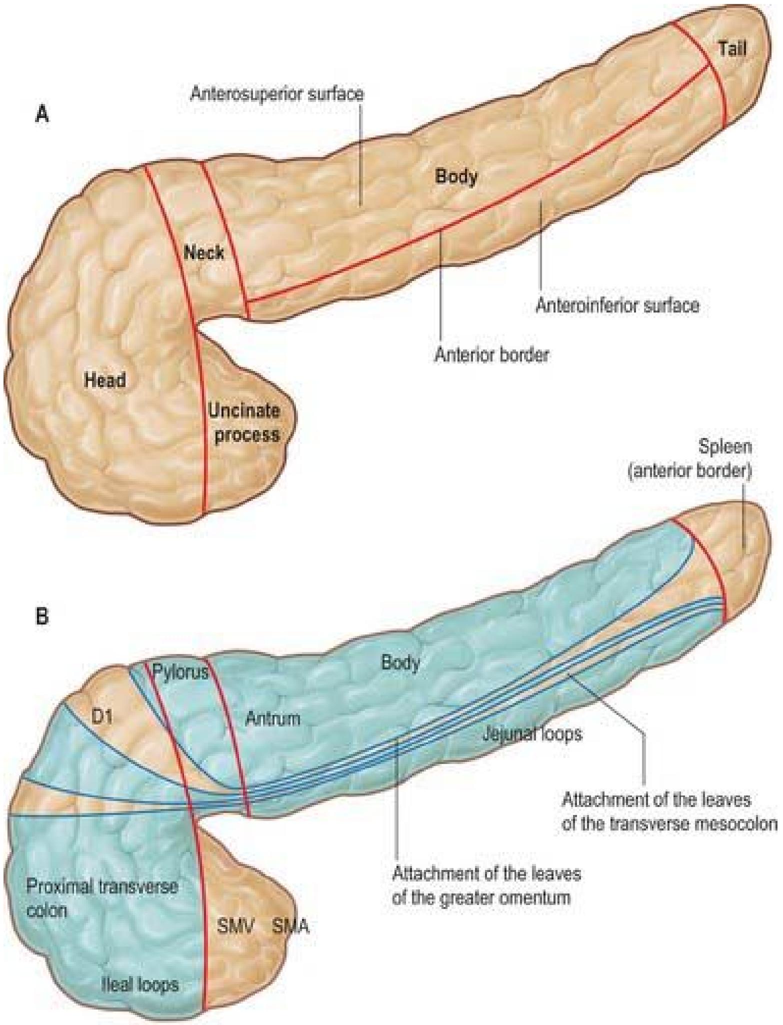
A
Anterosuperior surface
Tail
Body
Neck
Anteroinferior surface
Anterior border
Head
Uncinate process
B
Spleen (anterior border)
Body
Pylorus
D1
Antrum
Jejunal loops
Attachment of the leaves of the transverse mesocolon
Attachment of the leaves of the greater omentum
Proximal transverse colon
SMV
SMA
Ileal loops

Fig. 70.3 **A**, Regions and anterior surfaces and borders of the pancreas. **B**, Anterior relations of the pancreas. Areas covered in peritoneum are shown in blue and structures overlying these areas are separated from the pancreas by peritoneal ‘spaces’. The spleen in relation to the tail lies anterior to the anterior leaf of the splenorenal ligament and not in direct contact with the pancreatic tissue. D1, first part of the duodenum; SMA, superior mesenteric artery; SMV, superior mesenteric vein.

Posterior surface

The posterior surface of the head is related to the inferior vena cava, which ascends behind it and covers almost all of this aspect. It is also related to the right renal vein, the right crus of the diaphragm and usually the origin of the right gonadal vein (see Ch. 76, Fig. 76.7).

NECK

The neck of the pancreas is approximately 2 cm wide and links the head and body. It is often the most anterior portion of the gland and is defined as the portion of the pancreas that lies anterior to the portal vein, which is closely related to the upper posterior surface (see Fig. 70.8). The lower part of the neck lies anterior to the superior mesenteric vein just before the formation of the portal vein. These are important relations during surgery for pancreatic cancer because malignant involvement of these vessels may make resection impossible. The anterior surface of the neck is covered with peritoneum and lies adjacent to the pylorus just inferior to the epiploic foramen. The gastroduodenal and anterior superior pancreaticoduodenal arteries descend in front of the gland in the region of the junction of the neck and head.

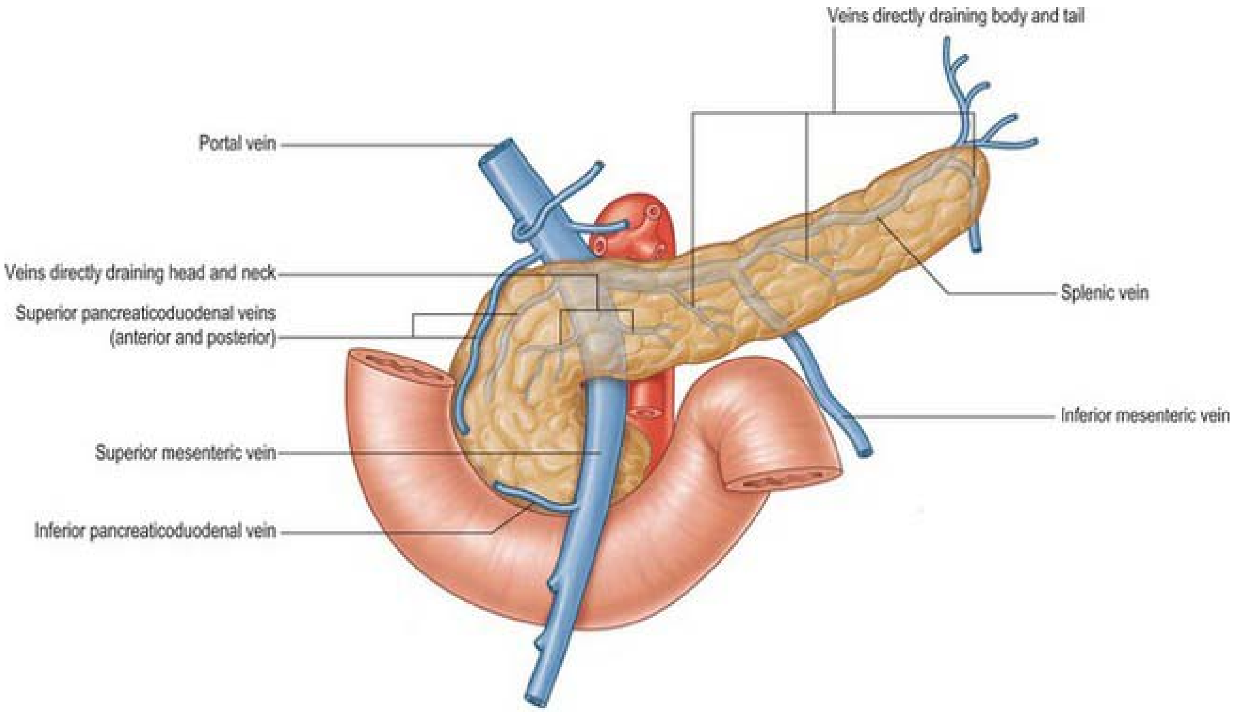
Veins directly draining body and tail
Portal vein
Veins directly draining head and neck
Superior pancreaticoduodenal veins (anterior and posterior)
Splenic vein
Inferior mesenteric vein
Superior mesenteric vein
Inferior pancreaticoduodenal vein

Fig. 70.8 Venous drainage of the pancreas.

(Adapted from Drake, Vogl and Mitchell 2005.)

BODY

The body of the pancreas is the longest portion of the gland and runs from the left side of the neck to the tail. It is slightly triangular in cross-section, becoming progressively thinner and less broad towards the tail. The body is described as having three surfaces, anterosuperior, posterior and anteroinferior.

Anterosuperior surface

The anterosuperior surface of the pancreas makes up most of the anterior aspect of the gland close to the neck. Laterally, it narrows and lies slightly more superiorly to share the anterior aspect with the anteroinferior surface. It is covered by peritoneum, which runs anteroinferiorly from the surface of the gland to be continuous with the anterior, ascending layer of the greater omentum (see Fig. 64.4). The superior leaf of the transverse mesocolon is reflected and is continuous with the descending, posterior leaf of the greater omentum just above the anterior border and so forms virtually none of the covering of the anterosuperior surface. It is separated from the stomach by the lesser sac.

Posterior surface

The posterior surface of the pancreas is devoid of peritoneum. It lies anterior to the aorta and the origin of the superior mesenteric artery, the left crus of the diaphragm, left suprarenal gland and the left kidney and renal vessels, particularly the left renal vein (Fig. 70.4). It is closely related to the splenic vein which lies between the posterior surface and the other posterior relations and runs from left to right forming anything from a shallow groove to a near enveloped ‘tunnel’ in the substance of the gland. The left kidney is also separated from the posterior surface by perirenal fascia and fat.

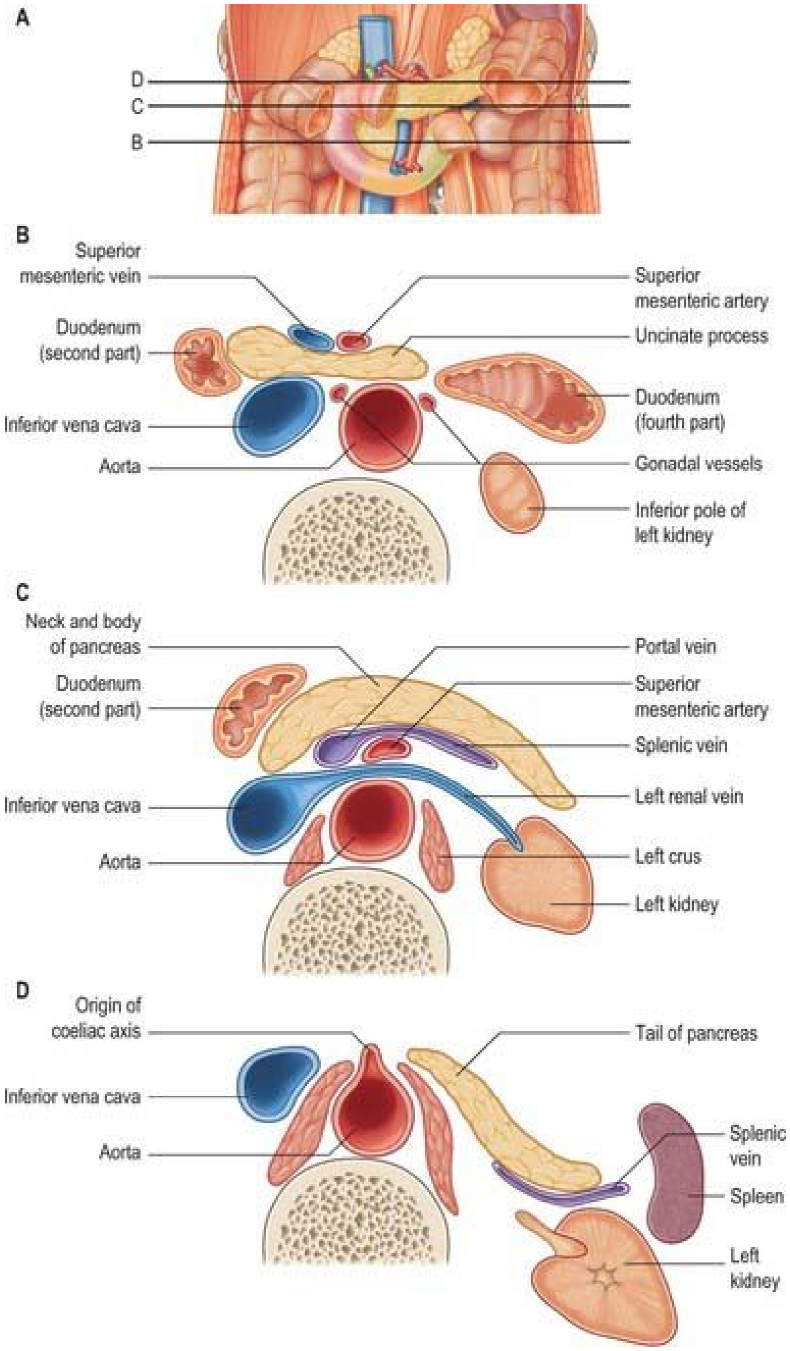
A
D
C
B
B
Superior mesenteric vein
Duodenum (second part)
Inferior vena cava
Aorta
Superior mesenteric artery
Uncinate process
Duodenum (fourth part)
Gonadal vessels
Inferior pole of left kidney
C
Neck and body of pancreas
Duodenum (second part)
Inferior vena cava
Aorta
Portal vein
Superior mesenteric artery
Splenic vein
Left renal vein
Left crus
Left kidney
D
Origin of coeliac axis
Inferior vena cava
Aorta
Tail of pancreas
Splenic vein
Spleen
Left kidney

Fig. 70.4 **A**, Posterior relations of the pancreas. Cross sections taken at the mid level of the uncinate process (**B**), head and neck (**C**), and tail (**D**) of the pancreas. See the coronal view for reference of transverse sections.

Anteroinferior surface

The anteroinferior surface of the pancreas begins as a narrow strip just to the left of the neck. As the body runs laterally, it broadens out to form more of the anterior aspect of the body. It is covered by peritoneum which is continuous with that of the posteroinferior layer of the transverse mesocolon. The fourth part of the duodenum, the duodenojejunal flexure and coils of jejunum all lie inferiorly. The lateral end of the inferior border often lies superior and posterior to the splenic flexure. The peritoneum of the anterosuperior layer of the transverse mesocolon is reflected onto the upper part of the anteroinferior surface at the line of the anterior border where it is continuous with the posterior leaf of the greater omentum. The apex of the ligament of Treitz may form an anterior relation of this surface of the body laterally.

Superior border

On the right side, the superior border of the pancreas is initially blunt and somewhat flat, but as the gland is followed to the left, the surface changes to become narrower and sharper. An omental tuberosity usually projects from the right end of the superior border above the level of the lesser curvature of the stomach, in contact with the posterior surface of the lesser omentum. The superior border is related to the coeliac artery. The common hepatic artery runs to the right just above the gland. The splenic artery runs a course that is often highly tortuous to the left along the superior border; it tends to rise above the level of the superior border at several points along its course.

Anterior border

The anterior border of the pancreas separates the anterosuperior from the anteroinferior surfaces. The two layers of the transverse mesocolon diverge along this border. The upper is reflected inferiorly after a very short distance into the descending (posterior) leaf of the greater omentum whilst the other runs downwards and backwards over the anteroinferior surface.

Inferior border

The inferior border of the pancreas separates the posterior from the anteroinferior surfaces. At the medial end of the inferior border, adjacent to the neck of the pancreas, the superior mesenteric vessels emerge from behind the gland. More laterally, the inferior mesenteric vein runs under the border to join the splenic vein on the posterior surface. This is a useful site of identification of the inferior mesenteric vein during left-sided colonic resections and on CT imaging.

TAIL

The tail of the pancreas is the narrowest, most lateral portion of the gland and lies between the layers of the splenorenal ligament. It is continuous medially with the body and is between 1.5 and 3.5 cm long in adults. It may finish at the base of the splenorenal ligament or extend up nearly as far as the splenic hilum, in which case it is prone to injury at splenectomy during ligation of the splenic vessels. Posteriorly it is related to the splenic branches of the splenic artery and the splenic vein and its tributaries. The tip of the tail may lie in contact with the splenic hilum.

UNCINATE PROCESS

The uncinate process of the pancreas extends from the inferior lateral end of the head of the gland (Fig. 70.5). Embryologically it is separate from the rest of the gland, and so it lies posterior to the superior mesenteric vein and occasionally the artery as they descend and run forward into the root of the ileal mesentery, in close contact with its anterior surface. Posteriorly it lies in front of the aorta, and inferiorly it lies on the upper surface of the third part of the duodenum. Tumours of the uncinate process do not cause obstruction to the common bile duct, but frequently compress the third part of the duodenum as a result of this close relationship.

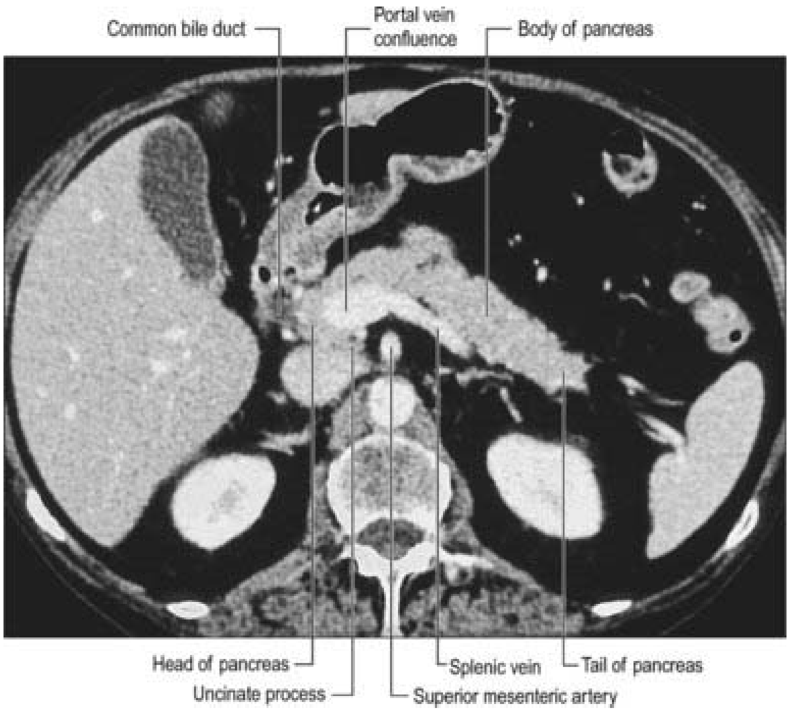
Common bile duct
Portal vein confluence
Body of pancreas
Head of pancreas
Uncinate process
Splenic vein
Tail of pancreas
Superior mesenteric artery

Fig. 70.5 Cross sectional CT scan of pancreas at the level of the uncinate process (cross sectional level between those shown in **Fig. 70.4B,C**).

PANCREATIC DUCTS

The exocrine pancreatic tissue drains into multiple small lobular ducts. The arrangement of the main ducts draining the pancreas is subject to some variation but the commonest arrangement is a single main and a single accessory duct (Fig. 70.6). This arrangement reflects the embryological development of the dorsal and ventral pancreatic ducts (see Ch. 73). The main duct is derived from the distal part of the dorsal duct in the body and tail but fuses with the more posteriorly placed ventral duct in the region where the dorsal bud fuses with the ventral bud (because the latter forms the posterior portion of the head of the pancreas and uncinate process). The accessory duct is the remnant of the duct of the dorsal pancreatic bud lying in the anterior pancreatic head after the principle part has joined with the ventral bud duct.

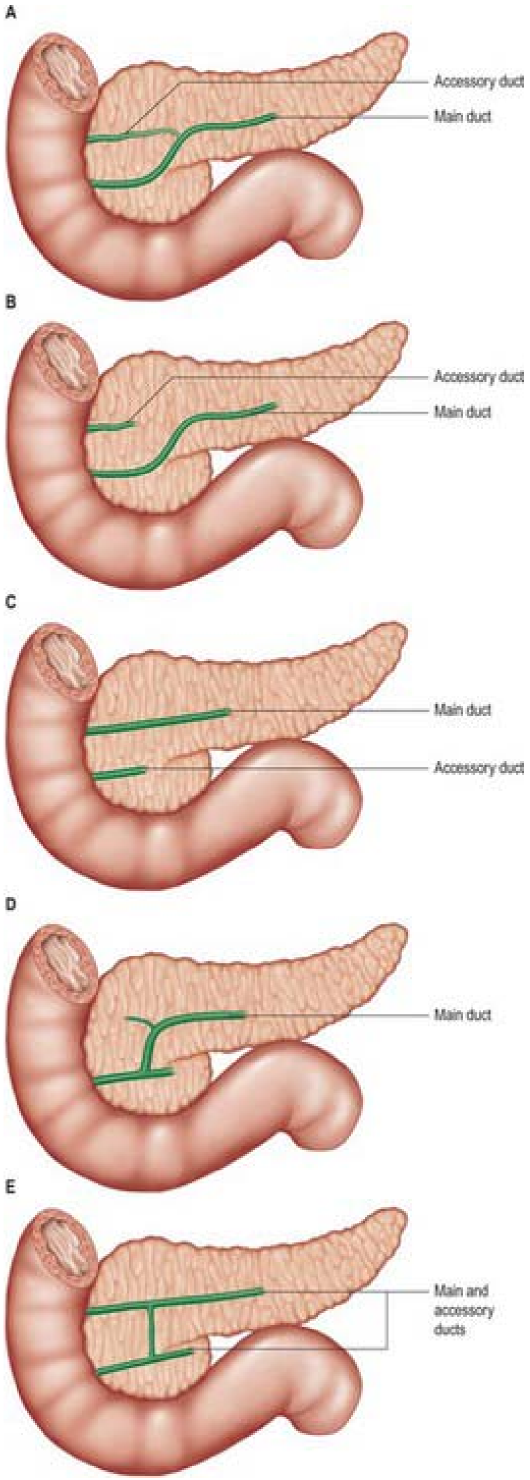
A
Accessory duct
Main duct
B
Accessory duct
Main duct
C
Main duct
Accessory duct
D
Main duct
E
Main and
accessory
ducts

Fig. 70.6 Variations in the ductal anatomy of the pancreas. **A**, Normal (50%). **B**, Absence of communication between normally sited accessory duct and main ducts (10%). **C**, Persistance of complete ventral and dorsal ducts with separate drainage (5%). **B** and **C** are both forms of ‘pancreas

divisum’. **D**, Absence of accessory duct (20%). **E**, Conjoined drainage of persistant ventral and dorsal ducts (<5%).

The main pancreatic duct (of Wirsung) usually runs within the substance of the gland from left to right. It tends to lie more towards the posterior than the anterior surface and is formed by the junction of several lobular (secondary) ducts in the tail. It increases in calibre as it runs within the body because it receives further lobular ducts which join it almost at right angles to its axis, forming a ‘herringbone pattern’. On ultrasound the duct can often be demonstrated, measuring approximately 3mm in diameter in the head, 2mm in the body, and 1mm in the tail in adults. As it reaches the neck of the gland it usually turns inferiorly and posteriorly towards the bile duct, which lies on its right side. The two ducts enter the wall of the descending part of the duodenum obliquely and unite in a short dilated hepatopancreatic ampulla (see Ch. 69).

The accessory pancreatic duct (of Santorini) usually drains the upper part of the anterior portion of the head of the pancreas. Much smaller in calibre than the main duct, it is formed within the substance of the head from several lobular ducts and ascends anterior to the main duct; it usually communicates with it through several small branches although these are rarely large enough to fill the accessory duct on a pancreatogram via the main ampulla. The accessory duct usually opens onto a small rounded minor duodenal papilla, which lies about 2cm anterosuperior to the major papilla. If the duodenal end of the accessory duct fails to develop, the lobular ducts drain via a small channel(s) into the main duct.

The main and accessory pancreatic ducts demonstrate some variability in their anatomy reflecting variations in the development and fusion of the dorsal and ventral ducts (Fig. 70.6). One clinically important variation is ‘pancreas divisum’, where entirely separate drainage occurs for different portions of the pancreas and which may allow some forms of pancreatitis to affect only one portion of the gland.

VASCULAR SUPPLY AND LYMPHATIC DRAINAGE

Arteries

The pancreas has a rich arterial supply derived from the coeliac axis and superior mesenteric artery via both named vessels and multiple small unnamed vessels (Fig. 70.7).

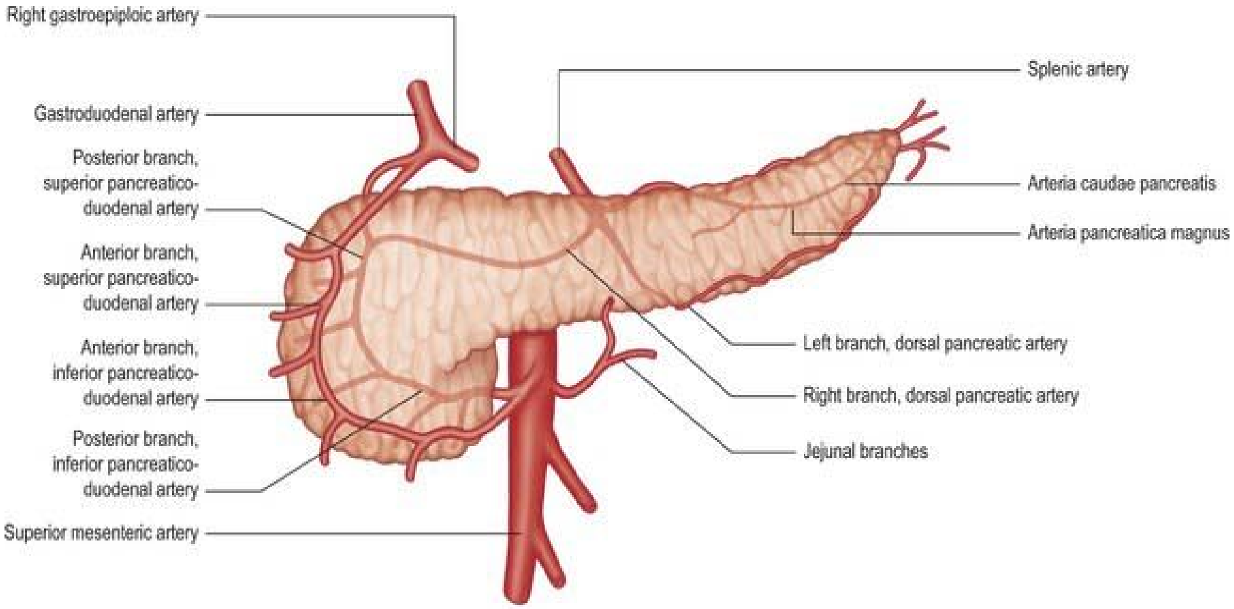
Right gastroepiploic artery
Gastroduodenal artery
Posterior branch, superior pancreatico-duodenal artery
Anterior branch, superior pancreatico-duodenal artery
Anterior branch, inferior pancreatico-duodenal artery
Posterior branch, inferior pancreatico-duodenal artery
Superior mesenteric artery
Splenic artery
Arteria caudae pancreatis
Arteria pancreatica magnus
Left branch, dorsal pancreatic artery
Right branch, dorsal pancreatic artery
Jejunal branches

Fig. 70.7 Arterial supply of the pancreas.

Inferior pancreaticoduodenal artery

The inferior pancreaticoduodenal artery arises from the superior mesenteric artery or its first jejunal branch, near the superior border of the third part of the duodenum. It usually divides directly into anterior and posterior branches. The anterior branch passes to the right, anterior to the lower border of the head of the pancreas, and runs superiorly to anastomose with the anterior superior pancreaticoduodenal artery. The posterior branch runs posteriorly and superiorly to the right, lying posterior to the lower border of the head of the pancreas and anastomoses with the posterior superior pancreaticoduodenal artery. Both branches supply the pancreatic head, its uncinate process and the second and third parts of the duodenum.

Superior pancreaticoduodenal artery

The superior pancreaticoduodenal artery is usually double. The anterior artery is a terminal branch of the gastroduodenal artery and descends in the anterior groove between the second part of the duodenum and head of the pancreas. It supplies branches to the head of the pancreas and anastomoses with the anterior division of the inferior pancreaticoduodenal artery. The posterior artery is usually a separate branch of the gastroduodenal artery arising at the upper border of the first part of the duodenum. It descends to the right, anterior to the portal vein and common bile duct, where the duct passes behind the first part of the duodenum. The artery next runs posterior to the head of the pancreas and crosses posterior to the common bile duct embedded in the head of the pancreas. It enters the duodenal wall and anastomoses with the posterior division of the inferior pancreaticoduodenal artery. The posterior superior artery supplies branches to the head of the pancreas and the first and second parts of the duodenum. (See Kimura 2000.)

Pancreatic branches

The pancreas is supplied by numerous small arterial branches which usually run into the gland directly from their arteries of origin. They are particularly numerous in the region of the neck, body and tail. Most originate from the splenic artery as it runs along the superior border of the gland and supply the left part of the body and tail. A dorsal branch descends posterior to the pancreas, dividing into right and left branches. It sometimes arises from the superior mesenteric, middle colic, hepatic or rarely, the coeliac artery. The right branch is often double and runs between the neck and uncinate process to form a prepancreatic arterial arch as it anastomoses with a branch from the anterior superior pancreaticoduodenal artery. The left branch runs along the inferior border to the pancreatic tail where it anastomoses with the greater pancreatic artery (*arteria pancreatica magna*) and the artery to tail of the pancreas (*arteria caudae pancreatis*).

Small un-named branches also arise from the first jejunal arcade of the superior mesenteric artery and the arterial branches of the retroperitoneal vessels.

Small arteries characteristically run along the inferior and superior borders of the gland, either lying in a deep groove or within the tissue of the gland. They receive contributions from many of the arteries supplying the gland, but mainly from the inferior and superior pancreaticoduodenal arteries, and supply branches which penetrate the substance of the gland at right angles to the vessel. They may bleed profusely on cutting the parenchyma of the gland during resection and usually require ligation.

Veins

The venous drainage of the pancreas is primarily into the portal system (Fig. 70.8). The head and neck drain primarily via superior and inferior pancreaticoduodenal veins. The body and tail drain mostly via small veins that run directly into the splenic vein along the posterior aspect of the gland, or occasionally directly into the portal vein. The veins are numerous and short, features that may lead to troublesome bleeding during surgical mobilization of the head and neck of the gland. Small venous channels exist between all parts of the gland and the retroperitoneal veins, and ultimately drain into the lumbar veins: they may hypertrophy and become clinically significant in cases of portal hypertension.

Lymphatics

The lymphatic drainage of the pancreas is extensive; multiple groups of nodes may receive drainage from each region of the gland (see Fig. 65.12B) which in part explains the poor prognosis following resection of pancreatic tumours. Lymph capillaries commence around the pancreatic acini. The larger lymph vessels follow the arterial supply and drain into the lymph nodes around the pancreas and adjacent node groups. Lymphatics from the tail and body drain mostly into the pancreaticosplenic nodes, although some drain directly to pre-aortic nodes. Lymphatics from the neck and head drain more widely into nodes along the pancreaticoduodenal, superior mesenteric and hepatic arteries, and some also drain to the pre-aortic nodes and coeliac axis nodes. There is no evidence of lymphatic channels within the pancreatic islets.

INNERVATION OF THE EXOCRINE PANCREAS

The exocrine lobules of the pancreas are innervated by a fine network of sympathetic and parasympathetic fibres. The sympathetic supply originates from the sixth to tenth thoracic spinal segments and is mainly distributed to the pancreas via the sympathetic contribution to the coeliac ganglia. The postganglionic fibres are distributed to the gland via the arterial supply as periarterial plexuses. The parasympathetic supply is from the posterior vagus nerve and the parasympathetic component of the coeliac plexus. The supply to the gland is both vasomotor (sympathetic) and parenchymal (sympathetic and parasympathetic). The exocrine lobules are innervated by a fine network of parasympathetic and sympathetic fibres. Sensory fibres running from the gland run in both the sympathetic and parasympathetic systems: they mediate the sensation of pain arising from the gland and may also carry other sensory information. In chronic inflammation or inoperable tumours of the gland, thermal or chemical ablation of the coeliac plexus may be required to control chronic pain mediated by these fibres.

Referred pain

Pain arising in the pancreas is poorly localized. In common with other foregut structures, the majority of pain arising from the pancreas is referred to the epigastrium. Inflammatory or infiltrative processes arising from the gland rapidly involve the tissues of the retroperitoneum that are innervated by somatic nerves: pain is referred to the posterior paravertebral region around the lower thoracic spine.

PANCREATITIS AND PSEUDOCYST

Pancreatitis is one of the major pathological processes affecting the pancreas. Gallstones lying within the common bile duct are associated with pancreatitis. The presence of a common drainage for the common bile duct and the pancreatic duct may allow reflux of bile or pancreatic enzymes into the pancreatic duct during the passage of a gallstone through the ampulla. Reflux may also occur if the wall of the common bile duct becomes oedematous even though the gallstones have not entered the common ampulla.

Inflammation in the pancreas may cause a range of secondary pathologies. The course of the superior mesenteric artery and vein behind the neck and between the inferior border and uncinate process makes these vessels vulnerable to compression and secondary inflammation, which may result in an inflammatory aneurysm of the superior mesenteric artery or thrombosis of the superior mesenteric vein. Inflammatory aneurysms may rupture producing major haemorrhage. Thrombosis of the superior mesenteric vein may cause potentially lethal venous ischaemia of the small intestine. Thrombosis of smaller arterial branches such as the origin of the middle colic artery may cause ischaemia of individual organs such as the transverse colon.

In acute episodes, the profuse arterial and venous supply to the gland makes it particularly prone to haemorrhage. The extravasated blood collects in the retroperitoneal tissues because the neck and body of the gland lie largely in the loose connective tissue of the retroperitoneum. The pancreas lies anterior to the thoracolumbar and perirenal fasciae and the blood-stained fluid can track freely in the retroperitoneal tissues to appear in either the flanks (Grey–Turner’s sign), groins, or above the iliac crest where the iliac fascia is attached. Blood-stained fluid tracking laterally from the head of the pancreas may enter the lesser omentum and the ‘bare area’ of the liver, from where it may run forward into the falciform ligament and appear around the skin of the umbilicus (Cullen’s sign).

During acute episodes of inflammation, the close anterior relationship of the stomach may contribute to gastric stasis and vomiting. The origin of the superior mesenteric plexus also lies close to the pancreas and secondary inflammation in the tissues around the pancreas may affect the autonomic supply to the midgut and contribute to the paralytic ileus that frequently develops.

In severe cases, pancreatic inflammation may cause the collection of fluid within and around the pancreatic tissue. Intrapancreatic collections frequently resolve spontaneously over time, but coalescence of the fluid may occur anterior to the pancreas beneath the layer of peritoneum covering its anterior surfaces (although this actually lies beneath the posterior wall of the lesser sac). If this collection persists and grows, the peritoneum anterior and superior to the pancreas is stretched and comes to lie in contact with the anterior wall of the lesser sac. This collection is referred to as a pseudocyst. The anterior wall of the pseudocyst is formed of the twin layers of peritoneum lying adjacent to the posterior wall of the stomach, the lesser omentum and, occasionally, the gastrosplenic ligament. The lateral wall of the pseudocyst includes the splenorenal ligament. The posterior wall is a mixture of fibrous tissue resulting from previous inflammation, the anterior surface of the pancreas and the retroperitoneal tissues. Treatment of the pseudocyst usually involves drainage of the contents into the lumen of the stomach. This may be established endoscopically by placement of a drain through the posterior stomach wall and the two thickened layers of peritoneum into the cyst. Alternatively, the drain may be placed using radiological guidance, via the anterior abdominal wall and the anterior stomach wall.

PANCREATIC RESECTION

Resection of the pancreas is complicated by several factors. The extensive vascular supply requires careful haemostasis. Spleen-preserving resections may be undertaken if the underlying pathology does not involve the splenic vein where it lies in the groove on the posterior surface of the gland, although the multiple small pancreatic veins draining into it may cause troublesome bleeding. Resection of the head and neck is possible provided the plane between the neck and the portal vein has not been involved by disease. Occasional small venous branches may enter the portal vein directly and may also cause bleeding during this mobilization. Resection of the head and neck are almost always accompanied by resection of the distal first and second parts of the duodenum because of the dense adherence between the two and the common arterial supply. Resection without removal of the proximal part of the first part of the duodenum and pylorus, pylorus-preserving pancreatectomy, may be possible provided there is an adequate arterial supply to the pylorus from the stomach, and directly from the pre-pyloric vessels.

MICROSTRUCTURE

The pancreas is composed of two different types of glandular tissue. The main tissue mass is exocrine, in which pancreatic islets of endocrine cells are embedded (Figs 70.9-70.11).

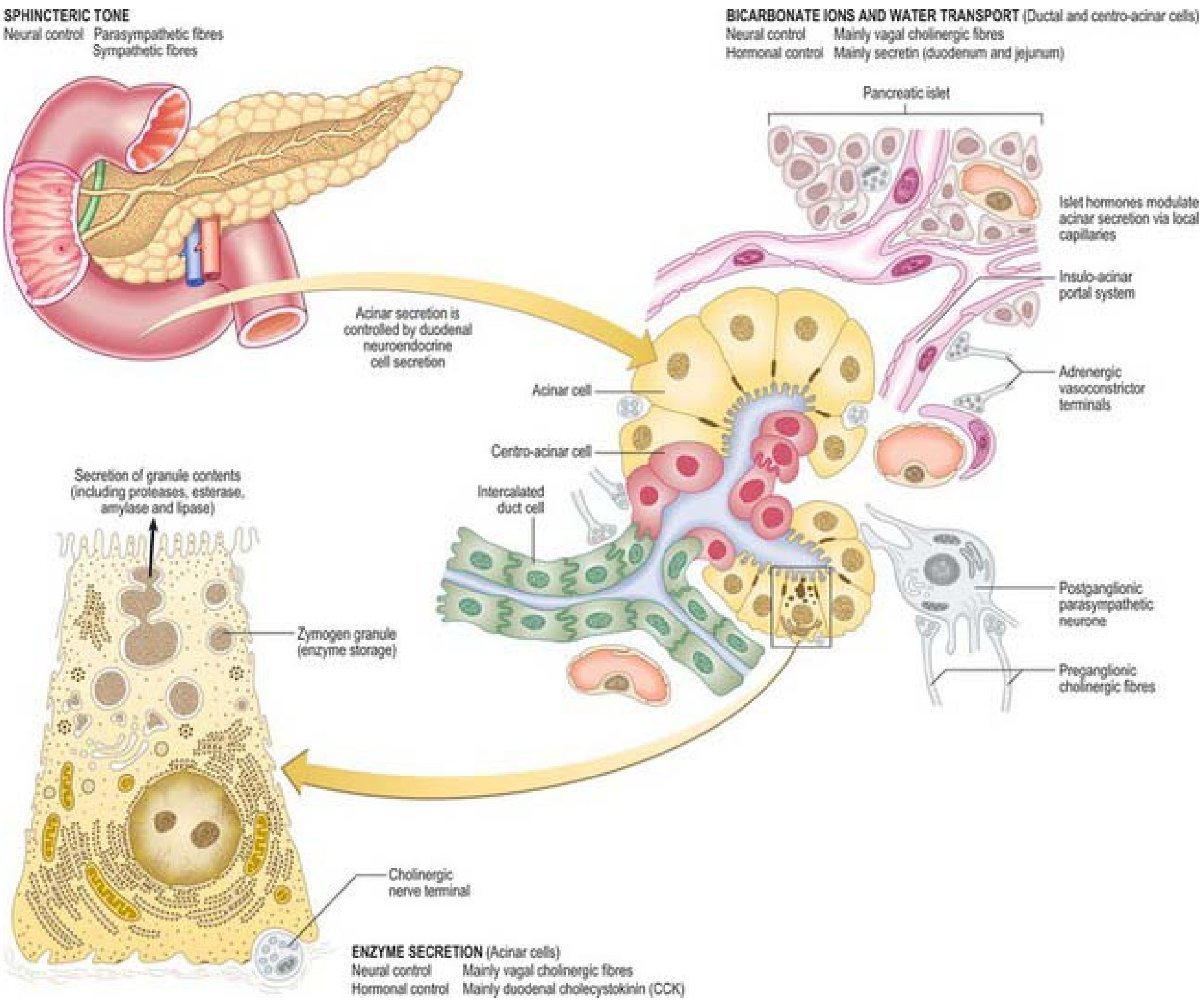
SPHINCTERIC TONE
Neural control Parasympathetic fibres
Sympathetic fibres
BICARBONATE IONS AND WATER TRANSPORT (Ductal and centro-acinar cells)
Neural control Mainly vagal cholinergic fibres
Hormonal control Mainly secretin (duodenum and jejunum)
Pancreatic islet
Islet hormones modulate acinar secretion via local capillaries
Insulo-acinar portal system
Adrenergic vasoconstrictor terminals
Acinar secretion is controlled by duodenal neuroendocrine cell secretion
Acinar cell
Centro-acinar cell
Intercalated duct cell
Postganglionic parasympathetic neurone
Preganglionic cholinergic fibres
Secretion of granule contents (including proteases, esterase, amylase and lipase)
Zymogen granule (enzyme storage)
Cholinergic nerve terminal
ENZYME SECRETION (Acinar cells)
Neural control Mainly vagal cholinergic fibres
Hormonal control Mainly duodenal cholecystokinin (CCK)

Fig. 70.9 Microstructure of the exocrine pancreas and the mechanisms by which its secretion is controlled. Pancreatic stellate cells (see text) are not shown.

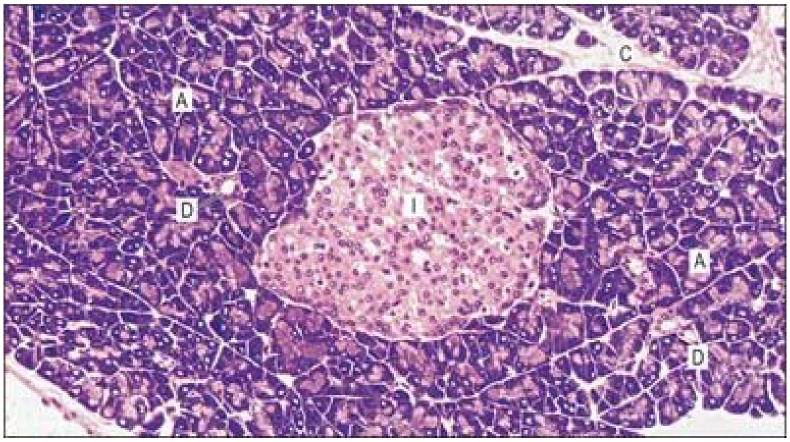

Fig. 70.10 Pancreatic tissue. Exocrine acinar cells (A) are deeply stained basally, indicating the high ribosomal concentration. Small ducts (D) are shown. An endocrine islet (of Langerhans) (I) is shown centrally, with pale-staining cells surrounded by a network of capillaries, seen as clear spaces. Connective tissue septa (C) separate lobules.

(By permission from Dr JB Kerr, Monash University, from Kerr JB 1999 Atlas of Functional Histology. London: Mosby.)

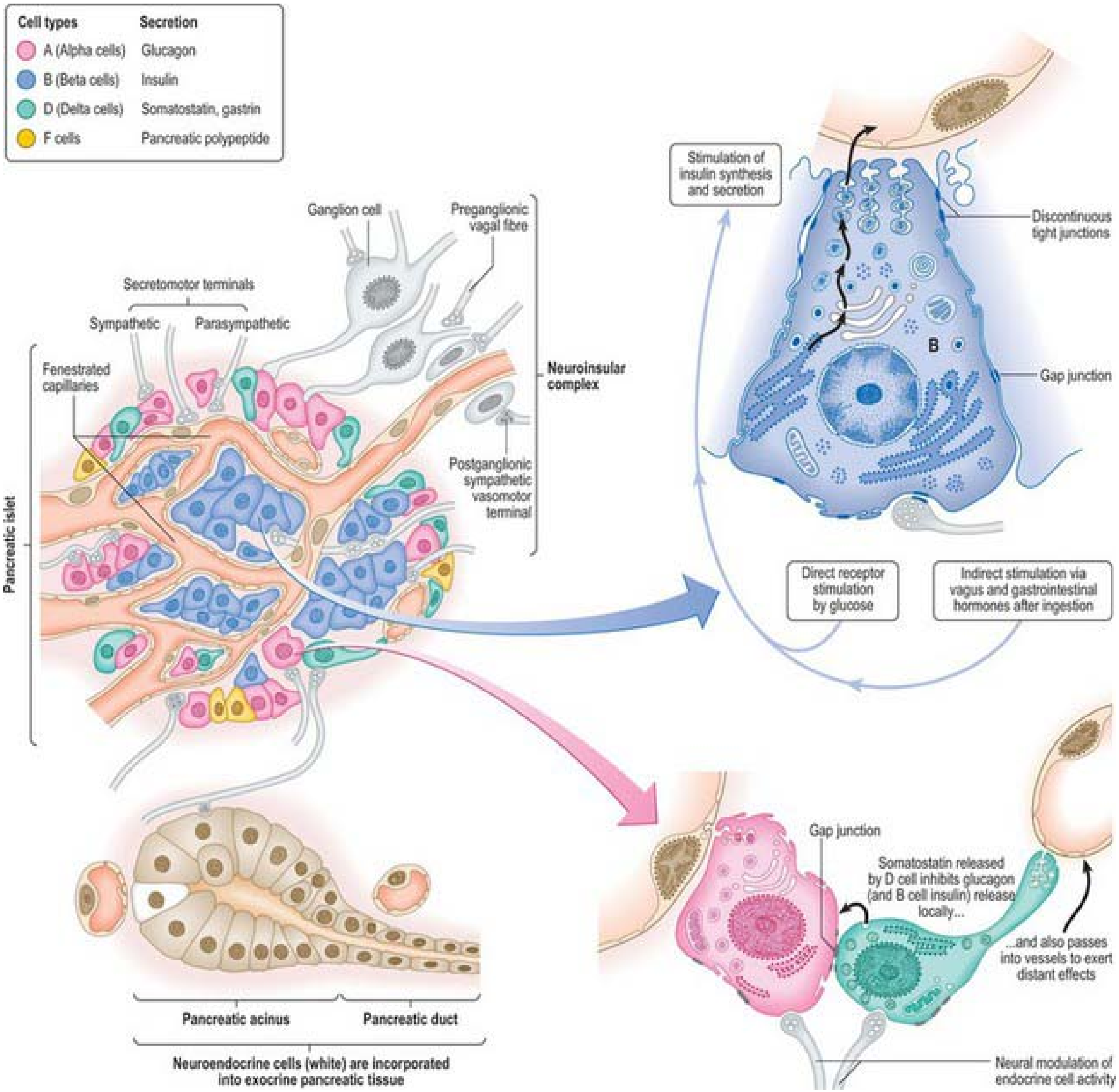
Cell types
Secretion
A (Alpha cells)
Glucagon
B (Beta cells)
Insulin
D (Delta cells)
Somatostatin, gastrin
F cells
Pancreatic polypeptide
Ganglion cell
Preganglionic vagal fibre
Secretomotor terminals
Sympathetic
Parasympathetic
Fenestrated capillaries
Neuroinsular complex
Postganglionic sympathetic vasomotor terminal
Pancreatic islet
Pancreatic acinus
Pancreatic duct
Neuroendocrine cells (white) are incorporated into exocrine pancreatic tissue
Stimulation of insulin synthesis and secretion
Discontinuous tight junctions
B
Gap junction
Direct receptor stimulation by glucose
Indirect stimulation via vagus and gastrointestinal hormones after ingestion
Gap junction
Somatostatin released by D cell inhibits glucagon (and B cell insulin) release locally...
...and also passes into vessels to exert distant effects
Neural modulation of endocrine cell activity

Fig. 70.11 Microstructure and control of function of the endocrine pancreas.

Exocrine pancreas

The exocrine pancreas isa branched acinar gland, surrounded and incompletely lobulated by delicate loose connective tissue. It is formed of pyramidal, secretory cells arranged mainly as spherical clusters, or acini. A narrow intercalated, intralobular duct originates within each secretory acinus, lined initially by flattened or cuboidal centro-acinar cells. These small ductules form branching links which run within and between adjacent acini, explaining why structurally distinct intralobular pancreatic ducts are infrequent (see Kerr 1999, for details). More distally, these are replaced by taller cuboidal and eventually columnar epithelium in the larger interlobular ducts. The latter are surrounded by loose connective tissue of the septa, containing smooth muscle and autonomic nerve fibres. Neuroendocrine cells are present amongst the columnar ductal cells and mast cells are numerous in the surrounding connective tissue.

Acinar cells

Acinar cells of the exocrine pancreas have a basal nucleus and, in their basal cytoplasmic domain, abundant rough endoplasmic reticulum which results in their basophilic staining characteristics. Dense secretory zymogen granules stain deeply with eosin in the apical region. A prominent supranuclear Golgi complex is surrounded by large, membrane-bound granules containing the proteinaceous constituents of pancreatic secretion, including enzymes which are only active after release. Ganglionic neurones and cords of undifferentiated epithelial cells are also found within the acini. The structure of the exocrine pancreas and its functional regulation are summarized in Fig. 70.9.

Stellate cells

Pancreatic stellate cells, PaSCs, are one of several resident cells in the exocrine pancreas. They are regulated by autocrine and paracrine stimuli and share many features with their hepatic counterparts. PaSCs are myofibroblast-like cells and are found in the periacinar space, where their long cytoplasmic processes encircle the base of the acinus, and in perivascular and periductal regions of the pancreas. They have been implicated as key players in the pathobiology of the major disorders of the exocrine pancreas, including chronic pancreatitis and pancreatic cancer (Bishr Omary et al 2007).

Endocrine pancreas

The endocrine pancreas consists of pancreatic islets of Langerhans, composed of spherical or ellipsoid clusters of cells embedded in the exocrine tissue. The human pancreas may contain more than a million islets, usually most numerous in the tail. An islet is a mass of polyhedral cells, each in close proximity to fenestrated capillaries and a rich autonomic innervation. Specialized staining procedures or immunohistochemical techniques are necessary to distinguish the three major types of cell, designated alpha, beta and delta. Their general organization is shown in Fig. 70.11.

The most numerous cells, types alpha and beta, secrete glucagon and insulin respectively. Alpha cells tend to be concentrated at the periphery of islets, and beta cells more centrally. A third type, the delta cell, secretes somatostatin and gastrin, and like alpha cells, is peripherally placed within the islets. A minor cell type, the F cell, secretes pancreatic polypeptide (PP), which is stored in smaller secretory granules. The autonomic neurotransmitters acetylcholine (ACh) and noradrenaline affect islet cell secretion: ACh augments insulin and glucagon release, noradrenaline inhibits glucose-induced insulin release, and they may also affect somatostatin and PP secretion.

Innervation of endocrine pancreas

The innervation of the endocrine islets is almost exclusively from the parasympathetic system. Fine branches ramify among the cells and form plexuses around the islets. Fibres frequently synapse with acinar cells before innervating the islets, suggesting a close linkage between neural control of exocrine and endocrine components. Many fibres enter the islets with the arterioles. Parasympathetic ganglia lie in the connective tissue within and between lobules, and in the former case are frequently associated with islet cells, forming neuroinsular complexes. Both alpha and beta cells are involved in these neuroinsular complexes. Three types of nerve terminal are seen in islets. Cholinergic terminals have agranular vesicles with a diameter of 30–50 nm, adrenergic terminals have dense-cored vesicles with a diameter of 30–50 nm and a third, uncharacterized, type have dense-cored vesicles with a diameter of 60–200 nm (Smith & Porte 1976).

No selective link with any one type of insular cell has been found. Sometimes more than one type of terminal contacts a single cell and some of the chemical synapses between axon terminals and islet cells show narrow areas in the synaptic clefts suggesting an electrical synapse or gap junction. Such junctions also occur between islet cells, and electrical coupling of nerve supply to a functional network of islet cells may occur (Orci 1974).

REFERENCES

shr Omary M, Lugea A, Lowe AW, Pandol SJ. The pancreatic stellate cell: a star on the rise in pancreatic diseases. *J Clin Invest*. 2007;117:50-59.

err JB. Atlas of Functional Histology, Chapter 14. London: Mosby, 1999.

mura W. Surgical anatomy of the pancreas for limited resection. *J Hepatobiliary Pancreat Surg*. 2000;7:473-479.

agai H. Configurational anatomy of the pancreas: its surgical relevance from ontogenetic and comparative-anatomical viewpoints. *J Hepatobiliary Pancreat Surg*. 2003;10:48-56.

rci L. A portrait of a pancreatic B-cell. *Diabetologia*. 1974;10:163-187.

nith PH, Porte DJr. Neuropharmacology of the pancreatic islets. *Annu Rev Pharmacol Toxicol*. 1976;16:269-285.

CHAPTER 71

Spleen

The spleen consists of a large encapsulated mass of vascular and lymphoid tissue situated in the upper left quadrant of the abdominal cavity between the fundus of the stomach and the diaphragm. Its shape varies from a slightly curved wedge to a ‘domed’ tetrahedron. The shape is mostly determined by its relations to neighbouring structures during development. The superolateral aspect is shaped by the left dome of the diaphragm with the inferomedial aspect being influenced mostly by the neighbouring splenic flexure of the colon, the left kidney and stomach. Its long axis lies approximately in the plane of the tenth rib. Its posterior border is approximately 4 cm from the mid-dorsal line at the level of the tenth thoracic vertebral spine. Its anterior border usually reaches the mid-axillary line.

The size and weight of the spleen vary with age and sex. It can also vary slightly in the same individual under different conditions. In the adult it is usually 12 cm long, 7 cm broad, and 3–4 cm wide. It is comparatively largest in the young child, and although its weight increases during puberty, by adulthood it is relatively smaller in comparison to the neighbouring organs. It tends to diminish in size and weight in senescence. Its average adult weight is about 150 g, although the normal range is wide, between 80 g and 300 g, in part reflecting the amount of blood it contains. The normal-sized adult spleen fits comfortably in a cupped hand; the spleen has to be at least three times its normal size before it can be palpated.

Additional collections of fully functional splenic tissue may exist near the spleen, especially within the gastrosplenic ligament and greater omentum. These accessory spleens, or splenunculi, are usually isolated but can be connected to the spleen by thin bands of similar tissue. They may be numerous and widely scattered in the abdomen. The spleen may retain its fetal lobulated form or show deep notches on its diaphragmatic surface and inferior border in addition to those usually present on the superior border.

RELATIONS

The spleen has a superolateral diaphragmatic and an inferomedial visceral surface (Fig. 71.1). There are superior and inferior borders and anterior and posterior extremities or poles. The diaphragmatic surface is convex and smooth and faces mostly superiorly and laterally although the posterior part may face posteriorly and almost medially as it approaches the inferior border. The diaphragmatic surface is related to the abdominal surface of the left dome of the diaphragm which separates it from the basal pleura, the lower lobe of the left lung and the ninth to eleventh left ribs (Fig. 71.2). The pleural costodiaphragmatic recess extends down as far as its inferior border. The visceral surface faces inferomedially towards the abdominal cavity, and is irregular and marked by gastric, renal, pancreatic and colic impressions. The gastric impression faces anteromedially and is broad and concave where the spleen lies adjacent to the posterior aspect of the fundus, upper body and upper greater curvature of the stomach. It is separated from the stomach by a peritoneal recess, which is limited by the gastrosplenic ligament. The renal impression is slightly concave and lies on the lowest part of the visceral surface, separated from the gastric impression above by a raised strip of splenic tissue and the splenic hilum. It faces inferomedially and slightly backwards, being related to the upper and lateral area of the anterior surface of the left kidney and sometimes to the superior pole of the left suprarenal gland. The colic impression lies at the inferior pole of the spleen and is usually flat. It is related to the splenic flexure of the colon and the phrenicocolic ligament. The pancreatic impression is often small when present and lies between the colic impression and the lateral part of the hilum. It is related to the tail of the pancreas which lies in the splenorenal ligament. The hilum of the spleen is a long fissure pierced by several irregular apertures through which the branches of the splenic artery and vein as well as nerves and lymphatics enter and leave the spleen; it lies in the visceral surface closer to the inferior border and anterior border.

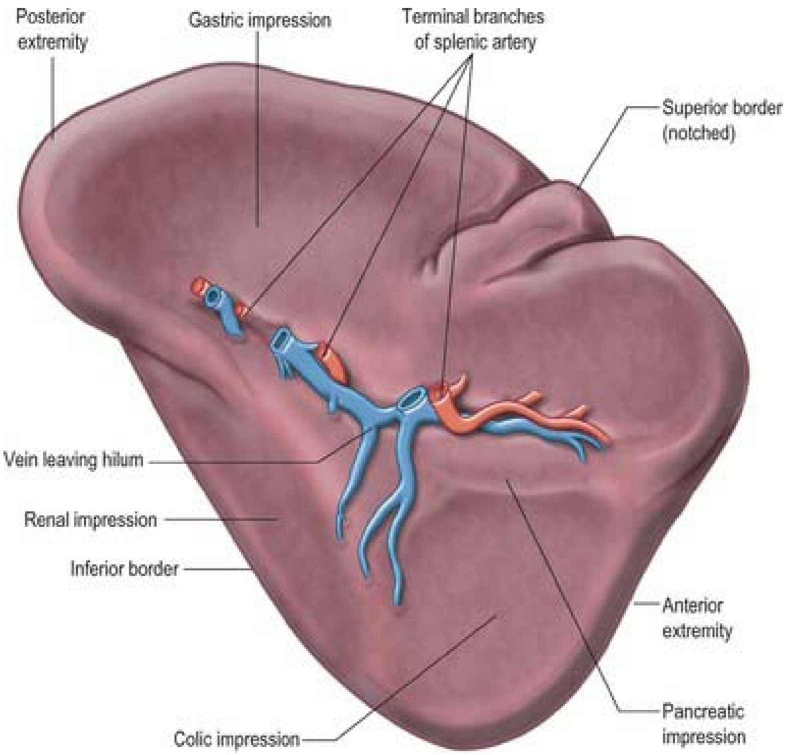
Posterior extremity
Gastric impression
Terminal branches of splenic artery
Superior border (notched)
Vein leaving hilum
Renal impression
Inferior border
Anterior extremity
Pancreatic impression
Colic impression

Fig. 71.1 The visceral surface of the spleen.

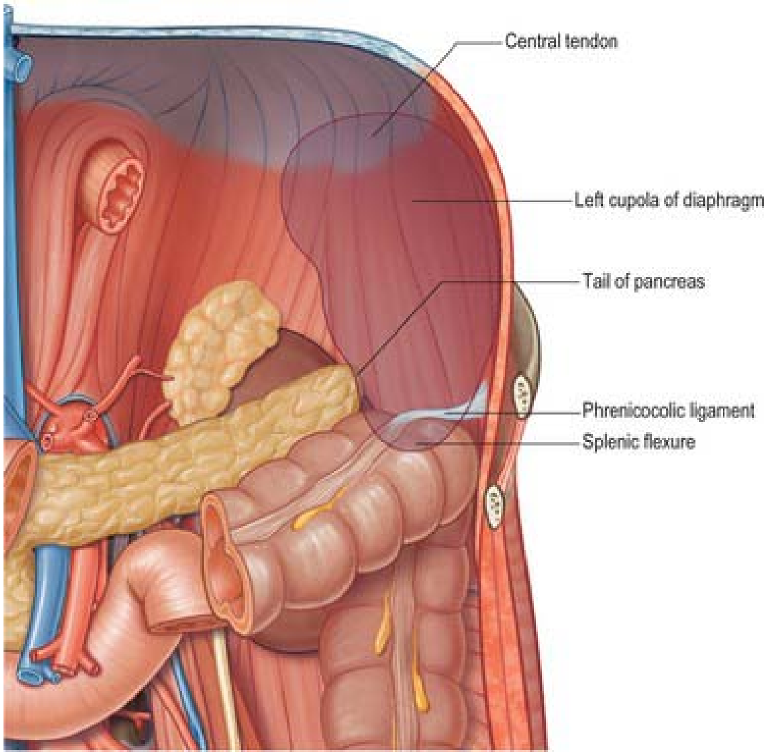
Central tendon
Left cupola of diaphragm
Tail of pancreas
Phrenicocolic ligament
Splenic flexure

Fig. 71.2 The posterior relations (‘bed’) of the spleen.

(Adapted from Drake, Vogl and Mitchell 2005.)

The superior border separates the diaphragmatic surface from the gastric impression and is usually convex. Near the anterior extremity there may be one or two notches that have persisted from the lobulated form of the spleen in early fetal life. However, they are often absent and are not a reliable guide to the identification of the spleen during clinical examination. The inferior border separates the renal impression from the diaphragmatic surface and lies between the diaphragm and the upper part of the lateral border of the left kidney. It is more blunt and rounded than the superior border and corresponds in position to the lower margin of the eleventh rib. The posterior extremity, or superior pole, usually faces the rounded vertebral column. The anterior extremity, or inferior pole, is larger and less angulated than the posterior extremity and connects the lateral ends of the superior and inferior borders: it is related to the colic impression and may lie adjacent to the splenic flexure and the phrenicocolic ligament.

PERITONEAL CONNECTIONS OF THE SPLEEN

The spleen is almost entirely covered by peritoneum that adheres firmly to its capsule, and is separated from the stomach and left kidney by recesses of the greater sac. It develops in the upper dorsal mesogastrium (see Figs 73.6 to 73.7), and remains connected via folds of peritoneum to the posterior abdominal wall (by the splenorenal, phrenicocolic and phrenicosplenic ligaments) and to the anterolateral abdominal wall and stomach (by the gastrosplenic ligament) (Fig. 71.3A). The splenorenal ligament is formed from two layers of peritoneum. The anterior layer is continuous with the peritoneum of the posterior wall of the lesser sac over the left kidney and with peritoneum of the splenic hilum where it runs into the posterior layer of the gastrosplenic ligament. The posterior layer of the splenorenal ligament is continuous with the peritoneum over the inferior surface of the diaphragm and runs onto the splenic surface over the renal impression. The splenic vessels lie between the layers of the splenorenal ligament: the tail of the pancreas is usually present in its lower portion (see Fig. 64.5B). The length of the splenorenal ligament may vary. Longer ligaments tend to make the spleen more mobile and may predispose the spleen to injury due to rotational shear forces during trauma, however they also make the mobilization of the spleen easier during surgery. The presence of the pancreatic tail within the splenorenal ligament must be remembered because it can be injured during ligation of the splenic vessels, causing pancreatitis or a pancreatic duct fistula to form.

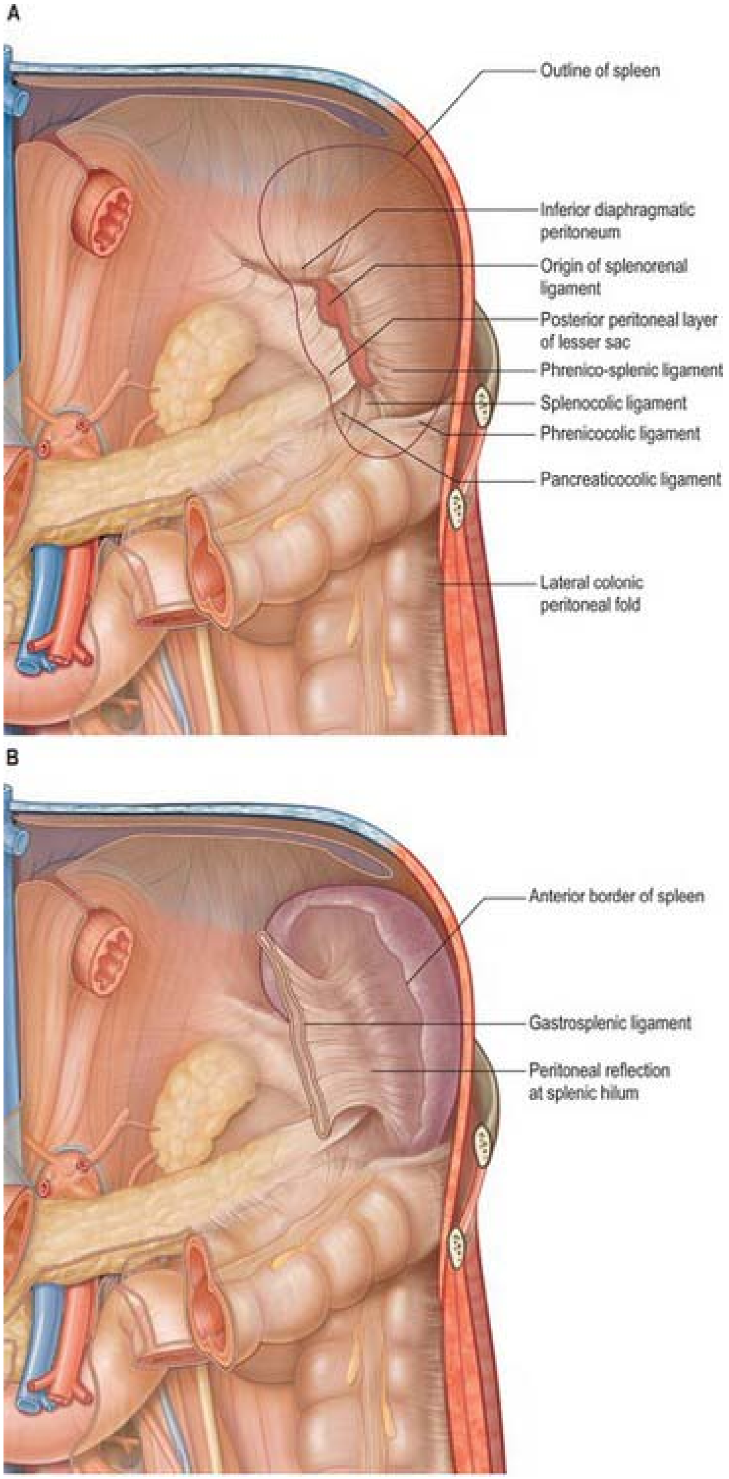
A
Outline of spleen
Inferior diaphragmatic peritoneum
Origin of splenorenal ligament
Posterior peritoneal layer of lesser sac
Phrenico-splenic ligament
Splenocolic ligament
Phrenicocolic ligament
Pancreaticocolic ligament
Lateral colonic peritoneal fold
B
Anterior border of spleen
Gastrosplenic ligament
Peritoneal reflection at splenic hilum

Fig. 71.3 The peritoneal connections of the spleen. **A**, The posterior peritoneal connection seen as if the spleen has been removed with the folds fixed in their ‘normal’ positions. **B**, The anterior peritoneal connections

seen with the spleen in place as if the stomach and greater omentum have been removed with the folds fixed in their ‘normal’ positions.

*(**A** and **B** adapted from Drake, Vogl and Mitchell 2005.)*

The gastrosplenic ligament also has two layers (Fig. 71.3B). The posterior layer is continuous with the peritoneum at the splenic hilum and over the posterior aspect of the stomach. The anterior layer is formed from the peritoneum that is reflected off the gastric impression and reaches the greater curvature of the stomach anteriorly. The short gastric and left gastroepiploic branches of the splenic artery pass between its layers. Division of the gastrosplenic ligament during surgery may be hazardous if the ligament is short because ligation of the short gastric vessels may risk injury to the greater curvature of the stomach.

The phrenicocolic ligament extends from the splenic flexure of the colon to the diaphragm at the level of the eleventh rib. It extends inferiorly and laterally and is continuous with the peritoneum of the lateral end of the transverse mesocolon at the lateral margin of the pancreatic tail, and the splenorenal ligament at the hilum of the spleen.

If the peritoneal attachments of the spleen are not recognized during surgery, the splenic capsule may be injured, with subsequent serious bleeding. Downward traction on the phrenicocolic ligament during handling of the descending colon, especially during mobilization of the splenic flexure, may cause rupture of the splenic capsule. This is less likely if traction on the phrenicocolic ligament is made laterally or medially. The superior border and anterior diaphragmatic surface are often adherent to the peritoneum of the greater omentum. Medial traction on the omentum during surgery may cause capsular injury, but this is less likely if any limited traction required is applied inferiorly. The diaphragmatic surface of the spleen is occasionally adherent to the peritoneum over the inferior surface of the diaphragm: these adhesions often occur after inflammation in the spleen, but may also be present congenitally.

SPLENOMEGALY

Splenic enlargement may accompany any massive immune response and occurs in many other systemic inflammatory and degenerative conditions. In splenomegaly, the anterior border, anterior diaphragmatic surface and notched superior border may become clearly palpable below the left costal margin. The notches are often exaggerated and may be clearly palpable, and the transverse colon and splenic flexure are displaced downward.

SPLENIC TRAUMA

The spleen is particularly prone to rotational injury during rapid deceleration or compression. Because it has relatively mobile peritoneal connections, tearing injuries to the splenic vessels at the hilum or burst injuries of the splenic pulp may occur. Fractures of the overlying lower left ribs may cause sharp penetrating injuries to the splenic capsule and pulp. The spleen may also be injured during surgical procedures by tearing of its capsule through peritoneal adhesions and connections (see above). Minor capsular tears may be treated by conservative management if from blunt trauma or by application of various haemostatic substances to the exposed pulp. Direct sutured repair of more extensive tears of the spleen is rarely successful because the splenic pulp is fragile. Moderately severe injuries may be treated by conservative management if from blunt trauma or by compression of the splenic tissue until haemostasis occurs if encountered at surgery, but extensive burst injuries or major injuries to the hilar vessels usually require splenectomy.

SPLENECTOMY

Partial splenectomy is followed by rapid regeneration of lost tissue and there is no significant loss in any of the functions of the spleen. Total splenectomy has few haematological consequences since the functions of the spleen are largely assumed by the liver. There is, however, a loss in immune function, particularly in the antibody response to systemic infections with encapsulated bacteria. This is referred to as ‘overwhelming post-splenectomy sepsis syndrome’, and is particularly a problem when the spleen is lost in early childhood, but is still a significant risk even if the spleen is lost in late adult life. Splenectomy in adults is usually followed by an increased white blood cell count with increased lymphocytic, neutrophil, eosinophil and platelet counts in the peripheral blood: these effects fade and disappear within a few weeks.

VASCULAR SUPPLY AND LYMPHATIC DRAINAGE

Splenic artery

The spleen is supplied exclusively from the splenic artery (see Fig. 70.7). This is the largest branch of the coeliac axis and its course is among the most tortuous in the body. From its origin the artery runs a little way inferiorly, then turns rapidly to the left to run initially horizontally above the level of the neck of the pancreas, before ascending as it passes more laterally. It is less steeply inclined than the body and tail of the pancreas and so comes to lie posterior to the superior border of the gland. It lies in multiple loops or even coils which appear above the superior border of the pancreas and descend to lie behind the gland. The splenic artery lies anterior to the left kidney and left suprarenal gland and runs in the splenorenal ligament posterior to the tail of the pancreas. It divides into two or three main branches before entering the hilum of the spleen (Fig. 71.1). As these branches enter the hilum they divide further into four or five segmental arteries that each supply a segment of the splenic tissue. There is relatively little arterial collateral circulation between the segments, which means that occlusion of a segmental vessel often leads to infarction of part of the spleen. There is, however, considerable venous collateral circulation between the segments, making segmental resection of the spleen practically impossible. The splenic artery gives off various branches to the pancreas in its course and gives off short gastric arteries to the stomach just prior to dividing or from its terminal branches.

Splenic vein

The splenic vein is formed within the splenorenal ligament, close to the tip of the tail of the pancreas, by five or six tributaries that emerge from the hilum of the spleen (Fig. 71.4). The tributaries are thin walled and often spread over several centimetres because the hilum is long and thin (Fig. 71.1). This must be remembered during surgical removal of the spleen because the venous tributaries must be divided close to the hilum to avoid injury to the pancreatic tail. They should be ligated in several groups to prevent the risk of avulsion of the veins from the splenic hilum and consequent profuse bleeding before the resection is complete.

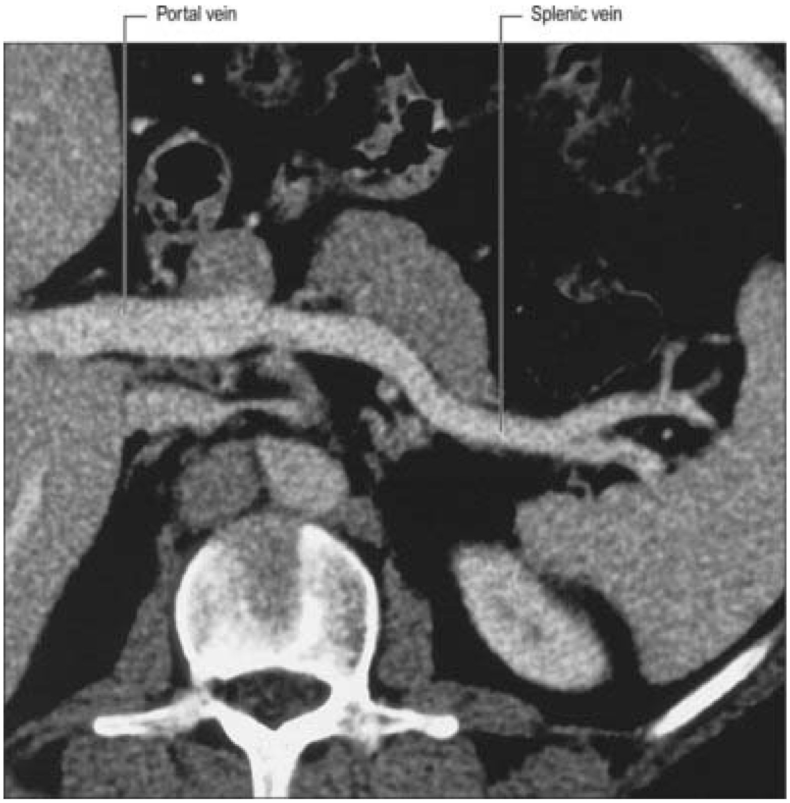

Fig. 71.4 Axial oblique CT slice of the portal vein and splenic vein.

The splenic vein runs in the splenorenal ligament below the splenic artery and posterior to the tail of the pancreas. It descends to the right, and crosses the posterior abdominal wall inferior to the splenic artery and posterior to the body of the pancreas, receiving numerous short tributaries from the gland as it does so. It crosses anterior to the left kidney and renal hilum and is separated from the left sympathetic trunk and left crus of the diaphragm by the left renal vessels, and from the abdominal aorta by the superior mesenteric artery and left renal vein. It ends behind the neck of the pancreas, where it joins the superior mesenteric vein to form the portal vein. The short gastric and left gastro-epiploic veins drain into the splenic vein through the folds of the gastrosplenic ligament near its origin.

Lymphatics

Lymphatic vessels drain along the splenic trabeculae and pass out of the hilum into lymphatic vessels that accompany the splenic artery and vein. They run posterior to the pancreas, close to the splenic artery, and drain into nodes at the hilum and along the splenic artery and into the coeliac nodes.

INNERVATION

The spleen is innervated by the splenic plexus, which consists of branches of the coeliac plexus, left coeliac ganglion and right vagus that accompany the splenic artery. The fibres are mainly sympathetic and terminate around blood vessels and in the non-striated muscle of the splenic capsule and trabeculae. Most appear to be noradrenergic, vasomotor, and are concerned with the regulation of blood flow through the spleen. Adrenergic agonists inhibit the concentration of red cells in the splenic blood (so called ‘plasma skimming’) indicating that sympathetic activity causes an increase in the ‘fast’ circulation of the spleen as opposed to slow filtration (Reilly 1985).

Referred pain

The sensation of pain arising from the pulp of the spleen is poorly localized and referred to the central epigastrium, as is the case for other structures derived from the foregut. Distension of the splenic capsule stretches the parietal layers of the peritoneum and produces pain that is localized to the posterior left upper quadrant.

MICROSTRUCTURE

The spleen is essentially concerned with phagocytosis and immune responses. In the fetus it is also an important site of haemopoiesis. Postnatally it may become haemopoietic in certain pathological conditions. Although important to the defence of the body it is not absolutely essential: if the spleen is removed, many of its functions can be assumed by the liver and by other lymphoid tissues.

Microscopically, the parenchymal tissue of the spleen consists of two major components, white pulp and red pulp, named on the basis of their appearance when a fresh spleen is transected (Fig. 71.5). The white pulp is composed of lymphoid tissue in which B and T lymphocytes mature and proliferate under antigenic stimulation (Fig. 71.6). The red pulp is a unique filtration device that enables the spleen to clear particulate material from the blood as it perfuses the spleen. It is composed of a complex system of interconnected spaces populated by large numbers of phagocytic macrophages that remove effete red blood cells, microorganisms, cellular debris and other particulate matter from the circulation.

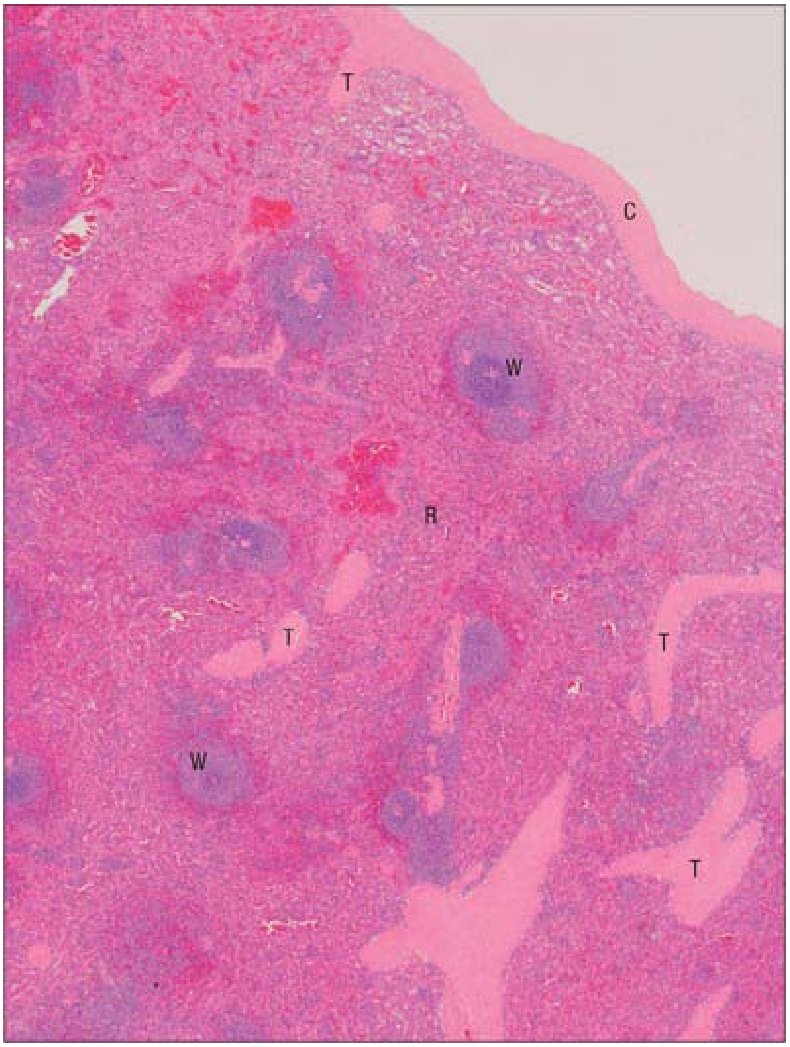

Fig. 71.5 A section through the spleen. White pulp (W) is present as ovoid areas of basophilic tissue. Red pulp (R) lies between white pulp tissue and consists of splenic sinusoids and intervening cellular cords. Part of the capsule (C) is seen top right, from which trabeculae (T) extend into the splenic tissue.

(By courtesy of Mr Peter Helliwell and Dr Joseph Mathew, Department of Histopathology, Royal Cornwall Hospitals Trust, UK.)

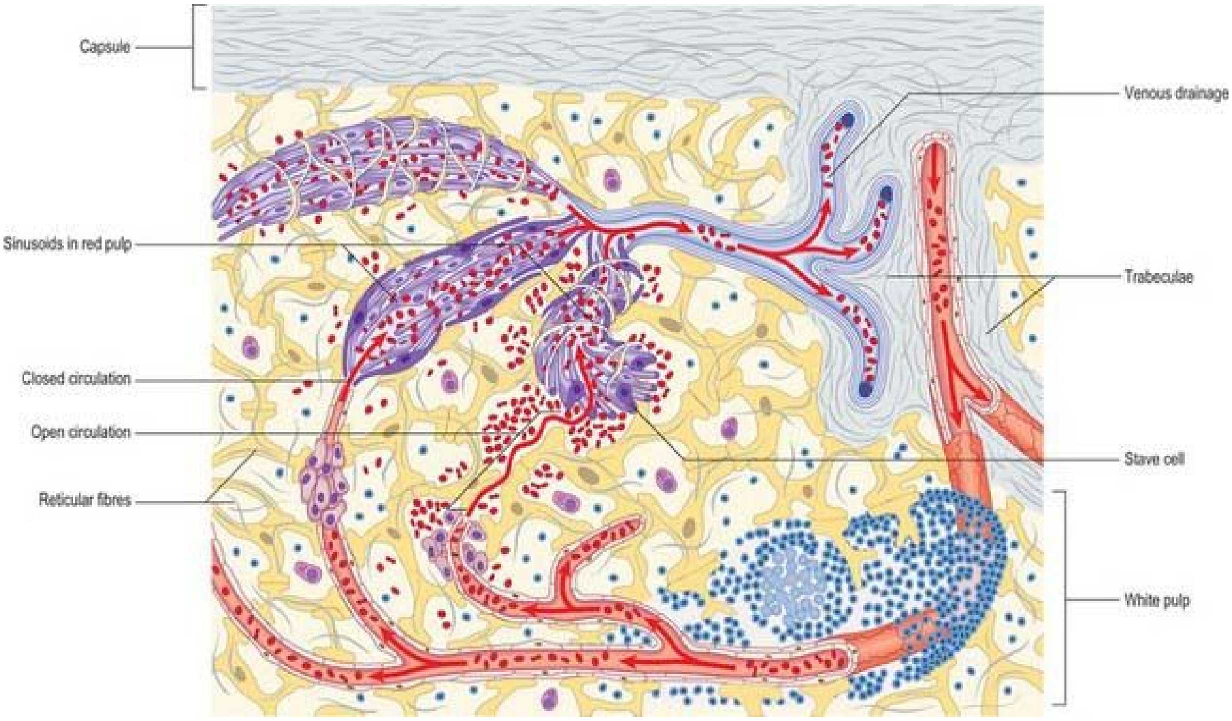
Capsule
Sinusoids in red pulp
Closed circulation
Open circulation
Reticular fibres
Venous drainage
Trabeculae
Stave cell
White pulp

Fig. 71.6 The main features of splenic structure, not to scale. Shown are the capsule, trabeculae, reticular fibres and cells, the perivascular lymphoid sheaths and follicles (white pulp), and the cellular cords and venous sinusoids of the red pulp. The 'open' and 'closed' theories of splenic circulation are illustrated: it is likely that most of the circulation is of the open form. The venous sinusoids are lined by specialized endothelial 'stave' cells, the intercellular gaps of which have been over-emphasized for clarity.

Fibrous framework of the spleen

The serosa of the peritoneum covers the entire organ except at its hilum and along the lines of reflexion of the splenorenal and gastrosplenic ligaments. Deep to this layer is the connective tissue capsule, a continuous layer approximately 1.5 mm thick, containing abundant type I collagen fibres and some elastin fibres. The capsule has an outer and an inner lamina in which the directions of the collagen fibres differ, thereby increasing its strength. Numerous trabeculae extend from the capsule into the substance of the spleen, where they branch to form a supportive framework. The largest trabeculae enter at the hilum and provide a conduit for the splenic vessels and nerves, dividing into branches in the splenic pulp (Figs 71.6 and 71.7). Within the spleen, these branches become continuous with a delicate network of type III (reticular) collagen fibres that pervades both red and white pulps and is secreted by fibroblasts within its meshes.

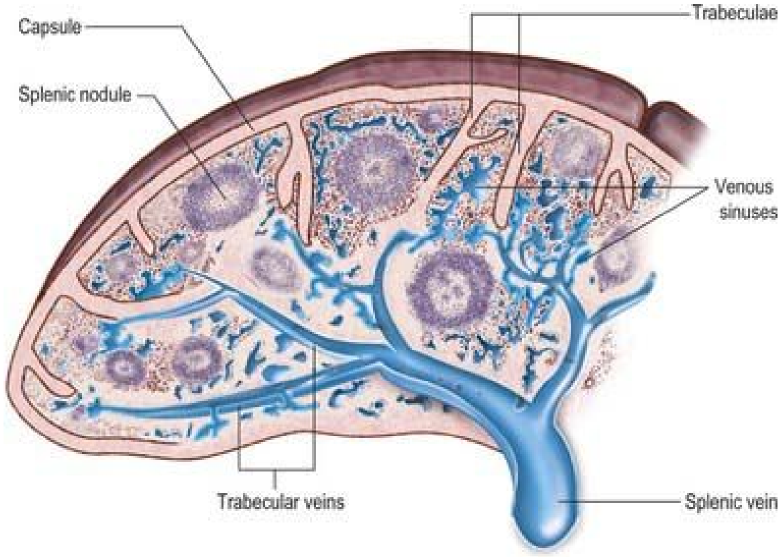

Fig. 71.7 Transverse section through the spleen, showing the trabecular tissue and the splenic vein and its tributaries.

White pulp

In the spleen parenchyma, branches of the splenic artery radiate out from the hilum within trabeculae, ramifying and narrowing to arterioles. In their terminal few millimetres, their connective tissue adventitia is replaced by a sheath of T-lymphocytes, the periarteriolar lymphatic sheath (PALS). This sheath is enlarged in places by lymphoid follicles, which are aggregations of B-lymphocytes, 0.25–1 mm in diameter and visible to the naked eye on the freshly cut spleen surface as white semi-opaque dots: they contrast with the surrounding deep reddish-purple of the red pulp. Follicles are usually situated near the terminal branches of arterioles and typically protrude to one side of a vessel, which consequently appears eccentrically placed within the follicle. Arterioles branch laterally within follicles to form a series of parallel terminal arterioles, called penicilli, or penicillar arterioles, from their resemblance to the penicillium mould.

Like the periarteriolar sheaths, follicles are centres of lymphocyte proliferation as well as aggregation, and when antigenically stimulated, the white pulp increases in size as lymphocytes proliferate. The primary follicles become intensely active in B-cell proliferation, and they develop germinal centres similar to those found in lymph nodes: the presentation of antigen by follicular dendritic cells is involved in this process. The germinal centres regress when the infection subsides. Follicles generally atrophy with increasing age and may be absent in the very elderly.

Red pulp

The red pulp constitutes the majority (75%) of the total splenic volume. It contains large numbers of venous sinusoids that ultimately drain into tributaries of the major splenic veins. The sinusoids are separated from each other by a fibrocellular network consisting of small bundles of delicate collagen type III fibres, the reticulum, and numerous reticular fibroblasts and splenic macrophages. Seen in two-dimensional sections, these intersinusoidal regions appear as strips of tissue, the splenic cords, which alternate with splenic sinuses (Fig. 71.6). In reality, they form a three-dimensional continuum around the venous spaces.

Venous sinusoids

Venous sinusoids are elongated ovoid vessels approximately 50 μm in diameter, lined by a characteristic, ‘incomplete’ endothelium that is unique to the spleen. Their endothelial cells are long and narrow, and aligned with the long axis of the sinusoid; they are often called stave cells, because they are reminiscent of planks in a barrel (Fig. 71.6). Stave cells are attached to their neighbours at intervals along their length by short stretches of intercellular junctions. These junctions alternate with intercellular slits which allow blood cells to squeeze into the lumen of the sinusoid from the surrounding splenic cords. A discontinuous basal lamina is present on the abluminal aspect of the sinus. The sinusoids are supported externally by circumferentially and longitudinally disposed reticular fibres, which are components of the fibrous reticulum.

Reticular tissue of the splenic cords

Large, stellate fibroblasts called reticular cells lie around the sinusoids. They synthesis the matrix components of the reticulum, including collagen and proteoglycans, and their cytoplasmic processes compartmentalize the reticular space. Blood is released from the ends of capillaries originating from penicillar arterioles and percolates through the reticular spaces within the splenic cords. As it does so, macrophages within the reticulum remove blood-borne particulate material, including ageing and damaged erythrocytes. When numbers of damaged erythrocytes increase, the reticular cells proliferate and the size of the red pulp increases considerably: this causes enlargement of the whole spleen, and in extreme cases, splenomegaly.

Marginal zone

The marginal zone lies at the interface between the white and red pulp. It is a region of great functional importance because it is where blood is delivered into the red pulp, and where many lymphocytes leave the circulation to migrate into their respective T- and B-lymphocyte areas in the white pulp. The lymphocytes are more loosely arranged than they are in the white pulp, and are held in a dense network of reticular fibres and cells. The arterioles leaving the white pulp are surrounded by a small aggregation of macrophages, the periarteriolar macrophage sheath.

Splenic microcirculation

The segmental splenic arteries enter the hilum and ramify in the trabeculae throughout the organ. The splenic vein forms in the splenorenal ligament from tributaries emerging from the hilum; they are similar in number to the arterial branches. Small arteries tapering to arterioles pass through the white pulp then turn abruptly to form penicillar branches which, after a course of approximately 0.5 mm, pass out of the white pulp into the marginal zone and red pulp. The passage of blood through the vascular compartments between the arterioles and splenic veins is referred to collectively as the intermediate circulation of the spleen. Ultimately, blood is passed to the venous sinusoids from which it enters venules leading to small veins that run within trabeculae, and thence into larger veins that drain the spleen at its hilum

Open and closed splenic circulations

Views on the intermediate circulation of the spleen differ on whether blood passes from the arterioles (or their terminal capillaries) directly into the venous sinuses (a closed circulation), or is instead discharged into a network of spaces in the splenic cords before entering the sinuses through the minute slits in their walls (an open circulation). In humans, evidence favours the presence of an anatomically and physiologically open circulation, in which blood percolates slowly through the reticular tissue of the splenic cords and filters through slits in the sinus walls before joining the majority of the blood flow (see Fig. 71.6). There is thought to be an additional closed vascular route, but this is likely to provide only a minor contribution to splenic circulation.

REFERENCES

eilly FD. Innervation and vascular pharmacodynamics of the mammalian spleen. *Experientia*. 1985;41:187-192.

CHAPTER 72

Suprarenal (adrenal) gland

The suprarenal (adrenal) glands lie immediately superior and slightly anterior to the upper pole of either kidney (see Fig. 74.5A,B). Golden yellow in colour, each gland possesses two functionally and structurally distinct areas, an outer cortex and an inner medulla. The glands are surrounded by connective tissue containing perinephric fat, enclosed within the renal fascia, and separated from the kidneys by a small amount of fibrous tissue.

The dimensions of the suprarenal glands in adults *in vivo* have been defined by Vincent and colleagues (1994) using computed tomography (CT). The mean transverse dimensions of the body of the suprarenal gland are 61 mm (right) and 79 mm (left) and the mean transverse dimensions of suprarenal limbs are 28 mm (right) and 33 mm (left). No individual suprarenal limb should measure more than 6.5 mm in transverse section. The suprarenal glands each weigh approximately 5 g (the medulla contributes about one-tenth of the total weight).

The glands are macroscopically slightly different in external appearance (Fig. 72.1). The right gland is pyramidal in shape and has two well developed lower projections (limbs) giving a cross-sectional appearance similar to a broad-headed arrow. The left gland has a more semilunar form and is flattened in the anteroposterior plane. The left gland is marginally larger than the right. The bulk of the right suprarenal sits on the apex of the right kidney and usually lies slightly higher than the left gland, which sits on the anteromedial aspect of the upper pole of the left kidney.

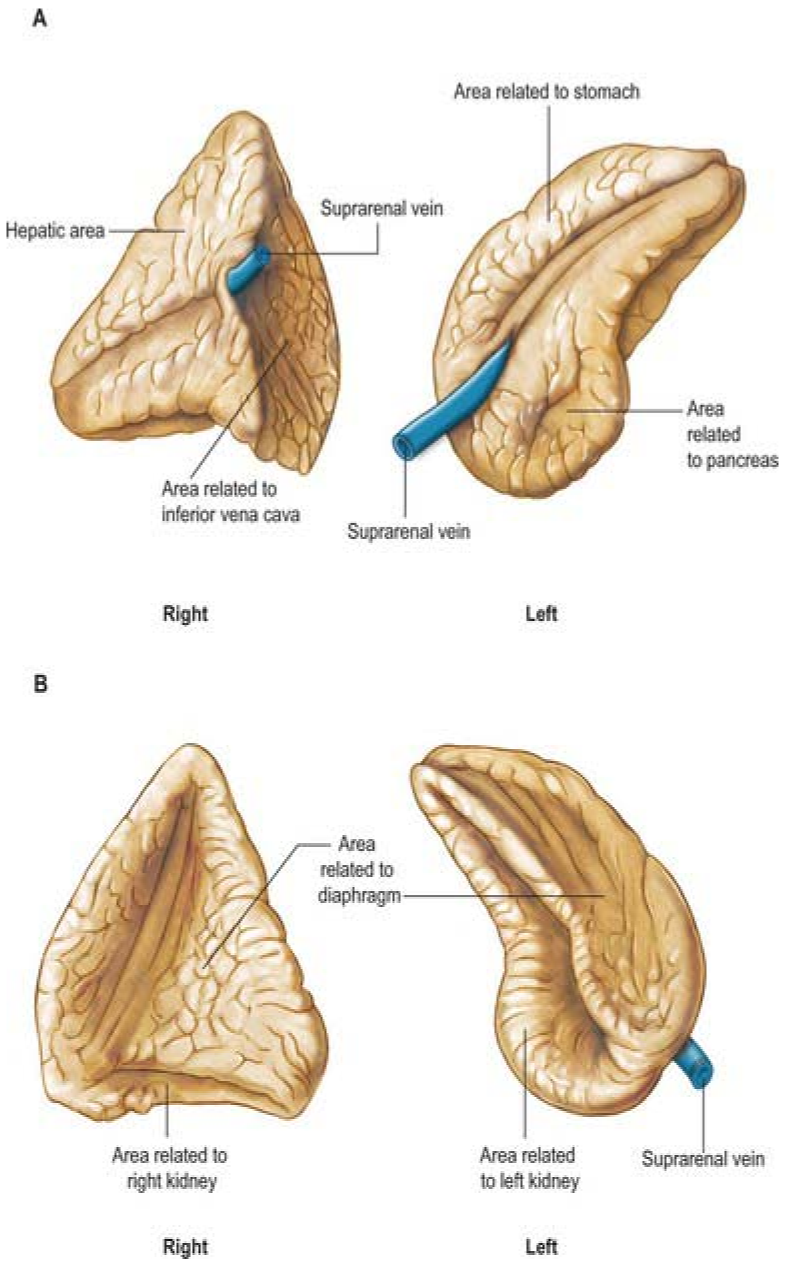
A
Area related to stomach
Hepatic area
Suprarenal vein
Area related to inferior vena cava
Suprarenal vein
Area related to pancreas
Right
Left
B
Area related to diaphragm
Area related to right kidney
Area related to left kidney
Suprarenal vein
Right
Left

Fig. 72.1 Suprarenal glands: anterior (**A**) and posterior (**B**) aspects.

At birth the glands are proportionately larger and are approximately one-third the size of the ipsilateral kidney. The cortex of each gland reduces in size immediately after birth and the medulla grows comparatively little. By the end of the second month the weight of the suprarenal has reduced by 50%. The glands begin to grow by the end of the second year and regain their weight at birth by puberty. There is little further weight increase in adult life.

Small accessory suprarenal glands, composed mainly of cortical tissue, may occur in the areolar tissue near the main suprarenal glands. Accessory glands, termed cortical bodies, may also occur in the spermatic cord, epididymis and broad ligament of the uterus.

RIGHT SUPRARENAL GLAND

The right suprarenal gland lies posterior to the inferior vena cava, from which it is only separated by a thin layer of fascia and connective tissue. It lies posterior to the right lobe of the liver and anterior to the right crus of the diaphragm and superior pole of the right kidney (Fig. 72.2). Its inferior surface is referred to as the base and adjoins the anterosuperior aspect of the superior pole of the right kidney. It often overlaps the apex of the upper pole of the right kidney as the two lower projections (limbs) straddle the renal tissue. The anterior surface faces slightly laterally and possesses two distinct facets. The medial facet is somewhat narrow, runs vertically and lies posterior to the inferior vena cava. The lateral facet is triangular and lies in contact with the bare area of the liver. The lowest part of the anterior surface may be covered by peritoneum, reflected onto it from the inferior layer of the coronary ligament. At this point it may lie posterior to the lateral border of the second part of the duodenum. Below the apex, near the anterior border of the gland, the hilum lies in a short sulcus from which the right suprarenal vein emerges to join the inferior vena cava. This vein is particularly short, which makes surgical resection of the gland potentially hazardous, because ligation may be difficult. The vein may be avulsed from the inferior vena cava during surgery or occasionally by high-energy deceleration injuries. The posterior surface is divided into upper and lower areas by a curved transverse ridge. The large upper area is slightly convex and rests on the diaphragm. The small lower area is concave and lies in contact with the superior aspect of the upper pole of the right kidney. The medial border of the gland is thin and lies lateral to the right coeliac ganglion and the right inferior phrenic artery as the artery runs over the right crus of the diaphragm.

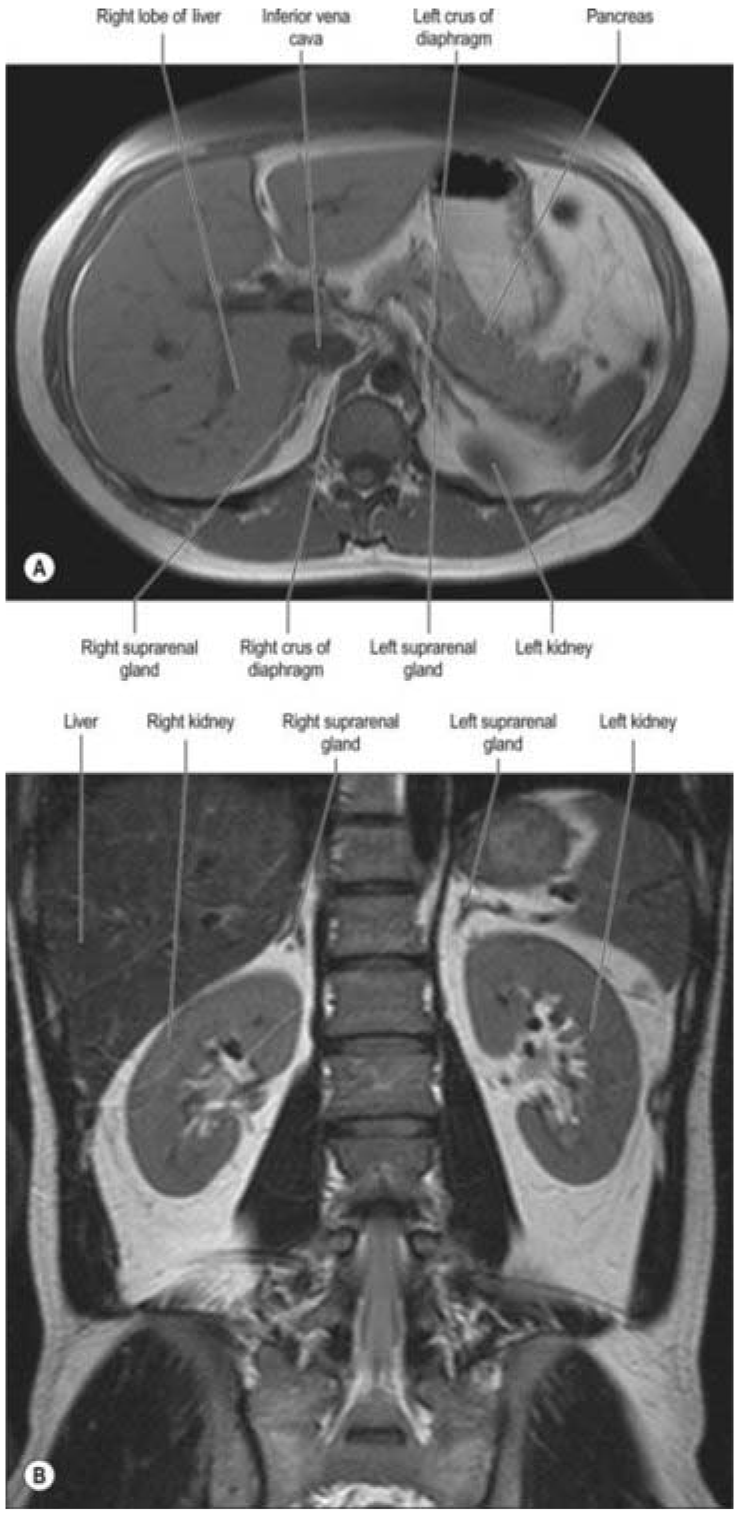
Right lobe of liver
Inferior vena cava
Left crus of diaphragm
Pancreas
A
Right suprarenal gland
Right crus of diaphragm
Left suprarenal gland
Left kidney
Liver
Right kidney
Right suprarenal gland
Left suprarenal gland
Left kidney
B

Fig. 72.2 **A**, Axial T1 weighted and **B**, Coronal T2 weighted MRI of the suprarenal glands. (Supplied by Dr Louise Moore, Chelsea & Westminster Hospital.)

LEFT SUPRARENAL GLAND

The left suprarenal gland lies closely applied to the left crus of the diaphragm and is separated from it only by a thin layer of fascia and connective tissue (Fig. 72.2). The medial aspect is convex whilst the lateral aspect is concave since it is shaped by the medial side of the superior pole of the left kidney. The superior border is sharply defined while the inferior surface is more rounded. The anterior surface has a large superior area covered by peritoneum on the posterior wall of the lesser sac, which separates it from the cardia of the stomach and sometimes from the posterior aspect of the spleen. The smaller inferior area is not covered by peritoneum and lies in contact with the pancreas and splenic artery. The hilum faces inferiorly from the medial aspect and is near the lower part of the anterior surface. The left suprarenal vein emerges from the hilum and runs inferomedially to join the left renal vein. The posterior surface is divided by a ridge into a lateral area adjoining the kidney and a smaller medial area which lies in contact with the left crus of the diaphragm. The convex medial border lies lateral to the left coeliac ganglion, and the left inferior phrenic and left gastric arteries, which ascend on the left crus of the diaphragm.

VASCULAR SUPPLY AND LYMPHATIC DRAINAGE

Arteries

The suprarenal glands have an extensive vascular supply in relation to their size. Each gland is supplied by superior, middle and inferior suprarenal arteries, whose main branches may be duplicated or even multiple (Fig. 72.3). They ramify over the capsule before entering the gland to form a subcapsular plexus, from which fenestrated sinusoids pass around clustered glomerulosal cells and between columns in the zona fasciculata to a deep plexus in the zona reticularis. Venules from this plexus pass between medullary chromaffin cells to medullary veins, which they enter between prominent bundles of smooth muscle fibres. Some relatively large arteries bypass this indirect route and pass directly to the medulla (Fig. 72.4). At operation the arteries are rarely obvious, but the veins deserve specific attention (see below).

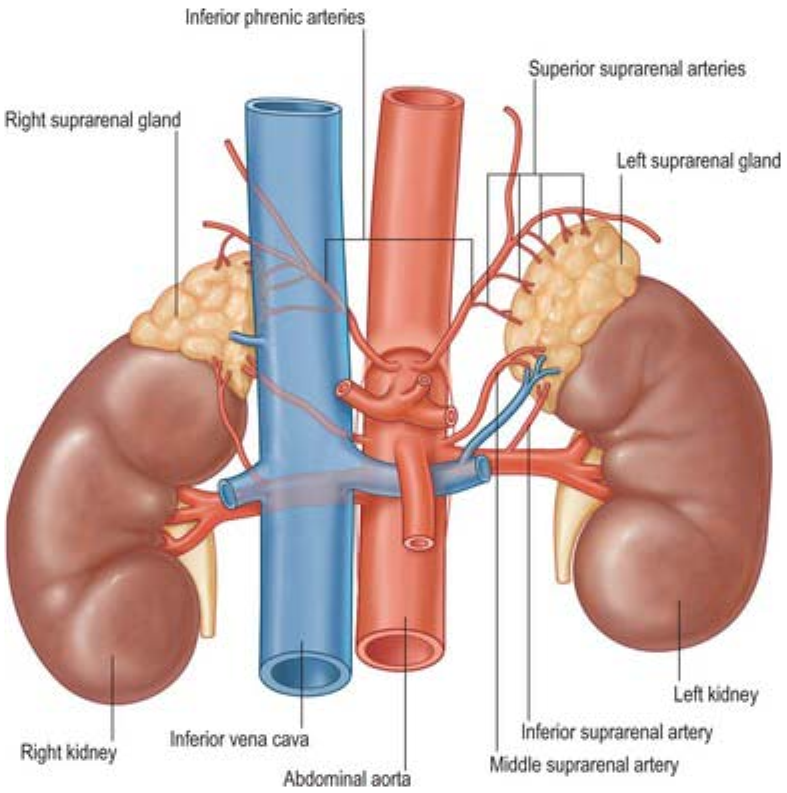
Inferior phrenic arteries
Superior suprarenal arteries
Right suprarenal gland
Left suprarenal gland
Left kidney
Inferior suprarenal artery
Right kidney
Inferior vena cava
Middle suprarenal artery
Abdominal aorta

Fig. 72.3 Arterial supply and venous drainage of the suprarenal glands.

(From Drake, Vogl and Mitchell 2005.)

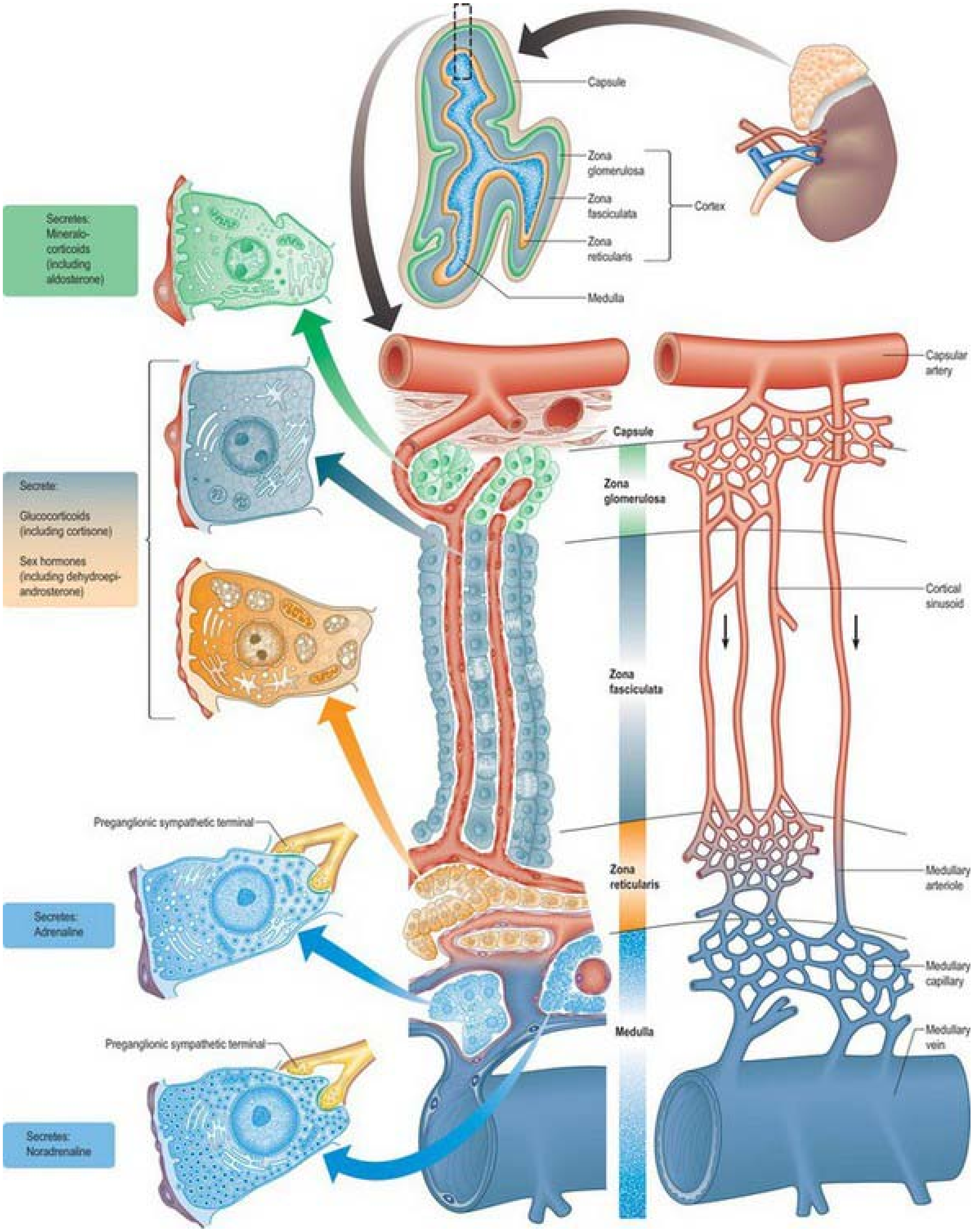
Capsule
Zona glomerulosa
Zona fasciculata
Zona reticularis
Cortex
Medulla
Secretes: Mineralo-corticoids (including aldosterone)
Secrete:
Glucocorticoids (including cortisone)
Sex hormones (including dehydroepi-androsterone)
Capsular artery
Capsule
Zona glomerulosa
Zona fasciculata
Cortical sinusoid
Preganglionic sympathetic terminal
Zona reticularis
Medullary arteriole
Secretes: Adrenaline
Medullary capillary
Medulla
Medullary vein
Preganglionic sympathetic terminal
Secretes: Noradrenaline

Fig. 72.4 The gross sectional appearance, microstructure, vasculature and ultrastructure of the suprarenal gland. Brief functional summaries are included.

Superior suprarenal arteries

The superior suprarenal artery arises from the inferior phrenic artery, a branch of the abdominal aorta: it is often small and may be absent.

Middle suprarenal arteries

The middle suprarenal artery arises from the lateral aspect of the abdominal aorta at the level of the superior mesenteric artery. It ascends slightly and runs over the crura of the diaphragm to the suprarenal glands, where it anastomoses with the suprarenal branches of the inferior phrenic and renal arteries. The right middle suprarenal artery passes behind the inferior vena cava and near the right coeliac ganglion and is frequently multiple. The left middle suprarenal artery passes close to the left coeliac ganglion, splenic artery and the superior border of the pancreas.

Inferior suprarenal arteries

The inferior suprarenal arteries arise from the renal arteries, usually from the main renal artery but occasionally from its upper pole branches.

Veins

Medullary veins emerge from the hilum to form a suprarenal vein, which is usually single. The right vein is very short, passing directly and horizontally into the posterior aspect of the inferior vena cava. An accessory vein is occasionally present and runs from the hilum superomedially to join the inferior vena cava above the right suprarenal vein. Their short course renders both right vessels liable to injury or even avulsion from the inferior vena cava during surgery if undue traction is applied, producing a side hole in the cava. The left suprarenal vein descends medially, anterior and lateral to the left coeliac ganglion. It passes posterior to the pancreatic body and drains into the left renal vein. Since the venous drainage from each gland is usually via a single vein, infarction of that gland is more likely to be caused by damage to a suprarenal vein than to one of the suprarenal arteries.

Lymphatic drainage

Small lymphatic channels from both cortex and medulla drain to the hilum, from where larger calibre lymphatics emerge to drain directly into the lateral groups of para-aortic nodes.

INNERVATION: SUPRARENAL PLEXUS

The suprarenal gland, relative to its size, has a larger autonomic supply than any other organ. On each side, the suprarenal plexus lies between the medial aspect of the gland and the coeliac and aorticorenal ganglia. It contains mostly preganglionic sympathetic fibres, which originate in the lower thoracic spinal segments and which reach the plexus via branches from the coeliac ganglion and plexus, and via the greater splanchnic nerve. These fibres synapse, often in deep invaginations, on large medullary chromaffin cells, which may therefore be considered to be homologous with postganglionic sympathetic neurones. A preponderance of non-myelinated axons has been described in the human suprarenal plexus. Both cortex and medulla also contain acetylcholinesterase (AChE)-positive axons that presumably reach the gland from the coeliac plexus: some synapse with ganglion cells in the zonae fasciculata and reticularis.

MICROSTRUCTURE

In section, the suprarenal gland has an outer cortex, which is yellowish in colour and forms the main mass, and a thin medulla, forming about one-tenth of the gland, which is dark red or greyish, depending on its content of blood (see Figs 72.4, 72.5). The medulla is completely enclosed by cortex, except at the hilum. The gland has a thick collagenous capsule from which trabeculae extend deep into the cortex. The capsule contains a rich arterial plexus which supplies branches to the gland.

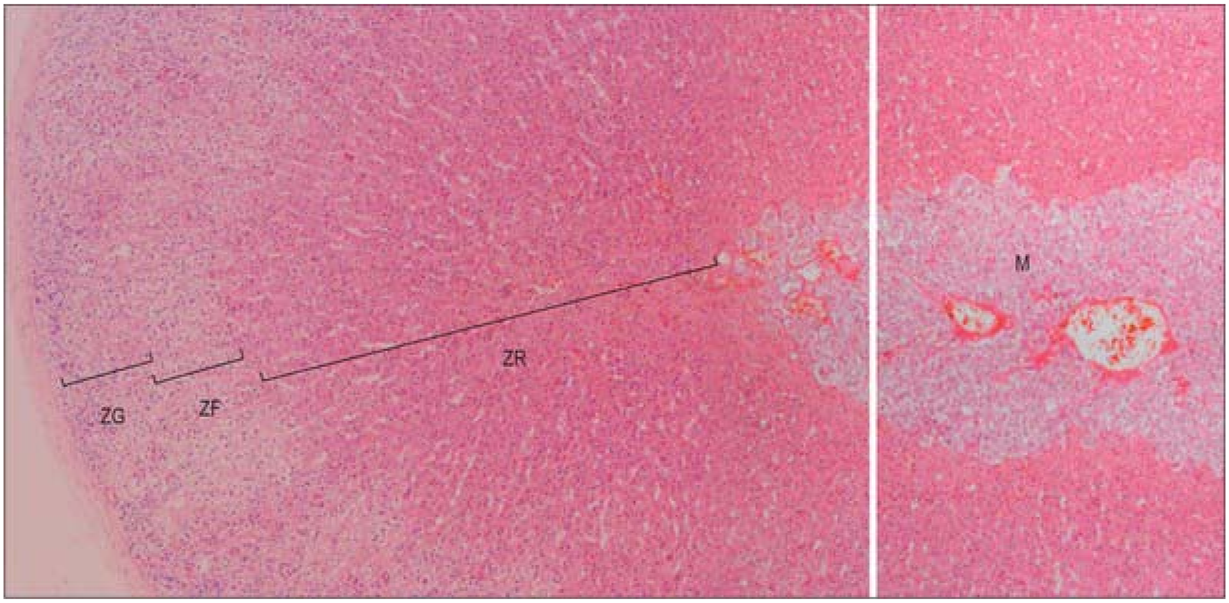

Fig. 72.5 Cross section through an adult suprarenal gland showing the zona granulosa (ZG), zona fasciculata (ZF), zona reticularis (ZR), and the highly vascular medulla (M).

(By courtesy of Mr Peter Helliwell and Dr Joseph Mathew, Department of Histopathology, Royal Cornwall Hospitals Trust, UK.)

Suprarenal cortex

The suprarenal cortex consists of the zona glomerulosa, zona fasciculata and zona reticularis (Figs 72.4, 72.5). The outer subcapsular zona glomerulosa consists of a narrow region of small polyhedral cells in rounded clusters. The cells have deeply staining nuclei and a basophilic cytoplasm containing a few lipid droplets. Ultrastructurally, the cytoplasm displays abundant smooth endoplasmic reticulum, a feature typical of cells that synthesize steroids. The broader intermediate zona fasciculata consists of large polyhedral basophilic cells arranged in straight columns, two cells wide, with parallel fenestrated venous sinusoids between them. The cells contain many lipid droplets and large amounts of smooth endoplasmic reticulum. The innermost part of the cortex, the zona reticularis, consists of branching interconnected columns of rounded cells whose cytoplasm also contains smooth endoplasmic reticulum, many lysosomes and aggregates of brown lipofuscin pigment that accumulate with age.

Cortical cells produce several hormones and the cells of the zonae fasciculata and reticularis are also rich in ascorbic acid. Cells in the zona glomerulosa produce mineralocorticoids, e.g. aldosterone, which regulates electrolyte and water balance; cells in the zona fasciculata produce hormones maintaining carbohydrate balance (glucocorticoids) e.g. cortisol (hydrocortisone); cells in the zona reticularis produce sex hormones (progesterone, oestrogens and androgens). The cortex is essential to life and its complete removal is lethal without replacement therapy. It exerts considerable control over lymphocytes and lymphoid tissue: an increased secretion of corticosteroids can result in a marked reduction in lymphocyte numbers.

The deeper part of the zona fasciculata widens in pregnancy and in women of childbearing age in summer. Cortical atrophy in elderly males is greatest in the same region.

Suprarenal medulla

The suprarenal medulla is composed of groups and columns of chromaffin cells (phaeochromocytes) separated by wide venous sinusoids and supported by a network of reticular fibres. Chromaffin cells, so-called from their colour reaction to dichromate fixatives, form part of the neuroendocrine system and are functionally equivalent to postganglionic sympathetic neurones. They are neural crest derivatives and synthesize, store (as granules) and release the catecholamines noradrenaline (norepinephrine) and adrenaline (epinephrine) into the venous sinusoids. Release is under preganglionic sympathetic control, mediated by the sympathetic neurones that occur either singly or in small groups in the medulla.

The majority of chromaffin cells synthesize adrenaline and store it in small granules with a dense core. Less numerous noradrenaline-secreting cells have larger granules with a dense eccentric core. Some cells synthesize both hormones. Chromogranin proteins package catecholamines within the granules, which also contain enkephalins, opiate-like proteins that may have endogenous analgesic effects in some circumstances. All of the cells are large, with large nuclei and basophilic, faintly granular cytoplasm. They form single rows along the venous sinusoids. Sympathetic axon terminals synapse with the chromaffin cells on the surfaces that face away from the sinusoids.

The sinusoids are lined by fenestrated endothelium and drain to the central medullary vein and hilar suprarenal vein. Under normal circumstances, little adrenaline or noradrenaline is released; secretion is increased in response to fear, anger or stress. Unlike the cortex, the suprarenal medulla is not essential to life.

SUPRARENAL GLAND EXCISION

Removal of one or both suprarenal glands may be performed either through ‘open surgery’ or via a laparoscopic approach. There are essentially three ‘open surgical’ methods for removing the suprarenal glands. The posterior and lateral approaches involve removal of either the eleventh or twelfth ribs. The surgeon remains in the retroperitoneal plane and accesses the gland via the perirenal fat. This approach can be performed laparoscopically, but is difficult: landmarks are not easily identified because of the surrounding fat and the ‘workspace’ is frequently small. Not surprisingly, few surgeons employ this approach.

During laparoscopic surgery the anterior, transperitoneal approach is most commonly used. The patient is placed in the lateral decubitus position. On the left side, the splenic flexure is mobilized inferiorly, revealing the kidney. The lateral phrenicocolic ligament is then fully divided, which allows the spleen to be mobilized medially exposing the splenorenal ligament. Division of the splenorenal ligament (when the patient is in the lateral decubitus position) allows the spleen to ‘drop’ medially. This exposes the plane between the splenic hilum and medial border of the left kidney, and is where the pancreatic tail is identified as it runs to the hilum of the spleen. The renal fascia is divided to expose the suprarenal gland lying over the superomedial aspect of the upper pole of the kidney. On the right side, the right triangular ligament of the liver is divided, which allows the liver to be retracted caudally. In most individuals the inferior vena cava is easily identified behind the peritoneum lateral to the second part of the duodenum. The peritoneal reflection on the inferior border of the liver is divided from the inferior vena cava to the lateral border of the liver, exposing the suprarenal gland in the angle between the inferior vena cava and liver. The peritoneal reflection along the lateral aspect of the inferior vena cava is divided and the gland is then mobilized laterally exposing the suprarenal vein, which often emerges from the posterior aspect of the inferior vena cava. Once the suprarenal vein has been divided, the small middle suprarenal arteries, which run from the aorta to the gland behind the inferior vena cava, are easily identified. The gland is then usually mobilized very easily in a lateral direction. However, it can lie either behind the inferior vena cava or under the liver, in which case dissection at the junction of the liver and inferior vena cava often becomes very difficult.

In obese (or Cushingoid) patients, identification of a relatively normal sized suprarenal gland can be extremely difficult and time consuming. The suprarenal vein emerges from the lower medial border of the gland and it is often a very substantial structure. In contrast, the supplying arteries tend to be rather smaller in size and individual arteries are often difficult to identify during surgery.

The anterior open approach follows the procedure as described above through either a subcostal or a midline incision.

REFERENCES

ncent JM, Morrison ID, Armstrong P, Reznek RH. The size of normal adrenal glands on computed tomography. *Clin Radiol*. 1994;49:453-455.

CHAPTER 73

Development of the peritoneal cavity, gastrointestinal tract and its adnexae

POSTPHARYNGEAL FOREGUT

The primitive gut is divided by head and tail folding into three main compartments. The foregut extends from the buccopharyngeal membrane to its continuation into the central midgut region via the cranial intestinal portal. The midgut extends between the intestinal portals, and in the early embryo is in wide communication with the yolk sac. The hindgut extends from the caudal intestinal portal to the cloacal membrane. The cranial end of the foregut, the embryonic pharynx, is intimately associated with head and neck development (see Ch. 35). The portion of foregut that passes dorsal to the pericardial cavity gives rise to the respiratory diverticulum and oesophagus within the thorax (see Chs 35 and 59). Caudal to the developing diaphragm, the enteric gut is conventionally subdivided into three embryological portions, fore- mid- and hindgut. There are no corresponding fundamental morphological and cytological distinctions between the three parts (Fig. 73.1), and so the foregut produces a portion of the duodenum, as does the midgut, and the midgut similarly produces large intestine, as does the hindgut. The differences between the portions of the gut develop as a result of interactions between the three embryonic tissue layers which give rise to the gut, namely the endodermal inner epithelium, the thick layer of splanchnopleuric mesenchyme, and the outer layer of proliferating splanchnopleuric coelomic epithelium.

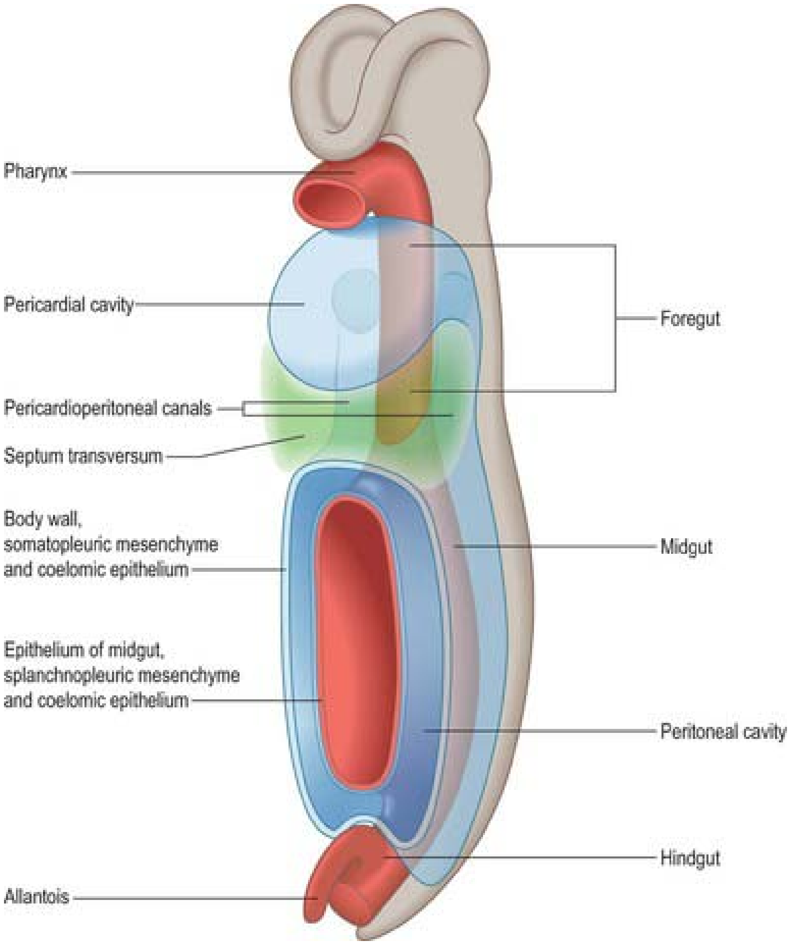
Pharynx
Pericardial cavity
Pericardioperitoneal canals
Septum transversum
Body wall, somatopleuric mesenchyme and coelomic epithelium
Epithelium of midgut, splanchnopleuric mesenchyme and coelomic epithelium
Allantois
Foregut
Midgut
Peritoneal cavity
Hindgut

Fig. 73.1 Major epithelial populations within the early embryo. The early gut tube is close to the notochord and neural tube dorsally. The splanchnopleuric layer of the intraembryonic coelomic epithelium is in contact with the foregut ventrally and laterally, with the midgut laterally and the hindgut ventrally and laterally.

The epithelial layer of the mucosa and connected ducts and glands are derived from the endodermal epithelium. The lamina propria and muscularis mucosa, the connective tissue of the submucosa, the muscularis externa and the external connective tissue are all derived from the splanchnopleuric mesenchyme. The outer peritoneal epithelium is derived from the splanchnopleuric coelomic epithelium.

Throughout the gut, blood vessels, lymphatics and lymph nodes develop from local populations of angiogenic mesenchyme. The nerves, which are distributed within the enteric and autonomic systems, are derived from the neural crest. There is a craniocaudal developmental gradient along the gut in that the stomach and small intestine develop in advance of the colon.

Figure 73.2 shows the gut in a stage 12 embryo in relation to the other developing viscera, especially the heart and liver. Figure 73.3 shows the overall development of the gut from stages 13–17. These diagrams should be compared. Figure 73.1 shows the fundamental relationship of the intraembryonic coelom to the developing gut.

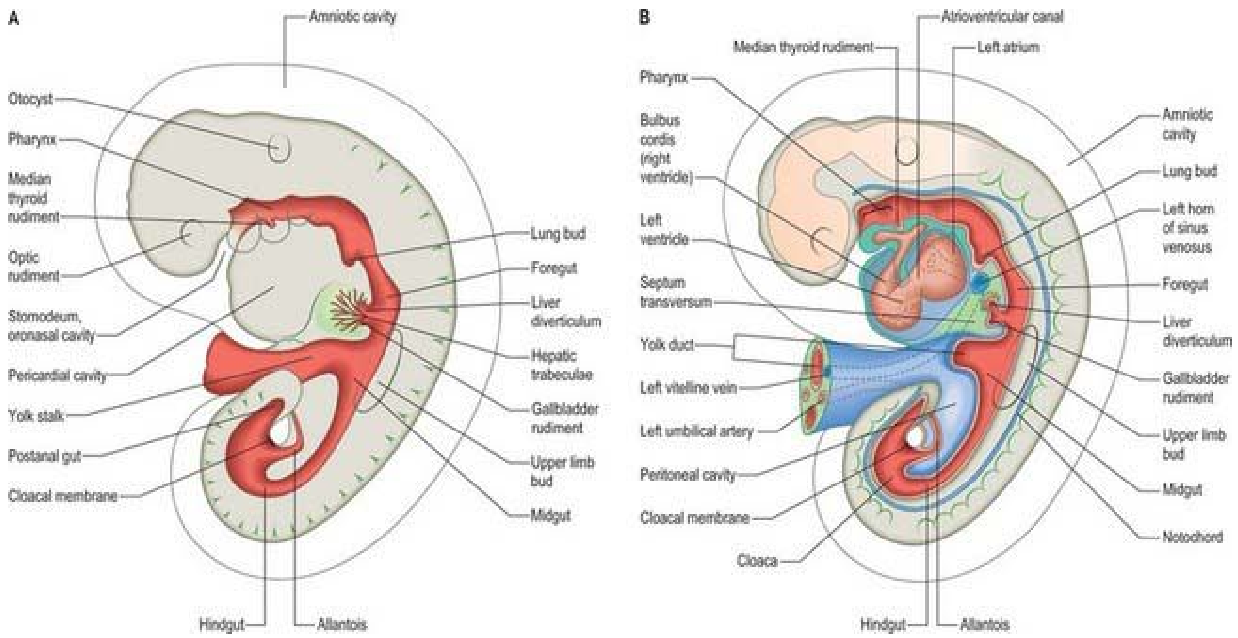
A
Amniotic cavity
Otocyst
Pharynx
Median thyroid rudiment
Optic rudiment
Stomodeum, oronasal cavity
Pericardial cavity
Yolk stalk
Postanal gut
Cloacal membrane
Lung bud
Foregut
Liver diverticulum
Hepatic trabeculae
Gallbladder rudiment
Upper limb bud
Midgut
Hindgut
Allantois
B
Atrioventricular canal
Median thyroid rudiment
Left atrium
Pharynx
Bulbus cordis (right ventricle)
Left ventricle
Septum transversum
Yolk duct
Left vitelline vein
Left umbilical artery
Peritoneal cavity
Cloacal membrane
Cloaca
Amniotic cavity
Lung bud
Left horn of sinus venosus
Foregut
Liver diverticulum
Gallbladder rudiment
Upper limb bud
Midgut
Notochord
Hindgut
Allantois

Fig. 73.2 **A**, The digestive tube of a human embryo at stage 12, with 29 paired somites, a CR length of 3.4 mm and an estimated age of 27 days. Note pharyngeal development. **B**, Reconstruction of a human embryo at the end of the fourth week. The alimentary canal and its outgrowths are shown in median section. The brain is shown in outline, but the spinal cord is omitted. The heart is shown in perspective, the left horn of the sinus venosus having been divided. The somites are indicated in outline.

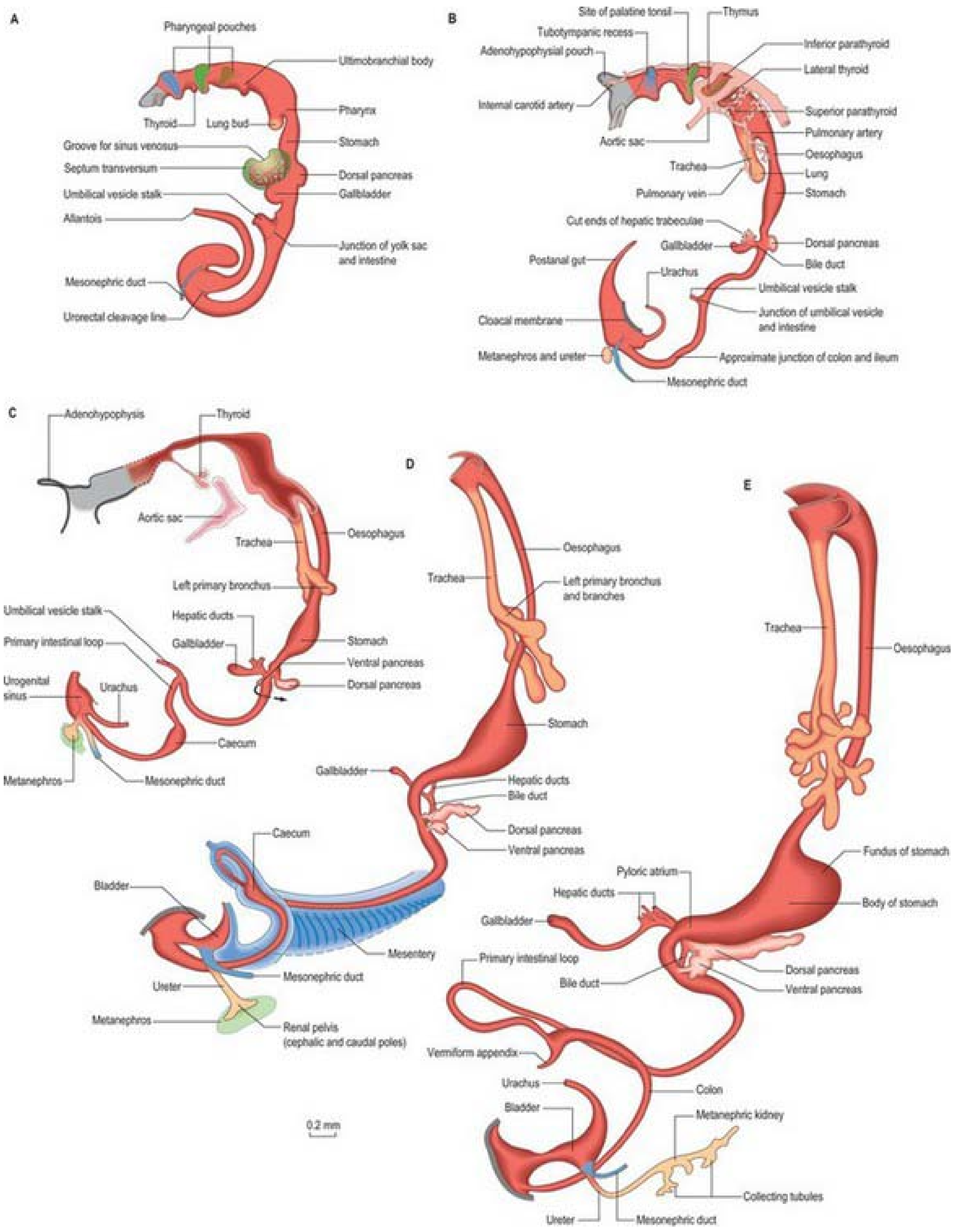
A
Pharyngeal pouches
Ultimobranchial body
Thyroid
Lung bud
Pharynx
Groove for sinus venosus
Stomach
Septum transversum
Dorsal pancreas
Umbilical vesicle stalk
Gallbladder
Allantois
Junction of yolk sac and intestine
Mesonephric duct
Urorectal cleavage line
B
Site of palatine tonsil
Thymus
Tubotympanic recess
Inferior parathyroid
Adenohypophysial pouch
Lateral thyroid
Internal carotid artery
Superior parathyroid
Pulmonary artery
Aortic sac
Oesophagus
Trachea
Lung
Pulmonary vein
Stomach
Cut ends of hepatic trabeculae
Gallbladder
Dorsal pancreas
Postanal gut
Bile duct
Urachus
Umbilical vesicle stalk
Junction of umbilical vesicle and intestine
Cloacal membrane
Metanephros and ureter
Approximate junction of colon and ileum
Mesonephric duct
C
Adenohypophysis
Thyroid
Aortic sac
Trachea
Oesophagus
Left primary bronchus
Umbilical vesicle stalk
Hepatic ducts
Primary intestinal loop
Gallbladder
Stomach
Ventral pancreas
Urogenital sinus
Urachus
Dorsal pancreas
Caecum
Metanephros
Mesonephric duct
D
Oesophagus
Trachea
Left primary bronchus and branches
Stomach
Gallbladder
Hepatic ducts
Bile duct
Dorsal pancreas
Ventral pancreas
Caecum
Bladder
Mesentery
Ureter
Mesonephric duct
Metanephros
Renal pelvis (cephalic and caudal poles)
0.2 mm
E
Trachea
Oesophagus
Fundus of stomach
Pyloric atrium
Hepatic ducts
Body of stomach
Gallbladder
Primary intestinal loop
Dorsal pancreas
Bile duct
Ventral pancreas
Vermiform appendix
Urachus
Colon
Bladder
Metanephric kidney
Collecting tubules
Ureter
Mesonephric duct

Fig. 73.3 The shape of the endodermal epithelium of the gut at succeeding stages. The scale is constant illustrating the enormous growth of the gut over a 13-day period. **A**, stage 13; **B**, stage 14; **C**, stage 15; **D**, stage 16; and **E**, stage 17. Note the separation of the respiratory diverticulum, the

elongation of the foregut and expansion of the stomach, the formation of the hepatic and pancreatic diverticula, the lengthening of the midgut loop which protrudes into the umbilical cord, and the separation of the cloaca into enteric and allantoic portions.

(Modified from O'Rahilly and Müller. Developmental Stages in Human Embryos 1987 Carnegie Institution of Washington. Pub 637.)

All regions of the gut develop from epithelial/mesenchymal interactions which are dependent on the sequential expression of a range of basic and specific genes; on the regulation of the developmental clock, seen in all areas of development; on endogenous regulatory mechanisms and local environmental influences (Lebenthal 1989). Although all these factors pertain to the whole range of developing tissues, local differences in any one of these factors along the length of the developing gut promotes the differentiation of, for example, the gastric mucosa and hepatocytes; the rotation of the midgut; and the final disposition of the sessile portions of the fully formed gastrointestinal tract. The gut is functional prior to birth and able to interact with the extrauterine environment in preterm infants.

OESOPHAGUS

The oesophagus can be distinguished from the stomach at stage 13 (embryo 5 mm). It elongates during successive stages and its absolute length increases more rapidly than the embryo as a whole. Cranially it is invested by splanchnopleuric mesenchyme posterior to the developing trachea, and more caudally between the developing lungs and pericardioperitoneal canals posterior to the pericardium. (For details of tracheo-oesophageal fistulae see p. 1037). Caudal to the pericardium, the terminal, pregastric segment of the oesophagus has a short thick dorsal meso-oesophagus (from splanchnopleuric mesenchyme), while ventrally it is enclosed in the cranial stratum of the septum transversum mesenchyme. Each of the above are continuous caudally with their respective primitive dorsal and ventral mesogastria. Thus the oesophagus has only limited areas related to a primary coelomic epithelium. However, note the subsequent development of the para-oesophageal right and left pneumatoenteric recesses (see Fig. 73.7), the relation of the ventral aspect of the middle third of the oesophagus to the oblique sinus of the pericardium, and the relation of its lateral walls in the lower thorax to the mediastinal pleura. All the foregoing are secondary extensions from the primary coelom.

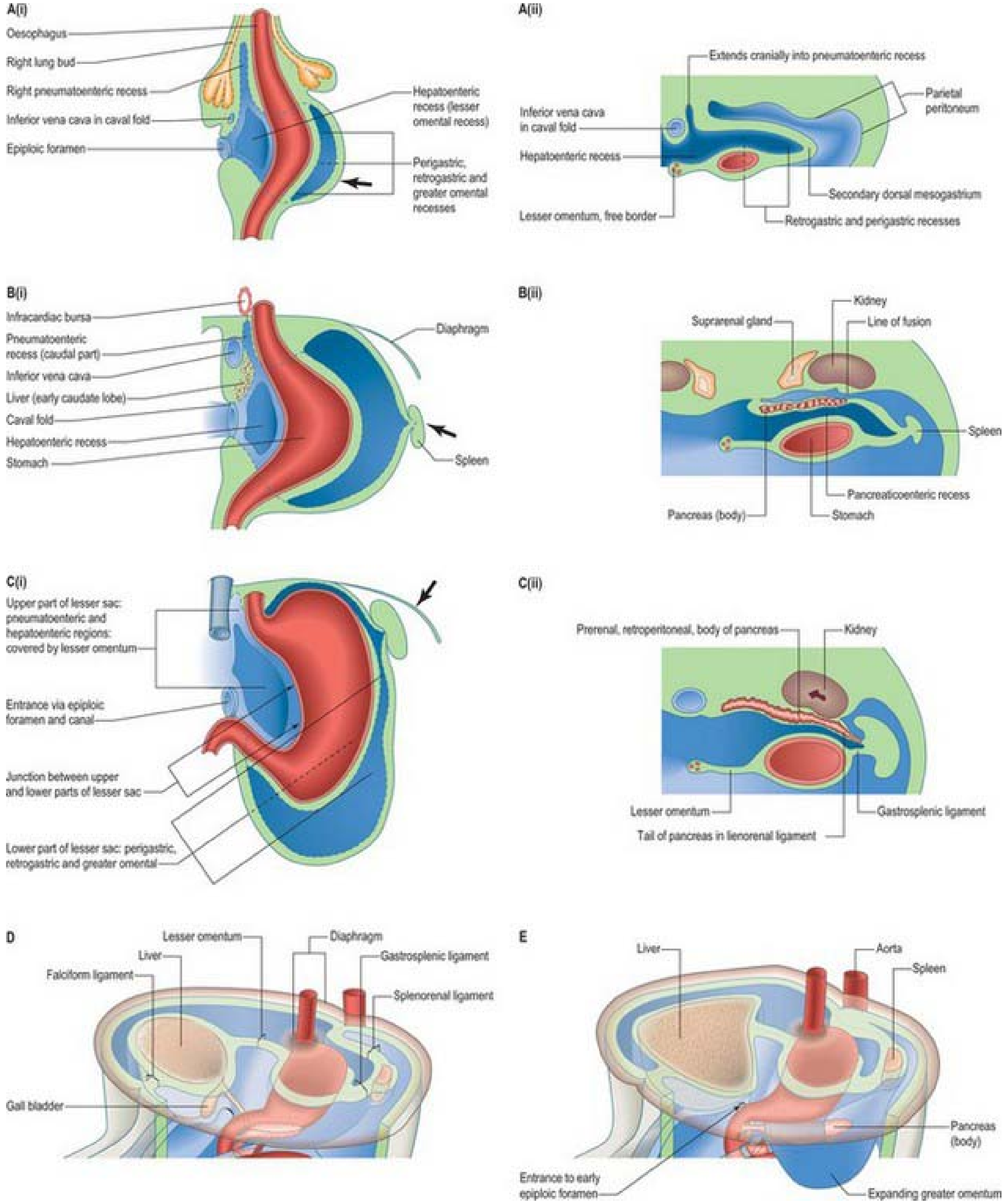
A(i)
Oesophagus
Right lung bud
Right pneumatoenteric recess
Inferior vena cava in caval fold
Epiploic foramen
Hepatoenteric recess (lesser omental recess)
Perigastric, retrogastric and greater omental recesses
A(ii)
Extends cranially into pneumatoenteric recess
Parietal peritoneum
Inferior vena cava in caval fold
Hepatoenteric recess
Secondary dorsal mesogastrium
Lesser omentum, free border
Retrogastric and perigastric recesses
B(i)
Infracardiac bursa
Pneumatoenteric recess (caudal part)
Inferior vena cava
Liver (early caudate lobe)
Caval fold
Hepatoenteric recess
Stomach
Diaphragm
Spleen
B(ii)
Kidney
Suprarenal gland
Line of fusion
Spleen
Pancreaticoenteric recess
Pancreas (body)
Stomach
C(i)
Upper part of lesser sac: pneumatoenteric and hepatoenteric regions: covered by lesser omentum
Entrance via epiploic foramen and canal
Junction between upper and lower parts of lesser sac
Lower part of lesser sac: perigastric, retrogastric and greater omental
C(ii)
Prerenal, retroperitoneal, body of pancreas
Kidney
Lesser omentum
Gastrosplenic ligament
Tail of pancreas in lienorenal ligament
D
Lesser omentum
Liver
Falciform ligament
Diaphragm
Gastrosplenic ligament
Splenorenal ligament
Gall bladder
E
Liver
Aorta
Spleen
Pancreas (body)
Entrance to early epiploic foramen
Expanding greater omentum

Fig. 73.7 **A–C**, Stages of development of the subdiaphragmatic foregut and the right and left pericardioperitoneal/pleuroperitoneal canals, with particular reference to the terminal oesophagus, stomach, duodenum, spleen, the lesser sac of peritoneum and omenta: seen in semicoronal

section (left column) and transverse section at the levels indicated by the arrows (right column). **D**, **E**, Three dimensional schematization of the lesser sac, dorsal and ventral mesogastria.

The oesophageal mucosa consists of two layers of cells by stage 15 (week 5), but the proliferation of the mucosa does not occlude the lumen at any time. The mucosa becomes ciliated at 10 weeks, and stratified squamous epithelium is present at the end of the 5th month: occasionally patches of ciliated epithelium may be present at birth. Circular muscle can be seen at stage 15 but longitudinal muscle has not been identified until stage 21. Neuroblasts can be demonstrated in the early stages; the myenteric plexuses have cholinesterase activity by 9.5 weeks and ganglion cells are differentiated by 13 weeks. It has been suggested that the oesophagus is capable of peristalsis in the first trimester. Oesophageal atresia is one of the more common obstructive conditions of the alimentary tract: fetuses swallow amniotic fluid, and so the condition may be indicated by polyhydramnios.

Oesophagus at birth

At birth the oesophagus extends 8–10 cm from the cricoid cartilage to the gastric cardiac orifice. It starts and ends one to two vertebrae higher than in the adult, extending from between the fourth to the sixth cervical vertebra to the level of the ninth thoracic vertebra (see Fig. 14.5). Its average diameter is 5 mm and it possesses the constrictions seen in the adult. The narrowest constriction is at its junction with the pharynx, where the inferior pharyngeal constrictor muscle functions to constrict the lumen: this region may be easily traumatized with instruments or catheters. In the neonate the mucosa may contain scattered areas of ciliated columnar epithelium, but these disappear soon after birth. Peristalsis along the oesophagus and at the lower oesophageal sphincter is immature at birth and results in frequent regurgitation of food in the newborn period. The pressure at the lower oesophageal sphincter approaches that of the adult at 3–6 weeks of age.

STOMACH

At the end of the fourth and beginning of the fifth week the stomach can be recognized as a fusiform dilation cranial to the wide opening of the midgut into the yolk sac (Figs 73.2 and 73.3). By the fifth week this opening has narrowed into a tubular vitelline intestinal duct, which soon loses its connection with the digestive tube. At this time the stomach is median in position and separated cranially from the pericardium by the septum transversum (see Fig. 73.5A), which extends caudally on to the cranial side of the vitelline intestinal duct and ventrally to the somatopleure. Dorsally, the stomach is related to the aorta and, reflecting the presence of the pleuroperitoneal canals on each side, is connected to the body wall by a short dorsal mesentery, the dorsal mesogastrium (see Fig. 73.6). The latter is directly continuous with the dorsal mesentery (mesenteron) of almost all of the remainder of the intestine, except its caudal short segment.

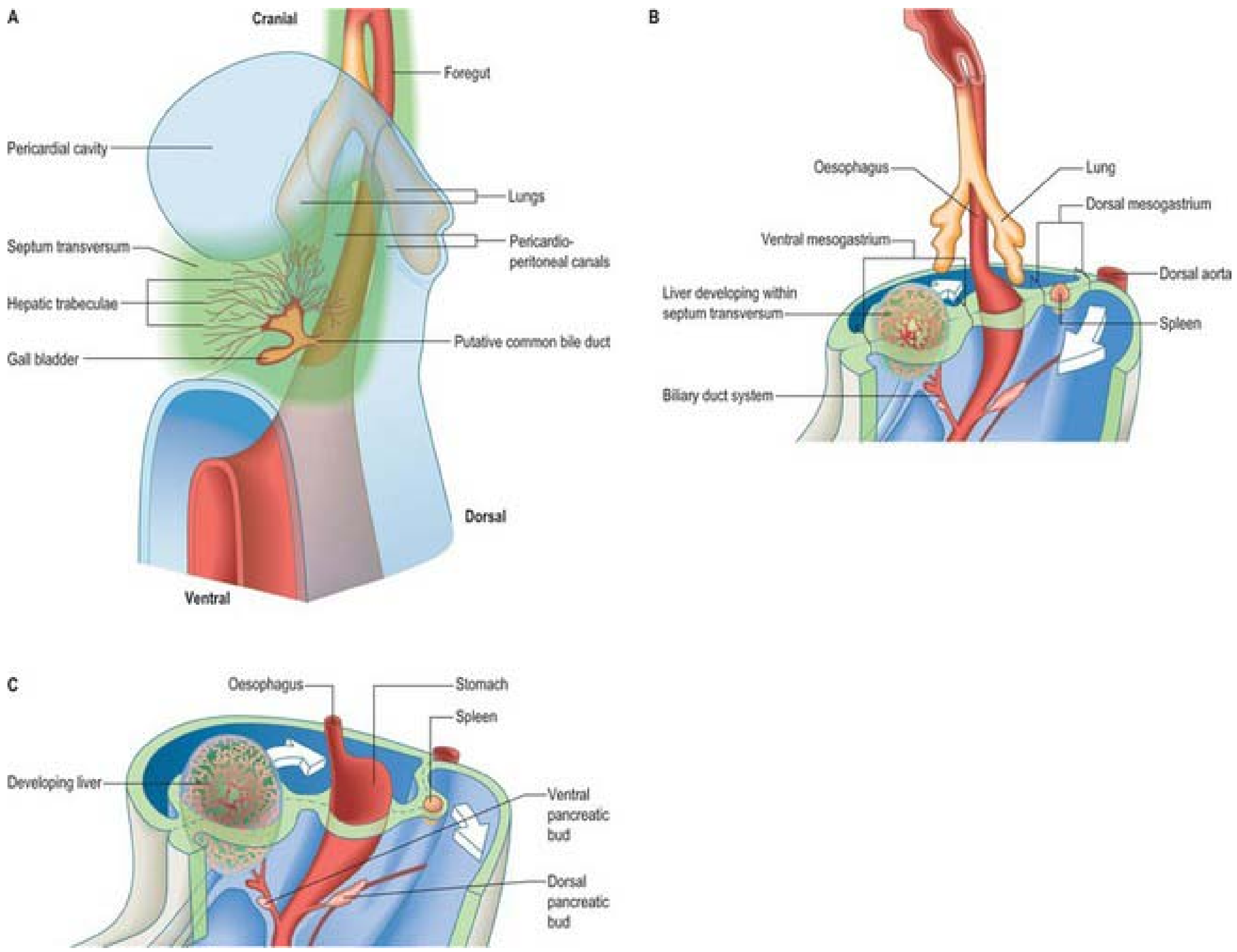
A
Cranial
Foregut
Pericardial cavity
Lungs
Pericardio-
peritoneal canals
Septum transversum
Hepatic trabeculae
Gall bladder
Putative common bile duct
Dorsal
Ventral
B
Oesophagus
Lung
Dorsal mesogastrium
Ventral mesogastrium
Dorsal aorta
Liver developing within
septum transversum
Spleen
Biliary duct system
C
Oesophagus
Stomach
Spleen
Developing liver
Ventral
pancreatic
bud
Dorsal
pancreatic
bud

Fig. 73.5 Early development of the liver and the supra-umbilical peritoneal cavities. **A**, The hepatic endodermal primordium proliferates ventrally into the septum transversum mesenchyme. The endodermal cells forming the hepatic trabeculae will become hepatocytes; the septum transversum mesenchymal cells will become the endothelium of the liver sinusoids and early blood cells. The developing lung buds can be seen expanding into the pericardioperitoneal cavities. **B**, The septum transversum mesenchyme and the stomach become enclosed by the right and left pericardioperitoneal canals (shown on transverse section). The apposition of the medial pericardioperitoneal walls form the dorsal and ventral mesogastria. The proximity of the lung buds to the developing stomach can be seen. The pleural and supra-umbilical peritoneal cavities are transiently, and bilaterally, symmetrical above the umbilicus. **C**, The lower border of the ventral mesogastrium denotes the connection between the supra-umbilical peritoneal cavities (pleuro-peritoneal canals) can be identified by the position of the ventral pancreatic bud and common bile duct. White arrows indicate the direction of movement of the dorsal and ventral mesogastria.

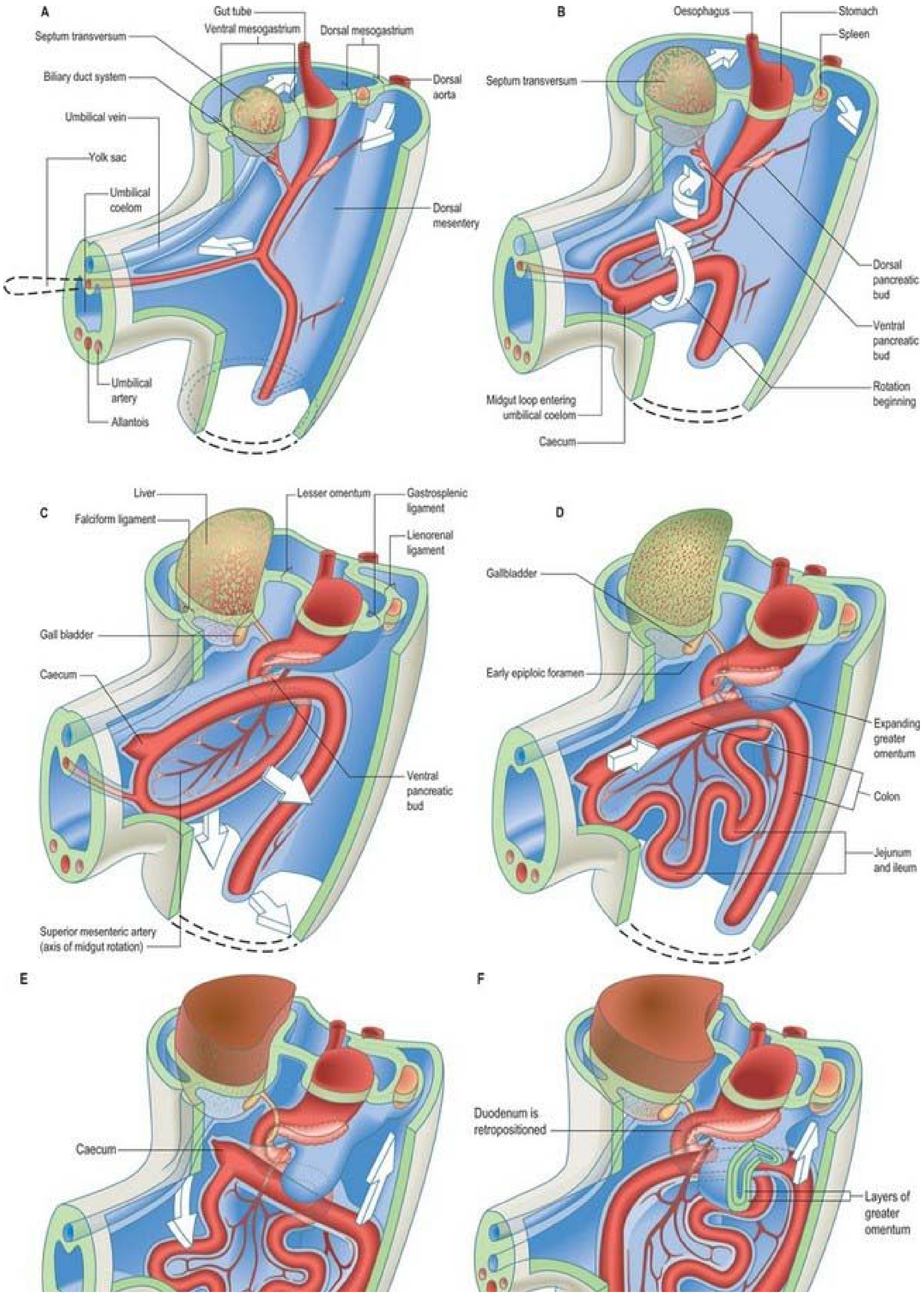
A
Gut tube
Ventral mesogastrium
Dorsal mesogastrium
Septum transversum
Biliary duct system
Dorsal aorta
Umbilical vein
Yolk sac
Umbilical coelom
Dorsal mesentery
Umbilical artery
Allantois
B
Oesophagus
Stomach
Spleen
Septum transversum
Dorsal pancreatic bud
Ventral pancreatic bud
Rotation beginning
Midgut loop entering umbilical coelom
Caecum
C
Liver
Falciform ligament
Lesser omentum
Gastrosplenic ligament
Lienorenal ligament
Gall bladder
Caecum
Ventral pancreatic bud
Superior mesenteric artery (axis of midgut rotation)
D
Gallbladder
Early epiploic foramen
Expanding greater omentum
Colon
Jejunum and ileum
E
Caecum
F
Duodenum is retropositioned
Layers of greater omentum

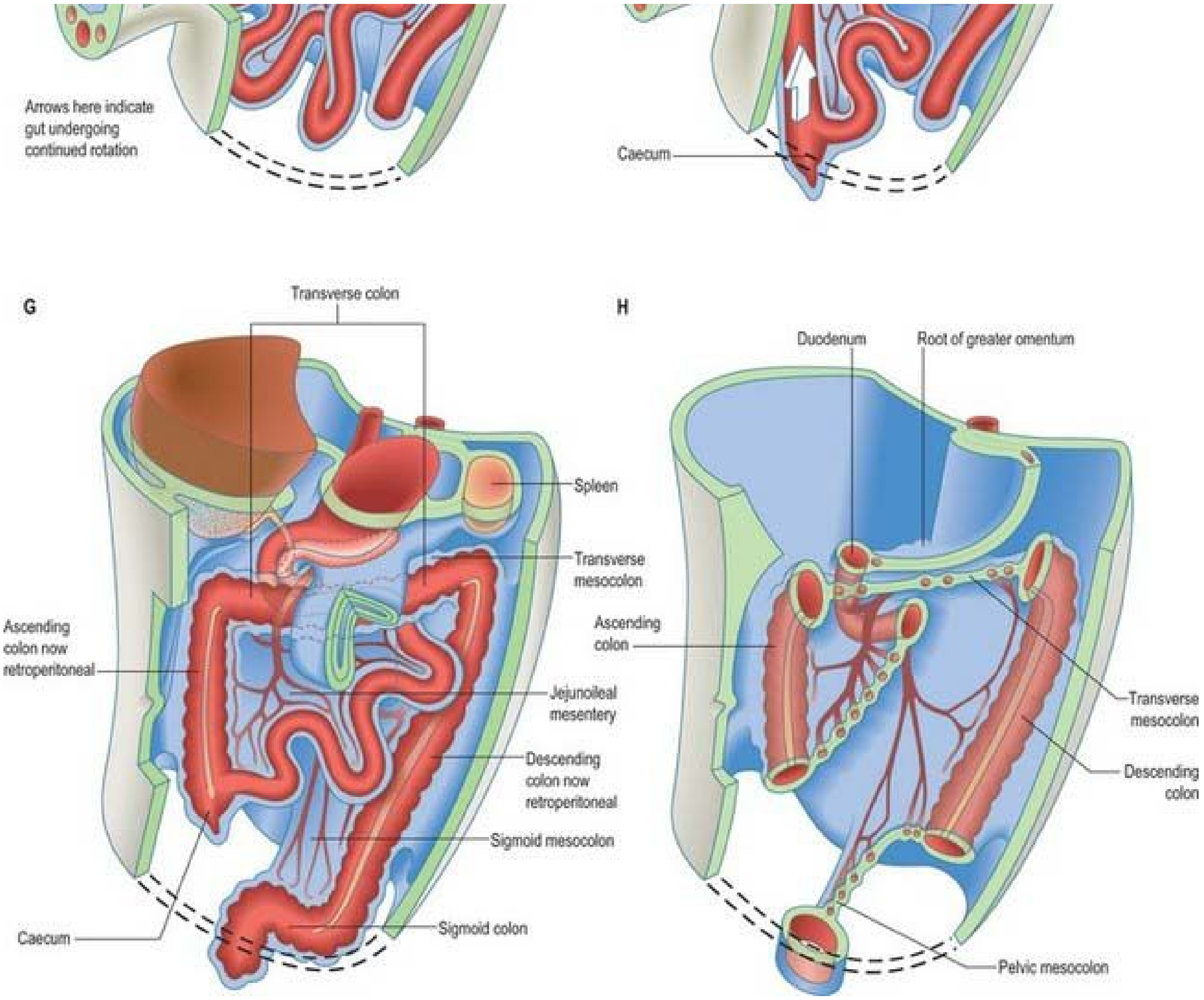
Arrows here indicate gut undergoing continued rotation
Caecum
G
Transverse colon
H
Duodenum
Root of greater omentum
Spleen
Transverse mesocolon
Ascending colon now retroperitoneal
Ascending colon
Jejunoileal mesentery
Transverse mesocolon
Descending colon now retroperitoneal
Descending colon
Sigmoid mesocolon
Caecum
Sigmoid colon
Pelvic mesocolon

Fig. 73.6 Three-dimensional schematization of the major developmental sequences of the subdiaphragmatic embryonic and fetal gut, together with its associated major glands, peritoneum and mesenteries: left anterolateral aspect. The development sequence **A–F** spans 1.5 months to the perinatal period. Three-dimensional schematization of the major developmental sequences of the subdiaphragmatic embryonic and fetal gut, together with its associated major glands, peritoneum and mesenteries: left anterolateral aspect. The development sequence **A–F** spans 1.5 months to the perinatal period. **H** denotes the general disposition of the remaining viscera and mesenteric roots with their lines of attachment and principal contained vessels, which approximate to the adult state for comparison.

In human embryos of 10 mm (stage 15–16), the characteristic gastric curvatures are already recognizable. Growth is more active along the dorsal border of the viscus: its convexity markedly increases and the rudimentary fundus appears. Because of more rapid growth along the dorsal border, the pyloric end of the stomach turns ventrally and the concave lesser curvature becomes apparent (Fig. 73.3; see also Fig. 73.6). The stomach is now displaced to the left of the median plane and apparently becomes physically rotated, which means that its original right surface becomes dorsal and its left surface becomes ventral. Accordingly the right vagus is distributed mainly to the dorsal, and the left vagus mainly to the ventral, surfaces of the stomach. The dorsal mesogastrium increases in depth and becomes folded on itself. The ventral mesogastrium becomes more coronal than sagittal. The pancreaticoenteric recess (see Fig. 73.7B(ii)), hitherto usually described as a simple depression on the right side of the dorsal mesogastrium, becomes dorsal to the stomach and excavates downwards and to the left between the folded layers. It may now be termed the inferior recess of the bursa omentalis. Put simply, the stomach has undergone two ‘rotations’. The first is 90° clockwise, viewed from the cranial end, the second is 90° clockwise, about an anteroposterior axis. The displacement, morphological changes and apparent ‘rotation’ of the stomach have been attributed variously to its own and surrounding differential growth changes, extension of the pancreaticoenteric recess with changes in its mesenchymal walls, and pressure, particularly that exerted by the rapidly growing liver.

Mucosa

Mucosal and submucosal development can be seen in the eighth to ninth weeks. No villi form in the stomach, unlike other regions of the gut; instead glandular pits can be seen in the body and fundus. These develop in the pylorus and cardia by weeks 10 and 11 when parietal cells can be demonstrated. Although acid secretion has not been demonstrated in the fetal stomach before 32 weeks’ gestation, preterm infants from 26 weeks’ gestation onwards are able to secrete acid soon after birth. Intrinsic factor has been detected after 11 weeks. This increases from the 14th to 25th week, at which time the pylorus, which contains more parietal cells than it does in the adult, also contains a relatively larger quantity of intrinsic factor. The significance of the early production of intrinsic factor and the late production of acid by the parietal cells is not known. Chief cells can be identified after weeks 12–13, although they cannot be demonstrated to contain pepsinogen until term. Mucous neck cells actively produce mucus from week 16. Gastrin-producing cells have been demonstrated in the antrum between 19 and 20 weeks and gastrin levels have been measured in cord blood and in the plasma at term. Cord serum contains gastrin levels 2–3 times higher than those in maternal serum.

Muscularis

The stomach muscularis externa develops its circular layer at 8–9 weeks, when neural plexuses are developing in the body and fundus. The longitudinal muscle develops slightly later. The pyloric musculature is thicker than the rest of the stomach: in general, the thickness of the total musculature of the stomach at term is reduced compared to the adult.

Serosa

The serosa of the stomach is derived from the splanchnopleuric coelomic epithelium. No part of this serosa undergoes absorption. The original left side of the gastric serosa faces the greater sac, the right side faces the lesser sac.

Stomach at birth

The stomach exhibits fetal characteristics until just after birth when the initiation of pulmonary ventilation, the reflexes of coughing and swallowing, and crying, cause the ingestion of large amounts of air and liquid. Once postnatal swallowing has started the stomach distends to four or five times its contracted state, and shifts its position in relation to the state of expansion and contraction of the other abdominal viscera, and to the position of the body. In the neonate, the anterior surface of the stomach is generally covered by the left lobe of the liver, which extends nearly as far as the spleen (see Fig.

14.4). Only a small portion of the greater curvature of the stomach is visible anteriorly. The capacity of the stomach is 30–35 ml in the full-term neonate, rising to 75 ml in the second week and 100 ml by the fourth week (adult capacity is on average 1000 ml). The mucosa and submucosa are relatively thicker than in the adult, however, the muscularis is only moderately developed and peristalsis is not coordinated. At birth gastric acid secretion is low, which means that gastric pH is high for the first 12 postnatal hours. It falls rapidly with the onset of gastric acid secretion, usually after the first feed. Acid secretion usually remains low for the first 10 days postnatally. Gastric emptying and transit times are delayed in the neonate.

DUODENUM

The duodenum develops from the caudal part of the foregut and the cranial part of the midgut. A ventral mesoduodenum, which is continuous cranially with the ventral mesogastrium, is attached only to the foregut portion. Posteriorly the duodenum has a thick dorsal mesoduodenum which is continuous with the dorsal mesogastrium cranially and the dorsal mesentery of the midgut caudally. Anteriorly the extreme caudal edge of the ventral mesentery of the foregut extends onto the short initial segment of the duodenum. The liver arises as a diverticulum from the ventral surface of the duodenum at the foregut–midgut junction, i.e. where the midgut is continuous with the yolk sac wall (the cranial intestinal portal). The ventral pancreatic bud also arises from this diverticulum. The dorsal pancreatic bud evaginates posteriorly into the dorsal mesoduodenum slightly more cranially than the hepatic diverticulum. The rotation, differential growth, and cavitations related to the developing stomach and omenta cause corresponding movements in the duodenum, which forms a loop directed to the right, with its original right side now adjacent to the posterior abdominal wall (see Fig. 73.6). This shift is compounded by the migration of the bile duct and ventral pancreatic duct around the duodenal wall. Their origin shifts until it reaches the medial wall of the second part of the fully formed duodenum: the bile duct passes posteriorly to the duodenum and travels in the free edge of the ventral duodenum and ventral mesogastrium. Local adherence and subsequent absorption of part of the duodenal serosa and the parietal peritoneum results in almost the whole of the duodenum, other than a short initial segment, becoming retroperitoneal (sessile).

Duodenal atresia is a developmental defect found in 1 in 5000 live births (Whittle 1999). It may be associated with an annular pancreas which may compress the duodenum externally (20% of duodenal atresia), or with abnormalities of the bile duct. In 40–60% of cases the atresia is complete and pancreatic tissue fills the lumen. The condition can be diagnosed on ultrasound examination, which reveals a typical double bubble appearance caused by fluid enlarging the stomach and the proximal duodenum.

Polyhydramnios is invariably present and often the indication for the scan. Duodenal atresia commonly occurs with other developmental defects, e.g. cardiac and skeletal anomalies and in Down’s syndrome.

DORSAL AND VENTRAL MESENTERIES OF THE FOREGUT

The epithelium of the stomach and duodenum does not rotate relative to its investing mesenchyme. The rotation includes the coelomic epithelial walls of the pericardioperitoneal canals, which are on each side of the stomach and duodenum and form its serosa, and the elongating dorsal mesogastrium or the much shorter dorsal mesoduodenum. A ventral mesogastrium can be seen when the distance between the stomach and liver increases. Whereas the dorsal mesogastrium takes origin from the posterior body wall in the midline, its connection to the greater curvature of the stomach, which lengthens as the stomach grows, becomes directed to the left as the stomach undergoes its first rotation. With the second rotation a portion of the dorsal mesogastrium now faces caudally (see Fig. 73.6). The ventral mesogastrium remains as a double layer of coelomic epithelium which encloses mesenchyme and forms the lesser omentum (see Fig. 73.7).

Movement of the stomach is associated with an extensive lengthening of the dorsal mesogastrium, which becomes the greater omentum, and which now, from its posterior origin, droops caudally over the small intestine, then folds back anteriorly and ascends to the greater curvature of the stomach. The greater omentum is therefore composed of a fold containing, technically, four layers of peritoneum. The dorsal mesoduodenum, or suspensory ligament of the duodenum, is a much thicker structure, and it fixes the position of the duodenum when the rest of the midgut and its dorsal mesentery elongate and pass into the umbilical cord. For a more detailed account of this process see page 1216.

SPECIAL GLANDS OF THE POSTPHARYNGEAL FOREGUT

Pancreas

The pancreas develops from two evaginations of the foregut which fuse to form a single organ. A dorsal pancreatic bud can be seen in stage 13 embryos as a thickening of the endodermal tube which proliferates into the dorsal mesogastrium (Figs 73.3 and 73.4). A ventral pancreatic bud evaginates in close proximity to the liver primordium but cannot be clearly identified until stage 14, when it appears as an evagination of the bile duct itself. At stage 16 (5 weeks) differential growth of the wall of the duodenum results in movement of the ventral pancreatic bud and the bile duct to the right side and ultimately to a dorsal position. It is not clear whether there is a corresponding shift of mesenchyme during this rotation. However, the ventral pancreatic bud and the bile duct rotate from a position within the ventral mesogastrium (ventral mesoduodenum) to one in the dorsal mesogastrium (dorsal mesoduodenum) which is destined to become fixed onto the posterior abdominal wall. By stage 17 the ventral and dorsal pancreatic buds have fused, although the origin of the ventral bud from the bile duct is still obvious. Three-dimensional reconstruction of the ventral and dorsal pancreatic buds have confirmed that the dorsal pancreatic bud forms the anterior part of the head, the body and the tail of the pancreas and the ventral pancreatic bud forms the posterior part of the head and the posterior part of the uncinate process. The ventral pancreatic bud does not form all of the uncinate process (Collins 2002).

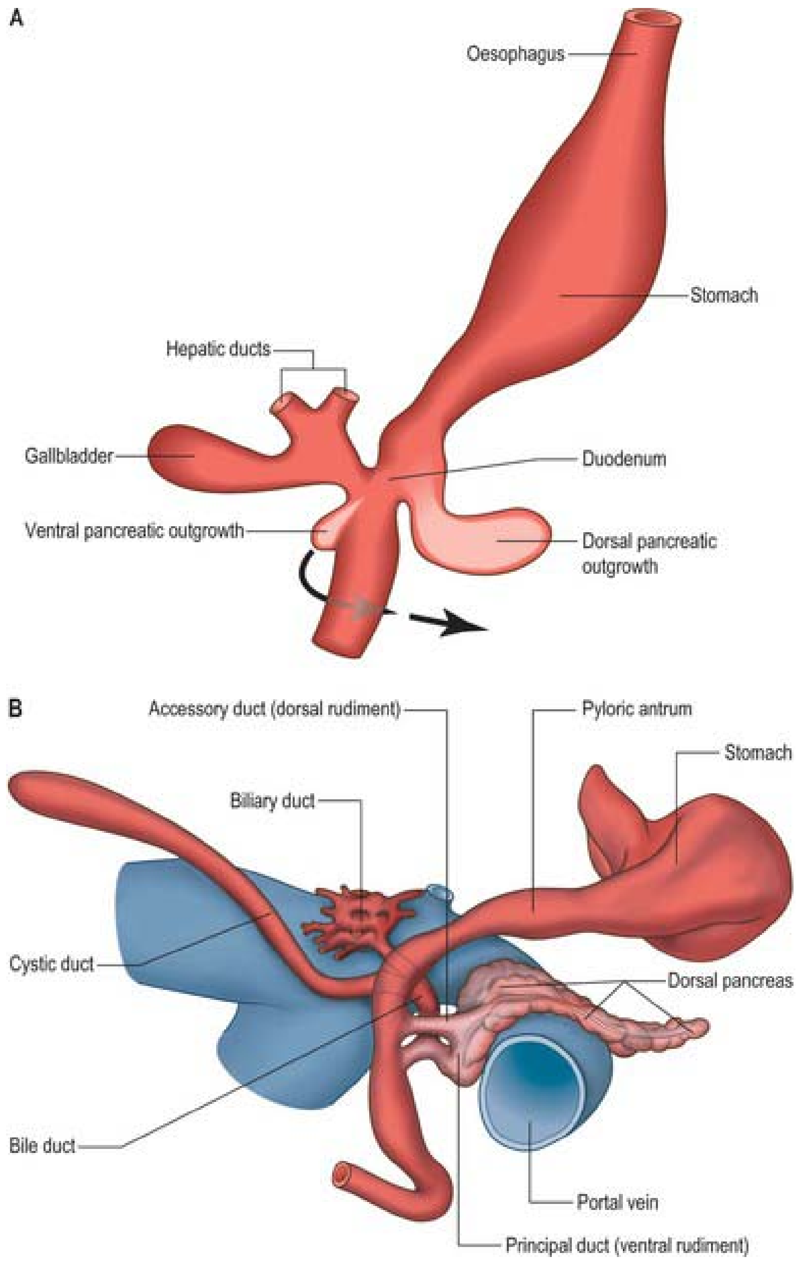
A
Oesophagus
Stomach
Hepatic ducts
Gallbladder
Duodenum
Ventral pancreatic outgrowth
Dorsal pancreatic outgrowth
B
Accessory duct (dorsal rudiment)
Pyloric antrum
Stomach
Biliary duct
Cystic duct
Dorsal pancreas
Bile duct
Portal vein
Principal duct (ventral rudiment)

Fig. 73.4 Development of the pancreas in a human embryo. **A**, An early stage, 7.5 mm embryo; lateral view. **B**, A later stage, 14.5 mm embryo; ventral view.

The developing pancreatic ducts usually fuse in such a way that most of the dorsal duct drains into the proximal part of the ventral duct (Figs 73.3 and 73.4). The proximal portion of the dorsal duct usually persists as an accessory duct. The fusion of the ducts takes place late in development or in the postnatal period: 85% of infants have patent accessory ducts as compared to 40% of adults. Fusion may not occur in 10% of individuals, in which case separate drainage into the duodenum is maintained, so-called pancreatic divisum. Failure of the ventral pancreatic diverticulum to migrate will result in an annular pancreas which may constrict the duodenum locally.

The ventral pancreas does not always extend anterior to the superior mesenteric vein but remains related to its right lateral surface. Initially the body of the pancreas extends into the dorsal mesoduodenum and then cranially into the dorsal mesogastrium. As the stomach rotates, this portion of the dorsal mesogastrium is directed to the left forming the posterior wall of the lesser sac. The posterior layer of this portion of dorsal mesogastrium fuses with the parietal layer of the coelom wall (peritoneum) and the pancreas becomes mainly retroperitoneal (see Fig. 73.7C). The region of fusion of the dorsal mesogastrium does not extend so far left as to include the tail of the pancreas which passes into the lienorenal (splenorenal) ligament. The anterior border of the pancreas later provides the main line of attachment for the posterior leaves of the greater omentum.

Cellular development of the pancreas

The early specification of pancreatic endoderm involves the proximity of the notochord to the dorsal endoderm, which locally represses the expression of Shh transcription factor. Endoderm caudal to the pancreatic region does not respond to notochordal signals. The ventral pancreatic endoderm does not seem to undergo the same induction. Pancreatic mesenchyme is derived from two regions. The mesenchyme which surrounds the dorsal pancreatic bud proliferates from the splanchnopleuric coelomic epithelium of the medial walls of the pericardioperitoneal canals, whereas the ventral pancreatic bud is invested by septum transversum mesenchyme and by mesenchyme derived from the lower ventral walls of the pericardioperitoneal canals.

The primitive endodermal ductal epithelium provides the stem cell population for all the secretory cells of the pancreas. Initially these endocrine cells are located in the duct walls or in buds developing from them, and later they accumulate in pancreatic islets. The remaining primitive duct cells will differentiate into definitive ductal cells. In the fetus they develop microvilli and cilia but lack the lateral interdigitations seen in the adult. Branches of the main duct become interlobular ductules which terminate as blind ending acini or as tubular, acinar elements.

The ductal branching pattern and acinar structure of the pancreas is determined by the pancreatic mesenchyme. This mesenchyme gives rise to connective tissue between the ducts which, in the fetus, appears to be important in stimulating pancreatic proliferation and maintaining the relative proportions of acinar, α and β cells during development. It also provides cell lines for smooth muscle within the pancreas. Angiogenic mesenchyme invades the developing gland to produce blood and lymphatic vessels.

The process of islet differentiation is divided into two phases (Collins 2002). Phase I, characterized by proliferation of polyhormonal cells, occurs from weeks 9–15. Phase II, characterized by differentiation of monohormonal cells, is seen from week 16 onwards. The β cells, producing insulin and amylin, differentiate first, followed by α-cells which produce glucagon. The δ cells which produce somatostatin are seen after 30 weeks. The dorsal bud gives rise mostly to α cells, and the ventral bud to most of the pancreatic polypeptide producing cells. The β cells develop from the duct epithelium throughout development and into the neonatal period. Later, in weeks 10–15, some of the primitive ducts differentiate into acinar cells in which zymogen granules or acinar cell markers can be detected at 12–16 weeks.

The pancreas in the neonate has all of the normal subdivisions of the adult. The head is proportionately large in the newborn and there is a smooth continuation between the body and the tail. The inferior border of the head of the pancreas is found at the level of the second lumbar vertebra. The body and tail pass cranially and to the left, and the tail is in contact with the spleen (see Fig. 14.4).

Liver

The liver is one of the most precocious embryonic organs and is the main centre for haemopoiesis in the fetus. It develops from an endodermal evagination of the foregut and from septum transversum mesenchyme, which is derived from the proliferating coelomic epithelium in the protocardiac region. The development of the liver is intimately related to the development of the heart. The vitelline veins, succeeded by the umbilical veins passing to the sinus venosus are disrupted by the enlarging septum transversum to form a hepatic plexus, the forerunner of the hepatic sinusoids. (See Collins, 2002 for a detailed account of hepatic development.)

Early liver development

As the head fold and early intraembryonic coelom form, the ventral parietal wall of the pericardial cavity gives rise to populations of cells termed precardiac or cardiac mesenchyme. Hepatic endoderm is induced to proliferate by this mesenchyme, although all portions of the early heart tube, truncus arteriosus, atria, ventricle, both endocardium and myocardium, have hepatic induction potency which is tissue-specific, but not species-specific. As the heart and foregut become separated by the accumulation of the cardiac mesenchyme, the mesenchyme itself is renamed septum transversum. It is seen as a ventral mass, caudal to the heart, which passes dorsally on each side of the developing gut to join the mesenchyme proliferating from the walls of the pericardioperitoneal canals. The majority of the cells within the septum transversum are destined to become hepatic mesenchyme.

In the stage 11 embryo the location of the hepatic endoderm has been identified at the superior boundary of the rostral intestinal portal. By stage 12, the hepatic endodermal primordium is directed ventrally and begins to proliferate as a diverticulum. There are two parts: a caudal part, which will produce the cystic duct and gallbladder, and a cranial part which forms the liver biliary system (Figs 73.3, 73.5A). The cells start to express liver-specific molecular markers and glycogen storage.

Around the cranial portion of the hepatic diverticulum the basal lamina is progressively disrupted and individual epithelial cells migrate into the surrounding septum transversum mesenchyme. The previously smooth contour of the diverticulum merges into columnar extensions of endoderm, the epithelial trabeculae, which stimulate the hepatic mesenchymal cells to form blood islands and endothelium. The advance of the endodermal epithelial cells promotes the conversion of progressively more hepatic mesenchyme into endothelium and blood cells, and only a little remains to form the scanty liver capsule and interlobular connective tissue. This invasion by the hepatic epithelium is completed in stage 13, when it approaches the caudal surface of the pericardial cavity, and is separated from it only by a thin lamina of mesenchyme which will give rise to part of the diaphragm.

During this early phase of development the liver is far more highly vascularized than the rest of the gut. The hepatic capillary plexus is connected bilaterally with the right and left vitelline veins. Dorsolaterally they empty by multiple channels into enlarged hepatocardiac channels, which lead to the right and left horns of the sinus venosus (see Fig. 73.9); usually the channel on the right side is most developed. Both left and right channels bulge into the pericardioperitoneal canals, forming sites for the exchange of fluid from the coelom into the vascular channels. The growth of the hepatic tissue in these regions is sometimes referred to as the left and right horns of the liver.

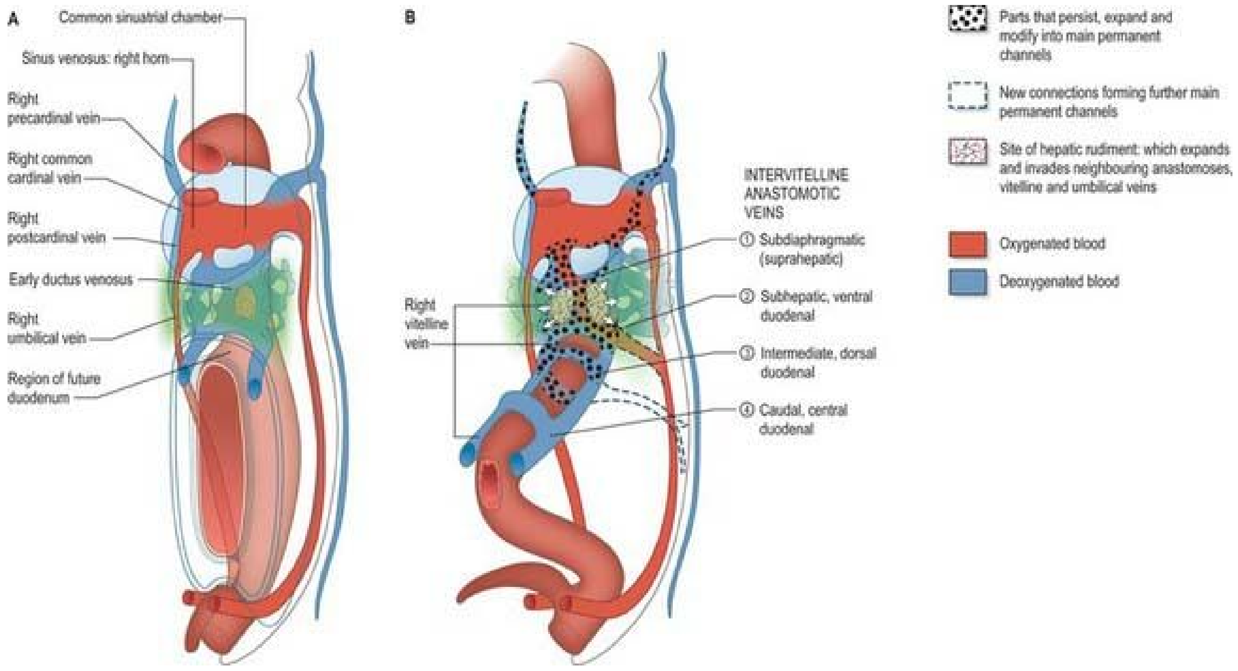
A
Common sinuatrial chamber
Sinus venosus: right horn
Right precardinal vein
Right common cardinal vein
Right postcardinal vein
Early ductus venosus
Right umbilical vein
Region of future duodenum
B
Right vitelline vein
INTERVITELLINE ANASTOMOTIC VEINS
① Subdiaphragmatic (suprahepatic)
② Subhepatic, ventral duodenal
③ Intermediate, dorsal duodenal
④ Caudal, central duodenal
Parts that persist, expand and modify into main permanent channels
New connections forming further main permanent channels
Site of hepatic rudiment: which expands and invades neighbouring anastomoses, vitelline and umbilical veins
Oxygenated blood
Deoxygenated blood

Fig. 73.9 Development of the vitelline, umbilical and terminal cardinal vein complexes: the early symmetric condition. **A**, Early symmetrical arrangement of cardinal and umbilical veins entering the sinus venosus, and blood from the yolk sac passing via vitelline veins through anastomoses forming in the septum transversum mesenchyme (green). **B**, The developing duodenum is surrounded by transverse duodenal intervitelline anastomoses. Changes in the developing gut and umbilical veins cause shifts in the routes taken by venous blood flowing to the sinus venosus.

The liver remains proportionately large during its development and constitutes a sizeable organ dorsal to the heart at stage 14 then more caudally placed by stage 16. By this stage hepatic ducts can be seen separating the hepatic epithelium from the extrahepatic biliary system, but even at stage 17 the ducts do not penetrate far into the liver.

Maturation of the liver

At 3 months' gestation, the liver almost fills the abdominal cavity and its left lobe is nearly as large as its right. When the haematopoietic activity of the liver is assumed by the spleen and bone marrow, the left lobe undergoes some degeneration and becomes smaller than the right. The liver remains relatively larger than in the adult throughout the remainder of gestation. In the neonate it constitutes 4% of the body weight, compared to 2.5–3.5% in adults. It is in contact with the greater part of the diaphragm and extends below the costal margin anteriorly, and in some cases to within 1 cm of the iliac crest posteriorly. The left lobe covers much of the anterior surface of the stomach and constitutes nearly one-third of the liver (see Fig. 14.4). Although its haemopoietic functions cease before birth its enzymatic and synthetic functions are not completely mature at birth.

Development of intrahepatic biliary ducts

The development of the intrahepatic biliary ducts follows the branching pattern of the portal vein radicles (Collins 2002). The cranial hepatic diverticulum gives rise to the liver hepatocytes, the intrahepatic large bile ducts (right and left hepatic ducts, segmental ducts, area ducts and their first branches) and the small bile ducts (septal bile ducts, interlobular ducts and bile ductules). The portal and hepatic veins arise together from the vitelline veins. Early in development the accumulation of mesenchyme around these veins is similar, whereas later mesenchyme increases around the portal veins. This is a prerequisite for bile duct development. Primitive hepatocytes surround the portal vein branches and associated mesenchyme and form a sleeve of cells termed the ductal plate. Portions of the ductal plate divide to produce lines of epithelial cells which migrate close to a portal vein branch where they differentiate into bile ducts. As the bile ducts develop, angiogenic mesenchymal cells form blood vessels which connect to the hepatic artery from 10 weeks. Thus the portal triads are patterned by the portal vein radicles which initially induce bile duct formation and then artery formation. The development of the biliary system extends from the hilum to the periphery. Abnormalities of the biliary tree are associated with abnormalities of the branching pattern of the portal vein. The developing bile ducts remain patent throughout development; the solid stage of ductal development previously promulgated has been refuted. Atresia of the extrahepatic bile ducts has been noted, often in association with extrahepatic atresia. The cause of this condition is not clear; inflammatory process may be involved, although some cases have features of ductal plate malformation (Howard 2002).

Development of extrahepatic biliary ducts

The caudal part of the hepatic endodermal diverticulum forms the extrahepatic biliary system, the common hepatic duct, gallbladder, cystic duct and common bile duct.

The bile duct, which originated from the ventral wall of the foregut (now duodenum), migrates with the ventral pancreatic bud first to the right and then dorsomedially into the dorsal mesoduodenum. The right and left hepatic ducts arise from the cranial end of the common hepatic duct from 12 weeks’ gestation.

Atresia of the extrahepatic bile ducts in neonates occurs alone or in conjunction with a range of other anomalies, including situs inversus, malrotation, polysplenia and cardiac defects. In such cases the intrahepatic bile ducts have a mature tubular shape but also show features of ductal plate malformation.

In the neonate the gallbladder has a smaller peritoneal surface than in the adult, and its fundus often does not extend to the liver margin. It is generally embedded in the liver and in some cases may be covered by bands of liver. After the second year the gallbladder assumes the relative size it has in the adult.

MIDGUT

The midgut forms the third and fourth parts of the duodenum, jejunum, ileum and two-thirds of the way along the transverse colon: its development produces most of the small and a portion of the large intestine. In embryos of stages 10 and 11 it extends from the cranial to the caudal intestinal portals and communicates directly with the yolk sac over its entire length. Although it has a dorsal wall, at these stages the lateral walls have not yet formed. By stage 12 the connection with the yolk sac has narrowed such that the midgut has ventral walls cranially and caudally. This connection is reduced to a yolk stalk containing the vitellointestinal duct during stage 13, at which time the yolk sac appears as a sphere in front of the embryo. Posterior to the midgut the splanchnopleuric coelomic epithelia converge forming the dorsal mesentery. Ventrolaterally the intraembryonic coelom is in wide communication with the extraembryonic coelom. At stage 14 the midgut has increased in length more than the axial length of the embryonic body and, with elongation of the dorsal mesentery, it bulges ventrally, deviating from the median plane. For all these stages see Figure 73.3.

PRIMARY INTESTINAL (OR MIDGUT) LOOP

The midgut loop can first be seen at stage 15 when a bulge, the caecal bud, can be discerned on the lower limb of the loop, caudal to the yolk stalk (which arises from the apex or summit of the loop) (Fig. 73.3). Later, the original proximal limb of the loop moves to the right and the distal limb to the left (Fig. 73.3C). The longest portion of the dorsal mesentery is at the level of the yolk stalk: there is less relative lengthening near the caudal end of the duodenum or the cranial half of the colon. The midgut extends into the umbilical coelom having already rotated through an angle of 90° (anticlockwise viewed from the ventral aspect). This relative position is approximately maintained so long as the protrusion persists, during which time the proximal limb which forms the small intestine elongates greatly. It becomes coiled, and its adjacent mesentery adopts a pleated appearance. The origin of the root of the mesentery is initially both median and vertical, while at its intestinal attachment it is elongated like a ruffle and folded along a horizontal zone. The mesenteric sheet and its contained vessels has spiralled through 90°. The distal, colic, part of the loop elongates less rapidly and has no tendency to become coiled. By the time the fetus has attained a length of 40 mm (10 weeks), the peritoneal cavity has enlarged and the relative size of the liver and mesonephros is much less. The re-entry of the gut occurs rapidly and in a particular sequence during which it continues the process of rotation. The proximal loop returns first, with the jejunum mainly on the left and the ileum mainly on the right of the subhepatic abdominal cavity. As they re-enter the abdominal cavity the coils of jejunum and ileum slide inwards over the right aspect of the descending mesocolon, and so displace the descending colon to the left. The transverse colon passes superiorly to the origin of the root of the mesentery (Fig. 73.6). The caecum is the last to re-enter and at first lies on coils of ileum on the right. Later development of the colon leads to its elongation and to the establishment of the hepatic and splenic flexures. A timetable for intestinal rotation in staged human embryos is given by Kim et al (2003).

Anomalies of midgut rotation

If the midgut loop fails to return to the abdominal cavity at the appropriate time a range of ventral defects can result. Failure of obliteration of the vitello-intestinal duct connecting the midgut to the yolk sac results in Meckel’s diverticulum. This may present as a short segment of vitelline duct attached to the original ventral side of the ileum; it may remain attached to the umbilicus as a fistula; or it may remain as a ligamentous attachment to the umbilicus.

An umbilical hernia occurs when loops of gut protrude into a widened umbilical cord at term. The degree of protuberance may increase when the infant cries, which raises the intra-abdominal pressure: these hernias usually resolve without treatment. Exomphalos is a ventral wall defect with midline herniation of the intra-abdominal contents into the base of the umbilical cord. Herniated viscera are covered by the peritoneum internally and amnion externally. The omphalocele so formed ranges in size from a large umbilical hernia to a very large mass containing most of the visceral organs. Even after the exomphalos has been repaired these babies will still have a deficient anterior abdominal wall.

Gastroschisis is a para-umbilical defect of the anterior abdominal wall associated with evisceration of the abdominal organs. The organs are not enclosed in membranes, thus gastroschisis can be detected by prenatal ultrasonography and differentiated from exomphalos. Gastro-schisis is thought to result from periumbilical ischaemia caused by vascular compromise of either the umbilical vein or arteries. The incidence of this condition appears to be increasing, especially in babies born to young women less than 20 years old (Whittle 1999).

Congenital volvulus arises if the midgut loop does not rotate appropriately. A number of types of this condition are identified. Left-sided colon occurs if the midgut loop has not rotated at all; mixed rotation results in the caecum lying inferior to the pylorus; failure of attachment of the peritoneum appropriately may result in the small intestine being attached at only two points on the posterior abdominal wall. All of these arrangements lead to a risk of volvulus, which may result in necrosis of the gut.

The position and configuration of the duodenal loop are of particular importance in children. The normal duodenal loop has a U-shaped configuration. The suspensory ligament of the duodenum (ligament of Treitz) is usually found to the left of the body of the first or second lumbar vertebral body after normal gut rotation: any other position of this ligament may indicate some degree of gut malrotation. On barium studies the duodenojejunal flexure should thus lie to the left of the upper lumbar spine at the level of the pylorus.

If the caecum has remained in the right upper quadrant it may become fixed in that position by peritoneal attachments passing to the right, the so called Ladd's bands. These may compress the underlying duodenum and give rise to duodenal stenosis. The high positioning of the caecum close to the duodenal jejunal flexure, in some cases in the midline, is associated with later development of volvulus.

The identification of intestinal malrotation can be made by X-ray investigation. However, ultrasonography has the advantage of showing the position of the superior mesenteric vein and artery. The vein should lie to the right of the artery. Most cases of volvulus will show inversion of this normal relationship, but malrotation can occur with apparently normally related vessels, particularly in malrotation with bowel obstruction due to Ladd's bands and not volvulus.

UMBILICAL CORD

During the period when the midgut loop protrudes into the umbilical coelom, the edges of the ventral body wall are becoming relatively closer, forming a more discrete root for the umbilical cord. Somatic mesenchyme, which will form the ventral body wall musculature, migrates into the somatopleuric mesenchyme and passes ventrally toward the midline. The umbilical cord (see p. 181) forms all of the ventral body wall between the pericardial bulge and the developing external genitalia. It encloses a portion of the extraembryonic coelom, the umbilical coelom, into which midgut loop protrudes. When the midgut loop is abruptly returned to the abdominal cavity the more recognizable umbilical cord forms. The vitellointestinal duct and vessels involute. The cranial end of the allantois becomes thinned and its lumen partially obliterated, and it forms the urachus. The mesenchymal core of the umbilical cord is derived by coalescence from somatopleuric amniotic mesenchyme, splanchnopleuric vitellointestinal (yolk sac) mesenchyme, and splanchnopleuric allantoic (connecting stalk) mesenchyme. These various layers become fused and are gradually transformed into the viscid, mucoid connective tissue (Wharton’s jelly) which characterizes the more mature cord. The changes in the circulatory system result in a large cranially oriented left umbilical vein (the right umbilical vein regresses), and two spirally disposed umbilical arteries (see p. 181).

MATURATION OF THE SMALL INTESTINE

Mucosa

The exact timing of the cellular morphogenesis of the gut is difficult to establish, especially as it undergoes a proximodistal gradient in maturation. Developmental differences between parts of the small intestine or colon have not yet been correlated with age. The endodermal cells of the small intestine proliferate and form a layer some three to four cells thick with mitotic figures throughout. From 7 weeks, blunt projections of the endoderm have begun to form in the duodenum and proximal jejunum; these are the developing villi which increase in length until in the duodenum the lumen becomes difficult to discern. The concept of occlusion of the lumen and recanalization which is described in many accounts of development does not match the cytodifferentiation which occurs in the gut epithelia. Thus it is no longer thought that there is secondary recanalization of the gut lumen. By 9 weeks the duodenum, jejunum and proximal ileum have villi and the remaining distal portion of ileum develops villi by 11 weeks. The villi are covered by a simple epithelium. Primitive crypts, epithelial downgrowths into the mesenchyme between the villi, appear between 10 and 12 weeks similarly along a craniocaudal progression. Brunner’s glands are present in the duodenum from 15 weeks and the muscularis mucosa can be seen in the small intestine from 18 weeks.

Whereas mitotic figures are initially seen throughout the endodermal layer of the small intestine prior to villus formation, by 10–12 weeks they are limited to the intervillous regions and the developing crypts. It is believed that an ‘adult’ turnover of cells may exist when rounded-up cells can be observed at the villus tips, in position for exfoliation. The absorptive enterocytes have microvilli at their apical borders before 9 weeks. An apical tubular system appears at this time composed of deep invaginations of the apical plasma membrane and membrane-bound vesicles and tubules; many lysosomal elements (meconium corpuscles) appear in the apical cytoplasm. These latter features are more developed in the ileum than jejunum, are most prominent at 16 weeks, and diminish by 21 weeks. There are abundant deposits of glycogen in the fetal epithelial cells, and it has been suggested that prior to the appearance of hepatic glycogen the intestinal epithelium serves as a major glycogen store. Goblet cells are present in small numbers by 8 weeks, Paneth's cells differentiate at the base of the crypts in weeks 11 and 12, and enteroendocrine cells appear between weeks 9 and 11. M cells (membrane or microfold cells) are present from 14 weeks.

Meconium can be detected in the lumen of the intestine by the 16th week. It is derived from swallowed amniotic fluid, which contains vernix and cellular debris, salivary, biliary, pancreatic and intestinal secretions, and sloughed enterocytes. As the mixture passes along the gut, water and solutes are removed and cellular debris and proteins concentrated. Meconium contains enzymes from the pancreas and proximal intestine in higher concentrations in preterm than full-term babies.

Muscularis layer

The muscularis layer is derived from the splanchnopleuric mesenchyme as it is in other parts of the gut. Longitudinal muscle can be seen from 12 weeks. At 26–30 weeks the gut shows contractions without regular periodicity; from 30–33 weeks repetitive groups of regular contractions have been seen in preterm neonates.

Serosa

The small intestine possesses only a dorsal mesentery. The movement of the root of this dorsal mesentery, and the massive lengthening of its enteric border in order to match the longitudinal growth of the gut tube, reflect the spiralizing of the midgut loop in the umbilical coelom. The specific regions of adherence of the serosa and parietal peritoneum of the small intestine in the peritoneal cavity are given on page 1216.

Small intestine at birth

In the neonate the small intestine forms an oval-shaped mass with its greater diameter transversely orientated in the abdomen, rather than vertically as in the adult. The mass of the small intestine inferior to the umbilicus is compressed by the urinary bladder, which is anterior at this point. The small intestine is 300–350 cm long at birth and its width when empty is 1–1.5 cm. The ratio between the length of the small and large intestine at birth is similar to the adult ratio. The mucosa and submucosa are fairly well developed and villi are present throughout the small intestine, however, some epithelial differentiation is incomplete. The muscularis is very thin, particularly the longitudinal layer, and there is little elastic tissue in the wall. There are few or no circular folds in the small intestine, and the jejunum and ileum have little fat in their mesentery.

PRIMITIVE HINDGUT

Just as the foregut has an extensive, ventral endodermal diverticulum which contributes to a system separate from the gut, so too the hindgut has a ventral diverticulum, the allantois, destined for a different system. However, unlike the respiratory diverticulum of the foregut, the allantois is formed very early in development, prior even to formation of the embryonic endoderm and tail folding. With the reorganization of the caudal region of the embryo at stage 10, part of the allantois is drawn into the body cavity. The early embryonic hindgut thus consists of a dorsal tubular region extending from the caudal intestinal portal to the cloacal membrane, and a ventral blind-ending allantois extending from the cloacal region into the connecting stalk. The slightly dilated cavity, lined by endoderm, that cranially receives the enteric hindgut proper and the root of the allantoenteric diverticulum is termed the endodermal cloaca. It is closed ventrally by the cloacal membrane (endoderm opposed to proctodeal ectoderm), and it also has, transiently, a small recess of endoderm in the root of the tail, the postanal gut. As elsewhere, the hindgut, allantois and endodermal cloaca are encased in splanchnopleuric mesenchyme. Proliferation of the mesenchyme and endoderm in the angle of the junction of hindgut and allantois produces a urorectal septum (see Fig. 78.4B). Continued proliferation of the urorectal septum and elongation of the endodermal structures thrusts the endodermal epithelium towards the cloacal membrane with which it fuses centrally, separating the presumptive rectum and upper anal canal (dorsally) from the presumptive urinary bladder and urogenital sinus (ventrally) (see Fig. 78.4C). The cloacal membrane is thus divided into anal (dorsal) and urogenital (ventral) membranes. The nodal centre of division is the site of the future perineal body, the functional centre of the perineum. Details of the development of the allantoic hindgut are given on page 1322.

ENTERIC HINDGUT

The development of the large intestine, whether derived from mid- or hindgut, seems to be similar. The proximal end of the colon can be first identified at stage 15 when an enlargement of a local portion of gut on the caudal limb of the midgut loop defines the developing caecum. An evagination of the distal portion of the caecum forms the vermiform appendix at stage 17 (Fig. 73.3). Apart from the embryonic studies of Streeter (1942) there is little information about the development of the large intestine in humans. The early endodermal lining of the colon appears stratified, and mitoses occur throughout the layers. A series of longitudinal folds arise initially at the rectum and caecum and later in the regions of colon between these two points. The folds segment into villi with new villi forming between. The developing mucosa invaginates into the underlying mesenchyme between the villi to form glands which increase in number by splitting longitudinally from the base upwards. The villi gradually diminish in size and are absent by the time of birth.

MATURATION OF THE LARGE INTESTINE

The similarity of development of the small and large intestines is further mirrored in their cytological differentiation. Fetal gut from 11 weeks shows dipeptidase activity in the colon as well as in the small intestine. Throughout preterm development meconium corpuscles are seen in the colon and in the small intestine: they are believed to be the phago-cytosed remains of neighbouring cells which have died as a result of programmed cell death.

There is little direct evidence of colonic function in the human fetus and neonate. However, the specific results of mammalian studies are being correlated to human studies where possible. A number of distinct and important differences between the function of adult and fetal colon have been reported.

Mucosa

The absorption of glucose and amino acids does not take place through the colonic mucosa in adult life, but there is evidence of direct absorption of these nutrients during development. At birth the normal cycle of bile acids is not mature. In the adult, bile is secreted by the liver, stored in the gallbladder and then secreted into the intestine, where it is absorbed by the jejunum and ileum. In the fetus and neonate, the transport of bile acids by an active process from the ileum does not occur, and so bile salts pass on into the colon. In the adult the presence of bile salts in the colon stimulates the secretion of water and electrolytes which results in diarrhoeal syndrome; however, the fetal and neonatal colon seems protected from this effect. The colon is not considered a site of significant nutrient absorption in the adult, and yet neonates are unable to assimilate the full lactose load of a normal breast feed from the small intestine and a large proportion of it may be absorbed from the colon. Thus it appears that the colon fulfills a slightly different role in the preterm and neonatal period, conserving nutrient absorption and minimizing fluid loss until the neonate has adjusted to extrauterine life, oral feeding, and the establishment of the symbiotic bacterial flora.

Muscularis

The muscularis is present and functioning by the eighth week, when peristaltic waves have been observed. The specific orientation of the longitudinal muscle layer into taeniae coli occurs in the 11th to 12th weeks when haustra appear. The enteric nerves are present in Meissner’s and Auerbach’s plexuses at 8 and 12 weeks respectively: there is a craniocaudal migration of neurones into the gut wall. A normal distribution of ganglion cells has been noted in preterm babies of 24 weeks, although there is a region devoid of ganglia just above the anal valves. Abnormal migration of neural crest cells to the gut may give rise to Hirschsprung’s disease (see below). Puborectalis appears in 20–30 mm embryos, following opening of the anal membrane.

Serosa

The development of the serosa of the intestine is considered with the development of the peritoneal cavity (see below).

Colon at birth

In the neonate the colon is typically 66 cm long and averages 1 cm in width. The caecum is relatively smaller than in the adult; it tapers into the vermiform appendix. The ascending colon is shorter in the neonate, reflecting the shorter lumbar region. The transverse colon is relatively long, whereas the descending colon is short, but twice the length of the ascending colon (see Fig. 14.4), The sigmoid colon may be as long as the transverse colon; it often touches the inferior part of the anterior body wall on the left and, in about 50% of neonates, part of the sigmoid colon lies in the right iliac fossa. The muscularis, including the taeniae coli, is poorly developed in the colon as it is in the small intestine. Appendices, epiploicae and haustra are not present, which gives a smooth external appearance to the colon. Haustra appear within the first 6 months. The rectum is relatively long; its junction with the anal canal forms at nearly a right angle.

ANAL CANAL

Mesenchymal proliferation occurs around the rim of the ectodermal aspect of the anal membrane which thus comes to lie at the bottom of a depression, the proctodeum (see Figs 78.4, 78.7E). With the absorption and disappearance of the anal membrane the anorectum communicates with the exterior. The lower part of the anal canal is formed from the proctodeal ectoderm and underlying mesenchyme, but its upper part is lined by endoderm. The line of union corresponds with the edges of the anal valves in the adult. The dual origin of the anal canal is reflected in its innervation: the endodermal portion is innervated by autonomic nerves, and the ectodermal proctodeum is innervated by spinal nerves.

In the fourth and fifth weeks a small part of the hindgut, the postanal gut, projects caudally beyond the anal membrane (Fig. 73.3B); it usually disappears before the end of the fifth week.

Imperforate anus is a term used to describe many different anorectal malformations. The most common is anal agenesis, which is found in almost 50% of all cases of imperforate anus. The condition is usually associated with a fistula, which opens into the vulva (females) or into the urethra (males). It is more rare for the anal membrane to fail to perforate. The condition cannot reliably be diagnosed prenatally by ultrasound diagnosis, and it may be confused with Hirschsprung’s disease (see below) and colonic atresia. The prognosis is good for low lesions of the anal canal. The principal concern in all cases is the degree of bowel control, urinary control and in some cases sexual function, which is compromised by the condition. Anorectal malformations may be indicators of other abnormalities, for example those forming the ‘VATER’ syndrome (Vertebral, Anal, Tracheo-Oesophageal and Renal abnormalities).

ENTERIC NERVOUS SYSTEM

Enteric neurones are derived from trunk neural crest cells at somite levels 1–7 and from 28 onwards (see Fig. 24.19 and p. 374). After neurulation the crest cells begin their ventral migration and invade the gut via the dorsal mesentery (see Fig. 24.11). Glial cells associated with the gut have been identified as arising from similar levels. The local splanchnopleuric mesenchyme patterns the crest cells such that those which enter the gut layers attain an enteric fate, whereas those that remain outside the gut become committed as parasympathetic postganglionic neurones. The enteric neurones also migrate to the glands of the gut, e.g. the pancreas.

Hirschsprung’s disease

Hirschsprung’s disease is usually characterized by an aganglionic portion of gut which does not display peristalsis, and a dilated segment of colon proximal to this site. Histologically there is either an absence or a reduction in the number of ganglia and postganglionic neurones in the myenteric plexus; postganglionic innervation of the muscle layers is also often defective. It is believed that the condition is caused by a failure of neural crest cells to colonize the gut wall appropriately. An overabundance of basal laminal components, perhaps at the mesothelial/mesenchyme interface, may prevent the early migrating neural crest cells from penetrating the gut wall; their new position outside the gut does not confer on them the environmental stimuli for enteric nerve differentiation and so non-enteric development occurs in local ganglia adjacent to the gut (Gershon 1987). A variable length of large intestine may be affected: the lower and midrectum are the most common sites, but in severe cases the rectum, sigmoid, descending and even proximal colon can be aganglionic. The chronic dilatation of the colon or rectum proximal to the affected segment gives rise to the common name, megacolon. It occurs as a consequence of functional obstruction due to the failure of peristalsis within the affected segment, and the dilated colon is structurally normal. Occasionally aganglionosis affects only a very short length of rectum proximal to the anorectal junction and the degree of functional obstruction is minimal: in these cases of ‘ultra-short segment Hirschsprung’s disease’, clinical abnormalities arise later in life. Infants with Hirschsprung’s disease show delay in the passage of meconium, constipation, vomiting and abdominal distension.

GUT-ASSOCIATED LYMPHOID TISSUE

Individual lymphocytes appear in the lamina propria of the gut from approximately week 12 of development, and lymphoid aggregates, Peyer's patches, have been noted between 15 and 20 weeks: it is not clear whether these cells migrate in from distant sources or differentiate from the investing mesenchyme. The endodermal epithelium overlying the lymphoid aggregates is often distorted into a dome shape. The cells within the dome are a mixed population of enterocytes, endocrine cells, goblet cells and M cells. M cells are specialized to provide a mechanism for the transport of micro-organisms and intact macromolecules across the epithelium to the intraepithelial space and lamina propria. They have been observed in the fetus by 17 weeks; it is believed that they are formed by a specialized epithelial/mesenchymal interaction of the endoderm and underlying lymphoid type mesenchyme.

There are similarly specialized epithelial cells between the enterocytes. Intraepithelial leukocytes typically account for 15% of the epithelial cells of the gut in the adult. They have been observed at 11 weeks, with a distribution of 2–3 intraepithelial leukocytes/100 gut epithelial cells. Both T and B lymphocytes have been described in the developing gut wall. For an account of the development of the immune cells of the gut consult Butzner & Befus (1989). The neonatal gut becomes colonized by a range of bacterial flora, some of which exist in a symbiotic relationship with their host, some of which may be considered pathogenic.

FUNCTIONAL MATURITY OF THE GUT AT BIRTH

After birth the first passage of stool of the newborn is termed meconium. This is a dark, sticky, viscid substance formed from the passage of amniotic fluid, sloughed cells, digestive enzymes and bile salts along the fetal gut. Meconium becomes increasingly solid as gestation advances but does not usually pass out of the fetal body while *in utero*. Fetal distress produced by anoxia may induce the premature defecation of meconium into the amniotic fluid, with the risk of its inhalation. At birth the colon contains 60–200 g of meconium. The majority of neonates defecate within the first 24 hours after birth. Delayed passage of stool beyond this time is associated with Hirschsprung’s disease (see above) or imperforate anus. The normal passage of meconium continues for the first 2 or 3 days after birth, and is followed by a transition to faecal stools by day 7.

PERITONEAL CAVITY

The early development of the intraembryonic coelom which gives rise to the peritoneal cavity is described on pages 189 and 199. Figure 12.2 shows a scheme of the shape of the early peritoneal cavity and indicates the mesenchymal populations derived from its epithelial walls. Initially the peritoneal cavity associated with the lower end of the foregut has separate right and left components, the pleuroperioneal canals (Fig. 73.1). At the level of the midgut, the pleuroperitoneal canals join a confluent cavity surrounding the developing gut, which transitorily is in communication with the extraembryonic coelom.

The description of the development of the peritoneal cavity which follows pertains to changes which occur as a consequence of the differential growth of the gut.

PERITONEUM

Peritoneum develops from a specific portion of the intraembryonic coelomic walls (pp. 189, 199). Initially the intraembryonic coelomic epithelium is a pseudostratified germinal layer from which cellular progeny with different fates arise in specific sites and at specific developmental times. The portion which will give rise to the peritoneum is derived from the lower portion of the pericardioperitoneal canals and the somatopleure and splanchnopleure associated with the lower foregut, midgut and upper portions of the hind gut (see Figs 12.2, 73.1).

The proliferative splanchnopleuric epithelium produces cell populations for the mucosa and muscularis of the gut and also the lamina propria and epithelium of the visceral peritoneum (the serosa of the gut wall). The somatopleuric epithelium gives rise to the lamina propria and epithelium of the parietal peritoneum. The visceral and parietal peritoneal layers constitute a mesothelium, which denotes their origin from the intraembryonic mesoderm of the coelomic wall.

As the gut grows, splanchnic mesenchyme accumulates around the endodermal epithelium and the whole unit generally moves ventrally. There is a concomitant enlargement of the caudal ends of the developing pericardioperitoneal (pleuroperitoneal) canals and developing peritoneal cavity. The medial walls of the intraembryonic coelom move closer and there is a relative decrease in the mesenchyme between them. The regions where the medial portions of the intraembryonic coelom come together are termed mesenteries. They are composed of two layers of peritoneum with intervening mesenchyme and contain the neurovascular structures which pass to and from the gut. At the caudal ends of the pleuroperitoneal canals the gut has both ventral and dorsal mesenteries, whereas caudal to this there is only a dorsal mesentery (Figs 73.6, 73.7).

The mesenteries attached to the gut lengthen to permit large movements or rotations of the gut tube. Later, when part or the whole of the mesentery lies against the parietal peritoneum, their apposed surfaces fuse and are absorbed, i.e. they become sessile. Only those viscera developed in direct apposition to one of the primary coelomic regions, or a secondary extension of the latter, retain a partial or almost complete visceral serous cover. Thus the original line of reflexion of mesenteries becomes altered, or in some cases the organ may become retroperitoneal. These mechanisms are significant throughout the subdiaphragmatic gut, but are predominant in the small and large intestine. All serous membranes may vary their thickness, lines of reflexion, disposition, 'space' enclosed and their channels of communication, by a process of areal and thickness growth on one aspect combined with cavitation (leading to expanding embryonic recess formation) on the other (Figs 73.6, 73.7).

Although all of the gut tube and its derived glands are associated with mesenteries formed as described above, the nomenclature for some portions of the gut and glands is different. Thus the mesenteries of the stomach are called omenta and the reflections of peritoneum around the liver, which develop from a confluence of splanchnopleuric, somatopleuric and septum transversum-derived portions, are called ligaments.

The movements of the developing viscera within the peritoneal cavity occur with associated movements of the mesothelia which surround them. The descriptions of peritoneal cavity development which follow are thus describing a sequence of changes which affect a complex space and its boundaries.

Mesenteries of the developing gut

The cervicothoracic oesophagus develops between the pericardioperitoneal canals (Fig. 73.1). It is encased in prevertebral, retrotracheal and retrocardiac mesenchyme. As the pericardioperitoneal canals expand with the developing lung buds, and the diaphragm forms immediately below them, the oesophagus at this level has no true dorsal or ventral mesentery. At superior and intermediate thoracic levels parts of the lateral aspects of the oesophagus are closely related to the secondary, mediastinal, parietal pleura. In the lower thorax the oesophagus inclines ventrally anterior to the descending thoracic aorta. The dorsocaudally sloping midline diaphragm between oesophageal and aortic orifices may be homologized with part of a dorsal meso-oesophagus, and is used in that context in descriptions of diaphragmatic development (see p. 1013). A ventral midline diaphragmatic strip may also be considered to be a derivative of a ventral meso-oesophagus, however, this region is more usually thought of as septum transversum.

The alimentary tube, from the diaphragm to the start of the rectum, initially possesses a sagittal dorsal mesentery. Its line of continuity with the dorsal parietal peritoneum (i.e. its ‘root’ or ‘line of reflexion’) is initially also midline.

The abdominal foregut, from the diaphragm to the future hepatopancreatic duodenal papilla, also has a ventral mesentery. This extends from the ventrolateral margins of the abdominal oesophagus and as yet ‘unrotated’ primitive stomach and proximal duodenum, cranially to the future diaphragm and anteriorly to the ventral abdominal wall (to the level of the cranial rim of the umbilicus). Caudally, between umbilicus and duodenum, it presents a crescentic free border.

The midgut and hindgut have no ventral mesentery; thus the pleural and supra-umbilical peritoneal cavities are initially, and transiently, bilaterally symmetrical above the umbilicus. Below the umbilicus, the peritoneal cavity is freely continuous across the midline ventral to the gut (Fig. 73.5A).

Foregut mesenteries

The ventral and dorsal foregut mesenteries are relatively large compared with the slender endodermal tubes they encase; they are composed of mesenchyme sandwiched between two layers of splanchnopleuric coelomic epithelium. A complex series of recesses develop in the splanchnopleuric mesenchyme and become confluent. As a result of foregut rotation, differential growth of stomach, liver, pancreas and spleen, and completion of the diaphragm, the territories of the greater sac and lesser sac (omental bursa) are delimited, and the mesenteric complexes of these organs (omenta and ‘ligaments’) are defined (Figs 73.6, 73.7).

Consequences of rotation of the stomach

A number of processes occur concurrently which conceptually can be visualized as the movement of the right pleuroperitoneal canal to a position posterior to the stomach such that its communication with the remainder of the peritoneal cavity is reduced. These processes include the differential growth of the walls of the stomach, the formation and specific local extension of the omenta (dorsal and ventral mesogastria), the growth of the liver and particularly of the vessels and ducts which enter and leave the liver. These developments permit stomach expansion both anteriorly and posteriorly when food is ingested and free movement of peristalsis. The right pleuroperitoneal canal forms a discrete region of the peritoneal cavity, the lesser sac, and the remaining left pleuroperitoneal canal and the remainder of the peritoneal cavity form the greater sac. The entrance to the original right pleuroperitoneal canal (lesser sac) becomes reduced in size. It is called the epiploic foramen, foramen of Winslow, or the aditus of the omental bursa (bursa omentalis) (Figs 73.6, 73.7).

Early stages of lesser sac development

The lesser sac is first indicated by the appearance of multiple clefts in the para-oesophageal mesenchyme on both left and right aspects of the oesophagus. Although they may become confluent, the left clefts are transitory and soon atrophy. The right clefts merge to form the right pneumatoenteric recess that extends from the oesophageal end of the lesser curvature of the stomach as far as the caudal aspect of the right lung bud. At its gastric end it communicates with the general peritoneal cavity and lies ventrolateral to the gut; more rostrally it lies directly lateral to the oesophagus. It is not, as commonly stated, a simple progressive excavation of the right side of the dorsal mesogastrium. The right pneumatoenteric recess undergoes further extension, subdivision and modification (Fig. 73.7 A(i), B(i)). From its caudal end a second process of cleft and cavity formation occurs which produces the hepatoenteric recess. This thins and expands the splanchnopleure between the liver and the stomach and proximal duodenum, and reaches the diaphragm (Fig. 73.7A(i), C(i)). The resulting, structurally bilaminar, mesenteric sheet is the lesser omentum. It is derived, cranially to caudally, from the small meso-oesophagus; the much larger ventral mesogastrium and the most caudal free border, is from the ventral mesoduodenum. As differential growth of the duodenum occurs, the biliary duct is repositioned and most of the duodenum becomes sessile. The duodenal attachment of the free border and a continuous neighbouring strip of the lesser omentum become confined to the upper border of a short segment of its superior part. The contrasting growth and positioning of its attached viscera cause the free border to change gradually from the horizontal to the vertical. It carries the bile duct, portal vein and hepatic artery, and its hepatic end is reflected around the porta hepatis. An alternative name for this part of the lesser omentum is the hepatoduodenal ligament: it forms the anterior wall of the epiploic foramen. The floor of the foramen is the initial segment of the superior part of the duodenum, its posterior wall is the peritoneum covering the immediately subhepatic part of the inferior vena cava, and its roof the peritonealized caudate process of the liver. The major part of the lesser omentum from the lesser gastric curvature passes in an approximately coronal plane to reach the floor of the increasingly deep groove for the ductus venosus on the hepatic dorsum: this part is sometimes called the hepatogastric ligament.

Ligaments of the liver

The liver is precociously large during development because of its early role in haematopoiesis. Thus the liver mass projects into the abdominal cavity with equal growth on the two sides of the peritoneal cavity. The ligaments associated with the liver develop from the ventral mesogastrium – which passes from the foregut to the ventral abdominal wall down to the cranial rim of the intestinal portal – and from the reflections of peritoneum from the liver to the diaphragm.

The medial portions of the germinative coelomic epithelial walls, containing splanchnopleuric mesenchyme, septum transversum mesenchyme and developing liver, constitute the early ventral mesogastrium (Fig. 73.5A). The mesenchyme between these layers is continuous superiorly with the septum transversum mesenchyme of the diaphragm. The coelomic epithelial layers of the ventral mesogastrium almost touch anterior and posterior to the liver, and are separated by a slender lamina of mesenchyme. They form the falciform ligament and the lesser omentum respectively, and where they are in contact with the liver directly they form visceral peritoneum (Fig. 73.7D).

When the diaphragm is formed above the liver, local cavities coalesce and open into the general coelomic cavity as extensions of the greater (and lesser) sacs. In this way almost all the ventrosuperior, visceral and some of the posterior aspects of the liver become peritonealized. The process of extending the greater sac continues over the right lobe and stops when the future superior and inferior layers of the coronary ligament and the right triangular ligament are defined. Those, plus a medial boundary provided by an extension of the lesser sac, enclose the ‘bare area’ of the liver where loose areolar tissue of septum transversum origin persists. Later in development, when the haematopoietic function of the liver declines, the left lobe becomes relatively smaller than the right, which presumably accounts for the smaller size of the left triangular ligament.

Where the superior layers of the coronary and left triangular ligaments meet they continue as a (bilaminar) ventral mesentery attached to the ventrosuperior aspects of the liver. Its somewhat arched umbilicohepatic free caudal border carries the left umbilical vein. As the ventral body wall develops this falciform ligament, which initially attaches to the early cranial intestinal portal, is drawn to the diminishing cranial rim of the umbilicus. It may be considered the final ventral part of the ventral mesogastrium, although its free border has a ventral mesoduodenal origin. Its passage to the ventral body wall becomes increasingly oblique, curved and falciform (sickle-shaped) as the umbilicus becomes more defined.

In the early embryo the connection between one pericardioperitoneal canal and the other was directly across the ventral surface of the cranial midgut, immediately caudal to the developing primitive ventral mesogastrium. By stage 14 the passage from one side of the falciform ligament to the other necessitates passing below the greatly enlarged liver, or the curved lower edge of the falciform ligament, or the lesser omentum. The position of the falciform ligament is of clinical interest in the neonate in diagnosing pneumoperitoneum because it is silhouetted by air on abdominal X-rays.

Caval fold

The caval fold is a linear eminence, with divergent cranial and caudal ends, which passes from the upper abdominal to the lower thoracic region and protrudes from the dorsal wall of the pleuroperitoneal canal. Cranially it becomes continuous, lateromedially, with the root of the pulmonary anlage and pleural coelom, the uppermost portion of the septum transversum mesenchyme, and the retrocardiac mediastinal mesenchyme. Caudally it forms an arch with dorsal and ventral horns. The dorsal horn merges with the primitive dorsal mesentery and the mesonephric ridge and associated gonad and suprarenal (adrenal) gland. The ventral horn is confluent with the dorsal surface of the septal mesenchyme.

Thus the caval fold is a zone where intestinal, mesenteric, intermediate, hepatic, pericardial, pulmonary and mediastinal mesenchymes meet and blend. It provides a mesenchymal route for the upper abdominal, transdiaphragmatic and transpericardial parts of the inferior vena cava, and it is also prominent in the development of parts of the liver, lesser sac of peritoneum, and certain mesenteries. The left fold regresses whereas the right fold enlarges rapidly (Fig. 73.7A).

The pneumatoenteric recess continues to expand to the right into the substance of the caval fold. It stops near the left margin of the hepatic part of the inferior vena cava, which remains extraperitoneal and crosses the base of the now roughly triangular bare area of the liver and this new expanded line of reflexion. With closure of the pleuroperitoneal canals the rostral part of the right pneumatoenteric recess is sequestered by the diaphragm but often persists as a small serous sac in the right pulmonary ligament. The remaining caval fold mesenchyme to the left of the inferior vena cava – which forms the right wall of the upper part of the lesser sac – becomes completely invaded by embryonic hepatic tissue and is transformed into the caudate lobe of the liver. This smooth, vertically elongated mass projects into the cavity of the lesser sac: both its posterior, and much of its anterior, surfaces become peritonealized as a result of the increasing depth of the groove for the ductus venosus and the attachment of the lesser omentum to its floor.

Later stages of lesser sac development

The lower (inferior) part of the lesser sac can be first seen in embryos of 8–9 mm CR length and the early pneumatoenteric and hepatoenteric recesses are well established. Progressive differential gastric growth produces an elliptical transverse sectional profile, with a right-sided lesser curvature, which corresponds to the original ventral border of the gastric tube. The lesser omental gastric part of the ventral mesogastrium remains attached to this border. The greater curvature of the stomach is a new, rapidly expanding, region: its convex profile projects mainly to the left, but also cranially and caudally (Fig. 73.7 A(i), B(i), C(i)). The original dorsal border of the gastric tube now traverses the dorsal aspect of the expanding rudiment, curving along a line near the lesser curvature. The primitive dorsal mesogastrium is transiently attached to it, and blends with the thick layer of compound gastric mesenchyme clothing the posterior aspect and greater curvature of the miniature stomach. Because of its thickness, the mesenchyme projects cranially, caudally, and particularly to the left, beyond the ‘new’ greater curvature of the endodermal lining of the stomach.

The processes already described in relation to the ventral mesenteries now supervene. Multiple clefts appear at various loci in the mesenchyme, and there are local mesenchyme to epithelial transitions. The groups of clefts rapidly coalesce to form transiently isolated closed spaces which soon join with each other and with the preformed upper part of the lesser sac; the newly formed epithelia join the coelomic epithelium. In sequence, the initial loci occur in the compound posterior gastric mesenchyme nearer the lesser curvature and along its zone of blending with the primitive dorsal mesogastrium; in the dorsal mesoduodenum; and independently in the caudal rim, where greater curvature mesenchyme and dorsal mesogastrium blend. As these cavities become confluent and their ‘reniform’ expansion follows, matches and then exceeds that of the gastric greater curvature, there are several major sequelae. The primitive dorsal mesogastrium increases in area by intrinsic growth, and, as cavitation proceeds, by incorporating substantial contributions from the dorsal lamella separated by cleavage of the posterior gastric mesenchyme: it is now called the secondary dorsal mesogastrium (Fig. 73.7A(ii)). The gastric attachment of the secondary dorsal mesogastrium changes progressively. It may be regarded as a set of somewhat spiral lines, longitudinally disposed, that move with time to the left, from near the lesser curvature, towards and finally reaching, the definitive greater curvature. The parietal mesogastrial and (cleaving) mesoduodenal attachment remains in the dorsal midline for a time, but it later undergoes profound changes. With the confluence of the cavities that collectively form the lower part of the lesser sac, its communication with the upper part (which corresponds to the lesser gastric curvature and right and left gastropancreatic folds) becomes better defined. Ventral to the lower part of the cavity, postcleavage splanchnopleure covers the posteroinferior surface of the stomach and a short proximal segment of the duodenum. This ventral wall is continued beyond the greater curvature and duodenum as the splanchnopleuric strip of visceral attachment of the secondary dorsal mesogastrium and mesoduodenum. The radial width of the strip is relatively short cranially (gastric fundus) and gradually increases along the descending left part of the greater curvature. It is longest throughout the remaining perimeter of the greater curvature as far as the duodenum: this prominent part shows continued marginal (caudoventral and lateral) growth with extended internal cavitation (its walls constitute the expanding greater omentum; Fig. 73.6H; see Fig. 3.6E). The margins of the cavity of the inferior part of the lesser sac are limited by the reflexed edges of the ventrally placed strata derived from the secondary dorsal mesogastrium just described. These converge to form the splanchnopleuric dorsal wall, which is initially ‘free’ throughout except at its midline dorsal root. At roughly midgastric levels, the pancreatic rudiment grows obliquely encased in this dorsal wall; its tail ultimately reaches the left limit of the lesser sac at the level of the junction between gastric fundus and body (Fig 73.7C(ii)).

Greater omentum

The greater omentum continues to grow both laterally, and particularly caudoventrally. It covers and is closely applied to the transverse mesocolon, transverse colon and inframesocolic and infracolic coils of small intestine (Fig. 73.6D–G). At this stage the quadrilaminar nature of the dependent part of the greater omentum is most easily appreciated. ‘Simple’ mesenteries are bilaminar: they possess two mesothelial surfaces derived from splanchnopleuric coelomic epithelium, which enclose a connective tissue core derived from splanchnopleuric mesenchyme. In the greater omentum, the gastric serosa covering its posteroinferior surface (single mesothelium) and the anterosuperior serosa (single mesothelium) converge to meet at the greater curvature and initial segment of the duodenum. The resulting bilaminar mesentery continues caudoventrally as the ‘descending’ stratum of the omentum. This, on reaching the omental margins, is reflexed and now passes craniodorsally to its parietal root as the ‘ascending’ posterior bilaminar stratum. The two bilaminar strata are initially in fairly close contact caudally, but separated by a fine, fluid-containing, cleft-like extension of the lower part of the lesser sac. The posterior mesothelium of the posterior stratum makes equally close contact with the anterosuperior surface of the transverse colon, starting at the taenia omentalis, and with its transverse mesocolon.

Maturation of the lesser sac

At this stage, and subsequently, it is convenient to designate the lower part of the lesser sac as consisting of three subregions: retrogastric, perigastric and greater omental (Fig. 73.7C(ii)). The names are self-explanatory but their confines are all modified by various factors. Two phenomena are particularly prominent, namely, gastric ‘descent’ relative to the liver, and fusion of peritoneal layers with altered lines of reflexion, adhesion of surfaces and loss of parts of cavities.

After the third month, hepatic growth, particularly of the left lobe, diminishes and the whole organ recedes into the upper abdomen. Meanwhile the stomach elongates and some descent occurs, despite its relatively fixed cranial and caudal ends. This produces the angular flexure of the stomach which persists postnatally. The concavity of the lesser curvature is now directed more precisely to the right, the lesser omentum is more exactly coronal and its free border vertical. Ventral to the liver the free border of the falciform ligament passes steeply craniodorsally from umbilicus to liver (see disposition in neonate in Figs 14.4 and 14.5). The mesenchymal dorsal wall of the lower part of the lesser sac, which is crossed obliquely by the growing pancreas, has hitherto remained free and retained its original dorsal midline root. Substantial areas now fuse with adjacent peritonealized surfaces of retroperitoneal viscera, the parietes, or another mesenteric sheet or fold. Where sheets fuse there is a variable loss of apposed mesothelia and some continuity of their mesenchymal cores, but they remain surgically separable and no vascular anastomosis develops across the interzone. Above the pancreas the posterior secondary dorsomesogastrial wall of the sac becomes closely applied to the peritoneum covering the posterior abdominal wall and its sessile organs, the diaphragm, much of the left suprarenal gland, the ventromedial part of the upper pole of the left kidney, the initial part of the abdominal aorta, the coeliac trunk and its branches, and other vessels, nerves, and lymphatics (see Fig. 14.4). Their peritoneal surfaces fuse. However, albeit with some tissue loss, a single mesothelium remains covering these structures, intercalated as a new secondary dorsal wall for this part of the lesser sac.

The pancreas grows from the duodenal loop, penetrating the substance of the dorsal mesoduodenum and secondary dorsal mesogastrium; their mesenchymes and mesothelia initially clothe its whole surface, except where peritoneal lines of reflexion exist. Its posterior peritoneum becomes closely applied to that covering all the posterior abdominal wall structures it crosses (the inferior vena cava, abdominal aorta, splenic vein, superior mesenteric vessels, inferior mesenteric vein, portal vein, left renal vessels, the caudal pole of the left suprarenal, a broad ventral band on the left kidney and various muscles (see Figs 14.4, 14.5). The intervening peritoneal mesothelia fuse and atrophy, and the mesenchymal cores form fascial sheaths and septa. The pancreas is now sessile. The peritoneum covering the upper left part of its head, neck and the anterosuperior part of its body forms the central part of the dorsal wall of the lesser sac. The pancreatic tail remains peritonealized by a persisting part of the secondary dorsal mesogastrium as it curves from the ventral aspect of the left kidney towards the hilum of the spleen. The infracolic parts of the pancreas are covered with greater sac peritoneum. In the greater omental subregion of the lower part of the lesser sac two contrasting forms of mesenteric adhesion occur. The posterior ‘returning’ bilaminar stratum of the omentum undergoes partial fusion with the peritoneum of the transverse colon at the taenia omentalis and with its mesocolon. The layers remain surgically separable; no anastomosis occurs between omental and colic vessels.

The original dorsal midline attachment to the parietes of the foregut dorsal mesentery is profoundly altered during the development of the lesser sac and its associated viscera. However, despite the extensive areas of fusion, virtually the whole of the gastric greater curvature (other than a small suboesophageal area) and its topographical continuation (the inferior border of the first 2–3 cm of the duodenum), retain true mesenteric derivatives of the secondary dorsal mesogastrium and its continuation, the dorsal mesoduodenum. Although regional names are used to assist identification and description, it must be emphasized that they are all merely subregions of one continuous sheet.

The upper (oesophagophrenic) part of the lesser omentum arches across the diaphragm. As this bilaminar mesentery approaches the oesophageal hiatus its laminae diverge, skirting the margins of the hiatus. They then descend for a limited distance and with variable inclination, to enclose reciprocally shaped areas on the dorsum of the gastric fundus and diaphragm. The area may be roughly triangular to quadrangular; it contains areolar tissue and constitutes the bare area of the stomach or, when large, the left extraperitoneal space. Its right lower angle is the base of the left gastropancreatic fold, and its left lower angle reconstitutes the bilaminar mesentery. The root of the latter arches downwards and to the left across the diaphragm and suprarenal gland and gives the gastrophrenic ligament to the gastric fundus. It continues to arch across the ventral surface of the upper part of the left kidney, and its layers part to receive the pancreatic tail: they initially extend to the hilum of the spleen as the lienorenal (splenorenal) ligament (see Figs 73.6C, 73.7D),. The left half of this bilaminar ‘ligament’ provides an almost complete peritoneal tunic for the spleen. It then reunites with its fellow at the opposite rim of the splenic hilum, and continues to the next part of the gastric greater curvature as the gastrosplenic ligament. The remaining part (perhaps two-thirds) of the gastric greater curvature and its short duodenal extension provide attachment for the anterior, ‘descending’, bilaminar stratum of the greater omentum. Its returning, posterior, bilaminar stratum continues to its parietal root (which extends from the inferior limit assigned to the splenorenal ligament), and curves caudally and to the right along the anterior border of the body of the pancreas, immediately cranial to the line of attachment of the transverse mesocolon. Crossing the neck of the pancreas, the same curve is followed for a few centimetres on to its head; the omental root then sharply recurves cranially and to the left, to reach the inferior border of the duodenum. Thus it reaches that part of the lesser sac provided by cleavage of the dorsal mesoduodenum from the greater sac. It enters the epiploic foramen, traverses the epiploic canal between the caudate hepatic process and proximal duodenum, then crosses the right gastropancreatic fold, and descends behind the proximal duodenum to enter the right marginal strip enclosed by the greater omentum. The definitive origins of the peritoneum from the posterior abdominal wall are shown in the adult in Figures 64.1, 69.4 and 64.5B.

Peritoneum associated with the mid- and hindgut

It is convenient to consider the mesenteries of the small and large intestine after rotation and the principal growth patterns have been achieved and the developing pancreas is becoming retroperitoneal.

Small intestine

Most of the duodenal loop encircles the head of the pancreas and is retroperitoneal. The peritoneum principally covers its ventral and convex aspects. Areas not covered are a short initial segment of the superior (first) part, which is more completely peritonealized because it gives attachment to the right margins of the greater and lesser omenta; the sites where the transverse colon is closely apposed to the descending (second) part, or where the latter is crossed by the root of the transverse mesocolon; and the sites where the mesentery crosses the transverse (third) part, and descends across the ascending (fourth) part from its upper extremity at the duodenojejunal flexure. These regions are illustrated in the adult in Figure 64.1. In addition, one or more of up to six different duodenal recesses may develop. Their variations in shape and size, their intestinal, mesenteric and vascular relations, and, when adequately recorded, the frequencies and disposition of their orifices, are given on page 1108–1109.

From a mesenteric standpoint, the succeeding small intestine, from the duodenojejunal flexure to the ileocaecal junction, undergoes less modification of its embryonic form than other gut regions. Its early dorsal mesentery is a continuous, single (but structurally bilaminar) sheet, with a midline parietal attachment (line of reflexion, or ‘root’). The attachment of the root becomes an oblique narrow band from the left aspect of the second lumbar vertebra to the cranial aspect of the right sacroiliac joint (Fig. 73.6H; see Fig. 64.1).

Ascending colon

The caecum and vermiform appendix arise as a diverticulum from the antimesenteric border of the caudal limb of the midgut loop, consequently the caecum does not possess a primitive mesocaecum. These regions of the gut undergo long periods of growth, often asymmetrical, and their final positions, dimensions and general topography show considerable variation. The vermiform appendix is almost wholly clothed with visceral peritoneum, derived from the diverging layers of its rather diminutive mesoappendix. The latter should perhaps be regarded as a direct derivative of the primitive dorsal mesentery, and perhaps a similar status for the vascular fold of the caecum should be considered.

The colonic gut retains its primitive dorsal mesentery, the meso-colon, until the differential growth, rotation and circumabdominal displacement of this part of the gut tube nears completion. Its original root is still vertical in the dorsal midline, although the mesocolon diverges from it widely as an incomplete, flattened pyramid, to reach its colonic border at the future taenia mesocolica. During the fourth and fifth months substantial areas of the primitive mesocolon adhere to, then fuse with, the parietal peritoneum. In this way, some colonic segments become sessile while others have a shorter mesocolon with an often profoundly altered parietal line of attachment. The mesocolon of the transverse and sigmoid segments normally persists, while the ascending colon, right (hepatic) flexure and descending colon become sessile: the ascending or descending, or both, colonic segments may also retain a mesocolon which varies from a localized ‘fold’ to a complete mesocolon. When sessile, the ventral, medial and lateral aspects of the ascending or descending colon are clothed with peritoneum, and the protrusion of the viscus produces medial and lateral peritoneal paracolic gutters on each side. This form of apposition to underlying structures (zygosis) proceeds from the ascending colon to include the right colic (hepatic) flexure, and thence continues anteroinferiorly to the left, so involving the right-sided initial segment of the transverse colon.

Transverse colon

The right extremity of the transverse colon is sessile, and is separated by fibroareolar tissue from the anterior aspect of the descending (second) part of the duodenum and the corresponding aspect of most of the head of the pancreas. The remainder of the transverse colon, up to and including the left (splenic) colic flexure, is almost completely peritonealized by the diverging layers of the transverse mesocolon. The root of the latter reaches the neck and whole extent of the anterior border of the body of the pancreas. The long axis of the definitive pancreas lies obliquely. The splenic colonic flexure is considerably more rostral than the hepatic flexure and consequently the root of the mesocolon curves obliquely upwards as it crosses the upper abdomen from right to left. As it expands, the posteroinferior wall of the greater omental part of the lesser sac gradually covers, and becomes closely applied to, the transverse mesocolon and its contained colon, finally projecting beyond the latter. Craniocaudal adherence now occurs between the omental wall and the pericolonic and mesocolonic layers.

Descending colon

The left colic flexure receives much of its peritoneal covering from the left extremity of the transverse mesocolon. It is also often connected to the parietal peritoneum of the diaphragm over the 10th and 11th ribs by a phrenicocolic ligament. The latter sometimes blends with a presplenic fold that radiates from the gastrosplenic ligament. The descending colon becomes sessile. The process of fusion and obliteration of both ascending and descending mesocolons starts laterally and progresses medially.

Sigmoid colon

The sigmoid colon is most variable in its length and disposition. It retains its dorsal mesocolon, but the initial midline dorsal attachment of its root is considerably modified in its definitive state.

Rectum

The rectum continues from the ventral aspect of the third sacral vertebra to its anorectal (perineal) flexure anteroinferior to the tip of the coccyx: the distance changes with age. All aspects of the rectum are encased by mesenchyme, and the early dorsally placed mass is named, by some authorities, the dorsal mesorectum. However, the latter does not form a true mesentery: with progressive skeletal development it is reduced to a woven fibroareolar sheet which displays patterned variations in thickness and fibre orientation. The sheet is closely applied to the ventral concavity of the sacrum and coccyx, and encloses numerous fibromuscular and neurovascular elements. The rectum therefore becomes sessile, and visceral peritoneum is restricted to its lateral and ventral surfaces (see Fig. 78.4).

With the disappearance of the postanal gut by the end of the fifth week, the ventrolateral peritoneum reaches the superior surface of the pelvic floor musculature: this condition persists until late in the fourth month. In the male the ventral rectal peritoneum is reflected over the posterior surface of the prostate, bladder trigone and associated structures. In the female the ventral peritoneum initially receives a reflection which covers almost the whole posterior aspect of the vagina, and is continued over the uterus. Subsequently, the closely apposed walls of these deep peritoneal pouches fuse over much of their caudal extent, their mesothelia are lost, and the viscera are separated by an intervening, bilaminar (surgically separable), fibrous stratum. In the male this becomes the rectovesical fascia and posterior wall of the prostatic sheath (see Fig. 78.10). In the female it becomes the rectovaginal septum between the lower part of the vagina and the rectum (see Fig. 78.9). The proximal third of the rectum is covered by peritoneum ventrolaterally: the lateral extensions of this tunic are triangular and deep proximally, but taper to an acute angle by the middle third of the rectum. The middle third of the rectum is covered by peritoneum only on its ventral surface, where it forms the posterior wall of the shallower rectovesical or rectovagino-uterine pouch. The remaining rectum and anal canal are extraperitoneal.

NEONATAL PERITONEAL CAVITY

The fully formed peritoneal cavity, although complex topographically, remains a single cavity with numerous intercommunicating regions, pouches and recesses (see Fig. 14.5). The only small peritoneal sacs to separate completely from the main cavity are the infracardiac bursa (Fig. 73.7(B(i)) and the tunica vaginalis testis (see Fig. 78.17).

In fetal life the greater omental cavity extends to the internal aspect of the lateral and caudal edges of the omentum. Postnatally a slow but progressive fusion of the internal surfaces occurs with obliteration of the most dependent part of the cavity: this proceeds rostrally and, when mature, the cavity does not usually extend appreciably beyond the transverse colon. Transverse mesocolon–greater omentum fusion begins early while the umbilical hernia of the midgut has not returned. It starts between the right margin of the early greater omentum and near the root of the presumptive mesocolon, and later spreads to the left.

In the neonate the peritoneal cavity is ovoid (see Fig. 14.4). It is fairly shallow from anterior to posterior because the bilateral posterior extensions on each side of the vertebral column, which are prominent in the adult, are not present. Two factors lead to the protuberance of the anterior abdominal wall in the neonate and infant. The diaphragm is flatter in the newborn, which produces a caudal displacement of the viscera. The pelvic cavity is very small in the neonate, which means that organs which are normally pelvic in the adult, i.e. urinary bladder, ovaries and uterus, all extend superiorly into the abdomen (see Figs 14.5, 78.9, 78.10). The pelvic cavity is joined to the abdominal cavity at less of an acute angle in the neonate because there is no lumbar vertebral curve and only a slight sacral curve.

The peritoneal attachments are similar to the adult. However, the greater omentum is relatively small: its constituent layers of peritoneum may not be completely fused, and it does not extend much below the level of the umbilicus (see Fig. 14.5). Generally the length of the mesentery of the small intestine and of the transverse and sigmoid mesocolons are longer than in the adult, whereas the area of attachment of the ascending and descending colons is relatively smaller. The peritoneal mesenteries and omenta contain little fat.

SPLEEN

The spleen appears about the sixth week as a localized thickening of the coelomic epithelium of the dorsal mesogastrium near its cranial end (Figs 73.6, 73.7). The proliferating cells invade the underlying angiogenetic mesenchyme, which becomes condensed and vascularized. The process occurs simultaneously in several adjoining areas which soon fuse to form a lobulated spleen of dual origin (from coelomic epithelium and from mesenchyme of the dorsal mesogastrium). The enlarging spleen projects to the left, so that its surfaces are covered by the peritoneum of the mesogastrium on its left aspect, which forms a boundary of the general extrabursal (greater) sac. When fusion occurs between the dorsal wall of the lesser sac and the dorsal parietal peritoneum, it does not extend to the left as far as the spleen, which remains connected to the dorsal abdominal wall by a short lienorenal ligament. Its original connection with the stomach persists as the gastrosplenic ligament. The earlier lobulated character of the spleen disappears, but is indicated by the presence of notches on its upper border in the adult.

The histogenesis of the spleen has attracted relatively little attention. The vascular reticulum is well developed at 8–9 weeks, and contains immature reticulocytes and numerous closely spaced thin-walled vascular loops. Differentiation of blood cells, macrophages, and of arteries, veins, capillaries and sinusoids has occurred by the eleventh to twelfth week. Initially the capsule consists of cuboidal cells bearing cilia and microvilla.

The spleen displays various developmental anomalies, including complete agenesis, multiple spleens or polysplenia, isolated small additional spleniculi and persistent lobulation. Asplenia and polysplenia are associated with other anomalies, especially those involving the cardiac and pulmonary systems. Accessory spleens are very common in neonates, located in the greater omentum. At birth the spleen weighs, on average, 13 g (see Fig. 14.4). It doubles its weight in the first postnatal year and triples it by the end of the third year.

SUPRARENAL GLANDS

The suprarenal (adrenal) cortex is formed during the second month by a proliferation of the coelomic epithelium. Cells pass into the underlying mesenchyme between the root of the dorsal mesogastrium and the mesonephros (see Fig. 24.11). The proliferating tissue, which extends from the level of the sixth to the 12th thoracic segments, is soon dis-organized dorsomedially by invasion of neural crest cells from somite levels 18–24, which form the medulla, and also by the development of venous sinusoids. The latter are joined by capillaries, which arise from adjacent mesonephric arteries and penetrate the cortex in a radial manner. When proliferation of the coelomic epithelium stops, the cortex is enveloped ventrally, and later dorsally, by a mesenchymal capsule which is derived from the mesonephros. The subcapsular nests of cortical cells are the rudiment of the zona glomerulosa: they proliferate cords of cells which pass deeply between the capillaries and sinusoids. The cells in these cords degenerate in an erratic fashion as they pass towards the medulla, becoming granular, eosinophilic and ultimately autolysed. These cords of cells constitute the fetal cortex, which undergoes rapid involution during the first two years after birth. The fascicular and reticular zones of the adult cortex are proliferated from the glomerular zone after birth.

The most common abnormality of suprarenal gland development is congenital hyperplasia, which occurs in 1 : 5000–1 : 15,000 births. This condition is caused by a group of autosomal recessive disorders in which there are deficiencies in enzymes required for the synthesis of cortisol. In 90% of cases the cause is deficiency of the enzyme 21-hydroxylase, producing an accumulation of 17-hydroxyprogesterone, which is converted to androgens. The levels of androgens increase by several hundred times, causing female embryos and fetuses to undergo external genital masculinization ranging from clitoral hypertrophy to formation of a phallus and scrotum: masculinization of the brain has also been suggested. In male embryos the levels do not cause any changes in external genitalia. Signs of androgen excess may appear in childhood with precocious masculinization and accelerated growth (Lewis, Yaron & Evans 1999).

SUPRARENAL GLANDS IN THE NEONATE

The suprarenal glands are relatively very large at birth (see Figs 14.4 and 78.8) and constitute 0.2% of the entire body weight, compared with 0.01% in the adult. The left gland is heavier and larger than the right, as it is in the adult. At term each gland usually weighs 4 g; the average weight of the two glands is 9 g (average in the adult is 7–12 g). The glands involute rapidly in the neonatal period when each gland loses 25% of its mass; the average weight of both glands is 5 g by the end of the second week, and 4 g by 3 months. Birth weight is not regained until puberty. The cortex of the suprarenal gland is thicker than in the adult and the medulla of the gland is small. Early studies on fetal suprarenal glands described extensive degeneration and necrosis of fetal zone cells; however, it is believed that these studies showed disease processes rather than the normal involution of the gland. With normal involution the fetal zone cells of the postnatal gland become smaller and they assume the appearance and organization typical of zona fasciculata.

INFERIOR VENA CAVA, PORTAL CIRCULATION AND UMBILICAL VESSELS

INFERIOR VENA CAVA

The inferior vena cava of the adult is a composite vessel which develops on the posterior abdominal wall dorsal to the developing peritoneal cavity. It forms as a consequence of the temporal remodelling of successive venous complexes (see Fig. 13.4). The precise mode of development of its postrenal segment (caudal to the renal vein) is still somewhat uncertain. Its function is initially carried out by the right and left postcardinal veins (Fig. 73.8; see also Fig. 13.4), which receive the venous drainage of the lower limb buds and pelvis and run in the dorsal part of the mesonephric ridges, receiving tributaries from the body wall (intersegmental veins) and from the derivatives of the mesonephroi.

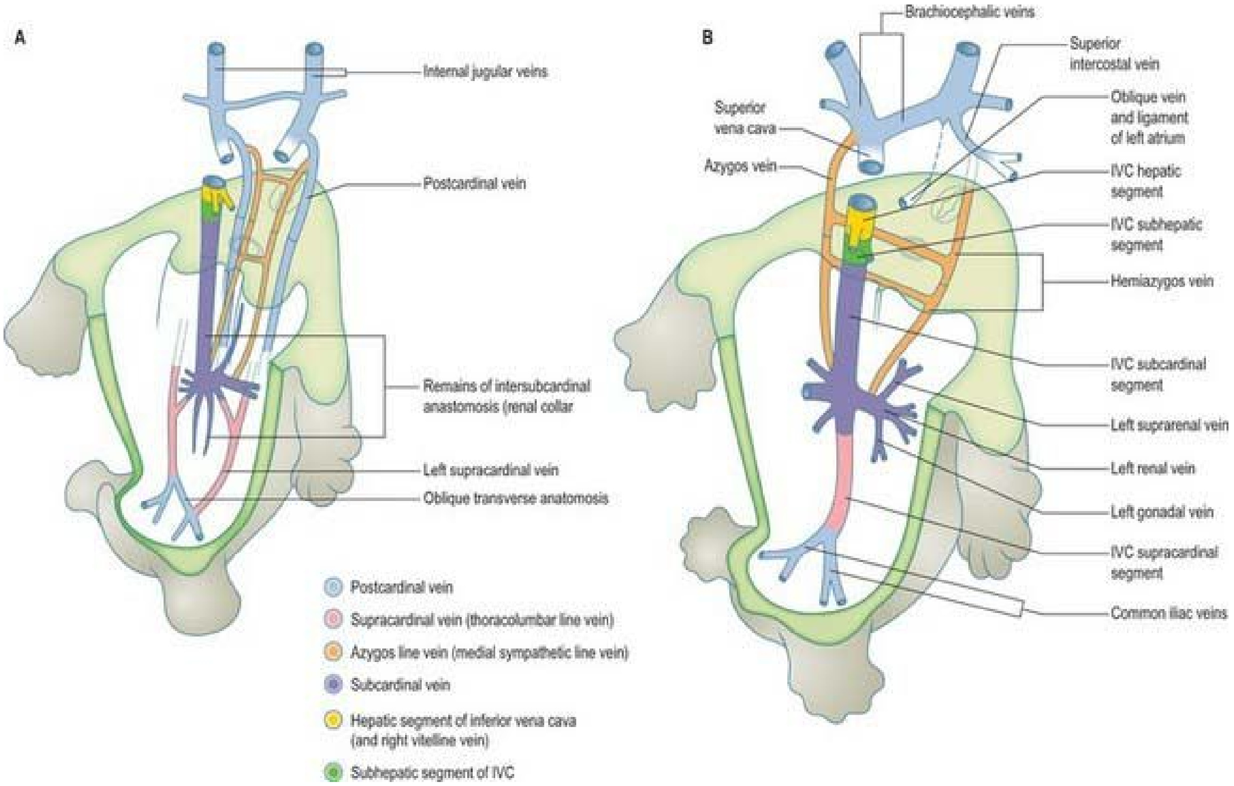
A
Internal jugular veins
Postcardinal vein
Remains of intersubcardinal anastomosis (renal collar
Left supracardinal vein
Oblique transverse anatomosis
Postcardinal vein
Supracardinal vein (thoracolumbar line vein)
Azygos line vein (medial sympathetic line vein)
Subcardinal vein
Hepatic segment of inferior vena cava (and right vitelline vein)
Subhepatic segment of IVC
B
Brachiocephalic veins
Superior intercostal vein
Superior vena cava
Azygos vein
Oblique vein and ligament of left atrium
IVC hepatic segment
IVC subhepatic segment
Hemiazygos vein
IVC subcardinal segment
Left suprarenal vein
Left renal vein
Left gonadal vein
IVC supracardinal segment
Common iliac veins

Fig. 73.8 The inferior vena cava develops within the posterior abdominal wall. It is a composite vessel formed by temporal remodelling of successive somatic venous anastomoses. (For early venous development see **Fig. 13.4**.)

The early postcardinal veins communicate across the midline via an interpostcardinal anastomosis. This remains as an oblique transverse anastomosis between the iliac veins, and becomes the major part of the definitive left common iliac vein. It diverts an increasing volume of blood into the right longitudinal veins, which accounts for the ultimate disappearance of most of those on the left.

The supracardinal veins receive the larger venous drainage of the growing body wall. The right supracardinal vein persists and forms the greater part of the postrenal segment of the inferior vena cava. The continuity of the vessel is maintained by the persistence of the anastomosis between the right supracardinal and the right subcardinal in the renal collar. The left supracardinal disappears, but some of the renal collar formed by the left supracardinal–subcardinal anastomosis persists in the left renal vein. Both supracardinal veins drain cranially into the subcardinal veins. On the right side, the subcardinal vein comes into intimate relationship with the liver. An extension of the vessel takes place in a cranial direction and meets and establishes continuity with a corresponding new formation that is growing caudally from the right vitelline hepatocardiac (common hepatic) vein. In this way, on the right side a more direct route is established to the heart and the prerenal (cranial) segment of the inferior vena. In summary, the inferior vena cava is formed from below upwards by the confluence of: the common iliac veins, a short segment of the right postcardinal vein, the postcardinal–supracardinal anastomosis, part of the right supracardinal vein, the right supracardinal–subcardinal anastomosis, right subcardinal vein, a new anastomotic channel of double origin (the hepatic segment of the inferior vena cava), and the cardiac termination of the right vitelline hepatocardiac vein (common hepatic vein).

Only the supracardinal part of the inferior vena cava receives intersegmental venous drainage. The postrenal (caudal) segment of the inferior vena cava is on a plane that lies dorsal to the plane of the prerenal (cranial) segment. Thus the right phrenic, suprarenal and renal arteries, which represent persistent mesonephric arteries, pass behind the inferior vena cava, whereas the testicular or ovarian artery, which has a similar developmental origin, passes anterior to it.

In some animals, the right postcardinal vein constitutes a large part of the postrenal segment of the inferior vena cava. In these cases the right ureter, on leaving the kidney, passes medially dorsal to the vessel and then, curving round its medial side, crosses its ventral aspect. Rarely, a similar condition is found in humans, and indicates the persistence of the right postcardinal vein and failure of the right supracardinal to play its normal part in the development of the inferior vena cava.

PORTAL CIRCULATION

The heart first differentiates in splanchnopleure that, after head fold formation, forms the dorsal wall of the primitive pericardial cavity (floor of the rostral foregut) and may therefore be considered a highly specialized vitelline vascular derivative. At the caudal extremity of the splanchnopleuric gut tube (the future lower rectum and upper anal canal) the vitelline venous drainage makes connections with the internal iliac radicles of the postcardinal complex.

The development of the gut occurs contemporaneously with changes to the early symmetrical embryonic circulation (see Ch. 13). A symmetrical, segmental system of somatic arteries remains and supplies the body wall of the trunk. The underlying arrangement of these vessels is only slightly modified by subsequent development. The main changes to the embryonic arrangement occur with the growth of the foregut, liver and paired viscera, i.e. kidneys and suprarenal glands.

The early development of the ventral splanchnic arteries is outlined in Chapter 13. Three main arterial trunks, the coeliac trunk, superior mesenteric and inferior mesenteric arteries, supply the fore- mid- and hind gut respectively. From the gastric terminal segment of the future oesophagus to the upper rectum, the developing endodermal epithelium is surrounded by splanchnopleuric mesenchyme permeated by a capillary plexus which drains into an anastomosing network of veins. This plexus is particularly dense ventrally associated with the central midgut region where, for a while, it receives a network of small veins from the definitive yolk sac. Later, in normal development, these vessels atrophy as the yolk sac diminishes. More rostrally the splanchnopleuric capillaries associated with the foregut and upper portions of the yolk sac form longitudinal channels anterolateral to the gut and these become increasingly well defined as the embryonic abdominal vitelline veins. Entering the septum transversum, the right and left vitelline veins incline slightly, becoming parallel to the lateral aspects of the gut. They establish connections with capillary plexuses in the septal mesenchyme, then continue, finally curving to enter the medial part of the cardiac sinual horn of their corresponding side. The parts of the gut closely related to the presinual segments of the vitelline veins are the future subdiaphragmatic end of the oesophagus, primitive stomach, the superior (first) and descending (second) regions of the duodenum, and the remainder of the duodenal tube.

The principal ascending vitelline veins flanking the sides of the abdominal part of the foregut receive venules from its splanchnopleuric capillaries, and those of the septal mesenchyme. Within these venular nets, enlarged (but still plexiform) anastomoses connect the two vitelline veins (Fig. 73.9; see Fig. 13.1C). A subdiaphragmatic intervitelline anastomosis develops in the rostral septal mesenchyme, lying a little caudal to the cardiac sinuatrial chamber, connecting the veins near their sinual terminations. (The channel is sometimes termed suprahepatic because of the position of the hepatic primordium; with expansion of the latter it becomes partly intrahepatic.) The presumptive duodenum is crossed by three transverse duodenal intervitelline anastomoses. Their relation to the gut tube alternates so that the most cranial, the subhepatic, is ventral, the intermediate is dorsal and the caudal is ventral (Fig. 73.9B). It has become customary to describe the paraduodenal vitelline veins and their associated anastomoses as forming a figure 8. At this early stage when left and right embryonic veins are still symmetric, the cranial duodenal anastomosis becomes connected with the subdiaphragmatic anastomosis by a median longitudinal channel, the primitive median ductus venosus, which is dorsal to the expanding hepatic primordium, but ventral to the gut. The further development of the vitelline veins and anastomoses is, as indicated, closely interlocked, with rapid hepatic expansion and gut changes, and umbilical vein disposition and modification is closely involved.

CHANGES IN THE VITELLO-UMBILICAL VEINS

Progressive changes in the vitello-umbilical veins are rapid, profound and closely linked with regional modifications in shape and position of the gut, expansion and invasion of venous channels by hepatic tissue, asymmetry of the heart and cardiac venous return. The principal events are summarized in Figs 73.9, 73.10 and 73.11.

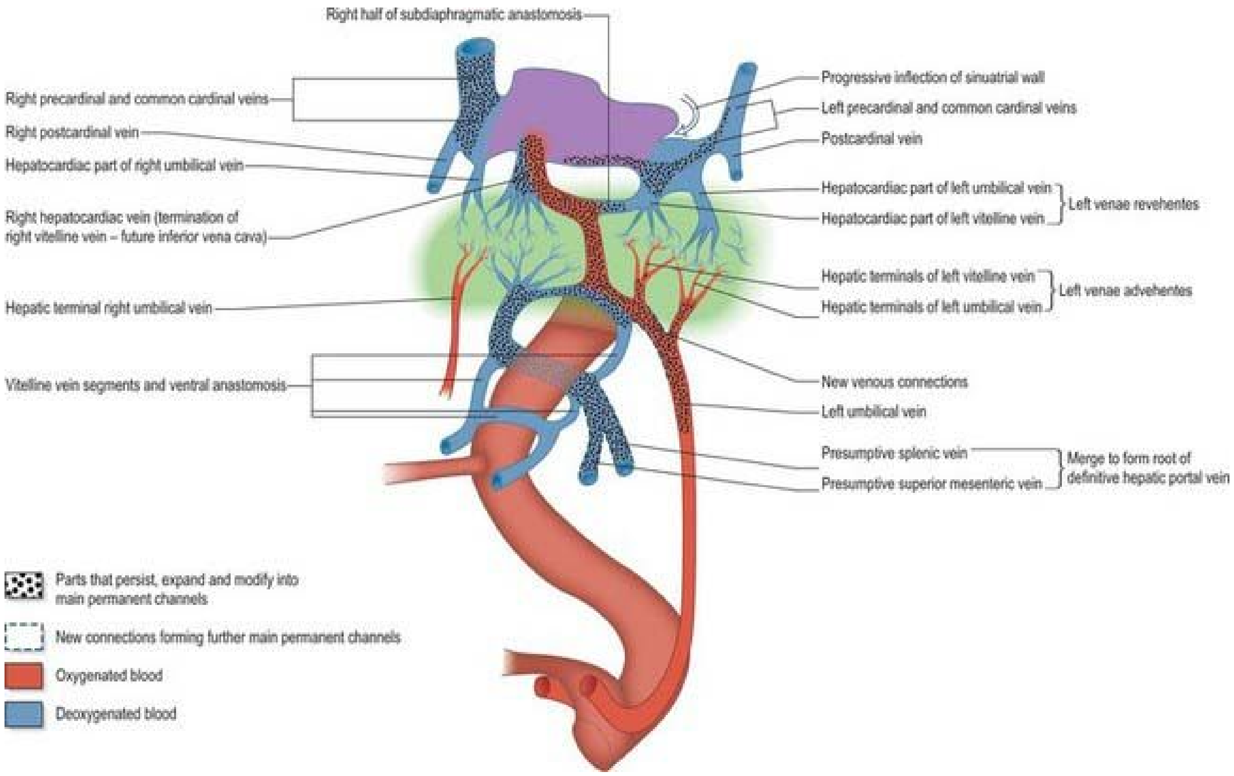
Right half of subdiaphragmatic anastomosis
Right precardinal and common cardinal veins
Right postcardinal vein
Hepatocardiac part of right umbilical vein
Right hepatocardiac vein (termination of right vitelline vein – future inferior vena cava)
Hepatic terminal right umbilical vein
Vitelline vein segments and ventral anastomosis
Progressive inflection of sinuatrial wall
Left precardinal and common cardinal veins
Postcardinal vein
Hepatocardiac part of left umbilical vein
Hepatocardiac part of left vitelline vein
Left venae revehentes
Hepatic terminals of left vitelline vein
Hepatic terminals of left umbilical vein
Left venae advehentes
New venous connections
Left umbilical vein
Presumptive splenic vein
Presumptive superior mesenteric vein
Merge to form root of definitive hepatic portal vein
Parts that persist, expand and modify into main permanent channels
New connections forming further main permanent channels
Oxygenated blood
Deoxygenated blood

Fig. 73.10 Development of the vitelline, umbilical and terminal cardinal vein complexes: a mid-stage of asymmetry has been reached between the early symmetric condition (see **Fig. 73.9**) and the definitive late prenatal state. The extent of the liver within the septum transversum mesenchyme is shown in green.

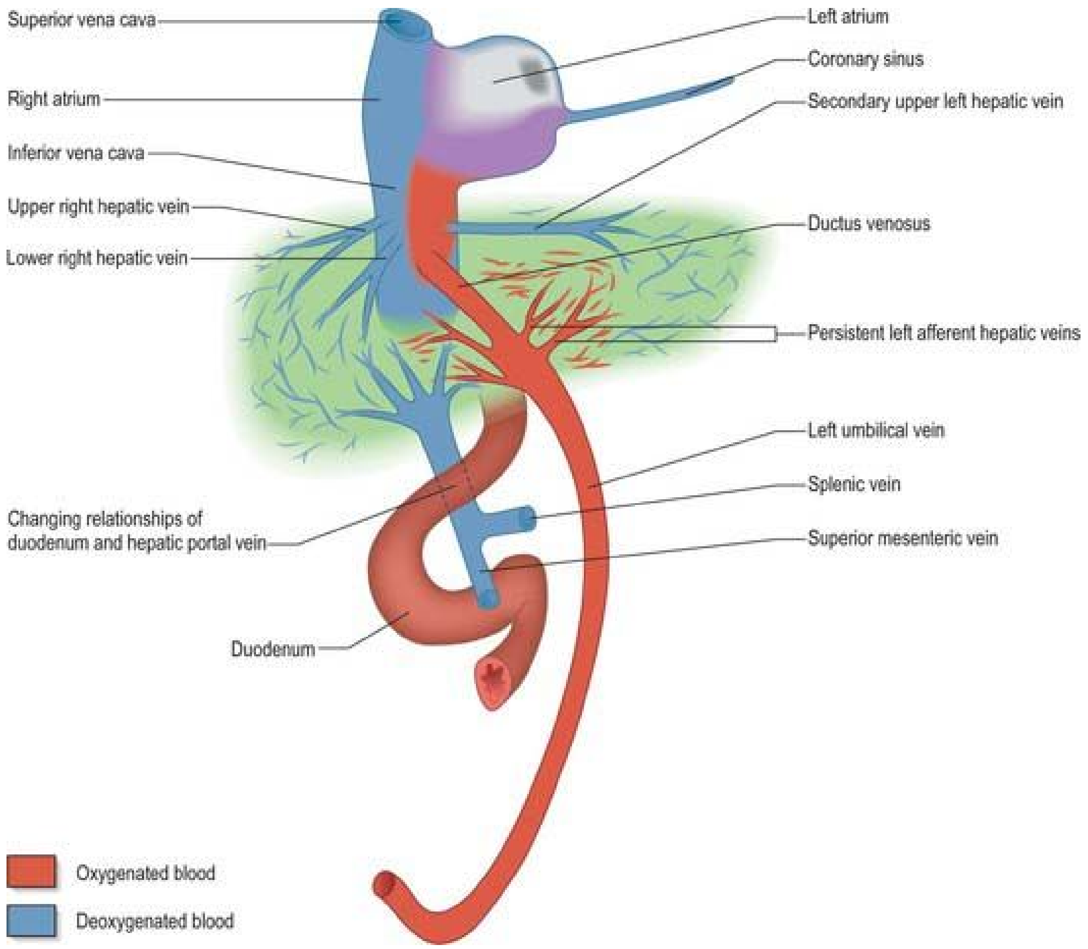
Superior vena cava
Right atrium
Inferior vena cava
Upper right hepatic vein
Lower right hepatic vein
Changing relationships of duodenum and hepatic portal vein
Duodenum
Left atrium
Coronary sinus
Secondary upper left hepatic vein
Ductus venosus
Persistent left afferent hepatic veins
Left umbilical vein
Splenic vein
Superior mesenteric vein
Oxygenated blood
Deoxygenated blood

Fig. 73.11 The condition of some main upper abdominal and intrathoracic right atrial terminal veins in the later prenatal months. The rotation of the stomach and movement of the duodenum produce relative changes in the final arrangement of duodenal intervitelline anastomoses which form the hepatic portal vein.

From the cranial portion of the early hepatic evagination of the foregut, interconnected sheets and ‘cords’ of endodermal cells, the presumptive hepatocytes, penetrate the septum transversum mesenchyme. Hepatic mesenchyme is composed of a mixed population of cells with endothelial/angiogenic and connective tissue lineages. Capillary plexuses develop within this mesenchyme and, possibly under the influence of the endodermal hepatic sheets, the plexuses become more profuse by further addition of angioblastic septal mesenchyme, which also forms masses of perivascular intrahepatic haemopoietic tissue. These processes extend along the plexiform connections of the vitelline, and later the umbilical, veins until their intrahepatic (trans-septal) zones themselves become largely plexiform. Initially capillary in nature, they transform into a mass of rather wider, irregular, sinusoidal vessels with a discontinuous endothelium containing many phagocytic cells. The lengths of vitelline veins involved in these processes are the intermediate parts of the segments extending from the subhepatic (cranioventral duodenal) to the suprahepatic (subdiaphragmatic) transverse intervitelline anastomoses, and the corresponding lengths of the umbilical veins. Thus at this early stage the liver sinusoids are perfused by mixed blood reaching them through a series of branching vessels collectively called the venae advehentes, or afferent hepatic veins: they are, deoxygenated from the gut splanchnopleure via vitelline vein hepatic terminals and oxygenated from the placenta via hepatic terminals of the umbilical veins (Fig. 73.10). Blood leaves the liver through four venae revehentes (efferent hepatic veins); two on each side reach and open into their respective cardiac sinual horns. This full complement of four hepatocardiac veins is only transient, and becomes reduced to one dominant, rapidly enlarging channel. The originally bilaterally symmetric cardinal vein complexes, both rostral and caudal, develop transverse or oblique anastomoses so that the cardiac venous return is ultimately restricted to the definitive right atrium.

These cardiac and concomitant hepatoenteric changes are accompanied by events in supra-, intra- and subhepatic parts of the vitello-umbilical veins. Some vessels enlarge, persisting as definitive vessels to maturity and, in places, they are joined later by other channels that become defined in already established capillary plexuses. Other vessels retrogress, either disappearing completely or remaining as vestigial tags and, occasionally, vessels of fine calibre. Some vessels of crucial importance in the circulatory patterns of embryonic and fetal life become obliterated postnatally and transformed to substantial fibrous cords. Both right and left umbilical hepatocardiac and the left vitelline hepatocardiac veins continue, for a time, to discharge blood into their sinual horns; however, they begin to retrogress (Figs 73.9 and 73.10). The right umbilical channel atrophies completely. The left channels also disappear, but their cardiac terminals may, on occasion, be found as conical fibrous tags attached to the inferior wall of the coronary sinus. The right vitelline hepatocardiac vein continues enlarging and ultimately forms the terminal segment of the inferior vena cava. The latter receives the right efferent hepatic veins and new channels draining the territories of the left efferent hepatic veins. These collectively form the upper and lower groups of right and (secondary) left hepatic veins. The terminal caval segment also shows the orifice of the right half of the intervitelline subdiaphragmatic anastomosis, and a large new connection with the right subcardinal vein.

The hepatic terminals of the right and left duodenal parts of the vitelline veins are destined to form the corresponding branches of the hepatic portal vein, the left branch incorporating the cranial ventral intervitelline anastomosis. With rotation of the gut and formation of the duodenal loop, segments of the original vitelline veins and the caudal transverse anastomosis atrophy (indicated in Fig. 73.10 and 73.10), while new splanchnopleuric venous channels, the superior mesenteric and splenic veins, converge and join the left end of the dorsal intermediate anastomosis. The numerous other radicles of the portal vein and its principal branches, including the inferior mesenteric vein, are later formations.

For a period, placental blood returns from the umbilicus via right and left umbilical veins, both discharging through afferent hepatic veins into the hepatic sinusoids, where admixture with vitelline blood occurs. At approximately 7 mm crown–rump length, the right umbilical vein retrogresses completely. The left umbilical vein retains some vessels discharging directly into the sinusoids, but new enlarging connections with the left half of the subhepatic intervitelline anastomosis emerge. The latter is the start of a bypass channel for the majority of the placental blood, which continues through the median ductus venosus and finally the right half of the subdiaphragmatic anastomosis, to reach the termination of the inferior vena cava (Fig. 73.11).

FETAL/NEONATAL UMBILICAL VESSELS

Umbilical vein

The umbilical vein in the neonate is 2–3 cm long and 4–5 mm in diameter when distended. It passes from the umbilicus, within the layers of the falciform ligament, superiorly and to the right, to the porta hepatis. Here it gives off several large intrahepatic branches to the liver and then joins the left branch of the portal vein and the ductus venosus. The umbilical vein is thin walled; it possesses a definite internal lamina of elastic fibres at the umbilical ring, but not in its intra-abdominal course. The tunica media contains smooth muscle fibres, collagen and elastic fibres. When the cord is severed, the umbilical vein contracts, but not so vigorously as the arteries. The rapid decrease in pressure in the umbilical vein after the cord is clamped means that the elastic tissue at the umbilical ring is sufficient to arrest any retrograde flow along the vessel. Before birth there is a subintimal proliferation of connective tissue. After birth, the contraction of the collagen fibres in the tunica media and the increased subintimal connective tissue contribute to the transformation of the vessel into the ligamentum teres. Obliteration occurs from the umbilical ring towards the hepatic end. No thrombi are formed in the obliteration process. For up to 48 hours after birth, the intra-abdominal portion of the umbilical vein can be easily dilated. In most adults the original lumen of the vein persists through the ligamentum teres and can be dilated to 5–6 mm in diameter.

Ductus venosus

The ductus venosus is a direct continuation of the umbilical vein and arises from the left branch of the portal vein, directly opposite the termination of the umbilical vein. It passes for 2–3 cm within the layers of the lesser omentum, in a groove between the left lobe and caudate lobe of the liver, before terminating in either the inferior vena cava, or in the left hepatic vein immediately before it joins the inferior vena cava. The tunica media of the ductus venosus contains circularly arranged smooth muscle fibres, an abundant amount of elastic fibres and some connective tissue.

The ductus venosus is already closed in about one-third of newborn infants. It shuts down by an unknown mechanism. Obliteration begins at the portal vein end in the second postnatal week and progresses to the vena cava; the lumen has been completely obliterated by the second or third month after birth. The fibrous remnant of the ductus venosus is the ligamentum venosum.

Umbilical vein catheterization

The umbilical vein may be catheterized in the neonate to enable exchange and transfusion of blood, for central venous pressure measurement and, usually in an emergency, for vascular access. The catheter is inserted into the cut end of the umbilical vein and is advanced along the length of the vein, through the ductus venosus and into the inferior vena cava, the tip being placed between the ductus venosus and the right atrium. Positioning of the catheter tip is confirmed radiologically and it should be located just above the diaphragm at a point which is level with the ninth or tenth thoracic vertebrae (T9/T10). As with umbilical arterial catheters, estimation of the required catheter length can be determined from standard charts.

Umbilical arteries

The fetal umbilical arteries are in direct continuation with the internal iliac arteries. Their lumen is 2–3 mm in diameter at their origin, when distended. This narrows as they approach the umbilicus, where there is a reciprocal thickening of the tunica media, as a result, in particular, of an increase in the number of longitudinal smooth muscle fibres and elastic fibres. Before birth there is a proliferation of connective tissue within the vessel wall. The umbilical vessels constrict in response to handling, stretching, cooling and altered tensions of oxygen and carbon dioxide. Umbilical vessels are muscular, but devoid of a nerve supply in their extra-abdominal course. After the cord is severed the umbilical arteries contract, preventing significant blood loss; thrombi often form in the distal ends of the arteries. The arteries obliterate from their distal ends until, by the end of the second or third postnatal month, involution has occurred at the level of the superior vesical arteries. The proximal parts of the obliterated vessels remain as the medial umbilical ligaments.

Umbilical arterial catheterization

Insertion of an umbilical catheter is undertaken to provide direct access to the arterial circulation. Arterial blood can be withdrawn repeatedly for measurement of oxygen and carbon dioxide partial pressures, pH, base excess and many other parameters of blood biochemistry and haematology. The indwelling catheter also enables the continuous measurement of arterial blood pressure.

The catheter is inserted directly into either the cut end or the side of one of the two umbilical arteries in the umbilical cord stump that remains attached to the baby after transection of the umbilical cord at the time of delivery. The catheter tip is then advanced along the length of the umbilical artery, through the internal iliac artery, into the common iliac artery and from there into the aorta. In order to keep the catheter patent, a small volume of fluid is continuously infused through it. It is important that the tip of the catheter should be located well away from arteries branching from the aorta, to avoid potentially harmful perfusion of these arteries with the catheter fluid. Thus umbilical arterial catheter tips are placed in the descending aorta either in a 'high' position, above the coeliac artery but well below the ductus arteriosus, or in a 'low' position, below the renal and inferior mesenteric arteries but above the point where the aorta bifurcates into the two common iliac arteries. The length of catheter to be inserted can be estimated from charts relating the required catheter length to external body measurements, or from birth weight. Positioning of the catheter is assessed by means of radiographs of the abdomen or chest: a 'high' catheter tip should be located in the descending aorta somewhere between the levels of the sixth and ninth thoracic vertebrae (T6–9), while a 'low' catheter tip should be at a level between the third and fourth lumbar vertebrae (L3–4). Relevant anatomical reference points are given in Table 73.1.

Table 73.1 Key anatomical reference points for umbilical arterial catheterization

Structure	**Vertebral level**
Ductus arteriosus	T4–5
Coeliac artery	T12
Superior mesenteric artery	T12–L1
Renal artery	L1
Inferior mesenteric artery	L3
Aortic bifurcation	L4–5

REFERENCES

tzner JD, Befus AD. Interactions among intraepithelial leucocytes and other epithelial cells in intestinal development and function. In: Lebenthal E, editor. *Human Gastrointestinal Development, Chapter 37*. New York: Raven Press, 1989.

llins P. Embryology of the pancreas. In: Howard ER, Stringer MD, Colombani PM. *Surgery of the Liver, Bile Ducts and Pancreas in Children, Part 8*. London: Arnold; 2002:479-492.

Covers pancreatic morphogenesis, the timescale of development, the origin of pancreatic cell lines and factors that regulate pancreatic development..

llins P. Embryology of the liver and bile ducts. In: Howard ER, Stringer MD, Colombani PM. *Surgery of the Liver, Bile Ducts and Pancreas in Children, Part 3*. London: Arnold; 2002:91-102.

Covers morphogenesis of the liver and early hepatic circulation, the origin of hepatic cell lines and the development of the extra- and intrahepatic biliary systems..

rshon MD. Phenotypic expression by neural crest-derived precursors of enteric neurons and glia. In: Madreson PFA, editor. *Developmental and Evolutionary Aspects of the Neural Crest*. New York: John Wiley, 1987.

Describes a mouse model of Hirschsprung’s disease..

oward ER. Biliary atresia: aetiology, management and complications. In: Howard ER, Stringer MD, Colombani PM. *Surgery of the Liver, Bile Ducts and Pancreas in Children, Part 3*. London: Arnold; 2002:103-132.

Reviews the aetiology and clinical presentation of biliary atresia, including the congenital, infective and anatomical factors that are related to the condition..

ebenthal E. Concepts in gastrointestinal development. In: Lebenthal E, editor. *Human Gastrointestinal Development, Chapter 1*. New York: Raven Press, 1989.

This chapter is the first in a volume dedicated to the development of structure and function of the gut, liver and pancreas. Includes the development of the immunological surveillance mechanisms and gastrointestinal flora..

ewis P, Yaron Y, Evans MI. Fetal endocrine disorders. In: Rodeck CH, Whittle MJ. *Fetal Medicine: Basic Sciences and Clinical Practice, Chapter 62*. Edinburgh: Churchill Livingstone; 1999:829-834.

Reviews the diagnosis and treatment of common fetal endocrine disorders, particularly of the suprarenal and thyroid glands..

reeter GL. Developmental horizons in human embryos. Descriptions of age group XI, 13 to 20 somites and age group XII, 21 to 29 somites. *Contrib Embryol Carnegie Inst Washington*. 1942;30:211-245.

hittle MJ. Gastrointestinal abnormalities. In: Rodeck CH, Whittle MJ. *Fetal Medicine: Basic Sciences and Clinical Practice, Chapter 54*. Edinburgh: Churchill Livingstone; 1999:703-714.

Reviews the diagnosis and treatment of abnormalities of the gastrointestinal tract..

CHAPTER 74

Kidney and ureter

KIDNEY

The kidneys excrete the end products of metabolism and excess water. These actions are essential for the control of concentrations of various substances in the body, maintaining electrolyte and water balance approximately constant in the tissue fluids. The kidneys also have endocrine functions, producing and releasing erythropoietin, which affects red blood cell formation; renin, which influences blood pressure; 1,25-di-hydroxycholecalciferol (the metabolically active form of vitamin D), which is involved in the control of calcium absorption and mineral metabolism; and various other soluble factors with metabolic actions.

In the fresh state, the kidneys are reddish-brown. They are situated posteriorly behind the peritoneum on each side of the vertebral column and are surrounded by adipose tissue. Superiorly they are level with the upper border of the 12th thoracic vertebra, inferiorly with the third lumbar vertebra. The right is usually slightly inferior to the left, reflecting its relationship to the liver. The left is a little longer and narrower than the right and lies nearer the median plane (Fig. 74.1). The long axis of each kidney is directed inferolaterally and the transverse axis posteromedially, which means that the anterior and posterior aspects usually described are in fact anterolateral and posteromedial. An appreciation of this orientation is important in percutaneous and endo-urologic renal surgery.

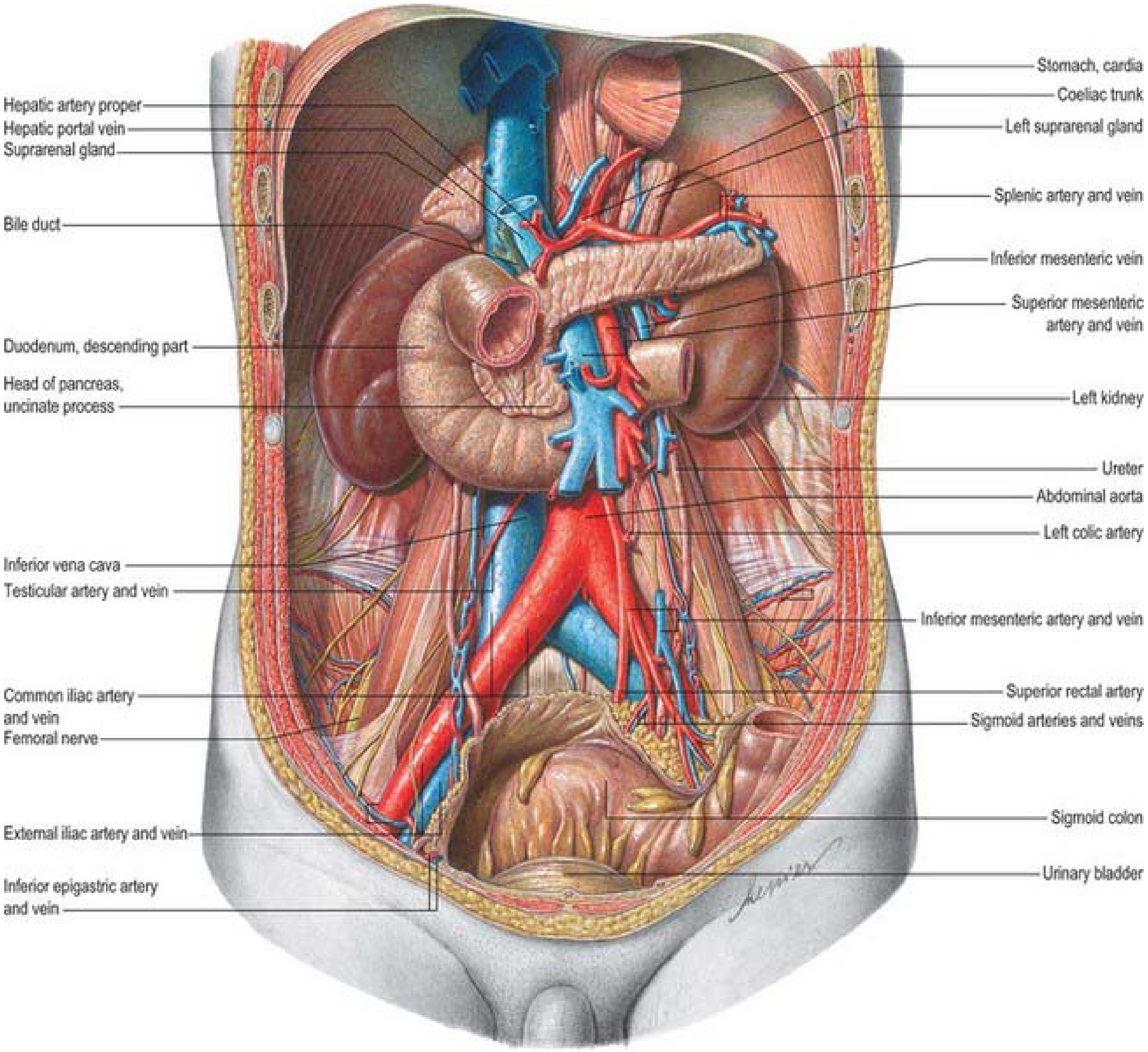
Hepatic artery proper
Hepatic portal vein
Suprarenal gland
Bile duct
Duodenum, descending part
Head of pancreas, uncinate process
Inferior vena cava
Testicular artery and vein
Common iliac artery and vein
Femoral nerve
External iliac artery and vein
Inferior epigastric artery and vein
Stomach, cardia
Coeliac trunk
Left suprarenal gland
Splenic artery and vein
Inferior mesenteric vein
Superior mesenteric artery and vein
Left kidney
Ureter
Abdominal aorta
Left colic artery
Inferior mesenteric artery and vein
Superior rectal artery
Sigmoid arteries and veins
Sigmoid colon
Urinary bladder

Fig. 74.1 Relationships of the kidneys and ureters in the male retroperitoneum.

(From Sobotta 2006.)

Each kidney is typically 11 cm in length, 6 cm in breadth and 3 cm in anteroposterior dimension. The left kidney may be 1.5 cm longer than the right; it is rare for the right kidney to be more than 1 cm longer than the left. The average weight is 150 g in men and 135 g in women. In thin individuals with a lax abdominal wall the lower pole of the lower right kidney may just be felt in full inspiration by bimanual lumbar examination, but this is unusual.

In the fetus and newborn, the kidney normally has 12 lobules. These are fused in adults to present a smooth surface although traces of lobulation may remain.

Absent and ectopic kidneys

A single absent kidney is seen in 1 in 1200 individuals and results from failure of metanephric blastema to join with a ureteric bud on the affected side. It has no clinical sequelae but may frequently be associated with absence of the ipsilateral vas deferens and/or epididymis and may be associated with other congenital anomalies including imperforate anus, cardiac valvular anomalies and oesophageal atresia. A single kidney often shows compensatory hypertrophy. The life expectancy of individuals with a single kidney is the same as those with two kidneys.

Failure of the kidney to ascend into the renal fossa *in utero* results in renal ectopia. Most commonly the kidney is found in the pelvis: this occurs in 1 in 2500 live births. Kidneys so placed often have associated malrotation anomalies, and may have marked fetal lobulation. Pelvic kidneys frequently become hydronephrotic as a result of an anterior placed ureter and an anomalous arterial supply. An associated pelviureteric junction obstruction is often present.

Very rarely, and despite the normal location of the ureteric orifices within the bladder, the two renal masses may be on the same side. This is termed crossed renal ectopia and usually the two renal masses are fused in such circumstances. A solitary crossed renal ectopia may be associated with skeletal and other genitourinary anomalies. A number of different anatomical patterns can result, all of which are extremely rare (Fig. 74.2).

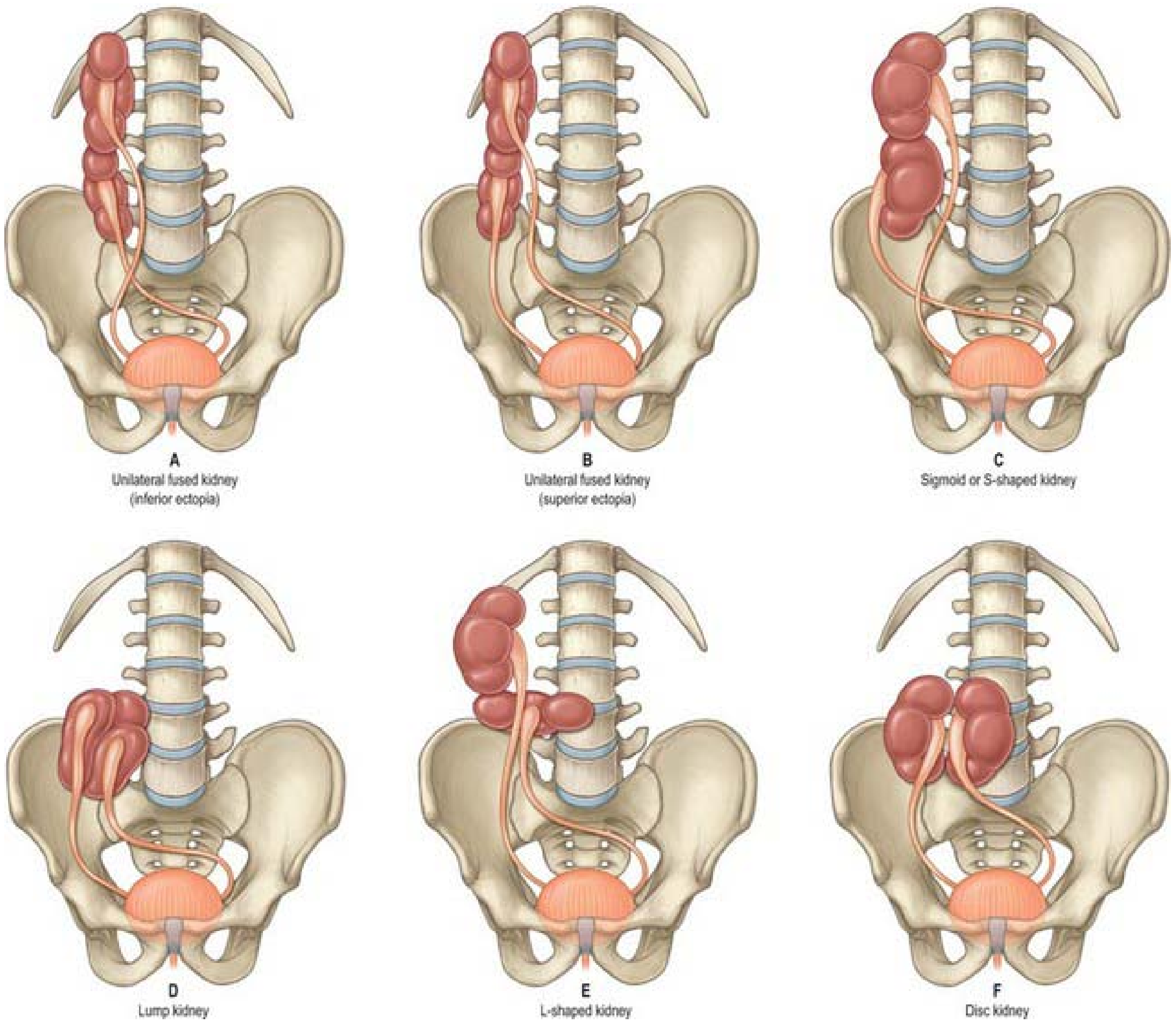
A
Unilateral fused kidney
(inferior ectopia)
B
Unilateral fused kidney
(superior ectopia)
C
Sigmoid or S-shaped kidney
D
Lump kidney
E
L-shaped kidney
F
Disc kidney

Fig. 74.2 Crossed renal ectopia: diagram showing the possible arrangements of crossed ectopic kidneys.

Horseshoe kidney

Horseshoe kidneys are found in 1 in 400 individuals. A transverse bridge of renal tissue, the isthmus, which usually but not invariably contains functioning renal substance, connects the two renal masses. The isthmus lies between the inferior poles, most commonly anterior to the great vessels. The ureters curve anterior to the isthmus and often have a high insertion into the renal pelvis (Fig. 74.3A,B).

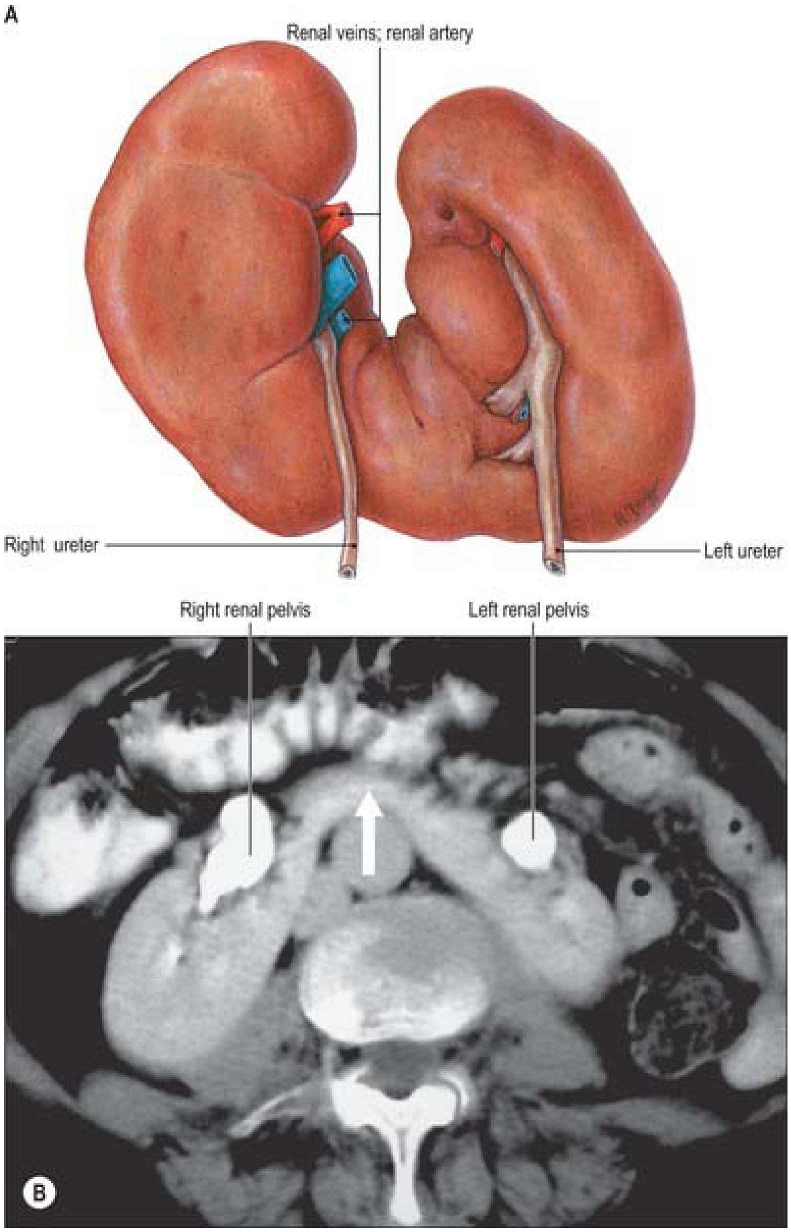
A
Renal veins; renal artery
Right ureter
Left ureter
Right renal pelvis
Left renal pelvis
B

Fig. 74.3 **A**, Horseshoe kidney. Note the ureters pass anterior to the isthmus. Note also the relatively high insertion of the ureters into the renal pelvis. **B**, Late phase post-contrast axial CT scan showing a horseshoe kidney. Both lower poles are directed medially and fused by an isthmus (arrowed). Note that the renal pelves (seen here filled with contrast) are directed anteriorly.

(From Sobotta 2006.)

The blood supply to horseshoe kidneys is variable. One vessel to each moiety is seen in 30% of horseshoe kidneys, but multiple anomalous vessels are common; the isthmus may be supplied by a vessel directly from the aorta or from branches of the inferior mesenteric, common iliac or external iliac arteries. In view of this variable arterial anatomy, angiography or CT scanning with vascular reconstruction is very helpful when planning renal surgery on horseshoe kidneys. Horseshoe kidneys can have an associated congenital pelviureteric junction obstruction in up to 30% of cases. Anomalous vessels crossing the ureter and the abnormal course of the ureter as it passes over renal substance may also cause obstruction. Horseshoe kidneys have an increased incidence of stone disease, probably as a consequence of areas of inefficient drainage.

PERIRENAL FASCIA

The perirenal fascia is a dense, elastic connective tissue sheath which envelops each kidney and suprarenal gland together with a layer of surrounding perirenal fat (Fig. 74.4A,B; see Fig. 62.1). The kidney and its vessels are embedded in perirenal fat, which is thickest at the renal borders and extends into the renal sinus at the hilum.

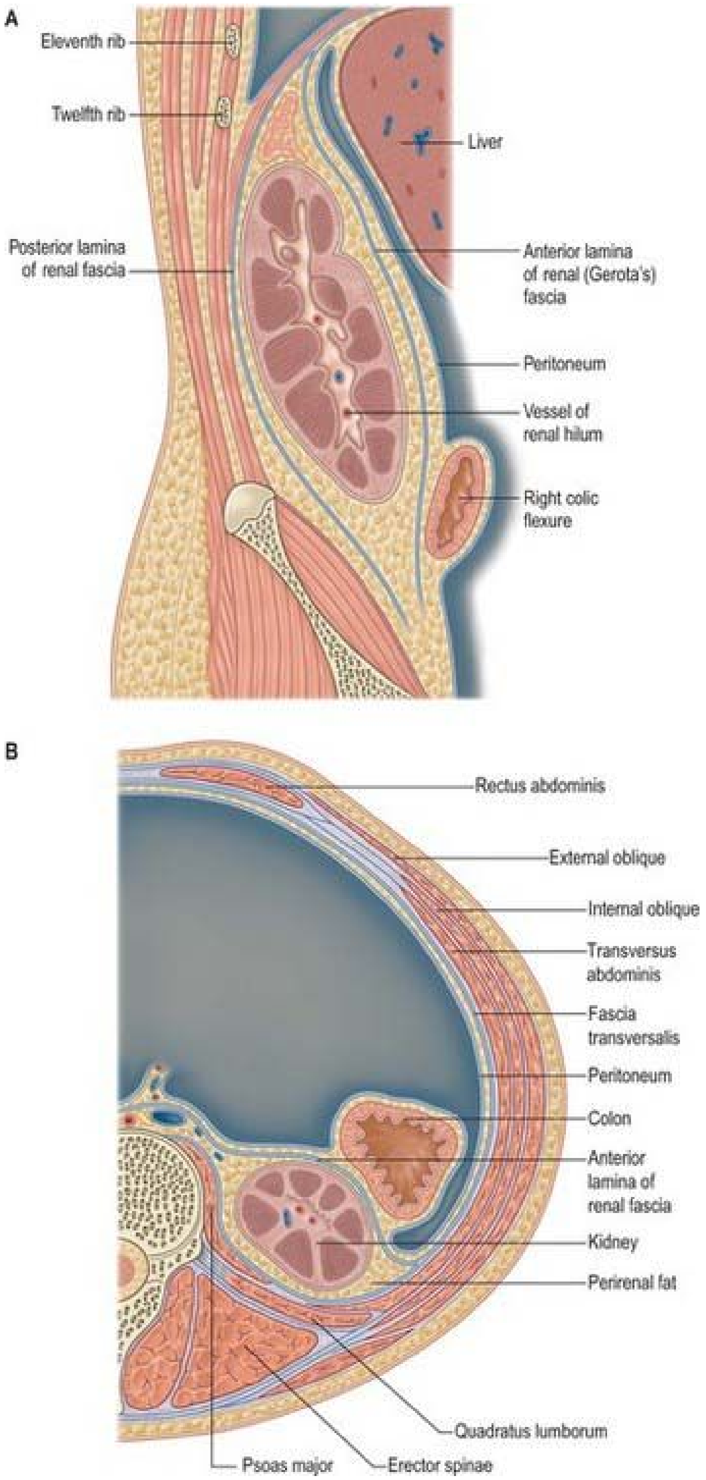
A
Eleventh rib
Twelfth rib
Liver
Posterior lamina of renal fascia
Anterior lamina of renal (Gerota's) fascia
Peritoneum
Vessel of renal hilum
Right colic flexure
B
Rectus abdominis
External oblique
Internal oblique
Transversus abdominis
Fascia transversalis
Peritoneum
Colon
Anterior lamina of renal fascia
Kidney
Perirenal fat
Quadratus lumborum
Psoas major
Erector spinae

Fig. 74.4 **A**, Sagittal section through the posterior abdominal wall showing the relations of the renal fascia of the right kidney. **B**, Transverse section, showing the relations of the renal fascia.

The perirenal fascia was originally described as being made up of two separate entities, the posterior fascia of Zuckerkandl and the anterior fascia of Gerota, which fused laterally to form the lateral conal fascia. According to this view, the lateral conal fascia continued anterolaterally behind the colon to blend with the parietal peritoneum. However, work by Mitchell (1950) showed that the perirenal fascia is not made up of distinct fused fasciae, but is in fact a single multilaminated structure which is fused posteromedially with the muscular fasciae of psoas major and quadratus lumborum. It then extends anterolaterally behind the kidney as a bilaminated sheet, which at a variable point divides into a thin anterior lamina, passing around the front of the kidney as the anterior perirenal fascia, and a thicker posterior lamina which continues anterolaterally as the lateral conal fascia, fusing with the parietal peritoneum.

Classically, the anterior perirenal fascia was thought to blend into the dense mass of connective tissue surrounding the great vessels in the root of the mesentery behind the duodenum and pancreas, thereby preventing communication between perirenal spaces across the midline. However inspection of CT images or of anatomical sections of cadavers, following injection of contrast or coloured latex respectively, into the perirenal space, revealed that fluid could extend across the midline at the third to fifth lumbar levels through a narrow channel measuring 2–10 mm in AP dimension. In the midline superiorly, the anterior and posterior renal fasciae fuse and are attached to the crura of their respective hemidiaphragms. Inferiorly the fasciae separate for a variable craniocaudal distance. The posterior perirenal fascia fuses with the muscular fascia of psoas major while the anterior perirenal fascia extends across the midline in front of the great vessels and so communication between the two sides is permitted although very rarely of clinical significance. Below this level the two fasciae once again merge and are attached to the great vessels or iliac vessels. The containment of fluid to one side of the perirenal space that is observed in over two thirds of clinical cases is attributed to the presence of fibrous septae.

Above the suprarenal glands the anterior and posterior perirenal fasciae were previously said to fuse with each other and to the diaphragmatic fascia.

This description of a closed superior cone is not universally accepted. Cadaveric experiments have shown the superior aspect of the perirenal space to be open and in continuity with the bare area of the liver on the right and the subphrenic extraperitoneal space on the left. The posterior fascial layer blends bilaterally with the fascia of psoas major and quadratus lumborum as well as the inferior phrenic fascia. The anterior fascial layer on the right blends with the right inferior coronary ligament at the level of the upper pole of the kidney and bare area of the liver. On the left the anterior layer fuses with the gastrosplenic ligament at the level of the suprarenal gland.

There is some debate concerning the inferior fusion of the perirenal fascia. Many investigators believe that inferiorly the anterior and posterior leaves of the perirenal fascial fuse to produce an inverted cone which is open to the pelvis at its apex. Laterally the anterior and posterior leaves fuse with the iliac fascia, and medially they fuse with the periureteric connective tissue. The inferior apex of the cone is open anatomically towards the iliac fossa but rapidly becomes sealed in inflammatory disease. An alternative view is based on the dissection of recently deceased cadavers after injections of coloured latex into the perirenal space: these have shown that the anterior and posterior perirenal fasciae merge to form a single multilaminar fascia which contains the ureter in the iliac fossa. Anteriorly this common fascia is loosely connected to the parietal peritoneum, and so denies free communication between the perirenal space and the pelvis, and also denies communication between the perirenal and pararenal spaces.

A simple nephrectomy for benign disease removes the kidney from within perirenal fascia; a radical nephrectomy (for cancer) removes the entire contents of the perirenal space including the perirenal fascia, in order to give adequate clearance around the tumour.

RELATIONS

The superior poles of both kidneys are thick and round and each is related to its suprarenal gland (Fig. 74.5A,B). The inferior poles are thinner and extend to within 2.5 cm of the iliac crests. The lateral borders are convex. The medial borders are convex adjacent to the poles, concave between them and slope inferolaterally. In each a deep vertical fissure opens anteromedially as the hilum, which is bounded by anterior and posterior lips and contains the renal vessels and nerves and the renal pelvis. The relative positions of the main hilar structures are the renal vein (anterior), the renal artery (intermediate) and the pelvis of the kidney (posterior). Usually an arterial branch from the main renal artery runs over the superior margin of the renal pelvis to enter the hilum on the posterior aspect of the pelvis, and a renal venous tributary often leaves the hilum in the same plane. Above the hilum the medial border is related to the suprarenal gland and below to the origin of the ureter.

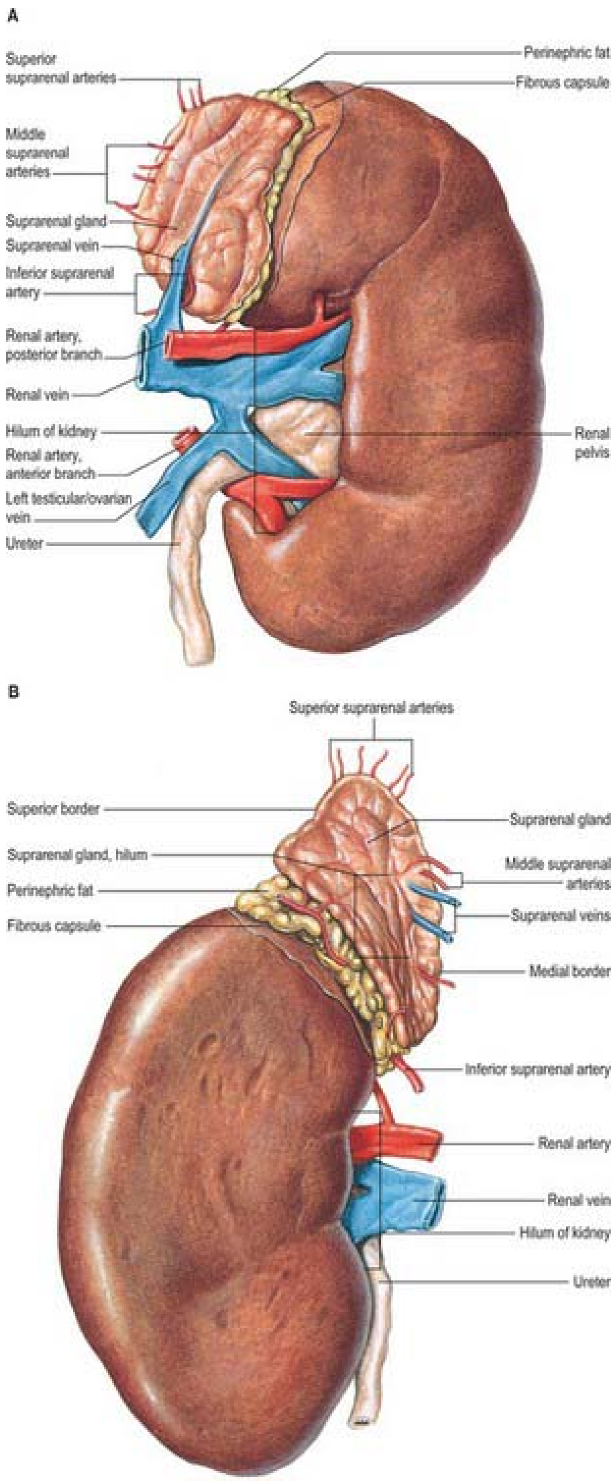
A
Superior suprarenal arteries
Middle suprarenal arteries
Suprarenal gland
Suprarenal vein
Inferior suprarenal artery
Renal artery, posterior branch
Renal vein
Hilum of kidney
Renal artery, anterior branch
Left testicular/ovarian vein
Ureter
Perinephric fat
Fibrous capsule
Renal pelvis
B
Superior suprarenal arteries
Superior border
Suprarenal gland, hilum
Perinephric fat
Fibrous capsule
Suprarenal gland
Middle suprarenal arteries
Suprarenal veins
Medial border
Inferior suprarenal artery
Renal artery
Renal vein
Hilum of kidney
Ureter

Fig. 74.5 Ventral aspect of left kidney and suprarenal gland (**A**), and of right kidney and suprarenal gland (**B**). Note the left suprarenal vein enters the left renal vein. This is an important relationship to identify when performing a left nephrectomy.

(From Sobotta 2006.)

The convex anterior surface of the kidney actually faces anterolaterally and its relations differ on the right and left. Likewise the posterior surface of the kidneys in reality faces posteromedially. Its relations are similar on both sides of the body (Fig. 74.6A–D).

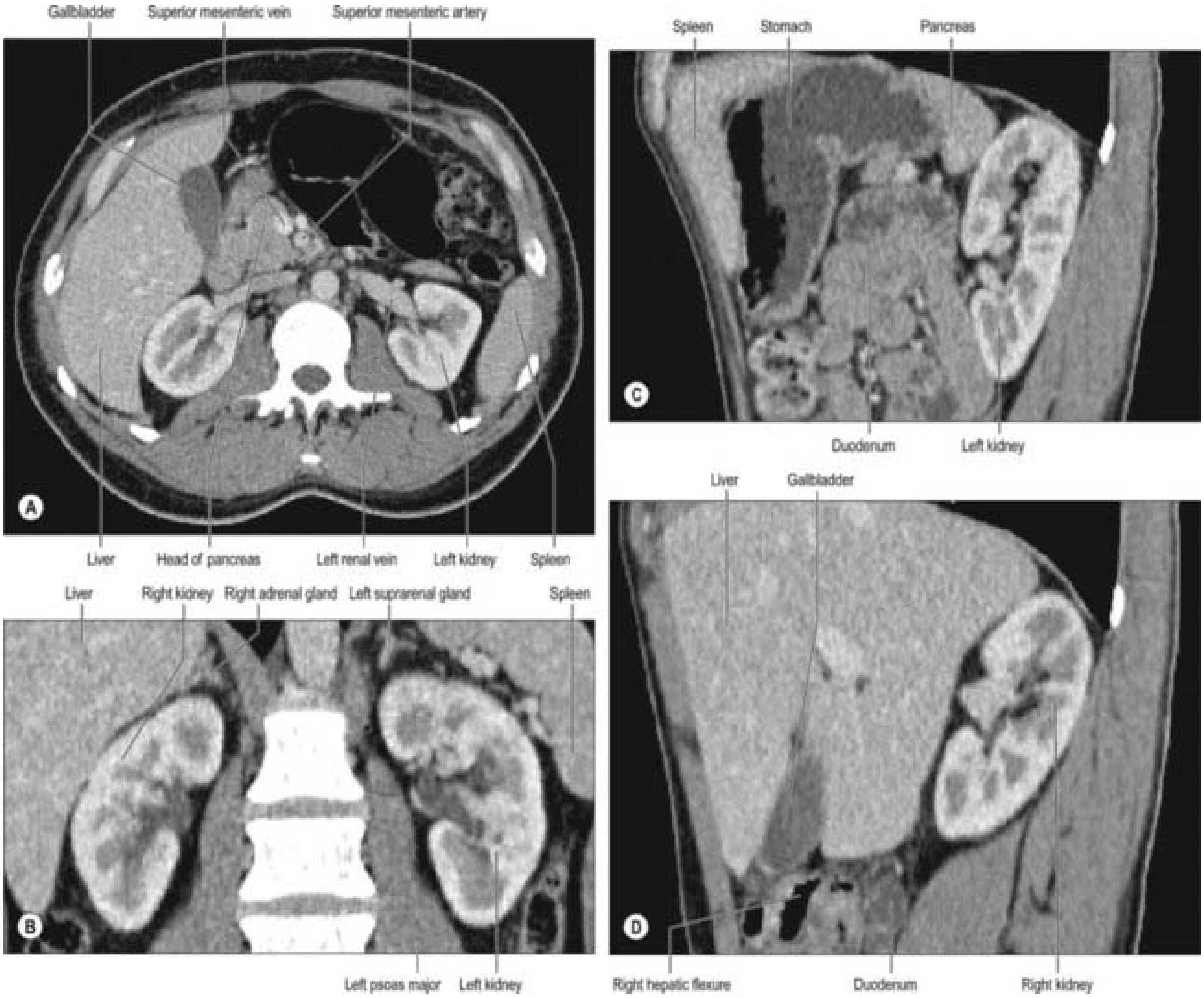
Gallbladder
Superior mesenteric vein
Superior mesenteric artery
A
Liver
Head of pancreas
Left renal vein
Left kidney
Spleen
Spleen
Stomach
Pancreas
C
Duodenum
Left kidney
Liver
Right kidney
Right adrenal gland
Left suprarenal gland
Spleen
B
Left psoas major
Left kidney
Liver
Gallbladder
D
Right hepatic flexure
Duodenum
Right kidney

Fig. 74.6 Multislice CT scan of the kidneys. **A**, Axial CT scan of the kidneys showing the anatomical relationships of the kidneys at the renal hilum. **B**, Coronal reformat showing both kidneys and the suprarenal glands. **C**, Sagittal reformat of the left kidney lying posterior to the stomach, spleen and pancreas. **D**, Sagittal reformat of the right kidney lying posterior to the right lobe of the liver, hepatic flexure and duodenum.

A small area of the superior pole is in contact with the right suprarenal gland, which may overlap the upper part of the medial border of the superior pole. A large area below this is immediately related the right lobe of the liver separated by a layer of peritoneum. A narrow medial area is directly related to the retroperitoneal descending part of the duodenum. Inferiorly the anterior surface is directly in contact laterally with the retroperitoneal right colic flexure and medially with part of the intraperitoneal small intestine.

A small medial area of the superior pole is related to the left suprarenal gland. The lateral half of the anterior surface is related to the spleen from which it is separated by a layer of peritoneum. A central quadrilateral area lies in direct contact with the retroperitoneal pancreas and the splenic vessels. Above this a small variable triangular region, between the suprarenal and splenic areas, is in contact with the stomach separated by a layer of peritoneum. Below the pancreatic and splenic areas, a narrow lateral strip which extends to the lateral border of the kidney is directly related to the retroperitoneal left colic flexure and the beginning of the descending colon. An extensive medial area is related to intraperitoneal loops of jejunum. The gastric area is covered with the peritoneum of the lesser sac (omental bursa) and the splenic and jejunal areas are covered by the peritoneum of the greater sac. Behind the peritoneum covering the jejunal area, branches of the left colic vessels are related to the kidney (Fig. 74.7A,B).

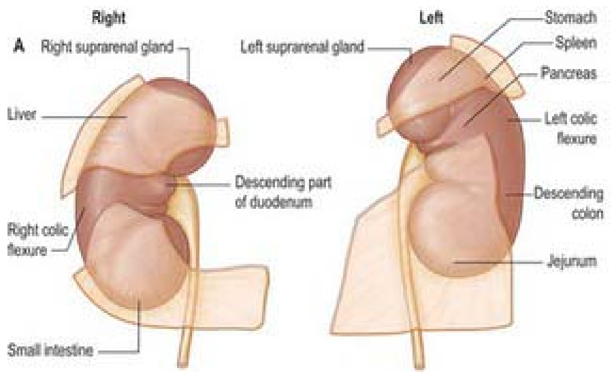
Right
A
Right suprarenal gland
Liver
Descending part of duodenum
Right colic flexure
Small intestine
Left
Left suprarenal gland
Stomach
Spleen
Pancreas
Left colic flexure
Descending colon
Jejunum

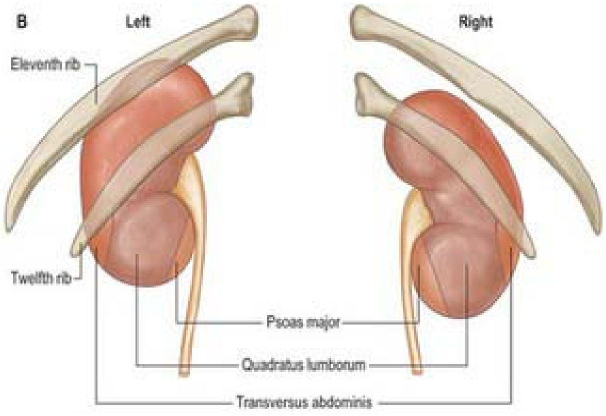
B
Left
Right
Eleventh rib
Twelfth rib
Psoas major
Quadratus lumborum
Transversus abdominis

Fig. 74.7 Surfaces of the kidneys. **A**, Anterior, showing the areas related to neighbouring viscera. The areas where overlying viscera are separated from the kidney by peritoneum are shown. **B**, Posterior, showing the areas of relation to the posterior abdominal wall.

(From Drake, Vogl, Mitchell, Tibbitts and Richardson 2008.)

The posteromedial surface of the kidneys is embedded in fat and devoid of peritoneum. The right and left kidneys are related to similar structures. Superiorly are the diaphragm and the medial and lateral arcuate ligaments. More inferiorly, moving in a medial to lateral direction, are psoas major, quadratus lumborum and the aponeurotic tendon of transversus abdominis, the subcostal vessels and the subcostal, iliohypogastric, and ilioinguinal nerves. The upper pole of the right kidney is level with the 12th rib, and that of the left with the 11th and 12th ribs. The diaphragm separates the kidney from the pleura, which descends to form the costodiaphragmatic recess: diaphragmatic muscle is sometimes defective or absent in a triangle immediately above the lateral arcuate ligament, and this allows perirenal adipose tissue to contact the diaphragmatic pleura.

INTERNAL MACROSTRUCTURE

The postnatal kidney has a thin fibrous capsule composed of collagen-rich tissue with some elastic and smooth muscle fibres. In renal disease the capsule may become adherent (Fig. 74.8A,B).

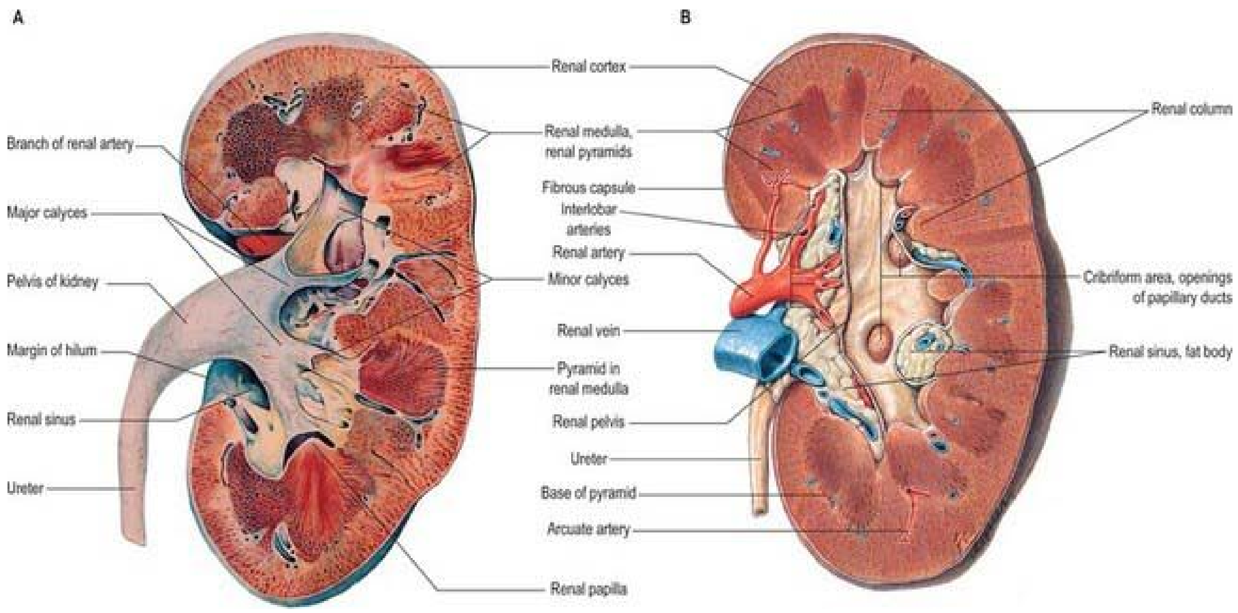
A
B
Branch of renal artery
Major calyces
Pelvis of kidney
Margin of hilum
Renal sinus
Ureter
Renal cortex
Renal medulla, renal pyramids
Fibrous capsule
Interlobar arteries
Renal artery
Minor calyces
Renal vein
Pyramid in renal medulla
Renal pelvis
Ureter
Base of pyramid
Arcuate artery
Renal papilla
Renal column
Cribriform area, openings of papillary ducts
Renal sinus, fat body

Fig. 74.8 Left kidney, oblique vertical hemisection: normal macroscopic appearance of the renal cortex and renal medulla and the major structures at the hilum of the kidney. In **A**, the fat body of the renal sinus and most of the major vessels at the hilum have been removed, and the renal pelvis has not been opened. In **B**, the renal pelvis has been opened to reveal the interlobar arteries.

*(**B** from Sobotta 2006.)*

The kidney itself can be divided into an internal medulla and external cortex. The renal medulla consists of pale, striated, conical renal pyramids, their bases peripheral, their apices converging to the renal sinus. At the renal sinus they project into calyces as papillae.

The renal cortex is subcapsular, arching over the bases of the pyramids and extending between them towards the renal sinus as renal columns. Its peripheral regions are termed cortical arches and are traversed by radial, lighter-coloured medullary rays, separated by darker tissue, the convoluted part. The rays taper towards the renal capsule and are peripheral prolongations from the bases of renal pyramids. The cortex is histologically divisible into outer and inner zones. The inner zone is demarcated from the medulla by tangential blood vessels (arcuate arteries and veins), which lie at the junction of the two, however a thin layer of cortical tissue (subcortex) appears on the medullary side of this zone. The cortex close to the medulla is sometimes termed the juxtamedullar cortex.

Renal pelvis and calyces

The hilum of the kidney leads into a central renal sinus, lined by the renal capsule and almost filled by the renal pelvis and vessels, the remaining space being filled by fat. Dissection into this plane can be challenging but is important in surgery on the renal pelvis, particularly open stone surgery. Within the renal sinus, the collecting tubules of the nephrons of the kidney open onto the summits of the renal papillae to drain into minor calyces, which are funnel-shaped expansions of the upper urinary tract. The renal capsule covers the external surface of the kidney and continues through the hilum to line the sinus and fuse with the adventitial coverings of the minor calyces. Each minor calyx surrounds either a single papilla or, more rarely, groups of two or three papillae. The minor calyces unite with their neighbours to form two or possibly three larger chambers, the major calyces. There is wide variation in the arrangement of the calyces. As the posterior aspect of the kidney rotates laterally during its ascent *in utero*, the calyces which were lateral *in utero* become positioned anteriorly, and the medial calyces move more posteriorly. The calyces drain into the infundibula. The renal pelvis is normally formed from the junction of two infundibula, one from the upper and one from the lower pole calyces, but there may be a third, which drains the calyces in the mid-portion of the kidney. The calyces are usually grouped so that three pairs drain into the upper pole infundibulum and four pairs into the lower pole infundibulum. If there is a middle infundibulum, the distribution is normally three pairs at the upper pole, two in the middle, and two at the lower pole. There is considerable variation in the arrangement of the infundibula and in the extent to which the pelvis is intrarenal or extrarenal. The funnel-shaped renal pelvis tapers as it passes inferomedially, traversing the renal hilum to become continuous with the ureter (Fig. 74.8A,B; see Fig. 74.9). It is rarely possible to determine precisely where the renal pelvis ceases and the ureter begins: the region is usually extrahilar and normally lies adjacent to the lower part of the medial border of the kidney. Rarely, the entire renal pelvis has been found to lie inside the sinus of the kidney so that the pelviureteric region occurs either in the vicinity of the renal hilum or completely within the renal sinus.

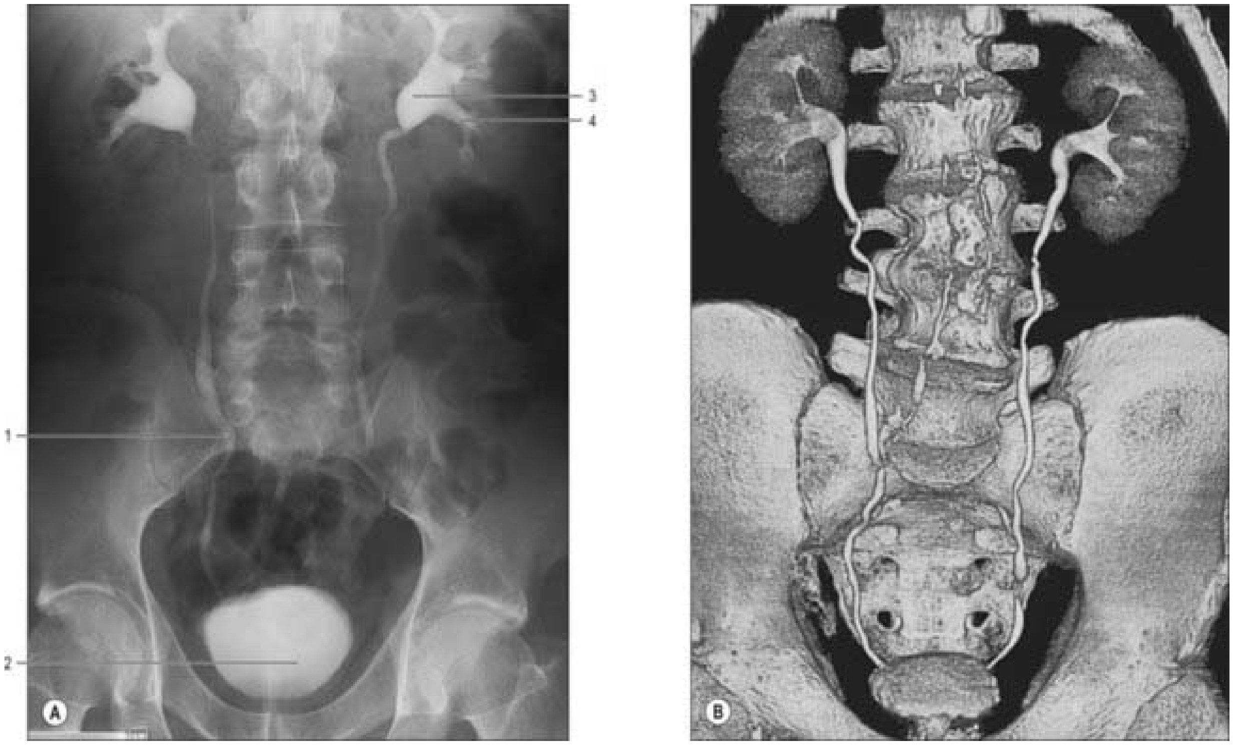

Fig. 74.9 **A**, Conventional intravenous urogram showing the renal calyces, pelves and both ureters. **1**. Ureter. **2**. Bladder. **3**. Renal pelvis. **4**. Calyces. **B**, Multislice CT urogram. 3D-surface shaded reformat showing the kidneys, ureters, bladder and surrounding bony anatomy.

The calyces, renal pelvis and ureter are well-demonstrated radiologically following an intravenous injection of radio-opaque contrast which is excreted in the urine (intravenous urography – IVU) (Fig. 74.9A,B); or after the introduction of radio-opaque contrast into the ureter by catheterization through a cystoscope (ascending or retrograde pyelography. Normal cupping of the minor calyces by projecting renal papillae may be obliterated by conditions that cause hydronephrosis, chronic distension of the ureter and renal pelvis due to upper or lower urinary tract obstruction resulting in elevated intrapelvic pressure. An appreciation of the rotation of the kidneys which results in the posterior calyces lying relatively medially and the anterior calyces lying laterally is essential when interpreting contrast imaging of the collecting system of the kidneys.

VASCULAR SUPPLY AND LYMPHATIC DRAINAGE

Renal arteries

The paired renal arteries take about 20% of the cardiac output to supply organs that represent less than one-hundredth of total body weight. They branch laterally from the aorta just below the origin of the superior mesenteric artery (see Fig. 62.8; Fig. 74.10A). Both cross the corresponding crus of the diaphragm at right angles to the aorta. The right renal artery is longer and often higher, passing posterior to the inferior vena cava, right renal vein, head of the pancreas, and descending part of the duodenum. The left renal artery is a little lower and passes behind the left renal vein, the body of the pancreas, and splenic vein. It may be crossed anteriorly by the inferior mesenteric vein.

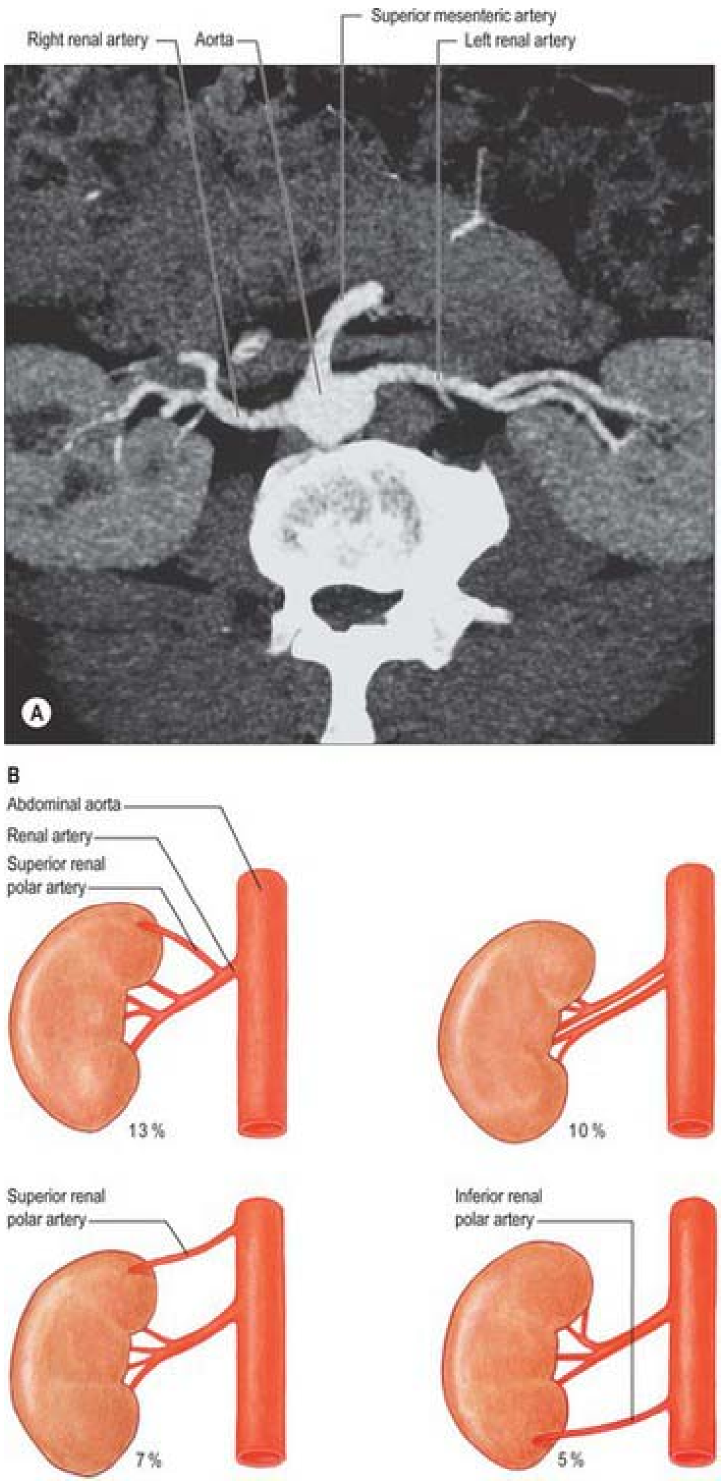
Right renal artery
Aorta
Superior mesenteric artery
Left renal artery
A
B
Abdominal aorta
Renal artery
Superior renal polar artery
13 %
10 %
Superior renal polar artery
7 %
Inferior renal polar artery
5 %

Fig. 74.10 **A**, Axial multislice CT renal angiogram. **B**, Variations in the number and patterns of branching of the renal artery (percentages are approximate).

*(**B** from Sobotta 2006.)*

A single renal artery to each kidney is present in approximately 70% of individuals (Fig. 74.11). The arteries vary in their level of origin and in their calibre, obliquity and precise relations (Fig. 74.10B). In its extrarenal course each renal artery gives off one or more inferior suprarenal arteries, a branch to the ureter and branches which supply perinephric tissue, the renal capsule, and the pelvis. Near the renal hilum, each artery divides into an anterior and a posterior division, and these divide into segmental arteries supplying the renal vascular segments. Accessory renal arteries are common (30% of individuals), and usually arise from the aorta above or below (most commonly below) the main renal artery and follow it to the renal hilum. They are regarded as persistent embryonic lateral splanchnic arteries. Accessory vessels to the inferior pole cross anterior to the ureter and may, by obstructing the ureter, cause hydronephrosis. Rarely, accessory renal arteries arise from the coeliac or superior mesenteric arteries near the aortic bifurcation or from the common iliac arteries.

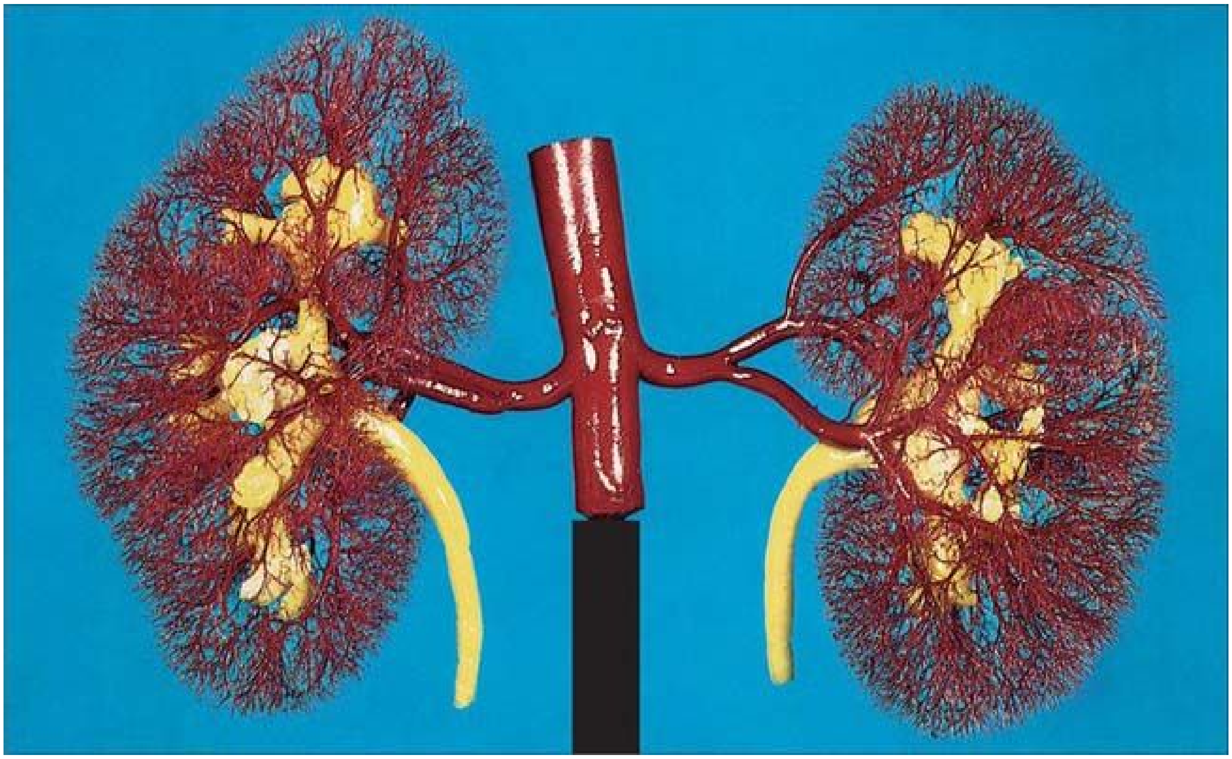

Fig. 74.11 Resin corrosion cast of human kidneys. Ureters, pelves and calyces are yellow; aorta, renal arteries and their branches are red.

(Prepared by the late DH Tompsett of the Royal College of Surgeons of England. By permission of the Museums of The Royal College of Surgeons.)

The subdivisions of the renal arteries are described sequentially as segmental, lobar, interlobar, arcuate and interlobular arteries and afferent and efferent glomerular arterioles (see Fig. 74.14).

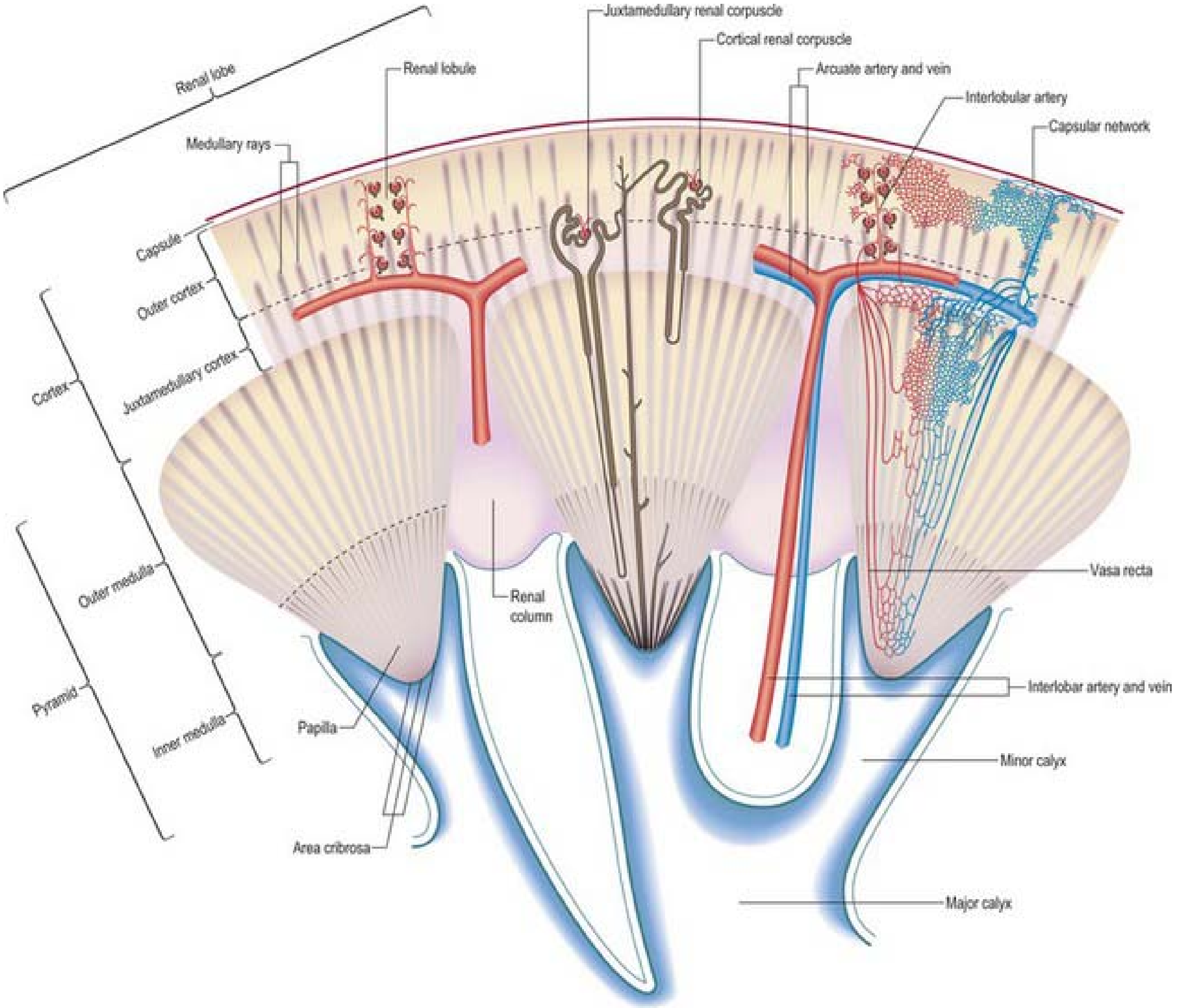
Renal lobe
Medullary rays
Capsule
Outer cortex
Juxtamedullary cortex
Cortex
Outer medulla
Pyramid
Inner medulla
Papilla
Area cribrosa
Renal lobule
Juxtamedullary renal corpuscle
Cortical renal corpuscle
Arcuate artery and vein
Interlobular artery
Capsular network
Renal column
Vasa recta
Interlobar artery and vein
Minor calyx
Major calyx

Fig. 74.14 The major structures in the kidney cortex and medulla (left), the position of cortical and juxtamedullary nephrons (middle) and the major blood vessels (right).

Segmental arteries

Renal vascular segmentation was originally recognized by John Hunter in 1794, but the first detailed account of the primary pattern was produced in the 1950s from casts and radiographs of injected kidneys. Five arterial segments have been identified (Fig. 74.12). The apical segment occupies the anteromedial region of the superior pole. The superior (anterior) segment includes the rest of the superior pole and the central anterosuperior region. The inferior segment encompasses the whole lower pole. The middle (anterior) segment lies between the anterior and inferior segments. The posterior segment includes the whole posterior region between the apical and inferior segments. This is the pattern most commonly seen, and although there can be considerable variation it is the pattern that clinicians most frequently encounter when performing partial nephrectomy. Whatever pattern is present, it must be emphasized that vascular segments are supplied by virtual end arteries. In contrast, larger intrarenal veins have no segmental organization and anastomose freely.

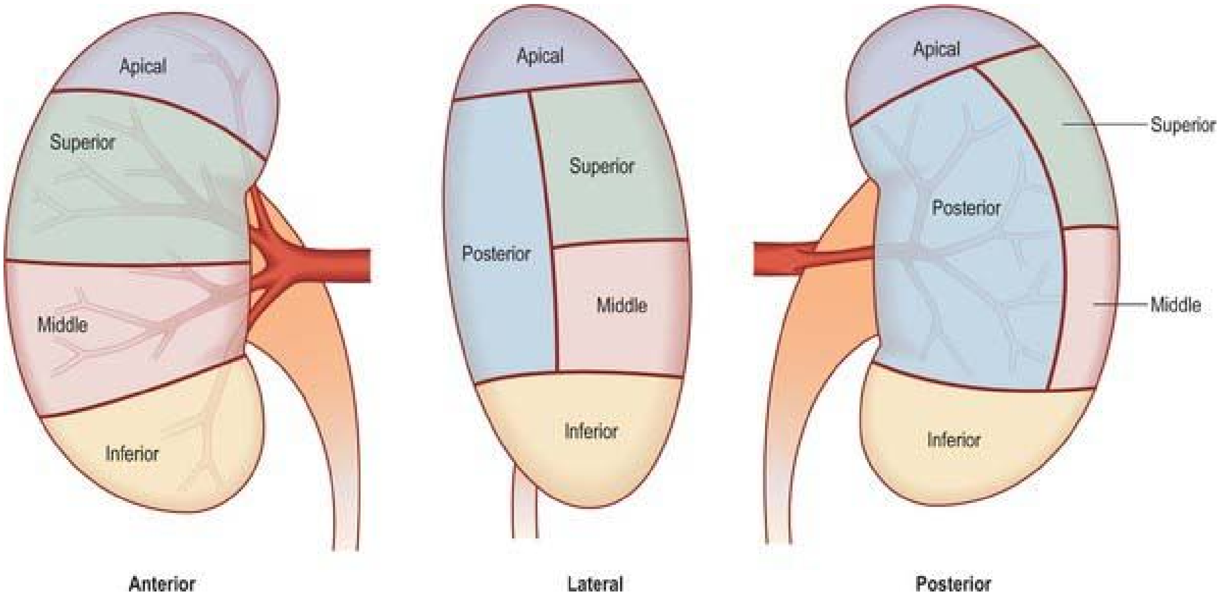
Apical
Superior
Middle
Inferior
Anterior
Apical
Superior
Posterior
Middle
Inferior
Lateral
Apical
Superior
Posterior
Middle
Inferior
Posterior

Fig. 74.12 Segmental arterial anatomy of the right kidney: the posterior division branches near the hilum before the anterior division divides into the other segmental arteries.

Brödel (1911) described a relatively avascular longitudinal zone (the ‘bloodless’ line of Brödel) along the convex renal border, which was proposed as the most suitable site for surgical incision. However, many vessels cross this zone, and it is far from ‘bloodless’: planned radial or intersegmental incisions are preferable. Knowledge of the vascular anatomy of the kidney is important when undertaking partial nephrectomy for renal cell cancers. In this surgery the branches of the renal artery are defined so that the surgeon may safely excise the renal substance containing the tumour while not compromising the vascular supply to the remaining renal tissue.

Lobar, interlobar, arcuate and interlobular arteries

The initial branches of segmental arteries are lobar, usually one to each renal pyramid. Before reaching the pyramid they subdivide into two or three interlobar arteries, extending towards the cortex around each pyramid. At the junction of the cortex and medulla, interlobar arteries dichotomize into arcuate arteries which diverge at right angles. As they arch between cortex and medulla, each divides further, ultimately supplying interlobular arteries which diverge radially into the cortex. The terminations of adjacent arcuate arteries do not anastomose but end in the cortex as additional interlobular arteries. Though most interlobular arteries come from arcuate branches, some arise directly from arcuate or even terminal interlobar arteries (see Fig. 74.14). Interlobular arteries ascend towards the superficial cortex or may branch occasionally en route. Some are more tortuous and recurve towards the medulla at least once before proceeding towards the renal surface. Others traverse the surface as perforating arteries to anastomose with the capsular plexus (which is also supplied from the inferior suprarenal, renal and gonadal arteries).

Afferent and efferent glomerular arterioles

Afferent glomerular arterioles are mainly the lateral rami of interlobular arteries. A few arise from arcuate and interlobar arteries when they vary their direction and angle of origin: deeper ones incline obliquely back towards the medulla, the intermediate pass horizontally, and the more superficial approach the renal surface obliquely before ending in a glomerulus (see Fig. 74.14). Efferent glomerular arterioles from most glomeruli (except at juxtamedullary and, sometimes, at intermediate cortical levels) soon divide to form a dense peritubular capillary plexus around the proximal and distal convoluted tubules: there are thus two sets of capillaries, glomerular and peritubular, in series in the main renal cortical circulation, linked by efferent glomerular arterioles. The vascular supply of the renal medulla is largely from efferent arterioles of juxtamedullary glomeruli, supplemented by some from more superficial glomeruli, and ‘aglomerular’ arterioles (probably from degenerated glomeruli). Efferent glomerular arterioles passing into the medulla are relatively long, wide vessels, and contribute side branches to neighbouring capillary plexuses before entering the medulla, where each divides into 12–25 descending vasa recta. As their name suggests, these run straight to varying depths in the renal medulla, contributing side branches to a radially elongated capillary plexus (see Fig. 74.14) applied to the descending and ascending limbs of renal loops and to collecting ducts. The venous ends of capillaries converge to the ascending vasa recta, which drain into arcuate or interlobular veins. An essential feature of the vasa recta (particularly in the outer medulla) is that both ascending and descending vessels are grouped into vascular bundles, within which the external aspects of both types are closely apposed, bringing them close to the limbs of renal loops and collecting ducts. As these bundles converge centrally into the renal medulla they contain fewer vessels: some terminate at successive levels in neighbouring capillary plexuses. This proximity of descending and ascending vessels with each other and adjacent ducts provides the structural basis for the countercurrent exchange and multiplier phenomena (see countercurrent exchange mechanism later in chapter (see Fig. 74.17)). These complex renal vascular patterns show regional specializations which are closely adapted to the spatial organization and functions of renal corpuscles, tubules and ducts (see below).

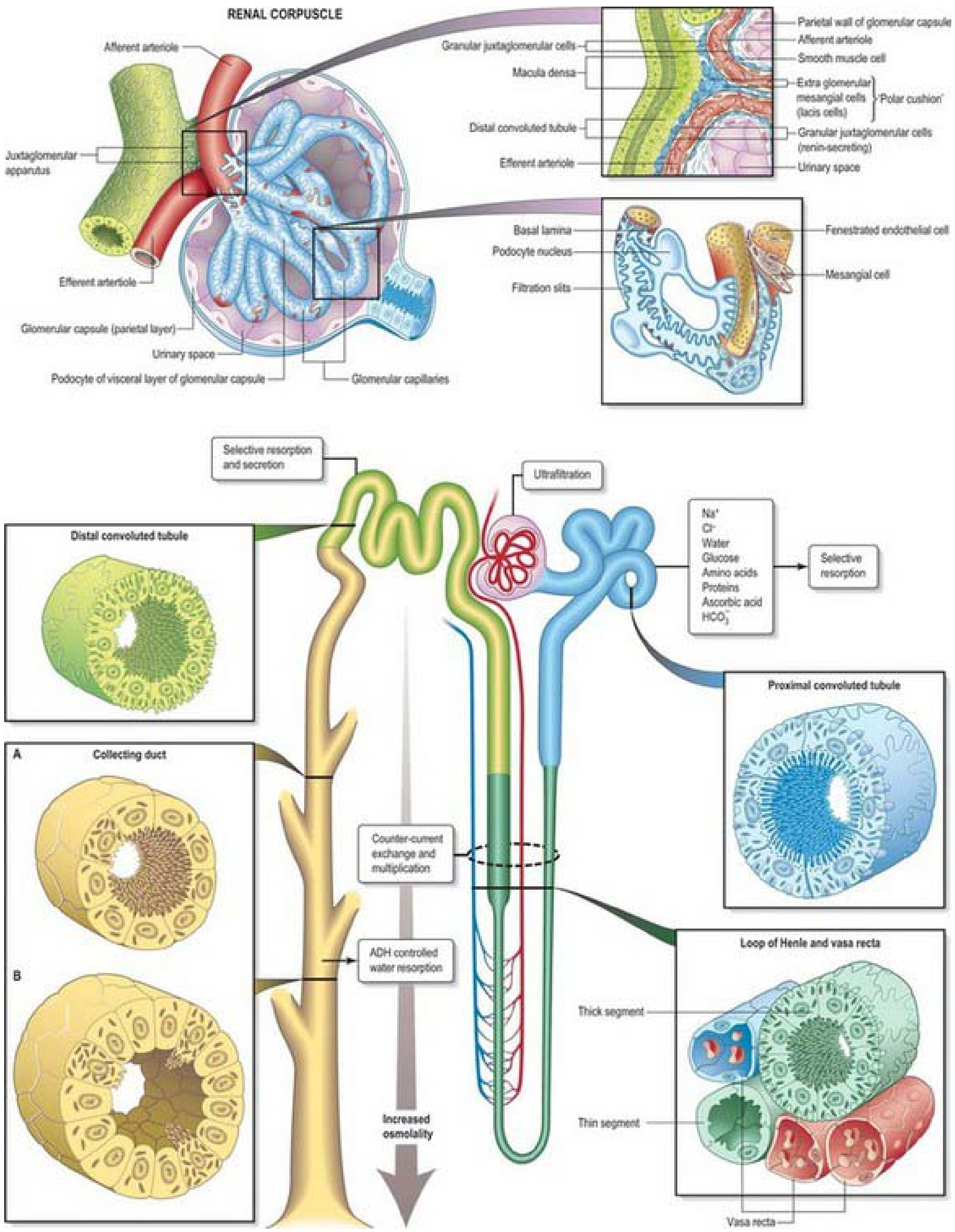
RENAL CORPUSCLE
Afferent arteriole
Juxtaglomerular apparutus
Efferent artertiole
Glomerular capsule (parietal layer)
Urinary space
Podocyte of visceral layer of glomerular capsule
Glomerular capillaries
Granular juxtaglomerular cells
Macula densa
Distal convoluted tubule
Efferent arteriole
Parietal wall of glomerular capsule
Afferent arteriole
Smooth muscle cell
Extra glomerular mesangial cells (lacis cells)
'Polar cushion'
Granular juxtaglomerular cells (renin-secreting)
Urinary space
Basal lamina
Podocyte nucleus
Filtration slits
Fenestrated endothelial cell
Mesangial cell
Selective resorption and secretion
Ultrafiltration
Distal convoluted tubule
Na+
Cl-
Water
Glucose
Amino acids
Proteins
Ascorbic acid
HCO3-
Selective resorption
Proximal convoluted tubule
A
Collecting duct
B
Counter-current exchange and multiplication
ADH controlled water resorption
Increased osmolality
Loop of Henle and vasa recta
Thick segment
Thin segment
Vasa recta

Fig. 74.17 The regional microstructure and principal activities of a kidney nephron and collecting duct. For clarity, a nephron of the long loop (juxtamedullary) type is shown.

Renal veins

Fine radicles from the venous ends of the peritubular plexuses converge to join interlobular veins, one with each interlobular artery. Many interlobular veins begin beneath the fibrous renal capsule by the convergence of several stellate veins, which drain the most superficial zone of the renal cortex and so are named from their surface appearance. Interlobular veins pass to the corticomedullary junction and also receive some ascending vasa recta before ending in arcuate veins (which accompany arcuate arteries), and anastomose with neighbouring veins. Arcuate veins drain into interlobar veins, which anastomose and form the renal vein.

The large renal veins lie anterior to the renal arteries and open into the inferior vena cava almost at right angles. The left is three times longer than the right (7.5 cm and 2.5 cm respectively) and for this reason, the left kidney is the preferred side for live donor nephrectomy. The left renal vein runs from its origin in the renal hilum, posterior to the splenic vein and the body of pancreas, and then across the anterior aspect of the aorta, just below the origin of the superior mesenteric artery. The left gonadal vein enters it from below and the left suprarenal vein, usually receiving one of the left inferior phrenic veins, enters it above but nearer the midline. The left renal vein enters the inferior vena cava a little superior and to the right. The right renal vein is behind the descending duodenum and sometimes the lateral part of the head of the pancreas. It can be extremely short (<1 cm) such that safe nephrectomy may require excision of a cuff of the inferior vena cava (Fig. 74.13).

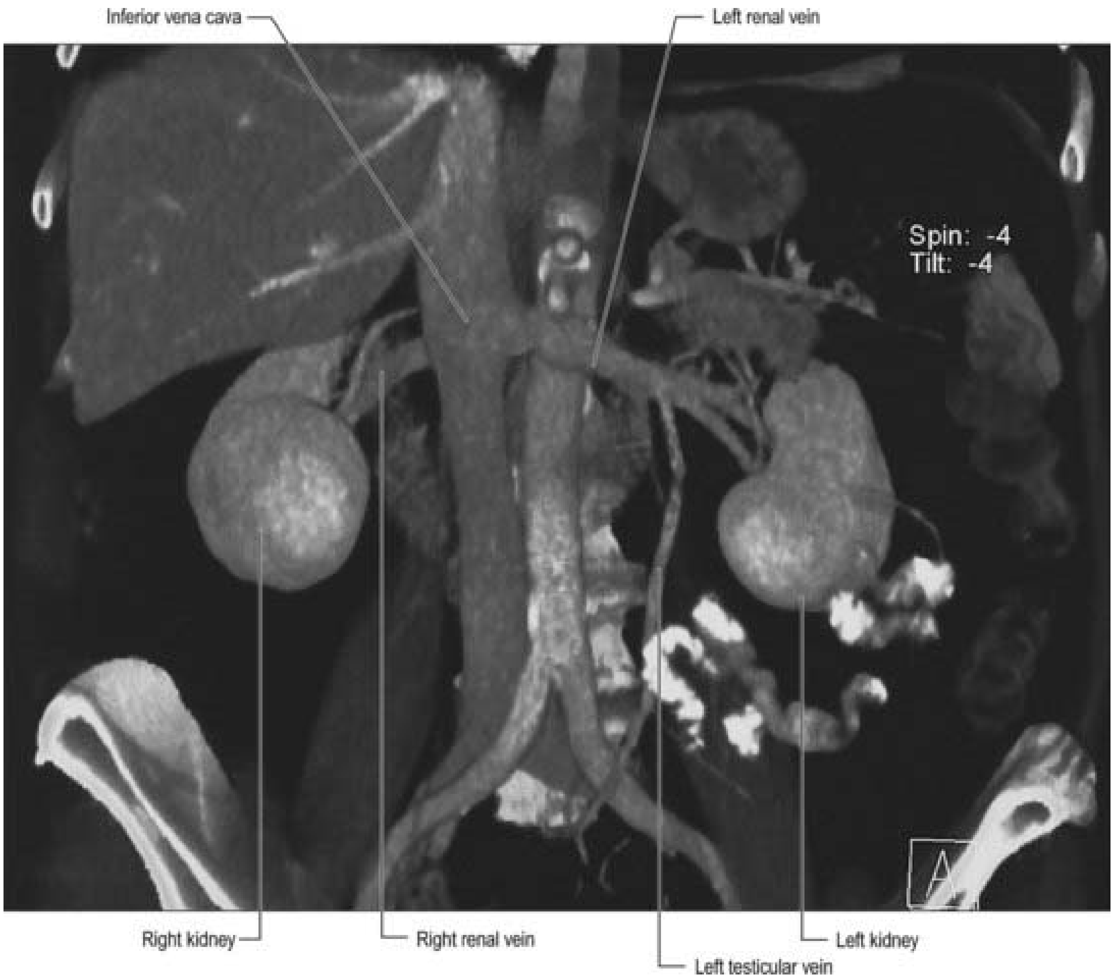
Inferior vena cava
Left renal vein
Spin: -4
Tilt: -4
A
Right kidney
Right renal vein
Left testicular vein
Left kidney

Fig. 74.13 CT renal venogram. Acquired from a multislice CT examination and reconstructed as a 3D surface shaded reformat.

The left renal vein may be double, one vein passing posterior, the other anterior, to the aorta before joining the inferior vena cava. This is sometimes referred to as persistence of the ‘renal collar’. The anterior vein may be absent so that there is a single retroaortic left renal vein. The left renal vein may be ligated during surgery for aortic aneurysm because it has such a close relationship with the aorta: this seldom results in any harm to the kidney, provided that the ligature is placed to the right of the draining gonadal and suprarenal veins, since these usually provide adequate collateral venous drainage. The right renal vein has no significant collateral drainage and cannot be ligated with impunity.

Lymphatic drainage

Renal lymphatic vessels begin in three plexuses, around the renal tubules, under the renal capsule, and in the perirenal fat (the latter two connect freely). Collecting vessels from the intrarenal plexus form four or five trunks which follow the renal vein to end in the lateral aortic nodes; the subcapsular collecting vessels join them as they leave the hilum. The perirenal plexus drains directly into the same nodes.

INNERVATION

Rami from the coeliac ganglion and plexus, aorticorenal ganglion, lowest thoracic splanchnic nerve, first lumbar splanchnic nerve and aortic plexus form a dense plexus of autonomic nerves around the renal artery.

Small ganglia occur in the renal plexus, the largest usually behind the origin of the renal artery. The plexus continues into the kidney around the arterial branches and supplies the vessels and renal glomeruli, and especially the cortical tubules. Axons from plexuses around the arcuate arteries innervate juxtamedullary efferent arterioles and vasa recta, which control the blood flow between the cortex and medulla without affecting the glomerular circulation. Axons from the renal plexus contribute to the ureteric and gonadal plexuses.

MICROSTRUCTURE

The kidney is composed of many tortuous, closely packed uriniferous tubules, bounded by a delicate connective tissue in which run blood vessels, lymphatics and nerves. Each tubule consists of two embryologically distinct parts, the nephron, which produces urine, and the collecting duct, which completes the concentration of urine and through which urine passes out into the calyces of the kidney, the renal pelvis, the ureter and urinary bladder (see p. 1305).

Nephron

The nephron consists of a renal corpuscle, concerned with filtration from the plasma, and a renal tubule, concerned with selective resorption from the filtrate to form the urine (Fig. 74.14). Collecting ducts carry fluid from several renal tubules to a terminal papillary duct, opening into a minor calyx at the apex of a renal papilla. Papillary surfaces show numerous minute orifices of these ducts and pressure on a fresh kidney expresses urine from them.

Renal corpuscle

Renal corpuscles are small rounded structures averaging 0.2 mm in diameter, visible in the renal cortex deep to a narrow peripheral cortical zone (Fig. 74.15A,B). Each has a central glomerulus of vessels and a glomerular (Bowman's) capsule, from which the renal tubule originates.

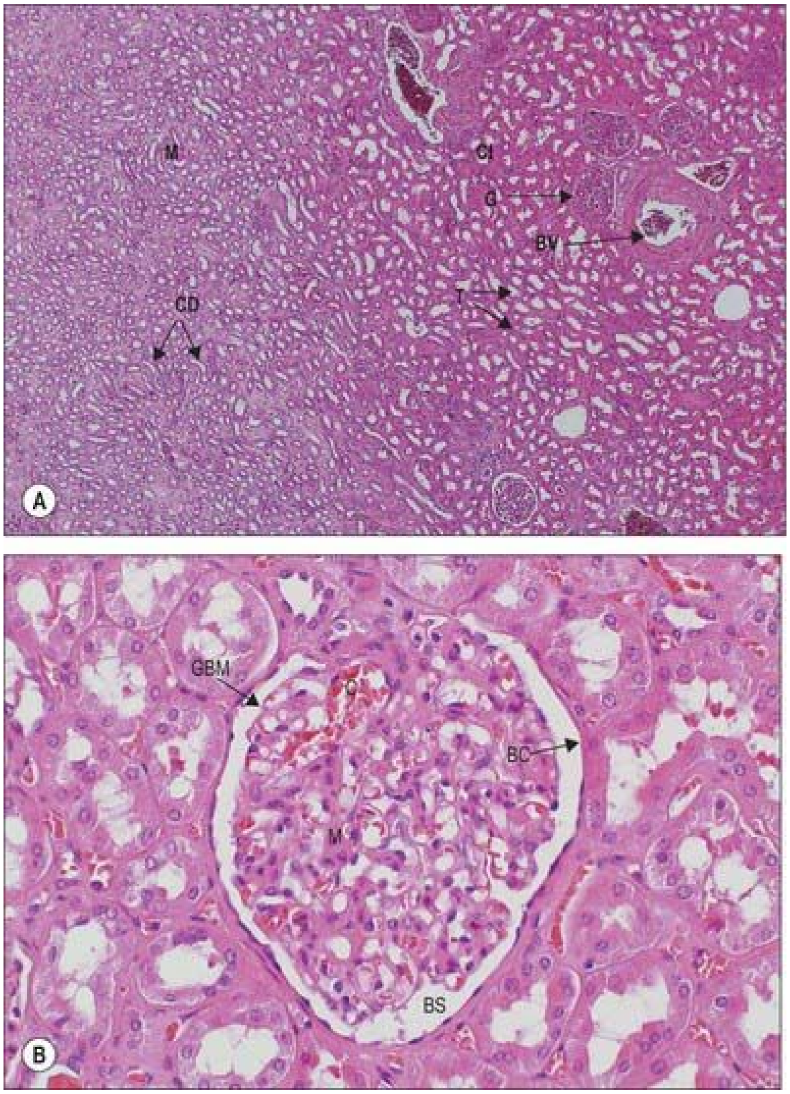

Fig. 74.15 **A**, Low power view of the kidney showing renal cortex (Ct) comprising glomeruli (G), proximal and distal convoluted tubules (T) and blood vessels (BV). The medulla (M) contains loops of Henle and collecting ducts (CD) (× 20, H&E stain). **B**, A glomerulus with a network of capillaries (C) set within a small amount of connective tissue, the mesangium (M). The glomerular basement membrane (GBM) of the capillaries is continuous with the Bowman's capsule (BC) of the glomerulus, and is separated from it by Bowman's space (BS) (× 200, H&E stain).

There are about one million renal corpuscles in each kidney, their number (which may be determined in part by intra-uterine factors) decreases with age; this process is accelerated by raised blood pressure. After birth new nephrons cannot be developed – a lost nephron can never be replaced. The decrease in corpuscular numbers with age is reflected in a corresponding reduction in the rate of glomerular filtration from the fourth decade onwards.

Glomerulus

A glomerulus is a collection of convoluted capillary blood vessels, united by a delicate mesangial matrix and supplied by an afferent arteriole which enters the capsule opposite the urinary pole, where the filtrate enters the tubule. (The term glomerulus is used most frequently to describe the entire renal corpuscle.) An efferent arteriole emerges from the same point, the vascular pole of the corpuscle. Glomeruli are simple in form until late prenatal life; some remain so for about 6 months after birth, the majority maturing by 6 years and all by 12 years (see p. 1305).

Bowman’s capsule

Bowman’s capsule is the blind expanded end of a renal tubule, and is deeply invaginated by the glomerulus. It is lined by a simple squamous epithelium on its outer (parietal) wall; its glomerular, juxtacapillary (visceral) wall is composed of specialized epithelial podocytes. Between the two walls of the capsule is a flattened urinary (Bowman’s) space, continuous with the proximal convoluted tubule (Fig. 74.15B; see Fig. 74.17).

Podocytes are stellate cells. Their major (primary) foot processes curve around the capillary loops and branch to form secondary processes which are applied closely to the basal lamina; secondary or tertiary processes give rise to terminal pedicels (Fig. 74.16A). Pedicels of one cell alternate with those of an adjacent cell and interdigitate tightly with each other, separated by narrow (25 nm) gaps, the filtration slits (Fig. 74.16B). The latter are covered by a dense, membranous slit diaphragm, through which filtrate must pass to enter the urinary space. The differentiation of the adult podocyte phenotype is associated with the presence of several specific proteins, including nephrin, podocin, synaptopodin and GLEPP-1. Mutations in these proteins can cause important functional problems, e.g. the classical Finnish form of congenital nephritic syndrome is caused by a mutation of NHPS1 coding for nephrin. The luminal membrane and the slit diaphragm are covered by a dense surface coat rich in sialoglycoproteins, which gives this surface a very high negative charge and is one of the key characteristics of the perm-selectivity barrier. Differentiated podocytes cannot replicate.

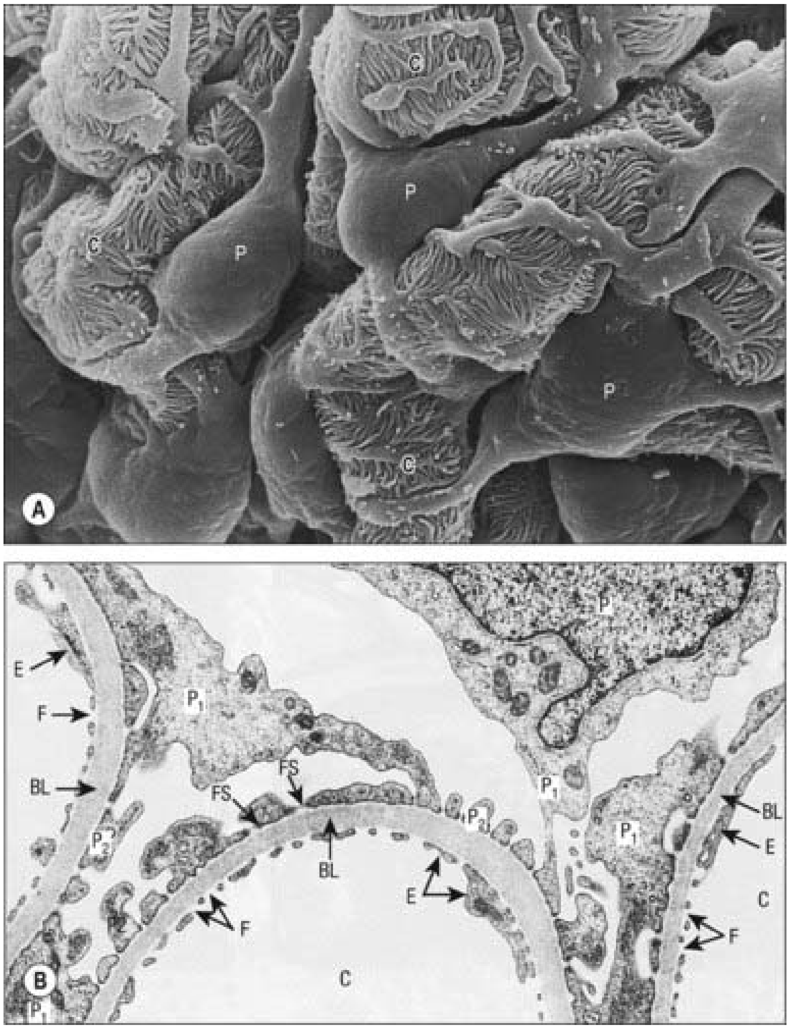

Fig. 74.16 **A**, Podocytes forming the visceral layer of Bowman's capsule in the renal corpuscle. Their cell bodies (P) send out primary processes which branch several times and end in fine pedicels which wrap tightly around the glomerular capillaries (C), and interdigitate with similar pedicels from a neighbouring podocyte. **B**, The glomerular filtration apparatus is

formed by the endothelial cells of fenestrated capillaries, the filtration slits between podocyte pedicels and their thick shared basal lamina. BL, basal lamina; C, capillary loops; E, endothelial cell cytoplasm; F, fenestrations; FS, filtration slits; P, podocyte, P_1 and P_2, primary and secondary foot processes which rest on the glomerular basal laminae.

(By permission of Igaku-Shoin, Tokyo, from Fujita T, Tanaka K, Tokunaga J 1981 SEM Atlas of Cells and Tissues). (By permission from Young B, Heath JW 2000 Wheater's Functional Histology. Edinburgh: Churchill Livingstone.)

The glomerular endothelium is finely fenestrated. The principal barrier to the passage of fluid from capillary lumen to urinary space is the glomerular basal lamina, the fused endothelial and podocyte basal laminae. This is usually 0.33 μm thick in man, and acts as a selective filter, allowing the passage from blood, under pressure, of water and various small molecules and ions in the circulation. Haemoglobin may cross the filter, but larger molecules and those of similar size with a negative charge, are largely retained. Most protein that does enter the filtrate is selectively resorbed and degraded by cells of the proximal convoluted tubule.

The glomerular basement membrane (GBM) serves as the skeleton of the glomerular tuft. Its outer aspect is completely covered by podocytes, and the interior is filled by capillaries and a delicate mesangial matrix (mesangium). The major components of the GBM are laminin and type IV collagen (both of which are expressed as unique isoforms) and heparin sulphate proteoglycans.

Irregular mesangial cells, with phagocytic and contractile properties, lie within and secrete the glomerular mesangium, a specialized connective tissue which binds the loop of glomerular capillaries and fills the spaces between endothelial surfaces that are not invested by podocytes (Fig. 74.15B; see Fig. 74.17). Mesangial cells are related to vascular pericytes and are concerned with the turnover of glomerular basement membrane. They clear the glomerular filter of immune complexes and cellular debris, and their contractile properties help to regulate blood flow. Similar cells, the extraglomerular mesangial (lacis) cells, lie outside the glomerulus at the vascular pole and form part of the juxtaglomerular apparatus.

Renal tubule

A renal or uriniferous tubule consists of a glomerular capsule that leads into a proximal convoluted tubule connected to the capsule by a short neck and continuing into a sinuous or coiled convoluted part (Fig. 74.17). This straightens as it approaches the medulla, and becomes the descending thick limb of the loop of Henle and then the ascending limb by an abrupt U-turn. The limbs of the loop of Henle are narrower and thin-walled within the deeper medullary tissue where they become the descending and ascending thin segments. The ascending thick limb continues into the distal tubule. The tubule wall shows a focal thickening, the macula densa, where it comes close to the vascular pole of its parent glomerulus at the start of the convoluted part of the distal tubule. The nephron finally straightens once more as the connecting tubule, which ends by joining a collecting duct.

Collecting ducts originate in the cortical medullary rays and join others at intervals. They finally open into wider papillary ducts which open on to a papilla, their numerous orifices forming a perforated area cribrosa on the surface at its tip (Fig. 74.14).

Renal tubules are lined throughout by a single-layered epithelium (Figs 74.17, 74.18). The type of epithelial cell varies according to the functional roles of the different regions, e.g. active transport and passive diffusion of various ions and water into and out of the tubules; reabsorption of organic components such as glucose and amino acids; uptake of any proteins which leak through the glomerular filter.

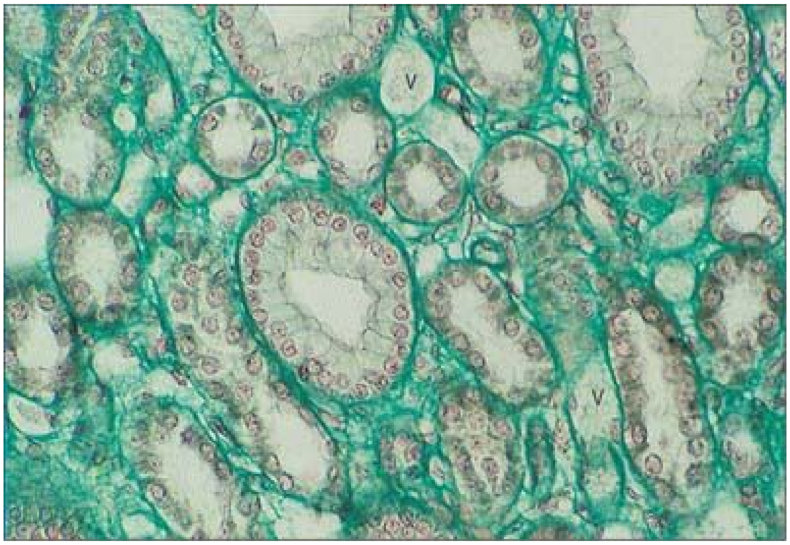

Fig. 74.18 Part of the renal medulla in cross-section. Note large collecting ducts and small thin segments of the loop of Henle, interspersed with vasa recta (V) (trichrome stained).

The proximal convoluted tubule is lined by cuboidal or low columnar epithelium and has a brush border of tall microvilli on its luminal surface. The shape of the cells depends on tubular fluid pressure, which in life distends the lumen and flattens the cells (they become taller when glomerular blood pressure falls postmortem or at biopsy). The cytoplasm of proximal tubular cells is strongly eosinophilic and the nuclei are euchromatic and central. The basal cytoplasm is rich in mitochondria, orientated perpendicularly, and the basal plasma membrane is highly infolded. The lateral surfaces of adjacent epithelial cells interdigitate, increasing the complexity of the basolateral plasma membrane. The microvilli on the luminal surfaces significantly increase the area of plasma membrane in contact with tubular fluid and the extratubular space, facilitating the transport of ions and small molecules against steep concentration gradients. The abundant mitochondria supply the energy, as ATP, needed for this process. Sodium/potassium adenosine triphosphatase (Na/K ATPase) is located in apical and basal membranes, and the cytoplasm contains numerous other enzymes concerned with ion transport. Water and other solutes pass between cells (paracellular transport) passively along osmotic and electrochemical gradients, probably through leaky apical tight junctions. Pinocytotic vesicles are found near the apical surface, and represent the means by which small proteins and peptides from the filtrate are internalized and degraded by associated lysosomes. Peroxisomes and lipid droplets abound in the cytoplasm.

The loop of Henle consists of a thin segment (30 μm in diameter), lined by low cuboidal to squamous cells, and a thick segment (60 μm in diameter) composed of cuboidal cells like those in the distal convoluted tubule. The thin segment forms most of the loop in juxtamedullary nephrons which reach deep into the medulla. Few organelles appear in cells lining the thin segment, indicating that these cells play a passive, rather than an active, role in ion transport. The thick segment is composed of cuboidal epithelium with many mitochondria, deep basolateral folds and short apical microvilli, indicating a more active metabolic role. The thick limb of the loop of Henle is the source of Tamm–Horsfall protein in normal urine.

Cells of the distal tubule are cuboidal and resemble those in the proximal tubule. They have few microvilli, and so the tubular lumen has a more distinct outline. The basolateral folds containing mitochondria are deep, almost reaching the luminal aspect (Fig. 74.17). Enzymes concerned in active transport of sodium, potassium and other ions are abundant. At the junction of the straight and convoluted regions the distal tubule comes close to the vascular pole of its parent renal corpuscle. Here, tubular cells form the macula densa, a sensory structure which is concerned with the regulation of blood flow and thus filtration rate. Cells in the terminal part of the distal tubule have fewer basal folds and mitochondria and constitute a connecting duct formed from metanephric mesenchyme during embryogenesis. Collecting ducts are lined by simple cuboidal or columnar epithelium. This increases in height from the cortex, where the ducts receive the contents of distal tubules, to the wide papillary ducts which discharge at the area cribrosa. The pale-staining principal cells have relatively few organelles or lateral interdigitations and only occasional microvilli. A second cell type, intercalated or dark cells (also present in smaller numbers in the distal convoluted tubule), have longer microvilli and more mitochondria and secrete H^+ into the filtrate; they function in the maintenance of acid–base homeostasis.

Renal vessels

Renal, interlobar and arcuate arteries are typical large muscular arteries and the interlobular vessels resemble small muscular arteries. Afferent glomerular vessels have a typical arteriolar structure with a muscular coat two to three cells thick: this coat and the connective tissue components of the wall diminish near a glomerulus until a point 30–50 μm proximal to it where arteriolar cells begin to show modifications typical of the juxtaglomerular apparatus. The efferent arterioles from most cortical glomeruli have thicker walls and a narrower calibre than corresponding afferents. Although the afferent arteriole is generally considered to be solely responsible for tubuloglomerular feedback, the peritubular and medullary capillaries possess a well-defined basal lamina and their endothelial cells have typically fenestrated cytoplasm, as do the ascending vasa recta, whereas the descending vasa recta have a thicker, continuous endothelium.

Other renal cells

Other cells essential to renal structure and function lie between the renal tubules and blood vessels. Connective tissue is inconspicuous in the cortex but prominent in the medulla, particularly in the papillae. Medullary interstitial cells, which may be modified fibroblasts, form vertical stacks of tangentially orientated cells between the more distal collecting ducts, like the rungs of a ladder. These cells secrete prostaglandins and may contribute, with cortical tubular cells, to the renal source of erythropoietin.

Calyces and pelvis

The wall of the proximal part of the urinary tract is composed of three layers, an outer connective tissue adventitia, an intermediate layer of smooth muscle and an inner mucosa. The mucosal lining of the renal calyces and pelvis is identical in structure to that of the ureter (see below). The adventitia consists of loose fibroelastic connective tissue which merges with retroperitoneal areolar tissue. Proximally the coat fuses with the fibrous capsule of the kidney lining the renal sinus.

The smooth muscle of the renal calyces and pelvis is composed of two distinct types of smooth muscle cell. One type of muscle cell is identical to that described for the ureter and can be traced proximally through the pelviureteric region and renal pelvis as far as the minor calyces. The other type of cell forms the muscle coat of each minor calyx and continues into the major calyces and pelvis where it forms a distinct inner layer. The cells also form a thin sheet of muscle which covers each minor calyx and extends across the renal parenchyma between the attachments of neighbouring minor calyces, thereby linking each minor calyx to its neighbours. This discrete inner layer of atypical smooth muscle ceases in the pelviureteric region so that the proximal ureter lacks such an inner layer. Pacemaker cells that initiate renal pelvic and ureteric peristalsis are sited within the calyces. These allow coordinated peristalsis of the ureter six times a minute.

PRODUCTION OF URINE

Glomerular filtration

Glomerular filtration (see Figs 74.14, 74.17) is the passage of water containing dissolved small molecules from the blood plasma to the urinary space in the glomerular capsule. Larger molecules, e.g. plasma proteins above 70 kilodaltons and those with a net negative charge, polysaccharides lipids and cells, are largely retained in blood by the selective permeability of the glomerular basal lamina.

Filtration occurs along a steep pressure gradient between the large glomerular capillaries and the urinary space, the principal structure separating the two being the glomerular basal lamina (Fig. 74.16B). This gradient far exceeds the colloid osmotic pressure of blood which opposes the outward flow of filtrate. In the peripheral renal cortex the arteriolar pressure gradient is enhanced because afferent glomerular arterioles are wider than efferent glomerular arterioles. In all glomeruli the rate of filtration can be altered by changes in the tone of the glomerular arterioles. When first formed, the glomerular filtrate is isotonic with glomerular blood and has an identical concentration of ions and small molecules.

The assessment of glomerular filtration is fundamental to the diagnosis of renal glomerular pathology and the management of drug therapy where clearance depends on the glomerular filtration, and in chronic kidney disease to facilitate timely management decisions. Measurements of glomerular filtration rate (GFR) are based on the renal clearance of a marker in plasma, expressed as the volume of plasma completely cleared of the marker per unit time. Markers used to measure GFR may be endogenous (creatinine, urea) or exogenous (inulin, iothalamate) substances. The ideal marker is endogenous, freely filtered by the glomerulus, neither reabsorbed nor secreted by the renal tubule, and eliminated only by the kidney.

Selective resorption

Selective resorption from the filtrate is an active process and occurs mainly in the proximal convoluted tubules, which resorb glucose, amino acids, phosphate, chloride, sodium, calcium and bicarbonate; they also take up small proteins (e.g. albumin) by endocytosis. Cells of the proximal tubules are permeable to water, which passes out of the tubules passively, so that the filtrate remains locally isotonic with blood. The rest of the tubule reabsorbs most of the water (to a variable extent up to 95%), so that when it reaches the calyces, urine is generally much reduced in volume and hypertonic to blood. The process depends on the establishment of high osmolality in the medullary interstitium, in order to exert sufficient osmotic pressure on water-permeable regions of the tubule, and is achieved by a countercurrent multiplier mechanism (see Figs 74.14, 74.17).

Countercurrent multiplier mechanism

The countercurrent multiplier mechanism is responsible for producing a high osmolality in the extratubular interstitial tissue of the renal medulla. Water passes freely from the tubular lumen into the adjacent medullary interstitium along the descending limb of the loop of Henle. This part of the tubule is less permeable to solutes. In the thick segment of the ascending limb, sodium and chloride ions are actively transported from the tubule lumen to interstitial spaces, while the tubular epithelium remains impermeable to water. It is in this segment of the tubule where furosemide and bumetamide act as diuretics. The increased interstitial osmolality causes water to be withdrawn from the descending part of the loop, thus concentrating the filtrate. Tubular fluid flows in a countercurrent on its descent into and ascent out of the medulla: it is augmented by new isotonic fluid entering the loop and depleted by hypotonic fluid leaving the loop, as solutes are actively resorbed.

In this way the osmotic gradient within the interstitium is multiplied from the corticomedullary boundary to the medullary pyramids, where it reaches an equilibrium of four to five times the osmolality of plasma. Although the tonicity of the tubular fluid changes during its passage through the steep osmotic gradient within the medulla, the osmotic gradient between ascending and descending limbs at each level never exceeds 200 mOsm/kg, a force which can be sustained by the cells of the tubular wall.

Countercurrent exchange mechanism

Rapid removal of ions from the renal medulla by the circulation of blood is minimized by another looped countercurrent system. This is the countercurrent exchange mechanism, in which arterioles entering the medulla pass for long distances parallel to the venules leaving it, before ending in capillary beds around tubules. This close apposition of oppositely flowing blood allows the direct diffusion of ions from outflowing to inflowing blood, so that the vasa recta (Fig. 74.14) conserve the high osmotic pressure in the medulla.

Concentration of urine

Because sodium and chloride ions are selectively resorbed by the cells of the ascending limbs and distal tubules under aldosterone control, the filtrate at the distal end of the convoluted tubules is hypotonic. As it reaches the collecting ducts, fluid descends again through the medulla and thus re-enters a region of high osmotic pressure. The cells lining the collecting ducts are variably permeable to water, under the influence of neurohypophysial ADH. Water follows an osmotic gradient into the adjacent extratubular spaces, so that the tonicity of the filtrate gradually rises along collecting ducts, until at the tip of the renal pyramids it is above that of blood. This complex system is highly flexible and the balance between the rate of filtration and absorption can be varied to meet current physiological demands.

Control of hydrogen and ammonium ion concentrations is essential to the regulation of acids and bases in the blood. Secretion of various ions occurs at several sites. Over 91% of ingested potassium is excreted in urine, largely through secretion by cells of the distal tubule and collecting duct. (For further details of renal physiology, see Madias & Adroque, 2005; Tannen & Hallows, 2005.)

Juxtaglomerular apparatus

The juxtaglomerular apparatus provides a tubuloglomerular feedback system which maintains systemic arterial blood pressure during a reduction in vascular volume and decrease in filtration rate. The elements of a juxtaglomerular apparatus are juxtaglomerular and lacis cells, and the macula densa.

The afferent and efferent arterioles at the vascular pole of a glomerulus and the macula densa of the distal tubule of the same nephron lie in close proximity, enclosing a small cone of tissue populated by extraglomerular mesangial (lacis) cells (Fig. 74.17). The cells of the tunica media of afferent and, to a lesser extent, efferent, arterioles differ from typical smooth muscle cells. These juxtaglomerular cells are large, rounded myoepithelioid cells and their cytoplasm contains many mitochondria and dense, renin-containing vesicles, 10–40 nm in diameter.

Each macula densa of the distal tubule is a cluster of up to 40 tightly packed cells in the tubule wall; the cells have large, oval nuclei and apically concentrated mitochondria. They are osmoreceptors, sensing the NaCl content of the filtrate after its passage through the loop of Henle.

When NaCl concentrations in the filtrate change, tubuloglomerular feedback mechanisms operate to maintain the inverse relationship between salt concentration and glomerular filtration rate. Juxtaglomerular cells release renin, an enzyme which acts on circulating angiotensinogen to activate the cascade whereby angiotensin II increases blood pressure (and therefore filtration rate), stimulates aldosterone and ADH release and increases sodium ion and water resorption, primarily from the distal tubule, to increase plasma volume. Macula densa cells are thought to respond to high salt concentration in the distal tubule by releasing nitric oxide, which inhibits the tubuloglomerular feedback response and reduces filtration rate. The role of macula densa cells in the stimulation of renin release to increase filtration rate is less well understood.

The third element of the juxtaglomerular apparatus is a population of extraglomerular mesangial cells which form a network (or lace, hence their alternative name of lacis cells) of stellate cells connecting the macula densa sensory cells with the juxtaglomerular effector cells. It is likely that extraglomerular mesangial cells transmit the sensory signal, possibly through gap junctions. They may also signal to contractile glomerular mesangial cells and effect vasoconstriction directly within the glomerulus. Adrenergic nerve fibres occur in small numbers among these cells.

URETER

The ureters are two muscular tubes whose peristaltic contractions convey urine from the kidneys to the urinary bladder (Fig. 74.9). Each measures 25–30 cm in length, is thick-walled and narrow, and is continuous superiorly with the funnel-shaped renal pelvis. Each descends slightly medially, anterior to psoas major, and enters the pelvic cavity where it curves initially laterally, then medially, to open into the base of the urinary bladder. The diameter of the ureter is normally 3 mm, but is slightly less at its junction with the renal pelvis, at the brim of the lesser pelvis near the medial border of psoas major, and where it runs within the wall of the urinary bladder, which is its narrowest part. These are the commonest sites for renal stone impaction.

RELATIONS

In the abdomen the ureter descends posterior to the peritoneum on the medial part of psoas major, which separates it from the tips of the lumbar transverse processes. During surgery on intraperitoneal structures, the ureter can be tented up as the peritoneum is drawn anteriorly, resulting in inadvertent ureteric injury. Anterior to psoas major it crosses in front of the genitofemoral nerve and is obliquely crossed by the gonadal vessels (Fig. 74.19). It enters the lesser pelvis anterior to either the end of the common iliac vessels or at the origin of the external iliac vessels (Fig. 74.20).

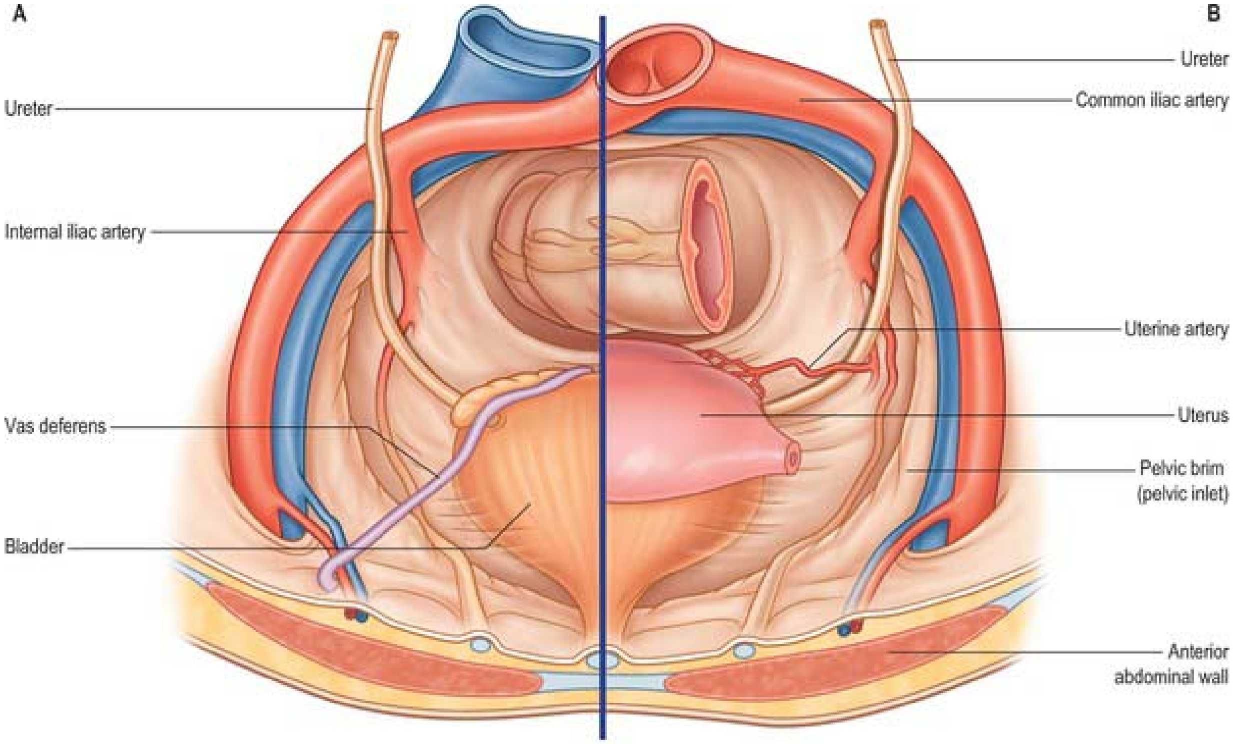
A
B
Ureter
Internal iliac artery
Vas deferens
Bladder
Ureter
Common iliac artery
Uterine artery
Uterus
Pelvic brim
(pelvic inlet)
Anterior
abdominal wall

Fig. 74.19 Relations of lower ureter. **A**, Male pelvis. **B**, Female pelvis.

(From Drake, Vogl and Mitchell 2005.)

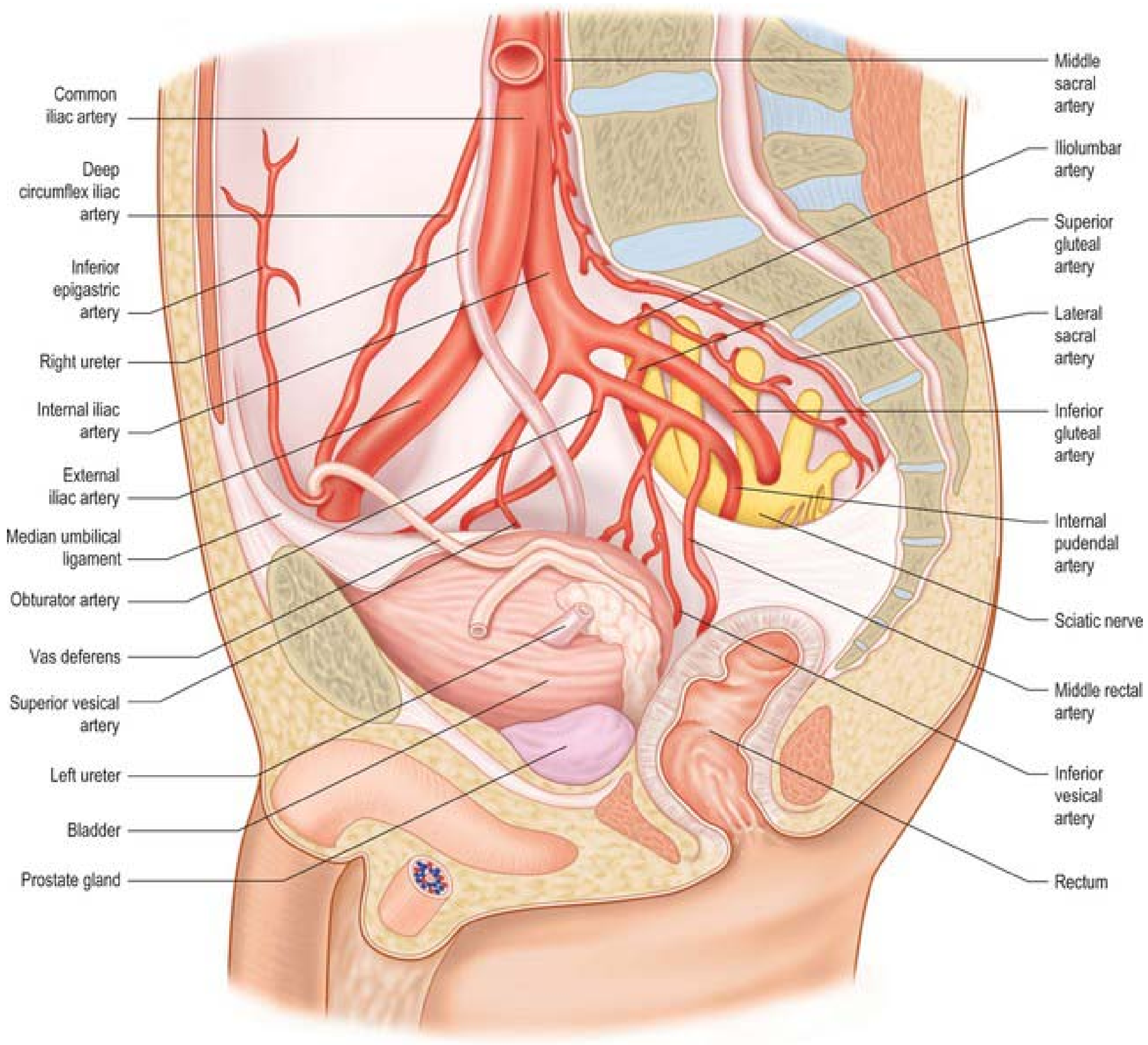
Common iliac artery
Deep circumflex iliac artery
Inferior epigastric artery
Right ureter
Internal iliac artery
External iliac artery
Median umbilical ligament
Obturator artery
Vas deferens
Superior vesical artery
Left ureter
Bladder
Prostate gland
Middle sacral artery
Iliolumbar artery
Superior gluteal artery
Lateral sacral artery
Inferior gluteal artery
Internal pudendal artery
Sciatic nerve
Middle rectal artery
Inferior vesical artery
Rectum

Fig. 74.20 Relations of male lower right ureter.

(By permission from Walsh PC, Retik AB, Vaughan ED et al (eds) 2002 Campbell's Urology, 8th edn. Philadelphia: Saunders.)

The inferior vena cava is medial to the right ureter while the left ureter is lateral to the aorta. The inferior mesenteric vein has a long retroperitoneal course lying close to the medial aspect of the left ureter.

At its origin the right ureter is usually overlapped by the descending part of the duodenum. It descends lateral to the inferior vena cava, and is crossed anteriorly by the right colic and ileocolic vessels. Near the superior aperture of the lesser pelvis it passes behind the lower part of the mesentery and terminal ileum. The left ureter is crossed by the gonadal and left colic vessels (see Fig. 74.24). It passes posterior to loops of jejunum and sigmoid colon and its mesentery in the posterior wall of the intersigmoid recess.

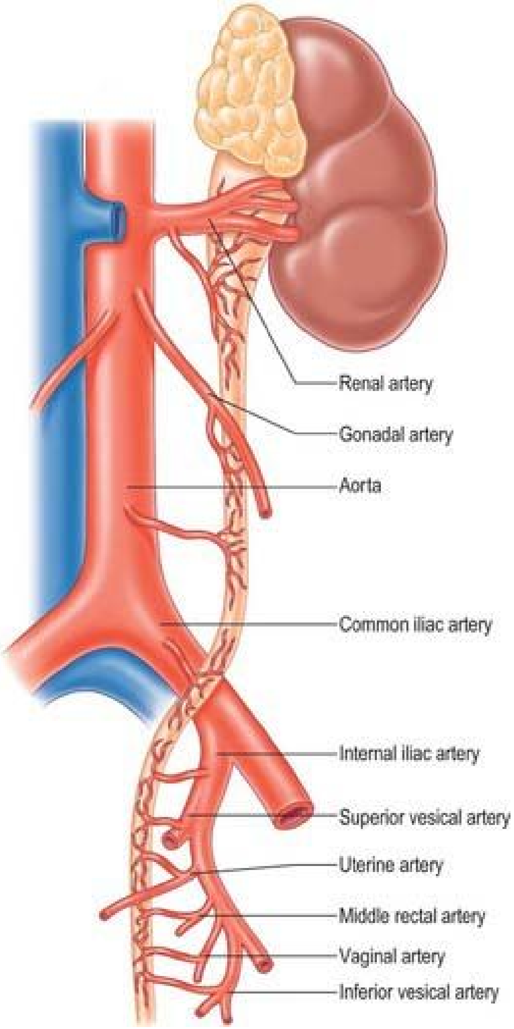
Renal artery
Gonadal artery
Aorta
Common iliac artery
Internal iliac artery
Superior vesical artery
Uterine artery
Middle rectal artery
Vaginal artery
Inferior vesical artery

Fig. 74.24 Arterial supply of the left ureter. The proximal part takes its blood supply medially, and the distal part is supplied laterally.

(By permission from Walsh PC, Retik AB, Vaughan ED et al (eds) 2002 Campbell's Urology, 8th edn. Philadelphia: Saunders.)

In the pelvis the ureter lies in extraperitoneal areolar tissue (see Fig. 75.3). At first it descends posterolaterally on the lateral wall of the lesser pelvis along the anterior border of the greater sciatic notch. Opposite the ischial spine it turns anteromedially into fibrous adipose tissue above levator ani to reach the base of the bladder. On the pelvic side-wall it is anterior to the internal iliac artery and the beginning of its anterior trunk, posterior to which are the internal iliac vein, lumbosacral nerve and sacroiliac joint. Laterally it lies on the fascia of obturator internus. It progressively crosses to become medial to the umbilical, inferior vesical, and middle rectal arteries.

In males, the pelvic ureter hooks under the vas deferens (Fig. 74.21), then passes in front of and slightly above the upper pole of the seminal vesicle to traverse the bladder wall obliquely before opening at the ipsilateral trigonal angle. Its terminal part is surrounded by tributaries of the vesical veins. In females, the pelvic part at first has the same relations as in males, but anterior to the internal iliac artery it is immediately behind the ovary, forming the posterior boundary of the ovarian fossa (see Ch. 77). In the anteromedial part of its course to the bladder it is related to the uterine artery, uterine cervix and vaginal fornices. It is in extraperitoneal connective tissue in the inferomedial part of the broad ligament of the uterus where it may be damaged during hysterectomy. In the broad ligament, the uterine artery is anterosuperior to the ureter for 2.5 cm and then crosses to its medial side to ascend alongside the uterus. The ureter turns forwards slightly above the lateral vaginal fornix and is generally 2 cm lateral to the supravaginal part of the uterine cervix in this location. It then inclines medially to reach the bladder, with a variable relation to the anterior aspect of the vagina. As the uterus is commonly deviated to one side, one ureter, usually the left, may be more extensively apposed to the vagina, and may cross the midline.

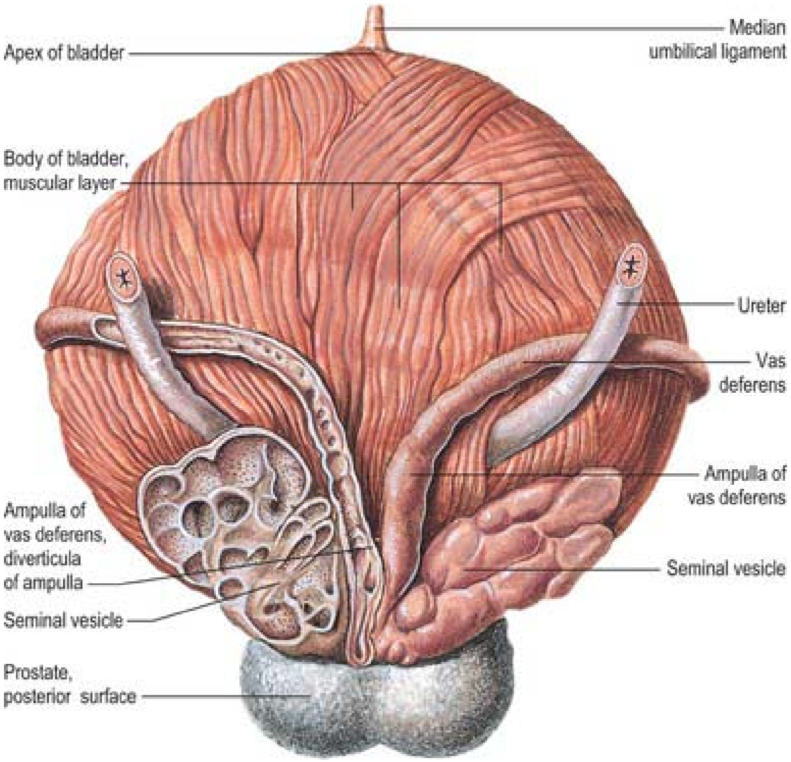
Apex of bladder
Median umbilical ligament
Body of bladder, muscular layer
Ureter
Vas deferens
Ampulla of vas deferens
Ampulla of vas deferens, diverticula of ampulla
Seminal vesicle
Seminal vesicle
Prostate, posterior surface

Fig. 74.21 Posterior aspect of the male urogenital organs, showing relationship of the lower ureter to the vas deferens and seminal vesicles.

(From Sobotta 2006.)

The distal 1–2 cm of each ureter is surrounded by an incomplete collar of non-striated muscle, which forms a sheath (of Waldeyer). The ureters pierce the posterior aspect of the bladder and run obliquely through its wall for a distance of 1.5–2.0 cm before terminating at the ureteric orifices (see Fig. 75.5B). This arrangement is believed to assist in the prevention of reflux of urine into the ureter, since the intramural ureters are thought to be occluded during increases in bladder pressure at the time of micturition. There is no evidence of a classic ureteral sphincter mechanism in man. The longitudinally oriented muscle bundles of the terminal ureter continue into the bladder wall and at the ureteric orifices become continuous with the superficial trigonal muscle. In the distended bladder, in both sexes, the ureteric openings are usually 5 cm apart, and 2.5 cm apart when the bladder is empty.

Duplex ureters

In 1 in 125 individuals, two ureters drain the renal pelvis on one side; this is termed a duplex system (Fig. 74.22). Bilateral duplex ureters occur in approximately 1 in 800 cases. The duplex ureters derive from two ureteric buds arising from the mesonephric duct. They are contained in a single fascial sheath and may fuse at any point along their course or may be separate until they insert through separate ureteric orifices into the bladder. Care must be taken not to compromise the blood supply of the second ureter when excising or reimplanting a single ureter of a duplex.

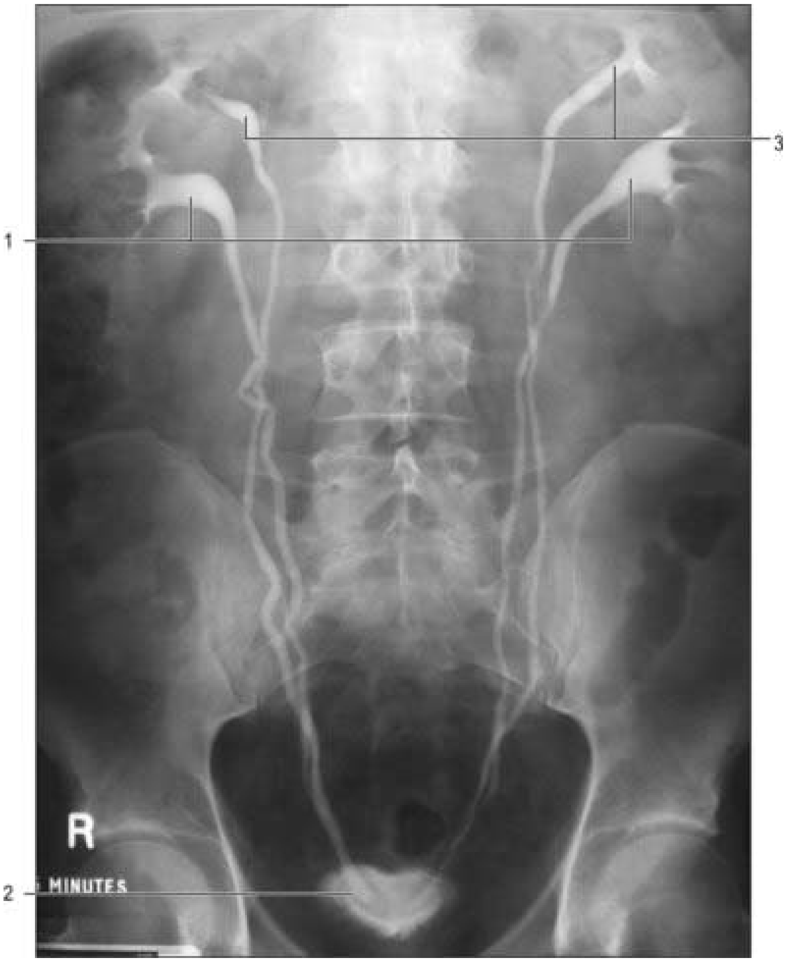

Fig. 74.22 Intravenous urogram showing bilateral duplex ureters and bilateral ureteroceles. Note that the ureters cross during their course. The right ureterocele can be clearly seen producing a halo appearance within the bladder surrounding the lower ureter. **1**. Contrast within lower moiety of

collecting system. **2**. ‘Cobra’s head’ halo around lower ureter showing ureterocele. **3**. Contrast within upper moiety of collecting system.

The ureter from the upper pole of the kidney (the longer ureter) inserts more medially and caudally in the bladder than the ureter from the lower pole (the shorter ureter). This reflects the embryological development of the ureter: the ureteric bud which is initially more proximal on the mesonephric duct has a shorter time to be pulled cranially in the bladder and so it inserts more distally in the mature bladder. The ureter from the lower pole has a shorter intramural course than the longer ureter and is prone to reflux.

Ectopic ureters

Single ureters, and more commonly the longer ureter of a duplex system, can insert more caudally and medially than normal in some individuals. In the male the ureter can insert at the bladder neck or posterior urethra, or rarely into the seminal vesicle, but it always inserts cranial to the external urethral sphincter. In the female, ectopic insertion can be distal to the external urethral sphincter in the urethra, or into the vagina, resulting in persistent childhood incontinence.

Ureteroceles

A ureterocele is a cystic dilatation of the lower end of the ureter: the ureteric orifice is covered by a membrane which expands as it is filled with urine and then deflates as it empties. Ureteroceles can vary in size, and although usually they have no influence on ureteric drainage they can be a cause of obstruction in the ureter and pelvicalyceal system more proximally. They usually do not cause bladder outflow obstruction except for the rare prolapsing ureterocele. Prolapsing ureteroceles, though small, prolapse from their position around the uretero-vesical junction region in to the urethra, causing intermittent bladder outflow obstruction. They are identified antenatally with ultrasound. In adults, ureteroceles tend to be bilateral and small and often found incidentally when the urinary tract is being imaged in the investigation of a coincidental pathology. Radiologically they classically result in a ‘cobra-head’ halo around the ureteric orifice following administration of contrast on intravenous urography (Fig. 74.22).

Retrocaval ureter

A persistence of the posterior cardinal vein, associated with high confluence of the right and left common iliac veins or a double inferior vena cava, may result in a retrocaval (or circumcaval) ureter which passes behind the inferior vena cava, usually at the level of the inferior edge of the third part of the duodenum, before it emerges in front of it to pass from medial to lateral. Retrocaval ureter occurs in 1 in 1500 individuals. Most commonly it has no clinical sequelae although it can result in upper ureteric obstruction (Fig. 74.23).

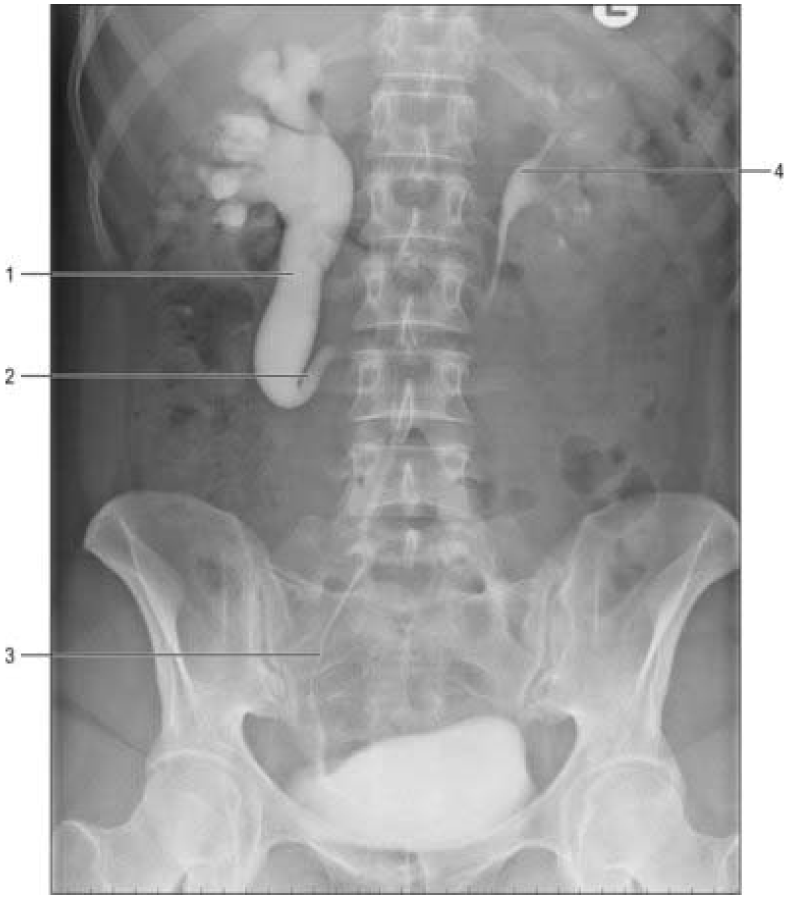

Fig. 74.23 Intravenous urogram showing a classical retrocaval (or circumcaval) ureter. A degree of obstruction has resulted in a markedly

dilated upper ureter. The ureter passes cranially, medially and then caudally, and can be followed into the pelvis. **1**. Contrast within dilated collecting system of right kidney and upper ureter. **2**. Contrast within ureter turning behind inferior vena cava. **3**. Contrast within normal calibre ureter seen below the obstruction. **4**. Contrast within normal collecting system of left kidney and upper ureter.

VASCULAR SUPPLY AND LYMPHATIC DRAINAGE

Arteries

The ureter is supplied by branches from the renal, gonadal, common iliac, internal iliac, vesical and uterine arteries, and the abdominal aorta (Fig. 74.24). The pattern of distribution is subject to much variation. The abdominal ureter is supplied from vessels originating medial to the ureter, while the pelvic ureter is supplied by vessels lateral to the ureter. There is a good longitudinal anastomosis between these branches on the wall of the ureter, which means that the ureter can be safely transected at any level intraoperatively, and a uretero-ureterostomy performed, without compromising its viability. The branches from the inferior vesical artery are constant in their occurrence and supply the lower part of the ureter as well as a large part of the trigone of the bladder. The branch from the renal artery is also constant and is preserved whenever possible in renal transplantation to ensure good vascularity of the ureter.

Veins

The venous drainage of the ureters generally follows the arterial supply.

Lymphatic drainage

Lymph vessels draining the ureter begin in submucosal, intramuscular and adventitial plexuses which all communicate. Collecting vessels from the upper abdominal ureter may join the renal collecting vessels or pass directly to the lateral aortic nodes near the origin of the gonadal artery, those from the lower abdominal ureter drain to the common iliac nodes, and those from the pelvic ureter drain to common, external or internal iliac nodes.

INNERVATION

The ureter is supplied from the lower three thoracic, first lumbar, and the second to fourth sacral segments of the spinal cord by branches from the renal and aortic plexuses, and the superior and inferior hypogastric plexuses. The ureteric nerves consist of relatively large bundles of axons which form an irregular plexus in the adventitia of the ureter. The plexus receives branches from the renal and aortic plexuses (in its upper part), from the superior hypogastric plexus and hypogastric nerve (in its intermediate part), and from the hypogastric nerve and inferior hypogastric plexus (in its lower part). Numerous small branches penetrate the ureteric muscle coat: some of the adventitial nerves accompany the blood vessels and branch with them as they extend into the muscle layer, others are unrelated to the vascular supply and lie free in the adventitial connective tissue around the circumference of the ureter.

The density of innervation increases gradually from the renal pelvis and upper ureter (where autonomic nerves are sparse) to a maximum density in the juxtavesical segment. At least three different neurotransmitter phenotypes, cholinergic, noradrenergic and peptidergic (substance P), are well known and others have been reported. The functional significance of these different types of autonomic nerve fibres in relation to ureteric smooth muscle activity is not fully understood: although they are thought to influence the inherent motility of the ureter, they are not essential for the initiation and propagation of ureteric contraction waves. A branching plexus of fine cholinergic, noradrenergic and peptidergic axons occurs throughout the lamina propria and extends from the inner aspect of the muscle coat towards the base of the urothelium. Some of these axons form perivascular plexuses, others lie in isolation from the vascular supply and may be sensory in function.

Ureteric peristalsis

Under normal conditions contraction waves originate in the proximal part of the upper urinary tract and are propagated in an anterograde direction towards the bladder. Atypical smooth muscle cells in the wall of the minor calyces act individually or collectively as pacemaker sites. A peristaltic wave begins at one (or possibly more) of these sites. Once initiated, the contraction is propagated through the wall of the adjacent major calyx and activates the smooth muscle of the renal pelvis. Contraction waves are propagated away from the kidney, and so undesirable pressure rises are not directed against the renal parenchyma. Since several potential pacemaker sites exist, the initiation of contraction waves is unimpaired by partial nephrectomy: the minor calyces spared by the resection remain *in situ* to continue their pacemaking function. Pressures within the ureter at the time of peristalsis reach 20–80 cm H_2O.

Experimental evidence indicates that autonomic nerves do not play a major part in the propagation of peristalsis. It seems more likely that they play a modulatory role on the contractile events occurring in the musculature of the upper urinary tract. The most likely mechanism to account for impulse propagation is myogenic conduction mediated by the electrotonic coupling of one muscle cell to its immediate neighbours by means of intercellular ‘gap’ junctions: there are numerous regions of close approach between ureteric smooth muscle cells and also between both types of muscle cell in the renal pelvis and calyces.

Referred pain

Excessive distension of the ureter or spasm of its muscle may be caused by a stone (calculus) and provokes severe pain (ureteric colic, which is commonly, but mistakenly, called renal colic). The pain is spasmodic and agonizing, particularly if the obstruction is gradually forced down the ureter by the muscle spasm. It is referred to cutaneous areas innervated from spinal segments which supply the ureter, mainly T11–L2, and shoots down and forwards from the loin to the groin and scrotum or labium majus; it may extend into the proximal anterior aspect of the thigh by projection to the genitofemoral nerve (L1, 2). The cremaster, which has the same innervation, may reflexly retract the testis.

RENAL AND URETERIC CALCULI

An understanding of intrarenal and ureteric anatomy is essential when managing patients with calculi, particularly now that minimally invasive techniques are widely used to treat this common pathology.

Smaller renal calculi are treated with extracorporeal shock wave lithotripsy. Stones in the lower pole of the kidney clear less well if the angle between the infundibulum of the calyx containing the stone and the ureter is acute, or if there is a particularly long and narrow infundibulum. Percutaneous stone extraction is most frequently achieved by puncturing a posterior calyx with a needle.

Ureteric calculi tend to be arrested in their descent in either the pelviureteric region, or the point where the ureter passes over the pelvic brim as it crosses the common iliac artery, or the vesico-ureteric junction, because these are the three areas where the ureter is narrowest. The vesico-ureteric junction is the narrowest of these areas and can be responsible for arresting the passage of stones of as little as 2–3 mm.

The kidney and upper ureter move with respiration within the perirenal fascia, and this can affect the visualization and tracking of a stone, both at the time of extracorporeal shock wave lithotripsy and at retrograde endoscopy.

MICROSTRUCTURE

Like the calyces and the renal pelvis, the wall of the ureter is composed of an external adventitia, a smooth muscle layer and an inner mucosal layer (Fig. 74.25). The mucosal layer consists of a urothelium and an underlying connective tissue lamina propria.

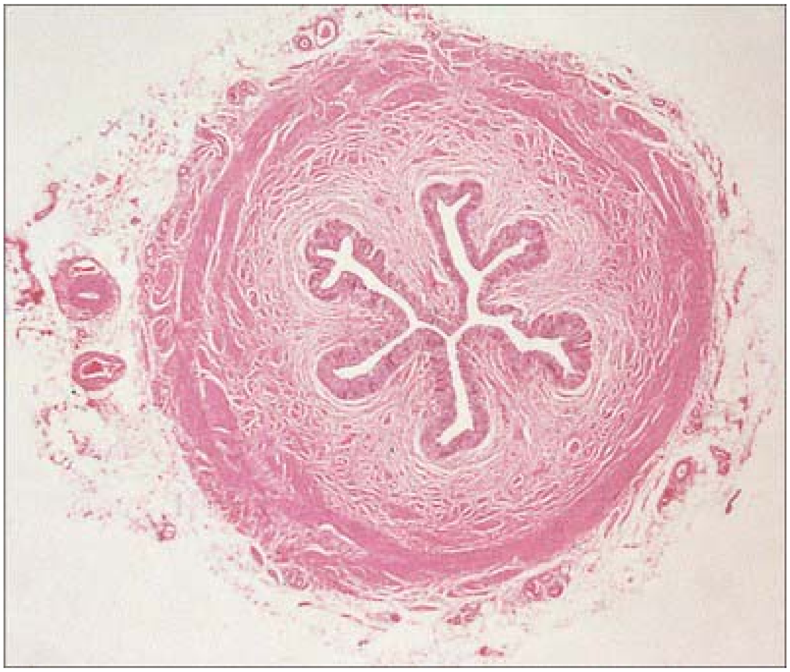

Fig. 74.25 Transverse section of ureter. The walls are muscular and are lined by a specialized urothelium.

(By permission from Stevens A, Lowe JS 1996 Human Histology, 2nd edn. London: Mosby.)

The ureteric adventitial blood vessels and connective tissue fibres are orientated parallel to the long axis of the ureter. Throughout its length, the muscle coat of the ureter is fairly uniform in thickness and in cross-section measures 750–800 µm in width. The muscle bundles which constitute this coat are frequently separated from one another by relatively large amounts of connective tissue. However, branches which interconnect muscle bundles are common and there is frequent interchange of muscle fibres between adjacent bundles. As a consequence of this extensive branching, individual muscle bundles do not spiral around the ureter, but form a complex meshwork of interweaving bundles. Moreover, unlike the gut (see Ch. 66), the muscle bundles are so arranged that morphologically distinct longitudinal and circular layers cannot be clearly distinguished. In the upper part of the ureter, the inner muscle bundles tend to lie longitudinally while those on the outer aspect have a circular or oblique orientation. In the middle and lower parts, there are additional outer longitudinally orientated fibres, and as the ureterovesical junction is approached, the muscle coat consists predominantly of longitudinally orientated muscle bundles.

The mucosa of the ureter consists of an epithelium, the urothelium, on the deep aspect of which is a layer of subepithelial fibroelastic connective tissue lamina propria. The latter varies in thickness from 350–700 µm and is a conduit for small blood vessels and bundles of non-myelinated nerve fibres. Occasional lymphocytes may be present in the lamina propria but their aggregation into definitive lymph nodules is rare. The urothelium is usually extensively folded, which gives the ureteric lumen a stellate outline.

REFERENCES

odel M. The intrinsic blood-vessels of the kidney and their significance in nephrotomy. *John Hopkins Hosp Bull*. 1911;12:10-13.

Original description of a relatively avascular longitudinal zone within the kidney, proposed as a site for surgical incision..

rkhill GJC, Healy JC. Anatomy of the retroperitoneum. *Imaging*. 2000;12:10-20.

Review of the imaging literature describing the contentious anatomy of the perirenal fascia..

avies A, Blakeley AGH, Kidd C. The renal system. In: *Human Physiology*. Edinburgh: Churchill Livingstone; 2001:713-797. Chapter 8.

avies JM. The role of the efferent arteriole in tubuloglomerular feedback. *Kidney Int (Suppl)*. 1991;32:S71-S73.

osling JA, Dixon JS. Species variation in the location of upper urinary tract pacemaker cells. *Invest Urol*. 1974;11:418.

Early paper describing the identification of pacemaker cells in various species..

erklin RJ, Michels NA. The variant renal and suprarenal blood supply with data on the inferior phrenic, ureteral, and gonadal arteries: a statistical analysis based on 185 dissections and a review of the literature. *J Int Coll Surg*. 1958;29:41-76.

A review of renal vascular anatomy in almost 11,000 kidneys..

itchell GAG. The renal fascia. *Br J Surg*. 1950;37:257-266.

Demonstrating that the perirenal fascia is a multilaminate structure rather than a single fused fascia..

ovick AC. Anatomic approaches in nephron-sparing surgery for renal cell carcinoma. *Atlas Urol Clin North Am*. 1998;6:39.

adias NE, Adrogué HJ. Hypo-hypernatraemia: disorders of water balance. Davison AM, Cameron JS, Grunfeld J-P, et al, editors. Oxford Textbook of Clinical Nephrology, Volume 1. Oxford University Press, 2005. Chapter 2.1

nnen RL, Hallows KR. Hypo-hyperkalaemia. Davison AM, Cameron JS, Grunfeld J-P, et al, editors. Oxford Textbook of Clinical Nephrology, Volume 1. Oxford University Press, 2005. Chapter 2.2;

CHAPTER 75

Bladder, prostate and urethra

URINARY BLADDER

The urinary bladder is a reservoir. Its size, shape, position and relations all vary according to its content and the state of neighbouring viscera. When the bladder is empty, it lies entirely in the lesser pelvis, but as it distends it expands anterosuperiorly into the abdominal cavity. An empty bladder is somewhat tetrahedral and has a base (fundus), neck, apex, a superior and two inferolateral surfaces.

RELATIONS

The base of the bladder is triangular and located posteroinferiorly. In females it is closely related to the anterior vaginal wall (Fig. 75.1; see Fig. 77.25B); in males it is related to the rectum although it is separated from it above by the rectovesical pouch, and below by the seminal vesicle and vas deferens on each side and Denonvillier's fascia (Fig. 75.2A,B). The neck, which is most fixed, lies most inferiorly, 3–4 cm behind the lower part of the symphysis pubis and just above the plane of the inferior aperture of the lesser pelvis. The bladder neck is essentially the internal urethral orifice, which lies in a constant position, independent of the varying positions of the bladder and rectum. In males the neck rests on, and is in direct continuity with, the base of the prostate; in females it is related to the pelvic fascia, which surrounds the upper urethra. In both sexes the apex of the bladder faces towards the upper part of the symphysis pubis. The median umbilical ligament (urachus) ascends behind the anterior abdominal wall from the apex to the umbilicus, covered by peritoneum to form the median umbilical fold (see below).

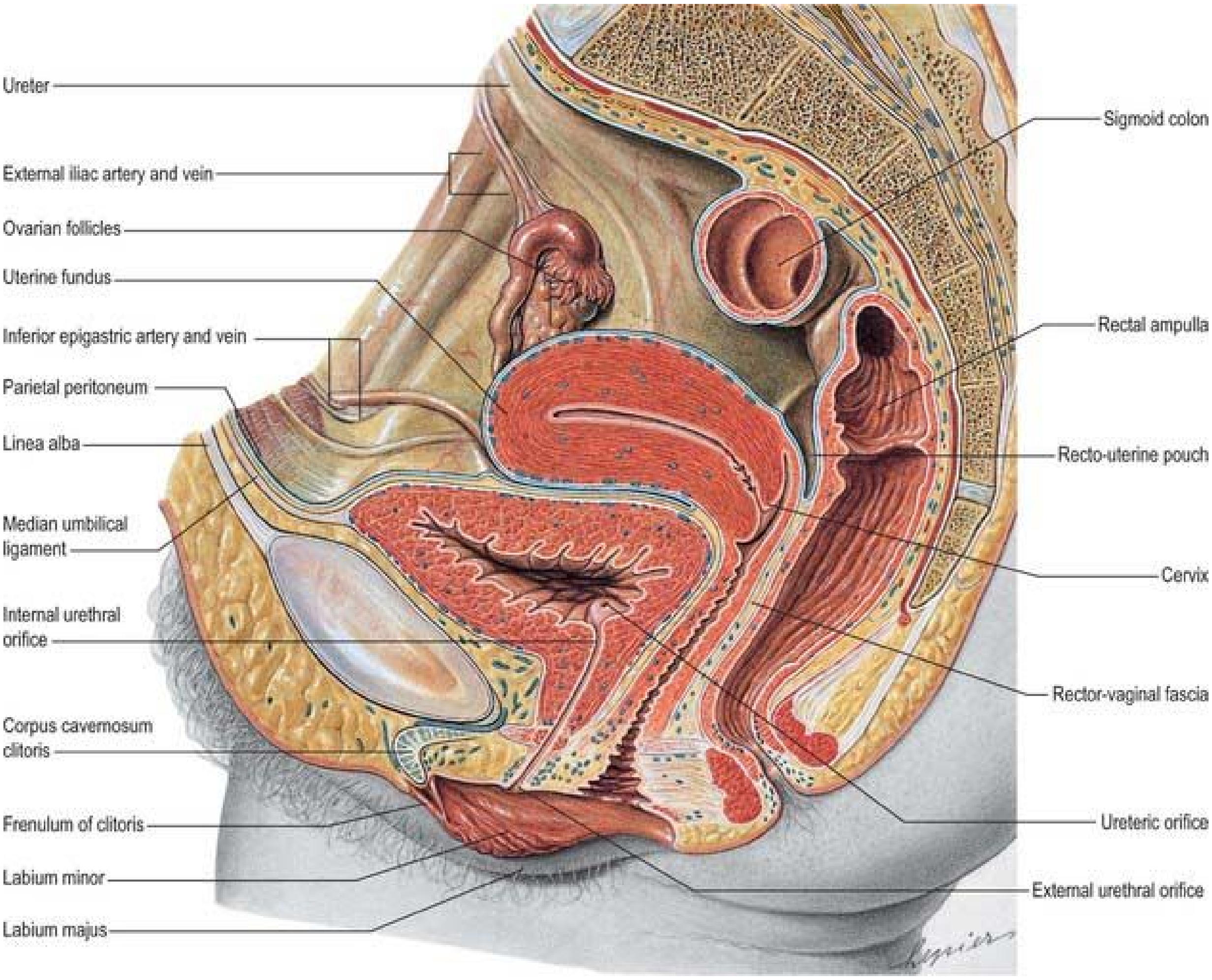
Ureter
External iliac artery and vein
Ovarian follicles
Uterine fundus
Inferior epigastric artery and vein
Parietal peritoneum
Linea alba
Median umbilical ligament
Internal urethral orifice
Corpus cavernosum clitoris
Frenulum of clitoris
Labium minor
Labium majus
Sigmoid colon
Rectal ampulla
Recto-uterine pouch
Cervix
Rector-vaginal fascia
Ureteric orifice
External urethral orifice

Fig. 75.1 Relations of the female bladder, sagittal section of the pelvis.

(From Sobotta 2006.)

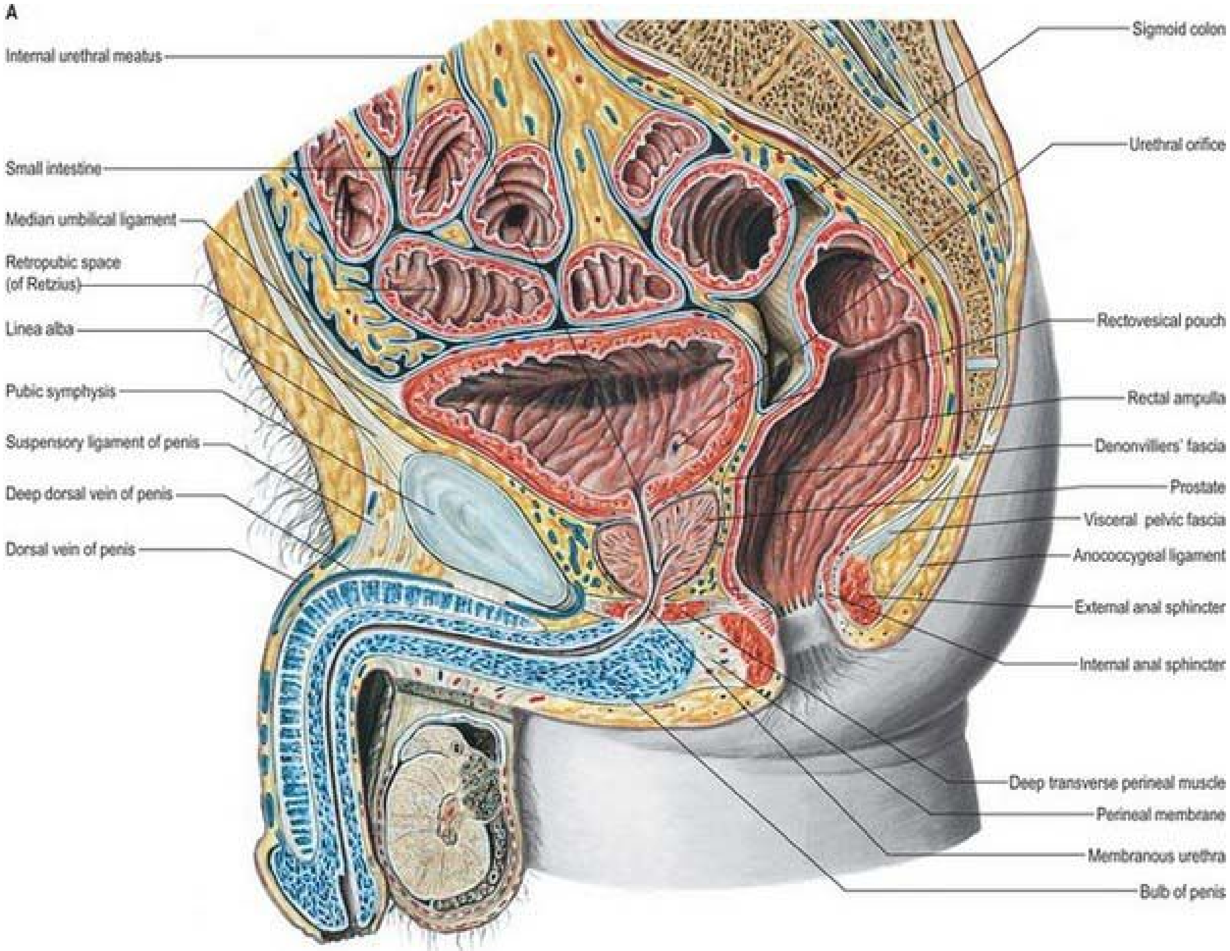
A
Internal urethral meatus
Small intestine
Median umbilical ligament
Retropubic space (of Retzius)
Linea alba
Pubic symphysis
Suspensory ligament of penis
Deep dorsal vein of penis
Dorsal vein of penis
Sigmoid colon
Urethral orifice
Rectovesical pouch
Rectal ampulla
Denonvilliers' fascia
Prostate
Visceral pelvic fascia
Anococcygeal ligament
External anal sphincter
Internal anal sphincter
Deep transverse perineal muscle
Perineal membrane
Membranous urethra
Bulb of penis

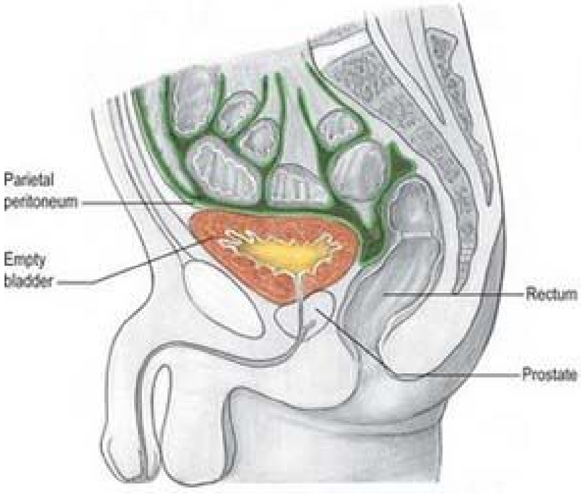
Parietal peritoneum
Empty bladder
Rectum
Prostate

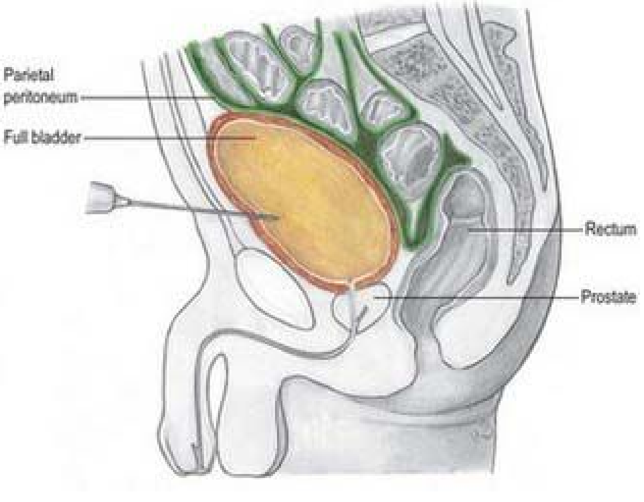
Parietal peritoneum
Full bladder
Rectum
Prostate

Rectus abdominis
Bladder
Seminal vesicle

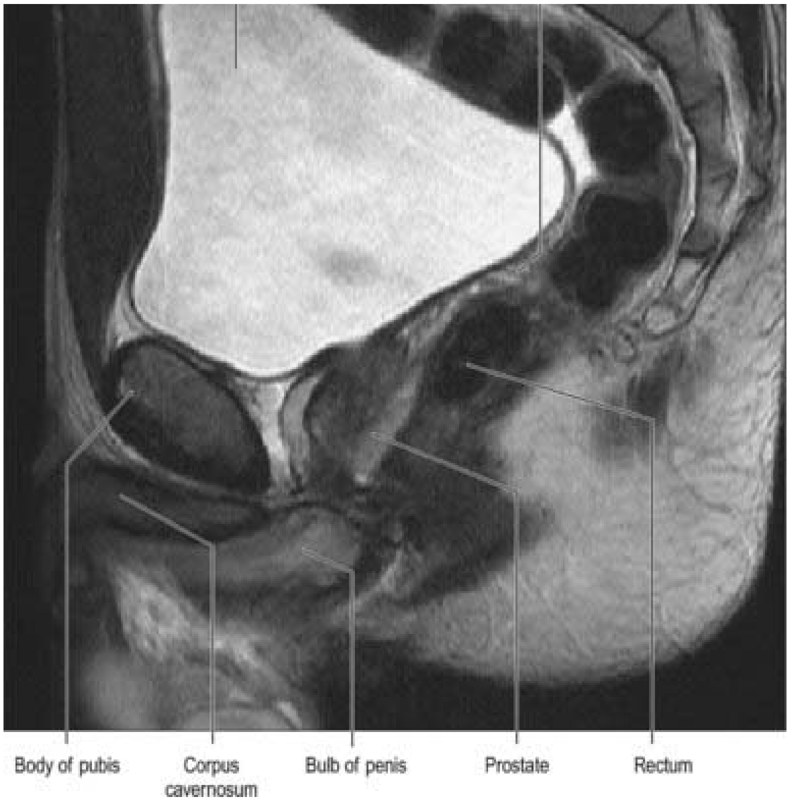

Fig. 75.2 **A**, The relationship of the bladder and prostate, sagittal section, male pelvis. The relationship of the bladder to the peritoneum and anterior abdominal wall on filling allows suprapubic cystotomy without intraperitoneal urinary leak. (**A**, From Sobotta 2006.) **B**, Sagittal T2 MRI of the male pelvis showing the bladder, prostate and relations.

The anterior surface of the bladder is separated from the transversalis fascia by fat in the potential retropubic space (of Retzius). This is more adherent to the bladder than to the anterior surface of the prostate, which aids reliable identification of the region of the bladder neck surgically. In males, each inferolateral surface is related anteriorly to the pubis and puboprostatic ligaments. In females the relations are similar, except that the pubovesical ligaments replace the puboprostatic ligaments. The inferolateral surfaces are not covered by peritoneum. The triangular superior surface is bounded by lateral borders from the apex to the ureteric entrances, and by a posterior border which joins them. In males the superior surface is completely covered by peritoneum, which extends slightly onto the base and continues posteriorly into the rectovesical pouch and anteriorly into the median umbilical fold: it is in contact with the sigmoid colon and the terminal coils of the ileum (Figs 75.1, 75.2 and 75.3; see page 1105). In females the superior surface is largely covered by peritoneum, which is reflected posteriorly onto the uterus at the level of the internal os (the junction of the uterine body and cervix), to form the vesicouterine pouch. The posterior part of the superior surface, devoid of peritoneum, is separated from the supravaginal cervix by fibroareolar tissue.

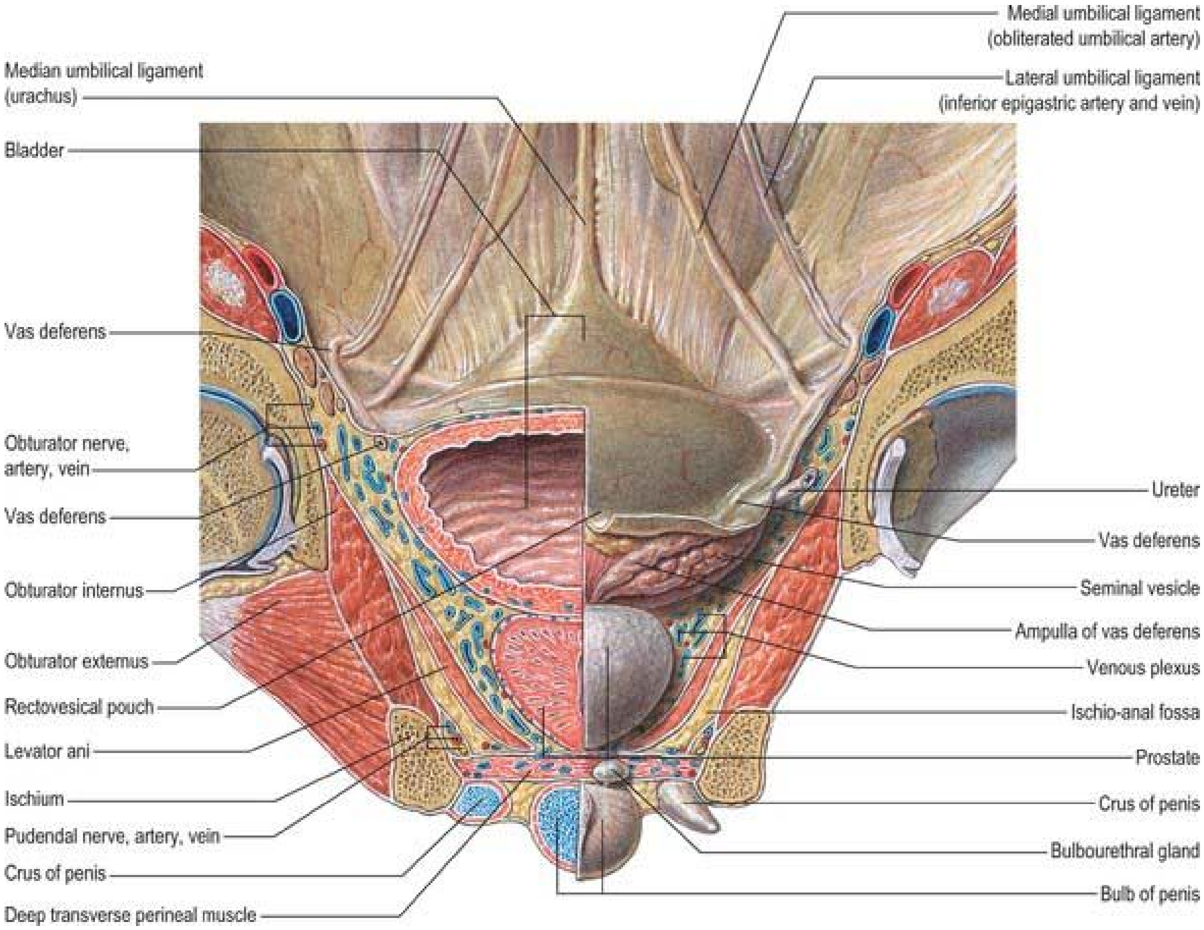
Median umbilical ligament (urachus)
Bladder
Vas deferens
Obturator nerve, artery, vein
Vas deferens
Obturator internus
Obturator externus
Rectovesical pouch
Levator ani
Ischium
Pudendal nerve, artery, vein
Crus of penis
Deep transverse perineal muscle
Medial umbilical ligament (obliterated umbilical artery)
Lateral umbilical ligament (inferior epigastric artery and vein)
Ureter
Vas deferens
Seminal vesicle
Ampulla of vas deferens
Venous plexus
Ischio-anal fossa
Prostate
Crus of penis
Bulbourethral gland
Bulb of penis

Fig. 75.3 Internal aspect of anterior abdominal wall and male anterior pelvic viscera.

(From Sobotta 2006.)

These relationships are important in managing bladder trauma. Extraperitoneal injuries can often be managed conservatively because urine is contained, whereas peritoneal injuries usually require surgical repair.

As the bladder fills it becomes ovoid. Anteriorly, it displaces the parietal peritoneum from the suprapubic region of the abdominal wall. Its inferolateral surfaces become anterior and rest against the abdominal wall without intervening peritoneum for a distance above the symphysis pubis which varies with the degree of distension, but is commonly 5–7 cm. The distended bladder may be punctured just above the symphysis pubis without traversing the peritoneum (suprapubic cystostomy): surgical access to the bladder through the anterior abdominal wall is usually by this route. The summit of the full bladder points up and forwards above the attachment of the median umbilical ligament, so that the peritoneum forms a supravesical recess of varying depth between the summit and the anterior abdominal wall: this recess often contains coils of small intestine. At birth, the bladder is relatively higher than in the adult because the true pelvis is shallow, and the internal urethral orifice is level with the upper symphysial border. The bladder is then abdominal rather than pelvic, and extends about two-thirds of the distance towards the umbilicus. Urine samples may therefore be obtained in children by performing suprapubic needle puncture. The bladder progressively descends with growth, and reaches the adult position shortly after puberty. Congenital abnormalities of the bladder are described on page 1312 (see also Fig. 78.11).

LIGAMENTS OF THE BLADDER

The bladder is anchored inferiorly by condensations of pelvic fascia which attach it to the pubis, lateral pelvic side-walls, and rectum.

In both sexes, stout bands of fibromuscular tissue, the pubovesical ligaments, extend from the bladder neck to the inferior aspect of the pubic bones. They are derived from the detrusor muscle, part of the detrusor apron (Fig. 75.4A,B). In the female, they constitute the superior extensions of the pubourethral ligaments. In the male, the detrusor apron is described as an extension of detrusor that extends over the anterior surface of the prostate, and condenses distally and anteriorly to form the puboprostatic ligaments.

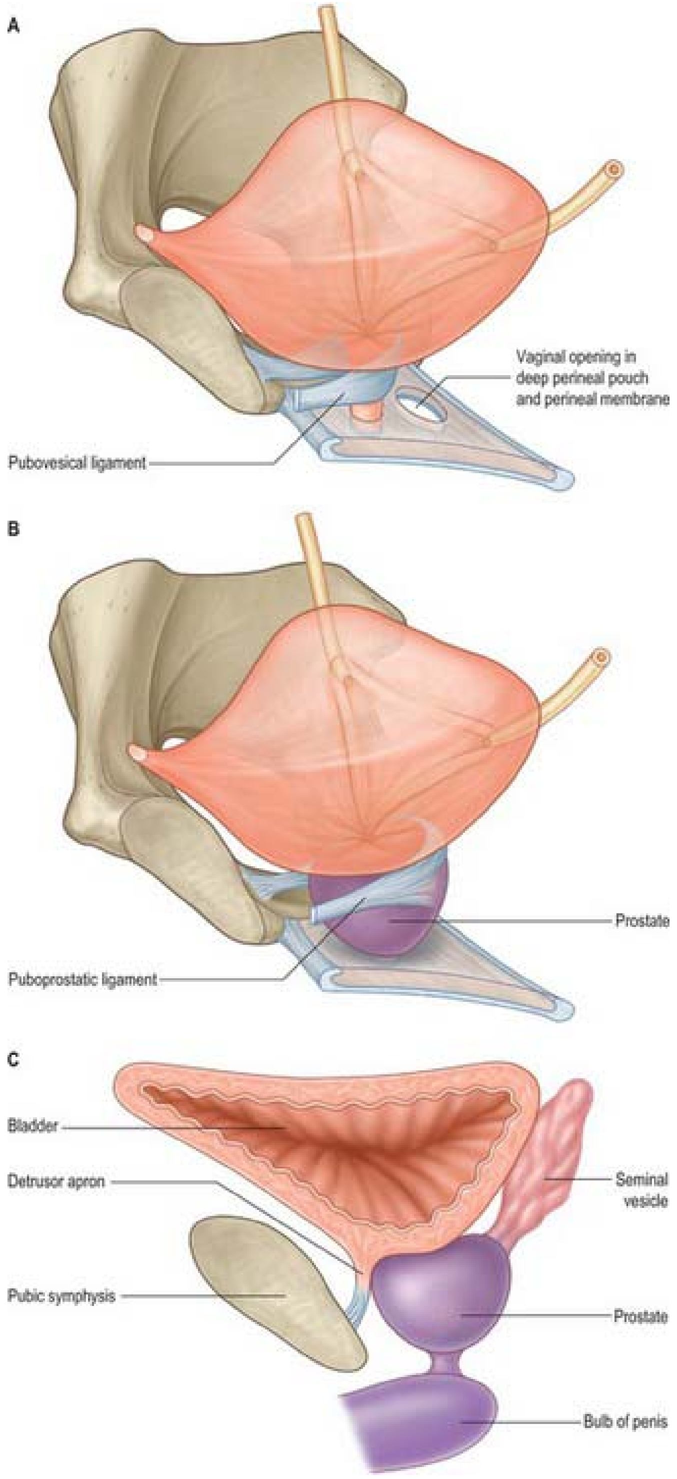
A
Vaginal opening in deep perineal pouch and perineal membrane
Pubovesical ligament
B
Prostate
Puboprostatic ligament
C
Bladder
Detrusor apron
Seminal vesicle
Pubic symphysis
Prostate
Bulb of penis

Fig. 75.4 Ligaments that anchor the neck of the bladder and pelvic part of the urethra to the pelvic bone. **A**, In the female. **B**, In the male. In males, the detrusor extends over the anterosuperior aspect of the prostate and inserts

into the pubic bone. It condenses to form pubovesical/puboprostatic ligaments (**B**,**C**).

*(**A**,**B** From Drake, Vogl, Mitchell, Tibbitts and Richardson 2008.)*

The pubovesical ligaments lie on each side of the median plane, leaving a midline hiatus through which numerous small veins pass. A number of other so-called ligaments have been described in relation to the base of the urinary bladder, namely the lateral and posterior vesical ligaments in the male and the cardinal and ureterosacral ligaments in the female. The reflections of the peritoneum from the bladder to the side-walls of the pelvis form the lateral ligaments, and the sacrogenital folds constitute the posterior ligaments. They are all condensations of connective tissue around major neurovascular structures rather than true ‘anatomical’ ligaments, nevertheless they are described as ligaments in routine clinical use.

The apex of the bladder is connected to the umbilicus by the remains of the urachus, which forms the median umbilical ligament (Fig. 75.3). It is composed of longitudinal muscle fibres derived from the detrusor, and becomes more fibrous towards the umbilicus. It usually maintains a lumen lined with epithelium which persists into adult life but is only rarely complicated by a urachal cyst, sinus, fistula or adenocarcinoma. From the superior surface of the bladder the peritoneum is carried off in a series of folds, the ‘false’ ligaments of the bladder. Anteriorly there are three folds, the median umbilical fold over the median umbilical ligament (urachus) and two medial umbilical folds over the obliterated umbilical arteries. The inferior epigastric vessels are lateral to these folds on the anterior abdominal wall.

BLADDER INTERIOR

Vesical mucosa

Almost all of the vesical mucosa (Fig. 75.5A–C) is attached only loosely to subjacent muscle: it folds when the bladder empties, and the folds are stretched flat as it fills. Over the trigone, immediately above and behind the internal urethral orifice, it is adherent to the subjacent muscle layer and is always smooth. The anteroinferior angle of the trigone is formed by the internal urethral orifice, its posterolateral angles by the ureteric orifices. The superior trigonal boundary is a slightly curved interureteric bar, which connects the two ureteric orifices and is produced by the continuation into the vesical wall of the ureteric internal longitudinal muscle. Laterally this ridge extends beyond the ureteric openings as ureteric folds, produced by the terminal parts of the ureters which run obliquely through the bladder wall. At cystoscopy the interureteric crest appears as a pale band and is a guide to the ureteric orifices.

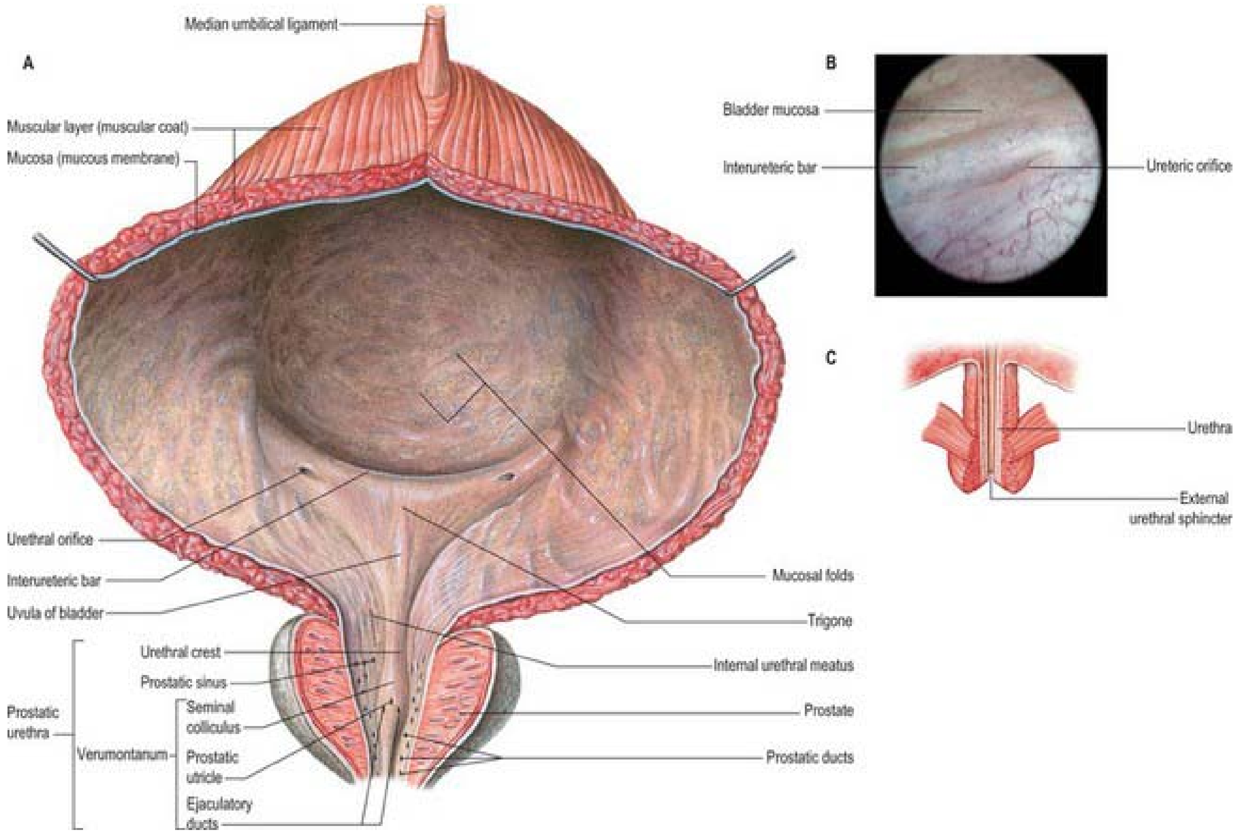
A
Median umbilical ligament
Muscular layer (muscular coat)
Mucosa (mucous membrane)
Urethral orifice
Interureteric bar
Uvula of bladder
Urethral crest
Prostatic sinus
Prostatic urethra
Verumontanum
Seminal colliculus
Prostatic utricle
Ejaculatory ducts
Mucosal folds
Trigone
Internal urethral meatus
Prostate
Prostatic ducts
B
Bladder mucosa
Interureteric bar
Ureteric orifice
C
Urethra
External urethral sphincter

Fig. 75.5 **A**, Coronal section of the urinary bladder in the male. The mucosal folds are dependent upon the state of filling. **B**, Ureteric orifice seen at endoscopy. **C**, Bladder neck in the female.

*(**A** from Sobotta 2006.)*

Trigone

The smooth muscle of the trigone consists of two distinct layers, sometimes termed the superficial trigonal muscle and deep trigonal detrusor muscle. The latter is composed of muscle cells, indistinguishable from those of the detrusor, and is simply the posteroinferior portion of the detrusor muscle proper. The superficial trigonal muscle represents a morphologically distinct component of the trigone, which, unlike the detrusor, is composed of relatively small diameter muscle bundles that are continuous proximally with those of the intramural ureters. The superficial trigonal muscle is relatively thin but is generally described as becoming thickened along its superior border to form the interureteric bar. Similar thickenings occur along the lateral edges of the superficial trigone. In both sexes the superficial trigone muscle becomes continuous with the smooth muscle of the proximal urethra, and extends in the male along the urethral crest as far as the openings of the ejaculatory ducts.

Ureteric orifices

The slit-like ureteric orifices are placed at the posterolateral trigonal angles (Fig. 75.5A). In empty bladders they are approximately 2.5 cm apart, and 2.5 cm from the internal urethral orifice: in distension these measurements may be doubled.

Internal urethral orifice

The internal urethral orifice is sited at the trigonal apex, the lowest part of the bladder, and is usually somewhat crescentic in section. There is often an elevation immediately behind it in adult males (particularly past middle age) which is caused by the median prostatic lobe.

BLADDER NECK

The smooth muscle of the bladder neck is histologically, histochemically and pharmacologically distinct from the detrusor muscle proper and so the bladder neck should be considered as a separate functional unit. The arrangement of smooth muscle in this region is quite different in males and females, and therefore will be described separately.

Female

The female bladder neck (Fig. 75.5C) consists of morphologically distinct smooth muscle. The large diameter fasciculi characteristic of the detrusor are replaced in the region of the bladder neck by small diameter fasciculi which extend obliquely or longitudinally into the urethral wall. In the normal female, the bladder neck sits above the pelvic floor supported predominantly by the pubovesical ligaments (Fig. 75.4A), the endopelvic fascia of the pelvic floor and levator ani. These support the urethra at rest; with elevated intra-abdominal pressure the levators contract, increasing urethral closure pressure to maintain continence. This anatomical arrangement commonly alters after parturition and with increasing age, such that the bladder neck lies beneath the pelvic floor, particularly when the intra-abdominal pressure rises, which means that the mechanism described above fails to maintain continence and women may experience stress incontinence as a result of urethral hypermobility.

Male

In the male (Fig. 75.4B), the bladder neck is completely surrounded by a circular collar of smooth muscle, with its own distinct adrenergic innervation, which extends distally to surround the preprostatic portion of the urethra. Distinct from the smooth muscle bundles which run in continuity from the bladder neck down to the prostatic urethra, and from the smooth muscle within the prostate, these smooth muscle bundles surround the bladder neck and preprostatic urethra. The bundles which form this ‘preprostatic sphincter’ are small in size compared with the muscle bundles of the detrusor and are separated by a relatively larger connective tissue component rich in elastic fibres.

The bladder neck is sometimes called the proximal sphincter mechanism, to distinguish it from the distal urinary sphincter mechanism. However, it is not a urinary sphincter and is not responsible for continence. It is a genital sphincter that allows antegrade ejaculation of semen. Unlike the detrusor and the rest of the urethral smooth muscle (common to both sexes), the preprostatic sphincter is richly supplied with sympathetic noradrenergic nerves and is almost totally devoid of parasympathetic cholinergic nerves. Contraction of the preprostatic sphincter serves to prevent the retrograde flow of ejaculate through the proximal urethra into the bladder. It is extensively disrupted in the vast majority of men undergoing bladder neck surgery, e.g. transurethral resection of the prostate, which results in retrograde ejaculation.

Whether this preprostatic sphincter replaces, or is additional to, the bladder neck muscle pattern seen in the female is unclear, but it is probably additional.

Bladder outflow obstruction

In progressive chronic obstruction to micturition, e.g. as a result of prostatic enlargement or urethral stricture, the muscle of the bladder hypertrophies. The muscle fasciculi increase in size and, because they interlace in all directions, a thick-walled ‘trabeculated bladder’ is produced. Mucosa between the fascicles forms ‘diverticula’. When outflow is obstructed, emptying is not complete: some urine remains and may become infected. Back pressure from a chronically distended bladder may gradually dilate the ureters and renal pelves and even the renal collecting tubules, which can result in progressive renal impairment.

VASCULAR SUPPLY AND LYMPHATIC DRAINAGE

Arteries

The bladder is supplied principally by the superior and inferior vesical arteries (see Fig. 77.3A,B), derived from the anterior trunk of the internal iliac artery, supplemented by the obturator and inferior gluteal arteries. In the female additional branches are derived from the uterine and vaginal arteries.

Superior vesical artery

The superior vesical artery supplies many branches to the fundus of the bladder. The artery to the vas deferens often originates from one of these and accompanies the vas deferens to the testis, where it anastomoses with the testicular artery. Other branches supply the ureter. The beginning of the superior vesical artery is the proximal, patent section of the fetal umbilical artery.

Inferior vesical artery

The inferior vesical artery often arises with the middle rectal artery from the internal iliac artery. It supplies the base of the bladder, prostate, seminal vesicles and lower ureter. Prostatic branches communicate across the midline. The inferior vesical artery may sometimes provide the artery to the vas deferens.

Veins

The veins which drain the bladder (see Fig. 77.3A,B) form a complicated plexus on its inferolateral surfaces and pass backwards in the lateral ligaments of the bladder to end in the internal iliac veins.

Lymphatics

Lymphatics which drain the bladder (see Fig. 77.3A,B) begin in mucosal, intermuscular and serosal plexuses. There are three sets of collecting vessels, most of which end in the external iliac nodes. Vessels from the trigone emerge on the exterior of the bladder to run superolaterally. Vessels from the superior surface of the bladder converge to the posterolateral angle and pass superolaterally to the external iliac nodes (some may go to the internal or common iliac group). Vessels from the inferolateral surface of the bladder ascend to join those from the superior surface or run to the lymph nodes in the obturator fossa. Minute nodules of lymphoid tissue may occur along the vesical lymph vessels.

INNERVATION

The nerves supplying the bladder arise from the pelvic plexuses, which are a mesh of autonomic nerves and ganglia on the lateral aspects of the rectum, internal genitalia and bladder base. They consist of both sympathetic and parasympathetic components, each of which contains both efferent and afferent fibres. The innervation of the bladder has been reviewed in some detail by Mundy (1999).

Efferent fibres

Parasympathetic fibres arise from the second to the fourth sacral segments of the spinal cord and enter the pelvic plexuses on the posterolateral aspects of the rectum as the pelvic splanchnic nerves. The sympathetic fibres are derived from neuronal cell bodies in the lower three thoracic and upper two lumbar segments of the spinal cord and form the coeliac and mesenteric plexuses around the great vessels in the abdomen, from which the hypogastric plexuses descend into the pelvis as fairly discrete nerve bundles within the extraperitoneal connective tissue posterior to the ureter on each side. The anterior part of the pelvic plexus is known as the vesical plexus. Small groups of autonomic neurones occur within the plexus and throughout all regions of the bladder wall. These multipolar intramural neurones are rich in acetylcholinesterase (AChE) and occur in ganglia consisting of up to 20 neuronal cell bodies. The majority of the preganglionic nerve terminals correspond morphologically to presumptive cholinergic fibres. Noradrenergic terminals also relay on cell bodies in the pelvic plexus: it is not known whether similar nerves synapse on intramural bladder ganglia.

The urinary bladder (including the trigonal detrusor muscle) is profusely supplied with nerves which form a dense plexus among the detrusor muscle cells. The majority of these nerves contain AChE and occur in abundance throughout the muscle coat of the bladder. Axonal varicosities adjacent to detrusor muscle cells possess features which are considered to typify cholinergic nerve terminals, and contain clusters of small (50 nm diameter) agranular vesicles, occasional large (80–160 nm diameter) granulated vesicles and small mitochondria. Terminal regions approach to within 20 nm of the surface of the muscle cells and may be partially surrounded by Schwann cell cytoplasm, or more often are naked nerve endings. The human detrusor muscle possesses a sparse supply of sympathetic noradrenergic nerves which generally accompany the vascular supply and only rarely extend among the myocytes. Non-adrenergic, non-cholinergic nerves have been identified, and a number of other neurotransmitters or neuromodulators have been detected in intramural ganglia, including the peptide somatostatin. The superficial trigonal muscle is associated with more noradrenergic (sympathetic) fibres than cholinergic (parasympathetic) nerves, a difference that supports the view that the superficial trigonal muscle should be regarded as ‘ureteric’ rather than ‘vesical’ in origin. However it must be emphasized that the superficial trigonal muscle forms a very minor part of the total muscle mass of the bladder neck and proximal urethra in either sex and is probably of little significance in the physiological mechanisms which control these regions.

The smooth muscle of the bladder neck in males is predominantly orientated obliquely or circularly. It is sparsely supplied with cholinergic (parasympathetic) nerves, but possesses a rich noradrenergic (sympathetic) innervation. A similar distribution of autonomic nerves also occurs in the smooth muscle of the prostate gland, seminal vesicles and vasa deferentia. Stimulation of sympathetic nerves causes contraction of smooth muscle in the wall of the genital tract resulting in seminal emission. Concomitant sympathetic stimulation of the proximal urethral smooth muscle causes sphincteric closure of the preprostatic sphincter, thereby preventing reflux of ejaculate into the bladder. Although this genital function of the bladder neck of the male is well established, it is not known whether the smooth muscle of this region plays an active role in maintaining urinary continence. In contrast, the smooth muscle of the bladder neck of the female receives relatively few noradrenergic nerves but is richly supplied with presumptive cholinergic fibres. The sparse supply of sympathetic nerves presumably relates to the absence of a functioning ‘genital’ portion of the wall of the female urethra.

The lamina propria of the fundus and inferolateral walls of the bladder is virtually devoid of autonomic nerve fibres, apart from some noradrenergic and occasional presumptive cholinergic perivascular nerves. However, the density of nerves unrelated to blood vessels increases closer to the urethral orifice. At the bladder neck and trigone a nerve plexus of cholinesterase positive axons extends throughout the lamina propria independent of blood vessels. Some of the larger diameter axons are myelinated and others lie adjacent to the basal urothelial cells. In the absence of any obvious effector target sites, the subepithelial nerve plexuses of the bladder and the ureter are assumed to subserve a sensory function.

Afferent fibres

Vesical nerves are also concerned with pain and awareness of distension and are stimulated by distension or spasm due to a stone, inflammation or malignant disease: they travel in sympathetic and parasympathetic nerves, but predominantly in the latter. Division of the sympathetic paths (e.g. ‘presacral neurectomy’), or of the superior hypogastric plexus, therefore does not materially relieve vesical pain, whereas considerable relief follows bilateral anterolateral cordotomy. Since nerve fibres mediating awareness of distension travel in the posterior columns (fasciculus gracilis), the patient still retains awareness of the need to micturate after anterolateral cordotomy. The nerve endings detecting noxious stimuli are probably of more than one type: a subepithelial plexus of fibres containing dense vesicles, which are probably afferent endings, has been described.

MICROSTRUCTURE

The bladder consists of four layers: a lining epithelium (urothelium), lamina propria, muscularis propria and serosa.

Lining epithelium or urothelium

Urothelium (transitional epithelium) is 4–7 cells thick; it may appear to be attenuated to 2–3 cells thick when the bladder is fully distended. It contains three distinctive cell layers, a basal layer, an intermediate layer and a superficial (‘umbrella’ cell) layer (see Fig. 75.8). The basal layer consists of small cuboidal cells from which the upper layers arise. The intermediate layers are polygonal and possess the capacity to stretch and flatten. The superficial layer forms a protective, almost impermeable surface for the bladder mucosa and consists of large, sometimes multinucleated, cells displaying degenerative changes in their cytoplasm; these cells are ultimately exfoliated into the urine. The apical surface of the umbrella cell layer is covered by 16 nm protein particles packed hexagonally to form 2D crystals of asymmetric unit membranes, (AUMs), that contribute to the permeability barrier function of the urinary bladder, preventing reabsorption of urine across the urothelium into the bloodstream. Islands or nests of urothelium may become separated from the surface during development and are found embedded in the underlying lamina propria. These are called von Brunn’s nests and may undergo central degeneration to form cysts (cystitis cystica).

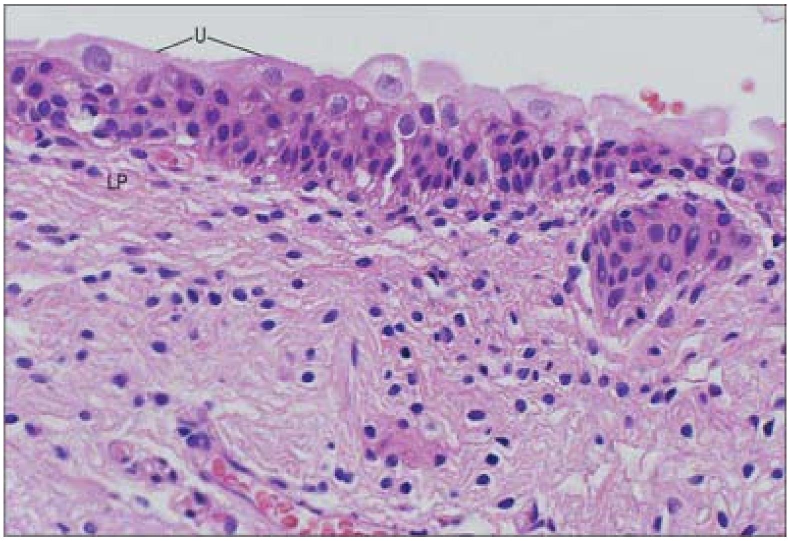

Fig. 75.8 The bladder is lined by urothelium with a surface ‘umbrella cell’ layer (U) and a layer of intermediate cells (3–5 cells thick). The lamina propria (LP) consists of stroma with blood vessels and von Brunn’s nests.

Lamina propria

The lamina propria forms a connective tissue bed supporting the overlying urothelium, from which it is separated by a basement membrane. It is rich in capillaries, lymphatics and nerve-endings. It contains elastic fibres and a thin, poorly defined layer of smooth muscle fibres, muscularis mucosae, that is variably distributed within the bladder. This layer is often very superficial, lying close beneath the urothelium, but is sometimes deeper in the lamina propria where it may be well developed, and must be distinguished from the muscularis propria.

Muscularis propria

The muscularis propria is the detrusor muscle of the bladder wall. It consists of three indistinct layers, an inner and outer longitudinal and an intermediate circular layer. In contrast to the muscularis mucosae, which consists of small wispy fibres, the muscularis propria is made up of larger, poorly defined bundles of smooth muscle that form well-defined inner circular and outer longitudinal layers at the neck of the bladder.

Serosa

The serosa partially covers the bladder. It is lined externally by mesothelium, beneath which there is a variable amount of vascularized adipose tissue that frequently extends into the muscularis propria and occasionally into the lamina propria.

MALE URETHRA

The male urethra (Fig. 75.6A,B) is 18–20 cm long, and extends from the internal orifice in the urinary bladder to the external opening, or meatus, at the end of the penis. It may be considered in two parts. The anterior urethra is approximately 16 cm long and lies within the perineum (proximally) and the penis (distally), surrounded by the corpus spongiosum. The posterior urethra is 4 cm long and lies in the pelvis proximal to the corpus spongiosum, where it is acted upon by the urogenital sphincter mechanisms. Functionally both parts act as a conduit.

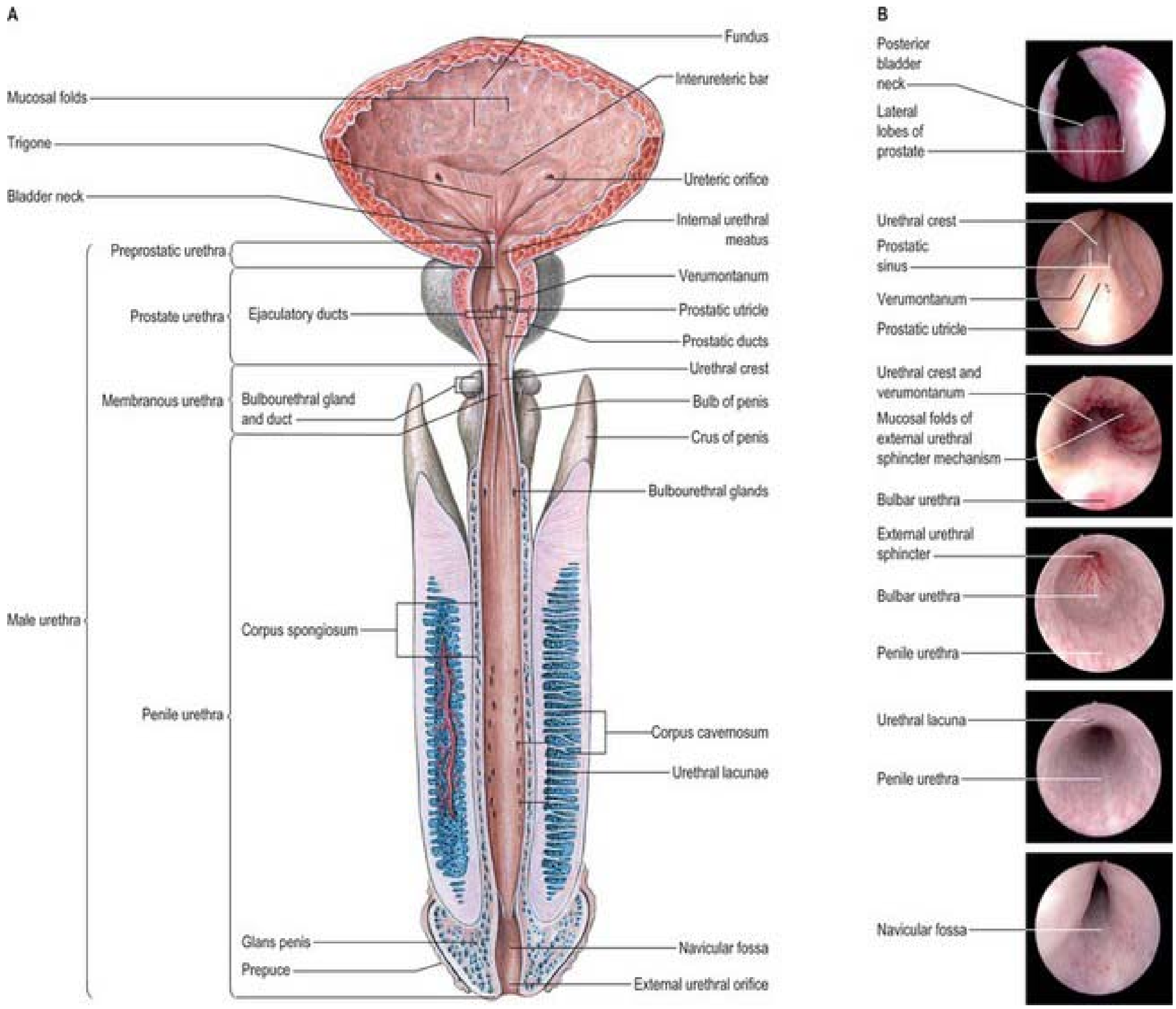
A
Fundus
Interureteric bar
Mucosal folds
Trigone
Ureteric orifice
Bladder neck
Internal urethral meatus
Preprostatic urethra
Verumontanum
Prostate urethra
Ejaculatory ducts
Prostatic utricle
Prostatic ducts
Urethral crest
Membranous urethra
Bulbourethral gland and duct
Bulb of penis
Crus of penis
Bulbourethral glands
Male urethra
Corpus spongiosum
Penile urethra
Corpus cavernosum
Urethral lacunae
Glans penis
Navicular fossa
Prepuce
External urethral orifice
B
Posterior bladder neck
Lateral lobes of prostate
Urethral crest
Prostatic sinus
Verumontanum
Prostatic utricle
Urethral crest and verumontanum
Mucosal folds of external urethral sphincter mechanism
Bulbar urethra
External urethral sphincter
Bulbar urethra
Penile urethra
Urethral lacuna
Penile urethra
Navicular fossa

Fig. 75.6 **A**, Male urethra. **B**, Endoscopic views (top to bottom): bladder neck, urethral crest, membranous urethra, bulbar urethra, penile urethra, navicular fossa.

*(**A** from Sobotta 2006.)*

The anterior urethra is subdivided into a proximal component, the bulbar urethra, which is surrounded by the bulbospongiosus and is entirely within the perineum, and a pendulous or penile component, which continues on to the tip of the penis. The posterior urethra is divided into preprostatic, prostatic, and membranous segments. In the flaccid penis, the urethra has a double curve. The urethral canal is a mere slit, except during the passage of fluid: in transverse section it is transversely arched in the prostatic part, stellate in the preprostatic and membranous portions, transverse in the bulbar and penile portions, and sagittal at the external orifice.

Posterior part

Preprostatic urethra

The preprostatic urethra (Fig. 75.6B; endoscopic views of bladder neck and urethral crest) is approximately 1 cm in length, and extends from the base of the bladder to the prostate. Small periurethral glands at this site may contribute to benign prostatic hyperplasia (BPH) and symptoms of outflow obstruction in older men.

Prostatic urethra

The prostatic urethra (Fig. 75.7; see Fig. 75.14) is 3–4 cm in length and tunnels through the substance of the prostate, closer to the anterior than the posterior surface of the gland. It is continuous above with the preprostatic part and emerges from the prostate slightly anterior to its apex (the most inferior point of the prostate). Throughout most of its length the posterior wall possesses a midline ridge, the urethral crest, which projects into the lumen causing it to appear crescentic in transverse section. On each side of the crest there is a shallow depression, the prostatic sinus, the floor of which is perforated by the orifices of 15–20 prostatic ducts. An elevation, the verumontanum (seminal colliculus), is seen at about the middle of the length of the urethral crest: it is used as a surgical landmark for the urethral sphincter during trans-urethral resection for benign enlargement of the prostate. At this point the urethra turns anteriorly by 35° and contains the slit-like orifice of the prostatic utricle. On both sides of, or just within, this orifice are the two small openings of the ejaculatory ducts. The prostatic utricle is a cul-de-sac 6 mm long, which runs upwards and backwards in the substance of the prostate behind its median lobe. Its walls are composed of fibrous tissue, muscular fibres and mucous membrane, the latter pitted by the openings of numerous small glands. The prostatic utricle develops from the paramesonephric ducts or urogenital sinus, and is thought to be homologous with the vagina of the female (p. 1338). It is sometimes called the ‘vagina masculina’, but the more usual view is that it is a uterine homologue and hence the term ‘utricle’. The lowermost part of the prostatic urethra is fixed by the puboprostatic ligaments and is therefore immobile.

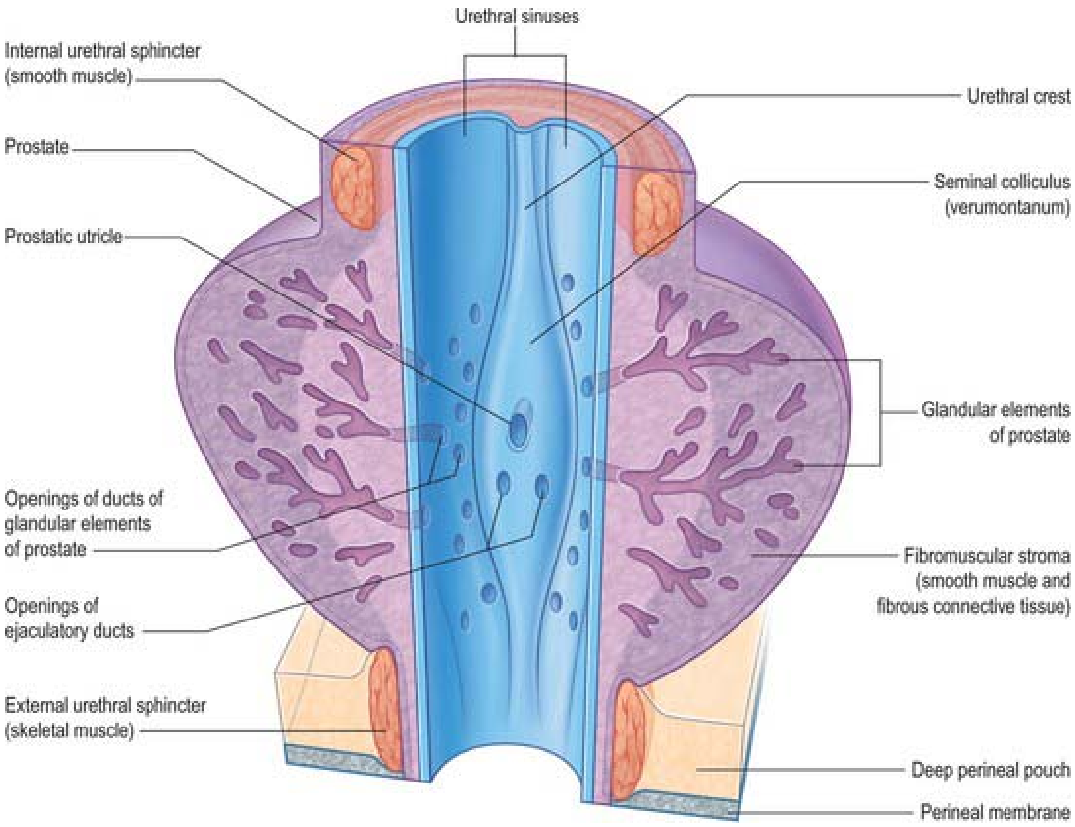
Urethral sinuses
Internal urethral sphincter (smooth muscle)
Urethral crest
Prostate
Seminal colliculus (verumontanum)
Prostatic utricle
Glandular elements of prostate
Openings of ducts of glandular elements of prostate
Fibromuscular stroma (smooth muscle and fibrous connective tissue)
Openings of ejaculatory ducts
External urethral sphincter (skeletal muscle)
Deep perineal pouch
Perineal membrane

Fig. 75.7 Prostatic part of the male urethra. The raised part of the urethral crest is the seminal colliculus, known clinically as the verumontanum.

(From Drake, Vogl and Mitchell 2005.)

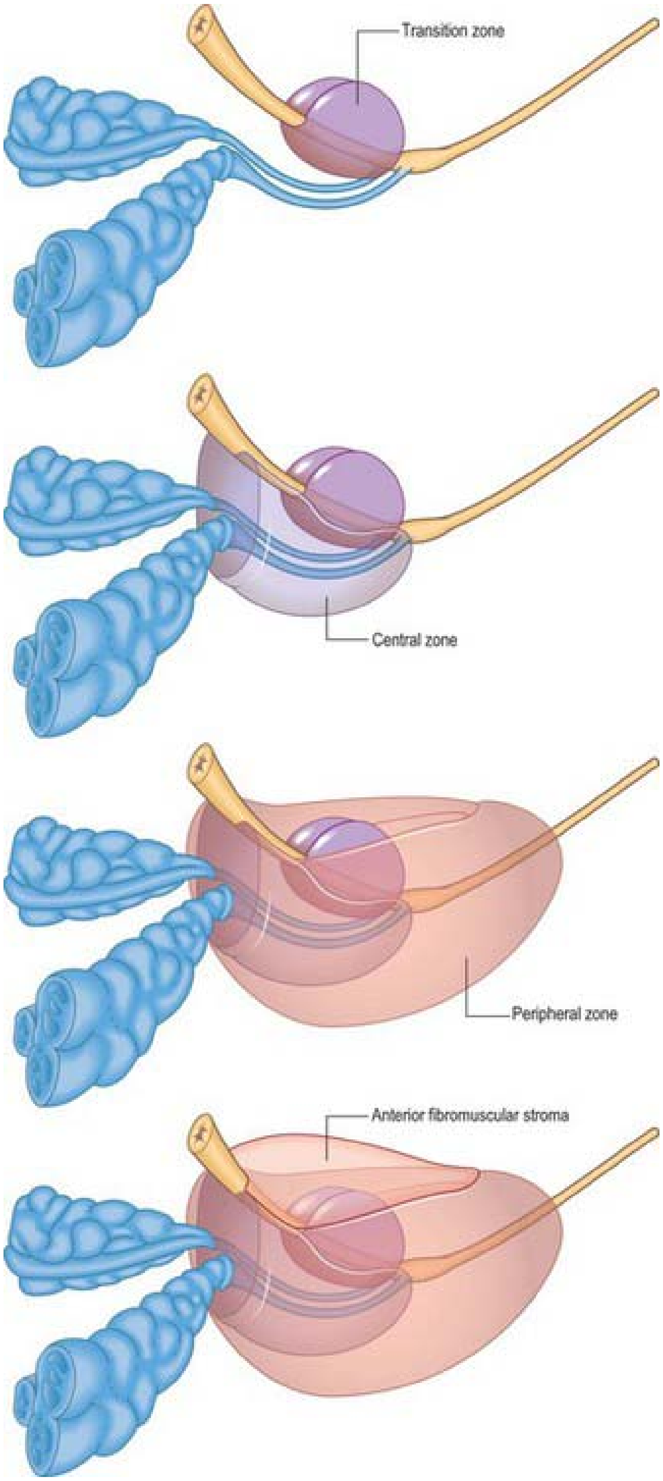
Transition zone
Central zone
Peripheral zone
Anterior fibromuscular stroma

Fig. 75.14 Zonal anatomy of the prostate.

(By permission from Walsh PC, Retik AB, Vaughan ED et al (eds) 2002 Campbell's Urology, 8th edition. Philadelphia: Saunders.)

Membranous urethra

The membranous part of the urethra is the shortest (2–2.5 cm), least dilatable and, with the exception of the external orifice, the narrowest, section of the urethra. It descends with a slight ventral concavity from the prostate to the bulb of the penis, passing through the perineal membrane, 2.5 cm posteroinferior to the pubic symphysis. The wall of the membranous urethra consists of a muscle coat which is separated from the epithelial lining by a narrow layer of fibroelastic connective tissue. The muscle coat contains a relatively thin layer of bundles of smooth muscle, which are continuous proximally with those of the prostatic urethra, and a prominent outer layer of circularly orientated striated muscle fibres, which together form the external urethral sphincter.

Urinary continence at the level of the membranous urethra is mediated by the radial folds of urethral mucosa, the submucosal connective tissue, the intrinsic urethral smooth muscle, the striated muscle fibres and the pubourethral component of levator ani. The muscle coat of the urethra and puborectalis surround the membranous urethra and are attached to the inner surface of the ischiopubic ramus; fibres also reach up to the lowest part of the neck of the bladder and lie on the surface of the prostate. The striated external urethral sphincter has a posterior fibrous defect and is inserted throughout its length into the perineal body. It is related to the dorsal vein complex anteriorly, levator ani laterally and the perineal body and rectourethralis posteriorly, and is suspended from the pubis by fibrous tissue that extends from its anterior and lateral parts to the puboprostatic liagaments posteriorly and to the suspensory ligament of the penis anteriorly. The bulbourethral glands are invested in sphincteric muscle and drain into the membranous urethra during sexual excitement.

Anterior part

The anterior or spongiose part of the urethra lies within the corpus spongiosum penis (p. 1271). In the flaccid penis it is about 15 cm long and extends from the end of the membranous urethra to the external urethral orifice on the glans penis. It starts below the perineal membrane at a point anterior to the lowest level of the symphysis pubis as the bulbar urethra, the widest part of the urethra, surrounded by bulbospongiosus. The bulbourethral glands open into the bulbar urethra approximately 2.5 cm below the perineal membrane. The urethra next curves downwards as the penile urethra. It is a narrow, transverse slit when empty, and has a diameter of approximately 6 mm when passing urine. It is dilated at its termination within the glans penis where it is known as the navicular fossa. The external urethral orifice is the narrowest part of the urethra, and is a sagittal slit, about 6 mm long, bounded on each side by a small labium.

The urethral epithelium, particularly in the bulbar and distal penile segments, presents the orifices of numerous small mucous urethral glands that lie in the submucosa. It also contains a number of small pit-like recesses, or lacunae, of varying sizes whose orifices are directed forwards. One, the lacuna magna, is larger than the rest and is situated in the roof of the navicular fossa.

Traumatic injury to the male urethra

The urethra may be ruptured by a fall-astride (straddle) injury to the bulbar urethra in the perineum, or by an injury related to a pelvic fracture. These injuries usually affect the junction of the membranous with the bulbar segments across the perineal membrane. One of the complications associated with such injuries is extravasation of urine. After an injury to the bulbar urethra, urine usually extravasates between the perineal membrane and the membranous layer of the superficial fascia (clinically known as Colles' fascia). As both of these are attached firmly to the ischiopubic rami, extravasated fluid cannot pass posteriorly because the two layers are continuous around the superficial transverse perineal muscles. Laterally, the spread of urine is blocked by the pubic and ischial rami. Urine cannot enter the lesser pelvis through the perineal membrane if this remains intact, and so it tracks anteriorly into the loose connective tissue of the scrotum and penis and thence to the anterior abdominal wall. If the posterior urethra is injured, urine is extravasated into the pelvic extraperitoneal tissue: if the perineal membrane is also torn then urine may be extravasated into the perineum.

Congenital anomalies of the male urethra

Hypospadias, found in one in 300 boys, most often results in the urethra opening in the distal penis, either on the ventral aspect of the penis or dorsally on to the perineum more proximally. There is also an associated abnormality of the prepuce, which is longer dorsally and lacking ventrally, and often an associated chordee which causes a ventral curvature of the penis. It is important that this anomaly be identified prior to circumcision, because the abnormal foreskin is sometimes used for surgical correction of the deformity.

Posterior urethral valves occur in one in 5000 to 8000 males and are the most common cause of urinary outflow obstruction in male infants. The commonest type (type I) is believed to occur if the Wolffian ducts open too anteriorly onto the primitive prostatic urethra: this abnormal migration of the ducts leaves behind thick vestigial tissue that forms rigid valve cusps extending caudally from the verumontanum.

Very rarely, urethral duplication occurs: the two urethrae almost invariably lie on top of each other rather than side-by-side. One of the urethrae, usually the more dorsal, may be blind ending.

VASCULAR SUPPLY AND LYMPHATIC DRAINAGE

Urethral artery

The urethral artery arises from the internal pudendal artery or common penile artery just below the perineal membrane and travels through the corpus spongiosum, to reach the glans penis. It supplies the urethra and erectile tissue around it. In addition, the urethra is supplied by the dorsal penile artery, via its circumflex branches on each side and retrogradely from the glans, by its terminal branches. The blood supply through the corpus spongiosum is so plentiful that the urethra can be divided without compromising its vascular supply.

Veins

The venous drainage of the anterior urethra is to the dorsal veins of the penis and internal pudendal veins, which drain to the prostatic plexus. The posterior urethra drains into the prostatic and vesical venous plexuses, which drain into the internal iliac veins.

Lymphatic drainage

Vessels from the posterior urethra pass mainly to the internal iliac nodes (see Fig. 77.3A,B); a few may end in the external iliac nodes. Vessels from the membranous urethra accompany the internal pudendal artery. Vessels from the anterior urethra accompany those of the glans penis, ending in the deep inguinal nodes. Some may end in superficial nodes, others may traverse the inguinal canal to end in the external iliac nodes.

INNERVATION

The prostatic plexus supplies the smooth muscle of the prostate and prostatic urethra. On each side it is derived from the pelvic plexus and lies on the posterolateral aspect of the seminal vesicle and prostate. Lesser cavernous nerves pierce the bulb of the corpus spongiosum proximally to supply the penile urethra. The greater cavernous nerves carry the sympathetic supply which causes contraction of the preprostatic sphincter during ejaculation and prevents reflux of ejaculate into the bladder. The parasympathetic preganglionic fibres are axons from neurones in the second to fourth sacral spinal segments. The nerve supply of the external urethral sphincter is controversial. It is generally believed to be supplied by neurones in Onuf’s nucleus and by perineal branches of the pudendal nerve lying on the perineal aspect of the pelvic floor; in both instances the axons arise from neurones in S2, 3 and 4. Fibres from Onuf’s nucleus (somatic) travel with the pelvic plexus on each side until they branch off and run on the pelvic aspect of the pelvic floor to enter the membranous urethra.

MICROSTRUCTURE

The epithelium lining the preprostatic urethra and the proximal part of the prostatic urethra is a typical urothelium (Fig. 75.8). It is continuous with that lining the bladder, and with the epithelium lining the ducts of the prostate and bulbourethral glands, the seminal vesicles, and the vasa deferentia and ejaculatory ducts. These relationships are important in the spread of urinary tract infections.

The epithelium changes below the openings of the ejaculatory ducts to a pseudostratified or stratified columnar type, which lines the membranous urethra and the major part of the penile urethra. Mucus-secreting cells are common throughout this epithelium and frequently occur in small clusters in the penile urethra. Branching tubular paraurethral glands secrete protective mucus onto the urethral epithelial lining and are especially numerous on its dorsal aspect. In older men, many of the deep recesses of the urethral mucosa contain concretions similar to those found within prostatic glands (see Fig. 75.15A). Towards the distal end of the penile urethra the epithelium changes once again, becoming stratified squamous in type with well-defined connective tissue papillae. This epithelium also lines the navicular fossa and becomes keratinized at the external meatus. The epithelial cells lining the navicular fossa are glycogen-rich. This may provide a substrate for commensal lactobacilli which, as in the female vagina provide a defence against pathogenic organisms.

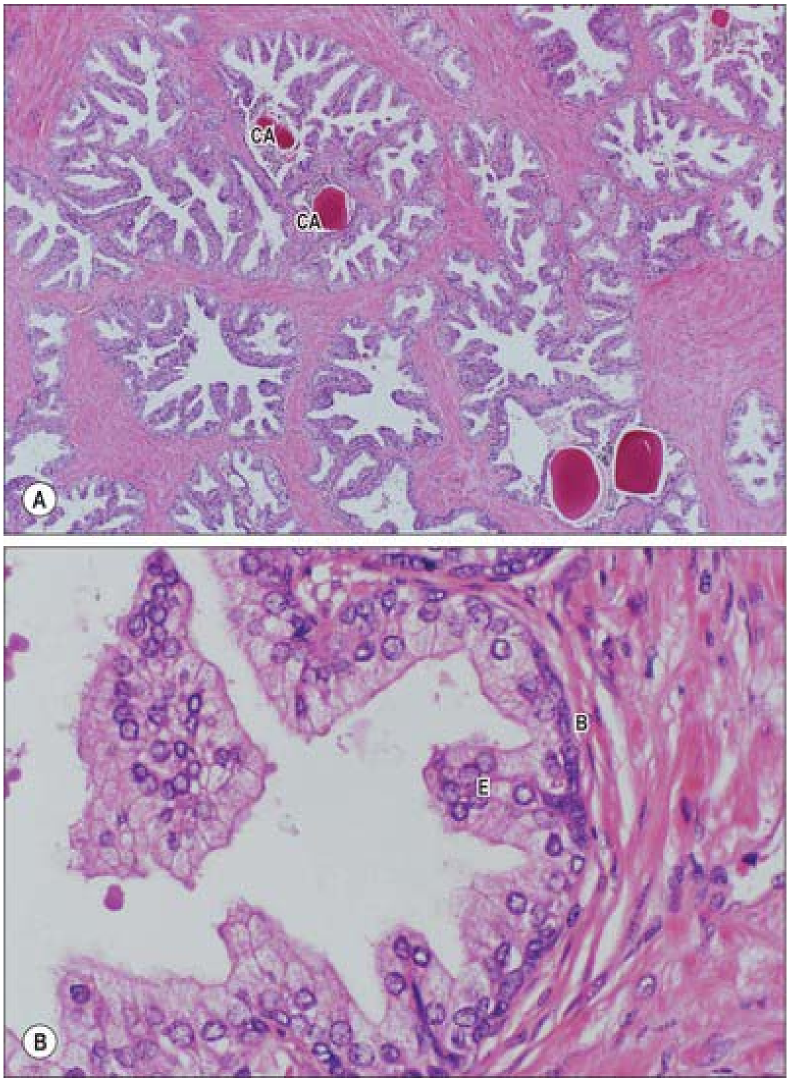

Fig. 75.15 **A**, Prostatic acini show papillary infoldings at the base of the gland (central zone). They are irregularly divided by fibromuscular stroma. Some acini contain eosinophilic (pink) secretions called corpora amylacea (CA) (×10, H&E stain). **B**, Prostatic acini consist of a double layer of epithelial cells (E), which line the lumen, and basal cells (B), which give rise to epithelial cells.

FEMALE URETHRA

The female urethra is approximately 4 cm long and 6 mm in diameter. It begins at the internal urethral orifice of the bladder, approximately opposite the middle of the symphysis pubis, and runs anteroinferiorly behind the symphysis pubis, embedded in the anterior wall of the vagina. It is suspended beneath the pubis by the posterior pubourethral ligaments and anteriorly by the suspensory ligament of the clitoris. It crosses the perineal membrane and normally ends at the external urethral orifice in the vestibule as an anteroposterior slit with rather prominent margins, directly anterior to the opening of the vagina, and 2.5 cm behind the glans clitoris. It sometimes opens into the anterior vaginal wall. Except during the passage of urine, the anterior and posterior walls of the urethra are in apposition and the epithelium is thrown into longitudinal folds, one of which, on the posterior wall of the canal, is termed the urethral crest. Many small mucous urethral glands and minute pit-like recesses or lacunae open into the urethra and may give rise to urethral diverticula. On each side, near the lower end of the urethra, a number of these glands, Skene’s glands, are grouped together and open into the para-urethral duct: each duct runs down in the submucous tissue and ends in a small aperture on the lateral margin of the external urethral orifice.

VASCULAR SUPPLY AND LYMPHATIC DRAINAGE

Urethral artery

The urethra is supplied principally by the vaginal artery, but also receives a supply from the inferior vesical artery.

Veins

The venous plexus around the urethra drains into the vesical venous plexus around the bladder neck, and into the internal pudendal veins. An erectile plexus of veins along the length of the urethra is continuous with the erectile tissue of the vestibular bulb.

Lymphatic drainage

The urethral lymphatics drain into the internal and external iliac nodes.

INNERVATION

Parasympathetic preganglionic fibres arise from neurones in the second to fourth segments of the sacral spinal cord and run in the pelvic splanchnic nerves; they synapse in the vesical plexus in or near the bladder wall. Postganglionic fibres are distributed to the smooth muscle of the urethral wall. Somatic fibres to the striated muscle are also derived from S2 to S4, and run in the pelvic splanchnic nerves but do not synapse in the vesical plexus. Sensory fibres run in the pelvic splanchnic nerves to the second to fourth segments of the sacral spinal cord. Postganglionic sympathetic fibres arise from the plexus around the vaginal arteries.

MICROSTRUCTURE

The mucosa lining the female urethra consists of a stratified epithelium and a supporting lamina propria of loose fibroelastic connective tissue. The latter is bulky and well-vascularized, and contains numerous thin-walled veins. Its abundant elastic fibres are orientated both longitudinally and circularly around the urethra. The lamina propria contains a fine nerve plexus, believed to be derived from sensory branches of the pudendal nerves. The proximal part of the urethra is lined by urothelium, identical in appearance to that of the bladder neck. Distally the epithelium changes into a non-keratinizing stratified squamous type which lines the major portion of the female urethra. This epithelium is keratinized at the external urethral meatus where it becomes continuous with the skin of the vestibule.

The wall of the female urethra consists of an outer muscle coat and an inner mucosa, which lines the lumen and is continuous with that of the bladder. The muscle coat consists of an outer sheath of striated muscle together with an inner coat of smooth muscle fibres. The female external urethral sphincter is anatomically separate from the adjacent periurethral striated muscle of the anterior pelvic floor. The muscle cells forming the external urethral sphincter are all small diameter, slow twitch, fibres.

The smooth muscle coat extends throughout the length of the urethra and consists of slender muscle bundles, the majority of which are orientated obliquely or longitudinally. A few circularly arranged muscle fibres occur in the outer aspect of the non-striated muscle layer and intermingle with the skeletal muscle fibres forming the inner part of the external urethral sphincter. Proximally the urethral smooth muscle extends as far as the bladder neck where it is replaced by fascicles of detrusor smooth muscle. This region in the female lacks a well-defined circular smooth muscle component comparable with the preprostatic sphincter of the male. Distally, urethral smooth muscle bundles terminate in the subcutaneous adipose tissue surrounding the external urethral meatus.

The smooth muscle of the female urethra receives an extensive presumptive cholinergic parasympathetic nerve supply, but contains relatively few noradrenergic nerves. In the absence of an anatomical bladder neck sphincter, competence of the female bladder neck and proximal urethra is unlikely to be totally dependent on smooth muscle activity, and is more probably related to the support provided by the ligamentous structures which surround them. The innervation and longitudinal orientation of most of the muscle fibres suggest that urethral smooth muscle in the female is active during micturition, serving to shorten and widen the urethral lumen.

MICTURITION AND URINARY CONTINENCE

The central integration of the nervous control of the bladder and urethra is essential for normal micturition (Fig. 75.9).

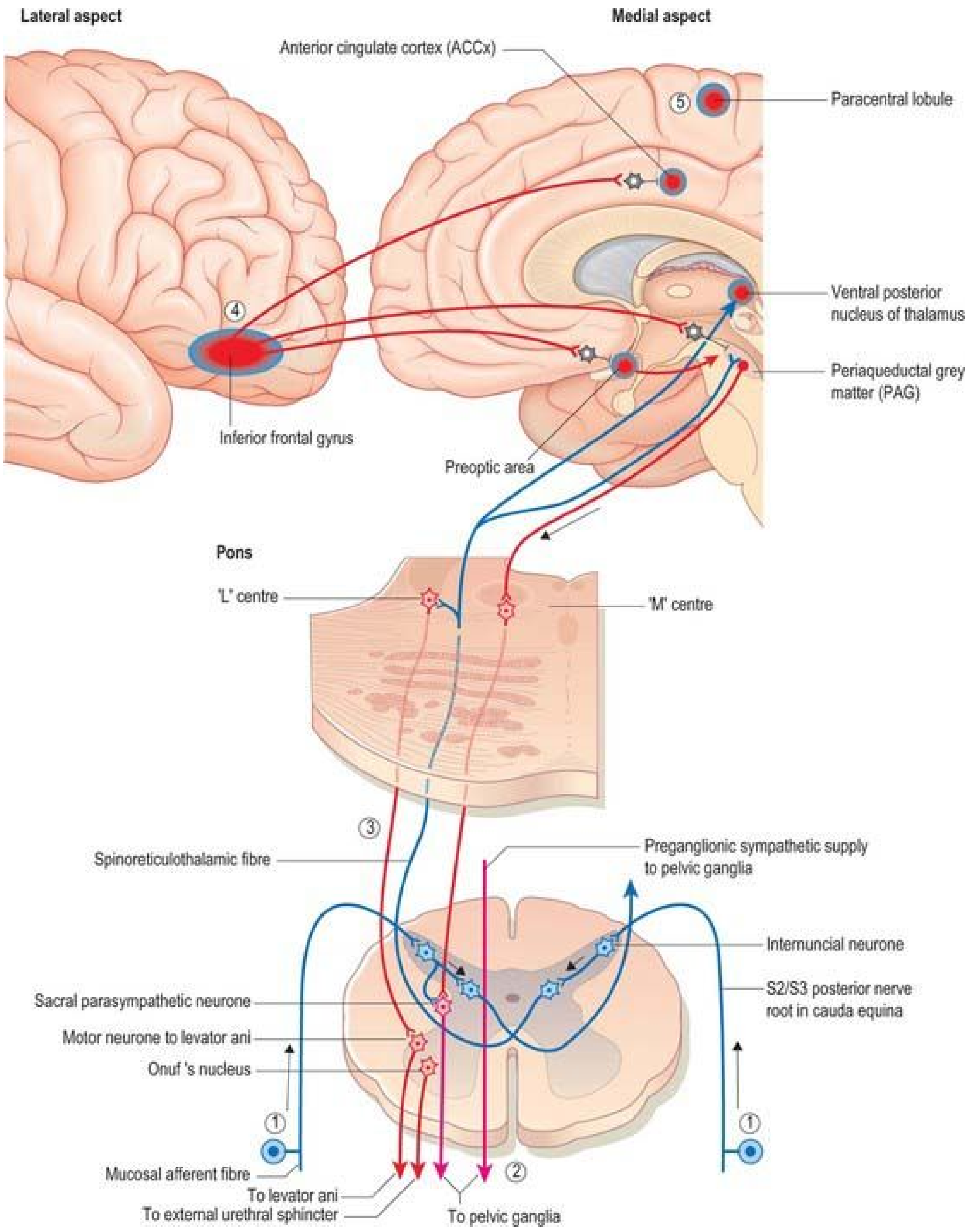
Lateral aspect
Medial aspect
Anterior cingulate cortex (ACCx)
⑤
Paracentral lobule
Ventral posterior nucleus of thalamus
④
Periaqueductal grey matter (PAG)
Inferior frontal gyrus
Preoptic area
Pons
'L' centre
'M' centre
③
Spinoreticulothalamic fibre
Preganglionic sympathetic supply to pelvic ganglia
Internuncial neurone
S2/S3 posterior nerve root in cauda equina
Sacral parasympathetic neurone
Motor neurone to levator ani
Onuf 's nucleus
①
①
Mucosal afferent fibre
②
To levator ani
To external urethral sphincter
To pelvic ganglia

Fig. 75.9 The micturition control centre is in the paramedian pontine reticular formation on each side and consists of a medially placed micturition centre, ‘M’ and a laterally placed storage centre, ‘L’. Neurones project from the ‘M’ centre and the storage centre ‘L’ to parasympathetic neurones in segments 2–4 of the sacral spinal cord, and to Onuf’s nucleus, which is in the same segments, and which innervates the external urethral sphincter. At higher levels, neurones in the right prefrontal and anterior cingulate cortex, right preoptic nucleus and periaqueductal grey matter, are involved in the control of micturition. Vesical afferents from stretch receptors in the detrusor and trigonal mucosa relay the extent of bladder filling to the brain stem and thalamus via spinoreticulothalamic fibres (1). Activity in the sympathetic system which maintains increases in bladder compliance (via β_2 receptors on detrusor fibres) and parasympathetic activity is inhibited (2). Spinoreticular fibres synapsing in the ‘L’ nucleus in the pons activate Onuf’s nucleus to increase the tone of the external sphincter (3). If micturition is deferred, fibres projecting from the inferior frontal gyrus inhibit the right anterior cingulate gyrus, preoptic area and periaqueductal grey matter) (4). Voluntary contraction of the pelvic floor musculature, controlled by the prefrontal cortex driving the perineal ‘area’ of the motor cortex (5) cannot be long sustained once filling is complete.

(By permission from FitzGerald MJT, Folan-Curren J 2001 Clinical Neuroanatomy, 4th edn. London: Saunders.)

Micturition consists of storage and voiding phases. During the storage phase the bladder accommodates an increasing volume of urine without any change in intravesical pressure, partly because of the viscoelastic properties of its walls, and partly because a gating mechanism operates in the spinal cord that reflexly inhibits preganglionic parasympathetic activity. A gating mechanism in the pelvic ganglia prevents the activation of postganglionic parasympathetic neurones until preganglionic activity has reached a threshold level.

Mean bladder capacity in adult males varies around 400 ml, but micturition commonly occurs at smaller volumes. Voluntary control is imposed from the inferior frontal gyrus of the cerebral cortex. Filling to 500 ml may be tolerated; beyond this level, pain caused by tension in the bladder wall leads to the urgent desire to micturate. The pain is referred to the cutaneous areas supplied by T10–L2, S2–4, including the lower anterior abdominal wall, perineum and penis. Threshold afferent stimulation activates the micturition centre in the rostral pons (the M-centre) (Fig. 75.9) which drives preganglionic parasympathetic neurones in the intermediolateral grey column of the second, third and fourth sacral spinal segments via descending spinal pathways. The axons of these neurones run to the inferior hypogastric plexus in the pelvic splanchnic nerves: they synapse on postganglionic neurones in ganglia lying within the plexus and in the wall of the bladder. Postganglionic axons ramify throughout the thickness of the detrusor smooth muscle coat. When stimulated, they release acetylcholine which activates muscarinic receptors in the detrusor layer of the bladder wall and produces the sustained bladder contraction required for micturition. The distal urethral sphincter maintains urethral closure.

Urinary continence in the male

Urinary continence at the level of the membranous urethra is mediated by the radial folds of urethral mucosa, the submucosal connective tissue, the intrinsic urethral smooth muscle, the striated external urethral sphincter and the pubourethral component of levator ani. The external urethral sphincter represents the point of highest intraurethral pressure in the normal, contracted state. The striated muscle component of the external urethral sphincter is devoid of muscle spindles. The striated muscle fibres themselves are unusually small in cross-section (15–20 μm diameter), and are physiologically of the slow twitch type, unlike the pelvic floor musculature, which is a heterogeneous mixture of slow and fast twitch fibres of larger diameter. The slow twitch fibres of the external sphincter are capable of sustained contraction over relatively long periods of time and actively contribute to the tone which closes the urethra and maintains urinary continence. They are innervated by neurones that lie in Onuf’s nucleus in the anterolateral grey matter of the second to fourth sacral spinal segments. Their firing is controlled centrally by a storage centre within the rostral pons (the L-centre) (Fig. 75.9). Just before the onset of voiding, the external urethral sphincter is relaxed by central inhibition of Onuf's nucleus. Relaxation of the urethra is currently believed to be due to the release of nitric oxide from parasympathetic nerves in the bladder neck and urethra.

Urinary continence in the female

The urethral sphincter mechanism consists of the intrinsic striated and smooth muscle of the urethra, the mucosa and submucosal connective tissue, and the puborectalis component of levator ani (which surrounds the urethra at the point of maximum concentration of those muscles). The striated muscle component of the urethral sphincter mechanism surrounds the middle and lower thirds of the urethra in the female. Proximally it forms a complete ring around the urethra, more distally it covers the anterior and lateral aspects of the urethra: it blends above with the smooth muscle of the bladder neck and below with the smooth muscle of the lower urethra and vagina. Contraction of this part of the sphincter compresses the urethra against the relatively fixed anterior vaginal wall. At its most distal point the striated sphincter encompasses the urethra and vagina as the urethrovaginal sphincter. The mucosa and submucosa are oestrogen dependent and atrophy postmenopausally, possibly resulting in stress incontinence.

PROSTATE

The prostate is a pyramidal fibromuscular gland which surrounds the prostatic urethra from the bladder base to the membranous urethra. It has no true fibrous capsule, but is enclosed by visceral fascia containing neurovascular tissue (Fig. 75.10A,B). The fascia is firmly adherent to the gland and is continuous with a median septum and with numerous fibromuscular septa which divide the glandular tissue into indistinct lobules.

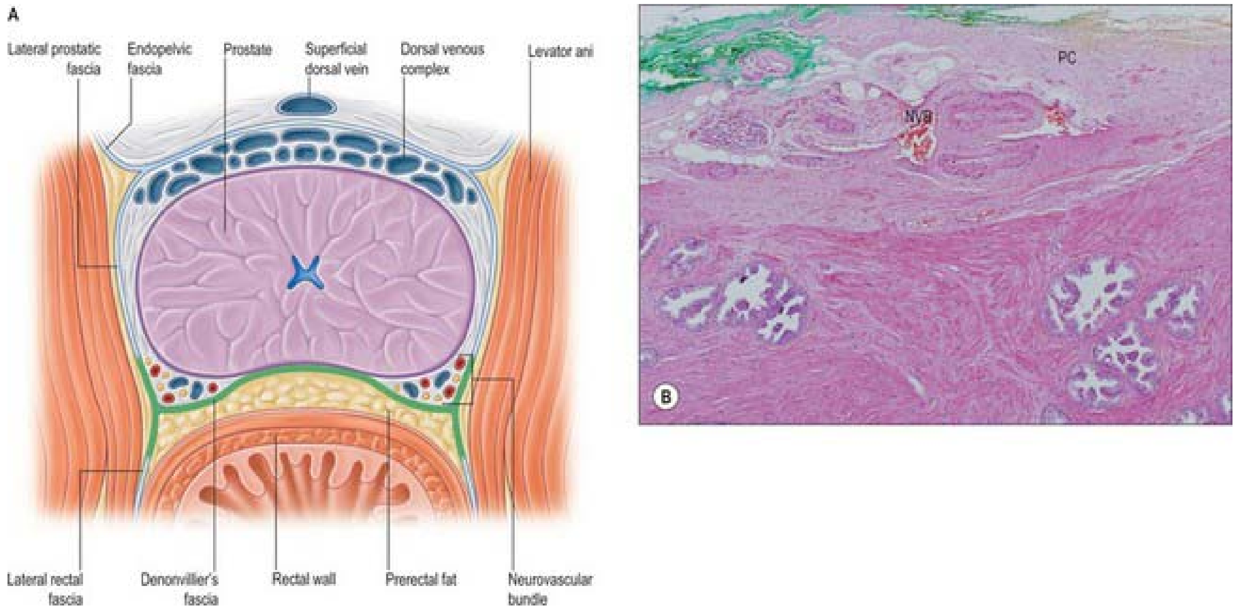
A
Lateral prostatic fascia
Endopelvic fascia
Prostate
Superficial dorsal vein
Dorsal venous complex
Levator ani
Lateral rectal fascia
Denonvillier's fascia
Rectal wall
Prerectal fat
Neurovascular bundle
PC
NVB
B

Fig. 75.10 **A**, The endopelvic fascia. The fascia covers the pelvic viscera and continues posteriorly over the lateral aspect of the prostate, as the lateral prostatic fascia and on the lateral aspect of the rectum as the lateral rectal fascia. Its relationship with Denonvilliers may be visualized as an ‘H’. The deep dorsal vein and lateral branches run deep to the endopelvic fascia and the lateral prostatic fascia, although communicating with perforators to the pelvic side wall. Denonvilliers is adherent to the prostate in the posterior midline, but like the lateral prostatic fascia is separated from the prostatic tissue by the neurovascular structures and fatty tissues elsewhere. Between Denonvilliers and the rectum is a fatty potential plane, the prerectal space. **B**, The prostatic capsule (PC) is a condensation of connective tissue on the

surface of the gland (green) and encloses the neurovascular bundle (NVB). The prostatic fibromuscular stroma and glands lie beneath the capsule.

The muscular tissue within the prostate is mainly smooth muscle. Anterior to the urethra a layer of smooth muscle merges with the main mass of muscle in the fibromuscular septa; it blends superiorly with vesical smooth muscle. Anterior to the layer of smooth muscle a transversely crescent-shaped mass of skeletal muscle is continuous inferiorly with the external urethral sphincter in the deep perineal pouch. Its fibres pass transversely internal to the capsule, and are attached to it laterally by diffuse collagen bundles; other collagen bundles pass posteromedially, merging with the prostatic fibromuscular septa and the septum of the urethral crest. This muscle, supplied by the pudendal nerve, probably compresses the urethra but it may pull the urethral crest back and the prostatic sinuses forwards, dilating the urethra. Glandular contents may be expelled simultaneously into the urethra when it has expanded in this way, so that it contains 3–5 ml seminal fluid prior to ejaculation.

The prostate lies at a low level in the lesser pelvis, behind the inferior border of the symphysis pubis and pubic arch (Figs 75.2A, 75.11) and anterior to rectourethralis and the rectal ampulla, through which it may be palpated. Being somewhat pyramidal, it presents a base or vesical aspect superiorly, an apex inferiorly, and posterior, anterior and two inferolateral surfaces. The prostatic base measures about 4 cm transversely. The gland is 2 cm in anteroposterior and 3 cm in its vertical diameters, and weighs about 8 g in youth, but almost invariably enlarges with the development of BPH: it usually weighs 40 g, but sometimes as much as 150 g or even more, after the first five decades of life. The small prostate without BPH is described as a croissant shape (short anterior commissure, prominent apical notch and posterior lip of prostatic tissue), and the enlarged gland is more doughnut-shaped. The shape of the prostate affects the relationship of the prostatic apex to the external urethral sphincter. This relationship is important when removing the prostate at radical prostatectomy for cancer, and anastomosing the bladder to the urethra to maintain sphincter integrity. The external urethral sphincter is flush to a large doughnut-type gland so a perpendicular incision will separate the prostate and external urethral sphincter accurately. In a small prostate the external urethral sphincter fills the defect in the anterior aspect of the prostate, so a perpendicular incision at the level of the posterior lip of the croissant shaped gland will excise much external urethral sphincter and leave the patient incontinent.

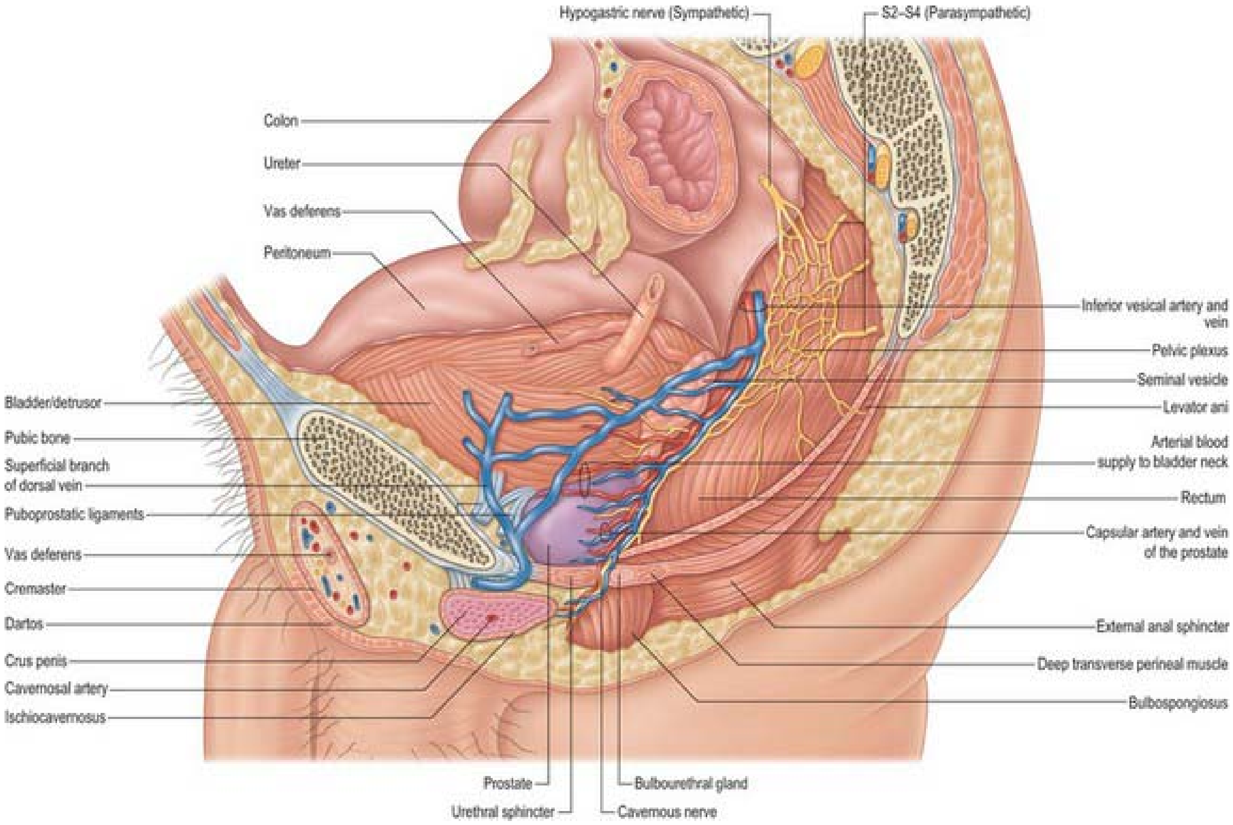
Hypogastric nerve (Sympathetic)
S2–S4 (Parasympathetic)
Colon
Ureter
Vas deferens
Peritoneum
Bladder/detrusor
Pubic bone
Superficial branch of dorsal vein
Puboprostatic ligaments
Vas deferens
Cremaster
Dartos
Crus penis
Cavernosal artery
Ischiocavernosus
Prostate
Urethral sphincter
Bulbourethral gland
Cavernous nerve
Inferior vesical artery and vein
Pelvic plexus
Seminal vesicle
Levator ani
Arterial blood supply to bladder neck
Rectum
Capsular artery and vein of the prostate
External anal sphincter
Deep transverse perineal muscle
Bulbospongiosus

Fig. 75.11 Sagittal section, male pelvis. The pelvic plexus lies with its midpoint level with the tip of the seminal vesicles. It gives branches to the prostate, bladder urethra, seminal vesicles, rectum and corpora cavernosa via the cavernous nerves. The cavernous nerves are the continuation of the neurovascular bundles, lying posterolateral to the prostate. These bundles may be damaged at radical prostatectomy resulting in impotence.

Superiorly the base is largely contiguous with the neck of the bladder. The apex is inferior, surrounding the junction of the prostatic and membranous parts of the posterior urethra. The apical posterior relation of the prostate and external urethral sphincter is rectourethralis, a Y-shaped muscle that originates from the outer longitudinal coat of the rectum. The upper limbs of the Y extend from the lateral rectal wall to the midline where rectourethralis inserts into the perineal body at the anorectal junction.

The anterior surface lies in the arch of the pubis, separated from it by the dorsal venous complex (Santorini's plexus) and loosely attached adipose tissue. It is transversely narrow and convex, extending from the apex to the base. Near its superior limit it is connected to the pubic bones by the puboprostatic ligaments. The urethra emerges from this surface anterosuperior to the apex of the gland. The anterior part of the prostate is relatively deficient in glandular tissue and is largely composed of fibromuscular tissue. The anterior and lateral aspects of the prostate are covered by a layer of fascia derived from the endopelvic fascia on each side, called the lateral prostatic fascia. This is adherent medially to the prostate, continues posteriorly over the lateral aspect of the prostate, neurovascular bundles and rectum (lateral rectal fascia) and passes distally over the urethra (Fig. 75.10A). The prostatic venous plexus (Fig. 75.11) lies between this extension of the endopelvic fascia and the prostate. Anteroinferiorly the parietal and visceral fasciae of the prostate merge and blend with the puboprostatic ligaments. The anterior surface of the prostate and associated vascular plexus is covered by the detrusor apron.

The inferolateral surfaces are related to the muscles of the pelvic sidewall: the anterior fibres of levator ani embrace the prostate in the pubourethral sling or pubourethralis. These muscles are separated from the prostate by a thin layer of connective tissue.

The posterior surface of the prostate is transversely flat and vertically convex. Near its superior (juxtavesical) border is a depression where it is penetrated by the two ejaculatory ducts. Below this is a shallow, median sulcus, usually considered to mark a partial separation into right and left lateral lobes. It is separated from prerectal fat in the prerectal space (Figs 75.2A, 75.10A), and rectum by Denonvillier's fascia, a condensation of pelvic fascia which develops by obliteration of the rectovesical peritoneal pouch, and by loose yellow fatty areolar tissue. The rectovesical pouch is obliterated from below upwards as fetal life progresses, forming Denonvillier’s fascia: at birth this fascia separates the prostate, the seminal vesicles and the ampullae of the vasa deferentia from the rectum. The superior limit of Denonvillier’s fascia is the peritoneum of the rectovesical pouch. Laterally Denonvillier’s fascia fuses with the lateral pelvic fascia: anterior to Denonvillier’s fascia, the fascia is called the lateral prostatic fascia, and posterior to Denonvillier’s fascia it is called the lateral rectal fascia.

The prostate is traversed by the urethra and ejaculatory ducts, and contains the prostatic utricle. The urethra enters the prostate near its anterior border and usually passes between its anterior and middle thirds. The ejaculatory ducts pass anteroinferiorly through its posterior region to open into the prostatic urethra (p. 1250).

ZONAL ANATOMY OF THE PROSTATE

The prostate gland was initially thought to be divided into five anatomical lobes, but it is now recognized that five lobes can only be distinguished in the fetal gland prior to 20 weeks' gestation. Between then and the onset of BPH, only three lobes are recognizable, two lateral and a median lobe. Clinicians refer to left and right 'lobes' when describing either what can be felt on rectal palpation, or endoscopically visible abnormalities in the diseased state when prostatic anatomy is distorted by BPH.

From an anatomical, and particularly from a morbid anatomical perspective, the glandular tissue may be subdivided into three distinct zones (Figs 75.12-75.14), peripheral (70% by volume), central (25% by volume), and transitional (5% by volume). Non-glandular tissue (fibromuscular stoma) fills up the space between the peripheral zones anterior to the preprostatic urethra. The central zone surrounds the ejaculatory ducts, posterior to the preprostatic urethra, and is more or less conical in shape with its apex at the verumontanum. The transitional zone lies around the distal part of the preprostatic urethra just proximal to the apex of the central zone and the ejaculatory ducts. Its ducts enter the prostatic urethra just below the preprostatic sphincter and just above the ducts of the peripheral zone. The peripheral zone is cup-shaped and encloses the central transitional zone and the preprostatic urethra except anteriorly, where the space is filled by the anterior fibromuscular stroma. Simple mucus-secreting glands lie in the tissue around the preprostatic urethra, above the transitional zone and surrounded by the preprostatic sphincter. These simple glands are similar to those in the female urethra and unlike the glands of the prostate.

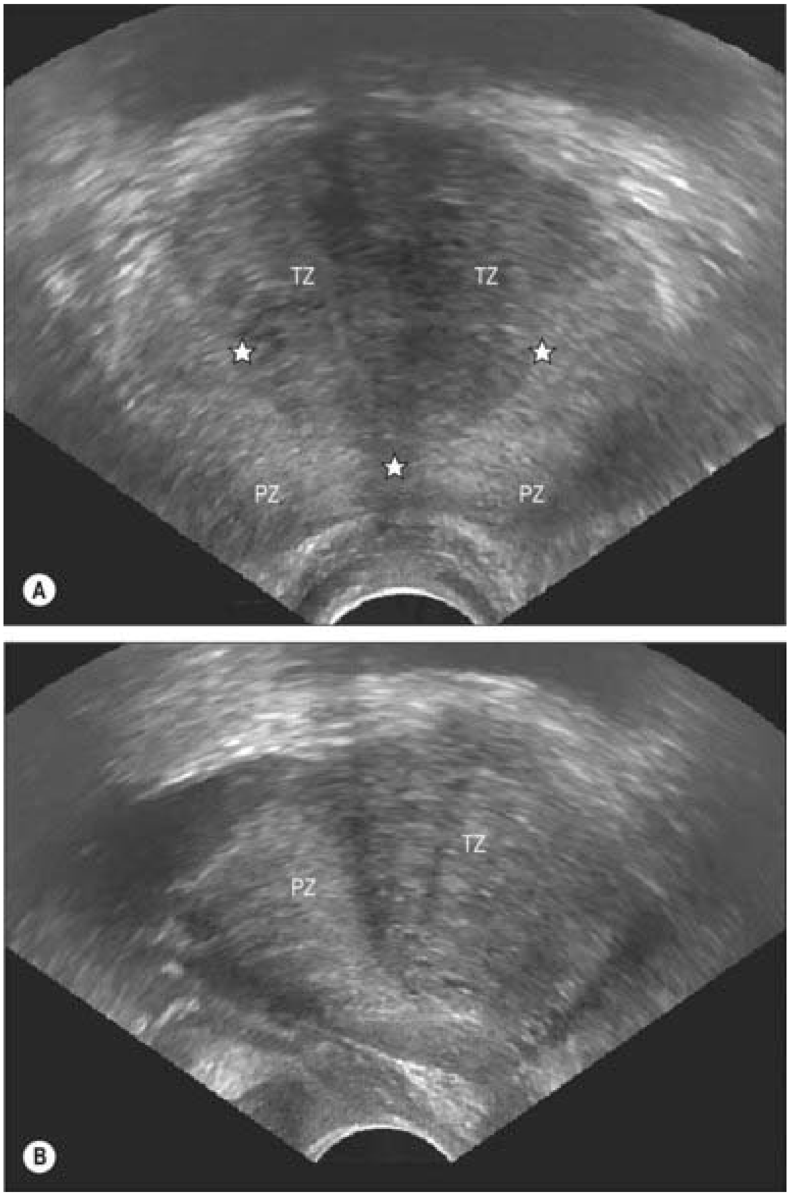

Fig. 75.12 Ultrasound of the prostate. **A**, Axial view showing the hypoechoic transition zone (TZ) and the more echogenic peripheral zone (PZ). Their interface is the surgical capsule (*). **B**, Sagittal view showing the hypoechoic transition zone (TZ) and the more echogenic peripheral zone (PZ).

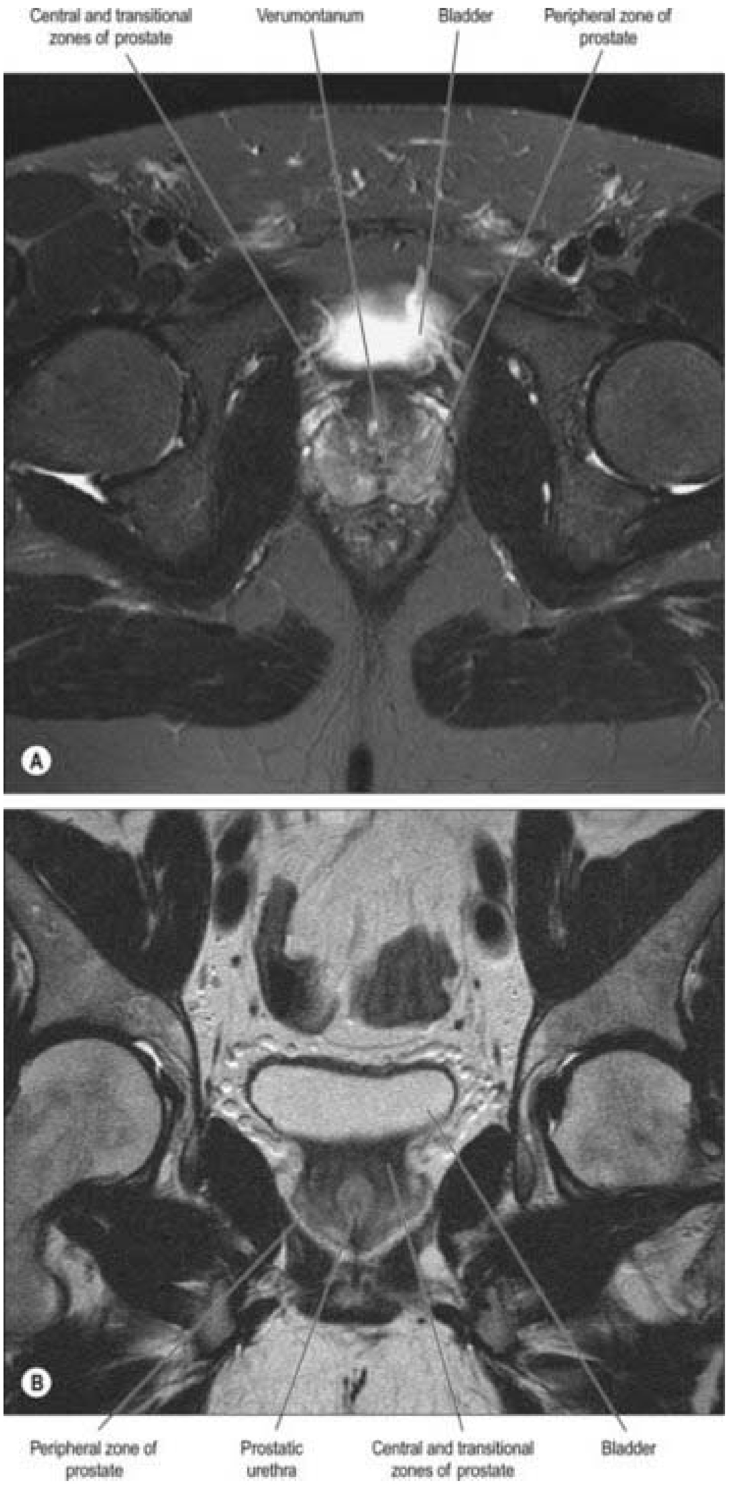
Central and transitional zones of prostate
Verumontanum
Bladder
Peripheral zone of prostate
A
B
Peripheral zone of prostate
Prostatic urethra
Central and transitional zones of prostate
Bladder

Fig. 75.13 MRI of the prostate. **A**, T2-weighted MRI scan showing the normal high signal of the peripheral zone and the intermediate signal of the central and transitional zones and the verumontanum in the central gland. **B**, T2-weighted coronal MRI scan of the prostate showing the zonal anatomy.

The zonal anatomy of the prostate is clinically important because most carcinomas arise in the peripheral zone, whereas BPH affects the transitional zone, which may grow to form the bulk of the prostate. BPH begins as micronodules in the transitional zone which grow and coalesce to form macronodules around the inferior margin of the preprostatic urethra, just above the verumontanum. Macronodules in turn compress the surrounding normal tissue of the peripheral zone posteroinferiorly, creating a ‘false capsule’ around the hyperplastic tissue which coincidentally provides a plane of cleavage for its surgical enucleation. As the transitional zone grows, it produces the appearance of ‘lobes’ on either side of the urethra. In due course, these lobes may compress or distort the preprostatic and prostatic parts of the urethra and produce symptoms. The central zone surrounding the ejaculatory ducts is rarely involved in any disease. It shows certain histochemical characteristics which differententiate it from the rest of the prostate: it is thought to be derived from the Wolffian duct system (much like the epididymi, vasa deferentia and seminal vesicles), whereas the rest of the prostate is derived from the urogenital sinus (p. 1323).

On magnetic resonance (MR) imaging the prostate gland has a zonal anatomy on T2-weighted images (Fig. 75.13). The normal peripheral zone has high signal intensity, as does fluid within the seminal vesicles. The central and transitional zones have relatively low signal and are often referred to as the ‘central gland’. The verumontanum may be seen as high signal within the central gland.

The relationship of the zones of the gland normally changes with age. The central zone atrophies, and the transitional zone enlarges secondary to BPH. This often produces a low signal band at the margin of the hypertrophied transitional and compressed peripheral zones, the surgical pseudocapsule, which is well seen on T2-weighted MR images.

VASCULAR SUPPLY AND LYMPHATIC DRAINAGE

Arteries

The prostate is supplied by branches from the inferior vesical, internal pudendal and middle rectal arteries (Fig. 75.11). They perforate the gland along a posterolateral line from the junction of the prostate with the bladder down to the apex of the gland.

The inferior vesical artery often arises from the internal iliac artery with the middle rectal artery. It gives rise to two groups of branches, the urethral and capsular. The urethral vessels enter at the prostatovesical junction principally posteriorly at the 5 and 7 o'clock positions, but also anteriorly at 1 and 11 o'clock. This bladder neck arterial anatomy is always apparent at transurethral resection of the prostate and open removal of BPH adenomas. The capsular arteries run posterolaterally and inferiorly in the neurovascular bundles, providing perpendicular perforating vessels to the prostate. The most constant in position and prominence is the apical perforator at the prostatourethral junction, an important landmark for this point and for the neurovascular bundle at radical prostatectomy.

Veins

The veins run into a plexus around the anterolateral aspects of the prostate, posterior to the arcuate pubic ligament and the lower part of symphysis pubis, anterior to the bladder and prostate (see Fig. 76.22). The chief tributary is the deep dorsal vein of the penis. The plexus also receives anterior vesical and prostatic rami (which connect with the vesical plexus and internal pudendal vein), and drains into vesical and internal iliac veins.

Lymphatic drainage

Collecting vessels from the vas deferens drain into the external iliac nodes, while those from the seminal vesicle drain to the internal and external iliac nodes. Prostatic vessels end mainly in internal iliac, sacral and obturator nodes. A vessel from the posterior surface accompanies the vesical vessels to the external iliac nodes, and another from the anterior surface reaches the internal iliac group by joining vessels which drain the membranous urethra.

INNERVATION

The prostate receives an abundant nerve supply from the inferior hypogastric (pelvic) plexus (Figs 75.10A, 75.11). The prostatic capsule is covered by numerous nerve fibres and ganglia posterolaterally, forming a crescenteric periprostatic nerve plexus. The greatest density of nerves is found in the preprostatic sphincter; fewer fibres are found in the anterior fibromuscular stroma, and the peripheral zone is the least densely innervated. Nerves containing neuropeptide Y and vasointestinal polypeptide (VIP) are localized in the subepithelial connective tissue, in the smooth muscle layers of the gland, and in the walls of its blood vessels. Neurovascular bundles containing autonomic nerves which supply the prostate, seminal vesicles, prostatic urethra, ejaculatory ducts, corpora cavernosa, corpus spongiosum, membranous and penile urethra and bulbourethral glands are closely applied to, but separable from, the posterolateral margins of the prostate. They are intimately related to the prostatic fascia. These nerves may be damaged during radical prostate surgery for organ-confined prostate cancer, producing impotence (p. 1277), or sacrificed as part of wide local excision of the prostate.

The somatic pudendal nerve (p. 1092) supplies the external urethral sphincter. The branches enter at the 5 and 7 o’clock positions, and must be avoided when placing anastomotic sutures to bring the bladder and urethra together during a radical prostatectomy. Sensory branches pass through the penile hilus in association with the dorsal venous complex and dorsal vein of the penis. They may be damaged during ligation of the dorsal vein during radical prostatectomy, which results in an anaesthetic penis.

MICROSTRUCTURE

The glandular tissue consists of numerous follicles with frequent internal papillae. Follicles open into elongated canals which join to form 12–20 main ducts. The follicles are separated by loose connective tissue, supported by extensions of the fibrous capsule and muscular stroma and enclosed in a delicate capillary plexus. Follicular epithelium is variable but predominantly columnar, and either single-layered or pseudostratified.

Prostatic ducts open mainly into the prostatic sinuses in the floor of the prostatic urethra. They have a bilayered epithelium, the luminal layer is columnar and the basal layer is populated by small cuboidal cells. Small colloid amyloid bodies (corpora amylacea) are frequent in the follicles (Fig. 75.15A,B). Prostatic and seminal vesicular secretions form the bulk of seminal fluid. Prostatic secretions are slightly acid, and contain acid phosphatase, amylase, prostate specific antigen, fibrinolysin and zinc. Numerous neuroendocrine cells, containing neuronespecific enolase, chromogranin and serotonin, are present in the glandular epithelium: their numbers decline after middle age and their function is unknown.

Histological sections just above the level of the verumontanum reveal two concentric, partially circumurethral, zones of glandular tissue. The larger outer zone is the peripheral zone and has long, branched glands, whose ducts open mainly into the prostatic sinuses. The inner zone is the transitional zone and consists of glands whose ducts open on the floor of the prostatic sinuses and colliculus seminalis, and a group of simple mucosal glands which surround the preprostatic urethra. Anteriorly, in the prostatic isthmus, the peripheral zone and submucosal glands are absent.

AGE CHANGES IN THE PROSTATE

At birth, the prostate has a system of ducts embedded in a stroma which forms a large part of the gland. Follicles are represented by small end-buds on the ducts. Before birth, the epithelium of the ducts, seminal colliculus and prostatic utricle display hyperplasia and squamous metaplasia, possibly due to maternal oestrogens in the fetal blood. This subsides after birth and is followed by a period of quiescence lasting for 12–14 years.

At puberty, between the ages of approximately 14 and 18 years, the prostate gland enters a maturation phase, and more than doubles in size during this time. Growth is almost entirely due to follicular development, partly from end-buds on ducts, and partly from modification of the ductal branches. Morphogenesis and differentiation of the epithelial cords starts in an intermediate part of the epithelial anlage and proceeds to the urethral and subcapsular parts of the gland; the latter is reached by the age of 17–18 years. The glandular epithelium is initially multilayered squamous or cuboidal, and is transformed into a pseudostratified epithelium consisting of basal, exocrine secretory (including mucous) and neuroendocrine cells. The mucous cells are temporary, and are lost as the gland matures. The remaining exocrine secretory cells produce a number of products including acid phosphatase, prostate-specific antigen and β-microseminoprotein. Growth of the secretory component is associated with a condensation of the stroma, which diminishes relative to the glandular tissue. These changes are probably a response to the secretion of testosterone by the testis.

During the third decade the glandular epithelium grows by irregular multiplication of the epithelial infoldings into the lumen of the follicles. After the third decade, the size of the prostate remains virtually unaltered until 45–50 years, when the epithelial foldings tend to disappear, follicular outlines become more regular, and amyloid bodies increase in number: all signs of prostatic involution. After 45–50 years the prostate tends to develop BPH: an age-related condition. If a man lives long enough then BPH is inevitable, although not always symptomatic.

REFERENCES

ooks JD, Eggener SE, Chao W-E. Anatomy of the rectourethralis muscle. *Eur Urol*. 2002;41:94-100.

ancellor MB, Yoshimura N. Physiology and pharmacology of the bladder and urethra. Walsh PC, et al. Campbell's Urology Study Guide, 2nd edn, Philadelphia: Saunders, 2002. Chapter 23.

utke CG, Siegel CL. Functional female pelvic anatomy. *Urol Clin North Am*. 1995;22(3):487-498.

eyers RP. Detrusor apron, associated vascular plexus, and avascular plane: Relevance to radical retropubic prostatectomy – Anatomic and surgical commentary. *Urology*. 2002;59:472-479.

undy AR, Fitzpatrick J, Neal D, George N. Structure and function of the lower urinary tract. In: *The Scientific Basis of Urology, Chapter 11*. Oxford: Isis Medical Media; 1999:217-242.

Explains the neurological components of bladder function from the higher cortical centres to molecular events within the cells of the detrusor muscle..

e prostate and benign prostatic hyperplasia. In: Mundy AR, Fitzpatrick J, Neal D, George N. *The Scientific Basis of Urology, Chapter 13*. Oxford: Isis Medical Media; 1999:257-276.

Includes a review of prostatic zonal anatomy..

CHAPTER 76

Male reproductive system

The male reproductive system consists of the spermatic cord and scrotum, testes and epididymes, vas deferens, prostate, seminal vesicles and penis.

SPERMATIC CORD

As the testis traverses the abdominal wall into the scrotum during early life, it carries its vessels, nerves and vas deferens with it. These meet at the deep inguinal ring to form the spermatic cord, which suspends the testis in the scrotum and extends from the deep inguinal ring to the posterior aspect of the testis (Fig. 76.1). The left cord is a little longer than the right. Between the superficial ring and testis the cord is anterior to the tendon of adductor longus. It is crossed anteriorly by the superficial external pudendal artery and posteriorly by the deep external pudendal artery. The ilioinguinal nerve lies inferior to the cord as it traverses the inguinal canal.

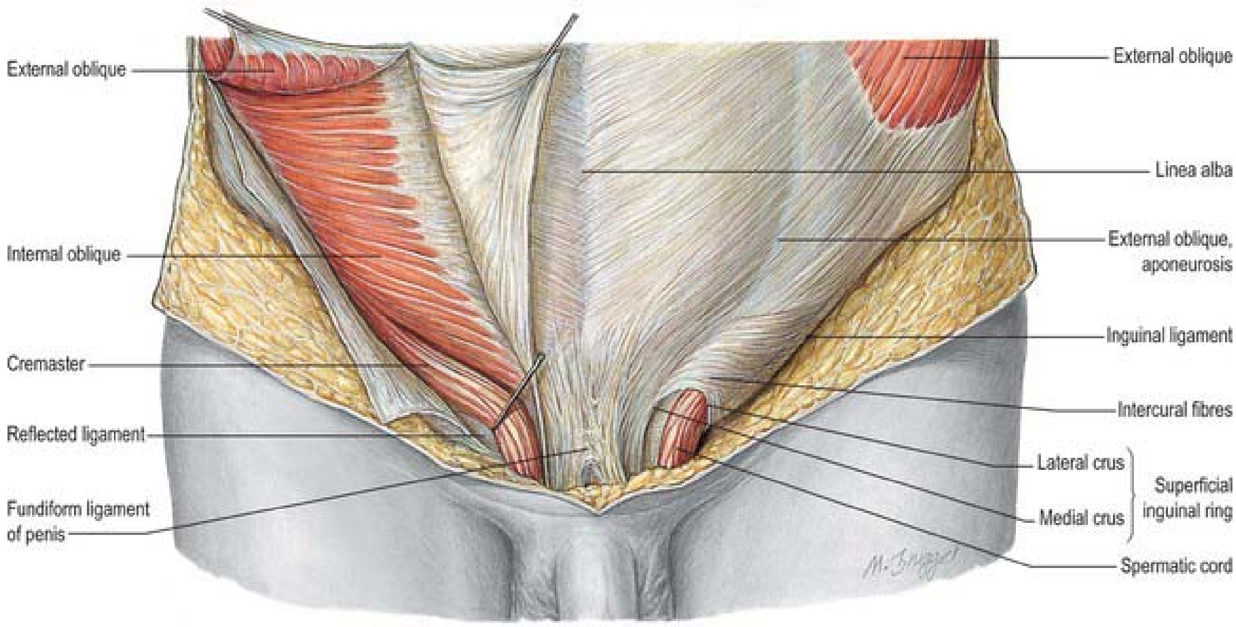
External oblique
Internal oblique
Cremaster
Reflected ligament
Fundiform ligament of penis
External oblique
Linea alba
External oblique, aponeurosis
Inguinal ligament
Intercural fibres
Lateral crus
Medial crus
Superficial inguinal ring
Spermatic cord

Fig. 76.1 Relationship of the spermatic cord to the anterior abdominal wall.

(From Sobotta 2006.)

In the canal the cord acquires coverings from the layers of the abdominal wall that extend into the scrotal wall as the internal spermatic, cremasteric and external spermatic fasciae (Fig. 76.2). The internal spermatic fascia is derived from the transversalis fascia and forms a thin, loose layer around the spermatic cord. The cremasteric fascia contains fasciculi of skeletal muscle united by loose connective tissue to form the cremaster muscle which is continuous with internal oblique. The external spermatic fascia descends from the crura of the superficial ring and is a thin fibrous stratum continuous above with the aponeurosis of external oblique. The spermatic cord contains the vas deferens; the testicular artery and veins, cremasteric artery (a branch of the inferior epigastric artery) and artery to the vas deferens (from the superior vesical artery); the genital branch of the genitofemoral nerve and cremasteric nerve and the sympathetic components of the testicular plexus (which are joined by filaments from the pelvic plexus accompanying the artery to the vas deferens); 4–8 lymph vessels draining the testis. All of these structures are conjoined by loose connective tissue (Figs 76.2, 76.3A).

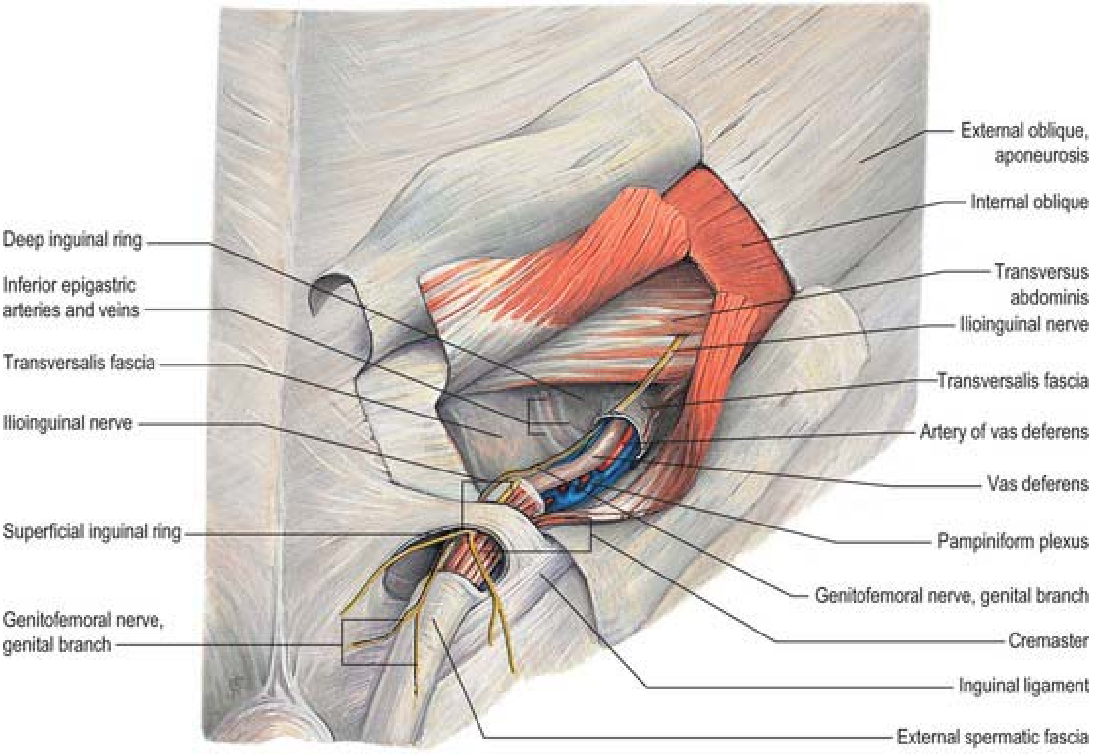
External oblique, aponeurosis
Internal oblique
Deep inguinal ring
Transversus abdominis
Inferior epigastric arteries and veins
Ilioinguinal nerve
Transversalis fascia
Transversalis fascia
Ilioinguinal nerve
Artery of vas deferens
Vas deferens
Superficial inguinal ring
Pampiniform plexus
Genitofemoral nerve, genital branch
Genitofemoral nerve, genital branch
Cremaster
Inguinal ligament
External spermatic fascia

Fig. 76.2 Structures contained within the spermatic cord.

(From Sobotta 2006.)

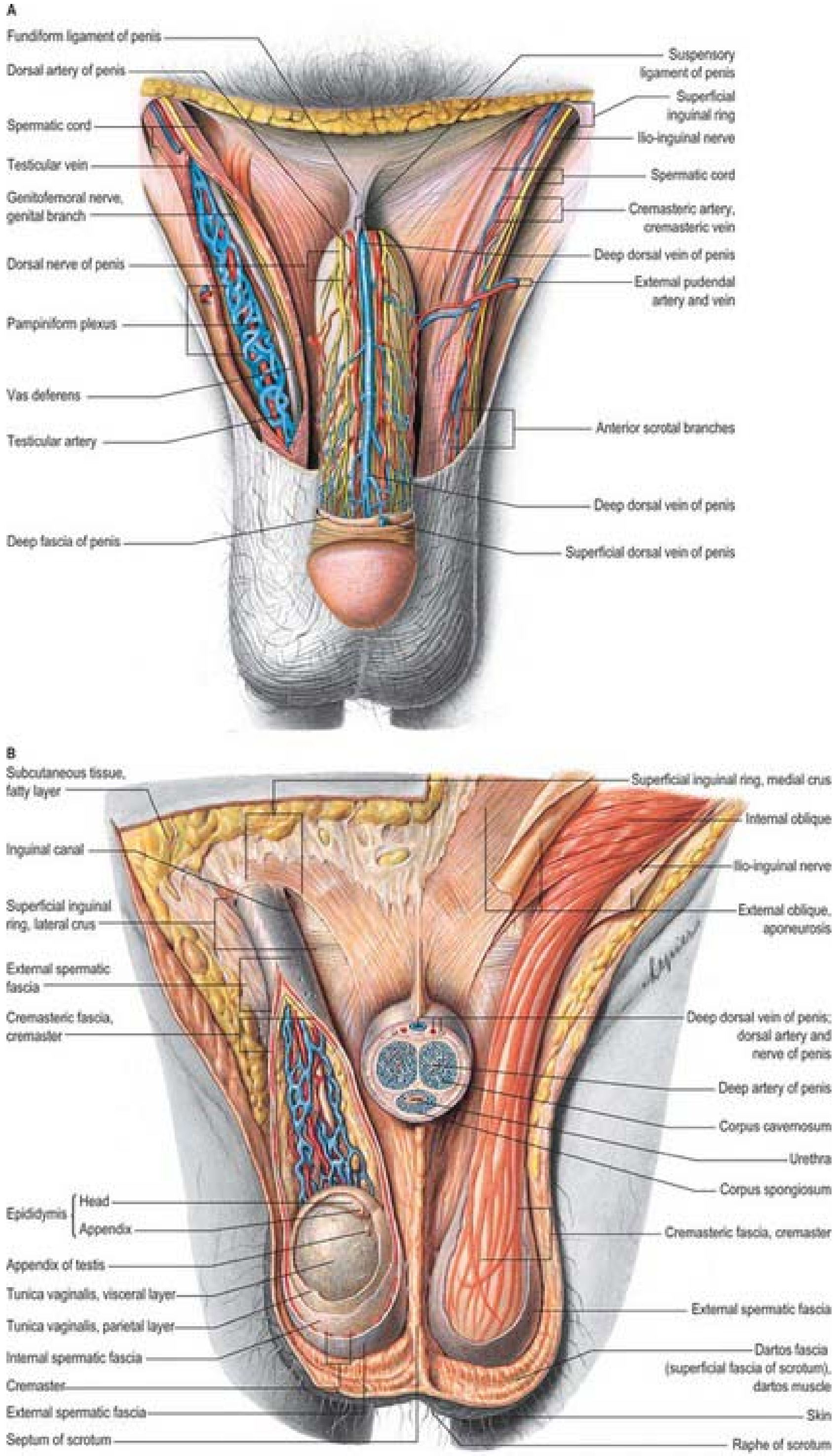
A
Fundiform ligament of penis
Dorsal artery of penis
Spermatic cord
Testicular vein
Genitofemoral nerve, genital branch
Dorsal nerve of penis
Pampiniform plexus
Vas deferens
Testicular artery
Deep fascia of penis
Suspensory ligament of penis
Superficial inguinal ring
Ilio-inguinal nerve
Spermatic cord
Cremasteric artery, cremasteric vein
Deep dorsal vein of penis
External pudendal artery and vein
Anterior scrotal branches
Deep dorsal vein of penis
Superficial dorsal vein of penis
B
Subcutaneous tissue, fatty layer
Inguinal canal
Superficial inguinal ring, lateral crus
External spermatic fascia
Cremasteric fascia, cremaster
Epididymis
Head
Appendix
Appendix of testis
Tunica vaginalis, visceral layer
Tunica vaginalis, parietal layer
Internal spermatic fascia
Cremaster
External spermatic fascia
Septum of scrotum
Superficial inguinal ring, medial crus
Internal oblique
Ilio-inguinal nerve
External oblique, aponeurosis
Deep dorsal vein of penis; dorsal artery and nerve of penis
Deep artery of penis
Corpus cavernosum
Urethra
Corpus spongiosum
Cremasteric fascia, cremaster
External spermatic fascia
Dartos fascia (superficial fascia of scrotum), dartos muscle
Skin
Raphe of scrotum

Fig. 76.3 External male genitalia, ventral aspect. **A**, Nerves and vessels exposed by extensive removal of the skin and the superficial fascia of the penis. The layers of the spermatic cord have been incised on the right: note the pampiniform venous plexus surrounding the testicular artery. **B**, The

skin of the abdomen and parts of the skin of the scrotum have been removed, and the body of the penis has been severed, revealing the internal structure of the penis. The layers of the spermatic cord and the coverings of the testis have been dissected on the right.

(From Sobotta 2006.)

SCROTUM

The scrotum is a cutaneous fibromuscular sac containing the testes and lower parts of the spermatic cords and hangs below the pubic symphysis between the anteromedial aspects of the thighs. It consists of skin, dartos muscle and external spermatic, cremasteric and internal spermatic fasciae. The internal spermatic fascia is loosely attached to the parietal layer of the tunica vaginalis (Fig. 76.3B). The scrotum is divided into right and left halves by a cutaneous raphe, which continues ventrally to the inferior penile surface and dorsally along the midline of the perineum to the anus. The raphe indicates the bilateral origin of the scrotum from the genital swellings. The left side of the scrotum is usually lower because the left spermatic cord is longer.

The scrotal skin is thin, pigmented and often rugose. It bears thinly scattered, crisp hairs, whose roots are visible through the skin. It has sebaceous glands, whose secretion has a characteristic odour, and also numerous sweat glands, pigment cells and nerve endings. These nerve endings respond to mechanical stimulation of the hairs and skin and to variations in temperature. There is no subcutaneous adipose tissue. The external appearance varies. When warm, and in the elderly and debilitated, the scrotum is smooth, elongated and flaccid. When cold, and in the young and robust, it is short, corrugated and closely applied to the testes because of the contraction of the dartos muscle.

The dartos muscle is a thin layer of smooth muscle continuous beyond the scrotum with the superficial inguinal and perineal fasciae. It extends into the scrotal septum, which connects the raphe to the inferior surface of the penile radix. The septum contains all the layers of the scrotal wall except the skin. The dartos muscle is closely united to the skin, but is connected to subjacent parts by delicate loose connective tissue. A fibromuscular ‘scrotal ligament’ extends from the dartos sheet to the inferior testicular pole, and may play a role in thermoregulation of the testis.

Vascular supply and lymphatic drainage

The arteries supplying the scrotum include the external pudendal branches of the femoral artery, the scrotal branches of the internal pudendal artery, and a cremasteric branch from the inferior epigastric artery. Dense subcutaneous plexuses of scrotal vessels carry a substantial blood flow, facilitating heat loss. Arteriovenous anastomoses of a simple but large-calibre type are also prominent. The veins follow the corresponding arteries. The skin of the scrotum is drained by vessels that accompany the external pudendal blood vessels to the superficial inguinal nodes (Fig. 76.3A).

Innervation

The scrotum is innervated by the ilioinguinal nerve, the genital branch of the genitofemoral nerve, the two posterior scrotal branches of the perineal nerve, and the perineal branch of the posterior femoral cutaneous nerve. The anterior third of the scrotum is supplied mainly from the first lumbar spinal segment (by way of the ilioinguinal and genitofemoral nerves), and the posterior two-thirds are innervated principally from the third sacral spinal segment (via the perineal and posterior femoral cutaneous nerves). The ventral axial line of the lower limb passes between these areas which means that a spinal anaesthetic must be injected much higher to anaesthetize the anterior region.

TESTES AND EPIDIDYMIS

TESTES

The testes are the primary reproductive organs or gonads in the male. They are ovoid, reproductive and endocrine organs responsible for sperm production and testosterone production. They are suspended in the scrotum by scrotal tissues including the dartos muscle and spermatic cords. Average testicular dimensions are 4–5 cm in length, 2.5 cm in breadth and 3 cm in anteroposterior diameter; their weight varies from 10.5–14 g. The left testis usually lies lower than the right testis. Each testis lies obliquely within the scrotum, the upper pole tilted anterolaterally and the lower posteromedially. The anterior aspect is convex, whereas the posterior aspect is nearly straight and has the spermatic cord attached to it. Anterior, medial and lateral surfaces and both poles are convex, smooth and covered by the visceral layer of the serosal tunica vaginalis, the parietal layer and the scrotal tissues, in that order from within outwards (Fig. 76.4). Each testis is separated from its fellow by a fibrous median raphe which is deficient superiorly. The posterior aspect of each testis is only partly covered by serosa; the epididymis adjoins its lateral part (see below). The testis is invested by three coats, which are, from outside inwards, the tunica vaginalis, tunica albuginea and tunica vasculosa (Fig. 76.4).

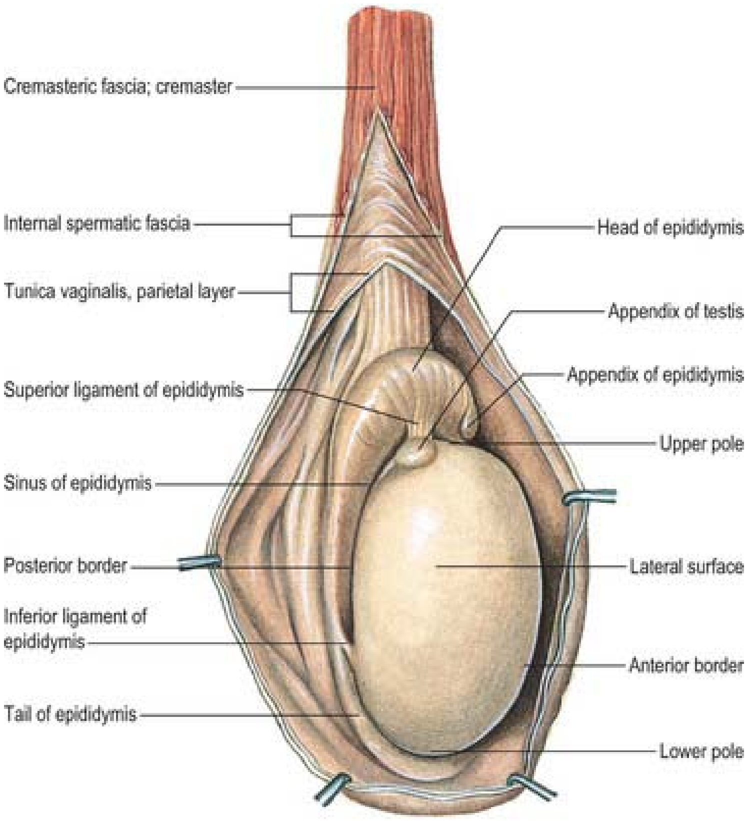
Cremasteric fascia; cremaster
Internal spermatic fascia
Tunica vaginalis, parietal layer
Superior ligament of epididymis
Sinus of epididymis
Posterior border
Inferior ligament of epididymis
Tail of epididymis
Head of epididymis
Appendix of testis
Appendix of epididymis
Upper pole
Lateral surface
Anterior border
Lower pole

Fig. 76.4 The left testis, exposed by incising and laying open the cremasteric fascia and parietal layer of the tunica vaginalis on the lateral aspect of the testis.

(From Sobotta 2006.)

Tunica vaginalis

The tunica vaginalis is the lower end of the peritoneal processus vaginalis, whose formation precedes the descent of the fetal testis from the abdomen to the scrotum (see p. 1320). After this migration, the proximal part of the tunica, from the internal inguinal ring almost to the testis, contracts and is obliterated, leaving a closed distal sac into which the testis is invaginated. The tunica is reflected from the testis onto the internal surface of the scrotum, so forming the visceral and parietal layers of the tunica. The visceral layer covers all aspects of the testis except most of the posterior aspect. Posteromedially it is reflected forwards to the parietal layer. Posterolaterally it passes to the medial aspect of the epididymis and lines the epididymal sinus, and then passes laterally to its posterior border where it is reflected forwards to become continuous with the parietal layer. The visceral and parietal layers are continuous at both poles, but at the upper pole the visceral layer surmounts the head of the epididymis before reflexion. There is always a very fine film of fluid between the two layers of the tunica vaginalis. This fluid layer can increase in inflammatory and neoplastic conditions of the testis, leading to a hydrocele (see below).

The more extensive parietal layer reaches below the testis and ascends in front of and medial to the spermatic cord. The inner surface of the tunica vaginalis has a smooth, moist mesothelium: the potential space between its visceral and parietal layers is termed the cavity of the tunica vaginalis.

Tunica albuginea

The tunica albuginea is a dense, bluish-white covering for the testis, composed mainly of interlacing bundles of collagen fibres. It is covered externally by the visceral layer of the tunica vaginalis, except at the epididymal head and tail and the posterior aspect of the testis, where vessels and nerves enter (Fig. 76.5A,B). The tunica vaginalis covers the tunica vasculosa and, at the posterior border of the testis, projects into the testicular interior as a thick, incomplete fibrous septum, the mediastinum testis, which extends from the upper to the lower end of the testis. Testicular vessels run within the mediastinum testis.

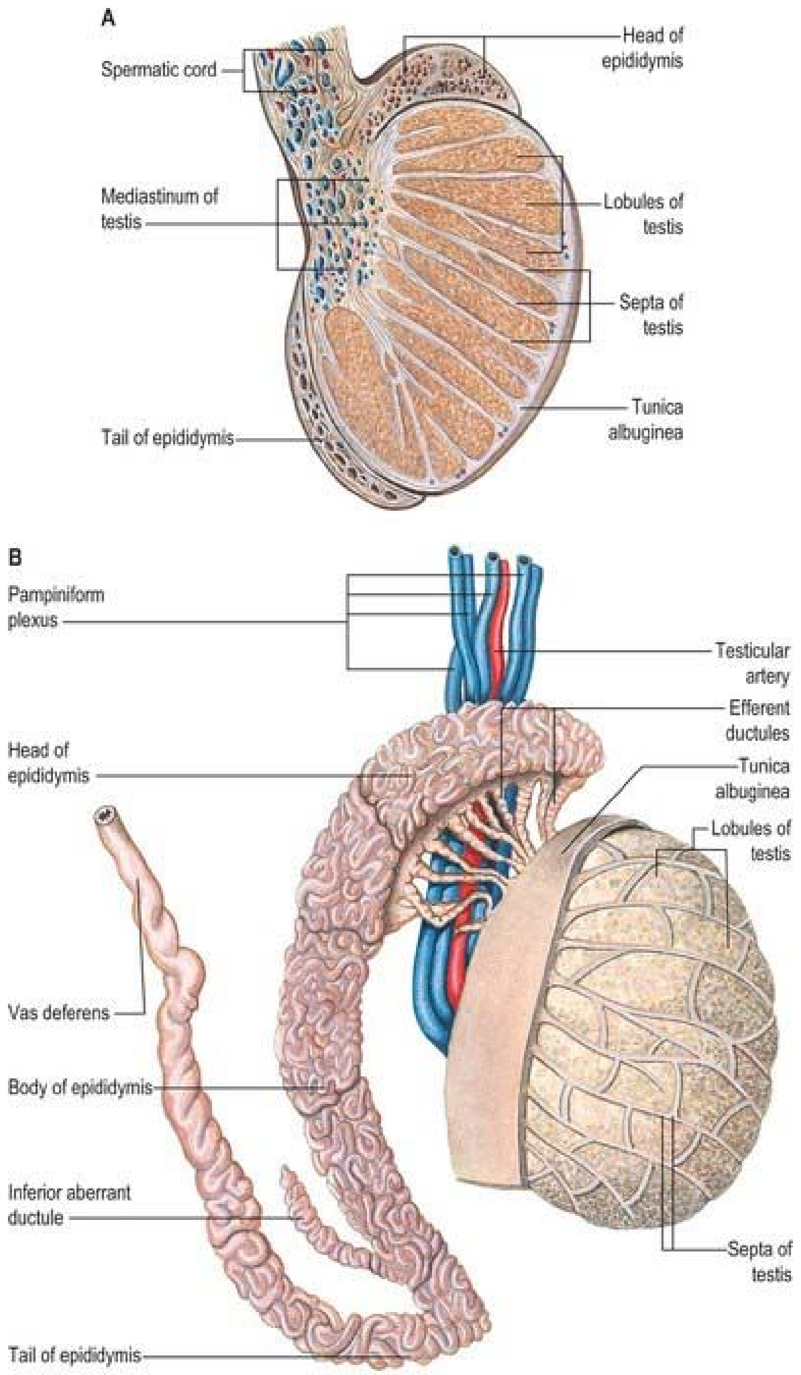
A
Spermatic cord
Head of epididymis
Mediastinum of testis
Lobules of testis
Septa of testis
Tunica albuginea
Tail of epididymis
B
Pampiniform plexus
Testicular artery
Efferent ductules
Head of epididymis
Tunica albuginea
Lobules of testis
Vas deferens
Body of epididymis
Inferior aberrant ductule
Septa of testis
Tail of epididymis

Fig. 76.5 **A**, Vertical section through the testis and epididymis, showing the arrangement of the ducts of the testis and the mode of formation of the vas deferens (**B**).

(From Sobotta 2006.)

Tunica vasculosa

The tunica vasculosa contains a plexus of blood vessels and delicate loose connective tissue, and extends over the internal aspect of the tunica albuginea, covering the septa and therefore all the testicular lobules.

Vascular supply and lymphatic drainage

Testicular arteries

The testicular arteries are two long, slender vessels which arise anteriorly from the aorta a little inferior to the renal arteries. Each passes inferolaterally under the parietal peritoneum on psoas major. The right testicular artery lies anterior to the inferior vena cava and posterior to the horizontal part of the duodenum, right colic and ileocolic arteries, root of the mesentery and terminal ileum. The left testicular artery lies posterior to the inferior mesenteric vein, left colic artery and lower part of the descending colon. Each artery crosses anterior to the genitofemoral nerve, ureter and the lower part of the external iliac artery and passes to the deep inguinal ring to enter the spermatic cord and travel via the inguinal canal to enter the scrotum (Figs 76.3A, 76.6). At the posterosuperior aspect of the testis the testicular artery divides into two branches on its medial and lateral surfaces: these pass through the tunica albuginea and ramify in the tunica vasculosa. Terminal branches enter the testis over its surface. Some pass into the mediastinum testis and loop back before reaching their distribution. Capillaries lying next to seminiferous tubules penetrate the layers of interstitial tissue and may form part of the ‘blood–testis’ barrier. They run either parallel to the tubules or across them but do not enter their walls. They are separated from germinal and supporting cells by a basement membrane and variable amounts of fibrous tissue containing interstitial cells: selective exchange phenomena involving androgens and immune substances occur here.

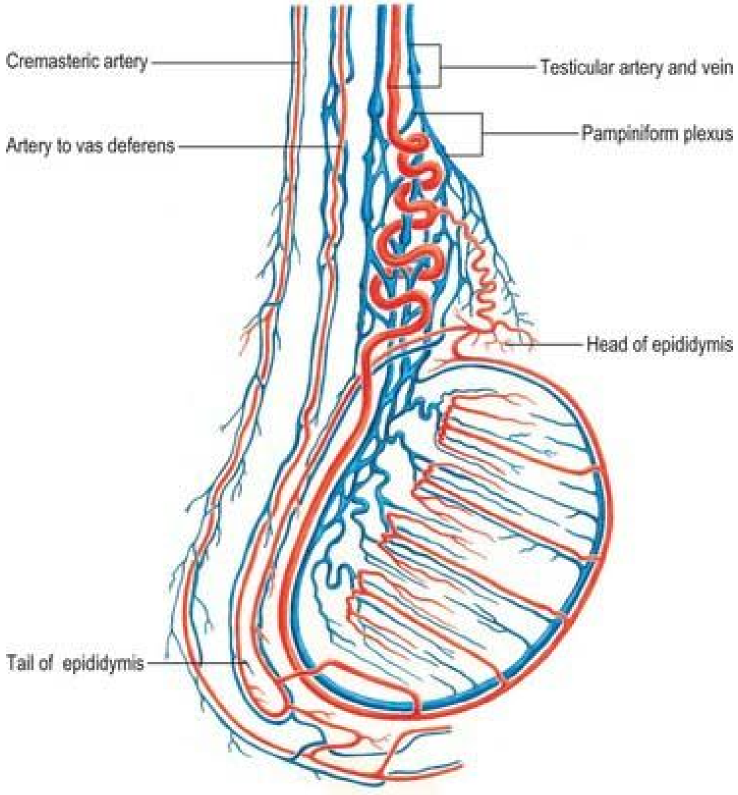
Cremasteric artery
Artery to vas deferens
Testicular artery and vein
Pampiniform plexus
Head of epididymis
Tail of epididymis

Fig. 76.6 Arterial blood supply and venous drainage of the testis.

(From Sobotta 2006.)

In the abdomen the testicular artery supplies perirenal fat, the ureter and iliac lymph nodes, and in the inguinal canal it supplies cremaster. Sometimes the right testicular artery passes posterior to the inferior vena cava. The testicular arteries represent persistent lateral splanchnic aortic branches that enter the mesonephros and cross ventral to the supracardinal vein, but dorsal to the subcardinal vein. Normally the lateral splanchnic artery – which persists as the right testicular artery – passes caudal to the suprasubcardinal anastomosis, which forms part of the inferior vena cava. When it passes cranial to the anastomosis, the right testicular artery lies behind the inferior vena cava.

The testis also receives blood from the cremasteric branch of the inferior epigastric artery, and from the artery to the vas deferens (Fig. 76.6). Interference with the testicular artery high in the abdomen therefore usually leaves the testis unharmed, whereas interruption in the region of the spermatic cord may interfere with all of these vessels and lead to infarction. Ligating both the testicular artery and vein high up interrupts the venae comitantes of the artery which anastomose with the internal spermatic veins and can be responsible for recurrence of a varicocele (see below).

Testicular veins

The testicular veins emerge posteriorly from the testis, drain the epididymis and unite to form the pampiniform plexus, a major component of the spermatic cord that ascends anterior to the vas deferens (Fig. 76.7). In the inguinal canal the pampiniform plexus is drained by three or four veins which run into the abdomen through the deep inguinal ring. Within the abdomen these veins coalesce into two veins, which ascend on each side of the testicular artery, anterior to psoas major and the ureter, and behind the peritoneum. The left veins pass behind the lower descending colon and inferior margin of the pancreas and are crossed by the left colic vessels, and the right veins pass behind the terminal ileum and horizontal part of the duodenum and are crossed by the root of the mesentery, ileocolic and right colic vessels. The veins join to form single right or left testicular veins: the right testicular vein opens into the inferior vena cava at an acute angle just inferior to the level of the renal veins, and the left testicular vein opens into the left renal vein at a right angle (Fig. 76.7). The testicular veins contain valves.

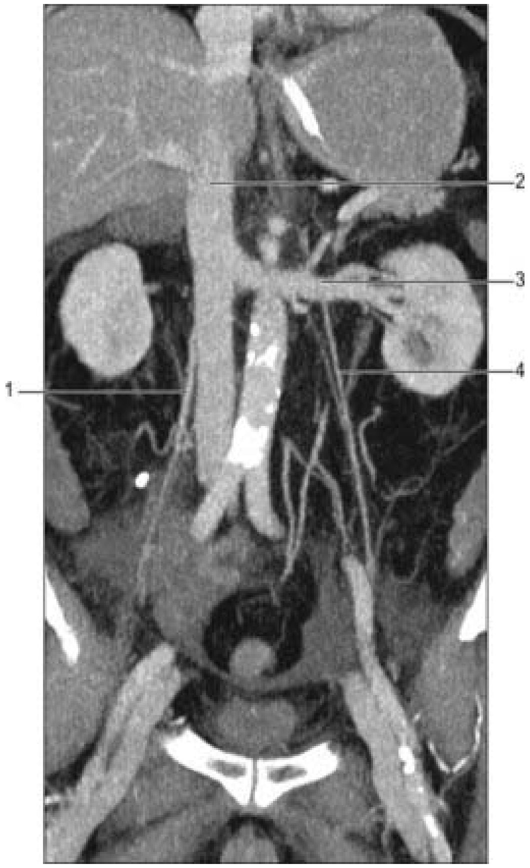

Fig. 76.7 Multislice CT of the inferior vena cava showing the left testicular vein draining to the left renal vein and the right testicular vein draining directly to the inferior vena cava. **1**. Right testicular vein. **2**. Inferior vena cava. **3**. Left renal vein. **4**. Left testicular vein.

The testicular veins in the scrotum and inguinal canal may be varicose in up to 15% of the male population. In fact between 25–35% of men with fertility problems may also have a varicocele. Varicocele formation, which is almost always on the left, may be due to the orthogonal junction of the left testicular and renal veins. There is evidence that the presence of a varicocele raises testicular temperature and impairs spermatogenesis. Varicoceles may also cause testicular pain, which is often a dragging type of pain experienced towards the end of the day after long periods of standing. Varicoceles may be treated surgically for pain but the role of varicocele surgery for treating male infertility is controversial. Varicoceles can also be treated by radiological embolization of the left testicular vein via a right femoral vein approach.

After ligation of a varicocele, venous return is by the small veins of the vas deferens, cremaster and scrotal tissues.

Lymphatic drainage

Testicular vessels start in a superficial plexus under the tunica vaginalis and a deep plexus in the substance of the testis and epididymis. Four to eight collecting trunks ascend in the spermatic cord and accompany the testicular vessels on psoas major, ending in the lateral aortic and pre-aortic nodes.

Innervation

Testicular nerves accompany the testicular vessels and are derived from the tenth and eleventh thoracic spinal segments via the renal and aortic autonomic plexuses. Catecholaminergic nerve fibres form plexuses around smaller blood vessels and among the interstitial cells in the testis and epididymis.

Microstructure

The surface of the testis is covered closely by the visceral tunica vaginalis, a layer of flat mesothelial cells similar to, and continuous with, the peritoneal lining. The visceral layer is separated from the parietal tunica vaginalis (the outer layer of the double fold of peritoneum that accompanies the descending testis (see p. 1320)), by a potential space containing serous fluid, which acts as a lubricant and allows movement of the testis within the scrotum. The testicular capsule proper, the tunica albuginea, is tough and collagenous and thickened posteriorly as the mediastinum testis. Beneath the tunica albuginea is a thin layer of connective tissue containing the superficial blood vessels. Blood vessels, lymphatics and the genital ducts enter or leave the body of the testis at the mediastinum (Fig. 76.8).

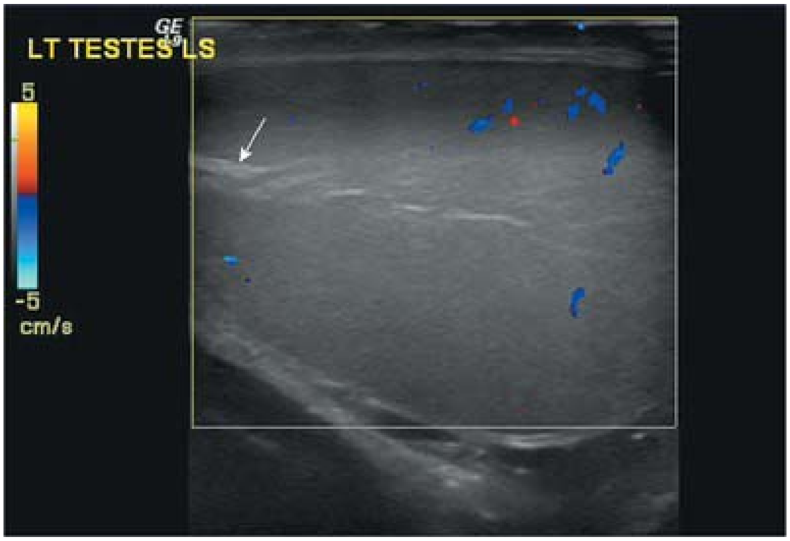

Fig. 76.8 Colour Doppler scan of the scrotal contents showing normal flow. The linear echogenic band (arrow) seen centrally represents the mediastinum testis composed of fibrofatty material.

Septa from the mediastinum extend internally to partition the testis into approximately 250 lobules (Fig. 76.5A). These differ in size, and are largest and longest in the centre. Each lobule contains one to four convoluted seminiferous tubules, much-coiled loops whose free ends both open into channels (the rete testis) within the mediastinum. The loose connective tissue between seminiferous tubules contains several layers of contractile peritubular myoid cells and clusters of androgen-producing interstitial (Leydig) cells.

There are 400–600 seminiferous tubules in each testis, each 70–80 cm long and 0.12–0.3 mm. in diameter. They are pale in early life, but in old age they contain much fat and are deep yellow. Each tubule is surrounded by a basal lamina, on which rests a complex, stratified seminiferous epithelium containing spermatogenic cells and supportive Sertoli cells (Fig. 76.9A). When active, the spermatogenic cells include basally situated spermatogonia and their progeny in the adluminal compartment, spermatocytes, spermatids and mature spermatozoa. Among the spermatids may be residual bodies, spherical structures derived from surplus spermatid cytoplasm shed during maturation and phagocytosed by Sertoli cells.

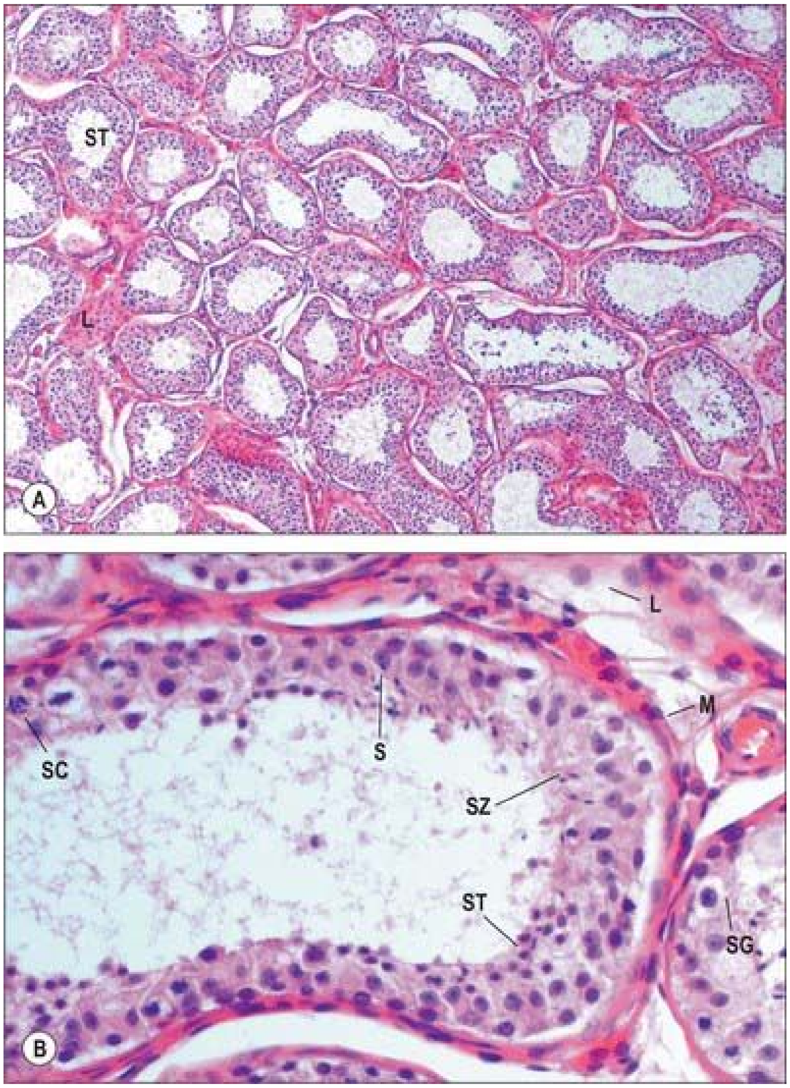

Fig. 76.9 **A**, Seminiferous tubules (ST; cut in various planes of section), and the interstitial tissue (Leydig cells, L) of the testis. The seminiferous tubules are highly convoluted and lined by a stratified epithelium which consists of cells in various stages of spermatogenesis and spermiogenesis (collectively referred to as the spermatogenic series). Non-spermatogenic cells are the Sertoli cells. **B**, Human seminiferous tubule showing the differentiation sequence of spermatozoa from basally situated spermatogonia (SG). Large primary spermatocytes (SC) have characteristic threadlike chromatin in various stages of prophase of the first meiotic division. Smaller haploid spermatids (ST) have round nuclei initially, but mature to possess the dense, elongated nuclei and flagellae of spermatozoa (SZ). Sertoli cells (S) are identified from their oval or pear-shaped nuclei

orientated perpendicular to the basal lamina, and prominent nucleoli. The tubule is surrounded by peritubular myoid cells (M). Clusters of large endocrine Leydig cells (L) are seen in the interstitial connective tissue.

Spermatogonia

Spermatogonia, the stem cells for all spermatozoa, are descended from primordial germ cells which migrate into the genital cords of the developing testis (Fig. 76.9B). In the fully differentiated testis they are located along the basal laminae of the seminiferous tubules. Several types of spermatogonia are recognized on the basis of cell and nuclear dimensions, distribution of nuclear chromatin (dark, condensed or pale, euchromatic) and histochemical and ultrastructural data. The three basic groups of spermatogonia are dark type A (Ad), pale type A (Ap), and type B. Ad cells divide mitotically to maintain the population of spermatogonia which, before puberty, is small but increases under androgenic stimulation. Some divisions give rise to Ap cells which also divide mitotically but remain linked in clusters by fine cytoplasmic bridges. These are the precursors of type B cells, which are committed to the spermatogenic sequence. At about the time that type B cells enter a final round of DNA synthesis, without undergoing cytokinesis, they leave the basal compartment and cross the blood–testis barrier to enter meiotic prophase as primary spermatocytes. These coordinated processes are under the control of Sertoli cells.

Primary and secondary spermatocytes

Primary spermatocytes have a diploid chromosome number but duplicated sister chromatids (DNA content is thus 4N, where N is the DNA content of haploid spermatozoa), and are all at some stage of a long meiotic prophase (p. 22) of approximately 3 weeks. Primary spermatocytes are large cells with large round nuclei in which the nuclear chromatin is condensed into dark, threadlike, coiled chromatids at different stages in the process of crossing over and genetic exchange between chromatids of maternal and paternal homologues. These cells give rise to secondary spermatocytes with a haploid chromosome complement (but 2N DNA content), the reduction division is designated as meiosis I. Few secondary spermatocytes are seen in tissue sections because they rapidly undergo the second meiotic (equatorial) division, where sister chromatids separate (DNA content now being N), to form haploid spermatids. Theoretically each primary spermatocyte produces four spermatids, but some degenerate during maturation so that the yield is lower.

Spermatids

Spermatids do not divide again but gradually mature into spermatozoa by a series of nuclear and cytoplasmic changes known as spermiogenesis. All of these maturational changes take place while the spermatids remain closely associated with Sertoli cells and linked by cytoplasmic bridges with each other. The first phase of spermiogenesis is the Golgi phase, when hydrolytic enzymes accumulate in Golgi vesicles that subsequently coalesce into a single large acrosomal vesicle close to the nucleus. The pair of centrioles migrates to the opposite posterior pole. The distal centriole begins to generate the axoneme, a circular arrangement of nine microtubule doublets surrounding a central pair. In the cap phase, the acrosomal vesicle flattens and envelops the anterior half of the nucleus to form an acrosomal cap which comes to occupy the presumptive anterior pole of the spermatozoon, furthest from the lumen of the tubule.

During the acrosome phase, nuclear chromatin condenses and the nucleus elongates into a spearhead shape. The anterior cytoplasmic volume is considerably reduced, so that the wall of the acrosomal vesicle is brought into contact with the plasma membrane. A perinuclear sheath of microtubules develops from the posterior edge of the acrosome to form the manchette, which extends towards the posterior pole. The axonemal complex continues to extend into the developing tail region, which now protrudes into the tubule lumen. The neck region forms at the posterior pole of the nucleus: it contains the centrioles. Mitochondria migrate through the neck region and along the axoneme into the developing middle piece. Here, they assemble into a helical sheath and surround a ring of nine coarse fibres forming along the length of the axonemal complex in the developing tail. In the final phase of maturation, excess cytoplasm is detached as a residual body that is phagocytosed and degraded by Sertoli cells. During the formation of residual bodies, spermatids lose their cytoplasmic bridges and separate from each other before being released into their tubule.

Spermatozoa

A spermatozoon that is released from the wall of the seminiferous tubule into the lumen is non-motile but structurally mature. Its expanded head contains little cytoplasm and is connected by a short constricted neck to the tail. The tail is a complex flagellum, divided into middle, principal and end pieces, that greatly exceeds the head region in volume. The head has a maximum length of approximately 4 μm and a maximum diameter of 3 μm. It contains an elongated, flattened nucleus with condensed, deeply staining chromatin, and is covered anteriorly by an acrosomal cap. The latter contains acid phosphatase, hyaluronidase, neuraminidase and proteases necessary for fertilization (see p. 168). The neck is approximately 0.3 μm long. In its centre is a well-formed centriole that corresponds to the proximal centriole of the spermatid from which it differentiated. The axonemal complex is derived from the distal centriole. A small amount of cytoplasm exists in the neck, covered by a plasma membrane continuous with that of the head and tail (Fig. 76.10).

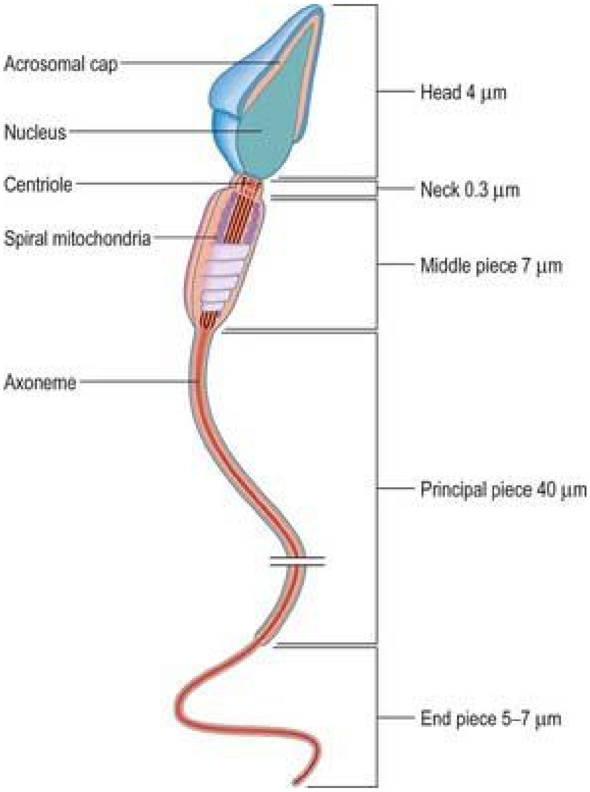
Acrosomal cap
Nucleus
Centriole
Spiral mitochondria
Axoneme
Head 4 µm
Neck 0.3 µm
Middle piece 7 µm
Principal piece 40 µm
End piece 5–7 µm

Fig. 76.10 The main ultrastructural features of a mature spermatozoon.

The middle piece of the tail is a long cylinder, approximately 1 µm in diameter and 7 µm long. It consists of an axial bundle of microtubules, the axoneme, outside which is a cylinder of nine dense outer fibres surrounded by a helical mitochondrial sheath. At the caudal end of the middle piece is an electron-dense body, the anulus. The principal piece of the tail becomes the motile part of the cell. It is approximately 40 µm long and 0.5 µm in diameter and forms the majority of the spermatozoon. The axoneme and the surrounding dense fibres are continuous from the neck region through the whole length of the tail except for its terminal 5–7 µm, in which the axoneme alone persists. The tail therefore has the typical structure of a flagellum, with a simple nine plus two arrangement of microtubules, in the terminal portion of the end piece.

Sertoli cells

Sertoli cells form a major cellular component of the tubule before puberty, and in the elderly. They are the supporting, non-spermatogenic cells of the seminiferous tubules. Variable in overall cell shape, they all contact the basal lamina and their cytoplasm extends to the tubule lumen where their apical plasma membranes form complex recesses which envelop spermatids and spermatozoa until the latter are mature enough for release. Long cytoplasmic processes also extend between the spermatogonia in the basal compartment and spermatocytes in the adluminal compartment of the tubule. Adjacent Sertoli cell processes are joined at this level by tight junctions, creating a diffusion barrier between the extratubular and intratubular compartments. This is the blood–testis barrier which, if breached by traumatic or inflammatory events, can allow immune responses to develop against sperm antigens, resulting in subfertility.

The Sertoli cell nucleus is euchromatic and irregular or pear-shaped, contains one or two prominent nucleoli, and is usually aligned perpendicular to the basal lamina. The cytoplasm is rich in lysosomes, consistent with its phagocytic phenotype. Sertoli cells provide trophic support for the surrounding germ cells, secrete androgen-binding protein and play an important role in controlling spermatocyte and spermatid differentiation and maturation. The proteinaceous fluid they secrete into the tubule lumen provides nutrients and facilitates the transport of spermatozoa into the excurrent duct system. Sertoli cells change considerably during the spermatogenic cycle and respond to the hypophysial hormones, luteinizing hormone (LH) and follicle-stimulating hormone (FSH). They also produce a hormonal substance, inhibin B, which is thought to be involved in local paracrine functions.

Spermatogenic cycle

At any locus in a seminiferous tubule, generation of germ cells occurs in a cycle with a periodicity of approximately 16 days. Stages in the cycle are characterized by the presence of different combinations of cells within the spermatogenic sequence. The generation of a mature spermatozoon from a spermatogonium takes four such cycles, or approximately 64 days. In cross-section, the seminiferous tubule shows more than one phase of the cycle around its circumference, because waves of progression through a spermatogenic cycle occur in spirals down the length of the tubule.

Testicular interstitial tissue

The tissues between the seminiferous tubules include various connective tissue components, peritubular myoid cells, vessels and nerves. The myoid cells are contractile: their rhythmic activity may propel non-motile spermatozoa through the tubule towards the rete testis and excurrent ductal system. Clusters of Leydig cells lie between the tubules. These large, polyhedral cells have eccentric nuclei with one to three nucleoli and pale staining cytoplasm containing a considerable amount of smooth endoplasmic reticulum, lipid droplets and unique needle-shaped crystalloid inclusions up to 20 μm long (crystals of Reinke), of unknown function. Leydig cells synthesize and secrete androgens and are stimulated by LH and by prolactin, which induces expression of the LH receptor. Their activity varies with age: they are active in fetal life in the development of the genital tract, but decline in function postpartum until the onset of puberty.

Age-related changes in the testis

Functionally, the fetal testis is predominantly an endocrine gland that produces testosterone and the anti-Müllerian hormone, a specifically fetal gonadal hormone. These two hormones play crucial roles in the induction and regulation of male sexual differentiation. Postnatally the testis gradually changes its role, but retains the ability to manufacture testosterone and other regulatory materials, e.g. the peptide hormone oxytocin, that act in either an endocrine or a paracrine fashion.

The seminiferous tubules do not become canalized until approximately the seventh month of gestation, although this may occur later. At puberty, the testis becomes primarily a source of spermatozoa. The fetal Leydig cells, responsible for the androgen-induced differentiation of the male genitalia, degenerate after birth, and are replaced, during puberty, by an adult population of androgen-producing cells that persist throughout adult life. The testes grow slowly until the age of 10 or 11 years, at which time there is a marked acceleration of growth rate, and spermatogenesis begins.

There is no definite age for the onset of the progressive testicular involution associated with advancing age. Testicular size, sperm quality and quantity, and the numbers of Sertoli cells and Leydig cells, have all been reported to decrease in the elderly. Leydig cell activity is driven by LH. The decrease in Leydig cell function in the elderly, as part of what has been described as the normal ageing process, may be affected by changes in the secretion of LH, which is controlled by the hypothalamus. The volume occupied by the seminiferous tubules decreases, whereas that occupied by interstitial tissue remains approximately constant. The most frequently observed histological change in the ageing testis is variation in spermatogenesis in different seminiferous tubules: it is complete, though reduced, in some, but absent in others, when sclerosis may occur. In tubules where spermatogenesis is complete, morphological abnormalities, e.g. multinucleation, may be observed in the germ cells.

Germ cell loss generally begins with the spermatids, but progressively affects the earlier germ cell types, i.e. the spermatocytes and spermatogonia. Sertoli cells are also affected by ageing, and show a range of morphological changes including dedifferentiation, mitochondrial metaplasia and multinucleation. In the Leydig cells, the quantity of smooth endoplasmic reticulum and mitochondria decrease, and lipid droplets, crystalline inclusions and residual bodies increase; some cells become multinucleate. Tubules in which the entire epithelium has been lost have been observed in testes where other tubules appeared normal. The development of tubular involution with advancing age is similar to that observed after experimental ischaemia, suggesting that vascular lesions may be involved in age-related testicular atrophy. However, there is no abrupt change in testicular function equivalent to the female climacteric.

Undescended testis

In the early fetal period the testes are located posteriorly in the abdominal cavity. Their descent to the scrotum appears to be under hormonal control (gonadotropins and androgens) (see p. 1320). Testicular descent may be arrested at any point along its route into the scrotum: a clinically undescended testis may be in the abdomen, at the deep inguinal ring, in the inguinal canal, or between the superficial inguinal ring and the scrotum. Occasionally, the testis may lie outside its normal path of descent and is termed an ectopic testis.

A unilateral undescended testis is present in 3% of boys at birth and 1% of boys by 3 months of age. Bilateral maldescent is seen in just over 1% of male births. Undescended testes can be associated with a higher risk of infertility and testicular tumours. There is evidence that surgical correction of an undescended testis at any age may not improve its spermatogenesis. Impairment of fertility can be seen in men with both bilateral and unilateral undescended testis. Leydig cell function is not usually affected by maldescent, so androgen production usually remains within the normal range. Patients with an undescended testis are at increased risk of developing testicular tumours, particularly seminoma. The risk is highest in abdominal testes. Surgery may not reduce the risk of tumour development, but maximizes the chance of early detection of any tumour. An undescended testis can usually be found by ultrasonography if it is in or close to the inguinal canal. Laparoscopy is more reliable in the pelvis. Magnetic resonance imaging may help localizing testis not seen on ultrasound. Retention in the inguinal canal is often complicated by congenital hernia, because the processus vaginalis remains patent. The testis may traverse the canal but reach an abnormal site.

Obliterated part of the processus vaginalis

The obliterated part of the processus vaginalis is often seen as a fibrous thread in the anterior part of the spermatic cord, extending from the internal end of the inguinal canal – where it is connected to the peritoneum – as far as the tunica vaginalis. Sometimes it disappears within the cord. However, its proximal part may remain patent, so that the peritoneal cavity communicates with the tunica vaginalis, or the proximal processus may persist, although it may be shut off distally from the tunica. Occasionally its cavity may persist at an intermediate level as a cyst. When patent, its cavity may admit a loop of intestine, to form an indirect inguinal hernia. The processus is usually obliterated by 18 months of age.

Hydrocele, spermatocele, epididymal cyst

In congenital hydrocele the fluid is in the tunical sac, which communicates with the peritoneal cavity through a non-obliterated processus vaginalis. Infantile hydrocele occurs when the processus is obliterated only at or near the deep inguinal ring. It resembles vaginal hydrocele, but fluid extends up the cord into the inguinal canal. If the processus is obliterated at both the deep inguinal ring and above the epididymis, leaving a central open part, this may distend as an encysted hydrocele of the cord. A spermatocele is a cyst related to the caput epididymis: it may contain spermatozoa and it is probably a retention cyst of one of the seminiferous tubules. Removal is usually unnecessary and may result in epididymal obstruction. The same applies to a simple epididymal cyst, which may have a similar aetiology to a spermatocele but remains free of sperm.

Testicular and epididymal appendices

At the upper extremities of the testis and epididymis are two small, stalked bodies, the appendix testis and appendix epididymis (Fig. 76.5A,B). They are developmental remnants of the paramesonephric (Müllerian) duct and the mesonephros, respectively. They may undergo torsion and produce symptoms that are difficult to differentiate from testicular torsion.

Testicular torsion

The testis and epididymis are usually fixed to their surrounding tissues. In some patients this fixation may be insufficient, so that the structures are able to twist within the tunica vaginalis. This is termed testicular torsion and normally results in severe scrotal pain, which is a surgical emergency.

Torsion produces an initial venous infarction followed by arterial occlusion: histopathological changes leading to gangrene occur in the testis if the twist is not reversed within 4–6 hours. Fertility may be affected by an episode of torsion. Other structures may also twist within the scrotum, e.g. the testicular appendix (otherwise termed the hydatid of Morgagni) and the appendix epididymis: torsion of these structures may also result in scrotal pain.

Male sub-fertility

Approximately one in seven couples will find difficulty in conceiving. In approximately 10% of couples the cause for their sub-fertility will be unknown: in 50% of couples, the reason will be due to male factors. A seminal analysis may demonstrate a spectrum of abnormalities from complete absence of sperm in the ejaculate (azoospermia) to too few sperm (oligozoospermia).

The causes of azoospermia are extensive but broadly can be classified into obstructive causes (rare) or testicular failure. Occasionally spermatogenesis may be arrested at a specific point in development, a condition known as maturation arrest.

Testicular failure is usually testicular in origin. It may have an underlying genetic aetiology, or may occur secondary to damage to the testis such as occurs following radiation therapy, torsion, trauma to the testis or undescended testis. Testicular failure resulting from these conditions may be associated with an increase in pituitary FSH and LH (hypergonadotrophic hypogonadism). Rarely, testicular failure may be the result of pituitary or hypothalamic damage leading to hypogonadotrophic hypogonadism. Histopathologically, testicular failure may be characterized by a spectrum of histopathological findings from Sertoli-cell-only syndrome (see Fig. 76.12) to varying degrees of hypospermatogenesis. Testicular sperm can be extracted from some men and injected into their partners’ eggs, a process known as intra-cytoplasmic sperm injection (ICSI).

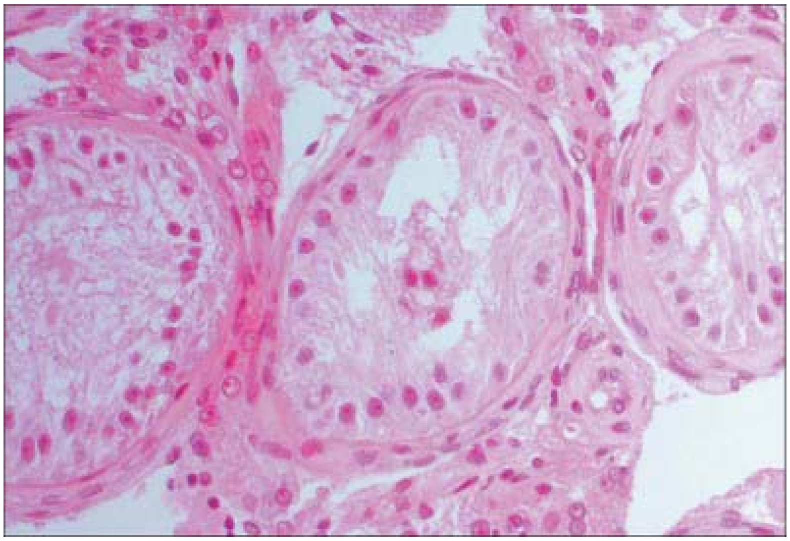

Fig. 76.12 Testis biopsy from a patient with azoospermia demonstrating Sertoli-cell-only syndrome. Only the Sertoli cells are present: this condition may also be caused by a deletion on the Y chromosome.

EPIDIDYMIS

The epididymis lies posteriorly and slightly lateral to the testis, and the vas deferens lies along its medial side (Fig. 76.5A,B). It has an expanded head or globus major superiorly, a body (corpus) and a tail (cauda or globus minor). The epididymis is invested by tunica vaginalis, somewhat less closely applied than it is to the testis, except at its posterior margin. Laterally there is a deep groove, the sinus epididymis, between the epididymis and the testis. The vas deferens ascends from the tail of the epididymis to the deep inguinal ring, lying within the spermatic cord (see below).

Microstructure

Spermatogenesis occurs in the highly coiled parts of the seminiferous tubules. As the latter reach the apical part of the lobule towards the mediastinum they become much less convoluted and form the short tubuli recti, lined by cuboidal epithelium that lacks spermatogenic cells. Tubuli recti enter the fibrous tissue of the mediastinum testis as a close network of anastomosing tubes, the rete testis, lined by a flat epithelium. At the upper pole of the mediastinum, 12–20 efferent ductules (ductuli efferentes) perforate the tunica albuginea and leave the testis for the epididymis. The efferent ductules are lined by a ciliated columnar epithelium that also contains shorter, actively endocytic, non-ciliated cells. External to the epithelium, the ductules are surrounded by a thin circular coat of smooth muscle (Fig. 76.11).

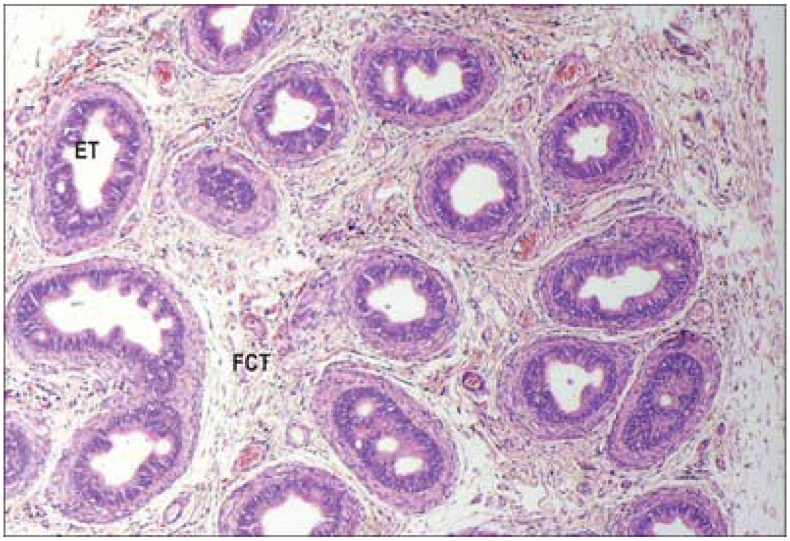

Fig. 76.11 Microstructure of the epididymis. ET, epididymal tubule; FCT, fibromuscular connective tissue.

Initially the ductules are straight. They become enlarged and very convoluted, forming the conical lobules of the epididymis that make up its head. Each lobular duct, 15–20 cm in length, opens into the single duct of the epididymis, whose coils form the epididymal body and tail. When the coils are unravelled, the tube measures more than 6 metres, increasing in thickness as it approaches the epididymal tail, where it becomes the vas deferens. The coils are held together by bands of fibrous connective tissue. In the epididymal duct the muscle is thicker and the epithelium is composed of columnar pseudostratified cells. The muscle undergoes peristaltic contractions to propel spermatozoa towards the tail region, where they are stored.

Epithelium

The epithelium contains two main cell types, principal and basal cells, and the less common apical and clear cells. Principal cells are tall columnar cells with basally located, elongated, oval nuclei. They bear long (15 µm) regular apical microvilli termed stereocilia, so named because they were once thought to be immotile cilia. These cells resorb fluid from the testicular secretions: approximately 90% of the total is absorbed in the epididymis.

They also secrete glycoproteins essential for the maturation of spermatozoa and endocytose various other components of the seminal fluid. Basal cells lie between the bases of the principal cells and are thought to be the precursors of principal cells. Apical cells have numerous mitochondria and are most abundant in the head of the epididymis. Clear cells are columnar cells, most numerous in the tail region, and have few microvilli but numerous endocytic vesicles and lipid droplets: their functions are unknown.

VAS DEFERENS, PARADIDYMIS AND EJACULATORY DUCT

VAS DEFERENS

The vas deferens is the distal continuation of the epididymis, starting as a muscular tube at the epididymal tail. It is 45 cm long and conveys sperm to the ejaculatory ducts (Fig. 76.5A,B). Initially very tortuous, the convoluted portion of the vas becomes straighter as it ascends along the posterior aspect of the testis, medial to the epididymis. From the superior pole of the testis it ascends in the posterior part of the spermatic cord, and traverses the inguinal canal. At the deep inguinal ring the vas deferens leaves the cord, curves round the lateral side of the inferior epigastric artery and ascends for approximately 2.5 cm anterior to the external iliac artery. It then turns back and inclines slightly down and obliquely across the external iliac vessels to enter the lesser pelvis. In the pelvis it is situated retroperitoneally, coursing posteriorly and medially to the obliterated umbilical artery, the obturator nerve and vessels, and the vesical vessels. It crosses the ureter and bends acutely to pass anteromedially between the posterior surface of the bladder and the upper pole of the seminal vesicle. It then descends in contact with the seminal vesicle, gradually approaching the opposite duct, lying between the base of the bladder and the rectum, from which it is separated by Denonvillier's fascia. At the base of the prostate, the vas deferens joins the duct of the seminal vesicle at an acute angle to form the ejaculatory duct. It feels cord-like when grasped because of its thick wall and small lumen. Posterior to the bladder the lumen becomes dilated and tortuous and is termed the ampulla; beyond this, where it joins the duct of the seminal vesicle, it is again greatly diminished in calibre. In men with azoospermia or no sperm in the ejaculate, testicular exploration may be undertaken to exclude an obstruction.

The vasa deferentia may be congenitally absent, a condition known as vasal aplasia. This can occur in association with cystic fibrosis: men with congenital absence of the vas deferens should be screened for cystic fibrosis mutations. This condition results in azoospermia, although spermatogenesis is usually normal.

Aberrant ductules

A narrow, blind, caudal aberrant ductule often occurs, usually connected with the caudal part of the epididymal duct or with the start of the vas deferens. Uncoiled, it varies in length from 5 to 35 cm; it may be dilated near its end, but is otherwise uniform in calibre and in structure is similar to the vas deferens. Occasionally it is not connected with the epididymis. A rostral aberrant ductule may occur in the epididymal head, connected with the rete testis. Aberrant ductules are derived from mesonephric tubules (see p. 1305).

PARADIDYMIS

The paradidymis is a small collection of convoluted tubules, found anteriorly in the spermatic cord above the epididymal head. The tubules are lined by ciliated columnar epithelium and probably represent the remains of the mesonephros (see p. 1305).

EJACULATORY DUCTS

The ejaculatory ducts are formed on each side by the union of the duct of the seminal vesicle with the ampulla of the vas deferens. Each is almost 2 cm in length, and starts from the base of the prostate, running anteroinferiorly between its median and right or left lobes. They skirt the prostatic utricle to end on the verumontanum at two slit-like orifices on, or just within, the utricular opening. The ducts diminish and converge towards their ends. Ejaculatory duct obstruction is rare and can lead to azoospermia or severe oligozoospermia: it may be caused by congenital cysts such as Müllerian duct cysts.

Vascular supply, lymphatic drainage and innervation

Each vas deferens has its own artery, usually derived from the superior vesical artery, which anastomoses with the testicular artery to supply the epididymis and testis. Veins drain from the vas deferens and seminal vesicles to the pelvic venous plexus. Lymphatic vessels drain to the external and internal iliac nodes. The vasa deferentia are innervated by a rich autonomic plexus composed mainly of sympathetic nerve fibres derived from the pelvic plexus.

Microstructure

The wall of the vas deferens has loose connective tissue externally, a thick middle muscular layer and an internal mucosal layer. The muscular layer is composed of smooth muscle fibres arranged in external longitudinal and internal circular sheets. An additional internal longitudinal layer is present at the origin of the duct where it leaves the tail of the epididymis, and all muscle layers intermingle. The mucosa is folded longitudinally and its epithelium is columnar and non-ciliated through most of the duct. Towards its distal end a pseudostratified columnar epithelium appears, the tallest cells of which bear non-motile stereocilia (elongated microvilli), similar to those of the epididymis. The connective tissue of the lamina propria contains elastic fibres (Fig. 76.13A,B).

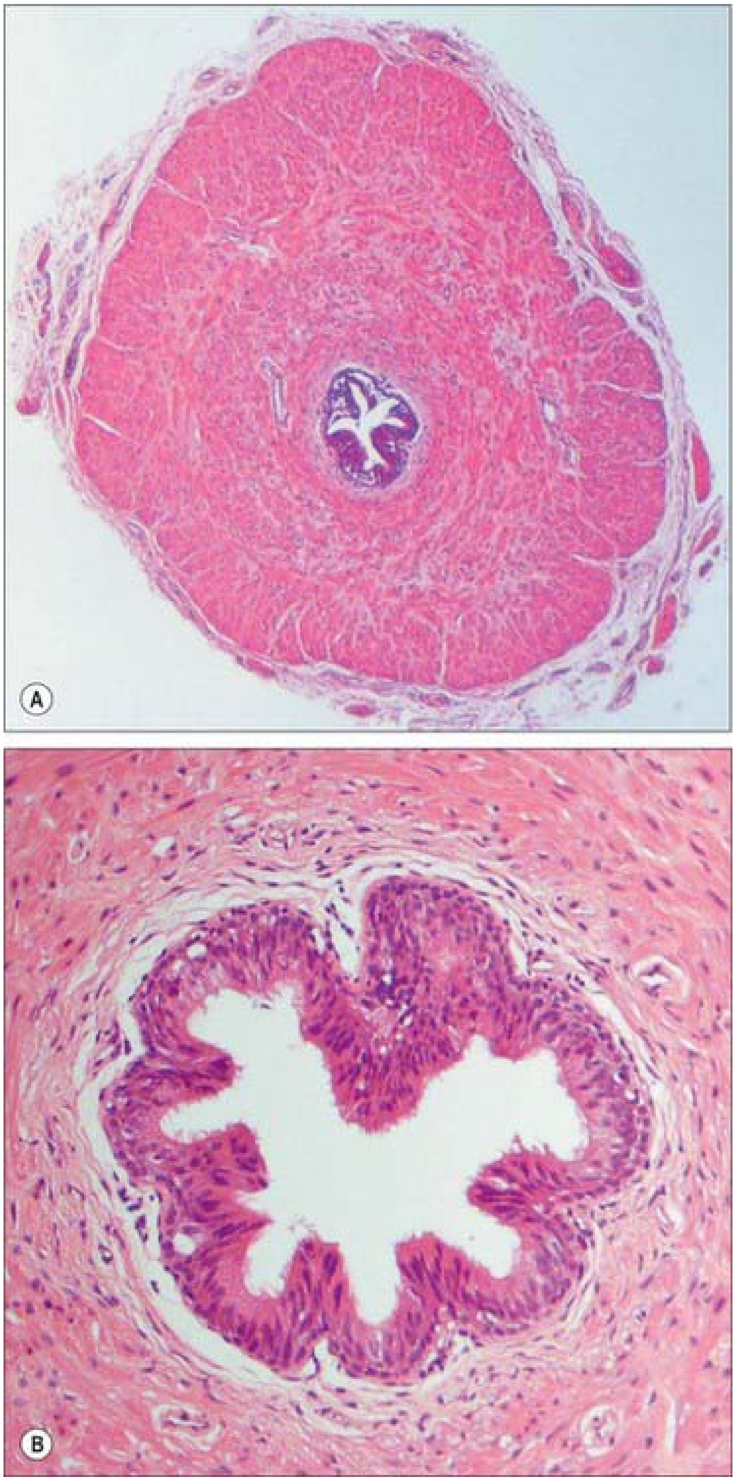

Fig. 76.13 Vas deferens. **A**, Low power view, transverse section. **B**, Higher power view. The convoluted lumen is lined by pseudostratified columnar epithelial cells.

The walls of the ejaculatory ducts are thin. They contain an outer fibrous layer, which is much reduced beyond their entrance into the prostate, a thin layer of smooth muscle fibres with an outer circular and inner longitudinal orientation, and a mucosa lined by columnar epithelium. The ducts dilate during ejaculation.

Maturation of spermatozoa

Functional maturation is a complex process. Spermatozoa show little independent motility while still in the male genital tract: when removed from the epididymis they may display circular or even forward directional movements if taken from the cauda epididymis near the beginning of the vas deferens. Apart from this immature motility, spermatozoa are largely transported through the genital tract initially by ciliary action and then by peristaltic contractions of the duct walls. Human spermatozoa do not undergo any demonstrable structural changes during their passage through the epididymis, but there is evidence of biochemical and functional modifications. Evidence from restorative surgery after vasectomy indicates that at least part of the human epididymis is essential for acquisition of mature motile activity.

ACCESSORY GLANDULAR STRUCTURES

SEMINAL VESICLES

The two seminal vesicles are sacculated, contorted tubes located between the bladder and rectum. Each vesicle is approximately 5 cm long, somewhat pyramidal, the base being directed up and posterolaterally. In essence, the seminal vesicle is a single coiled tube with irregular diverticula, the coils and diverticula being connected by fibrous tissue. The diameter of the tube is 3–4 mm and its uncoiled length is 10–15 cm. The upper pole is a cul-de-sac, the lower narrows to a straight duct which joins the vas deferens to form the ejaculatory duct. The anterior surface contacts the posterior aspect of the bladder, and extends from near the entry of the ureter to the prostatic base: the prostate is intimately located to the seminal vesicles (Fig. 76.14A,B; see Fig. 74.21). The posterior surface is related to the rectum, from which it is separated by Denonvillier’s fascia. The seminal vesicles diverge superiorly. On each side they are related to the vas deferens and the termination of the ureter, and they are partly covered by peritoneum. Each has a dense, fibromuscular sheath. The ampulla of the vas deferens lies along the medial margin of each seminal vesicle and the veins of the prostatic venous plexus, which drain posteriorly to the internal iliac veins, lie laterally.

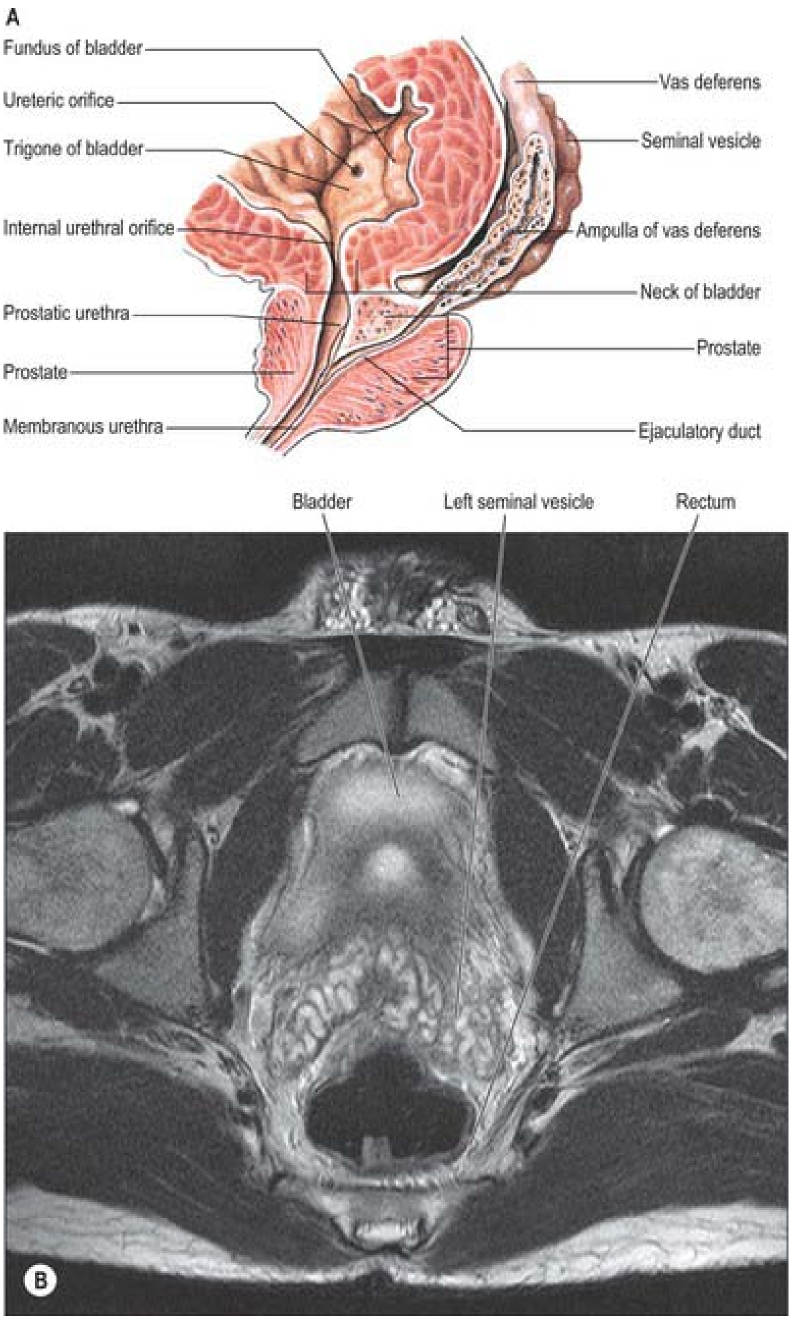
A
Fundus of bladder
Ureteric orifice
Trigone of bladder
Internal urethral orifice
Prostatic urethra
Prostate
Membranous urethra
Vas deferens
Seminal vesicle
Ampulla of vas deferens
Neck of bladder
Prostate
Ejaculatory duct
Bladder
Left seminal vesicle
Rectum
B

Fig. 76.14 **A**, Urinary bladder, prostate, vas deferens, seminal vesicles, oblique section to expose opening of the left ejaculatory duct into the urethra. The thickness of the muscular layer of the bladder indicates a contracted empty bladder. **B**, Axial MRI scan demonstrating the normal high signal in the seminal vesicles on a T2-weighted scan.

*(**A** from Sobotta 2006.)*

Vascular supply, lymphatic drainage and innervation

The arteries to the seminal vesicles are derived from the inferior vesical and middle rectal arteries. The veins and lymphatics accompany these arteries. The innervation of the seminal vesicles and bulbourethral glands is derived from the pelvic plexuses.

Microstructure

The paired seminal vesicles, together with the ampulla of the vas deferens and the ejaculatory ducts, form a functional unit which develops slowly until the onset of puberty. After puberty the vesicles form sac-like structures which contribute up to 85% of the seminal fluid. They are mainly concerned with secretion of seminal coagulating proteins, fructose, prostaglandins and other specific proteins in an alkaline, viscous yellowish fluid.

The wall of the seminal vesicle is composed of an external connective tissue layer, a middle smooth muscle layer (thinner than in the vas deferens and arranged in external longitudinal and internal circular layers) and an internal mucosal layer with a highly folded, labyrinthine structure (Fig. 76.15). The cuboidal to pseudostratified columnar epithelium of the mucosa shows features typical of protein-secreting cells. The vesicles are not reservoirs for spermatozoa as their name suggests, because spermatozoa are stored mainly in the epididymis. They contract during ejaculation, and their secretion forms most of the ejaculate.

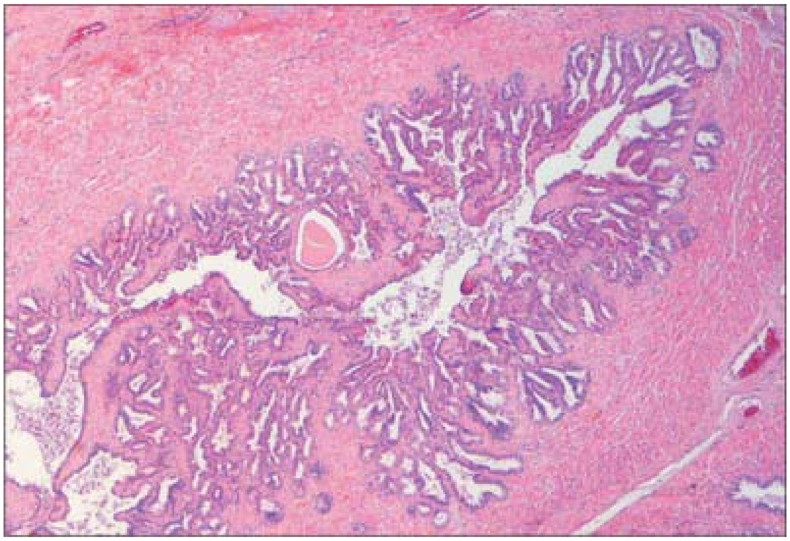

Fig. 76.15 Microstructure of the seminal vesicles showing tubulo-acinar structure.

BULBOURETHRAL GLANDS

The two bulbourethral glands are small, round, yellow, somewhat lobulated masses approximately 1 cm in diameter. They lie lateral to the membranous urethra above the perineal membrane and penile bulb and are enclosed by fibres of the urethral sphincter. The excretory duct of each, almost 3 cm long, passes obliquely forwards external to the mucosa of the membranous urethra and penetrates the perineal membrane. It opens by a minute orifice on the floor of the bulbar urethra, approximately 2.5 cm below the perineal membrane. In later decades the glands generally diminish in size.

Microstructure

Each bulbourethral gland consists of several lobules held together by a fibrous capsule. The secretory units are mainly tubulo-alveolar in form. The glandular epithelium is columnar and secretes acid and neutral mucins into the penile (spongiose) urethra prior to ejaculation: these have a lubricating function. The main secretory duct is lined by a stratified columnar epithelium. Diffuse mucosa-associated lymphoid tissue (MALT) is associated with the glands.

PENIS

The penis consists of an attached root (radix) in the perineum and a free, pendulous, body (corpus), which is completely enveloped in skin.

Skin

The penile skin is thin and loosely connected to the tunica albuginea. At the corona of the penis it is folded to form the prepuce or foreskin, which invariably overlaps the glans. The internal preputial layer is confluent at the neck with the thin skin covering and adhering firmly to the glans, and by this with the urethral mucosa at the external urethral orifice. On the urethral aspect of the glans a median fold, the frenulum, passes from the deep surface of the prepuce to the glans immediately proximal to the orifice. Cutaneous sensitivity is greatest over the glans penis. The prepuce and glans penis enclose a potential cleft, the preputial sac, and two shallow fossae flank the frenulum (Fig. 76.16).

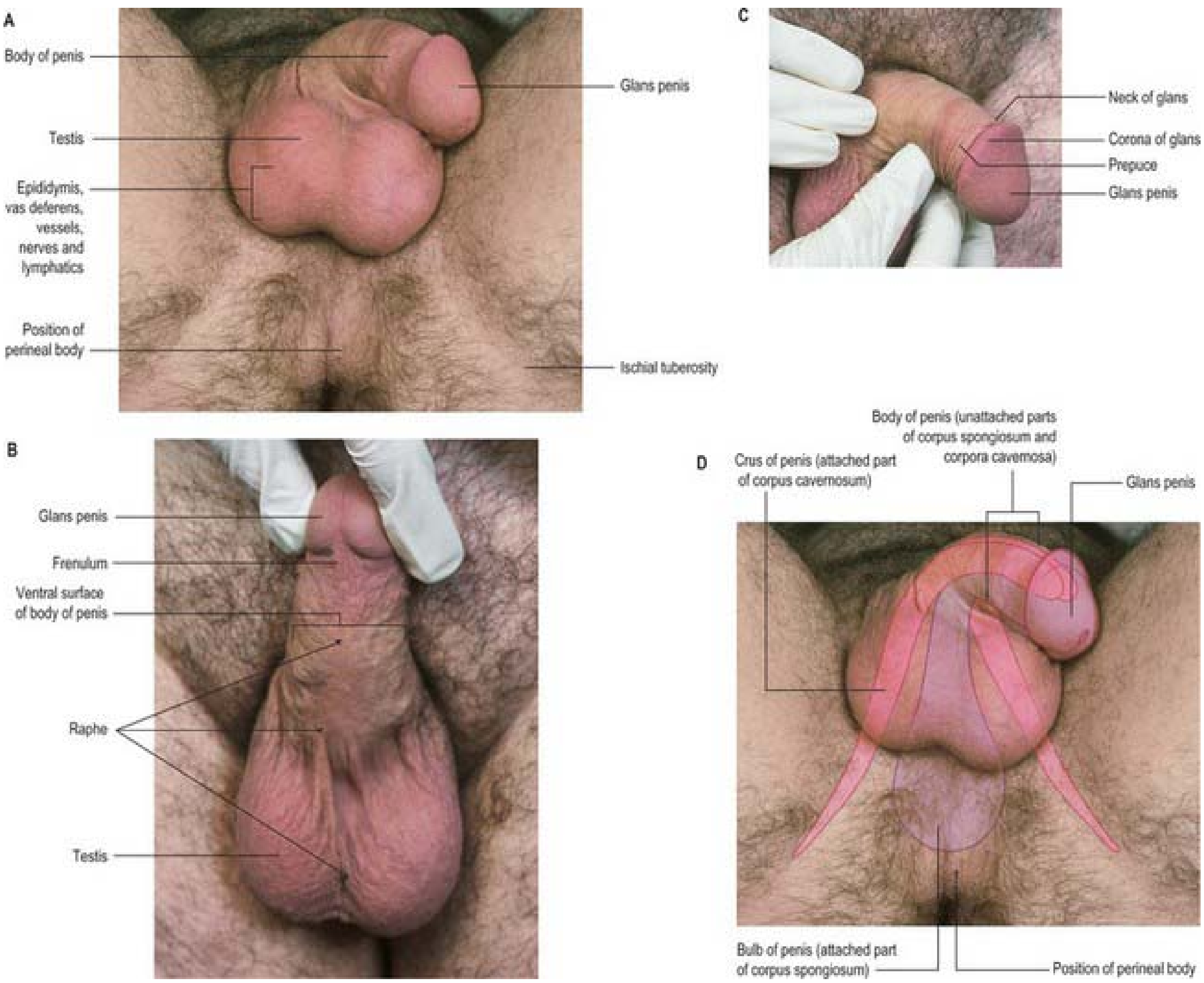
A
Body of penis
Testis
Epididymis, vas deferens, vessels, nerves and lymphatics
Position of perineal body
Glans penis
Ischial tuberosity
B
Glans penis
Frenulum
Ventral surface of body of penis
Raphe
Testis
C
Neck of glans
Corona of glans
Prepuce
Glans penis
D
Crus of penis (attached part of corpus cavernosum)
Body of penis (unattached parts of corpus spongiosum and corpora cavernosa)
Glans penis
Bulb of penis (attached part of corpus spongiosum)
Position of perineal body

Fig. 76.16 Structures in the male urogenital triangle. **A**, Inferior view. **B**, Ventral surface of the body of the penis. **C**, Lateral view of the body of the penis and glans. **D**, Inferior view of the urogenital triangle of a man with the erectile tissues of the penis indicated with overlays.

(From Drake, Vogl and Mitchell 2005.)

Root

The root of the penis consists of three masses of erectile tissue in the urogenital triangle, namely the two crura and the bulb, which are firmly attached to the pubic arch and perineal membrane respectively. The crura are the posterior extremities of the corpora cavernosa, and the bulb is the dilated posterior end of the corpus spongiosum.

Each penile crus starts behind as a blunt, elongated but rounded structure, attached firmly to the everted edge of the ischiopubic ramus and covered by ischiocavernosus (Fig. 76.17). Anteriorly it converges towards the contra-lateral crus and is slightly enlarged posterior to this. Near the inferior symphysial border the two crura come together and continue as the corpora cavernosa of the body of the penis.

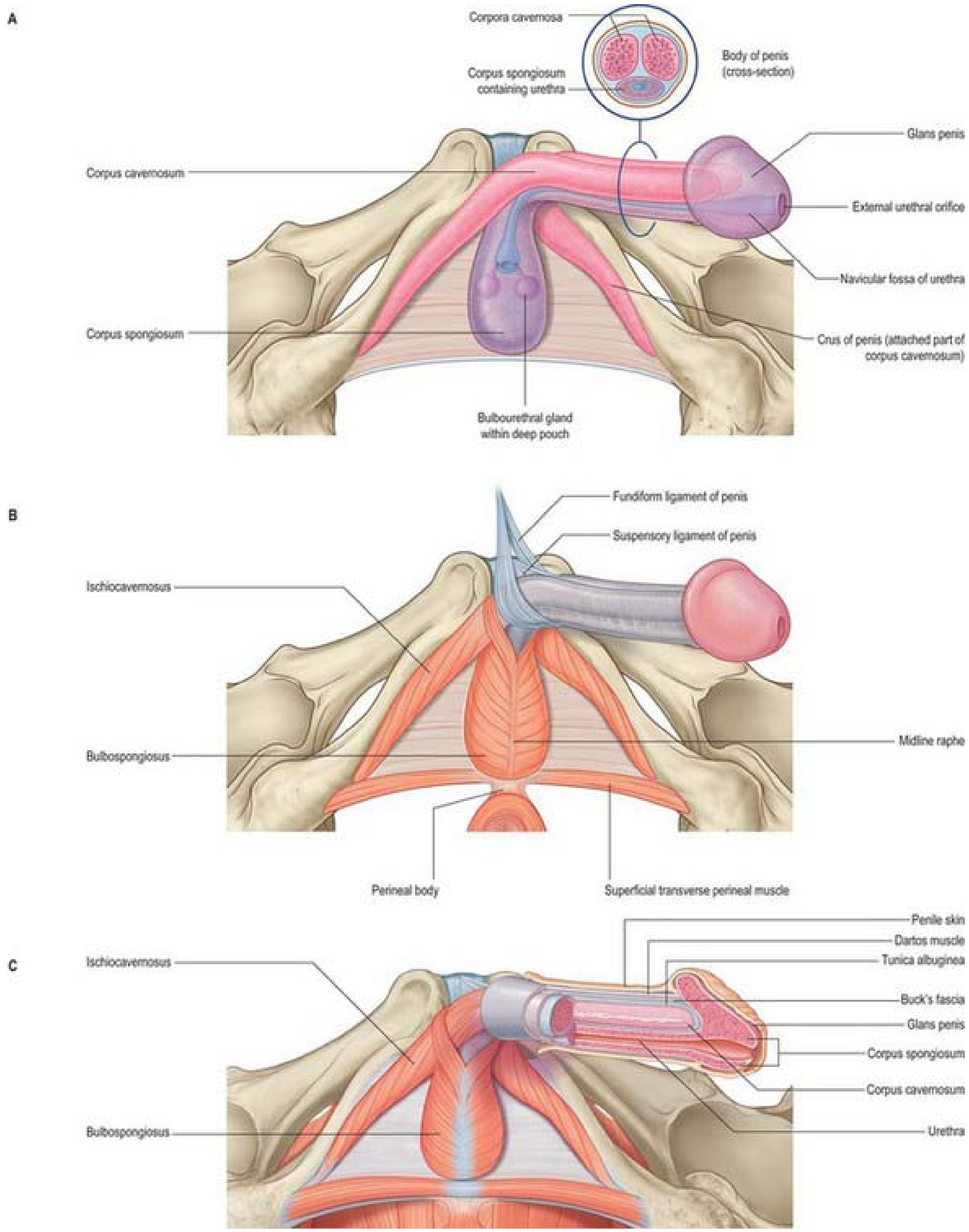
A
Corpora cavernosa
Corpus spongiosum containing urethra
Body of penis (cross-section)
Glans penis
Corpus cavernosum
External urethral orifice
Navicular fossa of urethra
Corpus spongiosum
Crus of penis (attached part of corpus cavernosum)
Bulbourethral gland within deep pouch
B
Fundiform ligament of penis
Suspensory ligament of penis
Ischiocavernosus
Bulbospongiosus
Midline raphe
Perineal body
Superficial transverse perineal muscle
C
Penile skin
Dartos muscle
Tunica albuginea
Ischiocavernosus
Buck's fascia
Glans penis
Corpus spongiosum
Corpus cavernosum
Bulbospongiosus
Urethra

Fig. 76.17 **A**, Erectile tissues of the penis. **B**, Muscles in the superficial perineal pouch. **C**, Muscles and erectile tissues of the penis in section.

*(**A** and **B** from Drake, Vogl and Mitchell 2005; **C** adapted from Drake, Vogl, Mitchell, Tibbitts and Richardson 2008.)*

The bulb of the penis lies between the crura and is firmly connected to the inferior aspect of the perineal membrane, from which it receives a fibrous covering (Figs 76.16D, 76.17). Oval in section, the bulb narrows anteriorly into the corpus spongiosum, down and forwards at this point. Its convex superficial surface is covered by bulbospongiosus and its flattened deep surface is pierced above its centre by the urethra, which traverses it to reach the corpus spongiosum.

Body

The main body of the penis consists of three masses of erectile tissue, the right and left corpora cavernosa, and the median corpus spongiosum, which are continuations of the crura and bulb of the penis respectively (Figs 76.17A, 76.18A,B). They become engorged with blood during penile erection (Fig. 76.19A). The penis is cylindrical when flaccid, but becomes triangular when erect. The surface which is posterosuperior during erection is termed the dorsum of the penis and the opposite aspect is the ventral surface.

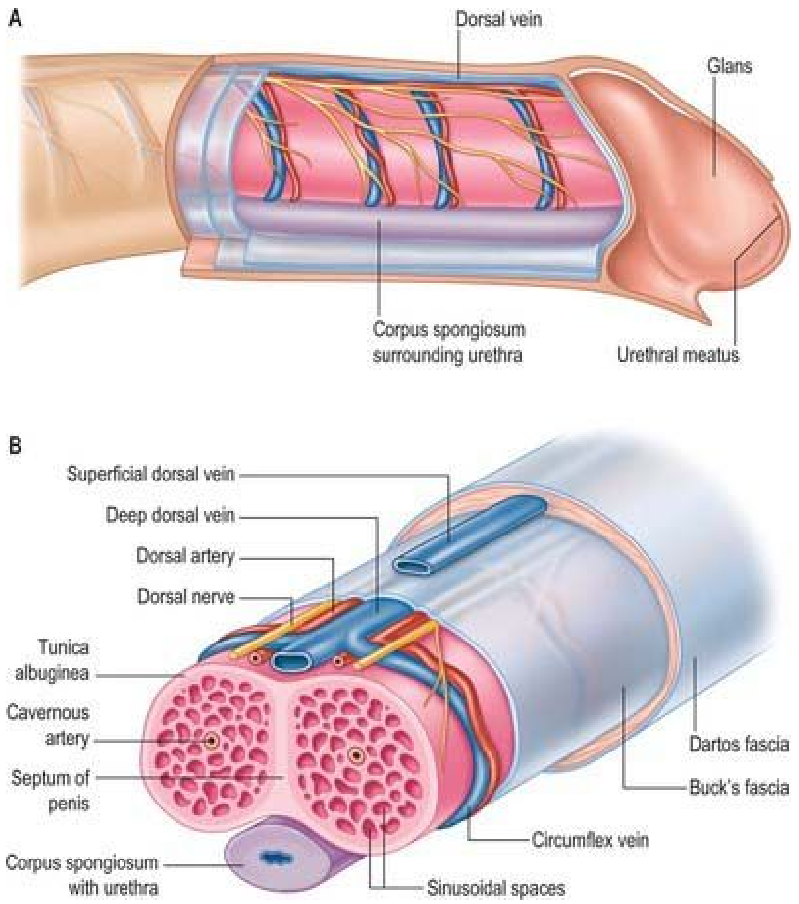
A
Dorsal vein
Glans
Corpus spongiosum surrounding urethra
Urethral meatus
B
Superficial dorsal vein
Deep dorsal vein
Dorsal artery
Dorsal nerve
Tunica albuginea
Cavernous artery
Septum of penis
Corpus spongiosum with urethra
Sinusoidal spaces
Circumflex vein
Dartos fascia
Buck's fascia

Fig. 76.18 **A**, Layers of the penis and main structures. **B**, Cross section of the body of the penis.

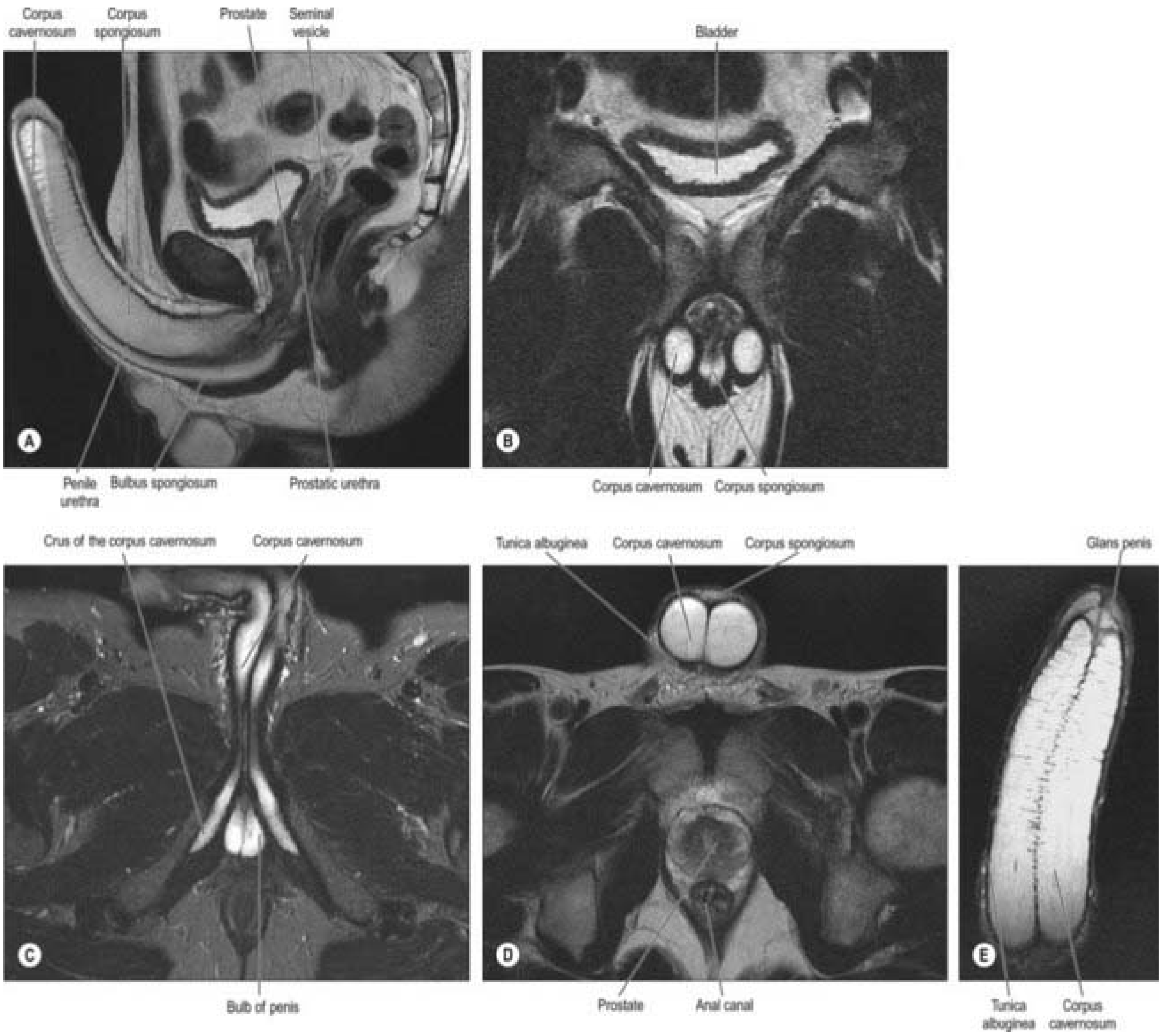
Corpus cavernosum
Corpus spongiosum
Prostate
Seminal vesicle
Bladder
A
B
Penile urethra
Bulbus spongiosum
Prostatic urethra
Corpus cavernosum
Corpus spongiosum
Crus of the corpus cavernosum
Corpus cavernosum
Tunica albuginea
Corpus cavernosum
Corpus spongiosum
Glans penis
C
D
E
Bulb of penis
Prostate
Anal canal
Tunica albuginea
Corpus cavernosum

Fig. 76.19 **A,B**, MRI scan of the penis showing the corpora cavernosum and spongiosum. Note the corpus spongiosum flaring posteriorly into the bulbus spongiosum. **C**, MRI scan showing the bulb of the penis and the attachment of the posterior portion of the corpora cavernosa, the crura. **D,E**, MRI scan of the penis showing the tunica albuginea.

Corpora cavernosa

The corpora cavernosa form most of the body of the penis. They share a common fibrous envelope, the tunica albuginea, and are in close apposition throughout their length, although separated by a median fibrous septum. On the urethral surface their combined mass has a wide median groove that adjoins the corpus spongiosum (Figs 76.17-76.19); dorsally a similar but narrower groove contains the dorsal neurovascular bundle. The corpora end distally within the proximal aspect of the glans penis in a rounded cone, in which each has a small terminal projection (Fig. 76.16D).

The strong fibrous tunica albuginea consists of superficial and deep strata. The superficial fibres run longitudinally, forming a single tube that surrounds both corpora, whereas the deep fibres are circularly arranged and surround each corpus separately. The deep fibres join to form the median septum of the penis. This is thick and complete proximally, so that the corporal bodies can be separated proximally for 5–7 cm. Distally the median septum consists of a pectiniform (comb-like) series of bands, the pectiniform septum, which is incomplete and allows cross-circulation of blood between the two corpora.

Corpus spongiosum

The corpus spongiosum of the penis is traversed by the urethra (Figs 76.17A, 76.18B, 76.19). It adjoins the median groove on the urethral surface of the conjoined corpora cavernosa. It is cylindrical, tapering slightly distally, and surrounded by a tunica albuginea. Near the end of the penis it expands into the glans penis which projects dorsally over the end of the corpora cavernosa and has a shallow concave surface to which they are attached. The corona glandis projects from its base, overhanging an obliquely grooved neck of the penis. Numerous small preputial glands on the corona glandis and penile neck secrete sebaceous smegma. The navicular fossa of the urethra is in the glans and opens by a sagittal slit on or near its apex.

Superficial penile fascia

The superficial penile fascia is devoid of fat, and consists of loose connective tissue invaded by fibres of the dartos muscle from the scrotum. Clinically, it is commonly referred to as the dartos layer. As in the suprapubic abdominal wall, the deepest layer is condensed to form a distinct tough fascial sheath, Buck’s fascia (Fig. 76.18B). It surrounds both corpora cavernosa and splits to enclose the corpus spongiosum, separating the superficial and deep dorsal veins. At the penile neck it blends with the fibrous covering of all three corpora. Proximally, it is continuous with the dartos muscle and with the fascia covering the urogenital region of the perineum (see p. 1094).

Suspensory ligaments of penis

The body of the penis is supported by two ligaments, the fundiform and triangular ligaments, which are continuous with its fascia and consist largely of elastin fibres (Fig. 76.17B). The fundiform ligament stems from the lowest part of the linea alba and splits into two lamellae which skirt the penis and unite below with the scrotal septum. The triangular suspensory ligament, deep to the fundiform ligament, is attached above to the front of the pubic symphysis and blends below with the fascia penis on each side. Damage to the suspensory ligament may occur after trauma and results in ventral angulation of the body of the penis.

Vascular supply and lymphatic drainage

Perineal artery

The perineal artery (Fig. 76.20) leaves the internal pudendal artery near the anterior end of its canal and approaches the scrotum in the superficial perineal region, between bulbospongiosus and ischiocavernosus. Beyond the perineal membrane, and near its base, a small transverse branch passes medially, inferior to the superficial transverse perineal muscle, to anastomose with its contralateral fellow and with the posterior scrotal and inferior rectal arteries; collectively these vessels supply tissues between the anus and the penile bulb. The posterior scrotal arteries, distributed to the scrotal skin, dartos and perineal muscles, are usually terminal branches of the perineal artery but may also arise from its transverse branch.

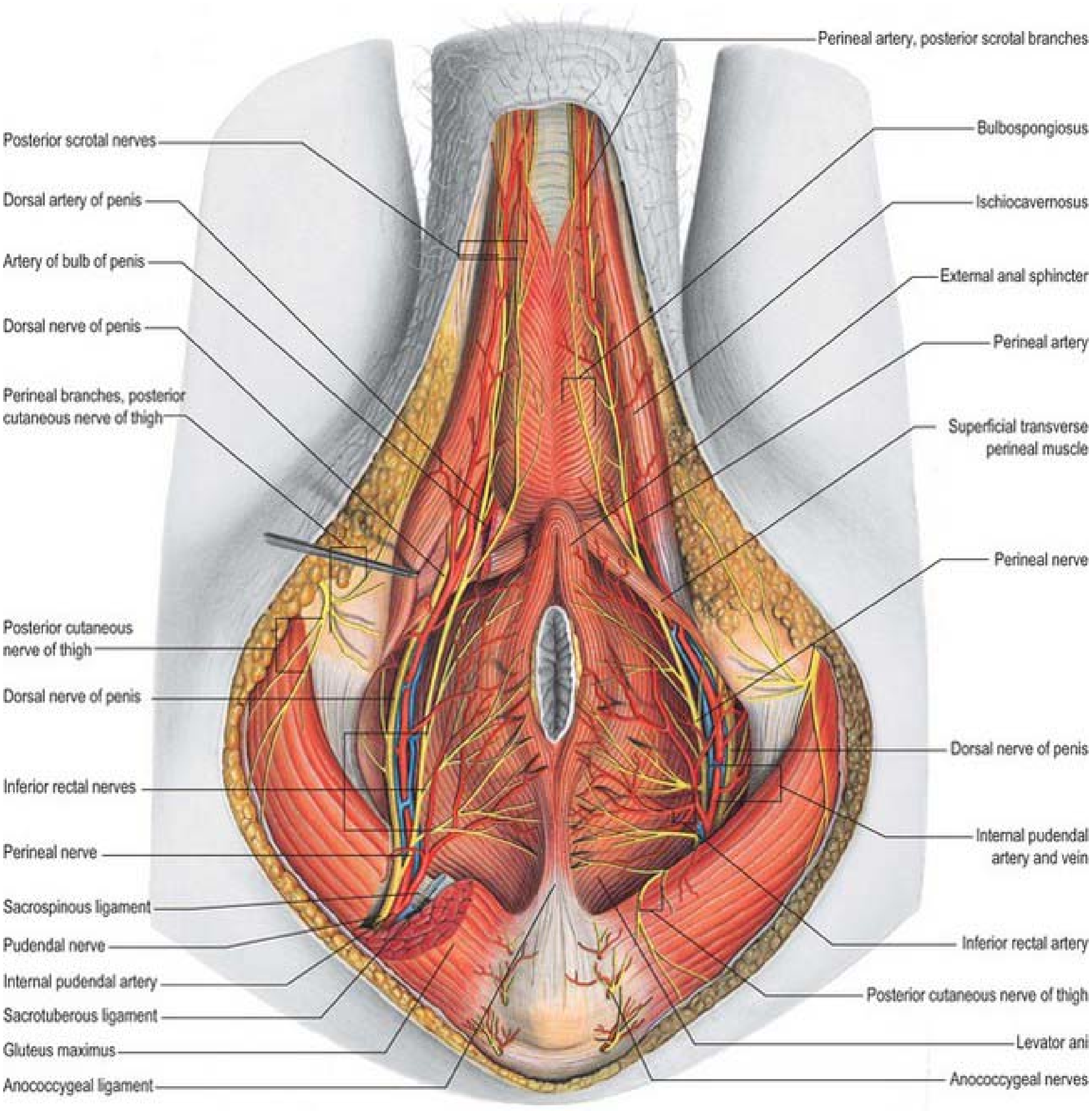

Perineal artery, posterior scrotal branches
Posterior scrotal nerves
Bulbospongiosus
Dorsal artery of penis
Ischiocavernosus
Artery of bulb of penis
External anal sphincter
Dorsal nerve of penis
Perineal artery
Perineal branches, posterior cutaneous nerve of thigh
Superficial transverse perineal muscle
Perineal nerve
Posterior cutaneous nerve of thigh
Dorsal nerve of penis
Dorsal nerve of penis
Inferior rectal nerves
Internal pudendal artery and vein
Perineal nerve
Sacrospinous ligament
Inferior rectal artery
Pudendal nerve
Posterior cutaneous nerve of thigh
Internal pudendal artery
Sacrotuberous ligament
Levator ani
Gluteus maximus
Anococcygeal nerves
Anococcygeal ligament

Fig. 76.20 Blood vessels and nerves of the perineal region and external genitalia in the adult male. The fat body of the ischio-anal fossa has been removed and gluteus maximus has been incised in order to expose the course of the pudendal nerve and internal pudendal artery.

(From Sobotta 2006.)

Artery of the bulb of the penis

The artery of the bulb of the penis is short but wide, and runs medially through the deep transverse perineal muscle to the penile bulb, which it penetrates (Fig. 76.20). It supplies the corpus spongiosum and the bulbourethral gland.

Cavernosal artery (deep artery of the penis)

The cavernosal artery is a terminal branch of the internal pudendal artery (Fig. 76.20). It passes through the perineal membrane, enters the crus penis on each side and runs the length of the corpus cavernosum, supplying the erectile tissue. Within the corpus, the cavernosal arteries divide into branches that either end directly in capillary networks which open into the cavernous spaces, or become convoluted and somewhat dilated helicine arteries, which also open into the cavernous spaces. Helicine arteries are most abundant in the posterior regions of the corpora cavernosa.

Dorsal artery of the penis

The dorsal artery of the penis is the other terminal branch of the internal pudendal artery (Figs 76.20, 76.21). It runs between the crus penis and pubic symphysis, and then pierces the suspensory ligament of the penis to run along its dorsum to the glans, where it forks into branches to the glans and prepuce. In the penis it lies deep to Buck’s fascia between the dorsal nerves and the deep dorsal vein, the latter being most medial. It supplies penile skin by branches that run through the dartos layer. It gives off circumflex branches that run laterally across the shaft of the penis, first deep to and then within Buck’s fascia, to supply the tunica albuginea of the corpus cavernosum, anastomosing through the tunica with the cavernosal system; these branches also supply the corpus spongiosum.

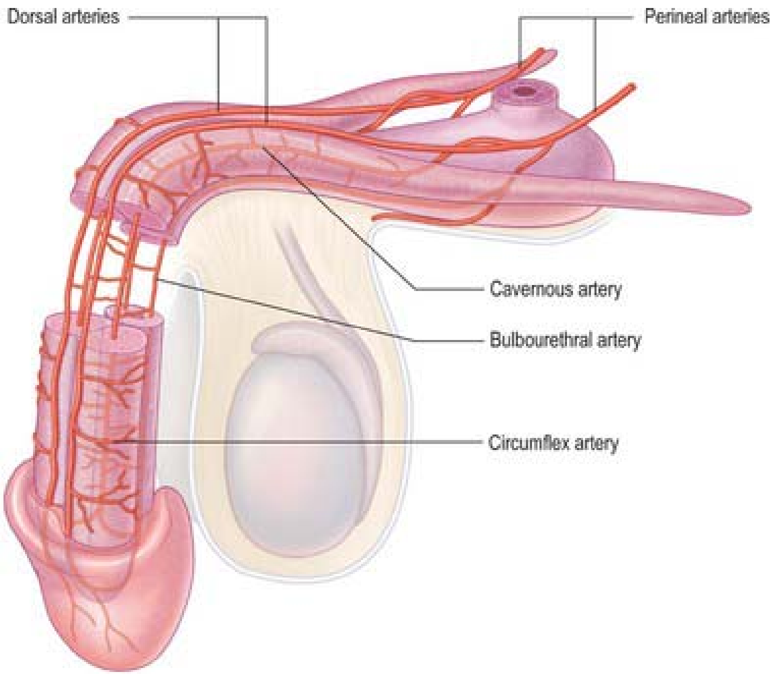

Fig. 76.21 Arterial blood supply to the body of the penis.

Dorsal veins of the penis

The veins that drain the corpora cavernosa leave the corpora by passing obliquely through the tunica albuginea via a series of small vessels called sub-tunical veins. These drain into the circumflex veins (Fig. 76.22) which run circumferentially around the shaft of the penis from its ventral aspect, where they receive tributaries from the corpus spongiosum, to its dorsal aspect, where they drain into the deep dorsal vein. The dorsal veins, superficial and deep, are unpaired. The superficial dorsal vein drains the prepuce and penile skin: it runs back in subcutaneous tissue and inclines either right or left before it opens into one of the external pudendal veins. The deep dorsal vein lies deep to Buck's fascia. It receives blood from the glans penis and corpora cavernosa penis, and courses back in the midline between the paired dorsal arteries. Near the root of the penis it passes deep to the suspensory ligament and through a gap between the arcuate pubic ligament and anterior margin of the perineal membrane. It divides into right and left branches that connect below the symphysis pubis with the internal pudendal veins and ultimately enter the prostatic plexus.

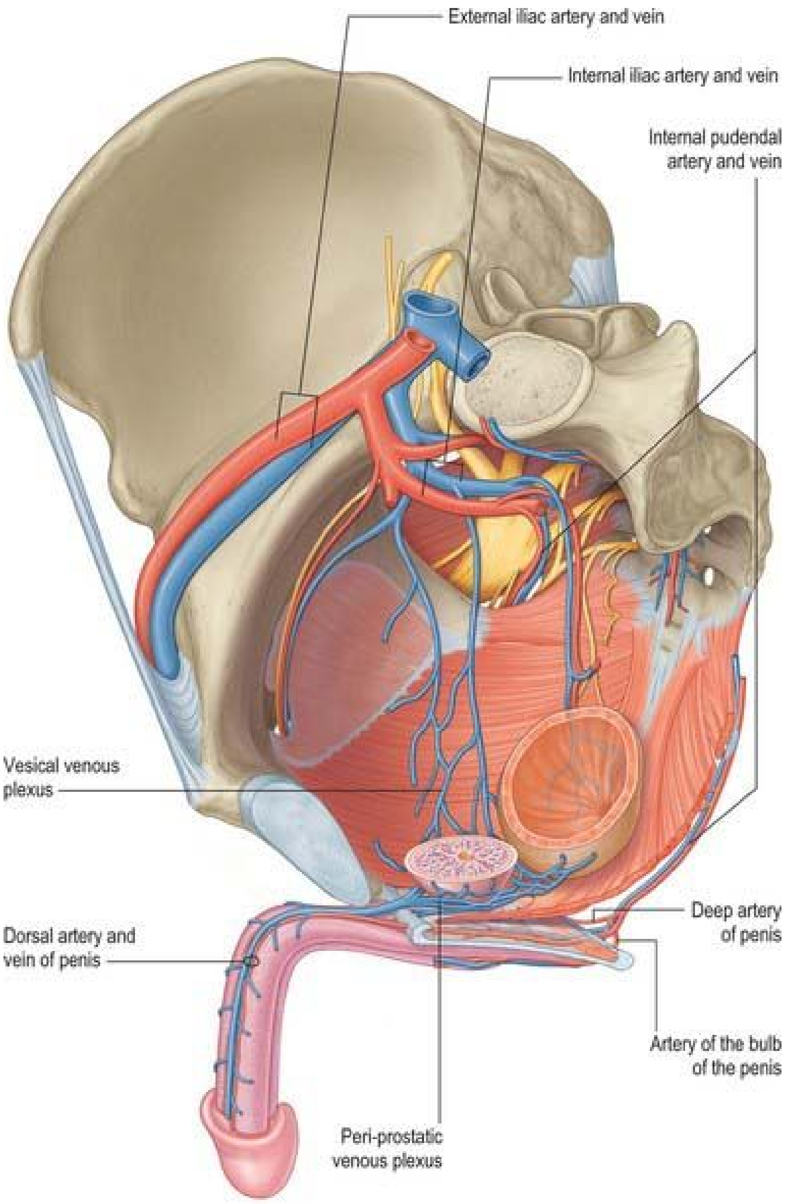
External iliac artery and vein
Internal iliac artery and vein
Internal pudendal artery and vein
Vesical venous plexus
Dorsal artery and vein of penis
Deep artery of penis
Artery of the bulb of the penis
Peri-prostatic venous plexus

Fig. 76.22 Perineal vessels.

(Adapted from Drake, Vogl and Mitchell 2005.)

Lymphatic drainage

The penile and perineal skin is drained by lymph vessels that accompany the external pudendal blood vessels to the superficial inguinal nodes. Lymph vessels from the glans pass to the deep inguinal and external iliac nodes.

Lymph vessels from the erectile tissue and penile urethra pass to the internal iliac lymph nodes.

Innervation

The nerves to the corpora cavernosa mainly consist of the cavernous nerves, which arise from the pelvic plexus and contain both sympathetic and parasympathetic components (Fig. 76.23). The cavernous nerves pierce the fibrous penile sheath proximally to supply the erectile tissue of the corpus spongiosum and penile urethra. During their course they run postero-laterally to the apex of the prostate. The sympathetic supply to the male genital organs is derived from spinal cord segments T11–L2: stimulation produces vasoconstriction, contraction of the seminal vesicles and prostate, and seminal emission. Parasympathetic fibres are derived from spinal cord segments S2–4 via the pelvic plexuses: stimulation produces vasodilatation.

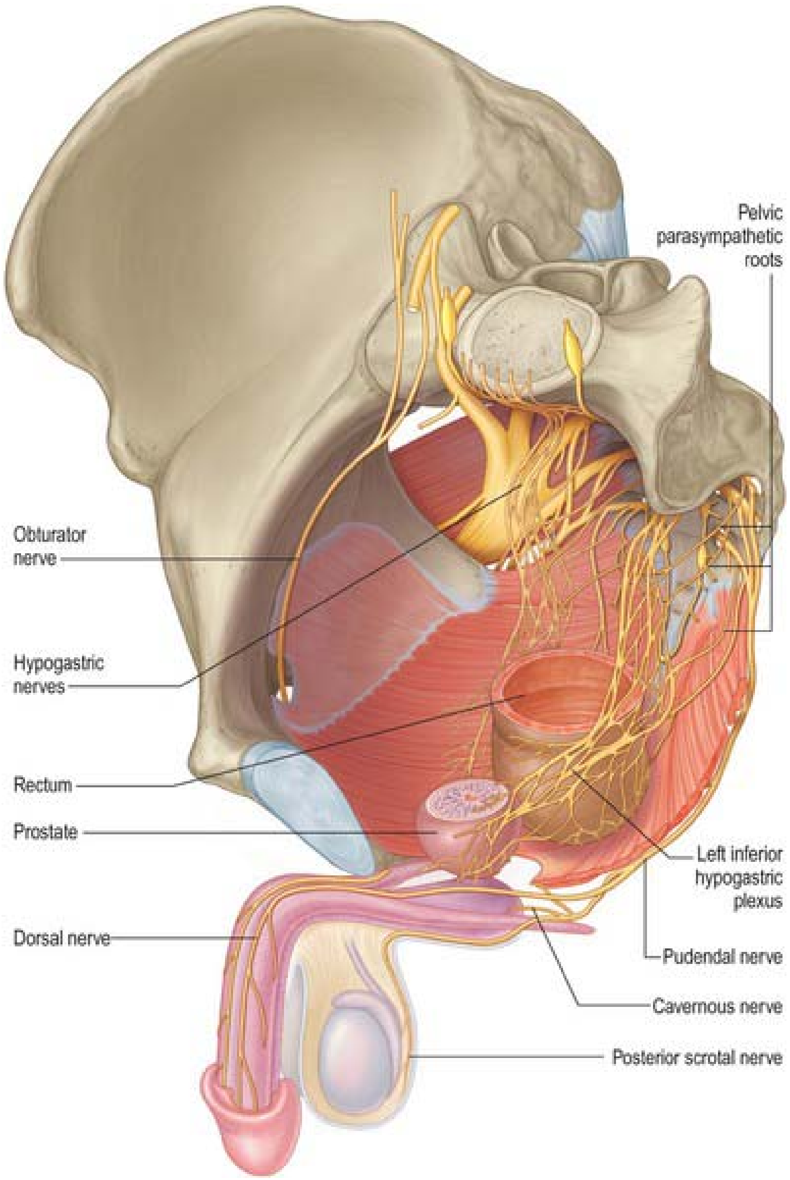
Pelvic parasympathetic roots
Obturator nerve
Hypogastric nerves
Rectum
Prostate
Dorsal nerve
Left inferior hypogastric plexus
Pudendal nerve
Cavernous nerve
Posterior scrotal nerve

Fig. 76.23 The nerve supply to the penis. The corpus cavernosum of penis receives both a parasympathetic and sympathetic innervation from the cavernous nerves. The afferent fibres from the glans pass via the dorsal nerves of the penis and via the pudendal nerve.

(Adapted from Drake, Vogl and Mitchell 2005.)

The main sensory nerve of the penis is the dorsal nerve of the penis. On the glans and bulb of the penis some cutaneous filaments innervate lamellated corpuscles. Afferent fibres from the glans penis and perigenital skin pass via the pudendal nerve to the spinal cord.

Microstructure

The internal surfaces of the fibrous sheaths of the corpora cavernosa and their dividing septum give rise to numerous trabeculae. These cross the corpora cavernosa in all directions and divide them into a series of cavernous spaces, giving them a spongy appearance. The trabeculae are composed of collagen and elastin fibres and smooth muscle and contain numerous vessels and nerves. The cavernous spaces are lined by an endothelium similar to that in other blood vessels. The spaces are empty in the flaccid state but become filled with blood during erection. The fibrous tunica albuginea of the corpus spongiosum is thinner, whiter and more elastic than that of the corpora cavernosa. It is formed partly of smooth muscle cells: a layer of the same tissue surrounds the urethral epithelium and the para-urethral glands.

ERECTION AND EJACULATION

Penile erection is a neurovascular process. The ischiocavernosi and bulbospongiosus may contribute to maximum rigidity although the main process is initiated by relaxation of the smooth muscle of the corpora cavernosa. Sexual arousal leads to rapid inflow from the helicine arteries following relaxation of the smooth muscle of the corpora cavernosa. This inflow of blood fills the cavernous spaces leading to tumescence. The resulting distension converts tumescence to an erection by pressure on the subtunical veins, which drain the erectile tissue, thereby obstructing them. This is known as the veno-occlusive mechanism. The smooth muscle of the corpora cavernosa relaxes in response to a number of neurotransmitters produced via the parasympathetic nerves and the endothelium. The most important neurotransmitter initiating penile erection appears to be nitric oxide, mainly produced from non-adrenergic, non-cholinergic nerves within the penis and acting via its second messenger, cyclic GMP.

Continuing cutaneous stimulation of the glans and frenulum contributes significantly to maintaining erection and initiating orgasm and ejaculation. Erection is thus dependent on a normal psychogenic response to stimulation, intact parasympathetic nerves, corporal smooth muscle capable of relaxation, patent arteries capable of delivering blood at the required rate, and a normal venous system. Following ejaculation the above process is reversed: smooth muscle contraction in response to sympathetic stimulation leads to penile detumescence.

Ejaculation consists of two processes, emission and ejaculation. Emission is the transmission of seminal fluid from the vasa, prostate and seminal vesicles into the prostatic urethra under sympathetic control. Ejaculation is the expulsion of seminal fluid from the prostatic urethra to the exterior, a phenomenon that has autonomic and somatic components. The first discernible part of the process is contraction of bulbospongiosus, which contracts about six times under somatic control. The way in which seminal fluid crosses the external urethral sphincter to enter the bulbar urethra is not clear, although it is known to be under autonomic control. It is timed so the ejaculate appears from the external meatus between the second to the final contraction of bulbospongiosus. In some younger men, ejaculation may be pulsatile.

Motility of spermatozoa

It is now generally accepted that the spermatic tail executes undulatory movements in one plane. It has been suggested that a helical component is superimposed upon these movements, and that there are perhaps two separable mechanisms to account for sperm motility, one involving flat waves travelling along the tail, the other associated with torsional activity. The latter type of movement has been linked with the unequal size and distribution of the dense fibres, and the asymmetry of the spermatozoon head. The central pair of fine fibrils may act as axial stiffeners.

As soon as they are ejaculated, spermatozoa display their full pattern of motility. The factors which trigger these movements are not yet clear: the other constituents of semen, which are derived from the epididymis, testis, seminal vesicle and prostate, are generally considered to exert an activating influence. Spermatozoa have been recovered in a motile state in human cervical mucus several days after insemination and will survive in this condition for as long as 7 days when implanted into such secretions *in vitro*. In view of the speed with which spermatozoa reach the infundibulum of the uterine tube, and the brevity of their fertilizing power, these survival periods may be of little significance. Spermatozoa have been shown to reach their tubal destination in a manner of minutes after ejaculation in some mammals; experiments on recently excised human uteri and tubes indicate a time of approximately 70 minutes. The conclusion must be that factors other than their own motility (1.5–3.0 mm/min) are responsible for the transport of spermatozoa from the site of deposition in the vaginal fornix to the ovarian end of the uterine tube, and there is considerable evidence that contraction of the uterine and tubal musculature is responsible.

Capacitation

After ejaculation into the female genital tract, spermatozoa undergo the final step in their maturation, a process known as capacitation. This normally requires exposure to the secretions of the uterine tube: a spermatozoon is unable to penetrate the corona radiata to fertilize an ovum until it has been within the female genital tract for a period of time, usually a few hours.

ERECTILE DYSFUNCTION AND PRIAPISM

Failure to achieve tumescence with adequate stimulation is termed erectile dysfunction. The mechanism of erection is complex: failure in any of the previously mentioned components can lead to erectile dysfunction. The commonest causes include psychogenic disturbance with failure to relax cavernous smooth muscle; arterial insufficiency as a result of atheromatous disease; and damage to the parasympathetic nervous system secondary to diabetes or following pelvic surgery such as radical prostatectomy, radical cystectomy or bowel resection. Oral pharmacotherapy is directed at achieving cavernosal smooth muscle relaxation by enhancing the effects of cyclic GMP.

Some men are prone to develop an erection which fails to subside after ejaculation and is termed a priapism. This can be either high flow or low flow, the latter condition being more common. Low flow priapism can occur spontaneously but is also seen in conditions such as sickle cell disease or leukaemia, or as a result of injection of drugs, such as intracavernosal prostaglandin E1, directly into the penis in men with erectile dysfunction. It leads to ischaemia of the corporal smooth muscle, which causes pain within the penis and will result in erectile dysfunction if left untreated. High flow priapism, where too much blood enters the penis, is usually secondary to an abnormal connection or fistula between the cavernosal arteries and sinusoidal spaces.

Peyronie’s disease may result in a bend in the erect penis that most commonly presents as a dorsal curvature that results from a localized thickening or plaque within the corpora cavernosa which prevents expansion of a segment during erection. Penile cancer is a rare malignancy of the penis and usually presents with a mass or ulceration of the penis. MRI scanning may be used in preoperative planning of Peyronie’s disease and local staging of penile cancer (see Fig. 76.19).

REFERENCES

undy AR. Male sexual function. In: *The Scientific Basis of Urology*. London: Taylor and Francis; 2004.

rhal P, Overton C. Clinical assessment and management of the infertile man. In: *Good Clinical Practice in Assisted Reproduction*. Cambridge: Cambridge University Press; 2004.

alsh PC. Campbell-Walsh Urology, 9th edn. Edinburgh: Elsevier, 2007.

CHAPTER 77

Female reproductive system

The female reproductive system consists of the lower genital tract (vulva and vagina) and the upper tract (uterus and cervix with associated uterine (Fallopian) tubes and ovaries).

LOWER GENITAL TRACT

VULVA

The female external genitalia or vulva include the mons pubis, labia majora, labia minora, clitoris, vestibule, vestibular bulb and the greater vestibular glands (Fig. 77.1A–D).

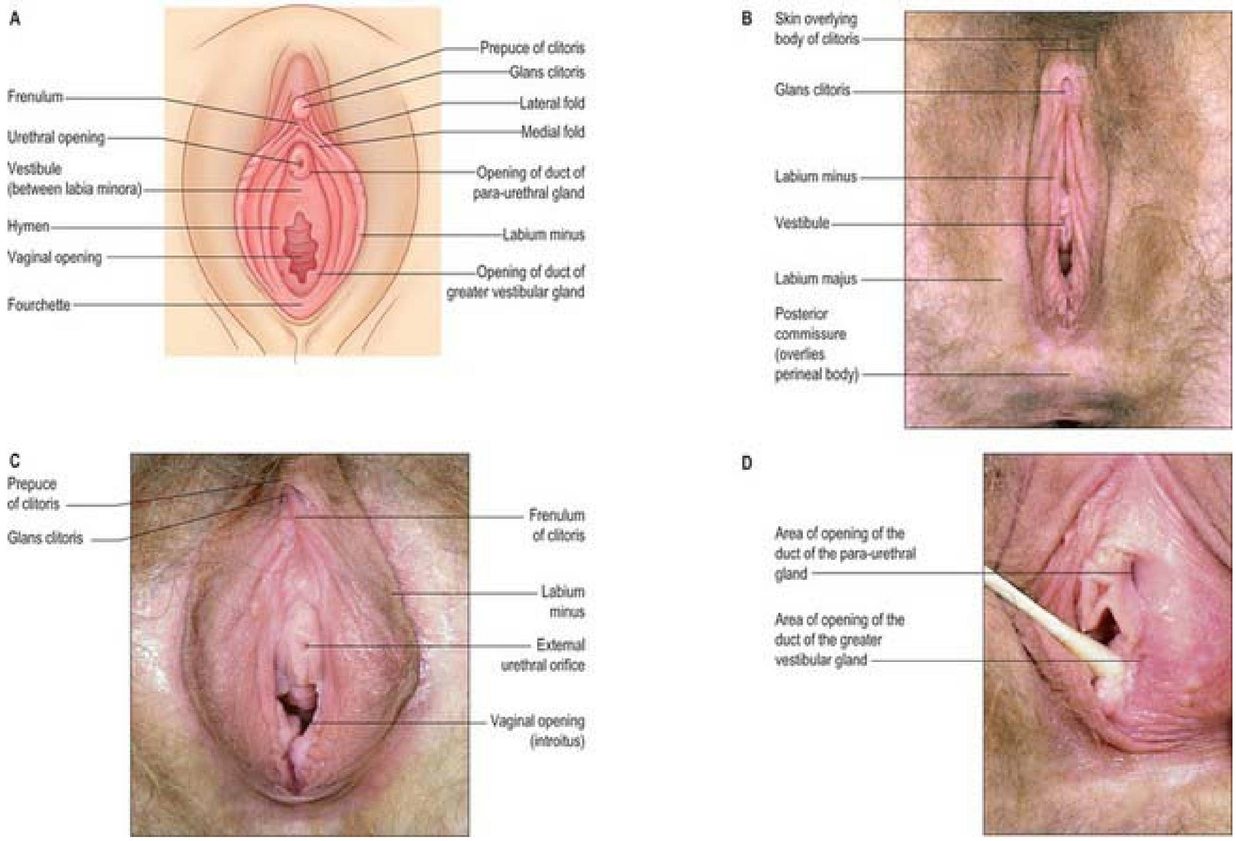
A
Frenulum
Urethral opening
Vestibule (between labia minora)
Hymen
Vaginal opening
Fourchette
Prepuce of clitoris
Glans clitoris
Lateral fold
Medial fold
Opening of duct of para-urethral gland
Labium minus
Opening of duct of greater vestibular gland
B
Skin overlying body of clitoris
Glans clitoris
Labium minus
Vestibule
Labium majus
Posterior commissure (overlies perineal body)
C
Prepuce of clitoris
Glans clitoris
Frenulum of clitoris
Labium minus
External urethral orifice
Vaginal opening (introitus)
D
Area of opening of the duct of the para-urethral gland
Area of opening of the duct of the greater vestibular gland

Fig. 77.1 **A**, Superficial features of the perineum. **B**, The labia majora and surrounding external genitalia. **C**, The labia minora. **D**, Inferior view of vestibule with the left labium minus pulled to one side to show the regions of the vestibule into which the greater vestibular and para-urethral glands open.

*(**A** from Drake, Vogl, Mitchell, Tibbitts and Richardson 2008. **B–D** from Drake, Vogl and Mitchell 2005.)*

Mons pubis

The mons pubis is the rounded hair-bearing area of skin over the pubic symphysis and adjacent pubic bone. It is formed by a mass of subcutaneous adipose connective tissue. Before puberty, the mons pubis is relatively flat and the labia minora are poorly formed. During adolescence, coarse hair forms over the mons and labia majora and the labia minora become more prominent and flap like. In adults, the mons is covered by coarse hair that is usually limited above by a horizontal boundary; in males there is a continuation of pubic hair to the umbilicus. After the menopause, pubic hair thins and labial tissue atrophies slightly.

Labia majora

The labia majora are two prominent, longitudinal folds of skin that extend back from the mons pubis to the perineum (Fig. 77.1B). They form the lateral boundaries of the vulva. Each labium has an external, pigmented surface covered with hairs and a smooth, pink internal surface with large sebaceous follicles. Between these surfaces there is loose connective and adipose tissue, intermixed with smooth muscle (resembling the scrotal dartos muscle), vessels, nerves and glands. The uterine round ligament may end in the adipose tissue and skin in the anterior part of the labium. A persistent processus vaginalis and congenital inguinal hernia may also reach a labium. The labia are thicker anteriorly, where they join to form the anterior commissure. Posteriorly they do not join, but instead merge into neighbouring skin, ending near and almost parallel to each other. The connecting skin between them posteriorly forms a ridge, the posterior commissure, that overlies the perineal body and is the posterior limit of the vulva. The distance between this and the anus is 2.5–3 cm thick and is termed the ‘gynaecological’ perineum.

Labia minora

The labia minora are two small cutaneous folds, devoid of fat, that lie between the labia majora. They extend from the clitoris obliquely down, laterally and back, flanking the vaginal orifice. Anteriorly, each labium minus bifurcates. The upper layer of each side passes above the clitoris to form a fold, the hood or prepuce, which overhangs the glans of the clitoris. The lower layer of each side passes below the clitoris to form the frenulum of the clitoris (Fig. 77.1A,C). Sebaceous follicles are numerous on the apposed labial surfaces. Sometimes an extra labial fold (labium tertium) is found on one or both sides between the labia minora and majora.

Vestibule

The vestibule is the cavity that lies between the labia minora. It contains the vaginal and external urethral orifices and the openings of the two greater vestibular (Bartholin's) glands and of numerous mucous, lesser vestibular glands. There is a shallow vestibular fossa between the vaginal orifice and the frenulum of the labia minora.

Urethra

The urethra opens into the vestibule about 2.5 cm below the clitoris and above the vaginal opening via a short, sagittal cleft with slightly raised margins, the urethral meatus. The meatus is very distensible and varies in shape: the aperture may be rounded, slit-like, crescentic or stellate. The ducts of the para-urethral glands (Skene's glands) open on each side of the lateral margins of the urethra.

Bulbs of the vestibule

The bulbs of the vestibule lie on each side of the vestibule. They are two elongated masses of erectile tissue, 3 cm long, which flank the vaginal orifice and unite anterior to it by a narrow commissura bulborum (pars intermedia). Their posterior ends are expanded and are in contact with the greater vestibular glands. Their anterior ends taper and are joined by a commissure and also to the clitoris by two slender bands of erectile tissue. Their deep surfaces contact the inferior aspect of the urogenital diaphragm, and superficially each is covered by bulbospongiosus posteriorly (Fig. 77.2A–C).

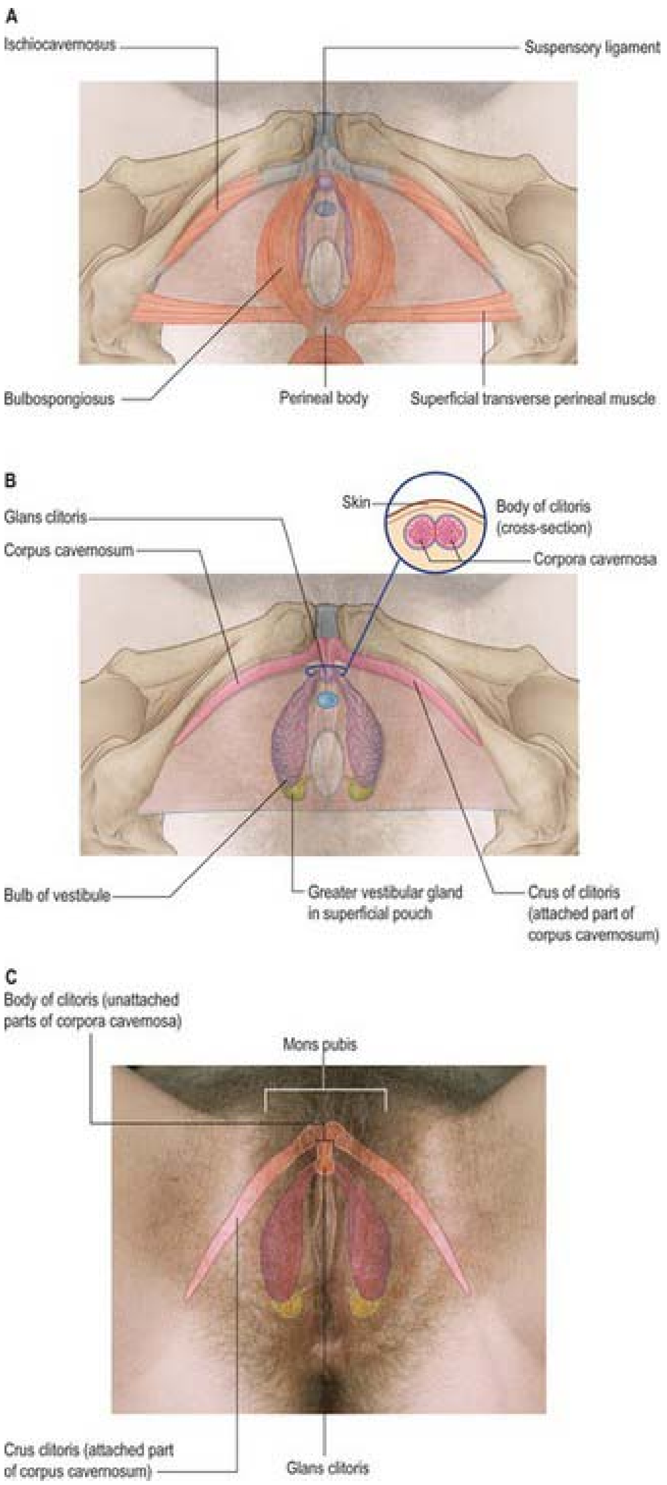
A
Ischiocavernosus
Suspensory ligament
Bulbospongiosus
Perineal body
Superficial transverse perineal muscle
B
Glans clitoris
Corpus cavernosum
Skin
Body of clitoris
(cross-section)
Corpora cavernosa
Bulb of vestibule
Greater vestibular gland
in superficial pouch
Crus of clitoris
(attached part of
corpus cavernosum)
C
Body of clitoris (unattached
parts of corpora cavernosa)
Mons pubis
Crus clitoris (attached part
of corpus cavernosum)
Glans clitoris

Fig. 77.2 **A**, Muscles of the vestibule and clitoris. **B**, Erectile tissues of the clitoris. **C**, Erectile tissues of clitoris, vestibule and greater vestibular gland with a surface anatomy overlay.

*(**A**, **B** adapted from Drake, Vogl and Mitchell 2005. **C** from Drake, Vogl and Mitchell 2005.)*

Greater vestibular glands (Bartholin’s glands)

The greater vestibular glands are homologues of the male bulbourethral glands. They consist of two small, round or oval, reddish-yellow bodies that flank the vaginal orifice, in contact with, and often overlapped by, the posterior end of the vestibular bulb. Each opens into the postero-lateral part of the vestibule by a 2 cm duct, situated in the groove between the hymen and the labium minus (Fig. 77.1D). The glands are composed of tubulo-acinar tissue. The secretory cells are columnar and secrete a clear or whitish mucus with lubricant properties. They are stimulated by sexual arousal.

Clitoris

The clitoris is an erectile structure partially enclosed by the anterior bifurcated ends of the labia minora. It has a root, a body, and a glans. The body can be palpated through the skin. It contains two corpora cavernosa, composed of erectile tissue and enclosed in dense fibrous tissue, and separated medially by an incomplete fibrous pectiniform septum. The fibrous tissue forms a suspensory ligament that is attached superiorly to the pubic symphysis. Each corpus cavernosum is attached to its ischiopubic ramus by a crus that extends from the root of the clitoris. The glans clitoris is a small round tubercle of spongy erectile tissue at the end of the body and connected to the bulbs of the vestibule by thin bands of erectile tissue. It is exposed between the anterior ends of the labia minora. Its epithelium has high cutaneous sensitivity, important in sexual responses (Fig. 77.2).

Vascular supply and lymphatic drainage of the vulva

Arteries

The arterial blood supply of the female external genitalia is derived from the superficial and deep external pudendal branches of the femoral artery and the internal pudendal artery on each side (Fig. 77.3A).

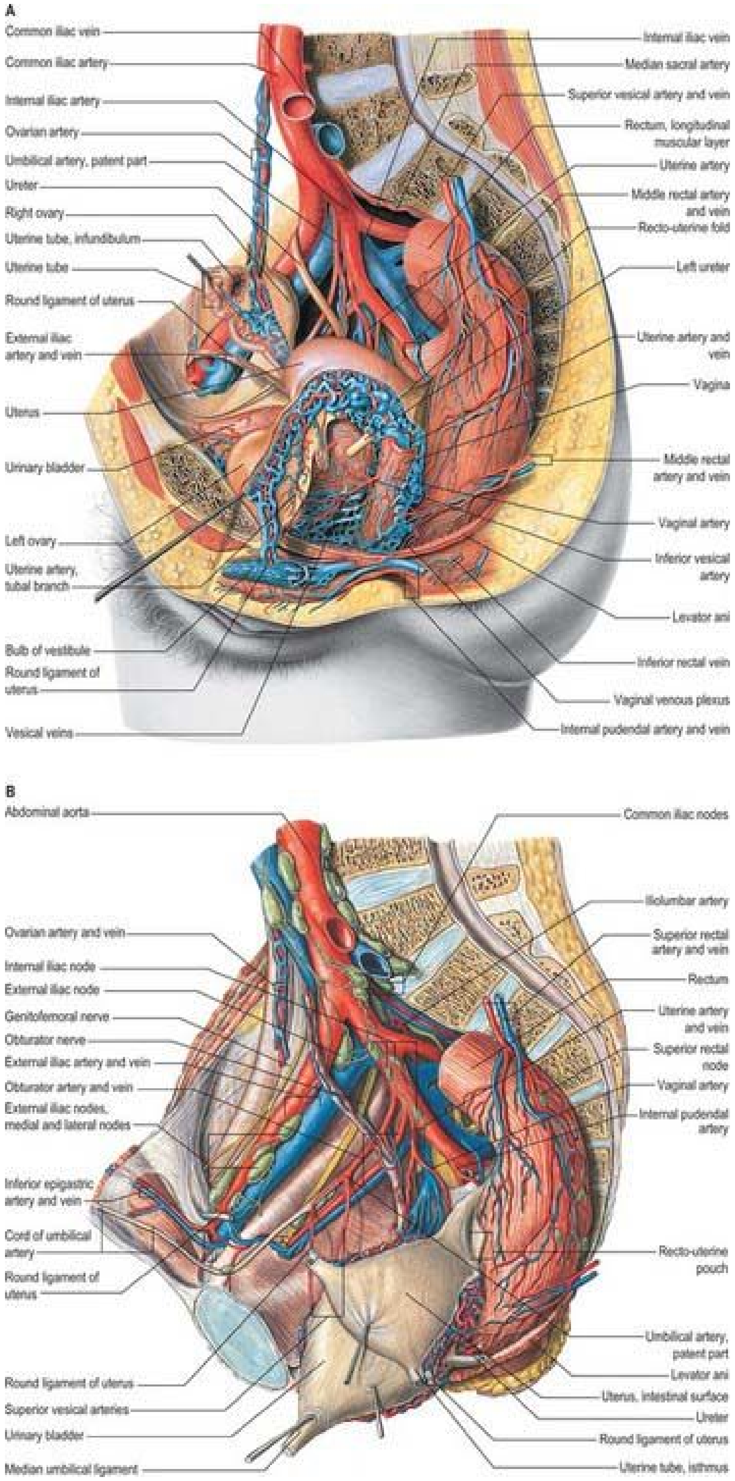
A
Common iliac vein
Common iliac artery
Internal iliac artery
Ovarian artery
Umbilical artery, patent part
Ureter
Right ovary
Uterine tube, infundibulum
Uterine tube
Round ligament of uterus
External iliac artery and vein
Uterus
Urinary bladder
Left ovary
Uterine artery, tubal branch
Bulb of vestibule
Round ligament of uterus
Vesical veins
Internal iliac vein
Median sacral artery
Superior vesical artery and vein
Rectum, longitudinal muscular layer
Uterine artery
Middle rectal artery and vein
Recto-uterine fold
Left ureter
Uterine artery and vein
Vagina
Middle rectal artery and vein
Vaginal artery
Inferior vesical artery
Levator ani
Inferior rectal vein
Vaginal venous plexus
Internal pudendal artery and vein
B
Abdominal aorta
Ovarian artery and vein
Internal iliac node
External iliac node
Genitofemoral nerve
Obturator nerve
External iliac artery and vein
Obturator artery and vein
External iliac nodes, medial and lateral nodes
Inferior epigastric artery and vein
Cord of umbilical artery
Round ligament of uterus
Round ligament of uterus
Superior vesical arteries
Urinary bladder
Median umbilical ligament
Common iliac nodes
Iliolumbar artery
Superior rectal artery and vein
Rectum
Uterine artery and vein
Superior rectal node
Vaginal artery
Internal pudendal artery
Recto-uterine pouch
Umbilical artery, patent part
Levator ani
Uterus, intestinal surface
Ureter
Round ligament of uterus
Uterine tube, isthmus

Fig. 77.3 Vessels (**A**), nerves and lymphatics (**B**) of the female pelvis. Sagittal view.

(From Sobotta 2006.)

Veins

Venous drainage of the vulval skin is via external pudendal veins to the long saphenous vein. Venous drainage of the clitoris is via deep dorsal veins to the internal pudendal vein and superficial dorsal veins to the external pudendal and long saphenous veins (Fig. 77.3A).

Lymphatic drainage

A meshwork of connecting vessels join to form three or four collecting trunks around the mons pubis which drain to superficial inguinal nodes lying on the cribriform fascia covering the femoral artery and vein; these nodes drain through the cribriform fascia to the deep inguinal nodes lying medial to the femoral vein. The deep inguinal nodes drain via the femoral canal to the pelvic nodes. The last of the deep inguinal nodes lies under the inguinal ligament within the femoral canal and is often called Cloquet's node. Lymph vessels in the perineum and lower part of the labia majora drain to the rectal lymphatic plexus. Lymph vessels from the clitoris and labia minora drain to deep inguinal nodes and direct clitoral efferents may pass to the internal iliac nodes (Fig. 77.3B).

Innervation

The innervation to the lower genital tract is shown in Fig. 77.5 and Table 77.1.

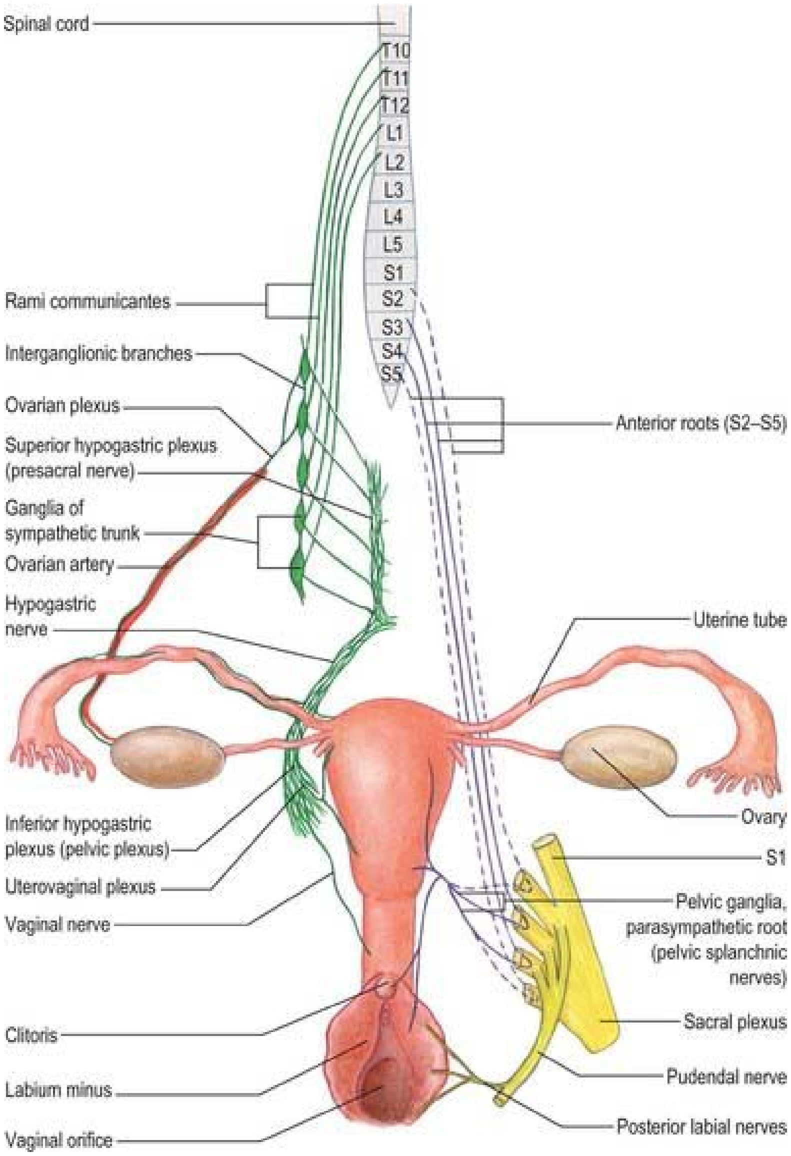
Spinal cord
T10
T11
T12
L1
L2
L3
L4
L5
S1
S2
S3
S4
S5
Rami communicantes
Interganglionic branches
Ovarian plexus
Superior hypogastric plexus (presacral nerve)
Ganglia of sympathetic trunk
Ovarian artery
Hypogastric nerve
Anterior roots (S2–S5)
Uterine tube
Ovary
S1
Inferior hypogastric plexus (pelvic plexus)
Uterovaginal plexus
Vaginal nerve
Pelvic ganglia, parasympathetic root (pelvic splanchnic nerves)
Sacral plexus
Clitoris
Labium minus
Pudendal nerve
Vaginal orifice
Posterior labial nerves

Fig. 77.5 Innervation of the female reproductive system.

(From Sobotta 2006.)

Table 77.1 Innervation of female genitalia.

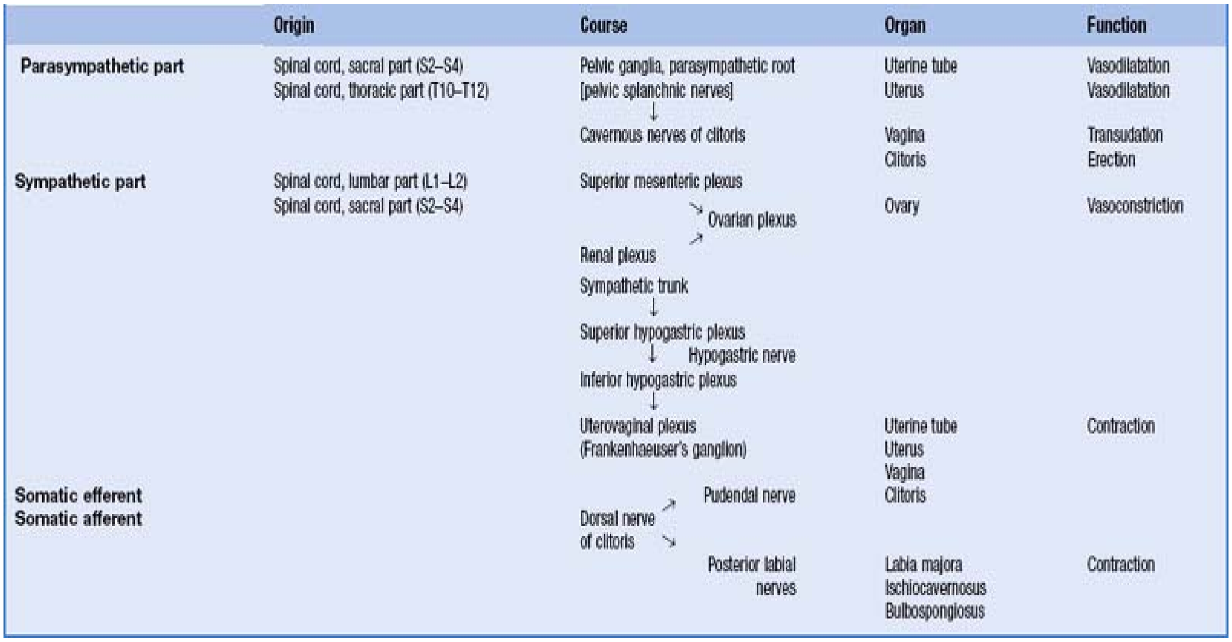

	Origin	Course	Organ	Function
Parasympathetic part	Spinal cord, sacral part (S2–S4) Spinal cord, thoracic part (T10–T12)	Pelvic ganglia, parasympathetic root [pelvic splanchnic nerves] ↓ Cavernous nerves of clitoris	Uterine tube Uterus Vagina Clitoris	Vasodilatation Vasodilatation Transudation Erection
Sympathetic part	Spinal cord, lumbar part (L1–L2) Spinal cord, sacral part (S2–S4)	Superior mesenteric plexus ↘ Ovarian plexus ↗ Renal plexus	Ovary	Vasoconstriction
		Sympathetic trunk ↓ Superior hypogastric plexus ↓ Hypogastric nerve Inferior hypogastric plexus ↓ Uterovaginal plexus (Frankenhaeuser's ganglion)	Uterine tube Uterus Vagina Clitoris	Contraction
Somatic efferent **Somatic afferent**		Pudendal nerve ↗ Dorsal nerve of clitoris ↘ Posterior labial nerves	Labia majora Ischiocavernosus Bulbospongiosus	Contraction

The sensory innervation of the anterior and posterior parts of the labium majus differ. The anterior third of the labium majus is supplied by the ilioinguinal nerve (L1), the posterior two-thirds are supplied by the labial branches of the perineal nerve (S3), and the lateral aspect is also innervated by the perineal branch of the posterior cutaneous nerve of the thigh (S2).

VAGINA

The vagina is a fibromuscular tube lined by non-keratinized stratified epithelium. It extends from the vestibule (the opening between the labia minora) to the uterus. The upper end of the vagina surrounds the vaginal projection of the uterine cervix. The annular recess between the cervix and vagina is the fornix: the different parts of this recess are given separate names, i.e. anterior, posterior and right and left lateral, but they are continuous (Fig. 77.6).

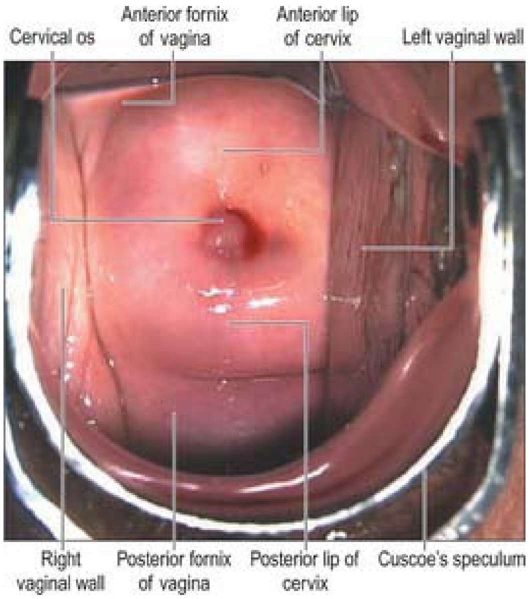
Cervical os
Anterior fornix of vagina
Anterior lip of cervix
Left vaginal wall
Right vaginal wall
Posterior fornix of vagina
Posterior lip of cervix
Cuscoe's speculum

Fig. 77.6 Cervix and vaginal fornices as seen via a Cuscoe's bivalve speculum.

The vagina ascends posteriorly and superiorly at an angle of over 90° to the uterine axis: this angle varies with the contents of the bladder and rectum. The width of the vagina increases as it ascends. Above the level of the hymen, the inner surfaces of the anterior and posterior vaginal walls are ordinarily in contact with each other forming a transverse slit. The vaginal mucosa is attached to the uterine cervix higher on the posterior cervical wall than on the anterior: the anterior wall is approximately 7.5 cm long and the posterior wall is approximately 9 cm long. The anterior wall of the vagina is related to the base of the bladder in its middle and upper portions and to the urethra (which is embedded in it) inferiorly. The posterior wall is covered by peritoneum in its upper quarter. It is separated from the rectum by the recto-uterine pouch superiorly, and by moderately loose connective tissue (Denonvillier's fascia) in its middle half. In its lower quarter it is separated from the anal canal by the musculofibrous perineal body. Laterally are levator ani and pelvic fascia (see Fig. 75.1A). As the ureters pass anteromedially to reach the fundus of the bladder, they pass close to the lateral fornices. As they enter the bladder the ureters are usually anterior to the vagina, and at this point, each ureter is crossed transversely by a uterine artery (Fig. 77.7).

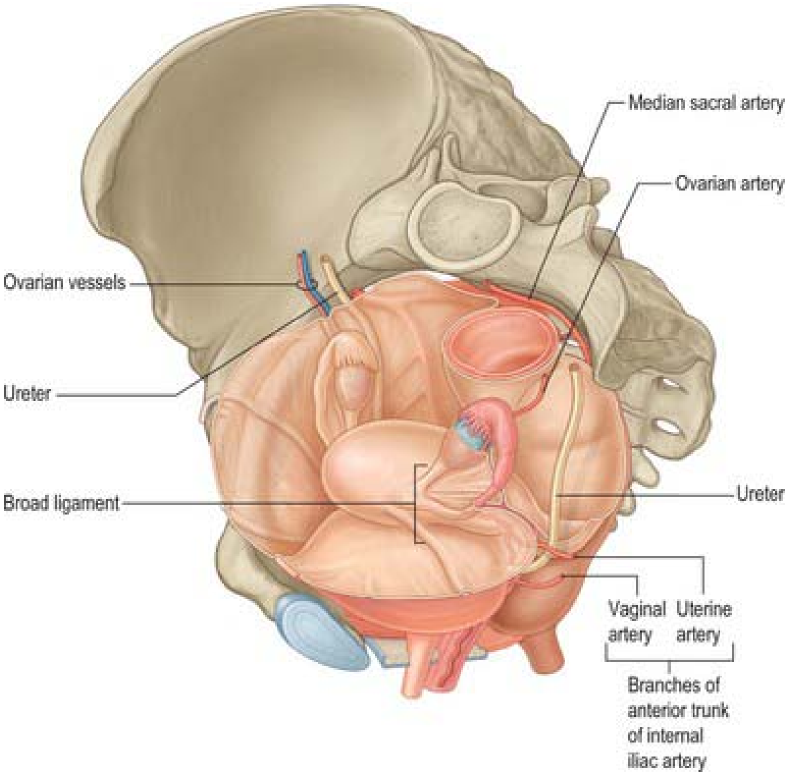
Median sacral artery
Ovarian artery
Ovarian vessels
Ureter
Broad ligament
Ureter
Vaginal artery
Uterine artery
Branches of anterior trunk of internal iliac artery

Fig. 77.7 Relationship of the ureter to the uterine and vaginal arteries.

(From Drake, Vogl and Mitchell 2005.)

The vagina opens externally via a sagittal introitus positioned below the urethral meatus. The size of the introitus varies: it is capable of great distension during childbirth and to a lesser degree during sexual intercourse. The hymen is a thin fold of mucous membrane situated just within the vaginal orifice. The internal surfaces of the folds are normally in contact each other and the vaginal opening appears as a cleft between them. The hymen varies greatly in shape and dimensions. When stretched, it is annular and widest posteriorly; it may also be semilunar and concave towards the mons pubis, cribriform, fringed, absent or complete and imperforate. The hymenal ring normally ruptures after first sexual intercourse, but can rupture earlier during non-sexual physical activity. Small round carunculae hymenales (also known as carunculae myrtiformis) are its remnants after it has been ruptured. It has no established function.

Remnants of the duct of Gartner (embryologically the caudal end of the mesonephric duct) (see Ch. 78), are occasionally seen protruding through the lateral fornices or lateral parts of the vagina; these can cause cysts (Gartner's cysts).

Vascular supply and lymphatic drainage

Arteries

The arterial supply of the vagina is derived from the internal iliac arteries. The vaginal arteries form two median longitudinal vessels, the azygos arteries of the vagina, which descend anterior and posterior to the vagina. They descend on the vagina and supply the mucous membrane. Branches are also sent to the vestibular bulb, fundus of the bladder, and adjacent part of the rectum. The uterine, internal pudendal and middle rectal branches of the internal iliac artery may also contribute to the blood supply.

Veins

The vaginal veins, one on each side, form from lateral plexuses that connect with uterine, vesical and rectal plexuses and drain to the internal iliac veins. The uterine and vaginal plexuses may provide collateral venous drainage to the lower limb.

Lymphatics

Vaginal lymphatic vessels link with those of the cervix, rectum and vulva. They form three groups but the regions drained are not sharply demarcated. Upper vessels accompany the uterine artery to the internal and external iliac nodes; intermediate vessels accompany the vaginal artery to the internal iliac nodes; vessels draining the vagina below the hymen, and from the vulva and perineal skin, pass to the superficial inguinal nodes.

Innervation

The lower vagina is supplied by the pudendal nerve (S2, S3 and S4). The upper vagina is supplied by the splanchnic nerves (S2, S3 and sometimes S4).

Microstructure

The vagina has an inner mucosal and an external muscular layer. The mucosa adheres firmly to the muscular layer. There are two median longitudinal ridges on its epithelial surface, one anterior and the other posterior. Numerous transverse bilateral rugae extend from these vaginal columns. They are divided by sulci of variable depth, giving an appearance of conical papillae, which are most numerous on the posterior wall and near the orifice, and which are especially well developed before parturition. The epithelium is non-keratinized, stratified, squamous similar to, and continuous with, that of the ectocervix. After puberty it thickens and its superficial cells accumulate glycogen, which gives them a clear appearance in histological preparations.

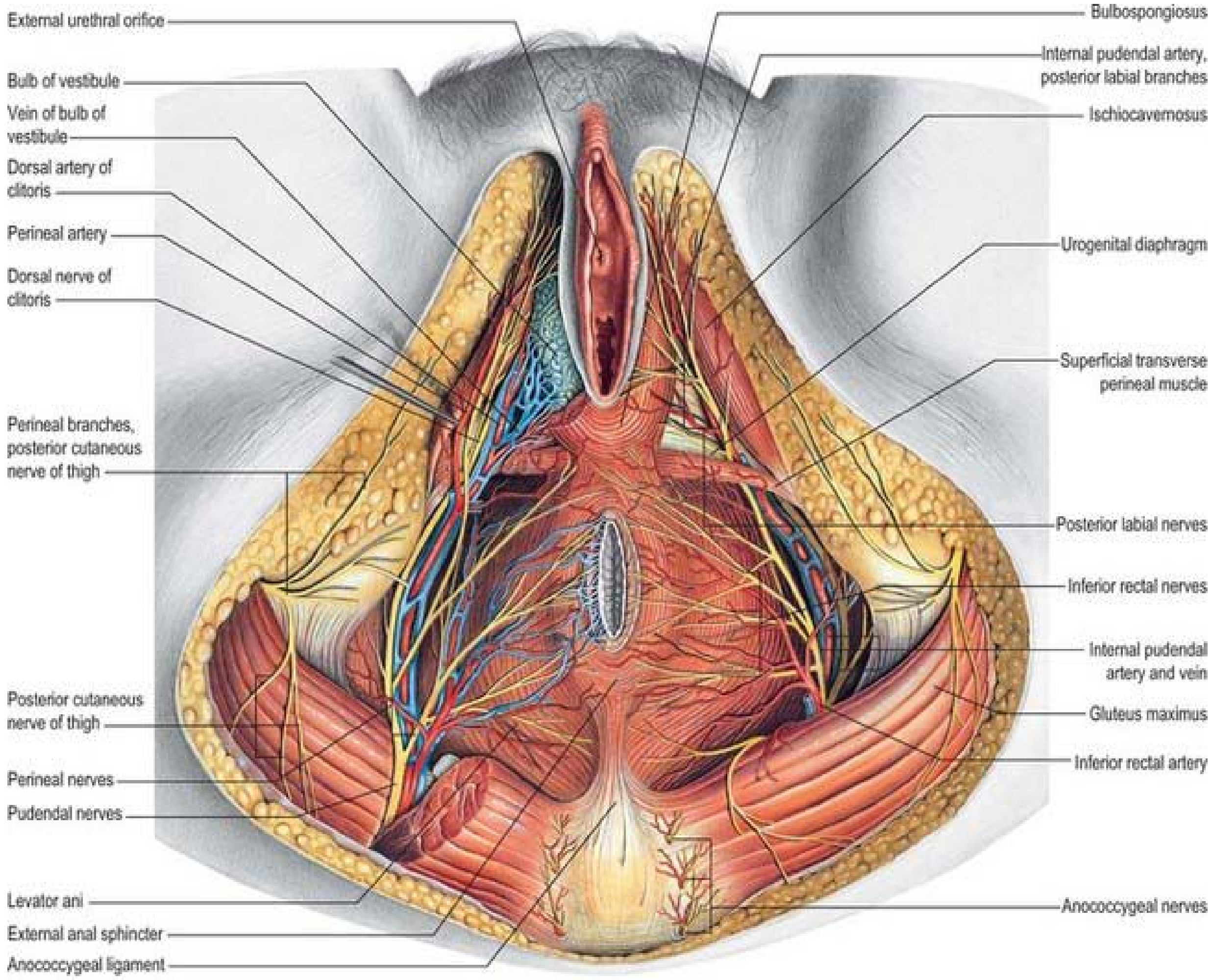
External urethral orifice
Bulb of vestibule
Vein of bulb of vestibule
Dorsal artery of clitoris
Perineal artery
Dorsal nerve of clitoris
Perineal branches, posterior cutaneous nerve of thigh
Posterior cutaneous nerve of thigh
Perineal nerves
Pudendal nerves
Levator ani
External anal sphincter
Anococcygeal ligament
Bulbospongiosus
Internal pudendal artery, posterior labial branches
Ischiocavernosus
Urogenital diaphragm
Superficial transverse perineal muscle
Posterior labial nerves
Inferior rectal nerves
Internal pudendal artery and vein
Gluteus maximus
Inferior rectal artery
Anococcygeal nerves

Fig. 77.4 Muscles, vessels and nerves of the female perineum. Inferior view.

(From Sobotta 2006.)

The vaginal epithelium does not change markedly during the menstrual cycle, but its glycogen content increases after ovulation and then diminishes towards the end of the cycle. Natural vaginal bacteria, particularly *Lactobacillus acidophilus*, break down glycogen in the desquamated cellular debris to lactic acid. This produces a highly acidic (pH 3) environment, which inhibits the growth of most other microorganisms. The amount of glycogen is less before puberty and after the menopause, when vaginal infections are more common. There are no mucous glands, but a fluid transudate from the lamina propria and mucus from the cervical glands lubricate the vagina (Fig. 77.8). The muscular layers are composed of smooth muscle and consist of a thick outer longitudinal and an inner circular layer. The two layers are not distinct but connected by oblique interlacing fibres. Longitudinal fibres are continuous with the superficial muscle fibres of the uterus. Half way along the vagina is a U-shaped muscular sling, called the pubo-vaginalis. The lower vagina is also surrounded by the skeletal muscle fibres of bulbospongiosus. A layer of loose connective tissue, containing extensive vascular plexuses, surrounds the muscle layers.

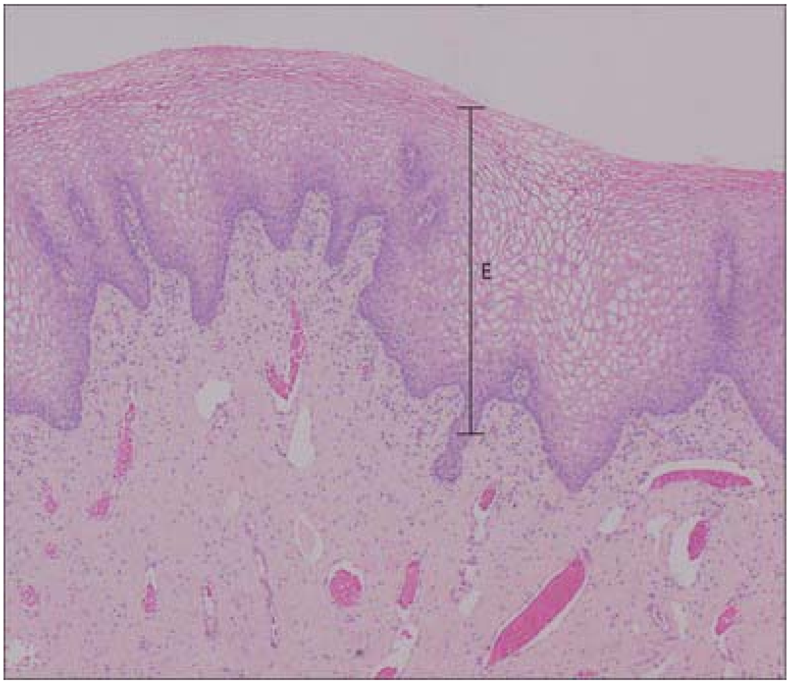

Fig. 77.8 Stratified squamous non-keratinizing epithelium (E) covering the ectocervix and vagina. The cells of the middle and upper layers appear clear due to their content of glycogen.

(By courtesy of Mr Peter Helliwell and Dr Joseph Mathew, Department of Histopathology, Royal Cornwall Hospitals Trust, UK.)

UPPER GENITAL TRACT

UTERUS

The uterus is a thick-walled, muscular organ situated in the pelvis between the urinary bladder and the rectum (Figs 77.9-77.11). It lies posterior to the bladder and uterovesical space and anterior to the rectum and recto-uterine pouch: it is mobile, which means that its position varies with distension of the bladder and rectum. The broad ligaments are lateral.

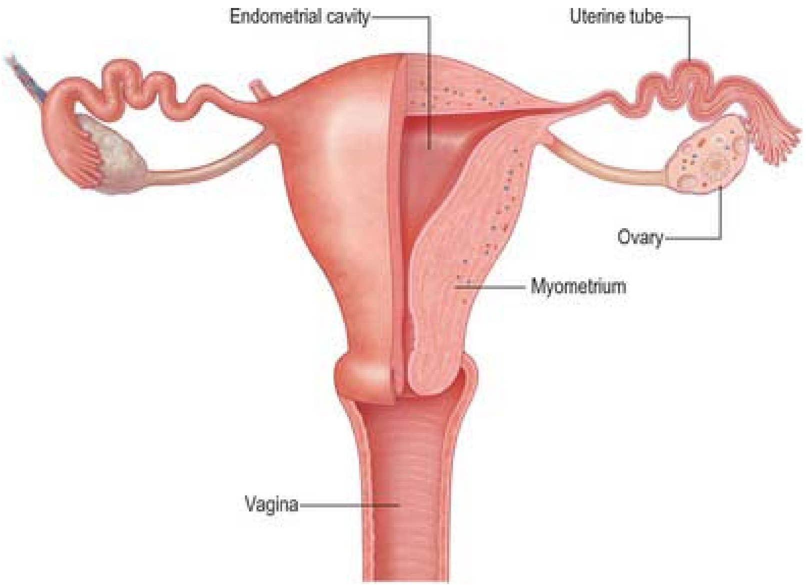

Fig. 77.9 Upper genital tract. Posterior view with the posterior half of the right part of the uterus, uterine tube, ovary and vagina cut away.

(From Drake, Vogl, Mitchell, Tibbitts and Richardson 2008.)

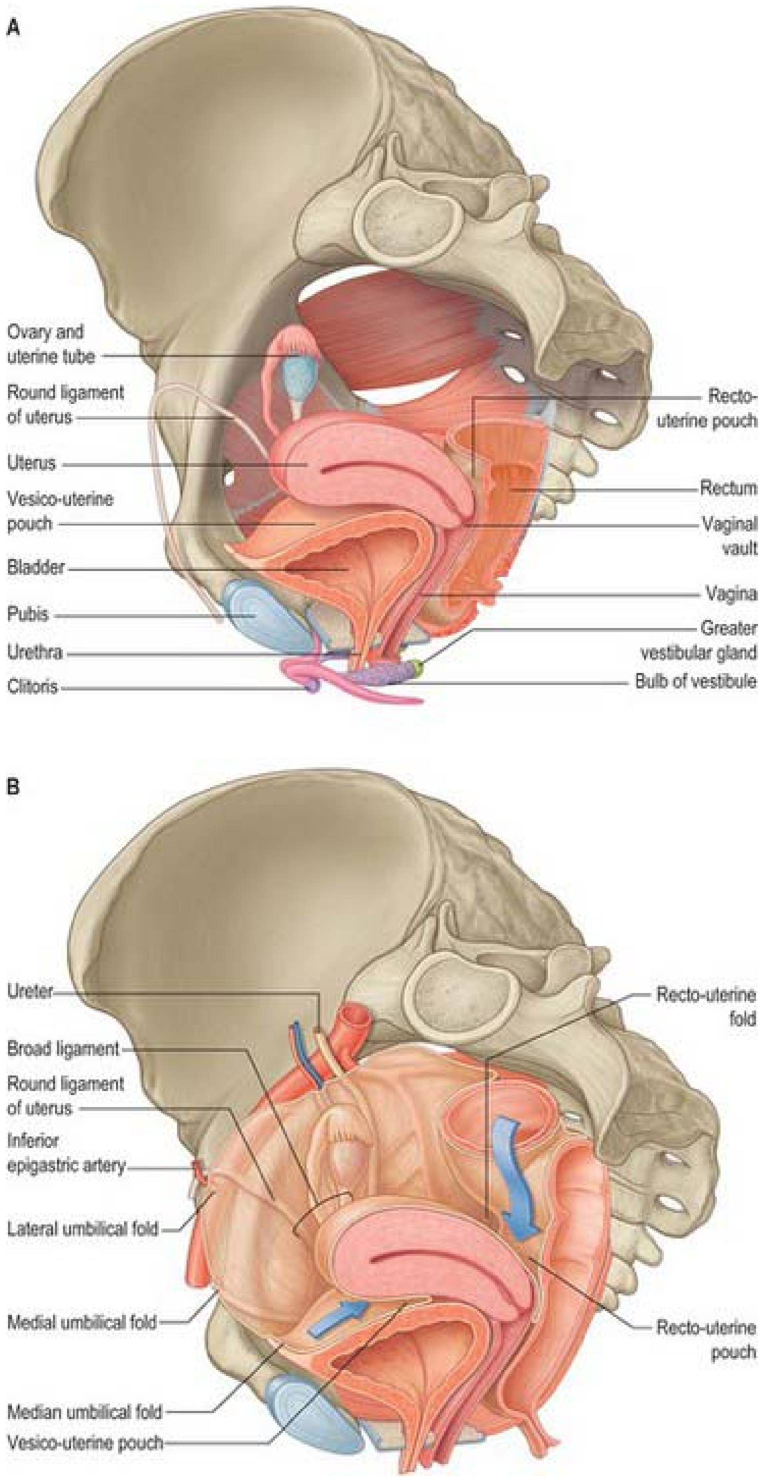
A
Ovary and uterine tube
Round ligament of uterus
Uterus
Vesico-uterine pouch
Bladder
Pubis
Urethra
Clitoris
Recto-uterine pouch
Rectum
Vaginal vault
Vagina
Greater vestibular gland
Bulb of vestibule
B
Ureter
Broad ligament
Round ligament of uterus
Inferior epigastric artery
Lateral umbilical fold
Medial umbilical fold
Median umbilical fold
Vesico-uterine pouch
Recto-uterine fold
Recto-uterine pouch

Fig. 77.10 **A**, Anatomical relations of the female genital tract and bladder and rectum. **B**, Pelvic peritoneal reflections showing broad ligament and its contents.

*(**A** from Drake, Vogl, Mitchell, Tibbitts and Richardson 2008. **B** from Drake, Vogl and Mitchell 2005.)*

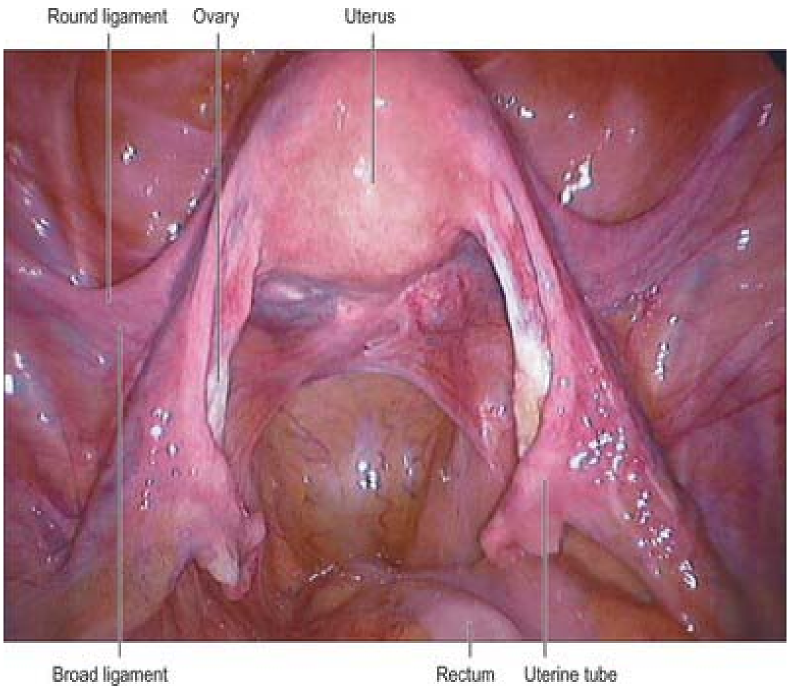

Fig. 77.11 Laparoscopic view of the uterus – the patient is tilted head down so that the small bowel is moved away from the uterus to give this view.

The uterus is divided into two main regions: the body of the uterus (corpus uteri) forms the upper two-thirds, and the cervix (cervix uteri) forms the lower third. In the adult nulliparous state the cervix tilts forwards relative to the axis of the vagina (anteversion), and the body of the uterus tilts forward relative to the cervix (anteflexion) (Fig. 77.12). In 10 to 15% of women the whole uterus leans backwards at an angle to the vagina and is said to be retroverted. A uterus that angles backwards on the cervix is described as retroflexed.

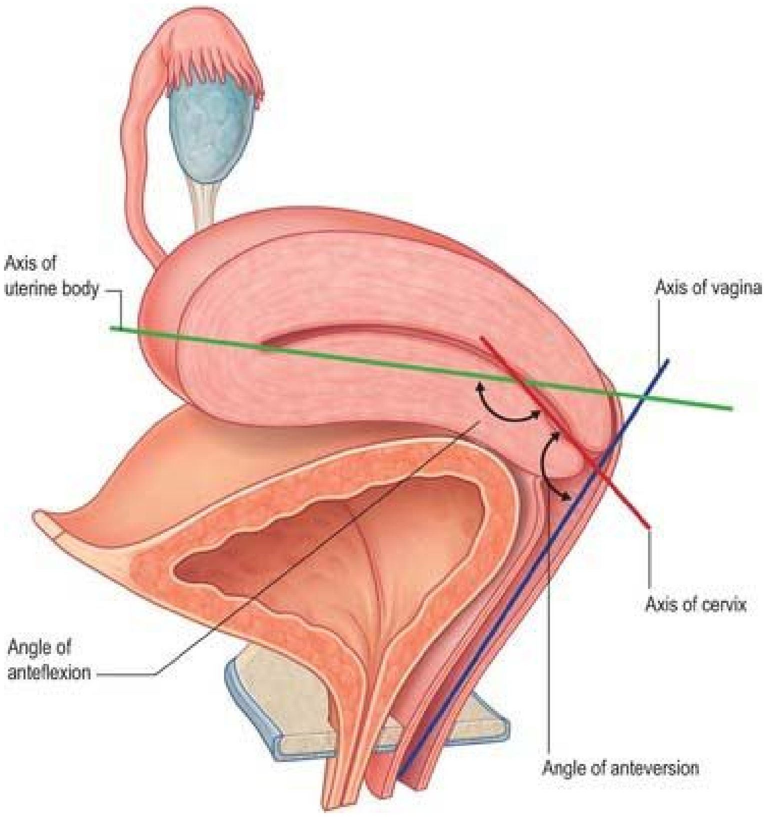

Fig. 77.12 Angles of anteflexion and anteversion.

(From Drake, Vogl and Mitchell 2005.)

Body

The body of the uterus is pear shaped and extends from the fundus superiorly to the cervix inferiorly. Near its upper end, the uterine tubes enter the uterus on both sides at the uterine cornua. Inferoanterior to each cornu is the round ligament and inferoposterior is the ovarian ligament. The dome-like fundus is superior to the entry points of the uterine tubes and covered by peritoneum which is continuous with that of neighbouring surfaces. The fundus is in contact with coils of small intestine and occasionally by distended sigmoid colon. The lateral margins of the body are convex, and on each side their peritoneum is reflected laterally to form the broad ligament, which extends as a flat sheet to the pelvic wall (Fig. 77.13). The anterior surface of the uterine body is covered by peritoneum which is reflected onto the bladder at the uterovesical fold (Fig. 77.14). This normally occurs at the level of the internal os, the most inferior margin of the body of the uterus. The vesico-uterine pouch between the bladder and uterus is obliterated when the bladder is distended, but may be occupied by small intestine when the bladder is empty. The posterior surface of the uterus is convex transversely. Its peritoneal covering continues down to the cervix and upper vagina and is then reflected back to the rectum along the surface of the recto-uterine pouch (of Douglas), which lies posterior to the uterus (Fig. 77.15). The sigmoid colon and occasionally the terminal ileum lie posterior to the uterus.

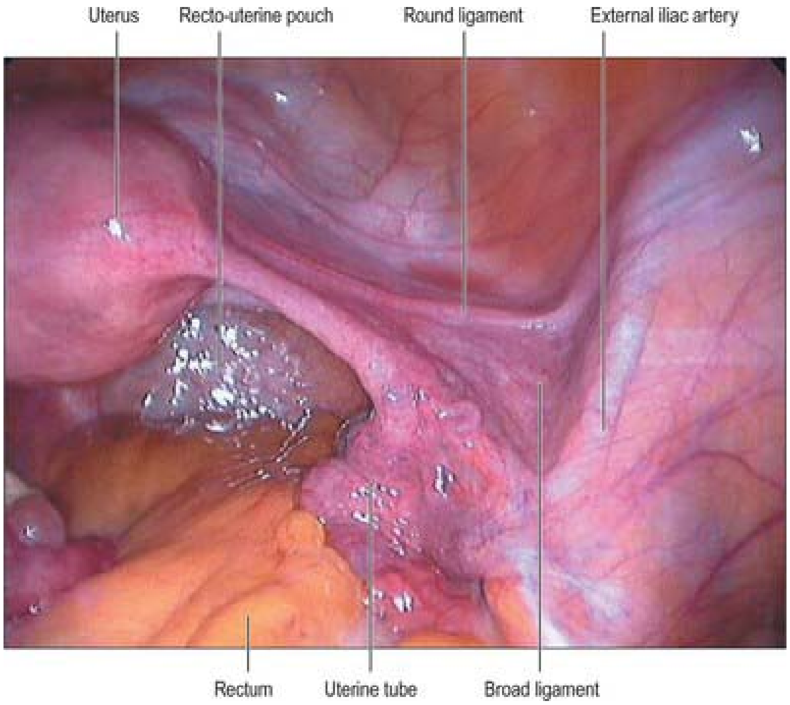
Uterus
Recto-uterine pouch
Round ligament
External iliac artery
Rectum
Uterine tube
Broad ligament

Fig. 77.13 Laparoscopic view of the broad ligament.

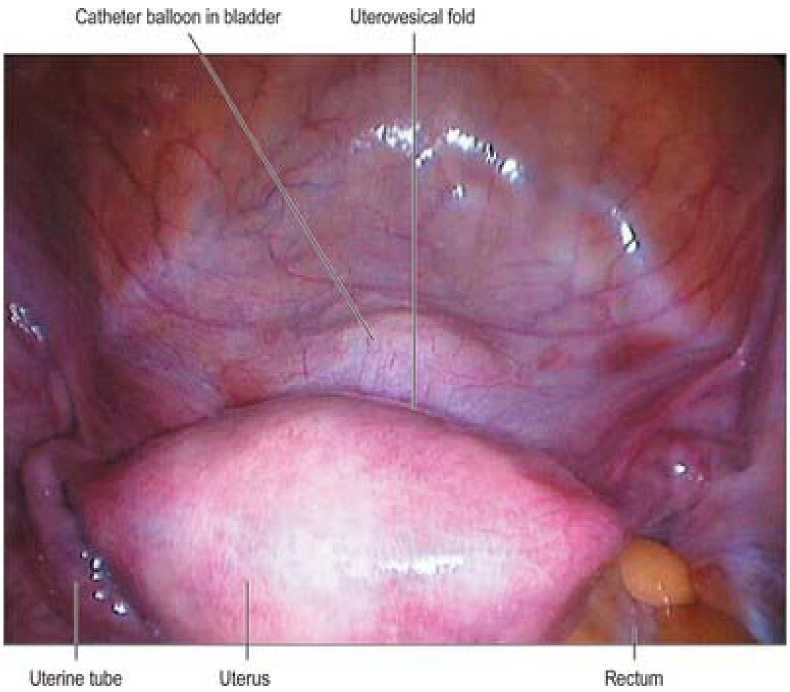
Catheter balloon in bladder
Uterovesical fold
Uterine tube
Uterus
Rectum

Fig. 77.14 Laparoscopic view of the anterior part of the pelvis showing uterovesical fold anterior to the uterus.

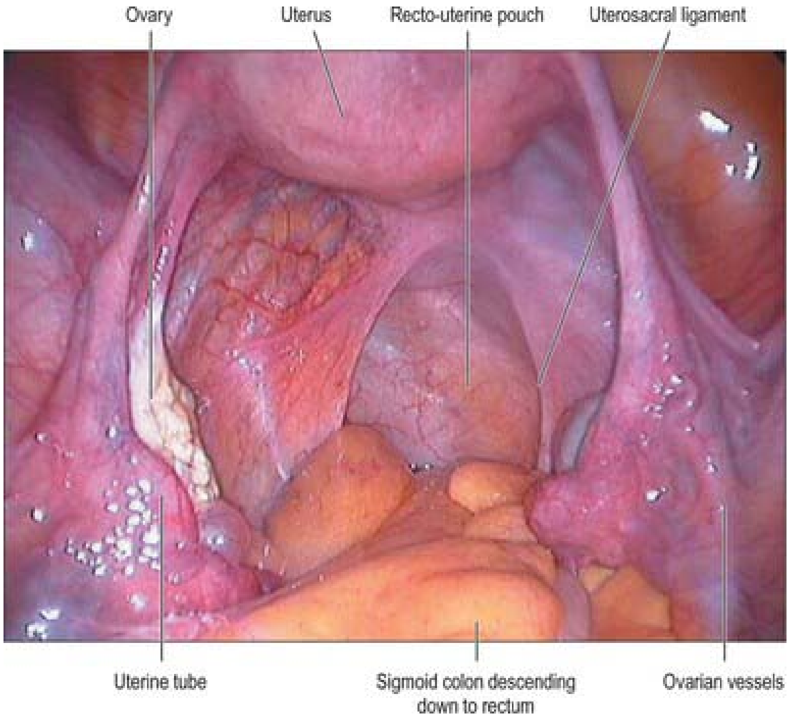
Ovary
Uterus
Recto-uterine pouch
Uterosacral ligament
Uterine tube
Sigmoid colon descending down to rectum
Ovarian vessels

Fig. 77.15 Laparoscopic view of the posterior pelvis showing the pouch of Douglas (recto-uterine pouch) with the sigmoid colon descending

towards the rectum.

The cavity of the uterine body usually measures 6 cm from the external os of the cervix to the wall of the fundus and is flat in its anteroposterior plane. In coronal section, it is triangular, broad above where the two uterine tubes join the uterus, and narrow below at the internal os of the cervix (Fig. 77.16).

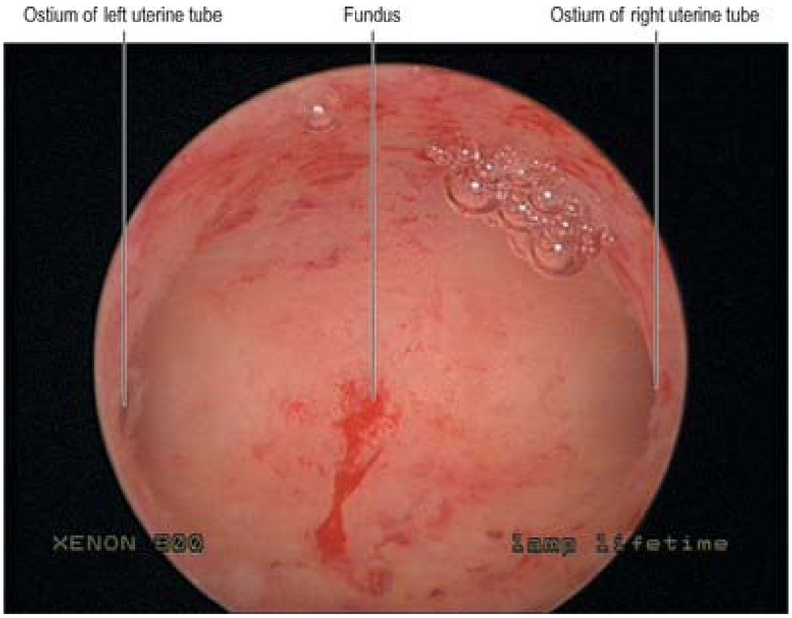

Fig. 77.16 Hysteroscopic view of the endometrial cavity of the uterus.

There may be failure in fusion of the paramesonephric (Müllerian) ducts, which results in a uterus that is not pear shaped. There may just be a septum (septate uterus) or partial clefting of the uterus (bicornuate uterus); the most extreme example is a septate vagina, two cervices, and two discrete uteri, each with one uterine tube (uterus didelphys).

Cervix

The adult, non-pregnant cervix is narrower and more cylindrical than the body of the uterus and is typically 2.5 cm long. The upper end communicates with the uterine body via the internal os and the lower end opens into the vagina at the external os. In nulliparous women, the external os is usually a circular aperture, whereas after childbirth it is a transverse slit. Two longitudinal ridges, one each on its anterior and posterior walls, give off small oblique palmate folds that ascend laterally like the branches of a tree (arbor vitae uteri): the folds on opposing walls interdigitate to close the canal. The narrower isthmus forms the upper third of the cervix. Although unaffected in the first month of pregnancy, it is gradually taken up into the uterine body during the second month to form the 'lower uterine segment' (see below). In non-pregnant women the isthmus undergoes menstrual changes, although these are less pronounced than those occurring in the uterine body. The external end of the cervix enters the upper end of the vagina, thereby dividing the cervix into supravaginal and vaginal parts. The supravaginal part is separated anteriorly from the bladder by cellular connective tissue, the parametrium, which also passes to the sides of the cervix and laterally between the two layers of the broad ligaments.

Pelvic ligaments and peritoneal folds

The uterus is connected to a number of 'ligaments'. Some are true ligaments in that they have a fibrous composition and provide support to the uterus, some provide no support to the uterus, and others are simply folds of peritoneum.

Peritoneal folds

The parietal peritoneum is reflected over the upper genital tract to produce anterior (uterovesical), posterior (rectovaginal) and lateral peritoneal folds. The lateral folds are commonly called the broad ligaments.

Uterovesical and rectovaginal folds

The anterior or uterovesical fold consists of peritoneum reflected onto the bladder from the uterus at the junction of its cervix and body. The posterior or rectovaginal fold consists of peritoneum reflected from the posterior vaginal fornix on to the front of the rectum, thereby create the deep recto-uterine pouch of Douglas. The pouch of Douglas is bounded anteriorly by the uterus, supravaginal cervix and posterior vaginal fornix, posteriorly by the rectum and laterally by the uterosacral ligaments.

Broad ligament

The lateral folds or broad ligaments extend on each side from the uterus to the lateral pelvic walls, where they become continuous with the peritoneum covering those walls (Figs 77.17, 77.18). The upper border is free and the lower border is continuous with the peritoneum over the bladder, rectum and pelvic side-wall. The borders are continuous with each other at the free edge via the uterine fundus and diverge below near the superior surfaces of levatores ani. A uterine tube lies in the upper free border on either side. The broad ligament is divided into an upper mesosalpinx, a posterior mesovarium and an inferior mesometrium.

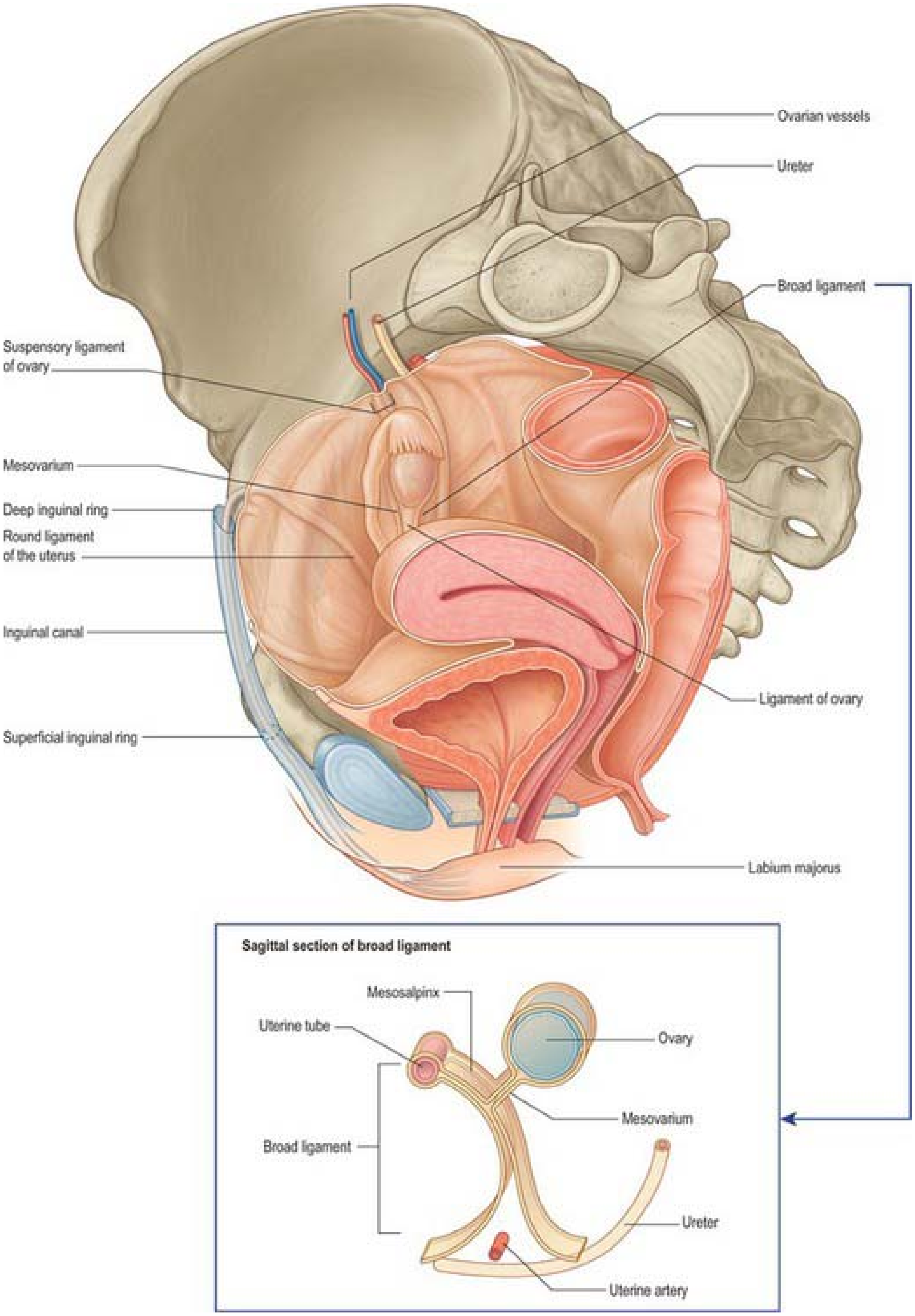
Ovarian vessels
Ureter
Broad ligament
Suspensory ligament of ovary
Mesovarium
Deep inguinal ring
Round ligament of the uterus
Inguinal canal
Superficial inguinal ring
Ligament of ovary
Labium majorus
Sagittal section of broad ligament
Mesosalpinx
Uterine tube
Ovary
Mesovarium
Broad ligament
Ureter
Uterine artery

Fig. 77.17 Pelvic peritoneal reflections, demonstrating the broad ligament and its contents.

(From Drake, Vogl and Mitchell 2005.)

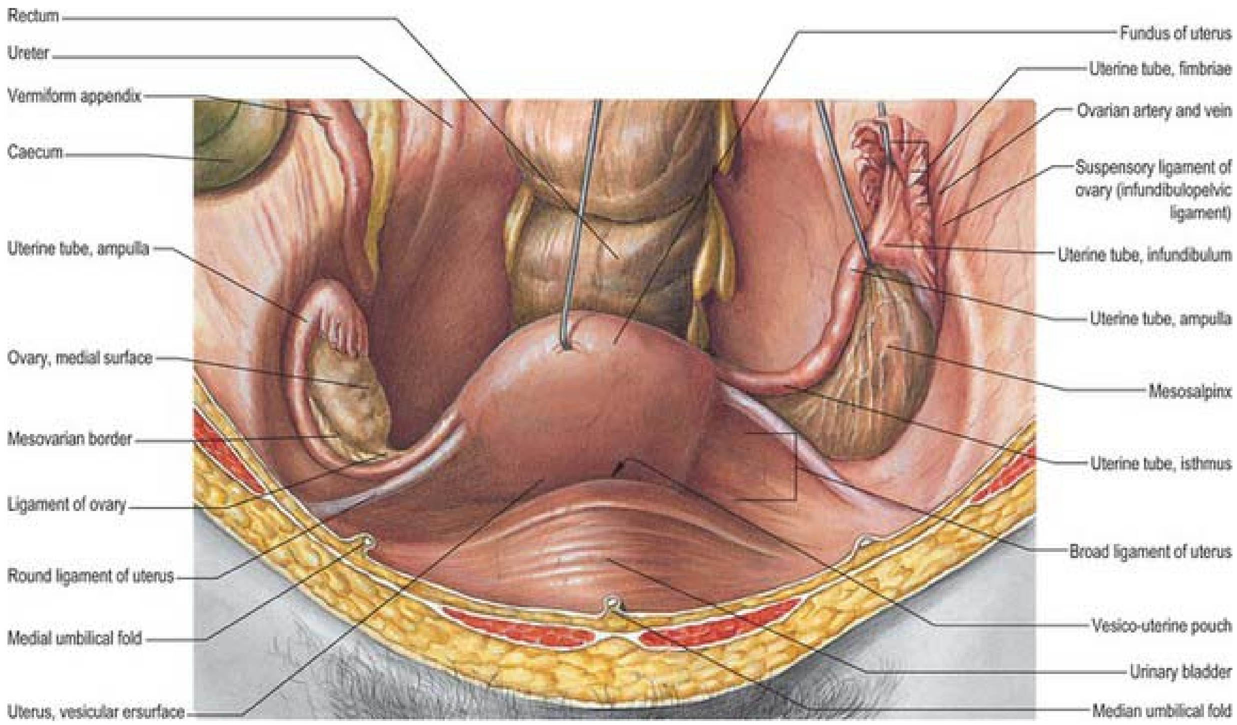
Rectum
Ureter
Vermiform appendix
Caecum
Uterine tube, ampulla
Ovary, medial surface
Mesovarian border
Ligament of ovary
Round ligament of uterus
Medial umbilical fold
Uterus, vesicular ersurface
Fundus of uterus
Uterine tube, fimbriae
Ovarian artery and vein
Suspensory ligament of ovary (infundibulopelvic ligament)
Uterine tube, infundibulum
Uterine tube, ampulla
Mesosalpinx
Uterine tube, isthmus
Broad ligament of uterus
Vesico-uterine pouch
Urinary bladder
Median umbilical fold

Fig. 77.18 Ovaries and broad ligament, superior view with the uterus lifted away from the bladder.

(From Sobotta 2006.)

Mesosalpinx

The mesosalpinx is attached above to the uterine tube and posteroinferiorly to the mesovarium. Superior and laterally it is attached to the suspensory ligament of the ovary and medially it is attached to the ovarian ligament. The fimbria of the tubal infundibulum projects from its free lateral end. Between the ovary and uterine tube the mesosalpinx contains vascular anastomoses between the uterine and ovarian vessels, the epoophoron, and the paroophoron (Fig. 77.19). The mesovarium projects from the posterior aspect of the broad ligament, of which it is the smaller part. It is attached to the hilum of the ovary and carries vessels and nerves to the ovary.

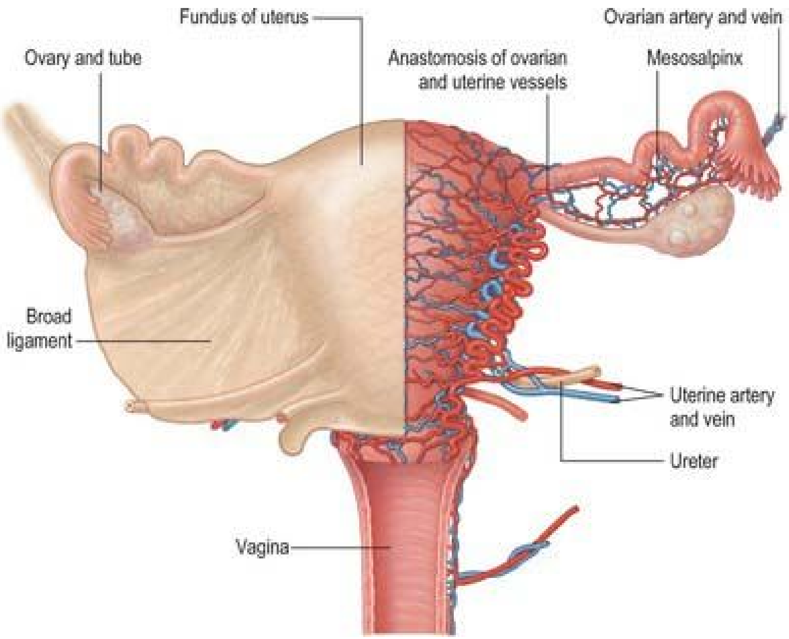
Fundus of uterus
Ovarian artery and vein
Ovary and tube
Anastomosis of ovarian and uterine vessels
Mesosalpinx
Broad ligament
Uterine artery and vein
Ureter
Vagina

Fig. 77.19 Broad ligament (left) and blood supply to the uterus and ovaries (right).

(From Drake, Vogl, Mitchell, Tibbitts and Richardson 2008.)

Mesometrium

The mesometrium is the largest part of the broad ligament, and extends from the pelvic floor to the ovarian ligament and uterine body. The uterine artery passes between its two peritoneal layers typically 1.5 cm lateral to the cervix: it crosses the ureter shortly after its origin from the internal iliac artery and gives off a branch that passes superiorly to the uterine tube, where it anastomoses with the ovarian artery (Fig. 77.19). Between the pyramid formed by the infundibulum of the tube, the upper pole of the ovary, and the lateral pelvic wall, the mesometrium contains the ovarian vessels and nerves lying within the fibrous suspensory ligament of the ovary (infundibulopelvic ligament). This ligament continues laterally over the external iliac vessels as a distinct fold. The mesometrium also encloses the proximal part of the round ligament of the uterus, as well as smooth muscle and loose connective tissue.

Ligaments of the pelvis

The ligaments of the pelvis consist of the round, uterosacral, transverse cervical and pubocervical ligaments.

Round ligament

The round ligaments are narrow, somewhat flattened bands 10–12 cm long. Each is attached medially to the upper part of the uterus just below and anterior to the lateral cornua. From here, each passes laterally within the upper part of the broad ligament to the pelvic side-wall. At the start of the inferior epigastric artery, the round ligament enters the deep inguinal ring. It traverses the inguinal canal and splits into strands that merge with the surrounding connective tissue before terminating in the mons pubis above the labium majus. Near the uterus the round ligament contains a considerable amount of smooth muscle but this gradually diminishes and the terminal portion is purely fibrous. The round ligament contains blood vessels, nerves and lymphatics. The latter drain the uterine region around the entry of the uterine tube to the superficial inguinal lymph nodes.

In the fetus a projection of peritoneum (processus vaginalis) is carried with the round ligament for a short distance into the inguinal canal. This is generally obliterated in adults, although it is sometimes patent even in old age. In the canal the ligament receives the same coverings as the spermatic cord, although they are thinner and blend with the ligament itself, which may not reach the mons pubis. The round and ovarian ligaments both develop from the gubernaculum and are continuous.

Uterosacral, transverse cervical and pubocervical ligaments

The uterosacral ligaments are recto-uterine folds and contain fibrous tissue and smooth muscle (Fig. 77.18). They pass back from the cervix and uterine body on both sides of the rectum, and they are attached to the front of the sacrum. The ligaments can be palpated laterally on rectal examination. On vaginal examination they can be felt as thick bands of tissue passing downwards on both sides of the posterior fornix. The transverse cervical ligaments (cardinal ligaments, ligaments of Mackenrodt) (Fig. 77.20) extend from the side of the cervix and lateral fornix of the vagina to attach extensively on the pelvic wall. At the level of the cervix, some fibres interdigitate with fibres of the uterosacral ligaments. They are continuous with the fibrous tissue around the lower parts of the ureters and pelvic blood vessels. Fibres of the pubocervical ligament pass forward from the anterior aspect of the cervix and upper vagina to diverge around the urethra (Fig. 77.20). These fibres attach to the posterior aspect of the pubic bones.

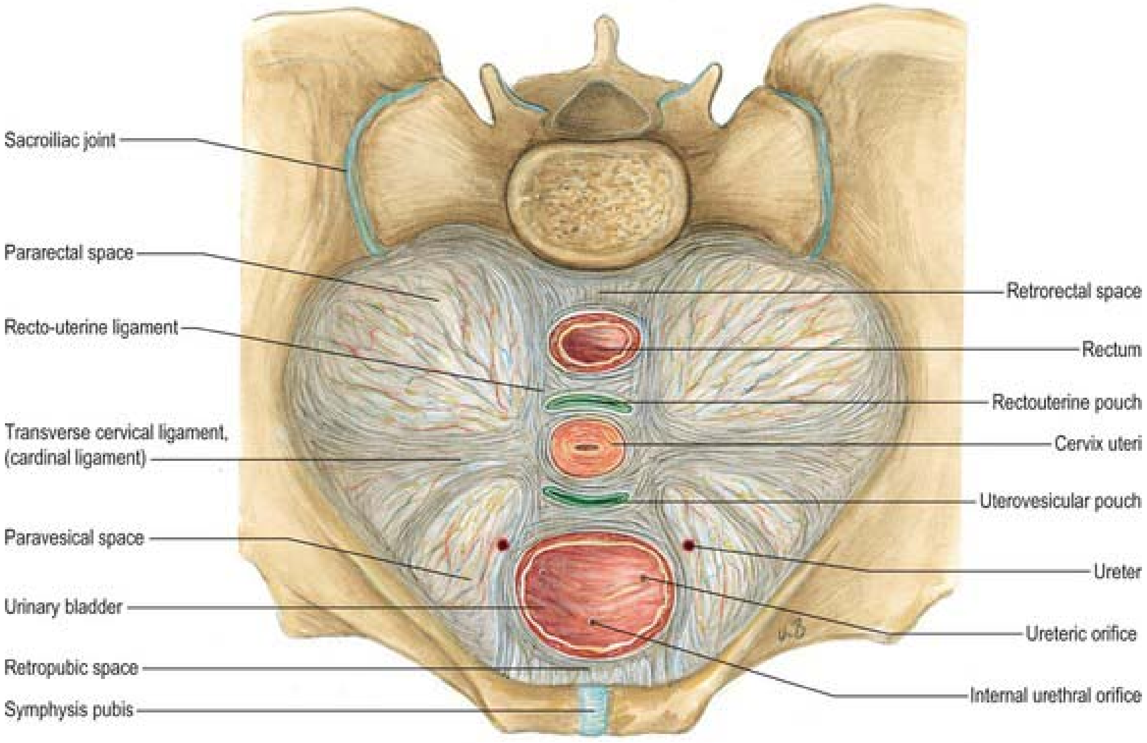
Sacroiliac joint
Pararectal space
Recto-uterine ligament
Transverse cervical ligament, (cardinal ligament)
Paravesical space
Urinary bladder
Retropubic space
Symphysis pubis
Retrorectal space
Rectum
Rectouterine pouch
Cervix uteri
Uterovesicular pouch
Ureter
Ureteric orifice
Internal urethral orifice

Fig. 77.20 Supporting ligaments of the pelvis showing the transverse cervical ligaments.

(From Sobotta 2006.)

While the uterosacral and transverse cervical ligaments may act in varying measure as mechanical supports of the uterus, levatores ani and coccygei, the urogenital diaphragm and the perineal body appear at least as important in this respect. There has been renewed interest in the supporting structures of the pelvis, and the subject has been reviewed in detail by Delancey (2000).

Vascular supply and lymphatic drainage

Arteries

The arterial supply to the uterus comes from the uterine artery (Fig. 77.21). This arises as a branch of the anterior division of the internal iliac artery. From its origin, the uterine artery crosses the ureter anteriorly in the broad ligament before branching as it reaches the uterus at the level of the cervico-uterine junction. One major branch ascends the uterus tortuously within the broad ligament until it reaches the region of the ovarian hilum, where it anastomoses with branches of the ovarian artery. Another branch descends to supply the cervix and anastomoses with branches of the vaginal artery to form two median longitudinal vessels, the azygos arteries of the vagina, which descend anterior and posterior to the vagina. Although there are anastomoses with the ovarian and vaginal arteries, the dominance of the uterine artery is indicated by its marked hypertrophy during pregnancy.

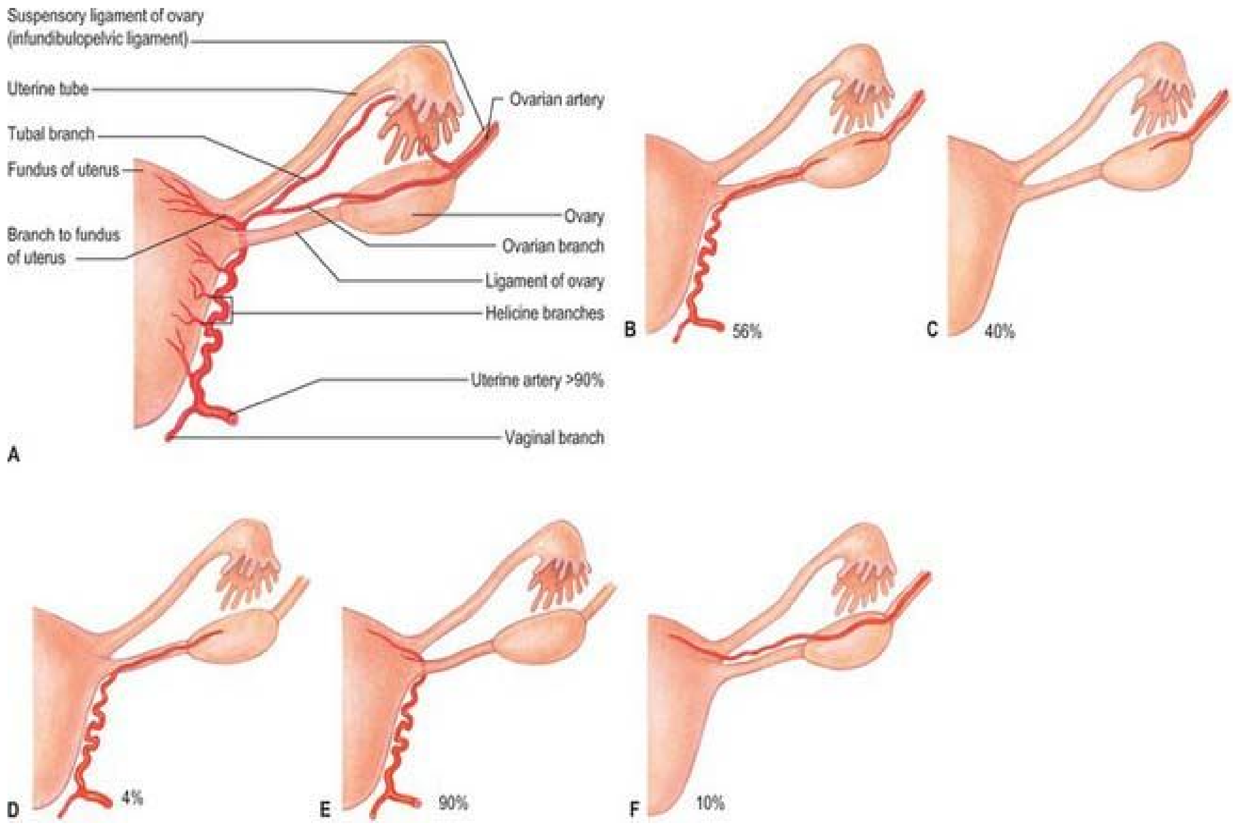
Suspensory ligament of ovary (infundibulopelvic ligament)
Uterine tube
Tubal branch
Fundus of uterus
Branch to fundus of uterus
Ovarian artery
Ovary
Ovarian branch
Ligament of ovary
Helicine branches
Uterine artery >90%
Vaginal branch
A
B
56%
C
40%
D
4%
E
90%
F
10%

Fig. 77.21 **A**, Normal arterial supply to uterus, uterine tubes and ovaries. **B–F**, Variant arterial supply.

(From Sobotta 2006.)

The tortuosity of the vessels as they ascend in the broad ligaments is repeated in their branches within the uterine wall. Each uterine artery gives off numerous branches. These enter the uterine wall, divide and run circumferentially as groups of anterior and posterior arcuate arteries. They ramify and narrow as they approach the anterior and posterior midline so that no large vessels are present in these regions. However, the left and right arterial trees anastomose across the midline and unilateral ligation can be performed without serious effects. Terminal branches in the uterine muscle are tortuous and are called helical arterioles. They provide a series of dense capillary plexuses in the myometrium and endometrium. From the arcuate arteries many helical arteriolar rami pass into the endometrium. Their detailed appearance changes during the menstrual cycle. In the proliferative phase helical arterioles are less prominent, whereas they grow in length and calibre, becoming even more tortuous in the secretory phase.

Veins

The uterine veins extend laterally in the broad ligaments, running adjacent to the arteries and passing over the ureters. They drain into the internal iliac veins (see Fig. 77.30). The uterine venous plexus anastomoses with the vaginal and ovarian venous plexuses.

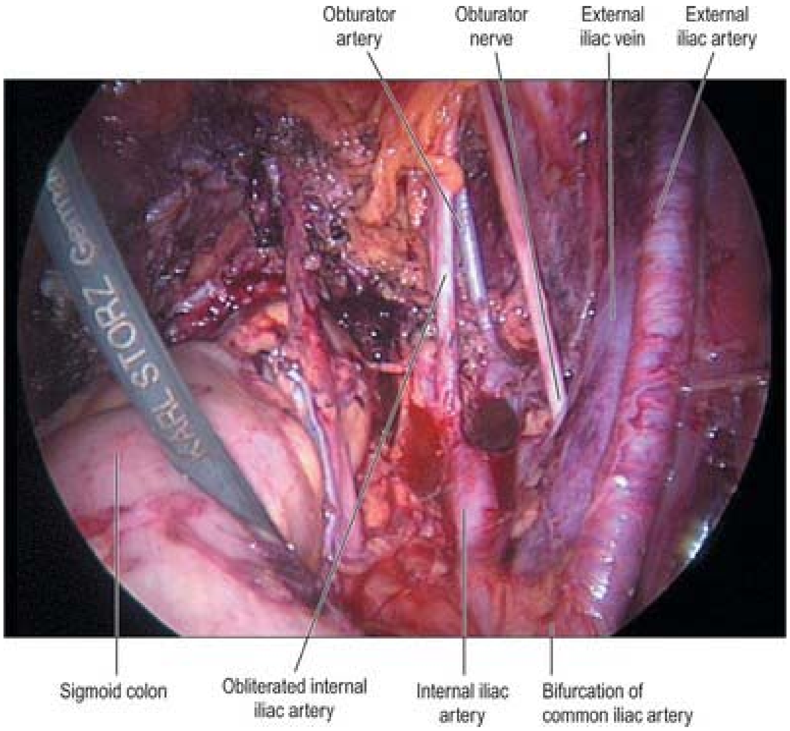
Obturator artery
Obturator nerve
External iliac vein
External iliac artery
KARL STORZ Germany
Sigmoid colon
Obliterated internal iliac artery
Internal iliac artery
Bifurcation of common iliac artery

Fig. 77.30 Broad ligament dissected and pelvic lymph nodes removed to reveal structures of the right-hand pelvic sidewall.

Lymphatic drainage

Uterine lymphatics exist in the superficial (subperitoneal) and deep parts of the uterine wall. Collecting vessels from the body of the uterus and cervix pass laterally in the parametrium to three main groups of lymph nodes: the external and internal iliac and the obturator nodes. The external and internal iliac nodes surround their corresponding arteries. The obturator nodes lie in the obturator fossa between the external and internal iliac vessels; the obturator nerve passes through the lower part of this group of lymph nodes.

Lymph vessels from the fundus of the uterus and the uterine tubes may accompany the lymph drainage of the ovaries to para-aortic nodes (Fig. 77.3B). The region surrounding the isthmus of the uterine tube may drain along the round ligament to the superficial inguinal nodes.

Innervation

The nerve supply to the uterus is predominantly from the inferior hypogastric plexus. Some branches ascend with, or near, the uterine arteries in the broad ligament. They supply the uterine body and tubes, and connect with tubal nerves from the inferior hypogastric plexus and with the ovarian plexus. The uterine nerves terminate in the myometrium and endometrium, and usually accompany the vessels. Nerves to the cervix form a plexus that contains small paracervical ganglia. Sometimes one ganglion is larger and is termed the uterine cervical ganglion. Branches may pass directly to the cervix uteri or may be distributed along the vaginal arteries.

Efferent preganglionic sympathetic fibres are derived from neurones in the last thoracic and first lumbar spinal segments; the sites where they synapse on their postganglionic neurones are unknown. Preganglionic parasympathetic fibres arise from neurones in the second to fourth sacral spinal segments and relay in the paracervical ganglia. Sympathetic activity may produce uterine contraction and vasoconstriction and parasympathetic activity may produce uterine inhibition and vasodilatation, but these activities are complicated by hormonal control of uterine functions.

Microstructure

Body of the uterus

The uterus is composed of three main layers. From its lumen outwards these are the endometrium (mucosa), myometrium (smooth muscle layer) and serosa (or adventitia) (Fig. 77.22).

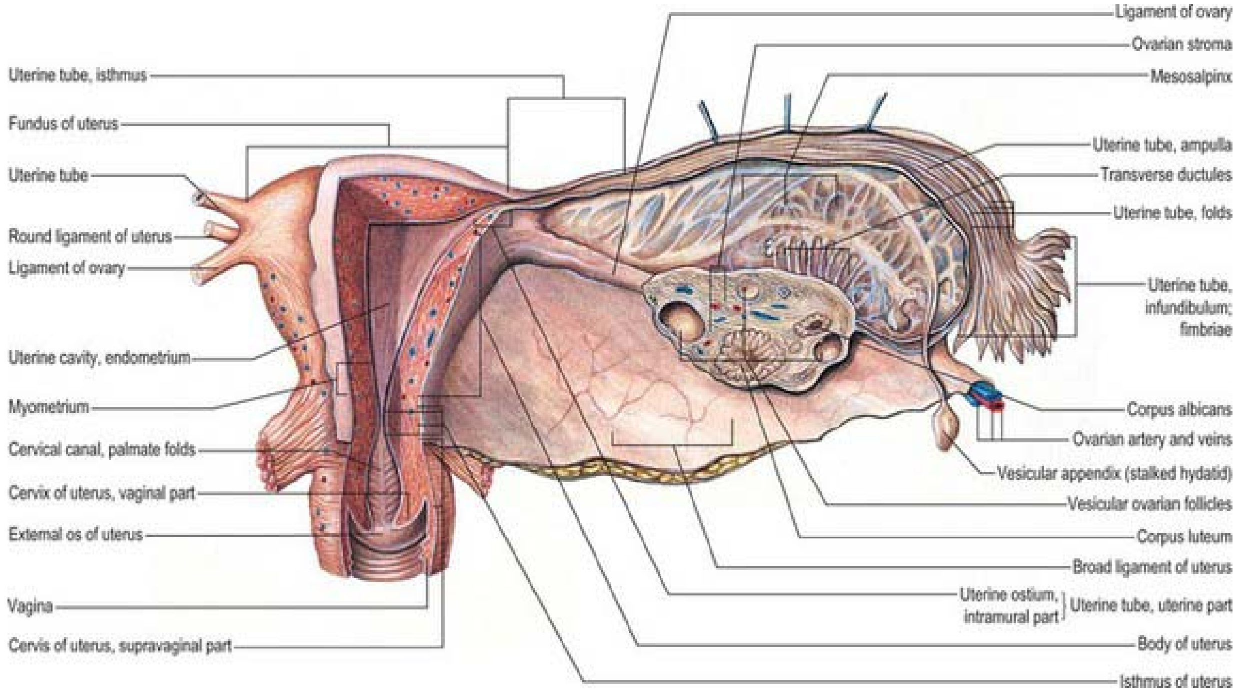
Uterine tube, isthmus
Fundus of uterus
Uterine tube
Round ligament of uterus
Ligament of ovary
Uterine cavity, endometrium
Myometrium
Cervical canal, palmate folds
Cervix of uterus, vaginal part
External os of uterus
Vagina
Cervix of uterus, supravaginal part
Ligament of ovary
Ovarian stroma
Mesosalpinx
Uterine tube, ampulla
Transverse ductules
Uterine tube, folds
Uterine tube, infundibulum; fimbriae
Corpus albicans
Ovarian artery and veins
Vesicular appendix (stalked hydatid)
Vesicular ovarian follicles
Corpus luteum
Broad ligament of uterus
Uterine ostium, intramural part
Uterine tube, uterine part
Body of uterus
Isthmus of uterus

Fig. 77.22 The uterus, uterine tubes and ovaries.

(From Sobotta 2006.)

Endometrium

The endometrium is formed by a layer of connective tissue, the endometrial stroma, which supports a single-layered columnar epithelium. Before puberty, the epithelium is ciliated and cuboidal. It contains glands which are composed largely of columnar cells secreting glycoproteins and glycogen. After puberty, the structure of the endometrium varies with the stage of the menstrual cycle (see below). The glands are tubular, run perpendicular to the luminal surface and penetrate up to the myometrial layer. The stroma consists of a highly cellular connective tissue between the endometrial glands, and contains blood and lymphatic vessels.

Myometrium

The myometrium is composed of smooth muscle and loose connective tissue and contains blood vessels, lymphatic vessels and nerves. It is dense and thick at the uterine midlevel and fundus but thin at the tubal orifices. The body of the uterus has four muscular layers. The submucosal (innermost) layer is composed of longitudinal and some oblique smooth muscle fibres. Where the lumen of the uterine tube passes through the uterine wall, this layer forms a circular muscle coat. The vascular layer is external to the submucosal layer and is rich in blood vessels as well as longitudinal muscle, it is succeeded by a layer of predominantly circular muscle, the supravascular layer. The outer, thin, longitudinal muscle layer, the subserosal layer, lies adjacent to the serosa.

The muscular fibres of the outer two layers converge at the lateral angles of the uterus, and continue into the uterine tubes. Some fibres enter the broad ligaments as the round and ovarian ligaments; others turn back into the uterosacral ligaments. At the junction between the body and the cervix, the smooth muscle merges with dense irregular connective tissue containing both collagen and elastin, and forms the majority of the cervical wall. Bilateral longitudinal fibres extend in the lateral submucosal layer from the fundal angle to the cervix. Their muscle fibres differ structurally from those of typical myometrium, and they may provide fast conducting pathways which coordinate the contractile activities of the uterine wall.

Serosa

The serosa is composed of peritoneum (mesothelium overlying a thin connective tissue lamina propria), which covers the uterine body. Posteriorly it continues downwards to cover the supravaginal cervix.

Cervix uteri

The cervix (Figs 77.23, 77.24) consists of fibroelastic connective tissue and contains relatively little smooth muscle. The elastin component of the cervical stroma is essential to the stretching capacity of the cervix during childbirth. The cervical canal is lined by a deeply folded mucosa with a surface epithelium of columnar mucous cells. There are branched tubular glands present amongst the mucosa, which are lined by a similar secretory epithelium. The glands extend obliquely upwards and outwards from the canal. They secrete clear, alkaline mucus, which is relatively viscous except at the midpoint of the menstrual cycle, when it becomes more copious and less viscous to encourage the passage of sperm. At the vaginal end of the cervix, the aperture of a gland may block and it then fills with mucus to form a Nabothian follicle (or cyst). None of the mucosa is shed during menstruation and so, unlike the body of the uterus, it is not divided into functional and basal layers and lacks spiral arteries. The surface of the intravaginal part of the cervix (ectocervix) is covered by non-keratinizing stratified squamous epithelium, which contains glycogen.

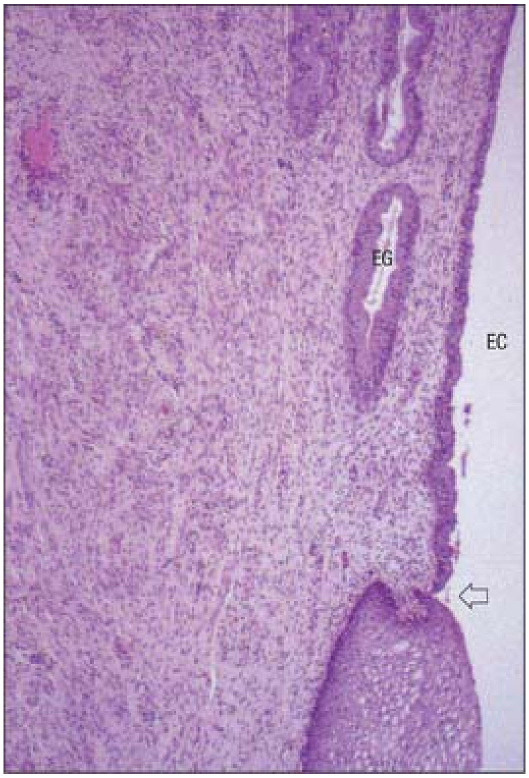

Fig. 77.23 Transformation zone of the uterine cervix. The single layered columnar epithelium lining the endocervical canal (EC) and its endocervical glands (EG) changes abruptly (arrow) to the stratified squamous non-keratinizing epithelium of the external os and ectocervix (below arrow).

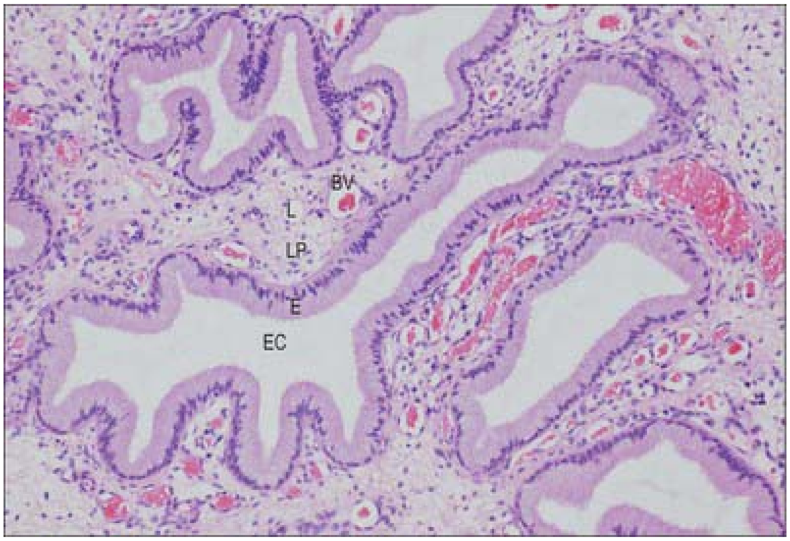

Fig. 77.24 Endocervical glands are deep infoldings of the lining of the endocervical canal (EC). The epithelium (E) is simple columnar and mucus-secreting. The underlying lamina propria (LP) is richly supplied with blood vessels (BV) and lymphatics (L).

(By courtesy of Mr Peter Helliwell and Dr Joseph Mathew, Department of Histopathology, Royal Cornwall Hospitals Trust, UK.)

The squamocolumnar junction, where the columnar secretory epithelium of the endocervical canal meets the stratified squamous covering of the ectocervix, is located at the external os before puberty. As oestrogen levels rise during puberty, the cervical os opens, exposing the endocervical columnar epithelium onto the ectocervix. This area of columnar cells on the ectocervix forms an area that is red and raw in appearance called an ectropion (cervical erosion). It is then exposed to the acidic environment of the vagina and through a process of squamous metaplasia transforms into stratified squamous epithelium. This area is thus known as the ‘transformation zone’. Other hyperoestrogenic states such as pregnancy and the use of oral contraceptive pills can also result in an ectropion. This area is the most usual site of cervical intraepithelial neoplasia (CIN) that may progress to malignancy. In postmenopausal women, the squamo-columnar junction recedes into the endocervical canal (Fig. 77.23).

Magnetic resonance imaging of the uterus

On T2-weighted magnetic resonance imaging (MRI), the uterus (Fig. 77.25A,B) displays a zonal anatomy, with three distinct zones: the endometrium; junctional zone; and myometrium. The endometrium and uterine cavity appear as a high-signal stripe; the thickness varies with the stage of the menstrual cycle. In the early proliferative phase it measures up to 5 mm, and widens to up to 1 cm in the mid-secretory phase. A band of low signal, the junctional zone, borders the endometrium. It represents the inner myometrium, which blends with the low-signal band of fibrous cervical stroma at the level of the internal os. The junctional zone appears low signal because the cells of the myometrium have low water content when compared to those of the outer myometrium. The junctional zone is of constant thickness and signal throughout the menstrual cycle, and usually measures 5 mm. The outer myometrium is of medium signal intensity in the proliferative phase, and of high signal intensity in the mid-secretory phase as a result of the increased vascularity and prominence of the arcuate vessels.

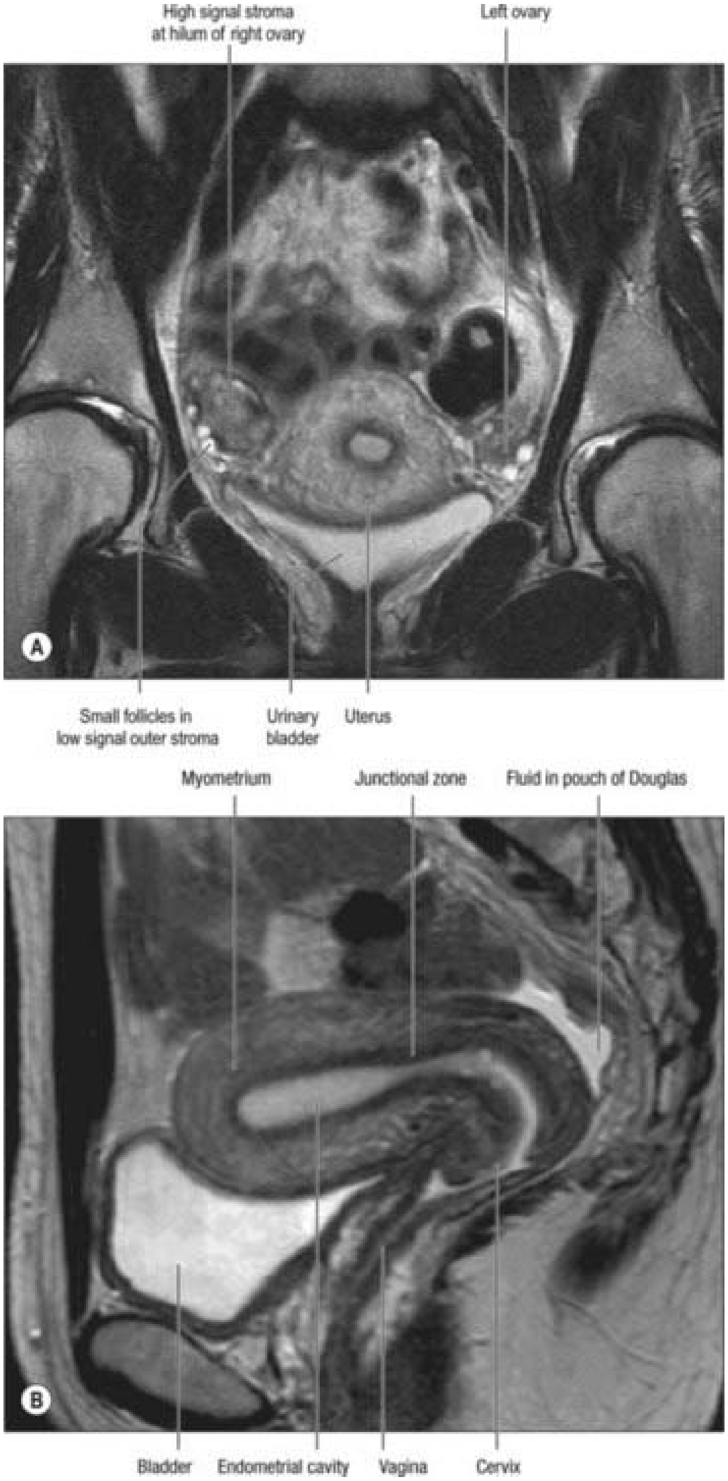
High signal stroma at hilum of right ovary
Left ovary
A
Small follicles in low signal outer stroma
Urinary bladder
Uterus
Myometrium
Junctional zone
Fluid in pouch of Douglas
B
Bladder
Endometrial cavity
Vagina
Cervix

Fig. 77.25 T2-weighted MRI scans of the uterus and ovaries. **A**, Coronal T2-weighted MRI through a female pelvis showing the uterus and both ovaries with the high signal central stroma and lower signal outer stroma. **B**,

Sagittal T2-weighted MRI through a female pelvis showing the zonal anatomy of the uterus.

In prepubertal females, the uterus is smaller (only 4 cm in length) and on T2-weighted images the endometrium is minimal or absent, and the junctional zone is indistinct. In postmenopausal women, the corpus decreases in size and the zonal anatomy is indistinct.

On T2-weighted MRI the cervix has an inner low-signal stroma continuous with the junctional zone of the uterus. Often this is surrounded by an outer zone of intermediate signal intensity, which is continuous with the outer myometrium. The appearances do not change with the menstrual cycle or oral contraceptive pill use. The central stripe is very high signal and is a consequence of the secretions produced by the endocervical glands.

UTERINE (FALLOPIAN) TUBES

The uterine tubes (Fig. 77.26) are attached to the upper part of the body of the uterus and their ostia open into the uterine cavity (Fig. 77.27). The medial opening of the tube (the uterine os) is located at the superior angle of the uterine cavity. The tube passes laterally and superiorly and consists of four main parts: intramural, isthmus, ampulla, fimbria. The intramural part is 0.7 mm wide, 1 cm long, and lies within the myometrium. It is continuous laterally with the isthmus, which is 1–5 mm wide and 3 cm long, and is rounded, muscular and firm. The isthmus is continuous laterally with the ampulla, the widest portion of the tube with a maximum luminal diameter of 1 cm. The ampulla is 5 cm long and has a thin wall and a tortuously folded luminal surface. Typically, fertilization takes place in its lumen. The ampulla opens into the trumpet-shaped infundibulum at the abdominal os. Fimbriae, numerous mucosal finger-like folds, 1 mm wide, are attached to the ends of the infundibulum and extend from its inner circumference beyond the muscular wall of the tube. One of these, the ovarian fimbria, is longer and more deeply grooved than the others, and is typically applied to the tubal pole of the ovary. At the time of ovulation, the fimbriae swell and extend as a result of engorgement of the vessels in the lamina propria, which aids capture of the released oocyte. All fimbriae are covered, like the mucosal lining throughout the tube, by a ciliated epithelium whose cilia beat towards the ampulla.

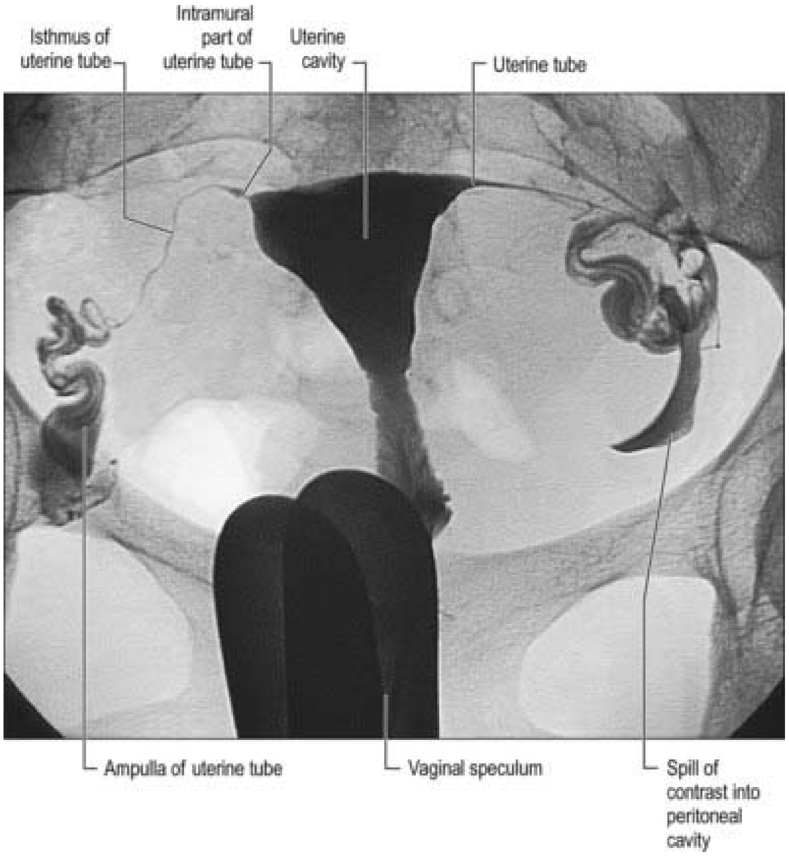
Isthmus of uterine tube
Intramural part of uterine tube
Uterine cavity
Uterine tube
Ampulla of uterine tube
Vaginal speculum
Spill of contrast into peritoneal cavity

Fig. 77.26 Digitally subtracted hysterosalpingogram. Radiopaque contrast is introduced via a catheter inserted through the cervical os: the catheter is introduced using a vaginal speculum. The contrast fills the triangular uterine cavity. The lumina of the narrow intramural and isthmic parts of the uterine tubes may be traced inferolaterally from the superior angles and they expand into the wider ampullae. Some contrast media has escaped into the pelvic cavity from the abdominal ostia.

(By courtesy of Dr Julia Hillier, Chelsea and Westminster Hospital, London.)

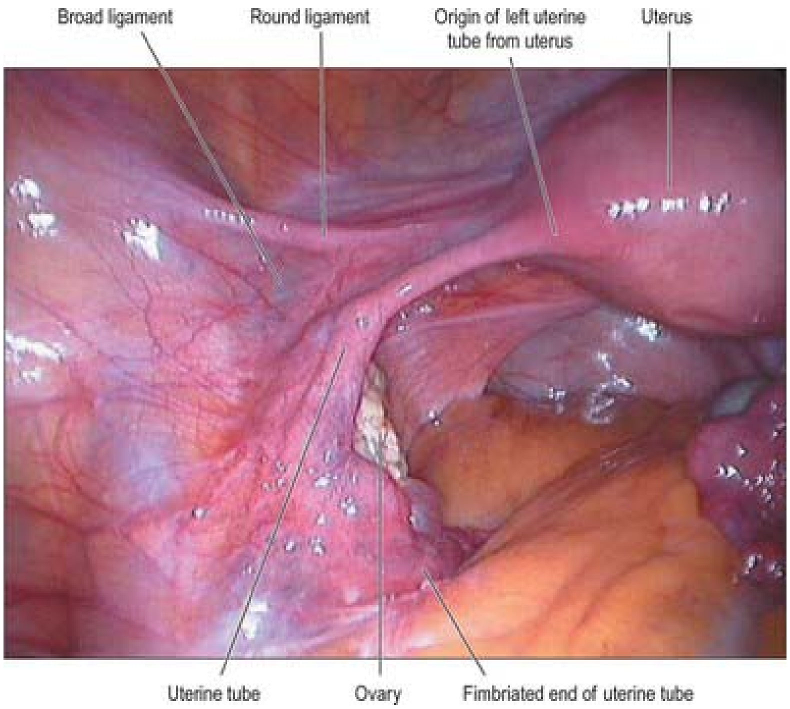
Broad ligament
Round ligament
Origin of left uterine tube from uterus
Uterus
Uterine tube
Ovary
Fimbriated end of uterine tube

Fig. 77.27 Laparoscopic view of the origin of the uterine tube from the uterus.

Vascular supply and lymphatic drainage

Arteries

The blood supply to the uterine tubes is derived from ovarian and uterine arteries. The lateral third of the tube is supplied by the ovarian artery, which continues in the mesosalpinx to anastomose with branches from the uterine artery. The medial two-thirds of the tube is supplied by the uterine artery.

Veins

Venous drainage is similar to the arterial supply. The venous drainage of the lateral two-thirds of the uterine tube is via the pampiniform plexus to the ovarian veins which open into the inferior vena cava on the right side and the renal vein on the left side. The medial two-thirds of the tube drain via the uterine plexus to the internal iliac vein.

Lymphatic drainage

Lymph drainage is via ovarian vessels to the para-aortic nodes and uterine vessels to the internal iliac chain. It is possible for lymph to reach the inguinal nodes via the round ligament.

Innervation

The uterine tube is innervated by autonomic fibres that are distributed mainly with the ovarian and uterine arteries. Most of the tube has a dual sympathetic and parasympathetic supply. Preganglionic parasympathetic fibres are derived from the vagus for the lateral half of the tube, and pelvic splanchnic nerves for the medial half. Sympathetic supply is derived from neurones in the tenth thoracic to the second lumbar spinal segments. Visceral afferent fibres travel with the sympathetic nerves, and enter the cord through corresponding dorsal roots: they may also travel with parasympathetic fibres. The ampullary submucosa contains modified Pacinian corpuscles.

Microstructure

The walls of the uterine tubes show typical visceral mucosal, muscular and serosal layers (Fig. 77.28). The mucosa is thrown into longitudinal folds, which are most pronounced distally at the infundibulum and decrease to shallow bulges in the intrauterine (intramural) portion. The mucosa is lined by a single-layered, tall, columnar epithelium, which contains mainly ciliated cells and secretory (peg) cells (so-called because they project into the lumen further than their ciliated neighbours), and occasional intraepithelial lymphocytes. In the tube, ciliated cells predominate distally and secretory cells proximally. Their activities vary with the stage in the menstrual cycle and with age. Secretory cells are most active around the time of ovulation. Their secretions include nutrients for the gametes and aid capacitation of the spermatozoa. Ciliated cells increase in height and develop more cilia in the oestrogenic first half of the menstrual cycle. Their cilia waft the oocyte from the open-ended infundibulum towards the uterus in fluids secreted by the peg cells. The epithelium regresses in height towards the end of the cycle and postmenopausally, when ciliated cells are reduced in number.

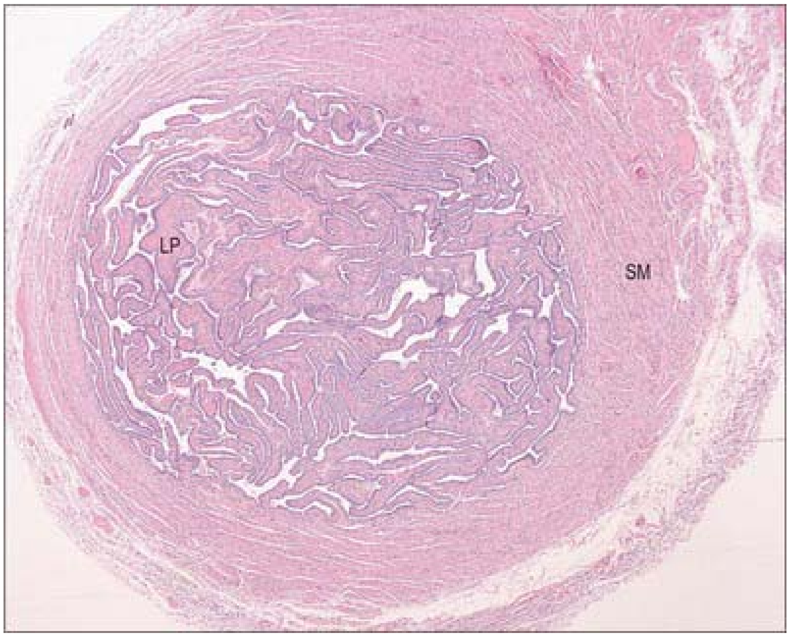

Fig. 77.28 Uterine tube (ampulla) with the mucosal lining thrown into extensive folds that fill the lumen. The superficial epithelium includes both secretory and ciliated cells, covering a lamina propria (LP). Smooth muscle (SM) occupies the wall of the tube.

(By courtesy of Mr Peter Helliwell and Dr Joseph Mathew, Department of Histopathology, Royal Cornwall Hospitals Trust, UK.)

The lamina propria provides vascular connective tissue support and abundant lymphatic drainage vessels. The smooth muscle of the muscularis is arranged as an inner circular, or spiral, layer and an outer, thinner, longitudinal layer. Together, their contractile activity produces peristaltic movements of the tube, which assist propulsion of the gametes and the fertilized ovum. The uterine tubes are covered externally by a highly vascular serosa.

OVARIES

In the adult non-pregnant state, the ovaries lie on each side of the uterus close to the lateral pelvic wall, suspended in the pelvic cavity by a double fold of peritoneum, the mesovarium, which is attached to the upper limit of the posterior aspect of the broad uterine ligament. They are dull white in colour and consist of dense fibrous tissue in which ova are embedded. Before regular ovulation begins they have a smooth surface, but thereafter their surfaces are distorted by scarring that follows the degeneration of successive corpora lutea (Fig. 77.29). Their average dimensions are 4 × 2 × 3 cm in reproductively mature women; they more than double their size during pregnancy. In the neonate, their dimensions are 1.3 × 0.6 × 0.4 cm. Prior to the first menstrual period (menarche) the ovaries are about a third of the normal reproductive adult size; they gradually increase in size with body growth. After the menopause, the average size of the ovary reduces to 2.0 × 1.5 × 0.5 cm and further to 1.5 × 0.75 × 0.5 cm in late menopause.

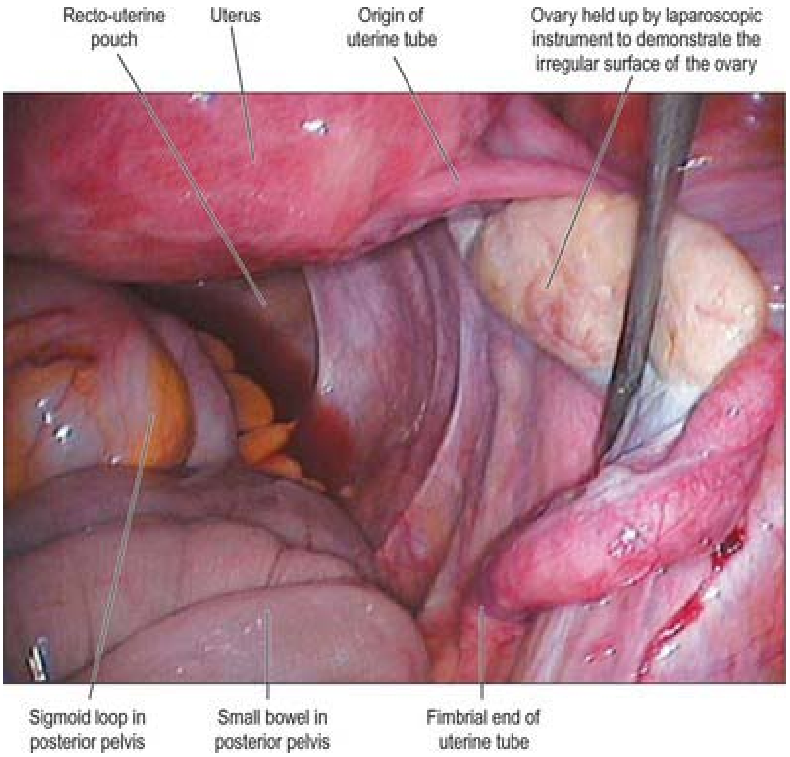
Recto-uterine pouch
Uterus
Origin of uterine tube
Ovary held up by laparoscopic instrument to demonstrate the irregular surface of the ovary
Sigmoid loop in posterior pelvis
Small bowel in posterior pelvis
Fimbrial end of uterine tube

Fig. 77.29 Laparoscopic picture of right ovary showing distorted surface.

The lateral surface of the ovary contacts parietal peritoneum in the ovarian fossa. Behind the ovarian fossa are retroperitoneal structures, including the ureter, internal iliac vessels, obturator vessels and nerve, and the origin of the uterine artery (Fig. 77.30). The medial surface faces the uterus and uterine vessels in the broad ligament, and the peritoneal recess here is termed the ovarian bursa. Above the superior extremity are the fimbria and distal section of the uterine tube. The inferior extremity points downwards towards the pelvic floor. The anterior border faces the posterior leaf of the broad ligament and contains the mesovarium. The posterior border is free and faces the peritoneum, which overlies the upper part of the internal iliac artery and vein, and the ureter. On the right side, superior and lateral to the ovary, are the ileocaecal junction, caecum and appendix. On the left side, the sigmoid colon passes over the superior pole of the ovary and joins the rectum, which lies between the medial surfaces of both ovaries. The mesosalpinx lies below the uterine tube. The ovarian ligament is inferior and medial. The mesovarium and ovary lie inferiorly at its fimbrial end. The round ligament is anterior to the tube. The superior and posterior surfaces of the tube lie free in the peritoneal cavity (Fig. 77.18).

In embryonic and early fetal life the ovaries are situated in the lumbar region near the kidneys. They gradually descend along the gubernaculum, stopping at the lesser pelvis. Accessory ovarian tissue may occur in the mesovarium or along the course of the gubernacula; rarely the ovaries may descend along the whole course of the gubernacula and are found in the labia majora. During pregnancy, the ovaries are lifted high in the pelvis and, by 14 weeks of gestation, become partly abdominal structures. By the third trimester they are totally abdominal structures and lie vertically behind and lateral to the parous uterus (see Ch. 78).

Peritoneal and ligamentous supports of the ovary

The peritoneal and ligamentous supports of the ovary consist of the infundibulopelvic, ovarian, and mesovarian ligaments.

Infundibulopelvic (suspensory) ligament

The suspensory or infundibulopelvic ligament of the ovary is a peritoneal fold, which is attached to the upper part of the lateral surface of the ovary. It contains the ovarian vessels and nerves. On the right side the infundibulopelvic ligament is attached to a fold of peritoneum that is posterior and inferior to the caecum and appendix. On the left side the peritoneal attachment is higher than on the right, and is lateral to the junction of the descending and sigmoid colons. As it joins the peritoneum which covers the psoas major, it passes superiorly over the external iliac vessels, genitofemoral nerve and ureter.

Ovarian ligament

The ovarian ligament attaches the uterine (inferiomedial) extremity of the ovary to the lateral angle of the uterus, posteroinferior to the uterine tube. It lies in the posterior leaf of the broad ligament and contains some smooth muscle cells. It is continuous with the medial border of the round ligament, both of which are remnants of the gubernaculum.

Mesovarium

The mesovarium is a short peritoneal fold which attaches the ovary to the back of the broad ligament. It carries blood vessels and nerves to the ovarian hilum. The uterine tube arches over the ovary, and ascends in relation to its mesovarian border, then curves over its tubal end and passes down on its posterior, free border and medial surface.

Vascular supply and lymphatic drainage

Arteries

The ovarian arteries are branches of the abdominal aorta and originate below the renal arteries. Each descends behind the peritoneum, and at the brim of the pelvis crosses the external iliac artery and vein to enter the true pelvic cavity. Here the artery turns medially in the ovarian suspensory ligament and splits into a branch to the mesovarium that supplies the ovary, and a branch that continues into the uterine broad ligament, below the uterine tube, and supplies the tube. There are variations in the site of the division to the ovary and tube (Fig. 77.21). On each side, a branch passes lateral to the uterus to unite with the uterine artery. Other branches accompany the round ligaments through the inguinal canal to the skin of the labium majus and the inguinal region. Early in intrauterine life the ovaries flank the vertebral column inferior to the kidneys, and so the ovarian arteries are relatively short, they gradually lengthen as the ovaries descend into the pelvis.

Veins

The ovarian veins emerge from the ovary as a plexus (pampiniform plexus) in the mesovarium and suspensory ligament (Fig. 77.3). Two veins emerge from the plexus and ascend with the ovarian artery: they usually merge into a single vessel before entering either the inferior vena cava on the right side, or the renal vein on the left side.

Lymphatic drainage

The main lymphatic drainage of the ovaries is along vessels that follow the ovarian veins to para-aortic nodes situated near the origin of the renal arteries. Drainage may also occur via pelvic nodes into lower para-aortic nodes, and rarely may follow the round ligament to the inguinal nodes.

Innervation

The ovarian innervation is derived from autonomic plexuses. The upper part of the ovarian plexus is formed from branches of the renal and aortic plexuses, and the lower part is reinforced from the superior and inferior hypogastric plexuses. These plexuses consist of postganglionic sympathetic, parasympathetic and visceral afferent fibres. The efferent sympathetic fibres are derived from the 10th and 11th thoracic spinal segments and are probably vasoconstrictor, whereas the parasympathetic fibres, from the inferior hypogastric plexuses, are probably vasodilator.

Microstructure

In young females the surface of the ovary is covered by a single layer of cuboidal epithelium, which contains some flatter cells. It appears dull white, in contrast to the shiny smooth peritoneal mesothelial covering of the mesovarium, with which it is continuous. A white line around the anterior mesovarian border usually marks the transition between peritoneum and ovarian epithelium. The surface epithelium is also termed the germinal epithelium, but this is a misnomer, because it is not the source of germ cells. Immediately beneath the epithelium there is a tough collagenous coat, the tunica albuginea. The ovarian tissue it surrounds is divisible into a cortex, which contains the ovarian follicles, and a medulla, which receives the ovarian vessels and nerves at the hilum.

Ovarian cortex

Before puberty, the cortex forms 35%, the medulla 20%, and interstitial cells up to 45%, of the volume of the ovary. After puberty the cortex forms the major part of the ovary, and encloses the medulla except at the hilum. It contains the ovarian follicles at various stages of development, and corpora lutea and their degenerative remnants, depending on age or stage of the menstrual cycle. The follicles and structures derived from them are embedded in a dense stroma composed of a meshwork of thin collagen fibres and fusiform fibroblast-like cells arranged in characteristic whorls. Stromal cells differ from fibroblasts in general connective tissue in that they contain lipid droplets, which accumulate in pregnancy. Stromal cells give rise to the thecal layers of maturing ovarian follicles. The theca interna becomes steroid-secreting in the corpus luteum.

Ovarian follicles

Primordial follicles

The development of ovarian follicles can be divided into different stages (Fig. 77.31). At birth, the ovarian cortex contains a superficial zone of primordial follicles. These consist of primary oocytes 25 μm in diameter, each surrounded by a single layer of flat follicular cells. The oocyte nuclei are slightly eccentric and have a characteristically prominent nucleolus. They contain the diploid number of chromosomes (duplicated as sister chromatids), arrested at the diplotene stage of meiotic prophase since before birth (Fig. 77.32). Many follicles degenerate either during prepubertal (including prenatal) life, or through atresia at some stage after beginning the process of cyclical maturation during the child-bearing period. Their remnants are visible as atretic follicles, the remains of which accumulate throughout the period of reproductive life. After puberty, cohorts of up to 20 primordial follicles become activated in each menstrual cycle (fewer are activated with advancing age). Their development takes a number of cycles. Of the follicles activated in each cohort, usually only one follicle from one or other ovary becomes dominant, reaches maturity and releases its oocyte at ovulation.

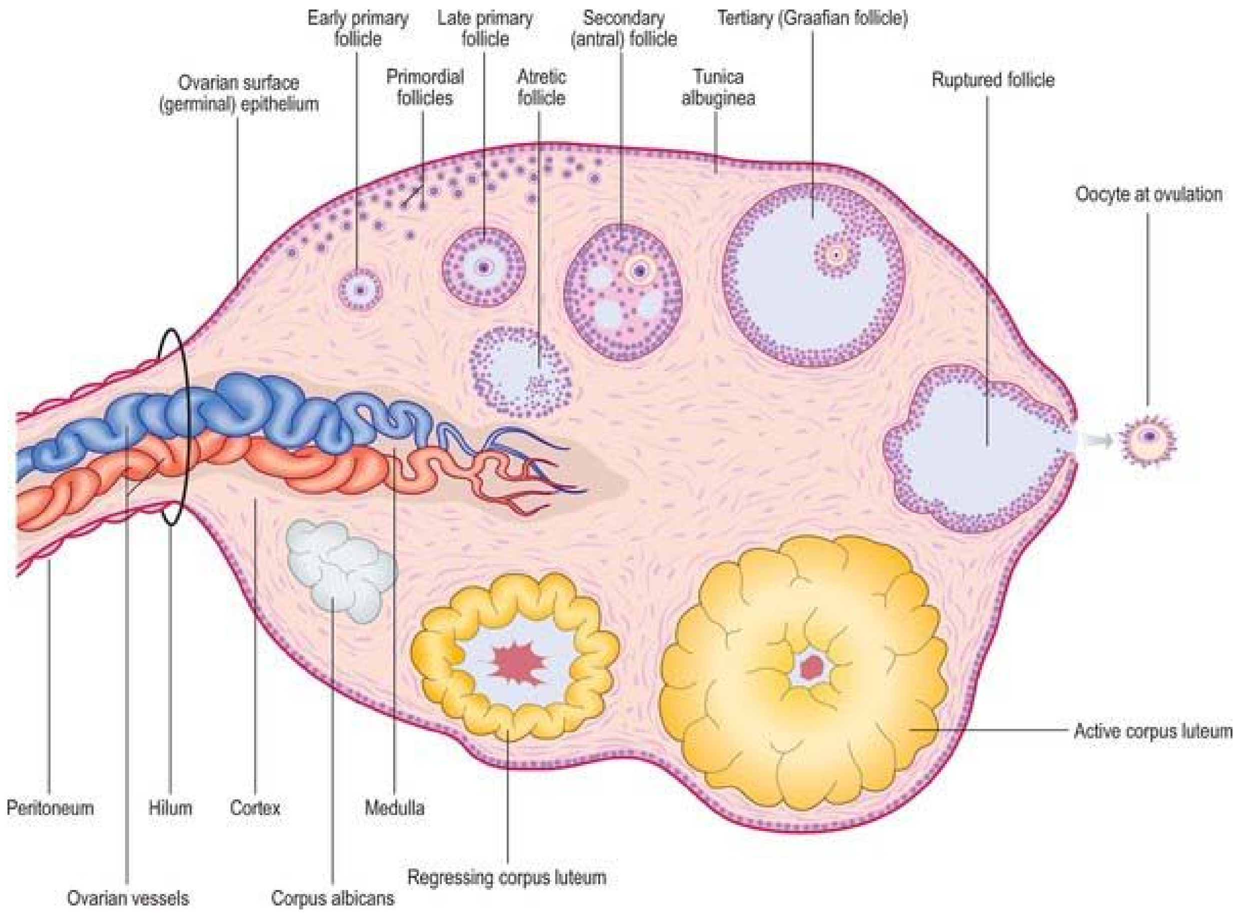
Early primary follicle
Late primary follicle
Secondary (antral) follicle
Tertiary (Graafian follicle)
Ovarian surface (germinal) epithelium
Primordial follicles
Atretic follicle
Tunica albuginea
Ruptured follicle
Oocyte at ovulation
Active corpus luteum
Peritoneum
Hilum
Cortex
Medulla
Regressing corpus luteum
Ovarian vessels
Corpus albicans

Fig. 77.31 The microstructure of the ovary and follicles at various stages in their cyclical development and the formation of corpora lutea and albicantes. Note that in the human ovary, developing follicles are rarely seen.

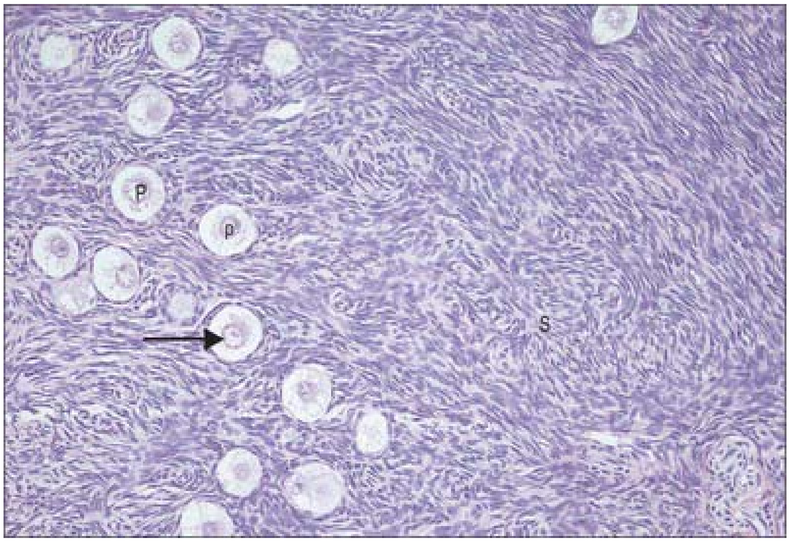

Fig. 77.32 High power ovarian cortex with primordial (p) and early primary (P) follicles within the stroma (S); stimulated primary follicles have cuboidal cells forming their wall. A large oocyte nucleus is visible in the plane of section of most of the follicles (arrow).

(By courtesy of Mr Peter Helliwell and Dr Joseph Mathew, Department of Histopathology, Royal Cornwall Hospitals Trust, UK.)

Primary follicles

Primary follicles develop from primordial follicles. The first sign is a change in the follicle cells from flattened to cuboidal. This is followed by their proliferation to give rise to a multilayered follicle consisting of granulosa cells surrounded by a thick basal lamina (Fig. 77.33). Stromal cells immediately surrounding the follicle begin to differentiate into spindle-shaped cells, which constitute the theca folliculi which will become the theca interna. They are later surrounded by a more fibrous layer called the theca externa. At the same time the oocyte increases in size and secretes a thick layer of extracellular proteoglycan-rich material, the zona pellucida, between its plasma membrane and the surrounding granulosa cells of the early follicle. This is important for the process of fertilization. The granulosa cells in contact with the zona pellucida send cytoplasmic processes radially inwards and these contact oocyte microvilli at gap junctions, indicating communication between them (see Motta et al 2003). The follicular cells, in particular the granulosa cells, which are in functional contact with each other through gap junctions, continue to proliferate and so the thickness of the late primary follicle wall increases.

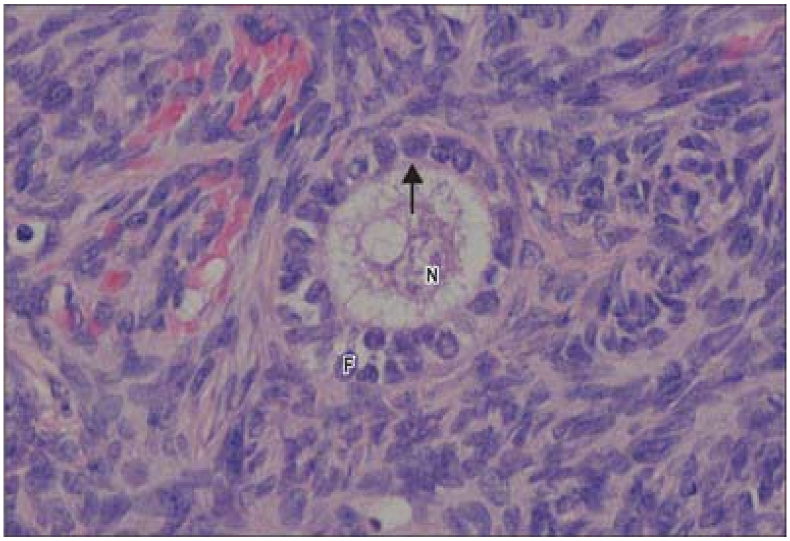

Fig. 77.33 High magnification micrograph of a primary follicle in a human ovarian cortex. The pale oocyte, with its eccentric nucleus (N) is separated from the follicle (F) by the zona pellucida (arrow). Cells of the follicle wall are in the early stages of proliferation to form a multilayered, late primary follicle.

(By courtesy of Mr Peter Helliwell and Dr Joseph Mathew, Department of Histopathology, Royal Cornwall Hospitals Trust, UK.)

Secondary (antral) follicles

Secondary (antral) follicles develop from primary follicles. The number of granulosa cells continues to increase. Cavities begin to form between them filled with a clear fluid (liquor folliculi) containing hyaluronate, growth factors, and steroid hormones secreted by the granulosa cells. The follicle is now about 200 μm in diameter and usually lies deep in the cortex. These cavities coalesce to form one large fluid-filled space, the antrum. This is surrounded by a thin, uniform layer of granulosa cells, except at one pole of the follicle where a thickened granulosa layer envelops the eccentrically placed oocyte, to form the cumulus oophorus. The oocyte has now reached its maximum size of about 80 μm and the inner and outer thecae are clearly differentiated (Fig. 77.34). As follicles mature, the theca interna becomes more prominent and its cells more rounded and typical of steroid-secreting endocrine cells. These cells produce androstenedione from which the granulosa cells synthesize oestrogens (primarily oestradiol). Follicular development is stimulated by follicle-stimulating hormone (FSH).

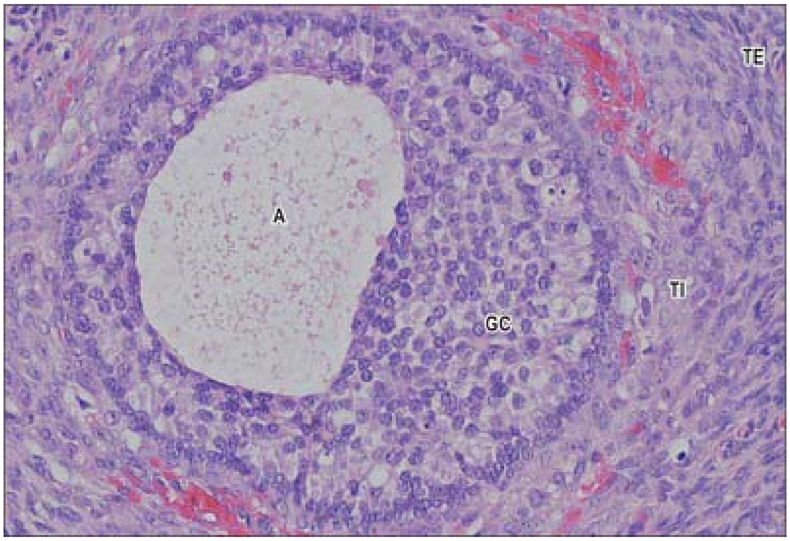

Fig. 77.34 Antral (secondary) follicle, showing the layers of the developing follicle wall. Granulosa cells (GC) enclose the antrum (A) filled with liquor folliculi and surround the oocyte (not seen in the plane of section) within an eccentric cellular mass (right). The outer theca interna (TI) is a highly vascular layer which develops steriod secretory activity and is enclosed by the outermost theca externa (TE).

(By courtesy of Mr Peter Helliwell and Dr Joseph Mathew, Department of Histopathology, Royal Cornwall Hospitals Trust, UK.)

Tertiary (Graafian) follicle

Although a number of follicles may progress to the secondary stage by about the first week of a menstrual cycle, usually only one tertiary follicle develops. The remainder become atretic. The surviving follicle increases considerably in size as the antrum takes up fluid from the surrounding tissues and expands to a diameter of 2 cm. The term Graafian follicle is often used to describe this mature follicular stage (Fig. 77.34). The oocyte and a surrounding ring of tightly adherent cells, the corona radiata, breaks away from the follicle wall and floats freely in the follicular fluid. The primary oocyte, which has remained in the first meiotic prophase since fetal life, completes its first meiotic division to produce the almost equally large secondary oocyte and a small first polar body with very little cytoplasm. The secondary haploid oocyte immediately begins its second meiotic division, but when it reaches metaphase, the process is arrested until fertilization has occurred. The follicle moves to the superficial cortex, causing the surface of the ovary to bulge. The tissues at the point of contact (the stigma) with the tough tunica albuginea and ovarian surface epithelium are eroded until the follicle ruptures and its contents are released into the peritoneal cavity for capture by the fimbria of the uterine tube. The oocyte at ovulation is still surrounded by its zona pellucida and corona radiata of granulosa cells. If fertilization does not occur, it begins to degenerate after 24 to 48 hours.

Corpus luteum

After ovulation, the remainder of the follicle becomes the corpus luteum (Fig. 77.35). The walls of the empty follicle collapse and fold. The granulosa cells increase in size and synthesize a cytoplasmic carotenoid pigment (lutein) giving them a yellowish colour (hence corpus luteum). These large (30–50 μm) granulosa lutein cells form most of the corpus luteum. The basal lamina surrounding the follicle breaks down, and numerous smaller theca lutein cells infiltrate the folds of the cellular mass, accompanied by capillaries and connective tissue. Extravasated blood from thecal capillaries accumulates in the centre as a small clot, but this rapidly resolves and is replaced by connective tissue. All lutein cells have a cytoplasm filled with abundant smooth endoplasmic reticulum, characteristic of steroid synthesizing endocrine cells. Granulosa lutein cells secrete progesterone and oestradiol (from aromatization of androstenedione, which is synthesized by theca lutein cells). The two cell types also respond differently to circulating gonadotropins. Theca lutein cells express receptors for human chorionic gonadotrophin (hCG). If the oocyte is not fertilized, the corpus luteum (of menstruation) functions for 12 to 14 days after ovulation, then atrophies. The lutein cells undergo fatty degeneration, autolysis, removal by macrophages and gradual replacement with fibrous tissue. Eventually, after 2 months, a small, whitish scar-like corpus albicans is all that remains.

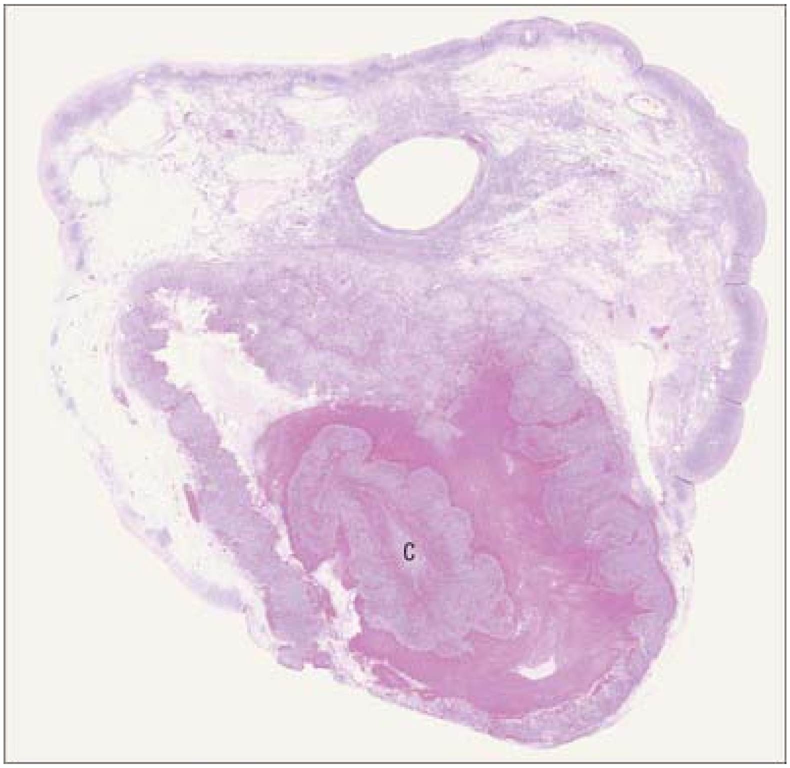

Fig. 77.35 Low power view of a section of a human ovary, containing a corpus luteum (C).

(By courtesy of Mr Peter Helliwell and Dr Joseph Mathew, Department of Histopathology, Royal Cornwall Hospitals Trust, UK.)

If fertilization does occur, implantation of the blastocyst into the uterine endometrium usually begins seven days later and the embryonic trophoblast then starts to produce hCG. The chorionic gonadotrophin stimulates the corpus luteum of menstruation to grow, and it becomes a corpus luteum of pregnancy. It normally increases in size from 10 mm in diameter to 25 mm at 8 weeks of gestation and can be seen clearly on ultrasound. It secretes progesterone, oestrogen and relaxin, and functions throughout pregnancy, although it gradually regresses as its endocrine functions are largely replaced by the placenta after 8 weeks gestation. Its diameter is reduced by the end of pregnancy to 1 cm. In the next few months it degenerates, like the corpus luteum of menstruation, to form a corpus albicans.

Ovarian medulla

The medulla is highly vascular. It contains numerous veins and spiral arteries, which enter the hilum from the mesovarium and lie within a loose connective tissue stroma. Small numbers of cells (hilus cells) with characteristics similar to interstitial (Leydig) cells in the testis are found in the medulla at the hilum, and they may be a source of androgens.

Menopause

At the menopause, ovulation ceases and various microscopic changes ensue within the ovarian tissues. The stroma becomes denser, the tunica albuginea thickens and the ovarian surface epithelium thins. However, many follicles persist within the cortex.

MENSTRUAL CYCLE

The uterus, ovaries and vagina undergo change during the menstrual cycle. The normal cycle is 28 days. A follicle begins a period of rapid development in the ovary on day 1 of the cycle, and matures and ruptures on day 14 to release a secondary oocyte. The wall of the follicle is then transformed into the corpus luteum, which secretes progesterone (luteal phase). About 10 days after ovulation the corpus luteum begins to regress, then ceases to function and is replaced by fibrous tissue. The breakdown of the endometrium that follows this cessation of function is due to the reducing levels of progesterone and oestrogen as the corpus luteum degenerates.

The changes that occur in the endometrium during the menstrual cycle may be divided into three phases: proliferative, secretory and menstrual (Fig. 77.36).

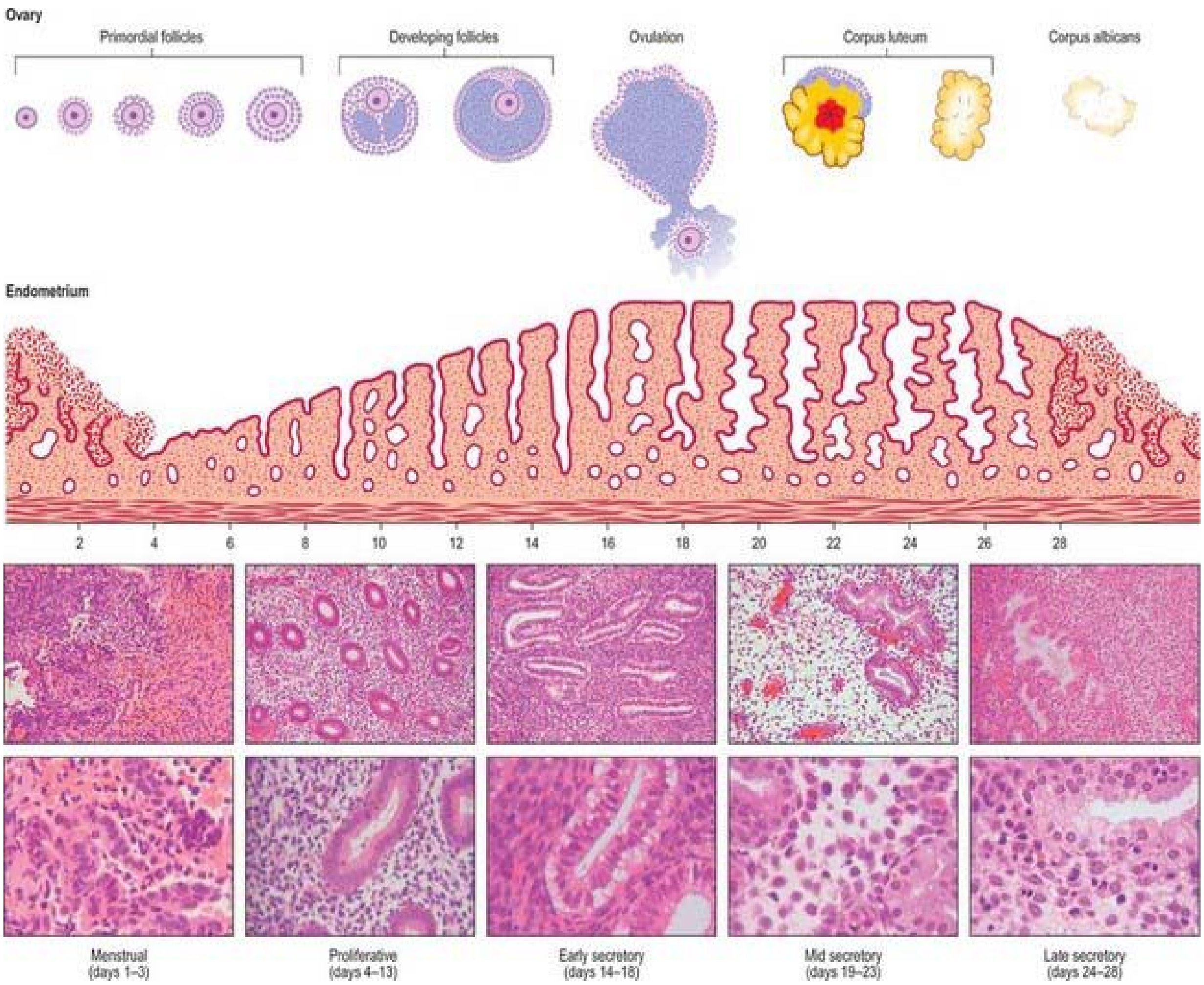
Ovary
Primordial follicles
Developing follicles
Ovulation
Corpus luteum
Corpus albicans
Endometrium
2
4
6
8
10
12
14
16
18
20
22
24
26
28
Menstrual (days 1–3)
Proliferative (days 4–13)
Early secretory (days 14–18)
Mid secretory (days 19–23)
Late secretory (days 24–28)

Fig. 77.36 Stages in the menstrual cycle with concomitant changes in the endometrium. Note that developing antral follicles are selected from cohorts of follicles recruited in earlier cycles. The ten lower panels are histological sections of endometrium at the cycle times indicated (low magnification on top and high magnification below in each case).

PROLIFERATIVE PHASE

In the early proliferative phase, even before the menstrual flow ceases, the epithelium from the persisting basal parts of the uterine glands grows over the surface of the endometrium which has been denuded by menstruation. Re-epithelialization is complete 5 to 6 days after the start of menstruation. Initially the tissue is only 1–2 mm thick and lined by low cuboidal epithelium. The glands are straight and narrow and their lining cells are short columnar. The apical cell surface contains microvilli; some cells are ciliated. The stroma is dense and contains small numbers of lymphocytes. During days 10 to12 of the proliferative phase, the endometrium thickens. Cells divide in response to rising levels of oestrogen which is produced by the ovary and which acts through receptors present on both the stromal and epithelial cells. The glands become tortuous and their lining epithelial cells become tall columnar in nature.

SECRETORY PHASE

The secretory phase coincides with the luteal phase of the ovarian cycle. The endometrial changes are driven by progesterone and oestrogen secreted by the corpus luteum. Steroid receptors in the endometrium activate a programme of new gene expression that produces, in the following 7 days, a highly regulated sequence of differentiative events, presumably required to prepare the tissue for blastocyst implantation. Part of the response is direct, but there is evidence that some of the effects may be mediated through growth factors. The first morphological effects of progesterone are evident 24 to 36 hours after ovulation (which occurs 14 days before the next menstrual flow). In the early secretory phase, glycogen masses accumulate in the basal cytoplasm of the epithelial cells lining the glands, where they are often associated with lipid. Giant mitochondria appear and are associated with semi-rough endoplasmic reticulum. There is an obvious increased polarization of the gland cells: nuclei are displaced towards the centre of the cells and Golgi apparatus and secretory vesicles accumulate in the supranuclear cytoplasm. The nuclear channel system is prominent and nuclei enlarge. Nascent secretory products may be detected immunohistochemically within the cells. Progestational effects on the stroma (known as the decidual reaction) are also evident in the early secretory phase. Nuclear enlargement occurs and the packing density of the resident stromal cells increases, due in part to the increase in volume of gland lumina and onset of secretory activity in the epithelial compartment.

By the mid-secretory phase the endometrium may be up to 6 mm deep. The basal epithelial glycogen mass is progressively transferred to the apical cytoplasm, and nuclei return to the cell bases. The Golgi apparatus becomes dilated and products including glycogen, mucin and other glycoproteins are released from the glandular epithelium into the lumen by a combination of apocrine and exocrine mechanisms: this activity reaches a maximum 6 days after ovulation. These secretory changes are considerably less pronounced in the basal gland cells and the luminal epithelium than in the glandular cell population of the stratum functionalis. There is a notable stromal oedema and a corresponding decrease in the density of collagen fibrils. At the same time the endoplasmic reticulum and Golgi apparatus become more prominent; there is evidence for collagen synthesis and degradation, presumably reflecting ongoing matrix remodelling.

In the late secretory phase, glandular secretory activity declines. Decidual differentiation occurs in the superficial stromal cells that surround blood vessels: this transformation includes nuclear rounding and an increased cytoplasmic volume, reflecting an increase in and dilatation of the rough endoplasmic reticulum and Golgi systems, and cytoplasmic accumulation of lipid droplets and glycogen. The cells begin to produce basal lamina components including laminin and type IV collagen.

Ultrasound is frequently used in the clinical evaluation of the endometrium. In the early secretory phase the endometrium is identified as a thin echogenic line, a consequence of specular reflection from the interface between opposing surfaces of endometrium. During the late proliferative phase the endometrium appears as a triple layer: a central echogenic line (due to the opposed endometrial surfaces), surrounded by a thicker hypoechoic functional layer, and bounded by an outer echogenic basal layer. During the secretory phase the functional layer surrounding the echogenic line becomes more hyperechoic as a result of the increased mucus and glycogen within the glands and the increased number of interfaces caused by the development of tortuous spiral arteries (Fig. 77.37).

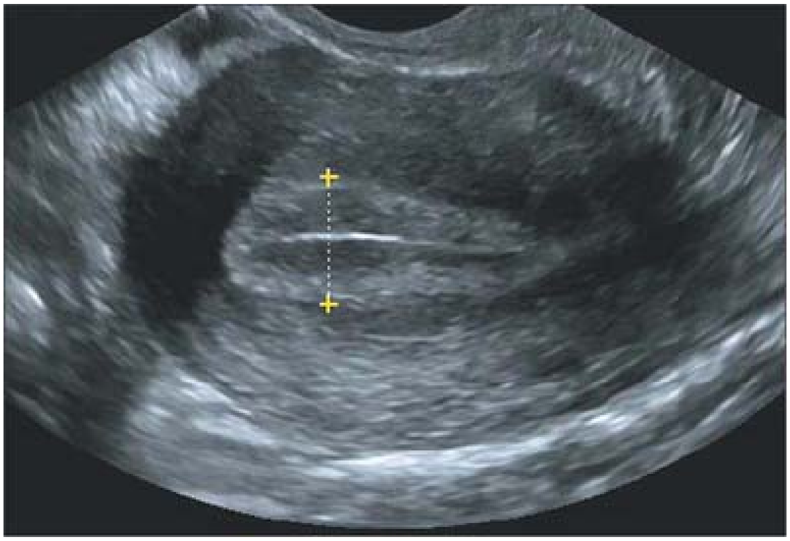

Fig. 77.37 Transvaginal ultrasound of the uterus showing the triple-layered endometrium. The central echogenic line is produced by the interface of the opposing surfaces of the endometrium. The functional layer of the endometrium surrounding the echogenic line is hypoechoic on the left, in keeping with late proliferative phase, but is becoming more hyperechoic on the right indicating the early secretory phase.

MENSTRUAL PHASE

Prior to menstruation three layers can be recognized in the endometrium: the strata compactum, spongiosum and basale. In the stratum compactum, which is next to the free surface, the necks of the glands are only slightly expanded and the stromal cells show a distinct decidual reaction. In the stratum spongiosum, the uterine glands are tortuous, dilated and ultimately only separated from one another by a small amount of interglandular tissue. The stratum basale, next to the uterine muscle, is thin and contains the tips of the uterine glands embedded in an unaltered stroma.

The two upper strata are often grouped together as the functional layer, stratum functionalis, of the endometrium; the lower (basal) layer is called the stratum basalis. As regression of the corpus luteum occurs, those parts of the stroma showing a decidual reaction, together with the glandular epithelium, undergo degenerative changes and the endometrium often diminishes in thickness. Blood escapes from the superficial vessels of the endometrium forming small haematomata beneath the surface epithelium (see below). The stratum functionalis, next to the free surface, is shed piecemeal, leaving mainly the stratum basalis, adjacent to the uterine muscle: 65–75% of the thickness of the endometrium may be shed. Blood and necrotic endometrium then begin to appear in the uterine lumen, to be discharged from the uterus through the vagina as the menstrual flow, which lasts from 3 to 6 days. The amount of tissue lost is variable, but usually the stratum compactum and most of the spongiosum are desquamated.

VASCULAR CHANGES WITHIN THE UTERUS DURING THE MENSTRUAL CYCLE

The vascular bed of the endometrium undergoes significant changes during the menstrual cycle. The arteries to the endometrium arise from a myometrial plexus and consist of short, straight vessels to the basal portion of the endometrium and more muscular spiral arteries to its superficial two-thirds. The venous drainage, consisting of narrow perpendicular vessels that anastomose by cross branches, is common to both the superficial and basal layers of the endometrium. The capillary bed consists of an endothelium with a basal lamina that is discontinuous in the proliferative phase, but becomes more distinct by the mid-secretory phase. Pericytes are present, some of which resemble smooth muscle cells, and these are sometimes enclosed within the basal lamina. The pericytes make contact with the endothelial cells by means of cytoplasmic extensions that project through the basal lamina. Enlargement of the pericytes starts in the early secretory phase, and leads to a conspicuous cuff of cells in the mid- and late-secretory phases. The arterial supply to the basal part of the endometrium remains unchanged during the menstrual cycle. However, the spiral arteries to the superficial strata lengthen disproportionately. They become increasingly coiled and their tips approach the uterine epithelium more closely. This leads to a slowing of the circulation in the superficial strata with some vasodilation. Immediately before the menstrual flow, these vessels begin to constrict intermittently, causing stasis of the blood and anaemia of the superficial strata. During the periods of relaxation of the vessels, blood escapes from the devitalized capillaries and veins, causing the menstrual blood loss. The breakdown of the endometrium is a consequence of the reducing levels of progesterone and oestrogen as the corpus luteum degenerates.

PREGNANCY AND PARTURITION

During pregnancy many morphological changes occur in the female reproductive system and associated abdominal structures. The uterus enlarges to accommodate the developing fetus and placenta, and various alterations take place in the pelvic walls, floor and contents which allow for this expansion, and which anticipate parturition. At the end of gestation, dramatic changes occur that facilitate the passage of the baby through the birth canal and subsequently allow the pelvic organs to return to the non-pregnant state (involution).

THE UTERUS IN PREGNANCY

The function of the uterus in pregnancy is to retain the developing fetus and to provide a protected environment until a stage at which the fetus is capable of surviving *ex utero*. The uterus must grow, facilitate delivery of the fetus and then involute. At the same time smooth muscle cells must be stretched by the growing fetus without producing miscarriage or premature labour.

The uterus grows dramatically during pregnancy, increasing in weight from about 50 g at the beginning of pregnancy to up to 1 kg at term. Most of the weight gain is the result of increased vascularity and fluid retention in the myometrium. The increased growth of the uterine wall is driven by a combination of mechanical stretching and endocrine input. The mechanical load that the growing fetus imposes on the uterine wall induces hypertrophy of uterine smooth muscle cells, and is the major stimulus that increases smooth muscle mass. Some hyperplasia occurs early on in pregnancy, mainly from the growth of the media of the myometrial arteries and veins. The myometrium is relatively unresponsive to additional endocrine stimulation during most of pregnancy, a relative quiescence that is in part attributed to progesterone. However, a number of growth factors, e.g. insulin-like growth factor-1 (IGF-1), have been identified which interact with oestrogen in promoting uterine growth. The myometrium thins with advancing gestation from 2–3 cm thick in early pregnancy to 1–2 cm at term.

The upper third of the cervix (isthmus) is gradually taken up into the uterine body during the second month to form the ‘lower segment’ (Fig. 77.38). The isthmus hypertrophies like the uterine body during the first trimester and triples in length to about 3 cm. From the second trimester the wall of the isthmus and that of the body are the same thickness and their junction is no longer visible externally. This condition persists until the middle of the third trimester when the junction between the body and the isthmus can sometimes be recognized as a transverse linear depression; the musculature above the depression is thicker than that below. The depression forms just below the vesico-uterine pouch and is thought to correspond to the level of the anatomical internal os (upper margin of lower segment). It is the anatomical landmark used at the time of a lower segment caesarean section to ensure that the uterine incision is not in the body of the uterus. The lower segment is less vascular than the upper part of the uterus. Moreover, the risk of rupture of a lower segment uterine scar in subsequent pregnancies is significantly reduced compared to rupture of a scar in the body of the uterus (classical caesarean section).

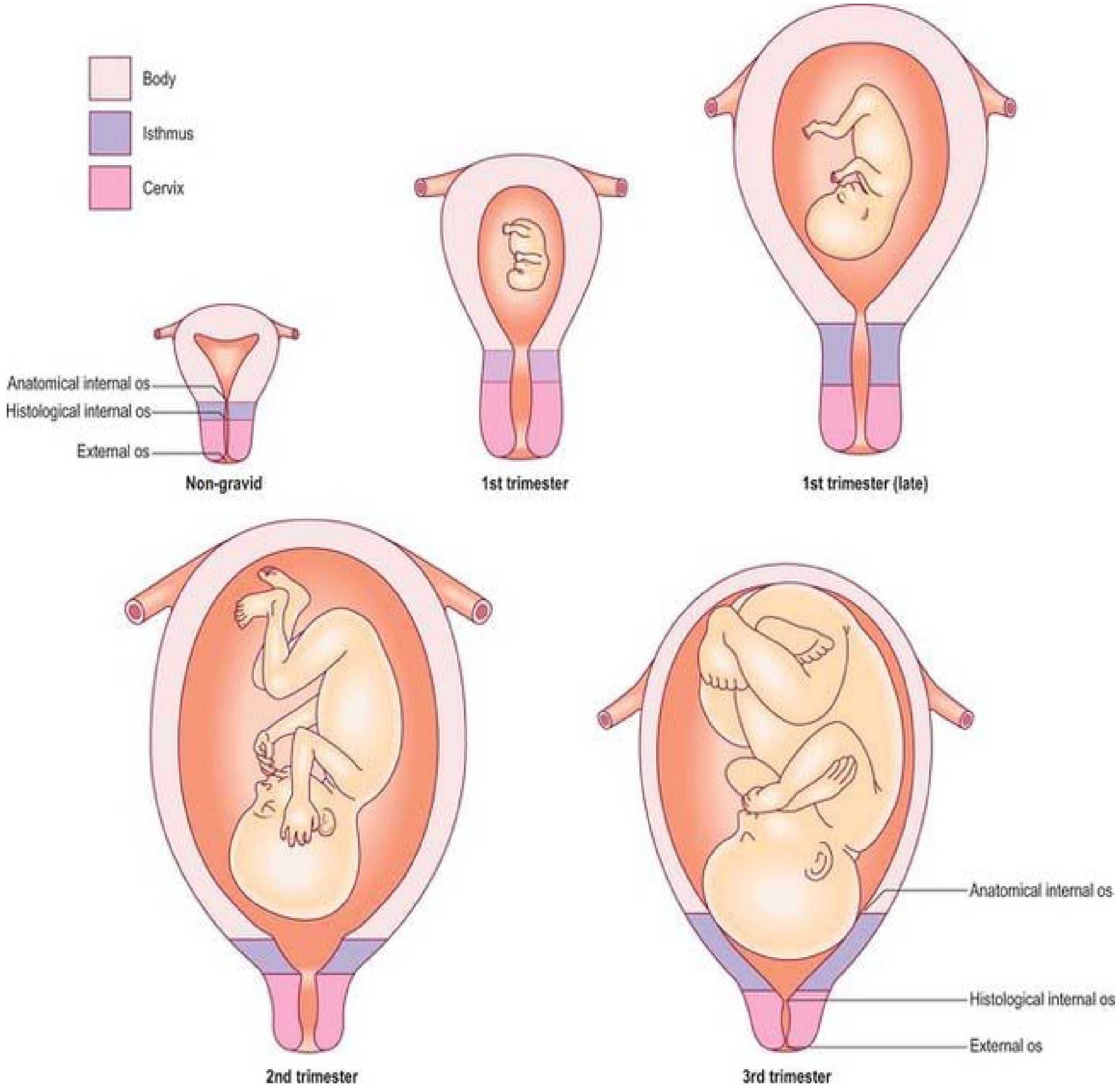
Body
Isthmus
Cervix
Anatomical internal os
Histological internal os
External os
Non-gravid
1st trimester
1st trimester (late)
2nd trimester
3rd trimester
Anatomical internal os
Histological internal os
External os

Fig. 77.38 Frontal view of the uterus showing the location and extent of the body, isthmus and cervix in the non-gravid and gravid uterus at different

stages in gestation. The isthmus forms the lower uterine segment with advancing gestation.

Growth of the uterus in pregnancy

Anatomical surface landmarks can be used to estimate uterine size and therefore gestational age. The uterus is usually palpable just above the pubic symphysis by the 12th week; if is retroverted it may not be palpable in the abdomen until a little later. By the 20th week of pregnancy the uterine fundus is at the level of the umbilicus, and by 36 weeks the fundus has reached the xiphisternum. In practice the gestational age is now calculated by ultrasound measurement of the fetal crown–rump length in the first trimester (Fig. 77.39). For women presenting after the first trimester, dating is less accurate and is based on measurement of the head circumference. Subsequent assessment of fetal size up to 24 weeks relies on abdominal palpation and correlating gestational age with anatomical landmarks. From 24 weeks of gestation serial measurement of the distance between the pubic symphysis and the uterine fundus is used. The symphysis–fundal height (SFH) measurement acts primarily as a screening method, and if there is a concern that the SFH is either above or below the normal range a more accurate assessment of fetal size and amniotic fluid volume is made using ultrasound. Dating of pregnancy based on fetal biometry rather than menstrual history has significantly reduced the number of pregnancies requiring induction of labour for post-term.

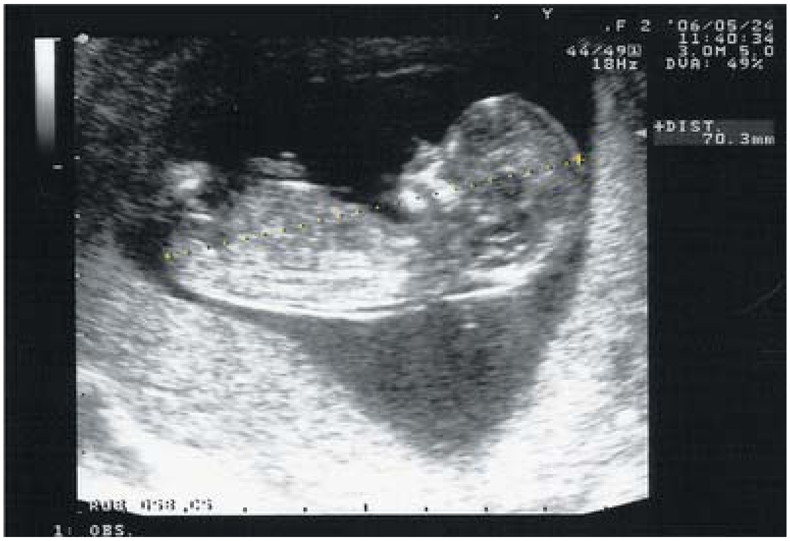

Fig. 77.39 Transabdominal ultrasound at 12 weeks showing measurement of the crown rump length to calculate the gestational age.

Doppler can be used to assess the placental and fetal circulations. Doppler assessment of the uterine arteries can play an important role in screening for impaired placentation and its complications of pre-eclampsia, intrauterine growth restriction and perinatal death, and assessment of the fetal circulation (e.g. umbilical artery, middle cerebral artery) can aid clinical management, such as timing of delivery in a growth restricted baby (Fig. 77.40A,B).

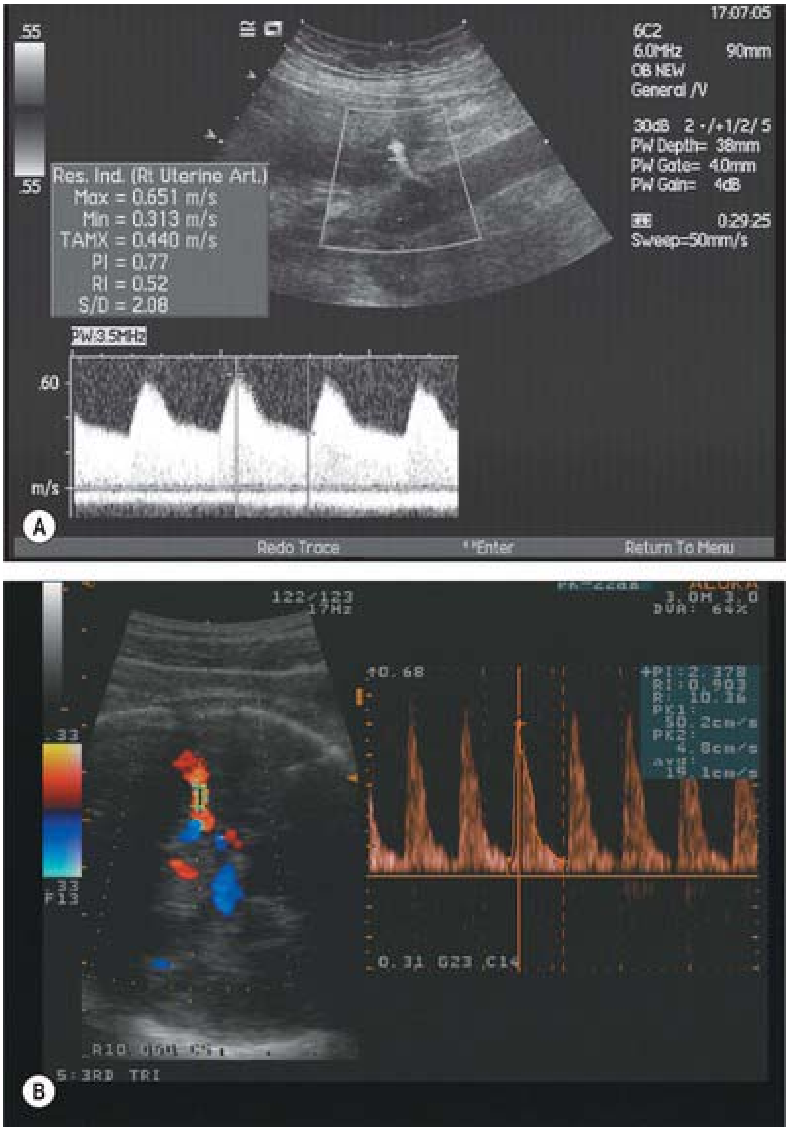
17:07:05
6C2
6.0MHz
90mm
OB NEW
General /V
30dB 2 •/+1/2/ 5
PW Depth= 38mm
PW Gate= 4.0mm
PW Gain= 4dB
0:29:25
Sweep=50mm/s
.55
.55
Res. Ind. (Rt Uterine Art.)
Max = 0.651 m/s
Min = 0.313 m/s
TAMX = 0.440 m/s
PI = 0.77
RI = 0.52
S/D = 2.08
PW:3.5MHz
.60
m/s
A
Redo Trace
Enter
Return To Menu
122/123
17Hz
ALOKA
3.0M 3.0
DUA: 64%
.33
.33
F13
+0.68
+PI:2.378
RI:0.903
R: 10.3
PK1:
50.2cm/s
PK2:
4.8cm/s
avg:
15.1cm/s
0.31 G23 C14
R10
S:3RD TRI
B

Fig. 77.40 Doppler examination of the maternal and fetal circulation in pregnancy. **A**, Pulsed Doppler showing a normal uterine artery waveform at 24 weeks. **B**, Pulsed Doppler showing normal waveforms in the middle cerebral artery at 32 weeks.

Cervix and pregnancy

The uterine cervix is required to serve two functions in relation to pregnancy and parturition. During pregnancy it is a relatively rigid fibromuscular structure which retains the developing fetus within the uterus. During active labour the cervix dilates to allow the fetus to descend through the birth canal.

Considerable softening and shortening of the cervix occurs in the weeks before the onset of labour; a corresponding increase in uterine activity is usually apparent during this pre-labour period. The rigidity of the cervix appears to be related to the orientation of its collagen fibres within a regular connective tissue matrix. The exact processes that allow softening, effacement and dilatation of the cervix are unclear, but are believed to include remodeling of the connective tissue matrix, probably mediated by an increase in the activity of enzymes such as matrix metalloproteinase 1, a reduction in collagen concentration, a significant increase in the water content in the cervix, an infiltration of macrophages and neutrophils, and an increased level of apoptosis.

The cervix can be viewed during pregnancy by transvaginal ultrasound examination. The cervical length, dilatation of the internal os and bulging of the membranes into the canal can be assessed (Fig. 77.41A,B). Measurement of cervical length on ultrasound appears to be a strong predictor of preterm labour: the shorter the cervix, the greater the risk of premature delivery. In clinical practice cervical length has been used to screen women at high risk of preterm labour or to screen symptomatic women in threatened preterm labour in order to plan appropriate management.

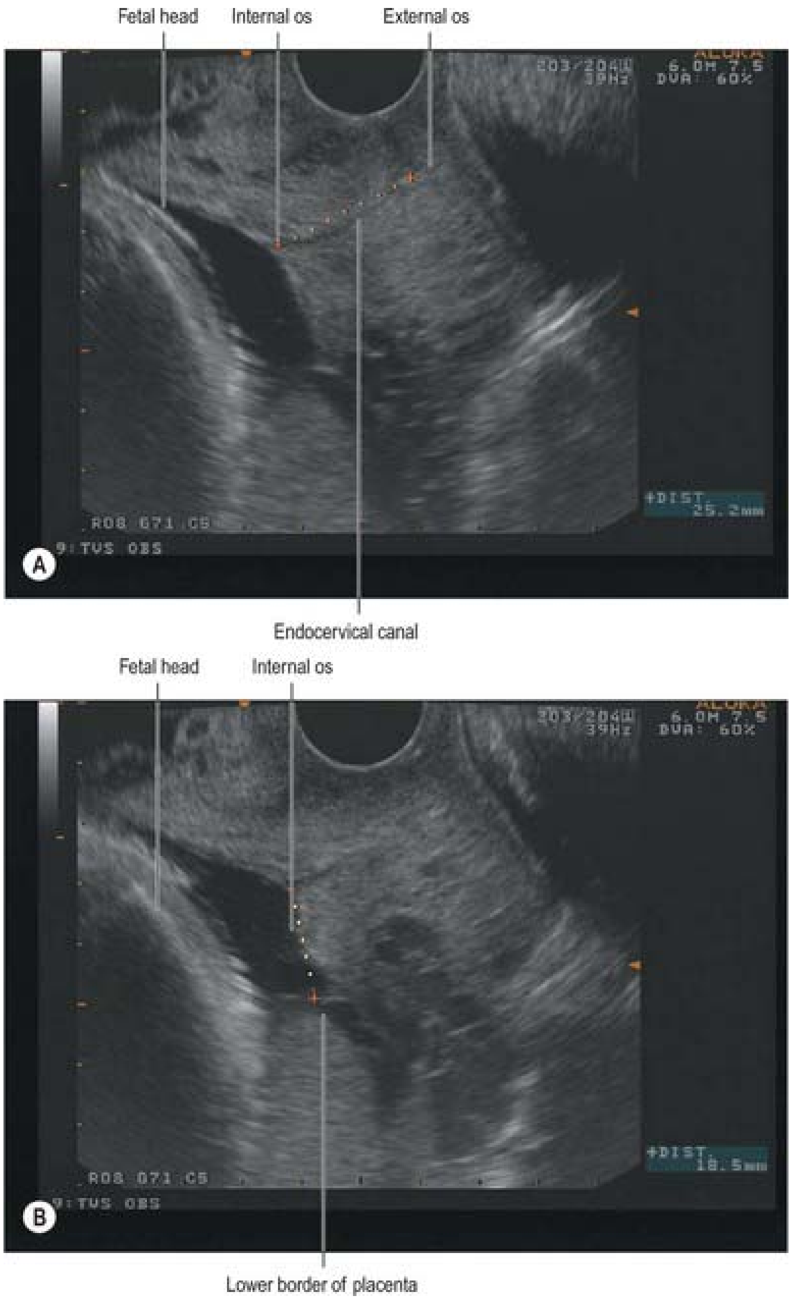
Fetal head
Internal os
External os
+DIST. 25.2mm
A
Endocervical canal
Fetal head
Internal os
+DIST. 18.5mm
B
Lower border of placenta

Fig. 77.41 Transvaginal ultrasound at 36 weeks showing (**A**) measurement of cervical length and (**B**) posterior placenta praevia 18.5 mm from the internal os.

Relations of the uterus in pregnancy

With uterine expansion, the ovaries and uterine tubes are displaced upwards and laterally. The round ligaments become hypertrophied and their course from the cornual regions of the uterus down to the internal inguinal ring becomes more vertical. The broad ligament tends to open out to accommodate the massive increase in the sizes of the uterine and ovarian vessels. The uterine veins in particular can reach about 1 cm in diameter and they appear to act as a significant reservoir for blood during uterine contractions. Lymphatics and nerves expand their territories (the significance of this increased innervation is not clear, because paraplegic women are able to labour normally, albeit painlessly). Later in pregnancy the increase in intra-abdominal pressure produced by the gravid uterus may produce eversion of the umbilicus. On the skin over the abdomen, a combination of stretching and hormonal changes may produce stretch marks (striae gravidarum). In multiparous patients, separation (diverification) of right and left rectus abdominis may occur allowing the uterine fundus to fall forwards to some extent. In the supine position, the pregnant woman in late pregnancy is vulnerable to aorto-caval compression, as the gravid uterus presses on, and reduces blood flow in, the great vessels. Aorto-caval compression can cause symptoms of nausea and faintness; these symptoms are minimized if the woman lies on her left side thereby reducing compression of the inferior vena cava.

The jejunum, ileum and transverse colon tend to be displaced upwards by the enlarging uterus, whereas the caecum and appendix are displaced to the right, and the sigmoid colon posteriorly and to the left. Upward and lateral displacement of the appendix in later pregnancy can cause difficulties in the diagnosis of appendicitis. The ureters are pushed laterally by the enlarging uterus and in late pregnancy can be compressed at the level of the pelvic brim, resulting in hydronephrosis and loin pain. However, mild ureteric dilatation is normal in pregnancy, and is caused by progesterone-induced relaxation of smooth muscle in the ureteric walls. The axis of the uterus is shifted or dextrorotated by the presence of the sigmoid colon which may lead to inadvertent incision into large uterine vessels at the time of lower segment caesarean section unless the operator is aware of any such rotation.

PELVIC CHANGES IN PREGNANCY

The presence of a pregnant uterus results in a change in the centre of gravity of the body, especially in late pregnancy (Fig. 77.42). In order to compensate for this, the mother tends to straighten her cervical and thoracic spine, and throw her shoulders back, resulting in a compensatory lumbar lordosis. There is also a softening of the pubic symphysis and sacroiliac joints, caused by production of relaxin and other pregnancy hormones. This increased mobility produces a form of pelvic instability, so that the pregnant woman tends to walk with a waddling gait. Softening also produces an increase in pelvic diameter, which is of benefit during the time of labour. Significant joint relaxation can be associated with pain, called symphysis pubis diastasis: in severe cases radiographs show that when a woman stands on one leg the two halves of the symphysis are at different levels.

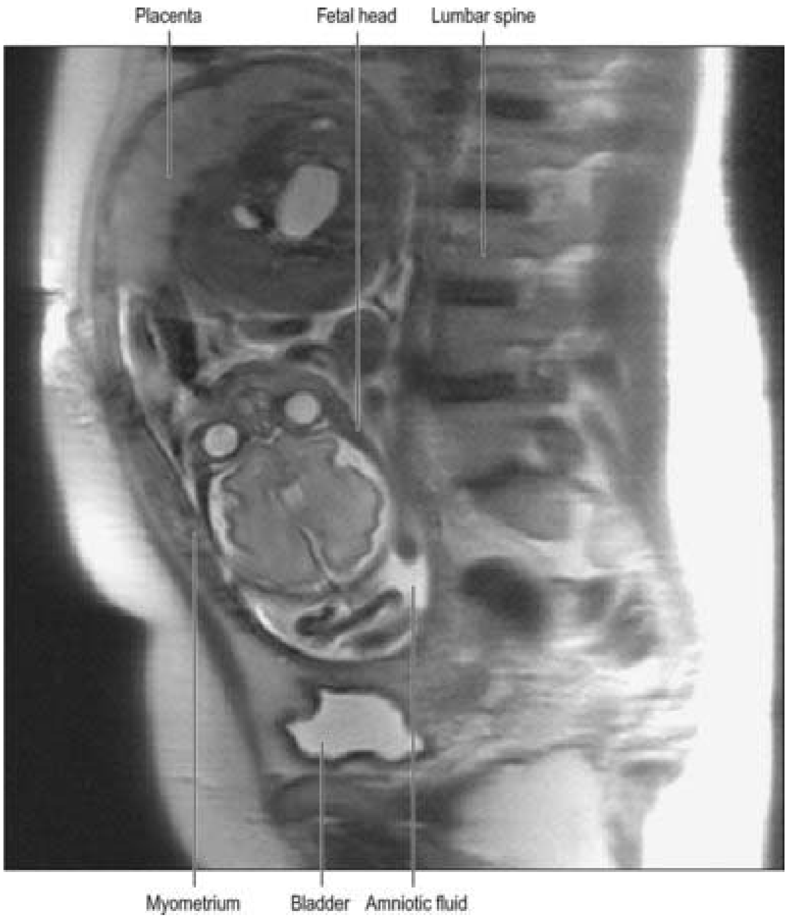

Fig. 77.42 Sagittal T2-weighted scan showing a normal cephalic presentation.

PLACENTAL LOCATION

The placenta may be attached at any point on the uterine wall. The site of attachment is determined by the point where the blastocyst becomes embedded: the factors on which this depends are not understood. In early pregnancy the placental disc occupies a large proportion of the uterine cavity and will often appear to be situated near the internal os. In the majority of cases growth and stretching of the uterus will usually draw the placenta upwards away from the cervix by the end of pregnancy.

In about 1% of pregnancies the position of the placenta will remain over, or in close proximity to, the internal cervical os at the end of pregnancy (Figs 77.41B, 77.43). This condition is called placenta praevia and is associated with vaginal bleeding during pregnancy and labour. If the placenta covers the internal os, or the lower edge is less than 2 cm from the internal os, delivery by caesarean section is likely to be needed. Women with placenta praevia are at an increased risk of having a morbidly adherent placenta if they have an anterior placenta praevia and have had previous uterine surgery, e.g. caesarean section. Pathological forms of adherence or penetration include placenta accreta, where the placenta displays exceptional adherence to the decidua basalis; placenta increta, where the myometrium is invaded; and placenta percreta, when the invasion by placental tissue passes completely through the uterine wall (Fig. 77.44).

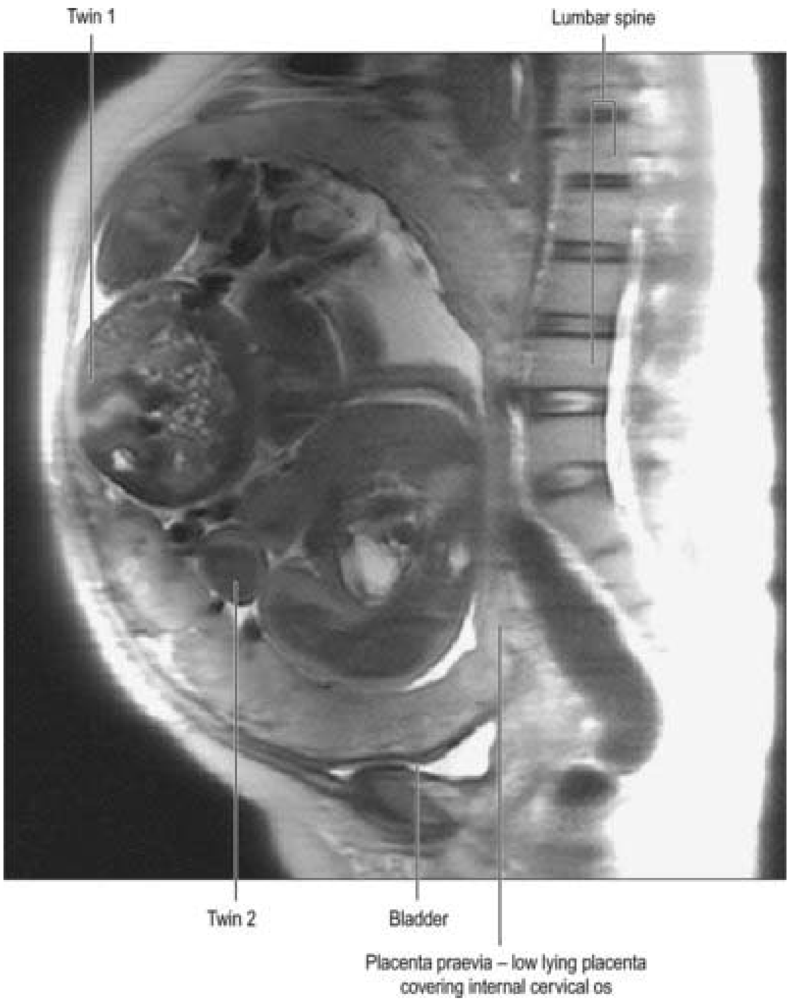
Twin 1
Lumbar spine
Twin 2
Bladder
Placenta praevia – low lying placenta covering internal cervical os

Fig. 77.43 Sagittal T2-weighted scan of a twin pregnancy with a placenta praevia overlying the internal cervical os.

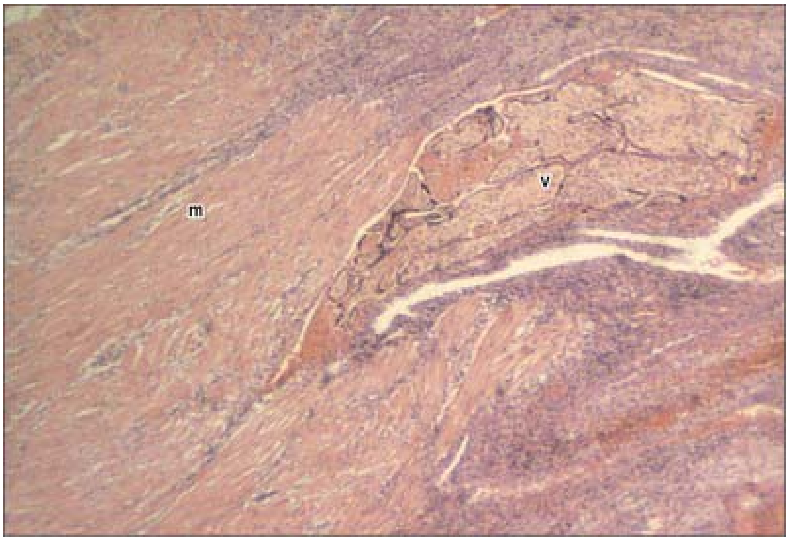

Fig. 77.44 Micrograph showing placental villi within the myometrium from a morbidly adherent placenta (increta): m, myometrium; v, villi.

(By courtesy of Professor Eric Jauniaux, Consultant in Fetal Medicine, University College Hospital, London.)

LABOUR

The onset of labour is defined as the combination of regular uterine contractions that are of sufficient intensity to produce progressive effacement and dilatation of the cervix. The process of labour is described in three main stages.

First stage

This is the period during which the cervix dilates as it is drawn up into the lower portion of the uterus until there is no longer any cervix palpable on vaginal examination. There is little change in the uterine volume, because myometrial contractions are isometric and so there is minimal shortening of the muscle fibres. Progress is determined by the equilibrium between forces generated by myometrial contractions, especially from the fundus, and the resistance of the cervix. The ‘give’ from a compliant cervix attenuates the tension generated by the myometrium, which means that a compliant cervix not only dilates quickly but does so with less uterine activity.

Second stage

This begins once the cervix is fully dilated, and ends with the delivery of the baby. Cervical resistance is lost and myometrial activity results in isometric contractions that aid descent of the baby in the birth canal. The second stage is usually divided into a passive phase where there is descent of the presenting part and an active phase which starts with maternal pushing and results in delivery of the baby. The head of the baby usually enters the pelvis with the occiput facing laterally. As the head descends further, the occiput contacts the gutter-shaped pelvic floor formed by levator ani and this promotes flexion and rotation of the occiput to the anterior position. With further descent the occiput escapes under the symphysis pubis and the head is born by extension. At this point, the baby’s head regains its normal relationship with its shoulders, and slight rotation (or restitution) of the head is seen. Further external rotation occurs as the leading shoulder is directed medially by the maternal pelvic floor. The body of the baby is now born by lateral flexion as one shoulder slips underneath the symphysis and the posterior shoulder is drawn over the frenulum.

Third stage

This is the time from delivery of the fetus until delivery of the placenta. Prior to separation of the placenta, a large proportion of the mother's cardiac output passes through the uterine circulation. After separation in the third stage of labour, maternal exsanguination is only prevented by marked uterine contraction: the criss-crossing myometrial fibres act as a tourniquet, restricting blood flow to the area that was the placental site. This process is usually expedited clinically by the administration of oxytocic drugs in an attempt to limit maternal blood loss. Any condition that predisposes to poor uterine contraction, such as retained placental tissue, will increase the likelihood of haemorrhage immediately after delivery (postpartum haemorrhage).

The placenta after delivery

Separation of the placenta from the uterine wall takes place along the plane of the stratum spongiosum. It extends beyond the placental area, detaching the villous placenta, with associated fibrinoid matrix and small amounts of decidua basale, the chorio-amnion, together with a superficial layer of the fused decidua capsularis, and the decidua parietalis. When the placenta and membranes have been expelled, a thin layer of stratum spongiosum is left as a lining for the uterus: it soon degenerates and is cast off in the early part of the puerperium. A new epithelial lining for the uterus is regenerated from the remaining stratum basale. The expelled placenta is a flattened discoid mass with an approximately circular or oval outline (Fig. 77.45). It has an average volume of 500 ml (range 200–950 ml), a weight of 470 g (range 200–800 g), a diameter of 185 mm (range 150–200 mm), a thickness of 23 mm (range 10–40 mm), and a surface area of approximately 30,000 mm^2. It is thickest at its centre (the original embryonic pole), and rapidly thins towards its periphery where it continues as the chorion laeve.

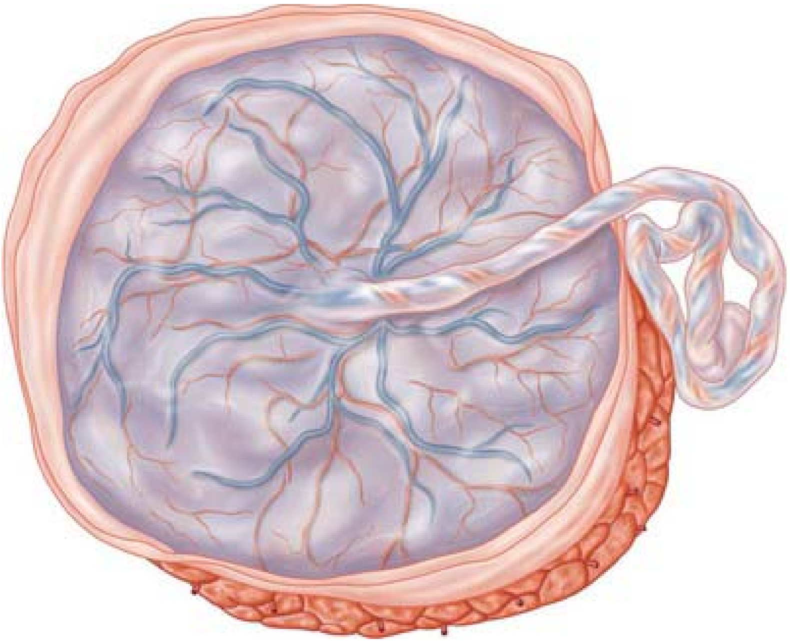

Fig. 77.45 The fetal surface of a recently delivered placenta. The spiral umbilical vessels in the umbilical cord and their radiating branches shine through the transparent amnion. The maternal surface is exposed in the lower and right corner of the figure. Note the fringes of amnion and chorion, the majority of which have been cut away near the placental margin.

Macroscopically, the fetal or inner surface, covered by amnion, is smooth, shiny and transparent, so that the mottled appearance of the subjacent chorion, to which it is closely applied, can be seen. The umbilical cord is usually attached near the centre of the fetal surface, and branches of the umbilical vessels radiate out under the amnion from this point; the veins are deeper and larger than the arteries. The maternal surface of the placenta is finely granular and mapped into some 15–30 lobes by a series of fissures or grooves. The placental lobes, which are often somewhat loosely termed cotyledons, correspond in large measure to the major branches of the umbilical vessels. The grooves correspond to the bases of incomplete placental septa, which become increasingly prominent from the third month onwards. They extend from the maternal aspect of the intervillous space (the basal plate) towards, but do not quite reach, the chorionic plate. The septa are complex structures composed of components of the cytotrophoblastic shell and residual syncytium, together with maternally derived material including decidual cells, occasional blood vessels and gland remnants, collagenous and fibrinoid extracellular matrix and, in the later months of pregnancy, foci of degeneration.

In multiple pregnancies the number of placentas is determined by the zygosity. Dizygotic pregnancies will always have two placentas (dichorionic); monozygotic pregnancies usually have a single placenta (monochorionic) but 33% will have two placentas. The number of placentas in monozygotic pregnancies is determined by the timing of splitting of the embryonic mass. If the single embryonic mass splits into two within 3 days of fertilization, each fetus will have its own placenta and amniotic sac (dichorionic diamniotic); splitting after the 3rd day following fertilization results in a monochorionic diamniotic (two amniotic sacs) pregnancy and vascular communication within the two placental circulations (Fig. 77.46); splitting after the 9th day results in a single placenta and single amniotic sac (monochorionic monoamniotic); and splitting after the 12th day results in conjoined twins.

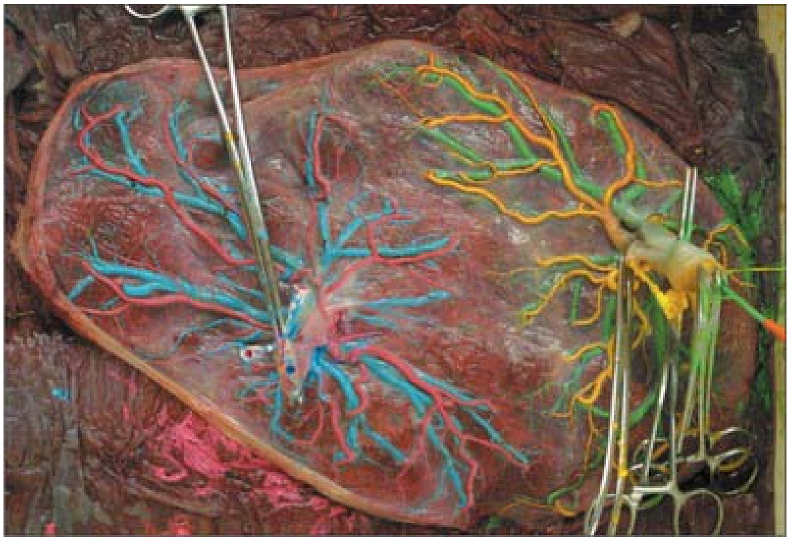

Fig. 77.46 Vascular cast from a monochorionic diamniotic twin pregnancy showing vascular communications between both placentas.

(By courtesy of Dr Ling Wee, University College London Hospital.)

Placental variations

The umbilical cord is usually attached near the centre of the placenta. It may insert at any point between its centre and margin, a condition known as a battledore placenta (Fig. 77.47). Occasionally the cord fails to reach the placenta itself and ends in the membranes as a velamentous insertion. When insertion of the cord is velamentous, the larger branches of the umbilical vessels traverse the membranes before they reach and ramify on the placenta (Fig. 77.48). They travel unprotected through the membranes to the placenta, which puts the fetus at risk because compression or tearing of the vessels can disrupt blood flow to and from the fetus. This can be particularly problematic when the vessels present themselves across the cervical os, a condition called vaso previa. A small accessory (succenturiate) placental lobe is occasionally present, connected to the main organ by membranes and blood vessels. It may be retained *in utero* after delivery of the main placental mass and cause postpartum haemorrhage. Other variations include placenta membranacea, in which villous stems and their branches persist over the whole chorion; and placenta circumvallate, where the placental margin is undercut by a deep groove (Fig. 77.49A,B).

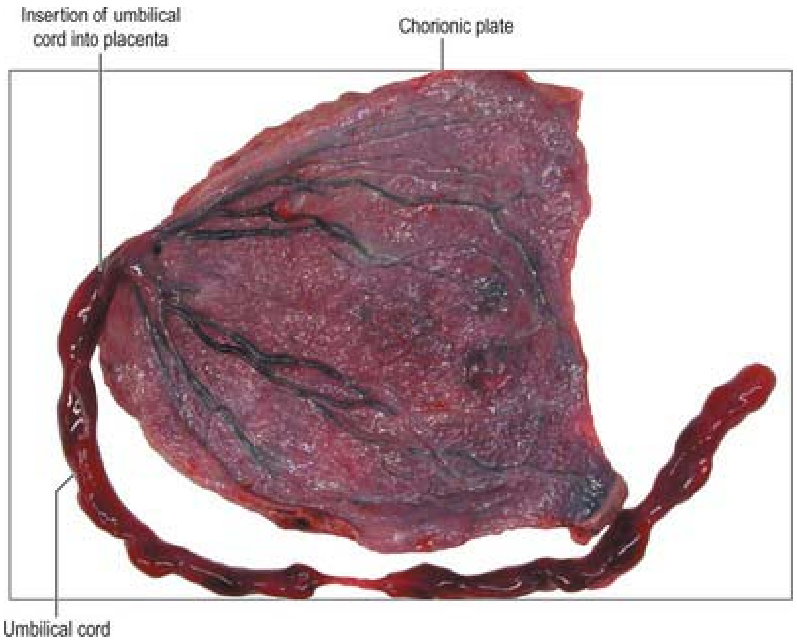

Fig. 77.47 A battledore placenta showing marginal insertion of the umbilical cord into the placenta.

(By courtesy of Dr Michael Ashworth, Consultant Histopathologist, Great Ormond Street Hospital for Children, London.)

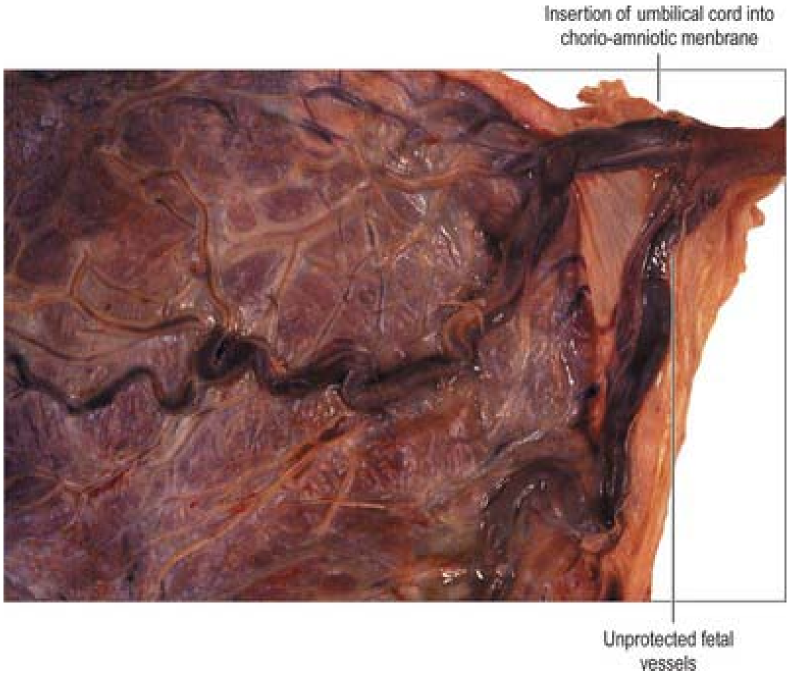
Insertion of umbilical cord into chorio-amniotic menbrane
Unprotected fetal vessels

Fig. 77.48 Velamentous insertion of the umbilical cord showing the cord inserting into the chorioamniotic membranes rather than the placental disk.

(By courtesy of Dr Michael Ashworth, Consultant Histopathologist, Great Ormond Street Hospital for Children, London.)

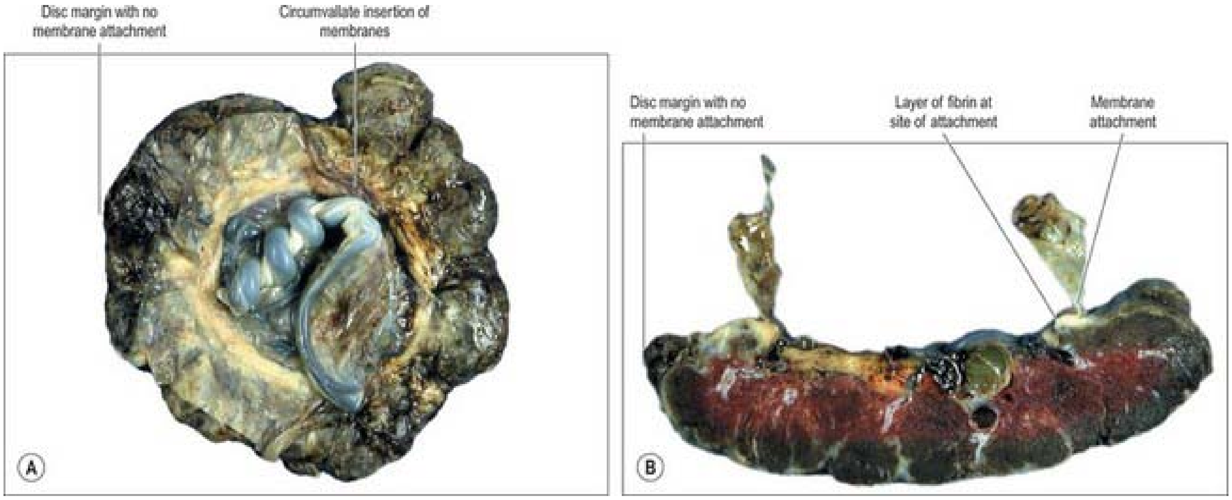
Disc margin with no membrane attachment
Circumvallate insertion of membranes
A
Disc margin with no membrane attachment
Layer of fibrin at site of attachment
Membrane attachment
B

Fig. 77.49 Placenta circumvallata. **A**, showing the fetal surface and a thick ring of membranes on the fetal surface of the placenta. **B**, A section through the placenta showing that the membranes insert central to the edge of the placental disk.

(By courtesy of Dr Michael Ashworth, Consultant Histopathologist, Great Ormond Street Hospital for Children, London.)

REFERENCES

len A, Creighton S, Davies M, MacDougall J, Stanhope R. Paediatric and adolescent gynaecology: a multi-disciplinary approach. Cambridge: Cambridge University Press, 2004.

lancey JO. Anatomy. Stanton SL, Monga A. Clinical Urogynaecology, 2nd edn., London: Churchill Livingstone, 2000.

CHAPTER 78

Development of the urogenital system

URINARY SYSTEM

The urinary and reproductive systems develop from intermediate mesenchyme and are intimately associated with one another especially in the earlier stages of their development. The urinary system develops ahead of the reproductive or genital systems.

Intermediate mesenchyme is disposed longitudinally in the trunk, subjacent to the somites (in the folded embryo), at the junction between the splanchnopleuric mesenchyme (adjacent to the gut medially) and the somatopleuric mesenchyme (subjacent to the ectoderm laterally) (Fig. 78.1). In lower vertebrates, intermediate mesenchyme typically develops serial, segmental epithelial diverticuli termed nephrotomes. Each nephrotome encloses a cavity, the nephrocele, which communicates with the coelom through a peritoneal funnel, the nephrostome (Fig. 78.2). The dorsal wall of a nephrotome evaginates as a nephric tubule. The dorsal tips of the cranial nephric tubules bend caudally and fuse to form a longitudinal primary excretory duct, which grows caudally and curves ventrally to open into the cloaca. The more caudally placed, and therefore chronologically later, tubules open secondarily into this duct or into tubular outgrowths from it. Glomeruli, specific arrangements of capillaries and overlying coelomic epithelium, arise from the ventral wall of the nephrocele (internal glomeruli) or the roof of the coelom adjacent to the peritoneal funnels (coelomic or external glomeruli), or in both situations (Fig. 78.2).

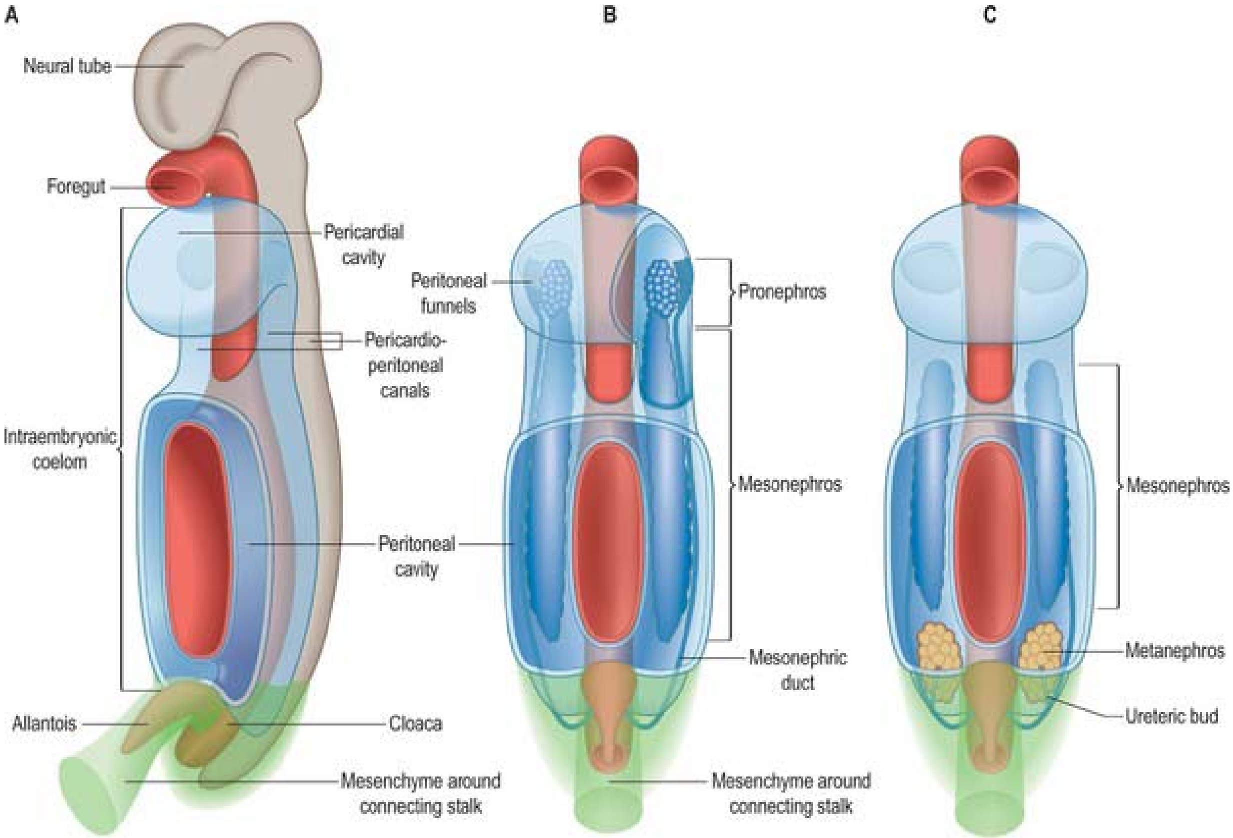
A
B
C
Neural tube
Foregut
Pericardial cavity
Peritoneal funnels
Pronephros
Pericardio-peritoneal canals
Intraembryonic coelom
Mesonephros
Mesonephros
Peritoneal cavity
Mesonephric duct
Metanephros
Ureteric bud
Allantois
Cloaca
Mesenchyme around connecting stalk
Mesenchyme around connecting stalk

Fig. 78.1 **A**, Major epithelial populations within a stage 11 embryo, viewed from a ventrolateral position. **B**, Position of pronephros and mesonephros on the posterior thoracic and abdominal walls. **C**, Position of mesonephros and metanephros.

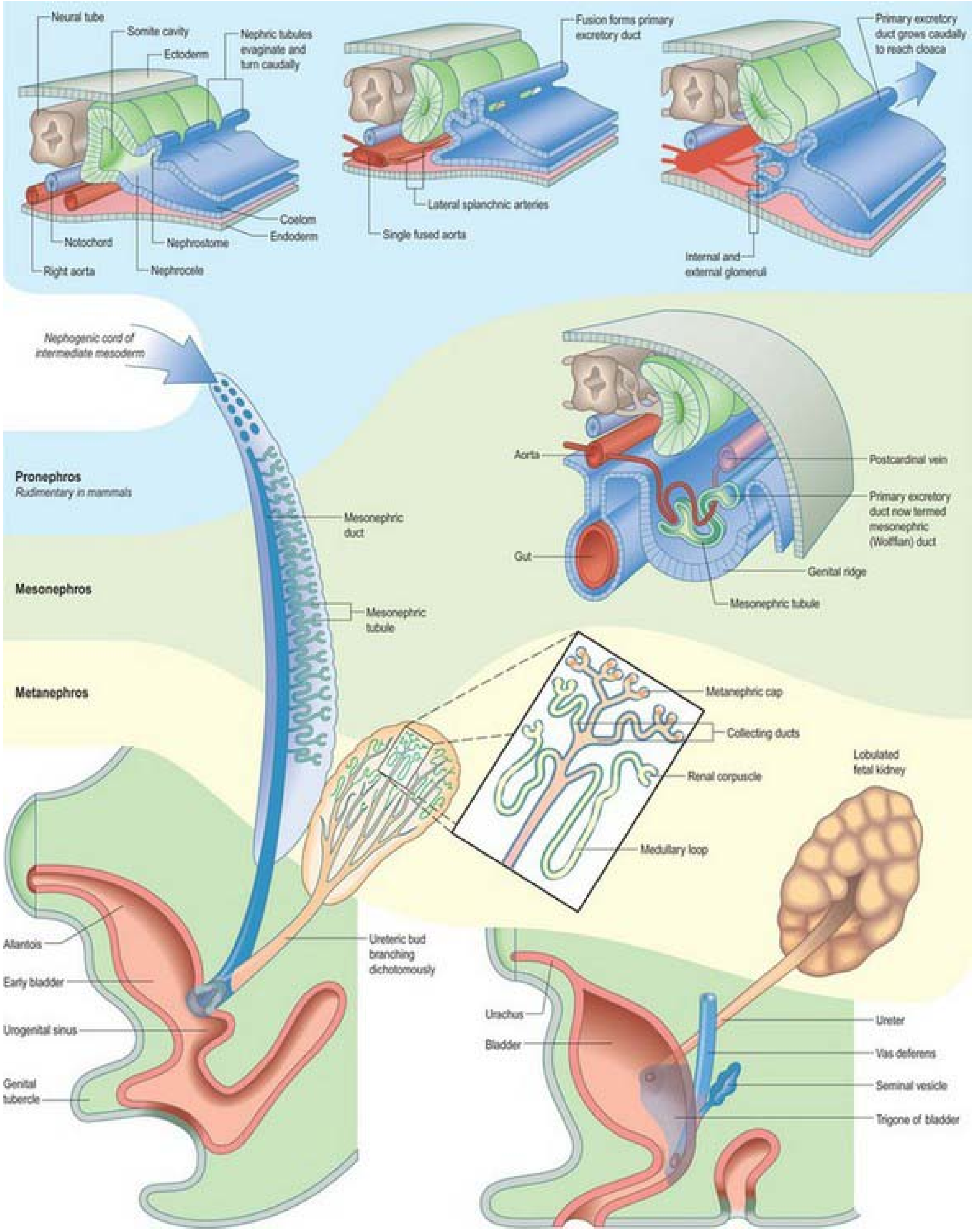
Neural tube
Somite cavity
Ectoderm
Nephric tubules evaginate and turn caudally
Coelom
Endoderm
Notochord
Nephrostome
Right aorta
Nephrocele
Fusion forms primary excretory duct
Lateral splanchnic arteries
Single fused aorta
Primary excretory duct grows caudally to reach cloaca
Internal and external glomeruli
Nephrogenic cord of intermediate mesoderm
Pronephros
Rudimentary in mammals
Mesonephros
Metanephros
Mesonephric duct
Mesonephric tubule
Aorta
Postcardinal vein
Primary excretory duct now termed mesonephric (Wolffian) duct
Gut
Genital ridge
Mesonephric tubule
Metanephric cap
Collecting ducts
Renal corpuscle
Medullary loop
Lobulated fetal kidney
Allantois
Early bladder
Urogenital sinus
Genital tubercle
Ureteric bud branching dichotomously
Urachus
Bladder
Ureter
Vas deferens
Seminal vesicle
Trigone of bladder

Fig. 78.2 Principal features of the primitive vertebrate nephric system for comparison with the development of the human nephric system. A considerable period of embryonic and fetal life has necessarily been compressed into a single diagram.

(Modified with permission from Williams PL, Wendell-Smith CP, Treadgold S 1969 Basic Human Embryology, 2nd edn. Philadelphia: Lippincott.)

It has been customary to regard the renal excretory system as three organs, the pronephros, mesonephros and metanephros, succeeding each other in time and space, such that the last to develop is retained as the permanent kidney (Figs 78.1, 78.2). However, it is difficult to provide reliable criteria by which to distinguish these stages or to define their precise limits in embryos.

Pronephros

The intermediate mesenchyme becomes visible in stage 10 embryos and can be distinguished as a nephrogenic cord when 10 somites are present. A pronephros is present in human embryos only as clusters of cells in the most cranial portions of the nephrogenic cord (Figs 78.1, 78.2). More caudally, similar groups of cells appear and become vesicular. The dorsal ends of the most caudal of the vesicles join the primary excretory duct. Their central ends are connected with the coelomic epithelium by cellular strands, which probably represent rudimentary peritoneal funnels. Glomeruli do not develop in association with these cranially situated nephric tubules, which ultimately disappear. It is doubtful whether external glomeruli develop in human embryos.

Primary excretory duct

In stage 11 embryos of approximately 14 somites, the primary excretory duct can be seen as a solid rod of cells in the dorsal part of the nephrogenic cord. Its cranial end is about the level of the ninth somite and its caudal tip merges with the undifferentiated mesenchyme of the cord. It differentiates before any nephric tubules, and when the latter appear it is at first unconnected with them. In older embryos the duct has lengthened and its caudal end becomes detached from the nephrogenic cord to lie immediately beneath the ectoderm. From this level it grows caudally, independent of the nephrogenic mesenchyme, and then curves ventrally to reach the wall of the cloaca. It becomes canalized progressively from its caudal end to form a true duct, which opens into the cloaca in embryos at stage 12 (Fig. 78.1C). Clearly, up to this stage the name ‘duct’ is scarcely appropriate.

Mesonephros

From stage 12 mesonephric tubules, which develop from the intermediate mesenchyme between somite levels 8–20, begin to connect to the primary excretory duct, which is now renamed the mesonephric duct. More caudally, a continuous ridge of nephrogenic mesenchyme extends to the level of somite 24. The mesonephric tubules (nephrons) are not metameric – there may be two or more mesonephric tubules opposite each somite.

Within the mesonephros, each tubule first appears as a condensation of mesenchyme cells, which epithelialize and form a vesicle. One end of the vesicle grows towards and opens into the mesonephric duct, while the other dilates and invaginates. The outer stratum forms the glomerular capsule, while the inner cells differentiate into mesonephric podocytes, which clothe the invaginating capillaries to form a glomerulus. The capillaries are supplied with blood through lateral branches of the aorta. It has been estimated that 70–80 mesonephric tubules and a corresponding number of glomeruli develop. However, these tubules are not all present at the same time, it is rare to find more than 30–40 in an individual embryo, because the cranial tubules and glomeruli develop and atrophy before the development of those situated more caudally.

By the end of the sixth week each mesonephros is an elongated, spindle-shaped organ that projects into the coelomic cavity, one on each side of the dorsal mesentery, from the level of the septum transversum to the third lumbar segment. This whole projection is called the mesonephric ridge, mesonephros, or Wolffian body (Figs 78.1B,C, 78.3). It develops subregions, and a gonad develops on its medial surface (p. 1311). There are striking similarities in structure between the mesonephros and the permanent kidney or metanephros, but the mesonephric nephrons lack a segment that corresponds to the descending limb of the loop of Henle. The mesonephros is believed to produce urine by stage 17. A detailed comparison of the development and function of the mesonephros and metanephros in staged human embryos is not available.

Rights were not granted to include this figure in electronic media.
Please refer to the printed publication.

Fig. 78.3 Arrangement of mesonephric duct from mesonephros to urogenital sinus. The duct runs within the tubal fold with the paramesonephric duct. For later development, see **Fig. 78.14**.

(Redrawn with permission from Tuchmann-Duplessis H, Haegel P 1972 Illustrated Human Embryology, Vol 2 Organogenesis. London: Chapman and Hall. With kind permission of Springer Science+Business Media.)

In stage 18 embryos (13–17 mm) the mesonephric ridge extends cranially to about the level of rib 9. In both sexes the cranial end of the mesonephros atrophies, and in embryos 20 mm in length (stage 19) a mesonephros is found only in the first three lumbar segments, although it may still possess as many as 26 tubules. The most cranial one or two tubules persist as rostral aberrant ductules (see Fig. 78.13); the succeeding five or six tubules develop into either the efferent ductules of the testis and lobules of the head of the epididymis (male), or the tubules of the epoöphoron (female);

the caudal tubules form the caudal aberrant ductules and the paradidymis (male), or the paroöphoron (female) (p. 1313).

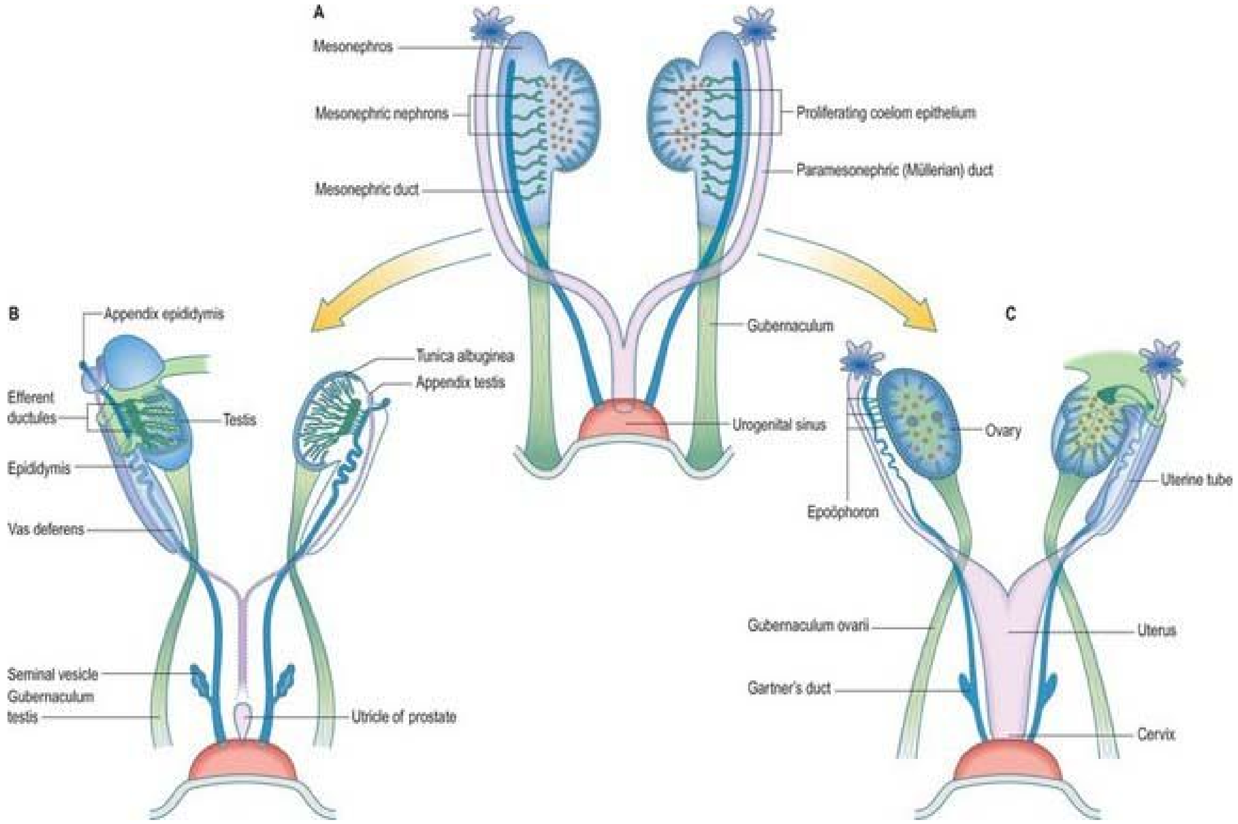
A
Mesonephros
Mesonephric nephrons
Mesonephric duct
Proliferating coelom epithelium
Paramesonephric (Müllerian) duct
Gubernaculum
Urogenital sinus
B
Appendix epididymis
Efferent ductules
Testis
Epididymis
Vas deferens
Tunica albuginea
Appendix testis
Seminal vesicle
Gubernaculum testis
Utricle of prostate
C
Ovary
Epoöphoron
Uterine tube
Gubernaculum ovarii
Uterus
Gartner's duct
Cervix

Fig. 78.13 **A**, Indifferent or ambisexual stage of development. **B**, Male. The mesonephric ducts are retained (left) and the paramesonephric ducts involute (right). **C**, Female. The paramesonephric (Müllerian) ducts are retained (right) and the mesonephric ducts involute (left).

Mesonephric duct

Once mesonephric nephrons connect to the primary excretory duct it is renamed the mesonephric duct. This runs caudally in the lateral part of the nephric ridge, and at the caudal end of the ridge it projects into the cavity of the coelom in the substance of a mesonephric fold (Fig. 78.3). As the mesonephric ducts from each side approach the urogenital sinus the two mesonephric folds fuse, between the bladder ventrally and the rectum dorsally, forming a transverse partition across the cavity of the pelvis, which is somewhat inappropriately called the genital cord (Fig. 78.3). In the male the peritoneal fossa between the bladder and the genital cord becomes obliterated, but it persists in the female as the uterovesical pouch. In the male the mesonephric duct itself becomes the canal of the epididymis, vas deferens and ejaculatory duct (p. 1317).

Urogenital sinus

The primitive hindgut ends in a cloacal region. This is connected ventrally with a blind-ending diverticulum, the allantois, which is intimately related to the development of the caudal portion of the urinary system. The enteric and allantoic portions of the hindgut are separated by the proliferation of the urorectal septum, a partition of mesenchyme and endoderm in the angle of the junction of hindgut and allantois (Fig. 78.4; see Fig. 78.7). The endodermal epithelium beneath the mesenchyme of the urorectal septum approaches but does not fuse with the cloacal membrane: it effectively divides the membrane into anal (dorsal) and urogenital (ventral) membranes, and the cloacal region into dorsal and ventral portions. The dorsal portion of the cloacal region is the putative rectum. The ventral portion can be further divided into: a cranial vesicourethral canal, continuous above with the allantoic duct; a middle, narrow channel, the pelvic portion; and a caudal, deep, phallic section, which is closed externally by the urogenital membrane. The second and third parts together constitute the urogenital sinus.

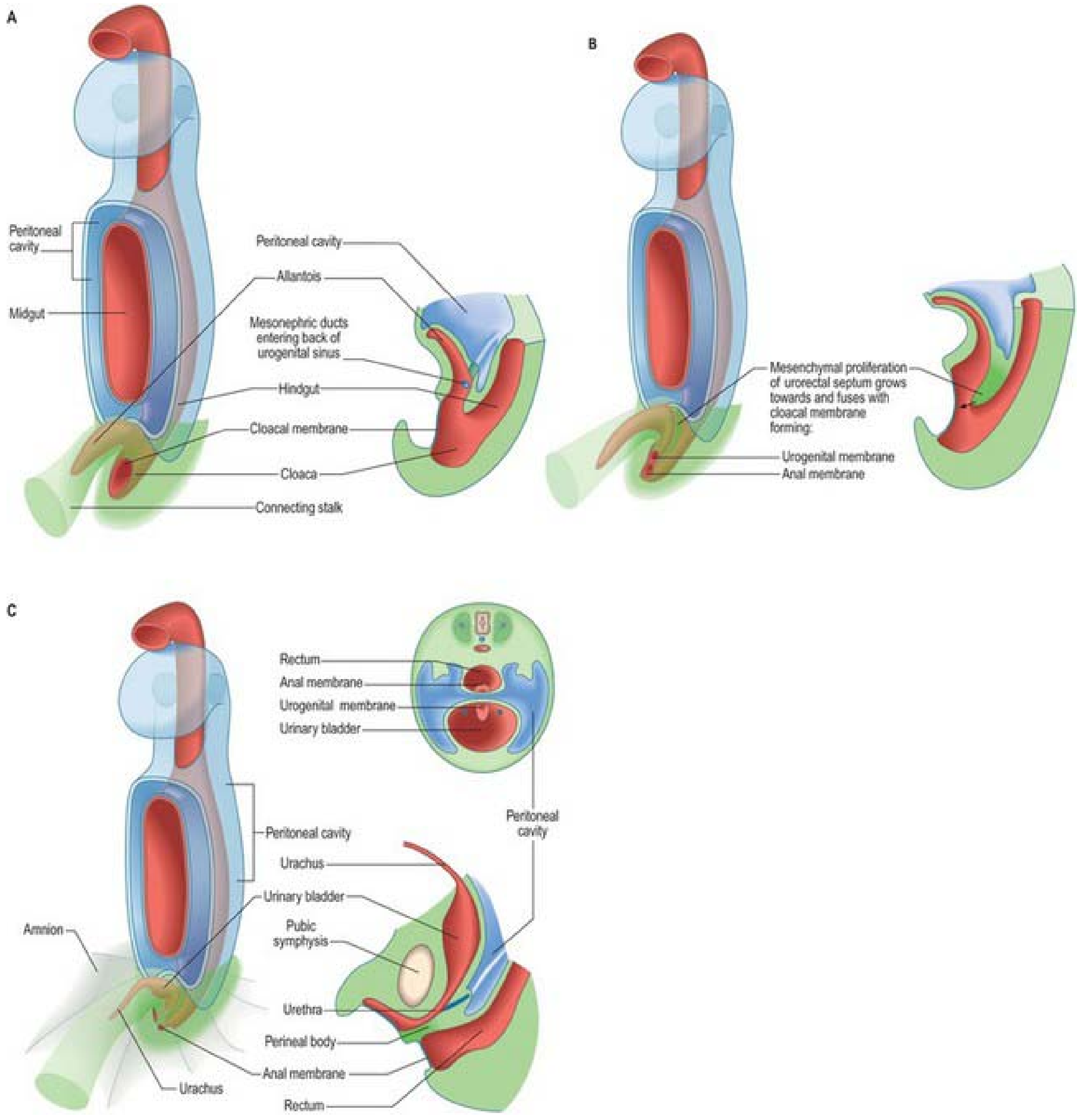
A
Peritoneal cavity
Midgut
Peritoneal cavity
Allantois
Mesonephric ducts entering back of urogenital sinus
Hindgut
Cloacal membrane
Cloaca
Connecting stalk
B
Mesenchymal proliferation of urorectal septum grows towards and fuses with cloacal membrane forming:
Urogenital membrane
Anal membrane
C
Rectum
Anal membrane
Urogenital membrane
Urinary bladder
Peritoneal cavity
Peritoneal cavity
Urachus
Urinary bladder
Amnion
Pubic symphysis
Urethra
Perineal body
Anal membrane
Rectum
Urachus

Fig. 78.4 The division of the hindgut into urinary and enteric parts. Left ventrolateral view of the intraembryonic coelom and corresponding midsagittal sections. **A**, Early cloaca. **B**, Proliferation of urorectal septum. **C**, Complete separation of urethra and anal canal, and position of perineal body.

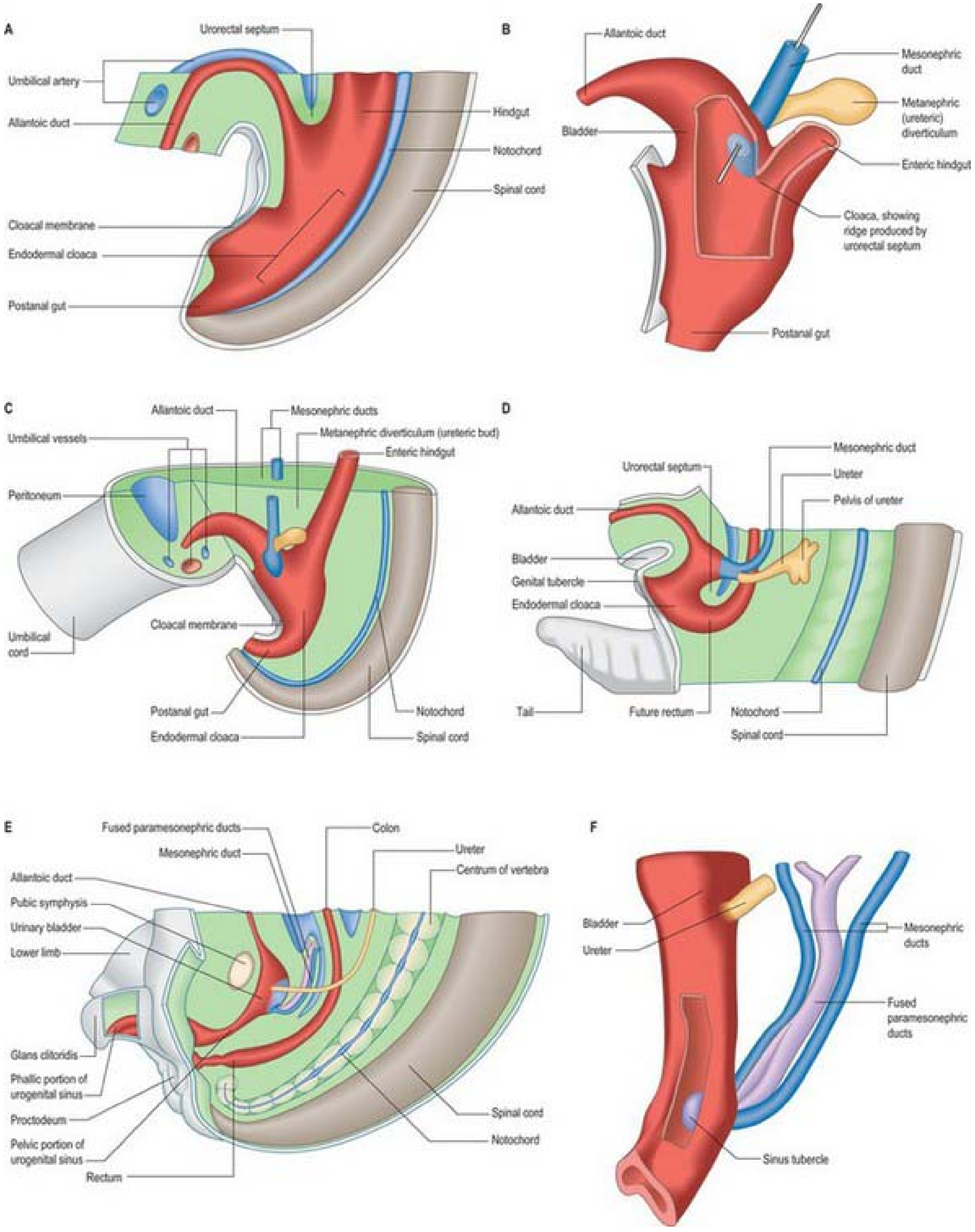
A
Urorectal septum
Umbilical artery
Allantoic duct
Hindgut
Notochord
Spinal cord
Cloacal membrane
Endodermal cloaca
Postanal gut
B
Allantoic duct
Mesonephric duct
Metanephric (ureteric) diverticulum
Bladder
Enteric hindgut
Cloaca, showing ridge produced by urorectal septum
Postanal gut
C
Allantoic duct
Mesonephric ducts
Metanephric diverticulum (ureteric bud)
Umbilical vessels
Enteric hindgut
Peritoneum
Umbilical cord
Cloacal membrane
Postanal gut
Endodermal cloaca
Notochord
Spinal cord
D
Mesonephric duct
Urorectal septum
Ureter
Pelvis of ureter
Allantoic duct
Bladder
Genital tubercle
Endodermal cloaca
Tail
Future rectum
Notochord
Spinal cord
E
Fused paramesonephric ducts
Colon
Mesonephric duct
Ureter
Centrum of vertebra
Allantoic duct
Pubic symphysis
Urinary bladder
Lower limb
Glans clitoridis
Phallic portion of urogenital sinus
Proctodeum
Pelvic portion of urogenital sinus
Rectum
Spinal cord
Notochord
F
Bladder
Ureter
Mesonephric ducts
Fused paramesonephric ducts
Sinus tubercle

Fig. 78.7 **A**, The caudal end of a human embryo, 4 weeks, showing the left lateral aspects of the spinal cord, notochord and endodermal cloaca. **B**, The endodermal cloaca of a human embryo, near the end of the fifth week. Part of the left wall of the cloaca, including the left mesonephric duct, has

been removed, together with the adjoining portions of the walls of the developing bladder and rectum. A piece of the ectoderm around the cloacal membrane has been left *in situ*. A wire is shown passing along the right mesonephric duct into the cloaca. **C**, The caudal end of a human embryo, 5 weeks, showing the endodermal cloaca. **D**, The caudal end of a human embryo, 6 weeks. The cloaca is becoming divided by the urorectal septum. **E**, The caudal end of a female human fetus, 8½–9 weeks, from the left-hand side showing structures in and near the median plane. The cloaca is now completely divided into urogenital and intestinal segments. **F**, Part of the vesicourethral portion of the endodermal cloaca of a female human fetus, 8½–9 weeks. The sinus tubercle is the elevation on the posterior wall of the urogenital sinus, caused by the fusion with the paramesonephric ducts.

Metanephros

The pronephros and mesonephros are linear structures. They both contain stacks of tubules distributed along the craniocaudal axis of the embryo, an arrangement that results in the production of hypotonic urine. In marked contrast, the tubules in the metanephric kidney are arranged concentrically, and the loops of Henle are directed towards the renal pelvis. This arrangement allows different concentration gradients to develop within the kidney and results in the production of hypertonic urine. Metanephric nephrons do not join with the existing mesonephric duct but with an evagination of that duct, which branches dichotomously to produce a characteristic pattern of collecting ducts.

The metanephric kidney develops from three sources. An evagination of the mesonephric duct, the ureteric bud, and a local condensation of mesenchyme, the metanephric blastema, form the nephric structure (Fig. 78.5). Angiogenic mesenchyme migrates into the metanephric blastema slightly later to produce the glomeruli and vasa recta. It is possible that an intact nerve supply is also required for metanephric kidney induction.

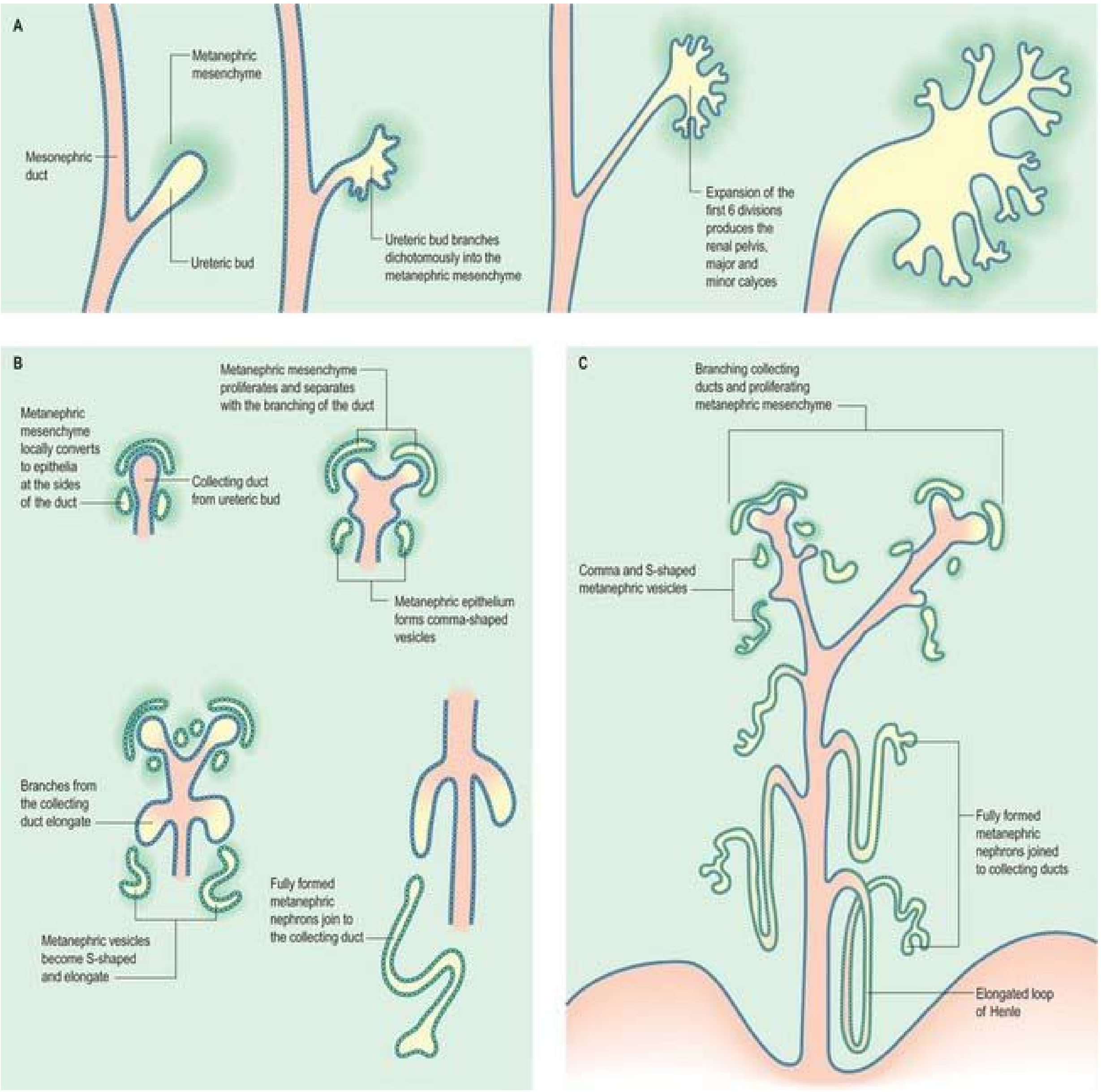
A
Metanephric mesenchyme
Mesonephric duct
Ureteric bud
Ureteric bud branches dichotomously into the metanephric mesenchyme
Expansion of the first 6 divisions produces the renal pelvis, major and minor calyces
B
Metanephric mesenchyme proliferates and separates with the branching of the duct
Metanephric mesenchyme locally converts to epithelia at the sides of the duct
Collecting duct from ureteric bud
Metanephric epithelium forms comma-shaped vesicles
Branches from the collecting duct elongate
Fully formed metanephric nephrons join to the collecting duct
Metanephric vesicles become S-shaped and elongate
C
Branching collecting ducts and proliferating metanephric mesenchyme
Comma and S-shaped metanephric vesicles
Fully formed metanephric nephrons joined to collecting ducts
Elongated loop of Henle

Fig. 78.5 Overview of metanephric kidney development. **A**, The ureteric bud arises from the mesonephric duct. The metanephric mesenchyme proliferates and separates with each subdivision of the ureteric bud. **B**, The metanephric mesenchyme converts to epithelia, forms comma and S-shaped vesicles which become metanephric nephrons. **C**, All stages of metanephric development are present concurrently. The most recently formed nephrons are on the outer aspect of the kidney.

An epithelial/mesenchymal interaction between the duct system and the surrounding mesenchyme occurs in both mesonephric and metanephric systems. In the mesonephric kidney, development proceeds in a craniocaudal progression, and cranial nephrons degenerate before caudal ones are produced. In the metanephric kidney a proportion of the mesenchyme remains as stem cells that continue to divide and which enter the nephrogenic pathway later when the individual collecting ducts lengthen. The temporal development of the metanephric kidney is patterned radially, such that the outer cortex is the last part to be formed. The following interactions occur in the development of the metanephric kidney (Fig. 78.5). The ureteric bud undergoes a series of bifurcations within the surrounding metanephric mesenchyme, and forms smaller ureteric ducts. At the same time the metanephric mesenchyme condenses around the dividing ducts to form S-shaped clusters, which transform into epithelia and fuse with the ureteric ducts at their distal ends. Blood vessels invade the proximal ends of the S-shaped clusters to form vascularized glomeruli.

The ureteric bud bifurcates when it comes into contact with the metanephric blastema in response to extracellular matrix molecules synthesized by the mesenchyme. Both chondroitin sulphate proteoglycan synthesis and chondroitin sulphate glycosaminoglycan processing are necessary for the dichotomous branching of the ureteric bud. In metanephric culture, incubation of fetal kidneys in β-D-xyloside, an inhibitor of chrondroitin sulphate synthesis, dramatically inhibits ureteric bud branching.

Subsequent divisions of the ureteric bud and associated mesenchyme define the gross structure of the kidney and the major and minor calyces, the distal branches of the ureteric ducts that will form the collecting ducts of the kidney. The proximal position of the ureteric bud elongates to form the developing ureter (Fig. 78.6). As the collecting ducts elongate the metanephric mesenchyme condenses around them. An adhesion molecule, syndecan, can be detected between the mesenchymal cells in the condensate. The cells switch off expression of N-CAM, fibronectin and collagen I, and start to synthesize L-CAM (also called E cadherin) and the basal lamina constituents laminin and collagen IV. The mesenchymal clusters are thus converted to small groups of epithelial cells, which undergo complex morphogenetic changes. Each epithelial group elongates, and forms first a comma-shaped, then an S-shaped, body, which continues to elongate and subsequently fuses with a branch of the ureteric duct at its distal end, while expanding as a dilated sac at its proximal end (Fig. 78.5). The latter involutes, and cells differentiate locally such that the outer cells become the parietal glomerular cells, while the inner ones become visceral epithelial podocytes. The podocytes develop in close proximity to invading capillaries derived from angiogenic mesenchyme outside the nephrogenic mesenchyme. This third source of mesenchyme produces the endothelial and mesangial cells within the glomerulus. The (metanephric-derived) podocytes and the angiogenic mesenchyme produce fibronectin and other components of the glomerular basement membrane. The isoforms of type-IV collagen within this layer follow a specific programme of maturation as the filtration of macromolecules from the plasma becomes restricted.

Rights were not granted to include this figure in electronic media.
Please refer to the printed publication.

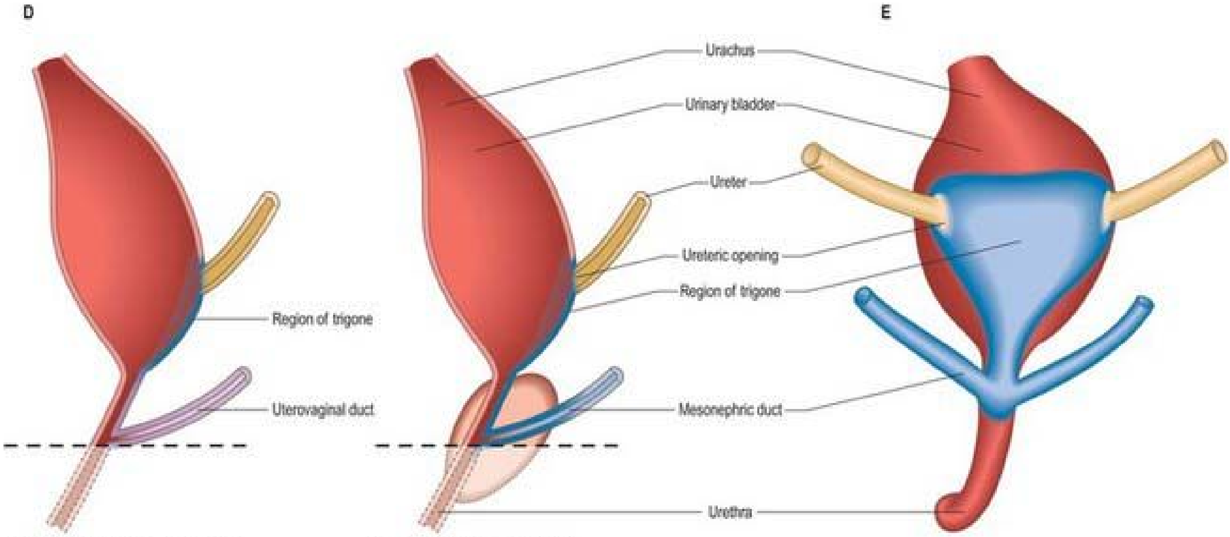
D
E
Urachus
Urinary bladder
Ureter
Ureteric opening
Region of trigone
Region of trigone
Uterovaginal duct
Mesonephric duct
Urethra

In the female the fused paramesonephric ducts form the uterovaginal duct. The mesonephric ducts degenerate.

In the male the mesonephric ducts form the vas deferens which enter the urethra through the prostate gland.

Fig. 78.6 Development of the urinary part of the urogenital sinus and formation of the trigone of the bladder. **A–C** and **E**, Posterior views. **D**, Male and female, median sagittal sections.

(Redrawn from Tuchmann-Duplessis H, Haegel P 1972 Illustrated Human Embryology, Vol 2 Organogenesis. London: Chapman and Hall. With kind permission of Springer Science+Business Media.)

Platelet derived growth factor (PDGF) β-chain and the PDGF receptor β-subunit (PDGFR β) have been detected in developing human glomeruli between 54 and 109 days' gestation. PDGF β-chain is localized in the differentiating epithelium of the glomerular vesicle during its comma and S-shaped stages, while PDGFR β is expressed in the undifferentiated metanephric blastema, vascular structures and interstitial cells. Both PDGF β-chain and PDGFR β are expressed by mesangial cells, which may promote further mesangial cell proliferation.

Metanephric mesenchyme will develop successfully *in vitro*, which makes experimental perturbation of kidney development comparatively easy to evaluate. Early experimental studies demonstrated that other mesenchymal populations, and spinal cord, were able to induce ureteric bud division and metanephric development. Nerves enter the developing kidney very early, travelling along the developing ureter. If developing kidney rudiments are incubated with antisense oligonucleotides, which neutralize nerve growth factor receptor (NGF-R) mRNA, nephrogenesis is completely blocked, suggesting that metanephric mesenchyme induction is a response to innervation. The powerful inductive effect of the spinal cord on metanephric mesenchyme may be a further expression of this phenomenon.

All stages of nephron differentiation are present concurrently in the developing metanephric kidney (Fig. 78.5). Antigens for the brush border of the renal tubule appear when the S-shaped body has formed. They appear first in the inner cortical area.

The metanephric kidney is lobulated throughout fetal life, but this condition usually disappears during the first year after birth (see Fig. 78.8). Varying degrees of lobulation occasionally persist throughout life.

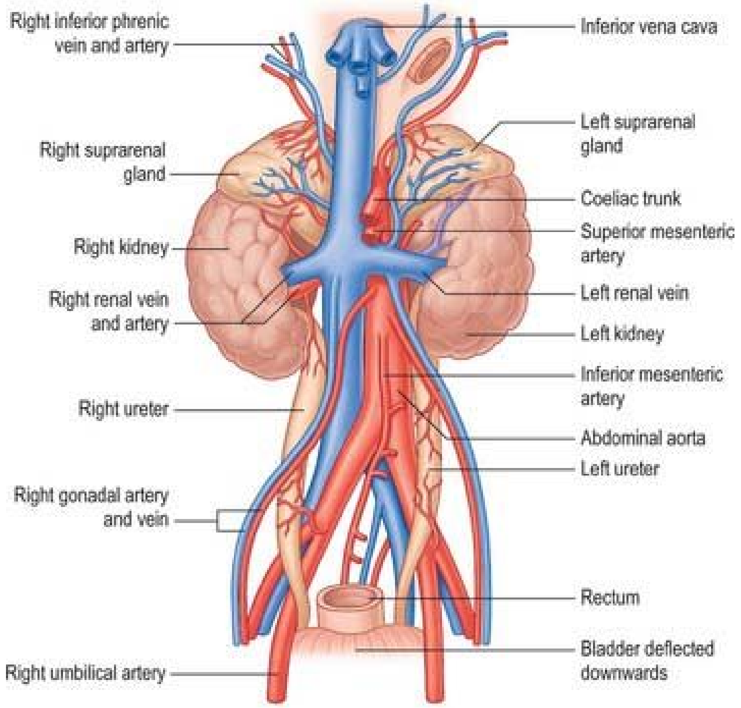
Right inferior phrenic vein and artery
Right suprarenal gland
Right kidney
Right renal vein and artery
Right ureter
Right gonadal artery and vein
Right umbilical artery
Inferior vena cava
Left suprarenal gland
Coeliac trunk
Superior mesenteric artery
Left renal vein
Left kidney
Inferior mesenteric artery
Abdominal aorta
Left ureter
Rectum
Bladder deflected downwards

Fig. 78.8 Posterior abdominal wall of a full-term neonate. Note the lobulated kidneys and relatively wide calibre of the ureters.

The growth of left and right kidneys is well matched during development. Fetal kidney volume increases most during the second trimester in both sexes. For reasons that are not understood, male fetuses show greater values for renal volume than female fetuses from the third trimester onwards.

Endocrine development of the kidney

The kidney functions not only as an excretory organ, but also as an endocrine organ, secreting hormones that are concerned with renal haemodynamics. Before birth homeostasis is controlled by the placenta. The fetal kidney produces amniotic fluid. The kidneys of premature babies of less than 36 weeks are immature. They contain incompletely differentiated cortical nephrons, which compromise their ability to maintain homeostasis. Problems of immaturity are further compounded by the effects of hypoxia and asphyxia, which modify renal hormones.

Renal hormones include the renin–angiotensin system, renal prostaglandins, the kallikrein–kinin system, and renal dopamine. Renin is found in the smooth muscle cells of arterioles, interlobular arteries and branches of the renal artery, and has also been described in the distal convoluted tubule cells. Kallikrein has been demonstrated in rat fetal kidney, and prostaglandins have been demonstrated in the renal medulla and renal tubule. Renal dopamine is produced (mainly) by the enzymatic conversion of L-dopa to dopamine in the early segments of the proximal convoluted tubule, and is also sourced locally from dopaminergic nerves. Other renal hormones include an antihypertensive lipid, which is produced in the interstitial cells of the renal medulla, and, possibly, histamine and serotonin. Growth factors produced by human embryonic kidney cells include erythropoietin and interleukin β (which stimulate megakaryocyte maturation) and transforming growth factor-β.

Ascent of the kidney

The metanephric kidney is initially sacral. As the ureteric outgrowth lengthens, it becomes positioned more and more cranially. The metanephric pelvis lies on a level with the second lumbar vertebra when the embryo reaches a length of about 13 mm. During this period the ascending kidney receives its blood supply sequentially from arteries in its immediate neighbourhood, i.e. the middle sacral and common iliac arteries. The definitive renal artery is not recognizable until the beginning of the third month. It arises from the most caudal of the three suprarenal arteries, all of which represent persistent mesonephric or lateral splanchnic arteries. Additional renal arteries are relatively common, and may enter at the hilum or at the upper or lower pole of the gland – they also represent persistent mesonephric arteries.

Ureter

The wall of the early ureter is initially highly permeable. Its lumen later becomes obliterated and is subsequently recanalized. Both of these processes begin in intermediate portions of the ureter and proceed cranially and caudally. Recanalization is not associated with metanephric function, but perhaps reflects the rapid elongation of the ureter as the embryo grows. Two fusiform enlargements appear at the lumbar and pelvic levels of the ureter at 5 and 9 months respectively (the pelvic enlargement is inconstant). As a result the ureter shows a constriction at its proximal end (pelviureteric region) and another as it crosses the pelvic brim. A third narrowing is always present at its distal end and is related to the growth of the bladder wall.

At first the distal end of the ureter is connected to the dorsomedial aspect of the mesonephric duct, but, as a result of differential growth, this connection comes to lie lateral to the duct.

Urinary bladder

The urinary bladder develops from the cranial vesicourethral canal, which is continuous above with the allantoic duct (Figs 78.4, 78.6, 78.7). The mesonephric ducts open into the urogenital sinus early in development. The ureters develop as branches of the mesonephric ducts, which attain their own access to the developing bladder, and their orifices open separately into the bladder on the lateral side of the opening of the mesonephric ducts. Later the two orifices become separated still further and, although the ureter retains its point of entry into the bladder, the mesonephric duct opens into that part of the urogenital sinus that subsequently becomes the prostatic urethra (Fig. 78.6). The triangular region of absorption of the mesonephric ducts contributes to the trigone of the bladder and dorsal wall of the proximal half of the prostatic urethra, i.e. as far as the opening of the prostatic utricle and ejaculatory ducts, or its female homologue, the whole female urethral dorsal wall. The remainder of the vesicourethral canal forms the body of the bladder and urethra, and its apex is prolonged to the umbilicus as a narrow canal, the urachus.

The fetal bladder can be identified by ultrasound examination at 9–11 weeks’ gestation and the absence of a bladder image is considered abnormal at 13 weeks or later.

Neonatal urinary system

At birth the two kidneys weigh approximately 23 g. They function early in development and produce the amniotic fluid that surrounds the fetus. The lobulated appearance of fetal kidneys is still present at birth (Fig. 78.8; see Fig. 14.4). Addition of new cortical nephrons continues in the first few months of postnatal life after which general growth of the glomeruli and tubules results in the disappearance of lobulation. The renal blood flow is lower in the neonate; adult values are attained by the end of the first year. The glomerular filtration rate at birth is approximately 30% of the adult value, which is attained by 3–5 months of age.

The neonatal urinary bladder is egg-shaped and the larger end is directed downwards and backwards (Figs 78.9, 78.10; see Figs 14.4, 14.5). Although described as an abdominal organ, nearly one half of the neonatal bladder lies below a line drawn from the promontory of the sacrum to the upper edge of the pubic symphysis, i.e. within the cavity of the true pelvis. From the bladder neck, the bladder extends anteriorly and slightly upwards in close contact with the pubis until it reaches the anterior abdominal wall. The apex of the contracted bladder lies at a point midway between the pubis and the umbilicus. When the bladder is filled with urine the apex may extend up to the level of the umbilicus. It is therefore possible to obtain urine by inserting a needle, connected to a syringe, into the bladder through the abdominal wall about 2 cm above the symphysis pubis and aspirating the contents into the sterile syringe. The success rate of the procedure is variable and depends upon the bladder being full: a much higher success rate has been reported by using an ultrasound scanner to locate the bladder and confirm that it contains urine prior to the insertion of the needle.

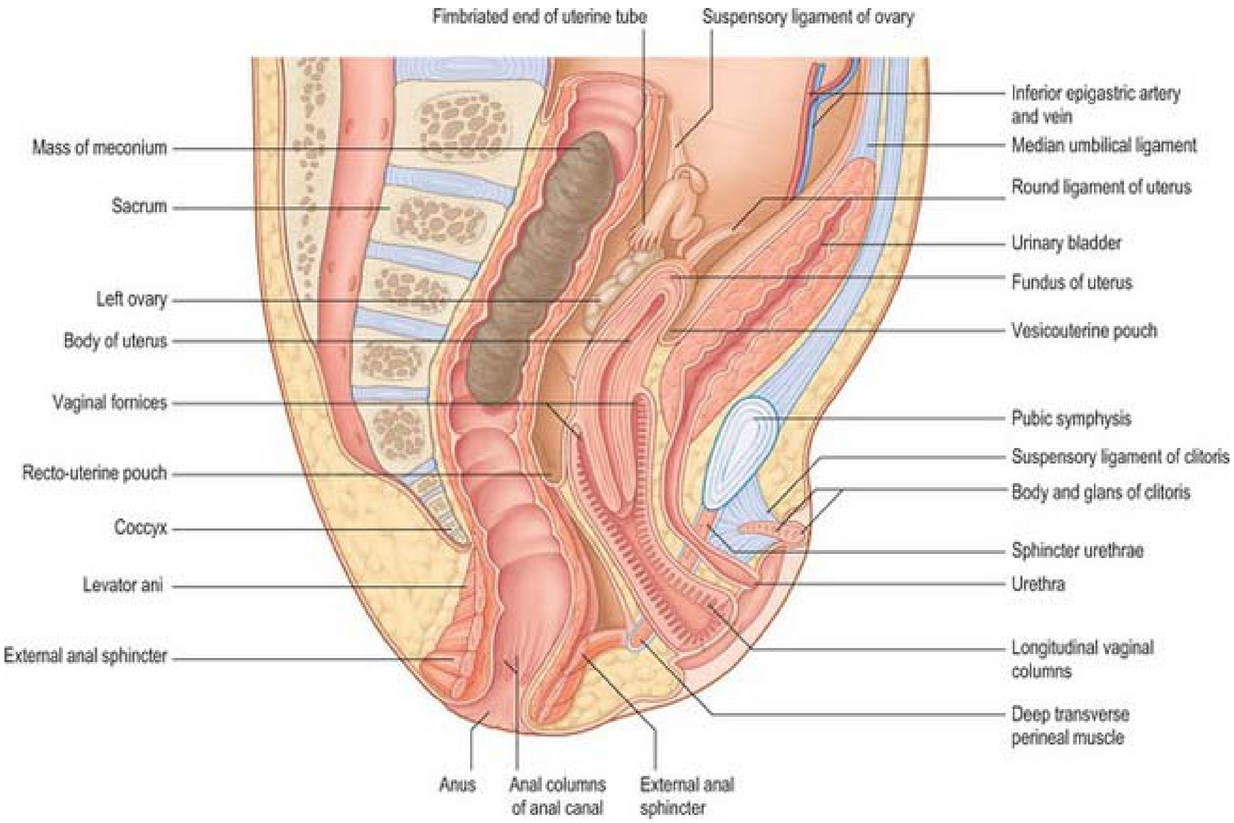
Fimbriated end of uterine tube
Suspensory ligament of ovary
Mass of meconium
Sacrum
Left ovary
Body of uterus
Vaginal fornices
Recto-uterine pouch
Coccyx
Levator ani
External anal sphincter
Inferior epigastric artery and vein
Median umbilical ligament
Round ligament of uterus
Urinary bladder
Fundus of uterus
Vesicouterine pouch
Pubic symphysis
Suspensory ligament of clitoris
Body and glans of clitoris
Sphincter urethrae
Urethra
Longitudinal vaginal columns
Deep transverse perineal muscle
Anus
Anal columns of anal canal
External anal sphincter

Fig. 78.9 Midsagittal section through the pelvis of a full-term female neonate. Note the abdominal position of the urinary bladder and uterus. (After Crelin ES 1969 Anatomy of the Newborn. Philadelphia: Lea and Febiger.)

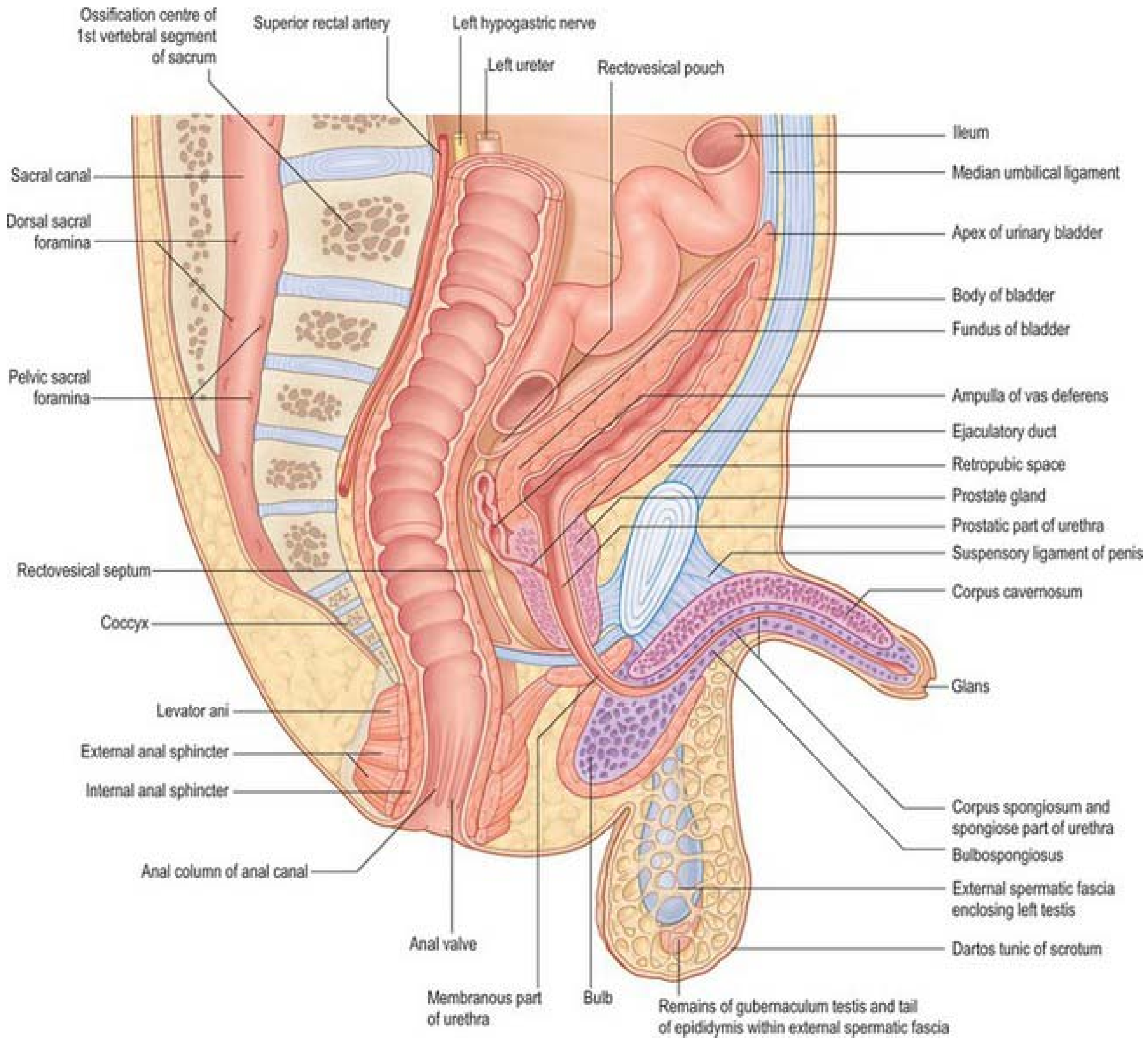
Ossification centre of 1st vertebral segment of sacrum
Superior rectal artery
Left hypogastric nerve
Left ureter
Rectovesical pouch
Sacral canal
Dorsal sacral foramina
Pelvic sacral foramina
Rectovesical septum
Coccyx
Levator ani
External anal sphincter
Internal anal sphincter
Anal column of anal canal
Anal valve
Membranous part of urethra
Bulb
Remains of gubernaculum testis and tail of epididymis within external spermatic fascia
Ileum
Median umbilical ligament
Apex of urinary bladder
Body of bladder
Fundus of bladder
Ampulla of vas deferens
Ejaculatory duct
Retropubic space
Prostate gland
Prostatic part of urethra
Suspensory ligament of penis
Corpus cavernosum
Glans
Corpus spongiosum and spongiose part of urethra
Bulbospongiosus
External spermatic fascia enclosing left testis
Dartos tunic of scrotum

Fig. 78.10 Midsagittal section through the pelvis of a full-term male neonate. Note the abdominal position of the urinary bladder. (After Crelin ES 1969 Anatomy of the Newborn. Philadelphia: Lea and Febiger.)

There is no true fundus in the fetal bladder as there is in the adult. Although the anterior surface is not covered with peritoneum, peritoneum extends posteriorly as low as the level of the urethral orifice. Because the apex of the bladder is relatively high, pressure on the lower abdominal wall will express urine from an infant bladder. Moreover, because the bladder remains connected to the umbilicus by the obliterated remains of the urachus (see Fig. 14.5), stimulation of the umbilicus can initiate micturition in babies.

The elongated shape of the bladder in neonates means that the ureters are correspondingly reduced in length and they lack a pelvic portion. The bladder does not gain its adult, pelvic, position until about the sixth year. A distinct interureteric fold is present in the contracted neonatal bladder.

Anomalies of the urinary system

Anomalies of the urinary system are relatively common (3% of live births). Renal agenesis is the absence of one or both kidneys. In unilateral renal agenesis, the remaining kidney exhibits compensatory hypertrophy and produces a nearly normal functional mass of renal tissue. Atresia of the ureter during development causes a non functional multicystic dysplastic kidney, thought to be secondary to urinary obstruction being present while the tubules are still forming. Problems with kidney ascent can result in a pelvic kidney. Alternatively, the kidneys may fuse together at their caudal poles producing a horseshoe kidney, which cannot ascend out of the pelvic cavity because the inferior mesenteric artery prevents further migration.

It was thought that renal cysts arose from clumps of vesicular cells, which persisted when the tips of branches from the ureteric diverticulum failed to fuse with metanephrogenic cap tissue. It is now believed that they are wide dilatations of a part of otherwise continuous nephrons. In most cases, autosomal dominant polycystic kidney disease results from mutations of *PKD1* or *PKD2* genes which are expressed in human embryos from 5–6 weeks of development within the mesonephros and later the metanephros (Chauvet et al 2002). In this condition the cystic dilatation may affect any part of the nephron, from Bowman’s capsule to collecting tubules. Less common is infantile cystic renal disease, inherited as a recessive trait, where the proximal and distal tubules are dilated to some degree but the collecting ducts are grossly affected.

Abnormalities of the ventral body wall caudal to the umbilicus, especially with inappropriate siting of the genital tubercle can result in exstrophy of the bladder (Fig. 78.11). In this condition the urorectal septum (internal) is associated with the genital tubercle (external), which means that the urogenital and anal membranes are widely separated. When the urogenital membrane involutes, the posterior surface of the bladder is exposed to the anterior abdominal wall. The lower part of the abdominal wall is therefore occupied by an irregularly oval area, covered with mucous membrane, on which the two ureters open. The periphery of this extroverted area, which is covered by urothelium, becomes continuous with the skin.

Rights were not granted to include this figure in electronic media.
Please refer to the printed publication.

Fig. 78.11 Bladder exstrophy. Misalignment of the genital tubercle and urogenital swellings with the urogenital membrane during early development results in subsequent malposition of the bladder, urethra and associated sphincters. The disappearance of the urogenital membrane exposes the posterior wall of the bladder, and the urethral opening is on the superior side of the penis or clitoris.

(Redrawn from Tuchmann-Duplessis H, Haegel P 1972 Illustrated Human Embryology, Vol 2 Organogenesis. London: Chapman and Hall. With kind permission of Springer Science+Business Media.)

The routine use of ultrasound as an aid to *in utero* diagnosis of abnormalities has revealed a prevalence of 1–2 abnormal fetuses per 1000 ultrasound procedures. Of these, 20–30% are anomalies of the genitourinary tract, and can be detected as early as 12–15 weeks' gestation. However, the decision to be made after such a diagnosis is by no means clear. Urinary obstruction is considered an abnormality, yet transient modest obstruction is considered normal during canalization of the urinary tract, and has been reported in 10–20% of fetuses in the third trimester. A delay in canalization, or in the rupture of the cloacal membrane, can produce a dilatation. Similarly, the closure of the urachus at 32 weeks may be associated with high-resistance outflow for the system, which again produces transient obstruction. The degree to which obstruction may cause renal parenchymal damage cannot be assessed in a developing kidney, which may have primary nephrogenic dysgenesis.

The volume of amniotic fluid is used as an indicator of renal function, but, because other sources produce amniotic fluid in early gestation, amniotic volume does not reflect fetal urinary output until the second trimester. Too little amniotic fluid is termed oligohydramnios, too much, polyhydramnios. Although variation in the amount of amniotic fluid may suggest abnormalities of either the gut or kidneys, it is not always possible to correlate even severe oligohydramnios with renal dysfunction. There is an important relationship between the volume of amniotic fluid, lung development and maturity, and oligohydramnios has been shown to be associated with pulmonary hypoplasia (see Ch. 59).

REPRODUCTIVE SYSTEM

Development of the reproductive organs from the intermediate mesenchyme starts from stage 14, about 10 days later than the urinary system. Bilateral paramesonephric (Müllerian) ducts develop alongside the mesonephric ducts, and the midportion of each mesonephros undergoes thickening to form the gonadal ridge. Although the primordial germ cells are delineated very early in development, they are sequestered in the extraembryonic tissues until the gonadal ridge is ready to receive them. It was thought that development to one or other sexual phenotype occurred after migration of the primordial germ cells to the indifferent gonads. However, it is now recognized that the development of male or female gonads, genital ducts and external genitalia is far more complicated, and is the result of a complex interplay between genetic expression, timing of development and the influence of sex hormones. As development proceeds, a significant proportion of early embryonic urinary tissue is incorporated into the reproductive tracts, especially in the male. The earliest stage of reproductive development, prior to the arrival of the primordial germ cells into the gonad, is termed the indifferent or ambisexual stage.

Early gonadal development (ambisexual or indifferent stage)

Essentially four different cell lineages contribute to the gonads. Cells are derived from: proliferating coelomic epithelium on the medial side of the mesonephros; underlying mesonephric mesenchyme; invading angiogenic mesenchyme already present in the mesonephros; and primordial germ cells that arise from the epiblast very early in development and later migrate from the allantoic wall.

The formation of the gonads is first indicated by the appearance of an area of thickened coelomic epithelium on the medial side of the mesonephric ridge in the fifth week, stage 16 (Figs 78.12, 78.13; see Fig. 78.16). Elsewhere on the surface of the ridge the coelomic epithelium is one or two cells thick, but over this gonadal area it becomes multilayered. Thickening rapidly extends in a longitudinal direction until it covers nearly the whole of the medial surface of the ridge. The thickened epithelium continues to proliferate, displacing the renal corpuscles of the mesonephros in a dorsolateral direction and forms a projection into the coelomic cavity, the gonadal ridge. Surface depressions form along the limits of the ridge, which is thus connected to the mesonephros by a broad mesentery, the mesogenitale. In this way the mesonephric ridge becomes subdivided into a lateral part, the tubal fold, containing the mesonephric and paramesonephric ducts, and a medial part, the gonadal fold. The tubal fold also contains the nephric tubules and glomeruli at its base (Fig. 78.3).

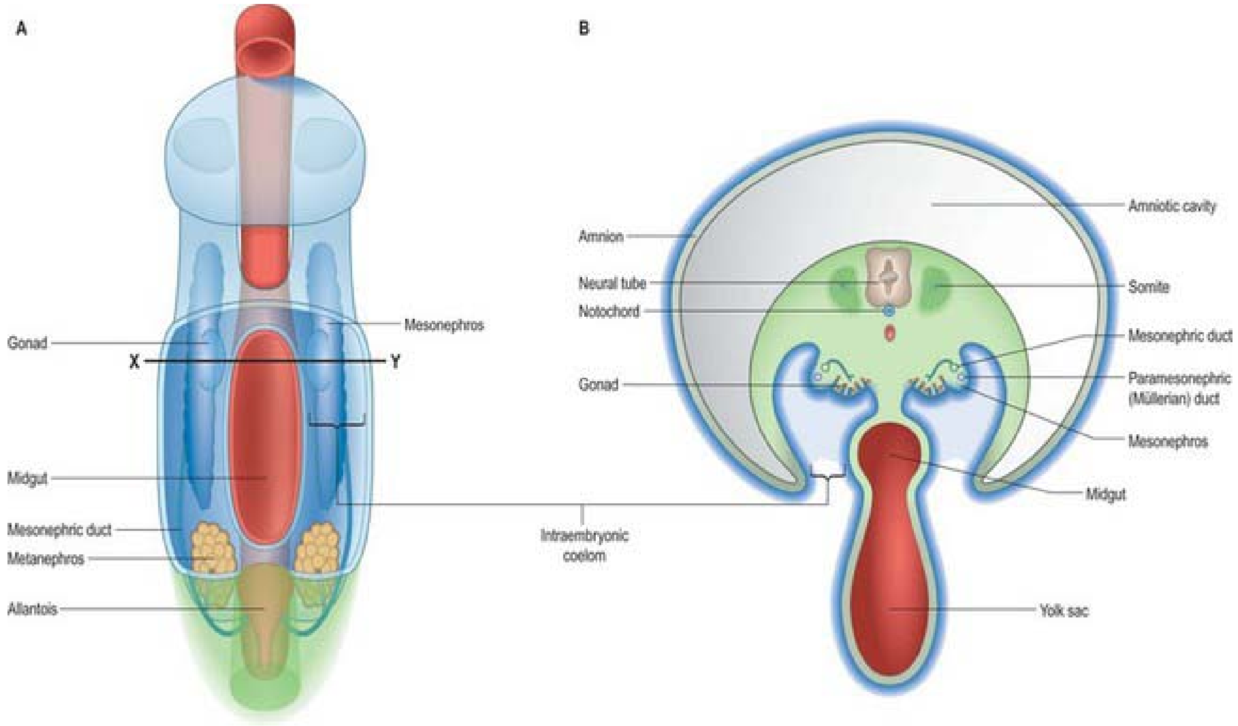
A
B
Gonad
X
Y
Mesonephros
Midgut
Mesonephric duct
Metanephros
Allantois
Amnion
Neural tube
Notochord
Gonad
Amniotic cavity
Somite
Mesonephric duct
Paramesonephric (Müllerian) duct
Mesonephros
Midgut
Intraembryonic coelom
Yolk sac

Fig. 78.12 **A**, Position of the gonads on the posterior abdominal wall, anteromedial to the mesonephros. **B**, Transverse section of figure **A**, through the line X–Y.

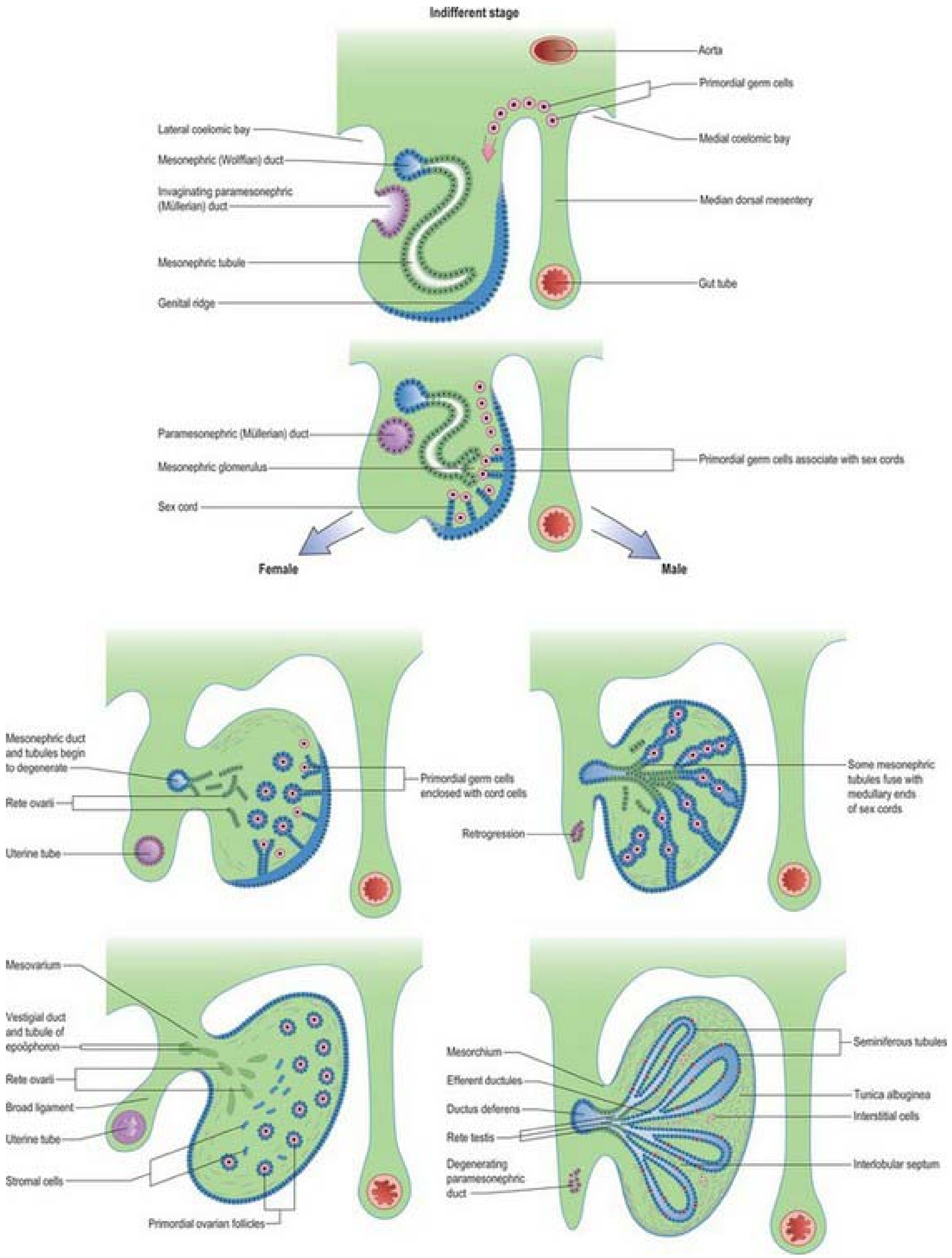
Indifferent stage
Aorta
Primordial germ cells
Lateral coelomic bay
Medial coelomic bay
Mesonephric (Wolffian) duct
Invaginating paramesonephric (Müllerian) duct
Median dorsal mesentery
Mesonephric tubule
Gut tube
Genital ridge
Paramesonephric (Müllerian) duct
Primordial germ cells associate with sex cords
Mesonephric glomerulus
Sex cord
Female
Male
Mesonephric duct and tubules begin to degenerate
Primordial germ cells enclosed with cord cells
Rete ovarii
Uterine tube
Some mesonephric tubules fuse with medullary ends of sex cords
Retrogression
Mesovarium
Vestigial duct and tubule of epoöphoron
Rete ovarii
Broad ligament
Uterine tube
Stromal cells
Primordial ovarian follicles
Seminiferous tubules
Mesorchium
Efferent ductules
Tunica albuginea
Ductus deferens
Interstitial cells
Rete testis
Interlobular septum
Degenerating paramesonephric duct

Fig. 78.16 Development of the gonads and associated ducts as seen in transverse section to show the fate of the primordial germ cells, mesonephric duct and tubules and paramesonephric duct in the two sexes.

(Modified with permission from Williams PL, Wendell-Smith CP, Treadgold S 1969 Basic Human Embryology, 2nd edn, Philadelphia: Lippincott.)

Up to the seventh week the ambisexual gonad possesses no sexually differentiating feature. From stage 16 the proliferating coelomic epithelium forms a number of cellular epithelial cords (sometimes called primary sex cords), separated by mesenchyme. The cords remain at the periphery of the primordium and form a cortex. Proliferation and labyrinthine cellular condensation of the mesonephric mesenchyme, including angiogenic mesenchyme, produces a central medulla (see Fig. 78.16).

Reproductive ducts

The paramesonephric, Müllerian, ducts develop in embryos of both sexes, but become dominant in the development of the female reproductive system. They are not detectable until the embryo reaches a length of 10–12 mm (early sixth week). Each begins as a linear invagination of the coelomic epithelium, the paramesonephric groove, on the lateral aspect of the mesonephric ridge near its cranial end. The blind caudal end continues to grow caudally into the substance of the ridge as a solid rod of cells, which becomes canalized as it lengthens. Throughout the extent of the mesonephros it is lateral to the mesonephric duct, which acts as a guide for it. The paramesonephric duct reaches the caudal end of the mesonephros in the eighth week. It turns medially and crosses ventral to the mesonephric duct to enter the genital cord, where it bends caudally in close apposition with its fellow from the opposite side (Fig. 78.13). The two ducts reach the dorsal wall of the urogenital sinus during the third month, and their blind ends produce an elevation called the Müllerian sinus tubercle (Fig. 78.7F; see Fig. 78.19).

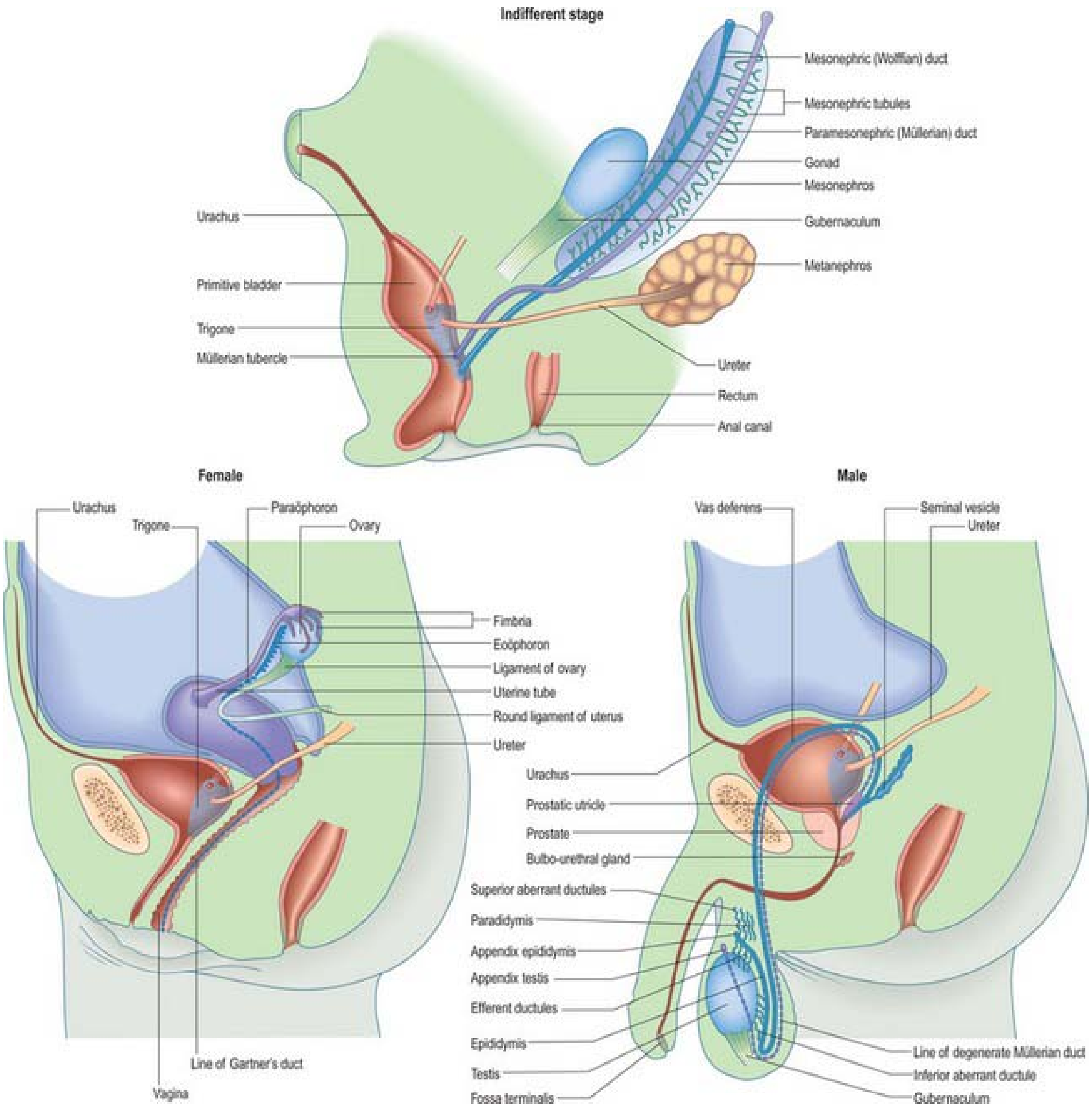
Indifferent stage
Mesonephric (Wolffian) duct
Mesonephric tubules
Paramesonephric (Müllerian) duct
Gonad
Mesonephros
Urachus
Gubernaculum
Metanephros
Primitive bladder
Trigone
Müllerian tubercle
Ureter
Rectum
Anal canal
Female
Male
Urachus
Trigone
Paraöphoron
Ovary
Vas deferens
Seminal vesicle
Ureter
Fimbria
Eoöphoron
Ligament of ovary
Uterine tube
Round ligament of uterus
Ureter
Urachus
Prostatic utricle
Prostate
Bulbo-urethral gland
Superior aberrant ductules
Paradidymis
Appendix epididymis
Appendix testis
Efferent ductules
Epididymis
Testis
Fossa terminalis
Line of degenerate Müllerian duct
Inferior aberrant ductule
Gubernaculum
Line of Gartner's duct
Vagina

Fig. 78.19 The development of the urogenital system from the indifferent stage to the definitive male and female conditions.

(Modified with permission from Williams PL, Wendell-Smith CP, Treadgold S 1969 Basic Human Embryology, 2nd edn. Philadelphia: Lippincott.)

At the end of the indifferent stage each paramesonephric duct consists of vertical cranial and caudal parts and an intermediate horizontal region. The mesonephric ducts course caudally, medial to the paramesonephric ducts, and both duct systems open into the urogenital sinus. The genital ducts possess an external serosa on some surfaces derived from coelomic epithelium, a smooth muscle muscularis derived from underlying mesenchyme, and an internal mucosa derived from either the mesonephric duct or from the invaginated tube of coelomic epithelium that forms the paramesonephic duct. The layers are invaded by angiogenic mesenchyme and by nerves.

Uterus and uterine tubes

In the female the mesonephric duct is vestigial. Cranially it becomes the longitudinal duct of the epoöphoron, while caudally it is referred to as Gartner's duct (Table 78.1). The cranial part of the paramesonephric ducts forms the uterine tubes, and the original coelomic invagination remains as the pelvic opening of the tube. The fimbriae become defined as the cranial end of the mesonephros degenerates. The caudal vertical parts of the two ducts fuse with each other to form the uterovaginal primordium (Figs 78.7, 78.13, 78.14; see Fig. 78.19). This gives rise to the lower part of the uterus and, as it enlarges, it takes in the horizontal parts to form the fundus and most of the body of the adult uterus. A constriction between the body of the uterus and the cervix can be found at 9 weeks. The stroma of the endometrium and the uterine musculature develop from the surrounding mesenchyme of the genital cord.

Table 78.1 Homologies of the parts of the urogenital system in male and female.

Gonad	**Testis**	**Ovary**
Gubernacular cord	Gubernaculum testis	Ovarian and round ligaments
Mesonephros (Wolffian body)	Appendix of epididymis (?)	Appendices vesiculosae (?)
	Efferent ductules	Epoöphoron
	Lobules of epididymis	
	Paradidymis	Paroöphoron
	Aberrant ductules	

Mesonephric duct (Wolffian duct)	Duct of epididymis	Duct of epoöphoron (Gartner’s duct)
	Vas deferens	
	Ejaculatory duct	
	Part of bladder and prostatic urethra	Part of bladder and urethra
Paramesonephric (Müllerian) duct	Appendix of testis	Uterine tube
		Uterus
	Prostatic utricle	Vagina (?)
Allantoic duct	Urachus	Urachus
Cloaca:		
Dorsal part	Rectum and upper part of anal canal	Rectum and upper part of anal canal
Ventral part	Most of bladder	Most of bladder and urethra
	Part of prostatic urethra	
Urogenital sinus	Prostatic urethra distal to utricle	
	Bulbo-urethral glands	Greater vestibular glands
	Rest of urethra to glans	Vestibule
Genital folds	Ventral penis	Labia minora
Genital tubercle	Penis	Clitoris
	Urethra in glans	

Rights were not granted to include this figure in electronic media.
Please refer to the printed publication.

Fig. 78.14 Relative movements of the gonads and associated tubes. **A**, Gonads and mesonephros move caudally, and the metanephros ascends. **B**, Posterior view of the mesonephric ducts (ureters) and the fused paramesonephric ducts (uterovaginal canal) in the female. For earlier development, see Fig. 78.3.

(Redrawn from Tuchmann-Duplessis H, Haegel P 1972 Illustrated Human Embryology, Vol 2 Organogenesis. London: Chapman and Hall. With kind permission of Springer Science+Business Media.)

Failure of fusion of the two paramesonephric ducts can lead to a range of anomalies summarized in Fig. 78.15. These fusions can also contribute to anomalies of vaginal development.

Rights were not granted to include this figure in electronic media.
Please refer to the printed publication.

Fig. 78.15 Uterovaginal malformations.

(Redrawn from Tuchmann-Duplessis H, Haegel P 1972 Illustrated Human Embryology, Vol 2 Organogenesis. London: Chapman and Hall. With kind permission of Springer Science+Business Media.)

At birth the uterus is 2.5–5 cm long (average 3.5 cm), 2 cm wide between the uterine tubes, and a little over 1 cm thick (Fig. 78.9; see Figs 14.4, 14.5). The body of the uterus is smaller than the uterine cervix, which forms two-thirds or more of the length. The isthmus between the body and the cervix is absent. The fetal female reproductive tract is affected by maternal hormones and undergoes some enlargement in the fetus. The endocervical glands are active before birth and the cervical canal is usually filled with mucus. The uterus is relatively large at birth, and subsequently involutes to about one-third of its length and more than half of its weight; it does not regain its neonatal size and weight until puberty. The uterine tubes are relatively short and wide.

The position of the uterus in the pelvic cavity depends to a great extent on the state of the bladder anteriorly and the rectum posteriorly. If the bladder contains only a small amount of urine the uterus may be anteverted but it is often in a direct line with the vagina (Fig. 78.9; see Fig. 78.19).

Vagina

At approximately 60 mm crown rump (CR) length an epithelial proliferation, the sinuvaginal bulb, arises from the dorsal wall of the urogenital sinus in the region of the sinus tubercle (Figs 78.7F, 78.14B),. Its origin marks the site of the future hymen. The proliferation gradually extends cranially as a solid anteroposteriorly flattened plate inside the tubular condensation of the uterovaginal primordium, which will eventually become the fibromuscular vaginal wall. The caudal tip of the paramesonephric duct epithelium recedes until, at about 140 mm (CR), its junction with the epithelial proliferation lies in the cervical canal.

Starting from its caudal end, and gradually extending cranially through its whole extent, the solid plate formed by the sinus proliferation enlarges into a cylindrical structure. Thereafter the central cells desquamate to establish the vaginal lumen. The extent to which mesonephric and paramesonephric ducts contribute directly to the formation of the vagina is controversial. As the upper end of the vaginal plate enlarges it grows up to embrace the cervix, and then is excavated to produce the vaginal fornices. Anomalies of paramesonephric duct fusion can produce related vaginal anomalies (Fig. 78.15). The urogenital sinus undergoes relative shortening craniocaudally to form the vestibule, which opens on the surface through the cleft between the genital folds. The lower end of the vaginal plate grows caudally so that in 109 mm embryos the vaginal rudiment approaches the vestibule. In fetuses of 162 mm the vaginal lumen is complete except at the cephalic end where the fornices are still solid; they are hollow by 170 mm. At approximately half way through gestation (180 mm) the genital canal is continuous with the exterior. During the later months of fetal life the vaginal epithelium is greatly hypertrophied, apparently under the influence of maternal hormones, but after birth it assumes the inactive form of childhood.

In the neonate, the vagina is 2.5–3.5 cm long and 1.5 cm wide at the fornices, and the uterine cervix extends into the vagina for about 1 cm. The posterior vaginal wall is longer than the anterior wall, giving the vagina a distinct curve (Fig. 78.9; see Fig. 78.19 and Fig. 14.5). The cavity is filled with longitudinal columns covered with a thick layer of cornified, stratified squamous epithelium. These cells slough off after birth when the effect exerted by maternal hormones is removed.

The orifice of the vagina is surrounded by a thick elliptical ring of connective tissue, the hymen (Fig. 78.9). During childhood the hymen becomes a membranous fold along the posterior margin of the vaginal lumen. Should the fold form a complete diaphragm across the vaginal lumen it is termed an imperforate hymenal membrane.

Reproductive ducts in the male

In the male, most of the paramesonephric ducts atrophy (Fig. 78.13) under the influence of anti-Müllerian hormone (AMH), which is released into the mesonephric duct by the Sertoli cells of the testis. Vestigial structures are therefore most likely to persist cranially and/or caudally, at the limits of the local exocrine effects of AMH. A vestige of the cranial end of the duct persists as the appendix testis (Fig. 78.13; see Fig. 78.19, Table 78.1). The fused caudal ends of the two ducts are connected to the wall of the urogenital sinus by a solid utricular cord of cells, which soon merges with a proliferation of sinus epithelium, the sinu-utricular cord. The latter is similar to, but less extensive than, the sinus proliferation in the female. The proliferating epithelium is claimed to be an intermingling of the endoderm of the urogenital sinus with the lining epithelia of the mesonephric and paramesonephric ducts, which have extended on to the surface of the sinus tubercle. As the sinu-utricular cord grows, so the utricular cord recedes from the tubercle. In the second half of fetal life the composite cord acquires a lumen and becomes dilated to form the prostatic utricle, the lining of which consists of hyperplastic stratified squamous epithelium (Fig. 78.13; see Fig. 78.19). The sinus tubercle becomes the colliculus seminalis.

The main reproductive ducts in the male are derived from the mesonephric ducts; the latter persist under the action of androgens that are probably secreted down the ducts themselves, and are subsumed into the male reproductive system as the metanephric kidney develops. The mesonephric duct gives rise to the canal of the epididymis, vas deferens and ejaculatory duct. The seminal vesicle and the ampulla of the vas deferens appear as a common swelling at the end of the mesonephric duct during the end of the third and into the fourth month. Their appearance coincides with degeneration of the paramesonephric ducts, although no causal relation between the two events has been established. Separation into two rudiments occurs at about 125 mm crown–heel length. The seminal vesicle elongates, its duct is delineated and hollow diverticula bud from its wall. About the sixth month (300 mm crown–heel length) the growth rate of both vesicle and ampulla is greatly increased. Figure 78.10 shows the position of the ampulla of the vas deferens in the neonate, possibly in response to increased secretion of prolactin by the fetal or maternal hypophysis, or to the effects of placental hormones. The tubules of the prostate show a similar increase of growth rate at this time.

Primordial germ cells

The primordial germ cells are formed very early from the epiblast (see Fig. 10.3). They are larger (12 to 20 μm in diameter) than most somatic cells, and are characterized by vesicular nuclei with well-defined nuclear membranes and by a tendency to retain yolk inclusions long after these have disappeared from somatic cells. It is not yet clear whether the primordial germ cells are derived from particular blastomeres during cleavage, if they constitute a clonal line from a single blastomere, or if they are the product of a progressive concentration of the nucleus of the fertilized ovum by unequal partition at successive mitoses. Primordial germ cells spend the early stages of development within the extraembryonic tissues near the end of the primitive streak and in the connecting stalk (see Fig. 10.4). In this situation they are away from the inductive influences to which the majority of the somatic cells are subjected during early development.

Primordial germ cells can be identified in human embryos in stage 11 when the number of cells is probably not more than 20–30. When the tail fold has formed they appear within the endoderm and the splanchnopleuric mesenchyme and epithelium of the hindgut as well as in the adjoining region of the wall of the yolk sac. They migrate dorsocranially in the mesentery, by amoeboid movements and by growth displacement, and pass around the dorsal angles of the coelom (medial coelomic bays) to reach the genital ridges from stage 15 (Fig. 78.16). It is believed that the genital ridges exert long-range effects on the migrating primordial germ cells, in terms of controlling their direction of migration and supporting the primordial germ-cell population.

Primordial germ cells proliferate both during and after migration to the mesonephric ridges. Cells which do not complete this migration degenerate. After segregation, when they are often termed primary gonocytes, they divide to form secondary gonocytes.

Development of the gonads

The factors that lead to formation of either testis or ovary are described below and in Fig. 78.16. The morphological events which occur in each type of gonadal development are presented first.

Testis

Most studies support the hypothesis that the seminiferous tubules are formed from cords of epithelial cells derived from the proliferating coelomic epithelium (Figs 78.13, 78.16). The cords lengthen, partly by addition from the coelomic epithelium, and encroach on the medulla, where they unite with a network of cells derived from the mesonephric mesenchyme destined to become the rete testis. Primordial germ cells are incorporated into the cords, which later become enlarged and canalized to form the seminiferous tubules. The cells derived from the surface of the early gonad form the supporting Sertoli cells. The latter proliferate throughout development and perhaps into childhood; when they stop dividing they mature and cannot be reactivated. Each Sertoli cell can only support a fixed number of germ cells during their development into spermatozoa, i.e. the number of Sertoli cells produced at this time determines the maximal limit of sperm output. Because the germ cells make up the bulk of the adult testis, the number of Sertoli cells is a major determinant of the size to which the testes will grow (factors which impair the process of spermatogenesis, resulting in the loss of germ cells, will also affect testicular size). Variation in Sertoli cell number is probably the most important factor in accounting for the enormous variation in sperm counts between individual men, whether fertile or infertile. Indeed, the available data for adult men indicate that Sertoli cell numbers vary across a fifty-fold range. Although some of this variation may result from attrition of Sertoli cell numbers because of ageing, the major differences in Sertoli cell numbers will have been determined by events in fetal and/or childhood life.

The interstitial cells of the testis are derived from mesenchyme and possibly also from coelomic epithelial cells that do not become incorporated into the tubules. Among other cell lines they form the embryonic and fetal cells of Leydig, which secrete testosterone and insulin-like factor 3 (Insl3). A later migration of mesenchyme beneath the coelomic epithelium forms the tunica albuginea of the testis.

The cords of the rete testis become connected to the glomerular capsules in the persisting part of the mesonephros. Ultimately they become connected to the mesonephric duct by the five to twelve most cranial persisting mesonephric tubules. These become exceedingly convoluted and form the lobules of the head of the epididymis. The mesonephric duct, which was the primitive ‘ureter’ of the mesonephros, becomes the canal of the epididymis and the vas deferens of the testis. The seminiferous tubules do not acquire lumina until the seventh month; the tubules of the testicular rete become canalized somewhat earlier.

Disorders of development of the testis and reproductive tract in the male fetus seem to be increasing in incidence. Testicular maldescent (cryptorchidism) and hypospadias appear to have doubled or trebled in incidence in the last 30–50 years, while testicular cancer has increased by an even greater margin and is now the commonest cancer of young men. Although testicular cancer is primarily a disease of young men (95% of cases affect 15- to 45-year-old males) it is now established that this age-incidence reflects activation of premalignant carcinoma-*in-situ* (CIS) cells, which are present at birth and which almost certainly arise during fetal life. It has been suggested that CIS cells are primordial germ cells that have failed to develop normally. Abnormalities of development of the testis and reproductive tract (e.g. gonadal dysgenesis, cryptorchidism, small testes) are important risk factors for the development of testicular cancer. However, the most dramatic change that appears to have occurred in the relatively recent past is a fall in sperm counts of around 40–50% (1% per year over the last 50 years). Although this dramatic decrease is obviously manifest only in adulthood, as is the case with testicular cancer, it is thought that it may reflect impaired testicular development during fetal or childhood life.

Ovary

The ovary closely resembles the testis early in development, except that its characteristically female features are slower to differentiate (Figs 78.13, 78.16). Few, if any, of the epithelial cords invade the medulla. The majority remain in the cortex, where they may be joined by a second proliferation from the coelomic epithelium overlying the gonad. In histological sections of ovaries from the third and subsequent months, the epithelial cords appear as clusters of cells, which may contain primitive germ cells, separated by fine septa of undifferentiated mesenchyme. An ovarian rete condenses in the medullary mesenchyme and some of its cords may join mesonephric glomeruli. The medulla subsequently regresses, and connective tissue and blood vessels from this region invade the cortex to form the ovarian stroma. During this invasion the clusters of epithelial cortical cells break into individual groups of supporting cells (now identified as granulosa cells), which surround the primordial germ cells (now identified as primary oocytes) that have entered the prophase of the first meiotic division. Primary oocytes are derived from a mitotic division of the primordial germ cells (naked oogonia). Their epithelial capsules consist of flattened pregranulosa cells derived from proliferations of coelomic epithelium. The ovary now has its full complement of primary oocytes. The majority undergo atresia, a hormonally controlled apoptotic process, but the remainder resume development after puberty, when they complete the first meiotic division shortly before ovulation (p. 1296). The granulosa cells at this time enlarge and multiply to form the stratum granulosum; as they do so, they become surrounded by thecal cells, which differentiate from the stroma.

Only the middle part of the gonadal ridge produces the ovary. Its cranial part is sterile and becomes the suspensory ligament of the ovary (infundibulopelvic fold of peritoneum). Its caudal region, also sterile, is incorporated into the ovarian ligament.

Sex determination in the embryo

It was believed that the gonads were indifferent or ambisexual until the arrival of the primordial germ cells in the gonadal ridge, at which point the sex of the embryo was ‘turned on’ by the presence of the male or female germ cells. It now seems that the germ cells may be essentially irrelevant to testis determination; embryos in which the genital ridges are devoid of germ cells may still have morphologically normal testis development. It is not clear if the germ cells are necessary for ovarian determination. They are required for the proper organization and differentiation of the ovary, and their absence results in the development of ‘streak gonads’, where only lines of follicular cells can be seen, as in Turner’s syndrome.

The processes of sex determination and differentiation involve interacting pathways of gene activity, which lead to the total patterning of the embryo as either male or female.

In the current, generally accepted model of sex determination in humans, the female pathway is considered to be the default pathway. According to this model, the Y chromosome of a male embryo diverts development into the testicular pathway, and the resulting changes that convert an indifferent gonad to a testis produce a range of local and widely acting hormones, which collectively generate all the secondary sexual characteristics.

The possession of a Y chromosome is usually associated with a male developmental pathway. Deletion mapping of the Y chromosome in a class of XX males arising from abnormal X:Y interchange at meiosis showed that the male-determining region of the chromosome was a conserved sequence located near its tip, termed the testis-determining factor (TDF). This sequence contains a gene that is regarded by some as the ‘master switch’ that programmes the direction of sexual development, the so-called SRY gene (sex-determining region on Y chromosome). It is believed to be genetically and functionally equivalent to the TDF. The SRY gene acts initially within the epithelial cords of cells derived from the coelomic epithelium of the ambisexual gonad. These cells can potentially differentiate into either Sertoli or granulosa cells (the supporting cells for the germ cells in the testis and ovary respectively). Studies indicate that SRY initiates testis formation from the indifferent gonad by directing the development of supporting-cell precursors as Sertoli rather than granulosa cells (Albrecht & Eicher 2001). Gene expression is seen first in cells designated as pre-Sertoli located centrally in the developing gonad and then later in the cranial and caudal poles. Once the developmental pathway of Sertoli cells is directed this influences the differentiation of the other cell types in the testicular pathway, so that Leydig cells appear later, and the connective tissue becomes organized into a male pattern. The germ cells are also affected by this environment. When they arrive they become enclosed within the Sertoli cells and enter mitotic arrest (which is characteristic of spermatogenesis), instead of entering meiosis and meiotic arrest (which characterizes oogenesis). Thus the development of male characteristics follows the expression of SRY, and female characteristics develop in its absence.

The possession of a Y chromosome expressing SRY may, therefore, underlie the switch to development of the male phenotype, by initiating Sertoli cell differentiation. An alternative view is that the possession of SRY accelerates the development of the gonads in XY embryos generally, so that testes are larger and more advanced than ovaries of the same age. Male human fetuses are generally bigger than females from 12 weeks’ gestation; indeed males are already slightly ahead of females at six weeks’ gestation, just prior to testicular differentiation. It has been suggested that this difference in the growth rate is encoded in the sex chromosomes. Once gonadal development has started, the difference in size between testes and ovaries becomes proportionately much greater than the overall size difference between XY and XX fetuses. (Interestingly, the right gonad develops slightly ahead of the left, an observation which may be correlated with the finding that testes are more often on the right side, and ovaries on the left, in hermaphrodites.)

Subsequent development of the male phenotype requires fetal secretion of both testosterone and anti-Müllerian hormone (AMH), (also called Müllerian inhibiting substance or MIS), and the development of the appropriate cytoplasmic testosterone-binding protein. Sertoli cells synthesize AMH, which causes the regression of the Müllerian ducts, and Leydig cells produce testosterone, which promotes the development of the mesonephric ducts, sets into process the development of male external genitalia, and sensitizes other tissues to testosterone. Absence of the testosterone-binding protein in the complete androgen insensitivity syndrome (CAIS) results in XY individuals who have testes and degenerated Müllerian ducts, but cannot respond to the circulating testosterone produced by their testes: they therefore develop female secondary sexual characteristics.

Although fetuses of either sex are exposed to maternal hormones, the accelerated development of the testis at early embryological stages ensures arrest of meiosis of the germ cells, and the production of hormones that masculinize the male embryo before the development of the reproductive tract and ovaries of the female. The range of intersex conditions, of phenotypic sex that is not correlated to genotype, and the effect of multiple X chromosomes in males, suggests that the male developmental pathway involves many testis determining genes, whereas only a single X chromosome determines the female default pathway. Once testicular differentiation and male hormone secretion have begun, other Y-chromosomal genes are required to maintain spermatogenesis and complete spermiogenesis. The consequences of impairment of oogenesis by other chromosomal abnormalities are much less severe than the impairment of spermatogenesis.

Descent of the gonads

The gonads develop on the posterior abdominal wall bilaterally along the central portion of the mesonephros. This region receives a rich blood supply, which is directed to the gonads as the mesonephros involutes. Both gonads descend, the testis to lie outside the abdominal cavity, and the ovary to the pelvis, however, they both retain their early blood supply from the dorsal aorta.

Descent of the testis

The mechanism of testicular descent is not completely understood, and to some extent remains controversial. Recent evidence suggests that it involves two phases, transabdominal and inguinoscrotal, that are regulated by distinct morphological and endocrine factors.

Transabdominal phase

Each testis initially lies on the dorsal abdominal wall. As it enlarges, its cranial end degenerates and the remaining organ therefore occupies a more caudal position. It is attached to the mesonephric fold by the mesorchium (the mesogenitale of the undifferentiated gonad), a peritoneal fold that contains the testicular vessels and nerves and a quantity of undifferentiated mesenchyme. It also acquires a secondary attachment to the ventral abdominal wall, which has a considerable influence on its subsequent movements. At the point where the mesonephric fold bends medially to form the genital cord (Fig. 78.3), it becomes connected to the lower part of the ventral abdominal wall by an inguinal fold of peritoneum. The mesenchymal cells occupying the core of the inguinal fold condense as another cord, the gubernaculum (Figs 78.3, 78.13, 78.17). This extends from the inguinal abdominal wall, at the site of the future inguinal canal, through the inguinal fold and the mesorchium to the caudal pole of the testis. The future inguinal canal is formed around it by the differentiating muscles of the abdominal wall. At the end of the second month the caudal part of the ventral abdominal wall is horizontal but, after the return of the intestine to the peritoneal cavity, it grows in length and becomes progressively more vertical. As the umbilical artery runs ventrally from the dorsal to the ventral wall, it pulls up a falciform peritoneal fold, which forms the medial boundary of a peritoneal fossa, the saccus vaginalis or lateral inguinal fossa, into which the testis projects. This lower end of the fossa protrudes down the inguinal canal, within the ventrosuperior aspect of the gubernaculum, as the processus vaginalis (Fig. 78.17; see Fig. 78.19).

Rights were not granted to include this figure in electronic media.
Please refer to the printed publication.

Fig. 78.17 The descent of the testis. The testis is retroperitoneal throughout development, **A**. It is held in apposition to the deep inguinal ring from the fourth month and descends into the scrotum surrounded by the processus vaginalis during the seventh month, after which time the proximal part of the processus vaginalis obliterates. The layers of the distal processus vaginalis which remain around the testis form the tunica vaginalis, **B–D**.

(Redrawn from Tuchmann-Duplessis H, Haegel P 1972 Illustrated Human Embryology, Vol 2 Organogenesis. London: Chapman and Hall. With kind permission of Springer Science+Business Media.)

Up to about 10 weeks the gubernaculum in male and female embryos is the same, but then production of insulin-like factor 3 (Insl3) from the Leydig cells stimulates enlargement (known as the ‘swelling reaction’) of the gubernaculum in males. This serves to anchor the fetal testis near the future inguinal canal as the abdominal cavity enlarges between 10 and 15 weeks. By comparison, the gubernaculum in females remains thin and subsequently develops into the round ligament (see below). The cranial attachment of the urogenital ridge, known as the cranial suspensory ligament, regresses in males under the action of androgens.

Inguinoscrotal phase

The caudal end of the gubernaculum initially remains embedded in the abdominal wall (hence the old name of genito-inguinal ligament). As the fetus grows, the distance between the future scrotum and the inguinal region increases. Between 25 and 35 weeks the male gubernaculum begins to bulge out from the abdominal muscles and the processus vaginalis elongates within it to create the inguinal canal. Elongation of the soft, gelatinous end of the gubernaculum, which in the early stage is formed mainly of hyaluronic acid, is controlled by androgens. The exact mechanism mediating elongation in humans is uncertain. In rodent models there is good evidence that androgens cause sexual dimorphism of the sensory branches of the genitofemoral nerve, which supplies the gubernaculum, the developing cremaster muscle within it, and part of the scrotum. The genital branch of the nerve releases calcitonin gene-related peptide (CGRP) which stimulates growth of the gubernacular tip along a chemotactic gradient to the scrotum.

The testis remains in apposition with the deep inguinal ring, held by the gubernaculum during the fourth to sixth months. During the inguinoscrotal phase the testis descends, surrounded by the elongating processus vaginalis, within the migrating gubernaculum. This occurs relatively rapidly about the seventh month, the left testis usually descending ahead of the right. In full-term male neonates over 95% have descended testes, although in premature babies descent may not be complete. After descent the distal processus vaginalis persists as a ‘tiny satellite peritoneal cavity’ around the testis as the tunica vaginalis, which becomes firmly attached to the surrounding scrotum within a few weeks. The proximal part of the processus vaginalis then obliterates, and there is evidence that this also is controlled by androgens indirectly via calcitonin gene-related peptide (CGRP) released from the genitofemoral nerve. Both exogenous CGRP and hepatocyte growth factor can cause obliteration *in vitro* of the processus vaginalis in hernial sacs excised from babies with indirect inguinal hernia.

At birth the processus vaginalis is narrowed and collapsed, but not necessarily completely obliterated. It remains patent for two weeks in nearly 70% of male infants, but by three weeks after birth it is at least partially obliterated in 80% of male infants, the left side before the right.

Persistent patency of the processus vaginalis leads to indirect inguinal hernia (widely patent and allowing prolapse of bowel), or hydrocele (narrow patency permitting only intraperitoneal fluid to trickle down into the tunica vaginalis). During obliteration fluid may trickle only part way down the processus vaginalis to produce an encysted hydrocele of the cord. This is a relatively common but transient state and usually resolves completely within a few weeks by further obliteration. Because of perinatal androgen exposure, the spermatic cord and scrotum are relatively large in the neonate, as are the seminal vesicles and adjacent ampullae of the vas deferens.

In aberrant testicular descent the testis may remain in the abdomen, although this is thought to be uncommon because the hormonal and morphological features of the transabdominal phase are relatively simple. By contrast, the indirect endocrine regulation and complex migratory process of the gubernaculum during the inguinoscrotal phase is frequently abnormal, leading to the testis lying in the inguinal or pubic region in 2–5% of neonates. Rarely the testis may lie in the perineum, upper part of the thigh or at the root of the penis. The cause for these aberrant locations is unknown, but is most likely to be secondary to aberrant migration of the gubernaculum, perhaps caused by a mislocated genitofemoral nerve.

Descent of the ovary

The relative movements of the ovary are less extensive than those of the testis and are not hormonally regulated. Like the testis, the ovary ultimately reaches a lower level than it occupies in the early months of fetal life, but it does not leave the pelvis to enter the inguinal canal, except in certain anomalies. The ovary is connected to the medial aspect of the mesonephric fold by the mesovarium (homologous with the mesorchium), and to the ventral abdominal wall by the inguinal fold (Figs 78.13, 78.18). A mesenchymatous gubernaculum develops in this fold but, as it traverses the mesonephric fold, it acquires an additional attachment to the lateral margin of the uterus near the entrance of the uterine tube. Its lower part, caudal to this uterine attachment, becomes the round ligament of the uterus and the part cranial to this becomes the ovarian ligament. Collectively these structures are homologous with the gubernaculum testis in the male (Figs 78.17-78.19). This new uterine attachment may be correlated with the restricted ovarian descent. At first the ovary is attached to the medial side of the mesonephric fold but, in accordance with the manner in which the two mesonephric folds form the genital cord, it is finally connected to the posterior layer of the broad ligament of the uterus (Figs 78.3, 78.13, 78.14B). The gubernacula thus develop in the female, unlike the male, as bilateral fibrous bands or ligaments in the absence of Insl3. They do not extend into the labia majora, but end in the connective tissue just external to the external ring of the inguinal canal, because, in the absence of androgens, there is no migratory phase analogous to inguinoscrotal migration in the male. The saccus vaginalis is present in the female. Its prolongation into the inguinal canal (sometimes termed the canal of Nuck) is normally completely obliterated, but may remain patent and form the sac of a potential indirect inguinal hernia.

Rights were not granted to include this figure in electronic media.
Please refer to the printed publication.

Fig. 78.18 Descent of the ovary. **A**, Early developing left ovary and uterine tube. **B**, Start of posterior movement of ovary. **C**, Left ovary in definitive posterior position. **D**, Sagittal section of the ligaments associated with the ovary viewed from a left lateral position.

(Redrawn from Tuchmann-Duplessis H, Haegel P 1972 Illustrated Human Embryology, Vol 2 Organogenesis. London: Chapman and Hall. With kind permission of Springer Science+Business Media.)

In the neonate the ovaries lie in the lower part of the iliac fossae. The long axis of the ovary is almost vertical. It becomes temporarily horizontal during descent, but regains the vertical when it reaches the ovarian fossa. The ovaries complete their descent into the ovarian fossae in early childhood. Thus, at birth the ovary and the lateral end of the corresponding uterine tube lie above the pelvic brim. They do not sink into the lesser pelvis until the latter enlarges sufficiently to contain both of them and the other pelvic viscera, including the bladder. The combined weight of the ovaries at birth is 0.3 g, which is relatively large, and much larger than the combined weight of the testes (Fig. 78.9; see Fig. 14.4). The ovaries double in weight during the first 6 postnatal weeks. They bear surface furrows, which disappear during the second and third postnatal months. All of the primary oocytes for the reproductive life of a female are present in her ovaries by the end of the first trimester of pregnancy. Of the 7,000,000 primary oocytes estimated to be present at the fifth month of gestation, 1,000,000 remain at birth, 40,000 by puberty, and only 400 are ovulated during reproductive life.

Cloaca and external genitalia

The cloaca is that region at the end of the primitive hindgut which is continuous with the allantois (Figs 78.4, 78.7). The allantois, a ventral diverticulum, passes into the connecting stalk of the early embryo prior to tail folding and is then drawn into the body cavity after stage 10. It retains an extension into the connecting stalk, and later into the umbilicus, throughout embryonic life. The cloaca is a slightly dilated cavity lined with endoderm. It is initially connected cranially to the enteric hindgut, and ventrocaudally is in contact with overlying ectoderm at the cloacal membrane. Proliferation of mesenchyme at the angle of the junction of the hindgut and allantois produces a urorectal septum, which grows caudally promoting the movement, but not the fusion, of the endodermal epithelium toward the cloacal membrane (Figs 78.4, 78.7, 78.20). The cloaca becomes separated into a presumptive rectum and anal canal dorsally, and a presumptive urinary bladder and urogenital sinus ventrally, and the cloacal membrane is divided into anal and urogenital parts respectively. The nodal centre of division is the site of the future perineal body. The urogenital sinus receives the mesonephric and paramesonephric ducts.

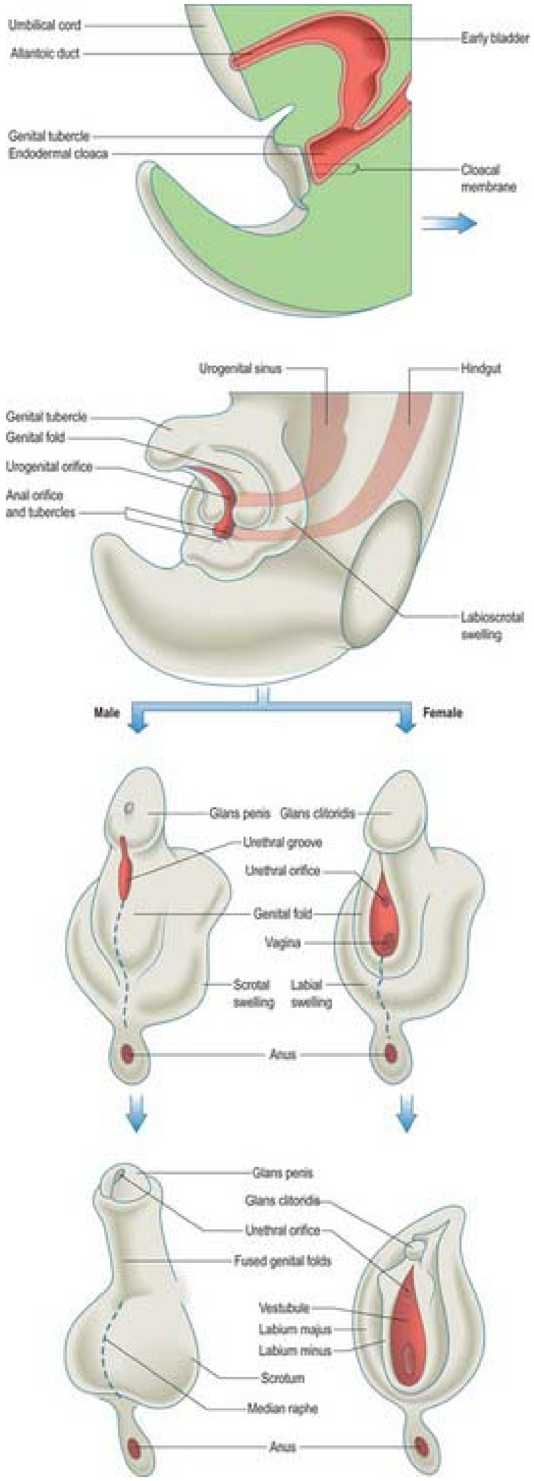
Umbilical cord
Allantoic duct
Early bladder
Genital tubercle
Endodermal cloaca
Cloacal membrane
Urogenital sinus
Hindgut
Genital tubercle
Genital fold
Urogenital orifice
Anal orifice and tubercles
Labioscrotal swelling
Male
Female
Glans penis
Glans clitoridis
Urethral groove
Urethral orifice
Genital fold
Vagina
Scrotal swelling
Labial swelling
Anus
Glans penis
Glans clitoridis
Urethral orifice
Fused genital folds
Vestubule
Labium majus
Labium minus
Scrotum
Median raphe
Anus

Fig. 78.20 The development of the external genitalia from the indifferent stage to the definitive male and female conditions.

Anomalies of cloacal development may result in a range of defects. In extroversion of the cloaca (ectopia cloacae), the urorectal septum does not develop and there is failure of mesenchymal migration around the ventral body wall to support the umbilical cord: this results in a large abdominal defect with a central colonic portion and bilateral bladder components. With only partial development of the urorectal septum, the urogenital sinus may remain with a high confluence of bladder, vagina and rectum. The cloacal membrane may be abnormally elongated and prematurely ruptured throughout its whole extent, prior to the formation of the urorectal septum, or, in some cases, there may be only a small sinus opening externally at the skin. The anal musculature is often present but not associated with the anal canal.

Pelvic floor

The pelvic floor consists of the ligamentous supports of the cervix, and the pelvic and urogenital diaphragms, and constitutes another partition that traverses the body cavity. Little is known about pelvic floor development in the human. The striated muscle is derived from the dermomyotomes in a similar manner to the muscles of the ventrolateral body wall. Puborectalis appears in 20–30 mm embryos, following opening of the anal membrane, and striated muscle fibres can be seen at 15 weeks. The smooth muscle of the urethral sphincter is also present at this time.

Urethra

The urethra is derived from endoderm, as are the prostate gland and vagina (both outgrowths of the lower urogenital sinus), and the other small glandular structures that develop around the caudal body orifices.

In the male, the prostatic urethra proximal to the orifice of the prostatic utricle is derived from the vesicourethral part of the cloaca and the incorporated caudal ends of the mesonephric ducts. The remainder of the prostatic part, the membranous part, and probably the part within the bulb, are all derived from the urogenital sinus. The anterior urethra, as far as the glans, is formed by canalisation of the urethral plate (see below). Secondary ingrowth of mesenchyme fuses the genital folds over the urethra (Fig. 78.20). The short section within the glans may be formed from ectoderm, which invaginates into the glans.

In the female, the urethra is derived entirely from the vesicourethral region of the cloaca, including the dorsal region derived from the mesonephric ducts. It is homologous with the part of the prostatic urethra proximal to the orifices of the prostatic utricle and the ejaculatory ducts. The region of the early urethra remains open to form the vestibule into which the definitive urethra and vagina open (Fig. 78.20). It is believed that these regions are invaded by ectoderm because they are innervated by somatic nerves.

Urethral defects caused by anomalous development are not uncommon in the male. In epispadias the urethra opens on the dorsal aspect of the penis at its junction with the anterior abdominal wall. This anomaly is considered to be a less severe form of exstrophy of the bladder. In the simplest form of hypospadias related to incomplete canalisation of the urethral plate, the urethra may open on the ventral (perineal) aspect of the penis at the base of the glans, and the part of the urethra that is normally within the glans is absent. In more severe cases the genital folds fail to fuse, and the urethra opens on the ventral aspect of a malformed penis just in front of the scrotum. A still greater degree of this malformation is accompanied by failure of the genital swellings to unite with each other. In these cases the scrotum is divided and, since the testes are also frequently undescended, the resemblance to the labia majora is very striking, leading to genital ambiguity. In such cases it is important to determine at the earliest time not only the chromosomal status of the infant but also the internal anatomy and state of development of the internal genital tract. Sex assignment and rearing will depend on these factors.

The urethral sphincter first forms as a mesenchymal condensation around the urethra in 12–15 mm (stage 18) embryos, after division of the cloaca. The mesenchyme proliferates and becomes defined at the bladder neck in 31 mm embryos, and along the anterior part of the urethra by 69 mm. The muscle fibres differentiate after 15 weeks’ development, at which time both smooth and striated fibres are present. In females there is continuity between the smooth muscle of the urethral wall and of the bladder. In males the muscle fibres are less abundant because of the local development of the prostate. Striated muscle fibres form around the smooth muscle initially in the anterior wall of the urethra and later encircle the smooth muscle layer. The origin of the striated muscle is not known: it could be derived from the myogenic cells that give rise to puborectalis. The smooth and striated components of the urethral sphincter are closely related, but there is no mixing of fibres as occurs in the anorectal sphincter.

Prostate gland

The prostate gland arises during the third month from interactions between the urogenital sinus mesenchyme and the endoderm of the proximal part of the urethra. Early outgrowths, some 14 to 20 in number, arise from the endoderm around the whole circumference of the tube, but mainly on its lateral aspects and excluding the dorsal wall above the utricular plate. They give rise to the outer glandular zone of the prostate. Later outgrowths from the dorsal wall above the mesonephric ducts arise from the epithelium of mixed urogenital, mesonephric and possibly paramesonephric, origin that covers the cranial end of the sinus tubercle. They produce the internal zone of glandular tissue. The outgrowths, which are at first solid, branch, become tubular and invade the surrounding mesenchyme. The latter differentiates into smooth muscle, associated blood and lymphatic vessels and connective tissue and is invaded by autonomic nerves.

Similar outgrowths occur in the female but remain rudimentary in the absence of androgenic stimulation. The urethral glands correspond to the mucosal glands around the upper part of the prostatic urethra, and the paraurethral glands correspond to the true prostatic glands of the external zone.

The bulbourethral glands in the male, and the greater vestibular glands in the female, arise as diverticula from the epithelial lining of the urogenital sinus.

External genitalia

Patterning of the external genitalia may be achieved by mechanisms similar to those that pattern the face and limb. In the cranial region neural crest mesenchyme makes an important contribution to the organization of the pharyngeal arches and the regions around the upper sphincters. Neural crest also arises from the tail-bud region, specifically from a population of cells termed the caudoneural hinge, which share the same molecular markers as the primitive node. The neural tube at this level is derived from a mesenchymal/epithelial transformation of caudoneural-hinge cells, which form a cylinder. Neural crest cells delaminate from the dorsal surface of the cylinder in a rostrocaudal direction. It is not known whether neuronal neural crest arising from secondary neurulation processes contributes to the caudal interface between endoderm and ectoderm.

The external genitalia, like the gonads, pass through an indifferent state before distinguishing sexual characters appear (Fig. 78.20). From stage 13, primordia of the external genitalia, composed of underlying proliferating mesenchyme covered with ectoderm, arise around the cloacal membrane, between the primitive umbilical cord and the caudal limit of the embryo. During stage 15 the cloacal membrane is divided by the urorectal septum into a cranial urogenital membrane and a caudal anal membrane (Figs 78.4, 78.14). Local ectodermal/mesenchymal interactions give rise to the anal sphincter, which will develop even without the presence of the anal canal. A surface elevation, the genital tubercle, appears at the cranial end of the urogenital membrane and two lateral ridges, the genital or urethral folds, form each side of the membrane (Fig. 78.20). The genital tubercle forms a distinct primordium, which will become the glans of either the penis or the clitoris. Elongation of the genital folds and urogenital membrane produces a primitive phallus. As this structure grows it is described as having a cranial surface analogous to the dorsum of the penis, and a caudal surface analogous to the perineal surface of both sexes. The urogenital sinus, contiguous with the internal aspect of the urogenital membrane, becomes attenuated within the elongating phallus forming the primitive urethra. The urogenital membrane breaks down at about stage 19, allowing communication of ectoderm and endoderm at the edges of the disrupted membrane and continuity of the urogenital sinus with the amniotic cavity. Urine can escape from the urinary tract from this time. The endodermal layer of the attenuated distal portion of the urogenital sinus, which is now displayed on the caudal aspect of the phallus, is termed the urethral plate. As mesenchyme proliferates within the genital folds, the urethral plate sinks into the body of the phallus forming a primary urethral groove. The genital folds meet proximally in a transverse ridge immediately ventral to the anal membrane.

While these changes are in progress two labioscrotal (genital) swellings appear, one on each side of the base of the phallus, and extend caudally, separated from the genital folds by distinct grooves (Figs 78.20, 78.21).

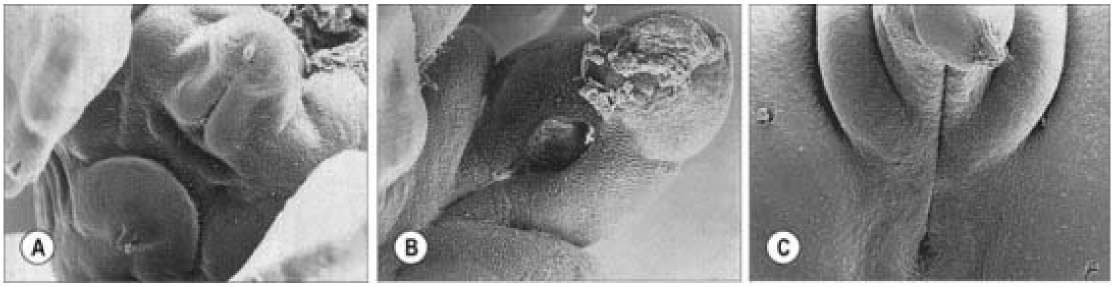

Fig. 78.21 Scanning electron micrographs of early human external genitalia. **A**, Indifferent stage in a human embryo estimated as 42 postovulatory days. **B**, A human female embryo at 12 weeks' development. The genital folds are not fused. **C**, A human male embryo at 12 weeks. Fusion of the genital folds has occurred.

(Photographs by P Collins.)

As a general rule, epithelium, which can be touched easily and has a somatic innervation, is derived from ectoderm. In the buccal cavity and pharynx the ectoderm/endoderm zone is towards the posterior third of the tongue – touch here usually elicits the gag reflex. In the anal canal the outer portion, distal to the anal valves, is derived from ectoderm and has a somatic innervation, whereas the epithelium proximal to the valves is derived from endoderm and has an autonomic innervation.

Homologies of the parts of the urogenital system are shown in Table 78.1.

Male genitalia

The growth of male external characteristics is stimulated by androgens regardless of the genetic sex. The male phallus enlarges to form the penis. The genital swellings meet each other ventral to the anus and unite to form the scrotum (Fig. 78.20). The genital folds fuse with each other from behind forwards, enclosing the phallic part of the urogenital sinus behind to form the bulb of the urethra and closing the definitive urethral groove in front to form the greater part of the spongiose urethra. Fusion of the folds results in the formation of a median raphe and occurs in such a way that the lining of the postglandular urethra is mainly, perhaps wholly, endodermal in origin, formed by canalisation of the urethral plate. Thus, as the phallus lengthens, the urogenital orifice is carried onwards until it reaches the base of the glans at the apex of the penis. From the tip of the phallus an ingrowth of surface ectoderm occurs within the glans to meet and fuse with the penile urethra. Subsequent canalisation of the ectoderm permits a continuation of the urethra within the glans.

The glans and shaft of the penis are recognizable by the third month. The prepuce also begins to develop in the third month, when the primary external orifice of the urethra is still at the base of the glans. A ridge consisting of a mesenchymal core covered by epithelium appears proximal to the neck of the penis and extends forwards over the glans. A solid lamella of epithelium deep to this ridge extends backwards to the base of the glans. The ventral extremities of the ridge curve backwards to become continuous with the genital folds at the margins of the urethral orifice. As the urethral folds meet to form the terminal part of the urethra, the ventral horns of the ridge fuse to form the frenulum. The epithelial lamella breaks down over the dorsum and sides of the glans to form the preputial sac, and thus free the prepuce from the surface of the glans. Thereafter the prepuce grows as a free fold of skin, which covers the terminal part of the glans. Although the prepuce and glans begin to separate from the fifth month *in utero*, they may still be joined at birth. The preputial sac may not be complete until 6–12 months or more after birth and, even then, the presence of some connecting strands may still interfere with the retractability of the prepuce.

The mesenchymal core of the phallus is comparatively undifferentiated in the first two months, but the blastemata of the corpora cavernosa become defined during the third month. Nerves are present in the differentiating mesenchyme from the seventh week. Despite containing less smooth muscle and elastic tissue than the adult, the neonatal penis is capable of erection.

The scrotum is formed by proliferation of the genital swellings. The genital swellings fuse across the midline covering the base of the penis. The testes descend into the scrotum prior to birth. The gelatinous matrix of the gubernaculum is then resorbed and the tunica vaginalis becomes adherent to the connective tissue of the scrotum. In the neonate the penis and scrotum are relatively large. The scrotum has a broad base which does not narrow until after the first year. Both the septum (i.e. the mesenchyme remaining between the tunica vaginalis on each side) and the walls of the scrotum are relatively thicker than in adults.

Female genitalia

The female phallus, which exceeds the male in length in the early stages, becomes the clitoris. The genital swellings remain separate as the labia majora and the genital folds also remain separate, forming the labia minora (Fig. 78.20). The perineal orifice of the urogenital sinus is retained as the cleft between the labia minora, above which the urethra and vagina open. The prepuce of the clitoris develops in the same way as its male homologue. By the fourth month the female external genitalia can no longer be masculinized by androgens.

At birth neonatal females have relatively enlarged labia minora, clitoris and labia majora. The labia majora are united by a posterior labial commissure. The distal end of the round ligament of the uterus, the gubernaculum ovarii, ends just outside the external inguinal ring.

There is evidence that in certain tissues, e.g. urogenital sinus and genital swellings, testosterone is converted into 5α-dihydrotestosterone. In XY individuals with a genetic deficiency of the enzyme responsible for this conversion, not only functioning testes but also female external genitalia with an enlarged clitoris and a small vaginal pouch, are present, suggesting that external genital development is under the control of 5α-dihydrotestosterone. Such individuals are often raised as girls, however, at puberty the external genitalia become responsive to testosterone, which causes masculinization at this time.

Maturation of the reproductive organs at puberty

Until the adolescent growth spurt the reproductive organs grow very slowly. Generally the changes occur over a time period termed puberty. The sequence of these events is much less variable than the age at which they take place. The sequence of puberty in girls and boys is shown in Fig. 78.22.

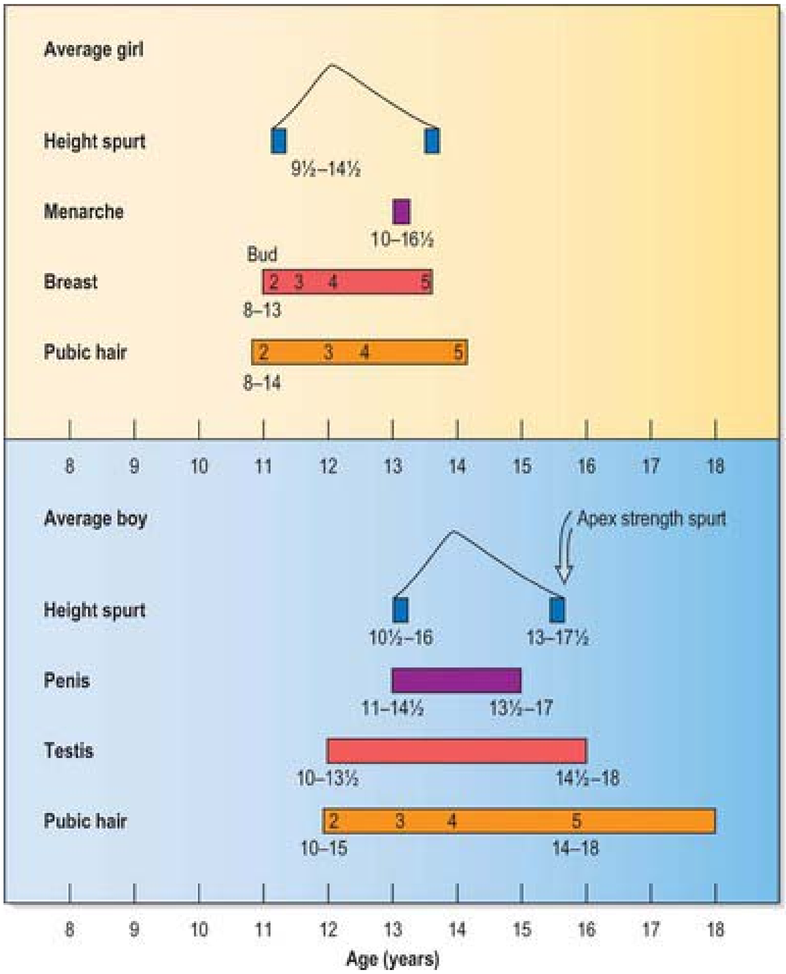

Fig. 78.22 Average ages at which maturation events occur in adolescent girls and boys. The figures beneath the bars indicate the range of ages within which each event may begin and end. Figures within the bars indicate the developmental stage.

(Adapted with permission from Tanner JM 1962 Growth at Adolescence, 2nd edn. Oxford: Blackwell Publishing.)

In girls the appearance of the breast bud is usually the first sign of puberty. The uterus and vagina develop simultaneously with the breast. Menarche occurs after the peak of the height spurt – onset is more closely related to radiological than to chronological age. It has been suggested that the menarche occurs as a critical weight of 50 kg is attained, and certainly sports and excessive restriction of diet, which may reduce weight below this level, can cause amenorrhoea in women who were previously menstruating normally. Tall girls reach sexual maturity earlier than short ones, but girls with a late adolescent growth spurt and later puberty are ultimately taller on the average than those who pass through the menarche early, for they have longer to grow. A girl who has begun to menstruate can be predicted to grow a further 7.5 cm at most. Menarche marks a definitive stage of uterine development but does not mean attainment of full reproductive function. Many of the early menstrual cycles may not involve ovulation.

The earliest sign of puberty in boys is the growth of the testes and scrotum. The volume of the testes may be estimated: the average adult volume is 20 ml, and a volume of 6 ml indicates that puberty has started. Later the penis, prostate and seminal vesicles begin to enlarge. Increased testosterone levels produced by the Leydig cells of the testes promote changes in the larynx, skin and distribution of bodily hair.

REFERENCES

brecht KH, Eicher EM. Evidence that SRY is expressed in pre-Sertoli cells and Sertoli and granulosa cells have a common precursor. *Dev Biol*. 2001;240:92-107.

rteczko KJ, Jacob MI. The testicular descent in human. Origin development and fate of the gubernaculum Hunteri, processus vaginalis peritonei and gonadal ligaments. *Adv Anat Embryol Cell Biol*. 2000;156:III-IIX. 1–98. Springer, Heidelberg

auvet V, Qian F, Boute N, et al. Expression of PKD1 and PKD2 transcripts and proteins in human embryo and during normal kidney development. *Am J Pathol*. 2002;160:973-983.

vorito LA, Klojda CA, Costa WS, Sampaio FJ. Is there a relationship with anomalous insertions of the distal gubernaculum testis and testicular ectopia? Analysis in human fetuses and patients with cryptorchidism. *J Urol*. 2003;170:554-557.

yns CF. The gubernaculum during testicular descent in the human fetus. *J Anat*. 1987;153:92-112.

tson JM, van der Putte SCJ, Penington E, Kluth D, Fiegel H. The embryology of anorectal malformations. In: Holschneider AM, Hutson JM. *Anorectal Malformations in Children. Embryology, Diagnosis, Surgical Treatment, Follow-up*. Heidelberg: Springer, 2006.

tson JM, Hasthorpe S. Testicular descent and cryptorchidism: the state of the art in 2004. *J Pediatr Surg*. 2005;40:297-302.

Connell HE, Hutson JM, Anderson CR, Plenter RJ. Anatomical relationship between urethra and clitoris. *J Urol*. 1998;159:1892-1897.

arpe RM, McKinnell C, Kivlin C, Fisher JS. Proliferation and functional maturation of Sertoli cells, and the relevance to disorders of testis function in adulthood. *Reproduction*. 2003;125:769-784.

Section 9

PELVIC GIRDLE AND LOWER LIMB

CHAPTER 79

Pelvic girdle and lower limb: overview and surface anatomy

This chapter is made up of two sections. The first is an overview of the general organization of the lower limb, with particular emphasis on the fascial skeleton, distribution of the major blood vessels and lymphatic channels, and the branches of the lumbar and sacral plexuses: it is intended to complement the detailed regional anatomy described in Chapters 80 to 84 Chapter 81 Chapter 82 Chapter 83 Chapter 84. The second section describes the surface anatomy of the lower limb.

The structure of the lower limb is determined by its adaptations for weightbearing, locomotion and the maintenance of equilibrium (stability). Indeed, the adaptations for weightbearing and for stability, and the differing developmental histories of the limbs account for the major structural and functional differences between the upper and lower limbs. The inguinal (pelvicrural) and gluteal (buttock) regions are important anatomical junctional zones between the trunk and the lower limb through which longitudinally running nerves and vessels may pass in either direction. The inguinal region includes the junctional zones between the limb and abdominal cavity via the myopectineal orifice (the gap between the inguinal ligament and hip bone), and between the limb and pelvic cavity via the obturator foramen. The gluteal region includes the junctional zones between the limb and the abdominopelvic cavity via the greater sciatic foramen, and between the limb and the perineum via the lesser sciatic foramen (Fig. 79.1).

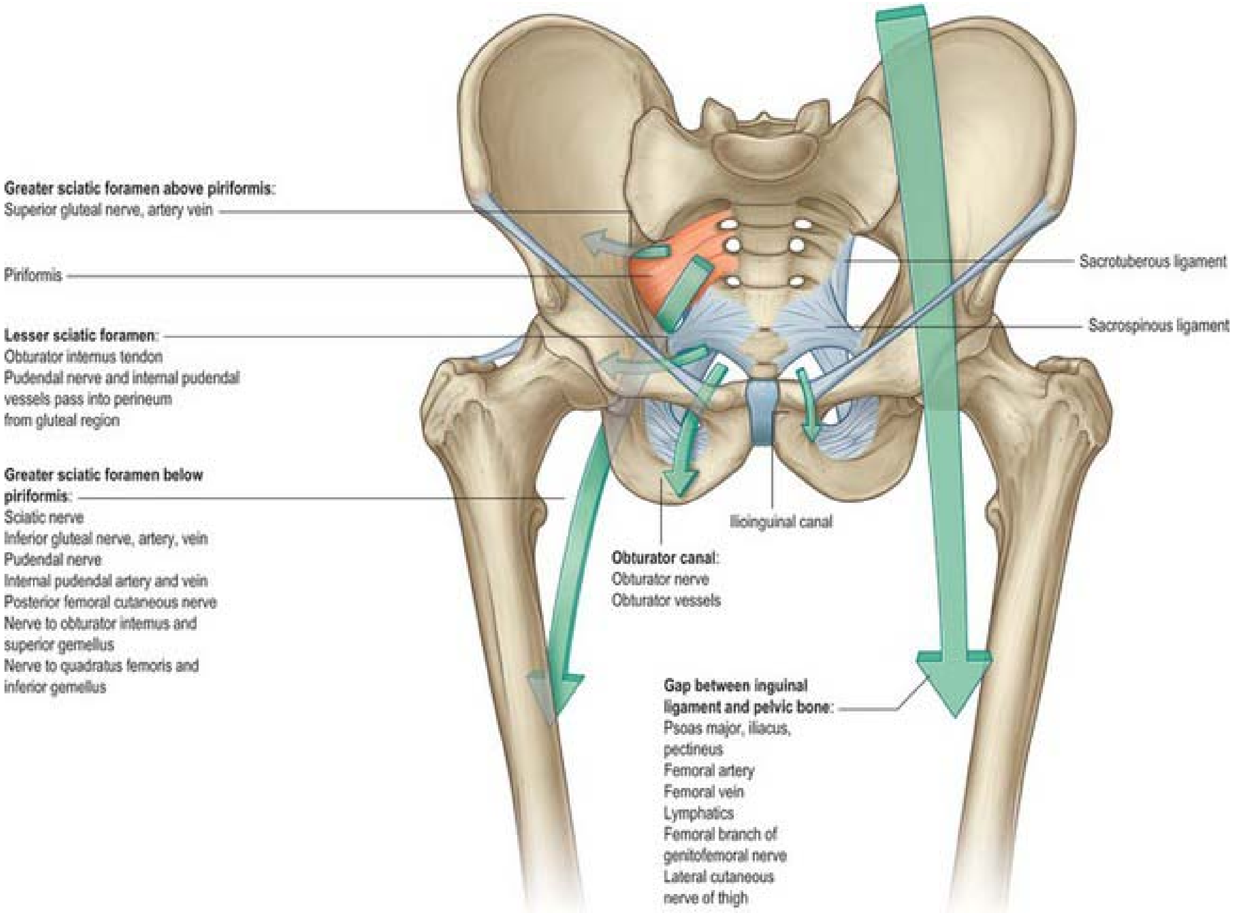
Greater sciatic foramen above piriformis:
Superior gluteal nerve, artery vein
Piriformis
Lesser sciatic foramen:
Obturator internus tendon
Pudendal nerve and internal pudendal vessels pass into perineum from gluteal region
Greater sciatic foramen below piriformis:
Sciatic nerve
Inferior gluteal nerve, artery, vein
Pudendal nerve
Internal pudendal artery and vein
Posterior femoral cutaneous nerve
Nerve to obturator internus and superior gemellus
Nerve to quadratus femoris and inferior gemellus
Sacrotuberous ligament
Sacrospinous ligament
Ilioinguinal canal
Obturator canal:
Obturator nerve
Obturator vessels
Gap between inguinal ligament and pelvic bone:
Psoas major, iliacus, pectineus
Femoral artery
Femoral vein
Lymphatics
Femoral branch of genitofemoral nerve
Lateral cutaneous nerve of thigh

Fig. 79.1 Gateways from the abdomen, pelvis and perineum to the lower limb.

(From Drake, Vogl and Mitchell 2005.)

SKIN, FASCIA AND SOFT TISSUES

In the young adult the skin of the lower limb is generally stronger and thicker than that of the upper limb: weightbearing skin, e.g. of the sole of the foot, is particularly thickened. The skin of the buttocks and posterior thigh bears weight in the sitting position, and consequently is relatively thick. The skin over the anteromedial aspect of the lower leg is particularly fragile and vulnerable in the elderly. Body hair is usually well developed in all areas except the sole and posterior ankle.

Fascial skeleton

The ‘fascial skeleton’ (deep fascia) of the lower limb is well-defined and forms a tough circumferential ‘stocking-like’ structure that constrains the musculature (Fig. 79.2). Septa pass from the deep surface of this fascial sheath to the bones within, confining the functional muscle groups within osteofascial compartments. The tough fascia gives additional areas of attachment to the muscles and ensures that they work to maximal effect. Thickenings in the ensheathing layer may act as additional tendons (e.g. iliotibial tract). Elsewhere, thickenings in the fascial skeleton form fibrous retinacula where tendons cross joints. Although they are particularly prominent in the embalmed cadaver, these fascial layers are also readily demonstrable in the living, and are of considerable functional significance. The pattern of soft-tissue organization has a bearing on the physiological effects of the muscles and is crucial for efficient venous return from the limb. The fascial planes also control and direct the spread of pathological fluids (blood, pus) within the limb and play an important part in determining the degree and direction of displacement seen in long bone fractures.

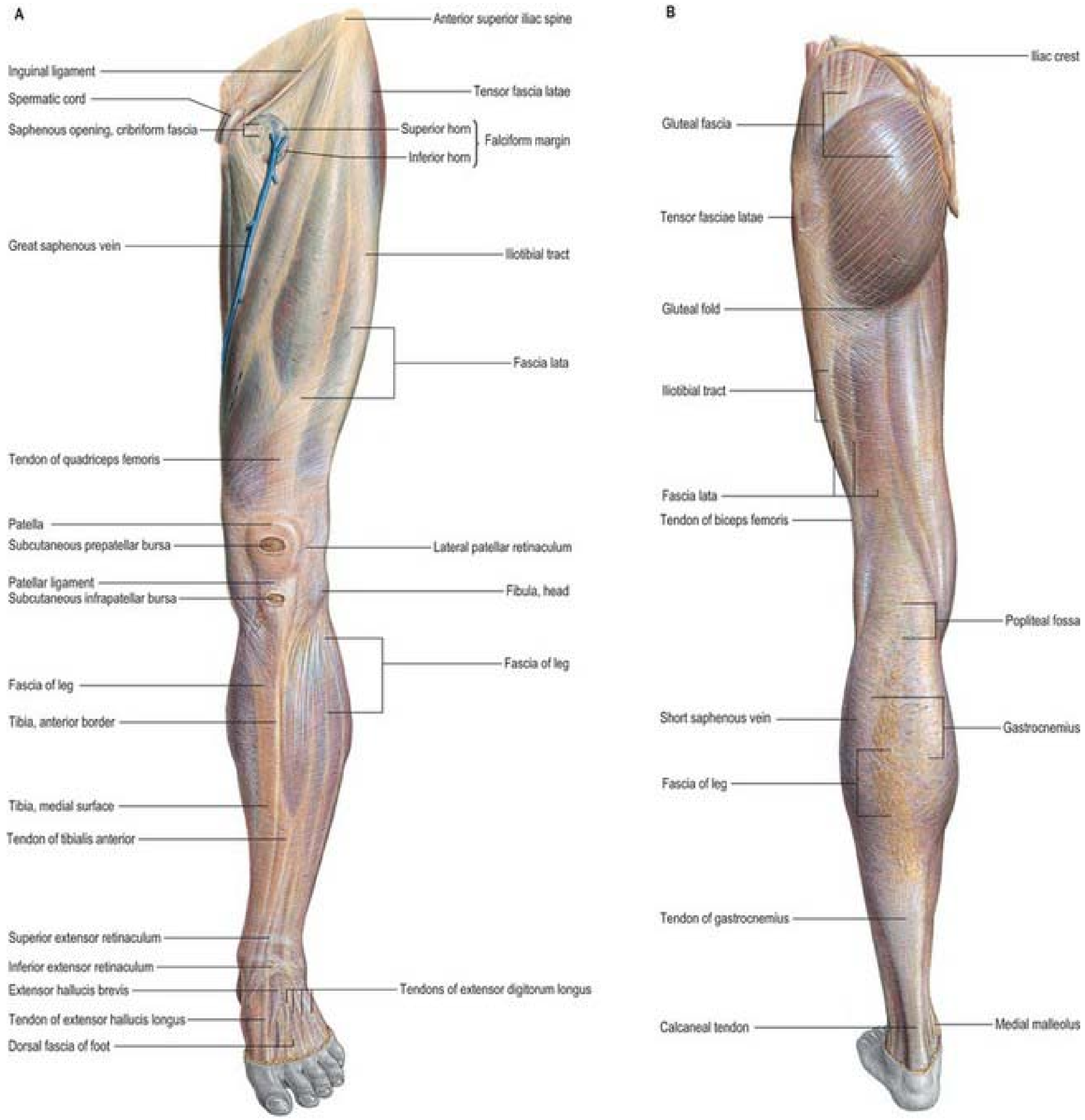
A
Anterior superior iliac spine
Inguinal ligament
Tensor fascia latae
Spermatic cord
Saphenous opening, cribriform fascia
Superior horn
Inferior horn
Falciform margin
Great saphenous vein
Iliotibial tract
Fascia lata
Tendon of quadriceps femoris
Patella
Subcutaneous prepatellar bursa
Lateral patellar retinaculum
Patellar ligament
Subcutaneous infrapatellar bursa
Fibula, head
Fascia of leg
Fascia of leg
Tibia, anterior border
Tibia, medial surface
Tendon of tibialis anterior
Superior extensor retinaculum
Inferior extensor retinaculum
Extensor hallucis brevis
Tendons of extensor digitorum longus
Tendon of extensor hallucis longus
Dorsal fascia of foot
B
Iliac crest
Gluteal fascia
Tensor fasciae latae
Gluteal fold
Iliotibial tract
Fascia lata
Tendon of biceps femoris
Popliteal fossa
Short saphenous vein
Gastrocnemius
Fascia of leg
Tendon of gastrocnemius
Calcaneal tendon
Medial malleolus

Fig. 79.2 Deep fascia of the lower limb. **A**, Anterior view. **B**, Posterior view.

(From Sobotta 2006.)

Fasciocutaneous system

The fascial septa dictate the pathways of cutaneous arteries, which subsequently perforate and ramify on the fascial ‘stocking’ before supplying the skin.

Osteofascial compartments in the lower limb

The muscles of the thigh may be grouped into three compartments according to their function, namely anterior (extensor), posterior (flexor) and medial (adductor): only the anterior and posterior compartments possess distinct fascial boundaries. A very definite fascial separation into anterior (extensor), posterior (flexor) and lateral (evertor) compartments exists in the leg, and compartment syndrome is most common in this region (see below). Osteofascial compartments in the foot are described in Chapter 84.

Vessels and nerves run through all the osteofascial compartments and supply the muscles contained within them. The muscles acting within these closed compartments assist in maintaining the anti-gravity flow of venous blood.

Compartment syndrome

The fascial boundaries that limit the osteofascial compartments are largely inelastic, which means that any condition that leads to an increase in the volume of the compartmental contents, e.g. muscle swelling caused by trauma or unaccustomed overuse, haemorrhage and local infection, is likely to cause an increase in intracompartmental pressure. If unrelieved, this increased pressure will lead to compressive occlusion of the vessels in the compartment and consequent ischaemic damage to the nerves and muscles of the compartment, a phenomenon known as compartment syndrome.

BONES AND JOINTS

The bones of the lower limb are the three fused components of the pelvic girdle; the femur and patella (thigh); the tibia and fibula (leg); the tarsus, metatarsus and phalanges (foot) (Fig. 79.3). The hip bones (especially the ilium and ischium), femur, tibia and bones of the hindfoot are strong and their external (cortical) and internal (trabecular) structure is adapted for weightbearing.

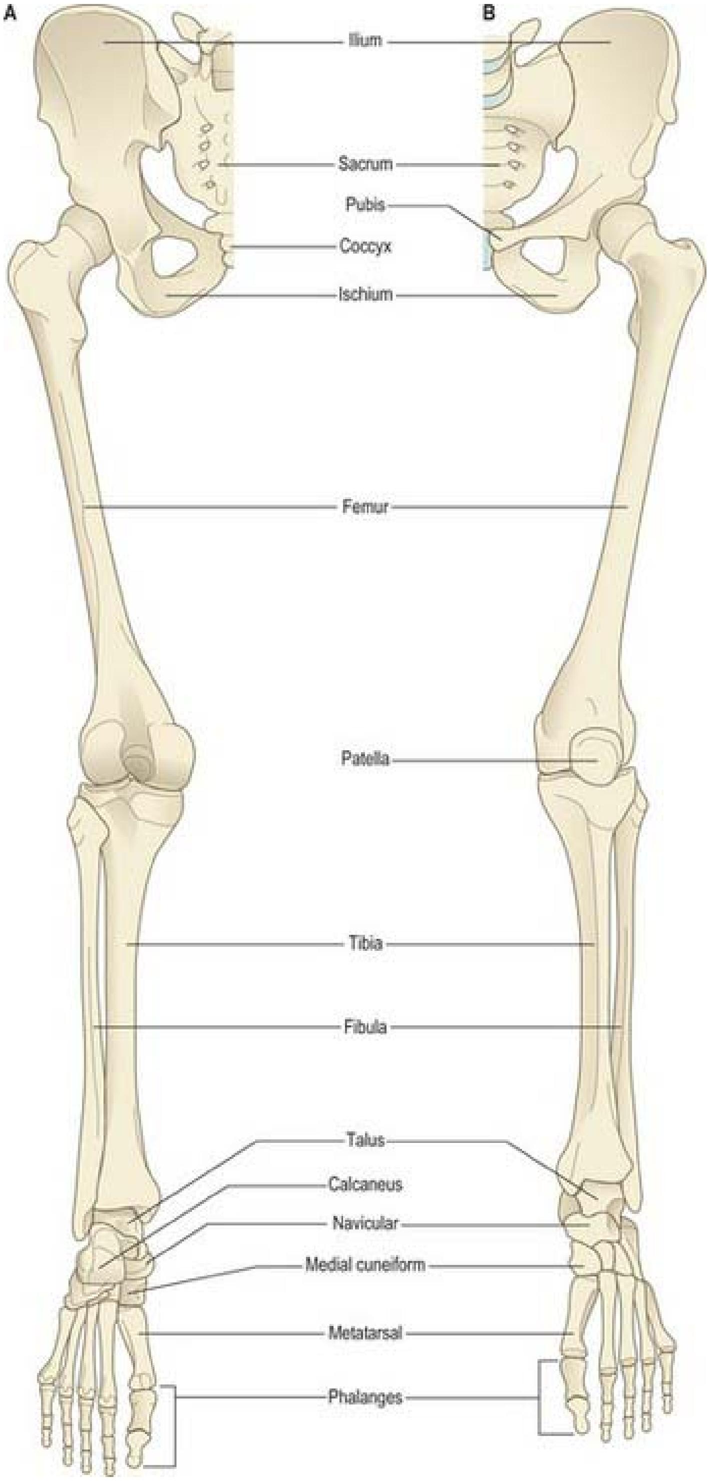
A
B
Ilium
Sacrum
Pubis
Coccyx
Ischium
Femur
Patella
Tibia
Fibula
Talus
Calcaneus
Navicular
Medial cuneiform
Metatarsal
Phalanges

Fig. 79.3 Overview of bones of the lower limb. **A**, posterior aspect. **B**, anterior aspect.

The pelvic girdle connects the lower limb to the axial skeleton via the sacroiliac joint, a synovial joint in which mobility has been sacrificed for stability and strength, to allow for effective weight transmission from the trunk to the lower limb. Anteriorly, the pelvic girdle articulates with the contralateral girdle at the pubic symphysis, a secondary cartilaginous joint that may display a slight degree of mobility during hip and sacroiliac movement and during childbirth. The hip joint, a synovial ball-and-socket joint, exhibits a very effective compromise between mobility and stability that allows movement in all three orthogonal planes. The more distal joints have gained mobility at the expense of stability. The knee joint includes the patellofemoral articulation, which allows the patella to glide over the distal femur. However, the main component of the knee joint is a bicompartmental synovial articulation between the femur and the tibia that allows flexion, extension and some medial and lateral rotation of the leg. It is not a true hinge joint because its axes of flexion and extension are variable and there is coupled rotation. The tibia and fibula articulate with each other at the superior and inferior tibiofibular joints. The superior joint, a plane synovial joint, allows slight gliding movement only. The inferior joint, a fibrous joint, lies just above the ankle and allows a degree of fibular rotation linked to ankle motion. The ankle (talocrural) joint is formed by the distal ends of the tibia and fibula ‘gripping’ the talus, and allows dorsiflexion and plantarflexion. There are multiple joints in the foot that may be classified topographically on the basis of whether they are in the hindfoot, midfoot or forefoot. Collectively, these joints allow the complex movements required as the foot fulfils its functional roles as a platform for standing and for shock absorption and propulsion in gait.

Both knee and ankle are commonly subject to closed injuries, and the relatively superficial location of the knee renders it susceptible to open injury and infection. Although the ankle is frequently injured and is a major loadbearing joint, the incidence of clinically significant degenerative arthritis is surprisingly low when compared with that found in the hip and knee.

MUSCLES

The effects of extension and medial rotation of the limb that occur during fetal development are manifest in the relative positions of the muscle groups in the thigh and the leg, and in the adult pattern of segmental innervation (dermatomes). In broad outline, the anterior aspect of the adult limb is the extensor aspect, while the flexors lie posteriorly; the reverse is true at the hip.

The role of the muscles of the lower limb in the maintenance of equilibrium during locomotion and in stance is rarely emphasized sufficiently. Many of the muscles act frequently or predominantly from their distal attachments. During both stance and locomotion, the distal attachment is often fixed and the proximal attachment is mobile, e.g. the predominant action of gluteus medius is as a pelvic stabilizer rather than as a hip abductor. (In contrast, in the upper limb the proximal muscle attachments are usually fixed and the distal attachments are mobile, an arrangement that is consistent with the prehensile function of the hand.) The lower limb contains many muscles that act upon more than one joint, and it is unusual for any joint of the lower limb to move in isolation.

Muscles of the lower limb may be subdivided into muscles of the iliac and gluteal regions, and of the thigh, leg and foot. (Note that in anatomical nomenclature, ‘leg’ refers to that part of the lower limb between the knee and ankle.) The main muscles of the iliac region are psoas major and iliacus, the major flexors of the hip that run from the lumbar spine and inner surface of the ilium respectively to the lesser trochanter of the femur. The much less important psoas minor (when present) runs from the lumbar spine to the pubis. The muscles of the gluteal region include the three named gluteal muscles and the deeper short lateral rotators of the hip joint. Gluteus maximus lies most superficially, running from the posterior pelvis to the proximal femur and fascia lata. It is a powerful extensor of the hip joint, acting more often to extend the trunk on the femur than to extend the limb on the trunk. Gluteus medius and minimus, attaching proximally to the outer iliac surface and distally to the greater trochanter of the femur, are abductors of the hip; their most important action is to stabilize the pelvis on the femur during locomotion, and they are helped in this function by tensor fasciae latae, a more anteriorly placed muscle that arises from the anterolateral ilium and inserts into the fascia lata. Two of the short lateral rotators of the hip, piriformis and obturator internus, arise from within the pelvic walls, while the others, obturator externus, the gemelli and quadratus femoris, are attached externally: all of these muscles are attached distally to the proximal femur.

The muscles of the thigh lie in three functional compartments. The anterior or extensor compartment includes sartorius and the quadriceps group. Sartorius and rectus femoris are attached proximally to the pelvis and can thus act on the hip joint as well as on the knee, whereas the vasti are attached proximally to the femoral shaft, and, acting as a unit, are powerful knee extensors. The medial or adductor compartment contains the named adductor muscles and gracilis; pectineus may also be included. These muscles are attached proximally to the anterior aspect of the pelvis, and distally to the femur; gracilis has no femoral attachment, being attached distally to the proximal tibia, while a part of adductor magnus has a proximal attachment to the ischial tuberosity. The posterior (‘hamstring’) compartment includes semitendinosus, semimembranosus and biceps femoris. These muscles are attached proximally to the ischial tuberosity and act both to extend the trunk on the femur and to flex and rotate the knee. Adductor magnus, as may be inferred from the extent of its proximal attachment and its dual innervation, shares the first of these functions with the hamstrings. Biceps femoris is the only muscle of the thigh that is attached distally to the fibula, and has no tibial attachment.

In the leg the anterior or extensor compartment includes the extensors (dorsiflexors) of the ankle and the long extensors of the toes. Tibialis anterior, the main ankle dorsiflexor, also inverts the foot at the subtalar joint, while the smallest muscle of the compartment, fibularis (peroneus) tertius, is a dorsiflexor that everts the foot. The posterior or flexor (plantarflexor) compartment has superficial and deep components. The superficial component contains gastrocnemius and soleus, powerful plantar flexors of the ankle, and the slender plantaris. Gastrocnemius and soleus are attached distally via the calcaneal (Achilles) tendon. The deep component of the flexor compartment contains popliteus, a rotator of the knee, the long flexors of the toes and tibialis posterior, the main invertor of the foot. The lateral compartment contains the main evertors of the foot, fibularis (peroneus) longus and brevis; both muscles are also plantar flexors at the ankle.

Gastrocnemius, plantaris and popliteus are the only muscles of the leg that are attached proximally to the femur and they can therefore act on the knee as well as at the ankle. The remaining leg muscles are attached proximally to the tibia, fibula or both, and to the interosseous membrane. The intrinsic muscles of the sole of the foot are arranged in layers. They facilitate the actions of the long flexors of the toes, and by effecting subtle changes in the shape of the foot they help control foot posture in stance and locomotion.

VASCULAR SUPPLY AND LYMPHATIC DRAINAGE

ARTERIAL SUPPLY

The femoral artery (the continuation of the external iliac artery) provides the principal arterial supply to the lower limb distal to the inguinal ligament and the gluteal fold (Figs 79.4, 79.5). The femoral artery courses within the anteromedial aspect of the thigh, becoming the popliteal artery on entering the posterior compartment of the thigh and dividing into its terminal branches in the posterior compartment of the leg. The obturator and inferior gluteal vessels also contribute to the supply of the proximal part of the limb. In the embryo the inferior gluteal artery supplied the main axial artery of the limb, which is represented in the adult by the arteria comitans nervi ischiadici (artery to the sciatic nerve).

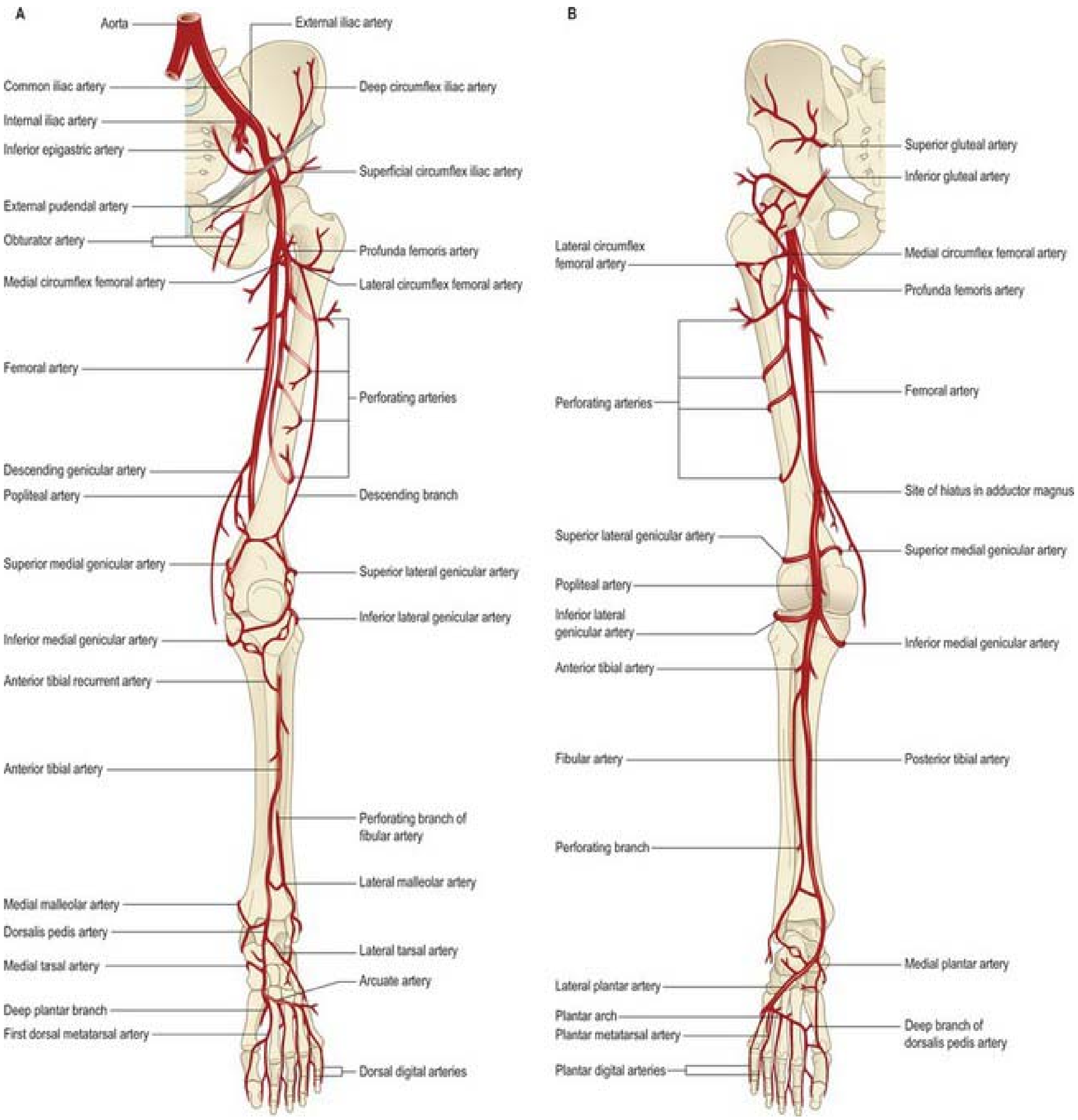
A
Aorta
External iliac artery
Common iliac artery
Deep circumflex iliac artery
Internal iliac artery
Inferior epigastric artery
Superficial circumflex iliac artery
External pudendal artery
Obturator artery
Profunda femoris artery
Medial circumflex femoral artery
Lateral circumflex femoral artery
Femoral artery
Perforating arteries
Descending genicular artery
Popliteal artery
Descending branch
Superior medial genicular artery
Superior lateral genicular artery
Inferior lateral genicular artery
Inferior medial genicular artery
Anterior tibial recurrent artery
Anterior tibial artery
Perforating branch of fibular artery
Lateral malleolar artery
Medial malleolar artery
Dorsalis pedis artery
Lateral tarsal artery
Medial tarsal artery
Arcuate artery
Deep plantar branch
First dorsal metatarsal artery
Dorsal digital arteries
B
Superior gluteal artery
Inferior gluteal artery
Lateral circumflex femoral artery
Medial circumflex femoral artery
Profunda femoris artery
Femoral artery
Perforating arteries
Site of hiatus in adductor magnus
Superior lateral genicular artery
Superior medial genicular artery
Popliteal artery
Inferior lateral genicular artery
Inferior medial genicular artery
Anterior tibial artery
Fibular artery
Posterior tibial artery
Perforating branch
Medial plantar artery
Lateral plantar artery
Plantar arch
Plantar metatarsal artery
Deep branch of dorsalis pedis artery
Plantar digital arteries

Fig. 79.4 Overview of arteries of the lower limb. **A**, Anterior aspect. **B**, Posterior aspect.

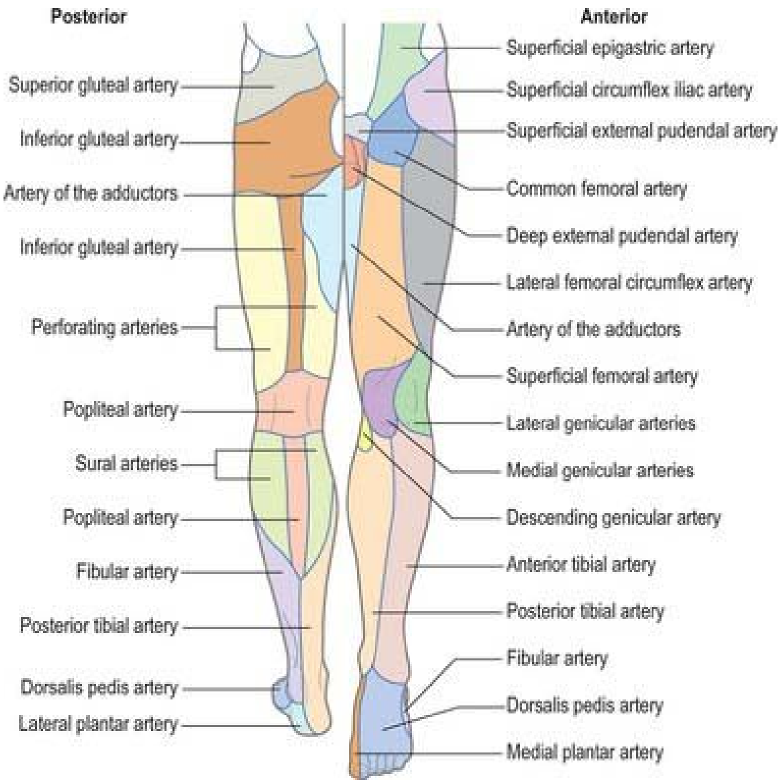
Posterior
Superior gluteal artery
Inferior gluteal artery
Artery of the adductors
Inferior gluteal artery
Perforating arteries
Popliteal artery
Sural arteries
Popliteal artery
Fibular artery
Posterior tibial artery
Dorsalis pedis artery
Lateral plantar artery
Anterior
Superficial epigastric artery
Superficial circumflex iliac artery
Superficial external pudendal artery
Common femoral artery
Deep external pudendal artery
Lateral femoral circumflex artery
Artery of the adductors
Superficial femoral artery
Lateral genicular arteries
Medial genicular arteries
Descending genicular artery
Anterior tibial artery
Posterior tibial artery
Fibular artery
Dorsalis pedis artery
Medial plantar artery

Fig. 79.5 The anatomical territories served by the cutaneous blood supply to the lower limb.

The bones of the lower limb receive their arterial supply from nutrient vessels, metaphysial arterial branches of the peri-articular anastomoses, and the arteries supplying the muscles that attach to their periosteum. The pattern of arterial supply is particularly relevant to fracture healing, the spread of infection and malignancy, and to the planning of reconstructive surgical procedures. For further details consult Cormack & Lamberty (1994), Taylor & Razaboni (1994) and Crock (1996).

Arterial perforators of the lower limb

Achieving adequate and aesthetically satisfactory skin and soft tissue cover for large, superficial tissue defects is a perennial challenge in the field of plastic and reconstructive surgery, and accounts for a substantial part of the plastic surgeon’s workload. Generally, split-thickness and full-thickness skin grafts are suitable only for very superficial defects. To achieve tissue cover for deeper and larger tissue defects, the plastic surgeon employs one of a variety of autologous tissue flaps. The viability of a flap transplanted from one part of the body to another is crucially dependent on the blood supply of the flap. An appreciation of the angiosome concept (see Ch. 6), coupled with technological advances in reconstructive microsurgery, has stimulated the development and use of perforator (or perforator-based) flaps. These are flaps of skin or subcutaneous tissue supplied by one or more fascial ‘perforators’, i.e. arteries which reach the suprafascial plexus either directly from a source vessel, or indirectly from some other neighbouring tissue (Fig. 79.6). Perforator-based flaps are typically harvested with sparing of underlying muscle tissue and minimal trauma: their use is said to reduce postoperative pain, donor site morbidity and functional loss.

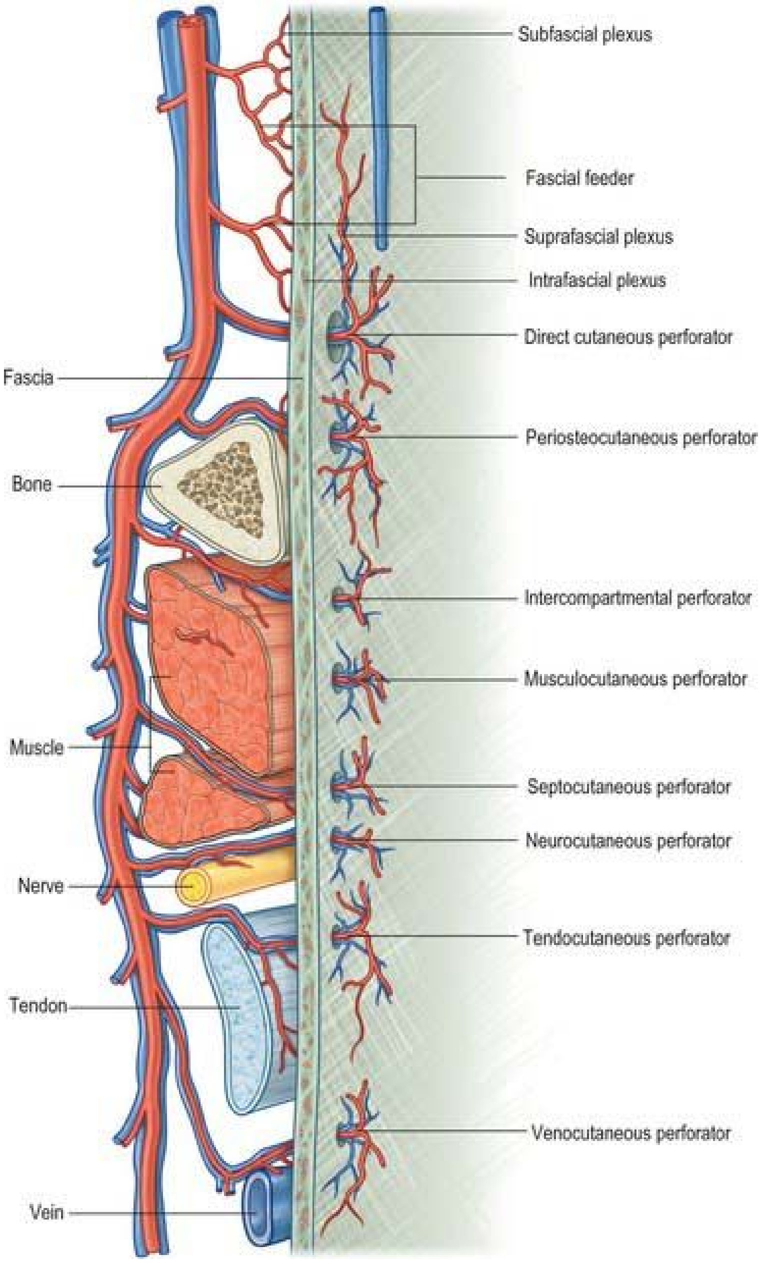
Subfascial plexus
Fascial feeder
Suprafascial plexus
Intrafascial plexus
Direct cutaneous perforator
Fascia
Periosteocutaneous perforator
Bone
Intercompartmental perforator
Musculocutaneous perforator
Muscle
Septocutaneous perforator
Neurocutaneous perforator
Nerve
Tendocutaneous perforator
Tendon
Venocutaneous perforator
Vein

Fig. 79.6 Types of arterial perforators.

The lower limb is the largest donor site in the body for perforator-based flaps. Commonly used flaps are antero-lateral thigh flaps which provide a large amount of skin; superior and inferior gluteal artery perforator flaps used in breast reconstruction; vascularized fibula flaps for reconstruction of deficient bone; vascularized tensor fasciae latae flaps for tendon reconstruction; vascularized sural nerve flaps for nerve reconstruction; and the gracilis muscle flap, used in reanimation of paralysed muscle.

In the context of perforator flap surgery, the lower limb may be considered in terms of four anatomic regions: gluteal; anterior hip and thigh; knee and leg; ankle and foot. Each lower limb accounts for approximately 23% of the total body surface area (thigh 10.5%, leg 6.5%, buttock 2.5% and foot 3.5%) and contains an average of 90 arterial perforators (Fig. 79.7).

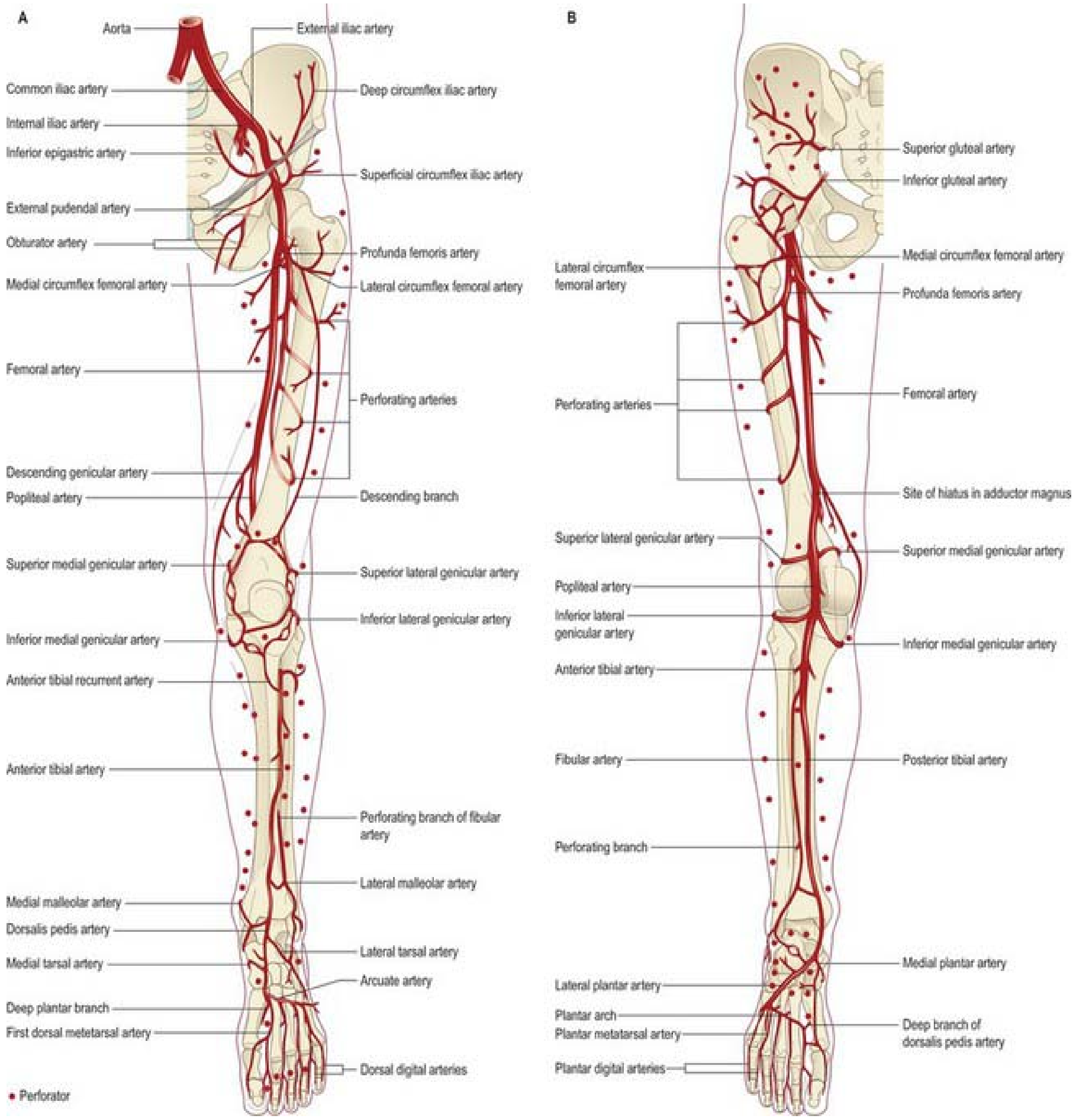
A
Aorta
External iliac artery
Common iliac artery
Deep circumflex iliac artery
Internal iliac artery
Inferior epigastric artery
Superficial circumflex iliac artery
External pudendal artery
Obturator artery
Profunda femoris artery
Medial circumflex femoral artery
Lateral circumflex femoral artery
Femoral artery
Perforating arteries
Descending genicular artery
Popliteal artery
Descending branch
Superior medial genicular artery
Superior lateral genicular artery
Inferior lateral genicular artery
Inferior medial genicular artery
Anterior tibial recurrent artery
Anterior tibial artery
Perforating branch of fibular artery
Lateral malleolar artery
Medial malleolar artery
Dorsalis pedis artery
Lateral tarsal artery
Medial tarsal artery
Arcuate artery
Deep plantar branch
First dorsal metatarsal artery
Dorsal digital arteries
• Perforator
B
Superior gluteal artery
Inferior gluteal artery
Medial circumflex femoral artery
Lateral circumflex femoral artery
Profunda femoris artery
Perforating arteries
Femoral artery
Site of hiatus in adductor magnus
Superior lateral genicular artery
Superior medial genicular artery
Popliteal artery
Inferior lateral genicular artery
Inferior medial genicular artery
Anterior tibial artery
Fibular artery
Posterior tibial artery
Perforating branch
Medial plantar artery
Lateral plantar artery
Plantar arch
Plantar metatarsal artery
Deep branch of dorsalis pedis artery
Plantar digital arteries

Fig. 79.7 Source and location of arterial perforators of the lower limb. **A**, Anterior aspect. **B**, Posterior aspect.

VENOUS DRAINAGE

The veins of the lower limb can be subdivided, like those of the upper limb, into superficial and deep groups (Figs 79.8, 79.9). The superficial veins are subcutaneous and lie in the superficial fascia; the deep veins (beneath the deep fascia) accompany the major arteries. Valves are present in both groups, but are more numerous in the deep veins. (Valves are more numerous in the veins of the lower limb than in the veins of the upper limb.) Venous plexuses occur within and between some of the lower limb muscles. The principal named superficial veins are the long and short saphenous veins; their numerous tributaries are mostly unnamed. For details and variations consult Kosinski (1926).

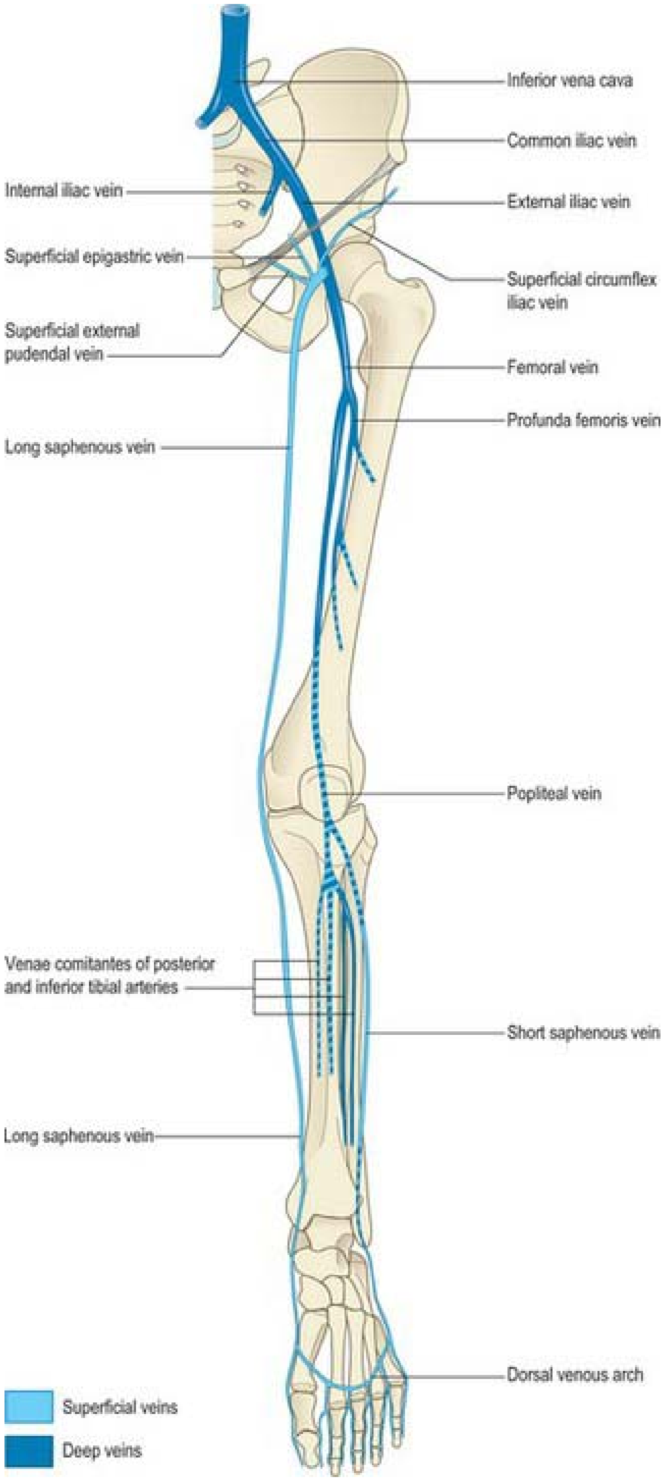
Inferior vena cava
Common iliac vein
Internal iliac vein
External iliac vein
Superficial epigastric vein
Superficial circumflex iliac vein
Superficial external pudendal vein
Femoral vein
Profunda femoris vein
Long saphenous vein
Popliteal vein
Venae comitantes of posterior and inferior tibial arteries
Short saphenous vein
Long saphenous vein
Dorsal venous arch
Superficial veins
Deep veins

Fig. 79.8 Overview of veins of the lower limb.

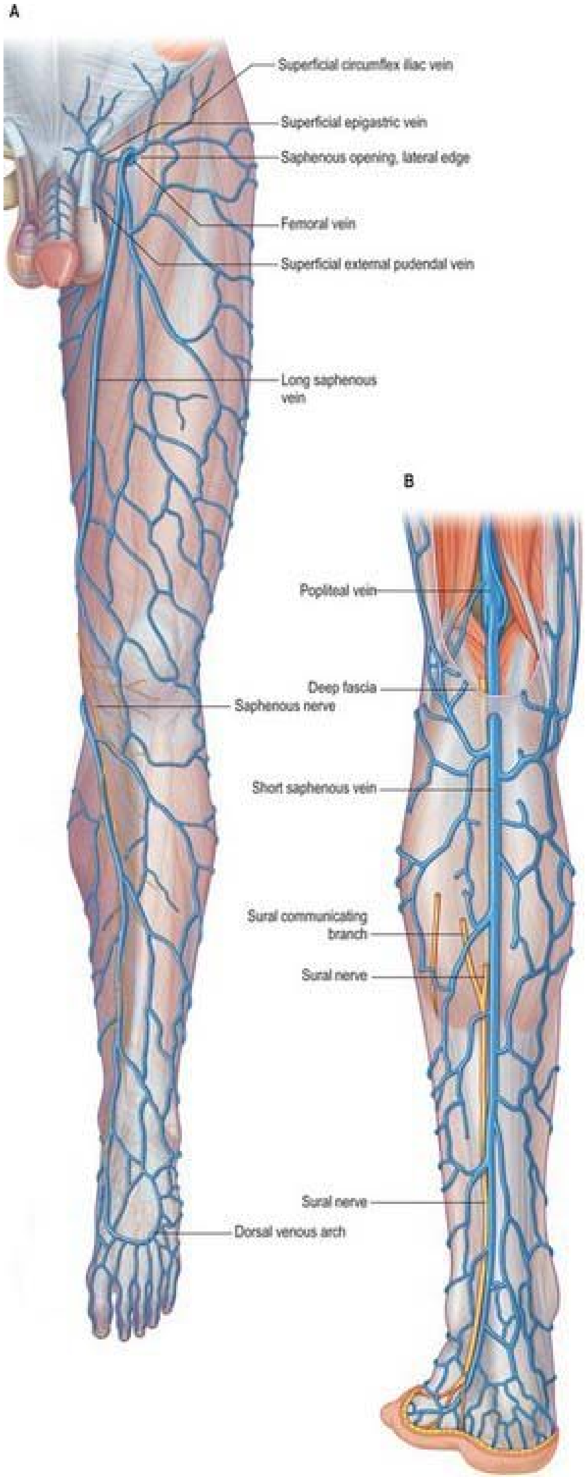
A
Superficial circumflex iliac vein
Superficial epigastric vein
Saphenous opening, lateral edge
Femoral vein
Superficial external pudendal vein
Long saphenous vein
Saphenous nerve
Dorsal venous arch
B
Popliteal vein
Deep fascia
Short saphenous vein
Sural communicating branch
Sural nerve
Sural nerve

Fig. 79.9 **A**, The long saphenous vein and its tributaries. **B**, The short saphenous vein and its tributaries.

Deep veins of the lower limbs accompany the arteries and their branches. Plantar digital veins arise from plexuses in the plantar regions of the toes, connect with dorsal digital veins and unite to form four plantar metatarsal veins. These run in the intermetatarsal spaces and connect with dorsal veins by means of perforating veins. They then connect with each other to constitute a deep plantar venous arch adjacent to the plantar arterial arch. From this arch, medial and lateral plantar veins run near the corresponding arteries: they communicate with the long and short saphenous veins before forming the posterior tibial veins behind the medial malleolus. The posterior tibial veins accompany the posterior tibial artery. They receive veins from the calf muscles, especially the venous plexus in soleus, and connect with superficial veins and with the fibular veins. The latter, running with their artery, receive tributaries from soleus and from superficial veins.

The anterior tibial veins are continuations of the venae comitantes of the dorsalis pedis artery. They leave the extensor region between the tibia and fibula, pass through the proximal end of the interosseous membrane, and unite with the posterior tibial veins, at the distal border of popliteus, to form the popliteal vein.

Venous (muscle) pumps

In a standing position, venous return from the lower limb depends largely on muscular activity, especially contraction of the calf and foot muscles, known as the ‘muscle pump’, whose efficiency is aided by the tight sleeve of deep fascia. ‘Perforating’ veins connect the long saphenous vein with the deep veins, particularly near the ankle, distal calf and knee. Their valves are arranged so as to prevent flow of blood from the deep to the superficial veins. At rest, pressure in a superficial vein is equal to the height of the column of blood extending from that vein to the heart. When calf muscles contract, blood is pumped proximally in the deep veins and is normally prevented from flowing into the superficial veins by the valves in the perforating veins. During muscular relaxation, blood is drawn into the deep veins from the superficial veins. If the valves in the perforating veins become incompetent, these veins become sites of ‘high pressure leaks’ during muscular contraction, and the superficial veins become dilated and varicose. Similar perforating connections occur in the anterolateral region, where varicosities may also occur. Valvar incompetence in the connecting veins between the long saphenous vein and femoral vein in the adductor canal may predispose to superficial varicosities in the medial aspect of the thigh (Dodd & Cockett 1976).

Venous plexuses

Venous plexuses may be intramuscular (soleus) or intermuscular (in the foot and gluteal region). The plexuses communicate with the axially running deep veins and are components of the ‘muscle pump’ mechanism.

LYMPHATIC DRAINAGE

Most lymph from the lower limb traverses a large intermediary inguinal group of nodes (Fig. 79.10). Peripheral nodes are few and all are deeply sited. Except for an inconsistent node lying proximally on the interosseous membrane near the anterior tibial vessels, they occur only in the popliteal fossa. Enlarged popliteal nodes may be palpated along the line of the popliteal vessels while the passively supported knee is gradually moved from extension to semi-flexion. Inguinal nodes are found superficial and deep to the deep fascia. The deep nodes are few and lie alongside the medial aspect of the femoral vein. The superficial nodes may be divided into a lower vertical group that clothe the proximal part of the long saphenous vein, and an upper group that lie parallel to, but below, the inguinal ligament and which are related to the superficial circumflex iliac and superficial external pudendal vessels. Lymph from the lower limb passes from the inguinal nodes to the external and common iliac nodes, and ultimately drains to the lateral aortic group. Deep gluteal lymph reaches the same group through the internal and common iliac chains.

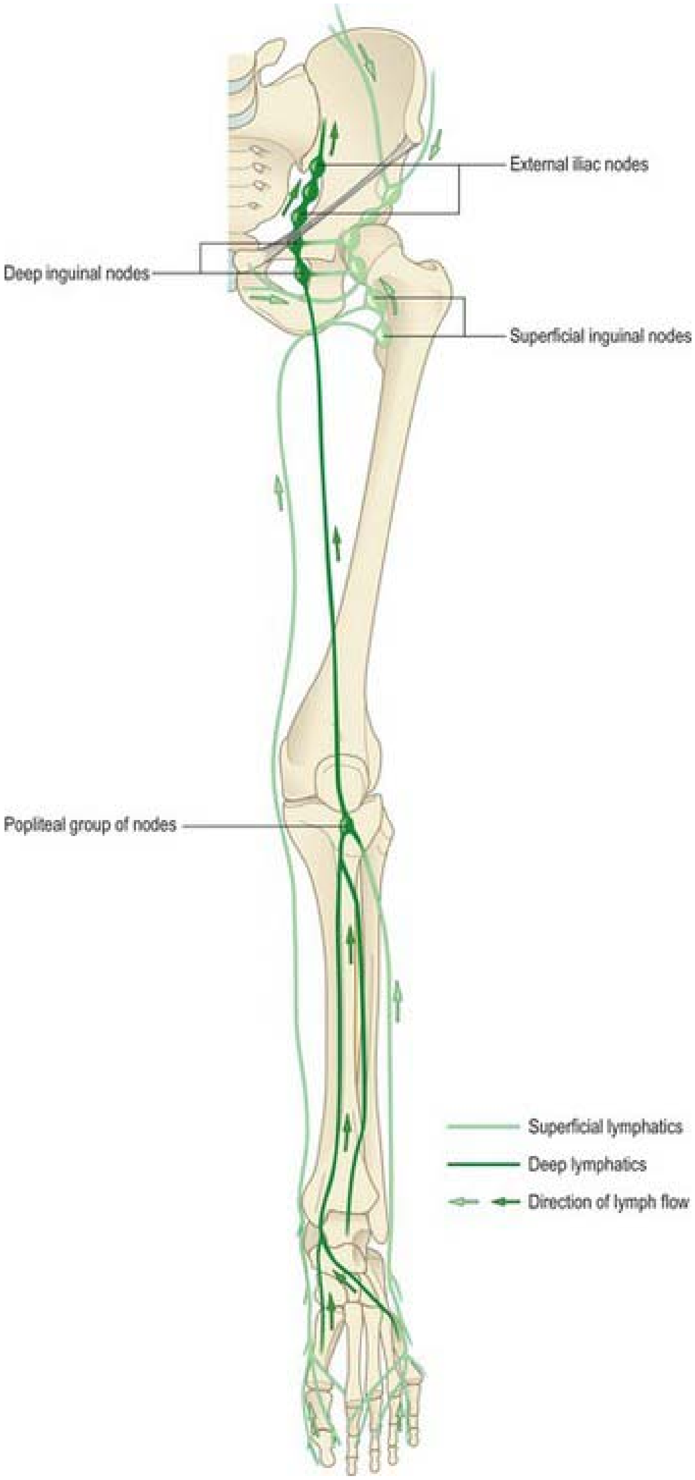
External iliac nodes
Deep inguinal nodes
Superficial inguinal nodes
Popliteal group of nodes
Superficial lymphatics
Deep lymphatics
Direction of lymph flow

Fig. 79.10 Overview of lymphatics of the lower limb.

Superficial tissues

The superficial lymph vessels begin in subcutaneous plexuses. Collecting vessels leave the foot medially, along the long saphenous vein, or laterally with the short saphenous vein. Medial vessels are larger and more numerous; they start on the tibial side of the dorsum of the foot, ascend anterior or posterior to the medial malleolus and accompany the long saphenous vein. They drain to the distal superficial inguinal nodes. Lateral vessels begin on the fibular side of the dorsum of the foot; some cross anteriomedially in the leg to join the medial vessels and so pass to the distal superficial inguinal lymph nodes, others accompany the short saphenous vein and drain to the popliteal nodes. Superficial lymph vessels from the gluteal region run anteriorly to the proximal superficial inguinal nodes.

Deeper tissues

The deep lymph vessels accompany the anterior and posterior tibial, fibular, popliteal and femoral vessels. The deep vessels from the foot and leg are interrupted by popliteal nodes; those from the thigh pass to the deep inguinal nodes. The deep vessels of the gluteal and ischial regions follow their corresponding blood vessels. Those accompanying the superior gluteal vessels end in a node near the intrapelvic part of the superior gluteal artery, adjacent to the superior border of the greater sciatic foramen, while those which follow the inferior gluteal vessels traverse one or two of the small nodes below piriformis and pass to the internal iliac nodes.

INNERVATION

OVERVIEW OF THE LUMBAR AND SACRAL PLEXUSES

Nerves derived from the lumbar and sacral plexuses innervate the lower limb (Figs 79.11). The lumbar plexus lies deep within psoas major, anterior to the transverse processes of the first three lumbar vertebrae. The sacral plexus lies in the pelvis on the anterior surface of piriformis, external to the pelvic fascia, which separates it from the inferior gluteal and pudendal vessels. The lumbosacral trunk (L4 and L5) emerges medial to psoas major on the posterior abdominal wall and lies on the ala of the sacrum before crossing the pelvic brim to join the ventral ramus of S1.

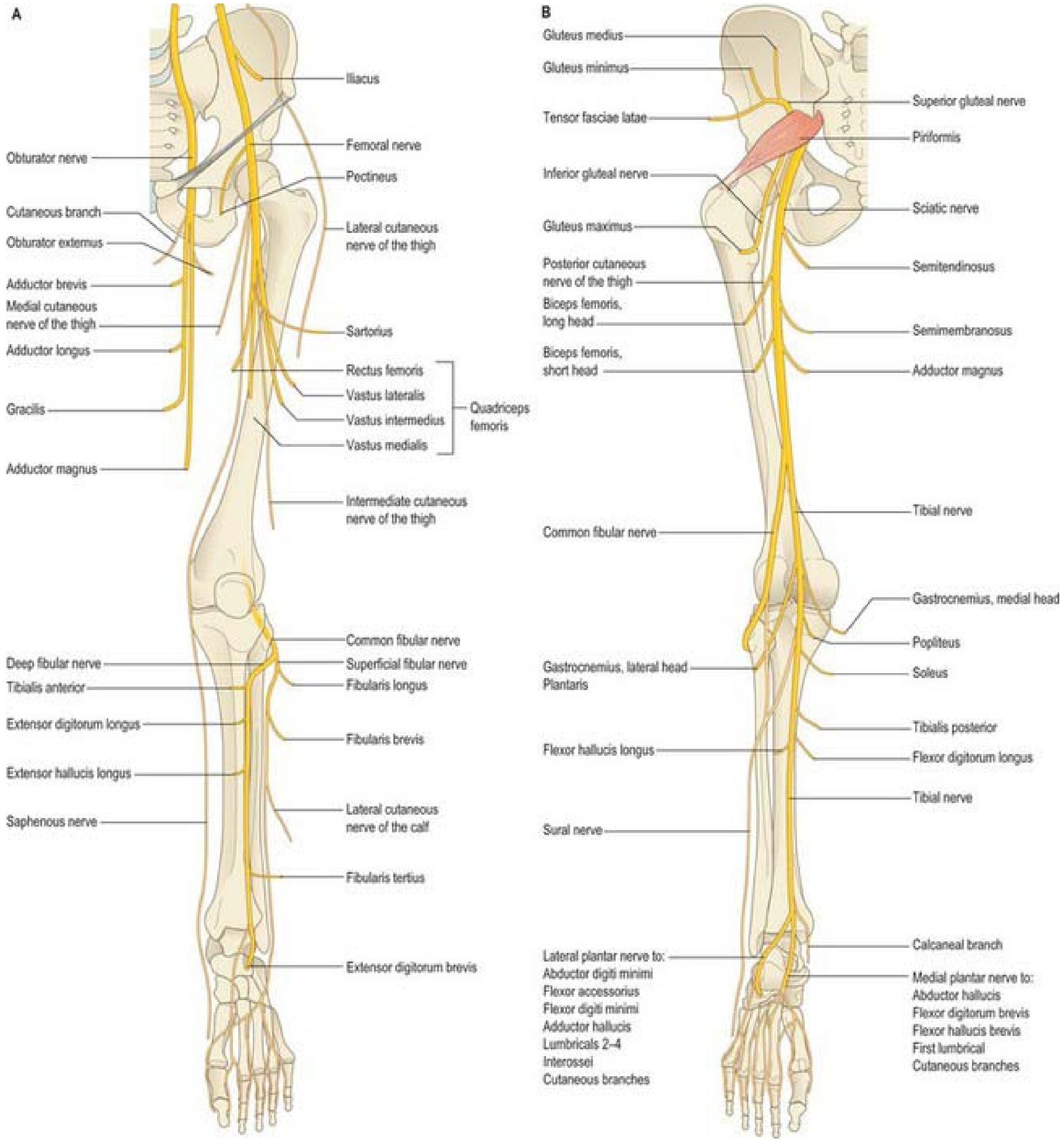
A
Iliacus
Femoral nerve
Pectineus
Obturator nerve
Cutaneous branch
Obturator externus
Lateral cutaneous nerve of the thigh
Adductor brevis
Medial cutaneous nerve of the thigh
Sartorius
Adductor longus
Rectus femoris
Vastus lateralis
Vastus intermedius
Vastus medialis
Quadriceps femoris
Gracilis
Adductor magnus
Intermediate cutaneous nerve of the thigh
Common fibular nerve
Deep fibular nerve
Superficial fibular nerve
Tibialis anterior
Fibularis longus
Extensor digitorum longus
Fibularis brevis
Extensor hallucis longus
Lateral cutaneous nerve of the calf
Saphenous nerve
Fibularis tertius
Extensor digitorum brevis
B
Gluteus medius
Gluteus minimus
Superior gluteal nerve
Tensor fasciae latae
Piriformis
Inferior gluteal nerve
Sciatic nerve
Gluteus maximus
Semitendinosus
Posterior cutaneous nerve of the thigh
Biceps femoris, long head
Semimembranosus
Biceps femoris, short head
Adductor magnus
Tibial nerve
Common fibular nerve
Gastrocnemius, medial head
Popliteus
Gastrocnemius, lateral head
Plantaris
Soleus
Tibialis posterior
Flexor hallucis longus
Flexor digitorum longus
Tibial nerve
Sural nerve
Calcaneal branch
Lateral plantar nerve to:
Abductor digiti minimi
Flexor accessorius
Flexor digiti minimi
Adductor hallucis
Lumbricals 2–4
Interossei
Cutaneous branches
Medial plantar nerve to:
Abductor hallucis
Flexor digitorum brevis
Flexor hallucis brevis
First lumbrical
Cutaneous branches

Fig. 79.11 Nerves of the lower limb, their cutaneous branches and muscular branches. **A**, anterior aspect. **B**, Posterior aspect. Adductor magnus has dual innervation.

Lesions of the lumbar and sacral plexuses

The deep and protected situation of the plexuses means that lesions are not common. The lumbar plexus may be involved in retroperitoneal pathology, and the sacral plexus may be invaded by spreading pelvic malignancy. Both may be involved in the reticuloses, affected by plexiform neuromas, or damaged in fractures of the lumbar spine and pelvis or in other conditions that cause severe retroperitoneal and pelvic haemorrhage. Temporary lesions may occur after pregnancy and childbirth, e.g. after difficult forceps delivery of a large baby. Pain, which may be diffuse, is the most common feature, and there is often clinical involvement of several roots.

OVERVIEW OF THE PRINCIPAL NERVES OF THE LOWER LIMB

Femoral nerve (L2–4)

The femoral nerve is the nerve of the anterior compartment of the thigh. It arises from the posterior divisions of the second to fourth lumbar ventral rami, descends through psoas major and emerges on its lateral border to pass between psoas and iliacus. It enters the thigh behind the inguinal ligament and lateral to the femoral sheath. Its terminal branches form in the femoral triangle about 2 cm distal to the inguinal ligament. In the abdomen the nerve supplies small branches to iliacus and a branch to the proximal part of the femoral artery. It subsequently supplies a large cutaneous area on the anterior and medial thigh, medial leg and foot, and gives articular branches to the hip and knee. The femoral nerve is described in detail on page 1383.

Obturator nerve (L2–4)

The obturator nerve is the nerve of the medial compartment of the thigh. It arises from the anterior divisions of the second to fourth lumbar ventral rami, descends through psoas major and emerges from its medial border at the pelvic brim. It crosses the sacroiliac joint behind the common iliac artery and lateral to the internal iliac vessels, runs along the lateral pelvic wall medial to obturator internus, and enters the thigh through the upper part of the obturator foramen. Near the foramen it divides into anterior and posterior branches which are separated at first by part of obturator externus and more distally by adductor brevis. It gives articular branches to the hip and knee, and may supply skin on the medial thigh and leg. The obturator nerve is described in detail on page 1383.

Sciatic nerve (L4, L5, S1–3)

The sciatic nerve is the nerve of the posterior compartment of the thigh and, via its major branches, of all the compartments of the leg and foot. Formed in the pelvis from the ventral rami of the fourth lumbar to third sacral spinal nerves, it is typically 2 cm wide at its origin and is the thickest nerve in the body. It enters the lower limb via the greater sciatic foramen below piriformis and descends between the greater trochanter and ischial tuberosity. The nerve passes along the back of the thigh, where it is crossed by the long head of biceps femoris, and divides into the tibial and common fibular (peroneal) nerves proximal to the knee: the level of bifurcation is variable. The tibial and common fibular nerves are structurally separate and only loosely held together within the sciatic nerve. The tibial nerve is derived from the anterior divisions of the sacral plexus and the common fibular nerve is made up of the posterior divisions of the plexus. The sciatic nerve gives off articular branches that supply the hip joint through its posterior capsule (these are sometimes derived directly from the sacral plexus) and the knee joint. All the hamstring muscles, including the ischial part of adductor magnus, but not the short head of biceps femoris, are supplied by the medial (tibial) component of the sciatic nerve. The short head of biceps is supplied by the lateral (common fibular) component. The sciatic nerve is described in detail on page 1384.

Tibial nerve (L4, L5, S1–3)

The tibial nerve is derived from the anterior divisions of the sacral plexus. It descends along the back of the thigh and popliteal fossa to the distal border of popliteus, then passes anterior to the arch of soleus with the popliteal artery and continues into the leg. In the popliteal fossa it lies lateral to the popliteal vessels, becomes superficial to them at the knee and crosses to the medial side of the artery. In the leg it is the nerve of the posterior compartment and descends with the posterior tibial vessels to lie between the heel and the medial malleolus. It ends beneath the flexor retinaculum by dividing into the medial and lateral plantar nerves. The tibial nerve supplies articular branches to the knee and ankle. Its cutaneous area of supply, including its terminal branches, includes the back of the calf, the whole of the sole, the lateral border of the foot and the medial and lateral sides of the heel. The tibial nerve is described in detail on page 1427.

Common fibular nerve (L4, L5, S1, S2)

The common fibular nerve (common peroneal nerve) is derived from the posterior divisions of the sacral plexus. In the leg it is the nerve of the anterior and lateral compartments. It descends obliquely along the lateral side of the popliteal fossa to the fibular head, lying between the tendon of biceps femoris and the lateral head of gastrocnemius, then curves lateral to the neck of the fibula lying on the bone deep to fibularis longus and divides into superficial and deep fibular (peroneal) nerves. Before it divides, it gives off articular branches to the knee and the superior tibiofibular joints, and cutaneous branches. The cutaneous area supplied by the common fibular nerve and its terminal branches includes the anterolateral and lateral surfaces of the leg and most of the dorsum of the foot. The common fibular nerve is described in detail on page 1427.

Gluteal nerves

The gluteal nerves arise from the posterior divisions of the sacral plexus. The superior gluteal nerve (L4, L5, S1) leaves the pelvis through the greater sciatic notch above piriformis and supplies gluteus medius, gluteus minimus, tensor fasciae latae and the hip joint. The inferior gluteal nerve (L5, S1, S2) passes through the greater sciatic notch below piriformis and supplies gluteus maximus. The gluteal nerves are described in detail on page 1384.

AUTONOMIC INNERVATION

The autonomic supply to the limbs is exclusively sympathetic. The preganglionic sympathetic inflow to the lower limb is derived from neurones in the lateral horn of the lower thoracic (T10, T11 and T12) and upper lumbar (L1, L2) spinal cord segments. Fibres pass in white rami communicantes to the sympathetic chain and synapse in the lumbar and sacral ganglia. Postganglionic fibres pass in grey rami communicantes to enter the lumbar and sacral plexuses, and many are distributed via the cutaneous branches of the nerves derived from these plexuses. The blood vessels to the lower limb receive their sympathetic supply via adjacent peripheral nerves. Postganglionic fibres accompanying the iliac arteries are destined mainly for the pelvis but may supply vessels in the upper thigh.

Surgical or chemical lumbar sympathectomy may be indicated in arterial disease and in the management of plantar hyperhidrosis, and may be used to treat rest pain or other troublesome sensory symptoms in arterial disease or in causalgia. The segment of the chain including the second and third lumbar ganglia is removed: preservation of the first lumbar ganglion is said to lessen the risk of ejaculatory problems.

MOVEMENTS, MUSCLES AND SEGMENTAL INNERVATION

Most limb muscles are innervated by neurones which are derived from more than one segment of the spinal cord. The predominant segmental origin of the nerve supply for each of the muscles of the lower limb and for the movements which take place at the joints of the lower limb is summarized in Tables 79.1-79.4. Red has been used in Table 79.3 to highlight those muscles or movements which have diagnostic value (see below): damage to these segments or to their motor roots results in maximum paralysis. Data are based chiefly on clinical evidence (Sharrad 1995). The following caveats should be borne in mind when consulting these tables.

Table 79.1 Segmental innervation of the muscles of the lower limb

L1	Psoas major, psoas minor
L2	Psoas major, iliacus, sartorius, gracilis, pectineus, adductor longus, adductor brevis
L3	Quadriceps, adductors (magnus, longus, brevis)
L4	Quadriceps, tensor fasciae latae, adductor magnus, obturator externus, tibialis anterior, tibialis posterior
L5	Gluteus medius, gluteus minimus, obturator internus, semimembranosus, semitendinosus, extensor hallucis longus, extensor digitorum longus, finularis tertius, popliteus
S1	Gluteus maximus, obturator internus, piriformis, biceps femoris, semitendinosus, popliteus, gastrocnemius, soleus, fibularis longus and fibularis brevis, extensor digitorum brevis
S2	Piriformis, biceps femoris, gastrocnemius, soleus, flexor digitorum longus, flexor hallucis longus, some intrinsic foot muscles
S3	Some intrinsic foot muscles (except abductor hallucis, flexor hallucis brevis, flexor digitorum brevis, extensor digitorum brevis)

Table 79.2 Segmental innervation of joint movements of the lower limb

Hip	Flexors, adductors, medial rotators	L1–3
	Extensors, abductors, lateral rotators	L5, S1
Knee	Extensors	L3,4
	Flexors	L5, S1
Ankle	Dorsiflexors	L4, 5
	Plantarflexors	S1, 2
Foot	Invertors	L4, 5
	Evertors	L5, S1
	Intrinsic muscles	S2, 3

Table 79.3 Movements, muscles and segmental innervation in the lower limb. Muscles and movements that have diagnostic value are marked in red

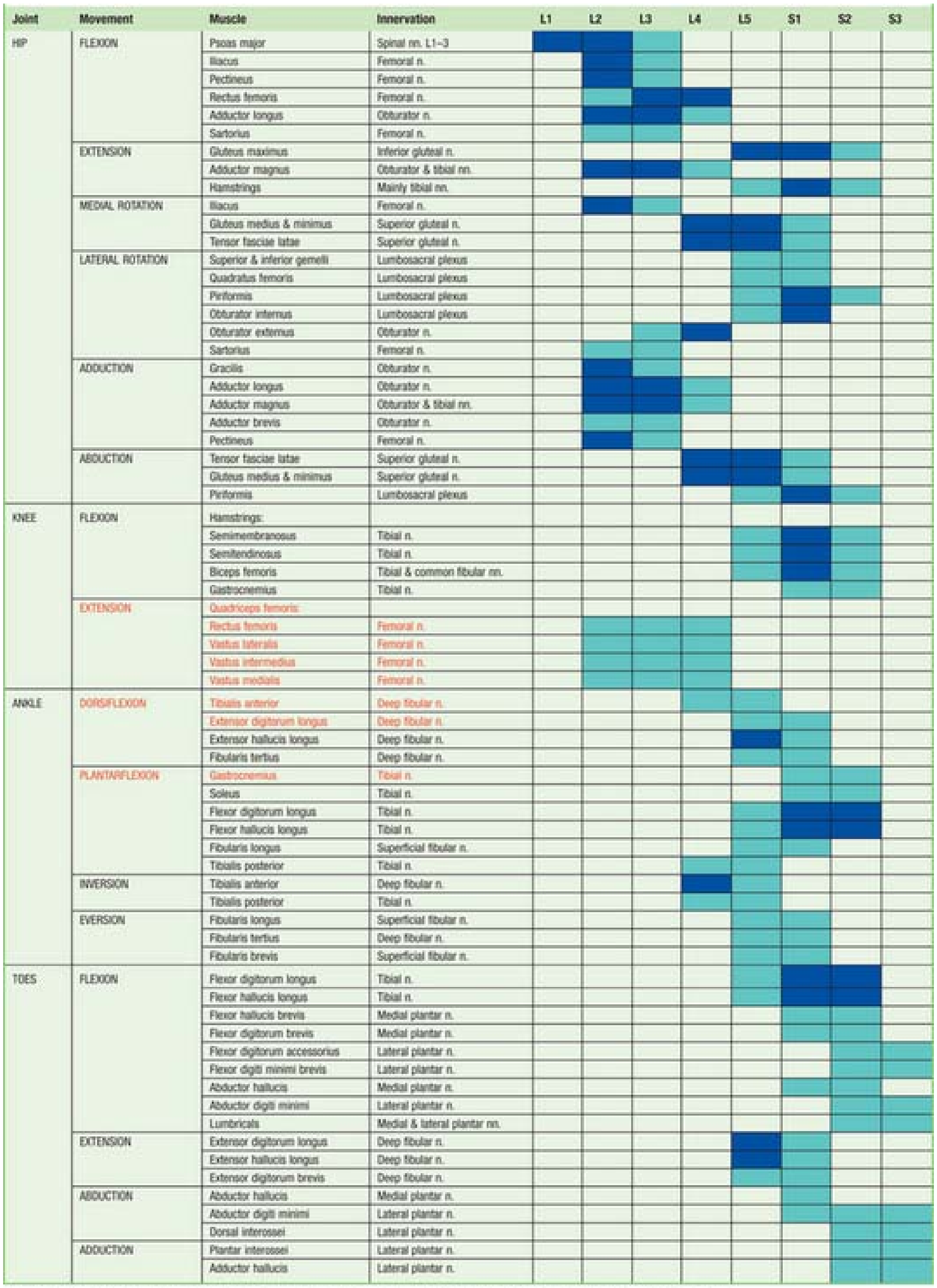

Joint	Movement	Muscle	Innervation	L1	L2	L3	L4	L5	S1	S2	S3
HIP	FLEXION	Psoas major	Spinal nn. L1–3	■	■	▨					
		Iliacus	Femoral n.		■	▨					
		Pectineus	Femoral n.		■	▨					
		Rectus femoris	Femoral n.		▨	■	■				
		Adductor longus	Obturator n.		■	■	▨				
		Sartorius	Femoral n.		▨	▨					
	EXTENSION	Gluteus maximus	Inferior gluteal n.					■	■	▨	
		Adductor magnus	Obturator & tibial nn.		■	■	▨				
		Hamstrings	Mainly tibial nn.					▨	■	▨	
	MEDIAL ROTATION	Iliacus	Femoral n.		■	▨					
		Gluteus medius & minimus	Superior gluteal n.				■	■	▨		
		Tensor fasciae latae	Superior gluteal n.				■	■	▨		
	LATERAL ROTATION	Superior & inferior gemelli	Lumbosacral plexus					▨	▨		
		Quadratus femoris	Lumbosacral plexus					▨	▨		
		Piriformis	Lumbosacral plexus					▨	■	▨	
		Obturator internus	Lumbosacral plexus					▨	■		
		Obturator externus	Obturator n.			▨	■				
		Sartorius	Femoral n.		▨	▨					
	ADDUCTION	Gracilis	Obturator n.		■	▨					
		Adductor longus	Obturator n.		■	■	▨				
		Adductor magnus	Obturator & tibial nn.		■	■	▨				
		Adductor brevis	Obturator n.		▨	▨					
		Pectineus	Femoral n.		■	▨					
	ABDUCTION	Tensor fasciae latae	Superior gluteal n.				■	■	▨		
		Gluteus medius & minimus	Superior gluteal n.				■	■	▨		
		Piriformis	Lumbosacral plexus					▨	■	▨	
KNEE	FLEXION	Hamstrings:									
		Semimembranosus	Tibial n.					▨	■	▨	
		Semitendinosus	Tibial n.					▨	■	▨	
		Biceps femoris	Tibial & common fibular nn.					▨	■	▨	
		Gastrocnemius	Tibial n.						▨	▨	
	EXTENSION	Quadriceps femoris:									
		Rectus femoris	Femoral n.		▨	▨	▨				
		Vastus lateralis	Femoral n.		▨	▨	▨				
		Vastus intermedius	Femoral n.		▨	▨	▨				
		Vastus medialis	Femoral n.		▨	▨	▨				
ANKLE	DORSIFLEXION	Tibialis anterior	Deep fibular n.				▨	▨			
		Extensor digitorum longus	Deep fibular n.					▨	▨		
		Extensor hallucis longus	Deep fibular n.					■	▨		
		Fibularis tertius	Deep fibular n.					▨	▨		
	PLANTARFLEXION	Gastrocnemius	Tibial n.						▨	▨	
		Soleus	Tibial n.						▨	▨	
		Flexor digitorum longus	Tibial n.					▨	■	■	
		Flexor hallucis longus	Tibial n.					▨	■	■	
		Fibularis longus	Superficial fibular n.					▨	▨		
		Tibialis posterior	Tibial n.				▨	▨			
	INVERSION	Tibialis anterior	Deep fibular n.				■	▨			
		Tibialis posterior	Tibial n.				▨	▨			
	EVERSION	Fibularis longus	Superficial fibular n.					▨	▨		
		Fibularis tertius	Deep fibular n.					▨	▨		
		Fibularis brevis	Superficial fibular n.					▨	▨		
TOES	FLEXION	Flexor digitorum longus	Tibial n.					▨	■	■	
		Flexor hallucis longus	Tibial n.					▨	■	■	
		Flexor hallucis brevis	Medial plantar n.						▨	▨	
		Flexor digitorum brevis	Medial plantar n.						▨	▨	
		Flexor digitorum accessorius	Lateral plantar n.							▨	▨
		Flexor digiti minimi brevis	Lateral plantar n.							▨	▨
		Abductor hallucis	Medial plantar n.						▨	▨	
		Abductor digiti minimi	Lateral plantar n.							▨	▨
		Lumbricals	Medial & lateral plantar nn.							▨	▨
	EXTENSION	Extensor digitorum longus	Deep fibular n.					■	▨		
		Extensor hallucis longus	Deep fibular n.					■	▨		
		Extensor digitorum brevis	Deep fibular n.					▨	▨		
	ABDUCTION	Abductor hallucis	Medial plantar n.						▨		
		Abductor digiti minimi	Lateral plantar n.						▨	▨	▨
		Dorsal interossei	Lateral plantar n.							▨	▨
	ADDUCTION	Plantar interossei	Lateral plantar n.							▨	▨
		Adductor hallucis	Lateral plantar n.							▨	▨

Royal blue shading denotes nerve roots from which there is a known dominant contribution. Turquoise shading denotes nerve roots from which the contribution is of similar degree.

Table 79.4 The movements and muscles tested to determine the location of a lesion in the lower limb

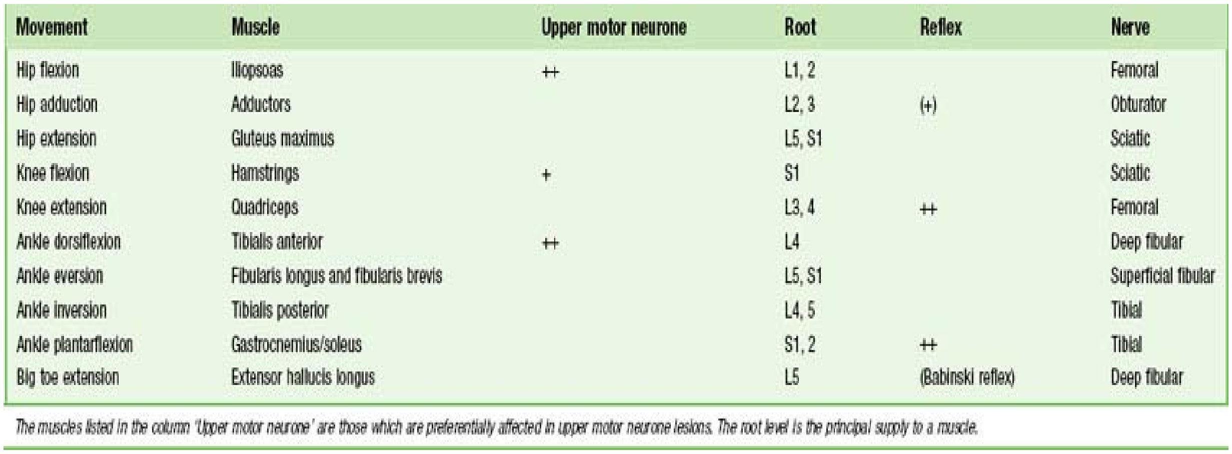

Movement	Muscle	Upper motor neurone	Root	Reflex	Nerve
Hip flexion	Iliopsoas	++	L1, 2		Femoral
Hip adduction	Adductors		L2, 3	(+)	Obturator
Hip extension	Gluteus maximus		L5, S1		Sciatic
Knee flexion	Hamstrings	+	S1		Sciatic
Knee extension	Quadriceps		L3, 4	++	Femoral
Ankle dorsiflexion	Tibialis anterior	++	L4		Deep fibular
Ankle eversion	Fibularis longus and fibularis brevis		L5, S1		Superficial fibular
Ankle inversion	Tibialis posterior		L4, 5		Tibial
Ankle plantarflexion	Gastrocnemius/soleus		S1, 2	++	Tibial
Big toe extension	Extensor hallucis longus		L5	(Babinski reflex)	Deep fibular

The muscles listed in the column 'Upper motor neurone' are those which are preferentially affected in upper motor neurone lesions. The root level is the principal supply to a muscle.

Movements

At the central nervous level of control, muscles are not recognized as individual actuators but as components of movement, and may therefore contribute to several types of movement, acting variously as prime movers, antagonists, fixators or synergists. Some muscles have been included in more than one place in Table 79.3, on the basis that a muscle which acts across one joint can produce a combination of movements (e.g. flexion with medial rotation, or extension with adduction) and a muscle which crosses two joints can produce more than one movement. It must also be remembered that these listings are not exhaustive.

Nerve roots

There is no universal consensus concerning the contribution that individual spinal roots make to the innervation of individual muscles: the most positive identifications, which are limited, have been obtained by electrically stimulating spinal roots and recording the evoked electromyographic activity in the muscles. Much of the information in Tables 79.1-79.4 is therefore based on neurological experience gained in examining the effects of lesions, and some of it is far from new. Spinal roots have been given turquoise shading when they innervate a muscle to a similar extent, or when differences in their contribution have not been described. Royal blue has been used to indicate roots from which there is known to be a dominant contribution. Minor contributions have been retained in the table in order to increase its utility in other contexts, such as electromyography and comparative anatomy.

Neurological localization of a lesion

In clinical practice it is only necessary to test a relatively small number of muscles in order to determine the location of a lesion. Any muscle to be tested must satisfy a number of criteria. It should be visible, so that wasting or fasciculation can be observed, and the muscle consistency with contraction can be felt. It should have an isolated action, so that its function can be tested separately. It should help to differentiate between lesions at different levels in the neuraxis and in the peripheral nerve, or between peripheral nerves. It should be tested in such a way that normal can be differentiated from abnormal, so that slight weakness can be detected early with reliability. Some preference should be given to muscles with an easily elicited reflex. Table 79.4 gives a list of movements and muscles chosen according to these criteria: in practice, these tests would be combined with tests of sensory function. Knowledge of the sequence in which motor branches leave a peripheral nerve to innervate specific muscles is very helpful in localizing the level of a lesion.

SURFACE ANATOMY

SKELETAL LANDMARKS

Pelvis

An oblique skin crease, the fold of the groin, marks the junction of the front of the thigh with the anterior abdominal wall, and lies distal to the inguinal ligament (Fig. 79.12). The anterior superior iliac spine lies above the lateral end of the fold and can always be palpated. At its medial end, the fold reaches the pubic tubercle. From the anterior superior iliac spine, the iliac crest is easily palpable along its entire length. It terminates posteriorly as the posterior superior iliac spine, which may be felt in the depression seen just above the buttock. This depression lies at the level of the second sacral segment, at the level of the middle of the sacroiliac joint and the termination of the spinal dural sac. The ischial tuberosity may be palpated in the lower part of the buttock. It is covered by gluteus maximus when the hip joint is extended, but can be identified without difficulty when the hip is flexed, e.g. in the sitting position, when the tuberosity emerges from under cover of the lower border of gluteus maximus and becomes subcutaneous, separated from the skin only by a pad of fat and the ischial bursa. In this position, the weight of the body is supported by the ischial tuberosities.

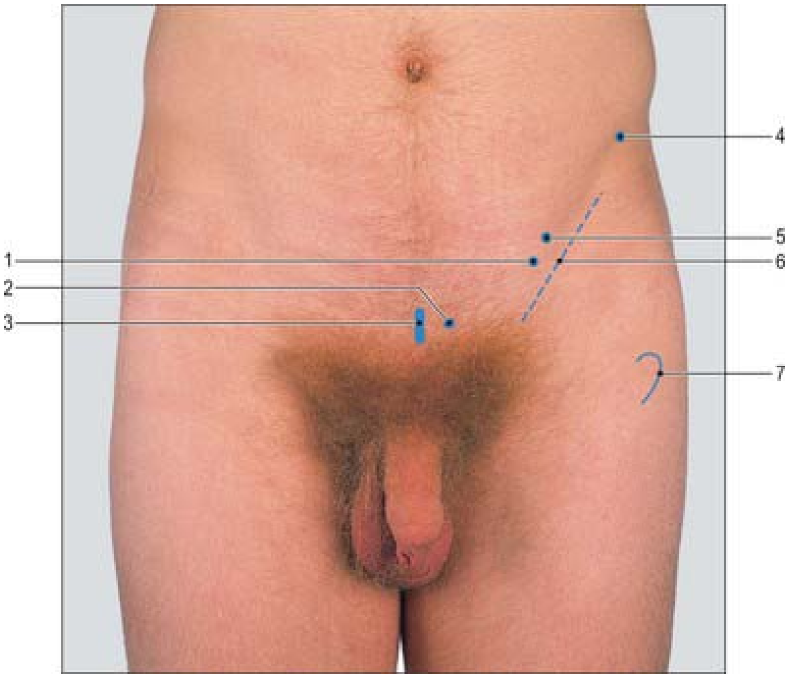

Fig. 79.12 Inguinal region. **1**. Mid-inguinal point. **2**. Pubic tubercle. **3**. Pubic symphysis. **4**. Anterior superior iliac spine. **5**. Midpoint of inguinal ligament. **6**. Groin crease. **7**. Greater trochanter.

(With permission from Lumley JSP, 2002, Surface Anatomy, The Anatomical Basis of Clinical Examination, 3rd edn. Edinburgh: Churchill Livingstone.)

Femur

The greater trochanter of the femur, which is the only palpable part of the proximal portion of the femur, lies the breadth of the subject's hand below the midpoint of the iliac crest. It can be both seen and felt as a prominence in front of the hollow on the side of the gluteal region. The lower end of the femur is less deeply placed. When the knee is flexed passively, the medial surface of the medial condyle and the lateral surface of the lateral condyle of the femur may both be palpated, and portions of the femoral articular surface can be examined on each side of the lower part of the patella.

Patella

The patella can be readily identified. When the quadriceps is relaxed in the fully extended knee, the patella can be tilted and moved on the lower end of the femur. The lower limit of the patella lies more than 1–2 cm above the line of the knee joint (Figs 73.13 and 73.14).

Knee

The patella and the medial and lateral condyles of the femur have been described above. The tibial condyles form visible and palpable landmarks at the medial and lateral sides of the patellar tendon (Fig. 79.13). The latter may be traced downwards from the apex of the patella to the tibial tubercle, which is easily seen as well as felt. When the knee is flexed, the anterior margins of the tibial condyles can be felt: each forms the lower boundary of a depression at the side of the patellar tendon. The lateral condyle is the more prominent of the two. The joint line of the tibiofemoral joint corresponds to the upper margins of the tibial condyles and can be represented by a line drawn round the limb at this level. The anterior horns of the menisci lie in the angles between this line and the edges of the patellar tendon. The iliotibial tract is attached to a prominence, Gerdy’s tubercle, on the anterior aspect of the lateral condyle that is usually 1 cm below the joint line and 2 cm lateral to the tibial tubercle.

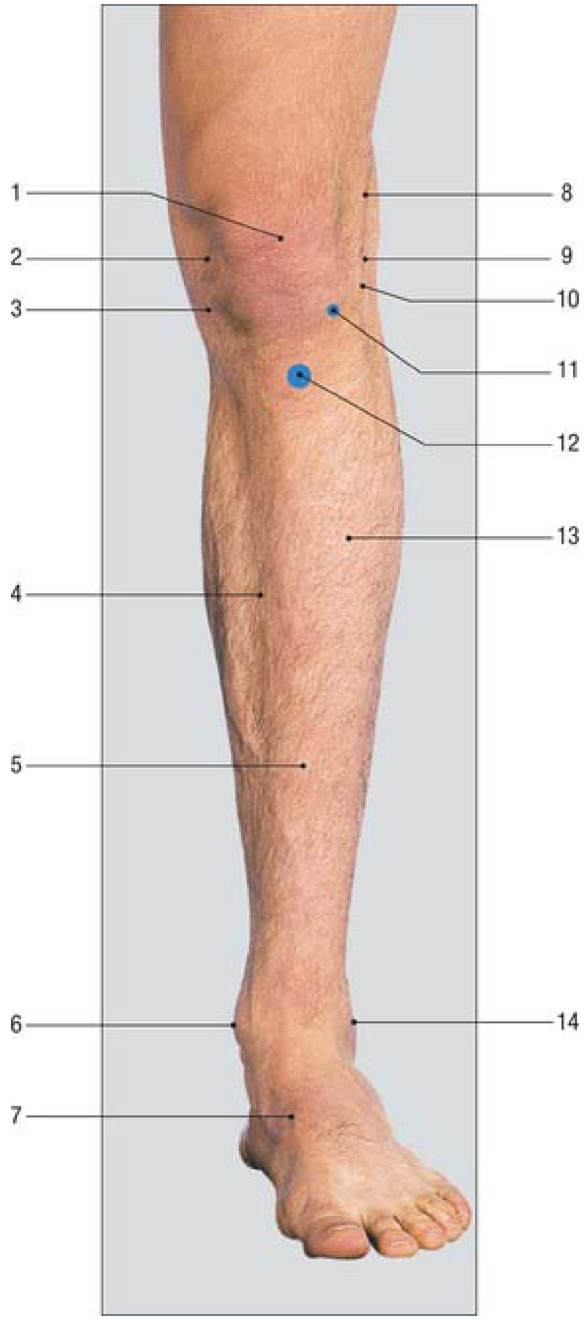

Fig. 79.13 Anterior aspect of the knee and leg. **1**. Patella. **2**. Medial femoral condyle. **3**. Medial tibial condyle. **4**. Medial surface of tibial shaft. **5**. Anterior border of tibia. **6**. Medial malleolus. **7**. Tibialis anterior tendon. **8**. Iliotibial tract. **9**. Lateral femoral condyle. **10**. Joint line of knee. **11**. Gerdy's tubercle on anterior aspect of lateral tibial condyle. **12**. Tibial tubercle. **13**. Anterior compartment of leg. **14**. Lateral malleolus.

(With permission from Lumley JSP, 2002, Surface Anatomy, The Anatomical Basis of Clinical Examination, 3rd edn. Edinburgh: Churchill Livingstone.)

The head of the fibula forms a slight surface elevation on the upper part of the posterolateral aspect of the leg. It lies vertically below the posterior part of the lateral condyle of the femur, not less than 1 cm below the level of the knee joint.

Leg and ankle

The subcutaneous medial surface of the tibia corresponds to the flat anteromedial aspect of the leg. Above, this surface merges with the medial condyle of the tibia, and below it is continuous with the visible prominence of the medial malleolus of the tibia (Fig. 79.14A). The sinuous anterior border of the tibia can be felt distinctly throughout most of its extent, but inferiorly it is somewhat masked by the tendon of tibialis anterior, which lies to its lateral side. The lateral malleolus of the fibula forms a conspicuous projection on the lateral side of the ankle: it descends to a more distal level than the medial malleolus and is placed on a more posterior plane (Fig. 79.14B). The lateral aspect of the lateral malleolus is continuous above with an elongated, subcutaneous, triangular area of the lower shaft of the fibula. The lateral part of the anterior margin of the lower end of the tibia can be detected immediately in front of the base of the lateral malleolus; the line of the ankle joint can be gauged from it.

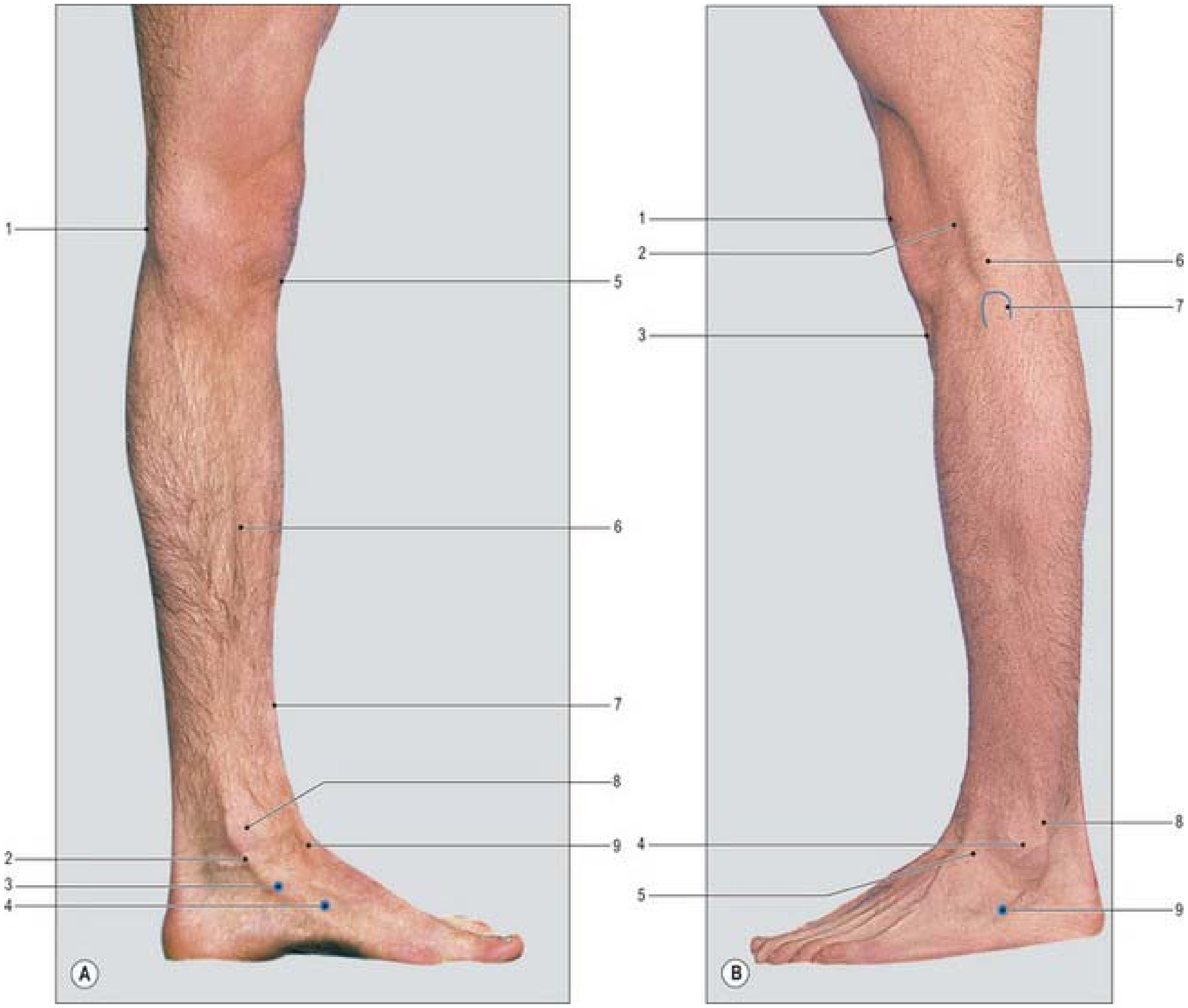

Fig. 79.14 **A**, Medial aspect of the knee, leg and foot. **1**. Knee joint line. **2**. Tibialis posterior tendon. **3**. Navicular tuberosity. **4**. Medial cuneiform. **5**. Patellar tendon. **6**. Medial surface of tibia. **7**. Anterior border of tibia. **8**. Medial malleolus. **9**. Tibialis anterior tendon. **B**, Lateral aspect of the knee. **1**. Patella. **2**. Iliotibial tract. **3**. Patellar tendon. **4**. Lateral malleolus. **5**. Tendon of fibularis tertius. **6**. Tendon of biceps femoris. **7**. Head of fibula. **8**. Tendons of fibularis longus and brevis. **9**. Styloid process of 5th metatarsal.

*(**A** and **B** with permission from Lumley JSP, 2002, Surface Anatomy, The Anatomical Basis of Clinical Examination, 3rd edn. Edinburgh: Churchill Livingstone.)*

Foot

The anterior part of the upper surface of the calcaneus can be identified a little in front of the lateral malleolus on the dorsum of the foot. When the foot is passively inverted, the upper and lateral part of the head of the talus can be both seen and felt 3 cm anterior to the distal end of the tibia; it is obscured by the extensor tendons when the toes are dorsiflexed.

The dorsal aspects of the bodies of the metatarsal bones can be felt more or less distinctly, although they tend to be obscured by the extensor tendons of the toes. The tuberosity on the base of the fifth metatarsal bone forms a distinct projection, which can be both seen and felt, half-way along the lateral border of the foot.

The flat lateral surface of the calcaneus can be palpated on the lateral aspect of the heel and can be traced forwards below the lateral malleolus, where it is hidden by the tendons of fibularis longus and brevis. The peroneal tubercle (fibular tubercle), when sufficiently large, can be felt 2 cm below the tip of the lateral malleolus. A palpable depression just anterior to the lateral malleolus leads to the lateral end of the sinus tarsi.

On the medial side of the foot, the sustentaculum tali of the calcaneus can be felt 2 cm vertically below the medial malleolus. The medial aspect of the calcaneus can be felt (indistinctly) below and behind the sustentaculum tali. The most conspicuous bony landmark on the medial side of the foot is the tuberosity of the navicular bone, which is usually visible and can always be felt 2.5 cm anterior to the sustentaculum tali. Anterior to this, the medial cuneiform bone can be identified by tracing the tendon of tibialis anterior into it. The upper and medial parts of the joint between the medial cuneiform and the first metatarsal can be felt as a narrow groove.

When the foot is placed on the ground, it rests on the posterior part of the inferior surface of the calcaneus, the heads of the metatarsal bones and, to a lesser extent, on its lateral border. The instep, which corresponds to the medial longitudinal arch of the foot, is elevated from the ground. The medial and lateral tubercles of the calcaneus can be identified on the posterior part of the inferior surface of the calcaneus, but they are obscured by the tough fibro-fatty pad that covers them. The heads of the metatarsal bones are similarly covered by a thick pad, which forms the ball of the foot. The foot is at its widest at this level, reflecting the slight splay of the metatarsal bones as they pass anteriorly.

The calcaneocuboid joint lies 2 cm behind the tubercle on the base of the fifth metatarsal bone and is practically in line with the talonavicular joint, whose position may be gauged from the position of the head of the talus. The tarsometatarsal joints lie on a line joining the tubercle of the fifth metatarsal bone to the tarsometatarsal joint of the great toe. When the latter joint cannot be felt on the medial border of the foot, its position may be indicated 2.5 cm in front of the tuberosity of the navicular bone. The joint between the second metatarsal and the intermediate cuneiform lies some 2–3 mm behind the line of the other tarsometatarsal joints. The metatarsophalangeal joints lie 2.5 cm behind the webs of the toes.

MUSCULOTENDINOUS AND LIGAMENTOUS LANDMARKS

Buttock and hip

The bulky prominence of the buttock is caused by the forward tilt of the pelvis (which throws the ischium backwards), the size of gluteus maximus, and the large amount of subcutaneous fat.

The horizontal gluteal fold marks the upper limit of the posterior aspect of the thigh. It does not correspond to the lower border of gluteus maximus but is caused by fibrous connections between the skin and the deep fascia. The natal cleft, which separates the buttocks inferiorly, starts above at the third or fourth sacral spine. The upper border of gluteus maximus begins on the iliac crest some 3 cm lateral to the posterior superior iliac spine and runs downwards and laterally to the apex of the greater trochanter. Its lower border corresponds to a line drawn from the ischial tuberosity, through the midpoint of the gluteal fold, to a point about 9 cm below the greater trochanter (Fig. 79.15). Although gluteus maximus overlaps the ischial tuberosity in the standing position, on sitting it slides superiorly posterior to the tuberosity, leaving it free to bear weight. The muscle can be felt to contract when the hip is extended against resistance.

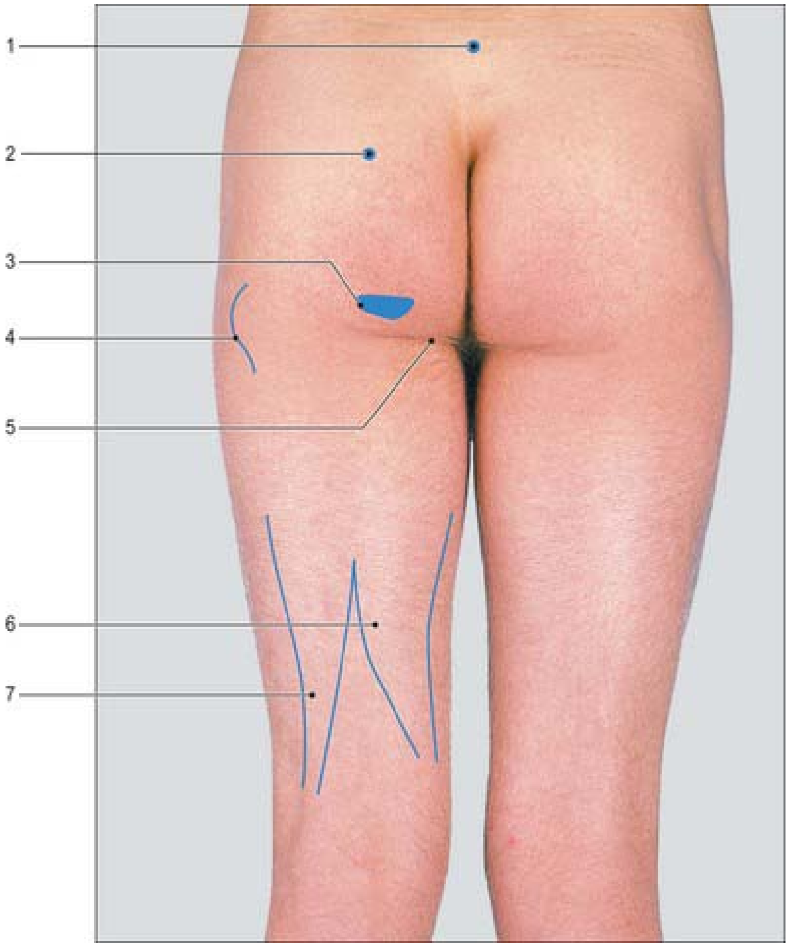

Fig. 79.15 Gluteal region and posterior aspect of the thigh. **1**. 4th lumbar spinous process. **2**. Posterior superior iliac spine. **3**. Ischial tuberosity. **4**. Greater trochanter. **5**. Gluteal crease. **6**. Semitendinosus and semimembranosus. **7**. Biceps femoris.

(With permission from Lumley JSP, 2002, Surface Anatomy, The Anatomical Basis of Clinical Examination, 3rd edn. Edinburgh: Churchill Livingstone.)

Gluteus medius completely covers the underlying gluteus minimus. Both muscles lie in a slight depression superolateral to gluteus maximus and inferior to the anterior portion of the iliac crest. They constitute the major abductors of the hip and are demonstrated by asking the subject to stand on one limb. The ipsilateral muscles contract and tilt the pelvis in order to stabilize the centre of gravity, and the contralateral gluteal fold will rise. If the hip abductors are paralysed, e.g. in congenital dislocation of the hip or in a long-standing fracture of the neck of the femur, this mechanism is disturbed and the normal tilting of the pelvis does not occur. Indeed, when the patient stands on the affected hip, the pelvis tilts downwards on the contralateral side (Trendelenburg’s sign).

Thigh

The inguinal ligament can be felt running between the anterior superior iliac spine and the pubic tubercle when the thigh is abducted and externally rotated. Just distal to the inguinal ligament, but running horizontally, is the hip flexure line (Holden’s line), where the deep layer of superficial fascia of the abdominal wall meets the fascia lata of the thigh.

The shallow depression lying immediately below the fold of the groin corresponds to the femoral triangle. It is bounded on its lateral side by the strap-like sartorius which can be both seen and felt in a reasonably thin and muscular subject when the hip is flexed in the sitting position, while keeping the knee extended, especially when the thigh is slightly abducted and rotated laterally. Sartorius can be traced downwards and medially from the anterior superior iliac spine to approximately half-way down the medial side of the thigh; distally, it may be identified as a soft longitudinal ridge passing towards the posterior part of the medial femoral condyle. The adductor group of muscles forms the bulky, fleshy mass at the upper part of the medial side of the thigh. The medial border of adductor longus forms the medial boundary of the femoral triangle and can be felt as a distinct ridge when the thigh is adducted against resistance. At its upper end, its tendon of origin immediately below the pubic tubercle can be identified and felt between the finger and thumb, which is a useful guide to this bony landmark.

The forward convexity of the front of the thigh is caused by the curvature of the femur covered by the fleshy mass of quadriceps femoris. Rectus femoris appears as a ridge passing down the anterior aspect of the thigh when the sitting subject flexes the hip with the knee extended. Vastus medialis constitutes the bulge above and medial to the patella. Vastus lateralis forms the elevation above and lateral to the patella, more proximal and less pronounced than that of vastus medialis. Vastus intermedius is hidden by the other three muscles.

The flattened appearance of the lateral aspect of the thigh is produced by the iliotibial tract, which is a thickened portion of the deep fascia of the thigh (fascia lata). It stands out as a strong, visible ridge on the lateral aspect of the knee when the knee is either extended against gravity or when the opposite limb is lifted from the floor while standing.

Knee

The large depression that can be seen at the back of the knee when the joint is actively flexed against resistance corresponds to the popliteal fossa (Fig. 79.16). The transverse skin crease of the popliteal fossa is 2–3 cm above the tibiofemoral joint line. The fossa is bounded on the lateral side by the prominent tendon of biceps femoris, which can be felt between the finger and thumb and can be traced downwards to the head of the fibula. Three tendons can be felt on the medial side of the fossa. Semitendinosus is the most lateral and posterior, and gracilis is the most medial and anterior. These two tendons stand out sharply and can be seen when the knee is flexed against resistance and the limb actively adducted. The third tendon is that of semimembranosus: it is more deeply situated and can be felt in the interval between the tendons of semitendinosus and gracilis. It is much thicker than the other two tendons and broadens rapidly as it is traced upwards. Distally, in thin individuals, the upper border of the pes anserinus can be palpated. The upper borders of the two heads of gastrocnemius form the medial and lateral inferior boundaries of the popliteal fossa.

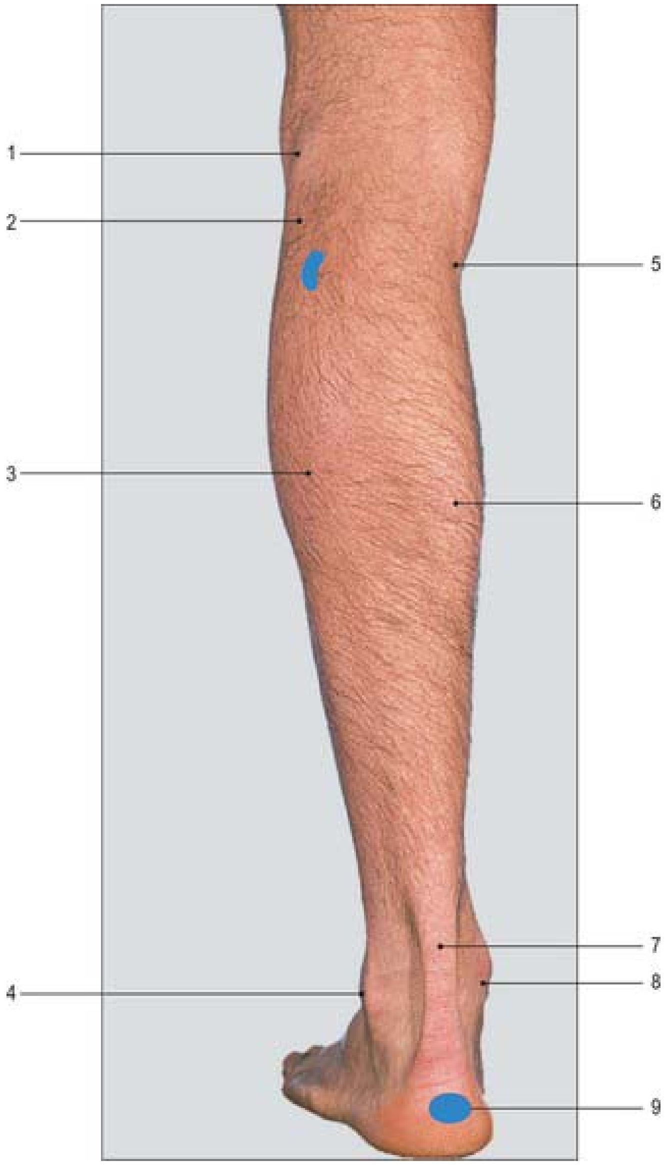

Fig. 79.16 Posterior aspect of the leg and heel. **1**. Tendon of biceps femoris. **2**. Head of fibula. **3**. Lateral head of gastrocnemius. **4**. Lateral malleolus. **5**. Semitendinosus. **6**. Medial head of gastrocnemius. **7**. Calcaneal tendon. **8**. Medial malleolus. **9**. Calcaneus.

(With permission from Lumley JSP, 2002, Surface Anatomy, The Anatomical Basis of Clinical Examination, 3rd edn. Edinburgh: Churchill Livingstone.)

The lateral collateral ligament may be felt passing from the tip of the fibular head to the lateral epicondyle of the femur when the knee is flexed and laterally directed pressure is applied to the medial side of the knee. The medial patellofemoral ligament may be felt overlying the medial femoral condyle in the flexed knee, running between the midpoint of the medial patella and medial femoral epicondyle.

Leg

The muscles in the anterior osteofascial compartment of the leg form a gentle prominence over the upper two-thirds of its anterolateral aspect: this prominence is accentuated when the foot is actively dorsiflexed. In the lower third of the leg these muscles are replaced by their tendons. The tendon of tibialis anterior can be seen just lateral to the anterior border of the tibia and traced downwards and medially across the front of the ankle (Fig. 79.14A). The other tendons cannot be examined satisfactorily above the ankle. Immediately above the medial malleolus and close to the medial border of the tibia, the tendons of tibialis posterior and flexor digitorum longus can be felt (rather indistinctly) when the foot is actively inverted and plantar flexed.

On the lateral aspect of the leg, fibularis longus can be seen as a narrow ridge during active eversion and plantarflexion of the foot. It covers and hides fibularis brevis. Both muscles cover the lateral aspect of the fibula, which means that the shaft of the fibula can only be palpated indistinctly between its neck and its lower subcutaneous triangular area.

The bulky prominence of the calf of the leg is formed by gastrocnemius and soleus, both of which can be identified either when the foot is plantar flexed against resistance, or when the heel is raised from the ground by standing on tiptoes. The two heads of gastrocnemius unite to form the inferior angle of the popliteal fossa. The medial head of gastrocnemius descends to a lower level than the lateral head. Soleus lies deep to gastrocnemius; when tensed, it bulges from under gastrocnemius, particularly on the lateral side, and its fleshy belly extends to a more distal level. Both muscles end below in the conspicuous calcaneal tendon which can be gripped between the finger and thumb and followed downwards to its insertion into the posterior aspect of the calcaneus (Fig. 79.16).

Foot

When the toes are actively dorsiflexed, the belly of extensor digitorum brevis forms a small elevation on the dorsum of the foot, a little in front of the lateral malleolus. It is the only intrinsic muscle of the foot to arise from the dorsum of the foot. The tendon of tibialis anterior stands out conspicuously on the medial side when active dorsiflexion of the toes is combined with inversion: it can be traced downwards and medially to the medial cuneiform bone. Also in dorsiflexion, the tendon of extensor hallucis longus can be identified lateral to tibialis anterior. Still more laterally, and immediately in front of the lateral part of the inferior end of the tibia, the tendons of extensor digitorum longus and fibularis tertius are crowded together as they pass through the fibrous loop of the inferior extensor retinaculum. More distally, these tendons diverge to their insertions.

The tendon of tibialis posterior winds posterior to the medial malleolus and then curves forwards in the interval between this bony landmark and the sustentaculum tali to reach the tuberosity of the navicular bone. The tendon is thrown into relief when the foot is forcibly plantar flexed and inverted. The tendon of flexor digitorum longus lies midway between the medial margin of the calcaneal tendon and the margin of the medial malleolus. It curves forwards below tibialis posterior and lies on the medial aspect of the sustentaculum tali. From there, it passes forwards and laterally to the centre of the sole of the foot, where it breaks up into tendons for the lateral four toes. The tendon of flexor hallucis longus lies inferior to, and grooves, the sustentaculum tali. As it passes forward to the great toe, it crosses the line of the flexor digitorum longus opposite the interval between the sustentaculum tali and the tuberosity of the navicular bone. Abductor hallucis may be seen in some subjects as a fleshy mass across the instep of the foot, passing from the medial calcaneal tubercle to the ball of the great toe.

The plantar fascia is most easily palpated along its medial border, in the sole of the foot when the toes are maximally dorsiflexed. Its precise origin is difficult to palpate because of the thickness of the heel pad, but it is easily palpated just distal to the heel pad as far as the ball of the foot.

VESSELS, PULSES AND NERVES

Arteries

The femoral artery enters the thigh at a point midway between the anterior superior iliac spine and the pubic symphysis, directly anterior to the hip joint. Its course can be represented by the upper two-thirds of a line joining that point to the adductor tubercle when the flexed thigh is abducted slightly and rotated laterally.

The popliteal artery may be represented approximately by a line extending from the junction of the middle and lower thirds of the thigh, 2.5 cm medial to its posterior midline, to the midpoint between the femoral condyles, and continuing inferolaterally to the level of the tibial tuberosity, medial to the fibular neck. The artery bifurcates into the anterior and posterior tibial arteries at the lower border of popliteus.

The anterior tibial artery may be represented by a line extending from a point half-way between the tibial tuberosity and fibular head to a point midway between the anterior borders of the two malleoli.

The posterior tibial artery corresponds to a line drawn from a mid-axial point on the calf at the level of the neck of the fibula to a point a third of the way between the posterior border of the medial malleolus and the calcaneal tendon. The same line represents the course of the tibial nerve. At first the nerve lies lateral to the popliteal artery, then gradually crosses the vessel to gain its medial side. The trunk of the medial plantar artery begins midway between the medial malleolus and heel (medial calcaneal tubercle) and extends towards the first interdigital cleft as far as the navicular bone.

Pulses

Femoral artery

The pulsations of the femoral artery can be felt at its origin, where the vessel can be compressed against the superior ramus of the pubis or the head of the femur. Like the carotid pulse, the femoral pulse is of value in assessing whether there is any significant cardiac output in cases of circulatory collapse. It is a common site for radiological catheter insertion and for arterial puncture for blood gas analysis.

Popliteal artery

The pulse of the popliteal artery is the most difficult of the peripheral pulses to feel because the artery lies deep in the popliteal fossa. It is best examined with the subject lying supine or prone, with the knee flexed, in order to relax the tense popliteal fascia that roofs the popliteal fossa. The popliteal pulse is then felt by deep pressure over the midline of the fossa against the popliteal surface of the femur.

Posterior tibial artery

The pulse of the posterior tibial artery can be felt by gentle palpation behind the medial malleolus as the artery lies between the tendons of flexor hallucis longus and flexor digitorum longus.

Dorsalis pedis arterial

The dorsalis pedis arterial pulse is found by palpation against the underlying tarsal bones immediately lateral to the tendon of extensor hallucis longus.

Veins

The surface marking for the femoral vein is immediately medial to the femoral pulse. The long saphenous vein usually terminates 2 cm inferior to the femoral pulse. Its course may be marked out in the thigh by a line passing from this point downwards and backwards to a point the breadth of the subject’s hand behind the medial border of the patella.

The long saphenous vein can often be seen as it runs upwards and backwards across the medial surface of the tibia a little above and in front of the medial malleolus: this is a useful site for obtaining surgical venous access or for harvesting vein for cardiac bypass surgery. The vein is accompanied in this region by the saphenous nerve, which is usually anterolateral, but may be posterior, to the vein. The vein and nerve then run proximally and posteriorly along the medial border of the tibia to reach a point the breadth of the subject’s hand posterior to the medial border of the patella. The short saphenous vein may be represented by a line that runs from the posterior surface of the lateral malleolus up the midline of the calf to the popliteal fossa; together with the sural nerve, it is the key anatomical guide to surgical dissection of the popliteal fossa.

The dorsal venous arch is often a conspicuous feature on the dorsum of the foot and curves, convex forwards, across the metatarsus. The long saphenous vein arises from its medial end and runs upwards and backwards immediately in front of the medial malleolus. The short saphenous vein arises from the lateral end of the arch and passes backwards and inferior to, and then upwards and posterior to, the lateral malleolus.

Femoral venous cannulation

While femoral venous puncture is relatively easy and supplies ready access to the right atrium, the use of this approach is relatively unpopular for long-term cannulation because of a higher incidence of thrombosis and sepsis. However, it is a useful site for venous sampling in a patient with collapsed veins. For femoral venous cannulation the skin puncture site is approximately 1 cm medial to the femoral artery and just below the inguinal ligament. After skin puncture the needle is advanced with the syringe at an angle of 30° to the skin, aiming cephalad.

Nerves

The areas of distribution and spinal segments of origin of the cutaneous nerves of the lower limb are shown in Figure 79.17.

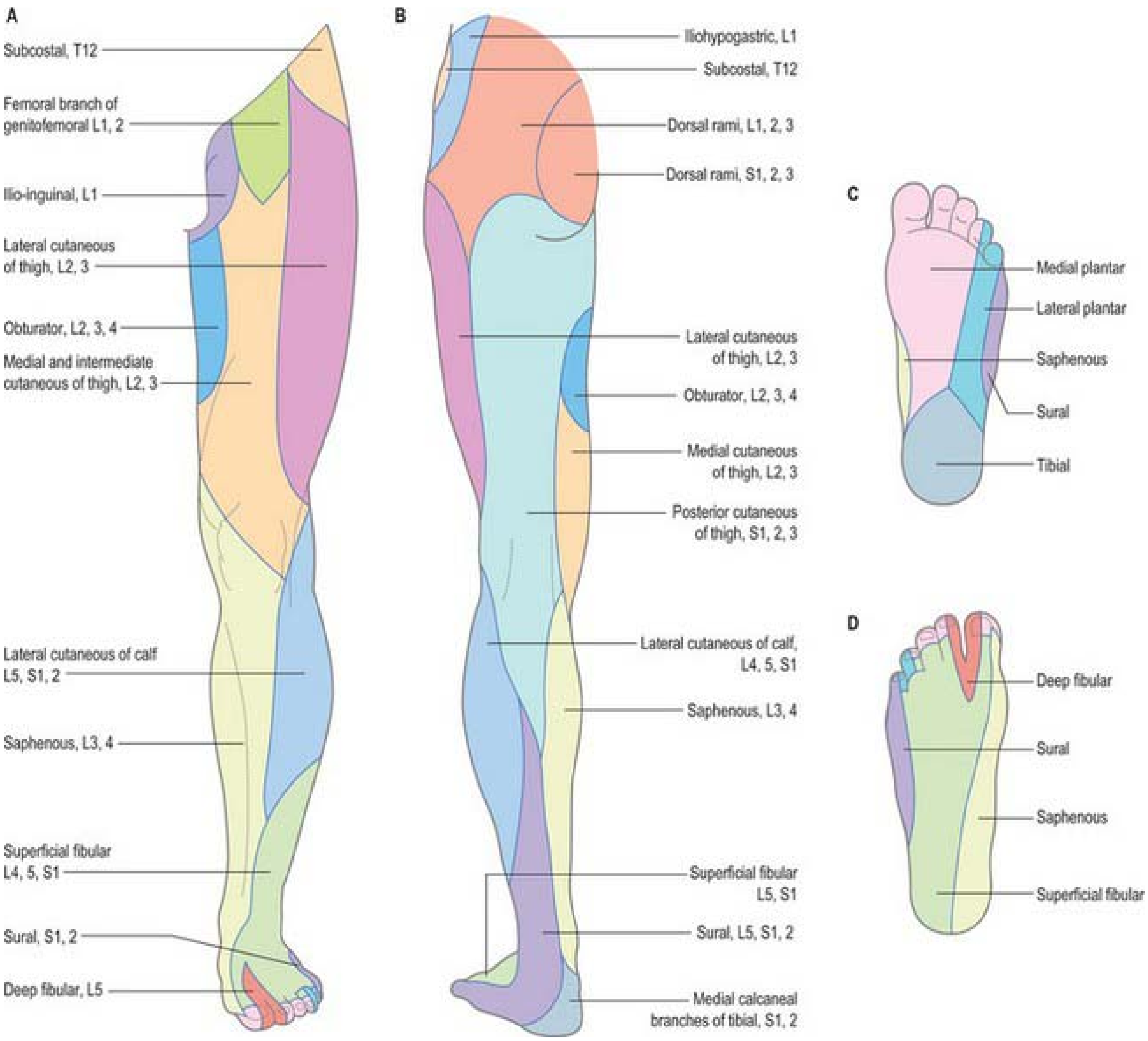
A
Subcostal, T12
Femoral branch of genitofemoral L1, 2
Ilio-inguinal, L1
Lateral cutaneous of thigh, L2, 3
Obturator, L2, 3, 4
Medial and intermediate cutaneous of thigh, L2, 3
Lateral cutaneous of calf L5, S1, 2
Saphenous, L3, 4
Superficial fibular L4, 5, S1
Sural, S1, 2
Deep fibular, L5
B
Iliohypogastric, L1
Subcostal, T12
Dorsal rami, L1, 2, 3
Dorsal rami, S1, 2, 3
Lateral cutaneous of thigh, L2, 3
Obturator, L2, 3, 4
Medial cutaneous of thigh, L2, 3
Posterior cutaneous of thigh, S1, 2, 3
Lateral cutaneous of calf, L4, 5, S1
Saphenous, L3, 4
Superficial fibular L5, S1
Sural, L5, S1, 2
Medial calcaneal branches of tibial, S1, 2
C
Medial plantar
Lateral plantar
Saphenous
Sural
Tibial
D
Deep fibular
Sural
Saphenous
Superficial fibular

Fig. 79.17 The cutaneous nerves of the lower limb: areas of distribution and spinal segments of origin. **A**, Anterior aspect; **B**, posterior aspect; **C**, sole of foot; **D**, dorsum of foot.

The surface marking for the femoral nerve in the inguinal region is immediately lateral to the femoral pulse. The surface marking for the course of the saphenous nerve is described with the course of the long saphenous vein (see above).

The course of the sciatic nerve can be represented by a line that starts at a point midway between the posterior superior iliac spine and ischial tuberosity, curves outwards and downwards through a point midway between the greater trochanter and the ischial tuberosity (Fig. 79.18), and then continues vertically downwards in the midline of the posterior aspect of the thigh to the upper angle of the popliteal fossa, where it divides into the tibial and common fibular nerves (if it has not already done so at a higher level).

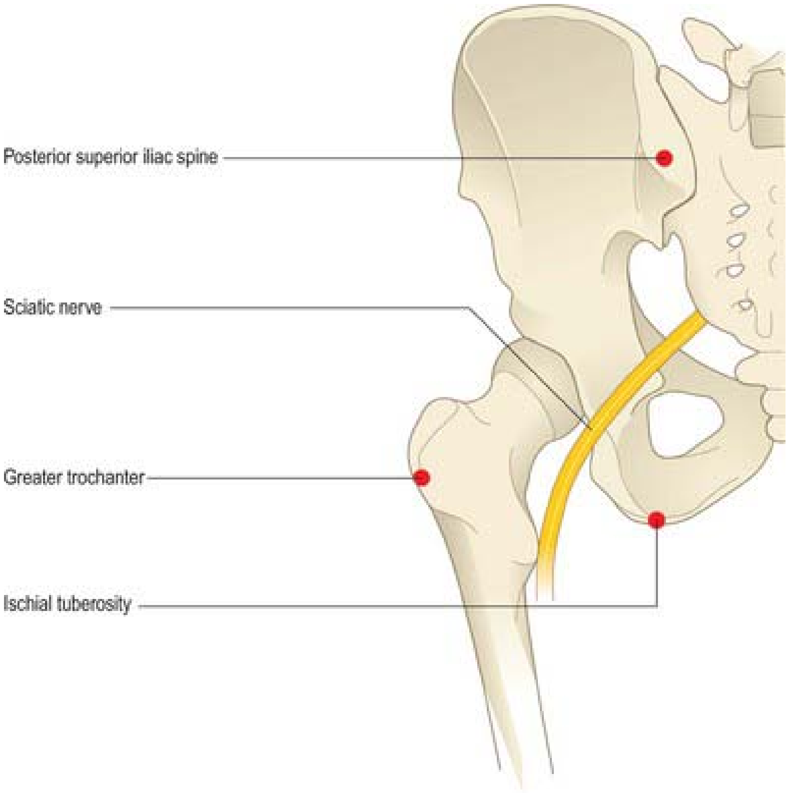

Fig. 79.18 Surface marking of the sciatic nerve. The line of the nerve joins the midpoint between the ischial tuberosity and the posterior superior iliac spine with the midpoint between the ischial tuberosity and the greater trochanter and then continues vertically down the back of the thigh.

The course of the common fibular nerve can be indicated by a line that runs from the upper angle of the popliteal fossa, along the medial side of the tendon of biceps femoris and then curves downwards and forwards around the neck of the fibula. The nerve is palpable medial and, more distally to the tendon of biceps and over the neck of the fibula, although here it is less distinct as it passes deep to the origin of fibularis longus. At the neck of the fibula the nerve is at particular risk of damage either from a tightly applied plaster cast or from a fracture.

The deep fibular nerve starts on the lateral aspect of the neck of the fibula, passes downwards and medially, and rapidly becomes associated with the anterior tibial artery, which it accompanies to the ankle. The superficial fibular nerve also begins on the lateral aspect of the neck of the fibula. It descends to a point on the anterior border of fibularis longus, at the junction of the middle and lower thirds of the leg, where it pierces the deep fascia and divides into medial and lateral branches. The latter gradually diverge as they descend to reach the dorsum of the foot and may be seen if the foot is pulled into maximal plantarflexion and adduction.

With one exception, the cutaneous nerves of the foot are not normally visible. The superficial fibular nerve is frequently seen and palpated over the dorsolateral aspect of the ankle and midfoot when the ankle is plantar flexed and the fourth toe passively flexed. This is particularly true in individuals with little subcutaneous fat. While the lateral branch is often seen, the medial branch is rarely visible. These superficial nerves are at risk from surgery in the anterior ankle region (especially during arthroscopy): they can be identified reliably by passive plantarflexion and inversion of the foot whilst running the blunt end of a ballpoint pen across the anterior ankle. An easily palpable click will localize the nerves, even in patients who are not thin.

Dermatomes

Our knowledge of the extent of individual dermatomes, especially in the limbs, is largely based on clinical evidence. The dermatomes of the lower limb arise from spinal nerves T12 to S3 (Fig 79.19 and 79.20).

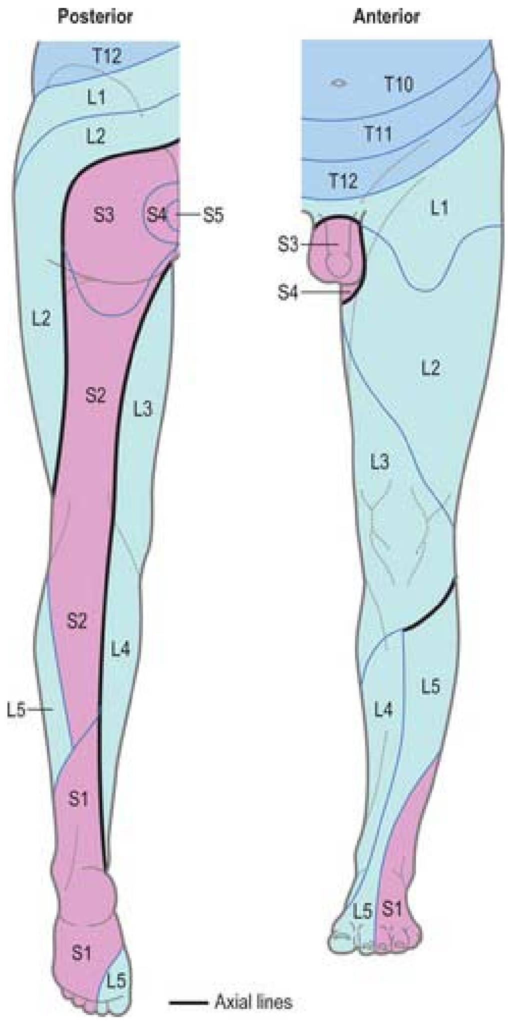
Posterior
Anterior
T12
L1
L2
S3
S4
S5
L2
S2
L3
S2
L4
L5
S1
S1
L5
Axial lines
T10
T11
T12
L1
S3
S4
L2
L3
L5
L4
L5
S1

Fig. 79.19 Dermatomes of the lower limb. There is considerable variation and overlap between dermatomes, but the overlap across axial lines (heavy black) is minimal.

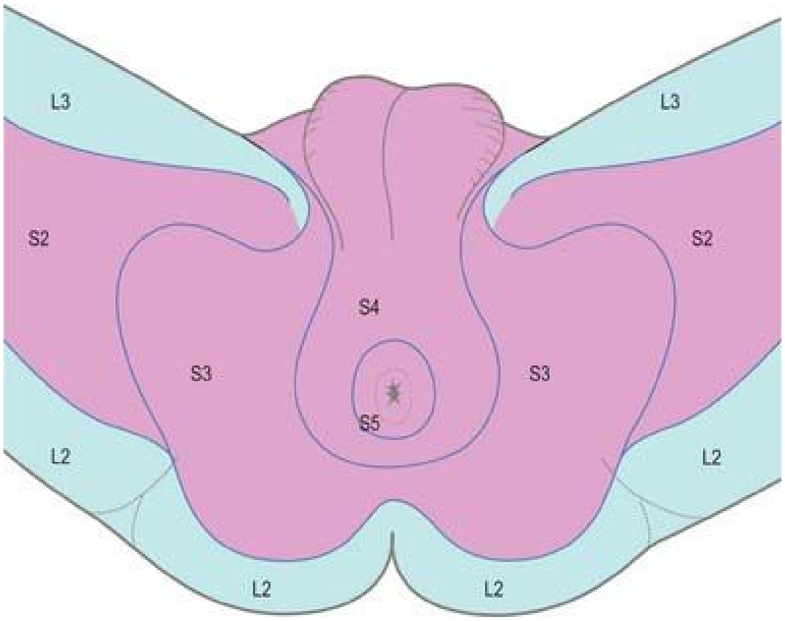

Fig. 79.20 Dermatomes of the perineum.

The preaxial border starts near the midpoint of the thigh and descends to the knee. It then curves medially, descending to the medial malleolus and the medial side of the foot and hallux. The postaxial border starts in the gluteal region and descends to the centre of the popliteal fossa, then deviates laterally to the lateral malleolus and the lateral side of the foot. The ventral and dorsal axial lines exhibit corresponding obliquity. The ventral starts proximally at the medial end of the inguinal ligament and descends along the posteromedial aspect of the thigh and leg to end proximal to the heel. The dorsal axial line begins in the lateral gluteal region and descends posterolaterally in the thigh to the knee; it inclines medially and ends proximal to the ankle. Considerable overlap exists between adjacent dermatomes innervated by nerves derived from consecutive spinal cord segments.

Myotomes

The predominant segmental origin of the nerve supply for each of the muscles of the lower limb and for the movements which take place at the joints of the lower limb are summarized in Tables 79.1-79.4.

Reflexes

Knee jerk (L2–4)

With the patient supine and the knee supported and partially flexed, the patellar tendon is struck at its midpoint: this should elicit contraction of the quadriceps, which extends the knee.

Ankle jerk (S1, 2)

With the patient supine and the lower limb externally rotated and partially flexed at hip and knee, the foot is passively dorsiflexed to stretch the calcaneal tendon, which is then struck with a percussion hammer. Contraction of the calf muscles plantar flexes the ankle. The reflex can also be examined with the patient kneeling on a chair.

Plantar reflex

The plantar reflex is a superficial reflex whose elicitation forms an important part of the clinical examination of the central nervous system. With the foot relaxed and warm, the outer edge of the sole is stroked longitudinally with a hard object (traditionally the examiner’s nail or a key). This should elicit flexion of the toes, although the normal adult response varies with the strength of the stimulus. In adults with upper motor neurone lesions, the response includes extension of the great toe (Babinski’s sign).

Nerve blocks

Nerves can be effectively blocked with local anaesthetic injection for surgical or post-injury pain relief. The useful blocks in the lower limb are around the hip, for thigh and knee pain, and around the ankle, for foot surgery. For the deeper nerves around the hip, the use of a nerve stimulator needle is very helpful to localize the nerve precisely before infiltration of local anaesthetic. For example, blockade of the sciatic nerve in the buttock, femoral nerve in the anterior groin, and obturator nerve in the medial groin may be undertaken to provide pain relief for total knee replacement; the tibial nerve at the posteromedial ankle, the sural nerve at the posterolateral ankle and the superficial fibular nerves at the anterior ankle may all be blocked at the ankle to allow ‘awake foot surgery’.

CLINICAL PROCEDURES

Intramuscular injection

Intramuscular injections into the buttock should be avoided to prevent iatrogenic damage to the sciatic nerve. If the buttock is to be used, the safe area is the true upper and outer quadrant, which is identified with the whole buttock exposed. The injection is then given mainly into gluteus medius rather than into gluteus maximus, provided a sufficiently long needle is used: most so-called ‘intramuscular’ injections given into the buttock are actually given into the fat. A safe alternative is to inject into the lateral aspect of the thigh (vastus lateralis).

Joint injection and aspiration

Careful aseptic technique is essential for all joint aspirations and injections.

Hip

With the patient lying supine, and after the positions of the femoral artery and the anterior superior iliac spine have been marked out, the needle is introduced anteriorly approximately 5 cm distal to the anterior superior iliac spine and 4 cm lateral to the femoral pulse, and passed posteriorly, a little proximally (cephalad), and medially.

Knee

The lateral retropatellar approach is used. With the patient supine and the knee extended, the needle is introduced at the level of the superior border of the patella and guided towards the suprapatellar pouch.

Ankle

The anterior approach entails introducing the needle between the tendons of tibialis anterior and extensor hallucis longus with the ankle partially plantar flexed, keeping the needle tangential to the curve of the talus.

Arthroscopy portals

The placement of portals for arthroscopy is critical, partly to maximize surgical access for visualization and for surgical instruments, but to also avoid damage to structures such as nerves and blood vessels.

Hip

Hip arthroscopy is not yet a common procedure but is increasingly being used. A variety of entry portals have been described. The anterolateral portal is sited on the skin approximately 4 cm lateral to the femoral pulse and 4 cm inferior to the inguinal ligament. A needle traversing the skin 30–45° cephalad is passed under X-ray control into the joint. Once the synovial cavity is entered the ‘vacuum’ is lost and the joint can be distracted. Other more lateral portals can be used: the lateral cutaneous nerve of the thigh and the sciatic nerve are potentially at risk.

Knee

The knee is the joint most frequently examined in this way. The standard portals are anterior. When the knee is flexed at a right angle, ‘soft triangles’ bordered by the patellar tendon, the femoral condyles and the tibia and anterior horns of the menisci are palpable on either side of the superior third of the patellar tendon. Small ‘stab’ incisions can be made in the apices of these triangular areas at about the level of the inferior pole of the patella for the anterolateral portal, and slightly lower for the anteromedial portal. These portals will allow passage of an arthroscope and instruments, with good access to most of the joint. The fat pad is close by and passage through it will hamper the view and subsequent surgery. The patellar tendon and the infrapatellar branch of the saphenous nerve are at risk from the incisions. The nerve is less vulnerable than the tendon: its position is variable but it usually lies below the appropriate portal sites. However, in the days of open meniscal surgery, the nerve was usually divided and painful neuroma formation was not uncommon.

Posteromedial and posterolateral portals are useful when better access to the posterior knee is required. The saphenous and common fibular nerves respectively are at risk with these approaches, and anatomical knowledge is vital to safe portal placement. Laterally the incision should be anterior to the tendon of biceps, which can easily be palpated. Medially the situation is more difficult because the saphenous nerve and vein run over the medial epicondylar region of the knee, a hand’s breadth posterior to the medial border of the patella. It is essential that sharp incision includes the skin only, and that dissection down to the joint capsule is undertaken bluntly. If the medial meniscus is sutured, the capsule must be exposed before tying off sutures to avoid ensnaring the nerve. In lateral meniscal repair a useful guide to avoid injury to the common fibular nerve is never to allow needles or sutures to pass medial to the tendon of popliteus whilst viewing arthroscopically.

Ankle

The use of ankle arthroscopy is well established, especially in treating sports-related injuries. Anterior portals are standard. The anteromedial portal can be placed to pass just medial to the tendon of tibialis anterior, in the palpable soft spot. However, this comes close to the long saphenous vein and nerve, and limiting the sharp incision to the skin, followed by blunt deeper dissection, reduces the risk. Alternatively the anteromedial portal can be chosen to pass between the lateral edge of tibialis anterior and extensor hallucis longus. The anterolateral portal is placed with the help of the arthroscope in the joint to check the position of a preliminary needle passed into the joint. The portal should pass lateral to fibularis tertius and extensor digitorum longus. The intermediate dorsal cutaneous branch of the superficial fibular nerve is at risk as it crosses the ankle anterior to the lateral malleolus, and therefore it is wise to ink in the nerves and blood vessels before making any incision. The nerves can be felt at the front of the ankle even in obese patients. They are often seen if the ankle is maximally pulled into plantarflexion and are seen to flick as the barrel of a pen is pulled across the front of the ankle. Posterior ankle arthroscopy is controversial: there is a view that the proximity of the neurovascular bundle (medially) and the sural nerve (laterally) renders it too hazardous. Keeping lateral to the tendon of flexor hallucis will safeguard the medial neurovascular bundle.

Surgical incisions

Hip

Hip joint surgery is usually undertaken for paediatric problems, trauma, or arthroplasty in arthritis. Anterior and anterolateral approaches, often used in children, put the lateral cutaneous nerve of the thigh at considerable risk. Even in more lateral approaches, the lateral cutaneous nerve of the thigh and the femoral and sciatic nerves are all at risk through traction. A popular anterolateral approach to the hip joint involves splitting and separating forwards the anterior part of gluteus medius and vastus lateralis as a single sheet of tissue for subsequent reattachment to the greater trochanter. This technique relies on the anatomical continuity of the tissue. If the splitting of gluteus medius is more than a few centimetres superior to the tip of the greater trochanter then the superior gluteal nerve and vessels are at risk, and weakness of hip abduction and a limp may result. In the posterior approach to the hip joint, gluteus maximus is incised in the line of its fibres. This is followed by division of the tendons of the short lateral rotators (piriformis, obturator internus and gemelli) near their trochanteric attachments to reveal the joint capsule. The sciatic nerve is protected by reflecting medially the cut ends of the divided short lateral rotators.

Knee

Most open knee surgery can be undertaken through an anterior midline longitudinal incision, which gives good access and means that any future surgery can usually be undertaken via the same wound. New incisions run the risk of skin necrosis and poor wound healing as a consequence of interfering with the cutaneous blood supply. Inevitable interruption of the cutaneous nerves, including the infrapatellar branch of the saphenous nerve, means that there is always numbness lateral to a longitudinal incision.

The extensile approach to the posterior knee is extensive. The key is to expose the sural nerve and short saphenous vein and to trace them proximally. This will lead the surgeon into the popliteal fossa and, after opening the deep fascia, safely to the neurovascular bundle. The wound crosses a flexure crease. A scar perpendicular to the crease might induce a fixed flexion contracture of the joint and therefore, as at the anterior elbow, an S-shaped incision is employed where the transverse segment runs in the line of the flexure crease.

Ankle and foot

Incisions around the foot and ankle frequently put cutaneous nerves at risk and such an injury can cause a distressing painful neuroma. The sural nerve at the ankle has a notorious tendency to form neuromas, often after repair of a ruptured calcaneal tendon. Bunion surgery is also problematic and can be undertaken through an internervous plane with a dorsomedial incision over the first metatarsophalangeal joint, rather than the traditional dorsal approach.

REFERENCES

rmack GC, Lamberty BGH 1994, see Bibliography.

ock HV. Atlas of Vascular Anatomy of the Skeleton and Spinal Cord. London: Martin Dunitz, 1996.

dd H, Cockett FB. The Pathology and Surgery of the Veins of the Lower Limb, 2nd edn. Edinburgh: Churchill Livingstone, 1976.

sinski C. Observations on the superficial venous system of the lower extremity. *J Anat*. 1926;60:131-142.

arrard WJW. The distribution of the permanent paralysis in the lower limb in poliomyelitis; a clinical and pathological study. *J Bone Joint Surg Br*. 1955;37-B(4):540-558.

ichel Salmon: Anatomic Studies, Book 1. In: Taylor GI, Razaboni RM. *Arteries of the Muscles of the Extremities and Trunk*. St. Louis: Quality Medical Publishing, 1994.

CHAPTER 80

Pelvic girdle, gluteal region and thigh

The pelvic girdle consists of the paired hip bones (each consisting of the ilium, ischium and pubis) and a single sacrum. The two pubic bones articulate anteriorly at the pubic symphysis and the sacrum articulates posteriorly with the two iliac bones: however, the bones are virtually incapable of independent movement except in the female during parturition. The pelvic girdle is massively constructed and serves as a weightbearing and protective structure, as an attachment for trunk and limb muscles, and as the skeletal framework of a birth canal capable of accommodating a large-headed fetus.

The gluteal region or buttock is an area demarcated by the gluteal fold inferiorly, a line joining the greater trochanter and the anterior superior iliac spine laterally, the iliac crest superiorly and the midline medially. It contains a large bulk of skeletal muscle that covers several vulnerable neurovascular structures, and incorporates junctional zones between the lower limb, pelvis and perineum at the sciatic foramina. Direct and indirect musculoskeletal injuries in this region may damage the sciatic nerve and gluteal vessels.

The thigh consists of a cylinder of compact bone, the femoral shaft, surrounded by muscle groups traversed by important neurovascular structures. The muscles are grouped according to function and lie within osteofascial compartments that are defined by fascial septa running between the femur and an enveloping tube of tough fascia, the fascia lata. The femoral artery gives off its major branch, the profunda femoris, in the anterior compartment, and the sciatic nerve usually divides into its main branches, the tibial and common fibular nerves, as it passes through the posterior compartment. The femoral nerve divides soon after entering the anterior compartment beneath the inguinal ligament; the obturator nerve enters the region proximally and medially from the pelvis and divides into its main branches which run anterior and posterior to adductor brevis.

SKIN AND SOFT TISSUES

SKIN

See also Chapter 79.

Vascular supply and lymphatic drainage

Buttock

Most of the skin of the buttock is supplied by musculocutaneous perforating vessels from the superior and inferior gluteal arteries. There are also small peripheral contributions from similar branches of the internal pudendal, iliolumbar and sacral arteries.

Cutaneous veins are tributaries of vessels that correspond to the named arteries. Cutaneous lymphatic drainage is to the superficial inguinal nodes.

Thigh

The skin of the thigh distal to the inguinal ligament and gluteal fold is supplied mainly by branches of the femoral and profunda femoris arteries. There is some contribution from the obturator, inferior gluteal and popliteal arteries and from direct cutaneous, musculocutaneous and fasciocutaneous vessels. For further details consult Cormack & Lamberty (1994).

Cutaneous veins are tributaries of vessels that correspond to the named arteries. Cutaneous lymphatic drainage is to the superficial inguinal nodes, mainly via collecting trunks accompanying the long saphenous vein.

Innervation

See page 1346 and Figs 79.17B, 79.19.

SOFT TISSUE

Fascia

Superficial fascia

The superficial fascia of the buttock is continuous superiorly with that over the low back, and contains a variable quantity of coarse fat. The superficial fascia of the thigh consists, as elsewhere in the limbs, of loose areolar tissue containing fat. In some regions, particularly near the inguinal ligament, it splits into recognizable layers, between which may be found the branches of superficial vessels and nerves. It is thick in the inguinal region, where its two layers enclose the superficial inguinal lymph nodes, long saphenous vein and other smaller vessels. Here the superficial layer is continuous with that of the abdominal fascia. The deep layer, a thin fibroelastic stratum, is most marked medial to the long saphenous vein and inferior to the inguinal ligament, and is interposed between the subcutaneous vessels and nerves and the deep fascia, fusing with the latter a little below the ligament. (The line of fusion lies in the floor of the ventral flexure line, otherwise known as the groove associated with the hip joint.) This membranous layer of superficial fascia overlies the saphenous opening, blending with its circumference and with the femoral sheath. Over the opening it is perforated by the long (great) saphenous vein, by the superficial branches of the femoral artery other than the superficial circumflex iliac (which perforates the fascia lata separately), and lymphatic vessels, hence the term cribriform fascia (Latin *cribrum* = a sieve).

Deep fascia

The deep fascia covering the gluteal muscles varies in thickness. Over the maximus it is thin, but over the anterior two-thirds of the medius it forms the thick, strong gluteal aponeurosis. This is attached to the lateral border of the iliac crest superiorly, and splits anteriorly to enclose tensor fasciae latae and posteriorly to enclose gluteus maximus.

Fascia lata

The fascia lata, the wide deep fascia of the thigh, is thicker in the proximal and lateral parts of the thigh where tensor fasciae latae and an expansion from gluteus maximus are attached to it. It is thin posteriorly and over the adductor muscles, but thicker around the knee, where it is strengthened by expansions from the tendon of biceps femoris laterally, sartorius medially, and quadriceps femoris anteriorly. The fascia lata is attached superiorly and posteriorly to the back of the sacrum and coccyx, laterally to the outer margin of the iliac crest, anteriorly to the inguinal ligament and superior ramus of the pubis, and medially to the inferior ramus of the pubis, the ramus and tuberosity of the ischium, and the lower border of the sacrotuberous ligament. From the iliac crest it descends as a dense layer over gluteus medius to the upper border of gluteus maximus, where it splits into two layers, one passing superficial and the other deep to the muscle, the layers reuniting at the lower border of the muscle.

Iliotibial tract

Over the flattened lateral surface of the thigh, the fascia lata thickens to form a strong band, the iliotibial tract. The upper end of the tract splits into two layers, where it encloses and anchors tensor fasciae latae and receives, posteriorly, most of the tendon of gluteus maximus. The superficial layer ascends lateral to tensor fasciae latae to the iliac crest; the deeper layer passes up and medially, deep to the muscle, and blends with the lateral part of the capsule of the hip joint. Distally, the iliotibial tract is attached to a smooth, triangular facet (Gerdy’s tubercle) on the anterolateral aspect of the lateral condyle of the tibia where it is superficial to, and blends with, an aponeurotic expansion from vastus lateralis. When the knee is extended against resistance it stands out as a strong, visible ridge on the anterolateral aspect of the thigh and knee.

Distally, the fascia lata is attached to all exposed bony points around the knee joint, such as the condyles of the femur and tibia, and the head of the fibula. On each side of the patella the deep fascia is reinforced by transverse fibres, which receive contributions from the lateral and medial vasti. The stronger lateral fibres are continuous with the iliotibial tract.

Intermuscular septa

The deep surface of the fascia lata yields two intermuscular septa, which are attached to the whole of the linea aspera and to its proximal and distal prolongations. The lateral septum, thicker and stronger than the medial one, extends from the attachment of gluteus maximus to the lateral femoral condyle, and lies between vastus lateralis in front and the short head of biceps femoris behind and provides partial attachment for them. The medial, thinner and weaker septum lies between vastus medialis and the adductors and pectineus. Numerous smaller septa, such as that separating the thigh adductors and flexors, pass between the individual muscles, ensheathing them and sometimes providing partial attachment for their fibres.

Saphenous opening

The saphenous opening is an aperture in the deep fascia, inferolateral to the medial end of the inguinal ligament, which allows passage to the long saphenous vein and other smaller vessels (Fig. 80.1). The cribriform fascia, which is pierced by these structures, fills in the aperture and must be removed to reveal it. Adjacent subsidiary openings may exist to transmit venous tributaries. In the adult the approximate centre of the opening is 3 cm lateral to a point just distal to the pubic tubercle. The length and width of the opening vary considerably. The fascia lata in this part of the thigh displays superficial and deep strata (not to be confused with the superficial and deep layers of the superficial fascia described above). They lie, respectively, anterior and posterior to the femoral sheath; with the saphenous opening situated where the two layers are in continuity. This serves to explain the somewhat oblique and spiral configuration of the saphenous opening.

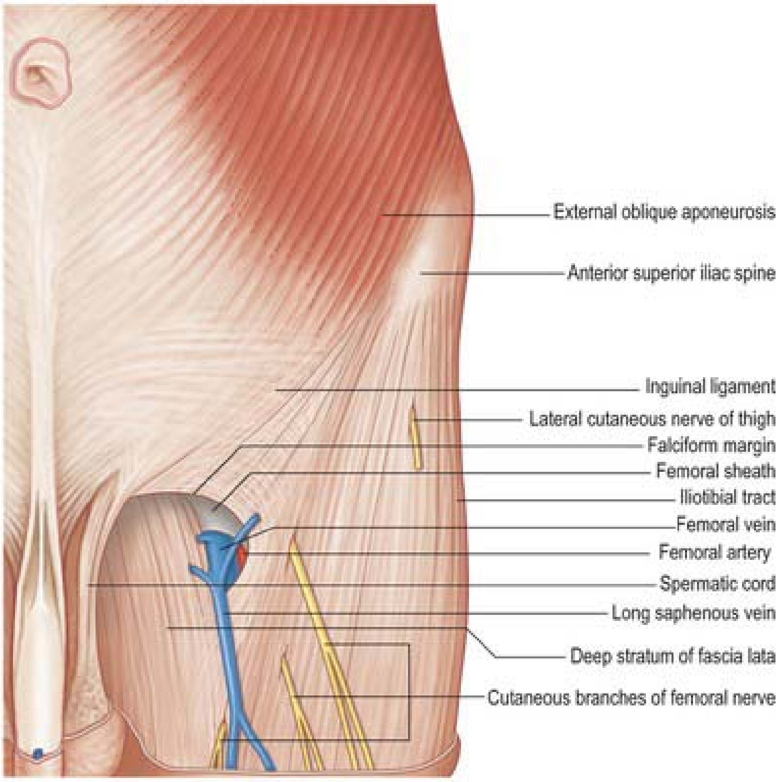
External oblique aponeurosis
Anterior superior iliac spine
Inguinal ligament
Lateral cutaneous nerve of thigh
Falciform margin
Femoral sheath
Iliotibial tract
Femoral vein
Femoral artery
Spermatic cord
Long saphenous vein
Deep stratum of fascia lata
Cutaneous branches of femoral nerve

Fig. 80.1 The saphenous opening, after removal of the cribriform fascia.

The superficial stratum, lateral and superior to the saphenous opening, is attached, in continuity, to the crest and anterior superior spine of the ilium, to the whole length of the inguinal ligament, and to the pecten pubis and lacunar ligament. It is reflected inferolaterally from the pubic tubercle as the arched falciform margin, which forms the superior, lateral and inferior boundaries of the saphenous opening: this margin adheres to the anterior layer of the femoral sheath, and the cribriform fascia is attached to it. The falciform margin is considered to have superior and inferior cornua. The inferior cornu is well defined, and is continuous behind the long saphenous vein with the deep stratum of the fascia lata.

The deep stratum is medial to the saphenous opening and is continuous with the superficial stratum at its lower margin. Traced upwards, it covers pectineus, adductor longus and gracilis, passes behind the femoral sheath, with which it is blends, and continues to the pecten pubis.

Fascial compartments

There are three functional groups of muscle in the thigh, namely, anterior (extensor), posterior (flexor) and medial (adductor). The anterior and posterior groups occupy separate osteofascial compartments that are limited peripherally by the fascia lata and separated from each other by the femur and the medial and lateral intermuscular septa (Fig. 80.2). The adductor muscles, though distinct in terms of function and innervation, do not possess a separate compartment limited by fascial planes. Nevertheless it is customary to speak of three compartments: anterior, posterior and medial. The muscles of the three compartments are described below. Adductor magnus, adductor longus and pectineus could each be considered to be constituents of two compartments, i.e. adductor magnus in the posterior and the medial compartments, and adductor longus and pectineus in the anterior and the medial compartments.

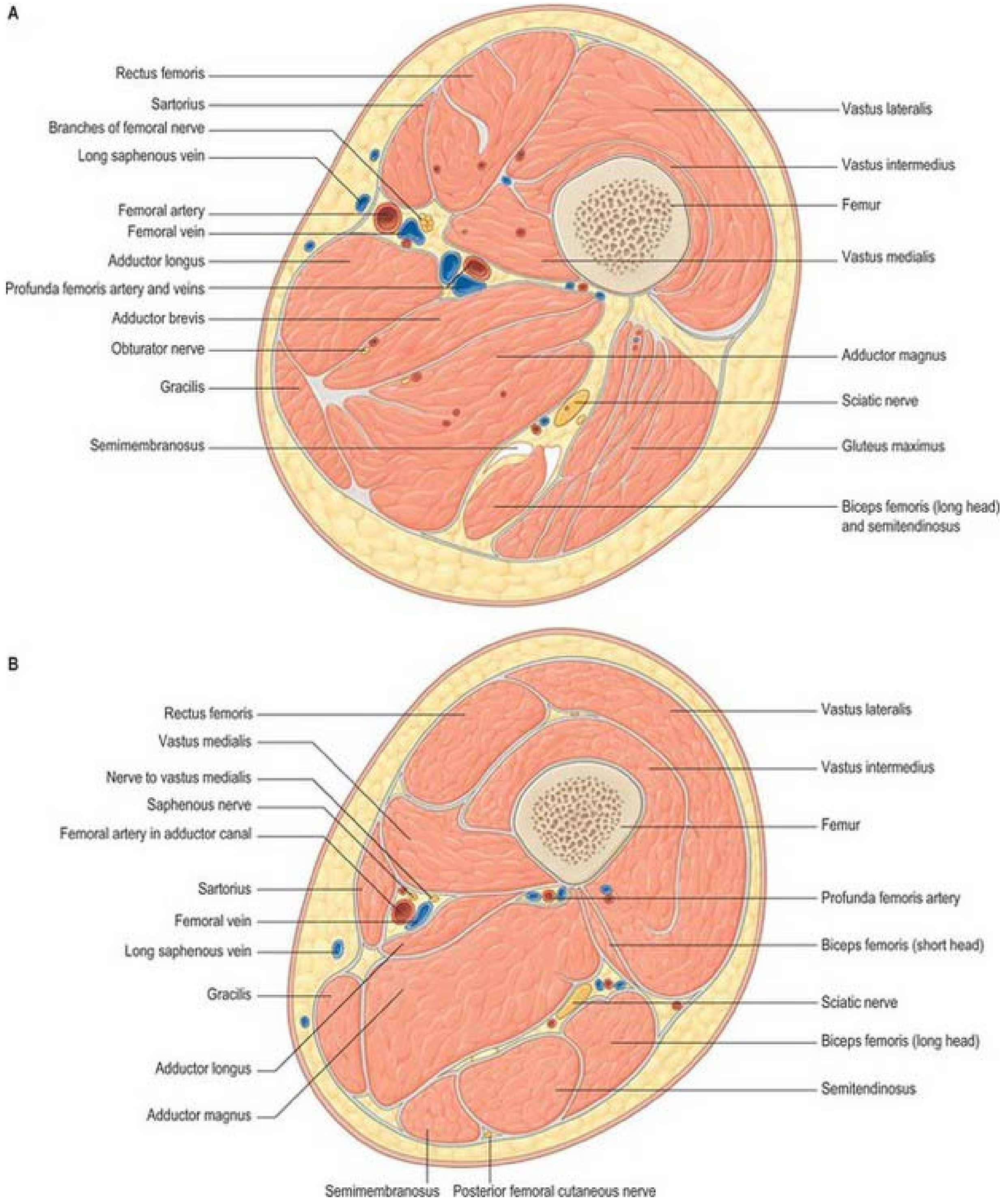
A
Rectus femoris
Sartorius
Branches of femoral nerve
Long saphenous vein
Femoral artery
Femoral vein
Adductor longus
Profunda femoris artery and veins
Adductor brevis
Obturator nerve
Gracilis
Semimembranosus
Vastus lateralis
Vastus intermedius
Femur
Vastus medialis
Adductor magnus
Sciatic nerve
Gluteus maximus
Biceps femoris (long head) and semitendinosus
B
Rectus femoris
Vastus medialis
Nerve to vastus medialis
Saphenous nerve
Femoral artery in adductor canal
Sartorius
Femoral vein
Long saphenous vein
Gracilis
Adductor longus
Adductor magnus
Semimembranosus
Posterior femoral cutaneous nerve
Vastus lateralis
Vastus intermedius
Femur
Profunda femoris artery
Biceps femoris (short head)
Sciatic nerve
Biceps femoris (long head)
Semitendinosus

Fig. 80.2 Transverse (axial) section through the thigh. **A**, At the level of the apex of the femoral triangle; **B**, at the level of the mid-thigh.

The nerve supply to the compartments of the thigh mainly follows the ‘one compartment – one nerve’ principle. Thus the femoral nerve supplies the anterior compartment muscles, the obturator nerve supplies the medial compartment muscles, and the sciatic nerve supplies those in the posterior compartment. The dual functional and compartmental attribution of adductor magnus and adductor longus and pectineus are reflected in their dual nerve supplies.

In contrast to the motor innervation, the arterial supply to the compartmental muscle groups does not exhibit such a direct relationship. All groups receive a supply from the femoral system, particularly from the profunda femoris and its branches. The adductors receive a contribution from the obturator artery, and the hamstrings receive a proximal supply from the inferior gluteal artery. Further details are given in the descriptions of the individual muscles.

Femoral sheath

The femoral sheath is a funnel-shaped distal prolongation of extraperitoneal fascia, formed of transversalis fascia anterior to the femoral vessels, and of the iliac fascia posteriorly (Fig. 80.3). It is wider proximally and its tapered distal end fuses with the vascular adventitia 3 or 4 cm distal to the inguinal ligament. At birth the sheath is shorter; it elongates when extension at the hips becomes habitual. The femoral branch of the genitofemoral nerve perforates its lateral wall. The medial wall slopes laterally and is pierced by the long (great) saphenous vein and lymphatic vessels. Like the carotid sheath, the femoral sheath encloses a mass of connective tissue in which the vessels are embedded. Three compartments are described: a lateral one containing the femoral artery, an intermediate one for the femoral vein, and a medial compartment, the femoral canal, which contains lymph vessels and an occasional lymph node embedded in areolar tissue. The presence of this canal allows the femoral vein to distend. The canal is conical and approximately 1.25 cm in length. Its proximal (wider) end, termed the femoral ring, is bounded in front by the inguinal ligament, behind by pectineus and its fascia and the pectineal ligament, medially by the crescentic, lateral edge of the lacunar ligament and laterally by the femoral vein. The spermatic cord, or the round ligament of the uterus, is just above its anterior margin, while the inferior epigastric vessels are near its anterolateral rim. It is larger in women than in men: this is due partly to the relatively greater width of the female pelvis and partly to the smaller size of the femoral vessels in women. The ring is filled by condensed extraperitoneal tissue, the femoral septum, which is covered on its proximal aspect by the parietal peritoneum. The femoral septum is traversed by numerous lymph vessels that connect the deep inguinal to the external iliac lymph nodes.

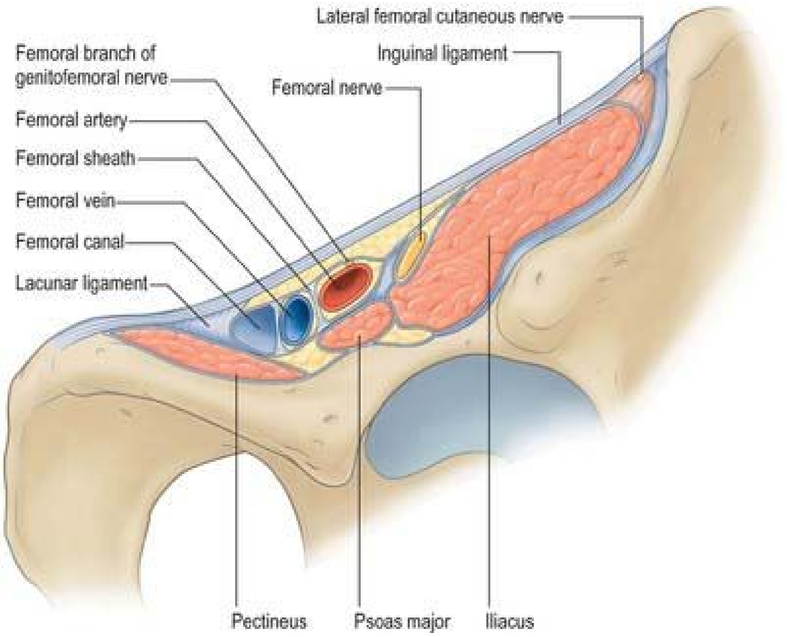
Lateral femoral cutaneous nerve
Femoral branch of genitofemoral nerve
Inguinal ligament
Femoral nerve
Femoral artery
Femoral sheath
Femoral vein
Femoral canal
Lacunar ligament
Pectineus
Psoas major
Iliacus

Fig. 80.3 Structures passing beneath the inguinal ligament.

Femoral hernia

Femoral hernia is described with other groin hernias on page 1067.

Iliac fascia

The iliac fascia covers psoas and iliacus. It is thin above, but thickens progressively towards the inguinal ligament. The part covering psoas is thickened above as the medial arcuate ligament. Medially, the fascia over psoas is attached by a series of fibrous arches to the intervertebral discs, the margins of vertebral bodies, and the upper part of the sacrum. Laterally, it blends with the fascia anterior to quadratus lumborum above the iliac crest, and with the fascia covering iliacus below the crest.

The iliac part is connected laterally to the whole of the inner lip of the iliac crest and medially to the pelvic brim, where it blends with the periosteum. It is attached to the iliopubic ramus, where it receives a slip from the tendon of psoas minor, when that muscle is present. The external iliac vessels are anterior to the fascia but the branches of the lumbar plexus are posterior. The fascia is separated from the peritoneum by loose extraperitoneal tissue. Lateral to the femoral vessels, the iliac fascia is continuous with the posterior margin of the inguinal ligament and the transversalis fascia. Medially it passes behind the femoral vessels to become the pectineal fascia, attached to the pecten pubis. At the junction of its lateral and medial parts it is attached to the iliopubic ramus and the capsule of the hip joint. It thus forms a septum between the inguinal ligament and the hip bone, dividing the space here into a lateral part, the muscular space, containing psoas major, iliacus and the femoral nerve, and a medial part, the vascular space, transmitting the femoral vessels (Fig. 80.3). The iliac fascia continues downward to form the posterior wall of the femoral sheath.

Obturator membrane

The obturator membrane (Fig. 80.4) is a thin aponeurosis that closes (obturates) most of the obturator foramen, leaving a superolateral aperture, the obturator canal, through which the obturator vessels and nerve leave the pelvis and enter the thigh. The membrane is attached to the sharp margin of the obturator foramen except at its inferolateral angle, where it is fixed to the pelvic surface of the ischial ramus, i.e. internal to the foramen. Its fibres are arranged mainly transversely in interlacing bundles; the uppermost bundle, which is attached to the obturator tubercles, completes the obturator canal. The outer and inner surfaces of the obturator membrane provide attachment for the obturator externus and internus respectively. Some fibres of the pubofemoral ligament of the hip joint are attached to the outer surface.

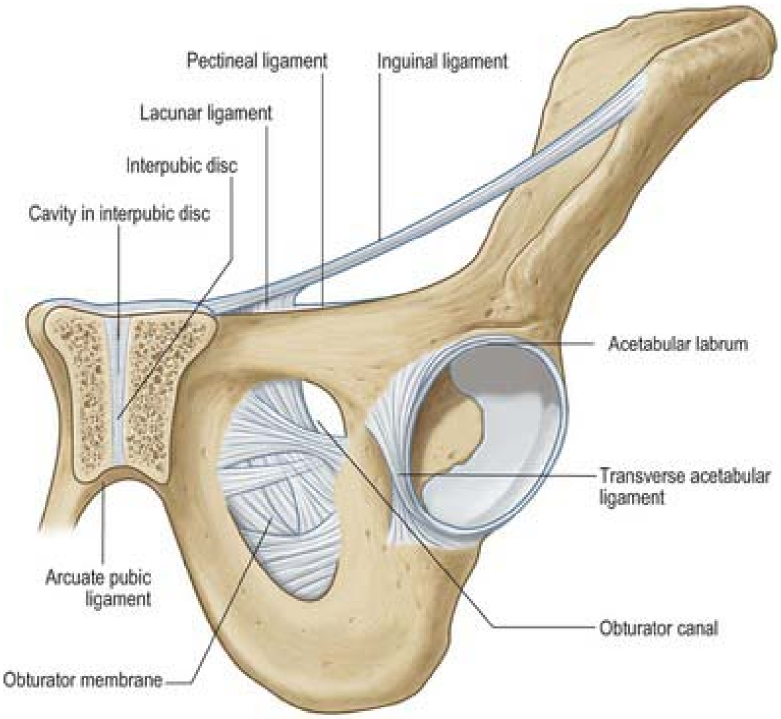
Pectineal ligament
Inguinal ligament
Lacunar ligament
Interpubic disc
Cavity in interpubic disc
Acetabular labrum
Transverse acetabular ligament
Arcuate pubic ligament
Obturator canal
Obturator membrane

Fig. 80.4 Anterolateral view of left bony pelvis, showing associated ligaments and obturator membrane. Note internal structure of pubic symphysis.

BONE

The pelvic girdle is an entity consisting of the two hip bones and the sacrum (strictly speaking, the sacrum is part of the vertebral column). These bones are virtually incapable of independent movement except in the female during parturition. The pelvic girdle is massively constructed and serves as a weightbearing and protective structure, an attachment for trunk and limb muscles, and as the skeletal framework of the birth canal.

HIP BONE

The hip bone is large, irregular, constricted centrally and expanded above and below (Fig. 80.5A,B). Its lateral surface has a deep, cup-shaped acetabulum, articulating with the femoral head, anteroinferior to which is the large, oval or triangular obturator foramen. Above the acetabulum the bone widens into an undulant plate surmounted by a sinuously curved iliac crest.

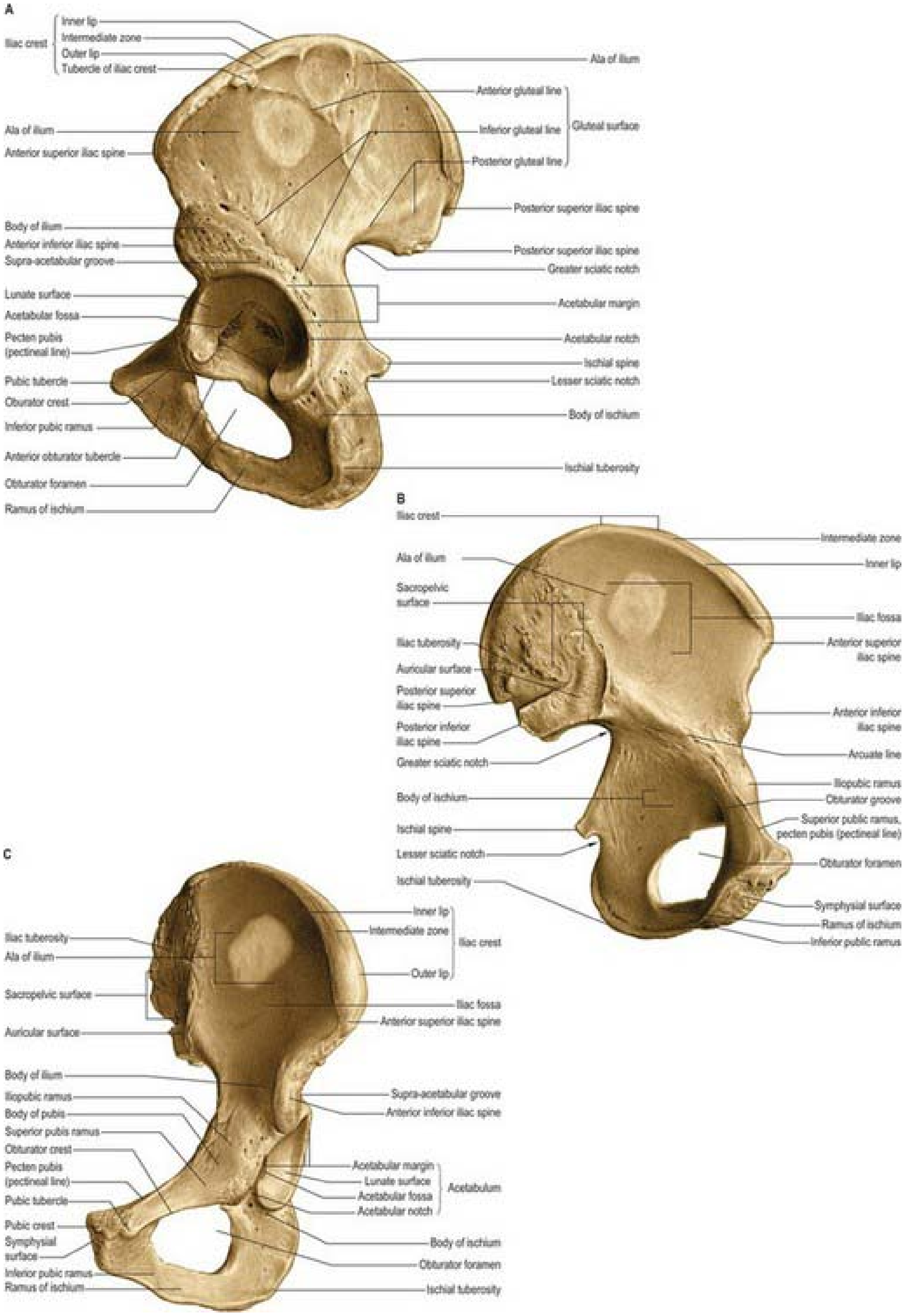
A
Iliac crest
Inner lip
Intermediate zone
Outer lip
Tubercle of iliac crest
Ala of ilium
Anterior superior iliac spine
Body of ilium
Anterior inferior iliac spine
Supra-acetabular groove
Lunate surface
Acetabular fossa
Pecten pubis (pectineal line)
Pubic tubercle
Obturator crest
Inferior pubic ramus
Anterior obturator tubercle
Obturator foramen
Ramus of ischium
Ala of ilium
Anterior gluteal line
Inferior gluteal line
Posterior gluteal line
Gluteal surface
Posterior superior iliac spine
Posterior superior iliac spine
Greater sciatic notch
Acetabular margin
Acetabular notch
Ischial spine
Lesser sciatic notch
Body of ischium
Ischial tuberosity
B
Iliac crest
Ala of ilium
Sacropelvic surface
Iliac tuberosity
Auricular surface
Posterior superior iliac spine
Posterior inferior iliac spine
Greater sciatic notch
Body of ischium
Ischial spine
Lesser sciatic notch
Ischial tuberosity
Intermediate zone
Inner lip
Iliac fossa
Anterior superior iliac spine
Anterior inferior iliac spine
Arcuate line
Iliopubic ramus
Obturator groove
Superior pubic ramus, pecten pubis (pectineal line)
Obturator foramen
Symphysial surface
Ramus of ischium
Inferior pubic ramus
C
Iliac tuberosity
Ala of ilium
Sacropelvic surface
Auricular surface
Body of ilium
Iliopubic ramus
Body of pubis
Superior pubis ramus
Obturator crest
Pecten pubis (pectineal line)
Pubic tubercle
Pubic crest
Symphysial surface
Inferior pubic ramus
Ramus of ischium
Inner lip
Intermediate zone
Iliac crest
Outer lip
Iliac fossa
Anterior superior iliac spine
Supra-acetabular groove
Anterior inferior iliac spine
Acetabular margin
Lunate surface
Acetabular fossa
Acetabular notch
Acetabulum
Body of ischium
Obturator foramen
Ischial tuberosity

Fig. 80.5 Left hip bone. **A**, Outer aspect. **B**, Inner aspect. **C**, Anterosuperior view.

(From Sobotta 2006.)

The bone articulates in front with its fellow and posteriorly with the side of the sacrum to form the pelvic girdle. Each hip bone has three parts, ilium, ischium and pubis, connected to each other by cartilage in youth but united as one bone in adults. The principal union is in the acetabulum. The ilium includes the upper acetabulum and expanded area above it; the ischium includes the lower acetabulum and bone posteroinferior to it; the pubis forms the anterior acetabulum, separating the ilium from ischium, and the anterior median region where the pubes meet.

Acetabulum

The acetabulum (Fig. 80.5A,C) is an approximately hemispherical cavity situated about the centre of the lateral aspect of the hip bone. It faces anteroinferiorly and is circumscribed by an irregular margin deficient inferiorly at the acetabular notch. The acetabular fossa forms the central floor and is rough and non-articular. The articular lunate surface is widest above (the ‘dome’), where weight is transmitted to the femur. Consequently, fractures through this region tend to be associated with unsatisfactory outcomes. All three components of the hip bone contribute to the acetabulum, although unequally. The pubis forms the anterosuperior fifth of the articular surface, the ischium forms the floor of the fossa and rather more than the posteroinferior two-fifths of the articular surface, and the ilium forms the remainder. Occasionally a linear defect may be seen to cross the acetabular surface from the superior border to the acetabular fossa This does not correspond to any junction between the main morphological parts of the hip bone.

Obturator foramen

The obturator foramen lies below and slightly anterior to the acetabulum, between the pubis and ischium. It is bordered above by the grooved obturator surface of the superior pubic ramus, medially by the pubic body and its inferior ramus, below by the ischial ramus, and laterally by the anterior border of the ischial body, including the margin of the acetabulum. The foramen is almost closed by the obturator membrane (see above), which is attached to its margins, except superolaterally, where a communication remains between the pelvis and thigh. This free edge of the membrane is attached to an anterior obturator tubercle at the anterior end of the inferior border of the superior pubic ramus, and a posterior obturator tubercle on the anterior border of the acetabular notch; these tubercles are sometimes indistinct. Since the tubercles lie in different planes and the obturator groove crosses the upper border of the foramen, the acetabular rim is in fact a spiral. The foramen is large and oval in males, but smaller and nearly triangular in females.

Structure

The thicker parts of the hip bone are trabecular, encased by two layers of compact bone, while the thinner parts, as in the acetabulum and central iliac fossa, are often translucent and consist of a single lamina of compact bone. In the upper acetabulum and along the arcuate line, i.e. the route of weight transmission from the sacrum to the femur, the amount of compact bone is increased and the subjacent trabecular bone displays two sets of pressure lamellae. These start together near the upper auricular surface and diverge to meet two strong buttresses of compact bone, from which two similar sets of lamellar arches start and converge on the acetabulum. The anterior part of the iliac crest has been much studied with regard to distribution of cortical and trabecular bone. For a survey of these studies consult Whitehouse (1977). Additionally, Whitehouse's observations, based on scanning electron micrography, indicate that the cortical bone is very porous, being only 75% bone, decreasing to 35% near the anterior superior iliac spine. Denser cortical bone starts at the margins of the crest and thickens rapidly below it on both aspects of the iliac blade.

Studies of the internal stresses within the hip bone have revealed a pattern of trabeculae that corresponds well with the theoretically expected patterns of stress trajectories (Holm 1980). These patterns are considerably more complex than in any other major bone. Stresses are higher in the acetabular than in the iliac region. In the ilium, the pelvic surface is subjected to considerably less stress than is the gluteal surface.

Muscle attachments

See individual bones.

Vascular supply

In the infant, nutrient arteries are clearly demonstrable for each component of the hip bone. Each nutrient artery branches in fan-like fashion within its bone of supply (Crock 1996). Later, a periosteal arterial network develops, with contributions from numerous local arteries (see under individual bones).

Innervation

Periosteal innervation is by a network of nerves derived from branches of local nerves. These nerves also supply muscles attaching to the periosteum and the joints involving the hip bone. Autonomic nerves accompany nutrient arteries and branch within the bone.

Ossification

Ossification (Figs 80.6, 80.7) is by three primary centres, one each for the ilium, ischium and pubis. The iliac centre appears above the greater sciatic notch prenatally at about the ninth week; the ischial centre in its body in the fourth month, and the pubic centre in its superior ramus between the fourth and fifth months. At birth the whole iliac crest, the acetabular floor and inferior margin are cartilaginous. Gradual ossification of the three components of the acetabulum results in a triradiate cartilaginous stem extending medially to the pelvic surface as a Y-shaped epiphysial plate between the ilium, ischium and pubis, and including the anterior inferior iliac spine. Cartilage along the inferior margin also covers the ischial tuberosity, forms conjoined ischial and pubic rami, and continues to the pubic symphysial surface and along the pubic crest to its tubercle.

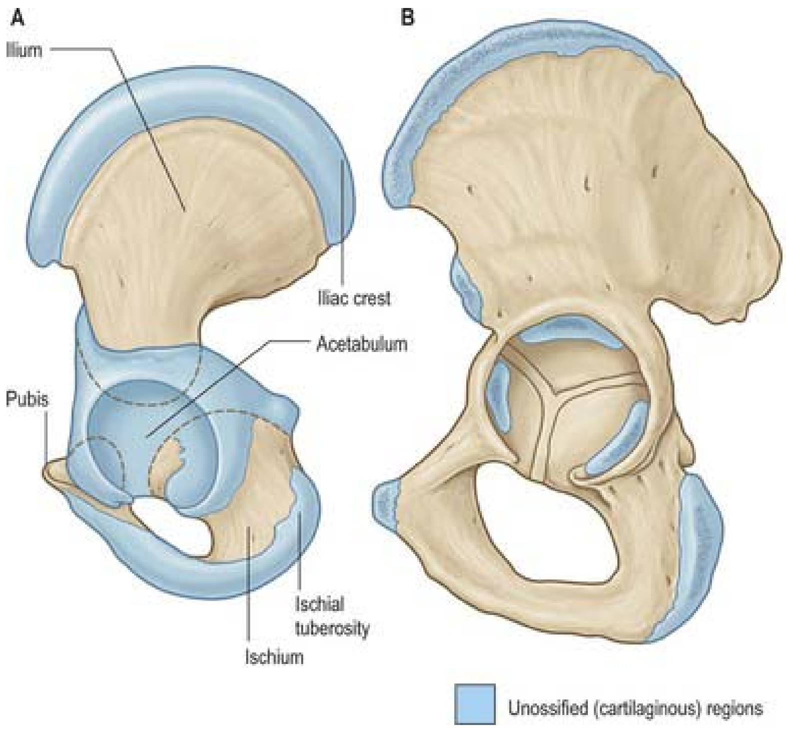
A
Ilium
Iliac crest
Acetabulum
Pubis
Ischial tuberosity
Ischium
B
Unossified (cartilaginous) regions

Fig. 80.6 The hip bone. **A**, At birth. **B**, In adolescence; more heavily stippled areas indicate the secondary centres of ossification.

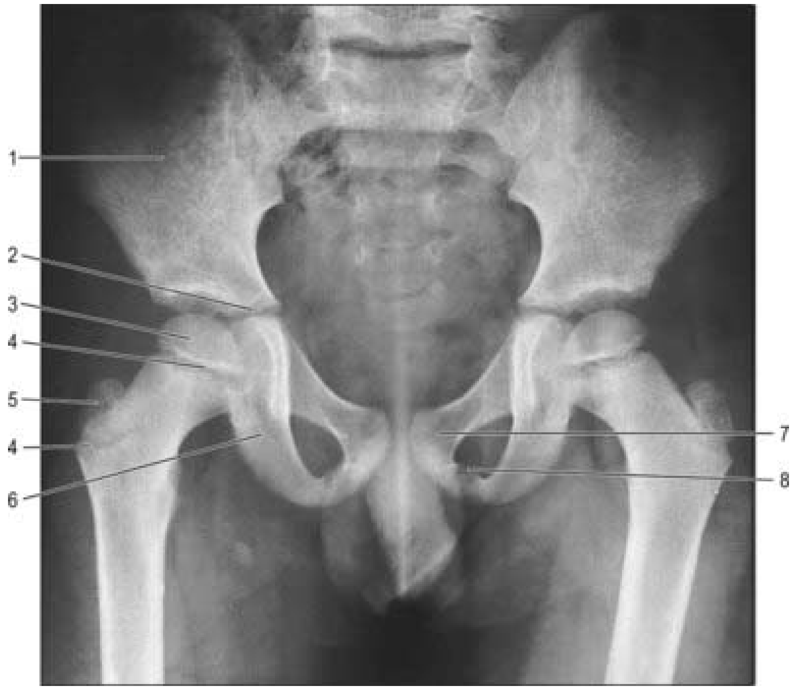

Fig. 80.7 Anteroposterior radiograph of the pelvis of a boy aged 7. **1**. Ilium. **2**. Part of triradiate growth cartilage. **3**. Superior femoral epiphysis. **4**.

Cartilaginous growth plates. **5**. Ossifying greater trochanter. **6**. Ischium. **7**. Pubis. **8**. Cartilage between pubic and ischial rami.

The ossifying ischium and pubis fuse to form a continuous ischiopubic ramus at the seventh or eighth year. Secondary centres, other than for the acetabulum, appear about puberty and fuse between the 15th and 25th years. There are usually two for the iliac crest (which fuse early), and single centres for the ischial tuberosity (in cartilage close to the inferior acetabular margin and spreading forwards), anterior inferior iliac spine (although it may ossify from the triradiate cartilage), and symphysial surface of the pubis (the pubic tubercle and crest may have separate centres). Progression of ossification of the iliac crest in girls is an index of skeletal maturity and is useful in determining the optimal timing of surgery for spinal deformity.

Between the ages of 8 and 9 years three major centres of ossification appear in the acetabular cartilage. The largest appears in the anterior wall of the acetabulum and fuses with the pubis, the second in the iliac acetabular cartilage superiorly, fusing with the ilium, and the third in the ischial acetabular cartilage posteriorly, fusing with the ischium. At puberty these epiphyses expand towards the periphery of the acetabulum and contribute to its depth (Ponseti 1978). Fusion between the three bones within the acetabulum occurs between the 16th and 18th years. Delaere et al (1992) have suggested that ossification of the ilium is similar to that of a long bone, possessing three cartilaginous epiphyses and one cartilaginous process, although it tends to undergo osteoclastic resorption comparable with that of cranial bones. During development the acetabulum increases in breadth at a faster rate than it does in depth.

Avulsion fractures of pelvic apophyses may occur from excessive pull on tendons, usually in athletic adolescents. The most frequent examples of such injuries are those to the ischial tuberosity (hamstrings) and anterior inferior iliac spine (rectus femoris).

Pubis

Topography

The pubis (Figs 80.5, 80.6) is the ventral part of the hip bone and forms a median cartilaginous pubic symphysis with its fellow. The body of the pubis occupies the anteromedial part of the bone, and from the body a superior ramus passes up and back to the acetabulum and an inferior ramus passes back, down and laterally to join the ischial ramus inferomedial to the obturator foramen.

Body

The body, anteroposteriorly compressed, has anterior, posterior and symphysial (medial) surfaces and an upper border, the pubic crest. The anterior surface also faces inferolaterally; it is rough superomedially and smooth elsewhere, giving attachment to medial femoral muscles. The smooth posterior surface faces upwards and backwards as the oblique anterior wall of the lesser pelvis and is related to the urinary bladder. The symphysial surface is elongated and oval, united by cartilage to its fellow at the pubic symphysis. Denuded of cartilage it has an irregular surface of small ridges and furrows or nodular elevations, varying considerably with age, features which are of forensic interest. The pubic crest is the rounded upper border of the body which overhangs the anterior surface; its lateral end is the rounded pubic tubercle. Both crest and tubercle are palpable, the latter partly obscured in males by the spermatic cord that crosses above it from the scrotum to the abdomen. The pubic rami diverge posterolaterally from the superolateral corners of the body.

The anterior surface of the pubic body faces the femoral adductor region. The anterior pubic ligament attaches to its medial part along a rough strip, which is wider in females. The posterior surface is separated from the urinary bladder by retropubic fat. The puboprostatic ligaments are attached to this surface medial to levator ani.

Superior pubic ramus

The superior pubic ramus passes upwards, backwards and laterally from the body, superolateral to the obturator foramen, to reach the acetabulum. It is triangular in section and has three surfaces and borders. Its anterior, pectineal surface, tilted slightly up, is triangular in outline and extends from the pubic tubercle to the iliopubic ramus. It is bounded in front by the rounded obturator crest and behind by the sharp pecten pubis (pectineal line) which, with the crest, is the pubic part of the linea terminalis (i.e. anterior part of the pelvic brim). The posterosuperior, pelvic surface, medially inclined, is smooth and narrows into the posterior surface of the body, which is bounded above by the pecten pubis and below by a sharp inferior border. The obturator surface, directed down and back, is crossed by the obturator groove sloping down and forwards. Its anterior limit is the obturator crest and its posterior limit is the inferior border.

Inferior pubic ramus

The inferior pubic ramus, an inferolateral process of the body, descends inferolaterally to join the ischial ramus medial to, and below, the obturator foramen. The union may be locally thickened, but not obviously so in adults. The ramus has two surfaces and borders. The anterolateral surface, continuous above with that of the pubic body, faces the thigh and is marked by muscles. It is limited laterally by the margin of the obturator foramen and, medially, by the rough anterior border. The posteromedial surface is continuous above with that of the body and is transversely convex: its medial part is often everted in males and gives attachment to the crus of the penis. This surface faces the perineum medially, its smooth lateral part tilted up towards the pelvic cavity.

The internal surface is indistinctly divided into medial, intermediate and lateral areas. The medial area faces inferomedially in direct contact with the crus of the penis or clitoris and is limited above and behind by an indistinct ridge for attachment of the fascia overlying the superficial perineal muscles. The medial margin of the ramus, strongly everted in males, provides attachment for the fascia lata and the membranous layer of the superficial perineal fascia.

Pubic tubercle

The pubic tubercle provides attachment to the medial end of the inguinal ligament. It forms part of the floor of the superficial inguinal ring and is crossed by the spermatic cord.

Pecten pubis

The pecten pubis is the sharp, superior edge of the pectineal surface. The conjoint tendon and lacunar ligament are attached at its medial end and a strong, fibrous, pectineal ligament is attached along the rest of its surface. The smooth pelvic surface is separated from parietal peritoneum only by areolar tissue, in which the lateral umbilical ligament descends forwards across the ramus and, laterally, the vas deferens passes backwards. The obturator groove, which is converted to a canal by the upper borders of the obturator membrane and obturator muscles, transmits the obturator vessels and nerve from the pelvis to the thigh. Some fibres of the pubofemoral ligament are attached to the lateral end of the obturator crest.

Muscle attachments

The tendon of adductor longus is attached on the anterior (external) surface of the body, below the pubic crest. Below adductor longus, gracilis is attached to a line near the lower margin extending down onto the inferior ramus. Above gracilis, adductor brevis is attached to the body and inferior ramus. Above again, obturator externus is attached to the anterior surface, spreading onto inferior pubic and ischial rami. Adductor magnus usually extends from the ischial ramus on to the lower part of the inferior pubic ramus between adductor brevis and obturator externus. Pectineus is attached to the pectineal surface of the superior ramus along its upper part. Ascending loops of cremaster are attached to the pubic tubercle. The lateral part of rectus abdominis and, inferiorly, pyramidalis, are attached lateral to the tubercle, on the pubic crest. Medially the crest is crossed by the medial part of rectus abdominis, ascending from ligamentous fibres that interlace in front of the pubic symphysis. Anterior fibres of levator ani are attached on the posterior (internal) surface of the body near its centre. More laterally, obturator internus is attached on this surface, extending onto both rami. Psoas minor, when present, is attached near the centre of the pecten pubis.

Vascular supply

The pubis is supplied by a periosteal anastomosis of branches from the obturator, inferior epigastric and medial circumflex femoral arteries. The superficial and deep external pudendal arteries may also contribute. Multiple vascular foramina are present, mainly at the lateral (acetabular) end of the bone, but there is no consistently placed nutrient foramen.

Innervation

The periosteum of the pubis is innervated by branches of nerves that supply muscles attached to the bone, the hip joint and the symphysis pubis.

Ossification

Ossification of the pubis is described on page 1354.

Ilium

Topography

The ilium has upper and lower parts and three surfaces (Figs 80.5, 80.6). The smaller, lower part forms a little less than the upper two-fifths of the acetabulum. The upper part is much expanded, and has gluteal, sacropelvic and iliac (internal) surfaces. The posterolateral gluteal surface is an extensive rough area; the anteromedial iliac fossa is smooth and concave; the sacropelvic surface is medial and posteroinferior to the fossa, from which it is separated by the medial border.

Iliac crest

The iliac crest is the superior border of the ilium. It is convex upwards but sinuous from side to side, being internally concave in front, and convex behind. Its ends project as anterior and posterior superior iliac spines. The anterior superior iliac spine is palpable at the lateral end of the inguinal fold; the lateral end of the inguinal ligament is attached to the anterior superior iliac spine. The posterior superior iliac spine is not palpable but is often indicated by a dimple, approximately 4 cm lateral to the second sacral spinous process, above the medial gluteal region (buttock).

The crest has ventral and dorsal segments. The ventral occupies slightly more than the anterior two-thirds of the crest and its prominence is associated with changes in iliac form as a result of the emergence of the upright posture; the dorsal segment, which occupies approximately the posterior third in man, is a feature of all land vertebrates. The ventral segment of the crest has internal and external lips and the rough intermediate zone is narrowest centrally. The tubercle of the crest projects outwards from the outer lip approximately 5 cm posterosuperior to the anterior superior spine. The dorsal segment has two sloping surfaces separated by a longitudinal ridge ending at the posterior superior spine. The summit of the crest, a little behind its midpoint, is level with the fourth lumbar vertebral body. The interosseous and posterior sacroiliac ligaments arise from the medial margin of the dorsal segment.

Anterior border

The anterior border descends to the acetabulum from the anterior superior spine. Superiorly it is concave forwards. Inferiorly, immediately above the acetabulum, is a rough anterior inferior iliac spine, which is divided indistinctly into an upper area for the straight part of rectus femoris and a lower area extending laterally along the upper acetabular margin to form a triangular impression for the proximal end of the iliofemoral ligament.

Posterior border

The posterior border is irregularly curved and descends from the posterior superior spine, at first forwards, with a posterior concavity forming a small notch. At the lower end of the notch is a wide, low projection, the posterior inferior iliac spine. Here the border turns almost horizontally forwards for approximately 3 cm, then down and back to join the posterior ischial border. Together these borders form a deep notch, the greater sciatic notch, that is bounded above by the ilium and below by the ilium and ischium. The upper fibres of the sacrotuberous ligament are attached to the upper part of the posterior border. The superior rim of the notch is related to the superior gluteal vessels and nerve. The lower margin of the greater sciatic notch is covered by piriformis and related to the sciatic nerve.

Medial border

The medial border separates the iliac fossa and the sacropelvic surface. It is indistinct near the crest, rough in its upper part, then sharp where it bounds an articular surface for the sacrum, and finally rounded. The latter part is the arcuate line, which inferiorly reaches the posterior part of the iliopubic ramus, marking the union of the ilium and pubis.

Gluteal surface

The gluteal surface, facing inferiorly in its posterior part and laterally and slightly downwards in front, is bounded above by the iliac crest, below by the upper acetabular border and by the anterior and posterior borders. It is rough and curved, convex in front, concave behind, and marked by three gluteal lines. The posterior gluteal line is shortest, descending from the external lip of the crest approximately 5 cm in front of its posterior limit and ending in front of the posterior inferior iliac spine. Above, it is usually distinct, but inferiorly it is ill-defined and frequently absent. The anterior gluteal line, the longest, begins near the midpoint of the superior margin of the greater sciatic notch and ascends forwards into the outer lip of the crest, a little anterior to its tubercle. The inferior gluteal line, seldom well-marked, begins posterosuperior to the anterior inferior iliac spine, curving posteroinferiorly to end near the apex of the greater sciatic notch. Between the inferior gluteal line and the acetabular margin is a rough, shallow groove. Behind the acetabulum the lower gluteal surface is continuous with the posterior ischial surface, the conjunction marked by a low elevation.

The articular capsule is attached to an area adjoining the acetabular rim, most of which is covered by gluteus minimus. Posteroinferiorly, near the union of the ilium and ischium, the bone is related to piriformis.

Iliac fossa

The iliac fossa, the internal concavity of the ilium, faces anterosuperiorly. It is limited above by the iliac crest, in front by the anterior border and behind by the medial border, separating it from the sacropelvic surface. It forms the smooth and gently concave posterolateral wall of the greater pelvis. Below it is continuous with a wide shallow groove which is bounded laterally by the anterior inferior iliac spine and medially by the iliopubic ramus.

The wide groove between the anterior inferior iliac spine and the iliopubic ramus is occupied by the converging fibres of iliacus laterally and the tendon of psoas major medially: the tendon is separated from the underlying bone by a bursa. The right iliac fossa contains the caecum, and often the vermiform appendix and terminal ileum. The left iliac fossa houses the terminal part of the descending colon and the proximal sigmoid colon.

Sacropelvic surface

The sacropelvic surface, the posteroinferior part of the medial iliac surface, is bounded posteroinferiorly by the posterior border, anterosuperiorly by the medial border, posterosuperiorly by the iliac crest and anteroinferiorly by the line of fusion of the ilium and ischium. It is divided into iliac tuberosity, auricular and pelvic surfaces. The iliac tuberosity, a large, rough area below the dorsal segment of the iliac crest, shows cranial and caudal areas separated by an oblique ridge and connected to the sacrum by the interosseous sacroiliac ligament. The sacropelvic surface gives attachment to the posterior sacroiliac ligaments and, behind the auricular surface, to the interosseous sacroiliac ligament. The iliolumbar ligament is attached to its anterior part. The auricular surface, immediately anteroinferior to the tuberosity, articulates with the lateral sacral mass. Shaped like an ear, its widest part is anterosuperior, its ‘lobule’ posteroinferior and on the medial aspect of the posterior inferior spine. Its edges are well defined, but the surface, though articular, is rough and irregular. It articulates with the sacrum and is reciprocally shaped. The anterior sacroiliac ligament is attached to its sharp anterior and inferior borders. The narrow part of the pelvic surface, between the auricular surface and the upper rim of the greater sciatic notch, often shows a rough preauricular sulcus (that is usually better defined in females) for the lower fibres of the anterior sacroiliac ligament. For the reliability of this feature as a sex discriminant, refer to Finnegan (1978) and Brothwell & Pollard (2001). The pelvic surface is anteroinferior to the acutely recurved part of the auricular surface, and contributes to the lateral wall of the lesser pelvis. Its upper part, facing down, is between the auricular surface and the upper limb of the greater sciatic notch. Its lower part faces medially and is separated from the iliac fossa by the arcuate line. Anteroinferiorly it extends to the line of union between the ilium and ischium. Though usually obliterated, it passes from the depth of the acetabulum to approximately the middle of the inferior limb of the greater sciatic notch.

Muscle attachments

The attachment of sartorius extends down the anterior border below the anterior superior iliac spine. The iliac crest gives attachment to the anterolateral and dorsal abdominal muscles, and to the fasciae and muscles of the lower limb. The fascia lata and iliotibial tract are attached to the outer lip and tubercle of its ventral segment. Tensor fasciae latae is attached anterior to the tubercle. The lower fibres of external oblique and, just behind the summit of the crest, the lowest fibres of latissimus dorsi are attached to its anterior two-thirds. A variable interval exists between the most posterior attachment of external oblique and the most anterior attachment of latissimus dorsi, and here the crest forms the base of the lumbar triangle. Internal oblique is attached to the intermediate area of the crest. Transversus abdominis is attached to the anterior two-thirds of the inner lip of the crest, and behind this to the thoracolumbar fascia and quadratus lumborum. The highest fibres of gluteus maximus are attached to the dorsal segment of the crest on its lateral slope. Erector spinae arises from the medial slope of the dorsal segment. The straight part of rectus femoris is attached to the upper area of the anterior inferior spine. Some fibres of piriformis are attached in front of the posterior inferior spine on the upper border of the greater sciatic notch.

The gluteal surface is divided by three gluteal lines into four areas. Behind the posterior line, the upper rough part gives attachment to the upper fibres of gluteus maximus and the lower, smooth region to part of the sacrotuberous ligament and iliac head of piriformis. Gluteus medius is attached between the posterior and anterior lines, below the iliac crest, and gluteus minimus is attached between the anterior and inferior lines. The fourth area, below the inferior line, contains vascular foramina.

The reflected head of rectus femoris attaches to a curved groove above the acetabulum. Iliacus is attached to the upper two-thirds of the iliac fossa and is related to its lower third. The medial part of quadratus lumborum is attached to the anterior part of the sacropelvic surface, above the iliolumbar ligament. Piriformis is sometimes partly attached lateral to the preauricular sulcus, and part of obturator internus is attached to the more extensive remainder of the pelvic surface.

Vascular supply

Branches of the iliolumbar artery run between iliacus and bone; one or more enter large nutrient foramina lying posteroinferiorly in the iliac fossa. The superior gluteal, obturator and superficial circumflex iliac arteries contribute to the periosteal supply. The obturator artery may supply a nutrient branch. Vascular foramina on the iliac gluteal aspect may lead into large vascular canals in the bone.

Innervation

The periosteum is innervated by branches of nerves that supply muscles attached to the bone, the hip joint and the sacroiliac joint.

Ossification

Ossification of the ilium is described on page 1354.

Ischium

Topography

The ischium, the inferoposterior part of the hip bone, has a body and ramus. The body has upper and lower ends and femoral, posterior and pelvic surfaces (Figs 80.5, 80.6). Above, it forms the posteroinferior part of the acetabulum; below, its ramus ascends anteromedially at an acute angle to meet the inferior pubic ramus, thereby completing the boundary of the obturator foramen. The ischiofemoral ligament is attached to the lateral border below the acetabulum.

The femoral surface faces downwards, forwards and laterally towards the thigh. It is bounded in front by the margin of the obturator foramen. The lateral border, indistinct above but well defined below, forms the lateral limit of the ischial tuberosity. At a higher level the femoral surface is covered by piriformis, from which it is partially separated by the sciatic nerve and the nerve to quadratus femoris. The posterior surface, facing superolaterally, is continuous above with the iliac gluteal surface, and here a low convexity follows the acetabular curvature. Inferiorly, this surface forms the upper part of the ischial tuberosity, above which is a wide, shallow groove on its lateral and medial aspects. Above the ischial tuberosity the posterior surface is crossed by the tendon of obturator internus and the gemelli. The nerve to quadratus femoris lies between these structures and the bone. The ischial tuberosity is a large, rough area on the lower posterior surface and inferior extremity of the ischium. Though obscured by gluteus maximus in hip extension, it is palpable in flexion. It is 5 cm from the midline and about the same distance above the gluteal fold. It is elongated, widest above, and tapers inferiorly. The ischial posterior aspect lies between the lateral and posterior borders. The posterior border blends above with that of the ilium, helping to complete the inferior rim of the greater sciatic notch, the posterior end of which has a conspicuous ischial spine. Below this, the rounded border forms the floor of the lesser sciatic notch, between the ischial spine and tuberosity. The pelvic surface is smooth and faces the pelvic cavity; inferiorly it forms part of the lateral wall of the ischio-anal fossa.

Ischial ramus

The ischial ramus has anteroinferior and posterior surfaces continuous with the corresponding surfaces of the inferior pubic ramus: the anteroinferior surface is roughened by the attachment of the medial femoral muscles. The smooth posterior surface is partly divided into perineal and pelvic areas, like the inferior pubic ramus. The upper border completes the obturator foramen; the rough lower border, together with the medial border of the inferior pubic ramus, contributes to the pubic arch. The fascia overlying the superficial perineal muscles is attached below the ridge between the perineal and pelvic areas of the posterior surface of the ischial ramus. Above the ridge areas give attachment to the crus of the penis or clitoris and the sphincter urethrae. The lower border of the ramus provides an attachment for the fascia lata and a membranous layer of the superficial perineal fascia.

Ischial tuberosity

The ischial tuberosity is divided nearly transversely into upper and lower areas. The upper area is subdivided by an oblique line into a superolateral and an inferomedial part. The lower area, narrowing as it curves onto the inferior ischial aspect, is subdivided by an irregular vertical ridge into lateral and medial areas. The medial is covered by fibroadipose tissue that usually contains the ischial bursa of gluteus maximus, which supports the body in sitting. Medially the tuberosity is limited by a curved ridge that passes on to the ramus and which gives attachment to the sacrotuberous ligament and its falciform process.

Ischial spine

The ischial spine projects downwards and a little medially (Fig. 80.8). The sacrospinous ligament is attached to its margins, separating the greater from the lesser sciatic foramen. The ligament is crossed posteriorly by the internal pudendal vessels, pudendal nerve and the nerve to obturator internus.

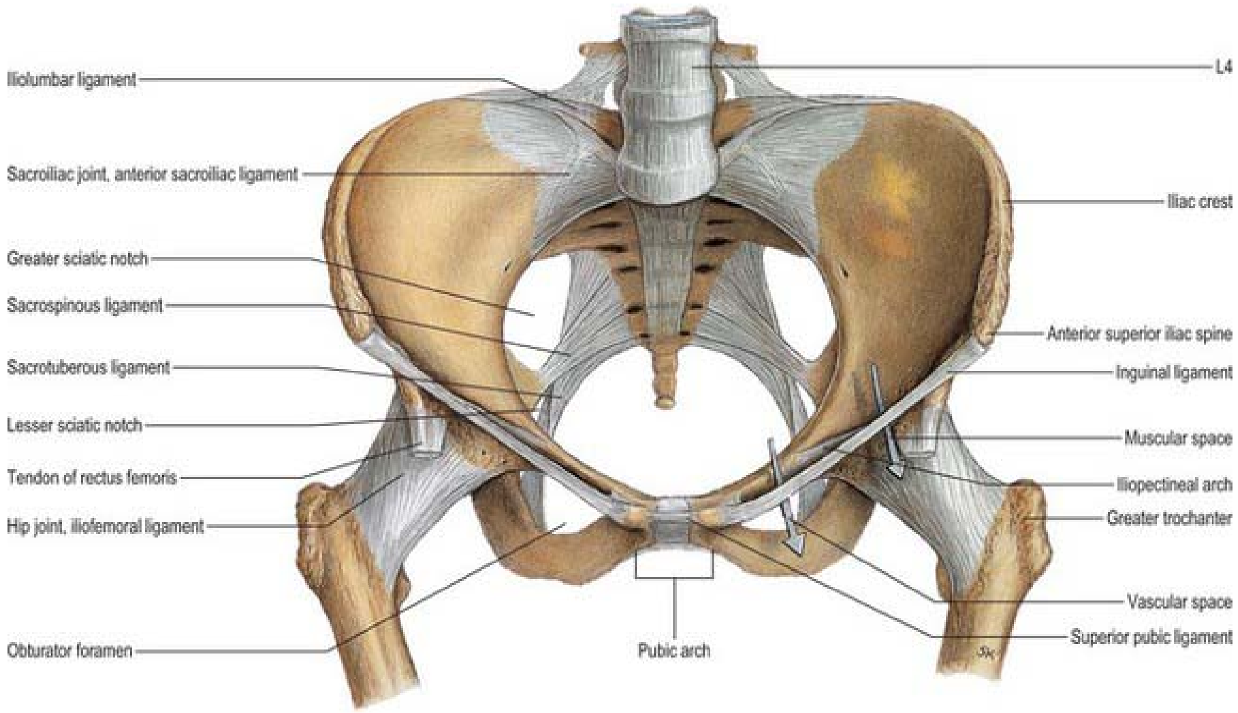
Iliolumbar ligament
L4
Sacroiliac joint, anterior sacroiliac ligament
Iliac crest
Greater sciatic notch
Sacrospinous ligament
Anterior superior iliac spine
Sacrotuberous ligament
Inguinal ligament
Lesser sciatic notch
Muscular space
Tendon of rectus femoris
Iliopectineal arch
Hip joint, iliofemoral ligament
Greater trochanter
Vascular space
Superior pubic ligament
Obturator foramen
Pubic arch

Fig. 80.8 Joints and ligaments of the pelvis: anterior aspect. Note arrows indicating vascular and muscular spaces.

(From Sobotta 2006.)

Muscle attachments

Part of obturator externus is attached to the lower femoral surface of the ischial body. Part of obturator externus, the anterior fibres of adductor magnus and, near the lower border, gracilis, are all attached to the anterior surface of the ischial ramus. Between adductor magnus and gracilis the attachment of adductor brevis may descend from the inferior pubic ramus. The posterior surface is divided into pelvic and perineal areas. The pelvic area, facing back, has part of obturator internus attached to it. The perineal area faces medially; its upper part is related to the crus of the penis or clitoris, and its lower part gives attachment to sphincter urethrae, ischiocavernosus and the transverse superficial perineal muscle.

The ischial tuberosity gives attachment to the posterior femoral muscles. Quadratus femoris is attached along the upper part of its lateral border. The upper area of the tuberosity is subdivided by an oblique line into a superolateral part for semimembranosus and an inferomedial part for the long head of biceps femoris and semitendinosus. The lower area is subdivided by an irregular vertical ridge into lateral and medial areas. The larger lateral area is for part of adductor magnus. Superomedial to the tuberosity the posterior surface has a wide, shallow groove, usually covered by hyaline cartilage, with a bursa between it and the tendon of obturator internus. Gemellus inferior is attached to the lower margin of the groove, near the tuberosity. Gemellus superior is attached to the upper margin, near the ischial spine.

The pelvic surface of the ischial spine gives attachment to coccygeus (coextensive with the sacrospinous ligament) and to the most posterior fibres of levator ani. Obturator internus is attached to the upper part of the smooth pelvic ischial surface and converges on the lesser sciatic notch, covering the rest of this surface other than the pelvic aspect of the ischial spine: the muscle and its fascia separate the bone from the ischiorectal fossa.

Vascular supply

There are multiple vascular foramina at the acetabular margins, and a few are usually present on the pelvic surface. The bone is supplied by branches of the obturator, medial circumflex femoral and inferior gluteal arteries.

Innervation

The periosteum is innervated by branches of nerves that supply the hip joint and muscles attached to the bone.

Ossification

Ossification of the ischium is described on page 1354.

SACRUM

See page 724.

COCCYX

See page 728.

SKELETAL PELVIS AS A WHOLE

The term pelvis (‘basin’) is applied variously to the skeletal ring formed by the hip bones and the sacrum, the cavity therein, and even the entire region where the trunk and lower limbs meet. It is used here in the skeletal sense, to describe the irregular osseous girdle between the femoral heads and fifth lumbar vertebra. It is large because its primary function is to withstand the forces of body weight and musculature. In this section, its obstetric, forensic and anthropological significance will be considered.

The pelvis can be regarded as having greater and lesser segments, the true and false pelves. The segments are arbitrarily divided by an oblique plane passing through the sacral promontory posteriorly and the lineae terminales elsewhere. Each linea terminalis includes the iliac arcuate line, pectineal line (pecten), and pubic crest. The segments are continuous, and the parts of the body cavity that they enclose are also continuous through the pelvic inlet (pelvic inlet).

Greater pelvis

The greater pelvis consists of the ilium and pubis above the lineae terminales and the sacral base. This junctional zone is structurally massive and forms powerful arches from the acetabular fossae to the vertebral column around the visceral cavity, which is part of the abdomen. It has little anterior wall because of the pelvic inclination.

Pelvic inlet (superior pelvic aperture)

The pelvic inlet or brim may be round or oval, and is indented posteriorly by the sacral promontory. The pelvic brim is obstetrically important and has also long been measured for anthropological reasons, as has the pelvic cavity.

By convention, the pelvic inlet is described in three dimensions. The anteroposterior diameter (true conjugate) is measured between the midpoints of the sacral promontory and upper border of the symphysis pubis and on average is 10 cm in the adult male and 11.2 cm in the adult female. The transverse diameter is the maximum distance between similar points (assessed by eye) on opposite sides of the pelvic brim and is on average 12.5 cm in the male and 13.1 cm in the adult female. The oblique diameter is measured from the iliopubic ramus to the opposite sacroiliac joint and is on average 12 cm in the adult male and 12.5 cm in the adult female. These measurements vary with the individual and racial group.

Articulated bony pelvis

The lesser pelvis encloses a true basin when soft tissues of the pelvic floor are in place. Skeletally it is a narrower continuation of the greater pelvis, with irregular but more complete walls around its cavity. Of obstetric importance, it has a curved median axis, and superior and inferior openings. The superior opening is occupied by viscera. The pelvic floor, viscera and subjacent perineal sphincters close the inferior opening.

Cavity of the lesser pelvis

The cavity of the lesser pelvis is short, curved, and markedly longer in its posterior wall. Anteroinferiorly it is bounded by pubic bones, their rami and symphysis. Posteriorly it is bounded by the concave anterior sacral surface and coccyx. Laterally on each side its margins are the smooth quadrangular pelvic aspect of the fused ilium and ischium. The region so enclosed is the pelvic cavity proper, through which pass the rectum, bladder and parts of the reproductive organs. The cavity in females must also permit passage of the fetal head.

The pelvic cavity diameters are measured at approximately the mid level. The anteroposterior diameter is measured between the midpoints of the third sacral segment and posterior surface of the symphysis pubis and is about 10.5 cm in the male and 13 cm in the adult female. The transverse diameter is the widest transverse distance between the side walls of the cavity, and often the greatest transverse dimension in the whole cavity. It measures about 12 cm in the adult male and 12.5 cm in the adult female. The oblique diameter is the distance from the lowest point of one sacroiliac joint to the midpoint of the contralateral obturator membrane and measures about 11 cm in the male and 13.1 cm in the adult female. All measurements vary with the individual and racial group.

Pelvic outlet (inferior pelvic aperture)

Less regular in outline than the pelvic inlet, the pelvic outlet is indented behind by the coccyx and sacrum and bilaterally by the ischial tuberosities. Its perimeter thus consists of three wide arcs. Anteriorly is the pubic arch, between the converging ischiopubic rami. Posteriorly and laterally on both sides are the sciatic notches between the sacrum and ischial tuberosities. These are divided by the sacrotuberous and sacrospinous ligaments into greater and lesser sciatic foramina.

With ligaments included, the pelvic outlet is rhomboidal. Its anterior limbs are the ischiopubic rami (joined by the inferior pubic ligament) and its posterior margins are the sacrotuberous ligaments, with the coccyx in the midline. The outlet is thus not rigid in its posterior half, being limited by ligaments and the coccyx, all slightly yielding. Even with the sacrum taken as the posterior midline limit (more reliable for measurement), there may be slight mobility at the sacroiliac joints. Note also that a plane of the pelvic outlet is merely conceptual. The anterior, ischiopubic part has a plane which is inclined down and back to a transverse line between the lower limits of the ischial tuberosities, and the posterior half has a plane approximating to the sacrotuberous ligaments, sloping down and forwards to the same line.

Three measurements are made for the pelvic outlet. The anteroposterior diameter is usually measured from the coccygeal apex to the midpoint of the lower rim of the symphysis. The lowest sacral point may also be used (on average male 8 cm, female 12.5 cm). The transverse (bituberous) diameter is measured between the ischial tuberosities at the lower borders of their medial surfaces (on average male 8.5 cm, female 11.8 cm). The oblique diameter extends from the midpoint of the sacrotuberous ligament on one side to the contralateral ischiopubic junction (on average male 10 cm, female 11.8 cm). All measurements vary with the individual and racial group.

Other measurements

Apart from these main measurements, by consensus the basis of pelvic osteometry, other planes and measurements are used in obstetric practice. The plane of greatest pelvic dimensions is an obstetric concept. It represents the most capacious pelvic level, between the pelvic brim and midlevel plane, and corresponds with the latter anteriorly at the middle part of the symphysis pubis and posteriorly at the level of the second and third sacral segments.

The plane of least dimensions is said to be at about midpelvic level. Its transverse diameter is between the apices of the ischial spines. This measurement is about 9.5 cm in an adult female and is just wide enough to allow passage of the biparietal diameter of a fetal head (about 9 cm). Not surprisingly, most difficulty in parturition occurs here.

The above measurements are sometimes made in clinical practice using X-ray or MRI pelvimetry. Precise measurement is not possible without radiological techniques, and even these do not take into account the soft tissues. In the past, measurements were made at physical and vaginal examination. However, these manual measurements have proved to be of little clinical value and are now obsolete.

Morphological classification of pelves

Interest in the dimensions described above is primarily obstetric and, less frequently, forensic. All pelvic measurements display individual variation and the values quoted are means from limited surveys. Sexual and racial differences also occur. These measurements have been analysed by many anatomists, anthropologists, obstetricians and radiologists in attempts to classify human pelves, especially female. The four most common terms used today are gynaecoid, anthropoid, platypelloid and android. The gynaecoid pelvis is the traditional Western female pelvis with a heart-shaped brim and the range of measurements quoted above. An anthropoid pelvis has a larger midcavity and a wide anteroposterior inlet which is oval in shape: it is more common in women of African origin and may be associated with a ‘high assimilation’ pelvis where there is an additional lumbar vertebra. A platypelloid pelvis is flat and oval from side to side at the brim: it is a contracted pelvis that is rarely seen nowadays, having previously been associated with rickets. An android pelvis has a triangular brim and is the shape of a male pelvis.

Pelvic axes and inclination

The axis of the superior pelvic aperture traverses its centre at right angles to its plane, directed down and backwards (Fig. 80.9). When prolonged (projected) it passes through the umbilicus and midcoccyx. An axis is similarly established for the inferior aperture: projected upwards it impinges on the sacral promontory. Axes can likewise be constructed for any plane, and one for the whole cavity is a concatenation of an infinite series of such lines (Fig. 80.9). The fetal head, however, descends in the axis of the inlet as far as the level of the ischial spines; it is then directed forwards into the axis of the vagina at right angles to that axis. The form of this pelvic axis and the disparity in depth between the anterior and posterior contours of the cavity are prime factors in the mechanism of fetal transit in the pelvic canal.

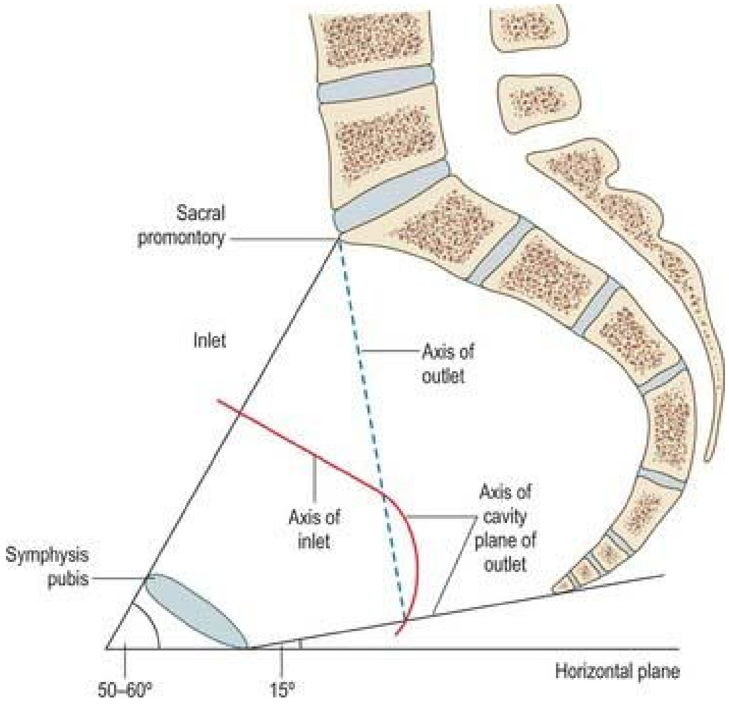
Sacral promontory
Inlet
Axis of outlet
Axis of inlet
Axis of cavity plane of outlet
Symphysis pubis
50–60°
15°
Horizontal plane

Fig. 80.9 Median sagittal section through the female pelvis, showing the planes of the inlet and outlet and the axis of the pelvic cavity.

In the standing position the pelvic canal curves obliquely backwards relative to the trunk and abdominal cavity. The whole pelvis is tilted forwards, the plane of the pelvic brim making an angle of 50–60° with the horizontal. The plane of the pelvic outlet is tilted to about 15°. Strictly, the pelvic outlet has two planes, an anterior passing backwards from the pubic symphysis and a posterior passing forwards from the coccyx, both descending to meet at the intertuberous line. In standing, the pelvic aspect of the symphysis pubis faces nearly as much upwards as backwards and the sacral concavity is directed anteroinferiorly. The front of the symphysis and anterior superior iliac spines are in the same vertical plane. In sitting, body weight is transmitted through inferomedial parts of the ischial tuberosities, with variable soft tissues intervening. The anterior superior iliac spines are in a vertical plane through the acetabular centres, and the whole pelvis is tilted back with the lumbosacral angle somewhat diminished at the sacral promontory.

Pelvic mechanism

The skeletal pelvis supports and protects the contained viscera, but is primarily part of the lower limbs, affording wide attachment for leg and trunk muscles. It constitutes the major mechanism for transmitting the weight of the head, trunk and upper limbs to the lower limbs. It may be considered as two arches divided by a coronal transacetabular plane. The posterior arch, chiefly concerned in transmitting weight, consists of the upper three sacral vertebrae and strong pillars of bone from the sacroiliac joints to the acetabular fossae. The anterior arch, formed by the pubic bones and their superior rami, connects these lateral pillars as a tie beam to prevent separation; it also acts as a compression strut against medial femoral thrust. The sacrum, as the summit of the posterior arch, is loaded at the lumbosacral joint. Theoretically this force has two components, one thrusting the sacrum downwards and backwards between the iliac bones, the other thrusting its upper end downwards and forwards. Sacral movements are regulated by osseous shape and massive ligaments. The first component therefore acts against the wedge, its tendency to separate iliac bones resisted by the sacroiliac and iliolumbar ligaments and symphysis pubis.

Vertical coronal sections through the sacroiliac joints suggest division of the (synovial) articular region of the sacrum into three segments. In the anterosuperior segment, involving the first sacral vertebra, the articular surfaces are slightly sinuous and almost parallel. In the middle segment the posterior width between the articular markings is greater than the anterior, and centrally a sacral concavity fits a corresponding iliac convexity, an interlocking mechanism relieving the strain on the ligaments produced by body weight. In the posteroinferior segment the anterior sacral width is greater than the posterior and here its sacral surfaces are slightly concave. Anteroinferior sacral dislocation by the second component (of force) is prevented, therefore, mainly by the middle segment, owing to its cuneiform shape and interlocking mechanism. However, some rotation occurs, in which the anterosuperior segment tilts down and the posteroinferior segment up. ‘Superior’ segmental movement is limited to a small degree by wedging but primarily by tension in the sacrotuberous and sacrospinous ligaments. In all movements the sacroiliac and iliolumbar ligaments and symphysis pubis resist separation of the iliac bones.

SEXUAL DIFFERENCES IN THE PELVIS

The pelvis provides the most marked skeletal differences between male and female. Distinction can be made even during fetal life, particularly in the subpubic arch. In infancy, dimensions of the whole pelvis are greater in males than in females, but the size of the pelvic cavity is usually greater in females. This distinction prevails in childhood, but the difference is maximal at about 22 months. Sexual differences in adults are divisible into metrical and non-metrical features: the range of most features overlaps between the sexes.

Differences are inevitably linked to function. While the primary pelvic function in both sexes is locomotor, the pelvis, particularly the lesser pelvis, is adapted to parturition in females, and these changes variably affect the proportions and dimensions of the greater pelvis. Since males are distinctly more muscular and therefore more heavily built, overall pelvic dimensions, such as the intercristal measurement (distance between the iliac crests), are greater, markings for muscles and ligaments more pronounced, and general architecture heavier. The male iliac crest is more rugged and more medially inclined at its anterior end; in females the crests are less curved in all parts. The iliac alae are more vertical in females, but do not ascend so far; the iliac fossae are therefore shallower and each iliopectineal line more vertical. These iliac peculiarities probably account for the greater prominence of female hips.

The male is relatively and absolutely more heavily built above the pelvis, with consequent differences at the lumbosacral and hip joints. The sacral basal articular facet for the fifth lumbar vertebra and intervening disc is more than a third of the total sacral basal width in males but less than a third in females, in whom the sacrum is also relatively broader, accentuating this difference. The female has relatively broader sacral alae. The male acetabulum is absolutely larger, and its diameter is approximately equal to the distance between its anterior rim and symphysis pubis. In females, acetabular diameter is usually less than this distance, not only because it is absolutely smaller but also because the anterolateral wall of the cavity is comparatively and often absolutely wider. The height of the female symphysis and adjoining parts of the pubis and ischium, which form the anterior pelvic wall, are also absolutely less, producing a somewhat triangular obturator foramen, which is more ovoid in males. Differing pubic growth is also expressed in the subpubic arch below the symphysis and between the inferior pubic rami. It is more angular in males, being 50–60°; in females it is rounded, less easy to measure and usually 80–85°. A greater separation of the pubic tubercles in females contributes to the pubic width. The ischiopubic rami are also much more lightly built and narrowed near the symphysis; in males they bear a distinctly rough, everted area for attachment of the penile crura, the corresponding attachment for the clitoris being poorly developed. Ischial spines are closer in males and are more inturned. The greater sciatic notch is usually wider in females: mean values for males and females are 50.4° and 74.4°, respectively. The greater female values for angle and width are associated with increased backward sacral tilt and greater anteroposterior pelvic diameter, especially at lower levels.

The sacrum also displays metrical sexual differences. Female sacra are less curved, the curvature being most marked between the first and second segments and the third and fifth, with an intervening flatter region. Male sacra are more evenly curved, relatively long and narrow and more often exceeding five segments (by addition of a lumbar or coccygeal vertebra). The sacral index compares sacral breadth (between the most anterior points on the auricular surfaces) with length (between midpoints on the anterior margins of the promontory and apex): average values for males and females are 105% and 115%. Auricular surfaces are relatively smaller and more oblique in females, but extend onto the upper three sacral vertebrae in both sexes. The dorsal auricular border is more concave in females. Many differences may be summarized in the generalization that the pelvic cavity is longer and more conical in males, shorter and more cylindrical in females; the axis is curved in both. Differences are greater at the inferior aperture than at the brim, where in absolute measurements males are not as different from females as sometimes stated. The superior aperture is more likely to be anthropoid or android in males and gynaecoid or android in females.

In forensic practice, identification of human skeletal remains (which are sometimes fragmentary) usually involves determination of sex, and this is most reliably established from an examination of the pelvis. Even fragments of the pelvis may be useful in this respect. Several studies of metrical characteristics in various pelvic regions have been made, leading to the establishment of various indices. The ilium has received particular attention, e.g. one index compares the pelvic and sacroiliac parts of the bone. A line is extended back from the iliopubic ramus to the nearest point on the anterior auricular margin and thence to the iliac crest. The auricular point divides this chilotic line into anterior (pelvic) and posterior (sacral) segments, each expressed as a percentage of the other. Chilotic indices display reciprocal values in the sexes: the pelvic part of the chilotic line is predominant in females, and the sacral part in males. Detailed metrical studies of the ilium have indicated its limited reliability in ‘sexing’ pelves. However, the higher incidence and definition of the female preauricular sulcus is recognized. The desirability of correlating all available metrical data is to be emphasized; when a range of pelvic data can be combined, especially if they are metrical, 95% accuracy should be achieved. Complete accuracy has been claimed when the rest of the skeleton is available. Assessment of sex from isolated and often incomplete human remains is less reliable. For further details, consult Mays (1998) and Brothwell & Pollard (2001).

FEMUR

Topography

The femur is the longest and strongest bone in the human body (Figs 80.10, 80.11). Its length is associated with a striding gait, its strength with the weight and muscular forces it is required to withstand. Its shaft, almost cylindrical along most of its length, is bowed forward. It has a proximal rounded, articular head projecting medially from its short neck, which, in turn, is a medial extension of the proximal shaft. The distal extremity is wider and more substantial, and presents a double condyle that articulates with the tibia. In standing, the femoral shafts show an inclination upwards and outwards from their tibial articulations, with the femoral heads being separated by the pelvic width. Since the tibia and fibula descend vertically from the knees, the ankles are also in the line of body weight in standing or walking. The degree of femoral obliquity varies between individuals, but is generally greater in women, reflecting the relatively greater pelvic breadth and shorter femora. Proximally the femur consists of a head, neck, and greater and lesser trochanters.

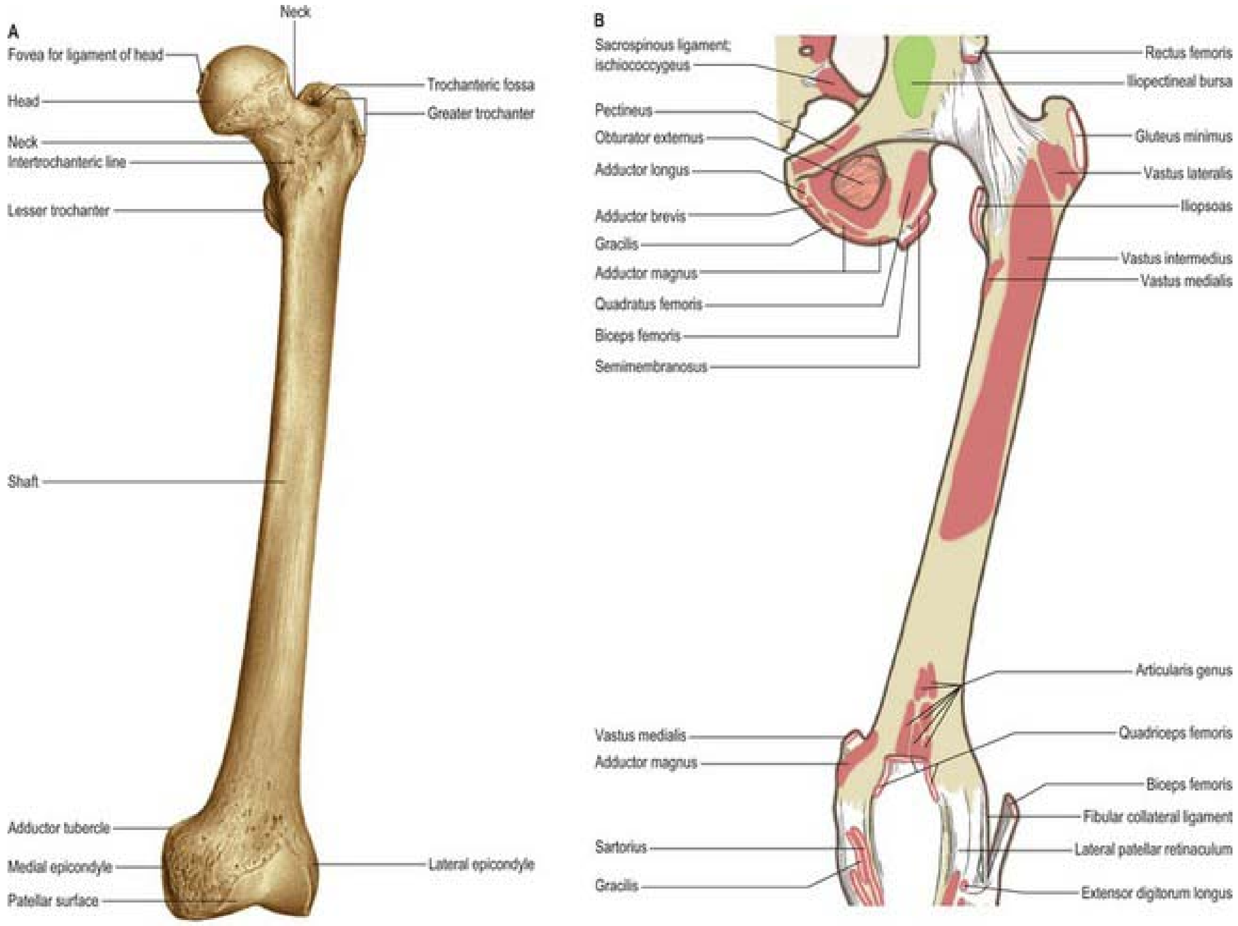
A
Neck
Fovea for ligament of head
Head
Neck
Intertrochanteric line
Lesser trochanter
Trochanteric fossa
Greater trochanter
Shaft
Adductor tubercle
Medial epicondyle
Patellar surface
Lateral epicondyle
B
Sacrospinous ligament; ischiococcygeus
Pectineus
Obturator externus
Adductor longus
Adductor brevis
Gracilis
Adductor magnus
Quadratus femoris
Biceps femoris
Semimembranosus
Rectus femoris
Iliopectineal bursa
Gluteus minimus
Vastus lateralis
Iliopsoas
Vastus intermedius
Vastus medialis
Articularis genus
Quadriceps femoris
Vastus medialis
Adductor magnus
Biceps femoris
Fibular collateral ligament
Lateral patellar retinaculum
Sartorius
Gracilis
Extensor digitorum longus

Fig. 80.10 Femur: anterior aspect. **A**, Osseous features. **B**, Muscle attachments.

(From Sobotta 2006.)

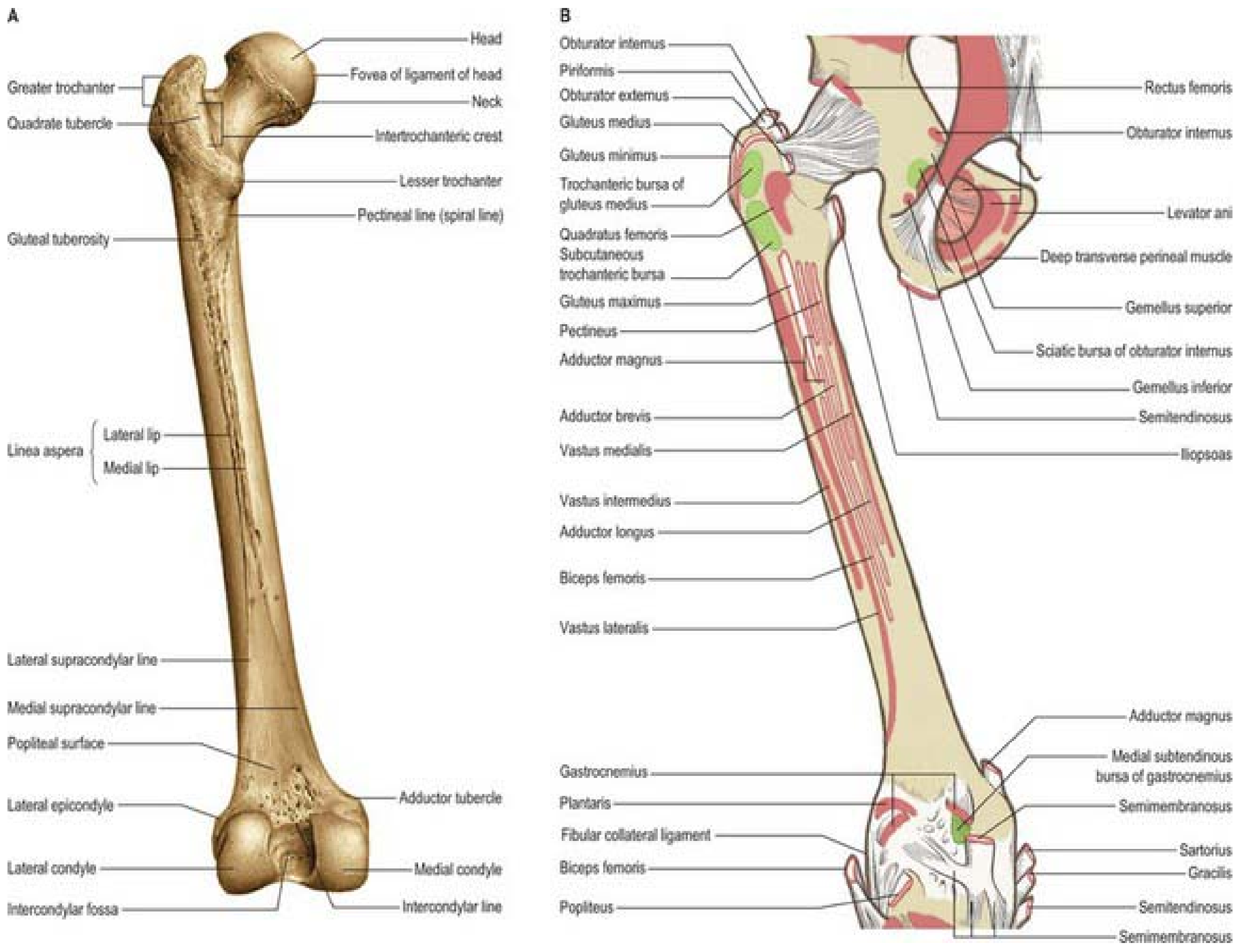
A
Head
Greater trochanter
Fovea of ligament of head
Neck
Quadrate tubercle
Intertrochanteric crest
Lesser trochanter
Pectineal line (spiral line)
Gluteal tuberosity
Linea aspera
Lateral lip
Medial lip
Lateral supracondylar line
Medial supracondylar line
Popliteal surface
Lateral epicondyle
Adductor tubercle
Lateral condyle
Medial condyle
Intercondylar fossa
Intercondylar line
B
Obturator internus
Piriformis
Obturator externus
Rectus femoris
Gluteus medius
Obturator internus
Gluteus minimus
Trochanteric bursa of gluteus medius
Levator ani
Quadratus femoris
Subcutaneous trochanteric bursa
Deep transverse perineal muscle
Gluteus maximus
Gemellus superior
Pectineus
Sciatic bursa of obturator internus
Adductor magnus
Gemellus inferior
Adductor brevis
Semitendinosus
Vastus medialis
Iliopsoas
Vastus intermedius
Adductor longus
Biceps femoris
Vastus lateralis
Adductor magnus
Medial subtendinous bursa of gastrocnemius
Gastrocnemius
Plantaris
Semimembranosus
Fibular collateral ligament
Sartorius
Gracilis
Biceps femoris
Popliteus
Semitendinosus
Semimembranosus

Fig. 80.11 Femur: posterior aspect. **A**, Osseous features. **B**, Muscle attachments.

(From Sobotta 2006.)

Femoral head

The femoral head faces anterosuperomedially to articulate with the acetabulum (Fig. 80.12). The head, often described as rather more than half a ‘sphere’, is not part of a true sphere but is spheroidal. Its smoothness is interrupted posteroinferior to its centre by a small, rough fovea. The head is intracapsular and is encircled, distal to its equator, by the acetabular labrum. Its articular margin is distinct, except anteriorly, where the articular surface extends on to the neck. The ligamentum teres is attached to the fovea. The anterior surface of the head is separated inferomedially from the femoral artery by the tendon of psoas major, the psoas bursa, and the articular capsule.

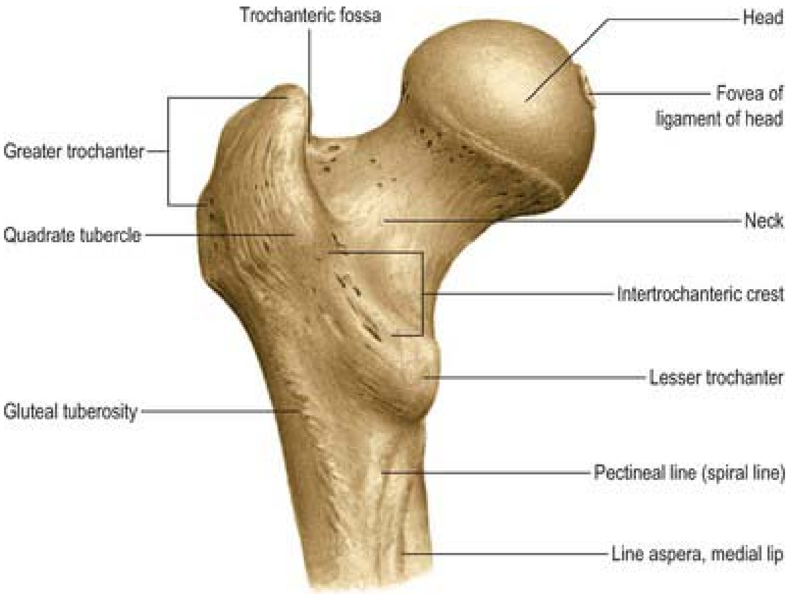
Trochanteric fossa
Head
Fovea of ligament of head
Greater trochanter
Quadrate tubercle
Neck
Intertrochanteric crest
Lesser trochanter
Gluteal tuberosity
Pectineal line (spiral line)
Line aspera, medial lip

Fig. 80.12 Proximal end of femur: posterior aspect.

(From Sobotta 2006.)

Femoral neck

The femoral neck (Fig. 80.12) is approximately 5 cm long, narrowest in its mid part and widest laterally, and connects the head to the shaft at an average angle of 135° (angle of inclination; neck–shaft angle): this facilitates movement at the hip joint, enabling the limb to swing clear of the pelvis. The neck also provides a lever for the action of the muscles acting about the hip joint, which are attached to the proximal femur. The neck–shaft angle is widest at birth and diminishes gradually until adolescence; it is smaller in females. The neck is laterally rotated with respect to the shaft (angle of anteversion) some 10–15°, although values of this angle vary between individuals and between populations (Eckhoff et al 1994). The contours of the neck are rounded: the upper surface is almost horizontal and slightly concave, the lower is straighter but oblique, directed inferolaterally and backwards to the shaft near the lesser trochanter. On all aspects the neck expands as it approaches the articular surface of the head. The anterior surface of the neck is flat and marked at the junction with the shaft by a rough intertrochanteric line. The posterior surface, facing posteriorly and superiorly, is transversely convex, and concave in its long axis; its junction with the shaft is marked by a rounded intertrochanteric crest. There are numerous vascular foramina, especially anteriorly and posterosuperiorly.

The anterior surface is intracapsular, the capsule attaching laterally to the intertrochanteric line. Facets, often covered by extensions of articular cartilage, and various imprints frequently occur here. These facets may sometimes be associated with squatting. One such feature, the cervical fossa, may be a racial characteristic. On the posterior surface the capsule does not reach the intertrochanteric crest; little more than the medial half of the neck is intracapsular. The anterior surface adjoining the head and covered by cartilage is related to the iliofemoral ligament. A groove, produced by the tendon of obturator externus as it approaches the trochanteric fossa, spirals across the posterior surface of the neck in a proximolateral direction.

Greater trochanter

The greater trochanter is large and quadrangular, projecting up from the junction of the neck and shaft (Fig. 80.12). Its posterosuperior region projects superomedially to overhang the adjacent posterior surface of the neck and here its medial surface presents the rough trochanteric fossa. The proximal border of the trochanter lies approximately a hand’s breadth below the iliac tubercle, level with the centre of the femoral head. It has an anterior rough impression. Its lateral surface, continuous distally with the lateral surface of the femoral shaft, is crossed anteroinferiorly by an oblique, flat strip, which is wider above. This surface is palpable, especially when the muscles are relaxed. The trochanteric fossa occasionally presents a tubercle or exostosis.

Lesser trochanter

The lesser trochanter is a conical posteromedial projection of the shaft at the posteroinferior aspect of its junction with the neck. Its summit and anterior surface are rough, but its posterior surface, at the distal end of the intertrochanteric crest, is smooth. It is not palpable.

Intertrochanteric line

The intertrochanteric line, a prominent ridge at the junction of the anterior surfaces of the neck and shaft, descends medially from a tubercle on the upper part of the anterior aspect of the greater trochanter to a point on the lower border of the neck, anterior to the lesser trochanter, where there may also be a tubercle. This line is the lateral limit of the hip joint capsule anteriorly. The upper and lower bands of the iliofemoral ligament are attached to its proximal and distal ends and the associated tubercles. Distally it is continuous with the spiral line.

Intertrochanteric crest

The intertrochanteric crest, a smooth and prominent ridge at the junction of the posterior surface of the neck with the shaft, descends medially from the posterosuperior angle of the greater trochanter to the lesser trochanter. A little above its centre is a low, rounded quadrate tubercle. It is covered by gluteus maximus, from which it is separated, medial to the tubercle, by quadratus femoris and the upper border of adductor magnus.

Gluteal tuberosity

The gluteal tuberosity may be an elongated depression or a ridge. It may at times be prominent enough to merit the unofficial title of ‘third trochanter’.

Shaft

The shaft is surrounded by muscles and is impalpable (Figs 80.10, 80.11). The distal anterior surface, for 5–6 cm above the patellar articular surface, is covered by a suprapatellar bursa, between bone and muscle. The distal lateral surface is covered by vastus intermedius. The medial surface, devoid of attachments, is covered by vastus medialis.

The shaft is narrowest centrally, expanding a little at its proximal end, and substantially more at its distal end. Its long axis makes an angle of approximately 10° with the vertical, and diverges 5–7° from the long axis of the tibia. Its middle third has three surfaces and borders. The extensive anterior surface, smooth and gently convex, is between the lateral and medial borders, which are both round and indistinct. The posterolateral surface is bounded posteriorly by the broad, rough linea aspera, usually a crest with lateral and medial edges. Its subjacent compact bone is augmented to withstand compressive forces, which are concentrated here by the anterior curvature of the shaft. The linea aspera gives attachment to adductor longus, intermuscular septa and the short head of biceps femoris, all inseparably blended at their attachments. Perforating arteries cross the linea laterally under tendinous arches in adductor magnus and biceps femoris. Nutrient foramina, directed proximally, appear in the linea aspera, varying in number and site, one usually near its proximal end, a second usually near its distal end. The posteromedial surface, smooth like the others, is bounded in front by the indistinct medial border and behind by the linea aspera. In its proximal third the shaft has a fourth, posterior surface, bounded medially by a narrow, rough spiral line that is continuous proximally with the intertrochanteric line and distally with the medial edge of linea aspera. Laterally this surface is limited by the broad, rough, gluteal tuberosity, ascending a little laterally to the greater trochanter and descending to the lateral edge of the linea aspera. In its distal third the posterior surface of the shaft presents a further surface, the popliteal surface (see below) between the medial and lateral supracondylar lines. These lines are continuous above with the corresponding edges of the linea aspera. The lateral line is most distinct in its proximal two-thirds, where the short head of biceps femoris and lateral intermuscular septum are attached. Its distal third has a small rough area for the attachment of plantaris, often encroaching on the popliteal surface. The medial line is indistinct in its proximal two-thirds, where vastus medialis is attached. Distally, the medial line is crossed obliquely by the femoral vessels entering the popliteal fossa from the adductor canal. Further distally, the line is often sharp for 3 or 4 cm proximal to the adductor tubercle.

The popliteal surface, triangular in outline, lies between the medial and lateral supracondylar lines. In its distal medial part it is rough and slightly elevated. Forming the proximal part of the floor of the popliteal fossa, the popliteal surface is covered by a variable amount of fat that separates the popliteal artery from bone. The superior medial genicular artery, a branch of the popliteal artery, arches medially above the medial condyle. It is separated from bone by the medial head of gastrocnemius. The latter is attached a little above the condyle; further distally there may be a smooth facet underlying a bursa for the medial head of gastrocnemius. More medially, there is often an imprint proximal to the articular surface: in flexion this is close to a rough tubercle on the medial tibial condyle for the attachment of semimembranosus. The superior lateral genicular artery arches up laterally proximal to the lateral condyle but is separated from bone by the attachment of plantaris to the distal part of the lateral supracondylar line.

Distal end

The distal end of the femur is widely expanded as a bearing surface for transmission of weight to the tibia (Fig. 80.13). It bears two massive condyles, which are partly articular. Anteriorly the condyles are confluent and continue into the shaft; posteriorly they are separated by a deep intercondylar fossa and project beyond the plane of the popliteal surface. The articular surface is a broad area, like an inverted U, for the patella and the tibia. The patellar surface extends anteriorly on both condyles, especially the lateral. It is transversely concave, vertically convex and grooved for the posterior patellar surface. The tibial surface is divided by the intercondylar fossa but is anteriorly continuous with the patellar surface. Its medial part is a broad strip on the convex inferoposterior surface of the medial condyle, and is gently curved with a medial convexity. Its lateral part covers similar aspects of the lateral condyle but is broader and passes straight back. The tibial surfaces are convex in all directions. The medial and lateral tibial surfaces have dissimilar anteroposterior curvatures. However views differ as to the exact representation of these differences. One view holds that in both tibial portions of the femoral condyles the sagittal radius of curvature is ever decreasing (a ‘closing helix’). More recently it has been suggested that the medial articular surface describes arcs of two circles. The more posterior has a smaller radius. Laterally there may only be one arc of fixed curvature with a radius similar to that of the posterior arc of the medial femoral articular surface. These differences are believed to be important determinants of knee joint motion.

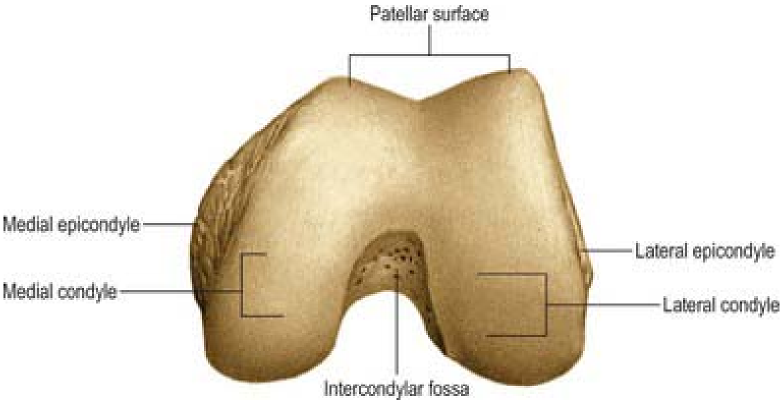

Fig. 80.13 Distal end of femur: articular surface.

(From Sobotta 2006.)

Patellar surface (trochlear groove)

The patellar surface extends more proximally on the lateral side. Its proximal border is therefore oblique and runs distally and medially, separated from the tibial surfaces by two faint grooves that cross the condyles obliquely. The lateral groove is the more distinct. It runs laterally and slightly forwards from the front of the intercondylar fossa and expands to form a faint triangular depression, resting on the anterior edge of the lateral meniscus when the knee is fully extended. The medial groove is restricted to the medial part of the medial condyle and rests on the anterior edge of the medial meniscus in full extension. Where it ceases, the patellar surface continues back to the lateral part of the medial condyle as a semilunar area adjoining the anterior region of the intercondylar fossa. This area articulates with the medial vertical facet of the patella in full flexion; its outline is indistinct in most femora. In habitual squatters articular cartilage may extend to the lateral aspect of the lateral condyle under vastus lateralis.

The trochlear groove helps to stabilize the patella. An abnormally shallow groove predisposes to instability.

Intercondylar fossa

The intercondylar fossa separates the two condyles distally and behind. In front it is limited by the distal border of the patellar surface, and behind by an intercondylar line, separating it from the popliteal surface. It is intracapsular but largely extrasynovial. Its lateral wall, the medial surface of the lateral condyle, bears a flat posterosuperior impression which spreads to the floor of the fossa near the intercondylar line for the proximal attachment of the anterior cruciate ligament. The medial wall of the fossa, i.e. the lateral surface of the medial condyle, bears a similar larger area, but far more anteriorly, for the proximal attachment of the posterior cruciate ligament. Both impressions are smooth and largely devoid of vascular foramina, whereas the rest of the fossa is rough and pitted by vascular foramina. A bursal recess between the ligaments may ascend to the fossa. The capsular ligament and, laterally, the oblique popliteal ligament, are attached to the intercondylar line. The ligamentum mucosum (infrapatellar synovial fold or plica) is attached to the anterior border of the fossa.

Lateral condyle

The lateral condyle (Figs 80.13, 80.14) is larger anteroposteriorly than the medial. Its most prominent point is the lateral epicondyle to which the lateral collateral ligament is attached. A short groove, deeper in front, separates the lateral epicondyle inferiorly from the articular margin. This groove allows the tendon of popliteus to run deep to the lateral collateral ligament and insert inferior and anterior to the ligament insertion. Adjoining the joint margin is a strip of condyle, 1 cm broad. It is intracapsular and covered by synovial membrane except for the attachment of popliteus.

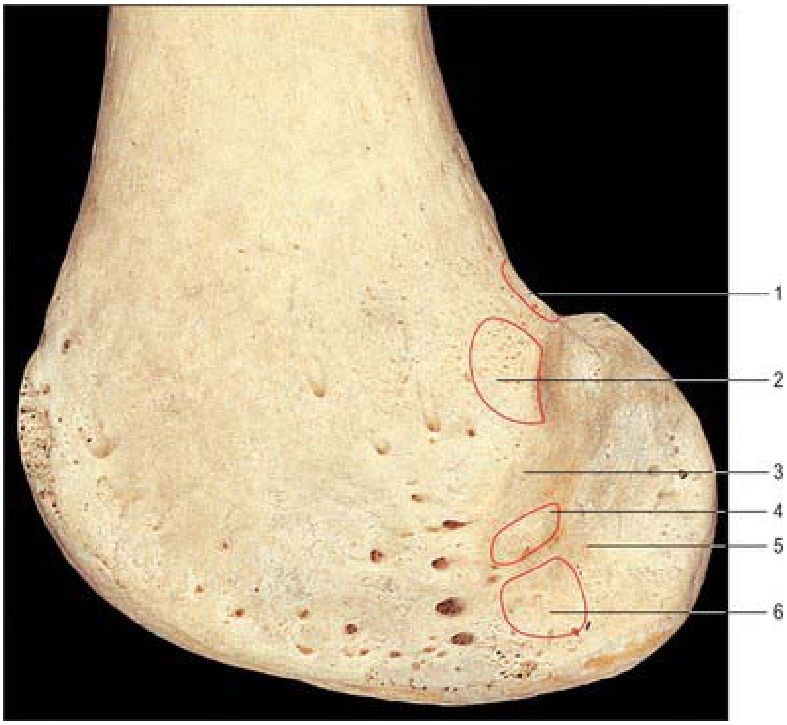

Fig. 80.14 Distal end of femur: lateral aspect. **1**. Attachment of plantaris. **2**. Attachment of lateral head of gastrocnemius. **3**. Lateral epicondyle. **4**. Attachment of lateral collateral ligament. **5**. Groove for popliteus in full flexion. **6**. Attachment of popliteus.

The medial surface is the lateral wall of the intercondylar fossa. Its lateral surface projects beyond the shaft. Part of the lateral head of gastrocnemius is attached to an impression posterosuperior to the lateral epicondyle.

Medial condyle

The medial condyle has a bulging, convex medial aspect which is easily palpable. Proximally its adductor tubercle, which may only be a facet rather than a projection, receives the tendon of adductor magnus. The medial prominence of the condyle, the medial epicondyle, is anteroinferior to the tubercle. The lateral surface of the condyle is the medial wall of the intercondylar fossa. The condyle projects distally so that, despite the obliquity of the shaft, the profile of the distal end is almost horizontal. A curved strip, 1 cm wide, adjoining the medial articular margin, is covered by synovial membrane and is inside the joint capsule. Proximal to this, the medial epicondyle receives the medial collateral ligament.

Structure

The femoral shaft is a cylinder of compact bone with a large medullary cavity. The wall is thick in its middle third, where the femur is narrowest and the medullary cavity most capacious. Proximally and distally the compact wall becomes progressively thinner, and the cavity gradually fills with trabecular bone. The extremities, especially where articular, consist of trabecular bone within a thin shell of compact bone, their trabeculae being disposed along lines of greatest stress. At the proximal end the main trabeculae form a series of plates orthogonal to the articular surface, converging to a central dense wedge, which is supported by strong trabeculae passing to the sides of the neck, especially along its upper and lower profiles (Fig. 80.15). Force applied to the femoral head is therefore transmitted to the wedge and thence to the junction of the neck and shaft. This junction is strengthened by dense trabeculae extending laterally from the lesser trochanter to the end of the superior aspect of the neck, thus resisting tensile or shearing forces applied to the neck through the head (Fig. 80.16). Tensile and compressive tests indicate that axial trabeculae of the femoral head withstand much greater stresses than peripheral trabeculae. A smaller bar across the junction of the greater trochanter with the neck and shaft resists shearing produced by muscles attached to it. These two bars are proximal layers of arches between the sides of the shaft and transmit to it forces applied to the proximal end. A thin vertical plate, the calcar femorale, ascends from the compact wall near the linea aspera into the trabeculae of the neck. Medially it joins the posterior wall of the neck; laterally it continues into the greater trochanter, where it disperses into general trabecular bone. It is thus in a plane anterior to the trochanteric crest and base of the lesser trochanter. Newell (1997), in a review of the calcar femorale, has described its three-dimensional anatomy in terms of the work of Dixon (1910), who was the first to recognize the deficiencies of the classic two-dimensional description of the architecture of the proximal femur. Dixon suggested that the trabecular framework of the proximal femur was spiral, and that the ‘arches’ were simplified sectional profiles of this spiral. At the distal end of the femur, trabeculae spring from the entire internal surface of compact bone, descending perpendicular to the articular surface. Proximal to the condyles these are strongest and most accurately perpendicular. Horizontal planes of trabecular bone, arranged like crossed girders, form a series of cubical compartments.

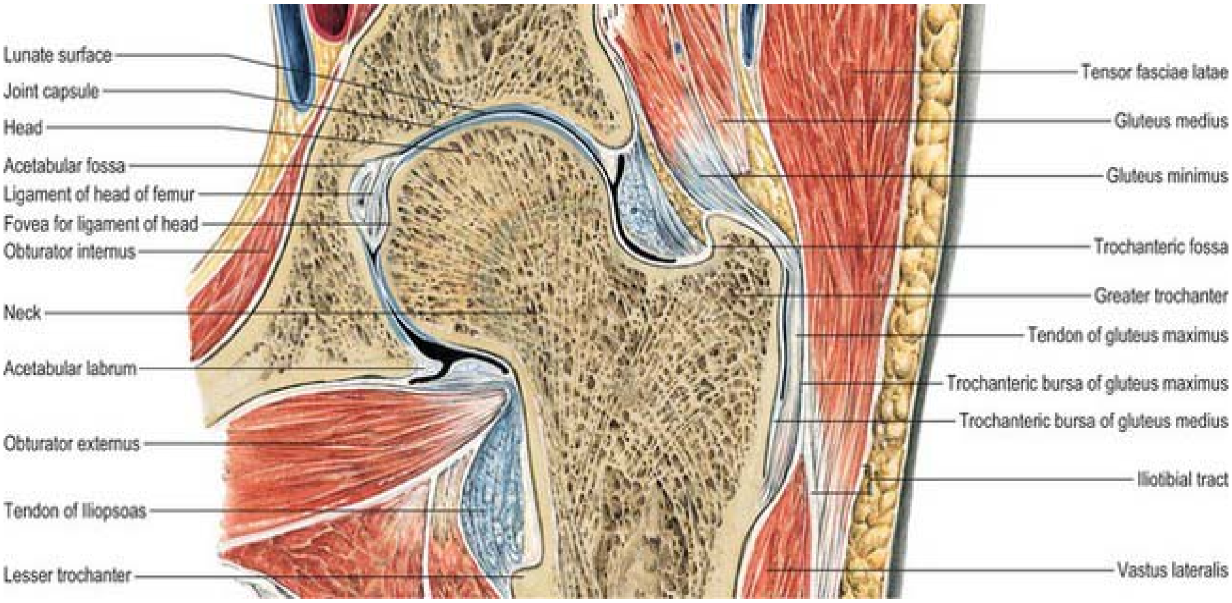
Lunate surface
Joint capsule
Head
Acetabular fossa
Ligament of head of femur
Fovea for ligament of head
Obturator internus
Neck
Acetabular labrum
Obturator externus
Tendon of iliopsoas
Lesser trochanter
Tensor fasciae latae
Gluteus medius
Gluteus minimus
Trochanteric fossa
Greater trochanter
Tendon of gluteus maximus
Trochanteric bursa of gluteus maximus
Trochanteric bursa of gluteus medius
Iliotibial tract
Vastus lateralis

Fig. 80.15 Coronal section through left hip joint.

(From Sobotta 2006.)

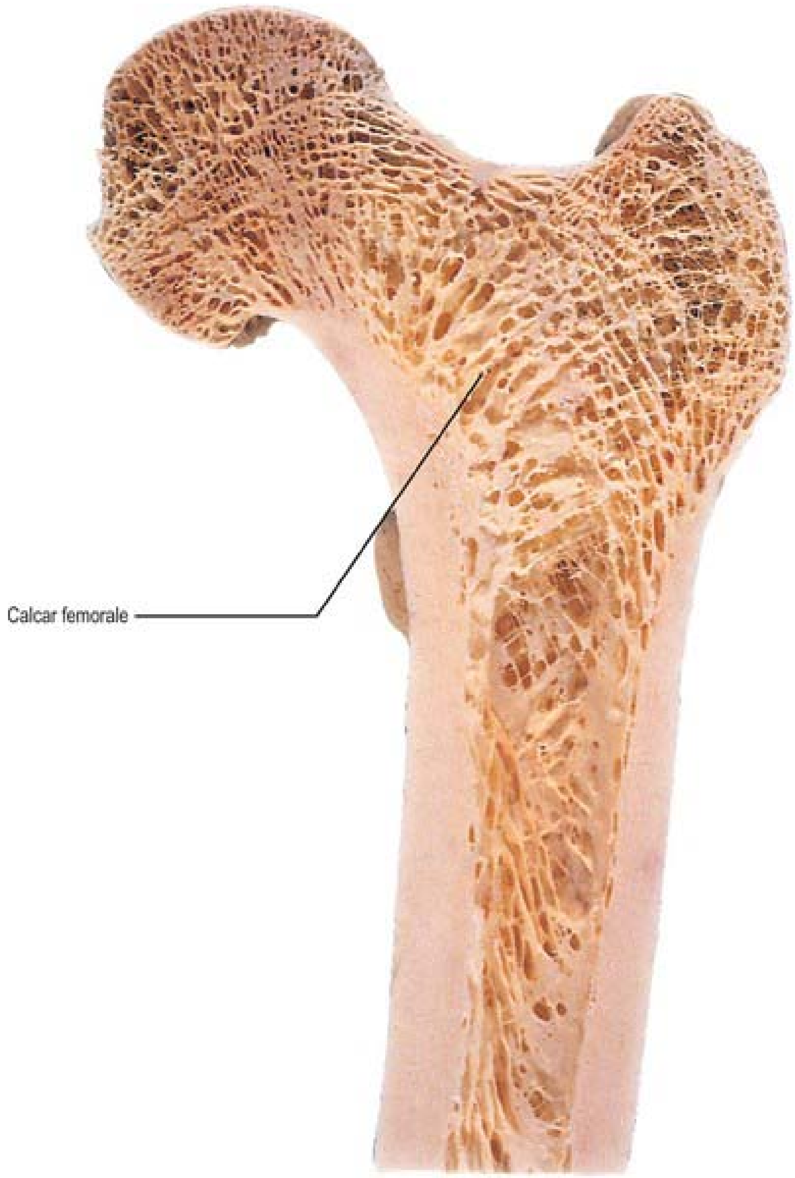

Fig. 80.16 Coronal section through the proximal end of the femur showing the trabecular architecture, calcar femorale, and variations in cortical thickness.

(From Sobotta 2006.)

Muscle attachments

The greater trochanter provides attachment for gluteus minimus and medius. Gluteus minimus is attached to its rough anterior impression and gluteus medius to its lateral oblique strip. The bone is separated from the tendon of gluteus medius by a bursa. The area behind is covered by deep fibres of gluteus maximus, with part of its trochanteric bursa interposed. The tendon of piriformis is attached to the upper border of the trochanter and the common (tricipital) tendon of obturator internus and the gemelli is attached to its medial surface. The trochanteric fossa receives the tendon of obturator externus. Psoas major is attached to the summit and anteromedial surface of the lesser trochanter. Iliacus is attached to the medial or anterior surface of its base, descending a little behind the spiral line as its tendon fuses with that of psoas. Adductor magnus (upper part) passes over its posterior surface, sometimes separated by an interposed bursa.

The most proximal fibres of vastus lateralis are attached to the proximal end of the intertrochanteric line, and those of vastus medialis to the distal end. Quadratus femoris is attached to the quadrate tubercle and the immediately distal bone. Vastus intermedius is attached to the anterior and lateral surfaces of the proximal three-quarters of the femoral shaft. Slips of articularis genu are attached distal to this.

The gluteal tuberosity receives the deeper fibres of the distal half of gluteus maximus and, at its medial edge, the uppermost fibres of adductor magnus. Distal to this, adductor magnus is attached to the linea aspera and, by an aponeurosis, to the proximal part of the medial supracondylar ridge. Its remaining fibres form a large tendon attached to the adductor tubercle, with an aponeurotic expansion to the distal part of the medial supracondylar ridge.

Pectineus and adductor brevis are attached to the posterior femoral surface between the gluteal tuberosity and spiral line. The pectineal attachment is a line, sometimes slightly rough, from the base of the lesser trochanter to the linea aspera. Adductor brevis is attached lateral to pectineus and beyond this to the proximal part of the linea aspera, medial to adductor magnus. Adductor longus, intermuscular septa and the short head of biceps femoris are attached to the linea aspera. Vastus lateralis has a linear attachment from the anterior surface of the base of the greater trochanter to the proximal end of the gluteal tuberosity, and along the lateral margin of the latter to the proximal half of the lateral edge of the linea aspera. Vastus medialis is attached from the distal end of the intertrochanteric line along the spiral line to the medial edge of the linea aspera and thence to the medial supracondylar line, which also receives many fibres from the aponeurotic attachments of adductor magnus.

The medial head of gastrocnemius is attached to the posterior surface a little above the medial condyle. The short head of biceps femoris is attached to the proximal two-thirds of the lateral supracondylar line. Plantaris attaches to the line distally. Vastus medialis is attached to the proximal two-thirds of the medial supracondylar line.

Part of the lateral head of gastrocnemius is attached posterosuperiorly to the lateral epicondyle. Popliteus is attached anteriorly in the groove on the outer aspect of the lateral epicondyle. Its tendon passes deep to the lateral collateral ligament (Fig. 80.14). The tendon lies in the groove in full knee flexion; in extension it crosses the articular margin and may form an impression on it.

Vascular supply

The blood supply of the femoral head (Fig. 80.17) is derived from an arterial ring around the neck, just outside the attachment of the fibrous capsule, constituted by the medial and lateral circumflex femoral arteries with minor contributions from the superior and inferior gluteal vessels (see trochanteric anastomosis). From this ring, ascending cervical branches pierce the capsule (under its zona orbicularis) to ascend the neck beneath the reflected synovial membrane. These vessels become the retinacular arteries and form a subsynovial intracapsular anastomosis. Here the vessels are at risk with a displaced fracture of the femoral neck. Interruption of blood supply in this way can lead to avascular necrosis of the femoral head. If the fracture is intracapsular, not only is the intraosseous blood supply damaged but the retinacular vessels are also vulnerable. If the fracture is extracapsular, the retinacular vessels will remain intact and avascular necrosis of the femoral head is much less likely. The ascending cervical vessels give off metaphysial branches that enter the neck, while the intracapsular ring gives off lateral and inferior epiphysial branches. A small medial epiphysial supply, of importance in early childhood, reaches the head along the ligamentum teres by the acetabular branches of the obturator and medial circumflex femoral arteries, which anastomose with the other epiphysial vessels. During growth, the epiphysial plate separates the territories of the metaphysial and epiphysial vessels; these vessels anastomose freely after osseous union of the head and neck. Observations on developmental patterns of this supply in late fetal and early postnatal periods have revealed that although medial and lateral circumflex femoral arteries at first contribute equally, two major branches of the medial provide the final supply, both posterior to the neck. The supply from the lateral circumflex artery diminishes and the arterial ring is interrupted. As the femoral neck elongates, the extracapsular circle becomes more distant from the epiphysial part of the head.

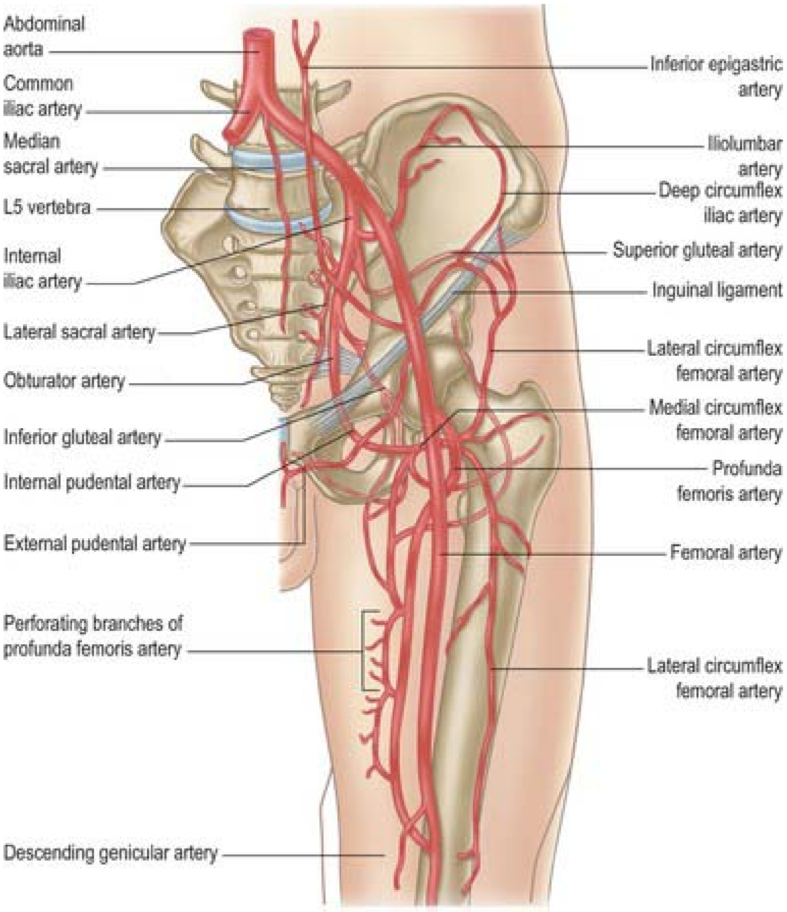
Abdominal aorta
Common iliac artery
Median sacral artery
L5 vertebra
Internal iliac artery
Lateral sacral artery
Obturator artery
Inferior gluteal artery
Internal pudental artery
External pudental artery
Perforating branches of profunda femoris artery
Descending genicular artery
Inferior epigastric artery
Iliolumbar artery
Deep circumflex iliac artery
Superior gluteal artery
Inguinal ligament
Lateral circumflex femoral artery
Medial circumflex femoral artery
Profunda femoris artery
Femoral artery
Lateral circumflex femoral artery

Fig. 80.17 Collateral circulation around the hip and upper thigh, anterior aspect.

The trochanteric regions and subtrochanteric shaft are supplied by the trochanteric and cruciate arterial anastomoses. More distally in the shaft, nutrient foramina, directed proximally, are found in the linea aspera, varying in number and site: one is usually near its proximal end and a second usually near its distal end. The main nutrient artery is usually derived from the second perforating artery (see profunda femoris). If two nutrient arteries occur, they may branch from the first and third perforators. Periosteal vessels arise from the perforators and from the profunda, and run circumferentially rather than longitudinally. The distal metaphysis has many vascular foramina. Arterial supply here is from the genicular anastomosis. For further details consult Crock (1980, 1996).

The pattern of venous drainage of the head and neck corresponds in general to that of the arteries, though there may be a single large cervical vein posteroinferiorly.

Innervation

The periosteal innervation is derived proximally from nerves that supply the hip joint, distally from those supplying the knee, and in all areas from nerves that innervate muscles attached to the bone.

Ossification

The femur ossifies from five centres: in the shaft, head, greater and lesser trochanters and the distal end (Figs 80.10, 80.11, 80.18). Other than the clavicle, it is the first long bone to ossify. The process starts in the midshaft in the seventh prenatal week and extends to produce a miniature shaft that is largely ossified at birth. Secondary centres appear in the distal end (from which the condyles and epicondyles are formed) during the ninth month, in the head during the first six months after birth, in the greater trochanter during the fourth year and in the lesser between the 12th and 14th year. The centre in the cartilaginous head is restricted to it until the tenth year, so that the epiphysial line (Fig. 80.7) is horizontal and the inferomedial part of the articular surface is on the neck. The medial epiphysial margin later grows over this part of the articular surface. Thus, the mature epiphysis is a hollow cup on the summit of the neck. The epiphysial line follows the articular margin except where it is separated superiorly from the articular surface by a non-articular area where blood vessels enter the head (Trueta 1957). The epiphyses fuse independently: the lesser trochanter soon after puberty followed by the greater trochanter. The capital epiphysis fuses in the 14th year in females and 17th year in males,. The epiphysis at the distal end fuses in the 16th year in females, and 18th year in males. The distal epiphysial plate traverses the adductor tubercle.

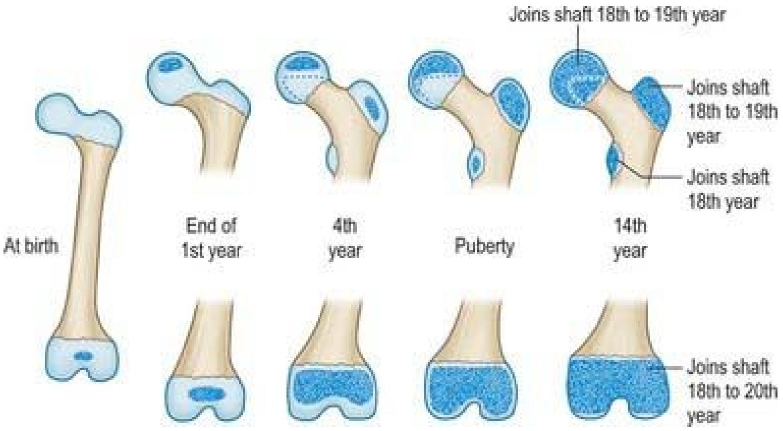
Joins shaft 18th to 19th year
Joins shaft 18th to 19th year
Joins shaft 18th year
At birth
End of 1st year
4th year
Puberty
14th year
Joins shaft 18th to 20th year

Fig. 80.18 Stages in ossification of the femur (not to scale).

Growth plate considerations

Trauma to any epiphysial plate can lead to bony union between epiphysis and metaphysis, and so cause premature cessation of growth. Any surgery in the hip region in children can injure the growth plate, resulting in abnormal proximal femoral development. In the case of fractures involving the epiphysis, expeditious restoration of normal bony alignment is essential in order to minimize the risk of subsequent abnormal growth.

The growth plate represents a line of weakness and predisposes to fracture from injury. Such acute injuries affecting the capital epiphysis are uncommon. However, a more chronic fracture through the capital epiphysis occurs in ‘slipped upper femoral epiphysis’. The condition affects pubescent adolescents, especially males. Endocrinological abnormality may be related.

The femoral head epiphysis displaces posteriorly off the femoral neck. If it heals in this position, lower limb deformity and restricted hip movement occur. A classic hallmark is obligatory external rotation of the femur as the hip is flexed. Treatment varies according to the time taken for the ‘slip’ to occur. Normal anatomical restoration is not attempted because of an increased incidence of avascular necrosis. The position of the femoral head may be accepted as it is and fixed with screws in this position to stop further displacement. This treatment will deliberately cause premature growth plate fusion and so prevent future ‘slippage’. Since the distal femoral growth plate accounts for most of the normal increase in longitudinal growth of the femoral shaft, an acceptable limb length difference usually results.

Infection of bone in neonates and young children tends to arise via bacteria in the blood stream which usually ‘seed’ in the metaphysial region, probably as a consequence of the vascular ‘arcade’ arrangement of arteries in this part of the bone. The proximal femoral growth plate is intra-articular. As a result infection in the proximal femoral metaphysis can spread into the joint and result in a septic arthritis that can destroy the hip joint permanently.

The distal end of the femur is the only epiphysis in which ossification consistently starts just before birth: the phenomenon therefore serves as a reliable indicator of the gestational maturity of a stillborn baby. Since the epiphysial plate is level with the adductor tubercle, the epiphysis is partly extra-articular. Operations here may damage the distal epiphysial cartilage in children and result in subsequent shortening of the leg.

JOINTS

PUBIC SYMPHYSIS

The pubic bones meet in the midline at the pubic symphysis, a secondary cartilaginous joint (Fig. 80.4).

Articulating surfaces

The articulating surfaces are the medial (symphysial) surfaces of the pubic bones, each covered by a thin layer of tightly adherent hyaline cartilage (surface growth cartilage in the young). The junction is not flat but marked by reciprocal crests and papillae. Theoretically this would resist shearing. The surfaces of hyaline cartilage are connected by fibrocartilage, varying in thickness and constituting the interpubic disc. The symphysis often contains a cavity, probably due to absorption. It rarely appears before the tenth year and is non-synovial. The cavity, which is better developed in females, is usually posterosuperior but may reach the front or even occupy most of the cartilage.

Ligaments

The interpubic disc is strengthened anteriorly by several interlacing collagenous fibrous layers, passing obliquely from bone to bone, decussating with fibres of the external oblique aponeuroses and the medial tendons of the recti abdominis. These layers constitute the anterior pubic ligament. There are less well-developed posterior fibres, sometimes named the posterior pubic ligament. The main ligaments of the joint are the superior and arcuate pubic ligaments. The superior pubic ligament connects the bones above, extending to the pubic tubercles. The arcuate pubic ligament, a thick arch of fibres, connects the lower borders of the symphysial pubic surfaces bounding the pubic arch. It blends superiorly with the interpubic disc and extends laterally attached to the inferior pubic rami. Its inferior edge is separated from the anterior border of the perineal membrane by an opening which is traversed by the deep dorsal vein of the penis or clitoris.

Vascular supply

The pubic symphysis is supplied by pubic branches of the obturator, superficial external pudendal and inferior epigastric arteries.

Innervation

The pubic symphysis is innervated by branches from the iliohypogastric, ilioinguinal and pudendal nerves.

Factors maintaining stability

The interpubic disc and the superior and arcuate ligaments are the main stabilizing factors of the pubic symphysis.

Movements

Angulation, rotation and displacement are possible but slight and are likely during movement at the sacroiliac and hip joints. Excessive movement may occur as a sports injury. Some separation occurs late in gestation and during childbirth: on occasion this is considerable.

Relations

Anteriorly the pubic symphysis is related to superficial fascia and skin. Because of the obliquity of the joint, the proximal ends of the penile or clitoral shafts lie anterior to the lower half of the joint. Inferiorly the urethra lies about 2.5 cm away in the male, and somewhat closer in the female, as it passes through the perineal membrane. Closer to the joint, the deep dorsal vein of the penis or clitoris passes between the arcuate ligament and the anterior border of the perineal membrane. Posteriorly the upper part of the joint is separated from the inferolateral surfaces of the bladder by the retropubic fat pad. Inferiorly in the male the prostatic venous plexus separates the prostate from the lower part of the joint. The region is sometimes termed the retropubic space. These relationships explain why traumatic disruption of the anterior bony pelvis may be associated with serious urogenital injury.

SACROILIAC JOINT

The sacroiliac joint is a synovial articulation between the sacral and iliac auricular surfaces. Fibrous adhesions and gradual obliteration occur in both sexes, earlier in males, and after the menopause in females. Radiological evidence of obliteration in normal subjects is occasionally seen before 50 years, but is not uncommon thereafter: in old age the joint may be completely fibrosed and occasionally even ossified.

Articulating surfaces

The surfaces are nearly flat in infants, whereas in adults they are irregular, often markedly so, and sometimes undulant. The curvatures and irregularities, greater in males, are reciprocal: they restrict movements and contribute to the considerable strength of the joint in transmitting weight from the vertebral column to the lower limbs. The sacral surface is covered by hyaline cartilage which is thicker anteriorly than posteriorly in adults. The thinner cartilage on the iliac surface is also hyaline in type, as confirmed by the presence of type II collagen.

Fibrous capsule

The capsule is attached close to both articular margins.

Ligaments

The ligaments of the sacroiliac joint are the anterior, interosseous and posterior sacroiliac, iliolumbar, sacrotuberous and sacrospinus ligaments.

Anterior sacroiliac ligament

The anterior sacroiliac ligament (Fig. 80.8), an anteroinferior capsular thickening, is particularly welldeveloped near the arcuate line and the posterior inferior iliac spine, where it connects the third sacral segment to the lateral side of the preauricular sulcus. It is thin elsewhere.

Interosseous sacroiliac ligament

The interosseous sacroiliac ligament is the major bond between the bones, filling the irregular space posterosuperior to the joint. It is covered superficially by the posterior sacroiliac ligament. Its deeper part has superior and inferior bands passing from depressions posterior to the sacral auricular surface to those on the iliac tuberosity. These bands are covered by, and blend with, a more superficial fibrous sheet connecting the posterosuperior margin of a rough area posterior to the sacral auricular surface to the corresponding margins of the iliac tuberosity. This sheet is often partially divided into superior and inferior parts, the former uniting the superior articular process and lateral crest on the first two sacral segments to the neighbouring ilium as a short posterior iliac ligament (see Fig. 42.52).

The posterior sacroiliac ligament

The posterior sacroiliac ligament (see Fig. 42.52) overlies the interosseous ligament: the dorsal rami of the sacral spinal nerves and vessels intervene. It consists of several weak fasciculi connecting the intermediate and lateral sacral crests to the posterior superior iliac spine and posterior end of the internal lip of the iliac crest. Inferior fibres, from the third and fourth sacral segments, ascend to the posterior superior iliac spine and posterior end of the internal lip of the iliac crest: they may form a separate long posterior sacroiliac ligament. This ligament is continuous laterally with part of the sacrotuberous ligament and medially with the posterior lamina of the thoracolumbar fascia.

Iliolumbar ligament

See page 735.

Sacrotuberous ligament

The sacrotuberous ligament (Fig. 80.8, see Fig. 42.52) is attached by its broad base to the posterior superior iliac spine., the posterior sacroiliac ligaments (with which it is partly blended), to the lower transverse sacral tubercles and the lateral margins of the lower sacrum and upper coccyx. Its oblique fibres descend laterally, converging to form a thick, narrow band that widens again below and is attached to the medial margin of the ischial tuberosity. It then spreads along the ischial ramus as the falciform process, whose concave edge blends with the fascial sheath of the internal pudendal vessels and pudendal nerve. The lowest fibres of gluteus maximus are attached to the posterior surface of the ligament; superficial fibres of the lower part of the ligament continue into the tendon of biceps femoris. The ligament is pierced by the coccygeal branches of the inferior gluteal artery, the perforating cutaneous nerve and filaments of the coccygeal plexus.

Sacrospinous ligament

The thin, triangular sacrospinous ligament (Fig. 80.8) extends from the ischial spine to the lateral margins of the sacrum and coccyx anterior to the sacrotuberous ligament, with which it blends in part. Its anterior surface is in fact the coccygeus muscle, i.e. muscle and ligament are coextensive. The sacrospinous ligament is often regarded as a degenerate part of coccygeus.

Sciatic foramina

The sacrotuberous and sacrospinous ligaments convert the sciatic notches into foramina (Fig. 80.8).

Greater sciatic foramen

The greater sciatic foramen is bounded anterosuperiorly by the greater sciatic notch, posteriorly by the sacrotuberous ligament and inferiorly by the sacrospinous ligament and ischial spine. It is partly filled by the emerging piriformis, above which the superior gluteal vessels and nerve leave the pelvis. Below it, the inferior gluteal vessels and nerve, internal pudendal vessels and pudendal nerve, sciatic and posterior femoral cutaneous nerves and the nerves to obturator internus and quadratus femoris all leave the pelvis.

Lesser sciatic foramen

The lesser sciatic foramen is bounded anteriorly by the ischial body, superiorly by its spine and sacrospinous ligament, and posteriorly by the sacrotuberous ligament. It transmits the tendon of obturator internus, the nerve to obturator internus, and the internal pudendal vessels and pudendal nerve.

Vascular supply

The arterial supply of the sacroiliac joint is derived from the iliolumbar, superior gluteal and superior lateral sacral arteries, with corresponding venous drainage. Lymphatic drainage follows the arteries, reaching the iliac and lumbar nodes.

Innervation

Nerve fibres ramify within the joint capsule and adjoining ligaments, but their source is uncertain. It is thought that the joint probably receives branches from the anterior and posterior rami of the first two sacral spinal nerves, and from the superior gluteal nerve, and there may also be contributions from the obturator nerve and the lumbosacral trunk: it would appear that Hilton's law is not readily applicable to this joint.

The sacro-iliac joint has been implicated as the source of pain in the lower back and buttocks in approximately 15% of the population. Diagnosing sacroiliac joint-mediated pain is difficult because the presenting complaints are similar to those of other causes of back pain. Patients with sacroiliac joint-mediated pain rarely report pain above L5; most localize their pain to the area around the posterior superior iliac spine.

Factors maintaining stability

The sacroiliac joint is one of the most stable joints in the body, and supports the weight of the trunk. The reciprocal irregularity of the joint surfaces allows very little movement. The tendency of the sacrum to be forced downwards by the trunk is resisted by the extremely strong posterior ligaments, while the iliolumbar ligaments help to resist displacement of the fifth lumbar vertebra over the sacrum. The sacrotuberous and sacrospinous ligaments oppose upward tilting of the lower part of the sacrum when downward thrust is applied at its upper end.

Movements

Primary movement of the sacroiliac joint is minimal. All muscles that cross the joint act on the lumbar spine or on the hip. Such movements as do occur are secondarily imposed on the joint as the pelvis moves. Data from living subjects are technically difficult to obtain, and those based on plain radiographs are unreliable. Studies using implanted tantalum spheres and biplanar radiography have shown mean rotational ranges of less than 2°. Even when there is recordable movement, the direction of movement is irregular. Biplanar radiography has also shown that the axes of movement of the sacroiliac joint during hip movement are oblique, and that the axes differ in flexion and extension.

During pregnancy the pelvic joints and ligaments loosen under the influence of the hormone relaxin. Movements in the joints increase. Relaxation renders the sacroiliac locking mechanism less effective, permitting greater rotation and perhaps allowing alterations in pelvic diameters at childbirth, although the effect is probably small. The impaired locking mechanism diverts the strain of weightbearing to the ligaments, with frequent sacroiliac strain after pregnancy.

Relations

The sacroiliac joints have many important anterior relations. The internal and external iliac veins join to form the common iliac veins immediately anteriorly, separating the joints from the bifurcations of the common iliac arteries and, more anteriorly, the ureters. The lumbosacral trunk and the obturator nerve cross the anterior aspect of the joint behind the vessels. Piriformis partly attaches to the anterior capsule, separating the joint from the upper part of the sacral plexus.

Variants

Accessory sacroiliac articulations are not uncommon. They develop behind the articular surface between the lateral sacral crest and posterior superior iliac spine and iliac tuberosity, and are acquired fibrocartilaginous joints resulting from the stresses of weightbearing. They have a joint capsule, are saddle-shaped, and may be single, double, unilateral or bilateral (Weisl 1954).

MUSCLES

MUSCLES OF THE ILIAC REGION

Although there is no ‘iliac region’ as such, this heading conveniently describes a group of three muscles that originate from the lumbar vertebral column (psoas major and minor) and the ilium (iliacus). Two (psoas major and iliacus) are attached together on the femur as flexors of the hip joint and are often considered as a functional unit, iliopsoas. Psoas minor only reaches the pubis, and acts on the spine and sacroiliac joint.

Psoas major

Attachments

Psoas major is a long muscle that lies on either side of the lumbar vertebral column and the pelvic brim (Fig. 80.19). Its proximal attachments are complex. They include the anterior surfaces and lower borders of the transverse processes of all the lumbar vertebrae. There are five digitations, each from the bodies of two adjoining vertebrae and their intervertebral disc. The highest of these arises from the lower margin of the body of the 12th thoracic vertebra, the upper margin of the body of the first lumbar vertebra and the interposed thoracolumbar disc. The lowest arises from the adjacent margins of the bodies of the fourth and fifth lumbar vertebrae and the interposed disc. A series of tendinous arches extend across the narrow parts of the bodies of the lumbar vertebrae between the digitations already described. The lumbar arteries and veins, and filaments from the sympathetic trunk, pass medial to these arches. The upper four lumbar intervertebral foramina bear important relations to these attachments of the muscle. The foramina lie anterior to the transverse processes and posterior to the attachments to vertebral bodies, discs and tendinous arches. Thus, the roots of the lumbar plexus enter the muscle directly, the plexus is lodged within it, and its branches emerge from its borders and surfaces.

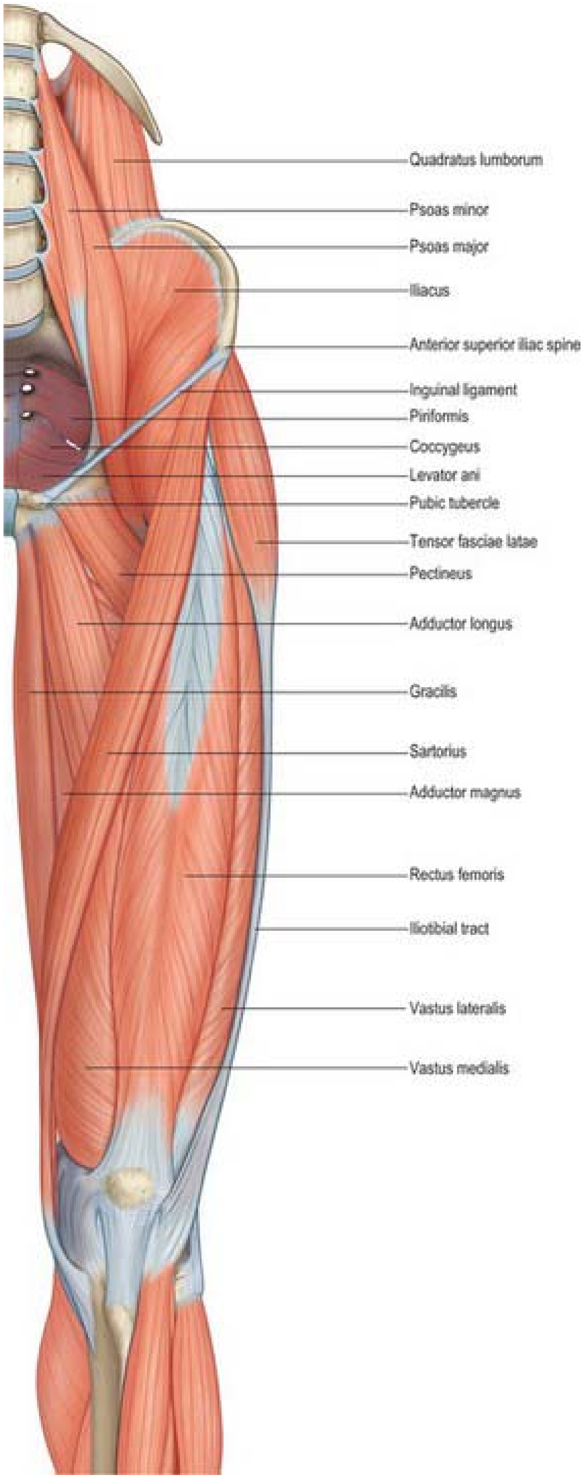
Quadratus lumborum
Psoas minor
Psoas major
Iliacus
Anterior superior iliac spine
Inguinal ligament
Piriformis
Coccygeus
Levator ani
Pubic tubercle
Tensor fasciae latae
Pectineus
Adductor longus
Gracilis
Sartorius
Adductor magnus
Rectus femoris
Iliotibial tract
Vastus lateralis
Vastus medialis

Fig. 80.19 The hip flexors and superficial muscles of the thigh.

The muscle descends along the pelvic brim, continues posterior to the inguinal ligament and anterior to the capsule of the hip joint, and converges to a tendon which, having received on its lateral side nearly all the fibres of iliacus, becomes attached to the lesser trochanter of the femur. The large subtendinous iliac bursa, which occasionally communicates with the cavity of the hip joint, separates the tendon from the pubis and the capsule of the joint.

The complex vertebral attachments of psoas major sometimes display minor numerical variations.

Relations

The upper limit of psoas major is posterior to the diaphragm in the lowest part of the posterior mediastinum. It may be in contact with the posterior extremity of the pleural sac. In the abdomen its anterolateral surface is related to the medial arcuate ligament (a linear arched thickening in the psoas fascia), extraperitoneal tissue and peritoneum, the kidney, psoas minor, renal vessels, ureter, testicular or ovarian vessels and genitofemoral nerve. Anteriorly, the right psoas is overlapped by the inferior vena cava and crossed by the terminal ileum; the left psoas is crossed by the colon. Its posterior surface is related to the transverse processes of the lumbar vertebrae and the medial edge of quadratus lumborum. The lumbar plexus is embedded posteriorly in the substance of psoas major. Medially the muscle is related to the bodies of the lumbar vertebrae and lumbar vessels. Along its anteromedial margin it is in contact with the sympathetic trunk, aortic lymph nodes and, along the pelvic brim, with the external iliac artery. This margin is covered by the inferior vena cava on the right side, and lies posterior and lateral to the abdominal aorta on the left side. In the thigh, psoas is related anteriorly to the fascia lata and the femoral artery, and posteriorly to the capsule of the hip joint from which it is separated by a bursa. At its medial border, it is related to pectineus and the medial circumflex femoral artery, and to the femoral vein, which may overlap it slightly. At its lateral border it is related to the femoral nerve and iliacus. The femoral nerve descends at first through the fibres of psoas major, and then in the furrow between it and iliacus.

Branches of the lumbar plexus diverge from the abdominal part of psoas. Emerging from the lateral border, from above downwards, are the iliohypogastric, ilioinguinal and lateral femoral cutaneous and femoral nerves. Emerging from the anterolateral surface is the genitofemoral nerve. The obturator and accessory obturator nerves and the upper root of the lumbosacral trunk all emerge from the medial border.

Vascular supply

Psoas major is supplied by a rich network of arteries derived from the lumbar, iliolumbar, obturator, external iliac and femoral arteries. In general terms, the upper part of the muscle is supplied by the lumbar arteries, the mid part by the anterior branch of the iliolumbar artery (the main artery to the muscle) with contributions from the deep circumflex and external iliac arteries, and the distal part by the femoral artery and its branches. The psoas sheath has an arterial supply independent from that of the muscle, though the same vessels contribute.

Innervation

Psoas major is innervated by the ventral rami of the lumbar spinal nerves, mainly L1 and 2 with some contribution from L3.

Actions

Psoas major acts together with iliacus; the combination is referred to as iliopsoas. See below with iliacus.

Testing

See below after iliacus.

Psoas minor

Attachments

Psoas minor (Fig. 80.19) is absent in almost 40% of subjects. When present, it lies anterior to psoas major, entirely within the abdomen. It arises from the sides of the bodies of the twelfth thoracic and first lumbar vertebrae and from the disc between them. It ends in a long, flat tendon which is attached to the pecten pubis and ilio-pubic ramus and, laterally, to the iliac fascia.

Relations

Psoas minor lies on psoas major, and its proximal anterior relations are those of the anterior or anteromedial surface of that muscle.

Vascular supply

The main arterial supply to psoas minor is from the lumbar arteries, though there may be minor contributions from other vessels of the network that supplies psoas major.

Innervation

Psoas minor is innervated by a branch from L1.

Action

Psoas minor is probably a weak flexor of the trunk.

Testing

Psoas minor cannot be tested clinically.

Iliacus

Attachments

Iliacus (Fig. 80.19) is a triangular sheet of muscle that arises from the superior two-thirds of the concavity of the iliac fossa, the inner lip of the iliac crest, the ventral sacroiliac and iliolumbar ligaments, and the upper surface of the lateral part of the sacrum (see Fig. 42.36). In front, it reaches as far as the anterior superior and anterior inferior iliac spines, and receives a few fibres from the upper part of the capsule of the hip joint. Most of its fibres converge into the lateral side of the strong tendon of psoas major, and the muscles then insert together into the lesser trochanter, but some fibres are attached directly to the femur 2.5 cm below and in front of the lesser trochanter.

Relations

In the abdomen, the anterior surface of iliacus is related to its fascia (which separates the muscle from extraperitoneal tissue and peritoneum), the lateral femoral cutaneous nerve, the caecum (on the right) and the iliac part of the descending colon (on the left). On its posterior surface is the iliac fossa; at its medial border, psoas major and the femoral nerve. In the thigh, its anterior surface is in contact with the fascia lata, rectus femoris, sartorius and profunda femoris artery, and its posterior surface is in contact with the capsule of the hip joint, from which it is partially separated by a bursa it shares with psoas major.

Vascular supply

Iliacus is supplied by the same arterial network as psoas major, and there is mutual overlap of the arterial territories of each muscle. The main supply is from the iliac branches of the iliolumbar artery, with contributions from the deep circumflex iliac and obturator arteries, and branches of the femoral artery.

Innervation

Iliacus is innervated by branches of the femoral nerve, L2 and 3.

Actions

Psoas major, acting from above together with iliacus, flexes the thigh upon the pelvis. Electromyographic studies do not support the common view that psoas major acts as a medial rotator of the hip joint, but activity has been described in lateral rotation, particularly in the young. When psoas major and iliacus of both sides act from below, they contract powerfully to bend the trunk and pelvis forwards against resistance, as in raising the trunk from the recumbent to the sitting posture when undertaking a ‘sit-up’ exercise.

Electromyography does not support the commonly held belief that unilateral action of psoas causes lateral and forward flexion of the trunk to that side.

In symmetrical upright stance, iliopsoas has some action from below to maintain the vertebral column upright. Psoas major is active in balancing the trunk while sitting.

Testing

Both psoas and iliacus may be the sites of pathological collections of fluid. An abscess (typically tuberculous) of vertebral origin may track down through psoas and present as a mass in the thigh. Haematoma or infection within the iliacus fascia may present as a mass or as a flexion deformity of the hip.

Iliopsoas may be tested clinically by actively flexing the hip against resistance, in the supine position with hip and knee flexed.

MUSCLES OF THE GLUTEAL REGION

Tensor fasciae latae

Attachments

Tensor fasciae latae (Fig. 80.19) arises from the anterior 5 cm of the outer lip of the iliac crest, from the lateral surface of the anterior superior iliac spine and part of the border of the notch below it, between gluteus medius and sartorius, and from the deep surface of the fascia lata. Proximal attachments may extend to the aponeurotic fascia superficial to gluteus medius. It descends between, and is attached to, the two layers of the iliotibial tract of the fascia lata and usually ends approximately one-third of the way down the thigh, although it may occasionally extend as far as the lateral femoral condyle.

Vascular supply

The muscle itself is supplied mainly by a large ascending branch of the lateral circumflex femoral artery. The tensor fasciae latae musculocutaneous flap is raised on this pedicle. The superior part of the muscle receives branches from the superior gluteal artery. The fascia surrounding the muscle is supplied on its superficial aspect by the superficial circumflex iliac artery and on its deep surface by the lateral circumflex femoral artery.

Innervation

Tensor fasciae latae is innervated by the superior gluteal nerve, L4, 5 and S1.

Actions

Tensor fasciae latae, acting through the iliotibial tract, extends the knee with lateral rotation of the leg; it may also assist in abduction and medial rotation of the thigh, though its role as an abductor is debatable. The muscle helps to maintain upright posture while minimizing energy expenditure on muscle activity: when the subject is standing it acts from below to steady the pelvis on the head of the femur and, through the iliotibial tract, to steady the condyles of the femur on the tibial condyles while the knee extensors are relaxed. The muscle aids gluteus medius in postural abduction at the hip. Postural control is its main function.

In the last 20° or so of extension the pull of the iliotibial tract is anterior to the flexion axis of the knee and so the tensor fasciae latae is a weak extensor. Flexion greater than 20° leads to the iliotibial tract passing posterior to the axis of flexion so that the muscle becomes a weak flexor.

Testing

When the thigh is flexed against gravity and the knee is extended, an angular depression appears immediately below the anterior superior iliac spine: its lateral boundary is tensor fasciae latae. If the thigh is then abducted against resistance, the muscle can be felt, and sometimes seen.

Gluteus maximus

Attachments

Gluteus maximus (Fig. 80.20) is the largest and most superficial muscle in the gluteal region. It is a broad, thick quadrilateral mass, which, with its overlying adipose fascia, forms the familiar prominence of the buttock. Gluteus maximus is thicker and more extensive in man than in any non-human primate, features that presumably correlate with the evolutionary transition to bipedality and a permanently upright posture. The muscle has a coarse fascicular architecture, with large bundles of fibres separated by fibrous septa. It arises from the posterior gluteal line of the ilium, and the rough area of bone, including the crest, immediately above and behind it; from the aponeurosis of erector spinae; the dorsal surface of the lower part of the sacrum and the side of the coccyx; the sacrotuberous ligament; and the fascia (gluteal aponeurosis) which covers gluteus medius. There may be additional slips from the lumbar aponeurosis or ischial tuberosity. The muscle may also be bilaminar. The fibres descend laterally; the upper part of the muscle, together with the superficial fibres of the lower part, ends in a thick tendinous lamina which passes lateral to the greater trochanter and is attached to the iliotibial tract of the fascia lata. The deeper fibres of the lower part of the muscle are attached to the gluteal tuberosity between vastus lateralis and adductor magnus.

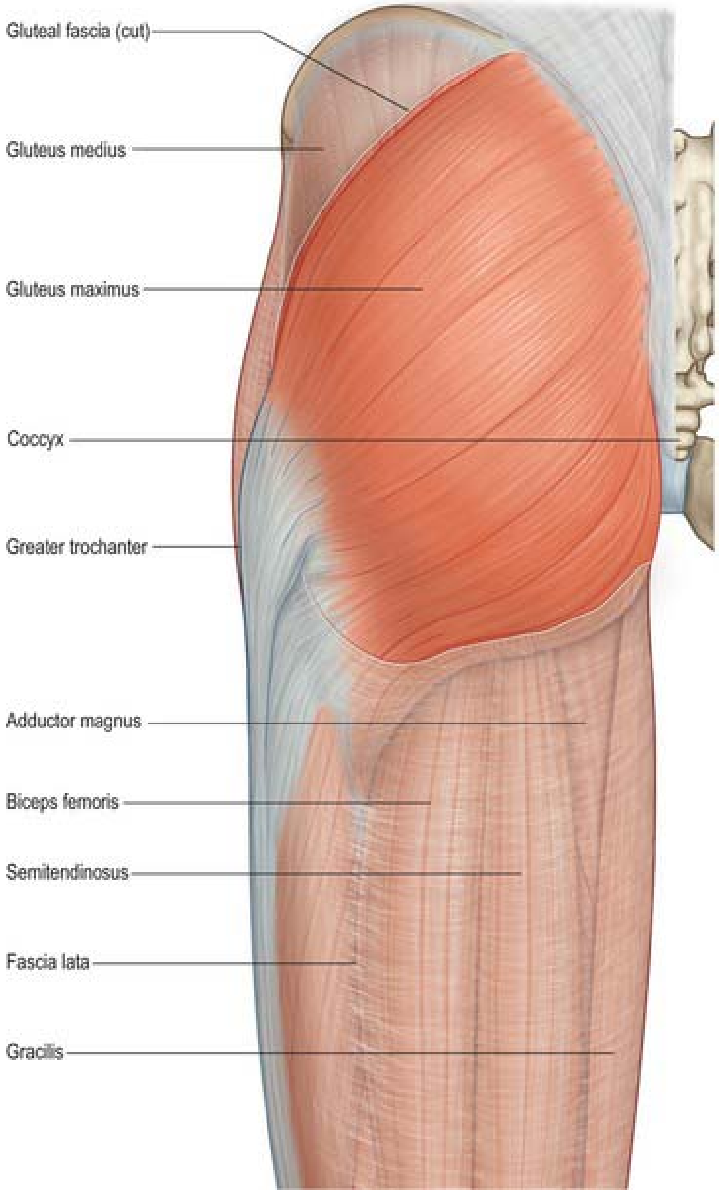
Gluteal fascia (cut)
Gluteus medius
Gluteus maximus
Coccyx
Greater trochanter
Adductor magnus
Biceps femoris
Semitendinosus
Fascia lata
Gracilis

Fig. 80.20 Gluteus maximus, posterior view.

Relations

A thin fascia separates the superficial surface of gluteus maximus from the overlying thick adipose subcutaneous tissue. The deep surface of the muscle is related to the ilium, sacrum, coccyx, sacrotuberous ligament, part of gluteus medius, piriformis, the gemelli, obturator internus, quadratus femoris, the ischial tuberosity, greater trochanter, and the attachments of biceps femoris, semitendinosus, semimembranosus and adductor magnus to the ischial tuberosity. Three bursae lie deep to gluteus maximus: trochanteric, over the greater trochanter; gluteofemoral, between the tendon of gluteus maximus and that of vastus lateralis; and ischiofemoral, over the gluteal tuberosity, which is less commonly present.

The superficial division of the superior gluteal artery reaches the deep surface of the muscle between piriformis and gluteus medius. The inferior gluteal and internal pudendal vessels, the sciatic, pudendal and posterior femoral cutaneous nerves, muscular branches from the sacral femoral cutaneous nerves, and muscular branches from the sacral plexus all leave the pelvis below piriformis. The first perforating artery and the terminal branches of the medial circumflex femoral artery are also deep to the lower part of gluteus maximus. Its upper border is thin and overlies gluteus medius. Its prominent lower border is free and slopes downwards and laterally. It is crossed by the horizontal gluteal fold (the posterior flexure line of the hip joint), which marks the upper limit of the back of the thigh on the surface.

Vascular supply

The dominant vascular pedicle is usually that of the inferior gluteal artery, which supplies approximately two-thirds of the muscle. The remainder is supplied mainly by the superior gluteal artery, though this may sometimes be the dominant vessel. The lateral and distal borders of the muscle receive a supply from the first profunda perforator and from the medial circumflex femoral artery. Minor branches may be derived from the lateral circumflex femoral, lateral sacral and internal pudendal arteries.

Gluteus maximus musculocutaneous flaps may be based on either of the gluteal vessels or on the first profunda perforator, depending on the site and size of the defect requiring coverage.

Innervation

Gluteus maximus is innervated by the inferior gluteal nerve, L5 and S1 and 2.

Actions

Acting from the pelvis, gluteus maximus can extend the flexed thigh and bring it into line with the trunk. Acting from its distal attachment, it may prevent the forward momentum of the trunk from producing flexion at the supporting hip during bipedal gait. The muscle is inactive during standing, when swaying forwards at the ankle joints, or when bending forwards at the hip joints to touch the toes. However, it acts with the hamstrings in raising the trunk after stooping, by rotating the pelvis backwards on the head of the femur. It is intermittently active in the walking cycle and in climbing stairs, and continuously active in strong lateral rotation of the thigh. Its upper fibres are active in powerful abduction of the thigh. It is a tensor of the fascia lata, and through the iliotibial tract it stabilizes the femur on the tibia when the knee extensor muscles are relaxed.

Testing

Extension of the hip against resistance, in the supine or prone position.

Gluteus medius

Attachments

Gluteus medius is a broad, thick muscle (Fig. 80.20, Fig. 80.21A). It arises from the outer surface of the ilium between the iliac crest and posterior gluteal line above, and the anterior gluteal line below, and also from the strong fascia superficial to its upper part. The fibres converge to a flat tendon that attaches to a ridge that slants downwards and forwards on the lateral surface of the greater trochanter.

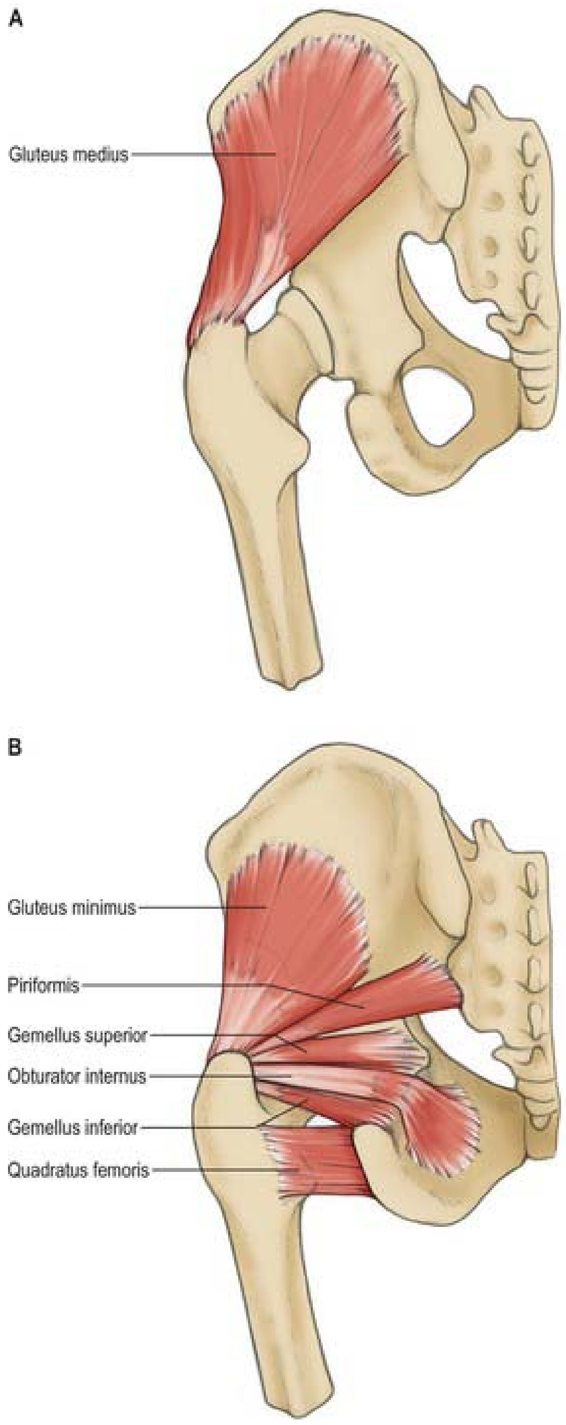
A
Gluteus medius
B
Gluteus minimus
Piriformis
Gemellus superior
Obturator internus
Gemellus inferior
Quadratus femoris

Fig. 80.21 **A**, Gluteus medius. **B**, Gluteus minimus and short external rotators of the hip.

(From Sobotta 2006.)

A deep slip of the muscle may be attached to the upper border of the trochanter. The posterior edge of gluteus medius sometimes blends with piriformis.

Relations

The posterior third of gluteus medius is covered by gluteus maximus, but it is superficial in its anterior two-thirds, where it is covered by a strong layer of deep fascia. Its deep surface is related to gluteus minimus. Branches of the deep divisions of the superior gluteal nerve and artery run between the medius and minimus muscles and are vulnerable during anterolateral and lateral approaches to the hip that involve splitting gluteus medius (see Fig. 80.22). Where the tendon glides on the anterosuperior part of the lateral surface of the trochanter, a bursa (trochanteric bursa of gluteus medius) separates it from the bone.

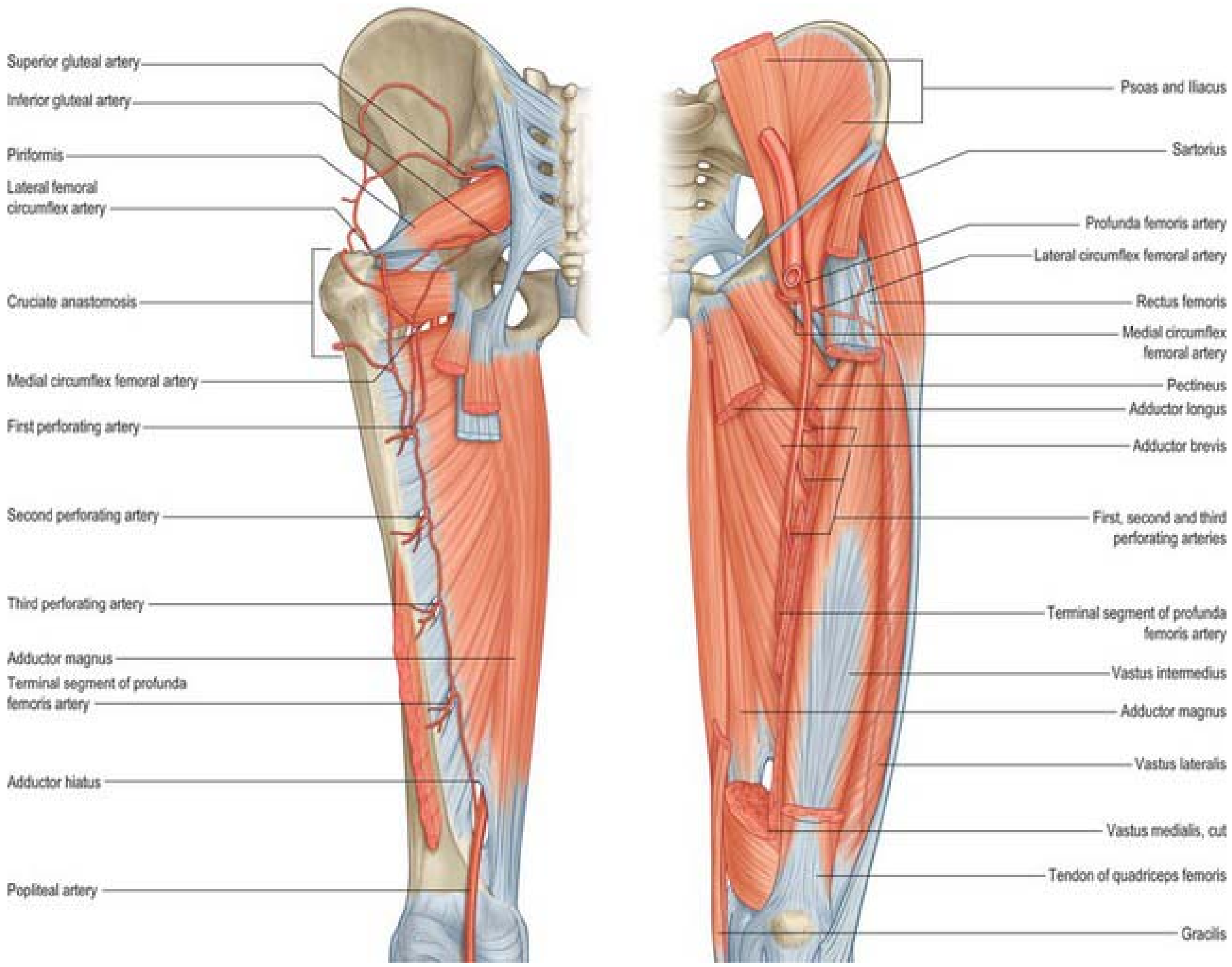
Superior gluteal artery
Inferior gluteal artery
Piriformis
Lateral femoral circumflex artery
Cruciate anastomosis
Medial circumflex femoral artery
First perforating artery
Second perforating artery
Third perforating artery
Adductor magnus
Terminal segment of profunda femoris artery
Adductor hiatus
Popliteal artery
Psoas and Iliacus
Sartorius
Profunda femoris artery
Lateral circumflex femoral artery
Rectus femoris
Medial circumflex femoral artery
Pectineus
Adductor longus
Adductor brevis
First, second and third perforating arteries
Terminal segment of profunda femoris artery
Vastus intermedius
Adductor magnus
Vastus lateralis
Vastus medialis, cut
Tendon of quadriceps femoris
Gracilis

Fig. 80.22 The arteries and muscles of the left gluteal and femoral regions. **A**, Posterior aspect. **B**, Anterior aspect.

(From Drake, Vogl and Mitchell 2005.)

Vascular supply

The main supply to gluteus medius is from the deep branch of the superior gluteal artery. The distal part of the muscle is supplied by the trochanteric anastomosis.

Innervation

Gluteus medius is innervated by the superior gluteal nerve, L4, 5 and S1.

Actions

Considered below with gluteus minimus.

Testing

Considered below with gluteus minimus.

Gluteus minimus

Attachments

Gluteus minimus lies deep to gluteus medius (Fig. 80.21B). The fan-shaped muscle arises from the outer surface of the ilium between the anterior and inferior gluteal lines and, behind, from the margin of the greater sciatic notch. The fibres converge below to the deep surface of an aponeurosis that ends in a tendon which is attached to an anterolateral ridge on the greater trochanter and contributes an expansion to the capsule of the hip joint.

The muscle may divide into anterior and posterior parts. Separate slips may pass to piriformis, gemellus superior, or vastus lateralis.

Relations

Branches of the deep division of the superior gluteal artery and nerve run on the superficial surface of the muscle. The reflected tendon of rectus femoris and the capsule of the hip joint are deep to gluteus minimus. A bursa (trochanteric bursa of gluteus minimus) separates the tendon from the medial part of the anterior surface of the greater trochanter.

Vascular supply

Gluteus minimus is supplied from both its surfaces, from the main trunk and the deep branch of the superior gluteal artery, with a contribution at its femoral attachment from the trochanteric anastomosis (Fig. 80.22).

Innervation

Gluteus minimus is innervated by the superior gluteal nerve, L4, 5 and S1.

Actions of gluteus medius and minimus

Both gluteus medius and minimus, acting from the pelvis, abduct the thigh, and their anterior fibres rotate it medially. Acting from the femur, they play an essential part in maintaining the trunk upright when the foot of the opposite side is raised from the ground in walking and running. In this phase the body weight tends to make the pelvis sag downwards on the unsupported side. This is counteracted by the gluteus medius and minimus of the supporting side, which, acting from below, exert such powerful traction on the hip bone that the pelvis is actually raised a little on the unsupported side. In symmetrical standing with the feet somewhat separated, the abductor muscles are usually ‘silent’ on electromyography, but with the feet placed parallel and close together they are active.

Testing

The supportive effect of the glutei (medius and minimus) on the pelvis when the contralateral foot is raised depends on the following conditions. The two muscles, and their innervation, must be functioning normally. The components of the hip joint, which forms the fulcrum, must be in their usual relation. The neck of the femur must be intact, with its normal angulation to the shaft.

When any one of these conditions is not fulfilled, e.g. in paralysis of the glutei, congenital dislocation of the hip, or coxa vara, the supporting mechanism is upset and the pelvis sinks on the unsupported side when the patient tries to stand on the affected limb. This is known clinically as Trendelenburg’s sign. Individuals with paralysis of gluteus medius and minimus have a characteristic lurching gait. Provided that these two muscles are intact, paralysis of other muscles acting on the hip joint produces remarkably little deficit in walking, or even in running.

Gluteus medius and minimus may be tested together by medial (internal) rotation of the thigh against resistance, in the supine position with hip and knee flexed. Both muscles may be tested together with tensor fasciae latae by abduction of the lower limb against resistance, in the supine position with the knee extended.

Piriformis

Attachments

Piriformis (see Fig. 63.1, Fig. 80.21B) occupies a central position in the buttock, where it lies in the same plane as gluteus medius. It arises from the anterior surface of the sacrum by three digitations, which are attached to the portions of bone between the pelvic sacral foramina, and to the grooves leading from the foramina (see Fig. 42.36). It also arises from the gluteal surface of the ilium near the posterior inferior iliac spine, from the capsule of the adjacent sacroiliac joint, and sometimes from the upper part of the pelvic surface of the sacrotuberous ligament. The muscle passes out of the pelvis through the greater sciatic foramen, which it substantially fills. Here it constitutes an important surgical landmark in the identification of structures that emerge above and below it. It inserts into the medial side of the upper border of the greater trochanter of the femur via a rounded tendon that lies behind and above, but is often partially blended with, the common tendon of obturator internus and the gemelli. The muscle itself may be fused with gluteus medius.

Relations

Within the pelvis, the anterior surface of piriformis is related to the rectum (especially on the left), the sacral plexus of nerves and branches of the internal iliac vessels. The posterior surface lies against the sacrum. Outside the pelvis, its anterior surface is in contact with the posterior surface of the ischium and capsule of the hip joint and its posterior surface with gluteus maximus. Its upper border is in contact with gluteus medius and the superior gluteal vessels and nerve, its lower border with coccygeus and gemellus superior. The inferior gluteal and internal pudendal vessels, the sciatic, posterior femoral cutaneous and pudendal nerves, and muscular branches from the sacral plexus appear in the buttock in the interval between piriformis and gemellus superior. The relationship between piriformis and the sciatic nerve is variable. The undivided nerve may emerge above the muscle or through the muscle. The major divisions of the nerve may lie either side of the muscle, or (the most common variant) one division passes between the heads of a divided muscle and one division either above or below.

Piriformis can occasionally cause entrapment of the sciatic nerve in the buttock, giving rise to the so-called ‘piriformis syndrome’.

Vascular supply

In the buttock, piriformis is supplied mainly from the superior gluteal artery, with contributions from the gemellar branches of the internal pudendal. There may be a separate branch from the inferior gluteal artery. In the pelvis the main supply is from the lateral sacral artery, with contributions from both gluteal vessels.

Innervation

Piriformis is innervated by branches from L5, S1 and 2.

Actions

Piriformis rotates the extended thigh laterally, but abducts the flexed thigh.

Testing

Clinically it is not possible to test piriformis alone; however, for suspected injury to piriformis the best provocative test is to ask the seated subject to abduct the thighs. Buttock pain suggests piriformis injury.

Obturator internus

Attachments

Obturator internus (see Fig. 63.1, Fig. 80.21B) is situated partly within the true pelvis and partly posterior to the hip joint. It arises from the internal surface of the anterolateral wall of the lesser pelvic cavity. Its attachments, which almost surround the obturator foramen, are to the inferior ramus of the pubis, the ischial ramus, and the pelvic surface of the hip bone below and behind the pelvic brim, to the upper part of the greater sciatic foramen above and behind, to the obturator foramen below and in front (Fig. 80.5B). It also arises from the medial part of the pelvic surface of the obturator membrane, from the tendinous arch that completes the obturator canal, and, to a small extent, from the obturator fascia that covers the muscle. The fibres converge towards the lesser sciatic foramen and end in four or five tendinous bands on the deep surface of the muscle. These bands make a lateral right-angled turn around the grooved surface of the ischium between its spine and tuberosity. The grooved surface is covered with a smooth layer of hyaline cartilage and is separated from the tendon by a bursa: ridges on the surface correspond to furrows between the tendinous bands. These bands leave the pelvis through the lesser sciatic foramen and unite to form a single flattened tendon that passes horizontally across the capsule of the hip joint. The gemelli fuse with this tendon before it inserts into an anterior impression on the medial surface of the greater trochanter anterosuperior to the trochanteric fossa. A long, narrow bursa is usually interposed between the tendon and the capsule of the hip joint, and occasionally communicates with the bursa between the tendon and the ischium.

Relations

Within the pelvis, the anterolateral surface of the muscle is in contact with the obturator membrane and inner surface of the lateral wall of the pelvis. Its posteromedial surface is related to the obturator fascia, the origin of levator ani, and the sheath that surrounds the internal pudendal vessels and pudendal nerve, and forms the lateral wall of the ischiorectal fossa. Outside the pelvis, the muscle is covered by gluteus maximus, is crossed posteriorly by the sciatic nerve and passes behind the hip joint. As the tendon of obturator internus emerges from the lesser sciatic foramen it is overlapped both above and below by the two gemelli, which form a muscular canal for it. Near its termination the gemelli pass anterior to the tendon and form a groove in which it lies.

Vascular supply

The main arterial supply of the extrapelvic part of obturator internus is from the gemellar branches of the internal pudendal artery. The intrapelvic part is supplied by the obturator artery, which gives branches to both surfaces of the muscle: it is also supplied by small branches from the internal pudendal artery.

Innervation

Obturator internus is innervated by the nerve to obturator internus, L5 and S1.

Actions

See below, with obturator externus.

Obturator externus

Attachments

Obturator externus (Fig. 80.23) is a flat, triangular muscle covering the external surface of the anterior pelvic wall. It arises from the anteromedial two-thirds of the external surface of the obturator membrane, and from the adjacent bone of the pubic and ischial rami, extending for a short distance onto their pelvic surfaces between the margin of the obturator foramen and the obturator membrane. The whole muscle, and the tendon into which its fibres converge, spirals backwards, laterally and upwards, and thus crosses the inferior aspect and then the back of the neck of the femur and lower part of the capsule of the hip joint to end in the trochanteric fossa of the femur.

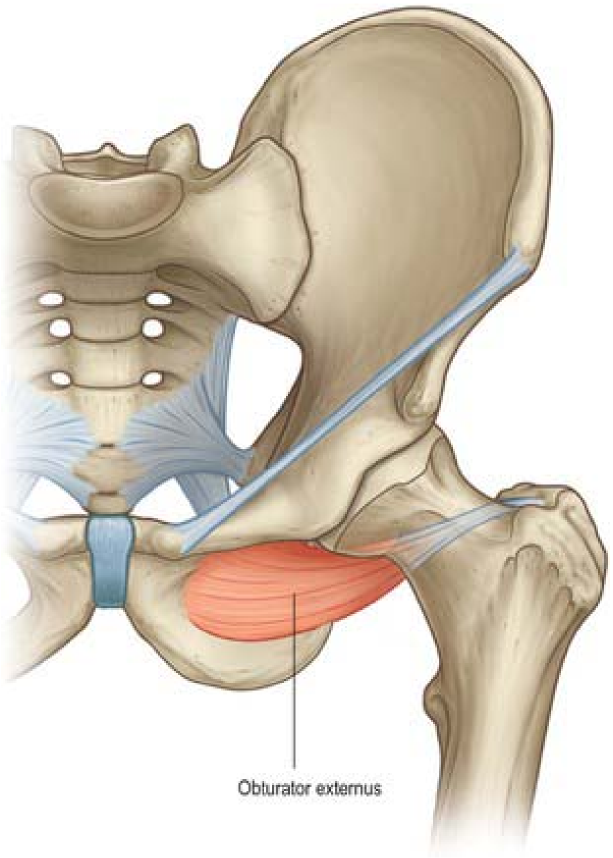

Fig. 80.23 Obturator externus: anteroinferior aspect.

(Adapted from Drake, Vogl and Mitchell 2005.)

Relations

A bursa, which communicates with the hip joint, may be interposed between the tendon and the hip joint capsule and femoral neck. The obturator vessels lie between the muscle and the obturator membrane. The anterior branch of the obturator nerve reaches the thigh by passing in front of the muscle, and the posterior branch by piercing it.

Vascular supply

Obturator externus receives a variable pattern of supply from the obturator and medial circumflex femoral arteries.

Innervation

Obturator externus is innervated by the posterior branch of the obturator nerve, L3 and 4.

Actions

It has been suggested that the short muscles around the hip joint, pectineus, piriformis, obturators, gemelli and quadratus femoris, are more important as postural muscles than as prime movers, acting as adjustable ligaments to maintain the stability and integrity of the hip. However, these muscles are largely inaccessible to direct observation, and because of the hazards presented by their close relationship to important neurovascular structures there is a total lack of electromyographic data in man. In both bipedal walking and vertical climbing obturator externus is recruited during the early part of swing phase: in climbing it effects lateral rotation of the thigh, and in walking it probably counteracts the tendency to medial rotation produced by the anterior adductor muscles at this stage of the cycle. Obturator internus differs from externus in its pattern of use but its role in bipedal walking remains unclear. Its attachments suggest that it, like the gemelli, is a lateral rotator of the extended thigh and an abductor of the flexed thigh. These actions may be used to antagonize unwanted components of movement produced by the primary locomotor muscles.

Testing

The short rotators cannot be tested individually, but external rotation of the extended hip and abduction of the flexed hip against resistance tests them as a group.

Gemellus inferior and gemellus superior

Attachments

Gemellus inferior arises from the upper part of the lateral surface of the ischial tuberosity, immediately below the groove for the tendon of obturator internus. It blends with the lower border of this tendon, and inserts with it into the medial surface of the greater trochanter.

Gemellus superior, the smaller of the two gemelli, arises from the dorsal surface of the ischial spine, blends with the upper border of the tendon of obturator internus, and inserts with it into the medial surface of the greater trochanter. It is sometimes absent.

The two gemelli can be regarded as accessory to obturator internus (see Fig. 80.21B).

Relations

The relations of the gemelli are as for the extrapelvic part of obturator internus.

Vascular supply

The superior gemellus is supplied by the internal pudendal artery and its gemellar branches; by the inferior gluteal and sometimes also by the superior gluteal artery. The inferior gemellus is supplied mainly by the medial circumflex femoral artery.

Innervation

Gemellus superior is innervated by the nerve to obturator internus, L5, S1 and S2. Gemellus inferior is innervated by the nerve to quadratus femoris,L4, L5 and S1.

Actions

The gemelli rotate the extended thigh laterally and abduct the flexed thigh.

Testing

See testing of obturator externus above.

Quadratus femoris

Attachments

Quadratus femoris (see Fig. 80.21B) is a flat, quadrilateral muscle lying between gemellus inferior and the upper margin of adductor magnus, from which it is separated by the transverse branch of the medial circumflex femoral artery. It arises from the upper part of the external aspect of the ischial tuberosity and inserts into a small tubercle a little above the middle of the trochanteric crest of the femur and into the bone for a short distance below. It may be absent.

Relations

The muscle passes behind the hip joint and the neck of the femur, separated from them by the tendon of obturator externus and the ascending branch of the medial circumflex femoral artery (which may cause troublesome bleeding if injured during the posterior approach to the hip). The sciatic nerve crosses the muscle posteriorly. A bursa is often present between the muscle and the lesser trochanter.

Vascular supply

Branches pass to the superficial surface of the muscle from the inferior gluteal artery and from the medial circumflex femoral artery. The latter vessel also supplies the deep surface.

Innervation

Quadratus femoris is innervated by the nerve to quadratus femoris, L5 and S1.

Action

Quadratus femoris produces lateral rotation of the thigh.

Testing

See testing of obturator externus.

MUSCLES OF THE THIGH

The presence and position of the femoral neck cause the femoral shaft to lie obliquely, which means that the anterior (extensor) muscle group, the quadriceps, runs obliquely distally and medially and so applies a pull to the patella which is both laterally and proximally directed. The adductor muscles occupy the region between the quadriceps and the medial margin of the thigh. They are attached distally to the posterior surface of the femur and lie more posteriorly than the quadriceps. The posterior (flexor) muscle group, the hamstrings, lie behind the adductors. The attachments of these muscles determine the nature and direction of displacement of femoral shaft fractures.

Anterior compartment

The muscles of the anterior compartment (Figs 80.2, 80.19) include sartorius and rectus femoris, which can act both at the hip and knee joints, and vasti medialis, lateralis, and intermedius, which act only at the knee. Articularis genu, a derivative of vastus intermedius, completes the group: it retracts the synovial capsule of the knee joint. Rectus femoris and the vasti extend the knee joint through a common tendon and hence are collectively termed the quadriceps femoris muscle. Adductor longus and pectineus are sometimes considered to be part of both the anterior and the adductor compartments.

Sartorius

Attachments

Sartorius is a narrow strap muscle, and is the longest muscle in the body. It arises by tendinous fibres from the anterior superior iliac spine and the upper half of the notch below it. It crosses the thigh obliquely over to the medial side, then descends more vertically to the medial side of the knee. The muscle fibres terminate at this point and a thin, flattened tendon curves obliquely forwards and expands into a broad aponeurosis. The aponeurosis is attached to the proximal part of the medial surface of the tibia in front of gracilis and semitendinosus, together forming the ‘pes anserinus’ (Fig.

80.24). A slip from its upper margin blends with the capsule of the knee joint, and another from its lower margin merges with the superficial layer of the deep fascia on the medial side of the leg. This sheet of tissue passes inferiorly to lie superficial to and over the distal insertions of gracilis and semitendinosus. It has to be split by sharp dissection to reveal these two tendons if they need to be harvested, e.g. in cruciate ligament surgery (Fig. 80.24).

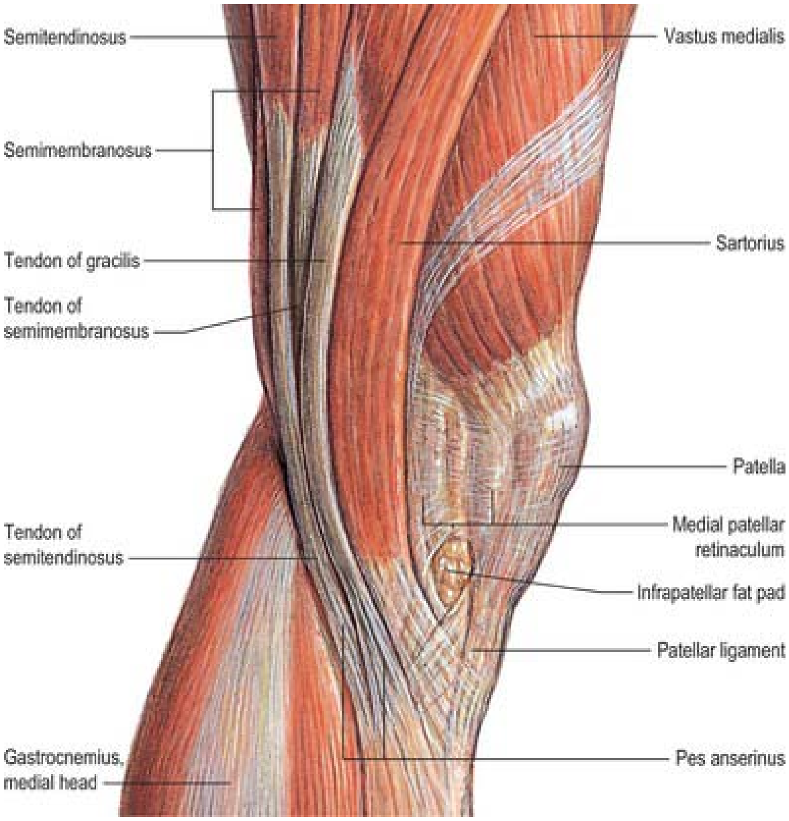
Semitendinosus
Semimembranosus
Tendon of gracilis
Tendon of semimembranosus
Tendon of semitendinosus
Gastrocnemius, medial head
Vastus medialis
Sartorius
Patella
Medial patellar retinaculum
Infrapatellar fat pad
Patellar ligament
Pes anserinus

Fig. 80.24 Distal attachment of muscles of the thigh: medial aspect.

(From Sobotta 2006.)

In some cases sartorius is absent, while in others the muscle may possess an extra head: when the latter occurs, the extra head is attached to the pectineal line or to the femoral sheath. Variations in the distal attachment of sartorius, in the vicinity of the knee, have been described.

Relations

The relations of sartorius are described in the femoral triangle (see below).

Vascular supply

The main arterial supply to sartorius is derived from multiple branches of the femoral system, and enters the medial half of the muscle from its deep surface. Vessels supplying the proximal third of sartorius may arise from the common femoral, the main trunk of the profunda, the artery of the quadriceps, the superficial femoral or the lateral circumflex femoral artery. There may be an additional proximal supply from the superficial circumflex iliac artery. Those supplying the middle third of the muscle arise from the superficial femoral artery. The distal vessels arise from the superficial femoral within the adductor canal and from the descending genicular artery.

Innervation

Sartorius is innervated by the femoral nerve, L2 and 3.

Actions

Sartorius assists in flexing the leg at the knee, and the thigh on the pelvis, particularly when these two movements are combined. It also helps to abduct the thigh and to rotate it laterally. (Together with inversion of the foot, these movements bring the sole of the foot into direct view.) The fact that sartorius represents only 1% of the physiological cross-sectional area of all muscles which cross the hip or knee joint would appear to suggest that its role in walking is a minor one. In a subject ascending steps, electromyographic activity of sartorius increases during lateral rotation of the thigh at the end of the swing phase immediately preceding heel strike, which presumably decelerates the limb. Sartorius may therefore have a significant involvement in climbing.

Testing

When it contracts against gravity, as it usually does, sartorius can be both seen and felt in the living subject.

Femoral triangle

The femoral triangle is a depressed, intermuscular space in the anteromedial aspect of the proximal thigh, lying immediately distal to the inguinal ligament. The latter constitutes the base of the femoral triangle’s inverted triangular outline. Its lateral boundary is the medial margin of sartorius. Its medial boundary is the medial margin of adductor longus. Its distal extremity, the apex, is where sartorius overlaps adductor longus. Its floor is provided laterally by iliacus and psoas major, medially by pectineus and adductor longus. Its roof is the overlying fascia lata. The femoral vessels, passing from midbase to apex, are in the deepest part of the triangle. Lying lateral to the artery and outside the femoral sheath is the femoral nerve, which, on entering the femoral triangle divides into multiple branches. The triangle also contains fat and lymph nodes.

Quadriceps femoris

Quadriceps femoris (Figs 80.2, 80.19), the great extensor muscle of the leg, covers almost all of the front and sides of the femur. It can be divided into four parts, each named individually. One, rectus femoris, arises from the ilium and travels straight down the middle of the thigh, its shape and path determining its name. The other three arise from the shaft of the femur and surround it (apart from the linea aspera) from the trochanters to the condyles: vastus lateralis is lateral to the femur, vastus medialis is medial to it, and vastus intermedius lies in front of the femur. Rectus femoris crosses both hip and knee joints, while the three vasti only cross the knee joint.

The tendons of the four components of quadriceps unite in the lower part of the thigh to form a single strong tendon attached to the base of the patella, and some fibres continue over it to blend with the patellar tendon. The patella is a sesamoid bone in the quadriceps tendon, and the patellar tendon, which extends from the patellar apex to the tubercle of the tibia, is the continuation of the main tendon. The medial and lateral patellar retinacula are expansions from its borders. The suprapatellar bursa (a synovial extension of the knee joint) lies between the femur and the suprapatellar part of the quadriceps tendon. The deep infrapatellar bursa lies between the patellar tendon and the proximal end of the tibia.

The arterial supply to the quadriceps group has been traditionally ascribed to a single branch of either the profunda femoris or of the lateral circumflex femoral, the ‘artery of the quadriceps’. This vessel, which may be large, occasionally arises directly from the femoral artery. However, according to Taylor & Razaboni (1994) this artery does not supply all four components of the quadriceps: vastus medialis is supplied directly from the (superficial) femoral artery. The supply of the individual muscle components is described below: their sheaths may have an additional and variable supply.

Quadriceps as a group shows little anatomical variation.

Rectus femoris

Attachments

Rectus femoris is fusiform. Its superficial fibres are bipennate, the deep fibres parallel. It has a double origin on the ilium: a straight tendon arises from the anterior inferior iliac spine, and a thinner, flatter reflected tendon from a groove above the acetabulum and from the fibrous capsule of the hip joint. The two unite at an acute angle and spread into an aponeurosis that is prolonged downwards on the anterior surface of the muscle: the muscular fibres arise from this aponeurosis. The fibres end in a broad, thick aponeurosis that forms over the lower two-thirds of its posterior surface and gradually narrows into the thick, flat tendon by which it is attached to the base of the patella. This constitutes the superficial central part of the quadriceps tendon.

Rectus femoris may arise from the anterior superior iliac spine, and its reflected head may be absent.

Relations

Proximally the muscle is covered by tensor fasciae latae, iliacus and sartorius. The reflected head lies beneath gluteus minimus. The capsule of the hip joint, vastus intermedius, the anterior borders of vasti lateralis and medius, the lateral circumflex femoral artery and some branches of the femoral nerve all lie deep to rectus femoris.

Vascular supply

There are two main pedicles, a superior and an inferior. The superior enters rectus femoris at the junction of its upper and middle thirds and arises from the ‘artery of the quadriceps’. The inferior and larger branch arises from the ‘artery of the quadriceps’ at about midthigh level and enters the muscle a few centimetres more distally. There are additional contributions from the lateral circumflex femoral and, less often, the superficial circumflex iliac arteries.

Vastus medialis and vastus medialis obliquus

Attachments

Vastus medialis arises from the lower part of the intertrochanteric line, spiral line, medial lip of the linea aspera, proximal part of the medial supracondylar line, the tendons of adductor longus and magnus, and the medial intermuscular septum. Its fibres pass downwards and forwards at an average angle of 15° to the long axis of the femur, most of them into an aponeurosis on the deep surface of the muscle which is attached to the medial border of the patella and quadriceps tendon. An expansion from this aponeurosis reinforces the capsule of the knee joint and is attached below to the medial condyle of the tibia.

The lowest fibres are nearly horizontal and form a bulge in the living subject, medial to the upper half of the patella. Some authors distinguish this part of the muscle as the vastus medialis obliquus, with fibres that originate largely from the tendon of adductor magnus and insert into the medial border of the patella. It plays an important role in the function of patellofemoral joint.

Relations

Vastus medialis is partly covered by rectus femoris and sartorius. In the central part of the thigh it forms the lateral wall of the adductor (Hunter’s) canal.

Vascular supply

Vastus medialis is supplied by three branches of the (superficial) femoral artery. The superior and middle branches arise, sometimes from a common trunk, proximal to the adductor canal, while the inferior arises within the canal. There may also be minor branches from the profunda femoris and descending genicular arteries.

Vastus lateralis

Attachments

Vastus lateralis is the largest component of quadriceps femoris. It arises by a broad aponeurosis from the upper part of the intertrochanteric line, the anterior and inferior borders of the greater trochanter, the lateral lip of the gluteal tuberosity, and the proximal half of the lateral lip of the linea aspera. This aponeurosis covers the proximal three-quarters of the muscle; many additional fibres arise from its deep surface. A few fibres also arise from the tendon of gluteus maximus and the lateral intermuscular septum between vastus lateralis and the short head of biceps femoris. The muscular mass thus formed is attached to a strong aponeurosis on the deep surface of the lower part of the muscle. This narrows to a flat tendon, which is attached to the base and lateral border of the patella and blends into the compound quadriceps femoris tendon. It contributes an expansion to the capsule of the knee joint which descends to the lateral condyle of the tibia and blends with the iliotibial tract.

Relations

Vastus lateralis is covered laterally by the fascia lata and the aponeurotic insertions of tensor fasciae latae and gluteus maximus. It is separated from vastus intermedius by branches of the femoral nerve and the lateral circumflex femoral artery. Posteriorly it is separated from biceps femoris by the lateral intermuscular septum.

Vascular supply

There are three main arteries of supply: the superior medial artery arises directly from the lateral circumflex femoral, the inferior medial (the largest of the three) from the ‘artery of the quadriceps’, and the lateral from the first perforating branch of the profunda femoris artery.

Vastus intermedius

Attachments

Vastus intermedius arises from the anterior and lateral surfaces of the upper two-thirds of the femoral shaft, and from the lower part of the lateral intermuscular septum. Its fibres end on the anterior surface of the muscle in an aponeurosis which forms the deep part of the quadriceps tendon and is attached to the lateral border of the patella and the lateral condyle of the tibia.

Vastus intermedius appears to be inseparable from vastus medialis. However, when rectus femoris is reflected a narrow cleft can be seen extending upwards from the medial border of the patella between the two muscles, sometimes as far as the lower part of the intertrochanteric line, proximal to which, the two muscles are frequently fused.

Relations

Vastus intermedius is almost completely covered by the other quadriceps components, except laterally where a small part becomes superficial behind vastus lateralis.

Vascular supply

Vastus intermedius receives a lateral artery of supply, which arises from the ‘artery of the quadriceps’, and a medial artery that arises directly from the profunda. Arteries to the other quadriceps components may also contribute. There is an anastomotic network deep to the muscle: this supplies the suprapatellar pouch and articularis genu and may form a collateral pathway when the (superficial) femoral artery is blocked.

Articularis genu

Articularis genu is a small muscle, usually distinct from vastus intermedius but occasionally blending with it. It consists of several muscular bundles that arise from the anterior surface of the lower part of the femoral shaft and are attached to a proximal reflection of the synovial membrane of the knee joint. It is visible during knee arthroscopy when viewed looking superiorly from within the suprapatellar pouch.

Innervation of quadriceps group

Quadriceps femoris and articularis genu are supplied by the femoral nerve, L2, 3 and 4.

Actions of quadriceps group

Quadriceps femoris extends the knee. Rectus femoris helps to flex the thigh on the pelvis; if the thigh is fixed, it helps to flex the pelvis on the thigh. Rectus can flex the hip and extend the knee simultaneously. Electromyographic studies indicate that the three vasti are not equally active in different phases of extension or rotation. There is little or no activity in quadriceps during standing. Rectus femoris pulls the patella along the line of the mechanical axis of the lower limb (i.e. the line connecting the centres of the hip, knee, and ankle) because its attachment is anterior to the hip joint. The remaining quadriceps are attached to the shaft of the femur and so the pull is lateral as well as proximal. An extremely important dynamic function of vastus medialis obliquus is to counter this lateral vector on the patella during knee motion. Other static factors that help are the depth of the femoral trochlear groove, the buttressing effect of the lateral femoral condyle in the groove, and the restraining action of the medial patellofemoral ligament. Inadequacy of vastus medialis obliquus is a factor in producing patellar instability and pain. Strengthening of this muscle to improve patellar ‘tracking’ on the femur and stability is an important part of physiotherapy regimens for patellofemoral problems.

Articularis genu retracts the synovial suprapatellar bursa proximally during extension of the leg, presumably to prevent interposition of redundant synovial folds between patella and femur.

Testing

The quadriceps group is tested by extending the knee against resistance, in the supine position with the hip flexed.

Adductor compartment

The muscles of the adductor compartment, gracilis, pectineus, adductor longus, adductor brevis, and adductor magnus (Fig. 80.25), have evolved, as their nerve supply suggests, both from flexor and extensor columns. All five muscles cross the hip joint, but only gracilis reaches beyond the knee. They are known collectively as the adductors of the thigh, although their actions are more complex than this, e.g. acting from below they have important roles in balancing the trunk on the lower limb during walking.

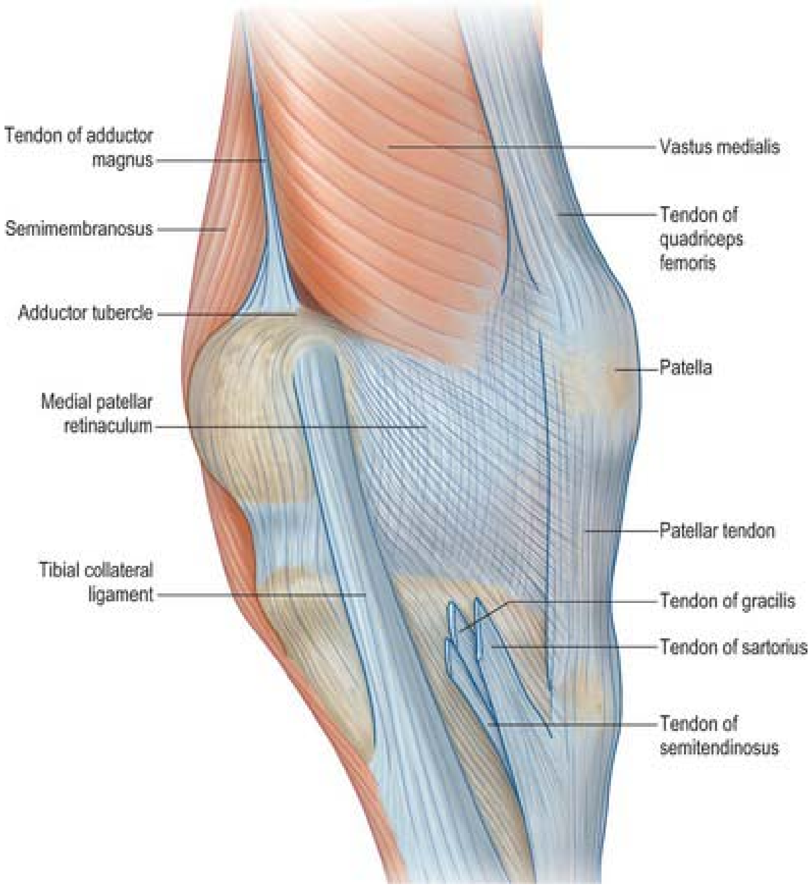
Tendon of adductor magnus
Semimembranosus
Adductor tubercle
Medial patellar retinaculum
Tibial collateral ligament
Vastus medialis
Tendon of quadriceps femoris
Patella
Patellar tendon
Tendon of gracilis
Tendon of sartorius
Tendon of semitendinosus

Fig. 80.25 Anteromedial aspect of the left knee region showing distal attachments of sartorius, gracilis, and semitendinosus.

Their blood supply is derived from the profunda, medial circumflex femoral, (superficial) femoral and obturator arteries. The profunda (or sometimes the first perforator) supplies a large branch, the ‘artery of the adductor muscles’.

Gracilis

Attachments

Gracilis (Figs 80.2, 80.19) is the most superficial of the adductor group. It is thin and flat, broad above, narrow and tapering below. It arises by a thin aponeurosis from the medial margins of the lower half of the body of the pubis, the whole of the inferior pubic ramus, and the adjoining part of the ischial ramus. The fibres descend vertically into a rounded tendon, often harvested as a knee ligament graft, which passes across the medial condyle of the femur posterior to the tendon of sartorius. It then curves around the medial condyle of the tibia, where it fans out and is attached to the upper part of the medial surface of the tibia, just below the condyle, forming part of the pes anserinus. A few fibres from the lower part of the tendon continue into the deep fascia of the lower leg. Often there is a slip that blends with the tendon of the medial head of gastrocnemius. Unless divided this can lead to problems during surgical harvesting of the gracilis tendon.

Relations

The muscle is covered medially by the fascia lata throughout most of its length. Deep to gracilis lie adductor brevis and adductor magnus. The tibial attachment is immediately proximal to that of semitendinosus, and its upper edge is overlapped by the tendon of sartorius, with which it is partly blended. It is separated from the medial collateral ligament of the knee joint by the tibial intertendinous bursa.

Vascular supply

The arterial supply to gracilis enters via its lateral surface. The main pedicle arises from the ‘artery to the adductors’ of the profunda and enters at the junction of the upper and middle thirds of the muscle. The gracilis musculocutaneous flap is based on this pedicle. A less important artery enters the distal third of the muscle from the femoral artery. There is a minor proximal supply from the medial circumflex femoral.

Innervation

Gracilis is innervated by the obturator nerve, L2 and 3.

Actions

Gracilis flexes the leg and rotates it medially. It may also act as an adductor of the thigh. When the foot is fixed, gracilis rotates the femur and pelvis laterally on the tibia, and helps balance the trunk during walking.

Testing

While palpating over the tendon posteromedially at the flexed knee, the knee is actively further flexed and the leg actively medially rotated. Gracilis can also be tested with the other adductors of the hip.

Adductor longus

Attachments

Adductor longus (Figs 80.2, 80.26), the most anterior of the three adductors, is a large, fan-shaped muscle that lies in the same plane as pectineus. It arises by a narrow tendon with a flattened (sometimes C-shaped) cross-section, which is attached to the front of the pubis in the angle between the crest and the symphysis. It expands into a broad fleshy belly which descends posterolaterally and inserts by an aponeurosis into the linea aspera in the middle third of the femur, between vastus medialis and adductors magnus and brevis, usually blending with all of them. Its proximal attachment is vulnerable to overload from sporting activity: this is one cause of sport-related groin pain.

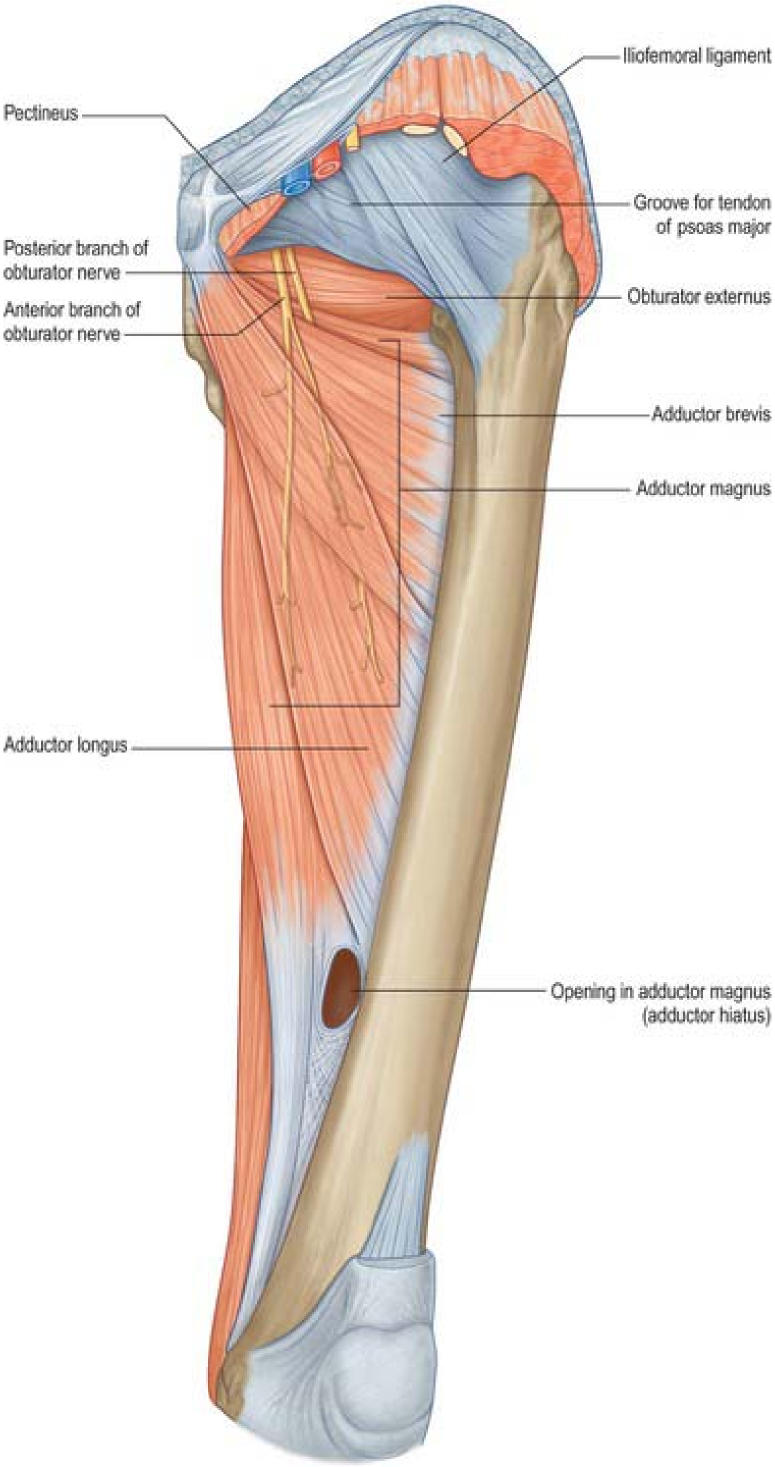
Pectineus
Posterior branch of obturator nerve
Anterior branch of obturator nerve
Adductor longus
Iliofemoral ligament
Groove for tendon of psoas major
Obturator externus
Adductor brevis
Adductor magnus
Opening in adductor magnus (adductor hiatus)

Fig. 80.26 Adductor muscles of the left thigh: anterior aspect.

Adductor longus is occasionally double.

Relations

Anterior to adductor longus are the spermatic cord, fascia lata (which separates it from the long saphenous vein) and, near its attachment, the femoral artery and vein and sartorius. Posterior to it are adductor brevis and adductor magnus, the anterior branch of the obturator nerve and, near its attachment, the profunda femoris vessels. Lateral and medial to adductor longus are, respectively, pectineus, and gracilis.

Vascular supply

The main supply to adductor longus is to the central part of the muscle from the ‘artery to the adductors’ of the profunda. There is an additional proximal supply from the medial circumflex femoral artery, and a more distal supply from the femoral artery and sometimes the descending genicular artery.

Innervation

Adductor longus is innervated by the anterior division of the obturator nerve, L2, 3 and 4.

Actions

The actions of the named adductors as a group are discussed below, after each muscle has been described.

Testing

The adductors are tested as a group by adduction of the thigh against resistance, in the supine position and with the knee extended.

Adductor brevis

Attachments

Adductor brevis (Figs 80.2A, 80.26) lies posterior to pectineus and adductor longus. It arises by a narrow attachment from the external aspect of the body and inferior ramus of the pubis, between gracilis and obturator externus. Like adductor longus it is somewhat triangular, and expands as it descends posterolaterally to insert via an aponeurosis into the femur, along a line from the lesser trochanter to the linea aspera, and on the upper part of the linea immediately behind pectineus and the upper part of adductor longus.

Adductor brevis often has two or three separate parts, or may be integrated into adductor magnus.

Relations

Anteriorly lie pectineus, adductor longus, the profunda femoris artery, and the anterior branch of the obturator nerve; posteriorly are adductor magnus and the posterior branch of the obturator nerve. The upper border of adductor brevis is related to the medial circumflex femoral artery, obturator externus, and the conjoined tendon of psoas major and iliacus. Its lower border is related to gracilis and adductor magnus. The second, or first and second perforating arteries pierce it near its femoral attachment.

Vascular supply

The vascular supply to adductor brevis is variable. Usually the main supply is directly from the profunda femoris distally and from the ‘artery to the adductors’ more proximally. There is an additional proximal supply from the medial circumflex femoral artery. The deep surface receives branches from the obturator artery.

Innervation

Adductor brevis is innervated by the obturator nerve, L2 and 3.

Actions

The actions of the named adductors as a group are discussed below, after each muscle has been described.

Testing

Adductor brevis is tested in the same way as adductor longus.

Adductor magnus

Attachments

Adductor magnus (see Figs 80.2, 80.26), a massive triangular muscle, arises from a small part of the inferior ramus of the pubis, from the conjoined ischial ramus, and from the inferolateral aspect of the ischial tuberosity. The short, horizontal fibres from the pubic ramus are inserted into the medial margin of the gluteal tuberosity of the femur, medial to gluteus maximus; this part of the muscle, in a plane anterior to the rest, is sometimes called adductor minimus. The fibres from the ischial ramus fan out downwards and laterally, to insert via a broad aponeurosis into the linea aspera and the proximal part of the medial supracondylar line. The medial part of the muscle, composed mainly of fibres from the ischial tuberosity, is a thick mass which descends almost vertically, and ends in the lower third of the thigh in a rounded tendon, which can be palpated proximal to its attachment to the adductor tubercle on the medial condyle of the femur. The tendon is connected by a fibrous expansion to the medial supracondylar line.

The long, linear attachment of the muscle is interrupted by a series of osseo-aponeurotic openings, bridged by tendinous arches attached to the bone. The upper four are small and transmit the perforating branches and the termination of the profunda femoris artery. The lowest is large and allows the femoral vessels to cross to the popliteal fossa.

The vertical, ischiocondylar part of the muscle varies in its degree of separation from the rest. The upper border of adductor magnus may fuse with quadratus femoris.

Relations

Anteriorly lie pectineus, adductor brevis and adductor longus, the femoral and profunda vessels, and the posterior branch of the obturator nerve. A bursa separates the proximal part of the muscle from the lesser trochanter of the femur. Posteriorly are the sciatic nerve, gluteus maximus, biceps femoris, semitendinosus and semimembranosus. The superior border is parallel with quadratus femoris, and the transverse branch of the medial circumflex femoral artery passes between the muscles. The medial border is related to gracilis, sartorius and the fascia lata.

Vascular supply

As expected from its position, adductor magnus is supplied from both its anterior and posterior aspects. The contribution from the anterior compartment is the more important. Here the obturator, profunda femoris and (superficial) femoral arteries contribute; the main supply is directly from the distal part of the profunda. Distally there may be contributions from the femoral and descending genicular arteries. Posteriorly there are branches from the medial circumflex femoral, the first and second perforating and the popliteal vessels.

Innervation

Adductor magnus is composite and is doubly innervated by the obturator nerve and the tibial division of the sciatic nerve (L2, 3 and 4); the latter supplies the ischiocondylar part. Both nerves are derived from anterior divisions in the lumbosacral plexus, indicating a primitive flexor origin for both parts of the muscle.

Actions of the adductors

Extensive or forcible adduction of the femur is not often required. Although the adductors can act in this way, they more commonly act as synergists in the complex patterns of gait activity, and to some degree as controllers of posture. They are active during flexion and extension of the knee. Magnus and longus are probably medial rotators of the thigh. The adductors are inactive during adduction of the abducted thigh in the erect posture (when gravity assists), but active in other postures, such as the supine position, or during adduction of the flexed thigh when standing. They are also active during flexion (longus) and extension (magnus) of the thigh at the hip joint. In symmetrical easy standing their activity is minimal.

Testing of the adductors

The adductors are usually tested as a group by adduction of the thigh against resistance, in the supine position with the knee extended. The tendon of adductor magnus can be felt just proximal to the adductor tubercle on the medial condyle of the femur. Clinical testing of the other actions mentioned above is not feasible for the individual muscles.

Pectineus

Attachments

Pectineus (Fig. 80.19) is a flat, quadrangular muscle in the femoral triangle. It may also be considered as part of the anterior compartment of the thigh. It arises from the pecten pubis, from the bone in front of it between the iliopubic ramus and the pubic tubercle, and from the fascia on its own anterior surface. The fibres descend, initially posteromedially and then posterolaterally to be attached along a line from the lesser trochanter to the linea aspera.

Pectineus may be bilaminar, in which case the two layers receive separate nerve supplies. Proximally it may be partially or wholly attached to the capsule of the hip joint.

Relations

Pectineus is related anteriorly to the deep lamina of the fascia lata, which separates it from the femoral vessels and long saphenous vein; posteriorly to the capsule of the hip joint, adductor brevis, obturator externus and the anterior branch of the obturator nerve; laterally to psoas major and the medial circumflex femoral vessels; and medially to the lateral margin of adductor longus.

Vascular supply

The main arterial supply to pectineus is derived from the medial circumflex femoral artery, which enters the superficial surface of the muscle. There may be a branch from the (common) femoral more proximally, and a deep supply from the obturator artery.

Innervation

Pectineus is innervated by the femoral nerve, L2 and 3, and accessory obturator nerve, L3, when present. Occasionally it receives a branch from the obturator nerve. The muscle may be incompletely divided into dorsal and ventral layers, which are supplied respectively by the obturator and femoral (or rarely accessory obturator) nerves.

Actions

Pectineus adducts the thigh and flexes it on the pelvis.

Testing

The action of pectineus cannot be tested clinically in isolation.

Adductor canal

The adductor canal (Hunter’s canal; subsartorial canal) is a trough-shaped intermuscular tunnel occupying the distal two-thirds of the medial aspect of the thigh (Fig. 80.2). It starts at the apex of the femoral triangle and extends distally as far as the distal attachment of the tendon of adductor magnus. It is triangular in section, and is bounded anterolaterally by vastus medialis, posteromedially by adductor longus, and distal to adductor longus, by adductor magnus. Its anteromedial boundary (often referred to as the roof) is a strong and dense fascia that extends from the medial surface of vastus medialis to the medial edge of the adductors longus and magnus, overlapping in its stride, the femoral vessels in the adductor canal. This fascia, on account of being overlain by sartorius, is termed the subsartorial fascia.

The adductor canal contains the femoral artery and vein, the descending genicular and muscular branches of the femoral artery and their corresponding venous tributaries, the saphenous nerve, and the nerve to vastus medialis (until it enters its muscle). The femoral vessels pass from the adductor canal into the popliteal fossa via the adductor hiatus, an opening in the tendon of adductor magnus adjacent to the femoral shaft, two-thirds of the way down the adductor canal.

Posterior compartment

The posterior femoral muscles, biceps femoris, semitendinosus, and semimembranosus, are colloquially termed the ‘hamstrings’. They cross both hip and knee joints, and integrate extension at the hip with flexion at the knee. As the muscles span the back of the knee, they form the proximal lateral and medial margins of the popliteal fossa. The actions of these muscles and their clinical anatomy will be considered as a group after they have been described individually.

The muscles of the posterior compartment (see Figs 80.2, 80.22) receive their blood supply from the perforating branches of the profunda femoris, most importantly through the first perforator. This vessel has important anastomoses with the inferior gluteal artery (on or within semitendinosus) and with the medial circumflex femoral artery, while the third perforator anastomoses with the medial superior genicular artery within the short head of biceps. This anastomotic chain forms an important collateral arterial pathway when the femoral artery is blocked.

Semitendinosus

Attachments

Semitendinosus (see Fig. 80.2B), notable for the length of its tendon, lies posteromedial in the thigh. It arises from an inferomedial impression on the upper area of the ischial tuberosity (Fig. 80.5), by a tendon it shares with the long head of biceps femoris, and from an aponeurosis connecting the adjacent surfaces of the two muscles for 7.5 cm from their common origin. The belly is fusiform and ends a little below midthigh in a long, rounded tendon that runs on the posterior surface of semimembranosus. The tendon curves around the medial condyle of the tibia, passes over the medial collateral ligament of the knee joint (from which it is separated by the bursa of the pes anserinus), and inserts into the upper part of the medial surface of the tibia behind the attachment of sartorius and distal to that of gracilis (Fig. 80.24). At its termination it is united with the tendon of gracilis and gives off a prolongation to the deep fascia of the leg and to the medial head of gastrocnemius. A tendinous intersection is usually present near the midpoint of the muscle, which may also receive a muscular slip from the long head of biceps femoris. These connections with the medial head of gastrocnemius and biceps can cause difficulty when harvesting the tendon surgically for a graft.

Relations

Semitendinosus lies on semimembranosus throughout its length. The relations of the distal part of the muscle are described above and with the pes anserinus.

Vascular supply

The two main arteries of supply to semitendinosus are superior and inferior. The superior is derived from either the medial circumflex femoral artery or from the first perforating artery. The inferior and larger branch arises from the first perforator distal to the origin of the superior branch. There is an accessory supply at the attachments of the muscle: at the ischial attachment this is derived from the inferior gluteal artery, and at the tibial attachment from the medial inferior genicular artery.

Innervation

Semitendinosus is innervated by the sciatic nerve, L5, S1 and 2, through its tibial division.

Semimembranosus

Attachments

Semimembranosus (see Fig. 80.2B), so named because of the flattened form of its upper attachment, is posteromedial in the thigh. It arises by a long, flat tendon from a superolateral impression on the ischial tuberosity (Fig. 80.5). Inferomedially the tendinous fibres intermingle to some extent with those of biceps femoris and semitendinosus. The tendon receives, from the ischial tuberosity and ramus, two fibrous expansions that flank adductor magnus. It then broadens and descends deep to semitendinosus and the long head of biceps femoris. Muscle fibres arise from the tendon at about midthigh and converge to a second aponeurosis on the posterior aspect of the lower part of the muscle, which tapers to the heavy, rounded tendon of the distal attachment. The tendon divides at the level of the knee into five components. The main one is attached to a tubercle (sometimes called the tuberculum tendinis) on the posterior aspect of the medial tibial condyle. The others are: a series of slips to the medial margin of the tibia, immediately behind the medial collateral ligament; a thin fibrous expansion to the fascia over popliteus; a cord-like tendon to the inferior lip and adjacent part of the groove on the back of the medial tibial condyle, deep to the medial collateral ligament; and a strong expansion which passes obliquely upwards to the femoral intercondylar line and lateral femoral condyle and forms much of the oblique popliteal ligament of the knee joint.

Semimembranosus varies considerably in size, and may be absent. It may be double, and arise mainly from the sacrotuberous ligament. Slips to the femur or to adductor magnus may occur.

Relations

Semimembranosus overlaps the popliteal vessels and is itself partly overlapped by semitendinosus throughout its extent (see Fig. 80.2). Its deep surface lies on adductor magnus. The sciatic nerve lies laterally and surprisingly close to the surface. The distal end of the muscle partially overlies the medial head of gastrocnemius before passing anteromedially to it. An important bursa lies between the semimembranosus tendon and gastrocnemius, and often communicates with the knee joint and with a smaller bursa between the tendon and the posterior tibial margin.

Vascular supply

Semimembranosus is supplied from the perforating arteries, usually from all, though predominantly from the first. Sometimes the predominant artery arises from the fourth perforator. A branch of the femoral or popliteal artery supplies the distal part of the muscle, and there may be a contribution from the inferior gluteal artery at the proximal attachment.

Innervation

Semimembranosus is innervated by the sciatic nerve, L5, S1 and 2, through its tibial division.

Biceps femoris

Attachments

Biceps femoris (see Fig. 80.2) occupies a posterolateral position in the thigh. It has two proximal attachments. One, the long head, arises from an inferomedial impression on the upper area of the ischial tuberosity (Fig. 80.5), via a tendon which it shares with semitendinosus, and from the lower part of the sacrotuberous ligament. The other, the short head, arises from the lateral lip of the linea aspera, between adductor magnus and vastus lateralis. This attachment extends proximally almost to gluteus maximus and distally along the lateral supracondylar line to within 5 cm of the lateral femoral condyle, and from the lateral intermuscular septum. The long head forms a fusiform belly that descends laterally across the sciatic nerve. The fibres end in an aponeurosis which covers the posterior surface of the muscle. This aponeurosis receives on its deep surface the fibres of the short head, and gradually narrows to a tendon (the lateral hamstring). The main part of the tendon splits round the fibular collateral ligament and is attached to the head of the fibula. The remainder splits into three laminae. The intermediate lamina fuses with the fibular collateral ligament, while the others pass superficial and deep to the ligament to attach to the lateral condyle of the tibia.

The short head may be absent. Additional slips may arise from the ischial tuberosity, linea aspera, or medial supracondylar line.

Relations

Proximally biceps femoris is covered by gluteus maximus, but elsewhere it lies relatively superficially. Deep to it lie semimembranosus proximally, and the sciatic nerve, adductor magnus and the lateral head of gastrocnemius more distally. Semitendinosus and semimembranosus lie medially. The common fibular nerve descends along the medial border of the tendon and separates it distally from the lateral head of gastrocnemius. As a guide during surgery, it is safest to find a nerve proximally and dissect it free distally. The common fibular nerve is found emerging posterior to the biceps tendon, which is thus a useful guide to locating the nerve and thereby, to avoiding injury to the nerve. For example, when the lateral meniscus is sutured arthroscopically, care must be taken that all needle passages are anterior to biceps. The nerve is adherent to the biceps tendon: if part of the fibular head or the biceps attachment, usually with the insertion of the lateral collateral ligament, is avulsed, then the tendon will exert proximal traction on the nerve. This may contribute to common fibular nerve traction injury. Also, the abnormal position of the nerve may render it vulnerable to inadvertent injury during surgical exploration. A proximal fibular fracture may result in the nerve being trapped in the fracture line. A bursa may lie between the tendon and the fibular collateral ligament.

Vascular supply

The long head of biceps femoris is supplied by the first and second perforating arteries, with accessory supplies at the ischial attachment from the inferior gluteal and medial circumflex femoral arteries and in the distal quarter from the lateral superior genicular artery. The short head is supplied superiorly by the second or third perforating artery and inferiorly by the lateral superior genicular artery.

Innervation

Biceps femoris is innervated by the sciatic nerve, L5, S1 and 2; the long head through the tibial division and the short head through the common fibular division, which reflects the composite derivation from flexor and extensor musculature.

Actions of posterior femoral muscles

Acting from above, the posterior femoral muscles flex the knee. Acting from below, they extend the hip joint, pulling the trunk upright from a stooping posture against the influence of gravity, biceps being the main agent. When the knee is semi-flexed, biceps femoris can act as a lateral rotator and semimembranosus and semitendinosus as medial rotators of the lower leg on the thigh at the knee. When the hip is extended, biceps is a lateral rotator and semimembranosus and semitendinosus are medial rotators of the thigh. As is the case with quadriceps femoris, the adductors and gluteus maximus, the hamstrings are quiescent in easy symmetrical standing. However, any action that takes the centre of gravity in front of a transverse axis through the hip joints, e.g. forward reaching, forward sway at the ankle joints, or forward bending at the hips, is immediately accompanied by strong contraction of the hamstrings. (This is in marked contrast to gluteus maximus, which contracts only when there is a call for powerful extension at the hip joint.)

When the knee is flexed against resistance, the tendon of biceps can be felt lateral to the popliteal fossa. Medial to the fossa, the tendons of gracilis (which is the more medial) and semitendinosus stand out sharply. The semimembranosus tendon is just palpable in the interval between them (and also by deep pressure from a ‘pincer’ grip beyond their margins). There is some evidence that semimembranosus, semitendinosus and biceps femoris, although they cross both hip and knee joints, may produce movement at one of these joints without resisting antagonists at the other. Usually, however, each of these muscles contracts as a whole, and whether or not movement takes place at hip or knee is determined by other muscles which act as fixators of these joints.

Testing

The posterior femoral muscles are tested clinically by active knee flexion against resistance in the supine or prone position. In the prone position the individual hamstring tendons can be identified more easily.

When relaxed, these muscles show considerable variation in length: in some individuals the muscles are so short as to impose a serious limitation on flexion of the trunk at the hip joints when the knees are kept extended. Movements such as stooping must then be accomplished by flexing the vertebral column or squatting. Perhaps the need for more stress on the lumbar spine accounts for the occurrence of hamstring tightness in adolescents who develop spondylolysis. These muscles are prone to tearing, which may be related to the relative complexity of muscles that cross two joints, or to the fact that they are subject to large forces including eccentric contractions.

VASCULAR SUPPLY AND LYMPHATIC DRAINAGE

Iliac vessels and external iliac arteries and veins

The iliac vessels are described on page 1086, and the external iliac arteries and veins on pages 1089, and page 1090 respectively.

ARTERIES

Gluteal vessels

The superior and inferior gluteal arteries (Fig. 80.27) are described on pages 1087, 1089.

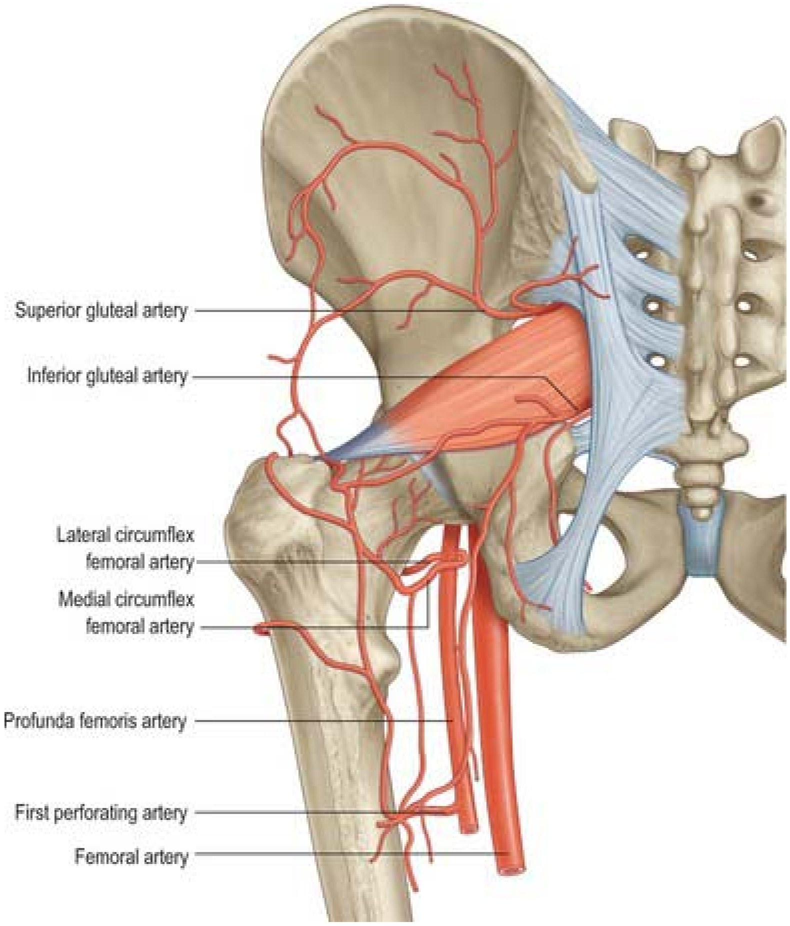
Superior gluteal artery
Inferior gluteal artery
Lateral circumflex femoral artery
Medial circumflex femoral artery
Profunda femoris artery
First perforating artery
Femoral artery

Fig. 80.27 The arteries of the gluteal region.

(From Drake, Vogl, Mitchell, Tibbitts and Richardson 2008.)

Arteria comitans nervi ischiadici (artery to sciatic nerve)

The arteria comitans nervi ischiadici is a branch of the internal iliac artery, and runs on the surface of, or within, the sciatic nerve. It represents the primitive axial artery of the lower limb. The artery is usually a very small vessel; occasionally it persists as a large vessel, in which case the femoral artery is correspondingly reduced in size. The artery may participate in collateral circulatory pathways.

Femoral artery

The femoral artery (Figs 80.2, 80.3, 80.28, 80.29) is a continuation of the external iliac artery. It begins behind the inguinal ligament, midway between the anterior superior iliac spine and the pubic symphysis, descends along the anteromedial part of the thigh in the femoral triangle, enters and passes through the adductor (subsartorial) canal, and becomes the popliteal artery as it passes through an opening in adductor magnus near the junction of the middle and distal thirds of the thigh. Its first three or four centimetres are enclosed, with the femoral vein, in the femoral sheath. The femoral artery gives off several branches in the proximal thigh, including the superficial epigastric, superficial circumflex iliac, superficial external pudendal, deep external pudendal and profunda femoris arteries. It gives off the descending genicular artery within the adductor canal. In clinical parlance, the part of the femoral artery proximal to the origin of profunda femoris is often termed the common femoral artery, while that distal to the origin of the profunda is termed the superficial femoral artery.

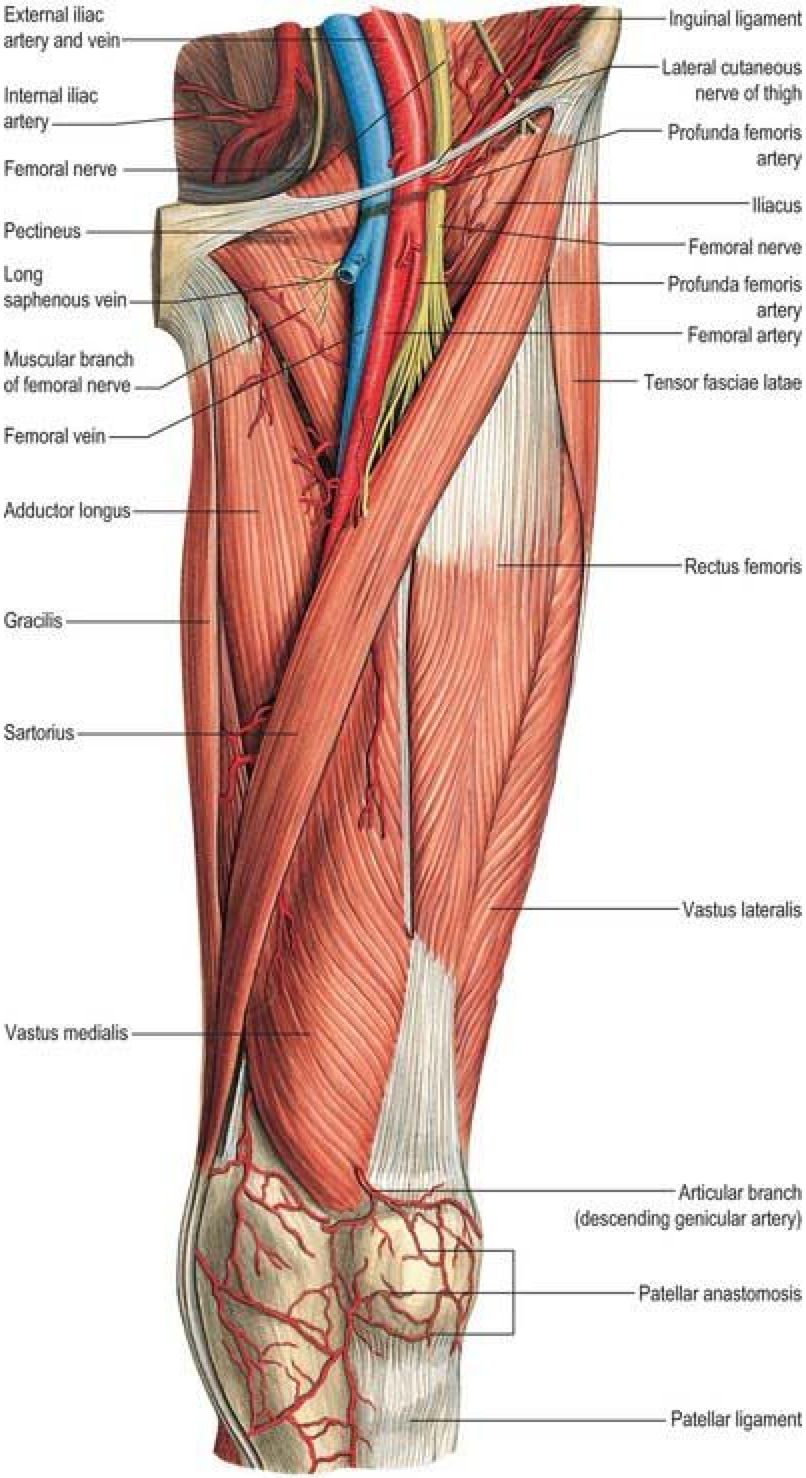
External iliac artery and vein
Internal iliac artery
Femoral nerve
Pectineus
Long saphenous vein
Muscular branch of femoral nerve
Femoral vein
Adductor longus
Gracilis
Sartorius
Vastus medialis
Inguinal ligament
Lateral cutaneous nerve of thigh
Profunda femoris artery
Iliacus
Femoral nerve
Profunda femoris artery
Femoral artery
Tensor fasciae latae
Rectus femoris
Vastus lateralis
Articular branch (descending genicular artery)
Patellar anastomosis
Patellar ligament

Fig. 80.28 The left femoral vessels.

(From Sobotta 2006.)

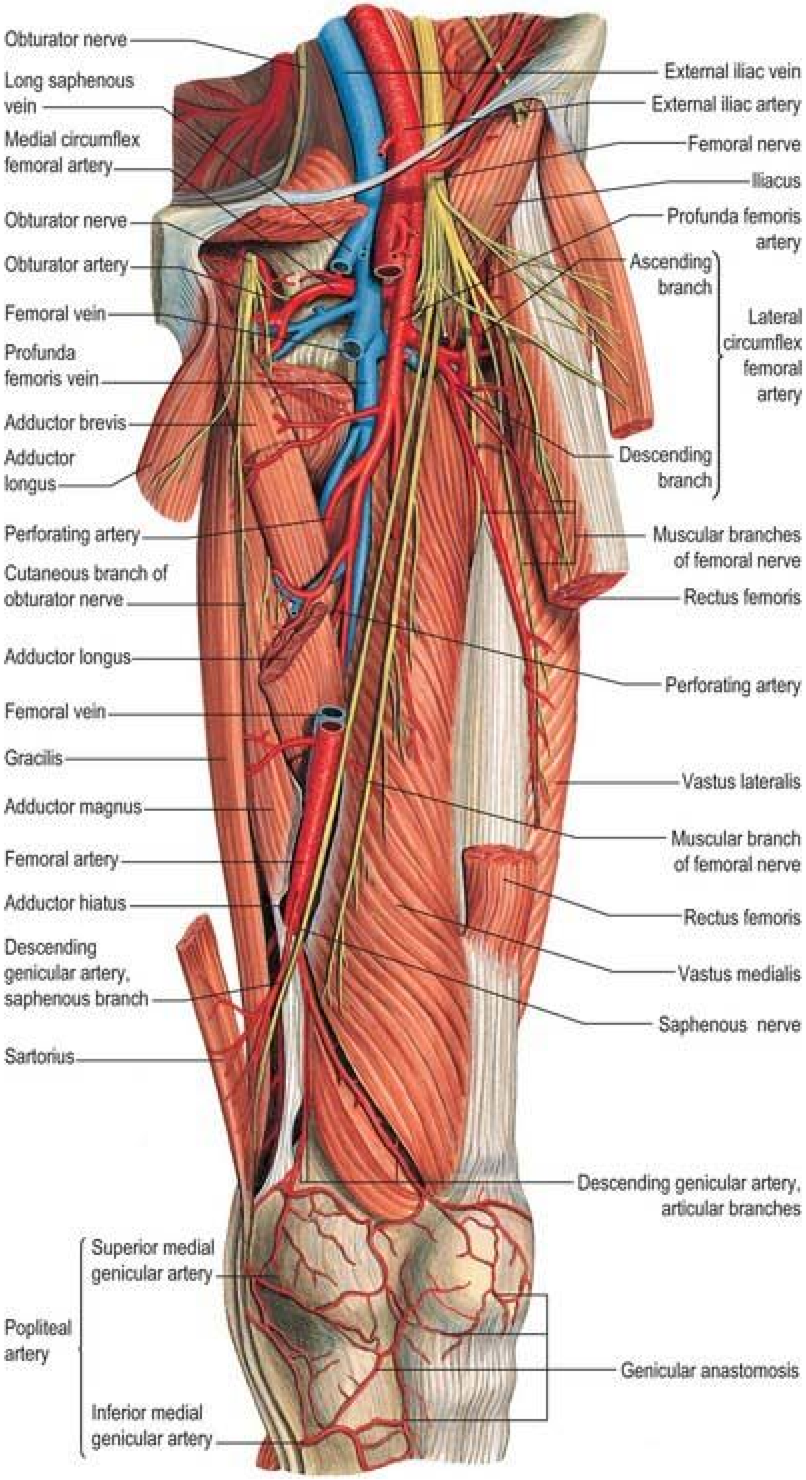
Obturator nerve
Long saphenous vein
Medial circumflex femoral artery
Obturator nerve
Obturator artery
Femoral vein
Profunda femoris vein
Adductor brevis
Adductor longus
Perforating artery
Cutaneous branch of obturator nerve
Adductor longus
Femoral vein
Gracilis
Adductor magnus
Femoral artery
Adductor hiatus
Descending genicular artery, saphenous branch
Sartorius
Popliteal artery
Superior medial genicular artery
Inferior medial genicular artery
External iliac vein
External iliac artery
Femoral nerve
Iliacus
Profunda femoris artery
Ascending branch
Lateral circumflex femoral artery
Descending branch
Muscular branches of femoral nerve
Rectus femoris
Perforating artery
Vastus lateralis
Muscular branch of femoral nerve
Rectus femoris
Vastus medialis
Saphenous nerve
Descending genicular artery, articular branches
Genicular anastomosis

Fig. 80.29 The profunda femoris artery and its branches.

(From Sobotta 2006.)

Rarely, the femoral artery divides, distal to the origin of the profunda femoris artery, into two trunks that reunite near the adductor opening. It may be replaced by the inferior gluteal artery, accompanying the sciatic nerve to the popliteal fossa and representing a persistence of the original axial artery. The external iliac artery is then small, ending as the profunda femoris artery.

Relations

Anterior to the artery in the femoral triangle are the skin, superficial fascia, superficial inguinal lymph nodes, fascia lata, femoral sheath, superficial circumflex iliac vein (crossing in the superficial fascia) and the femoral branch of the genitofemoral nerve (which is at first lateral then anterior). Near the apex of the triangle, the medial femoral cutaneous nerve crosses in front of the artery from the lateral to the medial side. Posteriorly, the posterior wall of the femoral sheath separates the artery from the tendons of psoas, pectineus and adductor longus. The artery is separated from the hip joint by the tendon of psoas major, from pectineus by the femoral vein and profunda vessels, and from adductor longus by the femoral vein. Proximally, the nerve to pectineus passes medially behind the artery. The femoral nerve lies lateral to the artery, outside the femoral sheath. The femoral vein is medial to the artery in the proximal part of the triangle and becomes posterior distally at the apex.

Within the adductor canal, the artery is covered by skin, superficial and deep fasciae, sartorius and the fibrous roof (subsartorial fascia) of the canal. The saphenous nerve lies at first lateral, then anterior and finally medial to the artery. Adductor longus and adductor magnus are posterior, vastus medialis and its nerve are anterolateral, and the femoral vein is also posterior proximally, but it becomes lateral distally (Fig. 80.28).

Compression of the femoral artery is most effective just distal to the inguinal ligament, where it is superficial and separated from the bone (iliopubic ramus) only by the psoas tendon. For this reason arterial injury proximal to the inguinal ligament, such as laceration by a knife, cannot be controlled simply by compression. Gaining proximal control of bleeding involves major exposure of the more proximal arteries as a life-saving manoeuvre.

Branches

Superficial epigastric artery

The superficial epigastric artery arises anteriorly from the femoral artery approximately 1 cm distal to the inguinal ligament and traverses the cribriform fascia to ascend anterior to the ligament and run in the abdominal superficial fascia almost to the umbilicus. It supplies the superficial inguinal lymph nodes and superficial fascia and skin, and anastomoses with branches of the inferior epigastric artery and its contralateral fellow (Fig. 80.28).

Superficial circumflex iliac artery

The superficial circumflex iliac artery is the smallest superficial branch of the femoral artery and arises near or with the superficial epigastric artery. It usually emerges through the fascia lata, lateral to the saphenous opening, and turns laterally distal to the inguinal ligament towards the anterior superior iliac spine. It supplies the skin, superficial fascia and superficial inguinal lymph nodes, anastomosing with the deep circumflex iliac, superior gluteal and lateral circumflex femoral arteries.

The superficial circumflex iliac artery is the basis for the important axial-pattern pedicled groin skin flap. Free flaps based on the vessel may also be raised.

Superficial external pudendal artery

The superficial external pudendal artery arises medially from the femoral artery, close to the preceding branches. Emerging from the cribriform fascia, it passes medially, usually deep to the long saphenous vein, across the spermatic cord (or round ligament) to supply the lower abdominal, penile, scrotal or labial skin, and anastomoses with branches of the internal pudendal artery.

Deep external pudendal artery

The deep external pudendal artery passes medially across pectineus and anterior or posterior to adductor longus, covered by fascia lata which it pierces to supply the skin of the perineum and scrotum or labium majus. Its branches anastomose with the posterior scrotal or labial branches of the internal pudendal artery.

Muscular branches

These branches supply sartorius, vastus medialis and the adductors.

Profunda femoris

The profunda femoris artery (deep femoral artery) (Figs 80.2B, 80.22, 80.28, 80.29) is a large branch that arises laterally from the femoral artery about 3.5 cm distal to the inguinal ligament. At first lateral to the femoral artery, it spirals posterior to this and the femoral vein to reach the medial side of the femur. It passes between pectineus and adductor longus, then between the latter and adductor brevis, before it descends between adductor longus and adductor magnus. It pierces adductor magnus and anastomoses with the upper muscular branches of the popliteal artery. This terminal part is sometimes named the fourth perforating artery.

The profunda is the main supply to the adductor, extensor and flexor muscles, and also anastomoses with the internal and external iliac arteries above and with the popliteal artery below.

The origin of the profunda femoris is sometimes medial, or rarely posterior on the femoral artery; if the former, it may cross anterior to the femoral vein and then pass backwards around its medial side.

Relations

Posteriorly, in proximodistal order, lie iliacus, pectineus, adductor brevis and adductor magnus. Anteriorly, the femoral and profunda veins, and distally, adductor longus, separate the profunda femoris from the main femoral artery. Laterally vastus medialis separates the proximal part of the artery from the femur.

Branches

The profunda femoris artery gives off the lateral and medial circumflex arteries in the proximal thigh, and perforating and muscular branches more distally.

Lateral circumflex femoral artery

The lateral circumflex femoral artery (Figs 80.27, 80.29) is a laterally running branch given off near the root of the profunda. It passes between the divisions of the femoral nerve, posterior to sartorius and rectus femoris and divides into ascending, transverse and descending branches. The ascending branch ascends along the intertrochanteric line, under tensor fasciae latae, lateral to the hip joint. It anastomoses with the superior gluteal and deep circumflex iliac arteries, supplying the greater trochanter, and, with branches of the medial circumflex femoral, forms an anastomotic ring round the femoral neck, from which ring the femoral neck and head are supplied. The descending branch, sometimes direct from the profunda or the femoral, descends posterior to rectus femoris, along the anterior border of vastus lateralis, which it supplies: a long branch descends in vastus lateralis to the knee, anastomosing with the lateral superior genicular branch of the popliteal, accompanied by the nerve to vastus lateralis. The transverse branch, the smallest, passes laterally anterior to vastus intermedius and pierces vastus lateralis to wind round the femur, just distal to the greater trochanter. It anastomoses with the medial circumflex, inferior gluteal and first perforating arteries (cruciate anastomosis).

The ascending branch forms the pedicle of the tensor fasciae latae musculocutaneous flap. The descending branch supplies the anterolateral thigh fasciocutaneous flap, which is based on the fasciocutaneous perforators that arise from the descending branch.

The lateral circumflex femoral artery may arise from the femoral artery.

Medial circumflex femoral artery

The medial circumflex femoral artery (Figs 80.27, 80.29) usually originates from the posteromedial aspect of the profunda, but often originates from the femoral artery itself. It supplies the adductor muscles and curves medially round the femur between pectineus and psoas major and then obturator externus and adductor brevis, finally appearing between quadratus femoris and the upper border of adductor magnus, dividing into transverse and ascending branches. The transverse branch takes part in the cruciate anastomosis. The ascending branch ascends on the tendon of obturator externus, anterior to quadratus femoris, to the trochanteric fossa, where it anastomoses with branches of the gluteal and lateral circumflex femoral arteries. An acetabular branch at the proximal edge of adductor brevis enters the hip joint under the transverse acetabular ligament with one from the obturator artery. It supplies the fat in the fossa, and reaches the femoral head along its ligament. For details of the blood supply of the proximal end of the femur consult Crock (1996).

Perforating arteries

The perforating arteries (Fig. 80.22) perforate the femoral attachment of adductor magnus to reach the flexor aspect of the thigh. There are three perforating branches, and the terminal part of the profunda itself becomes the fourth perforator. They pass close to the linea aspera under small tendinous arches and give off muscular, cutaneous and anastomotic branches. Diminished, they pass deep to the short head of biceps femoris (the first usually through the attachment of gluteus maximus), traverse the lateral intermuscular septum and enter vastus lateralis. The first arises proximal to adductor brevis, the second anterior and the third distal to the muscle. The first perforating artery passes back between pectineus and adductor brevis (sometimes through the latter), pierces adductor magnus near the linea aspera to supply adductor brevis, adductor magnus, biceps femoris and gluteus maximus, and anastomoses with the inferior gluteal, medial and lateral circumflex femoral and second perforating arteries. The larger second perforating artery, often arising with the first, pierces the attachments of adductor brevis and magnus, divides into the ascending and descending branches supplying the posterior femoral muscles and anastomoses with the first and third perforating arteries. The femoral nutrient artery usually arises from it. When two nutrient arteries exist they usually arise from the first and third perforators. The third perforating artery starts distal to adductor brevis, pierces the attachment of adductor magnus and divides into branches to the posterior femoral muscles. It anastomoses proximally with the perforating arteries, and distally with the end of the profunda and muscular branches of the popliteal. The femoral nutrient artery may arise from it. Side branches of the diaphysial nutrient and other branches of the profunda provide subsidiary cortical arteries.

The perforating arteries form a double chain of anastomoses, initially in the adductor muscles and subsequently near the linea aspera.

Muscular branches

Numerous muscular branches arise from the profunda femoris artery. Some end in the adductors, and others pierce adductor magnus, supply the flexors and anastomose with the medial circumflex femoral artery and superior muscular branches of the popliteal artery. The profunda is thus the main supply to the femoral muscles.

Descending genicular artery

The descending genicular artery (see Fig. 82.1), the distal branch of the femoral artery, arises just proximal to the adductor opening and immediately supplies a saphenous branch. It then descends in vastus medialis, anterior to the tendon of adductor magnus, to the medial side of the knee, where it anastomoses with the medial superior genicular artery. Muscular branches supply vastus medialis and adductor magnus and give off articular branches that anastomose round the knee joint (Ch. 82). One articular branch crosses above the femoral patellar surface, forming an arch with the lateral superior genicular artery and supplying the knee joint. The saphenous branch (saphenous artery) emerges distally through the roof of the adductor canal to accompany the saphenous nerve to the medial side of the knee. It passes between sartorius and gracilis and supplies the skin of the proximomedial area of the leg, and anastomoses with the medial inferior genicular artery.

Arterial anastomoses around the hip

Anastomoses on the back of the thigh

An important chain of anastomoses extends on the back of the thigh from the gluteal region to the popliteal fossa. It is formed in proximodistal order by anastomoses between the gluteal arteries and terminals of the medial circumflex femoral artery; the circumflex femoral arteries and the first perforating artery; the perforating arteries themselves; and between the fourth perforating artery and the superior muscular branches of the popliteal artery (Fig. 80.17). The trochanteric and cruciate anastomoses are the proximal elements of this chain.

Trochanteric anastomosis

The trochanteric anastomosis lies near the trochanteric fossa of the femur and is an anastomosis between the ascending branch of the medial circumflex femoral artery and descending branches of the superior and inferior gluteal arteries (Fig. 80.17). The lateral circumflex femoral artery and the first perforating artery from the profunda may also contribute, creating an extracapsular 'arterial ring of the femoral neck' (Crock 1996). Branches from this ring, the retinacular vessels, pierce the capsule and ascend along the femoral neck to give the main blood supply to the head of the femur.

Cruciate anastomosis

The cruciate anastomosis lies at the level of the lesser trochanter, near the lower edge of the femoral attachment of quadratus femoris and is an anastomosis between the transverse branches of the medial and lateral circumflex femoral arteries, a descending branch of the inferior gluteal artery and an ascending branch from the first perforating artery.

Collateral circulation in proximal femoral artery occlusion

After occlusion of the femoral artery proximal to the origin of the profunda femoris artery, five main anastomotic channels are available. These are between branches of the superior and inferior gluteal arteries, the medial and lateral circumflex femoral arteries and the first perforating branch of the profunda femoris artery; the obturator branch of the internal iliac artery and the medial circumflex femoral artery; the internal pudendal branch of the internal iliac artery and the superficial and deep external pudendal branches of the femoral artery; a deep circumflex iliac branch of the external iliac artery, the lateral circumflex femoral branch of the profunda femoris artery and the superficial circumflex iliac branch of the femoral artery; the inferior gluteal branch of the internal iliac artery and perforating branches of the profunda femoris artery.

Perforator flaps in the hip and thigh

Gluteal region

The gluteal region of the lower limb has an average of 21 perforators which arise from three main source arteries, namely the superior and inferior gluteal and internal pudendal arteries. The flaps which are based on these perforators are used as free flaps for breast reconstruction and as local flaps for covering defects in the sacral and perineal region.

Hip and thigh region

The hip and thigh region has six source arteries and an average of 50 arterial perforators. The thigh can be divided into four areas: antero-medial; antero-lateral and trochanteric; postero-medial; postero-lateral. The perforators that supply the antero-medial thigh are derived from the femoral artery, and those for the antero-lateral thigh are derived from branches of the lateral circumflex femoral artery. Perforators that supply the skin over the posteromedial and posterolateral thigh regions are derived from the profunda femoris and the popliteal arteries. Skin flaps based on the superficial circumflex iliac, superficial external pudendal and superficial inferior epigastric arteries have been used as local flaps, tube pedicles and free tissue transfers. Other popular skin flaps are TFL (tensor-fasciae latae) perforator flaps, ALT (anterolateral thigh) and AMT (anteromedial thigh) flaps, gracilis perforator flap and posterior thigh flaps.

VEINS

Femoral vein

The femoral vein accompanies its artery, beginning at the adductor opening as the continuation of the popliteal vein, and ending posterior to the inguinal ligament as the external iliac vein (Figs 80.3, 80.28). The vein is posterolateral to the femoral artery in the distal adductor canal. More proximally in the canal, and in the distal femoral triangle (i.e. at its apex), the vein lies posterior to the artery and proximally, at the base of the triangle, the vein lies medial to the artery. The vein occupies the middle compartment of the femoral sheath, between the femoral artery and femoral canal; fat in the canal permits expansion of the vein.

The femoral vein has numerous muscular tributaries. The profunda femoris vein joins the femoral vein posteriorly 4–12 cm distal to the inguinal ligament, and the long saphenous vein then enters anteriorly. Veins accompanying the superficial epigastric, superficial circumflex iliac and external pudendal arteries join the long saphenous vein before it enters the saphenous opening. Lateral and medial circumflex femoral veins are usually tributaries of the femoral vein. There are usually four or five valves in the femoral vein: the two most constant are just distal to the entry of the profunda femoris vein and near the inguinal ligament.

Profunda femoris vein

The profunda femoris vein lies anterior to its artery, and receives tributaries corresponding to the branches of the artery. Through these tributaries it connects distally with the popliteal and proximally with the inferior gluteal veins. It sometimes drains the medial and lateral circumflex femoral veins and has a valve just before it empties into the femoral vein.

Long saphenous vein

The long saphenous vein (great saphenous vein) (see Fig. 79.9A), the longest vein in the body, starts distally as a continuation of the medial marginal vein of the foot, and ends in the femoral vein a short distance distal to the inguinal ligament. It ascends immediately anterior to the tibial malleolus, crosses the distal third of the medial surface of the tibia obliquely in an anteroposterior direction to reach its medial border, then ascends a little behind the border to the knee. Proximally it is posteromedial to the medial tibial and femoral condyles (lying the breadth of the subject's hand posterior to the medial edge of the patella), and then ascends the medial aspect of the thigh. It passes through the saphenous opening and finally opens into the femoral vein. The 'centre' of the opening is often said to be 2.5–3.5 cm inferolateral to the pubic tubercle, and the vein is then represented by a line drawn from this point to the femoral adductor tubercle. However, the saphenous opening varies greatly in size and disposition so that this 'centre' is not a reliable surface marking for the saphenofemoral junction.

In its course through the thigh the long saphenous vein is accompanied by branches of the medial femoral cutaneous nerve. At the knee the saphenous branch of the descending genicular artery (the saphenous artery) and, in the leg and foot, the saphenous nerve, are all anterior to the vein. The vein is often duplicated, especially distal to the knee. It has from 10 to 20 valves, which are more numerous in the leg than in the thigh. One is present just before the vein pierces the cribriform fascia, another at its junction with the femoral vein. In almost its entire extent the vein lies in superficial fascia, but it has many connections with the deep veins, especially in the leg.

Tributaries

At the ankle the long saphenous vein drains the sole by medial marginal veins. In the leg it often connects with the short saphenous vein and with deep veins via perforating veins. Just distal to the knee it usually receives three large tributaries: from the front of the leg, from the tibial malleolar region (connecting with some of the 'perforating' veins) and from the calf (communicating with the short saphenous vein). The tributary draining the tibial malleolar region is formed distally from a fine network or 'corona' of delicate veins over the medial malleolus, and then ascends the medial aspect of the calf as the posterior arch vein (Dodd & Cockett 1976). This vein was first illustrated by Leonardo da Vinci, whose name is sometimes given to it. It connects with posterior tibial venae comitantes by a series of perforating (communicating) veins. There are usually three, equally spaced between the medial malleolus and the midcalf. More than three such perforators are uncommon, and an arch vein perforator above midcalf is only very rarely found.

Above the posterior crural arch vein, perforating veins join the long saphenous vein or one of its main tributaries at two main sites. The first is at a level in the upper calf indicated by its name, the tibial tubercle perforator; the second is in the lower/intermediate third of the thigh where it perforates the deep fascial roof of the subsartorial canal to join the femoral vein.

In the thigh the long saphenous vein receives many tributaries. Some open independently, while others converge to form large named channels that frequently pass towards the basal half of the femoral triangle before joining the long saphenous near its termination. These may be grouped as follows: one or more large posteromedial tributaries, one or more large anterolateral tributaries, four or more peri-inguinal veins. The posteromedial vein of the thigh, large and sometimes double, drains a large superficial region indicated by its name: it has (as have the other tributaries) radiological and surgical significance. One of its lower radicles is often continuous with the short saphenous vein. The posteromedial vein is sometimes named the accessory saphenous vein, though some restrict the term accessory to a lower (more distal) posteromedial tributary when two (or more) are present. Another large vessel, the anterolateral vein of the thigh (anterior femoral cutaneous vein), usually commences from an anterior network of veins in the distal thigh and crosses the apex and distal half of the femoral triangle to reach the long saphenous vein. As the latter traverses the saphenous opening, it is joined by the superficial epigastric, superficial circumflex iliac and superficial external pudendal veins. Their mode of union varies. Superficial epigastric and circumflex iliac veins drain the inferior abdominal wall, the latter also receiving tributaries from the proximolateral region of the thigh. The superficial epigastric or the femoral vein may connect with the lateral thoracic veins by means of a thoracoepigastric vein that runs superficially on the anterolateral aspect of the trunk. This vein connects the inferior and superior caval areas of drainage and may be dilated and visible in cases of inferior caval obstruction. Superficial external pudendal veins drain part of the scrotum/labia; one is joined by the superficial dorsal vein of the penis/clitoris. The deep external pudendal veins join the long saphenous vein at the saphenous opening.

The long saphenous vein is often harvested for grafts used both in peripheral and coronary arterial surgery.

LYMPHATIC DRAINAGE

Superficial inguinal nodes

The superficial inguinal nodes form proximal and distal groups. The proximal group usually consists of five or six nodes just distal to the inguinal ligament. Its lateral members receive afferent vessels from the gluteal region and the adjoining infra-umbilical anterior abdominal wall. Medial members receive superficial vessels from the external genitalia (including the inferior vagina), inferior anal canal and perianal region, adjoining abdominal wall, umbilicus and uterine vessels accompanying the round ligament. The distal group usually consists of four or five nodes along the termination of the long saphenous vein. They receive all the superficial vessels of the lower limb, except those from the posterolateral calf. All superficial inguinal nodes drain to the external iliac nodes, some via the femoral canal and others anterior or lateral to the femoral vessels. Numerous vessels interconnect individual nodes.

Superficial inguinal nodes are frequently enlarged in disease or injury in their region of drainage. Thus the proximal inguinal nodes are almost invariably affected in malignant or infective disease of the prepuce, penis, labia majora, scrotum, perineum, anus and lower vagina, or in diseases affecting the skin and superficial structures in these regions, in the infra-umbilical part of the abdominal wall or in the gluteal region. The distal group is implicated only in disease or injury of the limb.

Deep inguinal nodes

The deep inguinal nodes vary from one to three, and are situated medial to the femoral vein. One lies just distal to the saphenofemoral junction, another in the femoral canal, and the most proximal node lies laterally in the femoral ring. The middle node is the most inconstant and the proximal node is often absent. All receive deep lymphatics that accompany the femoral vessels, lymph vessels from the glans penis or clitoris and a few efferents from the superficial inguinal nodes. Their own efferents traverse the femoral canal to the external iliac nodes.

INNERVATION

LUMBAR PLEXUS AND BRANCHES

The lumbar plexus is formed by the first three and most of the fourth, lumbar ventral rami (see p. 1078). The iliohypogastric, iliolingual and genitofemoral nerves are described on pages 1080.

Lateral cutaneous nerve of the thigh

The lateral cutaneous nerve of the thigh arises from the dorsal branches of the second and third lumbar ventral rami and emerges from the lateral border of psoas major, crossing the iliacus obliquely towards the anterior superior iliac spine. It supplies the parietal peritoneum in the iliac fossa. The right nerve passes posterolateral to the caecum, separated from it by the fascia iliaca and peritoneum; the left passes behind the lower part of the descending colon. Both pass behind or through the inguinal ligament, variably medial to the anterior superior iliac spine (commonly 1 cm) and anterior to or through sartorius into the thigh, where they divide into anterior and posterior branches. The anterior branch becomes superficial approximately 10cm distal to the anterior superior iliac spine and supplies the skin of the anterior and lateral thigh as far as the knee. It connects terminally with the cutaneous branches of the anterior division of the femoral nerve and the infrapatellar branch of the saphenous nerve, forming the peripatellar plexus. The posterior branch pierces the fascia lata higher than the anterior, and divides to supply the skin on the lateral surface from the greater trochanter to about midthigh. It may also supply the gluteal skin.

Lesions of the lateral cutaneous nerve of the thigh

The lateral cutaneous nerve of the thigh may become entrapped at three sites along its course: close to the vertebral column; within the abdominal cavity as the nerve travels across the pelvis; as it leaves the pelvis. This last site is where the nerve is most commonly damaged, and entrapment is thought to occur as the nerve passes through or deep to the inguinal ligament just medial to the anterior superior iliac spine. The angulation of the nerve as it crosses the iliac crest means that it is vulnerable to compression during movement, e.g. hip extension may increase angulation and tension on the nerve.

Injury produces an area of impaired sensation, often with pain and paraesthesia on the anterolateral aspect of the thigh (meralgia paraesthetica) in the distal cutaneous distribution of the nerve. This area does not extend across the midline anteriorly, it does not extend below the knee and it does not extend behind the hamstring tendons laterally. Symptoms may be exacerbated when wearing tight belts or tight-waisted clothes or as a result of a recent weight gain or pregnancy. Exceptionally the posterior branch of the lateral cutaneous nerve of the thigh, which supplies a thin strip from the greater trochanter of the femur down about two-thirds of the way to the knee, may be affected separately. This branch leaves the main trunk of the nerve, usually distal to the inguinal ligament, and it then turns laterally to pierce tensor fasciae latae, where it may become entrapped.

Femoral nerve

The femoral nerve is the largest branch of the lumbar plexus and arises from the dorsal branches (posterior divisions) of the second to fourth lumbar ventral rami (Fig. 80.30). It descends through psoas major, emerging low on its lateral border, and then passes between psoas and iliacus, deep to the iliac fascia. Passing behind the inguinal ligament into the thigh, it is split into anterior and posterior divisions by the lateral circumflex femoral artery. Behind the inguinal ligament it is separated from the femoral artery by part of psoas major. In the abdomen the nerve supplies small branches to iliacus and pectineus and a branch to the proximal part of the femoral artery; the latter branch sometimes arises in the thigh.

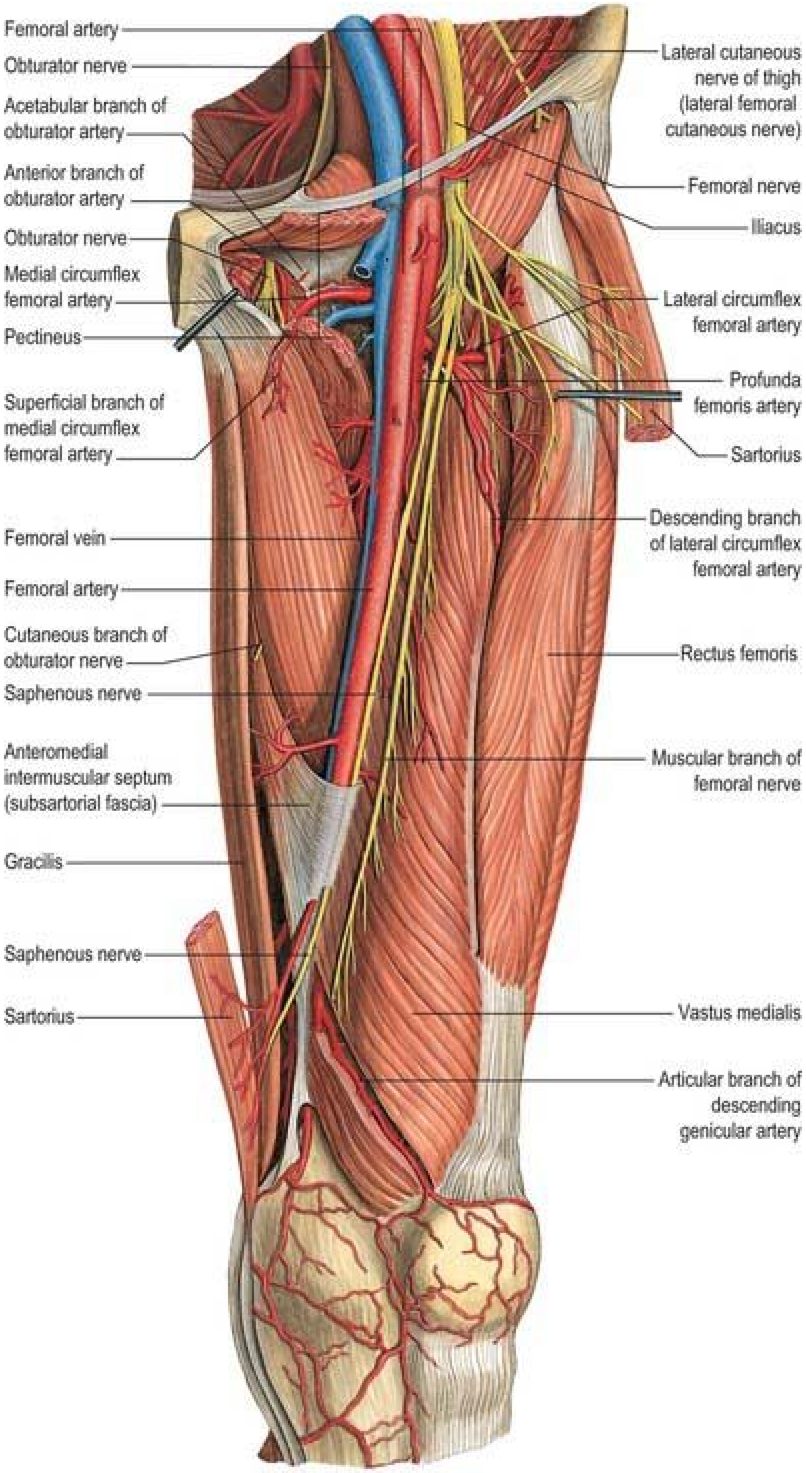
Femoral artery
Obturator nerve
Acetabular branch of obturator artery
Anterior branch of obturator artery
Obturator nerve
Medial circumflex femoral artery
Pectineus
Superficial branch of medial circumflex femoral artery
Femoral vein
Femoral artery
Cutaneous branch of obturator nerve
Saphenous nerve
Anteromedial intermuscular septum (subsartorial fascia)
Gracilis
Saphenous nerve
Sartorius
Lateral cutaneous nerve of thigh (lateral femoral cutaneous nerve)
Femoral nerve
Iliacus
Lateral circumflex femoral artery
Profunda femoris artery
Sartorius
Descending branch of lateral circumflex femoral artery
Rectus femoris
Muscular branch of femoral nerve
Vastus medialis
Articular branch of descending genicular artery

Fig. 80.30 The nerves of the left thigh: anterior aspect.

(From Sobotta 2006.)

Nerve to pectineus

The nerve to pectineus branches from the medial side of the femoral nerve near the inguinal ligament. It passes behind the femoral sheath and enters the anterior aspect of the muscle.

Anterior division of the femoral nerve

The anterior division of the femoral nerve supplies intermediate and medial cutaneous nerves of the thigh and branches to sartorius.

Medial cutaneous nerve of the thigh

The medial cutaneous nerve of the thigh is at first lateral to the femoral artery. It crosses anterior to the artery at the apex of the femoral triangle, and divides into anterior and posterior branches. Before doing so, it sends a few rami through the fascia lata to supply the skin of the medial side of the thigh, near the long saphenous vein: one ramus emerges via the saphenous opening, another becomes subcutaneous about midthigh. The anterior branch descends on sartorius, perforates the fascia lata beyond midthigh, and divides into a branch which supplies the skin as low as the medial side of the knee, and another which runs lateral to the former and connects with the infrapatellar branch of the saphenous nerve. The posterior branch descends along the posterior border of sartorius to the knee, pierces the fascia lata, connects with the saphenous nerve, and gives off several cutaneous rami, some as far as the medial side of the leg. The nerve contributes to the subsartorial plexus (see below).

Intermediate cutaneous nerve of the thigh

The intermediate cutaneous nerve of the thigh usually pierces the fascia lata 8 cm below the inguinal ligament, either as two branches or as one trunk that quickly divides into two. These descend on the front of the thigh, supplying the skin as far as the knee and ending in the peripatellar plexus. The lateral branch of the intermediate cutaneous nerve communicates with the femoral branch of the genitofemoral nerve, frequently piercing sartorius and sometimes supplying it.

Nerve to sartorius

The main nerve to sartorius arises from the femoral nerve in common with the intermediate cutaneous nerve of the thigh.

Posterior division of the femoral nerve

The branches of the posterior division of the femoral nerve are the saphenous nerve and branches to quadriceps femoris and the knee joint.

Saphenous nerve

See page 1409.

Muscular branches

The muscular branches of the posterior division of the femoral nerve supply quadriceps femoris. A branch to rectus femoris enters its proximal posterior surface and also supplies the hip joint. A larger branch to vastus lateralis forms a neurovascular bundle with the descending branch of the lateral circumflex femoral artery in its distal part and also supplies the knee joint. A branch to vastus medialis descends through the proximal part of the adductor canal, lateral to the saphenous nerve and femoral vessels, and enters the muscle at about its midpoint, sending a long articular filament distally along the muscle to the knee. Two or three branches to vastus intermedius enter its anterior surface about midthigh; a small branch from one of these descends through the muscle to supply articularis genu and the knee joint.

Vascular branches

Vascular branches of the femoral nerve supply the femoral artery and its branches.

Lesions of the femoral nerve

The main trunk of the femoral nerve is not subject to an entrapment neuropathy, but it may be compressed by retroperitoneal tumours or retroperitoneal haemorrhage in patients on anticoagulants or with a bleeding diathesis. A localized lesion of the femoral nerve may occur in diabetes mellitus (one of the forms of diabetic amyotrophy). The most striking feature of femoral neuropathy is wasting and weakness of quadriceps femoris, which results in considerable difficulty in walking and a tendency for the leg to collapse. Pain and paraesthesia may occur on the anterior and medial aspect of the thigh, extending down the medial aspect of the leg in the distribution of the saphenous branch of the femoral nerve.

Obturator nerve

The obturator nerve arises from the ventral branches of the second to fourth lumbar ventral rami. The branch from the third is the largest while that from the second is often very small. The nerve descends in psoas major, emerging from its medial border at the pelvic brim to pass behind the common iliac vessels and lateral to the internal iliac vessels. It then descends forwards along the lateral wall of the lesser pelvis on obturator internus, anterosuperior to the obturator vessels, to the obturator foramen, entering the thigh by its upper part. Near the foramen it divides into anterior and posterior branches, separated at first by part of obturator externus and lower down by adductor brevis.

Anterior branch

The anterior branch (Fig. 80.30) leaves the pelvis anterior to obturator externus, descending in front of adductor brevis, behind pectineus and adductor longus. At the lower border of adductor longus it communicates with the medial cutaneous and saphenous branches of the femoral nerve, to form a subsartorial plexus that supplies the skin on the medial side of the thigh (see below). It descends on, and supplies, the femoral artery. Near the obturator foramen the anterior branch supplies the hip joint. Behind pectineus it supplies adductor longus, gracilis, usually adductor brevis and often pectineus, and connects with the accessory obturator nerve (when this nerve is present). Occasionally the communicating branch to the femoral medial cutaneous and saphenous branches continues as a cutaneous branch to the thigh and leg. When this occurs, the nerve emerges from behind the distal border of adductor longus to descend along the posterior margin of sartorius to the knee, where it pierces the deep fascia and connects with the saphenous nerve to supply the skin halfway down the medial side of the leg.

Subsartorial nerve plexus

The medial cutaneous nerve of the thigh forms a subsartorial plexus with branches of the saphenous and obturator nerves, deep to the fascia lata, at the lower border of adductor longus. When the communicating branch of the obturator nerve is large and reaches the leg, the posterior branch of the medial cutaneous nerve is small, and ends in the plexus from which it gives rise to a few cutaneous filaments.

Posterior branch

The posterior branch pierces obturator externus anteriorly, supplies it and passes behind adductor brevis to the front of adductor magnus, dividing into branches to this and adductor brevis when the latter is not supplied by the anterior division. It usually sends an articular filament to the knee joint which either perforates adductor magnus distally or traverses its opening with the femoral artery to enter the popliteal fossa. Within the fossa the nerve descends on the popliteal artery to the back of the knee, pierces its oblique posterior ligament and supplies the articular capsule. It gives filaments to the popliteal artery.

Lesions of the obturator nerve

Isolated lesions of the obturator nerve are extremely rare, but may occasionally occur as a result of direct trauma (sometimes during parturition) or in anterior dislocations of the hip. The nerve may also be damaged by a rare obturator hernia, or be involved together with the femoral nerve in retroperitoneal lesions that occur close to the origins of the lumbar plexus. A nerve entrapment syndrome causing chronic medial thigh pain is described in athletes with large adductor muscles.

Accessory obturator nerve

Occasionally present (10%), the accessory obturator nerve is small and arises from the ventral branches of the third and fourth lumbar ventral rami. It descends along the medial border of psoas major, crosses the superior pubic ramus behind pectineus and divides into branches: one branch enters the deep surface of pectineus, another supplies the hip joint, and a third connects with the anterior branch of the obturator nerve. Sometimes the accessory obturator nerve is very small and only supplies pectineus. Any branch may be absent and others may occur: an additional branch sometimes supplies adductor longus.

SACRAL PLEXUS AND BRANCHES

The branches of the sacral plexus (see Fig. 79.11) are:

	Ventral divisions	**Dorsal divisions**
To quadratus femoris and gemellus inferior	L4, 5, S1	
To obturator internus and gemellus superior	L5, S1, 2	
To piriformis		S(1), 2
Superior gluteal		L4, 5, S1
Inferior gluteal		L5, S1, 2
Posterior femoral cutaneous	S2, 3	S1, 2
Tibial (sciatic)	L4, 5, S1, 2, 3	
Common fibular (sciatic)		L4, 5, S1, 2
Perforating cutaneous		S2, 3
Pudendal	S2, 3, 4	
To levator ani, coccygeus and sphincter ani externus	S4	
Pelvic splanchnic	S2, 3, (4).	

Sciatic nerve

The sciatic nerve is 2 cm wide at its origin and is the thickest nerve in the body. It leaves the pelvis via the greater sciatic foramen below piriformis and descends between the greater trochanter and ischial tuberosity, along the back of the thigh, dividing into the tibial and common fibular nerves at a varying level proximal to the knee. Superiorly it lies deep to gluteus maximus, resting first on the posterior ischial surface with the nerve to quadratus femoris between them. It then crosses posterior to obturator internus, the gemelli and quadratus femoris, separated by the latter from obturator externus and the hip joint. It is accompanied medially by the posterior femoral cutaneous nerve and the inferior gluteal artery. More distally it lies behind adductor magnus and is crossed posteriorly by the long head of biceps femoris. It corresponds to a line drawn from just medial to the midpoint between the ischial tuberosity and greater trochanter to the apex of the popliteal fossa.

Articular branches arise proximally to supply the hip joint through its posterior capsule; these are sometimes derived directly from the sacral plexus. Muscular branches are distributed to biceps femoris, semitendinosus, semimembranosus and the ischial part of adductor magnus.

The point of division of the sciatic nerve into its major components (tibial and common fibular) is very variable. The common site is at the junction of the middle and lower thirds of the thigh, near the apex of the popliteal fossa, but the division may occur at any level above this point, and rarely may occur below it. It is not uncommon for the major components to leave the sacral plexus separately, in which case the common fibular component usually passes through piriformis at the greater sciatic notch while the tibial component passes below the muscle.

Lesions of the sciatic nerve

The sciatic nerve supplies the knee flexors and all the muscles below the knee, which means that a complete palsy of the sciatic nerve results in a flail foot and severe difficulty in walking. Fortunately complete sciatic nerve palsy is very rare. The nerve is vulnerable in posterior dislocation of the hip. As it leaves the pelvis it passes either behind piriformis or sometimes through the muscle and at that point it may very rarely become entrapped or tethered: the piriformis syndrome is a controversial condition in which an anomalous relationship between piriformis and the sciatic nerve is thought to cause pain in the buttocks and along the course of the sciatic nerve. External compression over the buttock, e.g. in patients who lie immobile on a hard surface for a considerable length of time, can injure the nerve. However, the most common cause of serious sciatic nerve injury (and of the resulting major medicolegal claims) is iatrogenic. The nerve may be damaged in misplaced therapeutic injections into gluteus maximus (Ch. 79). Sciatic nerve palsy occurs after total hip replacement or similar surgery in 1% of cases, and may be caused by sharp injury, burning from bone cement, traction from instruments, manipulation of the hip, inadvertent lengthening of the femur, or haematoma surrounding the nerve. For some reason, possibly anatomical, the common fibular component of the sciatic nerve is more usually affected: the patient has a foot drop and a high stepping gait.

Inferior gluteal nerve

The inferior gluteal nerve arises from the dorsal branches of the fifth lumbar and first and second sacral ventral rami. It leaves the pelvis via the greater sciatic foramen below piriformis, and divides into branches that enter the deep surface of gluteus maximus.

Superior gluteal nerve

The superior gluteal nerve arises from the dorsal branches of the fourth and fifth lumbar and first sacral ventral rami. Accompanied by the superior gluteal vessels, the nerve leaves the pelvis via the greater sciatic foramen above piriformis, and divides into superior and inferior branches. The superior branch accompanies the upper branch of the deep division of the superior gluteal artery to supply gluteus medius and occasionally gluteus minimus. The inferior branch runs with the lower ramus of the deep division of the superior gluteal artery across gluteus minimus, supplies the glutei medius and minimus and ends in tensor fasciae latae.

Pudendal nerve

See Fig. 62.15 and page 1081.

Perforating cutaneous nerve

The perforating cutaneous nerve usually arises from the posterior aspects of the second and third sacral ventral spinal rami. It pierces the sacrotuberous ligament, curves round the inferior border of gluteus maximus and supplies the skin over the inferomedial aspect of this muscle. The nerve may arise from the pudendal nerve or it may be absent, in which case it may be replaced either by a branch from the posterior femoral cutaneous nerve or from the third and fourth, or fourth and fifth, sacral ventral rami.

Nerve to quadratus femoris and gemellus inferior

The nerve to quadratus femoris and gemellus inferior arises from the ventral branches of the fourth lumbar to the first sacral ventral rami. It leaves the pelvis via the greater sciatic foramen below piriformis, descends on the ischium deep to the sciatic nerve, the gemelli and the tendon of obturator internus, and supplies gemellus inferior, quadratus femoris and the hip joint.

Nerve to obturator internus and gemellus superior

The nerve to obturator internus and gemellus superior arises from the ventral branches of the fifth lumbar and first and second sacral ventral rami. It leaves the pelvis via the greater sciatic foramen below piriformis, supplies a branch to the upper posterior surface of gemellus superior, crosses the ischial spine lateral to the internal pudendal vessels, re-enters the pelvis via the lesser sciatic foramen, and enters the pelvic surface of obturator internus.

Posterior cutaneous nerve of the thigh

The posterior cutaneous nerve of the thigh arises from the dorsal branches of the first and second, and the ventral branches of the second and third sacral rami. It leaves the pelvis via the greater sciatic foramen below piriformis and descends under gluteus maximus with the inferior gluteal vessels, lying posterior or medial to the sciatic nerve. It descends in the back of the thigh superficial to the long head of biceps femoris, deep to the fascia lata. It pierces the deep fascia behind the knee and accompanies the short saphenous vein to midcalf, its terminal twigs connecting with the sural nerve. Its branches are all cutaneous and are distributed to the gluteal region, perineum and the flexor aspect of the thigh and leg.

Three or four gluteal branches curl round the lower border of gluteus maximus to supply the skin over the inferolateral portion of the muscle. The perineal branch supplies the superomedial skin in the thigh, curves forwards across the hamstrings below the ischial tuberosity, pierces the fascia lata and then runs in the superficial perineal fascia to the scrotal or labial skin. It communicates with the inferior rectal and posterior scrotal or labial branches of the perineal nerve, and gives numerous branches to the skin of the back and medial side of the thigh, the popliteal fossa and the proximal part of the back of the leg.

Nerve to piriformis

The nerve to piriformis usually arises from the dorsal branches of the first and second sacral ventral rami (sometimes only the second) and enters the anterior surface of piriformis.

Visceral and pelvic muscular branches of sacral plexus

Visceral branches of the sacral plexus are described on page 1092. For pelvic muscular branches, see page 1083.

REFERENCES

ɔgduk N. Clinical Anatomy of the Lumbar Spine and Sacrum, 3rd edn. Edinburgh: Churchill Livingstone, 1997.

ʻothwell DR, Pollard AM. Handbook of Archaeological Sciences. Chichester: Wiley, 2001.

ɔrmack GC, Lamberty BGH 1994; see Bibliography.

ʻock HV. An atlas of the arterial supply of the head and neck of the femur in man. *Clin Orthop*. 1980;152:17-25.

ʻock HV. Atlas of Vascular Anatomy of the Skeleton and Spinal Cord. London: Martin Dunitz, 1996.

ɛlaere O, Kok V, Nyssen-Behets C, Dhem A. Ossification of the human fetal ilium. *Acta Anat*. 1992;143:330-334.

.xon AF. The architecture of the cancellous tissue forming the upper end of the femur. *J Anat Physiol*. 1910;44:223-230.

A neglected and original work with far-reaching implications for the understanding of femoral structure..

ɔdd H, Cockett FB. The Pathology and Surgery of the Veins of the Lower Limb, 2nd edn. Edinburgh: Churchill Livingstone, 1976.

:khoff DG, Kramer RC, Watkins JJ, Alongi CA, van Gerven DP. Variation in femoral anteversion. *Clin Anat*. 1994;7:72-75.

nnegan M. Non-metric variation of the infracranial skeleton. *J Anat*. 1978;125:33-37.

A reference text for forensic and osteo-archaeological work..

ıss FK, Bacher A. New aspects of the morphology and function of the human hip joint ligaments. *Am J Anat*. 1991;192:1-13.

ɔlm NJ. The internal stress pattern of the os coxae. *Acta Orthop Scand*. 1980;51:421-428.

Biomechanical information, relevant to the function of the hip and pelvis..

seph J. Movements at the hip joint. *Ann R Coll Surg Eng*. 1975;56:192-201.

ays S. The Archaeology of Human Bones. London: Routledge, 1998.

well RLM. The calcar femorale: a tale of historical neglect. *Clin Anat*. 1997;10:27-33.

nseti IV. Growth and development of the acetabulum in the normal child. *J Bone Joint Surg*. 1978;60A:575-585.

ichael Salmon: Anatomic Studies. In: Taylor GI, Razaboni RM. *Book 1, Arteries of the Muscles of the Extremities and the Trunk*. St Louis: Quality Medical Publishing, 1994.

A translated, updated and edited version of a classic French text, first published in 1933. Now a major source-book in plastic surgery..

ueta J. The normal vascular anatomy of the femoral head during growth. *J Bone Joint Surg*. 1957;39B:353-358.

eisl H. The articular surfaces of the sacro-iliac joint and their relation to the movements of the sacrum. *Acta Anat*. 1954;22:1-14.

hitehouse WJ. Cancellous bone in the anterior part of the iliac crest. *Calcif Tissue Res*. 1977;23:67-76.

Detailed information on the internal structure of a site that is commonly used for marrow biopsy..

CHAPTER 81

Hip

The hip joint is a synovial joint of ball-and-socket (multiaxial spheroidal, cotyloid) type (Figs 81.1-81.3).

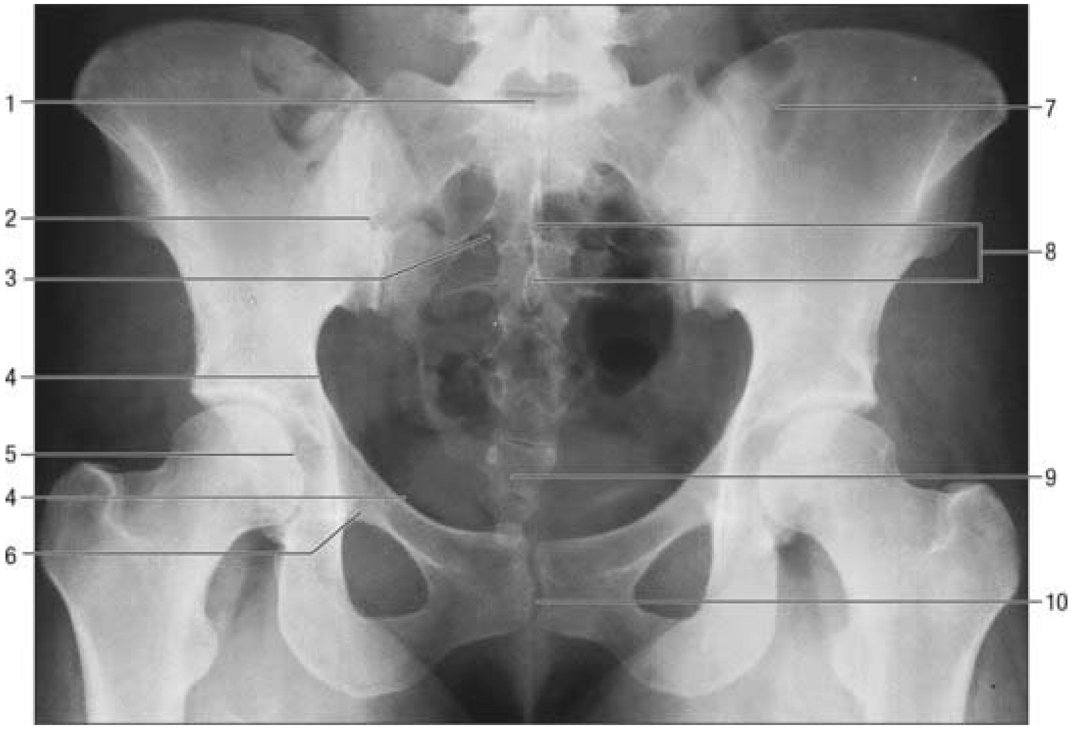

Fig. 81.1 Anteroposterior radiograph of an adult female pelvis. **1**. Sacral promontory. **2**. Sacroiliac joint. **3**. Margin of anterior sacral foramen. **4**. Pelvic brim. **5**. Fovea of femoral head. **6**. Obturator groove. **7**. Gas in pelvic colon. **8**. Sacral spines. **9**. Coccyx. **10**. Symphysis pubis.

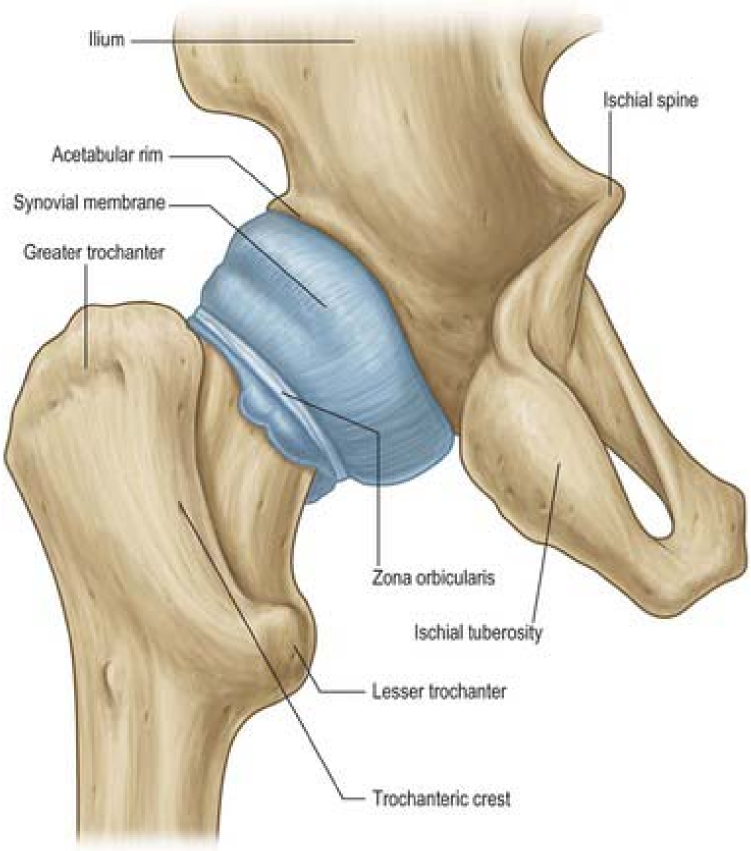
Ilium
Ischial spine
Acetabular rim
Synovial membrane
Greater trochanter
Zona orbicularis
Ischial tuberosity
Lesser trochanter
Trochanteric crest

Fig. 81.2 Synovial cavity of left hip joint (distended): posterior aspect.

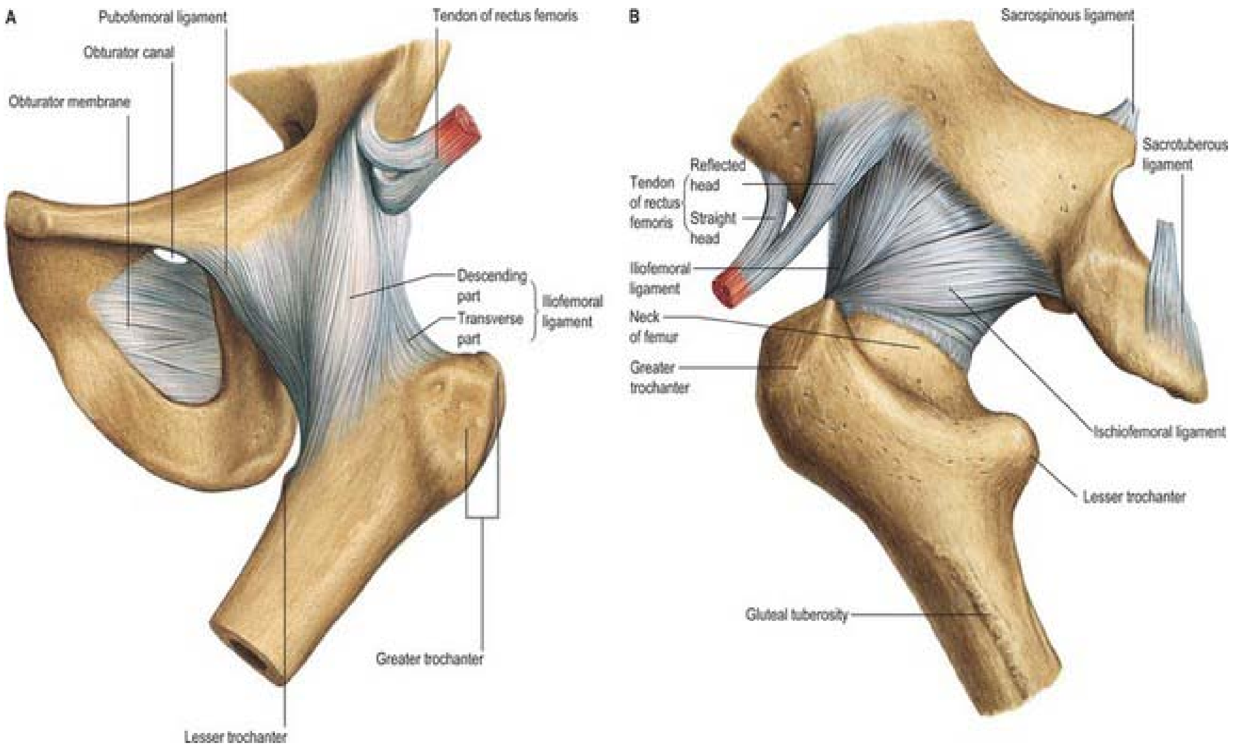
A
Pubofemoral ligament
Tendon of rectus femoris
Obturator canal
Obturator membrane
Descending part
Transverse part
Iliofemoral ligament
Greater trochanter
Lesser trochanter
B
Sacrospinous ligament
Sacrotuberous ligament
Reflected head
Tendon of rectus femoris
Straight head
Iliofemoral ligament
Neck of femur
Greater trochanter
Ischiofemoral ligament
Lesser trochanter
Gluteal tuberosity

Fig. 81.3 The ligaments of the hip joint: **A**, anterior aspect; **B**, posterior aspect.

(From Sobotta 2006.)

ARTICULAR SURFACES

The femoral head articulates with the cup-shaped (cotyloid) acetabulum, its centre lying a little below the middle third of the inguinal ligament. (The profile of the anterior margin of the joint is parallel to the middle third of the inguinal ligament.) The articular surfaces are reciprocally curved but neither coextensive nor completely congruent (Fig. 81.2; see Figs 80.4, 80.15). The close-packed position of the hip joint is one of full extension, with slight abduction and medial rotation. As in the shoulder joint, the surfaces are considered ovoid or spheroidal rather than spherical, but this view is controversial. Evidence appears to suggest that the articular surface on the femoral head is a spheroidal, or slightly ovoid, surface in youth but that it tends to become almost spherical with advancing age. The femoral head is covered by articular cartilage, except over the rough pit where the ligamentum teres is attached. In front the cartilage extends laterally over a small area on the adjoining neck. Articular cartilage is, generally, thicker centrally than at the periphery. Cartilage thickness is maximal anterosuperiorly in the acetabulum and anterolaterally on the femoral head, the two areas that correspond to the principal load-bearing areas within the joint The acetabular articular surface, the lunate surface, is an incomplete ring, broadest anterosuperiorly where the pressure of body weight falls in the erect posture, and narrowest in its pubic region. It is deficient inferiorly opposite the acetabular notch. The lunate surface is covered by articular cartilage, which is thickest where the surface is broadest. The acetabular fossa, the central non-articular area in the floor of the acetabulum, is devoid of cartilage but contains fibroelastic fat largely covered by synovial membrane. The acetabular labrum, a fibrocartilaginous rim attached to the acetabular margin, serves to deepen the acetabulum and bridges the acetabular notch by attaching to the peripheral edge of the transverse acetabular ligament. The labrum is triangular in section; it is attached by its base to the acetabular margin and its acute free edge projects beyond the acetabular margin. The diameter of the acetabular cavity is constricted by the labral rim which embraces the femoral head, maintaining joint stability both as a static restraint and by providing proprioceptive information.

FIBROUS CAPSULE

The capsule is strong and dense. It is attached above to the acetabular margin 5–6 mm medial to the labral attachment, in front to the outer labral aspect and, near the acetabular notch, to the transverse acetabular ligament and the adjacent rim of the obturator foramen. From its acetabular attachment it extends laterally to surround the femoral head and neck, and is attached anteriorly to the intertrochanteric line, superiorly to the base of the femoral neck, posteriorly 1 cm superomedial to the intertrochanteric crest, and inferiorly to the femoral neck near the lesser trochanter. Anteriorly many fibres ascend along the neck as longitudinal retinacula, containing blood vessels for both the femoral head and neck. The capsule is thicker anterosuperiorly, where maximal stress occurs, particularly in standing. Posteroinferiorly it is relatively thin and loosely attached. It has two sets of fibres, circular and longitudinal. The circular fibres (zona orbicularis) are internal and form a collar round the femoral neck; although partly blended with the pubofemoral and ischiofemoral ligaments, these fibres are not directly attached to bone. Externally, longitudinal fibres are most numerous in the anterosuperior region, where they are reinforced by the iliofemoral ligament. The capsule is also strengthened inferiorly by the pubofemoral ligament, and posteriorly by the ischiofemoral ligament. Externally it is rough, covered by muscles and tendons and separated anteriorly from psoas major and iliacus by a bursa (see below). The capsular attachment to the femur lies well distal to the growth plate of the femoral head both anteriorly and posteriorly. Thus the upper femoral epiphysis is entirely intracapsular. The capsular attachment intersects the growth plate of the greater trochanter on the upper surface of the base of the neck (see Fig. 80.18).

Relations

The joint capsule is surrounded by muscles (Fig. 81.4). Anteriorly, lateral fibres of pectineus separate it from the femoral vein. Lateral to this the tendon of psoas major, with iliacus lateral to it, descends across it, partly separated from the capsule by a bursa. The femoral artery is anterior to the tendon of psoas major, and the femoral nerve lies deep in a groove between the tendon and iliacus. More laterally the straight head of rectus femoris crosses the joint with a deep layer of the fascial iliotibial tract, which blends with the capsule under the lateral border of the muscle. Superiorly, the reflected head of rectus femoris contacts the capsule medially, while gluteus minimus covers it laterally, being closely adherent. Inferiorly, medial fibres of pectineus adjoin the capsule and, more posteriorly, obturator externus spirals obliquely to its posterior aspect. Posteroinferiorly, the capsule is covered by the tendon of obturator externus, separating it from quadratus femoris and accompanied by an ascending branch of the medial circumflex femoral artery. Above this the tendon of obturator internus and the gemelli contact the joint capsule, separating it from the sciatic nerve. The nerve to quadratus femoris is deep to the obturator internus tendon, and descends medially on the capsule. Above this, the posterior surface of the joint is crossed by piriformis.

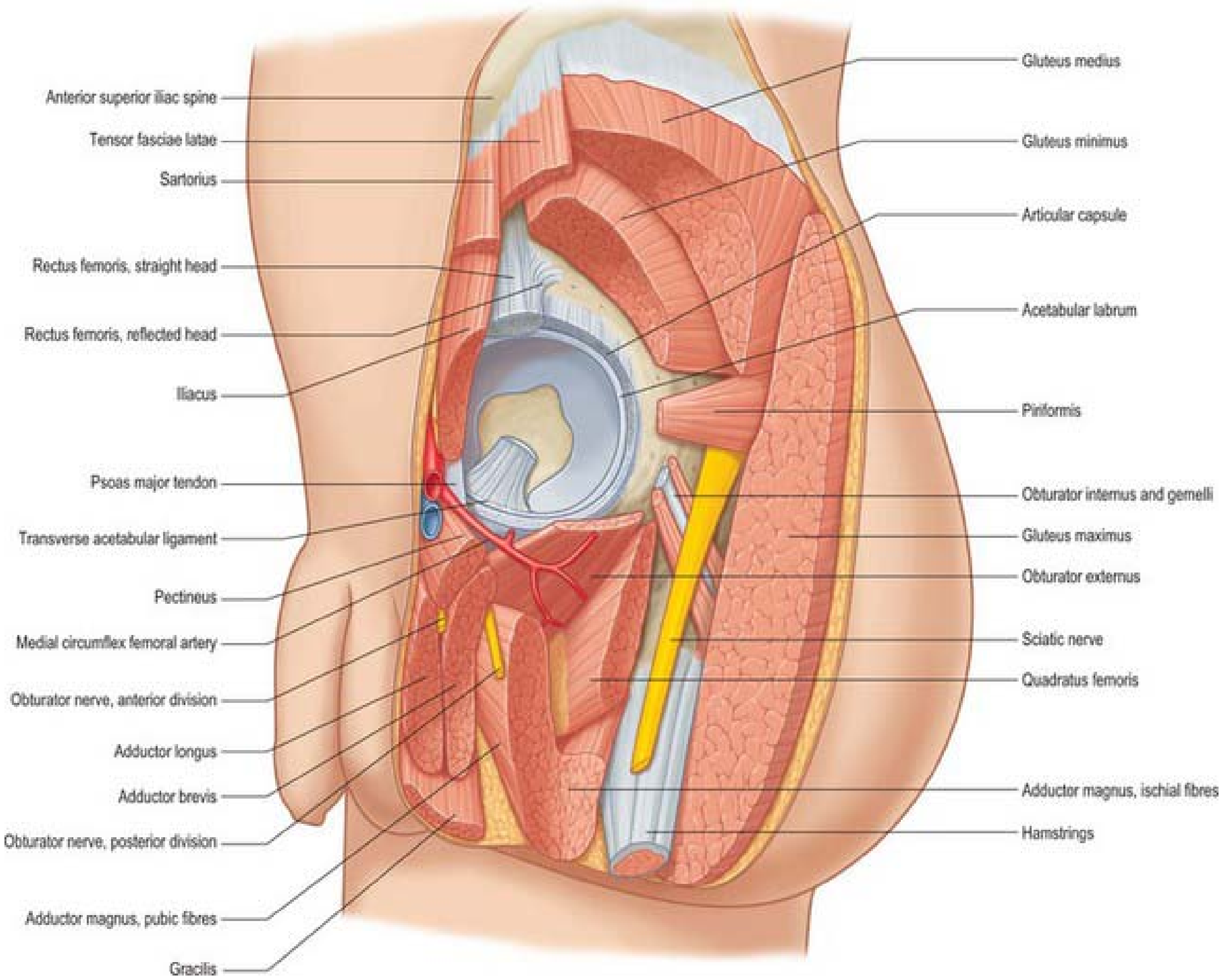
Anterior superior iliac spine
Tensor fasciae latae
Sartorius
Rectus femoris, straight head
Rectus femoris, reflected head
Iliacus
Psoas major tendon
Transverse acetabular ligament
Pectineus
Medial circumflex femoral artery
Obturator nerve, anterior division
Adductor longus
Adductor brevis
Obturator nerve, posterior division
Adductor magnus, pubic fibres
Gracilis
Gluteus medius
Gluteus minimus
Articular capsule
Acetabular labrum
Piriformis
Obturator internus and gemelli
Gluteus maximus
Obturator externus
Sciatic nerve
Quadratus femoris
Adductor magnus, ischial fibres
Hamstrings

Fig. 81.4 Dissection to display the structures surrounding the hip joint. The femoral head has been disarticulated and removed.

LIGAMENTS

The ligaments of the hip joint (Fig. 81.3) are the iliofemoral, pubofemoral, ischiofemoral and transverse acetabular ligaments and the ligamentum teres. As the hip moves so the capsular ligaments, as capsular thickenings, wind and unwind, tightening around the hip, affecting stability, excursion and joint capacity. Joint capacity is maximal when the hip is held in a partially flexed and abducted position: a patient with an effusion in the hip joint is therefore most comfortable when the joint is held in a position of flexion and abduction. See Fuss & Bacher (1991) for details.

Iliofemoral ligament

The iliofemoral ligament is very strong and shaped like an inverted Y, lying anteriorly and intimately blended with the capsule. Its apex is attached between the anterior inferior iliac spine and acetabular rim, its base to the intertrochanteric line. Fuss & Bacher describe a relatively weaker central portion, the greater iliofemoral ligament, with thicker and stronger marginal portions which they refer to as the lateral and medial iliofemoral ligaments. The obliquely disposed lateral ligament is attached to a tubercle at the superolateral end of the intertrochanteric line, while the vertically oriented medial ligament reaches the inferomedial end of the line.

Pubofemoral ligament

The pubofemoral ligament is triangular, its base attaching to the iliopubic eminence, superior pubic ramus, obturator crest and obturator membrane. It blends distally with the capsule and deep surface of the medial iliofemoral ligament. Fuss & Bacher describe this ligament as consisting of multiple crura.

Ischiofemoral ligament

The ischiofemoral ligament thickens the back of the capsule and consists of three distinct parts. The central part, the superior ischiofemoral ligament, spirals superolaterally from the ischium, where it is attached posteroinferior to the acetabulum, behind the femoral neck to attach to the greater trochanter deep to the iliofemoral ligament. Some fibres blend with the zona orbicularis. Lateral and medial inferior ischiofemoral ligaments embrace the posterior circumference of the femoral neck.

Transverse acetabular ligament

The transverse acetabular ligament (see Fig. 80.4) is continuous peripherally with the labrum but does not, itself, possess any cartilage cells. Its strong, flat fibres cross the acetabular notch forming a foramen through which vessels and nerves enter the joint.

Ligamentum teres (ligament of the head of the femur)

The ligamentum teres (Fig. 81.5) is a triangular and somewhat flattened band. Its apex is attached anterosuperiorly in the fovea on the femoral head and its base is attached principally to both edges of the acetabular notch, between which it blends with the transverse ligament. It also receives weaker contributions from the margins of the acetabular fossa. The ligamentum teres is ensheathed by synovial membrane, and varies in strength. Occasionally the synovial sheath exists by itself in the absence of the ligament; rarely both ligament and sheath are absent. The ligament appears to become tense when the hip joint is semi-flexed and adducted, and appears to relax when the joint is abducted.

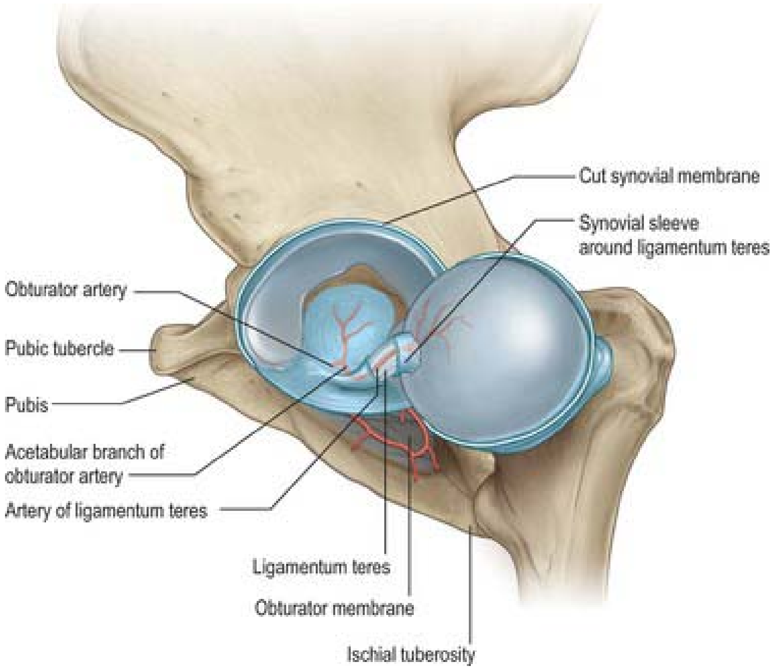
Cut synovial membrane
Synovial sleeve
around ligamentum teres
Obturator artery
Pubic tubercle
Pubis
Acetabular branch of
obturator artery
Artery of ligamentum teres
Ligamentum teres
Obturator membrane
Ischial tuberosity

Fig. 81.5 Interior of hip joint to show the ligamentum teres.

(From Drake, Vogl, Mitchell, Tibbitts and Richardson 2008.)

SYNOVIAL MEMBRANE

Starting from the femoral articular margin, the synovial membrane covers the intracapsular part of the femoral neck, then passes to the internal surface of the capsule to cover the acetabular labrum, ligamentum teres and fat in the acetabular fossa. It is thin on the deep surface of the iliofemoral ligament where it is compressed against the femoral head and sometimes is even absent here.

BURSAE

The hip joint may communicate with the subtendinous iliac (psoas) bursa through a circular aperture between the pubofemoral ligament and the vertical band of the iliofemoral ligament. More distant bursae are associated with the tendons of attachment of glutei medius and minimus at the greater trochanter, and between gluteus maximus and vastus lateralis.

VASCULAR SUPPLY AND LYMPHATIC DRAINAGE

Articular arteries are branches from the obturator, medial circumflex femoral, and superior and inferior gluteal arteries, with corresponding venous drainage. They form the cruciate and trochanteric anastomoses (Ch. 80). Lymphatics from the anterior aspect of the hip joint drain to the deep inguinal nodes, while those from the medial and posterior aspects run with the obturator and gluteal arteries respectively to reach the internal iliac nodes.

INNERVATION

The nerve supply to the hip is from the femoral nerve or its muscular branches, the obturator and accessory obturator nerves, the nerve to quadratus femoris and the superior gluteal nerve.

Hip and groin pain

Pain in the hip and groin may be due to any of a number of possible causes. True hip joint pain is usually felt deep in the crease of the groin. Pain over the lateral aspect of the hip usually suggests a local problem such as trochanteric bursitis. Pain in the buttock is only occasionally from the hip joint: most frequently it is referred from the lumbosacral spine or may be caused by vascular claudication pain. Pain in the groin may be due to inguinal or femoral hernias (see Ch. 61). In the younger age group groin pain afflicts those engaged in sport, especially running ball sports. Here the pain is sometimes due to a hernia but more commonly related to adductor tendinitis secondary to acute or chronic overload of the adductor longus tendon. Another common problem is attritional chronic overload of the anterior abdominal wall at its attachments to the pubis and inguinal ligament, or of external oblique at the external inguinal ring. Rarely problems may occur at the symphysis pubis.

FACTORS MAINTAINING STABILITY

The hip joint is very stable. The femoral head is closely fitted to the acetabulum in an area exceeding half a sphere, and is embraced closely by the acetabular labrum, which restrains it in the socket. In addition a ‘vacuum effect’ is present. The thick capsule is reinforced by the three major ligaments, of which the iliofemoral is the strongest, and is progressively tightened when the femur extends to the line of the trunk. The pubofemoral and ischiofemoral ligaments also tighten and, as the joint approaches the close packed position, resistance to an extending torque increases rapidly. The transverse ligament and the ligament of the head also contribute to stability. Only slight separation of the articular surfaces can be achieved by strong traction on the joint, and to aid insertion of an arthroscope, a needle is first inserted into the joint to eliminate the suction effect; with traction, the joint will then open sufficiently. Traumatic dislocation usually occurs only when the joint is subjected to extreme force.

BIOMECHANICS OF THE HIP JOINT

The transition from quadrapedal to bipedal gait was a considerable biomechanical milestone in the evolution of *Homo sapiens*. The biomechanical features of the human lower limb, whose function is primarily to allow stance and bipedal propulsion, are very different from those of the quadraped lower limb, and these differences are reflected in the anatomy and biomechanics of the human hip, knee, ankle and foot joints.

The acetabulum and femoral head form a multiaxial spheroidal (‘ball and socket’) joint, which allows relatively unhindered motion in three degrees of freedom, i.e. flexion/extension, abduction/adduction, medial (internal) and lateral (external) rotation. This articulation is innately limited in its capacity for translational motion in anteroposterior, transverse and vertical planes.

FEMUR

The femur is essentially a tubular structure with distortions that consist of bows and twists. The most notable is the anterior bow in its mid-portion, where the radius of curvature is relatively constant along the length of the femoral shaft. In the coronal plane, the femoral neck is inclined obliquely to the shaft at an angle of 135° (range 120–145°; Fig. 81.6). Although the neck/shaft angle and neck length are variable, the centre of the neck in the coronal plane is at the level of the apex of the greater trochanter. In the axial plane the femoral neck is anteverted, i.e. rotated anteriorly relative to the posterior surfaces of the femoral condyles: in the adult, this angle is 10–15º (Fig. 81.7). The degree of anteversion affects many aspects of lower limb biomechanics, including the abductor moment arm (the perpendicular distance from the centre of rotation of the femur to the line of action of the resultant abductor muscle force); patellar tracking (the motion of the patella relative to the femur or femoral groove on knee flexion and extension); foot orientation.

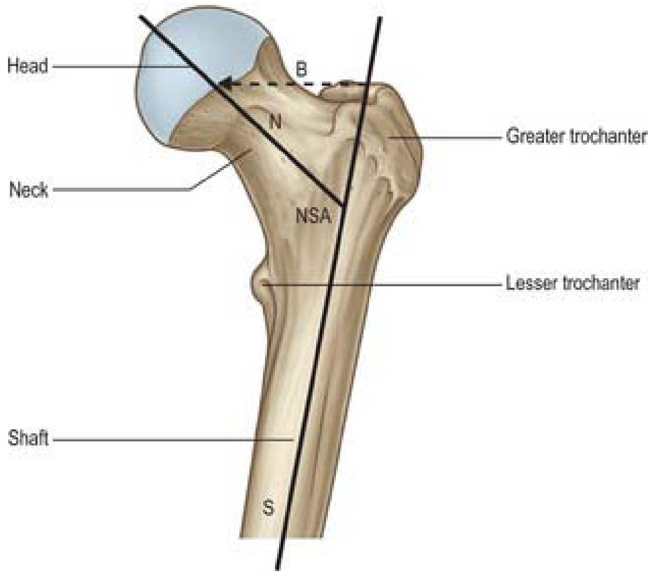

Fig. 81.6 The angle (NSA) between the long axis of the femoral shaft (S) and the axis of the femoral neck (N) is on average 135° (range 125–140°). In addition, in most hips, a line perpendicular to S from the tip of the greater trochanter (B) passes through the centre of the femoral head. This

approximation can be utlilized in judging the position of the femoral osteotomy in hip arthroplasty.

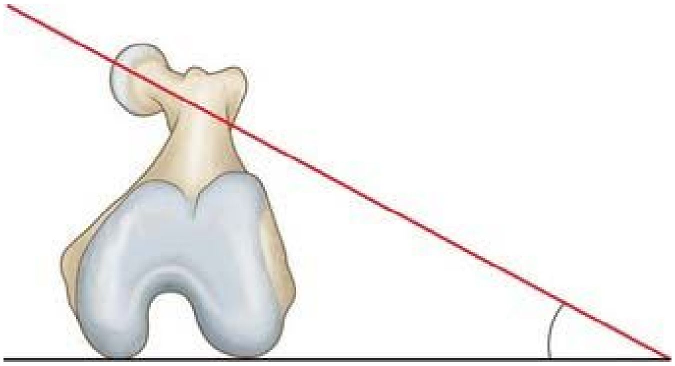

Fig. 81.7 The femoral anteversion angle is the angle subtended between the femoral neck and a line touching the posterior borders of the femoral condyles in the axial plane. This is 10–15° in the adult (greater in adult females than in males and children).

ACETABULUM

The acetabulum consists of the confluence of the ilium, ischium and pubis at the triradiate cartilage. By itself, the acetabulum covers an area slightly less than a hemisphere: it is deepened by the acetabular labrum. The degree of acetabular anteversion in the erect position is 14° (men) and 19° (women). In the coronal plane, the acetabular axis is inclined approximately 45° from the horizontal.

MOVEMENTS

When femoral movements are considered in relation to the articular surfaces, the length and angulation of the neck in relation to the shaft must be remembered. When the thigh is flexed or extended, the femoral head ‘spins’ in the acetabulum on an approximately transverse axis. Conversely, the acetabula rotate around similar axes in flexion and extension of the trunk on stationary femoral heads.

With the foot stationary on the ground, medial and lateral femoral rotation occur around a vertical axis through the centre of the femoral head and medial condyle. This axial medial rotation is the inevitable conjunct rotation that accompanies terminal extension of the knee and is often referred to as ‘screw-home’. The reverse occurs in initial flexion at the knee joint. The ‘screw-home’ phenomenon allows achievement of a ‘close packed position’ for the tibiofemoral joint, so aiding stability in the extended knee. The relationship of this axis to the whole femur (which has an angulated neck and oblique shaft) means that the medial condyle moves very little on the medial tibial condyle during medial rotation, while the lateral condyle moves forward on its tibial surface, and the greater trochanter moves simultaneously in a forward arc: converse movements occur during lateral rotation. With the foot either free or in loose contact with the ground, medial and lateral adjunct rotation of the whole lower limb occur around variable axes, all of which pass through the femoral head and any part of the foot. Conversely, with one foot stationary and the other free, the whole trunk may rotate on one femoral head, as in cross-kicking. Abduction and adduction occur about an anteroposterior axis through the femoral head, but since the latter is not strictly spherical, the axis is not a fixed one. Some kinesiologists refer to a mechanical axis coincident with the topographical long axis of the femoral neck, impinging on the approximate centre of the articular surface of the head, making extension and flexion of the thigh relatively pure ‘spins’ at the hip joint and most effective in tightening or relaxing the capsular ligaments. All other movements are regarded as pure or impure swings. While this permits analysis closer to actual articular function than a cardinal triaxial system related arbitrarily to the ‘anatomical’ position, the mechanical axis is itself regarded (incorrectly) by some as dynamic because forms of apparent dynamic ‘spin’ may occur in many positions. This view stems from an imprecise definition of the varieties of axes employed in arthrokinematics. The mechanical axis is not dynamic relative to the femur. It is stationary during pure spins, and moves relative to its coarticular surface in chordal or arcuate paths during pure or impure swings respectively.

Simple flexion is possible to 110–120° from the vertical; extension beyond the vertical is limited (perhaps 10–20°). Both movements are augmented by adjustments of the spinal column and pelvis, flexion of the knee and concomitant medial or lateral hip rotation. For example, knee flexion (lessening tension in the posterior femoral muscles) increases hip flexion to 120°; the thigh can be drawn passively to the trunk, though with some spinal flexion. Extension in walking and running is increased by forward inclination of the body, pelvic tilting and rotation and lateral rotation of the hip (Joseph 1975). Abduction and adduction can be similarly increased.

MUSCLES PRODUCING MOVEMENTS

Flexion is produced by psoas major and iliacus, assisted by pectineus, rectus femoris and sartorius. The adductors, particularly adductor longus, also assist, especially in early flexion following full extension.

Extension is produced by gluteus maximus and the hamstring (posterior femoral) muscles. In the fully erect posture with pendent arms a vertical line through the centre of gravity of the body passes behind a line joining the centres of the femoral heads. The body therefore tends to incline backwards but this is counterbalanced by ligamentous tension and congruence and compression of the articular surfaces with the hip joints in the close-packed position. Under increased loading of the trunk or leaning backwards, these resistive but passive factors are assisted by active contraction of the hip flexors. In swaying forwards at the ankles, or when the arms are stretched forward, and also in forward bending at the hip, the line of body weight moves in front of the transverse axis. The posture adopted, or the rate of change of posture, is largely controlled by the hamstrings which, besides being powerful flexors of the knee, are strong extensors of the hip. Gluteus maximus only becomes active when the thigh is extended against resistance, as in rising from a bending position or during climbing.

Abduction is produced by gluteus medius and minimus, assisted by tensor fasciae latae and sartorius; it is limited by adductor tension, the pubofemoral ligament and the medial band of the iliofemoral ligament. The muscles are consistently involved in walking or running, and contract periodically at precise phases of the walking or running cycle.

Adduction is produced by adductors longus, brevis and magnus, assisted by pectineus and gracilis; it is limited when the moving limb contacts the contralateral limb. The range of adduction is enhanced with the thigh flexed, when it is limited by the increasing tension in the abductor muscles, the lateral band of the iliofemoral ligament and ligament of the femoral head.

Medial rotation is produced by tensor fasciae latae and the anterior fibres of gluteus minimus and medius. It is a relatively weak movement and is limited by the lateral rotators, the ischiofemoral ligament and the posterior part of the capsule. Electromyographic data suggest that the adductors usually assist in medial rather than lateral rotation, but this is, of course, dependent on the primary position.

Lateral rotation is produced by the obturator muscles, the gemelli and quadratus femoris, assisted by piriformis, gluteus maximus and sartorius. It is a powerful action which is limited by tension in the medial rotators and the lateral band of the iliofemoral ligament.

FORCES ACTING ON THE HIP

Under bipedal loading conditions, the femoral heads support the weight of the body minus the weight of both legs (approximately one-third body weight) and the resultant vectors are vertical. When viewed in the sagittal plane, minimal muscle forces are required to maintain equilibrium and balance when the weight of the upper body is directly over the femoral heads. If the upper body is tilted posteriorly such that the body weight vector lies behind the femoral heads, the anterior hip structures (rectus femoris, iliopsoas and iliofemoral ligament) will act to counter the rotational moment causing hip extension.

The range of motion of the hip far exceeds that required for normal walking. The muscles of the joint are the major stabilizing factors: the ligaments of the hip joint provide little rotational stability when walking. During normal gait the hip is subjected to wide variations in load bearing, ranging from one third of body weight in the double-leg support phase to four times body weight in the single-leg support phase. The walking cycle is characterized by two load peaks (see p. 1460) at heel strike (see Fig. 81.9) and toe off, corresponding to maximal acceleration and deceleration respectively in single-leg stance (see Fig. 84.25). Between these two peaks the body translates smoothly with little vertical acceleration.

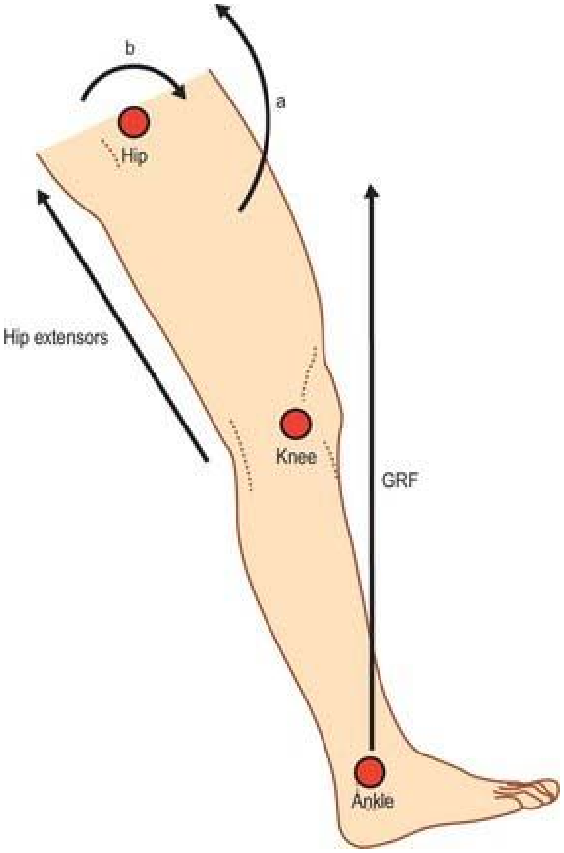

Fig. 81.9 Simplified kinetics of heel strike. At heel strike the ground reaction force (GRF) exerts a flexion (anticlockwise) moment about the hip (arrow a). The hip extensors counteract this moment with a clockwise moment (arrow b).

The factors influencing both the magnitude and direction of the compressive forces acting on the hip are the position of the centre of gravity; the abductor moment arm, which is a function of neck length (offset) and neck-shaft angle; the magnitude of body weight. Shortening of the abductor arm, e.g. in coxa valga or excessive femoral anteversion, will increase abductor demand and therefore increase joint reaction force. If the muscles cannot meet this demand, compensation takes place either in the form of a gluteus lurch (leaning towards the affected side to shorten the body weight lever arm), or a Trendelenburg gait (where the pelvis tilts away from the affected side).

Single-leg stance

In single-leg stance, the effective centre of gravity moves away from the supporting leg as the unsupported leg contributes to body weight. Body weight will exert a turning moment around the centre of the supporting femoral head: in order to maintain equilibrium, an equal but opposite turning moment is provided by the abductor muscles (primarily gluteii medius and minimus, tensor fasciae latae, piriformis and obturator internus). Since the lever arm of the abductors is much shorter than that of body weight acting through the centre of gravity, an abduction force greater than body weight is required to maintain equilibrium (Fig. 81.8). The vectors of these two forces produce a resultant compressive load on the femur that is oriented approximately 16° obliquely, laterally and distally. The joint reaction vector is exactly equal and opposite to this vector and is approximately four times body weight.

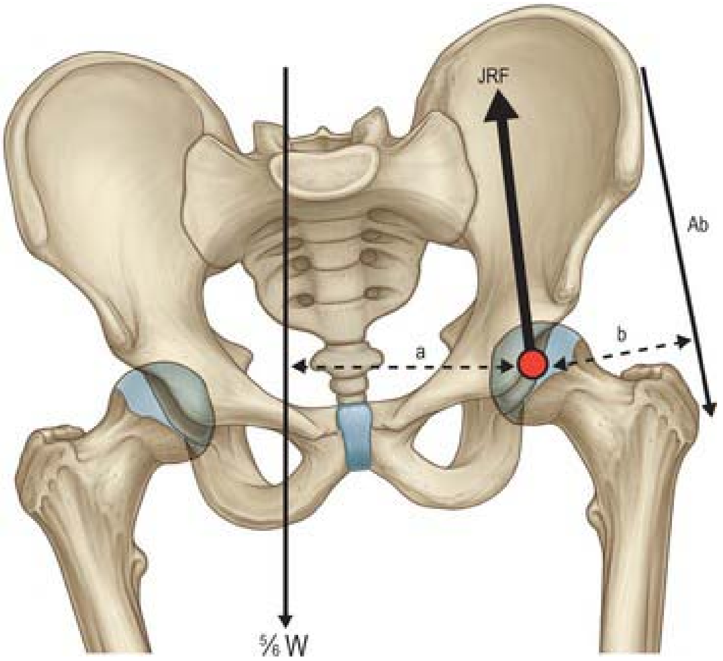

Fig. 81.8 In single-leg stance, 5/6 of total body weight (W) passes just lateral to the midline, exerting a clockwise moment on the pelvis; this is counteracted by the pull of the abductors, whose lever arm (a) is approximately half that of the body centre (b). Thus the abductor force (Ab) required to maintain equilibrium is approximately twice that of body

weight, resulting in a joint reaction force (JRF) approximately 3 to 4 times that of body weight.

Simplified kinetics of heel strike

Contact with the ground produces a reaction force equal to body weight multiplied by acceleration (see p. 1443). This ground reaction force acting at the foot produces a flexion moment about the hip which is approximately 3.3 times body weight, and is counterbalanced by the hip extensors (gluteus maximus and hamstrings) (Fig. 81.9).

REFERENCES

ıss FK, Bacher A. New aspects of the morphology and function of the human hip joint ligaments. *Am J Anat*. 1991;192:1-13.

seph J. Movements at the hip joint. *Ann R Coll Surg Eng*. 1975;56:192-201.

CHAPTER 82

Knee

The knee is the largest synovial joint in the body. It consists of three distinct and partially separated compartments that collectively form a complex ‘hinge’ joint. This arrangement offers a fulcrum for the powerful extensor and flexor muscles that act on the joint during propulsion. A number of stabilizing factors counter the considerable biomechanical demands that are imposed upon the joint: most important is a complex arrangement of intracapsular and extracapsular ligaments. Our understanding of the anatomy of the knee has improved considerably in recent years, due in large measure to significant technological advances in diagnostic imaging and surgery.

SKIN AND SOFT TISSUE

SKIN

Cutaneous vascular supply and lymphatic drainage

The arterial supply of the skin covering the knee is derived from genicular branches of the popliteal artery, the descending genicular branch of the femoral artery, and the anterior recurrent branch of the anterior tibial artery, with small contributions from the arteries to vastus medialis and the hamstrings (Fig. 82.1). For further details consult Cormack & Lamberty (1994).

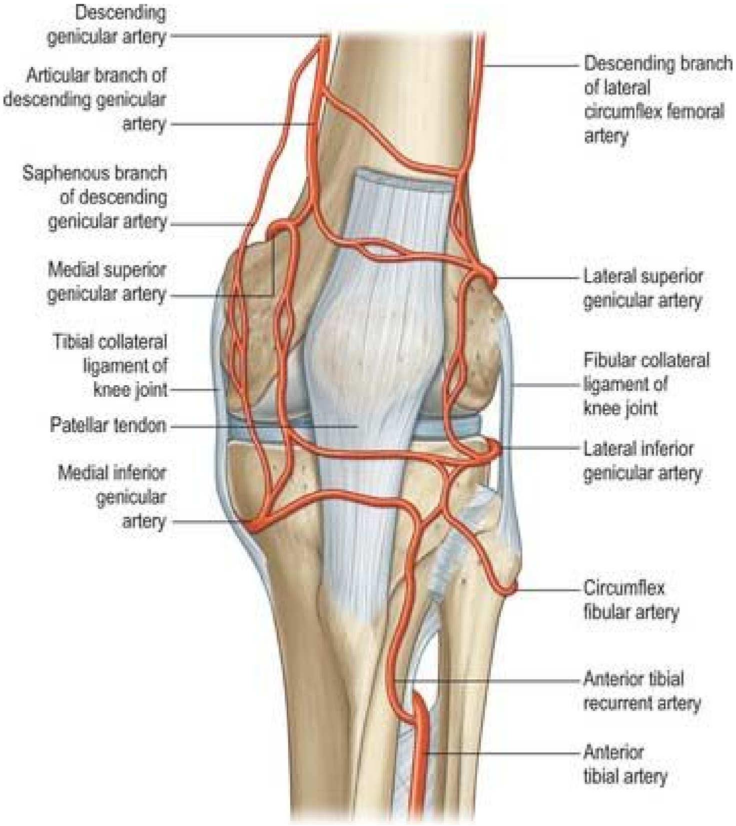
Descending genicular artery
Articular branch of descending genicular artery
Saphenous branch of descending genicular artery
Medial superior genicular artery
Tibial collateral ligament of knee joint
Patellar tendon
Medial inferior genicular artery
Descending branch of lateral circumflex femoral artery
Lateral superior genicular artery
Fibular collateral ligament of knee joint
Lateral inferior genicular artery
Circumflex fibular artery
Anterior tibial recurrent artery
Anterior tibial artery

Fig. 82.1 The arterial anastomoses around the knee joint.

Cutaneous veins are tributaries of the vessels that correspond to the named arteries. Cutaneous lymphatic drainage is initially to the superficial inguinal nodes, and possibly also to the popliteal nodes and thence to the deep inguinal group of lymph nodes.

Cutaneous innervation

Infrapatellar branch of the saphenous nerve

The infrapatellar branch of the saphenous nerve reaches the anterior aspect of the knee from the medial side. It is invariably divided in the medial approach to the knee, which accounts for the numbness that inevitably occurs lateral to the scar of a medial knee incision. A painful neuroma may form if the nerve is partially sectioned, e.g. by the incision for an arthroscopy portal or a small medial arthrotomy. Unfortunately the position of the nerve relative to the line of the joint is variable. In most cases it crosses just below the joint line, passing over the patellar tendon at its insertion into the tibia. For further details see Tennant et al (1998).

Peripatellar plexus

Proximal to the knee, the infrapatellar branch of the saphenous nerve connects with branches of the medial and intermediate femoral cutaneous nerves, and lateral femoral cutaneous nerve. Distal to the knee it connects with other branches of the saphenous nerve. This fine, subcutaneous network of communicating nerve fibres over and around the patella is termed the peripatellar plexus.

SOFT TISSUE

Popliteal fossa

The popliteal fossa (Figs 82.2, 82.3) is a narrow intermuscular space posterior to the knee joint, with a diamond-shaped outline that is rendered more apparent when its boundaries are artificially separated during dissection. The boundaries are biceps femoris proximolaterally; semimembranosus and the overlying semitendinosus proximomedially; the lateral head of gastrocnemius with the underlying plantaris distolaterally, and the medial head of gastrocnemius distomedially. The anterior boundary (or floor) of the fossa is formed, in proximodistal sequence, by the popliteal surface of the femur, the oblique popliteal ligament (overlying the posterior surface of the capsule of the knee joint), and the posterior aspect of the proximal tibia covered by popliteus and the fascia overlying popliteus. The fossa is covered posteriorly by the popliteal fascia, which is referred to as the roof of the fossa. The popliteal fascia is continuous with the fascia lata proximally and with the fascia cruris distally. It is a dense layer that is strongly reinforced by transverse fibres and is often perforated by the short saphenous vein and sural nerve; these two structures are useful landmarks in the direct posterior approach to the knee joint. (Note that ‘popliteal fascia’ refers to the deep fascia that forms the ‘roof’ of the fossa, in contradistinction to the ‘fascia overlying popliteus’, which forms part of the floor.)

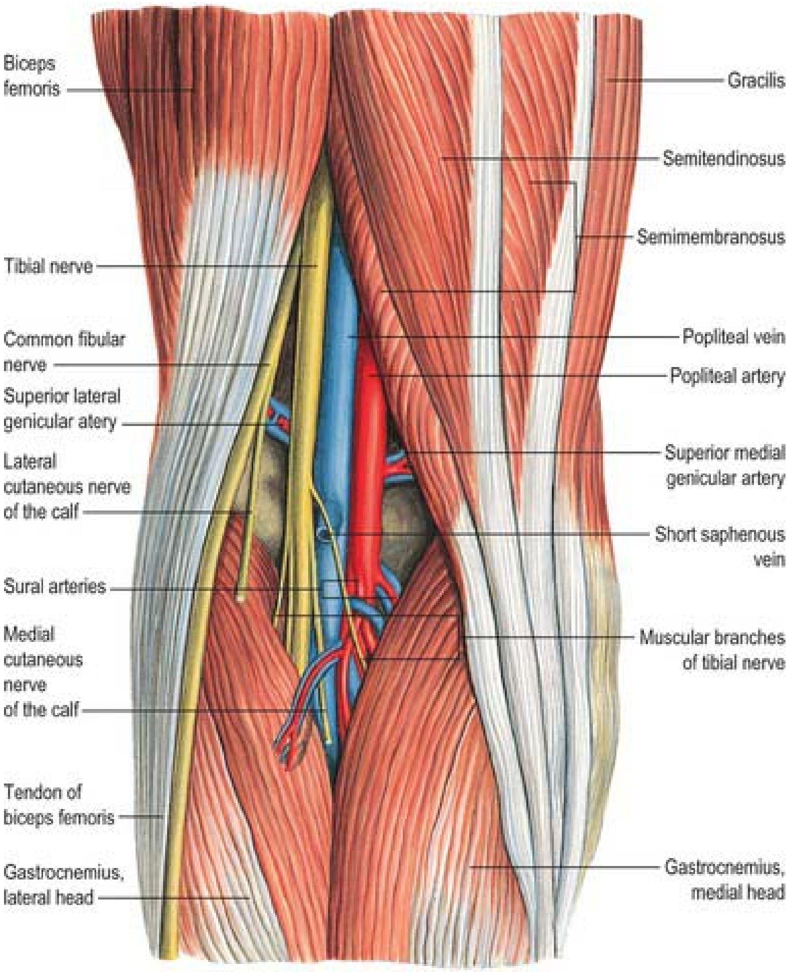
Biceps femoris
Tibial nerve
Common fibular nerve
Superior lateral genicular atery
Lateral cutaneous nerve of the calf
Sural arteries
Medial cutaneous nerve of the calf
Tendon of biceps femoris
Gastrocnemius, lateral head
Gracilis
Semitendinosus
Semimembranosus
Popliteal vein
Popliteal artery
Superior medial genicular artery
Short saphenous vein
Muscular branches of tibial nerve
Gastrocnemius, medial head

Fig. 82.2 Left popliteal fossa.

(From Sobotta 2006.)

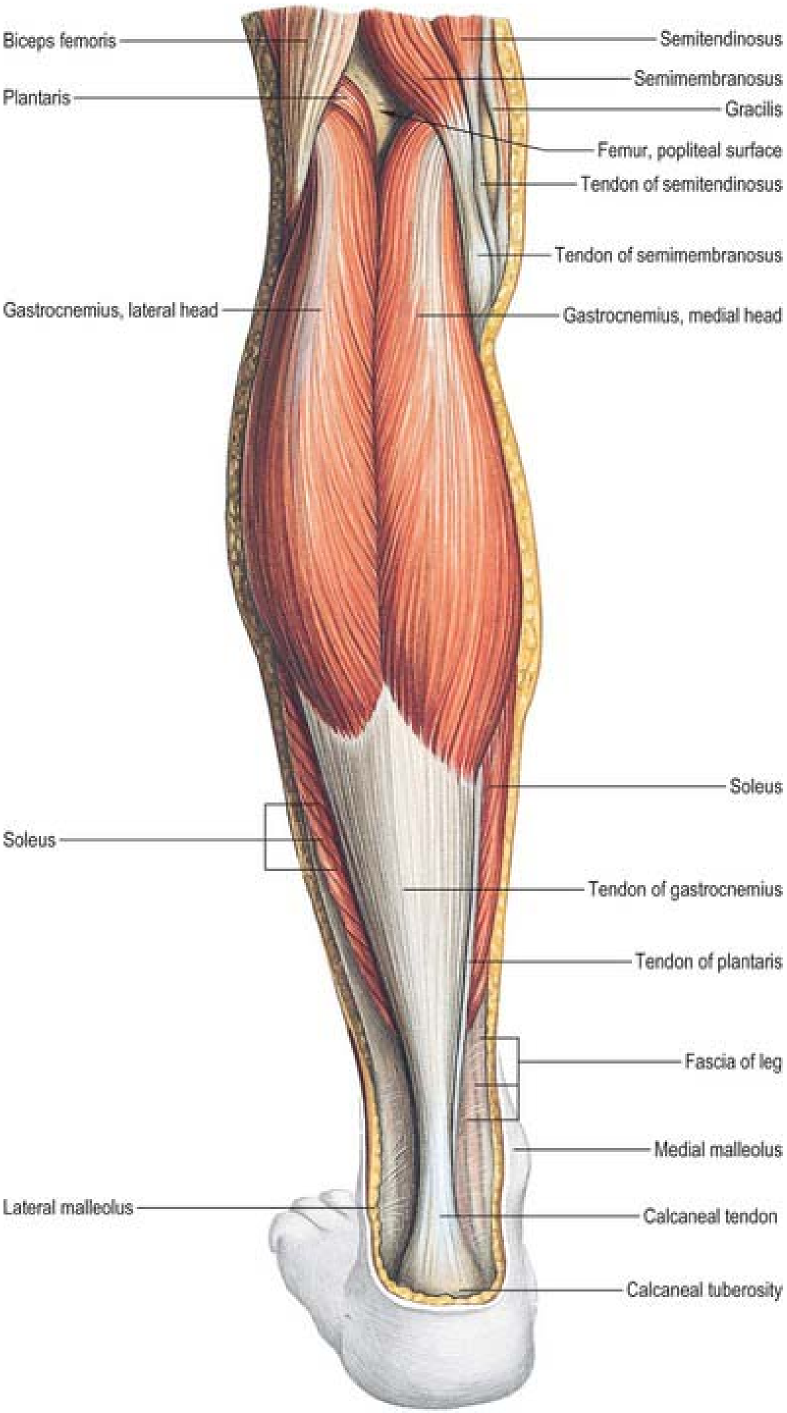
Biceps femoris
Plantaris
Semitendinosus
Semimembranosus
Gracilis
Femur, popliteal surface
Tendon of semitendinosus
Tendon of semimembranosus
Gastrocnemius, lateral head
Gastrocnemius, medial head
Soleus
Soleus
Tendon of gastrocnemius
Tendon of plantaris
Fascia of leg
Medial malleolus
Lateral malleolus
Calcaneal tendon
Calcaneal tuberosity

Fig. 82.3 Muscles of the calf: superficial view including boundaries of popliteal fossa.

(From Sobotta 2006.)

Contents

With its boundaries undisturbed, the popliteal fossa is typically 2.5 cm wide. Its contents are largely hidden, especially in its distal part, where the heads of gastrocnemius are in contact with each other. When its boundaries are separated, its contents are revealed as the popliteal vessels (Figs 82.2, 82.4), tibial and common fibular nerves, short saphenous vein, sural nerve, posterior femoral cutaneous nerve, an articular branch from the obturator nerve, lymph nodes, fat and a variable number of collapsed bursal sacs. The tibial nerve descends centrally immediately anterior to the popliteal fascia, crossing the vessels posteriorly from lateral to medial. The common fibular nerve descends laterally immediately medial to the tendon of biceps femoris. Popliteal vessels are deeply located and held together by dense areolar tissue. They lie on the floor of the fossa, the popliteal vein being superficial to the artery. Proximally, the thick-walled vein lies lateral to the artery, crossing to its medial side distally. At times the popliteal vein is duplicated, and the artery lies between the two veins, which are usually bridged by connecting channels. An articular branch from the obturator nerve descends on the artery to the knee. Six or seven popliteal lymph nodes are embedded in the fat, one under the popliteal fascia near the termination of the short saphenous vein, one between the popliteal artery and knee joint, the others around the popliteal vessels.

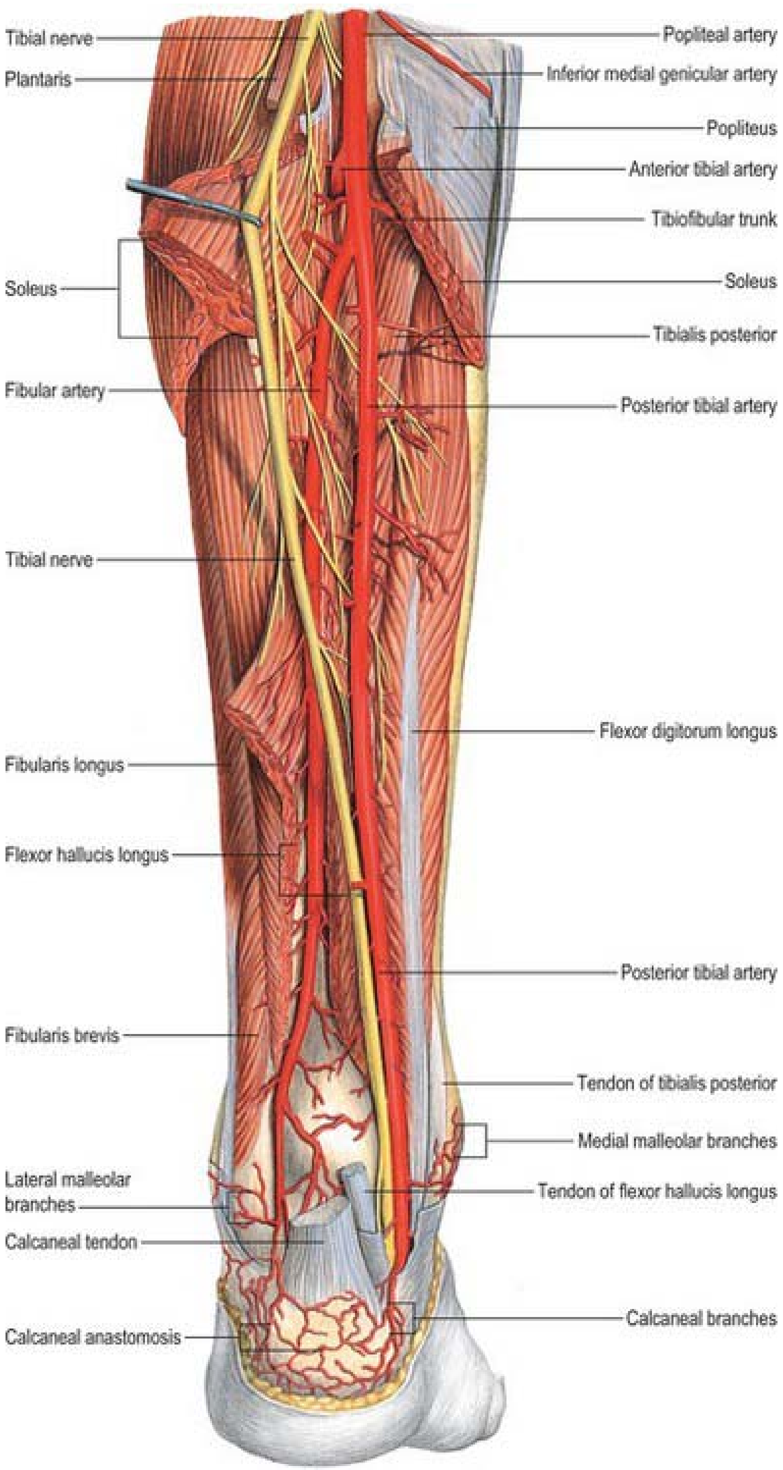
Popliteal artery
Tibial nerve
Inferior medial genicular artery
Plantaris
Popliteus
Anterior tibial artery
Tibiofibular trunk
Soleus
Soleus
Tibialis posterior
Fibular artery
Posterior tibial artery
Tibial nerve
Flexor digitorum longus
Fibularis longus
Flexor hallucis longus
Posterior tibial artery
Fibularis brevis
Tendon of tibialis posterior
Medial malleolar branches
Lateral malleolar branches
Tendon of flexor hallucis longus
Calcaneal tendon
Calcaneal branches
Calcaneal anastomosis

Fig. 82.4 Left popliteal, posterior tibial and fibular arteries: posterior aspect.

(From Sobotta 2006.)

BONE

FEMUR, TIBIA AND FIBULA

The femur is described in Chapter 80 and the tibia and fibula are described in Chapter 83.

PATELLA

Topography

The patella is the largest sesamoid bone (Figs 82.5, 82.6) and is embedded in the tendon of quadriceps femoris, anterior to the distal femur (femoral condyles). It is flat, distally tapered, proximally curved, and has anterior and posterior surfaces, three borders and an apex which is the distal end of the bone. With the knee in extension, the apex is just proximal to the line of the knee joint.

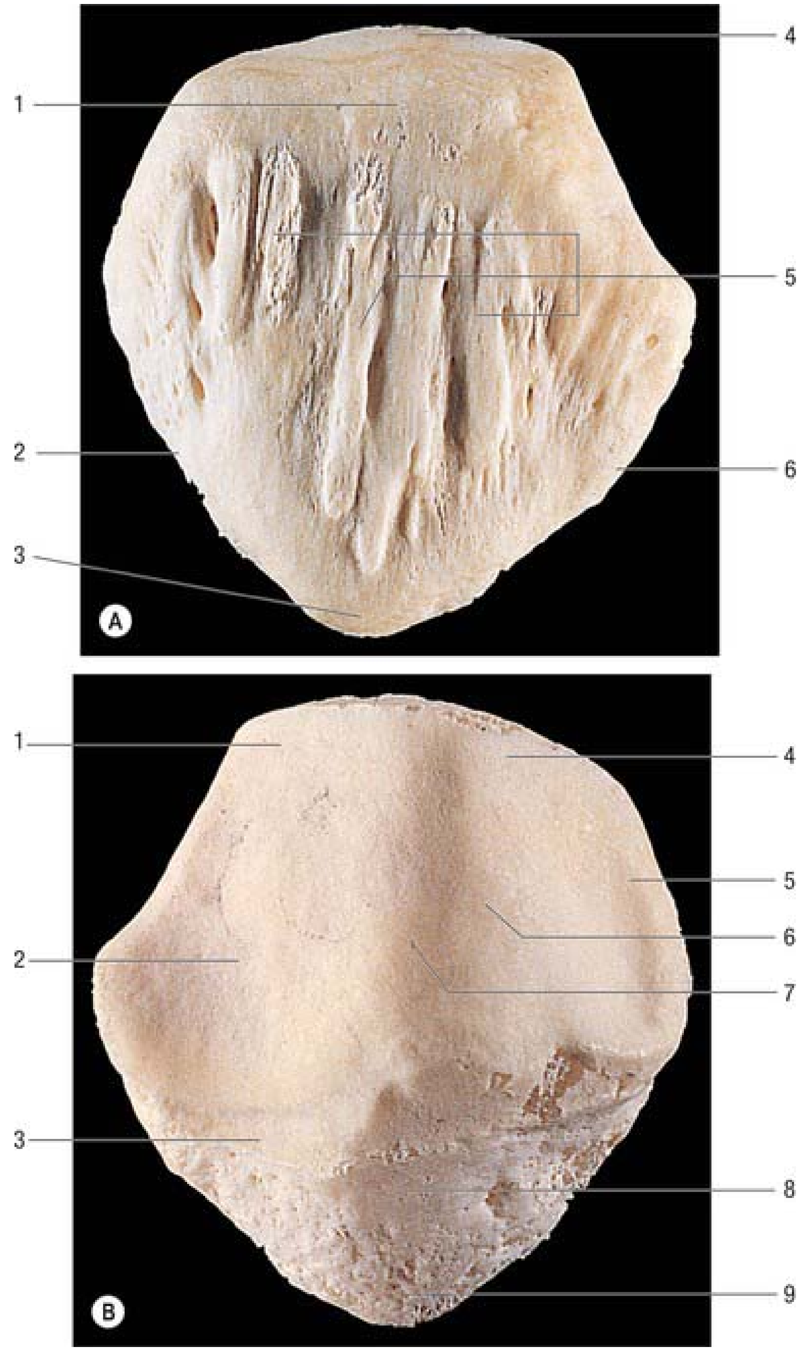

Fig. 82.5 **A**, Left patella: anterior aspect. **1**. Area of attachment of rectus femoris. **2**. Medial border: attachment of medial retinaculum (expansion). **3**. Apex. **4**. Area of attachment of vastus intermedius. **5**. Markings of attachment of quadriceps tendon. **6**. Lateral border: attachment of lateral retinaculum (expansion). **B**, Left patella: articular (posterior) surface. **1**. Upper lateral facet: in contact with femur in flexion. **2**. Lower lateral facet: in contact with femur in extension. **3**. Area overlain by edge of

circumferential fat pad. **4**. Upper medial facet: in contact with femur in flexion. **5**. Medial vertical (‘odd’) facet: in contact with femur in extreme flexion. **6**. Lower medial facet: in contact with femur in extension. **7**. Ridge. **8**. Area covered by infrapatellar fat pad. **9**. Area for attachment of patellar tendon.

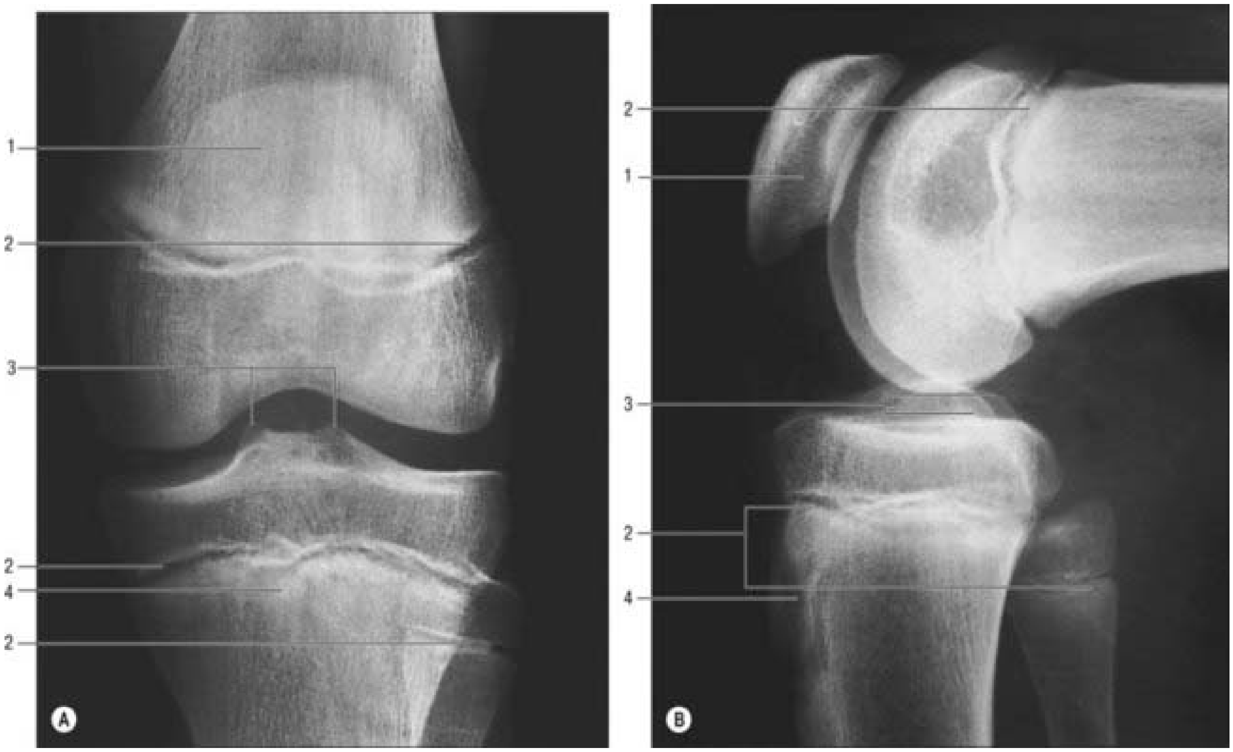

Fig. 82.6 Anteroposterior (**A**) and lateral (**B**) radiographs of the knee in a boy aged 14 years. **1**. Patella. **2**. Cartilaginous growth plates. **3**. Intercondylar eminence. **4**. Prolongation of proximal tibial epiphysis and growth plate forming the tibial tuberosity.

The subcutaneous, convex anterior surface is perforated by nutrient vessels. It is longitudinally ridged, separated from the skin by a prepatellar bursa, and covered by an expansion from the tendon of quadriceps femoris, which blends distally with superficial fibres of the patellar tendon (patellar ligament), the continuation of the tendon of quadriceps. The posterior surface has a proximal smooth, oval articular area, crossed by a smooth vertical ridge, which fits the intercondylar groove on the femoral patellar surface and divides the patellar articular area into medial and lateral facets; the lateral is usually larger. Each facet is divided by faint horizontal lines into equal thirds. A seventh ‘odd’ facet is present as a narrow strip along the medial border of the patella; it contacts the medial femoral condyle in extreme flexion. Distal to the articular surface, the apex is roughened by the attachment of the patellar tendon. Proximal to this, the area between the roughened apex and the articular margin is covered by an infrapatellar pad of fat. The articular cartilage is the thickest in the body, reflecting the magnitude of the stresses to which it is subjected.

The thick superior border (surface) slopes anteroinferiorly. The medial and lateral borders are thinner and converge distally; the expansions of the tendons of vastus medialis and lateralis (medial and lateral patellar retinacula respectively) are attached to them. The lateral retinaculum receives contributions from the iliotibial tract. Ossification occasionally extends from the lateral margin of the patella into the tendon of vastus lateralis.

The shape of the patella can vary, and certain configurations are associated with patellar instability. Not infrequently a bipartite patella is seen on radiographs. The bone seems to be in two parts, usually with a smaller superolateral fragment: this has long been attributed to the presence of a separate ossification centre, but in some cases could represent failed union following a stress fracture.

Structure

The patella consists of more or less uniformly dense trabecular bone, covered by a thin compact lamina. Trabeculae beneath the anterior surface are parallel to the surface; elsewhere they radiate from the articular surface into the substance of the bone.

Muscle attachments

Quadriceps femoris is attached to the superior surface, except near its posterior margin; the attachment extends distally onto the anterior surface. The attachment for rectus femoris lies anteroinferior to that for vastus intermedius. Rough markings can be traced in continuity around the periphery of the bone from the anterosuperior surface to the deep surface of the apex. Those at the lateral and medial borders represent the attachments of the lateral and medial vasti, and those at the apex represent the attachment of the patellar tendon.

Vascular supply

The arterial supply of the patella is derived from the genicular anastomosis, particularly from the genicular branches of the popliteal artery and from the anterior tibial recurrent artery.

Ossification

Several centres appear during the third to sixth years and these coalesce rapidly. Accessory marginal centres appear later and fuse with the central mass.

JOINTS

SUPERIOR TIBIOFIBULAR JOINT

The superior (proximal) tibiofibular joint is an almost plane synovial joint between the lateral tibial condyle and fibular head.

Articulating surfaces

The articulating surfaces vary in size, form and inclination. The joint line may be transverse or oblique. The fibular facet is usually elliptical or circular, almost flat or slightly grooved. The surfaces are covered with hyaline cartilage.

Fibrous capsule

The capsule is attached to the margins of the tibial and fibular articular, and is thickened anteriorly and posteriorly.

Ligaments

The ligaments of the superior tibiofibular joint are not entirely separate from the capsule. The anterior ligament is made up of two or three flat bands which pass obliquely up from the fibular head to the front of the lateral tibial condyle: it is closely related to the tendon of biceps. The posterior ligament is a thick band that ascends obliquely between the posterior aspect of the fibular head and the lateral tibial condyle: it is covered by the popliteal tendon.

Synovial membrane

The synovial membrane of the superior tibiofibular joint is sometimes (in approximately 10% of subjects) continuous with that of the knee joint via the subpopliteal recess.

Vascular supply and lymphatic drainage

The superior tibiofibular joint receives an arterial supply from the anterior and posterior tibial recurrent branches of the anterior tibial artery. Lymphatics follow the arteries and drain to the popliteal nodes.

Innervation

The superior tibiofibular joint is innervated by branches from the common fibular nerve and from the nerve to popliteus.

Factors maintaining stability

Stability of the superior tibiofibular joint is maintained by the fibrous capsule and the anterior and posterior ligaments, assisted by the biceps tendon and the interosseous membrane.

Movements

Very little movement other than limited gliding takes place at the superior tibiofibular joint. Some movement must occur in conjunction with movement occurring at the inferior tibiofibular joint, however, surgical fusion (arthrodesis) of the superior tibiofibular joint seems to have no effect on movements of the ankle joint.

Relations

The common fibular nerve runs posterior to the fibular head, medial to the tendon of biceps, which is closely associated with the anterior capsule. The anterior and posterior tibial branches of the popliteal artery, and the fibular artery, are all vulnerable inferomedial to the joint.

PATELLOFEMORAL JOINT

The patellofemoral joint is a synovial joint and is part of the knee joint.

Articulating surfaces

The articular surface of the patella is adapted to that of the femur. The latter extends onto the anterior surfaces of both femoral condyles like an inverted U. Since the whole area is concave transversely and convex in the sagittal plane, it is an asymmetrical sellar surface. The ‘odd’ facet on the articular surface of the patella contacts the anterolateral aspect of the medial femoral condyle in full flexion, when the highest lateral patellar facet contacts the anterior part of the lateral femoral condyle. As the knee extends, the middle patellar facets contact the lower half of the femoral surface; in full extension only the lowest patellar facets are in contact with the femur. In summary, on flexion the patellofemoral contact point moves proximally. The contact area also broadens to cope with the increasing stress that accompanies progressive flexion.

Patellar tendon sheath and patellar tendon

The patellar tendon (patellar ligament) is the central band of the tendon of quadriceps femoris, and is continued distally from the patella to the tibial tuberosity (see Fig. 80.25). It is strong, flat and 6 to 8 cm in length. Proximally it is attached to the patellar apex and adjoining margins, to roughened areas on the anterior surface and to a depression on the distal posterior patellar surface. Distally it is attached to the superior smooth area of the tibial tuberosity. This insertion is oblique, and is more distal laterally. Its superficial fibres are continuous over the patella with the tendon of quadriceps femoris, the medial and lateral parts of which descend, flanking the patella, to the sides of the tibial tuberosity, where they merge with the fibrous capsule as the medial and lateral patellar retinacula. The patellar tendon is separated from the synovial membrane by a large infrapatellar fat pad and from the tibia by a bursa, and lies within its own well-defined sheath.

In the procedure of tibial osteotomy, the tibia is cut transversely just above the patellar tendon insertion. Failure to appreciate the obliquity of the tibial attachment of the tendon may lead to inadvertent division of the tendon during this procedure, with unfortunate consequences.

All other aspects of the patellofemoral joint are described with the tibiofemoral joint.

TIBIOFEMORAL JOINT

The tibiofemoral joint is a complex synovial joint and is part of the knee joint.

Articulating surfaces

Proximal tibial surface

The proximal tibial surface (often referred to as the tibial plateau) slopes posteriorly and downwards relative to the long axis of the shaft (Fig. 82.7). The tilt, which is maximal at birth, decreases with age, and is more marked in habitual squatters. The tibial plateau presents medial and lateral articular surfaces (facets) for articulation with the corresponding femoral condyles. The posterior surface, distal to the articular margin, displays a horizontal, rough groove to which the capsule and posterior part of the medial collateral ligament are attached. The anteromedial surface of the medial tibial condyle is a rough strip, separated from the medial surface of the tibial shaft by an inconspicuous ridge. The medial patellar retinaculum is attached to the medial tibial condyle along its anterior and medial surfaces, which are marked by vascular foramina.

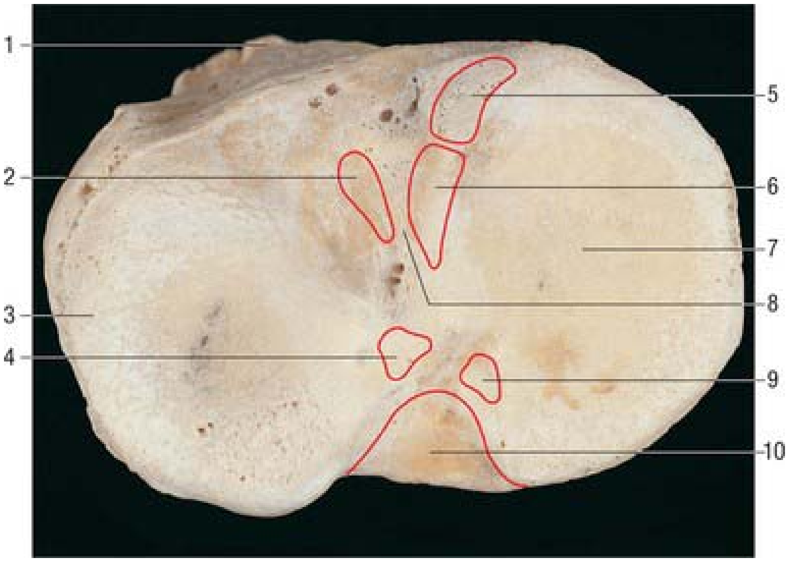

Fig. 82.7 The left tibial plateau. **1**. Tibial tuberosity. **2**. Attachment of anterior horn, lateral meniscus. **3**. Lateral condyle. **4**. Attachment of posterior horn, lateral meniscus. **5**. Attachment of anterior horn, medial meniscus. **6**. Attachment of anterior cruciate ligament. **7**. Medial condyle. **8**. Intercondylar eminence. **9**. Attachment of posterior horn, medial meniscus. **10**. Attachment of posterior cruciate ligament.

The medial articular surface is oval (long axis anteroposterior) and longer than the lateral articular surface. Around its anterior, medial, and posterior margins, it is related to the medial meniscus; the meniscal imprint, wider posteriorly and narrower anteromedially, is often discernible. The surface is flat in its posterior half and the anterior half slopes upwards about 10°. Much of the posterior surface is covered by the meniscus, so that overall a concave surface is presented to the medial femoral condyle. Its lateral margin is raised as it reaches the intercondylar region.

The lateral tibial condyle overhangs the shaft posterolaterally above a small circular facet for articulation with the fibula. The lateral articular surface is more circular and coapted to its meniscus. In the sagittal plane the articular surface is fairly flat centrally, and anteriorly and posteriorly the surface slopes inferiorly. Overall this creates a rather convex surface, so that, with the lateral femoral condyle in contact, there are anterior and posterior recesses (triangular in section), which are occupied by the anterior and posterior meniscal horns. Elsewhere the surface has a raised medial margin that spreads to the lateral intercondylar tubercle. Its articular margins are sharp, except posterolaterally, where the edge is rounded and smooth: here the tendon of popliteus is in contact with bone.

Intercondylar area

The rough-surfaced area between the condylar articular surfaces is narrowest centrally where there is an intercondylar eminence, the edges of which project slightly proximally as the lateral and medial intercondylar tubercles.

The intercondylar area widens behind and in front of the eminence as the articular surfaces diverge (Fig. 82.8).

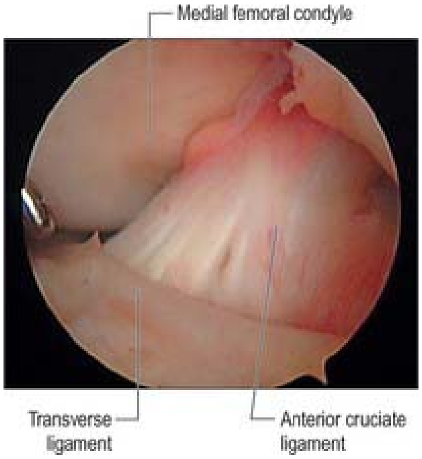

Fig. 82.8 The intercondylar notch at arthroscopy, showing the anterior cruciate and intermeniscal ligaments.

(By courtesy of Smith and Nephew Endoscopy.)

The anterior intercondylar area is widest anteriorly. Anteromedially, anterior to the medial articular surface, a depression marks the site of attachment of the anterior horn of the medial meniscus. Behind this a smooth area receives the anterior cruciate ligament. The anterior horn of the lateral meniscus is attached anterior to the intercondylar eminence, lateral to the anterior cruciate ligament. The eminence, with medial and lateral tubercles, is the narrow central part of the area. The raised tubercles are thought to provide a slight stabilizing influence on the femur.

The posterior horn of the lateral meniscus is attached to the posterior slope of the intercondylar area. The posterior intercondylar area inclines down and backwards behind the posterior horn of the lateral meniscus. A depression behind the base of the medial intercondylar tubercle is for the posterior horn of the medial meniscus. The rest of the area is smooth and provides attachment for the posterior cruciate ligament, spreading back to a ridge to which the capsule is attached.

Femoral surface

The femoral condyles, bearing articular cartilage, are almost wholly convex. Opinions as to the contours of their sagittal profiles tend to vary. One view is that they are spiral with a curvature increasing posteriorly (‘a closing helix’); that of the lateral condyle being greater. An alternative view is that the articular surface for contact with the tibia on the medial femoral condyle describes the arcs of two circles. According to this view, the anterior arc makes contact with the tibia near extension and is part of a virtual circle of larger radius than the more posterior arc, which makes contact during flexion. The lateral femoral condyle is believed to describe a single arc and thus to possess a single radius of curvature.

Tibiofemoral congruence is improved by the menisci, which are shaped to produce concavity of the surfaces presented to the femur; the combined lateral tibiomeniscal surface is deeper. The lateral femoral condyle has a faint groove anteriorly which rests on the peripheral edge of the lateral meniscus in full extension. A similar groove appears on the medial condyle, but does not reach its lateral border, where a narrow strip contacts the medial patellar articular surface in full flexion. These grooves demarcate the femoral patellar and condylar surfaces. The differences between the shapes of the articulating surfaces correlate with the movements of the joint.

Menisci

The menisci (semilunar cartilages) are crescentic, intracapsular, fibrocartilaginous laminae (Figs 82.9, 82.10). They serve to widen and deepen the tibial articular surfaces that receive the femoral condyles. Their peripheral attached borders are thick and convex and their free, inner borders thin and concave. Their peripheries are vascularized by capillary loops from the fibrous capsule and synovial membrane, while their inner regions are avascular. Tears of the menisci are common. Most occur in the avascular, inner zones and seldom heal spontaneously; if surgery is indicated, these menisci are best resected. Peripheral tears (i.e. in the vascularized zone) have the potential to heal satisfactorily if repaired surgically. The meniscal horns are richly innervated compared with the remainder of the meniscus. The central thirds are devoid of innervation (Gronblad et al 1985). The proximal surfaces are smooth and concave and in contact with the articular cartilage on the femoral condyles. The distal surfaces are smooth and flat, resting on the tibial articular cartilage. Each covers approximately two-thirds of its tibial articular surface. Canal-like structures open onto the surface of menisci in infants and young children and may transport nutrients to deeper avascular areas.

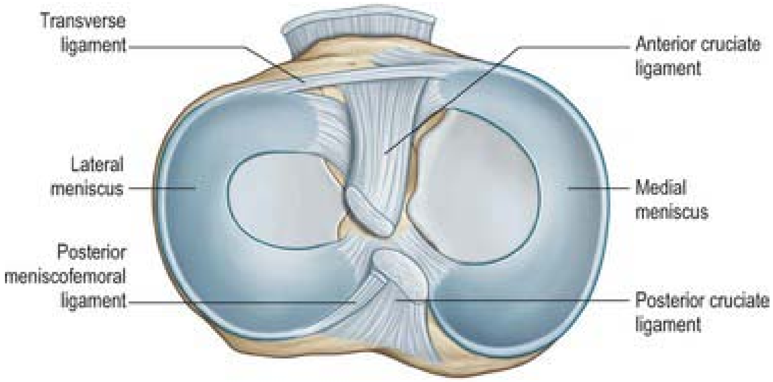
Transverse ligament
Anterior cruciate ligament
Lateral meniscus
Medial meniscus
Posterior meniscofemoral ligament
Posterior cruciate ligament

Fig. 82.9 Superior aspect of the left tibia, showing the menisci and the attachments of the cruciate ligaments.

(From Drake, Vogl, Mitchell, Tibbitts and Richardson 2008.)

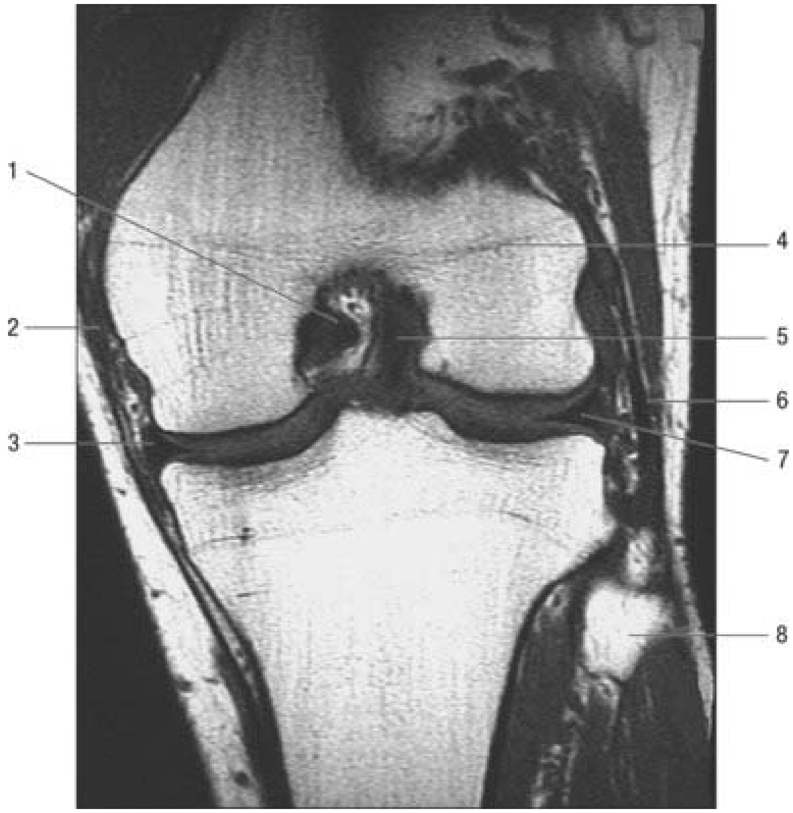

Fig. 82.10 Coronal T1-weighted magnetic resonance image (MRI) of the knee in an adult male. **1**. Posterior cruciate ligament. **2**. Medial collateral ligament. **3**. Medial meniscus. **4**. Epiphysial line. **5**. Anterior cruciate ligament. **6**. Lateral collateral ligament. **7**. Lateral meniscus. **8**. Head of fibula.

(By courtesy of Dr Justin Lee, Chelsea and Westminster Hospital, London.)

Two structurally different regions of the menisci have been identified. The inner two-thirds of each meniscus consists of radially organized collagen bundles, and the peripheral third consists of larger circumferentially arranged bundles (Ghadially et al 1983). The articular surfaces of the inner part are lined by thinner collagen bundles parallel to the surface, while the outer portion is covered by synovium. This structural arrangement suggests specific biomechanical functions for the two regions: the inner portion of the meniscus is suited to resisting compressive forces while the periphery is capable of resisting tensional forces. With ageing and degeneration, compositional changes occur within the menisci which reduce their ability to resist tensional forces. Outward displacement of the menisci by the femoral condyles is resisted by firm anchorage of the peripheral circumferential fibres to the intercondylar bone at the meniscal horns.

Menisci spread load by increasing the congruity of the articulation; give stability by their physical presence and as providers of proprioceptive feedback; probably assist lubrication; and may cushion the underlying bone from the considerable forces generated during extremes of flexion and extension.

Medial meniscus

The medial meniscus broader posteriorly, is almost a semicircle in shape (Fig. 82.9). It is attached by its anterior horn to the anterior tibial intercondylar area in front of the anterior cruciate ligament; the posterior fibres of the anterior horn are continuous with the transverse ligament. The anterior horn is in the floor of a depression medial to the upper part of the patellar tendon. The posterior horn is fixed to the posterior tibial intercondylar area, between the attachments of the lateral meniscus and posterior cruciate ligament. Its peripheral border is attached to the fibrous capsule and the deep surface of the medial collateral ligament. The tibial attachment of the meniscus is known as the ‘coronary ligament’. Collectively these attachments ensure that the medial meniscus is relatively fixed and moves much less than the lateral meniscus.

Lateral meniscus

The lateral meniscus forms approximately four-fifths of a circle, and covers a larger area than the medial meniscus. Its breadth, except at its short tapered horns, is more or less uniform. It is grooved posterolaterally by the tendon of popliteus, which separates it from the fibular collateral ligament. Its anterior horn is attached in front of the intercondylar eminence, posterolateral to the anterior cruciate ligament, with which it partly blends. Its posterior horn is attached behind this eminence, in front of the posterior horn of the medial meniscus. Its anterior attachment is contorted so that the free margin faces posterosuperiorly, and the anterior horn rests on the anterior slope of the lateral intercondylar tubercle. Near its posterior attachment it commonly sends a posterior meniscofemoral ligament superomedially behind the posterior cruciate ligament to the medial femoral condyle. An anterior meniscofemoral ligament may also connect the posterior horn to the medial femoral condyle anterior to the posterior cruciate ligament. The meniscofemoral ligaments are often the sole attachments of the posterior horn of the lateral meniscus. More laterally, part of the tendon of popliteus is attached to the lateral meniscus, and so mobility of its posterior horn may be controlled by the meniscofemoral ligaments and by popliteus. A meniscofibular ligament occurs in most knee joints. There is a tibial attachment via a coronary ligament, but the meniscus has no peripheral bony attachment in the region of popliteus: in surgical literature this gap is referred to as the popliteus hiatus.

Discoid lateral meniscus

A discoid lateral meniscus occurs in up to 5% of the population, often bilaterally. The distinguishing features of a discoid lateral meniscus are its shape and posterior ligamentous attachments. The following classification of the abnormality is based on Watanabe et al (1979). In its mildest form, the partial discoid meniscus is simply a wider form of the normal lateral meniscus. The acute, medial free edge is interposed between femoral and tibial condyles, but it does not completely cover the tibial plateau. A complete discoid meniscus appears as a biconcave disc with a rolled medial edge and totally covers the lateral tibial plateau. The Wrisberg type of meniscus has the same shape as a complete discoid meniscus, but its only peripheral posterior attachment is by the meniscofemoral ligaments. The normal tibial attachment of the posterior horn of the lateral meniscus is lacking, but the posterior meniscofemoral ligament persists. As a result, this type of meniscus is attached anteriorly to the tibia and posteriorly to the femur, which renders the posterior horn unstable. Under these circumstances, the meniscus is liable to get caught between the femur and tibia: this accounts for the classic presenting symptom of the ‘clunking knee’ in some patients.

The aetiology of discoid meniscus is not clear. Most are asymptomatic, and are often found by chance at arthroscopy. However, they may cause difficulty in gaining access to the lateral compartment at arthroscopy.

Discoid medial meniscus is extremely rare.

Transverse [intermeniscal] ligament

The transverse ligament connects the anterior convex margin of the lateral meniscus to the anterior horn of the medial meniscus (Figs 82.8, 82.9). It varies in thickness and is often absent. Its exact role is conjectural; presumably it helps to decrease tension generated in the longitudinal circumferential fibres of the menisci when the knee is subjected to load. A posterior meniscomeniscal ligament is sometimes present.

Meniscofemoral ligaments

The two meniscofemoral ligaments (MFLs) connect the posterior horn of the lateral meniscus to the inner (lateral) aspect of the medial femoral condyle (Figs 82.11, 82.12). The anterior MFL (aMFL; ligament of Humphry) passes anterior to the posterior cruciate ligament. The posterior MFL (pMFL; ligament of Wrisberg) passes behind the posterior cruciate ligament and attaches proximal to the margin of attachment of the posterior cruciate.

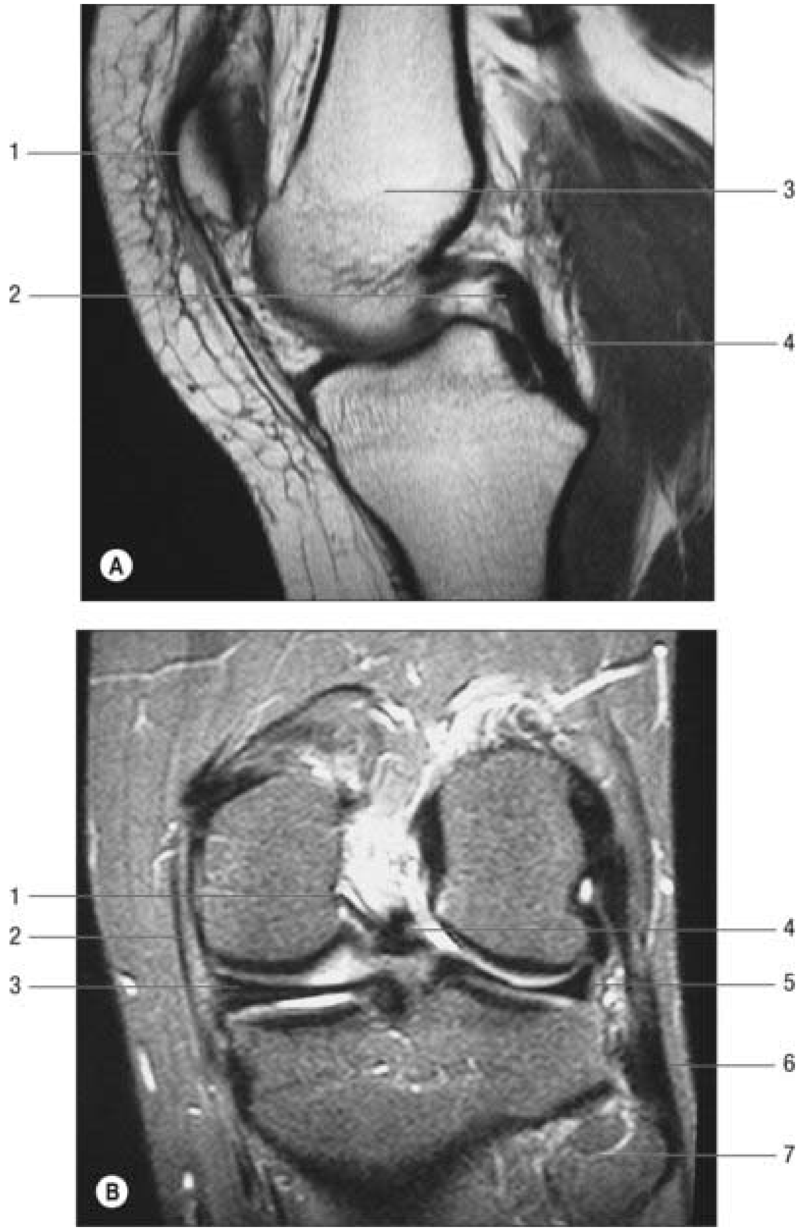

Fig. 82.11 **A**, Sagittal T1-weighted and **B**, coronal STIR magnetic resonance images (MRI) of the knee in an adult male showing the anterior meniscofemoral ligament. **A:** **1**. Patella. **2**. Anterior meniscofemoral ligament of Humphry. **3**. Epiphysial line. **4**. Posterior cruciate ligament. **B:** **1**. Anterior meniscofemoral ligament of Humphry. **2**. Medial collateral ligament. **3**. Medial meniscus. **4**. Posterior cruciate ligament. **5**. Lateral meniscus. **6**. Lateral collateral ligament. **7**. Head of fibula.

(By courtesy of Dr Justin Lee, Chelsea and Westminster Hospital, London.)

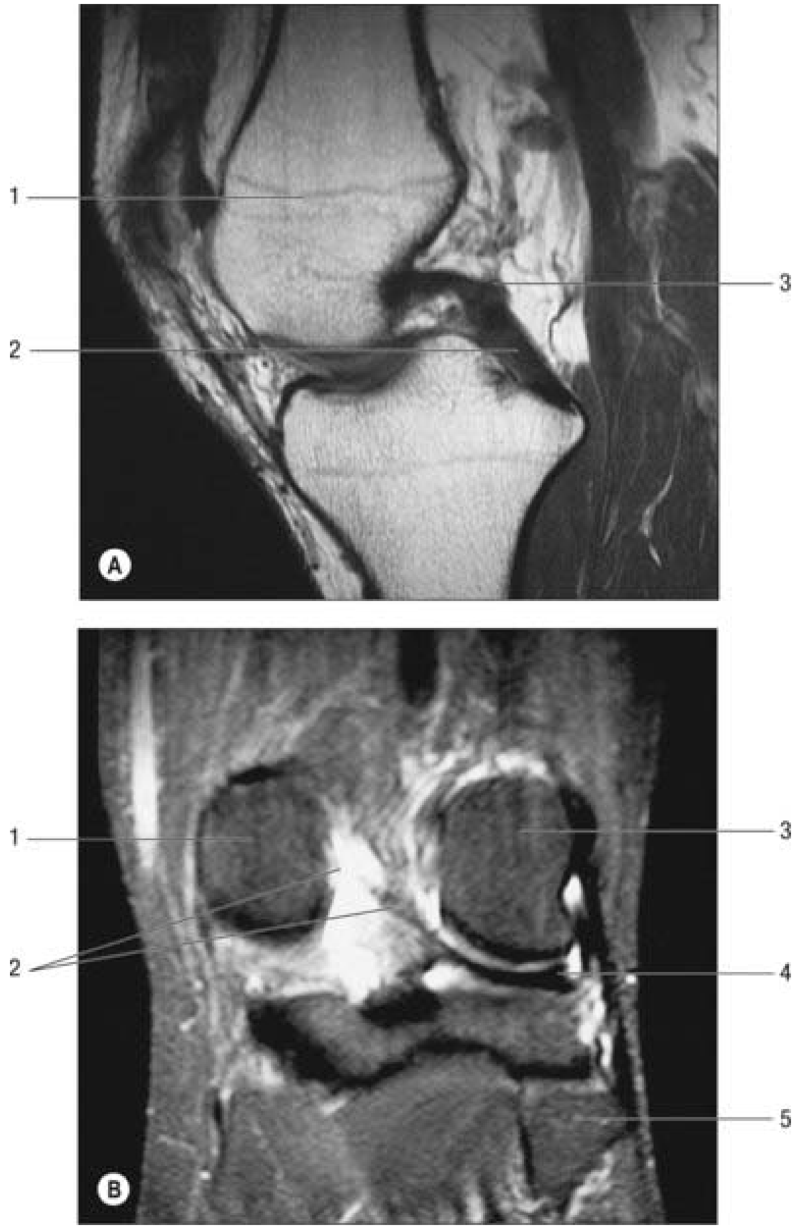

Fig. 82.12 **A**, Sagittal T1-weighted and **B**, coronal STIR magnetic resonance images (MRI) of the knee in an adult male showing the posterior meniscofemoral ligament. **A: 1**. Epiphysial line. **2**. Posterior cruciate ligament. **3**. Posterior meniscofemoral ligament of Wrisberg. **B: 1**. Medial femoral condyle. **2**. Posterior meniscofemoral ligament of Wrisberg. **3**. Lateral femoral condyle. **4**. Lateral meniscus. **5**. Head of fibula.

(By kind permission from Dr Justin Lee, Chelsea and Westminster Hospital, London.)

Anatomical studies found that at least one meniscofemoral ligament was present in 92% of cadaveric knees examined, whilst both coexisted in 32% (Gupte et al 2003). Biomechanical studies have revealed the cross-sectional area and strength of the meniscofemoral ligaments to be comparable to those of the posterior fibre bundle of the posterior cruciate ligament.

The meniscofemoral ligaments are believed to act as secondary restraints, supporting the posterior cruciate ligament in minimizing displacement caused by posteriorly directed forces on the tibia. These ligaments are also involved in controlling the motion of the lateral meniscus in conjunction with the tendon of popliteus during flexion.

Soft tissues

Recent advances in knee ligament surgery have contributed to a better understanding of the anatomy of the medial and lateral soft tissues of the knee.

Capsule and retinacula

The capsule is a fibrous membrane of variable thickness. Anteriorly it is replaced by the patellar tendon and does not pass proximal to the patella or over the patellar area. Elsewhere it lies deep to expansions from vasti medialis and lateralis, separated from them by a plane of vascularized loose connective tissue. The expansions are attached to the patellar margins and patellar tendon, extending back to the corresponding collateral ligaments and distally to the tibial condyles. They form medial and lateral patellar retinacula, the lateral being reinforced by the iliotibial tract.

Posteriorly the capsule contains vertical fibres that arise from the articular margins of the femoral condyles and intercondylar notch and from the proximal tibia. The fibres mainly pass downwards and somewhat medially. The oblique popliteal ligament is a well-defined thickening across the posteromedial aspect of the capsule, and is essentially an extension from the tendon of insertion of semimembranosus.

Medial soft tissues

The medial soft tissues (see Fig. 80.25, Fig. 82.13) are arranged in three layers (Warren & Marshall 1979).

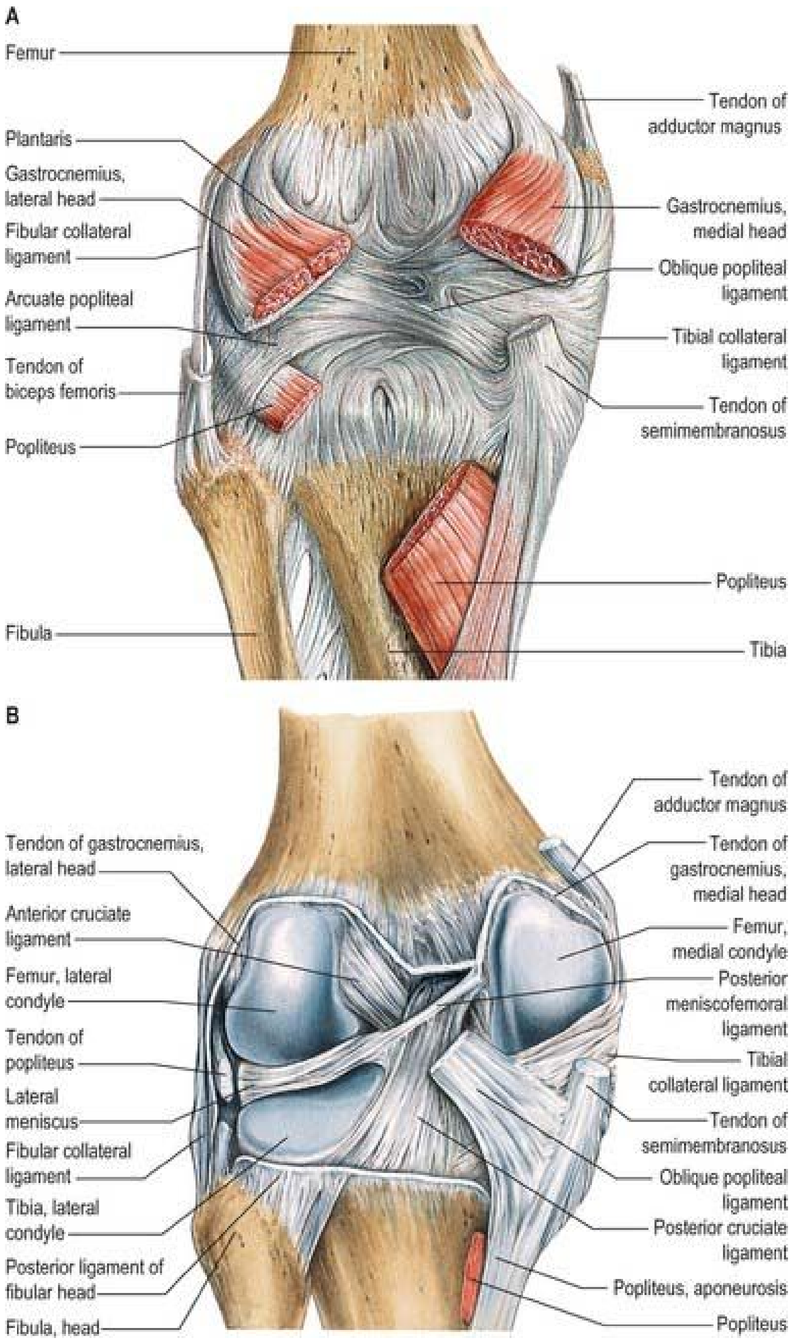
A
Femur
Plantaris
Gastrocnemius, lateral head
Fibular collateral ligament
Arcuate popliteal ligament
Tendon of biceps femoris
Popliteus
Fibula
Tendon of adductor magnus
Gastrocnemius, medial head
Oblique popliteal ligament
Tibial collateral ligament
Tendon of semimembranosus
Popliteus
Tibia
B
Tendon of gastrocnemius, lateral head
Anterior cruciate ligament
Femur, lateral condyle
Tendon of popliteus
Lateral meniscus
Fibular collateral ligament
Tibia, lateral condyle
Posterior ligament of fibular head
Fibula, head
Tendon of adductor magnus
Tendon of gastrocnemius, medial head
Femur, medial condyle
Posterior meniscofemoral ligament
Tibial collateral ligament
Tendon of semimembranosus
Oblique popliteal ligament
Posterior cruciate ligament
Popliteus, aponeurosis
Popliteus

Fig. 82.13 Posterior dissection of the knee. **A**, Capsule intact. **B**, Capsule removed.

(From Sobotta 2006.)

Layer 1

Layer 1 is the most superficial and is the deep fascia that invests sartorius. The saphenous nerve and its infrapatellar branch are superficial to the fascia. Sartorius inserts into the fascia as an expansion rather than as a distinct tendon. The layer 1 fascia spreads inferiorly and anteriorly to lie superficial to the distinct and readily identifiable tendons of gracilis and semitendinosus and their insertions. The latter two tendons are commonly harvested for surgical reconstruction of damaged cruciate ligaments. To gain access to them the upper edge of sartorius can be identified. The sartorius (layer 1) fascia is then incised to reveal the tendons. Deep to the tendons is the pes bursa, which overlies the superficial medial collateral ligament: this bursa is sometimes the seat of inflammation, especially in track and field athletes. Posteriorly, layer 1 overlies the tendons of gastrocnemius and the structures of the popliteal fossa. Anteriorly, layer 1 blends with the anterior limit of layer 2 and the medial patellar retinaculum. More inferiorly, layer 1 blends with periosteum.

A condensation of tissue passes from the medial border of the patella to the medial epicondyle of the femur (the medial patellofemoral ligament), the anterior horn of the medial meniscus (the meniscopatellar ligament), and the medial tibial condyle (the patellotibial ligament).

Layer 2

Layer 2 is the plane of the superficial medial collateral ligament, which means that the tendons of gracilis and semitendinosus lie between layers 1 and 2. The superficial medial collateral ligament has vertical and oblique portions. The former contains vertically orientated fibres that pass from the medial epicondyle of the femur to a large insertion on the medial surface of the proximal end of the tibial shaft. It extends to an area about 5 cm distal to the joint line. Its anterior edge is rolled and easily seen just posterior to the insertions of gracilis and semitendinosus once layer 1 has been opened. The posteriorly placed oblique fibres run posteroinferiorly from the medial epicondyle of the femur to blend with the underlying layer 3 (capsule), effectively to insert on the posteromedial tibial articular margin and posterior horn of the medial meniscus. This area is reinforced by a part of the insertion of semimembranosus. There is a vertical split in layer 2 anterior to the superficial medial collateral ligament. The fibres anterior to the split pass superiorly to blend with vastus medialis fascia and layer 1 in the medial patellar retinaculum. The fibres posterior to the split pass superiorly to the medial epicondyle and thence anteriorly as the medial patellofemoral ligament.

Layer 3

Layer 3 is the capsule of the knee joint and can be separated from layer 2 everywhere except anteriorly close to the patella, where it blends with the more superficial layers. Deep to the superficial medial collateral ligament it is thick and has vertically orientated fibres that make up the deep medial collateral ligament. It sends fibres to the medial meniscus. Anteriorly, the separation of the superficial and deep parts of the medial collateral ligament is distinct. Posteriorly, layers 2 and 3 blend to form a conjoined posteromedial capsule.

Lateral soft tissues

The lateral soft tissues (Figs 82.13, 82.15) are also arranged in three layers (Seebacher et al 1982). Most superficial is the lateral patellar retinaculum. The middle layer consists of the lateral collateral ligament, popliteofibular ligament, fabellofibular ligament and arcuate ligament. The deep layer is the lateral part of the capsule.

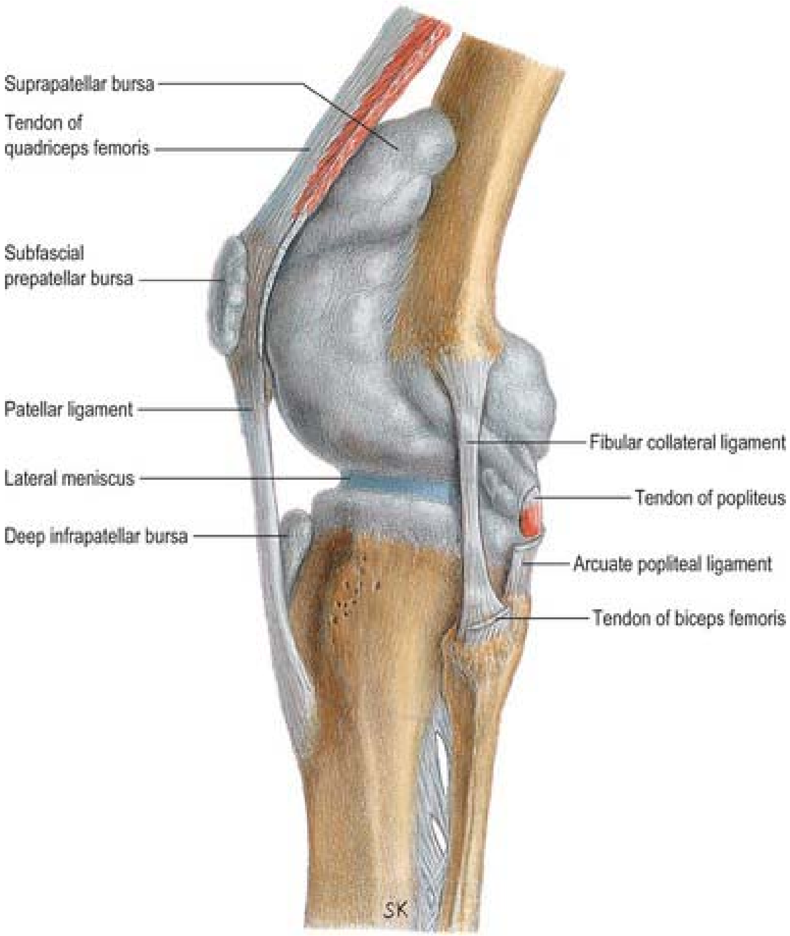
Suprapatellar bursa
Tendon of quadriceps femoris
Subfascial prepatellar bursa
Patellar ligament
Lateral meniscus
Deep infrapatellar bursa
Fibular collateral ligament
Tendon of popliteus
Arcuate popliteal ligament
Tendon of biceps femoris
SK

Fig. 82.15 Knee joint (lateral aspect); the synovial cavity is distended and synovial membrane appears grey.

(From Sobotta 2006.)

The lateral patellar retinaculum consists of superficial oblique and deep transverse portions. The former runs from the iliotibial band to the patella. The latter is thicker and subdivided into three parts: the lateral patellofemoral ligament, running from the lateral patellar border to the lateral epicondyle of the femur; the transverse retinaculum, running from the iliotibial band to the mid patella; and the patellotibial band, running from the patella to the lateral tibial condyle.

The fascia lata and the iliotibial band lie posterior to the lateral retinaculum. They come together distally to insert onto the tibia at Gerdy's tubercle on the anterolateral proximal tibia, and some fibres continue to the tibial tuberosity. Proximally the fascia lata merges with the lateral intermuscular septum. Posteriorly it blends with the biceps fascia. Here, as it emerges from behind the biceps tendon, the common fibular nerve lies in a thin layer of fat bound by the fascia.

The lateral collateral ligament arises from the lateral epicondyle of the femur posterior to the popliteus insertion and just proximal to the popliteus groove. It is a cord-like structure that passes distally, superficial to the popliteus tendon and deep to the lateral retinaculum, to attach to the fibular head, where it blends with the biceps tendon just anterior to the apex of the fibular head. It is separated from the capsule by a thin layer of fat and the inferior lateral genicular vessels.

The single most important stabilizer of the posterolateral knee is the popliteofibular ligament. It passes from the popliteus tendon at a level just below the joint line, posteriorly, laterally and inferiorly, to the fibular head. It is probably what was previously described as the short lateral genual ligament. As a passive ‘tether’ combined with the popliteus tendon proximal to it, it resists external rotation of the tibia. Its connection to the tendon of popliteus also allows ‘dynamic’ tensioning.

The fabellofibular ligament is a condensation of fibres that runs from the fabella, or from the lateral head of gastrocnemius if the fabella is absent, to the fibular styloid. The arcuate ligament is a condensation of fibres that runs from the fibular styloid, posteromedially over the emerging tendon of popliteus below the level of the tibial joint surface, to the tibial intercondylar area. The lateral joint capsule is thin and blends posteriorly with the arcuate ligament. Anteriorly it forms the weak, lax coronary ligament, which attaches the inferior border of the meniscus to the lateral tibia.

Ligaments

Cruciate ligaments

The cruciate ligaments, so named because they cross each other, are very strong intracapsular structures. The point of crossing is located a little posterior to the articular centre. They are named anterior and posterior with reference to their tibial attachments (Fig. 82.14). Synovial membrane almost surrounds the ligaments but is reflected posteriorly from the posterior cruciate to adjoining parts of the capsule: the intercondylar part of the posterior region of the fibrous capsule therefore has no synovial covering.

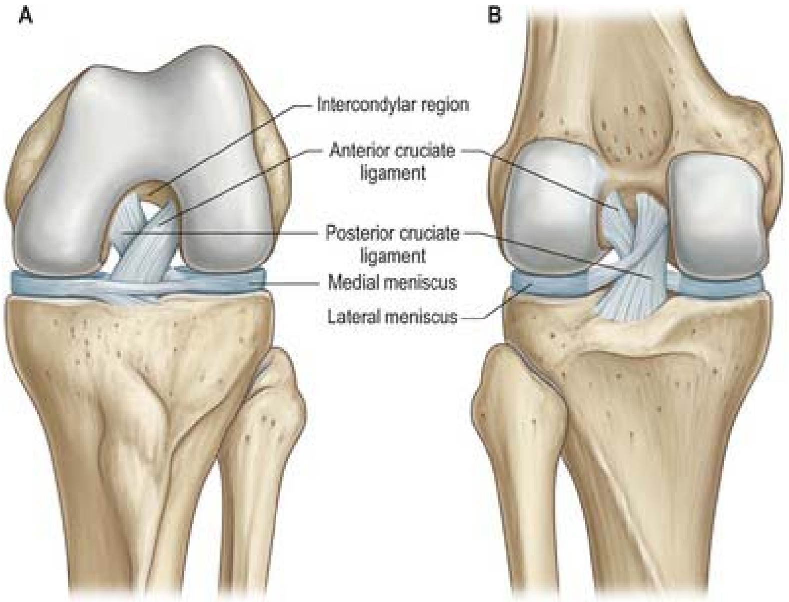

Fig. 82.14 The left knee joint. **A**, Anterior aspect in full flexion. **B**, Posterior aspect in extension.

(From Drake, Vogl, Mitchell, Tibbitts and Richardson 2008.)

Anterior cruciate ligament

The anterior cruciate ligament is attached to the anterior intercondylar area of the tibia, just anterior and slightly lateral to the medial tibial eminence, partly blending with the anterior horn of the lateral meniscus (Figs 82.8, 82.9). It ascends posterolaterally, twisting on itself and fanning out to attach high on the posteromedial aspect of the lateral femoral condyle (Girgis et al 1975). The average length and width of an adult anterior cruciate ligament are 38 mm and 11 mm respectively. It is formed of two, or possibly three, functional bundles that are not apparent to the naked eye, but can be demonstrated by microdissection techniques. The bundles are named anteromedial, intermediate, and posterolateral, according to their tibial attachments (Amis and Dawkins 1991).

Absent anterior cruciate ligament

Congenital absence of the anterior cruciate ligament is rare. The condition is usually associated with lower limb dysplasia (Thomas et al 1985), and may be a cause of instability of the knee.

Posterior cruciate ligament

The posterior cruciate ligament is thicker and stronger than the anterior cruciate ligament (Fig. 82.9), the average length and width of an adult posterior cruciate ligament being 38 mm and 13 mm respectively. It is attached to the lateral surface of the medial femoral condyle and extends up onto the anterior part of the roof of the intercondylar notch, where its attachment is extensive in the anteroposterior direction. Its fibres are adjacent to the articular surface. They pass distally and posteriorly to a fairly compact attachment posteriorly in the intercondylar region and in a depression on the adjacent posterior tibia. This gives a fan-like structure in which fibre orientation is variable. Anterolateral and posteromedial bundles have been defined: they are named (against convention) according to their femoral attachments. The anterolateral bundle tightens in flexion whilst the posteromedial is tight in extension of the knee. Each bundle slackens as the other tightens. Unlike the anterior cruciate ligament, it is not isometric during knee motion, i.e. the distance between attachments varies with knee position. The posterior cruciate ligament ruptures less commonly than the anterior cruciate; rupture is usually better tolerated by patients than that of the anterior cruciate ligament.

Synovial membrane, plicae and fat pads

The synovial membrane of the knee is the most extensive and complex in the body. It forms a large suprapatellar bursa between quadriceps femoris and the lower femoral shaft proximal to the superior patellar border (Fig. 82.16). The bursa is an extension of the joint cavity. The attachment of articularis genu to its proximal aspect prevents the bursa from collapsing into the joint. Alongside the patella the membrane extends beneath the aponeuroses of the vasti, especially under vastus medialis. It extends proximally a hand's breadth above the superior pole of the patella. Distal to the patella, the synovial membrane is separated from the patellar tendon by an infrapatellar fat pad. Where it lies beneath the fat pad, the membrane projects into the joint as two fringes, alar folds, which bear villi. The folds converge posteriorly to form a single infrapatellar fold or plica (ligamentum mucosum), which curves posteriorly to its attachment in the femoral intercondylar fossa (Fig. 82.17). This fold may be a vestige of the inferior boundary of an originally separate femoropatellar joint. The extent of the infrapatellar plica ranges from a thin cord to a complete sheet that can obstruct the passage of instruments during knee arthroscopy. When substantial, it has been mistaken for the anterior cruciate ligament, which is directly posterior to it. The medial plica extends in the midline anteriorly from the medial alar fold medially to the suprapatellar pouch. Occasionally it can be thickened and inflamed, usually following acute or chronic trauma.

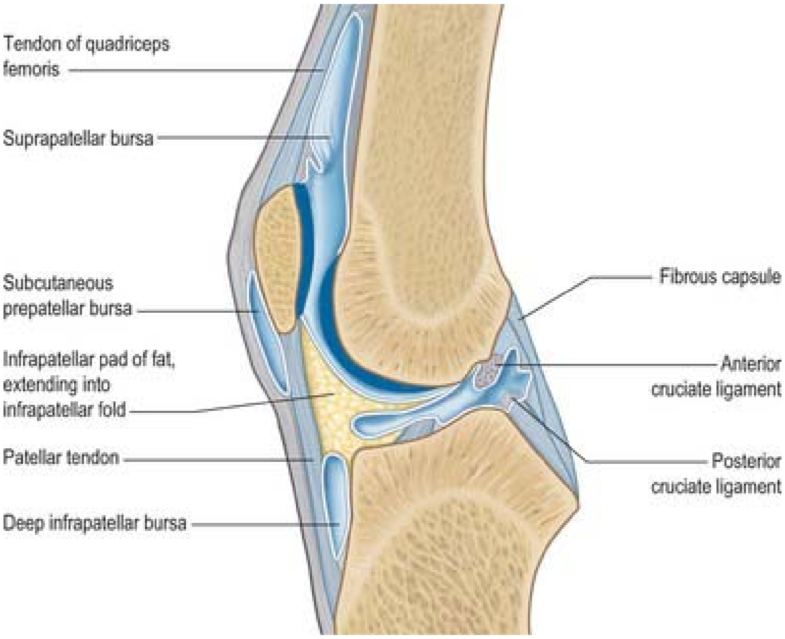
Tendon of quadriceps femoris
Suprapatellar bursa
Subcutaneous prepatellar bursa
Infrapatellar pad of fat, extending into infrapatellar fold
Patellar tendon
Deep infrapatellar bursa
Fibrous capsule
Anterior cruciate ligament
Posterior cruciate ligament

Fig. 82.16 Sagittal section through the left knee joint: lateral aspect.

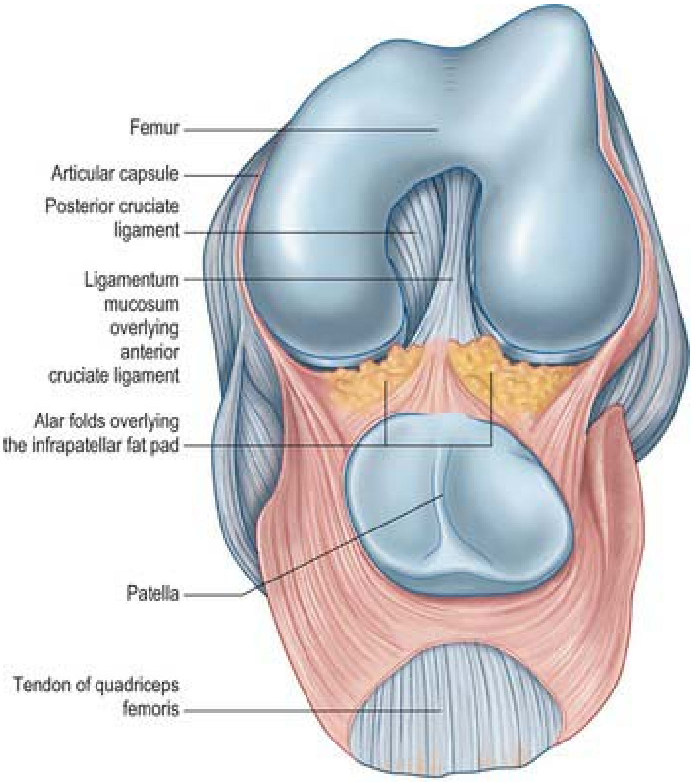
Femur
Articular capsule
Posterior cruciate ligament
Ligamentum mucosum overlying anterior cruciate ligament
Alar folds overlying the infrapatellar fat pad
Patella
Tendon of quadriceps femoris

Fig. 82.17 Left knee joint in full flexion: the quadriceps tendon has been sectioned and the patellar flap retracted distally. Compare with **Fig. 82.14A**.

The suprapatellar plicae are remnants of an embryonic septum that completely separates the suprapatellar pouch from the knee joint. Very occasionally a septum persists, either in its entirety, or perforated by a small peripheral opening. Loose bodies can lie hidden above this septum.

The infrapatellar fat pad is the largest part of a circumferential extrasynovial fatty ring which extends around the patellar margins (Newell 1991).

At the sides of the joint the synovial membrane descends from the femur and lines the capsule as far as the menisci, whose surfaces have no synovial covering. Posterior to the lateral meniscus the membrane forms a subpopliteal recess between a groove on the meniscal surface and the tendon of popliteus which may connect with the superior tibiofibular joint. The relationship of the synovial membrane to the cruciate ligaments is described above.

Bursae

Numerous bursae are associated with the knee. Anteriorly, there is a large subcutaneous prepatellar bursa between the lower half of the patella and skin; a small deep infrapatellar bursa between the tibia and patellar tendon; a subcutaneous infrapatellar bursa between the distal part of the tibial tuberosity and skin; and a large suprapatellar bursa which is the superior extension of the knee joint cavity (Fig. 82.16). Posterolaterally, there are bursae between the lateral head of gastrocnemius and the joint capsule (this bursa is sometimes continuous with the joint cavity); the fibular collateral ligament and the tendon of biceps femoris; the fibular collateral ligament and the tendon of popliteus; the tendon of popliteus and the lateral femoral condyle, which is usually an extension of the synovial cavity of the joint. The last two bursae may communicate with each other.

Medially, the arrangement of bursae is complex. The bursa between the medial head of gastrocnemius and the fibrous capsule is prolonged between the medial tendon of gastrocnemius and the tendon of semimembranosus (the semimembranosus bursa) and usually communicates with the joint. The bursa between the tendon of semimembranosus and the medial tibial condyle and the medial head of gastrocnemius may communicate with this bursa. There is a bursa between the medial collateral ligament and the tendons of sartorius, gracilis and semitendinosus (the ‘pes bursa’). Bursae that vary both in number and position lie deep to the medial collateral ligament between the capsule, femur, medial meniscus, tibia or tendon of semimembranosus. Occasionally there may be a bursa between the tendons of semimembranosus and semitendinosus.

Posteriorly, bursae associated with the knee are variable.

The clinically important bursae are the anterior group, the pes bursa, and the semimembranosus bursa. Inflammation of the subcutaneous prepatellar bursa and infrapatellar bursa are referred to colloquially as ‘housemaid’s knee’ and ‘clergyman’s knee’, respectively. The pes bursa can become inflamed in athletes. In adults, bursal inflammation producing a popliteal fossa swelling commonly occurs secondary to degeneration within the knee joint: regardless of size and position, it almost always arises from the plane between semimembranosus and the medial tendon of gastrocnemius.

Movements

Movements at the knee are customarily described as flexion, extension, internal (medial) and external (lateral) rotation. Flexion and extension differ from true hingeing in that the articular surface profiles of the femoral and tibial articular surfaces produce a variably placed axis of rotation during the flexion arc, and when the foot is fixed, flexion entails corresponding conjunct (coupled) external (lateral) rotation. These conjunct rotations are a product of the complex geometry of the articular surfaces and, to an extent, the disposition of the associated ligaments. There is differential motion in the medial and lateral tibiofemoral compartments. Laterally, there is considerable displacement of the femur on the tibia, with rolling as well as sliding at the joint surface. In contrast, medially, for most of the flexion arc there is minimal relative motion of the femur and tibia, and the motion almost exclusively involves one joint surface sliding on the other. In full flexion, the lateral femoral condyle is close to posterior subluxation off the lateral tibial articular surface. Medially, significant posterior femoral displacement only occurs when flexion exceeds 120°. The menisci move with the femoral condyles, the anterior horns more than the posterior, and the lateral meniscus considerably more than the medial.

The axial rotations have a smaller range than the arc of flexion and extension. These rotations are conjunct, and integral with flexion and extension, i.e. they are obligatory. They can also be adjunct and independent, i.e. voluntary, and are best demonstrated with the knee semi-flexed. The degree of axial rotation therefore varies with flexion and extension.

The range of extension is 5–10° beyond the ‘straight position’. Active flexion is approximately 120° with the hip extended, 140° when it is flexed, and 160° when aided by a passive element, e.g. sitting on the heels. Voluntary rotation is 60–70°, but conjunct rotation only 20°.

Conjunct medial rotation of the femur on the tibia in the later stages of extension is part of a ‘locking’ mechanism, the so-called ‘screw-home movement’, which is an asset when the fully extended knees are subjected to strain. Full extension results in the close-packed position, with maximal spiralization and tightening of the ligaments. The roles of the articular surfaces, musculature and ligaments in generating conjunct rotations remain controversial (Girgis et al 1975, Rajendran 1985), but the following points can be made. The lateral combined meniscotibial ‘receiving surface’ is smaller, more circular and more deeply concave. Since the articular surface is virtually convex in sagittal section the depth of the receiving surface is largely due to the presence of the lateral meniscus. The lateral femoral articular surface is also smaller. Consequently, the lateral femoral condyle approaches full congruence with the opposed surface some 30° before full extension (well before the medial condyle). Simple extension cannot continue, but medial rotation of the femur occurs on a vertical axis through its head and medial condyle: the medial femoral condyle moves very little in the sagittal plane and is stabilized by the ‘upslope’ of the anterior half of the medial tibia, while rotation of the lateral femoral condyle and meniscus brings the anterior horn of the latter onto the anterior ‘downslope’ of the lateral tibial condyle. Rotation and extension follow simultaneously and smoothly until final close packing of both condyles is accomplished. At the beginning of flexion from full extension (with the foot fixed) lateral femoral rotation occurs, which ‘unlocks’ the joint. While joint surfaces and many ligaments are involved, electromyographic evidence reveals that contraction of popliteus is important, and that it pulls down and backwards on the lateral femoral condyle, lateral to the axis of femoral rotation. It also retracts the posterior horn during lateral rotation and continuing flexion, via its attachment to the lateral meniscus, and so prevents traumatic compression.

Any position of extension adopted is a balance between forces (torque) extending the joint and passive mechanisms resisting them. The range near to close packing is functionally important. In symmetrical standing, the line of body weight is anterior to the transverse axes of the knee joints, but the passive mechanisms noted above preserve posture with minimal muscular effort (Joseph 1960). Active contraction of the extensors and a close-packed position only occur in asymmetrical postures, e.g. in leaning forward, heavy loading, or when powerful thrust is needed.

In extension, parts of both cruciate ligaments, the tibial and fibular collateral ligaments, the posterior capsular region, the oblique popliteal ligament, skin and fasciae are all taut. Passive and sometimes active tension exists in the hamstrings and gastrocnemius, and the anterior part of the medial meniscus is compressed between the femoral and tibial condyles. During extension the patellar tendon is tightened by quadriceps femoris but is relaxed in the erect attitude. When the knee flexes, the fibular collateral ligament and the posterior part of the medial collateral ligament relax but the cruciate ligaments and the anterior part of the medial collateral ligament remain taut: the posterior parts of the menisci are compressed between the femoral and tibial condyles. Flexion is checked by quadriceps femoris, anterior parts of the capsule, posterior cruciate ligament and compression of soft tissues behind the knee. In extreme passive flexion, contact of the calf with the thigh may be the limiting factor and parts of both cruciate ligaments are also tense. In addition to conjunct rotation with terminal extension or initial flexion, relaxed collateral ligaments also allow independent medial and lateral rotation (adjunct rotation) when the joint is flexed.

Accessory movements

Wider rotation can be obtained by passive movements when the knee is semi-flexed. To a limited extent, the tibia can also be translated backwards and forwards on the femur. Abduction and adduction are prevented in full extension by the collateral ligaments and secondary restraints such as the cruciate ligaments. With the knee slightly flexed, limited adduction and abduction are possible, both passive and active. Slight separation of the femur and tibia can be achieved by strong traction on the leg with countertraction applied to the thigh.

Muscles producing the movements

Flexion

Biceps femoris, semitendinosus and semimembranosus, assisted by gracilis, sartorius and popliteus. With the foot stationary, gastrocnemius and plantaris also assist (See Fig. 82.3).

Extension

Quadriceps femoris, assisted by tensor fasciae latae.

Medial rotation of the flexed leg

Popliteus, semimembranosus and semitendinosus, assisted by sartorius and gracilis.

Lateral rotation of the flexed leg

Biceps femoris.

Relations and ‘at risk’ structures

Anteriorly are the tendon of quadriceps femoris (which encloses and is attached to the non-articular surfaces of the patella), the patellar tendon, tendinous expansions from vastus medialis and lateralis (which extend over the anteromedial and anterolateral aspects of the capsule respectively), and the patellar retinacula. Posteromedial is sartorius, and the tendon of gracilis which lies along its posterior border, both descending across the joint. Posterolaterally, the tendon of biceps and the common fibular nerve (which lies medial to the tendon) are in contact with the capsule, and thereby separated from the tendon of popliteus. Posteriorly the popliteal artery and associated lymph nodes lie posterior to the oblique popliteal ligament; the popliteal vein is posteromedial or medial, and the tibial nerve is posterior to both. The nerve and vessels are overlapped by both heads of gastrocnemius and laterally by plantaris. Gastrocnemius contacts the capsules on either side of the vessels. Semimembranosus lies between the capsule and semitendinosus, medial to the medial head of gastrocnemius.

Factors maintaining stability

The control of the stability of the knee is of considerable importance.

Patellofemoral joint

The alignment of the femoral and tibial shafts is such that the pull of the quadriceps on the patella imparts a force on the patella that is directed both superiorly and laterally. The static bony factors that counter this tendency to move laterally are the congruity of the patellofemoral joint and the buttressing effect of the larger lateral part of the trochlear groove. Instability may result if the patella is small, or resides too high above the trochlea, or if the trochlear groove is too shallow. The static ligamentous factors are the medial patellofemoral ligament and medial patellar retinaculum.

Dynamic muscular control is important. The most distal part of vastus medialis (vastus medialis obliquus) consists of transverse fibres that are attached directly to the medial edge of the patella: these pull the patella medially, countering the tendency to lateral movement. This is the muscle that is preferentially strengthened in a physiotherapy programme aimed at treating patellofemoral problems.

Tibiofemoral joint

The tibiofemoral joint surfaces are inherently unstable, especially laterally. Medially some stability is afforded by the relatively concave tibial surface and the relatively fixed posterior horn of the medial meniscus. Both medially and laterally the menisci are helpful, particularly as they move with the femoral condyles. Ligaments play a major role in providing stability: their function is partly static, in that they bind the bones in positions of extreme stress, but they also provide proprioceptive feedback which aids coordination of stabilizing muscle activity. Taking a somewhat ‘two-dimensional’ view, the medial and lateral collateral ligaments may be considered as resistors of valgus and varus forces on the knee respectively, and the anterior and posterior cruciate ligaments as resistors of anterior and posterior tibial translation respectively. However in reality the situation is more complex than this. The stresses are rarely applied in orthogonal planes and so a combination of forces, especially rotational, is involved. Moreover, many structures other than the collateral and cruciate ligaments are involved in stabilizing the joint. The ‘posterolateral corner’, which resists tibial external rotation, consists of the popliteofibular, fabellofibular, arcuate, and lateral collateral ligaments and iliotibial band, together with popliteus, the lateral head of gastrocnemius and biceps femoris. The ‘posteromedial corner’, which resists tibial rotation, consists of the posterior oblique portion of the superficial medial collateral ligament, the capsule (including the oblique popliteal ligament) and semimembranosus. Since stresses are often a combination of force plus rotation, structures usually operate together rather than in isolation.

Loading at the knee

During level walking, the force across the tibiofemoral joint for most of the cycle is between two and four times body weight, and can be more. In contrast, the force across the patellofemoral joint is no more than 50% body weight. Peak force transmission across the joint increases sequentially as the menisci, articular cartilage and subchondral bone are damaged or removed. Walking up or down stairs has little influence on tibiofemoral forces, but significantly increases patellofemoral forces to two (walking up) or three (walking down) times body weight, reflecting the changed angle of the quadriceps tendon and patellar tendon during flexion. There are two mechanisms for ameliorating forces transmitted across the patella: the extensor lever arm is lengthened as the axis of rotation moves posteriorly during flexion, and the contact area between the patella and femur almost triples between 30° and 90°. To cope with the potential large forces generated by activities such as running, the patella has the thickest articular cartilage in the body.

BIOMECHANICS OF THE KNEE

The knee joint is a complex synovial joint consisting of the tibiofemoral and patellofemoral articulations. It functions to control centre of body mass and posture in the activities of daily living. This necessitates a large range of movement in three dimensions coupled with the ability to withstand high forces. These conflicting parameters of mobility and stability are only achieved by the interactions between the articular surfaces, the passive stabilizers and the muscles that cross the joint.

The relatively incongruent nature of the joint surfaces makes the knee joint *inherently* unstable. In addition, because it acts as a pivot between the longest bones in the body, and is subjected to considerable loads in locomotion, the joint is also *potentially* unstable. The long bones may act as levers, increasing the stresses on the stabilizing ligaments.

KNEE JOINT KINEMATICS

The surfaces of the tibia and femur are not as conforming as those of the relatively congruent hip joint. Although this variation in geometry permits motion to occur in six degrees of freedom (Fig. 82.18), the primary motion of the knee occurs in the sagittal plane, and a relatively minor degree of movement occurs in the transverse plane. The knee joint may therefore be described simplistically as a modified hinge joint allowing flexion–extension and a measure of rotatory motion. Knee motion is normally defined as starting from 0° (the neutral position), when the tibia and femur are in line in the sagittal plane. Biomechanically, it is important that the knee reaches the neutral position in extension, because that allows the leg to support the body weight like a simple strut when standing still. When standing upright, if the knee is flexed, the vertical line of action of the body weight passes posterior to the centre of rotation of the knee, tending to cause the body to tilt posteriorly. To counterbalance this, continuous quadriceps contraction is required, causing expenditure of energy.

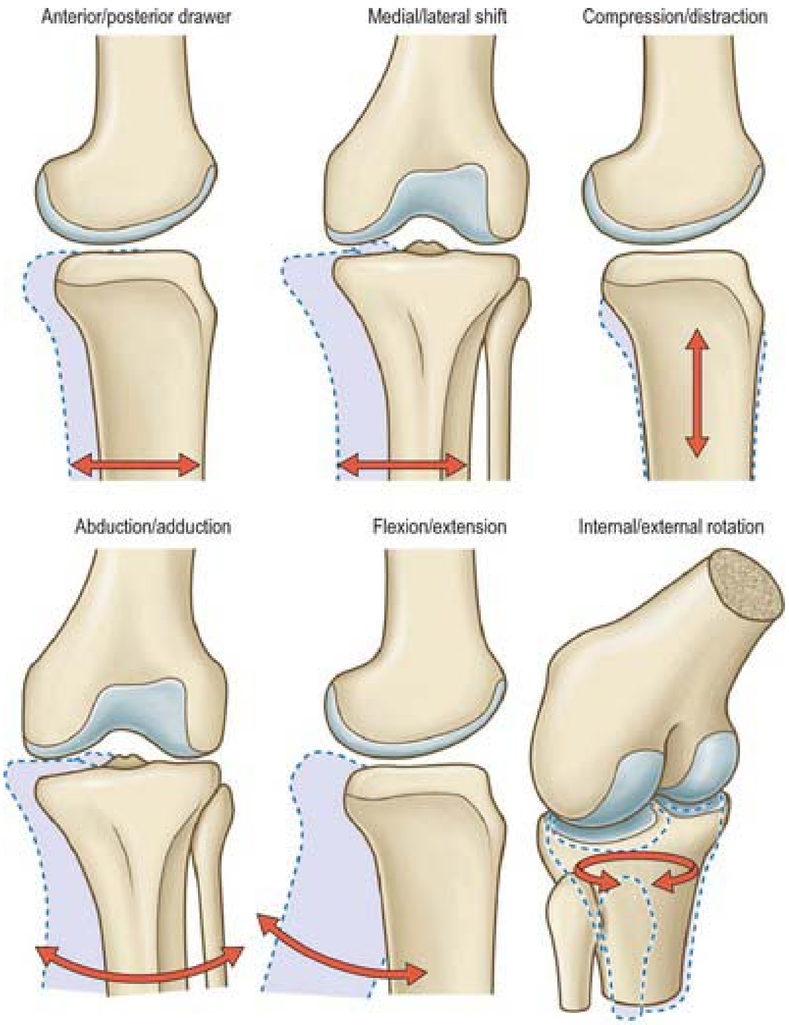
Anterior/posterior drawer
Medial/lateral shift
Compression/distraction
Abduction/adduction
Flexion/extension
Internal/external rotation

Fig. 82.18 Knee joint motion in three dimensions, which is described using six independent variables. These six variables are termed degrees of freedom.

Active knee flexion leads to approximately 130° flexion. The active motion is limited by apposition of the posterior soft tissue masses (thigh and calf). Passive flexion may reach 160°. This is required in people who habitually kneel as part of daily life, and is a challenge for designers of knee prostheses. It can be observed that such deep flexion is often accompanied by tibial internal rotation, so that when kneeling the buttocks can rest on the feet. This movement carries the lateral tibial plateau anteriorly, so that it does not engage with the femoral lateral condyle in deep knee flexion. The femoral condyle passes posteriorly and rides over the horn of the lateral meniscus.

The most frequently employed knee movement occurs when walking (Fig. 82.19). When the leg is swinging past the supporting leg, the knee must be flexed in order to avoid dragging the toes on the ground; this requires approximately 67° knee flexion. When the swinging leg approaches the first contact with the ground, the knee extends, to move the foot forwards for heel strike. If the knee remained extended, this would then cause the body to move in a circular arc, centred at the ankle, causing the centre of gravity to move upwards and then back down again, leading to more energy expenditure. It would also increase the forces on the knee, because the leg would act more like a rigid strut unable to dissipate the impact forces when the foot hit the ground. All these problems are overcome by the knee flexing 15° in the mid stance phase: the centre of gravity of the body can move forwards at approximately constant height, and the impact energy is absorbed by stretching the quadriceps (Fig. 82.19).

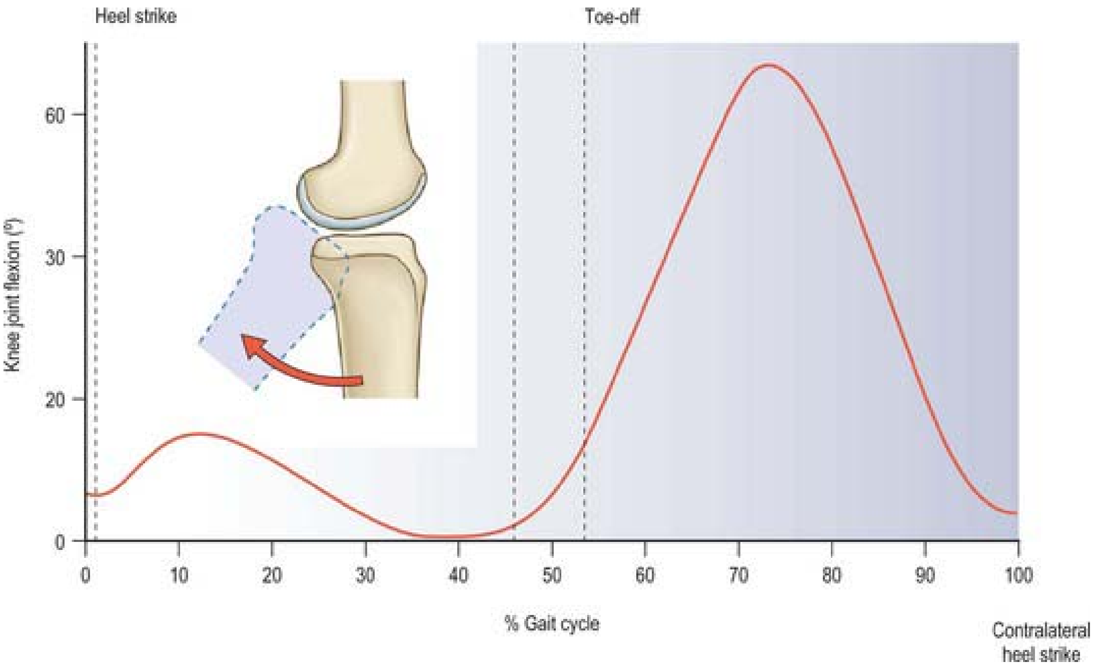

Fig. 82.19 Knee flexion–extension motion during gait.

Tibial internal-external rotation also occurs during gait: the tibia rotates externally during terminal extension, a phenomenon known as ‘screw home’ (Fig. 82.20). It is surmised that this rotation helps to lock the geometry and tighten the soft tissues, thereby maintaining the knee in a stable position prior to the impact load of weight bearing. The knee acts as one link in a chain of limb segments, and this screw-home relates to rotation of both foot and hip. When the foot is swung forwards for heel strike, the pelvis rotates so that the hip is moved forwards, a movement that entails external rotation of the hip. During stance, the femur is internally rotated against the locked knee. Tibial external rotation also causes inversion of the foot at the subtalar joint, raising the arch and locking the structure of the foot. The knee flexion that occurs after the impact on the ground allows the tibia to rotate internally so that the foot everts, softening its structure and allowing it to deform and absorb energy. Conversely, towards toe-off, the knee extends, rotating the tibia externally, so the foot is again a rigid lever with which to push the body forwards.

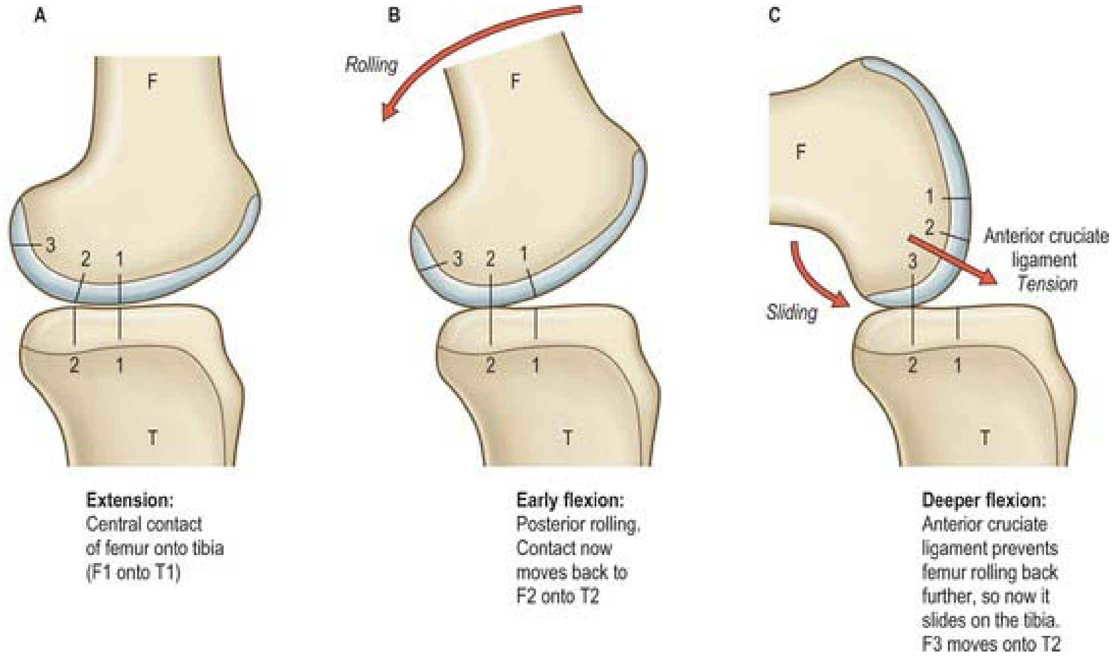

Extension: Central contact of femur onto tibia (F1 onto T1)

Early flexion: Posterior rolling. Contact now moves back to F2 onto T2

Deeper flexion: Anterior cruciate ligament prevents femur rolling back further, so now it slides on the tibia. F3 moves onto T2

Fig. 82.20 Knee joint kinematics during gait: rolling and gliding (flexion, anterior translation).

Articular kinematics

We now consider knee motion at a smaller scale, within the joint. This, of course, is difficult to separate from the actions of the ligaments that act as passive restraints to tibiofemoral joint movements, and are discussed below.

Sagittal sections of the knee reveal that the arcs of the femoral condyles are much longer than the anterior–posterior length of the tibial plateau. This means that if the knee flexed with a purely rolling motion, then the femur would roll off of the back of the tibia long before the knee reaches full flexion (Fig. 82.20). This does not happen because the femur slides anteriorly at the same time as it rolls posteriorly, and thus remains in correct articulation. If the knee were to possess a fully conforming roller-in-trough geometry, as in the humeroulnar joint, then flexion would occur by pure sliding movement between the joint surfaces. This conformity is not possible at the knee because it would inhibit the tibial internal-external rotation that is needed during locomotion.

In the locked, fully-extended knee, the anterodistal femoral articular surfaces press onto the anterior horns of the menisci. This tends to cause the femur to slide posteriorly, tensing the ACL and slackening the PCL. With knee flexion, the femur lifts off of the anterior horns of the menisci, leading to contact between the smaller radii of the posterior parts of the femoral condyles, and the tibial plateau plus posterior horns of the menisci. This means that the centre of contact moves posteriorly in early knee flexion. After this, the femoral condyles have approximately circular sagittal sections. The femur is now prevented from rolling back any further by tension in the ACL. The action of the ACL is similar to that of a rope attaching the back of a car to the ground: when the car tries to drive away, the wheels roll until the rope tightens, and then spin in one position (sliding motion).

Articular mechanics

The combined effect of the external and internal loads on the knee is to impose considerable forces on the articular cartilage. This may be analysed into a vertical (compressive) component and a horizontal (shear or friction) component. The friction component is a combination of the compressive force and the friction characteristics of the joint surfaces.

Compression

The compressive force is distributed over an area to produce a contact pressure (contact stress). The contact pressure is, therefore, dependent on the area of contact as well as the load itself. Fully-conforming articular surface geometry would allow the greatest area of contact, and thus would minimize contact pressure, however, this is not present in the knee. The medial compartment of the knee is semi-conforming with a convex femoral condyle articulating over a concave medial tibial plateau. The lateral compartment has less conformity: the lateral tibial plateau is flat or slightly convex in sagittal sections. These different shapes reflect the differential movement of the medial and lateral compartments. In normal movement, the screw home rotation of the tibia occurs about a medial axis which means that most of the rotation of the tibia is due to an anterior–posterior translation of the lateral compartment (Fig. 82.21).

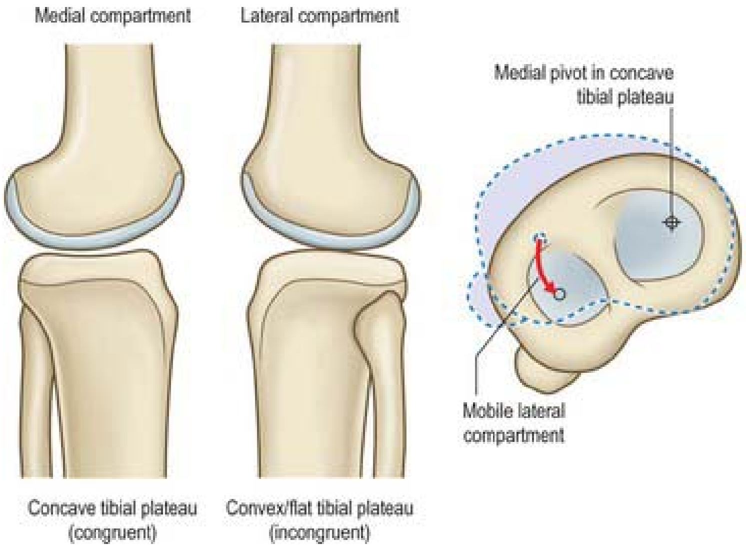
Medial compartment
Lateral compartment
Medial pivot in concave tibial plateau
Mobile lateral compartment
Concave tibial plateau (congruent)
Convex/flat tibial plateau (incongruent)

Fig. 82.21 The shape of the articular surfaces providing mobility of the lateral compartment.

In order to maintain some degree of conformity, and thus minimize contact pressure, the menisci have wedge-shaped cross-sections that fit between the femur and tibia around the bones. This serves to increase the area over which the compressive force on the knee is distributed. In the absence of the menisci, the load is carried by a much smaller area of cartilage, resulting in higher contact stresses on the articular cartilage. This explains the prevalence of osteoarthrosis following meniscectomy (Fig. 82.22).

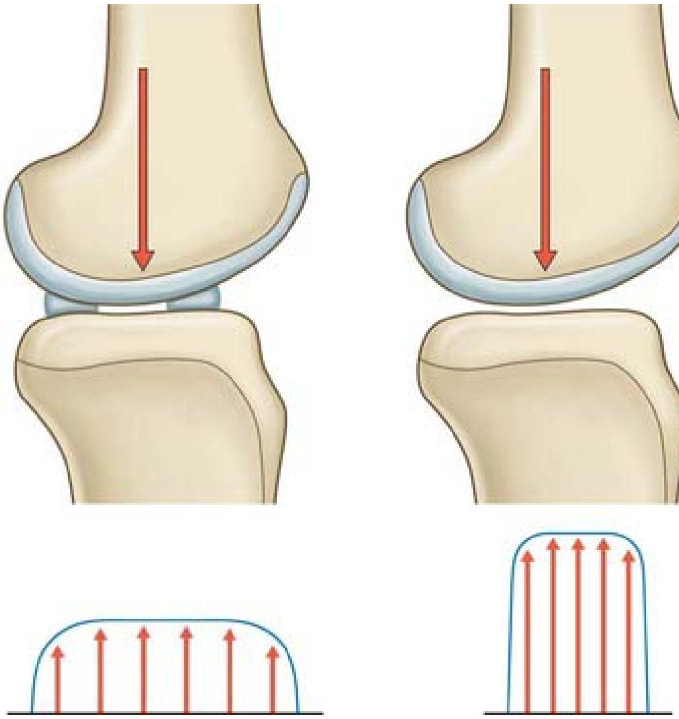

Fig. 82.22 The function of the menisci in increasing articular conformity, with increased peak pressure after meniscectomy.

The menisci are most firmly attached at the tibial intercondylar eminence and so they can translate anteriorly and posteriorly to ‘follow’ the femoral rollback. The lateral meniscus is more mobile, because it is attached to the capsule less tightly than the medial meniscus. The anterior–posterior movement of the menisci is approximately half the magnitude of the anterior–posterior movement of the femur, suggesting that the conformity of the joint changes during knee joint flexion.

The distal aspect of the femur, resting on the menisci in the extended knee, has a large radius of curvature, and so it fits against the entire area of the menisci. However, as the knee flexes, the smaller radii of the posterior parts of the femoral condyles cause the femur to lift off the anterior horns of the menisci, and the femoral contact is now solely on the posterior horns in the flexed knee. This, combined with the large joint forces that are generated when arising from a seated position, explains why there are often spontaneous tears of the posterior horns in older patients, when standing up from a squatting position.

The load-carrying mode of the menisci is shown in Fig. 82.23. When the femoral condyle presses down on the meniscus, it tends to squeeze the meniscus out of the joint, because of its tapered cross-section. This causes the diameter of the circular shape of the meniscus (and therefore the meniscal circumference) to increase. This is resisted by ‘hoop tension’ in strong fibres that pass around the periphery of the meniscus, and transmit the tension to the tibial plateau via strong insertional ligaments. Because the tissue is adapted to resist hoop stresses, it has much greater hoop strength (approximately 100 MPa) than radial strength (approximately 3 MPa), which explains why bucket handle tears occur. It also explains why a circumferential tear does not have such a serious effect on meniscal function, because the circumferential fibres can still transmit the loads, whereas a radial tear breaks the load-carrying fibres.

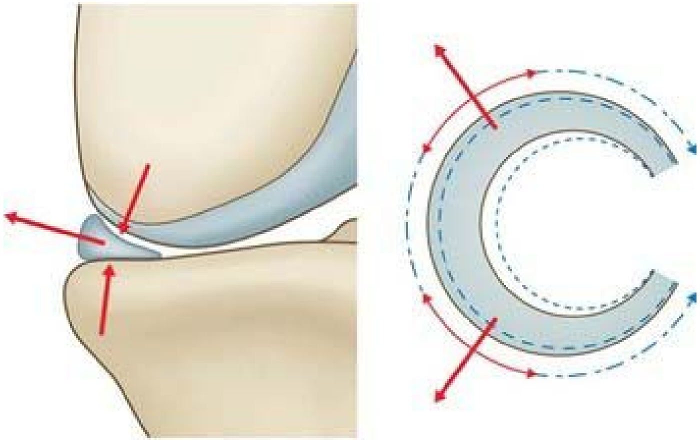

Fig. 82.23 The load-carrying mode of the menisci – conversion of axial load into meniscal hoop stresses.

Friction

The knee acts as a bearing that transmits forces and movements between the limb segments. Load-bearing synovial joints move with remarkably little friction, and their surfaces must withstand many millions of impact loads which tend to cause fatigue failure and breakdown of the surfaces.

During walking, every step involves phases of action that vary the loading and velocity conditions at the knee joint. A variety of lubrication mechanisms normally prevent joint surface damage. Thus, in the swing phase, when the foot is off the ground, the joint surfaces are loaded lightly, and have high relative velocity while the knee flexes and extends. This allows the synovial fluid to separate the surfaces, giving fluid film lubrication, with very low friction and no wear (Fig. 82.24). At the time of heel strike, a large impact load acts to compress the surfaces together. At a microscopic level, the surfaces do not come into contact, because of the squeeze film effect: in essence, the impact occurs so rapidly (less than 0.1 sec) that the synovial fluid cannot all be squeezed out of the joint space, because of its viscosity and the narrowness of the space. In the mid stance phase, the flexion–extension motion again entrains the synovial fluid in between the joint surfaces, producing what is known as a hydrodynamic effect: the fluid is trapped between the surfaces by the motion, and therefore it acts to separate them. Finally, when the foot is pushing off the body weight, there is little motion, and the thin fluid film diminishes under the compressive load. If the squeeze-film effect is insufficient, then the joint surfaces would now come into direct contact, were it not for the fact that the synovial fluid contains large protein molecules that are trapped on the cartilage surfaces when the fluid is expelled. This molecular layer acts as a boundary lubricant, protecting the cartilage in the same way that grease protects a synthetic bearing.

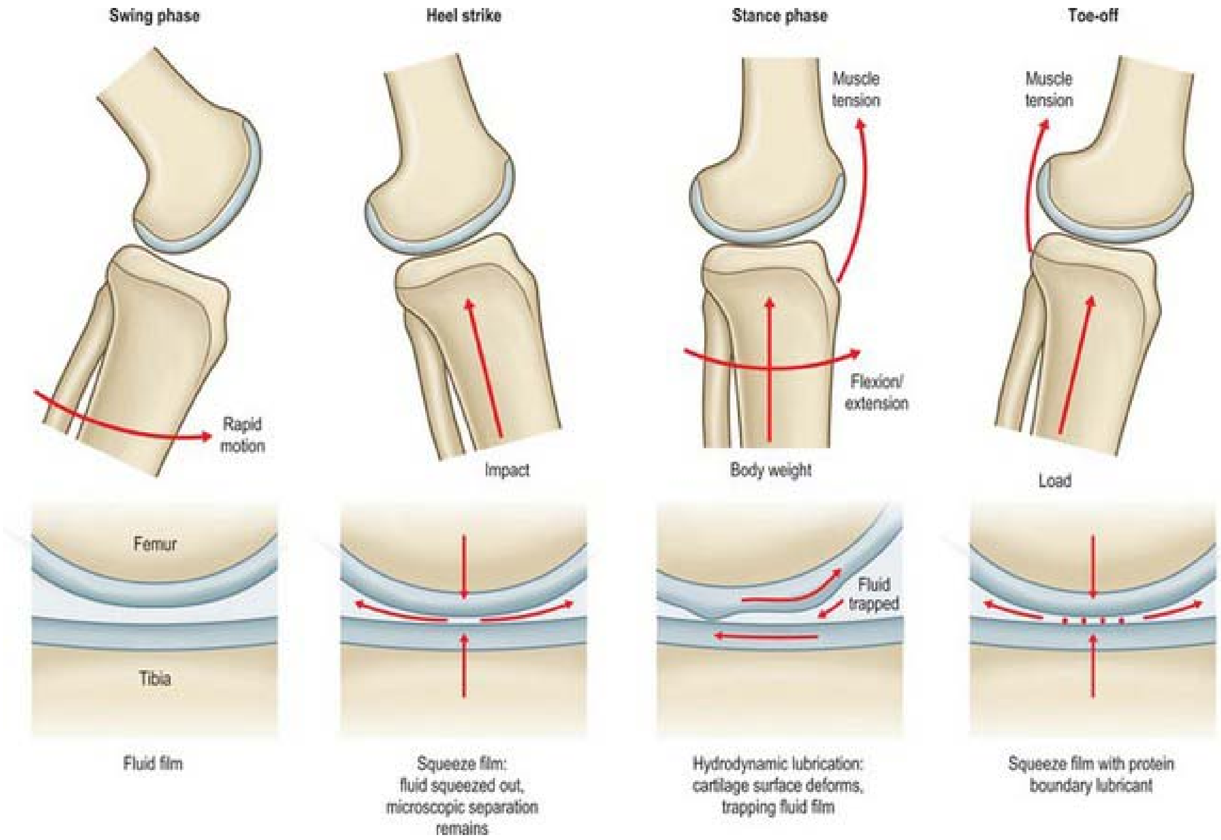
Swing phase
Heel strike
Stance phase
Toe-off
Muscle tension
Muscle tension
Flexion/ extension
Rapid motion
Impact
Body weight
Load
Femur
Tibia
Fluid trapped
Fluid film
Squeeze film: fluid squeezed out, microscopic separation remains
Hydrodynamic lubrication: cartilage surface deforms, trapping fluid film
Squeeze film with protein boundary lubricant

Fig. 82.24 The different modes of knee joint motion and lubrication when walking.

Many aspects of the arthritic breakdown of the cartilage can be explained on the basis of lubrication biomechanics. Thus, in joints affected by osteoarthrosis, synovial fluid is known to have a lower viscosity than that in normal joints. The viscosity is lower still in rheumatoid joints, and unable to prevent attritional damage to the cartilage surfaces.

SOFT-TISSUE MECHANICS

The knee joint relies on active (musculotendinous) and passive (ligamentous) restraints to maintain its stability. The muscles provide the loading to move the joint. The quadriceps, hamstrings and gastrocnemius control both flexion/extension and internal–external rotation. However, they also cause anterior–posterior shear forces that are resisted primarily by the cruciate ligaments. This tethering effect is critical in allowing the joint to move physiologically, maintaining congruency and stability.

The passive stabilizers of the joint act by resisting unwanted displacements between the bones. This may be to control the path of motion, or to limit the range of motion. When the muscles or some other external force (due to bodyweight or impact) cause the bones to displace, the ligaments are stretched, and so develop tensile forces that resist the displacement and allow the joint to maintain its stability. Disruption of any of these passive restraints may cause a mechanical instability, which is an abnormally increased displacement due to an applied force (in biomechanical terms this is called excess laxity).

Primary and secondary restraints

On testing the laxity in any of the degrees of freedom of the joint (e.g. in the anterior drawer test, a bedside clinical test in which the subject is placed in the supine position with the knee to be tested flexed to 80–90° before passive forward traction is applied to the tibia), there are usually combinations of ligaments that are tensed. Some of these are better aligned to resist the applied load or displacement. These are termed primary restraints, and are exemplified by the cruciate ligaments and the medial and lateral collateral ligaments. Secondary restraints are less well-aligned, but still have a significant restraining effect. These are exemplified by the menisci, and by the meniscofemoral ligaments. In the example in Fig. 82.25, the ACL is well-aligned to resist the applied anterior drawer force. With an absent ACL, the superficial MCL can resist the applied force, however, it does so by being loaded to a much higher level than the original loading on the ACL. The size of the lines in the vector diagram demonstrate this principle: although joint laxity may remain normal initially following rupture of a primary restraint, it may subsequently result in the overload of a secondary restraint, and ultimately, in further soft-tissue failure.

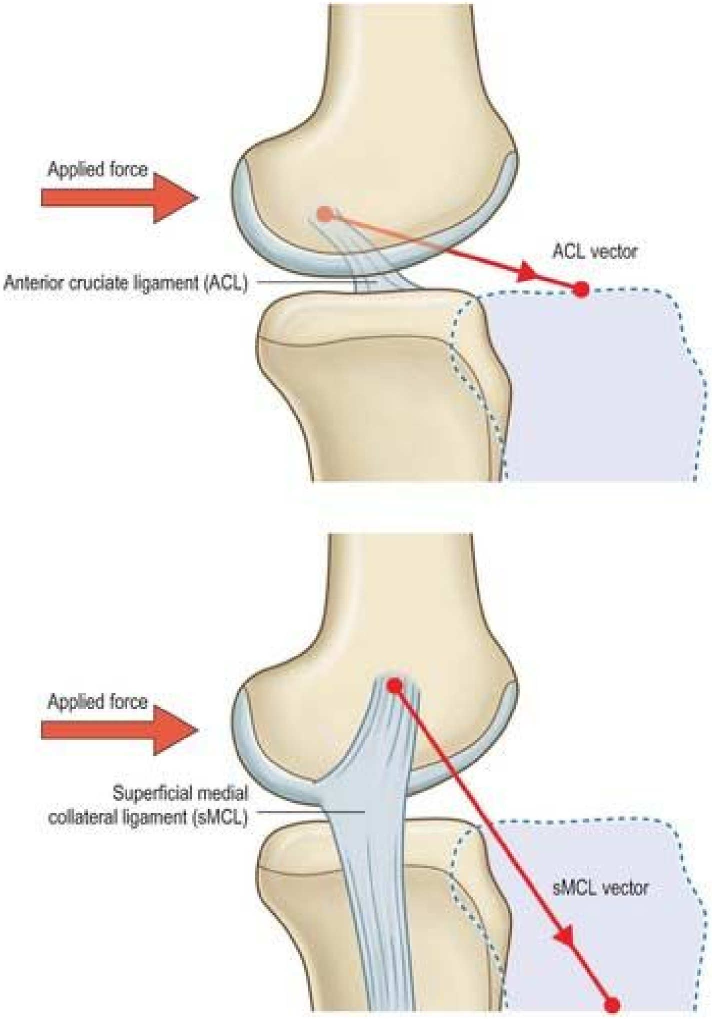
Applied force
ACL vector
Anterior cruciate ligament (ACL)
Applied force
Superficial medial collateral ligament (sMCL)
sMCL vector

Fig. 82.25 Primary and secondary restraints to anteroposterior forces – example of the ACL and superficial MCL.

The patellofemoral joint is most heavily loaded during weight-bearing activities when the knee is flexed. Analyses of rising from a chair have predicted that the patellar tendon tension at 90° flexion may then be 2.9 BW, and so the joint force will be 5.5 BW. This is higher than the tibiofemoral joint, which is loaded to 3.3 BW at the same time (Amis & Farahmand 1996).

In the frontal plane the quadriceps muscles and patellar tendon tensions combine to cause a lateralizing force vector termed the Q-angle effect. The Q angle is defined as the difference between the resultant force vector of the quadriceps, which is normally parallel to the femoral shaft, and the patellar tendon (Fig. 82.26). Clinically, the Q angle is changed by the position of hip rotation, tibial rotation, and quadriceps tension. The clinical Q-angle is 12–15° (males) and 15–18° (females), which means that there is a greater lateralizing force vector on the patellofemoral joint in females. Contraction of the quadriceps, therefore, tends to displace the patella laterally; this is resisted by the geometry of the joint and by the passive stabilizers. Vastus medialis obliquus (VMO) acts medially and posteriorly as much as it acts proximally, and so its tension helps to resist the Q angle effect.

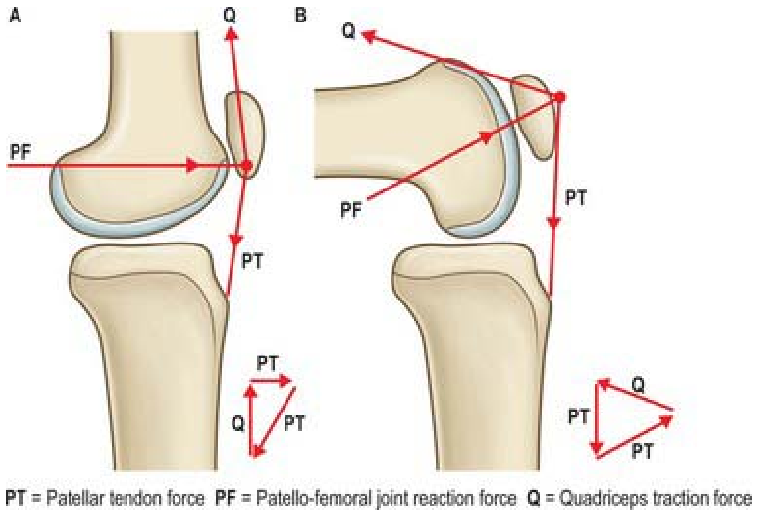
A
Q
B
Q
PF
PF
PT
PT
PT
Q
PT
Q
PT
PT
PT = Patellar tendon force PF = Patello-femoral joint reaction force Q = Quadriceps traction force

Fig. 82.26 Patellofemoral joint force at extension (**A**) and at 90° flexion (**B**).

MUSCLES

The majority of muscles that act on the knee joint are described in either Chapter 80 (quadriceps femoris, semimembranosus, biceps femoris, semitendinosus, articularis genu) or Chapter 83 (gastrocnemius). Popliteus is described below.

Popliteus

Attachments

Popliteus is a flat muscle that forms the floor of the lower part of the popliteal fossa. It arises within the capsule of the knee joint by a strong tendon, 2.5 cm long, which is attached to a depression at the anterior end of the groove on the lateral aspect of the lateral condyle of the femur. Medially this tendon is joined by collagenous fibres from the arcuate popliteal ligament, from the fibrous capsule adjacent to the lateral meniscus, and from the outer margin of the meniscus.

Popliteus is attached to the medial aspect of the fibular head by the popliteofibular ligament, which passes laterally and inferiorly from the popliteus tendon in a sheet of tissue that is normally about 2 cm^2. This ligament is the single most important stabilizer of the posterolateral region of the knee and resists external rotation of the tibia on the femur. Failure to recognize and reconstruct damage to this ligament and to the related ligamentous structures is the most common reason for a poor result from an otherwise well-performed operation for repair of ruptured cruciate ligaments.

Fleshy fibres expand from the inferior limit of the tendon to form a somewhat triangular muscle that descends medially to be inserted into the medial two-thirds of the triangular area above the soleal line on the posterior surface of the tibia, and into the tendinous expansion that covers its surface.

An additional head may arise from the sesamoid in the lateral head of gastrocnemius. Very rarely, two other muscles may be found deeply situated behind the knee. Popliteus minor runs from the posterior surface of the lateral tibial condyle, medial to plantaris, to the oblique popliteal ligament.

Peroneotibialis runs deep to popliteus from the medial side of the fibular head to the upper end of the soleal line.

Relations

Popliteus is covered posteriorly by a dense aponeurotic expansion, which is largely derived from the tendon of semimembranosus. Gastrocnemius, plantaris, the popliteal vessels and the tibial nerve all lie posterior to the expansion. The popliteal tendon is intracapsular and is deep to the fibular collateral ligament of the knee and the tendon of biceps femoris. It is invested on its deep surface by synovial membrane, and grooves the posterior border of the lateral meniscus and the adjoining part of the tibia before it emerges inferior to the posterior band of the arcuate ligament. This region is called the ‘popliteus hiatus’: the lateral meniscus has no peripheral bony attachment here, and is therefore rather mobile.

Vascular supply

The arterial supply of popliteus is derived mainly from the medial and lateral inferior genicular arteries. The latter may cross superficial or deep to the muscle. There are additional contributions from the nutrient artery to the tibia, the proximal part of the tibial artery and from the posterior tibial recurrent artery.

Innervation

Popliteus is innervated by a branch of the tibial nerve (L4 and 5 and S1) which winds around the distal border of popliteus and enters the anterior surface of the muscle; this nerve also innervates the superior tibiofibular joint and the crural interosseous membrane.

Actions

Popliteus rotates the tibia medially on the femur or, when the tibia is fixed, rotates the femur laterally on the tibia. It is usually regarded as the muscle that ‘unlocks’ the joint at the beginning of flexion of the fully extended knee: electromyography supports this view. Its connection with the arcuate popliteal ligament, fibrous capsule and lateral meniscus has led to the suggestion that popliteus may retract the posterior horn of the lateral meniscus during lateral rotation of the femur and flexion of the knee joint, thus protecting the meniscus from being crushed between the femur and the tibia during these movements. The muscle is markedly active in crouching, perhaps to provide stability as the tibia rotates internally during flexion of the knee. However, the main function is likely to be provision of dynamic stability to the posterolateral part of the knee by preventing excessive external rotation of the tibia, partly by its direct action, but more significantly by tensing the popliteofibular ligament.

Testing

Popliteus plays a part in medially rotating the leg when the knee is flexed and non-weightbearing, but its individual actions cannot be isolated clinically. Damage to the popliteus complex of ligament and tendon is manifest as excessive external rotation of the tibia on the femur at 90° and especially at 30° of knee flexion., reflecting the function of the popliteus complex as a ‘static tether’.

VASCULAR SUPPLY AND LYMPHATIC DRAINAGE

ARTERIES

There is an intricate arterial anastomosis around the patella and femoral and tibial condyles. A superficial network spreads between the fascia and skin around the patella and in the fat deep to the patellar tendon. A deep network lies on the femur and tibia near the adjoining articular surfaces, and supplies the bone and marrow, the articular capsule, synovial membrane and the cruciate ligaments (Fig. 82.1). The vessels involved are the superior, middle and inferior genicular branches of the popliteal artery, descending genicular branches of the femoral artery, the descending branch of the lateral circumflex femoral artery, the circumflex fibular artery and the anterior and posterior tibial recurrent arteries. For details consult Scapinelli (1968).

Popliteal artery

The popliteal artery is the continuation of the femoral artery and crosses the popliteal fossa (Fig. 82.4). It descends laterally from the opening in adductor magnus to the femoral intercondylar fossa, inclining obliquely to the distal border of popliteus, where it divides into the anterior and posterior tibial arteries. This division usually occurs at the proximal end of the asymmetrical crural interosseous space between the wide tibial metaphysis and the slender fibular metaphysis. The artery is relatively tethered at the adductor magnus hiatus and again distally by the fascia related to soleus, and is therefore susceptible to traction damage in knee injuries, e.g. dislocation.

Variations in arterial anatomy of lower limb

Most anatomical variations in the arterial pattern of the lower limb arteries are apparently symptomless and cause no clinically detectable functional impairment. They are usually incidental findings in the dissection room, or may come to light in the course of angiographic examination. However, some variations in vascular anatomy may be the cause of symptoms and may necessitate surgical correction, and other variations, while asymptomatic, may influence technical considerations in vascular surgical procedures.

Anatomical variations in the femoral, profunda femoris, anterior tibial, posterior tibial and fibular arteries have been described elsewhere in this section.

Variations in the popliteal artery

Several cadaveric studies have shown that the pattern and level of termination of the popliteal artery described above occurs in the majority (90%) of subjects. However, the artery may occasionally (5%) show a high bifurcation, and divide into its terminal branches proximal to popliteus, or it may trifurcate into anterior and posterior tibial and fibular arteries. Either the anterior tibial or the posterior tibial artery may be reduced or increased in size. The size of the fibular artery is usually inversely related to the size of the anterior and posterior tibial arteries, either of whose functions the fibular artery may assume. Rarely, the anterior tibial artery is the source of the fibular artery; almost always this is associated with a high bifurcation of the popliteal artery.

The popliteal artery may be a continuation, not of the femoral artery, but of the sciatic artery (a branch of the inferior gluteal artery). When this occurs, the popliteal artery usually has an abnormal relationship to popliteus, running deep to the muscle before dividing into its terminal branches. The popliteal artery may pass medially beneath the medial head of gastrocnemius, or may pass beneath an aberrant band of muscle in the popliteal fossa: in either case, contraction of the muscles may occlude the artery. This condition, known as popliteal artery entrapment, may present with claudication on exercise in a young male patient. The popliteal vein is usually superficial and adjacent to the artery, but it may run deep to the artery, or be separated from it by a slip of muscle derived from the medial head of gastrocnemius.

Relations

Anteriorly, from proximal to distal, are fat covering the femoral popliteal surface, the capsule of the knee joint, and the fascia of popliteus. Posteriorly are semimembranosus (proximally) and gastrocnemius and plantaris (distally). In between, the artery is separated from the skin and fasciae by fat and crossed from its lateral to its medial side by the tibial nerve and popliteal vein: the vein lies between the nerve and artery and is adherent to the latter. Laterally are biceps femoris, the tibial nerve, popliteal vein and lateral femoral condyle (all proximal), and plantaris and the lateral head of gastrocnemius (distal). Medially are semimembranosus and the medial femoral condyle (proximal), and the tibial nerve, popliteal vein and medial head of gastrocnemius (distally). The relations of the popliteal lymph nodes are described below.

Branches (other than terminal)

Genicular anastomosis

There is an intricate arterial anastomosis around the patella and femoral and tibial condyles (Fig. 82.1). A superficial network spreads between the fascia and skin around the patella and in the fat deep to the patellar tendon. A deep network lies on the femur and tibia near the adjoining articular surfaces, and supplies the bone and marrow, articular capsule and synovial membrane. The vessels involved are the medial and lateral superior genicular, the medial and lateral inferior genicular, the descending genicular, the descending branch of the lateral circumflex femoral, the circumflex fibular and the anterior and posterior tibial recurrent arteries.

Superior genicular arteries

The superior genicular arteries branch from the popliteal artery, curving round proximal to both femoral condyles to reach the anterior aspect of the knee. The medial superior genicular artery lies under semimembranosus and semitendinosus, proximal to the medial head of gastrocnemius and deep to the tendon of adductor magnus. It divides into a branch to vastus medialis that anastomoses with the descending genicular and medial inferior genicular arteries, and a branch that ramifies on the femur and anastomoses with the lateral superior genicular artery. Its size varies inversely with that of the descending genicular artery. The lateral superior genicular artery passes under the tendon of biceps femoris and divides into superficial and deep branches. The superficial branch supplies vastus lateralis and anastomoses with the descending branch of the lateral circumflex femoral and lateral inferior genicular arteries, while the deep branch anastomoses with the medial superior genicular artery, forming an anterior arch across the femur with the descending genicular artery. The superficial branch is vulnerable if the lateral patellar retinaculum is divided surgically.

Middle genicular artery

The middle genicular artery is small. It arises from the popliteal artery near the midpoint of the posterior aspect of the knee joint. It pierces the oblique popliteal ligament to supply the cruciate ligaments and synovial membrane.

Inferior genicular arteries

The medial and lateral inferior genicular arteries arise from the popliteal artery deep to gastrocnemius. The medial is deep to the medial head of gastrocnemius. It descends along the proximal margin of popliteus, which it supplies, passes inferior to the medial tibial condyle, under the medial collateral ligament, and then ascends anteromedial to the joint at the anterior border of the medial collateral ligament. It supplies the joint and the tibia, and anastomoses with the lateral inferior and medial superior genicular arteries and with the anterior tibial recurrent artery and saphenous branch of the descending genicular artery. The lateral inferior genicular artery runs laterally across popliteus and forwards over the fibular head to the front of the knee joint, passing under the lateral head of gastrocnemius, the fibular collateral ligament and the tendon of biceps femoris. Its branches anastomose with the medial inferior and lateral superior genicular, anterior and posterior tibial recurrent and circumflex fibular arteries.

Cutaneous branches: the superficial sural arteries

The superficial sural arteries are three vessels which leave the popliteal artery, or its side branches, descend between the heads of gastrocnemius and perforate the deep fascia to supply the skin on the back of the leg. The central or median vessel is usually larger than the medial and lateral, and usually accompanies the sural nerve.

Fasciocutaneous free and pedicled flaps may be raised on the superficial sural arteries.

Superior muscular branches

The superior muscular branches are two or three vessels that arise proximally and pass to adductor magnus and the hamstrings. They anastomose with the termination of the profunda femoris artery.

Sural arteries

The two sural arteries are large and arise behind the knee joint to supply gastrocnemius, soleus and plantaris. They are used in gastrocnemius musculocutaneous flaps.

VEINS

The veins draining the knee correspond in name to the arteries and run with them; the named smaller veins drain into the popliteal and femoral veins.

Popliteal vein

The popliteal vein ascends through the popliteal fossa to the opening in adductor magnus where it becomes the femoral vein (see Fig. 79.9B). Its relationship to the popliteal artery changes as the vein ascends. Distally it is medial to the artery, between the heads of gastrocnemius it is superficial (posterior) to it, and proximal to the knee joint it is posterolateral to the artery. Its tributaries are the short saphenous vein, veins corresponding to branches of the popliteal artery, and muscular veins, including a large branch from each head of gastrocnemius. There are usually four or five valves in the popliteal vein.

Long saphenous vein

The course of the long saphenous vein is described in Chapter 80.

Short saphenous vein

The short saphenous vein (small saphenous vein) begins posterior to the lateral malleolus as a continuation of the lateral marginal vein (see Fig. 79.9B). In the lower third of the calf it ascends lateral to the calcaneal tendon, lying on the deep fascia and covered only by superficial fascia and skin. Inclining medially to reach the midline of the calf, it penetrates the deep fascia, within which it ascends on gastrocnemius, only emerging between the deep fascia and gastrocnemius gradually at about the junction of the intermediate and proximal thirds of the calf (usually well below the lower limit of the popliteal fossa). Continuing its ascent, it passes between the heads of gastrocnemius then proceeds to its termination in the popliteal vein in the popliteal fossa, 3–7.5 cm above the knee joint.

Tributaries

The short saphenous vein connects with deep veins on the dorsum of the foot, receives many cutaneous tributaries in the leg, and sends several communicating branches proximally and medially to join the long saphenous vein. Sometimes a communicating branch ascends medially to the accessory saphenous vein: this may be the main continuation of the short saphenous vein. In the leg the short saphenous vein lies near the sural nerve. It has 7–13 valves, one near its termination. Its mode of ending is variable: it may join the long saphenous vein in the proximal thigh or it may bifurcate, one branch joining the long saphenous, the other the popliteal or deep posterior femoral veins. Sometimes it ends distal to the knee in the long saphenous or deep sural muscular veins.

LYMPHATIC DRAINAGE

Lymphatic drainage is to the popliteal lymph nodes. Most of the lymph vessels accompany the genicular arteries; some vessels from the joint drain directly into a node between the popliteal artery and the posterior capsule.

Popliteal lymph nodes

There are usually six small lymph nodes embedded in the fat of the popliteal fossa. One, near the termination of the short saphenous vein, drains the superficial region served by the vein. Another lies between the popliteal artery and the posterior aspect of the knee joint, receiving direct vessels from the knee joint and those accompanying the genicular arteries. The remainder flank the popliteal vessels, receiving trunks that accompany the anterior and posterior tibial vessels. Popliteal efferents ascend close to the femoral vessels to reach the deep inguinal nodes; some may accompany the long saphenous vein to the superficial inguinal nodes.

Inflammation of the popliteal nodes is often caused by lateral lesions of the heel.

INNERVATION

The knee joint is innervated by branches from the obturator, femoral, tibial and common fibular nerves (Freeman & Wyke 1967). The genicular branch of the obturator nerve is the terminal branch of its posterior division. Muscular branches of the femoral nerve, especially to vastus medialis, supply terminal branches to the joint. Genicular branches from the tibial and common fibular nerves accompany the genicular arteries: those from the tibial nerve run with the medial and middle genicular arteries, while those from the common fibular nerve run with the lateral genicular and anterior tibial recurrent arteries.

The femoral and obturator nerves are described on page 1382–1383, and the tibial and common fibular nerves are described on page 1427).

Saphenous nerve

The saphenous nerve is the largest and longest cutaneous branch of the femoral nerve. It descends lateral to the femoral artery in the femoral triangle and enters the adductor canal, where it crosses in front of the artery to lie medial to the artery. At the distal end of the canal it leaves the artery and emerges through the aponeurotic covering with the saphenous branch of the descending genicular artery. As it leaves the adductor canal it gives off an infrapatellar branch that contributes to the peripatellar plexus (p. 1393) and then pierces the fascia lata between the tendons of sartorius and gracilis, becoming subcutaneous to supply the prepatellar skin. It descends along the medial tibial border with the long saphenous vein and divides distally into a branch which continues along the tibia to the ankle and a branch which passes anterior to the ankle to supply the skin on the medial side of the foot, often as far as the first metatarsophalangeal joint. The saphenous nerve connects with the medial branch of the superficial fibular nerve. Near midthigh, it gives a branch to the subsartorial plexus. The nerve may be subject to an entrapment neuropathy as it leaves the adductor canal.

REFERENCES

nis AA, Dawkins GP. Functional anatomy of the anterior cruciate ligament. Fibre bundle actions related to ligament replacements and injuries. *J Bone Joint Surg*. 1991;73B:260-267.

ormack GC, Lamberty BGH. The Arterial Anatomy of Skin Flaps. Edinburgh: Churchill Livingstone, 1994.

rock HV. The blood supply of the lower limb bones in man. London: Livingstone, 1967.

eeman MAR, Wyke B. The innervation of the knee joint. *J Anat*. 1967;101:505-532.

nadially FN, Lalonde J-M A, Wedge JH. Ultrastructure of normal and torn menisci of the human knee joint. *J Anat*. 1983;136:773-791.

rgis FG, Marshall JL, Al Monajem ARS. The cruciate ligaments of the knee joint. *Clin Orthop*. 1975;106:216-231.

ronblad M, Korkala O, Leisi P, Karaharju E. Innervation of synovial membrane and meniscus. *Acta Orthop Scand*. 1985;56:484-486.

upte CM, Bull AMJ, Thomas RD, Amis AA. A review of the function and biomechanics of the meniscofemoral ligaments. *Arthroscopy*. 2003;19:161-171.

A comprehensive review of the properties of these hitherto poorly understood ligaments..

seph J. Man’s Posture: Electromyographic Studies. Springfield, Illinois: Thomas, 1960.

ewell RLM. A complete intra-articular fat pad around the human patella. *J Anat*. 1991;179:232.

Shows that the infrapatellar and suprapatellar fat pads are not isolated and separate structures..

ajendran K. Mechanism of locking at the knee joint. *J Anat*. 1985;143:189-194.

apinelli R. Studies on the vasculature of the human knee joint. *Acta Anat*. 1968;70:305-331.

Primary source of detail, complementing the work of Crock (q.v.) on the vasculature of the bones of the lower limb..

ebacher JR, Inglis AE, Marshall JL, Warren RF. The structure of the posterolateral aspect of the knee. *J Bone Joint Surg*. 1982;64A:536-541.

Work that established the current interpretation of the anatomy of the soft tissues of the knee..

nnant TD, Birch NC, Holmes MJ, Birch R, Goddard NJ. Knee pain and the infrapatellar branch of the saphenous nerve. *J Roy Soc Med*. 1998;91:573-575.

Recognizes the clinical significance of this small but important nerve branch..

omas P, Jackson AM, Aichroth PM. Congenital absence of the anterior cruciate ligament. *J Bone Joint Surg*. 1985;67B:572-575.

A rare but important congenital anomaly..

arren LF, Marshall JL. The supporting structures and layers on the medial side of the knee: an anatomical analysis. *J Bone Joint Surg*. 1979;61A:56-62.

atanabe M, Takeda S, Ikeuchi H. Atlas of Arthroscopy. Berlin: Springer-Verlag, 1979.

CHAPTER 83

Leg

This chapter describes the shafts of the tibia and fibula, the soft tissues that surround them and the interosseous membrane between them. The superior (proximal) and inferior (distal) tibiofibular joints are described in Chapters 82 and 84 respectively.

SKIN AND SOFT TISSUE

SKIN

Vascular supply and lymphatic drainage

The cutaneous arterial supply is derived from branches of the popliteal, anterior tibial, posterior tibial and fibular vessels (see Fig. 79.5). Multiple fasciocutaneous perforators from each vessel pass along intermuscular septa to reach the skin; musculocutaneous perforators traverse muscles before reaching the skin. In some areas there is an additional direct cutaneous supply from vessels that accompany cutaneous nerves, e.g. the descending genicular artery (saphenous artery) and superficial sural arteries. Fasciocutaneous and direct cutaneous branches have a longitudinal orientation in the skin, whereas the musculocutaneous branches are more radially oriented. For further details consult Cormack & Lamberty (1994).

Cutaneous veins are tributaries of vessels that correspond to the named arteries. Cutaneous lymphatic vessels running on the medial side of the leg accompany the long saphenous vein, and drain to the superficial inguinal nodes, while those from the lateral and posterior sides of the leg accompany the short saphenous vein and pierce the deep fascia to drain into the popliteal nodes.

Innervation

The skin of the leg is supplied by branches of the saphenous, common fibular and tibial nerves (see below and Figs 79.17; 79.20).

SOFT TISSUE

Deep fascia

The deep fascia of the leg, the fascia cruris, is continuous with the fascia lata and is attached around the knee to the patellar margin, the patellar tendon, the tuberosity and condyles of the tibia, and the head of the fibula. Posteriorly, where it covers the popliteal fossa as the popliteal fascia, it is strengthened by transverse fibres and often perforated by the short saphenous vein and sural nerve. It receives lateral expansions from the tendon of biceps femoris and multiple medial expansions from the tendons of sartorius, gracilis, semitendinosus and semimembranosus. The deep fascia blends with the periosteum on the subcutaneous surface of the tibia and the subcutaneous surfaces of the fibular head and malleolus, and is continuous below with the extensor and flexor retinacula. It is thick and dense in the proximal and anterior part of the leg, where fibres of tibialis anterior and extensor digitorum longus are attached to its deep surface, and is thinner posteriorly where it covers gastrocnemius and soleus. On the lateral side it is continuous with the anterior and posterior crural intermuscular septa, which are attached to the anterior and posterior borders of the fibula respectively. A broad transverse intermuscular septum, the deep transverse fascia of the leg, passes between the superficial and deep muscles in the calf.

Deep transverse fascia

The deep transverse fascia of the leg is a fibrous stratum between the superficial and deep muscles of the calf. It extends transversely from the medial margin of the tibia to the posterior border of the fibula. Proximally, where it is thick and dense, it is attached to the soleal ridge of the tibia and to the fibula, inferomedial to the fibular attachment of soleus. Between these bony attachments it is continuous with the fascia covering popliteus which is, in effect, an expansion from the tendon of semimembranosus. At intermediate levels it is thin, but distally, where it covers the tendons behind the malleoli, it is thick and continuous with the flexor and superior fibular retinacula.

Interosseous membrane

The interosseous membrane connects the interosseous borders of the tibia and fibula (Fig. 83.1). It is interposed between the anterior and posterior groups of crural muscles; some members of each group are attached to the corresponding surface of the interosseous membrane. The anterior tibial artery passes forwards through a large oval opening near the proximal end of the membrane, and the perforating branch of the fibular artery pierces it distally. Its fibres are predominantly oblique and most descend laterally; those which descend medially include a bundle at the proximal border of the proximal opening. The membrane is continuous distally with the interosseous ligament of the distal tibiofibular joint. Tibialis anterior, extensor digitorum longus, extensor hallucis longus, fibularis tertius, the anterior tibial vessels and deep fibular nerve are all anterior to the membrane, and tibialis posterior and flexor hallucis longus are posterior.

Retinacula

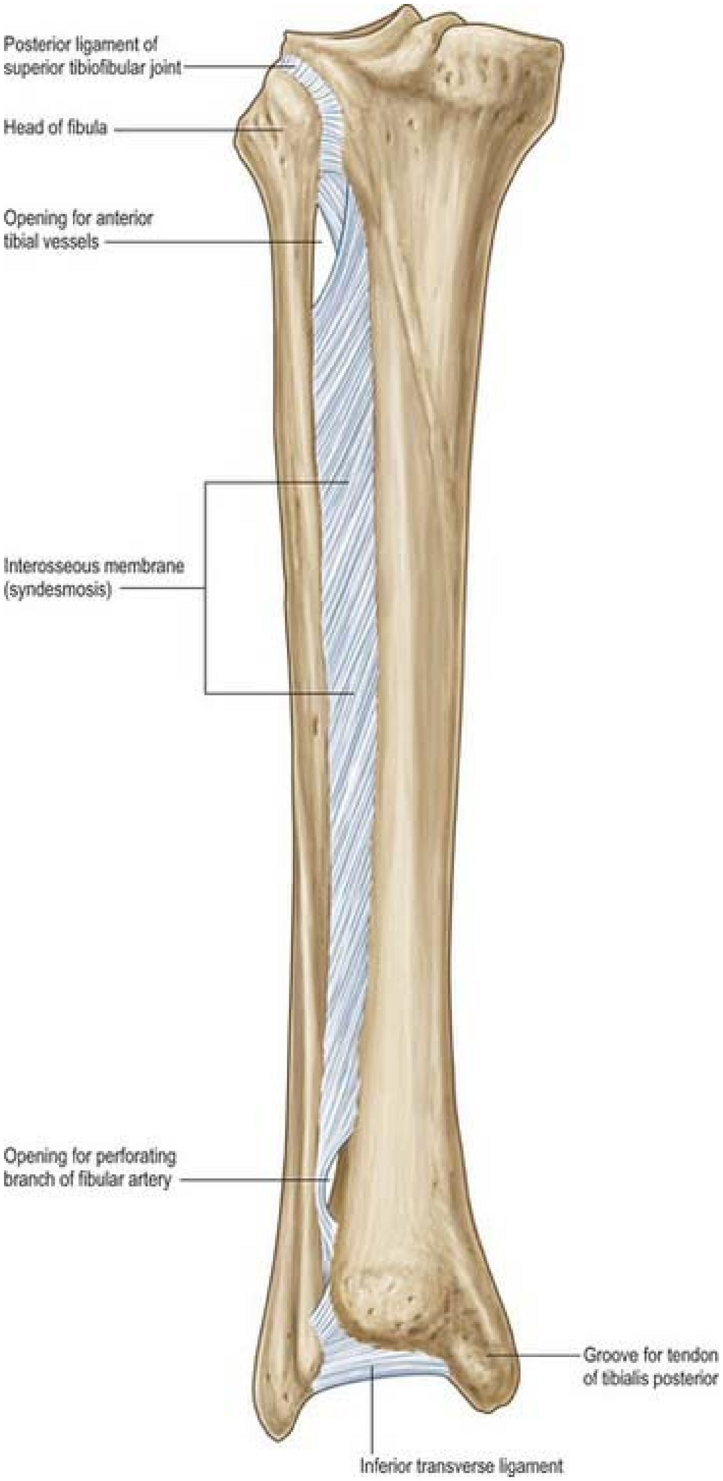
Posterior ligament of superior tibiofibular joint
Head of fibula
Opening for anterior tibial vessels
Interosseous membrane (syndesmosis)
Opening for perforating branch of fibular artery
Groove for tendon of tibialis posterior
Inferior transverse ligament

Fig. 83.1 Posterior aspect of the interosseous membrane. Note the contrasting direction of the fibre bundles around the vascular openings.

Retinacula

The retinacula at the ankle joint are described in Chapter 84.

Osteofascial compartments

The compartments of the leg are particularly well defined and are the most common sites at which osteofascial compartment syndromes occur. The three main compartments are anterior (extensor), lateral (fibular) and posterior (flexor). They are enclosed by the unyielding deep fascia (fascia cruris) and separated from each other by the bones of the leg and interosseous membrane and by the anterior and posterior intermuscular septa that pass from the deep fascia to the fibula. The anterior compartment, the least expansile of the three, is bounded by the deep fascia, the interosseous surfaces of the tibia and fibula, the interosseous membrane and the anterior intermuscular septum. The lateral compartment lies between the anterior and posterior intermuscular septa, and is bordered laterally by the deep fascia and medially by the lateral surface of the fibula. The posterior compartment is bounded by the deep fascia, the posterior intermuscular septum, the fibula and tibia and the interosseous membrane. Its relatively expansile superficial component is separated from the compacted deep component by the deep transverse fascia, reinforced by the deep aponeurosis of soleus.

The nerve supply of the muscles in the compartments follows the ‘one compartment – one nerve’ principle: the deep fibular nerve supplies the anterior compartment, the superficial fibular nerve supplies the lateral compartment, and the tibial nerve supplies the posterior compartment. Most of the muscles in the anterior compartment are supplied by the anterior tibial artery, with an additional contribution from the fibular artery to extensor hallucis longus. Muscles in the posterior compartment are supplied by the popliteal, posterior tibial and fibular arteries. Muscles in the lateral compartment are supplied by the anterior tibial and fibular arteries, and to a small extent proximally by a branch from the popliteal system.

Trauma and soft tissues of the leg

The relative paucity of soft tissue in the shin region and the subcutaneous position of the medial surface of the tibia means that even trivial soft tissue injury may lead to serious problems such as ulceration and osteomyelitis. In the elderly these soft tissues are often especially thin and unhealthy, reflecting the effects of ageing and venous stasis (see below). Tibial fractures are common in the young and, partly as a result of poor soft tissue coverage, they are often open injuries. Diminished blood supply to the bone, caused by traumatic stripping of attached soft tissues, and the risk of contamination add greatly to the risk of non-union and infection of the fracture. Healing of fractures at the junction of the middle and lower thirds of the tibia is compromised by the relatively poor blood supply to this region.

BONE

TIBIA

The tibia lies medial to the fibula and is exceeded in length only by the femur (Figs 83.2, 83.3). Its shaft is triangular in section and has expanded ends; a strong medial malleolus projects distally from the smaller distal end. The anterior border of the shaft is sharp and curves medially towards the medial malleolus. Together with the medial and lateral borders it defines the three surfaces of the bone. The exact shape and orientation of these surfaces show individual and racial variations.

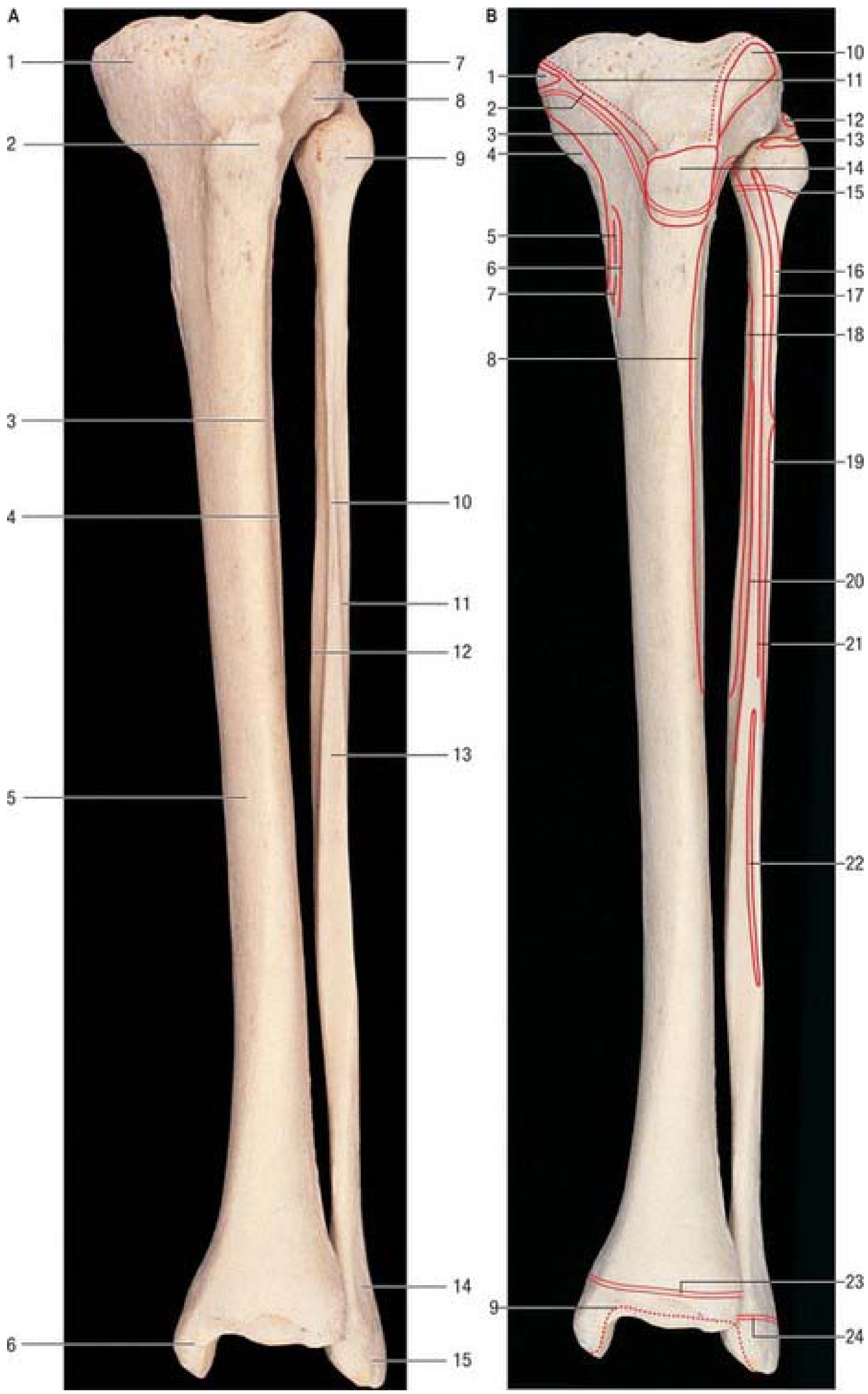
A
1
2
3
4
5
6
7
8
9
10
11
12
13
14
15
B
1
2
3
4
5
6
7
8
9
10
11
12
13
14
15
16
17
18
19
20
21
22
23
24

Fig. 83.2 **A**, Left tibia and fibula: anterior aspect. **B**, The muscle attachments. **A: 1**. Medial condyle. **2**. Tibial tuberosity. **3**. Anterior border of tibia. **4**. Interosseous border of tibia. **5**. Medial surface. **6**. Medial malleolus. **7**. Gerdy's tubercle. **8**. Lateral condyle. **9**. Head of fibula. **10**.

Interosseous border of fibula. **11**. Anterior border of fibula. **12**. Medial crest. **13**. Anterior surface. **14**. Subcutaneous area. **15**. Lateral malleolus. **B: 1**. Semimembranosus. **2**. Medial patellar retinaculum. **3**. Epiphysial line (growth plate). **4**. Medial collateral ligament. **5**. Gracilis. **6**. Sartorius. **7**. Semitendinosus. **8**. Tibialis anterior. **9**. Capsular attachment. **10**. Iliotibial tract. **11**. Capsular attachment. **12**. Lateral collateral ligament. **13**. Biceps femoris. **14**. Patellar tendon. **15**. Epiphysial line (growth plate). **16**. Fibularis longus. **17**. Extensor digitorum longus. **18**. Tibialis posterior. **19**. Fibularis brevis. **20**. Extensor hallucis longus. **21**. Extensor digitorum longus. **22**. Fibularis tertius. **23**. Epiphysial line (growth plate). **24**. Epiphysial line (growth plate).

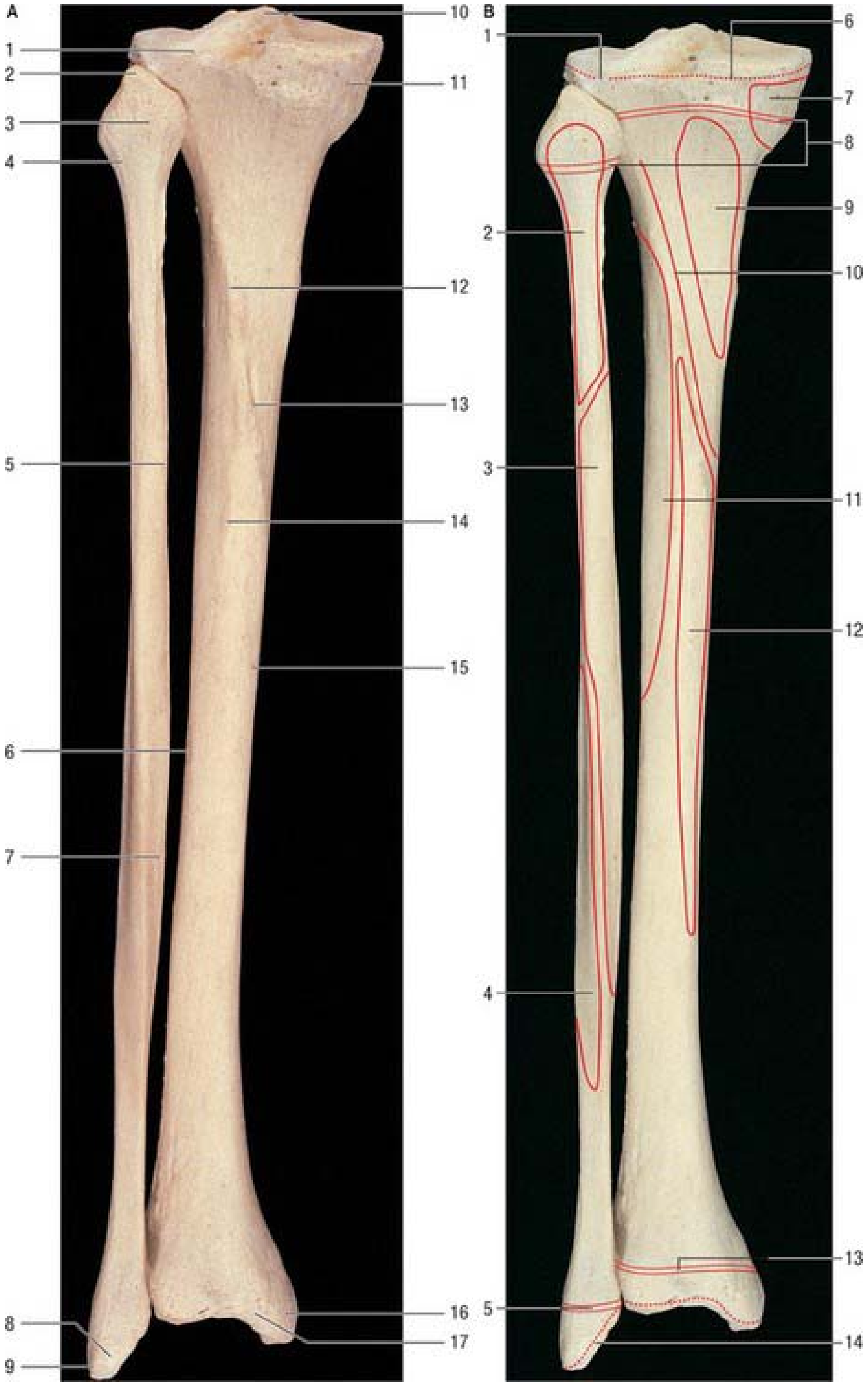
A
1
2
3
4
5
6
7
8
9
10
11
12
13
14
15
16
17
B
1
2
3
4
5
6
7
8
9
10
11
12
13
14

Fig. 83.3 **A**, Left tibia and fibula: posterior aspect. **B**, The muscle attachments. **A: 1**. Groove for tendon of popliteus. **2**. Styloid process (apex) of fibula. **3**. Head of fibula. **4**. Neck of fibula. **5**. Medial crest. **6**. Interosseous border of tibia. **7**. Posterior border. **8**. Groove for fibular

tendons. **9**. Lateral malleolus. **10**. Intercondylar eminence. **11**. Groove for semimembranosus attachment. **12**. Soleal line. **13**. Nutrient foramen. **14**. Vertical line. **15**. Medial border of tibia. **16**. Medial malleolus. **17**. Groove for tibialis posterior tendon. **B: 1**. Gap in capsule for popliteus tendon. **2**. Soleus. **3**. Flexor hallucis longus. **4**. Fibularis brevis. **5**. Epiphysial line (growth plate). **6**. Capsular attachment. **7**. Semimembranosus. **8**. Epiphysial lines (growth plates). **9**. Popliteus. **10**. Soleus. **11**. Tibialis posterior. **12**. Flexor digitorum longus. **13**. Epiphysial line (growth plate). **14**. Capsular attachment.

Proximal end

The expanded proximal end is a bearing surface for body weight, which is transmitted through the femur. It consists of medial and lateral condyles, an intercondylar area and the tibial tuberosity.

Condyles

The tibial condyles overhang the proximal part of the posterior surface of the shaft. Both condyles have articular facets on their superior surfaces that are separated by an irregular, non-articular intercondylar area. The condyles are visible and palpable at the sides of the patellar tendon, the lateral being more prominent. In the passively flexed knee the anterior margins of the condyles are palpable in fossae that flank the patellar tendon.

The fibular facet on the posteroinferior aspect of the lateral condyle faces distally and posterolaterally. The angle of inclination of the superior tibiofibular joint varies between individuals, and may be horizontal or oblique. Superomedial to it the condyle is grooved on its posterolateral aspect by the tendon of popliteus; a synovial recess intervenes between the tendon and bone. The anterolateral aspect of the condyle is separated from the lateral surface of the shaft by a sharp margin for the attachment of deep fascia. The distal attachment of the iliotibial tract makes a flat but definite marking, Gerdy's tubercle, on its anterior aspect. This tubercle, which is triangular and facet-like, is usually palpable.

The anterior condylar surfaces are continuous with a large triangular area whose apex is distal and formed by the tibial tuberosity. The lateral edge is a sharp ridge between the lateral condyle and lateral surface of the shaft. The condyles, their articular surfaces and the intercondylar area are described in Chapter 82.

Tibial tuberosity

The tibial tuberosity is the truncated apex of a triangular area where the anterior condylar surfaces merge. It projects only a little, and is divided into a distal rough and a proximal smooth region. The distal region is palpable and is separated from skin by the subcutaneous infrapatellar bursa. A line across the tibial tuberosity marks the distal limit of the proximal tibial growth plate (Fig. 83.2). The patellar tendon is attached to the smooth bone proximal to this, its superficial fibres reaching a rough area distal to the line. The deep infrapatellar bursa and fibroadipose tissue intervene between the bone and tendon proximal to its site of attachment. The latter may be marked distally by a somewhat oblique ridge, onto which the lateral fibres of the patellar tendon are inserted more distally than the medial fibres. (This knowledge is necessary to avoid damaging the tendon when sawing the tibia transversely just above the tibial tuberosity in a lateral to medial direction, e.g. in performing an osteotomy.) In habitual squatters a vertical groove on the anterior surface of the lateral condyle is occupied by the lateral edge of the patellar tendon in full flexion of the knee.

Shaft

The shaft is triangular in section and has (antero)medial, lateral and posterior surfaces separated by anterior, lateral (interosseous) and medial borders. It is narrowest at the junction of the middle and distal thirds, and expands gradually towards both ends. The anterior border descends from the tuberosity to the anterior margin of the medial malleolus and is subcutaneous throughout. Except in its distal fourth, where it is indistinct, it is a sharp crest. It is slightly sinuous, and turns medially in the distal fourth. The interosseous border begins distal and anterior to the fibular facet and descends to the anterior border of the fibular notch; it is indistinct proximally. The interosseous membrane is attached to most of its length, connecting tibia to fibula. The medial border descends from the anterior end of the groove on the medial condyle to the posterior margin of the medial malleolus. Its proximal and distal fourths are ill defined but its central region is sharp and distinct.

The anteromedial surface, between the anterior and medial borders, is broad, smooth and almost entirely subcutaneous. The lateral surface, between the anterior and interosseous borders, is also broad and smooth. It faces laterally in its proximal three-fourths and is transversely concave. Its distal fourth swerves to face anterolaterally, on account of the medial deviation of the anterior and distal interosseous borders. This part of the surface is somewhat convex. The posterior surface, between the interosseous and medial borders, is widest above, where it is crossed distally and medially by an oblique, rough soleal line. A faint vertical line descends from the centre of the soleal line for a short distance before becoming indistinct. A large vascular groove adjoins the end of the line and descends distally into a nutrient foramen. Deep fascia and, proximal to the medial malleolus, the medial end of the superior extensor retinaculum, are attached to the anterior border. Posterior fibres of the medial collateral ligament and slips of semimembranosus and the popliteal fascia are attached to the medial border proximal to the soleal line, and some fibres of soleus and the fascia covering the deep calf muscles are attached distal to the line. The distal medial border runs into the medial lip of a groove for the tendon of tibialis posterior. The interosseous membrane is attached to the lateral border, except at either end of this border. It is indistinct proximally where a large gap in the membrane transmits the anterior tibial vessels. Distally the border is continuous with the anterior margin of the fibular notch, to which the anterior tibiofibular ligament is attached.

The anterior part of the medial collateral ligament is attached to an area approximately 5 cm long and 1 cm wide near the medial border of the proximal medial surface. The remaining medial surface is subcutaneous and crossed obliquely by the long saphenous vein. Tibialis anterior is attached to the proximal two-thirds of the lateral surface. The distal third, devoid of attachments, is crossed in mediolateral order by the tendons of tibialis anterior (lying just lateral to the anterior border), extensor hallucis longus, the anterior tibial vessels and deep fibular nerve, extensor digitorum longus and fibularis tertius.

On the posterior surface, popliteus is attached to a triangular area proximal to the soleal line, except near the fibular facet. The popliteal aponeurosis, soleus and its fascia, and the deep transverse fascia are all attached to the soleal line: the proximal end of the line does not reach the interosseous border, and is marked by a tubercle for the medial end of the tendinous arch of soleus. Lateral to the tubercle, the posterior tibial vessels and tibial nerve descend on tibialis posterior. Distal to the soleal line, a vertical line separates the attachments of flexor digitorum longus and tibialis posterior. Nothing is attached to the distal quarter of this surface, but the area is crossed medially by the tendon of tibialis posterior travelling to a groove on the posterior aspect of the medial malleolus. Flexor digitorum longus crosses obliquely behind tibialis posterior; the posterior tibial vessels and nerve and flexor hallucis longus contact only the lateral part of the distal posterior surface.

Distal end

The slightly expanded distal end of the tibia has anterior, medial, posterior, lateral and distal surfaces. It projects inferomedially as the medial malleolus. The distal end of the tibia, when compared to the proximal end, is laterally rotated (tibial torsion). The torsion begins to develop *in utero* and progresses throughout childhood and adolescence till skeletal maturity is attained. Tibial torsion is approximately 30° in Caucasian and Asian populations, but is significantly greater in people of African origin (Eckhoff et al 1994). Some of the femoral neck anteversion seen in the newborn may persist in adult females: this causes the femoral shaft and knee to be internally rotated, and the tibia may develop a compensatory external torsion to counteract the tendency of the feet to turn inwards.

The smooth anterior surface projects beyond the distal surface, from which it is separated by a narrow groove. The capsule of the ankle joint is attached to an anterior groove near the articular surface. The medial surface is smooth and continuous above and below with the medial surfaces of the shaft and medial malleolus respectively: it is subcutaneous and visible. The posterior surface is smooth except where it is crossed near its medial end by a nearly vertical but slightly oblique groove, which is usually conspicuous and extends to the posterior surface of the malleolus. The groove is adapted to the tendon of tibialis posterior, which usually separates the tendon of flexor digitorum longus from the bone. More laterally, the posterior tibial vessels and nerve and flexor hallucis longus contact this surface. The lateral surface is the triangular fibular notch; its anterior and posterior edges project and converge proximally to the interosseous border. The floor of the notch is roughened proximally by a substantial interosseous ligament but is smooth distally and sometimes covered by articular cartilage. The anterior and posterior tibiofibular ligaments are attached to the corresponding edges of the notch. The distal surface articulates with the talus and is wider in front, concave sagittally and slightly convex transversely, i.e. it is saddle-shaped. Medially it continues into the malleolar articular surface which may extend into the groove that separates it from the anterior surface of the shaft. Such extensions, medial or lateral or both, are squatting facets, and they articulate with reciprocal talar facets in extreme dorsiflexion. These features have been used in the field of forensic medicine to identify the racial origins of skeletal material.

Medial malleolus

The short thick medial malleolus has a smooth lateral surface with a crescentic facet that articulates with the medial surface of the talus. Its anterior aspect is rough and its posterior aspect features the continuation of the groove from the posterior surface of the tibial shaft for the tendon of tibialis posterior. The distal border is pointed anteriorly, posteriorly depressed, and gives attachment to the deltoid ligament. The tip of the medial malleolus does not project as far distally as the tip of the lateral malleolus; the latter also being the more posteriorly located of the two malleoli. The capsule of the ankle joint is attached to the anterior surface of the medial malleolus, and the flexor retinaculum to its prominent posterior border.

Muscle attachments

The patellar tendon is attached to the proximal half of the tibial tuberosity. Semimembranosus is attached to the distal edge of the groove on the posterior surface of the medial condyle; a tubercle at the lateral end of the groove is the main attachment of the tendon of this muscle. Slips from the tendon of biceps femoris are attached to the lateral tibial condyle anteroproximal to the fibular facet. Proximal fibres of extensor digitorum longus and (occasionally) fibularis longus are attached distal to this area. Slips of semimembranosus are attached to the medial border of the shaft posteriorly, proximal to the soleal line. Some fibres of soleus attach to the posteromedial surface distal to the line. Semimembranosus is attached to the medial surface proximally, near the medial border, behind the attachment of the anterior part of the medial collateral ligament. Anterior to this area (in anteroposterior sequence), are the linear attachments of the tendons of sartorius, gracilis and semitendinosus: these rarely mark the bone. Tibialis anterior is attached to the proximal two-thirds of the lateral (extensor) surface. Popliteus is attached to the posterior surface in a triangular area proximal to the soleal line, except near the fibular facet. Soleus and its associated fascia are attached to the soleal line itself. Flexor digitorum longus and tibialis posterior are attached to the posterior surface distal to the soleal line, medial and lateral respectively to the vertical line (see above).

Vascular supply

The proximal end of the tibia is supplied by metaphysial vessels from the genicular arterial anastomosis. The nutrient foramen usually lies near the soleal line and transmits a branch of the posterior tibial artery; the nutrient vessel may also arise at the level of the popliteal bifurcation or as a branch from the anterior tibial artery. On entering the bone the nutrient artery divides into ascending and descending branches. The periosteal supply to the shaft arises from the anterior tibial artery and from muscular branches. The distal metaphysis is supplied by branches from the anastomosis around the ankle.

Innervation

The proximal and distal ends of the tibia are innervated by branches from the nerves that supply the knee joint and ankle joint respectively. The periosteum of the shaft is supplied by branches from the nerves that innervate the muscles attached to the tibia.

Ossification

The tibia ossifies from three centres, one in the shaft and one in each epiphysis. Ossification (Figs 83.2, 83.3, 83.4; see Fig. 82.6) begins in midshaft at about the seventh intrauterine week. The proximal epiphysial centre is usually present at birth: at approximately 10 years a thin anterior process from the centre descends to form the smooth part of the tibial tuberosity. A separate centre for the tuberosity may appear at about the twelfth year and soon fuses with the epiphysis. Distal strata of the epiphysial plate are composed of dense collagenous tissue in which the fibres are aligned with the patellar tendon. Exaggerated traction stresses may account for Osgood–Schlatter disease, where fragmentation of the epiphysis of the tuberosity occurs during adolescence and produces a painful swelling in the region of the tuberosity. Healing occurs once the growth plate fuses, leaving a bony protrusion. Prolonged periods of traction with the knee extended, both in children and adolescents, can lead to growth arrest of the anterior part of the proximal epiphysis, which results in bowing of the proximal tibia as the posterior tibia continues to grow. The proximal epiphysis fuses in the 16th year in females and the 18th in males. The distal epiphysial centre appears early in the first year and joins the shaft at about the 15th year in females and the 17th in males. The medial malleolus is an extension from the distal epiphysis and starts to ossify in the seventh year: it may have its own separate ossification centre. In 47% of females and 17% of males, an accessory ossification centre appears at the tip of the medial malleolus which fuses during the eighth year in females and the ninth in males: it should not be confused with an os subtibiale, which is a rare accessory bone found on the posterior aspect of the medial malleolus.

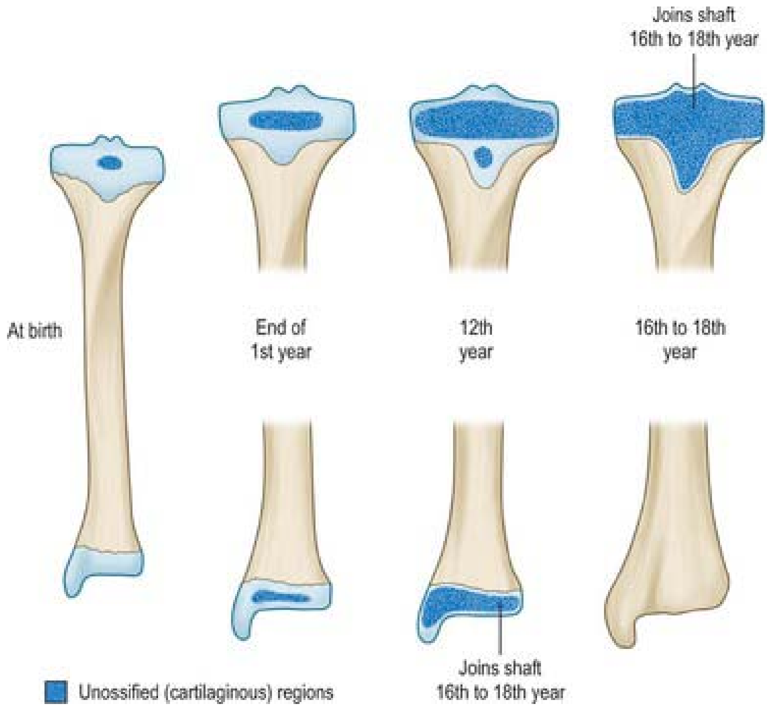
Joins shaft
16th to 18th year
At birth
End of
1st year
12th
year
16th to 18th
year
Joins shaft
16th to 18th year
Unossified (cartilaginous) regions

Fig. 83.4 Stages in the ossification of the tibia (not to scale).

FIBULA

The fibula (Figs 83.2, 83.3) is much more slender than the tibia and is not directly involved in transmission of weight. It has a proximal head, a narrow neck, a long shaft and a distal lateral malleolus. The shaft varies in form, being variably moulded by attached muscles: these variations may be confusing.

Head

The head of the fibula is irregular in shape and projects anteriorly, posteriorly, and laterally. A round facet on its proximomedial aspect articulates with a corresponding facet on the inferolateral surface of the lateral tibial condyle. It faces proximally and anteromedially and has an inclination which may vary among individuals from almost horizontal to an angle of up to 45°. A blunt apex (styloid process) projects proximally from the posterolateral aspect of the head and is often palpable approximately 2 cm distal to the knee joint. The fibular collateral ligament is attached in front of the apex, embraced by the main attachment of biceps femoris. The tibiofibular capsular ligament is attached to the margins of the articular facet. The common fibular nerve crosses posterolateral to the neck and can be rolled against bone at this location.

Shaft

The shaft has three borders and surfaces, each associated with a particular group of muscles. The anterior border ascends proximally from the apex of an elongated triangular area that is continuous with the lateral malleolar surface, to the anterior aspect of the fibular head. The posterior border, continuous with the medial margin of the posterior groove on the lateral malleolus, is usually distinct distally but often rounded in its proximal half. The interosseous border is medial to the anterior border and somewhat posterior. Over the proximal two-thirds of the fibular shaft the two borders approach each other, with the surface between the two being narrowed to 1 mm or less.

The lateral surface, between the anterior and posterior borders and associated with the fibular muscles, faces laterally in its proximal three-fourths. The distal quarter spirals posterolaterally to become continuous with the posterior groove of the lateral malleolus. The anteromedial (sometimes simply termed anterior, or medial) surface, between the anterior and interosseous borders, usually faces anteromedially but often directly anteriorly. It is associated with the extensor muscles. Though wide distally, it narrows in its proximal half and may become a mere ridge. The posterior surface, between the interosseous and posterior borders, is the largest and is associated with the flexor muscles. Its proximal two-thirds is divided by a longitudinal medial crest, separated from the interosseous border by a grooved surface that is directed medially. The remaining surface faces posteriorly in its proximal half; its distal half curves onto the medial aspect. Distally this area occupies the fibular notch of the tibia, which is roughened by the attachment of the principal interosseous tibiofibular ligament. The triangular area proximal to the lateral surface of the lateral malleolus is subcutaneous; muscles cover the rest of the shaft.

The anterior border is divided distally into two ridges that enclose a triangular subcutaneous surface. The anterior intermuscular septum is attached to its proximal three-fourths. The lateral end of the superior extensor retinaculum is attached distally on the anterior border of the triangular area and the lateral end of the superior fibular retinaculum is attached distally on the posterior margin of the triangular area. The interosseous border ends at the proximal limit of the rough area for the interosseous ligament. The interosseous membrane attached to this border does not reach the fibular head, which leaves a gap through which the anterior tibial vessels pass. The posterior border is proximally indistinct, and the posterior intermuscular septum is attached to all but its distal end. The medial crest is related to the fibular artery. A layer of deep fascia separating the tendon of tibialis posterior from flexor hallucis longus and flexor digitorum longus is attached to the medial crest.

Lateral malleolus

The distal end forms the lateral malleolus which projects distally and posteriorly (Figs 83.2, 83.3, 83.5). Its lateral aspect is subcutaneous while its posterior aspect has a broad groove with a prominent lateral border. Its anterior aspect is rough, round and continuous with the tibial inferior border. The medial surface has a triangular articular facet, vertically convex, its apex distal, which articulates with the lateral talar surface. Behind this facet is a rough malleolar fossa pitted by vascular foramina. The posterior tibiofibular ligament and, more distally, the posterior talofibular ligament, are attached in the fossa. The anterior talofibular ligament is attached to the anterior surface of the lateral malleolus; the calcaneofibular ligament is attached to the notch anterior to its apex. The tendons of fibularis brevis and longus groove its posterior aspect: the latter is superficial and covered by the superior fibular retinaculum.

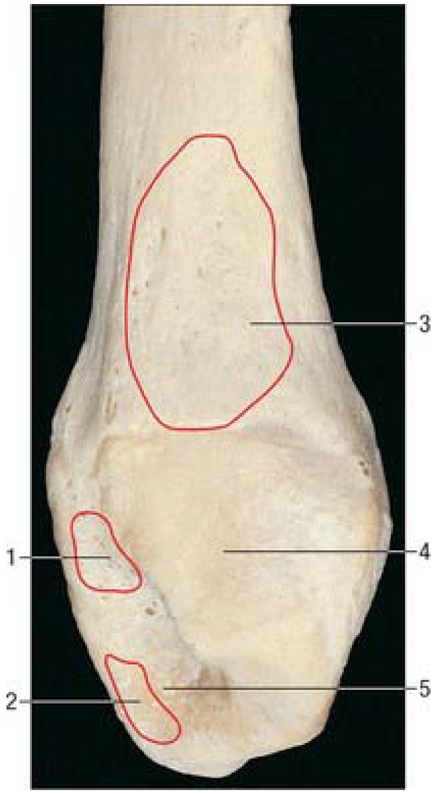

Fig. 83.5 Distal end of left fibula: medial aspect. **1**. Attachment of posterior tibiofibular ligament. **2**. Attachment of posterior talofibular

ligament. **3**. Area for attachment of interosseous tibiofibular ligament. **4**. Articular facet for talus. **5**. Malleolar fossa.

Muscle attachments

The main attachments of biceps femoris embrace the fibular collateral ligament in front of the apex (styloid process) of the fibular head. Extensor digitorum longus is attached to the head anteriorly, fibularis longus anterolaterally, and soleus posteriorly. Extensor digitorum longus, extensor hallucis longus and fibularis tertius are attached to the anteromedial (extensor) surface. Fibularis longus is attached to the whole width of the lateral (fibular) surface in its proximal third, but in its middle third only to its posterior part, behind fibularis brevis. The latter continues its attachment almost to the distal end of the shaft.

Muscle attachments to the posterior surface, which is divided longitudinally by the medial crest, are complex. Between the crest and interosseous border the posterior surface is concave. Tibialis posterior is attached throughout most (the proximal three-fourths) of this area; an intramuscular tendon may ridge the bone obliquely. Soleus is attached between the crest and the posterior border on the proximal fourth of the posterior surface; its tendinous arch is attached to the surface proximally. Flexor hallucis longus is attached distal to soleus on the posterior surface and almost reaches the distal end of the shaft.

Vascular supply

A little proximal to the midpoint of the posterior surface (14–19 cm from the styloid process), the fibular shaft is characterized by a nutrient foramen, directed distally, which receives a branch of the fibular artery. An appreciation of the detailed anatomy of the fibular artery in relation to the fibula is fundamental to the raising of osteofasciocutaneous free flaps incorporating segments of the bone. Free vascularized diaphysis grafts may also be taken on a fibular arterial pedicle. The proximal and distal ends receive metaphysial vessels from the arterial anastomoses at the knee and ankle respectively.

Innervation

The proximal and distal ends of the bone are supplied by branches of nerves that innervate the knee and superior tibiofibular joint and the ankle and inferior tibiofibular joints respectively. The periosteum of the shaft is supplied by branches from the nerves that innervate the muscles attached to the fibula.

Ossification

The fibula ossifies from three centres, one each for the shaft and the extremities (Fig. 83.6). The process begins in the shaft at about the eighth intrauterine week, in the distal end in the first year, and in the proximal end at about the third year in females and the fourth in males. The distal epiphysis unites with the shaft at about the 15th year in females and the 17th in males, whereas the proximal epiphysis does not unite until about the 17th year in females and the 19th in males.. An os subfibulare is an occasional and separate entity and lies posterior to the tip of the fibula, whereas the distal fibular apophysis lies anteriorly. An os retinaculi is rarely encountered; if present, it overlies the bursa of the distal fibula within the fibular retinaculum.

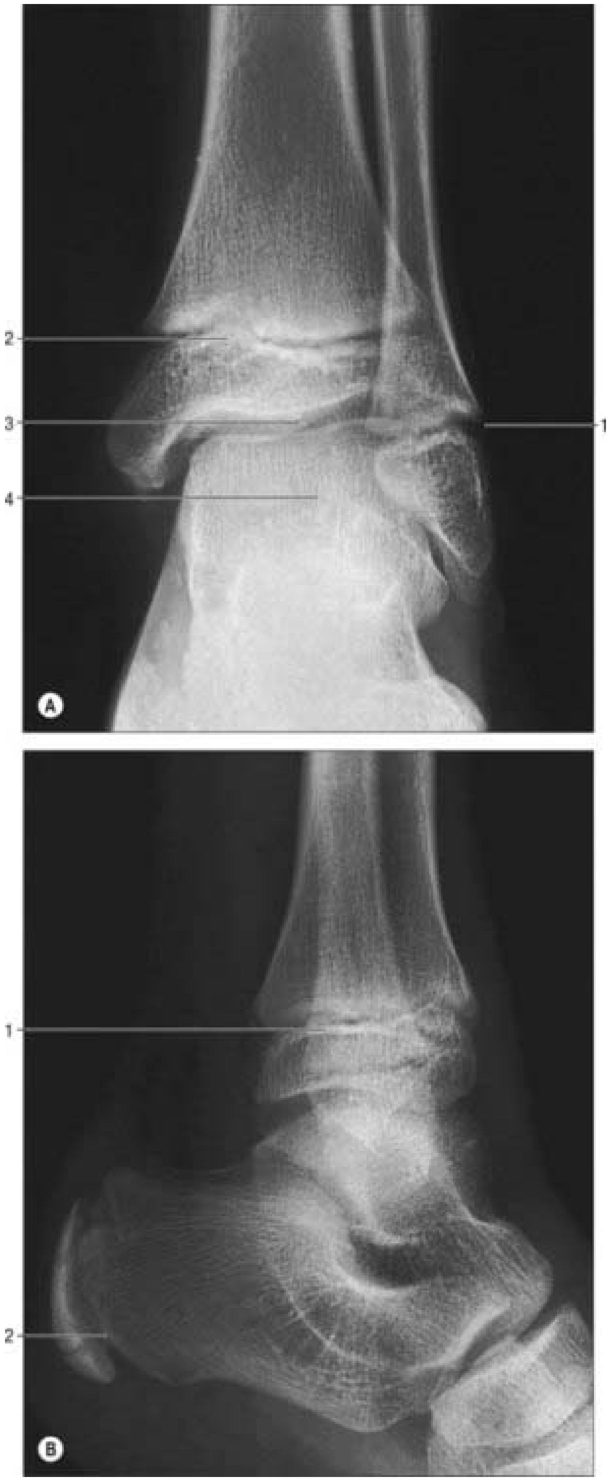

Fig. 83.6 Radiograph of an ankle in plantar flexion in a child aged 10 years. **A**, Oblique anteroposterior view. Note that the fibular growth plate is approximately at the level of the ankle joint. **1**. Inferior growth plate of fibula. **2**. Inferior growth plate of tibia. **3**. Ankle joint. **4**. Talus. **B**, Lateral

view. Note the trabecular pattern in the calcaneus. **1**. Tibial growth plate. **2**. Posterior growth plate of calcaneus.

MUSCLES

The muscles of the leg consist of an anterior group of extensor muscles, which produce dorsiflexion (extension) of the ankle; a posterior group of flexor muscles, which produce plantar flexion (flexion); and a lateral group of muscles, the fibulares, derived, embryologically, from the extensors. The greater bulk of the muscles in the calf is commensurate with the powerful propulsive role of the plantar flexors in walking and running.

ANTERIOR OR EXTENSOR COMPARTMENT

The anterior compartment contains muscles that dorsiflex the ankle when acting from above (Figs 83.7, 83.8, 83.9). When acting from below they pull the body forward on the fixed foot during walking. Two of the muscles, extensor digitorum longus and extensor hallucis longus, also extend the toes, and two muscles, tibialis anterior and fibularis tertius, have the additional actions of inversion and eversion respectively.

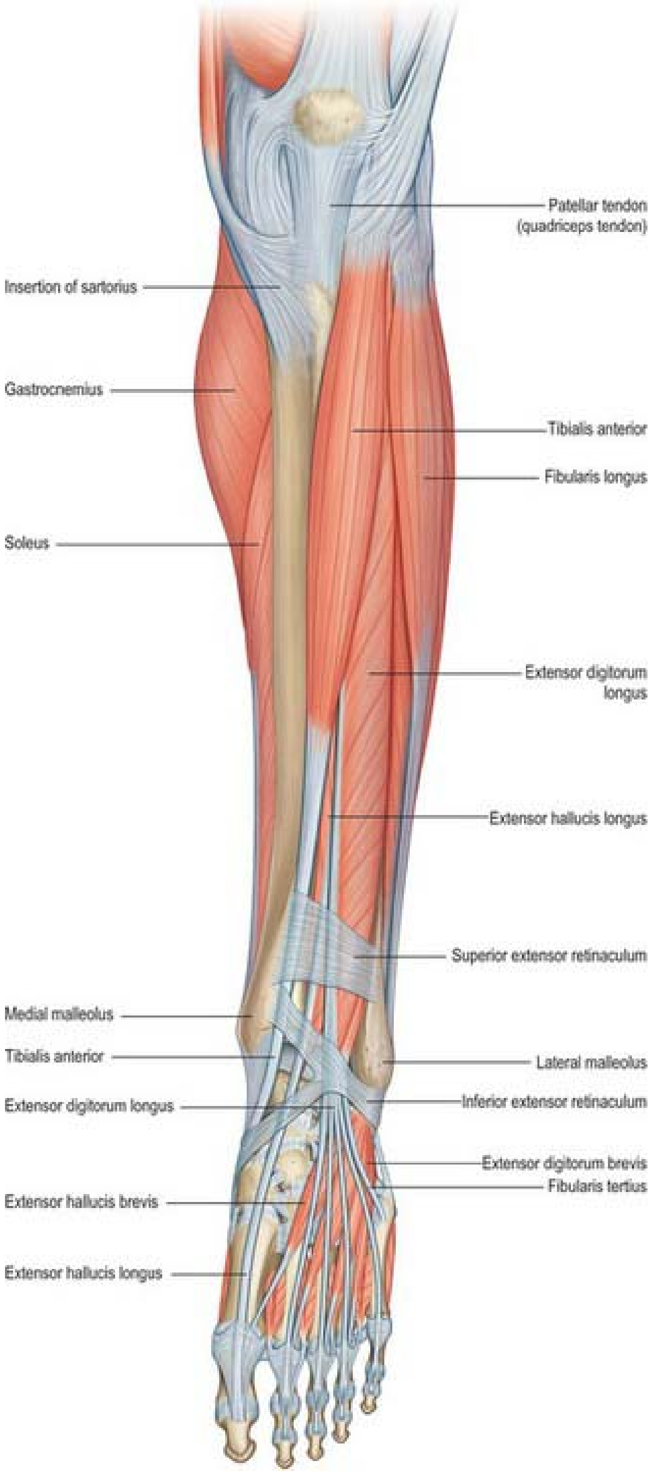
Patellar tendon (quadriceps tendon)
Insertion of sartorius
Gastrocnemius
Tibialis anterior
Fibularis longus
Soleus
Extensor digitorum longus
Extensor hallucis longus
Superior extensor retinaculum
Medial malleolus
Tibialis anterior
Lateral malleolus
Extensor digitorum longus
Inferior extensor retinaculum
Extensor digitorum brevis
Fibularis tertius
Extensor hallucis brevis
Extensor hallucis longus

Fig. 83.7 Muscles of the left leg: anterior aspect.

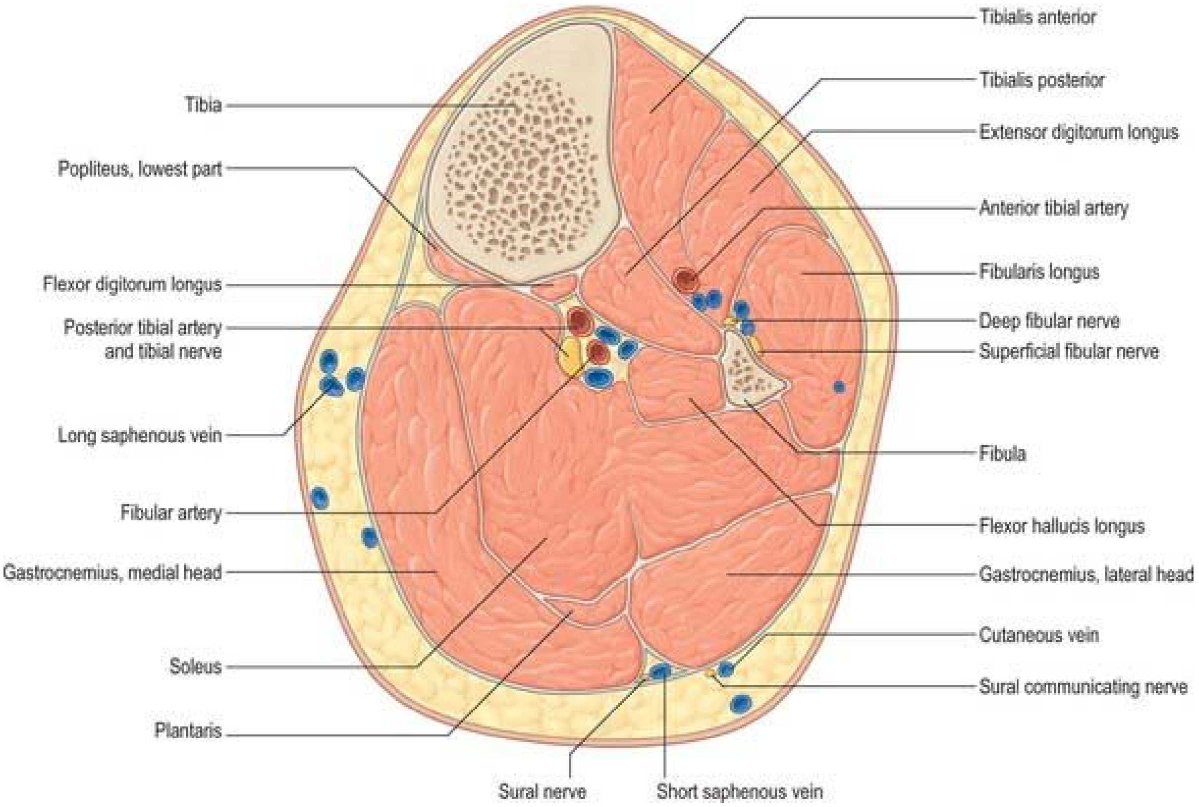
Tibialis anterior
Tibialis posterior
Extensor digitorum longus
Anterior tibial artery
Fibularis longus
Deep fibular nerve
Superficial fibular nerve
Fibula
Flexor hallucis longus
Gastrocnemius, lateral head
Cutaneous vein
Sural communicating nerve
Tibia
Popliteus, lowest part
Flexor digitorum longus
Posterior tibial artery
and tibial nerve
Long saphenous vein
Fibular artery
Gastrocnemius, medial head
Soleus
Plantaris
Sural nerve
Short saphenous vein

Fig. 83.8 Transverse (axial) section through the left leg, approximately 10 cm distal to the knee joint.

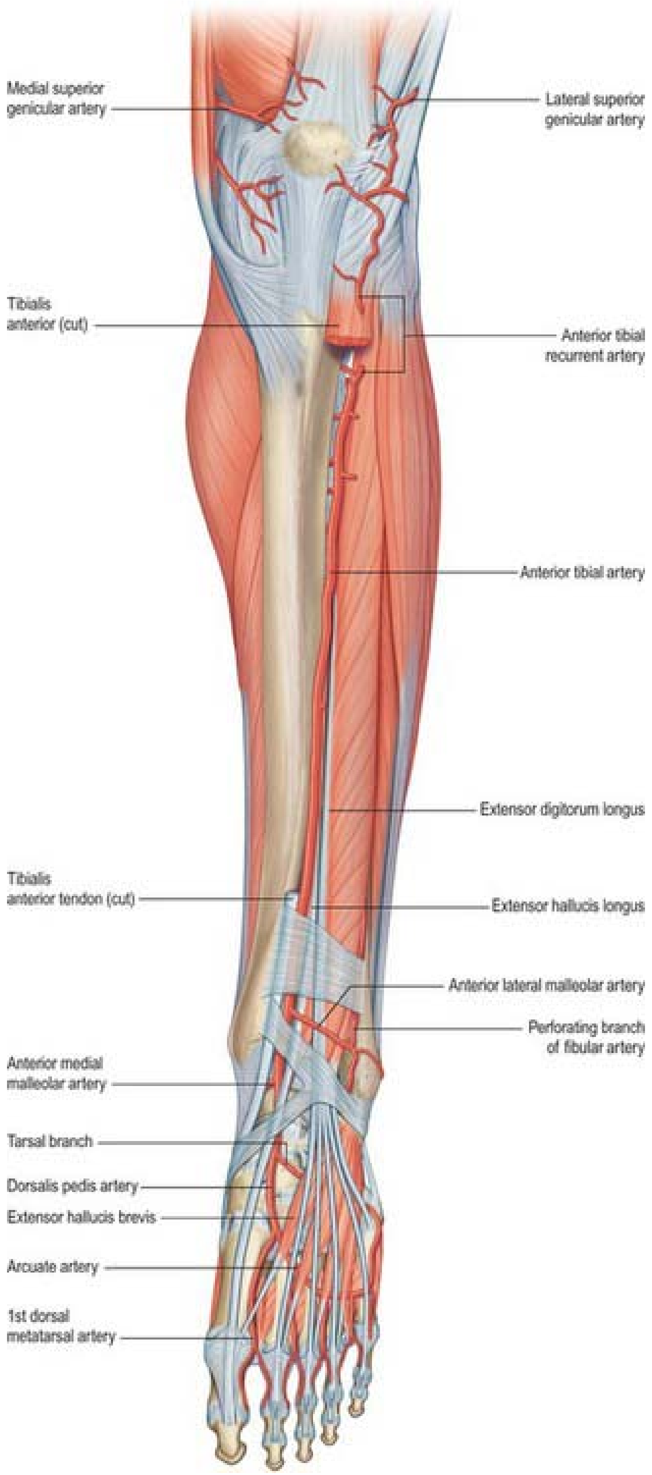
Medial superior genicular artery
Lateral superior genicular artery
Tibialis anterior (cut)
Anterior tibial recurrent artery
Anterior tibial artery
Extensor digitorum longus
Tibialis anterior tendon (cut)
Extensor hallucis longus
Anterior lateral malleolar artery
Perforating branch of fibular artery
Anterior medial malleolar artery
Tarsal branch
Dorsalis pedis artery
Extensor hallucis brevis
Arcuate artery
1st dorsal metatarsal artery

Fig. 83.9 The left anterior tibial and dorsalis pedis arteries. To expose the anterior tibial artery a large part of tibialis anterior has been excised and extensor hallucis longus is retracted laterally. Compare with **Fig. 83.7**.

Tibialis anterior

Attachments

Tibialis anterior is a superficial muscle and is therefore readily palpable lateral to the tibia. It arises from the lateral condyle and proximal half to two-thirds of the lateral surface of the tibial shaft; the adjoining anterior surface of the interosseous membrane; the deep surface of the deep fascia; and the intermuscular septum between itself and extensor digitorum longus. The muscle descends vertically and ends in a tendon on its anterior surface in the lower third of the leg. The tendon passes through the medial compartments of the superior and inferior retinacula, inclines medially, and is inserted into the medial and inferior surfaces of the medial cuneiform and the adjoining part of the base of the first metatarsal bone.

Attachments to the talus, first metatarsal head, base of the proximal phalanx of the hallux, and extensor retinaculum have been recorded.

Relations

Tibialis anterior overlaps the anterior tibial vessels and deep fibular nerve in the upper part of the leg. It lies on the tibia and interosseous membrane. Extensor digitorum longus and extensor hallucis longus lie laterally.

Vascular supply

The main body of tibialis anterior is supplied by a series of medial and anterior branches of the anterior tibial artery: the branches may occur in two columns. There is a proximal accessory supply from the anterior tibial recurrent artery. The tendon is supplied by the anterior medial malleolar artery and network, dorsalis pedis artery, medial tarsal arteries, and by the medial malleolar and calcaneal branches of the posterior tibial artery.

Innervation

Tibialis anterior is innervated by the deep fibular nerve, L4 and 5.

Actions

Tibialis anterior is a dorsiflexor of the ankle joint and invertor of the foot. It is most active when both movements are combined, as in walking. Its tendon can be seen through the skin lateral to the anterior border of the tibia and can be traced downwards and medially across the front of the ankle to the medial side of the foot. Tibialis anterior elevates the first metatarsal base and medial cuneiform and rotates their dorsal aspects laterally.

The muscle is usually quiescent in a standing subject, since the weight of the body acts through a vertical line that passes anterior to the ankle joints. Acting from below, it helps to counteract any tendency to overbalance backwards by flexing the leg forwards at the ankle. It has a role in supporting the medial longitudinal arch of the foot: although electromyographically detectable activity is minimal during standing, it is manifest during any movement that increases the arch, such as toe-off in walking and running.

Testing

Tibialis anterior can be seen to act when the foot is dorsiflexed against resistance.

Extensor hallucis longus

Attachments

Extensor hallucis longus lies between, and partly overlapped by, tibialis anterior and extensor digitorum longus. It arises from the middle two-fourths of the medial surface of the fibula, medial to extensor digitorum longus, and from the adjacent anterior surface of the interosseous membrane. Its fibres run distally and end in a tendon that forms on the anterior border of the muscle. The tendon passes deep to the superior extensor retinaculum and through the inferior extensor retinaculum, crosses anterior to the anterior tibial vessels to lie on their medial side near the ankle, and is inserted into the dorsal aspect of the base of the distal phalanx of the hallux. At the metatarsophalangeal joint a thin prolongation from each side of the tendon covers the dorsal surface of the joint. An expansion from the medial side of the tendon to the base of the proximal phalanx is usually present.

Extensor hallucis longus is sometimes united with extensor digitorum longus and may send a slip into the second toe.

Relations

The anterior tibial vessels and deep fibular nerve lie between extensor hallucis longus and tibialis anterior. Extensor hallucis longus lies lateral to the artery proximally, crosses it in the lower third of the leg, and is medial to it on the foot.

Vascular supply

Extensor hallucis longus is supplied by the anterior tibial artery via obliquely running branches, with a variable contribution from the perforating branch of the fibular artery. More distally, the tendon is supplied via the anterior medial malleolar artery and network, the dorsalis pedis artery, and the plantar arteries of the first ray via perforating branches.

Innervation

Extensor hallucis longus is innervated by the deep fibular nerve, L5.

Actions

Extensor hallucis longus extends the phalanges of the hallux and dorsiflexes the foot. When the hallux is actively extended, relatively little external force is required to overcome the extension of the distal phalanx, whereas considerable force is needed to overcome the extension of the proximal phalanx.

Testing

When the hallux is extended (dorsiflexed) against resistance, the tendon of extensor hallucis longus can be seen and felt on the lateral side of the tendon of tibialis anterior. This is a useful and very specific test of the integrity of the L5 spinal nerve.

Extensor digitorum longus

Attachments

Extensor digitorum longus arises from the inferior surface of the lateral condyle of the tibia, proximal three-quarters of the medial surface of the fibula, adjacent anterior surface of the interosseous membrane, deep surface of the deep fascia, anterior crural intermuscular septum, and from the fascial septum between itself and tibialis anterior. These origins form the walls of an osseo-aponeurotic tunnel. Extensor digitorum longus becomes tendinous at about the same level as tibialis anterior, and the tendon passes deep to the superior extensor retinaculum and within a loop of the inferior extensor retinaculum with fibularis tertius (see Figs 83.7, 84.2). It divides into four slips which run forward on the dorsum of the foot and are attached in the same way as the tendons of extensor digitorum in the hand. At the metatarsophalangeal joints the tendons to the second, third and fourth toes are each joined on the lateral side by a tendon of extensor digitorum brevis. The dorsal digital expansions thus formed on the dorsal aspects of the proximal phalanges, as in the fingers, receive contributions from the appropriate lumbrical and interosseous muscles. The expansion narrows as it approaches a proximal interphalangeal joint, and divides into three slips. These are a central (axial) slip, attached to the base of the middle phalanx, and two collateral (coaxial) slips, which reunite on the dorsum of the middle phalanx and are attached to the base of the distal phalanx.

The tendons to the second and fifth toes are sometimes duplicated, and accessory slips may be attached to metatarsals or to the hallux.

Relations

Extensor digitorum longus lies on the lateral tibial condyle, fibula, lower end of the tibia, ankle joint and extensor digitorum brevis. Tibialis anterior and extensor hallucis longus lie medially in the leg, and the fibular muscles lie laterally. In the upper part of the leg the anterior tibial vessels and deep fibular nerve lie between extensor digitorum longus and tibialis anterior; the nerve runs obliquely and medially beneath its upper part.

Vascular supply

The main blood supply to extensor digitorum longus is derived from anteriorly and laterally placed branches of the anterior tibial artery, supplemented distally from the perforating branch of the fibular artery. Proximally there may also be a supply from the lateral inferior genicular, popliteal or anterior tibial recurrent arteries. At the ankle and in the foot, the tendons are supplied by the anterior lateral malleolar artery and malleolar network, and by lateral tarsal, metatarsal, plantar and digital arteries.

Innervation

Extensor digitorum longus is innervated by the deep fibular nerve, L5, S1.

Actions

Extensor digitorum longus extends the lateral four toes. Acting synergistically with tibialis anterior, extensor hallucis longus and fibularis tertius, it is a dorsiflexor of the ankle. Acting with extensor hallucis longus it helps tighten the plantar aponeurosis.

Testing

The tendons of extensor digitorum longus can be seen when the toes are extended (dorsiflexed) against resistance.

Fibularis tertius

Attachments

Fibularis tertius (peroneus tertius) is a muscle unique to humans. It often appears to be part of extensor digitorum longus, and might be described as its ‘fifth tendon’. The muscle fibres of fibularis tertius arise from the distal third or more of the medial surface of the fibula, the adjoining anterior surface of the interosseous membrane, and the anterior crural intermuscular septum. The tendon passes deep to the superior extensor retinaculum and within the loop of the inferior extensor retinaculum alongside the extensor digitorum longus (see Figs 83.7, 84.2). It is inserted into the medial part of the dorsal surface of the base of the fifth metatarsal bone; a thin expansion usually extends forwards along the medial border of the shaft of the bone.

Relations

Fibularis tertius lies lateral to extensor digitorum longus.

Vascular supply

Fibularis tertius is supplied by the same vessels as extensor digitorum longus. In the foot it receives an additional supply from the termination of the arcuate artery and the fourth dorsal metatarsal artery.

Innervation

Fibularis tertius is innervated by the deep fibular nerve, L5, S1.

Actions

Electromyographic studies show that during the swing phase of gait (see Fig. 84.26), fibularis tertius acts with extensor digitorum longus and tibialis anterior to produce dorsiflexion of the foot, and with fibularis longus and fibularis brevis to effect eversion of the foot (Jungers et al 1993). This levels the foot and helps the toes to clear the ground, an action that improves the efficiency and enhances the economy of bipedal locomotion. Fibularis tertius is not active during the stance phase, a finding that is at variance with the suggestion that the muscle acts primarily to support the lateral longitudinal arch and to transfer the centre of pressure of the foot medially.

Testing

Fibularis tertius cannot be tested in isolation, but its tendon can sometimes be seen and felt when the foot is dorsiflexed against resistance.

LATERAL (FIBULAR OR PERONEAL) COMPARTMENT

The lateral compartment contains fibularis (peroneus) longus and fibularis (peroneus) brevis (Figs 83.7, 83.8). Both muscles evert the foot and are plantar flexors of the ankle, and both probably play a part in balancing the leg on the foot in standing and walking.

Fibularis longus

Attachments

Fibularis longus is the more superficial of the two muscles of the lateral compartment. It arises from the head and proximal two-thirds of the lateral surface of the fibula, the deep surface of the deep fascia, the anterior and posterior crural intermuscular septa, and occasionally by a few fibres from the lateral condyle of the tibia. The muscle belly ends in a long tendon that runs distally behind the lateral malleolus in a groove it shares with the tendon of fibularis brevis. The groove is converted into a canal by the superior fibular retinaculum, so that the tendon of fibularis longus, and that of fibularis brevis which lies in front of the longus tendon, are contained in a common synovial sheath. If the fibular retinaculum is ruptured by injury and fails to heal, the tendons can dislocate from the groove. The fibularis longus tendon runs obliquely forwards on the lateral side of the calcaneus, below the fibular trochlea and the tendon of fibularis brevis, and deep to the inferior fibular retinaculum. It crosses the lateral side of the cuboid and then runs under the cuboid in a groove that is converted into a canal by the long plantar ligament (see Fig. 84.19). It crosses the sole of the foot obliquely and is attached by two slips, one to the lateral side of the base of the first metatarsal bone and one to the lateral aspect of the medial cuneiform; occasionally a third slip is attached to the base of the second metatarsal bone. The tendon changes direction below the lateral malleolus and on the cuboid bone. At both sites it is thickened and at the second a sesamoid fibrocartilage (sometimes a bone, the os peroneum) is usually present. A second synovial sheath invests the tendon as it crosses the sole of the foot.

Relations

Proximally fibularis longus lies posterior to extensor digitorum longus and anterior to soleus and flexor hallucis longus. Distally in the leg it lies posterior to fibularis brevis. Between its attachments to the head and shaft of the fibula there is a gap through which the common fibular nerve passes.

Vascular supply of lateral compartment

Usually the predominant supply of the lateral compartment muscles is derived from superior and inferior branches of the anterior tibial artery; the superior is commonly the larger. There is also a lesser, variable, contribution from the fibular artery in the distal part of the leg. A fibular branch may replace the inferior branch of the anterior tibial artery; less commonly the fibular artery provides the main supply to the whole compartment. The upper part of fibularis longus is also supplied by the circumflex fibular artery, which is usually a branch of the anterior tibial artery. The companion artery to the common fibular nerve, a branch of the popliteal artery, provides a minor contribution proximally. Distally the tendons are supplied by the fibular perforating, anterior lateral malleolar, lateral calcaneal, lateral tarsal, arcuate, lateral and medial plantar arteries (see Fig. 84.9).

Innervation

Fibularis longus is innervated by the superficial fibular nerve, L5, S1.

Actions

There is little doubt that fibularis longus can evert the foot and plantar flex the ankle, and possibly act on the leg from its distal attachments. The oblique direction of its tendon across the sole would also enable it to support the longitudinal and transverse arches of the foot. With the foot off the ground, eversion is visually and palpably associated with increased prominence of both tendon and muscle. It is not clear to what extent this helps to maintain plantigrade contact of the foot in normal standing, but electromyographic records show little or no fibular activity under these conditions. Fibular activity is necessary to stand plantigrade with the legs crossed. Fibularis longus and brevis come strongly into action to maintain the concavity of the foot during toe-off and tip-toeing. If the subject deliberately sways to one side, the fibulares contract on that side, but their involvement in influencing postural interactions between the foot and leg remains uncertain.

Testing

Fibularis longus and brevis are tested together by eversion of the foot against resistance: the tendons can be identified laterally at the ankle and in the foot.

Fibularis brevis

Attachments

Fibularis brevis arises from the distal two-thirds of the lateral surface of the fibula, anterior to fibularis longus, and from the anterior and posterior crural intermuscular septa. It passes vertically downwards and ends in a tendon that passes behind the lateral malleolus together with, and anterior to, that of fibularis longus. The two tendons run deep to the superior fibular retinaculum in a common synovial sheath. The tendon of fibularis brevis then runs forwards on the lateral side of the calcaneus above the fibular trochlea and the tendon of fibularis longus, and is inserted into a tubercle on the lateral side of the base of the fifth metatarsal bone.

Relations

Anteriorly lie extensor digitorum longus and fibularis tertius. Fibularis longus and flexor hallucis longus are posterior. On the lateral surface of the calcaneus the tendons of fibularis longus and fibularis brevis occupy separate osteofascial canals formed by the calcaneus and the inferior fibular retinaculum; each tendon is enveloped in a separate distal prolongation of the common synovial sheath (see Fig. 84.2).

Vascular supply

See under fibularis longus.

Innervation

Fibularis brevis is innervated by the superficial fibular nerve, L5, S1.

Actions

Fibularis brevis may limit inversion of the foot and so relieve strain on the ligaments that are tightened by this movement (lateral part of interosseous talocalcaneal, lateral talocalcaneal and calcaneofibular ligaments). It participates in eversion of the foot and may help to steady the leg on the foot. See also under fibularis longus.

Testing

See under fibularis longus.

Variants of fibular muscles

Tendinous slips from fibularis longus may extend to the base of the third, fourth or fifth metatarsal bone, or to adductor hallucis. Fusion of fibularis longus and brevis has been reported, but is rare. Fibularis tertius is highly variable in its form and bulk but is seldom completely absent; its distal attachment may be to the fourth metatarsal rather than the fifth. Two other variant fibular muscles, arising from the fibula between fibularis longus and fibularis brevis, have been described. These are fibularis accessorius, whose tendon joins that of fibularis longus in the sole, and fibularis quartus, which arises posteriorly and inserts into the calcaneus or into the cuboid.

POSTERIOR (FLEXOR) COMPARTMENT

The muscles in the posterior compartment of the lower leg form superficial and deep groups, separated by the deep transverse fascia.

Superficial flexor group

The superficial flexors gastrocnemius, plantaris and soleus (Figs 83.8, 83.10; see Figs 82.2, 80.25) form the bulk of the calf. Gastrocnemius and soleus, collectively known as the triceps surae, constitute a powerful muscular mass whose main function is plantar flexion of the foot, although soleus in particular has an important postural role (see below). Their large size is a defining human characteristic, and is related to the upright stance and bipedal locomotion of the human. Gastrocnemius and plantaris act both on the knee and ankle joints; soleus on the latter alone.

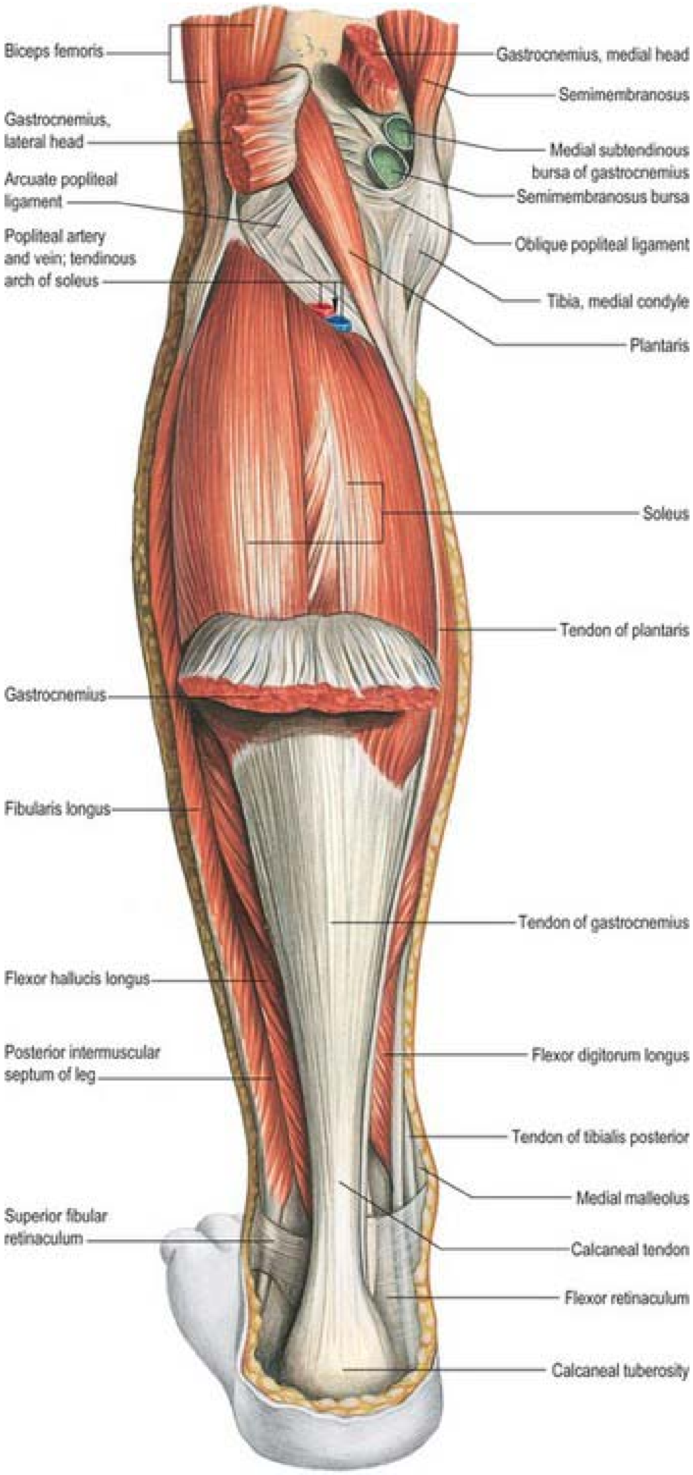
Biceps femoris
Gastrocnemius, medial head
Semimembranosus
Gastrocnemius, lateral head
Medial subtendinous bursa of gastrocnemius
Semimembranosus bursa
Arcuate popliteal ligament
Oblique popliteal ligament
Popliteal artery and vein; tendinous arch of soleus
Tibia, medial condyle
Plantaris
Soleus
Tendon of plantaris
Gastrocnemius
Fibularis longus
Tendon of gastrocnemius
Flexor hallucis longus
Flexor digitorum longus
Posterior intermuscular septum of leg
Tendon of tibialis posterior
Medial malleolus
Superior fibular retinaculum
Calcaneal tendon
Flexor retinaculum
Calcaneal tuberosity

Fig. 83.10 Muscles of the left leg, posterior aspect. Gastrocnemius partially removed.

(From Sobotta 2006.)

Gastrocnemius

Attachments

Gastrocnemius is the most superficial muscle of the group and forms the ‘belly’ of the calf. It arises by two heads, connected to the condyles of the femur by strong, flat tendons. The medial, larger, head is attached to a depression at the upper and posterior part of the medial condyle behind the adductor tubercle, and to a slightly raised area on the popliteal surface of the femur just above the medial condyle. The lateral head is attached to a recognizable area on the lateral surface of the lateral condyle and to the lower part of the corresponding supracondylar line. Both heads also arise from subjacent areas of the capsule of the knee joint. The tendinous attachments expand to cover the posterior surface of each head with an aponeurosis, from the anterior surface of which the muscle fibres arise. The fleshy part of the muscle extends to about midcalf. The muscle fibres of the larger medial head extend lower than those of the lateral head. As the muscle descends, the muscle fibres begin to insert into a broad aponeurosis that develops on its anterior surface; up to this point the muscular masses of the two heads remain separate. The aponeurosis gradually narrows and receives the tendon of soleus on its deep surface to form the calcaneal tendon (for a detailed description of the calcaneal tendon see Ch. 84).

On occasion the lateral head, or the whole muscle, is absent. A third head, arising from the popliteal surface of the femur, is sometimes present.

Relations

Proximally, the two heads of gastrocnemius form the lower boundaries of the popliteal fossa. The lateral head is partially overlaid by the tendon of biceps femoris, the medial head by semimembranosus. Over the rest of its length the muscle is superficial, and the two heads can easily be seen in the living subject. The superficial surface of the muscle is separated by the deep fascia from the short saphenous vein and the fibular communicating and sural nerves. The common fibular nerve crosses behind the lateral head of the muscle, partly under cover of biceps femoris. The deep surface lies posterior to the oblique popliteal ligament, popliteus, soleus, plantaris, popliteal vessels and the tibial nerve. A bursa, which communicates with the knee joint, is located anterior to the tendon of the medial head; if the bursa expands into the popliteal fossa it does so in the plane between the medial head of gastrocnemius and semimembranosus. The tendon of the lateral head frequently contains a fibrocartilaginous or bony sesamoid, the fabella, where it moves over the lateral femoral condyle. A sesamoid may occasionally occur in the tendon of the medial head. These can be seen on radiographs and may be mistaken for loose bodies in the knee joint.

Vascular supply

Each head of gastrocnemius is supplied by its own sural artery. These arteries are branches of the popliteal artery, and arise at variable levels, usually at the level of the tibiofemoral joint line. The medial sural artery almost always arises more proximally than the lateral: the medial may arise proximal to the joint line, the lateral sometimes distal to the line. Each sural artery enters the corresponding muscle head with its nerve of supply, the pedicle entering the muscle near its axial border at the level of the middle of the popliteal fossa. Medial or lateral gastrocnemius musculocutaneous flaps may be raised, each based on its neurovascular pedicle. Minor accessory sural arteries arise from the popliteal or from the superior genicular vessels.

The blood supply to the calcaneal tendon is described in Chapter 84.

Innervation

Gastrocnemius is innervated by the tibial nerve, S1 and 2.

Actions

The action of gastrocnemius is considered with soleus.

Testing

Gastrocnemius is tested by plantar flexion of the foot against resistance, in the supine position and with the knee extended.

Plantaris

Attachments

Plantaris arises from the lower part of the lateral supracondylar line and the oblique popliteal ligament. Its small fusiform belly is 7–10 cm long and ends in a long slender tendon which crosses obliquely, in an inferomedial direction, between gastrocnemius and soleus, then runs distally along the medial border of the calcaneal tendon and inserts on to the calcaneus just medial to the calcaneal tendon. Occasionally it ends by fusing with the tendon.

The muscle is sometimes double, and is absent in approximately 10% of cases. Occasionally, its tendon merges with the flexor retinaculum or with the fascia of the leg.

Vascular supply

Plantaris is supplied superficially by the lateral sural and popliteal arteries, and deeply by the lateral superior genicular artery. The distal tendon shares a blood supply with the calcaneal tendon.

Innervation

Plantaris is innervated by the tibial nerve, often from the ramus that supplies the lateral head of gastrocnemius, S1 and 2.

Actions

Plantaris is the lower limb equivalent of palmaris longus, and in many mammals is well developed and inserts directly or indirectly into the plantar aponeurosis. In man the muscle is almost vestigial and is normally inserted well short of the plantar aponeurosis, usually into the calcaneus. It is therefore presumed to act with gastrocnemius.

Soleus

Attachments

Soleus is a broad flat muscle situated immediately deep (anterior) to gastrocnemius. It arises from the posterior surface of the head and proximal quarter of the shaft of the fibula; the soleal line and the middle third of the medial border of the tibia; and from a fibrous band between the tibia and fibula (the soleal arch) that arches over the popliteal vessels and tibial nerve. This origin is aponeurotic: most of the muscular fibres arise from its posterior surface and pass obliquely to the tendon of insertion on the posterior surface of the muscle. Other muscle fibres arise from the anterior surface of the aponeurosis. They are short, oblique and bipennate in arrangement, and converge on a narrow, central intramuscular tendon that merges distally with the principal tendon. The latter gradually becomes thicker and narrower, and joins the tendon of gastrocnemius to form the calcaneal tendon. The muscle is covered proximally by gastrocnemius, but below midcalf it is broader than the tendon of gastrocnemius and is readily accessible on either side of the tendon.

An accessory part of the muscle is sometimes present distally and medially. It may be inserted into the calcaneal tendon, the calcaneus or the flexor retinaculum.

Relations

The superficial surface of soleus is in contact with gastrocnemius and plantaris. Its deep surface is related to flexor digitorum longus, flexor hallucis longus, tibialis posterior and the posterior tibial vessels and tibial nerve, from all of which it is separated by the deep transverse fascia of the leg.

Vascular supply

Soleus is supplied by two main arteries: the superior arises from the popliteal artery at about the level of the soleal arch, and the inferior from the proximal part of the fibular artery or sometimes from the posterior tibial artery. A secondary supply is derived from the lateral sural, fibular or posterior tibial vessels.

There is a venous plexus within the muscle belly that is important physiologically as part of the muscle pump complex (see below). Pathologically, it is a common site of deep vein thrombosis.

Innervation

Soleus is innervated by two branches from the tibial nerve, S1 and 2.

Actions

See under triceps surae.

Testing

Soleus is tested by plantar flexion of the foot against resistance in the supine position, with hip and knee flexed: the muscle belly can be palpated separately from those of gastrocnemius.

Actions of triceps surae

Gastrocnemius and soleus are the chief plantar flexors of the foot; gastrocnemius is also a flexor of the knee. The muscles are usually large and correspondingly powerful. Gastrocnemius provides force for propulsion in walking, running and leaping. Soleus, acting from below, is said to be more concerned with steadying the leg on the foot in standing. This postural role is also suggested by its high content of slow, fatigue-resistant (type 1) muscle fibres. In many adult mammals the proportion of this type of fibre in soleus approaches 100%. However, such a rigid separation of functional roles seems unlikely in man: soleus probably participates in locomotion, and gastrocnemius in posture. Nevertheless, the ankle joint is loose-packed in the erect posture, and since the weight of the body acts through a vertical line that passes anterior to the joint, a strong brace is required behind the joint to maintain stability. Electromyography shows that these forces are supplied mainly by soleus: during symmetrical standing, soleus is continuously active, whereas gastrocnemius is recruited only intermittently. The relative contributions of soleus and gastrocnemius to phasic activity of the triceps surae in walking have yet to be satisfactorily analysed.

Deep flexor group

The deep flexor group (Fig. 83.8, Fig. 83.11), lies beneath (anterior to) the deep transverse fascia, and consists of popliteus, which acts on the knee joint, and flexor digitorum longus, flexor hallucis longus and tibialis posterior, which all produce plantar flexion at the ankle in addition to their specific actions on joints of the foot and digits.

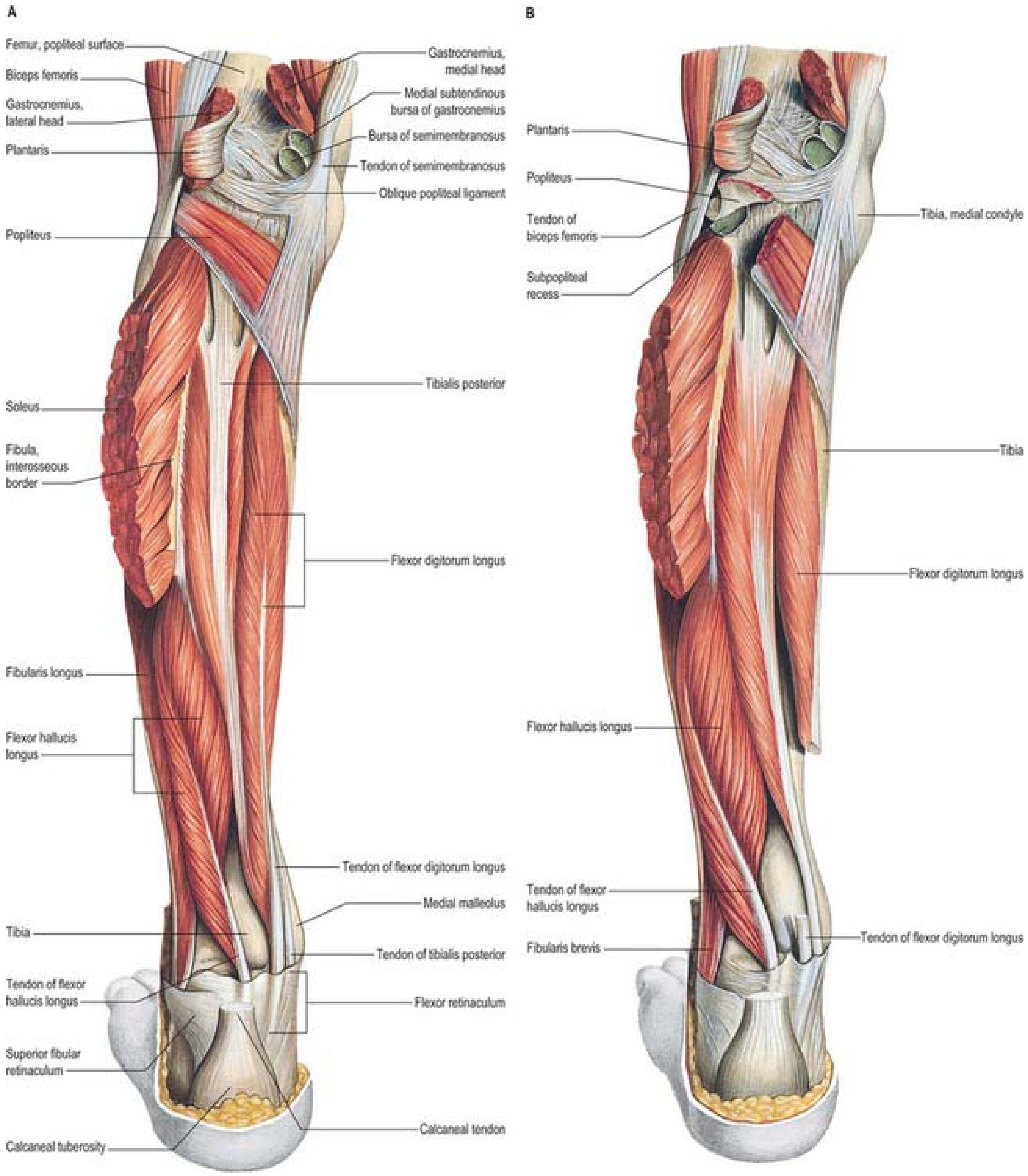
A
Femur, popliteal surface
Biceps femoris
Gastrocnemius, lateral head
Plantaris
Popliteus
Soleus
Fibula, interosseous border
Fibularis longus
Flexor hallucis longus
Tibia
Tendon of flexor hallucis longus
Superior fibular retinaculum
Calcaneal tuberosity
Gastrocnemius, medial head
Medial subtendinous bursa of gastrocnemius
Bursa of semimembranosus
Tendon of semimembranosus
Oblique popliteal ligament
Tibialis posterior
Flexor digitorum longus
Tendon of flexor digitorum longus
Medial malleolus
Tendon of tibialis posterior
Flexor retinaculum
Calcaneal tendon
B
Plantaris
Popliteus
Tendon of biceps femoris
Subpopliteal recess
Flexor hallucis longus
Tendon of flexor hallucis longus
Fibularis brevis
Tibia, medial condyle
Tibia
Flexor digitorum longus
Tendon of flexor digitorum longus

Fig. 83.11 Muscles of the left leg, posterior aspect. **A**, Superficial muscles extensively removed. **B**, Superficial muscles extensively removed,

popliteus sectioned and the tendon of flexor digitorum longus removed as it crosses the tendon of tibialis posterior.

(From Sobotta 2006.)

Popliteus

Popliteus is described in Chapter 82.

Flexor digitorum longus

Attachments

Flexor digitorum longus is thin and tapered proximally, but widens gradually as it descends. It arises from the posterior surface of the tibia medial to tibialis posterior from just below the soleal line to within 7 or 8 cm of the distal end of the bone; it also arises from the fascia covering tibialis posterior. The muscle ends in a tendon that extends along almost the whole of its posterior surface. The tendon gradually crosses tibialis posterior on its superficial aspect and passes behind the medial malleolus where it shares a groove with tibialis posterior, from which it is separated by a fibrous septum, i.e. each tendon occupies its own compartment lined by a synovial sheath. The tendon of flexor digitorum longus then curves obliquely forwards and laterally, in contact with the medial side of the sustentaculum tali, passes deep to the flexor retinaculum, and enters the sole of the foot on the medial side of the tendon of flexor hallucis longus (see Fig. 84.18). It crosses superficial to that tendon and receives a strong slip from it (and may also send a slip to it). The tendon of flexor digitorum longus then passes forward as four separate tendons, one each for the second to fifth toes, deep to the tendons of flexor digitorum brevis. After giving off the lumbricals, it passes through the fibrous sheaths of the lateral four toes. The tendons of flexor accessorius insert into the long flexor tendons of the second, third and fourth digits; flexor hallucis longus makes a variable contribution through the connecting slip mentioned above. The long flexor tendons of the lateral four digits are attached to the plantar surfaces of the bases of their distal phalanges; each passes between the slips of the corresponding tendon of flexor digitorum brevis at the base of the proximal phalanx.

A supplementary head of the muscle, flexor accessorius longus, with its own tendon, may arise from the fibula, tibia or deep fascia and insert into the main tendon or into flexor accessorius in the foot. It may send communicating slips to tibialis anterior or to flexor hallucis longus.

Relations

Flexor digitorum longus lies medial to flexor hallucis longus. In the leg its superficial surface is in contact with the deep transverse fascia, which separates it from soleus, and distally from the posterior tibial vessels and tibial nerve. Its deep surface is related to the tibia and to tibialis posterior. In the foot it is covered by abductor hallucis and flexor digitorum brevis and it crosses superficial to flexor hallucis longus.

Vascular supply

A series of transversely running branches of the posterior tibial artery enters the lateral border of flexor digitorum longus. There may be a secondary supply from fibular branches to flexor hallucis longus. The tendons are supplied by the vessels of the ankle and sole.

Innervation

Flexor digitorum longus is innervated by branches of the tibial nerve, L5, S1 and S2.

Actions

See under flexor hallucis longus.

Testing

Flexor digitorum longus is tested by flexing the toes against resistance. Aberrant function of flexor digitorum longus is implicated in toe deformities such as hammer toe, claw toe and mallet toe. It may be used in tendon transfer procedures for the surgical treatment of tibialis posterior tendon dysfunction.

Flexor hallucis longus

Attachments

Flexor hallucis longus arises from the distal two-thirds of the posterior surface of the fibula (except for the lowest 2.5 cm of this surface); the adjacent interosseous membrane and the posterior crural intermuscular septum; and from the fascia covering tibialis posterior, which it overlaps to a considerable extent. Its fibres pass obliquely down to a tendon that occupies nearly the whole length of the posterior aspect of the muscle. This tendon grooves the posterior surface of the lower end of the tibia, then, successively, the posterior surface of the talus and the inferior surface of the sustentaculum tali of the calcaneus (see Fig. 84.2B). Fibrous bands convert the grooves on the talus and calcaneus into a canal lined by a synovial sheath. In dancers, overuse causes thickening of the tendon in this region, and pain and even ‘triggering’ can occur (hallux saltans). In the sole of the foot, the tendon of flexor hallucis longus passes forward in the second layer (Ch. 84) like a bowstring. It crosses the tendon of flexor digitorum longus from lateral to medial, curving obliquely superior to it. At the crossing point (knot of Henry) it gives off two strong slips to the medial two divisions of the tendons of flexor digitorum longus and then crosses the lateral part of flexor hallucis brevis to reach the interval between the sesamoid bones under the head of the first metatarsal. It continues on the plantar aspect of the hallux, and runs in an osseo-aponeurotic tunnel to be attached to the plantar aspect of the base of the distal phalanx. The tendon is retained in position over the lateral part of flexor hallucis brevis by the diverging stems of the distal band of the medial intermuscular septum.

The distal extent of the muscle belly is a distinctive characteristic: in the posteromedial surgical approach to the ankle, flexor hallucis longus is readily identifiable by the fact that muscle fibres are evident almost to calcaneal level. In athletes the muscle fibres may be present so far inferiorly into the tendon as to be susceptible to impingement when pulled into the tunnel at the talus.

The connecting slip to flexor digitorum longus varies in size: it usually continues into the tendons for the second and third toes but is sometimes restricted to the second and occasionally extends to the fourth.

Relations

Soleus and the calcaneal tendon lie superficial (i.e. posterior) to flexor hallucis longus, separated by the deep transverse fascia. Deeply situated are the fibula, tibialis posterior, fibular vessels, distal part of the interosseous membrane and the talocrural joint. Laterally lie fibularis longus and fibularis brevis; medially are tibialis posterior, posterior tibial vessels and the tibial nerve. Flexor hallucis longus is an important surgical landmark at the ankle: staying lateral to it prevents injury to the neurovascular bundle.

Vascular supply

Flexor hallucis longus is supplied by numerous branches of the fibular artery. The tendon is supplied by arteries of the ankle and foot.

Innervation

Flexor hallucis longus is innervated by branches of the tibial nerve, L5, S1 and 2 (mainly S1).

Testing

Flexor hallucis longus is tested by flexion of the hallux against resistance.

Actions of deep digital flexors

Both flexor hallucis longus and flexor digitorum longus can act as plantar flexors but this action is weak compared with that of gastrocnemius and soleus. When the foot is off the ground, both muscles flex the phalanges of the toes, acting primarily on the distal phalanges. When the foot is on the ground and under load, they act synergistically with the small muscles of the foot and, especially in the case of flexor digitorum longus, with the lumbricals and interossei to maintain the pads of the toes in firm contact with the ground, enlarging the weightbearing area and helping to stabilize the heads of the metatarsal bones, which form the fulcrum on which the body is propelled forwards. Activity in the long digital flexors is minimal during quiet standing, so they apparently contribute little to the static maintenance of the longitudinal arch, but they become very active during toe-off and tip-toe movements.

Tibialis posterior

Attachments

Tibialis posterior is the most deeply placed muscle of the flexor group. At its origin it lies between flexor hallucis longus and flexor digitorum longus, and is overlapped by both, but especially by the former. Its proximal attachment consists of two tapered processes, separated by an angular interval that is traversed by the anterior tibial vessels. The medial process arises from the posterior surface of the interosseous membrane, except at its most distal part, and from a lateral area on the posterior surface of the tibia between the soleal line above and the junction of the middle and lower thirds of the shaft below. The lateral part arises from a medial strip of the posterior fibular surface in its upper two-thirds. The muscle also arises from the deep transverse fascia, and from the intermuscular septa that separate it from adjacent muscles. In the distal quarter of the leg its tendon passes deep to that of flexor digitorum longus, with which it shares a groove behind the medial malleolus, each enclosed in a separate synovial sheath. It then passes deep to the flexor retinaculum and superficial to the deltoid ligament to enter the foot. In the foot it is at first inferior to the plantar calcaneonavicular ligament, where it contains a sesamoid fibrocartilage. The tendon then divides into two. The more superficial and larger division, which is a direct continuation of the tendon, is attached to the tuberosity of the navicular, from which fibres continue to the inferior surface of the medial cuneiform. A tendinous band also passes laterally and a little proximally to the tip and distal margin of the sustentaculum tali. The deeper lateral division gives rise to the tendon of origin of the medial limb of flexor hallucis brevis, and then continues between this muscle and the navicular and medial cuneiform to end on the intermediate cuneiform and the bases of the second, third and fourth metatarsals; the slip to the fourth metatarsal is the strongest.

The slips to the metatarsals vary in number. Slips to the cuboid and lateral cuneiform may also occur. An additional muscle, the tibialis secundus, has been described running from the back of the tibia to the capsule of the ankle joint.

Relations

The superficial surface of tibialis posterior is separated from soleus by the deep transverse fascia, and is related to flexor digitorum longus, flexor hallucis longus, the posterior tibial vessels, the tibial nerve and the fibular vessels. The deep surface is in contact with the interosseous membrane, tibia, fibula and talocrural joint.

Vascular supply

Tibialis posterior is supplied by numerous branches of small calibre arising from the posterior tibial and fibular arteries. The tendon is supplied by arteries of the medial malleolar network and by the medial plantar artery.

Innervation

Tibialis posterior is innervated by the tibial nerve, L4 and 5.

Actions

Tibialis posterior is a powerful muscle which, on contraction, describes an excursion of only 1–2 cm. It is the principal invertor of the foot and also initiates elevation of the heel: it is responsible for the hindfoot varus that occurs during a single heel raise. By reason of its insertions into the cuneiform bones and the bases of the metatarsals, it has long been thought to assist in elevating the longitudinal arch of the foot, although electromyography shows that it is actually quiescent in standing. It is phasically active in walking, during which it probably acts with the intrinsic foot musculature and the lateral calf muscles to control the degree of pronation of the foot and the distribution of weight through the metatarsal heads. It is said that when the body is supported on one leg, the invertor action of tibialis posterior, exerted from below, helps to maintain balance by resisting any tendency to sway laterally.

Tibialis posterior is also important in the maintenance of the medial longitudinal arch. In overweight individuals with pes planus, unaccustomed activity can result in inflammation and degeneration of the terminal portion of the tendon, which leads to elongation of the tendon, attenuation of the spring ligament and progressive collapse of the medial longitudinal arch. As the excursion is so short, the muscle cannot compensate for the lengthening of its tendon, a failure that results in tibialis posterior tendon dysfunction.

Testing

Tibialis posterior is tested by asking the individual to perform a single heel raise and by moving the foot into a position of maximal plantar flexion and inversion against the resistance of the examiner’s hand: the tendon can be seen and felt just proximal to the medial malleolus.

VASCULAR SUPPLY

ARTERIES

Anterior tibial artery

The anterior tibial artery arises at the distal border of popliteus (Figs 83.9, 83.12, 83.13; see Figs 82.1, 82.4, 84.9). At first in the flexor compartment, it passes between the heads of tibialis posterior and through the oval aperture in the proximal part of the interosseous membrane to reach the extensor (anterior) compartment, passing medial to the fibular neck: it is vulnerable here during tibial osteotomy. Descending on the anterior aspect of the membrane it approaches the tibia and, distally, lies anterior to it. At the ankle the anterior tibial artery is midway between the malleoli, and it continues on the dorsum of the foot as the dorsalis pedis artery.

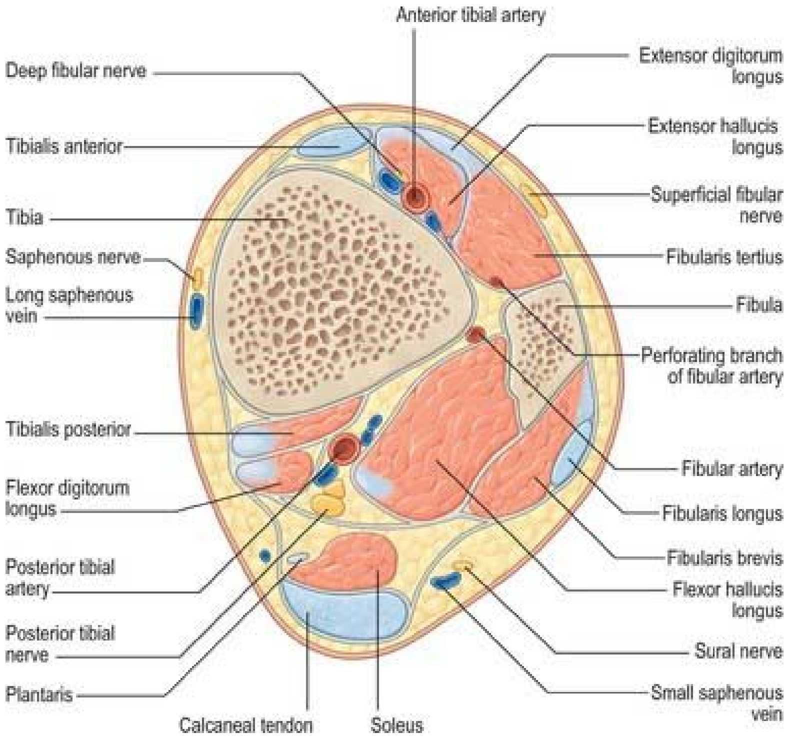
Anterior tibial artery
Deep fibular nerve
Extensor digitorum longus
Tibialis anterior
Extensor hallucis longus
Superficial fibular nerve
Tibia
Fibularis tertius
Saphenous nerve
Long saphenous vein
Fibula
Perforating branch of fibular artery
Tibialis posterior
Fibular artery
Flexor digitorum longus
Fibularis longus
Fibularis brevis
Posterior tibial artery
Flexor hallucis longus
Posterior tibial nerve
Sural nerve
Plantaris
Small saphenous vein
Calcaneal tendon
Soleus

Fig. 83.12 Transverse section through the left leg, approximately 6 cm proximal to the tip of the medial malleolus.

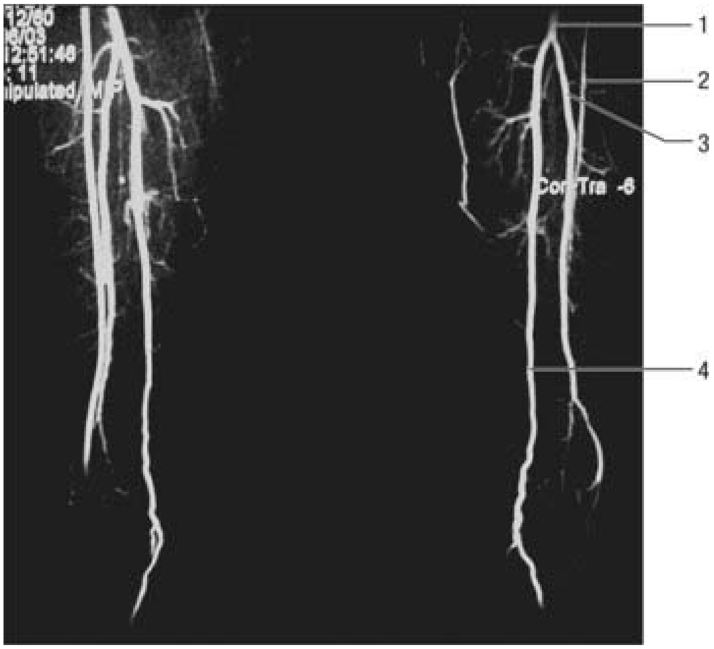

Fig. 83.13 Magnetic resonance angiogram of major branches of the popliteal artery. **1**. Tibiofibular trunk. **2**. Anterior tibial artery. **3**. Fibular artery. **4**. Posterior tibial artery.

(By courtesy of Dr Justin Lee, Chelsea and Westminster Hospital, London.)

The anterior tibial artery may, on occasion, be small but it is rarely absent. Its function may be replaced by perforating branches from the posterior tibial artery or by the perforating branch of the fibular artery. It occasionally deviates laterally, regaining its usual position at the ankle. It may also be larger than normal, in which case its territory of supply in the foot may be increased to include the plantar surface.

Relations

In its proximal two-thirds the anterior tibial artery lies on the interosseous membrane, and in its distal third it is anterior to the tibia and ankle joint. Proximally it lies between tibialis anterior and extensor digitorum longus, then between tibialis anterior and extensor hallucis longus. At the ankle it is crossed superficially from the lateral side by the tendon of extensor hallucis longus and then lies between this tendon and the first tendon of extensor digitorum longus. Its proximal two-thirds are covered by adjoining muscles and deep fascia, its distal third by the skin, fasciae and extensor retinacula. It is accompanied by venae comitantes. The deep fibular nerve, curling laterally round the fibular neck, reaches the lateral side of the artery where it enters the extensor region, is then anterior to the artery in the middle third of the leg, and becomes lateral again distally.

Branches

The named branches of the anterior tibial artery are the posterior and anterior recurrent tibial, muscular, perforating, and anterior medial and lateral malleolar arteries.

Posterior tibial recurrent artery

The posterior tibial recurrent artery is an inconstant branch that arises before the anterior tibial reaches the extensor compartment. It ascends anterior to popliteus with the recurrent nerve to that muscle, anastomosing with the inferior genicular branches of the popliteal artery. It supplies the superior tibiofibular joint.

Anterior tibial recurrent artery

The anterior tibial recurrent artery arises near the posterior tibial recurrent artery. It ascends in tibialis anterior, ramifies on the front and sides of the knee joint and joins the patellar network, anastomosing with the genicular branches of the popliteal and circumflex fibular arteries.

Muscular branches

Numerous branches supply the adjacent muscles. Some then pierce the deep fascia to supply the skin, while others traverse the interosseous membrane to anastomose with branches of the posterior tibial and fibular arteries.

Perforating branches

Most of the fasciocutaneous perforators pass along the anterior fibular fascial septum behind extensor digitorum longus before penetrating the deep fascia to supply the skin.

Anterior medial malleolar artery

The anterior medial malleolar artery arises approximately 5 cm proximal to the ankle. It passes posterior to the tendons of extensor hallucis longus and tibialis anterior medial to the joint, where it joins branches of the posterior tibial and medial plantar arteries.

Anterior lateral malleolar artery

The anterior lateral malleolar artery runs posterior to the tendons of extensor digitorum longus and fibularis tertius to the lateral side of the ankle and anastomoses with the perforating branch of the fibular artery and ascending branches of the lateral tarsal artery.

Posterior tibial artery

The posterior tibial artery begins at the distal border of popliteus, between the tibia and fibula (Fig. 83.13; see Figs 82.1, 82.4). It descends medially in the flexor compartment and divides under abductor hallucis, midway between the medial malleolus and the medial tubercle of the calcaneus, into the medial and lateral plantar arteries. The artery may be much reduced in length or in calibre: the fibular artery then takes over its distal territory of supply and may consequently be increased in size.

Relations

The posterior tibial artery is successively posterior to tibialis posterior, flexor digitorum longus, the tibia and the ankle joint. Proximally, gastrocnemius, soleus and the deep transverse fascia of the leg are superficial to the artery, and distally it is covered only by skin and fascia. It is parallel with and approximately 2.5 cm anterior to the medial border of the calcaneal tendon; terminally it is deep to the flexor retinaculum and abductor hallucis. The artery is accompanied by two veins and the tibial nerve. The nerve is at first medial to the artery but soon crosses behind it and subsequently becomes largely posterolateral.

Branches

The named branches of the posterior tibial artery are the circumflex fibular, nutrient, muscular, perforating, communicating, medial malleolar, calcaneal, lateral and medial plantar, and fibular arteries.

Circumflex fibular artery

The circumflex fibular artery, which sometimes arises from the anterior tibial artery, passes laterally round the neck of the fibula through the soleus to anastomose with the lateral inferior genicular, medial genicular and anterior tibial recurrent arteries. It supplies bone and articular structures.

Nutrient artery of the tibia

The nutrient artery of the tibia arises from the posterior tibial near its origin. After giving off a few muscular branches it descends into the bone immediately distal to the soleal line. It is one of the largest of the nutrient arteries.

Muscular branches

Muscular branches are distributed to the soleus and deep flexors of the leg.

Perforating branches

Approximately five fasciocutaneous perforators emerge between flexor digitorum longus and soleus and pass through the deep fascia, often accompanying the perforating veins that connect the deep and superficial venous systems. The arterial perforators then divide into anterior and posterior branches to supply periosteum and skin. These vessels are utilized in raising medial fasciocutaneous perforator flaps in the leg.

Communicating branch

The communicating branch runs posteriorly across the tibia approximately 5 cm above its distal end, deep to flexor hallucis longus, to join a communicating branch of the fibular artery.

Medial malleolar branches

The medial malleolar branches pass round the tibial malleolus to the medial malleolar network, which supplies the skin.

Calcaneal branches

Calcaneal branches arise just proximal to the terminal division of the posterior tibial artery. They pierce the flexor retinaculum to supply fat and skin behind the calcaneal tendon and in the heel, and muscles on the tibial side of the sole; the branches anastomose with medial malleolar arteries and calcaneal branches of the fibular artery.

Medial plantar artery

The medial plantar artery is the smaller terminal branch of the posterior tibial artery and passes distally along the medial side of the foot, medial to the medial plantar nerve (see Fig. 84.24). At first deep to abductor hallucis, it runs distally between this muscle and flexor digitorum brevis, and supplies both. Near the first metatarsal base, its size, already diminished by muscular branches, is further reduced by a superficial stem that divides to form three superficial digital branches. These accompany the digital branches of the medial plantar nerve and join the first to third plantar metatarsal arteries. The main trunk of the medial plantar artery then runs on to reach the medial border of the hallux, where it anastomoses with a branch of the first plantar metatarsal artery.

Lateral plantar artery

The lateral plantar artery is the larger terminal branch of the posterior tibial artery (see Fig. 84.24). It passes distally and laterally to the fifth metatarsal base, lateral to the lateral plantar nerve. (The medial and lateral plantar nerves lie between the corresponding plantar arteries.) Turning medially with the deep branch of the lateral plantar nerve, it reaches the interval between the first and second metatarsal bases, and unites with the dorsalis pedis artery to complete the plantar arch. As it passes laterally, it is first between the calcaneus and abductor hallucis, then between flexor digitorum brevis and flexor accessorius. Running distally to the fifth metatarsal base, it passes between flexor digitorum brevis and abductor digiti minimi and is covered by the plantar aponeurosis, superficial fascia and skin.

Branches

Muscular branches supply the adjoining muscles. Superficial branches emerge along the lateral intermuscular septum to supply the skin and subcutaneous tissue lateral in the sole. Anastomotic branches run to the lateral border of the foot, joining branches of the lateral tarsal and arcuate arteries. A calcaneal branch sometimes pierces abductor hallucis to supply the skin of the heel.

Fibular artery

The fibular artery arises from the posterior tibial artery approximately 2.5 cm distal to popliteus and passes obliquely to the fibula, descending along its medial crest either in a fibrous canal between tibialis posterior and flexor hallucis longus or within flexor hallucis longus (Figs 83.9, 83.12, 83.13; see Fig. 82.4). Reaching the inferior tibiofibular syndesmosis, it divides into calcaneal branches that ramify on the lateral and posterior surfaces of the calcaneus. Proximally it is covered by soleus and the deep transverse fascia between soleus and the deep muscles of the leg, and distally it is overlapped by flexor hallucis longus.

The fibular artery may branch high from the posterior tibial artery or may even branch from the popliteal artery separately, giving a true ‘trifurcation’. It may also branch more distally from the posterior tibial artery, sometimes 7 or 8 cm distal to popliteus. Its size tends to be inversely related to the size of the other arteries of the leg. It may be reduced in size but is more often enlarged, when it may join, reinforce or even replace the posterior tibial artery in the distal leg and foot. An enlarged perforating branch may replace the dorsalis pedis artery: the dorsalis pedis pulse will then be absent.

Branches

The fibular artery has muscular, nutrient, perforating, communicating and calcaneal branches.

Muscular branches

Multiple short branches supply soleus, tibialis posterior, flexor hallucis longus and the fibular muscles.

Nutrient artery

The nutrient artery branches from the main trunk approximately 7 cm from its origin and enters the fibula 14–19 cm from the styloid process.

Perforating branches

The main perforating branch traverses the interosseous membrane approximately 5 cm proximal to the lateral malleolus to enter the extensor compartment, where it anastomoses with the anterior lateral malleolar artery. Descending anterior to the inferior tibiofibular syndesmosis, it supplies the tarsus and anastomoses with the lateral tarsal artery. This branch is sometimes enlarged and may replace the dorsalis pedis artery.

Fasciocutaneous perforators from the lateral muscular branches pass along the posterior fibular fascial septum to penetrate the deep fascia and reach the skin. These vessels are utilized in raising fasciocutaneous posterolateral leg flaps (see below).

Communicating branch

The communicating branch connects to a communicating branch of the posterior tibial artery approximately 5 cm proximal to the ankle.

Calcaneal branches

Calcaneal (terminal) branches anastomose with the anterior lateral malleolar and calcaneal branches of the posterior tibial artery.

Perforator flaps in the knee and leg

The perforators which arise from the rich vascular anastomosis around the patella generally traverse the quadriceps tendon to supply the skin over the patella and the peri-patellar region (see Fig. 79.7). The skin flaps based on these perforators may be used as distally based or proximally based flaps to cover defects over the knee and popliteal region. The direct cutaneous branch of the popliteal artery and a superficial sural artery which accompanies the sural nerve provide additional perforators to the skin over the back of the knee. The posterior tibial artery gives out an average of ten perforators to the skin covering the anteromedial and posterior parts of the leg. In the upper third of the leg the perforating vessels are predominantly muscular and periosteocutaneous, while in the lower third, the perforating vessels are mainly direct subcutaneous types. They anastomose with the perforating branches of the anterior tibial artery anteriorly and fibular artery posteriorly. Inferiorly, the posterior tibial artery forms a rich anastomotic circle around the ankle joint with the fibular and anterior tibial arteries. Perforators from these vessels supply the calcaneal tendon and the overlying skin. The posterior tibial artery gives off three direct cutaneous perforators in the lower part of the leg: a distally based skin or adipo-fascial flap based on one of these perforators may be used to reconstruct a defect over the anterior or the posterior aspect of the lower leg. The anterior tibial artery gives off an average of six perforators which supply the antero-lateral part of the leg. They emerge in two longitudinal rows; one perforator is fairly large and accompanies the superficial fibular nerve. A small skin flap based on any one of these perforators may be used to cover small defects over the tibia and a neurocutaneous flap that includes the superficial fibular nerve may be used.

The fibular artery has an average of five perforators. A constant perforator pierces the deep fascia approximately 5 cm above the lateral malleolus and divides into an ascending and descending branch. A vascularized fibula graft based on the fibular artery is now the standard graft used in reconstruction of the mandible, while small fascio-cutaneous and adipo-fascial flaps based on the perforators of the fibular artery are useful in covering soft tissue defects over the heel and proximal part of the foot region.

DEEP AND SUPERFICIAL VENOUS SYSTEM

Posterior tibial veins

The posterior tibial veins accompany the posterior tibial artery (see Fig. 79.8). They receive tributaries from the calf muscles (especially from the venous plexus in the soleus) and connections from superficial veins and the fibular veins.

Fibular veins

The fibular veins, running with their artery, receive tributaries from soleus and from superficial veins.

Anterior tibial veins

The anterior tibial veins, continuations of the venae comitantes of the dorsalis pedis artery, leave the anterior compartment between the tibia and fibula and pass through the proximal end of the interosseous membrane. They unite with the posterior tibial veins to form the popliteal vein at the distal border of popliteus.

Long and short saphenous vein

The long and short saphenous veins are described on pages 1381 and 1409.

Venous disease

Chronic venous disease is common. Sustained overdistension of the superficial veins of the lower limb may result in the development of short, dilated venous segments or varicosities. Varicose veins can occur as a consequence of venous valve failure at the proximal end of the long saphenous vein at the saphenofemoral junction, or in the perforating veins that pass from the superficial system to the high-pressure deep veins. Varicose veins have thin walls and ‘leak’ red blood cells into adjacent soft tissues. As these cells are broken down haemosiderin is deposited in the soft tissues causing a brown pigmentation. This phenomenon, together with the fact that venous stasis produces oedema, renders the soft tissues of the leg unhealthy and prone to ulceration, particularly after minor trauma.

Acute venous disease occurs most commonly in the posterior compartment of the leg. This is attributed to the sluggish blood flow that occurs, at times, in the deep veins of the calf. This relative stasis predisposes to the formation of venous thrombi. Fragments of these thrombi may become dislodged and carried in the circulation to cause life-threatening pulmonary embolism. Blockage of the normal venous system may contribute to increased local venous pressure and oedema.

INNERVATION

Tibial nerve

The tibial nerve, the larger component of the sciatic nerve (see Chs 79 & 80), is derived from the ventral branches (anterior divisions) of the fourth and fifth lumbar and first to third sacral ventral rami. It descends along the back of the thigh and popliteal fossa to the distal border of popliteus. It then passes anterior to the arch of soleus with the popliteal artery and continues into the leg. In the thigh it is overlapped proximally by the hamstring muscles but it becomes more superficial in the popliteal fossa, where it is lateral to the popliteal vessels. At the level of the knee the tibial nerve becomes superficial to the popliteal vessels and crosses to the medial side of the artery. In the distal popliteal fossa it is overlapped by the junction of the two heads of gastrocnemius.

In the leg the tibial nerve descends with the posterior tibial vessels to lie between the heel and the medial malleolus. Proximally it is deep to soleus and gastrocnemius, but in its distal third is covered only by skin and fasciae, overlapped sometimes by flexor hallucis longus. At first medial to the posterior tibial vessels, it crosses behind them and descends lateral to them until it bifurcates. It lies on tibialis posterior for most of its course except distally, where it adjoins the posterior surface of the tibia. The tibial nerve ends under the flexor retinaculum by dividing into the medial and lateral plantar nerves.

Branches

The branches of the tibial nerve are articular, muscular, sural, medial calcaneal and medial and lateral plantar nerves. The medial and lateral plantar nerves are described in Chapter 84.

Articular branches

Articular branches to the knee joint accompany the superior, and inferior medial genicular arteries, and the middle genicular artery. They form a plexus with a branch from the obturator nerve and supply the oblique popliteal ligament. The branches accompanying the superior and inferior genicular arteries also supply the medial part of the capsule. Just before the tibial nerve bifurcates it supplies the ankle joint.

Muscular branches

Proximal muscular branches arise between the heads of gastrocnemius and supply gastrocnemius, plantaris, soleus and popliteus. The nerve to soleus enters its superficial aspect. The branch to popliteus descends obliquely across the popliteal vessels, curling round the distal border of the muscle to its anterior surface. It also supplies tibialis posterior, the proximal tibiofibular joint and the tibia, and gives off an interosseous branch that descends near the fibula to reach the distal tibiofibular joint.

Muscular branches in the leg, either independently or by a common trunk, supply soleus (on its deep surface), tibialis posterior, flexor digitorum longus and flexor hallucis longus. The branch to flexor hallucis longus accompanies the fibular vessels.

Sural nerve

The sural nerve descends between the heads of gastrocnemius, pierces the deep fascia proximally in the leg, and is joined at a variable level by the sural communicating branch of the common fibular nerve. Some authors term this branch the lateral sural cutaneous nerve, and the main trunk (from the tibial nerve) the medial sural cutaneous nerve. The sural nerve descends lateral to the calcaneal tendon, near the short saphenous vein, to the region between the lateral malleolus and the calcaneus and supplies the posterior and lateral skin of the distal third of the leg. It then passes distal to the lateral malleolus along the lateral side of the foot and little toe, supplying the overlying skin. It connects with the posterior femoral cutaneous nerve in the leg and with the superficial fibular nerve on the dorsum of the foot.

The surface marking at the ankle is a line parallel to the calcaneal tendon half-way between the tendon and the lateral malleolus. However, its position is variable and it is at risk from any surgery in this region. Rather like the radial nerve at the wrist, the sural nerve, when injured, has a tendency to form painful neuromas. The nerve is often used as an autologous peripheral nerve graft on the grounds that it is easily harvested, easily identified and exclusively sensory.

Lesions of the tibial nerve

The tibial nerve is vulnerable to direct injury in the popliteal fossa, where it lies superficial to the vessels at the level of the knee. It may be damaged in compartment syndrome that affects the deep flexor compartment of the calf. The nerve may be entrapped beneath the flexor retinaculum at the ankle, resulting in tarsal tunnel syndrome.

Common fibular nerve

The common fibular nerve (common fibular nerve) is approximately half the size of the tibial nerve and is derived from the dorsal branches of the fourth and fifth lumbar and first and second sacral ventral rami. It descends obliquely along the lateral side of the popliteal fossa to the fibular head, medial to biceps femoris. It lies between the bicipital tendon, to which it is bound by fascia, and the lateral head of gastrocnemius. The nerve then passes into the anterolateral compartment of the leg through a tight opening in the thick fascia overlying tibialis anterior. It curves lateral to the fibular neck, deep to fibularis longus, and divides into superficial and deep fibular nerves.

The course of the common fibular nerve can be indicated by a line drawn from the apex of the popliteal fossa, passing distally, medial to the biceps tendon, to the back of the head of the fibula, where the nerve can be rolled against the bone.

Branches

The common fibular nerve has articular and cutaneous branches and terminates as the superficial and deep fibular nerves.

Articular branches

There are three articular branches. Two accompany the superior and inferior lateral genicular arteries, and may arise in common. The third, the recurrent articular nerve, arises near the termination of the common fibular nerve. It ascends with the anterior recurrent tibial artery through tibialis anterior and supplies the anterolateral part of the knee joint capsule and the proximal tibiofibular joint.

Cutaneous branches

The two cutaneous branches, often from a common trunk, are the lateral sural and sural communicating nerves. The lateral sural nerve (lateral cutaneous nerve of the calf) supplies the skin on the anterior, posterior and lateral surfaces of the proximal leg. The sural communicating nerve arises near the head of the fibula and crosses the lateral head of gastrocnemius to join the sural nerve. It may descend separately as far as the heel.

Lesions of the common fibular nerve

The common fibular nerve is relatively unprotected as it traverses the lateral aspect of the neck of the fibula and is easily compressed at this site, e.g. by plaster casts or ganglia. The nerve may also become entrapped between the attachments of fibularis longus to the head and shaft of the fibula. Traction lesions can accompany dislocations of the lateral compartment of the knee, and are most likely to occur if the distal attachments of biceps and the ligaments that insert into the fibular head are avulsed, possibly with a small part of the fibular head: because the nerve is tethered to the bicipital tendon by dense fascia, it is pulled proximally. Patients with such injury present with a foot drop which is usually painless. Examination reveals weakness of ankle dorsiflexion, extensor hallucis longus and eversion of the foot, but inversion and plantar flexion are normal and the ankle reflex is preserved. Since the common fibular nerve divides at the fibular neck into the superficial and deep fibular nerves, injuries to the nerve at this level may damage either the main trunk or its branches.

Superficial fibular nerve

The superficial fibular nerve (superficial fibular nerve) begins at the bifurcation of the common fibular nerve. It lies at first deep to fibularis longus, then passes anteroinferiorly between fibularis longus and brevis and extensor digitorum longus and pierces the deep fascia in the distal third of the leg. It divides into a large medial dorsal cutaneous nerve and a smaller, more laterally placed, intermediate dorsal cutaneous nerve, usually after piercing the crural fascia, but sometimes while it is still deep to the fascia. As the nerve lies between the muscles it supplies fibularis longus, fibularis brevis and the skin of the lower leg. The deep course, i.e. the compartmental localization, and the peripheral digital distribution of the superficial fibular nerve are subject to considerable variation (see Kosinksi's classification; Kosinski 1926; Solomon et al 2001).

Branches

The medial dorsal cutaneous nerve passes in front of the ankle joint, and divides into two dorsal digital branches, one of which supplies the medial side of hallux and the other supplies the adjacent side of the second and third toes. It communicates with the saphenous and deep fibular nerves. The smaller intermediate branch traverses the dorsum of the foot laterally. It divides into dorsal digital branches that supply the contiguous sides of the third to fifth toes and the skin of the lateral aspect of the ankle, where it connects with the sural nerve. Both branches, especially the intermediate, are at risk during the placement of portal incisions for arthroscopy and during surgical approaches to the lateral malleolus. Branches of the superficial fibular nerve supply the dorsal skin of all the toes except that of the lateral side of the fifth toe (supplied by the sural nerve) and the adjoining sides of the great and second toes (supplied by the medial terminal branch of the deep fibular nerve). Some of the lateral branches of the superficial fibular nerve are frequently absent and are replaced by sural branches.

Accessory fibular nerves

An accessory superficial fibular nerve and an accessory deep fibular nerve have been described as anomalous branches of the superficial fibular nerve;

both are probably the product of atypical branching of the parent nerve deep to the crural fascia (see above).

Lesions of the superficial fibular nerve

A lesion of the superficial fibular nerve causes weakness of foot eversion and sensory loss on the lateral aspect of the leg that extends onto the dorsum of the foot. The nerve can be subject to entrapment as it penetrates the deep fascia of the leg and it may also be involved in compartment syndrome that affects the lateral compartment of the leg.

Deep fibular nerve

The deep fibular nerve (deep fibular nerve) begins at the bifurcation of the common fibular nerve, between the fibula and the proximal part of fibularis longus. It passes obliquely forwards deep to extensor digitorum longus to the front of the interosseous membrane and reaches the anterior tibial artery in the proximal third of the leg. It descends with the artery to the ankle, where it divides into lateral and medial terminal branches. As it descends, the nerve is first lateral to the artery, then anterior, and finally lateral again at the ankle.

Branches

The deep fibular nerve supplies muscular branches to tibialis anterior, extensor hallucis longus, extensor digitorum longus and fibularis tertius, and an articular branch to the ankle joint.

The lateral terminal branch crosses the ankle deep to extensor digitorum brevis, enlarges as a pseudoganglion and supplies extensor digitorum brevis. From the enlargement three minute interosseous branches supply the tarsal and metatarsophalangeal joints of the middle three toes.

The medial terminal branch runs distally on the dorsum of the foot lateral to the dorsalis pedis artery, and connects with the medial branch of the superficial fibular nerve in the first interosseous space. It divides into two dorsal digital nerves which supply adjacent sides of the great and second toes. Before dividing, it gives off an interosseous branch which supplies the first metatarsophalangeal joint. The deep fibular nerve may end as three terminal branches.

Lesions of the deep fibular nerve

Damage to the deep fibular nerve, e.g. in compartment syndrome that affects the anterior compartment of the leg, results in weakness of ankle dorsiflexion and extension of all toes; sensory impairment is confined to the first interdigital cleft.

Saphenous nerve

The saphenous nerve is described on page 1409.

REFERENCES

rmack GC, Lamberty BGH 1994; See Bibliography.

khoff DG, Kramer RC, Watkins JJ, Burke BJ, Alongi CA, Stamm ER, van Gerven DP. Variation in tibial torsion. *Clin Anat*. 1994;7:76-79.

ngers WL, Meldrum DJ, Stern JTJr. The functional and evolutionary significance of the human peroneus tertius muscle. *J Hum Evol*. 1993;25:377-386.

sinksi C. The course, mutual relations and distribution of the cutaneous nerves of the metazonal regions of the leg and foot. *J Anat Physiol*. 1926;60:274-297.

lomon LB, Ferris L, Tedman R, Henneberg M. Surgical anatomy of the sural and superficial fibular nerves with an emphasis on the approach to the lateral malleolus. *J Anat*. 2001;199:717-723.

ichael Salmon: Anatomic Studies. In: Taylor GI, Razaboni RM. *Book 1, Arteries of the Muscles of the Extremities and the Trunk*. St Louis: Quality Medical Publishing, 1994.

A translated, unpaid and edited version of a classic French text, first published in 1933. Now a major source-book in plastic surgery..

CHAPTER 84

Ankle and foot

The ankle joint (talocrural joint) is a diarthrodial articulation involving the distal tibia and fibula and the body of the talus: it is the only example in the human body of a true mortise joint. The human foot is a complex structure adapted to allow orthograde bipedal stance and locomotion and is the only part of the body which is in regular contact with the ground. There are 28 separate bones in the human foot, including the sesamoid bones of the first metatarsophalangeal joint and 31 joints, including the ankle joint.

SKIN AND SOFT TISSUE

SKIN

Vascular supply and lymphatic drainage

The skin around the ankle is supplied by anterior lateral and anterior medial malleolar arteries from the anterior tibial artery, medial malleolar branches from the posterior tibial artery, and fasciocutaneous perforators from the anterior and posterior tibial and fibular arteries. The main blood supply to the medial side of the heel is from the medial calcaneal branches of the lateral plantar artery passing through the flexor retinaculum; the skin of the lateral side of the heel is supplied by calcaneal branches of the fibular artery and the lateral tarsal artery. The arterial supply to the skin of the foot is rich and is derived from branches of the dorsalis pedis (the direct continuation of the anterior tibial artery), posterior tibial and fibular arteries. The skin covering the dorsum of the foot is supplied by the dorsalis pedis artery, and by its continuation, the first dorsal metatarsal artery, with smaller contributions from the anterior perforating branch of the fibular artery and the marginal anastomotic arteries on the medial and lateral borders of the foot. The plantar skin is supplied by perforating branches of the medial and lateral plantar arteries (the terminal branches of the posterior tibial artery). The skin of the forefoot is supplied by cutaneous branches of the common digital arteries.

Cutaneous venous drainage is via dorsal and plantar venous arches, which drain into medial and lateral marginal veins. On the plantar aspect, a superficial venous network forms an intradermal and subdermal mesh that drains to the medial and lateral marginal veins. Branches that accompany the medial and lateral plantar arteries arise from a deep venous network. Uniquely within the lower limb, venous flow in the foot is bidirectional. However, when valves are present, flow is from the plantar to the superficial dorsal system. From here, blood leaves the foot in the superficial and deep veins of the lower limb.

Superficial lymphatic drainage is via vessels that accompany the long saphenous vein medially and the short saphenous vein laterally and drain via the inguinal lymph nodes. Deep lymphatic vessels accompany the dorsalis pedis, posterior tibial and fibular arteries and pass via the popliteal lymph nodes.

Cutaneous innervation

The skin covering the ankle and foot is supplied by the fourth and fifth lumbar and first sacral spinal nerves (see Figs 79.18, 79.20). Innervation of the dorsum of the foot is provided medially by the saphenous nerve, centrally by the superficial fibular nerve and laterally by the sural nerve; the deep fibular nerve supplies the dorsum of the first web space. Dorsal branches of the medial and lateral plantar nerves supply the nail beds. The plantar aspect of the foot is supplied by the medial and lateral plantar nerves, which arise as terminal branches of the tibial nerve. The medial plantar nerve supplies sensation to the plantar aspect of the hallux, the second, the third and the medial half of the fourth toes. The lateral plantar nerve supplies the remaining lateral aspect of the fourth and the entire fifth toe. The heel is innervated by calcaneal branches of the tibial nerve. Injury to any of these nerves can lead to painful neuromata and loss of protective sensation. The sural nerve is especially prone to neuroma formation.

SOFT TISSUES

The tendons that cross the ankle joint are all deflected to some degree from a straight course, and must therefore be held down by retinacula and enclosed in synovial sheaths.

Retinacula at the ankle

In the vicinity of the ankle joint, the tendons of the muscles of the leg are bound down by localized, band-shaped thickenings of the deep fascia termed retinacula which collectively serve to prevent bowstringing of the underlying tendons. There are superior and inferior extensor retinacula, superior and inferior fibular retinacula, and a flexor retinaculum.

Extensor retinacula

Superior extensor retinaculum

The superior extensor retinaculum binds down the tendons of tibialis anterior, extensor hallucis longus, extensor digitorum longus and fibularis tertius immediately proximal to the anterior aspect of the talocrural joint (see Fig. 83.7; Fig. 84.1). The anterior tibial vessels and deep fibular nerve pass deep to the retinaculum and the superficial fibular nerve passes superficially. The retinaculum is attached laterally to the distal end of the anterior border of the fibula and medially to the anterior border of the tibia. Its proximal border is continuous with the fascia cruris, and dense connective tissue connects its distal border to the inferior extensor retinaculum. The tendon of tibialis anterior is the only extensor tendon that possesses a synovial sheath at the level of the superior extensor retinaculum.

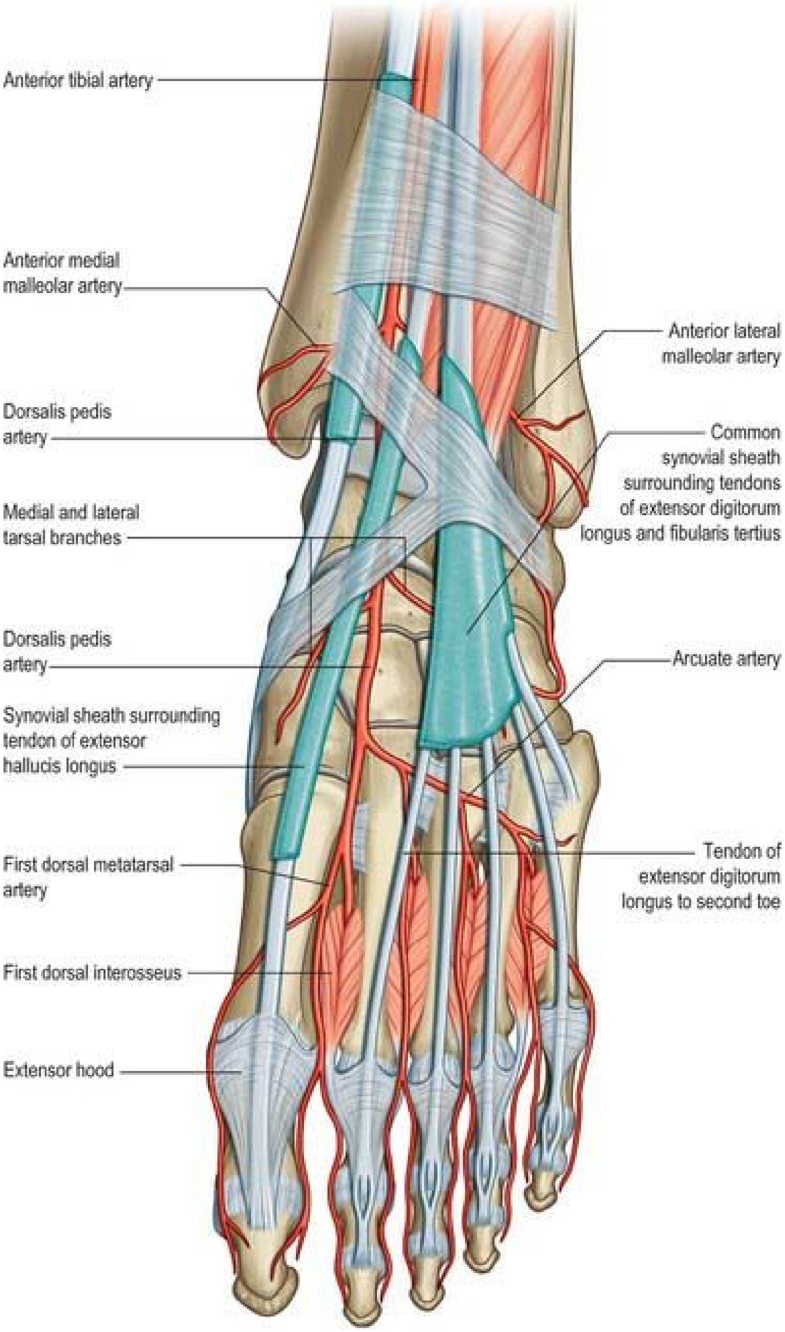
Anterior tibial artery
Anterior medial malleolar artery
Dorsalis pedis artery
Medial and lateral tarsal branches
Dorsalis pedis artery
Synovial sheath surrounding tendon of extensor hallucis longus
First dorsal metatarsal artery
First dorsal interosseus
Extensor hood
Anterior lateral malleolar artery
Common synovial sheath surrounding tendons of extensor digitorum longus and fibularis tertius
Arcuate artery
Tendon of extensor digitorum longus to second toe

Fig. 84.1 The synovial sheaths of the tendons of the ankle, anterior aspect.

(From Drake, Vogl and Mitchell 2005.)

Inferior extensor retinaculum

The inferior extensor retinaculum is a Y-shaped band lying anterior to the talocrural joint (see Fig. 83.7; Fig. 84.2A,B). The stem of the Y is at the lateral end, where it is attached to the upper surface of the calcaneus, in front of the sulcus calcanei. The band passes medially, forming a strong loop around the tendons of fibularis tertius and extensor digitorum longus (Fig. 84.2A). From the deep surface of the loop, a band passes laterally behind the interosseous talocalcaneal ligament and the cervical ligament and is attached to the sulcus calcanei. At the medial end of the loop, two diverging limbs extend medially to complete the ‘Y’ shape of the retinaculum. The proximal of the two limbs consists of two layers. The deep layer passes deep to the tendons of extensor hallucis longus and tibialis anterior, but superficial to the anterior tibial vessels and deep fibular nerve, to reach the medial malleolus. The superficial layer crosses superficial to the tendon of extensor hallucis longus and then adheres firmly to the deep one; in some cases it continues superficial to the tendon of tibialis anterior, before blending with the deep layer. The distal limb extends downwards and medially and blends with the plantar aponeurosis. It is superficial to the tendons of extensor hallucis longus and tibialis anterior, the dorsalis pedis artery and the terminal branches of the deep fibular nerve.

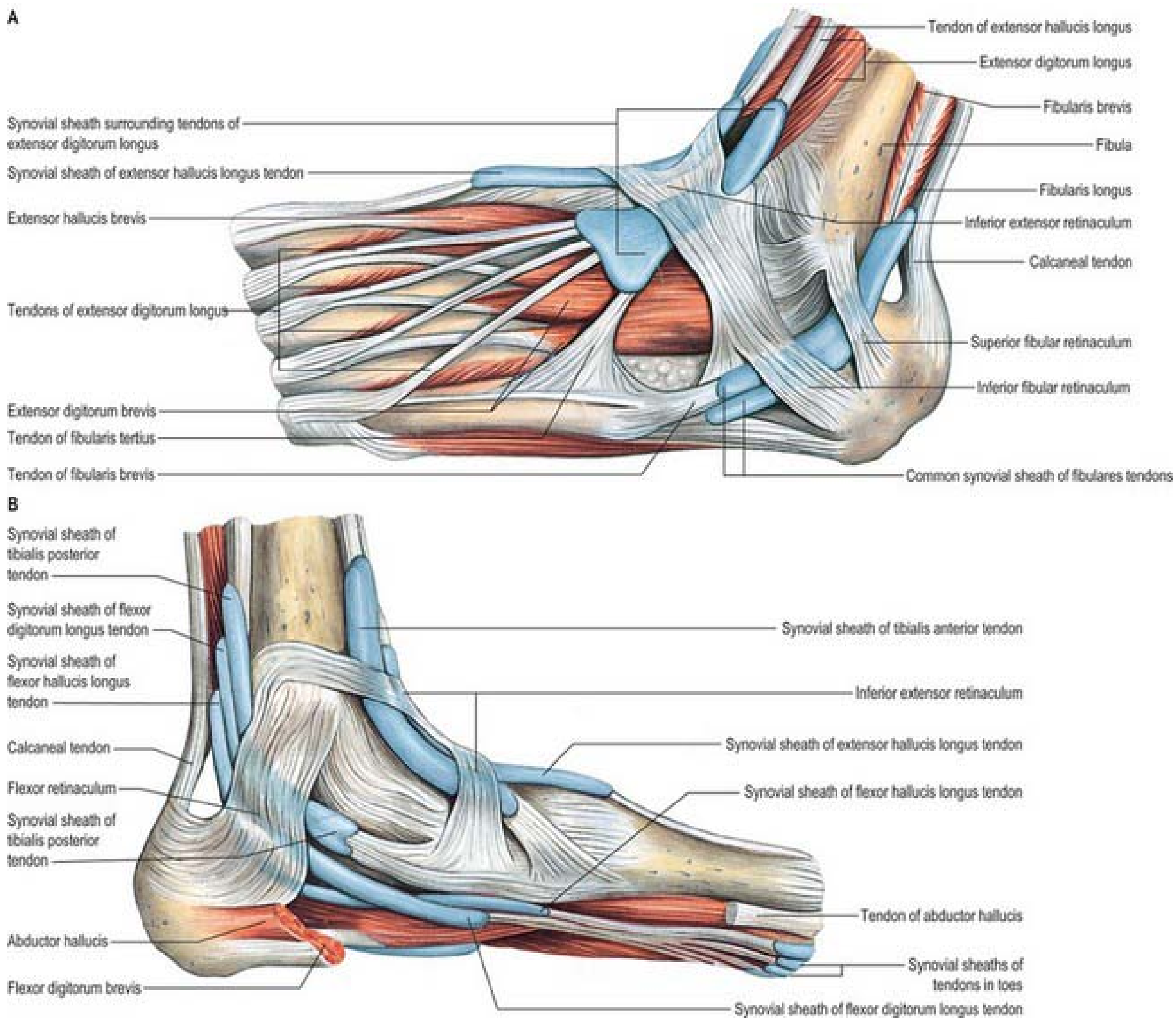
A
Tendon of extensor hallucis longus
Extensor digitorum longus
Fibularis brevis
Fibula
Fibularis longus
Inferior extensor retinaculum
Calcaneal tendon
Superior fibular retinaculum
Inferior fibular retinaculum
Common synovial sheath of fibulares tendons
Synovial sheath surrounding tendons of extensor digitorum longus
Synovial sheath of extensor hallucis longus tendon
Extensor hallucis brevis
Tendons of extensor digitorum longus
Extensor digitorum brevis
Tendon of fibularis tertius
Tendon of fibularis brevis
B
Synovial sheath of tibialis posterior tendon
Synovial sheath of flexor digitorum longus tendon
Synovial sheath of flexor hallucis longus tendon
Calcaneal tendon
Flexor retinaculum
Synovial sheath of tibialis posterior tendon
Abductor hallucis
Flexor digitorum brevis
Synovial sheath of tibialis anterior tendon
Inferior extensor retinaculum
Synovial sheath of extensor hallucis longus tendon
Synovial sheath of flexor hallucis longus tendon
Tendon of abductor hallucis
Synovial sheaths of tendons in toes
Synovial sheath of flexor digitorum longus tendon

Fig. 84.2 The synovial sheaths of the tendons of the ankle. **A**, Lateral aspect. **B**, Medial aspect.

(From Sobotta 2006.)

Flexor retinaculum

The flexor retinaculum is attached anteriorly to the tip of the medial malleolus, distal to which it is continuous with the deep fascia on the dorsum of the foot (Fig. 84.2B). From its malleolar attachment it extends posteroinferiorly to the medial process of the calcaneus and the plantar aponeurosis. Proximally, there is no clear demarcation between its border and the deep fascia of the lower leg, especially the deep transverse layer of the deep fascia. Distally, its border is continuous with the plantar aponeurosis, and many fibres of abductor hallucis are attached to it. The flexor retinaculum converts grooves on the tibia and calcaneus into canals for the tendons, and bridges over the posterior tibial vessels and tibial nerve. As these structures enter the sole they are, from medial to lateral, the tendons of tibialis posterior and flexor digitorum longus, the posterior tibial vessels, the tibial nerve and the tendon of flexor hallucis longus (see Fig. 84.14).

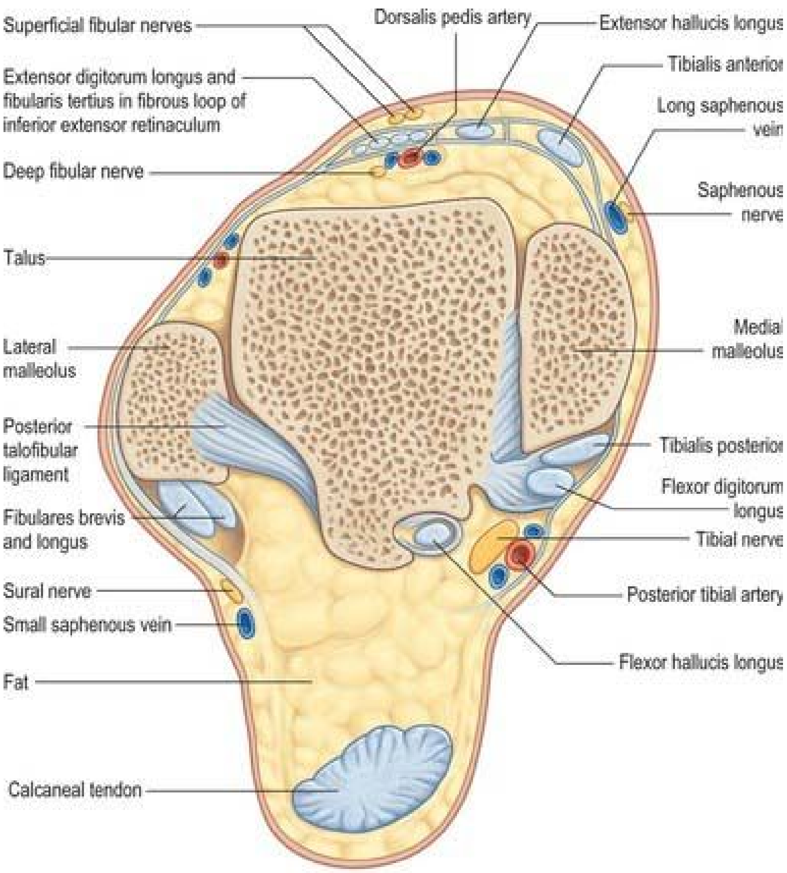
Superficial fibular nerves
Dorsalis pedis artery
Extensor hallucis longus
Tibialis anterior
Extensor digitorum longus and fibularis tertius in fibrous loop of inferior extensor retinaculum
Long saphenous vein
Deep fibular nerve
Saphenous nerve
Talus
Medial malleolus
Lateral malleolus
Posterior talofibular ligament
Tibialis posterior
Flexor digitorum longus
Fibulares brevis and longus
Tibial nerve
Sural nerve
Posterior tibial artery
Small saphenous vein
Flexor hallucis longus
Fat
Calcaneal tendon

Fig. 84.14 Transverse section through the lower part of the left ankle joint: superior aspect.

Fibular retinacula

The fibular retinacula are fibrous bands that retain the tendons of fibularis longus and brevis in position as these tendons cross the lateral aspect of the ankle region (Fig. 84.2A).

Superior fibular retinaculum

The superior fibular retinaculum is a short band which extends from the back of the lateral malleolus to the deep transverse fascia of the leg and the lateral surface of the calcaneus. Damage to the retinaculum can lead to instability of the fibular tendons.

Inferior fibular retinaculum

The inferior fibular retinaculum is continuous in front with the inferior extensor retinaculum, and is attached posteriorly to the lateral surface of the calcaneus. Some of its fibres are fused with the periosteum on the fibular trochlea (peroneal tubercle) of the calcaneus, forming a septum between the tendons of fibularis longus and brevis.

Synovial sheaths at the ankle

Anterior to the ankle, the sheath for tibialis anterior extends from the proximal margin of the superior extensor retinaculum to the interval between the diverging limbs of the inferior retinaculum (Figs 84.1, 84.2A,B). A common sheath encloses the tendons of extensor digitorum longus and fibularis tertius, starting just above the level of the malleoli, and reaching to the level of the base of the fifth metatarsal bone (Figs 84.1, 84.2A). The sheath for extensor hallucis longus starts at a level just distal to that for extensor digitorum longus and extends as far as the base of the first metatarsal bone (Figs 84.1, 84.2A,B).

Posteromedial to the ankle, the sheath for tibialis posterior starts approximately 4 cm above the medial malleolus and ends just proximal to the attachment of the tendon to the tuberosity of the navicular (Fig. 84.2B). The sheath for flexor hallucis longus starts at the level of the medial malleolus, and extends distally as far as the base of the first metatarsal bone (Fig. 84.2B). Occasionally, as a result of overuse, particularly in ballet dancers where balance on the tips of the toes en pointe involves sustained extreme plantar flexion of the ankle and first toe in the weight-bearing position, a fibrous nodule may develop in the tendon, just proximal to the tendon sheath.

This may result in the thickened tendon being caught intermittently in the sheath, causing pain and ‘triggering’ of the great toe, a condition referred to as hallux saltans. Surgical opening of the sheath may be required. In athletes, the muscle belly of flexor hallucis longus may be abnormally large and may extend more distally than usual; it can also catch at the opening of the sheath. The sheath for flexor digitorum longus starts slightly above the level of the medial malleolus and ends at the level of the navicular (Fig. 84.2B).

Posterolateral to the ankle, the tendons of fibularis longus and brevis are enclosed in a sheath that is single proximally but double distally (Fig. 84.2A). From the tip of the lateral malleolus it extends for about 4 cm both proximally and distally.

Plantar fascia

The plantar fascia or aponeurosis is composed of densely compacted collagen fibres orientated mainly longitudinally, but also transversely (Fig. 84.3). Its medial and lateral borders overlie the intrinsic muscles of the hallux and fifth toe respectively, while its dense central part overlies the long and short flexors of the digits.

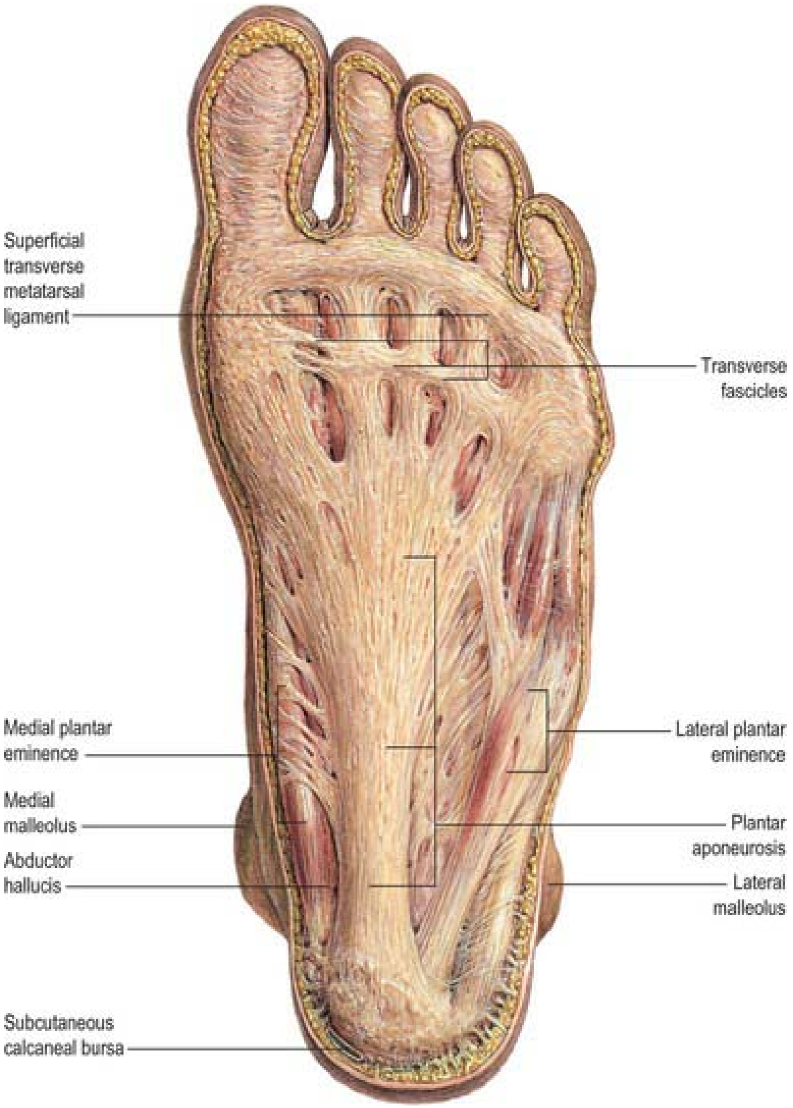
Superficial transverse metatarsal ligament
Transverse fascicles
Medial plantar eminence
Lateral plantar eminence
Medial malleolus
Plantar aponeurosis
Abductor hallucis
Lateral malleolus
Subcutaneous calcaneal bursa

Fig. 84.3 The plantar aponeurosis.

(From Sobotta 2006.)

The central part is the strongest and thickest. The fascia is narrow posteriorly, where it is attached to the medial process of the calcaneal tuberosity proximal to flexor digitorum brevis, and traced distally it becomes broader and somewhat thinner. Just proximal to the level of the metatarsal heads it divides into five bands, one for each toe. As these five digital bands diverge below the metatarsal shafts, they are united by transverse fibres (Fig. 84.3). Proximal, plantar and a little distal to the metatarsal heads and the metatarsophalangeal joints, the superficial stratum of each of the five bands is connected to the dermis by skin ligaments (retinacula cutis). These ligaments reach the skin of the ball of the foot proximal to, and in the floors of, the furrows that separate the toes from the sole: Dupuytren’s disease may involve these ligaments resulting in contractures of the affected digits. The deep stratum of each digital band of the aponeurosis yields two septa that flank the digital flexor tendons and separate them from the lumbricals and the digital vessels and nerves. These septa pass deeply to fuse with the interosseous fascia, the deep transverse metatarsal ligaments (which run between the heads of adjacent metatarsals), the plantar ligaments of the metatarsophalangeal joints, and the periosteum and fibrous flexor sheaths at the base of each proximal phalanx. Pads of fat develop in the webs between the metatarsal heads and the bases of the proximal phalanges; they cushion the digital nerves and vessels from adjoining tendinous structures and extraneous plantar pressures. Just distal to the metatarsal heads, a plantar interdigital ligament (superficial transverse metatarsal ligament) blends progressively with the deep aspect of the superficial stratum of the plantar aponeurosis where it enters the toes (Fig. 84.3). The central part of the plantar aponeurosis thus provides an intermediary structure between the skin and the osteoligamentous framework of the foot via numerous cutaneous retinacula and deep septa that extend to the metatarsals and phalanges. The central part is also continuous with the medial and lateral parts: at the junctions, two intermuscular septa, medial and lateral, extend in oblique vertical planes between the medial, intermediate and lateral groups of plantar muscles to reach bone. Thinner horizontal intermuscular septa, derived from the vertical intermuscular septa, pass between the muscle layers.

The lateral part of the plantar aponeurosis, which covers abductor digiti minimi, is thin distally and thick proximally, where it forms a strong band, sometimes containing muscle fibres, between the lateral process of the calcaneal tuberosity and the base of the fifth metatarsal bone. It is continuous medially with the central part of the aponeurosis, and with the fascia on the dorsum of the foot around its lateral border. The medial part of the plantar aponeurosis, which covers abductor hallucis, is thin. It is continuous proximally with the flexor retinaculum, medially with the fascia dorsalis pedis, and laterally with the central part of the plantar aponeurosis.

Fascial compartments of the foot

There are four main compartments of the plantar aspect of the foot (Jones 1949) (Fig. 84.4). The medial compartment contains abductor hallucis and flexor hallucis brevis, and is bounded inferiorly and medially by the medial part of the plantar aponeurosis and its medial extension, laterally by an intermuscular septum, and dorsally by the first metatarsal. The central compartment contains flexor digitorum brevis, the lumbricals, flexor accessorius and adductor hallucis, and is bounded by the plantar aponeurosis inferiorly, the osseofascial tarsometatarsal structures dorsally and intermuscular septa medially and laterally. The lateral compartment contains abductor digiti minimi and flexor digiti minimi brevis, and its boundaries are the fifth metatarsal dorsally, the plantar aponeurosis inferiorly and laterally, and an intermuscular septum medially. The interosseous compartment contains the seven interossei and its boundaries are the interosseous fascia and the metatarsals.

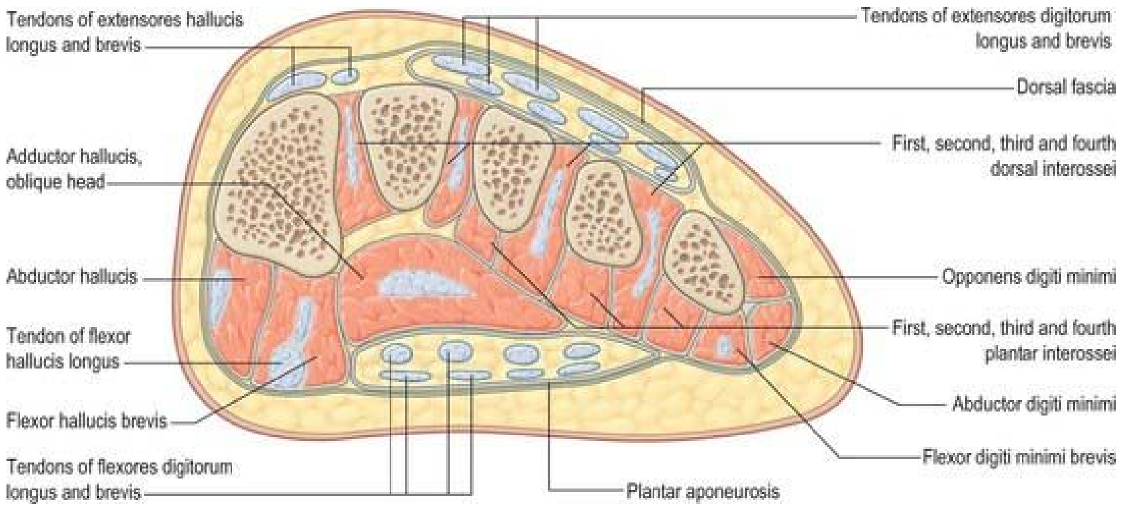
Tendons of extensores hallucis longus and brevis
Adductor hallucis, oblique head
Abductor hallucis
Tendon of flexor hallucis longus
Flexor hallucis brevis
Tendons of flexores digitorum longus and brevis
Tendons of extensores digitorum longus and brevis
Dorsal fascia
First, second, third and fourth dorsal interossei
Opponens digiti minimi
First, second, third and fourth plantar interossei
Abductor digiti minimi
Flexor digiti minimi brevis
Plantar aponeurosis

Fig. 84.4 Transverse section through the midfoot showing the main fascial compartments.

The dorsal aspect of the foot effectively contains a single compartment which is occupied by the extensor tendons and extensor digitorum brevis, and which is roofed by the deep dorsal fascia (see below).

Lateral intermuscular septum

The lateral intermuscular septum is incomplete, especially at its proximal end. Distally, its deep attachments are to the fibrous sheath of fibularis longus and to the fifth metatarsal bone.

Medial intermuscular septum

The medial intermuscular septum is incomplete and divides into three bands, proximal, intermediate and distal, each of which displays lateral and medial divisions as it approaches its deep attachment. The proximal band is attached laterally to the cuboid and blends medially with the tendon of tibialis posterior. The middle band is attached laterally to the cuboid and the long plantar ligament and medially to the medial cuneiform bone. The distal band divides to enclose the tendon of flexor hallucis longus and is attached to the fascia over flexor hallucis brevis.

Deep dorsal fascia

The deep fascia on the dorsum of the foot (fascia dorsalis pedis) is a thin layer, continuous above with the inferior extensor retinaculum; it covers the dorsal extensor tendons and extensor digitorum brevis.

Compartment syndrome in the foot

A compartment syndrome results from an increase in intracompartmental pressure sufficient to impair venous outflow from that compartment. As blood enters at arterial pressure, the compartment pressure increases further until it exceeds arterial pressure, at which point inflow of arterial blood ceases, leading to muscle and nerve ischaemia. Failure to relieve the increased pressure in the compartment surgically results in necrosis of the soft tissues within the compartment. The most common cause of compartment syndrome in the foot is trauma, usually of high-energy (high impact) type: crush injuries, calcaneal fractures and disruption of the tarsometatarsal joints are the usual antecedents associated with compartment syndrome in the foot.

Specialized adipose tissue (heel and metatarsal pad)

The heel pad is subject to repeated high impacts and is anatomically adapted to withstand these pressures. The adult heel pad has an average thickness of 18 mm and a mean epidermal thickness of 0.64 mm (dorsal epidermal thickness averages 0.069 mm). The heel pad contains elastic adipose tissue organized as spiral fibrous septa anchored to each other, to the calcaneus and to the skin. The septa are U-shaped fat-filled columns designed to resist compressive loads and are reinforced internally with elastic diagonal and transverse fibres, which separate the fat into compartments.

In the forefoot, the subcutaneous tissue consists of fibrous lamellae arranged in a complex whorl containing adipose tissue attached via vertical fibres to the dermis superficially and the plantar aponeurosis deeply. The fat is particularly thick in the region of the metatarsophalangeal joints, which cushions the foot during the toe-off phase of gait (see below). Like the heel pad, the metatarsal fat pad is designed to withstand compressive and shearing forces. Atrophy of either may be a cause of persistent pain in the distal plantar region.

BONE

Functionally, the skeleton of the foot may be divided into tarsus, metatarsus and phalanges. With regard to nomenclature of the surfaces of the foot, the terms ‘plantar’ and ‘dorsal’ are used, to denote the inferior and superior surfaces respectively. The terms ‘proximal’ and ‘distal’ are used with the same significance as in limbs generally. Rotation of the limb buds that occurs in the early stages of the development of the limbs results in a laterally directed thumb in the hand, and a medially directed great toe in the foot.

DISTAL TIBIA

The distal end of the tibia has anterior, medial, posterior, lateral and distal surfaces, and projects inferomedially as the medial malleolus (see Figs 83.2A,B; 83.3A,B). The distal surface articulates with the talus and is wider anteriorly than posteriorly. It is concave sagittally and slightly convex transversely and continues medially into the malleolar articular surface. The medial malleolus is short and thick and has a smooth lateral surface with a crescentic facet that articulates with the medial surface of the talar body. The distal end of the tibia, including its ossification, is described in detail in Chapter 83.

Attachments

No muscles are attached to the distal tibia. The interosseous ligament, the deltoid ligament, and the anterior and posterior tibiofibular ligaments are attached to the distal tibia.

Vascular supply

The distal tibia is supplied by an arterial network formed by branches of the dorsalis pedis, posterior tibial and fibular arteries.

Innervation

The distal tibia is innervated by branches from the deep fibular, posterior tibial, saphenous and sural nerves.

DISTAL FIBULA

The distal end of the fibula or lateral malleolus projects distally and posteriorly relative to the medial malleolus (see Figs 83.2A,B; 83.3A,B). Its lateral aspect is subcutaneous, the posterior surface has a broad groove with a prominent lateral border, and the anterior surface is rough and somewhat rounded and articulates with the anteroinferior aspect of the tibia. The medial surface has a triangular articular facet, vertically convex with its apex directed distally. It articulates with the lateral talar surface. Behind the facet is a rough malleolar fossa. The distal end of the fibula, including its ossification, is described in detail in Chapter 83.

Attachments

No muscles are attached to the distal fibula below the level of the interosseous ligament. The ligamentous attachments are those of the lateral ligament complex, i.e. the anterior talofibular, the calcaneofibular and the posterior talofibular ligaments. The interosseous ligament is attached on its medial aspect.

Vascular supply

The distal fibula is supplied by an arterial network made up of branches of the dorsalis pedis, posterior tibial and fibular arteries.

Innervation

The distal fibula is innervated by the deep fibular, tibial, saphenous and sural nerves.

TARSUS

The seven tarsal bones occupy the proximal half of the foot (Figs 84.5A,B; 84.6). The tarsus and carpus are homologous, but the tarsal elements are larger, reflecting their role in supporting and distributing body weight. As in the carpus, tarsal bones are arranged in proximal and distal rows, but medially there is an additional single intermediate tarsal element, the navicular. The proximal row is made up of the talus and calcaneus; the long axis of the talus is inclined anteromedially and inferiorly, its distally directed head is medial to the calcaneus and at a higher level. The distal row contains, from medial to lateral, the medial, intermediate and lateral cuneiforms and the cuboid. Collectively these bones display an arched transverse alignment that is dorsally convex. Medially, the navicular is interposed between the head of the talus and the cuneiforms. Laterally, the calcaneus articulates with the cuboid.

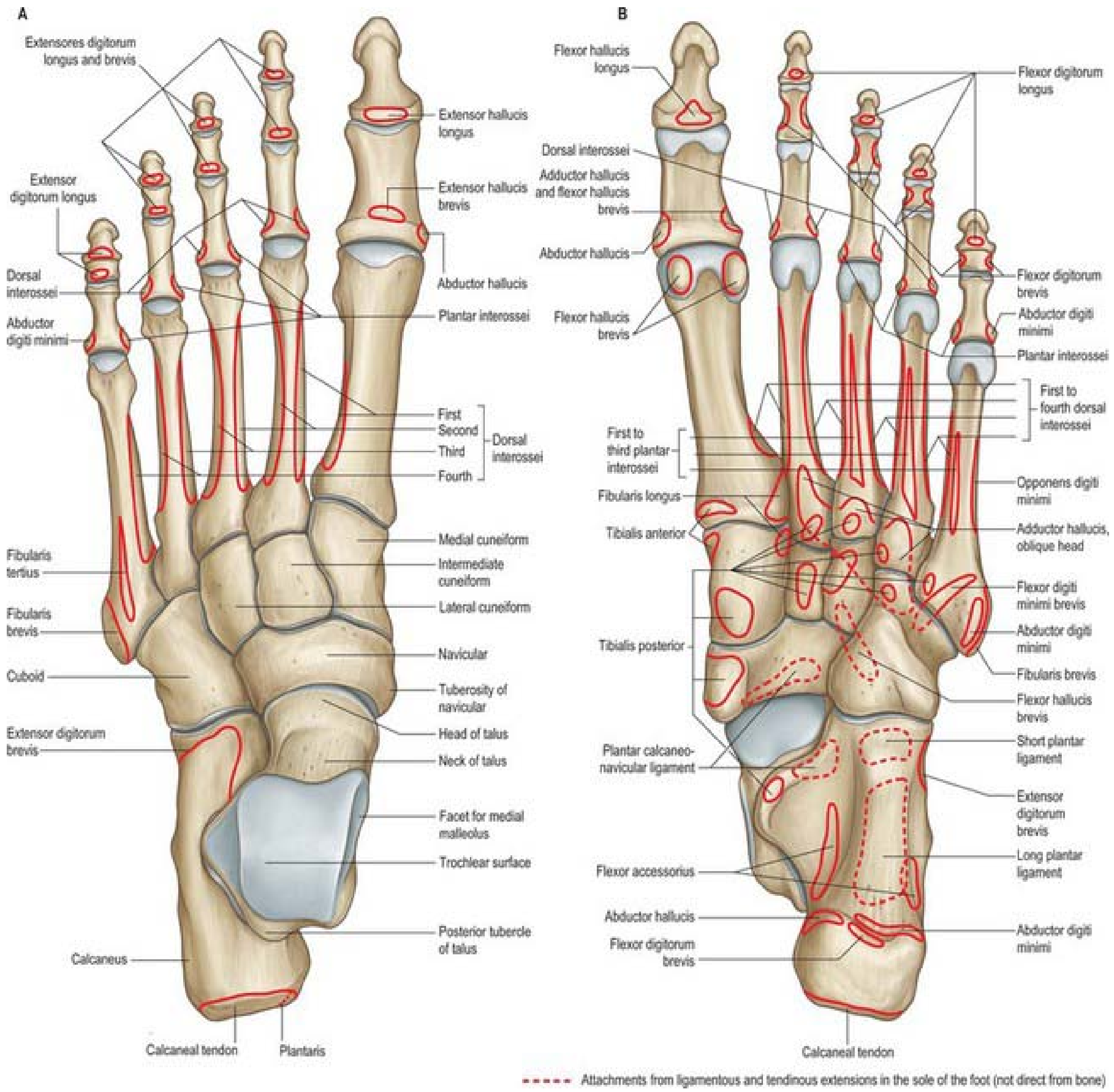
A
Extensores digitorum longus and brevis
Extensor digitorum longus
Dorsal interossei
Abductor digiti minimi
Fibularis tertius
Fibularis brevis
Cuboid
Extensor digitorum brevis
Calcaneus
Calcaneal tendon
Plantaris
Extensor hallucis longus
Extensor hallucis brevis
Abductor hallucis
Plantar interossei
First
Second
Third
Fourth
Dorsal interossei
Medial cuneiform
Intermediate cuneiform
Lateral cuneiform
Navicular
Tuberosity of navicular
Head of talus
Neck of talus
Facet for medial malleolus
Trochlear surface
Posterior tubercle of talus
B
Flexor hallucis longus
Dorsal interossei
Adductor hallucis and flexor hallucis brevis
Abductor hallucis
Flexor hallucis brevis
First to third plantar interossei
Fibularis longus
Tibialis anterior
Tibialis posterior
Plantar calcaneo-navicular ligament
Flexor accessorius
Abductor hallucis
Flexor digitorum brevis
Calcaneal tendon
Flexor digitorum longus
Flexor digitorum brevis
Abductor digiti minimi
Plantar interossei
First to fourth dorsal interossei
Opponens digiti minimi
Adductor hallucis, oblique head
Flexor digiti minimi brevis
Abductor digiti minimi
Fibularis brevis
Flexor hallucis brevis
Short plantar ligament
Extensor digitorum brevis
Long plantar ligament
Abductor digiti minimi
Attachments from ligamentous and tendinous extensions in the sole of the foot (not direct from bone)

Fig. 84.5 Skeleton of the left foot, with muscle attachments. **A**, Dorsal aspect. **B**, Plantar aspect. The attachments of tibialis posterior to the metatarsals vary; those to the third and fifth are sometimes absent.

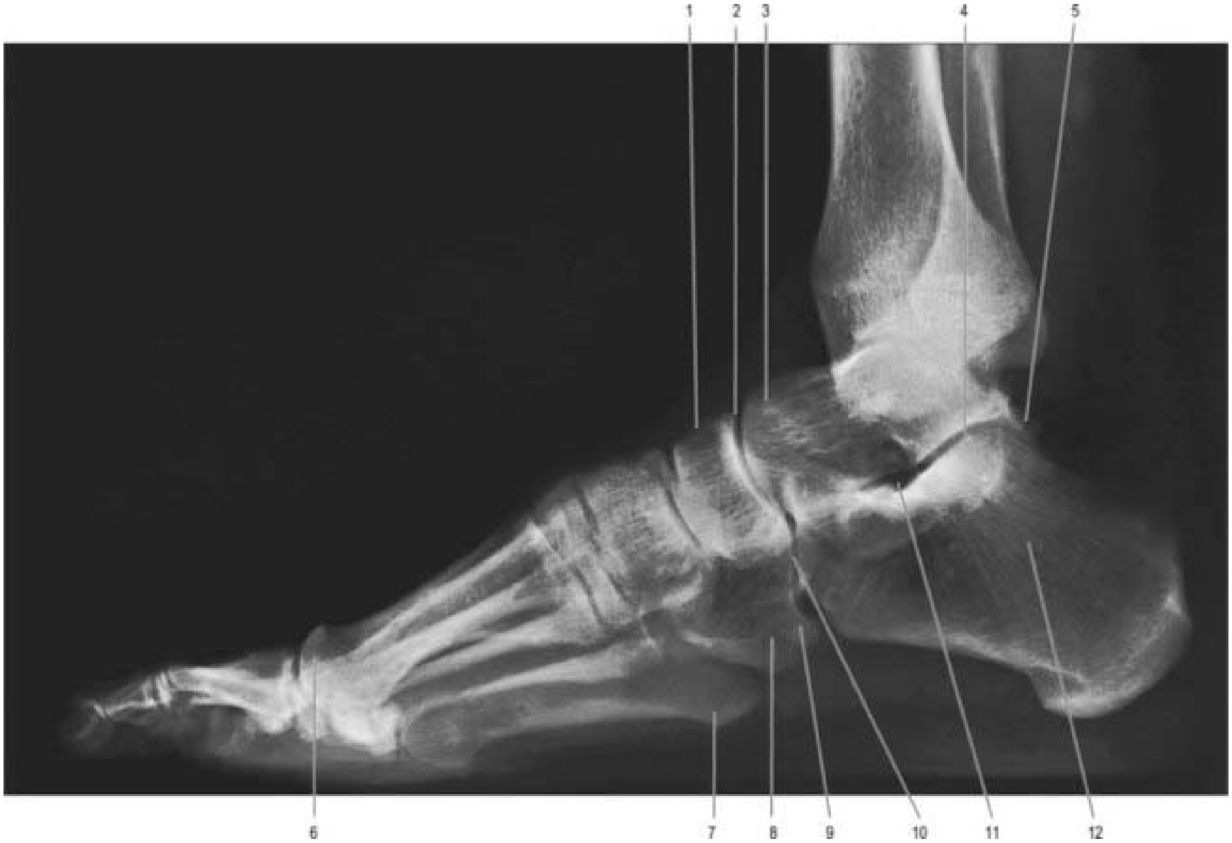

Fig. 84.6 Lateral radiograph of adult ankle and foot in full plantigrade contact with the ground, during symmetrical standing, in a man aged 44 years. **1**. Navicular. **2**. Talonavicular joint. **3**. Head of talus. **4**. Subtalar joint. **5**. Os trigonum. **6**. Head of first metatarsal. **7**. Tuberosity on base of fifth metatarsal. **8**. Cuboid. **9**. Sesamoid bone in tendon of fibularis longus. **10**. Calcaneocuboid joint. **11**. Sinus tarsi. **12**. Calcaneus (note trabecular pattern).

The tarsus and metatarsus are arranged to form intersecting longitudinal and transverse arches. Hence thrust and weight are not transmitted from the tibia to the ground (or *vice versa*) directly through the tarsus, but are distributed through the tarsal and metatarsal bones to the ends of the longitudinal arches. For the purposes of description, each tarsal bone is arbitrarily considered to be cuboidal in form, with six surfaces. The ossification sites and dates are summarized in Fig. 84.7.

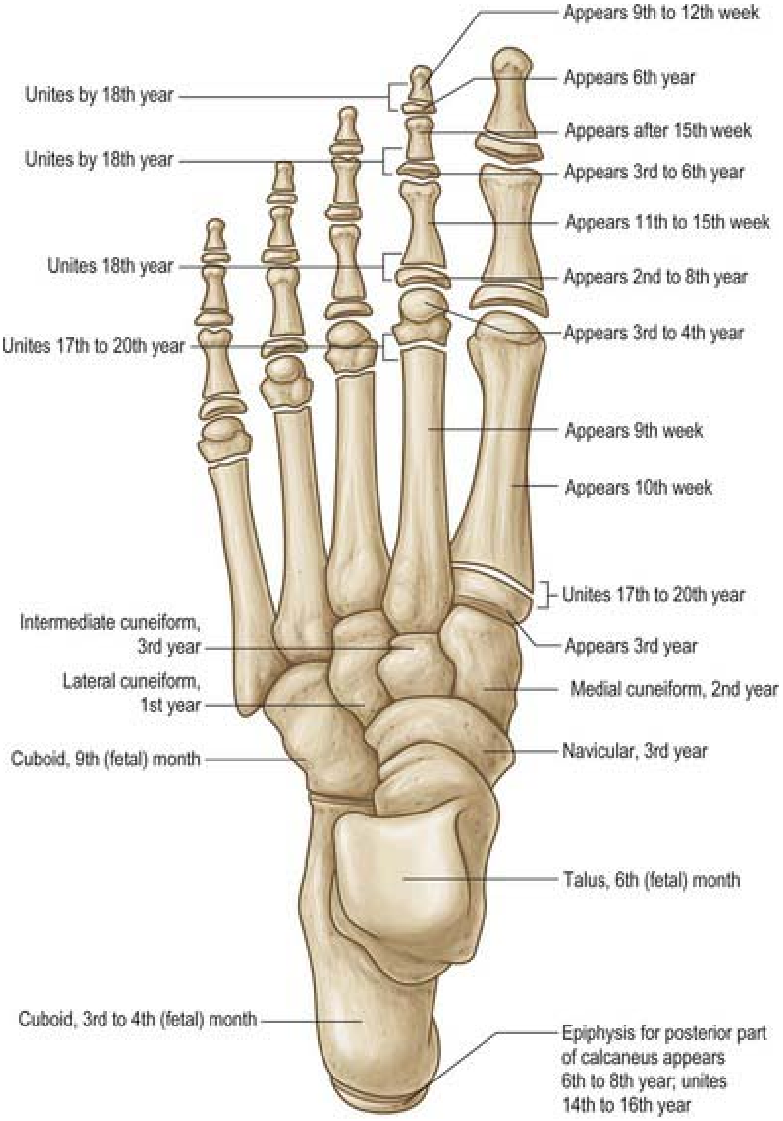
Appears 9th to 12th week
Unites by 18th year
Appears 6th year
Appears after 15th week
Unites by 18th year
Appears 3rd to 6th year
Appears 11th to 15th week
Unites 18th year
Appears 2nd to 8th year
Appears 3rd to 4th year
Unites 17th to 20th year
Appears 9th week
Appears 10th week
Unites 17th to 20th year
Intermediate cuneiform, 3rd year
Appears 3rd year
Lateral cuneiform, 1st year
Medial cuneiform, 2nd year
Cuboid, 9th (fetal) month
Navicular, 3rd year
Talus, 6th (fetal) month
Cuboid, 3rd to 4th (fetal) month
Epiphysis for posterior part of calcaneus appears 6th to 8th year; unites 14th to 16th year

Fig. 84.7 Ossification of the bones of the foot.

Talus

The talus is the link between the foot and leg, through the ankle joint (see Figs 84.16 and 84.18).

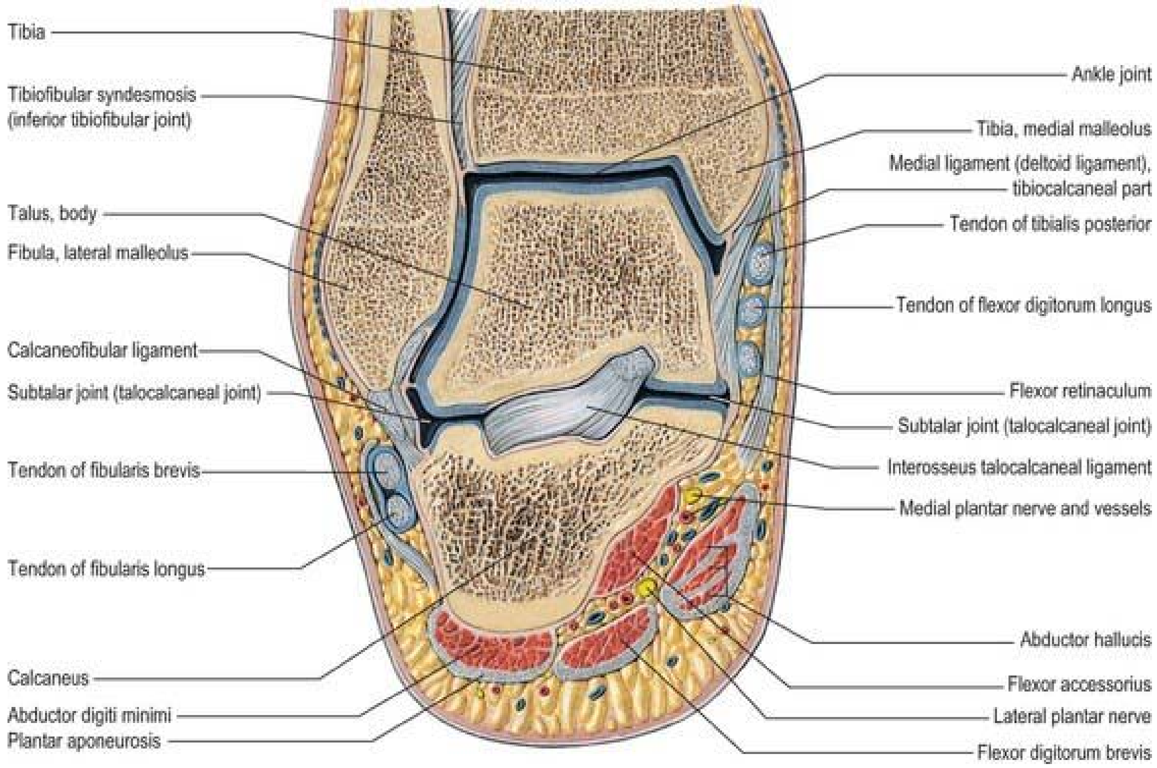
Tibia
Tibiofibular syndesmosis (inferior tibiofibular joint)
Talus, body
Fibula, lateral malleolus
Calcaneofibular ligament
Subtalar joint (talocalcaneal joint)
Tendon of fibularis brevis
Tendon of fibularis longus
Calcaneus
Abductor digiti minimi
Plantar aponeurosis
Ankle joint
Tibia, medial malleolus
Medial ligament (deltoid ligament), tibiocalcaneal part
Tendon of tibialis posterior
Tendon of flexor digitorum longus
Flexor retinaculum
Subtalar joint (talocalcaneal joint)
Interosseus talocalcaneal ligament
Medial plantar nerve and vessels
Abductor hallucis
Flexor accessorius
Lateral plantar nerve
Flexor digitorum brevis

Fig. 84.16 Coronal section through the left ankle and talocalcaneal joint (seen from behind).

(From Sobotta 2006.)

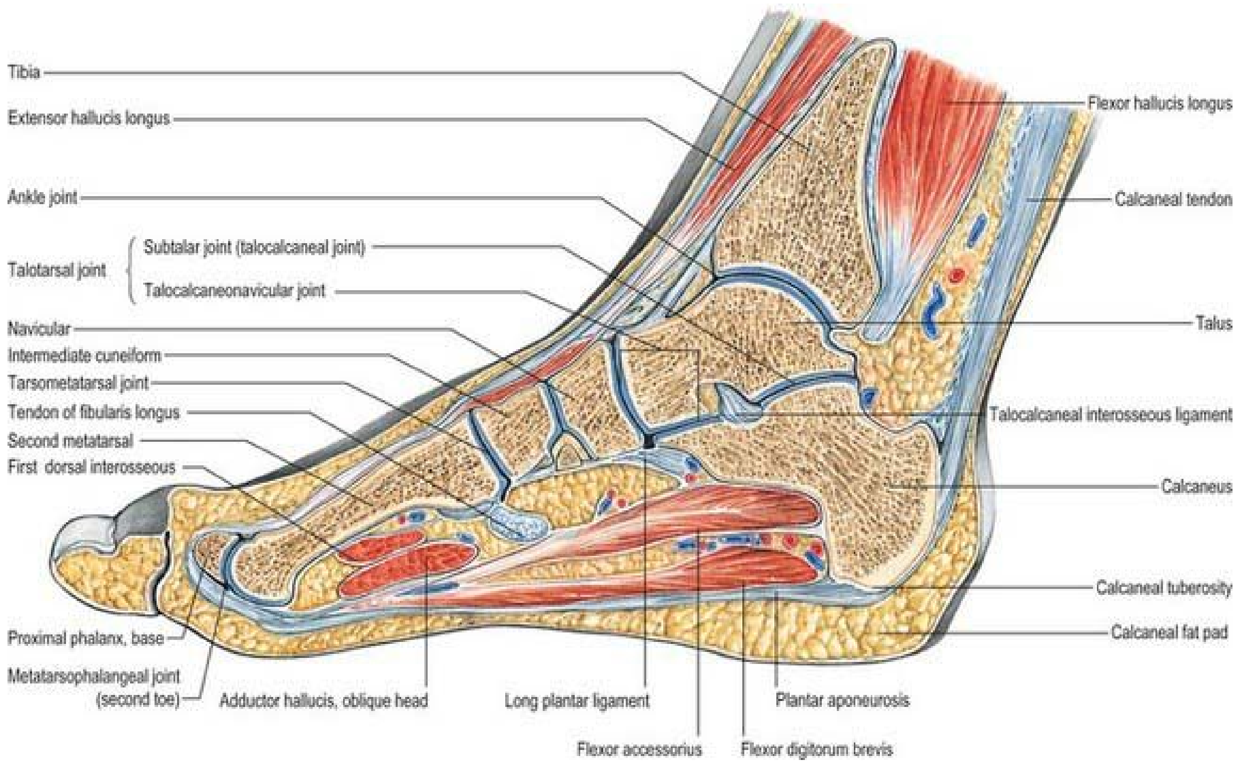
Tibia
Extensor hallucis longus
Ankle joint
Talotarsal joint
Subtalar joint (talocalcaneal joint)
Talocalcaneonavicular joint
Navicular
Intermediate cuneiform
Tarsometatarsal joint
Tendon of fibularis longus
Second metatarsal
First dorsal interosseous
Proximal phalanx, base
Metatarsophalangeal joint (second toe)
Adductor hallucis, oblique head
Long plantar ligament
Flexor accessorius
Flexor digitorum brevis
Plantar aponeurosis
Flexor hallucis longus
Calcaneal tendon
Talus
Talocalcaneal interosseous ligament
Calcaneus
Calcaneal tuberosity
Calcaneal fat pad

Fig. 84.18 Sagittal section of the foot showing talocrural and tarsal joints.

(From Sobotta 2006.)

Head

Directed distally and somewhat inferomedially, the head has a distal surface which is ovoid and convex; its long axis is also inclined inferomedially to articulate with the proximal navicular surface. The plantar surface of the head has three articular areas, separated by smooth ridges. The most posterior and largest is oval, slightly convex and rests on a shelf-like medial calcaneal projection, the sustentaculum tali. Anterolateral to this and usually continuous with it, a flat articular facet rests on the anteromedial part of the dorsal (proximal) calcaneal surface; distally it continues into the navicular surface. Between the two calcaneal facets, a part of the talar head, covered with articular cartilage, is in contact with the plantar calcaneonavicular ligament, which is covered here, superiorly, by fibrocartilage (see Fig. 84.15A,B). When the foot is inverted passively, the dorsolateral aspect of the head is visible and palpable approximately 3 cm distal to the tibia; it is hidden by extensor tendons when the toes are dorsiflexed.

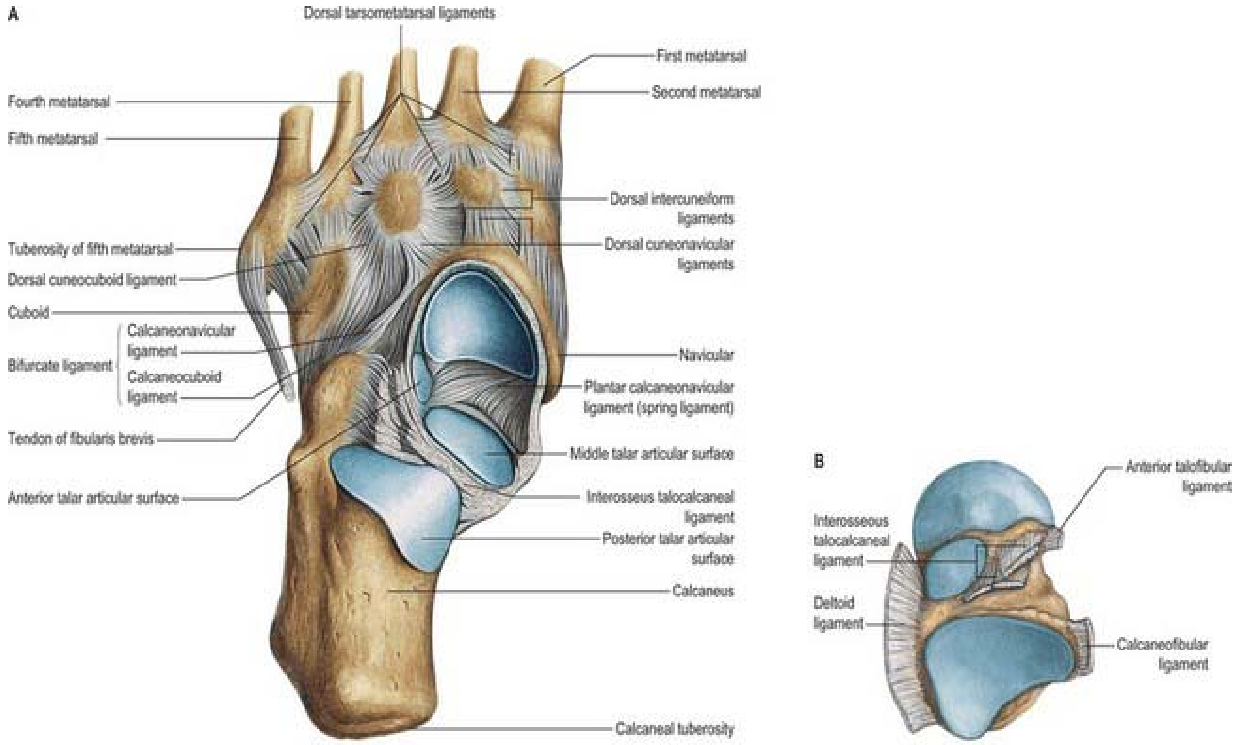
A
Dorsal tarsometatarsal ligaments
First metatarsal
Second metatarsal
Fourth metatarsal
Fifth metatarsal
Dorsal intercuneiform ligaments
Dorsal cuneonavicular ligaments
Tuberosity of fifth metatarsal
Dorsal cuneocuboid ligament
Cuboid
Bifurcate ligament
Calcaneonavicular ligament
Calcaneocuboid ligament
Navicular
Plantar calcaneonavicular ligament (spring ligament)
Tendon of fibularis brevis
Middle talar articular surface
Anterior talar articular surface
Interosseus talocalcaneal ligament
Posterior talar articular surface
Calcaneus
Calcaneal tuberosity
B
Anterior talofibular ligament
Interosseous talocalcaneal ligament
Deltoid ligament
Calcaneofibular ligament

Fig. 84.15 **A**, Disarticulated talocalcaneal and talocalcaneonavicular joints, seen from above. **B**, Disarticulated talus (seen from below).

(From Sobotta 2006.)

Neck

The neck is the narrow, medially inclined region between the head and body. Its rough surfaces are for ligaments. The medial plantar surface has a deep sulcus tali which, when the talus and calcaneus are articulated, forms a roof to the sinus tarsi, which is occupied by inter-osseous talocalcaneal and cervical ligaments.

The long axis of the neck, inclined downwards, distally and medially, makes an angle of approximately 150° with that of the body; it is smaller (130–140°) at birth, accounting in part for the inverted foot in young children. The dorsal talonavicular ligament and ankle articular capsule are attached distally to its dorsal surface. Thus the proximal part of this surface lies within the capsule of the ankle joint. The medial articular facet of the talar body and part of the trochlear surface may extend onto the neck. The anterior talofibular ligament is attached on the lateral aspect of the neck, spreading along the adjacent anterior border of the lateral surface. The interosseous talocalcaneal and cervical ligaments are attached to the inferior surface of the neck. A dorsolateral, so-called ‘squatting facet’ is commonly present on the talar neck in those individuals who habitually adopt the squatting position: it articulates with the anterior tibial margin in extreme dorsiflexion and may be double.

Body

The body is cuboidal, covered dorsally by a trochlear surface articulating with the distal end of the tibia. It is anteroposteriorly convex, gently concave transversely, widest anteriorly and, therefore, sellar. The triangular lateral surface is smooth and vertically concave for articulation with the lateral malleolus. Superiorly, it is continuous with the trochlear surface; inferiorly its apex is a lateral process. Proximally, the medial surface is (posterosuperiorly) covered by a comma-shaped facet, which is deeper in front and articulates with the medial malleolus. Distally, this surface is rough and contains numerous vascular foramina. The small posterior surface features a rough projection termed the posterior process. The process is marked by an oblique groove between two tubercles which lodges the tendon of flexor hallucis longus. The lateral tubercle is usually larger; the medial is less prominent and immediately behind the sustentaculum tali (Fig. 84.8A). The plantar surface articulates with the middle one-third of the dorsal calcaneal surface by an oval concave facet, its long axis directed distolaterally at an angle of approximately 45° with the median plane. The medial edge of the trochlear surface is straight, but its lateral edge inclines medially in its posterior part and is often broadened into a small elongated triangular area which is in contact with the posterior tibiofibular ligament in dorsiflexion.

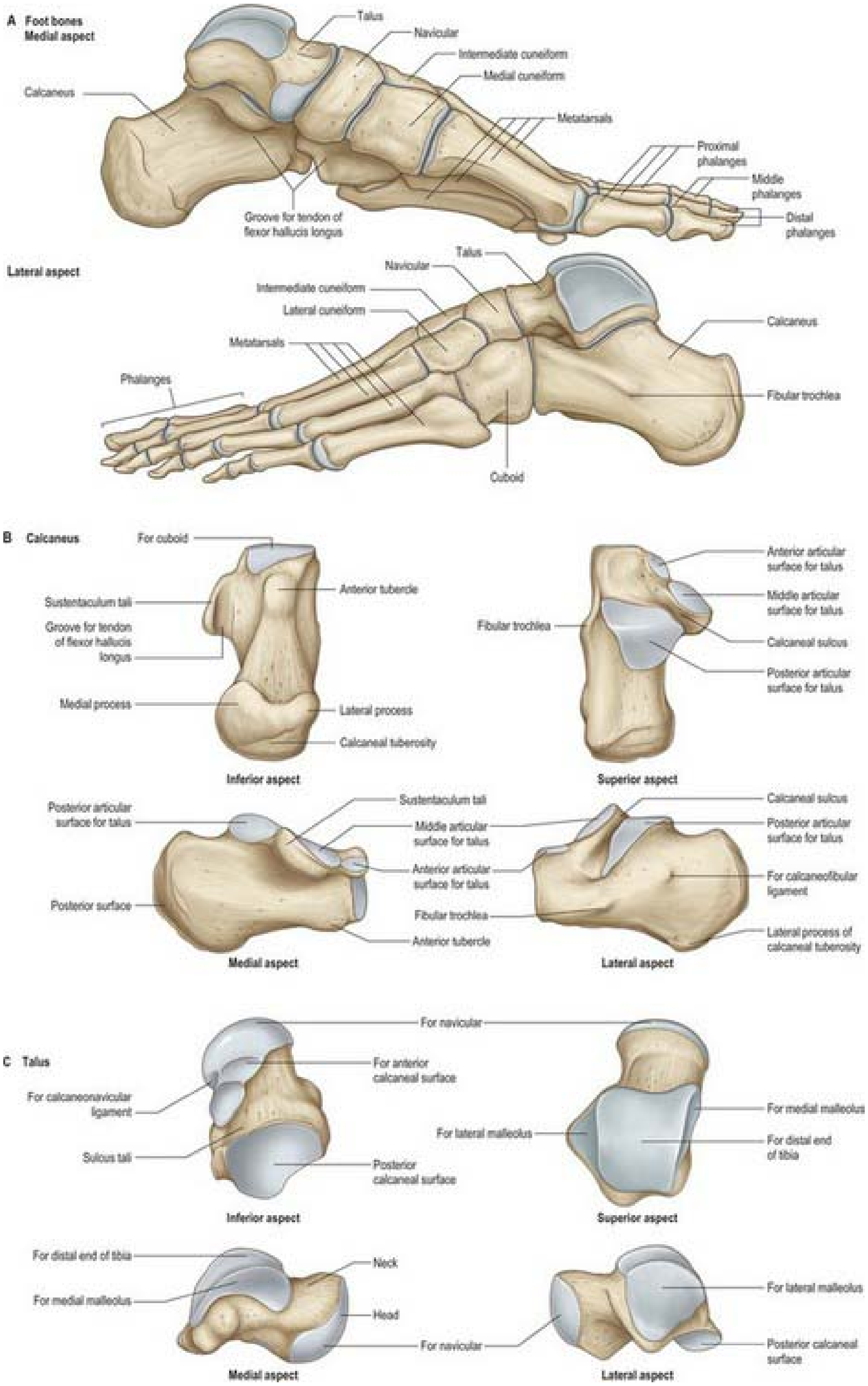
A Foot bones
Medial aspect
Talus
Navicular
Intermediate cuneiform
Medial cuneiform
Calcaneus
Metatarsals
Proximal phalanges
Middle phalanges
Distal phalanges
Groove for tendon of flexor hallucis longus
Lateral aspect
Talus
Navicular
Intermediate cuneiform
Lateral cuneiform
Metatarsals
Calcaneus
Phalanges
Fibular trochlea
Cuboid
B Calcaneus
For cuboid
Sustentaculum tali
Anterior tubercle
Groove for tendon of flexor hallucis longus
Medial process
Lateral process
Calcaneal tuberosity
Inferior aspect
Anterior articular surface for talus
Middle articular surface for talus
Fibular trochlea
Calcaneal sulcus
Posterior articular surface for talus
Superior aspect
Posterior articular surface for talus
Sustentaculum tali
Middle articular surface for talus
Anterior articular surface for talus
Posterior surface
Fibular trochlea
Anterior tubercle
Medial aspect
Calcaneal sulcus
Posterior articular surface for talus
For calcaneofibular ligament
Lateral process of calcaneal tuberosity
Lateral aspect
C Talus
For navicular
For anterior calcaneal surface
For calcaneonavicular ligament
Sulcus tali
Posterior calcaneal surface
Inferior aspect
For lateral malleolus
For medial malleolus
For distal end of tibia
Superior aspect
For distal end of tibia
Neck
For medial malleolus
Head
For navicular
Medial aspect
For lateral malleolus
Posterior calcaneal surface
Lateral aspect

Fig. 84.8 Skeleton of the foot. **A**, Foot bones. **B**, Calcaneus. **C**, Talus.

(From Drake, Vogl, Mitchell, Tibbitts and Richardson 2008.)

The posterior talofibular ligament is attached to the lateral tubercle of the posterior process. Its attachment extends up to the groove, or depression, between the process and posterior trochlear border. The posterior talocalcaneal ligament is attached to the plantar border of the posterior process. The groove between the tubercles of the process contains the tendon of flexor hallucis longus and continues distally into the groove on the plantar aspect of the sustentaculum tali. The medial talocalcaneal ligament is attached below to the medial tubercle, whereas the most posterior superficial fibres of the deltoid ligament are attached above the tubercle. The deep fibres of the deltoid ligament are attached still higher to the rough area immediately below the comma-shaped articular facet on the medial surface (Fig. 84.8A,C).

Muscle attachments

No muscles are attached to the talus. However, many ligaments are attached to the bone, and these confer stability to the ankle, subtalar and talocalcaneonavicular joints (Fig. 84.8A–C).

Vascular supply

The talar blood supply is rather tenuous because of the lack of muscle attachments. The first comprehensive account of talar blood supply was provided by Wildenauer in 1950. The extraosseous blood supply is via the posterior tibial, dorsalis pedis and fibular arteries (Fig. 84.9). The ‘artery of the tarsal canal’ arises from the posterior tibial artery approximately 1cm proximal to the origin of the medial and lateral plantar arteries (Fig. 84.10) and passes anteriorly between the sheaths of flexor digitorum longus and flexor hallucis longus to enter the tarsal canal in which it lies anteriorly, close to the talus. (The ‘tarsal canal’ is the term that is commonly used to describe the tunnel-shaped medial end of the sinus tarsi.) Branches from the arterial network in the tarsal canal enter the talus. The artery continues through the tarsal canal into the lateral part of the tarsal sinus, where it anastomoses with the artery of the tarsal sinus, forming a vascular sling under the talar neck. A branch of the artery of the tarsal canal known as the deltoid branch passes deep to the deltoid ligament and supplies part of the medial aspect of the talar body. Sometimes it arises from the posterior tibial artery; rarely, it arises from the medial plantar artery. In talar fractures it may be the only remaining arterial supply to the talus to maintain the viability of the talar body. The dorsalis pedis artery supplies branches to the superior aspect of the talar neck and also gives off the artery of the tarsal sinus. This large vessel is always present and anastomoses with the artery of the tarsal canal. The artery of the tarsal sinus receives a contribution from the anterior perforating branch of the fibular artery and supplies direct branches to the talus. The fibular artery provides small branches which form a plexus of vessels posteriorly with branches of the posterior tibial artery, however, the contribution that the fibular artery makes to the talar blood supply is thought to be insignificant.

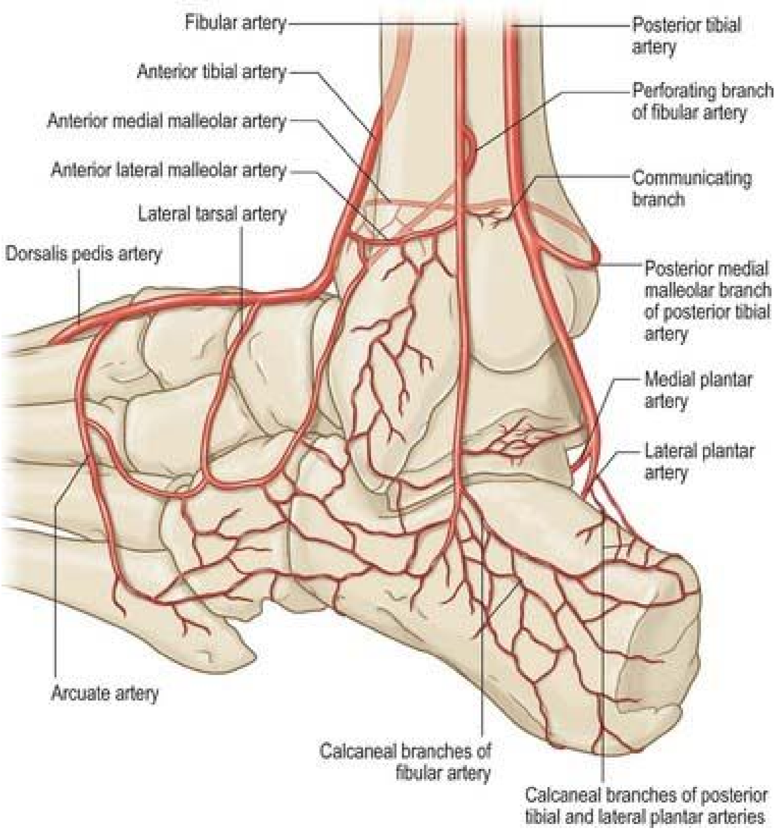
Fibular artery
Anterior tibial artery
Anterior medial malleolar artery
Anterior lateral malleolar artery
Lateral tarsal artery
Dorsalis pedis artery
Arcuate artery
Calcaneal branches of fibular artery
Calcaneal branches of posterior tibial and lateral plantar arteries
Posterior tibial artery
Perforating branch of fibular artery
Communicating branch
Posterior medial malleolar branch of posterior tibial artery
Medial plantar artery
Lateral plantar artery

Fig. 84.9 The arterial anastomoses of the ankle, tarsus and metatarsus.

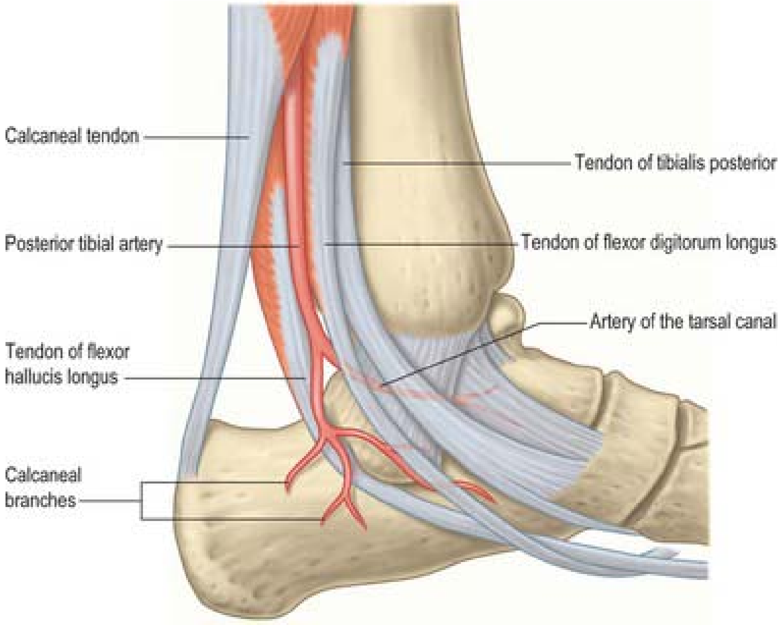
Calcaneal tendon
Posterior tibial artery
Tendon of flexor hallucis longus
Calcaneal branches
Tendon of tibialis posterior
Tendon of flexor digitorum longus
Artery of the tarsal canal

Fig. 84.10 Branches of the posterior tibial artery, posteromedial view of ankle.

The intraosseous blood supply of the talar head comes medially from branches of the dorsalis pedis and laterally via vessels that arise from the anastomosis between the arteries of the tarsal canal and tarsal sinus. The middle one-third of the talar body, other than its most superior aspect, and the lateral one-third, other than its posterior aspect, are supplied mainly by the anastomotic arcade in the tarsal canal. The medial one-third of the talar body is supplied by the deltoid branch of the artery of the tarsal canal.

Innervation

The talus is innervated by branches from the deep fibular, posterior tibial, saphenous and sural nerves.

Ossification

A single ossification centre appears prenatally at 6 months (Fig. 84.7). The posterior process (Stieda’s process) is a separate bone in 5% of individuals and arises from a separate ossification centre, which appears between 8 and 11 years. In athletes and dancers, it may be susceptible to impingement against the posterior tibia, resulting in pain and sometimes requires surgical removal. Another accessory bone (although rare) is the os supratalare, which lies on the dorsal aspect of the talus; it rarely measures more than 4 mm in length.

Talar fractures

The talus has no muscular attachments and 70% of its surface is covered by articular cartilage: displaced talar neck fractures, where the blood supply to the talar body is interrupted, can therefore result in avascular necrosis and non-union. In general, these complications do not occur in undisplaced fractures. If a subchondral lucency is seen in the talar dome on radiographs at 8 weeks after fracture of the talar neck (Hawkin's sign), it may be assumed that vascularity to the talar body is intact and that the fracture is likely to heal satisfactorily.

Calcaneus

The calcaneus is the largest tarsal bone and projects posterior to the tibia and fibula as a short lever for muscles of the calf attached to its posterior surface. It is irregularly cuboidal, its long axis being inclined distally upwards and laterally (Fig 84.8A,B). The superior or proximal surface is divisible into three areas. The posterior one-third is rough and concavo-convex; the convexity is transverse and supports fibroadipose tissue (Kager's fat pad) between the calcaneal tendon and ankle joint. The middle one-third carries the posterior talar facet, which is oval and convex anteroposteriorly. The anterior one-third is partly articular; distal (anterior) to the posterior articular facet, a rough depression, the sulcus calcanei, narrows into a groove on the medial side and completes the sinus tarsi with the talus. (The sinus tarsi is a conical hollow bounded by the talus medially, superiorly and laterally, with the superior surface of the calcaneus below. Its medial end is narrow and tunnel-shaped, and is often referred to as the tarsal canal.) Distal and medial to this groove, an elongated articular area covers the sustentaculum tali and extends distolaterally on the body of the bone. This facet is often divided into middle and anterior talar facets by a non-articular interval at the anterior limit of the sustentaculum tali (the incidence of this subdivision varies with sex, race and occupation). Rarely, all three facets on the upper surface of the calcaneus are fused into one irregular area. A detailed analysis of patterns of anterior talar articular facets in a series of 401 Indian calcanei revealed four types. Type I (67%) showed one continuous facet on the sustentaculum extending to the distomedial calcaneal corner; type II (26%) presented two facets, one sustentacular and one distal calcaneal; type III (5%) possessed only a single sustentacular facet; and type IV (2%) showed confluent anterior and posterior facets.

The anterior surface is the smallest, and is an obliquely set concavo-convex articular facet for the cuboid. The posterior surface is divided into three regions: a smooth proximal (superior) area separated from the calcaneal tendon by a bursa and adipose tissue; a middle area, which is the largest, limited above by a groove and below by a rough ridge for the calcaneal tendon; a distal (inferior) area inclined downwards and forwards, vertically striated, which is the subcutaneous weight-bearing surface.

The plantar surface is rough, especially proximally as the calcaneal tuberosity, the lateral and medial processes of which extend distally, separated by a notch. The medial process is longer and broader (Fig. 84.8B). Further distally, an anterior tubercle marks the distal limit of the attachment of the long plantar ligament.

The lateral surface is almost flat. It is proximally deeper and palpable on the lateral aspect of the heel distal to the lateral malleolus. Distally, it presents the fibular trochlea (Fig. 84.8A,B), which is exceedingly variable in size and palpable 2 cm distal to the lateral malleolus when well developed. It bears an oblique groove for the tendon of fibularis longus and a shallower proximal groove for the tendon of fibularis brevis. About 1 cm or more behind and above the fibular trochlea, a second elevation may exist for attachment of the calcaneofibular part of the lateral ligament.

The medial surface is vertically concave, and its concavity is accentuated by the sustentaculum tali, which projects medially from the distal part of its upper border (Fig. 84.8B). Superiorly, the process bears the middle talar facets and inferiorly a groove which is continuous with that on the talar posterior surface for the tendon of flexor hallucis longus (Fig. 84.8A,B). The medial aspect of the sustentaculum tali can be felt immediately distal to the tip of the medial malleolus; occasionally it is also grooved by the tendon of flexor digitorum longus.

Muscle and ligament attachments

The interosseous talocalcaneal and cervical ligaments and the medial root of the inferior extensor retinaculum are attached in the calcaneal sulcus. The non-articular area distal to the posterior talar facet is the site of attachment of extensor digitorum brevis (in part), the principal band of the inferior extensor retinaculum and the stem of the bifurcate ligament.

Abductor hallucis and the superficial part of the flexor retinaculum and, distally, the plantar aponeurosis and flexor digitorum brevis, are all attached to the medial process of the calcaneal tuberosity at its prominent medial margin. Abductor digiti minimi is attached to the lateral process, extending medially to the medial process. The long plantar ligament is attached to the rough region between the processes proximally, and extends to the anterior tubercle distally. The short plantar ligament is attached to the tubercle and the area distal to it. The lateral tendinous head of flexor accessorius is attached distal to the lateral process near the lateral margin of the long plantar ligament. Plantaris is attached to the posterior surface near the medial side of the calcaneal tendon. The anterior part of the lateral surface is crossed by the fibular tendons, but is largely subcutaneous. The calcaneofibular ligament is attached 1–2 cm proximal to the fibular trochlea, usually to a low, rounded elevation.

The dorsal surface of the sustentaculum tali is part of the talocalcaneonavicular joint; its plantar surface is grooved by the tendon of flexor hallucis longus and margins of the groove give attachment to the deep part of the flexor retinaculum. The plantar calcaneonavicular ligament is attached distally to the medial margin of the sustentaculum, which is narrow, rough and convex. A slip from the tendon of tibialis posterior, and superficial fibres of the deltoid ligament and medial talocalcaneal ligaments, are attached proximally. Distal to the attachment of the deltoid ligament, the tendon of flexor digitorum longus is related to the margin of the sustentaculum and may groove it. The large medial head of flexor accessorius is attached distal to the groove for flexor hallucis longus.

Vascular supply

The calcaneus receives its arterial supply from the medial and lateral calcaneal arteries (arising from the posterior tibial and fibular arteries, respectively), fibular artery, posterior calcaneal anastomosis (formed from the posterior tibial and fibular arteries), medial and lateral plantar arteries, artery of the tarsal sinus and tarsal canal, branches of the lateral tarsal artery and perforating fibular arteries.

Innervation

The calcaneus is innervated by branches of the tibial, sural and deep fibular nerves.

Ossification

The calcaneus is the only tarsal bone that always has two ossification centres (Fig. 84.7). In addition to the main ossification centre, there is a scale-like posterior apophysis that covers most of the posterior, and part of the plantar, surfaces. The main centre appears prenatally in the third month, whereas the posterior apophysis appears in the sixth year in females and the eighth in males, fusing in the 14th and 16th years, respectively.

An os calcaneus secondarius, an accessory bone rather than a secondary ossification centre, occurs in 2% of individuals. When present, it is located on the dorsal beak or anterior process of the calcaneus in an interval between the anteromedial aspect of the calcaneus, the proximal ends of the cuboid and navicular, and the head of the talus. Other rare accessory bones of the calcaneus include the calcaneus accessorius in the region of the fibular trochlea, the os sustentaculi on the posterior aspect of the sustentaculum, the os subcalcis on the plantar aspect of the calcaneus slightly posterior to the origin of the plantar aponeurosis, and the os aponeurosis plantaris, which lies within the plantar aponeurosis in close proximity to the medial process of the calcaneal tuberosity.

Navicular

The navicular articulates with the talar head proximally and with the cuneiform bones distally (Figs 84.8A,B; 84.11). Its distal surface is transversely convex and divided into three facets (the medial being the largest) for articulation with the cuneiforms. The proximal surface is oval and concave and articulates with the talar head. The dorsal surface is rough and convex. The medial surface is also rough and projects proximally as a prominent tuberosity, palpable approximately 2.5 cm distal and plantar to the medial malleolus. The plantar surface, rough and concave, is separated from the tuberosity medially by a groove. The lateral surface is rough, irregular and often bears a facet for articulation with the cuboid.

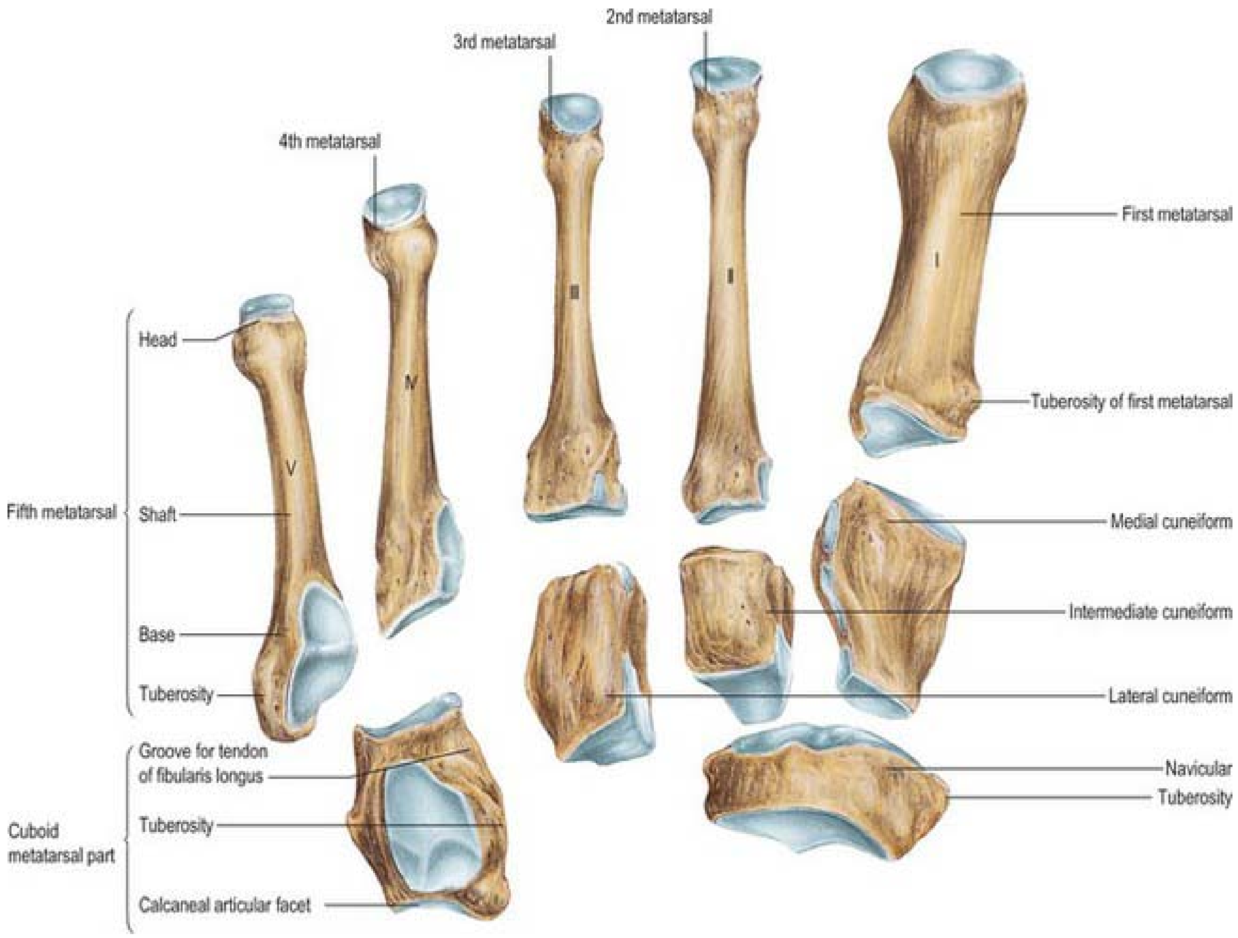
2nd metatarsal
3rd metatarsal
4th metatarsal
First metatarsal
I
II
III
IV
V
Tuberosity of first metatarsal
Medial cuneiform
Intermediate cuneiform
Lateral cuneiform
Navicular
Tuberosity
Head
Fifth metatarsal
Shaft
Base
Tuberosity
Groove for tendon of fibularis longus
Cuboid
metatarsal part
Tuberosity
Calcaneal articular facet

Fig. 84.11 Skeleton of the tarsals and metatarsals, dorsal aspect.

(From Sobotta 2006.)

The facet for articulation with the medial cuneiform is roughly triangular, its rounded apex is medial and its ‘base’, facing laterally, is often markedly curved; the articular facets for the intermediate and lateral cuneiforms are also triangular, with plantar facing apices. The facet for the lateral cuneiform may approach a wide crescent or a semicircle rather than a triangle (Fig. 84.11). Dorsal talonavicular, cuneonavicular and cubonavicular ligaments are attached to the dorsal navicular surface.

Muscle and ligament attachments

The navicular tuberosity is the main attachment of tibialis posterior and a groove lateral to it transmits part of the tendon distally to the cuneiforms and middle three metatarsal bases. The plantar calcaneonavicular ligament is attached to a slight projection lateral to the groove and adjacent to the proximal surface. The calcaneonavicular part of the bifurcate ligament is attached to the rough part of the lateral surface (Fig. 84.5B).

Vascular supply

The dorsal aspect of the navicular is supplied either from a branch of, or directly from, the dorsalis pedis artery. Its plantar aspect is supplied from the medial plantar artery, and the tuberosity is supplied by an anastomosis from the dorsalis pedis and medial plantar arteries.

Innervation

The navicular is innervated by the deep fibular and medial plantar nerves.

Ossification

The navicular ossification centre appears during the third year (Fig. 84.7). It is sometimes affected by avascular necrosis between the ages of 4 and 7 years (Köhler’s disease). An accessory navicular bone, which is considered an anatomic variant, occurs in approximately 5% of individuals. It arises from a separate ossification centre in the region of the navicular tuberosity. There are three distinct types of accessory navicular. Type I is probably a sesamoid bone within the plantar aspect of the tendon of tibialis posterior at the level of the inferior calcaneonavicular ligament. In type II, the accessory bone is separated from the body of the navicular by a synchondrosis. Type III is commonly called ‘the cornuate navicular,’ where the accessory bone is united to the navicular by a bony ridge, and may represent the possible end stage of type II. An accessory navicular may be the source of pain in athletes. Type II is the most commonly symptomatic variant: it has been suggested that the pull of the tendon of tibialis posterior, the degree of foot pronation, and the location of the accessory bone in relation to the undersurface of the navicular may produce tension, shear, and/or compression forces on the synchondrosis.

Rarely, the navicular is bipartite and it arises from two distinct centres of ossification. This can lead to premature degeneration within the talocalcaneonavicular joint (Muller–Weiss disease). Occasionally, a small bone is found within the talocalcaneonavicular joint on its dorsal aspect. Referred to as an os talonaviculare dorsale, it represents either a separate accessory bone or a fractured osteophyte of the proximal dorsal aspect of the navicular.

Cuboid

The cuboid, the most lateral bone in the distal tarsal row, lies between the calcaneus proximally and the fourth and fifth metatarsals distally (Fig. 84.11). Its dorsolateral surface is rough for the attachment of ligaments. The plantar surface is crossed distally by an oblique groove for the tendon of fibularis longus and bounded proximally by a ridge that ends laterally in the tuberosity of the cuboid, the lateral aspect of which is faceted for a sesamoid bone or cartilage that is frequently found in the tendon of fibularis longus. Proximal to its ridge, the rough plantar surface extends proximally and medially because of the obliquity of the calcaneocuboid joint, making its medial border much longer than the lateral. The lateral surface is rough; the groove for fibularis longus extends from a deep notch on its plantar edge. The medial surface, which is much more extensive and partly non-articular, bears an oval facet for articulation with the lateral cuneiform, and proximal to this another facet (sometimes absent) for articulation with the navicular: the two form a continuous surface separated by a smooth vertical ridge. The distal surface is divided vertically into a medial quadrilateral articular area for the fourth metatarsal base and a lateral triangular area, its apex lateral, for the fifth metatarsal base. The proximal surface, triangular and concavo-convex, articulates with the distal calcaneal surface; its medial plantar angle projects proximally and inferior to the distal end of the calcaneus.

Muscle (and ligament) attachments

The dorsal calcaneo-cuboid, cubonavicular, cuneocuboid and cubometatarsal ligaments are attached to the dorsal surface. Deep fibres of the long plantar ligament are attached to the proximal edge of the plantar ridge. Slips from the tendons of tibialis posterior and flexor hallucis brevis are attached to the projecting proximomedial part of the plantar surface. Interosseous, cuneocuboid and cubonavicular ligaments are attached to the rough part of the medial cuboidal surface. Proximally, the medial calcaneocuboid ligament, which is the lateral limb of the bifurcate ligament, is also attached to this surface.

Vascular supply

The cuboid is supplied by deep branches of the medial and lateral plantar arteries and by branches from the dorsal arterial network.

Innervation

The cuboid is innervated by branches from the lateral plantar, sural and deep fibular nerves.

Ossification

The cuboid frequently begins to ossify before birth, the primary ossification centre appearing just before birth (Fig. 84.7). An os cuboides secundarium is a rare accessory bone situated on the plantar aspect of the cuboid.

Cuneiforms

The wedge-like cuneiform bones articulate with the navicular proximally and with the bases of the first to third metatarsals distally; the medial cuneiform is the largest, the intermediate the smallest. The dorsal surfaces of the intermediate and lateral cuneiforms form the base of the wedge. The wedge is reversed in the medial cuneiform, which is a prime factor in shaping the transverse arch. The proximal surfaces of all three form a concavity for the distal surface of the navicular. The medial and lateral cuneiforms project distally beyond the intermediate cuneiform and so form a recess for the second metatarsal base.

Medial cuneiform

The medial cuneiform (Figs 84.5A,B; 84.11) articulates with the navicular and first metatarsal base. It has a rough, narrow dorsal surface. The distal surface is a reniform facet for the first metatarsal base, its ‘hilum’ being lateral. The proximal surface bears a piriform facet for the navicular, which is concave vertically and dorsally narrowed. The medial surface, rough and subcutaneous, is vertically convex; its distal plantar angle carries a large impression which receives the principal attachment of the tendon of tibialis anterior (Fig. 84.5B). The lateral surface is partly non-articular; there is a smooth right-angled strip along its proximal and dorsal margins for the intermediate cuneiform. Its distal dorsal area is separated by a vertical ridge from a small, almost square, facet for articulation with the dorsal part of the medial surface of the second metatarsal base. Plantar to this, the medial cuneiform is attached to the medial side of the second metatarsal base by a strong ligament. Proximally, an interosseous intercuneiform ligament connects this surface to the intermediate cuneiform. The distal and plantar area of the surface is roughened by attachment of part of the tendon of fibularis longus (Fig. 84.5B).

Muscle attachments

The plantar surface receives a slip from the tendon of tibialis posterior, in addition to part of the insertion of the tendon of fibularis longus. The medial surface receives the attachment of most of the tendon of tibialis anterior.

Vascular supply

The medial cuneiform is supplied via its dorsal, medial and lateral surfaces, mainly from the dorsal arterial network.

Innervation

The medial cuneiform is supplied by the deep fibular and medial plantar nerves.

Ossification

The medial cuneiform may have two separate ossification centres, which appear during the second year of life (Fig. 84.7). Very rarely, the medial cuneiform is bipartite and there is a horizontal cleavage plane between the two moieties.

The os cuneo-1 metatarsale-I plantare is a rare accessory bone that occurs on the plantar aspect of the foot at the base of the first metatarsal and articulates with the plantar base of the first metatarsal and the medial cuneiform.

Intermediate cuneiform

The intermediate cuneiform articulates proximally with the navicular and distally with the second metatarsal base (Figs 84.5A; 84.11). It has a narrow, plantar surface that receives a slip from the tendon of tibialis posterior. The distal and proximal surfaces are both triangular articular facets and articulate with the second metatarsal base and the navicular, respectively. The medial surface is partly articular: it articulates via a smooth, angled strip that is occasionally double with the medial cuneiform along its proximal and dorsal margins. The lateral surface is also partly articular: along its proximal margin a vertical strip, usually indented, abuts the lateral cuneiform. Strong interosseous ligaments connect non-articular parts of both surfaces to the adjacent cuneiforms.

Muscle attachments

Part of the tendon of tibialis posterior is attached to the intermediate cuneiform.

Vascular supply

The intermediate cuneiform is supplied via its dorsal, medial and lateral surfaces, mainly from the dorsal arterial network.

Innervation

The intermediate cuneiform is innervated by the deep fibular and medial plantar nerves.

Ossification

The ossification centre appears during the third year of life (Fig. 84.7). The os cuneo-2 metatarsale-II dorsale, a rare accessory bone, lies on the dorsal aspect of the joint between the intermediate cuneiform and the second metatarsal. It is wedge-shaped with its base orientated dorsally.

Lateral cuneiform

The lateral cuneiform is between the intermediate cuneiform and cuboid, and also articulates with the navicular and, distally, with the third metatarsal base (Figs 84.5A; 84.11). Like the intermediate cuneiform, its dorsal surface, which is rough and almost rectangular, is the base of a wedge. The plantar surface is narrow and receives a slip from tibialis posterior and sometimes part of flexor hallucis brevis. The distal surface is a triangular articular facet for the third metatarsal base. The proximal surface is rough on its plantar aspect, but its dorsal two-thirds articulate with the navicular by a triangular facet. The medial surface is partly non-articular and has a vertical strip, indented by the intermediate cuneiform, on its proximal margin; on its distal margin, a narrower strip (often two small facets) articulates with the lateral side of the second metatarsal base. The lateral surface, also partly non-articular, bears a triangular or oval proximal facet for the cuboid; a semilunar facet on its dorsal and distal margin articulates with the dorsal part of the medial side of the fourth metatarsal base. Non-articular areas of the medial and lateral surfaces receive intercuneiform and cuneocuboid ligaments, respectively, which are important in the maintenance of the transverse arch.

Muscle attachments

The plantar surface of the lateral cuneiform receives a slip from the tendon of tibialis posterior and, occasionally, part of flexor hallucis brevis.

Vascular supply

The lateral cuneiform is supplied via its dorsal, medial and lateral surfaces, mainly from the dorsal arterial network.

Innervation

The lateral cuneiform is innervated by branches of the deep fibular and lateral plantar nerves.

Ossification

The lateral cuneiform ossifies during the first year of life (Fig. 84.7).

Tarsal coalition

Tarsal coalition is a hereditary condition in which there is a fibrous, cartilaginous or osseous union of two or more tarsal bones, and is believed to arise as a result of a failure of segmentation of primitive mesenchyme. Harris & Beath (1948) were the first to recognize an association between tarsal coalitions and ‘peroneal (fibular) spastic flat foot’. The two most common examples are talocalcaneal and calcaneonavicular coalitions, which usually present with symptoms early in the second decade of life. They are often, but not invariably, associated with flat feet (see below). A talonavicular coalition is rare, but when present is often associated with a ‘ball and socket’ ankle joint. Surgical resection of tarsal coalitions may eradicate associated pain but seldom improves the range of movement.

METATARSALS

The five metatarsal bones lie in the distal half of the foot and connect the tarsus and phalanges. Like the metacarpals, they are miniature long bones, and have a shaft, proximal base and distal head. Except for the first and fifth, the shafts are long and slender, longitudinally convex dorsally, and concave on their plantar aspects. Prismatic in section, they taper distally. Their bases articulate with the distal tarsal row and with adjacent metatarsal bases. The line of each tarsometatarsal joint, except the first, inclines proximally and laterally, metatarsal bases being oblique relative to their shafts. The heads articulate with the proximal phalanges, each by a convex surface that passes farther on to its plantar aspect, where it ends on the summits of two eminences. The sides of the heads are flat, with a depression surmounted by a dorsal tubercle for a collateral ligament of the metatarsophalangeal joint.

On occasion, an os intermetatarseum is encountered between the medial cuneiform and the bases of the first and second metatarsal bones and represents a rare accessory bone in this region.

Individual metatarsals

First metatarsal

The first metatarsal (Fig. 84.5A,B; 84.11) is the shortest and thickest, and has a strong shaft, of marked prismatic form. The base sometimes has a lateral facet or ill-defined smooth area as a result of contact with the second metatarsal. Its large proximal surface, usually indented on the medial and lateral margins, articulates with the medial cuneiform. Its circumference is grooved for tarsometatarsal ligaments and, medially, part of the tendon of tibialis anterior is attached; its plantar angle has a rough, oval, lateral prominence for the tendon of fibularis longus. The medial head of the first dorsal interosseous is attached to the flat lateral surface of the shaft. The large head has a plantar elevation, the crista, which separates two grooved facets (of which the medial is larger), on which sesamoid bones glide.

Muscle attachments

The first metatarsal receives attachments from the tendon of tibialis anterior medially, and the tendon of fibularis longus on its plantar aspect. It gives origin to the medial head of the first dorsal interosseus on the proximal aspect of the lateral surface.

Vascular supply

The first metatarsal is supplied by the first dorsal and first plantar metatarsal arteries and a superficial branch of the medial plantar artery, which together form a periosteal network. A nutrient artery enters the lateral surface of the mid-diaphysis. The head receives a medial, lateral and plantar supply from these arteries.

Innervation

The first metatarsal is innervated by the deep fibular and medial plantar nerves.

Ossification

The first metatarsal has two centres of ossification, one in the shaft, the other in the base (unlike the other metatarsals, in which the secondary ossification centre is distal). They appear during the tenth week of prenatal life and the third year of life, respectively (Fig. 84.7) and fuse between the 17th and 20th years. There may be a third centre in the first metatarsal head.

Second metatarsal

The second metatarsal is the longest (Figs 84.5A,B; 84.11). Its cuneiform base bears four articular facets. The proximal one, concave and triangular, is for the intermediate cuneiform. The dorsomedial one, for the medial cuneiform, is variable in size and usually continuous with that for the intermediate cuneiform. Two lateral facets, dorsal and plantar, are separated by non-articular bone, each divided by a ridge into distal demifacets, which articulate with the third metatarsal base, and a proximal pair (sometimes continuous) for the lateral cuneiform. The areas of these facets vary, particularly the plantar facet, which may be absent. An oval pressure facet, caused by contact with the first metatarsal, may appear on the medial side of the base, plantar to that for the medial cuneiform. Because of its length, its steep inclination, and the position of its base recessed in the tarsometatarsal joint, it is at risk of stress overload; perhaps this is why it is a common site for stress fractures in athletes and an avascular phenomenon in its head (Freiberg's infraction).

Muscle attachments

The lateral head of the first dorsal interosseous and the medial head of the second, are attached to the medial and lateral surfaces of the shaft, respectively.

Vascular supply

The blood supply of the second, third and fourth metatarsals follows the same pattern as that described for the first metatarsal, i.e. the bones are all supplied by branches of the dorsal and plantar metatarsal arteries. The nutrient artery enters the diaphysis on its lateral side near the metatarsal base. A constant plantar vessel supplies the head.

Innervation

The second metatarsal is innervated by branches of the deep fibular and branches of medial plantar nerve.

Ossification

There are two centres of ossification, one in the shaft and one distally in the metatarsal head (Fig. 84.7). Ossification of the shaft starts during the ninth prenatal week and ossification of the metatarsal head starts between the third and fourth years; fusion occurs between the 17th and 20th years.

Third metatarsal

The third metatarsal (Figs 84.5A,B; 84.11) has a flat triangular base, articulating proximally with the lateral cuneiform, medially with the second metatarsal, via dorsal and plantar facets, and laterally, via a single facet, with the dorsal angle of the fourth metatarsal. The medial plantar facet is frequently absent. The third tarsometatarsal joint is relatively immobile and predisposes the third metatarsal to stress fracture.

Muscle attachments

The lateral head of the second dorsal interosseous and first plantar are attached to the medial surface of the shaft. The medial head of the third dorsal interosseous is attached to its lateral surface.

Vascular supply

The blood supply of the third metatarsal is the same as that of the second metatarsal, described above.

Innervation

The third metatarsal is innervated by the deep fibular and lateral plantar nerves.

Ossification

There are two centres of ossification, one in the shaft and one distally in the metatarsal head (Fig. 84.7). Ossification of the shaft starts during the ninth prenatal week and ossification of the metatarsal head starts between the third and fourth years; fusion occurs between the 17th and 20th years.

Fourth metatarsal

The fourth metatarsal is smaller than the third (Figs 84.5A,B; 84.11). Its base has proximally, an oblique quadrilateral facet for articulation with the cuboid; laterally, a single facet for the fifth metatarsal; medially, an oval facet for the third metatarsal. The latter is sometimes divided by a ridge, in which case the proximal part articulates with the lateral cuneiform.

Muscle attachments

The lateral head of the third dorsal and second plantar interossei are attached to the medial surface. The medial head of the fourth dorsal interosseous is attached to the lateral surface.

Vascular supply

The blood supply of the fourth metatarsal is the same as that of the second and third metatarsals, described above.

Innervation

The fourth metatarsal is innervated by the deep fibular and lateral plantar nerves.

Ossification

There are two centres of ossification, one in the shaft and one distally in the metatarsal head (Fig. 84.7). Ossification of the shaft starts during the ninth prenatal week and ossification of the metatarsal head commences between the third and fourth years; fusion occurs between the 17th and 20th years.

Fifth metatarsal

The fifth metatarsal has a tuberosity (styloid process) on the lateral side of its base (Figs 84.5A,B; 84.11). The base articulates proximally with the cuboid by a triangular, oblique surface, and medially with the fourth metatarsal. The tuberosity can be seen and felt midway along the lateral border of the foot; in acute inversion it may be fractured. The metaphysial–diaphysial junction of the fifth metatarsal base is prone to traumatic or stress fractures, and these have a tendency to delayed and non-union, and often require surgical fixation. It is believed that fractures at this level damage the nutrient artery and the extraosseous plexus, resulting in compromised vascularity of the fracture site and consequent poor fracture healing.

Muscle attachments

The tendon of fibularis tertius is attached to the medial part of the dorsal surface and medial border of the shaft, and that of fibularis brevis to the dorsal surface of the tuberosity. A strong band of the plantar aponeurosis, sometimes containing muscle, connects the apex of the tuberosity to the lateral process of the calcaneal tuberosity. It is this attachment, and not that of fibularis brevis, which is responsible for avulsion fractures of the tuberosity.

The plantar surface of the base is grooved by the tendon of abductor digiti minimi, and flexor digiti minimi brevis is attached here. The lateral head of the fourth dorsal and the third plantar interossei are attached to the medial side of the shaft.

Vascular supply

The fifth metatarsal is supplied by dorsal and plantar metatarsal arteries and an inconstant fibular marginal artery. The nutrient artery enters the diaphysis proximally and medially.

Innervation

The fifth metatarsal is innervated by branches from the sural, superficial fibular and lateral plantar nerves.

Ossification

There are three centres of ossification, one at the base in the region of the tuberosity (an apophysis), one in the shaft and one distally in the metatarsal head. Ossification of the shaft starts during the tenth prenatal week and ossification of the metatarsal head starts between the third and fourth years (Fig. 84.7). Fusion of the distal and shaft centres occurs between the 17th and 20th years, the proximal apophysis fuses earlier. An os vesalianum is a rare variant that should not be confused with the basal apophysis. (Fig. 84.12)

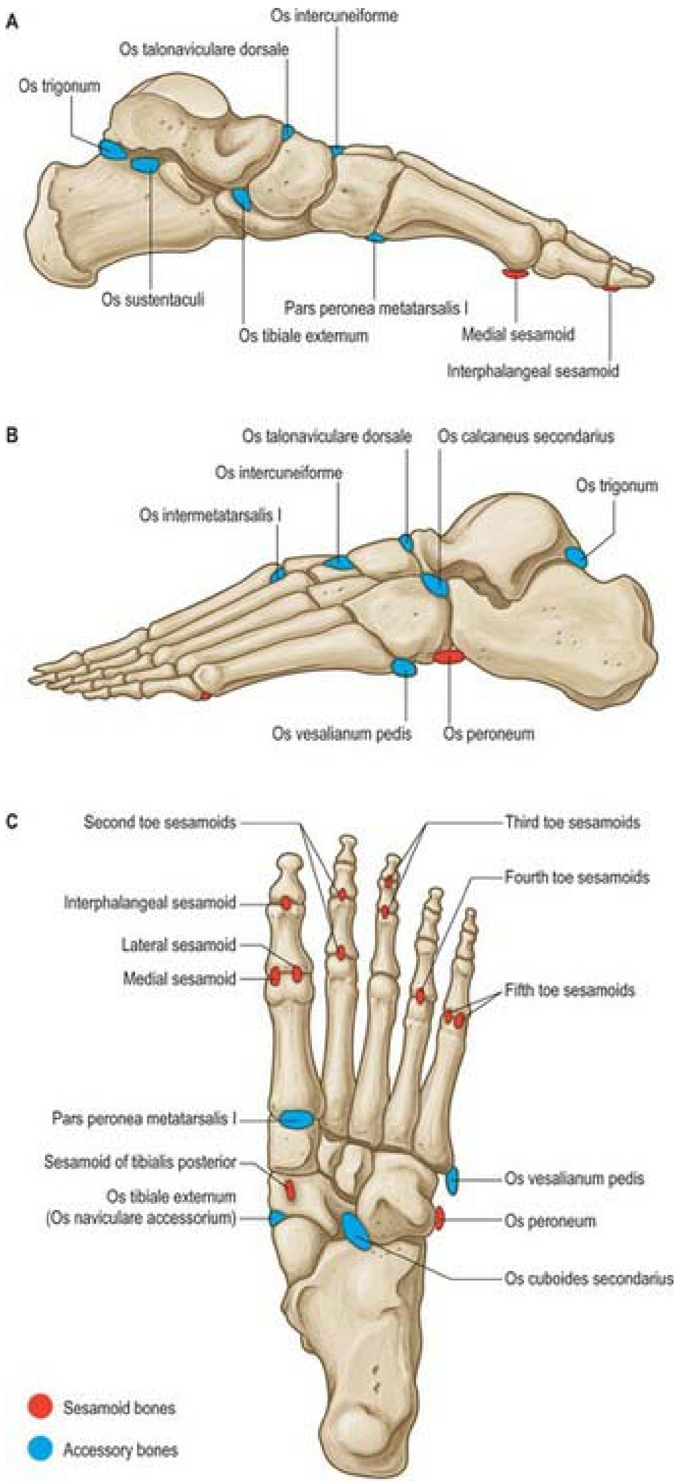
A
Os intercuneiforme
Os talonaviculare dorsale
Os trigonum
Os sustentaculi
Pars peronea metatarsalis I
Os tibiale externum
Medial sesamoid
Interphalangeal sesamoid
B
Os talonaviculare dorsale
Os calcaneus secondarius
Os intercuneiforme
Os trigonum
Os intermetatarsalis I
Os vesalianum pedis
Os peroneum
C
Second toe sesamoids
Third toe sesamoids
Fourth toe sesamoids
Interphalangeal sesamoid
Lateral sesamoid
Medial sesamoid
Fifth toe sesamoids
Pars peronea metatarsalis I
Sesamoid of tibialis posterior
Os tibiale externum
(Os naviculare accessorium)
Os vesalianum pedis
Os peroneum
Os cuboides secondarius
Sesamoid bones
Accessory bones

Fig. 84.12 Sites of sesamoid and accessory bones found in the left foot. **A**, Medial aspect; **B**, lateral aspect; **C**, plantar aspect.

PHALANGES OF THE FOOT

In general, the phalanges of the foot resemble those of the hand: there are two in the hallux, and three in each of the other toes (Fig. 84.5A,B). On occasion there are only two phalanges in the little toe and, rarely, this is the case with the other lesser toes. The phalanges of the toes are much shorter than their counterparts in the hand and their shafts, especially those of the proximal set, are compressed from side to side. In the proximal phalanges, the compressed shaft is convex dorsally, with a plantar concavity. The base is concave for articulation with a metatarsal head and the head is a trochlea for a middle phalanx. Middle phalanges are small and short, but broader than their proximal counterparts. Distal phalanges resemble those in the fingers, but are smaller and flatter. Each has a broad base for articulation with a middle phalanx and an expanded distal end. A rough tuberosity on the plantar aspect of the latter supports the pulp of the toe, and provides a weight-bearing area.

Muscle attachments

Tendons of the long digital flexors and extensors are attached to the plantar and dorsal aspects of the bases of the distal phalanges of the lateral four toes. Flexor hallucis longus and extensor hallucis longus are similarly attached to the hallux. The bases of the middle phalanges receive the tendons of flexor digitorum brevis and extensor digitorum brevis. The proximal phalanges of the second, third, fourth and fifth toes each receive a lumbrical on their medial side; those of the second, third and fourth toes also receive an interosseous muscle on both sides. For further details of muscular, capsular and ligamentous arrangements in the toes refer to Fig. 84.5A,B. The terminal phalanx of the hallux normally shows a small degree of valgus (lateral) deviation, as may the proximal phalanx. This is presumed to be unrelated to footwear, because this degree of. deviation has also been observed in fetal specimens.

Vascular supply

The proximal phalanges receive most of their blood supply from the dorsal digital arteries. The middle phalanges are supplied by plantar and dorsal digital arteries. The distal phalanges receive their supply mainly from plantar digital arteries.

Innervation

The phalanges are innervated by the plantar and dorsal digital nerves.

Ossification

Phalanges are ossified from a primary centre for the shaft and a basal epiphysis (Fig. 84.7). Primary centres for the distal phalanges appear between the ninth and twelfth prenatal weeks, somewhat later in the fifth digit. Primary centres for the proximal phalanges appear between the 11th and 15th weeks, and later for intermediate phalanges, but there is wide variation. Basal centres appear between the second and eighth years (usually second or third in the hallux), and union with the shaft occurs by the 18th year. There is considerable variation in ossification and fusion dates.

SESAMOIDS

Galen is believed to have been the first to use the term ‘sesamoid’ because of the resemblance of these bones to sesame seeds. Most sesamoid bones are only a few millimetres in diameter and their shape is variable. Some have a predictable location (see below), but many others vary in terms of location and frequency of occurrence (Fig. 84.12). Some sesamoids ossify, whereas others remain cartilaginous. Most sesamoid bones are embedded in tendons in close proximity to joints. Their precise role is not understood; it is believed that they may alter the direction of muscle pull, decrease friction and modify pressure.

Medial and lateral sesamoids of the first metatarsophalangeal joint

The two constant sesamoid bones within the foot are those of the first metatarsophalangeal articulation. The medial sesamoid is generally larger than the lateral sesamoid and lies slightly more distally. During dorsiflexion of the hallux, the sesamoids lie below the first metatarsal head, offering protection to the otherwise exposed plantar aspect of the first metatarsal head. The medial (tibial) sesamoid is approximately 10 mm wide and 14 mm long and the lateral (fibular) sesamoid is usually smaller (approximately 8 mm wide and 10 mm long): the overall sizes vary considerably.

The sesamoids are embedded within the double tendon of flexor hallucis brevis and articulate on their dorsal surfaces with the plantar facets of the first metatarsal head. They are separated by the crista or intersesamoidal ridge, which provides stability to the sesamoid complex. (This ridge can be eroded to the point of obliteration in severe cases of hallux valgus.) The sesamoids are connected to the plantar base of the proximal phalanx through the plantar plate, which is an extension of the tendon of flexor hallucis brevis. The plantar surface of each sesamoid is covered by a thin layer of the tendon of flexor hallucis brevis, whereas the dorsal or superior surface is covered by hyaline cartilage. The sesamoids are suspended by a sling-like mechanism made up of the collateral ligaments of the first metatarsophalangeal joint and the sesamoid ligaments on either side of the joint. The plantar aponeurosis also has an attachment to the sesamoids.

Approximately 30% of these sesamoid bones are bipartite. The medial is much more commonly affected and may have two, three or four parts, but the fibular sesamoid rarely has more than two. The condition may be bilateral. The sesamoids may be absent congenitally.

Muscle attachments

The medial sesamoid receives an attachment from abductor hallucis, which provides a medial stabilizing influence on the sesamoid complex. The lateral sesamoid receives some fibres from the tendon of adductor hallucis, and this provides lateral stabilization. The medial and lateral sesamoids are connected by the intersesamoid ligament, which forms the floor of the tendinous canal for the tendon of flexor hallucis longus.

Vascular supply

There are three patterns of blood supply to the sesamoid bones. In 50% of cases the arterial supply is derived from the medial plantar artery and the plantar arch, in 25% of cases it is predominantly from the plantar arch and in 25% of cases it is from the medial plantar artery alone. The major arterial blood supply to the sesamoids enters from the proximal and plantar aspects, and only a minor contribution enters through the distal pole. The pattern of vascular supply determines the vulnerability of a sesamoid to avascular necrosis after injury to the bone.

Innervation

The medial and lateral sesamoids are innervated by the plantar digital nerves.

Ossification

The ossification centres of the sesamoids can be multiple or single.

Other sesamoid and accessory bones

Accessory or inconstant sesamoid bones may occur under any weight-bearing surface of the foot, but are most common under the second to fifth metatarsal heads. They are extremely variable in size and their incidence is difficult to determine.

A true sesamoid occurs in the tendon of tibialis posterior in about 10% of individuals. It lies on the plantar aspect of the navicular tuberosity within the tendon at the level of the inferior border of the calcaneonavicular ligament (see above, accessory navicular bones). Very rarely, a sesamoid is found within the tendon of tibialis anterior near its insertion at the level of the anteroinferior corner of the medial cuneiform, where there is an articular facet. An os peroneum is a sesamoid bone within the tendon of fibularis longus that articulates with the lateral surface of the calcaneum, the calcaneocuboid joint or, more frequently, the plantar aspect of the cuboid where there is an articular facet. The bone is situated where the tendon of fibularis longus angles around the plantar aspect of the lateral border of the cuboid and is probably present in 95% of cases; it is usually cartilaginous.

JOINTS

ANKLE (TALOCRURAL) JOINT

The talocrural joint is a hinge joint, approximately uniaxial. The lower end of the tibia and its medial malleolus, together with the lateral malleolus of the fibula and inferior transverse tibiofibular ligament, form a deep recess (‘mortise’) for the body of the talus. Although it appears to be a simple hinge, its axis of rotation is dynamic, shifting during dorsi- and plantar flexion. Starting from the plantigrade position the normal range of dorsiflexion is 10° when the knee is straight, and 30° with the knee flexed (when the calcaneal tendon will be relaxed). The range of normal plantar flexion is 30°. (The values of these ranges are all approximate.) Dorsiflexion results in the joint adopting the ‘close-packed’ position, with maximal congruence and ligamentous tension; from this position, all major thrusting movements are exerted, in walking, running and jumping. The malleoli grip the talus, and even in relaxation no appreciable lateral movement can occur without stretch of the inferior tibiofibular syndesmosis and slight bending of the fibula. The superior talar surface is broader in front, and in dorsiflexion the malleolar gap is increased by slight lateral rotation of the fibula, by ‘give’ at the inferior tibiofibular syndesmosis and gliding at the superior tibiofibular joint.

Articulating surfaces

Articular surfaces are covered by hyaline cartilage. The talar trochlear surface, which is convex parasagittally and gently concave transversely, is wider in front; the distal tibial articular surface is reciprocally curved. The talar articular surface for the medial malleolus is a proximal area on the medial talar surface, and is fairly flat, comma-shaped and deeper anteriorly. The larger lateral talar articular surface is triangular and vertically concave, while the articular surface on the lateral malleolus is reciprocally curved. Posteriorly, the edge between the trochlear and fibular articular surfaces of the talus is bevelled to a narrow, flat triangular area that articulates with the inferior transverse tibiofibular ligament (Fig. 84.13A); all surfaces are contiguous. The bones are held together by a fibrous capsule, and by medial (deltoid), anterior and posterior talofibular and calcaneofibular ligaments.

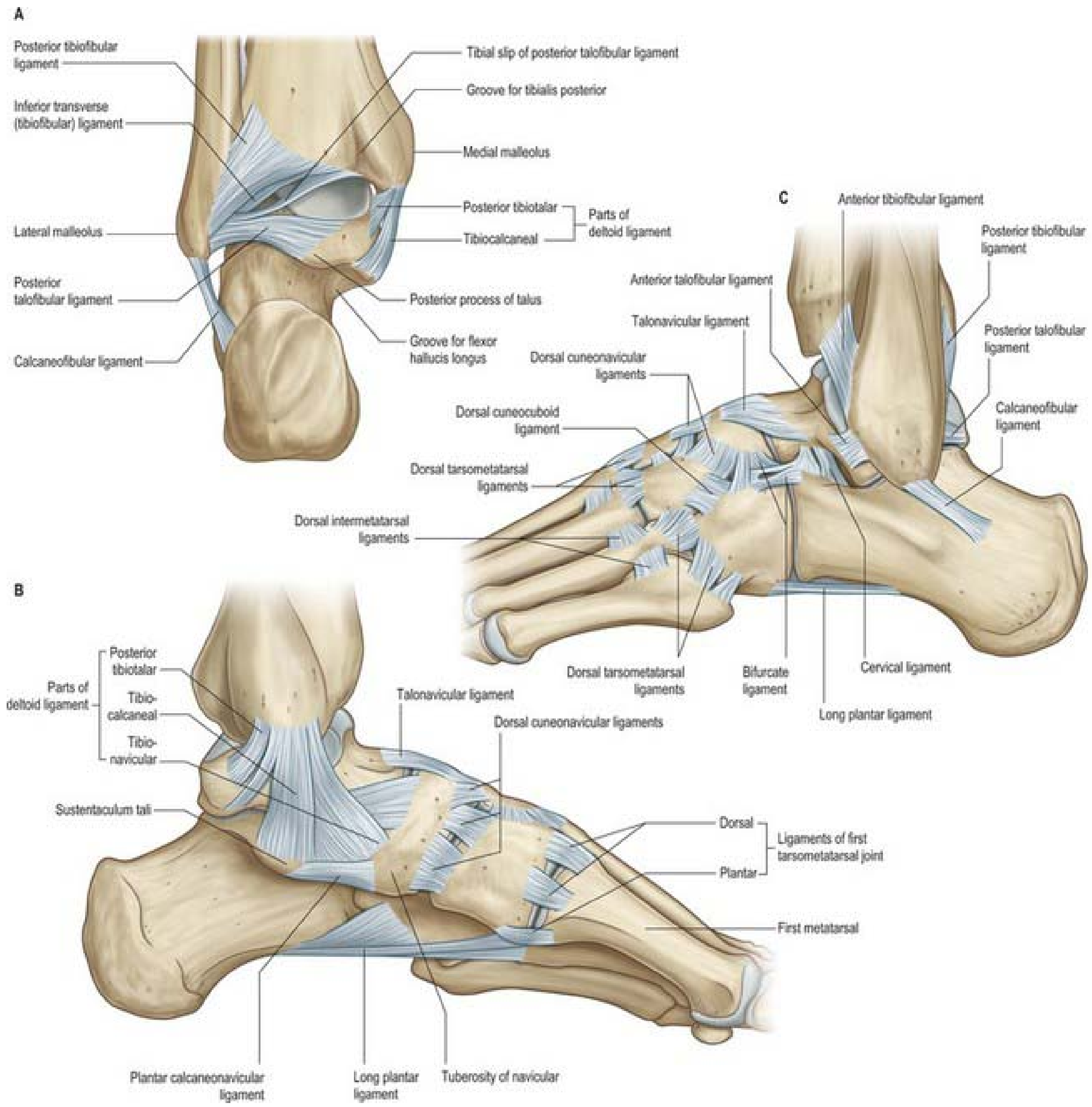
A
Posterior tibiofibular ligament
Inferior transverse (tibiofibular) ligament
Lateral malleolus
Posterior talofibular ligament
Calcaneofibular ligament
Tibial slip of posterior talofibular ligament
Groove for tibialis posterior
Medial malleolus
Posterior tibiotalar
Tibiocalcaneal
Parts of deltoid ligament
Posterior process of talus
Groove for flexor hallucis longus
C
Anterior tibiofibular ligament
Posterior tibiofibular ligament
Anterior talofibular ligament
Talonavicular ligament
Posterior talofibular ligament
Dorsal cuneonavicular ligaments
Calcaneofibular ligament
Dorsal cuneocuboid ligament
Dorsal tarsometatarsal ligaments
Dorsal intermetatarsal ligaments
Dorsal tarsometatarsal ligaments
Bifurcate ligament
Cervical ligament
Long plantar ligament
B
Parts of deltoid ligament
Posterior tibiotalar
Tibio-calcaneal
Tibio-navicular
Sustentaculum tali
Talonavicular ligament
Dorsal cuneonavicular ligaments
Dorsal
Plantar
Ligaments of first tarsometatarsal joint
First metatarsal
Plantar calcaneonavicular ligament
Long plantar ligament
Tuberosity of navicular

Fig. 84.13 The left ankle and tarsal joints. **A**, Posterior aspect. **B**, Medial aspect. **C**. Lateral aspect.

Fibrous capsule

Around the joint, the fibrous capsule is thin in front and behind. It is attached proximally to the borders of the tibial and malleolar articular surfaces, and distally to the talus near the margins of its trochlear surface, except in front where it reaches the dorsum of the talar neck. The capsule is strengthened by strong collateral ligaments. Its posterior part consists mainly of transverse fibres. It blends with the inferior transverse ligament and is thickened laterally where it reaches the fibular malleolar fossa.

Ligaments

The ligaments of the talocrural joint are the medial and lateral collateral ligaments.

Medial collateral ligament (deltoid ligament)

The medial collateral ligament (deltoid ligament) is a strong, triangular band, attached to the apex and the anterior and posterior borders of the medial malleolus (Fig. 84.13B). Of its superficial fibres, the anterior (tibionavicular) pass forwards to the navicular tuberosity, behind which they blend with the medial margin of the plantar calcaneonavicular ligament; inter-mediate (tibiocalcaneal) fibres descend almost vertically to the entire length of the sustentaculum tali; posterior fibres (posterior tibiotalar) pass posterolaterally to the medial side of the talus and its medial tubercle. The deep fibres (anterior tibiotalar) pass from the tip of the medial malleolus to the non-articular part of the medial talar surface. The ligament is crossed by the tendons of tibialis posterior and flexor digitorum longus. It is rarely injured alone, and when torn, is commonly associated with a fracture of the distal fibula. Chronic instability is rare.

Lateral ligament

The lateral ligament has three discrete parts. The anterior talofibular ligament extends anteromedially from the anterior margin of the fibular malleolus to the talus, attached in front of its lateral articular facet and to the lateral aspect of its neck (Fig. 84.13C). The posterior talofibular ligament runs almost horizontally from the distal part of the lateral malleolar fossa to the lateral tubercle of the posterior talar process (Fig. 84.13A); a ‘tibial slip’ of fibres connects it to the medial malleolus. The calcaneofibular ligament, a long cord, runs from a depression anterior to the apex of the fibular malleolus to a tubercle on the lateral calcaneal surface and is crossed by the tendons of fibularis longus and brevis (Fig. 8.13A,C). The lateral ligament complex is injured most commonly with inversion sprains, often during sport; the posterior talofibular ligament is almost always spared. Although the resulting increased laxity is tolerated in most cases, some require surgical reconstruction.

Synovial membrane

The joint is lined by synovial membrane which projects into the inferior (distal) tibiofibular joint.

Vascular supply and lymphatic drainage

The talocrural joint is supplied by malleolar branches of the anterior and posterior tibial and fibular arteries. Lymphatic drainage is via vessels accompanying the arteries and via the long and short saphenous veins superficially.

Innervation

The talocrural joint is innervated by branches from the deep fibular, saphenous, sural and tibial nerves (or medial and lateral plantar nerves, depending on the level of division of the tibial nerve). Occasionally, the superficial fibular nerve also supplies the ankle joint.

For a comprehensive account of the innervation of the ankle joint (and other foot joints) see Gardner & Gray (1968).

Relations

Anteriorly, from medial to lateral, are tibialis anterior, extensor hallucis longus, the anterior tibial vessels, deep fibular nerve, extensor digitorum longus and fibularis tertius; posteromedially from medial to lateral, are tibialis posterior, flexor digitorum longus, the posterior tibial vessels, tibial nerve, flexor hallucis longus; in the groove behind the lateral malleolus are the tendons of fibularis longus and brevis. The tendon of fibularis brevis lies anterior to the tendon of fibularis longus at this level (Fig. 84.14). The long saphenous vein and saphenous nerve cross the ankle joint medial to the tendon of tibialis anterior and anterior to the medial malleolus, the nerve lying posterior to the vein.

All of the above structures are at risk during surgery on the ankle: the main structures at risk are the neurovascular structures anteriorly and posteromedially. Branches of the superficial fibular nerve are at risk on the anterolateral aspect of the ankle, particularly during ankle arthroscopy.

Factors maintaining stability

Passive stability is conferred upon the ankle mainly by the medial and lateral ligament complexes, the distal tibiofibular ligaments, the tendons crossing the joint, the bony contours and the capsular attachments. Dynamic stability is conferred by gravity, muscle action and ground reaction forces. Stability requires the continuous action of soleus assisted by gastrocnemius: it increases when leaning forward, and decreases when leaning backwards. If backward sway takes the projection of the centre of gravity (‘weight line’) posterior to the transverse axes of the ankle joints, the plantar flexors relax and the dorsiflexors contract.

Failure of the fibular muscles can lead progressively to varus instability, whereas long-standing failure of the tendon of tibialis posterior, which is relatively common in the elderly female, can result in valgus instability of the ankle and particularly a planovalgus foot deformity.

Muscles producing movement

Dorsiflexion is produced by tibialis anterior, assisted by extensors digitorum longus and hallucis longus, and fibularis tertius. Plantar flexion is produced by gastrocnemius and soleus, assisted by plantaris, tibialis posterior, flexors hallucis longus and digitorum longus.

Ankle fractures

Ankle fractures are common and of importance because failure to achieve accurate anatomical alignment in the treatment of ankle fractures often results in significant long term morbidity. Except for very simple and undisplaced fractures, most ankle fractures are associated with a ligamentous injury. The direction and nature of forces applied to the ankle correlate with the fracture pattern and concomitant ligament injury. The Lauge–Hansen classification, although slightly cumbersome, classifies injuries according to two components: the position of the foot at the time of injury and the direction of the force applied. In a supination/adduction type injury, the foot is supinated and an adduction force is applied, resulting in a transverse fracture of the distal fibula (stage 1), followed by an oblique fracture of the medial malleolus (stage 2). In a supination/external rotation type injury, the first structure to rupture is the anterior inferior tibiofibular ligament, followed in order by a spiral fibular fracture, a posterior malleolar fracture and then a medial malleolar fracture (or deltoid ligament rupture). In pronation/abduction injuries, a transverse medial malleolar fracture is followed by rupture of the anterior and posterior inferior tibiofibular ligaments and interosseous ligament, and then by an oblique fibular fracture. Pronation/external rotation injuries commence with a medial malleolar fracture (or deltoid ligament rupture), followed in turn by rupture of the anterior inferior tibiofibular ligament, the interosseous ligament, the interosseous membrane, a high fibular fracture and fracture of the posterior tibial plafond ('posterior malleolus').

Inferior (distal) tibiofibular joint

The inferior (distal) tibiofibular joint is usually considered a syndesmosis. It consists of the anterior and posterior tibiofibular ligaments and the interosseous ligament.

Articulating surfaces

The distal tibiofibular joint is between the rough, medial convex surface on the distal end of the fibula and the rough concave surface of the fibular notch of the tibia. These surfaces are separated distally for approximately 4 mm by a synovial prolongation from the ankle joint, and may be covered by articular cartilage in their lowest parts.

Fibrous capsule

The distal tibiofibular joint does not have a capsule.

Ligaments

The ligaments of the inferior (distal) tibiofibular joint are the anterior, interosseous and posterior ligaments.

Anterior tibiofibular ligament

The anterior tibiofibular ligament is a flat band which descends laterally between the adjacent margins of the tibia and fibula, anterior to the syndesmosis (Fig. 84.13C). Bassett's ligament is a variant that presents as a low lying slip of the ligament which is inserted so far distally on the fibula that it may cause irritation of the lateral dome of the talus: it is amenable to arthroscopic removal.

Interosseous tibiofibular ligament

The interosseous tibiofibular ligament is continuous with the interosseous membrane and contains many short bands between the rough adjacent tibial and fibular surfaces; it is the strongest bond between the bones.

Posterior tibiofibular ligament

The posterior tibiofibular ligament is stronger than the anterior, and is disposed similarly on the posterior aspect of the syndesmosis (Fig. 84.13A). Its distal, deep part is the inferior transverse ligament, a thick band of yellow fibres which crosses from the proximal end of the lateral malleolar fossa to the posterior border of the tibial articular surface almost to the medial malleolus. The ligament projects distal to the bones, in contact with the talus. Its colour reflects its content of yellow elastic fibres.

Synovial membrane

The synovial membrane of the ankle joint projects into the distal 4 mm or so of the inferior tibiofibular joint.

Vascular supply and lymphatic drainage

The inferior tibiofibular joint is supplied by the perforating branch of the fibular artery and the medial malleolar branches of the anterior and posterior tibial arteries. Lymphatic drainage is via vessels corresponding to the arteries, and via vessels that accompany the long and short saphenous veins.

Innervation

The inferior tibiofibular joint is innervated by branches from the deep fibular and sural nerves.

Relations

No significant structures pass anterior to the anterior aspect of the inferior tibiofibular joint, but the superficial fibular nerve is at risk during surgery to this area. Posteriorly, the fibular artery passes over the posterior tibiofibular ligament and is at risk in the posterolateral approach to the fibula.

Factors maintaining stability

Stability is maintained in part by the bone contours, but mainly by the dense anterior and posterior tibiofibular and the interosseous ligaments.

Muscles producing movement

No muscles act on the inferior tibiofibular joint, which moves only slightly. Because of the varying slope of the lateral surface of the body of talus, the fibula undergoes a small degree of lateral rotation during dorsiflexion at the ankle, and this results in slight widening of the interval between the bones. Testing for a significant disruption of this joint is usually carried out with the patient under anaesthetic and involves applying an external rotation and abduction force, looking for abnormal widening of the syndesmosis. Excessive anterior/posterior glide of the fibula relative to the tibia also indicates a disruption of the joint.

Talocalcaneal joint

Anterior and posterior articulations between the calcaneus and talus form a functional unit often termed the ‘subtalar joint’. The posterior articulation is referred to as the talocalcaneal joint and the anterior articulation is regarded as part of the talocalcaneonavicular joint. The talocalcaneal joint is modified multiaxial and its permitted movements are considered together with those at other tarsal joints. The bones are connected by a fibrous capsule, and by lateral, medial, interosseous talocalcaneal and cervical ligaments.

Articulating surfaces

The subtalar joint proper involves the concave posterior calcaneal facet on the posterior part of the inferior surface of the talus and the convex posterior facet on the superior surface of the calcaneus (Fig. 84.15A,B).

Fibrous capsule

The fibrous capsule envelops the joint, its fibres are short and attached to its articular margins.

Ligaments

The ligaments of the talocalcaneal joint are the lateral, medial and interosseous talocalcaneal ligaments and the cervical ligament.

Lateral talocalcaneal ligament

The lateral talocalcaneal ligament is a short flat fasciculus that descends obliquely back from the lateral talar process to the lateral calcaneal surface and is attached anterosuperior to the calcaneofibular ligament.

Medial talocalcaneal ligament

The medial talocalcaneal ligament connects the medial talar tubercle to the back of the sustentaculum tali and adjacent medial surface of the calcaneus. Its fibres blend with the medial (deltoid) ligament of the ankle joint; the most posterior fibres line the groove for flexor hallucis longus between the talus and calcaneus.

Interosseous talocalcaneal ligament

The interosseous talocalcaneal ligament is a broad, flat, bilaminar transverse band in the sinus tarsi (Figs 84.15A; 84.16). It descends obliquely and laterally from the sulcus tali to the calcaneal sulcus. The posterior lamina of the ligament is associated with the talocalcaneal joint, and the anterior lamina with the talocalcaneonavicular joint. Its medial fibres are taut in eversion.

Cervical ligament

The cervical ligament is just lateral to the tarsal sinus and attached to the superior calcaneal surface (Fig. 84.13C). It is medial to the attachment of extensor digitorum brevis, from where it ascends medially to an inferolateral tubercle on the talar neck (Barclay-Smith 1896). It is considered to be taut in inversion.

Synovial membrane

The synovial cavity of the talocalcaneal joint is usually quite separate and does not communicate with those of other tarsal joints. However, direct communication with the ankle joint has been observed in rare instances.

Innervation

The talocalcaneal joint is innervated by branches of the posterior tibial, medial plantar and sural nerves.

Relations

Posteromedially, in the region of the posterior aspect of the talocalcaneal joint, and viewed from anterior to posterior, lie the veins on either side of the posterior tibial artery, the tibial nerve and the tendon of flexor hallucis longus. These neurovascular structures are at risk in posteromedial approaches to the ankle and talocalcaneal joints. On the lateral side, the tendon of fibularis brevis lies anterior to the tendon of fibularis longus, both passing behind the fibular malleolus in proximity to the talocalcaneal joint. The sural nerve lies just posterior to the fibular tendons and is at risk during lateral exposure of the joint.

Factors maintaining stability

Stability is conferred by the bony contours of the hindfoot plus the above mentioned ligaments; it is not known which ligaments provide the most stability. An additional ligamentous restraint is provided by the calcaneofibular component of the lateral ligament complex. The tendons crossing the articulation also aid stability.

Muscles producing movement

Heel inversion is controlled by tibialis anterior, tibialis posterior and the gastrocnemius–soleus complex via the calcaneal tendon; the long flexors of the toes also contribute. Heel eversion results from the pull of fibularis longus, brevis and tertius in addition to the long extensors of the toes.

Talocalcaneonavicular joint

An eloquent account of the talocalcaneonavicular joint was provided by Barclay-Smith in 1896. In terms of function, and in clinical practice, it is helpful to regard this complex joint as comprising two articulations, i.e. the anterior part of the ‘subtalar’ joint and the talonavicular joint. It is a compound, multiaxial articulation.

Articulating surfaces

The ovoid talar head is continuous with the triple-faceted anterior area of its inferior surface. The whole fits the concavity formed collectively by the posterior surface of the navicular, the middle and anterior talar facets of the calcaneus, and the superior fibrocartilaginous surface of the plantar calcaneonavicular ligament (spring ligament). The bones are connected by a fibrous capsule and by the talonavicular and plantar calcaneonavicular ligaments, and the calcaneonavicular part of the bifurcate ligament.

Fibrous capsule

The fibrous capsule is poorly developed, except posteriorly, where it is thick and blends with the anterior part of the interosseous ligament filling the tarsal sinus.

Ligaments

The ligaments of the talocalcaneonavicular joint are the talonavicular and plantar calcaneonavicular (spring) ligaments.

Talonavicular ligament

The talonavicular ligament is a broad, thin band (Fig. 84.13B,C). It connects the dorsal surfaces of the neck of the talus and the navicular, and is covered by extensor tendons. The plantar calcaneonavicular ligament and the calcaneonavicular part of the bifurcate ligament (Fig. 84.13C) are the plantar and lateral ligaments of the joint, respectively. Although the calcaneus and navicular do not articulate directly, they are connected by calcaneonavicular and plantar calcaneonavicular ligaments.

Plantar calcaneonavicular (spring) ligament

The plantar calcaneonavicular (spring) ligament is a broad, thick band connecting the anterior margin of the sustentaculum tali to the plantar surface of the navicular (Figs 84.13B; 84.15A; 84.17). It ties the calcaneus to the navicular below the head of the talus as part of its articular cavity and it sustains the medial longitudinal arch of the foot. The dorsal surface of the ligament has a triangular fibrocartilaginous facet on which part of the talar head rests (Fig. 84.15A). Its plantar surface is supported medially by the tendon of tibialis posterior and laterally by the tendons of flexors hallucis longus and digitorum longus; its medial border is blended with the anterior superficial fibres of the medial (deltoid) ligament. The calcaneonavicular ligament is described below as the medial band of the bifurcate ligament.

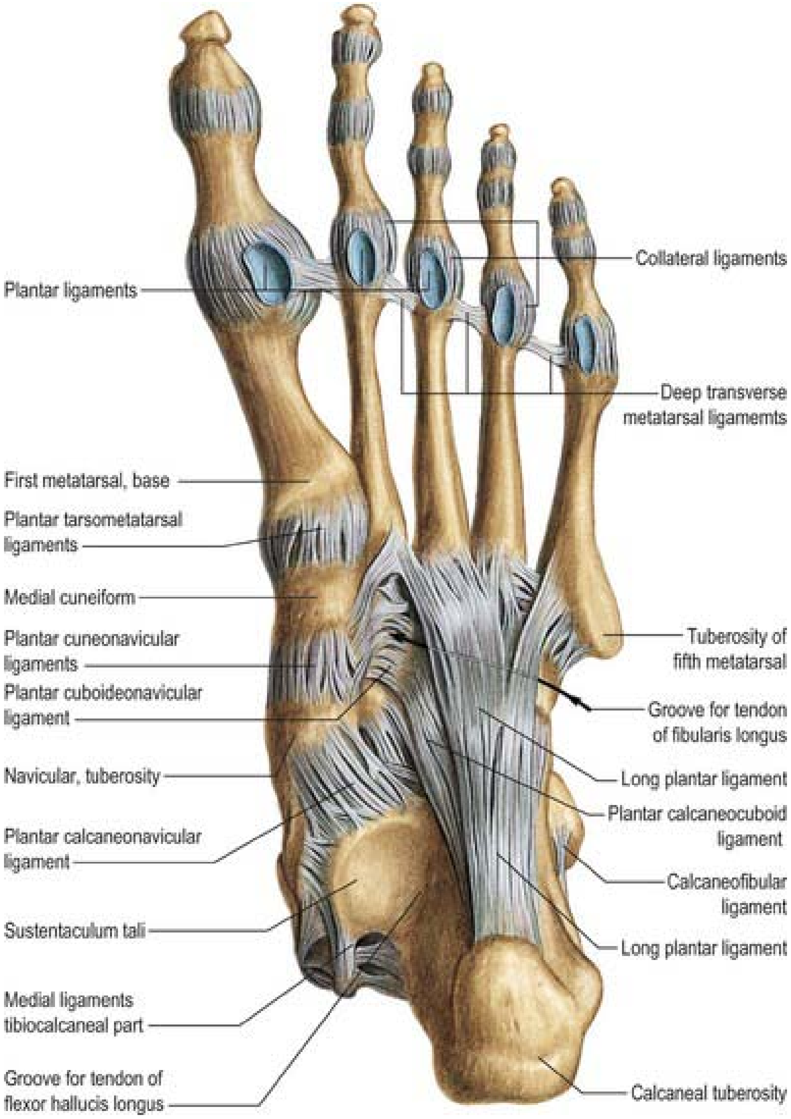
Collateral ligaments
Plantar ligaments
Deep transverse metatarsal ligamemts
First metatarsal, base
Plantar tarsometatarsal ligaments
Medial cuneiform
Plantar cuneonavicular ligaments
Tuberosity of fifth metatarsal
Plantar cuboideonavicular ligament
Groove for tendon of fibularis longus
Navicular, tuberosity
Long plantar ligament
Plantar calcaneocuboid ligament
Plantar calcaneonavicular ligament
Calcaneofibular ligament
Sustentaculum tali
Long plantar ligament
Medial ligaments tibiocalcaneal part
Groove for tendon of flexor hallucis longus
Calcaneal tuberosity

Fig. 84.17 Ligaments on the plantar aspect of the foot.

(From Sobotta 2006.)

Synovial membrane

The talocalcaneonavicular joint is a synovial joint whose cavity sometimes communicates with that of the talocalcaneal joint.

Innervation

The talocalcaneonavicular joint is innervated by the deep fibular and medial plantar nerves.

Relations

On the medial side from dorsal to plantar lie the tendon of tibialis posterior and the tendon of flexor digitorum longus above the sustentaculum tali, and the flexor hallucis longus tendon below. At this point, flexor hallucis longus lies deep to the medial and lateral plantar branches of the posterior tibial artery and nerve. The latter structures are at risk during medial approaches to the joint, e.g. resection of talocalcaneal coalition. Dorsally from medial to lateral lie the tendons of tibialis anterior and extensor hallucis longus, the deep fibular nerve and the dorsalis pedis artery, the muscle belly of extensor hallucis brevis passing medially and deep to the tendons of extensor digitorum longus and fibularis tertius. Structures at risk during the dorsal approach to the talonavicular joint include the branches of the superficial fibular nerve superficially and the dorsalis pedis artery and deep fibular nerve deep to the inferior extensor retinaculum.

Factors maintaining stability

Stability of the joint is due to a combination of factors: bony contours, the strong plantar calcaneonavicular (spring) ligament, and the calcaneonavicular component of the bifurcate ligament.

Muscles producing movement

The muscles producing movement are as described above for the talocalcaneal joint.

Calcaneocuboid joint

The calcaneocuboid joint is at the same level as the talonavicular joint and, together, they represent the transverse tarsal joint. It is a saddle (sellar) or biaxial joint with concavo-convex surfaces.

Articulating surfaces

The articular surfaces of the calcaneocuboid joint, which is 2 cm proximal to the tubercle on the fifth metatarsal base, are between the anterior (distal) surface of the calcaneus and the posterior (proximal) surface of the cuboid.

Fibrous capsule

The fibrous capsule is thickened dorsally as the dorsal calcaneocuboid ligament. The synovial cavity of this joint is separate, and does not communicate with those of other tarsal articulations (Fig. 84.6).

Ligaments

The ligaments of the calcaneocuboid joint are the bifurcate, long plantar and plantar calcaneocuboid ligaments.

Bifurcate ligament

The bifurcate ligament is a strong Y-shaped band (Fig. 84.13C). It is attached by its stem proximally to the anterior part of the upper calcaneal surface, and distally it divides into calcaneocuboid and calcaneonavicular parts. The (lateral) calcaneocuboid ligament extends to the dorsomedial aspect of the cuboid, forming a main bond between the two rows of tarsal bones; the (medial) calcaneonavicular ligament is attached to the dorsolateral aspect of the navicular.

Long plantar ligament

The long plantar ligament is the longest ligament associated with the tarsus (Figs 84.13C; 84.17; 84.18). It extends from the plantar surface of the calcaneus (anterior to the processes of its tuberosity) and from its anterior tubercle, to the ridge and tuberosity on the plantar surface of the cuboid. Deep fibres are attached to the cuboid and more superficial fibres continue to the bases of the second to fourth, and sometimes fifth, metatarsals. This ligament, together with the groove on the plantar surface of the cuboid, makes a tunnel for the tendon of fibularis longus. It is a most powerful factor limiting depression of the lateral longitudinal arch.

Plantar calcaneocuboid ligament

This short plantar ligament (Fig. 84.17) is deeper than the long plantar ligament, from which it is separated by areolar tissue. It is a short, wide band of great strength, stretching from the anterior calcaneal tubercle and the depression anterior to it, to the adjoining part of the plantar surface of the cuboid; it also sustains the lateral longitudinal arch.

Synovial membrane

A synovial membrane lines the calcaneo-cuboid joint.

Innervation

The calcaneocuboid joint is innervated on its plantar aspect by the lateral plantar nerve, and dorsally by the sural and deep fibular nerves.

Relations

Fibularis longus and abductor digiti minimi pass in proximity to the joint, and the lateral plantar nerve passes medially. Extensor digitorum brevis overlies the lateral aspect of the joint. The sural nerve and the tendon of fibularis longus are at risk during approaches to an os peroneum.

Factors maintaining stability

The calcaneocuboid joint only permits a small amount of movement; its stability reflects the bony contours and strong ligaments described above.

Muscles producing movement

Gliding occurs between the calcaneus and cuboid, with conjunct rotation upon each other during inversion and eversion of the entire foot. The movements are brought about by the same muscles that act on the talocalcaneal and talocalcaneonavicular joints.

Naviculocuneiform joints

The naviculocuneiform joint is a compound joint, often described as plane.

Articulating surfaces

The navicular articulates distally with the cuneiform bones where the distal navicular surface is transversely convex and divided into three facets by low ridges that are adapted to the proximal, slightly curved surfaces of the cuneiforms.

Fibrous capsule

The fibrous capsule is continuous with those of the intercuneiform and cuneocuboid joints and it is also connected to the second and third cuneometatarsal joints and intermetatarsal joints between the second to fourth metatarsal bones.

Ligaments

The ligaments of the naviculocuneiform joint are the dorsal and plantar ligaments.

Dorsal and plantar ligaments

The dorsal and plantar ligaments connect the navicular to each cuneiform; of the three dorsal ligaments, one is attached to each cuneiform. The fasciculus from the navicular to the medial cuneiform is continued as the capsule of the joint around its medial aspect, and then blends medially with the plantar ligament. Plantar ligaments have similar attachments and receive slips from the tendon of tibialis posterior.

Synovial membrane

The synovial membrane lines the fibrous capsule in the manner outlined above.

Innervation

The naviculocuneiform joint is innervated dorsally by branches from the deep fibular nerve. The medial and intermediate naviculocuneiform joints receive a plantar innervation from the medial plantar nerve, and the lateral naviculocuneiform joint is innervated from the lateral plantar nerve.

Relations

The tendon of tibialis posterior sends fibres to the medial cuneiform and crosses the joint on its medial side; it is vulnerable to injury when a medial surgical approach is used, as are the dorsal venous arch and the saphenous nerve. The tendon of tibialis anterior passes over the dorsomedial aspect of the joint and the tendon of extensor hallucis longus is lateral. Running over the intermediate cuneiform, from medial to lateral, are the deep fibular nerve, the dorsalis pedis artery and the muscle belly of extensor hallucis brevis, all of which are vulnerable during dorsal exposure of the joint. On the lateral aspect of the joint, the superficial structures at risk are the superficial fibular nerve and the dorsal venous arch.

Muscles producing movement

Movements at the naviculo-cuneiform, cuboideonavicular, intercuneiform and cuneocuboid joints are slight and subtle gliding and rotational movements that occur during pronation or supination of the foot: when alterations occur in a loaded foot in contact with the ground, they increase suppleness when the forefoot is stressed, e.g. in the initial thrust of running and jumping. The muscles responsible for these slight movements are tibialis anterior, tibialis posterior, fibularis longus and brevis and the long flexors and extensors of the toes.

Cuboideonavicular joint

The cuboideonavicular joint is usually a fibrous joint, the bones being connected by dorsal, plantar and interosseous ligaments. This syndesmosis is often replaced by a synovial joint that is almost plane; its articular capsule and synovial lining are continuous with that of the naviculocuneiform joint. The dorsal ligament extends distolaterally, the plantar nearly transversely from the cuboid to the navicular. The interosseous ligament is made of strong transverse fibres and connects non-articular parts of adjacent surfaces to the two bones (Fig. 84.13C).

Intercuneiform and cuneocuboid joints

The intercuneiform and cuneocuboid joints are all synovial and approximately plane or slightly curved. Their articular capsules and synovial linings are continuous with those of the naviculocuneiform joints. The bones are connected by dorsal, plantar and interosseous ligaments (Fig. 84.13B,C; 84.15A).

Ligaments

The ligaments of the intercuneiform and cuneocuboid joints are the dorsal, plantar and interosseous ligaments.

Dorsal and plantar ligaments

The dorsal and plantar ligaments each have three transverse bands that pass between the medial and intermediate cuneiform, the intermediate and lateral cuneiform, and the lateral cuneiform and cuboid. The plantar ligaments receive slips from the tendon of tibialis posterior.

Interosseous ligaments

The interosseous ligaments connect non-articular areas of adjacent surfaces and are strong agents in maintaining the transverse arch.

Innervation

The intercuneiform and cuneocuboid joints are innervated dorsally via the deep fibular nerve. The plantar aspect of the medial two joints is innervated from the medial plantar nerve, and the plantar aspect of the lateral joints is innervated from the lateral plantar nerve.

Muscles producing movement

The muscles producing movement are as described above for the naviculocuneiform joint.

Tarsometatarsal articulations

Tarsometatarsal articulations are approximately plane synovial joints.

Articulating surfaces

The first metatarsal articulates with the medial cuneiform; the second is recessed between the medial and lateral cuneiforms and articulates with the intermediate cuneiform; the third articulates with the lateral cuneiform; the fourth articulates with the lateral cuneiform and the cuboid; the fifth articulates with the cuboid. The joints are approximately on a line from the tubercle of the fifth metatarsal to the tarsometatarsal joint of the hallux, except for that between the second metatarsal and intermediate cuneiform, which is 2–3 mm proximal (Figs 84.5A; 84.11).

Fibrous capsule

The hallucal joint has its own capsule. The articular capsules and cavities of the second and third are continuous with those of the intercuneiform and naviculocuneiform joints, but are separated from the fourth and fifth joints by an interosseous ligament between the lateral cuneiform and fourth metatarsal base.

Ligaments

The bones are connected by dorsal and plantar tarsometatarsal and interosseous cuneometatarsal ligaments.

Dorsal ligaments

The dorsal ligaments are strong and flat. The first metatarsal is joined to the medial cuneiform by an articular capsule and the other tarsometatarsal capsules blend with the dorsal and plantar ligaments. The second metatarsal receives a band from each cuneiform, the third from the lateral cuneiform, the fourth from the lateral cuneiform and the cuboid, the fifth from the cuboid alone.

Plantar ligaments

The plantar ligaments are longitudinal and oblique bands, and are less regular than the dorsal ligaments. Those for the first and second metatarsals are strongest. The second and third metatarsals are joined by oblique bands to the medial cuneiform, the fourth and fifth by a few fibres to the cuboid.

Interosseous cuneometatarsal ligaments

There are three interosseous cuneometatarsal ligaments. One (the strongest) passes from the lateral surface of the medial cuneiform to the adjacent angle of the second metatarsal (Fig. 84.17). Known as Lisfranc’s ligament, it is crucial to the stability of the tarsometatarsal joint complex. Disruption of this ligament can lead to instability and deformity and subsequent degenerative changes. A second ligament connects the lateral cuneiform to the adjacent angle of the second metatarsal: it does not divide the joint between the second metatarsal and lateral cuneiform and is inconstant. A third ligament connects the lateral angle of the lateral cuneiform to the adjacent fourth metatarsal base.

Synovial membrane

The first tarsometatarsal joint has its own capsule, with a synovial lining. The other joints are similarly arranged, but there is a communication between the second and third and between the fourth and fifth tarsometatarsal joints.

Innervation

The interosseous cuneometatarsal ligaments are innervated dorsally via the deep fibular nerve. The plantar aspects of the medial two joints are innervated from the medial plantar nerve, and the plantar aspects of the lateral joints are innervated by the lateral plantar nerve.

Relations

From medial to lateral, the following structures cross the dorsal aspect of the tarsometatarsal joints: the saphenous nerve, the dorsal venous arch, the tendon of extensor hallucis longus, the dorsalis pedis artery, the deep fibular nerve, extensor hallucis brevis, the tendons of extensor digitorum longus, extensor digitorum brevis, fibularis tertius and fibularis brevis. Branches of the superficial fibular nerve are variable in location on the dorsum. The sural nerve lies just inferior to the tendon of fibularis brevis in the subcutaneous tissues. Surgery involving the tarsometatarsal joints is performed through a dorsal approach, and therefore all of these structures are potentially at risk.

Factors maintaining stability

The major stabilizers of the tarsometatarsal joints are the associated ligaments. However, despite the strength of the ligaments, this joint complex is vulnerable to injury because of the lack of ligamentous connection between the first and second metatarsal bases. The medial interosseous ligament or

Lisfranc’s ligament is responsible for the tell-tale avulsion fracture of the second metatarsal base, which may be the only radiographic indication of abnormality after injury to this part of the foot. It is a highly significant injury that is often missed: failure to recognize and treat this injury by surgical reduction and fixation can lead to long-term disability.

Muscles producing movement

Movements between the tarsal and metatarsal bones are limited to flexion and extension, except in the first tarsometatarsal joint, where some abduction and rotation also occur. The muscles that produce this motion are tibialis anterior and fibularis longus. Flexion and extension are brought about by the long and short flexors and extensors of the toes. Movement between the medial cuneiform and first metatarsal, and between the fourth and fifth metatarsal bases and the cuboid, is moderate and allows the foot to adapt to uneven surfaces, whereas movement between the second and third metatarsal bases and their corresponding cuneiforms is very limited.

Intermetatarsal joints

The intermetatarsal interosseous ligaments are very strong and are present between all the lateral four metatarsals; they are absent between the first and second metatarsals. The base of the second metatarsal is joined to the first tarsometatarsal joint by the medial interosseous ligament (Lisfranc’s ligament) which connects the plantar aspect of the second metatarsal to the medial cuneiform.

Ligaments

The ligaments of the intermetatarsal joints include the dorsal and plantar intermetatarsal ligaments.

Dorsal and plantar intermetatarsal ligaments

As with their dorsal counterparts, the plantar intermetatarsal ligaments are longitudinal, oblique or transverse and they vary considerably in both number and organization. The plantar ligaments are significantly stronger than the corresponding dorsal ligaments. The strongest is the second oblique plantar ligament, which connects the medial cuneiform to the second and third bases (Fig. 84.17).

Other ligaments

All the metatarsal heads are connected indirectly by deep transverse metatarsal ligaments. Dorsal and plantar ligaments pass transversely between adjacent bases; interosseous ligaments are strong transverse bands that connect non-articular parts of the adjacent surfaces (Fig. 84.17).

Metatarsophalangeal articulations

Metatarsophalangeal articulations are ovoid or ellipsoid joints between the rounded metatarsal heads and shallow cavities on the proximal phalangeal bases. They are usually 2.5 cm proximal to the webs of the toes.

Articulating surfaces

Articular surfaces cover the distal and plantar, but not the dorsal, aspects of the metatarsal heads. The plantar aspect of the first metatarsal head has two longitudinal grooves separated by a ridge (the crista). Each articulates with a sesamoid bone embedded in the capsule of the joint, formed here by the two tendons of flexor hallucis brevis. The sesamoids are connected to each other by the intersesamoid ligament, which forms the floor of the tendinous canal for the tendon of flexor hallucis longus. The medial sesamoid receives an attachment from abductor hallucis and the lateral sesamoid receives an attachment from adductor hallucis.

Articular areas on the proximal phalangeal bases are concave. The ligaments are capsular, plantar, deep transverse metatarsal and collateral.

Fibrous capsules

Fibrous capsules are attached to their articular margins. They are thin dorsally, and may be separated from the long extensor tendons by small bursae, or they may be replaced by the tendons, but they are inseparable from the plantar and collateral ligaments. The plantar aponeurosis blends with the plantar capsule to form the so-called ‘plantar plate’ which inserts distally into the base of the proximal phalanx via medial and lateral bundles. Proximally, the plate is attached to the metatarsal head via a thin synovial fold. It also receives an attachment from the accessory collateral ligament.

Ligaments

The ligaments of the metatarsophalangeal joints are the plantar, deep transverse metatarsal and collateral ligaments.

Plantar ligaments

The plantar ligaments are thick and dense. They lie between and blend with the collateral ligaments, being loosely attached to the metatarsals, and firmly attached to the phalangeal bases. Their margins blend with the deep transverse metatarsal ligaments. Their plantar surfaces are grooved for the flexor tendons, the fibrous sheaths of which connect with the edges of the grooves, and their deep surfaces extend the articular areas for metatarsal heads.

Deep transverse metatarsal ligaments

The deep transverse metatarsal ligaments are four short, wide, flat bands that unite the plantar ligaments of adjoining metatarsophalangeal joints. The interossei are dorsal to, and the lumbricals, digital vessels and nerves are plantar to, these ligaments. They resemble the deep transverse metacarpal ligaments except that, in the foot, there is a deep transverse metacarpal ligament between the plantar ligament of the second metatarsophalangeal joint and that of the hallucal metatarsophalangeal joint (Fig. 84.17).

Collateral ligaments

The collateral ligaments are strong cords flanking each joint. They are attached to the dorsal tubercles on the metatarsal heads and the corresponding side of the phalangeal bases and they slope downwards and forwards. The first metatarsophalangeal joint also contains metatarso-sesamoid ligaments. On either side, the ligaments arise from the metatarsal head with a narrow origin and then fan out to insert on the border of the proximal phalanx and the plantar plate. Each collateral ligament consists of the phalangeal collateral ligament, which inserts into the base of the proximal phalanx, and the accessory collateral ligament, which inserts into the plantar plate.

Synovial membrane

Each metatarsophalangeal joint is a separate synovial joint.

Innervation

The main nerve supply of the metatarsophalangeal joints is from the plantar interdigital nerves, which supply the first, second, third and medial half of the fourth metatarsophalangeal joint on their plantar aspects. Digital branches of the lateral plantar nerve supply the lateral half of the fourth joint, and both medial and lateral aspects of the fifth joint, on their plantar sides. The dorsomedial side of the hallucal metatarsophalangeal joint is supplied by the medial dorsal cutaneous branch of the superficial fibular nerve. The deep fibular nerve supplies the dorsolateral side of the hallucal metatarsophalangeal joint and the medial side of the metatarsophalangeal joint of the second toe.

Relations

Dorsally, the tendon of extensor hallucis longus lies medial to the tendon of extensor hallucis brevis. The same arrangement occurs in the lesser toes with the tendons of extensor digitorum longus and brevis. The interossei are plantarmedial and plantarlateral, dorsal to the intermetatarsal ligament, whereas the lumbrical tendons and the digital artery and nerve are plantar to the intermetatarsal ligament. The long and short flexors lie on the plantar aspect of the joint in the midline. If approaching the metatarsophalangeal joint surgically from the plantar surface, it is important not to stray from the midline.

Factors maintaining stability

The first metatarsophalangeal joint owes its stability to its capsuloligamentous structures, and to flexor and extensor hallucis brevis, with a small contribution from flexor and extensor hallucis longus or the bony contours. The metatarsophalangeal joints of the lesser toe are stabilized principally by the collateral ligaments and plantar plates. Rupture of the plantar plate leads to hammer toe deformity.

Muscles producing movement

The types of movements that occur at these joints are like those that occur at the corresponding joints in the hand, but the range of movement is quite different. In contrast to the metacarpophalangeal joints, the range of active extension that can occur at the metatarsophalangeal joints (50–60°) is greater than that of flexion (30–40°): this is an adaptation to the needs of walking, and is most marked in the hallucal joint, where flexion is a few degrees while extension may reach 90°. When the foot is on the ground, metatarsophalangeal joints are already extended to at least 25° because the metatarsals incline proximally in the longitudinal arches of the foot (Fig. 84.8A). The range of passive movements in these joints is 90° (extension) and 45° (flexion), according to Kapandji (1974). The following muscles produce movements at the metatarsophalangeal joints:

Flexion

Flexor digitorum brevis, lumbricals and interossei, assisted by flexores digitorum longus and accessorius. In the fifth toe, flexor digiti minimi brevis assists. In the hallux, flexores hallucis longus and brevis are the only flexors.

Extension

Extensores digitorum longus and brevis, extensor hallucis longus.

Adduction

Adductor hallucis; in the third to fifth toes, the first, second and third plantar interossei, respectively.

Abduction

Abductor hallucis; in the second toe, the first and second dorsal interossei; in the third and fourth toes, the corresponding dorsal interossei; in the fifth toe, abductor digiti minimi.

Note: The line of reference for adduction and abduction is along the second digit, which has the least mobile metatarsal. The second toe may therefore be ‘abducted’ medially and laterally by the first and second dorsal interossei respectively.

Hallux valgus

Hallux valgus is a common condition, occurring mainly in individuals who have a genetic predisposition. Footwear is implicated in the condition, which presumably accounts for the greater incidence in females. Metatarsus primus varus, an adduction deformity of the first metatarsal, is commonly associated with hallux valgus.

The more spheroidal the shape of the first metatarsal head, the more likely it is to be unstable. Conversely, a flat metatarsal head is less likely to be associated with hallux valgus. No muscle inserts into the first metatarsal head, and therefore its position is determined by the position of the proximal phalanx. As the proximal phalanx moves laterally on the metatarsal head, it pushes the head medially. This leads to attenuation of the medial soft tissue structures and contracture of the lateral ones. The sesamoid sling, which is anchored laterally by adductor hallucis, remains in place as the head moves medially, displacing the sesamoids from beneath the metatarsal head. As this happens, the weakest point of the medial capsule fails, so that abductor hallucis slips under the metatarsal head. This leads to failure of the intrinsic muscles to stabilize the joint, and the pull of abductor hallucis leads to spinning of the proximal phalanx, which results in a pronation deformity. Failure to intervene surgically inevitably results in a progressive deformity.

Interphalangeal articulations

Interphalangeal articulations are almost pure hinge joints, in which the trochlear surfaces on the phalangeal heads articulate with reciprocally curved surfaces on adjacent phalangeal bases. Each has an articular capsule and two collateral ligaments, as occurs in the metatarsophalangeal joints. The plantar surface of the capsule is a thickened fibrous plate, like the plantar metatarsophalangeal ligaments, and is often termed the plantar ligament.

Innervation

The interphalangeal articulations are innervated by branches from the plantar interdigital nerves. The medial dorsal cutaneous branch of the superficial fibular nerve also supplies the hallucal interphalangeal joint. Branches of the deep fibular, intermediate dorsal cutaneous and sural nerves sometimes supply the joints of the lesser toes.

Muscles producing movement

Movements are flexion and extension, which are greater in amplitude between the proximal and middle phalanges than between the middle and distal. Flexion is marked, but extension is limited by tension of the flexor muscles and plantar ligaments. Abduction, adduction and rotation occur to a minor extent.

Flexion

Flexores digitorum longus and brevis, flexor hallucis longus. Flexor accessorius assists flexor digitorum longus.

Extension

Extensores digitorum longus and brevis, extensor hallucis longus.

ARCHES OF THE FOOT

Three main arches are recognized in the foot. They are the medial longitudinal, the lateral longitudinal and the transverse arch. The roles of the arches of the foot in standing, walking and running are discussed later in this chapter.

MEDIAL LONGITUDINAL ARCH

The medial margin of the foot arches up between the heel proximally and the medial three metatarsophalangeal joints to form a visible arch (Fig. 84.8A). It is made up of the calcaneus, talar head, navicular, the three cuneiforms and the medial three metatarsals. The posterior and anterior pillars are the posterior part of the inferior calcaneal surface and the three metatarsal heads, respectively. The bones themselves contribute little to the stability of the arch, whereas the ligaments contribute significantly. The most important ligamentous structure is the plantar aponeurosis, which acts as a tie beam between the supporting pillars (Hicks 1953). Dorsiflexion, especially of the hallux, draws the two pillars together, thus heightening the arch: the so-called 'windlass' mechanism. Next in importance is the spring ligament, which supports the head of the talus. If this ligament fails, the navicular and calcaneus separate, allowing the talar head, which is the highest point of the arch, to descend. The talocalcaneal ligaments and the anterior fibres of the deltoid ligament, from the tibia to the navicular, also contribute to the stability of the arch.

Muscles play a role in the maintenance of the medial longitudinal arch. Flexor hallucis longus acts as a bowstring. Flexor digitorum longus, abductor hallucis and the medial half of flexor digitorum brevis also contribute, but to a lesser extent. Tibialis posterior and anterior invert and adduct the foot, and so help to raise its medial border. The importance of tibialis posterior is manifest by the collapse of the medial longitudinal arch that accompanies failure of its tendon (see below).

LATERAL LONGITUDINAL ARCH

The lateral longitudinal arch is much less pronounced arch than the medial one. The bones making up the lateral longitudinal arch are the calcaneus, the cuboid and the fourth and fifth metatarsals: they contribute little to the arch in terms of stability (Fig. 84.8B). The pillars are the calcaneus posteriorly, and the lateral two metatarsal heads, anteriorly. Ligaments play a more important role in stabilizing the arch, especially the lateral part of the plantar aponeurosis and the long and short plantar ligaments. However, the most important contribution to the maintenance of the lateral arch is made by the tendon of fibularis longus. The lateral two tendons of flexor digitorum longus (and flexor accessorius), the muscles of the first layer (lateral half of flexor digitorum brevis and abductor digiti minimi) and fibularis brevis and peronius tertius also contribute to the maintenance of the lateral longitudinal arch.

TRANSVERSE ARCH

The bones involved in the transverse arch are the bases of the five metatarsals, the cuboid and the cuneiforms (Fig. 84.5B). The intermediate and lateral cuneiforms are wedge-shaped and thus adapted to maintenance of the transverse arch. The stability of the arch is mainly provided by the ligaments, which bind the cuneiforms and the metatarsal bases, and also by the tendon of fibularis longus, which tends to approximate the medial and lateral borders of the foot. A shallow arch is maintained at the metatarsal heads by the deep transverse ligaments, transverse fibres that bind together the digital slips of the plantar aponeurosis, and, to a lesser extent, by the transverse head of adductor hallucis.

PES PLANUS AND PES CAVUS

The term pes planus denotes an excessively flat foot. There is no precise degree of flatness that defines pes planus, but it may be either physiological or pathological. In physiological pes planus, the feet are flexible and rarely problematic. In marked contrast, pathological pes planus is often associated with stiffness and pain. The windlass (or 'Jack's great toe') test involves passively dorsiflexing the hallux at the metatarsophalangeal joint. This tightens the plantar aponeurosis and, in flexible pes planus, results in accentuation of the medial longitudinal arch. In pathological pes planus, no accentuation of the arch is seen. This test can also be carried out by asking the individual to stand on tiptoe and viewing the hindfoot from behind. In flexible flat feet, the calcaneus swings into a varus position; in pathological pes planus it does not. Causes of pathological pes planus include tarsal coalition, disruption of the tendon of tibialis posterior, rupture of the spring ligament, tarsometatarsal arthritis (and subsequent collapse) and hindfoot (talo-calcaneal or subtalar joint) degenerative or inflammatory arthritis.

Pes cavus denotes an excessively high-arched foot. The majority of cases arise as a result of a neurological disorder (e.g. Charcot–Marie–Tooth disease, diastematomyelia, poliomyelitis). According to the anatomical location of the deformity, pes cavus may be classified into hindfoot, midfoot or forefoot cavus. When pes cavus involves all three parts of the foot it is called 'global' cavus.

In Charcot–Marie–Tooth disease, an overactive fibularis longus leads to plantar hyperflexion of the first metatarsal. To keep the forefoot in contact with the ground, the affected individual develops a progressive compensatory hindfoot varus. If ignored, the hindfoot varus, which is initially flexible, becomes fixed. The Coleman block test involves standing with the lateral part of the forefoot on a wooden block (Coleman & Chesnut 1977). This effectively balances the forefoot supination and the hindfoot deformity corrects itself spontaneously, provided the hindfoot varus is flexible. If the hindfoot is still flexible, surgery need only address the forefoot supination. If fixed, however, the hindfoot deformity also needs to be surgically corrected.

MUSCLES

The muscles acting on the foot may be divided into extrinsic and intrinsic groups.

EXTRINSIC MUSCLES

The extrinsic muscles are described in Chapter 83. Their tendons cross the ankle, and move and stabilize this joint. Distally, the tendons also act on the small joints of the foot and help to stabilize these joints. The muscles can be grouped according to their arrangement in the leg. The extensors arise in the anterior compartment of the leg and their tendons pass anterior to the ankle, where they are bound down by the extensor retinacula. The lateral group arises in the relatively narrow lateral compartment of the leg and their tendons pass posterior to the lateral malleolus, bound down by the fibular retinacula. The flexors arise in the posterior compartment of the leg and their tendons pass posterior to the ankle, where the tendons of the superficial group of flexors are inserted into the calcaneus (see below) and the tendons of the deep group of flexors are bound down by the flexor retinaculum.

Anterior group

Tibialis anterior, extensor hallucis longus, extensor digitorum longus and fibularis tertius are all described in Chapter 83.

Lateral group

Fibularis longus and fibularis brevis are described in Chapter 83.

Posterior group

Superficial group

Gastrocnemius and soleus are described in Chapter 83; the calcaneal tendon is described below.

Calcaneal (Achilles) tendon

The calcaneal tendon is the thickest and strongest tendon in the human body (see Fig. 82.3). It is approximately 15 cm long, and begins near the middle of the calf, although its anterior surface receives muscle fibres from soleus almost to its lower end. It gradually becomes more rounded until approximately 4 cm above the calcaneus, below this level it expands and becomes attached to the midpoint of the posterior surface of the calcaneus. The fibres of the calcaneal tendon are not aligned strictly vertically and they display a variable degree of spiralization (Cummins et al 1946).

Vascular supply

The blood supply to the calcaneal tendon is poor: the predominant artery is a recurrent branch of the posterior tibial artery which mainly supplies peritendinous tissues (Taylor & Razaboni 1994). There is an additional supply proximally from intramuscular arterial branches and distally from the calcaneus. The vascularity of the mid-substance of the tendon is relatively poor, although some blood enters the tendon at this point through its anterior surface. During surgery, the paratenon is therefore best left intact in this region.

The calcaneal tendon is not the only plantar flexor of the ankle, which is one of the reasons ruptures of the calcaneal tendon may not always be clinically apparent. However, it is a frequent site of pathology because of its susceptibility to rupture, degenerative change (tendinosis) and inflammation (paratendonitis): the area of relative avascularity in the mid-substance of the tendon is where the majority of problems occur.

Relations

The calcaneal tendon is subcutaneous. The sural nerve crosses its lateral border about 10 cm above its insertion: the nerve is especially vulnerable here to iatrogenic injury during surgery. Distally, there are bursae superficial and deep to the tendon. The muscle belly of flexor hallucis longus lies deep to the deep fascia on the anterior surface of the tendon.

Action

Plantar flexion of the ankle joint. The tendon fibres spiral laterally through 90° as they descend, so that the fibres associated with gastrocnemius come to insert on the bone more laterally, and those associated with soleus more medially.

Heel bursae

There are three locations about the heel where bursae occur. The most common is the retrocalcaneal bursa, which lies between the calcaneal tendon and the posterior surface of the calcaneus. An almost constant finding, it has an anterior bursal wall composed of fibrocartilage and a thin posterior wall which blends with the thin epitenon (epitendineum) of the calcaneal tendon. Dorsiflexion of the ankle results in compression of the bursa. Less common are an adventitious bursa superficial to the calcaneal tendon, and a subcalcaneal bursa between the inferior surface of the calcaneus and the origin of the plantar aponeurosis. A prominent superolateral calcaneal tuberosity may impinge on the deep aspect of the calcaneal tendon where it inserts onto the calcaneus (Haglund’s disease). It is often associated with a retrocalcaneal bursa, and symptoms are exacerbated by dorsiflexion of the ankle, because this movement increases the pressure within the bursa and causes impingement of calcaneus against the tendon insertion.

Plantaris

Plantaris is described in Chapter 83.

Deep group

The deep flexors of the calf include popliteus, which acts on the knee joint, and flexor hallucis longus, flexor digitorum longus and tibialis posterior, which all act on the ankle joint and joints of the foot.

Flexor hallucis longus

Flexor hallucis longus is described in Chapter 83. The tendon of flexor hallucis longus is described below.

Flexor digitorum longus

Flexor digitorum longus is described in Chapter 83.

Tibialis posterior

Tibialis posterior is described in Chapter 83.

INTRINSIC MUSCLES

The intrinsic muscles, i.e. those contained entirely within the foot, follow the primitive limb pattern of plantar flexors and dorsal extensors.

The plantar muscles in the foot can be divided into medial, lateral and intermediate groups. The medial and lateral groups consist of the intrinsic muscles of the hallux and minimus, respectively, and the central or intermediate group includes the lumbricals, interossei and short digital flexors. It is customary to group the muscles in four layers, because this is the order in which they are encountered during dissection. However, in clinical practice and in terms of function, the former grouping is often more useful.

Plantar muscles of the foot: first layer

This superficial layer includes abductor hallucis, abductor digiti minimi and flexor digitorum brevis (Fig. 84.19A). All three extend from the calcaneal tuberosity to the toes, and all assist in maintaining the concavity of the foot.

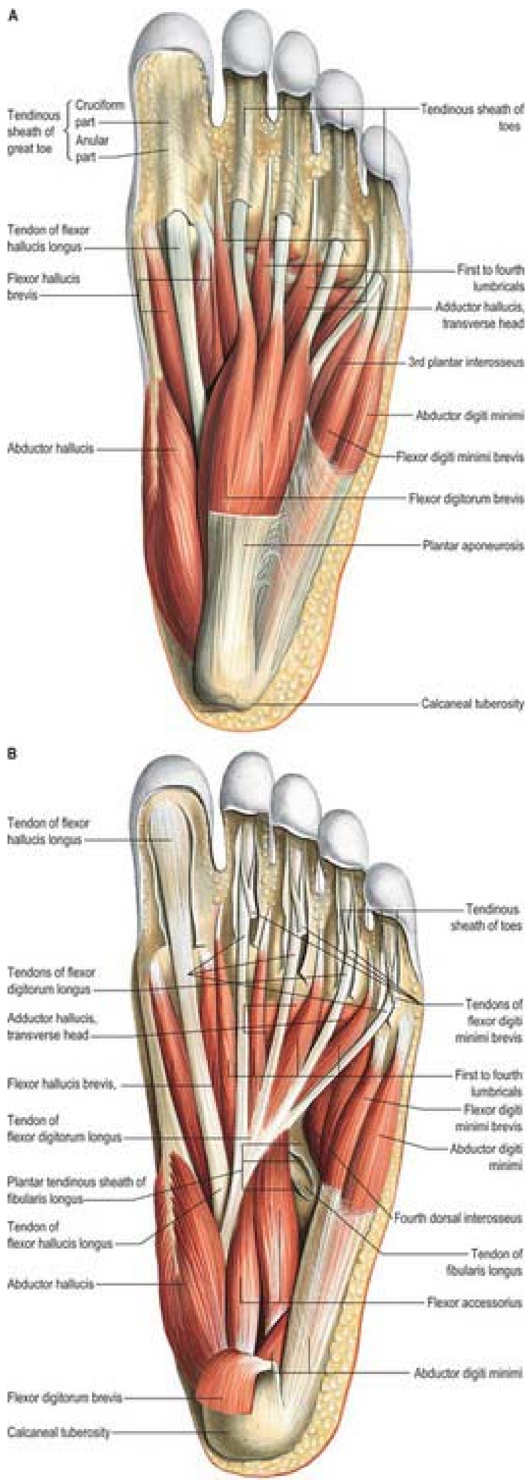
A
Tendinous sheath of great toe
Cruciform part
Anular part
Tendon of flexor hallucis longus
Flexor hallucis brevis
Abductor hallucis
Tendinous sheath of toes
First to fourth lumbricals
Adductor hallucis, transverse head
3rd plantar interosseus
Abductor digiti minimi
Flexor digiti minimi brevis
Flexor digitorum brevis
Plantar aponeurosis
Calcaneal tuberosity
B
Tendon of flexor hallucis longus
Tendons of flexor digitorum longus
Adductor hallucis, transverse head
Flexor hallucis brevis,
Tendon of flexor digitorum longus
Plantar tendinous sheath of fibularis longus
Tendon of flexor hallucis longus
Abductor hallucis
Flexor digitorum brevis
Calcaneal tuberosity
Tendinous sheath of toes
Tendons of flexor digiti minimi brevis
First to fourth lumbricals
Flexor digiti minimi brevis
Abductor digiti minimi
Fourth dorsal interosseus
Tendon of fibularis longus
Flexor accessorius
Abductor digiti minimi

Fig. 84.19 Muscles of the sole of the foot. **A**, First layer. **B**, Second layer.

(From Sobotta 2006.)

Abductor hallucis

Attachments

Abductor hallucis arises principally from the flexor retinaculum, but also from the medial process of the calcaneal tuberosity, the plantar aponeurosis, and the intermuscular septum between this muscle and flexor digitorum brevis. The muscle fibres end in a tendon that is attached, together with the medial tendon of flexor hallucis brevis, to the medial side of the base of the proximal phalanx of the hallux. Some fibres are attached more proximally to the medial sesamoid bone of this toe. The muscle may also derive some fibres from the dermis along the medial border of the foot.

Relations

Abductor hallucis lies along the medial border of the foot and covers the origins of the plantar vessels and nerves (Fig. 84.20).

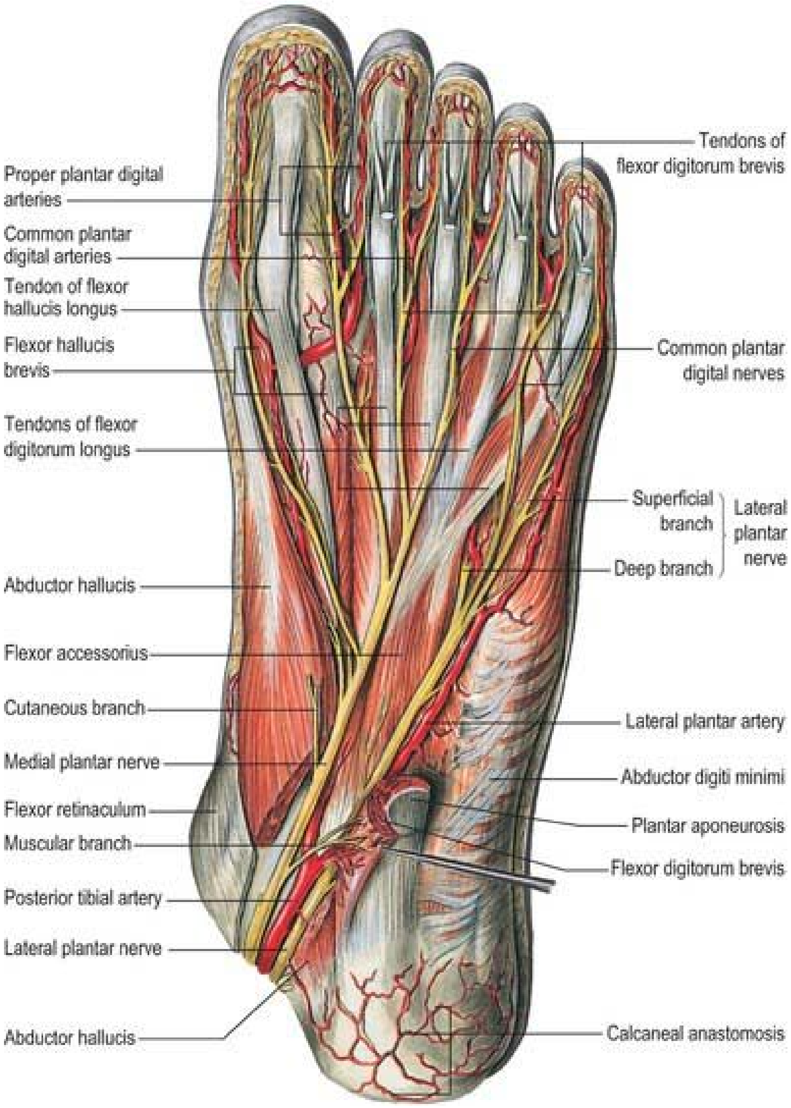
Proper plantar digital arteries
Common plantar digital arteries
Tendon of flexor hallucis longus
Flexor hallucis brevis
Tendons of flexor digitorum longus
Abductor hallucis
Flexor accessorius
Cutaneous branch
Medial plantar nerve
Flexor retinaculum
Muscular branch
Posterior tibial artery
Lateral plantar nerve
Abductor hallucis
Tendons of flexor digitorum brevis
Common plantar digital nerves
Superficial branch
Deep branch
Lateral plantar nerve
Lateral plantar artery
Abductor digiti minimi
Plantar aponeurosis
Flexor digitorum brevis
Calcaneal anastomosis

Fig. 84.20 Plantar nerves and vessels in relation to muscle layers.

(From Sobotta 2006.)

Vascular supply

Abductor hallucis is supplied by the medial malleolar network, medial calcaneal branches of the lateral plantar artery (Fig. 84.9), the medial plantar artery (directly and via superficial and deep branches), the first plantar metatarsal artery and perforators from the plantar arterial arch.

Innervation

Abductor hallucis is innervated by the medial plantar nerve, S1 and S2. Contraction of the muscle confirms an intact medial plantar nerve when the integrity of this nerve is in question.

Action

Abductor hallucis produces abduction of the hallux.

Testing

Abductor hallucis is tested clinically by instructing the subject to resist a forcibly applied lateral deviation of the proximal phalanx.

Clinical anatomy

The deep fascia has been implicated in chronic heel pain, because it can cause entrapment of the first branch of the lateral plantar nerve that lies immediately deep to it. The abductor hallucis fascia is strong and can be used in soft tissue augmentation following correction of hallux valgus. Rarely, persistent, exaggerated tonus in the muscle may be a cause of varus deformity of the foot, necessitating surgical intervention. An abductor hallucis flap is sometimes used for provision of soft tissue cover.

Flexor digitorum brevis

Attachments

Flexor digitorum brevis arises by a narrow tendon from the medial process of the calcaneal tuberosity, from the central part of the plantar aponeurosis, and from the intermuscular septa between it and adjacent muscles. It divides into four tendons, which pass to the lateral four toes; the tendons enter digital tendon sheaths accompanied by the tendons of flexor digitorum longus, which lie deep to them. At the bases of the proximal phalanges, each tendon divides around the corresponding tendon of flexor digitorum longus; the two slips then reunite and partially decussate, forming a tunnel through which the tendon of flexor digitorum longus passes to the distal phalanx. The short flexor tendon divides again and attaches to both sides of the shaft of the middle phalanx. The way in which the tendons of flexor digitorum brevis divide and attach to the phalanges is identical to that of the tendons of flexor digitorum superficialis in the hand. The slip to a given toe may be absent, or it may be replaced by a small muscular slip from the long flexor tendon or from flexor accessorius. Conversely, the slip may be joined by a second, supernumerary slip.

Relations

Flexor digitorum brevis lies immediately deep to the central part of the plantar aponeurosis (Fig. 84.19A). Its deep surface is separated from the lateral plantar vessels and nerves by a thin layer of fascia.

Vascular supply

Flexor digitorum brevis is supplied by the lateral and medial plantar arteries, the plantar metatarsal arteries and the plantar digital arteries to the lateral four toes.

Nerve supply

Flexor digitorum brevis is innervated by the medial plantar nerve, S1 and S2.

Actions

Flexor digitorum brevis flexes the lesser toes at the proximal interphalangeal joint, with equal effect in any position of the ankle joint.

Testing

To test the action of flexor digitorum brevis, the examiner passively extends the distal interphalangeal joint and asks the individual to flex the toes at the proximal interphalangeal joint. Contracture of the flexor tendon can lead to toe deformities, and release or lengthening procedures may be required. The muscle belly is sometimes excised as a flap to cover a soft tissue defect.

Abductor digiti minimi

Attachments

Abductor digiti minimi arises from both processes of the calcaneal tuberosity, from the plantar surface of the bone between them, from the plantar aponeurosis and from the intermuscular septum between the muscle and flexor digitorum brevis. Its tendon glides in a smooth groove on the plantar surface of the base of the fifth metatarsal and is attached, with flexor digiti minimi brevis, to the lateral side of the base of the proximal phalanx of the fifth toe; hence it is more a flexor than an abductor. Some of the fibres arising from the lateral calcaneal process usually reach the tip of the tuberosity of the fifth metatarsal (Figs 84.8B; 84.11) and may form a separate muscle, abductor ossis metatarsi digiti quinti. An accessory slip from the base of the fifth metatarsal is not infrequent.

Relations

Abductor digiti minimi lies along the lateral border of the foot, and its medial margin is related to the lateral plantar vessels and nerve (Fig. 84.20).

Vascular supply

Abductor digiti minimi is supplied by the medial and lateral plantar arteries (Fig. 84.20; see Fig. 84.24A), the plantar digital artery to the lateral side of minimus, branches from the plantar arch, the fourth plantar metatarsal artery and end twigs of the arcuate and lateral tarsal arteries (Fig. 84.9).

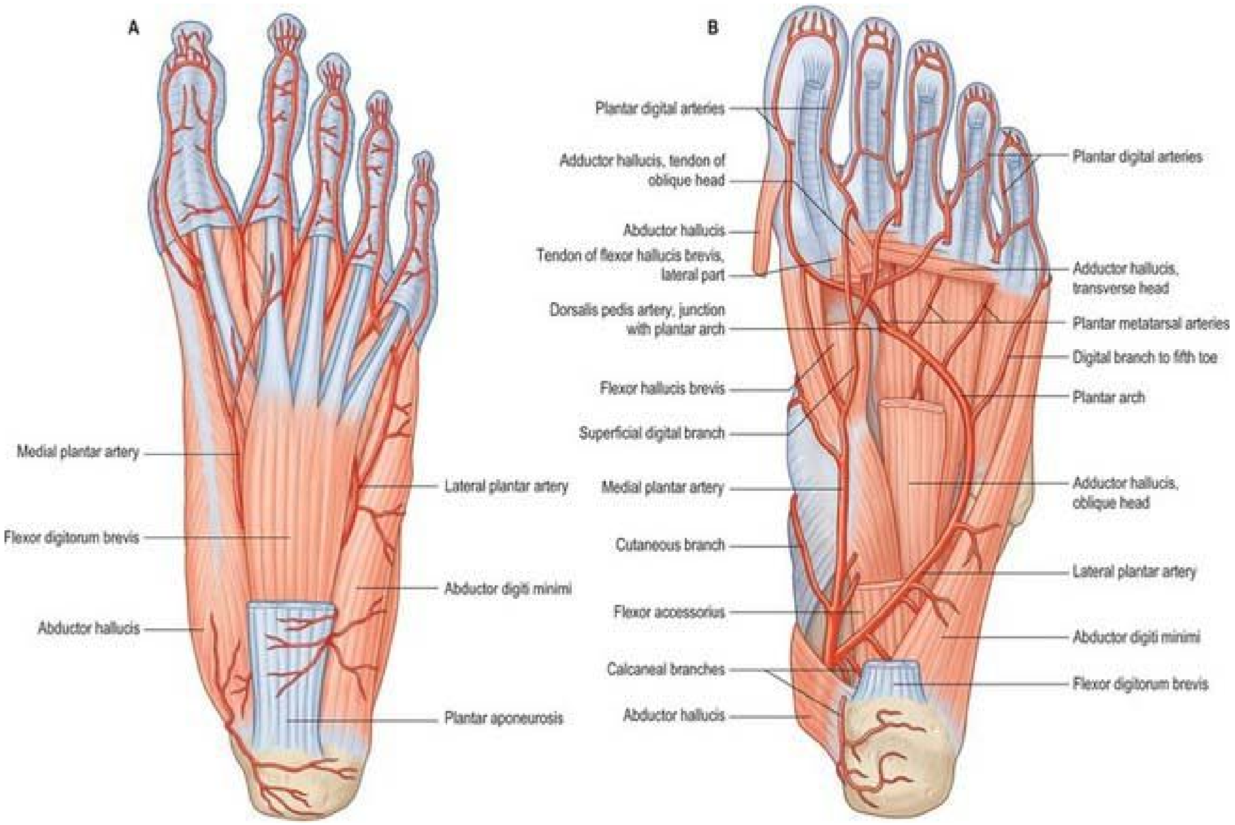
A
Medial plantar artery
Flexor digitorum brevis
Abductor hallucis
Lateral plantar artery
Abductor digiti minimi
Plantar aponeurosis
B
Plantar digital arteries
Adductor hallucis, tendon of oblique head
Abductor hallucis
Tendon of flexor hallucis brevis, lateral part
Dorsalis pedis artery, junction with plantar arch
Flexor hallucis brevis
Superficial digital branch
Medial plantar artery
Cutaneous branch
Flexor accessorius
Calcaneal branches
Abductor hallucis
Plantar digital arteries
Adductor hallucis, transverse head
Plantar metatarsal arteries
Digital branch to fifth toe
Plantar arch
Adductor hallucis, oblique head
Lateral plantar artery
Abductor digiti minimi
Flexor digitorum brevis

Fig. 84.24 The plantar arteries of the left foot. **A**, Superficial dissection. **B**, Deep dissection.

Innervation

Abductor digiti minimi is innervated by the lateral plantar nerve, S1, S2 and S3.

Action

Despite its name, abductor digiti minimi is more a flexor than an abductor of the metatarsophalangeal joint of the little toe.

Plantar muscles of the foot: second layer

The second layer consists of flexor digitorum accessorius and four lumbrical muscles. The tendons of flexor hallucis longus and flexor digitorum longus run in the same plane as the muscles of the second layer (Fig. 84.19B): flexor hallucis longus and flexor digitorum longus are described in Chapter 83.

Flexor tendon sheaths

The terminations of the tendons of the long and short flexor muscles are contained in osseo-aponeurotic canals similar to those which occur in the fingers. These canals are bounded above by the phalanges, and below by fibrous bands, the digital fibrous sheaths, which arch across the tendons and attach on either side to the margins of the phalanges (Fig. 84.19B). Along the proximal and intermediate phalanges, the fibrous bands are strong, and the fibres are transverse (anular part); opposite the joints they are much thinner and the fibres decussate (cruciform part). Each osseo-aponeurotic canal has a synovial lining, which is reflected around its tendon; within this sheath, vincula tendinum are arranged as they are in the fingers.

Flexor digitorum accessorius

Attachments

Flexor digitorum accessorius (Fig. 84.19B), also known as quadratus plantae, arises by two heads, with the long plantar ligament situated deeply in the interval between the two heads. The medial head is larger and more fleshy and is attached to the medial concave surface of the calcaneus, below the groove for the tendon of flexor hallucis longus. The lateral head is flat and tendinous and is attached to the calcaneus distal to the lateral process of the tuberosity, and to the long plantar ligament. The muscle belly inserts into the tendon of flexor digitorum longus at the point where it is bound by a fibrous slip to the tendon of flexor hallucis longus and where it divides into its four tendons.

The muscle is sometimes absent altogether. Its distal attachment to the tendons of flexor digitorum longus may vary, which means that the fourth and fifth long flexor tendons may, at times, fail to receive slips from the accessorius.

Relations

The medial plantar nerve passes medial to and the lateral plantar nerve passes superficial to flexor accessorius.

Vascular supply

Flexor digitorum accessorius is supplied by the stem of the medial plantar artery (to the medial head), the lateral plantar artery and the plantar arch.

Innervation

Flexor digitorum accessorius is innervated by the lateral plantar nerve, S1, S2 and S3.

Action

By pulling on the tendons of flexor digitorum longus, flexor digitorum accessorius provides a means of flexing the lateral four toes in any position of the ankle joint.

Lumbrical muscles

Attachments

The lumbrical muscles are four small muscles (numbered from the medial side of the foot) which are accessory to the tendons of flexor digitorum longus (Fig. 84.19A,B). They arise from these tendons as far back as their angles of separation, each springing from the sides of two adjacent tendons, except for the first lumbrical, which arises only from the medial border of the first tendon. The muscles end in tendons that pass distally on the medial sides of the four lesser toes and are attached to the dorsal digital expansions on their proximal phalanges.

Relations

The lumbricals are intimately related to the tendons of flexor digitorum longus before the latter enter their corresponding fibrous flexor sheaths. The lumbricals remain outside the fibrous flexor sheaths and cross the plantar aspects of the deep transverse metatarsal ligaments before reaching the dorsal digital expansions.

Vascular supply

The lumbricals are supplied by the lateral plantar artery and plantar arch, and by four plantar metatarsal arteries (four distal perforating arteries joined by three proximal perforating arteries). Their tendons are supplied by twigs from the dorsal digital arteries (and their parent dorsal metatarsal arteries) to the lateral four toes.

Innervation

The first lumbrical is supplied by the medial plantar nerve, and the remainder are supplied by the deep branch of the lateral plantar nerve, S2 and S3.

Action

The lumbricals help to maintain extension of the interphalangeal joints of the toes. In injuries of the tibial nerve, and in conditions such as the hereditary motor–sensory neuropathies (e.g. Charcot–Marie–Tooth disease), lumbrical dysfunction contributes to clawing of the toes.

Plantar muscles of the foot: third layer

The third layer of the foot contains the shorter intrinsic muscles of the hallux and minimus, i.e. flexor hallucis brevis, adductor hallucis and flexor digiti minimi brevis (Fig. 84.21).

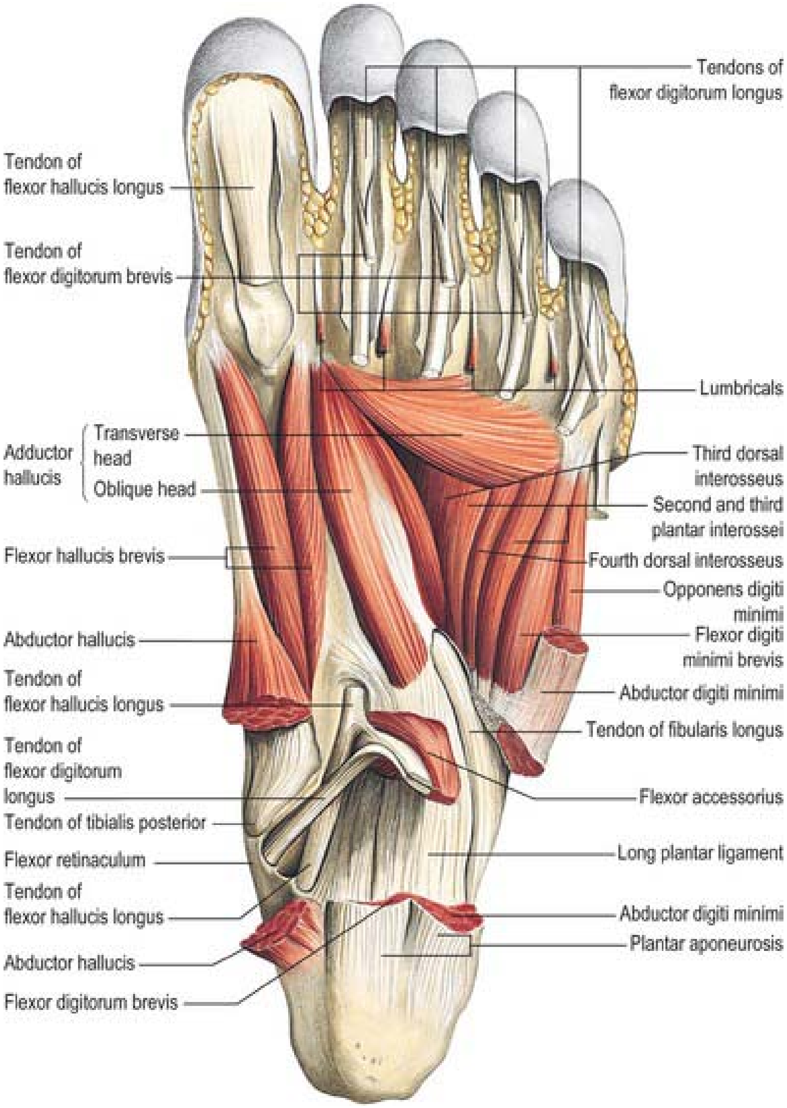
Tendons of flexor digitorum longus
Tendon of flexor hallucis longus
Tendon of flexor digitorum brevis
Lumbricals
Adductor hallucis
Transverse head
Oblique head
Third dorsal interosseus
Second and third plantar interossei
Flexor hallucis brevis
Fourth dorsal interosseus
Opponens digiti minimi
Flexor digiti minimi brevis
Abductor hallucis
Abductor digiti minimi
Tendon of flexor hallucis longus
Tendon of fibularis longus
Tendon of flexor digitorum longus
Flexor accessorius
Tendon of tibialis posterior
Long plantar ligament
Flexor retinaculum
Tendon of flexor hallucis longus
Abductor digiti minimi
Plantar aponeurosis
Abductor hallucis
Flexor digitorum brevis

Fig. 84.21 Muscles of the sole of the foot, third layer.

(From Sobotta 2006.)

Flexor hallucis brevis

Attachments

Flexor hallucis brevis has a bifurcate tendon of origin (Figs 84.19A,B; 84.21). The lateral limb arises from the medial part of the plantar surface of the cuboid, posterior to the groove for the tendon of fibularis longus, and from the adjacent part of the lateral cuneiform. The medial limb has a deep attachment directly continuous with the lateral division of the tendon of tibialis posterior, and a more superficial attachment to the middle band of the medial intermuscular septum. The belly of the muscle divides into medial and lateral parts, the twin tendons of which are attached to the sides of the base of the proximal phalanx of the hallux. The medial part blends with the tendon of abductor hallucis, and the lateral with that of adductor hallucis, as they reach their terminations.

A sesamoid bone usually occurs in each tendon near its attachment. Clinical problems with flexor hallucis brevis are usually related to the associated sesamoid bones. However, excision of both sesamoids leads to disruption of both tendons and a subsequent extension deformity at the first metatarsophalangeal joint: such surgery is therefore not recommended.

Accessory slips may arise proximally from the calcaneus or long plantar ligament. A tendinous slip may extend to the proximal phalanx of the second toe.

Relations

Flexor hallucis brevis lies on the underside of the first metatarsal shaft; abductor hallucis lies medially. The medial digital nerve to the hallux and the tendon of flexor hallucis longus pass to the hallux on its plantar surface. The medial plantar nerve lies more superficially on its lateral side.

Vascular supply

Flexor hallucis brevis is supplied by branches of the medial plantar artery, the first plantar metatarsal artery, the lateral plantar artery and the plantar arch.

Innervation

Flexor hallucis brevis is supplied by the medial plantar nerve, S1 and S2.

Action

Flexor hallucis brevis flexes the proximal phalanx of the hallux.

Testing

The individual is asked to flex the first metatarsophalangeal joint with the interphalangeal joint extended, thereby eliminating the action of flexor hallucis longus.

Adductor hallucis

Attachments

Adductor hallucis arises by oblique and transverse heads (Figs 84.19B; 84.21). The oblique head springs from the bases of the second, third and fourth metatarsal bones, and from the fibrous sheath of the tendon of fibularis longus. The transverse head, a narrow, flat fasciculus, arises from the plantar metatarsophalangeal ligaments of the third, fourth and fifth toes (sometimes only from the third and fourth), and from the deep transverse metatarsal ligaments between them. The oblique head has medial and lateral parts. The medial part blends with the lateral part of flexor hallucis brevis and is attached to the lateral sesamoid bone of the hallux. The lateral part joins the transverse head and is also attached to the lateral sesamoid bone and directly to the base of the first phalanx of the hallux. There is no phalangeal attachment for the transverse part of the muscle; fibres that fail to reach the lateral sesamoid bone are attached with the oblique part.

The transverse part of adductor hallucis is sometimes absent; part of the muscle may be attached to the first metatarsal, constituting an opponens hallucis; a slip may also extend to the proximal phalanx of the second toe.

Relations

Adductor hallucis lies plantar to the metatarsal shafts and interossei and the long and short toe flexors. The medial and lateral plantar arteries and nerves are superficial, and flexor hallucis brevis is proximal and medial.

Vascular supply

Adductor hallucis is supplied by branches of the medial plantar artery, the lateral plantar artery, the plantar arch and the first to fourth plantar metatarsal arteries.

Innervation

Adductor hallucis is innervated by the deep branch of the lateral plantar nerve, S2 and S3.

Action

Adductor hallucis partly flexes the proximal phalanx of the hallux, but also stabilizes the metatarsal heads.

Clinical anatomy

Adductor hallucis is one of the deforming forces in hallux valgus and needs to be released during a distal soft tissue release when there is a fixed deformity.

Flexor digiti minimi brevis

Attachments

Flexor digiti minimi brevis arises from the medial part of the plantar surface of the base of the fifth metatarsal bone, and from the sheath of fibularis longus (Figs 84.19B; 84.21). It has a distal tendon that inserts into the lateral side of the base of the proximal phalanx of the minimus; this tendon usually blends laterally with that of abductor digiti minimi. Occasionally, some of its deeper fibres extend to the lateral part of the distal half of the fifth metatarsal bone, constituting what may be described as a distinct muscle, opponens digiti minimi.

Relations

The fifth metatarsal shaft lies on the deep surface of flexor digiti minimi brevis, the interossei lie medially and abductor digiti minimi is lateral. The most lateral branch of the lateral plantar nerve lies superficially and just medial to flexor digiti minimi brevis.

Vascular supply

Flexor digiti minimi brevis is supplied by end twigs of the arcuate and lateral tarsal arteries, and the lateral plantar artery and its digital (plantar) branch to the lateral side of minimus.

Innervation

Flexor digiti minimi brevis is innervated by the super-ficial branch of the lateral plantar nerve, S2 and S3.

Action

Flexor digiti minimi brevis flexes the metatarsophalangeal joint of the little toe.

Plantar muscles of the foot: fourth layer

The fourth layer of muscles of the foot consists of the plantar and dorsal interossei and the tendons of tibialis posterior and fibularis longus (tibialis posterior and fibularis longus are described in Ch. 83). The interossei resemble their counterparts in the hand except that, when describing adduction and abduction of the toes, the axis of reference is a longitudinal axis corresponding to the shaft of the 2nd metatarsal (unlike the hand where reference is made to the long axis of the third metacarpal).

Dorsal interossei

Attachments

The dorsal interossei (Fig. 84.22A) are situated between the metatarsal bones. They consist of four bipennate muscles, each arising by two heads from the sides of the adjacent metatarsal bones. Their tendons are attached to the bases of the proximal phalanges and to the dorsal digital expansions. The first inserts into the medial side of the second toe; the other three pass to the lateral sides of the second, third and fourth toes.

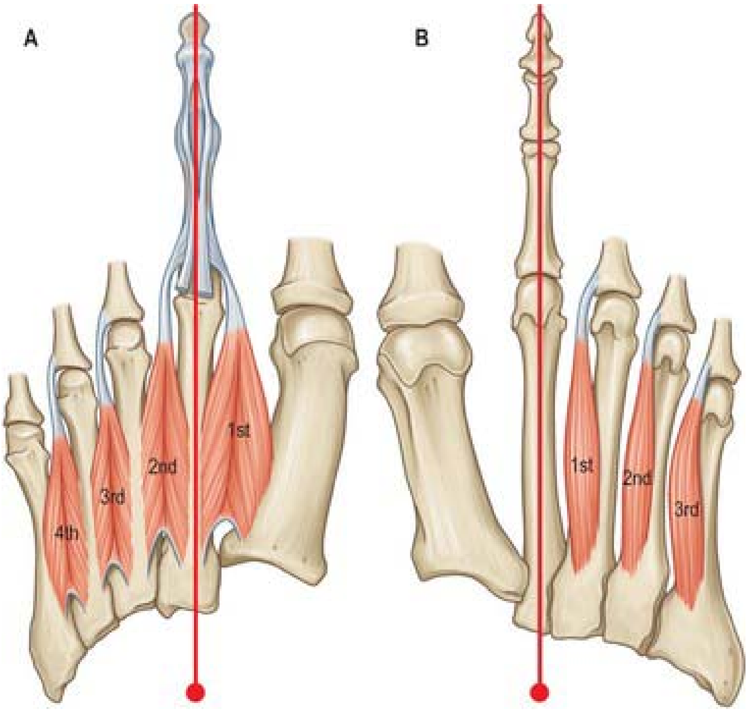

Fig. 84.22 The interossei of the left foot. **A**, Dorsal interossei viewed from the dorsal aspect. **B**, Plantar interossei viewed from the plantar aspect. The axis to which the movements of abduction and adduction are referred is indicated.

Relations

Between the heads of each of the three lateral muscles, there is an angular space through which a perforating artery passes to the dorsum of the foot. Between the heads of the first muscle, the corresponding space transmits the terminal part of the dorsalis pedis artery to the sole (see Fig. 84.1).

Vascular supply

Dorsal interossei are supplied by the arcuate artery, lateral and medial tarsal arteries, the first to fourth plantar arteries and the first to fourth dorsal metatarsal arteries (receiving proximal and distal perforating arteries), and by the dorsal digital arteries of the lateral four toes.

Innervation

Dorsal interossei are supplied by the deep branch of the lateral plantar nerve (S2 and S3), except that of the fourth interosseous space, which is supplied by the superficial branch of the lateral plantar nerve.

Action

Dorsal interossei abduct the toes relative to the longitudinal axis of the second metatarsal. They also flex the metatarsophalangeal joints and extend the interphalangeal joints of the lesser toes. The hallux and little toe have their own abductors.

Clinical anatomy

Denervation of the interossei leads to claw-toe deformities. Development of claw toes should alert the clinician to the possibility of a neuropathic process (e.g. Charcot–Marie–Tooth disease, diastematomyelia).

Plantar interossei

There are three plantar interossei (Fig. 84.22B). They lie below, rather than between, the metatarsal bones, and each is connected to one metatarsal bone only. They arise from the bases and medial sides of the third, fourth and fifth metatarsal bones, and insert into the medial sides of the bases of the proximal phalanges of the numerically corresponding toes, and into their dorsal digital expansions.

Relations

The plantar interossei lie plantar to the dorsal interossei and deep to the muscles of the third layer.

Vascular supply

Plantar interossei are supplied by the lateral plantar artery, the plantar arch, the second to fourth plantar metatarsal arteries and the dorsal digital arteries of the lateral three toes.

Innervation

Plantar interossei are supplied by the deep branch of the lateral plantar nerve (S2 and S3), except that of the fourth interosseous space, which is supplied by the superficial branch of the lateral plantar nerve.

Action

Plantar interossei adduct the third, fourth and fifth toes, flex the metatarsophalangeal joints and extend the interphalangeal joints.

Clinical anatomy

The clinical anatomy of the plantar interossei is similar to that of the dorsal interossei.

Extensor muscles of the foot

Extensor digitorum brevis and extensor hallucis brevis

Attachments

Extensor digitorum brevis (Fig. 84.2A) is a thin muscle which arises from the distal part of the superolateral surface of the calcaneus in front of the shallow lateral groove for fibularis brevis, from the interosseous talocalcaneal ligament, and from the deep surface of the stem of the inferior extensor retinaculum. It slants distally and medially across the dorsum of the foot, and ends in four tendons. The medial part of the muscle is usually a more or less distinct slip, ending in a tendon that crosses the dorsalis pedis artery superficially to insert into the dorsal aspect of the base of the proximal phalanx of the hallux; this slip is sometimes termed extensor hallucis brevis. The other three tendons attach to the lateral sides of the tendons of extensor digitorum longus for the second, third and fourth toes.

The muscle is subject to much variation, e.g. accessory slips from the talus and navicular, an extra tendon to the fifth digit, an absence of one or more tendons. It may be connected to the adjacent dorsal interosseous muscles.

Relations

The most medial tendon, that of extensor hallucis brevis, courses dorsomedially and passes superficial to the dorsalis pedis artery and the deep fibular nerve. The remaining three tendons pass obliquely deep to the corresponding tendons of extensor digitorum longus.

Vascular supply

Extensor digitorum brevis is supplied by the anterior perforating branch of the fibular artery, the anterior lateral malleolar artery, lateral tarsal arteries, dorsalis pedis arteries, arcuate artery, the first, second and third dorsal metatarsal arteries, proximal and distal perforating arteries, and the dorsal digital arteries to the medial four toes (including the hallux).

Innervation

Extensor digitorum brevis is supplied by the lateral terminal branch of the deep fibular nerve, L5, S1.

Actions

The muscle assists in extending the phalanges of the middle three toes via the tendons of extensor digitorum longus; in the hallux, it assists in extension of the metatarsophalangeal joint.

Clinical anatomy

Laceration of extensor digitorum brevis leads to little in the way of functional impairment, because the long extensors can compensate for the loss of the muscle. The proximal part of the muscle can be used as interposition material to prevent bone fusion after resection of a calcaneonavicular bar (a common tarsal coalition). The muscle belly and tendon of extensor hallucis brevis serve as guides to the location of the dorsalis pedis artery and deep fibular nerve. The tendon of extensor hallucis brevis can be used as a local graft.

VASCULAR SUPPLY

ARTERIES

Dorsalis pedis artery

The dorsalis pedis artery is the dorsal artery of the foot (Figs 84.1; 84.23), and is the continuation of the anterior tibial artery distal to the ankle. It passes to the proximal end of the first intermetatarsal space, where it turns into the sole between the heads of the first dorsal interosseous to complete the plantar arch, and provides the first plantar metatarsal artery.

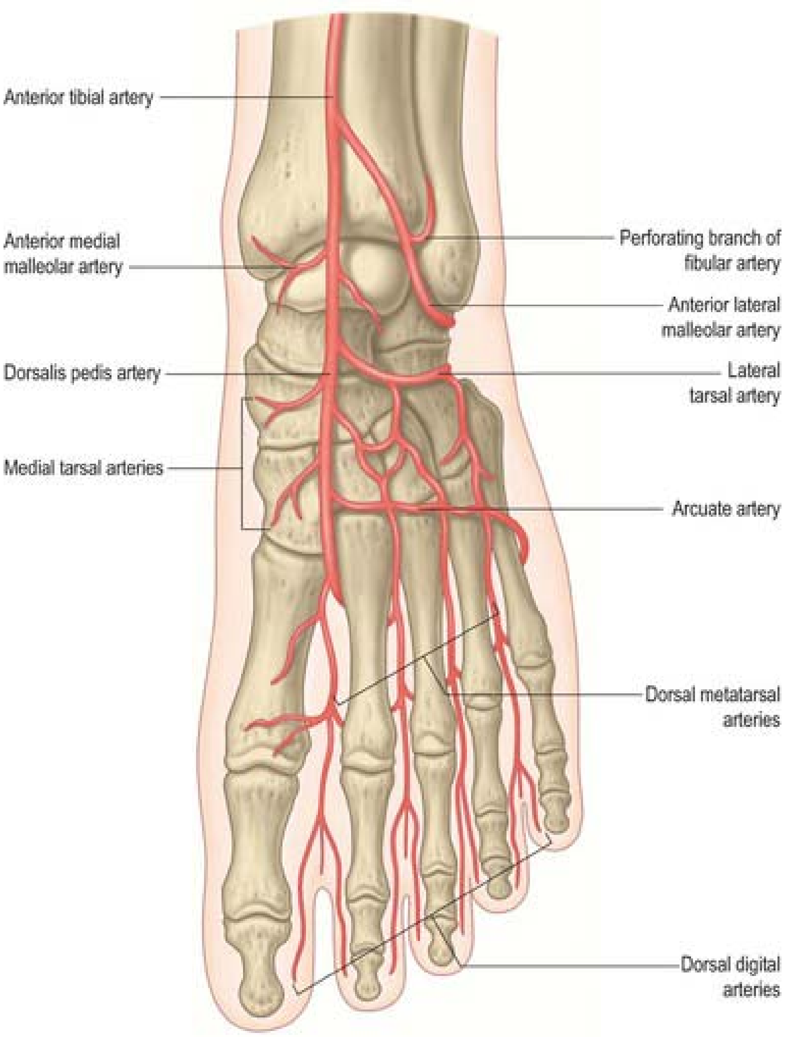

Anterior tibial artery
Anterior medial malleolar artery
Dorsalis pedis artery
Medial tarsal arteries
Perforating branch of fibular artery
Anterior lateral malleolar artery
Lateral tarsal artery
Arcuate artery
Dorsal metatarsal arteries
Dorsal digital arteries

Fig. 84.23 Dorsal arteries of the foot.

The artery may be larger than normal, to compensate for a small lateral plantar artery. It may be absent, in which event it is replaced by a large perforating branch of the fibular artery. It often diverges laterally from its usual route.

Relations

The dorsalis pedis artery crosses, successively, the talocrural articular capsule, talus, navicular and intermediate cuneiform and their ligaments; superficial to it are the skin, fasciae, inferior extensor retinaculum and, near its termination, extensor hallucis brevis. Medial to it is the tendon of extensor hallucis longus and lateral to it are the medial tendon of extensor digitorum longus and medial terminal branch of the deep fibular nerve. The tendons are useful landmarks in the planning of safe anatomical approaches in surgery of the ankle and foot.

Surface anatomy

The pulsation of the dorsal artery of the foot is palpable from the midpoint between the malleoli to the proximal end of the first intermetatarsal space.

Branches

The dorsalis pedis artery gives off the tarsal, arcuate and first dorsal metatarsal arteries.

Tarsal arteries

There are two tarsal arteries, lateral and medial (Fig. 84.23). They arise as the dorsalis pedis artery crosses the navicular. The lateral runs laterally under extensor digitorum brevis; it supplies this muscle and the tarsal articulations, and anastomoses with branches of the arcuate, anterior lateral malleolar and lateral plantar arteries, and the perforating branch of the fibular artery. Two or three medial tarsal arteries ramify on the medial border of the foot and join the medial malleolar network.

Arcuate artery

The arcuate artery (Fig. 84.23) arises near the medial cuneiform, passes laterally over the metatarsal bases, deep to the tendons of the digital extensors, and anastomoses with the lateral tarsal and plantar arteries. It supplies the second to fourth dorsal metatarsal arteries, running distally superficial to the corresponding dorsal interossei, and divides into two dorsal digital branches for the adjoining toes in the interdigital clefts. Proximally, in the interosseous spaces, these branches receive proximal perforating branches from the plantar arch. Distally, they are joined by distal perforating branches from the plantar metatarsal arteries. The fourth dorsal metatarsal artery sends a branch to the lateral side of the fifth toe.

First dorsal metatarsal artery

The first dorsal metatarsal artery (Fig. 84.23) arises just before the dorsalis pedis artery enters the sole. It runs distally on the first dorsal interosseous and divides at the cleft between the first and second toes. One branch passes under the tendon of extensor hallucis longus and supplies the medial side of the hallux; the other bifurcates to supply the adjoining sides of the hallux and the second toe.

Cutaneous vessels from the dorsalis pedis artery

The dorsalis pedis artery and its first dorsal metatarsal branch give rise to small direct cutaneous branches that supply the dorsal foot skin between the extensor retinaculum and the first web space. This vessel provides the basis for a fasciocutaneous flap raised from this region, and which may be used to cover superficial defects elsewhere.

Plantar arch

The plantar arch (Fig. 84.24) is deeply situated, extending from the fifth metatarsal base to the proximal end of the first interosseous space. Convex distally, it is plantar to the bases of the second to fourth metatarsal bones and corresponding interossei, but dorsal to the oblique part of adductor hallucis.

Branches

The plantar arch gives off three perforating and four plantar metatarsal branches, and numerous branches that supply the skin, fasciae and muscles in the sole. Three perforating branches ascend through the proximal ends of the second to fourth intermetatarsal spaces, between the heads of dorsal interossei, and anastomose with the dorsal metatarsal arteries. Four plantar metatarsal arteries extend distally between the metatarsal bones in contact with the interossei (Fig. 84.24). Each divides into two plantar digital arteries, supplying the adjacent digital aspects. Near its division, each plantar metatarsal artery sends a distal perforating branch dorsally to join a dorsal metatarsal artery. The first plantar metatarsal artery springs from the junction between the lateral plantar and dorsalis pedis arteries, and sends a digital branch to the medial side of the hallux. The lateral digital branch for the fifth toe arises directly from the lateral plantar artery near the fifth metatarsal base. Haemorrhage from the plantar arch is difficult to stem, because of the depth of the vessel and its important close relations.

Surface anatomy

The lateral plantar artery begins between the heel and medial malleolus, and crosses obliquely to a point 2.5 cm medial to the tuberosity of the fifth metatarsal. With a slight distal convexity, it reaches the proximal end of the first intermetatarsal space.

Posterior tibial artery

Before the posterior tibial artery divides into its two main terminal branches, it gives off a communicating branch which runs posteriorly across the tibia approximately 5 cm above its distal end, deep to flexor hallucis longus, and joins a communicating branch of the fibular artery; calcaneal branches, which arise just proximal to the termination of the posterior tibial artery, pierce the flexor retinaculum and supply the skin and fat behind the calcaneal tendon; the artery of the tarsal canal. The terminal branches of the posterior tibial artery are the medial and lateral plantar arteries.

Branches

Medial plantar artery

The medial plantar artery is the smaller terminal branch of the posterior tibial artery (Fig. 84.24). It arises midway between the medial malleolus and the medial calcaneal tubercle and passes distally along the medial side of the foot, with the medial plantar nerve lateral to it. At first deep to abductor hallucis, it runs distally between abductor hallucis and flexor digitorum brevis, supplying both. Near the first metatarsal base, when its calibre is already diminished as a result of supplying numerous muscular branches, it is further diminished by a superficial stem. It passes to the medial border of the hallux, where it anastomoses with a branch of the first plantar metatarsal artery. Its superficial stem then trifurcates and supplies three superficial digital branches that accompany the digital branches of the medial plantar nerve and join the first to third plantar metatarsal arteries.

Lateral plantar artery

The lateral plantar artery is the larger terminal branch of the posterior tibial artery (Fig. 84.24). It passes distally and laterally to the fifth metatarsal base; the lateral plantar nerve is medial. The plantar nerves lie between the plantar arteries. Turning medially, with the deep branch of the nerve, it gains the interval between the first and second metatarsal bases, and unites with the dorsalis pedis artery to complete the plantar arch. As it passes laterally, it is first between the calcaneus and abductor hallucis, then between flexor digitorum brevis and flexor accessorius. Running distally to the fifth metatarsal base, it passes between flexor digitorum brevis and abductor digiti minimi and is covered by the plantar aponeurosis, superficial fascia and skin.

Muscular branches supply the adjoining muscles. Superficial branches emerge along the intermuscular septum to supply the skin and subcutaneous tissue over the lateral part of the sole. Anastomotic branches run to the lateral border, and join branches of the lateral tarsal and arcuate arteries. Sometimes, a calcaneal branch pierces abductor hallucis to supply the skin of the heel.

Perforator flaps in the ankle and foot region

The arteries around the ankle and in the foot are the medial and lateral calcaneal artery, medial and lateral plantar artery and the dorsalis pedis artery. In the foot the two plantar arteries with communicating arteries from dorsalis pedis give out multiple small perforators. In the sole of the foot the perforators emerge on either side of the plantar aponeurosis, and also pass through it, to supply the skin. ‘Island flaps’ from these perforators may be advanced to reconstruct small defects in the weight bearing area. The skin of the sole of the foot is highly specialized and therefore ideally defects in this region should be reconstructed using local skin.

DEEP AND SUPERFICIAL VENOUS SYSTEMS IN THE FOOT

Plantar digital veins arise from plexuses in the plantar regions of the toes. They connect with dorsal digital veins to form four plantar metatarsal veins which run proximally in the intermetatarsal spaces and connect via perforating veins with dorsal veins, then continue to form the deep plantar venous arch which is situated alongside the plantar arterial arch. From this venous arch, medial and lateral plantar veins run near the corresponding arteries and, after communicating with the great and small saphenous veins, form the posterior tibial veins behind the medial malleolus.

The principal named superficial veins are the great and small saphenous. Their numerous tributaries are mostly (but not wholly) unnamed; named vessels will be noted (see Fig. 79.9A,B). As in the upper limb, the vessels will be described centripetally from peripheral to major drainage channels.

Dorsal digital veins receive rami from the plantar digital veins in the clefts between the toes and then join to form dorsal metatarsal veins, which are united across the proximal parts of the metatarsal bones in a dorsal venous arch. Proximal to this arch, an irregular dorsal venous network receives tributaries from deep veins and is continuous proximally with a venous network in the leg. At each side of the foot, this network connects with medial and lateral marginal veins, which are both formed mainly by veins from more superficial parts of the sole. In the sole, superficial veins form a plantar cutaneous arch across the roots of the toes and also drain into the medial and lateral marginal veins. Proximal to the plantar arch there is a plantar cutaneous venous plexus, especially dense in the fat of the heel. It connects with the plantar cutaneous venous arch and other deep veins, but drains mainly into the marginal veins. The veins of the sole are an important part of the lower limb ‘venous pump’ system aiding propulsion of blood up the limb. Intermittent foot compression devices are available to enhance this flow and so reduce the risk of deep vein thrombosis during periods of increased risk, e.g. after surgery.

INNERVATION OF THE FOOT

Superficial fibular nerve

The superficial fibular nerve is described in Chapter 83.

Deep fibular nerve

The deep fibular nerve is described in Chapter 83.

Tibial nerve

The branches of the tibial nerve that innervate structures in the ankle and foot are articular, muscular, sural, medial calcaneal and medial and lateral plantar nerves. The course and distribution of the tibial nerve in the calf are described in Chapter 83.

Medial calcaneal nerve

The medial calcaneal nerve arises from the tibial nerve and perforates the flexor retinaculum to supply the skin of the heel and medial side of the sole.

Medial plantar nerve

The medial plantar nerve is the larger terminal division of the tibial nerve, and lies lateral to the medial plantar artery. From its origin under the flexor retinaculum, it passes deep to abductor hallucis, then appears between it and flexor digitorum brevis, gives off a medial proper digital nerve to the hallux, and divides near the metatarsal bases into three common plantar digital nerves.

Cutaneous branches pierce the plantar aponeurosis between abductor hallucis and flexor digitorum brevis to supply the skin of the sole of the foot. Muscular branches supply abductor hallucis, flexor digitorum brevis, flexor hallucis brevis and the first lumbrical. The first two arise near the origin of the nerve and enter the deep surfaces of the muscles. The branch to flexor hallucis brevis is from the hallucal medial digital nerve, and that to the first lumbrical from the first common plantar digital nerve. Articular branches supply the joints of the tarsus and metatarsus.

Three common plantar digital nerves pass between the slips of the plantar aponeurosis, each dividing into two proper digital branches. The first supplies adjacent sides of the hallux and second toe and the second supplies adjacent sides of the second and third toes; the third supplies adjacent sides of the third and fourth toes, and also connects with the lateral plantar nerve. The first gives a branch to the first lumbrical. Each proper digital nerve has cutaneous and articular branches: near the distal phalanges a dorsal branch supplies structures around the nail, and the termination of each nerve supplies the ball of the toe.

The common digital branches of the medial plantar nerve are distributed in a manner similar to those of the median nerve, as are the motor branches of the two nerves. In the hand, the median nerve supplies abductor and flexor pollicis brevis, opponens pollicis and the first and second lumbricals. An opponens is absent in the foot, but abductor hallucis, flexor hallucis brevis and the first lumbrical are all supplied by the medial plantar nerve. Flexor digitorum brevis and flexor digitorum superficialis (innervated by the median nerve) correspond, but the innervation of the second lumbrical of the foot does not mirror the arrangement in the hand.

Lateral plantar nerve

The lateral plantar nerve supplies the skin of the fifth toe, the lateral half of the fourth toe, and most of the deep muscles of the foot (Fig. 84.20). Its distribution therefore closely resembles that of the ulnar nerve in the hand. It passes laterally forwards medial to the lateral plantar artery, towards the tubercle of the fifth metatarsal. Next, it passes between flexores digitorum brevis and accessorius, and ends between flexor digiti minimi brevis and abductor digiti minimi by dividing into superficial and deep branches. Before division, it supplies flexor digitorum accessorius and abductor digiti minimi and gives rise to small branches that pierce the plantar fascia to supply the skin of the lateral part of the sole (Fig. 84.25). The superficial branch splits into two common plantar digital nerves: the lateral supplies the lateral side of the fifth toe, flexor digiti minimi brevis and the two interossei in the fourth intermetatarsal space; the medial connects with the third common plantar digital branch of the medial plantar nerve and divides into two to supply the adjoining sides of the fourth and fifth toes. The deep branch accompanies the lateral plantar artery deep to the flexor tendons and adductor hallucis and supplies the second to fourth lumbricals, adductor hallucis and all the interossei (except those of the fourth intermetatarsal space). Branches to the second and third lumbricals pass distally deep to the transverse head of adductor hallucis, and curl round its distal border to reach them.

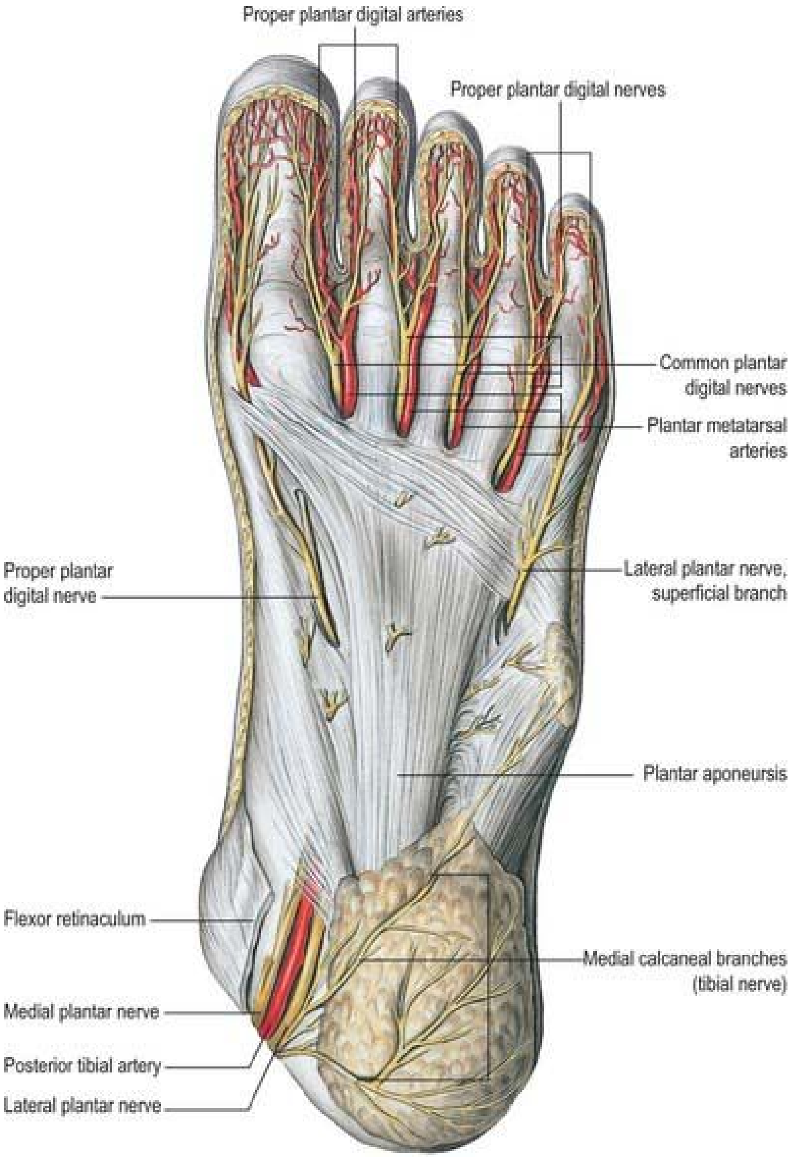
Proper plantar digital arteries
Proper plantar digital nerves
Common plantar digital nerves
Plantar metatarsal arteries
Proper plantar digital nerve
Lateral plantar nerve, superficial branch
Plantar aponeursis
Flexor retinaculum
Medial calcaneal branches (tibial nerve)
Medial plantar nerve
Posterior tibial artery
Lateral plantar nerve

Fig. 84.25 Plantar digital nerves.

(From Sobotta 2006.)

Nerve entrapment syndromes in the foot

All nerves of the foot can be affected by entrapment, leading classically to a burning sensation in the distribution of that nerve. Tarsal tunnel syndrome is much less common than carpal tunnel syndrome. The flexor retinaculum may compress the tibial nerve or either of its branches (medial and lateral plantar nerves). However entrapment at this level is most commonly due to a space-occupying lesion, e.g. ganglion, or compression by a leash of vessels or the deep fascia associated with abductor hallucis. Compression of the first branch of the lateral plantar nerve by the deep fascia of abductor hallucis can lead to heel pain. The medial plantar nerve can be compressed at the 'knot of Henry': this is usually related to jogging. The 'knot of Henry' is the anatomical landmark where the tendon of flexor hallucis longus crosses deep to the tendon of flexor digitorum longus, to reach its medial side in the sole of the foot. The superficial fibular nerve can be damaged in severe inversion injuries of the ankle, and the deep fibular nerve is sometimes compressed by osteophytes in the region of the second tarsometatarsal joint. Sural nerve entrapment is usually not due to compression by fascial elements; rather, it is secondary to distal fibular trauma and subsequent scar formation around the nerve. Entrapment of the common digital nerve as it passes under the intermetatarsal ligament of the third (or less commonly the second) webspace can result in a Morton's neuroma, which is probably the most common form of nerve entrapment in the foot.

BIOMECHANICS OF STANDING, WALKING AND RUNNING

PLANES OF MOTION

Much confusion surrounds the descriptive terms for movement in the foot and ankle. Plantar flexion and dorsiflexion refer to movement in the sagittal plane and occur principally, but not exclusively, at the ankle, metatarsophalangeal and interphalangeal joints. Inversion is tilting of the plantar surface of the foot towards the midline, and eversion is tilting away from the midline. This is motion in the coronal plane and takes place principally in the talocalcaneal and transverse tarsal joints. Adduction is movement of the foot towards the midline in the transverse plane; abduction is movement away from the midline. This movement occurs at the transverse tarsal joints and, to a limited degree, the first tarsometatarsal joint and the metatarsophalangeal joints.

Supination describes a three-dimensional movement and is a combination of adduction, inversion and plantar flexion. Pronation is the opposite motion, i.e. a combination of abduction, eversion and dorsiflexion. Pronation and supination are usually better terms than eversion and inversion, as the latter rarely occur in isolation and the former describe the ‘compound’ motion that usually occurs.

Active movements occur at the ankle, talocalcaneonavicular and subtalar joints. Movements at the ankle joint are almost entirely restricted to dorsi- and plantar flexion, but slight rotation may occur in plantar flexion. The ranges of movement at the talocalcaneonavicular and subtalar joint are greater: inversion and eversion mainly occur here.

STANDING

Humans are bipedal: we stand and walk with an erect trunk and knees which are almost straight. Moreover, we are plantigrade, i.e. we set the whole length of the foot down on the ground, whereas most medium to large mammals are digitigrade, i.e. they stand and walk on their toes, and ungulates stand on hooves on the tips of their toes.

When we stand motionless, the ground exerts a force on the feet called the ‘ground reaction force’, which is equal and opposite to body weight. The latter acts at the ‘centre of gravity’, a point a little above the hip joints and anterior to the vertebral column. The force on the ground is centred vertically below it, at the centre of pressure. When we stand comfortably, the centre of pressure is usually midway between the insteps of our two feet. We do not remain absolutely still, but sway slightly. As we age, our postural control deteriorates, which is a factor in the development of unsteadiness and risk of falling.

When considering the distribution of load in the lower limb, a knowledge of limb alignment is important. The ‘anatomic axis’ is produced by lines passing along the shafts of the femur and tibia, and is therefore angled at the knee by 5° to 7°. The ‘mechanical axis’ is a straight line connecting the centres of the femoral head and ankle. Exactly where the line passes through the knee has yet to be defined: for convenience it is usually taken to pass through the centre, but may well lie more medially. For the tibia, the lines of the mechanical and anatomic axes coincide. Whilst the weight of the body acts in a vertical line from the centre of gravity to the ground, the line of the mechanical axis of the lower limbs is inclined 3° to this in normal stance, with the ankles closer than hips.

In the sagittal plane, body weight acts along a line which passes a few centimetres anterior to the tibiotalar joint, exerting a moment that must be balanced by the plantar flexor muscles. Some electromyographic investigations of standing have found activity mainly in soleus, but others have found moderate activity in gastrocnemius as well. In either case it seems likely that the activity is mainly in type I (slow oxidative) fibres, since these can maintain tension more economically than faster fibres could do under the same conditions. Soleus contains mostly type I fibres, and gastrocnemius contains approximately 50%.

In normal standing, the weight of the body above the knee joint acts slightly anteriorly to the axes of the knees: it exerts a moment that is balanced passively by tension in the ligaments and posterior capsule which prevent hyperextension. If the knees are kept straight, there is little or no electrical activity in the hamstrings and only moderate levels in the quadriceps. Generally, the combined weight of the trunk, arms and head seems to act slightly behind the hip joints, exerting a small moment that is balanced largely by iliopsoas. Thus a relaxed stance, with trunk erect and knees straight, requires very little activity in thigh muscles. This demands low energy consumption and permits long periods of standing. In single leg stance the weight of the upper parts of the body exerts a moment about the supporting hip which must be balanced by the abductor muscles, especially tensor fasciae latae and glutei medius and minimus. Damage to the glutei or their nerve supply, e.g. during hip surgery, is a potent cause of a limp.

PROPULSION

The contraction of tibialis posterior, gastrocnemius and soleus is the chief factor responsible for propulsion in walking, running and jumping. The propulsive action of these calf muscles is enhanced by arching of the foot and flexion of the toes. In walking, the weight of the foot is taken successively on the heel, lateral border and the ball of the foot. The last part of the foot to leave the ground is the anterior pillar of the medial longitudinal arch and the medial three toes. In the act of running, the heel does not touch the ground, but the point of take-off is still the anterior pillar of the medial longitudinal arch. As the heel leaves the ground, the toes gradually extend. Extension, of the hallux particularly, tightens the plantar aponeurosis and thus heightens the arch. At the same time, flexor hallucis longus and flexor digitorum longus elongate, which increases their subsequent contraction. The long and short toe flexors increase the force of take-off by exerting pressure on the ground. The most important muscle in this respect is flexor hallucis longus, which is strongly assisted by the short toe flexors. The lumbricals provide a balancing action to the long toe flexors and prevent buckling of the toes during the toe-off phase of gait.

Walking

In walking, each foot is on the ground (stance phase) for approximately 60% of the stride, and off the ground (swing phase) for approximately 40% (Fig. 84.26). Thus single-support phases (one foot on the ground) alternate with double-support phases (two feet on the ground). The knee is straight at heel strike and remains nearly straight (10–30°) for most of the stance phase of that leg, bending more only immediately before toe-off. During the swing phase the knee flexes to a maximum of 60° at mid-swing.

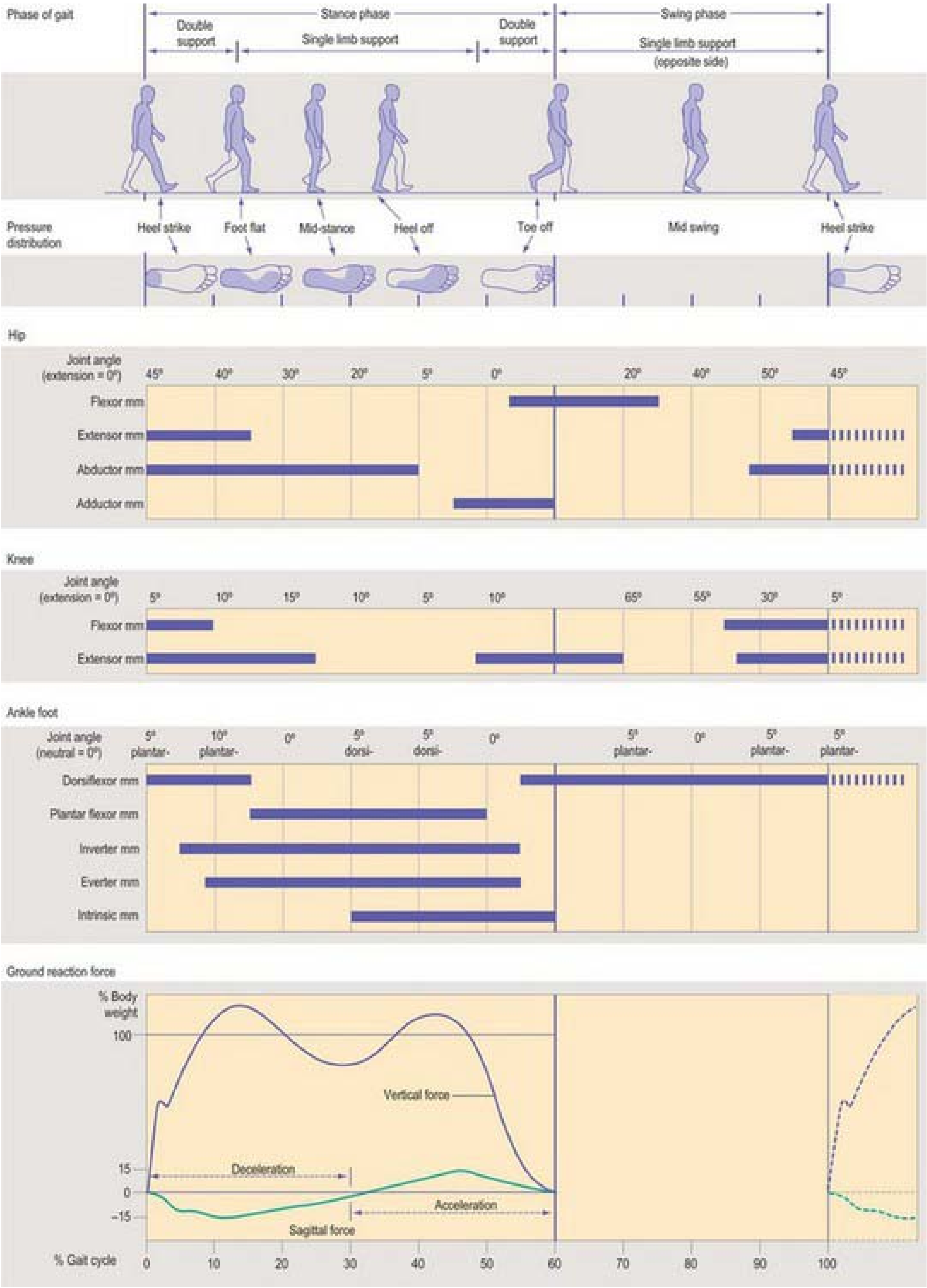

Fig. 84.26 The events that occur during the different phases of a normal gait cycle. Depicted are: distribution of pressure on the plantar surface of the foot; changes in the angles of hip, knee and ankle joints, together with activity in the corresponding muscle groups; and vertical and horizontal

(sagittal plane) components of the ground reaction force during stance phase. (Chart collated from various sources by Michael Gunther, Department of Human Anatomy and Cell Biology, University of Liverpool.)

Stance phase starts with ‘heel strike’. With the foot still planted in front of the body, ‘foot flat’ is reached, and becomes ‘mid-stance’ when the body comes to be directly above the planted foot. The heel then rises as the contralateral foot makes contact with the ground (the ‘double stance’ phase). The last event of stance is ‘toe off ’ when the ‘swing phase’ starts. Early in the stance phase, while it is ‘foot flat’ in front of the trunk, the foot pushes downwards and forwards on the ground, decelerating the body as well as supporting it. Later, when the foot is behind the trunk, it pushes downwards and backwards, re-accelerating the body (Fig. 84.26). The speed, and therefore the kinetic energy, of the body passes through a maximum in each double-support phase, and a minimum in each single-support phase.

The height of the centre of gravity, and therefore the potential energy of the body, also fluctuates. This is inevitable if the knee is kept nearly straight, making the hip move in a near-circular arc about the ankle of the supporting foot. The vertical component of the total force exerted by both feet on the ground in the double-support phase is greater than body weight, giving the body an upward acceleration. The vertical component of the ground force during the single-support phase is less than body weight, giving the body a downward acceleration. The force fluctuations have to be larger at higher speeds, to give the same vertical movement in less time.

During walking, the potential energy of the body is high when its kinetic energy is low, and *vice versa*. Energy can thus be swapped back and forth between the two forms, as in a swinging pendulum. A frictionless pendulum would continue swinging forever with no fresh input of energy. In walking, the exchange of potential and kinetic energy is less perfect, and the leg muscles have to do work to replace the energy which is lost at each impact of a foot with the ground. Even so, much less work is needed because of the pendulum principle. A second pendulum effect can be seen in the forward swing of the legs. If the leg were a rigid rod swinging from a fixed pivot, it would swing forward too slowly for normal walking: because it is free to bend at the knee, and because the hip from which it swings rises and falls, the leg swings forward faster with very little need for muscular work.

These pendulum effects ensure that relatively little work is needed to drive the fluctuations of kinetic and potential energy which occur in walking. The additional work needed to overcome air resistance and joint friction is very small, because we travel slowly and have well-lubricated joints. Human walking is economical of energy. Measurements of oxygen consumption show that 70-kg men use only 230 joules of metabolic energy for every metre they walk at their most economical speed (approximately 1.3 metres per second), which is 140 J/m more than they would use if they stood still. Running uses 260 J/m more than standing. Walking is economical only near the optimum speed, and the energy cost of fast walking overtakes that of running at 2 m/s, at which speed adults usually break into a run. Children, with their shorter legs, start running at lower speeds: the theoretical expectation is that the critical speed should be proportional to the square root of leg length.

The function of arm swinging in walking is not fully understood but it aids postural stability. For further discussion of standing and walking see Alexander (1992).

Development of walking

The average child sits at 6 months, crawls at 9 months, walks with support at 12 months, and without support at 18 months. The characteristic early gait matures rapidly and is similar to that of the adult by 3 years. Some minor changes occur up to 7 years which are largely a reflection of neurological development, but are also related to stature. Early gait is jerky, unsteady, and wide-based. The arms are held abducted at the shoulder and initially flexed at the elbows. Initial ground contact varies, and heel-toe, whole foot, and toe-heel are all possible. Generally a plantarflexed posture is adopted which contrasts with the adult pattern. In adults, heel strike is accompanied by a straight knee which then flexes. A child strikes the ground with a flexed knee which is then extended in response to weight-bearing, and a short time is spent in single leg stance (Fig. 84.27). Maturation is associated with diminution of base width, and increase in step length and velocity. The earliest changes are development of heel-strike, knee flexion during stance, and reciprocal upper limb swing. The period of single leg stance increases.

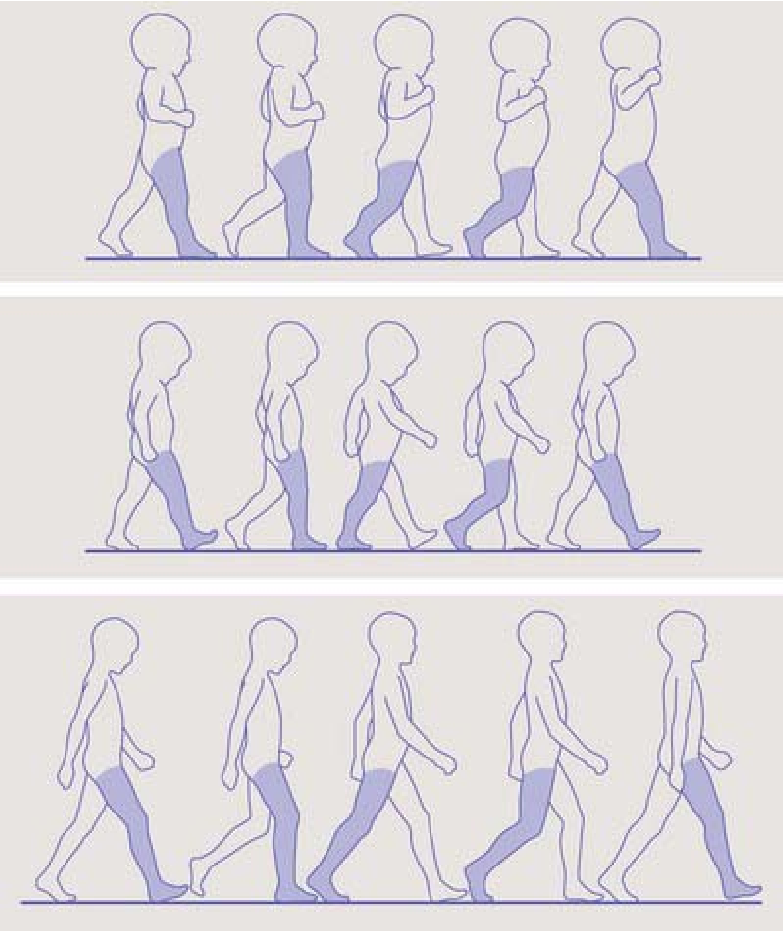

Fig. 84.27 Development of a mature gait. Top: 1-year-old. Note the flexed elbows and lack of arm swing. The foot is plantar flexed at contact. Middle: 3-year-old. Arm swing is now present as is heel strike. Bottom: 6-year-old. There is now an adult-type gait.

(By permission from Benson MKD, Fixsen JA, MacNicol MF (eds) 2001 Development of a mature gait. In: Children's Orthopaedics and Fractures, 2nd edn. Edinburgh: Churchill Livingstone.)

Running

Walking involves dual-support phases, but in running each foot is on the ground for 40% (jogging) to 27% (sprinting) of the stride, so there is an aerial phase, the ‘double float’ phase, when neither foot is on the ground. The faster the subject runs, the shorter the stance phase: world-class sprinters spend approximately 22% of the gait cycle in stance. During each aerial phase the body rises and then falls under gravity, which means that its height and potential energy are maximal in the middle of this phase and minimal at mid-stance, when, in marked contrast to walking, the knee of the supporting leg bends. Walking has been described as ‘controlled falling’, as the centre of gravity falls from a peak in mid-stance to a low during double support. The analogy that is used for running is an individual on a ‘pogo stick’. The runner propels himself from a low point in mid-stance to a peak during double float. During walking, efficiency is maintained by the interchange of potential and kinetic energy. During running, when potential and kinetic energies are in phase, efficiency is maintained in two ways: storage and release of potential energy in the elastic structure of tendons, and transfer of energy between limb segments via muscles which cross two joints (e.g. rectus femoris and hamstrings). The changes in muscle belly lengths are relatively slight during running. The muscles are acting as tensioners of the tendons, indeed, most of the change of length is produced by the stretch and recoil of the tendons. It has been estimated that, of the kinetic and potential energy lost and regained in each stance phase, 35% is stored temporarily as elastic strain energy in the calcaneal tendon, and 17% in the ligaments of the arch of the foot. Together these springs approximately halve the work required from the muscles.

A tendon is capable of withstanding stresses (force per unit cross-sectional area) of at least 100 N/mm^2 (10 kg force/mm^2). It stretches elastically by approximately 8% before breaking, and its recoil returns 93% of the energy used to stretch it. This high energy return is important, not only because it reduces the work required from the muscles, but also because the lost mechanical energy becomes heat: leg tendons with poor energy return would overheat in running, and be damaged. The calcaneal tendon is the most important ‘spring’ in the leg. Most runners strike the ground first with the heel, and the centre of pressure moves rapidly forward to the distal heads of the metatarsals, where it remains for most of the stance phase. A large force is then required in the calcaneal tendon to balance the moments about the tibiotalar joint. For a 70-kg man running at middle-distance speed, the peak force in the tendon is 5000 N (0.5 tonne force), which is enough to stretch it by approximately 6%. The parts of the tendon that run alongside the muscle bellies of gastrocnemius and soleus must be stretched, as well as the free distal part.

The mean vertical force on the ground during a complete stride cycle of any gait must equal body weight. If the foot is on the ground for only a small fraction of the stride, the forces must then be high. Peak vertical forces on one foot are approximately 1.0 times body weight in walking, 2.5 times in jogging, and 3.5 times in sprinting. Leg muscles have to exert much larger forces in running than in walking because the ground reaction forces are higher and also because, for a given ground force, flexion of the knee increases the moments about it. The main sources of power are the gastrocnemius–soleus complex at push-off; quadriceps femoris after ‘stance phase reversal’ (when the lower limb muscles change from a decelerating role to one of generating power, the generation phase); the hip extensors during late swing and early stance; the hip abductors just after stance phase reversal.

As in walking, the ground force acts more or less in line with the leg, so the body is decelerated and reaccelerated during each stance phase. The stance phase starts with deceleration and absorption of energy. Power is generated after stance phase reversal as the limb pushes up with the knee extending and foot plantarflexed, and this continues in the swing phase as the limb is accelerated forward. Once the limb is ahead of the trunk, the final phase of swing phase absorption is initiated, during which the limb is decelerated.

The ground force acts upward on the metatarsal heads, and the calcaneal tendon pulls upwards on the calcaneus. The necessary balancing reaction occurs at the ankle, where the tibia presses downwards on the talus. Together these three forces flatten the longitudinal arch of the foot, forcing the ankle 10 mm nearer to the ground than it would be if the foot was rigid.

Mechanical tests on amputated feet have shown that the foot is a reasonably good spring, giving an energy return of nearly 80%. The plantar aponeurosis, long and short plantar ligaments and the plantar calcaneonavicular ligament are all involved in the spring action: they are predominantly collagenous, and presumably have elastic properties similar to those of tendon.

A runner’s foot is still moving, typically at about 1.5 m/s, when the heel hits the ground. The impact is cushioned by the subcalcaneal foot pad, supplemented (when shoes are worn) by the compliance of the heel of the shoe. On contact the foot is supinated, which ‘locks’ the foot as a rigid structure, and is ideal for shock absorption. Immediately after heel strike the trunk progresses over the foot: passive pronation is initiated which makes the foot more flexible and therefore able to adapt to the running surface. As the foot approaches push-off, it becomes supinated again and as a consequence stiffens, which provides an excellent lever. These changes in foot posture cause rotational changes in the leg, and these in turn impact on the knee.

Eighty per cent of runners heel strike, and 20% have a mid foot strike. In sprinting the forefoot makes contact first to provide the greatest leverage. The knees never fully extend during running: at first contact, the knee is 25° flexed, increasing to a maximum during stance of 45° at stance phase reversal, and decreasing to 20° at toe-off. In running, the swing phase knee flexion increases 90° at the end of swing phase generation (up to 125° in sprinting), then decreases until contact with the ground again. (All values are approximate.)

Movements of the foot

With the foot on the ground, body weight causes some supination and flattening of the longitudinal arches; about one-third of the weight borne by the forefoot is taken by the head of the first metatarsal. When a resting position becomes active, as occurs on starting to walk, the foot is pronated by muscular effort, and the first metatarsal is depressed (the second less so), which accentuates the longitudinal arch to its maximum height (Hicks 1953). Similar changes can be imposed on a weight-bearing foot by active lateral femoral rotation, which is transmitted through the tibia to the talus and entails passive supination of the foot. Medial femoral rotation has an opposite effect. When the foot is grounded and immobile, muscles which move it when it is freely suspended may exert effects on the leg, e.g. the dorsiflexors can then pull the leg forwards at the ankle joint.

The foot has two major functions: to support the body in standing and progression, and to lever it forwards and absorb shock in walking, running and jumping. To fulfil the first function, the pedal platform must be able to spread the stresses of standing and moving and be pliable enough to accommodate walking or running over uneven and sloping surfaces. To fulfil the second function, the foot must be transformable into a strong adjustable lever in order to resist inertia and powerful thrust: a segmented lever can best meet such stresses if it is arched.

In infants and young children, fatty, connective tissue on the plantar aspect may give the foot a flat appearance, indeed, soft tissues modify its appearance to varying degrees at all ages. However, the skeleton of the human foot is normally arched, and the sole of the foot is usually visibly concave. This curvature is customarily analysed into longitudinal and transverse arches. These arches vary individually in height, especially the longitudinal in its medial part. Since they are dynamic, their heights also differ in different phases of activity.

The medial longitudinal arch contains the calcaneus, talus, navicular, cuneiform and medial three metatarsal bones. Its summit, at the superior talar articular surface, takes the full thrust from the tibia and passes it backwards to the calcaneus, and forwards through the navicular and cuneiforms to the metatarsals. When the foot is grounded, these forces are transmitted through the three metatarsal heads and calcaneus (especially its tuberosity). The medial arch is higher, and more mobile and resilient than the lateral arch; its flattening progressively tightens the plantar calcaneonavicular ligament and plantar fascia. The lateral arch is adapted to transmit weight and thrust rather than to absorb such forces: the long plantar and plantar calcaneocuboid ligaments tighten as it flattens.

The lateral arch makes contact with the ground more extensively than the medial arch. As the foot flattens, an increasing fraction of load traverses soft tissues which are inferior to the entire arch. The whole lateral border usually touches the ground, whereas the medial border does not. However the medial border is visibly concave, usually even in standing, which explains the familiar outline of human footprints (though this varies with the position of the feet (Fig. 84.28), the development of associated soft tissues, and the nature of the surface). In any activity, as soon as the heel rises, the toes are extended and muscular structures (including the plantar aponeurosis) tighten up in the sole, accentuating the longitudinal arches. It has been suggested that tension diminishes in the deeper plantar ligaments in this phase.

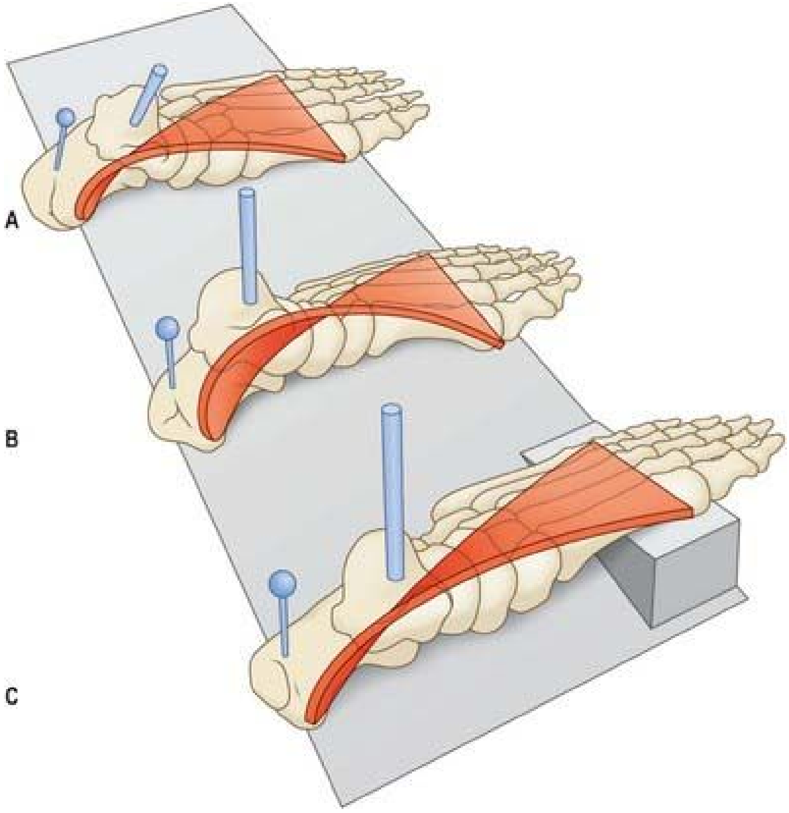

Fig. 84.28 The concept of the foot skeleton as a twisted plate which may be untwisted (supination) or further twisted (pronation) during the maintenance of a plantigrade stance in various positions of the foot. (Based upon MacConaill 1945, 1950.) **A**, The foot skeleton in supination, as in standing with the feet widely separated. Note the marked medial tilting of the talus and, to a lesser degree, of the calcaneus and the depression of the medial longitudinal arch. **B**, Relative pronation of the foot, as in standing

with the feet close together. **C**, Supination of the foot when standing on an inclined surface; if the position of the wedge had been reversed, the foot skeleton would, of course, approach maximal pronation.

The sole is transversely concave, both in skeletal form and usually in external appearance, and serial transverse arches are most developed inferior to the metatarsus and adjoining tarsus. Transmission of force occurs at the metatarsal heads, to some degree along the lateral border of the foot, and through subjacent soft tissues.

In standing, with only body weight to support, both the intrinsic and extrinsic muscles appear to relax. If the longitudinal arches are allowed to sink as a result of muscular relaxation, the plantar ligaments tie the bones into an arched form. The medial arch is more elevated when the feet are together than when they are apart, i.e. inversion with supination increases as the feet are separated. This medial sag can be countered by voluntary contraction of muscles such as tibialis anterior. Pronation and supination ensure that in standing, whatever the position of the feet, a maximal weight-bearing area is grounded, from the metatarsal heads along the lateral border of the foot to the calcaneus. The twist imparted by pronation (which is partly undone in supination) prompts the likening of the foot to a twisted but resilient plate (Fig. 84.28), where adequate ground contact was ensured whatever the angle between the foot and leg, and adaptable resilience was imparted in standing and progression.

REFERENCES

exander R McN. The Human Machine. London: Natural History Museum Publications, 1992.

rclay-Smith E. The astragalo-calcaneo-navicular joint. *J Anat Physiol*. 1896;30:390-412.

This paper gave the first description of the astragalo-calcaneo-navicular joint and explained the importance of the joint complex in terms of hindfoot motion..

ɔleman S, Chesnut W. A simple test for hindfoot flexibility in the cavovarus foot. *Clin Orthop*. 1977;123:60-62.

ımmins JE, Anson JB, Carr WB, Wright RR, Hauser DWE. The structure of the calcaneal tendon (of Achilles) in relation to orthopedic surgery with additional observations on the plantaris muscle. *Surg Gynecol Obstet*. 1946;83:107-116.

ırdner E, Gray DJ. The innervation of the joints of the foot. *Anat Rec*. 1968;161:141-148.

ırris RI, Beath T. Etiology of peroneal spastic flat foot. *J Bone Joint Surg [Br]*. 1948;30:624-634.

.cks JH. The mechanics of the foot II. The plantar aponeurosis and the arch. *J Anat*. 1953;88:25-30.

nes FW. Structure and Function as Seen in the Foot, 2nd edn., London: Baillière, Tindall and Cox; 1949:63-65.

One of the classic texts on the foot..

ıpandji IA. The Physiology of the Joints. Annotated Diagrams of the Mechanics of the Human Joints, 2nd edn (3 vols translated by LH Honoré: Vol 1 Upper Limb. Vol 2 Lower Limb. Vol 3 The Trunk and the Vertebral Column.). Edinburgh: Churchill Livingstone, 1970–1974.

ırrafian SK. Anatomy of the Foot and Ankle, Descriptive, Topographic, Functional, 2nd edn. Philadelphia: Lippincott, 1993.

.ylor GI, Razaboni RM. Arteries of the Muscles of the Extremities and the Trunk. St Louis: Quality Medical Publishing Inc, 1994.

ildenauer F. Die Blutversorgung des Talus. *Z Anat Entwicklungsgesch*. 1950;115:32-36.

The first comprehensive account of talar blood supply and the identification of the important artery of the tarsal canal..

CHAPTER 85

Development of the pelvic girdle and lower limb

STAGES OF LOWER LIMB DEVELOPMENT

The lower limb is first recognizable as a laterally projecting ridge at stage 13 and by stage 14 it is closely associated with the wide umbilical cord. During stages 15–17 the limb projects laterally and outgrowth is fairly symmetrical.

By stage 17 the lower limb still has a flattened foot plate and although a hip region can be identified, there is no true knee as yet. In stage 18 the lower limb appears to be flexed and abducted at the hip with the knee bent, giving the appearance that the knee is facing laterally. Very little skin of the thigh is visible. The soles of the feet face the umbilical cord, and the foot plate has digit rays. During stages 20–23 the digit rays separate, and toes are clearly defined by stage 23. The feet can finally touch at stage 21, when the umbilical cord becomes proportionally smaller and the embryo larger.

The pelvis forms from two hemipelves each of which develops from one cartilaginous focus. Ossification of the pelvis starts with the ilium, which undergoes endochondral ossification at 9.5 weeks. The femur and tibia form in cartilage and the sciatic nerve extends distally to the tibia by stage 18. Cavitation of the hip joint has been reported at 7–8 weeks. The sacroiliac joint can be recognized from 7 weeks; its development is slightly different from that of other synovial joints in that the development of the ilium is ahead of that of the sacrum.

VESSELS IN THE LOWER LIMB

The axial artery of the lower limb arises from the dorsal root of the umbilical artery and courses along the dorsal surface of the thigh, knee and leg (Fig. 85.1). Below the knee it lies between the tibia and popliteus, and in the leg it lies between the crural interosseous membrane and tibialis posterior. It gives off a perforating artery that traverses the sinal tarsus to form a dorsal network and ends distally in a plantar network. The femoral artery passes along the ventral surface of the thigh, opening a new channel to the lower limb. It arises from a capillary plexus that is connected proximally with the femoral branches of the external iliac artery and distally with the axis artery. At the proximal border of popliteus the axis artery splits into primitive posterior tibial and fibular branches which run distally on the dorsal surface of popliteus and tibialis posterior to gain the sole of the foot. At the distal border of popliteus the axis artery gives off a perforating branch which passes ventrally between the tibia and the fibula and then courses to the dorsum of the foot, forming the anterior tibial and dorsalis pedis arteries. The primitive fibular artery communicates with the axis artery at the distal border of popliteus and in its course in the leg.

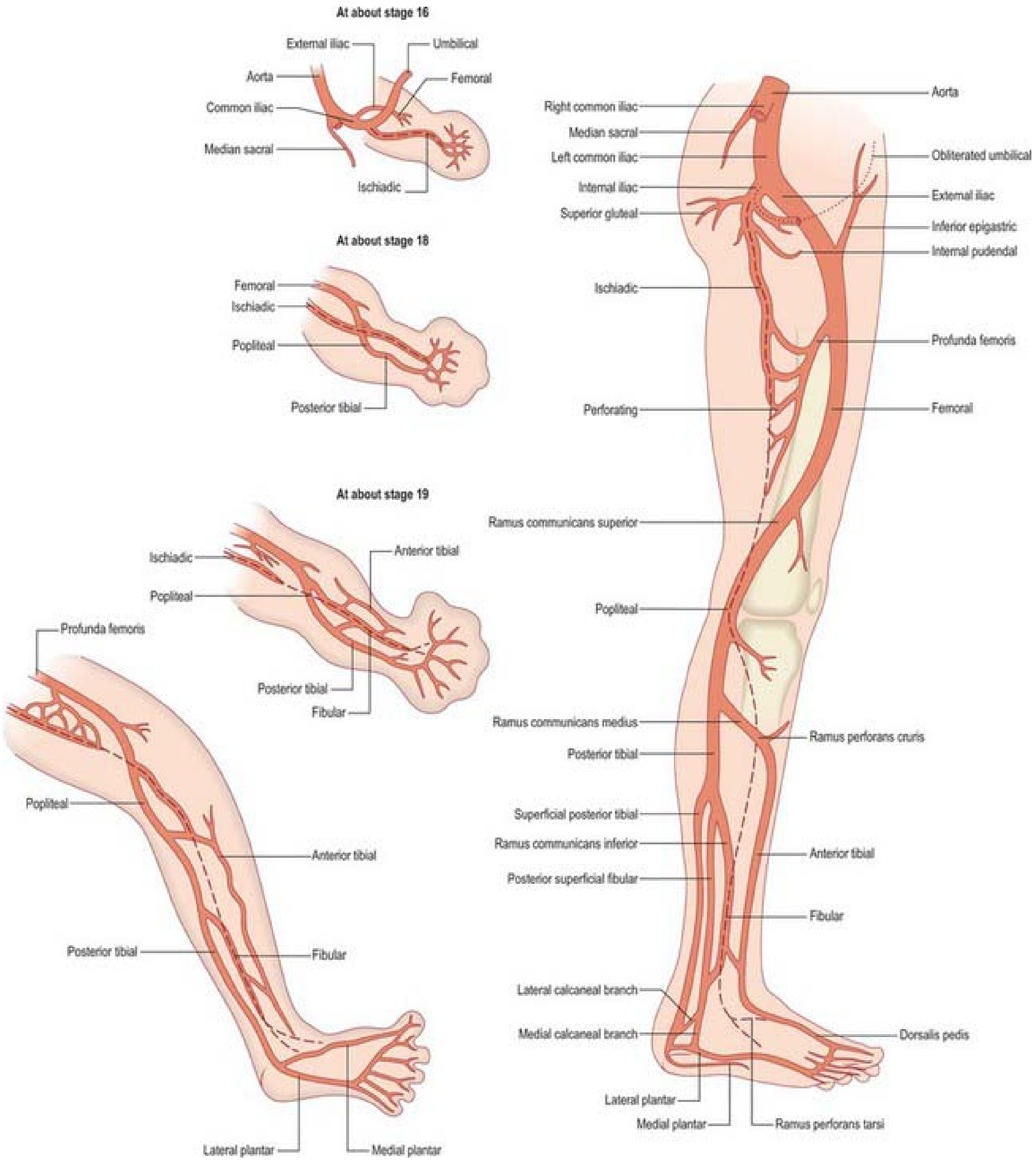
At about stage 16
External iliac
Umbilical
Aorta
Femoral
Common iliac
Median sacral
Ischiadic
At about stage 18
Femoral
Ischiadic
Popliteal
Posterior tibial
At about stage 19
Ischiadic
Anterior tibial
Popliteal
Profunda femoris
Posterior tibial
Fibular
Popliteal
Anterior tibial
Posterior tibial
Fibular
Lateral plantar
Medial plantar
Aorta
Right common iliac
Median sacral
Left common iliac
Obliterated umbilical
Internal iliac
External iliac
Superior gluteal
Inferior epigastric
Internal pudendal
Ischiadic
Profunda femoris
Perforating
Femoral
Ramus communicans superior
Popliteal
Ramus communicans medius
Ramus perforans cruris
Posterior tibial
Superficial posterior tibial
Ramus communicans inferior
Anterior tibial
Posterior superficial fibular
Fibular
Lateral calcaneal branch
Medial calcaneal branch
Dorsalis pedis
Lateral plantar
Medial plantar
Ramus perforans tarsi

Fig. 85.1 Stages in the development of the arteries of the leg. The original path of the axis artery is indicated by a dashed line.

The femoral artery gradually increases in size. Coincidentally, most of the axis artery disappears, but proximal to its communication with the femoral artery, the root of the axis artery persists as the inferior gluteal artery and the arteria comitans nervi ischiadici.

The proximal parts of the primitive posterior tibial and fibular arteries fuse but they remain separate distally. Ultimately, much of the primitive fibular artery disappears; a part of the axis artery is incorporated in the permanent fibular artery. The same considerations apply to anomalies and variations as were described for the developing forelimb (see Ch. 52).

The preaxial vein becomes the long saphenous vein, which drains into the femoral vein at the saphenous opening. The postaxial vein becomes the short saphenous vein, which passes deep and joins the popliteal vein.

NEONATAL LOWER LIMB

In the neonate the pelvis is cone-shaped. The transverse diameter of the true pelvis is 2.2 cm, its anteroposterior diameter 2.8 cm, and the length between the inlet and outlet is 2 cm. The sacrum is proportionately larger than in the adult and the sacral promontory is higher. When walking begins, the sacrum descends between the ilia and the promontory develops. The ilia, ischia and pubic bones are variably ossified at birth: they meet at the acetabulum, which in the neonate is cartilaginous, relatively large and shallow.

The lower limbs are underdeveloped in the neonate when compared to the upper limbs. They are retained in a flexed position and the leg is proportionately shorter than the thigh. Although the legs appear to be bowed, the tibia and fibula are straight: the illusion of bow legs is caused by the shape of the soft tissues and the slightly more advanced development of the lateral head of gastrocnemius compared to its medial head. The femoral neck is much shorter and forms an acute angle with the shaft. The latter is quite straight, because the adult curvature is acquired with walking. The head of the femur is larger than the acetabular fossa and nearly one-third remains external, which means that the ligamentum teres is relatively very long. Dislocation of the hip joint is relatively easy; the femoral head can be removed from the acetabular fossa laterally, but not posteriorly. The calcaneus and the talus have an ossification centre at birth, and a centre is present in the cuboid in 50% of neonates.

The muscles of the lower limb are much less developed than those in the upper limb. The fetal position often assumed by postnatal babies keeps the thighs in continuous abduction, stretching the adductors. The muscles that will be used for walking are weak; the lack of gluteal development in particular gives the typically diminutive buttocks of the neonate.

In neonates, the feet are usually inverted and they have a greater degree of dorsiflexion, caused by the relatively greater area of the trochlea of the talus. Plantar flexion is limited, in part reflecting the shortness of the extensor muscles of the foot. At birth the footprint outlines the whole plantar surface, reflecting the deposition of subcutaneous fat beneath the longitudinal and transverse arches, and so most babies appear flat-footed.

LOWER LIMB ANOMALIES

The categories of limb defects described by Swanson (1976) are given in Chapter 52. Although devised for the upper limb, they apply in the same manner to the lower limb.

Developmental dysplasia of the hip is a term that covers an alteration in hip development before and after birth. The term is now preferred to ‘congenital dislocation of the hip’. In the most extreme cases, the femoral head is completely dislocated out of the acetabulum. This condition occurs in approximately 1 in 100 live births; the ratio of females to males is 6 : 1. The aetiology is considered to be multifactorial and is associated with first pregnancies, suggesting that both maternal and uterine musculature restrict fetal movement and put postural strain on the fetal hips. Developmental dysplasia of the hip is seen more frequently in breech delivery, especially if the child’s knees are extended. The left hip is more frequently affected than the right, which may be because in breech presentation the fetus lies with the right shoulder anterior and the left thigh closest to the maternal sacrum. The physiological effects that cause the maternal ligaments to become temporarily lax prior to delivery are also considered to affect the fetus and to contribute to laxity of the hip capsule.

Congenital talipes equinovarus, or club foot, derives its name from a combination of *talus* and *pes*, together with terms describing an elevated heel resembling that of a horse (*equino*), which is also turned inwards (*varus*). It is a common neonatal anomaly and occurs in approximately 1 per 1000 live births, with males affected twice as often as females. There is some degree of inheritance, so it is not entirely an effect of intrauterine positioning or of oligohydramnios (abnormally little amniotic fluid). Both bones and soft tissues are affected and it is difficult to tell which are primary effects and which are secondary. A number of theories have been proposed to explain the underlying pathogenetic mechanism(s), including abnormal tendon and ligament attachments and delayed muscle maturation. The most widely held theory is that the talus undergoes defective development and that all the other deformities arise as a consequence of this initial defect. The talus is decreased in size by up to 25%. It has a foreshortened neck and decreased body/neck angle, and the subtalar facets are medially rotated. The navicular is small and medially deviated relative to the talus. The calcaneus is also small and shows varus displacement and equinus tilt: the anterior facets correspond to those of the talus (Barlow & Clarke 1994). The entire affected foot and calf are smaller than their normal counterparts. The foot is inverted and supinated and the forefoot is adducted. The heel is small, rotated inwards and elevated. The calcaneus is inverted beneath the talus. Treatment varies between splintage and repeated complex surgery, which reflects the highly variable severity of the condition and individual response to therapy.

‘Flat feet’ are common in childhood. The majority are ‘flexible’ and simply related to posture, whereas ‘rigid’ flat feet are caused by structural abnormalities. The description of ‘rocker bottom’ foot is associated with many congenital syndromes. The foot is flat and rigid and the plantar surface appears curved with the apex of the curve at the midtarsal joint. The condition shows an equinus position of the hindfoot. The talus may be vertical and palpable on the plantar surface. A majority of infants with this condition have neurological abnormalities.

REFERENCES

rlow I, Clarke NMP. Congenital talipes equinovarus. *Surgery*. 1994;12:211-215.

vanson AB. A classification for congenital limb malformations. *J Hand Surg*. 1976;1:8-22.

INDEX

Note:

Index structure

This index is in a *classified* form, i.e. arteries, ducts, muscles, nerves, veins, etc. are all listed under these respective main entries, e.g. 'arteries (named)'. This includes subjects/structures such as cells, connections, diseases, syndromes and tracts, e.g. lymphocytes are to be found under 'cells (named)'. Bones are an exception, and specific bones are listed as main entries, e.g. tibia is listed as tibia, not under 'bones'.

Organs and regional structures have their own main entries and subentries (e.g. oesophagus). Cross-references to individual arteries, veins, muscles, etc. are assumed, not explicit.

In most cases structures are listed under singular nouns, with the plural in brackets.

Index entry order

This index is in a *letter-by-letter* order, whereby hyphens and spaces between words are excluded from the alphabetization (e.g. 'lymphatic' precedes 'lymph node'). Characters in brackets are excluded from alphabetization. For example: arc(s) precedes arcade or arch(es).

Terms such as first, second, third (as in arch(es), pharyngeal) are in numerical order ahead of alphabetical sub (or sub-sub) entries.

Page numbers

Page numbers suffixed with 'f' refer to figures; those suffixed with 't' refer to tables.

A

abdomen
  arterial supply, 1047, 1047(f)
  autonomic supply, 1041-7, 1043(f)
    ganglia, 1045-6
    parasympathetic, 1044-5
    plexuses, 1044(f), 1045-6, 1045(f), 1046(f)
    sympathetic, 1042-4
  cavity, 1101(f)
    structure and function, 1041
  landmarks, skeletal, 1052-3
  muscles, 1060-6, 1070-2, 1071(f)
    expulsive efforts, 1008, 1061
  musculoskeletal framework, 1041, 1042(f)
  planes, 1052, 1052(f)
  regions, 1052, 1052(f)
  role in breathing, 1012, 1071, 1085
  sagittal section, 1102(f)
  surface anatomy, 1052-4
    planes, 1052, 1052(f)
    regions, 1052, 1052(f)
    viscera
      intra-abdominal, 1053-4
      retroperitoneal, 140
  tone, 1061, 1064
  transverse section, 71(f)
  visceral landmarks, 1053-4, 1053(f) *See also* abdominal wall

abdominal wall
  anterior, 1041, 1055-67
    arteries, 1056-9, 1057(f), 1059(f)
    boundaries, 1052
    connective tissue, 1060, 1099
    CT, 1062(f)
    hernias, 1066-7
    inguinal canal, 1064

    - lower, peritoneum, 1104-5, 1105(f)
    - lymphatic drainage, 1059
    - muscles, 1055(f), 1056(f), 1060-6, 1062(f)
        - functions, 1041, 1060-1
        - posterior attachment, 1065(f)
    - segmental nerves, 1057(f), 1060
    - skin and soft tissues, 1055-9
    - surface anatomy, 1052-4, 1053(f)
        - skeletal, 1052
        - soft tissue, 1052-3
    - tone, 1060, 1064
    - veins, 1056-9
- defects, 1209
- neonate, 1313(f)
- posterior, 1069-81, 1219(f), 1225(f)
    - anterolateral abdominal wall muscle attachment, 1065(f)
    - arteries, 1072-4 *See also* aorta, abdominal
    - bones, 1070
    - connective tissue, 1070, 1099
    - hernias, 1072
    - inflammation, 1080
    - lower, fascia, 1070
    - lymphatic drainage, 1077-8, 1077(f)
    - MRI, 1071(f)
    - muscles, 1070-2, 1071(f), 1078(f)
    - nerves, 1070(f), 1078-81, 1078(f), 1079(f)
    - skin and soft tissues, 1069-70, 1069(f)
    - veins, 1074-6, 1075(f)

abduction (movement), 103
- of arm, 122(f)

ABO blood group, 68

abscess
- axillary, incision for, 791
- Bezold’s, 626
- dental, 524(f), 525, 543
- epidural, 744

  peritonsillar (quinsy), 405, 567
  psoas, 1368
  submandibular, 538 *See also* infection

acalculia, 358

acardia, 172

acceleration
  angular, 643
    eye movements, 663
  linear, 643
    eye movements, 663

accommodation, of eye, 680

acetabulum, 1352, 1353(f), 1390
  dome, 1352
  in hip joint, 1387
  ossification, 1354
  sex differences, 1359

acetylcholine (ACh), 47, 111, 233
  bipolar cells, 339
  effect on pancreas, 1190
  in striatum, 328

acetylcholinesterase (AChE), 46(t), 111, 1249
  in striatum, 328

achalasia, cardia, 953

achondroplasia, 527, 1014

acid
  bile, cycle, 1212
  gastric
    secretion in fetus, 1206
    secretion in neonate, 1206
  hyaluronic *See* hyaluronic acid *see also specific acids*

acinus (acini)
  of breast, 933, 933(f)

  glandular, 31
  of lacrimal glands, 673
  of lung, 995, 1004
  mucous, sublingual gland, 523(f)
  of pancreas, development, 1207
  of prostate, 1259(f)
  of salivary glands, 523(f), 605
  of sebaceous glands, 151(f), 153
  secretory, parotid gland, 523(f)
  serous, 522, 523(f)

acne, 153

acoustic neuroma, 495

acromegaly, 96

acromion, 785, 786, 795, 803
  surface anatomy, 785

acrosomal cap, 1266, 1266(f)

acrosome, 1266

ACTH (adrenocorticotrophin), 149, 321

actin, 3(f), 7, 14, 14, 18, 764
  cardiac muscle, 142
  epithelial somite cells, 764
  fibrillar, 14
  globular, 14
  neuroblast cells, 369
  skeletal muscle, 106-7, 117
  smooth muscle, 127, 128, 129(f)

actin-binding proteins, 15

α-**actinin**, 7, 14(f), 107, 764
  smooth muscle, 127

action potential, 63-4, 110, 111, 225
  skeletal muscle, 110, 111

Adam’s apple, 405, 579

adaptin, 9, 12

addiction, drug, 331

adduction (movement), 103

adenohypophysis, 321-3
  development, 367
  hormone products, 321
  microstructure, 321, 322(f)
  secretion, 322 *See also* gland(s), pituitary

adenoid (nasopharyngeal tonsil), 563-4, 563(f)
  age-related changes, 563
  arteries, 563
  development, 604
  function, 564
  lymphatics, 563
  microstructure, 564
  removal, 564
  veins, 563

adhesion(s)
  interthalamic, 239, 380
  peritoneal, 1099

adhesion molecules *See* cell adhesion molecules

adhesion plaques, focal, 7

aditus
  laryngis (laryngeal), 573, 582, 1006
  to lesser sac (bursa omentalis) *See* foramen (foramina), epiploic (of Winslow)
  mastoid, 622, 626
    surgical access, 622

adminiculum lineae albae, 1062

adolescence, puberty changes in, 1325, 1325(f)

adrenal gland *See* gland(s), suprarenal

adrenaline (epinephrine), 46, 47, 56, 142, 1029

dental anaesthesia, 520
production, 1199(f), 1200

adrenocorticotrophin (ACTH), 149, 321

adventitia, 1051
of heart, 977

aganglionosis, 1213 *See also* Hirschsprung’s disease

age
coital, 211
estimation from teeth, 516
fertilization, 211
gestational, 211, 216, 216(f)
menstrual, 211

age-related changes
adenoid (nasopharyngeal tonsil), 563
aortic arch, 984
articular surfaces, 99(f), 100
bone, 87, 91
breast, 934-5, 935(f)
ciliary body, 681
costal cartilage, 81, 922
hip bone, 1354(f)
hyaline cartilage, 82, 83
lens (of eye), 686
lumbar vertebrae, 714
mandible, 532-3, 532(f)
meniscus of knee, 1398
muscle, 112, 117
natural synostosis, 614
ovary, 1294
palatine tonsil, 566
pancreas, 1183
paranasal sinuses, 556
parathyroid glands, 464
prostate, 1257, 1259
skin, 161-2

- spermatogenesis, 1267
- testis, 1267

agenesis
- anal, 1212
- of lungs, 1037
- renal, 1035, 1312

agger nasi, 477, 555, 557, 558

agglutination, 68, 72

agnosia
- apperceptive visual, 358
- associative visual, 358
- tactile/visual, 358

agraphia, 358

agrin, 62

AIDS (acquired immunodeficiency syndrome), 71

air, humidification in respiratory tract, 1005

air sac *See* alveolus (alveoli)

air sinuses *See* sinus(es), paranasal

airways, conducting
- arteries, 999(f)
- congenital malformations, 1036-7, 1037(f)
- development, 1033(f), 1034
    - cartilage, 1034
- veins, 999(f) *See also* bronchus (bronchi); *See also* trachea

akinesia, 230

ala(e)
- nasi, 548
- of sacrum, 724
- of vomer, 415, 475, 529, 530

albinism, 149

aldosterone, 154

- functions, 1238
- saliva composition affected by, 523

alexia, 358, 359

allantois, 173, 174, 180, 181(f), 207, 1203(f), 1205(f), 1209, 1212, 1305(f)
- cloaca relationship, 1322
- definition, 180, 186, 1212, 1307
- development, 174, 180, 183
- urachus formation, 1209

Allen’s test, 787

allocortex, 338, 358, 382

alpha-fetoprotein (AFP), 180

alveolar bone, 500, 513, 517-18, 532-3

alveolus (alveoli)
- of breast, 933, 933(f), 936
  - development, 934
- dental, 514, 517, 518
- glandular, 31
- of lungs, 992, 995-6, 998
  - area and number, 998
  - development, 998, 1033, 1034-5
  - interalveolar pores of Köhn, 998, 1000(f)
  - mouths of (sacs), 995
  - structure, 998, 999(f), 1000(f)
  - surface tension, 1000
  - surfactant *See* surfactant
- mandibular, 478, 480
- maxillary, 476, 477

alveus, 350, 351(f), 352(f)

Alzheimer’s disease, pathophysiology, 358

amastia, 934

amazia, 934

amelogenins, 514

amenorrhoea, 1325

ametropia, 688

amino acids, 48

D-amino-acid oxidase, 13

ammonium ions, regulation of levels, 1238

amnesia
- anterograde, 358
- retrograde, 358

amnion (chorio-amnion), 180-1, 1302
- uses/applications, 180-1

amphetamines, 331

ampulla
- hepatopancreatic, 1178
- rectal, 1137, 1151
- of semicircular canals, 633, 633(f), 636
- of uterine tube, 1293
- of vas deferens, 1269, 1314(f), 1317
- of Vater, 1178

amygdala, 320, 325, 353-4, 353(f)
- connections, 353-4
  - afferent, 343-4
  - efferent, 354
- development, 382, 383
- ‘extended’, 353
- functions, 354
- lesions, 358
- nuclei, 346, 353
  - accessory basal, 346, 353
  - basal, 353, 354
  - central, 353
  - development, 383
  - lateral, 353
  - medial, 353

relations, 353 *See also* complex, amygdaloid nuclear

amylin, 1207

analgesia
- local, dental, 519-20
- naturally occurring opiates, 48

anaphase
- cellular division, 21-2
- meiosis, 23

anaphylactic shock, 36

anastomosis (anastomoses)
- arterial, 134
    - brain, development, 392
    - bronchopulmonary, 1003
    - circulus arteriosus, 249(f), 251-2
    - of colon, 1140, 1146
    - convergence, 134
    - coronary, 978, 980-1
    - cruciate, 1380
    - end-to-end, 134
    - gastroepiploic vessels, 1103(f), 1104
    - of gastrointestinal tract, 1048
    - in heart, 141
    - hip region, 1380-1
    - Hyrtl’s, 177
    - of knee joint, 1408
    - palmar, 787
    - splanchnic, dorsal, 207
    - of stomach, 1268
    - transverse, 134
    - trochanteric, 1380
    - of vertebral column, 715(f), 732
- arteriovenous, 134, 135(f)
    - coronary, 980-1
    - glomera, 134
    - newborn, 134

        - of skin, 156
    - genicular, 1394, 1408
    - interpostcardinal, 1219
    - intraosseous, of bone, 91
    - of knee joint, 1394, 1395(f), 1408
    - lumbar veins, 1075
    - nervous, vestibulofacial, 643
    - venous
        - cardiac, 982
        - common cardinal-left superior vena cavae, 959
        - duodenal, 1220
        - subdiaphragmatic intervitelline, 1220
        - supracardial-subcardinal, 1219
        - of vitelline veins, 1220

anatomical snuffbox, 786, 787, 789, 851

anatomical territory, 134-5

anatomy ***see individual structures***

androgens
    - descent of testes, 1320
    - masculinization of female fetus, 1219 *See also* hormones, testosterone

anencephaly, 181, 364, 365(f)

aneuploidy, 23

aneurysms
    - aortic, 985
        - abdominal, 1074
        - renal vein ligation, 1233
    - cerebral, 252, 252(f)
    - inflammatory, superior mesenteric artery, 1187

angina
    - Ludwig’s, 543
    - pectoris, 236

angiogenesis, 136, 600
    - allantois, 180

  brain, 391
  coronary arteries, 1026
  dermal repair, 162-3

angiogram, aortoiliac, 1073(f)

angioplasty, balloon, 981

angiosomes, 110(f), 134-5

angiotensin II, 1238

angiotensinogen, 1238

angle(s)
  abdominal aorta bifurcation, 1072
  acromial, 795
  anorectal, 1150, 1155, 1160
  canthal, medial, 674
  carrying, 786, 833
  cerebellopontine, 240, 242, 279, 284, 286, 295
  cranial base, 420, 481
  of femur, 1360
  ‘filtration’ *See* angle, iridocorneal
  frontal (anteriosuperior), of parietal bone, 469
  inferior lateral (sacrum), 725
  iridocorneal (of anterior chamber), 675, 677(f)
    development, 702
  of Louis, 909
  of Lovibond (proximal nail fold), 155, 155(f), 159
  of mandible, 412, 413(f), 418
    fracture, 480
  mandibular, 402
  mastoid (posteroinferior), 469, 617
  of mouth, 467
  occipital (posterosuperior), 470
  of pennation, 113, 114
  posteroinferior, of parietal bone, 412
  of rib
    anterior, 919

        - posterior, 919
    - of sacrum, 725
    - scapular, 795, 800, 812
        - inferior, 785, 795, 812, 817
        - lateral, 795
        - superior, 795, 811, 814
    - sphenoidal (anteroinferior), of parietal bone, 469, 470(f)
    - sternal, 909, 917, 917(f)
    - subarachnoid, 752

angulation (movement), 103

anhydramnios, 181

ankle *See* joints (named), ankle

ankylosing spondylitis, 744, 745

ankyrin, 15

annulus *See* anulus

anodontia, 517

anophthalmia, 699

anorectum, 1212 *See also* anus; *See also* rectum

anosmia, 555

anotia, 618

ansa
- cervicalis, 456, 460
- lenticularis, 323, 331
- of Maubrac, 459
- subclavia, 448, 457(f), 461

antagonists (muscle), 114, 115, 121

antibodies, 68
- to nerve growth factor, 370
- opsonization, 69 *See also* immunoglobulin

antibody-dependent cell-mediated cytotoxicity (ADCC), 72, 78

antigen(s)
- of erythrocytes, 68
- human leukocyte (HLA), 68, 176
- Rhesus, 68
- very late, 137

antigen-presenting cells (APC), 78-80, 79(f), 80(f)

antihelix, 618, 619, 620

antitragus, 618, 620

antrum
- mastoid, 403, 615, 618, 623(f), 626
  - aditus, 622, 626
  - development, 652
  - surgical access, 622
- prepyloric, 1115
- pyloric, 1112, 1112(f), 1207(f)

anulus
- fibrosus, 730(f)
- stapedius, 652
- of valves, 1027
  - aortic, 969(f), 972, 983
  - mitral, 970, 974
  - pulmonary, 967, 969(f), 983
  - tricuspid, 967, 974
- of Vieussens, 978

anus
- agenesis, 1212
- development, 1212-13
- fissure, 1157
- fistula, 1158
- imperforate, 1212-13
- nerves, 1212
- sphincter *See* sphincter(s)

aorta, 980
- abdominal, 1072-4, 1072(f), 1073(f)

    - bifurcation, 1072, 1072(f), 1086
    - branches, 1073-4, 1073(f)
    - course, 1072
    - CT angiogram, 1074(f)
    - MR angiogram, 1073(f)
    - relations, 1072-3
    - surface anatomy, 1054
- aneurysm, 985, 1074
- arch, 984, 1030(f)
    - age-related changes, 984
    - arteries of, 600, 601(f)
    - branches, 984
    - chest radiography, 954(f), 957
    - development, 1027, 1027(f), 1030(f), 1032
    - embryonic, 206, 1027, 1027(f), 1030(f), 1032
        - first, 390, 1027
        - second, 390
        - third, 390, 600, 1027
        - fourth, 1032
        - sixth, 601, 1033, 1034
    - hypoplasia, 984
    - interrupted, 575
    - magnetic resonance angiography, 984(f)
    - relations, 984
    - right, 1032
    - surface anatomy, 912, 913
    - variation, 984
- ascending, 962, 963, 964, 978
    - relations, 961(f), 983, 984
    - thoracic, 983-4
- ‘baffle’, 971
- bifurcation, 1072, 1073(f), 1074, 1086
    - angle, 1072
- calcification, 986
- coarctation, 975, 984-5, 1030, 1032
- CT angiogram, 1074(f)
- descending, 954, 955(f), 957

  - development, 205
  - dimensions (diameter), 130
  - dissection, 985
  - dorsal, 1027
  - embryonic, 206
  - interruption, 984
  - knuckle, 914, 954, 984
  - ‘nipple’, 954
  - orifice, 913
  - regurgitation, 985
  - root, 970(f), 974, 1026
  - rupture, 985
  - sclerosis, 986
  - surface anatomy, 919
  - thoracic, 983-5
    - descending, 985
      - branches, 985
      - relations, 985
      - surface anatomy, 985

aorto-caval compression, 1300

aperture(s), 86, 100
  - of diaphragm *See* diaphragm, thoracic, apertures
  - of frontal sinus, 556-7
  - nasal, 404, 409
    - posterior (choanae), 415, 547, 549, 550(f)
  - palpebral, 659
  - pelvic
    - inferior, 1358
    - superior, 1358
  - of sphenoidal sinuses, 557
  - of ventricles, of brain
    - lateral (of Luschka), 237, 240, 242
      - development, 377
    - median (of Magendie), 237, 242
      - development, 377 *See also* aditus; *See also* hiatus; *See also* opening(s); *See also* orifice

apex
  of bladder (urinary), 1245, 1312
  of femoral triangle, 1373
  of gastric fundus, 1112
  of heart, 913, 962-3, 980
  of lung, 465, 993
  moduli, 489
  of patella, 1394
  of sacrum, 725
  of tooth, 517

apex beat, of heart, 913

aphasia, 358
  semantic (trans-cortical), 358

apical ectodermal ridge maintenance factor, 900, 901, 902

aplasia
  of lungs, 1037
  of thymus, 949

apnoea
  periodic, 1012
  sleep, 561

aponeurosis
  aponeurosis, 857
  bicipital, 778, 786, 787, 789, 825, 825(f), 826
    surface anatomy, 786
  bilaminar (concept), 1061, 1063, 1063(f)
  central tendon of diaphragm, 1007
  epicranial, 397, 467, 481-2, 538
  of external oblique muscles, 1063
    hiatus (superficial inguinal ring), 1065
  of genioglossus, 503
  gluteal, 1368
  of internal oblique, 1062(f), 1064
  of levator palpebrae superioris, 658, 659, 670-1, 672
  palatine, 565

palmar, 778, 859(f)
    anchorage system, 80
    transverse fibres, 859
plantar *See* fascia, plantar
of transversus abdominis, 1062(f), 1064, 1070

apoptosis, 24-5, 24(f), 181
in digit formation, 902
menstrual cycle, breast changes, 935-6
in synaptogenesis, 370
T cells
    cytotoxic, 71
    progenitors, 77, 947
and terminal differentiation, 193

apparatus
Golgi, 1297
    somitogenesis, 764
juxtaglomerular, 1237(f), 1238
lacrimal, development, 703
nasolacrimal, 674
pharyngeal
    development, 595, 596(f) *See also* arch, pharyngeal
subneural, 110
vestibular, 636-9, 661, 663 *See also* organ; *See also* systems

appendicitis, 1143-4
in pregnancy, 1300

appendicoliths, 1143

appendix (appendices)
of epididymis, 1264(f), 1267, 1268
epiploicae, 1137, 1138, 1138(f), 1151, 1162
of testis, 1263(f), 1264(f), 1267, 1268, 1315(f), 1316(t), 1317
vermiform, 1142-4, 1143(f)
    arteries, 1144-5
    development, 1212, 1217
    epithelium, 1137
    lumen, 1142-3

        lymphatics, 1145
        lymphoid aggregates, 1143
        microstructure, 1143, 1143(f)
        nerves, 1143-4, 1146
        pain, 1143-4, 1146
        peritoneum, 1217
        positional variation, 1142, 1143(f)
            in pregnancy, 1300
        surface anatomy, 1053
        veins, 1145

apraxia, ideomotor, 358

aqueduct
    cerebral, 239-40, 240(f)
    cochlear, 634
    vestibular, 425, 431, 617, 633, 634
        opening, 425, 617

arachnoid mater, 426, 427, 434
    cranial, development, 389
    spinal, 752, 752(f)
    villi, 243-4, 244(f)

arbor vitae
    of cerebellum, 298, 299(f)
    uteri, 1285

arc(s), 102
    monosynaptic reflex, 287
    painful, 807
    reflex, 261
    of Riolan, 1140
    spinal reflex, 8, 389

arcade
    arterial, of hand, 894, 894(f)
    of Fröhse, 835(f), 855
    palpebral, 665, 672

arch(es)

alveolar, 477
    superior, 414
aortic *See* aorta, arch
arterial
    aortic *See* aorta arch
    carpal
        dorsal, 890, 894
        palmar, 890, 892(f), 893
    of colon, 1146, 1149
    palmar, 890, 892(f)
        deep, 890, 891, 892(f), 894
        superficial, 890, 892(f), 893(f), 894
    pollicial, 892
    prepancreatic, 1186
of atlas
    anterior, 719, 770
    posterior, 719, 770
axillary, 811
branchial (gill), 532, 596 *See also* arch(es), pharyngeal
coracoacromial, 807
cortical (renal), 1229
cricoid, 579
crural
    deep, 1060
    superficial *See* ligaments (named), inguinal
dental
    lower, 511(f)
    upper, 511(f)
of foot, 1450
    lateral longitudinal, 1450
    medial longitudinal, 1450
    transverse, 1450
hyoid, 595, 596(f), 597, 652
jugular, 451, 465
lumbocostal, 1007 *See also* ligaments (named) (ligamentum), arcuate
mandibular, 595, 595(f), 597, 652
maxillomandibular *See* arch(s), pharyngeal

- neural, 767, 768, 769(f)
- occipital, 611
- palatoglossal, 501, 503(f), 565, 604
- palatopharyngeal, 503(f), 565
- palmar
  - superficial, 857(f)
  - surface anatomy, 787
- of pelvis, 1358
- pharyngeal
  - first (mandibular), 595(f), 597, 652
  - second (hyoid), 595, 596(f), 652
  - blood supply, 600-2, 601(f)
  - derivatives of, 597(t)
  - development, 595
    - nerve supply, 374
  - embryonic, 596-602, 597(f)
  - muscles of, 599-600, 599(f), 600(f)
  - nerves of, 600
  - skeletal elements, 598-9, 598(f)
- plantar, 1456-7, 1456(f)
- pubic, 1358, 1365
- subpubic, sex differences, 1359
- superciliary, 404, 409, 416, 470, 471(f)
- tendinous
  - of levator ani, 1086
  - of pelvic fascia, 1086
- thoracic duct, 942
- venous, of foot, dorsal, surface anatomy, 1344
- venous, of hand, palmar
  - deep, 894
  - superficial, 894
- vertebral, 716, 721, 727, 734, 768
- zygomatic, 403, 412, 416, 527, 538, 615

archenteron, 184

archicortex (archipallium), 338, 350, 382 *See also* formation (formatio), hippocampal

area
- aortic, 913
- bare, of liver, 1163, 1164(f), 1165, 1168
- cochlear, of internal acoustic meatus, 636
- cortical, visual, V5 (middle temporal), 664
- cortical (cerebral)
    - area, 8, 343
    - area, 17, 315
    - association, 335, 340-1, 341(f), 344, 358
    - auditory, 345-6, 345(f)
    - Broca’s (area 44, 45), 335, 343(f), 349
    - Brodmann’s, 340
        - area 1, 344
        - area 2, 344
        - area 3a and 3b, 344
        - area 4, 342, 344
        - area 5, 344
        - area 6, 341, 343, 343(f), 344, 664
        - area 7a, 343, 345
        - area 7b, 343, 344, 345
        - area 8, 343, 343(f), 664
        - area 9, 343, 343(f)
        - area 10, 343, 344
        - area 17, 346, 696
            - V1, 346, 696
            - V2 and V3, 346
        - area 18, 346, 347
        - area 19, 346, 347
        - area 20, 340, 345
        - area 21, 345
        - area 22, 343(f), 345
        - area 24, 343, 345
        - area 25, 347, 348
        - area 28, 348, 351
        - area 29, 348
        - area 35, 352
        - area 36, 354

        - area 37, 343(f)
        - area 38, 345
        - area 39, 341(f), 343(f), 345, 664
        - area 40, 343(f), 345
        - area 41, 345, 357
        - area 42, 345, 357
        - area 44, 335, 343 *See also* area, cortical (cerebral), Broca's
        - area 45, 335, 343, 358
        - area 46, 343, 345, 664
    - cingulate motor, 343
    - entorhinal, 348, 349, 356
    - frontal eye field (area 8), 343, 343(f)
    - insular, 346, 346(f)
    - motor
        - primary (MI), 342, 342(f)
        - supplementary (SMA; MII), 343
    - multimodal, 386
    - occipitotemporal, 345
    - parastriate, 340
    - piriform, 382
        - development, 383-4
    - precommissural, 385
    - prefrontal, 341, 343
    - premotor, 343
    - somatic sensory *See* cortex, cerebral
    - striate, 346, 347
    - subcallosal (parolfactory gyrus), 335
    - visual, 346, 354
        - V1, 347
        - V2-V4, 347
        - V5 (middle temporal), 347
    - Wernicke's speech, 343(f) *See also* cortex, cerebral
- intercondylar, of knee joint, 1397, 1397(f)
- Little's, 553, 554
- mitral, 913
- paraspinal, 957

- pelvic, of ischial ramus, 1356
- perineal, of ischial ramus, 1356
- polymodal sensory, temporal lobe, 354
- postrema, 51, 240, 241, 241(f)
- pulmonary, 913
- reticular, 294
- supramammillary, 350
- vestibular
  - of fourth ventricle, 240, 269, 275
  - of internal acoustic meatus, 633, 633(f), 636
- vestibular cortical, 286

areae gastricae, 1115

areola(e)
- of breast, 930, 930(f), 932(f)
  - innervation, 932
  - nerves, 932
  - vascular supply, 931
- male, 937
- primary, of bone, 93

arginine vasopressin, 317

arm, 823-30
- arteries, 827-8
- hypoplasia, 808
- innervation, 828-30
- lymphatics, 828
- movements, 122(f)
- muscles, 778, 824-7, 824(f), 825(f)
  - anterior compartment, 824-6
  - posterior compartment, 826-7
- neonatal, 905-6
- nerves, 828-30
- skin, 823-4
  - blood supply, 823
  - innervation, 823
  - nerves, 823

- soft tissue, 823-4
- veins, 828 *See also* forearm; *See also* limb, upper

armpit, 791, 814

Arnold-Chiari malformation, 770

arrhythmia, cardiac, atrial fibrillation, 1020

arteries (general), 130
- blood supply, 138
- cerebral, 134, 138-9
  - development, 390, 391(f)
- classification, 131
- conducting, 131
- development
  - cerebral, 390, 391(f)
  - in limbs, 903
- distributing, 131
- distribution, 130-1
- elastic, 131-2, 132(f), 137
- embryonic, 205-6, 206(f)
  - aortic arches *See* aorta, arches
- heat exchange, 131
- innervation, 138
- muscular, 131, 132, 132(f)
- nerves, 131-2, 133, 138
- resistance, 131
- structure, 130-1

arteries (named)
- aberrant, 985
- accessory
  - meningeal, 431, 540, 541, 544
  - of muscle, 109
  - pudendal, 1098
  - renal, 1231
- acromio-thoracic, 817
- alveolar (dental)
  - branches, 518

- inferior, 518, 540, 600
  - lingual branch, 518
  - mylohyoid branch, 518
  - perforating branches, 500
- superior, 518
  - anterior, 518
  - middle, 544
  - posterior, 518, 543-4

anastomotic, of Kugel, 980
angular, 490, 490(f)
aorta *See* aorta
aortic arch *See* aorta, arch
appendicular, 1145
- accessory, 1145
- thrombosis, 1145

arcuate, 1289
- of foot, 1455(f), 1456
- of kidney, 1232

auditory, internal (labyrinthine), 251, 642
auricular, 491
- deep, 540, 541, 628
- posterior, 490(f), 491, 609, 619, 620, 621
- superior, 620

axial, of embryonic limb, 903, 905, 906(f), 1463
axillary, 778, 815-17, 816(f), 986
- branches, 817
- relations, 815, 817

azygos, 1284, 1289
basilar, 242, 248, 248(f), 251, 449, 461
- development, 390

basisphenoid, 563
brachial, 778, 823, 827-8, 831(f), 835, 835(f)
- branches, 827-8
- pulse points, 787
- puncture of, 981

brachiocephalic, 914, 984, 985
- branches, 985

  - relations, 985
- bronchial, 950, 985, 991, 999(f), 1035
  - capillary/mucosal plexuses, 1003
  - left, 1003
  - right, 1003
- buccal, 491, 540, 541
- of bulb, of penis, 1273
- caecal (anterior/posterior), 1145
- calcaneal
  - of fibular, 1425, 1426
  - of lateral plantar, 1425
  - of posterior tibial, 1425
- callosomarginal, 248
- caroticotympanic, 247
- carotid, 406
  - common, 98, 397, 400, 406, 444-5
    - development, 600
    - left, 984, 986
    - relations, 986
    - right, 984, 986
  - external, 406, 445-7
    - branches, 445-6, 490, 496, 496(f)
    - development, 600
    - pulse, 445
  - internal, 247-8, 247(f), 400, 406, 430, 444(f), 445, 447
    - caroticotympanic branches, 601
    - cavernous part, 248
    - development, 390
    - intracranial part, 248
    - petrous part, 247-8
    - pulse, 437, 444
- cavernosal, 1098, 1273
- central
  - of brain, 252, 252(f)
    - of anterior cerebral, 248, 248(f)
    - of middle cerebral, 248, 248(f)
- central, of retina, 667

centrifugal, 392
centripetal, 392
cerebellar
    development, 390
    inferior, 242
        anterior, 249(f), 251
        posterior, 249(f), 250, 251
    superior, 249(f), 251
cerebral
    anterior, 248-50
        branches, 249, 249(f)
    middle, 250
    posterior, 242, 251
        development, 390
cervical
    ascending, 445(f), 465, 714
    deep, 449, 451, 708, 714
    transverse, 438, 453(f), 457, 816(f), 817
Charcot's, of cerebral haemorrhage, 253
choroidal
    anterior, 248, 253, 390
    posterior, 390
ciliary, 665, 681
    long, 682(f)
    short, 682(f)
cilioretinal, 694
circumflex, 978, 980
    anterior, 980
    coronary artery bypass graft, 981
    deep, 1057(f), 1065(f)
    humeral
        anterior, 817, 818(f)
        posterior, 817, 818(f)
    iliac, deep, 1089
    left, 977
    scapular, 804(f), 815(f), 816(f), 817
coeliac *See* trunk (arterial), coeliac

colic, 207
    left, 1140, 1146, 1149(f)
    middle, 1140, 1146, 1147(f)
    right, 145(f), 1140, 1145, 1146
        accessory, 1145, 1145(f)
collateral *See* circulation, collateral
collateral
    middle, 823(f), 827, 827(f)
    radial, 824(f), 827, 827(f)
    ulnar
        inferior, 828, 829(f)
        middle, 828
        superior, 828, 829(f)
comitans nervi ischiadici, 1378
communicating
    of brain
        anterior, 248, 252, 252(f)
        posterior, 247(f), 248, 248(f), 252
            fetal, 248
    of fibular artery, 1426
    of posterior tibial, 1425
conus (arteria coni arteriosi), 978
    left, 980
coronary, 978
    accessory, 1026
    anastomoses, 978, 980-1
    angiography, 981
    bypass graft, 981
    calibre of, 978
    development, 1026
    disease, 978, 981
    distribution, 978, 980
    dominant, 978
    left, 978, 980
    revascularization, 981
    right, 977, 978, 980
        branches, 980

    - stenosis, 981
    - third, 978
- cortical, of middle cerebral, 249-50
- cranial, development, 390
- cremasteric, 1056-7, 1064, 1262
    - pubic branch, 1056-7
- cricothyroid, 446, 588
- cubital, inferior, 839, 852
- cystic, 1179-80
    - accessory, 1180
- deep, of penis, 1098, 1273
- dental *See* arteries (named), alveolar
- diagonal, left, 980
- digital
    - dorsal, of hand, 894
    - palmar, 894
        - common, 892(f), 894
    - ulnar, 894
    - ulnodorsal, of thumb, 890
    - ulnopalmar, of thumb, 890
- dorsal
    - digital (of hand), 894
    - lingual, 505
    - lumbar, 1074
    - metacarpal *See* arteries (named), metacarpal
    - nasal, 491
    - of penis, 1252, 1273
    - perforating, 811
    - scapular *See* arteries (named), scapular
- dorsalis pedis, 1419(f), 1455-6, 1455(f)
    - cutaneous vessels, 1456
    - pulse, 1344
- epigastric
    - inferior, 1056, 1059, 1063, 1064, 1089
        - branches, 1088
        - inguinal canal relations, 1066
        - pubic branch, 1067

    - superficial, 1379
    - superior, 985, 1056
- epiphysial, 91
    - subclavian, pulse, 438
- ethmoidal, 544
    - anterior, 665
    - posterior, 665
- of external auditory meatus, 621
- facial, 444(f), 445(f), 446-7, 490, 538, 541, 671
    - ascending palatine branch, 505, 539
    - branches, 447, 478, 505
    - infraorbital, 541
    - submandibular gland relation, 520
    - tonsillar branch, 505
    - transverse, 490-1, 671
- femoral, 1351(f), 1378-80, 1379(f), 1388
    - branches, 1379-80
    - circumflex
        - lateral, 1380
        - medial, 1380
    - deep *See* arteries (named), profunda femoris
    - lateral, 1364(f)
    - medial, 1364(f)
    - proximal occlusion, 1381
    - pudendal branches (superficial and deep), 1280, 1282(f)
    - pulse, 1344
    - puncture of, 981
    - relations, 1378-9
    - surface anatomy, 1344
- fibular, 1425-6
    - branches, in leg, 1426
- frontal
    - of anterior cerebral, 249
    - of superficial temporal, 491
- ganglionic, 249(f), 252
- gastric, 1111
    - anastomoses, 1268

    left, 1007, 1116
        variations, 1116
    posterior, 1111, 1117
    right, 1117
    short, 1116-17
gastroduodenal, 1126
    retroduodenal branch, 1180
gastroepiploic
    anastomoses, 1268
    left, 1104, 1117
    right, 1104, 1117
genicular
    descending, 1380
    inferior, 1409
    lateral, 1362
    medial, 1362
    middle, 1409
    superior, 1408-9
glandular, of facial, 447
gluteal
    branches, 1087
    inferior, 1054, 1089
    superior, 1054, 1087
    surface anatomy, 1054
gonadal, 1074
great
    abnormal connections, 1030, 1031-2, *1032*
    transposition, 1030, 1031
helicine, of penis, 1273, 1274
haemorrhoidal *See* arteries (named), rectal
hepatic, 1169-70, 1169(f), 1180
    accessory, 1169
    arteriogram, 1170(f)
    common, 1169
    replaced, 1169
    right, 1169
    variants, 1169

Heubner’s (arteria recurrens anterior), 392
hyaloid, 702
  atrophy, 702
  development, 699, 702
hypoglossal, presegmental, 390
hypophysial
  inferior, 323
  superior, 323, 1057(f), 1059
ileal, 1130, 1145
ileocolic, 1140, 1144-5, 1145(f)
  branches, 1144
iliac, 1054
  circumflex
    deep, 1088
    superficial, 1379
  common, 1086
    branches, 1086
    left, 1086
    right, 1086
  external, 206, 1086, 1089
    collateral circulation, 1059
  internal, 206, 1086-7, 1087(f), 1140, 1284
    fetus/neonate, 1087
iliolumbar, 1087
  lumbar branch, 1071, 1074
incisive, perforating branches, 500
infrahyoid, 446
infraorbital, 491, 518, 544, 559, 600, 666, 671
innominate *See* arteries (named), brachiocephalic
insular, 250
intercostal
  anterior, 926
  dorsal branches, 915
  posterior, 98, 714, 927, 927(f), 928, 940, 984, 985, 987, 1056, 1059, 1064
    branches, 109, 855(f), 915, 927
    dorsal branches, 927

- superior, 451, 461, 926, 990(f), 993, 1003

interdental, 518
interlobar, of kidney, 1230(f), 1232
interlobular, of kidney, 1231, 1232
interosseous
- anterior, 778, 839, 852-3
- common, 778, 846(f), 852
- posterior, 778, 839(f), 853
  - development, 905

intersegmental, 1027
interventricular
- anterior, 980
- posterior, 978, 980

intramedullary, 757
intraparenchymal (medullary), 392 *See also* arteries (named), medullary
jejunal, 1048, 1127(f), 1128, 1130, 1131(f), 1132(f)
labial
- inferior, 490(f)
- superior, 490, 490(f), 544

labyrinthine, 251, 642
lacrimal, 491, 541, 665
laryngeal
- inferior, 449, 588
- posterior, 588
- superior, 446, 587
  - epiglottic branches, 505

lenticulostriate, 250, 252, 254
lingual, 445(f), 446, 500, 505, 505(f)
- deep, 505
- dorsal, 505

lobar, of kidney, 1232
lumbalis ima, 1071, 1074
lumbar, 714, 985, 1059, 1074
- dorsal branches, 1074
- posterior, 1061, 1063, 1064

malleolar

        - lateral, anterior, 1425
        - medial, anterior, 1425
- mammary *See* arteries (named), thoracic
- marginal
    - of colon (of Drummond), 1140, 1140(f)
    - of heart
        - left, 980
        - right, 980
- masseteric, 538, 540, 541
- maxillary, 517, 527, 529, 533, 538, 539, 540-1, 540(f), 543-4, 660
    - branches, 628
        - buccal, 499, 500
        - facial, 488, 491
        - oral mucosa supply, 500
    - in pterygopalatine fossa, 540, 559
- median, 852, 855(f), 857, 905
- medullary, 250-1, 392
    - of Adamkiewicz, 757
    - of bone, 90(f), 91
    - segmental, 757
- meningeal, 250, 432(f), 446, 461, 665
    - accessory, 431, 540, 541, 544
    - development, 390, 600
    - infratentorial, 390
    - long circumferential, 390
    - middle, 404, 412, 415, 424, 429(f), 431, 433, 535, 540, 541, 541(f), 600
        - development, 600
    - paramedian, 390
    - perforating branches, 390
    - posterior, 446
    - short circumferential, 390
    - supratentorial, 390
- mental, 491, 500, 518
- mesencephalic, primitive, 390
- mesenteric

    - inferior, 1047, 1048, 1072(f), 1074, 1074(f), 1140, 1140(f), 1149, 1149(f), 1220
        - ligation, 1141
        - occlusion, 1140-1
    - superior, 1047, 1048, 1072(f), 1074, 1074(f), 1130, 1132(f), 1140, 1140(f), 1209, 1210(f), 1220
- mesonephric, persistent, 1310
- metacarpal
    - dorsal, 890-1
        - first, 858(f), 890-1
        - second, 890, 891
        - third, 891
        - fourth, 891
    - palmar, 892(f), 893
- metaphysial, 91
- metatarsal, dorsal, 1456
- muscular
    - of anterior tibial, 1425
    - of fibular, 1426
    - of posterior tibial, 1425
    - of radial, 852, 855(f)
    - of ulnar, 852-3, 855(f)
- musculophrenic, 926, 985
- mylohyoid, 518
- nasal
    - dorsal, 666
    - dorsal (external), 491, 666
    - lateral, 490, 490(f)
- nutrient
    - of bone, 91
    - of femur, 1364, 1380
    - of fibula, 1426
    - of fibular artery, 1426
    - of hip bone, 1352
    - of humerus, 827-8
    - of scaphoid, 862
    - of tibia, 1425

of vertebrae, 714
obturator, 1041, 1088
  aberrant, 1059
  branches, 1088
  variations, 1067
occipital, 444(f), 445(f), 447, 491
oesophageal, 950, 1111
  anastomoses, 1268
olfactory, primitive, 390
ophthalmic, 248, 600, 656, 659, 660, 665-6, 665(f), 667
  branches, 491
  facial branches, 491
origin, lumbar, number and relations, 1074
otic, presegmental, 390
ovarian, 207, 1288, 1289, 1293, 1295
palatine
  ascending, 446, 544
  greater (descending), 544, 559
  lesser, 559
palmar, 894
  common, 892(f), 894
  metacarpal, 892(f), 893
palpebral
  lateral, 671
  medial, 491, 665, 671
pancreatic, greater, 1186
pancreaticoduodenal
  inferior, 1048, 1128, 1184, 1186
  superior, 1048, 1128, 1184, 1186
parathyroid, 464
paricallosal, 248
parietal
  of anterior cerebral, 249
  of middle cerebral, 249
  of superficial temporal, 491
penile, dorsal, 1252, 1273
of penis, 1098

perforating, 252
    of ankle and foot, 1457
    of anterior tibial artery, 1425
    dorsal, of shoulder region, 811
    of femoral artery, 1380
    of hand, 891, 893
    of internal thoracic artery, 915, 926
    meningeal, 390
    of oral cavity, 500
    of posterior tibial artery, 1425
pericardiacophrenic, 985
perineal, 1273, 1275(f)
    in female, 1098
    scrotal, 1093(f), 1098
peroneal *See* arteries (named), fibular
pharyngeal, 446, 544, 1025
    ascending, 446, 544
        branches, 446
    ventral, 600
phrenic, 1008(f), 1009-10
    inferior, 1010, 1074
    left, 1009
    medial and lateral branches, 1010
    origin, 1009
    right, 1010
pineal, 324
plantar
    lateral, 1425, 1456-7
    medial, 1425, 1457
        surface anatomy, 1344
pontine, 251
popliteal, 1044, 1394
    branches, 1408-9
    entrapment, 1408
    pulse, 1344
    relations, 1408
    surface anatomy, 1344

    - variations, 1408
- posterior, auricular, 441, 445, 447
- premasseteric, 490
- princeps pollicis, 891-2
- profunda brachii, 778, 824(f), 825(f), 826, 827, 828, 829(f)
- profunda femoris, 1379-80, 1379(f)
- profunda linguae, 446
- pterygoid, 247, 540, 541
- pudendal
    - external
        - deep, 1379
        - superficial, 1379
    - internal, 1088-9, 1280, 1282(f), 1284
        - accessory, 1098
        - branches, 1275(f)
        - in perineum, 1097-8
- pulmonary, 980, 983, 996-7, 999(f), 1028
    - bifurcation, 996
    - branches, 996
    - development, 1035
        - postnatal, 1036
    - fetal, 983
    - left, 996-7
        - lingular branches, 996-7
    - relations, 983
    - right, 982, 996
- pulse, 446
- pyloric, 1268
- radial, 778, 857, 890-3, 891(f)
    - at elbow, 835, 835(f)
    - at wrist, 890
    - development, 905
    - in forearm, 839, 839(f), 842(f), 845, 846(f), 848, 852
    - in hand, 890-3
    - pulse points, 787
    - puncture of, 981
    - recurrent, 827, 827(f), 835

radialis indicis, 857, 891(f), 892-3
radicular
    anterior, 757
    posterior, 757
rectal
    accessory, 1231
    branches, 1231
    inferior, 1098, 1140, 1154
    left, 1231
    middle, 1088, 1140, 1154, 1284
    right, 1231
    superior, 1140, 1154, 1159
recurrens anterior (Heubner's), 392
recurrent
    interosseous, posterior, 835, 852, 853
    radial, 827, 827(f), 835
    tibial
        anterior, 1425
        posterior, 1425
    ulnar
        anterior, 827
        posterior, 827
renal, 207, 1054, 1074, 1225(f), 1228, 1228(f), 1230(f), 1231, 1231(f), 1310
    branches, 1231(f)
    characteristics, 1231
    left, 1225(f)
    right, 1225(f)
retinacular, 1364
retinal, central, 665, 693, 695
retroportal, 1180
sacral
    lateral, 708, 714, 1087
    median, 1074, 1154
scapular
    circumflex, 804(f), 815(f), 816(f), 817
    dorsal, 450, 451, 816(f), 817

        - variants, 816(f)
- scrotal, 1273
- segmental
    - of kidney, 1231-2, 1232(f)
    - spinal, 757
- septal, posterior, 980
- sigmoid, 1140, 1141, 1148, 1149
- sinu-atrial nodal, 980
- somatic, 206
- sphenoidal, of middle cerebral, 250
- sphenopalatine, 544, 558, 665
- spinal, 714, 715(f)
    - anterior, 148, 757
    - posterior, 250, 253, 757
- splanchnic
    - lateral, 206-7, 1263
        - development, 1310
        - persistence, 1231
    - ventral, 207, 1220
- splenic, 1193
    - pancreatic branches, 1186
    - segmental, 1193
- stapedial, 600, 629
    - branches, 600
    - haemorrhage of, 607
- sternocleidomastoid, 446
- striate, 252, 253
    - development, 392
    - lateral, 249(f), 250
    - medial, 249(f), 250, 252, 253
- stylomastoid, 628, 629
- subclavian, 400, 406-7, 435, 438, 443, 447-8, 600, 986, 991, 993
    - branches, 444, 447-8
    - development, 601, 905
    - left, 448, 449, 984, 986
    - pulse, 448
    - relations, 986

- right, 98, 446-7, 1032
    - development, 600
- subcostal, 985, 1059, 1063, 1064
  - branches, 1071
- sublingual, 505
- submental, 444(f), 446-7
- subscapular, 816(f), 817, 984
- supraclavicular, 791, 815
- supraduodenal, 1127
- suprahyoid, 446
- supraorbital, 59, 491, 600, 660, 665
- suprarenal, 207, 1074, 1310
  - inferior, 1198, 1232
  - middle, 1198
  - superior, 1198
- suprascapular, 449-50, 814
- supratrochlear, 491, 665-6, 828, 829(f)
- sural, 1409
  - superficial, 1409
- to tail of pancreas, 1186
- tarsal, 1456
- temporal
  - deep, 540, 541
  - middle, 491
    - parietal (posterior) branch, 491
    - pulse point, 490
  - superficial, 490(f), 491, 496(f), 538, 671
    - frontal (anterior), 491
    - pulse, 405
- testicular, 207, 1262-3
- thoracic
  - alar, 817
  - coronary artery bypass graft, 981
  - internal, 449, 926, 939, 985
    - collateral circulation, 1059
    - perforating branches, 915, 926
    - relations, 926

    - sternal branches, 926
  - lateral, 817, 915, 984
  - superior, 817
- thoracoacromial, 803, 817, 984
- thoracodorsal, 811, 817
- thyroid
  - ima, 462, 984, 985
  - inferior, 443, 444(f), 449-50, 466, 946, 950, 951(f)
  - superior, 445-6, 462, 946
    - branches, 445-6
- tibial
  - anterior, 1411, 1415, 1417, 1418(f), 1419(f), 1424-5
    - branches, 1425
  - posterior, 1425, 1457
    - branches, 1425, 1457
    - pulse, 1344
  - surface anatomy, 1344
- tonsillar, 446, 566, 566(f), 567
- trigeminal, primitive, 390
- tympanic
  - anterior, 540, 541, 628
  - inferior, 446
  - superior, 430
- ulnar, 778, 857
  - at elbow, 827
  - development, 905
  - in forearm, 839, 839(f), 842(f), 846(f), 847, 852-3
    - branches, 852-3
  - in hand, 891(f), 892(f), 893-4
  - pulse points, 787
  - superficial, 790(f)
- umbilical, 182, 206, 1222-3
  - catheterization, 1222-3
  - descent of testes and, 1320
  - development, 1087
  - embryonic circulation, 205, 205(f), 206(f)
  - obliterated, 1062, 1105, 1106

urethral, 1252
uterine, 1088, 1284, 1289, 1290(f), 1293, 1294(f)
vaginal, 1088, 1088(f), 1284
to vas deferens, 1269
ventricular, anterior, 980
ventriculofugal, 391, 391(f)
ventriculopetal, 391, 391(f)
vertebral, 250-1, 251(f), 449, 449(f), 714, 719, 721, 734
    cervical branches, 449
    left, 984
vertebrobasilar, 250-1
vesical
    inferior, 1088, 1249
    superior, 1088, 1249
Vidian’s, 544
visceral, 1054
zygomatic, 491
zygomatico-orbital, 491, 665
zygomaticofacial, 490(f), 491
zygomaticotemporal, 491

arteries (of organs, or regions)
of abdomen, 1047, 1047(f)
of abdominal wall
    anterior, 1056-9
    posterior, 1072-4, 1073(f)
of adenoid, 563
of anal canal, 1159-60
of ankle, 1442
of aortic arch, 600, 601(f)
of appendix, 1144-5
of arm, 827-8
    cutaneous, 823
of auricle, of ear, 620
of back, cutaneous, 708, 708(f)
of bladder, urinary, 1249
of bone, 90(f), 91*see also individual bones*
of brain, 247-56, 247(f), 248(f)

    - development, 390
- of breast, 931
    - cutaneous, 931
- of bronchi, 985, 991, 999(f), 1003
- of bulbourethral glands, 1273
- of caecum, 1144-5
- of cerebellum, 253
- of cheeks, 499
- of choroid plexus, 242
- of colon
    - ascending, 1146
    - descending, 1147, 1147(f)
    - sigmoid, 1148-9, 1148(f), 1149(f)
    - transverse, 1146
- of common bile duct, 1180
- of conjunctiva, 672
- of diaphragm, 1009-10, 1056
- of duodenum, 1127-8, 1186
- of ear
    - external, 620
    - inner, 642
    - middle, 628-9
- of elbow, cutaneous, 831
- of elbow region, 835
- of embryo, 206-7, 207(f)
- of external genitalia, male, 1098, 1262-4, 1273, 1275(f)
- of external oblique muscle, 1064
- of eyelids, 671
- of face, 489-91
- of female perineum, 1283(f)
- of femur, 1364-5, 1364(f)
- of floor of mouth, 501
- of foot, 1344, 1455-7, 1455(f), 1456(f)
    - cutaneous, 1429
- of forearm, 852-3
    - cutaneous, 839, 839(f)
- of gallbladder, 1179-80

of gastrointestinal tract, 1047-8
of gluteal region, 1378, 1378(f)
  cutaneous, 1349
of hand, 620, 890-3
  cutaneous, 857, 858(f)
of hard palate, 502
of head, 397-400, 398(f), 444-51, 539(f), 540(f)
of heart, 978-81, 979(f)
  cardiac muscle, 141
of hepatic ducts, 1180
of hip joint, 1390
of ileum, 1129-30, 1131(f)
of ilium, 1087, 1356
of internal oblique muscle, 1063
of intestine, large, 1140, 1140(f), 1144-5
of iris, 685
of ischium, 1357
of jejunum, 1129-30, 1131(f)
of joints, 101*see also individual joints*
of kidney, 1225(f), 1231-3, 1232(f), 1233(f)
of knee joint, 1408-9
  cutaneous, 1393
of lacrimal gland, 673
of larynx, 587-8, 587(f)
of leg, 1424-6
  cutaneous, 1411
of lips, 500
of liver, 1169-70, 1169(f), 1174
of lungs, 996-7, 997(f), 1035
  left, 996
  right, 996-7
of muscle
  skeletal, 109-10
  smooth, 128*see also individual muscles*
of nasal cavity, 553
of neck, 444-51
  cutaneous, 435

of neonate, 1032
of nose, external, 549
nutrient, of bone, 91
of oesophagus, 950, 1111
  cervical, 465
of optic chiasma, 253
of optic nerve head, 695
of oral mucosa, 500
of orbit, 665-6
of ovary, 1295, 1295(f)
of palatine tonsil, 567
of pancreas, 1186, 1187(f)
of paranasal sinuses, 557
of parathyroid glands, 464
of parotid gland, 497
of pelvis, 1041, 1047, 1047(f), 1086-9, 1087(f), 1088(f)
of penis, 1098, 1273, 1275(f)
of pericardium, 959
of perineum, 1097-8
of periodontal ligament, 518
of pharyngotympanic tube, 564
of pharynx, 561
of pineal gland, 324
of pituitary gland, 323
of pleura, 991
of prostate, 1257
rectum, 1154, 1154(f)
of retina, 693, 693(f), 694
of scalp, 470-1
of scrotum, 1273
of seminal vesicles, 1270
of shoulder region, cutaneous, 791
of skin, 156
  arm, 823
  back, 708, 708(f)
  breast, 931
  elbow, 831

    - of foot, 1429
    - forearm, 839, 839(f)
    - gluteal region, 1349
    - hand, 857, 858(f)
    - knee, 1393
    - leg, 1411
    - neck, 435
    - shoulder region, 791
    - thorax, 915, 915(f)
    - wrist, 857, 858(f)
- of spinal cord, 757, 758(f)
- of spleen, 1193
- of sternum, 918
- of stomach, 1116-18, 1116(f), 1117(f)
- of sublingual salivary gland, 521
- of submandibular salivary gland, 521
- of suprarenal gland, 1198, 1198(f), 1199(f)
- of teeth, 518
- of temporomandibular joint, 535-6
- of tendons, 112
- of testis, 1262-4, 1265(f)
- of thoracic wall, 926-7
- of thorax, 910
- of thorax, cutaneous, 915, 915(f)
- of thymus, 946
- of thyroid gland, 462
- of tongue, 505, 505(f)
- of trachea, cervical part, 466
- of tympanic cavity, 628-9
- of upper limb, 778, 779, 814-17
- of ureter, 1241, 1241(f)
- of urethra
    - female, 1253
    - male, 1252
- of uterine tube, 1293
- of uterus, 1284(f), 1289, 1290(f)
- of uveal tract, 682(f)

  of vagina, 1284, 1284(f)
  of vas deferens, 1269
  of vertebral column, 714, 715(f)
  of vulva, 1280
  of wrist, cutaneous, 857, *858*

arteriography, pulmonary, 997

arterioles, 130, 131, 132, 133(f), 134, 135(f), 136, 137, 138, 139
  afferent, glomerular, 1232-3, 1236(f)
  efferent, glomerular, 1232-3, 1236(f)
  helical, of uterus, 1289
  penicillar, 1194, 1195

arthroscopy *See* surgical procedures and approaches

arthroses *See* joints (general)

ascites
  chylous (lymphatic) recurrent, 1077
  drainage, 1109 *See also* fluid, peritoneal

aspartate, 46, 47
  hippocampal formation, 351

asphyxiating thoracic dystrophy, 1014

aspiration, fine-needle, mediastinal lymph nodes, 953

asplenia, 1218

asterion, 404, 414, 417, 470

astigmatism, 688

astrogliosis, 48

asymmetry, cerebral, 358

asynergia, 309

ataxia
  gait, 309
  truncal, 309

athelia, 934

atherosclerosis, 981, 985
    of aorta, 986

athletes, cardiac hypertrophy, 970

atlanto-axial region, 770

atlas (C1 vertebra), 397, 719-20
    arch, 719
    at birth, 720
    defects, 770
    development, 770
    muscle attachments, 720
    ossification, 720

atresia
    biliary, 1208
    bronchial, 1037
    duodenum, 1206
    extrahepatic bile ducts, 1208
    mitral, 1030
    oesophageal, 953, 1015, 1037(f), 1203
    pulmonary, 1031
    pupil, 702
    tricuspid, 1030
    uterus, 1317(f)

atrial fibrillation, 1020

atrial natriuretic factor, 140, 142, 1020, 1021, 1022

atrium (atria)
    of heart
        development, 1018, 1019
        left, 960, 961(f), 962, 963, 967-8
            development, 1019-20
            isomerism, 974
        right, 960, 962, 963, 964
            development, 1019
            external features, 964
            interior surface, 964

            isomerism, 974
        septal defects, 974-5, 1030-1
        septation, 1023, *1024*
    of lateral ventricle (collateral trigone), 237
    of middle nasal meatus, 551

atrophy
    epidermal, 161
    hyaloid artery, 702
    mesonephros, 1307
    paramesonephric duct, 1317
    thoracic diaphragm, 1012
    vitelline veins, 1220

attic (epitympanic recess), 623

auricle
    of ear, 618-20
        abnormalities, 618-19
        arteries, 620
        cartilage, 619
        development, 580-1, 652-3
        ligaments, 619
        lymphatics, 621
        muscles, 619-20
        nerves, 621
        skin, 619
        veins, 620
    of heart
        left, 968, 980
        right, 964, 977

automaticity, of heart, 1017-18

autophagy, 12

autosomal dominant polycystic kidney disease, 1312

avis, calcar, 238

axial loading, 872

axilla, 814
  boundaries, 814, 815(f)
  contents, 814
  infection, 791
  lymph nodes, 818

axis (axes)
  anatomical, 1458
  arterial, thoracoacromial, 915
  coeliac *See* trunk (arterial), coeliac (coeliac axis)
  embryonic
    cephalocaudal, 197
    of division, 171
    dorsoventral, 197
    laterolateral, 197
  of femoral shaft, 1362
  of joints, 103, 104
  of limb buds, 899-902, 900(f)
    craniocaudal, 900
    dorsoventral, 900
    proximodistal, 900
  mechanical, 1458-9
    of bone, 121, 122(f)
  neuroendocrine, thymus, 946
  ocular, 661
  pelvic, 1358-9
  for pronation, 868
  of rotation, 102
  for supination, 868
  of tendons, 113(f), 114
  visual, 661

axis (C2 vertebra), 397, 720-1
  arch, posterior, 770
  arterial supply, 721
  defects, 770
  muscle attachments, 721
  ossification, 721

axolemma, 43

axon(s), 41, 43-6, 225, 225(f), 228, 234
  conduction, 63-4, 64(f)
  corticospinal, 269
  α-efferent, 110
  growth cone, 369-70
    guidance cues, 370
  hillock, 42, 42(f), 43, 44, 46, 64(f), 338
  injury, 44, 53
  microtubules, 44
  α-motor, 110, 111
  myelinated, 53-4, 54(f)
  postganglionic, 234
  preganglionic, 234
  terminals, 225, 226(f)
  termination, 44
  transport mechanisms, 42, 44
  unmyelinated, 53, 54(f)
  varicosities, 328 *See also* neurone

axoneme, 17
  of spermatozoa, 1265-6

axoplasmic flow, 44

azoospermia, 1268

B

Babinski reflex, 230, 261, 389

Babinski's sign, 269, 1346

back, 707-48
  bones, 710-28
  clinical examination, 747
  dermatomes, 707-8, 708(f)
  fascia, 707-9
  muscles, 736-43, 737(f)
    actions of, 742
    extrinsic, 736, 925-6, 926(f)
    intrinsic, 736
    stability, 744-5
    vascular supply, 742
  pain, 732, 745
  skin, 707-9, 1069
    hair tracts, 707(f)
    innervation, 707-8
    lymphatic drainage, 708, 709(f)
    nerves, 707-8
    tension lines, 707(f)
    vascular supply, 708, 708(f) *See also* column(es), vertebral; *See also* vertebra(e)

balance, anatomy, 643-4, 643(f)

ball, of foot, 1341

ballism (ballismus), 332

band(s)
  of Baillarger, 339, 339(f)
  of Broca, 356
  of Giacomini, 350
  iliotibial, 1400
  intertendinous, 849
  Ladd's, 1209

  moderator, 966
  onychodermal, 155
  outer, of Baillarger, 339
  patellotibial, 1400
  sagittal, 880
  septal, 966
  of skeletal muscle
    A (anisotropic), 104, 105, 106, 108(f), 115
    I (isotropic), 104, 105, 106, 115
  spiral, of Gosset, 859
  vestibular, 605

bar, of cervical vertebrae, 718

barium meal, 953, 954(f), 957, 1115(f)

barium studies, oesophagus, 953

baroreceptors, 58

barotrauma, oesphageal rupture, 953

Barr body, 19, 69

Barrett's oesophagus, 1114, 1115

barrier(s)
  blood-brain, 48-9, 226
  blood-CSF, 242
  blood-testis, 1263, 1265, 1266
  blood-thymus, 947

basal ganglia, 227, 229, 230, 325-34, 325(f), 326(f)
  arterial supply, 253
  disorders, 230, 326, 332-4, 333(f), 334(f)
  functions, 332
  input structure (striatum), 325
  output connections, 331(f)
  output structure (globus pallidus), 325, 326(f) *See also* claustrum; *See also* complex, lentiform; *See also* corpus (corpora), striatum; *See also* nucleus, basal

basal lamina *See* lamina, basal

base
- cranial, 415-16 *See also* calvaria
- of lungs, 993
- moduli, 489
- of sacrum, 724
- of skull *See* skull, base

basement membrane *See* membrane (membrana)

basilar invagination, 770

basiocciput, 770

battledore placenta, 1303, 1304(f)

Battle's sign, 481

Becker muscular dystrophy, 107

bed
- of liver, 1165
- microvascular, 131, 134
- nail, 155

behavioural disorders, basal ganglia dysfunction, 332-3

Bell's palsy, 286, 495, 520, 630

Bennet shift, 536

Bernoulli effect, 591

beta-endorphin, 48

Bezold's abscess, 626

biglycan, 86, 87

bile, 68
- secretion, 1173

biliary colic, 1179

biliary tree, 1177-81, 1177(f)
- extrahepatic, 1178-9
- intrahepatic, 1173, 1175, 1177-8 *See also* duct(s), bile (biliary)

biomechanics, 117-24
  running, 1459-62, 1460(f), 1461(f)
  walking, 1458-9*see also various joints*

Birbeck granules, 149

bivalents, 22

bladder
  gall *See* gallbladder
  lymphatic drainage, 1145(f)
  neurogenic, 271
  referred pain, 235
  suprapubic puncture, 1106
  urinary, 1245-59, 1245(f)
    apex, 1245, 1312
    arteries, 1249
    at birth, 1246
    development, 1308(f), 1310, 1312, 1313(f), 1314(f)
    distended, 1245, 1246, 1312
    empty, 1245
    exstrophy, 1312, 1314(f), 1323
    female, relations, 1286(f)
    fetus, 1312
    internal structures, 1247-8
    ligaments, 1246-7
    lymphatic drainage, 1249
    microstructure, 1250, 1250(f), 1251(f)
    mucosa, 1245, 1247
    muscles, 1247-8
    neck, 1248-9
      female, 1245, 1248
      male, 1245, 1248
    neonate, 1246, 1312, 1313(f), 1314(f)
    nerves, 1249-50
      afferent, 1250
      efferent, 1249-50
    orifices, 1248
    outflow obstruction, 1248-9

        - referred pain, 1254
        - sex differences, 1245, 1245(f), 1246(f), 1247(f), 1248
        - trabeculated, 1248
        - trigone, 1312, 1322(f)
        - veins, 1249

blastema
- metanephric, 1307, 1309(f)
    - failure, 1226

blastocyst, 171-2, 171(f), 175, 176, 180

blastopore, 184

bleeding
- from superior epigastric vessels, 1056
- nose, 554
- oesophageal varices, 951, 1118 *See also* haemorrhage

‘blind spot’, 694

blood, 67-72
- cells, 67-72
    - formation, 74-5, 75(f)
    - red *See* erythrocytes
    - white, 69-72
- clot formation, 67, 68(f), 72, 135
- clot retraction, 72, 135
- groups, 68
- plasma, 67
- platelets, 72
- vessels *See* vessels, blood

blood flow
- cerebral
    - pain-evoked changes, 348
    - regulation, 254
- dental pulp, 514
- renal, 1237, 1310
- vitello-umbilical, 1019

Bochdalek’s hernia, 1015

body (bodies)
- amyloid, of prostate, 1259
- aortic, 986
- aorticopulmonary, 984
- Barr, 19, 69
- basal, 16, 17(f)
- carotid, 447-8, 448(f)
  - nerves, 458
- central fibrous, of heart, 974
- chromaffin, 986
- ciliary, 668, 675, 677(f), 680-9, 680(f), 689(f)
  - development, 699, 700
  - functions, 680
  - structure, 680-1
- foreign, inhaled, 1001
- of gallbladder, 1177
- geniculate
  - lateral, 311, 357
  - medial, 277(f), 289(f), 291, 313(f), 314, 357
- glomus, tumours of, 894
- of incus, 627
- of ischium, 1356
- juxtarestiform, 298, 305, 308
- lamellar, 1035
- of lateral ventricle, 237, 237(f)
- mammillary, 239, 317(f), 318(f), 319, 320
  - development, 380
- of mandible, 409, 480, 481, 505, 530
  - fracture, 480
- of maxilla, 476-7
- Nissl, 41, 43(f)
- Odland, 148, 158(f)
- Pacchionian, 243
- of pancreas, 1184-5, 1184(f)
- para-aortic, 1046-7, 1081
  - development, 374
- of penis, 1271-3, 1271(f), 1272(f), 1273(f)

- perineal, 250, 252, 1096, 1098, 1151, 1155, 1159, 1284
    - development, 1212, 1322
    - lacerations, 1096
- of pubis, 1354
- restiform, 298, 300
- of sphenoid bone, 415, 424, 429
- of sternum, 917-18, 917(f)
- trapezoid, 281(f), 282(f), 285
- tympanic, 452
- ultimobranchial, 602, 609
- vertebral, 716, 718, 744
    - of axis, 720
    - cervical, 718
    - development, 768, 770
    - ossification, 769(f)
    - thoracic, 721, 984
- vitreous, development, 702
- Weibel-Palade, 136, 137
- Wolffian, 1306(f), 1307, 1322(f) *See also* mesonephros

body height, 744

bone (general), 85-97
- anatomy, macroscopic, 85-6, 85(f)
- bundle (woven bone), 86, 87, 88, 88(f), 89, 93, 95
- calcification, 94(f), 95
- canaliculi, 88, 88(f), 89, 90(f), 93, 124
- cancellous (trabecular), 85, 85(f), 89, 89(f), 91, 95
- cartilage bone, 93, 96
- cells of, 87-9
- compact, 85, 87, 90, 91, 92, 93, 95
- cortical, 85, 86, 88, 91, 92, 96, 113(f), 120(t)
- crystal, 86, 87, 93
- degeneration, 124
- demineralization, 88
- deposition, 87
- development, 92-7
    - in limbs, 902-3

diploë, 409, 416, 417
endosteum, 86, 90-1
fracture repair, 91
growth, 92-7
    postnatal, 95-7
injury, 124
lacuna, 87, 88, 88(f), 90(f), 93, 94(f), 95
lamellar, 86, 87, 88, 88(f), 89(f), 90(f), 92(f), 95
long, mechanical properties of, 120-1, 121(f)
lymphatics, 91
maintenance, 95-7
marking, 85-6
marrow *See* marrow, of bone
material properties of, 120, 120(f)
matrix, 86-7, 86(f)
mechanical axes, 121, 122(f)
membrane, 92
metaplastic, 95
microstructure, 86-91
minerals, 87
modelling, 86, 93, 95
movements, 121-3
muscle attachment, 86
nerves, 91-2
ossification, 92 *See also* ossification
periosteum, 86, 89(f), 90-1, 91(f), 93, 97, 98(f), 112, 467
pneumatized, 85
remodelling, 90, 91, 91(f), 93(f), 94(f), 95
    adaptive, 123, 124(f)
repair, frustrated, 124
resorption, 87, 88, 88(f), 89(f), 90, 93, 95, 96
spongy (cancellous), 85, 89, 95
tendon attachment, 86
trabecular (cancellous), 85(f), 86(f), 88, 88(f), 89-90, 89(f), 90(f), 91, 92, 95, 96
vasculature, 91-2, 92(f)
woven, 86, 87, 88, 88(f), 89, 93, 95

bone marrow *See* marrow, of bone

bone morphogenetic proteins (BMP), 87, 370, 699, 1026, 1034

bones (named) ***see individual bones***

bones (of regions)
- of cheek, 409, 412, 420
- of ear, 627-8
  - inner, 633
- of foot, 1432-42, 1435(f)
- of forearm, 840-3
- of hand, 861-8
- of knee, 1394-5
- of lower limb, 1331, 1412-17
- of nose, 547
- of pelvic girdle, 1352-65, 1353(f)
- of pharyngeal arch, 598-9, 598(f)
- of shoulder region, 791-800
- of skull, 409-21
- of thigh, 1360-5
- of thoracic wall, 909, 917-22, 917(f)
- of upper limb, 777-8, 777(f)
- of vertebral column, 710-28

borders
- of greater omentum, 1104
- of heart, 961(f)
  - surface anatomy, 913
- of iliac crest, 1355
- inferior, of costodiaphragmatic recess, 991
- interosseous
  - of radius, 840
  - of ulna, 844
- of lesser omentum, 1102
- of limb bud
  - postaxial, 899
  - preaxial, 899
- of lower limb

        postaxial, 1346
        preaxial, 1346
    of lung, 993
    predentine-dentine, 514
    of scapula, 794-5, 814, 817

botulinum toxin, 954

bouton, 45-6, 45(f)
    presynaptic, 44, 45(f), 46, 62
    terminal, 45, 45(f)

bouton de passage, 45

Boutonnièrre deformity, 878

brachium, quadrigeminal
    inferior, 288, 289
    superior, 291, 292, 311
        inferior, 311, 314

brachycephaly, 418, 613

brachydactyly, 906

bradykinin, 1028

brain, 226-7, 227(f), 228(f)
    arteries, 247-8, 247(f), 248(f)
    asymmetry *See also* cerebral hemisphere
    blood flow regulation, 254
    development, 375-6, 375(t)
        elongation, 362, 362(f)
        induction, 370-1
        patterning, 370-1 *See also* mesencephalon (midbrain); *See also* prosencephon (forebrain); *See also* rhombencephalon (hindbrain)
    dimensions, 388
    ischaemic/hypoxic lesions, 392
    lymphocyte entry, 52
    neonatal, 388-9
    ‘sand’, 324

  structure, 226-7, 228(f)
  vascularization, 391
  veins, 254-6, 255(f)
  venous drainage, development, 392-3, 393(f) *See also* cerebral hemisphere; *See also* cerebrum; *See also* cortex, cerebral

brain derived neurotrophic factor (BDNF), 370

brain stem, 225-6, 229, 230, 275-96
  arteries, 253
  connections, 330(f)
  death, 275, 295
  development, 369(f), 371
  lesions, 275-6
  neonate, 377
  projections to amygdala, 354
  spinothalamic tract inhibition, 264
  veins, 254

breast, 929-37
  absent, 934
  age-related changes, 934-5, 935(f)
  anomalies, 934
  arteries, 931
  at birth, 934
  bud, 934, 1325
  cancer, 933-4
    lymphatics, 932
    male, 933
    reconstructive surgery, 933-4
    surgery, 932
  development, 934
  epithelium, 27
  lactation, 936, 936(f)
  lymphatics, 932
  male, 934, 936
  microstructure, 932-3, 933(f)
  nerves, 932
  postlactation, 937

- in pregnancy, 931, 932, 936, 937
- secretion from, 32
- skin, 930-1
- soft tissue, 930-1
- structure, 929-30, 930(f)
- supernumerary, 934
- surface anatomy, 912
- veins, 932

breathing, 989, 1011-12
- abdomen role, 1012, 1071
- ‘abdominal’, 1012
- accessory muscles, 924-6
- anatomy, 1011-12
- diaphragm role, 1011-12
- expiration, 1012
    - abdomen role, 1012
    - forced, 1007
    - lung movements, 914
    - muscles, 1012
- fetal, 1013
- inspiration, 1011-12, 1011(f)
    - deep, 1012
        - before expulsive efforts, 1009
    - forced, 1007, 1012
    - lung movements, 914
    - muscles, 1011, 1071, 1085
    - quiet, 991, 1012, 1085
        - pulmonary border, 993
- intercostal muscle role, 1012
- nasal reflex in neonate, 389
- pharyngeal muscle role, 1012
- during sleep, 1012
- ‘thoracic’, 1012

bregma, 412, 469

bridge, nasal, 471, 475, 479

Brodmann’s area *See* area, cortical (cerebral)

bronchial atresia, 1037

bronchiectasis, 1035

bronchioles
  microstructure, 1004
  respiratory, 995, 998, 1001(f), 1004
  terminal, 995, 999(f)

bronchocoele, 1037

bronchodilation, 1004

bronchogenic cyst, 1037

bronchogram, 1002(f)

bronchomalacia, 1036-7

bronchopulmonary segments *See* segment(s), bronchopulmonary

bronchoscopy, 1001, 1006
  virtual, 1005(f)

bronchospasm, 1004

bronchus (bronchi), 994(f), 996(f), 1000-6
  accessory cardiac, 1002
  anatomical variants, 1002
  arteries, 1003
  bronchogram, 1002(f)
  cartilage, 996(f), 1005
  congenital malformations, 1002, 1036-7, 1037(f)
  connective tissue, 1004
  development, 1000
  extrapulmonary, 1003, 1004
    cartilage, 1004, 1005(f)
  glands of, 1035
  intrapulmonary, 995, 1005
    cartilage, 1004, 1005(f)
  left main, 992(f), 1003, 1030(f)
    branches, 1003

    - radiograph, 954(f)
  - lingular, 1003
  - lobar, 994
    - inferior, 1002
      - left, 1003
      - right, 1003
    - middle, right, 1003
    - superior, 994, 1002
      - left, 1003
      - right, 1002-3
  - lymphatic drainage, 1003
  - muscle, 1004
  - principal, 994, 995
  - right main, 992(f), 1001-3
    - branches, 1002-3
  - segmental, 994-5, 995(f)
    - anterior, 1002
    - apical (superior), 1002
      - left, 1003
      - right, 1003
    - apicoposterior (left), 1003
    - basal
      - anterior, 996(f), 1003
      - medial, 996(f), 1003
      - posterior, 1003
    - posterior, 996(f), 1002
  - subsuperior (subapical), 1003
  - surface anatomy, 914
  - tracheal, 1001
  - veins, 1003

bronchus-associated lymphoid tissue (BALT), 74

Brown-Séquard syndrome, 273(f)

bud(s)
  - breast, 934, 1325
  - caecal, 1205(f), 1209
  - limb, 95, 115

    - axis, axes, 899-902, 900(f)
    - upper, 905
  - lung, 601, 1013-14, 1033, 1034
  - mammary, 934, 1325
  - osteogenic, 93, 94(f)
  - pancreatic
    - dorsal, 1206, 1207
    - ventral, 1206, 1207
  - taste *See* taste buds
  - tubular, lacrimal apparatus development, 703
  - ureteric, 1240, 1307, 1308, 1309(f)
    - absent kidney and, 1226

bulb
  - aortic, 984
  - hair, 151, 152(f)
  - of internal jugular vein
    - inferior, 451
    - superior, 451, 452, 461
  - olfactory, 44, 45(f), 55, 349, 351, 353, 356, 553
    - centrifugal inputs, 349
    - development, 382-3
    - organization of, 349(f)
  - of penis, 1271, 1271(f)
  - sinuvaginal, 1316
  - of vestibule, 1280, 1281(f)

bulbus, 1020

bulbus cordis, 1020
  - formation, 1020

bulge(s)
  - cerebellum (bilateral), 379
  - follicular, 151

bulla ethmoidalis, 473, 551, 551(f)

bullous pemphigoid, 33

bundle(s)

atrioventricular (of His), 974, 975, 976, 977-8, 1022
ciliary, 482
circumolivary, 377
dorsal ascending
  cholinergic, 290
  noradrenergic, 290
forebrain, medial, 320
of His *See* bundle(s), atrioventricular
hook (uncinate fasciculus), 298, 308
keratin filament, 147
neurovascular, 131
  mylohyoid, 530
noradrenergic, dorsal, 290
reticulin, lymph node, 72, 73, 74, 75
spiral, of cochlear nerve, 645
ventral ascending
  cholinergic, 290
  noradrenergic, 290
  serotoninergic, 290

bursa(e)
heel, 1461
infracardiac, 950, 1215(f), 1218
of Luschka, 563
obturator externus, 1372
olecranon, 833
omentalis (omental, omentis), 1214
  inferior recess of, 1204
ovarian, 1294
pharyngeal, 563
psoas, 1389
subacromial, 795
suprapatellar, 1401(f), 1402
synovial, 100
  extensor tendons, of hand, 880
  gastrocnemius, 1420
  gluteofemoral, 1369
  gluteus maximus, 1357

    - of hip joint, 1389
    - infrapatellar, 1401(f), 1402, 1412
        - subcutaneous, 1402
    - ischiofemoral, 1369
    - of knee joint, 1402
    - obturator
        - externus, 1371
        - internus, 1371
    - pes, 1402
    - prepatellar, 1394, 1402
    - quadratus femoris, 1372
    - semimembranous, 1402
    - subacromial, 804(f), 806, 810, 812
    - subscapular, 794, 812
    - subtendinous iliac (psoas), 1389
    - suprapatellar, 1401, 1401(f), 1402
    - trochanteric, 1369
  - tensor veli palatini, 569 *See also* sac(s), lesser

bursitis, trochanteric, 1390

burst-forming units, erythroid line (BFU-E), 77

buttock, region(s), gluteal

C

cadherins, 5, 7
  embryonic, 194

caecum, 1141-2, 1212
  arteries, 1144-5
  at birth, 1142
  development, 1142, 1209, 1217
  epithelium, 1137
  fetal, 1142
  haustrations, 1138
  length, 1142
  lymphatics, 1141
  malformations, 1209
  nerves, 1141
  peritoneum, 1142
  recesses, 1109, 1142
  relations, 1141-2
  veins, 1145
  volvulus, 1142 *See also* intestine, large

calcaneus, 1433, 1437
  accessory, 1437
  club foot, 1463
  innervation, 1437
  muscle/ligament attachments, 1437
  ossification, 1437
  surface anatomy, 1340-1, 1437
  vascular supply, 1437

calcar avis, 336
  development, 385

calcar femorale, 1363, 1364(f)

calcification
  aorta, 986
  bone, 94(f), 95

- choroid plexus, 51

calcitonin gene-related peptide (CGRP), 508
- descent of testes and, 1320-1

calcium, 8
- deficiency, 95
- muscle contraction
    - cardiac muscle, 141, 142
    - skeletal muscle, 111
    - smooth muscle, 130
- in nails, 154

calcospherites, 514

calculi
- renal, 1242
- ureteric, 1242

caldesmon, 128

calluses, 148

calmodulin, 18

calponin, 128

calsequestrin, 142

calvaria, 416, 417, 418

calyx (calyces)
- glycocalyx, 4
- renal, 1230-1, 1230(f)
    - cupping, 1231
    - development, 1308, 1309(f)
    - major, 1230, 1237, 1242
    - microstructure, 1236(f)
    - minor, 1230, 1234, 1237, 1242

cAMP, 8, 9

camptodactyly, 906

canal(s)

adductor (Hunter’s), 1373, 1376
Alcock’s (pudendal), 1092, 1097
alimentary
    microstructure, 1049-52, 1050(f) *See also* tube(s), digestive/gut; *specific regions*
alveolar, 476, 558
    inferior, 517(f), 519
anal, 1155-60, 1156(f), 1308(f), 1322, 1323, 1324
    arteries, 1159-60
    continence, 1160
    development, 1212-13
    dissection, 1094, 1098
    fibromuscular structures, 1159
    fissure, 1157
    fistula, 1158
    lining, 1155-6
    lymphatics, 1160
    muscles, 1158-9, 1158(f)
    nerves, 1160
    referred pain, 1160
    resections, 1094
    veins, 1160
atrioventricular, 1022
    formation, 1016-17, 1018-19, 1021, 1022-4, 1025(f)
    septation, 1023-4
auditory *See* meatus, acoustic
of bone, 85, 85(f), 86
carotid, 415, 416
    opening, 617
cartilage, 81
central, of spinal cord, 41, 226, 227(f), 257, 258, 259(f), 260, 275, 277, 278(f), 749
cervico-axillary, 814
cochlear, 634, 639-40
condylar, 415
    anterior *See* canal(s), hypoglossal
    posterior, 415, 425, 432

craniopharyngeal, 367, 530
dental *See* canal(s), alveolar
Dorello’s, 429, 667
of epididymis, 1317
ethmoidal, 471, 472
    anterior, 472
    posterior, 423, 472
facial (Fallopian), 624, 625, 628, 629, 630
    dehiscences, 630
of facial nerve, 625
Fallopian (facial), 624, 625, 628, 629, 630
femoral, 1350, 1351(f), 1381, 1382
    sex differences, 1350
frontonasal, 472
Haversian, 85(f), 88, 89, 89(f), 90(f), 91, 93
Hunter’s (adductor), 1373, 1376
hyaloid, 702
hypoglossal, 415, 420, 424, 446, 460
incisive, 414, 472(f), 473(f), 475, 476, 477
    lateral, 477
infraorbital, 474(f), 476, 656
inguinal, 1064, 1320, 1321
    boundaries, 1066
    deep structures, 1065-6
    ‘floor’, 1064
    position and relations, 1065-6
mandibular, 518, 532
nasolacrimal, 475, 476, 550
nasopalatine, 550
    fetal, 502
neurenteric, 184
notochordal, 184
of Nuck, 1321
obturator, 1058(f), 1352, 1372
optic, 529, 655, 656, 660, 667
osteoligamentous, 206
palatine

    greater, 502, 543
    lesser, 502
palatovaginal, 479, 529, 550
pericardioperitoneal, 189, 197, 198, 199(f), 201, 205, 1013, 1013(f), 1014, 1034, 1213, 1214, 1215
    connections between, 1215
    enlargement, 1213, 1214
    foregut development, 1206
    pancreas development, 1207
pharyngeal (palatovaginal), 479, 550
pilary
    dermal, 151-2
    intraepidermal, 151-2
pleuropericardial, 207, 1213
    development, 1014
pleuroperitoneal, 1214
    closure, 1216
    development, 1014
    stomach rotation and, 1214
portal, 1168, 1173, 1174, 1175
pterygoid, 247, 402, 415, 528, 529, 543, 557
pudendal (Alcock's), 1092, 1097
radicular (root), 717, 749, 754
reuniens *See* duct(s) (or ductus), reuniens
root (radicular), 717, 749, 754
Rosenthal's, 634
sacral, 725, 727(f)
of Schlemm (scleral venous sinus), 675, 676, 686, 702
semicircular, 633-4, 633(f), 637-8, 663
    balance and posture, 643-4, 643(f)
    head movements, 638
    lateral (horizontal), 634
    posterior, 634
    superior (anterior), 633-4
sinuosus, 476, 518
sphenoparietal (of Trolard), 431
spiral, of modiolus, 634

  tarsal, 1436, 1437
  for tensor tympani, 617, 626
  urethral, 1250
  uterovaginal, 1316(f)
  vertebral, 712-15, 715(f), 717
  vesicourethral, 1307, 1310, 1312
  Volkmann’s, 89, 89(f), 90(f), 517
  vomerovaginal, 475, 550

canaliculus (canaliculi), 88, 88(f), 89, 90(f), 93, 124
  bile, 1173, 1174(f), 1175
  for chorda tympani
    anterior, 623
    posterior, 623
  cochlear, 424, 431, 617, 635, 642
  dental, 516
  inferior, 703
  lacrimal, 672, 674, 703
  mastoid, 415, 617, 624
  for tympanic nerve, 617

canalis sinuosus, 476, 518

cancer
  breast, 933-4
  of head, 454
  lung, staging, 957
  of neck, 454
  pancreatic, 1184, 1185, 1186, 1187
  prostate, 1258
  rectal, 1154
  uterine cervix, 1292
  vertebral, 744 *See also* tumours

canines *See* teeth

canthus
  lateral, 669
  medial, 669

cap
  acrosomal, 1266
  duodenal, 1125
  Phrygian, 1177

capacitation, 167

capillary (capillaries), 132-3
  cerebral, 238-9
  continuous, 133
  dimensions, 132
  fenestrated, 133
  of lung, 998
  lymphatic, 139
  medullary (of kidney), 1233
  of mesonephros, 1307
  peritubular, 1233
  permeability, 133
  pulmonary, 998

capitate, 863, 863(f)
  ossification, 864

capitulum, 796, 799, 799(f)

capsule(s)
  Bowman's, 1234-5, 1235(f), 1236(f)
  external, cerebral hemisphere, 326
  extreme, 326
  fibrous (of joints)
    of acromioclavicular joint, 801
    development, 902
    of elbow joint, 832, 832(f)
    of glenohumeral joint, 804(f), 805
    of hip joint, 1366, 1387-8
    of knee joint, 1395, 1396, 1402
    of prostate gland, 1258
    of sternoclavicular joint, 801
    of synovial joints, 100
    of temporomandibular joint, 533

        - of wrist, 870
    - of Glisson, 1060, 1061
    - glomerular, mesonephros, 1307
    - internal (of cerebrum), 326, 357-8
        - anterior limb, 357
        - arterial supply, 253
        - of cerebral cortex, 227, 228, 229(f), 230(f)
        - development, 380, 383, 385
        - fibres of, 357
        - genu, 357
        - posterior limb, 357
        - retrolentiform part, 357
        - stroke, 253, 254(f)
        - structure and relations, 357
        - sublenticular part, 357
    - of kidney, 1230, 1233
    - of lens, 686, 702
    - of liver, 1163
    - lymph node, 72, 73, 73(f), 74, 74(f)
    - nasal, 611
    - otic, 611
    - parotid, 397, 469, 496
    - renal, 1230, 1233
    - splenic, 1193-4
        - injuries, 1104
        - rupture, 1192
    - of suprarenal gland, 1200, 1218
    - Tenon’s, 657, 671-2
    - of thyroid gland, 463
    - of tonsils, 566
    - vascular, of developing lens, 702

caput, 86

caput medusae, 1059

caput succedaneum, 416

carbohydrates, plasma membrane, 4

cardia, achalasia, 953

cardiac defects
  acyanotic, 974-5
  congenital, 974-5
  cyanotic, 975

cardiac jelly, 142

cardiac myosin heavy chain, 1016

cardiac output, embryonic, 206

cardiac pacing, 978

‘cardiac seat belt’, 959

cardiac tamponade, 960, 985

cardiomyopathy, hypertrophic, 969

carpal bones, 861-4, 861(f), 862(f), 874(f)
  at birth, 864
  distal row, 872
  instability, 872
  kinematics, 872
  movements, 872, 873(f)
  ossification, 93(f), 864, 864(f)
  proximal row, 872*see also individual named bones*

carpus *See* carpal bones

carrier proteins, 4

cartilage (general), 81-5
  articular, 82-3, 99, 100(f), 124
  calcification, 95(f)
  canals, 81
  cells of, 81
  collagen fibres, 81
  condylar, 532
    remodelling, 534
  cricoid, 610
  cuneiform, of axis, 721

development, 84-5
elastic, 86, 86(f)
    material properties of, 120
embryonic, 81, 84, 84(f)
fibrocartilage, 83-4, 84(f), 533
    intra-articular, 101
    material properties of, 120
growth, 84-5
hyaline, 81, 82-4, 82(f), 83(f), 533
    material properties of, 120
matrix, 81-2
microstructure, 81-4
nutrition, 81, 99
zones, 83

cartilage (named)
of acoustic meatus, 619
arytenoid, 578(f), 579, 599, 610
of auditory tube, 564
basisphenoid, 611
bronchial, 996(f), 1005
condylar, 533
corniculate, 578(f), 579, 610
costal, 82, 96, 919(f), 922, 963
    ageing, 81, 322
    attachments, 922
    left, 983, 984
    right, 987
    surface anatomy, 909, 1052
cricoid, 405, 577(f), 579, 599
    malformation, 579
cuneiform, of larynx, 579
epiglottic *See* epiglottis
exoccipital, 611
interorbitonasal, 611
intrathyroid, 579
laryngeal, 397
of larynx, 577-80, 577(f), 578(f), 996(f)

            calcification, 579-80
            infant, 584
            levels, 577
    Meckel’s, 532, 598, 599, 604, 607, 627, 652
    nasal, 82, 409
            alar, 547-8
            lateral (superior), 547
            septal, 547
    orbital, 611
    palatopterygoquadrate, 598
    parachordal, 611
    pharyngeal arch, 598-9, 598(f)
            derivatives of, 598(f)
    of pharyngtotympanic tube, 564
    precartilage, of clavicle, 793
    Reichert’s, 599
    semilunar *See* meniscus (menisci), of knee
    of sternum, 917, 918
    thyroid, 405, 577(f), 578-9, 610
            sex differences, 579
    of trachea, 405, 406, 996(f), 1005, 1034
            complete rings, 1037
            incomplete rings, 1005
    tritiate, 579
    unciform, 530
    of xiphoid process, 918

cartilago triticea, 504

caruncle, lacrimal, 669, 703

carunculae
    hymenales, 1284
    myrtiformis, 1284

caspases, 25

catalase, 13

cataract, 686

catechol-O-methyltransferase, 244

catecholamines, 47, 56
  production, 1199(f), 1200 *See also* adrenaline (epinephrine); *See also* dopamine; *See also* noradrenaline (norepinephrine)

catheterization
  central venous, 1032
  umbilical artery, 1222-3, 1223(t)
  umbilical vein, 1222

cauda equina, 750(f), 754
  lesions, 759-60, 1074

caudate, 325, 326

caudate nucleus *See* nucleus, caudate

cauliflower ear, 84

caveolae, 12, 128, 129(f), 130

cavity (cavities)
  abdominal, 1101(f)
  amniotic, 172-3
  buccal *See* cavity (cavities), oral
  cardiac, primitive, 1016
  chorionic *See* coelom, extraembryonic
  cranial, 397, 414, 423, 425(f), 426, 431
    brain volume, 388
  glenoid, 794, 795(f), 796, 805
  head
    caudal, 702
    premandibular, 702
  implantation, 175
  laryngeal, 582-4
  lesser sac *See* sac, lesser
  middle, 623-30
  nasal, 547, 549-56
    development, 603-4 *See also* nose, cavity
  oral, 499-525, 499(f), 604-7
    after birth, 606-7

    development, 604
    mucosa, 500-1
    primitive *See* stomodeum *See also* mouth
orbital *See* orbit
pelvic, 1358
pericardial, 181(f), 959-60, 960(f)
    development, 189, 1013, 1013(f), 1018
peritoneal, 1099-110, 1214
    below umbilicus, 1214
    compartments, 1107-8
    development, 1013, 1013(f), 1213-18, 1305(f)
        fetus (10 weeks), 1208(f), 1209
    embryo, 1013, 1013(f)
    fluid, 1099, 1109-10
    general arrangement, 1107-10
    greater sac *See* sac, greater
    inframesocolic compartment, 1108-9
    neonatal, 1218
    recesses, *See also* recess(es)
    supra-umbilical, 1208(f), 1214
    supramesocolic compartment, 1107-8
pleural, 189, 989
pulp, of teeth, 513, 514-15
synovial, 99(f), 101
thoracic, 910
tympanic, 617, 623-6
    arteries, 628-9
    at birth, 623
    boundaries, 623-7
    development, 652
    fetal, 623
    floor, 623
    function, 623
    lateral wall, 623-4
    lymphatics, 628-9
    medial wall, 624-5
    movement, 628

    - muscles, 628
    - nerves, 629-30
    - posterior wall, 625-6
    - roof, 623
    - veins, 628-9

cell adhesion molecules, 5-7, 137
- amniotic, 175(f), 180, 181, 182
- calcium-dependent, 5
- calcium-independent, 5-6
- in embryo, 137
- intracellular, 6
- kidney development, 1308
- podocytes, epithelial, in metanephros, 1308

cell junction, 3(f), 6(f)

cells (general)
- coat, 4, 5(f)
- cycle, 20-3
    - ventricular zones, 367, 369(f)
- death, 27
    - programmed *See* apoptosis
- determined, 193
- differentiation, 23-4
- division, 20-3, 193-4
- domains, 4
    - apical, 4
    - basal, 4
- function, 3-26
- fusion, 24
- of heart, development, 1016-18
- hyperplasia, 217(f)
- membrane, 3(f), 4-9
- migration, inter-kinetic nuclear, 369
- motility, 3
- nucleus, 3, 3(f), 18-20
- organelles, 5(f)
- organization, 3(f), 4, 10

- polarity, 4
- shape, 3
- signalling *See* signals (signalling), cellular
- size, 3
- structure, 3-23
- surface
  - contacts, 4-5
  - folds, 3(f)
  - invagination, 3(f)
  - lateral, 4
  - projections, 3(f), 17-18, 18(f)
- turnover, small intestine, 1210

cells (named)

- acinar, 1188(f), 1189-90, 1189(f)
  - polyhedral, 603
- adipocytes, 14, 34-5, 38
- agger nasi, 557, 558
- air
  - ethmoidal, 471, 472, 473
    - anterior, 558
    - middle, 473, 558
    - ossification, 473-4
    - posterior, 472, 473, 558
  - mastoid, 623, 626
    - arteries, 629
    - development, 626
    - innervation, 626
    - nerves, 626
- alar plate, 377
- alpha (A), of pancreas, 1189(f), 1190, 1207
- alveolar epithelial (pneumocytes), 998
- alveolar squamous, lifespan, 1005
- amacrine, 688, 691, 692
  - development, 700
- amine precursor uptake and decarboxylation *See* cells (named), APUD
- amniotic, 181
  - pluripotency of, 181

angioblasts (angioblastic)
    development, 772
    heart development, 1016
angiogenic, 1020
antigen-presenting (APC), 78-80, 79(f), 80(f)
apical, of epididymis, 1268
APUD, 463
    development, 374
argentaffin, 374
astrocytes, 48-9, 367, 370
    ependymal, 51
    fibrous, 48
    protoplasmic, 48
    of retina, 692
atrial muscle, 140, 142, 975
B lymphocytes, 7, 19, 24, 35, 36, 72, 673
    development, 75, 77
band, 69
basal
    of cochlear duct, 640
    of epididymis, 1268
    globose, 552(f), 553
    horizontal, 553
    of respiratory tract, 1004
    rounded, 603
basket, 27, 339
    of cerebellar cortex, 206 *See also* cells (named), myoepithelial
basophils, 69-70, 69(f), 71, 77
    development, 76(f)
Bergmann glia, 367, 386
beta (B), of pancreas, 1189(f), 1190, 1207
Betz, 268, 268(f), 342
bipolar (cerebral cortex), 339
bipolar (retinal), 688, 691-2
    blue cone, 691
    cone, 691
    diffuse cone, 691

        midget cone, 691
        rod, 691
blood *See* blood; *specific cell types (in this section)*
boundary cap, 63
brush, of conducting airways, 1004
‘burst’, 663
C (clear; parafollicular), of thyroid gland, 463
of Cajal (interstitial), 1051, 1160
carcinoma-in-situ (CIS), testes, 1319
cardiac, 975
cementoblasts, 516
cementocytes, 516
centre, germinal, of spleen, 1194
chandelier, 339
chief
        development, 1204
        of parathyroid glands, 464
chief (peptic), 1121
chondroblasts, 36, 81
        formation, 764(f)
chondrocytes, 81-2, 82(f), 83, 84(f), 87, 93, 94, 94(f), 95, 99, 100
chromaffin (phaeochromocytes), 235(f), 236, 911, 986
        development, 374
        of suprarenal medulla, 1200
chromophils, 322, 322(f)
chromophobes, 322, 322(f)
ciliated, 1294
Clara, 1000, 1004, 1034
Claudius’, 635(f), 641
clear, 145, 149, 150, 154
        of epididymis, 1268
clump, 682
CNS, development, 367
columnar, 28, 29(f), 30
        absorptive, 1161
        ciliated, of respiratory system, 1004
complex (of striate cortex), 347

cone (retinal), 685, 689-91, 690(f), 691(f), 692(f)
    bipolar, 691
    types, 691(f)
cuboidal, 28, 1034
dark, 154, 634, 639, 640
    endolymphatic duct, 639
    intercalated, 1237
    sweat glands, 154
decidua, 175-6
Deiter’s, 635(f), 640, 641, 641(f)
delta (D), of pancreas, 1189(f), 1190, 1207
dendritic, 79, 79-80
    follicular, 79-80, 80(f)
    interdigitating, 79, 947
    Langerhans, 79, 80(f)
    myeloid, 79
    thymic, 79
dense-core *See* cells (named), neuroendocrine
double bouquet, 339
dust, 78
endocrine, of pancreas, 1207
endothelial, 136
enterocytes, 1133, 1135
    development, 1210
    in intestinal crypts, 1135
eosinophils, 34, 36, 69
    development, 76(f)
    of parathyroid glands, 464
ependyma, 41, 51, 51(f), 239(f), 240, 240(f)
epiblast, 186, 361
epiblasts, 763
    migration, 763
epithelial
    electrolyte transport, 522, 522(f)
    rests, 517
    of somites, 832 *See also* epithelium
epithelial glial (Bergmann), 302

erythroblasts, 75, 76(f), 77
erythrocytes *See* erythrocytes
F, of pancreas, 1190
fat (adipocytes), 14, 34-5, 38
fibroblasts, 15, 34, 34(f), 91(f), 675
    coronary, 1026
    mesothelial cell transformation, 1099
    thymus, 947
fibrocysts, 34, 38
follicular dendritic cells (FDC), 79-80, 80(f)
follicular, of thyroid gland, 463
ganglion, 688
    of heart, 982
ganglion (retinal), 692
    axons, 693(f)
    midget cells, 692
    parasol cells, 692
gastrin-producing, 1204
germ, primordial, 184, 186, 1317, 1318(f)
    development, 1317
    sex determination, 1319
glia (neuroglia), 225, 367, 692
    central nervous system, 48-52, 49(f)
    development, 367
    enteric, 55
    olfactory ensheathing, 55
    radial, 364(f), 367
    retinal, 692-3
glioblasts, 367, 369
glomerular, parietal, 1308
glomus, 448
goblet, 28, 29(f), 31, 39
    conjunctiva, 672
    small intestine, 1133-4, 1134(f), 1210
    trachea and bronchi, 1004 *See also* cells (named), mucous
Golgi, of cerebellar cortex, 302, 303
granule, 300, 302, 303

of cerebellar cortex, 300
    development, 378(f), 379
of cerebral cortex, 338
of dentate gyrus, 350
extroversion, 379 *See also* cells (named), stellate
granulocytes, 36, 69-70, 77
    CNS entry, 52
    eosinophil *See* cells (named), eosinophils
    formation, 77
    neutrophil *See* cells (named), neutrophil
granulosa, 1296, 1319
hair, 636, 637(f), 638, 647, 648(f)
    cochlear, 635(f), 640-1
    damage, 648
    development, 652
    of organ of Corti, 640
    vestibular, 639(f)
Haller’s, 551, 558
‘heart-failure’, 78
Hensen’s, 635(f), 642
of hepatic sinusoids, 1175
hepatocytes, 24, 1163, 1173, 1174, 1175
    development, 1208
    presumptive, development, 59
    zonal arrangement, 1175
hilus, 1298
Hofbauer, 178(f), 179, 180
horizontal, 688, 691
hyalocytes, 688
hypercomplex, 347
intercalated (dark), renal collecting ducts, 1237
intercalated duct, salivary gland, 522, 522(f)
interneurones, 225, 229, 236
interplexiform, 692
interstitial (of Cajal), 1051
interstitial (of Leydig), 1297
juxtaglomerular, 1238

keratinocytes, 14(f), 29, 30(f), 145, 146-7
keratocytes, 678(f)
Kulchitsky, 1004 *See also* cells (named), neuroendocrine
Kupffer, 1175
lacis, 1235, 1236(f), 1238
Langerhans, 79, 80(f), 145, 149-50, 150(f), 157-8, 158(f), 163
Langerhans, in oesophageal epithelium, 952
Langhans, 179
leukocytes, 69-72
    intraepithelial, 1213
    lifespan, 70
    mononuclear, 70-2
    polymorphonuclear (polymorphs) *See* cells (named), leukocytes
Leydig, 1265, 1266(f), 1267
    development, 1319, 1320
    in testis, 1266(f), 1267
    testosterone production, 1325
light, 639
lipocytes, 35-6
lymphoblasts, 75
lymphocytes, 19, 35-6, 70-1, 71(f), 603
    B lymphocytes *See* cells (named), B lymphocytes
    development, 947, 947(f)
    entry into brain, 52
    formation, 75-7, 76(f)
    gut-associated lymphoid tissue, 1213
    in small intestine, 1134
    in spleen, 1194
    T lymphocytes *See* cells (named), T lymphocytes
    thymus, 946, 947, 947(f), 948(f)
lymphoid, 605
M *See* cells (named), microfold (M)
macroglia, 41, 48
macrophages *See* macrophages
macula densa, 1238
mast, 36, 1004
    granule release, 36

medullary interstitial, of kidney, 1237
megakaryoblasts, 77
megakaryocytes, 67, 72, 75, 76(f), 77
melanocytes (pigment cells), 30(f), 38, 145, 146, 147(f), 148-9, 149(f), 150(f), 152, 155, 157, 158, 158(f), 159, 162, 365, 675, 679
    in breast, 930
    fetal, 158
melanosomes, 689
memory, 70, 74, 80
Merkel, 57, 58(f), 59, 145, 146, 147(f), 150, 158(f)
mesangial, 1235
    extraglomerular (lacis), 1235, 1236(f), 1238
mesenchymal *See* mesenchyme
mesoblast, 190(f), 191, 199(f), 201
mesothelial, of pleura, 991
metamyelocytes, 69, 77
microfold (M), 1161
    gut-associated lymphoid tissue, 1213
    small intestine, 1134, 1210
microglia, 48, 52-3, 52-3, 52(f), 78
    phagocytic role, 52
    of retina, 692
microvillar, 553
monocytes, 70, 367
    phagocytosis, 70
    production, 77
    thymus, 947
mucous, 1161, 1161(f)
    salivary glands, 522, 522(f)
    small intestine, 1135 *See also* cells (named), goblet
mucous acinar, 523(f)
mucous neck, of stomach, 1121, 1204
myeloblasts, 77
myoblasts, 104, 115-16, 116(f), 117, 130, 142, 143, 607, 903
    development, 772
    migration, 115, 116(f)
    postmitotic embryonic, 772

- skeletal muscle, 115, 116(f)
myocytes, 103, 974, 976
- cardiac, 142, 1017-18, 1018(t), 1022
- primitive cardiac, 1016 *See also* fibre(s), muscle

myoepithelial, 27, 28, 29(f), 153, 154, 157, 158
- lacrimal glands, 673
- salivary glands, 522, 522(f), 523

myofibroblasts, 162(f)
myogenic, 903
- development, 373

myoid, 1265, 1266(f), 1267
- thymus, 947

myotome, 772
natural killer (NK), 72, 176
neural crest *See* neural crest
neural tube, heart development, 1017(f)
neuroblasts, 369, 372
- apolar, 374
- bipolar, 374, 376(f)
- cerebral cortex development, 379, 382, 387(f)
- cranial nerve development, 372-3
- migration during development, 372
  - dynamics, 387(f)
- peripheral nervous system, 372
- spinal cord development, 374
- unipolar, 374

neuroendocrine, 1122
- large intestine, 1161
- respiratory tract, 1004
- small intestine, 1135

neurogliaform (spiderweb), 339
neuroglial *See* cells (named), glia
neurone *See* neurone
neutrophils, 36, 69, 69(f)
- development, 77
- phagocytosis, 69

non-pyramidal (of cerebral cortex), 338, 339

odontoblasts
  cell bodies, 515, 517(f)
  cytoplasmic process, 514
odontoclasts, 517
olfactory ensheathing, 553
oligodendrocytes, 49, 49(f), 50, 367, 375
  development, 375
  interfascicular, 49
oocytes *See* oocyte(s)
osteoblasts, 36, 91(f), 92, 93, 93(f), 95
  alveolar bone, 517
osteoclasts, 36, 76(f), 77, 88
osteocytes, 87-8, 88(f)
oxyphil, of parathyroid glands, 464, 465(f)
pacemaker, 975, 977
pacemaker, renal, 1237
Paneth, 1135
  development, 1210
parafollicular (C), 463, 608, 609
parietal (oxyntic), 1121
  development, 1204
peg (secretory), 1294
pericardial, 1026
pericytes, 132, 133, 136, 137, 138, 138(f), 139, 179, 680, 1299
perilymphatic, 634
phaeochromocytes *See* cells (named), chromaffin
phagocytes, 682
phalangeal (Deiter’s), 635(f), 640, 641, 641(f)
photoreceptor *See* photoreceptors
pigment *See* cells (named), melanocyte (pigment cell)
pillar, 635(f), 640-1, 645
pinealocytes, 324
pituicytes, 48, 321
plasma, 35, 36, 70, 71(f), 74, 76(f), 80, 673
platelets, 72
  production, 77
pneumocytes (alveolar epithelial), 998, 1034

- podocytes, 1234
  - Bowman’s capsule, 1234, 1235, 1235(f), 1236(f)
  - mesonephric, 1307
- pre-Sertoli, 1319
- prechondroblasts, 85
- premyoblasts, 115
- principal, 1268
- proerythroblasts, 77
- progenitor, 193
- prolymphocytes, 75
- promegakaryocytes, 77
- promonocytes, 77
- promyelocytes, 77
- proplatelets, 77
- Purkinje, 225
  - activation, 303
    - control, 7
  - axons, 297, 300, 301(f)
  - of cerebellar cortex, 300, 302, 303, 307
    - development, 379
  - dendrites, 302
  - dimensions, 302
  - tumours of, 978
- pyramidal, 338
  - hippocampus, 351, 352(f)
- radial (Müller), of retina, 367, 690, 692, 700
  - development, 700
- red blood *See* erythrocytes
- relay, vestibulo-ocular, 308
- Renshaw, 375
- reticular, 34, 75
  - of spleen, 1195
- reticulocytes, 77
- of retina
  - radial (Müller), 367, 690, 692, 700 *See also* cells (named), bipolar
- rod (retinal), 685, 689-91, 690(f), 691(f)

    - bipolar, 691
    - types, 691(f)
- satellite, 55, 55(f)
    - development, 372
    - skeletal muscle, 116(f), 117
- Schwann, 43, 44, 50, 50(f), 51, 53
    - development, 367, 369, 372, 375
- sclerotomal, 764, 765(f), 767
- sebocytes, 153
- secretory (peg), 1294
- seromucous, salivary glands, 522, 522(f)
- serosal, 39
- serous acinar, 523(f)
- serous, salivary glands, 522, 522(f)
- Sertoli, 1266-7
    - development, 1317, 1319, 1320
- small granule *See* cells (named), neuroendocrine
- small intensely fluorescent (SIF), 374
- smooth muscle, development, 772
- somitocoeles, 764, 768, 770
- spermatids, 1265-6
- spermatocytes, 24
    - primary, 1265
    - secondary, 1265
- spermatogonia, 1265
    - types, 1265
- spermatozoa *See* spermatozoa
- spiderweb, 339
- splanchnopleuric coelomic, 1203, 1203(f)
- squames, 27, 145, 147(f), 148, 151, 154, 155, 157, 158(f), 160
- stab, 69
- stave, 1194(f), 1195
- stellate
    - of cerebellar cortex, 300, 302, 303
    - of cerebral cortex, 338-9
        - non-spiny, 339
        - spiny, 338-9

    hepatic, 1175
    pancreatic, 1190
stem, 24, 193, 1121
    haemopoietic, 75, 75(f), 76(f)
    human embryonic, 193
    intestinal crypts, 1135
    of large intestine, 1161
    mesenchymal, 35
    myeloid, 77
    osteoprogenitor, 87, 91, 92, 93, 96
    in skin, 146, 147, 153, 158
    in thymus, 947
striated duct, salivary glands, 522, 523(f)
sustentacular, 447, 448(f), 552, 553, 603
sympathochromaffin, 372
syncytia (giant), 78
synovial
    type A, 100
    type B, 100
T lymphocytes (thymus-derived), 35, 36, 67, 68, 71, 72, 73, 74, 75, 78, 79
    CD nomenclature, 71
    in conducting airways, 1004
    cytotoxic, 71
    delayed type hypersensitivity, 71
    development, 72, 77, 946, 947, 947(f)
    helper, 71, 74, 77, 78, 80
    regulatory, 71, 72, 77
    thymus, 946
tanycytes, 48(f), 51, 240, 367, 380, 386
terminally differentiated, 193
theca lutein, 1297
thrombocytes *See* cells (named), platelets
thymocytes, 946, 947-8, 948(f)
    development, 947
transiently amplifying, 193
transit amplifying, 20

  transitional, 975
  trilaminar, of dentate gyrus, 350
  vascular muscle, 137
  veiled, 74, 79, 79(f)
  ventricular muscle, 975
  white cells, 69-72

cells (of organs, or regions) *See* microstructure *under specific organs/regions*

cellular oncogene, 8

cellulitis, in neck, 439-40

cementoblasts, 517

cementum, 515-16, 516(f)
  formation, 515

central alveolar hypoventilatory syndrome, 1011

central pattern generator, 574

centre
  gaze, 303, 308
  germinal, of appendix, 1143
  optokinetic, 305, 308
  ossification *See* ossification
  salivatory, 523
  subcoracoid, 796

centrioles, 4, 16(f), 42

centrosomes, 16

centrum (centra), of vertebrae
  axis, 770
  cartilaginous, 769(f), 770
  development, 768, 769(f), 770
  neural arch relationship, 770
  occipitocervical region, 770
  ossification, 768
  spinal nerves/ganglia relationship, 768

  - tethering of cord and, 772

‘cerebellar cognitive affective syndrome’, 309

cerebellum, 226, 228(f), 230, 232, 297-309
  - anterior/posterior localization, 303
  - arterial supply, 253
  - bilateral bulges, 380
  - commissure, 298, 308
  - connections, 303-5
    - afferent, 303-5
    - efferent, 307-8
  - cortex, 300-3
    - excitatory inputs (climbing and mossy fibres), 303
    - histiogenesis, 379
    - layers, 300
    - organization, 378(f), 379
  - development, 377-9, 377(f), 378(f)
    - cellular, 379
    - extroversion, 379
  - disorders, 309
  - dysfunction, 309
  - external features and relations, 298
  - extraventricular part, 379
  - fissures, 298
    - development, 378
    - fissura prima, 379
    - fissura secunda, 379
    - posterolateral, 378
    - postpyramidal, 379
    - prepyramidal, 379
  - folium, 298, 301, 305, 308
  - functional divisions, 298
  - functions, 308-9
    - anticipatory, 308-9
    - eye movement control, 664
  - hemispheres, 298, 301(f)
    - development, 379

- hilum, 298
- internal structure, 298-308
- intraventricular part, 379
- lesions, 309
    - midline, 309
- lingula, 298, 300(f)
- lobes
    - anterior, 298, 303, 304, 305, 307
    - disorders/damage, 309
    - flocculonodular, 298, 304(f), 306(f), 379
    - posterior, 298, 303, 304, 307
- magnetic resonance imaging, 299(f)
- nodule, 298, 305
- nuclei, 298, 300, 301, 303, 305, 306, 308
    - development, 378(f), 379
- peduncles, 275, 277, 278, 298-9
- peduncles *See* peduncle(s)
- pyramis, 298, 300(f), 304, 305(f)
- structural/functional localization, 303
- synaptic glomerulus, 301(f), 302
- tonsil, 298, 303
- tuber, 298, 303, 306
- uvula, 298, 300(f), 305, 307
- vallecula, 379
- venous drainage, 255
- vermis *See* vermis, of cerebellum

cerebral hemisphere, 226, 227, 228(f), 229(f), 335-59, 336(f), 356(f)
- arterial supply, 253-4, 254(f)
- association fibres, 354, 355(f)
- asymmetry, 358
- commissural fibres, 354-6, 355(f) *See also* corpus (corpora), callosum
- cortex *See* cortex, cerebral
- development, 369, 382-8, 382(f)
- gyri, 335-8
    - development, 383, 385, 388 *See also* gyrus (gyri)
- lesions, 358
- limbic lobe *See* lobe(s), limbic

lobes, 335-8
neonates, 388-9
neuropsychological functions, 358-9, 358(f)
projection fibres, 357, 357(f)
sulci, 335-8
    development, 385
    neonatal, 388-9 *See also* sulcus (sulci)
surface anatomy, 335-8
surfaces
    inferior (basal), 335, 338
        orbital, 335
        tentorial, 335
    medial, 335
        anterior, 335
        posterior, 335-6
    superolateral, 335
white matter, 354-8 *See also* cortex, cerebral

cerebrospinal fluid *See* fluid, cerebrospinal (CSF)

cerebrum, 226, 227, 233
arteries, development, 390-2
cellular development, 385(f), 386-7
cortex *See* cortex, cerebral
development, 381-8, 382(f)
ischaemia and reperfusion, 392

cerumen (ear wax), 619

cervix (uterine), 1283(f), 1285
cancer, 1292
changes at puberty, 1292
erosion, 1292
glands, 1292, 1292(f)
length, 1285
magnetic resonance imaging, 1292, 1292(f)
microstructure, 1291-2, 1291(f), 1292(f)
in pregnancy and parturition, 1285, 1299
supravaginal part, 1285

  transformation zone, 1291(f), 1292
  vaginal part, 1285

cGMP, 8, 9

chalazion, 671

chamber(s)
  anterior, 675
    development, 702
    iridocorneal angle *See* angle, iridocorneal
  aqueous, development, 702
  posterior, 675
    development, 702
  sinuatrial, formation, 1019
  utriculosaccular, 122
  vitreous, 675

channel(s)
  calcium, cardiac muscle, 142
  coelomic, 189
  hepatocardiac, 205
  lymphatic *See* lymphatic drainage (of organs, or regions)
  suprahepatic, 1220

channel proteins, 4

cheek(s), 467, 499-500
  arteries, 499
  bones, 409, 412, 420
  innervation, 499
  mucosa, 499
  muscles, 486-8

chemokines, recognition, 137

chemoreflex, upper airway, 389

chest *See* thorax

chest wall *See* thorax, wall

chiasma, optic, 239, 240(f), 242, 685

  arterial supply, 253
  development, 380, 700

chiasmata, 22, 23

chickenpox, 55, 56

childbirth trauma, 1096

children
  thymus, 948, 948(f), 949
  trachea, 1000, 1005(f) *See also* neonate

chilotic indices, 1360

chin, 486, 527

chloride ions, resorption by renal tubules, 1238

choanae, 415, 547, 549
  development, 604

cholecystokinin (CCK), 1181

cholecystokinin (CCK)-immunoreactivity, hippocampal formation, 352

cholesteatoma, 630

cholesterol, plasma membrane, 4

choline, 47

choline acetyltransferase (CAT), striatum, 328

cholinergic input, basolateral complex (amygdala), 353

cholinesterase, 982

chondrocranium, 598(f), 610-11, 611(f)
  neonate, 611

chondroectodermal dysplasia, 1014

chondrogenesis
  limb development, 902
  pharyngeal arches, 598
  skull, 611
  sphenoid bone, 530

chondroitin sulphate, 534, 1016
  metanephros, 1308

chordae
  tendineae, 966
    of mitral valve, 971, 972
    of tricuspid valve, 966-7

chordamesoderm *See* notochord

chordin, 370

chorio-amnion (amnion) *See* amnion (chorio-amnion)

chorion, 176, 177, 180
  at term, 180
  frondosum, 177(f), 180
  laevae, 177(f), 180

choroid (eye), 675, 679-80, 679(f), 690(f)
  development, 702

choroid plexus *See* plexus, choroid

chromaffin tissue, 1046, 1081 *See also* cells (named), chromaffin

chromatin, 19

chromogranins, 1200

chromosomes, 3, 19-20
  classification, 19-20
  drumstick formation, 19, 69
  non-disjunction, 23
  X, 1319
  Y, 1319
    male-determining region, 1319
    sex-determining region, 1319

chuck grip, 875

chyle, 139
  leakage, 943

chylomicrons, 1135

chylothorax, 991

chyme, storage, 1142

cilia, 3(f), 4, 16, 17-18, 17(f)
  of bronchial tree, 1034
    development, 1034
    dysfunction, 989
    functions, 1004
  nodal, 1034
  of olfactory neurones, 553
  of uterine tube, 1294

ciliary neurotrophic factor (CNTF), 370

cingulum, 354

circle
  vascular, of synovial joints, 99
  of Willis *See* circulus arteriosus (circle of Willis)
  of Zinn/Haller, 695

circuit, Papez, 347, 358

circulation
  collateral
    in inferior vena cava occlusion, 1076
    of spinal cord arteries, 1074
    superior/inferior epigastric arteries, 1056 *See also* arteries (named), collateral
  embryonic, 205-9, 205(f), 206(f)
  fetal, 176, 178, 181, 205, 1027-8, 1028(f), 1301(f)
    changes after birth, 205, 1028 *See also* ducts (or ductus), arteriosus
    persistent, 1036
    primitive, 176
  maternal, 1301(f)
  portal, 131, 950, 1220
  pulmonary, 127, 130, 131, 1030
  system, 130

circulus arteriosus (circle of Willis), 242, 249(f), 251-2

development, 390

circulus arteriosus major, 685

circulus tonsillaris, 567

circumduction, 103

cirrhosis, 950

cisterna(e) (cistern)
  chyli, 209, 940, 941(f), 942, 1077
  interpeduncular, 242
  of lamina terminalis, 239
  magna, 242, 760
  pontine, 242, 243(f)
  pontis, 284
  postchiasmatic, 242
  prechiasmatic, 242
  subarachnoid, 242, 243(f)
  terminal, 107(f), 108, 110(f), 111

citric acid (Krebs’, tricarboxylic acid) cycle, 13

classification
  arteries, 131
  bony pelvis, 1358
  chemical synapses, 44-5
  chromosomes, 19-20
  epithelium, 27-31, 27-31, 28(f)
  exocrine glands, 31, 31, 32(f)
  joints *See* joints (general)
  Lauge-Hansen, of ankle fractures, 1443-4
  muscles, 103-4, 105(f)
  nerve fibres, 53
  neurones, 41
  receptors, 57-8
  skin, 145
  skull types, 418
  spinal cord lesions, 271-3
  spinal nerves, 753-4

  synapses, 44-6
  tissues, 27, 38-9

clathrin, 12

clathrin-coated pits, 9, 12

claustrum, 325, 326, 346
  connections, 353

clavicle, 405, 792(f), 800-2
  development, 905
  fracture, 792
  ossification, 793
  sex differences, 791-2
  structure, 791
  surface anatomy, 785, 912

claw hand, 888

clearance, interocclusal, 219

cleavage (ovum), 168-71, 169(f)

cleft
  hypophysial, 321
  intratonsillar, 566, 605
  natal, 747, 1341
  para-oesophageal mesenchyme, 1214
  pharyngeal, 596, 602
    first, 652
  primary, 61
  secondary, 62
  synaptic, 44, 46, 47, 62, 63

cleidocranial dysplasia, 608, 613

clergyman's knee, 1402

clinodactyly, 906

clitoris, 1280, 1281(f)
  arteries, 1280
  development, 1325

  lymphatics, 1280
  muscles, 1281(f)
  nerves, 1280, 1280(t)
  prepuce of, 1325
  veins, 1280

clivus, 424, 431, 527

cloaca, 1205(f), 1305(f), 1307, 1308(f), 1311(f), 1322-3
  endodermal, 1212, 1311(f), 1323(f)
  male *vs* female, 1324(f)
  subdivision, 1322
    anomalies, 1322-3

club foot, 1463

coats
  cellular, 4, 5(f)
  conjoint longitudinal, 1159 *See also* tunica

cocaine, 331

coccyx, 728
  ligament attachments, 728
  muscle attachments, 728
  ossification, 728, 728(f)
  surface anatomy, 728

cochlea, 634-6, 635(f), 636(f)
  duct *See* duct(s), cochlear
  innervation, autonomic, 646
    nerves, autonomic, 646

coelom, 189
  disposition of, 185(f)
  extraembryonic, 175(f), 180, 181(f), 1209
  intraembryonic, 205, 1203, 1209, 1213, 1305(f), 1308(f)
    compartments, 189
    epithelium, 198, 198(f), 199
    formation, 185(f), 189, 1016
    heart development, 1016
    lung development, 1015(f)

    - peritoneum development, 1213
  - splanchnopleuric, 1016
  - umbilical, 1209
  - yolk sac within, 180

cognitive processes
  - cerebellum role, 309
  - Papez circuit, 347, 358

coital age, 211

colchicine, 22

colic
  - renal, 1242
  - ureteric, 1242

collagen, 5, 33(f), 34(f), 36, 37, 51, 53, 55, 59, 60, 60(f), 62
  - banding patterns, 37
  - basal lamina, 34
  - blood vessels, 137-8
  - of bone, 86
  - of cartilage, 81
  - dermal, 150, 161
  - in embryo, 194, 195
  - of lens, 686
  - mutations, 33
  - placental villi, 178
  - scleral, 675
  - type I, 37, 178, 606
    - dental pulp, 515
    - neonatal lung, 1036
    - periodontal ligament, 517
  - type II, 37, 178
    - perinotochordal sheath, 767, 768
  - type III, 34, 37
    - dental pulp, 515
    - neonatal lung, 1036
    - periodontal ligament, 517
  - type IV, 33, 1298

        neonatal lung, 1036
    type V, 37, 178
    type VI, 178
    type VII, 34
    type VIII, 33
    type XI, 37

collar
    periosteal, 93, 94(f)
    renal, 208, 1219, 1233

collaterals
    cortical projection formation via, 388
    Schaffer, 351, 352 *See also* arteries (named), collateral

colliculus (colliculi)
    of brain stem, arterial supply, 253
    deep superior, 331
    facial, 240, 241(f)
    inferior, 291, 647
    seminalis, 1259, 1317
    superior, 291-2, 305, 308, 331, 332
        afferents, 291, 308
        efferents, 305
        structure, 291
        thalamus relation, 311
        visual responses, 291

coloboma, congenital, 699

colon
    aganglionic, 1213 *See also* Hirschsprung’s disease
    arteries, 1144-5, 1146-7, 1148(f), 1149(f)
    ascending, 1138, 1138(f), 1144-6, 1212
        development, 1217
        mesentery, 1217
    at birth/neonate, 1212
    chronic dilatation, 1213
    descending, 1147, 1212
        development, 1209

        - peritoneum, 1218
    - development, 1212
    - diverticula, 1148
    - epithelium, 1161
    - flexure, left (splenic) *See* flexure, splenic
    - flexure, right (hepatic) *See* flexure, hepatic
    - functions, preterm/neonate, 1212
    - haustration, 1138, 1139(f)
    - lymphatics, 1145, 1147, 1150
    - nerves, 1146, 1147, 1150
    - peritoneum, 1144, 1146, 1147, 1218
    - radiographic appearance, 1138-9, 1139(f)
    - sigmoid, 1147-50, 1148(f), 1212
        - mesocolon of, 1147, 1218
        - volvulus, 1148
    - structure, 1138, 1139(f)
    - transverse, 1146-7, 1147(f), 1212
        - development, 1137, 1209
        - displacement in pregnancy, 1300
        - mesentery, 1102, 1104, 1107, 1217-18
        - mesocolon of, 1104-5, 1218
        - surgical mobilization, 1104
    - veins, 1145, 1146-7, 1148-9, 1148(f), 1149(f) *See also* intestine, large

colony-forming units, 75, 77

columella, 547

column(s)
- anal, 1156
- cerebral cortex, 8, 341-57
- nervous, 225-6
    - branchial motor, 225, 227(f)
    - Clarke’s, 258, 259(f), 260, 262, 263, 264(f)
    - grey, of spinal cord, 258, 259(f), 260, 265, 266, 270(f)
        - anterior (ventral), 372, 375, 376
            - development, 375
        - lateral, development, 375
        - posterior (dorsal), development, 375

- intermediate, 376
- somatic motor, 225, 227(f), 286
- somatic sensory
    - general, 225, 227(f)
    - special, 225, 227(f)
- vertebral
    - development, 763-73
    - dorsoventral patterning, 764
- visceral motor, 225, 227(f)
- visceral sensory
    - general, 225, 227(f)
    - special, 15.1, 15.3(f)20.
- white, of spinal cord, 226, 262-71
    - dorsal, 262-3

ocular dominance, 341
orientation, 341, 347
parasympathetic (visceral efferent), 275
renal, 1229, 1230(f)
somatic motor, 286
spinal *See* column(s), vertebral
vaginal, 1284
vertebral, 712-16, 712(f)
- arteries, 714, 715(f)
- bones, 710-28
- conus medullaris relationship, 375
- curvatures, 712(f), 713-14
- in elderly, 714
- function, 712
- injury, 759-60
- joints, 728-34
- length, 772
- ligaments, 728-30
    - instability, 730
    - stability, 744-5
- lymphatics, 715
- movements, 743-4
    - muscles involved, 744

- nerves, 715-16
- segments, 712
- spinal cord relationship, 375
- stability, 744-5
- structural defects, 713
- veins, 714-15, 715(f) *See also* back; *See also* spine (or spina); *See also* vertebra(e)

‘comb’ system, 329

comedone, 153

commissure(s), 227
- anteroinferior, 966, 967
- anteroseptal, 966
- of brain, 227
    - anterior, 239, 240(f), 241, 326, 356-7
        - development, 385
        - white, 749
    - cerebellar, 298, 308
    - of fornix, 385
    - hippocampal, 385
    - posterior, 239, 380, 385(f)
        - of epithalamus, 324
    - supraoptic, 385
- bulborum, 1280
- cerebral, 383
    - development, 383 *See also* corpus (corpora), callosum
- of external anal sphincter, 1159
- grey, of spinal cord
    - dorsal, 257
    - ventral, 257, 258
- habenular, 380, 385(f)
- inferoseptal, 966, 967
- labial, 467
- of larynx, 582, 583
- of mitral valve, 970
- posterior, 380

communicantes, grey/white rami *See* rami communicantes

compaction, embryo, 170

compartment(s)
- of cytoplasm, 10
- of femoral sheath, 1350, 1351(f)
- of leg, 1330-1, 1411-12
- of neck, 439
- osteofascial, of lower limb, 1329
- of thigh, 1330

complement cascade, 69

complex(es)
- amygdaloid nuclear, 325, 353
    - basal nucleus, 353, 354
    - basolateral area (nuclear group), 353
    - central nucleus, 353
    - development, 383
    - lateral nucleus, 353 *See also* amygdala
- anterior thalamic nuclear, 352
- cardinal venous, 1220(f), 1221, 1221(f)
- caudal pharyngeal, 602
- centromedial amygdaloid, 353
- crease-line
    - of hand, 657
    - of wrist, 657
- fascial
    - digital, 859(f), 860
    - palmar, 859, 859(f)
- habenular, 331
- hepatic primordial, 1220
- lacunar ligament, 1064, 1066
- lentiform (nucleus), 325, 326, 356, 357
    - arterial supply, 253
    - development, 380, 383
- mammillary, subiculum projections to, 352
- nasoethmoidal, fracture, 479-80

neuroinsular, 1190
olivary
    cerebellar fibres/connections, 305
    inferior, 279, 283, 293, 305, 308
    superior, 285
ostiomeatal, 559
perihypoglossal, 283, 663
pharyngeal, caudal, 609
septal
    hippocampal projections, 352
    medial, 352
subicular, 347, 349, 351, 352
triangular fibrocartilage (TFCC), 869(f), 871, 872, 873, 874
venous, somatic, 1220
XYZ, 770
zygomaticomaxillary, fracture, 480

computed tomography
abdominal aorta, 1074(f)
anterior abdominal wall, 1062(f)
colon
    ascending, 1144(f)
    descending, 1148(f)
heart, 973(f)
inferior vena cava, 1075(f)
kidney, 1227(f), 1229(f)
mediastinal spaces, 955(f), 957
pleural effusion, 989, 990(f)
retroperitoneal region, 1070(f)
thymus, 945

conceptus, 175(f), 176, 177, 177(f), 181(f)
development, 177(f)

concha(e)
of auricle, 618
bullosa, 550
nasal
    highest/supreme, 551

    - inferior, 474-5, 550
        - ossification, 475
    - middle, 473, 477, 478, 550-1
    - mucosa, 602
    - obstruction, 551
    - superior, 473, 478, 551
  - sphenoidal, 472, 475, 528, 529-30

condensins, 19

conduction
  - axonal, 63-4, 64(f)
  - saltatory, 64

condyles, 84, 86, 101
  - femoral
    - lateral, 1361(f), 1362-3
    - medial, 1362, 1363
    - surface anatomy, 1341(f), 1342
  - humerus, 798
  - occipital, 415, 425, 770
    - defects, 770
    - dissociated, 770
  - tibial, 1412
    - surface anatomy, 1340, 1341(f), 1412

cone(s)
  - ‘closing’, 90, 91(f), 95
  - ‘cutting’, 90, 91(f), 95
  - growth, of axon, 369-70
  - of retina *See* cells (named), cone (retinal)

congenital adrenal hyperplasia, 1219

congenital malformations *See* malformations

conjunctiva, 671-2, 672(f)
  - bulbar, 671-2
  - innervation, 672
  - limbal, 672
  - lymphatic drainage, 672

  - marginal, 671
  - orbital, 671
  - structure, 672
  - tarsal, 671
  - vascular supply, 672

connections (neural)
  - callosal, visual areas, 347
  - cerebellovestibular, 308
  - contralateral corticocortical (commissural), 402-3, 402(f), 403(f)
    - fibres, 354-6, 355(f) *See also* corpus (corpora), callosum
    - somatosensory cortex, 345
  - dendrodendritic, 42, 45
    - dendrosomatic, 41, 42
  - ipsilateral corticocortical (association), 340
    - fibres, 354, 355(f)
    - frontal eye field, 343
    - insula, 346
    - occipital lobe, 347
  - somatotopic pattern, 329
  - thalamic
    - of auditory cortex, 346
    - of extralimbic cortex, 348
    - of frontal eye field, 343
    - of insula, 346
    - of motor cortex, 342, 342(f)
    - of prefrontal cortex, 343-4
    - of premotor cortex, 343
    - of supplementary motor cortex, 343
    - of visual cortex, 347 *See also* fibre(s), nerve

connexins, 7, 977, 1020, 1022

connexons, 7

conotruncus, 1023

constriction(s), of external auditory meatus, 620

continence

- anorectal, 1085, 1160
- faecal, 1160
- urinary, 1085, 1095, 1251, 1254
  - female, 1254
  - male, 1254 *See also* incontinence

contraction, heart *See* heart

contraction, muscular
- cardiac muscle, 141-2
- concentric, 114
- eccentric, 114
- isometric, 114
- skeletal muscle, 111-12
  - range, 114
- smooth muscle, 127-8

contracture
- congenital, multiple, 903
- Dupuytren's, 860
- Volkmann's ischaemic, 840

conus, 1020

conus arteriosus, 964, 966, 983, 1020

conus elasticus, 581

conus medullaris, 257, 749
- development, 375
- lesions, 759-60

convolutions *See* gyrus (gyri)

copula (hypobranchial eminence), 604

cord(s)
- of brachial plexus, 815, 819(f)
- caudal end, 1311(f)
- epithelial (primary sex cords), 1313, 1317, 1319
- genital, 1307, 1307(f)
  - formation in females, 1321
  - formation in males, 1320

gubernacular, 1316(t)
haemopoietic, 75
hepatic, 1174-5
lacrimal, 602
medullary, lymph node, 74
nephrogenic, 1305
oblique, of forearm, 839
sex, primary, 1313, 1317, 1319
sinu-utricular, 1317
spermatic, 1064, 1065(f), 1261, 1261(f), 1321
    fascia, 1060, 1065
    muscle fasciculi (cremaster) along, 1064
spinal, 226, 227(f), 257-73, 749-50, 750(f)
    arteries, 757, 758(f)
    canal, 41, 226, 226(f), 230, 257, 275, 277, 278(f), 749
    cerebellum connections, 303-5
    changes in embryo/fetus, 375
    columns *See* column(s), nervous
    development, 364(f), 369, 374-6
        induction, 370-1
        patterning, 370-1
    enlargements, 749
    external features, 257, 749
    fissure, 749
    horns
        dorsal, 226, 227(f), 228, 257, 258(f), 259, 260, 263, 267, 268, 269, 270
        lateral, 226, 227(f), 228
        ventral, 226, 257, 258
    injury, 757, 759
    intermediate layer, 752
    internal organization, 257
    ischaemia, 757
    laminae, 375
    length, 749
    lesions, 271-3, 272(f), 273(f)
        classification, 271-3

- extradural, 271, 758
- ganglionic, 759
- intradural, 271
- intramedullary, 271
- lumbar region, development, 375
- maturation, 375
- meninges, 751-2
- neurones, 257-8
- pain, 759
- relations, 257
- split (diastematomyelia), 772
- sulci *See* sulcus (sulci)
- termination, 749
- tethering, 772
- thoracic region, development, 375
- tracts *See* tract(s)
- veins, 757, 759(f)
- vertebral column relationship, 375
- splenic, 1195
- tendinous *See* chordae, tendinae
- of testis, 1319
- umbilical, 181-2, 1028
  - anatomy, 182
  - degeneration, 181
  - development, 181, 1209
  - length and diameter, 182
  - velamentous insertion, 1303, 1303(f)
- utricular, 1317
- vocal, 583, 584(f)
  - cadaveric position, 589
  - infant, 584
  - ligaments, 583
  - microstructure, 582
  - nodules, 583
  - in speech, 590

cornea, 668, 675, 676, 678, 678(f)
- curvature, 678

  - development, 702
  - dimensions, 676, 678
  - functions, 678
  - innervation, 7
  - microscopic structure (layers), 678, 678(f)
  - reflex action, 286, 287(f)
  - thickness, 678

cornification, 145, 146, 147, 147(f), 148, 148(f), 149, 151, 152, 154, 155, 157

corns (on foot), 148

cornu (cornua, cornus), 85
  - ammonis, 386
  - coccygeal, 22(f), 42, 725, 736
  - of falciform margin, 1350
  - of hyoid bone
    - greater, 436
    - lesser, 436, 436(f)
  - of lateral ventricles, 383
  - of modiolus
    - inferior, 489
    - superior, 489
  - sacral, 725, 747
  - of thyroid cartilage, 579 *See also* hamulus; *See also* horns

corona
  - ciliaris, 680-1
  - of glans penis, 1271, 1271(f), 1273
  - radiata
    - of brain, 355, 357
    - of oocyte, 1296

corpus (corpora)
  - albicans, 1297
  - amylaceae, 42
    - rostrum, development, 386
  - bigemina, 379
  - callosum, 227, 229(f), 237, 326, 335, 354-6, 355(f), 648

        - destruction of, 359
        - development, 383, 385-6
        - dimensions, 354
        - genu, 335, 354
        - surgical division, 358
        - trunk, 355
    - cavernosum (cavernosa)
        - arteries, 1098
        - of clitoris, 1280
        - development, 1325
        - of penis, 1271-2, 1272(f), 1273(f), 1274(f)
            - vascular supply, 1273
    - luteum, 175, 1296-7, 1297(f)
    - pontobulbare, 377
    - quadrigemina, 288 *See also* colliculus (colliculi), superior
    - spongiosum, 1272(f), 1273, 1273(f), 1274(f)
        - vascular supply, 1273
    - striatum, 325
        - development, 380, 383
        - functions, 332 *See also* globus pallidus; *See also* nucleus, caudate; *See also* putamen; *See also* striatum
    - uteri, 1285

corpuscle(s)
- Hassall's, 609, 947, 947(f)
- lamellated, 101
- meconium, 1210, 1212
- Meissner's, 58(f), 59, 59(f), 150, 155, 157, 159
- Pacinian, 57, 58(f), 59, 61, 146(f), 157, 159
- red blood *See* erythrocytes
- renal, 1234, 1234(f), 1235(f)
    - cortical, 1234(f)
    - filtration apparatus, 1234(f), 1236(f)
    - juxtamedullary, 1234(f)
- of Ruffini (Ruffini endings), 59, 101
- of Vater-Pacini (Pacinian), 57, 58(f), 59, 61, 146(f), 157, 159, 1293
- white, 69-71

cortex
- auditory, 345-6, 345(f)
    - projections from amygdala, 354
- auditory association, 345
- cerebellar *See* cerebellum, cortex
- cerebral, 226, 227, 228, 229(f), 338-54
    - agranular, 340
    - areas *See* area, cortical (cerebral)
    - arterial supply, 253-4, 254(f), 390
    - of cerebrum *See* cortex, cerebral
    - columns and modules, 341
    - connectivity, 340-1, 340(f), 341(f)
        - contralateral corticocortical (commissural), 340-1, 340(f), 341(f)
        - ipsilateral corticocortical (association), 340-1, 340(f), 341(f)
        - lamination and, 341
        - patterns, 341
        - to subcortical regions, 341
    - development, 379
        - organizational models, 386
    - granular, 340
    - gyri *See* gyrus (gyri)
    - ischaemia and reperfusion, 392
    - laminar organization, 339-40
    - layers *See* lamina, of cerebral cortex
    - microstructure, 338-40, 338(f), 339(f)
    - organization
        - cell death role, 388
        - cellular, mechanisms, 386-388458387(f)
        - malformations, 388
        - modelling theories, 386
    - sulci *See* sulcus (sulci)
    - types, 340
        - agranular, 340, 342
        - frontal, 340
        - granular, 340, 346

        parietal, 340
        polar, 340
        trilaminar, 350 *See also* lobe(s); specific cerebral cortex regions (below)
    veins, 392-3, 393(f) *See also* lobe(s); *specific cerebral cortex regions (below)*
entorhinal, 348, 349, 351-2
    boundaries, 351
    connections, 351, 352
    enkephalin, 352
    layers, 352
frontal, 340, 341-4 *See also* lobe
frontal association, dorsolateral, 329
of frontal pole, 343
of hair, 151, 152(f)
infralimbic, 348
insular, 314, 354
limbic, 347-8
of lymph node, 72, 73, 73(f), 74
motor, 335
    projections to putamen, 329
occipital, 346-7 *See also* lobe(s)
orbital, projections to amygdala, 354
orbitofrontal, 344
    projections to ventral striatum, 329
orbitofrontal association, 329
of ovary, 1295-7, 1296(f)
parietal, 340, 345 *See also* lobes
perirhinal, 354
prefrontal, 343-4
    auditory cortex connections, 345
    dorsolateral, 343
    medial, 343
    ventrolateral, 343
premotor, 343
    connectivity, 343
    dorsal and ventral areas, 343

- prepiriform, 356
- presupplementary motor (preSMA), 343
- primary motor, 342
  - connectivity, 342
- primary (SI), 228
- renal, 1228-9, 1230(f), 1232, 1235(f)
- sensory, 341
- somatosensory, 342, 344
  - commissural connections, 345
  - connectivity, 341, 345
  - ipsilateral projections, 342, 345
  - primary (SI), 314, 341, 342, 345
  - projections to putamen, 329
  - second (SII), 314, 342, 345
- striate, 346
  - connectivity, 347
  - sublayers, 346
- supplementary motor (SMA), 343
- of suprarenal gland, 1197, 1199(f), 1200, 1201(f)
- temporal, 345-6
  - inferior, 345-6
  - middle, 345 *See also* lobe(s), temporal
- of temporal pole, 346
- of thymus, 947-8, 948(f)
- visual, 315, 346, 388
  - columns, 341
  - connections, 346
  - projections from amygdala, 354
  - V1, 346, 347
  - V2, V3 and V4, 346, 347
- volume, 335 *See also* area, cortical (cerebral); *See also* cerebral hemisphere

Corti, organ of *See* organ, of Corti

costal, ageing, 81

coughing, 284, 284(f)
- anatomy, 1005-6

countercurrent exchange mechanism, 1238

countercurrent multiplier mechanism, 1238

coverings, of spermatic cord, 1261

coxa valga, 1391

coxa vara, 1371

cranial capacity, 388

craniorachischisis, 772

craniorachischisis totalis, 364, 365(f)

cranioschisis, 364, 365(f)

craniosynostosis, 418, 612, 613

cranium, 414
  development, 390 *See also* skull

cranium bifidum, 613

creases
  digital, 657
  palmar, 160, 657, 657(f)
  skin, 160-1
    of fingers, 785, 857
    palmar, 160, 657, 657(f)
    of wrist, 785

crescent, cardiac, 1016, 1016(f), 1018

crest (or crista(e)), 85, 85(f)
  alveolar, 500, 517(f), 543
  ampullary, 638, 638(f)
  basilaris, 640
  conchal, 474, 476, 477(f), 478, 478(f)
  ethmoidal, 473(f), 477, 477(f), 478
  frontal, 423, 471
  galli, 410(f), 423, 426, 428, 472, 472(f), 473(f), 668
  iliac, 1340, 1355
    borders, 1355

- infratemporal, 415, 529
- interosseous, of ulna, 843
- intertrochanteric, 1361
- interureteric, 1247
- jugal, 476
- lacrimal, 409, 474(f), 475, 476
  - anterior, 404
  - posterior, 655
- of maxilla, 476
- nasal, 475, 477, 478
  - of maxilla, 475
  - of palatine bone, 478
- neglecta, 643
- neural *See* neural crest
- obturator, 1354, 1355
- occipital
  - external median, 416, 713, 739
  - internal, median, 425, 426
- palatine, 415, 478
- pubic, 1354, 1355
- radial, 840
- rib, 919
- sacral, 725
- sphenoidal, 528, 529
- of spine, of scapula, 795, 809
- supinator, 844
- supramastoid, 412, 420, 615, 626
- supraventricular, 964, 965(f), 966, 983, 1025
- temporal, 532
- terminalis, 964
- urethral, 1250, 1251, 1252(f), 1253, 1254
- vestibular, 633, 633(f)
- vomerovaginal, 475

cristae, 13
- terminalis, 1019

cross-bridge cycling, 111, 112, 113

crossed acoustic response, 620

crossed renal ectopic kidneys, 1226, 1226(f)

crown, of teeth, 513, 513(f), 514, 517
    dentine, 514
    peg-shaped, 509, 513

crow's feet, 486

crus (crura)
    ampullaris, 637
    of antihelix, 618
    cerebri, 288(f), 289, 332, 357
        arterial supply, 253
    of clitoris, 1280
    commune, 634, 637
    dextrum, 977
    of diaphragm, 1007, 1008(f), 1010
        apertures in, 1007-9
        external oesophageal sphincter function, 953
        left, 1007
        right, 1007, 1012
        in vomiting, 953
    of fornix, 355
    of helix, 618
    nasal, 547, 551
    of penis, 1097, 1271
    sinistrum, 977
    of stapes, 627
    of superficial inguinal ring, 1065

crutch palsy, 829

crux, of heart, 962, 963, 964, 968

crypt(s)
    anal, 1156
    intestinal, 1131, 1134, 1134(f), 1161, 1161(f)
    of Lieberkühn, 1131, 1134, 1134(f)
    of palatine tonsil, 566, 567

small intestine development, 1210
tonsillar, 605

cryptorchidism, 1319

cryptotia, 618

crystallins, lens, 687, 701

crystals, of Reinke, 1267

CT *See* computed tomography

cuboid bone, 1438

Cullen’s sign, 1100, 1188

culmen, 298, 305(f)

cuneiform bones, 1349(f), 1438-9
innervation, 1438, 1439
intermediate, 1438-9
lateral, 1439
medial, 1438, 1439(f)
surface anatomy, 1341
muscle attachments, 1438, 1439
ossification, 1438, 1439
vascular supply, 1438, 1439

cuneus, 336, 336(f), 346

cup, optic, 681, 699
development, 699, 701

cupula (cupola; cupolae)
of cochlea, 633(f), 634
of diaphragm, 1007
of semicircular canal, 638

curtain, subaortic, 969, 971(f), 972

curvatures
of rectum, 1150, 1154
of spine, 713-14
adult, 714

        cervical, 714
        embryonic, 713-14
        fetal, 713-14
        lateral, 745, 768
        lumbar, 714
        movement, 744
        neonatal, 714
        pelvic, 714
        sacral, 714
        sagittal, 714
        thoracic, 714 *See also* kyphosis; *See also* lordosis
    of stomach, development, 1216

cushion(s)
    anal, 1156, 1157
        enlargement, 1157
    atrioventricular, 1023
        inferior, 1019, 1023
    endocardial, 1016-17, 1022
        atrioventricular, 1030
        conotruncal, 1023

cusp(s)
    of aortic valve, 972
    of mitral valve, 970-2
    of pulmonary valve, 967
    of teeth, 509, 513, 513(f)
        bicuspid, 510
        of Carabelli, 510, 513
        molars, 510
            deciduous, 510
    of tricuspid valve, 966

cusplet, of Carabelli, 510

cuticle
    of hair, 151, 152(f)
    of nail, 155, 159
    of teeth (enamel) *See* enamel (teeth)

Cx40 protein, 1020

cycle
  bile acids/salts, 1212
  cardiac, 975
  hair growth, 152-3
  menstrual, 1297-9, 1298(f)
    breast changes, 935-6
    endometrial changes, 1291
    menstrual phase, 1298-9
    proliferative phase, 1297
    secretory phase, 1297-8, 1297(f)
    vaginal changes, 1284
    vascular changes, 1299
  nasal, 555-6
  spermatogenic, 1267
  uterine *See* cycle, menstrual

cyclin-dependent protein kinases, 20

cymba conchae, 618, 626

cyst(s)
  auricular, 619
  branchial, 441
  bronchogenic, 1037
  carinal, 1037
  cervical, lateral, 602
  dental, 517
  epididymal, 1267
  Gartner’s, 1284
  hilar, 1037
  pancreatic pseudocysts, 1187-8
  para-oesophageal, 1037
  para-tracheal, right, 1037
  para-vertebral, 1037
  pericardial, 1037
  protoepithelial, primitive, 170
  renal, 1312

  retention, sublingual gland, 521
  retrosternal, 1037
  sebaceous, 467
  thymus, 949

cytitis cystica, 1250

cytokines, 35, 36, 71, 75, 77, 78, 79

cytokinesis, 21(f)

cytoplasm, 3-4, 10-18

cytoskeleton, 4, 10, 14(f)

cytosol, 3(f), 4
  organelles, 14-17

cytotactin (tenascin), 36, 38

cytotrophoblast, 172, 173(f), 175, 176, 177, 177(f), 179

D

dandruff, 148

De Quervain’s tenovaginitis, 879-80

dead tract, dentine, 514

deafness, 648-9

death
  brain stem, 275, 295
  cellular, 27
  perinatal, 1299

decidua
  basalis, 176, 177, 178
  capsularis, 176, 177
  maternal, 176, 179, 181
  parietalis, 176, 177, 180 *See also* endometrium

decidualization, 175-6, 1297

decorin, 86, 87

decussation
  lemniscal, 279, 292
  pyramidal, 268, 268(f), 270(f), 276(f), 277, 278(f), 280
  superior cerebellar peduncles, 289

defecation, 1160

deformation, 119, 119(f)

deformity
  Boutonnièrre, 878
  nose, 547
  Satiro’s, 618-19
  Sprengel’s, 608
  Stahl’s, 618-19
  swan neck, 878

degeneration

dental follicles, 510
dopaminergic neurone, 332
substantia nigra pars compacta, 332
transneuronal, 370
umbilical cord, 181

deglutition *See* swallowing

dehiscence, of Killian, 572

Delta-Notch signalling, 24

dementia, semantic, 358

dendrite(s), 41, 42-3, 43(f), 225, 226(f), 370
- of Golgi neurones, 302
- growth/development, 370
- of Purkinje cells, 302
- of pyramidal cells, 338
  - formation, 386
- spiny, 328
- tree structure, 43(f)

denervation, sympathetic, of lower limb, 1093

dens, of axis, 718(f), 719, 770
- abnormalities, 721
- fusion abnormalities, 770
- ossification, 721
- size reduction, 770

dentine, 514, 517
- components, 514
- formation, 514
- intertubular, 514
- mantle, 514
- peritubular, 514
- primary, 514
- secondary, 514
- spindles, 514, 515(f)
- tertiary, 514, 515(f)

deoxyribonucleic acid *See* DNA

derangement, internal, of temporomandibular joint, 537

dermal bones, 611

dermatomes, 157, 231, 231(f)
  of back, 707-8, 708(f)
  of face, 405
  of lower limb, 1346, 1346(f)
  of perineum, 1346(f)
  of upper limb, 789, 789(f)

dermis, 147(f), 150-1, 154(f)
  cells of, 150-1
  development, 157-8
  embryonic, 158(f), 159
  layers of, 150-1
  of nail bed, 155

dermomyotomes, 766(f), 772, 832(f)
  development, 772

descendens hypoglossi, 456, 460

descent
  of ovary, 1321-2, 1321(f)
  of testis *See* testis (testes)

desmin, 7, 106, 115, 127, 137, 138, 1051

desmocollin, 7

desmocranium, 612(f)

desmoglein, 7

desmoplakin, 7

desmosomes, 3(f), 6(f), 7
  in skin, 146, 147, 149(f), 150, 153, 154, 157, 163

desquamation, 148

detumescence, 1274

development *See* embryo; *See also* neural crest; *specific organs/regions*

deviation
  nasal septum, 551
  radial and ulnar, 871

dextrocardia, 974

diabetes mellitus
  femoral nerve lesion, 1383
  third nerve palsy, 252

diabetic amyotrophy, 1383

diacylglycerol, 8

diakinesis, 22

dialysis, peritoneal, 1110

diaphragm, 910, 963
  pelvic, fascia, 1086
  role in speech, 590
  thoracic, 1007-12
    anterior, defect, 1009
    apertures, 910, 1007-9, 1008(f)
      aortic, 1007, 1008(f)
      defects, 1009
      oesophageal, 1007-8
      vena caval, 1008
    arteries, 1009-10, 1056
    atrophy, 1012
    attachments and components, 1007, 1008(f)
    in breathing, 1012
    central tendon, 1007, 1008(f)
      in breathing, 1012
      folia, 1007
      relationship to phrenic nerve, 1010
    costal part, 1007
    crus *See* crus (crura), of diaphragm
    depression, 1007
    development, 1014-15, 1015(f), 1217

        domes (cupolae), 1007, 1012
        electrical stimulation, 1011
        eventration, 1015
        hernia, 181, 1015, 1034
        incisions, radial, 1010
        inferior surface, 1008, 1008(f)
        level affected by posture, 1012
        lumbar part, 1007
        lung position/length, 993
        lymphatics, 928
        movements, 926, 1012
            paradoxical, 1011, 1012
        neonatal, 1015-16, 1218
        nerves, 1010-11
        paralysis, 1012
            unilateral, 1007
        posterior, defect, 1009
        rupture/laceration, 1009
        shape and relationships, 910
        sternal part, 1007
        surface anatomy, 910
        trauma, 1009
        veins, 1010
    thoracoabdominal interface, 1041
    urogenital, inferior fascia, 1094

diaphragma sellae, 424, 426, 527

diarthroses *See* joints (general), classification, synovial

diastema, 500

diastematomyelia, 772

diastole, CSF movement, 243

diencephalon, 226, 227, 228(f), 311-24, 368(f), 372(f)
    arterial supply, 253
    caudal, 602, 611
    connections, 330(f)

development, 362(f), 380, 595
    telencephalon wall fusion, 383
dorsal and ventral parts, 380

Dieu la Foy lesions, 1268

digits
of foot *See* hallux; *See also* toes
of hand
    anomalies in number, 902, 906
    development, 905
supernumerary, development, 902 *See also* finger(s); *See also* thumb

5α-dihydrotestosterone, 1325

diploë, 95

diplopia, 656

diplosomes, 16

diplotene, 22

disc(s)
articular
    of acromioclavicular joint, 803
    of distal radio-ulnar joint, 868, 868(f)
    of sternoclavicular joint, 801
    of synovial joints, 101
    of temporomandibular joint, 533, 534-5, 535(f)
        functions of, 534-5
        position changes during movement, 536
    of wrist joint, 870
embryonic, 197
    bilaminar, 173, 183
    trilaminar, 186
epiphysial, 96
intercalated, 139, 140(f), 141, 141(f)
interpubic, 1365
intervertebral, 81, 83, 84(f), 118, 119, 121, 124, 730-3
    development, 766(f), 768, 769(f)
    levels, segmental, 768

        - load-bearing capacity, 744
        - lumbar, 771
        - mechanical properties of, 121, 122(f)
        - movement, 743
        - prolapse, 731-2, 732(f)
        - relations, 731
        - structure, 730
        - water loss, 744
    - optic, 695
        - development, 700
        - oedema, 695
    - perichordal, 768
    - temporary, occipitocervical junction, 770
    - Z (Zwischenscheiben), 106

disease(s)
    - Alzheimer’s, 358
    - autosomal dominant polycystic kidney, 1312
    - Becker muscular dystrophy, 107
    - Charcot-Marie-Tooth, 1450, 1453
    - coronary artery, 978
    - diverticular, 1148
    - Duchenne muscular dystrophy, 107, 114
    - Dupuytren’s, 860
    - Graves’, 658
    - haemolytic, of newborn, 68
    - Hirschsprung’s, 374, 1213
        - ultrashort segment, 1213
    - Huntington’s, 332
    - infantile cystic renal, 1312
    - inflammatory, of vertebrae, 744
    - Köhler’s, 1438

disease, Ménière’s, 649

disease(s)
    - Muller-Weiss, 1438
    - Osgood-Schlatter, 1415
    - Parkinson’s, 193, 253, 289, 290, 313, 314, 326, 332

        - medical therapy, 332-4
        - neurosurgery, 333
        - pathophysiology, 332, 333(f)
    - Peyronie’s, 1276
    - sickle-cell, 68
    - venous, of leg, 1426
    - vestibular, 663
    - Wartenberg’s, 855
    - ‘wearing-off’ and ‘wearing-on’ phenomenon, 333

DISH (diffuse idiopathic skeletal hyperostosis), 744

dislocations
    - elbow, 786
    - elbow joint, 835
    - glenohumeral joint, 807
    - shoulder, 786

disomy, uniparental, 167

diverticular disease, 1148

diverticulum (diverticula)
    - allantoenteric, 180
    - duodenal, 1126
    - hepatic, 1206, 1207, 1208
        - biliary duct development, 1208
    - hypopharyngeal, 572
    - lateral, of prosencephalon, 380
    - Meckel’s (ileal), 1129, 1209
    - median, 608
    - respiratory, 1032, 1033, 1205, 1212
    - ventral
        - foregut, 1212
        - hindgut, 1212 *See also* allantois

division
    - cleavage, 168-71, 169(f)
    - embryo, cell populations, 193-4

DNA, 19

  synthesis, 20

dome
  of acetabulum, 1352
  cervical pleura, 406
  glial, 63
  of liver, 1163, 1164, 1164(f)
    cardiac, 1163
  nasal, 548

dominance (of cardiac blood supply)
  balanced, 980
  left, 980
  right, 980

dopamine, 47
  actions, 332, 333(f)
  cell groups, 329, 329(f), 331, 332
  cells secreting, development, 374
  D2 receptors, 303
    striatum, 328
  D3 receptors, 303
  deficit, Parkinson’s disease, 332
  nucleus accumbens innervation and, 331
  pathways
    mesolimbic, 331, 332
    mesostriatal, 329, 332
  renal, 1310 *See also* neurone, dopaminergic

dorsiflexion, 103

dorsum
  nasi, 547, 549
  sellae, 420, 424, 426, 527, 530
  of tongue, 503, 503(f), 507-9

dowager’s hump, 714

drugs, of abuse, 331

drum, ear *See* membrane (membrana), tympanic

drüsen, 680

Duchenne muscular dystrophy, 107, 114

duct(s) (or ductus)
- aberrans, 1269, 1307
- allantoic, 180, 181, 182, 1316(t)
- of apocrine gland, 153
- arteriosus, 601, 984, 1023, 1028-30, 1030(f)
  - closure, 602, 1029-30
    - stages, 1029-30
  - development, 1028
  - dimensions, 1028
  - fetal circulation, 1028-9
  - neonate, 1028
  - patent, 974
    - persistent, 1028, 1032
  - recurrent laryngeal nerve relation, 1028
  - reopening, 1036
  - tunica media, 1028
- Bartholin’s, 521
- bile (biliary), 1177(f), 1185
  - arteries, 1180
  - atresia, 1208
  - common, 1178, 1178(f)
  - development, 1206, 1207
  - extrahepatic
    - atresia, 1208
    - development, 1208-9
  - hepatic, 1178
  - innervation, 1180-1
  - lymphatics, 1180
  - microstructure, 1181
  - referred pain, 1181
  - sphincter, 1178
  - variations, 1178(f)
  - veins, 1180
- of bulbourethral gland, 1270

cochlear, 634, 639-40
    development, 652
collecting
    of kidney, 1235, 1236(f), 1237
        development, 1308
        microstructure, 1238
    of salivary glands, 522
of Cuvier *See* veins or venae (named), cardinal, common
cystic, 1177, 1178
    development, 1207
    lymphatics, 1180
    variations, 1178, 1178(f)
deferens *See* vas (vasa), deferens
ejaculatory, 1269, 1317
    microstructure, 1269
endolymphatic, 617, 633, 636, 639
    development, 652
of epididymis, 1268
excretory, primary, 1305, 1306(f), 1307
extralobar, salivary gland, 522
frontonasal, 473, 479
fusion, 1316(f)
of Gartner, 1284, 1313, 1315(f), 1316(t), 1322(f)
genital, 1312, 1313
hepatic
    accessory, 1178
    arteries, 1180
    common, 1178
    development, 1208
    left, 1166
    lymphatics, 1180
    veins, 1180
intercalated, salivary gland, 522, 523(f)
intestino-vitelline, 1129
intrahepatic, development, 1208
lacrimal, 671, 672, 674
lactiferous, 933

  development, 933, 934
  obstruction, 933
lymphatic, 139
  right, 449, 451, 454, 455, 455(f), 941, 941(f), 942
mesonephric, 1307, 1309(f), 1310, 1313, 1316(f)
  ambisexual stage of development, 1315(f), 1318(f)
  fate in males/females, 1318(f)
  involution, 1313, 1315(f)
  male reproductive ducts, 1317
  male *vs* female, 1316(t) *See also* ureter
Müllerian *See* duct(s), paramesonephric (Müllerian)
nasolacrimal, 476, 547(f), 672, 674, 703
pancreatic, 1185-6, 1189
  accessory, 1185, 1248, 1249(f)
  development, 1205(f), 1206, 1207, 1207(f)
  dorsal, 1207
  variations, 1185-6
para-urethral, 1253
paramesonephric (Müllerian), 1267, 1285, 1312, 1313, 1315(f), 1318(f)
  atrophy in male, 1317
  development, 1313
  failure of fusion, 1316, 1317, 1319
  fusion, 1316, 1317(f)
  male *vs* female, 1316(f)
parotid, 405, 496, 497, 499, 523(f), 605
  accessory, 496, 497
  sialogram, 497
perilymphatic, 617
pharyngobranchial, 609
prostatic, 1259
reproductive, male, 1317
reproductive, development, 1313-17, 1318(f)
  female, 1313-17, 1318(f)
  male, 1315(f), 1317, 1318(f)
reuniens, 636, 637, 640
  development, 652
saccular, 652

salivary glands, 522-3
    minor, 502
    striated, 522, 523
    sublingual, 502(f), 521
    submandibular, 501, 521, 598(f), 605
sebaceous, 151, 152
semicircular, 638
    development, 651(f)
striated, salivary gland, 522, 523
sublingual, 501, 502(f), 521
submandibular, 501, 502(f), 605
submucosal glands, 1135
sweat
    intradermal, 154
    intraepidermal, 154
sweat gland, 154, 154(f)
thoracic, 139, 941(f), 942-4, 985
    abdominal confluence of lymph trunks, 1077
    abdominal origin, 1077
    anomalies, 943
    arch, 942
    bifurcation, 942
    dimensions, 942
    injury, 978
        during oesophageal surgery, 943-4
    length, 942
    ligation, 943
    microstructure, 942
    relations, 942
    rupture, 943
    termination and patterns, 942
    tributaries, 943
thyroglossal, 462, 608
tubular, formation, 195
ureteric, 1308
utriculosaccular, 636, 637, 652
venosus, 1220, 1222

        - depth of groove for, 1216
    - vitellointestinal, 1209
        - obliteration, 1209
            - failure, 1209
    - Wolffian, 1316(t) *See also* duct(s), mesonephric
    - yolk, 182

ductules
- aberrant, 1269, 1307
- efferent, of testes, 1268
- interlobular, of pancreas, 1207
- mesonephric tubules persisting as, 1307

duodenum, 1125-8, 1125(f)
- arteries, 1127-8, 1186
- atresia, 1206
- development, 1203, 1206, 1210, 1216
    - intervitelline anastomoses, 1220
- diverticula, 1126
- ligaments, 1127
- loop, 1217
    - position/configuration, 1210
- lymphatics, 1128
- nerves, 1128, 1173
- papillae, 1126, 1127(f), 1185
- peritoneum over, 1099
- referred pain, 1128
- relations, 1125-7
- retroperitoneal (sessile), 1206, 1217
- stenosis, 1209
- surface anatomy, 1053
- suspensory muscle, 1127
- veins, 1128

Dupuytren’s disease(s), 860

dura mater
- cranial, 425-33
    - arterial supply, 431-3

        - cranial nerve sheaths, 426
        - head injury, 426
        - innervation, 433
        - partitions of, 426-7
        - venous plexus, 392-3
        - venous sinuses, 427-31
    - development, 390
    - spinal, 751-2

dwarfism, 96
    - thanatrophic, 1014

dyads, 140(f), 141

dynamin, 16

dyneins, 16, 17, 17(f)

dynorphin, 48
    - dentate gyrus, 352
    - globus pallidus, 331
    - striatum, 328

dysarthria, ‘cerebellar’, 309

dysdiadochokinesia, 309

dyskinesia, 230, 326
    - levodopa-induced, 332, 333
    - pathophysiology, 332

dysphagia, 953
    - lusoria, 1032

dysplasia, ectodermal, 159

dyspnoea, posture affecting, 1012

dystonia, 332
    - pallidal stimulation for, 333-4, 334(f)

dystrophin, 107

E

E-cadherin, 170, 1308

ear, 615-31
- development, 615-17 *See also* auricle; *See also* meatus, acoustic
- external, 618-20
  - development, 652-3
- inner, 633-50
  - arteries, 642
  - bone, 633-6
  - development, 634
  - fluids, 634-6
  - function, 633
  - nerves, 642-9
  - veins, 642 *See also* meatus, acoustic, internal
- middle, 623-30
  - development, 652 *See also* cavity (cavities), tympanic
- surgery *See* surgical procedures and approaches, ear surgery

ear wax, 619

echocardiography, 969, 973, 973(f), 978

ectocervix, 1284, 1292

ectoderm
- dysplasia, 159
- embryonic, 186
- epithelium derived from, 1324
- neural, 198, 361
- pharyngeal, 602
- surface, 157, 186, 198
  - eye development, 699

ectoderm/endoderm zone, 1324

ectomeninx, 612

ectomesenchyme, 534, 534(f) *See also* neural crest

ectopia (ectopic organs)

cloacae, 1322
  cordis, 974
  kidney, 1226, 1226(f)
  sebaceous glands, 499
  thymus, 946
  ureter, 1240

ectopic pregnancy, 172, 175

ectropion, 669

effusion, pleural, 989, 990(f), 993

eight-cell stage, 171, 171(f)

Eisenmenger complex, 1031

ejaculation, 1274-5

elastin, 1035, 1111
  in blood vessels, 137-8
  dermal, 151, 154, 159
  in extracellular matrix, 36(f), 37

elderly, lung appearance, 992

electrocardiography, 977(f), 978, 1022

electrodes, deep-brain, implantation, 333, 333(f), 334(f)

electrolyte transport, epithelial cells, 522, 522(f)

electromyography (EMG), 114

electron transport (cytochrome) pathway, 13

elements
  costal, 717, 718, 723, 724, 725, 727
  skeletal, limb development, 902-3

elevation, tubal, 563, 564

elliptocytosis, 67

embolism
  pulmonary, 997
    prevention by inferior vena caval filters, 1076

embolization, pulmonary, 997

embryo
  caudal end, 1311(f)
  cell populations, 197-203
    at organogenesis, 197-203
    determination, 193
    differentiation, 193
    division, 193-4
    epithelial, 1203(f), 1306(f)
    epithelial-mesenchyme transitions, 194
    induction, 193
  cell-tissue signalling, 194
  chimeric, 195
  circulation, 205-9, 205(f), 206(f)
  cranial nerves, 372-3
  definition, 170
  developmental stages, 168(f), 169(f), 211, 212(f)
    head, 595(f)
    internal, 211
  digestive tube, 1203, 1203(f), 1204(f), 1205(f), 1209 *See also* foregut; *See also* hindgut; *See also* midgut
  eye development, 699, 700(f), 701(f)
  facial development, 603(f)
  folding, 186-9, 187(f), 188(f)
    head, 187(f), 189
    tail, 187(f), 189
  formation, 175(f), 176
  frozen, 168
  head, 595(f)
    arterial supply, 600(f)
  heart, 205, 964, 1013, *1013*
    cardiac output, 206
  hiccups, 604
  horizons, 211
  implantation, 172, 175-6
  lungs, 1013
  lymph nodes, 209

lymphatic vessels, 205, 209
mandible, 532(f)
mesenteron, 197
metenteron, 197
movements, 903
mucoid tissue, 38-9
occipitocervical junction, 769
oesophagus, 1203
ovary, 1294
paramesonephric (Müllerian) ducts, 1313
peritoneal cavity, 1013, 1013(f)
pharyngeal arches, 596-602, 597(f)
pharyngula stage, 597
pharynx, 596-602, 597(f)
pneumatoenteric recess, 1214, 1215(f)
preimplantation, 168-72, 175
proenteron, 197
pronuclei, 167
sex determination, 1319-20
somite formation, 764, 764(f) *See also* somites
staging, 167, 168(f), 169(f), 170, 764
    stage, 10, 197, 198, 199
stomach, 1204, 1206
tenascin, 38
testing, 168
thorax, 1013, 1013(f)
urinary system, 1305, 1306(f)
vertebral curvatures, 713-14

embryogenesis
axes specification, 197
    body-plan stage, 197
embryo folding, 186-9, 187(f), 188(f)
experimental approaches, 195
extraembryonic tissue formation, 173-4, 175, 176
intraembryonic coelom formation, 189
intraembryonic tissue formation, 183-6
morphogenesis, 194-5

pattern formation, 194-5
  preimplantation development, 168-72, 175
  protein synthesis, 170 *See also* embryo

eminence
  arcuate, 424, 617, 633, 649
  articular (tubercle), 412, 416, 533, 615
  canine, 404, 476, 510
  caudal, 184
  collateral, 238
  conchae, 619, 620
  hypobranchial (hypopharyngeal), 604, 610
  hypothenar, 787, 857
  medial, 240
  parietal (tuber), 412, 469
  pyramidal, 625, 628, 629
  scaphae, 619, 620
  thenar, 787 *See also* tuber; *See also* tubercle

emission of seminal fluid, 1274-5

emmetropia, 681, 687

emotional behaviour
  amygdala role, 353
  disturbances, 347

emphysema, 1007
  congenital lobar, 1037

empyema, 991

enamel (teeth), 513-14
  components, 513-14
  incremental lines, 513(f), 514
  prismless, 514
  prisms, 514, 515(f)
  spindles, 514
  striae, 513(f), 514, 515(f)
  striation, 514, 515(f)
  thickness, 514

enamelins, 514

encephalon *See* brain

end plate, motor, 110, 111

endings, nerve *See* nerves (general), endings

endocardium, 966, 974
  development, 1016, 1017

endocytosis, 3, 4, 9

endoderm, 199
  derived from ectoderm, 1324
  embryonic, 184-5
    hepatic, 1207, 1208(f)
    prostate gland, development, 1323-4
    small intestine, 1210
  of gut, 1205(f)
  pharyngeal, 602-3, 603(f), 609(f)
  urethra, development, 1323

endolymph, 634-6, 640, 643, 646

endometrium, 175, 1291
  magnetic resonance imaging, 1292, 1292(f)
  menstrual cycle, 1291, 1297, 1299
  ultrasound, 1298, *1298* *See also* decidua

endomysium, 86, 107(f), 108, 109, 121, 974

endoneurium, 52(f), 53

endoplasmic reticulum, 10(f)
  muscular *See* sarcoplasmic reticulum
  rough, 3(f), 4, 10, 11(f)
  smooth, 3(f), 4, 10(f)

endoreduplication, 24

β-**endorphin**, 48

endosomes, 12
  late, 12

endosteum, 86, 90-1

endothelin, 1036

endothelium, 4, 135-7, 136(f)
  of blood vessels, 135-7, 136(f)
  of cornea, 69
  development, 1207
  fenestrated, 133
  glomerular, 1235
  leukocyte interactions, 136-7
  of lymph vessels, 139, 139(f)
  markers, 1017
  secretions, 137

endotracheal intubation, neonate, 1033

energy, 119

enkephalins, 48, 1200
  entorhinal cortex, 352
  striatum, 328

enlargement
  of anal cushions, 1157
  fusiform, of ureter, 1310
  gangliform, 52, 59
  of pericardioperitoneal canal, 1213, 1214
  pseudoganglion, 52
  of spinal cord, 749
    cervical, 749
    lumbar, 749
  splenic, 1192, 1198
  ventricles of brain, 244

enophthalmos, 656

entactin, 33, 38

entropion, 669

envelope
  of motion, 537

syncytiotrophoblastic, 176

enzymes
distal renal tubules, 1237
lysosomal, 12*see also individual enzymes*

eosinophilia, 69

ependyma
cells, 41, 51, 51(f), 239(f), 240, 240(f)
of spinal cord, 257, 374

epiblast, 172-3, 175, 180, 181, 183-4, 183(f), 1317

epicanthus, 670

epicardium, 959, 1026
development, 1016, 1026

epicondyle, 85
femoral, 1360(f), 1361(f), 1363
humeral, 778, 786, 796, 799-800

epicondylitis
lateral, 848
medial, 845

epidermal growth factor, 8

epidermis, 145-8, 146(f), 147(f)
abnormalities, 159
cells of, 145-8
development, 157-8
interfollicular, 145, 146(f), 151, 152, 153, 157-8
layers of, 145
of lips, 467
of nail bed, 155
regeneration, 145-8 *See also* skin

epidermolysis bullosa simplex, 15

epididymis, 1263(f), 1268
canal, 1317
development, 1317

  epithelium, 1268
  microstructure, 1268

epigastrium, 1053

epiglottis, 503(f), 577-8, 605
  fetal, taste buds, 508
  functions, 578
  infant, 584
  neonatal, 574
  in neonate, 606(f), 607

epilepsy, split-brain syndrome, 358-9

epimyocardium, 1016

epimysium, 86, 108, 121

epinephrine *See* adrenaline

epineurium, 53

epiphora, 669

epiphyses
  anular, of vertebrae, 768
  odontoid, dissociated apical, 770
  ‘ring’, 768*see also specific bones*

epiphysis cerebri *See* gland(s), pineal

epipteric bones, 418

episiotomy, 1096

epispadias, 1323

epithalamus, 226, 311, 323-4
  development, 380, 385(f)

epithelial transition, 194
  somites, 195

epithelium, 4, 27-31
  alveolar, 998, 1000(f), 1005
  amnion, 180-1

Barrett’s, 1114
characteristics, 27
ciliary, 681
ciliated, 28
classification, 27-31, 28(f)
coelomic, 199
    gonad development, 1312, 1318(f)
    intraembryonic, 1203
    somatopleuric, 189, 1014, 1213
    splanchnopleuric, 189, 1016, 1018, 1034, 1203, 1206, 1212
    spleen development, 1218
    suprarenal gland development, 1218
of colon, 5(f)
columnar
    cells *See* cells (named), columnar
    simple (unilaminar), 28, 29(f)
    stratified (multilaminar), 29-31
corneal, 678
development, 27
embryonic, 189-90, 1203(f), 1306(f)
    body-plan stage, 197
endodermal, of gut in embryo, 1205(f)
of endometrium, 1291
of epididymis, 1268
follicle-associated, 74
function, 27
germinal, 190, 191, 1295
hepatic, 1207
of iris, 682
keratinized, 29-30
lamella of, penis development, 1325
of lens, 686, 686(f)
of lips, 467
mesenchymal interactions *See* mesenchyme
mucous, 28
multilaminar *See* epithelium, stratified
non-keratinized, 30

of oesophagus, 951-2, 952(f), 1113
    functions, 951-2
olfactory, 551, 552, 552(f)
orthokeratinized, 30
parakeratinized, 30
pseudostratified, 28, 29(f)
    cerebral hemisphere wall, 386
regeneration, in oesophagus, 952
of renal tubules, 1234, 1236(f)
respiratory, 28, 551, 1005
reticulated, 567
retinal pigment, 688, 689, 689(f)
    development, 700
seminiferous, 27, 28(f), 31
sensory, 28
simple (unilaminar), 27-9
    columnar, 28, 29(f)
    cuboidal, 28, 29(f)
    squamous, 27-8, 29(f)
small intestinal, 1210
somatopleuric, 189, 1213
splanchnopleuric coelomic, 189, 1016, 1203, 1206, 1212, 1213
of stomach, 1120, 1121(f)
stratified (multilaminar), 29-31
    columnar, 30, 30(f)
    cuboidal, 30, 30(f)
stratified, squamous, 29-31
    oral mucosa, 500
    of tongue, 507
of thymus, 947, 947(f)
transitional *See* urothelium
unilaminar *See* epithelium, simple
urinary *See* urothelium
of uterine tube, 1294
vaginal, 1281, 1316 *See also* cells (named), epithelial

epithelium/mesenchymal interactions (transition) *See* **mesenchyme**

eponychium, 155, 155(f), 159

epoophoron, 1285, 1315(f), 1316(t), 1318(f)
  tubules, 1307

Erb-Duchenne paralysis, 822

erection, 1274-5
  dysfunction, 1276

ergonomics, 745

eruption, of teeth *See* teeth, eruption

erythrocytes, 67-9, 68(f), 70(f), 77
  antigens, 68
  deformation, 67
  fetal, 67
  life span, 68
  plasma membrane, 67
  production, 77
  red cell ghosts, 67
  removal, in spleen, 1195

erythropoiesis, 77

erythropoietin, 77
  secretion by kidney, 1225

ethmoid bone, 411, 415, 417, 420, 423, 472-4, 528
  cribriform plate, 423, 471, 472, 527, 611
  ethmoidal labyrinths, 472-3
  in nasal cavity, 550
  orbital plate, 471, 472, 474, 558
  ossification, 473-4

eventration, 1009
  of diaphragm, 1015

examination
  laryngeal, 584, 584(f)
  lower limb, 1340(t), 1346

excitation-contraction coupling, 111, 141-2

  - electromechanical, 130
  - hormonal influence, 142
  - pharmacomechanical, 130
  - regulation, 130

executive functions, 358

exocytosis, 3, 4, 9

exomphalos, 181, 182, 1209
  - giant, 1014

exophthalmos, 658

expansion, extensor, 880, 882(f)

expiration *See* breathing

extension, joints, 103, 103(f)

exteroception, nerve fibres, 263, 264

extracorporeal shock wave lithotripsy, 1242

extroversion, cerebellum, 378

eye and eyeball, 675-97
  - absence of (anophthalmia), 699
  - development, 699-703
    - functional components, 699-703
  - embryonic components, 699
  - fibrous tissue layer
    - cornea *See* cornea
    - sclera, 675-6, 702
  - movements, 660-5, 661(f), 662(f)
    - control of, 664(f)
    - gaze shift/stabilization, 661, 663
    - pursuit, 663, 664
    - saccades, 661, 663, 664
  - muscles of, extraocular, 482-6, 655, 658-65, 659(f), 662(f), 663(f)
  - neural layer *See* retina
  - optic disc *See* disc, optic
  - refractive media

        vitreous body, 702 *See also* humour, aqueous; *See also* lens (of eye)
    retina *See* retina
    small (microphthalmia), 699
    structures around, 702-3 *See also* body (bodies), ciliary; *See also* choroid; *See also* iris

eyebrows, 467
    muscles, 659

eyelashes, 669
    development, 703

eyelids, 669-71, 669(f), 670(f)
    arteries, 671
    blinking, 669
    ciliary part, 669
    development, 701, 701(f), 702-3
    innervation, 671
    lacrimal part, 669
    lymphatic drainage, 671
    muscles, 482, 659, 660, 703
    skin, 669-70
    structure, 670-1, 670(f)
    veins, 671

F

fabella, 1420

face, 467-97
  adult, 603(f)
  approximation (reconstruction), 420-1
  arteries, 469-71
  clefts of, 607, 607(f)
  development, 602-3, 603(f)
  developmental anomalies, 607
  embryonic, 603(f)
  fascia, 397, 468-9
  fracture, 479-81
  growth of, 417-18
  lymphatics, 492
  membrane bones, 613
  modiolus, 489
  movements, 488-9
  muscles, 481-9
  nerves, 492-7
  postnatal growth, 417-18
  skeleton *See* skeleton, facial
  skin, 397, 467-8
  skin flaps, 468
  superimposition, 421
  surface anatomy, 403-4
    dermatomes, 405
  tissue plane, 397, 468-9
  veins, 491-2

facet(s), 86
  articular, vertebral
    axis, 719
    cervical, 719
  clavicular, 795
  costocapitular, 721
  costotubercular, 721

- joints *See* joints (named), zygapophysial
- odd, of patella, 1394, 1395(f)
- ‘squatting’, 1434
- of suprarenal glands, 1197
- sustentacular, 1437
- talar, 1437
- of third metacarpal, 865

factors
- growth *See* growth factors
- intrinsic, 1204
- transcription *See* transcription factors *see also individual factors*

Fallot’s tetralogy, 975, 1030, 1031, 1032

falx
- cerebelli, 426
- cerebri, 335, 355, 397, 423, 426
  - development, 393
- inguinalis (conjoint tendon), 1064, 1065(f), 1066

fascia, 39-40
- abdominal wall, anterior
  - deep/membranous layer, 1060
  - superficial, 1060
  - transversalis, 1060
- abdominal wall, posterior, 1069, 1069(f), 1070(f)
- acetabular, 1389
- adherens, 7
- of anal triangle, 1094
- antebrachial, 840, 845
- anterior, of Gerota, 1226
- of arm, 823-4
- of axilla, 791
- of back, 708-10
- brachial, 823-4
- buccopharyngeal, 469, 568
- Buck’s, 1273
- bulbi, 657, 658, 672

cervical, 438-40
    deep, 438-40, 533, 708, 709-10, 791
    superficial, 438
clavipectoral, 791, 793, 917
Colles’, 1095, 1252
conal, lateral, 1226-7
cremasteric, 1064
cribriform, 1280, 1349
cruris, 1411
deep, 40
    cervical, 438-40, 709-10, 791
    of forearm, 778, 840
    of gluteal region, 1349-50
    of leg, 1411
    of lower limb, 1329-30
    of perineum, 1095
    of thorax, 917
    transverse, of leg, 1411
deltoid (over), 791
Denonvillier’s, 1151, 1245, 1269, 1270, 1272(f), 1284
dentata, 350
digital, of hand, 860
dorsalis pedis, 1431
endopelvic, 1256(f)
endothoracic, 989, 999(f)
    subpleural, 1111
of face, 397, 468-9
of foot, 1344, 1431-2, 1431(f)
of forearm, 840
of gluteal region, 1349-50
of hand, 860
iliac, 1070, 1070(f), 1351-2
infraspinous, 791
investing, 39
of knee joint, 1399-400
lacrimal, 655, 674
lata, 1349-50

  - of knee joint, 1394, 1400, 1409
- lateroconal, 1070
- longitudinal, medial (MLF), 306, 308
- masseteric, 397, 469
- materials properties of, 120
- mesorectal, 1151, 1151(f), 1152(f), 1154
- muscular, 657
- of neck, 438-40
- obturator, 1085
- ocular, 658
- orbital, 658, 658(f)
- palmar, 859(f), 860
- parietal, of rectum, 1153
- parotid, 397, 469
- parotid-masseteric, 397, 469
- pectoral, 791
- of pectoral girdle, 791
- pelvic, 1085-6, 1085(f)
  - parietal, 1085-6
- of pelvic diaphragm, 1086
- of penis, 1273
- of perineum, 1093-7, 1093(f), 1095(f), 1097(f)
  - deep, 1095
  - superficial, 1095
- perirenal, 1070, 1226-8, 1227(f)
  - anterior, 1227
  - fusion, 1227-8
  - posterior, 1227
- pharyngobasilar, 529, 568
- of pharynx, 568
- piriformis (over), 1086
- plantar, 1430-1, 1432(f)
  - surface anatomy, 1344
- popliteal, 1394, 1411
- posterior, of Zuckerkandl, 1226
- presacral, 1086, 1151, 1152(f), 1154
- pretracheal, 439, 589

prevertebral, 439
propria, 1067
    of rectum, 1151
of prostate, 1254
psoas, 1070
rectovesical, 1218
of rectum, 1151-3, 1152(f), 1153(f)
of sartorius, 1400
of scalp, 397, 468
Scarpa’s, 1095
of shoulder region, 791
spermatic, 1064, 1065, 1066
    cremasteric, 1261, 1261(f)
    external, 1261, 1261(f)
    internal, 1060, 1261, 1261(f)
subscapular, 791
superficial, 39-40
    of abdominal wall, anterior, 1060
    cervical, 397, 438
    of gluteal region, 1349
    of penis, 1273
    of perineum, 1095
    temporal, 397, 469
    of thigh, 1349
    of thorax, 916
    of upper limb, 778
supraspinous, 791
temporal, 397, 469, 538, 622
    deep, 397, 469
    superficial, 397, 469
temporo-parietal, 397, 469
of thoracic wall, 916-17
thoracolumbar (lumbodorsal), 708-9, 744, 1069-70, 1069(f), 1070(f)
of thyroid gland, 462, 589
transversalis, 1060, 1111
of upper limb, 778
    deep, 778

        superficial, 778
    of urogenital diaphragm, inferior, 1094
    of wrist, 778

fascia adherens, 7

fascicle(s)
    of atrioventricular bundle, 977
    of cochlear nerve, 634
    of olfactory neurones, 553
    subendocardial, 977
    vestibulocochlear, 633

fasciculus (fasciculi)
    circumolivary, 285
    cuneatus, 228, 262, 262(f), 263, 264, 275, 277, 278, 278(f), 280, 305, 749
    from medial side of left crus, 1007
    fronto-occipital, 354
    gracilis, 228, 262, 262(f), 263, 263(f), 275, 277, 278(f), 749
    intrafusal, 53, 59, 60, 61(f), 62
    lenticularis, 323, 331
    of Lissauer, development, 375
    long association, of cerebral hemisphere, 354
    longitudinal
        inferior, 354
        medial (MLF), 278, 279, 281(f), 285-6, 285(f), 288(f), 289(f), 291, 645(f), 663
        superior, 354
    medial longitudinal, 664
    papillomacular, 692
    peripheral nerves, 53
    proprii, 271
    retroflexus (habenulointerpeduncular tract), 293, 323, 353
    subcallosal, 326
    subthalamic, 323
    sulcomarginal, 262, 268, 270
    tegmental, central, 281(f), 283, 288(f), 290, 294, 308
    thalamic, 331

  uncinate, 298, 308, 354 *See also* bundle(s); *See also* tract(s)

fascin, 18

fat
  brown, 35
  cells, 34-5
  mobilization, 35
  palmar, 860
  perirenal, 1226
  subcutaneous, 40
    abdominal wall (anterior), 1055, 1060
    distribution, 150
  subepicardial, 974, 977 *See also* lipids

fat pads
  articular, of synovial joints, 99(f), 100, 101
  of Bichat, 467
  buccal, 467, 538
  of elbow joint, 832
  foot, 1432, 1432(f)
  heel, 1432, 1432(f)
  infrapatellar, 1402, 1402(f)
  Kager’s, 1437
  malar, 468
  metatarsal, 1432, 1432(f)
  oesophageal, 1111
  retropubic, 1365
  temporal, superficial, 469
  temporo-parietal, 469

fate map, nervous system development, 366(f)

fauces *See* arch(es), palatopharyngeal; *See also* arche(es), palatoglossal

feedback, tubuloglomerular, 1237, 1238

feet *See* foot

feet, ‘junctional’ (pillars), 108

felon, 861

femur, 1360-5, 1360(f), 1361(f), 1390
  arteries, 1364-5, 1364(f)
  distal end, 1362-3, 1362(f), 1363(f)
  fracture, 1342, 1364
  growth plate, 1365
    trauma, 1365
  head of, 1360, 1361(f)
  in hip joint, 1365, 1387
  infection, 1365
  muscle attachments, 1363-4
  neck, 1360-1, 1361(f)
    anteversion, 1414
  neonate, 1365
  nerves, 1365
  ossification, 1360(f), 1361(f), 1365, 1365(f)
  patellar surface, 1362
  structure, 1363-4
  surface anatomy, 1340, 1341(f)
  trochanter
    greater, 1361, 1361(f)
    lesser, 1361
  veins, 1365
  weight bearing, 1362

fenestra(ae), 85
  of capillaries, 133
  cochlea (round window), 624, 625(f), 634, 646
  vestibuli (oval window), 602, 624, 625(f), 634

fertilization, 167-8, 170(f), 175, 1293, 1294
  in vitro, 168

fertilization age, 211

α-**fetoprotein**, 180

fetus
  in amnion, 180-1
  aortic bodies, 986
  bladder, 1312

blood vessels, 179
bone marrow, 75
breathing movements, 1013, 1035
caecum, 1142
caudal end, 1311(f)
circulation, 176, 178, 181, 205, 1027-8, 1028(f), 1301(f)
    changes after birth, 205, 1028
    persistent, 1036
    primitive, 176
crown-rump length, 211, 1299, 1300(f)
definition, 211
dermis, 158(f), 159
developmental staging, 211, 213, 213(f)
distress, premature defecation of meconium, 1213
erythrocytes, 67, 68
Eustachian valve, 964
female, masculinization, 1219
gestational age, 211, 216, 216(f), 1299
haemoglobin (HbF), 68
heart, 1030
insulin-like growth factors, 218
internal iliac artery, 1087
kidney, 1225
large intestine, 1212
length, 211, 213, 216, 216(f)
liver, 1173
lungs, 206(f), 992
melanocytes, 158
membranes, 180-2
movements, 213, 903
nutritional requirements, 218
ossification centres, 92(f)
ovary, 1294
prostate, 1257, 1259
pulmonary artery, 983
sex determination, 1319-20
size, male *vs* female, 1319

  - swallowing of amniotic fluid, 181
  - symphysis-fundal height, 1299
  - umbilicus, 1062
  - vertebral curvatures, 713-14
  - weight, 213, 216(f)

fibre(s)
  - ‘clasp’, 1114
  - collagen
    - blood vessels, 137-8 *See also* collagen
  - cruciate, of hand, 879
  - elastin, blood vessels, 137-8
  - Henle, 693
  - lens, 686, 686(f), 687, 687(f)
    - development, 701(f)
    - microstructure, 687
  - muscle, 122(t)
    - adaptive capacity, 111-12
    - fast twitch (white), 111
    - formation, 115-16, 116(f)
    - growth, 116-17
    - length regulation, 116-17
    - skeletal, 103-17
    - slow twitch (red), 111
    - smooth, 127, 128(f)
    - tonic, 110, 111, 112(t)
    - type development, 115, 116(f)
    - type I, 111, 112(t)
    - type II, 111, 112(t)
    - type transformation, 111-12 *See also* muscles (general)
  - nerve
    - A, 53
    - A B C classification, 53
    - adrenergic, 138, 141
      - of heart, 982
    - afferent
      - groups I, II, III, IV, 53, 60, 60(f)
      - gustatory, 283

  - primary, termination, 257, 258
- arcuate
  - anterior, 278(f), 279(f)
  - external, 279(f), 281
  - interior, 278(f)
- association, 354, 355(f)
  - long, 354, 355(f)
  - short (arcuate; ‘U’), 354
- B, 53
- beta efferent, 60, 60(f)
- C, 53, 110
- cerebelloreticular, 307-8
- cerebellorubral, 290, 308
- cerebellothalamic, 308
- cerebellovestibular, 307-8
- cholinergic, 138, 141
  - of heart, 982
  - salivary secretion control, 522(f), 523
- climbing, 283, 300, 302, 303, 305, 306, 308 *See also* fibres(s), nerve, olivocerebellar
- commissural, 354-6, 355(f)
- corticobulbar (corticonuclear), 228, 230(f), 284, 286, 287, 307, 357
- corticocortical, 341
- corticofugal, 228, 357
  - development, 380, 385
- corticonigral, 290
- corticonuclear *See* fibre(s), nerve, corticobulbar (corticonuclear)
- corticopetal, 380, 385
  - development, 380
- corticopontine, 230, 284, 289, 306, 357
  - development, 377, 388
- corticorubral, 290
- corticospinal, 229, 284, 286, 289, 343, 357
  - development, 377
- corticothalamic, 341
- corticovestibular, 307

cuneocerebellar, 304, 305
efferent
    beta, 60, 60(f)
    fusimotor (gamma), 60, 110
    thoracic vagus nerve, 945
fastigial, 308
fastigiobulbar, 298
frontopontine, 284, 288(f), 289, 357
functions, 309
fusimotor, 60, 110, 258
gamma-efferents, 60, 110
hypothalamospinal, 270
intrafusal, 53, 59, 60, 61(f), 62
intramuscular, 130
mossy, 264, 300, 302, 303, 305, 306, 308, 350, 351
    input to cerebellum, 303-5, 379
    origin, 302
    vestibulocerebellum, 305
motor, cranial nerves, 372
nigrostriatal, 290
noradrenergic, of cerebellar cortex, 303
occipitopontine, 289, 357
occipitotectal, 357
olivocerebellar climbing, 300, 305, 309
    input to cerebellum, 305
parallel, of cerebellar cortex, 300, 302, 303
parasympathetic, thoracic vagus, 945
parietopontine, 289, 357
peripheral, 53
pontocerebellar, 284, 285, 306
postganglionic
    to oesophagus, 951
    to sacral plexus, 1093
projection, 357, 357(f)
Purkinje, 975, 976 *See also* cells (named), Purkinje; *See also* layer(s), Purkinje
reticular, 37

        reticulocerebellar, 306
        secretomotor, 32
        serotoninergic, of cerebellar cortex, 303
        of spinal nerves
            somatic, 755
            visceral, 755
        spinocerebellar, 304-5
        spinoreticular, 267, 306
        striatopallidal (direct pathway), 331, 332
        striatopallidal (indirect pathway), 331, 331(f), 332
        tectopontine, 292
        temporopontine, 289, 357
        trigeminocerebellar, 304-5
        vasomotor sympathetic, oesophagus, 951
        vestibulocerebellar, 282(f), 286, 305-6
        of white matter, 355 *See also* connections (neural); *See also* projection
    nuclear bag, 60, 60(f), 61
    nuclear chain, 60, 60(f), 61
    olivocerebellar, 305
    olivocerebellar climbing, 305
    of palmar aponeurosis, transverse, 859
    preganglionic, for lower limb, 1093
    Sharpey's, 91, 515, 516, 517, 518(f)
    of Skoog, 859 *See also* connections (neural)

fibrils
    collagen, 37, 1298
    elastic, 37
    muscle *See* myofibrils

fibrin, clot formation, 67, 68(f), 72

fibroblast growth factor (FGF), 8, 370, 612, 763, 1026, 1034

fibroid, striae, Nitabuch's, 177

fibronectin, 5, 38, 606, 1016, 1033
    embryo development, 194
    placental villi, 178

fibula, 1389(f), 1414(f), 1415-17
  distal, 1432
  head, 1340, 1415
  muscle attachments, 1416-17
  ossification, 1417
  shaft, 1343, 1415-16
  surface anatomy, 1340, 1343
  vascular supply, 1417

field(s)
  of Forel (subthalamic), 323, 327(f), 329, 331, 331(f)
  frontal eye (FEF), 343, 343(f), 664
  ‘H’, of Forel, 331
  heart-forming
    primary, 1016
    second, 1016, 1018
  hippocampal *See* hippocampus
  nail, 159
  supplementary eye (SEF), 664
  visual, 315

fila coronaria, 966, 974

filament(s)
  actin, 3(f), 14, 18, 127, 128
  fibronectin, 38
  intermediate, 3(f), 6(f), 15
    glial, 48
    keratin, 28
  long sarcomeric, 106
  myosin, 128, 129(f)
  sliding, 111
  thick, 106
  thin, 106

film, tear, 671, 672, 673-4

filopodia, 3, 14, 18

filters, inferior vena caval, 1076

filum (fila)
- terminale, 375, 725, 749
  - externum, 750(f), 751(f)
  - internum, 750(f), 751(f)

fimbria(e), 238(f), 239(f)
- of fornix, 348(f), 352, 352(f)
- ovarian, 1293
- of uterine tube, 1285, 1293, 1294, 1313

fimbrin, 15, 18

finger(s)
- bones, 866, 867(f)
- drop, 829
- joints, 875-8
- little, phalanges of, 866
- muscles, 885-6
- webbing, 906

fingerprints, 161, 161(f), 857, 857(f)

fissure(s)
- anal, 1157
- antitragohelicina, 619
- azygos, 993
- of cerebellum *See* cerebellum
- of cerebral hemisphere, 335
  - great longitudinal, 335
  - lateral (Sylvian), 335
    - rami, 335
  - rhinal, 338 *See also* sulcus (sulci)
- choroid, 239(f), 311
  - development, 384, 385(f)
- choroidal (of eye), 237, 239(f)
  - development, 702
- of Gans, 1166
- hepatic, 1165
- horizontal, of cerebellum, 298
- interlobar (lung), 989

intervertebral, 772
lateral (Sylvian), 335, 412
for ligamentum teres, 1164(f), 1165
for ligamentum venosum, 1164(f), 1165
of lungs, 914, 990(f), 993-4
    horizontal, 992(f), 993
    incomplete, 993
    inferior accessory, 993
    interlobar, 989
    oblique, 992(f), 993-4
    superior accessory, 993
median
    of medulla oblongata, ventral, 277(f), 278
    of spinal cord, anterior, 749
optic, failure to close, 699
oral, 467
orbital
    inferior, 404, 415, 475, 476, 478, 479, 480, 518, 520, 544, 656
    superior, 410(f), 424, 429, 430, 431, 529, 656, 666
palpebral, 669, 671
petro-occipital, 424
petrosquamous, 416, 615, 618
petrotympanic, 416, 527, 541, 615, 616(f), 617, 624, 627, 629
portal, 1165, 1166
posterolateral, of cerebellum, 298
precentral, of cerebellum, 298
preculminary, of cerebellum, 298
primary, of cerebellum, 298
pterygoid, angular, 529
pterygomaxillary, 412, 415, 527, 529, 540, 543
of Santorini, 620
secunda (postpyramidal), 379
squamotympanic, 416, 533, 534, 615, 617
of Sylvian, 412
transverse, 242
umbilical, 1166
venous, 1166

  von Ebner’s, 763(f), 765(f), 767

fistula
  in ano, 1158
  aorto-caval, 1073, 1076
  branchial, 441
  tracheo-oesphageal, 1015, 1032, 1037, 1037(f)

fixation (of gaze), 661, 663

fixators, 114, 115

flagella, 3, 4, 16, 17-18

flail foot, 1384

flap(s), formation/structure, 163-4, 468
  ankle/foot perforator flaps, 1457
  anterolateral thigh perforator flaps, 1381
  anteromedial thigh perforator flaps, 1381
  deep inferior epigastric artery perforator flap (DIEP), 934
  deltopectoral, 926
  fasciocutaneous, 164
  forehead, 468
  free, 164
  gluteal perforator flaps, 1381
  hip and thigh perforator flaps, 1381
  lateral arm, 827
  musculocutaneous, 164
    latissimus dorsi, 811
    pectoralis major, 807-8
    trapezius, 809
  myocutaneous, rectus abdominis, 1061
  nasolabial, 468
  parascapular, 817
  posterior interosseous artery, 853
  radial forearm fasciocutaneous, 852
  scalp, 467
  scapular, 817
  skin *See* skin flap(s), formation

    tensor-fasciae latae perforator flaps, 1381
    transverse rectus abdominis musculocutaneous flap (TRAM), 934

flexion (movement), 104

flexure(s)
    cervical, 362, 363(f)
    colic
        left (splenic), 1137, 1146, 1209, 1217
        right (hepatic), 1137, 1144, 1144(f), 1209, 1217
    colonic
        left *See* flexure(es), splenic
        right *See* flexure(es), hepatic
    duodenal
        inferior, 1126
        superior, 1125-6
    duodenojejunal, 1073, 1126, 1126(f), 1209, 1217
    hepatic, 1137, 1144, 1144(f), 1209, 1217
    mesencephalic, 362, 363(f)
    perineal, of rectum, 1150
    pontine, 362, 363(f), 376, 377, 381(f)
        development, 381(f)
    sacral, of rectum, 1150, 1154
    splenic, 1137, 1146, 1209, 1217

flocculus, cerebellum, 305, 306, 308, 664

floor
    inguinal canal, 1064
    mouth *See* mouth, floor
    nasal cavity, 550
    pelvic *See* pelvis, floor
    pharyngeal, development, 605(f)
    plate, neural tube, 363(f), 364(f), 372(f)

fluid
    amniotic, 181, 1035, 1312
        abnormal volume, 181
        composition, 181
        fetal swallowing, 181

        - sources, 181
        - volume, 181
    - aqueous, 681
    - cerebrospinal (CSF), 41, 52(f), 242-4, 277
        - access to, 760
        - circulation, 243, 377
        - composition, 242
        - drainage, 242-3
        - endoneurial, 53
        - mixing, 243
        - obstruction of, 244, 296
            - hydrocephalus, 244, 244(f), 295, 418
        - otorrhoea, 623
        - secretion, 242
            - by choroid plexus, 242, 380
        - spinal cord, 257, 752
        - subarachnoid space development, 390
        - volume, 243
    - coelomic, 189
    - exocoelomic, 189
    - of inner ear, 634-6
    - lacrimal *See* tears
    - peritoneal, 1099
        - accumulation site, 1107, 1109
        - management, 1109-10 *See also* ascites
    - seminal, 1259, 1270
    - synovial, 81, 82, 99, 100-1, 100(f), 120, 120(f)
        - of flexor tendon sheaths, 861

fold(s)
- alar, of knee, 1401, 1402(f)
- aryepiglottic, 577, 581, 581(f), 582
    - development, 610
- axillary
    - anterior, 786, 808
    - posterior, 778, 779, 811, 813
- basolateral, distal renal tubules, 1237
- bloodless, of Treves, 1109

caval, 1215(f), 1216
circular, of small intestine, 135(f)
crescentic, atrial septation, 1023, 1030
duodenal, 1126, 1126(f), 1127(f)
failure to fuse, 1323
falciform, 1100, 1320
gastropancreatic, 1107, 1216
genital, 1323, 1323(f), 1324
    fusion, 1323, 1324(f), 1325
    male *vs* female, 1316(t)
glossoepiglottic, 503, 577
gluteal, horizontal, 1341, 1369
gonadal, 1307(f), 1313
of groin, 1340
head, 187(f), 189
horizontal, of rectum, 1151
infrapatellar, 1401, 1401(f)
infundibulopelvic, of peritoneum, 1319
inguinal, lateral, 1307, 1320
inter-ureteric, 1312
malleolar, 624, 627, 630
mesonephric, 1307, 1320, 1321
    genital cord formation, 1321
nail, 155, 858, 861
nasolabial, 467
neural *See* neural crest
palatoglossal, 501(f)
palatopharyngeal, 501(f)
peritoneal, 1285, 1288, 1319
peritoneal *See* peritoneum, folds (ligaments)
recto-uterine, 1106
rectovaginal, 1285
of rectum, 1151
    horizontal, 1151
sacrogenital, 1105
salpingopalatine, 562(f), 563
salpingopharyngeal, 563

- of stomach (magenstrasse; rugae), 1051, 1115, 1116(f)
- sublingual, 521
- synovial, of elbow joint, 832
- tail, 187(f), 189
- tubal, 1307(f), 1313
- umbilical, 1105, 1245, 1247
  - lateral, 1056, 1105
  - medial, 1105
  - median, 1105, 1106(f)
- ureterovesical, 1285, 1287(f)
- urethral *See* fold(s), genital
- ventriculosaccular, 583
- vestibular, 581(f), 582
- vocal *See* cord(s), vocal *See also* plica

folium, of cerebellum, 298, 301, 305, 308

follicle(s)
- anagen, 151
- antral, 1296
- dental, 510
  - cystic degeneration, 510
- endocrine glands, 31
- Graafian, 1296
- hair, 146(f), 151, 151(f), 152(f), 602
- lymphoid, 74
  - bronchial, 1005
  - of large intestine, 1143, 1161, 1161(f)
  - of palatine tonsil, 567, 605
  - of tongue, 505
- Nabothian, 1292
- ovarian, 1295-6
  - atretic, 1295-6
  - primary, 1296
  - primordial, 1295-6, 1295(f)
  - secondary (antral), 1296
  - tertiary (Graafian), 1296
- prostatic, 1259

  splenic, 1194, 1194(f)
  thyroid, 463, 608

follistatin, 370

fontanelle(s), 613
  anterior, 402, 412, 416, 417, 420, 469
  anterolateral, 613
  closure, 418, 613
  mastoid (posterolateral), 404, 417
  of maxilla, 550
  posterior, 412, 416, 418, 470, 613
  size of, 613
  sphenoidal (anterolateral), 412

fonticuli *See* fontalle(s)

foot, 1429-62
  adipose tissue, 1432, 1432(f)
  arches, 1450
  arteries, 1455-7, 1455(f), 1456(f)
  bones, 1432-42, 1435(f)
    accessory, 1441(f), 1442
    sesamoids, 1441-2
  compartment syndrome, 1431-2
  drop, 1384
  fascia, 1344, 1431-2, 1431(f)
  flail, 1384
  flat, 1450, 1463, 1464
  instep, 1341
  joints, 1331, 1442-50
  lymphatics, 1336
  muscles, 1331, 1450-5
    plantar, 1451-5, 1452(f), 1453(f)
  neonatal, 1463
  nerve entrapment syndromes, 1458
  nerves, 1453(f), 1457-8, 1458(f)
  planes of motion, 1458
  propulsive movements, 1459

- rocker bottom, 1464
- running, 1459-62, 1460(f), 1461(f)
- skin, 1429
    - lymphatics, 1429
    - nerves, 1429
    - vascular supply, 1429
- soft tissue, 1429-32
- standing, 1458-9
- surface anatomy, 1340-1, 1342(f), 1343-4
- veins, 1457
    - as venous pump, 1457
- walking, 1459

foramen (foramina), 86, 93, 409
- accessory, of mandible, 532
- basivertebral, 718
- bulboventricular, 1024
- caecum, 423, 428, 432, 471, 472, 605, 608
    - of medulla oblongata, 183, 276(f)
    - of tongue, 503
- carotico-clinoid, 424, 529
- costovertebral, 923(f)
- emissary, 415
    - sphenoidal, 415, 430, 432, 529, 541
- epiploic (of Winslow), 1049, 1101(f), 1102, 1107-8, 1214
- ethmoidal (anterior and posterior), 655, 656, 668
- frontal (frontal notch), 470, 471(f), 491
- genial (lingual), 505
- of Huschke, 420, 615, 618
- incisive
    - anterior, 477
    - lateral, 414
    - median, 414
    - posterior, 477
- inconstant, 423
- infraorbital, 404, 409, 475, 476, 477(f), 480, 656
- interventricular, 237, 237(f), 239, 242, 1024
    - development, 383, 1021

    slow growth, 383
intervertebral, 713, 716, 717, 718(f), 927
    boundaries, 716, 717, 718(f)
    cervical, 717
    lumbar, 719
    thoracic, 719
jugular, 415, 416, 424, 425, 431
lacerum, 415, 424, 430, 432, 529, 541, 611
lingual, 505, 530
lumbosacral, 717
of Luschka, 237, 240, 242, 276, 295
of Magendie, 237, 242
magnum, 414, 415, 424, 425, 426, 427, 433, 532, 611, 613, 710, 770
    Arnold-Chiari malformation, 770
    in occiput anomalies, 770
    sagittal canal diameter, 770
mandibular, 530, 539
mastoid, 412, 416, 425, 431, 615, 629
mental, 402, 409, 481, 486, 491, 494, 530, 533(f)
nutrient
    of clavicle, 793
    of femur, 1362, 1364
    of fibula, 1417
    of humerus, 798
    of radius, 840, 841
    of tibia, 1412, 1413(f)
    of ulna, 844
obturator, 1041, 1352
ovale
    of heart, 964, 968, 1023, 1030
        closure of, 1028
        patent, 964
        reopening, 1036
    of sphenoid bone, 415, 424, 430, 432, 527, 529, 541, 611
palatine
    greater, 414, 415
    lesser, 415, 478, 544, 546

- parietal, 412, 432, 469, 470(f), 491
- postglenoid, 615
- primum, 1023
- rotundum, 424, 529, 543, 544, 557(f)
- sacral, 724
- sciatic
    - greater, 1041, 1366
    - lesser, 1041, 1366
- secundum, 1023
- singulare, 636, 637(f), 643
- sphenoidal emissary, 415, 424
- sphenopalatine, 473(f), 474(f), 543, 551
- spinosum, 415, 424, 431, 433, 527, 529, 541
- squamosal, 615
- sternal, 917, 918
- stylomastoid, 416, 617, 618, 620, 624, 626, 629, 630
- supraorbital, 493
- of suprascapular nerve, 795
- transversarium, 397, 400, 718, 719(f), 720, 721
    - of axis (C2 vertebra), 720
    - of C3-C7, 770
    - of C7, 721
- vertebral, 716, 718
- of Vesalius (sphenoidal emissary), 415, 424
- of Winslow (epiploic), 1101(f), 1102, 1107-8, 1107-8, 1214
- zygomatico-facial, 665
- zygomatico-orbital, 475, 476(f)
- zygomaticofacial, 409
- zygomaticotemporal, 475, 476(f) *See also* opening(s); *See also* orifice

forced vital capacity, 1036

forceps
- major, 238
- minor, 355

forces, 117-18, 118(f)
- acting on, hip, 1391-2
- internal, of muscles, 121, 122(f)

Fordyce’s spots, 499

forearm, 839-56
- arteries, 852-3
- bones, 840-4
- compartments, 840, 840(f)
- development, 905
- muscles, 845-52
  - anterior compartment, 845-8
    - deep flexors, 847-887848
    - superficial flexors, 845-7, 846(f)
  - posterior compartment, 848-52
    - deep extensors, 850-2, 850(f)
    - superficial extensors, 848-50, 848(f)
- neonatal, 905-6
- nerves, 853-6
- rotation, 871
- skin, 839
  - innervation, 839
  - nerves, 839
  - vascular supply, 839, 839(f)
- soft tissue, 839-40 *See also* arm

forebrain *See* prosencephalon

foregut
- mesenteries, 1206
- postpharyngeal, 1203-9, 1203(f), 1204(f), 1205(f), 1215(f)
  - development gradient, 1203
  - glands, 1206-9
  - ventral mesentery, 1214 *See also* duodenum; *See also* oesophagus; *See also* stomach
- primitive, 189

forehead (frons), bones of, 404, 470

foreign bodies, inhaled, 1001

foreskin *See* prepuce, of penis

formants, 593

reticular, 303

formation (formatio)
  hippocampal, 347, 349-52
    chemical anatomy, 352
    connections, 352
      from amygdala, 354
    development, 384
    neurotransmitters, 352
    peptide-containing neurones, 352
    subcortical projections of, 351 *See also* complex(es), subicular; *See also* cortex, entorhinal; *See also* gyrus (gyri), dentate; *See also* hippocampus
  paramedian pontine reticular, 663
  reticular, 275, 278(f), 286, 292, 303, 307, 308
    brain stem, 292-5
    cerebellum connections, 307-8
    medullary, 303, 308
    paramedian pontine (PPRF), 308

fornix (fornices), 237, 320
  of brain
    commissure of, 385
    development, 383, 385
    fibre number, 354
    fimbriae of, 348(f), 352, 352(f)
  conjunctival, 658
    superior, 671, 703
  vaginal, 1281, 1283(f), 1313(f), 1316
  vestibuli, 500, 524(f)

fossa(e), 85, 100(f), 101
  acetabular, 1352, 1353(f), 1387
  articular, 412, 533, 615, 617, 618
  canine, 476, 477(f)
  cerebral, lateral, 383, 384(f)
  cervical, of femur, 1361
  condylar, 415, 745
  coronoid, 796, 800

cranial, 397, 414, 415, 423-5, 425(f)
    anterior, 414, 423-4
    fracture, 623
    middle, 424, 429(f), 529, 535, 541
    posterior, 414, 415, 424-5
cubital, 831, 831(f)
    content, 831
digastric, 415, 530
femoral, 1105
gallbladder, 1177
glenoid (mandibular), 412, 533, 615, 617, 618
hyaloid, of vitreous body, 686, 688
hypophysial (pituitary), 424, 527, 530, 611
iliac, 1356
incisive, 404, 414, 476, 477, 486, 488
incudis, 625, 626, 627, 628, 630
infraclavicular, 785, 786
infraspinous, 794, 795
infratemporal, 412, 415, 424, 529, 538, 541, 656
    boundaries, 412
    infection, 439, 543
    nerve blocks, 520
inguinal, lateral, 1105
intercondylar, 1362
interpeduncular, 288, 288(f), 289(f), 316
intratemporal, 412, 415, 416, 527-43
    bones, 527-33
    relations, 527
ischioanal, 1094, 1154, 1155, 1158
    sepsis, 1158
jugular, 415, 416, 459, 617, 624, 793
lacrimal, 471(f), 477, 655, 674
for lacrimal gland, 471
lunate, of wrist, 872
mandibular (glenoid), 412, 533, 615, 617, 618
nasal, 415
for nasolacrimal sac, 655

navicular, 1252
olecranon, 796, 800
ovale, 964
ovarian, 1106, 1321
pararectal, 1105
paravesical, 1105
piriform, 567
pituitary 2, 424, 426, 427
popliteal, 1393-4, 1393(f)
    content, 1394
    surface anatomy, 1343, 1343(f)
    swelling, 1402
posterior, diminished volume, 770
pterygoid, 415, 529
pterygopalatine, 412, 415, 474(f), 476, 478, 479, 480, 527, 527(f), 529, 540, 543-6, 544(f), 551, 553, 656
radial, 799, 800
retromandibular, 403
retromolar, 519, 532
rhomboid, 284, 1058
of Rosenmüller, 563
scaphoid, 529
    of auricle, 618, 619
    of wrist, 872
subarcuate, 425, 617, 618, 629
sublingual, 530
submandibular, 520, 530
supraclavicular, 406
    greater, 438
    lesser, 407, 440
supraspinous, 794, 795
suprasternal, 986
supratonsillar, 566
supravesical, 1105
temporal, 412, 527
tonsillar, 565, 566, 605
trochanteric, 1361

trochlear, 660
vermian, 711, 713

fountains, of microglia, 367

fovea
of bone, 86 *See also* fossa(e)
of femoral head, 1360
of fourth ventricle (superior/inferior), 240, 241(f)
oblonga, 579
palatini, 564
pterygoid, 532, 538
of retina, 661, 688, 693, 693(f)
triangularis, 579
trochlear, 471, 471(f), 655

foveola(e)
granular, 423, 469, 471
of retina, 688, 693

fracture(s)
ankle joint, 1443-4
avulsion, of pelvic apophyses, 1354
blow-out, 480, 656
clavicle, 792
cranial fossa, 623
facial, 479-81
of femur, 1342, 1364
Guerin’s, 480
humeral shaft, 798
of humerus, 798, 835
Le Fort, 480
mandibular, 480, 532
metatarsal bones, 1440
midface, 529
nasal bones, 547
orbital, 480, 656
pyramidal, 480
repair/healing, 91

- ribs, 922
- scaphoid, 862
- second metatarsal base, 1448
- skull, 409
- supracondylar, 798, 835
- talus, 1336-7
- tibia, 1411-12
- zygomatic arch, 538
- zygomatic bone, 538

freckles, 149

frenulum (frenula)
- of clitoris, 1280
- of ileocaecal valve, 1142
- of labia minora, 1280
- labial, 500
- lingual, 505
- major, 500
- minor, 500
- of penis, 1271, 1271(f)
- of prepuce, 1325
- veli, 379

frenum, lingual, 501

fringes, choroid vascular, 242

frons (forehead), bones of, 470

frontal bone, 409, 410(f), 470-2, 529, 613
- during birth, 613
- blood supply, 491
- cranial surface, 423
- development, 612
- nasal part, 471
- orbital part, 471-2, 655
- ossification, 472
- squamous part, 412, 470-1

frostbite, 156

fundus
  of gallbladder, 1177, 1181
  oculi, 688
  of stomach, development, 1204
  striati, 326, 329, 331
  of urinary bladder, 1245

funiculus
  of medulla oblongata, ventral, 275
  separans, 240, 241(f)
  of spinal cord
    anterior, 749
      development, 372(f), 375
    anterolateral, 749
    dorsal, 258(f), 259(f), 262, 266(f)
    lateral, 749
    posterior, 749
      development, 375
    ventral, 275, 280 *See also* columns, nervous; *See also* cords, spinal; *See also* fasciculus (fasciculi)

furrows
  malar, 670
  median, 747
  naso-jugal, 670
  vascular, of skull, 423

fusion, sperm and oolemma, 167

G

G-protein(s), 9

G-protein-coupled receptors, 8

GABA *See* gamma-aminobutyric acid (GABA)

gag reflex, 283, 401, 458, 573, 1324

gait, 1391, 1392(f)
  ataxia, 309
  gluteus lurch, 1391
  gluteus medius/minimus paralysis, 1371
  heel strike, 1392, 1392(f)
  high stepping, 1384
  muscle involvement, 118
  in pregnancy, 1301
  single-leg stance, 1391(f), 1392
  Trendelenburg, 1391 *See also* walking

gait cycle, 1460(f)

galactocerebroside, 51

galactosylglycerides, 51

galea aponeurotica, 467, 469

gallbladder, 1177-81
  anatomy, 1177, 1177(f)
  arteries, 1179-80
  development, 1207, 1207(f)
  duplication, 1177
  inflammation, 1179
  lymphatics, 1180
  microstructure, 1181, 1181(f)
  mucosa, 1181
  neonate, 1209
  nerves, 1172, 1180-1
  referred pain, 1181
  secretions, 1181

  surface anatomy, 1054, 1179
  veins, 1180

gallstones, 1179
  pancreatitis, 1187-8

GALT *See* gut-associated lymphoid tissue (GALT)

gamekeeper's thumb, 877

gamete(s)
  fusion, 167 *See also* oocytes; *See also* spermatozoa

gamma-aminobutyric acid (GABA), 46, 47, 48
  cerebellar cortex, 302, 303, 305, 307
  of non-spiny cells, 339
  receptors, hippocampus, 351
  striatal neurones, 328

ganglion (ganglia), 55-6, 57(f)
  accessory nerve, development, 373
  acoustic, development, 367
  aorticorenal, 1045
  autonomic, 56
    cranial, development, 373
  basal *See* basal ganglia; *See also* nucleus (nuclei – nervous), basal
  cardiac, 982
  cervical, 461, 754
    inferior *See* ganglion (ganglia), cervicothoracic
    middle, 407, 449, 457(f), 460, 461, 944(f)
    superior, 407, 456(f), 458, 460, 461, 515, 521, 646
      branches, 461
    sympathetic, 142, 234, 235(f)
  cervicothoracic, 407, 449, 455, 461, 779, 944, 944(f), 993
  ciliary, 401, 668-9, 668(f), 669(f), 684
    ramus communicans, 668
    roots, 669
  cochlear (spiral), 425(f), 634, 642, 646(f)
  coeliac, 911, 1045
  conarii (nervus), 324

cranial
    development, 373
    sensory, development, 373
dorsal root, development, 372, 375
enteric, 56, 57(f)
facial, 546
of facial nerve *See* ganglion (ganglia), geniculate
geniculate, of facial nerve, 626, 629, 630
    development, 367, 373
of glossopharyngeal nerve, 235
    inferior, 458
    superior, 458
of hypoglossal nerve, development, 373
inferior
    of glossopharyngeal nerve, 458
    of vagus nerve, 458-9
lumbar, 1078, 1081
mesenteric, superior, 1045, 1131
otic, 402, 527, 542, 543, 543, 564, 565
    branches, 543
    development, 374
paracervical, 1291
parasympathetic
    development, 373-4
    neural anlage, of heart, 374
    submandibular, 521
in pineal gland, 324
primordial spinal, 372
proximal, facial, development, 373
pterygopalatine, 402, 503, 529, 544-6, 558, 559, 656
    nasal branches, 519
    pharyngeal branches, 563, 564, 565
    postganglionic sympathetic fibres, 213, 559
    preganglionic parasympathetic fibres, 559
    rami orbitales, 559, 669
sacral, 712, 1044
Scarpa's *See* ganglion (ganglia), vestibular

sensory, 55-6
spinal, 750(f), 752, 754, 768, 769, 771(f)
    centra of vertebrae relationship, 771(f)
    development, 372
    experimental removal, 768
    lesions, 759
spinal accessory, development, 373
spiral (of cochlea), 425(f), 634, 642, 646(f)
splanchnic, 945
statoacoustic *See* ganglion (ganglia), vestibulocochlear
stellate *See* ganglion (ganglia), cervicothoracic
submandibular, 232(t), 234, 401-2, 506, 521
    development, 374
    removal, 506
superior
    glossopharyngeal, development, 373
    of glossopharyngeal nerve, 458
    of vagus nerve, 458
sympathetic
    cervical, 142, 234, 235(f)
    development, 374
    lumbar, 1078, 1081
terminal, 234
thoracic, 461, 944, 945
    first, 944
    second, 942(f), 944, 944(f), 945
    sympathetic, 710
trigeminal, 541, 595, 602, 610, 617, 667
    development, 367, 373
uterine cervical, 1291
of vagus nerve
    afferent, 235
    inferior (nodose), 458-9
    superior (jugular), 433, 458
vertebral, 461
vestibular (Scarpa’s), 642, 642(f)
    development, 367, 373

vestibulocochlear, 602, 652
    development, 373

gangliosides, 51

gastrin, 1204

gastro-oesophageal reflux, 1114

gastroschisis, 181, 182, 1209

gastrulation, 197
embryonic cell populations, 183-91, 197-203

gaze, neural control, 308, 332, 663-5, 664(f) *See also* eye and eyeball, movements

gelatinoreticulum, 1016, 1017(f)

gene(s)
bHLH (basic helix-loop-helix), 115
EFNB1, 607
homeobox *See* gene(s), *HOX*
HOX, 195, 596, 1032
    expression, 371
    eye development, 699
    limb development, 902
    neural development, 371, 371(f)
imprinted, 167
Notch, 763
Pax, neural development, 371
PAX2, 699
PAX6, 699
PKD1 and *PKD2*, 1312
RUNX2, 613
Sonic hedgehog, 901, 906
Sox9, 902
TCOF1, 607
tenascin, 38
Wnt7a, 902

genitalia, external

development, 1323(f), 1324-5
    5α-dihydrotestosterone role, 1325
female, 1060, 1323(f), 1324(f), 1325
indifferent stage, 1323(f), 1324, 1324(f)
male, 1060, 1323(f), 1324-5, 1324(f), 1325 *See also* penis; *See also* testis (testes)
maturation at puberty, 1325, 1325(f)

genu
of corpus callosum, 335
of internal capsule, 357

germ, hair, 158

germ cells *See* cells (named), germ

gestation
ectopic, 172, 175
period, 211

gestational age, 211, 216, 216(f), 1299

gigantism, 96

gingiva(e), 500, 501, 513
attached, 500
buccal, 500
development, 605-6
free, 500
labial, 500
palatal, 500
tooth eruption, 606

girdle(s)
pectoral
    development, 905
    joints, 800-7
    movements, 803
    muscles
        anterior, 778, 807
        posterior, 778
pelvic, 1331, 1349-85

        - bones of, 1352-65, 1353(f)
        - joints, 1365-7, 1387-92

glabella, 404, 409, 416, 420, 470, 471(f), 479, 481

glabellar tap, 389

gland(s), 31-3
    - adrenal *See* gland(s), suprarenal
    - anal, 1156, 1156(f), 1158
        - infection, 1158
    - apocrine, 31, 153
        - development, 158
    - arytenoid, 582
    - Bartholin’s (greater vestibular), 1280
    - of Bowman, 552, 552(f), 553, 603
    - of bronchial tree, 1004
    - Brunner’s (submucosal), 1134(f), 1135, 1210
    - buccal, 522
    - bulbourethral, 1270, 1280
        - arteries, 1273
        - development, 1324
        - innervation, 1270
        - microstructure, 1270
        - secretion, 1270
    - cardiac, 1122
    - cardiac, oesophageal, 952
    - ceruminous, 153, 602, 619
    - ciliary, 153
    - endocervical, 1292, 1292(f)
    - endocrine, 31
        - secretion control, 31
    - epicrine (merocrine), 31
    - exocrine, 31
        - classification, 31
        - secretion control, 31
        - secretion mechanism, 31
        - tubuloacinar, 520
    - gastric, 1121-2, 1122(f)

greater vestibular (Bartholin’s), 1280
holocrine, 31
intestinal (crypts), 1131, 1134, 1134(f), 1161, 1161(f)
of Krause, 673
labial, 522
lacrimal, 544, 545, 672-3, 672(f), 673(f)
  accessory, 673
  innervation, 673
  microstructure, 673
  orbital part, 672
  palpebral part, 672
  secretion, 672, 673(f)
  vascular supply, 673
of larynx, 582
lingual, 509, 659
mammary *See* breast
Meibomian *See* gland(s), tarsal (Meibomian)
merocrine, 31
of Moll, 153, 671
of Montgomery (areolar), 930
mucous, 27, 28, 31
  of bronchi, 1035
  of larynx, 582
  of palate, 564
  of trachea, 1035
multicellular, 31
of neck, 608-9, 609(f)
oesophagus, 952
olfactory, 552, 552(f), 553
palatine, 415
para-urethral, 1280
parathyroid, 464-5, 465(f), 608-9, 609(f)
  adenoma, 949
  age-related changes, 464
  lymphatics, 464
  microstructure, 464
  nerves, 463

    - tumours, 463
    - variations, 463
    - vascular supply, 463
- paraurethral, 1253
- parotid, 405, 495-7, 496, 520, 605
    - accessory, 495
    - content, 496
    - lymphatics, 497
    - nerves, 232(t), 233(f), 497
    - relations, 496(f)
    - secretory acini, 523(f)
    - secretory ‘endpieces’, 522, 522(f)
    - structure, 496
    - tumours, 496
    - vascular supply, 497
- pineal, 241, 324
    - arterial supply, 253
    - calcification, 324, 324(f)
    - development, 380
    - hypothalamic control, 318
    - secretions, 324
    - vascular supply, 324
- pituitary, 321-3, 322(f), 424, 527, 611
    - arteries, 253, 323
    - at birth, 367
    - development, 367
    - fetal, 322
    - microstructure, 321
    - posterior *See* neurohypophysis
    - veins, 323
- preputial, 1273
- prostate *See* prostate
- pyloric, 1122
- salivary, 520-3, 520(f), 521(f), 522(f), 605
    - activity control, 523
    - buccal, 522
    - labial, 522

  - major, 520-2
  - microstructure, 522-3, 523(f)
  - minor, 501, 522-3
  - palatoglossal, 522
  - parotid *See* glands, parotid
  - secretory ‘endpieces’, 522
  - sublingual *See* gland(s), sublingual
  - submandibular *See* gland(s), submandibular
- sebaceous, 146(f), 153, 153(f), 602
  - development, 158
  - ectopic, cheek, 499
- secretion control, 31
- seromucous
  - of adenoid, 563
  - nasal, 551
  - sublingual, 521
  - submandibular, 520-1
- serous, 31
  - parotid *See* gland(s), parotid
  - of respiratory tract, 1005
  - sublingual, 500, 521, 522(f), 605
  - of von Ebner, 508, 508(f), 522
- Skene’s, 1280
- of stomach *See* gland(s), gastric
- sublingual, 500, 521, 522(f), 605
  - arteries, 521
  - lymphatic drainage, 521
  - nerves, 232(t), 233(f), 521
  - retention cysts, 521
- submandibular, 406, 437, 438(f), 446, 451, 462, 520-1, 522(f), 530, 605
  - arteries, 520, 521
  - deep part, 521
  - lymphatic drainage, 521
  - nerves, 232(t), 233(f), 521
  - secretary units, 523
  - superficial part, 520-1
- submucosal, 1134(f), 1135

suprarenal, 206, 1196-201, 1197(f), 1198(f), 1218-19, 1226, 1227(f)
    abnormal development, 1219
    accessory, 1197
    in adult, 1197
    arteries, 1198, 1198(f)
    at birth, 1197, 1219
    computed tomography, 1229(f)
    cortex, 1197, 1199(f), 1200, 1201(f), 1218
    development, 374, 375, 1218-19
    dimensions, 1197
    excision, 1200-1
    left, 1197-8, 1197(f)
    lymphatics, 1198
    medulla, 1081, 1197, 1199(f), 1200, 1218
        development, 374, 375
    microstructure, 1199(f), 1200, 1201(f)
    neonates, 1197, 1219
    nerves, 234, 1200
    relations, 1197
    relations to the kidney, 1226, 1227(f)
    right, 1197, 1197(f)
    secretions, 1200
    veins, 1198, 1198(f)
    weight, 1219
sweat (sudorific), 31, 154, 154(f)
    development, 158-9
tarsal (Meibomian), 153, 158, 669, 671, 674(f)
    development, 703
thoracic, abdominal origin, 1077
thymus *See* thymus
thyroid, 406, 462-4, 608, 609(f)
    accessory, 462
    arteries, 462
    C cells, 463
    development, 605
    fascia, 462, 589
    follicles, 463

growth, 608
imaging, 462-3, 463(f)
isthmus, 406
lingual, 503, 605
lobes, 406, 462
lymphatics, 462
microstructure, 463
neonate, 608
nerves, 462
relations, 462
removal, 463
surfaces, 462
veins, 462
tubular, 31
unicellular, 31
urethral, 1251, 1252, 1253
of uterus, 1297
vestibular, greater *See* gland(s), of Bartholin
of Wolfring, 673
of Zeis, 671

glans
clitoris, 1280
penis, 1271, 1271(f)

glaucoma, 675, 686, 697, 702

glenoid, 794

***Gli* proteins**, 1032

glia *See* cells (named), glia

glia limitans, 48, 49(f), 55, 63, 368, 379

glial fibrillary acidic protein (GFAP), ventricular zone, 392

gliogenesis, 369

Glisson, capsule of, 1060, 1169

globus pallidus, 229(f), 230, 323, 325, 326, 326(f), 331
arterial supply, 253

- cell density, 331
- development, 383
- dorsal, 326
- medial, underactivity, dyskinesia, 332
- segments, 326, 331
- stimulation, for dystonia, 333
- striatal efferents to, 329, 331
- ventral, 326

glomera, 134

glomerular filtration, 1237-8
- rate, 1238, 1312

glomerulus (glomeruli)
- of cerebellum, 302
- coelomic (external), 1305, 1306(f)
- internal, 1305, 1306(f)
- renal, 1234, 1236(f)
  - capillary loops, 1234, 1235(f)
  - endothelium/basal lamina, 1235
  - filtration, 1237-8
  - mesonephros, 1307
  - metanephros, 1307
  - structure, 1234, 1236(f)
  - vascular supply, 1232-3, 1234, 1234(f)

glomus, 452
- tumours, 458, 460, 894

glomus jugulare, 452

glucagon, 1207

glucose, absorption, 1212

glutamate, 47
- cerebellar cortex, 302
- hippocampal formation, 351
- subthalamic nucleus, 332

glutamic acid decarboxylase (GAD), striatum, 328

glutamine synthetase, 244

glutathione, 10

glycine, 46, 47

glycocalyx (cell coat), 4, 18(f)

glycogen, 14, 1297
  skeletal muscle, 107, 111
  small intestinal epithelium, 1210
  trophoblast, 179
  in vaginal epithelium, 1284

glycolipids
  myelin, 51
  plasma membrane, 4

glycoprotein, 5-6, 8
  adhesive, 36, 38
  myelin-associated, 51

glycosaminoglycans, 37
  in cartilage, 81, 82

glycosylation, 10

goitre, 463

Golgi apparatus (complex), 3(f), 4, 9, 11(f), 12
  cis-Golgi network, 12
  cisternae, 11(f), 12
  trans-Golgi network, 12

Golgi tendon organs, 53, 57, 59-60, 60(f)

gomphosis, 97

gonads
  cell lineages, 1312
  descent, 1320-2, 1320(f), 1321(f)
  development, 1316(f), 1317-20, 1318(f)
    ambisexual stage, 1312-13, 1315(f), 1318(f)
    early, 1312-13, 1318(f)

        positioning, 1312, 1318(f)
    female *See* ovary (ovaries)
    male *See* testis (testes)
    ‘streak’, 1319

goose bumps, 154

grafting
    pedicled bone, 842
    skin, 164

granulation (of tissue), 34, 163

granulations, arachnoid, 243-4, 244(f)

granules
    azurophilic, 69
    basophilic, 70, 77
    Birbeck, 149
    eosinophilic, 69
    heart, 142
    keratohyalin, 147(f), 148, 151, 154, 155, 158, 159
    lipofuscin, 140
    neutrophilic, 69
    Nissl, 43, 43(f)
    pigment, 42
    of platelets
        alpha, 71
        delta, 71
        lambda, 71
    zymogen, 522, 1207

granulopoiesis, 609

granzymes, 71, 72

Gremlin, 902

grey matter *See* matter, grey

Grey-Turner’s sign, 1188

grips, power, 872

groin
  pain, 1375, 1390 *See also* region(s), inguinal

groove(s), 83, 85, 86, 97, 98(f)
  for anterior ethmoidal nerve, 472, 475
  aortic, 993
  atrioventricular (coronary), 962, 963, 964, 974, 980
    diaphragmatic part, 962
    sternocostal part, 962
  bicipital (intertubercular), 797
  for brachiocephalic vein, 993
  buccolabial, 467
  carotid, 424
  carpal, 861
  caval, of liver, 1075, 1165
  circumalar, 467
  costal, 919
  deltopectoral, 807(f), 978
  gingival, 500
  for greater petrosal nerve, 617
  hyomandibular, 652
  for inferior petrosal sinus, 424, 430, 617
  for inferior vena cava, 1075, 1165
  infraorbital, 474(f), 476, 477(f), 544, 656
  inguinal, 1064
  interatrial, 962, 964
  intersphincteric, 1156, 1157
  interventricular, 962, 974
    posterior, 962, 963
  labiomarginal, 467
  laryngotracheal, 610, 1033
  for lesser petrosal nerve, 617
  linguogingival, 604, 605, 606
  mentolabial, 467, 487, 489
  mylohyoid, 530, 532, 539
  nail, 159
  nasolabial, 467
  nasolacrimal, 475, 476

- neural, 184, 187, 190(f), 361
- oblique, of femur, 1362
- for obturator externus, 1361
- palatine, greater, 478, 478(f)
- paramesonephric, 1313
- pharyngeal, 596, 602
    - first (hyomandibular), 652
- of placenta, 1302
- for popliteus, 1363, 1363(f)
- primitive, 184
- radial, 798(f)
- for sigmoid sinus, 424, 428
- spiral, 797
- sub-tarsal, 671
- subclavian, 793
    - of first rib, 921
- for subclavius, 791, 792
- for superior petrosal sinus, 617, 628
- for superior sagittal sinus, 427, 469, 470(f)
- for superior vena cava, 993
- for transverse sinus, 425
- trochlear, 1362
- vertebral, 716 *See also* sulcus (sulci)

growth, 211-21
- adolescent spurt, 219-20, 219(f), 220(f)
- allometric, 217, 217(f)
- appositional, 220
- of bone, 92-7
- of cartilage, 84-5
- children, 218-19
- compensatory, 214
- of face, 417-18
- of hair, 152-3
- *in utero*, 217-18
- isometric, 217
- multiplicative, 217, 217(f)
- patterns, 217, 219

- postnatal, 218-20
- prenatal, 211-12
- rate *See* growth rate
- of skull, 416-17
- spurts, 1325
- symphysial, 99
- of tissues/organs, subcutaneous fat, 217
- types of, 217
- weight gain, 220

growth charts, 220(f)

growth curves, 219(f)

growth factors
- in embryo, 194
- epidermal, 8
- fibroblast (FGF), 8, 370
  - FGF8, 763
- insulin-like *See* insulin-like growth factors (IGF)
- nerve (NGF), 370
  - receptor, 1309
- platelet-derived (PDGF), 8, 72, 1308
- renal production, 1310
- transforming (TGF-β), 86
- vascular endothelial *See* vascular endothelial growth factor

growth hormone *See* hormones, growth

growth rate
- effects of maternal environment, 213
- hair, 153
- of tissues/organs, head, 217, 217(f)

growth table, of embryos, 167

gubernaculum
- of ovary, 1289, 1294, 1321, 1321(f)
- of testis, 1320, 1320(f)
  - descent of testes and, 1320-1
  - extensions, 1320

Guerin’s fracture, 480

gullet *See* oesophagus

gums *See* gingiva(e)

gustatory sweating, 497

gut
  development, 1220
  functional maturity at birth, 1213
  postanal, 1212
    disappearance, 1218
  postdiaphragmatic, 1203 *See also* foregut; *See also* hindgut; *See also* midgut
  wall, microstructure, 1049-52, 1050(f) *See also* tube(s), digestive/gut; *specific anatomical regions*

gut-associated lymphoid tissue (GALT), 74
  development, 1213

‘gutter’, paracolic
  left, 1102, 1108
    right, 1102, 1104, 1107, 1108
  paravertebral, 1041

gynaecomastia, 937

gyrus (gyri)
  ambiens, 346
  angular, 344
  of cerebral hemispheres, 227, 335-8, 385, 423
    angular, 344, 358
    anterior transverse temporal, 345
    inferior frontal, 335, 341
    inferior temporal, 345
    lateral occipitotemporal, 338
    lingual, 338
    medial frontal, 335, 341
    medial occipitotemporal, 338
    middle temporal, 345
    orbital, 338

        - paraterminal, 348(f), 355
        - postcentral, 228, 344
        - precentral (area 4), 340, 341
        - superior frontal, 335
        - superior temporal, 345, 354
        - supramarginal, 344
        - transferse temporal, of Heschl, 345
    - cingulate, 335, 344, 345, 355
        - areas, 347-8
        - connections, 348
        - functions, 347-8
    - dentate, 347, 348(f), 349, 350, 351, 351(f), 352, 355
        - connections, 351, 351(f)
        - development, 384
        - granule cell layer, 350
            - dynorphin, 352
            - GABAergic neurons, 351
        - polymorphic layer (hilus), 350
            - tail, 350
        - trilaminar cortex, 350, 351(f)
    - fasciolaris, 355
    - frontal *See* gyrus (gyri), of cerebral hemispheres
    - Heschl’s, 648
    - parahippocampal, 288, 295(f), 335, 338, 348, 356
        - development, 384
        - projections, 348
    - parolfactory, 335
    - postcentral, 228, 344
    - rectus, 338, 527
    - supramarginal, 344
    - temporal, 345
        - inferior, 356, 617
        - middle, 356
        - superior, 357
        - transverse, 357

H

habenula perforata, 634, 635(f), 640

habenula, projections from, 353

haematoma
- extradural, 404, 426
- retrobulbar, 520
- subdural, 434

haematopoiesis, 74-7
- fetus, 1208, 1214
- liver, 1214

haemoglobin, 67-8
- adult (HbA), 67
- fetal (HbF), 68
- H (HbH), 68
- S (HbS), 68

haemoptysis, 1035

haemorrhage
- antepartum, 172
- cerebral, 253
- intraperitoneal, 172
- intraventricular, 239
- pancreatic, 1187
- plantar arch, 1456
- postpartum, 1302, 1305
- purpuric, 162
- retroperitoneal, 1100
- subarachnoid, 244, 252
- subpial, 244 *See also* bleeding

haemorrhoids, 1157

haemostasis, platelets, 72

haemothorax, 991

hair, 151-4
  bulb, 151, 152(f)
  colour, 152
  cortex, 151, 152(f)
  cuticle, 151, 152(f)
  cycle, 152-3
  development, 158-9
  follicle, 146(f), 151, 151(f), 152(f), 602
  growth, 152-3
  lanugo, 158, 213
  medulla, 151
  placode, 158
  pubic, development, 1325, 1325(f)
  rudiment, 152
  sheaths, 151-2
  structure, 151-2
  terminal, 151, 153
  vellus, 151, 153, 158

hallux, saltans, 1423, 1430

hallux valgus, 1441, 1449

hamate bone, 863-4, 863(f)
  ossification, 864
  surface anatomy, 786

hammer action, 874-5

hamulus, 85, 861
  of hamate, 786, 787, 863
  lacrimal, 475, 656
  pterygoid, 415, 472(f), 473(f), 474(f), 475, 529, 563, 564
  of spiral lamina, 634 *See also* cornu

hand(s), 857-98
  anatomical position, 887
  anomalies, 906
  arteries, 620, 778, 890-3
  bones, 861-8, 866(f)

clawing, 837, 888, 898
development, 905
fascia, 857-61
    function, 860
functions, 887-90
grips, 889-90, 890(f)
infection, 861
‘intrinsic minus’, 888
joints, 868-78, 869(f)
left, preference, 358
ligaments, 869(f)
movements, 871-2, 873(f)
    closure, 887
    coordinated, 886-7
    fist making, 888
    opening, 888
muscles, 878-86
    extensor, 778
    intrinsic (small), 778, 881-6
neonatal, 905
nerves, 895-8, 896(f)
palm, 778
position of rest, 889
pulley systems, 879, 880(f)
right, preference, 358
simian, 898
skin, 857-61, 857(f), 858(f)
    creases, 857, 857(f)
    dorsal, 857
    innervation, 858, 858(f)
    lines, 857, 857(f)
    nerves, 858, 858(f)
    palmar, 857
    tightness, 860
    vascular supply, 857-8, 858(f)
soft tissue, 857-8, 857(f), 858(f)
surface anatomy, 787

  veins, 857, 858(f), 893(f), 894-5, 895(f)
  as venous pump, 860

handedness, 358

handle, of malleus, 624, 627

hare lip, 607

haustra, of large intestine, 1138, 1139(f), 1212

haustrations, of large intestine, 1137, 1138, 1139(f)

head
  arterial supply, 397-400, 398(f), 444-51, 539(f), 540(f)
    embryonic, 600(f)
  cancers, 454
  development, 595-614
    cranial nerves, 372-3
  fold, formation, 187(f), 189
  growth rate, 217, 217(f)
  innervation, 401-2, 539(f), 540(f), 541-3, 542(f)
  lymphatics, 400(f), 401, 453-5
  mesenchyme, 699
  movements, 638
  muscles, 397
  neural crest, 201
  reflexes, 401
  of sperm/spermatozoa, 167
  surface anatomy, 402-5
    dermatomes, 405
    nerves, 405
    pulses, 405
    skeletal landmarks, 402-4, 403(f), 404(f)
    soft tissues and viscera, 404-5
  trauma, 397
  turning in neonates, 389
  of ulna, 844
  veins, development, 392-3, 393(f)
  venous drainage, 399(f), 400, 540(f)

head (of bones or organs), 85(f), 86, 93, 97, 102, 103, 104, 111
  of femur, 1360, 1361(f)
  of fibula, 1340, 1415
  of humerus, 786, 796
  of malleus, 627
  of metacarpal, 864
  of pancreas, 1183-4, 1207
  of phalanges, 866
  of radius, 786, 840, 841(f)
  of rib, 919
  of spermatozoa, 1266
  of stapes, 627
  of talus, 1340
  of ulna, 786

headache, cervicogenic, 435

hearing
  anatomy, 646-8, 647(f), 648(f)
  loss, 648-9

heart, 959-87
  acute margin, 963, 981
  apex, 913, 962-3, 980
  apex beat, 913
  arteries, 978-81, 979(f)
    development, 1026
  atria *See* atrium (atria)
  auscultation sites, 913
  base, 962-3
  borders, 913, 961(f), 962-3
  chambers, 960
  compression (cardiac tamponade), 960
  conducting system, 975-8, 975(f), 976(f), 977(f)
    abnormalities, 978
    automaticity, 1017-18
    development, 1017-18, 1021-3, 1022(f)
    fast and slow, 1018
    ventricular, 1018

conduction studies, 978
congenital defects, 974-5, 1030-1
  acyanotic, 974-5
  cyanotic, 975
  septal
    atrial, 1028, 1030-1
    ventricular, 1030
connective tissue, 973-4
contractions, 975-6, 1017-18, 1030
  embryo, 1030
crux, 962, 963, 964, 968
development, 186, 205-6, 1016-32
  cardiac muscle, 142
  cells giving rise to, 1016-18
  conducting system, 1017-18, 1021-3, 1022(f)
  fibrous skeleton and valves, 1017
  formation and twisting of heart tube, 1018
  impulse conducting tissue, 143
  inflow and outflow regions, 1018-21, 1019(f), 1020(f)
  positioning, 1030
  septation, 1023-5, 1024(f)
  stage, 11, 1013(f)
  stage, 12, 1032, 1033
  stage, 13, 1020(f), 1022(f), 1032, 1032(f), 1034
  stage, 15, 1026, 1027(f), 1034
  stage, 16, 1028, 1034
echocardiography, 969, 973, 973(f)
embryonic, 205, 964, 1013, *1013*, *1021*
external features, 961(f), 962
fetal, 1030
fibrous skeleton, 973-4
grooves, 962
imaging, 969, 973(f)
left, 960, 962
lymphatic drainage, 982
margins, 963, 981
muscle, 139-43

        - hypertrophy, 969-70 *See also* muscles (general), cardiac; *See also* muscles (named), papillary
    - neonatal, 1029(f), 1030
    - nerves, 982-3, 983(f)
    - organization, 960-2, 961(f)
    - orifices *see specific orifices under ‘orifice(s)’*
    - pacing, 978, 1017
    - pericardium, 959-60 *See also* pericardium
    - position, 962, 1030
        - abnormalities of, 974
    - positioning, 1025-6
    - rate
        - embryonic, 206
        - hormonal influence, 142
        - neonatal, 1030
    - referred pain, 236
    - relations, 966(f)
    - rhythm, 1020
    - right, 960, 962
    - rotation to left
    - septa *See* septum (septa)
    - shape, 962
    - size, 962, 1030
    - surface anatomy, 913
    - surfaces, 962-3
    - veins, 981-2, 982(f)
        - development, 1026
    - ventricle *See* ventricle(s), of heart
    - weight, 962, 1030

heel
- bursae, 1451
- pad, 1432, 1432(f)
- strike, 1459

helicotrema, 634, 636(f), 652

helix, 618, 619, 620, 653

hemianopia, 697

hemicapsule, tonsillar, 566, 567

hemidesmosomes, 6(f), 7
  in skin, 159

hemidiaphragm, 1007

hemifacial microsomia, 418-19, 607

hemiplegia, contralateral, 269

hemisphere
  cerebellar *See* cerebellum, hemispheres
  cerebral *See* cerebral hemisphere

hemivertebra, 768, 772, 1014

Hensen's cells, 635(f), 642

Hensen's node, 184

Hensen's stripe, 642

heparin, 67

hepatocyte nuclear factor 3 β, 1032

herculin, 115

herculin/MRF 4, 772

hernia
  of anterior abdominal wall, 1066-7
  Bochdalek's, 1015
  congenital, 1009
  diaphragmatic, 1015, 1034
    congenital, 181
  femoral, 1067
    strangulation, site, 1067
    surgery, aberrant obturator artery damage, 1059
  hiatus, 953, 1009, 1114
    type I (sliding), 1009
    type II (para-oesophageal), 1009
  inguinal, 1066-7, 1279

        - acquired indirect, 1066
        - clinical features, 1066-7
        - complete congenital, 1066
        - direct, 1066, 1080
        - incomplete congenital, 1066
        - indirect, 1066
        - oblique, 1321
    - Morgagni, 1015
    - oesophageal, 1009
    - paraumbilical, 1063
    - of posterior abdominal wall, 1072
    - posterolateral (Bochdalek), 1009
    - subcostosternal (Morgagni), 1009
    - surgery, inferior epigastric artery damage, 1056
    - umbilical, 1063, 1209
        - acquired, 1063
        - congenital, 1063
        - infantile, 1063

herniation, medial temporal lobe (uncus), 295

herpes zoster, 44, 55, 56

heterochromatin, 18, 19
    - constitutive, 19
    - facultative, 19

heterophagy, 12

hexabrachion (tenascin), 36, 38

hiatus, 85
    - diaphragmatic, 1114
    - for greater petrosal nerve, 424, 431, 617
    - for lesser petrosal nerve, 424, 617
    - maxillary, 12, 473(f), 476, 477(f), 558
    - popliteus, 1408
    - sacral, 717, 725
    - semilunaris, 472, 551 *See also* aperture(s); *See also* opening(s)

hiccups, embryo, 604

high endothelial venules (HEV), 72, 73(f)

hillock, axon, 42, 42(f), 43, 44, 46, 64

Hilton’s law, 101

hilum (hila; hilus), 72, 73, 73(f)
  of cerebellum, 298
  of kidney, 1228, 1231
  of lung *See* lung(s), hilum
  neurovascular, 109
    of skeletal muscle, 109
  of ovary, 1285
  pulmonary, 985, 986
  splenic, 1184(f), 1185, 1191
  of suprarenal gland, 1198

hindbrain *See* rhombencephalon

hindgut, 1308(f)
  allantoic/urinary, 1307, 1308(f)
  development, 1203, 1212-13
  enteric, 1212, 1307, 1308(f)
  peritoneum associated, 1217
  primitive, 1212-13, 1307

hinge
  caudoneural, 184, 361, 1324
  joints, 101
  point, of neural plate, 361

hip bone, 1352-7, 1353(f)
  acetabulum, 1352
  age-related changes, 1354(f)
  at birth, 1354(f)
  nerves, 1354
  nutrient arteries, 1352
  ossification, 1354, 1354(f)
  structure, 1352, 1353(f) *See also* ilium; *See also* ischium; *See also* pubis

hip joint *See* joint(s) (named), hip

hippocampus, 347, 349-52
  commissure of fornix, 385
  connections, 348, 351
    projections to ventral striatum, 329
  development, 383-4
  fields (CA1, CA2, CA3), 351
    CA1, 351, 351(f), 352, 354
    CA2, 351, 352
    CA3, 351, 352
  GABA receptor, 351
  pyramidal cell layers, 351
  strata, 350-1
  structure and position, 347, 350-1 *See also* formation (formatio), hippocampal

hirsutism, 151

histaminase, 69

histamine, 47, 1122
  bronchi, 1004

histology *See* cells (general); *See also* cells (named), tissue

Hjortso's crook, 1177

homeobox genes *See* gene(s), *HOX*

homeorhesis, 219

homocysteinuria, 985

homunculus
  map, 342(f), 344
  motor, 342, 342(f)

hood, extensor, of hand, 880

hook, of hamate, 863
  surface anatomy, 786

hordeolum
  external, 671
  internal, 671

hormones, 322
- acetylcholine (ACh), 47, 111, 233
  - effect on pancreas, 1190
- adrenaline *See* adrenaline
- adrenocorticotrophin (ACTH), 149, 321
- aldosterone *See* aldosterone
- anti-Müllerian (AMH), 1267, 1317, 1319
- antidiuretic (ADH), functions, 1238
- atrial natriuretic factor, 140, 142
- calcitonin (thyrocalcitonin), 463
- catecholamines *See* catecholamines
- cholecystokinin (CCK), 1181
- corticotrophin-releasing (CRH), 319
- epinephrine *See* adrenaline
- follicle-stimulating (FSH), 319, 320, 1296
- gastrin, 1122
- growth, 321
  - bone growth regulation, 95
  - resistance to, 218
- growth hormone releasing (GHRH), 318
- histamine, 47
- human chorionic gonadotrophin (hCG), 168, 175, 1297
- luteinizing, 321
- melatonin, 318
- noradrenaline *See* noradrenaline
- norepinephrine *See* noradrenaline
- oestrogen, 95, 153, 1297
  - hair growth, 153
- oxytocin, 319, 320, 321
- pancreatic, development, 1207
- pancreatic polypeptide, 1190
- parathyroid (PTH), 464
  - excess, 95
- progesterone, 1297
- prolactin, 321
  - decidual cells producing, 176
- relaxin, 1297, 1301

- renal, 1310
- sex, 1200
- somatostatin, 319, 1122
- steroid, 8
- testosterone, 1267, 1319
  - production, 1325
- thymic, 946
- thyrocalcitonin, 463
- thyroid, 8, 463
- thyrotrophin-releasing (TRH), 319
- vasopressin, 319, 320, 321

horns
- Ammon’s, 347
- dorsal
  - of caval fold, 1216
  - of septum primum, 1023
  - of spinal cord, 226, 227(f), 228, 257, 258-60
  - of ventricular septum, 1024
- of lateral meniscus, 1398
- of lateral ventricle
  - anterior (frontal), 237, 238(f)
  - inferior (temporal), 237-8
  - posterior (occipital), 238
- of liver, 1207
- of medial meniscus, 1398
- sinus (of heart), 265, 1018
  - left, 1018, 1019, 1020, 1021(f)
  - right, 101, 1018, 1021(f), 1023, 1220(f)
- of spinal cord
  - dorsal, 226, 227(f), 228, 257, 258-60
  - lateral, 226, 227(f), 228, 257, 258, 260
  - ventral, 226, 257, 260
- ventral
  - of caval fold, 1216
  - of septum primum, 1023
  - of spinal cord, 226, 257, 260
  - of ventricular septum, 1024 *See also* cornu (cornua, cornus)

horseshoe kidney, 1226, 1227(f), 1312

housemaid's knee, 1402

human leukocyte antigens (HLA), 68

humerus, 796-800, 797(f), 798(f), 799(f)
- amputation, 800
- anatomical neck, 796
- blood supply, 827
- fracture, 798, 835
- head, 786, 796, 798(f)
- ossification, 96, 800, 800(f)
- shaft, 786, 797-8
- surgical neck, 796

humour
- aqueous, 675, 685-6
    - composition, 685-6
    - drainage, 675, 686
- vitreous, 675, 688

Hurler's syndrome, 13

hyaluronan, 36, 37, 38, 82, 101, 604, 688

hyaluronate, 1296

hyaluronic acid, 1016

hyaluronidase, 1016

hyaluronidase, and morphogenesis, 195

hydatid, of Morgagni (appendix testis), 1263(f), 1264(f), 1267, 1268, 1315(f), 1316(t), 1317

hydramnios, 1312

hydrocele, 1267

hydrocephalus, 244, 244(f), 295, 418
- communicating, 244

hydrodynamic hypothesis, 519

hydrogen ion, regulation of levels, 1238

hydronephrosis, 1231, 1300

hydrops, endolymphatic, 639, 649

hydrothorax, 991

hydroxyapatite, 86, 87, 120, 514

1,25-**hydroxycholecalciferol**, 1225

21-**hydroxylase, deficiency**, 1219

hymen vaginae, 1284, 1316
  development, 1317

hyoid bone, 397, 405, 436
  cornua, 436
    lesser, 599
  elevation, 502
  movements
    in speech, 592
    in swallowing, 573
  neonate, 610
  ossification, 436
  surface anatomy, 436

hyperactive child syndrome, 332

hyperacusis, 630

hypercolumns, 341

hyperdontia, 513

hypergonadism, 95

hyperkeratinization, 153

hyperopia, 688

hyperparathyroidism, primary, 95

hyperplasia
  benign prostatic, 1250, 1259
  cellular, 217(f)

congenital adrenal, 1219

hypertelorism, 530
traumatic, 418, 479

hypertension
portal, 950, 1118
‘caput medusae’, 1059
transjugular intraparenchymal porto-systemic shunt, 1172
pulmonary, 1015

hypertonia, 326

hypertrophy
heart, 970
kidney, 1226
masseter, 538

hypoalgesia, 315

hypoblast, 173, 175(f), 180, 181, 183, 197
parietal (extraembryonic), 173, 180
visceral (embryonic), 173, 180

hypodermis, 146(f), 150-1

hypodontia, 513

hypogastrium, 1053

hypogonadism, 95

hyponychium, 154-5

hypopharynx *See* laryngopharynx

hypophosphatasia, familial, 418

hypophysis cerebri *See* gland(s), pituitary

hypoplasia
arm, 808
pulmonary, 181
of thymus, 949

hypospadias, 1252, 1319, 1323

hypothalamus, 226, 228(f), 229(f), 232(t), 233, 316-23
  anterior part, development, 380
  autonomic system control, 317
  connections, 320-3
    afferent, 320, 354
    amygdaloid projections to, 354
    efferent, 320
  damage, 317
  development, 367, 368(f), 380
  endocrine system control, 316
  lesions, 316
  nuclei, 317-20
  pituitary control, 319, 320
  relations, 316
  zones, 317

hysteroscopy, 1287(f)

I

I-CAM, 6

icthyosis, 159

ileum, 1129-31, 1129(f), 1130(f)
  arteries, 1129-30
  development, 1210
  displacement in pregnancy, 1300
  lymphatics, 1130-1
  lymphoid aggregates, 1129
  nerves, 1131
  referred pain, 1131
  terminal, 1129
  veins, 1130

ilium, 1041, 1353(f), 1355-6
  in acetabulum, 1352
  arteries, 1087, 1356
  muscle attachments, 1356
  nerves, 1356
  ossification, 1354
  sex differences, 1356
  structure, 1352
  surface anatomy, 1340
  surfaces, 1356
  topography, 1355 *See also* hip bone

imaging
  kidney, 1227(f), 1229(f)
  large intestine, 1138, 1139(f)
  mediastinum *See* mediastinum, imaging
  mesorectum, 1151, 1153
  paranasal sinuses, 559
  pleura, 989, 990(f)
  prostate, 1215, 1257(f)
  of prostate, 1258(f)

    thyroid gland, 462-3, 463(f) *See also* computed tomography (CT); *See also* magnetic resonance imaging (MRI)

immune system, development, gut-associated lymphoid tissue, 1213

immunoglobulin A (IgA), 71, 74
    secretion, salivary glands, 522
    in tears, 672

immunoglobulin D (IgD), 71, 73(f), 77

immunoglobulin E (IgE), 71

immunoglobulin G (IgG), 68, 71, 75

immunoglobulin M (IgM), 68, 71

impingement position, 807

implantation, 172, 175-6
    ectopic, 172, 175
    interstitial, 175
    site, 172, 180

importins, 19

impotence, 1276

impression
    of liver
        cardiac, 1163
        oesophageal, 1164(f), 1165
    on lung, cardiac, 992(f), 993
    of spleen
        colic, 1191
        gastric, 1191
        pancreatic, 1191
        renal, 1191
    trigeminal, 424, 617

***in vitro* fertilization**, 168

Inca bone, 411, 418, 711

incisors *See* teeth

incisura(e) (incisure), 85
  angularis, 1112
  cardiaca, 1112
  mandibulare, 412, 532, 538, 541, 542
  Schmidt-Lanterman, 50, 55
  tentorial, 427 *See also* notch

incontinence, 1160
  stress, 1248, 1254 *See also* continence

incus, 621(f), 627
  development, 598, 652
  movements, 628
  ossification, 627 *See also* ossicles, auditory

index (indices)
  chilotic, 1360
  sacral, 1359

indusium griseum, 355, 383
  development, 386

infantile cystic renal disease, 1312

infants
  aortic coarctation, 984
  bony pelvis, 1359
  cartilage of larynx, 584
  epiglottis, 584
  larynx, 584
  lumbar puncture, 760
  lungs, 992
  premature, 213, 216
    gut function, 1203
    kidney, 1309
    myelination, 389
    testicular descent, 1321
  running, 1461
  subglottis, 584
  supraglottis, 584

umbilical hernia, 1063
vocal cords, 584 *See also* neonate

infection
axilla, 791
carotid sheath, 568
dental, 517, 518(f), 524
of hand, 861
infratemporal fossa, 439, 543
maxillary sinus, 525
neck, 439-40
paranasal sinus, 559
parapharyngeal space, 568
pharynx, 568
prevertebral space, 568
retropharyngeal space, 568
submasseteric space, 538
vertebrae, 744 *See also* abscess

infertility, male, 1268

inflammation
dermal repair, 163
mast cells, 36
neurogenic, 236
peritoneal fluid, 1107

infundibulum
of ethmoid bone, 473, 551
of hair follicle, 151, 153
of hypophysis, 380
of hypothalamus, 319, 321
of kidney, 1231, 1242
of right ventricle, 964, 966, 984
of uterine tube, 1285

inion, 745

injury *see specific anatomical structures*; *See also* trauma

inlet(s)

- laryngeal, 567, 582
- pelvic, 1083, 1358
- thoracic, 909

innervation *See* nerves (of organs, or regions); *specific anatomical structures*

innominate bone *See* hip bone

insertion, of muscles, 121, 122(f)

inspiration *See* breathing

instep, of foot, 1341

insula, 335, 346, 346(f)
- caudal, 354
- development, 383
- functions, 346
- gyri, 346
- opercula, 335, 346, 383
- projections to amygdala, 354
- rostral, 354
- zones, 346

insulin, 1207

insulin-like growth factors (IGF), 8, 1299
- decidual cells producing, 176
- fetal, 218

integrins, 5, 7, 128, 129, 137

interbrain *See* diencephalon

interface, thoracoabdominal, 1041

interferon(s), 8

interleukin(s), 8

interneurones, 225
- of cerebral cortex, 339
- of spinal cord, development, 375
- of subthalamic nucleus, 332

internode, 43, 50, 53, 54

interosseous muscle paralysis, 849

interparietal bone, 411, 613, 713

intersex conditions, 1319

interval, rotator, 805, 806

intestine, large, 1137-62, 1137(f), 1138(f)
  arteries, 1140-1, 1141(f), 1144-5
    occlusion, 1140-1
  comparison with small intestine, 1137
  development, 1137, 1209, 1212-13
  fetus, 1212
  haustrations, 1137
  lymphatics, 1141, 1141(f), 1145, 1147
  malrotation, 1209
  maturation, 1212
  mesentery, 1138, 1140
  microstructure, 1160-2
  mucosa, 1212
  muscularis, 1212
  neonate, 1212
  nerves, 1141, 1146, 1147, 1150
  radiographic appearance, 1138, 1139(f)
  serosa, 1212
  size, 1137
  smooth muscle, 8-1050
  structure
    external, 1138, 1139(f)
    internal, 1138, 1139(f)
  veins, 1141, 1141(f), 1145, 1150 *See also* caecum; *See also* colon; *See also* rectum

intestine, small, 1052, 1125-35
  at birth, 1211-12
  development, 1137, 1209
  epithelium, 1133-4

- malrotation, 1209
- maturation, 1209-11
- mesentery, 1053, 1105, 1217, 1218
- microstructure, 1125-35
- microvilli, 1210
- mucosa, 1133-5, 1134(f)
  - development, 1209-11
- muscularis layer, development, 1211
- peritoneum, 1217
- serosa, development, 1211
- submucosa, 1135
- surface anatomy, 1053 *See also* duodenum; *See also* ileum; *See also* jejunum

intima
- synovial, 100
- tunica *See* tunica

intrauterine growth restriction, 216, 216(f), 1299

intrinsic factor, 1121

introitus
- laryngeal, 582
- vaginal, 1284

intubation, endotracheal, neonate, 1033

ions
- selective resorption, kidney, 1238
- transport, 9
  - kidney, 1237

iris, 668, 675, 681-5, 684(f)
- arteries, 682(f)
- coloboma, 699
- colour, 682, 684(f), 701
- development, 699, 701
- innervation, 684-5
- microstructure, 684(f), 685(f)
- muscles of, 682, 684-5

  - photosensory, 675
  - vascular supply, 685
  - veins, 682(f)

ischaemia
  - cerebral cortex, 392
  - peri-umbilical, 1209
  - spinal cord, 757

ischium, 1041, 1353(f), 1356-7
  - in acetabulum, 1352
  - arteries, 1357
  - muscle attachments, 1357
  - nerves, 1357
  - ossification, 1354
  - surface anatomy, 1340, 1356 *See also* hip bone

island
  - blood, of embryo, 203, 1207
  - haemopoietic, 75
  - parathyroid, 464

islet, of Langerhans, 1190
  - development, 1207

isomerism, 974

isthmus
  - aortic, 984, 1027
  - of cervix uteri, 1299
  - of external auditory meatus, 620
  - of hair follicle, 151, 152
  - of kidney, 1226, 1227(f)
  - oropharyngeal, 500, 564, 604
  - pharyngeal, 563, 564
  - of pharyngtotympanic tube, 564
  - of thyroid gland, 463(f), 465
  - of uterine tube, 1293

isthmus rhombencephali, 376, 377, 379

J

Jacoby, border tissue of, 694

jaundice
- blood-brain barrier, 49
- obstructive, 1179

jaw
- clicking, 536
- closing, 536, 537
- locking, 536
- movements, 513, 536-7, 537(f)
- opening, 537(f)
  - eccentric, 536-7
  - symmetrical, 536
- tissue spaces around, 524, 524(f)
- tooth-bearing region, quadrants, 509 *See also* mandible; *See also* maxilla

jejunum, 1128, 1128-9, 1129(f)
- arteries, 1129-30, 1131(f)
- development, 1209, 1210
- displacement in pregnancy, 1300
- feeding, 1129
- lymphatics, 1130-1
- lymphoid aggregates, 1128
- nerves, 1131
- referred pain, 1131
- veins, 1130

jelly
- cardiac, 1016
- Wharton’s, 177, 182, 1209

joints (general), 97-103
- blood supply, 101
- capsule *See* capsule(s)
- classification

ball and socket, 101(f), 102
biaxial, 101, 102
bicondylar, 101
cartilaginous, 98-9, 99(f)
    primary, 98
    secondary, 98-9
complex, 99(f), 102
compound, 102
ellipsoid, 101
fibrous, 97, 98(f)
    development, 902
ginglymi (hinge), 101
gomphosis, 97
hinge, 101
membrane, 100-1, 100(f)
multiaxial, 101, 102, 103(f), 114
pivot, 101
plane, 101
saddle, 101
schindylesis, 97, 97(f)
spheroidal, 101
sutures, 97
synarthroses, 97, 98(f)
synchondroses, 95, 98, 98(f), 99
syndesmosis, 97
synovial, 99-103
    adipose tissue, 100
    articular surfaces, 99-100, 99(f), 121-2, 121(f)
    classification, 102-3
    degrees of freedom, 102
    development, 902
    erosion, 100
    fibrous capsule, 100
    lubrication, 100, 101, 120-1, 120(f)
    mechanical properties of, 121
    membrane, 82, 83, 99, 99(f), 100, 100(f)
    movements, 102-3

        - uniaxial, 101, 102, 114 *See also* sutures
    - congruence, 99, 101
    - development, 103, 902
    - ‘dry’, 100
    - lymphatics, 101
    - movements, 102-3
        - lever systems, 121, 122(f)
        - limitation, 101
    - position
        - close-packed, 114, 121, 123, 123(t)
        - locked, 123
        - loose-packed, 123, 123(t)
    - reaction at, 115
    - stability, 114, 120, 120(f)
        - dynamic, 114
        - static, 114
    - sutures, 97, 409, 410(f), 411 *See also* suture(s) *See also* suture(s)
    - symphysis, 98, 98(f), 99
        - pubis, 98
    - vascular supply, 101

joints (named)
- acromioclavicular, 801-3
    - articulating surface, 801, 802(f)
    - fibrous capsule, 801
    - innervation, 803
    - movements, 803, 806
    - stability, 803
    - surface anatomy, 785
    - vascular supply, 803
- ankle, 1331, 1442-4, 1443(f), 1444(f), 1447(f)
    - arteries, 1457
    - articulating surfaces, 1442
    - clinical procedure, 1347
    - fibrous capsule, 1442
    - fractures, 1443-4
    - innervation, 1442
    - ligaments, 1442

    - lymphatic drainage, 1442
    - movements, 103, 1339(t)
    - muscles, 1339(t)
    - muscles producing movement, 1443
    - reflex, 1346
    - relations, 1442
    - stability, 1443
    - surface anatomy, 1340, 1342(f)
    - synovial membrane, 1442
    - synovial sheaths, 1430, 1430(f)
    - vascular supply, 1442
- arytenocorniculate, 580
- atlanto-axial, 409, 425, 734-5, 734(f)
    - articulating surfaces, 734
    - fibrous capsules, 734
    - innervation, 735
    - ligaments, 734-5
    - movements, 735, 743
    - muscles acting on, 735
    - relations, 735
    - stability, 730, 735
    - synovial membranes, 735
    - vascular supply, 735
- atlanto-occipital, 409, 416, 733-4, 734(f)
    - articulating surfaces, 733
    - fibrous capsules, 733
    - innervation, 734
    - ligaments, 733-4
    - movements, 734, 743
    - muscles acting on, 734
    - relations, 734
    - stability, 734
    - synovial membrane, 734
    - vascular supply, 734
- calcaneocuboid, 1446-7
    - articulating surfaces, 1446
    - fibrous capsule, 1446

    - innervation, 1446
    - ligaments, 1446
    - muscles producing movement, 1447
    - relations, 1446
    - stability, 1446
    - surface anatomy, 1341
    - synovial membrane, 1446
- carpal, 857, 870-1
    - arteries, 870
    - innervation, 870
    - synovial membrane, 870
- carpometacarpal, 875-6
    - movements, 875
    - muscles acting on, 875
- chondrosternal, 924, 924(f)
- chondrosternal (junctions), 924
- costochondral (junctions), 98(f)
- costocorporeal, 922
- costotransverse, 769(f), 770, 923-4, 923(f)
    - movements, 923-4
- costovertebral, 922(f), 923(f)
    - capitular, 770
    - development, 768, 770
    - movement during breathing, 1011
- craniovertebral, 733-5
- cricoarytenoid, 580
    - movement, 580
    - nerves, 580
- cricothyroid, 577(f), 580
    - nerves, 580
- cubital *See* joints (named), elbow
- cuboideonavicular, 1448
- cuneocuboid, 1448
- elbow, 831-7, 832(f), 833(f)
    - arteries, 835
    - articulating surfaces, 831
    - dislocation, 835

- fibrous capsule, 832, 832(f)
- injuries, 835
- innervation, 830, 836-7
- movements, 778, 833-4
  - accessory, 833
- neonatal, 905
- pulled, 835
- skin, 831
  - blood supply, 831
  - nerves, 831
- surface anatomy, 786
- synovial membrane, 832-3, 832(f), 833(f)
- veins, 836

facet *See* joints (named), zygapophyseal
glenohumeral, 803-7, 804(f)
- articulating surfaces, 803, 804(f), 805
- dislocation, 786, 807
- fibrous capsule, 804(f), 805
- innervation, 806
- movements, 778, 806-7
  - muscles of, 807
- stability, 806
- synovial membrane, 805
- vascular supply, 806

hamate-triquetral, force transmission, 874
hip, 1331, 1387-92, 1387(f), 1388(f)
- arterial anastomoses, 1380-1
- arteries, 1390
- articulating surfaces, 1352, 1365, 1366, 1387, 1387(f)
- biomechanics, 1390-2
- bursae, 1389
- clinical procedure, 1346
- development, 1463
- developmental dysplasia, 1463
- dislocation, 1342
- fibrous capsule, 1387-8
- forces acting on, 1391-2

  - innervation, 1382-4, 1382(f), 1390
  - ligaments, 1388-9
  - lymphatic drainage, 1381
  - lymphatics, 1390
  - movements, 1339(t), 1390-1
  - muscles, 1339(t)
  - muscles acting on, 1391-2, 1392(f)
  - pain, 1366, 1390
  - range of motion, 1391
  - relations, 1387-8
  - stability, 1390
  - surface anatomy, 1341-2
  - synovial membrane, 1388(f), 1389
  - veins, 1381-2
- incudomalleolar, 628
- intercarpal, movements, 871-2
- interchondral, 924
- intercoccygeal, 736
- intercuneiform, 1448
- intermetacarpal, 876
  - movements, 876
  - muscles acting upon, 876
- intermetatarsal, 1448-9
- interphalangeal
  - of foot, 1449-50
    - innervation, 1450
    - muscles producing movement, 1450
  - of hand, 857, 877-8, 878(f)
    - movements, 878
      - accessory, 878
      - muscles acting upon, 878
    - stability, 878
    - surface anatomy, 786
- intervertebral, 99, 730-3
  - innervation, 731-2
  - vascular supply, 731
- knee, 1331, 1393-410, 1393(f), 1394(f), 1402

arteries, 1408-9
articulating surfaces *see individual joints*
biomechanics, 1403-7
    articular, 1405-6, 1406(f)
    soft-tissue, 1407, 1407(f)
bones, 1394-5
bursae, 1402
capsule, 1400
clergyman's, 1402
clinical procedure, 1346-7
clunking, 1398
compression, 1405-6, 1405(f), 1406(f)
fat pads, 1401-2
friction, 1406
housemaid's, 1402
kinematics, 1403-5, 1404(f)
    articular, 1404-5, 1405(f)
ligaments, 1398-9, 1401
loading, 1403
lymphatics, 1409
menisci, 1340, 1397-8, 1398(f)
movements, 1339(t), 1402-3
    accessory, 1403
muscles, 1339(t), 1407-8, 1407(f)
muscles producing movement, 1403
nerves, 1409-10
plicae, 1401-2
reflex, 1346
relations, 1403
restraints (primary and secondary), 1407, 1407(f)
screw-home mechanism, 1404
skin, 1393
    innervation, 1393
    lymphatics, 1393
    nerves, 1393
    vascular supply, 1393
soft tissue, 1393-4, 1393(f)

        stability, 1403
        surface anatomy, 1340, 1341(f), 1342-3, 1342(f)
        synovial membrane, 1396, 1401-2
        veins, 1409
    of Luschka, 730
    mandibular *See* joints (named), temporomandibular
    manubriosternal, 99, 909, 910, 917, 922
        movements, 922
        surface anatomy, 913, 917, 917(f)
    metacarpal, first, movements, 778
    metacarpophalangeal, 857, 876-7, 876(f)
        movements, 778, 877
            accessory, 877
            muscles, 877
        surface anatomy, 786
    metatarsophalangeal, 1449
        articulating surfaces, 1449
        fibrous capsules, 1449
        innervation, 1449
        ligaments, 1449
        muscles producing movement, 1449
        relations, 1449
        stability, 1449
        surface anatomy, 1341
        synovial membrane, 1449
    midcarpal, 870
        force transmission, 874
        movements, 871-2, 873(f)
    naviculocuneiform, 1447-8
        articulating surfaces, 1447
        fibrous capsule, 1447
        innervation, 1447
        ligaments, 1447
        muscles producing movement, 1447
        relations, 1447
        synovial membrane, 1447
    patellofemoral, 1396-7, 1403

    - articulating surfaces, 1396 *See also* joints (named), knee
- radio-ulnar
    - distal, 835, 868
        - arteries, 868
        - articular disc, 868
        - force transmission, 874
        - innervation, 868
        - movements, 868
        - stability, 871
    - movements, 778
    - proximal (superior), 834-5
        - stability, 835
        - synovial membrane, 834
- radiocarpal *See* joints (named), wrist
- rotator cuff, 778, 806, 807, 812
- sacrococcygeal, 736
- sacroiliac, 97, 1331, 1366-7
    - arteries, 1366
    - articulating surfaces, 1366
    - development, 1366
    - innervation, 1366
    - lymphatics, 1366
    - movements, 1366
    - relations, 1366
    - stability, 1366
    - surface anatomy, 1340
    - variants, 1366
- scaphotrapeziotrapezoid, force transmission, 874
- shoulder *See* joints (named), glenohumeral
- sternochondral *See* joints (named), sternocostal
- sternoclavicular, 800-1, 801(f), 986
    - articular disc, 801
    - articular surfaces, 800-1, 801(f)
    - fibrous capsule, 801
    - innervation, 801
    - movements, 778, 803
    - stability, 801

    vascular supply, 801
sternocostal, 924, 984
    variations, 104
symphysis, menti, 99
talocalcaneal, 1444-6, 1445(f)
    articulating surfaces, 1444
    fibrous capsule, 1444
    innervation, 1445
    ligaments, 1444-5
    muscles producing movement, 1446
    relations, 1445-6
    stability, 1446
    synovial membrane, 1445
talocalcaneonavicular, 1437, 1445(f), 1446
    articulating surfaces, 1446
    fibrous capsule, 1446
    innervation, 1446
    ligaments, 1446
    muscles producing movement, 1446
    relations, 1446
    stability, 1446
    synovial membrane, 1446
talocrural *See* joints (named), ankle
talonavicular, surface anatomy, 1341
tarsal, 1443(f), 1447(f)
tarsometatarsal, 1448
    articulating surfaces, 1448
    fibrous capsule, 1448
    innervation, 1448
    ligaments, 1448
    muscles producing movement, 1448
    stability, 1448
    surface anatomy, 1341
    synovial membrane, 1448
temporomandibular, 533-40, 534(f), 535(f)
    articular surfaces, 534
    development, 534, 534(f)

    - dysfunction syndrome, 539
    - imaging, 537
    - innervation, 535-6
    - ligaments, 533-4
    - lymphatic drainage, 536
    - movements, 536
    - relations, 535
    - synovial membrane, 534
    - vascular supply, 535-6
- tibiofibular, 1403
    - inferior, 97, 1331, 1444
        - articulating surfaces, 1444
        - fibrous capsule, 1444
        - innervation, 1444
        - ligaments, 1444
        - lymphatic drainage, 1444
        - muscles producing movement, 1444
        - relations, 1444
        - stability, 1444
        - synovial membrane, 1444
        - vascular supply, 1444
    - superior, 1331, 1395-6
        - articulating surfaces, 1395
        - fibrous capsule, 1395
        - innervation, 1396
        - ligaments, 1395
        - lymphatic drainage, 1396
        - movements, 1396
        - relations, 1396
        - stability, 1396
        - synovial membrane, 1396
        - vascular supply, 1396
    - surface anatomy, 1340
- uncovertebral, 730
- wrist, 857, 869(f), 870
    - actions, 874
    - arteries, 857, 858(f), 870

        - articulating surfaces, 868, 870, 872
        - drop, 829
        - fibrous capsule, 870
        - force transmission, 872-3
        - in hand movements, 887
        - innervation, 870
        - instability, 875
        - ligaments, 870-1
        - loading, 872-3
        - magnetic resonance imaging, 869(f)
        - movements, 778, 871-2, 873(f), 874
        - muscles, 778, 887
        - surface anatomy, 786
    - xiphisternal, 922
        - surface anatomy, 912
    - zygapophysial, 732-3, 768
        - articulating surfaces, 732
        - fibrous capsule, 732
        - innervation, 733
        - ligaments, 732
        - lumbar tropism, 733
        - relations, 733
        - vascular supply, 732-3
    - zygopophysial, sites, 768

joints (of regions)
- of auditory ossicles, 628
- of ear, middle, 628
- of fingers, 875-8
- of foot, 1331
- of hand, 868-78, 869(f)
- of larynx, 580
- of lower limb, 1331
- of pectoral girdle, 800-3
- of pelvic girdle, 1365-7
- of sternum, 917-18, 922
- of thoracic wall, 800-1, 922-4
- of thumb, 875-7

- of upper limb, 778
- of vertebral column, 730-6
- of wrist, 868-70

jugum sphenoidale, 423, 424, 527, 530

junction(s)
- anorectal, 1151, 1157(f)
- anterior (prevascular), of lungs, 957
- atrioventricular, 962, 966, 1030
- bulboventricular, 1025
- corneoscleral, 672, 675, 678, 679
- corticomedullary, 77, 946, 947
- costochondral, 98(f), 924
- craniovertebral *See* junction(s), occipitocervical
- dermo-epidermal, 146, 150, 157, 161
- enamel-dentine, 514
- fascia adherens, 7, 140(f), 141, 141(f)
- gap, 7
    - in embryo, 186, 194
    - in heart, 976
    - smooth muscle, 127, 128(f)
- gastro-oesophageal, 1008, 1113-14
- ileocaecal, 1294
- intracellular
    - adhesive, 7
    - communicating, 7
    - occluding, 6-7, 6(f) *See also* junction(s), gap; *See also* junction(s), tight
- lumbosacral, 735-6
- manubriosternal, 99, 909, 910, 917
- mucogingival, 500
- neuromuscular (myoneural), 41, 61-3, 225
    - autonomic, 62-3
    - development, 115, 116(f)
    - skeletal, 61-3, 111
    - smooth muscle, 128, 132
- occipitocervical, 771(f)

        - development, 769-70
        - embryos (stages 12-15), 769
    - oesophago-gastric (squamocolumnar), 1008
    - pelviureteric, obstruction, 1226
    - pharyngo-oesophageal, 561
    - pontomedullary, 240
    - posterior, mediastinal, 957
    - primary, 1025
    - sacrococcygeal, 736
    - spinomedullary *See* junction(es), occipitocervical
    - squamocolumnar, of uterine cervix, 1292
    - tight, 6-7, 6(f)
    - ventriculoatrial, 962

‘junctional feet’ (pillars), 108

juncturae tendinae, 849, 880

juxtamedullary, definition, 1232

K

kallikrein, 1310

Kartagener's immotile cilia syndrome, 17

karyotype, 19-20, 20(f)

keratinization, 145, 148, 153, 158(f)

keratins, 7, 14(f), 15, 145, 147, 147(f), 148, 149(f), 150, 152, 153, 154, 157, 159

keratoconus, 688

kidney, 1225-38, 1225(f)
- absent, 1226
- agenesis, 1035, 1312
- arteries, 1225(f), 1231-3, 1232(f)
  - segmentation, 1231-2
- calyces *See* calyx (calyces), renal
- colour, 1225
- cortex, 1228-9, 1230(f), 1232, 1235(f)
- cysts, 1312
- development, 1309-10
  - anomalies, 1312
  - ascent, 1310
    - failure, 1226
  - endocrine, 1309-10
  - mesonephric, 1308
  - metanephric, 1308, 1309(f) *See also* mesonephros; *See also* metanephros
- dimensions, 1225
- ectopia, 1226, 1226(f)
  - crossed, 1226, 1226(f)
- endocrine function, 1225
- fetus, 1225
- functions, 1225
  - indicators, 1312
- hilum, 1228, 1231

hormones secreted, 1310
horseshoe, 1226, 1227(f), 1312
hypertrophy, compensatory, 1226
imaging, CT, 1227(f), 1229(f)
innervation, 1233
left, surfaces, 1228, 1228(f)
lobulated, 1312
lobules, 1225, 1312, 1313(f)
location, 1225
lymphatic drainage, 1233
medulla, 1228-9, 1230(f), 1232-3, 1234(f), 1237(f), 1238
microstructure, 1233-7, 1236(f) *See also* glomerulus (glomeruli); *See also* renal; *See also* tubule(s), renal
neonatal, 1225, 1312, 1313(f)
organization, 1234(f)
pelvic, 1226, 1312
pelvis of *See* pelvis, renal
perirenal fascia *See* fascia, perirenal
pleural relationship, 1009
postnatal, 1228
relations, 1228, 1228(f), 1229(f)
right, surfaces, 1228
stones, 1242
structure, 1228, 1228(f)
surface anatomy, 1054, 1225, 1225(f), 1227(f), 1228
    antolateral, 1228
    posteromedial, 1228
surgical approach, 991
veins, 1233
weight, 1225, 1312

kinesins, 15, 16

kinetochore, 16, 19

kinocilium, 638, 638(f)

Klumpke's paralysis, 822

knee *See* joints (named), knee

knot of Henry, 1458

knuckle(s)
  aortic, 914, 954
  of hand, 786, 864

Korsakoff psychosis, 358

kyphosis, 714, 744, 745
  in spina bifida, 772

L

L-CAM, 1308

L-selectin, 175

labial tractors, direct, 467, 488-9

labium (labia)
- majus (majora), 1279, 1279(f)
  - age-related changes, 1279
  - development, 1325
  - lymphatics, 1280
  - nerves, 1280
- minus (minora)
  - age-related changes, 1279
  - development, 1279-80, 1279(f), 1325
  - lymphatics, 1280
- tertium, 1280
- tympanic, 640
- vestibular, 640, 642

labour (childbirth), 1301-3
- first stage, 1301
- second stage, 1301-2
- third stage, 1302
- onset, 1301

labrum (labra), 101
- acetabular, 1387
- glenoid, 805

labyrinth(s)
- bony, 633-42, 633(f)
  - development, 652
  - microstructure, 634-6, 636(f)
- ethmoidal, 472-3, 528
- membranous, 633, 633(f), 634, 636-42, 636(f)
  - development, 651(f), 652

lacrimal bone, 475, 655

- lesser, 475
- orbital surface, 475
- ossification, 475

lactation, 936, 936(f)

lacteals, 139, 1130-1, 1134(f), 1135

lactic acid, 62

lactoferrin, 672

lactose, 1212

lacuna(e)
- of bone, 87, 88, 88(f), 90(f), 93, 94(f), 95
- of cartilage, 81
- Howship’s, 88
- magna, 1252
- of urethra, 1252, 1253

lake, lacrimal, 669

lambda, 412, 418, 470

lamella(e)
- of bone, 86, 87, 88, 88(f), 89, 89(f), 90, 90(f), 91, 92(f), 95
- corneal stroma, 678-9
- elastic, 131
- epithelial, penis development, 1325

lamellipodia, 3, 50

lamina(e), 83, 86
- alar *See* plate(s), alar
- basal, 27, 31, 33-4, 33(f)
  - of bone, 89, 101, 105, 107, 108, 111, 116, 117
  - of epithelial somite cells, 764
  - functions, 34
  - glomerular, 1235
  - muscular, 107, 108, 110(f), 111, 115, 116, 116(f), 117, 117(f)
  - of oesophagus, 952
  - of renal corpuscle, 1235, 1236(f)

    - of skin, 146-7, 147(f)
    - spinal cord development, 375
- of cerebral cortex, 300, 339-41, 379
    - agranular type, 340
    - connections, 341-2
    - geniculate, 347
    - granular, 340
    - heterotypical variants, 340
    - homotypical variants, 340
    - I (plexiform) layer, 339
    - II (external granular) layer, 326, 339
    - III (pyramidal) layer, 329, 339
    - IIIa (pyramidal) layer, 339
    - IIIb (pyramidal) layer, 339
    - IIIc (pyramidal) layer, 339
    - IV (internal granular) layer, 339
        - striate cortex, 346
        - sublayers, 346-7
    - V (internal pyramidal [ganglionic]) layer, 329, 339
    - VI (multiform [fusiform/pleiomorphic]) layer, 329, 339-40
- of costoclavicular ligament, 801, 801(f)
- cribrosa, 667, 693, 694, 695
- cribrosa sclerae, 675
- cricoid, 577(f), 579, 610, 952
- densa, 33, 33(f)
    - of skin, 146, 147, 159
- dental, 605, 606
- Descemet’s, 33
- dissecans, 351
- dura, 517
- elastic, 137
    - arterial, 131, 132(f), 137
    - fenestrations, 137
- fibroreticularis, 146
- fibrosa, 970
- of flexor retinaculum, 879
- fusca, 679

labiogingival, 605, 606
lacrimal, 602
limiting
    anterior (Bowman’s layer), 677(f), 678
    posterior (Descemet’s membrane), 33, 675, 678(f), 679, 702
limiting (Descemet’s), of cornea, 33
lucida, 33
    of skin, 146, 159
marginalis, 257, 259
medial
    of globus pallidus, 383
    of lentiform nucleus, 383
medullary
    external, 311
    internal, 311, 312, 313, 316
    of thalamus, 311
nuclear, 18
of palatine bone, 478
papyracea, 655
of pectoralis major, 807-40
prevertebral, pus behind, 525
propria, 38, 39, 127, 1122
    GALT development, 1213
    of gut wall, 1050-1
    of large intestine, 1161
    of oesophagus, 952
    of pleura, 991
    of tongue, 507
    of urethra, 1250, 1253
reticular, 34
    of cochlea, 640
Rexed’s, 257
    IX, 258, 269, 271
    VII, 258, 263, 264, 265, 266, 267, 269, 270, 271
of small intestine, 1135
spiral, of cochlea, 634, 639, 640, 652
splendens, 199

- subintimal, 100
- superciliaris, 675
- of superior colliculus, 291
- terminalis, 356, 380, 381(f), 385
    - arterial supply, 253
    - development, 364-5
- of thyroid cartilage, 579
- of uterine tube, 1294
- ventral, spinal cord development, 375
- ventrolateral (basal) *See* plate, basal
- of vertebrae, 716, 770
    - cervical, 719
- vitrea (Bruch's membrane), 679, 680 *See also* layers(s); *See also* plate(s)

laminin, 5, 38, 194, 205
- placental villi, 178

lamins, 15, 18

landmarks
- musculotendinous, 747
- posterior pelvic, 747
- sacrococcygeal, 747
- scapular, 746-7

language, cerebral areas
- asymmetry, 358
- lesions, 358

laryngocoele, 583

laryngopharynx, 561(f), 567-8
- boundaries, 567

larynx, 577-94
- arteries, 587-8, 587(f)
- cartilage, 577-80, 577(f), 578(f), 996(f)
- cavity, 582-4
- examination, 584, 584(f)
- glands, 582

- infant, 584
- inflammation, 584
- inlet, 567, 582
- joints, 580
- ligaments, 580-2
- lymphatics, 588
- membranes, 580-2
- microstructure, 582
- muscles, 583, 585-7, 586(f)
  - extrinsic, 585
  - intrinsic, 585-7
- neonate, 574, 610
- nerves, 588-9, 588(f)
  - anomalies, 589
  - autonomic, 589
- obstruction, 584
- paralumenal spaces, 584-5
- size, 577
- skeleton, 577-80, 577(f), 578(f)
- soft tissue, 580-2
- speech, 589-93
- swallowing, 573
  - neonatal, 574
- taste buds, 582
- trauma, 584
- tumours, 585, 588
- veins, 588

laws
- Hilton’s, 101
- Newton’s second, 121
- Semon’s, 589

layer(s)
- anterior border, of iris, 682
- aponeurotic, 467
- Bowman’s, 677(f), 678
- cambial, 97, 97(f)

of cerebellar cortex *See* lamina, of cerebral cortex
choriocapillaris, 679(f), 680
dartos, 1273
dermal
    hypodermis, 146(f), 150-1
    papillary, 150
    reticular, 150
entorhinal cortex, 351
epicardial, 1026
granular, of cerebellar cortex, development, 379
Haller’s, 680
Henle’s, 151, 152, 152(f)
of hippocampal formation, 350-1
Huxley’s, 151, 152, 152(f)
intermediate, of spinal cord, 752
investing, of deep cervical fascia, 439
longitudinal, of anal canal, 1159
of mesoblast
    somatopleuric, 183
    splanchnopleuric, 183
molecular, of cerebellar cortex, 300, 302, 303
    development, 379
Nitabuch’s, 177
of oesophagus, 951-2, 952(f)
plexiform, of subicular complex, 350-1
Purkinje, of cerebellar cortex, 303
    development, 379 *See also* cells (named), Purkinje
retinal, 688-9, 689(f)
    modification in macular area, 688-9
Sattler’s, 680
of scalp, 467
of skin, 145
suprachoroid, 679
of urinary bladder, 1250
vitelline, 167 *See also* lamina(e); *See also* stratum (strata)

Le Fort fractures, 480

learning, motor, inferior olivary complex role, 309

leg, 1411-28
  arteries, 1424-6
    cutaneous, 1411
  bones, 1412-18
  compartments, 1330-1, 1411-12
    anterior (extensor), 1411
    lateral (fibular), 1411
    posterior (flexor), 1411
  muscles, 1331-3, 1417-24
    anterior (extensor) compartment, 1417-19, 1418(f), 1419(f)
    arterial supply, 1411
    innervation, 1411
    lateral (peroneal/fibular) compartment, 1418(f), 1419-20
    nerves, 1411
    posterior (flexor) compartment, 1418(f), 1420-4
  nerves, 1426-8
  skin, 1411
    lymphatics, 1411
    vascular supply, 1411
  soft tissue, 1411
  surface anatomy, 1340-1, 1341(f), 1342(f), 1343, 1343(f)
  trauma, 1411-12
  veins, 1426
  venous drainage, 1090

lemniscus
  lateral, 281(f), 285
    trigeminal, 282, 285, 287
  medial, 228, 229(f), 263, 263(f), 264, 264(f), 265(f), 267, 267(f), 270, 277-8, 278(f), 279
  trigeminal, 282, 285, 287 *See also* tract(s)

lens (of eye), 675, 676(f), 686-8, 686(f), 687(f)
  adult, 686, 686(f)
  age-related changes, 686
  development, 699, 701-2, 701(f)
  dimensions, 686

- dislocation, 688
- fetus, 686
- microstructure, 686(f), 687
- nucleus, 687
- nutrition, 702
- refraction, 687
  - disorders, 687-8
- shape, 681, 686

leptomeninges *See* arachnoid mater; *See also* pia mater

leptotene, 22

lesions ***see specific nerves or anatomical structures***

leukaemia inhibitory factor, 8

leukomalacia, periventricular (PVL), 391

leukotrienes, bronchi, 1004

lever systems, movement, 121-2, 122(f)

levodopa, 332

ligaments (general), 98, 98(f), 99(f), 119
- material properties of, 120
- movement limitation, 103

ligaments (named) (ligamentum(a))
- accessory, 99, 100, 923
  - functions, 100
- acetabular, transverse, 1352(f), 1380, 1387
- acromioclavicular, 801
- alar, of dens, 735
- anococcygeal, 1094, 1154, 1155, 1158(f), 1159
- anterior
  - of auricle, 619
  - cruciate, 1397, 1397(f), 1398, 1398(f), 1401
  - of malleus, 624, 627, 628
  - pubic, 1365
  - of tibiofibular joint, superior, 1395
- anular, 834

        of stapes, 627, 628
apical, of dens, 735
arcuate
        of knee, 1400, 1401, 1408
        lateral, of diaphragm, 985, 1007, 1069
        medial, of diaphragm, 1007, 1041, 1070
        pubic, 1365
        of wrist, 870, 871
arteriosum, 982, 984, 1030
aryepiglottic, 581
atlantal, transverse, 735
bifurcate, 1446
broad, of uterus, 1106, 1285, 1286(f), 1288, 1288(f), 1289(f), 1321(f)
        development, 1321
        laparoscopic view, 1287(f)
Broyles’, 583, 584
calcaneocuboid, plantar, 1446
calcaneonavicular, plantar (spring), 1437, 1446
cardinal, 1289
caroticoclinoid, 530
cervical, 1445
        transverse, 1289, 1290(f)
check, 656, 657, 658(f), 661
check-rein, 877
Cleland’s, 859, 894
cochlear, 639
collateral
        of interphalangeal joints, 877
        lateral (of knee), 1398(f), 1399(f), 1400, 1403, 1407
                surface anatomy, 1343
        medial (of knee), 1398(f), 1399(f), 1400, 1402, 1407
        of metacarpophalangeal joints, 876(f), 877, 882(f)
        of metatarsophalangeal joints, 1449
        radial, 832, 862, 870, 872
        ulnar, 832, 832(f), 870, 877
commissural
        distal, 859, 859(f)

    proximal, 859, 859(f)
conus, of heart, 964, 974
coracoacromial, 795
coracoclavicular, 792, 792(f), 793, 801
coracohumeral, 806
corniculopharyngeal, 581
coronary
    of knee joint, 1398, 1401
    of liver, 1100, 1164(f), 1168, 1214
costoclavicular, 801, 801(f)
costocoracoid, 791
costotransverse, 923
    lateral, 923-4
    superior, 923
costoxiphoid, 924
cricoarytenoid, 577(f), 578(f), 580
cricothyroid, 581
    anterior (median), 405
cricotracheal, 577(f), 581
cruciate (of knee), 1398(f)
    anterior, 1397, 1397(f), 1398, 1398(f), 1401
        absent, 1401
    posterior, 1397(f), 1398, 1398(f), 1399(f), 1401
cruciform, 735
cuneometatarsal, interosseous *See* ligaments (named) (ligamentum(a)), Lisfranc’s
cystoduodenal, 1102
deltoid, 1436, 1442
    rupture, 1444
denticulatum, 752
dorsal
    of carpometacarpal joints, 875, 876
    of intercuneiform and cuneocuboid joints, 1448
    of intermetacarpal joints, 876
    of naviculocuneiform joints, 1447
    of tarsometatarsal joints, 1448
duodenocolic, 1104

fabellofibular, 1401
falciform, 1028, 1099-100, 1103(f), 1167-8
    development, 1099, 1214-15, 1216
‘false’, of bladder, 1247
flavum, 729, 730(f)
fundiform, 1273
gastrocolic, 1104, 1146
gastrohepatic, 1100, 1102
gastrophrenic, 1111, 1112, 1113
gastrosplenic, 1104, 1112, 1191, 1192, 1218
glenohumeral, 805-6
    inferior, 802(f), 806
    middle, 802(f), 806
    superior, 802(f), 805(f), 806
Grayson’s, 859(f), 860, 894
of head of femur (teres), 1100, 1164(f), 1165, 1167, 1389, 1463
hepatocolic, 1104
hepatoduodenal, 1100, 1107, 1214
hepatogastric, 1214
hepatorenal, 1101
humeral, transverse, 806
of Humphry, 1398-9, 1399(f)
hyoepiglottic, 581
iliac, posterior, 1366
iliofemoral, 1388, 1391
iliolumbar, 735-6
infundibulopelvic, 1285, 1288, 1294, 1319
inguinal, 1064
    surface anatomy, 1053, 1340, 1341(f), 1342
interchondral, 924
interclavicular, 801
interclinoid, 530
intercornual, 736
interfoveolar, 1064, 1066(f)
intermeniscal, 1397(f), 1398
of intermetacarpal joints, 876
intermetatarsal (dorsal and plantar), 1448

interosseous, 97, 97(f)
    of carpometacarpal joints, 876
    distal row, 871
    of intermetacarpal joints, 876
    proximal row, 871
interspinous, 729-30
intertransverse, 730
intra-articular
    of costotransverse joint, 923
    of sternocostal joint, 924
ischiofemoral, 1388-9
lacunar, 1066
Landsmeer, 860, 881, 888
lateral
    of ankle joint, 1442
    arcuate, 1007, 1069, 1070
    of bladder, 1247
    of carpometacarpal joints, 875, 876
    collateral (of knee), 1343, 1398(f), 1399(f), 1400, 1403, 1407
    costotransverse, 923
    of malleus, 628
    patellofemoral, 1400
    rectal, 1153, 1154
    sacrococcygeal, 728, 736
    of thyroid gland, 589
leinorenal *See* ligaments (named), splenorenal
Lisfranc’s, 1448
longitudinal
    anterior, 713, 728-9
    posterior, 729, 729(f)
lumbocostal, 921, 923
lunotriquetral, 871
of Mackenrodt, 1289
malleolar, anterior, 598, 627, 628
mammillo-accessory, 723, 741
mandibular, 469
mandibulostylohyoid, 469

meningovertebral, 751
meniscofemoral (MFLs), 1398-9, 1399(f)
meniscofibular, 1398
meniscopatellar, 1400
metacarpal, transverse, 859
  deep, 859, 877, 882(f)
  superior, 859
metatarsal
  deep transverse, 1449
  superficial transverse, 1430
mucosum (infrapatellar fold), 1401, 1401(f)
natatory, 859
nuchae, 737, 745
oblique popliteal, 1394, 1399, 1399(f), 1403
occipital, transverse, 735
ovarian, 1294, 1321(f)
  development, 1321
palmar
  of carpometacarpal joints, 875, 876
  of metacarpophalangeal joints, 877
palpebral
  lateral, 656, 657
  medial, 57
palpebral (canthal), 670, 671(f)
patellar, 1340, 1394, 1396, 1401(f)
patellofemoral
  lateral, 1400
  medial, 1400, 1403
    surface anatomy, 1343
patellotibial, 1400
pectineal, of Astley Cooper, 1066
pelvic, 1285, 1288
of penis, superficial, 1060
perineal, transverse, 1094
periodontal, 513, 514(f), 517
  arterial supply, 518
peritoneal *See* mesentery;

petrosphenoidal (of Gruber), 424
phrenicocolic, 1104, 1191, 1192
phreno-oesophageal, 1008, 1009, 1111
pisohamate, 862, 884
pisometacarpal, 862, 869(f)
plantar
    of intercuneiform and cuneocuboid joints, 1448
    long, 1446
    of metatarsophalangeal joints, 1449
    of naviculocuneiform joints, 1447
    of tarsometatarsal joints, 1448
popliteal, oblique, 1394, 1399, 1399(f), 1403
popliteofibular, 1400, 1403, 1407, 1408
posterior
    of auricle, 619
    of bladder, 1247
    cruciate, 1397(f), 1398, 1398(f), 1399(f), 1401
    iliac, 1366
    of incus, 628
    pubic, 1365
    tibiofibular, 1395
pterygospinous, 530, 540
pubic
    anterior, 1365
    arcuate, 1365
    posterior, 1365
    superior, 1365
pubocervical, 1289
pubofemoral, 1388
pubourethral, 1094
pubovesical, 1247
pulmonary, inferior, 991, 992(f)
quadrate, 834
radiate, 924
radio-ulnar, distal, 871
radiolunate (long, short), 870-1
radiolunotriquetral, dorsal, 871

radioscaphocapitate, 870
radioscapholunate, 871
rectal, lateral, 1153, 1154
retaining, of face, 469
retinacular, of Landsmeer
    oblique, 860, 881, 888
    transverse, 859(f), 881
round
    of liver, 1062
    of uterus, 1288-9, 1321(f)
        development, 1320, 1321, 1322(f)
sacrococcygeal
    anterior, 736
    dorsal, deep, 736
    lateral, 736
    posterior, superior, 736
sacroiliac
    anterior, 1356, 1357(f), 1366
    interosseous, 1356, 1366
    posterior, 1366
sacrospinous, 1083(f), 1084, 1366
sacrospinous, 1366
sacrotuberous, 1366
scaphocapitate, 871
scaphocapitate-trapezoid, palmar, 871
scapholunate, 871
scaphotrapeziotrapezoidal, 871
scapular, 794(f)
    inferior, 796
    transverse, superior, 795, 796
‘scrotal’, 1262
sphenomandibular, 519, 529, 530, 533, 534(f), 536, 539, 541, 542, 598, 627
of spinal cord
    dorsal, 752
    dorsolateral, 752
    ventral, 752

spinoglenoid, 796
splenorenal (lienorenal), 1104, 1112, 1191, 1206, 1207(f), 1217, 1218
sternoclavicular
    anterior, 801
    posterior, 801
of sternocostal joints, 924
sternocostal, radiate, 923
sternopericardial, 959
of Struthers, 836
stylohyoid, 397, 469, 504, 599
stylomandibular, 469, 533
superior
    of incus, 628
    of malleus, 628
    pubic, 1365
suprascapular, 796
supraspinus, 729(f), 730
suspensory
    of axilla, 791
    of breast, 931
    of duodenum, 1099-100, 1103(f), 1127, 1167-8, 1206
    of eye, 658
    of lens, 681
    of ovary, 1285, 1294, 1319
    of penis, 1273
sutural, 97(f)
talocalcaneal
    interosseous, 1445
    lateral, 1444
    medial, 1444
talofibular
    medial, 1436
    posterior, 1436
talonavicular, 1446
temporomandibular (lateral), 533-4, 536
teres, 1049, 1100, 1164(f), 1165, 1167, 1222, 1389, 1463
of Testus, 871

thyroepiglottic, 581
thyrohyoid, 577(f), 579
tibiofibular
  anterior, 1444
  posterior, 1444
transforaminal, 718
transverse
  acetabular, 1352(f), 1380, 1387
  atlantal, 735
  humeral, 806
  inferior, spinoglenoid, 796
  of knee joint, 1397(f), 1398, 1398(f)
  metacarpal *See* ligaments (named), metacarpal
  metatarsal *See* ligaments (named), metatarsal
  occipital, 735
  perineal, 1094
  retinacular, 859(f), 860, 881
  scapular, 795, 796
  superior, suprascapular, 796
  of vertebral column, 730
of Treitz (suspensory, of duodenum), 1099-100, 1103(f), 1127, 1167-8, 1184, 1206
trequetrocapitate, 871, 874(f)
triangular, of liver, 1100, 1168, 1214
triquetrohamate, 871, 874(f)
ulnolunate, 871
ulnotriquetral, 871
umbilical
  medial, 1062, 1087
  median, 1062, 1247
uterosacral, 1285, 1289
venosum, 1102, 1164, 1165, 1168, 1222
vestibular, 578(f), 581(f), 582
vocal, 583
of Wrisberg, 1399
zonular, 681
zygomatic, 469

ligaments (of organs, or regions)
- of anal canal, 1155, 1158, 1158(f)
- of auditory ossicles, 628
- of auricle, 619
- of bladder, urinary, 1246-7, 1248(f)
- of carpometacarpal joints, 875, 876
- of costotransverse joints, 923-4, 924(f)
- of duodenum, 1099-100, 1103(f), 1127, 1167-8, 1206
- of ear, middle, 628
- of elbow joint, 832-3
- of face, 469
- of foot, 1447(f)*see also individual ligaments and joints*
- of glenohumeral joint, 805, 805(f)
- of hip joint, 1388-9
- of incus, 628
- of intermetacarpal joints, 876
- of interphalangeal joints, 877
- of knee joint, 1398-9, 1401
- of larynx, 580-2, 583
- of liver, 1167-8, 1214-15
- of malleus, 628
- of neck, 436, 438
- of ovary, 1294-5, 1294(f)
- of pelvis, 1288-9, 1289(f)
- of penis, 1273
- of pericardium, 959
- of pubic symphysis, 1365
- of rectum, 1153, 1154
- of sacroiliac joint, 1366
- of scapula, 795, 796
- of stapes, 628
- of sternoclavicular joint, 801
- of synovial joints, 99
- of thyroid gland, 589
- of tibiofibular joint, superor, 1395
- of vertebral column, 728-30
- of wrist, 870-1

ligands, 7-8

limb(s)
- development, 899-902
    - skeletal elements, 902-3
- lower, 759, 1331-47
    - anomalies, 1463-4
    - arterial perforators, 1333-4, 1333(f), 1334(f)
    - arteries, 1332(f), 1333, 1333(f)
        - development, 1463, 1464(f)
    - bones, 1331, 1331(f)
        - arterial supply, 1333
    - clinical procedures, 1346-7
    - compartments, 1330-1
    - examination, 1340(t), 1346
    - fascia, 1329-30
    - gateways to, 1329(f)
    - joints, 1331
    - lymphatics, 1336, 1336(f)
    - muscle pumps, 1334-5
    - muscles, 1331-3
    - nerves, 260, 1093, 1336-40, 1338(t)
        - autonomic, 1338
        - lesions, 1340(t)
        - segmentation, 1339(t), 1340(t)
    - pelvic interface, 1041
    - pulses, 1344
    - reflexes, 1346
    - skin and soft tissues, 1329-30
    - surface anatomy, 1340-6
        - arteries, 1344
        - ligaments, 1341-4
        - muscles, 786-7
        - nerves, 1344-6, 1345(f), 1346(f)
        - skeletal, 1340-1, 1341(f)
        - veins, 1334-5, 1335(f), 1344 *See also* leg
- reduction defects, 906
- upper, 777

- anomalies, 906
- arteries, 778, 778, 779, 779(f), 814-17
  - anomalies, 906
- bones, 777-8
- clinical procedures, 787-8, 788(f)
- development, 905-6
- fascia, 778
- joints, 778
- lymphatics, 779, 781(f), 818
- movements, 784(t)
- muscles, 784(t), 785(t)
- neonatal, 905-6
- nerves, 779-85, 784(t), 785(t), 818-22
  - autonomic, 781-2
- pulses, 787
- reflexes, 789
- skin, 778
- soft tissue, 778
- surface anatomy, 785-8, 788(f)
  - arteries, 787-9
  - bones, 785-6
  - joints, 785-6
  - lymph nodes, 789
  - muscles, 778, 786-7
  - nerves, 789
  - skin/fascia/soft tissue, 785
  - veins, 789
- veins, 778, 781(f), 817-18 *See also* arm *See also* arm

limb girdles *See* girdle(s)

limbic associated membrane protein (LAMP), 386, 387

limbus, 669, 672, 675, 678, 679

limen insulae, 346

limen nasi, 551

line(s) (linea), 89, 91, 91(f)

alba, 499, 1053, 1057(f), 1061-2, 1099
    characteristics, 1061-2
    tensing, pyramidalis role, 1063
Andresen, 514
anterior costomediastinal, of pleural reflection, 991
arcuate
    of ilium, 1083, 1352
    of rectus sheath, 1061
aspera, 1362, 1364
axial, of lower limb, 1346
axillary, anterior, 981
azygo-oesophageal, 957
Blaschko, 161
‘bloodless’, of Brödel, 1231
cement, 89, 90
chilotic, 1360
contour, 160
of costodiaphragmatic reflection of pleura, 989
dentate, 1155, 1156, 1157
epiphysial, 95
of expression, 160
of femur, 1362, 1364
flexure, 160
    of hand, 857, 857(f)
    of wrist, 857, 857(f)
of Gennari, 340
gluteal, 1353(f)
grey, of eyelid, 669
growth, 96, 525
Harris’, 96, 525
hip flexure, 1342, 1349
Holden’s, 1342
iliopectineal, posterior, 736
incision, 161
incremental
    enamel, 513(f), 514
    von Ebner, 514

interischial, 1093
intertrochanteric, 1361-2
intraperiod, 50
joint, 160
of Kraissl, 161, 468
of Langer, 161
lateral, 1052
M (Mittelscheibe), 105, 106, 107(f)
mammary, 1052
of mesenteric reflexion, 1214
midclavicular, 1052
mucogingival, 500
mylohyoid, 520, 530
nuchal, 420
    highest, 481, 712, 712(f), 713
    inferior, 412, 416
    superior, 406, 412, 414, 415, 416
    supreme, 416
oblique
    of ischium, 1357
    of mandible, 486, 487
    of thyroid cartilage, 579
    of ulna, 844
occupational, 160
palmar, 857
paraspinal, 957
parietovisceral, of serosal reflection, 959
pectinate, 1156
pectineal, 1066, 1353(f), 1354
pericraniocervical, 402, 405
period, 50
of posterior azygo-oesophageal reflection, 989
precostal/lumbocostal, 208
relaxed skin tension (RSTLs), 161, 468
retrosternal, 954(f)
of retrosternal pleural reflection, 989
reversal, 88, 89, 95

  - semilunaris, 1053, 1061
  - skin, 145, 160-2
  - skin surface patterns, 160
  - skin tension
    - of back, 707(f)
    - of upper limb, 778
  - snowdrift, 636
  - soleal, 1412, 1413, 1414(f), 1415
  - spiral, 1361(f), 1362, 1364
  - supracondylar, 1364, 1376
  - surface reversal, 95
  - temporal
    - of frontal bone, 470, 471(f)
    - inferior, 412, 413(f), 469, 470
    - superior, 412, 469, 470
  - tension, 160
  - terminalis, 1357
    - pubic part, 1354
  - trapezoid, 792
  - Voigt, 161
  - von Ebner, 514
  - white, of Gennari, 340
  - wrinkle, 160
  - Z (Zwischenscheiben), 105, 1113

lingual bone, 518

lingula, 992(f), 994
  - of cerebellum, 298, 300(f)
  - of mandible, 530
  - of sphenoid, 424, 528

lip(s), 467-8, 499-500
  - arteries, 500
  - cleft, 607, 608(f)
  - innervation, 500
  - lower, 467
  - movements, 488-9
  - mucosa, 499

  - rhombic
    - cerebellum development, 377
    - inferior, myelencephalon, 377
    - superior, metencephalon, 377
  - of rostral neuropore, 361
  - upper, 467
  - vermilion of, 467, 487, 488, 602

lipid(s)
  - epidermal, 148, 150, 153
  - plasma membrane, 4 *See also* fat

lipid bilayer, 4, 9

lipid ‘rafts’, 4

lipids, antihypertensive, 1310

lipocalin, tear, 672

lipofuscin, 12

liquids, biomechanics, 119

liquor amnii *See* fluid, amniotic

liquor folliculi, 1296

LIS-1 protein, 388

lissencephaly, 388

liver, 1163-75
  - arteries, 1169-70, 1169(f), 1174
  - bare area, 1163, 1164(f), 1165, 1168
  - ‘bed’ of, 1165
  - capsule, 1163
  - cells of, 1175
  - development, 1206, 1207-9, 1208(f)
    - early, 1207-8
    - extrahepatic biliary ducts, 1208-9
    - intrahepatic biliary ducts, 1208
    - maturation, 1208, 1216-17
  - fatty, 1163

- fetal, 1173
- functions, 1163, 1207
- horns, 1207
- innervation, 1172-3
- ligaments, 1167-8, 1214-15
- lobes, 1173, 1174(f)
- lobules, 1173, 1174(f)
- lymphatics, 1172
- microstructure, 1173-5, 1174(f)
- peritoneal connections, 1100-2, 1103(f)
- peritoneum, 1163, 1164, 1167-8
  - reflections around, 1100, 1214
- porta hepatis, 1165, 1168-9
- referred pain, 1173
- regeneration, 1175
- resection, 1166, 1169, 1170
- segments, 1166-7
- sinusoids *See* sinusoid, hepatic
- size (fetus, neonate and adult), 1163, 1208
- steatosis, 1163
- supports of, 1167
- surface anatomy, 1053-4, 1163-5, 1163(f), 1164(f)
- surfaces, 1163-5, 1163(f), 1164(f)
- transplant, 1170, 1172
- veins, 1171, 1171(f), 1174
- ventral mesentery, 1214

load transmission, in palm, 860

lobe(s)
- of cerebellum
  - anterior, 298, 303, 304, 305, 307
  - flocculonodular, 298, 304(f), 306(f), 379
  - posterior, 298, 303, 304, 307
- of cerebral hemispheres, 335-8 *See also* cortex, cerebral; *specific lobes (below)*
- frontal, 341-4
  - frontal eye field, 343, 343(f)

    prefrontal cortex, 343-4
    premotor cortex, 343
    primary motor cortex, 342
    supplementary motor cortex, 343
    surface anatomy, 341-2
    syndrome, 358
hippocampal, 382
limbic, 347-54
    development, 383-4
    septum, 352-3 *See also* formation, hippocampal
of liver, 1173, 1174(f)
of lungs, 992(f), 993-4
of mammary gland, 931, 933
occipital, 346-7
    connections, 346-7
    surface anatomy, 346
‘of azygos vein’, 993
olfactory, development, 382
parietal, 344-5
    inferior lobule, 345
    somatosensory cortex, 345
    sulci, 345
    superior lobule, 344-5
    surface anatomy, 344-5
piriform, 338, 386
of placenta, 1302
    accessory (succenturiate), 1303
of prostate, 1254
pyramidal, of thyroid, 462
temporal, 345-6
    asymmetry, 358
    auditory cortex, 345-6
    development, 383
    input to amygdala, 354
    lesions, 358
    polymodal sensory areas, 354
    surface anatomy, 345

- of thymus, 946(f), 947, 948
- of thyroid gland, 462

lobectomy, of lung, inferior, 1003

lobule(s)
- of auricle, 618(f), 653
- of carotid body, 447
- central, of cerebellum, 298
- of kidney, 1225, 1236(f)
- of liver, 1173, 1174(f)
- of lungs, 995
- of mammary gland, 930-1, 931(f), 933
- paracentral, of cerebral hemisphere, 335
- of parietal lobe, 344-5
- posterior biventral, of cerebellum, 303
- of salivary glands, 522
- of testis, 1264(f), 1265

locus coeruleus, 240, 241, 291, 292, 294, 315, 316, 320

loop(s)
- capillary, 147(f), 150, 152(f), 156, 157(f), 160, 162
- duodenal, 1217
    - position/configuration, 1209
- of heart tube, 1018
- of Henle, 1235, 1235(f), 1236(f), 1237
    - functions and permeability, 1238
    - in metanephros, 1307
- interperitoneal, 1099
- Meyer’s, 696
- primary intestinal (midgut), 1209
- sigmoid, 1147
- ventricular, 1018

lordosis, 714, 743, 744, 745, 1041
- lumbar, in pregnancy, 1300

Ludwig’s angina, 543

lumen

  - of vermiform appendix, 1142-3 *See also* cavity (cavities); *See also* space(s); *See also* tube(s)

lunate bone, 862, 863(f)
  - ossification, 864

lung(s), 989, 992-1000
  - agenesis, 1037
  - alveoli *See* alveolus (alveoli), of lungs
  - anatomical defects, 989
  - anatomical defences, 989, 1005-6
  - apex, 465, 993
    - surface anatomy, 993
  - aplasia, 1037
  - appearance (external), 992-3
  - arteries, 996, 997(f)
    - development, 1035
      - postnatal, 1036
  - base, 993
  - borders, 993
  - bronchopulmonary segments, 994, 995(f), 996, 996(f)
    - naming/numbering, 994, 995(f)
    - pulmonary vessels, 994
  - buds, 601, 1013-14, 1033, 1034
  - cancer, staging, 957
  - chest wall relationship, 989
  - congenital malformations, 1036-7, 1037(f)
  - development, 1013-14, 1032, 1033-5, 1033(f)
    - alveolar phase, 1034-5
    - canalicular phase, 1034
    - embryonic phase, 1034
    - postnatal, 1036, 1036(f)
    - pseudoglandular phase, 1034
    - saccular phase, 1034
    - sexual dimorphism, 1032
  - elastic recoil, 1011
  - fetal, 206(f), 992, 1013
  - fissures, 914, 992(f), 993-4

functions, 989
    changes around time of birth, 1035-6
hilum, 963
hilum (hila), 963, 993, 994-5
hypoplasia, 181, 1014, 1015, 1035
infants, 992
innervation, 998
intra-uterine maturation, 1035
left, 992(f)
    arteries, 996-7
    bronchopulmonary segments, 994
    cardiac impression, 992(f), 993
    fissures and lobes, 992(f), 994
    hilum, 995
    relations, 964
    surface anatomy, 992-3
    veins, 997-8, 997(f)
lobes, 992(f), 993-4
    congenital large hyperlucent, 1037
lobules, 995
lymphatic drainage, 998, 999(f), 1035
microstructure, 998-1000, 999(f) *See also* alveolus (alveoli), of lungs
movements during quiet ventilation, 1012
nerves, 998
overinflation, 1007
pleura covering *See* pleura
radiography, 993
resections, right-sided, 994, 996
right, 992(f)
    arteries, 993
    bronchopulmonary segments, 993
    cardiac impression, 992(f), 993
    fissures and lobes, 992(f), 993-4
    hilum, 995
    relations, 964
    surface anatomy, 992-3, 992(f)
    veins, 997-8, 997(f)

- root, 991, 994
- sequestration, 997
- sequestration segments, 997
- surface anatomy, 914, 989, 992-3, 992(f)
  - apex, 993
  - base, 993
  - cardiac impression, 992(f), 993
  - costal, 993
  - medial, 993
- veins, 997-8, 997(f)
  - development, 1035
- weight, 992

lunule, of nail, 155

lutein, 693, 1297

lymph, 73, 131, 139

lymphadenopathy, subcarinal, 1006

lymphangitis, 139

lymphatic drainage (of organs, or regions)
- of abdominal wall
  - anterior, 1059
  - posterior, 1077-8, 1077(f)
- of adenoid, 563
- of anal canal, 1160
- of ankle, 1442
- of appendix, 1145
- of arm, 828
- of auricle, of ear, 620
- of back, cutaneous, 708, 709(f)
- of bile ducts, 1180
- of bladder, urinary, 1090, 1249
- of bone, 91
- of breast, 932, 932(f)
  - cutaneous, 932
- of bronchi, 1003

of caecum, 1141
of cardiac muscle, 141
of colon
  ascending, 1146
  descending, 1147
  sigmoid, 1150
  transverse, 1147
of conjunctiva, 672
of diaphragm, 928
of duodenum, 1128
of ear
  external, 620
  middle, 628-9
of elbow, 836
embryonic, 205, 209
of external acoustic meatus, 657
of eyelids, 671
of face, 492
of foot, 1336, 1429
of gallbladder, 1180
of gluteal region, 1336
  cutaneous, 1349
of hard palate, 502
of head, 400(f), 401, 453-5
heart, 982
of hepatic ducts, 1180
of hip, 1390
of hip and thigh, 1381
of ileum, 1130-1
of iliac region, 1336
of intestine, large, 1141, 1141(f), 1145, 1147
of jejunum, 1130-1
of joints, 101
of kidney, 1233
of knee joint, 1393
of larynx, 588
of leg, cutaneous, 1411

of liver, 1172
of lower limb, 1336, 1336(f)
of lungs, 998, 999(f), 1035
of mediastinum, 941, *941*, 941(f)
of nasal cavity, 554
of neck, 400(f), 401, 454
  cutaneous, 454
of nose, external, 549
of oesophagus, 951
  cervical, 465
of oral mucosa, 500
of orbit, 666
of ovary, 1295
of palatine tonsil, 567
of pancreas, 1186
of paranasal sinuses, 557, 558
of parathyroid glands, 464
of parotid gland, 497
of pelvis, 1090-1, 1091(f)
of penis, 1273
of pericardium, 959
of perineum, 1098
of pharynx, 567
of pleura, 991
of prostate, 1258
of rectum, 1155, 1155(f)
of scalp, 492
of scrotum, 1262
of seminal vesicles, 1270
of skeletal muscle, 110
of skin, 156-7
  of back, 708, 709(f)
  of breast, 932
  of gluteal region, 1349
  of knee, 1393
  of leg, 1411
  of neck, 454

- of spleen, 1193
- of stomach, *658*, 1119-20
- of sublingual salivary gland, 521
- of submandibular salivary gland, 521
- of suprarenal gland, 1198
- of teeth, 519
- of temporomandibular joint, 536
- of testis, 1264
- of thigh, 1336
- of thoracic wall, 928
- of thorax, 911
- of thymus, 946
- of thyroid gland, 462
- of tongue, 505-6, 506(f)
  - central vessels, 506
  - dorsal vessels, 506
  - marginal vessels, 506
- of trachea, cervical part, 466
- of tympanic cavity, 628-9
- of upper limb, 779, 818
- of ureter, 1241
- of urethra
  - female, 1253
  - male, 1252
- of uterine tube, 1293
- of uterus, 1290
- of vagina, 1284, 1284(f)
- of vas deferens, 1269
- of vertebral column, 715
- of vulva, 1280
- vulva, 1280, 1282(f)

lymphatic vessels
- anterior abdominal wall, 1059
- pulmonary, 998

lymph nodes (general), 72-4
- cells/cellular zones, 73-4

- distribution, 72
- lung cancer staging, 957
- lymphatics, 73
- microstructure, 72-3, 73(f)
- tracheobronchial, inferior, 983
- vasculature, 73

lymph nodes (named)

- aortic, 1077-8
- apical, 779, 932
- axillary, 911, 932
    - apical, 818
    - central, 818
    - lateral, 779, 818
    - posterior, 818
    - subscapular, 779
- bronchopulmonary, 985
- buccal, 492
- central, 779, 932
- cervical, 406, 454
    - anterior, 454
    - deep, 454, 951
        - inferior, 454, 779
        - lower, 492
        - superior, 454
        - upper, 492
    - superficial, 454(f), 492
    - upper, deep, 492, 497
- Cloquet’s, 1280
- coeliac, 1077, 1172
- colic, 1141, 1141(f)
    - intermediate, 1141
    - preterminal, 1141
- cystic, 1077, 1180
- diaphragmatic
    - anterior, 928
    - lateral, 928
    - posterior, 928

epicolic, 1141
epigastric, inferior, 1090
epirectal, 1155
gastric, 1077, 1111
    left, 951
hepatic, 1077, 1172, 1180
    common, 1126
hepatoduodenal, 1126
hilar, 72, 73, 73(f)
ileocolic, 1145
iliac
    circumflex, 1090
    common, 1090
    external, 1090, 1290
    internal, 1090-1, 1091(f), 1280, 1284, 1290
infraclavicular, 779, 818, 819(f), 932
infrahyoid, 454
inguinal, 1293, 1295
    deep, 1280, 1336, 1382
    superficial, 1059, 1280, 1284, 1336, 1382
intercostal, 928
interpectoral, 932
jugular
    lower, 454
    middle, 454
    upper, 454
jugulo-omohyoid, 492
jugulodigastric, 454, 567
lateral aortic, 1077-8
lingual, 454, 492
mediastinal, 941, 941(f)
    assessment, 952-3
    posterior, 951
    sampling, 952-3
mesenteric
    inferior, 1077
    superior, 1077, 1141

obturator, 1290
occipital, 492
    submandibular, 454
pancreatic, 1128
pancreaticosplenic, 1077, 1186
para-aortic, 941, 1111, 1198, 1293, 1295
para-oesophageal, 941
paracardiac, 1172
paracardial, 1111
paracolic, 1141
pararectal, 1155, 1155(f)
parasternal, 928, 932, 1059
paratracheal, 454, 941, 951
    lower, 941
    upper, 941
parotid, 497
    deep, 671
    superficial, 492, 671
pectoral, 779, 928, 932
pelvic, 1280, 1295
pericaval, 1172
popliteal, 1336, 1393, 1409
pre-aortic, 1077, 1186
pre-auricular, 672
preauricular, 497
prelaryngeal (Delphian), 454, 588
pretracheal, 372, 454
pulmonary, 941
pulmonary ligament, 941
retro-aortic, 1078
retro-auricular, 492
retropharyngeal, 454
sigmoid, 1150
subaortic, 941
subcarinal, 941
submandibular, 492, 500, 520, 672
submental, 454, 492

        median, 506
    subscapular, 928, 932
    supraclavicular, 818
    supratrochlear, 779, 836
        surface anatomy, 789
    thoracic, internal (parasternal), 928, 932, 1059
    tracheobronchial, 939, 941, 941(f), 963(f)
        inferior, 982, 998
        superior, 998

lymph nodes (of organs, or regions)
    of anal canal, 1160
    of bile ducts, 1180
    of breast, 932
    of bronchi, 1003
    of caecum, 1141, 1141(f)
    of cystic duct, 1180
    of diaphragm, 928
    of duodenum, 1128
    of elbow, 836
    of embryo, 209
    of face, 492
        of skin, of back, 708, 709(f)
    of foot, 1336
    of gallbladder, 1180
    of head, 401
    of heart, 982
    of hip and thigh, 1381
    of intestine, large, 1141, 1141(f), 1145, 1147
    of larynx, 588
    of liver, 1172
    of lower limb, 1336
    of lungs, 998, 999(f)
    of neck, 20, 28, 401, 454
        grouping, 454
    of oral cavity and pharynx, 605
    of ovary, 1295
    of palatine tonsil, 567

  of pancreas, 1186
  of parotid gland, 497
  of rectum, 1155, 1155(f)
  of scalp, 492
  of thoracic wall, 928
  of tongue, 505-6, 506(f)
  of trachea, 1003
  of upper limb, 779, 781(f), 818
  of uterine tube, 1293
  of uterus, 1291
  of vagina, 1284
  of vertebral column, 715
  of vulva, 1280

lymphoid aggregations
  gut, 1213
  pulmonary, 998

lymphoid follicles *See* follicle(s), lymphoid

lymph trunk *See* trunk (lymphatic)

lysosomal storage diseases, 13

lysosomes, 3(f), 4, 10, 12-13, 682
  tertiary, 12

lysozyme, 522, 672, 952, 1135
  secretion, from submucous glands of airways, 1004

M

M-cadherin, 116

macrodontia, 513

macrophages, 9, 35, 36(f), 73, 78-80, 79(f), 80(f), 609, 981
  alveolar, 78, 78(f), 998, 1000, 1000(f)
  greater omentum, 1104
  hepatic, 1175
  phagocytosis, 78, 78(f)
  secretions, 78, 80
  in spleen, 1195
  thymus, 947

macula(e)
  cribrosa, 634
  densa, of renal tubules, 1235, 1236(f), 1237, 1238
  of eye, 688, 688(f), 689(f), 693
  of inner ear **icthyosis**, 644
  of saccule, 637
  of utricle, 636, 636(f)

macula adherens (maculae adherents) *See* desmosomes

macular sparing, 254

magenstrasse, 1115, 1116(f)

magnetic resonance angiography, 975(f), 984(f)

magnetic resonance imaging (MRI)
  anal canal, 1157(f)
  aorta, 986
  cerebellum, 299(f)
  diaphragmatic trauma, 1009
  functional, cerebellum function, 309(f)
  heart, 969
  mediastinal spaces, 956(f), 957
  orbit, 655(f)
  posterior abdominal wall, 1073

  rectum, 1150(f), 1151(f), 1152(f), 1153(f)
  temporomandibular joint, 536(f), 537
  thymus, 945
  uterus, 1292, 1292(f)
  wrist, 869(f)

major histocompatibility complex (MHC), 68, 77, 78
  gene mutations, 970
  restriction, 79-80

male developmental pathway, 1319

male pattern baldness, 153

malformations
  Arnold-Chiari, 770
  of caecum, 1209
  congenital cystic adenomatous, 1037
  of cricoid cartilage, 579
  of ductal plate, 1208
  of face, 607
  of heart, 974-5
  of vertebrae (lumbosacral), 772

malleolus
  lateral, 1416
    surface anatomy, 1340
  medial, 1412, 1413, 1413(f), 1415
    surface anatomy, 1340

mallet finger, 878

malleus, 621(f), 623, 624, 627
  development, 598, 652
  movements, 628
  ossification, 627 *See also* ossicles, auditory

MALT *See* mucosa-associated lymphoid tissue (MALT)

mamelons, 509

mandible, 517(f), 527, 530-3, 531(f), 613
  accessory foramina, 532

- age changes, 532-3, 532(f)
- angle of, 480, 532
- body, 409, 480, 505, 530
  - alveolar part, 478, 480
  - fracture, 480
- development, 604
- edentulous, 525, 533(f)
- fracture, 480
- innervation, 501
- ossification, 533
- ramus, 402, 412, 418, 530-1, 538
- surface anatomy, 402-3
- tissue spaces around, 524, 524(f)

mandibulofacial dysostosis, 419, 607

manoeuvre(s)
- Epley's, 639
- Pringle, 1168
- Valsalva, 407, 1118

manometry, oesophageal, 953

manubrium
- of malleus, 627
- of sternum, 407, 917, 917(f), 918, 984, 986

margin
- acute, of heart, 963
- costal, 909, 912
  - surface anatomy, 1052
- falciform, 1350
- infraorbital, 409, 476, 476(f)
- obtuse, of heart, 963
- parietal, 470, 471(f)
- supraorbital, 409, 470, 471(f), 486

marrow, of bone, 74-5, 75(f), 85, 87, 88, 88(f), 90-1
- gelatinous, 74
- red, 75

  replacement therapy, 75
  vasculature, 75
  yellow, 74-5

Martin-Gruber connection, 854

masculinization, of female fetus, 1219

mass
  lateral, of cervical vertebrae, 718, 719, 720
  premuscle, 903

massa intermedia, 239, 239(f), 244(f), 380

mastication, 499
  muscles of, 489, 538-40, 539(f)
  teeth, 513

mastitis, 934

mastoiditis, 626

mater
  arachnoid *See* arachnoid mater
  dura *See* dura mater
  pia *See* pia mater

materials, properties of, 119, 120(t)
  bone, 120, 120(f)
  cartilage
    elastic, 120
    fibrocartilage, 120
    hyaline, 120
  fascia, 120
  ligaments, 120
  tendons, 120

matrix
  of bone, 86-7, 86(f)
  of cartilage, 81-3, 82(f)
  extracellular, 34, 36-8
    embryonic, 190-1
    heart development, 1016

        - mutations, 194
    - fibrillar, 37
    - germinal
        - of brain *See* zone(s), ventricular
        - of hair, 151, 152, 152(f)
        - of nail, 155
        - nervous *See* zone(s), ventricular
    - interfibrillar, 37-8
    - mesangial, 1234
    - myocardial, 974
    - of nail, 155
    - sterile, of nail, 155
    - subsarcolemmal, 108

matrix metalloproteinases, 175, 1299

matter
- grey, 41, 225-6, 227(f)
    - of cerebral cortex, 382
    - of medulla oblongata, 277-8
    - of spinal cord, 226, 257-63
- white, 41, 225, 226, 227(f)
    - of cerebral hemisphere, 354-8
    - of medulla oblongata, 227
    - of spinal cord, 226, 262-71

maxilla, 409, 412, 476-8, 527, 613
- age related changes, 478
- alveolar process, 477
- anterior surface, 404
- at birth, 478
- body, 476-7
    - anterior surface, 476
    - infratemporal surface, 476
    - nasal surface, 476
    - orbital surface, 476
- edentulous, 525
- frontal process, 476-7, 547
- innervation, 501

- in nasal cavity, 549
- ossification, 478, 613
- postnatal growth, 418
- zygomatic process, 476

measurements
- intercristal, 1359
- neonate length, 216
- pelvic diameters, 1358, 1366
- sacral, 1359
- of skull, 419-21

meatus
- acoustic
  - external, 403, 412, 416, 469, 494(f), 615, 617, 620-2
    - arteries, 621
    - cartilaginous part, 620
    - development, 602, 652-3
    - injury, 621
    - lymphatics, 621
    - nerves, 621-2
    - osseous part, 620-1
    - relations, 621
  - internal, 425, 636
    - at birth, 617
    - neonatal, 618
  - veins, 621
- external, *See also* ear, external
- internal, 633, 634, 636
  - surgical access, 649 *See also* ear, inner
- nasal
  - inferior, 550
  - middle, 550-1
  - superior, 551
  - supreme, 551
- urethral, 1280 *See also* ear, external

mechanical properties, 118

mechanobiology, 124, 124(f)

mechanotransduction, 124

Meckel's diverticulum, 1129, 1209

meconium, 1210-11, 1213
- delayed passaage, 1213
- normal passage, 1213
- premature defecation, 1213

medial pallidum, 331

mediastinoscopy, 941

mediastinostomy, anterior, 941

mediastinum, 910, 939-57, 939(f), 942(f), 989
- definition, 939
- imaging, 954-7
  - CR and MRI, 955(f), 956(f), 957
  - radiography, 954, 954(f)
- inferior, 939, 955(f)
  - anterior, 910, 939, 955(f), 956(f)
  - middle, 910, 939, 955(f), 956(f)
  - posterior, 910, 939, 955(f), 956(f)
- lymph nodes *See* lymph nodes (named), mediastinal
- right lymphatic trunk, 944
- shift, 1009
- superior, 910, 939, 956(f), 984
- thoracic duct course *See* duct(s), thoracic
- thymus *See* thymus
- tumours, 949
- vagus nerve course, 945
- vascular supply, 939-41, 940(f), 941(f)

medulla
- of hair, 151
- of kidney, 1228-9, 1230(f), 1232-3, 1234(f)
  - vascular supply, 1231-3
- of lymph node, 72, 73, 73(f), 74, 77
- oblongata, 226, 228(f), 275-84

        arterial supply, 253
        development, 376(t), 377
        external features, 275-7
        herniation, 296
        internal structure, 277-84
        lateral reticular nucleus, 304, 306
        lesions, 295
        pyramid formation, 377
        relations, 275-7
        transverse section, 277(f), 278-80, 279(f)
        venous drainage, 254
    ovary, 1297
    spinalis *See* cord(s), spinal
    of suprarenal gland, 1081, 1197, 1199(f), 1200
        development, 375
    of thymus, 947-8, 948(f)

medulloblastoma, roof of fourth ventricle, 309

megacolon, 1213

meiosis, 19, 22-3, 23(f)

meiosis II, 23

melanin, 145, 148, 149
    ciliary body, 681

melanism, 159

melanogenesis, 149

melanopsin, 692

melanosomes, 149, 152, 682

membrane bone, 92

membrane (membrana)
    anal, 1212, 1307
    atlanto-occipital
        anterior, 733
        posterior, 733-4

basement, 33-4
    glomerular, 1235
    myocardial, 1016
basilar, of cochlea, 634, 635(f), 640
    vibration, 646
Bruch’s, 679, 680
buccopharyngeal, 185(f), 186, 189, 367, 368(f)
cloacal, 186, 1212, 1307, 1308(f), 1311(f), 1322, 1323(f)
    rupture, 1312, 1323
cricothyroid, 581
cricovocal, 581
Descemet’s, 33, 675, 678(f), 679, 702
‘detergent’-resistant, 4
of Elschnig, 694
exocoelomic, 173
fetal, 180-2
glassy, 151, 152(f)
glial limiting *See* glia limitans
Heuser’s, 173
imperforate hymenal, 1317
intercostal
    external, 924, 926, 929
    internal, 919, 925
internal limiting, of retina, 692-3
interosseous, 871
    of forearm, 839-40
    of leg, 1411, 1412(f)
Jackson’s, 1104
mucous *See* mucosa
myelin, 50
nuclear, 18-19, 18(f)
obturator, 1352, 1352(f)
oropharyngeal, 604
otolithic, 636, 637, 637(f), 639, 643
perineal, 1094
phreno-oesophageal, 1009
plasma, of cell *See* plasma membrane

- pleuropericardial, 1014, 1014(f)
- pleuroperitoneal, 1014, 1014(f), 1015
- prosencephalon, 189
- pupillary
  - development, 702
  - persistence, 702
- quadrangular, 581
- Reissner’s, 634, 640
- serous, 1213
  - peritoneum *See* peritoneum
  - pleura *See* pleura *See also* serosa
- statoconial, 636, 637
- suprapleural, 989, 993
- sutural, 97
- synaptic, 46, 47
- synovial, 82, 83, 99, 99(f), 100, 100(f)
  - of individual joints *see individual joints*
- tectorial, 635(f), 640, 641-2, 720, 734, 735
- thyrohyoid, 579
- tympanic, 404, 602, 617, 618, 622(f), 624
  - development, 602
  - in hearing, 646
  - microstructure, 624
  - nerves, 624
- urogenital, 1307, 1312, 1318(f)
- vestibular, 634, 640

memory
- lateralization, 358
- loss of *See* amnesia
- mnemonic, Papez circuit, 347
- non-verbal, right hemisphere, 358
- semantic, 358
- verbal, left hemisphere, 358

menarche, 1325

meninges, 389-90
- cranial, 425-34

development, 389-90
spinal, 751-2

meningitis, 52

meningocoele, 772

meningomyelocoele, 772

meninx
primary, 389
primitiva, 389

meniscus (menisci), 101, 102
homologue, 871
of knee, 1340, 1397-8, 1398(f)
age-related changes, 1398
lateral, 1398
discoid, 1398
medial, 1398, 1398(f)
nerves, 1398
tears, 1397
Wrisberg type, 1397
of Kuhnt, 694
of wrist joint, 870

menopause
breast changes, 936
ovarian changes, 1297

menstrual age, 211

meralgia paraesthetica, 1381

merosin, 33, 107

mesangium, 1235

mesaxons, 50, 50(f), 51

‘mesencephalic locomotor region’, 331, 334

mesencephalon (midbrain), 226, 228(f), 288-92
arterial supply, 253

- development, 362, 362(f), 380
- external features, 288
- internal structure, 288-92
- lesions, 295-6
- pain perception, 267
- relations, 288
- splanchnopleuric, 610
- venous drainage, 255

mesenchyme, 186, 189-90, 534
- angioblastic, 203, 367
  - heart development, 1016
- angiogenic
  - biliary duct development, 1208
  - facial development, 602
  - foregut development, 1203
  - lung development, 1034
  - pancreas development, 1207
  - thymus development, 609
- axial, 198-9
- body-plan stage, 197
- cardiac, 1016, 1017, 1207
  - formation, 1016, 1023 *See also* mesenchyme, precardiac; *See also* mesenchyme, septum transversum
- caval fold, 1216
- cranial, 596
- epithelial interactions, 194, 194(f)
  - gut development, 1203
  - metanephros, 1308
- epithelial transition, 702, 764, 1324
  - neural crest, 365
  - peritoneal lesser sac, 1216
  - sclerotome formation, 764
  - somites, 764-7, 767(f)
- extraembryonic, coating yolk sac, 180
- frontonasal, 602, 613
- head, 699
- hepatic, 1221

intermediate, 203, 1305
interzonal, of developing joints, 902
lateral plate (somatopleuric), 186, 187(f), 201, 899, 903
mediastinal, 1016, 1023
metanephric, 1308, 1309, 1309(f)
neural crest
    external genitalia development, 1324
    eye development, 699
    eyelid development, 702-3
    non-neuronal, 365
    pituitary gland development, 367 *See also* neural crest
non-neuronal, of neural crest, 365
pancreatic, 1207
para-oesophageal, 1214
paraxial, 186, 201, 361, 361(f), 365
    development, 763-4, 763(f), 764(f)
    meninges development, 389
    segmentation, 763-4
    somite formation, 763
    somitic, 365
periotic, 651, 652
pia mater development, 389
precardiac, 201, 1207
prechordal, 184, 186, 201, 373, 702
    muscular derivatives, 599(f)
presomitic, 199, 201, 763
presomitic *See* mesenchyme, paraxial
primary, 596
sclerotomal, 767, 768
septum transversum, 1013, 1203
    liver development, 1207, 1208(f)
somatic, 1209
somatopleuric, 201, 772, 1209 *See also* mesenchyme, lateral plate
splanchnic, peritoneum development, 1213
splanchnopleuric, 203, 207, 772, 1220
    enteric nervous system development, 1213
    gut development, 1203

    - lung development, 1013-14, 1032, 1033, 1034
    - oesophageal development, 1203-4
  - unsegmented, 201, 763
  - urogenital sinus, 1324
  - vascular, vitreous body development, 702

mesenteron *See* mesentery, dorsal (mesenteron)

mesentery
  - of appendix, 1105, 1217
  - bilaminar, 1099, 1216, 1217
  - development, 1210(f), 1214
  - dorsal (mesenteron), 1099, 1204, 1206, 1208
    - development, 1214
    - lesser sac development, 1216
    - mesocolon, 1217
    - midline parietal attachment, 1217
    - root, origin, 1209, 1211, 1217
  - of foregut, 1214
  - functions, 1214
  - of gonadal ridge, 1313
  - lines of reflexion, 1214
  - midline parietal attachment, 1206
  - nomenclature, 1214
  - of oesophagus (embryonic) *See* meso-oesphagus
  - root, 1099
  - root, origin, 1208, 1217
  - of small intestine, 1099, 1105, 1217, 1218
  - of stomach *See* mesogastrium; *See also* omentum
  - of transverse colon, 1104-5, 1217-18
  - ventral, 1099, 1206, 1214, 1216
    - persistence, 1099 *See also* peritoneum

meshwork, trabecular, 675, 677(f)

mesiodens, 513

meso-oesophagus, 1203, 1214
  - ventral, 1214 *See also* septum (septa), transversum *See also* mediastinum

mesoappendix, 1105, 1145, 1217

mesoblast
  cardiogenic, 186
  extraembryonic, 173-4, 175, 180, 181(f), 183, 183(f)
  intraembryonic, 186

mesocardium, dorsal, 1016, 1018

mesocolon, 1217
  greater omentum fusion, 1218
  sigmoid, 1105
  transverse, 1104-5, 1146

mesoderm, 189, 190

mesoduodenum
  dorsal, 1206, 1208
  ventral, 1206, 1214, 1216

mesogastrium, 1099, 1216
  dorsal, 1204, 1206, 1208(f), 1215(f), 1216
    fusion with peritoneum, 1216
    secondary, 1215(f), 1216
    spleen development, 1218
  ventral, 1102, 1204, 1206, 1208(f), 1216
    ligaments of liver development, 1214

mesogenitale, 1313, 1320

mesometrium, 1285, 1288

mesonephros, 206, 1263, 1267, 1269, 1305, 1305(f), 1306(f), 1307
  atrophy, 1307
  male *vs* female, 1316(t)

mesorchium, 1320

mesorectum, 1151-3, 1152(f), 1153(f), 1155, 1218
  MRI imaging, 1151, 1152(f), 1153

mesosalpinx, 1285, 1293, 1294

mesosigmoid, 1148, 1155

mesosternum, 917
  subcostal (twelfth thoracic), 916, 921

mesothelia, 4

mesothelium
  peritoneum, 1099, 1110
  yolk sac, 180

mesovarium, 1285, 1294-5, 1321

metacarpal bones, 864-6
  first, 864-5, 867(f)
  second, 865, 867(f)
  third, 865, 867(f)
  fourth, 865-6, 867(f)
  fifth, 866, 867(f)
  ossification, 864(f), 865(f), 866, 866(f)
  surface anatomy, 786

metamerism, 763

metanephros, 206, 1305(f), 1306(f), 1307-12, 1309(f)
  ascent of kidney, 1310, 1316(f)

metaphase
  cellular division, 21
  meiosis, 23

metaplasia, 39

metarterioles, 134

metasternum *See* process (or processus), xiphoid

metatarsal bones, 1433, 1439-40
  first, 1439-40, 1439(f)
  second, 1439(f), 1440
  third, 1439(f), 1440
  fourth, 1439(f), 1440
  fifth, 1439(f), 1440
  fracture, 1440
  innervation, 1440

muscle attachment, 1440
ossification, 1440
surface anatomy, 1341
vascular supply, 1440

metatarsal pad, 1432, 1432(f)

metathalamus, development, 380

metencephalon, 226, 228(f)
development, 362(f), 377

microdontia, 513

microfilaments, 6(f), 7, 14

micrognathia, 607

microphthalmia, 699

microspikes, 14

microtia, 618

microtubules, 3(f), 14(f), 16(f)
disassembly, 16
stability, 16

microvilli, 3, 14, 18(f)
cell coat, 1133
of endometrium, 1297
of enterocytes, 1133

micturition, 1253, 1254
control centre, 1255(f)

midbrain *See* mesencephalon

middle ear *See* cavity (cavities), tympanic; *See also* ear, middle

midgut
development, 1203, 1205(f), 1209-12, 1210(f)
loop (primary intestinal), 1209
duodenum, 1206
peritoneum associated, 1217
rotation, 1209

        anomalies, 1209
        mixed, 1209

milk, witch’s, 934

milklines, 934, 935(f)

‘milky-spots’, 1104

mineralization
    osteoid, 87, 89(f), 91, 93, 95(f), 96
    teeth, 514

miosis, 685

mitochondria, 3(f), 4, 13-14, 13(f)
    cardiac muscle, 13(f), 140(f), 141, 142
    endometrium, 1297
    renal tubule epithelium, 1237
    skeletal muscle, 107, 107(f), 110(f), 111
    smooth muscle, 13

mitosis, 19, 21-2, 21(f), 22(f)
    quantal, 193

modiolus
    of cochlea, 634, 652
    of facial muscles, 487, 488, 489

molars *See* teeth

mole, 159

molecules
    cell adhesion *See* cell adhesion molecules
    extracellular matrix, 36-8

moments, 117-18, 118(f)

monoamines, 47

mons pubis, 1279, 1279(f)

Morgagni hernia, 1015

morphogenesis, 194-5

    neural tube segmentation, 371

Morton’s neuroma, 1458

morula, 171, 171(f)

motor end-plate, 110, 111

motor learning, olivocerebellar climbing fibre role, 309

motor unit, 111, 112(t)

mound, aortic, 964

mouth, 505(f)
    floor, 499, 501-2
    functions, 499
    lateral walls, 499
    muscles, 501
    primitive *See* stomodeum
    regions, 499
    roof, 499
    trauma, 521 *See also* cavity (cavities), buccal; *See also* cavity (cavities), oral

movement(s)
    of ankle joint, 1443
    of auditory ossicles, 628, 646
    of bones, 122, 123(f)
    of cilia, 17-18
    control
        basal ganglia role, 332
        supplementary motor cortex, 343
    disorders, of basal ganglia, 326
    embryonic, 903
    execution of, 358
    of eye *See* eye and eyeball, movements
    of face, 488-9
    of feet *See* foot, movements
    fetal, 903
    fine, coordination
        cerebellum role, 308-9

    - incoordination in neocerebellar lesions, 309
  - of flagella, 17-18
  - of hand, 871-2, 873(f)
  - head tilt, 644(f)
  - incoordination, neocerebellar lesions, 309
  - of jaw, 513
  - of joints
    - abduction/adduction, 103
    - angulation, 103
    - axial rotation, 103
    - biomechanics, 117-20
    - circumduction, 103, 806
    - dorsiflexion, 103
    - extension, 103, 103(f)
    - flexion, 104
    - opposition, 864
    - ovoid of, 102, 103
    - plantarflexion, 103
    - pronation, 868-70
    - spin, 121, 122(f), 123, 123(f)
    - supination, 868, 872(f)
    - translation, 102*see also individual joints*
  - of lips, 488-9
  - modiolar, 489
  - of pectoral girdle, 803
  - preparation, premotor cortex role, 343
  - primary motor cortex role, 342
  - respiration *See* breathing
  - of spermatozoa, 1275
  - of thoracic cage, 926
  - of thumb, 864, 888-9, 889(f)
  - of vertebral column, 743-4
  - of vocal cords, 591
  - walking *See* gait; *See also* walking *see also other specific movements*

MPTP, parkinsonism due to, 333

mucins, 39, 1297

mucociliary escalator (rejection current), 989

mucosa, 39
  alveolar, 499(f)
  Barrett's, 952
  of bladder, 1245, 1247
  of cervix, 1292
  of cheek, 499
  dorsal lingual, 507
  of gallbladder, 1181
  of intestine, 1050
    large, 1160-1
    small, 1133-5
  of larynx, 582
  of lips, 467
  lips, 499
  nasal, 551-2
  oesophageal, 951-2, 952(f), 1113-14
    development, 1203
    neonate, 1204
  oral, 500-1
    arterial supply, 500
    gingival, 500
    innervation, 501
    lining, 500
    lymphatic drainage, 500-1
    masticatory, 500-1
      dorsal lingual, 500
      gingival, 500
      palatal, 500 *See also* gingivae
  of paranasal sinuses, 556
  of pharyngotympanic tube, 564
  of small intestine, 1133-5, 1134(f)
    development, 1209-11
  of stomach, 1113-14, 1115, 1116(f), 1120, 1121(f), 1206
    development, 1204
  of tongue, 503
    dorsal lingual, 507

  tympanic, 629
  of urethra, 1252, 1253
  vaginal, 1281
  vesical, of bladder, 1245, 1247

mucosa-associated lymphoid tissue (MALT), 74, 74(f), 401, 671, 1135
  lymphocytes, 74
  venules, 133

mucus, 39

Müllerian inhibiting substance (MIS; anti-Müllerian hormone), 1317, 1319

multiple sclerosis, 52, 64

muscles (acting upon)
  atlanto-axial joint, 735
    atlanto-occipital joint, 734
  auricle, 619-20
  carpometacarpal joints, 875, 876
  elbow joint, 834
  hip joint, 1391-2, 1392(f)
  intermetacarpal joints, 876
  interphalangeal joints, of hand, 878
  knee, 1403
  metacarpophalangeal joints, 877
  wrist, 778, 887

muscles (general), 103-17
  antagonists, 114, 115, 121
  architecture, 104, 121
    collagenous, 121
  bipennate, 104, 105(f), 113
  cardiac, 104, 139-43
    development, 142
    excitation-contraction coupling, 141-2
    innervation, 141
    lymphatic drainage, 141
    microstructure, 139-40

        - nerves, 141
        - regeneration, 143
        - vasculature, 141 *See also* myocardium
    - circumpennate, 104
    - classification, 103-4, 105(f)
    - embryonic development, 772
    - epaxial, 260
    - epiaxial, 772
    - fixators, 114, 115
    - force of contraction, 113-14
    - fusiform, 104, 105(f), 113
    - hypaxial, 260
    - insertion, 121, 122(f)
    - internal forces, 121, 122(f)
    - involuntary *See* muscles (general), smooth
    - multipennate, 104, 113, 114
    - nomenclature, 104, 105(t)
    - origin, 115
    - pennate, 104, 114
    - power, 113-14, 114(f)
    - prime movers, 114-15
    - quadrilateral, 104, 105(f)
    - repair, 117
    - short, 104
    - skeletal, 104-17
        - attachments, 112-13
        - classification, by vascular supply, 109
        - connective tissue, 108
        - contraction
            - physiology, 111-13
            - range, 114
        - development, 115-17
            - in limbs, 903
            - nerve connection failure, 370
        - direction of action, 114, 114(f)
        - fibres *See* fibre(s), muscle
        - form, 113-15

    function, 113-15
    innervation, 110-11
    lymphatic drainage, 110
    microstructure, 104-9
    movement, 114
    nerves, 110-11
    neuromuscular junction, 61-3
    proteins, 106-7 *See also* protein(s)
    regeneration, 143
    striations, 106, 116
    vascular supply, 109-10, 110(f)
smooth, 104, 127-43
    blood supply, 128
    contraction, 128
    development, 130
    distribution, 127
    excitation-contraction coupling, 130
    function, 127
    innervation, 128
    intestinal, 1051
    microstructure, 127-8, 128(f), 129(f)
    multi-unit, 128
    of renal calyces and pelvis, 1237
    unitary, 128, 130
    urethral sphincter, 1323
    vascular, 137
spindle, sensory innervation, 60-1
spiral, 104, 113
strap-like, 104, 105(f), 113, 114
strength, 114, 118
striated, 104
    urethral sphincter, 1323 *See also* muscles (general), cardiac; *See also* muscles (general), skeletal
synergists, 114
triangular, 104, 105(f), 105(t)
twisted, 104, 123
unipennate, 104, 105(f), 113

voluntary *See* muscles (general), skeletal *See also* fibre(s), muscle

muscles (named)

- of abdomen, anterolateral, 1060-6
- abductor digiti, minimi
  - of foot, 1452
  - of hand, 883-4, 883(f), 884
- abductor hallucis, 1451
  - surface anatomy, 1344
- abductor pollicis
  - brevis, 883-4, 883(f)
  - longus, 848(f), 850-1, 850(f), 879
- adductor
  - magnus, 1332, 1332(f), 1375(f), 1376, 1391
  - pollicis, 787, 883(f), 884
- adductor brevis, 1375-6, 1375(f), 1391
- adductor hallucis, 1454
- adductor longus, 1375, 1375(f), 1391
  - surface anatomy, 1052, 1342
- anconeus, 778, 850
- antitragicus, 620
- arrector pili, 146(f), 150, 151, 152, 153-4
- articularis cubiti, 827
- articularis genu, 1374
  - actions, 1374
- aryepiglottic, 585
- arytenoid
  - oblique, 585
  - transverse, 585
- auriculares, 600, 619-20
  - anterior, 538
  - obliquus, 620
  - superior, 538
  - transversus, 620
- axillary arch, 811
- biceps brachii, 778, 786, 823(f), 825-6
  - surface anatomy, 786
  - testing, 826

biceps femoris, 1332, 1377
    surface anatomy, 1343
brachialis, 823(f), 826
    testing, 826
brachioradialis, 786, 848-9, 848(f)
    surface anatomy, 786
branchial, 225
buccinator, 405, 484(f), 485(f), 487, 530, 538, 541, 573
bulbospongiosus, 1095, 1095(f), 1096-7, 1098, 1280, 1284
    actions, 1096-7
    ejaculation, 1275
ceratocricoid, 585
chondroglossus, 504
ciliary, 669, 681, 683(f)
cleidohyoid, 442
coccygeus (ischiococcygeus), 1046, 1083-4
constrictor, of pharynx
    inferior, 569(f), 570(f), 572
    middle, 569(f), 570(f), 571
    superior, 565, 566, 569(f), 570(f), 571
coracobrachialis, 778, 824-5, 827, 828, 829(f)
    surface anatomy, 786
    testing, 825
corrugator, supercilii, 486
cremaster, 1064, 1261(f)
    functions, 1064
cricoarytenoid, 578(f), 579
    lateral, 578(f), 579, 585-7
    posterior, 585
cricopharyngeus, 572, 951, 953
    relaxation impairment, 953
cricothyroid, 578(f), 579, 587
    development, 600
    paralysis, 592
cucullaris *See* muscles (named), trapezius
dartos, 1060, 1262
deltoid, 778, 786, 807(f), 809-10

    - surface anatomy, 786
- depressor anguli oris, 485(f), 486, 487, 607
- depressor labii inferioris, 484(f), 485(f), 486-7
- depressor septi, 302(f), 476, 482, 483(f), 549
- detrusor, trigonal, 1247-8
- diaphragm, 1007
- digastric, 441, 539
    - development, 600
- digital palmar, common, 857
- dilator naris
    - anterior, 549
    - posterior, 549
- dilator pupillae, 668, 684, 685(f), 701
- epicranius, 481-2, 600
- erector spinae, 738-40, 738(f), 1072
    - surface anatomy, 738
- extensor carpi radialis
    - brevis, 848(f), 849
    - longus, 848(f), 849
    - synovial sheath, 879
- extensor carpi ulnaris, 787, 848(f), 850, 878(f), 879, 887
- extensor digiti minimi, 849-50, 879
    - synovial sheath, 879, 882(f)
- extensor digitorum, 787, 848(f), 849, 887, 888
    - brevis, 1343, 1455
        - surface anatomy, 1344
    - longus, 1418-19
        - surface anatomy, 1344
    - synovial sheath, 879, 882(f)
- extensor hallucis
    - brevis, 1455
    - longus, 1332, 1343, 1417-18
        - surface anatomy, 1344
- extensor indicis, 778, 850(f), 851
    - brevis, manus, 851
    - synovial sheath, 879
- extensor pollicis

  - brevis, 778, 848(f), 850(f), 851
    - synovial sheath, 879
  - longus, 778, 786, 787, 788(f), 789, 848(f), 850(f), 851
    - synovial sheath, 879
- extensor retinaculum, 857
- extraocular, 482-6, 655, 658-65, 659(f), 660, 662(f), 663(f)
  - actions, 661
  - development, 702
- facial, 600
- fibularis
  - brevis, 1416, 1417(f), 1418(f), 1419, 1420
    - synovial sheath, 1420
  - longus, 1416, 1419-20
    - synovial sheath, 1419-20
  - surface anatomy, 1343
  - tertius, 1332, 1417(f), 1418(f), 1419
  - variants, 1420
- flexor accessorius, 1423
  - longus, 1423
- flexor carpi radialis, 783(f), 784(t), 845-6, 846(f)
  - testing, 846
- flexor carpi ulnaris, 783(f), 784(t), 846(f), 847
  - testing, 847
- flexor digiti minimi, brevis, 1454
- flexor digitorum
  - accessorius, 1453
  - brevis, 1451-2
  - longus, 1423
    - surface anatomy, 1344
  - pollicis, synovial sheath, 678
  - profundus, 783(f), 784(t), 785(t), 847-8, 853(f), 886
    - testing, 848
  - superficialis, 778, 783(f), 846-7, 846(f), 886
    - synovial sheath, 868(f), 878(f), 879-80
    - testing, 847
- flexor hallucis
  - brevis, 1453-4

    - longus, 1423, 1451
        - surface anatomy, 1344
- flexor pollicis
    - brevis, 881, 883, 883(f)
    - longus, 778, 783(f), 784(t), 785(t), 848
        - synovial sheath, 868(f), 879-80
        - testing, 848
- flexor retinaculum, 857
- gastrocnemius, 1332, 1420-1
    - blood supply, 109, 1420-1
    - surface anatomy, 1343
- gemellus, 1331, 1391
    - inferior, 1372
    - superior, 1372
- genioglossus, 503, 530
- geniohyoid, 501, 530, 539
- gluteus maximus, 1331, 1369, 1369(f), 1389, 1391
    - actions, 1369
    - attachments, 1368
    - blood supply, 109, 1369
    - relations, 1368-9
    - vascular supply, 1369
- gluteus medius, 1331, 1369-70, 1369(f), 1389, 1391
    - actions, 1370
    - attachments, 1369
    - surface anatomy, 1342
- gluteus minimus, 1331, 1370, 1388, 1389, 1391
    - actions, 1370
    - attachments, 1370
    - relations, 1370
    - vascular supply, 1370
- gracilis, 1332, 1374-5, 1374(f), 1391
    - actions, 1375
    - attachments, 1374-5
    - blood supply, 109
    - relations, 1375
    - surface anatomy, 1343

  - vascular supply, 1375
- hamstrings, 1332, 1377
- helicis major and minor, 620
- hyoglossus, 503-4, 504(f)
- hypothenar, 884-6
- iliacus, 1072, 1331, 1368, 1387, 1391
- iliococcygeus, 1083-4
- iliocostalis, 739
  - cervicis, 739
  - lumborum, 739
  - thoracis, 739
- iliopsoas, 1367, 1368, 1391
- incisivus labii
  - inferioris, 482(f), 483(f), 488
  - superioris, 482(f), 483(f), 488
- infrahyoid, 442
- infraspinatus, 778, 812, 813(f)
- intercostal, 924-5, 925(f)
  - external, 924, 1011
  - innermost, 925
  - internal, 925, 1011
  - role in breathing, 1012
  - role in speech, 590
- interossei
  - dorsal
    - of foot, 1454-5, 1454(f)
    - of hand, 877, 883(f), 885-6, 885(f)
  - palmar, 883(f), 885, 885(f)
  - plantar, 1454(f), 1455
- interspinales, 741
- intertransversarii, 741
  - laterales, 741
  - mediales, 741
- ischiocavernosus, 1096
- ischiococcygeus, 1083-4
- latissimus dorsi, 747, 778, 786, 811
  - blood supply, 109, 811

    surface anatomy, 786, 910, 912, 912(f)
laxator tympani, 628
levator anguli oris, 482(f), 483(f), 484(f), 485(f), 486
levator ani, 1046, 1078, 1083-4, 1092, 1092(f), 1289
levator coccygei, 1289
levator labii superioris, 482, 483(f), 484(f), 486, 486(f), 607
    alaeque nasi, 486, 549, 607
levator palpebrae
    superioris, 656, 657, 658-9, 661, 667, 671(f), 703
levator scapulae, 810
levator, of thyroid, 462
levator veli palatini, 541, 568-9, 569(f), 570(f)
levatores, costarum, 925
    breves, 925
    longi, 925
longitudinal
    of large intestine, 1212
    of small intestine, 1211
    of stomach, 1204
    of tongue, 504
        inferior, 504
        superior, 504
        transverse, 504
        vertical, 504
longus
    capitis, 443
    colli, 443
lumbricals
    of foot, 1453
    of hand, 883(f), 886
        variations, 886
malaris, 486
masseter, 532, 538, 538(f)
    actions, 538
    hypertrophy, 538
    innervation, 538
    relations, 538

    - vascular supply, 538
- masticatory, 532, 600
- mentalis, 482(f), 483(f), 484(f), 485(f), 486
- Müller’s, 545, 660
- multifidus, 740(f)
- muscularis
    - large intestine, 1212
    - small intestine, 1211
- muscularis externa (of mucosa), 39
- muscularis mucosae, 39
- mylohyoid, 501
    - development, 600
    - innervation, 501
    - vascular supply, 501
- nasalis, 482(f), 483(f), 484(f), 486, 549
    - transverse, 607
- oblique, 660
    - external, 1041, 1061, 1063
        - aponeurosis, 1058(f), 1060, 1062(f), 1063
        - arteries and nerves, 1063
        - attachments, 1063
        - surface anatomy, 910, 912(f), 913
    - inferior, 657, 658, 660
    - internal, 1041, 1061, 1064
        - arteries and nerves, 1064
        - attachments, 1064
        - variations/defects, 1064
    - superior, 657, 660, 661
- obliquus
    - auriculae, 620
    - capitis, inferior, 742
    - superior, 742
- obturator, 1391
    - externus, 1331, 1369(f), 1371-2, 1388
        - actions, 1372
        - attachments, 1371-2, 1371(f)
        - relations, 1372

- internus, 1046, 1083, 1085, 1331, 1369(f), 1371
  - attachments, 1371
  - relations, 1371
  - vascular supply, 1371

occipitofrontalis, 481, 659
oculogyric, 307
omohyoid, 442
opponens
- digiti, minimi, of hand, 884-5
- pollicis, 883(f), 884

orbicularis oculi, 482, 486, 535, 655, 658, 659, 669, 670, 674, 703
- development, 703

orbicularis oris, 484(f), 487-8, 573, 607
orbitalis, 545, 660
palatoglossus, 504, 506, 570
- development, 600

palatopharyngeus, 570-1, 570(f)
palmaris brevis, 857, 883(f), 885, 885(f)
palmaris longus, 846(f), 847
- surface anatomy, 786
- testing, 847

panniculus carnosus (remnant), 607
papillary, 966, 967, 972
Passavant’s, 563, 565(f), 571
pectinate, of right atrium, 964
pectineus, 1332, 1376, 1387, 1391
pectoralis
- major, 778, 786, 807-8, 809(f)
  - blood supply, 109
  - surface anatomy, 786
- minimus, 808
- minor, 808

peroneotibialis, 1408
peroneus *See* muscles, named, fibularis
pharyngeal
- inferior, 1204
- superior, constrictor, 530

    ventilatory role, 1012
piriformis, 1331, 1369(f), 1371, 1391
    attachments, 1371
    fascia over, 1086
    relations, 1371
    vascular supply, 1371
plantaris, 1332, 1421
platysma, 257, 436, 437, 438, 440, 483(f), 484(f), 488, 538, 607
popliteus, 1332, 1407-8
    minor, 1408
posterior mass, 1071
preprostatic, 1248, 1250, 1253
prevertebral, 442, 453
princeps, pollicis, 857
procerus, 486, 548-9
pronator quadratus, 846(f), 848
    testing, 848
pronator teres, 778, 840(f), 845, 846(f)
    testing, 845
psoas
    abscess, 1368
    major, 259(f), 1041, 1070, 1071, 1331, 1367-8, 1367(f), 1387, 1391
    minor, 1072, 1331, 1367(f), 1368
pterygoid, 610
    lateral, 527, 532, 538-9, 539(f), 540
        actions, 539
        innervation, 539
        relations, 538-9
        vascular supply, 539
    medial, 527, 532, 539
puboanalis, 1083, 1084
pubococcygeus, 1083-4
    innervation, 1085
puborectalis, 1083, 1085
    development, 1323
pubourethralis, 1083

pubovaginalis, 1083
pyloric, 1204
pyramidalis, 1056(f), 1057(f), 1063
quadratus femoris, 1331, 1369(f), 1372, 1391
    attachments, 1070-1, 1372
quadratus lumborum, 985, 1041, 1070-1, 1071(f)
    actions, 1071
    innervation, 1071
    perirenal fascia relations, 1227, 1228
    relations, 1071
    variations, 1071
    vascular supply, 1071
quadriceps femoris, 1373
    actions, 1374
    surface anatomy, 1342
recto-urethralis, 1151
rectococcygeal, 1151
rectus abdominis, 1041, 1056(f), 1057(f), 1058(f), 1061, 1062(f)
    arteries, 1061
    attachments, 1061
    diverication, 1063
    innervation, 1061
    separation of, 1300
    sheath, 1061
    surface anatomy, 912(f), 913, 1053
rectus capitis
    anterior, 442-3, 442(f)
    lateralis, 442(f), 443
    posterior (major and minor), 742
rectus of eyeball, 659-60
    inferior, 657, 658, 660, 671
    lateral, 656, 658, 659(f), 660
    medial, 658, 660
    relations, 659
    superior, 660
rectus femoris, 1332, 1373, 1388
    attachments, 1373

- relations, 1373
- surface anatomy, 1342
- vascular supply, 1373

rectus sternalis, 808
rhomboid
- major, 722, 736(f), 810, 810(f)
- minor, 736, 736(f), 737, 810-11, 810(f)
- occipitalis, 810
- testing, 811

risorius, 488, 538
rotator cuff, 778, 806, 812
- disease, 807

rotatores, 740
- capitis, 740
- cervicis, 740
- thoracis, 740

salpingopharyngeus, 571
sartorius, 1332, 1372-3, 1374(f), 1391
- actions, 1373
- surface anatomy, 1342
- vascular supply, 1372-3

scalenus
- anterior, 407, 443, 986
- medius, 443
- posterior, 443-4

semimembranosus, 1332, 1377
- surface anatomy, 1343

semispinalis, 741
- capitis, 741
- cervicis, 741
- thoracis, 741

semitendinosus, 1332, 1374(f), 1377
- surface anatomy, 1343

serratus
- anterior, 808, 809(f), 811-12
  - surface anatomy, 786, 913
  - testing, 812

    - posterior
        - inferior, 925-6, 926(f)
        - superior, 925
- soleus, 1332, 1421-2
    - surface anatomy, 1343
- sphincter
    - anal
        - damage to, 1160
        - external, 1159
            - sex differences in, 1159, 1159(f)
    - oesophageal, upper, 572, 573
    - palatopharyngeal, 571
    - pupillae, 669, 682, 684
    - urethral
        - distal, 1254
        - external, 1251, 1252
- spinalis, 738-9
    - capitis, 738
    - cervicis, 738
    - thoracis, 738
- splenius
    - capitis, 737
    - cervicis, 737-8
- stapedius, 600, 628
    - development, 652
- sternalis, 808
- sternocleidomastoid, 406, 407, 440-1, 607, 614
    - innervation, 460
    - nerves, 460
    - surface anatomy, 440
- sternocostal, 963
- sternocostalis, 918, 925
- sternohyoid, 442, 985
- sternothyroid, 442, 985
- styloglossus, 504, 504(f), 539
- stylohyoid, 441-2, 504(f), 600
- stylopharyngeus, 539, 569(f), 571, 600

subclavius, 808, 809(f)
subcostales, 925
suboccipital, 742-3
subscapularis, 778, 807, 809(f), 812
supinator, 850(f), 851-2
    attachments, 841(f), 851
suprahyoid, 263, 438(f), 440, 501
supraspinatus, 778, 812, 813(f)
    paralysis, 806
    testing, 812
suspensory, of duodenum, 1127
tarsal
    inferior, 658
    superior, 659, 661
temporal, 610
temporalis, 404-5, 532, 538, 538(f)
    actions, 538
    innervation, 538
    relations, 538
    vascular supply, 538
temporoparietalis, 482
tensor fasciae lata, 1331, 1367(f), 1368, 1374, 1391
    actions, 1368
    blood supply, 109, 1368
    perforator flaps, 1381
tensor palati, 50
tensor tympani, 617, 623, 626, 628
    development, 600, 652
tensor veli palatini, 529, 539, 541, 543, 569-70, 569(f), 570(f)
    development, 600
teres
    major, 778, 786, 812-13
        surface anatomy, 786
        testing, 813
    minor, 778, 813-14
thenar, 881-4
thyroarytenoid, 582(f), 585, 587

  - superior, 587
- thyroepiglotticus, 587
- thyrohyoid, 442
- thyropharyngeus, 572
- tibialis
  - anterior, 1332, 1343, 1417-18
  - posterior, 1423-4
  - secundus, 1424
  - surface anatomy, 1343
- tongue, intrinsic, 767, 772
- tragicus, 620
- transverse perinei
  - deep, 1094
  - superficial, 1096
- transversospinalis, 744
- transversus abdominis, 985, 1041, 1061, 1062(f), 1064, 1070
  - attachments, 1064
  - thoracis, 925, 925(f)
  - variations/defects, 1064
- trapezius, 406, 607, 746, 747, 809
  - innervation, 460
  - nerves, 460
  - surface anatomy, 912(f), 913
- triceps, 778, 823(f), 825(f), 826-7
  - brachii, 113, 795
  - surae, 1420, 1421, 1422
    - actions, 1422
  - surface anatomy, 786
  - testing, 827
- trigonal
  - deep, 1248
  - superficial, 1248
- uvulae, 571
- vastus
  - intermedius, 1332, 1374
  - lateralis, 1332, 1374, 1389
  - medialis, 1332, 1373-4

            obliquus, 1373-1374, 1403
    vocalis, 586(f), 587
    zygomaticus
        major, 486, 538
        minor, 486

muscles (of organs, or regions)
    of abdomen
        anterolateral, 1060-6
        development, 772
    of abdominal wall
        anterior, 1060-5
        posterior, 1070-2, 1071(f)
    accessory, of ventilation, 924-6
    of anal canal, 1158-9, 1158(f)
    of arm, 778, 823(f), 824-8, 824(f)
        anterior compartment, 824-6
        posterior compartment, 826-7
    of auricle, of ear, 619-20
    of back, 736-43, 737(f)
    of bladder, 1247-8
    of cheeks, 482-6
    of chest wall, 909-10
    of clitoris, 1281(f)
    craniofacial, 397, 481-9
        buccolabial, 486-8
        circumorbital, 482-6
        epicranial, 481-2
        nasal, 486-8
        palpebral, 482-6
    of duodenum, 1127
    of ear, middle, 628
    of external nose, 548-9
    of eye, extraocular, 482-6, 655, 658-65, 659(f), 660, 661, 662(f), 663(f), 702
    of eyelid, 482, 659, 660, 703
    of face, 481-9, 607
    of facial expression, 40, 481-9

of female perineum, 1283(f)
of floor of mouth, 501
of foot, 1331, 1332, 1450-5
of forearm, 845-52
    anterior compartment, 845-8
    posterior compartment, 848-52
of gluteal region, 1331, 1368-72, 1369(f), 1391-2
of hand, 878-86
    extensor, 778
    small (intrinsic), 778
hypothenar, 884-6
of iliac region, 1331, 1367-8, 1391-2
of iris, 682, 684-5
of knee, 1332, 1407-8
of larynx, 583, 585-7, 586(f)
    extrinsic, 585
    intrinsic, 585-7, 585(f)
of leg, 1332, 1417-24
of lower limb, 1331-3
of mastication, 489, 538-40, 539(f)
of neck, 440-4
    anterior triangle, 441-3
    cervical, 440-1
    infrahyoid, 442
of oesphagus, 1114(f)
of pectoral girdle
    anterior, 778, 807-8
    posterior, 778, 807-8
of pelvis, 1083-5, 1083(f)
    female, 1084(f)
of perineum, 55(f), 1093-7, 1093(f), 1095(f)
of pharyngeal arch, 599-600, 599(f), 600(f)
of pharynx, 561, 561(f), 568-72, 569(f), 570(f)
of prostate, 1259
of scrotum, 145(f), 1262
of shoulder region, 778, 807-12
of soft palate, 568-72

  - of stomach, 1114(f), 1204, 1206
  - thenar, 881-4
  - of thigh, 1332, 1372-8, 1373(f)
    - adductor compartment, 1374-6
    - anterior compartment, 1372-4
    - posterior compartment, 1376-8
  - of thoracic wall, 924-6
  - of tongue, 503-5, 504(f)
    - extrinsic, 503
    - intrinsic, 503
  - trunk, dorsal, development, 772
  - of tympanic cavity, 628
  - of upper limb, 778
    - of wrist, 778
  - of urethra, 1250, 1252, 1311
  - ventrolateral, development, 772
  - of vestibule, 1281(f)

muscularis externa, 1050, 1051
  - of large intestine, 1161-2
  - mallei, 628
  - of oesophagus, 952
  - of small intestine, 1135
  - of stomach, 1050, 1122, 1204, 1206

muscularis mucosae, 1050, 1051
  - of anal canal, 1157
  - of large intestine, 1161
  - of rectum, 1051, 1157-8
  - of small intestine, 1135
  - of stomach, 1122

muscularis submucosae ani, 1157

myasthenia gravis, 948

mydriasis, 685

myelencephalon, 605
  - development, 362(f), 376(t), 377 *See also* medulla, oblongata

myelin, 41, 42, 50-1, 50(f)
  CNS/PNS differences, 50
  mutations, 51
  secretion, 5
  ultrastructure, 51, 51(f)

myelination, 50-1, 50(f)
  cranial nerves, 389
  in neonate/infants, 389
  spinal cord, 375

myelocoele, 772

myelopathy, 271

Myf 5, 772

myocardial infarction, 981

myocardium, 139, 141, 142, 143
  development, 1016
  primary, 1022

myocytes *See* cells (named), myocytes

MyoD, 772

myofibrils, 110(f)
  cardiac muscle, 140(f)
  skeletal muscle, 106, 106(f), 107(f), 108(f), 110(f)

myogenesis, 115-17
  determination factors, 115
  development, 115-17

myogenic determination factors, 115

myogenin, 115, 117(f), 772

myoglobin, 111

myomesin, 106

myometrium, 1291
  magnetic resonance imaging, 1292, 1292(f)

myopia, 688

myosin light chain, gene mutations, 970

myosins, 15
    cardiac muscle, 143
    skeletal muscle, 106, 111, 112, 112(t)
    smooth muscle, 127, 128, 129(f)

myotomes, 231, 764, 764(f), 772
    formation, 766(f), 772
    lower limb, 1338(t), 1339(t), 1340(t), 1346

myotonic dystrophy, 1013

myotubes, 115-16, 116(f)
    heterokaryotic, 772
    primary, 115, 116(f)
    secondary, 115, 116(f)
    tertiary, 115, 116(f)

N

N-CAM, 6, 1308

naevus, 159
  pigmented, spinal cord disorders, 772

nail, 154-6, 155(f), 858
  at birth, 905
  bed, 155
  cuticle, 155, 159
  development, 159
  field, 159
  folds, 155, 861
  growth, 156
  matrix, 155
  plate, 155

nares (naris)
  external, 547, 549
  posterior, 561(f), 563

nasal bone, 409, 410(f), 475, 547, 613
  fractures, 547
  ossification, 475

nasion, 409

nasopharynx, 544, 561(f), 563-4, 610
  boundaries, 563
  microstructure, 563-4
  nerves, 563

navicular bone, 1433, 1437-8
  accessory, 1438
  bipartite, 1438
  club foot, 1463
  innervation, 1438
  muscle/ligament attachments, 1437-8
  ossification, 1438
  surface anatomy, 1341

  - vascular supply, 1438

nebulin, 106, 115

neck, 435-66
  - arterial supply, 397-400, 398(f), 444-51
  - blood vessels, 610
  - cancers, 454
  - cellulitis, 439-40
  - compartments, 439
  - development, 595-614
  - fascia, 438-40
  - formation of, 607-10
  - infection spread, 439-40
  - innervation, 401-2
  - ligaments, 436, 438
  - lymphatics, 400(f), 401, 454
  - muscles, 397, 440-4
    - anterior triangle, 441-3
    - cervical, 440-1
    - infrahyoid, 442
    - vertebral, anterior, 442-3
      - vertebral, lateral, 443
  - nerves, 455-62
  - radial, 840, 841(f)
  - reflexes, 401
  - root of, 406, 438, 439, 443, 465-6
  - skin, 435-6
    - innervation, 435-6
    - lymphatics, 454
    - nerves, 435-6
    - vascular supply, 435
  - surface anatomy, 397, 405-7
    - arteries, 406-7
    - nerves, 407
    - skeletal landmarks, 405
    - soft tissues and viscera, 406
    - veins, 407

tissue spaces, 439-40
triangles, 436-8 *See also* triangle(s)
veins, 451-2
    development, 393(f)
venous drainage, 399(f), 400
viscera, 462-5

neck (of bones, or organs)
femoral, 1360, 1361(f)
of gallbladder, 1177
of malleus, 627
of rib, 919
of scapula, 794
of stapes, 627
of urinary bladder, 1245, 1248

necrosis, 24

neocortex, 335, 382
anterior temporal, 358
axons to striatum, 329
commissures, 385
connectivity, 340-1, 340(f), 341(f)
laminar organization, 339-40 *See also* cortex, cerebral

neonate, 214-16
abdominal wall, 1313(f)
anatomy, 214(f), 215(f)
arteries, 1032
brain, 388-9
brain stem, 376(t), 377
brown fat, 35
chondrocranial ossification, 611
colon, 1212
congenital heart disease, 974
dentition, 512(f)
diaphragm, 1015-16, 1218
ductus arteriosus, 1028
endotracheal intubation, 1033

Eustachian valve, 964
female external genitalia, 1325
femur, 1365
functional maturity of gut, 1213
gallbladder, 1209
heart, 1029(f), 1030
hip bone, 1354(f)
hyoid bone, 610
inguinal rings, 1066
internal iliac artery, 1087
kidney, 1225, 1312, 1313(f)
large intestine, 1212
larynx, 574, 610
length measurement, 216
limb(s), lower, 1463-4
lumbar puncture, 760
lung function, 1035-6
mandible, 532
myelination, 389
occipital bone, 711(f)
oesophagus, 1203-4
    mucosa, 1204
oral cavity, 606-7
ovary, 1294, 1321
peritoneal cavity, 1218
pharynx, 610
post-term, 213
preterm (premature), 213, 216 *See also* infants, premature
reflexes, 389
REM sleep, 1015-16
respiratory distress, 1035
skeleton, 215, 215(f)
skull, 611(f)
small intesting, 1211-12
sphenoid bone, 530
stomach, 1206
suckling, 606-7

  - suprarenal gland, 1219
  - swallowing, 573(f), 574
  - testes, 1325
  - thorax, 1015-16
  - thymus, 947(f), 948
  - thyroid gland, 608
  - ureter, 1312, 1313(f)
  - urinary bladder, 1312, 1313(f)
  - urinary system, 1312, 1313(f)
  - urine sampling, 1312
  - uterus, 1313, 1313(f), 1316
  - vagina, 1316
  - veins, 1032
  - vertebral curvatures, 714
  - vitreous humour, 688
  - weight, 216 *See also* infants

neostriatum, 325 *See also* striatum

nephrectomy
- live donor, 1233
- partial, 1231
- simple *vs* radical, 1228

nephrocoele, 1306(f)

nephron(s), 1234-7, 1236(f)
- mesonephros, 1307
- metanephric, 1309, 1309(f)
- neonates, 1310
- structure, 1234, 1236(f) *See also* glomerulus; *See also* tubule(s), renal

nephrostome, 1305, 1306(f)

nephrotomes, 1305

nerve block
- alveolar nerve
  - inferior, 520
  - superior, 539
- brachial nerve plexus, 790

        - administration routes, 790
    - digital nerve, 790
    - lower limb, 1346
    - pudendal nerve, in perineum, 1098
    - radial nerve, 790
    - ulnar nerve, 790

nerve growth factor, 8, 370

nerves (general)
- adrenergic, 138, 141
- adrenergic, salivary secretion control, 522(f), 523
- blood supply, peripheral nerves, 55-6
- cholinergic, 56, 138, 141
    - salivary secretion control, 522(f), 523
- dopaminergic *See* neurone
- endings, Ruffini-like, 517
- endings, sensory, 57-61
    - en grappe, 110
    - en plaque, 110
    - encapsulated, 59-60
    - flowerspray, 60, 60(f)
    - free, 58-9
    - joint receptors, 61
    - Merkel tactile, 59
    - motor, 60
    - neurosecretory, 46
    - paciniform (encapsulated), 59
    - primary (anulospiral), 60, 60(f)
    - Ruffini, 59(f), 101
- impulse conduction, 63-4, 64(s)
- mixed, 236
    - phrenic nerve, 1010
- motor, 110-11
- peripheral, 53
- rami *See* ramus (rami)
- root *See* root(s)
- secretomotor, salivary secretion control, 522(f), 523

sensory
    cutaneous, 157, 159
    development, 157, 159
    of tongue, 506
sensory-motor, 236 *See also* fibre(s), nerve; *See also* neurone; *See also* pathway(s); *See also* plexus (nervous)

nerves (named)
abducens, 275, 429, 655, 656, 660, 666-7, 667(f)
    accessory, 275
    lesion, 295
    origin, 275
accessory, 459-60, 600
    cranial root, 459
    lesions, 460
    spinal, 752
    spinal root, 459-60
alveolar (dental)
    inferior, 501, 519, 532, 540, 542, 543
        anaesthesia, 519
        fascicular organization, 519
        incisive branch, 519
        mental branch, 519
        mylohyoid branch, 519
        nerve block, 520
    superior, 519
        anterior, 519
        inferior, 554
        middle, 519
        nerve block, 539
        posterior, 519, 559
ampullary, 643
ansa(e) *See* ansa
auricular, 458
    great, 435-6, 496, 622
auriculotemporal, 496, 497, 533, 535, 538, 540, 542-3
axillary, 780, 781(f), 813(f), 814, 821
    lesions, 821

to brachialis, 833
branchial efferent
    development, 373
    special, 600
buccal, 487, 493(f), 494, 539, 540, 542
calcaneal, medial, 1457
cardiac, 236
caroticotympanic, 626, 629
carotid, internal, 234, 460
carotid sinus, 447
cavernous
    greater, 1252, 1273
    lesser, 1252, 1273
cervical, 493, 495, 756
    cutaneous branches, 436, 915, 916
    development, 767(f)
    first (suboccipital), 450(f), 455, 755
    lesions, 759
    lower, 709
    rami *See* ramus (rami)
    roots, 754
chorda tympani, 506, 508, 509, 521, 529, 533, 541, 542(f), 543, 600, 605, 629-30
ciliary
    long, 668, 684
    short, 668, 669, 681, 684
of clitoris, dorsal, 1098
coccygeal, 754
    rami, dorsal, 756, 757
    roots, 754
cochlear, 634, 641, 642, 644-6, 646(f)
    afferent fibres, 645
    efferent fibres, 645-6
collateral, ulnar, 829
cranial, 225, 226, 227, 228(f), 230-1, 275, 401, 457-60
    compression, 568
    development, 372-3

- myelination, 389
- palsy, 295*see also individual nerves*

cutaneous
- of arm
  - lateral, 829
  - medial, 821, 830
  - posterior, 829
- of forearm
  - lateral, 856
  - medial, 821, 830, 856
  - posterior, 829, 856
- of neck, transverse, 436
- perforating, 1384
- posterior, 1280
- sural
  - lateral, 1427
  - medial, 1427
- of thigh, 1080
  - intermediate, 1383
  - lateral, 1080, 1382
    - lesions of, 1382
  - medial, 1383
  - posterior, 1384
- of thorax
  - anterior, 929
  - lateral, 929

dental (alveolar) *See* nerves (named), alveolar

descendens cervicalis, 456, 460

digital
- dorsal
  - of foot, 1427, 1428
  - of hand, 855, 858, 858(f), 895(f), 897, 898
- nerve block, 790
- palmar, 895
  - common, 895
- pollicial, 898

dorsal

    - of clitoris, 1098
    - of penis, 1098, 1274
    - scapular, 820
- dorsolumbar, 929, 1060
- ethmoidal
    - anterior, 433, 668
    - posterior, 433, 668
- facial, 275, 405, 433, 494-5, 543, 600, 610, 617, 620, 622, 625, 626, 629-30
    - branching patterns, 495, 495(f)
    - chorda tympani branch, 506, 508, 509, 521, 527
    - complications, 495
    - lesions, 295, 495
    - origins, 286
    - paralysis, 495, 630
    - parasympathetic fibres, 234
    - roots, 279
    - surgery, 495(f)
        - complications, 495
    - in tympanic cavity, 629-30
- femoral, 1080, 1336, 1382-3, 1382(f), 1390
    - anterior division, 1383
    - lesions, 1383
    - posterior division, 1383
    - surface anatomy, 1344
- fibular
    - common, 1338, 1427
        - surface anatomy, 1344
    - deep, 1411, 1427-8
        - lesions of, 1428
        - surface anatomy, 1344
    - superficial, 1427
        - surface anatomy, 1344
- frontal, 667
- furcal, 1078
- ganglionic, 544
- gastric

    - anterior, greater, 1120
    - posterior, 1120
- to gemellus inferior, 1384
- to gemellus superior, 1384
- to geniohyoid, 456, 460
- genitofemoral, 1080, 1294, 1321
    - distribution, 1080
    - genital branch, 1064
- glossopharyngeal, 275, 457-8, 506, 543, 600, 605
    - branches, 458, 572
    - carotid branch, 458
    - gangion, 458
    - ganglion, visceral afferent fibres, 236
    - lesions, 458
    - pharyngeal branches, 458
    - tympanic branch, 458, 629, 629(f)
- gluteal
    - inferior, 1338, 1384
    - superior, 1338, 1384, 1390
- gustatory, 508
- hepatic, 1120, 1172
- hypogastric, 1046
    - inferior, 1043, 1044, 1046, 1154
- hypoglossal, 275, 433, 460, 611
    - branches, 433, 460
    - communications, 460
    - lesions, 405, 460
    - origin, 275
    - rootlets, 275, 283, 770
- iliohypogastric, 1064, 1078
    - branches and distribution, 1080
    - distribution, 1080
    - entrapment, 1080
    - injuries, 1080
- ilioinguinal, 1064, 1078, 1080, 1280
- incisive, 532
- infraorbital, 404, 494, 544, 554, 559, 656, 668, 671

infratrochlear, 493, 657, 668, 671
intercostal, 911, 928-9, 928(f), 1060
  7th and 8th, 1060
  9th to 11th, 1060
  cutaneous branches, 916, 929, 1060
  lesions, 929, 1067
  lower, 1060, 1172
  pleura innervation, 991
  posterior branches, 1060
intercostobrachial, 791, 829, 830, 916, 929
intermedius, 425, 546, 624, 629
interosseous
  anterior, 780, 781(f), 854-5
    palsy, 854
  posterior, 780, 781(f), 856
    palsy, 854
    surface anatomy, 789
jugular, 461
labial, 1098
lacrimal, 493, 657, 667, 671
laryngeal
  external, 445(f), 459, 588-9
    surgical damage risk, 589
  inferior, 589
  internal, 459, 588
  lesions, 589
  non-recurrent, 589
  recurrent, 459, 589, 600, 949, 951, 984
    left, 984
    paralysis, 589
    relation with ductus arteriosus
  superior, 459, 588
to lateral pterygoid, 542
lingual, 506, 521, 541, 542, 543
  anaesthesia, 519, 539
  risk at molar removal, 506, 510
lowest (least), 945

lumbar, 754, 756(f), 1064
    lesions, 759
    rami, dorsal, 756
    roots, 759, 1071
lumbosacral trunk, 1078, 1091-2, 1093
mandibular, 494, 501, 527, 538, 539, 541-2, 545(f), 600, 653
    anterior trunk, 542
    medial pterygoid branch, 539
    nerve block, 519
    posterior trunk, 506, 542
to masseter, 542
masseteric, 535, 538, 542
maxillary, 493, 544, 545(f), 600, 656, 668, 668(f)
    greater palatine branch, 501
    nasopalatine branch, 501, 544
    nerve block, 519
    pharyngeal branches, 563
    in pterygopalatine fossa, 559
to medial pterygoid, 542
median, 780, 783(f), 787, 821, 822, 823(f), 827, 828, 895-7
    branches
        muscular, 895
        palmar cutaneous, 895
        palmar digital, 895
    compression, 854, 895
    in cubital fossa, 828, 836-7
    division, at wrist, 897
    in forearm, 846(f), 847, 853-5, 854(f)
    surface anatomy, 789
meningeal, 544
    recurrent, 754
meningeus medius, 433
mental, 494, 519, 525, 532
musculocutaneous, 780, 782(f), 821, 828-9
    in cubital fossa, 837
    lesions, 821
nasal, 554-5

    - external, 493, 554
    - superior, posterior, 544, 545
- nasociliary, 554, 666, 667, 668, 684
- nasopalatine, 501, 502, 503, 544, 545, 546, 555, 555(f)
- obturator, 1080, 1337, 1383
    - accessory, 1080-1, 1383-4
    - lesions, 1383
- to obturator internus, 1384
- occipital
    - greater, 435, 493(f), 495, 755
        - neuralgia, 755
    - lesser, 435, 493(f), 495, 620
    - third, 755-6
- oculomotor, 81, 275, 427, 429, 655, 656, 659, 660, 666, 667(f)
    - development, 702
    - inferior, 666
    - palsy, 252, 295
    - roots, 288
    - superior, 666
- olfactory, 230, 232(t), 275, 401, 555
    - development, 383-4
    - injury, 555
    - sheath, 555
- ophthalmic, 67, 493, 656, 667-8
- optic, 230, 232(t), 275, 401, 655, 667, 675, 694
    - development, 700
    - head, 694-6, 694(f), 695(f)
    - postlaminar zone, 695
    - prelaminar zone, 694, 695(f)
    - vascular supply, 695
- orbital, 544-5
- palatine
    - greater (anterior), 502, 544, 545-6, 554
    - lesser (posterior), 544, 545-6, 565
- to pectineus, 1383
- pectoral
    - lateral, 821

    - medial, 821
- pelvic, 235
- of penis, dorsal, 1098
- perineal, 1098, 1280
- peroneal *See* nerves (named), fibular
- petrosal
    - deep, 544, 673
    - external, 461
    - greater, 544, 600, 629, 630
    - lesser, 543, 629
- pharyngeal, 544, 546, 553
    - ascending, 565
- phrenic, 270, 456-7, 959, 1010, 1014, 1015
    - accessory, 457, 1010
    - diaphragmatic relationship, 1010
    - left, 963, 1010, 1010(f)
    - lesions, 1010-11
    - ‘pacing’, 1011
    - pleural innervation, 991
    - right, 964, 1010, 1010(f)
- to piriformis, 1385
- plantar
    - lateral, 1458
    - medial, 1457-8
- to popliteus, 1338, 1427
- pterygoid, lateral, 542
- of pterygoid canal, 629
- pudendal
    - in pelvis, 1092
    - in perineum, 1098
- pyloric, 1120
- to quadratus femoris, 1384
- to quadriceps, 1079(f)
- radial, 780, 782(f), 814, 822, 824(f), 825(f), 826, 829
    - at elbow, 835(f), 837
    - branches
        - cutaneous, 829

            muscular, 829
            superficial terminal, 855-6
        compression/entrapment, 855-6
        in forearm, 855-6, 855(f)
        in hand, 898
        lesions, 829
        nerve block, 790
        surface anatomy, 789
rectal, inferior, 1098
renal, 455, 1045
sacral, 754
        fourth, perineal branch, 1092
        lesions, 759
        rami, dorsal, 756
        roots, 754
saphenous, 1409-10
        infrapatellar branch, 1393
        short, 1394
to sartorius, 1383
scapular, dorsal, 820
sciatic, 1079, 1079(f), 1091, 1337-8, 1384
        artery to, 1378
        lesions, 1384
        surface anatomy, 1344
scrotal, posterior, 1098
of shoulder region, cutaneous, 791
sinuvertebral, 25, 42, 715-16, 718, 731, 754, 755(f)
of skin, shoulder region, 791
somatic
        development, 371-3 *See also* nerves (named), cranial; *See also* nerves (named) spinal
spinal, 225, 226, 227(f), 230, 257, 258, 262, 401, 712, 715, 753(f), 757
        accessory, 407
        arteries, 757, 758(f)
        centra of vertebra relationship, 771(f)
        classification, 754
        compression, 717, 759

    - covering, 752, 752(f)
    - development, 371-2, 766(f)
    - fibres (somatic/visceral), 755
    - injury, 730, 731
    - lesions, 757, 759
    - rami, 713-15
    - relations, 752
    - surface anatomy, 757
    - typical, 754, 754(f)
    - variations, 755
    - ventral, rootlet development, 375
- spinal accessory, 752
    - development, 376
- spinosus, 433, 542
- splanchnic, 985
    - greater, 945, 1042, 1045
        - aperture in crus of diaphragm, 1008
    - lesser, 945, 1042, 1045
        - aperture in crus of diaphragm, 1008
    - lowest (least), 1042-3
    - lumbar, 1043, 1081, 1141, 1150, 1155
    - pelvic, 375, 1044-5, 1081, 1092, 1141, 1147, 1150, 1155, 1160
    - sacral, 1160
- to stapedius, 629
- to subclavius, 820
- subcostal (twelfth thoracic), 911, 929, 1060, 1063
    - centra and neural arch relationship, 771(f)
- suboccipital, 455, 457, 755
- subscapular
    - inferior (lower), 821
    - superior (upper), 821
- supraclavicular, 436, 916
- supraorbital, 493, 657, 665, 668, 671
- suprascapular, 820-1
    - lesions, 821
- supratrochlear, 493, 657, 668, 671
- sural, 1394, 1427

  surface anatomy, 1427
temporal, deep, 542
of tendons, 113
tentorii (is ‘nervus tentorii’), 433
to teres major, 822
testicular, 1264
thoracic, 754, 779, 781(f)
  12th (subcostal) *See* nerves (named), subcostal
  cutaneous branches, 916, 929
  lesions, 759
  long, 820
  rami
    dorsal, 756, 929
    ventral, 755, 928-9, 928(f), 1060
  spinal, 911 *See also* nerves (named), intercostal
thoracodorsal, 821
to thyrohyoid, 461
tibial, 1092, 1093, 1338, 1426-7, 1457
  branches, 1426-7
  lesions, 1427
  surface anatomy, 1344
trigeminal, 287, 404(f), 429, 433, 493-4, 527, 600, 602, 667, 671
  lesion, 295
  origins, 284
trochlear, 275, 288, 427, 429, 655, 656, 660, 666
tympanic, 458
ulnar, 780-1, 822, 823(f), 829, 897-8
  at elbow, 837
    division, 837
  branches, in hand, 896(f), 897-8
  compression, 837, 898
  division, at wrist, 898
  in forearm, 855, 855(f)
  in hand, 897-8
  nerve block, 790
  palpation, 787, 799
  paralysis, 888

        - surface anatomy, 789
    - utricular, 643
    - vagus, 275, 458-9, 600, 605, 1044, 1081, 1120, 1120(f)
        - anterior, 1044, 1111
        - branches, 572, 1120
            - auricular, 459, 617, 620, 621, 624
            - cardiac, 945, 982
            - intestinal, 945
            - in neck, 459
            - pulmonary (bronchial), 945
        - branches, gastric, 945
        - bronchial innervation, 1003
        - course in mediastinum, 945
        - development, 1204
        - ganglion, 458-9
            - visceral afferent fibres, 236
        - left, 141, 945, 984, 1120, 1204
        - lesions of, 589
        - oesophageal relations, 951, 1120
        - posterior, 1044, 1111, 1187
        - right, 141, 945, 985, 1204
        - thoracic, 911-12, 945
    - vestibular, 642-3
        - infratemporal, 642-3, 644
    - vestibulocochlear, 285, 286, 291, 295, 610, 642, 642(f)
        - lesion, 295, 642
    - Vidian’s, 543, 544, 629
    - Voit’s, 643
    - zygomatic, 544, 549, 667, 668
    - zygomaticofacial, 494, 656, 668
    - zygomaticotemporal, 493-4, 538, 544, 656, 668 *See also* plexus (nervous); *See also* ramus (rami); *specific anatomical regions/structures*

nerves (of organs, or regions)
- of abdominal wall
    - anterior, 1060
    - posterior, 1078-81, 1078(f), 1079(f)
- of abominal wall, posterior, 1071(f)

of adenoid, 563
of anal canal, 1160
of ankle, 1442
of anus, 1212
of appendix, 1143-4, 1146
of areola, of breast, 932
of arm, 818-22
    cutaneous, 823
of auricle, of ear, 620
of back, cutaneous, 707-8
of bone, 91-2*see also individual bones*
of breast, 932
of bronchi, 1003-4
of bulbourethral glands, 1270
of caecum, 1141
of calcaneus, 1437
of cheek, 499
of colon
    ascending, 1146
    descending, 1147
    sigmoid, 1150
    transverse, 1147
of common bile duct, 1180-1
of conjunctiva, 672
of cornea, 679
of cuneiform bones, 1438, 1439
of diaphragm, 1010-11
of duodenum, 1128, 1173
of ear
    external, 620
    inner, 642-9
    middle, 621-2, 629-30
of elbow, cutaneous, 831
of external acoustic meatus, 621-2
of external oblique muscle, 1065
of eyelids, 671
of face, 492-4

of female perineum, 1283(f)
of female reproductive system, 1283(f)
of floor of mouth, 501, 502
of foot, 1457-8, 1458(f)
    cutaneous, 1429
of forearm, 853-6
of gallbladder, 1172, 1180-1
of hand, 895-8, 896(f)
    cutaneous, 858, 858(f)
of hard palate, 502-3
of head, 401-2, 539(f), 540(f), 541-3, 542(f)
of heart, 141, 982-3, 983(f)
of hip and thigh, 1382-4, 1382(f)
of ileum, 1131
of internal oblique muscle, 1064
of intestine, large, 1141, 1146, 1147, 1150
of iris, 684-5
of jejunum, 1131
of joints *see individual joints*
of kidney, 1233
of knee joint, 1409-10
    cutaneous, 1393
of lacrimal gland, 673
of larynx, 588-90, 588(f)
of leg, 1426-8
of lips, 500
of liver, 1172-3
of lower limb, 1093, 1336-40, 1337(f), 1338(t), 1339(t)
of lung, 998
of mastoid air cells, 626
of muscle
    skeletal, 110-11
    smooth, 128*see also individual muscles*
of nasal cavity, 554-5, 555(f)
of nasopharynx, 563
of navicular bone, 1438
of neck, 401-2, 407, 455-62

    - cutaneous, 435-6
- of nipple, 932
- of nose, external, 549
- of oesophagus, 951
    - cervical, 465
- of oral mucosa, 501
- of orbit, 666-9, 667(f), 668(f)
- of ovary, 1295
- of palatine tonsil, 567
- of pancreas, 1173
    - endocrine, 1190
    - exocrine, 1187
- of paranasal sinuses, 557
- of parathyroid, 464
- of parotid gland, 497
- of pelvis, 1091-3
- of penis, 1215-16
- of pericardium, 959
- of perineum, 1098
- of peritoneum, 1010, 1106-7
- of pharyngeal arches, 600
- of pharynx, 563
- of pleura, 991, 1010
- of prostate, 1258-9
- of pylorus, 1172
- of rectum, 1141, 1155
- of rectus abdominis, 1061
- of retina, 694
- of salivary glands
    - salivary secretion control, 522(f), 523
    - sublingual, 521
    - submandibular, 521
- of scalp, 492
- of seminal vesicles, 1270
- of sesamoid bones, 1442
- of skin, 157, 159
    - of arm, 823

    - of back, 707-8
    - of elbow, 831
    - of foot, 1429
    - of hand, 858, 858(f)
    - of knee, 1393
    - of neck, 435-6
    - of thorax, 916
    - of wrist, 858, 858(f)
- of soft palate, 565
- of spleen, 1193
- of sternum, 918
- of stomach, 1120, 1120(f)
- of suprarenal gland, 234
- of talus, 1436
- of taste buds, 508
- of teeth, 519, 519(t)
    - dental pulp, 515
- of temporomandibular joint, 535-6
- of testis, 1264
- of thoracic wall, 928-9
- of thorax, 911-12
    - cutaneous, 916
- of thymus, 946
- of thyroid gland, 462
- of tongue, 506-7
- of trachea, cervical part, 466
- of tympanic cavity, 629-30
- of tympanic membrane, 624
- of upper limb, 779-85, 818-22
- of ureter, 1241
- of urethra, 1098
    - female, 1253
    - male, 1251
- of uterine tube, 1293
- of uterus, 1290-1
- of vagina, 1284
- of vas deferens, 1269

    of vulva, 1280, 1280(t), 1282(f)

nervi vasorum, 138

nervus furcalis, 1078

nestin, 15

network(s)
- inframedullary, of sinuses, 918
- sinusoidal, of bone, 91, 92(f)
- of veins, gut tube, 1220

neural crest, 186, 187(f), 188, 188(f), 189, 201, 361, 364-6, 595, 596(f), 613, 1324
- autonomic nerve development, 373-4
- cardiac, 374
- cell populations from, 365, 369
- cranial, 373
- cranial sensory ganglia development, 373
- derivatives, in trunk, 373
- development, 595, 596(f)
- diencephalic, 699
- enteric nervous system development, 374, 1213
- head, 201
- heart development, 1016
- large intestine development, 1212
- lumbosacral, 373
- malformations, 607
- migration patterns, 365, 371, 373, 374
- preotic myelencephalic, 374
- segmentation, 371
    - in hindbrain, 371
- spinal nerve development, 371-2
- trunk, 201, 373
- vagal, 374 *See also* mesenchyme, neural crest

neuralgia
- greater occipital nerve, 494, 755
- trigeminal, 281

neurites, 603
    formation, 367

neurobiotaxis, 377

neurocranium, 409, 416, 610
    cartilaginous components, development, 768, 769(f)

neuroectoderm, of forebrain, 699

neuroepithelium
    cranial motor fibre development, 372
    pluripotential, 368

neurofibrillary tangles, 15

neurofibromatosis, 1014

neurofilaments, 14(f), 15

neurogenesis, monophyletic theory, 369

neuroglia *See* cells (named), glia (neuroglia)

neurohormones, 46-7

neurohypophysis, 241, 321
    development, 367
    secretions, 321 *See also* gland(s), pituitary

neuroma, acoustic, 497

neuromediation, 47

neuromediators, 47

neuromelanin, 12, 42, 44, 44(f), 47, 149, 290

neuromeres, 362, 362(f), 371

neuromodulators, 47

neuromuscular spindles, 60-1, 60(f)

neuronal migration disorders (NMDs), 388

neurone, 41-8, 225-7
    adrenergic, 138, 141, 523

afferent (sensory), 225-6
    primary, 226, 228(f), 236
    secondary, 228
    tertiary, 228
ageing, 42
axon *See* axon(s)
basket cells, 339
bipolar, 41, 43(f), 48, 339
cell body (soma), 41-2, 42(f)
centrioles, 42
chandelier cells, 339
cholinergic, 56, 138, 141, 522(f), 523
classification, 41
cytoskeleton, 42
dendrite *See* dendrite(s)
development, 370
dopaminergic, 331, 353
    cerebellar cortex, 303
    degeneration, 332
    groups, 329
    nucleus accumbens, 331 *See also* dopamine
double bouquet (bitufted) cells, 339
α-efferent, 110
efferent (motor), 110, 225, 226
enkephalinergic, 328
GABAergic, 290
    dentate gyrus, 351
    globus pallidus, 331
    hippocampus, 351
    subthalamic nucleus, 332
gamma-motor, of spinal cord, 261(f)
ganglionic
    autonomic, 56
    enteric, 56
    sensory, 55-6
giant pyramidal, 268
Golgi, 302

histaminergic, 47
interneurones *See* interneurones
monoaminergic, 56
motor, 372
    alpha-, 110, 261, 261(f)
    cranial nerves, 372
    lower, lesions, 230
    spinal cord, 257-8
    upper, lesions, 230
multipolar, 41, 43(f), 56
of neocortex, 339-40
neurites, 225
neurogliaform (spiderweb), 339
olfactory receptor, 552-3
pallidosubthalamic, inhibition, 332
pause, 663
peptidergic, 53, 56
pontocerebellar, 664
postganglionic, 234, 374, 375
    enteric nervous system, 1213
    sympathetic, 234, 374, 375
preganglionic, 234
    parasympathetic, 373
    sympathetic, 234
        development, 374
        of spinal cord, 260
projection, 340, 357, 357(f)
protein synthesis, 41, 42
purinergic, 62, 63
pyramidal, 340, 386
resting potential, 63
second-order, 264
serotoninergic, groups, 303, 329
size, 41
soma (cell body), 41-2, 42(f)
of spinal cord, 257-8
    ventral horn, 260

of spinothalamic tracts, 264-5
        inhibition, 266
    stellate
        non-spiny, 339
        spiny, 338-9
    of striatum, 328
    unipolar, 41, 43(f), 55, 231
    ventral horn, development, 375
    vestibulo-abducens, 664

neuropeptide Y, 319, 353, 982

neuropeptides, 47-8
    development of sympathetic ganglia, 374

neuropil, 41

neuropores
    caudal, 361
        somite level, 361
    primary, 361
    rostral, 361
    secondary, 361-2

neuropsychological functions, 358-9

neurotransmitters, 41, 47-8, 63, 225, 233, 234
    autonomic, 234
    excitatory, 351-2 *See also* aspartate; *See also* glutamate
    of non-spiny cells, 339
    striatum, 328*see also individual neurotransmitters*

neurotrophic factor, in amniotic fluid, 181

neurotrophins, 370

neurulation, 187(f), 188, 188(f), 361-4
    defects, spina bifida, 772
    failure, 184, 364, 365(f)
    primary, 186, 187, 361, 365
    secondary, 184, 361, 365, 1324
    segmentation of paraxial mesenchyme, 763, 763(f)

nipple, 930, 930(f), 931
  absent, 934
  aortic, 954
  development, 934
  innervation, 932
  inversion, 934
  male, 937
  microstructure, 930, 931(f)
  supernumerary, 934
  surface anatomy, 912

nitric oxide, 8, 47, 136, 138, 1114, 1160

nitric oxide synthase, 1036

Nkx2–5, **cardiac transcription factor**, 1016, 1022

nociception, 261, 266, 267, 271, 348
  control, 271

node(s)
  atrioventricular, 966, 975, 976, 977, 1022
    blood supply, 980
  clergyman's, 583
  Hensen's, 183-4, 183(f), 763 *See also* streak, primitive
  lymph *See* lymph nodes (general); *See also* lymph nodes (named)
  PNS-CNS compound, 63
  primitive, 183-4, 183(f)
  of Ranvier
    central nervous system, 43, 50, 50(f), 54, 55, 56
    peripheral nervous system, 54-5, 54(f)
  singer's, 583
  sinoatrial, 977
    blood supply, 980
  sinuatrial (sinus), 964, 975, 976, 982, 1017, 1022

nodule(s)
  of Arantius, 967
  of cerebellum, 298, 305
  lymphoid *See* follicle(s), lymphoid

- vocal cord, 583

noggin, 370

non-disjunction, 23

noradrenaline (norepinephrine), 47, 138, 142, 233, 234, 986, 1029
- cells secreting, development, 374
- cerebellar cortex, 303
- effect on pancreas, 1190
- production, 1200

nose, 547-59
- airflow, 555-6
- bleeding, 554
- cavity, 547, 549-56
  - arteries, 553, 554(f)
  - floor, 550
  - lateral wall, 550-1
  - lymphatics, 554
  - medial wall, 550
  - nerves, 554-5, 555(f)
    - olfactory, 555
    - of ordinary sensation, 554-5
  - roof, 550, 550(f)
  - soft tissue, 551-2
  - veins, 553, 554(f)
- congenital deformities, 550
- external
  - arteries, 549
  - lymphatics, 549
  - muscles, 548-9, 548(f)
  - nerves, 549
  - skin, 547
  - soft tissue, 547
  - veins, 549
- fracture, 547
- obstruction, 551
- skeleton, 547-8

- bony, 547
- cartilaginous, 547-8
- vestibule, 551

nostril *See* nares (naris), external

notalgia paraesthetica, 929

notch
- cardiac, 989, 992(f), 993, 994
- clavicular, 917
- costal, 917(f), 918
- ethmoidal, 471, 472
- fibular, 1412, 1413, 1414
- frontal, 470, 471(f), 491, 493
- interarytenoid, 582
- intervertebral, 721
- jugular (suprasternal), 617, 713, 912, 912(f), 914, 917, 917(f)
- lacrimal, 476, 477(f)
- mandibular *See* incisura(e) (incisure(s)), mandibulare
- mastoid, 415, 416, 615
- nasal, 409, 471, 476, 477(f)
- radial, 843
- sciatic
  - greater, 1353(f), 1355-6
  - lesser, 1353(f), 1356, 1357
- sphenopalatine, 477(f), 478, 479
- spinoglenoid, 794, 795
- supraorbital, 409, 470, 471(f), 491, 493, 668
- suprascapular, 795
- suprasternal (jugular), 405, 617, 713, 912, 912(f), 914, 917, 917(f)
- thyroid, 405
- trigeminal, 424
- trochlear, 799, 843
  - in elbow joint, 831
- ulnar, 841
- vertebral, 708, 717 *See also* cleft; *See also* fossa(e); *See also* incisura(e) (incisure(s))

notochord, 184, 198-9, 362, 371, 611
  caudal end, 1311(f)
  centrum enclosing, 767
  excision, effect, 768
  expansion between vertebrae, 766(f), 768
  neural tube development, 371
  pancreatic endoderm development, 1207
  removal, 184
  segmental nature of vertebrae, 768
  segmentation, 371

nuclear localization sequence, 19

nuclear membrane (envelope), 3(f), 18-19, 18(f)

nuclear pore, 3(f)

nucleolus, 3, 3(f), 20

nucleoporins, 19

nucleus (nuclei)
  of cells, 3, 3(f), 18-20, 225, 227, 228
    skeletal muscle, 110(f), 116(f), 121
  ‘clock-face’, 19
  ‘open face’, 19
  pedunculopontine, 334
  pontine cuneiform, 334
  pulposus, 731
    ageing, 731
    at birth, 731
    development, 768, 771
  spinal
    of accessory nerve, 277
    of trigeminal nerve, 276(f), 278
  subcuneiform, 334
  suprachiasmatic, 692
  supraspinal, 277
  tegmenti pedunculopontinus, 334
  of tractus solitarius, 574

nucleus (nuclei – nervous), 41
  abducens, 276(f), 282(f), 286, 376, 663
  accessory, 291
  accumbens, 316, 319(f), 320, 326, 331
    dopaminergic innervation, 331
    projections from amygdala, 353, 353(f)
    projections to ventral striatum, 329
  ambiguus, 275, 276(f), 277(f), 281(f), 283-4, 376, 377, 945, 951, 982
  amygdaloid nuclear complex, 312, 353 *See also* amygdala
  arcuate, 279, 281(f), 283, 285, 318, 319
    accessory, 283
  association, 312
  basal, 383
    arterial supply, 391
    development, 381(f), 383 *See also* basal ganglia
  basalis, magnocellular (of Meynert), 353
  bed, of stria terminalis, 356
  branchial (special visceral) efferent, 376
  of Cajal, 270, 324, 664
  caudate, 229(f), 230, 237
    aminergic input to, 329
    arterial supply, 253
    development, 383
    nucleus accumbens relation, 331
    overactivity associated with, 332
    structure, 326
    ventromedial, 329
  central, caudal, 290
  central medial, 352
  centromedian, 316, 342, 343
  cerebellar, 298
  cerebelloreceptive nucleus centralis lateralis, 329
  cervical, lateral, 267, 270
  of circumolivary bundle, 377
  cochlear, 276(f), 281(f), 285
    dorsal, 276(f), 281(f), 285
    ventral, 276(f), 281(f), 285

cranial nerve, 275
    development, 376
cuneate, 228, 263, 264, 264(f), 279(f), 280
    development, 377
of Darkschewitsch, 289, 324
Deiter’s, 286, 305
dentate, 298, 305, 306, 307
of dorsal column, 280 *See also* nucleus (nuclei – nervous), cuneate
dorsal raphe, 329
dorsal vagal, 242
Edinger-Westphal, 275, 290, 291, 669, 681, 685
emboliform, 305, 306
facial, 282(f), 286, 377
    neurobiotaxis, 377
fastigial, 298, 305, 306, 307-8, 664
general somatic afferent, 376
general visceral (general splanchnic)
    afferent, 376, 376(f)
    efferent, 376
geniculate
    lateral, 314-15, 685, 696
    medial, 314
gigantocellular, 267, 270, 293, 293(f), 294, 312
globose, 298, 305, 306, 308
gracilis, 228, 263, 263(f), 265(f), 279(f)
    development, 377
gustatory, 279, 546
habenular, 324, 380
    lesions, 324
hypoglossal, 276(f), 279, 282-3, 376
inferior olivary, 300, 303, 308
interpeduncular, 316, 323
interstitial, 290
    of Cajal, 291
    of Darkschewitsch, 289, 308
intralaminar, 316
    spinothalamic tract projections, 264

Kölliker-Fuse, 294
lateral dorsal, 315
lateral geniculate, 388
lateral lemniscus, 286
lateral posterior, 315
lateral reticular, 304, 306
lentiform *See* complex, lentiform
magnocellular (gigantocellular), 267, 270, 293, 293(f), 294, 312 *See also* nucleus (nuclei – nervous), basalis
mammillary
    lateral, 312, 320
    medial, 312, 320
mesencephalic, 287
midline, 316
oculomotor, 275, 289, 290-1, 376, 663, 664
    accessory (Edinger-Westphal), 275, 290, 291
olfactory, anterior, 356
olivary
    accessory, 278(f), 279(f), 281, 283, 292, 305
    inferior, 275, 279(f), 281(f), 283
    principal, 305
    superior, 285
of Onuf, 260, 285, 1253, 1254
pallidoreceptor centromedian, 329
parabigeminal, 291
parabrachial, 353
parabrachialis pigmentosus, 290
parafascicular, 316, 343
paragigantocellular, 294
paralaminar basal, 353
paramedian reticular, 306
paranigral, 332
parasolitarius, 283
parataenial, 352
paraventricular, 241, 319-20
pedunculopontine, 331, 332
peripeduncular, 353

periventricular, 319
phrenic, 260
pontine (pontis), 284, 306, 346, 347, 357, 377
pontine reticular, 267(f), 270
pontine tegmental reticular, 308
of posterior commissure, 324
posterior thoracic, 305(f)
precerebellar, 280, 283, 295
prepositus hypoglossi, 663
pretectal, 292, 685
propositus hypoglossi, 664
proprius, of dorsal spinal horn, 257, 259(f), 260
pulvinar, 315
raphe, 292, 316
    dorsal, 292
    magnus, 271, 282, 292, 293(f)
    obscurus, 271
    pallidus, 271
    pontine, 293(f)
    superior, central, 293(f)
raphe interpositus, 663
red, 290
    development, 379, 380
    parvicellular, 305, 308, 309
relay, 312
    precerebellar, 308
    vestibulo-ocular, 308
reticular, 316, 320
    development, 380
    lateral, cerebellar connections, 306
    lateral column, 294
    of lower medulla, 377
    medial column, 293-4
    median column, 292-3
reticularis tegmenti pontis, 308
retroambiguus, 294
retrorubral, 329, 332

reuniens, 352
salivary (salivatory), 287, 521
    inferior, 543
solitarius, 283
special somatic afferent, 376
special visceral (special splanchnic) afferent, 376
spinal tract, of trigeminal nerve, 280-1
subthalamic, 323, 332
    functions, 332
    inhibition, 332
    lesions, effects, 332
    overactivity, 332
    projections, from motor cortex, 343
    stimulation, 332
    striatal efferents to, 331
suprachiasmatic, 317-19
supraoptic, 241, 319-20
tegmental reticular, 306, 308
thalamic, 311-16, 341, 349
    anterior, 312
    lateral, 313-15
    medial, 312-13
thalamic mediodorsal, 331
trapezoid, 281(f), 285, 286
trigeminal brain stem, 305
trigeminal nerve
    mesencephalic, 287(f), 288(f), 289
    motor, 287
    sensory, 228, 275, 280-1, 286, 287(f)
    spinal, 276(f), 278(f), 281, 282
trochlear, 288(f), 289, 291, 376, 664
vagal, 235, 279(f), 282
ventral
    anterior, 313
    lateral, 313-14
    posterior, 314
vestibular, 269, 270(f), 279, 280(f), 286, 663

        inferior, 279(f), 280, 286
        lateral, 281(f), 286, 306(f), 307, 308
        medial, 279(f), 286
        superior, 286, 305
    vestibulocochlear, 279
    Z, 280

nystagmus, 309, 663
    optokinetic, 663

O

obesity
  breathing during sleep, 1012
  divarication of recti, 1063
  identification of suprarenal gland, 1201
  and steatosis, 1163

obex, 240, 241(f)

object recognition, V4 visual area, 347, 358

obsessive-compulsive disorder (OCD), 332

obstetric staging, 213

occipital bone, 409, 411, 412, 414, 415, 431
  basilar part, 409, 414, 415, 416, 424
  lateral (condylar) part, 424
  neonate, 711(f)
  squamous part, 412, 415, 416, 423, 424, 425

occipitocervical region *See* junction(s), occipitocervical

occiput
  anomalies, 770
  development, 770

odontoblasts *See* cells (named), odontoblasts

odynophagia, 952

oedema, Reinke's, 583

oesophageal atresia, 181

oesophagoscopy, 952-3

oesophagus, 949-54, 950(f)
  abdominal, 950, 1111, 1111(f)
    peritoneum of, 1099
  arteries, 950, 951(f), 1111
  at birth/neonate, 1203-4
  atresia, 953, 1015, 1037(f), 1203

barium studies, 953
Barrett’s, 952, 1114, 1115
cervical, 465, 949
    arteries, 465
    lymphatics, 465
    nerves, 465
    perforation, 953
    relations, 465
    veins, 465
cervicothoracic, development, 1203(f), 1214
development, 610, 1014, 1015-16, 1032, 1203-4, 1215(f)
    abnormal, 953
    mucosa, 1203
    normal, 1203-4
dimensions, 949
dysmotility, 953-4
epithelium, 1050
fat pads, 1111
glands, 952
innervation, 951
length, 949
lymphatic drainage, 951, 1111
microstructure, 951-2, 952(f), 1050(f)
motor dysfunction, 953-4
muscles, 1114(f)
oesophagoscopy and ultrasound, 953
relations, 949
rupture, 953
spasm (diffuse), 954
speech, 590
sphincters, 953
swallowing, 573-4
thoracic, 949-50, 1111(f)
    perforation, 953
varices, 950-1, 1118-19, 1177(t)
veins, 950, 951(f), 1111
wall, 951, 952

of sacroiliac joint, 1366

olecranon, 786, 790, 843, 844
    ossification, 844

olfaction
    epithelium, 551, 552(f), 553
    loss, 555

oligodactyly, 902

oligohydramnios, 181, 1013, 1035, 1313

oligosaccharides, 4

oligozoospermia, 1268

olive, 275, 276(f), 277, 285, 286, 293(f)

omentum, 1099, 1214, 1215(f)
    greater, 1099, 1102, 1104, 1216, 1218
        development, 1206, 1210(f), 1216, 1218
        right border, 1104
        structure, 1102, 1104
    lesser, 1099, 1102, 1168, 1215(f), 1216
        development, 1206, 1215(f)
        left border, 1102
        upper (oesophagophrenic) part, 1217

omphalocoele, 1013, 1209

oncogenes, 8

Ondine's curse, 1011

oocyte(s)
    collection, 168
    development, 1322
    meiosis II completion, 167
    numbers, 1322
    primary, 1319

oogonia, naked, 1319

oolemma, 167

ootids, 167

opening(s)
- accessory, of maxillary sinus, 551
- aortic (diaphragm), 913, 1007, 1008(f)
- of aortic valve, 973
- atrioventricular, 964, 965(f)
- of bulbourethral glands, 1252
- of carotid canal, 617
- of frontal sinuses, 471-2, 471(f)
- of glenohumeral joint capsule, 805
- of internal acoustic meatus, 617
- of jaw *See* jaw
- of maxillary sinus, 551, 559
- of mitral valve, 972
- oesophageal (diaphragm), 1007-8, 1044
- orbital, 404, 409
- of pharyngotympanic tube, 563, 564
- of pulmonary valve, 967, 967(f)
- puncta lacrimalia, 703
- saphenous, 1067, 1350, 1350(f)
- stomodeal, 602
- of tricuspid valve, 967, 967(f)
- vena caval (diaphragm), 1008
- of vestibular aqueduct, 424, 617 *See also* aditus; *See also* aperture(s); *See also* foramen (foramina); *See also* orifice

operculum (opercula)
- frontal, 346
- frontoparietal, 346
- of insula, 335, 346, 383
- temporal, 345

ophthalmoplegia, 656
- internuclear, 663

ophthalmoscopy, 688(f), 693, 697

opiates, naturally occurring, 48

opposition (movement), 875-6

opsin, 690

opsonization, 69

optic neuropathy, 656

ora serrata, 675, 680, 681(f), 688-9

orbicularis ciliaris, 681

orbit, 404, 529, 655-74, 655(f)
  arteries, 665-6
  bones, 655-6
  connective tissue, 656-8
  contents, 655, 657(f)
  fat, 658, 658(f)
  floor, 656, 656(f)
  fracture, 480
  innervation, 666-9, 667(f), 668(f)
  lateral margin, 404
  lateral wall, 656
  lymphatic drainage, 666
  medial wall, 655-6, 655(f), 656(f)
  roof, 655, 655(f)
  venous drainage, 666, 666(f)

orbital bones, 613

organ(s)
  circumventricular, 49, 51, 240-2, 241(f), 367, 380
  of Corti, 634, 635(f), 640-1, 641(f), 652
    innervation, 644
    nerves, 644
  Golgi tendon, 53, 57, 59-60, 60(f), 101, 110, 113
  of lamina terminalis, 319
  lymphoid, 72-4
  parapineal, 380
  spiral, innervation, 285, 286
  subcommissural, 241
  subfornical, 241, 241(f)

vascular, 241
vomeronasal, 550, 604*see also individual organs*

organell(es), cytosolic, 14-17

organogenesis, cell populations, 197-203

organum vasculosum, 241

orifice(s)
- aortic, 913 *See also* diaphragm, thoracic, apertures
- of aortic valve, 971(s)
- of appendix, 1142, 1143(f)
- atrioventricular, 1025, 1026
  - left, 960, 969
  - right, 960
- for basivertebral vein, 715
- of bulbourethral gland, 1270
- cardiac, 1113-14
  - embryonic circulation, 205-6
- of ejaculatory ducts, 1251, 1269
- of external auditory meatus, 618
- of ileocaecal valve, 1142
- of lactiferous duct, 933
- of lymphatic trunks, 455
- of mitral valve, 913, 970
- of pharyngotympanic tube, 564
- of prostatic utricle, 1251
- pulmonary, 913, 962, 966
- pyloric, 1114
- sinuatrial, 1019
- of tricuspid valve, 913, 966
- ureteric, 1226, 1240, 1245(f), 1248
- urethral
  - external, male, 1252
  - internal, 1248, 1250, 1252(f)
- urogenital, 1323(f)
- of vagina, 1284

- ventricular, left, 962 *See also* aditus; *See also* aperture(s); *See also* hiatus; *See also* opening(s)

oropharynx, 561(f), 564-7, 605, 610
- anterior wall (postsulcal part of tongue), 503
- boundaries, 561(f), 562(f), 564
- pillars of fauces, 565

orthopantomograms, at birth, 512(f)

os
- aponeurosis plantaris, 1437
- calcaneus secondarius, 1437
- centrale, 864
- cuneo-1 metatarsale-I plantare, 1438
- cuneo-2-metatarsale-II dorsale, 1439
- incisivum, 416
- intermetatarseum, 1439
- odontoideum, 770
- peroneum, 1420
- subcalcis, 1437
- sustentaculi, 1437
- talonaviculare dorsale, 1438
- uterine, 1292
- vesalianum, 1440, 1441(f)

Osgood-Schlatter disease, 1415

osmolality, urine formation, 1238

osmoreceptors, macular densa cells, 1238

ossicles
- auditory, 627-8
  - articulations, 628
  - development, 652
  - ligaments, 628
  - ossification, 88, 96
- Goethe's, 418, 711, 713
- mental, 532
- pterion, 418

suprasternal, 918
sutural, 418*see also individual bones*

ossiculum terminale, 770

ossification, 92-5
  centres, 93(f), 96, 98(f)
    vertebrae, 768, 769(f)
      cervical, 768
      lumbar, 768
      secondary, 768, 770
      thoracic, 768, 770
  endochondral, 83, 93-5, 93(f), 94(f)
  epiphysial, 96
  of individual bones *see under individual named bones*
  intramembranous, 92-3
  mandible, 533
  metaphysial, 95
  rates of, 96
  skull, 611
  sphenoidal bone, 530
  vertebrae, 768, 770
    centres *see above*

osteitis fibrosa cystica, 95

osteocalcin, 86, 87

osteodifferentiation, cranial vault, 390

osteogenesis imperfecta, 194

osteoid, mineralization, 87, 89(f), 91, 93, 95(f), 96

osteomalacia, 95

osteonectin, 86, 87

osteons, 88-9
  primary, 88, 93

osteophytes, vertebral, 714

osteopontin, 86, 87

osteoporosis, 95, 96, 714

ostium (ostia: opening(s))
  arteriosum, 969
  arteriosum *See* valve(s), aortic
  of coronary sinus, 964
  lacrimalis, 674
  of maxillary sinus, 472
  of nasolacrimal duct, 550
  primum, 1023
    defect, 1030
  secundum, 1023
  venosum, 969
  venosum *See* valve(s), mitral
  venous, of right atrium, 964

otitis media, 624, 626-7

otoconia *See* otoliths

otoconial crystals, 644

otocyst, 610, 651, 652, 1204(f) *See also* vesicle(s), optic

otoliths, 636, 663

otosclerosis, 628

outlet
  double, of ventricle, 1031
  pelvic
    inferior, 1358
    planes, 1358
    superior, 1358 *See also* pelvis, floor ('outlet')
  thoracic, 909, 910

ovary (ovaries), 1289(f), 1291(f), 1294-7, 1294(f), 1295(f)
  accessory, 1294
  age-related changes, 1294
  arteries, 1295, 1295(f)
  descent, 1294, 1321-2, 1321(f)
  development, 213, 1315(f), 1319, 1321(f), 1322(f)

        similarities to testes, 1316(t)
    embryo, 1294
    innervation, 1295
    ligaments, 1294-5, 1294(f)
    lymphatics, 1295
    menopause, 1294, 1297
    microstructure, 1295-7, 1296(f), 1297(f)
    neonatal, 1294, 1321
    peritoneal attachments, 1294-5
    in pregnancy, 1294
    relations, 1294
    sex determination, 1319
    size, 1294
    stroma, 1319
    surface anatomy, 1294
    veins, 1295
    weight, 1322

overbite, 500(f), 511

overjet, 513

oxidative phosphorylation, 13

oxycephaly, 418

P

pacemakers
  artificial, 978
  of heart *See* node(s), sinuatrial

pachymeninx *See* dura mater

pachyonychia, 156

pachytene, 22

pads, fat *See* fat pads

pain
  appendix, 1143-4, 1146
  back, 732, 745
  buttock, 1371
  cardiac *vs*, 951
  control
    local, dental, 519-20
    naturally occurring opiates, 48
  dental, 519
  gluteal region, 1390
  groin, 1390
  hip, 1390
  mechanisms, 266-7, 266(f)
  neuropathic, 348
  perception, 267, 270, 348
  pericardial, 959
  referred *See* referred pain
  sensation, teeth, 519
  spinal
    radicular, 759
    referrred, 759
  spinal cord, 759
  thigh, 1383
  uterine, 235
  visceral, 53, 58, 235-6

palate, 502-3
  bony, 414
  cleft, 571, 573, 607, 607(f), 608(f)
  development, 603-4, 604(f)
  hard, 500, 502-3, 604
    arteries, 502
    innervation, 502
    lymphatic drainage, 502
  primitive, 603, 604
  soft, 502, 565, 604
    arteries, 565
    muscles, 568-72
    nerves, 565
    taste buds, 508-9, 565
    veins, 565

palatine bone, 478-9, 529
  in nasal cavity, 550
  plate
    horizontal, 478
    perpendicular, 478
  process
    orbital, 478-9
    pyramidal, 415, 478, 529
    sphenoidal, 479

paleocortex (paleopallium), 335, 382

palisades, 94, 94(f)

pallidotomy, 253, 333

pallidum *See* globus pallidus

pallium, 382
  development, 383 *See also* cortex, cerebral

palm, of hand, 778

palpebrae *See* eyelids

palsy

- Bell’s, 286, 495, 520, 630
- cranial nerves, 295
    - oculomotor nerve, 252, 295
- crutch, 829
- interosseous nerve, 854
- progressive supranuclear, 332
- Saturday night, 829, 854

Pancoast tumour, 822

pancreas, 1170, 1183-90, 1183(f)
- age-related changes, 1183
- annular, 1206
- arteries, 1186, 1187(f)
- body, 1183-4
- development, 1203-17, 1249(f)
    - cellular, 1206-7
- divisum, 1185-6, 1207
- ducts, 1185-6
    - development, 1207
- endocrine, 1183, 1190
    - development, 1207
- exocrine, 1183, 1185, 1188(f)
- fetal alpha cells, 1207
- fetal beta cells, 218, 1207
- fetal delta cells, 1207
- haemorrhage, 1187
- head of, 1183-4, 1207
- inflammation, 1187
- lymphatics, 1186
- microstructure, 1188-90, 1188(f), 1189(f)
- neck, 1184
- nerves, 1173, 1187
    - endocrine, 1190
    - exocrine, 1187-8
- pseudocyst, 1187-8
- relations, 1183, 1183(f), 1184(f)
- resection, 1183, 1188

- retroperitoneal position, 1207
- rudiment, 1216
- secretion mechanisms, 1188(f)
- surface anatomy, 1054
- tail of, 1185, 1192
  - development, 1207, 1216
- veins, 1186, 1187(f)
- ventral, development, 1207

pancreatic polypeptide, 1190

pancreatitis, 1187-8
- acute haemorrhagic, 1100

pannexins, 48

panniculus carnosus, 457

papilla(e)
- dental, 606
- dermal, 146(f), 152, 157, 158(f), 160
- duodenal, 1126, 1127(f), 1185
- incisive, 502
- interdental, 500
- lacrimal, 669
- lingual, 503(f), 507
- of oesophagus, 952
- of tongue, 503, 507, 508(f)
  - circumvallate, 503, 507, 508, 508(f)
  - filiform, 503, 507
  - foliate, 503, 507
  - fungiform, 503, 507
- of vagina, 1284
- vallate, 605

papilloedema, 695

paracellular transport, 1237

paradidymis, 1269, 1307

parafovea, of retina, 693

paraganglia, 236, 374
  development, 374

paralysis *See* palsy

paranode, 43, 50, 51, 54, 54(f)

paraoophoron, 1307

paraplegia, 759

parasubiculum, 351, 351(f), 352

parenchyma, liver, 1172

parental imprinting, 167

parietal bone, 412, 416, 469-70, 470(f), 615, 617
  during birth, 613
  development, 612
  ossification, 470

parietes, 1216, 1217

parkinsonism, toxins causing, 333

Parkinson's disease *See* disease(s), Parkinson's

paronychia, 861

paroophoron, 1285

pars
  caudalis, 313
  compacta, 290
  dorsalis diencephali, 380
  externa
    of cochlea, 636
    of external auditory meatus, 620
    of saccule, 637
  flaccida, of tympanic membrane, 624, 630
  intermedia, 305, 367, 1280
    of pituitary gland, 322
  interna
    of cochlea, 636

      - of external auditory meatus, 620
      - of saccule, 637
  - media, of external auditory meatus, 620
  - oralis, 313
  - palatina, 566
  - plana, of ciliary body, 681, 686
  - plicata, 680-1
  - reticulata (reticularis), 290
  - tensa, of tympanic membrane, 624, 630
  - triangularis, 280
  - tuberalis, of pituitary gland, 321, 322
  - ventralis diencephali, 380

parturition, bladder changes, 1248

patch(es)
  - McGregor’s, 469
  - Peyer’s, 1051, 1133(f), 1135, 1213

patella, 1394-5, 1395(f)
  - bipartite, 1394
  - muscle attachments, 1394
  - ossification, 1395
  - structure, 1394
  - surface anatomy, 1340, 1394
  - vascular supply, 1394

pathway(s)
  - auditory, 314, 649(f)
      - central, 647-8
      - peripheral, 646-7
  - autonomic *See* systems, nervous (specific)
  - bulbar reflex, 294
  - cholinergic, from forebrain to cortex, 341, 352
  - contralateral (commissural), 402-3, 402(f), 403(f)
  - corticopontine, 230, 284, 289, 306
  - corticopontocerebellar, 298
  - corticoreticular, 230
  - direct, of striatum, 329, 331, 332

dopamine
    mesolimbic, 331, 332
    'mesostriatal', 329, 332
dorsal column-medial lemniscus, 280
gustatory, 508
indirect, of striatum, 329, 329(f), 331, 332
    underactive, 332
ipsilateral (association), 402-3, 402(f), 403(f)
motor, descending, 228-9
nucleo-olivary, 308
olfactory, 348-357349
pain control, 292
perforant, 351
propriospinal, 271
reticulospinal, 230
sensory, ascending, 227-8
serotoninergic, 293
somatosensory, 314
spinal, monoaminergic, 270-1
spino-reticulo-thalamo-cortical, 267
spinocerebellar, disease, 309
spinocervicothalamic, 267
spinomesencephalic, 267
spinoreticular, 267
subcoeruleospinal, 294
subcorticospinal, myelination, 389
thalamocortical, 326
trigeminothalamic, 314
uveo-scleral, 676, 686
vestibulospinal, 230
visceral
    afferent, 235-6, 235(f)
    efferent, 231, 232(t), 233
visual, 314, 347, 696-7, 696(f) *See also* fibre(s); *See also* tract(s)

patterning/pattern formation, 194-5
dorsoventral, of vertebral column, 764
spinal cord, 370-1

paxillin, 15

peau d’orange, 933

pecten pubis, 1355

pectin, 1156

pectus
- carinatum, 918
- excavatum, 918

pedicel, terminal, Bowman’s capsule, 1234, 1235(f)

pedicle
- pulmonary (roots), 992(f), 994
- of vertebrae, 716, 718, 721
    - cervical, 718
    - development, 768

peduncle(s)
- cerebellar, 275, 277, 278, 298-9
    - inferior, 277, 278(f), 279(f), 281, 285, 298
        - afferents, 285, 286
        - development, 377
    - middle, 298, 306
    - superior, 281, 285, 288, 290, 298-9
- superior, lesions, 309

peg
- bulbous, 158
- hair, 158

pelvis
- angle of, 1041
- arteries, 1041, 1047, 1047(f), 1086-9, 1087(f), 1088(f)
- autonomic supply, 1041-7, 1043(f)
    - ganglia, 1045-6
    - parasympathetic, 1044-5
    - plexuses, 1044(f), 1045-6, 1045(f)
    - sympathetic, 1042-4
- bones, 1352-65

bony, 1041, 1083-93, 1357-9
    android, 1358, 1359
    anthropoid, 1358
    axes, 1083, 1358-9
    classification, 1358
    greater (true), 1358
    gynaecoid, 1358
    inclination, 1358-9
    in infants, 1359
    lesser (false), 1358
        cavity, 1358
    measurements, 1358, 1366
    platypelloid, 1358
    sex differences, 1359-60
    surface anatomy, 1340, 1341(f)
    weight bearing, 1359
development, 903
diaphragm, fascia of, 1086
extrarenal, 1231
false, 1041, 1083
fasciae, 1085-6, 1085(f)
    parietal, 1085-6
floor (‘outlet’), 1083
    development, 1323 *See also* outlet, pelvic
inlet, 1083, 1358
innervation, 1041, 1091-3
intrarenal, 1231
ligaments of, 1289-90, 1290(f)
lower limb interface, 1041
lymphatic drainage, 1041, 1090-1, 1091(f)
male, 1256(f)
muscles, 1083-5, 1083(f), 1084(f)
musculoskeletal framework, 1041, 1042(f)
ossification, 902, 1463
peritoneum of *See* peritoneum, pelvic
in pregnancy, 1300-1
renal, 1230-1, 1230(f)

            microstructure, 1231
    structure and function, 1041
    surface anatomy, 1052-4, 1053(f)
    true, 1041, 1083
    veins, 1041, 1089-90, 1090(f)

pemphigoid, bullous, 33

penicilli, 1194, 1195

penis, 1271-4
    arteries, 1098, 1273
    body, 1271-3, 1271(f), 1272(f), 1273(f)
    bulb, 1271, 1271(f)
    crus, 1097, 1271
    development, 1323(f)
    ejaculation, 1274-5
    erection, 8, 1096, 1274-5
    fascia, 1060, 1273
    glans, 1271, 1271(f)
    ligaments, 1273
    lymphatics, 1275
    maturation at puberty, 1325(f)
    microstructure, 1274
    nerves, 1273-4
    root, 1271, 1271(f)
    skin, 1271
    veins, 1273

pepsinogen, 1204

peptides
    atrial natriuretic, 142
    latency-associated, 194 *See also* neuropeptides

perception
    pain, 267, 270, 348
    V4 visual area, 347

perforin, 71, 72

periarteriolar lymphatic sheath (PALS), 1194

pericardium, 959-60, 960(f), 963, 993
  development, 186
  fibrous, 959, 1014
  innervation, 959
  lymphatic drainage, 959
  pain originating from, 959
  relations, 959
    to diaphragm, 1007
  serosal, 959, 1014
    reflections, 959, 960(f)
  vascular supply, 959
  visceral layer *See* epicardium

perichondrium, 81, 82, 85, 91, 93, 98(f)

pericoronitis, 510

pericranium, 426, 428

periderm, 157, 158(f), 198

‘perihypoglossal grey’ (complex), 283

perikymata, 514, 515(f)

perilymph, 633(f), 634-6, 635(f)
  movement, 628

perimysium, 86, 108, 121, 657

perineum, 1093-8
  arteries, 1097-8
  fasciae, 55(f), 1093-7, 1093(f), 1095(f), 1109(f)
    deep, 1095
    superficial, 1095
  female, 1094, 1095(f), 1097(f)
    muscles, 1283(f)
    nerves, 1283(f)
    vasculature, 1283(f)
  ‘gynaecological’, 1279
  innervation, 1098
  lymphatic drainage, 1098

- male, 1093(f), 1094
- muscles, 55(f), 1093-7, 1095(f), 1109(f)
- surface anatomy, 1093
- veins, 1098

period
- embryonic, 167, 211, 212(f)
- fetal, 167, 211, 213, 213(f)
- gestation, 211
- neonatal, 214-16
- perinatal, 214
- refractory, 64

periosteum, 86, 89(f), 90-1, 91(f), 93, 97, 98(f), 112, 467
- orbital, 658

peristalsis
- of epididymis, 1268
- large intestine, 1213
- oesophageal, 954
    - at birth, 1204
    - fetus, 1203
- stomach, at birth, 1206
- ureteric, 1241, 1242

peritoneum, 1107-14, 1213-14, 1286(f), 1288(f)
- adhesions, 1099
- cavity *See* cavity (cavities), peritoneal
- covering colon, 1099, 1104-5, 1217
- covering duodenum, 1099
- covering kidney, 1228, 1229(f)
- covering pancreas, 1217
- covering posterior bladder, 1105-6, 1312
- covering rectum, 1099, 1218
- covering small intestine, 1105, 1217
- covering spleen, 1104, 1191, 1192(f)
- covering stomach, 1099
- development, 1099, 1213-18
- folds (ligaments), 1214, 1216, 1319

        - falciform, 1099-100, 1319
        - liver connections, 1101-2
        - mesorchium, 1319
        - presplenic, 1104
        - splenic connections, 1104 *See also* fold(s); *See also* omentum
    - greater sac *See* sac(s), greater
    - innervation, 1106-7
    - lesser sac *See* sac(s), lesser
    - liver connections, 1070-2, 1073(f)
    - of lower abdomen, 1104-5
    - mesenteries *See* mesentery
    - microstructure, 1099
    - nerves, 1010
    - omentum *See* omentum
    - parietal, 1099, 1104, 1213, 1214, 1215(f), 1217
        - innervation, 1106
    - pelvic (of pelvis), 1105-6
        - female, 1106
        - male, 1105-6, 1106(f)
    - posterior, 1217
    - pouches
        - rectovagino-uterine, 1218
        - rectovesical, 1105, 1218
    - reflections, 1107-14
        - around liver (ligaments), 1070(f), 1071(f), 1099-100, 1214 *See also* peritoneum, folds
    - relationship to diaphragm, 1007
    - structure, 1099
    - of upper abdomen, 1099-104, 1103(f) *See also* ligaments (named), falciform
    - ventriculoperitoneal shunts, 1110
    - visceral, 1099, 1217
        - innervation, 1106 *See also* serosa

perlecan, 33, 38

peroxisomes, 3(f), 4, 10, 12, 13

pes

- anserinus, 494, 1343
- bursa, 1402
- cavus 2450
- hippocampi, 349
- planus, 1450, 1463, 1464

Peyronie’s disease, 1276

phaeochromocytoma, 1047, 1081

phagocytosis, 3, 9, 69, 70, 78, 78(f)

phagosomes, 12

phalanx (phalanges)
- of foot, 1441 *See also* toes
- of hand, 866
  - muscle attachment sites, 866
  - ossification, 864(f), 865(f), 866-7, 866(f) *See also* finger(s)

phallus
- development, 1323(f) *See also* penis

pharyngula stage, 597

pharynx, 561-75
- arteries, 561
- development, 610, 1204(f)
  - rhombencephalon relationship, 376
- ectoderm, 48
- embryo, 202, 596-602, 597(f)
- endoderm, 602-3, 603(f), 609(f)
- fascia, 568
- floor, 597
- infection, 568
- lymphatics, 563-4
- muscles, 561, 568-72, 569(f), 570(f)
- neonate, 610
- nerves, 563, 572
- relations, 561
- swallowing, 572-4
- tissue spaces, 568

- tumours, 568
- veins, 561

phenomenon, ‘screw-home’, 1391

pheromones, 153

philtrum, 467, 602

phocomelia, 906

phonation, 590-2

phonemes, 592, 593

phonocardiogram, 975

phosphatidylinositol, 9

phospholipids, plasma membrane, 4

photoageing, 162

photoreceptors, 675, 685, 688
- development, 700 *See also* cells (named), cone (retinal); *See also* cells (named), rod (retinal)

pia mater, 244, 427, 434
- cranial, 244
- development, 244, 383, 389
- spinal, 751
- vascular (tela choroidea) *See* tela choroidea

pigeon chest, 918

pigment
- bile, 49
- cells *See* cells (named), pigment; *See also* substantia, nigra
- macular, 693
- senility, 42

pigmentation
- constitutive, 149
- facultative, 149
- naevus, 772
- skin, 149

- of substantia nigra, 290

pillars
- of fauces, 565
- junctional, 108

pinch grip, 875, 889-90, 890(f)

pinna *See* auricle

pinocytosis, 9

pisiform, 861, 861(f), 862
- ossification, 864
- surface anatomy, 786

pit(s)
- gastric, 1122(f)
- glandular, of stomach, 1204
- mammary, 934, 934(f)
- otic, 651

placenta, 1027
- accreta, 1301
- battledore, 1303, 1304(f)
- chorio-allantoic, 176
- circumvallate, 1303, 1304(f)
- development, 176-8
- endocrine functions, 180
- fetal surface, 1302, 1303(f)
- growth, 176-7
- haemochorial, 176, 178
    - formation, 176
- increta, 1301
- intervillous space, 178-9
- lobes, 1302
    - accessory (succenturiate), 1303
- location, 1301
- membranacea, 1303
- percreta, 1301, 1302(f)
- plates

        - basal, 177-8
        - chorionic, 177
    - post-delivery, 1302-3
    - praevia, 172, 182, 1301
    - respiratory function, 1035
    - size, 1302
    - syncytium, 179
    - transport across, 180
    - twin pregnancy, 172, 173(f), 1303, 1303(f)
    - variations, 1303-4, 1303(f), 1304(f)
    - weight, 1302

placode(s)
    - ectodermal, 186, 188, 366-7, 595-6
    - epibranchial, 367, 602
    - epipharyngeal, 596
    - hair, 158
    - hypophysial, 366, 367
    - lens, 699
    - nasal, 602
    - neurogenic, 366
        - ventrolateral (epibranchial), 367
    - neuronal, 198
    - nodose, 374
    - non-neurogenic, 366, 367
    - olfactory, 366(f), 382, 604
    - optic, 366(f), 595(f)
    - otic, 367, 651, 652
    - profundal, 367
    - trigeminal, 366(f), 367

plagiocephaly, 418, 613

plakoglobin, 7

plane(s)
    - of abdomen, 1052, 1052(f)
        - interspinous, 1052
        - paramedian, 1052

        - of pubic crest, 1052
        - subcostal, 1052
        - supracristal, 1052
        - transpyloric, 1052
        - transtubercular, 1052
        - xiphisternal, 1052
    - anatomical, thoracic, transverse, 913
    - of face, 468-9
    - prevertebral, 708

plantarflexion, 103

planum semilunatum, 637

planum temporale, asymmetry, 358

plaque, atheromatous, 137, 981

plasma, 67

plasma fibronectin, 38

plasma membrane, 3(f), 4-9, 17(f)
    - axonal, 43
    - P face, 4
    - potential, 63
    - transport mechanisms, 9
    - urothelial cells, 28(f)

plasma skimming, 1193

plasmin, 72

plate(s)
    - alar, 377
        - cell columns, 376-7
        - cells, 377
        - cerebellum development, 377
        - development, 375, 376-7
    - alveolar, 517
    - basal, 177-8
        - cells, 376
        - cranial nerve development, 372

    hindbrain development, 376
    of metencephalon, 377
    of midbrain (mesencephalon), 379
    of neural tube, 363, 364
    of placenta, 1303
    spinal cord development, 375
buccal, 530
cartilaginous, intrapulmonary bronchi, 995, 1005
chorionic, 177
cortical, 369
cribriform, 423, 425(f), 471, 472, 472(f), 517, 611, 665
digital, 902
ductal, 1208
    malformation, 1208
epiphysial, 94(s), 96
epithelial, of somites *See* somites
floor, of neural tube, 363(f), 364(f)
growth, 81, 83, 91, 94, 95, 96, 98, 98(f)
hand, 905
hepatic, 1174-5
hilar, 1168-9
horizontal, of palatine bone, 414, 415, 478
lingual, 480
motor end, 110, 111
nail, 155
neural, 186, 186(f), 187, 188, 361
notochordal, 184, 185
orbital
    of ethmoid bone, 472, 474, 655
    of frontal bone, 471
perpendicular
    of ethmoid bone, 471, 472
    of palatine bone, 478
postanal, 1094
prechordal, 184, 389, 390
primitive, 184
pterygoid, 412, 415, 539

        - lateral, 412, 415, 529
        - medial, 415, 529, 530
    - sole, 61, 62, 110
    - tarsal, 657, 671(f)
        - inferior, 670-1
        - superior, 670-1
    - tympanic, 412, 414, 416
    - vaginal, 1316
    - ventrolateral *See* plate(s), basal
    - volar, 877 *See also* lamina(e)

plateau, cardiac, 1007

platelet-activating factor (PAF), 388

platelet-derived growth factor (PDGF), 8, 72, 1308-9, 1332-3
- receptor β-subunit, 1309

platelets *See* cells (named), platelets

plectrin, 106

pleura, 963, 989-92, 990(f)
- arteries, 991
- chest radiography, 989, 990(f)
- computed tomography, 989, 990(f)
- development, 991
- diaphragm relationship, 1007
- dome of, 465, 989
- kidney relationship, 1009
- lymphatic drainage, 991
- mediastinal
    - left, 984
    - parietal, 1014
- microstructure, 991
- nerves, 991, 1010
- parietal, 989, 991
    - arteries, 991
    - cervical (apical), 465, 989, 990(f)
    - costovertebral, 989, 990(f)

        - diaphragmatic, 989, 991
        - mediastinal, 989, 991
        - surface anatomy, 914
    - reflections, 914
    - shadowing, 989
    - surface anatomy, 914
    - veins, 991
    - visceral (pulmonary), 991, 996
        - arteries, 991

pleural drainage, 989

pleural effusion, 989, 990(f), 991, 993

plexus
- basilar, 431
- choroid, 41, 52, 52(f), 227, 228(f), 242
    - calcification, 51
    - development, 377, 380, 383
    - fourth ventricle, 242
    - lateral ventricle, 242
    - microstructure, 51
    - third ventricle, 242
    - vasculature, 242
- endocardial, 1016
- epicardial, 982
- infraclavicular branches, 821-2
- myocardial, 982
- subendocardial, 982

plexus (arterial)
- capsular, of kidney, 1232
- deep, of pituitary gland, 323
- Kiesselbach’s, 553, 554
- mantle, 323
- mediastinal, subpleural, 926
- palmar, development, 905
- periosteal, of bone, 91
- pial, 757

        - development, 391
    - of skin
        - dermal, 156
        - development, 159
        - subcutaneous, 156
        - subpapillary, 156
    - subsynovial, 101

plexus (capillary)
- of bronchial arteries, 1003
- hepatic, 205, 1207
- internal carotid development, 390
- of lung, 1003
- peritubular (renal), 1233
- primary of head, 392
- of renal arteries, 1233
- of splanchnopleuric mesenchyme, 1220
- termina, of embryonic limb, 903
- vitelline vein development, 1220

plexus (lymphatic)
- abdominal, 928
- digital, 779
- dorsal, 779
- of eyelids, 671
- intrarenal, 1233
- palmar, 779
- perianal, 1160
- perirenal, 1233
- subareolar, 932
- submucosal, 1180
- subpleural, superficial, 998
- subserosal, 1180
- of synovial subintima, 101
- thoracic, 928

plexus (nervous), 58, 1180
- abdominal, 1081
- aortic

  - abdominal, 1043, 1045-6, 1150
  - thoracic, 943(f), 944, 944(f)
- atrial, 983
- Auerbach’s (myenteric), 953, 1044, 1122
  - development, 1051, 1203, 1212
- autonomic, 951
- brachial, 401(f), 407, 457, 779-81, 781(f), 818-22, 819(f)
  - arrangement, 779
  - central and neural arch relationship, 771(f)
  - injury, 978
  - lesions
    - lower, 822
    - upper, 822, 1010
  - nerve block, 790
  - supraclavicular branches, 820-1
  - surface anatomy, 790
- cardiac, 461, 912, 939, 945, 982-3, 983(f)
  - deep, 982-3, 984
  - superficial, 982, 983
- carotid autonomic, 247
- cervical, 401(f), 407, 435, 437, 439, 455-7
  - branches, 456-7
  - centra and neural arch relationship, 771(f)
- coccygeal, 1092-3
  - centra and neural arch relationship, 771(f)
- coeliac, 1043, 1044, 1045, 1111, 1120, 1187
- coronary
  - left, 983
  - right, 982, 983
- cystic, 1172
- dental, superior, 519
- gonadal, 1046, 1233
- hepatic, 1044, 1120, 1172-3
- hypogastric
  - inferior (pelvic), 1044, 1046, 1141, 1153, 1159, 1160, 1249, 1291
    - development, 374

    superior, 986, 1043, 1044, 1046, 1150, 1155
iliac, 1046
incisor, 519
on inferior thyroid artery, 462
infraorbital, 494
intercostal, centra and neural arch relationship, 771(f)
intermesenteric, 986, 1043, 1045-6
intragemmal, 508
lumbar, 1078-80, 1079(f), 1336
    branches, 1079, 1079(f), 1080
    centra and neural arch relationship, 771(f)
    irritation, 1080
    lesions, 1336
lumbosacral, 1081, 1091-2
Meissner’s (submucosal), 1044, 1051, 1122, 1212
mesenteric
    inferior, 1043, 1046, 1141, 1147, 1150, 1151, 1155
    superior, 1045, 1131, 1141, 1143, 1144, 1146, 1147
mucosal, 1051
myenteric, 953, 1051, 1213
    development, 1203
oesophageal, 912, 951, 1044, 1111
ovarian, 1295
papillary, superficial, 157
parotid (pes anserinus), 494, 1343
pelvic, 1044, 1046
pelvic *See* plexus (nervous), hypogastric, inferior (pelvic)
peri-oesophageal, 951, 1111
perigemmal, 508
peripatellar, 1393
pharyngeal, 452(f), 458, 459, 460, 572
phrenic, 1045
postfixed, 1078
prefixed, 1078
preprostatic, 1258
prevertebral, 98
prostatic, 1252

- pulmonary, 912, 945, 991, 994, 998
  - anterior, 982, 998
  - posterior, 944, 998
- Raschkow’s, 515
- rectal, 1155
- renal, 1233
- reticular, deep, 157
- retro-orbital, 545
- sacral, 1091-2, 1336, 1384-5
  - branches, 1092, 1384-5
  - centra and neural arch relationship, 771(f)
  - lesions, 1336
  - muscular branches, 1092
  - visceral branches, 1092
- solar (coeliac), 1187
- splenic, 1193
- subclavian, 461
- submucosal (Meissner’s), 1044, 1051, 1122, 1212
- subsartorial, 1383
- subserosal, 1051
- suprarenal, 1200
- thoracic aortic, 943(f), 944, 944(f)
- tympanic, 629
- ureteric, 1233
- vertebral, 461
  - external, 715
  - internal, 714, 715
- vesical, 1249, 1253, 1257

plexus (venous)
- conchal, 553
- coronal, 757
- dorsal, of hand, 894
- of dura mater, development, 392-3
- dural, development, 392-3
- pampiniform, 131, 1264, 1293, 1295
- pharyngeal, 452, 561, 563-4
- prostatic, 1252

- pterygoid, 431, 500, 502, 527, 540(f), 541, 656, 666
- sagittal, 393
- subpapillary, 157
- uterine, 1284, 1293
- vaginal, 1284
- vertebral, 452, 987, 1075
    - external, 453
    - internal, 452
- vesical, 1252

plica(e)
- ciliary, 681
- circulares, 1128(f), 1129, 1133(f)
- fimbriata, 503
- infrapatellar, 1401
- lacrimalis, 674
- semilunaris, 669, 703
- suprapatellar, 1401
- triangularis, 566 *See also* fold(s)

pneumoperitoneum, 1216

pneumothorax, 406, 914, 978, 991
- tension, 991

point(s)
- datum, 509
- Erb's, 406(f), 407
- hinge, of neural plate, 361
- mid-inguinal, 1053
- motor, 110
- pivot, 118, 122(f)

pole
- frontal, 343, 344
    - development, 383
- of spleen, 1191
- temporal, 338, 345-6
    - cortex, 346
    - development, 383

  use of term, 383

polydactyly, 902

polyhydramnios, 181, 953, 1015, 1203, 1206

polymastia, 934

polymicrogyria, 388

polyotia, 618

polysaccharides, 4

polysomes, 10

polysplenia, 1218

polythelia, 934

pons, 226, 228(f), 229(f), 284-7
  arterial supply, 253
  basilar, 306
  cortical projection fibres, 357(f)
  development, 377
  external features, 284
  lesions, 295
  micturition control, 1254
  relations, 284
  tegmental reticular nucleus, 306, 308
    cerebellar connections, 306
  ventral, 284

ponticles, 720

ponticulus, 619, 625

pontine flexure *See* flexure(s), pontine

pore(s)
  gustatory, 508
  interalveolar (of Köhn), 998, 1000(f)
  nuclear, 19
  skin, 146(f), 154, 161(f)

porins, 13

porta hepatis, 1049, 1165, 1168-9

portals, lymphovenous, 455-6

positron emission tomography, 358

posture, 745
- abnormal, basal ganglia dysfunction, 334
- affecting level of diaphragm, 1012
- anatomy, 643-4, 643(f)
- anticipatory function of cerebellum, 308
- ‘beach’, breathing while holding, 1012
- fixation, role of cerebellum, 309
- muscles of, 744, 745

potassium, excretion, 1238

potential
- action *See* action potential
- end-plate, 111
- endolymphatic, 647
- graded, 64
- membrane, 64
- nervous, receptor, 57
- receptor, in hearing, 647
- resting, 63

pouch
- adenohypophysial, 602, 611
- of Douglas (recto-uterine), 1106, 1151, 1285, 1287(f)
- Hartmann’s, 1177
- hepatorenal (of Morison), 1101, 1108
- hypophysial, 611
- inguinal, superficial, 1060
- perineal
  - subcutaneous, 1095-6
  - superficial, 1096
- peritoneal, rectovesical, 1257
- pharyngeal, 596, 608, 1205(f)
  - development, 598(f), 602

        - placode thickening, 367
    - of Rathke (hypophysial recess), 198, 321, 367, 368(f)
    - recto-uterine (of Douglas), 1106, 1151, 1285, 1287(f)
    - rectovagino-utero, 1218
    - rectovesical, 1105, 1151, 1218
    - Seesel’s, 367
    - vesico-uterine, 1245, 1285, 1299

power, grip, 874

praxis, 358

pre-eclampsia, 176, 1299

precuneus, 336, 336(f)

predentine, 514, 517(f)

pregnancy, 1299-304
- abdominal, 172, 175
- appendicitis, 1300
- breast changes, 931, 932, 936, 936
- cervix uteri in, 1299
- decidua of, 176, 179, 181
- duration, 211, 213
- ectopic, 172, 175
- femoral ring changes, 1067
- hair growth, 153
- miscarriage, 213
- multiple, 172, 173(f)
- ovarian, 172, 175
- pelvic changes, 1300-1, 1301(f)
- pelvic floor shape, 1085
- pelvic joint changes, 1366
- pre-eclampsia, 176
- rhesus antigen, 68
- skin changes, 149
- starvation, 218
- suprarenal gland changes, 1200
- twin, *1302*

- undernutrition, 218
- uterine size, 1299, 1300(f)
- uterus relations, 1299-300

preimplantation genetic diagnosis, 168

premaxilla, ossification, 613

premolars *See* teeth

prenatal diagnosis, oesophageal atresia, 953

prepuce
- of clitoris, 1325
- of penis, 1271
  - abnormalities, 1252

presbyacusis, 648

presbyoesophagus, 954

presbyopia, 687

pressure
- intra-abdominal, elevated, deep inguinal ring action, 1066
- intraocular, 680
  - increased, 680, 686, 695
- negative, pleural space, 989
- pleural, rise during coughing, 1005
- portal, 950, 1118

presubiculum, 347, 351, 352

priapism, 1276

prime movers, 114-15

primordium
- chiasmatis, 699
- uterovaginal, 1313, 1316(f), 1318(f)

pro-epicardium, 1026

proatlas, 770
- remnants, 770

process (or processus), 88
- accessory, of lumbar vertebrae, 723, 724
- articular, of vertebrae *See* zygapophyses
- blastemal articular *See* zygapophyses
- caudate, 1168
- ciliary, 686
- clinoid, 248
  - anterior, 423, 424, 427, 529
  - middle, 424, 527, 529, 530
  - posterior, 424, 425, 427
- cochleariformis, 626, 628
- condylar, mandibular, 412, 530, 532, 533
  - fracture, 480
- coracoid, 786
  - of scapula, 794, 794(f), 795
- coronoid
  - of mandible, 412, 530, 532, 533, 538
    - fracture, 480
  - of ulna, 843
- costal, 770
  - development, 768, 769(f)
- falciform, 1366
- frontal
  - of maxilla, 476-7
  - of zygomatic bone, 409, 475
- frontonasal, 602
- head, of embryo *See* notochord
- of incus, 627
- intrajugular, 713
- jugular, of occipital, 415, 425, 428
- junctional, 141
- lacrimal, 474
  - of inferior nasal concha, 474, 475, 476
- lenticular, 627
- of malleus, 627
- mammillary, 723, 724
- mandibular, 602

mastoid, 403, 411, 412, 416, 417, 419, 615, 617, 618, 619, 620, 622, 626
    of temporal bone, 415, 428
maxillary, 602
    alveolar, 409, 477
    of inferior nasal concha, 478
nasal
    lateral, 602
    medial, 602
neural, 767, 770
notochordal, 702
odontoid *See* dens, of axis
orbital, of palatine bone, 478-9
palatal, 604
palatine, maxillary, 404, 414, 477
palpebral, 703
paramastoid, 713
petrosal, 527
petrous, 414, 415
phalangeal, of organ of Corti, 641
pterygoid, of sphenoid bone, 415, 417(f), 529
pyramidal, of palatine bone, 415, 478, 529
septal, 547
sphenoidal, 551
    of palatine bone, 479
spinous, of vertebrae, 716, 716(f), 719, 720-1, 723, 768
    of axis (C2 vertebra), 721
    of C7 vertebra, 721
    cervical, 718
    development, 768
    palpation, 912
    thoracic, 721
Stieda’s, 1436
styloid, 403
    of fibula, 1415
    of radius, 840
    of temporal bone, 412, 416, 615, 617

        of third metacarpal, 865
        of ulna, 786, 844
    supracondylar, 798
    transverse, of vertebrae, 716-17, 770
        atlas, 405
        axis, 405
        cervical, 717, 718(f), 721
        coccygeal, 728
        development, 768, 770
        lumbar, 716
        sacral, 724
        thoracic, 716-17
    trochleariformis, 626
    tubarius, 529
    uncinate
        of cervical vertebrae, 718
        of ethmoid bone, 472, 473(f), 475
        of pancreas, 1183, 1185
            development, 1207
    vaginal, of sphenoid bone, 416, 529
    vaginalis
        females, 1289
        males, 1320, 1320(f), 1322(f)
            obliteration, 1311
            persistence, 1279, 1320
        obliterated part, 1262
    vocal, 579
    xiphoid, 909, 912, 917(f), 918, 1007, 1009, 1052, 1053
        ossification, 918
    zygomatic
        of frontal bone, 404, 409, 470
        of maxilla, 409, 412, 476
        of temporal bone, 615 *See also* prominence

procollagen, type I, 1017

proctodeum, 1212

proctography, 1160

progeria, 18

progressive supranuclear palsy (PSP), 332

projection(s)
- development, 388
- nervous, 357, 357(f)
  - coeruleospinal, 271
  - corticofugal, 357, 380, 385
  - corticopetal, 380, 385, 388
  - corticopontine, development, 388
  - development, 388
  - striatonigral, 329, 332
- neurosecretory
  - magnocellular, 316, 319
  - parvocellular, 316, 318
- rubro-olivary, 290
- tecto-olivary, 292
- ulnar, 861 *See also* connections (neural); *See also* fibre(s), nerve

prolapse
- intervertebral disc, 731-2, 732(f)
- rectal, 1153-4

prometaphase, cellular division, 21

prominence
- cardiac (pericardial), 197
- facial, 624, 625(f)
- laryngeal (Adam’s apple), 405, 577, 578(f), 579
- spiral, 640 *See also* process (or processus)

promontory
- of middle ear, 625
- sacral, 724, 1046, 1052

pronation (movement), 868-70
- muscles involved, 868, 872, 872(f)

pronephros, 1305, 1305(f), 1306(f)

pronuclei, 167

prophase, cellular division, 21

proprioception, nerve fibres, 263, 271, 273(f), 535

prosencephalon (forebrain), 226, 228(f), 362(f)
  amygdaloid projections, 354
  cholinergic system, 352
  development, 362, 380
  neuroectoderm, 699
  projections to cortex, 341 *See also* diencephalon; *See also* telencephalon

prosopagnosia, 358

prostaglandins
  in patent ductus arteriosus, 975, 984, 1028-9
  secretion by renal cells, 1237

prostate, 1255-9
  age-related changes, 1257, 1259
  arteries, 1257
  carcinoma, 1258
  fascia, 1254
  fetal, 1257
  hyperplasia, benign, 1250, 1259
  imaging, 1258(f)
  lobes, 1254
  lymphatics, 1258
  microstructure, 1258-9
  nerves, 1258-9
  relations, 1254
  urethra in, 1254, 1266-7
  veins, 1257
  zonal anatomy, 1256-7, 1257(f), 1258(f)

protease(s), inhibitors, 176

proteasomes, 12, 13

protein(s)
  actin-binding, 15
  bone morphogenetic, 87, 370
  bundling, 15

carrier, 4
channel, 4
extracellular matrix, 36-8
filament severing, 15
G-protein, 92
gel-forming, 15
Gli, 902
glial fibrillary acidic, 392
guanosine triphosphate-binding, 16
histone, 19
housekeeping (primary), 193
iodothyroglobulin, 463
kinesin family, 44
kinetochore, 16
M-cadherin, 116
microtubule-associated, 16, 42
mitochondrial, 14
of muscle, 106-7
  actin *See* actin
  α-actinin, 7, 14(f), 106
  desmin, 7, 106, 114, 127, 137, 138
  dystrophin, 106, 107
  merosin, 107
  myomesin, 106
  myosin *See* myosins
  nebulin, 106, 115
  plectrin, 106
  titin, 106, 115, 124
  tropomyosin, 106, 111
  troponin, 106, 111
myelin *See* myelin
myelin basic, 51
myelin-associated glycoprotein (MAG), 51
nexin-linking, 17(f)
olfactory marker, 553
pannexins, 48
perforin, 71, 72

  plasma membrane, 4
  primary, of embryo, 193
  profilaggrin, 148, 158
  proteolipid (PLP), 51
  receptor, 8-9
  secondary, of embryo, 193
  Tamm-Horsfall, 1237
  testosterone-binding, 1319
  transmembrane, 4, 15 *See also* glycoprotein

protein kinases, 20

proteoglycans, 38, 675
  in cartilage, 81, 82(f), 83, 84, 86, 87, 89, 96, 108, 120
  synthesis, metanephros, 1308

proto-oncogene, 8

‘protocortex’ model, 386

‘protomap’ hypothesis, 386

protrusion, of lip, 489

protuberance, 409
  mental, 409, 527
  occipital
    external, 411, 412, 415, 416, 481, 745
    internal, 425, 426, 428

pseudocyst, pancreatic, 1187-8

pseudoganglion, of posterior interosseous nerve, 856

pseudopodia, 3

psoriasis, 147

pterion, 403, 412, 418, 469, 529

ptosis, 252, 295, 659, 661, 671

puberty
  bone growth, 96
  breast changes, 934-5, 935(f), 1325

  - hair growth, 153
  - prostate gland changes, 1259
  - reproductive organ maturation, 1325, 1325(f)
  - sebaceous glands, 153
  - voice changes, 592

pubis, 1041, 1353(f), 1354-5
  - in acetabulum, 1352
  - innervation, 1355
  - muscle attachments, 1061, 1355
  - ossification, 1354
  - sex differences, 1355
  - surface anatomy, 1354
  - vascular supply, 1255 *See also* hip bone

pudendum *See* vulva

pulled elbow, 835

pulmonary defence mechanisms, 989

pulmonary defensive mechanisms, 1005

pulmonary hypertension, 1015

pulmonary sequestration, 997

pulmonary vascular resistance, 1035-6

pulp
  - dental, 514-15
    - infections, 517, 518(f)
  - of spleen, red, 1194-5, 1194(f)
  - white, 1194, 1194(f)

pulse(s)
  - arterial
    - brachial, 787
    - dorsalis pedis, 1344
    - external carotid, 445
    - facial, 446
    - femoral, 1344
    - internal carotid, 437, 444

        posterior tibial, 1344
        radial, 787
        subclavian, 407, 438, 448
        superficial temporal, 405
        ulnar, 787
    facial, 405
    head, 405
    neck, 405
    venous, jugular, 407

pulvinar, 311, 315, 357

pump(s), calcium-ATPase, 108, 111

punctum lacrimale, 669

puncture
    suprapubic, 1106
    venepuncture, 790

pupil (of eye), congenital atresia, 702

Purkinje fibres/cells *See* cells (named), Purkinje; *See also* fibre(s), nerve

pursuit (eye movements), 663, 664

putamen, 229(f), 230, 325, 326
    aminergic input to, 329, 329(f)
    development, 383
    projections to, 329

pyelogram
    ascending, 1231
    retrograde, 1231

pylorus, innervation, 1172

pyramid(s) (pyramis), 265(f), 268, 275-7, 276(f)
    of cerebellum, 298, 300(f), 304, 305(f)
    of kidney, 1232, 1234(f)
    of medulla oblongata, 377
    vestibular, 633

Q

quadriplegia, 759

quickening, 903

R

‘radial unit’ model, 386

radiation
- auditory, 357
- optic, 346, 357, 696
  - arterial supply, 253
  - lesions of, 697
- somaesthetic, 357
- thalamic, posterior, 357

radicles, vitelline, 1019

radiography
- chest, 989, 990(f), 991, 993, 1002
  - endotracheal intubation, neonate, 1033
  - mediastinal contours, 954, 954(f)
- colon, 1138-9, 1139(f)

radius, 840-4, 840(f), 841(f)
- attachment sites, 840(f), 841-2, 841(f)
- congenital absence, 906
- development, 905
- distal end, 841
- head, 786
- head subluxation, 835
- ossification, 842-3, 843(f)
- shaft, 778, 786, 840-1, 840(f)
- surface anatomy, 786
- vascular supply, 842, 842(f), 852

rami communicantes
- grey, 234, 753, 944
  - cervical, 460
  - lumbar, 754, 1043, 1078, 1081
  - pelvic, 1093
- ‘mixed’, 944
- white, 234, 753, 755, 944

        development, 375
        lumbar, 754, 1043
        thoracic, 754, 911, 944

‘ramus cristae terminalis’, 979

ramus (rami)
    communicans, to ciliary ganglion, 668
    to facial nerve, 542-3
    of gastric arteries, 1268
    of gastroepiploic arteries, 1268
    iliopubic, 1378
    ischial, 1356-7
    ischiopubic, 1280
    of lateral fissure (cerebral cortex), 335
    lingualis vagi, 459, 572
    of mandible, 402, 412, 418, 530-1, 538
        fracture, 480
    orbitales, of pterygopalatine ganglion, 669
    of phrenic nerve, 1010
    pubic
        inferior, 1355
        superior, 1354-5
    of somatic arteries, 206

ramus (rami), of spinal nerves
    dorsal, cervical, 457
    dorsal (posterior primary), 230, 755, 755-7, 756(f)
        cervical, 457, 755-6
        coccygeal, 757
        lumbar, 756
        sacral, 756
        thoracic, 756, 929
    intermedius, 754
    ventral (anterior primary), 230, 455-7, 755, 911
        7th–12th thoracic, 1060
        cervical, 460, 755
        first thoracic nerve, 993
        lumbar, 754, 1078, 1081

        - sacral, 755
        - thoracic, 47, 928-9, 928(f), 1060

ranula, 521-2

raphe
    - of iliococcygeus, 1083
    - of levator ani plate, 1155
    - median
        - development, 377
        - fibrous, 501
    - palatine, 500, 502
    - palpebral, lateral, 482
    - perineal, 1096
    - pharyngeal, 561, 568
    - pterygomandibular, 415, 487, 499, 530, 543, 565, 565(f)
    - of scrotum, 1262
    - serotoninergic cell groups, 329, 329(f)
    - of soft palate, 565

rays
    - digit, 905
    - medullary, of kidney, 1229, 1234(f), 1235

receptor(s)
    - baroreceptors, 58
    - chemoreceptors, 58, 59
    - classification, 57-8
    - cutaneous, 58, 59
    - epithelial, 57, 58
    - ionotropic, 46
    - mechanoreceptors, 535
    - nociceptors, 535
    - olfactory, 28
    - proprioceptors, 535
    - sensory, 57-8
        - baroreceptors, 58
        - chemoreceptors, 57, 58
        - classification, 57-8

        - cutaneous, 57
        - epithelial, 57
        - exteroceptors, 57
        - general, 57
        - interoceptors, 57-8
        - irritant, 58
        - joint, 61
        - mechanoreceptor, 53, 57, 58(f), 59, 61
        - neuroepithelial, 57
        - neuronal, 57
        - nociceptors, 57, 58, 58(f), 63
        - peritrichial, 58
        - proprioceptors, 57
        - taste, 57
        - thermoreceptors, 53, 57, 58
        - visual, 57
    - special, 59
    - stretch, 261

recess(es)
- adenohypophysial, 367
- aortic, 959
- azygo-oesophageal, 957
- caecal, 1109
- cochlear, 633, 634
- costodiaphragmatic, 910, 914, 991, 1015(f), 1228
        - inferior border, 991, 992(f)
- costomedial, 991
- duodenal, 1217
- duodenojejunal, 1109
- elliptical, 633, 636
- epitympanic, 621, 626, 627, 628
- hepatoenteric, 1216
- hypophysial (pouch of Rathke), 198, 321, 367, 368(f)
- ileocaecal (superior and inferior), 1109
- inferior, of bursa omentalis, 1204
- infundibular, of third ventricle, 239
- intersigmoid, 1109

  - lateral, of fourth ventricle, 240
  - mesentericoparietal, 1109
  - optic, 239
  - pancreaticoenteric, development, 1204, 1215(f)
  - para-oesophageal, 1203, 1215(f)
  - paraduodenal, 1109
  - pericardial, 959
  - pharyngeal, 563
  - pharyngotympanic, 604
  - pineal, 239
  - pleural, 991
  - pneumatoenteric, 1203, 1214, 1215(f), 1216
  - prestyloid, of wrist joint, 870
  - pulmonary, 959
  - retrocaecal, 1109, 1142
  - retrocaval, 986
  - retroduodenal, 1109
  - sacciform, of distal radio-ulnar joint, 868, 868(f)
  - sphenoethmoidal, 529, 551
  - splenic, 1107
  - subpopliteal, 1396, 1402
  - suprapineal, 239
  - tubotympanic, 604, 652
  - of tympanic membrane, 630
  - zygomatic, 558

rectocele, 1154

rectum, 1150-5, 1150(f)
  - arteries, 1154, 1154(f)
  - epithelium, 1050, 1161
  - haustrations, 1138, 1139(f)
  - ligaments, 1153, 1154
  - lymphatics, 1155, 1155(f)
  - nerves, 1141, 1155
  - peritoneum, 1151, 1218
  - prolapse, 1153-4
  - putative, 1307

  - relations, 1153
    - to female genital tract, 1286(f)
  - tumour extension, 1086
  - veins, 1155

referred pain
  - in anus, 1160
  - from appendix, 1146
  - from bladder, 235, 1254
  - from common bile duct, 1181
  - from diaphragm, 1011
  - from duodenum, 1128
  - from spleen, 1193
  - from ureter, 1242
  - from gallbladder, 1181
  - from heart, 236
  - from ileum, 1131
  - from jejunum, 1131
  - from liver, 1173
  - from Meckel’s diverticulum, 1129
  - from palatine tonsil, 567
  - from pancreas, 1187
  - from pleura, 991
  - from spine, 759
  - from stomach, 1120

reflections
  - peritoneal *See* peritoneum
  - pleural, 914

reflex(es)
  - accommodation, 681
  - ankle jerk, 1346
  - at birth, 389
  - Babinski, 230, 261, 389
  - biceps jerk, 789
  - blink, 401
  - corneal, 286, 287(f)
  - cough, 284

- cremasteric, 1064
- diving, 389
- extensor plantar, 261, 271, 272(f),
- extrusion, 389
- Ferguson's, 319
- flexor, 261-2, 261(f)
- gag, 283, 401, 458, 573, 1324
- gamma, 261, 261(f)
- glabellar tap, 389
- jaw-jerk, 287
- knee jerk, 1346
- lacrimal, 673, 674(f)
- milk ejection, 319
- nasal, 389
- neck righting, 389
- optokinetic, 663
- peristaltic, 1051
- plantar, 1346
- pupillary light, 389, 683(f), 685
- radial jerk, 790
- recto-anal inhibitors (RAIR), 1160
- sneeze, 284, 284(f)
- spinal, 266(f), 272(f), 273(f), 389
- stapedius, 287, 401, 628
- stretch, 261
- swallowing, 283
- tensor tympani, 287, 628
- torsional tilt, 663
- traction response, 389
- triceps jerk, 789-90
- vestibulo-ocular, 663
- visual, 644

reflux
- gastro-oesophageal, 1114
- oesophageal, 953, 1009

refraction of lens, 687

- disorders, 687-8

regeneration
- cardiac muscles, 143
- epidermis, 145-8
- epithelium (oesophageal), 952
- liver, 1175
- skeletal muscles, 143
- skin, 162

region(s)
- abdominal, 1052
- aorta-gonad-mesonephros, 207
- elbow, 831-8
  - arteries, 835
  - injuries, 835
  - innervation, 836-7
  - skin
    - blood supply, 831
    - innervation, 831
- gluteal, 1349-85
  - arteries, 1378, 1378(f)
  - fascia, 1349-50
  - lymphatic drainage, 1336
  - muscles, 1331, 1368-72, 1369(f), 1391-2
  - pain, 1390
  - perforator flaps, 1381
  - skin, 1349
  - soft tissue, 1349-52
  - surface anatomy, 1341-2, 1343(f)
- hip *See* girdle(s), pelvic; *See also* joints (named), hip; *See also* region(s), gluteal
- iliac
  - lymphatic drainage, 1336
  - muscles, 1332, 1367-8, 1367(f), 1391-2
- inguinal, 1064-6
  - surface anatomy, 1053, 1340, 1341(f)
- joints, 868-70

- nerves
  - paranodal, 43, 54, 54(f)
  - perinuclear (mid-internodal), 54
- occipitocervical *See* junction(s), occipitocervical
- shoulder
  - bones, 791-800
  - joints *See* joints (named), glenohumeral
  - muscles, 778, 807-14
  - skin, 791
    - innervation, 791
    - vascular supply, 791
- wrist
  - ligaments, 870-1
    - extrinsic, 870-1
    - intrinsic, 871
      - rupture, 871
  - skin, 857-61
    - innervation, 858, 858(f)
    - nerves, 858, 858(f)
    - vascular supply, 857, 858(f)

relaxin, 1366

relay, synaptic, vagus nerve, 945

‘renal collar’, 208, 1219, 1233

renin, 1225, 1310
- release, 1238

residual bodies, 12

respiration *See* breathing

rete
- ovarian, 1319
- pegs, 146, 147, 150, 154, 161
- ridges, 146, 147(f), 150, 162
- testis, 1265, 1268
  - development, 1319

reticulin, 72, 73, 74, 75

reticulum
- endoplasmic *See* endoplasmic reticulum
- myoepicardial, 1016, 1017(f)
- sarcoplasmic *See* sarcoplasmic reticulum
- splenic, 1195

retina, 688-96
- arteries, 693, 693(f), 694
- capillaries, 694
- colour, 688, 695
- degenerative disease, 680
- detachment, 699
- development, 699
    - neural, 700
- dimensions, 688
- fluorescence angiography, 688, 689(f)
- innervation, 694
- microstructure, 688-9
    - cells, 689-93, 689(f)
    - layers, 688-9
- optical coherence tomography, 690(f)
- photoreceptors, 675, 685
- quadrants (inferior and superior), 346
- sensory, development, 700
- veins, 693, 693(f)

retinaculum
- cutis, 1430
- extensor
    - of ankle
        - inferior, 1429, 1430(f)
        - superior, 1429, 1430(f)
    - of wrist, 879-80, 882(f)
- fibular, of ankle
    - inferior, 1430, 1431(f)
    - superior, 1430, 1431(f)
- flexor
    - of ankle, 1429-30

        upperlimb, surface anatomy, 785
        of wrist, 878-9, 878(f)
    patellar, 1400, 1403, 1409
        lateral, 1400

retinoic acid, 1020, 1035

retinoids, 8

retrohyoid depression, 602

retroperitoneal structures, 1069, 1099

retroperitoneum, 1069-81, 1137
    spaces, 1069

reverse transcriptase, 19

Rhesus antigen system, 68

Rhesus factor incompatibility, 68

rheumatoid arthritis, 69, 78, 744

rhodopsin, 8, 690

rhombencephalon (hindbrain), 226, 227, 228(f)
    cells giving rise to heart, 1016
    development, 362, 362(f), 376-9, 595
        cell columns of alar plate, 376-7
        cell columns of basal plate, 376
        derivatives, 412(t)
    pain perception, 267
    segmentation, 371 *See also* cerebellum; *See also* isthmus rhombencephali; *See also* metencephalon; *See also* myelencephalon

rhombomeres, 194, 362, 365, 371, 376, 595, 596
    segmentation, 376

ribbon, synaptic, 45, 46(f)

ribosomes, 4, 10, 12
    mitochondrial, 14

ribs, 918-22, 919(f)
    abnormalities, 1014

attachments, 919-20
atypical, 920-2
cervical, 465, 770, 822, 920
counting, 913
development, 768(f), 770
elevation during breathing, 1012
eleventh, 909, 921-2, 1054
false, 918
first, 920-1, 920(f)
    intrathoracic, 993
floating (11, 12), 770, 918
fractures, 922
innervation, 920, 921
lowest palpable, 991
lumbar, 724
lumbar vertebra associated, 770
movements during breathing, 1011
    ‘bucket handle’, 1011
    ‘pump handle’, 1011, 1011(f)
ninth, 1054
ossification, 921, 922
palpation, 912
precartilaginous, 770
relations, 918-19
second, 921
seventh, 909
size, 919
structure, 919
surface anatomy, 909, 1054
tenth, 909, 921-2, 1054
thoracic, 717
true, 919
twelfth, 909, 921-2
typical, 918-19, 919(f)
vascular supply, 921
vertebrochondral (8–10), 770
vertebrosternal (1–7), 770

rickets, 95, 418

ridge(s), 227
- apical ectodermal (AER), 198, 201, 900, 901(f)
    - removal, 900
- crescentic, ventricular septation, 1024
- epidermal, 159
- genital, 1317, 1318(f)
- gonadal, 1312, 1313
- intersesamoidal, 1441
- mammary, 934
- mesonephric, 1014, 1307, 1312, 1313
- nasolacrimal, 703
- papillary, 160, 160(f)
- Passavant’s, 571, 573
- ponticulus, 619
- pulmonary, 1014
- sinutubular, 967
- supracondylar
    - lateral, 786, 797, 798
    - medial, 786, 797, 798
- trabecular, 1026
- of trapezium, 862
- zygomaticoalveolar, 476

rigor mortis, 111

rim, acetabular, 1352, 1356

rima glottidis, 583-4
- in speech, 592

ring
- anorectal, 1159
- aortic, 977
- arterial, 1032
- circumpharyngeal lymphoid, 567
- common tendinous, of orbit, 656, 657(f)
- ectodermal, 198
    - intramembral part, 198

- femoral, 1058(f), 1059, 1067
- hymenal, 1284
- inguinal, 1320, 1320(f)
  - deep, 1056, 1060, 1065-6, 1289, 1320
    - neonate, 1066
    - position and actions, 1065-6
    - transversalis fascia at, 1060
  - superficial, 1065
    - neonate, 1066 *See also* hernia, inguinal
- intra-articular, of femoral head, 1364
- lymphatic, 602
- tympanic, 613, 617-18, 621
- Waldeyer's, 401, 564, 567

RNA

- messenger (mRNA), 10
- ribosomal (rRNA), 10
- small interfering (siRNA), 12

rods, of retina *See* cells (named), rod (retinal)

root(s)

- ansa cervicalis
  - inferior, 445(f), 456
  - superior, 437, 445(f), 456
- of aorta, 970(f), 974
- dorsal, 226
- of lungs, 991, 994
- of mesentery, 1099
  - dorsal, 1209, 1211, 1217
- of neck, 438, 439, 443, 465-6
- of nerves
  - accessory
    - cranial, 459
    - spinal, 459-60
  - of ciliary ganglion, 669
  - facial, 279
  - hypoglossal, 276(f), 281
  - lumbar, 754

    - myelination, 389
    - oculomotor, 288
    - olfactory, 554-5
    - sacral, 754
    - spinal
      - appearance, 754
      - arteries, 757, 758(f)
      - compression, 759
      - coverings, 751(f), 752, 752(f)
      - dorsal, 227(f), 230, 751, 754
        - development, 371-2
      - lesions, 759
      - orientation, 754
      - variations, 755
      - ventral, 226, 227(f), 230, 260, 754
        - development, 371
    - thoracic, 754
  - omental, 1217
  - of penis, 155, 1271(f)
  - of teeth, 513, 514(f), 516(f)
    - canines, 510
    - incisors, 509
    - molars, 510
    - premolars, 510
  - of tongue, 503

rootlets, of spinal nerves, 257, 754, 769, 770

rosette(s), mossy fibre, 303

rostrum
  - of corpus callosum, 355, 386
  - sphenoidal, 98(f), 529

rotation (movement), 103, 122(f), 123
  - adjunct, 102, 103
  - axial, 103
  - axis of, 103
  - centre of, 123

conjunct (coupled), 102, 103, 123

rotator cuff, 778, 806, 807, 812
    disease, 807

rouleaux, 67

rugae
    of mouth, 606-7
    of stomach, 1051, 1115, 1116(f)
    of vagina, 1284

running, 1459-62, 1460(f), 1461(f)

S

sac(s)

- alveolar (air), 995, 996, 998, 999(f)
- aortic, 1020, 1025
    - development, 390, 601
    - of embryo, 206
- dental, 606
- endolymphatic, 634, 636, 639, 651
    - surgical access, 649
- greater, peritoneal, 1107, 1108, 1214, 1228
- infundibular, 367
- lacrimal, 404, 672, 674, 703
- lesser, peritoneal, 1104, 1107-8, 1113, 1215(f), 1216, 1228
    - aditus to (epiploic foramen), 1101(f), 1102, 1107-8, 1217
    - anterior/posterior walls, 1107
    - borders, 1107
    - early development, 1216
    - greater omental region, 1104
    - inferior recess, 1107
    - later development stages, 1214
    - ligaments of liver, 1214
    - maturation, 260-1
    - perigastric region, 1216
    - peritoneal connection, 1104
    - retrogastric region, 1216
    - secondary dorsal wall, 1216
    - vestibule, 1108
- lymph, 209, 209(f)
    - cisterna chyli, 209
    - jugular, 209
    - posterior, 209
    - retroperitoneal, 209
    - subclavian, 209
- meningeal, 772
- nasolacrimal, 655
- pericardial serosal, 960(f)

- peritoneal, lesser, greater omental region, 1216
- pharyngeal, *See also* pouch, pharyngeal
- pleural, 989, 990(f), 1014
    - formation, 989
- preputial, 1271
- yolk, 180
    - primary, 173, 180
    - secondary, 173, 175(f), 180, 184, 185, 190(f)

saccade (movement of eye), 661, 663

saccule(s) (sacculus (sacculi))
- of ear, 633, 636, 637
    - development, 652
    - head movement, 638
    - microstructure, 638-9, 639(f)
- of larynx, 583
- of lungs, development, 1034

saccus
- endolymphaticus, 617
- vaginalis, 1320, 1321

sacral index, 1359

sacralization, 724, 728

sacrum, 724-8, 726, 726(f), 727(f)
- agenesis, 771
- alar (anterolateral), 771
- apex, 725
- base, 724
- development, 771-2
- in elderly, 725
- facet tropism, 728
- measurements, 1359
- muscle attachments, 725
- ossification, 727, 728(f)
- sex differences, 1359
- structure, 724

- surfaces
    - dorsal, 724-5
    - lateral, 725
    - pelvic, 724
- variants, 728
- weight bearing, 1359

saliva, 520
- composition, 523
- flow rates, 520
- hypotonic, 522
- secretion, 520, 522
    - control, 523

salivation, nerve impulses, 523

sarcolemma
- cardiac muscle, 140-1
- skeletal muscle, 104, 106, 108, 110, 110(f), 111, 115, 116, 117

sarcomere, 105, 106, 106(f), 108, 109(f), 111
- cardiac muscle, 139, 140(f), 141
- skeletal muscle, 107(f), 108(s), 111, 112, 113, 115, 117

sarcoplasmic reticulum, 10
- cardiac muscle, 140, 140(f), 141, 142
- curbular, 141
- junctional, 108, 141
- skeletal muscle, 107(f), 108, 110(f), 111, 112, 115

Satiro’s ears, 618-19

Saturday night palsy, 829

scala
- media, 634
- tympani, 634, 652
- vestibuli, 634, 652

scalp, 467
- arteries, 489-91
- fascia, 397, 468

flaps, 467, 468
lacerations, 467
layers, 467
lymphatics, 492
nerves, 492

scaphocephaly, 418

scaphoid, 862
  fractures, 862
  ossification, 864
  surface anatomy, 786

scapula, 793-6, 793(f), 794(f)
  costal surface, 794
  development, 905
  dorsal surface, 794
  landmarks, 746-7
  ossification, 796, 796(f)
  structure, 793-4
  surface anatomy, 785
  ‘winged’, 786, 812, 820

scar
  epiphysial, 95
  glial, 48
  skin, 161, 162-3

SCIWORA, 759

sclera, 675-6, 676(f)
  development, 702
  thickness, 675

sclerosant, oesophageal varices, 951

sclerotomes, 763(f), 764, 770
  central, 767
  cervical, malfusions/defects, 770
  development, 765(f), 767-8, 768(f), 770
  dorsal, 767
  lateral, 767

occipital, 73-770
        malfusions/defects, 770
    occipitocervical junction, 769-70
    rib development, 768-9, 770
    rostral, 371
    vertebrae development, 767, 770

scoliosis, 745, 768, 770, 1014

scrotum, 1060, 1261(f), 1262
    arteries, 1262
    divided, 1323
    formation, 1320, 1325
    lymphatics, 1262
    nerves, 1262
    skin, 1262
    testicular descent, 1320
    veins, 1262

sebum, 153, 153(f)
    fetal, 213

second messengers, 8-9

segment(s)
    bronchopulmonary, 994, 995(f), 996, 996(f)
        naming/numbering, 994, 995(f)
        pulmonary vessels, 994
    Couinaud’s, 1165, 1166(f)
    of liver, 1165, 1166-7, 1166(f)
    pulmonary sequestration, 997
    spinal, 751

segmentation
    lower limb nerves, 1339(t), 1340(t)
    neural crest, 371
    neural tube, 371
    notochord, 371
    paraxial mesenchyme, 763, 763(f)
    renal vascular, 1231-2, 1232(f)

- rhombencephalon (hindbrain), 371
- rhombomeres, 376

segmentation clock, 763

selectins, 5, 137, 175

sella turcica, 424, 426, 427, 527, 530, 611

Semon's law, 589

senile elastosis, 162

senility pigment, 12

senses, special ***see specific senses/sense organs***

sepsis, cryptoglandular, 1158

septum (septa)
- aorticopulmonary, 601
- atrial, 964, 1029
  - defects, 974-5, 1030-1, 1031(f)
- atrioventricular, 964
  - defects, 1030
- dorsal median, of spinal cord, 257
- femoral, 1067, 1350
- inter-radicular, 530
- interalveolar, 998, 1000(f), 1001(f)
- interatrial (atrial), 964, 980 *See also* septum (septa), atrial
- interdental, 516(f), 530
- intermuscular
  - of arm, 824
  - crural, 1411
  - of foot
    - lateral, 1431
    - medial, 1431
  - of gluteal region
    - lateral, 1350
    - medial, 1350
- interventricular, 962, 963, 977, 980
- Körner's, 626

- lateral (cerebral hemisphere), projections from, 352
- of limbic lobe, 352-3
- median, of penis, 1272
- membranous
  - of heart, 969, 974
  - of nose, 550
- nasal, 409, 415, 418, 471, 472, 472(f), 475, 528, 550
  - bony, 550
  - cartilaginous, 550
  - displacement, 551
  - ossification, 604
- orbital, 656-7, 657(f)
- pectiniform, 1272, 1280
- pellucidum, 237, 352, 355
  - development, 386
- perimysial, 108, 109, 110
- placental (cotyledonary), 178
- primum (of atria), 964, 1023, 1028
- rectovaginal, 1151, 1153, 1154, 1218
- secundum (of atria), 964
- sinus, 1019
- of spinal cord
  - median
    - dorsal, 257
    - posterior, 749
  - posterointermediate, 262
- spurium, 1019
- transversum (of embryo), 201, 207, 1013, 1014, 1015, 1018
  - hepatic mesenchyme development, 1207
  - stomach/pericardium separation, 1204, 1208(f) *See also* mesenchyme, cardiac
- transversum, of semicircular canal, 637
- urorectal, 1212, 1307, 1308(f), 1311(f), 1322, 1324
  - partial development, 1323
  - prostate gland development, 1324
- ventricular, 964, 967, 969
  - defects, 974-5, 1030, 1031

        of heart, ‘Swiss’-cheese, 1031
    vertical, of palmar fascial complex, 860

serosa, 39, 1050, 1050(f), 1051
    of appendix, 1143
    of large intestine, 1161, 1212
    of lung, 991
    of small intestine, 1135, 1211
    of stomach, 1122
        development, 1206
    of uterus, 1291

serotonin, 46, 47
    ascending/descending pathways, 293
    bronchi, 1004
    cerebellar cortex, 303
    neurone, groups, 329, 329(f)
    striatum, 328

sesamoid bones
    accessory, 1442
    bipartite, 1441-2
    fibular, 1441
    of foot, 1441-2
    of hand, 862, 865, 865(f), 884
    innervation, 1442
    muscle attachments, 1442
    ossification, 1442
    patella *See* patella
    tibial, 1441
    of tibialis posterior, 1442
    vascular supply, 1442

seven-pass transmembrane receptors, 8

sex determination, 1320-1

sex differences
    acetabulum, 1359
    bladder, 1245, 1245(f), 1246(f), 1247(f), 1248

  - bony pelvis, 1359-60
  - clavicle, 791-2
  - external anal sphincter, 1159
  - femoral canals, 1350
  - ilium, 1356
  - pubis, 1355
  - sacrum, 1359
  - skull, 419-20
  - subpubic arch, 1359
  - thyroid cartilage, 579
  - tibia, 1414

sex hormones, 1200

sex vesicle, 22

shadow
  - cardiac, 957
  - mediastinal, 957
  - pleural, 989

shaft
  - of femur, 1361(f), 1362
  - of fibula, 1343, 1415-16
  - of humerus, 786, 797-8
  - of metacarpals, 864
    - first, 84
    - second, 865
  - of phalanges, 866
  - of radius, 778, 786, 840-1, 840(f)
  - of rib, 919
  - of tibia, 1412-13
  - of ulna, 840(f), 841(f), 844

sheath(s)
  - axillary, 439, 465, 815
  - carotid, 407, 439
    - infection, 568
  - connective tissue, peripheral nerves, 53
  - endomysial, 108, 110

  - epimysial, 108, 110
  - of eyeball, fascial, 657-8, 657(f), 658(f)
  - femoral, 1060, 1350, 1351(f)
    - at birth, 1350
    - compartments, 1350
  - fibrous, of flexor tendons, of fingers, 879
  - flexor tendon, of foot, 1452
  - Glissonian, 1166, 1167, 1169
  - hair, 151-2
  - myelin, 43, 49, 49(f), 50, 51, 53, 54, 54(f), 55, 59, 64
  - of olfactory nerve, 555
  - perimysial, 108, 110
  - perinotochordal, 198, 767
  - prostatic, posterior wall, 1218
  - psoas, 1367
  - rectus (abdominis), 1061, 1062(f)
  - spinal nerve (root), 755
  - of styloid process (vaginal process), 617
  - synovial
    - of ankle, 1430, 1430(f)
    - of extensor tendons, of fingers, 879-80, 882(f)
    - of flexor tendons, of fingers, 878(f), 879
  - of Waldeyer, 1240

sheet, digital, lateral, 859

shelf, palatal
  - elevation, 604
  - fusion, 604, 604(f)
  - rotation, 604

shingles, 56

shock absorption, 119

shoulder *See* joints (named), glenohumeral

shunts
  - left-right, 974
  - right-left, fetal, 974

- transjugular intraparenchymal porto-systemic, 1172
- vascular, 134-5
  - porto-systemic, 1171
    - common sites, 1171, 1171(f)
- ventriculoperitoneal, 1110

sialic acid, 1005

sialogram
- parotid duct, 497
- sublingual duct, 521, 521(f)
- submandibular duct, 521, 521(f)

sialoliths, 405

sickle-cell disease, 68

sign
- Babinski’s, 269, 1346
- Battle’s, 481
- Cullen’s, 1100, 1188
- Grey-Turner’s, 1188
- Hawkin’s, 1437
- pterygoid, 539
- Romberg’s, 309
- Trendelenburg’s, 1342, 1371

signals (signalling)
- cellular, 7-9
  - adhesive glycoprotein, 36, 38
  - astrocytes, 48
  - autocrine, 7, 8(f)
  - contact-dependent, 7, 8(f)
  - embryonic, 194
  - endocrine, 7, 8(f)
  - juxtacrine, 7, 8(f)
  - ‘organizer’, of nervous tissue, 370
  - paracrine, 7, 8(f)
  - receptor proteins, 8-9
  - synaptic, 8(f)

  - endocrine *See* hormone; *See also* hormones
  - heart formation, 1018
  - intracellular, 8-9
  - neurocrine, 7, 8(f)

sinus(es)
  - air, 527, 626 *See also* sinus(es), paranasal
  - aortic bulbous, 974
  - aortic (of Valsalva), 962, 972-3, 981, 984
    - anterior, 978
    - posterior, left, 980
  - basilar, 431
  - bullar, 558
  - caroticocavernous, fistula, 430
  - carotid, 447-8, 448(f)
  - cavernous, 424, 429-30, 527, 541, 666
    - development, 393
    - middle fossa triangles, 430
    - thrombosis, 430, 492
  - central, of bone, 91
  - cervical, 602
  - conchal, 550
  - coronary, 960, 964, 965(f), 981-2, 986, 1019
    - ‘unroofing’, 1032
  - dural venous, 427-31
    - development, 427
    - variation, 427
  - epididymis, 1262
  - ethmoidal, posterior, 529
  - frontal, 470, 471(f), 472, 473(f), 479
  - imaging, 559
  - inframedullary network, 918
  - infundibular, 550
  - intracavernous, 430
  - jugular, external, 451
  - lactiferous, 933
  - of larynx, 583
  - lymphatic, 73, 74(f)

marginal, 431, 433
maxillary
    infections, 525
    relation to teeth, 519, 525
oblique, 959, 960(f)
    of pericardium, 1203
occipital, 429
paranasal, 477, 479, 556-8, 602, 614
    age-related changes, 556
    arteries, 557, 558
    ethmoidal, 558
        anterior, 473, 558
        middle, 556(f), 558
        pneumatization, 558
        posterior, 558 *See also* cells (named), air, ethmoidal
    frontal, 556-7, 556(f)
        aperture, 556-7
        variations, 557
    functions, 556
    imaging, 557(f), 559
    infection spread, 559
    lymphatics, 557
    maxillary, 477, 557(f), 558-9
        relations, 558
        tumours, 559
    nerves, 557, 558
    sphenoidal, 544, 557-8
        aperture, 557
        relations, 557
    veins, 557, 558
peri-infundibular, 558
pericardial, 960(f), 968
pericranii, 432
petrosal
    inferior, 429, 430-1, 451, 457, 460
        development, 393
    superior, 429, 430, 617, 629

                development, 393
    - petrosquamous, 428
    - pre-auricular, 619
    - pro-otic, development, 393
    - prostatic, 1267
    - renal, 1228, 1230, 1230(f), 1231
    - sagittal
        - inferior, 428
        - superior, 427-8
    - scleral venous (canal of Schlemm), 702
    - sigmoid, 393, 428-9
    - sphenoidal, 424, 528, 529, 557
        - pneumatization, 557
    - sphenoparietal, 431
    - splenic, 1195
    - straight, 428
    - tarsi, 1341, 1437
    - tonsillar, 565
    - transitory tentorial, 393
    - transverse, 428
        - of pericardium, 959, 960(f), 1018
    - tympani, 625
    - urogenital, 1311(f), 1312, 1313, 1316(f), 1323
        - in cloacal anomalies, 1323
        - male *vs* female, 1316(t)
        - mesonephric duct to, 1307, 1307(f)
    - of Valsalva (aortic) *See* sinus(es), aortic (of Valsalva)
    - venarum, 1019
    - venosus, 205, 610, 963, 964, 1016, 1018
        - defects, 1030, 1031(f)
        - developmental changes, 1021(f)
    - venous, dural *See* sinus(es), dural venous

sinusoid, 131, 133
- of bone, 91, 92(f)
- of bone marrow, 75, 95
- hepatic, 1173, 1174, 1174(f)
    - development, 1207, 1208(f)

        - embryonic blood supply, 1221
    - myocardial, 981
    - of suprarenal medulla, 1200
    - venous, of spleen, 1194(f), 1195

sitting
- ergonomics, 745
- pelvic position, 1359

situs inversus, 974

skeleton
- facial, 409, 416, 417, 418
    - fracture, 479-81
- fascial, of lower limb, 1329-30, 1330(f)
- of larynx, 577-80, 577(f), 578(f)
- nasal, 547-8
- neonate, 215, 215(f)*see also specific bones*

skin, 145-64
- of abdominal wall
    - anterior, 1055-9
    - posterior, 1069-70, 1069(f)
- age-related changes, 162
- appendages, 145-77
- of arm *See* arm
- arteries *See* arteries (of organs, or regions), of skin
- of auricle of ear, 619
- of back *See* back, skin
- of breast, 930-1
- cells, 146-8
    - turnover time, 147
- changes in pregnancy, 149
- classification, 145
- colour, 145
- creases *See* creases, skin
- development, 157-8, 767
    - epithelial-mesenchymal interactions, 159
- dorsal, of hand, 857

embryonic, 157, 159
facial, 467-8
flaps *See* skin flap(s), formation
of foot *See* foot
of forearm *See* forearm
functions, 145
glabrous, 145, 146(f)
grafts, 164
hirsute, 145, 146(f)
innervation, 157, 159
of leg *See* leg
lines, 145, 160-2
lymphatics, 156-7, 159
of neck *See* neck, skin
neonatal growth, 159-60
nerves of *See* nerves (of organs, or regions)
over joints *see specific joints under* joints (named)
palmar, 778
    of hand, 857
of penis, 1271
pigmentation, 149
regeneration, 162
remodelling, 163
repair, 161-3
of scalp, 467
of scrotum, 1262
types, 145
vascular supply, 156-7, 159
venous drainage *See* veins or venae (of organs, or regions) *See also* epidermis

skin flap(s), 164, 468
anterolateral thigh perforator flaps, 1381
anteromedial thigh perforator flaps, 1381
deep inferior epigastric artery perforator flap (DIEP), 934
deltopectoral, 926
fasciocutaneous, 164
forehead, 468

- free, 164
- gluteal region perforator flaps, 1381
- hip and thigh perforator flaps, 1381
- lateral arm, 827
- musculocutaneous, 164
  - pectoralis major, 808
- nasolabial, 468
- parascapular, 817
- posterior interosseous artery, 853
- radial forearm fasciocutaneous, 852
- scalp, 467
- scapular, 817
- tensor fasciae latae perforator flaps, 1381
- transverse rectus abdominis musculocutaneous flap (TRAM), 934

skull, 397, 409-21

- age differences, 420
- at birth, 416, 417(f)
- base, height decreased, 770
- binding, 418, 419(f)
- bones of, 397, 409
  - ossification, 95, 97
- congenital anomalies, 418-19
- development, 390, 409, 610-14
- external appearance, 409-21
  - frontal (anterior view), 409-10
  - inferior (basal) view, 414-16
  - lateral view, 412-13
  - posterior view, 410-11
  - superior view, 411
- fracture, 409
- fronto-occipital diameter, 613
- geographic variation, 420
- identification from, 419-20
- internal surface, 423
- moulding, 416
- neonatal, 416-18, 611(f)
- ossification, 611

- paediatric, 416-18
- postnatal growth, 416-19, 613-14, 613(f)
- premature baby, 903
- sex differences, 419-20
- shape/size measurement, 419-21
- surface anatomy, 402-3
- surgical access, 481
- sutures *See* suture(s)
- type classification, 419-20
- vault *See* vault, of skull

skull cap *See* calvaria

sleep
- apnoea, 561
- breathing during, 1012
- REM
  - locus coeruleus, 284
  - neonates, 1015-16
  - reduced tonic intercostal activity, 1016-17

sling, mental, 487

slip (lateral or central), of hand, 881, 888

slit filtration, Bowman's capsule, 1234, 1235(f)

smegma, 1273

smoking, lung appearance, 992, 998

snoring, 561

sockets, teeth, 476, 477, 480

sodium ions
- resorption by renal tubules, 1238
- transport, renal medulla, 1238

somatopleure, 197, 1204, 1213

somatostatin (ST), 48, 1207

somatotopic maps, 386

somatotopic pattern, 329

somites, 365, 368(f), 763
  autonomic nervous system development and, 374
  boundary
    formation, 763
    occipitocervical junction, 769-70
  development, 201, 764-7, 764(f), 765(f)
    staging embryos from, 767
  digestive tube development, 1204(f)
  epithelial, 764
    intervertebral disc formation, 768
  epithelial plate, 764, 767
    cranial nerve development, 372-3
    dermomyotome formation, 772
    sclerotome formation, 767
  epithelial-mesenchyme transition, 195, 764 *See also* mesenchyme
  neural crest cell migration, 371
  number, control, 763
  occipitocervical junction, 769-70
  pre-otic, 702
  structures derived from, 772
  thoracic, 1013
  vertebrae development, 767, 767(f), 768, 768(f)

somitocoele *See* cells (named), somitocoeles

somitogenesis, 201, 764-7, 765(f), 766(f)
  compaction, 764, 764(f)
  stages, 764, 764(f)
    numbering, 767

somitomeres, 200(f), 201

sonic hedgehog, 1032

space(s)
  apical, at fingertip, 861
  around jaws, 524, 524(f)
    lower jaw, 524, 524(f)

  - upper jaw, 524, 524(f)
- Bowman's, 1234, 1235(f)
- buccal tissue, 469, 524
- canine (infraorbital), 525
- carotid, 439
- cavernous, of penis, 1274
- digital, 861
- of Disse, 1174
- epidural, 751-2, 751(f)
  - access to, 760-1
- extraperitoneal/subperitoneal tissues, 1099
- freeway, 513
- infracolic (left and right), 1108
- infraorbital, 469
- infratemporal, 524, 535
- intercostal, 918, 962, 963, 1030
- interseptovalvular, 1023
- intersphincteric, 1159
- intervillous, 176, 177, 178, 1303
- intrapharyngeal, 524, 568
- intraretinal, 699
- intratonsillar, 568
- lacunar, conceptus, 176, 177(f)
- mediastinal, CT and MRI, 955(f), 956(f), 957
- of Nuel, 640
- palatal, 524
- palmar, 861
  - deep, 861
- paraglottic, 584-5
- paralumenal, of larynx, 584-5
- parapharyngeal, 568
  - infection spread, 568
  - tumours, 568
- pararenal
  - anterior, 1069
  - posterior, 1069
- paratracheal, 957

parotid, 524, 524(f)
perianal, 1159
perihepatic, left, 1108
perilymphatic, 634, 652
perineal
    deep, 1094-5
    superficial, 1095-6
peripharyngeal, 568
perirenal, 1069
peritonsillar, 524
perivascular, 244
perivitelline, 167
pleural, 989
    fluid in, 991
of Poirier, 871
postanal, 1155
pre-epiglottic, 584
pretracheal, 439, 957
prevertebral, 439, 713
    infection, 568
Prussak’s, 630
pterygomandibular, 524
pulp, digital, 861
quadrangular, 813(f), 814, 823, 826
Reinke’s, 583
retrocardiac, 957
retrocrural, 957
of retroperitoneum, 1069
retropharyngeal, 439, 524, 568
    infection, 568
retropubic, 1245, 1365
retrovisceral, 439
subacromial, 807
subarachnoid, 749, 751(f), 752
    development, 389
subcarinal, 957
subdural, 752

  - subepicardial, 1026
  - subglottic, 585
  - subhepatic, right (hepatorenal recess), 1107
  - sublingual, 524
  - submammary, 930
  - submandibular, 524
  - submasseteric, 524
    - infections of, 538
  - submental, 524
  - subperitoneal, 1138, 1149
  - subphrenic
    - extraperitoneal, 1108
    - left, 1108
    - right, 1107
  - subpial, 244, 752
  - suprachoroidal, 676, 686
  - supraciliary, 676, 686
  - suprasternal, 435, 438, 454
  - tracheal, posterior, 957
  - triangular, 813(f), 814, 826
  - urinary (Bowman’s), 1234, 1235(f)
  - Virchow-Robin, 244
  - web, 861

spans, subaortic, 974

spasm, diffuse, oesophageal, 954

spasmodic torticollis, 460

spasticity, 230

spectrin, 15, 18, 67, 77

speech, 589-93
  - articulation, 592-3
  - consonant production, 593
  - harmonics, 592
  - muscular control, 590
  - oesophageal, 590

- phonation, 590-2
- pitch, 592
- production, 590
- vowel production, 593

spermatocele, 1267

spermatogenesis, 133, 1320-1
- age-related changes, 1267

spermatozoa, 167, 1266, 1266(f)
- capacitation, 167, 1276
- counts, 1319
- intracytoplasmic injection, 168
- maturation, 1269
- motility, 3, 1275

spermiogenesis, 1265, 1266(f)

sphenoid bone, 423, 424, 426, 431, 527, 527-30, 527(f), 528(f)
- at birth, 530
- body, 415, 424, 429, 527-9
- chondrogenic centres, 530
- conchae, 417, 472, 475, 528, 529-30
- in nasal cavity, 556, 558
- ossification, 530
- wings
  - greater, 424, 431, 527, 529, 599, 611
    - in orbit, 529
  - lesser, 423, 431, 529, 611
    - in orbit, 529

spherocytosis, 67

sphincter(s)
- anal
  - damage, 1160
    - during pregnancy, 1160
  - development, 1324
  - external, 1094, 1159
    - sex differences, 1159, 1159(f)

        - internal, 1156, 1156(f), 1157(f), 1158(f), 1159
    - bile duct, 1178
    - cardio-oesophageal, 953
        - failure of relaxation, 953
    - hepatopancreatic ampulla, 1178
    - of Oddi, 1178
    - oesophageal, 952, 953, 954(f)
        - control, 953
        - lower, 953, 954, 954(f), 1111, 1114
            - at birth, 1204
        - mechanisms, 953
        - pharyngeal, 953
        - upper, 572, 573
        - in vomiting, 953
    - palatopharyngeal, 563, 565(f), 571
    - pancreatic duct, 1178
    - precapillary, 142-3
    - pyloric, 1115
    - urethral, 1094-5, 1323
    - urethrovaginalis, 1095, 1095(f)

sphingomyelin, 4

spin (movement), 121, 122(f), 123, 123(f)

spina bifida, 364, 772
    - cystica, 772
    - occulta, 713, 772

spinal muscular atrophy, 1013

spindle
    - dentine, 514
    - enamel, 514
    - neuromuscular, 60-1, 60(f)

spine (or spina), 85
    - curvature *See* curvature, of spine
    - dendritic, 42
    - of helix, 619

- iliac
    - inferior
        - anterior, 1353(f), 1354, 1356
        - posterior, 1353(f), 1355
    - superior
        - anterior, 1340
        - posterior, 1340
- ischial, 1357, 1357(f)
- mental (genial tubercle), 503
- nasal, 409, 420, 471, 471(f), 472, 473(f), 475
    - anterior, 473(f), 476, 477(f)
    - posterior, median, 415, 478
- scapular, 746-7, 785, 795
- of sphenoid, 414(f), 415
- trochlear, 471
- vertebral, 405, 745-6, 746(f)
    - cervical, deformations, 770
    - fusion, 770
    - injury, breathing affected by, 1012
    - as landmarks for viscera, 747(t)
    - sacral, 724 *See also* column(s), vertebral; *See also* vertebra(e)
- vestibular, 1023

splanchnopleure, 1213, 1216, 1220
- postcleavage, 1216

spleen, 1191-5
- absence of (asplenia), 974
- accessory, 1191, 1218
- arteries, 1193
- circulation, 1195
    - closed, 1195
    - intermediate, 1195
    - open, 1195
- development, 1215(f), 1218
    - anomalies, 1218
- dimensions, 1191
- enlargement, 1192

  fibrous framework, 1193-4
  histiogenesis, 1218
  lymphatics, 1241
  microstructure, 1193-4, 1194(f)
  nerves, 1241
  peritoneal connection, 1191-2, 1192(f)
  polysplenia, 974
  referred pain, 1199
  relations, 1191
  surface anatomy, 1054
  trauma, 1192-3
  veins, 1193
  weight, 1218

splenium, 335, 355

splenomegaly, 1192

splenunculi, 1191

Splotch mutation, 371

spondylolisthesis, 713, 718

spondylolysis, 713, 718, 744

spongiosa, primary, 92

sprouts, mammary, 934

spur(s)
  of malleus, 627
  scleral, 675, 676, 677(f), 680

squama(s), 86

Stahl's bar, 618-19

stalk
  connecting, of embryo, 174, 180, 181, 181(f), 182, 185(f), 186, 1305(f), 1308(f), 1322
    development of, 181
  of epiglottis, 577
  optic, 699

  pineal, 324
  yolk, 181, 1209 *See also* peduncle(s)

standing, 1458-9
  centre of gravity, 1458
  pelvic position, 1358-9
  single leg stance, 1459

stapes, 599, 621(f), 627
  development, 652
  movements, 628
  ossification, 627
  otosclerosis, 628 *See also* ossicles, auditory

statoliths, 636

steatosis, 1163

stem(s)
  dural, development, 393
  infundibular, 321

Stener's lesion, 877

stenosis
  duodenal, 1209
  pulmonary, 1030
  spinal, 717
  subglottic, 579

stereocilia, 18, 637(f), 638, 643, 646, 648(f), 1268
  of cochlear hair cells, 640-1

sternebrae, 917, 918

sternum, 917-18, 917(f), 963
  arteries, 918
  innervation, 918
  joints, 917-18, 922
  manubrium, 917, 917(f), 918, 984, 986
  muscle attachments, 918
  ossification, 918, 918(f)
  structure, 917

  - surface anatomy, 909
  - veins, 918

stillbirth, 213

‘stimulus-bound’ behaviour, 332

stirrup *See* stapes

stomach, 1112-20
  - antrum, 1204
  - arteries, 1116-18, 1116(f), 1117(f)
  - at birth/neonate, 1206
  - body, 1112
  - capacity, 1112, 1114, 1206
  - curvatures, 1112
    - development, 1214
  - development, 1204, 1205(f), 1206
    - angular flexure, 1216
    - rotations, 1204, 1206
      - consequences, 1214
  - Dieu la Foy lesions, 1268
  - endoscopy, 1114, 1115(f)
  - filling, 1114
  - form, 1114
  - fundus, 1112
    - development, 1204
    - greater, 1112
  - glands, 1121-2, 1122(f)
  - innervation, 1120, 1120(f)
  - internal appearances, 1114-15, 1114(f), 1115(f)
  - lymphatic drainage, 1119-20, 1119(f)
  - microstructure, 1120-2
  - mucosa, 1113-14, 1115, 1116(f), 1120, 1121(f)
  - mucosa and submucosa, 1206
    - development, 1204
  - mucosal rosette, 1115
  - muscles, 1114(f)
  - muscularis

        - development, 1204, 1206
        - mucosae, 1122
    - orifices, 1113-14
    - parts of, 1112, 1112(f)
    - peritoneum of, 1099, 1112
    - pyloric antrum, 1112
    - pylorus, 1112
    - referred pain, 1120
    - relations, 1112-13, 1112(f), 1113(f)
    - rugae, 1115, 1120
    - serosa, 1122
    - serosa, development, 1206
    - submucosa, 1122
    - surface anatomy, 1053
    - surfaces, 1113, 1113(f)
    - veins, 1268-9
    - volvulus, 1113

stomodeum, 367
    - development, 367, 380

stratum (strata)
    - basale
        - of endometrium, 1299
        - of skin, 145, 147(f)
    - cinereum, 291
    - compactum, 1299
    - corneum, 145, 147(f), 148
        - of skin, 29, 145, 146(f), 147
    - deep, of fascia lata, 1349
    - functionalis, of endometrium, 1299
    - granulosum, 1319
        - of skin, 145, 147(f), 155
    - lacunosum, 351, 351(f), 352
    - lemnisci, 291
    - lucidum, 857
        - of skin, 145, 147(f)
    - moleculare, 351, 352

oriens, 351
pyramidalis, 350
radiatum, 351
spinosum, of skin, 145, 147(f)
spongiosum, 1302
superficial, of fascia lata, 1349
of tympanic membrane, 624
zonale, 311 *See also* layer(s); *See also* zone(s)

‘streak’ gonads, 1319

streak, primitive, 172, 180
epithelial-mesenchyme transition, 194
formation, 173, 183-4
ingression, 184, 197

stress fibres, 7

stria(e)
albae, 161
of Gennari, 346
gravidarum, 161, 1300
longitudinal, 386
medullaris, 239, 277(f), 279(f), 281(f), 323-4
Nitabuch’s, 177
of olfactory tract, 383
rubrae, 161
terminalis, 237, 238, 238(f), 239, 311, 320, 326
bed nucleus, 356
vascularis, of cochlear duct, 640

striation, cross, teeth, 514, 515(f)

striatopallidal system, ventral, projections from amygdala, 354

striatum, 325, 326-31, 326(f), 327(f)
afferents and terminals of, 328, 329
aminergic inputs, 331
amygdaloid projections to, 354
connections, 329, 329(f), 330(f)
development, 328, 383

  - dorsal, 326, 328-9
    - afferents to, 328
    - connections, 329, 329(f), 330(f)
    - efferents, 329
  - efferents, 329, 329(f), 331
  - neurones, 328
  - ventral, 326, 329, 354
    - afferents to, 329-30
    - connections, 329, 330(f)
    - continuity with dorsal striatum, 330
    - efferents, 331 *See also* nucleus (nuclei – nervous), accumbens; *See also* tubercle(s), olfactory *See also* nucleus, caudate; *See also* putamen

stridor, ventilatory, 949

striola
  - of saccule, 638
  - of utricle, 636, 637

strip
  - dorsal, of metacarpals, 865, 866
  - palmar, of metacarpals, 865, 866

stripe
  - Hensen's, 642
  - paratracheal, 954

stroke, 230, 253, 269

stroma
  - of bone marrow, 75
  - of breast, 931, 933
  - of choroid, 79-80
  - ciliary, 681, 682(f)
  - of cornea (substantia propria), 72, 678-9
  - of endometrium, 1291
  - of iris, 682
  - or iris, 701
  - of ovary, 1319

subcortex, connections, somatosensory cortex, 345

subglottis, 584
  infant, 584
  in speech, 590

subiculum, 351
  juxtallocortex, 349
  projections, 352
  projections to, 354

subluxation, vertebral ligaments, 730

submucosa, 39, 1050, 1051
  anal, 1159, 1160
  of appendix, 1143
  of hard palate, 502
  of large intestine, 1161
  of oesophagus, 952
  oral, 500
  of small intestine, 1135
  of stomach, 1122

subnucleus
  caudalis, 282, 282(f)
  interpolaris, 282
  oralis, 282
  rectus, 290, 291

substance P (SP), 48, 508
  globus pallidus, 331
  striatum, 328

substance, perforated
  anterior, 317(f), 356, 383, 391
  posterior, 288(f), 289(f), 316

substantia
  gelatinosa, 257, 259(f), 260, 266
  nigra, 42, 44(f), 290, 332
    development, 379, 380
    pars compacta, 330, 332

        - degeneration in Parkinson’s disease, 332
    - pars lateralis, 332
    - pars reticulata, 325, 332
        - efferents, 332
        - striatal efferents to, 328, 329, 331
- propria, 672, 678-9

subthalamus, 226, 230, 323
- development, 380

succussion splash, 1053

sucking, in neonate, 389
- difficulties, 389

suckling, 606-7

sulcus (sulci), 85
- antihelicis transversus, 619
- buccal, 539
- carotid, 527
- of cerebellum, 297, 298
- of cerebral hemispheres, 227, 335-8
    - anterior parolfactory, 335
    - calcarine, 335-6, 346, 696
        - development, 385
    - callosal, 335
    - central, 335, 344
        - development, 385
        - neonates, 388-9
    - cingulate, 335
    - collateral, 338
    - development, 385
    - fimbriodentate, 349, 351(f)
    - hippocampal, 349, 350(f)
    - inferior polar, 347
    - inferior temporal, 345, 347
    - insular, 346
    - intraparietal, 344
    - lateral occipital, 347

        medial frontal, 335
        neonatal, 388-9
        occipitotemporal, 336(f), 338
        olfactory, 337
        orbital, 337
        paracentral, 335
        parieto-occipital, 335, 344, 385
        postcentral, 344
            development, 385
        posterior parolfactory, 335
        precentral, development, 385
        rhinal, 336(f), 338
        superior temporal, 345
    chiasmatis, 424, 527
    collateral, 238
    coronary, 913
    cruciform, 288
    gingival, 500, 513
    hippocampal, 384, 385
    hypothalamic, 239, 312, 380
    infraorbital, 656
    interligamentous, 871
    intermedius, 1112
    intertuberculous, 797
    limitans, 240
        development, 361, 363, 372(f), 374
    linguogingival, 606
    malleolar, 617
    of medulla oblongata, posterolateral, 275
    nasolabial, 467
    optic, 699
    paramedian, of cerebellum, 298
    preauricular, 1356
    preauricular, of ilium, 1360, 1366
    precentral, 341
    preotic, 595(f), 596, 596(f)
    sagittal, 423

- superior, 713
- for sagittal sinus, 471
- sigmoid, 425, 615
- of spinal cord
  - median
    - anterior, 757
    - posterior, 749
    - ventral, 258(f), 268
  - posterolateral, 749
- spiral
  - external, 640
  - internal, 640
- superior temporal, 238
- terminalis, 326, 503, 605, 963
- transverse, 425
- tympanic, 617, 621, 624, 627
- ventrolateral, 275 *See also* groove(s)

summation
- spatial, 225
- temporal, 225

summit, of trapezium, 862

sunburn, 148

superficial musculo-aponeurotic system (SMAS), 397, 468

supination (movement), 852, 868, 872(f)
- muscles involved, 868

supraglottis, 582
- infant, 584
- in speech, 593

surface(s)
- articular
  - movement, 121-2, 121(f)
  - ovoid, 83, 101, 103(f)
  - shape of, 102, 121(f)
  - of synovial joints, 99-100, 100(f)

- basal, epihelium, 27
- of bladder, 1245
- buccal, 510(f)
- of humerus, 797-8, 798(f)
- of ilium, 1356
- labial, 510(f)
- lingual, 509
- of liver, 1163-5, 1163(f), 1164(f)
- respiratory *See* alveolus (alveoli)
- of scapula, 794, 794(f)
- of spleen, 1191-2, 1191(f)
- temporal, of frontal bone, 470, 471(f)
- volar, of nail, 155

surface anatomy *see* specific anatomical structures

surfactant, 1000
- composition, 1000
- development, 1000
- production, 1035
    - Clara cells, 1000, 1004
- storage, 1000, 1035

surgical procedures and approaches
- abdominoperineal excision, 1154
- access to peritoneal spaces, 1110
- adenoidectomy, 564
- ankle arthroscopy, 1347
- ankle aspiration, 1347
- ankle injection, 1347
- ankle surgery, 1443
- aortic, 1074, 1077
- of appendix, iliohypogastric nerve injury, 1080
- arthroscopy, 1347
- axillary abscess incision, 791
- axillary lymph node dissection, 932
- axillary lymph node sampling, 932
- balloon angioplasty, 981
- bleeding from superior epigastric vessels, 1056

breast conservation, 933
breast reconstruction, 933-4
caecostomy, 1054
caesarian section, 1299, 1300
Caldwell-Luc procedure, 404
cannulation
    bile duct, 1179
    femoral vein, 1344
    internal jugular vein, 453
    upper arm arteries, 787
cardiac, phrenic nerve injury, 1010-11
cauda equina, 1074
central venous catheterization, 1032
chest drain insertion, 937
choledochoduodenostomy, 1126
cisternal puncture, 760
colonic resection, vascular ligation, 1149
colostomy, 1054
commissurotomy, 358
cordotomy, dorsolateral, 264
coronary angiography, 981
coronary artery bypass graft, 981
craniofacial, 467
craniotomy, frontotemporal, 479, 481
cricothyroid puncture, 405
cricothyroidotomy, 405
deltoid-splitting, posterior, 821
dental implant, 532
distraction osteogenesis, 419
ear surgery
    endaural approach, 622
    inner ear, 649
    permeatal approach, 622
    postauricular approach, 622
    transmeatal approach, 622
    tympanotomy, 622*see also individual procedures* under surgical procedures and approaches

endoscopic cholangiography, 1179
epidural, 751-2
    caudal, 759-60, 760(f)
    lumbar, 760
epiglottopexy, 574
episiotomy, 1096
Epley's manoeuvre, 639
facelift, 469
facial nerve dissection, 494
flap formation *See* flap(s), formation
gallbladder drainage, 1179
gallbladder excision, 1178
gastrectomy, 1120
gastric lymphadenectomy, 1120
gastrostomy, 1116
hepatectomy, 1170
hip arthroscopy, 1347
hip aspiration, 1346
hip injection, 1346
ileostomy, 1054
incisions, 161
    abdominal, 1054
    ankle surgery, 1347
    for axillary abscess, 791
    diaphragm (radial), 1010
    hip surgery, 1347
    knee surgery, 1347
    subxiphoid, 960
    thoracotomy *see below*
intramuscular injection, lower limb, 1346
jejunostomy, 1129
joint aspiration, 1346-7
joint injection, 1346-7
knee arthroscopy, 1347
knee aspiration, 1346-7
knee injection, 1346-7
laryngectomy, 590

laryngotomy, 584
liver resection, 1166, 1169, 1170
liver transplant, 1170, 1172
lobectomy (lung), 1003
lumbar puncture
    adult, 747, 760
    neonate/infant, 760
lumbar sympathectomy, 1338
lymphadenectomy, colorectal cancer, 1141
mandibular distraction, 419
mandibular swing procedure, 481
mastectomy, 933
mediastinostomy, 941
medullary tractotomy, 281
mesorectal excision, 1154
mini-thoracotomy, 981
myectomy, ventricular septal, 969
myotomy, ventricular septal, 969
myringoplasty, 622
myringotomy, 626
neck dissections, 455
nephrectomy *See* nephrectomy
oesophageal thoracic duct injury, 943-4
ossuloplasty, 622
osteotomy
    mandibular ramus, 481
    midfacial, 418
    zygomatic, 481
pallidotomy, 253, 333
pancreatectomy, pylorus preserving, 1188
for pancreatic pseudocyst, 1188
pancreatic resection, 1183, 1188
for Parkinson’s disease, 333-4, 334(f)
parotid gland surgery, complications, 497
parotidectomy, superficial, 495
pedicled bone grafts, 842
pericardiocentesis, 937

pharyngostomy, 574
plane of dissection, ischioanal fossa, 1094
pneumoperitoneum, 1054
port access surgery, 981
pyramidotomy, 269
rectal excision, 1154
refractive surgery, 688
saphenous vein harvesting, 1344
sentinel lymph node biopsy, 932
skin flap formation *See* skin flap(s), formation
skin grafts, 163-4
sphincterotomy, 1178
    duodenal, 1126
    pre-cut, 1179
splenectomy, 1192-3
    pancreatic tail injury, 1185, 1193
splenic capsule injuries, 791
stapedectomy, 622, 628
stapedotomy, 628
sternotomy, 937, 981
suprapubic catheterization, 1054
suprarenal gland excision, 1200-1
suprarenal gland resection, 1200-1
thalamotomy, 333
thoracic sympathectomy, 945
thoracocentesis (pleural aspiration), 937
    needle, 937
thoracotomy, 937, 960
    anterolateral, 937
    axillary, 937
    ‘clam shell’, 937
    posterolateral, 937
thymectomy, 949
thyroidectomy, 463
tibial osteotomy, 1396
tracheostomy, 405
tracheotomy, 584

- transjugular intraparenchymal porto-systemic shunt (TIPS), 1172
- transverse colon, 791
- tympanic neurectomy, 629
- tympanotomy, 622
  - posterior, 649
- uvulopalatopharyngoplasty, 565-6
- vitreo-retinal, 681

sustentaculum
- hepatis, 1104
- tali, 1434, 1437
- surface anatomy, 1341

sutural bones, 411, 412, 416, 417, 418

suture(s), 97, 409, 410(f), 411
- coronal, 412, 418, 423, 469, 470(f), 610, 611
  - growth at, 613
  - premature closure, 613
- cranial, development, 390
- frontal, 479
- fronto-ethmoidal, 423, 656
- frontonasal, 409
- frontosphenoid, 424
- frontozygomatic, 403, 412, 417, 475, 480
- fusion of *See* synostosis
- incisive, 477
- intermaxillary, 409, 414
- intermaxillary palatal, 477
- internasal, 409, 418
- lambdoid, 411, 412, 416, 423, 469, 470(f), 493, 613
  - synostosis, 613
- of lens, 687, 687(f)
- median, of frontal bone, 472
- metopic, 409, 472, 613
- obliteration, 418
- occipitomastoid, 411, 412, 416, 425
- palatine, median, 409, 414
- palatomaxillary, 550

  - parietomastoid, 411, 412
  - petro-occipital, 415, 417
  - petromastoid, 415
  - petrosphenoidal, 415
  - petrosquamosal, 615, 617, 623
  - petrosquamous, 424
  - sagittal, 409, 410(f), 412, 423, 469, 470(f), 611, 613
    - synostosis, 613
  - schindylesis, 97, 98(f)
  - serrated, 409
  - simple (butt-end), 409
  - spheno-occipital, 415, 530
  - sphenoethmoidal, 424
  - sphenosquamosal, 181, 412, 529
  - sphenozygomatic, 412
  - squamomastoid, 615, 626
  - squamosal, 417
  - zygomaticomaxillary, 409, 412
  - zygomaticotemporal, 403, 412

swallowing, 283, 561-75
- in neonate, 389, 573(f), 574
  - difficulties, 389
- neural control, 574
- oesophageal phase, 573-4
- oral phase, 573
- pharyngeal phase, 573
- postnatal, 1206
- pulsion diverticulum, 572
- transit phase, 573

swan neck deformity, 878

sweat, 154

swelling(s)
- of aryepiglottic folds, 582
- arytenoid, 610
- labioscrotal (genital), 1323(f), 1324

  - mandibular (lingual), 604
  - popliteal, 1402

switch, calcium-sensitive, 111

symphalangism, 906

symphysis, 98, 98(f), 99
  - intervertebral *See* disc(s), intervertebral; *See also* disc(s), intervertebral
  - menti, 98, 486, 530, 532
  - pubic, 98, 1280, 1331, 1353(f), 1365
    - diastasis, 1301
    - movements, 1365
    - in pregnancy, 1300-1
    - relations, 1365

symphysis-fundus height, 1299

synapses, 41, 44-8, 225-6
  - activity mechanism, 46
  - axoaxonic, 45, 225, 226(f)
  - axodendritic, 45, 225
  - axosomatic, 41, 45, 46(f), 56, 225, 226(f)
  - chemical, 44-6
    - classification, 44-6
  - dendroaxonic, 45
  - dendrodendritic, 45
  - depolarization, 46
  - development, 47
  - electrical, 46
  - hyperpolarization, 44, 46, 57, 63, 64(f)
  - plasticity, 42, 47
  - ribbon, 45, 46(f)
  - somatodendritic, 45
  - somatosomatic, 45
  - symmetrical, 45
  - type I, 46
  - type II, 46

synapsis, 22

synaptic ribbon, 45, 46(f)

synaptogenesis, 370, 374, 386

synaptonemal complex, 22

synchondroses, 95, 98, 98(f), 99
- development, 611, 902
- neurocentral, 770
    - thoracic, 770
- postcranial, 98, 99
- posterior, thoracic, 770
- spheno-occipital, 409, 417, 420, 424, 527

syncytia, 772

syncytial knots, 179

syncytial sprouts, 179

syncytiotrophoblast, 173(f), 175, 176, 177(f), 178(f), 179

syncytium, 24, 179, 1303

syndecan, 1308

syndrome(s)
- acquired immune deficiency (AIDS), 71
- Alport, 33
- anterior interosseous, 854-5
- Apert’s, 418
- auriculotemporal, 497
- Axenfeld-Rieger, 702
- Brown-Séquard, 273(f)
- Budd-Chiari, 1172
- carpal tunnel, 897
- Carpenter’s, 418
- central alveolar hypoventilatory, 1011
- central cord, 759
- Chilaiditi, 1146, 1164
- compartment
    - of foot, 1431-2
    - of forearm, 840

    - of leg, 1428
    - of lower limb, 1330-1
- craniofrontonasal, 607
- Crouzon’s, 418, 419
- cubital tunnel, 837
- Cushing’s, 1201
- diarrhoea, 1212
- DiGeorge, 371, 609
- Down’s, 160, 906
- Edward’s, 1015
- Ehlers-Danlos, 985
- Frey’s, 436, 497, 629
- Frölich, 319
- frontal lobe, 358
- Goldenhaar, 418-19, 607
- Goodpasture, 33
- Guillain-Barré, 1011
- Horner’s, 461, 659, 671, 759, 790, 822
- hyperactive child, 332
- internuclear ophthalmoplegia, 663
- Jeune’s, 1014
- jugular foramen, 458
- Kartagener’s, 974
- Klippel-Feil, 608, 770
- Marfan’s, 194, 688, 918, 985, 1014
- Mirizzi, 1179
- multiple pterygium, 903
- nerve entrapment, of foot, 1458
- overwhelming post-splenectomy sepsis, 1193
- Parkinson’s, 47, 52, 53
- Patau’s, 1015
- Pfeiffer’s, 418
- Pierre Robin, 607, 607(f), 609
- piriformis, 1371, 1384
- Poland, 808
- Potter’s, 1013, 1035
- pronator, 836-7

- ‘prune belly’, 1061
- radial tunnel, 855
- Ramsay Hunt, 56
- rectus abdominis, 929
- rotator cuff impingement, 807
- Saethre-Chotzen, 418
- split-brain, 358
- tarsal tunnel, 1427, 1458
- temporomandibular joint dysfunction, 539
- thoracic outlet, 822
- Treacher-Collins, 419, 607
- Turner’s, 1319
- ulnar tunnel, 898
- VATER, 1037, 1213
- Waardenburg, 371
- Waardenburg type II, 374
- Wallenberg’s, 281
- Williams-Campbell, 1037
- Wiskott-Aldrich, 50
- Wolff-Parkinson-White, 977-8
- Zellweger, 13

synergists, 114

synostosis, 97, 98(f), 99, 409, 418
- coronal, 418
- premature, 418
- treatment, 418

syphilis, 985

syringobulbia, 281

systems
- auditory, 648(f)
  - central, 647-8
  - cortical connectivity, 341
  - peripheral, 646-7
- biliary, liver, development, 1205(f), 1207(s)
- body, development of, 212(f)

cardiovascular, 130-9
    development, 205
    organization, 130-4 *See also* arteries (general); *See also* heart; *See also* veins or venae (general) *See also* arteries (general); *See also* heart; *See also* veins or venae (general)
circulation, embryonic, 189
conducting, of heart *See* heart
cruciform, of sutures, 414
digestive (alimentary) *See* canal(s), alimentary; *See also* tract(s), gastrointestinal
endogenous analgesic, 266
excretory *See* systems, urinary
extrapyramidal (motor), 230
fasciocutaneous, 1330
Haversian *See* osteons
hepatobiliary, 1163-75, 1181
internal carotid, 247-8, 247(f)
lacrimal, 672-3, 672(f)
limbic, 335, 347, 350(f) *See also* lobe(s), limbic
lymphatic, 130-9, 139
mononuclear phagocyte, 35, 67, 78
musculoskeletal, 81-125
nervous (general), 41-65, 225-30
    cells of, 225
    development, 361-94
        lineage and growth, 369-70
        mechanisms, 367-71
        Schwann cells, 53
nervous (specific)
    autonomic, 41, 225, 232-6
        development, 373-4
        of thorax, 944-5
        of thymus, 946
        of tongue, 509
    central (CNS), 41, 225-7
        development, 361, 373-4, 375-93
        injury, 48

        enteric, 41, 225, 235, 374
            development, 374, 1213
        parasympathetic, 234-5, 373-4, 401-2, 402(f)
            abdominopelvic region, 1044-5
            lumbar, 1081
            to stomach, 1120, 1120(f)
            thoracic, 945
        peripheral (PNS), 41, 225, 230-2
            development, 361, 371-4
            microstructure, 53
            myelination in neonate, 389
        sympathetic, 234, 374, 402
            abdominopelvic region, 1042-4
            dental pulp fibres, 515
            lumbar, 1043-4, 1081
                vascular branches, 1043-4
            pelvic part, 1044, 1093
                vascular branches, 1044
            to stomach, 1120
            structures innervated, 234
            thoracic, 945
    olivocochlear, 645
    palmar shock absorption, 860
    portal venous, 1048-9, 1049(f), 1171
    pyramidal (corticospinal), 230
    reproductive
        ambisexual stage, 1315(f), 1318(f)
        ambisexual state, 1312-13
        anomalies, 1316, 1317(f)
        development, 1314-25, 1322(f)
        female, 1279-304
        male, 1261-76 *See also* gonads
    respiratory, 989-1006
        defence mechanisms, 989
        defensive mechanisms, 1005 *See also* tract(s), respiratory
    Rhesus antigen, 68
    urinary

anomalies, 1312 *See also* bladder, urinary; *See also* kidney
urogenital, male/female homologies, 1316(f)
ventricular, 237-42, 237(f)
vestibular, microstructure, 638-9
visual, cortical connectivity, 341 *See also* apparatus; *individual structures/regions*

systole, CSF movement, 243

T

T-box transcription factors, heart development, 1016, 1019, 1022, 1023(f)

T-tubules
- cardiac muscle, 140, 141, 142
- skeletal muscle, 107, 108, 110(f), 111, 115
  - development, 111, 115

‘tabula rasa’, 386

taenia
- coli, 1137, 1138, 1143(f), 1212
  - of rectum, 1151
- libera, 1138, 1138(f)
- mesocolica, 1138, 1138(f)
- omentalis, 1138, 1138(f)
- thalami, 311

tail
- axillary, 929
- of dentate gyri, 350
- embryo, folding, 187(f), 189
- of epididymis, 1262, 1264(f), 1265(f)
- of helix, 619
- of pancreas *See* pancreas
- of spermatozoa, 1266

talin, 15, 127, 128

talipes equinovarus, 1463

talus, 1434, 1436-7
- anomalies, 1464
- body, 1436
- fractures, 1336-7
- head, 1340, 1434
- innervation, 1436
- muscle attachments, 1436
- neck, 1434, 1436

  ossification, 1436
  surface anatomy, 1340
  vascular supply, 1435(f), 1436

Tamm-Horsfall protein, 1237

tandem repeat, 19

tanning, 149

tapetum, 355, 357

tarsal bones, 1433-4, 1433(f), 1434(f)
  coalitions, 1439
  ossification, 96, 1434(f)*see also individual named bones*

tarsal tunnel syndrome, 1427, 1458

tarsus *See* tarsal bones

taste
  discrimination, 508-9
  impulses/nerves, 503, 508, 509
  and nutritive sucking in neonate, 389
  types of sensation, 508

taste buds, 508-9, 582
  distribution and number, 508
  of fetal epiglottis, 508
  innervation, 508
  of larynx, 582
  of soft palate, 508, 565
  of tongue, 508
    microstructure, 508

Taussig-Bing anomaly, 1031

taxol, 22

Tay-Sachs disease, 13

tears, 672
  film, 671, 672, 673-4
  functions, 374

volume, 672

tectum, 291-2
  posterius, 611

teeth, 509-20, 509(f), 515(f), 516(f)
  abscess, 506(s), 524(f), 525
  additional/supernumerary, 513
  alignment and occlusion, 513
    centric, 500(f), 511
    disharmony, 513
    ideal, 513
  arteries, 518
  at birth, 512(f)
  auditory (dentes acoustici of cochlear duct), 640
  bicuspid, 509
  canines, 404, 510
    morphology, 510, 510(f)
    socket, 476, 477
  chronology, 512(f), 512(t)
  crown *See* crown, of teeth
  cusps *See* cusp(s)
  deciduous (primary), 217(f), 510-11, 510(f)
    eruption, 218(f), 218(t), 511
  development, 605-6
  enamel formation, 606
  eruption, 218(f), 511, 606, 608(t)
    wisdom teeth, 510
  extraction, 510, 517
  forensic anatomy, 516-17, 517(f)
  formation, 606
  incisors, 509
    maxillary, retroclined, 500
    morphology, 509, 510(f)
    peg-shaped, 509, 513
    protrusion, 500
    roots, 509
    socket, 477

infection, 439
innervation, 519, 519(t)
lymphatic drainage, 519
malocclusion, 217, 219
mineralization, 514
molariform, 510
    molars, 513
        deciduous, 217
        impaction, 510, 519, 530
        lower third, removal risk (‘removal’), 506, 510, 519
        mandibular, 510
        maxillary, 510
        morphology, 510, 510(f)
        roots, 510, 530
        socket, 477, 530
    premolars, 510
        development failure, 510
        morphology, 510, 510(f)
        roots, 510, 530
        socket, 477, 530
Mongoloid *vs* African, 513
morphology, 509-18
number, size and form variations, 513
orthopantomogram at birth, 512(f)
pain sensation, 519
    analgesia, 519-20
permanent (secondary), 509-10, 511(f), 606
    eruption, 511, 512(f), 512(t), 513
    forensic, 517
postcanine, 509, 511
protrusion, 500
sockets, 476, 477
surface anatomy, 509
surfaces, 509
terminology, 509
tissue arrangement, 513-16
    cementum, 515-16, 516(f)

        - dental pulp, 514-15 *See also* dentine; *See also* enamel
    - veins, 518
    - wisdom, 510
        - missing, 510
        - removal, 510 *See also* dentine; *See also* enamel

tegmen tympani, 424, 535, 615, 617, 623, 626
- development, 652

tegmentum
- mesencephalic, 289
    - development, 379, 380
- pontine, 284-5, 294

tela choroidea, 242, 311
- arterial branches, 390
- development, 377
- of third ventricle, 355, 380

tela subcutanea, 1095

telecanthus, traumatic, 479

telencephalon (endbrain), 226, 228(f), 602
- development, 362(f), 369, 380-2, 381(f), 382(f), 595
    - diencephalon wall fusion, 383

telencephalon impar, 380

telomerase, 19

telomere, 19

telophase
- cellular division, 22
- meiois, 23

temporal bone, 411, 412, 415, 527, 614, 615-18
- at birth, 618(f)
- external acoustic meatus, 617
- mandibular fossa, 615
- mastoid part, 424, 425, 615, 617
- ossification, 617-18

  petromastoid part, 615
  petrous part, 415, 424, 425, 426, 428, 429, 430, 529, 613, 617, 626
  squamous part, 529, 611, 615, 626
  tympanic part, 617
  zygomatic process, 615

tenascin, 36, 38, 1033

tendinitis, adductor, 1390

tendon(s), 86, 92(f), 105(f), 112-13, 113(f), 115, 117, 119, 119(t), 120, 124
  attachments, to bone, 113
  axis of, 113(f), 114
  calcaneal (Achilles), 113, 1451
    action, 1451
    relations, 1451
    surface anatomy, 1344
    vascular supply, 1451
  carpal extensor, 879-80
  carpal flexor, 879
  central, of diaphragm, 926, 1007
    phrenic nerve relations, 1010
  conjoint, 1064, 1065(f), 1066
  extensor digitorum, 880-1
    expansion, 881, 881(f), 883(f)
  flexor, of hand, 879
  growth, 112
  innervation, 113
  material properties of, 120
  ocular, common anular, 529
  patellar, 1340, 1394, 1395(f), 1396-7
  of rectus abdominis, 1061
  structure, 112
  of temporalis, 538, 542
  of Todaro, 964, 965(s), 977, 1019
  vasculature, 113

tentorium cerebelli, 288, 295(f), 297, 298, 335, 355, 397, 424, 426-7

territory

  - anatomical, 134-5
  - vascular, 134-5

test(s)
  - abductor pollicis longus, 851
  - adductor brevis, 1376
  - adductor muscles, 1375, 1376
  - Allen’s, 787, 905
  - biceps brachii, 826
  - brachialis, 826
  - brachioradialis, 849
  - coracobrachialis, 825
  - deltoid, 810
  - extensor carpi radialis brevis, 849
  - extensor carpi radialis longus, 849
  - extensor carpi ulnaris, 850
  - extensor digiti minimi, 850
  - extensor digitorum, 849
  - extensor indicis, 851
  - extensor pollicis, 851
  - extensor pollicis brevis, 851
  - femoral muscles, 1377-8
  - flexor carpi radialis, 846
  - flexor carpi ulnaris, 847
  - flexor digitorum profundus, 848
  - flexor digitorum superficialis, 847
  - flexor hallucis, 1454
  - flexor pollicis longus, 848
  - gluteus maximus, 1369
  - gluteus medius, 1370-1
  - gluteus minimus, 1370-1
  - gracilis, 1375
  - latissimus dorsi, 811
  - median nerve lesions, 884
  - obturator externus, 1372
  - palmaris longus, 847
  - piriformis, 1371
  - popliteal, 1408

- pronator quadratus, 848
- pronator teres, 845
- quadriceps muscles, 1374
- rhomboid muscles, 811
- sartorius, 1373
- spinal nerves, L5, 1418
- supinator, 852
- supraspinatus, 812
- tensor fasciae latae, 1368
- teres major, 813
- trapezius, 809
- triceps, 827
- ulnar nerve integrity, 885
- wrist tenodesis, 887

testing
- lower limb muscles, 1340(t), 1346
- pectoralis major, 808
- pudenal nerve, 1155

testis (testes), 206
- age-related changes, 1267
- appendix, 1263(f), 1264(f), 1267, 1268, 1315(f), 1316(t), 1317
- arteries, 1262-3, 1265(f)
- cancer, 1319
- cremaster action, 1064
- descent, 213, 1320-1, 1320(f), 1325
  - abnormal, 1319, 1321
- development, 1315(f), 1318(f), 1319, 1322(f)
  - disorders, 1319
  - ovary homologies, 1325
- interstitial tissue, 1267
- involution, 1267
- lymphatics, 1264
- malpositioning, 1321
- maturation at puberty, 1325, 1325(f)
- microstructure, 1264-7, 1265(f), 1266(f)
- neonate, 1325

  - nerves, 1264
  - rete, 1319
  - retraction from scrotum, 1060
  - sex determination, 1319
  - thermoregulation, 1064
  - torsion, 1268
  - undescended, 1267, 1323
  - veins, 1264, 1265(f)
  - volume, 1325

testis-determining factor, 1319

testosterone-binding protein, 1319

thalamotomy, 333

thalamus, 226, 228, 229(f), 230, 311-16
  - arterial supply, 253
  - connections *See* connections
  - development, 380, 381(f), 383, 388
    - superior surface, 388
  - growth, 380
  - input from cerebellum, 308
  - intralaminar, afferents to striatum, 329
  - nuclei/nuclear groups
    - anterior, 312
    - intralaminar, 312, 316
    - lateral, 313-15
    - medial, 312-13
      - injury, 312-13
    - mediodorsal, 331, 354
    - midline, 312, 316
    - non-specific, 312
    - reticular, 316
    - specific, 312
    - ventral posterior, 344
  - projections from fastigial nucleus, 308
  - relations, 311-12, 312(f)

thalassaemia, 68

theca, 749
    externa, 1296
    folliculi, 1296
    interna, 1295, 1296

thelarche, 935

theories
    of carpal bone movement, 872
        column, 872
        four-unit, 872
        ring, 872
        row/rigid body, 872
    of cerebral cortex development, 386
    gate-control, 266
    of neurogenesis (monophyletic), 369
    resegmentation, 768

thermoregulation
    of scrotum, 1262
    skin involvement, 151, 154, 157

thigh
    arteries, 1378-81, 1378(f)
    bones, 1360-5, 1360(f), 1361(f)
    compartments, 1330
    innervation, 1382-4, 1382(f), 1390
    lymphatics, 1336, 1382
    muscles, 1332, 1372-8, 1373(f)
    pain, 1383
    surface anatomy, 1340, 1342, 1342(f)
    veins, 1381-2

thinking
    analytical, 358
    Gestalt, 358

thoracoabdominal interface, 1041

thoracoscopy, 989

thorax

- arterial supply, 910, 911(f)
- at birth, 909
- cage, 1013
- cavity, 910
  - viscera, 913
- embryo, 1013, 1013(f)
- innervation, 911
  - autonomic, 911-12
- lymphatic drainage, 911
- neonatal, 1015-16
- nerves, 911-12
- surface anatomy, 909-14
  - musculotendinous, 909-10
  - skeletal, 909
  - visceral, 913, 913(f)
- surgical access, 937
- variations, 909, 911
- venous drainage, 911, 911(f)
- wall, 915-38, 984
  - arteries, 926-7
  - bones, 791-3, 909, 909(f), 917-22
  - compliance, 1015
  - congenital disorders, 1014
  - development, 1013-14, 1013(f)
  - fascia, 916-17
  - joints, 800-1, 922-4
  - lymphatics, 928
  - muscles, 924-6
  - nerves, 928-9
  - pleura and lung relationship, 990(f)
  - skin, 915-16
    - innervation, 916
    - nerves, 916
    - vascular supply, 915, 915(f)
  - veins, 927-8

thrombosis
- appendicular artery, 1145

  - cavernous sinus, 492
  - deep vein, 1426
  - jugular bulb, 458
  - superior mesenteric vein, 1187
  - venous, leg, 47

thrombospondin, 86, 87

thumb
  - bones, 866
  - joints, 875-6
  - movements, 864, 875-7, 888-9, 889(f)
  - muscles
    - opposition, 889
    - pinch grip, 889-90
    - retroposition, 888, 889
  - ossification, 866
  - phalanges of, 866
  - pulley system, 879, 881(f)

thymectomy, 949

thymoma, 948

thymus, 609, 609(f), 945-9, 946(f), 947(f)
  - accessory nodules, 946
  - agenesis, 949
  - anatomy and relations, 946
  - aplasia and hypoplasia, 949
  - arteries, 946
  - blood barrier, 947
  - children, 948, 948(f), 949
  - congenital anomalies, 949
  - cortex and medulla, 947-8, 948(f)
  - development, 609, 609(f), 948-9, 948(f)
  - ectopic, 946
  - functions, 946
  - innervation, 946
  - lobes, 946(f), 947, 948
  - lymphatic drainage, 946

- microstructure, 946-8, 947(f), 948(f)
    - epithelial, 947
    - microcirculation, 947-8
    - non-lymphocytic cells, 947
- neonatal, 947(f), 948
- rudiments, 948
- size, 948
- tumours, 948
- veins, 946
- weight, 948

thyroid transcription factor, 1032

tibia, 1412-15, 1413(f), 1414(f)
- condyles, 1412
- distal, 1432
- growth, 95
- innervation, 1415
- muscle attachments, 1412
- ossification, 96, 1415
- racial differences, 1414
- sex differences, 1414
- shaft, 1412-13
- surface anatomy, 1340
- torsion, 1414
- trauma, 1411-12
- vascular supply, 1415

tip links, 640, 641

tissue, 27-49
- adipose, 34, 35(f), 38, 39
    - perirenal, 1226, 1228(f)
    - in thymus, 948
- areolar
    - of diaphragm, 1008-9
    - of heart, 974
- border, of Jacoby, 694
- buccolabial, 467

cartilage *See* cartilage (general)
chromaffin, 1081
classification, 27
connective, 34-9
    abnormalities, 985
    anterior abdominal wall, 1060, 1099
    areolar, 38
    cells, 35-6
    classification, 38-9
    extraperitoneal, 1070, 1099
    general, 34-5
    irregular, 38
        dense, 38
    loose, 38
    matrix, 37-8
    muscular, 108
    posterior abdominal wall, 1070, 1099
    regular, 38
    subendothelial, 131, 132, 137
    subperitoneal, 1099
dental, 513-16 *See also* teeth
ectodermal *See* ectoderm
endodermal *See* endoderm
endothelium *See* endothelium
epidermis *See* epidermis
epineurium, 53
epithelium *See* epithelium
extraperitoneal, 1060
formation, homophilic binding, 5
granulation, 34, 163
haematopoietic, 74-5, 75(f)
hypodermis, 146(f), 150-1
interactions *See* tissue interactions
lymphoid, 72-4
    development, 209
    thymus, 945-9, 946(f), 947(f) *See also* gut-associated lymphoid tissue (GALT); *See also* lymph nodes (general); *See also*

            mucosa-associated lymphoid tissue (MALT)
    mucoid, 38-9
    mucosa *See* mucosa
    muscle *See* muscles (general)
    neuroectoderm *See* neuroectoderm
    parenchyma, liver, 1172
    reticular, 34
    scar, dermal, 163
    soft *See* fascia; *specific anatomical structures*
    subcutaneous fibroadipose, 397, 468
    submucosa *See* submucosa
    subsynovial, 101
    tubulo-acinar, 1280
    urothelium *See* urothelium *See also* cells (named)

tissue interactions, 193-4
    competence, 193
    epithelium/mesenchymal *See* mesenchyme
    induction, 193
    instructive, 193
    permissive, 193
    restriction, 193

titin, 106, 115, 124

toes
    great *See* hallux
    movements, 1339(t)
    muscles, 1339(t)

tongue, 505-11, 604-5
    apex, 505, 506
    arteries, 505
    dorsum (posterosuperior surface), 503, 503(f), 507-9
    inferior (ventral) surface, 503
    innervation, 506-7
        autonomic, 509
        sensory, 506-7
    lymphatic drainage, 505-6, 506(f)

  - movements, in swallowing, 573
  - mucosa, 503
  - muscles, 503-5, 504(f)
    - extrinsic, 503
    - intrinsic, 503-5
  - oral (presulcal) part, 503
  - papillae, 503(f), 507, 508(f)
  - pharyngeal (postsulcal) part, 503
  - respiration obstruction, prevention, 503
  - root, 503
  - shape, 505
  - in speech, 593
  - surface anatomy
    - dorsum (posterosuperior surface), 503, 503(f), 506-7
    - inferior (ventral surface), 503, 503(f)
  - taste buds *See* taste buds
  - veins, 505

tonsil, 605
  - abscess (quinsy), 405
  - adenoid *See* adenoid (nasopharyngeal tonsil)
  - of cerebellum, 298, 303
  - lingual, 503, 505
  - nasopharyngeal *See* adenoid
  - palatine, 405, 501(f), 503(f), 566-7, 566(f)
    - age-related changes, 566
    - arteries, 567
    - crypts, 566, 567
    - development, 602, 605
    - lymphatics/lymphoid tissue, 567
    - microstructure, 567
    - nerves, 567
    - pits, 566
    - referred pain, 567
    - removal, 567
    - veins, 567
  - pharyngeal
    - development, 209, 604

        tubal, 564, 567 *See also* adenoid (nasopharyngeal tonsil) *See also* adenoid (nasopharyngeal tonsil)
    tubal, development, 209, 604

tonsillitis, 567

tooth *See* teeth

torques, 117-18, 118(f)

torsion
    testicular, 1268
    tibial, 1414

torticollis, spasmodic, 460

torus
    aorticus, 964
    mandibularis, 525, 530
    maxillary, 477, 525
    palatine, 477, 525

touch, failure of recognition by, 358

Tpt, planum temporale, asymmetry, 358

trabecula(e)
    of bone, 85, 85(f), 86, 90, 90(f), 92, 94, 95, 113(f)
    carneae, 966, 969, 971(f), 976(f)
    epithelial, liver development, 1207
    hepatic, 1207, 1208(f)
    of penis, 1274
    septomarginal, 966, 967, 977
    septoparietal, 966
    splenic, 1193, 1194(f), 1195, 1195(f)

trabecular meshwork, 675, 677(f)

trabeculations, ventricular, 1020

trachea, 996(f), 1000-5, 1002(f)
    arteries, 1003
    bifurcation, 983, 1000
    bronchogram, 1002(f)

- cartilage, 405, 406, 996(f), 1005, 1033
    - complete rings, 1037
    - incomplete rings, 1005
- cervical part, 405, 465-6, 1001
    - arteries, 466
    - lymphatics, 466
    - nerves, 466
    - relations, 465-6, 1001
    - veins, 466
- children, 1000, 1005(f)
- congenital malformations, 1036-7, 1037(f)
- connective tissue, 1004
- development, 610, 1032, 1033
- glands of, 1035
- innervation, 1003-4
- length and diameter, 465, 1000
- lymphatic drainage, 1003
- muscle, 1004
- relations, 465-6, 1001
- surface anatomy, 406, 909, 912, 914
- thoracic part, 1001
- veins, 1003

tracheomalacia, 1036-7

tract(s)
- gastrointestinal
    - arterial supply, 1047-8
    - development, 1203-23
    - microstructure, 1049-52, 1050(f) *See also* tube(s), digestive/gut
- genital *See* system(s), reproductive
- hair, of back, 707(f)
- iliotibial, 1340, 1342, 1349-50
- inflow, of heart, 1018-20
    - development, 1018-20
- olfactory, development, 383, 384
- optic
    - arterial supply, 253

        - development, 382
    - outflow, of heart, 1020-1
        - development, 1020-1
        - positioning, 1025-6
        - septation, 1025-6
    - portal, 1173, 1175
    - respiratory, 996(f), 1032-7
        - arteries, 996-7, 997(f)
        - defensive mechanisms, 989, 1005
        - development, 1032-3, 1033(f)
        - elastin *See* elastin
        - lymphatic drainage, 998
        - microstructure, 998-1000, 999(f)
        - nerves, 998, 1010-11
        - veins, 997-8 *See also* systems, respiratory
    - urinary
        - development, 1305-14, 1305(f), 1306(f)
        - obstruction, 1312
    - urogenital, development, 1305-25
    - uveal, 675, 679-85, 682(f)

tract(s) (tractus) (nerve)
- bulbospinal (medial reticulospinal), 293
- central tegmental, 281(f), 283, 285, 289(f), 290, 294, 305, 308
- corticobulbar, 229, 230(f), 280, 287
- corticospinal (pyramidal), 229-30, 230(f), 268-9, 343, 357
    - development, 385, 389
    - lateral, 266(f), 268, 268(f), 269(f), 280
    - lesions, 290
    - ventral, 262(f), 268, 280
- cuneocerebellar, 264, 264(f), 279, 280, 295, 304, 305
- dead, dentine, 514
- dorsolateral (of Lissauer), 257, 259, 262(f), 265(f), 271, 375
- habenulo-interpeduncular (fasciculus retroflexus), 293, 323, 329
- hypothalomohypophysial, 321
- interstitiospinal, 270, 306
- of Lissauer, 257, 259, 262(f), 265(f), 271, 375
- mammillotegmental, 320

mammillothalamic, 312, 320
nerve fibres, spinal cord, 257
olivocerebellar, 283, 298, 300, 302, 303, 305
optic, 275, 276(f)
pontospinal, 293
propriospinal, 271
pyramidal *See* tract(s), corticospinal
reticulocerebellar, 298, 306
reticulospinal, 230
    lateral, 293
    medullary, 293, 308
rubrospinal, 269, 279, 283, 290, 294, 306, 308
solitariospinal, 270
solitarius, 276(f), 279, 282, 283, 546, 574
    development, 373, 376, 377
spinal, 262-71
    ascending, 262-8
    descending, 268-71
spino-olivary, 267-8
spinocerebellar, 262(f), 263-4, 298, 304-5
    anterior, 304, 305
    dorsal (posterior), 260, 262, 263, 264(f), 268, 278, 279(f), 281(f)
    fibres, 304, 305
    posterior, 298, 304
    ventral (anterior), 262(f), 263, 264, 278(f), 281(f)
spinocervical, 267
spinomesencephalic, 267
spinotectal, 267, 279, 291
spinothalamic, 228, 229, 264-5
    lateral, 262, 264, 279, 281(f), 283, 285
    neurone, 264-5
    ventral, 262(f), 264
spiral, 634
spiralis foraminosus, 634
tectobulbar, 292
tectospinal, 258, 262(f), 269, 292, 306
trigeminocerebellar, 304-5

- trigeminothalamic, 228, 275, 287(f)
  - lesions, 230
- urinary, obstruction, 1312
- vestibulospinal, 269-70, 286
  - lateral, 269, 306, 308
  - medial, 269-70 *See also* fasciculus (fasciculi); *See also* fibre(s)

traction response, 389

tragus, 403, 618, 619, 620, 653

transcription factors
- Emx2 and Lhx2, 387
- neural tube development, 371
- Shh, 1207

transdifferentiation, 39

transferrin, 9

transforming growth factor beta, 8, 1033

transforming oncogene, 8

translation (movement), 102

transmitter, neurochemical *See* neurotransmitters

transplantation
- chimeric embryo, 195
- liver, 1170, 1172

transtentorial coning, 427

transverse nuchae, 289

transversus menti, 487

trapezium, 862, 863(f)
- attachment site, 862, 863(f)
- ossification, 864
- surface anatomy, 786

trapezoid, 863, 863(f)
- ossification, 864

trauma
- aorta, 985
- childbirth, 1096
- diaphragmatic, 1009
- foot, 1431-2
- laryngeal, 584
- leg, 1411-12
- mouth (floor of), 521
- splenic, 1192
- tibial, 1411-12
- vertebrae, 744 *See also* injury *under specific anatomical structures*

tree
- biliary *See* biliary tree
- respiratory *See* tract(s), respiratory

tremor, 309
- intention, 309

Trendelenburg's sign, 1342

triad
- muscle, 107(f), 108, 110(f)
- near, of eye, 681
- portal, 1173, 1173(f), 1174, 1174(f)
  - development, 1208

triangle(s)
- anal, 1093-4
- Calot's, 1179
  - contents, 1179
- carotid, 437
- cervical (neck), 406, 406(f), 436-8
  - anterior, 405, 437
    - carotid, 437
    - digastric, 437
    - muscular, 437
    - submental, 437
  - posterior, 406, 436-7
    - occipital, 436-7

supraclavicular, 438
deltopectoral, 785, 789
digastric, 520
female, 1094
femoral, 1080, 1351(f), 1373
surface anatomy, 1342
hypoglossal, 240
inguinal, 1066
Killian’s, 572
of Koch, 964, 965(f), 966, 977
Laimer’s, 572
lumbar, 747, 811, 1072
male, 1094
submandibular, 406
submental, 406
suboccipital, relations, 742
suprameatal (Macewen’s), 403, 412, 615, 618, 626
urogenital, 1093, 1094-5
female, 1093, 1094
male, 1093, 1094
vagal, 240 *See also* trigone (trigonum)

triangular fibrocartilage (TFC), 871, 872

trichiasis, 669

trigeminal neuralgia, 281

trigger finger, 879

trigone (trigonum)
of aortic valve, 972, 974
of bladder, 1247-8
collateral, 237
habenulae, 380
of mitral valve, 970
olfactory, 383 *See also* triangle(s)

trigonocephaly, 418

trigonometry, 106

trimesters, 213

triquetral bone, 862, 863(f)
    ossification, 864

trismus, 538, 539, 543

trochanter, 85, 85(f)
    greater, 1340, 1361, 1361(f)
    lesser, 1361
    ossification, 1365
    third, 1362

trochlea, 86, 657, 660, 799
    humeral, 799
        in elbow joint, 831

trophectoderm *See* trophoblast

trophoblast (trophectoderm), 172, 179
    mural, 173, 175
    polar, 172, 175
    syncytial, 175

tropomyosin, 106, 111

troponin, 106, 111

truncus, 1020

truncus arteriosus, 600
    formation, 1020(f), 1022(f), 1025

trunk (arterial)
    anterior, branches, 1087-9
    brachiocephalic, 984, 986
    coeliac (coeliac axis), 207, 1048, 1073, 1116, 1117(f), 1220
    coeliacomesenteric, 1047
    costocervical, 450-1, 984
    gastrocolic, 1145
    leinohepaticomesenteric, 1047
    phrenic, 1010-16
    posterior, branches, 1087

- pulmonary, 960, 962, 963, 964, 983
- thyrocervical, 449

trunk (lymphatic)

- abdominal, 1077-8, 1077(f)
- abdominal confluence, 1077
- bronchomediastinal, 455(f), 928
  - left, 455, 941, 941(f)
  - right, 455, 941, 941(f)
  - variations, 455
- cardiac, 982
- cisterna chyli, 209, 940, 941(f), 942, 1077
- intercostal, upper, 943
- intestinal, 1077
- jugular, 928
  - left, 455, 943
  - right, 455
  - variations, 455
- lumbar, 1077
- mediastinal, 943
- right, 941(f), 944
  - anomalies, 944
- subclavian, 818
  - left, 455, 943
  - right, 455
  - variations, 455
- thoracic
  - bilateral ascending, 943
  - bilateral descending, 943 *See also* duct(s), thoracic

trunk (nerve)

- callosal, 355
- cervicofacial, 494
- lumbosacral, 1078, 1091-2
- sympathetic, 234
  - cervical, 433, 460-1
  - lumbar, 944, 1043-4, 1081
  - pelvic part, 1044, 1093

thoracic, 911, 944-5, 944(f), 945
of teeth, 519
temporofacial, 494
vagal, 944(f), 945

trunk (of body), 746(f)
anterior flexion, 1061
paralysis, 1012

tube(s)
auditory *See* tube(s), pharyngotympanic
digestive/gut
embryo, 1203, 1203(f), 1204(f), 1205(f)
veins, 1219(f), 1220 *See also* canal(s), alimentary; *See also* foregut; *See also* hindgut; *See also* midgut
endocardial, 1016
epithelial, myocardial, 1026
Eustachian *See* tube(s), pharyngotympanic
Fallopian *See* tube(s), uterine; *See also* canal(s), facial
heart, 142, 1018, 1020
chambers, 1018
formation and twisting, 1018
looping, 1018, 1019(f)
primitive, 142
neural, 41, 187, 187(f), 189, 361, 768
cells in heart development, 1016
cellular arrangement, 362-3
closure, 362
development, 364(f)
failure to close, 772
flexures, 362
histogenesis, 368-9
segmentation, 371
vesicles, 362
pericardial, 959
pharyngotympanic, 529, 544, 564, 604, 617
arteries, 564
at birth, 564

        - blockage, 626
        - bony part, 564
        - cartilaginous part, 564
        - development, 652
        - neonate, 618
        - opening, 564
        - relations, 564
        - swallowing, 564
        - veins, 564
    - uterine, 1285, 1291(f), 1292-4, 1293(f)
        - arteries, 1293
        - development, 175, 1316(f)
        - fertilization *See* fertilization
        - imaging, 1293(f)
        - innervation, 1293-4
        - intramural part, 1293
        - lymphatics, 1293
        - menstrual cycle, 1294
        - microstructure, 1293-4
        - relations, 1293
        - veins, 1293

tuber
    - auricular, 618(f)
    - of cerebellum, 298, 303, 306
    - cinereum, 48, 239, 316, 318, 321, 367, 380
        - development, 380
    - frontal, 409
    - parietal, 412, 469 *See also* tuberosity

tubercle(s) (tuberculum(a)), 85, 96, 97
    - adductor, 1360(f), 1361(f), 1363
    - articular, of temporal bone, 615
    - of calcaneus, 1341
    - of Carabelli, 510, 513
    - carotid, of Chassaignac, 406, 444, 719
    - Chassaignac's, 406, 444, 719
    - conoid, 792

cuneate, 240, 277(f)
Darwin’s, 618
deltoid
    of clavicle, 792
    of humerus, 797
    of scapula, 795
of epiglottis, 577
fibular (peroneal), 1341
genial, 530
    genioglossi attachment, 503
genital
    development, 1324
    inappropriate siting, 1312, 1314(f)
    male *vs* female, 1316(t)
Gerdy’s, 1340, 1412, 1413(f)
gracile, 240, 277
of humerus
    greater, 797
    lesser, 796-7
infraglenoid, 795
intercondylar, 1397, 1398
ischial, surface anatomy, 1340
jugular, 424
Lister’s, 786, 841, 851
marginal, 475
mental, 402, 487, 530
Müllerian sinus, 1313, 1322(f)
obturator, 1352, 1353(f)
olfactory, 329, 331, 356
    development, 383
orbital, 656
pharyngeal, 414(f), 415
postglenoid, 533, 615, 617
pterygoid, 529
pubic, 1053, 1067, 1355
quadrate, 1361(f), 1362
of rib, 919

        - first, 921
    - scalene, 921
    - sellae, 424, 527, 530
    - sinus, 1316, 1317
    - sinuvaginal, 1316(f)
    - subcutaneous, of breast, 930
    - supraglenoid, 794
    - teeth, incisors, 509, 510(f)
    - thalamic, anterior, 312
    - tibial, 1340
    - ulnar, 844
    - vertebral
        - cervical, 718
        - twelfth thoracic, 723
    - Whitnall’s, 404, 475

tuberculum impar, 604

tuberosity, 85
    - frontal, 404, 470, 491
    - gluteal, 1362, 1364
    - of humerus
        - greater, 814(f)
        - lesser, 802(f)
    - iliac, 1356
    - ischial, 1357
        - surface anatomy, 1357
    - maxillary, 476, 477(f), 478, 539
    - metacarpal
        - fifth, 866
        - second, 865
    - metatarsal, fifth, 1341
    - of navicular bone, 1341
    - omental, 1184
    - radial, 839(f), 840
    - tibial, 1412, 1415
    - ulnar, 844 *See also* tuber

tubule(s)

- collecting *See* duct(s), collecting
- dentine, 514
- of epoophoron, 1307
- mesonephric (nephrons), 1307
- mucous, salivary glands, 522, 523(f)
- nephric, 1305, 1306(f)
- renal, 1235, 1236(f), 1237, 1237(f)
    - antigens, 1309
    - distal convoluted, 1232, 1235(f), 1236(f), 1237
    - functions, 1237-8
    - proximal convoluted, 1234, 1235, 1236(f), 1237, 1238
- seminiferous, 1265, 1266, 1266(f)
    - development, 1317
- uriniferous *See* tubule(s), renal

tubuli recti, 1268

tubulins, 10, 14, 16, 17(f)

tuft, dendritic, 339

tumescence, 1274

tumour necrosis factor (TNF-α), 8, 71, 78, 1135

tumours
- cerebral, 49
- glomus, 894
- laryngeal, 585, 588
- maxillary sinus, 559
- Pancoast, 822
- parathyroid gland, 464
- parotid, 496
- parotid gland, 496
- pharyngeal, 568
- retroperitoneal, 1383
- tympanic body, 452 *See also* cancer

tunica
- adventitia, 131, 139
    - arterial, 131, 132(f)

        - lymphatic, 139
        - venous, 131, 132(f)
    - albuginea
        - of ovary, 1295
        - of penis, 1271, 1272, 1272(f), 1273, 1274(f)
        - of testes, 1262, 1318(f), 1319
    - intima, 131, 132(f), 139
        - arterial, 131, 132(f)
        - lymphatic, 139
        - venous, 131, 132(f)
    - media, 130, 131, 132(f), 139, 205, 602, 1222
        - arterial, 131, 132(f), 139
        - juxtaglomerular apparatus, 1238
        - lymphatic, 139
        - venous, 131, 132(f)
    - vaginalis
        - of epididymis, 1262
        - of testes, 1218, 1262, 1321, 1325
    - vasculosa, 1262

tunnel
- carpal, 861, 895
    - surface anatomy, 785
- of Corti, 635(f), 640

turbinate *See* concha(e), nasal

turricephaly, 418

twins, 172, 173(f), 1302(f)
- conjoined, 173(f)
- dizygotic, 172, 173(f)
- monozygotic, 172, 173(f)
- placenta, 172, 173(f), 1303, 1303(f)

TWIST, 612

typhlitis, 1146

U

ubiquitin, 20

ubiquitin ligases, 20

ulcers, peptic, 1126

ulna, 840(f), 841(f), 843-4
  development, 905
  muscle attachments, 840(f), 841(f), 844
  ossification, 844, 845(f)
  proximal end, 843-4
  shaft, 840(f), 841(f), 844
  surface anatomy, 786
  vascular supply, 844, 852

ultrafiltration, 1236(f)

ultrasound
  endometrium, 1298, *1298*
  pleural effusion, 991
  transoesophageal, 952-3
  urinary system abnormalities, 1312

umbilicus, 1062(f), 1063
  discolouration around, Cullen’s sign, 1100, 1188
  eversion, 1300
  fetus, 1062
  neonatal, 213
  surface anatomy, 1052-3

umbo, 623, 624

uncus, 338, 383

unit
  burst-forming, 77
  colony-forming, 75, 77
  columnar proliferative, 147
  lamellar, 131
  motor, 111, 112(t)

- osteomeatal, 559
- pilosebaceous, 151-4, 152(f)
  - development, 158-9
- ‘radial unit’, model, 386
- secretory, submandibular glands, 523(f)

urachus, 1247
- closure, 1312
- formation, 1209
- remnants, 1062, 1312

urate oxidase, 13

ureter, 1238-42
- arteries, 1241
- calculi, 1242
- development, 1310, 1316(f)
- duplex, 1240
- ectopic, 1240
- female, 1239(f), 1240
- fusiform enlargements, 1310
- lymphatics, 1241
- male, 1239(f), 1240, 1240(f)
- microstructure, 1242, 1242(f)
- neonates, 1312, 1313(f)
- nerves, 1241
- orifice, 1226, 1240, 1245(f), 1248
- origin, 1238, 1239
- peristalsis, 1241, 1242
- in pregnancy, 1300
- referred pain, 1242
- relations, 1238-40, 1239(f), 1240(f)
  - abdominal, 1238-9
  - pelvic, 1239-40
- retrocaval, 1240-1
- smooth muscle, 1240
- surface anatomy, 1054
- ureterocoele, 1240
- veins, 1241

ureterocoele, 1240

urethra, 1250-4, 1251(f)
- arteries, 1252, 1253
- compressor, 1095, 1095(f)
- defects, 1323
- development, 1308(f), 1323
- female, 1095, 1253, 1280, 1323
  - microstructure, 1253
- glands, 1251, 1252, 1253
- lacunae, 1251(f), 1252, 1253
- lymphatics, 1252, 1253
- male, 1095, 1250-3, 1251(f), 1323
  - anomalies, congenital, 1252
  - anterior (spongiose) part, 1251-2
  - bulbar, 1250
  - duplication, 1252
  - injury, 1252
  - membranous part, 1095, 1251
  - microstructure, 1253
  - penile, 1251(f), 1252
  - posterior, 1250-1
  - preprostatic part, 1250
  - prostatic part, 1250-1, 1252(f), 1254, 1312, 1323
  - vascular supply, 1252
- in micturition, 1253
- nerves, 1098, 1253
- postglandular, 1325
- sphincter, 1323
- sphincter mechanism, 1094-5
- veins, 1252, 1253

urinary bladder *See* bladder, urinary

urine
- concentration, 1238
- extravasation, 1252
- production, 1237-8
  - mesonephros, 1307

- sampling, neonate, 1312

urography, intravenous, 1230(f), 1231

urothelium, 27, 30-1, 1242
- of bladder, 1250, 1253(f)
- female/male, 30
- of urethra, 1250, 1253

uterus, 1285-92, 1285(f), 1291(f)
- anomalies, 1316, 1317, 1317(s)
- anteflexed/anteverted, 1285, 1316
- arteries, 1284(f), 1289, 1290(f)
- at birth, 1313(f), 1317
- atresia, 1317(f)
- bicornis (bicornuate), 1285, 1317(f)
- bilocular, 1317(f)
- body, 1285, 1291
- development, 1313, 1316
- didelphine (didelphyd), 1285, 1317(f)
- hysteroscopy, 1287(f)
- innervation, 1290-1
- laparoscopic view, 1287(f)
- lymphatics, 1290
- magnetic resonance imaging, 1292, 1292(f)
- microstructure, 1291-2, 1291(f)
- neonate, 1313(f), 1317
- pain, 236
- peritoneum, 1285
- positions, 1285, 1316, 1322(f)
- in pregnancy, 1299-300, 1300(f)
- relations, 1285
- septate, 1285
- veins, 1289-90

utricle
- of ear, 633, 636-7, 637(f)
  - development, 652
  - microstructure, 638-9

  head movements, 636-7
  prostatic, 1251, 1317

uvula, 501(f)
  of cerebellum, 298, 300(f), 305, 307
  cleft, 607
  of soft palate, 564, 604
  of urinary bladder, 1249(f)

V

VACTERL association, 1014

vacuole, lipid, 14

vagina, 1281, 1284
  anomalies, 1317, 1317(f)
  arteries, 1284, 1284(f)
  bacteria, 1284
  in childbirth, 1284
  development, 1316-17
  double, 1317(f)
  epithelium, 1281, 1316
  fornices, 1281, 1283(f), 1313(f), 1316
  innervation, 1284
  lymphatics, 1284
  ‘masculina’, 1251
  microstructure, 1284
  muscular layers, 1284
  neonates, 1316
  peritoneum, 1284
  relations, 1281
  septate, 1285
  veins, 1284, 1284(f)
  vestibule, 1316

vallecula
  of cerebellum, 379
  of epiglottis, 577

Valsalva’s manoeuvre, 407, 1118

valve(s)
  anal, 1155, 1156, 1212
  aortic, 962, 968(f), 972-3, 1031
    cusps of, 972
    development, 1027
    opening of, 973

    - orifice of, 971(f)
    - stenosis, 975
- atrioventricular, development, 962, 966, 1026-7, 1027(f)
- bicuspid *See* valve(s), mitral
- Eustachian *See* valve(s), of inferior vena cava
- of external jugular veins, 451
- of Hoboken, 182
- ileocaecal, 1142, 1142(f)
- of inferior vena cava, 964, 965(s), 1019
    - fetus, 964
- lymphatic, 139, 139(f)
- mitral, 960, 962, 970-2
    - atresia, 1030
    - chordae tendineae, 972
    - ‘cleft’, 1030
    - cusps of, 970-2
    - development, 1027
    - opening of, 972
    - orifice of, 913, 970
    - stenosis, 975
- nasal, 549, 555
- pulmonary, 962, 964, 967, 968(f), 1026(f)
    - cusps of, 967
    - development, 1027
    - opening of, 967
    - stenosis, 975
- semilunar, 981
- of short saphenous vein, 1409
- sinuatrial, 1019
- testicular, 1264
- Thebesian, 964, 1019
- thoracic duct, 942
- tricuspid, 960, 962, 964, 965(f), 966-7, 967(f), 1031
    - atresia, 1030
    - chordae tendineae, 966-7
    - cusps of, 966
    - development, 1027

        - opening of, 967
        - orifices of, 913, 966
    - venous, of embryonic heart, 964

varices
- gastric, 1118-19, 1171(t)
- oesophageal, 950-1, 1118-19, 1171(t)
- rectal, 1171(t)

varicoceles, 1264

vas (vasa)
- aberrantia
    - brachial artery, 827
    - hepatic, 1060
- brevia, of colon, 1140
- deferens, 1268-9, 1269(f), 1317
    - absence, 1269
    - ampulla, 1314(f), 1317
    - arteries, 1269
    - lymphatics, 1269
    - microstructure, 1269
- longa, of colon, 1140
- nervorum, 53
- recta, 1140, 1232, 1233, 1236(f), 1237(f)
- vasorum, 138, 980, 982

vascular cell adhesion-1 molecule (VCAM-1), 137

vasculogenesis, 203, 600, 1026
- angiotrophic *See* angiogenesis

vaso previa, 1303

vasoactive intestinal polypeptide (VIP), 48, 317
- hippocampal formation, 352

vasopressin (ADH), 1238

VATER syndrome, 1037, 1213

vault, of skull, 409, 412, 416, 423
- development, 390, 611-13, 612(f)

growth, 390
    postnatal, 416-17

VCAM, 6

veins or venae (general), 130-1, 134, 134(f)
  blood pressure changes, 134
  blood supply, 137
  collateral, after renal vein ligation, 1233
  development, in limbs, 903
  embryonic, venous complexes, 1222
  heat exchange, 131
  innervation, 138
  satellite, 131
  structure, 134, 137
  valves, 134, 134(f)
  varicose, 1426

veins or venae (named)
  advehentes, 1221, 1221(f)
  alveolar (dental), 541
  anastomotic, of brain
    inferior (of Labbe), 255, 392
    superior (of Trolard), 255, 392
  angular, 451, 492
  appendicular, 1145
  arch *See* arch(es)
  arcuate, of kidney, 1233
  atrial, oblique, 986
  auricular, 620
    posterior, 492
  axillary, 778, 781(f), 817-18
  azygos, 484-5, 911, 928, 950, 964, 985, 986, 987, 991, 993, 1075, 1118
    development, 1027, 1219(f)
    lines of, 207, 208
    lumbar, 1075
    variations, 915, 940
  basal, 255
    common, 998

  - development, 393
  - inferior, surface anatomy, 1054
- basilic, 778, 779, 781(f), 853
  - development, 905
- basivertebral, 715
- brachial, 828, 853
- brachiocephalic, 400, 959, 986, 987
  - development, 1027, 1220(f)
  - left, 984, 987
  - right, 985, 987
  - surface anatomy, 914
- bronchial, 991, 1035
- buccal, 492, 541
- cardiac, 981-2, 982(f)
  - anastomoses, 982
  - anterior, 964, 981, 982
  - great, 964, 980, 981
  - middle, 981
  - small, 981, 982
  - variations, 981
- cardinal, 206, 207-8
  - common, 610, 959, 982, 1014, 1019
  - development, 1027, 1220(f)
  - further development, 208
- cardinal, common, 959
- cava
  - inferior, 959, 962, 963, 964, 986, 1075-7, 1075(f), 1076(f), 1219-20, 1219(f)
    - anomalies, 1075
    - collateral channels, 987
    - course, 1075
    - CT, 1075(f)
    - development, 1219
    - diaphragmatic aperture, 1008
    - double, 1075, 1076(f)
    - filters, 1076
    - obstruction, 1076

        - opening of, 964
        - relations (abdominal), 1075
        - tributaries, 1075-6
        - valve of, 964, 965(f)
        - visceral transposition, 1075
    - left, 982
    - superior, 962, 964, 980, 985, 986
        - congenital defects, 1030
        - development, 1028, 1219(f), 1222(f)
        - left, persistent, 1032
        - obstruction, 986
        - opening of, 964
        - relations, 986
        - right, persistent, 1032
        - surface anatomy, 914
        - tributaries, 986
        - variations, 986
- central, of retina, 666
- cephalic, 610, 778, 779, 781(f), 787, 828, 853
    - accessory, 853
    - development, 905
    - in hand, 894
    - surface anatomy, 789
- cerebellar
    - inferior, 255
    - superior, 255
- cerebral
    - anterior, 255
    - development, 392
    - external (superficial), 255
    - great, 255, 256, 256(f)
    - inferior, 255, 256(f)
    - internal, 255
    - middle, 392
        - deep/superficial, 255
    - posterior, 255
    - superior, 255

cervical, deep, 453
choroidal, 242, 255(f), 256
ciliary, 681
circumhepatic, 1028, 1219(f), 1220(f), 1221(f)
cochlear, 642
colic
    left, 1150
        ligation, 1149
    middle, 1145, 1147
    right, 1145
comitans nervi hypoglossi, 451
comitantes, 131
    of forearm, 853
    of upper limb, 778, 780, 781(f)
conjunctival, 672
coronary, development, 1026
cubital, median, 778, 781(f), 828, 853
    surface anatomy, 789
    venepuncture, 789
cystic, 1049, 1180
digital
    dorsal, of hand, 894
    palmar, 894
diploic, 431-2
    anterior, 541
dorsal
    of hand, 894
    lingual, 451
    metacarpal, 895, 895(f)
    of penis, 1273
embryonic, left and right, 1220
emissary, 392, 423, 425, 432-3, 492
    of bone, 91
    condylar, 432
    mastoid, 432
    occipital, 432
    parietal, 432

- sigmoid, 425
epigastric
  - inferior, 1056, 1059, 1090
    - ‘caput medusae’, 1059
  - superior, 1056

episcleral, 686
facial, 451, 492, 538, 666
  - anterior, 393
  - tributaries, 451, 492

femoral, 1350, 1351(f), 1352(f), 1378, 1381-2
  - cannulation, 1344
  - common, 1041
  - surface anatomy, 1344

fibular, 1426
gastric
  - left, 950, 1049, 1118, 1268
  - posterior, 1118, 1268
  - right, 1118, 1268
  - short, 1268

gastroepiploic
  - left, 1268
  - right, 1268

gluteal, inferior/superior, 1041, 1090
gonadal, 1075
  - left, 1233

great, abnormal connections, 1031-2
great cerebral, 255, 256, 256(f)
head, primary, 610
hemiazygos, 208, 911, 927, 928, 940, 951, 985, 987, 1075, 1118
  - accessory, 927, 928, 940

hepatic, 1048, 1171-2, 1172(f), 1174
  - afferent, 1221
  - common, 1171, 1220
  - development, 1028, 1208, 1221
  - left, 1172
  - middle, 1171
  - right, 1171

  - tributaries, 1172
- hepatocardiac, 1221
  - umbilical, 1221
  - vitelline
    - left, 1221
    - right, 1221
- hypophysial, 323
- ileocolic, 1145, 1146
- iliac
  - circumflex, deep, 1090
  - common, 987, 1089, 1090(f)
    - left, 1089, 1219
    - right, 1089
  - external, 1041, 1090
    - disease, 1090
  - internal, 1041, 1089-90, 1284
- infraorbital, 492, 666
- intercapitular, 894
- intercostal, 951
  - anterior, 928
  - development, 1028
  - posterior, 928, 940, 987
  - superior, 987
    - left, 927-8, 959, 984
    - right, 928
- interlobular, of kidney, 1233
- intersegmental, 1219, 1220
- intervertebral, 715
- intralobular, of liver, 1174
- intramedullary, 757
- intraparenchymal, 392
- jugular
  - anterior, 407, 451
  - external, 407, 451, 610
    - posterior, 451
    - tributaries, 451
  - internal, 400, 407, 451, 452, 610

        - cannulation, 453, 978
        - development, 392, 393
    - tributaries, 451
- labyrinthine, 642
- laryngeal, 588, 610
- lingual, 451, 505
    - deep, 451, 503, 505
    - dorsal, 451, 505
- linguofacial, 610
- lobar, middle, 997
- of lower limb, 1334-5, 1335(f)
- lumbar, 208, 715, 1075
    - anastomoses, 1075
    - ascending, 987, 1075
- mammary (thoracic, internal), 927
- marginal, 903
    - right, 964, 982
- masseteric, 541
- maxillary, 541, 541(f)
    - primitive, 392
- median, 853
    - anterior, 757
    - deep, 778, 779
    - surface anatomy, 789
- median medullary
    - anterior, 255
    - posterior, 255, 757
- medullary, of suprarenal gland, 1198
- meningeal, 431
    - middle, 431, 541
- mental, 492
- mesenteric
    - inferior, 1141, 1141(f), 1150, 1150(f)
        - ligation, 1149
        - surgical identification, 1184-5
    - superior, 1130, 1130(f), 1132(f), 1150, 1209
        - thrombosis, 1187

            tributaries, 1130
- metacarpal
  - dorsal, 895, 895(f)
  - palmar, 895
- metatarsal, plantar, 1334
- of nasal cavity, 553
- oblique
  - development, 1028
  - of forearm, 853
  - of left atrium, 964, 981-2, 982(f)
- obturator, 1041, 1089
- occipital, 490(f), 492
- oesophageal, 951, 1118
- ophthalmic, 433, 656, 671
  - inferior, 429, 541, 656, 666
  - superior, 429, 666
- ovarian, 208, 1293, 1295
- palatine
  - external, 563, 620, 620(f)
  - greater, 541
- palmar, metacarpal, 895
- pancreaticoduodenal
  - inferior, 1128
  - superior, 1128
- of paranasal sinuses, 557, 558
- paratonsillar *See* veins or venae (named), palatine; *See also* veins or venae (named), palatine, external
- pericardial, 987
- peroneal *See* veins or venae (named), fibular
- pharyngeal, 452
  - ventral, 610
- phrenic, 1010
  - inferior, 1076
  - left, 984
- pineal, 324
- pontine, 255
- popliteal, 1409

portal, 131, 1048-9, 1170-1
    abnormalities, 1208
    development, 1028
    fetus, 1048, 1208
    lack of valves, 1048
    tributaries, 1049, 1170
    variations, 1170
postaxial, of embryonic limb, 903, 905
postcardinal, 1219, 1219(f)
    development, 1028
    right, persistence, 1220
posterior, of left ventricle, 981, 982(f)
preaxial, of embryonic limb, 903, 905, 906(f), 1463
precardinal, 392, 610, 1220(f)
    development, 1027
profunda femoris, 1381
pterygoid, 541
pubic, 1090
pudendal
    external, 1280, 1282(f)
    internal, 1089, 1098
pulmonary, 962, 991, 997-8, 997(f), 1032
    development, 1020, 1035
    inferior left/right, 997
    right, 964, 968
    superior left/right, 997
radial, 853, 895
radicular, 254, 757, 759(f)
rectal
    middle, 1090, 1155
    superior, 1150, 1155, 1160
renal, 208, 1076, 1233, 1233(f), 1293, 1295
    left, 1233
    retroaortic left, 1233
    right, 1233
retinal, central, 696
retinociliary, 694

retromandibular, 428, 492, 494, 496, 496(f), 496(s), 541
sacral
    lateral, 1089-90
    median, 1089
saphenous
    coronary artery bypass graft, 981
    long (great), 1280, 1282(f), 1335(f), 1381, 1409
        surface anatomy, 1344
    long (great) tributaries, 1381-2
    short, 1409
        surface anatomy, 1344
        tributaries, 1409
sigmoid, emissary, 425
sinuses, dural *See* sinus(es), dural venous
sphenopalatine, 541, 553
spinal, 255
splenic, 1150, 1193
    pancreatic tributaries, 1186, 1193
stellate, of kidney, 1233
striate, 255
stylomastoid, 492
subarcuate, 629
subcardinal, 207, 1219, 1220, 1221
    development, 1219
    persistence (left), 1075
subcentral, 207
subclavian, 407, 452, 818
    cannulation, 978
    development, 1027
subcortical, 392
subependymal, 392
sublingual, 451, 505
subtunical, 1274
supracardinal, 207
    further development, 208
    left, 1219
    right, 1219

supraorbital, 491-2, 666
    primitive, 393
suprarenal, 1076
    accessory, 1198
    left, 1198, 1233
    right, 1198
supratrochlear, 491
temporal
    deep, 541
    middle, 491, 492
testicular, 208, 1264
    varicoceles, 1264
thalamostriate, 237, 255(f), 256, 311
Thebesian, 981, 982
thoracic, internal (mammary), 927, 987
thymic, 946, 987
thyroid
    inferior, 452(f), 453(f), 456(f), 462, 985, 987
    middle, 452, 462
    superficial, 490(f), 496(f)
    superior, 452, 462
tibial
    anterior, 1334, 1426
    posterior, 1334, 1426
tracheobronchial, 610
transcortical, of sternum, 918
ulnar, 853
umbilical, 182, 206, 207, 1019, 1028, 1028(f), 1049, 1221
    catheterization, 1222
    changes during development, 1209, 1221, 1222
    development, 1220(f), 1221
    fetal/neonatal, 1222
    left, 1170
        remnants, 1062
    retrogression, 1221-2
umbilicalis impar, 207
uterine, 1300

- vaginal, 1284
- vertebral, 452
  - accessory, 448, 452
  - anterior, 453
  - left, 987
  - tributaries, 453
- vitelline, 206, 207, 1220
  - anastomoses of, 1220
  - ascending, 1220
  - atrophy, 1221
  - changes during development, 1221-2, 1221(f), 1222(f)
  - development, 1220(f)
  - hepatocardiac, 1219, 1220
  - left, 1220
  - liver development, 1207
  - right, 1220
- vitello-umbilical, changes during development, 1221-2, 1221(f), 1222(f)
- vortex, of eyeball, 666, 682(f)

veins or venae (of organs, or regions), 1280
- of abdomen, 1047, 1048(f)
- of abdominal wall
  - anterior, 1055-9
  - posterior, 1075-7, 1076(f)
- of adenoid, 563
- of anal canal, 1160
- of appendix, 1145
- of arm, 828
- of auricle, of ear, 620
- of back, cutaneous, 708
- of bile duct, 1180
- of bladder, 1247(f), 1249
- of bone, 91
- of brain, 254-6, 255(f)
- of breast, 932
  - cutaneous, 932
- of bronchi, 1003
- of caecum, 1145

of cerebral cortex, 392
of choroid plexus, 242
of colon
    ascending, 1145
    descending, 1150
    sigmoid, 1150
    transverse, 1146-7
of conjunctiva, 672
of diaphragm, 1010
of duodenum, 1128
of ear
    external, 620
    inner, 642
    middle, 629
of elbow, 836
of embryo, 207-8, 208(f)
of external acoustic meatus, 621
of eyelids, 671
of face, 491-2
of female perineum, 1283(f)
of foot, 1457
    cutaneous, 1429
of forearm, 853
of gallbladder, 1180
of gluteal region, cutaneous, 1349
of hand, 858(f), 894-5
of head, 541, 541(f)
    development, 378(f), 392-3
of heart, 981-2, 982(f)
of hepatic ducts, 1180
of hip and thigh, 1381-2
of ileum, 1130
of intestine, large, 1141, 1141(f), 1145, 1150
of iris, 685
of jejunum, 1130
of kidney, 1233
of knee joint, 1409

    - cutaneous, 1393
- of lacrimal gland, 673
- of larynx, 588
- of leg, 1090, 1426
    - cutaneous, 1411
- of liver, 1170-2, 1174
- of lower limb, 1334-5, 1335(f)
- of lungs, 997-8, 1035
- of neck, 451-3
    - cutaneous, 435
- of neonate, 1032
- of nose, external, 549
- of oesophagus, 950, 951(f), 1111
    - cervical, 465
- of orbit, 666, 666(f)
- of ovary, 1295
- of palatine tonsil, 567
- of pancreas, 1186, 1187(f)
- of paranasal sinuses, 557, 558
- of parotid gland, 497
- of pelvis, 1047, 1048(f), 1089-90, 1090(f)
- of penis, 1273
- of pericardium, 959
- of perineum, 1098
- of pharyngotympanic tube, 564
- of pharynx, 561
- of pineal gland, 324
- of pleura, 991
- of prostate, 1257
- of rectum, 1155
- of retina, 693, 693(f)
- of ribs, 921
- of scrotum, 1262
- of seminal vesicles, 1270
- of skeletal muscle, 110
- of skin, 156-7
    - of back, 708

        - of breast, 932
        - of foot, 1429
        - of gluteal region, 1349
        - of knee, 1393
        - of leg, 1411
        - of neck, 435
    - of soft palate, 565
    - of spinal cord, 757, 759(f)
    - of spleen, 1193
    - of sternum, 918
    - of stomach, 1268-9
    - of suprarenal gland, 1198, 1198(f), 1199(f)
    - of teeth, 518
    - of temporomandibular joint, 535-6
    - of testis, 1264, 1265(f)
    - of thoracic wall, 927-8
    - of thorax, 911
    - of thymus, 946
    - of thyroid gland, 453(f), 456(f), 462
    - of tongue, 505
    - of trachea, cervical part, 466
    - of tympanic cavity, 629
    - of upper limb, 778, 781(f), 817-18
    - of ureter, 1241
    - of urethra
        - female, 1253
        - male, 1252
    - of uterine tube, 1293
    - of uterus, 1289-91
    - of uveal tract, 682(f)
    - of vagina, 1284
    - of vertebral column, 714-15, 715(f)

velocity curves, 220(f)

velum, medullary
- anterior, 298
- development, 362

- inferior, 240
- superior, 240, 281(f), 284, 288, 298

venepuncture, elbow, 789

venogram, renal, 1233(f)

ventilation *See* breathing

ventilation/perfusion mismatch, pulmonary embolism, 997

ventricle(s)
- of brain, 227
  - arterial supply, 253
  - development, 383
  - enlargement, 244
  - fourth, 227, 240, 240(f), 297, 298
    - development, 377
    - medulloblastoma in roof, 309
    - roof, 377
  - lateral, 227, 228(f), 237-9, 237(f), 238(f), 335
  - third, 227, 239
    - development, 380, 381(f)
- of heart, 965(f), 968(f), 971(f)
  - development, 1018, 1020
  - double inlet, 1030
  - double outlet, 1031
  - left, 962, 963, 968-70
    - at birth, 1030
  - right, 960, 962, 964, 966
    - at birth, 1030
    - external features, 964
    - internal features, 96, 964, 969
    - relations, 968 *See also* bulbus cordis
  - septal defects, 974-5, 1030, 1031
  - septation, 1024-5, *1025*
- of larynx, 582, 583
- terminal, of spinal cord, 257 *See also* bulbus cordis

venules, 131, 133

  - cerebral, 139
  - high endothelial (HEV), 72, 73(f), 133, 136, 136(f)
  - muscular, 133
  - postcapillary, 131, 133

verge, anal, 1155, 1156(f), 1158

vergence (movement of eye), 661

vermis, of cerebellum, 298, 426
  - anticipatory function, 308-9
  - efferent connections, 306(f)
  - inferior, 298
  - midline, 226, 298
  - posterior, 664

vernix caseosa, 157, 213

verrucae hippocampae, 351

version (movement of eye), 661

vertebra(e), 716-24
  - arterial supply, 91
  - blastemal centrum, 766(f), 767, 767(f)
  - block, 719, 1014
  - body *See* body (bodies), vertebral
  - cancer, 744
  - cervical, 397, 718-21
    - C1 *See* atlas (C1 vertebra)
    - C2 *See* axis (C2 vertebra)
    - C3-C7
      - anomalies, 770
      - development, 770
    - C7 *See* vertebra(e), prominens
    - first *See* atlas (C1 vertebra)
    - second *See* axis (C2 vertebra)
    - development, 770
    - fusion (inappropriate), 770
    - muscle attachments, 719
    - ossification, 719, 770

    typical, 718-19
    union of arches, 768
coccygeal, 728 *See also* coccyx
cuneiform, 768
development, 763, 768-72
    abnormal in spina bifida, 772
    blastemal stage, 768
    cartilaginous stage, 768
    ossification stage, 768
    somites, 767, 768
embryonic derivation, 769, 769(f)
infection, 744
inflammatory disease, 744
load-bearing capacity, 744
lumbar, 723-4, 724(f)
    age-related changes, 714
    development, 771
    embryonic derivation, 769, 769(f)
    fascial attachments, 723-4
    fifth, 724
    muscle attachments, 723-4
    ossification, 724, 771
    union of arches, 768
lumbosacral, malformations, 772
movements, 744
ossification, 771
    centres, 768, 769(f)
    cervical, 719, 770
    lumbar, 724, 771
processes *See* process (or processus)
prominens (C7 vertebra), 397, 721, 745, 746(f)
    muscle attachments, 721
    ossification, 721
    spine of, 405
sacral *See* sacrum
second *See* axis (C2 vertebral)
segmental nature, 768

- sexual dimorphism, 717
- size, 716
- structure, 716, 716(f)
- surface anatomy, 912, 914
- thoracic, 716(f), 721-3
  - first, 722, 722(f)
  - ninth, 722, 722(f)
  - tenth, 722, 722(f)
  - eleventh, 714-15, 722(f)
  - development, 770-1
  - embryonic derivation, 769, 769(f)
  - muscle attachments, 722
  - ossification, 722
- trauma, 744
- typical, 715-18, 716(f) *See also* column(s), vertebral; *See also* spine (or spina), vertebral

vertigo, 639, 649

verumontanum, 1251

vesicle(s), 3(f), 4
- auditory *See* otocyst
- cerebral, 362, 362(f)
- lens, 699
- metanephric, 1309(f)
- optic, 699, 700(f), 702
  - development, 380 *See also* otocyst
- pinocytotic, 128, 136, 137, 139, 676, 1237
  - of pleural mesothelial cells, 991
- seminal, 1270, 1317
  - innervation, 1270
  - lymphatics, 1270
  - microstructure, 1270
  - secretion, 1270
  - vascular supply, 1270
- synaptic, 44, 45, 46, 47, 48, 62, 62(f)
- umbilical, primary, 173
- zymogen, 28

vessels
  blood
    capacitance, 131
    cerebral, 138-9
    choke, 109, 135
    exchange, 131
    innervation, 138
    microstructure, 135-7
    resistance, 1312
    structures, 131, 132(f)
    vitelline, 182 *See also* arteries (named), arterioles; *See also* capillary (capillaries); *See also* veins or venae (named); *See also* venules
  choke, 109, 135
  development, 203
  fetal, 179, 181, 182
  great
    anomalies, 1030, 1031-2, *1032*
    transposition, 1030, 1031*see also individual vessels*
  lymphatic, 131, 139, 139(f)
    development, 203
    of small intestine (lacteals), 139, 1130-1, 1134(f), 1135

vestibule
  of labyrinth, of ear, 633-4, 633(f)
  of lesser sac, 1108
  membranous, 652
  nasal, 551
    hairs (vibrissae), 551
  oral, 499 *See also* cavity (cavities), buccal
  of vagina, 1279(f), 1280
    development, 1316

vestibulocerebellum, 303, 305, 308, 664
  connections, 308
  mossy fibre projections, 305
  Purkinje cell connections, 307

vestiges, notochordal, 768

vibrissae, 551

villi
  arachnoid, 243-4, 244(f)
  chorion frondosum, 177(f), 180
  duodenal, 1131
  jejunal, 1131
  large intestine, development, 1212
  placental, 176, 178-9
    specialization of, 176
    terminal, 176
    transport across, 180
  small intestine, 1133, 1133(f)
    development, 1210
    structure, 1135
  synovial, 100

villin, 15, 18

vimentin, 15, 127, 137, 1034, 1051

vincula tendinum, of fingers, 879, 881(f)
  brevis, 879
  longa, 879

vinculin, 7, 14(f), 15

viscera, vertebral levels, 746, 747(t)

viscerocranium, 409, 610
  membrane bones, 613 *See also* arch(es), pharyngeal

viscoelasticity, 119-20

vision
  colour, V4 visual area, 347
  direction selectivity, 347
  orientation selectivity, 347
  spatial, pathways, 345

visual field, 314
  defects, 697

visual hemifield, 347

visual neglect, 358

visual processing, 347

visuospatial discrimination, 347, 358

vital capacity, 1012

vitamin A
- deficiency, 30, 95
- excess, 95

vitamin C, deficiency, 34, 95, 533

vitamin D, 8
- deficiency 958, 533

Volkmann’s ischaemic contracture, 840

volvulus
- caecum, 1142
- congenital, 1209
- gastric, 1113
- sigmoid, 1148

vomer, 415, 420, 472(f), 475, 527, 613
- in nasal cavity, 549, 550, 611
- ossification, 475

vomiting, 242
- mechanism, 953

von Ebner’s fissure(s), 763(f), 765(f), 767

von Ebner’s line, 514

von Ebner’s serous glands, 508, 508(f), 522

von Willebrand factor, 135, 136, 137

vulva, 1279-81, 1279(f)
- age-related changes, 1279
- arteries, 1280
- innervation, 1280, 1280(t), 1282(f)

lymphatics, 1280, 1282(f)
veins, 1280

W

wad, mobile, 840

waist, of scaphoid, 862

walking, 1459
  centre of gravity, 1459
  development, 1459, 1461(f)
  energy use, 1459
  heel strike, 1459
  pendulum principle, 1459
  stance phase, 1459
  support phases, 1459
  swing phase, 1459
  toe-off, 1459 *See also* gait

wall
  abdominal *See* abdominal wall
  chest *See* thorax, wall
  gut, microstructure, 1049-52, 1050(f)
  somatopleuric, 1013, 1014, 1017(f)

Wartenberg's disease, 855-6

weight charts, 216(f)

Wharton's jelly, 38

white matter *See* matter, white

'Wilson's pencils', 328

window
  aortic, 984
  aortopulmonary, 957
  oval, 602, 624, 625(f), 633, 634, 649
  round, 624, 625(f), 634, 646

wing(s)
  presacral, of hypogastric sheath, 1151
  of sphenoid

greater, 424, 431, 527, 529, 599, 611
lesser, 423, 431, 529, 611

winged scapula, 786, 812, 820

wings
of sphenoid
greater, 424, 431
lesser, 423, 431

witch’s milk, 934

wormian bones, 411, 412, 416, 417, 418

wound repair
dermal injury, 161-3
embryonic, fibronectin, 38
fibroblasts, 34
scarless, 163

wounds, suicidal, on larynx, 584

wrinkles, on forehead, 468, 486

wrist *See* joints (named), wrist

wrist drop, 829

X

xerostomia, 520

xiphisternum *See* process (or processus), xiphoid

XYZ complexes, 770

Y

yolk sac *See* sac(s), yolk

Z

Z-discs, cardiac muscle, 140(f), 141

zeaxanthin, 693

Zellweger syndrome, 13

zona
  arcuate, of cochlea, 640
  fasciculata, of suprarenal gland, 1200, 1200(f), 1218
  glomerulosa, of suprarenal gland, 1200, 1200(f), 1218
  incerta, 323, 331
  orbicularis, of hip joint, 1387, 1388(f), 1389
  pectinata, of cochlea, 640
  pellucida, 167, 170, 170(f), 1296
  reticularis, of suprarenal gland, 1200, 1200(f)

zone(s)
  active, of synapse, 45
  anal transition, 1157
  antichondrogenic, of developing limb, 902
  articular cartilage, 83
  basement membrane zone (BMZ), of skin, 146, 146(f), 157, 158(f)
  of bone growth, 94, 95
  of calcified cartilage, 94(f), 95
  cellular, of lymph node, 73-4
  cruciate, of hand, 879
  H, of skeletal muscle, 105, 108(f)
  high pressure, of gastro-oesophageal junction, 1114
  intermediate, 363, 364(f), 369, 386
  mantle, 363, 364(f), 369
  marginal, 388
    of neural tube, 363, 363(f), 386
    of retina, 700
    of spleen, 1195
  of neural tube, 363, 363(f)
  nuclear, of retina, 700
  of polarizing activity, 900-1, 900(f)

- of preprogrammed cell death, digit formation, 902
- progress, of limb development, 900
  - states, 900
- proliferative, of bone, 94, 95, 534
- of prostate gland, 1257, 1257(f), 1258(f)
- resting, of bone, 94
- subependymal, 51
- subplate, 386
- subventricular, 386
- transformation, of uterine cervix, 1292, 1292(f)
- transition(al)
  - CNS-PNS, 63
  - of nasopharynx, 563
  - of prostate, 1259
- of tricuspid valve, 966
- ventricular, 369, 375, 386
  - cell cycle, 369
  - internal, 362, 368
  - vascularization, 392
- vermilion, of lips, 467, 487, 488, 602
- of vertebral canal, 717

zonula
- adherens, 6(f), 7, 18
  - of retinal glial cells, 690
- occludens, 6-7, 6(f)

zonules, ciliary, 686
- development, 702

zygapophyses, 716, 732
- development, 768

zygomatic bone, 404, 409, 410(f), 412, 419, 475-6, 529, 538, 656
- orbital surface, 475
- ossification, 476

zygote, cleavage, 168-71, 169(f)

zygotene, 22

zyxin, 15

Instructions for online access

Thank you for your purchase. Please note that your purchase of this Elsevier eBook also includes access to an online version. Please click here (or go to http://ebooks.elsevier.com) to request an activation code and registration instructions in order to gain access to the web version.